Can. J. Chem. Downloaded from www.nrcresearchpress.com by 210.87.254.105 on 09/05/12
For personal use only.

Canadian Journal of Chemistry

Published by THE NATIONAL RESEARCH COUNCIL OF CANADA

VOLUME 47 JANUARY 1, 1969 NUMBER 1

Studies of specifically fluorinated carbohydrates. Part I. Nuclear magnetic resonance studies of hexopyranosyl fluoride derivatives

L. D. HALL[1] AND J. F. MANVILLE[2]

Department of Chemistry, University of British Columbia, Vancouver 8, British Columbia

AND

N. S. BHACCA[3]

Varian Associates, 611 Hansen Way, Palo Alto, California

Received May 14, 1968

A detailed study has been made of both the ^1H and ^{19}F nuclear magnetic resonance (n.m.r.) spectra of a series of hexopyranosyl fluoride derivatives. Some of the ^1H spectra were measured at 220 MHz. The ^1H spectral parameters define both the configuration and the conformation of each of these derivatives. Study of the ^{19}F n.m.r. parameters revealed several stereospecific dependencies. The ^{19}F chemical shifts depend upon, (*a*) the orientation of the fluorine substituent with respect to the pyranose ring and, (*b*) the relative orientation of other substituents attached to the ring; for acetoxy substituents, these configurational dependencies appear to be additive. The *vicinal* ^{19}F–^1H coupling constants exhibit a marked angular dependence for which J_{trans} = ca. 24 Hz whilst J_{gauche} = 1.0 to 1.5 Hz for J_{F_a,H_e} and 7.5 to 12.6 Hz for J_{F_e,H_a}. The *geminal* ^{19}F–^1H couplings depend on the orientation of the substituent at C-2; when this substituent is equatorial $J_{F,H}$ is ca. 53.5 Hz and when it is axial the value is ca. 49 Hz.

Canadian Journal of Chemistry, 47, 1 (1969)

Introduction

During the past several years it has become apparent that the determination of the precise conformations of carbohydrate derivatives in solution, by proton magnetic resonance (p.m.r.) spectroscopy, is considerably more complex than was at first appreciated (1). Unfortunately, the confidence limit which can be placed on such determinations has been severely compromised by the lack of any independent, and generally applicable, check upon the accuracy of the p.m.r. method. A further shortcoming of this technique arises from the comparatively low sensitivity of most p.m.r. parameters with respect to changes in steric environment, which precludes the *facile* study of carbohydrate systems which are conformationally mobile.

In principle, these inherent disadvantages of the p.m.r. method could be eliminated if a second "magnetic" nuclear species, were to be included in the molecule under study. Investigation of the nuclear magnetic resonance (n.m.r.) parameters of this second nuclear species could, in principle, afford an independent check on the geometry of the compound under investigation. This second nuclear species could thus be effectively utilized as a "stereospecific probe" and, in the event that its parameters were more sensitive to changes in steric environment than are p.m.r. parameters, it could, in effect, be used as an "amplifier" for studying conformational distortions and mobilities which might otherwise be overlooked in a p.m.r. study.

For a variety of reasons, fluorine is an obvious choice for this second nuclear species. Thus, the natural abundance of the magnetic ^{19}F isotope

---

[1]All correspondence should be addressed to this author.

[2]Recipient of a MacMillan, Bloedel and Powell River Scholarship, 1965–1966 and a NRCC Studentship, 1966–1967. Present address: Forest Products Laboratory, S.W. Marine Drive, Vancouver 8, British Columbia.

[3]Present address: Department of Chemistry, Louisiana State University, Baton Rouge, Louisiana 70803.

Can. J. Chem. Downloaded from www.nrcresearchpress.com by 210.87.254.105 on 09/05/12
For personal use only.

(spin $\frac{1}{2}$) is 100% and its n.m.r. signals can be readily determined by essentially the same high-resolution techniques as are conventionally used for protons,[4] and with approximately the same sensitivity.

More important from the conformational viewpoint, is the fact that certain ^{19}F nuclear magnetic resonance (^{19}F n.m.r.) parameters are known to be extremely sensitive to the precise steric environment of the fluorine substituent under investigation. Illustration of this point with respect to the chemical shifts of fluorine attached to a six-membered ring system, follows from a comparison of the chemical shift separation (at low temperatures) between the axial and the equatorial proton resonances (δ_{ae}) of cyclohexane (0.47 p.p.m.) (2, 3), with the separation of the corresponding fluorine resonances of perfluorocyclohexane (18.2 p.p.m.) (4); thus for these two derivatives the ^{19}F shifts are ca. 40 times more sensitive than the proton shifts. Similarly, for cyclohexyl fluoride, Bovey *et al.* (5) showed that the δ_{ae} value for the H-1 resonances is only 0.46 p.p.m. whereas the δ_{ae} value for the F_1 resonances is 20.5 p.p.m. Thus, the fluorine chemical shift is ca. 45 times more sensitive to steric environment than is the shift of the proton attached to the *same* carbon. For many systems, the measurement of ^{19}F shifts at 94 MHz is equivalent, in terms of the "steric-sensitivity" to the measurement of ^{1}H shifts with a spectrometer operating at ca. 4000 MHz. Roberts and coworkers (6) have recently used this high steric sensitivity of ^{19}F n.m.r. shifts to facilitate the study of conformationally mobile 1,1-difluorocycloalkanes.

Although fluorine was an obvious choice for this "stereospecific probe" for studying the conformations of carbohydrate derivatives, its selection at the time we initiated these studies[5] created several attendant problems. The first of these was that only two classes of specifically fluorinated sugars were known at that time; these contained either a fluorine substituent at the terminal carbon atom, the so-called "primary" fluorides (8, 9) or a fluorine substituent attached to the anomeric carbon, the glycopyranosyl fluorides (10, 11). The second problem was that very little was known at that time of the precise angular and other dependencies of ^{19}F n.m.r. parameters.

The aim of the present study was an investigation of the stereospecific dependencies of ^{19}F n.m.r. parameters, with particular emphasis on the behavior of fluorine attached to six-membered ring systems. The glycopyranosyl fluorides were, for several reasons, chosen as model systems for these studies. Firstly, because a large variety of derivatives were readily available through either of two stereoselective routes, which had originally been studied by Brauns (10) and reviewed recently by Micheel and Klemer (11), and secondly because the configurations of these derivatives were predictable within certain limits and could be readily checked by the p.m.r. method. Finally, these derivatives each contain only one fluorine substituent and, therefore, simple ^{19}F n.m.r. spectra could be anticipated.

Results and Discussion

The glycopyranosyl fluoride derivatives were prepared by standard literature procedures, or were kindly donated to us by Dr. Christian Pedersen (12, and references listed in the Experimental). Originally, the anomeric configurations of these derivatives had been assigned on the basis of the method used for their synthesis, and by comparisons of optical rotations. The first stage of the present investigation involved a detailed study of the p.m.r. spectra of these derivatives which confirmed, in every case, the previously assigned anomeric configuration; this also established that the anhydrous HF, which had been used in several of the syntheses, had caused no configurational changes elsewhere in the molecule. Furthermore, the p.m.r. parameters showed that, to a first approximation, these derivatives all existed in the anticipated conformations. Details of the method used to assign these spectra are given in the Experimental section.

The fluorides ((**1**) and (**3**)) obtained from D-glucopyranose pentaacetate can be used to illustrate this aspect of the study. The observation of a 2.7 Hz coupling between H-1 and H-2 in the spectrum (See Figs. 1*a*, 2*a*) of the product obtained by reaction of the above pentaacetate with

[4]For a static magnetic field of 23,500 G, ^{1}H resonates at 100.000 MHz and ^{19}F at 94.071 MHz.

[5]These studies were started in 1964. Preliminary accounts were presented at the 3rd International Fluorine Symposium, Munich, Germany, August 30 to September 2, 1965 and at the 153rd meeting of the American Chemical Society, Miami Beach, Florida, April 9–14, 1967 (see also ref. (7)).

Can. J. Chem. Downloaded from www.nrcresearchpress.com by 210.87.254.105 on 09/05/12
For personal use only.

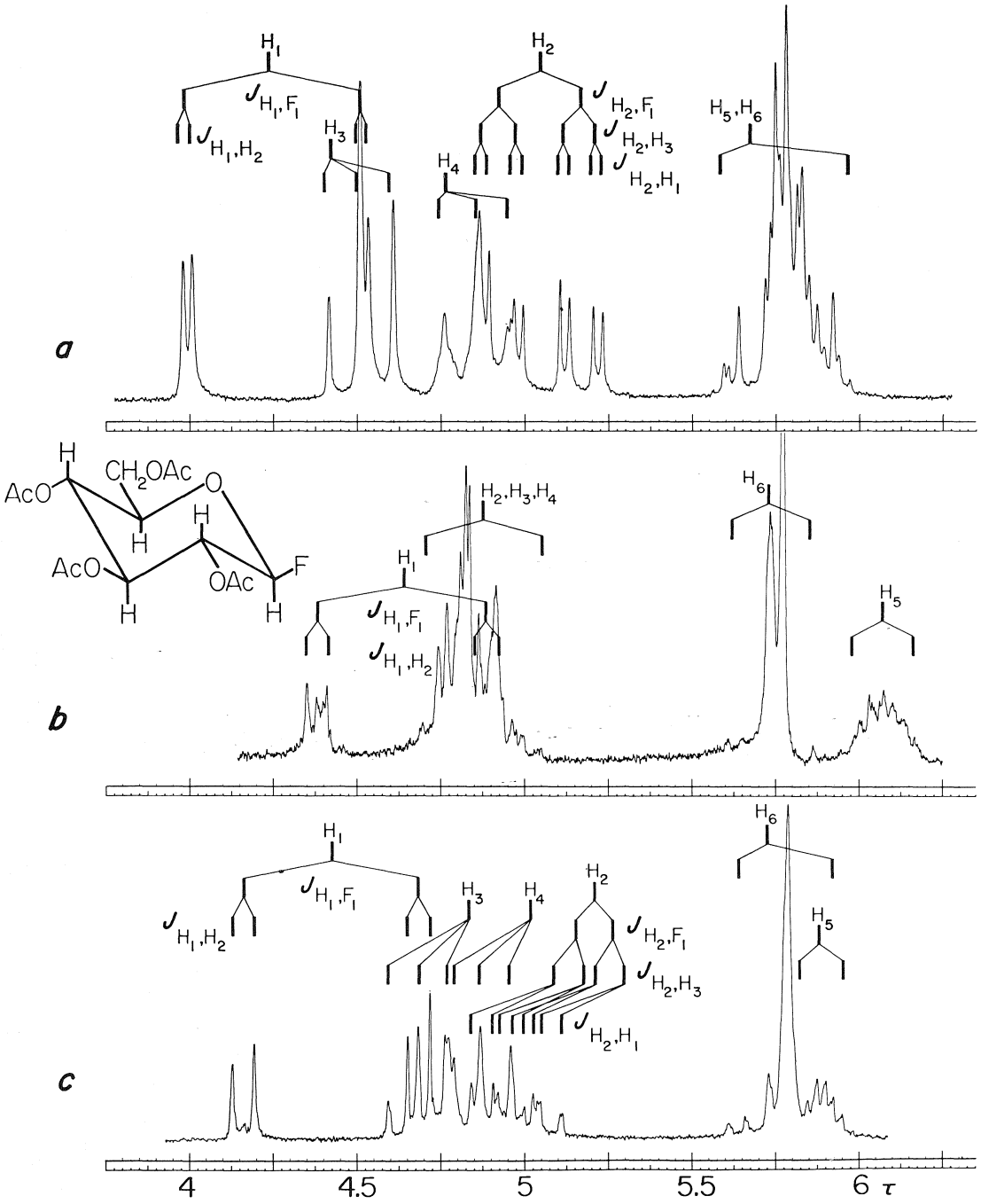

FIG. 1. Partial 100 MHz proton magnetic resonance spectrum of : (*a*), α-D-glucopyranosyl fluoride tetraacetate (**1**) in $CDCl_3$ solution; (*b*), β-D-glucopyranosyl fluoride tetraacetate (**3**) in $CDCl_3$ solution; (*c*), derivative (**3**) in $(CD_3)_2CO$ solution. The first-order assignments are depicted above the spectra.

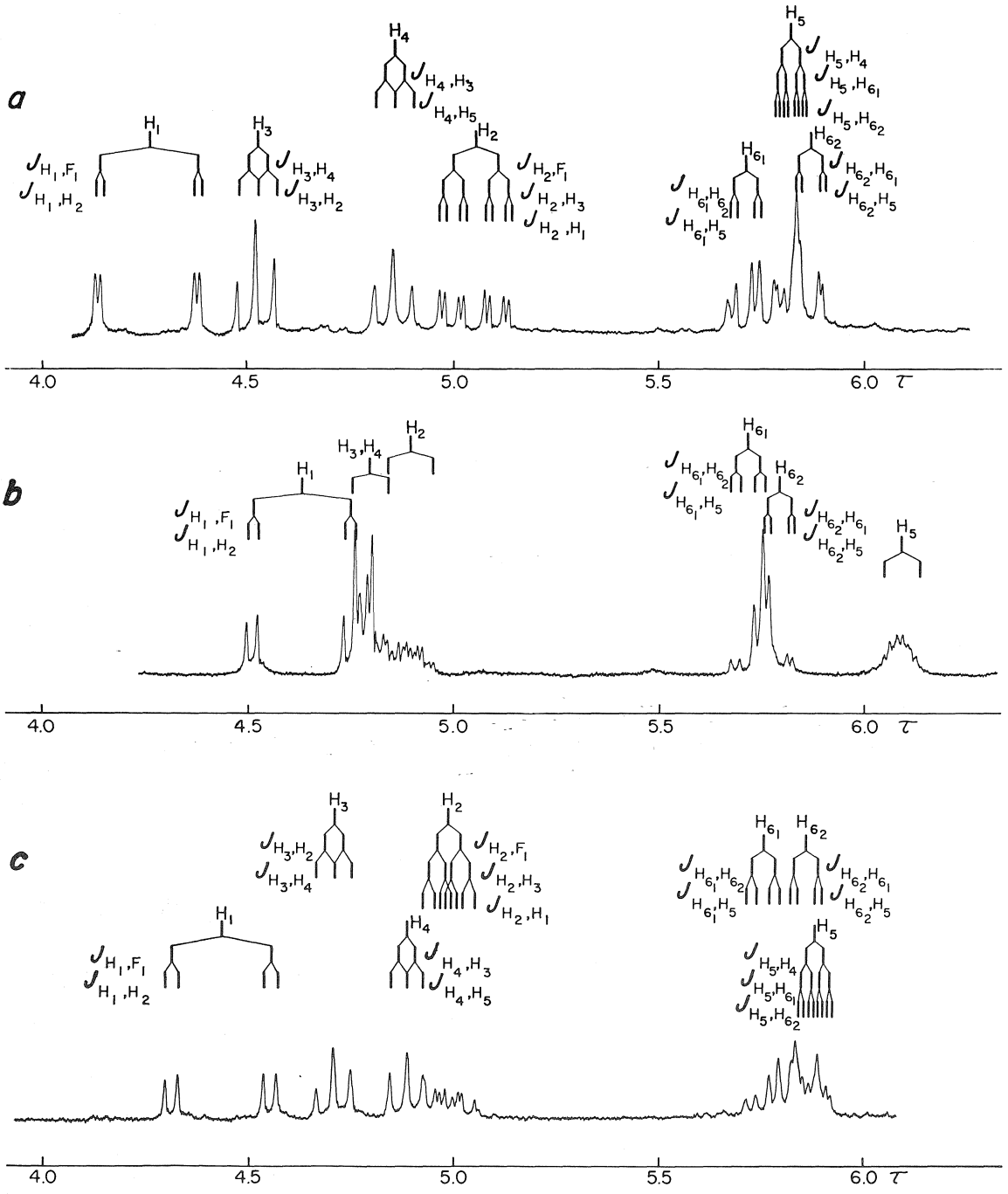

FIG. 2. Partial 220 MHz proton magnetic resonance spectrum of : (*a*), α-D-glucopyranosyl fluoride tetraacetate (**1**) in $CDCl_3$ solution; (*b*), β-D-glucopyranosyl fluoride tetraacetate (**3**) in $CDCl_3$ solution; (*c*), derivative (**3**) in $(CD_3)_2CO$ solution. The first-order assignments are depicted above the spectra.

Can. J. Chem. Downloaded from www.nrcresearchpress.com by 210.87.254.105 on 09/05/12
For personal use only.

Can. J. Chem. Downloaded from www.nrcresearchpress.com by 210.87.254.105 on 09/05/12
For personal use only.

HF, immediately confirms that these protons have a *gauche* relationship. This, together with the additional observation of large (ca. 9.5 Hz) ^1H–^1H couplings between each of the remaining pairs of *vicinal* protons shows unequivocally that this compound has the α-D-*gluco*-configuration; it also shows that the compound has a shape approximating the $^4C_1$ (D) conformation.[6] A similar interpretation of the spectrum of the fluoride obtained from α-D-glucopyranosyl bromide tetraacetate by AgF exchange, which shows large couplings between each of the pairs of *vicinal* ring protons, confirms that this derivative has the β-D-*gluco*- configuration (Figs. 1*b*, 2*b*, 1*c*, 2*c*). The conformation of this derivative will be discussed subsequently; for the present we shall assume that it also has the $^4C_1$ (D) conformation. The first-order parameters obtained for these and the other derivatives studied in this paper are listed in Tables I and II.

For compounds having an equatorially oriented hydrogen atom at C-2, it was not possible to assign the anomeric configuration solely on the basis of the H_1–H_2 coupling, since this proton would be *gauche* to both the fluorine and proton at C-1. However, the shift of the H-5, and in some instances the H-3 resonance could be related to an α- rather than a β-configuration. Furthermore, it was subsequently found that whilst the ^{19}F shifts of the α-anomers (**1**, **15**) were essentially temperature invariant, those of the β-anomers (**3**, **8**, **14**) were subject to large (4 to 8 p.p.m.) shifts for a temperature change from 190 °K to 330 °K (*vide infra*). On the basis of the data listed in the Tables it was felt that the structures and approximate conformations of the derivatives under investigation were known with some certainty, and at this point the ^{19}F n.m.r. parameters were considered.

Measurement of the ^{19}F n.m.r. spectra (for example, see Fig. 3) gave directly the ^{19}F–^1H couplings and also the ^{19}F chemical shifts, from which stereospecific dependencies of ^{19}F n.m.r. parameters were to be derived. In most instances there was no discrepancy between the magnitudes of the ^{19}F–^1H couplings derived from the ^1H and the ^{19}F spectra. For those compounds (**1**, **2**, **5**, **7**, **9**, **11**, **13**, **19**) which possess a *trans-diaxial* arrangement of fluorine at C-1 and hydrogen at C-2, a ^{19}F–^1H coupling of ca. 24 Hz is observed. This coupling was found to be essentially unaltered when the C-2 substituent was either OAc, OBz, OMe, or OH and is approximately 4 times larger than those *trans-diaxial* ^1H–^1H couplings observed as $J_{1,2}$ of the β-D-hexopyranosyl fluoride derivatives.

The magnitudes of *vicinal* ^{19}F–^1H couplings corresponding to a *gauche* relationship were found to fall in two distinct ranges which appear to reflect a "configurational" electronegativity dependence for such couplings, thus: (*a*) for compounds with an axial fluorine at C-1 and an equatorial proton at C-2 (compounds **15**, **16**, **17**, **18**) the coupling is 1.0–1.5 Hz. (*b*) for compounds with an equatorial fluorine at C-1, and an axial proton at C-2 (compounds **3**, **4**, **6**, **8**, **10**, **12**, **14**, **20**) the coupling is 7.5–12.6 Hz.

A similar configurational dependence has also been observed previously for ^1H–^1H couplings of pyranose carbohydrates (14, 27), steroidal alcohols (15) and claimed for other cyclic systems (16) and is also observed for the ^1H–^1H couplings of the derivatives under consideration. Thus, for derivatives (**15**, **17**, **18**) in which both H-1 and H-2 are equatorially oriented, the coupling is ca. 1.5 Hz, whereas, for derivatives (**1**, **5**, **7**, **9**, **11**, **13**, **19**) in which H-2 is axial, the coupling is ca. 2.7 Hz. On the basis of Booth's electronegativity hypothesis (16) the smaller magnitude of the couplings of the compounds in group (*a*) above compared with those in group (*b*), would be rationalized in terms of the anti-planar relationships (shown in **A**) of the O_2—C_2, C_1—F_1 and O_5—C_1, C_2—H_2 bonds; these anti-planar interactions are not present for the compounds in group (*b*) (shown in **B**).

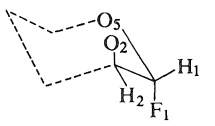

A

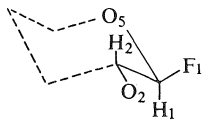

B

In spite of the rather wide range of *vicinal* ^{19}F–^1H couplings observed for the *gauche*

[6]The convention adopted for identification of the two possible chair conformations, is based on the suggestion of Hall (13); any four atoms of a pyranose ring system are used to define a reference plane and then the remaining atoms are indicated as superscript if they are "above" that plane or as a subscript if they are "below". Thus the "normal" chair conformation (C1-D) is referred to as $^4C_1$ indicating that C-4 is above and C-1 below the plane defined by C-2, C-3, C-5, and O-5. On this basis the (1C-D) conformation is $^1C_4$(D).

Can. J. Chem. Downloaded from www.nrcresearchpress.com by 210.87.254.105 on 09/05/12
For personal use only.

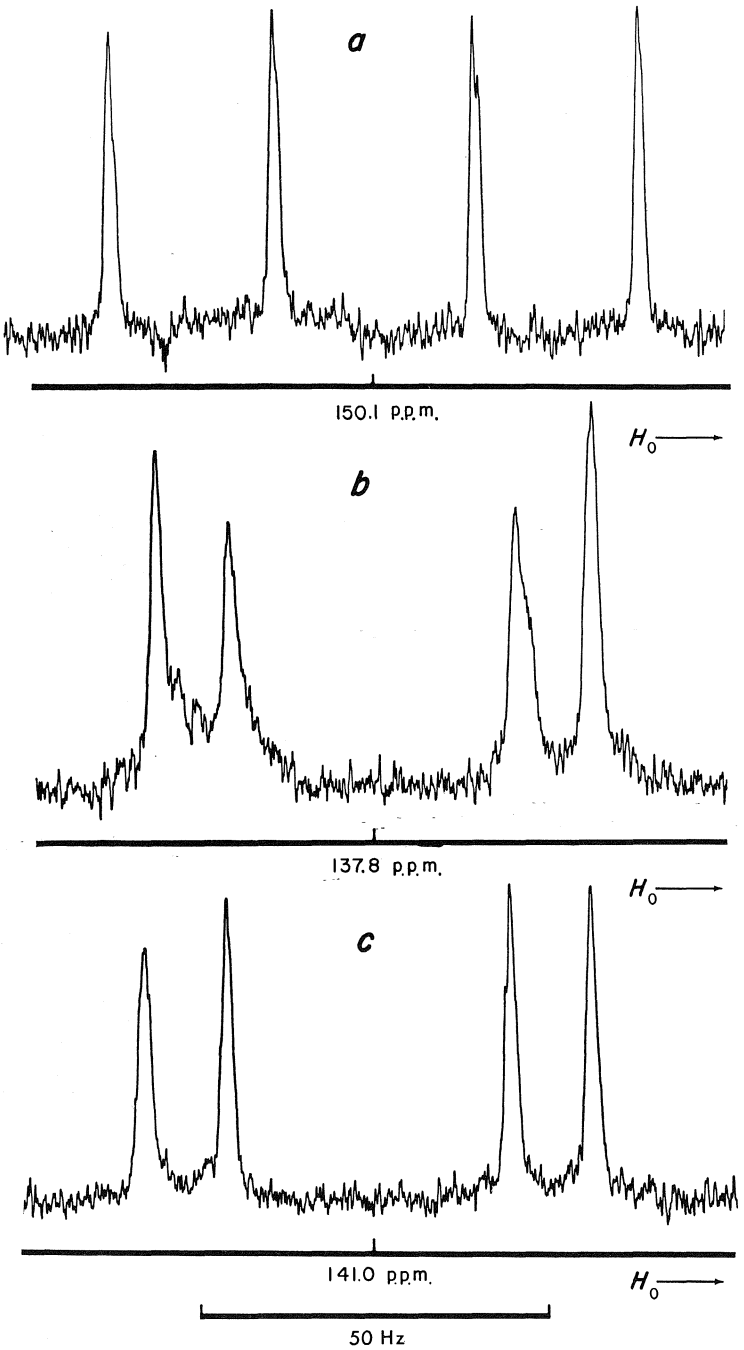

FIG. 3. ^{19}F Nuclear magnetic resonance spectrum of : (*a*), α-D-glucopyranosyl fluoride tetraacetate (**1**) in $CDCl_3$ solution; (*b*), β-D-glucopyranosyl fluoride tetraacetate (**3**) in $CDCl_3$ solution; (*c*), derivative (**3**) in $(CD_3)_2CO$ solution.

Can. J. Chem. Downloaded from www.nrcresearchpress.com by 210.87.254.105 on 09/05/12
For personal use only.

TABLE I

First-order chemical shifts (τ values, ϕ values) of the fully *O*-acylated hexopyranosyl fluorides

	Compound			H-1	H-2	H-3	H-4	H-5	H-6$_1$	H-6$_2$	—OAc				F
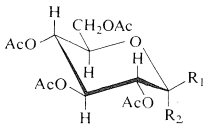			*c*	4.26	5.06	4.52	4.86	5.82[d]	5.72[d]	5.88	7.90	7.90	7.98	7.98	149.9
	1	α	*a*	4.23	5.02	4.57	4.85	—	5.80	—	7.96	7.99	8.00	8.04	149.5
			b	4.41	5.07	4.36	4.74	5.77	— 6.01 —		8.25	8.28	8.30	8.36	149.5
			c	4.60[d]	4.88[d]	— 4.80 —		6.08	5.70	5.78[d]	7.89	7.89	7.95	7.95	137.8
	3	β	*a*	~4.4	4.98	4.68	4.85	~5.9	— 5.8 —		7.97	7.98	8.00	8.04	141.0
			b	4.96	—	4.81	—	6.52	5.79	5.98	8.25	8.28	8.28	8.30	138.5
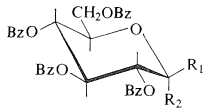			*c*	3.97	4.58	3.78	4.19	—	5.42	—					149.6
	5	α	*a*	3.81	4.36	3.77	4.01	5.20	5.26	5.42					148.6
			b	4.15	4.56	3.55	4.07	—	5.55	—					148.7
			c	4.26	4.35	— 4.10 —		—	5.40	—					134.8
	6	β	*a*	3.98	4.37	3.91	4.11	—	5.30	—					139.7
			b	4.74	4.25	3.77	4.16	6.13	5.38	5.60					136.4
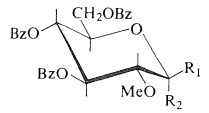			*c*	4.16	6.35	4.05	4.37	5.47	5.36	5.58					149.9
	7	α	*a*	3.97	6.10	4.12	4.32	—	5.44	—					149.9
			b	4.58	6.88	3.86	4.24	5.75[g]	5.42	5.75[g]					149.1
			c	4.52	6.38	4.30	4.39	5.75	5.35	5.55					135.2
	8	β	*a*	4.37	6.29	— 4.32 —		—	5.45	—					137.9
			b	4.96	6.74	4.22	4.35	6.43	5.45	5.70					136.2
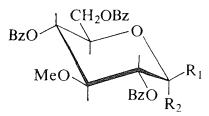			*c*	4.10	4.79	5.88	4.43	—	5.5	—					149.9
	9	α	*a*	4.04	4.77	5.80	4.30	—	5.5	—					148.6
			b	4.30	4.78	6.00	4.37	5.68[g]	5.45	5.68[g]					148.8
			c	4.37	4.55	6.10	4.40	5.65	5.38	5.45					131.8
	10	β	*a*	4.19	4.59	5.83	4.37	5.50	— 5.69 —						136.3
			b	5.20	4.55	6.35	4.61	5.92	5.32	5.52					131.2
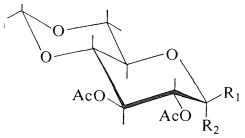			*c*	4.28	5.03	4.40	5.6	—	—	6.4		7.97	7.97		147.8
	11	α	*a*	4.35	5.12	4.57	5.7	—	—	6.4		7.96	8.00		147.5
			b	4.47	5.04	4.19	5.8	—	—	6.8		8.33	8.35		146.9
			c	4.60	4.94	4.75	5.4	—	—	6.4		7.93	7.94		134.7
	12	β	*a*	4.45	4.98	4.66	5.5	—	—	6.4		7.99	8.05		138.1
			b	4.95	— 4.70 —		5.9	—	—	6.8		8.32	8.34		134.6
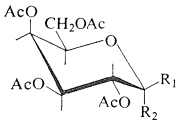			*c*	4.20	4.82	4.68	4.48	5.55	5.79	5.92	7.86	7.91	7.97	8.03	151.1
	13	α	*a*	4.17	4.84	4.63	4.47	5.47	5.79	5.91	7.87	7.94	8.01	8.06	150.5
			b	4.18	4.73	4.50	4.45	5.66	5.82	5.94	8.27	8.34	8.34	8.35	150.1
			c	4.72	4.69	4.93	4.58	—	5.8	—	7.85	7.93	7.97	8.03	142.$\frac{4}{9}$
	14	β	*a*	4.50	— 4.8 —		4.59	5.62	5.76	5.89	7.86	7.95	8.01	8.07	142.$\frac{4}{9}$
			b	4.94	4.45	4.91	4.59	6.31	— 5.85 —		8.24	8.24	8.27	8.27	141.$\frac{9}{9}$
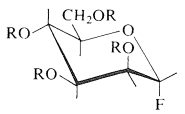			*c*	4.43	—	4.65	—	—	5.80	—	7.83	7.89	7.94	8.00	138.8
	15	α	*a*	4.34	4.74	— 4.66 —		—	5.82	—	7.87	7.96	7.97	8.05	138.2
	R = OAc		*b*	4.66	— 4.54 —		4.47	5.96[g]	5.72	5.96[g]	8.21	8.24	8.24	8.30	137.9
			c	4.16	4.14	4.10	3.78	5.39	5.23	5.51					138.7
	17	α	*a*	3.97	4.07	4.13	3.74	—	5.3	—					138.1
	R = OBz		*b*	4.58	4.04	3.99	3.55	5.44	— 5.75 —						137.7
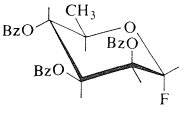			*c*	4.21	—	4.20	—	5.61				τCH$_3$, 8.57			137.6
	18[f]	α	*a*	4.04	—	4.20	—	5.54				τCH$_3$, 8.60			137.2
			b	4.50	—	4.01	—	5.76				τCH$_3$, 8.78			136.8
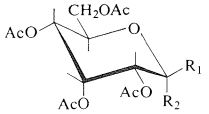			*c*	4.35	5.01	4.32	4.95	5.57	— 5.7 —		7.86	7.97	7.97	8.00	146.0
	19	α	*a*	4.29	4.95	4.31	4.94	5.57	— 5.8 —		7.91	7.98	7.98	8.02	145.0
			b	4.45	5.21	4.68	4.88	6.00	— 5.8 —		8.18	8.25	8.25	8.31	145.5
			c	4.45	5.01	4.31	4.92	—	5.7	—	7.86	7.94	7.91	7.99	146.6
	20	β	*a*	4.34	4.93	4.32	4.96	5.63	— 5.75 —		7.89	7.99	7.99	8.04	146.6
			b	4.59	4.93	4.62	4.95	6.04	— 5.8 —		8.31	8.39	8.31	8.39	146.3

NOTE: The compounds listed above were each measured in chloroform-*d* (*c*), acetone-d_6 (*a*), and benzene-d_6 (*b*) solution. The benzoate ester protons resonated at ., τ 2 and ca. τ 2.5. The methine proton of the benzylidene substituent was observed at ca τ 4.5, whilst the aromatic protons were observed at ca. τ 2.5. The methyl her protons resonated at ca. 6.5, (*d*) measured at 220 MHz in chloroform-*d* solution; (*e*) measured at 220 MHz in acetone-d_6 solution. R_1 = H, R_2 = F for anomers and R_1 = F, R_2 = H for β-anomers. [f]This compound was the L-enantiomer. [g]Overlapping resonances.

Can. J. Chem. Downloaded from www.nrcresearchpress.com by 210.87.254.105 on 09/05/12
For personal use only.

TABLE II

First-order coupling constants of the fully *O*-acylated hexopyranosyl fluorides (Hz)

Compound			$J_{1,2}$	$J_{2,3}$	$J_{3,4}$	$J_{4,5}$	$J_{5,6_1}$	$J_{5,6_2}$	$J_{6_1,6_2}$	J_{5,CH_3}	$J_{1,F}$	$J_{2,F}$
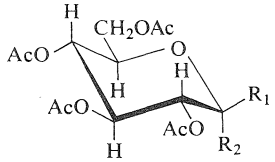		*c*	2.7	10.0	9.5	9.7	4.2[d]	2.0[d]	12.7[d]		52.8	23.8
1	α	*a*	2.9	9.9	9.3	9.3	—	—	—		53.0	24.1
		b	2.8	10.0	9.5	9.6	5.2	—	12.7		52.9	23.9
		c	6.6	—	—	—	5.0[d]	3.0[d]	12.8[d]		52.5	12.0
3	β	*a*	6.6	9.0[e]	9.0[e]	9.4[e]	—	—	—		52.6	12.0
		b	~7	—	—	—	5.0	2.7	12.2		~53	~9
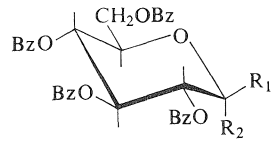		*c*	2.8	10.0	10.0	9.7	—	—	—		52.6	23.6
5	α	*a*	2.8	9.6	9.6	9.5	4.5	2.6	12.2		53.2	23.7
		b	2.9	10.0	10.0	9.5	—	—	—		53.0	23.6
		c	5.4	—	—	—	—	—	—		52.5	8.0
6	β	*a*	6.4	~8.5	~8.5	~8.5	—	—	—		51.2	12.0
		b	5.7	8.6	8.6	8.6	5.0	3.6	11.9		51.5	10.3
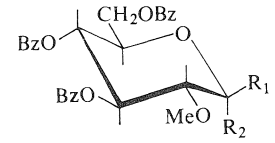		*c*	2.7	9.6	9.6	9.6	—	—	—		52.0	24.3
7	α	*a*	2.7	9.6	9.6	9.6	—	—	—		52.5	25.0
		b	2.6	9.7	9.7	9.7	4.3	3.7	12.6		52.2	24.3
		c	6.0	7.8	8.5	8.5	5.0	3.6	12.3		52.4	10.4
8	β	*a*	6.3	—	—	—	—	—	—		52.8	11.5
		b	6.0	8.0	~9	~9	5.0	3.0	12.2		52.3	11.0
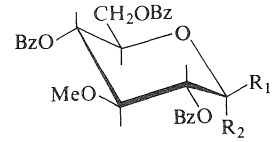		*c*	2.8	9.5	9.5	9.5	—	—	—		53.4	24.2
9	α	*a*	2.6	9.5	9.5	9.5	—	—	—		53.4	24.1
		b	2.7	9.5	9.5	9.5	—	—	—		53.4	24.3
		c	4.5	6.0	7.5	7.5	5.0	5.0	12.0		51.2	7.5
10	β	*a*	6.0	7.8	8.3	8.3	—	—	—		51.8	11.1
		b	4.7	6.4	6.4	6.5	5.2	5.3	12.0		53.5	8.0
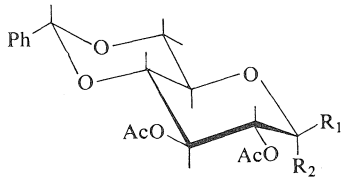		*c*	3.0	9.8	9.7	—	—	—	—		53.1	24.3
11	α	*a*	3.0	9.8	9.4	—	—	—	—		53.0	24.6
		b	3.0	9.9	9.9	—	—	—	—		53.0	24.4
		c	5.2	6.2	8.0	—	—	—	—		52.6	10.2
12	β	*a*	6.2	7.8	8.8	—	—	—	—		53.4	11.6
		b	5.8	—	—	—	—	—	—		~52	~10

Can. J. Chem. Downloaded from www.nrcresearchpress.com by 210.87.254.105 on 09/05/12
For personal use only.

TABLE II (*concluded*)

Compound				$J_{1,2}$	$J_{2,3}$	$J_{3,4}$	$J_{4,5}$	$J_{5,6_1}$	$J_{5,6_2}$	$J_{6_1,6_2}$	J_{5,CH_3}	$J_{1,F}$	$J_{2,F}$
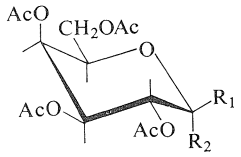	**13**	α	*c*	2.7	11.0	—	2.0	5.8	7.0	11.0		53.0	22.2
			a	2.8	10.8	2.3	1.8	5.5	7.3	10.7		53.0	21.7
			b	2.8	10.0	—	1.8	5.1	7.3	10.8		53.0	21.8
	14	β	*c*	6.6	10.0	3.4	~3	—	—	—		53.8	10.0
			a	7.4	—	—	1.3	4.9	8.0	11.4		~52	~12.5
			b	7.0	10.3	3.4	~2	—	—	—		52.0	12.6
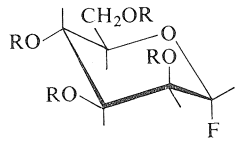	**15**	α	*c*	1.7	—	9.5	9.5	4.5	3.6	13.0		48.6	~1.5
			a	1.8	—	10.0	10.0	—	—	—		48.5	~1.5
	R = OAc		*b*	1.5	—	10.0	10.0	—	—	—		48.1	~1.5
			c	1.5	—	—	—	—	—	—		~49	—
	17	α	*a*	1.5	—	—	—	—	—	—		49.0	1.1
	R = OBz		*b*	1.1	—	9.5	9.5	4.9	2.0	12.5		48.5	~1
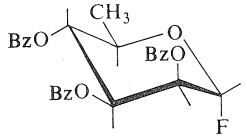	**18**[f]	α	*c*	~1	—	—	8.1				6.0	~49.0	1.0
			a	~1.5	—	—	~9				6.1	48.5	—
			b	1.5	—	—	—				6.1	48.4	—
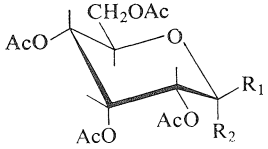	**19**	α	*c*	3.0	3.1	3.1	10.6	—	—	—		53.4	26.1
			a	3.0	3.1	3.1	10.4	—	—	—		53.4	26.3
			b	3.2	3.2	3.0	10.2	4.6	2.3	—		53.5	26.0
	20[g]	β	*c*	7.3	3.0	3.0	9	—	—	—		53.0	11.9
			a	7.4	3.0	3.0	9.2	—	—	—		53.4	12.0
			b	7.3	2.8	2.8	9.5	—	—	—		52.7	12.0

NOTE: The compounds listed above were each measured in chloroform-*d* (*d*), acetone-d_6 (*a*), and benzene-d_6 (*b*) solution. (*d*) measured at 220 MHz in chloroform-*d* solution; (*e*) measured at 220 MHz in acetone-d_6 solution. R_1 = H, R_2 = F for α-anomers and R_1 = F, R_2 = H for β-anomers. [f]This compound was the L-enantiomer. [g]The value of $J_{3,F}$ for this compound is +3.7 Hz.

Can. J. Chem. Downloaded from www.nrcresearchpress.com by 210.87.254.105 on 09/05/12
For personal use only.

relationships, it is noteworthy that those ^{19}F–^{1}H couplings corresponding to a *nominal* dihedral angle of ca. 180° are larger than those which correspond to a dihedral angle of ca. 60°. This angular dependence appears to be similar to that described by Karplus (17) for *vicinal* ^{1}H–^{1}H couplings. Furthermore, the ^{19}F–^{1}H couplings are several times greater in magnitude than the corresponding ^{1}H–^{1}H couplings, and are thus apt to be more sensitive, (absolutely) to changes in dihedral angle. This may prove to be one of the advantages of using ^{19}F n.m.r. spectroscopy for studying conformational distortions of cyclic systems. Other results from this (18) and other laboratories (19–22) further support the suggestion that *vicinal* ^{19}F–^{1}H and ^{1}H–^{1}H couplings exhibit a fundamentally similar angular dependence.

All of the derivatives showed a *geminal* coupling of ca. 50 Hz; however, there are clearly two distinct ranges for these couplings. For those molecules with an equatorial substituent at C-2, the *geminal* coupling is ca. 53.5 Hz, whereas, when the C-2 substituent is axially oriented, this coupling has a value of ca. 49 Hz. Again these couplings are *nominally* ca. 4 times those found for ^{1}H–^{1}H *geminal* couplings (23) in similar environments. A detailed discussion of these coupling constant dependencies will be reserved for a subsequent paper in this series.

Inspection of the ^{19}F chemical shifts obtained from the ^{19}F n.m.r. spectra (Table I) revealed several marked stereospecific dependencies and it is convenient to consider initially only those derivatives having equatorially oriented substituents (D-*gluco*-series). For such derivatives, a fluorine substituent having an equatorial orientation (**3**, **6**, **8**, **10**, **12**, **14**, **20**) has a shift within the range[7] ϕ_c +131.8 to ϕ_c +137.8, whilst for a corresponding axially oriented fluorine, the shift is ϕ_c +147.8 to ϕ_c +149.9 p.p.m. On this basis there is an average ^{19}F chemical shift difference of ca. 14 p.p.m. between the resonances of an axial and an equatorial fluorine substituent and in every case the equatorial fluorine gives a resonance to low field of its axial counterpart. This dependence thus parallels that already recognized for the p.m.r. shifts of anomeric (25, 26) and other ring proton (26) and indeed, for the anomeric proton shifts of the derivatives under discussion. The ^{19}F n.m.r. shifts of compounds in this class show a slight dependence upon the nature of the various *O*-substituents attached to the pyranose ring, at least when these are acetate, benzoate or methyl. Compare for example, the shifts of **1** and **3** which have acetoxy substituents at C-2 with the shifts of **9** and **10** which have a benzoyloxy substituent and **7** and **8** which have a methoxy substituent. When the non-acylated glucopyranosyl fluorides were measured in aqueous solutions with external Freon-11 as reference, the shift of the α-anomer (**2**) was found to be essentially unaltered from that of the fully acetylated derivative **1**, whereas, the shift of β-D-glucopyranosyl fluoride (**4**) came at significantly higher field (+8.1 p.p.m.) than that of derivative **3**. Thus, for all compounds having only equatorial oriented substituents, the ^{19}F chemical shift provides a convenient and unequivocal means for identifying the orientation of the fluorine substituent with respect to the pyranose ring.

A striking dependence of ^{19}F chemical shift on changes in the configuration of remote centers is noted when one considers that chemical shift of those *derivatives* possessing an axial *O*-substituent at C-2 (**15**, **17**, **18**) i.e. having typically the D-*manno* configuration. The shift of these derivatives, which also possess an axial fluorine at C-1, fall[8] within the range ϕ_c +137.6 to +138.8 which coincides with the range previously observed for the β-D-glucopyranosyl fluorides (**3**, **6**, **8**, **10**, **12**). There are two possible rationales for this observation; either, that all of the compounds in this group do not possess the α-D-configuration, or, that *fluorine chemical shifts are extremely sensi-*

[7]The ranges quoted are for chloroform solutions with ca. 20% $CFCl_3$ as internal reference (24) and are referred to as "ϕ_c" values. The ^{19}F chemical shifts are somewhat concentration dependent and also vary with solvent to a small extent, thus they are only quoted to four significant figures although they were measured to at least five significant figures. The concentration shift was greatest for the fully *O*-acetylated glucose derivatives (**1**) and (**3**). The shift of the α-anomer (**1**) varied by only 0.2 p.p.m. over a concentration range of 1.0–0.0 molal, whereas, that of the β-anomer (**3**) varied by 0.9 p.p.m. over the same concentration range.

[8]The shift of α-D-mannopyranosyl fluoride (**16**), measured in aqueous solution with external Freon-11 as reference, was found to be essentially the same as that of the tetraacetate. This result parallels that already found for the α-D-gluco derivatives (**1**, **2**). If this invariance of chemical shift is general for all *axially* oriented fluorine substituents, it may serve as a convenient method for establishing anomeric configurations of hexopyranosyl fluorides.

Can. J. Chem. Downloaded from www.nrcresearchpress.com by 210.87.254.105 on 09/05/12
For personal use only.

tive to the relative orientation of the substituent attached to the adjacent center. The latter explanation seemed the more appropriate; however, at the time of this study it had no precedent in the field of ^{19}F n.m.r. spectroscopy, although it had a counterpart in the carbohydrate p.m.r. field (25, 26) where it has been shown that changes in the orientation of a C—O bond can influence the shifts of protons at "remote" centers.

Further unpublished ^{19}F n.m.r. studies in this laboratory on sugars fluorinated at C-2 (18*b*) and C-3 (18*c*), together with specifically fluorinated cyclohexanes (18*d*) and published data from other fluorinated systems (22) have all confirmed the generality of the particular stereospecific shift outlined above.

The two D-galactopyranosyl fluorides (**8** and **14**) also exhibit the same general dependence as the D-*gluco* derivatives; however, the inherent axial:equatorial shift difference for these derivatives is only 8.7 p.p.m. Comparison of the chemical shift of **13** and **14** with those of the corresponding D-*gluco* derivatives (**1** and **3**) shows that inversion of an acetoxy group at C-4 of a pyranose carbohydrate induces an upfield shift on a fluorine atom at the anomeric center.

Measurement of the ^{19}F chemical shift of α-D-allopyranosyl fluoride tetraacetate (**19**) showed that the fluorine of this derivative now resonated to lower field of **1** by 3.9 p.p.m. Since the p.m.r. spectra showed this molecule to have the α-D-configuration, and to possess the $^4C_1$ (D) conformation, the shift to low-field was attributed solely to a deshielding effect of an axial acetoxy substituent on a *cis-axial* fluorine atom. A similar effect is well characterized in the field of p.m.r. spectroscopy (26, 27) and has also been observed for the p.m.r. parameters of the derivatives under consideration. When the ^{19}F chemical shift of the β-anomer (**20**) was measured, it was found to resonate to *higher* field than its axial counterpart by 0.6 p.p.m. Again, the difference between the behavior of these two derivatives and their D-*gluco* counterparts was attributable to a specific chemical shift contribution from the acetoxy substituents. The individual ^{19}F chemical shift changes induced by inversion of an acetoxy substituent from an equatorial to an axial orientation are summarized in Table III.

In order to test the possibility that these configurationally induced chemical shift changes might be strictly additive, an attempt to synthesize α-D-altropyranosyl fluoride tetraacetate and measure its ^{19}F n.m.r. spectrum was undertaken. Unfortunately the reaction resulted in a mixture of the two anomeric fluorides, which could not be separated.[9] Nevertheless the chemical shift of the α-anomer, which was identified by its ^{19}F–^1H coupling $J_{F,H} = 48.3$ Hz, $J_{F,H_2} = 2.7$ Hz was precisely that predicted on the assumption that these induced shift changes are truly additive.

TABLE III

Induced shifts for an axially oriented fluorine substituent, following inversion of a "remote" acetoxy substituent

Compound	Orientation of acetate at C-2	C-3	C-4	ϕ_c	Induced shift p.p.m.
D-*gluco* (**1**)	eq	eq	eq	+149.9	0.0
D-*manno* (**15**)	*ax*	eq	eq	+138.8	−11.1
D-*allo* (**19**)	eq	*ax*	eq	+146.0	−3.9
D-*galacto* (**13**)	eq	eq	*ax*	+151.1	+1.2

Calculated shift (ϕ_c − value) = Shift of α-D-*gluco* (**1**) − Δ(C_2-inversion) − Δ(C_3-inversion)

$$= +149.9 - 11.1 - 3.9 = +134.9$$

Observed Shift $= +134.9$

Deviation 0.0 p.p.m.

On the basis of the empirical "rules", summarized in Table III, for calculating the chemical shift of an axially oriented fluorine atom attached to the anomeric carbon of a pyranose carbohydrate, it is possible to predict the ^{19}F chemical shifts (ϕ_c-values) for the remaining pyranosyl fluorides of rare hexoses; assuming that these all exist exclusively in the $^4C_1$ (D) conformation the calculated values are:

α-D-idopyranosyl fluoride tetraacetate: $\phi_c = +149.9 - 11.1 - 3.9 + 1.2 = +136.1$

α-D-talopyranosyl fluoride tetraacetate: $\phi_c = +149.9 - 11.1 + 1.2 = +140.0$

α-D-gulopyranosyl fluoride tetraacetate: $\phi_c = +149.9 - 3.9 + 1.2 = +147.2$

It is not appropriate at this time to make similar predictions for equatorially oriented fluorine substituents since too small a selection of these

[9]Dr. C. Pedersen (private communication) has also synthesized these derivatives; his samples have also failed to crystallize so far.

Can. J. Chem. Downloaded from www.nrcresearchpress.com by 210.87.254.105 on 09/05/12
For personal use only.

derivatives is at present available and, furthermore, there is the possibility of conformational distortion for these anomers. We are currently investigating the synthesis of the above derivatives.

Whilst the above discussion has been primarily concerned with information associated with the ^{19}F parameters it is convenient to mention at this point, several further aspects which involve some of the ^{1}H parameters.

The *vicinal* ^{1}H–^{1}H couplings of the α-D-*gluco* derivative (**1**) appear to support quite successfully the original assumption that this derivative exists exclusively in the $^{4}C_1$ (D) conformation. Thus $J_{2,3}$ = 10.0 Hz, $J_{3,4}$ = 9.5 Hz, and $J_{4,5}$ = 9.7 Hz which indicates (17) that each of these pairs of protons have a *trans-diaxial* relationship. However, the *vicinal* ^{1}H–^{1}H couplings for the β-D-anomer (**3**) are generally smaller than their counterparts in the α-D-anomer (**1**). A similar behavior is observed for the couplings of each of the other anomeric pairs of D-glucopyranosyl fluorides. If it is accepted that the smaller couplings for the β-anomers are due either to time averaging between the two chair forms ($^{4}C_1 \leftrightarrows {}^{1}C_4$) or to some local or static distortions from the $^{4}C_1$ (D) chair conformation, it is unexpected that D-*gluco* derivatives would show this behavior. All arguments based on "repulsive" non-bonded interactions, would lead one to expect these derivatives, more than any other hexopyranoses, to exist in the "ideal" $^{4}C_1$ (D) chair conformation since this would have all the substituent groups equatorial. It is of further interest to note that those D-*gluco* derivatives (**6**, **10**) with a benzoyloxy substituent at C-2 exhibit the smallest *vicinal* couplings (i.e. the maximum deviation from "normality").

The driving force for either of the above conformational distortions could be the powerful "anomeric effect" (28–30) of the (nominally) equatorially oriented fluorine substituent, which would tend to force this substituent to adopt an *axial* orientation. There would be no necessity for such a distortion for an α-anomer where the fluorine substituent is already axially oriented in the $^{4}C_1$ (D) conformation. Further indication that the β-anomer (**3**) is apparently subject to a conformational mobility, not shown by the α-anomer (**1**) followed the measurement of the ^{19}F shift at different temperatures. In acetone solution, over the range 190 °K to 330 °K, the ^{19}F shift of the α-anomer was essentially invariant, whilst that of the β-anomer changed −8 p.p.m. (+143 to +135 p.p.m.). Over the same temperature range, the ^{1}H spectra of the α-anomer showed *only* minor chemical shift changes, whilst for the β-anomer, the *vicinal* couplings *increased* by ca. 10%. Although this evidence would appear to indicate the occurrence of a $^{4}C_1 \leftrightarrows {}^{1}C_4$ inversion process for the β-anomer, it was not possible to lower the temperature sufficiently to stop this inversion. This was unexpected, and bothersome, since the energy barrier for the above chair–chair interconversion was expected to be of the order of 10 Kcal/mole (2–6, 31).

The 4,6-*O*-benzylidene derivatives (**11**) and (**12**) were examined; they each have two *trans*-fused six-membered rings and should, by analogy with the *trans*-decalin system (6, 32), be incapable of undergoing a gross, chair–chair conformational inversion. In particular the pyranose ring of these derivatives should be locked in the $^{4}C_1$ (D) conformation. It was evident even before the low temperature spectra were run, that this anticipation was not entirely correct since the *vicinal* ^{1}H–^{1}H couplings of the β-anomer (**12**) were again significantly smaller than those of the α-anomer (**11**). The low temperature spectra indicated that these benzylidene derivatives had nearly the same characteristics as the parent glucosyl fluorides. However, the temperature-induced shift change of the β-anomer was smaller ($\Delta\ ^{19}F$ = 3.5 p.p.m.) than that of **3** ($\Delta\ ^{19}F$ = 8 p.p.m.).

It is known (33) that some ^{19}F shifts are *per se* temperature dependent. However, it seems highly improbable that the shift of an equatorially oriented fluorine substituent should be so markedly temperature dependent, whilst a chemically similar, but axially oriented fluorine should be essentially independent of temperature.

Two possible rationales for the source of this observation remain. The first is that the observed chemical shift dependencies reflect changes in the rotamer populations of the various ester substituents attached to the ring. However, it is difficult to see why such changes should be reflected in the shift of an equatorial, but not of an axial, fluorine substituent; in particular the C_2-acetoxy substituent which is *gauche* with respect to the fluorine substituent for both the α- and the β-series, would seem to be implicitly excluded from such an argument.

If we discount the above rationale, the final

Can. J. Chem. Downloaded from www.nrcresearchpress.com by 210.87.254.105 on 09/05/12
For personal use only.

alternative is that the β-D-anomers suffer a distortion about the O-5,C-1,C-2 region of the pyranose ring, into a conformational symmetry which is capable of undergoing conformational inversion process(es) with a very small activation energy barrier. This would appear to be consistent with all the observations we have made thus far; however, it should be emphasized that no unequivocal evidence to support this suggestion is available at this time. The search for such evidence is to be continued in this laboratory, (*a*) by measuring spectra at ultra-low temperatures (ca. 110 °K) in the hope of "freezing" out any low-barrier inversion processes and (*b*) by examining the n.m.r. behavior of other glycosyl fluoride derivatives. It is felt that unequivocal evidence for the existence of a conformational inversion process can only be obtained by actually "freezing out" the process and observing the separate resonances of the participating conformers. The only serious disadvantage of this conformational indeterminacy at this time, is that it detracts somewhat from the confidence which can be placed in the *vicinal* ^{19}F–^{1}H couplings found for the β-D-glucosyl fluorides. However, it seems highly improbable that a conformational distortion alone could account for the six-fold, or greater, difference between these *gauche* couplings and those of the α-D-mannosyl fluorides.

A detailed examination of the *vicinal* ^{1}H–^{1}H couplings arising from the C-5 and C-6 protons has revealed an interesting dependency. The *preferred* rotamer about the C_5—C_6 bond is different for those compounds having an equatorially oriented substituent at C-4 (typically, D-*gluco* derivatives) than for those having an axially oriented substituent (D-*galacto* derivatives). For simplicity, the effects of rotamer time-averaging will not be considered.

For compounds having the D-*gluco* configuration, it is observed that $J_{5,6_1} \simeq 4.5$ Hz and $J_{5,6_2} \simeq 2.5$ Hz. These values are consistent with a *preference* for the rotamer shown in **C** below,

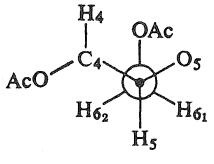

C

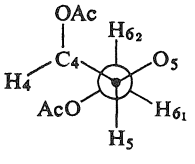

D

in which H-5 is *gauche* with respect to both $H\text{-}6_1$, and $H\text{-}6_2$. The difference in magnitude between these two couplings, both of which have the same nominal dihedral angle (60°) with H-5, is anticipated on the basis of the configurational dependence (14–16, 27) of *vicinal* couplings. It has been shown that any proton which is *antiparallel* to an electronegative substituent will give smaller (less positive) couplings than a proton which is *gauche* with respect to the same electronegative substituent. Thus $H\text{-}6_2$, which is anti-planar with respect to O-5 should give a smaller coupling than $H\text{-}6_1$.

The couplings observed for derivatives having the D-*galacto* configuration are $J_{5,6_2} = 7$ Hz and $J_{5,6_1} = 5.5$ Hz. These values are consistent with a preference for the rotamer shown in **D**, where $H\text{-}6_2$ is antiparallel ($\phi = 180°$) with respect to H-5, and $H\text{-}6_1$ is *gauche*. It is important to note that $H\text{-}6_1$ is not antiparallel with respect to any electronegative substituent, and hence would be expected to exhibit a fairly large coupling with H-5.

A simple rationale for the above conformational preferences can be offered as follows. Assume that steric or dipolar (or both) interactions between the C_4—OAc and C_6—OAc groups are of sufficient magnitude to eliminate any significant population of a rotamer having these substituents oriented as in (**E**) or (**F**); these involve the equivalent of a 1,3-*diaxial* interaction

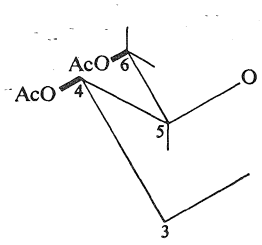

E

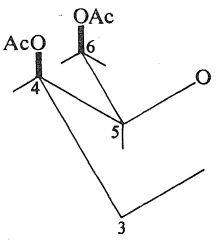

F

on a cyclohexane ring system. Although it is more difficult to effectively eliminate one remaining conformer for each of the two series, it is noteworthy that our interpretation implies that the conformer represented in **G** is particularly unfavored for both configurations at C-4. Possibly this is due to dipolar interactions with the ring oxygen substituent.

A parallel study (34), in this laboratory, of the above problem involved the measurement of the *vicinal* H_5–F_6 couplings of a series of 6-deoxy-6-fluoro carbohydrates. The observation of a ca. 30 Hz coupling for derivatives having the D-*gluco*

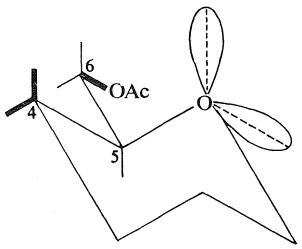

G

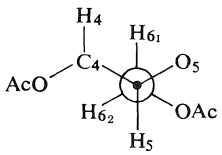

H

configuration implies a marked preference for the rotamer equivalent to **C** in which H-5 and F-6 are antiparallel. In like fashion the ca. 15 Hz coupling found for the D-*galacto* series is consistent with rotamer **D**.

The interpretation outlined above is at variance with that previously preferred by Lemieux and Stevens (26), who suggested that the rotamer depicted in **H** was preferred. The strongest argument in favor of their assignment is that it does not have OAc_6 *gauche* with respect to both C-4 and O-5, which is an apparent disadvantage of rotamer **C**. Nevertheless the further understanding of the dependencies of *vicinal* ^1H–^1H couplings, which has been gained since Lemieux and Stevens published their study, would appear to effectively eliminate their suggested rotamer. In particular, it would not seem reasonable to assign a coupling of ca. 4.5 Hz to an antiparallel relationship between two *vicinal* protons. Our conclusions are also at variance with those recently reported by Horton and co-workers (35). Unfortunately there seems little opportunity of resolving unequivocally these discrepancies at this time. However, two further points appear to be relevant. Firstly, the *geminal* H_{6_1}–H_{6_2} coupling constants of these derivatives are consistent with our interpretation. Thus, rotamer **C** requires (14, 23) the C_5—O_5 bond to be *external* to the H_{6_1}—C_6—H_{6_2} angle which would require a coupling of ca. 13 Hz, the observed value is ca. 12.8 Hz. In like fashion rotamer **D** which has the C_5—O_5 bond bisecting the H_{6_1}—C_6—H_{6_2} angle requires a coupling of ca. 11 Hz; the experimental value is ca. 10.8 Hz. Secondly, it has been found (18*c*) that for methyl 2-*O*-acetyl-4,6-*O*-benzylidene-3-deoxy-3-fluoro-β-D-glucopyranose $J_{5,6} = 4.8$ Hz. The 4,6-*O*-benzylidene substituent effectively requires one particular C_5—C_6 rotamer **C** and it would seem to be more than coincidence that the magnitude of this *gauche* coupling agrees so closely with that independently assigned to a pair of protons having the identical stereo-relationship ($J_{5,6_1}$ in rotamer **C**). Indeed, it is remarkable that a discussion which ignores the effects of rotamer time-averaging should be as adequate as appears to be the case.

In conclusion, our studies indicate that a combination of ^1H and ^{19}F n.m.r. studies provide a direct, and generally applicable, method for elucidating the structures of unknown fluorinated carbohydrates. It would also seem that the general characteristics of the stereospecific dependencies of ^{19}F n.m.r. parameters resemble those of the corresponding ^1H parameters, although their sensitivity towards changes in steric environment is much greater. As far as glycopyranosyl fluoride derivatives are concerned, our studies indicate that the "anomeric" effect of a fluorine substituent is appreciable, and the next paper in this series will be primarily concerned with an elaboration of this statement.

Experimental and Spectral Assignments

General Methods

All evaporations were carried out under reduced pressure. All optical rotations were measured for chloroform (ethanol-free) solutions, using a Bendix ETL-NPL Automatic Polarimeter (Type 143A) with either a 4 cm, or a 0.5 cm, cell. Melting points were determined on a Fisher–Johns melting point apparatus and are uncorrected. Microanalyses were determined by Mr. P. Borda of this Department.

All acetylations were performed at ca. 0° using excess acetic anhydride – pyridine (1:1). Excess reagent was decomposed by adding aqueous sodium bicarbonate. Evaporation of the dried (Na_2SO_4) chloroform solution generally afforded a syrup contaminated with pyridine, which was effectively removed by repeated evaporation with toluene. The pyridine-free syrup generally could be induced to crystallize from aqueous ethanol.

Fully acylated glycopyranosyl bromides were prepared by dissolving the fully esterified aldose in excess hydrogen bromide – acetic acid (35%, w/w). After the starting material had all dissolved, the solution was left at room temperature for ca. 2 h. This reaction mixture was then diluted with dichloromethane, washed with water, dried (Na_2SO_4), and evaporated. The syrupy glycopyranosyl bromide was either reacted directly or crystallized from diethyl ether at ca. −5°.

Synthesis of Glycopyranosyl Fluoride Derivatives

Since the preparation of these derivatives followed one or other of the two standard literature procedures (reviewed by Micheel and Klemer (11)), only one detailed example of each procedure will be given. All syntheses started from the fully *O*-acylated sugar.

α-D-Glucopyranosyl Fluoride Tetraacetate (1)

D-Glucose pentaacetate (5 g) was dissolved in anhydrous liquid HF (20 ml) which had been cooled in a polyethylene

Can. J. Chem. Downloaded from www.nrcresearchpress.com by 210.87.254.105 on 09/05/12
For personal use only.

Can. J. Chem. Downloaded from www.nrcresearchpress.com by 210.87.254.105 on 09/05/12
For personal use only.

vessel to −78° (solid CO_2/acetone). The resulting solution was left to warm to room temperature (ca. 20 min) and was then poured directly into a mixture of ether and aqueous sodium bicarbonate solution. The ether layer was washed with water and dried (Na_2SO_4). Evaporation of this solution produced a clear syrup which crystallized as needles from ethanol solution (3.3 g, 74%), m.p. 107–111°. Recrystallization from aqueous ethanol afforded pure (**1**), m.p. 110–112°, $[\alpha]_D^{23}$ +91.0° (*c*, 2.93) (lit. (10) m.p. 108°, $[\alpha]_D^{20}$ +90.1°).

A sample (3.3 g) of **1** was dissolved in absolute methanol (12 ml) and sodium methoxide (2.4 ml, 1%) was added. After 20 min the basic solution was neutralized with ion exchange resin (Amberlite 1R-120-H), filtered, and evaporated to give α-D-glucopyranosyl fluoride (**2**). It had a fluorine chemical shift (aqueous solution; external Freon-11) of +149.7 p.p.m. and $J_{1,F}$ 53.0 Hz; $J_{2,F}$ 26.8 Hz.

β-D-Glucopyranosyl Fluoride Tetraacetate (3)

α-D-Glucopyranosyl bromide (40) tetraacetate (5 g), prepared in the usual manner from D-glucose pentaacetate, was dissolved in acetonitrile (25 ml) containing powdered silver monofluoride (5 g). Light was excluded and the mixture was shaken overnight. The resulting solution was filtered and aqueous sodium chloride was added to precipitate any silver ions from solution. This mixture was filtered and concentrated to a mobile syrup which was dissolved in chloroform, extracted with water, dried (Na_2SO_4), evaporated, and dissolved in boiling diethyl ether. Crystallization was completed by the addition of light petroleum (b.p. 65–110°) to give (3.5 g, 80%) of **3** as sturdy prisms, m.p. 86–89°; recrystallization from diethyl ether afforded pure **3**, m.p. 89° (lit. (36) m.p. 88°, $[\alpha]_D$ +20°; (42) m.p. 98°, $[\alpha]_D$ +21.9°).

A sample of **3** was de-*O*-acetylated to give β-D-glucopyranosyl fluoride (**4**). The ^{19}F chemical shift (aqueous solution external Freon-11) was +142.9 p.p.m. and $J_{1,F}$ 52 Hz; $J_{2,F}$ 12.5 Hz.

α-D-Mannopyranosyl Fluoride Tetraacetate (15)

Synthesis by the method used for the preparation of either **1** or **3** afforded the same syrupy product (by nuclear magnetic resonance (n.m.r.)). This crystallized after seeding with a sample provided by C. Pedersen. The product (**15**) had m.p. and mixture m.p. 69–71° (lit. (37) m.p. 68–69°).

A sample of **5** was de-*O*-acetylated to give α-D-mannopyranosyl fluoride (**16**). The ^{19}F chemical shift (aqueous solution; external Freon-11) was +138.8 p.p.m. and $J_{1,F}$ 50.0 Hz, $J_{2,F}$ ca. 1.5 Hz.

α-D-Galactopyranosyl Fluoride Tetraacetate (13)

Preparation of this derivative followed the method described for **1**. However, the reaction yielded a syrup which failed to crystallize. The syrupy product was chromatographed on a column of silica gel, using 1% methanol in dichloromethane as eluant. The fastest moving component was shown to be pure (**13**), by inspection of both its ^1H and ^{19}F n.m.r. spectra $[\alpha]_D^{25}$ +106.6° (*c*, 0.84).

Anal. Calcd. for $C_{14}H_{19}O_9F$: C, 48.0; H, 5.45; F, 5.45. Found: C, 48.2; H, 5.6; F, 5.7.

Pedersen[10] has also mentioned that the above compound is non-crystalline.

[10]Dr. C. Pedersen. Private communication.

β-D-Galactopyranosyl Fluoride Tetraacetate (14)

The preparation of this derivative followed the conversion of D-galactose pentaacetate (5 g) to syrupy α-D-galactopyranosyl bromide tetraacetate (38) which was allowed to react, without purification, with silver monofluoride in acetonitrile. Inspection (^{19}F n.m.r.) of the crude, syrupy fluoride showed the presence of ca. 5% of the α-anomer, which was not isolated in the work-up. The crude product was crystallized from diethyl ether to yield 1.7 g (40% from the pentaacetate), of **14** m.p. 103–104° (lit. (39) m.p. 98–99°; $[\alpha]_D^{18}$ +22°).

α-D-Allopyranosyl Fluoride Tetraacetate (19) and β-D-Allopyranosyl Fluoride Tetraacetate (20)

When D-allose pentaacetate (0.75 g) was subjected to the conditions discussed above, for the formation of **1**, an almost equimolar mixture of **19** and **20** was obtained, (0.63 g, 91%). The β-fluoride (**20**) was also produced from the syrupy α-bromide and crystallized from diethyl ether. Recrystallization from aqueous ethanol afforded **20** as fine needles (m.p. 149–151°, $[\alpha]_D$ −1.3° (*c*, 1.55).

Anal. Calcd. for $C_{14}H_{19}O_9F$: C, 48.0; H, 5.45; F, 5.45. Found: C, 47.8; H, 5.4; F, 5.2.

Successive crystallization of the β-anomer from the mixture obtained from the HF reaction left mainly the α-anomer which was chromatographed (silica gel, 1% MeOH in CH_2Cl_2) to give impure **19**. It contained ca. 25% impurities by p.m.r.; thin-layer chromatography showed only one spot.

α-D-Altropyranosyl Fluoride Tetraacetate and β-D-Altropyranosyl Fluoride Tetraacetate

Reaction of methyl α-D-altropyranoside tetraacetate with anhydrous liquid HF yielded a mixture of the α- and β-fluorides, which has so far failed to crystallize. These fluorides have been characterized on the basis of their ^{19}F n.m.r. parameters which are given below. α-Anomer ϕ_c +134.9; $J_{1,F}$ 48.3 Hz; $J_{2,F}$ 2.7 Hz; β-anomer ϕ_c +138.5; $J_{1,F}$ 54 Hz; $J_{2,F}$ 20 Hz. Pedersen[10] has also mentioned that the benzoate analogues of these derivatives are non-crystalline.

2,3-Di-O-acetyl-4,6-O-benzylidene-α-D-glucopyranosyl Fluoride (11) and 2,3-Di-O-acetyl-4,6-O-benzylidene-β-D-glucopyranosyl Fluoride (12)

These two compounds were obtained by acetylation of the corresponding (40) 4,6-*O*-benzylidene compounds. These compounds were not, however, obtained in sufficient quantity or purity for detailed physical characterization. **11** had m.p. 137–143° after two recrystallizations from aqueous ethanol. **12** had m.p. 142–148°, also after recrystallization from aqueous ethanol. Nuclear magnetic resonance showed them to be at least 95% pure since no impurity peaks were discernable.

The following derivatives were kindly donated to us by Dr. Christian Pedersen and were used as received. Their ^1H and ^{19}F spectra provided confirmation of their structures and of their purity: *α-D-Mannopyranosyl Fluoride Tetrabenzoate (17) (37); α-L-Rhamnopyranosyl Fluoride Tribenzoate (18) (12); α-D-Glucopyranosyl Fluoride Tetrabenzoate (5) (41); β-D-Glucopyranosyl Fluoride Tetrabenzoate (6) (12); 2-O-Methyl-α-D-glucopyranosyl Fluoride Tribenzoate (7) (42); 2-O-Methyl-β-D-glucopyranosyl Fluoride Tribenzoate (8) (42); 3-O-Methyl-α-*

Can. J. Chem. Downloaded from www.nrcresearchpress.com by 210.87.254.105 on 09/05/12
For personal use only.

D-glucopyranosyl Fluoride Tribenzoate (9) (43); 3-O-Methyl-β-D-glucopyranosyl Fluoride Tribenzoate (10) (43).

Nuclear Magnetic Resonance Spectra

Most p.m.r. spectra were measured with a Varian HA-100 spectrometer operating in the "frequency-sweep" mode using tetramethylsilane as internal reference for the lock signal. Appropriate sweep-widths and sweep-times were used for optimal resolution and non-linearities of the sweep-widths were monitored by using the "difference 1" setting of the instrument. All ^1H–$\{^1H\}$ decoupling experiments were performed in the frequency-sweep mode, using a Hewlett Packard 200 CD, or a Hewlett Packard 204B, or a modified (14) Hewlett Packard 200 AB audio-oscillator.

All ^{19}F n.m.r. spectra were measured on the same spectrometer, which was tuned to 94.071 MHz for this purpose. The spectrometer was used either in the "unlocked" HR-mode, or in the "locked" field-sweep mode using the "infinite offset" modification of Douglas[11] (which was further modified by Mr. R. Burton of this Department). For either mode of operation, Freon-11 (trichlorofluoromethane) was used as internal reference (24); "ϕ_c" values are in p.p.m. and refer to a chloroform solution of the derivative, containing ca. 20% Freon-11.[12]

Some of the p.m.r. spectra were measured by Dr. N. S. Bhacca at the Varian Research Laboratories, Palo Alto, California, using a spectrometer operating at 220 MHz.

Spectral Assignments

Generally the spectral assignments were quite straightforward and followed the usual procedure of matching the splittings observed in the individual multiplets. The spectra were measured in three different solvents, (chloroform-*d*, acetone-d_6, benzene-d_6) to facilitate assignments and where appropriate, frequency-sweep spin decoupling experiments were also employed. To illustrate this general method of assignment, the spectra of the α- (1) and β- (3) anomers of D-glucopyranosyl fluoride tetraacetate are described in some detail below. The 100 MHz spectrum of the α-anomer (1) in $CDCl_3$ solution (Fig. 1*a*) shows, as the lowest field resonance, a doublet (2.7 Hz) which has an integrated intensity equivalent to 0.5 proton. This doublet can be assigned to the H-1 resonance if it is assumed that the other "half" of this resonance lies at ca. τ 4.6; the separation between the two "halves" corresponds to a *geminal* H_1–F_1 coupling of 52.8 Hz. The quartet centered at ca. τ 5.3 also integrates for 0.5 proton and since it exhibits a splitting equal to that observed in the resonance assigned H-1, it can tentatively be assigned to H-2. The remaining "half" of the H-2 resonance must then be partially concealed by the rather broad triplet at τ 4.86. It now remains to assign either this triplet, or the one centered at τ 4.52, to the H-3 resonance. It is not possible to make an assignment solely on the basis of spectral splittings since both of these triplets contain the splitting of ca. 9 Hz observed in the H-2 resonance. However, if the triplet at τ 4.86 had been due to H-3, the transitions assigned to H-1 and the triplet at τ 4.52 would then have been broadened by virtual coupling (44); in fact H-1 and the triplet at τ 4.52 are quite sharp. Thus, the triplet at τ 4.52 is assigned to H-3 and the triplet at τ 4.86 to H-4. This latter triplet is notably broadened as a result of virtual coupling resulting from the H-5 and the two H-6 resonances which are themselves observed as a complex multiplet centered at τ 5.6. The above assignment of the H-3 and H-4 resonances is also consistent with the α-anomeric configuration, insofar that one would expect an axial fluorine substituent at C-1 to deshield preferentially H-3 with respect to H-4. If this overall assignment is correct then, $J_{F,1}$ = 52.8 Hz and $J_{F,2}$ = 23.8 Hz, and this is confirmed by direct measurement of the ^{19}F n.m.r. spectrum (shown in Fig. 3*a*).

In $CDCl_3$ solution at 100 MHz, the β-anomer (3) gives a poorly resolved spectrum (Fig. 1*b*) which does, however, have some features consistent with the β-anomeric configuration. Most noteworthy is the observation of the H-5 resonance to higher field (ca. τ 6.1) than the H-5 resonance of the α-anomer (ca. 5.8); again, one would expect an axial fluorine substituent to have resulted in the preferential deshielding of H-5. The poorly resolved multiplet at ca. τ 4.4, intensity 0.5 proton, is assignable to part of the anomeric resonance. It is quite evident that the poor resolution of this resonance is due to virtual coupling between other ring protons, since the spectrum of the same sample measured in acetone solution (Fig. 1*c*) now exhibits one half of the H-1 resonance as a fairly sharply resolved doublet ($J_{1,2}$ 6.6 Hz) at ca. τ 4.3. At the time the H-2 and H-3 resonances are now seen to be chemically shifted from one another. The remaining assignment of this spectrum was straightforward. Confirmation of these assignments again followed from measurement of the ^{19}F n.m.r. spectra. For chloroform solution, the ^{19}F n.m.r. spectrum was obviously virtually coupled (see Fig. 3*b*) in the same fashion as the proton spectrum. However, in acetone solution (Fig. 3*c*) a sharp quartet was observed which confirmed that the magnitudes of $J_{F,1}$ and $J_{F,2}$ were respectively 52.6 and 12.0 Hz.

Although confident with the above assignments, it was a pleasure to accept the opportunity to confirm them by measurement of the spectra at 220 MHz. These p.m.r. spectra, shown in Fig. 2 were obtained by N. S. Bhacca using a 220 MHz spectrometer. The increase in dispersion as compared with the spectra measured at 100 MHz is quite revealing and fully confirms the former assignments. Noteworthy for the α-anomer, is the clear resolution of all four of the H-1 transitions and all eight of the H-2 transitions, besides the considerable simplification of the H-5 and the two H-6 resonances. It is apparent, however, that the triplet assigned to H-4 is still less well resolved than the H-3 triplet, which is a result of the H-5 and the two H-6 resonances still being fairly strongly coupled (44). In fact, the first-order assignments made for these resonances are not *strictly* justifiable. However, this in no way invalidates

[11]A. W. Douglas. Private communication.

[12]The preliminary communications of this work referred the ^{19}F shifts to neat trifluoroacetic acid, which was used in a capillary tube. All shifts quoted in this paper have been *remeasured* as outlined above. Some difficulties were experienced initially due to paramagnetic impurities in the Freon 11, which resulted in detectable line broadening; these impurities were removed by bulb-to-bulb distillation. Blank experiments indicated that the amount of Freon 11 added to the chloroform solution could be varied over wide limits without appreciably altering the ^{19}F shift.

the other assignments and is not required for the determination of the conformational symmetry of the molecule as a whole. In Fig. 2*b*, some of the spectral features are more clearly resolved, and in particular the virtual coupling of the H-1 resonance has been considerably diminished. Note, however, that even with this increased dispersion, the spectrum is less clearly resolved than that of the 100 MHz spectrum for acetone-d_6 solution. In Fig. 2*c*, the various ring proton resonances are now mutually shifted so that the assignment can be seen more clearly and this substantiates the assignment made at 100 MHz. Once again the assignment of the C-5 and C-6 proton resonances is beyond the limits of a first-order analysis; the H-5,H-6 resonances are usually best resolved in benzene solutions.

Although 220 MHz spectra were only measured for the above mentioned glucosyl fluorides, all of the other hexopyranosyl fluorides were subjected to a rigorous spectral assignment at 100 MHz in the solvents mentioned.

Acknowledgments

It is a pleasure to acknowledge the generous gifts of samples from Dr. Christian Pedersen, of the Technical University, Lyngby, Denmark, which helped us so much during the initial stages of this work. Financial assistance from the National Research Council of Canada and the National Cancer Institute of Canada is also gratefully acknowledged. This paper was written during the tenure (by L. D. H.) of a Royal Society and Nuffield Foundation Commonwealth Bursary at the University of New South Wales, Australia; it is a pleasure to acknowledge the hospitality of Professor S. J. Angyal during this period.

1. L. D. HALL. Advan. Carbohydrate Chem. **19**, 51 (1964), and references therein.
2. F. A. L. ANET, M. AHMAD, and L. D. HALL. Proc. Chem. Soc. 145 (1964).
3. F. A. BOVEY, E. W. ANDERSON, F. P. HOOD, and R. L. KORNEGAY. Proc. Chem. Soc. 146 (1964).
4. G. V. D. TIERS. Proc. Chem. Soc. 389 (1960).
5. F. A. BOVEY, E. W. ANDERSON, F. P. HOOD, and R. L. KORNEGAY. J. Chem. Phys. **40**, 3099 (1964).
6. J. D. ROBERTS. Chem. Brit. **2**, 529 (1966), and references given therein.
7. L. D. HALL and J. F. MANVILLE. Chem. Ind. London. 991 (1965).
8. N. F. TAYLOR and P. W. KENT. J. Chem. Soc. 872 (1958); P. W. KENT, A. MORRIS, and N. F. TAYLOR. J. Chem. Soc. 298 (1960).
9. N. F. TAYLOR. Nature, **182**, 660 (1958).
10. D. H. BRAUNS. J. Am. Chem. Soc. **45**, 833, 2381 (1923); **46**, 1484 (1924).
11. F. MICHEEL and A. KLEMER. Advan. Carbohydrate Chem. **16**, 85 (1961), and references given therein.
12. I. LUNDT and C. PEDERSEN. Michrochem. Acta, **1**, 125 (1966), and references given therein.
13. L. D. HALL. Chem. Ind. London. 950 (1963).
14. L. D. HALL and J. F. MANVILLE. *In* The chemistry of deoxy sugars. *Edited by* S. Hanessian. Advances in Chemistry Series No. 74, American Chemical Society. pp. 228–253 (1968).
15. N. S. BHACCA and D. H. WILLIAMS. J. Am. Chem. Soc. **86**, 2742 (1964).
16. H. BOOTH. Tetrahedron Letters, **7**, 411 (1965).
17. M. KARPLUS. J. Chem. Phys. **30**, 11 (1959); J. Am. Chem. Soc. **85**, 2870 (1963).
18. (*a*) L. D. HALL and J. F. MANVILLE. Can. J. Chem. **45**, 1299 (1966); Chem. Commun. 37 (1968); (*b*) L. D. HALL, I. JOHANSSON, and B. LINDBERG. To be published. (*c*) A. B. FOSTER, L. D. HALL, and R. HEMS. To be published. (*d*) L. D. HALL, D. L. JONES, and J. F. MANVILLE. To be published.
19. K. L. WILLIAMSON, Y. F. LI, F. H. HALL, and S. SWAGER. J. Am. Chem. Soc. **88**, 5678 (1966).
20. R. J. ABRAHAM and L. CAVALLI. Mol. Phys. **9**, 67 (1965).
21. R. J. ABRAHAM, L. CAVALLI, and K. G. R. PACHLER. Mol. Phys. **11**, 471 (1966).
22. G. ARANDA, J. JULLIEN, and J. A. MARTIN. Bull. Soc. Chim. France. 2850 (1966); J. M. JULLIEN and H. STAHL-LARIVIER. Bull. Soc. Chim. France. 99 (1967).
23. (*a*) J. A. POPLE and A. A. BOTHNER-BY. J. Chem. Phys. **42**, 1339 (1965); (*b*) A. A. BOTHNER-BY. Advan. Magn. Resonance, **1**, 195 (1965); (*c*) R. C. COOKSON, T. A. CRABB, J. J. FRANKEL, and J. HUDEK. Tetrahedron Supplement, **7**, 355 (1967).
24. G. FILIPOVICH and G. V. D. TIERS. J. Phys. Chem. **63**, 761 (1959).
25. L. D. HALL. Tetrahedron Letters. 1457 (1964).
26. R. U. LEMIEUX and J. D. STEVENS. Can. J. Chem. **43**, 2059 (1965).
27. B. COXON. Tetrahedron, **22**, 2281 (1966).
28. J. T. EDWARD. Chem. Ind. London. 1102 (1955).
29. R. U. LEMIEUX. *In* Molecular rearrangements. Part 2. *Edited by* P. de Mayo. Interscience, New York. 1964. p. 735–743.
30. S. J. ANGYAL. *In* Conformational analysis. E. L. ELIEL, N. L. ALLINGER, S. J. ANGYAL, and G. A. MORRISON. Interscience, New York. 1965. Chap. 6.
31. N. S. BHACCA and D. HORTON. J. Am. Chem. Soc. **89**, 5993 (1967).
32. R. K. HARRIS and N. SHEPPARD. Proc. Chem. Soc. 418 (1961); J. MUSHER and R. E. RICHARDS. Proc. Chem. Soc. 230 (1958).
33. D. F. EVANS. J. Chem. Soc. 877 (1960).
34. L. D. HALL and L. EVELYN. Chem. Ind. London. 183 (1968).
35. C. V. HOLLAND, D. HORTON, M. J. MILLER, and N. S. BHACCA. J. Org. Chem. **32**, 3077 (1967).
36. F. MICHEEL, A. KLEMER, M. NOLTE, H. NORDIEK, L. TORK, and H. WESTERMANN. Ber. **90**, 1612 (1957).
37. C. PEDERSEN. Acta Chem. Scand. **17**, 673 (1963).
38. H. OHLE, W. MARECEK, and W. BOURJAU. Ber. **62**, 833 (1929).
39. F. MICHEEL, A. KLEMER, G. BAUN, P. RISTIC and F. ZUMBULTE. Ber. **88**, 475 (1955).
40. F. MICHEEL. Ber. **90**, 1612 (1959).
41. B. HELFERICH, K. BAUERLEIN, and F. WEYGAND. Ann. Chem. **447**, 27 (1926).
42. C. PEDERSEN. Acta Chem. Scand. **20**, 963 (1966).
43. I. LUNDT, C. PEDERSEN, and B. TRONIER. Acta Chem. Scand. **18**, 1917 (1964).
44. J. I. MUSHER and E. J. COREY. Tetrahedron, **18**, 791 (1962).

Can. J. Chem. Downloaded from www.nrcresearchpress.com by 210.87.254.105 on 09/05/12
For personal use only.

Studies of specifically fluorinated carbohydrates. Part II. Nuclear magnetic resonance studies of pentopyranosyl fluoride derivatives

L. D. HALL[1] AND J. F. MANVILLE[2]
Department of Chemistry, University of British Columbia, Vancouver 8, British Columbia
Received May 14, 1968

Detailed studies, by ^{1}H and ^{19}F nuclear magnetic resonance spectroscopy, of a series of fully esterified pentopyranosyl fluorides, show that all such derivatives favor that conformer in which the fluorine substituent is axially oriented. This conclusion is supported by separate considerations of the *vicinal* and *geminal* ^{19}F–^{1}H and ^{1}H–^{1}H coupling constants, of the *long-range* (^{4}J) ^{1}H–^{1}H and ^{19}F–^{1}H coupling constants and of the ^{19}F chemical shifts. The limitations of the above conformational model are discussed.

Canadian Journal of Chemistry, 47, 19 (1969)

Can. J. Chem. Downloaded from www.nrcresearchpress.com by 210.87.254.40 on 09/05/12
For personal use only.

Introduction

In the previous paper of this series (1) we described the use of hexopyranosyl fluoride derivatives as models for an investigation of the stereospecific dependences of ^{19}F nuclear magnetic resonance (^{19}F n.m.r.) parameters. In the present paper we describe an essentially parallel investigation of a series of pentopyranosyl fluoride derivatives which, besides confirming some aspects of the previous ^{19}F n.m.r. study, indicates that an anomeric fluorine substituent can have a profound influence on the preferred conformation of a pyranose derivative.[3]

Results and Discussion

Our original intention in studying the proton and fluorine nuclear magnetic resonance (n.m.r.) spectra of a series of pentopyranosyl fluorides was to extend directly the studies which we had made of hexopyranosyl fluorides. However, it became apparent early in this study that the derivatives in this series all showed a most marked preference for that conformation in which the fluorine substituent had an axial orientation. In order to present most clearly the evidence which led to this conclusion, and supported it, the data obtained for the α- and β-D-xylopyranosyl fluoride systems, which are the limiting cases, will be discussed first in some detail; the remaining derivatives will then be discussed by analogy.

It is relevant to note that from both a conformational and an n.m.r. viewpoint, the D-xylopyranose and the D-glucopyranose systems are closely related, the sole difference being at C-5 where the D-glucose system has an equatorially oriented hydroxymethyl (or acetoxymethyl, benzoyloxymethyl, etc.) substituent in place of H-5e of the D-xylose system in the $^{4}C_{1}$(D) conformation. On this basis one would anticipate fundamentally similar n.m.r. spectra for the two systems.

Consider the partial 100 MHz spectrum for α-D-xylopyranosyl fluoride triacetate (**1**) shown in Fig. 1*a*. The resemblance between this spectrum and the one previously presented (1) for α-D-glucopyranosyl fluoride tetraacetate (**15**) is quite evident; noteworthy is the similarity between the H-1, H-2, and H-3 resonances. The transitions in the complex region at τ 5.0, which had not already been assigned to H-2, were assigned to H-4 since they had the same splitting (9.7 Hz) as that found in the H-3 resonance. The remaining resonances centered at τ 6.15 were assigned to the C-5 protons, the triplet at higher field (τ 6.29) being attributed to H-5a since it displayed a large splitting (10.8 Hz), characteristic of a *trans-diaxial, vicinal* coupling. This left the remaining transitions centered at τ 6.02 assignable to H-5e, which displayed the same *geminal* ^{1}H–^{1}H coupling (10.8 Hz) as H-5a and a smaller *vicinal* coupling (5.7 Hz) indicative of a *gauche* relationship with H-4. Measurement of the ^{19}F spectrum supported this overall assignment since the *geminal* (53.3 Hz) and

[1]All correspondence should be addressed to this author.
[2]Recipient of a British Columbia Sugar Refining Co. Scholarship, 1964–1965 and a NRCC Studentship 1966–1967. Present address: Forest Products Laboratory, N.W. Marine Drive, Vancouver 8, British Columbia.
[3]Preliminary accounts of these conclusions were presented at the 3rd International Fluorine Symposium Munich, Germany, August 30 to September 2, 1965 and at the 153rd meeting of the American Chemical Society, Miami Beach, Florida, April 9–14, 1967. See also references (2) and (3).

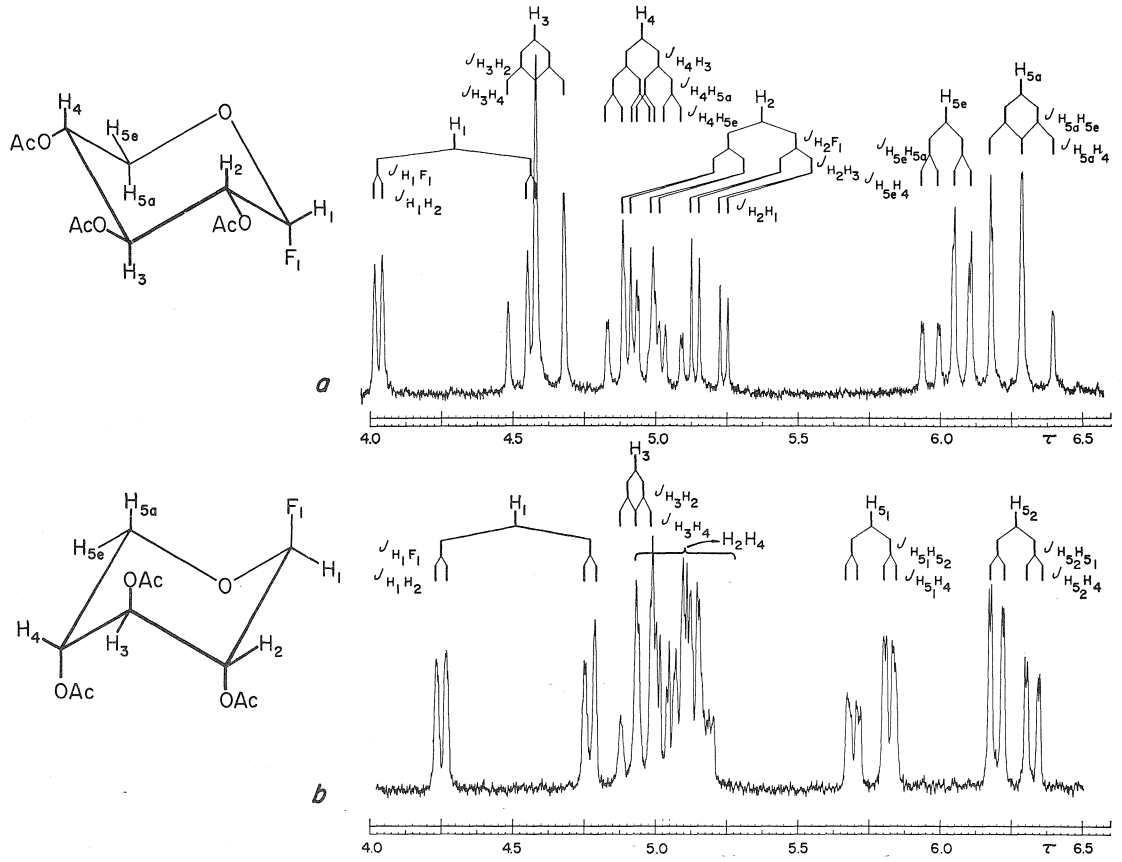

FIG. 1. Partial 100 MHz proton magnetic resonance spectra of: (*a*), α-D-xylopyranosyl fluoride triacetate (**1**) and (*b*), β-D-xylopyranosyl fluoride triacetate (**3**) in acetone-d_6 solutions.

vicinal (24.1 Hz) ^{19}F–^{1}H couplings are indicative of a *trans-diaxial* relation between H-2 and F-1. Hence, the conformation of (**1**) must approximate to the $^{4}C_{1}$(D) symmetry (**1***a*).

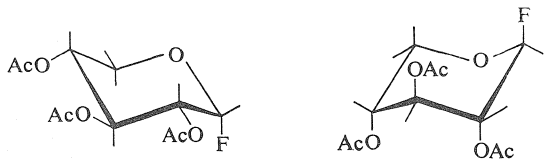

1*a*

3*a*

Consider now the spectrum (Fig. 1*b*) of β-D-xylopyranosyl fluoride triacetate (**3**), which was anticipated to resemble that of the corresponding β-D-glucosyl fluoride tetraacetate (**16**) (1) and to a certain extent that of the α-D-xylopyranosyl triacetate fluoride (**1**) (1). It is immediately apparent that this expectation is not fulfilled. The H-1 and H-5 resonances are particularly noteworthy in this respect. The *vicinal* H_1–H_2 coupling is only 3.5 Hz which is half the value found for the corresponding coupling of the β-D-*gluco* derivative (**16**). Furthermore, neither of the H-5 resonances exhibit the large (ca. 10Hz) splitting anticipated for the *trans-diaxial* coupling with H-4a. Since there seemed to be little chance that the halogen exchange reaction, used in the synthesis of this derivative from the known α-D-xylosyl bromide triacetate, could have effected simultaneously inversion at both C-4 and C-2, the only reasonable rationale for the proton n.m.r. data was based on a gross conformational inversion of the pyranose ring. Previous experience had already indicated (1, 5) the "anomeric effect" of a fluorine substituent to be significant, and it seemed possible that in this case it had caused the

Can. J. Chem. Downloaded from www.nrcresearchpress.com by 210.87.254.40 on 09/05/12
For personal use only.

Can. J. Chem. Downloaded from www.nrcresearchpress.com by 210.87.254.40 on 09/05/12
For personal use only.

β-D-xylosyl fluoride (**3**) to adopt a conformation approximating to the $^1C_4$(D) conformation (*3a*); this would allow the fluorine substituent to adopt an axial orientation but would also require the acetoxy substituents at C-2, C-3, and C-4 to be axially oriented. This inversion would account for the small magnitudes of the H_1–H_2 and H_4–H_5 couplings[4] together with the rather small *vicinal* ^{19}F–^1H coupling (ca. 7Hz) and the multitude of *long-range* ^1H–^1H couplings in the various resonances.

If it is accepted for the present that the β-D-*xylo* derivative (**3**), and its benzoate analogue (**4**) do exist in the $^1C_4$ conformation, then it is highly probable that *all of the other pentopyranosyl fluorides described in this paper adopt that chair conformation having the fluorine substituent axially oriented.* Inspection of the *vicinal* coupling constants listed in Table II indicates that, to a first approximation, this is correct.

Further evidence supporting the above view, which is *completely independent of any arguments based on the angular dependence of vicinal coupling constants*, follows a consideration of the ^{19}F chemical shifts (ϕ_c-values) of the fully acetylated derivatives. Using the empirical rules derived previously (1) for predicting the chemical shifts (ϕ_c-values) of an axial fluorine substituent attached to the anomeric carbon atom of a pyranose carbohydrate, it is possible to calculate the ϕ_c-values for all of the pentopyranosyl fluoride triacetates. Table III lists the experimental ϕ_c-values for these derivatives, together with the values calculated on the assumption that all derivatives exist exclusively in that conformation having the fluorine substituent axially oriented; the calculated values have been normalized with respect to the shift of the α-D-xylopyranosyl fluoride triacetate. It can be seen that the mean deviation between the experimental and calculated values is essentially the same for the α-($\pm$0.6 p.p.m.) and β-($\pm$0.8 p.p.m.) series of compounds.

Before the above evidence is acceptable it is necessary to show that calculations based on those conformations having an equatorially oriented fluorine substituent are less satisfactory than those listed in Table III. Although this is not possible in every instance due to the lack of suitable model compounds in the hexopyranose series, in the two cases where it is possible, the alternate conformations lead to ϕ_c-values seriously at variance with the experimental values. The inherent axial:equatorial ^{19}F shift difference ($\delta_{a,e}$) is known (1) to be 12.1 p.p.m. for the D-glucosyl fluoride tetraacetates (**15** and **16**) and −0.6 p.p.m. for the D-allosyl derivatives (**19** and **20**); these values can be used to calculate the shifts expected for the β-D-*xylo* (**3**) and β-D-*ribo* (**7**) derivatives if they were to adopt the $^4C_1$(D) conformation. For example, using the shift of α-D-xylopyranosyl fluoride triacetate (**1**) as reference, together with the $\delta_{a,e}$ value for the D-glucosyl fluorides (**15**) and (**16**), the β-D-xylopyranosyl fluoride triacetate (**3**) in the $^4C_1$(D) conformation should have a shift of 140.0 p.p.m.; this is +3 p.p.m. from the experimental value, whereas, the error in the value calculated for the $^1C_4$(D) conformation is −1.3 p.p.m. In like fashion, the calculated value for β-D-ribopyranosyl fluoride triacetate (**7**) in the $^4C_1$(D) conformation is 148.8 p.p.m., which is +7.4 p.p.m. from the observed value; in this case the error for the $^1C_4$(D) value is only −0.8 p.p.m.

A further set of ^{19}F shift comparisons can be formulated, in which each of the pentose derivatives is compared with the configurationally related hexose counterpart. This is shown in Table IV; from these comparisons it is clear that an equatorially oriented acetoxymethyl substituent at C-5 *deshields* an axially oriented fluorine substituent at C-1 by ca. 2.5 p.p.m. Clearly, it would be of some interest to obtain the glycosyl fluorides of the "rare" hexoses in order to complete this set of comparisons. Nevertheless, the comparisons which can be made at this time are consistent with the conformations postulated for the pentopyranosyl fluorides.

Several series of comparisons can be made between the ^1H chemical shifts of some of these derivatives in $CDCl_3$ solutions; these also support the anticipated conformational symmetries and, at the same time, help to confirm the assignments of the H-5e and H-5a resonances for those compounds (**3**, **4**, **7**, **8**, **9**) where the C_4—H_4 bond is *gauche* with respect to both of the C_5—H_5 bonds. Consider first those derivatives for which an unequivocal assignment of the

[4]The C-5 protons were assigned on the basis of the empirical rules advanced by Lemieux and Stevens (4) from consideration of shielding parameters of acetoxy substituents on remote protons. See also (5).

Can. J. Chem. Downloaded from www.nrcresearchpress.com by 210.87.254.40 on 09/05/12
For personal use only.

TABLE I

First-order chemical shifts (τ values, ϕ values) of the fully *O*-acylated-D-pentopyranosyl fluorides

Compound		H-1	H-2	H-3	H-4	H-5e	H-5a	OAc			F
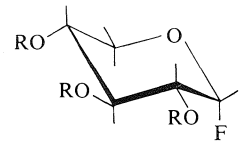		*c* 4.33	5.11	4.51	4.96	6.03	6.25	7.90	7.95	7.95	152.1
	1	*a* 4.30	5.07	4.58	4.97	6.02	6.29	7.98	8.02	8.02	151.3
	R = OAc	*b* 4.45	5.89	4.36	4.96	6.26	6.41	8.31	8.40	8.43	151.3
		c 4.05	4.63	3.82	4.50	5.42	5.92				151.6
	2	*a* 3.94	4.47	3.88	4.39	5.67	5.92				151.0
	R = OBz	*b* 4.24	4.65	3.64	4.57	6.00	6.21				150.9
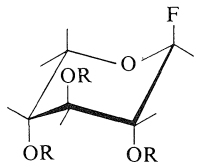		*c* 4.57	——5.04——			6.26	5.72	7.88	7.88	7.88	137.0
	3	*a* 4.54	5.10	4.94	5.10	6.27	5.76	7.95	7.98	7.98	136.6
	R = OAc	*b* 4.69	—4.85—		5.73	6.60	6.03	8.39	8.39	8.43	136.1
		c 4.25	4.70[d]	4.34	4.70[d]	5.80	5.40				137.3
	4	*a* 4.12	4.52[d]	4.28	4.52[d]	5.86	5.36				136.8
	R = OBz	*b* 4.42	4.58	4.23	4.87	6.27	5.76				136.7
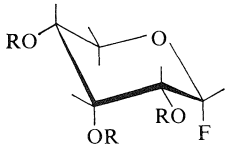		*c*									147.7
	5	*a*									
	R = OAc	*b*									
		c 4.12	4.65	3.79	4.52	5.95	5.58				148.1
	6	*a*									
	R = OBz	*b*									
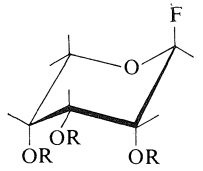		*c* 4.42	——4.75——			5.81	6.06	7.84	7.84	7.96	141.4
	7	*a* 4.40	4.85	4.70	4.80	5.79	6.08	7.92	7.94	8.06	140.4
	R = OAc	*b* 4.60	— 4.7 —		4.95	6.24	6.43	8.27	8.28	8.29	140.4
		c 4.13	——4.3——			5.57	5.77				140.4
	8	*a* 3.95	4.2[d]	4.14	4.2[d]	5.44	5.69				139.9
	R = OBz	*b* 4.44	— 4.33 —		4.53	6.12	6.26				139.9

Can. J. Chem. Downloaded from www.nrcresearchpress.com by 210.87.254.40 on 09/05/12
For personal use only.

TABLE I (*concluded*)

First-order chemical shifts (τ values, ϕ values) of the fully *O*-acylated-D-pentopyranosyl fluorides

Compound		H-1	H-2	H-3	H-4	H-5e	H-5a	OAc			F
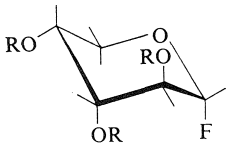		*c* 4.65		4.8		6.25	5.89	7.89	7.90	7.95	138.4
	9	*a*									138.8
	R = OAc	*b*									137.9
		c 4.51		4.3		5.91	5.44				137.8
	10	*a* 4.17		4.2		5.78	5.54				138.6
	R = OBz	*b* 4.47	4.21	4.1	4.29	6.14	5.70				137.7
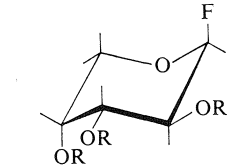		*c* 4.23	4.8	4.65		5.85	6.14	7.86	7.90	7.98	153.7
	11	*a* 4.28	4.83	4.6		5.79	6.72	7.92	7.97	8.07	153.0
	R = OAc	*b* 4.3	4.7	4.7	4.6	6.31	6.51	8.28	8.33	8.35	152.8
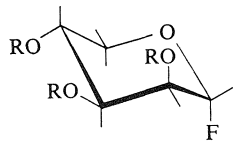		*c* 4.54		4.7		5.98	6.27	7.84	7.94	7.97	141.1
	13	*a* 4.40		4.7		5.97	6.28	7.87	8.00	8.05	140.7
	R = OAc	*b* 4.76		4.5		6.09	6.42	8.31	8.40	8.42	140.5
		c 4.22		4.2		5.65	5.96				140.7
	14	*a* 4.03		4.1		5.59	5.85				140.3
	R = OBz	*b* 4.56		4.0		5.89	6.18				140.0

NOTE: The compounds listed above were each measured in chloroform-*d* (*c*), acetone-d_6 (*a*), and benzene-d_6 (*b*) solutions. The fluorine chemical shifts are quoted in p.p.m. upfield from Freon-11 which was used as internal standard. The benzoate ester protons resonated at ca. τ 2 and ca. τ 2.5. [d]Overlapping resonances.

Can. J. Chem. Downloaded from www.nrcresearchpress.com by 210.87.254.40 on 09/05/12
For personal use only.

TABLE II

First-order coupling constants of the fully *O*-acylated-D-pentopyranosyl fluorides (Hz)

	Compound		$J_{1,2}$	$J_{2,3}$	$J_{3,4}$	$J_{4,5e}$	$J_{4,5a}$	$J_{5e,5a}$	$J_{1,F}$	$J_{2,F}$
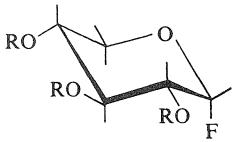		*c*	2.8	10.0	10.0	6.0	10.6	10.6	53.5	23.7
	1	*a*	2.8	9.7	9.7	5.7	10.8	10.8	53.3	24.1
	R = OAc	*b*	2.9	10.0	10.0	6.2	11.0	11.0	53.2	24.0
		c	2.8	10.2	10.1	6.0	10.8	10.8	53.1	23.5
	2	*a*	2.8	9.8	9.8	5.9	10.9	10.9	53.2	23.7
	R = OBz	*b*	2.6	10.1	9.8	6.0	10.7	10.7	53.1	23.6
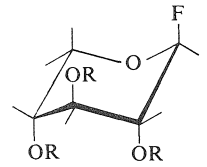		*c*	2.5	—	—	3.2	3.6	12.6	50.4	6.8
	3	*a*	3.5	5.7	5.7	3.1	4.3	12.5	52.1	7.9
	R = OAc	*b*	~2.5	—	—	3.0	3.6	12.7	~52	7.0
		c	~2.5	~3.5	~3.5	2.5	3.5	13.1	49	~6
	4	*a*	2.8	4.4	4.4	3.2	3.5	13.1	49.8	6.7
	R = OBz	*b*	2.5	3.6	3.6	~2.5	~3.4	~13	49.0	6.0
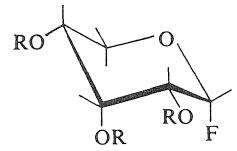		*c*							52.1	26.3
	5	*a*								
	R = OAc	*b*								
		c	3.5	3.1	2.9	5.5	10.6	10.9	53.5	25.3
	6	*a*								
	R = OBz	*b*								
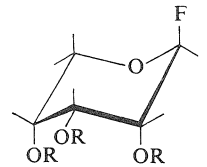		*c*	2.5	—	—	2.0	2.6	13.2	~49	<3
	7	*a*	2.6	3.8	2.0	2.0	3.0	13.0	49.5	~5
	R = OAc	*b*	2.3	—	—	2.5	2.7	13.2	49.2	~3
		c	~2	—	—	2.0	2.2	13.6	~49	<3
	8	*a*	~2	1.6	4.2	2.3	2.3	13.4	~48	<3
	R = OBz	*b*	1.5	—	—	~2	~2	~13	48.5	<3

Can. J. Chem. Downloaded from www.nrcresearchpress.com by 210.87.254.40 on 09/05/12
For personal use only.

TABLE II (*concluded*)

First-order coupling constants of the fully *O*-acylated-D-pentopyranosyl fluorides (Hz)

	Compound		$J_{1,2}$	$J_{2,3}$	$J_{3,4}$	$J_{4,5e}$	$J_{4,5a}$	$J_{5e,5a}$	$J_{1,F}$	$J_{2,F}$
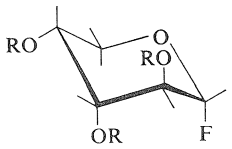		*c*	~2.5	—	—	5.3	~8	11.4	49.2	5.3
	9	*a*							50.0	9.5
	R = OAc	*b*							50.2	5.0
		c	2.5	4.5	—	4.7	9.0	11.5	~49	3.9
	10	*a*	3.6	—	—	3.9	6.9	11.7	50.9	6.1
	R = OBz	*b*	3.0	4.5	3.0	4.5	8.3	11.6	49.5	4.3
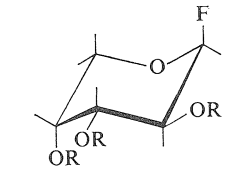		*c*	2.5	—	—	~2	1.8	13.0	53.4	22.2
	11	*a*	2.7	10.5	—	~2	1.8	13.4	54.0	23.9
	R = OAc	*b*	2.7	10.4	—	<2	1.9	13.1	~54	~25
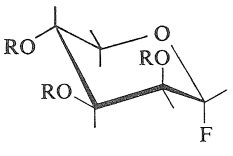		*c*	2.0	—	—	~5	~9.5	~11	49.1	<2
	13	*a*	1.9	—	—	4.5	~9	11.2	48.9	<2
	R = OAc	*b*	2.1	—	—	5.0	~9	~11	48.0	<2
		c	1.8	—	—	5.3	9.5	~10	48.6	<2
	14	*a*	1.9	—	—	4.5	~8	11.0	48.6	<2
	R = OBz	*b*	1.9	—	—	5.0	~9	11.0	48.6	<2

NOTE: The compounds listed above were each measured in chloroform-*d* (*c*) acetone-d_6 (*a*), and benzene-d_6 (*b*) solutions.

TABLE III

The ^{19}F chemical shifts (ϕ_c-values) of the fully *O*-acetylated pentopyranosyl fluorides

Compound		Conformation	Orientation of acetate at C-2	C-3	C-4	Calcd. ϕ_c	Obs. ϕ_c	Difference p.p.m.
α-D-xylo	(1)	$^4C_1$(D)	eq	eq	eq	—	152.1	—
α-D-lyxo	(13)	$^4C_1$(D)	ax	eq	eq	141.0	141.1	+0.1
α-D-ribo	(5)	$^4C_1$(D)	eq	ax	eq	148.2	147.7	−0.5
α-D-arabino	(9)	$^4C_1$(D)	ax	ax	eq	137.1	138.4	+1.3
β-D-xylo	(3)	$^1C_4$(D)	ax	ax	ax	138.3	137.0	−1.3
β-D-lyxo	(12)	$^1C_4$(D)	eq	ax	ax	149.4	—	—
β-D-ribo	(7)	$^1C_4$(D)	ax	eq	ax	142.2	141.4	−0.8
β-D-arabino	(11)	$^1C_4$(D)	eq	eq	ax	153.3	153.7	+0.4

H-5 resonances can be based on the *vicinal* couplings between H-4a and H-5a. Comparison of the H-5a shifts of **2** and **6**, shows that inversion of a benzoyloxy substituent at C-3 from an equatorial to an axial orientation shifts H-5a by −0.34 p.p.m.; however, a similar comparison for **14** and **10** gives a shift of −0.52 p.p.m. Only one comparison can be made for inversion of an acetoxy function, namely that of **13** with **9**, which gives a shift parameter of −0.38 p.p.m. Turning now to those derivatives having H-4 equatorially oriented, it can be seen that according to the assignments chosen for Table I, inversion of a C_3-benzoyloxy substituent (**8** and **4**) deshields H-5a by −0.37 p.p.m. whilst the shift for the corresponding acetates (**13** and **9**) is −0.38 p.p.m.; both of these shifts are in reasonable agreement with those listed earlier. For a similar inversion of acetoxy functions in the hexopyranose pentaacetate system, Lemieux and Stevens (4) report −0.25 p.p.m.

The remaining ^1H n.m.r. parameters of most of these pentopyranosyl fluoride derivatives appear to be reasonably consistent with the hypothesis that they all adopt either the $^1C_4$(D) or the $^4C_1$(D) conformational symmetry. Thus the *vicinal* couplings, $J_{a,a}$, fall within the range 9.5 to 10.8 Hz, in agreement with values observed for the hexose derivatives. The values for *vicinal* $J_{e,a}$ couplings fall in two distinct ranges, namely 2.0–3.5 Hz for couplings between H-1, H-2, H-3, and H-4, and 5.0–6.2 Hz for those couplings between H-4a and H-5e that have no associated *anti-planar* electronegative groups (derivatives in $^4C_1$(D) conformation). The observation of such large *vicinal* couplings (ca. 6 Hz) between two protons that are separated by a dihedral angle of 60° is at variance with that value anticipated from consideration of the known configurational dependencies (6, 7) in conjunction with the Karplus relationship (8). These large couplings occurred in spectra of the α-D-xylosyl fluorides (**1**, **2**), both of which appear to exist in the $^1C_4$(D) conformation as evidenced by the remaining couplings. This *vicinal* coupling is even larger than the one observed (9) in 2-deoxy-α-D-*arabino*-hexopyranosyl fluoride triacetate for which H-2e, H-3a is 5.2 Hz. It is therefore

TABLE IV

Comparison of the ^{19}F chemical shifts (ϕ_c-values) of the pentopyranosyl fluoride triacetates (axial fluorine) with the configurationally related α-D-hexopyranosyl fluoride tetraacetate

Pentose ϕ_c	Hexose ϕ_c	Difference (p.p.m.)	Pentose ϕ_c	Hexose ϕ_c	Difference (p.p.m.)
α-D-xylo (1) 152.1	α-D-gluco (15) 149.9	+2.2	β-D-xylo (3) 137.0	α-D-ido	
α-D-lyxo (13) 141.1	α-D-manno (17) 138.8	+2.3	β-D-lyxo (12)	α-D-gulo	
α-D-ribo (5) 147.7	α-D-allo (19) 146.0	+1.7	β-D-ribo (7) 141.4	α-D-talo	
α-D-arabino (9) 138.4	α-D-altro (21) 134.9	+3.5	β-D-arabino (11) 153.7	α-D-galacto (18) 151.1	+2.6

Can. J. Chem. Downloaded from www.nrcresearchpress.com by 210.87.254.40 on 09/05/12
For personal use only.

Can. J. Chem. Downloaded from www.nrcresearchpress.com by 210.87.254.40 on 09/05/12
For personal use only.

apparent that *vicinal* couplings associated with a $—CH_2—$ function, can vary over a considerable range.

Measurement of ^{19}F spectra showed that the *vicinal* $^{19}F–^{1}H$ couplings of these derivatives were also consistent with the anticipated symmetries. For a *trans-diaxial* relationship between F-1 and H-2, the coupling is 22.2 to 26.3 Hz, whilst for a *gauche* relationship between these substituents, a coupling of 2 to 5 Hz is observed. These values are similar to those reported previously (1) for the hexopyranosyl fluorides.

A further set of interesting comparisons concerns the *geminal* couplings, $F_1–H_1$ and $H_{5e}–H_{5a}$. For those derivatives that possess an axial substituent at C-2, the *geminal* $F_1–H_1$ coupling is 48.6–49.5 Hz, whilst those compounds having the C-2 substituent equatorial give couplings of 53.1 to 53.5 Hz. This same dependence was noted (1) in the $F_1–H_1$ couplings of the hexopyranosyl fluorides. However, it is in contrast with the dependence observed for the *geminal* $H_{5e}–H_{5a}$ couplings; compounds (**7**, **8**, **11**), which possess an *axial* acetoxy substituent at C-4, display a *larger* coupling (ca. 13Hz) than do those derivatives (**1**, **2**, **5**, **6**, **13**, **14**) having an equatorially oriented substituent, when the coupling is ca. 10.8 Hz. Previous studies in this laboratory have established that whilst the *absolute* sign of a *geminal* $^{19}F–^{1}H$ coupling is positive (10), that of a *geminal* $^{1}H–^{1}H$ coupling is negative (11). With this fact in mind it can be seen that the two sets of *geminal* couplings listed above do in fact demonstrate the same phenomenon; in each case, an axially oriented acetoxy group (and, possibly, other electronegative substituents) attached to a *vicinal* position results in a *geminal* coupling which is *absolutely more negative* than when that substituent is equatorially oriented. From a conformational viewpoint it is important to note that in all but two cases (*vide infra*) the magnitudes of the various *geminal* couplings are again in accord with that undistorted chair conformation having the anomeric fluorine substituent axially oriented.

These pentosyl fluoride derivatives also exhibit a wide selection of *long-range* $^{1}H–^{1}H$ coupling constants across four bonds (^{4}J), and in every case their occurrence was in accord (11, 12) with the anticipated conformational symmetry. In view of our recent finding (13) that *long-range* (^{4}J) couplings of ca. 4 Hz occur between a fluorine and a proton substituent having a 1,3-diequatorial orientation, it is particularly noteworthy that none of the derivatives included in this study show any couplings of this magnitude; this further supports our contention that these derivatives have the fluorine substituent axially oriented.

We shall now discuss in greater detail the two derivatives whose predicted ^{19}F chemical shifts showed the greatest deviation from the experimental values, namely β-D-xylopyranosyl fluoride triacetate (**3**) and α-D-arabinopyranosyl fluoride triacetate (**9**). It could be argued that since the calculated shifts for these two derivatives involve the summation of, respectively, three and two inversion contributions, these maximal deviations merely reflect the accumulation of the errors involved in these empirical shift parameters; certainly the minimal errors are observed for those two derivatives (**11**, **13**) for which the predicted shifts are obtained by considering a single inversion only. However, we consider that the deviations observed for **3** and **9**, do in fact reflect a genuine breakdown of the idealized conformational models considered thus far.

We shall now justify this statement. For α-D-mannopyranosyl fluoride tetraacetate (**17**), $J_{F_{1a}H_{1e}}$, = ca. 48.5 Hz, $J_{F_{1a}H_{2e}}$, = ca. 1.0 Hz and $J_{H_{1e}H_{2e}}$, = ca. 1.5 Hz. The corresponding couplings for derivatives **13** and **14**, which have nominally the same configurations at C-1 and C-2 are in good agreement with these values. However, the agreement is less good for those derivatives having *two* axially oriented acetoxy substituents and is poorest for β-D-*xylo* derivatives (**3**, **4**) and the α-D-*arabino* derivatives (**9**, **10**). The *geminal* H-5e, H-5a couplings of these derivatives also seem to be somewhat anomalous. The couplings for **3**, **4** are slightly less than that of **11**, ca. 13 Hz, which has only a single axial acetoxy function, and which we assume is close to the $^{1}C_4$(D) symmetry; in like fashion the couplings for **9**, **10** are somewhat larger than those of their counterparts (**1**, **2**) for which $J_{5e,5a}$ = ca. 10.8 Hz. Clearly some of the above "deviations" are somewhat small, but it does seem more than fortuitous that they all happen to be maximal for the same derivatives which are, furthermore, just those systems

Can. J. Chem. Downloaded from www.nrcresearchpress.com by 210.87.254.40 on 09/05/12
For personal use only.

having the maximal number of "axially" oriented acetoxy substituents. On this basis we suggest that whilst the powerful "anomeric-effect" (14, 15) of a fluorine substituent is sufficiently predominant to exert overall control of the conformational preference of these derivatives, classical, non-bonded interactions are capable of distorting the conformational symmetry of the system. This is the converse of the situation which we have previously (1) envisaged for the D-hexopyranosyl fluoride systems.

It would seem that for the pentopyranosyl fluorides *three* sets of repulsive non-bonded interactions are required to cause a detectable distortion from an "ideal" chair conformation; in this regard we consider only the following 1,3-interactions, OAc_a; H_a, OAc_a; F_a and OAc_a; OAc_a. Again it is necessary to consider whether the conformational deviations implied by the room-temperature n.m.r. data reflect a true distortion of a ground-state conformational symmetry, or whether they reflect some conformational time-averaging process(es). As found previously for the hexopyranosyl fluoride system, variable temperature studies with the equipment available at this time do not enable us to make an unequivocal distinction between these two possibilities. The ^{19}F shift of the β-D-xylo-derivative (**3**) changed by ca. 2 p.p.m. between 190 °K and 330 °K. We plan to reinvestigate this point at a future date.

It is of some interest to compare the parameters of the two triacetate derivatives (**3**, **9**) with those of the corresponding tribenzoates (**4**, **10**, respectively). In each case the parameters of the tribenzoate are closer to the values anticipated for undistorted chair conformations than are those of the triacetate. This observation could imply that the anomeric effect of a fluorine substituent is greater for the tribenzoates than for the triacetates. Alternatively, the *gauche* interaction between a pair of *vicinal* benzoyloxy substituents may be greater than that between a corresponding pair of acetoxy substituents. Although these isolated examples do not merit further discussion at this time it is interesting to note that the results previously quoted for hexopyranosyl fluoride derivatives appear to reflect a remarkable similarity to those outlined above.

Whilst the studies described in this paper were in progress two other groups of workers have reported results concerning the conformations of pentopyranose derivatives which are in accord with many of our observations. Coxon (5) studied a series of D-ribopyranose derivatives and concluded that ". . . . the operation, or non-operation of the anomeric effect appears to be the principal factor determining which particular chair conformation predominates." In a somewhat broader study, Horton and Turner (16*a*) investigated the "thermodynamically-favored" pentopyranosyl halides and also concluded that the anomeric effect of a halogen substituent is of predominant importance in controlling the conformations of pentopyranose derivatives. Of particular relevance to the present study was the observation (16*b*) that β-D-xylopyranosyl chloride triacetate favors the $^1C_4$(D) conformational symmetry. Unfortunately, it is not possible to make a detailed comparison of this derivative with the corresponding fluoride because insufficient coupling constants are available for the β-chloride.

It will be noted in the above discussions we have considered only "repulsive" non-bonded interactions and have ignored the possible existence of attractive forces between substituent groups (17). We do not feel that we have yet sufficient data to comment meaningfully on such forces; however, the possibility of an attraction between a pair of 1,3-diaxially related substituents would clearly stabilize further several of the conformations suggested in this paper. At this time it would seem reasonable to ascribe the conformational preferences of these pentopyranosyl fluoride derivatives to the various properties associated with the highly polar C_1–F bond and which would familiarly be termed the "anomeric-effect" of the fluorine substituent. However, it remains to be seen whether this phenomenon results solely from dipolar interactions between the polar bond at C-1 and the ring oxygen.

Experimental

The basic procedures used in this study were identical to those outlined previously for the hexopyranosyl fluoride derivatives (1).

α-D-Xylopyranosyl Fluoride Triacetate (1)

A sample of this derivative was synthesized by the method of Brauns (18). The crude reaction product contained ca. 5% of the corresponding β-isomer (**3**) as shown by ^{19}F n.m.r., which was not isolated in the work-up; **1** had m.p. 86–88°; (lit. (18), m.p. 87°).

Can. J. Chem. Downloaded from www.nrcresearchpress.com by 210.87.254.40 on 09/05/12
For personal use only.

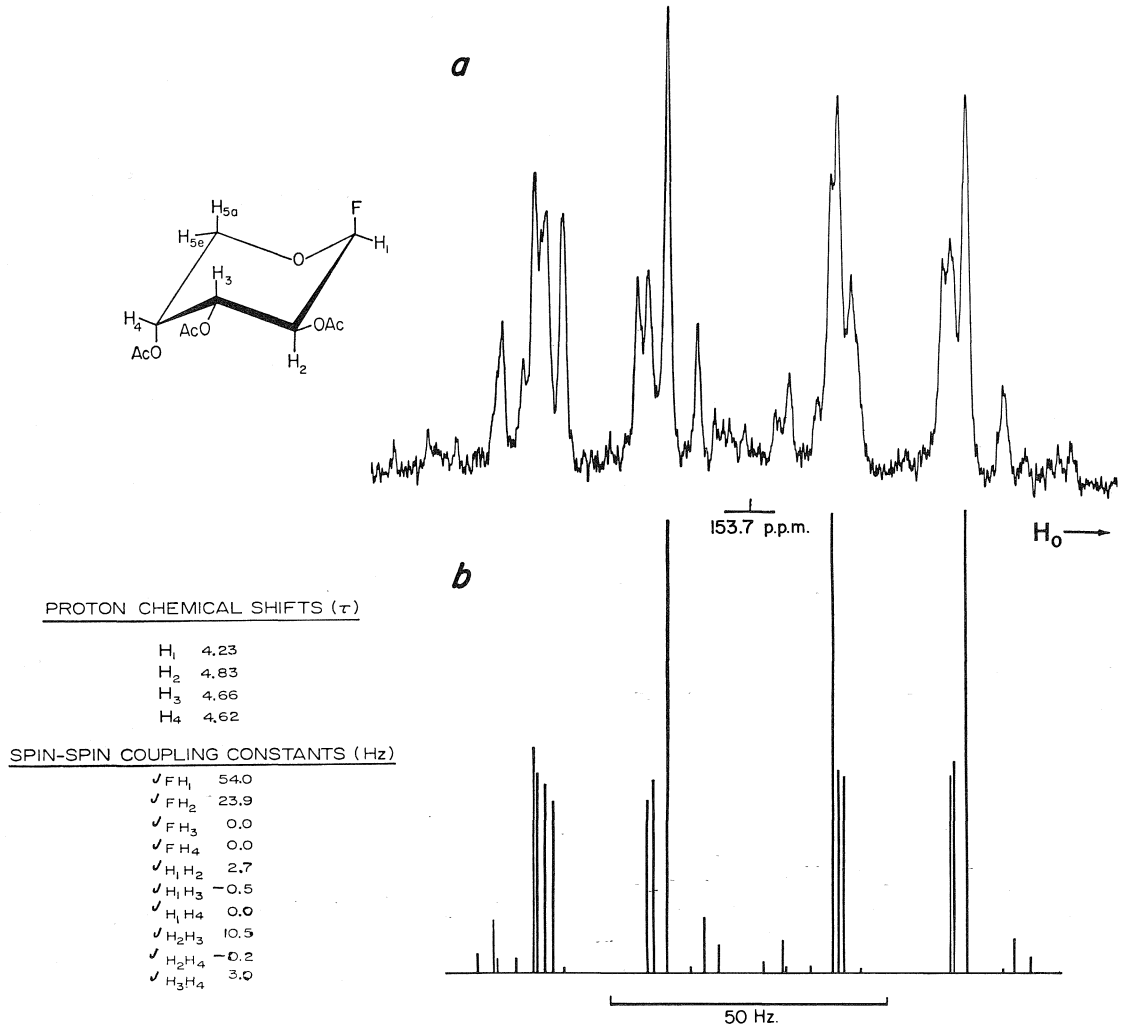

FIG. 2. (*a*) The ^{19}F nuclear magnetic resonance spectrum of β-D-arabinopyranosyl fluoride triacetate (**11**) in acetone-d_6 solution, and (*b*), the spectrum calculated from the estimated first-order parameters. The correlation between the two spectra is not perfect (*vide infra*).

β-D-*Xylopyranosyl Fluoride Triacetate (3)*

The preparation of this derivative followed the method of Lundt and Pedersen (19), except that crystalline α-D-xylopyranosyl bromide triacetate (20) was used. **3** had m.p. 52–55°; (lit. (19), m.p. 56–57°, $[\alpha]_D^{23}$ −56.4°).

β-D-*Ribopyranosyl Fluoride Triacetate (7)*

The preparation of this derivative also followed the method of Lundt and Pedersen (19). Examination by ^{19}F n.m.r. of the crude reaction product showed the presence of a second component which we assigned to the α-D-ribopyranosyl fluoride triacetate (**5**) on the basis of its chemical shift and first-order coupling constants. This compound was not isolated; however, its ^{19}F n.m.r. parameters were measured and found to be: ϕ_c + 147.7, $J_{1,F}$ 52.1 Hz, $J_{2,F}$ 26.3 Hz; (**7**) had m.p. 94–96°; (lit. (19), m.p. 93–95°).

α-D-*Ribopyranosyl Fluoride Tribenzoate (6) and* β-D-*Ribopyranosyl Fluoride Tribenzoate (8)*

These derivatives were prepared by the method of Pedersen and Fletcher (21), **6** had m.p. 202–204°; (lit. (21), m.p. 205–206°). **8** had m.p. 135–137°; (lit. (21), m.p. 139–140°).

α-D-*Lyxopyranosyl Fluoride Triacetate (13)*

This compound was synthesized in the manner of Lundt and Pedersen (19), (**13**) had m.p. 85–87°; (lit. (19), m.p. 87–89°).

The following derivatives were generously donated by Dr. Christian Pedersen of the Technical University, Lyngby, Denmark. These samples were used as received and inspection of their ^1H and ^{19}F n.m.r. spectra effectively constitutes further evidence for their purity and structure: α-D-*Xylopyranosyl fluoride tribenzoate* (**2**) (22);

β-D-*Xylopyranosyl fluoride tribenzoate* (**4**) (22); α-D-*Arabinopyranosyl fluoride triacetate* (**9**) (19); α-D-*Arabinopyranosyl fluoride tribenzoate* (**10**) (19); β-D-*Arabinopyranosyl fluoride triacetate* (**11**) (18, 19); α-D-*Lyxopyranosyl fluoride tribenzoate* (**14**) (23).

Generally the pentopyranosyl fluorides gave clearly resolved spectra, in at least one solvent, and the couplings were then easily extracted by a first-order analysis. However, for the β-D-*arabino* derivative (**9**) the spectrum was never first-order (see Fig. 2*a*) and consequently it was felt that some check was required to evaluate the accuracy of the estimated couplings that were extracted from the spectral splittings. These were tested by computing[5] the theoretical spectrum based on these estimated parameters. This result, for the ^{19}F spectrum, is given below the actual spectrum in Fig. 2*b*. It should be noted that the calculated spectrum is not in perfect agreement with the experimental spectrum. However, the agreement is sufficiently close to demonstrate that, even in a highly coupled spectrum ($J_{i,j}/\delta_{i,j} \rightarrow 1$), fairly accurate values for the couplings and chemical shifts can be obtained by first-order analysis.

Acknowledgments

This work was supported by grants from the National Research Council of Canada and the National Cancer Institute of Canada. It is a pleasure to acknowledge gifts of samples from Dr. Christian Pedersen. This paper was written during the tenure (by L. D. H.) of a Royal Society and Nuffield Foundation Commonwealth Bursary at the University of New South Wales, Australia; it is a pleasure to thank Professor S. J. Angyal for his hospitality during this period.

[5]Using the TWOSUM MODE B, program kindly supplied by Dr. J. Martin, Chemistry Department, University of Alberta, Edmonton, Alberta.

1. L. D. HALL, J. F. MANVILLE, and N. S. BHACCA. Can. J. Chem. This issue.
2. L. D. HALL and J. F. MANVILLE. Chem. Ind. London. 991 (1965).
3. L. D. HALL and J. F. MANVILLE. Carbohydrate Res. 512 (1967).
4. R. U. LEMIEUX and J. D. STEVENS. Can. J. Chem. **43**, 2059 (1965).
5. B. COXON. Tetrahedron, **22**, 2281 (1966).
6. N. S. BHACCA and D. H. WILLIAMS. J. Am. Chem. Soc. **86**, 2742 (1964).
7. H. BOOTH. Tetrahedron Letters, **7**, 411 (1965).
8. M. KARPLUS. J. Chem. Phys. **30**, 11 (1959); M. KARPLUS. J. Am. Chem. Soc. **85**, 2870 (1963).
9. L. D. HALL and J. F. MANVILLE. Can. J. Chem. **45**, 1299 (1967).
10. L. D. HALL and J. F. MANVILLE. Chem. Ind. London. 468 (1967), and references given therein.
11. L. D. HALL and J. F. MANVILLE. Carbohydrate Res. 271 (1967), and references given therein.
12. L. D. HALL, J. F. MANVILLE, and A. TRACEY. Carbohydrate Res. 514 (1967), and references therein; S. STERNHELL. Rev. Pure Appl. Chem. **14**, 15 (1964).
13. A. B. FOSTER, L. D. HALL, R. HEMS, and J. F. MANVILLE. Chem. Comm. 158 (1968).
14. R. U. LEMIEUX. *In* Molecular rearrangements. Part 2. *Edited by* P. de Mayo. Interscience Division. John Wiley and Sons, Inc., New York. 1964. pp. 735–743 and references therein.
15. S. G. ANGYAL. *In* Conformational analysis. E. L. ELIEL, N. L. ALLINGER, S. J. ANGYAL, and G. A. MORRISON. Interscience Division, John Wiley and Sons, Inc., New York. 1965. Chap. 6, and references therein.
16. (*a*) D. HORTON and D. W. TURNER. J. Org. Chem. **30**, 3387 (1965). (*b*) C. V. HOLLAND, D. HORTON, and J. S. JEWELL. J. Org. Chem. **32**, 1818 (1967).
17. R. U. LEMIEUX. Private communication. Gordon Conf. Chemistry of Carbohydrates. Tilton. New Hampshire. 1966.
18. D. H. BRAUNS. J. Am. Chem. Soc. **45**, 833, 2381 (1923); D. H. BRAUNS. J. Am. Chem. Soc. **46**, 1484 (1924).
19. I. LUNDT and C. PEDERSEN. Michrochem. Acta, **1**, 125 (1966).
20. J. K. DALE. J. Am. Chem. Soc. **37**, 2745 (1915).
21. C. PEDERSEN and H. G. FLETCHER. J. Am. Chem. Soc. **82**, 941, 945 (1960).
22. C. PEDERSEN. Acta Chem. Scand. **17**, 1269 (1963).
23. C. PEDERSEN. Acta Chem. Scand. **18**, 60 (1964).

Can. J. Chem. Downloaded from www.nrcresearchpress.com by 210.87.254.40 on 09/05/12
For personal use only.

Synthesis of 2,6-Di-*O*-methyl-D-mannose[1]

M. B. Perry and Ann C. Webb
Division of Biochemistry and Molecular Biology, National Research Council of Canada, Ottawa, Canada
Received August 22, 1968

2,6-Di-*O*-methyl-D-mannose was synthesized using the following sequence of reactions: 1,3,4,6-tetra-*O*-acetyl-2-*O*-methyl-β-D-mannopyranose → methyl 2-*O*-methyl-α-D-mannopyranoside → methyl 2-*O*-methyl-6-*O*-trityl-α-D-mannopyranoside → methyl 3,4-di-*O*-acetyl-2-*O*-methyl-6-*O*-trityl-α-D-mannopyranoside → methyl 3,4-di-*O*-acetyl-2-*O*-methyl-α-D-mannopyranoside → methyl 3,4-di-*O*-acetyl-2,6-di-*O*-methyl-α-D-mannopyranoside → 2,6-di-*O*-methyl-D-mannose. The preparation and properties of derivatives of the 2,6-di-*O*-methyl-D-mannose are recorded.

Canadian Journal of Chemistry, 47, 31 (1969)

Can. J. Chem. Downloaded from www.nrcresearchpress.com by 210.87.254.40 on 09/05/12
For personal use only.

2,6-Di-*O*-methyl-D-mannose has been tentatively identified as a fission product of several methylated glycans (1–3) suggesting the presence of either D-mannopyranosyl units substituted at positions-3 and -4 or D-mannofuranosyl units substituted at positions-3 and -5 in the original polymers. This note records the synthesis of 2,6-di-*O*-methyl-D-mannose which was required for the identification of a product obtained from methylated glycans produced by *Cryptococcus* and *Tremella* species.

1,3,4,6-Tetra-*O*-acetyl-2-*O*-methyl-β-D-mannopyranose (4) with hot methanolic hydrogen chloride afforded methyl 2-*O*-methyl-α-D-mannopyranoside which on treatment with one mole of triphenylchloromethane was converted to methyl 2-*O*-methyl-6-*O*-trityl-α-D-mannopyranoside. Subsequent acetylation of this compound gave methyl 3,4-di-*O*-acetyl-2-*O*-methyl-6-*O*-trityl-α-D-mannopyranoside which on treatment with hydrogen bromide – acetic acid mixture underwent detritylation to yield methyl 3,4-di-*O*-acetyl-2-*O*-methyl-α-D-mannopyranoside. The methyl 3,4-di-*O*-acetyl-2-*O*-methyl-α-D-mannopyranoside could be reconverted to methyl 3,4-di-*O*-acetyl-2-*O*-methyl-6-*O*-trityl-α-D-mannopyranoside indicating that no acetyl group migration had occurred during the detritylation process. The methyl 3,4-di-*O*-acetyl-2-*O*-methyl-α-D-mannopyranoside was methylated with diazomethane using boron trifluoride etherate catalyst (4) and the resulting methyl 3,4-di-*O*-acetyl-2,6-di-*O*-methyl-α-D-mannopyranoside on hydrolysis gave 2,6-di-*O*-methyl-D-mannose.

All the intermediates were pure by thin-layer chromatography and their nuclear magnetic resonance (n.m.r.) spectra and elemental analyses were consistent with the proposed structures.

The 2,6-di-*O*-methyl-D-mannose gave a single spot on paper chromatogaphy and had no mobility on electrophoresis in borate buffer. On methanolysis it gave a glycoside which gave a single peak on gas–liquid chromatography. On oxidation with bromine, the glycose was converted to 2,6-di-*O*-methyl-D-mannono-1,4-lactone which gave a single peak on gas–liquid chromatography and its infrared spectrum showed a single carbonyl absorption peak at 1780 cm^{-1} characteristic of hexono-1,4-lactones (5); the lactone was converted to crystalline 2,6-di-*O*-methyl-D-mannonic acid phenylhydrazide.

The 2,6-di-*O*-methyl-D-mannose on reduction with sodium borohydride gave 2,6-di-*O*-methyl-D-mannitol which on periodate oxidation released no formaldehyde but consumed approximately two moles of periodate and released one mole of formic acid per mole hexitol, a result consistent with the proposed structure.

Experimental

Paper chromatography was performed by the descending method (6) on Whatman No. 1 filter paper using pyridine – ethyl acetate – water (2:5:5 v/v, top layer) as the mobile phase. Glycoses were detected with *p*-anisidine hydrochloride (7) and their rates of movement are quoted relative to 2,3,4,6-tetra-*O*-methyl-D-glucose (R_G). Gas–liquid chromatography was carried out at 200 °C using a Hewlett–Packard model 402 gas chromatograph with a hydrogen flame detector and fitted with glass U tubes (4ft × 6mm × 3mm internal diameter) packed with 10% neopentylglycol sebacate polyester on 80–100 mesh acid-washed Chromosorb W. Retention times are quoted relative to methyl 2,3,4,6-tetra-*O*-methyl-α-D-glucoside (T_G). The purity of all intermediates was determined by thin-layer chromatography on silica gel G using acetone–benzene (1:4 v/v) mixture as the mobile

[1]Issued as NRCC No. 10418.

Can. J. Chem. Downloaded from www.nrcresearchpress.com by 210.87.254.40 on 09/05/12
For personal use only.

phase and detection was made by spraying the developed plates with sulfuric acid – ethanol (1:1 v/v) mixture and heating them for 10 min at 120 °C.

Nuclear magnetic resonance (n.m.r.) spectra were recorded at 60 MHz with a Varian A-60A spectrometer with tetramethylsilane (τ 10.00) as an internal standard for spectra measured in chloroform-*d*, and sodium 4,4-dimethy-4-silapentane-1-sulfonate (τ 10.00) as the internal standard for spectra measured in deuterium oxide.

Melting points were determined on a Fisher–Johns apparatus and are corrected. Solutions were concentrated under reduced pressure, below 40 °C. Optical rotations were determined at 20 °C using a Perkin–Elmer 141 polarimeter.

Methyl 2-O-Methyl-6-O-trityl-α-D-mannopyranoside

1,3,4,6-Tetra-*O*-acetyl-2-*O*-methyl-β-D-mannose (4) (20 g) in 2.5% methanolic hydrogen chloride solution (400 ml) was boiled under reflux for 4 h and the neutralized (Ag_2CO_3) solution was concentrated to yield methyl 2-*O*-methyl-α-D-mannopyranoside (11 g) as a syrup which had $[\alpha]_D$ +56° (*c*, 1.7 in methanol) (Calcd. OMe, 29.8. Found: OMe, 29.6.). The n.m.r. spectrum of the product in deuterium oxide showed two equal (3 protons each) signals for methoxyl groups at τ 6.53 and 6.57 and exhibited an H-1 doublet at τ 5.07 with a spacing of 1.7 c.p.s. No formaldehyde was produced on periodate oxidation of the compound indicating the absence of any furanoside derivatives.

Methyl 2-*O*-methyl-α-D-mannopyranoside (10 g) was dissolved in dry pyridine (70 ml) and after the addition of triphenylchloromethane (18.6 g) the mixture was heated at 90 °C for 1 h. The cooled mixture was added dropwise to a vigorously stirred ice-water mixture (1.5 l) and the collected precipitated product was washed with water and then dried under vacuum. The crystalline methyl 2-*O*-methyl-6-*O*-trityl-α-D-mannopyranoside (17.1 g) obtained from ethanol solution had m.p. 143–144 °C and $[\alpha]_D$ +2° (*c*, 1 in chloroform) and $[\alpha]_D$ +25° (*c*, 3 in methanol).

Anal. Calcd. for $C_{27}H_{30}O_6$: C, 71.98; H, 6.71; OMe, 13.77. Found: C, 71.5; H, 6.8; OMe, 14.0.

The n.m.r. spectrum of the product in $CDCl_3$ showed a complex multiplet for the triphenylmethyl group centered at τ 2.70, two equal methoxyl signals at τ 6.56 and 6.59 and an H-1 doublet at τ 5.23 with a spacing of 1.3 c.p.s.

Methyl 3,4-Di-O-acetyl-2-O-methyl-6-O-trityl-α-D-mannopyranoside

Methyl 2-*O*-methyl-6-*O*-triytyl-α-D-mannopyranoside (15 g) dissolved in dry pyridine (45 ml) was treated with acetic anhydride (45 ml) and the mixture was kept at 22 °C for 48 h. The reaction mixture was added dropwise to a vigorously stirred ice-water mixture (2 l) and the precipitated product was collected, washed with water, and dried to yield methyl 3,4-di-*O*-acetyl-2-*O*-methyl-6-*O*-trityl-α-D-mannopyranoside (15.2 g) (m.p. 59–61 °C) which after recrystallization from ethanol had m.p. 60–61 °C and $[\alpha]_D$ +44° (*c*, 2 in chloroform).

Anal. Calcd. for $C_{31}H_{34}O_8$: C, 69.63; H, 6.41; OMe, 11.6. Found: C, 69.9; H, 6.6; OMe, 11.4.

The n.m.r. spectrum of the product in $CDCl_3$ showed a complex multiplet for the triphenylmethyl group centered at τ 2.70, two equal methoxyl signals at τ 6.51 and 6.53, two equal acetoxyl signals at τ 7.96 and 8.26 and an H-1 doublet at τ 5.19 with a spacing of 2.1 c.p.s.

Methyl 3,4-Di-O-acetyl-2-O-methyl-α-D-mannopyranoside

Methyl 3,4-di-*O*-acetyl-2-*O*-methyl-6-*O*-trityl-α-D-mannopyranoside (14 g) dissolved in acetic acid (100 ml) was treated with a saturated solution of hydrogen bromide in acetic acid (15 ml) and after 20 min at 22 °C the reaction mixture was added dropwise with stirring to an ice-water mixture (2 l). The precipitated triphenylcarbinol was removed by filtration and the filtrate, kept at 0 °C, was neutralized with sodium bicarbonate. The solution was extracted with chloroform (3 × 400 ml) and the dried (anhydrous Na_2SO_4) extract was concentrated to a syrup (6.9 g) which slowly crystallized. Pure methyl 3,4-di-*O*-acetyl-2-*O*-methyl-α-D-mannopyranoside (6 g) obtained by recrystallization from ether had m.p. 91 °C and $[\alpha]_D$ +73° (*c*, 1 in chloroform).

Anal. Calcd. for $C_{12}H_{20}O_8$: C, 49.31; H, 6.90; OMe, 21.2. Found: C, 49.2; H, 7.0; OMe, 21.1.

The n.m.r. spectrum of the product in $CDCl_3$ showed two equal methoxyl signals at τ 6.51 and 6.57, two equal acetoxyl signals at τ 7.91 and 7.94, and an H-1 doublet at τ 5.20 with a spacing of 1.8 c.p.s.

A portion of the methyl 3,4-di-*O*-acetyl-2-*O*-methyl-α-D-mannopyranoside (0.1 g) in pyridine (1.5 ml) containing triphenylchloromethane (0.12 g) was kept at 80 °C for 1 h and the product isolated in the normal way was fractionated by preparative thin-layer chromatography to yield methyl 3,4-di-*O*-acetyl-2-*O*-methyl-6-*O*-trityl-α-D-mannopyranoside (0.12 g) which had m.p. and mixture m.p. 90 °C, $[\alpha]_D$ +72° (*c*, 1 in chloroform) and gave an n.m.r. spectrum identical with the authentic material.

Methyl 3,4-Di-O-acetyl-2,6-di-O-methyl-α-D-mannopyranoside

Methyl 3,4-di-*O*-acetyl-2-*O*-methyl-α-D-mannopyranoside (5.5 g) in dry dichloromethane (60 ml) containing boron trifluoride etherate (0.1 ml) kept at 0 °C was treated with diazomethane in dichloromethane until a faint yellow color persisted and after 30 min the white solid (polymethylene) was removed on a coarse sintered glass filter and the filtrate was concentrated to a syrup (5.2 g). The syrup was dissolved in an ether – light petroleum (b.p. 60–80 °C) mixture and on cooling to 10 °C crystalline methyl 3,4-di-*O*-acetyl-2,6-di-*O*-methyl-α-D-mannopyranoside (5 g) was obtained which had m.p. 61 °C and $[\alpha]_D$ +65.2° (*c*, 1.5 in chloroform).

Anal. Calcd. for $C_{13}H_{22}O_8$: C, 50.98; H, 7.24; OMe, 30.37. Found: C, 51.1; H, 7.3; OMe, 30.3.

The n.m.r. spectrum of the product in $CDCl_3$ showed three equal methoxyl signals at τ 6.57, 6.60, and 6.65, two equal acetoxyl signals at τ 7.96 and 8.00 and an H-1 doublet at τ 5.25 with a spacing of 1.8 c.p.s.

2,6-Di-O-methyl-D-mannose

Methyl 3,4-di-*O*-acetyl-2,6-di-*O*-methyl-α-D-mannopyranoside (5 g) in ethanol (5 ml) was treated with 2 *N* sulfuric acid (70 ml) and the mixture was heated on a boiling water bath for 5 h. The cooled reaction mixture after neutralization ($BaCO_3$) was passed down a column of mixed Rexyn 101(H^+) and Duolite A4(OH^-) ion-exchange resins (25 ml) and the eluate and washings were

concentrated to a syrup (3.1 g). Paper chromatographic analysis of the product showed a major component giving a red color with the *p*-anisidine hydrochloride spray reagent (R_G 0.72) together with a very faint spot corresponding in position with a mono-*O*-methylhexose. The syrup was fractionated on a cellulose column (5 × 40 cm) using butan-1-ol half saturated with water as the mobile phase and the fraction corresponding to 2,6-di-*O*-methyl-D-mannose was collected and concentrated to a syrup (2.8 g). The 2,6-di-*O*-methyl-D-mannose gave a single spot on paper chromatography (R_G 0.72) and had $[\alpha]_D$ +22.4° (*c*, 3.5 in water).

Anal. Calcd. for $C_8H_{16}O_6$: C, 46.15; H, 7.75; OMe, 29.8. Found: C, 46.1; H, 7.7; OMe, 30.0.

The n.m.r. spectrum of 2,6-di-*O*-methyl-D-mannose in deuterium oxide showed three methoxyl signals (total six protons) having τ 6.53, 6.58, and 6.61 and two doublets at τ 4.70 (spacing 1.5 c.p.s.) and τ 5.11 (spacing 2 c.p.s.) in the ratio 1:1.4 which are assigned to the respective α and β anomers of the glycose present in equilibrium.

Gas–liquid chromatographic analysis of the trimethylsilylated 2,6-di-*O*-methyl-D-mannose gave two peaks having T_G 0.77 (63%) and 0.96 (37%). The glycose had zero mobility on paper electrophoresis in 0.05 *M* sodium tetraborate.

2,6-Di-*O*-methyl-D-mannose (15 mg) was heated in a sealed tube at 90 °C for 5 h with 2% methanolic hydrogen chloride (2 ml) to yield the glycoside which on gas–liquid chromatography gave a single peak having T_G 3.24.

2,6-Di-O-methyl-D-mannonic Acid Phenylhydrazide

2,6-Di-*O*-methyl-D-mannose (0.1 g) was oxidized with bromine water at room temperature (48 h) and the 2,6-di-*O*-methyl-D-mannono-1,4-lactone (92 mg), isolated in the usual way, was a syrup which had $[\alpha]_D$ +58° (*c*, 5 in water) and on gas chromatography gave a single peak having T_G 3.68. Its infrared spectrum (smear on KBr disk) showed a carbonyl absorption at 1780 cm^{-1}. The lactone (80 mg) gave a phenylhydrazide derivative which after recrystallization from ethanol gave pure 2,6-di-*O*-methyl-D-mannonic acid phenylhydrazide (40 mg) which had m.p. 130 °C and $[\alpha]_D$ −40° (*c*, 0.5 in water).

Anal. Calcd. for $C_{14}H_{22}N_2O_6$: C, 53.49; H, 7.05; N, 8.91. Found: C, 53.5; H, 7.0; N, 9.0.

2,6-Di-O-methyl-D-mannitol (1,5-di-O-methyl-L-mannitol)

2,6-Di-*O*-methyl-D-mannose (0.1 g) in water (5 ml) was reduced by the addition of sodium borohydride (50 mg) and after 6 h the mixture was acidified with acetic acid and was passed down a column of Rexyn 101(H^+) ion-exchange resin (15 ml). The eluate and washings were concentrated to dryness and the residue was reconcentrated from methanol solution (5 × 25 ml) to remove boric acid to yield 2,6-di-*O*-methyl-D-mannitol (82 mg) as a syrup which had $[\alpha]_D$ +18.5° (*c*, 0.5 in water).

2,6-Di-*O*-methyl-D-mannitol (45 mg) was oxidized with 0.15 *M* sodium metaperiodate (5 ml) in a solution made up to 25 ml with distilled water. Samples were withdrawn at intervals for analysis; 1.88 moles of periodate were consumed and 0.85 mole of formic acid was released per mole of di-*O*-methylhexitol (constant value after 2 h oxidation at 22 °C). No formaldehyde was produced during the oxidation.

1. F. SMITH and H. C. SRIVASTAVA. J. Am. Chem. Soc. **81**, 1715 (1959).
2. P. A. J. GORIN and J. F. T. SPENCER. Can. J. Chem. **45**, 1543 (1967).
3. R. J. STOODLEY. Ph.D. Thesis. Queen's University, Kingston, Ontario. 1959.
4. J. O. DEFERRARI, E. G. GROS, and I. O. MASTRONARDI. Carbohydrate Res. **4**, 432 (1967).
5. W. BROCK NEELY. Advan. Carbohydrate Chem. **12**, 13 (1957).
6. L. HOUGH, J. K. N. JONES, and W. H. WADMAN. J. Chem. Soc. 1702 (1950).

Can. J. Chem. Downloaded from www.nrcresearchpress.com by 210.87.254.40 on 09/05/12
For personal use only.

Can. J. Chem. Downloaded from www.nrcresearchpress.com by 210.87.254.105 on 09/05/12
For personal use only.

Peak doubling in the nuclear magnetic resonance spectra of certain phosphorus esters

R. V. JARDINE, A. H. GRAY, AND J. B. REESOR
Chemistry Section, Defence Research Establishment Suffield, Ralston, Alberta

Received May 28, 1968

Doubling of nuclear magnetic resonances of certain mixed phosphorus esters has been observed and has been attributed to the presence of rotational conformers occupying "up" and "down" orientations of the ester moieties. Treatment of these esters with uranyl nitrate results in the expected resonances, although chemically shifted.

This is believed to be due to the "freezing" of rotational conformers by complex formation. Dependence of the observed resonances upon temperature supports this hypothesis. There appears to be some steric control over the relative population of the contributing conformers.

Canadian Journal of Chemistry, 47, 35 (1969)

Introduction

The literature contains several references to the doubling of absorptions in nuclear magnetic resonance (n.m.r.) spectra obtained on a variety of compounds. A number of explanations for this phenomena have been advanced, including partial bond hybridization (1), stereochemical nonequivalence of geminal protons (2), and hindered rotation (3, 4). Pertinent to this investigation is the work of Siddall and Prohaska (5) who reported doubling of resonances in a number of arylphosphinic and arylphosphonic esters and offered several alternative explanations. For example they attributed their findings to a different magnetic environment experienced by the phosphoryl alkoxy groups due to rotation about the P — O — C linkage, the observed resonances due then to contributions from one alkoxyl group "up", the other "down" with respect to the phosphoryl function. They also suggested, for the case of the isopropyl derivatives, a magnetic nonequivalence of the β methyl protons due to a "near to" and "far from" orientation with respect to the benzene ring, and they did not rule out the possibility of selective separation of diastereomers during preparation of the compound. It was concluded by these authors that a phenyl ring was a necessary structural feature.

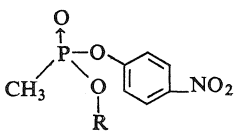

1

We have investigated mixed phosphorus esters of the general formula, **1**, and have observed doubling of resonances in a number of cases. Our choice of mixed esters, which include variation in asymmetry and in steric properties, has allowed a clear separation of the O—R moieties in the n.m.r. spectrum. With these compounds it has been possible to demonstrate that the O-alkyl function is occupying "up" and "down" conformations, a conclusion supported by temperature studies which show that peak doubling is not maintained at higher temperatures, i.e. 150 °C. We have further demonstrated that the conformation may be "frozen" probably in the "down" position by complex formation, utilizing uranyl nitrate. The alternative argument of "near to" and "far from" β methyl protons cannot be applied consistently to our compounds.

Results and Discussion

The spectra of isopropyl *p*-nitrophenyl methylphosphonate, (**2**), pinacolyl *p*-nitrophenyl methylphosphonate, (**3**), and pinacolyl *o*-chloro-*p*-nitrophenyl methylphosphonate, (**4**,) exhibited peak doubling.

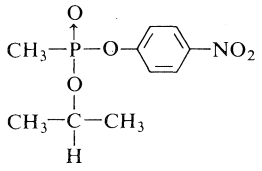

2

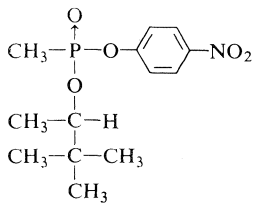

3

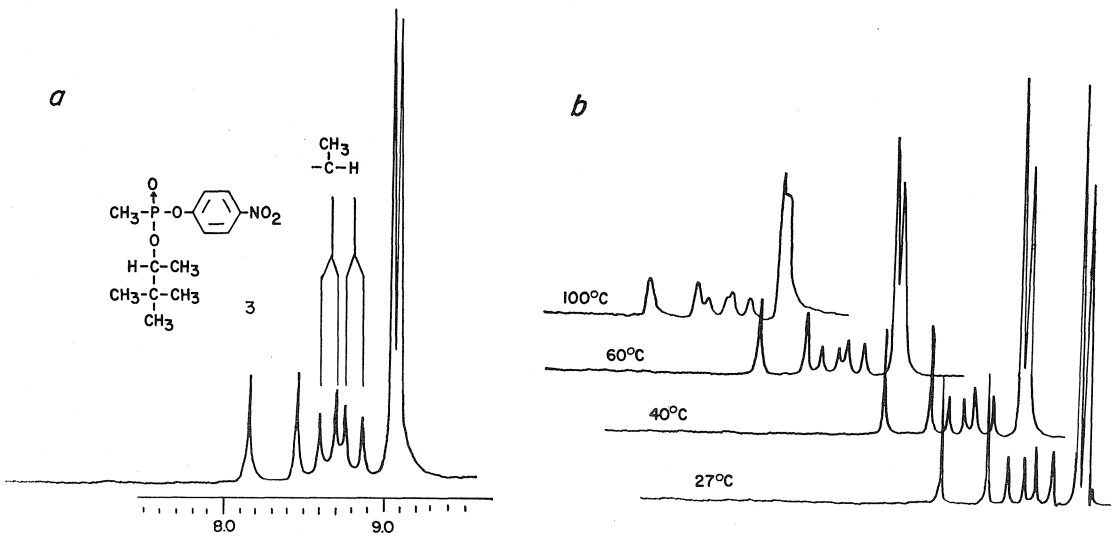

FIG. 1*a*. Partial nuclear magnetic resonance spectrum of pinacolyl *p*-nitrophenyl methylphosphonate, **3**, obtained in carbon tetrachloride using TMS as internal standard; *b*. Partial nuclear magnetic resonance spectra of pinacolyl *p*-nitrophenyl methylphosphonate, **3**, obtained in tetrachloroethylene at various temperatures.

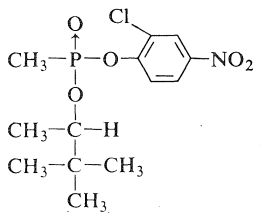

4

In isopropyl *p*-nitrophenyl methylphosphonate, (**2**), the β methyl protons appear as two doublets in solution. The β methyl protons of **3**, and **4**, appear as two doublets at $\tau = 8.83$ ($|J_{H-H}| = 6.5$ Hz); $\tau = 8.66$ ($|J_{H-H}| = 6.5$ Hz), (**3**): and $\tau = 8.65$ ($|J_{H-H}| = 6.5$ Hz); $\tau = 8.80$ ($|J_{H-H}| = 6.5$ Hz), (**4**): instead of the expected doublet (s) (see Table I). The tertiary butyl protons of the pinacolyl groups, normally singlets, as in pinacolyl methylphosphonochloridate, also appear as *two* singlets (see Fig. 1*a*).

The methine protons[1] of isopropyl *p*-nitrophenyl methylphosphonate, (**2**), and pinacolyl *p*-nitrophenyl methylphosphonate, (**3**,) revealed apparent 16 and 13 line spectra respectively (Figs. 4*a*, 4*b*). These resonances result from two sets of signals chemically shifted from each other by 1.9 Hz (**2**) and 2.05 Hz (**3**), which are split by phosphorus ($|J_{P-H}| = 8.0$ Hz) and resplit by the β methyl protons ($|J_{H-H}| = 6.4$ Hz), (**2**); ($|J_{H-H}| = 6.5$ Hz), (**3**).[2]

A computer programed for an A_6B system produced essentially the same pattern for the B region of **2** when four spectra were superposed 1.9, 8.0 and 9.9 Hz apart. Two superposed A_3BX spectra separated by 2.05 Hz produced the B portion of **3** (see Figs. 4*a*, 4*b*).

In all cases only one set of resonances due to the aromatic ring are present. We believe that this results from the fact that the aromatic protons lie well under the π electron cloud of the benzene ring, preventing operation of a through space mechanism (8). The *p*-nitrophenyl derivatives exhibit resplitting ($J = 1.0$ Hz) of the high field aromatic protons. This is probably due to

[1]The authors gratefully acknowledge Dr. T. H. Siddall III, Savannah River Laboratory, E. I. Dupont de Nemours & Co., Aiken, South Carolina, U.S.A., for drawing to our attention the significance of fully interpreting the methine proton signals.

[2]These spin systems may be regarded as superposed A_6BX, $A_6'B'X$ and A_3BX, $A_3'B'X$ respectively. As an approximation, the B portion of an A_6BX system has been calculated by superposing two parts of A_6B systems (6) in each of which there are 16 non zero lines. The system A_6B and A_6BX has been fully treated by Ranft (7). A note on the computer technique is to be published by A. Delaney.

Can. J. Chem. Downloaded from www.nrcresearchpress.com by 210.87.254.105 on 09/05/12
For personal use only.

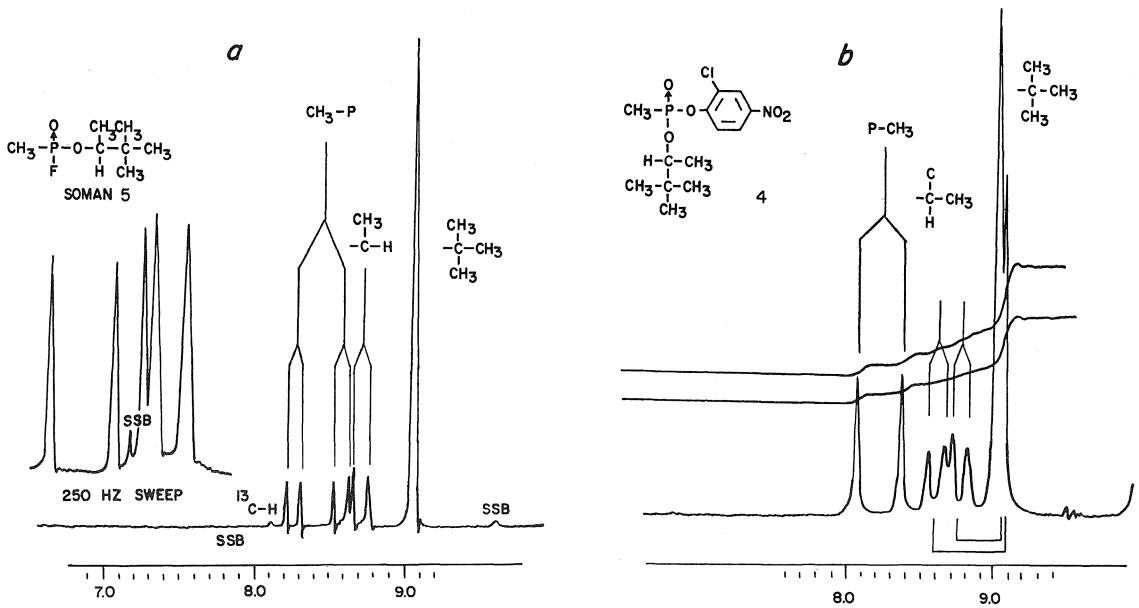

FIG. 2*a*. Partial nuclear magnetic resonance spectrum of Soman, **5**, obtained in carbon tetrachloride, using TMS as internal standard; *b*. Partial nuclear magnetic resonance spectrum of pinacolyl *o*-chloro-*p*-nitrophenyl methylphosphonate, using TMS as internal standard.

the proximity of the phosphorus atom. Long-range phosphorus coupling has recently been described in substituted benzyltriphenylphosphonium bromides. The magnitude of the coupling constant was found to be $p\text{-}CH_3 > o\text{-}CH_3 > m\text{-}CH_3$ (9).

Spectra of pinacolyl methylphosphonochloridate (neat and in CCl_4) also exhibited small doubling of the β methyl resonances ($\simeq 1$ Hz), which illustrates that a phenyl ring is not an essential structural feature. However, no similar doubling was noted in the spectrum of isopropyl methylphosphonochloridate or pinacolyl methylphosphonofluoridate (Soman, **5**). The complete spectrum of the latter, is presented in Fig. 2*a* for reference.

The dependence of the resonances of **2**, **3**, and **4** upon temperature was determined in tetrachloroethylene. Spectra of pinacolyl *p*-nitrophenyl methylphosphonate, (**3**), are presented in Fig. 1*b* and show that the peak separation for the β methyl and tertiary butyl groups are temperature dependent. As the temperature is increased, the peaks tend to coalesce.[3] The boiling point of the solvent did not allow higher temperature runs, however, in diphenyl ether complete coalescence of the peaks was observed at 150 °C, although the peaks were considerably broadened. Thus isopropyl *p*-nitrophenyl methylphosphonate, (**2**), pinacolyl *p*-nitrophenyl methylphosphonate, (**3**), and pinacolyl *o*-chloro-*p*-nitrophenyl methylphosphonate, (**4**), must exist in two rotameric conformations.

Moreover, compound **4** assumes "preferred" conformations in a ratio of about 2:3 (Fig. 2*b*). This is probably due to steric factors associated with the chlorine atom in close juxtaposition to the phosphorus. The n.m.r. spectra of compounds **2** and **3** did not reveal a similar preference (Fig. 1*a*).

Finally, isopropyl *p*-nitrophenyl methylphosphonate, **2**, pinacolyl *p*-nitrophenyl methylphosphonate, **3** and pinacolyl *o*-chloro-*p*-nitrophenyl methylphosphonate, **4**, were complexed with uranyl nitrate in pyridine. Burdett and Burger (10) have shown this to be a particularly useful technique for separating overlapping absorptions in n.m.r. spectra. They showed that the presence

[3]The same effect has been demonstrated in dimethyl formamide (3). At room temperature two absorptions are observed for the methyl protons, these coalesce at about 150 °C into a singlet.

Can. J. Chem. Downloaded from www.nrcresearchpress.com by 210.87.254.105 on 09/05/12
For personal use only.

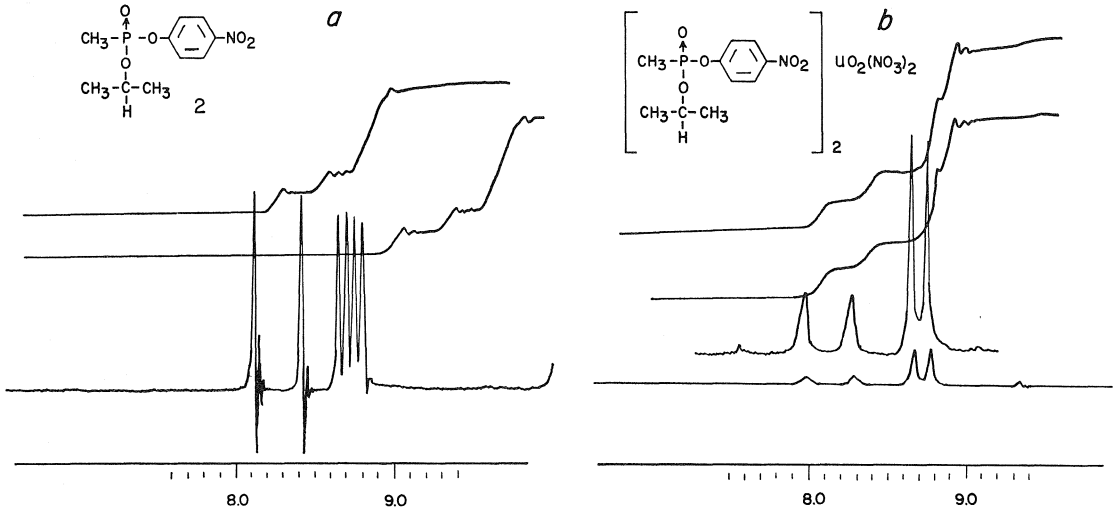

FIG. 3*a*. Partial nuclear magnetic resonance spectrum of isopropyl *p*-nitrophenyl methylphosphonate, **2**, obtained in pyridine using TMS as internal standard; *b*. Partial nuclear magnetic resonance spectrum of isopropyl *p*-nitrophenyl methylphosphonate uranyl nitrate complex obtained in pyridine, using TMS as internal standard.

of uranyl nitrate produced a significant downfield chemical shift[4] of the resonances of protons located on atoms as far as three bonds removed from phosphorus. All three compounds, **2**, **3**, and **4**, when complexed with uranyl nitrate[5] revealed this characteristic downfield shift. More significant, however, was the disappearance of peak doubling of the β methyl and tertiary butyl groups of the pinacolyl functions of **3** and **4** (Fig. 3*a*, 3*b*) and Table I. This is undoubtedly due to the fixation of the molecules into one conformation. The experimental technique does not permit a selective separation of diastereoisomers in the case of compounds **3** and **4**. The methine protons of **2** and **3** were simplified by complex formation. In pyridine **2** and **3** revealed broadened 8 and 5 line spectra respectively. Splitting of high-field aromatic protons is maintained after complex formation, confirming the integrity of the P—O—phenyl bond (acetone solution).

Our conclusion that certain organophosphorus esters exist in two forms, viz., "up" and "down" rotational conformers is well substantiated by our experimental results. It is consistent with the observations of doubling of spectra and changes which occur at high temperature. The use of mixed esters of vastly differing chemical shift has been used advantageously to observe the resonances of individual O—R moieties both in complexed and non-complexed forms.

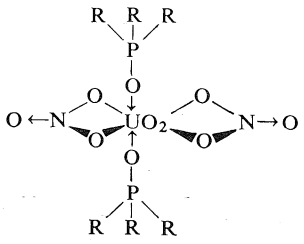

6

Experimental

Nuclear magnetic resonance (n.m.r.) spectra were determined on a Varian Associates A-60 instrument equipped with a V-6057 variable temperature system. Spectra were obtained as 20% w/v solutions in pyridine unless otherwise noted. Temperature experiments were cycled and spectra (n.m.r. and infrared (i.r.)) were obtained before and after, precluding decomposition during the experiment. On pertinent spectra the field was swept in both directions. Computed spectra were obtained on an IBM 1130 computer.

Thin-layer chromatography (t.l.c.) was carried out on Eastman Chromagram Sheet, type K 301 R (silica gel)

[4]While a downfield shift is normally observed, J. R. Ferraro (11) reports some cases of more highly shielded protons, as a result of complex formation with uranyl nitrate.

[5]X-ray crystallographic studies (12) have shown uranyl nitrate complexes of phosphoryl compounds to have the structure **6**.

Can. J. Chem. Downloaded from www.nrcresearchpress.com by 210.87.254.105 on 09/05/12
For personal use only.

TABLE I

Chemical shifts and coupling constants of compounds **2**, **3**, and **4** and their uranyl nitrate complexes

	PCH_3			P — O — C — H		P — O — C — CH_3			
		M*	J	M†	J		M	J	P — O — C — C — CH_3
2	8.30	2	18.0	5.10	6.4	8.73	2	6.0	—
						8.66	2	6.0	
2 Complex	8.02	2	18.0	4.68	6.4	8.63	2	6.0	—
3	8.22	2	18.0	5.62	6.5	8.83	2	6.5	9.10
						8.66	2	6.5	9.14
3 Complex	8.13	2	17.0	5.53	6.5	8.55	2	6.5	9.02
4‡	8.24	2	18.0	5.57	6.5	8.80	2	6.5	9.04
						8.65	2	6.5	9.09
4 Complex	8.32	2	17.0	5.59	6.0	8.71	2	6.0	9.16

*Resonances were observed at the multiplicity under M. Center of resonance is given in τ units relative to tetramethylsilane. Spectra run at 27 °C in pyridine unless noted otherwise.
†Complicated multiplet (see text).
‡Obtained in carbon tetrachloride.

with reagent chloroform as eluting solvent. Spots were visually located with iodine vapor. Elemental and n.m.r. analyses were in agreement with the proposed structures.

Column chromatography was carried out on Mallinckrodt silicic acid (chromatographic grade) eluting with benzene.

Isopropyl p-Nitrophenyl Methylphosphonate (2)[6]

Essentially the Fukuto (13) procedure was followed using 32.2 g (0.2 mole) of anhydrous sodium *p*-nitrophenoxide and 31.2 g (0.2 mole) of isopropyl methylphosphonochloridate in 250 ml of dry toluene. The yellow sodium salt had been previously dehydrated by azeotropic distillation of a toluene suspension to yield the red, anhydrous salt. After allowing the reagents to react for 15–20 min at room temperature the red color of the solution was discharged and a white precipitate (NaCl) formed. After refluxing 2 h the mixture was washed with 6 × 150 ml of distilled water and dried over anhydrous sodium sulfate. Distillation afforded the pure ester, b.p. 109°/0.005 mm; yield 31 g (61%); lit. (14) 130°/0.25 mm. Thin-layer chromatography of the material showed two spots of R_f 0.51 and 0.25. It was shown that with this and with a different solvent system, 5% MeOH/$CHCl_3$, the lower spot had an R_f value, identical with an authentic sample of *p*-nitrophenol. The n.m.r. spectra, however, showed no free phenol.

Pinacolyl p-Nitrophenyl Methylphosphonate (3)

Method a

A procedure similar to that used to prepare **2** was carried out on 32.2 g (0.2 mole) sodium *p*-nitrophenoxide and 39.7 g (0.2 mole) of pinacolyl methylphosphonochloridate in 250 ml toluene. The red color of the anhydrous salt disappeared after about 15–20 min. After further refluxing for 2 h the product was washed several times with water, dried over Na_2SO_4, and distilled to yield 33 g (55%) of yellow oil of b.p. 130–135°/0.03 mm, n_D^{25} 1.5092. Thin-layer chromatography showed two spots, an upper one of R_f 0.56 and a lower one of 0.25 corresponding to *p*-nitrophenol.

Anal. Calcd. for $C_{13}H_{20}NO_5P$: C, 51.82; H, 6.69; N, 4.65; P, 10.28. Found: C, 51.50; H, 6.67; N, 5.15; P, 10.10.

Method b

A run similar to Method *a* was carried out on 20 g (0.1 mole) of the chloridate and 16.1 g (0.1 mole) sodium *p*-nitrophenoxide. The red color of the salt disappeared after 10–15 min. Thin-layer chromatography of an aliquot taken after 1 h of refluxing showed the same two spot pattern as the distilled material from run *a*. The solution was refluxed 4 h more and let stand overnight. Thin-layer chromatography of an aliquot showed no further change had taken place. The toluene solution was then filtered through Celite and the solvent distilled. A fraction of this yellow residue (10.5 g) was chromatographed on 200 g of silicic acid eluting with benzene. The early fractions contained *p*-nitrophenol (note reverse order—the phenol is the lower spot on t.l.c.). After several hundred ml of eluent were collected, the desired material began to come off as shown by t.l.c. and inhibited cholinesterase preparation. In this way about 5 g of material were collected. The n.m.r. and t.l.c. results were identical to those obtained with the distilled material from Method *a*.

Pinacolyl o-Chloro-p-nitrophenyl Methylphosphonate (4)

Anhydrous sodium *o*-chloro-*p*-nitrophenoxide 12.65 g (0.073 mole) in 100 ml dry toluene was treated with 14.5 g (0.073 mole) pinacolyl methylphosphonochloridate in 50 ml dry toluene in a dropwise manner. An exothermic reaction ensued (28–42°). On completion of addition the products were refluxed 3 h, cooled and a quantity of Celite added. The products were then filtered through a Celite filter pad, followed by toluene. The resulting solution was then distilled yielding a viscous yellow oil (5 g, 21.8%) of b.p. 135–138°/0.01 mm.

[6]CAUTIONARY NOTE: The compounds described in this paper are toxic anticholinesterases and must be handled with requisite care.

Can. J. Chem. Downloaded from www.nrcresearchpress.com by 210.87.254.105 on 09/05/12
For personal use only.

Can. J. Chem. Downloaded from www.nrcresearchpress.com by 210.87.254.105 on 09/05/12
For personal use only.

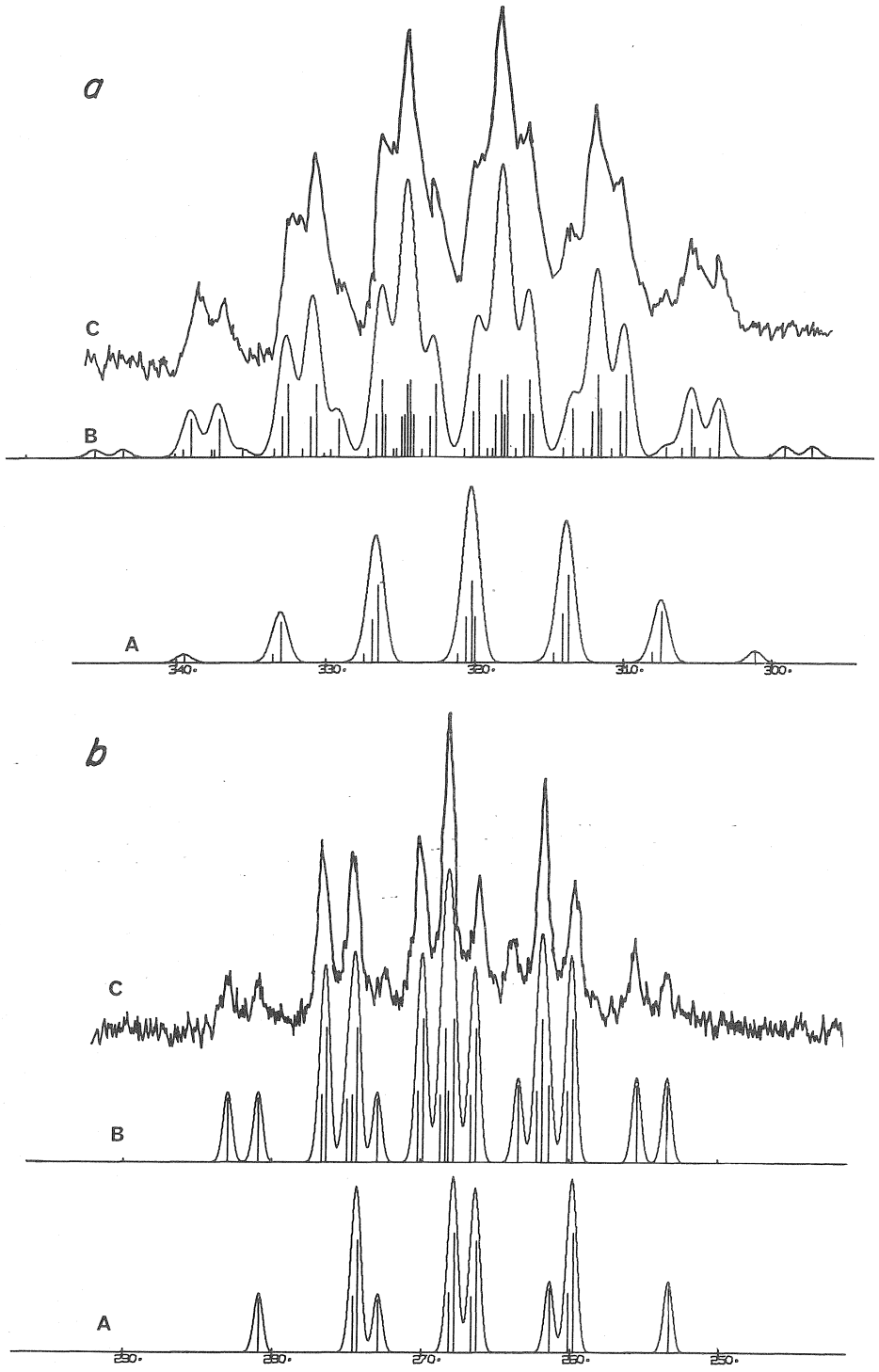

FIG. 4*a*. The methine proton of isopropyl *p*-nitrophenylmethylphosphonate, **2**, obtained in $CDCl_3$: (A) calculated A_6B spectrum; (B) calculated $A_6A'_6BB'X$ spectrum; (C) observed spectrum; *b*. The methine methine proton of pinacolyl *p*-nitrophenyl methylphosphonate obtained in $CDCl_3$; (A) calculated A_3BX spectrum; (B) calculated $A_3A_3'BB'X$ spectrum; (C) observed spectrum.

Anal. Calcd. for $C_{13}H_{19}O_5PNCl$: C, 46.51; H, 5.70; N, 4.17; P, 9.23; Cl, 10.56. Found: C, 46.45; H, 5.68; N, 4.13; P, 9.19; Cl, 10.55.

Uranyl Nitrate Complexes General

One molar equivalent of uranyl nitrate hexahydrate in sufficient pyridine to maintain solubility was treated with two equivalents of the phosphorus ester. The resulting solution was stirred 8 h and the n.m.r. spectrum obtained directly from an aliquot of the resulting yellow solution. When it was of interest to examine the aromatic region, the complexes were prepared in acetone.

Acknowledgments

The authors wish to thank Mr. A. S. Hansen, Miss L. E. Nelson, and Mr. L. R. Provost for assistance in the synthesis of the compounds described and for the n.m.r. spectra. Thanks are also extended to Mr. R. Hicken for the elemental analyses and to Mr. A. Delaney for programming computed spectra.

1. H. FINEGOLD. J. Am. Chem. Soc. **82**, 2641 (1960).
2. J. S. WAUGH and F. A. COTTON. J. Phys. Chem. **65**, 562 (1961).
3. H. S. GUTOWSKY and C. H. HOLM. J. Chem. Phys. **25**, 1228 (1956).
4. J. J. DRYSDALE and W. D. PHILLIPS. J. Am. Chem. Soc. **79**, 319 (1957).
5. T. H. SIDDALL and C. A. PROHASKA. J. Am. Chem. Soc. **84**, 3467 (1962).
6. K. D. BARTLE, R. S. EDMUNDSON, and D. W. JONES. Tetrahedron, **23**, 1701 (1967).
7. J. RANFT. Ann. Physik, **10**, 1 (1962).
8. J. S. WAUGH and R. W. FESSENDEN. J. Am. Chem. Soc. **79**, 846 (1957).
9. K. KHALEEDUDDIN and J. M. W. SCOTT. Chem. Commun. No. 15, 511 (1966).
10. J. L. BURDETT and L. L. BURGER. Can. J. Chem. **44**, 111 (1966).
11. J. R. FERRARO. J. Inorg. Nucl. Chem. **26**, 225 (1964).
12. J. E. FLEMING and H. LYNTON. Chem. Ind. 1409, (1959).
13. T. R. FUKUTO and R. L. METCALF. J. Am. Chem. Soc. **81**, 372 (1959).
14. A. M. DE ROOS. Rec. Trav. Chim. **78**, 145 (1959).

Can. J. Chem. Downloaded from www.nrcresearchpress.com by 210.87.254.105 on 09/05/12
For personal use only.

Reactions of ozonides. VIII. An examination of the possibility of reversible ozonide formation using ^{14}C labelling

DUNDAPPA R. KERUR AND DENNIS G. M. DIAPER
Department of Chemistry and Chemical Engineering, Royal Military College of Canada, Kingston, Ontario
Received May 15, 1968

Carboxyl-^{14}C-10-formyldecanoic acid was made by $^{14}CO_2$ carbonation of 10-undecenylmagnesium bromide and ozonolysis of the product. Attempts were made to equilibrate its methyl ester with

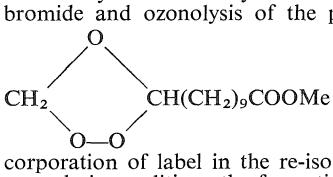

and

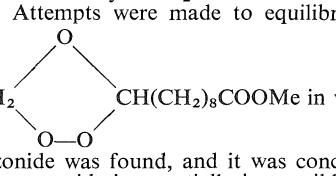

in various solvents. Little incorporation of label in the re-isolated ozonide was found, and it was concluded that under normal ozonolysis conditions the formation of ring ozonide is essentially irreversible. Slight incorporation in chloroform is explicable either by reversal of the Criegee mechanism of ozonide formation or by reversal of the recently suggested regenerative carbonyl – primary ozonide reactions.

Canadian Journal of Chemistry, 47, 43 (1969)

A recent interest in the mechanism of formation of ozonides from olefins has been sparked by a close examination of the stereochemistry of the reaction. The Criegee mechanism (1) accommodates stereospecificity by invoking a solvent cage which must be penetrated in cross-ozonide formation (2). To explain different *cis–trans* ozonide ratios in cross ozonides from *cis* and *trans* olefins, a mechanism has been proposed involving a carbonyl – primary ozonide interaction step (3). Recently, refinements have been added to the Criegee mechanism by advocating the formation of *syn* and *anti* zwitterions which combine stereospecifically with aldehydes or ketones to yield ozonides (4).

Two schools have studied ozonide ring formation using isotopic oxygen (3*b*, 5, 6). Incorporation of the label in both the ether and peroxidic oxygens of aliphatic ozonides was interpreted to mean simultaneous operation of the Criegee mechanism and a regenerative carbonyl – primary ozonide interaction as shown:

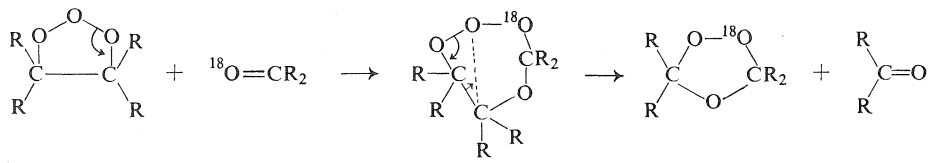

In the aromatic ^{18}O study, peroxide incorporation was very nearly negligible and the label appeared in the ether oxygen. This supports the Criegee mechanism, but does not exclude interactions of the type shown above, because it was pointed out that the same seven-membered intermediate can give ether-labelled ozonide by a C—O fission of the primary ozonide as shown below rather than O—O fission as shown above:

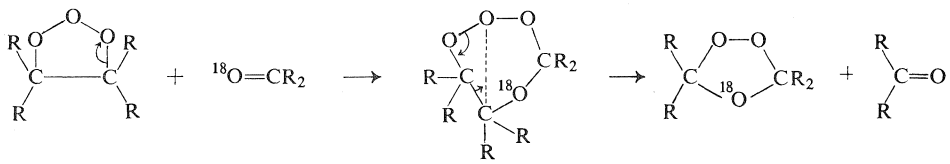

Can. J. Chem. Downloaded from www.nrcresearchpress.com by 210.87.254.105 on 09/05/12
For personal use only.

TABLE I

Radioactivity (*c*/min/ml) of fractions after equilibration

	Ozonide*		Aldehyde ester†		
	Fraction 1	Fraction 2	Fraction 3	Fraction 4	Fraction 5
Ether	45 ± 3‡	252 ± 7	3661 ± 56	5483 ± 6	1678 ± 15
	24 ± 3	114 ± 3	1440 ± 7	3744 ± 10	1456 ± 19
Methanol	23 ± 5	67 ± 6	1639 ± 48	3182 ± 21	805 ± 26
Chloroform	135 ± 6	587 ± 8	3642 ± 42	645 ± 4	
Acetone	64 ± 10	64 ± 4	6299 ± 82	816 ± 10	

*Eluted with 5% ether in petroleum ether (30–60°).
†Eluted with ether.
‡Counting errors were determined as standard deviations (7).

These results have prompted us to reexamine the reversibility of ozonide formation. Each of the mechanisms considered calls for nonreversible ozonide formation but the nonuniform ^{18}O incorporation in peroxide and ether oxygens could also be explained by reversal of the carbonyl–ozonide step. Early work was based on ozonolyses in the presence of foreign carbonyl compounds and indicated nonreversibility. We have used a ^{14}C tracer technique which is more sensitive and permits the "foreign" aldehyde to be chemically identical with that from the substrate.

For our studies we chose the ozonide of methyl 10-undecenoate. This ozonide is readily purified from peroxidic reaction products, is relatively stable and is easy to handle. The nonperoxidic decomposition product of interest obtained from this ozonide is the methyl ester of sebacic semialdehyde. In earlier experiments we prepared this compound labelled with ^{14}C on the ester methyl carbon by reacting ^{14}C-diazomethane with sebacic semialdehyde. However, it soon became evident that use of this compound in equilibration studies with the ozonide was obscured by considerable ester interchange.

We then decided to use the next higher homologue, the methyl ester of carboxyl-^{14}C-10-formyldecanoic acid. This was readily prepared from 11-bromo-1-undecene by the sequence of steps shown in the Experimental section.

Equilibration of methyl 10-undecenoate ozonide with the ^{14}C-labelled aldehyde ester was attempted at room temperature for 18–48 h in solvents which varied over a wide range of polarity. Solvents used were chloroform, methanol, ether, acetone, and dimethyl sulfoxide. Ozonide could be recovered in good yield from each of these solvents except the last.

Separation of the ozonide and the aldehyde ester was effected on a silica gel column. Advantage was taken of the fact that on elution with 5% ether in petroleum ether (30–60°), the ozonide moved considerably faster than the aldehyde ester. Once the ozonide fraction had been completely removed, recovery of the aldehyde ester fraction was expedited by washing the column with ether.

Under the experimental conditions used, the ozonide did not show any appreciable decomposition except in dimethyl sulfoxide. The latter proved to be unsuitable for our purposes and no ozonide was recovered after attempted equilibration. The effects of this solvent on ozonides will be the subject of a later communication.

Examination of Table I reveals that, in none of the solvents used except chloroform did we observe any significant amounts of radioactivity in the recovered ozonide fraction. Almost all of the activity could be accounted for in the non-ozonide fraction. In chloroform some equilibration does occur, negligible under normal ozonation conditions.

The chloroform experiment was repeated using the methyl ester of carboxyl-^{14}C-10-formyldecanoic acid and methyl 11-dodecenoate ozonide. After contact, specific activity of the recovered ozonide was 6.06 ± 0.13 *c*/min/mg and that of the recovered aldehyde ester was 147.8 ± 0.43 *c*/min/mg. The ozonide fraction was rechromatographed and found to have a specific activity of 7.09 ± 0.22 *c*/min/mg. The fact that purification did not decrease the specific activity but rather slightly increased it, shows that the radioactivity was not attributable to impurity. While negligible under ordinary

Can. J. Chem. Downloaded from www.nrcresearchpress.com by 210.87.254.105 on 09/05/12
For personal use only.

Can. J. Chem. Downloaded from www.nrcresearchpress.com by 210.87.254.105 on 09/05/12
For personal use only.

preparative conditions, this must mean that during prolonged contact, some formation of ozonide from the carbonyl moiety can occur.

A time study of aldehyde–ozonide reaction in chloroform showed that equilibrium was approximately half way attained in 0.5–4 h. There was no attempt to control catalyst traces (such as HCl from chloroform photooxidation in moist air) and no quantitative conclusions were drawn about reaction rate, but in this solvent, under ordinary ozonolysis conditions, exchange amounting to a few per cent may be possible.

If this reaction takes place by the reopening of the ozonide ring to form carbonyl and zwitterion fragments, this implies a finite lifetime for the zwitterion in chloroform during which a nonradioactive carbonyl fragment is replaced by a labelled carbonyl fragment which has diffused to the reaction site. Reaction of the zwitterion with itself or with solvents such as methanol or acetone, would prohibit labelled ozonide formation.

If the carbonyl – initial ozonide regenerative mechanism for ozonide formation can be reversed, the nature of the solvent should also affect the rate and extent of the reverse mechanism. Acetone would compete with the labelled carbonyl compound and lead to low incorporation. Polar solvents by encouraging charge separation would assist forward and reverse reactions. Incorporation of the label would therefore depend on reactions competing with the forward reaction. It was noticed that a purified ozonide during prolonged storage gives polymeric peroxidic products as well as the aldehyde and acid expected as decomposition products. The observed small incorporation of label when ozonide and aldehyde are contacted for prolonged periods in chloroform is therefore explicable by both types of ozonide formation mechanisms. Caution must be used in detailed quantitative interpretation of labelling mechanism studies if conditions permit reverse reaction.

Any quantitative study of ozonide formation, such as the recent ^{18}O work (5, 6) should be interpreted with the possibility of equilibration in mind. Aromatic compounds show less incorporation of ^{18}O in the peroxide oxygen of the ozonide ring than do the aliphatic compounds reported. It is not likely that the difference can be explained by equilibration, which our study shows to be near negligible under ordinary ozonolysis conditions, rather it is explicable by reactivity differences between the various intermediates involved. An aromatic zwitterion for example would be expected to be different from an aliphatic zwitterion because of resonance stabilization.

In view of these observations, it seems safe to conclude that there is no equilibrium established between the ozonide on the one hand and the zwitterion and the carbonyl moiety on the other, under customary ozonide preparation conditions when carbonyl concentration is low, temperature is low and contact time short. Moreover, significant fission of the ozonide ring to reform the zwitterion is also unlikely. Fliszar (8, 9) has shown that the zwitterion can change into carbonyl compound by bimolecular elimination of oxygen. Ozonide ring closure is thus essentially nonreversible in ozonide formation from this terminal olefin.

Experimental

Barium carbonate-^{14}C was from New England Nuclear Corp., Boston, Massachusetts. It had a specific activity of 5.0 millicuries/mmole.

"Baker Analyzed" reagent grade silica gel powder was used for column chromatography.

Thin-layer chromatography was performed on Eastman Chromagram sheets without fluorescent indicator.

3% Potassium iodide in 5% aqueous acetic acid was used for spraying.

Melting point was determined on a Fisher–Johns melting point apparatus and is uncorrected.

Counting of radioactive samples was done on a Nuclear-Chicago counter. Nuclear magnetic resonance (n.m.r.) spectrum was recorded on a Varian A-60A model spectrometer using tetramethylsilane as internal reference.

Microanalyses were carried out by Microanalyses Laboratory, Toronto.

10-Undecenoic acid, m.p. 21–23°, was from Brickman and Company, Montreal. Its methyl ester, b.p. 244–248°, n_D^{24} 1.4388, was prepared by refluxing with methanol in the presence of concentrated sulfuric acid.

The ozonide of methyl 10-undecenoate was prepared by passing a stream of ozone-oxygen mixture through a solution of the ester in carbon tetrachloride. After removing the solvent on a rotary evaporator, the residue was chromatographed on a silica gel column. A solution of 5% ether in petroleum ether (30–60°) was used for elution. Fractions were examined by thin-layer chromatography and those that reacted readily with the spray reagent to give single spots were pooled. Removal of the solvent gave the ozonide as a white powdery material. It was stored under nitrogen at −10° and was used as soon as feasible. Methyl 11-dodecenoate ozonide was similarly prepared and isolated using the corresponding olefinic ester as starting material. Its n.m.r. spectrum in $CDCl_3$

showed the expected $COOCH_3$ signal at $\delta = 3.63$ p.p.m. and the chain CH_2 protons as a broad peak at $\delta = 1.32$. The α-CH_2 triplet (position-2) was centered at $\delta = 2.28$. The characteristic terminal alkene ozonide signal was two singlets of the non-equivalent methylene located at $\delta = 4.98$ and 5.12 superimposed on the CH triplet centered at $\delta = 5.09$ with a coupling constant of 4.5 c.p.s.

^{14}C-Labelled aldehyde ester was prepared by the following sequence of reactions.

$$CH_2{=}CH(CH_2)_8CH_2Br \xrightarrow[2)\ {}^{14}CO_2\ 3)\ H^+\ 4)\ CH_2N_2]{1)\ Mg} CH_2{=}CH(CH_2)_8CH_2{}^{14}CO_2CH_3$$

$$CH_2{=}CH(CH_2)_8CH_2{}^{14}CO_2CH_3 \xrightarrow[2)\ Zn/CH_3CO_2H]{1)\ O_3} CHO(CH_2)_8CH_2{}^{14}CO_2CH_3$$

The n.m.r. spectrum of an undiluted sample of the aldehyde ester showed a singlet at $\delta = 3.63$ ascribed to $-COOCH_3$, two α-CH_2 triplets centered at $\delta = 2.05$ and $\delta = 2.29$. The chain $-CH_2$ protons gave a peak at $\delta = 1.30$ and the —CHO proton was observed at $\delta = 9.70$. The characteristic terminal ozonide signal at $\delta = 5$ p.p.m. was absent. Peaks due to ozonide were absent from the infrared spectrum. A nonradioactive sample of the aldehyde–ester and the radioactive sample had identical infrared spectra. The semicarbazone of the aldehyde ester melted at 112–114° (lit. (10) 114–115°).

Anal. Calcd. for $C_{13}H_{25}O_3N_3$: N, 15.49. Found: N, 15.04, 14.99.

The radioactive aldehyde–ester was dissolved in ether and aliquots were withdrawn for equilibration experiments. The ether solution registered about 20 000 *c*/min/ml.

The ozonide and the radioactive aldehyde ester were mixed in 1–5 ml each of methanol, chloroform, acetone, and dimethyl sulfoxide at room temperature for about 18–48 h. After standing, solvent was removed if necessary and the residue chromatographed on a silica gel column. Appropriate fractions corresponding to the ozonide and the aldehyde ester were pooled and evaporated. Residues were usually taken up in 10 ml of ether. One ml of this solution was evaporated on a planchet and counted. In order to clarify the slight incorporation observed when chloroform was used as a solvent a further experiment was conducted as follows: Methyl 11-dodecenoate ozonide and the methyl ester of carboxyl-^{14}C-10-formyldecanoic acid were mixed in 5 ml of chloroform and allowed to stand at room temperature for 24 h. The ozonide and aldehyde–ester fractions were separated using a silica gel column as described above and their specific activities determined. The recovered ozonide was repurified using a silica gel column and its specific activity was redetermined.

In another experiment 250 mg of methyl 11-dodecenoate ozonide and approximately 250 mg of the methyl ester of carboxyl-^{14}C-10-formyldecanoic acid (128.2 $\pm$ 0.71 *c*/min/mg) were mixed in 5 ml of chloroform at 28°. Separation was performed by silica gel chromatography as previously described after 30 min of contact. The specific activity of recovered ozonide was 4.79 $\pm$ 0.10 *c*/min/mg raised to 4.85 $\pm$ 0.09 *c*/min/mg on repurification. In a similar experiment with similar quantities but a contact time of 1 h, recovered ozonide had 3.42 $\pm$ 0.22 *c*/min/mg. After 8 h of further contact with an additional 250 mg of radioactive aldehyde–ester in 5 ml of chloroform, this sample was re-isolated and now had 8.32 $\pm$ 0.10 *c*/min/mg. In a similar experiment with 4 h of contact time, recovered ozonide had 3.44 $\pm$ 0.20 *c*/min/mg and after a further 14 h of contact with a fresh 250 mg sample of radioactive aldehyde–ester this was raised to 7.90 $\pm$ 0.19 *c*/min/mg.

Corrections were made for background counts (81–108 *c*/min.)

Acknowledgments

The authors wish to thank Prof. S. N. Naldrett of this department for the use of counting facilities. Financial assistance from Defence Research Board under Grant No. 9530–17 is gratefully acknowledged.

1. (*a*) R. Criegee. Record Chem. Progr. Kresge–Hooker Sci. Lib. **18**, 111 (1957). (*b*) P. S. Bailey. Chem. Rev. **58**, 925 (1958).
2. R. W. Murray, R. D. Youssefyeh, and P. R. Story. J. Am. Chem. Soc. **88**, 3143 (1966).
3. (*a*) P. R. Story, R. W. Murray, and R. D. Youssefyeh. J. Am. Chem. Soc. **88**, 3144 (1966). (*b*) P. R. Story, C. E. Bishop, J. R. Burgess, J. B. Olson, R. W. Murray, and R. D. Youssefyeh. Original Manuscripts submitted to International Oxidation Symposium, San Francisco, California. Aug. 28–Sept. 1. 1967. Vol. II. p. 325. (*c*) P. R. Story, C. E. Bishop, J. R. Burgess, R. W. Murray, and R. D. Youssefyeh. J. Am. Chem. Soc. **90**, 1907 (1968).
4. N. L. Bauld, J. A. Thompson, C. E. Hudson, and P. S. Bailey. J. Am. Chem. Soc. **90**, 1822 (1968).
5. S. Fliszar, J. Carles, and J. Renard. J. Am. Chem. Soc. **90**, 1364 (1968).
6. C. E. Bishop and P. R. Story. J. Am. Chem. Soc. **90**, 1905 (1968).
7. M. Calvin, C. Heidelberger, J. C. Reid, B. M. Tolbert, and P. F. Yankwich. Isotopic carbon. John Wiley and Sons, Inc., New York. 1949. p. 283.
8. S. Fliszar, D. Gravel, and E. Cavalieri. Can. J. Chem. **44**, 1013 (1966).
9. S. Fliszar and J. B. Chylinska. Can. J. Chem. **46**, 783 (1968).
10. G. C. Tomecko and R. Adams. J. Am. Chem. Soc. **49**, 522 (1927).

Can. J. Chem. Downloaded from www.nrcresearchpress.com by 210.87.254.105 on 09/05/12
For personal use only.

Synthesis of 3-(1,1-ethylenedioxyoctyl)-cyclopentanone

D. E. Orr and F. B. Johnson
Department of Chemistry, Lakehead University, Port Arthur, Ontario
Received August 12, 1968

1,4-Cyclohexanedione has been converted into compounds **8** and **9**. Treatment of **8** and **9** with base produces compound **10**, which has been converted into 3-(1,1-ethylenedioxyoctyl)-cyclopentanone.

Canadian Journal of Chemistry, 47, 47 (1969)

Can. J. Chem. Downloaded from www.nrcresearchpress.com by 210.87.254.105 on 09/05/12
For personal use only.

A number of publications have recently appeared (1–6) describing the syntheses of various naturally occurring prostaglandins and related compounds. With the exception of the elegant method of Corey *et al.* (1) all the syntheses described so far rely on the modification of a five-membered ring compound to produce the prostaglandin skeleton.

We have approached the problem by using a readily available six-membered carbocyclic ring compound as the starting material. A seven carbon atom side chain is added in the first step. At a later stage in the reaction sequence, the length of the seven carbon atom chain is increased by one carbon atom by the contraction of the six-membered ring to produce a suitably substituted five-membered ring. The ring contraction not only gives a side chain of the correct length but also generates a ketone function in the eight carbon side chain, in a position suitable for later introduction of the allyl alcohol function.

When a half-molar equivalent of *n*-heptyl magnesium bromide was added to 1,4-cyclohexanedione it was possible to separate 4-heptyl-4-hydroxycyclohexanone **1** as the mono-adduct from the reaction mixture.

The keto-alcohol **1** was quantitatively reduced to 1-heptyl-1,4-cyclohexanediol **2**. The nuclear magnetic resonance (n.m.r.) spectrum has broad multiplets at τ 6.15 and 6.5 of roughly equal area corresponding to epimeric alcohols. Thin-layer chromatography (t.l.c.) confirmed that two closely related compounds were present.

Acetylation of the epimeric mixture of diols with acetic anhydride – pyridine gave the monoacetate **3**. The acetate **3** was dehydrated by heating under reflux in acetic anhydride to give a product composed of two compounds (by t.l.c.). The n.m.r. spectrum has peaks due to a hydrogen atom on a double bond and a hydrogen atom attached to the same carbon atom as the acetoxy group. Also included in the spectrum are two sharp peaks at τ 8.06 and 8.02, due to two very similar acetate methyl groups. The chromatographic and n.m.r. evidence is compatible with the product being composed of exocyclic and endocyclic double bond isomers **4** and **5**, respectively.

Acid-catalyzed equilibration of this olefinic mixture converted it into the more stable endocyclic olefin **5** (7). The reaction could be followed conveniently by the disappearance of one of the spots on the t.l.c. plate. Further reactions in the synthetic sequence, and the broad peak in the n.m.r. spectrum at τ 4.7 indicate that the product is correctly represented by structure **5**.

cis-Hydroxylation of 1-heptyl-4-acetoxy-1-cyclohexene **5** was effected by treating it with OsO_4–pyridine in ether (8). The intermediate complex was decomposed on treatment with mannitol. The decomposition of the complex also resulted in partial hydrolysis of the acetoxy group. Complete hydrolysis occurred on treatment of the product with KOH in aqueous alcohol, to give the two possible epimeric triols **6** and **7**.

The triol epimers were converted into the corresponding secondary ditosylates by treating with tosyl chloride and pyridine. Two crystalline ditosylates **8** and **9** (R = Ts) could be isolated from the reaction product. Elemental analyses and almost identical infrared (i.r.) spectra were consistent with the fact that these two compounds were indeed epimeric at the secondary tosyl group in the 4-position.

Treatment of the mixture of crystalline tosylates with $CaCO_3$ in dimethyl formamide under reflux brought about the desired ring contraction, as was shown by the appearance of a peak at 1700 cm^{-1} in the i.r. spectrum of the product **10** (9). The secondary tosyl group was also lost in the work-up as was shown by the absence of characteristic peaks in the i.r. and n.m.r. spectra, and by

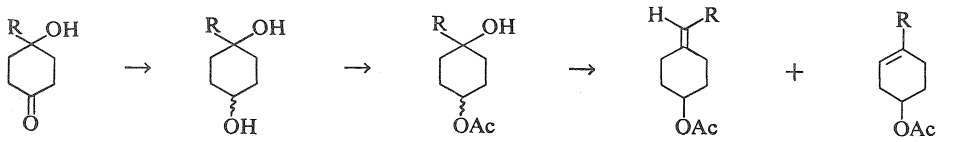

1 R = *n*-heptyl **2** R = *n*-heptyl **3** R = *n*-heptyl **4** R = *n*-hexyl **5** R = *n*-heptyl

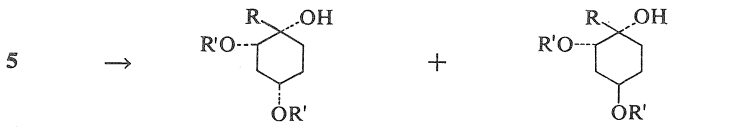

6 R = *n*-heptyl R′ = H
8 R = *n*-heptyl R′ = Ts
7 R = *n*-heptyl R′ = H
9 R = *n*-heptyl R′ = Ts

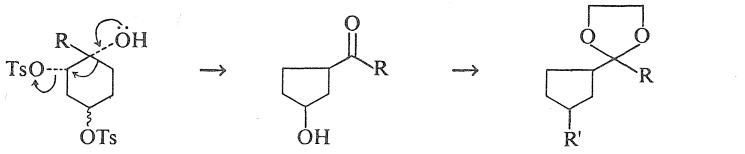

8 or **9** R = *n*-heptyl **10** R = *n*-heptyl **11** R = *n*-heptyl R′ = OH
12 R = *n*-heptyl R′ = =O

the presence of a peak at 3400 cm^{-1} in the i.r. spectrum of the product, due to the hydroxyl group.

The rearrangement product **10**, which was homogeneous on t.l.c., was converted into the ethylene ketal **11** by heating under reflux in benzene with ethylene glycol and a catalytic amount of *p*-toluenesulfonic acid.

The ketal was oxidized with chromium trioxide in pyridine to give the keto-ketal **12**. The product was homogeneous by t.l.c. analysis and had a peak in the i.r. spectrum at 1740 cm^{-1}, showing the presence of a five-membered ring ketone.

Elemental analyses and the n.m.r. spectrum were also in agreement with structure **12**. A sharp peak at τ 6.1 is indicative of the ethylene ketal protons and a broad multiplet centered at τ 7.8 is due to the hydrogen atoms α to the ketone. The remainder of the n.m.r. spectrum is in agreement with the presence of a large hydrocarbon side chain.

These results show that this approach to the prostaglandin skeleton is feasible and we are now in the process of incorporating the seven carbon atom side chain by direct alkylation or by rearranging the appropriately substituted cyclohexane ring.

Experimental

Infrared (i.r.) spectra were of chloroform or carbon tetrachloride solutions. Nuclear magnetic resonance (n.m.r.) spectra were of deuteriochloroform or carbon tetrachloride solutions with tetramethylsilane as internal standard.

4-Heptyl-4-hydroxycyclohexanone **1**

A solution of *n*-heptyl bromide (17.5 g; 0.1 mole) in anhydrous ether (150 ml) was added dropwise over a period of 2 h to a stirred mixture of magnesium (2.43 g; 0.1 mole) and ether (50 ml). During the addition, reflux was maintained by occasional warming of the reaction flask. After addition was complete, reflux was continued for 1 h. The Grignard reagent solution was cooled and transferred to a dry 250 ml dropping funnel while maintaining a nitrogen atmosphere. The Grignard reagent was then added dropwise to a stirred solution of 1,4-cyclohexanedione (10 g; 0.1 mole), in anhydrous ether (200 ml). Addition was completed in 2 h after which the reaction was heated under reflux for 1 h.

The reaction mixture was allowed to cool and then diluted to 600 ml with ether. The resulting organic layer was washed with a saturated solution of ammonium chloride until the aqueous washings were acidic. The organic layer was then washed with water, and after drying, the ether was removed by flash evaporation. The crude product was obtained as a clear, viscous, yellow oil (5.96 g). Thin-layer chromatography (silica–ether eluent) revealed the presence of four products, in an overall yield of 37%.

Vacuum distillation of the crude product gave 4-heptyl-4-hydroxycyclohexanone **1**; b.p. 0.9 mm 128°, in a 24% yield (3.84 g) as a clear, viscous, yellow oil; n_D^{25} 1.4741.

Can. J. Chem. Downloaded from www.nrcresearchpress.com by 210.87.254.105 on 09/05/12
For personal use only.

Can. J. Chem. Downloaded from www.nrcresearchpress.com by 210.87.254.105 on 09/05/12
For personal use only.

Thin-layer chromatography (silica–ether eluent) of the product showed the presence of one compound.

Infrared spectrum: 3600 cm^{-1}, 3400 cm^{-1}. Nuclear magnetic resonance spectrum: τ 6.4 (hydroxyl hydrogen, disappears when treated with D_2O), τ 8.1 (4 hydrogens α to the ketone) τ 8.6–9.1 (remaining methyl and methylene hydrogens).

1-Heptyl-1,4-cyclohexanediol **2**

1-Heptyl-4-hydroxycyclohexanone (1.80 g) was dissolved in methanol (50 ml). Sodium borohydride (1.50 g) was added in one portion to the solution. After 1 h, water (10 ml) was added to destroy the excess of sodium borohydride. The reaction mixture was diluted to 100 ml with ether and the organic layer was washed with 2% HCl solution followed by washing with water. The organic layer was dried over anhydrous magnesium sulfate, filtered, and the ether removed by flash evaporation to give 1.67 g of product (92% yield). Thin-layer chromatography (silica–ether eluent) indicated two products with no indication of starting material.

Infrared spectrum: 3600 cm^{-1}, 3400 cm^{-1}. Nuclear magnetic resonance spectrum: τ 6.15 and 6.5 (hydrogens on the same carbon atoms as the hydroxyls), τ 7.6 (hydroxyl hydrogen), τ 8.4–9.1 (methyl and methylene hydrogens).

A sample of the cyclohexanediol was recrystallized, to analytical purity (m.p. 74–77°) from petroleum ether (b.p. 30–60°) – ether. Thin-layer chromatography showed one spot.

Anal. Calcd. for $C_{13}H_{26}O_2$: C, 72.84; H, 12.23; O, 14.93. Found: C, 72.99; H, 12.24; O, 14.91.

1-Heptyl-4-acetoxy-1-cyclohexene **5**

1-Heptyl-1,4-cyclohexanediol (2.21 g) was dissolved in anhydrous pyridine (50 ml) to which acetic anhydride (30 ml) was added. The reaction was allowed to stand at room temperature for 24 h. The excess acetic anhydride and pyridine were removed by flash evaporator and the reaction residue was diluted to 150 ml with ether. The organic layer was washed with 2% HCl solution, sodium bicarbonate solution, followed by water. Removal of the dried ether gave 2.08 g of a clear, viscous, yellow oil in 80% yield. Thin-layer chromatography (silica–ether eluent) indicated that there were two new products.

The product mixture (2.08 g) was not further purified (i.r. and n.m.r. indicated mono-acetate), but was heated under reflux for 24 h in acetic anhydride (100 ml). The reaction was cooled and approximately one-half of the acetic anhydride was removed by flash evaporator. The residue was diluted to 250 ml with ether, then washed with a 1% sodium hydroxide solution until the aqueous extracts were basic then with water until neutral. Removal of the dried ether gave 1.85 g of a yellow, viscous oil, corresponding to a yield of 89%. Thin-layer chromatography (silica–benzene eluent) indicated the presence of two products.

The n.m.r. spectrum showed narrowly spaced singlets (τ 8.04, 8.06) probably due to the exocyclic and endocyclic forms of the alkene acetate **4** and **5** respectively.

The mixture of **4** and **5** (1.85 g) and *p*-toluenesulfonic acid (1.9 g) were dissolved in benzene (50 ml) heated under reflux for 2 h. The reaction was cooled and diluted to 150 ml with benzene. The benzene layer was washed with a 2% sodium bicarbonate solution followed by water. Removal of the dried benzene gave 1.85 g of 1-heptyl-4-acetoxy-1-cyclohexene as a viscous, yellow oil; n_D^{25} 1.4547. The yield was quantitative. Thin-layer chromatography (silica–benzene eluent) indicated one product.

Infrared spectrum: 1740 cm^{-1}, 1600 cm^{-1}. Nuclear magnetic resonance spectrum: τ 4.7 (hydrogen on double bond), τ 5.15 (hydrogen attached to the same carbon atom as the acetoxy group), τ 8.05 (singlet, acetoxy methyl hydrogens), τ 8.7–9.1 (remaining methyl and methylene hydrogens).

Anal. Calcd. for $C_{15}H_{26}O_2$: C, 75.58; H, 10.99; O, 13.42. Found: C, 75.88; H, 11.05; O, 13.15.

1-Heptyl-1,2,4-cyclohexanetriol **6** *and* **7**

Osmium tetroxide (7.0 g) was added to a cold solution of 1-heptyl-4-acetoxy-1-cyclohexene (6.97 g) in dry ether (150 ml) and dry pyridine (4.5 ml). The reaction was left for 6 days at room temperature. The dark colored reaction mixture was filtered to give 6.96 g of a brown complex.

The complex was decomposed by stirring overnight with a solution composed of mannitol (2 g) and KOH (10 g) in water (100 ml). Ether extraction gave 2.44 g of product which was a mixture of the desired triol and monoacetylated triol. Hydrolysis of this mixture with 5% KOH EtOH–H_2O solution (60 ml) converted it into 2.38 g of crude triol.

The above filtrate was similarly treated with mannitol–KOH solution to give a further 2.33 g of product identical with that obtained from the complex. Total product: 4.77 g–72% yield. Infrared spectrum had absorption peaks at 3600 cm^{-1} and 3400 cm^{-1} due to non-bonded and bonded —OH. The n.m.r. spectrum had peaks at τ 5.9 (1 H broad multiplet), τ 6.2 (1 H poorly resolved triplet), τ 7.4 broad peak due to hydroxyl hydrogens, τ 8.0–9.1 envelope due to remaining methylene and methyl hydrogens.

Anal. Calcd. for $C_{13}H_{26}O_3$: C, 67.79; H, 11.38; O, 20.84. Found: C, 67.67; H, 11.63; O, 20.92.

Tosylation of 1-Heptyl-1,2,4-cyclohexanetriol **6** *and* **7**

p-Toluenesulfonic acid chloride (4.6 g) and 2.0 g of a mixture of **6** and **7** were dissolved in dry pyridine (90 ml). The resulting solution was left at room temperature for 20 h.

The majority of the pyridine was removed under reduced pressure, and the residue was dissolved in benzene. The benzene solution was washed with 5% aqueous $NaHCO_3$, and after drying the benzene was removed under reduced pressure to give 4.3 g of crude product.

Crystallization of the residue from a mixture of ether – petroleum ether (b.p. 30–60°) yielded 500 mg of a compound, which after repeated crystallizations melted at 107°.

Infrared spectrum: 3500 cm^{-1}, 1600 cm^{-1}, 1180 cm^{-1}. Nuclear magnetic resonance spectrum: τ 2.15–2.7 (AB quartet, aromatic hydrogens), τ 5.6 (broad multiplet due to hydrogens on same carbon atoms as O-tosyl), τ 7.5 (singlet, aromatic methyl hydrogens), τ 8.0–9.1 (remaining methyl and methylene hydrogens).

Anal. Calcd. for $C_{27}H_{38}S_2O_7$: C, 60.19; H, 7.10; O, 20.79; S, 11.90. Found: C, 60.37; H, 7.32; O, 20.06; S, 11.98.

Can. J. Chem. Downloaded from www.nrcresearchpress.com by 210.87.254.105 on 09/05/12
For personal use only.

Crystallization of the material from the above mother liquors from ether – petroleum ether (b.p. 30–60°) yielded 400 mg of a second compound which after repeated crystallizations melted at 62°.

Infrared spectrum: 3500 cm^{-1}, 1600 cm^{-1}, 1180 cm^{-1}. Nuclear magnetic resonance spectrum: τ 2.15–2.7 (AB quartet, aromatic hydrogens), τ 5.4 (broad multiplet due to hydrogens on same carbon atoms as O-tosyl), τ 7.55 (singlet, aromatic methyl hydrogen), τ 8.1–9.1 (remaining methyl and methylene hydrogens).

Anal. Calcd. for $C_{27}H_{38}S_2O_7$: C, 60.19; H, 7.10; O, 20.79; S, 11.90. Found: C, 60.19; H, 7.14; O, 20.97; S, 11.99.

The two crystalline compounds had distinctly different R_f values -0.31 for the isomer melting at 107° and 0.59 for the isomer melting at 62°—on t.l.c. (silica – petroleum ether (b.p. 30–60°) eluent). The i.r. spectra were almost identical (small differences in 900–950 cm^{-1} range).

Rearrangement of 1-Heptyl-1,2,4-cyclohexanetriol-2,4-ditosylate ***8*** *and* ***9***

Crystalline ditosylate (500 mg) was dissolved in freshly distilled dimethyl formamide (30 ml) and dry $CaCO_3$ (500 mg) was added. The resulting suspension was heated under reflux with stirring for $2\frac{1}{2}$ h.

The reaction mixture was added to benzene (100 ml) and washed several times with water. Removal of the benzene gave 175 mg of an oily product **10**—88% yield. Thin-layer chromatography showed one spot. The i.r. spectrum showed absorption bands at 3600 cm^{-1}, 3400 cm^{-1}, and 1700 cm^{-1}. The n.m.r. spectrum showed peaks at τ 5.7 (broad multiplet, hydrogen on some carbon atom as the hydroxyl), τ 7.6 (broad multiplet, methine hydrogen α to ketone), τ 8.1 (poorly resolved triplet, methylene hydrogens α to ketone), τ 8.7–9.1 (broad envelope, due to remaining methylene and methyl hydrogens).

Preparation of Ethylene Ketal ***11***

The hydroxy ketone **10** (163 mg) and a catalytic amount of *p*-toluenesulfonic acid were dissolved in benzene (50 ml) in the presence of ethyleneglycol (1 ml). The resulting mixture was heated under reflux for 3 h. All traces of water were removed by means of a water separator.

After cooling, the benzene solution was washed with 5% $NaHCO_3$ and water. Removal of the benzene yielded 148 mg of ketal. The product gave one spot on t.l.c. examination, showed no ketone in the i.r. spectrum, and had a sharp peak at τ 6.15 in the n.m.r. spectrum due to the ethylene ketal hydrogens.

Preparation of Ketal–Ketone ***12***

The hydroxy ketal **11** (133 mg) dissolved in dry pyridine (2 ml) was added to a slurry of CrO_3 (500 mg) in dry pyridine (15 ml). The resulting mixture was stirred at room temperature for 24 h.

Ether extraction of the product yielded 98 mg of ketone found to be homogeneous by t.l.c. The i.r. spectrum had a band at 1740 cm^{-1}. The n.m.r. spectrum had a sharp peak at τ 6.1 (hydrogens of ethylene ketal), τ 7.8 (broad multiplet, hydrogens α to ketone), τ 8.7–9.1 (broad envelope, due to methylene, methine, and methyl hydrogens).

Anal. Calcd. for $C_{15}H_{26}O_3$: C, 70.82; H, 10.30; O, 18.87. Found: C, 71.28; H, 10.07; O, 17.97.

Acknowledgments

The authors are indebted to the National Research Council of Canada for generously supporting this work. We would also like to thank Dr. T. Griffith and Mr. W. Mettinen for running the nuclear magnetic resonance spectra.

1. (*a*) E. J. Corey, N. H. Andersen, R. M. Carlson, J. Paust, E. Vedejs, I. Vlattas, and R. E. K. Winter. J. Am. Chem. Soc. **90**, 3245 (1968); (*b*) E. J. Corey, I. Vlattas, N. H. Andersen, and K. Harding. J. Am. Chem. Soc. **90**, 3247 (1968).
2. E. Hardegger, H. P. Schenk, and E. Broger. Helv. Chim. Acta, **50**, 2501 (1967).
3. G. Just and C. Simonovitch. Tetrahedron Letters, 2093 (1967).
4. J. F. Bagli and T. Bogri. Tetrahedron Letters, 5 (1967).
5. P. F. Beal III, J. C. Babcock, and F. H. Lincoln. J. Am. Chem. Soc. **88**, 3131 (1966).
6. J. F. Bagli, T. Bogri, R. Deghengi, and K. Wiesner. Tetrahedron Letters, 465 (1965).
7. H. C. Brown, J. H. Brewster, and H. Shechter. J. Am. Chem. Soc. **76**, 467 (1954).
8. F. D. Gunstone. Advances in organic chemistry. Interscience Publishers, Inc., New York. Vol. 1. 103 (1960).
9. Y. Mazur and M. Nussim. J. Am. Chem. Soc. **83**, 3911 (1961).

Can. J. Chem. Downloaded from www.nrcresearchpress.com by 210.87.254.40 on 09/05/12
For personal use only.

The photochemical Beckmann rearrangement[1]

H. IZAWA,[2] P. DE MAYO, AND T. TABATA
Department of Chemistry, University of Western Ontario, London, Ontario

Received August 26, 1968

The direct irradiation of aryl aldoximes gives the amide (the photochemical Beckmann rearrangement) by intramolecular oxygen migration. This has been shown by the rearrangement of ^{18}O-labelled benzaldoxime in the presence of *p*-tolualdoxime: no exchange of label was observed.

The rearrangement usually gives the amide, but in the case of the anisyl derivative the anilide was also obtained. The highest quantum yield for benzamide formation noted (in acetic acid) was 0.034, but the figure is dependent on irradiation time. The results of low-temperature irradiation suggest that an oxazirane is an intermediate. Phenyl-*N*-methyl oxazirane is converted into the amide on irradiation (though not thermally) and it seems likely that the reaction is induced, under the conditions of the reaction, by benzylic hydrogen abstraction by thermally produced small amounts of benzaldehyde; a fact which may explain the variation in quantum yield of amide formation with extent of irradiation. An additional route from oxazirane to amide may also be available.

The activation of the oxime by high energy sensitizers under the most favorable conditions gives $\Phi_{amide} = 0.002$, and so a singlet pathway for oxazirane formation is preferred. The main route for energy degradation appears to be by *syn–anti* isomerism. This can be induced by a variety of sensitizers and so can be a triplet process. The direct irradiation of benzaldoxime leads to isomerism with $\Phi_{\alpha\beta} = 0.40$ and $\Phi_{\beta\alpha} = 0.38$. From these figures, together with the composition of the stationary state found, the composition of the sensitized stationary state can be calculated in fair agreement with the experimentally found value. This suggests that the isomerization following direct irradiation is also a triplet process.

In a single example of an aralkyl ketoxime (*p*-anisylmethyl ketoxime) irradiation products of both aryl and alkyl migration, were found.

Canadian Journal of Chemistry, 47, 51 (1969)

Many systems of the type (**1**) and its vinylogues have been found to undergo, on irradiation, an overall migration of C, a heteroatom, from B to A.

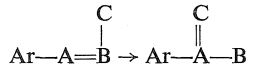

1

Included in this classification[3] are the following: the conversion of azoxybenzenes (A = N; B = $\overset{+}{N}$; C = O^-) to hydroxyazobenzenes (1, 2) and the recent transformation of **2** to **3** (3); the conversion of oxythiobenzoyl chloride (A = C; B = $\overset{+}{S}$; C = O^-) to benzoyl chloride (4) and of 2-methoxynaphthalene thiocarbaldehyde-5-oxide to the aromatic aldehyde (5); the conversion of *N*-oxides and nitrones (A = C; B = $\overset{+}{N}$; C = O^-) to amides (the largest group, of which refs. 6–15 are illustrative); the transformation of methyl isamate to a quinazoline derivative (16, 17) (A = C; B = $\overset{+}{N}$; C = N^-) and, essentially, **4** into **5** (18).[4]

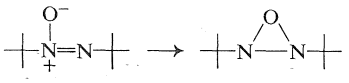

2 **3**

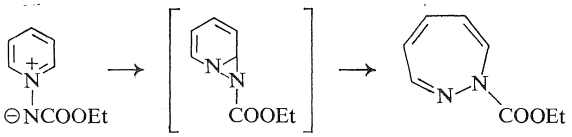

4 **5**

The most studied of these reactions, the nitrone rearrangement, was first reported by Alessandri (19) who noted the isolation of benzanilide from the products of irradiation of *N*-α-diphenylnitrone. An oxazirane intermediate was suspected (20) and later demonstrated (7) in certain cases. Instances have been recorded (22) where the oxazirane does not undergo further transformation to the amide, whilst in others (for example, see refs. 21, 23) the second step is so fast as to preclude the detection of an

[1]Photochemical Synthesis, Part 24. For Part 23 see B. D. Challand and P. de Mayo. Chem. Comm. 982 (1968).

[2]Present address: Kyoritsu College of Pharmacy, Tokyo.

[3]In view of the large literature which has accumulated in recent years on reactions of this type, only a few leading references can be given.

[4]For an analogous carbon transfer see Streith *et al.* (53).

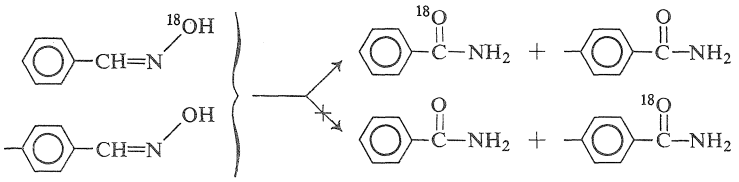

SCHEME I

intermediate whose participation must therefore be conjectural. Occasionally, as in the conversion of **4** to **5**, the intermediate in the heteroatom transfer finds an alternative breakdown pathway (see also ref. 24, and other papers in this series).

In all the instances cited the atom, C, has been such that the bond with A could be formed to give, in principle, a stable product as regards bonding, without necessitating the rupture of a further bond. This transformation appears to be rather general, and further examples of what may be termed a heteroatom transfer may be expected.

Some years ago we reported (25) that aromatic aldoximes gave, on irradiation, the Beckmann products, *viz*, the amides. Briefly, the results then available can be summarized as follows.

Benzamide was obtained from benzaldoxime by irradiation in several solvents. The highest yield (41%) was obtained in acetic acid, but fair yields, comparatively, (20–30%) were obtained in cyclohexane containing 0.5–2.0 equivalents of acetic or trifluoroacetic acids. Lower yields were obtained in dioxan, methanol, or cyclohexane. The reaction was shown to have some generality since rearrangement products were obtained with *p*-methyl-, *p*-chloro-, and *p*-methoxybenzaldoxime, and with α-naphthaldoxime. No amide was obtained with the oximes from *m*- and *p*-nitrobenzaldehyde, *p*-fluorobenzaldehyde, isonicotinic aldehyde, and *p*-cyanobenzaldehyde. The interconversion of the *syn* and *anti* oximes, amongst the earliest of reported photochemical reactions (26) was also observed. Subsequently the obtention of an amide by the irradiation of an alicyclic oxime was reported by Just and his collaborators (27).

This reaction bore at least a superficial resemblance to the nitrone–amide interconversion just discussed. There was, however, a difference of significance. In contrast to the generality of heteroatom transfer reactions an additional nuclear transfer—that of the proton attached to the oxygen—was necessary before an uncharged intermediate could be arrived at. Two other general observations suggested caution in drawing too close a parallel with the nitrone rearrangement. First, the quantum yield, though not known at that stage, was suspected of being very low because of the prolonged times of irradiation needed. Nitrones, on the other hand, rearrange, at least to the oxaziranes, with fair efficiency (28). Secondly, the rearrangement appeared to be best carried out in solvents containing acetic acid, an observation for which there was no analogy in the nitrone series. An analogy with the normal Beckmann itself could be conceived if the relevant excited state of the oxime were sufficiently basic to accept a proton from acids normally too weak to induce the Beckmann rearrangement. In this case reaction would have to follow very rapidly on protonation since collapse to the ground state would be expected to be followed very rapidly by ionization of the proton.

A distinction between the two main pathways available could be clearly made: a heteroatom transfer process would be intramolecular whilst the normal Beckmann is intermolecular (29). To decide, experimentally, between these alternatives, benzaldoxime labelled with ^{18}O was prepared from labelled hydroxylamine. This material was then irradiated in acetic acid in the presence of an equimolecular amount of *p*-tolualdoxime. The amide products were isolated, separated by vapor-phase chromatography, and the ^{18}O content of the individual amides determined. The results clearly indicated that, within the experimental error, all the ^{18}O was retained in the benzamide (1.54 atom % excess) and none found (0.034 atom % excess) in the *p*-toluamide (Scheme I). An intramolecular oxygen transfer, or at least one involving caged radicals or ions was indicated. The photochemical Beckmann, therefore, resembles the normal Beckmann only in so far as the products are concerned.[5]

[5]This was not unexpected since it was known (25) that the oxime acetate did not rearrange. See also ref. 30.

Can. J. Chem. Downloaded from www.nrcresearchpress.com by 210.87.254.40 on 09/05/12
For personal use only.

TABLE I
Decomposition of phenyloxazirane

Solvent	Temperature (°)	$h\nu$	% decomposition (h)	% amide
C_6H_{12}/HOAc*	25	+	100 (0.25)	71
C_6H_{12}/HOAc*	25	—	50 (8) 100 (24)	2
C_6H_{12}/HOAc*	60	—	90 (2)	3
C_6H_{12}/Et_2O†	25	—	0 (18)	—

*1:3.
†3% Et_2O.

In a migration of the oxygen atom from nitrogen to carbon, this atom must at some period be bonded to both origin and terminus. This could be, of course, in a transition state, in a reactive intermediate, such as an ion or radical, or as an, in principle, isolable intermediate. In the case of benzaldoxime this would be the presently unknown phenyloxazirane.[6] Despite the fact that simple oxaziranes of this kind were known not to rearrange, at least thermally, to amides, (22) a photochemical route through such species was not excluded (see ref. 32) and seemed attractive. A search for such an intermediate was, therefore, made. Phenyloxazirane[7] has absorption in an inconvenient part of the spectrum since there is much overlap with the starting material and product. The anisyl derivative, on the other hand, is more suitable since any oxazirane formed would be expected to absorb in the window between the main absorption bands of the oxime and of the amide (Fig. 1).

α-*p*-Anisaldoxime was irradiated in *n*-hexane solution at −88°, with light near 290 nm, (see Experimental) in an apparatus in which it was possible, simultaneously, to observe the changes induced in the absorption spectrum. On cooling the solution there was observed a shift in the absorption spectrum (Curve 2, Fig. 2). After irradiation for 50 min, a considerable decrease in absorption was noted in the 270 nm region indicating a decrease in oxime concentration in the beam path. At the same time a peak appeared near 235 nm, the region expected for the oxazirane absorption.[8] On allowing the mixture to warm to room temperature this peak disappeared and the absorption at 270 nm increased though it did not reach its original value. Part of the change must be attributed to slow diffusion in the viscous solution at low temperature and equilibration on warming up.

These results are consistent with the suggestion that, under the conditions of the experiment, an oxazirane was formed. They do not require that the oxazirane necessarily be an intermediate in amide formation.

Further evidence that an oxazirane was formed was obtained from the iodometric test used (22, 31) for quantitative oxazirane estimation. Iodine was liberated from iodide ion at low temperatures, indicating the presence of an oxidizing agent. Addition of iodide ion to the solution after it had warmed to room temperature did not result in iodine liberation. Further, although the amide was a product of this sequence of operations the yield of amide decreased by about 50% if the cold irradiated solution was treated with iodide ion. This suggested a relationship between the oxidizing agent and benzamide formation.

For the oxazirane to be a genuine intermediate in the conversion of the oxime to amide (and not a divergent pathway leading to other products) there must be a thermal or photochemical pathway from it to the amide. This possibility was next examined.

Solutions of phenyloxazirane were found to be very difficult to purify. They contained, as impurities, benzaldehyde and benzaldoxime as well as smaller amounts of unidentified substances. In a solvent mixture of cyclohexane – acetic acid (one of the irradiation media used) the substance was moderately stable, as compared with solutions in pure ether, and the decomposition could be followed. After 24 h (see Table I) little oxazirane, as estimated iodometrically, remained, but the yield of benzamide was about 2%. A similar solution irradiated with an

[6]Recent work by Schmitz (31) has indicated that solutions of this substance may be made, and that derivatives may be prepared, but that the substance itself is unstable. We have confirmed this.

[7]Assuming that this substance absorbs in the same region as the more stable *N*-methyl compound.

[8]Using 2-ethyl-3-*p*-methoxyphenyl oxazirane (9) as a model for the absorption spectrum: λ_{max}231 nm (ϵ = 13 800).

Can. J. Chem. Downloaded from www.nrcresearchpress.com by 210.87.254.40 on 09/05/12
For personal use only.

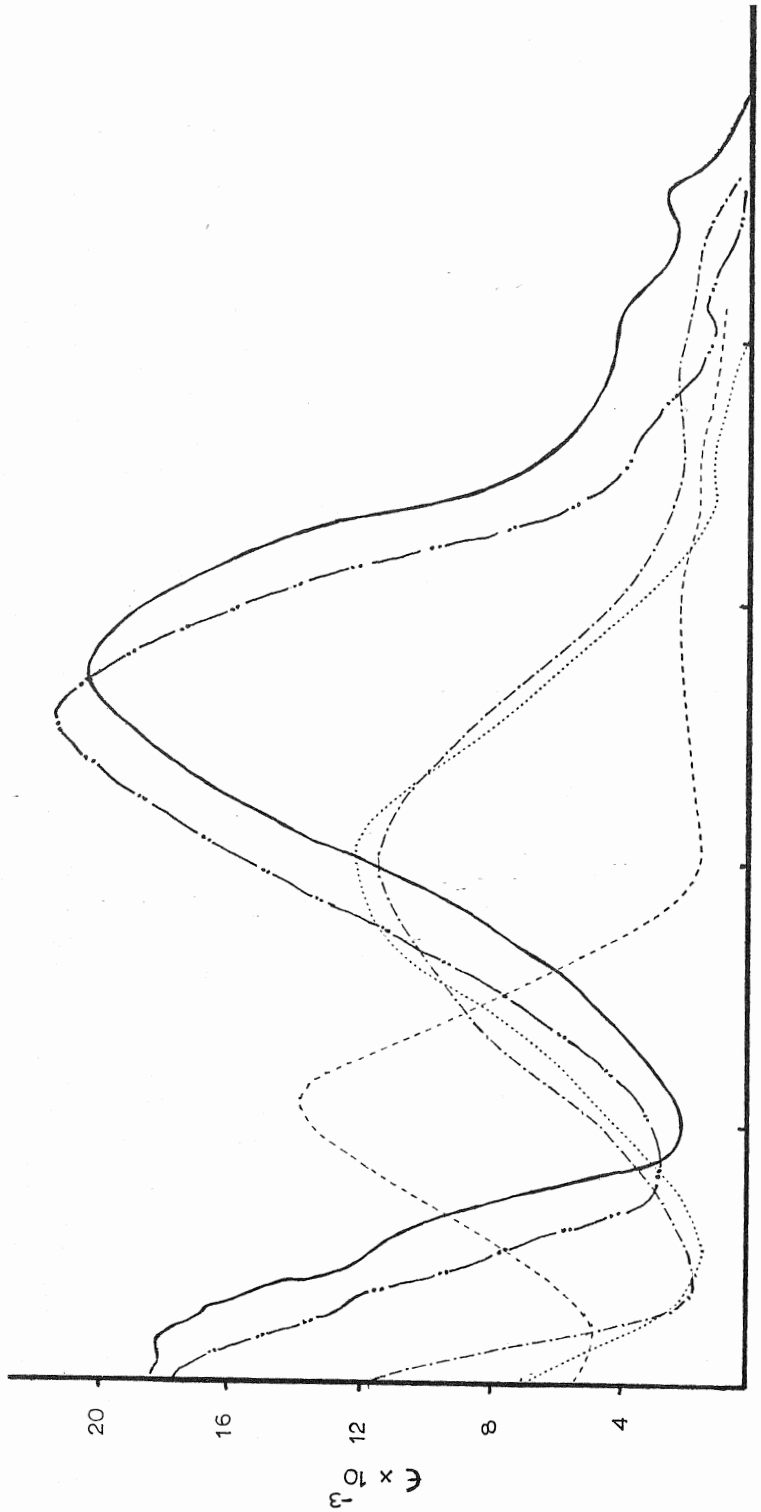

FIG. 1. Absorption spectra of α-*p*-anisaldoxime (——); β-*p*-anisaldoxime (—·—·—); *p*-anisamide (·····); *N*-*p*-methoxyformanilide (–·–·–·–); and 2-ethyl-3-phenyloxazirane (- - - -).

Can. J. Chem. Downloaded from www.nrcresearchpress.com by 210.87.254.40 on 09/05/12
For personal use only.

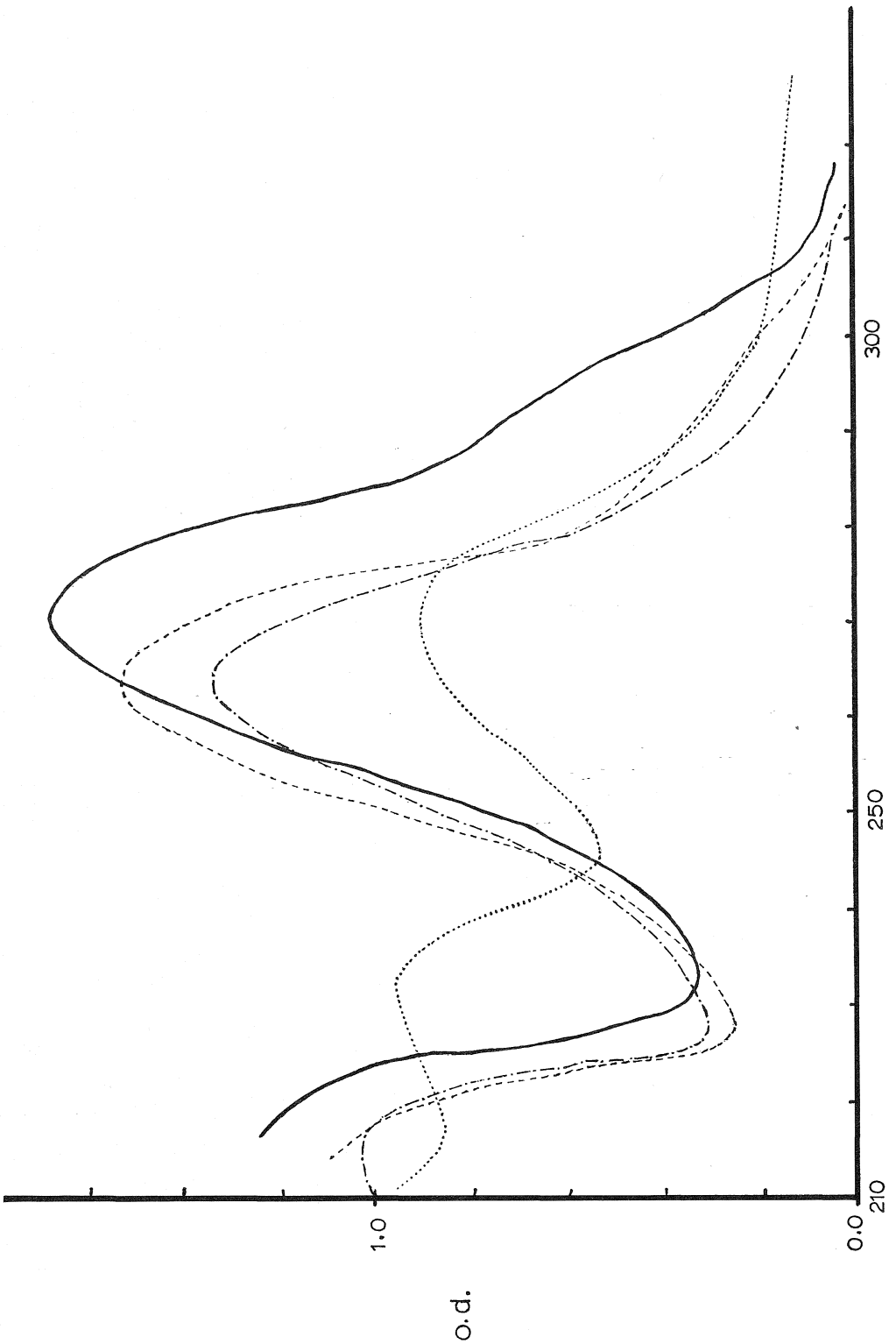

FIG. 2. Low-temperature irradiation of α-*p*-anisaldoxime (8.05×10^{-5} *M*). Curve 1 (- - - -) absorption at 20°; Curve 2 (——) absorption at −87°; Curve 3 (. . . . .) absorption after 50 min irradiation; Curve 4 (- . - . -) absorption at 20° after irradiation.

Can. J. Chem. Downloaded from www.nrcresearchpress.com by 210.87.254.40 on 09/05/12
For personal use only.

TABLE II

Quantum yields of benzamide formation

Concentration (M)	0.05	0.028	0.054	0.0071	0.0071
Solvent	HOAc	HOAc	HOAc	C_6H_{12}	C_6H_{12}/HOAc*
Wavelength (nm)	~289†	254‡	254	254	254
Quantum yield	0.034 ± .004	0.016 ± .002	0.015 ± .002	0.001§	0.004 ± .0015

*Cyclohexane containing an equimolar concentration of acetic with respect to oxime.
†Bausch and Lomb monochromator.
‡Resonance arc: 1 cm of nickel sulfate and of cobalt sulfate and 1 cm of cation X (52).
§The error in this value may be 100%.

unfiltered medium pressure mercury arc was decomposed rapidly and a yield of 71% amide obtained.

Clearly, then, a route from the oxazirane to the amide was available under the appropriate conditions, but, equally clearly, the problem was not resolved since it was required to be demonstrated that any oxazirane intermediate formed could indeed absorb the incident radiation. For meaningful results, therefore, it was necessary to put the irradiation data on a quantitative basis. Benzaldoxime was irradiated at 2537 Å and near 2900 Å and the quantum yields determined for acetic acid (the best solvent found), cyclohexane and for a mixture of the two. Near 2900 Å the quantum yield was about 3.4% (Table II) and a value of about half that found at 2537 Å. In cyclohexane (2537 Å) a quantum yield of near one-tenth % was obtained. The reaction is therefore very inefficient although the preparative yield is fair. The degradation of the energy was shown to take place mainly through *syn–anti* isomerism (see below)[9] and it thus appeared that if amide formation were a two or multistep process, all (including the rearrangement of the oxazirane) but the first must be quite efficient, at least in acetic acid solution.

That the situation was not simple was revealed when the quantum yield of benzamide was determined after the absorption of varying amounts of energy (Fig. 3).[10] It was found that in the early stages the quantum yield is even lower than found in the earlier determination (Table II) but rises to this value as the reaction proceeds. A tentative conclusion which may be drawn from these results would be that some step in the overall transformation is accelerated (or even induced) by the product itself (the amide) or by a by-product. Specifically, the oxazirane intermediate postulated might be so transformed; and indeed some such explanation is essential if the oxazirane be an intermediate. This is because although irradiation of the oxazirane with unfiltered light does induce the desired transformation, at 290 nm the amount of light absorbed by the oxazirane, especially in the presence of the oxime, is negligible. As has been seen, thermal and acid-catalyzed decay does not lead to the amide. Thus, if the results of the low-temperature experiments be accepted as implying that an oxazirane intermediate be involved in amide formation, then two routes from the oxazirane to the amide must be available. Evidence for a second route was now sought.

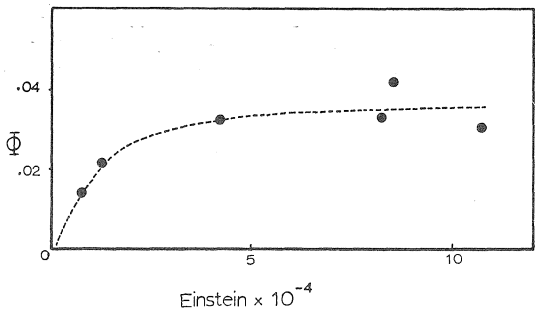

FIG. 3. Variation of quantum yield of benzamide formation in acetic acid solution (0.139 *M* in benzaldoxime) with quanta absorbed near 290 nm.

Of the substances present in the irradiated mixture the most likely candidate for the role of 'catalyst' in the oxazirane–amide conversion was benzaldehyde. The aldehydes are very frequently major products in the thermal breakdown of oxaziranes and their presence in these reactions seems unavoidable. In the present instance the selection of a thermal breakdown product of the oxazirane as the

[9]No emission could be detected at 77 °K.
[10]It was established that the destruction of the amide under these conditions was negligible.

Can. J. Chem. Downloaded from www.nrcresearchpress.com by 210.87.254.40 on 09/05/12
For personal use only.

TABLE III

Irradiation of *N*-methylphenyloxazirane (290 nm)

Light absorbed (Einstein × 10^{-5})	1.42	2.12	41.3	44.0	1.2–2.9*
[Oxazirane]	0.039	0.035	—	0.038	0.037
[Benzaldehyde]	—	0.0091	—	—	—
[Triphenylene]	—	—	—	—	0.0088
[β-Benzaldoxime]	—	—	0.139	0.139	—
$\Phi_{N\text{-Methylbenzamide}}$	1.36	2.23	—	0.006	0.05
$\Phi_{\text{Benzamide}}$	—	—	0.027	0.01	—

*Irradiation at 334 nm.

conjectural active agent had a further motivation. The accumulation of the oxazirane in detectable amounts in the low-temperature irradiation could be then explained by the absence of this supposed agent following the increased thermal stability of the oxazirane at low temperatures.

To perform even an approximately quantitative experiment to determine whether benzaldehyde could induce isomerization it was necessary to have a pure oxazirane. We were unable to prepare aldehyde-free solutions of phenyloxazirane itself, but in the hope that the *N*-methyl derivative was a suitable model this substance was prepared and purified such that the residual extinction at 290 nm was ~4.5 (corresponding to a maximum benzaldehyde content of about 0.34%). The absorption gradually increased on standing, decomposition being about 3% in 24 h in acetic acid solution. Irradiation of this solution at 290 nm gave a quantum yield of *N*-methylbenzamide greater than unity (Table III) suggesting a radical chain process. Addition of a small amount of benzaldehyde, such that the aldehyde absorbed 99% of the light, further increased the quantum yield. On the other hand the addition of benzaldoxime reduced the quantum yield dramatically (and led to the formation of some benzamide). Attempted sensitization with triphenylene was largely ineffective.[11]

The evidence available certainly does not lead compellingly to an unequivocal interpretation. One plausible pathway, however, in accord with the available facts, for the conversion of the phenyloxazirane to the amide is that indicated below.

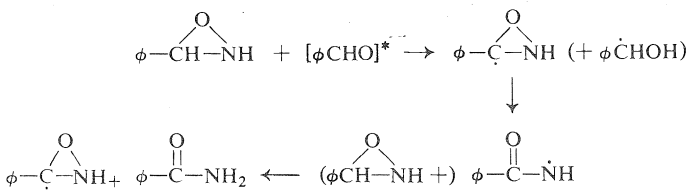

SCHEME II

An alternative pathway from the oxazirane has been suggested (33) as follows:

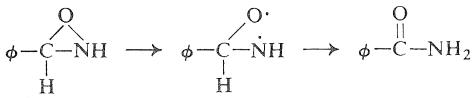

but whilst this may have relevance to the mechanism for a direct conversion of oxazirane to amide it is not that involved, it would seem, under circumstances when the oxazirane itself does not absorb the light.

The hydrogen-abstracting role of the benzaldehyde in Scheme II is unexceptional, as is the particular abstraction of the benzylic hydrogen atom. The overall scheme therefore favored at

[11]The triplet energy of the phenyloxazirane is not known, but might be expected to be close to that of toluene. Under those circumstances neither benzaldehyde nor triphenylene should be able to sensitize by triplet energy transfer. It does not seem likely that the phenyloxazirane triplet level could be lower than 72 kcal/mole, that of benzaldehyde, yet higher than 67 kcal/mole (triphenylene). Singlet sensitization, previously observed with triphenylene (40), seems the most likely explanation.

Can. J. Chem. Downloaded from www.nrcresearchpress.com by 210.87.254.40 on 09/05/12
For personal use only.

TABLE IV
Sensitized activation of benzaldoxime

Wavelength (nm)	Solvent	[HOAc]	[ϕCH = N · OH]	Sens.	[Sens.]	Φ amide
334	Dioxan	—	0.05	T*	0.016	0.000
334	C_6H_{12}	0.71	0.0089	T	0.013	0.002
334	Dioxan	—	0.05	P†	0.017	0.000
~290	Acetone	—	0.0078	A‡	—	0.000

*Triphenylene.
†Phenanthrene.
‡Acetone (solvent).

this time is the photochemical conversion of the oxime to the oxazirane, followed by the sequence in Scheme II. Although in the preparative runs unfiltered light was used it is computed that little light could be absorbed by the oxaziranes themselves, until towards the end of the irradiations. At that stage another mechanism may be operative, but we do not consider that, in the cases we have studied, that a direct pathway is unquestionably required. However, in view of our results with a ketoxime (see below) it seems probable. One rationalization would be that the "direct" route merely provided an alternative hydrogen-abstracting radical in a mechanism resembling that in Scheme II. Splitter and Calvin (42) have recently shown that the irradiation of **6** leads both to fragmentation and to rearrangement to the anilide **7**. They have shown that oxygen leads to some quenching of the fragmentation, but not of the anilide formation. In addition, acetone appeared to sensitize the fragmentation, but not the anilide formation,[12] and it is concluded that the anilide formation proceeds through a singlet.

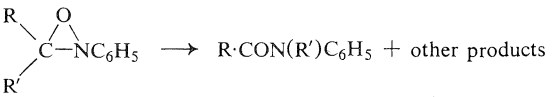

6 **7**

a) R = $(CH_3)_2N{\cdot}C_6H_4$—, R′ = H *b*) R = R′ = C_6H_5—

With a self-consistent and plausible chemical scheme for amide formation available, attention can be turned to the photochemistry of oxime excitation.

The ultraviolet absorption spectra of both the α- and β-oximes of benzaldehyde greatly resemble that of styrene. The O—O band, for instance, of the α-isomer appears to be at 2905 Å (98.0 kcal/mole) whilst that of styrene is, in cyclohexane, at 2915 Å. The origin of this absorption appears to be at about 3100 Å (92 kcal/mole). This absorption is attributed to a $\pi \rightarrow \pi^*$ transition (34, 35), and no absorption corresponding to a lower energy $n \rightarrow \pi^*$ transition has been observed.[13] Further support for the $\pi \rightarrow \pi^*$ assignment was found in the small bathochromic shift observed in polar solvents. The vibronic structure was not blurred. These effects contrast with the large hypsochromic shift expected of $n \rightarrow \pi^*$ absorption bands in general (36).

In styrene, Evans (37) has located the triplet O—O band at 61.7 kcal/mole whilst Hammond and his collaborators give β-methylstyrene as 59.8 kcal/mole (38). This large singlet–triplet splitting (~40 kcal/mole), common to $\pi \rightarrow \pi^*$ systems, if found in the oximes would place the benzaldoxime triplet in the 60 kcal/mole region. We have obtained evidence that it is most probably lower than that. In a rigid matrix at 77 °K the phosphorescence of benzophenone (0.035 *M*) and triphenylene (0.0074 *M*) were both quenched by benzaldoxime (0.17 and 0.018 *M* respectively). In fluid solution, in the presence of biacetyl (55–57 kcal/mole) when the concentration of benzaldoxime (0.099 *M*) exceeded that of biacetyl by 50%, total quenching was observed. The fluorescence of biacetyl was unaffected. Since the *n*, π* singlet–triplet splitting would be expected to be small it

[12]But benzene increases the yield of **7***a* from 10% (in diethylamine) to 24%, and **7***b* from nil to 5%. The fragmentation is also sensitized by *p*-dimethylaminobenzaldehyde which should have a triplet energy far below that of the isolated phenyl or aniline chromophores. The situation is not, therefore, entirely clear-cut.

[13]The $n \rightarrow \pi^*$ of imines appears near 245 nm (39), but is shifted to shorter wavelength in oximes. The C=N absorption in aliphatic oximes is in the 200 nm region, whatever its nature may be.

Can. J. Chem. Downloaded from www.nrcresearchpress.com by 210.87.254.40 on 09/05/12
For personal use only.

TABLE V

Photostationary states in *syn–anti* isomerism of the benzaldoxime

Irradiation (Å)	$\left[\frac{\beta}{\alpha}\right]$	Sensitizer	E_T (Kcal/mole)
Direct 2537	1.3±0.06	—	—
Sens. >3400	1.7±0.04	*p*-Hydroxyacetophenone	71.3
Sens. >3340	1.6±0.04	Triphenylene	67.2
Sens. >3400	1.8±0.14	Michlers Ketone	62.0

follows that the lowest triplet is π, π*. Hence the states which were most likely candidates for the photochemical Beckmann were the π, π* singlet and π, π* triplet.[14]

Since the phosphorescence quenching showed that triplet energy could be conveyed from triphenylene to benzaldoxime the means were available for testing whether T_1 was the excited species responsible for amide formation. In dioxan solution sensitization with triphenylene or phenanthrene did not lead to the formation of detectable amounts of amide, nor did the use of acetone as solvent (Table IV). The quantum yield on direct irradiation is low under these conditions, however, and sensitization was also attempted in the presence of acetic acid.[15] Under these circumstances a very small quantum yield (0.2%) of amide was detected, but this yield was about 8% of that obtained by direct irradiation at 290 nm under the same solvent conditions. Since, in view of the biacetyl experiment, energy transfer should have been diffusion controlled we are inclined to the view that the π, π* singlet is the photochemically active species leading to oxazirane formation and, hence, to amide. Similar conclusions have been reached by Tanaka and his colleagues with regards oxazirane formation from nitrones (28, 41). An explanation for the very small sensitized quantum yield can be conceived. If the triplet were sufficiently long-lived ($>10^{-3}$ s) the possibility of triplet–triplet annihilation, with concommitant singlet formation, could be considered. But the triplet is not quenched by oxygen (see below), nor does it phosphoresce, so this extended lifetime is improbable. Mixed sensitizer–oxime triplet quenching is also improbable in view of the large excess of acceptor. Just and collaborators (27) have suggested that the rearrangement of **8** to **9** may proceed through a triplet since this reaction is quenched by oxygen. However, as in the present instance, this

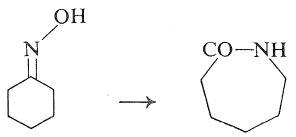

8 **9**

may merely mean that some radical intermediate is being trapped. As previously noted for the oxazirane[11] singlet sensitization seems, therefore, the most probable rationalization of this observation.

Geometrical isomerism in the oximes is induced by triplet excitation. Photostationary states in dioxan solution were reached with a number of sensitizers. These states were not identical (Table V) but $\left[\frac{\beta}{\alpha}\right]$ lay between 1.6 and 1.8. The photostationary state ratio obtained by direct irradiation in dioxan solution at 2537 Å was 1.3. The quantum yield for $\beta \rightarrow \alpha$ isomerization, near 2900 Å, was 0.40 ± .013 (dioxan) in the 6–7% reaction range. That for the $\alpha \rightarrow \beta$ was 0.38, and necessitated a small correction for the trace of β isomer contained therein. The photostationary state obtained by direct irradiation should be given by the following expression if the quantum yield of isomerization be independent of wavelength between 2537 and ca. 2900 Å.

$$\left[\frac{\beta}{\alpha}\right] = \left[\frac{\epsilon\alpha}{\epsilon\beta}\right]\left[\frac{\Phi\alpha\beta}{\Phi\beta\alpha}\right]$$

With the available data the right-hand side is estimated as 1.3, in good agreement with the

[14]Very recently (see, for instance, ref. 40) it has been shown that higher states may react chemically. It is not, therefore, excluded that a T_2, formed by intersystem-crossing from S_1, might be the excited state responsible for oxazirane formation.

[15]It was established that the presence of acetic acid did not interfere with energy transfer as indicated by the phosphorescence quenching.

Can. J. Chem. Downloaded from www.nrcresearchpress.com by 210.87.254.40 on 09/05/12
For personal use only.

Can. J. Chem. Downloaded from www.nrcresearchpress.com by 210.87.254.40 on 09/05/12
For personal use only.

experimentally found value of 1.3. Hammond's simple formula (38) for predicting the photostationary state, *viz.*

$$\left[\frac{\beta}{\alpha}\right] = \left[\frac{\beta}{\alpha}\right]_{sens}\left[\frac{\epsilon\alpha}{\epsilon\beta}\right]$$

does not hold in this instance. It requires that

$$\left[\frac{\beta}{\alpha}\right]_{sens} = \left[\frac{\Phi\alpha\beta}{\Phi\beta\alpha}\right]$$

and the former was found, in fact, to be greater than the latter by a factor of 1.6. One of the requirements for the applicability of this formula must, therefore, not hold—perhaps the identity of the intersystem crossing terms. Similar observations have been made with regards to azobenzene isomerization (43, see however 50). It would be reasonable to assume, in view of the closeness of the values, that the isomerization induced by direct irradiation is also passing through the triplet.[16] Such seems to be the case in the stilbenes (44, see however 45), whereas in the azobenzene isomerization the situation is more complex since a ratio of 15–30 was found (43).

Oxygen has no effect on $\Phi_{\alpha\beta}$ despite the fact that sufficient was available to destroy much of the oxime. This would suggest that the triplet has a short lifetime. This isomerization of azobenzene has also been reported to be unaffected by oxygen in solution (46).

In the course of these investigations some further observations were made requiring some modification of the results previously reported (25). *p*-Fluorobenzamide has now been shown to be formed by the irradiation of the oxime in cyclohexane – acetic acid solution through Corex. The yield was about 25%. Irradiation through quartz, as was previously reported, did not give isolable amounts of amide, and it seems probable that the amide produced was destroyed by the shorter wavelength radiation.

The irradiation of *p*-anisaldoxime through Corex gave, in addition to the previously reported anisamide, *p*-methoxyformanilide. Both amides were destroyed by further irradiation. A careful check of the oxime rearrangements previously reported confirmed that the anilides, the products of the alternative migration were absent.

We have investigated a single instance of a ketoxime irradiation. *p*-Methoxyacetophenone oxime in cyclohexane – acetic acid was irradiated through Corex. *N*-*p*-anisylacetamide, *N*-methylanisamide, and *p*-anisamide were obtained in the approximate ratio of 6:6:1.

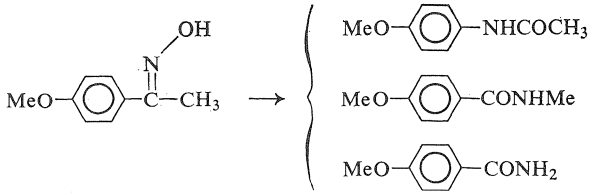

This reaction involves, together with a minor amount of bond cleavage, both aryl and alkyl migration. The ratio observed seems compatible neither with an ionic nor radical process, but at least one instance of abnormal migration has been observed in a radical process (47).

Experimental

Benzaldoxime-^{18}O

Isotopically enriched potassium nitrite was prepared by equilibration of potassium nitrite (8.5 g) and enriched water (12.5 ml, 1.82 atom % excess ^{18}O) adjusted to pH 4 with concentrated nitric acid. After four days the water was removed, the salt taken up in water and evaporated to dryness under reduced pressure. The residue was redissolved in the same medium at pH 4, left overnight and then diluted with 62 ml enriched water. Sulfur dioxide was passed in (temperature below 0°) and the precipitated potassium hydroxylamine disulfonate collected, washed and dried (19.6 g). The salt (13.44 g) was hydrolyzed with 0.5 *N* hydrochloric acid (62 ml: 100° for 2 h), cooled and barium chloride (60 g) added. After evaporation to dryness the residue was extracted with absolute ethanol to give 3.86 g hydroxylamine hydrochloride.

This product in ethanol (40 ml) containing pyridine (14 ml) and benzaldehyde (5.93 g) was allowed to stand overnight. The solvents were removed and the product isolated with ether.

The ether was removed and the oxime distilled. A small amount of a carbonyl compound was present which was removed by filtering an ethereal solution of the distillate through a thin layer of alumina. The benzaldoxime obtained was checked by comparison of its infrared spectrum with an authentic sample. It contained 1.54 atom % excess ^{18}O.[17]

Irradiation of Benzaldoxime-^{18}O and p-Tolualdoxime

Equimolar amounts (0.00414 *M*) of labelled benzaldoxime and normal *p*-tolualdoxime in acetic acid

[16]Though, indeed, as pointed out by a Referee, there is no *a priori* reason for requiring 'S and 'T states to partition differently.

[17]Analytica Corporation, 118 East 28th Street, New York 16, New York.

Can. J. Chem. Downloaded from www.nrcresearchpress.com by 210.87.254.40 on 09/05/12
For personal use only.

(200 ml) were irradiated in a quartz well (85 W mercury arc) under nitrogen for 8 h. The acetic acid was removed (< 35°) the residue dissolved in chloroform and the amides separated on a 5 ft × ¼ in. column (3% Craig and 1% Carbowax 20 M on Chromosorb W) at 190°; helium: 170 ml/min. The benzamide (21 min) and *p*-toluamide (35 min) were crystallized from benzene. The benzamide had 1.54 atom % excess ^{18}O and the *p*-toluamide 0.034 atom % excess.[17]

Benzamide Quantum Yields

The solution of β-benzaldoxime in the specified solvent was degassed by the freeze–thaw cycle (to a residual pressure of $< 10^{-4}$ mm). The absorption of light was checked before and after irradiation. After irradiation (using a beam-splitter with a transmittance–reflectance ratio in the region of 10:1) the solvent was removed at low pressure, the residue dissolved in chloroform and the concentration of amide determined by infrared spectroscopy (1676 cm^{-1} band). The conversion (0.5–3.5%) was determined by comparison with a calibration curve. The appropriate controls were carried out. The irradiation took about 24 h. The results are given in Table II.

The variation in quantum yield with total quanta absorbed is shown in Fig. 1.

All actinometry in this and following experiments was by the ferrioxalate method of Hatchard and Parker (48).

Low-Temperature Irradiation of α-p-Anisaldoxime

A cell as described by Hirshberg and Fischer (49) was used. An attachment was made such that degassing could be accomplished outside the rectangular cell. The temperature was measured with an Iron–Constantan thermocouple connected directly to a recorder. The cell was cooled by the passage of nitrogen (dried) precooled by passage through a copper coil immersed in liquid nitrogen. An Osram HBO-200 lamp was used as source and the ~290 nm light isolated by a Baird Atomic interference filter (No. A-21). Irradiations were carried out at right angles to the measuring beam.

Preparation and Irradiation of Phenyloxazirane Solution

To a mixture of 2.12 g benzaldehyde (0.02 *M*), 10 ml of sodium hydroxide (2 *N*), and 16 ml ether, was added a cold solution of 2.26 g (0.02 *M*) hydroxylamine-*o*-sulfonic acid in 20 ml water and 10 ml sodium hydroxide (2*N*) and the stirred solution maintained at 0° for 8 min. The yellow ethereal solution was separated and stirred at 0° for 20 min with a solution of hydroxylamine-*o*-sulfonic acid. The ethereal solution was again separated, washed with water, and dried (Na_2SO_4). The ether was removed with bubbling nitrogen and replaced in portions with cyclohexane. The cyclohexane was then diluted to one-third with acetic acid.

The oxazirane in this solution was estimated by iodide titration (22). After 30 min the original solution (1.3 mg/ml) had decreased to ~85%. After 2 h about half had decomposed and after 24 h about 15% remained. Both the original cyclohexane solution and the cyclohexane – acetic acid solution were examined for benzamide content. The solvents were removed at low temperature. The benzamide was separated by thin-layer chromatography (t.l.c.), extracted with cyclohexane-1-propanol (4:1), centrifuged, and the benzamide estimated spectrophotometrically. The appropriate controls were run. From a set of four experiments the amount of benzamide formed was 2 ± 1%.

The phenyloxazirane solution (63 ml; 5.2 mg/ml in cyclohexane) was diluted to 250 ml with acetic acid. The mixture was degassed with nitrogen and irradiated in an immersion vessel with an 85 W medium pressure mercury arc. After 15 min the irradiation was terminated. No phenyloxazirane remained in the solution. In the control 17% of the phenyloxazirane had been decomposed. Benzamide was estimated as described above. A yield of 71% was found in the irradiated solution and 2% in the non-irradiated control.

Preparation and Irradiation of N-Methyl-3-phenyloxazirane

The oxazirane was prepared by the method of Pews (51) from *N*-methylbenzylidene amine. The product in ethereal solution was washed with hydroxylamine-*o*-sulfonic acid solution to remove benzaldehyde and the solvent evaporated. The resultant material was 85% pure estimated iodometrically. Before use it was distilled four times through a short path distillation column (bath temperature 24°/0.005 mm) ϵ_{289} 4.5; ϵ_{297} 2.5; ϵ_{303} 1.0; ϵ_{313} 0.3, corresponding to a maximum benzaldehyde content of 0.34%.

The oxazirane was irradiated at 290 nm (interference filter) in acetic acid solution, in the presence and absence of added benzaldehyde and benzaldoxime. The results are given in Table III. The amide yields were estimated by thin-layer chromatography (eluent: cyclohexane–acetone 2:1), extraction with cyclohexane–propanol-2 (1:1), centrifugation and estimation by ultraviolet spectrometry. Controls were run. The separation of *N*-methylbenzamide from benzamide was adequate for the estimation of one in the presence of the other.

The Rearrangement of p-Methoxyacetophenone Oxime

The oxime (3.95 g) and acetic acid (24 ml) were dissolved in cyclohexane (200 ml) and the mixture irradiated under nitrogen through a Corex filter in an immersion apparatus (450 W) for 71 h. After removal of the solvent the amides were separated from polymer by preparative thin-layer chromatography (eluent: ethyl ether, light petroleum [35–60°] 1:5), sublimed and the individual amides isolated by thin-layer chromatography in the same solvent system. There was obtained *N*-*p*-anisylacetamide (R_f 0.27) (103 mg), *N*-methyl anisamide (R_f 0.19) (50 mg) and *p*-anisamide (10 mg) (R_f 0.12). All were identified by comparison (including mixture melting points) with authentic specimens.

Irradiation of p-Fluorobenzaldoxime

The oxime (204 mg), acetic acid (8.4 ml), and cyclohexane (200 ml) were irradiated through Corex in an immersion apparatus (450 W). After removal of the solvent the residue was chromatographed. Elution with ethyl ether – light petroleum (5:1) gave the amide, crystallized from ethanol (50 mg).

Irradiation of p-Anisaldoxime

80 ml of a solution of cyclohexane containing 94 mg α-*p*-anisaldoxime and 81 ml acetic acid were irradiated on an optical bench at 290 nm for 16 h. After evaporation of the solvent at low temperature, followed by t.l.c.

separation, *p*-anisamide (44 mg) was obtained together with (3 mg) *p*-methoxyformanilide.

Sensitized Benzaldoxime Equilibration

The relative amounts of α- and β- oximes were determined by taking aliquots periodically during the irradiation. The oximes were separated by t.l.c. (eluent: light petroleum [60–80°] – diethyl ether 4:1). The areas containing the oximes (detectable under ultraviolet light) were extracted with cyclohexane–*n*-propanol (4:1). Control experiments showed that this mixture extracted 99% of the oximes. Further, the silicic acid sedimented rapidly and permitted the obtention of reproducible results when this solvent mixture was used. With other solvents, such as methanol, large blanks were obtained and were variable.

The oximes were shown to be stable to this treatment, and the concentrations were computed from the separately determined molar extinction coefficients in the same solvent system.

The results are given in Table IV.

1. G. M. Badger and R. G. Buttery. J. Chem. Soc. 2243 (1954).
2. G. E. Lewis and J. A. Reiss. Australian J. Chem. **19**, 1887 (1966).
3. S. S. Hecht and F. D. Greene. J. Am. Chem. Soc. **89**, 6761 (1967).
4. J. F. King and T. Durst. J. Am. Chem. Soc. **85**, 2676 (1963).
5. J. Strating, L. Thijs, and B. Zwanenberg. Rec. Trav. Chim. **83**, 631 (1964).
6. J. Landquist. J. Chem. Soc. 2830 (1953).
7. J. Splitter and M. Calvin. J. Org. Chem. **20**, 1086 (1955); **23**, 651 (1958); **30**, 3427 (1965).
8. M. J. Haddadin and C. H. Issidorides. Tetrahedron Letters, 753 (1967).
9. F. Krohnke. Ann. **604**, 203 (1957).
10. A. Padwa. Tetrahedron Letters, 2001 (1964).
11. R. Bonnett, V. H. Clark, and A. Todd. J. Chem. Soc. 2102 (1959).
12. L. Brehm, K. G. Jensen, and B. Jerslev. Acta Chem. Scand. **20**, 915 (1966).
13. O. Buchardt, J. Becher, and C. Lohse. Acta Chem. Scand. **20**, 2467 (1966).
14. J. Streith, H. K. Darrah, and M. Weil. Tetrahedron Letters, 5555, (1966).
15. J. Streith and E. Sigwalt. Tetrahedron Letters, 1347 (1966).
16. P. de Mayo and J. J. Ryan. Tetrahedron Letters, 827 (1967).
17. P. de Mayo and J. J. Ryan. Can. J. Chem. **45**, 2177 (1967).
18. J. Streith and J.-M. Cassal. Angew. Chem. Intern. Ed. Engl. **7**, 129 (1968).
19. L. Alessandri. Atti. Accad. Lincei. **19**, 2, 122 (1910); Chem. Abstr. **5**, 276 (1911).
20. M. Kamlet and L. Kaplan. J. Org. Chem. **22**, 576 (1957).
21. C. Kaneko, I. Yokoe, S. Yamada, and M. Ishikawa. Chem. Pharm. Bull. Tokyo **14**, 1316 (1966).
22. W. D. Emmons. J. Am. Chem. Soc. **78**, 6208 (1956); **79**, 5739 (1957).
23. E. C. Taylor and G. G. Spence. Chem. Commun. 767 (1966).
24. C. Kaneko, S. Yamada, and I. Yokoe. Tetrahedron Letters, 4701 (1966).
25. J. H. Amin and P. de Mayo. Tetrahedron Letters, 1583 (1963).
26. G. Ciamician and P. Silber. Ber. **36**, 4268 (1903).
27. R. T. Taylor, M. Douek, and G. Just. Tetrahedron Letters, 4143 (1966).
28. K. Koyano and I. Tanaka. J. Phys. Chem. **69**, 2545 (1965).
29. P. A. S. Smith. *In* Molecular rearrangements. *Edited by* P. de Mayo Vol. 1. Interscience Publishers, Inc. New York. 1963. p. 457 *et seq.*
30. A. W. Chapman and C. C. Howis. J. Chem. Soc. 806 (1933).
31. E. Schmitz, R. Ohme, and S. Schramm. Tetrahedron Letters, 1857 (1965).
32. L. S. Kaminsky and M. Lamchen. J. Chem. Soc. 2295 (1966).
33. R. O. Kan. Organic photochemistry. McGraw–Hill Book Co., Inc., New York and London. 1966. p. 149.
34. T. Kubota, M. Yamakawa, and Y. Mori. Bull. Soc. Chem. Japan, **36**, 1552 (1963).
35. T. Kubota and M. Yamakawa. Bull. Soc. Chem. Japan, **36**, 1564 (1963).
36. J. W. Sidman. Chem. Rev. **58**, 689 (1958).
37. D. F. Evans. J. Chem. Soc. 1351 (1957).
38. G. S. Hammond, J. Saltiel, A. A. Lamola, N. J. Turro, J. S. Bradshaw, D. O. Cowan, R. C. Counsell, V. Vogt, and C. Dalton. J. Am. Chem. Soc. **86**, 3197 (1964).
39. R. Bonnett, N. J. David, J. Hamlin, and P. Smith. Chem. Ind. London, 1836 (1963).
40. P. de Mayo, J.-P. Pete, and M. Tchir. J. Am. Chem. Soc. **89**, 5712 (1967).
41. K. Shinazawa and I. Tanaka. J. Phys. Chem. **68**, 1205 (1964).
42. J. S. Splitter and M. Calvin. Tetrahedron Letters, 1445 (1968).
43. L. B. Jones and G. S. Hammond. J. Am. Chem. Soc. **87**, 4219 (1965).
44. K. A. Muszkat, D. Gegiou, and E. Fischer. J. Am. Chem. Soc. **89**, 4814 (1967).
45. J. Saltiel. J. Am. Chem. Soc. **89**, 1037 (1967).
46. G. Zimmerman, L.-Y. Chow, and N. J. Park. J. Am. Chem. Soc. **80**, 3528 (1958).
47. F. D. Greene, W. Adam, and A. Knudson. J. Org. Chem. **31**, 2087 (1966).
48. C. G. Hatchard and C. A. Parker. Proc. Roy. Soc. London Ser. **A235**, 518 (1956).
49. Y. Hirshberg and E. Fischer. Rev. Sci. Instr. **30**, 197 (1959).
50. E. Fischer. J. Am. Chem. Soc. **90**, 796 (1968).
51. G. Pews. J. Org. Chem. **32**, 1628 (1967).
52. M. Kasha. J. Opt. Soc. Am. **38**, 929 (1948).
53. J. Streith, B. Banner, and C. Sigwalt. Chem. Commun. 979 (1967).

Can. J. Chem. Downloaded from www.nrcresearchpress.com by 210.87.254.40 on 09/05/12
For personal use only.

Structure of "phytic acids"

L. F. JOHNSON
Spectroscopy Applications Laboratory, Varian Associates, Palo Alto, California

AND

M. E. TATE[1]
Department of Agricultural Biochemistry, Waite Agricultural Research Institute, University of Adelaide, South Australia, Australia

Received June 24, 1968

Evidence is presented to show that cereal grain phytic acid has the myoinositol hexaorthophosphate structure suggested by Anderson and not the hydrated myoinositol tripyrophosphate structure proposed by Neuberg. DL-Myoinositol 1,6:2,3:4,5-tripyrophosphate which is structurally related to the Neuberg formulation has been prepared. The "phytic acid" fraction from chicken blood has been shown to be predominantly 1,3,4,5,6-myoinositol pentaphosphate. The structures assigned to these compounds have been confirmed by ^{31}P nuclear magnetic resonance.

Canadian Journal of Chemistry, 47, 63 (1969)

Can. J. Chem. Downloaded from www.nrcresearchpress.com by 210.87.254.6 on 09/05/12
For personal use only.

Introduction

Myoinositol hexaphosphate or phytic acid as it is frequently called, has been the subject of several reviews (1–4). The name "phytic acid" has been used interchangeably in the literature with the term "phytin" which more correctly refers to the mixed calcium and magnesium salt of the acid (2).

The term "la phytine" was first employed by S. Posternak (5) to describe the major organic phosphate component of seeds, and at that time, he considered it to be an intermediate in the fixation of carbon dioxide by chlorophyll. Although this concept was later abandoned, the name was retained and subsequently applied to similar materials from soil (6) and the blood of birds and turtles (7).

By the application of ion exchange procedures, the heterogeneity of "phytic acid" from soil was revealed (8) and Cosgrove (1) has shown it to be a complex mixture of polyphosphates, which includes esters of inositols other than myoinositol.

The availability of an improved electrophoretic procedure (9) for establishing homogeneity and ^{31}P nuclear magnetic resonance (n.m.r.) for structure determination, has enabled us to reinvestigate the nature of the inositol polyphosphate fractions from cereal grains and chicken blood, with occasionally surprising results. In this paper, the term phytic acid (without quotation marks) will be restricted to signify the myoinositol hexaphosphate from cereal grains.

[1]All correspondence should be addressed to this author.

Results and Discussion

(a) Cereal Grain Phytic Acid

If the conformational aspects are neglected, the problem posed by the structure of cereal grain phytic acid simplifies to a consideration of the symmetrical hexaorthophosphate structure **1** proposed by Anderson (10) and the asymmetrical hydrated tripyrophosphate structure **2** proposed by Neuberg (11), to account for the apparently stable trihydrate of phytic acid.

There can be little doubt that many of the earlier studies were hampered by the paucity of criteria for establishing the purity of phytic acid. Several authors (12–14) have commented adversely on the quality of commercial phytate preparations and Fig. 1, lane 3 shows the complexity of one batch of "biochemical grade" sodium phytate. Considerable variation in composition was found among samples from different suppliers and even between batches from a single source. They ranged in purity from the example in Fig. 1 to almost homogeneous sodium phytate. The last traces of lower phosphates were removed from a commercial sample of calcium phytate (ex maize) by conversion to the sodium salt (1, 15) with repeated crystallization from aqueous methanol (16) until the material was chromatographically and electrophoretically homogeneous (Fig. 1, lane 2). At least two crystalline modifications were observed with 31 and 35

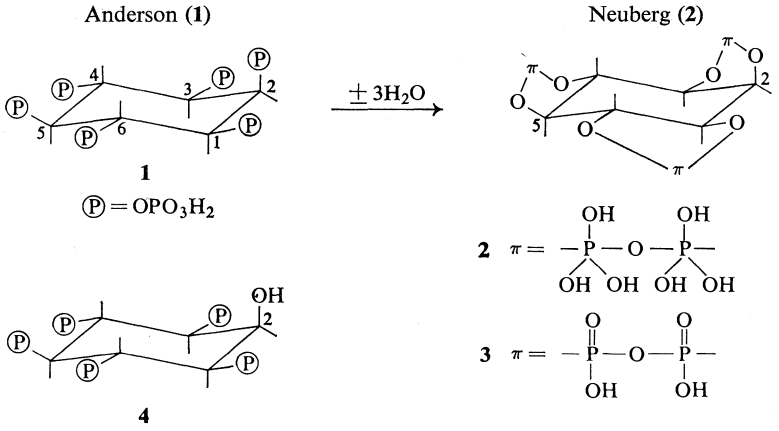

molecules of water of crystallization. They differ from the hydrates with 38 and 44 molecules of water described by Posternak (15) and do not melt, instead they display characteristic differential thermal analysis patterns. The stable crystalline sodium phytate with 31 molecules of water was used as the reference standard in this work.

Cogent arguments (2, 4) in favor of the Neuberg formulation **2**, rest mainly on studies indicating that salts of phytic acid form trihydrates, which it was thought (15) were not capable of further dehydration without decomposition, and secondly upon experiments (17) performed with material which analyzed for an octadecasodium salt of phytic acid.

In our work both crystalline hydrates of sodium phytate were found to have a sodium: phosphorus ratio of 2.0:1 in agreement with the observations of Posternak (15) and Hoff-Jorgensen (18). However, by subjecting the crystalline reference material to a precipitation with ethanol from strongly alkaline solution, according to the procedure of Brown, Heit, and Ryan (17), an amorphous product was obtained. It exhibited a high sodium:phosphorus ratio (2.2:1) and was found to be a mixture of sodium phytate and sodium carbonate. Brown, Heit, and Ryan have utilized the high sodium:phosphorus ratio (3:1) obtained for their material, as evidence for the existence of an octadecasodium salt of phytic acid, but as neither a carbon analysis nor an inositol estimation were given to corroborate this assumption, it and the subsequent potentiometric titration data must be considered of doubtful validity. The careful potentiometric titration results by Hoff-Jorgensen (18) on crystalline sodium phytate clearly show the presence of six strongly dissociated protons (pK's < 3.5) and six weakly dissociated protons (pK's 4.6–10) and are in accord with the Anderson structure **1**.

Both of the crystalline hydrates of sodium phytate were found to dehydrate readily at 100° to a product which analyzed for a trihydrate in agreement with previous work (15, 18). However, by prolonged heating *in vacuo* at 145° the trihydrate was found to dehydrate to at least a monohydrate, without detectable decomposition. At higher temperatures (150–210°) the decomposition mentioned by Posternak (15) was observed.

The dehydration of sodium phytate to a monohydrate, obviated the original necessity (11) to postulate the hydrated tripyrophosphate structure **2** for this material. It should not be construed that further dehydration is impossible. However, with standard analytical procedures it is technically very difficult to analyze such hygroscopic material.

It would seem that although the water molecules are strongly held to the phosphate anions, they are held by hydrogen bonds and are not covalently bound by the hydration of P=O groups. It should be noted that the known compounds (19, 20) with the sp^3d orbital arrangement for phosphorus, are unstable in hydroxylic solvents and revert to the the sp^3 arrangement. In the case of structure **2**, this would lead to the formation of the inositol tripyrophosphate structure **3**.

Treatment of phytic acid in aqueous pyridine,

Can. J. Chem. Downloaded from www.nrcresearchpress.com by 210.87.254.6 on 09/05/12
For personal use only.

Can. J. Chem. Downloaded from www.nrcresearchpress.com by 210.87.254.6 on 09/05/12
For personal use only.

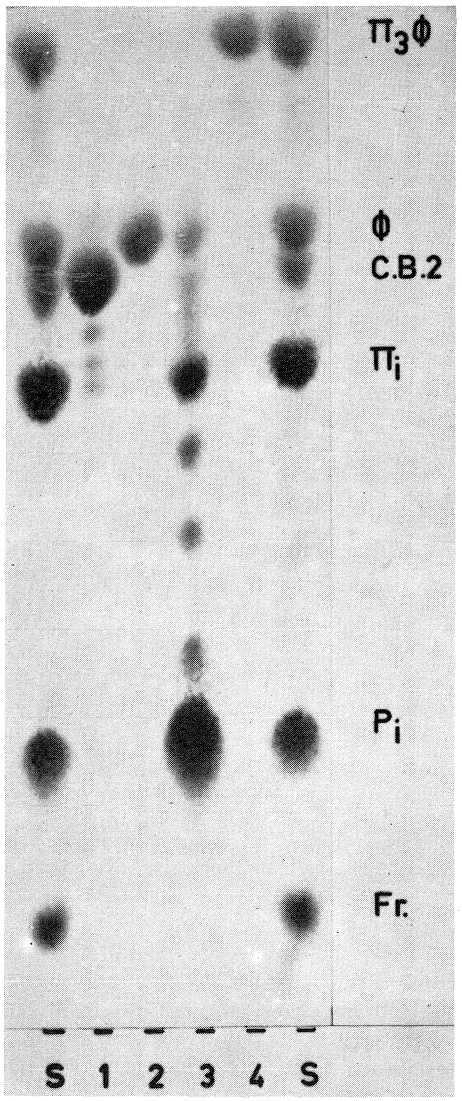

FIG. 1. Electrophoretogram (0.1 *M* oxalate, pH 1.5, 1 h, 1500 V, CCl_4 coolant, phosphomolybdate dip reagent). Components of Lane S in decreasing order of mobility are: myoinositol 1,6:2,3:4,5-tripyrophosphate ($\pi_3\phi$), cereal grain phytic acid (ϕ), major inositol polyphosphate from chicken blood (C.B.2), inorganic pyrophosphate (π_i), inorganic orthophosphate (P_i), uncharged marker (fructose, Fr.). Lane 1, crude inositol polyphosphates from chicken blood. Lane, 2, crystalline cereal grain sodium phytate. Lane 3, commercial sodium phytate. Lane 4, myoinositol 1,6:2,3:4,5-tripyrophosphate.

with dicyclohexylcarbodiimide gave products with electrophoretic mobilities greater than phytic acid. With increased reaction time at 60°, the fastest moving component ($\pi_3\phi$) predominated and is shown in Fig. 1, lane 4. It was rapidly hydrolyzed back to phytic acid under acid conditions and, unlike sodium phytate, the sodium salt showed a strong POO^- antisymmetric absorption at 1255 cm^{-1} (21) in the infrared spectrum. The analysis, chemical behavior, and spectroscopic properties of this product are consistent with the inositol tripyrophosphate structure **3**.

To examine the suggestion (17) that the hexaorthophosphate structure may be a degradation product of the Neuberg formulation, phytic acid was extracted from wheat under conditions which did not degrade the model inositol tripyrophosphate. The sodium salt of the major polyphosphate isolated under these conditions was found to be indistinguishable from the crystalline reference sample of sodium phytate. It appears that, in wheat, phytic acid is stored as the hexaorthophosphate *in situ* and is not an artifact of the usual acidic isolation procedures. In the course of the extraction, ferric ions were observed in those fractions associated with phytic acid and it seems likely that phytic acid is associated with these ions as well as with potassium, calcium, and magnesium in the wheat grain. The view that phytic acid is mainly localized in the aleurone grains, has recently been confirmed directly by Sobolev (22) in the case of the castor oil plant (*Ricinus communis*).

The asymmetry of the Neuberg structure **2** suggests that as phytic acid is a natural product, it would exhibit optical activity. However, no detectable rotation was observed with our material and the error in the molar rotation ($\pm 0.6°$) is well below the smallest molar rotation ($+15°$) which can be calculated for any recorded asymmetric inositol phosphate (23).

(b) Chicken Blood "Phytic Acid"

The occurrence of an unusually high concentration of an inositol polyphosphate in the acid-soluble phosphorus fraction of chicken blood was first observed by Rapoport (7). The term "phytic acid" was applied to this material on the basis of a similarity in properties to cereal grain phytic acid and the results of phosphorus and sodium analyses. This assignment was reexamined in 1964 by Oshima, Taylor, and Williams (24) who supported the hexaphosphate structure with evidence for a phosphorus to inositol ratio of 6:1 using a biological assay for the estimation of inositol.

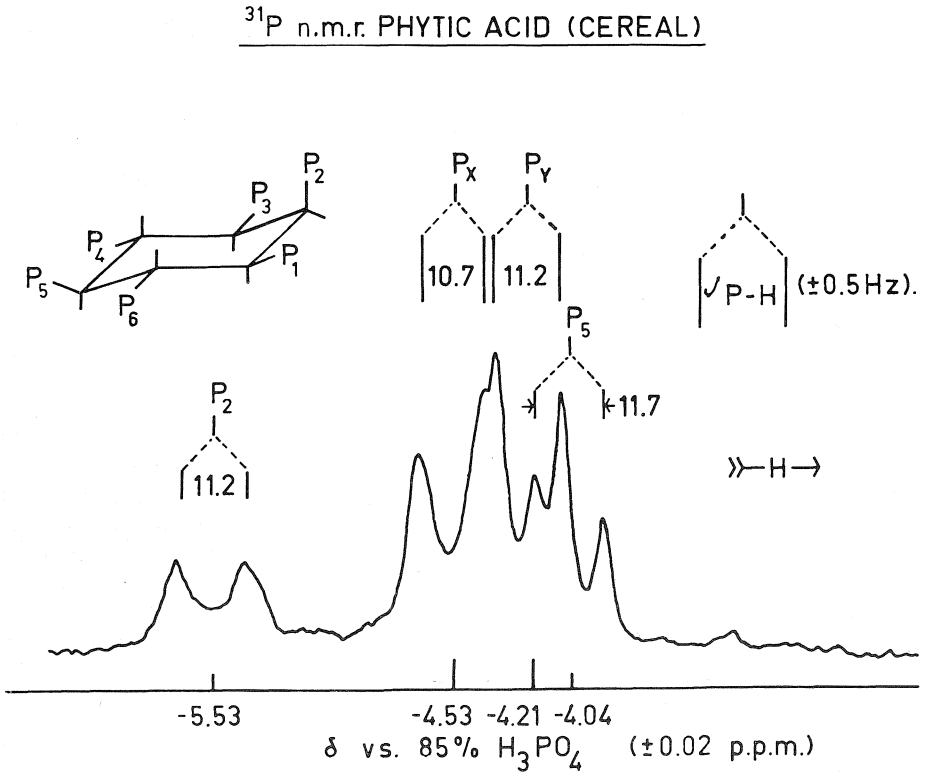

FIG. 2. Phosphorus magnetic resonance spectrum (40.5 MHz) of a saturated solution of crystalline cereal grain sodium phytate in D_2O. The signal to noise ratio has been enhanced by nine scans with a Varian C1024 time averaging computer. P_4O_6 in a sealed capillary was used as the external standard and δ-values have been calculated relative to 85% phosphoric acid.

Figure 1, lane 1, clearly shows that the "phytic acid" fraction of chicken blood is electrophoretically heterogeneous and that the major component is dissimilar to cereal grain phytic acid (lane 2). By ion-exchange chromatography a series of myoinositol polyphosphates was obtained. The sodium salt of the major component (C.B.2), which comprises 93% of the total phosphorus was found to be optically inactive, its analysis, electrophoretic, and ion-exchange behavior corresponded to an inositol pentaphosphate rather than the hexaphosphate structure. Ammonolysis gave myoinositol (1-, 4-, and 5-monophosphates) only. The absence of the axial 2-monophosphate led to the assignment of the symmetrical myoinositol 1,3,4,5,6-pentaphosphate structure **4**.

Of the minor inositol polyphosphates in the chicken blood extract, the fastest moving component (C.B.1) was found to be electrophoretically indistinguishable from cereal grain phytic acid and C.B.3 is probably an enantiomorph or racemate of myoinositol 1,4,5,6-tetraphosphate. The significance of these additional polyphosphates is not clear, they may be metabolically related to the major component (C.B.2) or alternatively it is possible that all the phosphates may arise as degradation products of some larger molecule containing acid labile linkages which are ruptured in the course of isolation.

Although Rapoport and Guest (25) have reported "phytic acid" in the blood of the snapping turtle (*Chelydra serpentina*) and a wide variety of birds, we have been unable to detect inositol penta- or hexaphosphates in the Murray River short-necked tortoise (*Emydura macquarii*).

The prior assignments (7, 24) of the hexaphosphate structure to chicken blood phytate exemplify the difficulty in distinguishing between inositol hexaphosphates and pentaphosphates

Can. J. Chem. Downloaded from www.nrcresearchpress.com by 210.87.254.6 on 09/05/12
For personal use only.

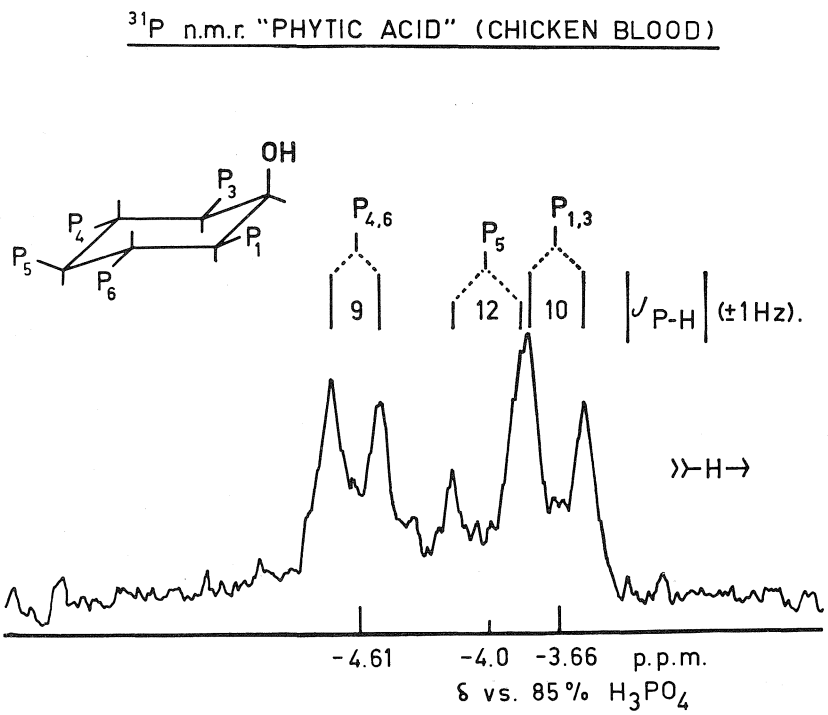

FIG. 3. Phosphorus magnetic resonance spectrum (40.5 MHz) of a saturated solution of the major component (C.B.2) of chicken blood "phytate" in D_2O.

on the basis of analytical values alone. The uncertainty in some methods of myoinositol estimation has led to a preference in this work for the elemental analysis of the sodium salts, whose homogeneity has been previously confirmed by both electrophoresis and paper chromatography.

(c) ^{31}P Nuclear Magnetic Resonance

Although the foregoing results were only compatible with the Anderson hexaorthophosphate structure **1** for cereal grain phytic acid and the myoinositol 1,3,4,5,6-pentaphosphate structure **4**, for chicken blood "phytic acid", there was no satisfactory confirmatory evidence for the structure of the myoinositol tripyrophosphate. The most convincing structural evidence for all these compounds has come from a study of their phosphorus magnetic resonance spectra.

Synthetic myoinositol 2-phosphate (26) was studied as a model compound of known structure. It was examined as the free acid and also as its disodium salt in D_2O at 40.5 MHz. The chemical shift (δ) for the free acid is essentially the same as the primary reference standard of 85% phosphoric acid and the characteristic (27, 28) downfield displacement of 5 p.p.m. for the complete transition from mono-anion to di-anion was observed. The signal is a doublet (J_{P-H} 7.5 Hz), and the splitting appears to be almost independent of the degree of ionization. The similar splitting (J_{H-P} 7.5 Hz) of the equatorial proton to a pair of triplets in the 100 MHz proton magnetic resonance spectrum, confirmed that the doublet formation observed in the phosphorus spectra was due to the ^{31}P nucleus of the axial phosphate group, coupling to the ^{1}H nucleus of the equatorial hydrogen.

An examination of the ^{31}P n.m.r. spectrum of the crystalline dodecasodium salt of cereal grain phytic acid gave the spectrum shown in Fig. 2. The single axial phosphate P_2 (δ −5.53 p.p.m.) appears as a well resolved doublet (J_{P-H} 11.2 Hz) at low field. The remaining five equatorial phosphorus nuclei appear as a sextet at higher field, a situation which is analogous to the methyl groups in the corresponding proton magnetic resonance spectrum of myoinositol hexaacetate (29). The sextet comprises two tall

Can. J. Chem. Downloaded from www.nrcresearchpress.com by 210.87.254.6 on 09/05/12
For personal use only.

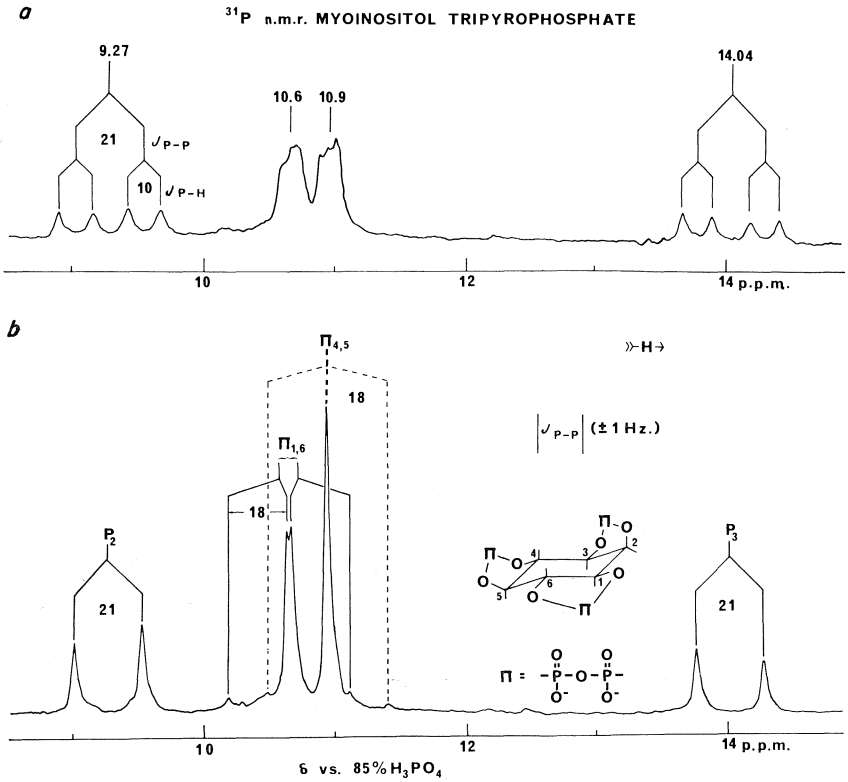

FIG. 4. (*a*) Phosphorus magnetic resonance spectrum (40.5 MHz) of a saturated solution of the hexasodium salt of myoinositol 1,6:2,3:4,5-tripyrophosphate in D_2O.
(*b*) ^{31}P Spectrum of the same sample after all phosphorus–proton couplings have been removed by the proton noise decoupling procedure of Ernst (30) using a Varian V-3512-1 heteronuclear noise decoupler. The signal has been enhanced in both cases by 19 scans with the Varian C1024 time averaging computer.

doublets P_x and P_y together with a smaller doublet (δ −4.04 p.p.m.) which may be assigned to the second meso position (P_5). These three doublets must arise from the phosphorus – axial proton coupling of the three remaining types of phosphorus nuclei. The correct assignment of each of the doublets P_x and P_y to the appropriate pair (P_1, P_3) or (P_4, P_6) of magnetically equivalent nuclei was not possible at this stage. The observed increase in doublet width from the monophosphate ($J_{P-H} \sim 8$ Hz) to the hexaphosphate ($J_{P-H} \sim 11$ Hz) was unexpected, but larger variations have been observed (20) between isomeric orthophosphates.

Confirmation of the 1,3,4,5,6-myoinositol pentaphosphate structure **4** for chicken blood "phytate" (C.B.2) is shown in Fig. 3. Comparison with Fig. 2 shows the absence of the axial phosphate signal at δ −5.53 p.p.m. and a marked upfield shift of the tall doublet (P_y, Fig. 2) from δ −4.21 p.p.m. to δ −3.66 p.p.m. in Fig. 3. The doublets P_x and P_5 in Fig. 2 are recognizable in Fig. 3 as signals located at δ −4.61 and δ −4.0 p.p.m. respectively. As the P_1 and P_3 nuclei have had their electronic environment drastically altered by the removal of the axial phosphate group from position-2, it is reasonable to assign P_y to this pair, whereas the P_x signal which is but little altered in chemical shift in both spectra, can now be assigned to the P_4, P_6 pair.

The ^{31}P n.m.r. spectrum for the racemic inositol tripyrophosphate obtained by the action of dicyclohexylcarbodiimide on cereal grain phytic acid is shown in Fig. 4*a*. The quartets (δ +9.27 p.p.m. and δ +14.04 p.p.m.) correspond to two phosphorus nuclei in unique environments and exhibit both P—P and P—H

Can. J. Chem. Downloaded from www.nrcresearchpress.com by 210.87.254.6 on 09/05/12
For personal use only.

Can. J. Chem. Downloaded from www.nrcresearchpress.com by 210.87.254.6 on 09/05/12
For personal use only.

coupling (J_{P-P} 21 Hz, J_{P-H} 10 Hz). Confirmation that the two nuclei concerned are coupled by a pyrophosphate bond, was obtained by phosphorus – phosphorus double resonance of the signal at δ +9.27 p.p.m., which gave the expected perturbation of the signal at δ +14.04 p.p.m.

The complexity of the remaining signals located between the two quartets and corresponding to four phosphorus nuclei was initially the subject of considerable conjecture. The problem was eventually solved by the noise decoupling technique of Ernst (30). Figure 4*b* displays the proton noise decoupled ^{31}P n.m.r. spectra with all the splittings due to proton–phosphorus couplings removed. The decoupled spectrum shows a near classical example of three pairs of AB spectra, ranging from the almost AX situation of the signals at δ 9.27 and 14.04 p.p.m. (J_{P-P} 21 Hz), through the intermediate AB case centered at δ 10.6 p.p.m. (J_{P-P} 18 Hz) to the almost A_2 situation centered at δ 10.9 p.p.m. (J_{P-P} 18 Hz).

By simultaneous P—P coherent and P—H noise irradiation of the small peak at δ 11.09 p.p.m. in Fig. 4*b*, the tall signal at δ 10.6 p.p.m. is split to a doublet (δ 10.55 and 10.71 p.p.m.) thus verifying the assignment of the AB pattern.

A completely unequivocal assignment of each AB pair to each corresponding pyrophosphate linkage is still not possible, although it seems reasonable to suggest that the low field signal at δ 9.27 p.p.m. derives from the axial P_2 nucleus and the second signal at δ 14.04 p.p.m. is consequently the P_3 nucleus of the myoinositol tripyrophosphate enantiomorph depicted in Fig. 4*b*. The two remaining AB systems have been tentatively assigned (Fig. 4*b*) on the grounds that the P nuclei of the pyrophosphate ($\pi_{4,5}$) with two *trans*-neighbors will be more equivalent than those of the pyrophosphate ($\pi_{1,6}$) with one *cis*- and one *trans*-neighbor. However, it is clear that the ^{31}P n.m.r. spectra, are compatible with the racemic myoinositol 1,6:2,3:4,5-tripyrophosphate structure **3**.

Conclusions

We have been unable to find any evidence, either physical or chemical, from crystalline samples of the dodecasodium salt of cereal grain phytic acid to support the Neuberg formulation **2** for this compound. The Anderson hexaorthophosphate structure **1** has been independently confirmed by Angyal and Russel[2] in a study of the crystalline dodecamethyl ester of cereal grain phytic acid. Cereal grain phytic acid appears to be present as the hexaorthophosphate **1**, *in situ* and is probably associated with ferric ions (31) as well as calcium, magnesium, and potassium cations.

The elucidation of the ^{31}P n.m.r. spectrum of DL-myoinositol 1,6:2,3:4,5-tripyrophosphate **3**, provided a good example of the simplification which can be achieved with the noise decoupling technique.

Although traces of material corresponding to cereal grain phytic acid were found in the acid-soluble phosphate fraction of chicken blood, the bulk of the phosphorus is undoubtedly present as myoinositol 1,3,4,5,6-pentaphosphate **4**, and not the hexaorthophosphate **1**.

From these studies and those on soil inositol polyphosphates (1) it is clear that in the past, the expression "phytic acid" has been employed to cover a whole range of different polyphosphates, which were indistinguishable from one another at that time. Now that the techniques for separating and identifying these compounds are available, it would seem desirable to restrict its usage to describe the myoinositol hexaorthophosphate **1**.

Experimental

Microanalyses for C, H, and P were made by the Australian Microanalytical Service. Sodium analyses were obtained with an Eel flame photometer. Water of crystallization was measured by dehydration *in vacuo* (140°/0.05 mm Hg/17 h). X-ray fluorescence analyses were obtained by courtesy of Mr. J. Hutton, C.S.I.R.O. Soils Division, Adelaide.

Differential thermal analysis (d.t.a.) patterns were obtained with an instrument supplied by A. R. Bolton and Co., Edinburgh, Scotland and fitted with matched chromel P alumel thermocouples. Samples (100 mg) were tightly packed around the thermocouple and covered with ignited alumina and were compared with ignited alumina in the reference well. The temperature gradient to 400° was at 10°/min.

Electrophoretograms were run by either the routine or moving paper electrophoresis (m.p.e.) techniques (9) in the 0.1 *M* oxalate buffer (pH 1.5) of Seiffert and Agranoff (32). Before electrophoresis or chromatography, samples of insoluble phosphate salts were converted to the free acids by addition of Dowex 50 H^+ (−400 mesh) to a

[2]S. J. Angyal and A. F. Russel. Personal communication.

Can. J. Chem. Downloaded from www.nrcresearchpress.com by 210.87.254.6 on 09/05/12
For personal use only.

suspension of the salt (10 mg) in water (0.5 ml). Phosphates were detected with the Harrap phosphomolybdate dip procedure (33). The papers were heated for 15 min at 65° before irradiation with ultraviolet light. The blue background fades as the paper regains its moisture content and the α-benzoinoxime treatment was only necessary in the case of chromatograms.

Reproducible results for inositol polyphosphates on paper chromatograms were only obtained with papers (Whatman 3 MM and No. 1) which had been chromatographically washed for 17 h with 0.1 *M* oxalic acid and then with 1.5 *M* ammonium hydroxide. The descending technique was used at 30° with the following solvent systems: (*a*) Isopropanol (80 ml), 15 *M* ammonia (20 ml), ethylenediamine – tetraacetic acid (EDTA) (100 mg). (*b*) Isopropanol (60 ml), 15 *M* ammonia (10 ml), water (30 ml), EDTA (100 mg). (*c*) Phenol (80 g), water (20 ml) (34).

Inositols were detected by the method of Anet and Reynolds (35).

Phosphorus magnetic resonance spectra were obtained with a Varian HA 100 instrument operated at 40.5 MHz. Samples whose homogeneity had been confirmed by electrophoresis and paper chromatography (solvent *b*) were prepared as saturated solutions of the sodium salts or the free acid in D_2O. A sealed capillary of phosphorus oxide P_4O_6 was used as the reference standard (36) and lock signal. Chemical shifts have been calculated using the observed separation for 85% phosphoric acid (4556.0 ± 0.2 Hz upfield from P_4O_6) at 40.48 MHz. The sample temperature was 35°. Where necessary the sample was also examined by proton magnetic resonance at 100 MHz. For clarity the signal to noise ratio was enhanced by processing multiple scans with a Varian C1024 time averaging computer. The proton noise decoupled spectra were obtained with the V-3512-1 heteronuclear noise decoupler. Infrared spectra were obtained with a Perkin–Elmer model 237 grating spectrophotometer, on solid samples at a concentration of 0.5% in potassium chloride disks.

Crystallization and Properties of Cereal Grain Sodium Phytate

It should be noted that crystallization of the sodium salt could only be achieved with samples containing only small amounts of both cationic and anionic impurities. Each sample should be examined by electrophoresis and where substantial impurities exist, they should be removed by ion exchange chromatography (12). Factors involved in the purification of calcium phytate and its conversion to sodium phytate have been discussed by Cosgrove (1).

Amorphous sodium phytate (10 g; P, 12%) was dissolved in distilled water (225 ml, 65°) and methanol (75 ml) was added. The hot solution was centrifuged and after decantation the clear supernatant was allowed to cool to 40°. Crystallization was initiated by scratching or seeding and the flask was set aside at ambient temperature (20–25°) for 72 h. A mixture of rhombohedra and clusters of needles were deposited, the crystals were filtered, washed with aqueous methanol (225:75), and air dried (6.4 g, 64%). The product was electrophoretically and chromatographically (solvent *b*) homogeneous and the two crystal types were hand separated. The large rhombohedra were efflorescent and analyzed for the dodecasodium salt with 35 molecules of water.

Anal. Calcd. for $C_6H_6O_{24}Na_{12}\cdot 35\ H_2O$: C, 4.65; H, 4.9; P, 12.0; Na, 17.8; H_2O, 40.6. Found: C, 4.95; H, 5.2; P, 12.2; Na, 18.0; H_2O, 40.3.

The rhombohedra do not melt, but show a loss of birefringence under plane polarized light at 50–57° on the Kofler melting point apparatus. The differential thermal analysis pattern showed endotherms at 63° m, 80° m, 133° s, and an exotherm at 325° w. The infrared spectrum showed the following absorption maxima; 740 w, 775 w, 835 s, 910 w, 940 sh, 975 s, 1010 sh, 1115 s, 1280 w, 1335 w, 1380 w, 1445 w, 1645 s, 2000–2400 w, 2550–3700 s, cm^{-1}. The needles analyzed for the dodecasodium salt with 31 molecules of water.

Anal. Calcd. for $C_6H_6O_{24}P_6Na_{12}\cdot 31\ H_2O$: C, 4.9; H, 4.6; P, 12.5; Na, 18.6; H_2O, 37.7. Found: C, 5.0; H, 4.9; P, 12.7; Na, 18.5; H_2O, 37.5.

The needles do not melt, but show a loss of birefringence at 50–57°. The differential thermal analysis pattern shows endotherms at 80° s, 123° s, and an exotherm at 327° w. An apparently homogeneous crop of needles was obtained by crystallization from the same solvent mixture at constant temperature (30°). The specific rotation for both forms was zero $[\alpha]_D^{20} = 0.00 \pm 0.04$ (*c*, 7; *l*, 4 in water).

Dehydration of either form (110°/0.1 mm Hg/10 h) gave an amorphous white solid corresponding to the trihydrate described by Hoff-Jorgensen (18).

Anal. Calcd. for $C_6H_6O_{24}P_6Na_{12}\cdot 3\ H_2O$: C, 7.4; H, 1.3; P, 19.0. Found: C, 7.6; H, 1.8; P, 19.1.

Further dehydration (145°/10^{-4} mm Hg/30 h) gave a hygroscopic white solid which was electrophoretically and chromatographically homogeneous and analyzed for the monohydrate of sodium phytate.

Anal. Calcd. for $C_6H_6O_{24}Na_{12}\cdot 1\ H_2O$: C, 7.7; H, 0.9; P, 19.7; Na, 29.3. Found: C, 7.7; H, 1.2; P, 19.8; Na, 29.0.

A sample of crystalline sodium phytate (1 g) was dissolved in 5 *M* sodium hydroxide (15 ml) and was precipitated once with ethanol (300 ml) according to the method outlined by Brown, Heit, and Ryan (17). The dried amorphous product (0.6 g) differed from the crystalline starting material in its infrared absorption maxima with peaks (1445 m, and 880 w, cm^{-1}) corresponding to the carbonate anion (37). The product analyzed for C, 8.7; P, 19.6; Na, 32.4% corresponding to Na:P:C ratio of 2.2:1:1.1 and appears to be a mixture of sodium phytate and sodium carbonate.

Using the above analytical figures a mixture of crystalline sodium phytate ($C_6H_6O_{24}P_6Na_{12}\cdot 31\ H_2O$, 135 mg) and anhydrous sodium carbonate (8 mg) was dried, and homogenized in an agate ball mill. The infrared spectrum (KCl disk) of this mixture was virtually superimposable with the amorphous product from the precipitation procedure.

Hexasodium Salt of Myoinositol 1,6:2,3:4,5-Tripyrophosphate

Crystalline sodium phytate (3 g) in water (30 ml) was converted to the free acid by passage through a column of Dowex 50 H^+. The column eluate was adjusted to pH 8 with pyridine and evaporated to dryness, the residue

TABLE I

Paper chromatographic and electrophoretic mobilities of some myoinositol polyphosphates relative to inorganic pyrophosphate

Substance	Symbol	Phosphorus/ myoinositol ratio	R_π solvent *b*	M_π oxalate buffer
Inorganic pyrophosphate	π		1.00	1.00
Inorganic orthophosphate	P_i		1.63	0.32
Cosgrove pentaphosphate fraction IB	α	5	0.34	1.21
Cosgrove pentaphosphate fraction IB	β	5	0.36	1.18
Cosgrove pentaphosphate fraction IC	γ	5	0.32	1.12
Cosgrove pentaphosphate fraction IC	δ	5	0.50	1.08
Cereal grain phytic acid	ϕ	6	0.25	1.26
Myoinositol tripyrophosphate	$\pi_3\phi$	6	1.78	1.65
Chicken blood fraction	C.B.1	6	0.25	1.26
	C.B.2	5	0.34	1.21
	C.B.3	4	0.49	1.10
	C.B.4	*	—	1.03
	C.B.5	*	—	0.98

*These compounds were not isolated and have not been examined for myoinositol content.

was dissolved in water (21 ml) and pyridine (84 ml) containing *N,N*-dicyclohexylcarbodiimide (5.25 g) was added. The reaction mixture was heated 6 h at 50° and evaporated to dryness. The residue was extracted with water (4 × 5 ml) filtered and the filtrate adjusted to pH 10 with 5 *M* sodium hydroxide. The sodium salt was precipitated by the addition of methanol (60 ml) and separated by centrifugation. The solid was redissolved in water (10 ml) and again precipitated, washed with 75% methanol (2 × 15 ml), methanol, and dried *in vacuo* (140°/0.1 mm Hg/8 h) to give the amorphous hexasodium salt of an inositol tripyrophosphate.

Anal. Calcd. for $C_6H_6O_{21}P_6Na_6$: C, 9.8; P, 25.2; Na, 18.7. Found: C, 9.8; P, 25.0; Na, 19.0.

Electrophoresis indicated the product contained a trace amount of an impurity M_π 1.49 which could not be removed by precipitation. The infrared spectrum showed the following absorption maxima: 685 w, 715 w, 742 w, 765 m, 810 m, 843 sh, 862 w, 892 w, 920 m, 955 m, 980 m, 995 sh, 1070 s, 1090 s, 1120 s, 1255 s, 1380 w, 1530 w, 1640 s, 2850 w, 2900 w, sh, 2925 w, 3580 sh, 2800–3800 s, br, cm^{-1}. Hydrolysis in 1 *M* hydrochloric acid (100°/15 min) gave the hexaorthophosphate with some lower phosphates and inorganic phosphate. Electrophoretic and chromatographic mobilities are listed in Table I.

Phytate Extraction from Wheat Bran

Wheat bran (50 g) in water (500 ml) was boiled for 10 min and filtered through muslin, the residue was washed with boiling water (6 × 250 ml). The residue was suspended in a solution of tetrasodium ethylenediaminetetraacetate (EDTA, 5 g) in water (500 ml) and stirred for 2 h. The mixture was filtered through muslin and the residue washed with water (5 × 100 ml). Aliquots of both the water and EDTA extracts were examined by electrophoresis, the bulk of the phytic acid was found in the EDTA extract. Neither extract showed evidence for phosphate compounds with mobilities greater than the crystalline sodium phytate reference marker. Crude barium phytate was recovered from the EDTA extract by the addition of excess 10% w/v barium acetate (100 ml). The flocculant precipitate was centrifuged, washed with water (4 × 100 ml) and dried (2.6 g; P, 8%). The crude barium salt was converted to the crystalline sodium salt (needles) and found to be chromatographically (solvent *b*) and electrophoretically indistinguishable from the crystalline dodecasodium salt ($31 \cdot H_2O$ obtained from commercial sodium phytate (ex maize). The infrared spectrum and d.t.a. patterns were superimposable.

Ultraviolet prints of electrophoretograms of the EDTA extract showed the presence of an ultraviolet absorbing spot M_π 1.73. This material was extracted and gave a positive spot test for ferric ions. The ultraviolet absorption spectra and electrophoresis mobility coincided with that for a dilute solution of ferric chloride in the oxalate buffer. The spot contained no phosphorus and is an anionic ferric oxalate complex. The original bran (oven dried) gave the following analysis, calculated from results obtained by X-ray fluorescence on the ashed sample: P, 1.19; S, 0.05; Si, 0.015; K, 1.6; Mg, 0.57; Ca, 0.10; Fe, 0.015; Mn, 0.014; Al, 0.002.

Isolation of Chicken Blood Inositol Polyphosphates

Crude inositol polyphosphate fractions were isolated by the procedures of Rapoport (7) and Oshima, Taylor, and Williams (24) and were similar to material isolated by the perchloric precipitation, which was simpler on a large scale separation.

Fresh chicken blood (10 l) was collected over a period of 15 min in a stainless steel vessel containing disodium citrate (100 g). Distilled water (2.5 l) and 60% w/v perchloric acid (1.25 l) were added and the mixture was stirred for 1 h. The thick suspension was filtered through a Buchner funnel and the residue was rinsed with a small volume of water. The combined filtrate and washings (8.1 l) contained total phosphorus (38) (153 μg P/ml) and free inorganic phosphorus (39) (34 μg P/ml).

To a portion of the filtrate (1 l), a solution of ferric chloride hexahydrate (2.7 g) and sodium chloride (200 g)

Can. J. Chem. Downloaded from www.nrcresearchpress.com by 210.87.254.6 on 09/05/12
For personal use only.

Can. J. Chem. Downloaded from www.nrcresearchpress.com by 210.87.254.6 on 09/05/12
For personal use only.

in water (1 l) was added, the mixture was boiled for 10 min and the flocculant white precipitate was allowed to settle overnight. The bulk of the clear yellow supernatant liquor was discarded. The residue was centrifuged and the crude ferric salt was washed with 0.5 *M* hydrochloric acid (2 × 30 ml) and finally with water (2 × 30 ml). The crude ferric salt was suspended in water (20 ml) and 5 *M* sodium hydroxide (1.5 ml) added. The suspension was boiled to coagulate the ferric hydroxide and centrifuged, the clear supernatant was then decanted and evaporated to dryness *in vacuo*. The crude sodium salt was dissolved in water (4 ml) and reprecipitated as an oil by the addition of methanol (8 ml). The two phases were separated by centrifugation and the oily lower solidified on trituration with methanol (13 ml). The hygroscopic solid was separated by centrifugation and dried *in vacuo* (2 h/0.1 mm Hg/100°/P_2O_5) to give the partially purified sodium salt (148 mg; P, 17.9%). The product was electrophoretically heterogeneous (see Fig. 1, lane 1) and showed five phosphate components (C.B. 1–5). The electrophoretic and chromatographic mobilities are listed in Table I.

The crude sodium salt (304 mg) in water (5 ml) was converted to the free acid by passage through a short column of Dowex 50 H^+. The eluate was applied to a second column of Dowex 1 × 2 (42 × 0.8 cm) packed in 0.1 *M* hydrochloric acid. The column was eluted with a gradient from a mixing vessel (11.7 cm I.D.) containing 0.1 *M* hydrochloric acid (1300 ml) connected by a siphon to a donor vessel (9.8 cm I.D.) containing 1.6 *M* hydrochloric acid (900 ml). The column eluate was collected in 20 ml fractions, aliquots (5 μl) were removed from each fraction with a wire loop and spotted onto a grid (10 × 10 cm) ruled on Whatman No. 1 filter paper. Phosphate compounds were detected on the grid by the phosphomolybdate test, and the relevant fractions were examined by electrophoresis.

Electrophoretically homogeneous fractions were combined, adjusted to pH 10 with ammonia, and precipitated by the addition of excess 10% w/v barium acetate solution (5–10 ml). The suspension was diluted with an equal volume of ethanol and allowed to stand overnight. The bulk of the clear supernatant was decanted and the residue was centrifuged, washed with 50% ethanol (2 × 30 ml) and dried *in vacuo*. The fractions, their electrophoretic designation and the weights of the barium salts obtained were as follows: 66–69, C.B.1 (18 mg); 52–59, C.B.2 (369 mg); 43–45, C.B.3 (12 mg). The components C.B.4 and C.B.5 were not detected by the grid procedure and were not isolated. The infrared spectra of all three barium salts (C.B.1–3) were similar and showed absorption maxima at 685 w, 825 w, sh, 853 s, 972 s, 1115 s, br, 1450 s, br, 1635 m, br, 2000–2500 w, 2500–3700 s cm^{-1}. The peaks at 685, 853, and 1453 were correlated with the presence of barium carbonate (37) which precluded the determination of the degree of phosphorylation from the C:P ratio. Hydrolysis (6 *M* hydrochloric acid/125°/40 h) of samples of each barium salt, followed by deionization of the hydrolyzate through a short column of a mixed bed resin (Amberlite M.B.1) with subsequent paper chromatography (solvents *a* and *c*) on the concentrated eluate, showed myoinositol to be the only detectable polyol in C.B.1, 2, and 3.

Table I shows that C.B.1 was indistinguishable from cereal grain phytic acid and that the major component (95% on a total P basis), C.B.2 was indistinguishable from the α component of Cosgrove's pentaphosphate fraction IB (9, 12). Table I also shows that C.B.3 is not electrophoretically (m.p.e.) identical with any of the known pentaphosphates and upon isomerization (1 *M* hydrochloric acid/110°/1 h 20 min), phosphates with the same or lower electrophoretic mobilities (M_π 1.08, 1.02, 0.97, 0.85 w, 0.31) were formed.

The phosphorus-inositol ratio for the crude barium salts of C.B.1 and C.B.3 (5.8:1 and 4.2:1 respectively) were determined by total P analyses (38) and gas chromatography of the acetylated hydrolysis products (40). Periodate oxidation (0.1 *M* periodic acid, pH 2, 25°, 24 h) of the free acid of fraction C.B.3 (10 mg) proceeded smoothly to give a product (M_π 1.04) which was reduced with excess sodium borohydride (pH 8, 24 h) to give an acyclic polyol polyphosphate. The phosphate groups were hydrolyzed (pH 5.0, 110°, 48 h) and the product was passed through a short column of Dowex 50 H^+ and evaporated to dryness with methanol (3 × 50 ml). A final deionization through a mixed bed resin gave material which was chromatographically indistinguishable (solvents *a* and *c*) from L-iditol. Acetylation (pyridine – acetic anhydride) of this product gave material which was indistinguishable by gas chromatography (40) from L-iditol acetate. Although insufficient material was available for the determination of optical activity, the available evidence suggests that C.B.3 is one of the enantiomorphs or alternatively the racemate of myoinositol 1,4,5,6-tetraphosphate. The other minor components C.B.4 and 5 were not detected by the grid procedure and were not isolated.

Identification of the Major Component C.B.2

The carbonate was removed from the major component C.B.2, by conversion to the sodium salt. The barium salt (347 mg) in water (35 ml) was stirred (2 h) with Dowex 50 H^+ (−400 mesh, 750 mg). The mixture was filtered and the residue washed with water (4 × 10 ml), the combined filtrates were passed through a column of Dowex 50 H^+ and the eluate was adjusted to pH 12 with 5 *M* sodium hydroxide. The solution was evaporated to dryness and the residue dissolved in water (2 ml) and the sodium salt was precipitated as an oil by the addition of methanol (3 ml), the phases were separated by centrifugation. The precipitation procedure was repeated until the lower layer was colorless and finally the oil was solidified by trituration with methanol and dried (140°/0.05 mm Hg/P_2O_5/17 h) to give an amorphous, hygroscopic decasodium salt of an inositol pentaphosphate (186 mg), $[\alpha]_D^{20} = 0.0 \pm 1°$ (*c* 3, *l* 0.5 in water). Infrared absorption maxima, 690 w, 780 w, 830 m, 865 sh, 975 s, 1008 w, sh, 1110 s, 1340 w, 1375 w, 1640 s, 2000–2400 w, 2500–3700 s, cm^{-1}.

Anal. Calcd. for $C_6H_7O_{21}P_5Na_{10}$: C, 9.0; P, 19.4; Na, 28.7. Found: C, 9.2; P, 19.6; Na, 28.5.

A solution of the purified sodium salt (20 mg) in 7.5 *M* ammonium hydroxide (1.0 ml) was heated in a sealed tube at 105° for 1 week. The reaction mixture was separated by electrophoresis and after developing guide strips with the phosphomolybdate reagent, the band

corresponding to inositol monophosphates was cut out and eluted with water. The eluates were concentrated and examined by prolonged paper chromatography (14 days) (41) on oxalate washed paper in solvent *a*, myo-inositol 1-, 4-, and 5-monophosphates were detected. The major product was the 4-phosphate but the axial 2-phosphate was not detectable. Thus C.B.2 is the deca-sodium salt of myoinositol 1,3,4,5,6-pentaphosphate.

Two attempts to isolate inositol penta- or hexaphosphates by a similar procedure from the blood of a female Murray River short-necked tortoise (*Emydura macquarii*) were unsuccessful.

Acknowledgments

Financial support of this work by the Commonwealth Wheat Industry Council and the Australian Research Grants Committee is gratefully acknowledged. Thanks are also due to Dr. D. J. Cosgrove of C.S.I.R.O. Division of Plant Industry, Canberra, for a gift of the inositol pentaphosphate fractions I*b* and I*c*. It is a pleasure to acknowledge the technical assistance of Mrs. June Oliphant in this work.

1. D. J. Cosgrove. Rev. Pure and Appl. Chem. **16**, 209 (1966).
2. T. Posternak. The cyclitols. Hermann, Paris; Holden-Day, Inc., San Francisco. 1965. p. 227.
3. G. Kimura. Yuki Gosei Kagaku Kyokai Shi **25**, 167 (1967); Chem. Abstr. **66**, 85963*b* (1967).
4. J. E. Courtois. Bull. Soc. Chim. Biol. **33**, 1075 (1951).
5. S. Posternak. Compt. Rend. Soc. Biol. **55**, 1190 (1903).
6. W. J. Dyer, C. L. Wrenshall, and G. R. Smith. Science, **91**, 319 (1940).
7. S. Rapoport. J. Biol. Chem. **135**, 403 (1940).
8. D. H. Smith and F. E. Clark. Soil Sci. **72**, 353 (1951).
9. M. E. Tate. Anal. Biochem. **23**, 141 (1968).
10. R. J. Anderson. J. Biol. Chem. **17**, 141 (1914).
11. C. Neuberg. Biochem. Z. **2**, 557 (1908).
12. D. J. Cosgrove. Biochem. J. **89**, 172 (1963).
13. J. Schormuller and G. Bressau. Z. Lebensm. Untersuch. Forsch. **113**, 484 (1960).
14. F. G. Peers. Biochem. J. **53**, 102 (1953).
15. S. Posternak. Helv. Chim. Acta, **4**, 150 (1921).
16. A. K. Smith and J. J. Rackis. J. Am. Chem. Soc. **79**, 633 (1957).
17. E. C. Brown, M. L. Heit, and D. E. Ryan. Can. J. Chem. **39**, 1290 (1961).
18. E. Hoff-Jorgensen. Kgl. Danske Videnskab. Selskab. **21**, No. 7 (1944).
19. J. R. Van Wazer. Phosphorus and its compounds. Vol. I. Interscience Publishers, Inc., New York. 1958. p. 14.
20. F. Ramirez. Bull. Soc. Chim. France, 2443 (1966).
21. D. F. Peppard and J. R. Ferraro. J. Inorg. Nucl. Chem. **10**, 275 (1959).
22. A. M. Sobolev. Fiziol. Rast. **13**, 193 (1966). A. M. Sobolev. Plant Physiol. USSR (English Transl.) **13**, 177 (1966).
23. F. L. Pizer and C. E. Ballou. J. Am. Chem. Soc. **81**, 4745 (1959).
24. M. Oshima, T. G. Taylor, and A. Williams. Biochem. J. **92**, 42 (1964).
25. S. Rapoport and G. M. Guest. J. Biol. Chem. **138**, 269 (1941).
26. B. M. Iselin. J. Am. Chem. Soc. **71**, 3822 (1949).
27. M. Cohn and T. R. Hughes. J. Biol. Chem. **235**, 3250 (1960).
28. C. Ho and R. J. Kurland. J. Biol. Chem. **241**, 3002 (1966).
29. R. U. Lemieux, R. K. Kullnig, H. J. Bernstein, and W. G. Schneider. J. Am. Chem. Soc. **79**, 1005 (1957).
30. R. R. Ernst. J. Chem. Phys. **45**, 3845 (1966).
31. S. Posternak. Compt. Rend. **137**, 202 (1903).
32. U. B. Seiffert and B. W. Agranoff. Biochim. Biophys. Acta, **98**, 574 (1965).
33. F. E. G. Harrap. Analyst, **85**, 452 (1960).
34. T. Posternak, D. Raymond, and W. Haerdi. Helv. Chim. Acta, **38**, 191 (1955).
35. E. F. L. J. Anet and T. M. Reynolds. Nature, **174**, 930 (1954).
36. A. C. Chapman, J. Homer, D. J. Mowthorpe, and R. T. Jones. Chem. Commun. 121 (1965).
37. F. A. Miller and C. H. Wilkins. Anal. Chem. **24**, 1253 (1952).
38. G. R. Bartlett. J. Biol. Chem. **234**, 466 (1959).
39. A. C. Jennings and R. K. Morton. Australian J. Biol. Sc. **16**, 332 (1963).
40. J. M. Oades. J. Chromatog. **28**, 246 (1967).
41. S. J. Angyal and M. E. Tate. J. Chem. Soc. 4122 (1961).

Can. J. Chem. Downloaded from www.nrcresearchpress.com by 210.87.254.6 on 09/05/12
For personal use only.

Syntheses related to the carbohydrate moiety in lincomycin

G. B. HOWARTH, D. G. LANCE, W. A. SZAREK, AND J. K. N. JONES
Department of Chemistry, Queen's University, Kingston, Ontario

Received August 15, 1968

Addition of nitroethane to 1,2:3,4-di-*O*-isopropylidene-α-D-*galacto*-hexodialdo-1,5-pyranose (**3**) gave a mixture of β-nitro alcohols (**4**), which was acetylated to afford a mixture of β-nitro acetates (**5**). Dehydroacetylation of the latter gave *cis*- and *trans*-6,7,8-trideoxy-1,2:3,4-di-*O*-isopropylidene-7-*C*-nitro-α-D-*galacto*-oct-6-enose (**6** and **7**) in a ratio of about 6:1, respectively. Addition of ammonia to the *cis*-nitroolefin (**6**) gave rapidly a mixture of two stereoisomeric *vic*-nitroamines (**8**), which was acetylated to furnish a mixture of two 6-acetamido-6,7-dideoxy-7-*C*-nitro derivatives (**9**). The same products (**9**) were obtained by the action of ammonia in aqueous tetrahydrofuran upon the preponderant β-nitro acetate, followed by acetylation. Vinylation of the aldehyde **3** gave a mixture of allylic alcohols (**10**); the preponderant epimer was obtained pure in crystalline form. The various 8-carbon sugar derivatives are of interest as potential intermediates in the synthesis of the carbohydrate moiety in lincomycin.

Canadian Journal of Chemistry, 47, 75 (1969)

Can. J. Chem. Downloaded from www.nrcresearchpress.com by 210.87.254.6 on 09/05/12
For personal use only.

Introduction

The carbohydrate obtained by cleavage of lincomycin, an important new antibiotic with activity against gram-positive organisms, has been shown (1) to be methyl 6-amino-6,8-dideoxy-1-thio-D-*erythro*-α-D-*galacto*-octopyranoside (**1**). The trivial name methyl thiolincosaminide (MTL) has been given to this compound. In the present paper we report the results of some experiments directed towards the synthesis of **1**. The addition of nitroethane to 1,2:3,4-di-*O*-isopropylidene-α-D-*galacto*-hexodialdo-1,5-pyranose (**3**) and conversion of the resulting β-nitro alcohols (**4**) to a mixture of two 6-acetamido-6,7-dideoxy-7-*C*-nitro derivatives (**9**) are described. The addition of vinylmagnesium bromide to compound **3** has been achieved also.

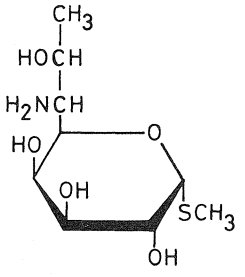

1

Results and Discussion

Oxidation of 1,2:3,4-di-*O*-isopropylidene-α-D-*galacto*-pyranose (**2**) (2) with the Pfitzner–Moffatt reagent (3) (methyl sulfoxide-*N*,*N*′-dicyclohexylcarbodiimide, with pyridine hydrochloride as the proton source) gave the aldehyde **3** (4) in a chromatographically homogeneous state in 83% yield. Our oxidation procedure is a significant improvement over that published earlier (5), by which compound **3** was obtained pure from **2** in 46% yield only after careful fractional distillation of a crude product. Addition of nitroethane to compound **3** in the presence of sodium methoxide gave a mixture of β-nitro alcohols (**4**), which was acetylated with acetic anhydride/sulfuric acid to afford a mixture of β-nitro acetates (**5**). Three stereoisomers were obtained analytically pure by fractional crystallization. Treatment of the nitro alcohols (**4**) with acetic anhydride/pyridine gave a dark solution; the infrared spectrum of the crude product showed strong absorption attributable to α-nitroolefins.

Attempts to dehydroacetylate the β-nitro acetates by sodium hydrogen carbonate in boiling benzene (Schmidt–Rutz reaction) (6) were unsatisfactory. Even after 48 h, very little elimination had occurred. Treatment of the nitro acetates with triethylamine in boiling benzene, however, rapidly gave *cis*-6,7,8-trideoxy-1,2:3,4-di-*O*-isopropylidene-7-*C*-nitro-α-D-*galacto*-oct-6-enose (**6**) and its *trans* isomer (**7**) in a ratio of approximately 6:1, respectively. Some dehydroacetylation occurred also during an attempted separation of the nitro acetates by preparative gas–liquid chromatography at 180°.

Configurational assignments of the *cis* and *trans* unsaturated nitro compounds are made on the basis of their ultraviolet (u.v.) and nuclear

Can. J. Chem. Downloaded from www.nrcresearchpress.com by 210.87.254.6 on 09/05/12
For personal use only.

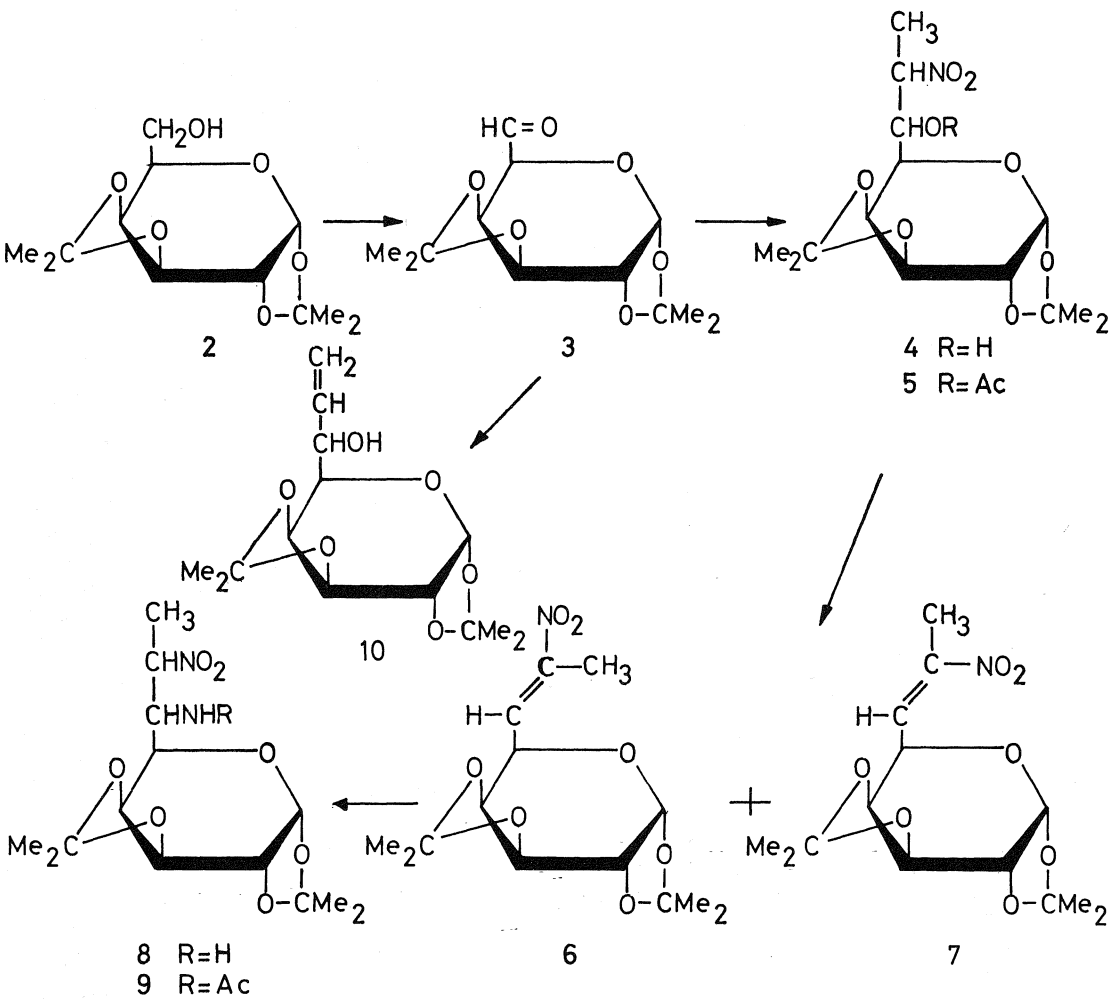

magnetic resonance (n.m.r.) spectra. Molecular models show that there is greater steric hindrance to the attainment of coplanarity of the conjugated system for the *trans* isomer (**7**). The u.v. absorption band for this isomer would be expected to occur at shorter wavelength. Thus, to the compound with λ_{max} (ethanol) 232 mμ (ε 4.7 × 10^3) the *trans* stereochemistry shown in **7** is assigned, and that with λ_{max} (ethanol) 245 mμ (ε 1.2 × 10^4) is the *cis* isomer (**6**). In the n.m.r. spectra of the two isomers the signal for the vinyl proton in the *cis* isomer is at lower field than in the *trans* isomer (see Experimental section). When either of the isomers is dissolved in ether containing a trace of triethylamine, isomerization occurs to give again a 6:1 mixture of *cis* and *trans* isomers, respectively. A photochemical *cis–trans* isomerization of **6** and **7** has been demonstrated also in this laboratory (7).

Treatment of the *cis*-nitroolefin (**6**) with saturated methanolic ammonia rapidly gave a mixture of two stereoisomeric *vic*-nitroamines (**8**). The same two nitroamines were formed by the action of ammonia in aqueous tetrahydrofuran upon the preponderant β-nitro acetate itself. These reactions have been previously applied in carbohydrate chemistry for similar syntheses of vicinal nitroamino sugars (8). *N*-Acetylation of the nitroamines (**8**) gave a crystalline, sharp-melting approximately 1:1 mixture of two 6-acetamido-6,7-dideoxy-7-*C*-nitro derivatives (**9**). Attempts to resolve this mixture by fractional crystalliza-

Can. J. Chem. Downloaded from www.nrcresearchpress.com by 210.87.254.6 on 09/05/12
For personal use only.

tion, thin-layer, and column chromatography have been unsuccessful.

A useful method for extension of sugar chains is the addition of acetylenic or vinylic Grignard reagents to *aldehydo* sugars (9). Vinylation of the aldehyde **3** with vinylmagnesium bromide (10) in tetrahydrofuran gave a mixture of allylic alcohols (**10**). The preponderant epimer was obtained pure in crystalline form. The stereochemistry at C-6 has not been established. The same compound has been prepared previously by Horton *et al.* (11) by ethynylation of **3** with ethynylmagnesium bromide in tetrahydrofuran, followed by hemihydrogenation of the preponderant acetylenic derivative over Lindlar catalyst.

Experimental

Melting points were determined on a Fisher–Johns melting point apparatus and are uncorrected. Optical rotations were measured with a Perkin–Elmer model 141 automatic polarimeter at $21 \pm 2°$ in chloroform containing 0.75% ethanol, unless otherwise stated. Infrared spectra were measured on a Beckman-IR5A spectrophotometer. Nuclear magnetic resonance (n.m.r.) spectra were measured on a Varian A-60A spectrometer in chloroform-*d* and tetramethylsilane as internal standard. Ultraviolet spectra were measured with a Unicam SP.800B spectrophotometer. Thin-layer chromatography (t.l.c.) was performed with Silica Gel G as the absorbent, and 2:3 ethyl acetate – petroleum ether as the developing solvent. The term "petroleum ether" refers to the fraction of b.p. 60–80°. Gas–liquid chromatography (g.l.c.) (F and M chromatograph, model 402) was carried out at a carrier gas flow rate of ca. 100 ml/min on a column of 1% (w/w) Apiezon L supported on 50–60 mesh acid washed DMCS treated Chromosorb W (115 × 0.4 cm) at 180°, unless otherwise stated. Retention times, *T*, are quoted relative to 1,3,5-trinitrobenzene (=1.00). The chromatograph was adapted for preparative separations as described previously (12).

1,2:3,4-Di-O-isopropylidene-α-D-galacto-hexodialdo-1,5-pyranose (3)

To a solution of 1,2:3,4-di-*O*-isopropylidene-α-D-galactopyranose (2) (25 g) in dry (molecular sieves) methyl sulfoxide (450 ml) were added pyridine hydrochloride (prepared by saturation of a solution of pyridine (5 ml) in ether (100 ml) with dry hydrogen chloride and concentration to dryness) and *N,N'*-dicyclohexylcarbodiimide (61 g). The mixture was stirred for 24 h at room temperature; a solution of oxalic acid (25 g) in methanol (50 ml) was then added, the stirring was continued to decompose the excess of *N,N'*-dicyclohexylcarbodiimide, and the mixture was poured into an aqueous saturated sodium chloride solution (1 l). *N,N'*-Dicyclohexylurea was removed by filtration, and the filtrate was extracted with chloroform (5 × 250 ml). The extracts were washed with aqueous sodium hydrogen carbonate (250 ml) and then with water (6 × 250 ml). The aqueous washings were extracted with chloroform, and the organic phases were combined, dried (magnesium sulfate), and concentrated to dryness. The syrupy residue was dissolved in warm acetone (250 ml), and a small amount of *N,N'*-dicyclohexylurea was removed by filtration. The filtrate was concentrated to give a colorless, chromatographically homogeneous (t.l.c. and g.l.c.) syrup (20.8 g, 83%), b.p. 96–100°/0.1 mm Hg, $[\alpha]_D$ −113° (*c*, 3.4); R_f 0.40 (t.l.c.), *T* 0.27 (g.l.c.). The product had the same infrared and n.m.r. spectral features as those previously reported (5) for compound **3**. For a fraction with b.p. 104–105°/0.5 mm Hg, $[\alpha]_D^{20}$ −131° (*c*, 0.9 in chloroform) has been reported (5).

Anal. Calcd. for $C_{12}H_{18}O_6$: C, 55.8; H, 7.03. Found: C, 55.4; H, 7.11.

An oxime of the syrupy aldehyde **3** was prepared essentially by the method of Horton *et al.* (5), which involves treatment with hydroxylamine hydrochloride in aqueous methanol containing pyridine as the acid acceptor, except that the solution was heated at reflux temperature for 5 h. The product was recrystallized from petroleum ether, and had m.p. 114–115°, $[\alpha]_D$ −132° (*c*, 2.3). For an oxime derivative of **3**, m.p. 107–108° and $[\alpha]_D^{20}$ −116° (*c*, 0.35 in chloroform) have been reported (5).

Anal. Calcd. for $C_{12}H_{19}NO_6$: C, 52.7; H, 7.01; N, 5.13. Found: C, 52.4; H, 7.10; N, 5.47.

Preparation of β-Nitro Acetates (5)

To a slurry of nitroethane (100 ml) in dry methanol (180 ml) containing sodium (2.7 g) was added aldehyde **3** (18.4 g) in methanol (30 ml) dropwise with stirring, and the mixture was allowed to stand at room temperature overnight. The solution was passed then through Rexyn-101 (H form) exchange resin, and the eluate and washings were concentrated to dryness under reduced pressure to give a viscous syrup (20 g) whose infrared spectrum (film) showed strong absorption at 6.4–6.5 μm attributable to C—NO_2, but no carbonyl absorption.

The syrupy product was dissolved in acetic anhydride (200 ml) containing sulfuric acid (2 ml). After 15 min at room temperature methanol (200 ml) was added with cooling, and the solution was poured into an excess of sodium hydrogen carbonate solution. Extraction with chloroform and concentration of the dried (magnesium sulfate) extracts gave a syrup which yielded from ethanol–water a crystalline product (10 g), m.p. 118–124°. Recrystallization of this first crop of crystals from chloroform – petroleum ether afforded large white prisms (6.4 g, 25%), m.p. 127–129°, $[\alpha]_D$ −73° (*c*, 2.4 in ethanol); *T* 2.27 (g.l.c.); λ_{max} (KBr) 5.70 (OAc), 6.45 (C—NO_2), 7.2, 7.25 μm (CMe_2); n.m.r. data: τ 4.49 (1-proton doublet, $J_{1,2}$ 5 Hz, H-1), τ 7.93 (3-proton singlet, OAc), τ 8.44 (3-proton doublet, *J* 7 Hz, C-7 Me), τ 8.46, 8.56, 8.68 (3-, 3-, and 6-proton singlets, CMe_2).

Anal. Calcd. for $C_{16}H_{25}NO_9$: C, 51.2; H, 6.7; N, 3.8. Found: C, 51.4; H, 6.9; N, 3.7.

A second crop of crystals (1.8 g), m.p. 104–110°, was obtained by the addition of more water to the ethanol–water mother liquors above and cooling to 5°. Recrystallization from chloroform – petroleum ether and then ether – petroleum ether gave crystals (1.2 g, 5%), m.p. 116–118°, $[\alpha]_D$ −72° (*c*, 2.6 in ethanol); *T* 1.98 (g.l.c.); λ_{max} (KBr) 5.68 (OAc), 6.43 (C—NO_2), 7.2–7.3 μm

Can. J. Chem. Downloaded from www.nrcresearchpress.com by 210.87.254.6 on 09/05/12
For personal use only.

(CMe_2); n.m.r. data: τ 4.50 (1-proton doublet, $J_{1,2}$ 5 Hz, H-1), τ 7.90 (3-proton singlet, OAc), τ 8.40, 8.57, 8.66, 8.90 (3-proton singlets, CMe_2), τ 8.43 (3-proton doublet, *J* 7 Hz, C-7 Me).

Anal. Calcd. for $C_{16}H_{25}NO_9$: C, 51.2; H, 6.7; N, 3.8. Found: C, 51.5; H, 7.0; N, 3.6.

A further crop was obtained from the chloroform – petroleum ether mother liquors remaining after recrystallization of the first crop of crystals, and was shown by g.l.c. to be a 3:2 mixture of the first component (*T* 2.27) and a new third component (*T* 1.64). Preparative g.l.c. of a small amount of this mixture gave a fraction which was mainly this third component. The fraction was recrystallized twice from chloroform – petroleum ether, and then used to nucleate a solution of the mixture in this solvent to yield finally a third crystalline β-nitro acetate (150 mg), m.p. 190–191°, $[\alpha]_D$ −69° (*c*, 3.0 in ethanol); λ_{max} (KBr) 5.7 (OAc), 6.45 (C—NO_2), 7.2, 7.25 μm (CMe_2); n.m.r. data: τ 7.94 (3-proton singlet, OAc), τ 8.40 (3-proton doublet, *J* 7 Hz, C-7 Me), τ 8.50, 8.54, 8.68 (3-, 3-, and 6-proton singlets, CMe_2).

Anal. Calcd. for $C_{16}H_{25}NO_9$: C, 51.2; H, 6.7; N, 3.8. Found: C, 51.3; H, 6.9; N, 3.5.

*cis- and trans-6,7,8-Trideoxy-1,2:3,4-di-O-isopropylidene-7-C-nitro-α-*D*-galacto-oct-6-enose (**6** and **7**)*

A solution of the preponderant β-nitro acetate (*T* 2.27) (2 g) in benzene (50 ml) containing triethylamine (5 ml) was heated at reflux temperature for 2 h. Concentration of the solution after it had been washed successively with sulfuric acid (2 *N*), sodium hydrogen carbonate solution, and water yielded a solid, which was recrystallized from petroleum ether to afford the *cis* isomer (**6**) as white prisms (1.25 g, 75%), m.p. 137–139°, $[\alpha]_D$ −109° (*c*, 2.6 in ethyl acetate); *T* 2.27 (g.l.c.); λ_{max} (KBr) 3.25 (vinylic C—H), 5.93 (C=C), 6.55 (olefinic NO_2), 7.2, 7.3 μm (CMe_2); λ_{max} (Ethanol) 245 mμ (ε 1.2×10^4); n.m.r. data: τ 2.63 (1-proton quartet, $J_{6,5}$ 8 Hz, $J_{6,8}$ 1.2 Hz, H-6), τ 4.27 (1-proton doublet, $J_{1,2}$ 5 Hz, H-1), τ 5.20 (1-proton quartet, $J_{3,2}$ 2.5 Hz, $J_{3,4}$ 8 Hz, H-3), τ 5.50 (1-proton quartet, $J_{2,1}$ 2.5 Hz, $J_{2,3}$ 2.5 Hz, H-2), τ 5.65 (1-proton quartet, $J_{4,3}$ 8 Hz, $J_{4,5}$ 2 Hz, H-4), τ 5.30 (1-proton quartet, $J_{5,4}$ 2 Hz, $J_{5,6}$ 8 Hz, H-5), τ 7.67 (3-proton singlet, C-7 Me), τ 8.40, 8.50, 8.60 (3-, 3-, and 6-proton singlets, CMe_2).

Anal. Calcd. for $C_{14}H_{21}NO_7$: C, 53.4; H, 6.7; N, 4.4. Found: C, 53.4; H, 6.9; N, 4.3.

Gas–liquid chromatographic examination of the petroleum ether mother liquors above showed the presence of a 2:3 mixture of the *cis* isomer (*T* 2.27) and a second component (*T* 1.00). A small amount of the second component was obtained pure by preparative g.l.c., and was used to nucleate a solution of the mixture in ethanol. The *trans* isomer (**7**) crystallized as prisms (40 mg), m.p. 99–100°, $[\alpha]_D$ −90° (*c*, 1.1 in ethyl acetate); λ_{max} (KBr) 3.25 (vinylic C—H), 6.02 (C=C), 6.50 (olefinic NO_2), 7.2, 7.25 μm (CMe_2); λ_{max} (Ethanol) 232 mμ (ε 4.7×10^3); n.m.r. data: τ 4.05 (1-proton broad doublet, $J_{6,5}$ 7.5 Hz, $J_{6,8}$ <1 Hz, H-6), τ 4.5 (1-proton doublet, $J_{1,2}$ 5 Hz, H-1), τ 4.95 (1-proton broad doublet, $J_{5,6}$ 7.5 Hz, H-5), τ 5.35 (1-proton quartet, $J_{3,4}$ 8 Hz, $J_{3,2}$ 2 Hz, H-3), τ 5.57 (1-proton quartet, $J_{4,3}$ 8 Hz, $J_{4,5}$ 2 Hz, H-4), τ 5.68 (1-proton quartet, $J_{2,1}$ 5 Hz, $J_{2,3}$ 2 Hz, H-2), τ 7.76 (3-proton singlet, C-7 Me), τ 8.50, 8.53, 8.68 (3-, 3-, and 6-proton singlets, CMe_2).

Anal. Calcd. for $C_{14}H_{21}NO_7$: C, 53.4; H, 6.7; N, 4.4. Found: C, 53.7; H, 6.9; N, 4.3.

*Preparation of 6-Acetamido-6,7-dideoxy-7-C-nitro Derivatives (**9**)*

*(a) By Addition of Ammonia to cis-Nitroolefin **6***

A solution of *cis*-nitroolefin **6** (0.5 g) in saturated methanolic ammonia (10 ml) was allowed to stand for 2 h at room temperature. Thin-layer chromatography showed the absence of starting material (R_f 0.58) and the presence of two new components (R_f 0.26 and 0.14). The solution was concentrated to a syrup, which was dissolved in a mixture of acetic anhydride (2 ml) and pyridine (3 ml). After standing for 5 h at room temperature, the mixture was poured into water, and a syrup was isolated in the usual manner. The product was crystallized from chloroform – petroleum ether as fine white needles (140 mg), m.p. 220–222°, $[\alpha]_D$ −41.3° (*c*, 0.9); λ_{max} (KBr) 3.1 (amide NH), 6.05 (amide I), 6.45 (C—NO_2) 7.2–7.3 μm (CMe_2); n.m.r. data: τ 4.52 (doublet, $J_{1,2}$ 5 Hz, H-1), τ 7.94, 8.00 (singlets, NAc). Gas–liquid chromatography at 215° showed the presence of two components (two stereoisomers **9**) in an approximately 1:1 ratio (*T* 2.80 and 3.85).

Anal. Calcd. for $C_{16}H_{26}N_2O_8$: C, 51.4; H, 6.95; N, 7.5. Found: C, 51.2; H, 7.08; N, 7.40.

*(b) By Reaction of Ammonia with Preponderant β-Nitro Acetate **5***

To a solution of the preponderant β-nitro acetate **5** (*T* 2.27) (100 mg) in tetrahydrofuran (1 ml) was added concentrated aqueous ammonia (0.5 ml). The mixture was stirred vigorously for two days; t.l.c. showed the presence of the same two *vic*-nitroamines as obtained in (*a*) (R_f 0.26 and 0.14). Acetylation as in (*a*) gave a mixture (40 mg) of the same two *N*-acetyl derivatives (**9**).

*7,8-Dideoxy-1,2:3,4-di-O-isopropylidene-*D*-glycero (and L-glycero)-α-*D*-galacto-oct-7-enopyranose (**10**)*

To a solution of vinylmagnesium bromide (**10**), prepared from magnesium (3 g) and vinyl bromide (12 ml) in tetrahydrofuran (100 ml), was added a solution of aldehyde **3** (3.6 g) in tetrahydrofuran (20 ml), and the mixture was heated at reflux temperature. After 3 h, g.l.c. (on a column of 10% (w/w) LAC-4R-886 wax on 100–120 mesh Chromosorb W at 200°) showed the presence of two components in a ratio of about 1:2. Ether (200 ml) was added and then water. The mixture was filtered, and the filtrate was concentrated to leave a syrup which was distilled under high vacuum. After several days the syrupy distillate crystallized. Two recrystallizations from ether – petroleum ether gave the preponderant epimer as white plates (1.24 g, 31%), m.p. 108–109°, $[\alpha]_D$ −53.5° (*c*, 1.7); λ_{max} (KBr) 2.85 (OH), 7.2, 7.3 μm (CMe_2); n.m.r. data: τ 4.45 (1-proton doublet, $J_{1,2}$ 5 Hz, H-1), τ 8.50, 8.65, 8.68 (6-, 3-, and 3-proton singlets, CMe_2).

Anal. Calcd. for $C_{14}H_{22}O_6$: C, 58.8; H, 7.7. Found: C, 59.0; H, 7.8.

Acknowledgments

The authors thank the National Research

Council of Canada for financial support and Dr. D. G. M. Diaper, Royal Military College, Kingston, Ontario for the use of the nuclear magnetic resonance spectrometer.

1. W. SCHROEDER, B. BANNISTER, and H. HOEKSEMA. J. Am. Chem. Soc. **89**, 2448 (1967).
2. O. T. SCHMIDT. *In* Methods in carbohydrate chemistry. Vol. II. Academic Press, Inc., New York. 1963. p. 324.
3. K. E. PFITZNER and J. G. MOFFATT. J. Am. Chem. Soc. **85**, 3027 (1963); **87**, 5661 (1965).
4. G. B. HOWARTH. M.Sc. Thesis. Queen's University, Kingston, Ontario. 1966.
5. D. HORTON, M. NAKADATE, and J. M. J. TRONCHET. Carbohydrate Res. **7**, 56 (1968).
6. A. SCHMIDT and G. RUTZ. Ber. **61**, 2142 (1928); J. C. SOWDEN. Advan. Carbohydrate Chem. **6**, 291 (1951).
7. G. B. HOWARTH, D. G. LANCE, W. A. SZAREK, and J. K. N. JONES. Can. J. Chem. This issue.
8. H. H. BAER and T. NEILSON. J. Org. Chem. **32**, 1068 (1967), and references therein.
9. D. HORTON, J. B. HUGHES, and J. K. THOMSON. J. Org. Chem. **33**, 728 (1968), and references therein.
10. I. N. NAZAROV, I. V. TORGOV, and G. P. VERKHOLETOVA. Dokl. Akad. Nauk SSSR, **112**, 1067 (1957); Chem. Abstr. **51**, 14647*d* (1957).
11. D. HORTON, J. B. HUGHES, and J. M. J. TRONCHET. Chem. Commun. 481 (1965).
12. D. G. LANCE and G. B. HOWARTH. Laboratory practice (London). To be published.

Can. J. Chem. Downloaded from www.nrcresearchpress.com by 210.87.254.6 on 09/05/12
For personal use only.

Can. J. Chem. Downloaded from www.nrcresearchpress.com by 210.87.254.105 on 09/05/12
For personal use only.

Photolysis of a carbohydrate nitroolefin[1]

G. B. HOWARTH, D. G. LANCE, W. A. SZAREK,[2] AND J. K. N. JONES
Department of Chemistry, Queen's University, Kingston, Ontario

Received August 15, 1968

Irradiation of an acetone solution of *cis*-6,7,8-trideoxy-1,2:3,4-di-*O*-isopropylidene-7-*C*-nitro-α-D-*galacto*-oct-6-enose (**4**) with ultraviolet light gives a complex mixture from which the three major products have been isolated: the *trans* isomer of the nitroolefin **4**, *cis*-6,8-dideoxy-1,2:3,4-di-*O*-isopropylidene-α-D-*galacto*-oct-5-enos-7-ulose (**5**), and the *trans* isomer of **5**. The structures of the compounds were established by spectroscopic methods. Signal assignments in the nuclear magnetic resonance spectra have been made by spin decoupling.

Canadian Journal of Chemistry, 47, 81 (1969)

The photochemistry of nitro compounds is of interest because of the similarity of their absorption characteristics to those of carbonyl compounds. Some studies of the action of ultraviolet light on unsaturated nitro compounds have been described (2, 3). Thus, irradiation of β-methyl-β-nitrostyrene (**1**) has been reported (2) to give 1-phenyl-1-oximinopropan-2-one (**2**). A rationalization for this novel photoisomerization has been suggested according to which the initial rearrangement is R—NO_2 to R—O—NO. Cleavage of the nitrite followed by readdition of nitrogen (II) oxide at the α-carbon would give a nitrosoketone which could isomerize to the oximinoketone (**2**).

During the course of our work (4) directed towards the synthesis of the carbohydrate moiety in lincomycin (5), methyl 6-amino-6,8-dideoxy-1-thio-D-*erythro*-α-D-*galacto*-octopyranoside (**3**), we prepared *cis*-6,7,8-trideoxy-1,2:3,4-di-*O*-isopropylidene-7-*C*-nitro-α-D-*galacto*-oct-6-enose (**4**) and its *trans* isomer. Compound **4** was irradiated in acetone with 2537 Å light in an attempt to achieve a photoisomerization of the type described above. The anticipated oximinoketone would be a valuable intermediate in the synthesis of **3**. In the present paper we report the results of the photochemical studies.

Irradiation of **4** gave a complex mixture from which the three major products were isolated. These are the *trans* isomer of the nitroolefin **4**, *cis*-6,8-dideoxy-1,2:3,4-di-*O*-isopropylidene-α-D-*galacto*-oct-5-enos-7-ulose (**5**), and the *trans* isomer of **5**. The isolation of the compounds was very difficult because of the similarity of their chromatographic mobilities (gas–liquid and thin-layer chromatography), and was complicated further by the facile isomerization of the *trans* αβ-unsaturated ketone to the *cis* isomer **5** in chloroform. A separation was eventually achieved by a combination of column and preparative gas–liquid chromatography (g.l.c.). The relative amounts of the compounds at the end of the irradiation, as determined by g.l.c., are shown in Table I.

TABLE I
Gas–liquid chromatographic data*

Compound	Relative retention time	Final relative peak area
4	1.00 = 3.4 min	3.3
trans Isomer of **4**	0.54	4.7
5	0.40	1.3
trans Isomer of **5**	0.26	1.0

*See Experimental section for details.

Configurational assignments of the *cis* and *trans* unsaturated nitro compounds have been made (4) on the basis of their ultraviolet (u.v.) and nuclear magnetic resonance (n.m.r.) spectra. Molecular models show that there is greater steric hindrance to the attainment of coplanarity of the conjugated system for the *trans* isomer. The u.v. absorption band for this isomer would be expected to occur at shorter wavelength. The *cis* and *trans* isomers have λ_{max} (Ethanol) 245 mμ (ε 1.2 × 10^4) and λ_{max} (Ethanol) 232 mμ (ε 4.7 × 10^3), respectively (4). In the n.m.r. spectra of the two isomers the signal for the vinyl proton in the *cis* isomer is at lower field than in the *trans* isomer (see Table II).

The signal assignments in the n.m.r. spectra of the *cis*- and *trans*- nitroolefins (Figs. 1 and 2,

[1]For a preliminary communication, see ref. 1.
[2]To whom inquiries should be addressed.

Can. J. Chem. Downloaded from www.nrcresearchpress.com by 210.87.254.105 on 09/05/12
For personal use only.

TABLE II

Chemical shifts (τ) and coupling constants (Hz)*

Compound	H-1	$J_{1,2}$	H-2	$J_{2,3}$	H-3	$J_{3,4}$	H-4	$J_{4,5}$	H-5	$J_{5,6}$	H-6	$J_{6,8}$	C-7Me	CMe_2
4	d, 4.27	5	q, 5.50	2.5	q, 5.20	8	q, 5.65	2	q, 5.30	8	q, 2.63	1.2	7.67	8.40–8.60 (12H)
trans Isomer of **4**	d, 4.50	5	q, 5.68	2	q, 5.35	8	q, 5.57	2	broad d, 4.95	7.5	broad d, 4.05	<1	7.76	8.50–8.68 (12H)
5	d, 4.18	3	q, 5.68	3	q, 5.36	7	d, 5.53	—	—	—	s, 4.50	—	7.67	8.52–8.62 (12H)
trans Isomer of **5**	d, 4.31	3	q, 5.78	3	q, 5.47	6	d, 4.15	—	—	—	s, 4.0	—	7.80	8.53–8.60 (12H)

*Data taken from spectra measured in chloroform-*d* at 60 MHz; s = singlet, d = doublet, q = quartet.

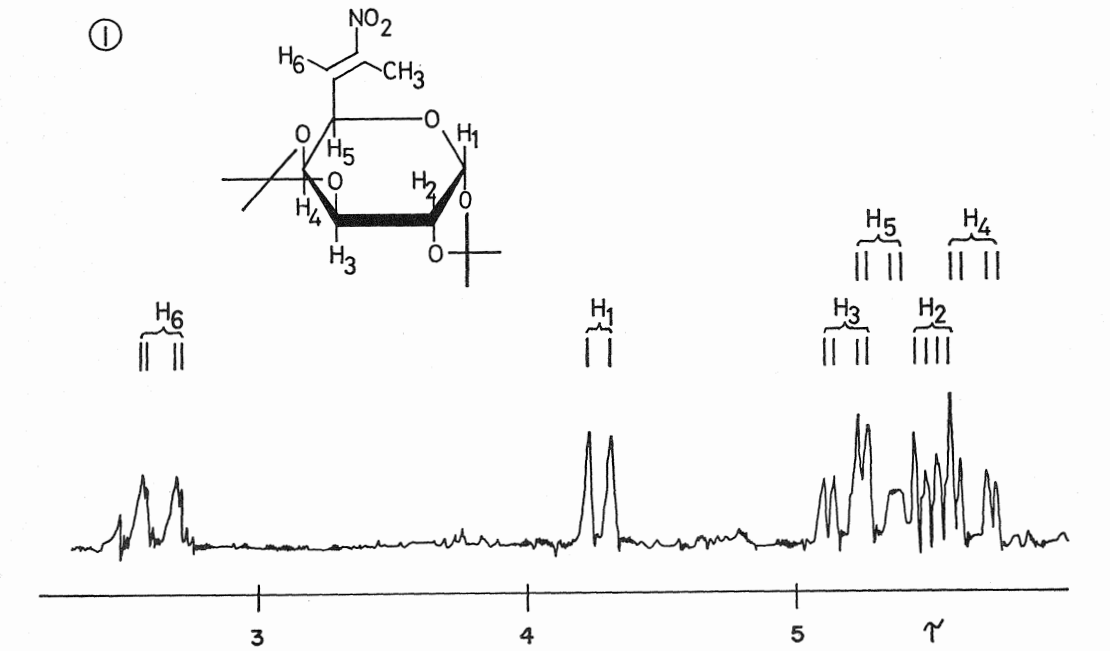

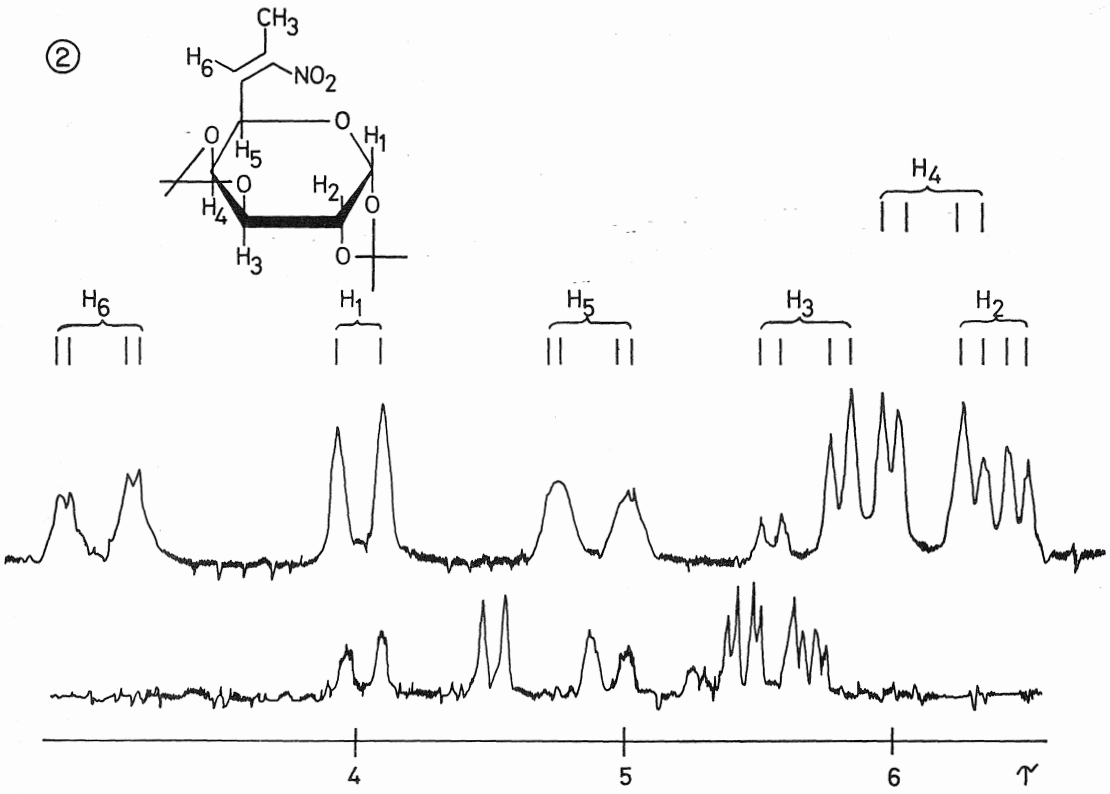

FIG. 1. The low-field portion of the 60 MHz nuclear magnetic resonance spectrum of *cis*-nitroolefin (**4**) in chloroform-*d*.

FIG. 2. The low-field portion of the 60 MHz nuclear magnetic resonance spectrum of the *trans*-nitroolefin in chloroform-*d*.

Can. J. Chem. Downloaded from www.nrcresearchpress.com by 210.87.254.105 on 09/05/12
For personal use only.

Can. J. Chem. Downloaded from www.nrcresearchpress.com by 210.87.254.105 on 09/05/12
For personal use only.

respectively) were made by spin decoupling. For the *cis* isomer **4**, irradiation at τ 4.27 (H-1) caused the quartet centered at τ 5.50 to collapse to a doublet with a splitting of 2.5 Hz. The quartet was assigned, therefore, to H-2, and the coupling constant $J_{2,3}$ = 2.5 Hz. Similarly, irradiation of H-1 in the *trans* isomer (τ 4.50) caused collapse of the quartet centered at τ 5.68 to a doublet, a result which shows that this signal is that of H-2, and $J_{2,3}$ = 2 Hz. Decoupling of H-2 from H-3, H-3 from H-4, and H-4 from H-5 in the *cis* isomer (**4**) was not possible because of the similarity of their chemical shifts. The assignment of the H-3 signal was made on the basis of $J_{2,3}$ = 2.5 Hz, which showed that the signal is the quartet at τ 5.20. The quartet at τ 2.63 was assigned to H-6 because of the small splitting (ca. 1 Hz) owing to long range coupling with the terminal methyl group. Irradiation of H-6 caused the quartet centered at τ 5.30 to collapse to a doublet with a splitting of 2 Hz. This signal is, therefore, that of H-5 with $J_{5,4}$ = 2 Hz. Finally, the quartet at τ 5.65 is assigned to H-4 with $J_{4,5}$ = 2 Hz.

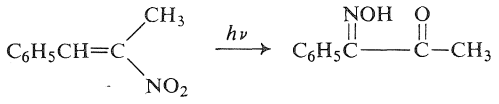

1 **2**

For the *trans*-nitroolefin, irradiation of H-2 caused the quartet centered at τ 5.35 to collapse to a doublet with a splitting of 8 Hz. This signal is, therefore, that of H-3 with $J_{3,4}$ = 8 Hz. The broad doublet at τ 4.05 was assigned to the vinyl proton H-6, since the signal simplified to a sharp doublet on irradiation of the terminal methyl group. Irradiation of H-6 caused the broad doublet at τ 4.95 to collapse to a broad band. The signal has been assigned to H-5. The coupling constant $J_{4,5}$ = 2 Hz was determined from the H-4 signal, which was identified as the quartet at τ 5.57, since it collapsed to a doublet on irradiation of H-5. The splitting of the doublet was 8 Hz, the same value as had been obtained earlier for $J_{3,4}$.

The structures of the two αβ-unsaturated ketones were established by spectroscopic methods. Elemental analysis of the two compounds corresponded in each case to a loss of one atom of nitrogen, oxygen, and hydrogen from the starting *cis*-nitroolefin (**4**). The infrared and u.v. spectra of both compounds showed absorptions attributable to an αβ-unsaturated ketone. The evidence for the configurational assignments of the isomers was their u.v. spectra. In this case molecular models show that there is greater steric hindrance to the attainment of coplanarity of the conjugated system for the *cis* isomer (**5**). Thus, the compound with λ_{max} (ethanol) 248 mμ (ε 1.6 × 10^4) is the *cis* isomer, and that with λ_{max} (ethanol) 256 mμ (ε 1.1 × 10^4) is the *trans* isomer. The n.m.r. spectra of the two isomers showed in each case a 3-proton singlet attributable to the terminal methyl group, a 1-proton singlet attributable to the vinyl proton, and signals assigned to the methyl groups of the isopropylidene rings (see Table II). The remainder of the proton assignments were made by spin decoupling experiments (Figs. 3 and 4). When the H-1 nuclei were irradiated (τ 4.18 for **5** and τ 4.31 for the *trans* isomer), the respective quartets at τ 5.68 and τ 5.78 collapsed in each case to a doublet with a splitting of 3 Hz. The quartets were assigned, therefore, to the H-2 protons with $J_{2,3}$ = 3 Hz. Irradiation of the H-2 protons in **5** and the *trans* isomer caused the respective quartets at τ 5.36 and τ 5.47 to collapse to doublets with splittings of 7 Hz and 6 Hz, respectively. These quartets are, therefore, those of the H-3 protons, and the splittings are the $J_{3,4}$ coupling constants. Irradiation of H-3 in the *trans* isomer caused the doublet at τ 4.15 to collapse to a singlet, indicating that this signal is that of H-4. Decoupling of H-3 from

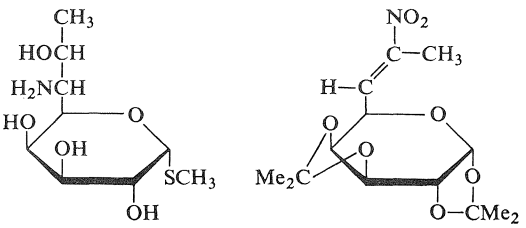

3 **4**

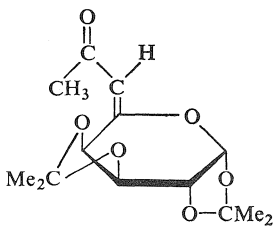

5

Can. J. Chem. Downloaded from www.nrcresearchpress.com by 210.87.254.105 on 09/05/12
For personal use only.

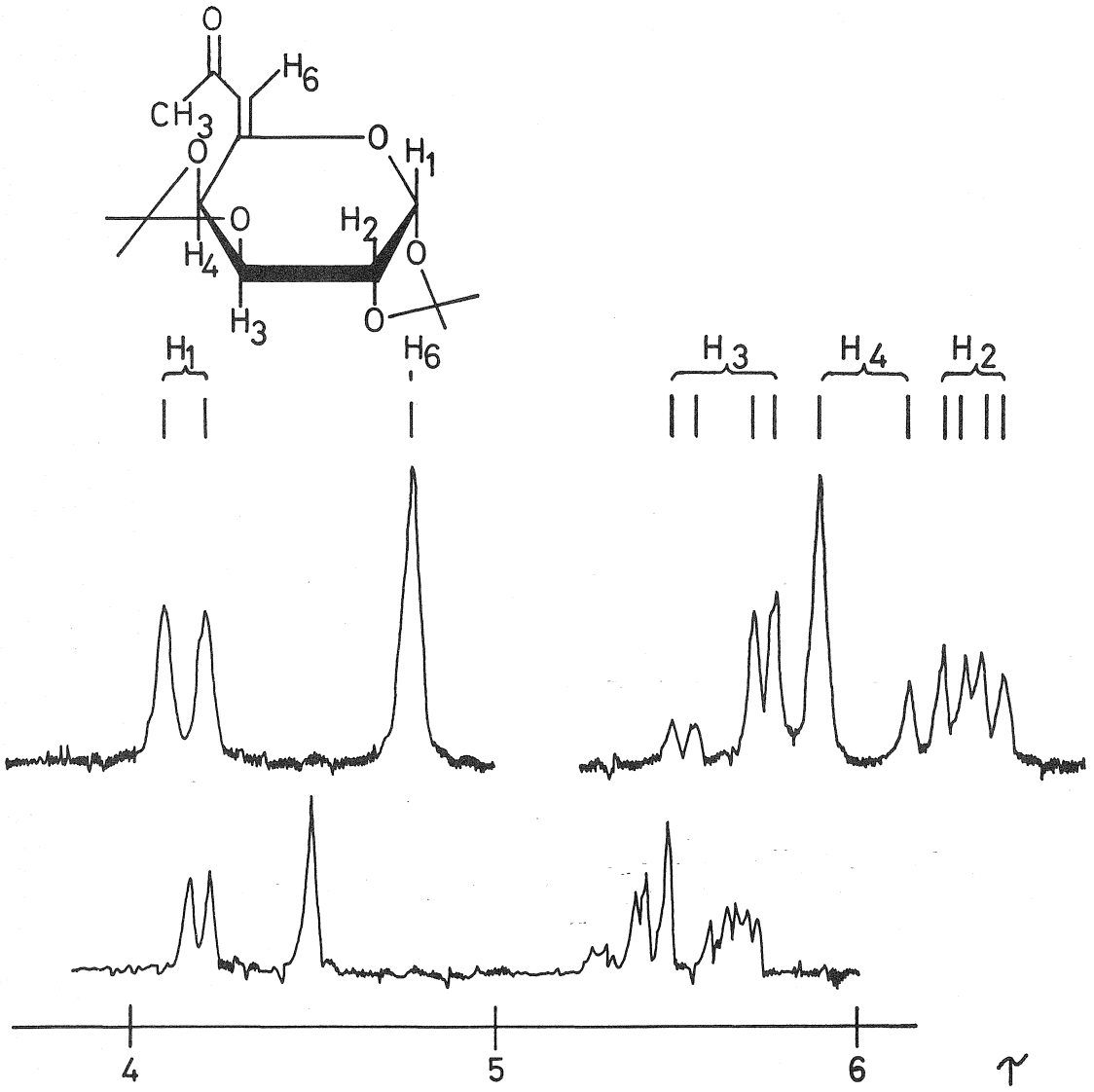

FIG. 3. The low-field portion of the 60 MHz nuclear magnetic resonance spectrum of the *cis* αβ-unsaturated ketone (**5**) in chloroform-*d*.

H-4 in the *cis* isomer (**5**) was not possible because of the similarity of their chemical shifts. In this case, however, the H-4 doublet was clearly seen at τ 5.53 with a splitting of 7 Hz ($J_{4,3}$). It is interesting to note the significantly greater deshielding of the H-4 proton in the *trans* isomer.

The formation of the αβ-unsaturated ketones is of particular interest to carbohydrate chemists, because of the resemblance to the Nef reaction, a procedure widely used in monosaccharide synthesis (6). Such a photochemical reaction has been reported previously (2, 3); irradiation of 6-nitro-Δ^5-cholesteryl 3β-acetate in hexane, aqueous dioxane, or acetone gives in low yield, in addition to other products, 6-oxo-Δ^4-cholesteryl 3β-acetate.

Experimental

Melting points were determined on a Fisher–Johns melting point apparatus and are uncorrected. Optical rotations were measured with a Perkin–Elmer model 141

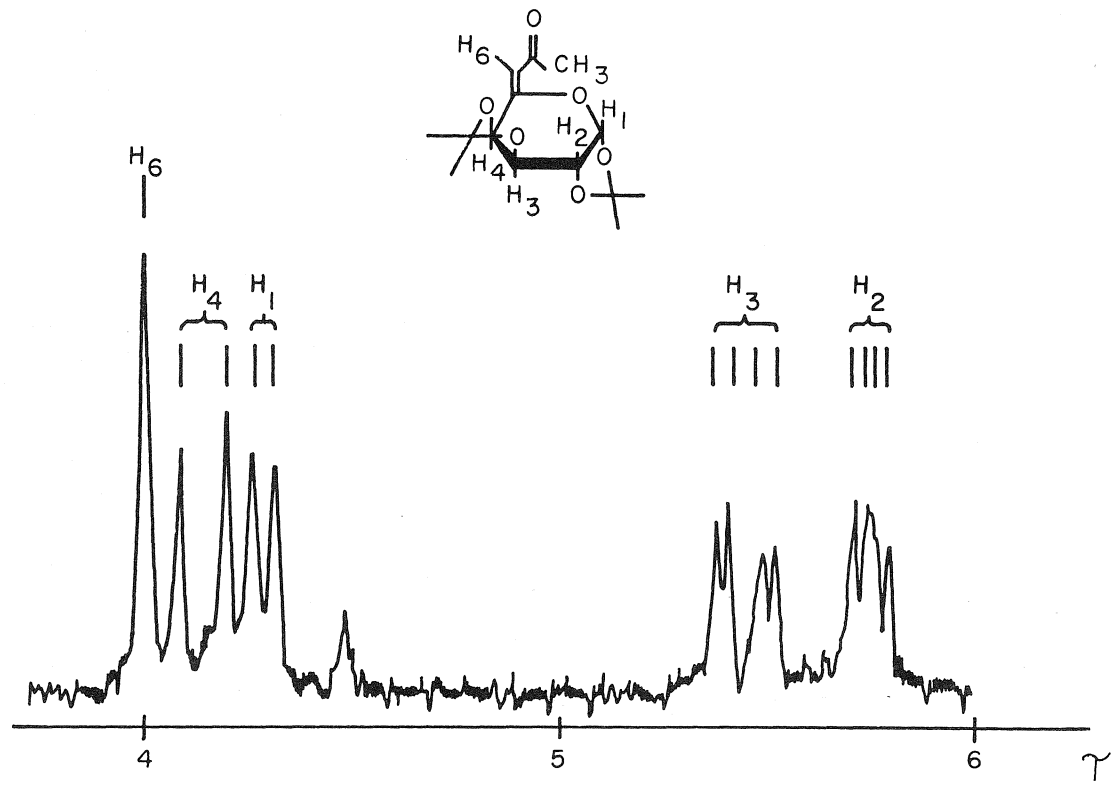

FIG. 4. The low-field portion of the 60 MHz nuclear magnetic resonance spectrum of the *trans* αβ-unsaturated ketone in chloroform-*d*.

automatic polarimeter at 21 ± 2°. Infrared spectra were measured on a Beckman-IR5A spectrophotometer. Ultraviolet spectra were measured with a Unicam SP. 800B spectrophotometer. Nuclear magnetic resonance (n.m.r.) spectra were measured on a Varian A-60A spectrometer in chloroform-*d* and tetramethylsilane as internal standard; a Varian homonuclear spin decoupler was used. Gas–liquid chromatography (g.l.c.) (F and M chromatograph, model 402) was carried out on a column of 1% (w/w) Apiezon L supported on 50–60 mesh acid washed DMCS treated Chromosorb W (115 × 0.4 cm) at 170° with a flow-rate setting of 3.4 at 46 p.s.i. of helium (ca. 100 ml/min). The chromatograph was adapted for preparative separations as described previously (7). Irradiations were performed in quartz tubes with a Rayonet Photochemical Chamber Reactor using a complete set (sixteen) of 2537 Å lamps. The term "petroleum ether" refers to the fraction of b.p. 60–80°.

Photolysis of cis-6,7,8-Trideoxy-1,2:3,4-di-O-isopropylidene-7-C-nitro-α-D-galacto-oct-6-enose (4)

A solution of *cis*-6,7,8-trideoxy-1,2:3,4-di-*O*-isopropylidene-7-*C*-nitro-α-D-*galacto*-oct-6-enose (**4**) (430 mg) in acetone (30 ml) was irradiated as described above. The progress of the reaction was followed by g.l.c.; four major components (see Table I) and a few minor ones were shown to be present. After 4 h the solution was concentrated to give a syrup, which was chromatographed on silica gel, with 2:3 ethyl acetate – petroleum ether as eluent. The fraction rich in the component with relative retention time 0.54 was chromatographed again to yield a syrup, which finally crystallized after a further purification by preparative g.l.c. (115 mg, 27%). Recrystallization from cold ethanol afforded, analytically pure, the *trans* isomer of the nitroolefin **4** (4).

A second column chromatographic separation of the fraction rich in the component with relative retention time 0.40 gave a crystalline product. Recrystallization from chloroform – petroleum ether at −10° afforded pure *cis*-6,8-dideoxy-1,2:3,4-di-*O*-isopropylidene-α-D-*galacto*-oct-5-enos-7-ulose (**5**) (31 mg, 8%), m.p. 142–143°, $[\alpha]_D$ −276° (*c*, 0.3 in ethyl acetate); λ_{max} (KBr) 6.03 (conjugated C=O), 6.08 (conjugated C=C), 7.20, 7.25 μm (CMe_2); λ_{max} (ethanol) 248 mμ (ε 1.6 × 10^4); n.m.r. data: (see Table II).

Anal. Calcd. for $C_{14}H_{20}O_6$: C, 59.2; H, 7.0. Found: C, 58.9; H, 7.0.

The fraction rich in the component with relative retention time 0.26 was purified by a second chromatographic separation using the original conditions, and then chromatography on neutral alumina with 1:4 ethyl acetate – petroleum ether as eluent. *trans*-6,8-Dideoxy-1,2:3,4-di-*O*-isopropylidene-α-D-*galacto*-oct-5-enos-7-ulose was obtained as a colorless syrup (23 mg, 6%);

Can. J. Chem. Downloaded from www.nrcresearchpress.com by 210.87.254.105 on 09/05/12
For personal use only.

λ_{max} (Film) 5.92 (conjugated C═O), 6.12–6.20 (conjugated C═C), 7.20, 7.25 μm (CMe_2); λ_{max} (ethanol) 256 mμ (ε 1.1×10^4); n.m.r. data (see Table II).

Anal. Calcd. for $C_{14}H_{20}O_6$: C, 59.2; H, 7.0. Found: C, 58.8; H, 7.1.

The *trans* isomer of **5** rapidly isomerized to the *cis* isomer in chloroform at room temperature, but was stable in ethyl acetate.

Acknowledgments

The authors thank the National Research Council of Canada and the Committee on Scientific Research at Queen's University for financial support. We are indebted to Dr. D. G. M. Diaper, Royal Military College, Kingston, Ontario for the use of the nuclear magnetic resonance spectrometer.

1. G. B. HOWARTH, D. G. LANCE, W. A. SZAREK, and J. K. N. JONES. Chem. Commun. To be published.
2. O. L. CHAPMAN, A. A. GRISWOLD, E. HOGANSON, G. LENZ, and J. REASONER. Pure Appl. Chem. **9**, 585 (1964); O. L. CHAPMAN, P. G. CLEVELAND, and E. D. HOGANSON. Chem. Commun. 101 (1966).
3. J. T. PINHEY and E. RIZZARDO. Chem. Commun. 362 (1965).
4. G. B. HOWARTH, D. G. LANCE, W. A. SZAREK, and J. K. N. JONES. Can. J. Chem. This issue.
5. W. SCHROEDER, B. BANNISTER, and H. HOEKSEMA. J. Am. Chem. Soc. **89**, 2448 (1967).
6. J. C. SOWDEN. Advan. Carbohydrate Chem. **6**, 291 (1951).
7. D. G. LANCE and G. B. HOWARTH. Laboratory practice (London). To be published.

Can. J. Chem. Downloaded from www.nrcresearchpress.com by 210.87.254.105 on 09/05/12
For personal use only.

Synthesis of 3-acetamido-2,3,6-trideoxy-D-*lyxo*-hexose (*N*-acetyl-D-daunosamine) and its D-*arabino* isomer

HANS H. BAER, KAREL ČAPEK,[1] AND MARTIN C. COOK
Department of Chemistry, University of Ottawa, Ottawa, Canada

Received July 15, 1968

Two syntheses of 3-acetamido-2,3,6-trideoxy-D-*lyxo*-hexose (*N*-acetyl-D-daunosamine, **14**) are described. The first one starts from methyl 3-acetamido-2,3-dideoxy-β-D-*arabino*-hexopyranoside (**1**) which is converted via its 6-*O*-tosylate (**2**) and 4-*O*-acetyl 6-*O*-tosylate (**3**) into methyl 3-acetamido-4-*O*-acetyl-2,3,6-trideoxy-6-iodo-β-D-*arabino*-hexopyranoside (**5**). Under certain conditions the last step involves a partial anomerization giving the α-anomer (**6**) as an additional product. Both **5** and **6** may be reductively dehalogenated to the corresponding 4-*O*-acetates having a 6-deoxy function (**7** and **8**). Preferably, **5** is reduced and simultaneously de-*O*-acetylated to methyl 3-acetamido-2,3,6-trideoxy-β-D-*arabino*-hexopyranoside (**9**). This glycoside is converted into its β-D-*lyxo* isomer (**13**) by solvolysis of the 4-*O*-mesylate (**12**). Hydrolyses of **9** give 3-acetamido-2,3,6-trideoxy-D-*arabino*-hexose (**10**) and the corresponding amino sugar hydrochloride (**11**), while hydrolyses of **13** give *N*-acetyl-D-daunosamine (**14**) and a syrupy amino sugar hydrochloride. The second synthesis of **14** departs from the D-*lyxo* isomer (**15**) of **1** and proceeds in a similar sequence via the 4-*O*-acetylated derivatives with 6-*O*-tosyl (**16**), 6-deoxy-6-iodo (**17**), and 6-deoxy (**18**) functions, the two last-mentioned compounds being α-glycosides due to anomerization in the step **16** → **17**.

Canadian Journal of Chemistry, 47, 89 (1969)

Can. J. Chem. Downloaded from www.nrcresearchpress.com by 210.87.254.40 on 09/05/12
For personal use only.

Previous work in this laboratory on the utility of nitro sugars for amino sugar syntheses has furnished methyl 3-amino-2,3-dideoxy-β-D-*arabino*-hexopyranoside (**1**) (1) and its β-D-*lyxo* isomer (**15**) (2). The present article describes the conversion of these two glycosides into derivatives of D-daunosamine, the optical antipode of an antibiotics constituent. The natural product (L-daunosamine) has been obtained by Arcamone and co-workers as a fragment of daunomycin, a *Streptomyces* metabolite showing antitumor activity, and has been demonstrated to be 3-amino-2,3,6-trideoxy-L-*lyxo*-hexose (3). A chemical synthesis of L-daunosamine hydrochloride has recently been accomplished (4), as has a synthesis of the *N*-benzoyl derivative of the D-enantiomer (5). In both instances the introduction of nitrogen at C-3 of the sugars was based on the action of sodium azide upon suitable hexose derivatives which were prepared departing from L-rhamnal and methyl 2,3-anhydro-4,6-*O*-benzylidene-α-D-allopyranoside, respectively. As our starting compounds **1** and **15** originate from deoxynitro glycosides that are available via the nitromethane method commencing with methyl β-D-glucopyranoside, the present work offers an alternative entry into the D-daunosamine series. In addition it has afforded the isomer with D-*arabino* configuration.[2]

Compound **1** was treated with 1 mole of *p*-toluenesulfonyl chloride in pyridine and underwent monotosylation in position-6 in high yield. This result accords with findings of Richardson (5) who has reported and discussed a highly selective monotosylation of the α-anomer of **1**. The crystalline 6-*O*-tosylate (**2**) was then acetylated to give the 4-*O*-acetyl 6-*O*-tosyl derivative (**3**). Alternatively, **1** was tosylated and subsequently acetylated without isolation of **2**. For successful monotosylation it proved essential that rigorously dried pyridine be employed. In an experiment neglecting this precaution a sulfur-free mono-*O*-acetate arose; the *O*-acetyl group was presumed to be located in position-6 (**4**) and to have entered there as a consequence of abortive tosylation.

Next, displacement in **3** of the tosyl group by iodine was effected with sodium iodide in refluxing butanone. This reaction was investigated rather thoroughly because it was discovered in initial experiments that the displacement at C-6

[1]On leave of absence from the Laboratory of Monosaccharides, Institute of Chemical Technology, Prague, Czechoslovakia.

[2]In principle, the reaction sequences to be reported could also be carried out in the L-series. The requisite L-enantiomers of **1** and **15**, which have not yet been described, would have to be prepared according to the directions given for the D-compounds (1, 2), from the known nitro precursors with β-L-configuration that have been synthesized starting from methyl β-L-arabinofuranoside (2).

Can. J. Chem. Downloaded from www.nrcresearchpress.com by 210.87.254.40 on 09/05/12
For personal use only.

was unexpectedly accompanied by partial anomerization at C-1. The presence of two anomeric iodo compounds in the crude reaction mixture was revealed by a nuclear magnetic resonance (n.m.r.) spectrum to be discussed in a later paragraph. Careful fractional crystallization of such a mixture ($[\alpha]_D$ +33°) yielded the pure β-anomer **5** (m.p. 196–198°, $[\alpha]_D$ +5°) and the pure α-anomer **6** (m.p. 175–177°, $[\alpha]_D$ +111°). From the rotation data was calculated a β:α ratio of 2.8:1 for that particular run, which does not necessarily represent an anomeric equilibrium.

It was considered that partial anomerization was caused by traces of acid liberated in a side reaction during the displacement. This conclusion, which appeared reasonable in view of the high reactivity at the anomeric center generally observed in deoxy sugar derivatives (6–9), received support from two facts. First, crystalline **5** was not anomerized but recovered unchanged when it was refluxed with sodium iodide in butanone under the conditions of the displacement. Secondly, the optical rotation of a solution of **5** in butanone slowly increased, signifying progressive anomerization, when the solution was refluxed together with a trace of *p*-toluenesulfonic acid. Consequently, in order to prevent anomerization, the iodide exchange in **3** was performed in the presence of sodium bicarbonate. This became the preferred modification as it proceeded with complete retention of the β-configuration, pure **5** being isolable in yields up to 93% on a preparative scale.

The conversion of the 6-iodo function into a 6-deoxy function, which was required next, was possible with Raney nickel (or platinum) and hydrogen in the presence of diethylamine. The methyl 3-acetamido-4-*O*-acetyl-2,3,6-trideoxy-β- and -α-D-*arabino*-hexopyranosides (**7** and **8**) were in this manner obtained from the iodides **5** and **6**, respectively. However, the reductions were accompanied to a considerable extent by de-*O*-acetylation.

Experiments designed to carry on the plan of synthesis in the α-series were discontinued when it was learned that Richardson (5) had successfully pursued the same course. Efforts were therefore concentrated on the β-series, which happened to be more convenient too, when the β-derivative **5** had become readily accessible in pure form as outlined above.

As it appeared difficult to avoid partial loss of the 4-*O*-acetyl group during the reductive dehalogenation of **5**, and as this group was to be removed later on anyway, compound **5** was hydrogenated with platinum in the presence of sodium methoxide which effected complete de-*O*-acetylation. Methyl 3-acetamido-2,3,6-trideoxy-β-D-*arabino*-hexopyranoside (**9**) was thereby obtained in 80–90% yields. This glycoside was hydrolyzed, with 25% acetic acid to give 3-acetamido-2,3,6-trideoxy-D-*arabino*-hexose (**10**), and with hydrochloric acid to give 3-amino-2,3,6-trideoxy-D-*arabino*-hexose hydrochloride (**11**), a hitherto unknown stereoisomer of daunosamine.

Mesylation of the glycoside **9** afforded the 4-*O*-mesyl derivative **12**, which was isolated in crystalline form in 70% yield and then subjected to solvolysis with sodium acetate in water-containing 2-methoxyethanol, in order to effect inversion of configuration at C-4 by neighboring group participation (10). Methyl 3-acetamido-2,3,6-trideoxy-β-D-*lyxo*-hexopyranoside (**13**) was produced, again in a yield of 70%.[3] Hydrolysis of **13** by dilute acetic acid led to crystalline 3-acetamido-2,3,6-trideoxy-D-*lyxo*-hexose (**14**, *N*-acetyl-D-daunosamine), whereas D-daunosamine hydrochloride, expected to arise by hydrolysis with hydrochloric acid, was obtained as an impure syrup only.

The second synthesis commenced with methyl 3-acetamido-2,3-dideoxy-β-D-*lyxo*-hexopyranoside (**15**) which, with *p*-toluenesulfonyl chloride and acetic anhydride, was in part converted into the 4-*O*-acetyl-6-*O*-tosyl derivative (**16**). Displacement of the tosyl group by sodium iodide produced the calculated amount of sodium *p*-toluenesulfonate. However, only half the expected weight of a syrup containing iodo sugar could be extracted. The syrup apparently contained both anomers of methyl 3-acetamido-4-*O*-acetyl-2,3,6-trideoxy-6-iodo-α-D-*lyxo*-hexopyranoside, and preparative thin-layer chromatography furnished the preponderant product in crystalline form (yield, 20% based on **16**). This product (**17**) was assigned the α-configuration on the basis of its high dextrorotation, $[\alpha]_D$ +155°, which contrasted with the lower rotation, $[\alpha]_D$ +64°, of a second material that was obtained, though as a

[3]Richardson (5) similarly mesylated the α-anomer of **9** but encountered difficulties in attempting to isolate the ester (α-anomer of **12**). However, he found isolation unnecessary and proceeded directly with a solvolysis leading in 42% overall yield to the α-anomer of **13**.

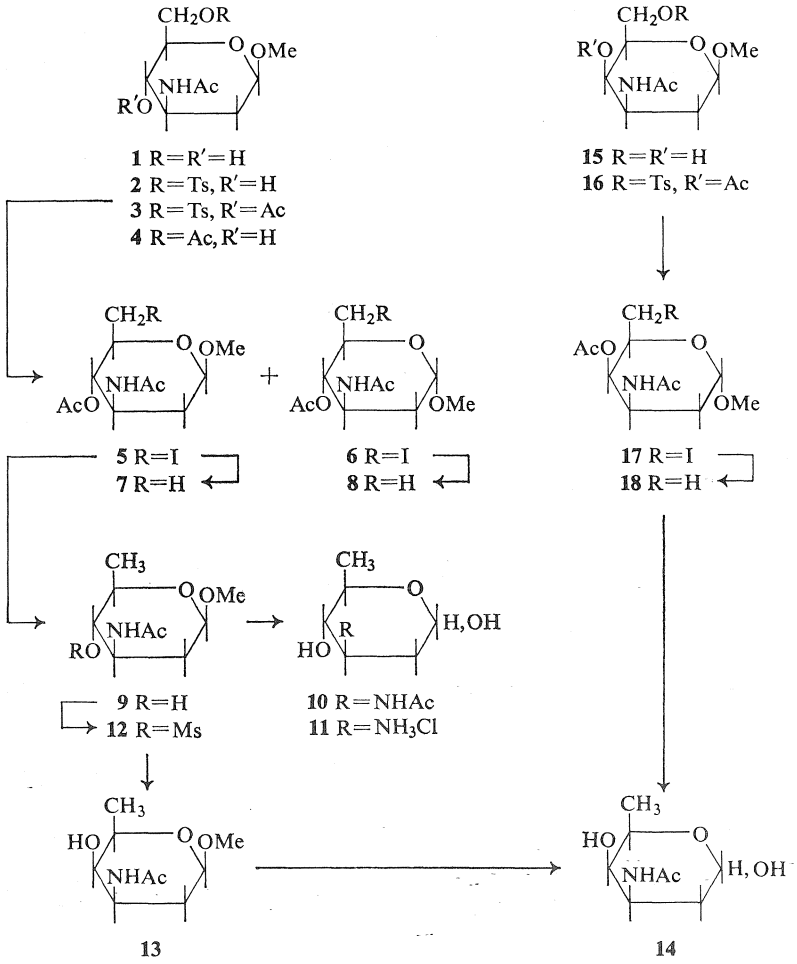

syrup only, and that was probably an α,β-mixture. Further points in support of this assignment will be discussed in a later paragraph. Raney nickel reduction of **17** afforded methyl 3-acetamido-4-*O*-acetyl-2,3,6-trideoxy-α-D-*lyxo*-hexopyranoside (**18**), and this glycoside was converted by alkaline de-*O*-acetylation followed by hydrolysis with an acidic resin into *N*-acetyl-D-daunosamine, identical with **14** obtained in the previous synthesis.

The synthesis of *N*-acetyl-D-daunosamine was thus accomplished in two independent ways involving stereochemically unambiguous reactions and employing starting compounds whose configurations had been rigorously established (1, 2). This fact makes it unnecessary to adduce further configurational proof for the new compounds described, except that the assignment of anomeric configuration to the products arisen in the iodide exchange processes requires justification.

The n.m.r. spectrum of the crude product obtained from **3** by sodium iodide treatment in the absence of bicarbonate displayed two singlets attributable to methoxy groups (τ 6.44 and 6.58). After the material was separated into isomers by fractional crystallization, the τ 6.44 signal was seen to be associated with the anomer (**5**) of low dextrorotation, and the τ 6.58 signal, with the anomer (**6**) of high dextrorotation. Assignment of the β-configuration to the former, and of the α-configuration to the latter, primarily based on the rotations, is in accord with these chemical shifts as, in comparable compounds, protons in equatorial anomeric methoxyls usually resonate at lower field than those in axial

Can. J. Chem. Downloaded from www.nrcresearchpress.com by 210.87.254.40 on 09/05/12
For personal use only.

TABLE I

Chemical shifts (τ) of substituent resonances in $CDCl_3$ solution (60 MHz spectra)

	1-OCH_3 equatorial	1-OCH_3 axial	4-OAc axial	4-OAc equatorial	3-NHAc equatorial	Others
3	6.60			8.01	8.11	7.57*
5	6.44			7.90	8.06	
6		6.58		7.90	8.08	
7	6.54			7.94	8.10	8.75†
8		6.67		7.95	8.11	8.80†
$\mathbf{8}_{4-OH}$‡		6.66			7.99	8.72†
9§	6.51				ca. 8.0	8.66†
12	6.54				8.02	8.62†; 6.96‖
16	6.53		7.95		8.10	7.55*
17	(6.45)¶	6.58	7.85		8.08	
18		6.67	7.84		8.09	8.88†

*Aromatic methyl. In addition, 4 triplets belonging to the aromatic A_2B_2 system were in the τ 2 region.
†Doublet for C-6 methyl; splitting, 6 c.p.s.
‡Refers to a sample of **8** that had been de-*O*-acetylated.
§Signals from a spectrum of de-*O*-acetylated **8** that contained a small amount of **9**. Because of poor solubility no spectrum using crystalline **9** was taken.
‖Sulfonyl methyl.
¶Signal attributed to admixed β-isomer; intensity, ca. 5% of the axial methoxy signal.

ones. Pertinent examples in the literature (11–13) are supplemented by data given in Table I, special note being taken of the values for the anomeric pair **7** and **8** and of the value for **17** together with that listed in parentheses. Finally, the specific rotations of the α-compounds **6** and **8** were very close in magnitude to those reported (5) for the corresponding derivatives lacking the 4-*O*-acetyl group.

In the D-*lyxo* series the crystalline iodo derivative (**17**), which was assigned α-configuration, exhibited its methoxyl resonance at τ 6.58, and a weak signal suggesting contamination by about 5% of the β-anomer occurred at τ 6.45. The 6-deoxy derivative (**18**) had its methoxyl resonance at τ 6.67, and its melting point and specific rotation were in satisfactory agreement with data reported for the same compound (5) and its enantiomorph (4).

The chemical shifts of the acetoxy and acetamido methyl protons in the compounds of Table I were all in the expected regions (14–16). It is noteworthy that the acetoxy signals of **3** and **16** occurred at higher than usual field, which is attributable (15) to a shielding effect of the aromatic substituent.

Experimental

Melting points were taken in capillaries in an electric aluminium block apparatus equipped with a calibrated thermometer. All evaporations were performed *in vacuo* at a bath temperature of 35–40°. Petroleum ether refers to the fraction of boiling range 30–60°. Thin-layer chromatography (t.l.c.) was done on silica gel G (E. Merck A. G., Darmstadt) with the solvent systems benzene–acetone (2:3, v/v), (solvent *a*) and benzene–acetone (3:7, v/v) (solvent *b*), and spots were made visible with ceric sulfate – sulfuric acid spray. Column chromatography was carried out on silicic acid, 100 mesh (Mallinckrodt Analytical Reagent). Nuclear magnetic resonance (n.m.r.) spectra were obtained from deuteriochloroform solutions on a Varian HA-60 instrument and were calibrated with tetramethylsilane as internal standard. Optical rotations were measured at about 23° in 1-dm tubes, most readings being taken on a Perkin–Elmer 141 automatic polarimeter. Infrared spectra were taken by the Nujol mull technique on a Beckman IR-8 instrument unless otherwise indicated, and the most characteristic frequencies of new compounds are listed in Table II at the end of this section.

*Methyl 3-Acetamido-2,3-dideoxy-6-O-p-tolylsulfonyl-*β*-*D*-arabino-hexopyranoside (2)*

A sample (510 mg) of methyl 3-acetamido-2,3-dideoxy-β-D-*arabino*-hexopyranoside (**1**) (1) in pyridine (10 ml; distilled from sodium hydride) was chilled in a dry ice – acetone bath, and *p*-toluenesulfonyl chloride (530 mg; 1.2 *M* equivalents) was added. The reaction mixture was then stored at 0° for 48 h and at room temperature for 6 h. Water (0.5 ml) was introduced, and after 1 h the solution was concentrated *in vacuo* with several additions of 1% sodium bicarbonate solution, in order to remove most of the pyridine. Finally, the largely aqueous concentrate (ca. 10 ml) was extracted with several portions of chloroform, and the combined extracts were washed once with a small amount of water and dried over sodium sulfate. Inspection by t.l.c. (solvent *a*) of the chloroform phase revealed a strong spot (**2**) accompanied by a much weaker, faster moving spot which presumably represented the 4,6-ditosylate of **1**; the aqueous phase was seen to contain unreacted **1**. The chloroform solution was evaporated to give a crystalline residue (752 mg). Recrystallization from ethyl acetate – petroleum ether afforded **2** (586 mg; m.p. 143–148°). A second recrystallization gave **2** (542 mg) of m.p. 145–148° which could not be raised

Can. J. Chem. Downloaded from www.nrcresearchpress.com by 210.87.254.40 on 09/05/12
For personal use only.

Can. J. Chem. Downloaded from www.nrcresearchpress.com by 210.87.254.40 on 09/05/12
For personal use only.

further. Work-up of the mother liquors yielded another 62 mg of chromatographically pure **2**, the total thus being 604 mg (70%). The remaining syrup contained the fast-moving by-product. Compound **2** showed $[\alpha]_D$ +25.5 (*c*, 1, chloroform).

Anal. Calcd. for $C_{16}H_{23}NO_7S$ (mol. wt., 373.4): C, 51.47; H, 6.21; S, 8.59. Found: C, 51.50; H, 6.13; S, 8.57.

It was possible and worthwhile to recover unreacted **1** by pooling the extracted, aqueous bicarbonate solutions from several runs, evaporating them to dryness, and eluting **1** with ethyl acetate.

Methyl 3-Acetamido-4-O-acetyl-2,3-dideoxy-6-O-p-tolylsulfonyl-β-D-arabino-hexopyranoside (3)

(a) From 2

A solution of **2** (542 mg) and acetic anhydride (0.5 ml) in pyridine (10 ml) was allowed to stand at 23° for 12 h, after which time t.l.c. (solvent *a*) indicated complete acetylation. Excess water was added, and the reaction mixture was evaporated with several further additions of water. When most of the pyridine and acetic acid was removed, **3** began to crystallize as a hydrate from the remaining aqueous solution and was collected (559 mg) after a few hours of storage at 4°. Upon concentration to about 3 ml and chloroform extraction the mother liquor gave another 25 mg of **3**; total yield, 93%. The hydrate melted at 77–80° (crude) and at 80–82° (recrystallized from ethanol–water). It exhibited infrared absorption at 3600 cm^{-1} (OH) and, in $CDCl_3$ solution, displayed an n.m.r. signal near τ 7.8, with concentration-dependent chemical shift (water). *Anhydrous* **3**, in which these spectral features were absent, crystallized readily from ethyl acetate – petroleum ether, especially when seeded with crystals obtained by repeated evaporation of the hydrate with benzene; m.p. 121–123°, $[\alpha]_D$ +10.5° (*c*, 1, chloroform). Yields of chromatographically pure anhydrous **3** averaging 86% could be obtained when mother liquors of crystallization were worked up.

Anal. Calcd. for $C_{18}H_{25}NO_8S$ (mol. wt., 415.5): C, 52.03; H, 6.07. Found: C, 51.80; H, 6.03.

Anal. Calcd. (for monohydrate): S, 7.38. Found: S, 7.43.

(b) From 1

Compound **1** (600 mg) was tosylated as described for the preparation of **2**, except that 1.1 mole of *p*-toluenesulfonyl chloride and a reaction time of 6 h at 0° followed by 15 h at 4° and 7 h at 23° were employed. Acetic anhydride (1 ml) was then added and the mixture was kept at 23° for 16 h. Addition of water (0.5 ml) was followed after 15 min by dilution with chloroform (50 ml) and consecutive washing with 5% sulfuric acid, water, 1% sodium bicarbonate solution, and water. The organic solution was dried over sodium sulfate and evaporated to leave a residue (824 mg) which was dissolved in ethyl acetate, treated with activated charcoal and recovered by evaporation of the solvent. The hydrate of **3**, m.p. 79–81°, then crystallized from ethanol–water and was converted into the anhydrous form by recrystallization from ethyl acetate – petroleum ether. The product (712 mg; 62%) melted at 121–123°, undepressed on admixture of **3** from (*a*).

Methyl 3-Acetamido-6(?)-O-acetyl-2,3-dideoxy-β-D-arabino-hexopyranoside (4)

In an early attempt at preparing compound **3** an experiment was performed similar to that described in the preceding section (*b*). The reactants were compound **1** (214 mg), *p*-toluenesulfonyl chloride (204 mg), and acetic anhydride (0.2 ml). However, the solvent, reagent grade pyridine, had not been specially dried with sodium hydride. No **3** was produced. Instead, the chloroform phase obtained after washing yielded crystals (60 mg) which melted at 152–154°, showed $[\alpha]_D$ +8.3° (*c*, 0.8, ethanol), and displayed an infrared band at 1733 cm^{-1} (ester carbonyl) but no bands attributable to hydroxyl or tosyl groups. This material was identical with the previously described (1) 4,6-di-*O*-acetate of **1**, m.p. 157.5–158°, $[\alpha]_D$ +9.9° (*c*, 0.6 in ethanol). The aqueous washing liquids were combined, neutralized with sodium bicarbonate, and evaporated to dryness. The solid residue was extracted with ethyl acetate and the extract, upon removal of the solvent, was chromatographed on a column of silica gel (17 g). Benzene–ethanol (20:1) eluted an additional crop (40 mg) of the 4,6-di-*O*-acetate. Subsequent elution with benzene–ethanol (10:1) gave monoacetate **4** (88 mg) which after recrystallization from ethyl acetate – petroleum ether had m.p. 185–187°, $[\alpha]_D$ −19.8° (*c*, 0.4, ethanol).

Anal. Calcd. for $C_{11}H_{19}NO_6$ (mol. wt., 261.3): C, 50.56; H, 7.33; N, 5.36. Found: C, 50.53; H, 7.12; N, 5.46.

Methyl 3-Acetamido-2,3,6-trideoxy-6-iodo-β-D-arabino-hexopyranoside (5) and Methyl 3-Acetamido-2,3,6-trideoxy-6-iodo-α-D-arabino-hexopyranoside (6)

(a) Displacement in the Absence of Sodium Bicarbonate

For purification, commercial butanone (60 ml) was refluxed 1 h with sodium iodide (3 g) and distilled in the presence of anhydrous magnesium sulfate. The distillate dissolved sodium iodide without producing a yellow color.

Compound **3** (200 mg) and sodium iodide (150 mg) were refluxed for 20 h in purified butanone (10 ml). The mixture was then chilled, and sodium *p*-toluenesulfonate (91 mg; 97.5%) was filtered off and washed with chloroform. The filtrate was evaporated to give a pale-yellow residue to which was added chloroform (25 ml), water (5 ml), and 2 drops of 0.1 *N* sodium thiosulfate solution. After thorough shaking the chloroform layer was allowed to separate and, upon drying with sodium sulfate and evaporation, it gave a colorless crystalline material (174 mg; $[\alpha]_D$ +33.4°, *c*, 1.7, chloroform) which was a mixture of **5** and **6**.

This mixture was fractionated in a process involving 20 recrystallizations, with the progress of separation being monitored polarimetrically and fractions of similar rotations being combined. Ether was used to recrystallize fractions of relatively low dextrorotation (rich in **5**), and ethyl acetate – petroleum ether was employed for fractions of relatively high dextrorotation (rich in **6**). The operation afforded 82 mg of pure **5**, m.p. 196–198° decomp., $[\alpha]_D$ +5.0°, (*c*, 1.5, chloroform), and 17 mg of pure **6**, m.p. 175–177° decomp., $[\alpha]_D$ +111°, (*c*, 1, chloroform), $[\alpha]_D$ +96° (*c*, 0.6, dimethyl sulfoxide[4]). In addition there remained mixed fractions totalling 65 mg. Nuclear magnetic resonance spectra of **5** and **6** (Table I)

[4]The rotation in this solvent was measured for comparison with the value, $[\alpha]_D$ +93° in DMSO, recorded (5) for the non-acetylated derivative of **6**.

Can. J. Chem. Downloaded from www.nrcresearchpress.com by 210.87.254.40 on 09/05/12
For personal use only.

indicated anomeric purity, whereas a spectrum of the combined mixed fractions showed a β:α ratio of roughly 2:1. Infrared spectra of **5** and **6** were extremely similar although there were minor differences in band positions and relative intensities (Table II).

(b) Displacement in the Presence of Sodium Bicarbonate

Compound **3** (484 mg), sodium iodide (370 mg) and sodium bicarbonate (100 mg) were refluxed with magnetic stirring in purified butanone (22 ml) for 17 h. After cooling, the insoluble matter (330 mg, sodium tosylate and bicarbonate) was filtered off and washed with chloroform, and work-up was proceeded with as described under (*a*). The crude crystalline product (456 mg) showed $[\alpha]_D$ +5.2° (*c*, 4.5, chloroform), i.e. virtually the value of pure **5**. Recrystallization from water (which proved superior to ether) gave **5** (310 mg) as long needles having m.p. 195–197° decomp. and $[\alpha]_D$ +4.9° (*c*, 1.5, chloroform). The yields in five experiments were 70–74%. Column chromatography on silicic acid, with benzene–ethanol (50:1) as eluent, of the material that had remained in the mother liquor of recrystallization furnished additional **5** (90 mg; $[\alpha]_D$ +5.9° in chloroform), thus increasing the yield to 93%.

Anal. Calcd. for $C_{11}H_{18}INO_5$ (mol. wt., 371.2): C, 35.59; H, 4.89; I, 34.19. Found: C, 35.81; H, 5.06; I, 34.00.

Methyl 3-Acetamido-4-O-acetyl-2,3,6-trideoxy-β-D-arabino-hexopyranoside (7)

A solution of **5** (500 mg) and diethylamine (0.14 ml) in methanol (30 ml) was shaken with Raney nickel-T4 (0.1 g) (17) in an atmosphere of hydrogen at room temperature for 5 h. The filtered solution was concentrated to a syrup which was dissolved in chloroform. The chloroform solution was washed successively with cold solutions of sodium thiosulfate, 0.5 *N* hydrochloric acid, sodium bicarbonate, and finally with water. It was then dried with magnesium sulfate and concentrated to a syrup that crystallized from ethyl acetate – petroleum ether. There was obtained 175 mg (53%) of **7**, m.p. 180°, $[\alpha]_D$ +23.4° (*c*, 1, chloroform). This preparation, made from a sample of **5** which was not entirely pure anomerically, contained as a consequence a small admixture of the α-anomer (**8**) accounting for too high a rotation. The n.m.r. spectrum showed a weak signal at τ 6.67 (α-OCH_3) beside the main OCH_3 signal at τ 6.54.

Anal. Calcd. for $C_{11}H_{19}NO_5$ (mol. wt., 245.3): C, 53.86; H, 7.81; N, 5.71. Found: C, 53.75; H, 7.67; N, 5.78.

A similar reduction was performed using *pure* **5** (116 mg), diethylamine (0.1 ml), and *platinum oxide* (50 mg) as catalyst; the solvent was methanol (10 ml). Hydrogen consumption (18 ml at room temperature) was rapid. After 2 h the filtered solution was shown by t.l.c. (solvent *a*) to contain 2 carbohydrate substances, namely fast-moving **7** and its slow-moving product of de-*O*-acetylation (**9**). In addition, diethylammonium iodide was present. The reaction solution was evaporated to give a residue which was treated with chloroform and water, the former dissolving most of **7** and the latter dissolving **9** and the ammonium salt. The chloroform solution was evaporated to yield crystalline **7** (48 mg; 62%), m.p. 177–180° after one and 185–186° after a second recrystallization from ethyl acetate – petroleum ether; $[\alpha]_D$ +7.4° (*c*, 0.4, chloroform). An n.m.r. spectrum showed no evidence for contamination by α-anomer.

The aqueous solution containing **9** was made alkaline by adding 0.35 ml of 1 *N* potassium hydroxide solution and was then evaporated to remove diethylamine. The dry residue (**9** plus potassium iodide) was extracted with ethyl acetate, which yielded 26 mg (40%) of **9**, m.p. 237–239°, identical in its infrared spectrum with **9** described in a subsequent section.

Methyl 3-Acetamido-4-O-acetyl-2,3,6-trideoxy-α-D-arabino-hexopyranoside (8)

A solution of **6** (190 mg) and diethylamine (0.075 ml) in methanol (15 ml) was shaken with Raney nickel-T4 (17) (40 mg) and hydrogen for 4.5 h at room temperature. The solution was evaporated, the residue taken up in chloroform and applied to 2 large t.l.c. plates which were irrigated with solvent *a*. The faster-moving band was scraped off and, upon elution with ethyl acetate, afforded the product **8** (61 mg), m.p. 162–163°, $[\alpha]_D$ +142° (*c*, 1, chloroform). In the n.m.r. spectrum a strong signal at τ 6.67 (α-OCH_3) was accompanied by a much weaker signal at τ 6.53 indicating a slight contamination by the β-anomer. The derivative of **8** lacking the 4-*O*-acetyl group has been reported (5) to show $[\alpha]_D$ +137° (methanol). Extraction of the slower-moving band from the t.l.c. plates afforded some of this derivative as a solid which was used without further purification for obtaining the n.m.r. spectrum ($\mathbf{8}_{4\text{-OH}}$ in Table I).

Methyl 3-Acetamido-2,3,6-trideoxy-β-D-arabino-hexopyranoside (9)

A solution of **5** (276 mg; 0.75 mmole) in methanol (11 ml) containing 1.1 mmole of sodium methoxide was shaken with hydrogen in the presence of platinum catalyst (70 mg of PtO_2). Hydrogen uptake (22 ml) was rapid, about 20 ml being consumed within the first 5 min. After 3.5 h the solution was filtered and its pH was adjusted to about 9 by careful titration with 0.1 *N* sulfuric acid (2.8 ml) against phenolphthalein. The solution, which must stay weakly alkaline at all times, was then evaporated to give a solid. Two ways of further work-up were employed from hereon. In some experiments the solid was dissolved in water and **9** was isolated by exhaustive extraction with chloroform although the distribution coefficient is not very favorable. The method might be convenient for larger scale runs when a liquid–liquid extractor can be used. The dried extract was evaporated and the residue crystallized from ethanol – petroleum ether to give **9** (e.g., 114 mg, 75%). Recrystallized from the same solvents, an analytical sample had m.p. 224–226° and $[\alpha]_D$ −57.6° (*c*, 0.95, water).

Anal. Calcd. for $C_9H_{17}NO_4$ (mol. wt., 203.2): C, 53.19; H, 8.43; N, 6.89. Found: C, 53.28; H, 8.61; N, 7.03.

In runs of the small scale described we preferred chromatographic isolation of **9**. To this end the crude solid was placed on a short column of silicic acid (8 g) and **9** was eluted with benzene–ethanol (20:1) after minor impurities had been eluted with benzene. The yields in **9** were good, e.g. 123 mg (81.5%) in a 0.75 mmole run. The crystals showed m.p. 200–210°, raised to 223–225° by one recrystallization from ethanol – petroleum ether; $[\alpha]_D$ −57.9° (*c*, 1.1, water).

Can. J. Chem. Downloaded from www.nrcresearchpress.com by 210.87.254.40 on 09/05/12
For personal use only.

Compound **9** appears to be capable of existing in two crystal modifications. While the melting points just recorded were found in several experiments and could not be raised by further recrystallization of the samples, in two cases a m.p. 237–239° was observed. Such a sample showed the same rotation ($[\alpha]_D$ −57.5°, *c*, 1.2, water) and gave an infrared spectrum identical to that of the lower-melting material. Moreover, both modifications yielded identical reaction products with methanesulfonyl chloride (see a later paragraph).

*3-Acetamido-2,3,6-trideoxy-*D*-arabino-hexose (**10**)*

A solution of **9** (63 mg) in water (3 ml) and acetic acid (1 ml) was boiled under reflux for 25 min. The hydrolysis was monitored by t.l.c. (solvent *b*), which revealed the disappearance of **9** and concomitant formation of more slowly-moving **10**. The hydrolyzate was evaporated and the residue crystallized from 2-propanol – ether. The product (42 mg; 71.5%) had m.p. 196–200°, raised to 199–201° (decomp., sealed capillary) by one recrystallization. The mother liquor gave crystals of m.p. 198–201° decomp. Compound **10** exhibited downward mutarotation: $[\alpha]_D$ +30.4° (4 min) → +18.3° (6 h, constant) (*c*, 0.8, water).

Anal. Calcd. for $C_8H_{15}NO_4$ (mol. wt., 189.2): C, 50.79; H, 7.99; N, 7.40. Found: C, 50.68; H, 7.80; N, 7.25.

*3-Amino-2,3,6-trideoxy-*D*-arabino-hexose Hydrochloride (**11**)*

A solution of **9** (50 mg) in 1 *N* hydrochloric acid (2 ml) was boiled under reflux for 65 min, during which period gradual disappearance of **9** and formation of **11** with intermediary occurrence of **10** was observed by t.l.c. (solvent *b*). The hydrolyzate was evaporated to a syrup which was dried *in vacuo* and then crystallized from 2-propanol – ether giving **11** (43 mg), m.p. 160–170° decomp. One recrystallization from the same solvents gave **11** (31 mg), m.p. 168–170° decomp., unchanged by a further recrystallization. No mutarotation was observed: $[\alpha]_D$ +81.7° (*c*, 0.7, water). A sample reduced hot Fehling solution strongly.

Elemental analysis of a sample dried *in vacuo* at 56° gave a high carbon value which suggested retention of solvent of crystallization. The data did not correspond perfectly to 1 mole of 2-propanol, but its presence was strongly supported by mass spectrometry. A sample heated up to 100° in the high vacuum of the spectrometer released volatile matter that gave a weak parent peak at 60 *m/e* and a strong fragment peak at 45 *m/e* attributable to 2-propanol. We thank Prof. J. L. Holmes for this determination.

Anal. Calcd. for $C_6H_{14}ClNO_3 \cdot C_3H_8O$ (mol. wt., 243.7): C, 44.35; H, 9.10. Found: C, 44.69; H, 8.44.

*Methyl 3-Acetamido-2,3,6-trideoxy-4-O-methylsulfonyl-β-*D*-arabino-hexopyranoside (**12**)*

A solution of **9** (109 mg) in pyridine (5 ml; dried over sodium hydride) was cooled to −70°, and methanesulfonyl chloride (0.3 ml) was added. The reaction mixture was allowed to stand for 2 days at −10–0°. Water (0.1 ml) was then added to the brown solution which, after 15 min, was evaporated with several additions of 1% sodium bicarbonate solution in order to remove most of the pyridine. The remaining aqueous solution was extracted with chloroform (40 ml in several portions), the extract was dried with sodium sulfate and evaporated to a dark, crystalline mass (154 mg). Passage through a column of silicic acid (8 g), which was eluted first with benzene and then with benzene–ethanol (50:1), gave unidentified impurities in the benzene fractions while the mixed solvent fractions furnished 26 mg of **12** containing a trace of a contaminant (faster moving on t.l.c.) and subsequently 100 mg of chromatographically pure **12** (total yield, 83%). Upon one or two recrystallizations from ethyl acetate – petroleum ether **12** had m.p. 153–155° decomp., $[\alpha]_D$ −16.5° (*c*, 1, chloroform), unchanged on further recrystallization. Omitting the column chromatography we obtained from crude **12**, by recrystallization with use of decolorizing carbon, pure **12** in somewhat lower yields.

Anal. Calcd. for $C_{10}H_{19}NO_6S$ (mol. wt., 281.3): C, 42.70; H, 6.81; S, 11.40. Found: C, 42.78; H, 7.34; S, 11.10.

*Methyl 3-Acetamido-2,3,6-trideoxy-β-*D*-lyxo-hexopyranoside (**13**)*

A solution of mesylate **12** (91 mg), sodium acetate trihydrate (170 mg), and water (0.5 ml) in 2-methoxyethanol (5 ml) was refluxed for 40 min. The reaction mixture was evaporated to dryness and the residue was chromatographed on silicic acid (5 g) by elution with benzene–ethanol (20:1). Crystalline **13** (46 mg; 70%) was obtained and melted, in a sealed capillary, at 208–212° after one and at 210–212° after a second and a third recrystallization from ethyl acetate; $[\alpha]_D$ +27.7° (*c*, 1, water). The compound sublimed *in vacuo*.

Anal. Calcd. for $C_9H_{17}NO_4$ (mol. wt., 203.2): C, 53.19; H, 8.43; N, 6.89. Found: C, 53.16; H, 8.40; N, 6.83.

*3-Acetamido-2,3,6-trideoxy-*D*-lyxo-hexose (**14**)*

*(a) From **13***

The glycoside **13** (37 mg) was hydrolyzed with acetic acid as described for the hydrolysis of **9** to **10**. The reducing sugar **14** crystallized from ethyl acetate in a yield of 28 mg (81%), m.p. 143–145°. After one recrystallization **14** had m.p. 145–146°, $[\alpha]_D$ +101° (ca. 4 min.) → +94.2° (10 min, constant) (*c*, 0.5, water). When the rotational sample was recovered by evaporation of the water, it melted at 151–153°.

Anal. Calcd. for $C_8H_{15}NO_4$ (mol. wt., 189.2): C, 50.79; H, 7.99. Found: C, 51.00; H, 7.99.

*(b) From **18***

The glycoside **18** (12 mg) was dissolved in 0.1 *N* sodium hydroxide solution (0.5 ml). After 15 min it was determined by t.l.c. (solvent *a*) that fast-moving **18** had disappeared completely, giving rise to a slower spot that travelled like the de-*O*-acetylated glycosides **9** and **13**. After another 10 min the solution was diluted with a few milliliters of water and stirred with 2 ml of cation exchanger, Rexyn 101(H^+), for 20 min at 60°. Thin-layer chromatography then revealed complete disappearance of the product of alkaline hydrolysis and showed the presence of a single spot moving at the still lower speed of **14**. The resin was filtered off and washed well with water, and the filtrate was treated with activated charcoal and evaporated to give 5 mg of white crystals. Recrystallization from ethyl acetate gave **14** (3 mg), m.p. 144–146°,

TABLE II

The most important infrared frequencies

Compound*	ν_{max} in cm^{-1} (group assignments in parentheses)
2†	3450 (NH); 3400–3200 (OH); 1655, 1510 (amide); 1590, 1360, 1170 (tosyl); 1070, 975.
3†‡	3450 (NH); 1740 (ester CO); 1670, 1515 (amide); 1595, 1370, 1175 (tosyl); 1050, 975; 1225 (ester C—O—C).
3‡	3400 (NH); 1750 (ester CO); 1670, 1555 (amide); 1610, 1380, 1180 (tosyl); 1245 (ester C—O—C); 1070, 1050, 1010–960, 930, 910, 880, 845, 820, 800.
3§	3600 (OH); 3400 (NH); 1740 (ester CO); 1660 and 1640, 1570 (amide); 1610, 1360, 1180 (tosyl); 1245 (ester C—O—C); 1070, 1050, 1010–975; 930, 910, 875, 840, 825, 803.
4	3400, 3280, 3120 (NH, OH); 1715 (ester CO); 1645, 1565 (amide); 1265 (ester C—O—C); 1140, 1075, 980, 950.
5	3250 (NH); 1730 (ester CO); 1635, 1535 (amide); 1230 (ester C—O—C); 1120, 1035, 970–940.
5†	3450 (NH); 1735 (ester CO); 1675, 1515 (amide); 1395 weak, 1375 strong; 1220 (ester C—O—C); 1285 strong singlet, 1150 weak, 1123, 1050.
6†	3450 (NH); 1735 (ester CO); 1675, 1515 (amide); 1375 strong (no band at 1395); 1220 (ester C—O—C); 1290–1275 weak doublet, 1130, 1040.
7	3400 (NH); 1750 (ester CO); 1660, 1560 (amide); 1245 (ester C—O—C); 1170, 1130, 1050, 965, 930.
8	3300 (NH); 1730 (ester CO); 1635, 1535 (amide); 1230 (ester C—O—C); 1120, 1040, 955, 920.
9	3400–3200, 3100 (NH, OH); 1642, 1560 (amide); 1300, 1070.
10	3400–3200, 3100 (NH, OH); 1640, 1560 (amide); 1310, 1120, 1090–1050, 990.
11	3450–3300 (OH); 3050, 1600, 1520 (NH_3^+); 1170–1100, 1065, 1010, 985.
12	3300 (NH); 1665, 1560 (amide); 1345, 1180 (mesyl); 1080, 1010, 970, 865, 730.
13	3480, 3310 (NH, OH); 1645, 1550 (amide); 1330, 1290–1220, 1195, 1150, 1080–1030, 980, 725.
14‖	3450, 3350 (NH, OH); 1650 and 1625, 1535 (amide); 1250, 1200, 1165, 1110–1025, 980, 800–700.
14¶	3430, 3320 (NH, OH); 1625, 1550 (amide); 1240, 1190, 1165, 1115, 1080, 1035, 990, 800–700.
16	3400 (NH); 1745 (ester CO); 1650, 1535 (amide); 1600, 1370, 1170 (tosyl); 1240 (ester C—O—C); 1070 1030, 990, 840, 815, 735.
17	3300 (NH); 1745 (ester CO); 1650, 1560 (amide); 1240 (ester C—O—C); 1125, 1050, 995, 955, 910, 885.
18	3400 (NH); 1745 (ester CO); 1645, 1530 (amide); 1240 (ester C—O—C); 1130, 1120, 1060, 1020, 990, 940.

*In Nujol unless indicated otherwise.
†In chloroform.
‡Anhydrous compound.
§Hydrate.
‖Melting point 145–146°.
¶Melting point 152–153°.

undepressed upon admixture of **14** from (*a*); $[\alpha]_D$ +117° → +95.7° (20 min, constant) (*c*, 0.11, water). Crystals recovered from the aqueous solution melted at 152–153°.

Attempted Preparation of D-*Daunosamine Hydrochloride*

The glycoside **13** (44 mg) was hydrolyzed, first with 0.2 *N* hydrochloric acid at 80° for 2 h and at 100° for 1.5 h, and thereafter with increased acid strength (0.43 *N*) at 100° for 1 h. Thin-layer chromatography (solvent *b*) then indicated complete conversion of **13** into material that remained at the starting point. Evaporation of the hydrolyzate gave a syrup which was dried to glassy consistency in a desiccator. The substance failed to crystallize from a variety of solvents. It reduced hot Fehling solution and showed $[\alpha]_D$ +63.7° (*c*, 1.7, water). Reported (4) for crystalline L-daunosamine hydrochloride, $[\alpha]_D$ −54.2° (water).

*Methyl 3-Acetamido-4-O-acetyl-2,3-dideoxy-6-O-p-tolylsulfonyl-β-*D*-lyxo-hexopyranoside (16)*

To a chilled solution of 1.12 g of methyl 3-acetamido-2,3-dideoxy-β-D-*lyxo*-hexopyranoside (**15**) (2) in dried pyridine (7.5 ml) was added a chilled solution of *p*-toluenesulfonyl chloride (1.02 g; 1.05 molar equivalents) in dry, ethanol-free chloroform (28 ml). The mixture was kept at −8° for 24 h. Acetic anhydride (0.53 ml) was then added, and the mixture was allowed to stand at −8° for another 24 h. It was then shaken briefly with a small quantity of water, diluted with excess chloroform, and washed successively with dilute sulfuric acid, sodium bicarbonate solution, and water. The organic phase was dried over magnesium sulfate and evaporated to give a syrup which was crystallized from ethyl acetate – petroleum ether. Crude **16** (1.06 g; 50%), m.p. 140–142°, was recrystallized from ethyl acetate to give fibrous needles

Can. J. Chem. Downloaded from www.nrcresearchpress.com by 210.87.254.40 on 09/05/12
For personal use only.

Can. J. Chem. Downloaded from www.nrcresearchpress.com by 210.87.254.40 on 09/05/12
For personal use only.

(0.84 g) of m.p. 148–149°, $[\alpha]_D$ +13.8° (*c*, 1, chloroform).

Anal. Calcd. for $C_{18}H_{25}NO_8S$ (mol. wt., 415.5): C, 52.03; H, 6.07; S, 7.72. Found: C, 51.94; H, 6.36; S, 7.24.

The mother liquor remaining in the crystallization of **16** gave 3 spots on t.l.c. (solvent *a*). Application to large plates allowed the separation into bands which were scraped off and extracted with acetone. The slowest band afforded crystals that were identified as the known (2) *4,6-di-O-acetate* of **15** by comparing infrared and n.m.r. spectra with those of an authentic sample. The middle band gave crystals of **16**, m.p. 148–150°. The third and fastest band furnished a syrupy *di-O-tosylate*. Its infrared spectrum showed peaks at 3350 (NH), 1650 and 1540 (amide I and II), and 1610, 1470, and 1180 cm^{-1} (tosyl). The last three bands were more intense with respect to the amide absorptions than the corresponding bands in the spectrum of **16** (Table II). There were no peaks attributable to *O*-acetyl in the 1730 and 1250 cm^{-1} regions. The n.m.r. spectrum exhibited methyl proton singlets at τ 6.60 (*O*—CH_3), 7.56 (arom. CH_3), and 8.09 (*N*—Ac). The signal at τ 7.56 was twice as intense as either one of the others. (Compare also the spectra of **3** and **16**, Table I.)

*Methyl 3-Acetamido-4-O-acetyl-2,3,6-trideoxy-6-iodo-α-*D*-lyxo-hexopyranoside (17)*

A solution of **16** (840 mg) and sodium iodide (610 mg) in dry acetone (6 ml) was heated in a bomb for 18 h at 100–110°. After the mixture had cooled, sodium *p*-toluenesulfonate (392 mg, 99%) was filtered off and the red filtrate concentrated. Water was added to the residue, and the mixture was extracted three times with chloroform. The combined extracts were washed with sodium thiosulfate solution and water, dried with magnesium sulfate, and evaporated to give a syrup (0.37 g) which did not crystallize. The syrup was dissolved in a small amount of chloroform and applied to 3 large t.l.c. plates which were developed with solvent *a*. Two bands separated. Extraction with acetone of the faster-moving, and major, band afforded a crystalline material which was recrystallized from ethyl acetate – petroleum ether to give **17** (152 mg) m.p. 167–169°, $[\alpha]_D$ +155° (*c*, 1.5, chloroform). A Beilstein test indicated the presence of halogen.

Anal. Calcd. for $C_{11}H_{18}NIO_5$ (mol. wt., 371.2): C, 35.59; H, 4.89. Found: C, 35.83; H, 5.02.

The slower band afforded a syrupy material (47 mg) that had $[\alpha]_D$ +64° (*c*, 1.5 in chloroform). It showed infrared bands at 3350 (NH), 1750 (ester CO), 1660 and 1530 cm^{-1} (amide I and II). Presumably this syrup contained the β-anomer of **17**; however, it was not investigated further.

*Methyl 3-Acetamido-4-O-acetyl-2,3,6-trideoxy-α-*D*-lyxo-hexopyranoside (18)*

A solution of **17** (130 mg) and diethylamine (0.04 ml) in methanol (8 ml) was shaken with Raney nickel-T4 (30 mg) and hydrogen for 3 h at room temperature. The solution was filtered and concentrated to a syrup which was dissolved in a small amount of chloroform and subjected to preparative t.l.c. (solvent *a*). As the main component a crystalline material (48 mg) was obtained. Recrystallization from ethyl acetate – petroleum ether gave **18** (25 mg), m.p. 189–190°, $[\alpha]_D$ +186° (*c*, 0.5, chloroform). Reported (5) for **18**: m.p. 183–185°, $[\alpha]_D$ +192° (chloroform); reported (4) for the L-enantiomer of **18**: m.p. 187–188°, $[\alpha]_D$ −204° (chloroform). A small amount of the β-anomer was present in our sample, causing low rotation and a (very weak) n.m.r. signal at τ 6.50.

Anal. Calcd. for $C_{11}H_{19}NO_5$ (mol. wt., 245.3): C, 53.86; H, 7.81. Found: C, 53.93; H, 7.85.

Acknowledgment

Support of this work by the Life Insurance Medical Research Fund, Rosemont, Pennsylvania, is gratefully acknowledged.

1. H. H. Baer and T. Neilson. Can. J. Chem. **43**, 840 (1965).
2. H. H. Baer and F. Kienzle. Can. J. Chem. **43**, 3074 (1965).
3. F. Arcamone, G. Cassinelli, P. Orezzi, G. Franceschi, and R. Mondelli. J. Am. Chem. Soc. **86**, 5335 (1964).
4. J. P. Marsh, Jr., C. W. Mosher, E. M. Acton, and L. Goodman. Chem. Commun. 973 (1967).
5. A. C. Richardson. Carbohydrate Res. **4**, 422 (1967).
6. F. Shafizadeh. Advan. Carbohydrate Chem. **13**, 9 (1958).
7. B. Capon and W. G. Overend. Advan. Carbohydrate Chem. **15**, 11 (1960).
8. J. N. BeMiller. Advan. Carbohydrate Chem. **22**, 25 (1967).
9. E. L. Eliel, N. L. Allinger, S. J. Angyal, and G. A. Morrison. Conformational analysis. Interscience Publishers, Inc., New York. 1965. p. 422.
10. L. Goodman. Advan. Carbohydrate Chem. **22**, 109 (1967).
11. S. A. Barker, J. Homer, M. C. Keith, and L. F. Thomas. J. Chem. Soc. 1538 (1963).
12. R. U. Lemieux and B. Fraser-Reid. Can. J. Chem. **42**, 532 (1964).
13. H. H. Baer and G. V. Rao. Ann. **686**, 210 (1965).
14. L. D. Hall. Advan. Carbohydrate Chem. **19**, 51 (1964).
15. D. Horton, J. B. Hughes, J. S. Jewell, K. D. Philips, and W. N. Turner. J. Org. Chem. **32**, 1073 (1967).
16. A. Hasegawa and H. Z. Sable. J. Org. Chem. **33**, 1604 (1968).
17. S. Nishimura. Bull. Chem. Soc. Japan, **32**, 61 (1959).

Can. J. Chem. Downloaded from www.nrcresearchpress.com by 210.87.254.6 on 09/05/12
For personal use only.

Cyclizations of dialdehydes with nitromethane. XIV. The isolation of four crystalline methyl 3,6-dideoxy-3-nitro-α-L-hexopyranosides[1]

HANS H. BAER AND KAREL ČAPEK[2]
Department of Chemistry, University of Ottawa, Ottawa, Canada

Received July 26, 1968

Cyclization of L′-methoxy-L-methyldiglycolic aldehyde (**1**) with nitromethane and sodium methoxide in methanol (40 min at room temperature) furnished four crystalline methyl 3,6-dideoxy-3-nitro-α-L-hexopyranosides in a combined yield of 75%. Chromatographic separation gave the *gluco* (**2**), *manno* (**3**), *talo* (**4**), and *galacto* (**5**) isomers in an approximate ratio of 18:8:3:1. Shortening of the reaction time to 25 min decreased the total yield to 53% at the expense of **2**, the ratio of isolated products being 8:8:2.3:1.7. The configurations of the new nitro glycosides **3**, **4**, and **5** were proven by catalytic hydrogenation followed by *N*-acetylation, which gave the known 3-acetamido derivatives.

Canadian Journal of Chemistry, 47, 99 (1969)

In the nitromethane cyclization of a periodate-oxidized methyl glycoside ("sugar dialdehyde") the resulting methyl deoxynitro glycoside contains three new asymmetric centers and consequently, eight stereoisomeric products can be expected *a priori*.[3] In practice, however, it has been found in all the cases which were examined in some detail as to the stereochemical composition of the products, that the reaction is endowed with a marked stereoselectivity. One or two of the eight configurations usually arise in considerable preponderance while another one or two occur to a minor extent, and the remaining ones are not encountered (2, 3). This picture will probably change little, and retain its general validity, even if reinvestigation of individual reactions should bring to light small proportions of additional isomers that have hitherto escaped detection. The observed stereoselectivity no doubt is governed by two factors, namely the conformational behavior of reaction intermediates and the thermodynamic stability of the final products. Stereochemical considerations (4–8) rationalizing some of the experimental results have been advanced as the latter gradually emerged over the past decade, but a comprehensive theory consistent with all observations is still lacking. It was felt that more data on the sugar dialdehyde–nitromethane cyclization need be gathered before such a theory may evolve, and the present work was undertaken in order to make a contribution in this regard.

The cyclization of L′-methoxy-L-methyldiglycolic aldehyde (**1**) (9) obtainable from methyl α-L-rhamnopyranoside was first performed by Richardson and McLauchlan (10) in whose hands it has served as a convenient preparative avenue to 3-amino-3,6-dideoxy sugars which command interest in connection with the chemistry of antibiotics (11). The authors (10) obtained from **1** and nitromethane a syrupy mixture of methyl 3,6-dideoxy-3-nitro-α-L-hexopyranosides which they reduced with Raney nickel without prior isolation of individual stereoisomers. The procedure furnished a single crystalline amine shown to possess the α-L-*gluco* configuration, and from its yields[4] of 25–31% one may realize the minimum extent to which the nitro precursor, methyl 3,6-dideoxy-3-nitro-α-L-glucopyranoside (**2**), must have been present. Repeating the nitromethane cyclization of **1**, Čapek *et al.* (12) succeeded in isolating **2** in crystalline form. In a more detailed investigation we have now isolated besides **2** the crystalline isomers with α-L-*manno*

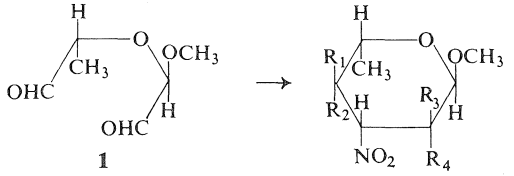

2 $R_1 = R_3 = OH$, $R_2 = R_4 = H$
3 $R_1 = R_4 = OH$, $R_2 = R_3 = H$
4 $R_2 = R_4 = OH$, $R_1 = R_3 = H$
5 $R_2 = R_3 = OH$, $R_1 = R_4 = H$

[1]For paper XIII in this series see reference 1.
[2]On leave of absence from the Laboratory of Monosaccharides, Institute of Chemical Technology, Prague, Czechoslovakia.
[3]The possibility of additional stereoisomerism will be mentioned later on.
[4]Here and subsequently, yields are based upon the original methyl α-L-rhamnopyranoside; no unacceptable error would be introduced by equating these figures with yields based upon the dialdehyde **1**, since the latter is engendered from the rhamnoside in a virtually quantitative reaction.

Can. J. Chem. Downloaded from www.nrcresearchpress.com by 210.87.254.6 on 09/05/12
For personal use only.

(**3**), α-L-*talo* (**4**), and α-L-*galacto* (**5**) configurations, determined their proportions, and come to the conclusion that any other products do not play a significant role in the reaction mixture.

In a cyclization performed under the conditions specified previously (10), i.e. with a reaction time of 40 min at room temperature, we obtained **2** in 26% yield by direct crystallization. A thin-layer chromatogram (t.l.c.) of the mother liquor showed five spots. Column chromatography on silicic acid made possible the separation of these components. The fastest spot was due to a yellow, ether-soluble oil which was eluted from the column first and appeared to be a minor impurity amounting to less than 1% of the mother liquor dry-weight. This oil was not investigated further. The second-fastest t.l.c. spot corresponded to the α-L-*talo* isomer (**4**) which was obtained from the column in crystalline form in a yield of 7.6%. The middle, and strongest, spot did not represent a single compound but a mixture of the α-L-*manno* (**3**) and α-L-*gluco* (**2**) isomers which were present in the mother liquor in nearly equal amounts. The column furnished both **3** and **2** in yields of about 20%, although either isomer was recovered in pure form only to the extent of two-thirds of that amount while the remainder was obtained as a noncrystalline mixture of both, with a component ratio of about 1:1 determined polarimetrically. The second-to-last t.l.c. spot was due to the α-L-*galacto* isomer (**5**). This isomer was eluted from the column in yields of 2–2.5%. Finally, the slowest t.l.c. spot represented a material which, when eluted from the column, amounted to a yield of 1.5% (calculated as an isomeric nitro glycoside). However, this material did not appear to be a uniform product; it gave several spots on rechromatography and only a small part of it could be crystallized. The crystals did show infrared bands characteristic of a nitro glycoside and may have been an additional isomer,[5] but their quantity was too small for further examination.

[5]Should this be verified, a choice among the α-L-*allo*, *altro*, *gulo*, and *ido* configurations would seem logical, although glycosides bearing an axial nitro group at C-3 have not been encountered in nitromethane cyclizations (1–8), with the notable exception (4) of the β-D- and β-L-ribopyranosides. However, one would also have to consider the possibility of stereoisomers arising from epimerization of C-5. Such rather unexpected epimerizations have recently been discovered in a cyclization with nitroethane (13) and have occurred to a small degree in one cyclization with nitromethane (14).

TABLE I

Methyl 3,6-dideoxy-3-nitro-α-L-hexopyranosides

Configuration	Melting point	$[\alpha]_D^{23}$ in H_2O	Yields, % 40 min	Yields, % 25 min
Gluco (**2**)	142–145°	−162.0°	45–46	22
Manno (**3**)	73–78°*	−23.9°	18–21	20
Talo (**4**)	105–107°	−89.8°	7–8	6
Galacto (**5**)	155–158°	−216.0°	2–3	5

*This compound crystallized as a monohydrate; it liquefied with loss of water on drying *in vacuo* at room temperature.

Physical constants and isolated yields of the four stereoisomeric methyl 3,6-dideoxy-3-nitro-α-L-hexopyranosides (**2**–**5**) are listed in Table I. The table contains also the yields, obtained after chromatographic separation, of a second cyclization experiment that was conducted under identical conditions except for a shorter reaction time of 25 min. The total of isolated, crystalline products was less in this case, namely 53% *versus* 75% in the 40 min experiment. Moreover, there was an interesting variation in the ratio of products, the *gluco* and *manno* isomers on the one hand and the *talo* and *galacto* isomers on the other being now found in equal amounts. It has been recognized previously (6, 15) that nitro glycosides formed initially may epimerize as the reaction in an alkaline medium goes on, and this circumstance explains variations in the product composition as a function of time. The course of the epimeric equilibration of the sodium nitronates of **2**, **3**, **4**, and **5** will be the subject of a later communication (16), but the result of the present study, namely the observed predominance of *gluco* and *manno* products in early stages of the cyclization and the occurrence of minor proportions of *talo* and *galacto* isomers, is in full harmony with the results obtained (6) in the series of methyl 3-deoxy-3-nitro-α-D-hexopyranosides. By contrast, in the analogous series of β-D-hexopyranosides the *gluco* and *galacto* configurations were strongly favored and the *manno* configuration arose to a subordinate extent (17).

Whereas the configuration of **2** had been established previously (10, 12), that of each of the new isomers had yet to be determined. Compounds **3**, **4**, and **5** were therefore hydrogenated catalytically with platinum in the presence of

Can. J. Chem. Downloaded from www.nrcresearchpress.com by 210.87.254.6 on 09/05/12
For personal use only.

acetic anhydride to give the corresponding methyl 3-acetamido-3,6-dideoxy-α-L-hexopyranosides. All of these were known, and identifications with authentic specimens were made by comparison of physical constants and infrared spectra.

Experimental

Unless otherwise indicated, thin-layer chromatography (t.l.c.) was performed on silica gel G (Merck A.G., Darmstadt) with the solvent system benzene–ethanol (20:1, v/v); spots were made visible by a ceric sulfate – sulfuric acid spray. Silic acid (analytical grade, 100 mesh) from Mallinckrodt was used for column chromatography. Petroleum ether refers to the fraction with boiling range 30–60°. Infrared spectra were taken from Nujol mulls on a Beckman IR-8 instrument. Optical rotations were measured at about 23° in a Perkin–Elmer 141 automatic polarimeter.

Nitromethane Cyclization[6]

Crystalline methyl α-L-rhamnopyranoside (18) (25 g, 0.14 mole) was prepared by an improved procedure (19) and oxidized with sodium metaperiodate as described (10). Examination by t.l.c. (acetone–benzene, 3:2) revealed that the oxidation was complete after 1 h. Treatment with nitromethane and sodium methoxide for 40 min was then conducted as described (10), and the syrupy mixture of nitro glycosides resulting after work-up was triturated with a few milliliters of chloroform and seeded with methyl 3,6-dideoxy-3-nitro-α-L-glucopyranoside (**2**) (12). Partial crystallization took place, and the crystals (**2**) were isolated after standing in the refrigerator overnight, washed with a small amount of cold chloroform, and recrystallized from chloroform – petroleum ether. The yield of **2** was 7.75 g (26%), m.p. 141–143°, $[\alpha]_D$ −164.3° (*c*, 1, water). Reported (12): m.p. 136–139°, $[\alpha]_D$ −164.5° (water).

Chromatographic Separation of Mother Liquor Components

The mother liquor remaining after the collection of crude **2** was evaporated to a brown syrup weighing 22.1 g.

A part (2.5 g) of the above syrup together with a small amount of benzene was absorbed in a lump of cotton wool and placed on a column (40 × 2 cm) containing 45 g of silicic acid. In the subsequent chromatography, 25-ml fractions were collected, evaporated and, if they left any residue, examined by t.l.c. Elution was started with pure benzene (250 ml), which produced no detectable residues in fractions 1–10. This was followed by benzene–ethanol (100:1) (450 ml). Fractions 11–20 were blank also and 21 and 22 contained a few milligrams of an oil that was discarded. Fraction 23 (146 mg) was a mixture of crystals and a yellow oil, and fractions 24–28 gave a total of 258 mg of dry, yellow crystals. The latter were recrystallized from ether – petroleum ether with the use of decolorizing carbon and afforded 177 mg of the *talo* isomer (**4**), m.p. 104–107°.

[6]Mr. C. W. Chiu is thanked for performing this preparation.

The mother liquor from this recrystallization was combined with the above fraction 23 and subjected to rechromatography on another (smaller) column, from which was obtained a brownish oil (60 mg, not uniform on t.l.c.), a partially crystalline fraction (62 mg, *talo* isomer + yellow, faster-moving oil, according to t.l.c.), and a crystalline fraction (73 mg, *talo* isomer **4** of m.p. 105–107°).

The main chromatography was continued with benzene–ethanol (100:1.5) to fraction 55, and benzene–ethanol (100:2) to fraction 63. Fractions 29–32 contained mixtures of **4** and (presumably) **3** totalling 23 mg; they were discarded. Fractions 33–63 all showed only the "middle" spot on t.l.c., the *manno* (**3**) and *gluco* (**2**) isomers being indistinguishable in the system employed. There were weight maxima in fractions 42 and 47. We combined fractions 33–39 (**A**, 220 mg), 40–43 (**B**, 337 mg) and 44–63 (**C**, 800 mg). Part **C**, whose individual portions had crystallized without difficulty, was recrystallized from chloroform–petroleum ether to give *gluco* isomer **2** (443 mg, m.p. 136–140°). The mother liquor therefrom was evaporated to give a syrup (**C′**, ca. 350 mg). Parts **A** and **B** did not crystallize upon seeding with **2**, but different crystals were obtained with initial difficulty. However, the materials crystallized well when triturated with a few drops of water, and the same was true for the syrup **C′**. The crystals were the monohydrate of the *manno* isomer **3**. Recrystallization from moist ethyl acetate (with careful, dropwise addition of petroleum ether) of the crude crystals obtained from **A**, **B** and **C′** gave a total of 433 mg of **3** (hydrate), m.p. 72–78°. The combined mother liquors were evaporated to a syrup which was dissolved in water, and the aqueous solution was decolorized with activated charcoal and evaporated again, to constant weight (427 mg). This residue showed only one spot on t.l.c. and had $[\alpha]_D$ −99.3° (*c*, 1.23, water). From the rotations of pure **2** and **3** (see below) it was calculated that the residue contained 207 mg of the former and 220 mg of the latter.

The chromatography was continued with benzene–ethanol (100:3). Fractions 64–73 contained the *galacto* isomer **5** only, according to t.l.c. The combined residues were treated with charcoal in ethyl acetate, and after filtration and addition of petroleum ether there crystallized **5** (82 mg), m.p. 154–158°.

Further elution with benzene–ethanol (100:5) gave, in fractions 74–80, 15 mg of a mixture of **5** and an unidentified, slow-moving component and, in addition, some material which did not move at all on t.l.c. The total dry-weight was 40 mg (syrup); crystallization and recrystallization from ethyl acetate – petroleum ether afforded 7 mg of the unidentified, slow-moving component, m.p. 193–197°, $[\alpha]_D$ −109.5° (*c*, 0.4, water).

A similar fractionation was carried out with a larger part (9.2 g) of the syrup (22.1 g) mentioned before, on a column containing 150 g of silicic acid. There was obtained crystalline **4** (694 mg,[7] m.p. 104–108°); crystalline **3** (1.756 g, as hydrate, m.p. 71–78°); crystalline **2**

[7]This was a yield of 5.7%. In contrast to the small-scale separation, which yielded 7.6%, no efforts were made here to isolate additional **4** by rechromatography of mixed fractions.

Can. J. Chem. Downloaded from www.nrcresearchpress.com by 210.87.254.6 on 09/05/12
For personal use only.

(1.634 g, m.p. 139–143°); a mixed fraction of **2** and **3** (1.726 g) which on the basis of its rotation, $[\alpha]_D$ −78° (*c*, 3.1 in water) was seen to contain 675 mg of the former and 1.05 g of the latter; and crystalline **5** (234 mg, m.p. 154–157°).

Short-time Experiment

A periodate oxidation of methyl α-L-rhamnopyranoside (3.56 g, 20 mmole) followed by nitromethane condensation was carried out exactly as described (10), except that the nitromethane cyclization was interrupted by deionization after 25 min. In this case, crystallization of **2** from the crude syrup could not be induced, probably because of its lower content in the reaction mixture. The syrup was chromatographed on silicic acid (40 g) in a manner similar to the example described. The following were obtained: **4** (276 mg, m.p. 104–107°); a mixed fraction (90 mg) containing **4** and (presumably) **3**; crystalline **3** (631 mg as monohydrate, m.p. 73–78°); **2** (668 mg, m.p. 137–142°); a mixed fraction of **2** and **3** which on the basis of its rotation of $[\alpha]_D$ −90° was calculated to contain 251 mg of the former and 274 mg of the latter; and **5** (166 mg, m.p. 152–156°) plus an estimated 25 mg of **5** in a mixed fraction containing an equally small amount of an unidentified, slow-moving component.

Characterization of Products

Methyl 3,6-Dideoxy-3-nitro-α-L-glucopyranoside (2)

The fractions of crude **2** obtained chromatographically were recrystallized from chloroform – petroleum ether and then melted at 142–145° and had $[\alpha]_D$ −162 ± 0.8° (*c*, 1, water). Infrared bands were at 3550–3450 (OH) and 1555 cm^{-1} (NO_2) and the compound was identical with **2** obtained by direct crystallization.

Methyl 3,6-Dideoxy-3-nitro-α-L-mannopyranoside (3)

The hydrate of **3** melted in the range of 73–78° even after several recrystallizations from moist ethyl acetate, whereby the rotation remained unchanged, $[\alpha]_D$ −23.9° (*c*, 1.3, water). Infrared bands were at 3500–3200 (OH), 1650 (H_2O), 1550 cm^{-1}(NO_2). The analytical sample was air-dried.

Anal. Calcd. for $C_7H_{13}NO_6 \cdot H_2O$ (mol. wt., 225.2): C, 37.33; H, 6.71; N, 6.22. Found: C, 37.23; H, 6.67; N, 6.18.

Drying *in vacuo* at room temperature caused a loss in weight of 7.3% (calcd. for 1 H_2O, 8.0%) and the sample became syrupy.

Anal. Calcd. for $C_7H_{13}NO_6$ (mol. wt., 207.2): C, 40.58; H, 6.32; N, 6.76. Found: C, 40.40; H, 6.41; N, 6.94.

Upon exposure to the atmosphere the anhydrous syrup began to crystallize slowly, reforming the hydrate.

Methyl 3,6-Dideoxy-3-nitro-α-L-talopyranoside (4)

The melting point (104–107°) and rotation ($[\alpha]_D$ −89.8°, *c*, 1.1, water) remained virtually unchanged in several recrystallizations from ether – petroleum ether. Infrared bands occurred at 3530–3400 (OH) and 1550 cm^{-1} (NO_2). The analytical sample was dried *in vacuo* at room temperature as **4** sublimed rapidly at 56°.

Anal. Calcd. for $C_7H_{13}NO_6$ (mol. wt., 207.2): C, 40.58; H, 6.32; N, 6.76. Found: C, 40.47; H, 6.22; N, 6.76.

Methyl 3,6-Dideoxy-3-nitro-α-L-galactopyranoside (5)

The melting point of crude **5** was raised to 155–158°, and then remained unchanged, by recrystallization from ethyl acetate – petroleum ether. Rotations of crude and recrystallized **5** were the same, $[\alpha]_D$ −216° (*c*, 1, water). Infrared bands were at 3500–3430 (OH) and 1550 cm^{-1} (NO_2).

Anal. Calcd. for $C_7H_{13}NO_6$ (mol. wt., 207.2): C, 40.58; H, 6.32; N, 6.76. Found: C, 40.51; H, 6.14; N, 6.61.

Hydrogenations

The nitro glycosides **3**, **4**, and **5** (50 mg) were hydrogenated in methanol (5 ml) in the presence of platinum oxide (50–150 mg) and acetic anhydride (0.3 ml), at ordinary temperature and pressure. The reaction proceeded smoothly with **4**, less so with **3**, and had to be repeated with fresh reagents in the case of **5**. Evaporation then gave the acetamido derivatives.

Compound **3** gave a syrup shown by t.l.c. (benzene–acetone, 3:7) to contain some starting material and unidentified impurities besides the *N*-acetyl derivative. Passage over a silicic acid column (benzene–ethanol, 100:1, with increasing ethanol content) afforded methyl 3-acetamido-3,6-dideoxy-α-L-mannopyranoside (17 mg) which after recrystallization from ethyl acetate – petroleum ether melted at 169–171°, $[\alpha]_D$ −47.3° (*c*, 0.4, ethanol). Reported (12): m.p. 169–171.5°, $[\alpha]_D$ −50.3° (ethanol); for the D-enantiomer (20), m.p. 168–170°, $[\alpha]_D$ +49° (ethanol). Our sample and an authentic specimen gave identical infrared spectra.

Compound **4** afforded a crystalline hydrogenation product (35 mg, m.p. 185–195°) which after recrystallization from acetone or acetone–petroleum ether melted at 201–203°, $[\alpha]_D$ −108.5° (*c*, 0.5, water). Reported for methyl 3-acetamido-3,6-dideoxy-α-L-talopyranoside (10): m.p. 195–196°, $[\alpha]_D$ −104° (water); for the D-enantiomer (21), m.p. 201–202°, $[\alpha]_D$ +106.1° (water). Our product and an authentic sample of the D-enantiomer gave superimposable infrared spectra.

Compound **5** gave a hydrogenation product that contained some starting material but afforded, by recrystallizations from ethyl acetate and then from ethyl acetate – petroleum ether, 18 mg of methyl 3-acetamido-3,6-dideoxy-α-L-galactopyranoside of $[\alpha]_D$ −234.5° (*c*, 0.4, water) and m.p. 200–202°. An authentic sample (12) did not depress the melting point on admixture and gave an identical infrared spectrum. Recorded data: m.p. 202–203°, $[\alpha]_D$ −238° (water) (12); and m.p. 199–200°, $[\alpha]_D$ −219° (water) (22).

Acknowledgments

Financial support of this work by the Life Insurance Medical Research Fund, Rosemont, Pennsylvania, and in part by the National Research Council of Canada is gratefully acknowledged.

1. H. H. BAER and A. AHAMMAD. Can. J. Chem. **44**, 2893 (1966).
2. H. H. BAER. Tetrahedron, **20**, Suppl. 1, 263 (1964).
3. F. W. LICHTENTHALER. Angew. Chem. **76**, 84 (1964).
4. H. H. BAER and H. O. L. FISCHER. J. Am. Chem. Soc. **81**, 5184 (1959); J. Am. Chem. Soc. **82**, 3709 (1960).

5. A. C. RICHARDSON and H. O. L. FISCHER. J. Am. Chem. Soc. **83**, 1132 (1961).
6. H. H. BAER. J. Am. Chem. Soc. **84**, 83 (1962).
7. G. BASCHANG. Ann. **663**, 167 (1963).
8. F. W. LICHTENTHALER and H. K. YAHYA. Tetrahedron Letters, 1805 (1965).
9. W. D. MACLAY, R. M. HANN, and C. S. HUDSON. J. Am. Chem. Soc. **61**, 1660 (1939).
10. A. C. RICHARDSON and K. A. MCLAUCHLAN. J. Chem. Soc. 2499 (1962).
11. J. D. DUTCHER. Advan. Carbohydrate Chem. **18**, 259 (1963).
12. K. ČAPEK, J. ŠTEFFKOVÁ, and J. JARÝ. Coll. Czech. Chem. Commun. **31**, 1854 (1966).
13. H. H. BAER and G. V. RAO. Ann. **686**, 210 (1965).
14. S. INOUYE. Chem. Pharm. Bull. **14**, 902 (1966).
15. H. H. BAER and F. KIENZLE. Ann. **695**, 192 (1966).
16. K. ČAPEK and H. H. BAER. In preparation.
17. H. H. BAER and F. KIENZLE. Can. J. Chem. **41**, 1606 (1963).
18. E. FISCHER. Ber. **28**, 1158 (1895).
19. J. JARÝ, K. ČAPEK, and J. KOVÁŘ. Coll. Czech. Chem. Commun. **28**, 2171 (1963).
20. J. D. DUTCHER, D. R. WALTERS, and O. WINTERSTEINER. J. Org. Chem. **28**, 995 (1963).
21. K. ČAPEK, J. ŠTEFFKOVÁ, and J. JARÝ. Coll. Czech. Chem. Commun. **33**, 1750 (1968).
22. A. C. RICHARDSON. Carbohydrate Res. **4**, 415 (1967).

Can. J. Chem. Downloaded from www.nrcresearchpress.com by 210.87.254.6 on 09/05/12
For personal use only.

Pyranoquinolines. Part I. Syntheses and ultraviolet absorption characteristics of 6-chloro-4*H*-pyrano[3,2-*h*]quinoline-4-ones

D. R. PATEL, C. S. CHOXI, AND S. R. PATEL
Department of Chemistry, Sardar Patel University, Vallabh Vidyanagar, District Kaira, Gujarat State, India
Received May 1, 1968

6-Chloro-2-phenyl and 2-*p*-anisyl-4*H*-pyrano[3,2-*h*]quinoline-4-ones, their 2,3-dihydro and 3-hydroxy derivatives, and 6-chloro-3-benzoyl-2-phenyl-4*H*-pyrano[3,2-*h*]quinoline-4-one are synthesized by the application of appropriate flavonoid syntheses to 5-chloro-7-acetyl-8-hydroxyquinoline (**5**). **5** was formed on Friedel–Crafts acetylation of 5-chloro-8-methoxy and -8-hydroxyquinolines. Ultraviolet spectra of **5** are studied at three different pH's in aqueous ethanol and those of the pyranoquinolines are studied in ethanolic solutions and compared with those of their corresponding simple flavonoids.

Canadian Journal of Chemistry, **47**, 105 (1969)

Can. J. Chem. Downloaded from www.nrcresearchpress.com by 210.87.254.105 on 09/05/12
For personal use only.

Survey of literature reveals that very few pyranoquinolines have been synthesized. Flindersine (1), isolated from *Flindersia australis* R.Br., is a pyrano[3,2-*c*]quinoline derivative (**1**) and

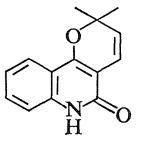

1

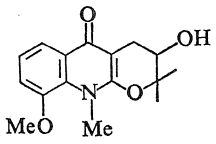

2

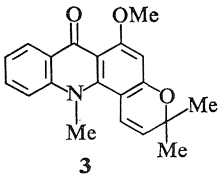

3

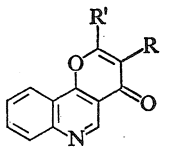

4

isobalfourodine (**2**) (2) isolated from *Balfouradendron riedelianum* is a pyrano[2,3-*b*]quinoline derivative. Acronycine (**3**), isolated from *A. bauerii* (3) can be regarded as a pyrano[2,3-*h*]-quinoline derivative. Elliott and Tittensor (4) have reported syntheses of 2R′-3R-4*H*-pyrano-[3,2-*c*]quinoline derivatives. The fact that the pyranoquinolines are rare was the main consideration in the selection of the work described in the present communication dealing with the syntheses of 6-chloro-2-phenyl and 2-*p*-anisyl-4*H*-pyrano[3,2-*h*]quinoline-4-ones. This provided an opportunity of studying the application of some of the well known methods of flavonoid synthesis to an *o*-hydroxyquinolinone derivative (**5**). The ultraviolet spectra of the pyranoquinolines described in this communication are studied with a view to revealing their characteristic spectral trends and correlating them with those of their parent bicyclic quinoline and flavonoid derivatives.

The Friedel–Crafts acetylation of 5-chloro-8-hydroxyquinoline (**6**), formed on chlorination of 8-hydroxyquinoline (5), was studied using different proportions of the reactants in absence of any solvent and also in presence of solvents like carbon disulfide or nitrobenzene. The product viz., 5-chloro-7-acetyl-8-hydroxyquinoline (**5**) was formed in 40% yield when the reaction was carried out by heating a mixture of 5-chloro-8-hydroxyquinoline (1 part), acetyl chloride (2 parts), and anhydrous aluminium chloride (3 parts) at 120–130° for 12 h. When Friedel–Crafts acetylation of 5-chloro-8-methoxyquinoline (**7**) was effected under similar conditions, **5** was formed in about 50% yield. **7** was formed by the application of Skraup synthesis to 2-methoxy-5-chloroaniline following the method described by Weizmann and Bograchov (6) with the only modification that acetic acid was used as a diluent. It may be interesting to note that 8-hydroxyquinoline on Friedel–Crafts acylation affords 5-acyl-8-hydroxyquinoline in 52% yield (7). The hydroxyquinolinone (**5**) dissolved in dilute alkali solution but was almost insoluble in dilute acid solution. It developed a violet color with aqueous Fe^{+3} solution.

The condensation of **5** with benzaldehyde in presence of alcoholic alkali solution was carried out at room temperature and also at 80°. The product (**8**) obtained did not respond to the characteristic color reactions of a chalcone (8) and remained unchanged on prolonged refluxing with alcoholic acid solution. This suggested that

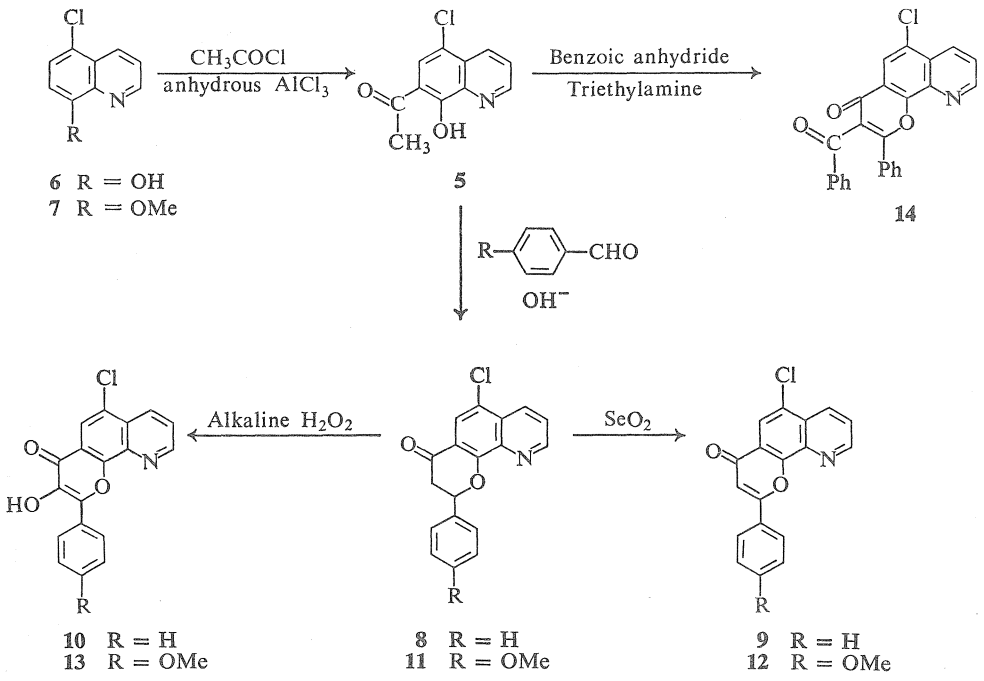

Chart I

the product **8** was not a chalcone but a flavanone derivative, 6-chloro-2-phenyl-4*H*-2,3-dihydropyrano[3,2-*h*]quinoline-4-one (**8**); this was also supported by the nature of its ultraviolet spectrum. The flavanone (**8**) was dehydrogenated on treatment with selenium dioxide (9) in dioxan solution to 6-chloro-2-phenyl-4*H*-pyrano[3,2-*h*]-quinoline-4-one (**9**). The Algar–Flynn oxidation (10) of **8** afforded 6-chloro-3-hydroxy-2-phenyl-4*H*-pyrano[3,2-*h*]quinoline-4-one (**10**). The latter compound (**10**) was also formed in very low yield when **8** was allowed to react with pentyl nitrite in alcoholic hydrochloric acid solution. These reactions have been summarized in Chart I.

6 - Chloro - 2 - *p* - anisyl - 4*H* - pyrano[3,2-*h*]-quinoline-4-ones **11**, **12**, and **13** (Chart I) were synthesized starting with **5** and anisaldehyde following the methods described for the synthesis of their corresponding desmethoxy analogues **8**, **9**, and **10** respectively. In this case too, the chalcone type of compound was not formed on condensing **5** with anisaldehyde but the flavanone derivative, 6-chloro-2-*p*-anisyl-4*H*-2,3-dihydropyrano[3,2-*h*]quinoline-4-one (**11**) was formed. All the reactions in this series ran much more smoothly giving better products than the corresponding reactions in the previous series.

Kostanecki–Robinson reaction of 5-chloro-7-acetyl-8-hydroxyquinoline (**5**) with benzoic anhydride in presence of triethylamine afforded 6-chloro-3-benzoyl-2-phenyl-4*H*-pyrano[3,2-*h*]-quinoline-4-one (**14**). The latter compound could not be deacylated when it was treated with hot 10% alkali solution. It is reported by Bhullar and Venkataraman (11) that 3-benzoyl-α-naphthoflavone having an angular structure analogous to that of **14** does not undergo deacylation on treatment with hot dilute alkali. A one-step Baker–Venkataraman transformation comprising a reaction between an *o*-hydroxyacetophenone derivative (12) with an acyl halide in presence of anhydrous potassium carbonate was applied to **5**. The latter (**5**) on treatment with benzoyl chloride in presence of anhydrous potassium carbonate in dry acetone afforded the flavone derivative (**9**). Some of these pyranoquinolines gave color reactions characteristic of flavonoids.

Thus all the above-mentioned flavonoid syntheses are applicable to 5-chloro-7-acetyl-8-hydroxyquinoline. The corresponding pyranoquinolines are formed in comparatively good yields. In this respect, **5** behaves like a simple *o*-hydroxyacetophenone derivative. This is not surprising as

Can. J. Chem. Downloaded from www.nrcresearchpress.com by 210.87.254.105 on 09/05/12
For personal use only.

TABLE I

Spectral data for 5-chloro-8-hydroxy and 5-chloro-7-acetyl-8-hydroxyquinolines

Compound	Medium	Band II λ_{max} (mμ) (log ε)	Band I λ_{max} (mμ) (log ε)
5	Acidic (pH = 1.2)	230* sh (4.10) 271 (4.49)	364 (3.50)
	Basic (pH = 14.0)	285 (4.39)	372–373 (3.95)
	Neutral (pH = 8.5)	230 In (4.10) 269 (4.41) 288 sh (3.87)	365–366 b (3.66)
6	Acidic (pH = 1.1)	226 In (3.98) 261 (4.66)	305 (3.34) 375–385 b (3.41)
	Basic (pH = 14.0)	258 (4.51)	346 (3.56) 380–385 (3.60)
	Neutral (pH = 8.4)	246 (4.56) 264 sh (3.70)	329 (3.56)

*Sh, shoulder; In, Inflection; b, broad.

the quinoline is a stable ring system and 8-hydroxyquinoline behaves like a true phenol (13). However, Pechmann condensation between 5-chloro-8-hydroxyquinoline and acetoacetic ester failed. The reaction was carried out both in presence of concentrated sulfuric acid and polyphosphoric acid. This seems to be due to absence of any activating group in a position para with respect to the point of cyclization (7-position) (14).

The ultraviolet spectra of 5-chloro-7-acetyl-8-hydroxyquinoline (**5**) were studied in aqueous alcoholic solution at three different pH's. The spectral curves are shown in Fig. 1 and the spectral data along with those of 5-chloro-8-hydroxyquinoline (**6**) are recorded in Table I. The ultraviolet spectrum of **6** was studied by Chakrabarty and co-workers (15) at different pH's for the determination of the acid dissociation constant. The ultraviolet spectrum of **5** in aqueous alcoholic solution at pH = 8.5 comprises two bands. The long wavelength band, designated as band I, forms a broad peak at 365 mμ (log ε = 3.66) and the short wavelength band, designated as band II, comprises an inflection at 230 mμ (log ε = 4.1), a sharp intense peak at 269 mμ (log ε = 4.41) and a shoulder at 288 mμ (log ε = 3.87). The spectrum of the compound **5** in the acidic medium (pH = 1.2) resembles very closely its spectrum at 8.5 pH. This suggested that the compound **5** exists mostly in the non-protonated form in acid solution and thereby indicating that it (**5**) is a very weak base. The spectrum of the compound **5** in the basic medium (pH = 14) however differs much from those in the acid and neutral media; the band II has suffered a bathochromic shift of 15 mμ and the band I has become broader and more intense than the corresponding bands in the spectra in the other two media. The bathochromic shift, broadening of the band and the increased intensity observed in the spectrum in the basic medium seems to be due to the anionic form in which the

TABLE II

Spectral data for pyranoquinoline derivatives and flavonoids

Compound	Band II λ_{max} (mμ) (log ε)	Band I λ_{max} (mμ) (log ε)
5	230* sh (4.10) 269 (4.40)	364–367 b (3.66)
8	224 In (4.19) 268 (4.43)	314 (3.93)
11	226 (4.45) 268 (4.51)	355–365 b (3.95)
9	241 (4.32) 282 (4.56)	
12	240 (4.30) 280–330 (4.2)	
10	235 (4.43) 280 (4.4)	335–338 sh (4.1)
13	236 (4.50) 284 (4.21)	340–370 b (3.63)
14	272 (4.58)	
15	220 (4.45) 246 sh (3.9) 284 In (3.4)	327 (3.62)
16	245 (4.22) 275–285 sh (3.76)	340–360 b (3.57)
17	255 (4.23)	298 (4.22)
18	275–280 (4.49)	

*Sh, shoulder; In, Inflection; b, broad.

Can. J. Chem. Downloaded from www.nrcresearchpress.com by 210.87.254.105 on 09/05/12
For personal use only.

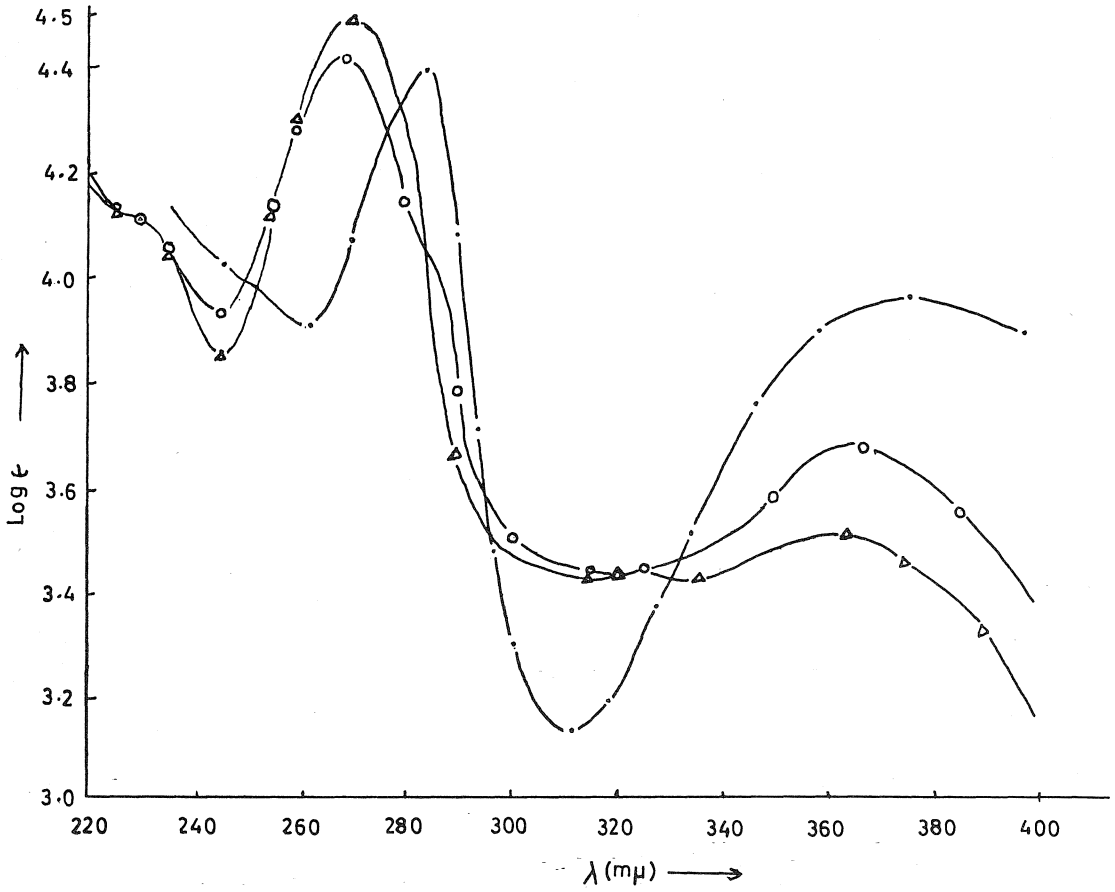

FIG. 1. The ultraviolet spectra of 5-chloro-7-acetyl-8-hydroxyquinoline (**5**) in acidic (—△—△—), basic (—•—•—), and neutral (—O—O—) media.

compound **5** would mostly exist in the basic medium. That the anionic form would prove a stronger chromophore than the neutral acid form has been observed in case of phenols and naphthols (16).

A comparative study of the spectrum of the compound **5** and its parent compound 5-chloro-8-hydroxyquinoline (**6**) reveals that all the bands in the spectrum of *o*-hydroxyquinolinone derivative (**5**) appear at longer wavelengths or are more intense than the corresponding bands in the spectrum of the compound **6**. This seems to be due to the strong hydrogen bond formation (chelation) between the hydroxy–hydrogen and the carbonyl–oxygen atoms (**5***a*).

The ultraviolet spectra of the pyranoquinolines (**8–14**) are studied in alcoholic solution. The

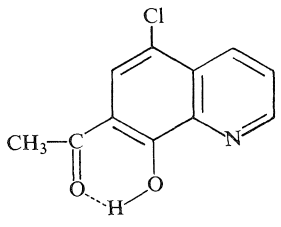

5*a*

spectral data are reported in Table II and the spectral curves are shown in Figs. 2 and 3.

It is reported that the spectrum of a flavanone comprises a strong absorption in 270–290 mμ region and a weak absorption in the form of inflection in the 320–330 mμ region; these bands have been designated as bands II and I respectively

Can. J. Chem. Downloaded from www.nrcresearchpress.com by 210.87.254.105 on 09/05/12
For personal use only.

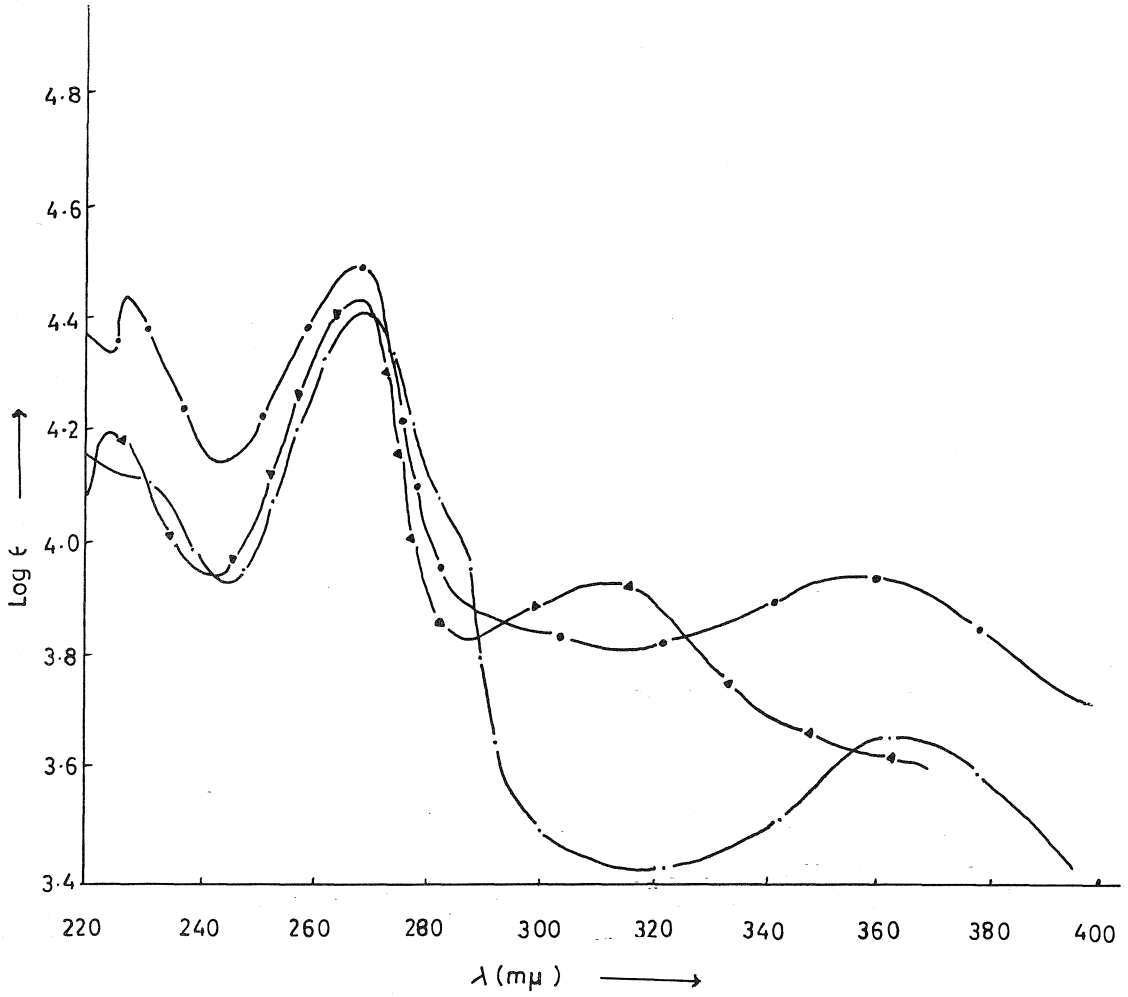

FIG. 2. The ultraviolet spectra of 5-chloro-7-acetyl-8-hydroxyquinoline (**5**) (—.—.—), 6-chloro-2-phenyl-4*H*-2,3-dihydropyrano[3,2-*h*]quinoline-4-one (**8**) (—▲—▲—), and 6-chloro-2-*p*-anisyl-4*H*-2,3-dihydropyrano[3,2-*h*]quinoline-4-one (**11**) (—.—.—).

(17). The spectrum of 6-chloro-2-phenyl-4*H*-2,3-dihydropyrano[3,2-*h*]quinoline-4-one (**8**) comprises two bands; band I appearing at 314 mμ ($\log \varepsilon = 3.93$) and band II comprising a sharp and more intense band at 268 mμ ($\log \varepsilon = 4.4$) and an inflection at 224 mμ ($\log \varepsilon = 4.19$). The band II in the spectrum of **8** resembles very closely the spectrum of the parent ketone 5-chloro-7-acetyl-8-hydroxyquinoline (**5**) (Fig. 2). This is not unexpected as in a flavanone there is no continuity of conjugation between the 2-phenyl and the carbonyl groups. The spectrum of 6-chloro-2-*p*-anisyl-4*H*-2,3-dihydropyrano[3,2-*h*]quinoline-4-one (**11**) also comprises two bands with the only difference that the band I in the spectrum of the compound **11** is more intense and appears at a longer wavelength than the corresponding band in the spectrum of its desmethoxy analogue (**8**).

The spectrum of 6-chloro-2-phenyl-4*H*-pyrano[3,2-*h*]quinoline-4-one (**9**) comprises a sharp inflection at 241 mμ and a prominent band of high intensity with a maxima near about 282 mμ. The low wavelength band II in the spectrum of a flavone has been attributed to the benzoyl grouping and any increase in conjugation in this grouping would result in a bathochromic shift and/or increase in the intensity of this band (18). In the flavone type pyranoquinoline **9**, the

Can. J. Chem. Downloaded from www.nrcresearchpress.com by 210.87.254.105 on 09/05/12
For personal use only.

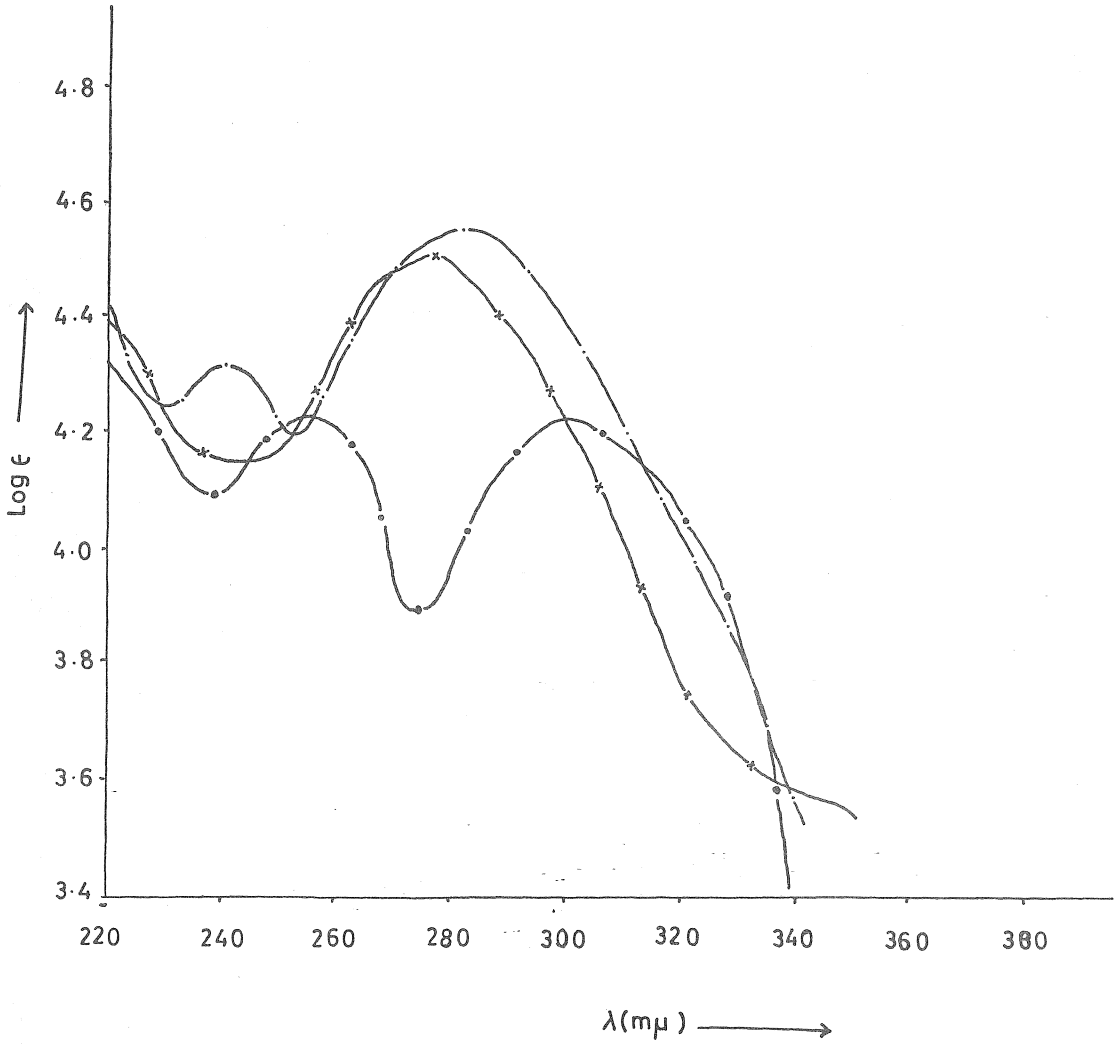

FIG. 3. The ultraviolet spectra of 6-chloroflavone (**17**) (—.—.—), 6-chloro-8-aminoflavone (**18**) (—×—×—), and 6-chloro-2-phenyl-4*H*-pyrano[3,2-*h*]quinoline-4-one (**9**) (—.—.—).

benzoyl grouping of a flavone is replaced by a quinonoyl grouping. This quinonoyl grouping being a stronger chromophore than the benzoyl grouping seems to be responsible for the prominent band II exhibited by the flavone type pyranoquinoline **9**. The long wavelength band which normally appears in the spectrum of a flavone in the region 320–380 mμ (19) is absent in the spectrum of **9**. It is likely that this band I has merged with the tail part of the intense band II and hence appears to have disappeared. The spectrum of 6-chloro-2-*p*-anisyl-4*H*-pyrano[3,2-*h*]quinoline-4-one (**12**) comprises a sharp inflection at 240 mμ and a very broad band ranging from 280 to 330 mμ with the log ε varying from 4.3 to 4.1. Due to the presence of the *p*-methoxy group in the cinnamoyl grouping, the band I in the spectrum of **12** would be more intense and would have undergone a red shift. Hence the broad 280–330 mμ band in the spectrum of **12** seems to be a continuous band comprising the end-part of the band II and whole of band I.

The spectra of the flavonol type of pyranoquinolines **10** and **13** comprise two bands. The band II in the spectra of each of these two compounds consists of an inflection at 235 mμ and a small peak at 280 mμ. The band I appears in the form of shoulder in the spectrum of **10** near

Can. J. Chem. Downloaded from www.nrcresearchpress.com by 210.87.254.105 on 09/05/12
For personal use only.

Can. J. Chem. Downloaded from www.nrcresearchpress.com by 210.87.254.105 on 09/05/12
For personal use only.

about 335 mμ and in the form of a broad band in the spectrum of **13**.

The spectrum of 6-chloro-3-benzoyl-2-phenyl-4*H*-pyrano[3,2-*h*]quinoline-4-one (**14**) comprises only one intense band appearing at 272 mμ (log ε = 4.58). The disappearance of one of the bands and the high intensity of the constituent band in the spectrum seems to be due to the additional —C—Ph group in 3-position.

‖
O

In order to bring forth the characteristics of the ultraviolet spectra of flavone and flavanone type pyranoquinolines which might distinguish them from their simple analogues, the ultraviolet spectra of 6-chloro, 6-chloro-8-aminoflavones, and flavanones and the corresponding pyrano-[3,2-*h*]quinoline derivatives are compared. The spectral data are given in Table II and spectral curves of only the flavone type of compounds are shown in Fig. 3. Comparative study of these spectral data reveals that in the flavanone type of compounds a continuous bathochromic shift and hyperchromic change is discernible as one passes from spectra of 6-chloro-2:3-dihydroflavone (**15**) to that of 6-chloro-2:3-dihydro-8-aminoflavone (**16**) and to that of 6-chloro-2-phenyl-4*H*-2,3-dihydropyrano[3,2-*h*]quinoline-4-one (**8**). In the flavone type of compounds, 6-chloroflavone (**17**) exhibits a two band spectrum—255 mμ (log ε = 4.23); 298 mμ (log ε = 4.22). The spectrum of 6-chloro-8-aminoflavone (**18**) comprises only one prominent and a comparatively more intense band at 275–280 mμ (log ε = 4.49). The spectrum of 6-chloro-2-phenyl-4*H*-pyrano[3,2-*h*]quinoline-4-one (**9**) comprises a similar but slightly more intense band appearing at a slightly longer wavelength and a characteristic distinguishing small peak at 241 mμ (log ε = 4.32).

This spectral analysis of pyranoquinoline derivatives thus reveals that the spectra do not exhibit any outstandingly distinguishing characteristics, except the ones which arise due to increased conjugation.

Experimental

The ultraviolet spectra of the compounds described in this communication are studied in ethanolic or aqueous ethanolic solution on Beckmann DU spectrophotometer. The ultraviolet spectra of 5-chloro-8-hydroxyquinoline and 5-chloro-7-acetyl-8-hydroxyquinoline are studied at three different pH's. The solvent composition was maintained constant in all the three media. The nearly neutral, acidic or basic solution of **5** (or **6**) was prepared by adding 20 ml of distilled water, 20 ml of 0.1 *M* HCl or 20 ml of 0.1 *M* NaOH to 80 ml of the pure ethanolic solution of the compound respectively. The ultraviolet spectra of other compounds were studied in pure ethanolic solution. In all these cases the concentrations of the reagent in solution were maintained accurately around 3×10^{-5} *M*.

5-Chloro-8-methoxyquinoline (7)

To a mixture of 2-methoxy-5-chloroaniline (20 g), arsenic oxide (18 g), glycerine (36 g), and acetic acid (40 ml) cooled in an ice-bath, concentrated sulfuric acid (50 g) was added in small lots over a period of 2 h. The reaction mixture was heated at 160–170° for 8 h, cooled, poured in ice-water, and filtered. The solid product obtained on rendering the filtrate alkaline was collected, washed, dried, and extracted in benzene. The solid product left on removal of benzene was purified by distillation under reduced pressure at 210–215° at 20 mm, m.p. 60–61° (6); yield 43%.

5-Chloro-7-acetyl-8-hydroxyquinoline (5)

A mixture of 5-chloro-8-hydroxyquinoline (1 g), acetyl chloride (2 g), and finely powdered anhydrous aluminium chloride (3 g) was left overnight at 0° and heated at 120–130° for 12 h, cooled, and decomposed with crushed ice and concentrated hydrochloric acid (2 ml). The solid product was collected, washed with water, dried in air and crystallized from aqueous ethanol (1:1) in yellow needles, m.p. 160–161°; yield 0.5 g.

5 was formed in about 50% yield when the reaction was carried out as described above using 5-chloro-8-methoxyquinoline in place of 5-chloro-8-hydroxyquinoline.

Anal. Calcd. for $C_{11}H_8O_2NCl$: C, 59.5; H, 3.6; N, 6.3; Cl, 16.0. Found: C, 59.3; H, 3.8; N, 6.0; Cl, 16.3.

6-Chloro-2-phenyl-4H-2,3-dihydropyrano[3,2-h]-quinoline-4-one (8)

A solution of **5** (0.5 g) and benzaldehyde (0.4 ml) in ethanol (15 ml) was mixed with sodium hydroxide solution (10 ml, 30%) with stirring and left at room temperature for 24 h. It was then decomposed with crushed ice and acidified with hydrochloric acid. The solid product was filtered, washed with bicarbonate solution, and then with water. It was crystallized from aqueous acetic acid (1:1) in yellow light needles, m.p. 191–192°; yield 0.3 g.

This product remained unchanged when it was refluxed with alcoholic hydrochloric acid solution for 48 h.

Anal. Calcd. for $C_{18}H_{12}O_2NCl$: C, 69.7; H, 3.87; N, 4.5; Cl, 11.5. Found: C, 69.6; H, 3.95; N, 4.7; Cl, 11.2.

6-Chloro-2-p-anisyl-4H-2,3-dihydro-pyrano[3,2-h]quinoline-4-one (11)

It was formed on condensing **5** (0.5 g) with anisaldehyde (0.4 ml) following the method described above. The product was crystallized from glacial acetic acid in yellow granules, m.p. 201–202°; yield 0.2 g.

This product remained unchanged on prolonged treatment with hot alcoholic hydrochloric acid.

Anal. Calcd. for $C_{19}H_{14}O_3NCl$: C, 67.1; H, 4.12; N, 4.1; Cl, 10.4. Found: C, 67.3; H, 4.35; N, 4.0; Cl, 10.2.

6-Chloro-2-phenyl-4H-pyrano[3,2-h]quinoline-4-one (9)

A suspension of **8** (0.25 g) and selenium dioxide (0.3 g) in dioxan (8 ml) was refluxed at 110–120° for 18 h, diluted with acetic acid (10) and refltouxed. The reac-mlatedlytion mixture was repefilte,red (thrice) remove

Can. J. Chem. Downloaded from www.nrcresearchpress.com by 210.87.254.105 on 09/05/12
For personal use only.

suspended selenium and concentrated on a water bath. The product which separated was collected and crystallized from acetic acid in pinkish white needles, m.p. 273–274°; yield 0.1 g.

Anal. Calcd. for $C_{18}H_{10}O_2NCl$: C, 70.2; H, 3.25; N, 4.5; Cl, 11.5. Found: C, 70.1; H, 3.0; N, 4.3; Cl, 11.8.

*6-Chloro-2-p-anisyl-4H-pyrano[3,2-h]quinoline-4-one (**12**)*

It was formed on treating **11** (0.25 g) with selenium dioxide (0.3 g) in dioxan (10 ml) as described above. It was crystallized from acetic acid in light-yellow needles, m.p. 303–304°; yield 0.08 g.

Anal. Calcd. for $C_{19}H_{12}O_3NCl$: C, 67.5; H, 3.55; N, 4.1; Cl, 10.5. Found: C, 67.8; H, 3.7; N, 4.0; Cl, 10.9.

*6-Chloro-3-hydroxy-2-phenyl-4H-pyrano[3,2-h]quinoline-4-one (**10**)*

It was synthesized by two methods.

*By Algar–Flynn Oxidation of **8** (Method a)*

A solution of **8** (0.2 g) in a mixture of methanol (10 ml) and 10% sodium hydroxide solution (6 ml) was cooled to 0° and mixed with hydrogen peroxide (5 ml, 20%). The reaction mixture was kept initially at 0° for 6 h and then at room temperature for 24 h. The product obtained on acidification was crystallized from acetic acid in light-yellow shining needles, m.p. 267–268°; yield 0.05 g.

*By the Action of Pentyl Nitrite on **8** (Method b)*

To a suspension of **8** (0.2 g) and pentyl nitrite (0.5 ml) in ethanol (5 ml), concentrated hydrochloric acid (5 ml) was added dropwise at room temperature and the mixture was left at room temperature for 6 h. More pentyl nitrite (0.5 ml) was added to the mixture and the reaction mixture was allowed to stand at room temperature for 6 h more. It was then diluted with water (10 ml), refluxed on a water-bath for 2 h, cooled, and neutralized with ammonia. The product was repeatedly crystallized from acetic acid in light-yellow shining needles, m.p. 267–268°; yield 0.02 g.

Anal. Calcd. for $C_{18}H_{10}O_3NCl$: C, 66.7; H, 3.09; N, 4.3; Cl, 10.9. Found: C, 66.5; H, 3.2; N, 4.3; Cl, 11.2.

*6-Chloro-3-hydroxy-2-p-anisyl-pyrano-[3,2-h]quinoline-4-one (**13**)*

It was formed on treatment of **11** (0.2 g) with hydrogen peroxide (5 ml, 20%) as described above in method *a*. It was crystallized from acetic acid in yellow powder, m.p. 295–296° (decomp.); yield 0.05 g.

Anal. Calcd. for $C_{19}H_{12}O_4NCl$: C, 64.4; H, 3.39; N, 3.9; Cl, 10.0. Found: C, 64.6; H, 3.5; N, 3.7; Cl, 10.3.

*6-Chloro-3-benzoyl-2-phenyl-4H-pyrano-[3,2-h]quinoline-4-one (**14**)*

A mixture of **5** (0.2 g), benzoic anhydride (0.8 g), and triethylamine (2 ml) was refluxed at 170–180° for 6 h, cooled and diluted with ether (10 ml). The product which separated out was collected, washed, dried, and crystallized from acetic acid in white shining needles, m.p. 281–282°; yield 0.1 g. It remained unchanged when treated with hot 10% alkali solution.

Anal. Calcd. for $C_{25}H_{14}O_3NCl$: C, 72.9; H, 3.4; N, 3.4; Cl, 8.6. Found: C, 73.1; H, 3.2; N, 3.6; Cl, 8.8.

*Baker–Venkataraman Transformation Reaction of 5-Chloro-7-acetyl-8-hydroxyquinoline: Formation of 6-chloro-2-phenyl-4H-pyrano[3,2-h]quinoline-4-one (**9**)*

A mixture of **5** (0.5 g), benzoyl chloride (0.5 ml), and anhydrous potassium carbonate (1 g) in dry acetone (35 ml) was refluxed for 24 h and distilled to remove acetone. The product which separated on treating the reaction mixture with water (25 ml) was collected, treated with concentrated sulfuric acid (15 ml) and poured on crushed ice. The solid product was filtered, washed, dried, and crystallized from acetic acid in pinkish white needles, m.p. 273–274°; yield 0.2 g. Mixture m.p. with the product obtained by the selenium dioxide dehydrogenation of the flavanone type pyranoquinoline (**8**) showed no depression.

1. R. F. C. Brown, J. J. Hobbs, G. K. Hughes, and F. Ritchie. Australian J. Chem. **7**, 348 (1954).
2. H. Rapoport and K. G. Holden. J. Am. Chem. Soc. **81**, 3738 (1959); H. Rapoport and K. G. Holden. J. Am. Chem. Soc. **82**, 4395 (1960).
3. L. J. Drummond, F. N. Lahey, and W. O. Thomas. Australian J. Sci. Research, Ser. **A2**, 622, 630 (1949); T. R. Govindachari, B. R. Pai, and P. S. Subramaniam. Tetrahedron, **22**, 3245 (1966).
4. K. Elliott and E. Tittensor. J. Chem. Soc. 484 (1959); 2796 (1961).
5. Rabindranath Sen Gupta. J. Indian Chem. Soc. **22**, 171 (1945).
6. M. Weizmann and E. Bograchov. J. Am. Chem. Soc. **69**, 1222 (1947).
7. E. Hodel and H. Gysin. U.S. Pat. 2,875,126 (Feb. 24, 1959); E. Hodel and H. Gysin. Chem. Abstr. **53**, 15101 (1959); K. Matsumara. J. Am. Chem. Soc. **52**, 4433 (1930); V. M. Thakor and R. C. Shah. J. Indian Chem. Soc. **31**, 597 (1954).
8. C. W. Wilson. J. Am. Chem. Soc. **61**, 2303 (1939).
9. A. Arcoleo, A. Bellino, and P. Venturella. Ann. Chim. Rome **47**, 66 (1957); H. S. Mahal, H. S. Rai, and K. Venkataraman. J. Chem. Soc. 866 (1935); H. S. Mahal, H. S. Rai, and K. Venkataraman. J. Chem. Soc. 569 (1936); S. N. Chakravarti and M. Swaminathan. J. Indian Chem. Soc. **11**, 873 (1934).
10. T. S. Wheller. Record Chem. Progr. Kresge-Hooker Sci. Lib. **18**, 133 (1957).
11. A. S. Bhullar and K. Venkataraman. J. Chem. Soc. 1165 (1931); A. S. Bhullar and K. Venkataraman. Chem. Abstr. **25**, 4267 (1931).
12. A. V. Rama Rao, S. A. Telang, and P. Madhavan Nair. Indian J. Chem. **2**, 431 (1964).
13. G. W. Ewing and E. A. Steck. J. Am. Chem. Soc. **68**, 2181 (1946).
14. R. D. Desai and M. Ekhlas. Proc. Indian Acad. Sci. **8A**, 567 (1938); R. D. Desai and M. Ekhlas. Chem. Abstr. **33**, 3356 (1939).
15. M. R. Chakrabarty, E. S. Hanrahan, N. D. Heindel, and G. F. Watts. Anal. Chem. **39**, 238 (1967).
16. L. Doub and J. M. Vandenbelt. J. Am. Chem. Soc. **69**, 2714 (1947).
17. The chemistry of flavonoid compounds. *Edited by* T. A. Geissman, Pergamon Press, Paris. 1962. p. 151.
18. L. Jurd and R. M. Horowitz. J. Org. Chem. **22**, 1618 (1957).
19. T. A. Geissman. Modern methods of plant analysis. *Edited by* K. Peach and M. V. Tracey, Vol. III, Julius Springer, Berlin. 1955. p. 485.

Can. J. Chem. Downloaded from www.nrcresearchpress.com by 210.87.254.6 on 09/05/12
For personal use only.

A quantum mechanical study of proton exchange in sulfoxides with retention and inversion of configuration

ARVI RAUK[1] AND SAUL WOLFE[2]
Department of Chemistry, Queen's University, Kingston, Ontario

AND

I. G. CSIZMADIA
Lash Miller Chemical Laboratories, University of Toronto, Toronto, Ontario

Received May 21, 1968

A survey of the experimental data on the structures of α-sulfonyl and α-sulfinyl carbanions is presented as an introduction to the present work, a theoretical study of hydrogen methyl sulfoxide (HMSO) and hydrogen methylsulfinyl anion ($HMSO^-$) by nonempirical self consistent field (s.c.f.) calculations using Gaussian basis sets. Calculations on dimethyl sulfoxide (DMSO) and its conjugate base ($DMSO^-$) are also presented and fully justify the choice of HMSO and $HMSO^-$ for the detailed work. A conformational energy surface (total energy as a function of rotation about the C—S bond and inversion of the carbanion angle) for $HMSO^-$ is presented and used to determine the stereochemical fate of a carbanion generated next to a sulfinyl group. Predictions are made concerning the probable course of proton exchange next to S—O and an explanation is offered for the experimental facts concerning exchange in sulfoxides. A very significant finding is that postulation of d-orbital conjugation is not essential to explain the asymmetry of α-sulfinyl carbanions.

Canadian Journal of Chemistry, **47**, 113 (1969)

Introduction

Although the synthetic capabilities of carbanions are well known, their structures and symmetry properties have aroused serious attention only during the last decade and mainly as a result of the systematic studies of Cram and his co-workers (1). The method of attack has usually involved base-catalyzed hydrogen–deuterium exchange at an asymmetric carbon, the ratio of k_e, the rate constant for isotopic exchange, to k_α, the polarimetric rate constant, being used to decide whether the process occurs with retention, racemization, inversion, or isoinversion. Several generalizations have been reached concerning the way in which data, obtained from one-point pseudo first order rate constants, depend upon the structure of the substrate and the nature of the solvent. In particular, carbanions stabilized by adjacent second row element functional groups have fallen into two distinct classes: (*i*) those which undergo substitution with high retention of configuration, i.e., via an intrinsically asymmetric intermediate ($k_e/k_\alpha \gg 1$); (*ii*) those which undergo substitution via an intrinsically symmetrical intermediate ($k_e/k_\alpha \simeq 1$). In all cases k_e/k_α is strongly dependent upon the solvent composition but, in nonaqueous media, no crossover is seen. Thus **1** behaves as if it were asymmetric with asymmetric solvation effects superimposed, and **2** behaves as if it were symmetric at carbon with asymmetric solvation effects superimposed (2).

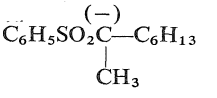

1

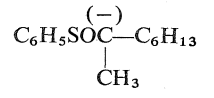

2

The α-sulfonyl system has been the most completely studied (3–10) without, however, general agreement having been reached on the origin of its asymmetry. Such a decision depends strongly upon the value taken for the carbanion angle as well as the conformational dependence of any interaction between the electron pair on carbon and the sulfur atom. A pyramidal configuration at carbon would retain asymmetry if there were a sufficiently high barrier to inversion irrespective of the form of the rotational energy function, i.e., **3** can protonate to give **4** but not **5** (it is assumed that protonation with inversion of configuration is indistinguishable from proton capture by an inverted carbanion).

[1]Holder of NRCC Studentships 1966–1968.
[2]To whom correspondence should be addressed.

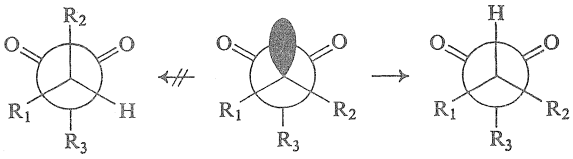

5 3 4

On the other hand, if the configuration at carbon is planar, asymmetry is possible if the structure is **6** and rotation to the symmetrical conformation **7** is restricted. Structures **6** and **7** are, respectively, the Case II and Case I conformations of Koch and Moffitt (11).

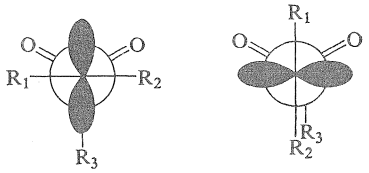

6 7

Corey and his co-workers have made a number of ingenious attempts to obtain experimental information about these possibilities. Base-catalyzed decarboxylation (6) of the α-carboxy sulfone **8**, which presumably proceeds via an α-sulfonyl carbanion that is free to adopt its most stable structure, affords phenyl 2-octylsulfone with at least 97% retention of configuration (7). In contrast, the α-carboxy sulfone **9** decarboxylates via a conformationally constrained α-sulfonyl carbanion that behaves as if it were symmetric (6) with asymmetric solvation effects superimposed (10). It was argued that the intermediate from **8** cannot be pyramidal,

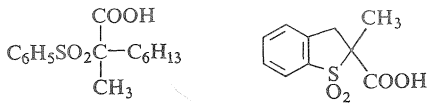

8 9

i.e., with a significant barrier to inversion, for the same degree of stereospecificity would then be expected from both **8** and **9**. However, this would be true only in the event that there were no conformational dependence of the inversion barrier.

The ratios of k_e/k_α were 58 and 41, respectively, for the H/D exchange of the sulfones **10** and **11** (6). It was argued that, if asymmetric sulfonyl

10, R = *t*-Bu

11, R = *n*-C_6H_{13}

carbanions possess the pyramidal structure, the rate of racemization of the carbanion from **10** should be far greater than that for the carbanion from **11** because of the ability of *t*-butyl to accelerate the pyramidal → planar conversion. However, if the pyramidal → planar conversion simply generated a Case II conformation, the two systems would retain asymmetry but for different reasons. Thus it seems that one is not compelled, as Corey suggests, to confer Case II planar geometry upon an α-sulfonyl carbanion.

Cram and Wingrove suggested (9) that the configuration at carbon is pyramidal and the electron pair is directed *anti* to the polar S—O bonds (electrostatic repulsion). However, in a beautifully conceived experiment, Corey and Lowry (8) demonstrated that protonation of anion **13**, generated by reverse aldol cleavage of the hydroxysulfone **12**, takes place with inversion of configuration, i.e., from the same side as the oxygen atoms. This is not shielding of the developing carbanion by the departing formyl group because similar shielding in the decarboxylation of **8** and related compounds should have led to predominant inversion rather than retention of configuration.

It seems then that the electron pair in **13** is directed along the acute bisector of the OSO angle. The result can be interpreted to mean either that there is highly asymmetric solvation of a planar (Case II) anion or spontaneous inversion of a pyramidal anion to that structure which has the electron pair directed along the bisector of the OSO angle. The results of Broaddus (12) may be consistent with the latter conclusion. In $NaOD/D_2O$ the most acidic proton in a mixture of **14***a* and **14***b* is the α-*vinyl* proton of

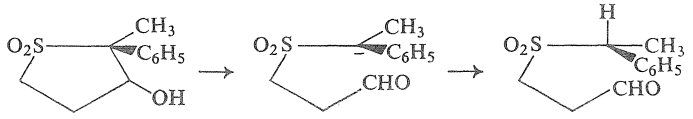

12 13

Can. J. Chem. Downloaded from www.nrcresearchpress.com by 210.87.254.6 on 09/05/12
For personal use only.

14*a*. It is not yet known whether this exchange occurs via the vinyl carbanion or by a reversible Michael addition. For the analogous exchange of the 4*H*-thiopyran-4-one 1,1-dioxide (**15***a* → **15***b*), the latter explanation is preferred (13).

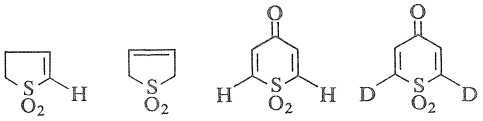

14*a* **14***b* **15***a* **15***b*

The data concerning α-sulfinyl carbanions are less detailed. Cram and Pine (14) used non-aqueous media for their studies with the diastereomeric phenyl 2-octylsulfoxides and, as mentioned earlier, they concluded that **2** is an intrinsically symmetrical species. Not only is the S—O grouping less able to confer asymmetry upon an adjacent carbanion than the SO_2 grouping, its acidifying effect upon α-protons is less. The second order rate constants for exchange of **11**-*d* at 25° were (4) 3.06×10^{-3} l mole^{-1} s^{-1} in MeOH/MeOK/DMSO and 1.45×10^{-2} l mole^{-1} s^{-1} in *t*-BuOH/*t*-BuOK. For the exchange of *R*:*S* phenyl 2-octyl sulfoxide-*d* (14, 15) *at 60°*, the rate constants were 8.5×10^{-4} l mole^{-1} s^{-1} in DMSO/MeOK and 1.8×10^{-5} l mole^{-1} s^{-1} in *t*-BuOH/*t*-BuOK. A number of earlier examples are summarized by Price and Oae (16).

In contrast to these results, dimethyl sulfoxide was found to undergo facile hydrogen exchange in NaOD/D_2O (17). Even more unexpected was the finding that benzyl methyl sulfoxide also undergoes facile hydrogen exchange in NaOD/D_2O via an asymmetric intermediate (18). It was demonstrated that at 15° *S*-benzyl methyl sulfoxide is converted sequentially, without loss of asymmetry at sulfur, to *S*,*S*-benzyl-α-*d* methyl sulfoxide, *S*-benzyl-α,α-d_2 methyl sulfoxide, and *S*-benzyl-α,α-d_2 methyl-d_3 sulfoxide (19). Analysis of the nuclear magnetic resonance (n.m.r.) spectrum of *S*-benzyl methyl sulfoxide led to the conclusions that its structure in NaOD/D_2O is **16** and that the structure of the derived asymmetric carbanion is **17**, i.e., carbanion electron pair along the bisector of the oxygen:sulfur:lone pair angle.

In this paper we show by nonempirical LCAO-MO-SCF calculations that an α-sulfinyl carbanion is intrinsically asymmetric, that the carbanion angle is pyramidal, that the most stable

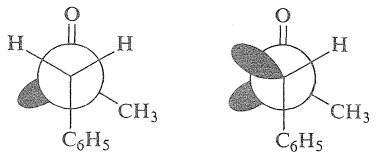

16 **17**

structure has the electron pair along the bisector of the oxygen:sulfur:lone pair angle, and that d-orbital conjugation is not a significant factor in determining the asymmetry. It is demonstrated further that the rate of proton abstraction and the stereochemistry of reprotonation will depend strongly upon the orientation of the exchanging proton relative to the groups on sulfur.

Method

For practical reasons, and because it had been shown previously that meaningful results can be obtained with a minimal basis set (20), the minimal basis set of Gaussian-type functions (GTF) was used in calculations on hydrogen methyl sulfoxide (HMSO, **18**) and its carbanion ($HMSO^-$, **19**). The basis set size for **18** was 33 and for **19** it was 32 consisting of sulfur 5^s, 2^p, 1^d, oxygen 3^s, 1^p, carbon 3^s, 1^p and hydrogen 1^s. The exponents for the GTF are listed in Table I.

18 **19**

The geometry of **18** paralleled as closely as possible the experimentally determined (22) geometry of dimethyl sulfoxide (∠CSH = 100°, ∠CSO = ∠HSO = 107°, C—S = 3.43935 bohr (1.82 Å); S—H = 2.5117 bohr (1.329 Å[3]); C—H = 2.04093 bohr (1.08 Å); ∠HCH = ∠SCH = 109° 28′). Rotation of the methyl group was treated as a variable.

The geometry of the anion **19** was the same as for **18** except that both rotation about the C—S bond (Θ) and variation of the anion angles (∠SCH = ∠HCH = ϕ) were treated as variables.

The mathematical formalism for the closed shell s.c.f. as well as other calculations (dipole moment, and electron population analysis) have been reviewed recently (23) in detail. Consequently only the computational results are given here. The computations were carried out on an IBM 7094-II computer using the POLYATOM system (23). The running time for a given conformation was about 30 min. It was assumed from the beginning that the results of the calculations would be meaningful despite the presence of an S—H bond in **18** and **19**. After the initial stage of the work was completed, calculations were performed on methyl sulfinyl carbanion to test the severity of this assumption.

[3]The S—H distance in mercaptans (22).

Can. J. Chem. Downloaded from www.nrcresearchpress.com by 210.87.254.6 on 09/05/12
For personal use only.

Can. J. Chem. Downloaded from www.nrcresearchpress.com by 210.87.254.6 on 09/05/12
For personal use only.

TABLE I

Exponents for Gaussian type functions

Center	Type	Exponent (α)	Reference
S	*s*	0.5581 3.151 17.79 100.44 567.05	20
	p	0.375 6.332	20
	d	5.42	20
O	*s*	1.20 9.45 74.7	20
	p	0.749	20
C	*s*	0.634 5.00 39.6	20
	p	0.382	20
H	*s*	0.283	21

Hydrogen Methyl Sulfoxide

Figure 1 shows the variation of the total energy of **18** as a function of rotation about the C—S bond. The positions of the energy minima and maxima correspond neither to those of ethane ($\Theta = 0°$ and 60°, respectively) nor to those of acetaldehyde ($\Theta = 60°$ and 0°, respectively (24)), but are about midway between, $\Theta = 21°$ and 81°.

Consideration of the components which make up the total energy reveals that for HMSO only

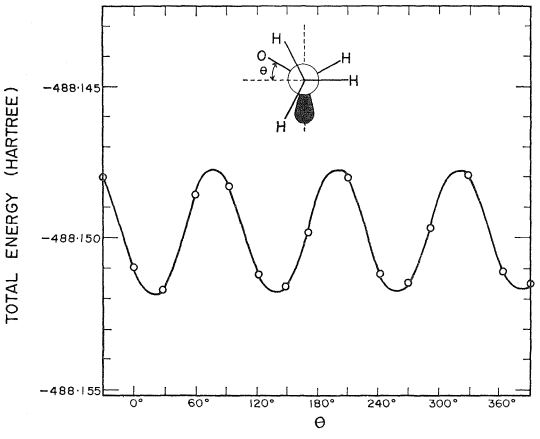

FIG. 1. Variation of the total energy of HMSO as a function of rotation about the C—S bond.

the nuclear–nuclear repulsion term displays ethane-type behavior. This can be seen in Fig. 2 where it is evident that the total energy reflects a balance between attractive (V_{ne} = nuclear–electron attraction) and repulsive (V_{ee} = electron–electron repulsion; V_{nn} = nuclear–nuclear repulsion; T = kinetic energy)[4] interactions. Although the compound exists because the large negative contribution from V_{ne} outweighs the other three, the phase of the total energy is that of the repulsive interactions which, together, counterbalance V_{ne} in deciding the geometry of the compound. The barrier heights associated with the individual terms are: V_{ne}, 58.0 kcal/mole; V_{ee}, 32.6 kcal/mole; V_{nn}, 12.6 kcal/mole, and T, 18.2 kcal/mole. For comparison purposes the corresponding quantities for ethane from s.c.f. calculations using Hartree–Fock atomic orbitals are (26): V_{ne}, 19.7 kcal/mole; V_{ee}, 9.5 kcal/mole; V_{nn}, 4.7 kcal/mole; and T, 8.2 kcal/mole. Whether the differences are due to the different basis sets used or to a property of the S—O grouping is not clear but it is noteworthy that the barrier height for the total energy of HMSO (2.68 kcal) does not differ significantly from that calculated for related systems, including ethane (26–28).

Allen and his co-workers (26–28) have proposed that the barriers in ethane, methylamine, methanol, hydrogen peroxide, hydrazine, and hydroxylamine can be understood by consideration of the one-electron ($V_{ne} + V_{nn} + T$) and two-electon (V_{ee}) components of the total energy. They find that in each case these two terms possess opposite phase. For ethane, methylamine, and methanol the phase of total energy is the same as that of the two-electron component. But for hydrazine, hydrogen peroxide, and hydroxylamine this is not the case, no simple relationship between the phase of total energy and that of either of the two components being apparent. Significantly the latter three compounds possess in each case at least one pair of electrons on each of two contiguous atoms. A very striking indication of the anomalous behavior produced by such a system is shown in Fig. 3, a reproduction of Allen's total energy data for hydrazine. *The*

[4]The kinetic energy term enters as a positive number and with the same phase as the repulsive interactions as a consequence of the virial theorem (25). According to this $-\Sigma V/2T = 1$ for an exact wave function, deviations from unity being taken as a measure of the inexactness of the actual wave function. For the minimal basis set used here, $-\Sigma V/2T = 1.0065$ (see Table II).

Can. J. Chem. Downloaded from www.nrcresearchpress.com by 210.87.254.6 on 09/05/12
For personal use only.

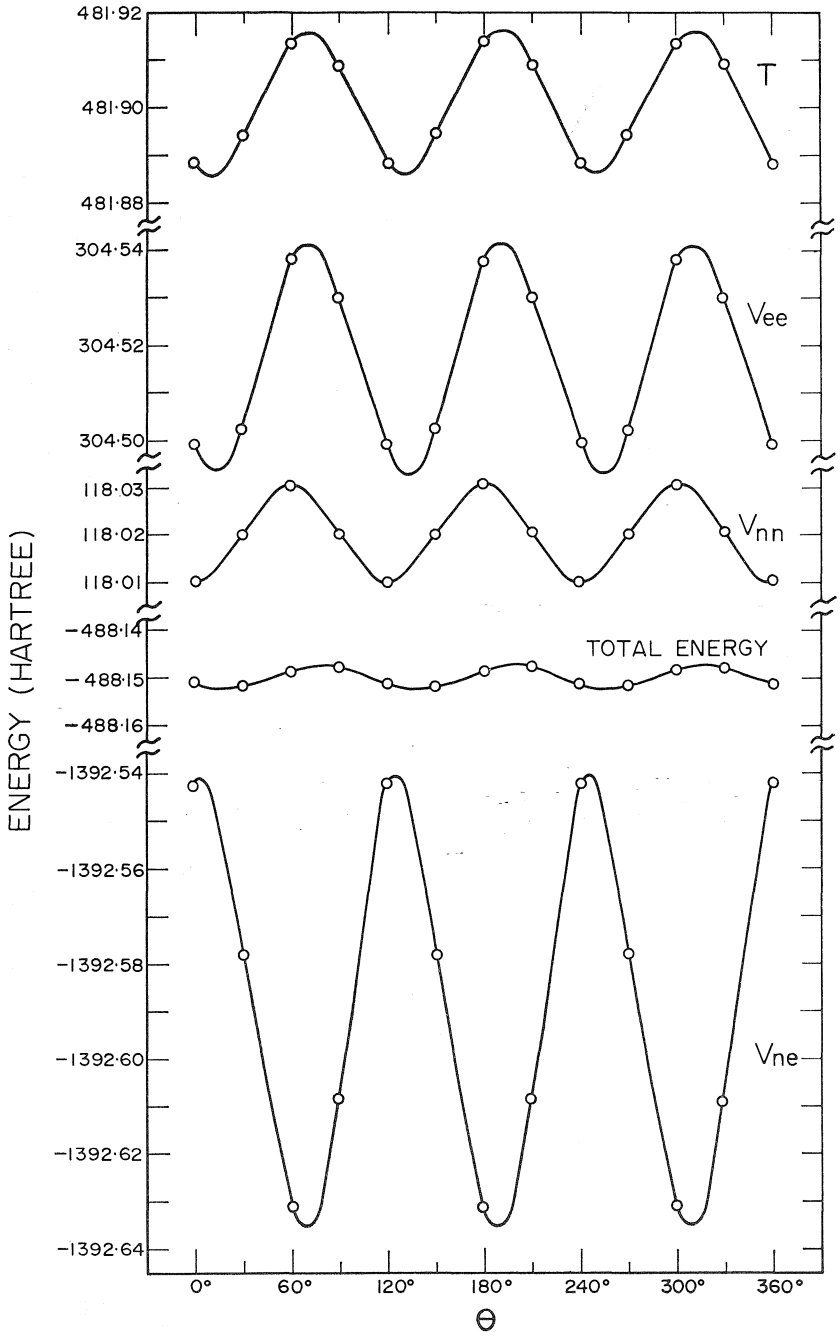

FIG. 2. The total energy of HMSO and the components of the total energy of HMSO as a function of rotation about the C—S bond.

Can. J. Chem. Downloaded from www.nrcresearchpress.com by 210.87.254.6 on 09/05/12
For personal use only.

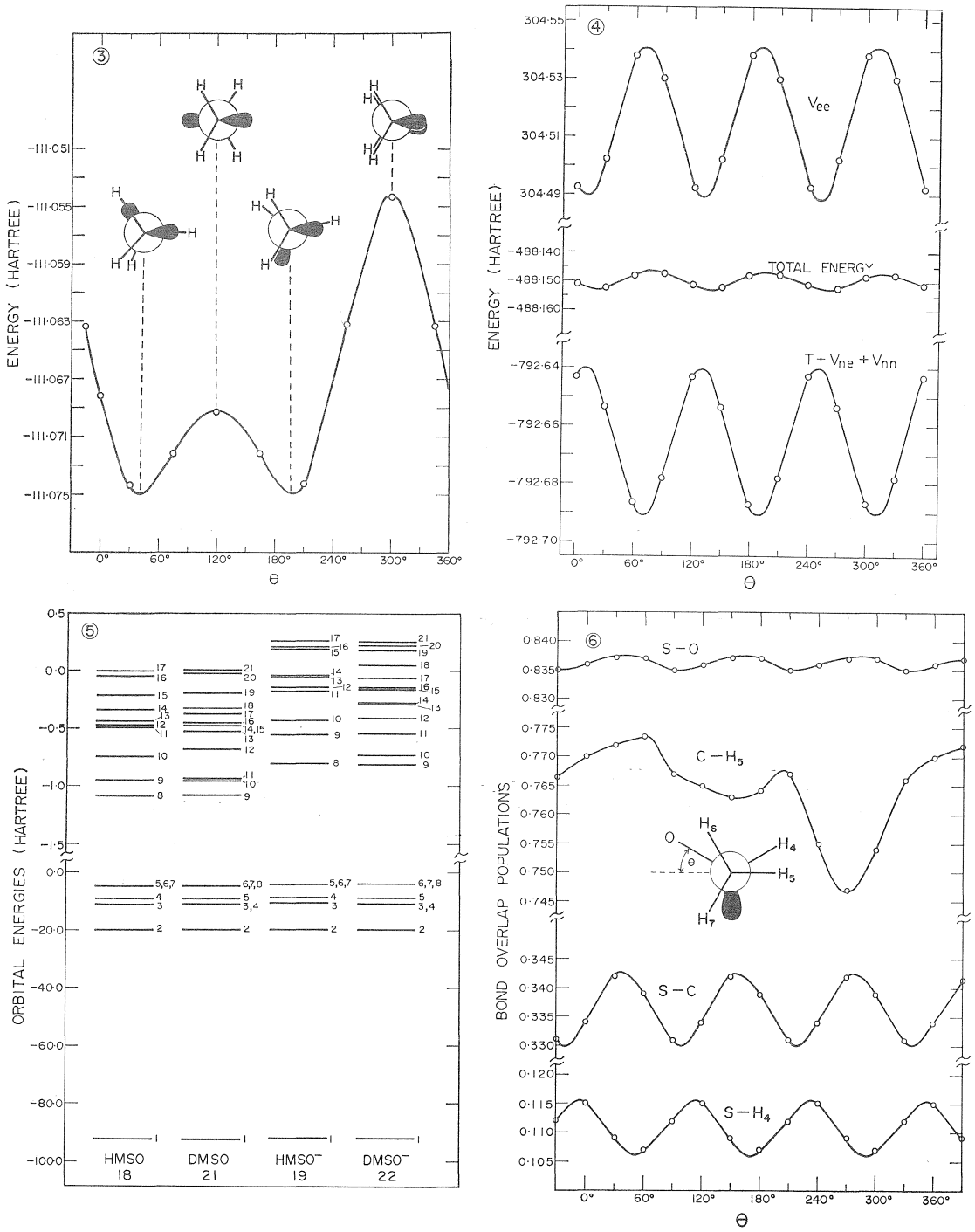

FIG. 3. The total energy of hydrazine as a function of rotation about the N—N bond (from ref. 28).
FIG. 4. The total energy of HMSO and the one- and two-electron components of the total energy of HMSO as for a function of rotation about the C—S bond.
FIG. 5. The orbital energies of HMSO and DMSO for the conformation $\Theta = 0°$, and of $HMSO^-$ and $DMSO^-$ the favored conformations (see text).
FIG. 6. Bond overlap populations for HMSO as a function of rotation about the C—S bond.

Can. J. Chem. Downloaded from www.nrcresearchpress.com by 210.87.254.6 on 09/05/12
For personal use only.

TABLE II

Total energy and molecular orbital energies of hydrogen methyl sulfoxide as a function of methyl rotational angle Θ

		Energy (Hartree)			
Θ		0°	30°	60°	90°
MO	1	−92.2275	−92.2329	−92.2310	−92.2257
	2	−19.9095	−19.9044	−19.9044	−19.9090
	3	−11.0604	−11.0618	−11.0605	−11.0592
	4	−9.0275	−9.0317	−9.0301	−9.0260
	5	−4.6152	−4.6195	−4.6179	−4.7137
	6	−4.6099	−4.6141	−4.6125	−4.6084
	7	−4.6038	−4.6081	−4.6064	−4.6023
	8	−1.0900	−1.0895	−1.0890	−1.0893
	9	−0.9382	−0.9386	−0.9380	−0.9377
	10	−0.7405	−0.7414	−0.7411	−0.7402
	11	−0.4960	−0.4976	−0.4971	−0.4955
	12	−0.4752	−0.4754	−0.4767	−0.4768
	13	−0.4307	−0.4308	−0.4278	−0.4278
	14	−0.3388	−0.3385	−0.3378	−0.3381
	15	−0.2146	−0.2136	−0.2136	−0.2144
	16	−0.0494	−0.0481	−0.0478	−0.0489
	17	−0.0009	−0.0000	+0.0012	+0.0006
T		481.8884	481.8940	481.9135	481.9091
V_{ee}		304.4922	304.5021	304.5382	304.5303
V_{nn}		118.0105	118.0201	118.0304	118.0207
V_{ne}		−1392.5421	−1392.5678	−1392.6307	−1392.6081
Total		−488.1510	−488.1516	−488.1486	−488.1479
$-\Sigma V/2T$		1.00650	1.00649	1.00647	1.00647
Geometry		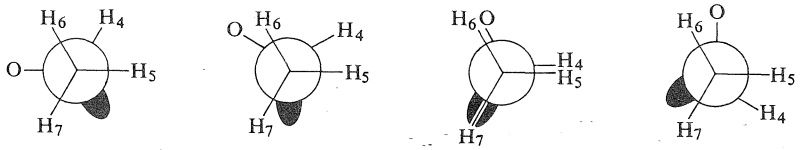			

conformation in which the electron pairs on nitrogen are trans to each other represents an energy maximum.

Figure 4 shows an Allen plot for HMSO. The compound resembles ethane, methanol, and methylamine with the difference that the minima and maxima for total energy are slightly shifted from those of the one- and two-electron components. On the basis of this plot it would appear that the form of the barrier is not greatly affected by the presence of the SO grouping or the availability of d-orbitals.

The orbital energies for the individual atoms of HMSO have been published previously (20, 29). Table II gives the total energy and orbital energies of HMSO for conformations in which the methyl group is rotated through 0°, 30°, 60°, and 90°, and the first column of Fig. 5 shows these orbital energies graphically for the 0° conformation.

The variation of the total energy with Θ is not attributable in any simple way to the behavior of the individual molecular orbital energies. The coefficient matrices reveal that the highest occupied molecular orbital, no. 17, is largely a lone pair in an oxygen p-type atomic orbital that is directed in the plane of the bisector of the CSH angle.[5] Molecular orbital no. 16 is largely made up of a lone pair in an oxygen p-type atomic orbital that is directed perpendicular to the plane of the bisector of the CSH angle and has a small but significant contribution from a sulfur p-type orbital, suggestive of π-type bonding. Electron density contour plots of the analogous molecular orbitals of dihydrogen sulfoxide (H_2SO) (orbitals

[5] i.e., as in 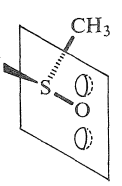

Can. J. Chem. Downloaded from www.nrcresearchpress.com by 210.87.254.6 on 09/05/12
For personal use only.

TABLE III

Dipole moment and electron distribution analysis of **18** as a function of methyl rotational angle Θ

Quantity	Site	Θ 0°	30°	60°	90°
Dipole moment (Debye)		2.40	2.41	2.33	2.32
Net charges	Carbon	−0.105	−0.110	−0.113	−0.109
	Sulfur	1.111	1.104	1.103	1.109
	Oxygen	−0.147	−0.136	−0.136	−0.147
	Hydrogen-4	−0.534	−0.536	−0.538	−0.536
	Hydrogen-5	−0.104	−0.095	−0.092	−0.100
	Hydrogen-6	−0.111	−0.114	−0.110	−0.106
	Hydrogen-7	−0.109	−0.113	−0.114	−0.110
Overlap populations	S—O Bond	0.836	0.837	0.837	0.835
	S—C Bond	0.334	0.342	0.339	0.331
	S—H_4 Bond	0.115	0.109	0.107	0.112
	C—H_5 Bond	0.770	0.772	0.773	0.767
	C—H_6 Bond	0.755	0.747	0.754	0.766
	C—H_7 Bond	0.765	0.763	0.764	0.767

no. 13 and 12) may be seen in Fig. 5 of ref. 20. Molecular orbital no. 15 is more highly delocalized but has largely the characteristics of a σ-type bond between sulfur and oxygen due to overlap of p-orbitals aligned with the S—O bond. Molecular orbital no. 14 is more delocalized still but is attributable, in large part, to the lone pair on sulfur. Molecular orbitals 13 and 8 constitute σ bonds between carbon and sulfur, and oxygen and sulfur respectively.

Table III contains the variation of dipole moment as a function of Θ as well as electron population analyses for the four conformations. Figures 6 and 7 display, respectively, the bond overlap populations and the net atomic charges as a function of Θ. From Fig. 6 the strength of the C—H bond, as judged from overlap populations, would be predicted to be least when it is situated approximately between oxygen and the lone pair. As Fig. 7 shows, there is a periodicity in net charge for all atoms except the hydrogens of the methyl group. Unfortunately, a quantitative estimation of the relative acidities of the hydrogens as a function of Θ cannot be inferred from the computed net charges because the minimal basis set used for hydrogen always gives the wrong sign (23, and references therein).

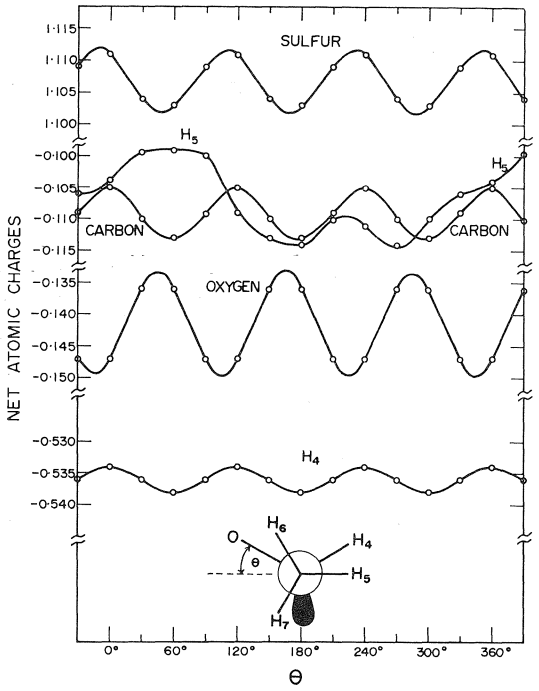

FIG. 7. Net atomic charges in HMSO as a function of rotation about the C—S bond.

Hydrogen Methyl Sulfinyl Anion

The conformation of $HMSO^-$ was defined by two independent parameters, the rotational angle Θ about the C—S bond, and the anion angle φ where $\angle H_6CH_7 = \angle SCH_6 = \angle SCH_7 = \phi$. Figure 8 shows the variation of the total energy of $HMSO^-$ as a function of Θ and φ. Horizontal

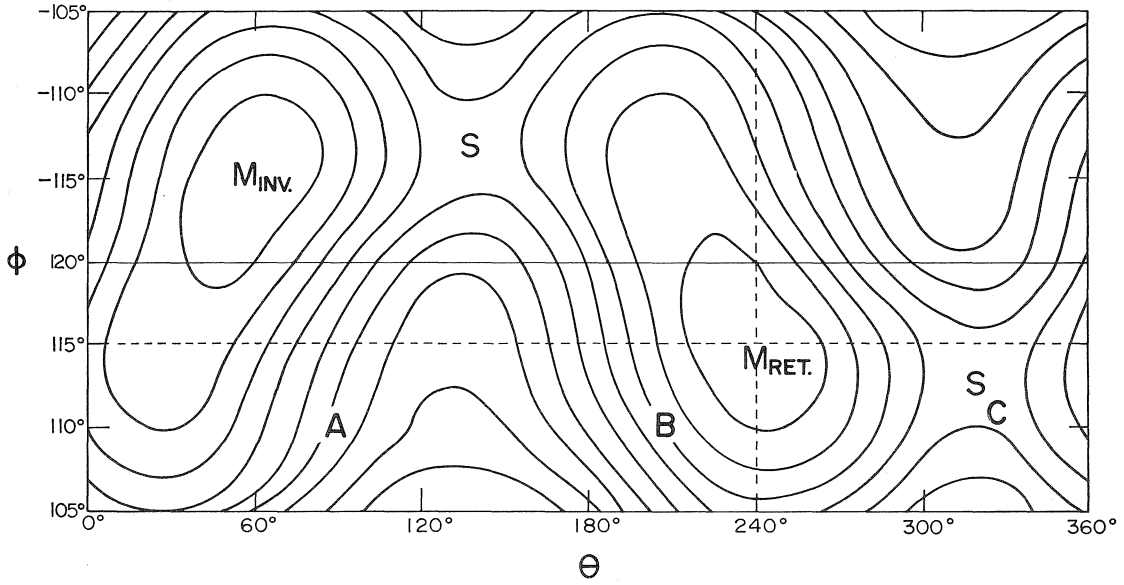

FIG. 8. Variation of the total energy of $HMSO^-$ as a function of rotation about the C—S bond (Θ) and inversion of the carbanion angle (ϕ).

movement across the surface corresponds to rotation about the C—S bond with anion angles fixed. A vertical movement across the center line represents inversion of the carbanion. Figure 9 is a projection of the three dimensional surface. Two cross-sections through the energy minimum, represented by the dashed lines of Figure 8, have already been published (Figs. 2 and 3 in ref. 30) and are reproduced in Figs. 10 and 11 along with their associated Allen plots. Figure 10 is the horizontal cross-section ($\phi = 115°$) and Fig. 11 the vertical cross-section ($\Theta = 240°$). The signs of the values of ϕ in Fig. 8 serve only to designate whether the location is on the upper or lower half of the energy surface. The signs of the ϕ values in Fig. 11 are consistent with this convention. The absolute values of ϕ represent the actual carbanion angles.

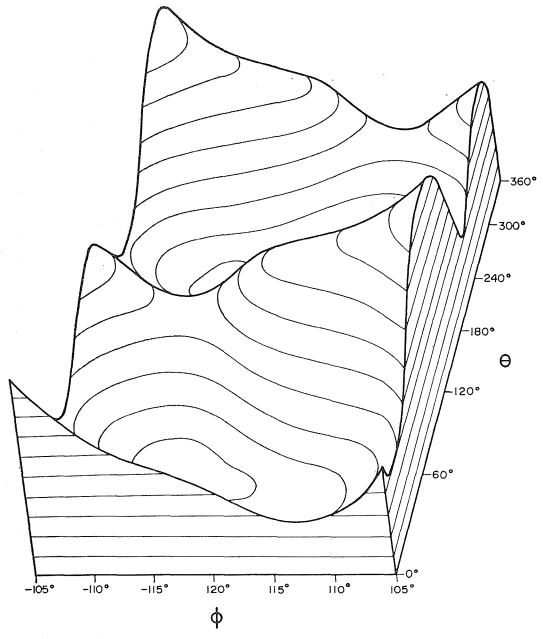

FIG. 9. A projection of the three dimensional surface of Fig. 8.

It is very clear from Fig. 11 that there is no barrier to inversion of the carbanion as was found in the case of $CH_3^{(-)}$ (31). This is, in fact, true of any of the vertical cross-sections of the energy surface as can be seen by inspection of the three-dimensional projection (Fig. 9). There are two identical minima (M) and two identical saddle points (S) on the surface so that a combination of rotation through 180° and inversion of the carbanion angle will reproduce any conformation. The energy barrier to rotation about the C—S bond in $HMSO^-$ is the difference in energy between S and M (Fig. 8) and is equal to 0.0121 Hartree (7.6 kcal/mole). This barrier is almost three times as high as the calculated barrier to

Can. J. Chem. Downloaded from www.nrcresearchpress.com by 210.87.254.6 on 09/05/12
For personal use only.

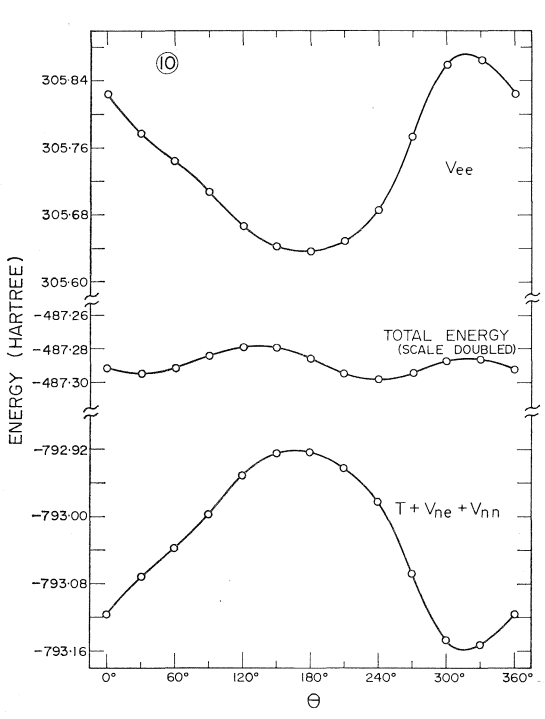

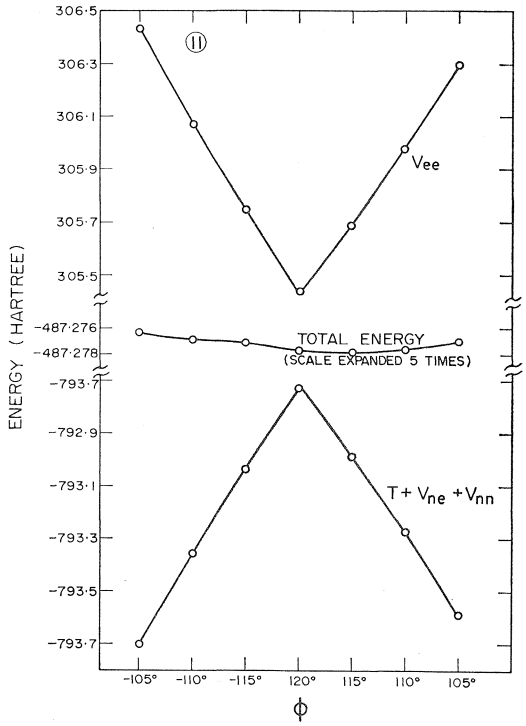

FIG. 10. Total energy of $HMSO^-$ as a function of rotation about the C—S bond ($\phi = 115°$), together with the one- and two-electron components of the total energy.

FIG. 11. Total energy of $HMSO^-$ as a function of the carbanion angle (ϕ) for the favored rotational conformer ($\Theta = 240°$), together with the one- and two-electron components of the total energy.

rotation in the hydrocarbon HMSO, and reflects increased electronic interaction between the carbanion and the sulfinyl grouping.

Probing of this interaction with the Allen plots is not very helpful. Like the systems mentioned earlier which contain electron pairs on contiguous atoms, no relationship is apparent between the phase of total energy and those of the one-electron and two-electron components. This is true for both rotation and inversion. In this respect $HMSO^-$ resembles hydrazine, methanol, and hydrogen peroxide despite the presence of the second row atom and the availability of d-orbitals.

The conformation of the anion with minimum energy is shown in Fig. 12*a*. The carbanion lone pair is situated in the plane of the bisector of the O:S:lone pair angle. The conformation which corresponds to the higher minimum of Fig. 10 has carbanion lone pair *trans* to oxygen; the two maxima of Fig. 10 correspond to carbanion lone pair *trans* to the sulfur lone pair (higher) and carbanion lone pair nearly eclipsed with the sulfur lone pair (lower).

From the energy surface (Fig. 9) it can be predicted that a carbanion generated in any conformation will spontaneously convert to that having the anion lone pair in the plane of the bisector of the O:S:lone pair angle. The ability to generate a carbanion at different points on the surface will depend on the orientation of the departing proton with respect to the groups on sulfur, as will be discussed in a following section.

Table IV lists the molecular orbital energies of the conformations of **19** shown in Figs. 12*a* and 12*b*. The latter has the conformation corresponding to the higher maximum of Fig. 10 (carbanion lone pair *trans* to the sulfur lone pair). Molecular orbitals 12, 14, and 17 have a significantly lower energy in the most stable conformation. These molecular orbitals correspond to a carbon–hydrogen bond, the sulfur–oxygen π-type bond and, surprisingly, the oxygen lone pair that is in the plane of the bisector of the HSC angle,

Can. J. Chem. Downloaded from www.nrcresearchpress.com by 210.87.254.6 on 09/05/12
For personal use only.

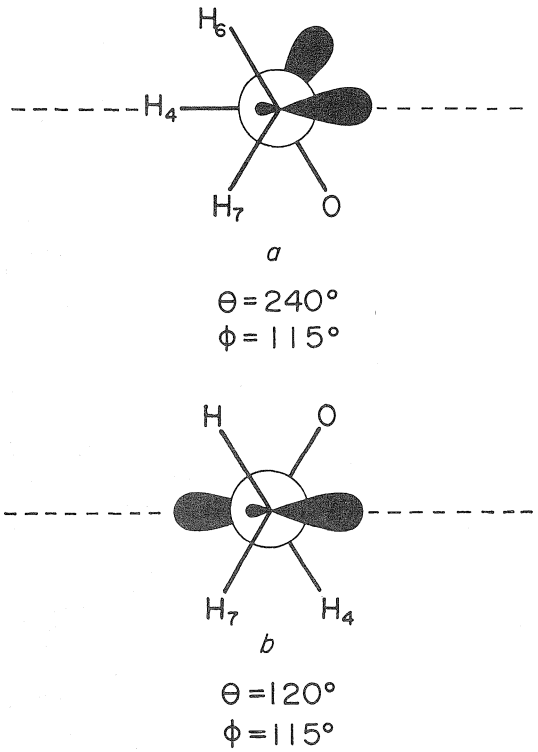

FIG. 12. (*a*) A Newman projection of the conformation of $HMSO^-$ which has minimum energy. (*b*) A Newman projection of the conformation of $HMSO^-$ which has maximum energy when $\phi = 115°$.

TABLE IV

A comparison of molecular orbital energies between conformations of $HMSO^-$ having energy minima ($\phi = 115°$, $\Theta = 240°$) and Maxima ($\phi = 115°$, $\Theta = 120°$)

	Energy (Hartree)	
MO	$\phi = 115°$, $\Theta = 240°$	$\phi = 115°$, $\Theta = 120°$
1	−91.9392	−91.9371
2	−19.6200	−19.6223
3	−10.5947	−10.5927
4	−8.7426	−8.7414
5	−4.3312	−4.3302
6	−4.3255	−4.3242
7	−4.3211	−4.3191
8	−0.8083	−0.8096
9	−0.5497	−0.5491
10	−0.4322	−0.4365
11	−0.1792	−0.1787
12	−0.1410	−0.1227
13	−0.0615	−0.0789
14	−0.0451	−0.0314
15	0.1904	0.1954
16	0.2125	0.2115
17	0.2575	0.2742
Total	−487.2979	−487.2784

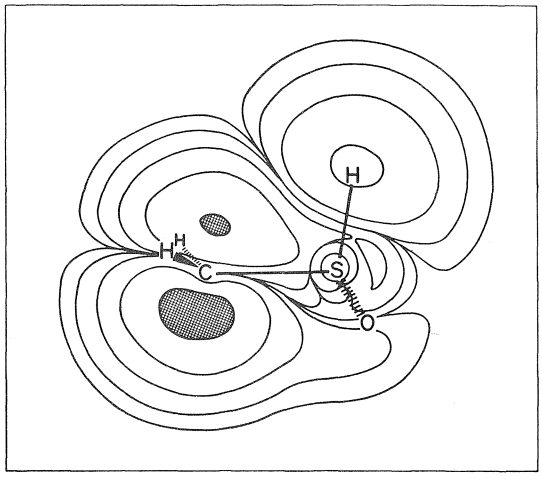

FIG. 13. An electron contour drawing of the third highest molecular orbital of $HMSO^-$ showing the elements of an sp^3 hybrid orbital on carbon.

respectively. Molecular orbital 15, which corresponds to the carbanion lone pair, is also lowered in energy, although not to the same extent as the three mentioned above. The electron contour drawing for this orbital in the plane containing the C—S bond and bisecting the HCH angle is shown in Fig. 13. Although this molecular orbital is completely delocalized, the elements of an sp^3 hybrid orbital on carbon can be recognized and are indicated by the shading of the areas of highest electron density.

The molecular orbital energies of the favored conformation of $HMSO^-$ are shown in the third column of Fig. 5.

Table V compares the electron population analyses of the conformations shown in Figs. 12*a* and 12*b*. The net charge on carbon is less and the overlap population of the S—C bond is greater in the more stable conformation. This suggests that when the carbanion lone pair is projected in a plane that bisects the oxygen:sulfur:lone pair angle there is particularly favorable delocalization of carbanionic charge into the sulfinyl group. This is qualitatively similar to the enolization process except that the anion is not flat as classical theory requires nor does the sulfinyl group need to become planar.

Figure 14 shows a contour map for the overlap population of the carbon–sulfur bond as a function of Θ and ϕ. The overlap population is maximum for the conformation ($\Theta = 240°$,

Can. J. Chem. Downloaded from www.nrcresearchpress.com by 210.87.254.6 on 09/05/12
For personal use only.

TABLE V

A comparison of electron population analyses between conformations having energy minima ($\phi = 115°$, $\Theta = 240°$) and maxima ($\phi = 115°$, $\Theta = 120°$)

Quantity	Site	$\phi = 115°$, $\Theta = 240°$	$\phi = 115°$, $\Theta = 120°$
Net charges	Sulfur	1.0093	1.0054
	Oxygen	−0.2869	−0.2785
	Carbon	−0.4092	−0.4223
	Hydrogen-4	−0.6314	−0.6233
	Hydrogen-6	−0.3399	−0.3416
	Hydrogen-7	−0.3418	−0.3397
Overlap populations	S—O Bond	0.7894	0.7963
	S—C Bond	0.5313	0.4706
	S—H_4 Bond	−0.0156*	−0.0092*
	C—H_6 Bond	0.6914	0.6809
	C—H_7 Bond	0.6754	0.6919

*A negative overlap population has no physical meaning and should be taken as zero.

$\phi = 115°$) and minimum in the region ($\Theta = 120°$, $\phi = 110°$). Figure 15 shows a similar contour map for the overlap population of the oxygen–sulfur bond. The S—O bond overlap population is minimum in the region $\Theta = 240°$ and $\Theta = 60°$ and maximum in the region $\Theta = 120°$ and $\Theta = 300°$.

The Role of the d-Orbitals

It has become customary to associate unusual structural or chemical effects arising from the introduction of a second or third row atom into a compound with the availability of d-orbitals for bonding. One simply chooses a set of coordinate axes such that the symmetry of an atomic d-orbital is correct for overlap with an adjacent p- or sp^3-hybrid orbital and then draws some diagram to illustrate the proposed interaction. We believed, at the outset of the present work, that inclusion of sulfur d-type GTF in the minimal basis set would permit an evaluation of the importance and, indeed, the *nature* of the d-orbital interaction in an α-sulfinyl carbanion.

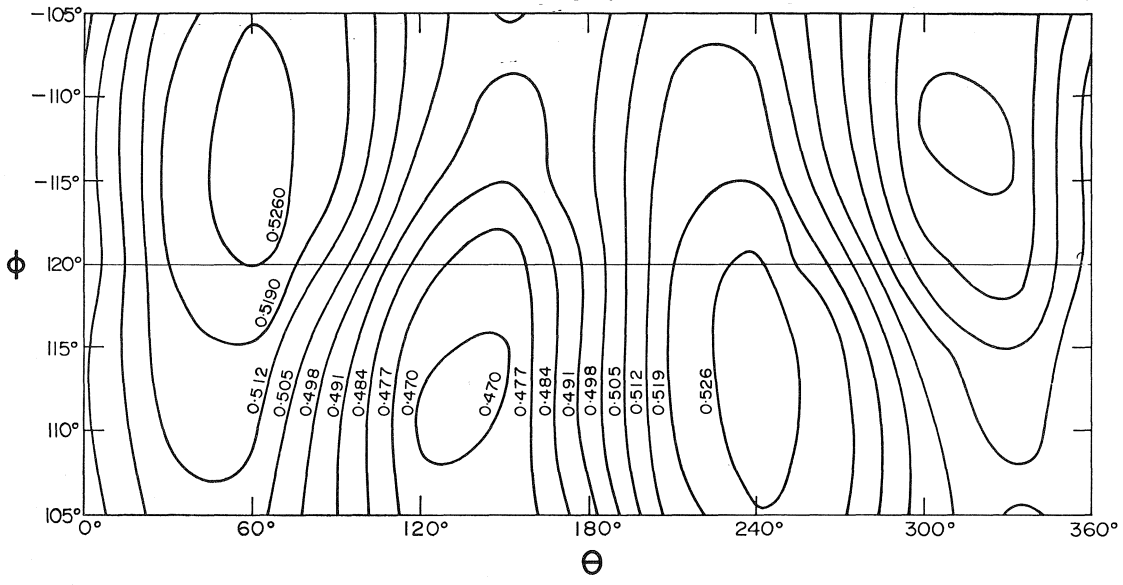

FIG. 14. A contour map for the overlap population of the C—S bond of $HMSO^-$ as a function of Θ and ϕ.

Can. J. Chem. Downloaded from www.nrcresearchpress.com by 210.87.254.6 on 09/05/12
For personal use only.

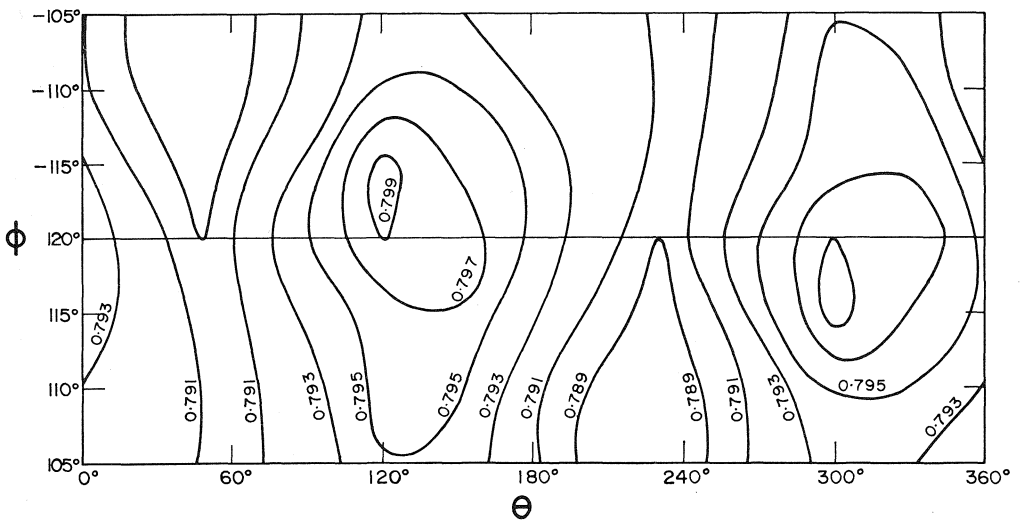

FIG. 15. A contour map for the overlap population of the S—O bond of $HMSO^-$ as a function of Θ and ϕ.

We were convinced that such an interaction would be found despite an intuitive prediction to the contrary (32). However, the intuitive prediction proved to be correct insofar as the present calculations are concerned, and we have had to revise our view to one of agnosticism. The situation is much more complicated than was originally thought, for reasons that will be discussed below.

Interestingly, the classical experimental bases for d-orbital conjugation are now also being critically reappraised for an array of structural types as new and more subtle criteria are devised (33–35), and disagreements are beginning to be made public (36–38).

Theoretical calculations on sulfur containing systems both with and without d-orbitals abound in the literature. A number of these are summarized in Table VI. The main surprise for one schooled in the pictorial approach is that there is as yet no real concensus of opinion either for or against the need to invoke contributions from the d-orbitals although the argument is a lively one. Thus, Bielefeld and Fitts (48) summarized the conclusions of Mangini and Zauli (58) as follows: "*d-orbital participation has never been proved and calculations based on the Longuet–Higgins model are fallacious.*"

In the present study six GTF have been used to describe the d-orbitals of sulfur atom rather than the usual five d-orbitals. This creates a problem because the six d-GTF do not have the proper symmetry characteristics of the spherical harmonics essential to the solutions of atomic problems. However, as explained in Appendix I of ref. 20, it is possible to effect a linear transformation of this set of six d-GTF to a single 3s-type and a set of five 3d-type (i.e. $d_{x^2-y^2}$, $d_{3z^2-r^2}$, d_{xy}, d_{xz}, and d_{yz}) functions. The same transformation can be used in any given molecular orbital to change the coefficients of the present six d-GTF to a set of one 3s and five 3d atomic orbitals.

The largest participation of d-GTF in occupied molecular orbitals occurs in the case of orbitals nos. 1 and 4 which can be associated with the sulfur 1s and 2s cores. Inspection of the virtual orbitals of the coefficient matrices for HMSO and $HMSO^-$ reveals that there are, as expected five nearly degenerate molecular orbitals which arise solely from linear combinations of the six d-type GTF. Although these are true molecular orbitals they can loosely and without ambiguity be referred to as the d-orbitals of sulfur. Table VII shows the energies of the d-orbitals of HMSO and $HMSO^-$ in the conformations indicated. It is apparent that the energies of the d-orbitals are not significantly disturbed upon formation of the carbanion.

The transformed coefficients of the two occupied (nos. 1 and 4) and the five nearly degenerate unoccupied (nos. 23–27) molecular orbitals of

Can. J. Chem. Downloaded from www.nrcresearchpress.com by 210.87.254.6 on 09/05/12
For personal use only.

TABLE VI

Survey of theoretical calculations of sulfur compounds with and without d-orbitals

Reference	Compound	Method	d-Orbitals	Conclusion
11	Diphenyl-sulfone	Symmetry considerations	Yes	Under some circumstances, expect strong conjugation with an α,β-unsaturated group
39	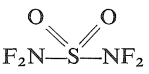	LCAO-MO Semi-empirical	Yes	The barrier to rotation arises from interaction of d-orbitals with p-orbitals of bonded atoms; there is competition of oxygen p's for the d-orbitals
40		Symmetry considerations	Yes	Unequal radicals compete for the d-orbitals of the central atom in tetrahedral anions
41	Thiophene, benzene	Simple HMO and symmetry considerations	Yes	(d-p)π overlap explains the "aromaticity" of thiophene
42	Thiophene	Simple HMO and symmetry considerations	Yes	—S— is about equivalent to —CH=CH—
43	Thiophene, 1,4-Dithiadiene	LCAO-MO (simple HMO)	Yes	Fairly good agreement with experiment
44		Evaluation of overlap integrels between s,p,d-orbitals using both radial and angular functions	Yes	Phosphorus and sulfur outer d-orbitals are much too diffuse for useful bonding; if used, e.g. as in SF_6, one must invoke contraction of d's
45	First row elements	Symmetry consider-ations and calculations using hydrogenic AO's and promotion energies from spectral data	Yes	Even carbon can use d-orbitals under certain circumstances, e.g., in the S_N2 transition state
46	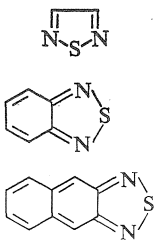	Simple HMO	Yes	Good agreement with experimental data
47	$SO_4^=$	Extended HMO (Wolfsberg-Helmholtz, and Cusachs)	Yes	Inclusion of d-orbitals is important; they affect ordering of the energy levels in a Wolfsberg-Helmholtz calculation
48	Thiophene	An extension of the SCF-MO method, π-orbital approx.	Yes	There is limited participation of d-orbitals in the π electronic structure and a large effect on calculated electronic properties
49		Atomic d-orbital size with respect to nuclear charge and octahedral field of (+) charges	Yes	d-Orbitals can contract enough to be important in PCl_5 and SF_6
50	Bivalent sulfur	Electrostatic treatment with exchange among valence shell orbitals	Yes	There is negligible use of d-orbitals in bivalent sulfur
51	SF_6	A.O. calculation on S^{6+} with F atom potential	Yes	d-Orbitals are contracted to half their size in the free atom

Can. J. Chem. Downloaded from www.nrcresearchpress.com by 210.87.254.6 on 09/05/12
For personal use only.

TABLE VI (*Concluded*)

Reference	Compound	Method	d-Orbitals	Conclusion
52		Electrostatic effect of H,C,F,Cl as ligand to sulfur; S core omitted	Yes	Insignificant changes in dδ and dπ orbitals, e.g. as in S—O bonds
53	Thiophene, Furan, Pyrrole	SCF-LCAO-MO (PPP)	No	Good agreement with experiment
54	Furan, Thiophene, 1,4-Dithiadiene	LCAO-MO(Pariser-Parr) self-consistent with respect to charge and electronegativity	No	No need to consider d-orbitals to explain differences in compounds studied
55	Dithienyl-thiophene	Semi-empirical SCMO (π electron and zero differential overlap)	No	Good calculated dipole moments
56	Thiophene	PPP-SCF-MO	Yes	3d, 4s, 4p Orbitals of sulfur have a negligible effect on the total energy
57	Disulfides	Semi-empirical LCAO-MO	No	The rotational energy barrier in disulfides had the correct order of magnitude

$HMSO^-$ clearly indicate (Table VIII) that in the low lying occupied molecular orbitals the d-GTF participate as s-type functions and that the five d-type functions are relegated to the virtual orbitals. Consequently, d-orbital conjugation such as structures **20** in valence bond notation, appears to be entirely out of the question.

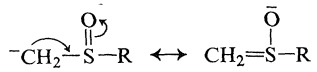

20

It would be proper to point out, however, that the exponent that we have used for the d-GTF ($\alpha = 5.42$) may be too large to permit efficient bonding since its maximum is close to the sulfur nucleus. This point was considered earlier (Appendix II of ref. 20) in connection with the question of d-orbital participation in the bonding of H_2S. It was shown there that inclusion of a second set of d-GTF with an exponent ($\alpha = 0.25$) chosen to permit more efficient overlap made no appreciable contribution to the ground state wave function. This might have been anticipated on intuitive grounds since the sulfur is bivalent in H_2S. Greater participation of d-orbitals is expected intuitively in compounds where the coordination number of sulfur is higher than 2. A second set of d-GTF, with an exponent of 0.25, was, therefore, added to the basis set (N = 38 GTF) and a complete calculation was performed for a number of conformations of $HMSO^-$. The transformed d-coefficients of the favored conformation ($\phi = 115°$, $\Theta = 240°$) (Table IX) indicate that d-orbitals of the lower orbital exponent do mix appreciably into the higher filled molecular orbitals.[6]

TABLE VII

Orbital energies for sulfur d-orbitals in HMSO ($\Theta = 0°$) and $HMSO^-$ ($\Theta = 240°$, $\phi = 115°$).

Energy (Hartree)			
MO	HMSO	MO	$HMSO^-$
24	8.3463	23	8.6311
25	8.3483	24	8.6319
26	8.3595	25	8.6417
27	8.3640	26	8.6486
28	8.3670	27	8.6516

This demonstrates the difficulty in assigning a proper role to the d-orbitals when a small basis set is used. The same energy minimum is obtained whether the d-orbitals participate in the higher occupied molecular orbitals or not. It is clearly desirable to improve the accuracy of the present calculations. Very recently Hartree–Fock Atomic Orbitals have been obtained for sulfur (59). We hope that by use of these it will be possible to bring calculations on HMSO and $HMSO^-$ closer to the Hartree–Fock limit and provide a more meaningful basis for discussion of the problem. Whatever the outcome of these further studies it is already clear that what is significant in deciding

[6]The $\phi = 115°$, $\Theta = 240°$ conformation has minimum energy with all basis sets used so far.

Can. J. Chem. Downloaded from www.nrcresearchpress.com by 210.87.254.6 on 05/05/12
For personal use only.

TABLE VIII

Transformed coefficients for d-GTF* in $HMSO^-$ ($\Theta = 240°$, $\phi = 115°$)

MO	s	x^2-y^2	$3z^2-r^2$	xy	xz	yz
1	0.379	—	—	—	—	—
2	—	—	—	—	—	—
3	—	—	—	—	—	—
4	−0.494	—	—	—	—	—
5	—	−0.002	−0.003	−0.001	—	−0.001
6	0.004	−0.002	0.002	0.001	−0.002	−0.002
7	−0.009	—	−0.002	0.002	−0.003	0.003
8	−0.102	0.001	—	—	0.001	−0.002
9	−0.067	—	0.002	−0.001	—	—
10	−0.067	0.002	0.001	−0.001	—	—
11	−0.056	−0.004	−0.001	0.001	0.001	−0.002
12	−0.004	−0.001	—	—	−0.001	−0.001
13	0.033	−0.002	0.002	−0.002	−0.001	0.002
14	−0.007	−0.001	0.005	−0.001	−0.003	0.004
15	0.021	0.004	0.001	−0.003	—	—
16	0.015	0.007	—	—	−0.001	−0.002
17	−0.046	—	−0.004	−0.001	−0.002	0.001
.	.	.	.	.	.	.
.	.	.	.	.	.	.
.	.	.	.	.	.	.
.	.	.	.	.	.	.
23	0.002	−0.650	0.202	−0.728	0.172	0.363
24	0.002	−0.767	−0.298	0.659	0.303	0.152
25	—	0.559	0.113	0.129	0.331	0.811
26	0.005	0.075	−0.759	0.084	−0.712	0.313
27	0.001	−0.414	0.884	0.111	−0.513	0.300
28	4.103	—	—	—	—	—

*Orbital exponent $\alpha = 5.42$; basis set size = 32.

structure is not the presence or absence of d-orbital conjugation but the conformational preference of an electron pair adjacent to another electron pair or to a dipole. As noted earlier, $HMSO^-$ closely resembles hydrazine, hydroxylamine, and hydrogen peroxide and similar results are obtained in calculations on $^-CH_2SHO_2$ and $^-CH_2SH$ (60) and in experimental (61) and theoretical (57) studies on CH_3SSCH_3.[7]

Comparison of HMSO and $HMSO^{(-)}$ with Dimethyl Sulfoxide (21) and Methylsulfinyl Carbanion (22)

The minimal basis set for DMSO consists of 41 GTF and that for $DMSO^-$ consists of 40 GTF. Because of the time required for the computations, a complete study of the dimethyl sulfoxide system was not undertaken. However, a sufficient number of calculations were performed to establish that the form of the energy surface for $DMSO^-$ would be very similar to that of $HMSO^-$ One cross-section of this surface is shown in Fig. 16 which has parallel curves representing the energies of the anions $HMSO^-$ and $DMSO^-$ as a function of rotational angle about the C—S bond with the anion angle fixed at $\phi = 115°$. The maxima and minima fall at nearly identical positions and the relative barrier heights are about the same. Figure 17 shows parallel curves representing the energies of $HMSO^-$ and $DMSO^-$ as a function of the anion angle where the rotational conformation is that corresponding to $\Theta = 240°$. The essential similarity in the shapes of the curves is clear. Both are asymmetric with a minimum at about $\phi = 115°$.

In Fig. 5, where the molecular orbital energies of **18**, **19**, **21**, and **22** are plotted next to each other, the close correspondence between the energy levels of **18** and **21** and of **19** and **22** is clear.

It is our conclusion, therefore, that the calculations are unaffected by the presence of a sulfur–

[7]The favored conformations are, respectively,

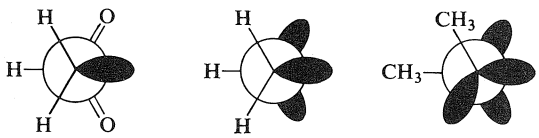

$^-CH_2SHO_2$ $^-CH_2SH$ CH_3SSCH_3

Can. J. Chem. Downloaded from www.nrcresearchpress.com by 210.87.254.6 on 09/05/12
For personal use only.

TABLE IX

Transformed coefficients of the two sets of d-GTF* for $HMSO^-$ ($\Theta = 240°$, $\phi = 120°$)

MO	s	x^2-y^2	$3z^2-r^2$	xy	xz	yz
1	−0.007	—	—	—	—	—
	0.380	—	—	—	—	—
2	—	—	—	—	—	—
	—	—	—	—	—	—
3	—	—	—	—	—	—
	—	—	—	—	—	—
4	−0.001	—	—	—	—	—
	−0.496	—	—	—	—	—
5	0.039	−0.037	−0.058	−0.020	−0.009	−0.028
	−0.001	−0.001	−0.002	−0.001	—	−0.002
6	—	0.079	−0.019	−0.004	0.009	−0.004
	−0.001	0.001	−0.001	−0.001	0.002	0.001
7	0.036	—	−0.007	0.003	—	0.006
	0.007	—	0.003	—	0.002	−0.001
8	0.271	−0.043	0.126	−0.049	−0.099	0.144
	0.066	−0.001	0.003	−0.001	−0.002	0.003
9	0.158	0.067	−0.139	0.045	0.075	−0.114
	0.093	0.001	0.003	0.001	0.001	−0.002
10	−0.038	0.051	0.011	−0.031	−0.038	0.077
	−0.067	0.003	—	−0.001	—	0.001
11	−0.095	0.080	0.126	−0.025	−0.091	0.009
	−0.032	−0.002	−0.001	0.001	−0.001	−0.003
12	0.093	0.011	−0.070	−0.036	−0.065	0.021
	0.008	—	−0.003	−0.001	−0.002	−0.001
13	−0.033	0.111	−0.111	−0.020	−0.060	−0.081
	0.004	−0.001	0.001	−0.002	−0.004	0.001
14	−0.173	0.064	0.165	0.068	0.022	−0.090
	−0.012	0.001	0.008	0.001	−0.002	0.001
15	−0.078	−0.365	−0.060	0.090	0.171	0.138
	−0.010	−0.015	−0.002	0.003	0.005	0.005
16	0.159	0.007	0.288	0.191	0.097	−0.083
	0.029	0.001	0.009	0.007	0.004	−0.004
17	0.115	0.067	0.135	−0.128	0.148	0.024
	0.016	—	0.007	−0.005	0.004	0.001

*For every MO the first row refers to the set of d-GTF which has exponents of 0.25 and the second row corresponds to d-GTF of $\alpha = 5.42$.

hydrogen bond in the model system HMSO and its anion.

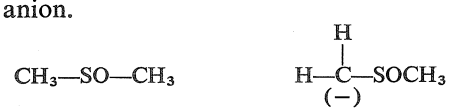

21 22

The Stereochemistry of Proton Exchange Alpha to a Sulfinyl Group

In every conformation of HMSO the three methyl protons occupy different positions with respect to the groups on sulfur. We postulate that the abstraction of any methyl proton proceeds by a vertical energy transition which generates a carbanion whose electron pair points initially in the direction of the departing proton. Then the carbanion proceeds to its most stable structure; depending on the position on the conformational energy surface where the carbanion appears initially, this structural change may involve rotation or inversion or both. The usefulness of this concept is that if the transition state for proton abstraction possesses considerable carbanion character then it can be stated at once for any conformation what the relative rates of abstraction of the three methyl protons will be, and whether the reprotonation will occur with retention or inversion of configuration.

Can. J. Chem. Downloaded from www.nrcresearchpress.com by 210.87.254.6 on 09/05/12
For personal use only.

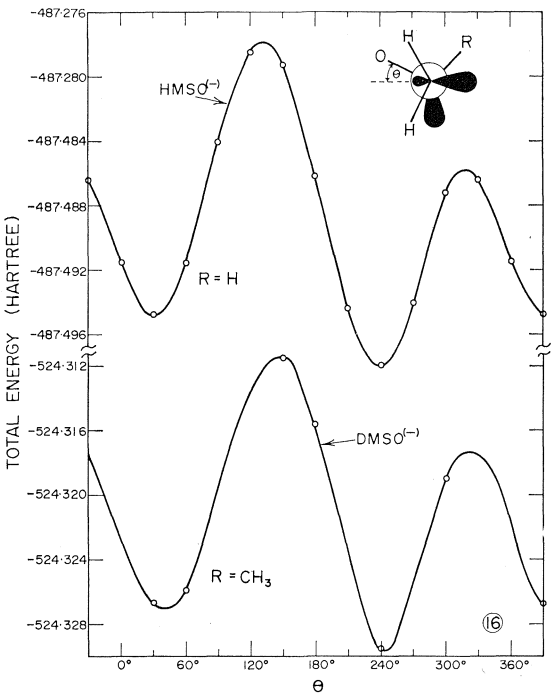

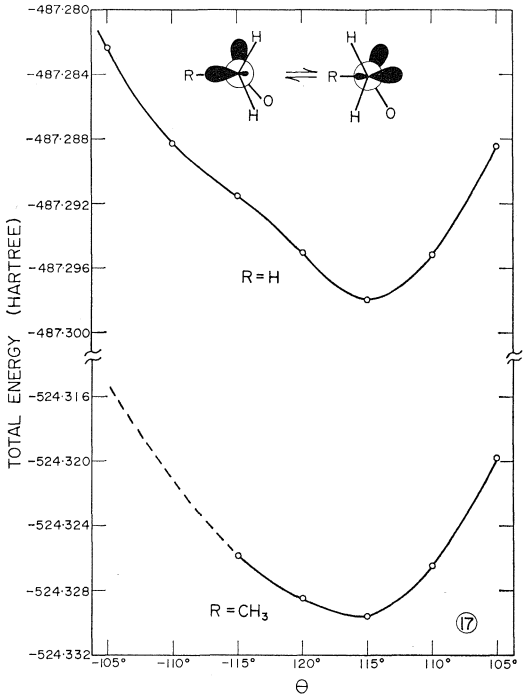

FIG. 16. Total energies of $HMSO^-$ (upper) and $DMSO^-$ (lower) as a function of rotation about the C—S bond ($\phi = 115°$).

FIG. 17. Total energies of $HMSO^-$ (upper) and $DMSO^-$ (lower) as a function of the carbanion angle ϕ for $\Theta = 240°$.

Stewart and Jones (62) have carried out hydrogen–tritium exchange studies on DMSO in water. These workers obtained a linear plot of log k against H^- with a slope of 0.939 over a range of rates varying by eight powers of ten. The result is consistent with a process in which proton transfer to the base is well advanced in the transition state. For the exchange of the methylene protons of benzyl methyl sulfoxide it has been found (63) that the kinetic isotope effect, k_H/k_D, for exchange of H_A is 1.4, and the solvent isotope effect, k_{D_2O}/k_{H_2O}, is 2.4. These effects are those expected for an unsymmetrical transition state (64) which resembles the products of an equilibrium ionization process (65). Thus, it seems valid to proceed with the assumption that the energy of the transition state for proton abstraction can be approximated by that of the carbanion (66).

$HMSO^-$ will be generated by the proton abstraction process somewhere along the cross-section of the energy surface (Fig. 9) through $\phi = 110°$. This cross-section, together with the potential curve for rotation about the C—S bond in HMSO, and the difference between the two are shown in Fig. 18, curves *a*, *b*, and *c*, respectively. From the reasoning given above, curve *c* ought to represent qualitatively the change of activation energy for the formation of $HMSO^-$ as the orientation of the proton with respect to the groups on sulfur varies. It is seen that if in HMSO one of the methyl protons were situated in the plane of the bisector of the O:S:lone pair angle ($\Theta = 240°$), this proton would be abstracted most readily.

To carry this further, consider HMSO in any conformation, say $\Theta = 90°$. Let the three different environments of the methyl protons be labelled A, B, and C as shown in Fig. 19. Abstraction of a proton from environment A generates $HMSO^-$ initially in conformation $\Theta = 90°$. Similarly abstraction from environments B and C generates $HMSO^-$ in conformations $\Theta = 210°$ and $\Theta = 330°$ respectively. Reference to curve *c*

Can. J. Chem. Downloaded from www.nrcresearchpress.com by 210.87.254.6 on 09/05/12
For personal use only.

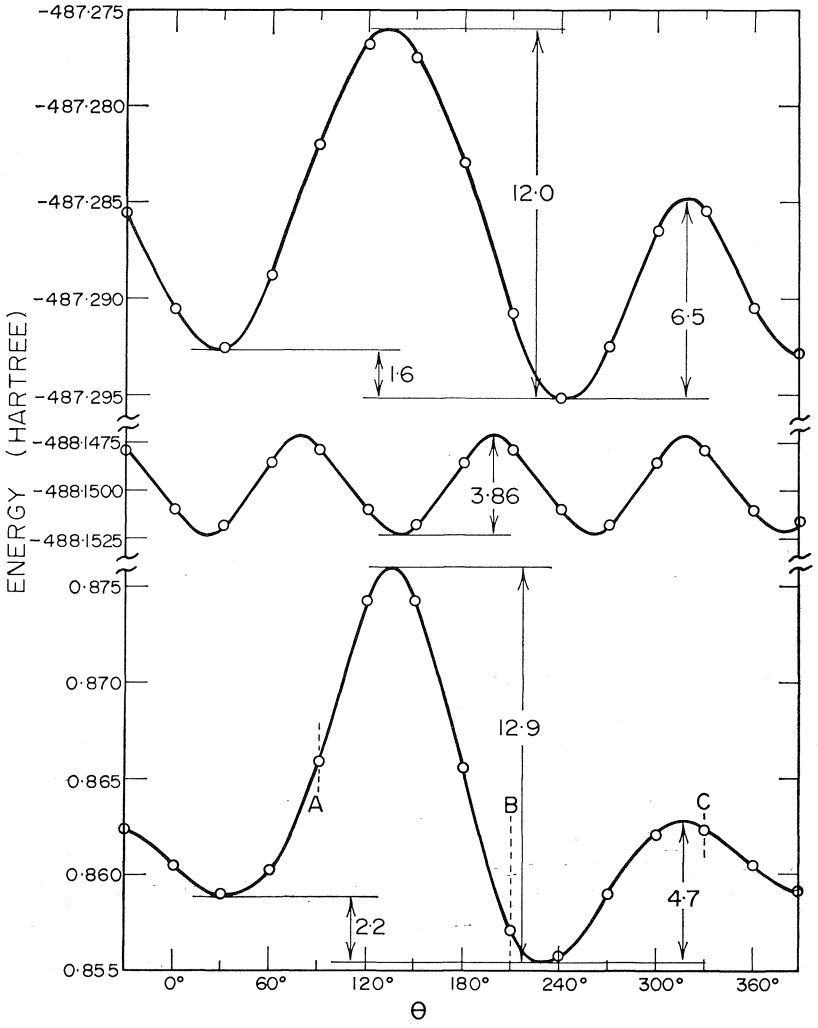

FIG. 18. Total energy of $HMSO^-$ as a function of rotation about the C—S bond for the cross-section through $\phi = 110°$ (upper curve) and the total energy of HMSO as a function of rotation about the C—S bond (middle curve). The lower curve is the difference between the upper and middle curves (energy differences are quoted in kcal/mole units).

of Fig. 18 permits the prediction that the ease of formation of $HMSO^-$ would be in the order B > C > A. The stereochemical fate of each of the resulting anions can be predicted by observing their location, labelled A, B, and C on the energy surface (Figs. 8 and 9). A will spontaneously invert, B would retain configuration, and C, being near a saddle point, may either retain or invert. These processes are shown in a three-dimensional projection in Fig. 20.

Figure 21 summarizes the procedure for predicting the stereochemical fate of a carbanion generated next to S—O. A carbanion generated in the shaded region would invert and one generated in the unshaded region would retain its configuration.

On the basis of these conclusions, we believe that hydrogen exchange in *S*-benzyl methyl sulfoxide (18, 19) can be discussed in the following manner. In conformation *a* of Fig. 22 the proton labelled A would be predicted to exchange rapidly and with retention of configuration. The

Can. J. Chem. Downloaded from www.nrcresearchpress.com by 210.87.254.6 on 09/05/12
For personal use only.

Can. J. Chem. Downloaded from www.nrcresearchpress.com by 210.87.254.6 on 09/05/12
For personal use only.

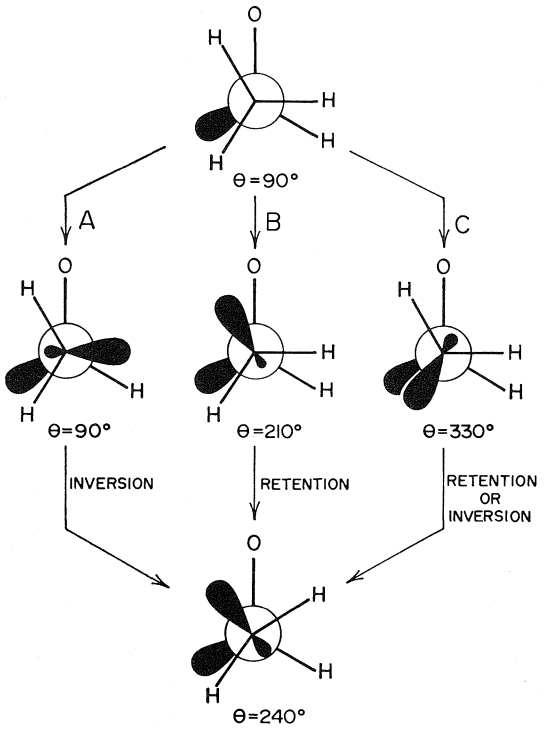

FIG. 19. A summary of the procedure for predicting the relative rates and the stereochemistry of exchange of the methyl protons of HMSO when the conformation corresponds to $\Theta = 90°$.

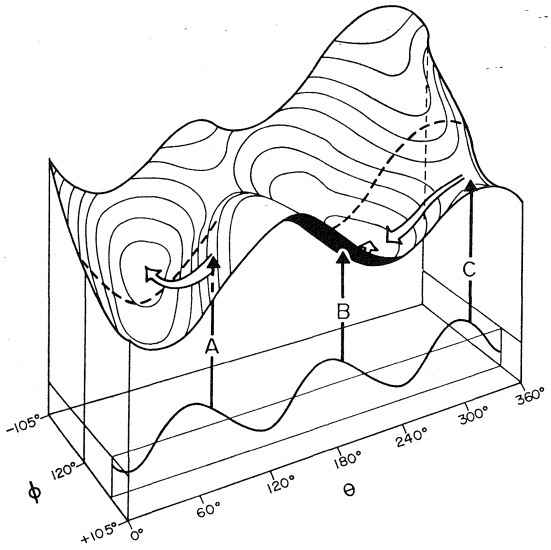

FIG. 20. A three dimensional projection to illustrate how the most stable carbanion structure would be generated by abstraction of each of H_A, H_B, and H_C of Fig. 19.

exchange of proton B would be slower and occur with inversion of configuration. In a deuterated medium the sequence of events would be,

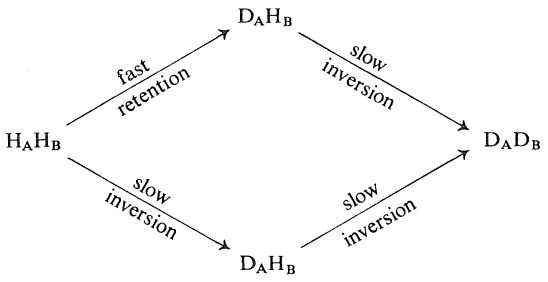

SCHEME *a*

In conformation *b*, proton B will exchange faster and with inversion; the slower exchange of proton A might occur with either retention or inversion. The sequence of events would then be

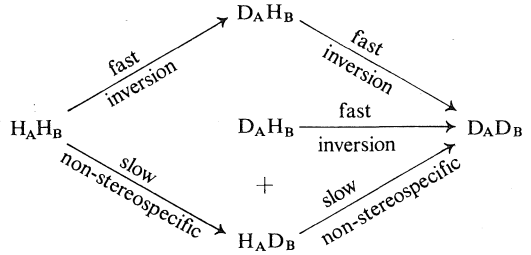

SCHEME *b*

In conformation *c*, proton B will exchange faster and with retention, while proton A will exchange more slowly and with inversion. The sequence of events would be

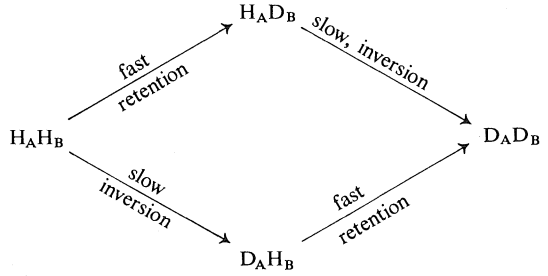

SCHEME *c*

Scheme *a* predicts that D_AH_B will accumulate in the medium. Scheme *c* predicts that H_AD_B will accumulate in the medium. Scheme *b* predicts that a monodeuterated species will be almost undetectable; any that would be detected would consist of H_AD_B. According to this treatment the

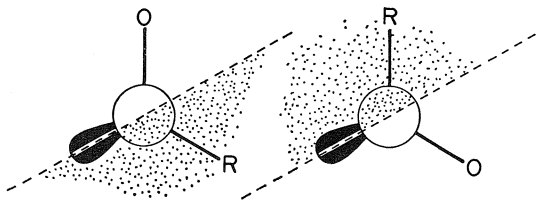

FIG. 21. A summary of the procedure for predicting the stereochemical fate of a carbanion generated next to S—O.

extent of reaction via schemes *a*, *b*, and *c* will depend upon the mole fractions of the conformations *a*, *b*, and *c* present in the medium. Since these will change as the solvent is changed the relative importance of the three schemes and thus the overall rate and stereochemistry of exchange will be affected by a change of solvent. The experimental finding, in NaOD–D_2O at 15°, is

$$H_AH_B \xrightarrow{\text{fast}} D_AH_B \xrightarrow{\text{slow}} D_AD_B$$

The result is thus consistent with Scheme *a* and with the conclusion expressed earlier (19). A forthcoming paper (63) will describe the results of experiments on conformationally constrained sulfoxides and an experiment on benzyl methyl sulfoxide which demonstrates that the conversion of D_AH_B to D_AD_B does proceed with inversion of configuration, as required by Scheme *a*.

Conclusions

Some understanding has been gained during the present work of the stereochemistry of an α-sulfinyl carbanion. Solvation effects have not been treated explicitly but, as noted in the preceding section some of the phenomena can be understood in terms of a dependence of conformer populations of the parent hydrocarbon upon the solvent. This is contrary to the view that solvation of the carbanion is a decisive factor in determining the stereochemistry of hydrogen exchange reactions.

It appears that, for a number of systems including α-sulfinyl carbanions, which contain directed electron lone pairs or highly polar bonds on adjacent atoms, conformations that place these substituents *syn or anti* to each other are energetically disfavored. The reasons for this are unknown but it is clear that the explanation of the effect is closely related to the question of the origin of rotational and inversion barriers. A result of the effect is that conformations that

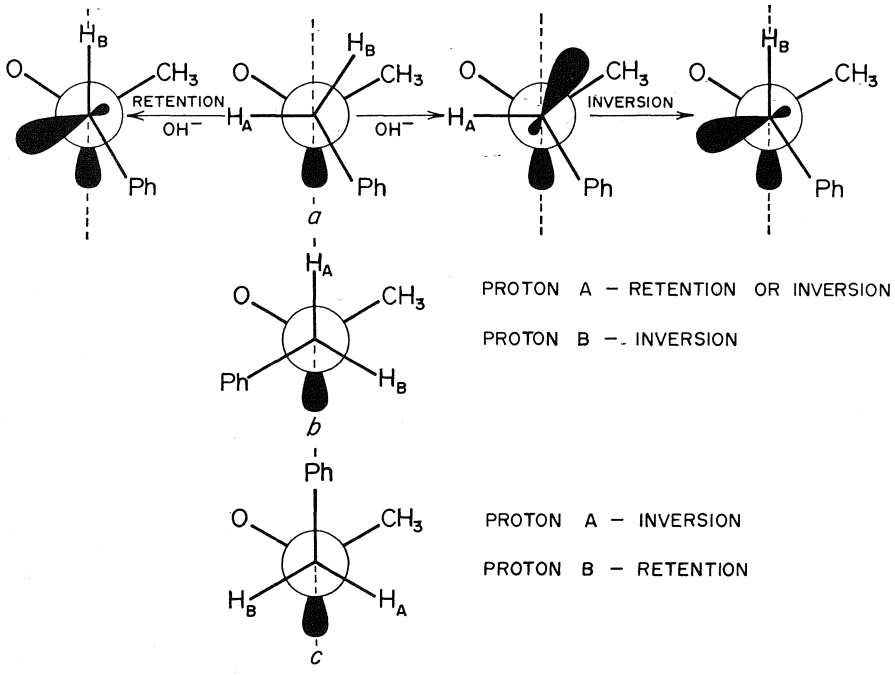

FIG. 22. Application of the theoretical results of this paper to the prediction of the rate and stereochemistry of exchange of the methylene protons of benzyl methyl sulfoxide.

Can. J. Chem. Downloaded from www.nrcresearchpress.com by 210.87.254.6 on 09/05/12
For personal use only.

place lone pairs *gauche* to each other often represent a minimum in the energy surface.

More extensive calculations than ours would be necessary to probe further the source of this anomalous behavior and to be certain of the relative positions on a conformational energy surface of structures other than the minimum. Throughout this work we have been conscious of the limitations of our basis set. The use of a minimal basis set was imposed upon us by the magnitude of the task we undertook. Even had exponents for sulfur been available from the beginning a near Hartree–Fock calculation on one conformation of $HMSO^-$ would have involved a basis set of about 120 GTF and about 24 h of 7094-II time. Forty-five separate conformations were calculated to obtain the surface shown in Fig. 9. Small basis set calculations were thus necessary forerunners to the more extensive and elaborate ones that now have to be done.

Acknowledgments

We thank the Institute of Computer Science of the University of Toronto for making their facilities available to us and the National Research Council of Canada for financial support. Special thanks go from S.W. and A.R. to Professor D. J. LeRoy for his kind hospitality.

1. D. J. Cram. Fundamentals of carbanion chemistry. Academic Press, Inc. New York. 1965.
2. D. J. Cram. *In* XIXth Intern. Congr. Pure Appl. Chem. 19th Congr. Butterworths, London. 1963. p. 155.
3. E. J. Corey and E. T. Kaiser. J. Am. Chem. Soc. **83**, 490 (1961).
4. D. J. Cram, D. A. Scott, and W. D. Nielsen. J. Am. Chem. Soc. **83**, 3696 (1961).
5. H. L. Goering, D. L. Townes, and B. Dittmer. J. Org. Chem. **27**, 736 (1962).
6. E. J. Corey, H. Konig, and T. H. Lowry. Tetrahedron Letters, 515 (1962).
7. E. J. Corey and T. H. Lowry. Tetrahedron Letters, 803 (1965).
8. E. J. Corey and T. H. Lowry. Tetrahedron Letters, 793 (1965).
9. D. J. Cram and A. S. Wingrove. J. Am. Chem. Soc. **85**, 1100 (1963).
10. D. J. Cram and T. A. Whitney. J. Am. Chem. Soc. **89**, 4651 (1967).
11. H. P. Koch and W. E. Moffitt. Trans. Faraday Soc. **47**, 7 (1951).
12. C. D. Broaddus. J. Am. Chem. Soc. **88**, 3863 (1966).
13. L. A. Paquette and L. D. Wise. J. Am. Chem. Soc. **90**, 807 (1968).
14. D. J. Cram and S. H. Pine. J. Am. Chem. Soc. **85**, 1096 (1963).
15. K. Mislow, M. M. Green, P. Laur, J. T. Melillo, T. Simons, and A. L. Ternay. J. Am. Chem. Soc. **87**, 1958 (1965).
16. C. C. Price and S. Oae. Sulfur bonding. The Ronald Press Co., New York. 1962. p. 136.
17. E. Buncel, E. A. Symons, and A. W. Zabel. Chem. Commun. 173 (1965).
18. A. Rauk, E. Buncel, R. Y. Moir, and S. Wolfe. J. Am. Chem. Soc. **87**, 5498 (1965).
19. S. Wolfe and A. Rauk. Chem. Commun. 778 (1966).
20. A. Rauk and I. G. Csizmadia. Can. J. Chem. **46**, 1205 (1968).
21. C. M. Reeves. J. Chem. Phys. **39**, 1 (1963).
22. Tables of interatomic distances. Chem. Soc. London, Spec. Publ. 11, (1958).
23. I. G. Csizmadia, M. C. Harrison, J. W. Moskowitz, and B. T. Sutcliffe. Theoret. Chim. Acta, **6**, 191 (1966); **7**, 156 (1967).
24. R. W. Kilb, C. C. Lin, and E. B. Wilson. J. Chem. Phys. **26**, 1695 (1957).
25. G. W. Wheland. Resonance in organic chemistry. John Wiley and Sons, Inc., New York. 1955. pp. 681–684.
26. W. H. Fink and L. C. Allen. J. Chem. Phys. **46**, 2261 (1967).
27. W. H. Fink and L. C. Allen. J. Chem. Phys. **46**, 2276 (1967).
28. W. H. Fink, D. C. Pan, and L. C. Allen. J. Chem. Phys. **47**, 895 (1965).
29. S. S. Seung, M. C. Harrison, and I. G. Csizmadia. Theoret. Chim. Acta, **8**, 281 (1967).
30. S. Wolfe, A. Rauk, and I. G. Csizmadia. J. Am. Chem. Soc. **89**, 5710 (1967).
31. R. E. Kari and I. G. Csizmadia. J. Chem. Phys. **46**, 4585 (1966).
32. P.-O. Löwdin. Private communication to S. Wolfe and I. G. Csizmadia.
33. L. Goodman, A. Konstam, and L. H. Sommer. J. Am. Chem. Soc. **87**, 1012 (1965).
34. L. Goodman and R. W. Taft. J. Am. Chem. Soc. **87**, 4385 (1965).
35. A. G. Brook, D. G. Anderson, J. M. Duff, P. F. Jones, and D. M. MacRae. J. Am. Chem. Soc. **90**, 1076 (1968).
36. E. W. Randall, J. J. Ellner, and J. J. Zuckerman. J. Am. Chem. Soc. **88**, 622 (1966).
37. E. A. V. Ebsworth. Chem. Commun. 530 (1966).
38. E. W. Randall and J. J. Zuckerman. Chem. Commun. 732 (1966).
39. T. Jordan, H. W. Smith, L. L. Lohr, and W. N. Lipscomb. J. Am. Chem. Soc. **85**, 846 (1963).
40. H. H. Jaffe. J. Phys. Chem. **58**, 185 (1954).
41. H. C. Longuet-Higgins. Trans. Faraday Soc. **45**, 173 (1949).
42. J. De Heer. J. Am. Chem. Soc. **76**, 4802 (1954).
43. M. M. Kreevoy. J. Am. Chem. Soc. **80**, 5543 (1958).
44. D. P. Craig, A. Maccoll, R. S. Nyholm, L. E. Orgel, and L. E. Sutton. J. Chem. Soc. 332 (1954).
45. R. J. Gillespie. J. Chem. Soc. 1002 (1952).
46. N. K. Ray and P. T. Narasimhan. Theoret. Chim. Acta, **5**, 401 (1966).
47. D. M. Bishop. Theoret. Chim. Acta, **8**, 285 (1967).
48. M. J. Bielefeld and D. D. Fitts. J. Am. Chem. Soc. **88**, 4804 (1966).
49. D. P. Craig and E. A. Magnusson. J. Chem. Soc. 4895 (1956).
50. G. L. Bendazzoli and C. Zauli. J. Chem. Soc. 6827 (1965).
51. D. P. Craig and C. Zauli. J. Chem. Phys. **37**, 601 (1962).

Can. J. Chem. Downloaded from www.nrcresearchpress.com by 210.87.254.6 on 09/05/12
For personal use only.

52. D. P. CRAIG and C. ZAULI. J. Chem. Phys. **37**, 609 (1962).
53. N. SOLONY, F. W. BIRSS, and J. B. GREENSHIELDS. Can. J. Chem. **43**, 1569 (1965).
54. D. S. SAPPENFIELD and M. M. KREEVOY. Tetrahedron, **19**, Suppl. **2**, 157 (1963).
55. A. J. H. WACHTERS and D. W. DAVIES. Tetrahedron, **20**, 2841 (1964).
56. D. T. CLARK. Tetrahedron Letters, 5257 (1967).
57. G. BERGSON. Arkiv Kemi, **18**, 409 (1961).
58. A. MANGINI and C. ZAULI. J. Chem. Soc. 2210 (1960).
59. J. W. MOSKOWITZ. Private communication.
60. A. RAUK, S. WOLFE, and I. G. CSIZMADIA. 51st Canadian Chemical Conference, Vancouver, British Columbia, June, 1968. Abstracts.
61. C. W. N. CUMPER, J. F. READ, and A. I. VOGEL. J. Chem. Soc. 5323 (1965).
62. R. STEWART and J. R. JONES. J. Am. Chem. Soc. **89**, 5069 (1967).
63. S. WOLFE and A. RAUK. 51st Canadian Chemical Conference, Vancouver, British Columbia. June, 1968. Abstracts.
64. F. H. WESTHEIMER. Chem. Rev. **61**, 265 (1961).
65. C. G. SWAIN, A. D. KETLEY, and R. F. W. BADER. Tetrahedron, **10**, 182 (1960).
66. G. S. HAMMOND. J. Am. Chem. Soc. **77**, 334 (1955).

Can. J. Chem. Downloaded from www.nrcresearchpress.com by 210.87.254.6 on 09/05/12
For personal use only.

Stereoselective synthesis of (±)-eremophil-3,11-diene and related compounds. Concerning the structure of eremophilene

EDWARD PIERS AND ROBERT J. KEZIERE
Department of Chemistry, University of British Columbia, Vancouver 8, British Columbia
Received August 6, 1968

An efficient, stereoselective synthesis of (±)-eremophil-3,11-diene (**3**) is described. The key step of the synthetic sequence involves the conjugate addition of lithium dimethylcopper to the octalone **7**, which produces (±)-eremophil-11-en-3-one (**12**) in good yield. The latter is converted, *via* the tosylhydrazone derivative **13**, into compound **3**. Comparison of **3** with eremophilene indicates that the initial structural proposal for the latter sesquiterpene is in error. Evidence is presented which demonstrates that eremophilene is correctly represented by structure **4**.

Canadian Journal of Chemistry, 47, 137 (1969)

Can. J. Chem. Downloaded from www.nrcresearchpress.com by 210.87.254.6 on 09/05/12
For personal use only.

The biogenetically interesting (1) eremophilane class of sesquiterpenes possess the basic carbon skeleton **1**. Since the isolation of eremophilone (2) by Simonsen and co-workers (3), the number of known, naturally occurring eremophilane-type sesquiterpenes has, particularly in recent years, grown rapidly.[1] Structurally, one of the simplest members of this class is eremophilene, a $C_{15}H_{24}$ hydrocarbon first isolated from *Petasites officinalis* Moench. (5) and from *P. albus* (L.) Gaertn. (6). In 1964, Hochmannová and Herout (7), on the basis of nuclear magnetic resonance (n.m.r.) spectra, a fairly extensive chemical degradation, and correlation with hydroxydihydroeremophilone (**2**) (2), assigned structure **3** to eremophilene.

In connection with an interest in developing general methods for the total synthesis of various eremophilane-type sesquiterpenes, we report in this paper an efficient and stereoselective total synthesis of racemic **3**, and present evidence which invalidates the original structural proposal (7) for eremophilene. It should be immediately noted, however, that very recently, after our synthetic work had appeared in preliminary form (8), Křepinský *et al.* (9) presented spectroscopic and structural evidence which also disagreed with the initial structural proposal for eremophilene (7) and, on the basis of this evidence, assigned structure **4** to this sesquiterpene.[2] This latter assignment has very recently been confirmed by a stereoselective total synthesis of (±)-**4**.[3] We also present, in this paper, evidence which confirms that eremophilene is indeed correctly represented by structure **4**.

The starting material for our synthesis, 3-isopropenylcyclohexanone (**5**), was readily prepared, essentially by the procedure of House and co-workers (10). Thus, cuprous chloride – catalyzed conjugate addition of isopropenyl magnesium bromide to 2-cyclohexen-1-one gave the desired cyclohexanone derivative (**5**) in 71% yield. Sodium methoxide – catalyzed condensation of ketone **5** with ethyl formate in dry benzene afforded, in 75% yield, the corresponding hydroxymethylene derivative **6**, b.p. 101–102° at 4 mm, λ_{max} 283 mμ. The latter, upon treatment with 1-diethylamino-3-pentanone methiodide in the presence of sodium methoxide in methanol gave, after deformylation, ring closure, and appropriate work-up (for a similar procedure, see ref. 11), a 64% yield of the desired substituted octalone **7**, b.p. 127–131° at 0.3 mm. The spectral data obtained for this compound were in complete agreement with the assigned structure. Of particular pertinence were the ultraviolet (u.v.) spectrum (λ_{max} 249 mμ, $\varepsilon = 14\,600$) and the n.m.r. spectrum, which exhibited signals at τ 5.26 (unresolved multiplet, $=C^{12}H_2$),[4] τ 8.22 (doublet of doublets, $-C^{14}H_3$), and τ 8.25 (triplet, $-C^{13}H_3$). The chemical shifts assigned to the vinylic methyl groups ($-C^{13}H_3$ and $-C^{14}H_3$) were confirmed by a frequency-sweep decoupling

[1]At the present time, there are approximately 45 known eremophilane-type sesquiterpenoids. For a recent tabulation, see ref. 4.

[2]We acknowledge private communications from Professors R. B. Bates and V. Herout regarding this matter. We are also grateful to Dr. J. Křepinský for a preprint of their communication.

[3]R. M. Coates and J. E. Shaw. Private communication from Professor Coates, to whom we are grateful for a preprint concerning their work.

[4]To avoid confusion, the numbering employed is that normally used for eremophilane-type sesquiterpenes.

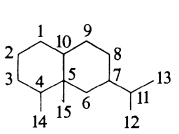

1

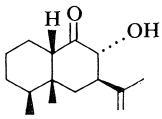

2

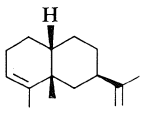

3

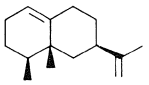

4

experiment in which the olefinic protons at C-12 were strongly irradiated, whereupon the triplet at τ 8.25 collapsed to a strong, sharp singlet, while the signal at τ 8.22 remained unaffected.

The stereochemistry of the octalone **7** was assigned as shown, since, under the basic conditions involved in the preparation of this compound, the bridgehead position at C-10 would be epimerizable. Obviously, therefore, the molecule would adopt a configuration which would allow the sterically bulky isopropenyl group to adopt an equatorial orientation, with ring B in the chair conformation. This requires that the isopropenyl group be *cis* to the hydrogen at C-10.

In order to produce the characteristic eremophilane-like skeleton from the octalone **7**, it was necessary, at this stage, to introduce an angular methyl group at C-5. In particular, we wished to carry out this introduction in a stereoselective manner such that the product would contain *cis*-fused six-membered rings. At the outset, it appeared that this might be conveniently accomplished by use of the copper salt – catalyzed conjugate addition of methyl magnesium bromide (or iodide) to the α,β-unsaturated ketone system of **7**. This type of reaction had been successfully employed (12, 13) in the case of a number of 1 (9)-octal-2-ones (e.g. **8**, **9**, and **10**) and, stereochemically, resulted in each case in the formation of the corresponding *cis*-fused decalone system. It should be noted, however, that a number of years ago, Ireland and co-workers (14) reported an unsuccessful attempt to introduce, by cuprous bromide – catalyzed 1,4-addition of methyl magnesium bromide, an angular methyl group into the octalone **11**. It thus appeared that, although the conjugate addition of methyl Grignard reagent was successful with 1 (9)-octal-2-ones bearing no substituent on C-1 (as in **8**, **9**, and **10**), this reaction failed when there was a methyl group (or, presumably, another alkyl group) present on C-1 (as in **11**). Indeed, we have found, in agreement with Ireland's observation (14), that the copper-salt – catalyzed conjugate addition of methyl magnesium iodide to the octalone **7** was extremely difficult to accomplish. In fact, even the use of the reportedly (12) superior catalyst, cupric acetate in tetrahydrofuran, gave no synthetically useful result. Thus, although the latter procedure (12) afforded a crude product which exhibited a significant saturated carbonyl absorption in the infrared (i.r.) (5.85 μ), analysis of this crude material by gas–liquid chromatography (g.l.c.) showed that it was a complex mixture consisting of at least ten components. One of these components, which was formed in varying amounts (approximately 10–25% of the mixture) depending upon the experimental conditions employed, exhibited a g.l.c. retention time and i.r. spectrum (after isolation by preparative g.l.c.) identical with those of the authentic desired decalone **12**, which was eventually prepared by another method (see below). Thus, although this reaction was partially successful, the low yield of the desired compound **12**, as well as the complex nature of the reaction product, precluded its further use in our synthetic work.

In view of the above situation, we considered other routes for the conversion of octalone **7** into the decalone **12** and were attracted by a recent report by House and co-workers (15) who found that the reagents lithium dimethylcopper and "methylcopper-tri-*n*-butylphosphine complex" very selectively add a methyl group to the β carbon of an α,β-unsaturated ketone system. We therefore explored the use of these reagents for the crucial introduction of an angular methyl group in the octalone **7** and found that lithium dimethylcopper, which is prepared simply by reaction of ethereal methyllithium with cuprous iodide (molar ratio 2:1, respectively) at 0° under nitrogen, was excellent for this purpose. Thus, reaction of octalone **7** with an excess of lithium dimethylcopper in ether at 0° and under nitrogen for 2 h gave, after appropriate work-up, a 77% yield of the desired ($\pm$)-eremophil-11-en-3-one (**12**). The spectral properties of the latter were in complete agreement with the assigned structure. The compound exhibited no strong

Can. J. Chem. Downloaded from www.nrcresearchpress.com by 210.87.254.6 on 09/05/12
For personal use only.

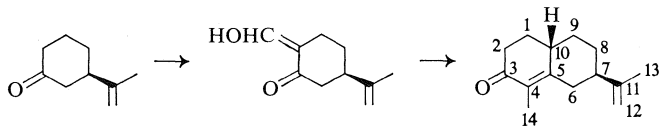

5 6 7

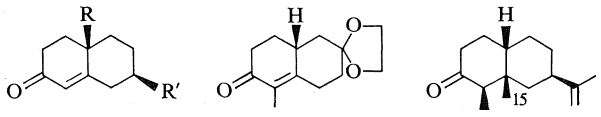

8, R = R′ = H
9, R = CH_3, R′ = H
10, R = CH_3, R′ = $CH(CH_3)_2$

11 12

u.v. absorption above 215 mμ, and showed a saturated carbonyl absorption (5.86 μ) in the i.r. The n.m.r. spectrum, when compared with that of the starting material (**7**), was particularly instructive, showing signals for two olefinic protons (τ 5.33, $=C^{12}H_2$), one vinyl methyl group (τ 8.29, $-C^{13}H_3$), one secondary methyl group (τ 9.11, $-C^{14}H_3$), and one tertiary methyl group (τ 9.21, $-C^{15}H_3$). In addition there appeared a one-proton quartet (1:3:3:1) at τ 7.17, readily attributable to the lone hydrogen on C-4.

The work-up procedure following the reaction of the octalone **7** with lithium dimethylcopper requires some comment. It had already been noted (15) that, in reactions of this type, hydrolysis of the excess organometallic reagent by addition of water to the ethereal reaction mixture led to the formation of significant amounts of di-addition products. This was attributed (15) to hydrolysis of the intermediate enolate formed from conjugate addition, followed by 1,2-addition of a residual unhydrolyzed "methylcopper" species to the resultant saturated ketone. These workers circumvented this difficulty by altering the isolation procedure so that the reaction mixture was poured into water or aqueous ammonium chloride with vigorous stirring. We found, however, that in the reaction of lithium dimethylcopper with octalone **7**, the latter work-up procedure did not eliminate di-addition and, in fact, produced a product which contained only a relatively small amount of the desired decalone **12**. Therefore, since we felt that the excess organometallic reagent would be destroyed much more rapidly by a stronger acid and would thus no longer be available for subsequent 1,2-addition to the saturated carbonyl of **12**, we carried out the hydrolysis by slowly pouring the reaction mixture into rapidly stirred dilute hydrochloric acid. This procedure proved successful and produced a clean product which contained, in addition to a small amount of starting material (**7**), the desired (±)-eremophil-11-en-3-one (**12**) as the only major component.

Having successfully introduced a methyl group at the bridgehead position of octalone **7**, it became important to determine the stereochemistry of the product (**12**). Although, as noted previously, the copper salt – catalyzed conjugate addition of methyl magnesium halides to various 1(9)-octal-2-ones had invariably resulted in the formation of the corresponding *cis*-fused decalone derivatives, the obscurity of the mechanism of the reaction of lithium dimethylcopper with α,β-unsaturated ketones (15, 16) required that caution be used in assuming that decalone **12** should also possess *cis*-fused six-membered rings. We therefore obtained independent and unambiguous evidence which showed that **12** had the stereochemistry shown.

(±)-Eremophil-11-en-3-one (**12**) was converted, by standard procedure, into the corresponding tosylhydrazone **13**, m.p. 159–161°. Treatment of the latter with sodium borohydride in dioxane (17) gave, in good yield, (±)-eremophil-11-ene (**15***a*). Alternatively, the hydrocarbon (**15***a*) was also obtained by Huang–Minlon reduction (18) of the semicarbazone derivative (**14**) of compound **12**. An analytically pure sample of **15***a* was obtained by preparative g.l.c. and exhibited, in the n.m.r. spectrum, signals at τ 5.38 (unresolved multiplet, $=C^{12}H_2$), τ 8.32 (triplet,

Can. J. Chem. Downloaded from www.nrcresearchpress.com by 210.87.254.6 on 09/05/12
For personal use only.

Can. J. Chem. Downloaded from www.nrcresearchpress.com by 210.87.254.6 on 09/05/12
For personal use only.

—$C^{13}H_3$), τ 9.18 (singlet, —$C^{15}H_3$), and τ 9.28 (doublet, —$C^{14}H_3$, $J_{4,14}$ = 6.5 Hz). Hydrogenation of compound **15***a* over platinum in ethanol gave, in 84% yield, (±)-7β-eremophilane (**16***a*).

Authentic (+)-eremophil-11-ene (**15***b*) and (+)-7β-eremophilane (**16***b*) were obtained by literature procedures (see ref. 19) from hydroxydihydroeremophilone (**2**),[5] a naturally occurring sesquiterpenoid of known absolute configuration (2). Thus, reduction of hydroxydihydroeremophilone acetate (**17**) with calcium in liquid ammonia afforded, in good yield, (+)-dihydroeremophilone (**18**), which, upon Huang–Minlon reduction (18), gave (+)-eremophil-11-ene (**15***b*).[6] The i.r. and n.m.r. spectra of the latter were identical with the corresponding spectra of synthetic (±)-eremophil-11-ene (**15***a*) obtained as described above. In addition, the two compounds exhibited identical g.l.c. retention times on a number of different columns. Hydrogenation of compound **15***b* over platinum in ethanol produced authentic (+)-7β-eremophilane (**16***b*) (6, 20)[7] which exhibited spectra (i.r., n.m.r.) and g.l.c. retention times identical with those of synthetic (±)-7β-eremophilane (**16***a*) (see above). These two comparisons (**15***a* with **15***b*, and **16***a* with **16***b*) conclusively demonstrated that the conjugate addition of lithium dimethylcopper to octalone **7** had, in fact, proceeded to give the desired, *cis*-fused (±)-eremophil-11-en-3-one (**12**).

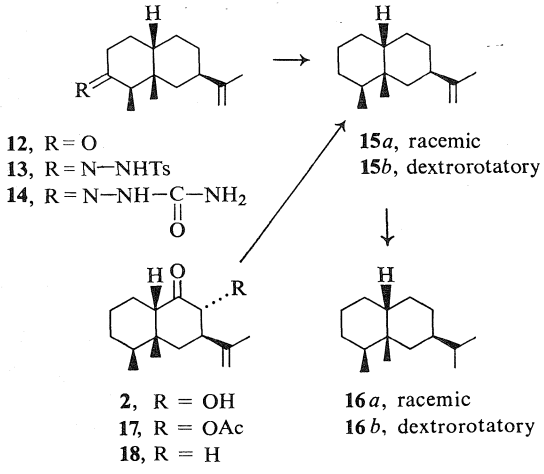

[5]We are very grateful to Professor L. H. Zalkow for a generous sample of hydroxydihydroeremophilone.

[6]Djerassi and co-workers (ref. 19) named this compound *cis*-desoxydihydroeremophilone.

[7]We thank Dr. H. Ishii for a copy of the i.r. spectrum of (+)-7β-eremophilane.

When the tosylhydrazone derivative **13** was heated with sodium ethylene glycolate (Bamford–Stevens reaction) (21), (±)-eremophil-3,11-diene (**3**) was formed in high yield. An analytical sample of this compound was obtained by preparative g.l.c. and exhibited n_D^{20} 1.5052. The n.m.r. spectrum showed a one-proton signal at τ 4.70 (unresolved multiplet, —C^3H), a two-proton signal at τ 5.35 (multiplet, =$C^{12}H_2$), and three 3-proton signals at τ 8.30 (triplet, —$C^{13}H_3$), τ 8.40 (multiplet, —$C^{14}H_3$), and τ 8.96 (singlet, —$C^{15}H_3$). The chemical shifts assigned to the vinylic methyl groups were confirmed by frequency-sweep decoupling experiments. Irradiation of the C-3 proton at τ 4.70 caused substantial sharpening of the multiplet at τ 8.40, while irradiation of the C-12 protons at τ 5.35 caused the poorly resolved triplet at τ 8.30 to collapse to a strong, sharp singlet.

Comparison of our synthetic (±)-eremophil-3,11-diene (**3**) with an authentic sample of eremophilene[8] clearly showed that the two compounds were different. Firstly, the two compounds exhibited different g.l.c. retention times. Secondly, the i.r. spectrum of (±)-eremophil-3,11-diene (**3**) differed, particularly in the "finger-print" region, from the i.r. spectrum of eremophilene. Finally, there were significant differences in the corresponding n.m.r. spectra. The n.m.r. spectrum (9) of eremophilene exhibited unresolved multiplets at τ 4.70 (1H) and τ 5.32 (2H), a triplet at τ 8.29 (3H), a singlet at τ 9.11 (3H), and a doublet (J = 6 Hz) at τ 9.15. Thus, although the n.m.r. spectra of (±)-eremophil-3,11-diene (**3**) and eremophilene were quite similar in the low-field region, the spectrum of **3** clearly showed, at high field,

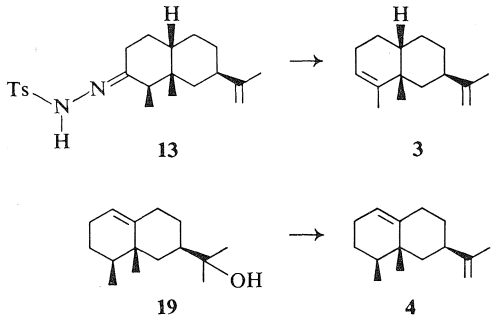

[8]We are very grateful to Dr. J. Křepinský for an authentic sample of eremophilene and to Professor R. B. Bates for a copy of the i.r. and n.m.r. spectrum of this compound.

Can. J. Chem. Downloaded from www.nrcresearchpress.com by 210.87.254.6 on 09/05/12
For personal use only.

two vinylic methyl groups and one tertiary methyl group, while the spectrum of eremophilene showed the presence of only one vinylic methyl group, one tertiary methyl group, and one secondary methyl group.

The stereoselective total synthesis of (±)-eremophil-3,11-diene (**3**), carried out as described above, clearly demonstrated that the original structural proposal (7) for the sesquiterpene eremophilene was incorrect. However, as already noted, Křepinský *et al.* (9), on the basis of new structural and spectroscopic evidence, recently assigned structure **4** to this compound. If this new proposal were correct, then eremophilene (**4**) should be related (by dehydration) to eremoligenol, a naturally occurring sesquiterpene which was isolated from *Ligularia fischeri* Turcz. and was shown to possess structure **19** (20). In fact, the dehydration of eremoligenol (**19**) had already been carried out (20) although the product was not compared with eremophilene (**4**). We were able to secure a sample of eremoligenol (**19**)[9] and found that, upon dehydration with thionyl chloride in pyridine, it gave a hydrocarbon which was identical (i.r., n.m.r., g.l.c.) with authentic eremophilene (**4**).[10] This experiment confirmed that eremophilene is indeed correctly represented by structure **4**.

It should be noted that the conjugate addition of lithium dimethylcopper to the octalone **7**, which stereoselectively produced the decalone **12**, is of particular significance, since this reaction provides a simple and efficient entry into the vicinal dimethyl system found in eremophilane-type sesquiterpenes. We are currently applying this reaction to the synthesis of sesquiterpenes belonging to the eremophilane group.

Experimental

Melting points, which were determined on a Kofler block, and boiling points are uncorrected. Ultraviolet spectra were measured in methanol solution on a Cary spectrophotometer, model 14. Routine i.r. spectra were recorded on a Perkin–Elmer Infracord model 137 spectrophotometer, while all comparison spectra were recorded on a Perkin–Elmer model 421 spectrophotometer. Nuclear magnetic resonance spectra were taken in deuteriochloroform solution on either a Varian Associates model A-60 spectrometer, a Jeolco C-60-H spectrometer, or a Varian Associates model HA-100 spectrometer, with the latter being used for decoupling experiments. Line positions are given in the Tiers τ scale, with tetramethylsilane as an internal standard; the multiplicity, integrated peak areas, and proton assignments are indicated in parentheses. Gas–liquid chromatography was carried out on an Aerograph Autoprep, model 700. The following columns (10 ft × 1/4 in.) were employed, with the inert, supporting material being 60/80 mesh Chromosorb W in each case: column A, 20% Apiezon J; column B, 20% FFAP; column C, 10% FFAP; column D, 15% QF-1; column E, 20% SE30; column F, 20% Carbowax 20M. The specific column used, along with the column temperature, are indicated in parentheses. The carrier gas (helium) flow-rate was 80–85 ml/min in each case. Microanalyses were performed by Mr. P. Borda, Microanalytical Laboratory, University of British Columbia, Vancouver.

3-Isopropenylcyclohexanone (5)

This compound was prepared by the reaction of 2-cyclohexen-1-one with isopropenyl magnesium bromide in the presence of anhydrous cuprous chloride in dry tetrahydrofuran. The procedure employed was essentially identical with that described by House and co-workers (10). From 24.2 g of 2-cyclohexen-1-one there was obtained 24.5 g (71%) of pure 3-isopropenylcyclohexanone as a clear colorless oil, b.p. 69–72° at 7.5 mm, n_D^{26} 1.4749; lit. b.p. 80.5–84° at 8 mm, n_D^{26} 1.4743–1.4749 (10). Infrared (film), λ_{max} 5.85, 6.12, 11.20 μ; n.m.r., τ 5.22 (unresolved multiplet, 2H, $=CH_2$), 8.24 (broadened singlet, 3H, vinyl methyl).

Preparation of Hydroxymethylene Derivative 6

To a stirred slurry of sodium methoxide (31.6 g) in 160 ml of dry benzene was added a solution of ethyl formate (43.3 g) in dry benzene (160 ml). The resulting mixture was cooled to 0° and then a solution of 3-isopropenylcyclohexanone (26.4 g) in 160 ml of benzene was added dropwise, over a period of 20 min. The mixture was allowed to warm to room temperature and then stirred, under an atmosphere of nitrogen, for 50 h. Water (500 ml) was added, the mixture was thoroughly shaken, and the layers separated. The organic layer was extracted with two portions of dilute aqueous sodium hydroxide. The combined aqueous layer and alkaline extracts were cooled, acidified with concentrated hydrochloric acid, and thoroughly extracted with ether. The combined extracts were washed with water and dried over anhydrous sodium sulfate. Removal of the solvent gave a red-brown oil which, upon distillation under reduced pressure, afforded 21 g (75%) of the hydroxymethylene derivative **6** as a light-yellow oil, b.p. 101–102° at 4 mm, n_D^{20} 1.5198. Ultraviolet, λ_{max} 283 mμ; i.r. (film), λ_{max} 6.02, 6.22, 11.15 μ. The instability of this compound precluded the acquisition of satisfactory analytical data.

Preparation of Octalone 7

To a stirred solution of sodium methoxide (2.4 g) in 60 ml of dry methanol was added 11.7 g of the hydroxymethylene derivative **6**. A solution of 1-diethylamino-3-pentanone methiodide (from 15.9 g of 1-diethylamino-3-pentanone and 14.6 g of methyl iodide) in 40 ml of dry methanol was then added dropwise over a period of 20

[9]We thank Dr. H. Ishii for a sample of this compound.

[10]This reaction has also been independently carried out by R. M. Coates and J. E. Shaw, who dehydrated (±)-eremoligenol to (±)-eremophilene. See footnote 3.

Can. J. Chem. Downloaded from www.nrcresearchpress.com by 210.87.254.6 on 09/05/12
For personal use only.

min and the resulting solution was stirred at room temperature, under an atmosphere of nitrogen, for 26 h. The solution was poured into ice-cold dilute hydrochloric acid which had been saturated with ammonium sulfate. The resulting mixture was extracted thrice with ether, and the combined ether extracts were concentrated under reduced pressure. The residual material was stirred for 1 h, under nitrogen with 630 ml of 2% aqueous sodium hydroxide (deformylation). The basic mixture was extracted with ether and the ether extract was dried over anhydrous sodium sulfate. Removal of the solvent afforded a yellow oil (14.5 g) which exhibited in the i.r., a strong saturated carbonyl absorption (5.86 μ) and only a weak α,β-unsaturated carbonyl absorption (6.02 μ). Therefore, the oil was dissolved in 125 ml of dry methanol containing 0.5 g of sodium methoxide and the resulting solution was refluxed for approximately 6 h, at which time the α,β-unsaturated carbonyl absorption, in the i.r., of an acid-quenched aliquot of the reaction solution, had attained a maximum intensity. After removal of the methanol under reduced pressure, the residual material was diluted with water (50 ml), acidified with dilute hydrochloric acid, and then extracted with ether. The combined ether extracts were washed once with water and dried (anhydrous sodium sulfate). Removal of the ether yielded a pale-yellow oil which, upon distillation under reduced pressure gave, in addition to a small amount (0.6 g) of 3-isopropenylcyclohexanone, 10 g (70%) of a pale-yellow oil, b.p. 127–131° at 0.3 mm. This material contained, as shown by g.l.c. (column A, 230°), approximately 92% of the desired octalone (**7**). An analytical sample of **7** was obtained by preparative g.l.c. (column A, 230°) and exhibited n_D^{24} 1.5320. Ultra violet, λ_{max} 249 mμ (ε = 14 600); i.r. (film), λ_{max} 6.00 6.19, 11.25 μ; n.m.r., τ 5.26 (unresolved multiplet, 2H, $=C^{12}H_2$), 8.22 (poorly resolved quartet, 3H, $-C^{14}H_3$, J = 1.2 and 1.8 Hz, homoallylic coupling (ref. 22 p. 110)), 8.25 (triplet, 3H, $-C^{13}H_3$, J = 1.2 Hz, allylic coupling (ref. 22 p. 108)). The chemical shifts assigned to $-C^{13}H_3$ and $-C^{14}H_3$ were confirmed by a frequency-sweep decoupling experiment in which the olefinic protons at C-12 were strongly irradiated, whereupon the triplet at τ 8.12 collapsed to a strong, sharp singlet, while the quartet at τ 8.22 remained unaffected.

Anal. Calcd. for $C_{14}H_{20}O$: C, 82.30; H, 9.87. Found: C, 82.43; H, 10.03.

The oxime derivative of octalone **7**, after recrystallization from methanol, exhibited m.p. 163–165°.

Anal. Calcd. for $C_{14}H_{21}NO$: C, 76.66; H, 9.65; N, 6.39. Found: C, 76.84; H, 9.55; N, 6.21.

*(±)-Eremophil-11-en-3-one (**12**) and Derivatives (**13**, **14**)*

The following reaction was carried out under an atmosphere of dry nitrogen. To a stirring, ice-cold (0°) slurry of cuprous iodide (6.0 g) in 120 ml of anhydrous ether was added, by injection from a dry syringe, 39.4 ml of 1.59 *M* ethereal methyllithium. The resulting tan-colored solution, containing the lithium dimethylcopper reagent, was stirred at 0° for 5 min, and then a solution of octalone **7** (2.0 g) in 80 ml of anhydrous ether was added dropwise over a period of 20 min. The reaction mixture was stirred for an additional 2 h at 0°, and then poured into 800 ml of vigorously stirred 1.2 *N* hydrochloric acid. The resulting mixture was extracted thoroughly with ether. The combined ether extracts were washed with water and dried over anhydrous sodium sulfate. Removal of the solvent gave a light-yellow oil which, upon distillation under reduced pressure, afforded 1.9 g of a clear colorless liquid, b.p. 123.5–124.5° at 0.03 mm. This material contained, as shown by g.l.c. (column B, 215°), approximately 5% starting material (octalone **7**), 82% of the desired (±)-eremophil-11-en-3-one (**12**), and a number of minor, unidentified components. Preparative g.l.c. (column B, 215°), allowed the isolation of an analytical sample of compound **12**, n_D^{20} 1.5041. Infrared (film), λ_{max} 5.86, 6.10, 11.27 μ; n.m.r., τ 5.33 (unresolved multiplet, 2H, $=C^{12}H_2$), 7.17 (quartet, 1H, $-C^4H$, $J_{4,14}$ = 6.7 Hz), 8.29 (poorly resolved triplet, 3H, $-C^{13}H_3$), 9.11 (doublet, 3H, $-C^{14}H_3$, $J_{4,14}$ = 6.7 Hz), 9.21 (singlet, 3H, $-C^{15}H_3$).

Anal. Calcd. for $C_{15}H_{24}O$: C, 81.76; H, 10.98. Found: C, 81.61; H, 10.71.

Reaction of (±)-eremophil-11-en-3-one (**12**) with *p*-toluenesulfonylhydrazine under standard conditions afforded a good yield of the tosylhydrazone (**13**), which, after recrystallization from methanol, exhibited m.p. 159–161°.

Anal. Calcd. for $C_{22}H_{32}N_2O_2S$: C, 68.00; H, 8.30; N, 7.21; S, 8.25. Found: C, 68.22; H, 8.41; N, 7.41; S, 8.11.

Reaction of compound **12** with semicarbazide afforded the corresponding semicarbazone **14**, which was recrystallized from methanol, m.p. 191.5–193.5°.

Anal. Calcd. for $C_{16}H_{27}N_3O$: C, 69.27; H, 9.81; N 15.15. Found: C, 69.20; H, 9.98; N, 15.05.

*(±)-Eremophil-11-ene (**15a**)*

*(a) From Tosylhydrazone **13***

A stirred solution of the tosylhydrazone **13** (0.5 g) and sodium borohydride (0.3 g) in 20 ml of dioxane was refluxed, under an atmosphere of nitrogen, for 20 h. The dioxane was removed under reduced pressure and the residue was diluted with water. The resulting mixture was extracted thoroughly with pentane. The combined extracts were washed with water, dried (anhydrous sodium sulfate), and concentrated. The residual colorless oil (0.27 g) was shown by g.l.c. (column D, 130°) to contain 95% of (±)-eremophil-11-ene (**15a**), with only minor impurities. An analytical sample of **15a** was collected by preparative g.l.c. (column D, 130°) and exhibited n_D^{24} 1.4933. Infrared (film), λ_{max} 6.10, 11.28 μ; n.m.r., τ 5.38 (unresolved multiplet, 2H, $=C^{12}H_2$), 8.32 (poorly resolved triplet, 3H, $-C^{13}H_3$), 9.18 (singlet, 3H, $-C^{15}H_3$), 9.28 (doublet, 3H, $-C^{14}H_3$, $J_{4,14}$ = 6.5 Hz). This material was shown to be spectroscopically (i.r., n.m.r.) identical with (+)-eremophil-11-ene (**15b**) obtained from hydroxydihydroeremophilone (**2**) (see below).

Anal. Calcd. for $C_{15}H_{26}$: C, 87.30; H, 12.70. Found: C, 87.02, H, 12.79.

*(b) By Huang–Minlon Reduction of Semicarbazone **14***

A stirred solution of the semicarbazone **14** (2.0 g), 85% hydrazine hydrate (1.8 ml), and potassium hydroxide (1.9 g) in 20 ml of diethylene glycol was heated to 190–195° and maintained at this temperature for 24 h. The cooled solution was poured into water (100 ml) and the resulting mixture was extracted thoroughly with ether. The combined extracts were washed with water, dried

Can. J. Chem. Downloaded from www.nrcresearchpress.com by 210.87.254.6 on 09/05/12
For personal use only.

(anhydrous sodium sulfate), and concentrated, yielding 1.47 g of a pale-yellow oil. The latter material showed virtually one component by g.l.c. (column C, 140°). An analytical sample, obtained by preparative g.l.c. (column C, 140°), was identical in all respects with (±)-eremophil-11-ene (**15***a*) obtained as described above.

*(±)-7β-Eremophilane (**16***a*)

This compound was obtained by hydrogenation (platinum oxide, ethanol) of (±)-eremophil-11-ene (**15***a*), at room temperature and atmospheric pressure. From 0.65 g of **15***a* there was obtained 0.6 g of (±)-7β-eremophilane. An analytical sample of the latter, obtained by preparative g.l.c. (column C, 135°), exhibited n_D^{24} 1.4820. Infrared (film), 6.82, 6.92, 7.25, 7.32 μ; n.m.r., τ 9.15 (doublet, 6H, —$C^{12}H_3$ and —$C^{13}H_3$, J = 6.0 Hz), 9.16 (singlet, 3H, —$C^{15}H_3$), 9.28 (doublet, 3H, —$C^{14}H_3$, $J_{4,14}$ = 6.8 Hz). The i.r. and n.m.r. spectra of this compound were found to be identical with the corresponding spectra of authentic (+)-7β-eremophilane (**16***b*) obtained from hydroxydihydroeremophilone (**2**) (see below).

*(+)-Dihydroeremophilone (**18**)*

Hydroxydihydroeremophilone acetate (**17**), which was obtained by acetylation (19) of hydroxydihydroeremophilone (**2**), was reduced with calcium in liquid ammonia. The procedure employed was identical with that reported by Djerassi and co-workers (19). The product, (+)-dihydroeremophilone (**18**), was obtained in 60% yield. Infrared (film), λ_{max} 5.86, 6.08, 11.20 μ; n.m.r., τ 5.26 (unresolved multiplet, 2H, =$C^{12}H_2$), 8.27 (poorly resolved triplet, 3H, —$C^{13}H_3$), 8.97 (singlet, 3H, —$C^{15}H_3$), 9.23 (doublet, 3H, —$C^{14}H_3$, $J_{4,14}$ = 5.9 Hz).

*(+)-Eremophil-11-ene (**15***b*)

This compound was obtained, according to a literature procedure (19), by Huang–Minlon reduction of (+)-dihydroeremophilone (**18**). An analytical sample of **15***b*, obtained by preparative g.l.c. (column C, 140°), gave spectra (i.r., n.m.r.) and g.l.c. retention times (four different columns: A, 180°; B, 168°; D, 120°; E, 180°) identical with those of synthetic (±)-eremophil-11-ene (**15***a*), obtained as described above.

*(+)-7β-Eremophilane (**16***b*)

Hydrogenation of (+)-eremophil-11-ene (**15***b*) (see ref. 20) at room temperature and atmospheric pressure over platinum in ethanol afforded (+)-7β-eremophilane (**16***b*). An analytical sample was obtained by preparative g.l.c. (column F, 140°). This material exhibited i.r. and n.m.r. spectra, as well as g.l.c. retention times on three different columns (D, 120°; E, 158°; B, 158°) identical with those of synthetic (±)-7β-eremophilane (**16***a*) prepared as described above.

*(±)-Eremophil-3,11-diene (**3**)*

The Bamford–Stevens reaction (21) on the tosylhydrazone **13** was carried out as follows. Sodium metal (10.0 g) was dissolved in ethylene glycol (100 ml). To this solution was added 1.5 g of the tosylhydrazone **13**, and the solution was then refluxed, under an atmosphere of nitrogen, for 2h. The solution was cooled and poured into ice-cold water. The resulting mixture was extracted thoroughly with ether. The combined extracts were washed twice with water and dried over anhydrous sodium sulfate. Removal of the ether gave a yellow oil, which upon distillation under reduced pressure afforded 0.75 g (95%) of a clear colorless liquid, b.p. 85–88° (bath temperature) at 0.38 mm, which was shown by g.l.c. (column C, 135°) to be approximately 90% pure. An analytical sample of the major component, (±)-eremophil-3,11-diene (**3**), was collected by preparative g.l.c. (column C, 135°) and exhibited n_D^{20} 1.5052. Infrared (film), λ_{max} 6.10, 6.95, 7.32, 11.28 μ; n.m.r., τ 4.70 (unresolved multiplet, 1H, —C^3H, width at half-height = 8 Hz), 5.35 (unresolved multiplet, 2H, =$C^{12}H_2$, width at half-height = 3.5 Hz), 8.30 (triplet, 3H, —$C^{13}H_3$), 8.40 (unresolved multiplet, 3H, —$C^{14}H_3$), 8.96 (singlet, 3H, —$C^{15}H_3$). The chemical shifts assigned to the vinylic methyl groups were confirmed by frequency-sweep decoupling experiments. Thus, strong irradiation of the olefinic signal at τ 4.70 (—C^3H) caused considerable sharpening of the multiplet at τ 8.40, while similar irradiation of the C-12 protons (τ 5.35) caused the triplet at τ 8.30 to collapse to a strong, sharp singlet. The i.r. and n.m.r. spectra of (±)-eremophil-3,11-diene (**3**) were clearly different from the corresponding spectra of an authentic sample of eremophilene (**4**). Also, the g.l.c. retention times (column C, 135°) of the two compounds were different.

Anal. Calcd. for $C_{15}H_{24}$: C, 88.16; H, 11.84. Found: C, 88.36; H, 11.98.

*Eremophilene (**4**) by Dehydration of Eremoligenol (**19**)*

The dehydration of eremoligenol (**19**) was carried out by a procedure identical with that described by Ishii, Tozyo, and Minato (20). From 44 mg of eremoligenol there was obtained 34 mg of crude product as a pale-yellow oil. An analytical sample of eremophilene was obtained from the crude product by means of preparative g.l.c. (column A, 180°). Infrared (film), λ_{max} 6.08, 6.85, 7.28, 11.30 μ; n.m.r., τ 4.70 (multiplet, 1H, —C^1H, width at half-height = 7 Hz), 5.32 (multiplet, 2H, =$C^{12}H_2$, width at half-height = 4 Hz), 8.29 (triplet, 3H, —$C^{13}H_3$), 9.11 (singlet, 3H, —$C^{15}H_3$), 9.15 (doublet, 3H, —$C^{14}H_3$, $J_{4,14}$ = 6 Hz). This material was shown to be identical (i.r., n.m.r., g.l.c. retention times on three different columns: A, 180°; C, 140°; F, 185°) with an authentic sample of natural eremophilene.

Acknowledgments

We very gratefully acknowledge financial support from the National Research Council of Canada and from the University of British Columbia Committee on Research.

1. W. Parker and J. S. Roberts. Quart. Rev. London, **21**, 331 (1967).
2. L. H. Zalkow, F. X. Markley, and C. Djerassi. J. Am. Chem. Soc. **82**, 6354 (1960), and references therein.
3. A. E. Bradfield, A. R. Penfold, and J. L. Simonsen. J. Chem. Soc. 2744 (1932).
4. G. Ourisson, S. Munavalli, and C. Ehret. International tables of selected constants. Vol. 15. Data relative to sesquiterpenoids. The Pergamon Press, Ltd., New York. 1966.
5. J. Hochmannová, L. Novotný, and V. Herout. Collection Czech. Chem. Commun. **27**, 1870 (1962).

6. J. HOCHMANNOVÁ, L. NOVOTNÝ, and V. HEROUT. Collection Czech. Chem. Commun. **27**, 2711 (1962).
7. J. HOCHMANNOVÁ and V. HEROUT. Collection Czech. Chem. Commun. **29**, 2369 (1964).
8. E. PIERS and R. J. KEZIERE. Tetrahedron Letters, 583 (1968).
9. J. KŘEPINSKÝ, O. MOTL, L. DOLEJŠ, L. NOVOTNÝ, V. HEROUT, and R. B. BATES. Tetrahedron Letters, 3315 (1968).
10. H. O. HOUSE, R. A. LATHAM, and C. D. SLATER. J. Org. Chem. **31**, 2667 (1966).
11. D. K. BANERJEE, S. CHATTERJEE, and S. P. BHATTACHARYA. J. Am. Chem. Soc. **77**, 408 (1955).
12. J. A. MARSHALL, W. I. FANTA, and H. ROEBKE. J. Org. Chem. **31**, 1016 (1966), and references therein.
13. J. A. MARSHALL and H. ROEBKE. J. Org. Chem. **33**, 840 (1968).
14. R. F. CHURCH, R. E. IRELAND, and D. R. SHRIDHAR. J. Org. Chem. **27**, 707 (1962).
15. H. O. HOUSE, W. L. RESPESS, and G. M. WHITESIDES. J. Org. Chem. **31**, 3128 (1966).
16. H. O. HOUSE and W. F. FISCHER, JR. J. Org. Chem. **33**, 949 (1968).
17. L. CAGLIOTI. Tetrahedron, **22**, 487 (1966), and references therein.
18. HUANG-MINLON. J. Am. Chem. Soc. **68**, 2487 (1946).
19. C. DJERASSI, R. MAULI, and L. H. ZALKOW. J. Am. Chem. Soc. **81**, 3424 (1959).
20. H. ISHII, T. TOZYO, and H. MINATO. J. Chem. Soc. C, 1545 (1966).
21. W. R. BAMFORD and T. S. STEVENS. J. Chem. Soc. 4735 (1952).
22. N. S. BHACCA and D. H. WILLIAMS. Applications of nuclear magnetic resonance spectroscopy in organic chemistry. Holden-Day, Inc., San Francisco. 1964.

Can. J. Chem. Downloaded from www.nrcresearchpress.com by 210.87.254.6 on 09/05/12
For personal use only.

Preparative conversion of oximes to parent carbonyl compounds by cerium(IV) oxidation[1]

J. W. Bird and D. G. M. Diaper
Department of Chemistry, Royal Military College of Canada, Kingston, Ontario
Received August 12, 1968

Oximes and semicarbazones are oxidized by ceric ammonium nitrate to the parent carbonyl compound in good yield. Suitable solvent systems include aqueous alcohols, acetonitrile, and acetic acid. The reaction is rapid at 0° or below. This procedure for regeneration of aldehydes and ketones from these derivatives may be preferable to the well-known hydrolytic procedures in some cases. The stoichiometry of the reaction was studied by isothermal calorimetry; two equivalents of oxidant are consumed by one mole of oxime evolving approximately 40 kcal/mole. A smaller consumption of oxidant by hexane-2,5-dione dioxime was attributed to stabilization of the monoxime as a nitroso chelate. Gaseous products were studied by infrared spectroscopy and nitrous oxide was identified as the sole product absorbing between 3 and 15 μ. A reaction mechanism is proposed involving one-electron oxidation to the iminoxy radical, oxidized by a second one-electron step to the α-hydroxy nitroso compound. Dimerization and elimination of hyponitrous acid gives the carbonyl compound. Nitrocyclohexane was absent from the oxidation product from cyclohexanone oxime. Carvone oxime was oxidized to carvone without racemization or significant attack of the olefin groups.

Canadian Journal of Chemistry, **47**, 145 (1969)

Can. J. Chem. Downloaded from www.nrcresearchpress.com by 210.87.254.42 on 09/05/12
For personal use only.

Introduction

The formation of oxime and semicarbazone derivatives is a common method of isolating, purifying, identifying, and characterizing carbonyl compounds. This is especially true with natural products, for example the separation of ketone hormone intermediates obtained by oxidation of sterols may be done by formation of the sparingly soluble semicarbazones (1). After purification the regeneration of the original ketone or aldehyde is then encountered.

A number of good procedures exist including direct acid hydrolysis (2), acid-catalyzed exchange with pyruvic acid (1), levulinic acid (6) or formaldehyde (7), nitrous acid in acetic acid (8–10), and most recently cleavage with bisulfite (11). These procedures are all hydrolytic and several involve equilibrium reaction of hydroxylamine with a more reactive carbonyl compound. They may take a number of hours to go to equilibrium or completion. Common hydrolytic procedures especially applicable to semicarbazones include sulfuric acid in ethanol (2), sulfuric acid in dioxane (3, 4) hydrochloric and acetic acids (5), and sodium nitrite and acetic acid (8). Some of the procedures are drastic and can lead to condensation products or hydrolysis of sensitive protecting groups such as acetoxy groups.

There are occasions when a mild procedure is required which is quick and will not affect other groups present in the molecule. We believe a fast, mild, and usually satisfactory procedure has now been found in the oxidation of oximes and semicarbazones by cerium(IV).

Diaper and Richardson (12) have used the discharge of alcohol – ceric ammonium nitrate orange colors as a colorimetric quantitative determination method for oximes and other easily oxidized compounds. There has been some literature on oxime oxidations but when carbonyl compounds have been recovered the yield is poor (13).

Oxidants of the donor or peroxide type give nitro compounds. Thus oxidations with manganese dioxide in acetic acid (14, 15) result in high yields of the nitro compound. Employing trifluoroacetic acid and hydrogen peroxide results also in 50–80% yields of the nitro compounds (16, 17). Recently much work has been done on the electron spin resonance identification of iminoxy radicals produced by oxime oxidation, the usual oxidant being lead tetraacetate (18–24), although ceric ammonium nitrate in methanol has also been used (19).

Ceric ammonium nitrate as an oxidant has attracted considerable attention lately. It can be used in aqueous solutions and partly organic solutions including aqueous acetic acid. It may be used in aqueous alcohols if the temperature is kept low to minimize attack on the solvent itself. Its power as an oxidant is evident from the fact

[1]Presented at the Vancouver meeting of The Chemical Institute of Canada, June 1968.

Can. J. Chem. Downloaded from www.nrcresearchpress.com by 210.87.254.42 on 09/05/12
For personal use only.

that the standard redox potential of Ce(IV)–Ce(III) is approximately 1.6 V. An interesting feature of its use as a preparative oxidant is the ability to oxidize benzyl alcohols smoothly to benzaldehydes (25) without significant further oxidation of the aldehyde to the aromatic acid. It was this fact and the earlier colorimetric work which recommended this reagent to our attention.

In our procedure low reaction temperatures were employed, but the solubility of the oxime or semicarbazone in the solvent became a factor limiting the temperature. Choice of solvents other than alcohols is limited by considerations of low-temperature solubility of reagent and substrate. Reactions were rapid and easy to follow, because the color was discharged or diminished and vigorous gas evolution occurred for a few minutes. Transient blue colors were often seen. After dilution with water, the carbonyl compound was recovered by solvent extraction.

Experimental

Solutions were concentrated under reduced pressure below 50° in a rotating evaporator. Melting points were determined on a Fisher–Johns hotstage apparatus and are uncorrected. Infrared (i.r.) spectra were determined using a Perkin–Elmer Infracord model 137. Nuclear magnetic resonance (n.m.r.) spectra were obtained using samples in $CDCl_3$ containing 6% of tetramethylsilane as an internal standard. The instrument was a Varian A-60-A spectrometer. Gas–liquid chromatography (g.l.c.) was performed on a Burrell "Kromotog" model KD gas chromatograph with a thermal conductivity detector. Columns were constructed of $\frac{3}{16}$ in. copper tubing 20 ft. long coiled with a diameter of approximately 4 in. The liquid phase was Carbowax 4000, 5% on Chromosorb P (60–80 mesh). Helium flow rates of 45–110 ml/min and temperatures of 105–170 °C were employed. Columns were conditioned for at least 18 h at 190° before use.

The internal standard method was used in the determination of the yields of recovered aldehydes and ketones. An appropriate ketone with a symmetrical, well resolved peak eluting reasonably close to the peak of interest was selected as an internal standard: thus cycloheptanone was used for determination of *d*-camphor or cyclohexanone yields, *d*-camphor for *l*-carvone, and cyclohexanone for cycloheptanone and heptaldehyde. Peak areas were measured by multiplying the peak height by the width at the middle.

A study of the stoichiometry of the reaction was made using an isothermal calorimeter. It was an all-glass ice calorimeter similar to that described by Vallee (26). In principle the reaction takes place in a tube surrounded by ice. Melting of the ice mantle causes a mercury meniscus to move along a graduated horizontal capillary, whose calibration, determined electrically, corresponded to 1.23 cal/cm. The aqueous solution of ceric ammonium nitrate (0.2–0.7 *M* in *N* HNO_3) was initially pipetted into the vessel containing methanol (25 ml) at 0°. A solution of the oxime in absolute alcohol of known concentration was sealed into a weighed fragile glass bulb and introduced. A steady drift (fore-drift) of approximately 0.1 cal/min was observed. The bulb was broken with a stirrer and rapid evolution of heat observed. At the end of 30–40 min the rate of drift (after-drift) was usually about the same as that of the fore-drift. The heat evolution was measured by finding the difference between the extrapolated fore-drift and after-drift lines at the time of mixing. Blanks (0.3–0.5 cal) were determined and subtracted from the heat measured (30–40 cal per determination). Results were expressed graphically for cyclohexanone oxime (Fig. 1) and heptaldoxime (Fig. 2). Benzophenone oxime similarly gave a graph indicating consumption of 1.87 equivalents of oxidant per mole evolving 39.8 kcal/mole. Hexane-2,5-dione dioxime used 3.47 equivalents or 1.735 equivalents of oxidant per oxime group; the evolved heat was 19 kcal per equivalent of Ce(IV). In all isothermal calorimeter experiments, solutions were so dilute that gas evolution did not occur.

Preparation of Oximes and Semicarbazones

Heptaldoxime was a commercial sample (Eastman No. 3001) and had constants in agreement with literature values. Other oximes were prepared from the carbonyl compound and hydroxylamine hydrochloride in aqueous or aqueous–alcoholic basic media as appropriate. Semicarbazones were similarly prepared using semicarbazide hydrochloride. Melting points agreed with literature values; α-*l*-carvoxime had m.p. 74–75° and $[\alpha]_D^{22}$ −39.1° (1.98 g in 18.88 g of 95% ethanol). Wallach (27) found m.p. 73.5°, $[\alpha]_D^{19}$ −43.5° (1.9799 g in 18.8826 g of 95% ethanol).

Oxidation of Oximes and Semicarbazones

In a typical experiment the oxime or semicarbazone (5 mmoles) was dissolved in ethanol (20 ml) and cooled

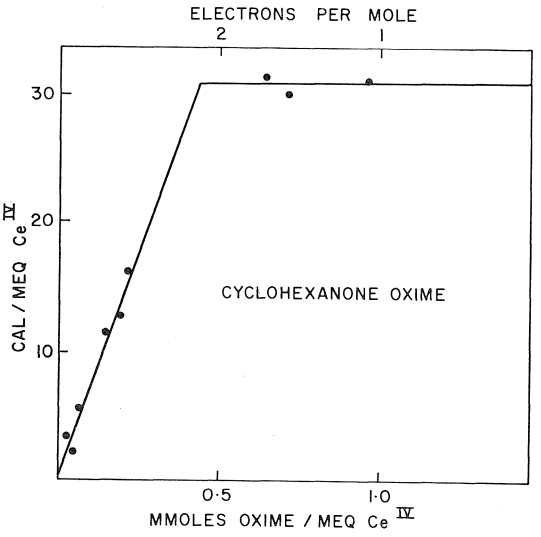

FIG. 1. Heat liberated in the reaction of ceric ammonium nitrate with cyclohexanone oxime.

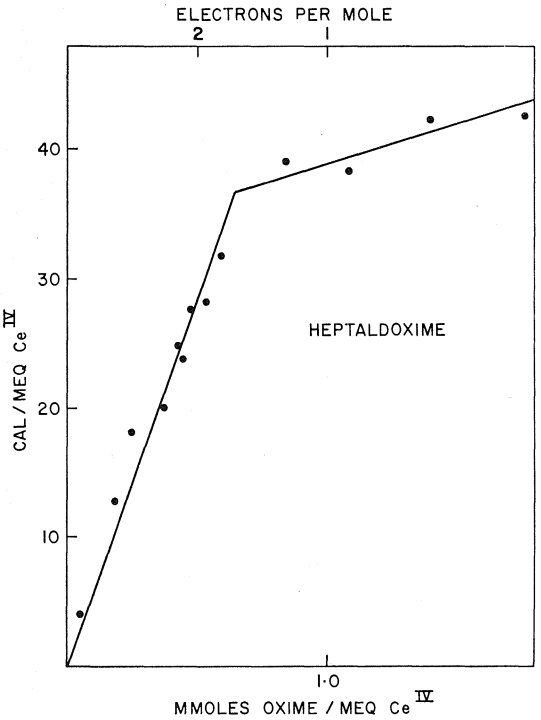

FIG. 2. Heat liberated in the reaction of ceric ammonium nitrate with heptaldoxime.

to the reaction temperature. The oxidant was prepared by mixing 20 mmoles (100% excess) of aqueous ceric ammonium nitrate (0.3 *M* in 0.5 or 1.0 *N* HNO_3, 67 ml) at 0 °C with ethanol at −40° and adjusting to the desired reaction temperature. A little care must be taken to avoid precipitation of ceric ammonium nitrate. The ceric solution was then mixed with the oxime solution, stirred manually, and maintained at the reaction temperature for 5 min. The mixture was diluted with an equal volume of ice water and immediately extracted with chloroform or other immiscible solvent (e.g. three portions of 50 ml). Extracts were dried over anhydrous $MgSO_4$, filtered, and the solvent was removed by distillation at atmospheric pressure. The yields of carbonyl compounds are summarized in Table I. Oxidation temperatures, solvents, and isolation methods were varied to attempt to optimize yields. Results are given in Table II.

Oxidation of Carvone Oxime

Carvone oxime (0.826 g, 5 mmoles) was dissolved in ethanol and cooled to −20°. To this was added the ceric oxidant solution prepared by mixing ceric ammonium nitrate (0.3 *M* in 0.5 *N* HNO_3, 40 ml, 10.2 meq) with ethanol (95%, 50 ml) at −40 °C and adjusted to −20 °C. The reaction mixture was held at −20±2° for 5 min then diluted with an equal volume of cold water and extracted immediately with pentane (three portions of 75 ml). The organic layer was washed with saturated sodium bicarbonate solution, water, dried ($MgSO_4$), and filtered. After removal of the pentane by distillation the resultant solution was divided into aliquots and analyzed by g.l.c. The average yield was 71%.

In a separate experiment to examine the purity of the recovered carvone the proportions of reactants above were doubled and the same procedure followed except that the pentane was removed by rotary evaporation below 40 °C. The resulting liquid was distilled at 10 mm and approximately 108 °C in a short-path distillation apparatus. The carvone had $[\alpha]_D^{24}$ −54.2° (*c*, 2.60, 95% ethanol). A sample of the carvone starting material was purified by vacuum distillation (123–125 °C, 33 mm) and found to have $[\alpha]_D^{24}$ −54.9° (*c*, 2.611, 95% ethanol). The n.m.r. spectra of the two carvone samples were identical with each other and with the published spectrum.

Examination of the Gaseous Product

Cyclohexanone oxime (10 mmoles) in 50% aqueous acetic acid (100 ml) was placed in a flask fitted with a dropping funnel and gas inlets and outlets. The solution was cooled to 0 °C and stirred magnetically while a solution of ceric ammonium nitrate (134 ml, 40 mmoles, 0.3 *M* in *N* HNO_3) was added dropwise. A stream of hydrogen was passed through the mixture to sweep out volatile products. They passed first into a trap cooled in solid CO_2/acetone and then into a trap cooled in liquid air (N_2O boils at −90°). After addition of the oxidant was complete (30–40 min) the reaction mixture was warmed to room temperature while stirring continued. One hour later the hydrogen stream was interrupted. The trap, cooled in liquid air, was connected to a gas cell for use with the i.r. spectrometer and flushed with hydrogen. This cell had NaCl windows 10 cm apart. The trap was allowed to warm slowly to room temperature and the volatilized contents were displaced by hydrogen into the cell. The spectrum had strong sharp absorption peaks at 4.48, 4.55, 7.75, and 7.9 μ. There were no other peaks. Similar peaks were seen in the spectra of the volatile products from cyclopentanone oxime and acetophenone oxime and from cyclohexanone oxime oxidized by ceric ammonium nitrate made up in aqueous acetic acid in place of nitric acid. A control experiment was

TABLE I

Cerium(IV) oxidation of oximes and semicarbazones

Oxime of	Ketone yield (%)§
Cyclohexanone	88
Cyclopentanone	83
Camphor	27
Carvone	71
Cycloheptanone	82
Acetophenone	90†, 74*
Heptanal	72‡
Benzophenone	79*
Semicarbazone of	
Cycloheptanone	81
Cyclohexanone	78

*By weight of 2,4-dinitrophenylhydrazone formed.
†Vacuum distilled and weighed.
‡Aldehyde yield.
§Yield determined by g.l.c.

Can. J. Chem. Downloaded from www.nrcresearchpress.com by 210.87.254.42 on 09/05/12
For personal use only.

TABLE II
Oxidation conditions

Compound	Temperature (°C)	Solvent	Isolation method¶	Ketone yield (%)*
Cyclohexanone oxime	−15 to −20	EtOH	A,B	77–80
	0	EtOH	A,B	73–81
	−20 to −30	MeOH	A,B	74, 82
	−15 to −20	EtOH	A,C	80–84
	− 7 to −12	EtOH	A,C	88
	− 7 to −12	CH_3CN	A,C	65–72
	− 7 to −12	CH_3CN	D,C	32–35
	−15 to −20	EtOH	A,B†	78–78.5
Cycloheptanone oxime	−12 to −17	EtOH	A,C	75–82
Acetophenone oxime	−10 to −15	EtOH	A,C,E	90‡,§
Heptaldoxime	− 5 to −10	EtOH	A,C	25–27‖
	0 to 4	EtOH	A,C	49‖
	0 to 2	CH_3CN	A,C	49–55‖
	0 to − 4	CH_3CN	D,C	69–75‖
Carvone oxime	−10	EtOH	A,C	62–63
	0	EtOH	A,C	66–66.5
	−20	EtOH	D,C	70–72§
Cyclopentanone oxime	−20	MeOH	A,B	83
Cycloheptanone semicarbazone	− 5 to −10	EtOH	A,C	79.5–82.5
Cyclohexanone semicarbazone	−12 to −17	EtOH	A,C	74–81

*Yield determined by g.l.c. except where noted.
†Oxidation by 0.295 *M* ceric ammonium nitrate in 0.5*N* acetic acid.
‡Yield determined by weight of recovered product.
§An n.m.r. spectrum was indistinguishable from the spectrum of an authentic sample.
‖Aldehyde yield.
¶NOTE: A, chloroform extraction; B, rotary evaporated below 30 °C; C, solvent removed by distillation; D, pentane extraction; E, product purified by vacuum distillation.

performed by flushing the cell with hydrogen and introducing authentic nitrous oxide from a cylinder. The spectrum was identical with that of the oxime product.

Results and Discussion

In most cases a reasonable recovery of carbonyl compound from the oxime or semicarbazone was obtained. Low yields from camphor oxime may be attributable to steric hindrance. The Ce(IV) oxidant appears to differ from oxidants of the donor type in that nitroalkane formation was not observed, and, for the cyclohexanone oxime case, it was shown by g.l.c. to be entirely absent. Identification of nitrous oxide evolved, earlier work on iminoxy radical formation, observation of blue-green colors, and the observed stoichiometry of two electrons per oxime group lead us to propose the reaction mechanism scheme outlined:

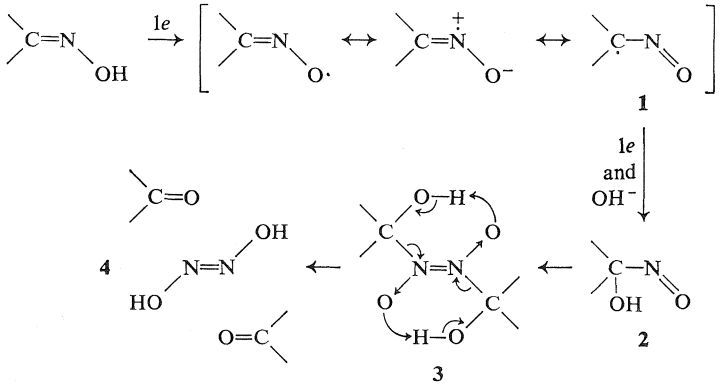

Can. J. Chem. Downloaded from www.nrcresearchpress.com by 210.87.254.42 on 09/05/12
For personal use only.

Can. J. Chem. Downloaded from www.nrcresearchpress.com by 210.87.254.42 on 09/05/12
For personal use only.

The iminoxy radical known to be the first product of oxime oxidation, is produced in a one-electron step, so a second oxidation process, involving one electron per mole, must be postulated. Hybridization of the radical has been discussed by other authors. The radical can be oxidized to a cation having a canonical structure positively charged on the carbon atom. The hydroxy-nitroso intermediate **2** has not been isolated, but an analogous compound, 4-*t*-butyl-1-acetoxy-1-nitrosocyclohexane, was observed by Lown (23) in the oxidation of 4-*t*-butylcyclohexanone oxime by lead tetraacetate. It was obtained as a blue oil and a white crystalline dimer. Compound **2** would dimerize to **3** shown in the *trans* type of structure discussed by Gowenlock (28) for dimeric unsubstituted nitroso-hydrocarbons. An α-hydroxy-nitroso compound, monomer or dimer, is analogous to other α-hydroxy chlorides and *gem* diols. By analogy with them, easy decomposition would be expected and could take place as shown to give hyponitrous acid (**4**) and the carbonyl compound. Compound **4** is a postulated intermediate in the oxidation of hydroxylamine itself to nitrous oxide.

Dimerization of the iminoxy radical through the oxygen atoms would not lead to nitrous oxide but to a peroxide; dimerization through nitrogen would violate the adjacent charge rule. Such mechanisms are therefore discarded. Another possible mechanism, hydrolysis to hydroxylamine and oxidation of the latter, is considered unlikely since oxime hydrolysis is known to be a much slower process than the oxidative cleavage studied.

While the examples given in the Tables are drawn from aliphatic, alicyclic, or aromatic classes, the reaction may be general. The carvone oxime experiment shows that it is possible for good recovery of the ketone to be achieved when the molecule contains other oxidizable groups. Moreover, retention of most of the optical activity indicated that the conditions of the reaction are sufficiently mild for general application in natural product work.

Semicarbazones in general are less rapidly oxidized than oximes and their lower solubility poses problems in the choice of solvent and conditions. The inorganic products of semicarbazone oxidation were not studied.

The stoichiometry of the oxidation was observed by isothermal calorimetry and indicated consumption of two equivalents of oxidant per mole of oxime. Slightly more than two equivalents for cyclohexanone (Fig. 1) was absorbed because of further attack on the ketone. Heptaldehyde (Fig. 2) also showed evidence of two or more simultaneous reactions in the isothermal calorimeter. The break in the curve was in the vicinity of two electrons per mole, but for high oxime to oxidant ratios the heat liberation increased. A similar slight rise, though less steep, was seen in the hexane-2,5-dione dioxime curve and consumption of the oxidant was less than two electrons per oxime group. No product isolation study was made in this case, but the solution was seen to have a strong and unusually persistent blue color. It would be expected that the product of the first stage of oxidation having one keto and one oximino group would be stabilized as structure **5** and possibly resist further oxidation.

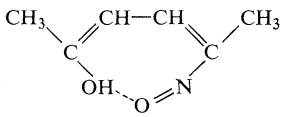

5

Acknowledgments

The authors are indebted to Dr. S. S. Barton for use of the isothermal calorimeter and to O/C J. C. Giroux for assistance with experimental work.

1. E. B. Hershberg. J. Org. Chem. **13**, 542 (1948).
2. L. Ruzicka and A. Wettstein. Helv. Chim. Acta, **18**, 986 (1935).
3. Kennedy, Coppock, and White. German medical targets. British Intelligence Objectives Sub-Committee, B.I.O.S. Final Report No. 449. Item 24. 1945. p. 228.
4. C. R. Addinall. Manufacture of synthetic hormones in Germany. Office of the Publication Board, Department of Commerce, FIAT Final Report 996. p. 42.
5. L. Ruzicka, M. W. Goldberg, and H. Brüngger. Helv. Chim. Acta, **17**, 1389 (1934).
6. C. H. DePuy and B. W. Ponder. J. Am. Chem. Soc. **81**, 4629 (1959).
7. M. P. Cava, R. L. Litle, and D. R. Napier. J. Am. Chem. Soc. **80**, 2257 (1958).
8. St. Goldschmidt and W. L. C. Veer. Rec. Trav. Chim. **65**, 796 (1946).
9. M. L. Wolfrom. Rec. Trav. Chim. **66**, 238 (1947).
10. St. Goldschmidt and W. L. C. Veer. Rec. Trav. Chim. **66**, 238 (1947).

11. S. H. PINES, J. M. CHEMERDA, and M. A. KOZLOWSKI. J. Org. Chem. **31**, 3446 (1966).
12. D. G. M. DIAPER and F. R. RICHARDSON. Can. J. Chem. **34**, 1835 (1956).
13. G. JUST and K. DAHL. Tetrahedron Letters, **22**, 2441 (1966).
14. L. CANONICA. Gazz. Chim. Ital. **79**, 738 (1949).
15. L. CANONICA. Gazz. Chim. Ital. **77**, 92 (1947).
16. FRANTISEK SIPOS. Chemie Svazek, **10**, 499 (1958).
17. W. D. EMMONS and A. S. PAGANO. J. Am. Chem. Soc. **77**, 4557 (1955).
18. M. BETHOUX, H. LEMAIRE, and A. RASSAT. Bull. Soc. Chim. France, 1985 (1964).
19. J. R. THOMAS. J. Am. Chem. Soc. **86**, 1446 (1964).
20. B. C. GILBERT and R. O. C. NORMAN. J. Chem. Soc. B, 86, 1966.
21. B. C. GILBERT and R. O. C. Norman. J. Chem. Soc. B, 722 (1966).
22. B. C. GILBERT and R. O. C. Norman. J. Chem. Soc. B, 123 (1968).
23. J. W. LOWN. J. Chem. Soc. B, 441 (1966).
24. J. W. LOWN. J. Chem. Soc. B, 644 (1966).
25. W. S. TRAHANOVSKY, L. B. YOUNG, and G. L. BROWN. J. Org. Chem. **32**, 3865 (1967).
26. R. E. VALLEE. Rev. Sci. Instr. **33**, 856 (1963).
27. O. WALLACH. Ann. **246**, 227 (1888).
28. B. G. GOWENLOCK. Quart. Rev. London, **12**, 321 (1958).

Can. J. Chem. Downloaded from www.nrcresearchpress.com by 210.87.254.42 on 09/05/12
For personal use only.

Can. J. Chem. Downloaded from www.nrcresearchpress.com by 210.87.254.105 on 09/05/12
For personal use only.

Action of some bases on the tropylium cation

S. G. McGeachin
Department of Chemistry, University of Alberta, Edmonton, Alberta

Received September 3, 1968

The tropylium cation has been treated with the hindered bases triphenylmethyl sodium, 2,6-dimethoxyphenyl lithium, and 2,4,6-tri-*t*-butylphenyl lithium to give substituted cycloheptatrienes. Where possible its reaction with tertiary amines follows Reaction Scheme 1 to give immonium salts which can be hydrolyzed to tropylated aldehydes and ketones. Its reaction with trimethylamine gives the quaternary ammonium salt which on exposure to the atmosphere is decomposed to trimethylammonium fluoborate and a mixture of tropone and ditropyl ether.

Canadian Journal of Chemistry, 47, 151 (1969)

Introduction

This study arose in attempts to deprotonate the tropylium cation with the formation of the cycloheptatrienyl carbene **1**. Two reports of the generation of this species by photochemical and thermal decomposition of the sodium salt of tropone *p*-toluene sulfonylhydrazone have appeared (1).

Cycloheptatrienylidene should be relatively stable among carbenes, for the same reasons as the tropylium cation is among carbonium ions. A number of such dipolar or nucleophilic carbenes have been generated in heterocyclic systems. Wanzlick has demonstrated, *inter alia*, the formation of the dimer **4** by reaction of benzthiazolium halides **2** with triethylamine in polar solvents (2). This reaction must proceed either by dimerization of the carbene **3** formed by deprotonation, or by its attack on a benzthiazolium cation followed by deprotonation of the resulting intermediate. The biological functions of thiamine have been shown to depend on the formation of a similar intermediate (3). It should be noted in passing that species of type **3** are better referred to as heterocyclic ylids in recognition of that major canonical form in which all atoms have formal electron octets. All the canonical forms of **1** have one atom with an electron sextet and hence the term carbene would seem appropriate in this case.

Olofson and co-workers have studied the rates of deprotonation of a wide range of five-membered heterocyclic 'olium ions (4). They have found that, aside from the positive charge, deprotonation is accelerated by an increasing number of electronegative atoms in the ring, and markedly by a sulfur atom adjacent to the carbon undergoing deprotonation. This latter is explained in terms of d–σ overlap in the resulting ylid. The tropylium cation lacking these features should therefore undergo deprotonation much more slowly than say the N,N^1-dimethylimidazolium ion ($t_{1/2}$ = 4.5 min for H—D exchange at pD8–9) (4). When it is also considered that the tropylium cation reacts very rapidly with all but the weakest bases, e.g. chloride ion, to form stable substituted cycloheptatrienes it would seem improbable that it can be deprotonated by ordinary means.

In the light of this our approach has been twofold. Firstly we have examined the action of strong bases in which the basic center is sterically hindered, in the hope that preferred attack on a ring proton rather than addition to a less accessible ring carbon atom might occur. In a similar vein we reasoned that reaction with a hindered

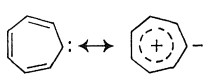

1

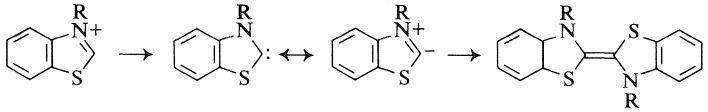

2 **3** **4**

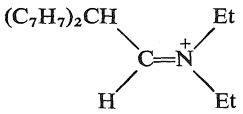

5

$(C_7H_7)_2CH\,CHO$

6

tertiary amine might result in direct deprotonation, or in the formation of an intermediate quaternary ammonium salt which might under certain conditions be unstable relative to the carbene and the protonated amine.

Results

Treatment of tropylium fluoborate with three increasingly hindered strong bases, triphenylmethyl sodium, 2,6-dimethoxyphenyl lithium, and 2,4,6-tri-*t*-butylphenyl lithium gave no evidence of deprotonation. The only isolated products were the corresponding substituted cycloheptatrienes in moderate yield. These were identified spectroscopically and by analysis. Addition of triethylamine to a solution of tropylium fluoborate in acetonitrile resulted in a rapid, mildly exothermic reaction. Removal of the solvent gave an oil from which there was obtained a fluoborate salt, $C_{20}H_{26}NBF_4$. The nuclear magnetic resonance (n.m.r.) spectrum of this salt, with appropriate decoupling studies, showed the presence of two tropyl groups (tropyl will be used to refer to the 1,3,5-cycloheptatrien-7-yl group), two chemically different deshielded ethyl groups, and a single low field vinylic proton coupled to a single aliphatic C—H which in turn was coupled to the C-7 protons of the tropyl groups. These findings are adequately met by the structure **5**. Confirmation of this structure came from hydrolysis either of the isolated salt or of the original reaction mixture. This resulted in a neutral substance, $C_{16}H_{16}O$, whose properties indicated it to be 2,2-ditropylacetaldehyde **6**. The formation of **5** must involve an oxidation step. The tropylium cation is well known to abstract hydride ion from suitable substrates (5). That this is operative here was demonstrated by the presence of cycloheptatriene in the reaction mixture when examined by gas–liquid chromatography.

We conclude that the tropylium cation abstracts a hydride ion from triethylamine to give the immonium salt **7**. This is then deprotonated by triethylamine to give the enamine **8** which then adds to a tropylium cation to generate a second immonium salt **9**. A further cycle of deprotonation and addition to the tropylium cation then gives the observed product. This is depicted in Reaction Scheme 1. Similar results were obtained by the use of the hindered ethyldiisopropylamine. From the reaction mixture the salt **10** was isolated. The salt **11** could not be isolated but was certainly present as hydrolysis of the reaction mixture gave two products which were separated chromatographically and found to be 2,2-ditropylacetaldehyde and 1,3-ditropyl-2-propanone, **12**.

$$C_7H_7^+ + Et_3N \rightleftharpoons C_7H_8 + CH_3CH{=}\overset{+}{N}Et_2$$

7

$$CH_3CH{=}\overset{+}{N}Et_2 + Et_3N \rightleftharpoons CH_2{=}CH{-}NEt_2 + Et_3\overset{+}{N}H$$

8

$$C_7H_7^+ + CH_2{=}CH{-}NEt_2 \rightleftharpoons C_7H_7CH_2CH{=}\overset{+}{N}Et_2$$

9

$$C_7H_7CH_2CH{=}\overset{+}{N}Et_2 + Et_3N \rightleftharpoons C_7H_7CH{=}CHNEt_2 + Et_3\overset{+}{N}H$$

$$C_7H_7CH{=}CHNEt_2 + C_7\overset{+}{H}_7 \rightleftharpoons (C_7H_7)_2CHCH{=}\overset{+}{N}Et_2$$

$$\text{Net } 3C_7H_7^+ + 3Et_3N \rightarrow (C_7H_7)_2CHCH{=}\overset{+}{N}Et_2 + C_7H_8 + 2Et_3\overset{+}{N}H$$

REACTION SCHEME 1

Excellent analogy for these processes exists in the reaction of tertiary amines with the triphenylmethyl carbonium ion. Damico and Broaddus (6) have shown that dodecyldimethylamine reacts with this ion to give triphenylmethane and the amine hydrochloride as the isolated products in good yield. These findings were interpreted in terms of repeated cycles of hydride abstraction from the base, and deprotonation of the immonium salt to an enamine, with the enamine then acting as substrate for the abstraction of a second hydride ion. The net result would be the formation of the above mentioned products along with a relatively small amount of polyenamines. Depending on the extent to which the first step in Reaction Scheme 1 takes place, one might expect exclusively cycloheptatriene or any of mono-, di-, or tritropyl-acetaldehyde after hydrolysis of the triethylamine reaction. With ethyldiisopropylamine the number of possible products is even greater. Careful thin-layer chromatographic examination of the products of

Can. J. Chem. Downloaded from www.nrcresearchpress.com by 210.87.254.105 on 09/05/12
For personal use only.

Can. J. Chem. Downloaded from www.nrcresearchpress.com by 210.87.254.105 on 09/05/12
For personal use only.

hydrolysis of these reaction mixtures has revealed only ditropylacetaldehyde in the case of triethylamine, and that plus the symmetrical ditropylacetone in the case of ethyldiisopropylamine. This result is independent of the way in which the reaction between base and tropylium cation is conducted. Slow addition over several hours of the tropylium cation to triethylamine, or the reverse, followed by the hydrolysis gave in comparable yields the product already obtained and no other.

Since all of the steps in Reaction Scheme 1 are presumably reversible it is probable that the observed products are derived from the most stable immonium salts. That steric effects are of importance is inferred from the formation of 1,3-ditropyl-2-propanone as against the 1,1-derivative and from the following. When the tropylium cation was allowed to react with tri-*n*-propylamine under identical conditions, there were obtained from the hydrolysis two products in the ratio of 1:15. The minor product proved to be 2,2-ditropylpropionaldehyde **13** and the major, the corresponding monotropyl derivative **14**. We ascribe this to the destabilizing effect of a quaternary carbon *cis* to the propyl group in the intermediate **15**.

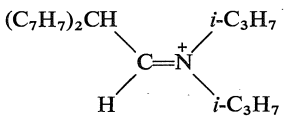

10

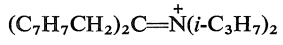

11

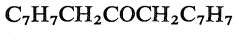

12

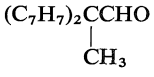

13

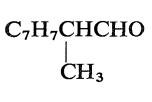

14

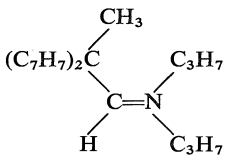

15

We have also investigated the action of trimethylamine since this cannot be converted to an enamine. This resulted only in formation of the quaternary ammonium salt. On the basis of the n.m.r. spectrum of the crude product, no compounds derived by hydride transfer were formed. The n.m.r. spectrum of the salt in deuteriodichloromethane was of interest in that it showed a sharp singlet at τ 7.12 for *N*-methyl protons and a slightly broadened singlet (half-width ca. 3 c.p.s.) for the seven protons of the ring at τ 3.75. In this solvent there must be an equilibrium between the quaternary salt and tropylium fluoborate – trimethylamine which makes the ring protons equivalent. The position of this absorption at considerably higher field than occurs for tropylium fluoborate in acetonitrile (τ 0.45) is in accord with this. This salt is stable in solution under nitrogen or dry air. Heating a sample under high vacuum to 150° resulted in decomposition without the formation of any volatile product. On exposure to the atmosphere the salt decomposed to trimethylammonium fluoborate and a mixture of tropone and ditropyl ether. We interpret this to be reaction with atmospheric moisture. It is reasonable that in the presence of water vapor some hydrolysis of the salt to ditropyl ether should occur. It is already known (7) that ditropyl ether disproportionates to tropone and cycloheptatriene in the presence of the tropylium cation.

Experimental

General

Melting points were taken on a Köfler melting point apparatus and are uncorrected. Analyses were performed by the Microanalytical Laboratory of this department.

7-Triphenylmethyl-1,3,5-cycloheptatriene

Triphenylmethyl sodium (8) (25 ml of a standard ethereal solution) was added to a stirred suspension of tropylium fluoborate (9) (0.353 g; 1 equivalent) in diethylene glycol dimethyl ether (25 ml) under nitrogen. The red color of the anion disappeared within a few minutes. The reaction mixture was poured into water after 10 min and the product isolated by extraction into pentane. It was chromatographed on Grade I alumina. Elution with 1:1 benzene–heptane gave triphenylmethane (50 mg) and 7-triphenylmethyl-1,3,5-cycloheptatriene (470 mg; 71%). The analytical sample recrystallized from dichloromethane–methanol and had m.p. 137–140°.

Anal. Calcd. for $C_{26}H_{22}$: C, 93.37; H, 6.63. Found: C, 93.35; H, 6.44.

Nuclear magnetic resonance spectrum ($CDCl_3$): τ 2.82 (15H, singlet), τ 3.15, 3.85, 4.73 (3 × 2H, multiplets), τ 7.07 (1H, triplet) assigned to the phenyl groups, the three pairs of vinylic protons and the C-7 proton of the cycloheptatriene ring respectively.

7-(2,6-Dimethoxyphenyl)-1,3,5-cycloheptatriene

Solid tropylium fluoborate (1.88 g) was added slowly in batches to a stirred suspension of 2,6-dimethoxyphenyl

Can. J. Chem. Downloaded from www.nrcresearchpress.com by 210.87.254.105 on 09/05/12
For personal use only.

lithium (1.55 g) in 50 ml of diethyl ether under nitrogen. After complete addition the mixture was stirred for a further 10 min, filtered, washed with water, dried, and the solvent removed. The resulting oil on crystallization from methanol gave 7-(2,6-dimethoxyphenyl)-1,3,5-cycloheptatriene (1.57 g; 65%). The analytical sample, recrystallized as plates from methanol, had m.p. 91–92°.

Anal. Calcd. for $C_{15}H_{16}O_2$: C, 78.92; H, 7.06. Found: C, 78.89; H, 6.94.

Nuclear magnetic resonance spectrum ($CDCl_3$): τ 2.77 (1H, multiplet), τ 3.36 (4H, multiplet), τ 3.82 (2H, multiplet), τ 4.59 (2H, multiplet), τ 6.23 (6H, singlet), τ 6.48 (1H, triplet).

7-(2,4,6-Tri-t-butylphenyl)-1,3,5-cycloheptatriene

Butyl lithium (2.3*M*, 0.72 ml) was added to a stirred solution of 2,4,6-tri-*t*-butylbromobenzene (10) (0.540 g) in ether (25 ml). The mixture was refluxed gently for 1 h, cooled, and solid tropylium fluoborate (0.355 g; 1.2 molar equivalents) added. After being stirred for a further 1 h the reaction mixture was filtered, and the filtrate washed with water, and dried. The crude material was filtered through a column of silica gel (50 g) in benzene, and the resulting product crystallized from chloroform–ethanol to give 7-(2,4,6-tri-*t*-butylphenyl)-1,3,5-cycloheptatriene (352 mg; 63%). The analytical sample had m.p. 150°.

Anal. Calcd. for $C_{25}H_{36}$: C, 89.22; H, 10.78. Found: C, 89.08; H, 10.82.

Nuclear magnetic resonance spectrum ($CDCl_3$): τ 2.58 (2H, singlet), τ 3.80 (4H, multiplet), τ 5.88 (2H, multiplet), τ 6.78 (1H, multiplet), τ 8.55 (18H, singlet), τ 8.68 (9H, singlet).

N,N-Diethyl-2,2-ditropylacetaldimine Fluoborate (5)

A stirred solution of tropylium fluoborate (5.16 g) in dry acetonitrile (50 ml) was treated with triethylamine (4.05 ml). A rapid mildly exothermic reaction ensued. The mixture was allowed to stand 2 h, and then evaporated *in vacuo* to a gum. This was taken up in dichloromethane, washed with water, to remove triethylammonium fluoborate, and dried. Removal of the solvent left an oil which was crystallized from dichloromethane – ethyl acetate to give the imine fluoborate salt (2.56 g; 72%). The analytical sample, m.p. 96–97°, formed prisms from dichloromethane – ethyl acetate.

Anal. Calcd. for $C_{20}H_{26}NBF_4$: C, 65.42; H, 7.14; N, 3.90. Found: C, 65.13; H, 7.00; N, 3.94.

Nuclear magnetic resonance spectrum ($CDCl_3$): (*1*) τ 1.82 (1H, doublet, J = 11 c.p.s.), (*2*) τ 3.40, 3.70, 4.65 (3 × 4H, multiplets), (*3*) τ 6.07, 6.35 (2 × 2H, quartets, J = 7 c.p.s.), (*4*) τ 6.69 (2H, multiplet), (*5*) τ 7.03 (1H, multiplet), (*6*) τ 8.56, 8.67 (2× 3H, triplets, J = 7 c.p.s.). Decoupling indicated that proton (*1*), assigned to the aldimine CH, is coupled to proton (*5*), the aliphatic CH, which in turn is coupled to protons (*4*), the C-7 protons of the cycloheptatriene rings, with J = 8 c.p.s. Protons (*2*) were assigned to the cycloheptatriene rings and (*3*) and (*6*) to the methylenes and methyls of the *N*-ethyl groups respectively.

N,N-Diisopropyl-2,2-ditropylacetaldimine Fluoborate (10)

This was prepared by the above process in 26% yield. No other product could be isolated from the mother liquors of the crystallization. The analytical sample from dichloromethane – ethyl acetate had m.p. 156–157°.

Anal. Calcd. for $C_{22}H_{30}NBF_4$: C, 66.83; H, 7.65; N, 3.54. Found: C, 67.07; H, 7.79; N, 3.55.

Nuclear magnetic resonance spectrum ($CDCl_3$): τ 1.53 (1H, doublet, J = 10 c.p.s.), τ 3.45, 3.75, 4.62 (3 × 4H, multiplets), τ 5.75 (2H, multiplet), τ 6.65 (3H, multiplet), τ 8.47, 8.55 (2 × 6H, doublets, J = 7 c.p.s.).

Ditropylacetaldehyde (6)

A solution of tropylium fluoborate (12 g) in acetonitrile (120 ml) was treated with triethylamine (11.4 ml). After 2 h, water (60 ml) was added and the solution left for ca. 18 h. It was then poured into water (600 ml), the product isolated by extraction into ether, and distilled to give ditropylacetaldehyde (3.5 g, 66%), b.p. 112–113° at 0.01 mm pressure.

Anal. Calcd. for $C_{16}H_{16}O$: C, 85.68; H, 7.19. Found: C, 85.54; H, 7.33.

Infrared spectrum: ν_{max} (film) 1725 cm^{-1}. Nuclear magnetic resonance spectrum ($CDCl_3$): τ 0.1 (1H, doublet, J = 3.5 c.p.s.), τ 3.37, 3.80, 4.75 (3 × 4H, multiplets), τ 7.03 (1H, triplet of doublets, J = 3.5 and 7.5 c.p.s.), τ 7.72 (2H, multiplet). The last two absorptions are assigned to the proton α to the carbonyl and the C-7 protons of the rings respectively.

1,3-Ditropyl-2-propanone (12)

By the same procedure as for the above aldehyde tropylium fluoborate (8 g) in acetonitrile (80 ml) was treated with ethyldiisopropylamine (7.85 ml). After 2 h, water (40 ml) was added to effect hydrolysis. The isolated crude product was chromatographed on silica gel (500 g). Elution with benzene gave firstly ditropylacetaldehyde (2.04 g) and then 1,3-ditropyl-2-propanone (1.80 g). The analytical sample of the ketone, m.p. 88–89°, was obtained by sublimation at 130–140°/0.05 mm.

Anal. Calcd. for $C_{17}H_{18}O$: C, 85.67; H, 7.61. Found: C, 85.39; H, 7.56.

Infrared spectrum: ν_{max} (Nujol) 1712 cm^{-1}. Nuclear magnetic resonance spectrum ($CDCl_3$): τ 3.39, 3.84, 4.86 (3 × 4H, multiplets), τ 7.27 (4H, doublet, J = 8 c.p.s.) τ 7.69 (2H, multiplet).

2-Tropylpropionaldehyde (14) and 2,2-Ditropylpropionaldehyde (13)

Tropylium fluoborate (2.1 g) in acetonitrile (20 ml) was treated with tri-*n*-propylamine (2.25 ml). The mixture was left 2 h, treated with water (10 ml), and left for a further 18 h. The crude product, isolated by dilution of the reaction mixture with water and extraction into ether, was chromatographed on silica gel (50 g). Elution with benzene gave firstly 2,2-ditropylpropionaldehyde (50 mg) followed by the more polar monotropyl-propionaldehyde (750 mg). An analytical sample of the former compound was prepared by sublimation at 130°/0.05 mm. It had m.p. 113–114.5°.

Anal. Calcd. for $C_{17}H_{18}O$: C, 85.67; H, 7.61. Found: C, 85.80; H, 7.79.

Infrared spectrum: ν_{max} (film) 1725 cm^{-1}. Nuclear magnetic resonance spectrum ($CDCl_3$): τ 0.15 (1H, singlet), τ 3.25, 3.75, 4.75 (3 × 4H, multiplets), τ 7.88 (2H, broad triplet), τ 8.59 (3H, singlet). An analytical sample of the latter compound was obtained by evaporative distillation at 80–85°/0.05 mm.

Anal. Calcd. for $C_{10}H_{12}O$: C, 81.04; H, 8.16. Found: C, 80.94; H, 8.31.

Infrared spectrum: ν_{max} (film) 1725 cm^{-1}. Nuclear magnetic resonance spectrum ($CDCl_3$): τ 0.30 (1H, doublet, $J = 2$ c.p.s.), τ 3.33, 3.75, 4.75 (3 × 2H, multiplets), τ 7.3 (1H, multiplet), τ 8.05 (1H, multiplet), τ 8.82 (3H, doublet, $J = 7$ c.p.s.).

Tropyltrimethylammonium Fluoborate

A solution of tropylium fluoborate (4.12 g) in acetonitrile (40 ml) under nitrogen was cooled in an acetone–CO_2 bath to −20°. Trimethylamine (2.52 *M*) in acetonitrile (9.5 ml) was added and the solution was allowed to rise to room temperature. Removal of the solvent *in vacuo* gave an oil which crystallized. It was recrystallized from dichloromethane – ethyl acetate under nitrogen to give tropyltrimethylammonium fluoborate, m.p. 73–78°. A satisfactory analysis was not obtained.

Nuclear magnetic resonance spectrum (CD_2Cl_2): τ 3.75 (7H, broad singlet), τ 7.12 (9H, singlet).

Acknowledgments

The author is grateful to Mr. G. Harvie for technical assistance. He also wishes to thank the National Research Council of Canada for financial assistance.

1. W. M. Jones and C. L. Ennis. J. Am. Chem. Soc. **89**, 3069 (1967); T. Mukai, T. Nakazawa, and K. Isobe. Tetrahedron Letters, 565 (1968).
2. H. W. Wanzlick, H. J. Kleiner, I. Lasch, and H. U. Füldner. Angew. Chem. Intern. Ed. Engl. **5**, 126 (1966).
3. R. Breslow. J. Am. Chem. Soc. **80**, 3719 (1958), and other papers.
4. R. A. Olofson, W. R. Thompson, and J. S. Michelman. J. Am. Chem. Soc. **86**, 1865 (1964); R. A. Olofson and J. M. Landesberg. J. Am. Chem. Soc. **88**, 4263 (1966).
5. T. Nozoe. *In* Progress in organic chemistry. Vol. V, Butterworths, London. 1961. p. 132.
6. R. Damico and C. D. Broaddus. J. Org. Chem. **31**, 1607 (1966).
7. T. Ikemi, T. Nozoe, and H. Sugiyama. Chem. Ind. London, 932 (1960).
8. W. B. Renfrow, Jr. and C. R. Hauser. Org. Syn. Coll. Vol. II. p. 607 (1943).
9. K. Conrow. Org. Syn. **43**, 101 (1963).
10. E. E. Betts and L. R. C. Barclay. Can. J. Chem. **33**, 1768 (1955).

Can. J. Chem. Downloaded from www.nrcresearchpress.com by 210.87.254.105 on 09/05/12
For personal use only.

Can. J. Chem. Downloaded from www.nrcresearchpress.com by 210.87.254.6 on 09/05/12
For personal use only.

Twofold alkylations of ketone and aldehyde phenylhydrazones with methylene halides by means of alkali amides to form bis-*N*-derivatives[1]

FRED E. HENOCH AND CHARLES R. HAUSER
Department of Chemistry, Duke University, Durham, North Carolina 27706

Received July 5, 1968

The phenylhydrazones of benzophenone, acetophenone, and benzaldehyde were converted by a molecular equivalent of an alkali amide in liquid ammonia to their mono-alkali derivatives, which underwent twofold alkylation with 1,3-dibromopropane or higher methylene halides or with α,α′-dichloro-*p*-xylene to form corresponding bis-*N*-derivatives. Two of the products were reduced by means of lithium in liquid ammonia to give corresponding substituted bis-hydrazines. These reactions furnish convenient methods of synthesis of such compounds.

Canadian Journal of Chemistry, 47, 157 (1969)

As an extension of a previous method for effecting certain *N*-alkylations of ketone and aldehyde phenylhydrazones with alkyl halides (1), we have now found that twofold *N*-alkylations of phenylhydrazones **1***a–c* can be accomplished with appropriate methylene bromides by means of alkali amides in liquid ammonia to form the bis-derivatives **2***a–f*, respectively. Similarly the intermediate alkali phenylhydrazones **1***a–b* underwent twofold alkylation with α,α′-dichloro-*p*-xylene to give the bis-derivatives **3***a–b*, respectively. The results are summarized in Tables I and II.

Table I shows that the yields of the analytically pure bis-derivatives **2***a–f* and **3***a–b* were quite satisfactory (48–81%). In certain cases the yields were slightly better with potassium amide than with sodium amide. The structures of the products were supported by analysis and absorption spectra (see Tables I and II). The most notable difference in the infrared (i.r.) spectra of the bis-derivatives from those of the starting phenylhydrazones is the lack of any absorption in the NH region. Otherwise, these spectra are similar to those of the starting phenylhydrazones except that the peaks appear at different frequencies. The nuclear magnetic resonance (n.m.r.) spectra of compounds **2***a–f* show an N—CH_2 triplet and those of **3***a–b* an N—CH_2 singlet. Their n.m.r. spectra are in complete agreement with the assigned structures.

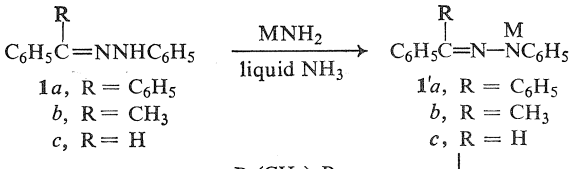

1*a*, R = C_6H_5
b, R = CH_3
c, R = H

1′*a*, R = C_6H_5
b, R = CH_3
c, R = H

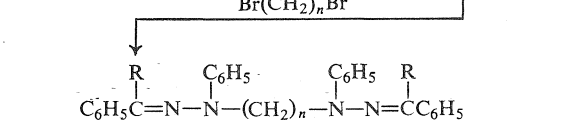

2*a*, R = C_6H_5, *n* = 3
b, R = C_6H_5, *n* = 4
c, R = CH_3, *n* = 4
d, R = H, *n* = 3
e, R = H, *n* = 4
f, R = H, *n* = 10

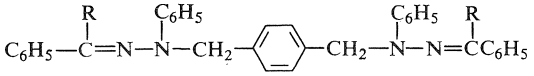

3*a*, R = C_6H_5
b, R = CH_3

This method of synthesis would probably be suitable with, not only other phenylhydrazones, but also with other methylene bromides higher than 1,3-dibromopropane and with α,α′-dichloro-*o*-xylene (see Table I). However, the method failed with phenylhydrazone **1***a* and ethylene or methylene bromide or chloride with which the starting phenylhydrazone **1***a* was largely recovered. The results with the ethylene halides may be accounted for by β-elimination.

[1]This investigation was supported by United States Public Health Service Research Grant No. CA 04455 from the National Cancer Institute.

Can. J. Chem. Downloaded from www.nrcresearchpress.com by 210.87.254.6 on 09/05/12
For personal use only.

TABLE I

Twofold *N*-alkylations of phenylhydrazones with methylene halides by alkali amides in liquid ammonia to form bis-derivatives

Phenyl hydrazone	Methylene halide	bis-Derivative	Yield, % $NaNH_2$	Yield, % KNH_2	Melting point (°C)	Emperical formula	Elemental analysis: Calculated C	Calculated H	Calculated N	Found C	Found H	Found N
1*a*	1,3-Dibromopropane	**2***a*	48	52	129–130*	$C_{41}H_{36}N_4$	84.21	6.21	9.58	84.41	6.09	9.40
1*a*	1,4-Dibromobutane	**2***b*	55	57	142–143†	$C_{42}H_{38}N_4$	84.24	6.40	9.36	84.04	6.41	9.28
1*b*	1,4-Dibromobutane	**2***c*	54	54	110–111*	$C_{32}H_{34}N_4$	80.97	7.22	11.81	80.93	7.18	11.69
1*c*	1,3-Dibromopropane	**2***d*	74	78	145.5–146.0*	$C_{29}H_{28}N_4$	80.52	6.53	12.95	80.34	6.46	12.74
1*c*	1,4-Dibromobutane	**2***e*	65	66	89.5–90.5*	$C_{30}H_{30}N_4$	80.68	6.77	12.55	80.50	6.88	12.44
1*c*	1,10-Dibromodecane	**2***f*	51	55	164–166*	$C_{36}H_{42}N_4$	81.47	7.98	10.56	81.31	7.91	10.71
1*a*	α,α′-Dichloro-*p*-xylene	**3***a*	—	81	158–159‡	$C_{46}H_{38}N_4$	85.41	5.92	8.66	85.15	5.81	8.73
1*b*	α,α′-Dichloro-*p*-xylene	**3***b*	—	73	145–146§	$C_{36}H_{34}N_4$	82.72	6.56	10.72	82.58	6.50	10.89

*Recrystallized from 95% ethanol.
†Recrystallized from methanol–hexane.
‡Recrystallized from hexane–benzene.
§Recrystallized from acetonitrile.

TABLE II

Infrared and nuclear magnetic resonance spectra of the bis-derivatives

bis-Derivative	C=N‡	γ*, cm^{-1} aromatic	C—N	Aromatic CH out-of-plane bend	Nuclear magnetic resonance data† (c.p.s. ± 1): Protons N—CH_2—	C—CH_2—C	C—CH_3	Aromatic
2*a*	1610	1595§, 1505	1250	755, 705	235 (t, 4.0)	122 (q, 2.0)		423–456 (m, 29.9)
2*b*	1620	1603, 1502	1270	760, 700	213 (t, 3.9)	106 (m, 4.0)		413–465 (m, 30.1)
2*c*	1610	1600, 1498	1300	765, 705	210 (t, 4.0)	107 (m, 4.0)	119 (s, 6.0)	405–473 (m, 20.0)
2*d*	1614	1600, 1500	1280	760, 701	236 (t, 4.1)	128 (q, 1.9)		420–460 (m, 22.0)
2*e*	1615	1598, 1500	1260	765, 690	230 (t, 4.1)	104 (m, 4.0)		414–470 (m, 22.1)
2*f*	1620	1605, 1505	1310	770, 705	228 (t, 4.1)	79–172 (m, 15.8)		415–458 (m, 21.7)
3*a*	1605	1595, 1495	1335	745, 690	272 (s, 4.0)			405–462 (m, 33.8)
3*b*	1615	1600, 1500	1345	755, 746, 685	296 (s, 3.9)		167 (s, 6.0)	428–474 (m, 24.1)

*All peaks are strong unless otherwise noted.
†Determined in deuteriochloroform; for n.m.r. descriptions see ref. 4.
‡Shoulders.
§Medium peak.

Can. J. Chem. Downloaded from www.nrcresearchpress.com by 210.87.254.6 on 09/05/12
For personal use only.

The bis-hydrazones **2***c* and **3***b* were reduced by means of lithium in liquid ammonia to form the corresponding substituted bis-hydrazines **4** and **5** in yields of 54 and 61%, respectively. The other bis-hydrazones could presumably be reduced similarly. This method has previously been employed for reduction of an α,β-unsaturated ketone (2).

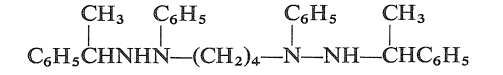

4

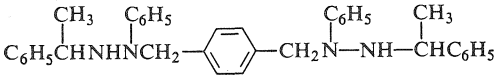

5

The structures of the bis-hydrazines **4** and **5** were supported by analysis and absorption spectra (see Experimental). The i.r. spectra of **4** and **5** lack the C=N peak observed in the spectra of starting bis-hydrazones **2***c* and **3***b* and have strong peaks for the NH and C—N groups. Although the n.m.r. spectrum of **4** is somewhat complicated by overlap of the methyl protons with the methylene protons and of the benzylic protons with the *N*-methylene protons, the n.m.r. spectrum for **5** shows the expected doublet for the methyl group and a quartet for the CH group adjacent to the methyl group.

The bis-hydrazones **2***c* and **3***b* were hydrolyzed with hot acid but the resulting bis-hydrazines or their acid salts appeared to be too unstable to isolate readily. For example, on refluxing a solution of **2***c* with 20% hydrochloric acid under nitrogen for 3 h, a dark tarry gum was obtained. That hydrolysis had occurred was shown by isolation of the ketone as its 2,4-dinitrophenylhydrazone (78%) and the bis-hydrazine **6** as its bis-benzaldehyde derivative **2***e* (12%) [eq. 1]:

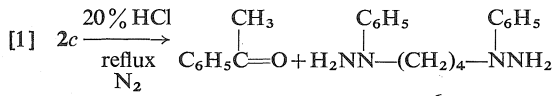

[1]

6

It may be concluded that the twofold alkylation of phenylhydrazones and subsequent reduction of the products furnish convenient methods for the synthesis of an apparently new class of bis-hydrazones and bis-hydrazines such as **2***a–f*, **3***a–b*, **4**, and **5**. The possible twofold condensation of a bis-hydrazine such as **6** with an aldehyde or ketone does not seem suitable, since **6** appears not readily available and too unstable for a satisfactory result (see above).

Experimental

Melting points, taken on a Thomas Hoover capillary melting point apparatus, are uncorrected. Infrared spectra were recorded on a Perkin–Elmer model 237 Infracord using samples prepared as potassium bromide pellets. Nuclear magnetic resonance spectra were recorded on a Varian A-60 spectrometer using deuteriochloroform solutions containing tetramethylsilane as an internal standard[2] Elemental analyses were performed by Paul Demoen, Janssen Pharmaceutical Laboratories, Beerse, Belgium, and M-H-W Laboratories, Garden City, Michigan.

The benzophenone phenylhydrazone (3), acetophenone phenylhydrazone (4), and the benzaldehyde phenylhydrazone (5) used in this study were prepared according to literature procedures. The acetophenone phenylhydrazone should be freshly prepared.

Twofold N-Alkylations of Phenylhydrazones

To a stirred suspension of 0.025 mole of sodium amide (6) or potassium amide (7) in 350 ml of commercial, anhydrous liquid ammonia was added a molecular equivalent of the phenylhydrazone **1***a*, **1***b*, or **1***c*. The solutions of the resulting alkali salt were colored blood-red, orange-tan, and brownish-yellow respectively. After 20 min, a solution of one half of a molecular equivalent of the appropriate dihalide in 15–20 ml of anhydrous ether was added during a 4–6 min period; the color of the solution was essentially discharged and a precipitate formed. After stirring for 45–60 min, a slight excess of a molecular equivalent of ammonium chloride was added. The ammonia was allowed to evaporate, and the residue was taken up in ether and water. The layers were separated and the aqueous layer was washed twice with 100 ml of ether. The ether layers were combined and dried ($MgSO_4$) and the solvent was removed. The residue was recrystallized from an appropriate solvent. The results are summarized in Tables I and II.

Reduction of bis-Derivative 2c

To a stirred, blue solution of 0.7 g (0.1 mole) of lithium in 250 ml of commercial, anhydrous liquid ammonia was added 2.30 g (0.005 mole) of **2***c* in 100 ml of dry THF (freshly distilled from lithium aluminium hydride) during a 10 min period. After 1 h, the color of the solution had changed to a darker blue. A slight excess of ammonium chloride was then added in small equal portions during a 20 min period. The ammonia was evaporated and the reaction mixture was worked up to give a yellowish solid which was recrystallized from ethanol to give 1.43 g (54%) of hydrazine **4** (yellowish crystals), m.p. 143–144°; i.r. 3420 cm^{-1} (NH), 1600 and 1500 cm^{-1} (aromatic), 1265 and 1335 cm^{-1} (C—N), 760 and 700 cm^{-1} (out-of-plane CH bend); n.m.r. ($CDCl_3$)

[2]In n.m.r. descriptions, s = singlet, d = doublet, t = triplet, qt = quartet, q = quintet, m = multiplet, b = broad.

105–129 c.p.s. (m, 10.0), 205–224 c.p.s. (m, 6.0), 284 c.p.s. (b, 1.8), 420–466 c.p.s. (m, 20.4).

Anal. Calcd. for $C_{32}H_{38}N_4$: C, 80.29; H, 8.00; N, 11.71. Found: C, 80.42; H, 7.93; N, 11.58.

Reduction of bis-Derivative 3b

This reaction was effected essentially as described above for **2c** to give, after recrystallization from methanol–acetonitrile, 1.60 g (61%) of hydrazine **5** (tan crystals), m.p. 126–127°; i.r. 3440 cm^{-1} (NH), 1603 and 1505 cm^{-1} (aromatic), 1270 and 1315 cm^{-1} (C—N), 765 and 690 cm^{-1} (out-of-plane CH bend); n.m.r. ($CDCl_3$) 124 c.p.s. (d, 6.0, $J = 9$), 215 c.p.s. (qt, 2.0, $J = 9$), 290 c.p.s. (s, 4.1), 355 c.p.s. (b, 2.1), 432–476 c.p.s. (m, 24.0).

Anal. Calcd. for $C_{36}H_{38}N_4$: C, 82.09; H, 7.27; N, 10.64. Found: C, 81.91; H, 7.32; N, 10.39.

1. W. G. KENYON and C. R. HAUSER. J. Org. Chem. **30**, 292 (1965).
2. H. O. HOUSE and H. W. THOMPSON. J. Org. Chem. **28**, 360 (1963).
3. S. G. COHEN and C. H. WANG. J. Am. Chem. Soc. **77**, 3628 (1955).
4. R. L. SHRINER, W. C. ASHLEY, and E. WELCH. Org. Syn. Coll. Vol. III. John Wiley and Sons, Inc., New York. 1955. p. 725.
5. K. A. JENSEN and B. BAK. J. Prakt. Chem. **151**, 187 (1938).
6. See C. R. HAUSER, F. W. SWAMER, and J. T. ADAMS. Org. Reactions, Vol. 8. John Wiley and Sons, Inc., New York. 1954. p. 122.
7. R. S. YOST and C. R. HAUSER. J. Am. Chem. Soc. **69**, 2325 (1947).

Steroid derivatives of cysteamine and cysteine

OWEN H. WHEELER AND CESAR REYES-ZAMORA
Puerto Rico Nuclear Center and Department of Chemistry, University of Puerto Rico, Mayaguez, Puerto Rico

Received July 8, 1968

A number of androstenone, estrone, and pregnenone derivatives of cysteamine have been prepared by reacting the steroid amines with ethylene monothiolcarbonate. The amides of androstenone carboxylic acid with mercaptoethylamine and cysteine have also been prepared.

Canadian Journal of Chemistry, 47, 160 (1969)

The only compounds which have shown any promise in affording protection against radiation in the animal body are cysteamine (2-mercaptoethylamine) and its simple derivatives (1). Cysteine, which was one of the first compounds reported to show radiation protection, is less effective (2). However, these compounds are relatively toxic and are also easily metabolized and eliminated from the body. The object of this work was to prepare derivatives which might be less toxic and less readily metabolized, by joining cysteamine and cysteine to a steroid molecule, while still leaving the mercapto group free, since this is essential for radiation protection. The following derivatives of cysteamine have been prepared: *N*-(2-mercaptoethyl)-3-ketopregn-4-en-20β-yl amine (**1**), *N*-(2-mercaptoethyl)-3-keto-androst-4-en-17β-yl amine (**2**), *N*-(2-mercaptoethyl)estra-1,3,5(10)-trien-3-ol-17β-yl amine (**3**), and *N*-(2-mercaptoethyl)-3-ketoandrost-4-ene 17β-carboxamide (**4**). A derivative of cysteine, *N*-(3-ketoandrost-4-ene 17β-carboxyl)cysteine (**5**), has also been synthesized.

The condensation of pregn-5-en-3-ol-20-amine with an excess of ethylene monothiolcarbonate gave a good yield of *N*-mercaptoethylpregn-5-en-3-ol-20β-yl amine. Although condensations with ethylene monothiolcarbonate are usually carried out (3, 4) with an excess of amine to avoid di-substitution, no *N,N*-dimercaptoethyl derivative was formed in the present case. This same compound was formed by using one equivalent of ethyl 2-mercaptoethylcarbonate (4). An Oppenauer oxidation of *N*-(2-mercaptoethyl)pregn-5-en-3-ol-20-yl amine under standard conditions gave *N*-(2-mercaptoethyl)-3-ketopregn-4-en-20β-yl amine (**1**), without oxidizing the mercapto group, although the yield was low. The molecular weight indicated that the compound was still in the free mercapto form.

As an alternative route pregn-5-en-3-ol-20β-yl amine was oxidized with chromium trioxide in pyridine (5) to 3-ketopregn-5-en-20β-yl amine, which was obtained in an impure state and in low yield, apparently due to the formation of chromium complexes. Oxidation of the corre-

Can. J. Chem. Downloaded from www.nrcresearchpress.com by 210.87.254.6 on 09/05/12
For personal use only.

105–129 c.p.s. (m, 10.0), 205–224 c.p.s. (m, 6.0), 284 c.p.s. (b, 1.8), 420–466 c.p.s. (m, 20.4).

Anal. Calcd. for $C_{32}H_{38}N_4$: C, 80.29; H, 8.00; N, 11.71. Found: C, 80.42; H, 7.93; N, 11.58.

Reduction of bis-Derivative 3b

This reaction was effected essentially as described above for **2c** to give, after recrystallization from methanol–acetonitrile, 1.60 g (61%) of hydrazine **5** (tan crystals), m.p. 126–127°; i.r. 3440 cm^{-1} (NH), 1603 and 1505 cm^{-1} (aromatic), 1270 and 1315 cm^{-1} (C—N), 765 and 690 cm^{-1} (out-of-plane CH bend); n.m.r. ($CDCl_3$) 124 c.p.s. (d, 6.0, $J = 9$), 215 c.p.s. (qt, 2.0, $J = 9$), 290 c.p.s. (s, 4.1), 355 c.p.s. (b, 2.1), 432–476 c.p.s. (m, 24.0).

Anal. Calcd. for $C_{36}H_{38}N_4$: C, 82.09; H, 7.27; N, 10.64. Found: C, 81.91; H, 7.32; N, 10.39.

1. W. G. KENYON and C. R. HAUSER. J. Org. Chem. **30**, 292 (1965).
2. H. O. HOUSE and H. W. THOMPSON. J. Org. Chem. **28**, 360 (1963).
3. S. G. COHEN and C. H. WANG. J. Am. Chem. Soc. **77**, 3628 (1955).
4. R. L. SHRINER, W. C. ASHLEY, and E. WELCH. Org. Syn. Coll. Vol. III. John Wiley and Sons, Inc., New York. 1955. p. 725.
5. K. A. JENSEN and B. BAK. J. Prakt. Chem. **151**, 187 (1938).
6. See C. R. HAUSER, F. W. SWAMER, and J. T. ADAMS. Org. Reactions, Vol. 8. John Wiley and Sons, Inc., New York. 1954. p. 122.
7. R. S. YOST and C. R. HAUSER. J. Am. Chem. Soc. **69**, 2325 (1947).

Can. J. Chem. Downloaded from www.nrcresearchpress.com by 210.87.254.42 on 09/05/12
For personal use only.

Steroid derivatives of cysteamine and cysteine

OWEN H. WHEELER AND CESAR REYES-ZAMORA
Puerto Rico Nuclear Center and Department of Chemistry, University of Puerto Rico, Mayaguez, Puerto Rico

Received July 8, 1968

A number of androstenone, estrone, and pregnenone derivatives of cysteamine have been prepared by reacting the steroid amines with ethylene monothiolcarbonate. The amides of androstenone carboxylic acid with mercaptoethylamine and cysteine have also been prepared.

Canadian Journal of Chemistry, 47, 160 (1969)

The only compounds which have shown any promise in affording protection against radiation in the animal body are cysteamine (2-mercaptoethylamine) and its simple derivatives (1). Cysteine, which was one of the first compounds reported to show radiation protection, is less effective (2). However, these compounds are relatively toxic and are also easily metabolized and eliminated from the body. The object of this work was to prepare derivatives which might be less toxic and less readily metabolized, by joining cysteamine and cysteine to a steroid molecule, while still leaving the mercapto group free, since this is essential for radiation protection. The following derivatives of cysteamine have been prepared: *N*-(2-mercaptoethyl)-3-ketopregn-4-en-20β-yl amine (**1**), *N*-(2-mercaptoethyl)-3-keto-androst-4-en-17β-yl amine (**2**), *N*-(2-mercaptoethyl)estra-1,3,5(10)-trien-3-ol-17β-yl amine (**3**), and *N*-(2-mercaptoethyl)-3-ketoandrost-4-ene 17β-carboxamide (**4**). A derivative of cysteine, *N*-(3-ketoandrost-4-ene 17β-carboxyl)cysteine (**5**), has also been synthesized.

The condensation of pregn-5-en-3-ol-20-amine with an excess of ethylene monothiolcarbonate gave a good yield of *N*-mercaptoethylpregn-5-en-3-ol-20β-yl amine. Although condensations with ethylene monothiolcarbonate are usually carried out (3, 4) with an excess of amine to avoid di-substitution, no *N,N*-dimercaptoethyl derivative was formed in the present case. This same compound was formed by using one equivalent of ethyl 2-mercaptoethylcarbonate (4). An Oppenauer oxidation of *N*-(2-mercaptoethyl)pregn-5-en-3-ol-20-yl amine under standard conditions gave *N*-(2-mercaptoethyl)-3-ketopregn-4-en-20β-yl amine (**1**), without oxidizing the mercapto group, although the yield was low. The molecular weight indicated that the compound was still in the free mercapto form.

As an alternative route pregn-5-en-3-ol-20β-yl amine was oxidized with chromium trioxide in pyridine (5) to 3-ketopregn-5-en-20β-yl amine, which was obtained in an impure state and in low yield, apparently due to the formation of chromium complexes. Oxidation of the corre-

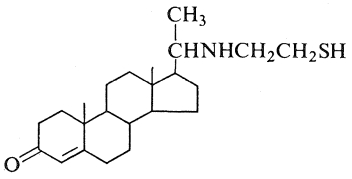

1

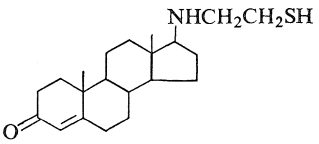

2

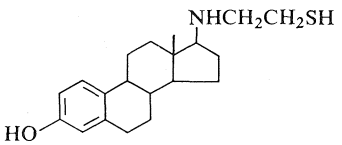

3

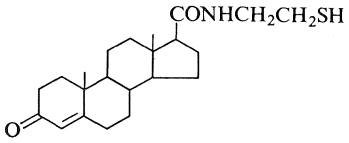

4

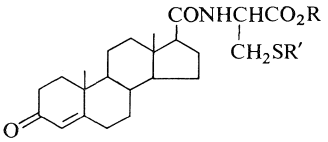

5 *a*; R = R′ = H
b; R = CH_3, R′ = $PhCH_2$

sponding amine hydrochloride following the method of Jones (6) gave only traces of the ketoamine. 3-Ketopregn-5-en-20β-yl amine could not be isomerized to 3-ketopregn-4-en-20β-yl amine with oxalic acid (7), but isomerization was achieved with alcoholic potassium hydroxide at room temperature.

Androst-5-en-3-ol-17β-yl amine also condensed with ethylene monothiolcarbonate to give *N*-(2-mercaptoethyl)androst-5-en-3-ol-17β-yl amine, which was oxidized under the conditions of Oppenauer to *N*-(2-mercaptoethyl)-3-ketoandrost-4-en-17β-yl amine (**2**). Estra-1,3,5(10)-trien-3-ol-17β-yl amine also reacted readily with ethylene monothiolcarbonate to give *N*-(2-mercaptoethyl)estra-1,3,5(10)-trien-3-ol-17β-yl amine (**3**).

3-Ketoandrost-4-ene 17β-carboxylic acid was converted to its acid chloride with oxalyl chloride and condensed with mercaptoethylamine to give *N*-(2-mercaptoethyl)-3-ketoandrost-4-ene 17β-carboxamide (**4**). The acid chloride was also reacted with cysteine in the presence of triethylamine to form *N*-(3-ketoandrost-4-ene 17β-carboxyl)cysteine (**5***a*). Condensation could not be effected in the presence of pyridine. Previously the acid chloride had been condensed with *S*-benzylcysteine methyl ester to afford *S*-benzyl-*N*-(3-ketoandrost-4-ene 17β-carboxyl)cysteine methyl ester (**5***b*). However, since the free cysteine derivative was prepared by direct condensation, hydrolysis and debenzylation of this last compound were not attempted.

Experimental

Analyses were performed by Dr. Jansen, Beerse, Belgium.

Pregn-5-en-3-ol-20β-yl Amine

Pregnenolone oxime (lit. (8) m.p. 218–219°) was reduced with sodium in *n*-propanol (9) to the amine hydrochloride, m.p. 304–305°. The free base was liberated with 30% aqueous sodium hydroxide, m.p. 165–167° (lit. (9) m.p. 163–166°).

N-(2-Mercaptoethyl)pregn-5-en-ol-20β-yl Amine

Pregn-5-en-3-ol-20β-yl amine (1.0 g) was dissolved in toluene (50 ml) and the solution dried by distilling off half the solvent. Ethylene monothiolcarbonate (0.165 g) was then added and the mixture refluxed for 15 h. Part of the solvent was evaporated at reduced pressure, when the product (0.97 g) crystallized and was then recrystallized from acetone, m.p. 152–154°.

As an alternative method, pregn-5-en-3-ol-20β-yl amine (0.765 g) in dry toluene (25 ml) was treated over 1 h at reflux with ethyl 2-mercaptoethylcarbonate (0.362 g) (4). The solution was refluxed for ½ h and the solvent removed *in vacuo*. The product (0.65 g) was recrystallized from acetone to m.p. 152–154°.

Anal. Calcd. for $C_{23}H_{39}NOS$: C, 73.25; H, 10.41. Found: C, 73.69; H, 10.60.

N-(2-Mercaptoethyl)-3-ketopregn-4-en-20β-yl Amine (1)

The above compound (0.55 g) was dissolved in toluene (200 ml) and cyclohexanone (30 ml). Part (70 ml) of the solvent was distilled off and aluminium isopropoxide (4.0 g) in toluene (30 ml) added dropwise while the solvent

Can. J. Chem. Downloaded from www.nrcresearchpress.com by 210.87.254.42 on 09/05/12
For personal use only.

Can. J. Chem. Downloaded from www.nrcresearchpress.com by 210.87.254.42 on 09/05/12
For personal use only.

(50 ml) was distilled off. The mixture was refluxed for 15 h, Rochelle salt (5 g) was then added and the mixture steam distilled. The product was extracted from the residue with ether and recrystallized from acetone – petroleum ether (0.23 g) m.p. 186–188° (decomp.); λ_{max} 242 mμ (log ε 4.03).

Anal. Calcd. for $C_{23}H_{37}NOS$ (mol. wt., 373): C, 73.54; H, 9.93. Found (mol. wt. (Rast), 363): C, 73.35; H, 9.71.

Androst-5-en-3-ol-17β-yl Amine

Phosphorus oxychloride (1.0 ml) was added dropwise to pregnenolone oxime (0.5 g) in pyridine (7.0 ml) with stirring and cooling to 0°. The mixture was maintained at 0–5° for 1½ h and then poured into ice and dilute hydrochloric acid. The acetylamino compound was filtered off, washed with water and recrystallized from methanol water, m.p. 245–247°. The hydrolysis was carried out by refluxing overnight with 20% potassium hydroxide in ethylene glycol. The product was extracted with ether and the amine hydrochlorides (0.2 g); m.p. 362° (lit. (10) m.p. 360°) precipitated by passing in hydrogen chloride. The free amine was liberated with 30% sodium hydroxide and recrystallized from acetone (0.11 g), m.p. 161–164° (lit. (10) m.p. 162°).

N-(2-Mercaptoethyl)androst-5-en-3-ol-17β-yl Amine

Androst-5-en-3-ol-17β-yl amine was condensed as above with ethylene monothiolcarbonate. The product, m.p. 150–152°, was recrystallized from acetone.

Anal. Calcd. for $C_{21}H_{35}NOS$: C, 72.15; H, 10.09. Found: C, 72.41; H, 9.93.

N-(2-Mercaptoethyl)-3-ketoandrost-4-en-17β-yl Amine (2)

N-Mercaptoethylandrost-5-en-3-ol-17β-yl amine (0.72 g) was subjected to an Oppenauer oxidation as before giving the product (0.31 g), m.p. 193–196° (decomp.), from acetone – petroleum ether; λ_{max} 241 mμ (log ε 4.02).

Anal. Calcd. for $C_{21}H_{33}NOS$ (mol. wt., 348): C, 72.57; H, 9.57. Found (mol. wt. (Rast), 343): C, 72.83; H, 9.82.

Estra-1,3,5(10)-trien-3-ol-17β-yl Amine

Estrone oxime (0.8 g) (m.p. 231–232°) (11) in *n*-propanol (50 ml) was refluxed with small pieces of sodium (1.48 g) until they dissolved. The solvent was evaporated at reduced pressure, water added, and carbon dioxide passed in. The precipitated solid was washed with hot water and recrystallized from methanol (0.3 g), m.p. 223–226° (lit. (11) m.p. 222–223°).

N-(2-Mercaptoethyl)estra-1,3,5(10)-trien-3-ol-17β-yl Amine (3)

Estratriene-3-ol-17β-yl amine (0.237 g) and ethylene monothiolcarbonate (0.041 g) in toluene (1.3 ml) under the usual conditions, gave mixed crystals (0.18 g) of the estratriene-3-ol-17β-yl amine and *N*-(2-mercaptoethyl)-estratrien-3-ol-17β-yl amine, recrystallized from acetone, m.p. 129–130°.

Anal. Calcd. for $C_{20}H_{29}NOS \cdot C_{18}H_{25}NO$: C, 75.70; H, 9.03. Found: C, 75.78; H, 8.97.

N-(2-Mercaptoethyl)-3-ketoandrost-4-ene 17β-carboxamide (4)

3-Ketoandrost-4-ene 17β-carboxylic acid (1.0 g) prepared by hypobromite oxidation of progesterone (12), was dissolved in 0.79 *N* sodium hydroxide (39 ml). The water was evaporated and the sodium salt dried at 170° and 1 mm for 5 h. The salt was suspended in anhydrous pyridine (0.16 g) and benzene (15 ml), cooled to 5°, and treated with oxalyl chloride (4.5 ml). The mixture was allowed to stand at room temperature for 5 min and evaporated *in vacuo* at 20°. Benzene (2 ml) was added and the solution reevaporated. The residue was dissolved in benzene (12 ml), cooled to 0°, and a suspension of freshly sublimed mercaptoethylamine (0.24 g) in benzene (5 ml) added with stirring. The solution was left at room temperature overnight and then evaporated. The residue was triturated with 10% sodium carbonate. The remaining solid was recrystallized from acetone–ether to crystals (0.66 g), m.p. 148–150° (decomp.); λ_{max} 242 mμ (log ε 4.08).

Anal. Calcd. $C_{22}H_{31}NO_2S \cdot H_2O$: C, 67.14; H, 8.96. Found: C, 67.33; H, 8.08.

N-(3-Ketoandrost-4-ene 17β-carboxyl)cysteine (5a)

3-Ketoandrost-4-ene 17β-carboxylic acid (0.33 g) was converted as above to its acid chloride, and this in benzene (4 ml) added dropwise at 0° with stirring to a solution of cysteine hydrochloride (0.16 g) in triethylamine (0.15 ml) and tetrahydrofuran (5 ml). A further amount of triethylamine (0.15 ml) was added during the addition. The reaction was stirred overnight, and then poured into water (10 ml) and acidified with a few drops of hydrochloric acid. The product was recovered by ether extraction, and recrystallized from acetone–hexane, m.p. 175–180° (decomp.); λ_{max} 242 mμ (log ε 4.10).

Anal. Calcd. for $C_{23}H_{33}NOS$: C, 65.84; H, 7.92. Found: C, 65.92; H, 7.68.

S-Benzyl-N-(3-ketoandrost-4-ene 17β-carboxyl)cysteine Methyl Ester (5b)

3-Ketoandrost-4-ene 17β-carboxylic acid (0.33 g) was converted to the acid chloride and added to *S*-benzyl-L-cysteine methyl ester (0.24 g (13)), m.p. 147°, and triethylamine (0.15 ml) in benzene (5 ml) cooled to 10°. Evaporation of the solvent and trituration with ether gave the product, m.p. 115–117°.

Anal. Calcd. for $C_{31}H_{41}NO_4S$: C, 71.09; H, 7.89. Found: C, 70.93; H, 7.75.

Acknowledgment

The authors acknowledge gifts of steroids from Syntex, S. A., Mexico City. The work was financed in part by a grant from the National Institutes of Health.

The Puerto Rico Nuclear Center is operated by the University of Puerto Rico for the United States Atomic Energy Commission.

1. J. F. Thompson. Radiation protection in mammals. Reinhold Publishing Corp., New York. 1962. Chap. 5.
2. H. M. Patt, E. B. Tyree, R. L. Straube, and D. E. Smith. Science **110**, 213 (1949).
3. D. D. Reynolds, M. K. Massad, D. L. Fields, and D. L. Johnson. J. Org. Chem. **26**, 5109 (1961).

4. D. D. REYNOLDS, D. L. FIELDS, and D. L. JOHNSON. J. Org. Chem. **26**, 5125 (1961).
5. G. I. POOS, G. E. ARTH, R. E. BEYLER, and L. H. SARETT. J. Am. Chem. Soc. **75**, 422 (1953).
6. K. BOWDEN, I. M. HEILBRON, E. R. H. JONES, and B. C. L. WEEDON. J. Chem. Soc. 39 (1946).
7. L. F. FIESER. J. Am. Chem. Soc. **75**, 5421 (1953).
8. A. BUTENANDT and U. WESTPHAL. Ber. **69**, 443 (1936).
9. R. A. LUCAS, D. F. DICKEL, R. L. DZIEMIAN, M. J. CEGLOWSKI, B. L. HENSLE, and H. B. MACPHILLAMY. J. Am. Chem. Soc. **82**, 5688 (1960).
10. J. SCHMIDT-THOMÉ. Ber. **88**, 895 (1955).
11. A. BUTENANDT and F. HILDEBRANDT. Z. Physiol. Chem., **199**, 243 (1937).
12. C. DJERASSI and J. STAUNTON. J. Am. Chem. Soc. **83**, 736 (1961).
13. R. A. BOISSONNAS, ST. GUTTMANN, P. A. JAQUENOUD, and J. P. WALLER. Helv. Chim. Acta, **38**, 1491 (1955).

Convenient *C*-alkylation of some acyloins

JOHAN H. VAN DE SANDE[1] AND KARL R. KOPECKY
Department of Chemistry, University of Alberta, Edmonton, Alberta

Received August 29, 1968

Acetoin, adipoin, and benzoin are conveniently alkylated by benzyl chloride and methyl iodide in 1,2-dimethoxyethane solution using sodium hydride as the base. Only alkylation at carbon is observed. Little or no alkylation occurs at oxygen.

Canadian Journal of Chemistry, 47, 163 (1969)

A large quantity of 3-benzyloxy-2-butanone was required in these laboratories. A possible route to this compound appeared to be the base-catalyzed benzylation of acetoin, eq. [1]. There

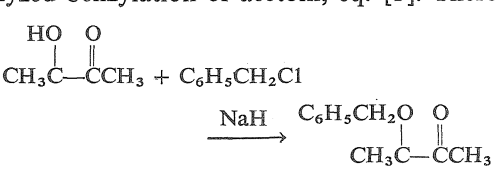

[1] $CH_3C(HO)(C{=}O)CH_3 + C_6H_5CH_2Cl \xrightarrow{NaH} CH_3C(OCH_2C_6H_5)(C{=}O)CH_3$

appear to be few studies of base-catalyzed alkylations of acyloins. There are a number of reports of alkylation at oxygen in reactions between dianions of enediols and alkyl halides (1–4). However, alkylation at carbon has also been observed in such systems (5, 6), and appears to be general in simple cases (6). Also, acyloins give products of reaction at carbon in the base-catalyzed aldol (7) and Michael (8–10) condensation reactions with aldehydes and activated olefins, respectively, presumably via the monoanion.

A convenient procedure for the methylation of alcohols (11, 12) was adapted for the benzylation of acetoin. Addition of sodium hydride in small portions to a 1,2-dimethoxyethane solution of equimolar amounts of acetoin and benzyl chloride at room temperature resulted in a rapid reaction. The product, isolated in 45% yield, did not have spectral properties expected for 3-benzyloxy-2-butanone. The infrared spectrum (CCl_4) showed strong hydroxyl absorption at 3480 cm^{-1}. No absorptions characteristic of the CH_3—CH— group could be detected in the nuclear magnetic resonance (n.m.r.) spectrum. The material was identified as 3-benzyl-3-hydroxy-2-butanone on the basis of its n.m.r. spectrum, taken in carbon tetrachloride, which showed singlet absorptions at τ 2.86 (5.0 H) for the phenyl protons, τ 6.15 (0.93 H) for the hydroxyl proton, τ 7.13 (1.85 H) for the methylene protons, and at τ 7.95 (2.84 H) and τ 8.76 (3.24 H) for the protons of the two methyl groups. Alkylation had thus occurred at the carbon atom and there was no evidence for any product resulting from alkylation at oxygen.

A brief extension of the alkylation of acyloins was made, using the same procedure, to include methylation and benzylation of acetoin, benzoin, and adipoin. Yields of alkylated products ranged from 40% to 70%. Alkylation at the ketol carbon appeared to be the exclusive reaction in all cases except in the methylation of adipoin. In this case the presence of a singlet at τ 6.9 in the n.m.r. spectrum (CCl_4) of the crude product indicates that some *O*-alkylation might have occurred. However, the major product resulted from carbon alkylation. In the other cases no n.m.r. spectral evidence was found for the formation of any *O*-alkylated materials.

[1]Holder of a NRCC Studentship, 1964–1968, and a University of Alberta Dissertation Fellowship, 1967–1968.

Can. J. Chem. Downloaded from www.nrcresearchpress.com by 210.87.254.42 on 09/05/12
For personal use only.

4. D. D. REYNOLDS, D. L. FIELDS, and D. L. JOHNSON. J. Org. Chem. **26**, 5125 (1961).
5. G. I. POOS, G. E. ARTH, R. E. BEYLER, and L. H. SARETT. J. Am. Chem. Soc. **75**, 422 (1953).
6. K. BOWDEN, I. M. HEILBRON, E. R. H. JONES, and B. C. L. WEEDON. J. Chem. Soc. 39 (1946).
7. L. F. FIESER. J. Am. Chem. Soc. **75**, 5421 (1953).
8. A. BUTENANDT and U. WESTPHAL. Ber. **69**, 443 (1936).
9. R. A. LUCAS, D. F. DICKEL, R. L. DZIEMIAN, M. J. CEGLOWSKI, B. L. HENSLE, and H. B. MACPHILLAMY. J. Am. Chem. Soc. **82**, 5688 (1960).
10. J. SCHMIDT-THOMÉ. Ber. **88**, 895 (1955).
11. A. BUTENANDT and F. HILDEBRANDT. Z. Physiol. Chem., **199**, 243 (1937).
12. C. DJERASSI and J. STAUNTON. J. Am. Chem. Soc. **83**, 736 (1961).
13. R. A. BOISSONNAS, ST. GUTTMANN, P. A. JAQUENOUD, and J. P. WALLER. Helv. Chim. Acta, **38**, 1491 (1955).

Convenient *C*-alkylation of some acyloins

JOHAN H. VAN DE SANDE[1] AND KARL R. KOPECKY
Department of Chemistry, University of Alberta, Edmonton, Alberta

Received August 29, 1968

Acetoin, adipoin, and benzoin are conveniently alkylated by benzyl chloride and methyl iodide in 1,2-dimethoxyethane solution using sodium hydride as the base. Only alkylation at carbon is observed. Little or no alkylation occurs at oxygen.

Canadian Journal of Chemistry, 47, 163 (1969)

A large quantity of 3-benzyloxy-2-butanone was required in these laboratories. A possible route to this compound appeared to be the base-catalyzed benzylation of acetoin, eq. [1]. There

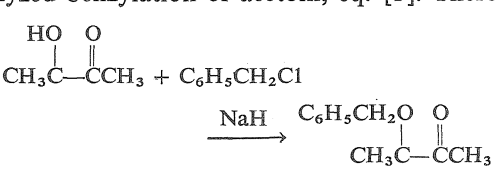

[1] $CH_3C(HO)(C{=}O)CH_3 + C_6H_5CH_2Cl \xrightarrow{NaH} CH_3C(OCH_2C_6H_5)(C{=}O)CH_3$

appear to be few studies of base-catalyzed alkylations of acyloins. There are a number of reports of alkylation at oxygen in reactions between dianions of enediols and alkyl halides (1–4). However, alkylation at carbon has also been observed in such systems (5, 6), and appears to be general in simple cases (6). Also, acyloins give products of reaction at carbon in the base-catalyzed aldol (7) and Michael (8–10) condensation reactions with aldehydes and activated olefins, respectively, presumably via the monoanion.

A convenient procedure for the methylation of alcohols (11, 12) was adapted for the benzylation of acetoin. Addition of sodium hydride in small portions to a 1,2-dimethoxyethane solution of equimolar amounts of acetoin and benzyl chloride at room temperature resulted in a rapid reaction. The product, isolated in 45% yield, did not have spectral properties expected for 3-benzyloxy-2-butanone. The infrared spectrum (CCl_4) showed strong hydroxyl absorption at 3480 cm^{-1}. No absorptions characteristic of the CH_3—CH— group could be detected in the nuclear magnetic resonance (n.m.r.) spectrum. The material was identified as 3-benzyl-3-hydroxy-2-butanone on the basis of its n.m.r. spectrum, taken in carbon tetrachloride, which showed singlet absorptions at τ 2.86 (5.0 H) for the phenyl protons, τ 6.15 (0.93 H) for the hydroxyl proton, τ 7.13 (1.85 H) for the methylene protons, and at τ 7.95 (2.84 H) and τ 8.76 (3.24 H) for the protons of the two methyl groups. Alkylation had thus occurred at the carbon atom and there was no evidence for any product resulting from alkylation at oxygen.

A brief extension of the alkylation of acyloins was made, using the same procedure, to include methylation and benzylation of acetoin, benzoin, and adipoin. Yields of alkylated products ranged from 40% to 70%. Alkylation at the ketol carbon appeared to be the exclusive reaction in all cases except in the methylation of adipoin. In this case the presence of a singlet at τ 6.9 in the n.m.r. spectrum (CCl_4) of the crude product indicates that some *O*-alkylation might have occurred. However, the major product resulted from carbon alkylation. In the other cases no n.m.r. spectral evidence was found for the formation of any *O*-alkylated materials.

[1]Holder of a NRCC Studentship, 1964–1968, and a University of Alberta Dissertation Fellowship, 1967–1968.

Can. J. Chem. Downloaded from www.nrcresearchpress.com by 210.87.254.42 on 09/05/12
For personal use only.

Can. J. Chem. Downloaded from www.nrcresearchpress.com by 210.87.254.42 on 09/05/12
For personal use only.

The procedure described offers a convenient method for the carbon alkylation of simple, unhindered acyloins in reasonable yield. The reaction conditions were not optimized and yields could probably be improved. The reaction appears to be general and leads to the same products as the alkylation of the dianions (6) which were generated by the acyloin condensation of esters. The present procedure is considerably more convenient.

Experimental

Melting points and boiling points are uncorrected. Infrared spectra were recorded on Perkin–Elmer model 421 and 337 spectrophotometers. Nuclear magnetic resonance spectra were determined with a Varian model A-60 analytical spectrometer using carbon tetrachloride as solvent and tetramethylsilane as an internal standard.

Sodium hydride dispersed in mineral oil was freed of the oil by washing with pentane. 1,2-Dimethoxyethane was allowed to reflux over lithium aluminium hydride for 2 h and then distilled through a 45 cm Vigreaux column.

3-Benzyl-3-hydroxy-2-butanone

The following procedure is typical of all the alkylation reactions.

Into a 500 ml 3-necked flask equipped with a dry ice condenser was placed a solution of 8.8 g (0.1 mole) of freshly distilled 3-hydroxy-2-butanone and 14.7 g (0.11 mole) of benzyl chloride in 200 ml of 1,2-dimethoxyethane. Sodium hydride, (2.5 g, 0.106 mole) was added in small portions to the stirred solution over a 20 min period. Vigorous hydrogen evolution occurred after the addition of each portion. The solution was stirred a further 2 h at room temperature and then the solvent was removed by distillation at atmospheric pressure. Ether (50 ml) was added to the residue to precipitate the remainder of the sodium chloride. The resulting mixture was filtered and the filtrate concentrated. Distillation of the residual oil afforded 7.9 g (45%) of a colorless oil, b.p. 88–91° (0.8 mm), n_D^{27} 1.5175. The features of the n.m.r. spectrum were given in the text.

Anal. Calcd. for $C_{11}H_{14}O_2$: C, 74.13; H, 7.92. Found: C, 74.24; H, 8.20.

3-Hydroxy-3-methyl-2-butanone

The procedure described above was used except that solvent was removed through an efficient distillation column. From 17.6 g (0.20 mole) of acetoin, 32.7 g (0.23 mole) of methyl iodide and 5.04 g (0.21 mole) of sodium hydride 12 g (63%) of product were obtained, b.p. 136–139°, $n_D^{27.5}$ 1.4096; reported (13) b.p. 140–141°, n_D^{21} 1.415.

Methylbenzoin

The reaction was carried out as described above. The reaction mixture was poured into one liter of water and the resulting mixture extracted with three 50 ml portions of chloroform. The combined extracts were washed twice with water and dried over magnesium sulfate. The chloroform was removed under reduced pressure and the residue was crystallized from pentane. From 10.6 g (0.05 mole) of benzoin, 15 g (0.105 mole) of methyl iodide and 1.25 g (0.050 mole) of sodium hydride there were obtained 7.6 g (67%) of white crystals, m.p. 63–65°; reported (14) m.p. 65–66°.

Benzylbenzoin

The procedure described for the preparation of methylbenzoin was used. From 5.3 g (0.025 mole) of benzoin, 3.4 g (0.027 mole) of benzyl chloride and 0.63 g (0.026 mole) of sodium hydride there was obtained 3.5 g (47%) of white crystals, m.p. 113–116°; reported (15) m.p. 115–118°.

2-Hydroxy-2-methylcyclohexanone

The procedure described for the preparation of 3-benzyl-3-hydroxy-2-butanone was used. From 11.4 g (0.1 mole) of adipoin (16), 20 g (0.14 mole) of methyl iodide and 2.4 g (0.1 mole) of sodium hydride there was obtained 5.3 g (41%) of a colorless oil, b.p. 82–85° (15 mm), n_D^{27} 1.4605; reported (17) b.p. 80–95° (15 mm), n_D^{20} 1.4644.

2-Benzyl-2-hydroxycyclohexanone

The procedure described for the preparation of methylbenzoin was used. From 11.4 g (0.1 mole) of adipoin, 12.6g (0.1 mole) of benzyl chloride and 2.4 g (0.1 mole) of sodium hydride there were obtained 9.5 g (46%) of light-yellow crystals, m.p. 65–67°. The n.m.r. spectrum showed peaks at τ 2.76 (singlet, 5.0 H) for the aromatic protons, τ 6.10 (singlet, 0.82 H) for the hydroxyl proton, τ 6.93 (singlet, 0.87 H), and τ 6.97 (singlet, 0.87 H) for the non-equivalent benzylic protons and broad absorption from 7.1 to τ 8.7 (8.35 H) for the protons of the cyclohexanone ring. The compound absorbed moderately at 3540 cm^{-1} in the infrared spectrum.

Anal. Calcd. for $C_{13}H_{16}O_2$: C, 76.44; H, 7.90. Found: C, 76.35; H, 8.02.

1. H. Staudinger and H. Binkert. Helv. Chim. Acta, **5**, 703 (1922).
2. H. Scheibler and R. Emden. Ann. **434**, 265 (1923).
3. W. E. Bachmann. J. Am. Chem. Soc. **56**, 963 (1934).
4. R. C. Fuson and E. C. Horning. J. Am. Chem. Soc. **62**, 2692 (1940).
5. M. S. Kharasch, E. Sternfield, and F. R. Mayo. J. Org. Chem. **5**, 362 (1940).
6. J. C. Speck and R. W. Bast. J. Org. Chem. **11**, 788 (1946).
7. J. Colonge and Y. Vaginay. Bull. Soc. Chim. France, 3140 (1965).
8. J. Szmuszkovicz and H. Bom. J. Am. Chem. Soc. **75**, 3350 (1953).
9. J. Colonge and P. Brison. Bull. Soc. Chim. France, 96 (1962).
10. J. Colonge and P. Brison. Bull. Soc. Chim. France, 175 (1962).
11. D. J. Cram and K. R. Kopecky. J. Am. Chem. Soc. **81**, 2748 (1959).
12. U. E. Diner, F. Sweet, and R. K. Brown. Can. J. Chem. **44**, 1591 (1966).
13. P. Freon. Ann. Chim. **11**, 453 (1939).
14. R. Roger. J. Chem. Soc. **127**, 523 (1925).
15. G. Schneing and A. Hensle. Ann. **440**, 82 (1924).
16. A. Kotz, K. Blendermann, R. Rosenbusch, and E. Sirringhaus. Ann. **400**, 62 (1913).
17. L. W. Butz, B. S. Davis, and A. M. Gaddis. J. Org. Chem. **12**, 122 (1947).

Synthesis of caerulomycin

S. RANGANATHAN AND B. B. SINGH
Department of Chemistry, Indian Institute of Technology, Kanpur, India

AND

P. V. DIVEKAR
Defence Research Laboratory (Materials), Kanpur, India

Received April 9, 1968

The synthesis of Caerulomycin starting from the known 4-methoxy-2,2′-bipyridyl-l-oxide, prepared from 2,2′-bipyridyl, is described.

Canadian Journal of Chemistry, 46, 165 (1968)

Can. J. Chem. Downloaded from www.nrcresearchpress.com by 210.87.254.40 on 09/05/12
For personal use only.

Caerulomycin (**1**), a secondary metabolite of *Streptomyces caeruleus* Baldacci, was isolated in 1959 (1) and its structure established in 1967 by Divekar, Read, and Vining (2). The 2,2′-bipyridyl along with an oxime attachment at the 6-position constitutes a novel arrangement for an antibiotic. Caerulomycin possesses powerful antifungal properties and it is also a potent plant-wilt toxin (3). Amongst a series of 2,2′-bipyridyls prepared by Jones and co-workers (4) for spectroscopic studies, was 4-methoxy-2,2′-bipyridyl-1-oxide (**2**). This timely information greatly simplified our efforts aimed at the synthesis of caerulomycin. 2,2′-Bipyridyl (5) was converted to the methoxy compound **2** (4). Compound **2** was reacted with methyl sulfate and the crude *O*-alkylated product, on treatment with potassium cyanide in aqueous dioxan, gave 6-cyano-4-methoxy-2,2′-bipyridine (**3**). Initial attempts to reduce the nitrile using sodium hypophosphite – Raney nickel (6) or lithium triethoxyaluminohydride (7) were not successful. Attention was then directed to the use of lithium aluminium hydride for this purpose. In a model experiment an ether solution of benzonitrile was treated with excess ethereal lithium aluminium hydride. The precipitated complex (believed to be $\overset{\phi}{\underset{H}{}}>=N—AlH_3Li$ (7)) on treatment with dilute sulfuric acid followed by 2,4-dinitrophenylhydrazine reagent gave a quantitative yield of benzaldehyde 2,4-dinitrophenylhydrazone. On the basis of the above experiment an ether solution of **3** was reacted with excess lithium aluminium hydride and the precipitated pink complex decomposed with 2 *N* sulfuric acid. The pH of the solution was adjusted to 8–9 with 2.5 *N* sodium hydroxide, mixed with excess neutralized hydroxylamine hydrochloride, and heated for 0.5 h, conditions which generally lead to *syn* oximes (8). Work up gave essentially pure caerulomycin; m.p. 165–169°. Two crystallizations from methanol gave a sample m.p. 174–175°, identical in all respects

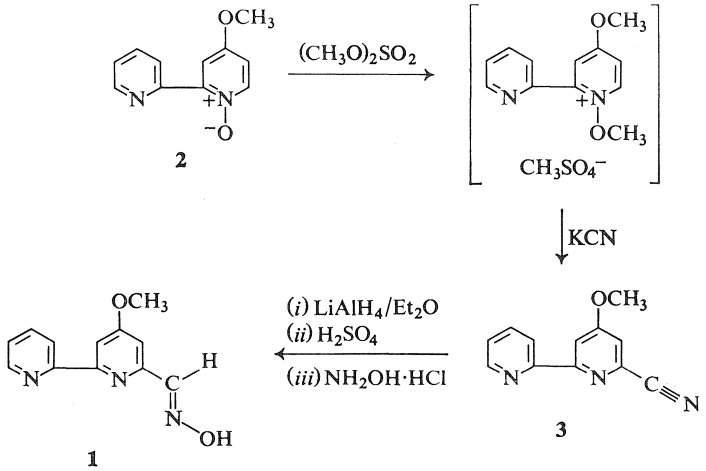

with natural caerulomycin. The synthetic antibiotic was also identical with the natural one in its ability to inhibit the growth of *Candida albicans* and *Curvularia lunata*. This synthesis should make caerulomycin more accessible for biological studies.

Experimental

Melting points were taken on a Kofler block and are uncorrected. Most infrared spectra were obtained with a Perkin–Elmer model 137 recording spectrophotometer. Samples were mixed with potassium bromide and pressed into wafers. The infrared spectra of synthetic and natural caerulomycin were obtained with a Perkin–Elmer model 521 instrument. Thin-layer chromatography was carried out on 0.2 mm layers of silica gel G (Stahl) which were dried for 0.5 h at 100 °C and were developed with iodine vapor. The solvent system used was benzene:ethyl acetate (3:1). The microanalysis (C, H) was done by Mr. A. H. Siddiqui, IIT, Kanpur. Nitrogen analysis was done at C.D.R.I., Lucknow. 4-Methoxy-2,2′-bipyridyl-1-oxide (**2**) was prepared according to the published procedure (4).

6-Cyano-4-methoxy-2,2′-bipyridine (3)

A stirred solution of 4-methoxy-2,2′-bipyridyl-1-oxide (30 mg, 0.15 mmole) and methyl sulfate (38 mg, 0.3 mmole) in dioxan (0.5 ml) was heated at 100° for 2 h. Dioxan and excess methyl sulfate were removed under reduced pressure at 100° and the crude *O*-alkylated product treated with excess potassium cyanide (29 mg, 0.45 mmole) in aqueous dioxan (pH of solution 8–9). The resulting pinkish reaction mixture was stirred at room temperature for 3 h and extracted with chloroform. The chloroform extract gave crude **3** (10 mg, 30% from **2**). Thin-layer chromatography showed one spot (R_f 0.6) corresponding to nitrile obtained from natural sources. The above material after two crystallizations from ethanol gave a product m.p. 171–172°, undepressed on admixture with caerulomycinonitrile, obtained from the natural product. The infrared spectra of synthetic and authentic samples were identical.

Caerulomycin (1)

Under dry nitrogen a solution of **3** (50 mg, 0.24 mmole) in dry ether (50 ml) was mixed with a standardized ether solution of lithium aluminium hydride (18 mg in 1.2 ml of ether; 0.47 mmole). The pinkish complex was allowed to settle and the supernatant liquid rejected. The residue was treated with 2 *N* sulfuric acid and the pH adjusted to 8–9 by addition of 2.5 *N* sodium hydroxide. The solution was treated with excess neutralized hydroxylamine hydrochloride (8) (from 100 mg of reagent) and the mixture heated on a water bath for 0.5 h. Extraction with ether gave crude caerulomycin m.p. 165–169° (15.5 mg, 28%). Thin-layer chromatography showed one spot (R_f 0.3) corresponding to the natural product. Two crystallizations from methanol gave a sample m.p. 174–175°, undepressed on admixture with natural caerulomycin. The infrared spectra of synthetic and natural samples were identical in all respects.

Anal. Calcd. for $C_{12}H_{11}N_3O_2$: C, 62.90; H, 4.80; N, 18.33. Found: C, 63.19; H, 4.83; N, 17.89.

Acknowledgment

We are pleased to acknowledge the help we have received from Dr. L. M. Pande of DRL(M), Kanpur.

1. A. Funk and P. V. Divekar. Can. J. Microbiol. **5**, 317 (1959).
2. P. V. Divekar, G. Read, and L. C. Vining. Can. J. Chem. **45**, 1215 (1967).
3. R. R. Chandran, R. Sankaran, and P. V. Divekar. J. Antibiotics, Tokyo, **21**, No. 3 (1968).
4. R. A. Jones, B. D. Roney, W. H. F. Sasse, and K. O. Wade. J. Chem. Soc. B, 106 (1967).
5. W. Karminski and Z. Kulichi. Chem. Abstr. **63**, 18018 (1965).
6. O. G. Backberg and B. Staskun. J. Chem. Soc. 3961 (1962).
7. H. C. Brown and C. P. Garg. J. Am. Chem. Soc. **86**, 1085 (1964).
8. S. Ginsburg and I. B. Wilson. J. Am. Chem. Soc. **79**, 481 (1957).

Can. J. Chem. Downloaded from www.nrcresearchpress.com by 210.87.254.40 on 09/05/12
For personal use only.

Can. J. Chem. Downloaded from www.nrcresearchpress.com by 210.87.254.42 on 09/05/12
For personal use only.

Canadian Journal of Chemistry

Published by THE NATIONAL RESEARCH COUNCIL OF CANADA

VOLUME 47 JANUARY 15, 1969 NUMBER 2

Normal coordinate analysis of titanium(IV) halide : monoethylenediamine complexes

P. J. ASHLEY[1] AND E. G. TORRIBLE[1]

Chemistry Department, Queen's University, Kingston, Ontario

Received July 16, 1968

A partial normal coordinate analysis was performed for the $Ti(en)X_4$ complexes, assuming *gauche* configuration of the ligand and overall symmetry of C_2 for the complex. Comparison of the calculated frequencies with the available experimental data supports the assumption of the chelate structure for the complexes and also confirms the previous assignments for the Ti—N stretching frequencies. Some new assignments are proposed in the 900–300 cm^{-1} region.

Canadian Journal of Chemistry, 47, 167 (1969)

Introduction

The preparation and infrared spectra of the compounds $Ti(en)Cl_4$ and $Ti(en)Br_4$ have been reported recently (1). The spectra were found to be qualitatively consistent with a chelate structure with the ethylenediamine in the *gauche* configuration. Assignments were made for both metal–nitrogen and metal–halide vibrational modes in the complex.

In this paper we report the results of a vibrational analysis based on the proposed chelate structure for the $Ti(en)Cl_4$ and $Ti(en)Br_4$ molecules.

Results

The skeleton of the proposed structure is shown in Fig. 1. In the model the ethylenediamine ligand has been coordinated in the *cis* configuration. This increased the symmetry of the complex from C_2 to C_{2v}. All the initial calculations were done for a molecule of this symmetry. However, in order to clarify certain assignments the final calculations were done for the ligand in the *gauche* configuration and hence for a molecule with C_2 symmetry, but all angles about the titanium atom were considered to be 90°. The results produced by this latter calculation are the ones reported in this paper.

[1]Present Address: Alcan Research and Development Ltd., P.O. Box 8400, Kingston, Ontario.

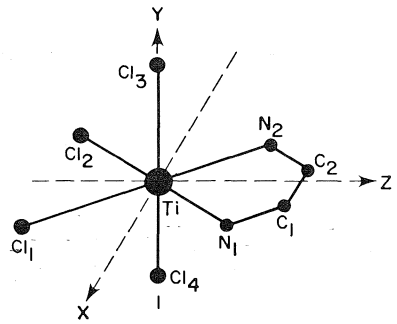

FIG. 1. C_{2v} model of $Ti(en)Cl_4$.

In the absence of known structural data, the bond lengths (Table I) used were based on corresponding dimensions in other comparable molecules.

To simplify further the calculation, the hydrogen frequencies were not calculated. There is evidence for probable coupling of the NH_2

TABLE I

Assumed bond lengths for the $Ti(en)X_4$ complexes

Bond	$Ti(en)Cl_4$ (Å)	$Ti(en)Br_4$ (Å)
Ti—X	2.34	2.40
Ti—N	2.00	2.00
N—C	1.66	1.50
C—C	1.54	1.70

TABLE II

Observed and calculated frequencies (cm^{-1}) and assignments for $Ti(en)X_4$ complexes

$Ti(en)Cl_4$			$Ti(en)Br_4$	
Observed	Calculated	Assignment	Observed	Calculated
1107	1092	Sym. C—N stretch	1105	1090
1053	1084	Asym. C—N stretch	1040	1070
880	849	C—C stretch	880*	872
520	533	N—C—C—N bend	515	521
442	497	Ti—X stretch	435	421
390	417	Ti—N stretch and ring deformation	365	359
372	364	Ti—Cl stretch		
350	345	Ti—N stretch	330	345
315	295	Ti—X stretch and ring deformation	280†	276

*A very weak band which was not previously reported (1).
†Observed, but just below the calibrated range of the spectrometer.

deformation modes with the low frequency skeletal modes (2). However, because we were unable to observe modes which absorb below 300 cm^{-1}, it was considered that for the present purpose no serious error was introduced by this simplification.

The skeleton contains nine atoms giving rise to 21 normal vibrations and 25 internal coordinates including 4 redundancies. The 25th order secular equation of the form $|\mathbf{GF} - \mathbf{E}\lambda| = 0$ was solved on an IBM 360/50 computer for the 21 normal vibrational frequencies. Four "zero frequencies" corresponding to the four redundancies were obtained. The potential function used was a simple Urey–Bradley potential function (3). The full details of the calculation are given elsewhere (4).

The calculated and observed frequencies for the complexes are listed in Table II. As an additional aid in assigning the calculated frequencies to specific vibrational modes, a potential energy distribution in each symmetry coordinate was also calculated. Table II includes an approximate description of each mode based on both the potential energy distribution and the normal coordinate analysis.

The force constants obtained from the calculation and corresponding to the calculated frequencies of Table II are listed in Table III.

Discussion

There is general agreement between the previously reported (1) and the present calculated frequencies (Table II), and the corresponding force constants are considered reasonable (5–7). However, because the observed spectra were obtained on an instrument with a lower limit of 300 cm^{-1}, only those frequencies observed above 300 cm^{-1} were available for comparison. Thus in general only the stretching force constants could be adjusted to give the best fit. The values of the bending force constants and those of the interaction terms cannot be considered final.

The assignments also agree with those previously reported (1) except for those at 442 and 315 cm^{-1} in the chloride complex and at 435 cm^{-1} in the bromide complex. For the chloride complex the calculated frequencies of 364 and 295 cm^{-1} were very sensitive to changes of the Ti—Cl stretching force constant, as also was the calculated frequency of 497 cm^{-1}. Thus the observed bands at 442, 370, and 315 cm^{-1} are assigned to Ti—Cl stretching modes. Horley and Torrible (1) originally assigned the bands at 520 and 442 cm^{-1} in the chloride to N—C—C—N bending modes on the basis of a qualitative comparison with the assignments made for free ethylenediamine (8). Our calculations now indicate that while the original assignment of the band at 520 cm^{-1} was probably correct, the band at 442 cm^{-1} in the chloride complex is a Ti—Cl stretching frequency associated with the chlorine atoms above and below the plane of molecule. A calculated Ti—Cl stretching frequency of 505 cm^{-1} for a five coordinate (C_{2v}) titanium complex, $TiCl_4.NMe_3$, has been reported (6). A shift to a lower frequency in a six coordinate complex would be expected. A comparable argument leads to a reassignment of the observed band at 435 cm^{-1} in the bromide complex to the out of plane Ti—Br stretching frequency.

Can. J. Chem. Downloaded from www.nrcresearchpress.com by 210.87.254.42 on 09/05/12
For personal use only.

TABLE III

Urey–Bradley force constants corresponding to values in Table II*

Stretching	Force constant	Bending	Force constant	Repulsion	Force constant
K(Ti—Cl)	1.55	H(Cl—Ti—Cl)	0.1	F(Cl—Cl)	0.18
K(Ti—N)	0.48	H(Cl—Ti—N)	0.1	F(Cl—N)	0.17
K(C—N)	4.1	H(N—Ti—N)	0.09	F(N—N)	0.02
K(C—C)	2.5	H(Ti—N—C)	0.09	F(Ti—C)	0.02
K(Ti—Br)	1.05	H(N—C—C)	0.32	F(N—C)	0.05
		H(Br—Ti—Br)	0.11	F(Br—Br)	0.18
		H(Br—Ti—N)	0.09	F(Br—N)	0.17

*Force constants are given in mdyn/Å.

A C—C stretching frequency was not assigned by Horley and Torrible (1). However, the bands they reported at 981 and 978 cm^{-1} for the chloride and bromide complex respectively, correspond closely to the band at 980 cm^{-1} assigned to the C—C stretching frequency by Sabatini and Califano (8) for free ethylenediamine. There is, however, some controversy regarding the assignment of the C—C stretching frequency in the ethylenediamine complexes. Bands at frequencies from 820 cm^{-1} to close to 1000 cm^{-1} have been assigned to this mode (2, 9–11). On the basis of our calculation the observed band at 880 cm^{-1} in both the Ti(en)Cl_4 and Ti(en)Br_4 complex is tentatively assigned as the C—C stretching frequency. The potential energy distribution indicated very little coupling between the C—C and C—N stretching modes, and consequently specific assignments for these vibrations have been made. A similar conclusion was also reached by Armendarez and Nakamoto for the nickel(II)oxamido complex (5).

The calculation based on the proposed chelate skeleton (Fig. 1) gives 21 possible frequencies. We have been able to compare only 9 of these values with observed values because of limited experimental data. The comparison of those frequencies indicates that the proposed chelate structure for the Ti(en)X_4 complexes is probable, and also supports the original assignments for the Ti—N stretching frequencies (1).

Acknowledgments

Grateful acknowledgement is made to the National Research Council of Canada for financial support and to the Government of the Province of Ontario for Fellowships (to P. J. A.).

The authors also wish to thank Dr. H. F. Shurvell for his assistance with the calculations and computer program.

1. D. Horley and E. G. Torrible. Can. J. Chem. **43**, 3201 (1965).
2. A. D. Allen and C. V. Senoff. Can. J. Chem. **43**, 888 (1965).
3. K. Nakamoto. Infrared spectra of inorganic coordination compounds. John Wiley and Sons, Inc., New York. 1963.
4. P. J. Ashley, Ph.D. Thesis, Queen's University, Kingston Ontario. 1968.
5. P. Armendarez and K. Nakamoto. Inorg. Chem. **5**, 796 (1966).
6. I. R. Beattie and T. Gilson. J. Chem. Soc. 6595 (1965).
7. J. F. Jacovitz and J. Walter. Spectrochim. Acta, **22**, 1393 (1966).
8. A. Sabatini and S. Califano. Spectrochim. Acta, **16**, 677 (1960).
9. K. Krishnan and R. A. Plane. Inorg. Chem. **5**, 852 (1966).
10. D. B. Powell and N. Sheppard. Spectrochim. Acta, **17**, 68 (1961).
11. G. W. Watt and D. S Klett. Inorg. Chem. **5**, 1278 (1966).

Can. J. Chem. Downloaded from www.nrcresearchpress.com by 210.87.254.42 on 09/05/12
For personal use only.

Can. J. Chem. Downloaded from www.nrcresearchpress.com by 210.87.254.5 on 09/05/12
For personal use only.

Nickel(II) complexes with substituted ureas[1]

R. A. BAILEY, I. R. FEINS[2], AND T. R. PETERSON[3]
Department of Chemistry, Rensselaer Polytechnic Institute, Troy, New York 12181

Received August 23, 1968

A number of nickel(II) complexes with methyl-, *n*-butyl-, phenyl-, and N,N′dimethylurea ligands were prepared with a variety of anions. All exhibited octahedral coordination geometry. Of the anions, only NCS^- was in the coordination sphere. Infrared spectral studies indicate coordination of the ligands through oxygen.

Canadian Journal of Chemistry, 47, 171 (1969)

Introduction

Complexes of Ni(II) with thiourea type ligands are well known, exhibiting a variety of formulas and stereochemistries (octahedral, tetragonal, tetrahedral, planar (1)). Bonding is generally through the sulfur atom of the ligand (2). Some Ni(II) complexes with the analogous urea ligands have been prepared and shown by X-ray analysis (3, 4) or infrared spectroscopy (5) to be oxygen coordinated. The latter technique has been used frequently in the study of the coordination of ureas and thioureas, and while not always unambiguous in its results, is a useful approach. The purpose of the present study was to consider some Ni(II) complexes of substituted ureas comparable to the substituted thioureas prepared previously in order to compare the complexing in these analogous systems. The compounds have been examined in somewhat close detail by infrared and visible spectroscopy, and magnetic susceptibility techniques.

Experimental

Chemicals

All substituted ureas, anhydrous nickel halides, and nickel perchlorate hexahydrate were obtained from K and K Laboratories, Inc., and were used without further purification. Nickel nitrate hexahydrate and all other chemicals used were Fisher Reagent grade materials.

Analyses

Nickel was determined by EDTA titration using murexide indicator (6). Halogens and sulfur were determined by a modification of the Schöringer method. C, H, and N analyses were performed on a commercial Perkin–Elmer C—H—N analyzer. Sulfur and some N analyses were performed by Schwartzkopf Microanalytical Laboratories.

Spectra

Infrared spectra were obtained by the KBr pellet technique on a Perkin–Elmer 621 spectrophotometer, and checked in mulls. Visible spectra were obtained by the reflectance technique, using $MgCO_3$ as standard in a Beckman DK 2 A spectrophotometer.

Magnetic Susceptibility

Magnetic data were obtained by the Guoy technique, using $Hg[Co(SCN)_4]$ as calibrant, and corrected for diamagnetism in the usual manner (7). Measurements at a number of field strengths all gave essentially identical results. Dewar flasks containing liquid nitrogen and dry-ice – acetone were used in low temperature measurements.

Preparation of Complexes

The yellow–green complexes prepared in this study and the analytical results for them are listed in Table I. They were prepared by mixing 0.01 mole of metal salt in 50 ml hot absolute ethanol with 0.06 mole of ligand dissolved in 35 ml ethanol, boiling for 10 min, and evaporating the filtered solution to 45 ml on a steam bath. Chilling produced pale yellow–green crystals which were recrystallized three times from absolute ethanol and vacuum dried. The perchlorate compound was formed and recrystallized similarly from a solvent of 50 ml chloroform – 15 ml ethanol. The thiocyanate was made from $Ni(SCN)_2$ formed in ethanol from $NiCl_2$ and NaSCN. Frequently in these preparations a waxy, rather intractable mass was produced on cooling. The addition of a small amount of chloroform or ether reduced this to readily workable crystalline form.

Results and Discussion

The solid state electronic spectra (reflectance spectra) of the Ni(II) substituted urea complexes, which are all very similar to one another, may be assigned satisfactorily on the basis of a ligand field of O_h symmetry. The energies of the bands assigned as the three spin allowed transitions; $^3A_{2g} \rightarrow {}^3T_{2g}$ (F) at 8000–8400 cm^{-1} (ν_1),

---

[1]This material is taken in part from theses presented to the Graduate School of Rensselaer Polytechnic Institute in partial fulfillment of the requirements for the Ph.D. degree: I. R. Feins, 1966; T. R. Peterson, to be presented.

[2]Present address: American Cyanamid Co., Stamford, Connecticut.

[3]Present address: Imperial Color and Chemical Department, Hercules Incorporated, Glens Falls, New York.

Can. J. Chem. Downloaded from www.nrcresearchpress.com by 210.87.254.5 on 09/05/12
For personal use only.

TABLE I

Analytical results (%) for Ni(II) urea complexes

Compound	Nickel		Carbon		Hydrogen		Nitrogen		Halogen		Yield (%)
	Calcd.	Found	Calcd.	Found	Calcd.	Found	Calcd.	Found	Calcd.	Found	
[Ni (N-methylurea)$_6$]Cl$_2$	10.2	10.3	25.1	24.9	6.3	6.4	29.3	29.2	12.4	12.4	74
[Ni (N-methylurea)$_6$]Br$_2$	8.9	8.9	21.7	21.8	5.5	5.5	25.4	25.8	24.1	23.9	68
[Ni (N-methylurea)$_6$]I$_2$	7.8	7.8	19.0	19.1	4.8	4.8	22.2	21.9	33.5	33.2	71
[Ni (N-methylurea)$_6$](NO$_3$)$_2$	9.4	9.5	23.0	22.8	5.8	5.9	31.3	31.0			80
[Ni (N-methylurea)$_4$ (NCS)$_2$]	12.5	12.4	25.5	25.7	5.1	5.1	29.7	29.6	13.6	13.7[a]	64
[Ni (N-methylurea)$_6$](ClO$_4$)$_2$	8.4	8.3	20.5	20.4	5.2	5.2	23.9	23.5	10.1	9.9	53
[Ni (*n*-butylurea)$_6$]Cl$_2$	7.1	7.2	43.6	42.8	8.8	8.8	20.3	20.3	8.6	8.8	61
[Ni (*n*-butylurea)$_6$]Br$_2$	6.4	6.5	39.4	39.5	7.9	8.1	18.4	18.4	17.5	17.5	58
[Ni (*n*-butylurea)$_6$]I$_2$	5.8	5.9	35.7	35.6	7.2	7.4	16.7	16.5	25.1	25.0	68
[Ni (*n*-butylurea)$_6$](NO$_3$)$_2$	6.7	6.6	41.0	41.0	8.3	8.2	22.3	22.0			91
[Ni (N-phenylurea)$_6$]Cl$_2$	6.2	6.3	53.3	52.9	5.1	5.0	17.8	17.5	7.5	7.5	68
[Ni (N-phenylurea)$_6$]Br$_2$	5.7	5.6	48.7	49.0	4.7	4.7	16.2	16.0	15.4	15.5	52
[Ni (N-phenylurea)$_6$]I$_2$	5.2	5.2	44.7	44.6	4.3	4.1	14.9	14.9	22.5	22.5	51
[Ni (N-phenylurea)$_6$](NO$_3$)$_2$	5.9	5.9	50.5	50.5	4.8	4.8	19.6	19.6			48
[Ni (N,N′dimethylurea)$_6$]Br$_2$	7.9	7.9	28.9	29.1	6.5	6.5	22.5	22.3	21.4	21.2	51

[a]Sulfur.

TABLE II

Reflectance spectra for Ni(II) urea complexes band positions in cm^{-1}

	ν_1 (Δ)	ν_2	ν_3	ν_4	ν_5	B (cm^{-1})	β
[Ni (N-methylurea)$_6$]Cl_2	8 200	13 400	21 300 sh	24 400		880	0.85
[Ni (N-methylurea)$_6$]Br_2	8 200	13 350	21 200 sh	24 250	32 500	870	0.84
[Ni (N-methylurea)$_6$]I_2	8 000	13 250	21 300 sh	24 400	34 600	900	0.87
[Ni (N-methylurea)$_6$]$(ClO_4)_2$	8 000	13 200	20 700 sh	24 250	30 900	900	0.87
[Ni (N-methylurea)$_6$]$(NO_3)_2$	8 000	13 200	20 800 sh	24 400	33 300	900	0.87
[Ni (*n*-butylurea)$_6$]Cl_2	8 100	13 350	21 800 sh	24 400		900	0.87
[Ni (*n*-butylurea)$_6$]Br_2	8 100	13 200	20 800 sh	24 250		880	0.85
[Ni (*n*-butylurea)$_6$]I_2	8 000	13 200	22 000 sh	24 400	28 000–35 100	890	0.86
[Ni (*n*-butylurea)$_6$]$(NO_3)_2$	8 100	13 200	20 800 w	24 200	33 000	880	0.85
[Ni (N-phenylurea)$_6$]Cl_2	8 265	13 400	21 200 sh	24 250		860	0.83
[Ni (N-phenylurea)$_6$]Br_2	8 300	13 600	21 300 sh	24 250		860	0.83
[Ni (N-phenylurea)$_6$]I_2	8 300	13 600	21 300 sh		29 300	860	0.83
[Ni (N-phenylurea)$_6$]$(NO_3)_2$	8 200	13 600	21 300 sh	24 800	32 900	920	0.88
[Ni (N,N′dimethylurea)$_6$]Br_2	8 500	13 350	21 400 sh	24 400		880	0.85
[Ni (N-methylurea)$_4$ $(NCS)_2$]	8 300	13 700	21 200 sh	24 400		880	0.85

$^3A_{2g} \rightarrow {}^3T_{1g}$ (F) at 13 200 – 13 700 cm^{-1} (ν_2), and $^3A_{2g} \rightarrow {}^3T_{1g}$ (P) at 24 200 – 24 800 cm^{-1} (ν_4), (Table II), agree well with those predicted from the energy level diagram of Liehr and Ballhausen (8) with 10 *Dq* about 8 100 cm^{-1}. Bands or shoulders at 20 700 – 22 000 cm^{-1} and 28 000 – 34 600 cm^{-1} are most probably spin-forbidden bands arising from transitions to the $^1A_{1g}$ or $^1T_{2g}$ (D), and $^1T_{2g}$ (G) or ^1E_g (G) levels which lie in these regions.

In the case of [Ni (N-methylurea)$_4$ $(NCS)_2$], the only compound of this series with fewer than six organic ligands, the 10 *Dq* value of 8300 cm^{-1} (Table II) is well within the range expected for octahedral Ni(II). The value of 10 *Dq* for this compound agrees with that predicted from the rule of average environments (9) for nitrogen bonded (but not sulfur bonded) thiocyanate (10). Further evidence for coordination of the thiocyanate group to the Ni(II) ion through nitrogen is provided by the infrared spectrum.

The Racah parameter, *B*, was calculated for each complex in the usual manner (11) from the observed positions of the three spin allowed transitions using the relation $15B = \nu_2 + \nu_3 - 3\Delta$ where Δ is the energy of the $^3A_{2g} \rightarrow {}^3T_{2g}$ transition. The values of *B* for the complexes calculated in this way (Table II) are of the order 850–900 cm^{-1}, and may be compared to the free Ni(II) ion value of 1030 cm^{-1} and a value of 880 cm^{-1} in the hexaquo complex (9). The values of *Dq* obtained for the substituted ureas in the present study are 880–850 cm^{-1}, very similar to the field strength of sulfur bonding thioureas with Ni(II) (2). The general order is found to be N,N′dimethylurea > N-phenylurea > *n*-butylurea ≈ N-methylurea.

The magnetic moments of the Ni(II) substituted urea complexes were studied at liquid nitrogen, dry-ice – acetone, and room temperatures (Table III). In no case was there a dependence of the susceptibility on field strength. The observed susceptibilities were corrected for diamagnetism and temperature independent paramagnetism (t.i.p.) in the usual manner from the relation t.i.p. = $8N\beta^2/10\,Dq$ c.g.s.u. The t.i.p. values are 200–250 $\times$ 10^{-6} c.g.s.u., approximately 6% of the room temperature susceptibility values. Plots of $1/\chi_m$ (corr.) vs. temperature gave straight lines in all cases. From these data θ values were obtained; these are small (Table III). As the significance of θ is uncertain, it has not been used in the calculation of the moment. The magnetic moments are in the range 2.9–3.2 B.M. normally found for octahedrally coordinated Ni(II) complexes (12, 13), and are close to the room temperature moments of 3.09 and 3.32 B.M. for [Ni(urea)$_6$] (ClO_4) and [Ni(N,N′dimethylurea)$_6$] $(ClO_4)_2$ previously reported by Stonestreet *et al.* (5). For most of these compounds the moments lead to values of the spin–orbit coupling constant λ' of approximately -150 to -200 cm^{-1} (from the relation $\mu = 2.83\,(1 - 4\lambda'/10\,Dq)$). Although not very accurate, these values are evidently slightly smaller than those observed with the thiourea complexes (2).

Penland *et al.* (14) and Shafer (15) have shown that urea and tetramethylurea complexes of

Can. J. Chem. Downloaded from www.nrcresearchpress.com by 210.87.254.5 on 09/05/12
For personal use only.

TABLE III

Magnetic properties of Ni(II) urea complexes

Compound	$\chi_m \times 10^6$ c.g.s.u.			Diamagnetic corrections $\times 10^6$ c.g.s.u.	θ (°K)	$\mu_{299°}$ (B.M.)
	299 °K	188 °K	77 °K			
[Ni (N-methylurea)$_6$]Cl_2	4 050	6 050	15 000	−192	−7	3.10
[Ni (N-methylurea)$_6$]Br_2	3 900	5 950	13 950	−214	−6	3.05
[Ni (N-methylurea)$_6$]I_2	3 850	5 800	13 900	−246	−5	3.04
[Ni (N-methylurea)$_6$] $(NO_3)_2$	3 850	5 550	14 100	−183	−9	3.02
[Ni (N-methylurea)$_6$] $(ClO_4)_2$	3 850	5 900	14 550	−209	−2	3.02
[Ni (N-methylurea)$_4$ $(NCS)_2$]	4 000	5 400	14 500	−163	−7	3.07
[Ni (N-phenylurea)$_6$]Cl_2	4 450	6 000	14 500	−217	−6	3.24
[Ni (N-phenylurea)$_6$]Br_2	3 850	5 400	15 200	−240	−5	3.06
[Ni (N-phenylurea)$_6$]I_2	4 100	5 900	14 450	−272	−7	3.16
[Ni (N-phenylurea)$_6$] $(NO_3)_2$	3 850	5 900	15 200	−208	+4	3.03
[Ni (*n*-butylurea)$_6$]Cl_2	3 750	5 800	15 050	−405	0	3.08
[Ni (*n*-butylurea)$_6$]Br_2	3 750	5 750	14 400	−428	−8	3.06
[Ni (*n*-butylurea)$_6$]I_2	3 950	6 050	15 500	−460	−4	3.16
[Ni (*n*-butylurea)$_6$] $(NO_3)_2$	4 500	6 400	16 250	−396	−10	3.34
[Ni (N,N′-dimethylurea)$_6$]Br_2	3 550	5 450	12 950	−346	−4	2.97

metal ions exhibit a decrease in the energy of the carbonyl stretching frequency of the ligand on coordination when oxygen-to-metal bonding is involved. Other carbonyl compounds, ketones, amides, etc., show similar behavior (16–18). On the other hand, coordination to the metal ion through the nitrogen atom of a urea type ligand shows a marked shift of the carbonyl stretching band to higher frequencies while the N—H stretching frequency of the bonded —NH_2 or —NHR group is decreased (14, 19). This has been shown to be the case for N-bonded Pt(II) and Pd(II) complexes containing urea ligands, as reported earlier by Penland *et al.* (14), and for a variety of Pd(II) substituted urea complexes (20). Recently Costamagna and Levitus (21) have examined the infrared spectra of a number of cobalt(II) complexes containing N-methylurea, N-ethylurea, N,N′ethyleneurea, N,N′diethylurea, and N,N′dimethylurea; and reported them to be oxygen bonded from the shifting of the carbonyl stretching band to lower frequencies along with no apparent change in position for the N—H stretching frequencies. A number of complexes of first row transition metals with N,N′dimethylurea have been reported by Stonestreet *et al.* (5) to be oxygen bonded to the metal ion, based on similar infrared evidence.

The infrared spectra of the Ni(II) complexes prepared in the present study (Table IV) suggest that in all cases oxygen is the coordinated atom. The N—H stretching frequencies are shifted slightly to higher values and sometimes split, probably because of differences in hydrogen bonding, while the carbonyl stretching frequency is usually decreased. The spectrum of the N,N′dimethylurea example is similar to those of [Co(N,N′dimethylurea)$_6$] $(NO_3)_2$ and [Co(N,N′dimethylurea)$_6$][$CoCl_4$] reported previously (21) and also considered to be oxygen bonded. This mode of bonding is further supported by the evidence of Cavalca *et al.* (23) which shows [Ni(N-methylurea)$_6$]Cl_2 to be isostructural with the oxygen bonded cobalt compound. Slight differences in the spectrum of a given complex with change of anion may be attributed to solid state effects (21, 22). Unfortunately, the infrared spectra of these organic ligands have not yet been assigned to permit bands other than the carbonyl stretching and N—H stretching frequencies to be considered unambiguously. It is probable that the C—N stretching bands in the free organic ligands lie at ca. 1150–1250 cm^{-1}. However, by analogy with the assigned spectra of urea (14) and N-methylthiourea (25), one would expect that the C—N stretching frequencies in the free ligand would shift to higher values if metal-to-oxygen bonds were present due to the increased double bond character of the C—N linkage, while metal-to-nitrogen bonding would lead to increased single bond character and decreased stretching frequency of this bond. In these complexes, this band appears shifted significantly to higher frequencies (Table IV) which would be in keeping with the presence of nickel-to-oxygen bonds if their origin is in fact due to C—N stretching.

Other significant bands in the spectra of the

Can. J. Chem. Downloaded from www.nrcresearchpress.com by 210.87.254.5 on 09/05/12
For personal use only.

TABLE IV

Significant bands in the infrared spectra of coordinated Ni(II) urea complexes

Compound	Band positions (cm^{-1})		
	N—H Str.	C=O Str.	C—N Str.[a]
N-methylurea	3420,3310 3200	1645	1160
[Ni (N-methylurea)$_6$]Cl_2	3420,3330 3315,3220	1635	1170
[Ni (N-methylurea)$_6$]Br_2	3430,3315	1635	1170
[Ni (N-methylurea)$_6$]I_2	3418,3330 3260,3220	1632	1168
[Ni (N-methylurea)$_6$] $(ClO_4)_2$	3420,3320 3260	1635	1170
[Ni (N-methylurea)$_6$] $(NO_3)_2$	3400,3340 3240	1635	1170
[Ni (N-methylurea)$_4$ $(NCS)_2$]	3490,3422 3370,3340 3230	1642	1170
n-Butylurea	3400,3322 3260,3185	1635	1160
[Ni (*n*-butylurea)$_6$]Cl_2	3410,3330 3260,3190	1632	1160
[Ni (*n*-butylurea)$_6$]Br_2	3420,3322 3260,3185	1635	1160
[Ni (*n*-butylurea)$_6$]I_2	3410,3330 3285,3215 3190	1635	1160
[Ni (*n*-butylurea)$_6$] $(NO_3)_2$	3418,3320 3260,3120	1635	1160
N-phenylurea	3420,3310 3200	1650	1248
[Ni (N-phenylurea)$_6$]Cl_2	3430,3410 3310,3270 3220	1640	1250
[Ni (N-phenylurea)$_6$]Br_2	3430,3410 3315,3270 3235	1640	1248
[Ni (N-phenylurea)$_6$]I_2	3400,3310 3270,3230	1638	1245
[Ni (N-phenylurea)$_6$] $(NO_3)_2$	3420,3320 3250,3190	1645	1245
N,N′dimethylurea	3320,3160	1610	1170
[Ni (N,N′dimethylurea)$_6$]Br_2	3400,3265 3120	1625	1178

[a]Tentative assignment.

substituted ureas are the amide(II) (N—H deformation plus C—N antisymmetric stretching), and amide(III) (N—H deformation and C—N stretching), which cannot be assigned at the present time. The former should shift to higher frequencies with either nitrogen or oxygen bonding, while the latter should increase in frequency with oxygen bonding but decrease if bonding is through nitrogen. None of the remaining free ligand bands decrease in frequency on coordination, but increases are noted in the 1535–1590 and 1100 cm^{-1} regions. Thus there is no evidence to support nitrogen bonding of the organic ligand in any of these compounds. While it should be emphasized that conclusions based on the infrared spectra of ligands of this complexity must always be regarded with caution, oxygen bonding is clearly indicated.

The thiocyanate groups in [Ni(N-methylurea)$_4$-$(NCS)_2$] are shown to be coordinated through the nitrogen atom by the C—N stretching frequency at 2070 cm^{-1}, the NCS bending mode at 482 cm^{-1}, and most significantly, the C—S stretching absorption at 850 cm^{-1} (24).

There are notable differences in the coordination of substituted ureas and thioureas to Ni(II). The tendency to form an octahedral NiO_6 coordination group is quite marked, while thioureas are prone to allow the anions to coordinate, and to permit other than octahedral

Can. J. Chem. Downloaded from www.nrcresearchpress.com by 210.87.254.5 on 09/05/12
For personal use only.

geometries. The ligand field strength of the O-bonding ureas is surprisingly similar to that of the S-bonding thioureas toward Ni(II). One may presume that while sulfur is a weaker electron donor than oxygen, as indicated by its usual position in the spectrochemical series, this effect is balanced by a greater covalency of the Ni—S bond in the thioureas.

Acknowledgments

We wish to thank Miss P. Mullun for the visible reflectance measurements, Mrs. J. Fornasar and Mrs. P. Stekman for the C—H—N halide determinations, and the American Cyanamid Company and Hercules Incorporated for permission to publish these results.

1. S. L. Holt, Jr., and R. L. Carlin. J. Am. Chem. Soc. **86**, 3017 (1964).
2. R. A. Bailey and T. R. Peterson. To be published.
3. M. Nardelli and L. Coghi. Ric. Sci. **29**, 134 (1959).
4. M. B. Cingi, L. Coghi, and C. Guastini. Gazz. Chim. Ital. **95**, 368 (1965).
5. B. C. Stonestreet, W. E. Bull, and R. J. Williams. J. Inorg. Nucl. Chem. **28**, 1895 (1966).
6. G. Schwarzenbach. Complexometric titrations. *Translated by* H. Irving. Interscience Publishers, Inc., New York. 1957. p. 79, and references therein.
7. B. N. Figgis and J. Lewis. *In* Modern coordination chemistry. *Edited by* J. Lewis and R. G. Wilkins. Interscience Publishers, Inc., New York. 1960. p. 415.
8. A. D. Liehr and C. J. Ballhausen. Ann. Phys. N.Y. **6**, 134 (1959).
9. B. N. Figgis. Introduction to ligand fields. Interscience Publishers, Inc., New York. 1966. Chap. 9.
10. D. Forster and D. M. L. Goodgame. Inorg. Chem. **4**, 823 (1965).
11. Y. Tanabe and S. Sugano. J. Phys. Soc. Japan, **9**, 753 (1954).
12. B. N. Figgis and J. Lewis. *In* Progress in inorganic chemistry. Vol. 6. *Edited by* F. A. Cotton. Interscience Publishers, Inc., New York. 1964. p. 197.
13. N. S. Gill and R. S. Nyholm. J. Chem. Soc. 3997 (1959).
14. R. B. Penland, S. Mizushima, C. Curran, and J. V. Quagliano. J. Am. Chem. Soc. **79**, 1575 (1957).
15. M. Shafer. 148th Natl. Meeting Am. Chem. Soc. Chicago. September 1964. Abstracts, p. 28.
16. G. F. Svatos, C. Curran, and J. V. Quagliano. J. Am. Chem. Soc. **77**, 6159 (1959).
17. L. J. Bellamy and R. F. Branch. J. Chem. Soc. 4491 (1954).
18. R. S. Drago, D. W. Meek, M. D. Joesten, and L. LaRoche. Inorg. Chem. **2**, 124 (1963).
19. F. A. Cotton. *In* Modern coordination chemistry. *Edited by* J. Lewis and R. G. Wilkins. Interscience Publishers, Inc., New York. 1960. p. 388.
20. R. Eskanazi, T. Raskovan, and R. Levitus. *Quoted in* J. A. Costamagna and R. Levitus. J. Inorg. Nucl. Chem. **28**, 2685 (1966).
21. J. A. Costamagna and R. Levitus. J. Inorg. Nucl. Chem. **28**, 2685 (1966).
22. F. A. Cotton, D. M. L. Goodgame, and M. Goodgame. J. Am. Chem. Soc. **83**, 4690 (1961).
23. L. Cavalca, M. Nardelli, and L. Coghi. Gazz. Chim. Ital. **87**, 903 (1957).
24. I. Bertini and A. Sabatini. Inorg. Chem. **5**, 1025 (1966).
25. T. J. Lane, A. Yamaguchi, J. V. Quagliano, J. A. Ryan, and S. Mizushima. J. Am. Chem. Soc. **81**, 3824 (1959).

Can. J. Chem. Downloaded from www.nrcresearchpress.com by 210.87.254.5 on 09/05/12
For personal use only.

The transmission of polar effects. Part IX.[1] The ionization and esterification with diazodiphenylmethane of 9-substituted 10-triptoic acids

KEITH BOWDEN AND D. C. PARKIN
Department of Chemistry, The University of Essex, Wivenhoe Park, Colchester, Essex, England

Received February 16, 1968

A series of 9-substituted 10-triptoic acids have been prepared. Their pK_a values in 80% 2-methoxyethanol–water and 50% ethanol–water at 25° and rate coefficients for esterification with diazodiphenylmethane in five alcohols at 30° have been measured. The results have been analyzed by linear free energy relations. The π-inductive effect is shown to be unimportant in such systems, while the field effect model can account for the transmission.

Canadian Journal of Chemistry, 47, 177 (1969)

Can. J. Chem. Downloaded from www.nrcresearchpress.com by 210.87.254.6 on 09/05/12
For personal use only.

Introduction

A number of model systems have been studied to attempt a real understanding of the mode of transmission of substituent polar effects (1–6). The most important problem remaining is the estimation of the relative importance of the field and the inductive modes of transmission (3, 4). While the field effect is the coulombic action of a charged or dipolar substituent on a reaction center (7), the inductive effect derives from the polarization of the bonds connecting them (3, 4, 8). The latter can be effected through the σ- or π-bonds. Most studies (1–6), though not all (9), appear to be in favor of the field effect dominating the transmission. However, it appears likely that a π-inductive transmission may augment the field effect in favorable cases (4).

The most interesting and informative model so far studied is that of Roberts and Moreland, the 4-substituted bicyclo(2,2,2)octane-1-carboxylic acids (**1**) (1). These studies have been extended by other workers (10, 11). Analyses of the results of these and related studies (1, 2, 10, 11) appear to be in favor of the field effect transmission. The present study presents an extension of this model to include the possibility of a π-inductive transmission. The reactivity of a series of 9-substituted 10-triptoic acids (**2**) was measured in their ionization and esterification with diazodiphenylmethane (DDM) in a number of alcohols. After this study had been completed, results for a similar model, the 4-substituted dibenzobicyclo(2,2,2)-octa-2,5-diene-1-carboxylic acids (**3**), were reported (12). Our triptoic acid model is more

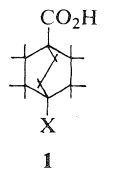

1

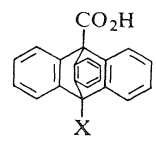

2

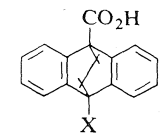

3

symmetrical and contains the maximum of 3 potential π-bonded transmissive links. The present report and the latter study appear to be both complimentary and consistent. In this work, the ionization and esterification with diazodiphenylmethane of a series of 9-substituted triptoic acids has been studied and the results have been correlated by linear free energy relations.

Results and Discussion

The rate coefficients for the esterification of the 9-substituted 10-triptoic acids with diazodiphenylmethane in five alcohols at 30.0° are shown in Table I. Table II shows the pK_a values of the acids in 50% w/w ethanol–water and 80% w/w 2-methoxyethanol–water.

These results have been analyzed by a linear free energy relation [1], similar to the Hammett equation and using the substituent constants σ_I (13). These constants have been derived from the pK_a values of the substituted acetic acids in

$$[1] \qquad \log (k/k_0) \text{ or } (K/K_0) = \rho_I \sigma_I$$

water at 25° as the standard reaction, with ρ_I equal to 3.95. The correlations found are shown

[1]For Part VIII; ref. 6.

Can. J. Chem. Downloaded from www.nrcresearchpress.com by 210.87.254.6 on 09/05/12
For personal use only.

TABLE I

Rate coefficients for the esterification of 9-substituted 10-triptoic acids with diazodiphenylmethane at 30.0°

	k*				
9-Substituent	Methanol	Ethanol	Isopropyl alcohol	2-Methoxy-ethanol	2-*n*-Butoxy-ethanol
H	10.1	3.47	2.03	1.78	0.917
Me	10.2	3.35	2.14	1.87	1.06
Cl	18.9	6.91	4.10	4.28	2.27
Br	18.2	6.67	4.24	4.09	2.24
NO_2	24.2	9.11	5.64	5.90	3.24

*The rate coefficients, k (l mole^{-1} min^{-1}), are reproducible to ±3% or better, and are the mean of at least two determinations.

TABLE II

pK_a values of the 9-substituted 10-triptoic acids in 50% w/w ethanol–water (50% EW) and in 80% w/w 2-methoxyethanol–water (80% MCS) at 25°

	pK_a*	
9-Substituent	50% EW	80% MCS
H	5.20	6.23
Me	5.23	6.27
Cl	4.67	5.70
Br	4.67	5.69
NO_2	4.40	5.43

*The pK_a values are the mean of at least two determinations and are reproducible to ±0.03 units.

in Table III and are excellent. Data for related systems (1, 10, 12) have been correlated with σ_I values and are shown in Table IV. These correlations are also very good.

The reaction constants obtained from the present study are contrasted with those available for the acetic and bicyclo(2,2,2)octane carboxylic acid systems in Table V. It is immediately obvious that there is *no* increased transmission of the substituent polar effect in the triptoic acids, compared with the bicyclo(2,2,2)octane carboxylic acids. The transmission is very similar for both systems and in both reactions. For the ionization reaction, the reaction constants for the 2 other bicyclo(2,2,2)octene systems studied recently by Stock's group (12) are also almost the same. Thus, it appears that the π-inductive transmissive route, available in the triptoic acids, has no major role in the relay of the polar effect. *However*, this does not exclude the intervention of this route when either or both the substituent and the reaction site are bonded *directly* to a π-bonded system. In these triptoic acids, both substituent and reaction site groups are bound to saturated carbons. The π-inductive effect would have to be originally generated by a field or σ-inductive effect. In substituted cinnamic acids, for example, it is possible, and indeed probable, that such an effect can and does exist (4, 6).

A number of other possibilities are excluded by this lack of increase in the susceptibility of the system to the substituent polar effect. An

TABLE III

Reaction constants, ρ_I, for triptoic acids

Reaction	ρ_I*	log k_0	r†	n†
Esterification with DDM at 30.0°				
in methanol	0.517	1.017	0.998	5
in ethanol	0.589	0.545	0.999	5
in isopropyl alcohol	0.593	0.332	0.996	5
in 2-methoxyethanol	0.703	0.277	0.996	5
in 2-*n*-butoxyethanol	0.707	0.009	0.991	5
Ionization at 25.0°				
in 50% w/w ethanol–water	1.102	5.20	0.999	5
in 80% w/w 2-methoxyethanol–water	1.114	6.23	1.000	5

*σ_I values (13) used are 0.0 (H), −0.03 (Me), 0.48 (Cl), 0.47 (Br), and 0.73 (NO_2). The last value is derived from the pK_a of nitroacetic acid in water at 25° (1.88) (14).
†r is the correlation coefficient; n is the number of substituents studied.

Can. J. Chem. Downloaded from www.nrcresearchpress.com by 210.87.254.6 on 09/05/12
For personal use only.

TABLE IV

Reaction constants, ρ_I, for octane systems*

System	Reaction	ρ_I	log k_0	r	n	Reference
4-Substituted bicyclo(2,2,2)octane-1-carboxylic acid	DDM esterification, ethanol at 30°	0.668	−0.620	0.984	5	1
4-Substituted bicyclo(2,2,2)octane-1-carboxylic acid	Ionization, 50% EW at 25°	1.481	6.87	0.997	9	1, 10
4-Substituted bicyclo(2,2,2)oct-2-ene-1-carboxylic acid	Ionization, 50% EW at 25°	1.691	6.54	0.997	5	12
4-Substituted dibenzobicyclo(2,2,2)octa-2,5-diene-1-carboxylic acid	Ionization, 50% EW at 25°	1.070	5.75	0.984	7	12

*Values of σ_I are those noted in Table III or those derived from reliable pK_a values of substituted acetic acids in water at 25° (13, 15).

TABLE V
Comparison of reaction constants, ρ_I

Reaction	ρ_I		ϕ*	
	Acetic	9,10-Triptoic	9,10-Triptoic	Bicyclo-octane carboxylic†
Esterification with DDM at 30.0°				
in methanol	2.34	0.52	0.22	—
in ethanol	2.44	0.59	0.24	0.27
in isopropyl alcohol	2.58	0.59	0.23	—
in 2-methoxyethanol	2.92	0.70	0.24	—
in 2-*n*-butoxyethanol	3.01	0.71	0.24	—
Ionization at 25.0°				
in 50% w/w ethanol–water	4.18	1.10	0.26	0.35
in 80% w/w 2-methoxyethanol–water	4.04	1.11	0.27	—

*ϕ equals ρ_I (system)/ρ_I(acetic).
†4-Substituted bicyclo(2,2,2)octane-1-carboxylic acids.

increased susceptibility could have arisen, in the ionization reaction, from increased dependence on polar substituent effects needed to replace sterically inhibited solvation of the carboxylate anion (4). In fact, triptoic acid does not appear to suffer significant steric inhibition of solvation, which causes strong acid-weakening for triphenylacetic acid (13*b*). This must be due to the "tying-back" of the bulky phenyl groups in triptycene. More importantly, the low dielectric cavity (7) in the triptoic acids is greatly increased compared to the bicyclo(2,2,2)octane carboxylic acids. As the transmission has not increased, a field effect must pass mainly through the core of the molecule. The medium surrounding the reaction site and substituent can still be involved in the transmission. It is important to point out that an inductive model could account for the transmission in this and related models; albeit that the transmissive coefficient, ε, (4) would have to equal about 0.44 for the triptoic acids. This is a rather large and unlikely value (3). It is important to attempt to see if the field effect model can account for the results satisfactorily. Numerous attempts (2, 4, 7, 10–12) have been made to relate the transmission of polar effects to the Kirkwood–Westheimer theory for the field effect (7). Most detailed attempts fail, but modifications to give a simpler relation have had some success. Such a model (4, 16) has been previously proposed to allow a calculation of the reaction constant ratio, ϕ, of the reaction constant of a system to that of the parent for the same reaction.

In Table VI, the field effect calculations are shown. These are based on the equation proposed by Kirkwood and Westheimer (7), shown below in eq. [2].

$$[2] \qquad \log (K/K_0) = \frac{e\mu \cos \theta}{2.303kTD'r^2}$$

When attempting a calculation of the reaction constant ratio this reduces to eq. [3], where D' is the effective dielectric constant, r the distance between the dipolar substituent and the reaction site, and θ the angle between the r and the dipolar axis. The subscript $_0$ refers to the reference system.

$$[3] \qquad \phi \text{ (calcd.)} = \frac{\cos \theta D'_0 r_0^2}{\cos \theta_0 D' r^2}$$

The chloro-substituted acids are taken as the models for the calculation (see (4, 17) for details). In Table VI, the results for a point dipole substituent spherical model are shown for 50% ethanol–water (ionization) and ethanol (DDM esterification). The important distance is that from the center of the dipole to the surface of the molecular cavity and this is taken as 1.5 Å in accordance with a suggestion by Tanford (18). The experimentally found values of the ratio, ϕ, are in good agreement with the calculations; especially considering the uncertainties involved. It is very interesting to note that these calculations predict a very small variation of the effective dielectric constant, D', with the medium for the acetic acid system. This would result in a very small variation in ρ_I for this system. This has been found especially for the ionization reaction for this system (13*b*).

The variation of the reaction constant for

Can. J. Chem. Downloaded from www.nrcresearchpress.com by 210.87.254.6 on 09/05/12
For personal use only.

Can. J. Chem. Downloaded from www.nrcresearchpress.com by 210.87.254.6 on 09/05/12
For personal use only.

TABLE VI

Field effect calculations (spherical model and point dipole approximations)

Acid	r (Å)	θ (degrees)	D'		$10^2 \cos\theta/r^2 D'$ (Å^{-2})		φ, calcd.		φ, found	
			50% EW	Ethanol	50% EW	Ethanol	50% EW	Ethanol	50% EW	Ethanol
Chloroacetic	2.83	53	2.78	2.72	2.70	2.76	1.00	1.00	1.00	1.00
4-Chlorobicyclo(2,2,2)-octane-1-carboxylic	5.87	0	4.25	3.98	0.68	0.73	0.25	0.26	0.35	0.27
9-Chloro-10-triptoic	6.22	0	4.33	4.07	0.60	0.64	0.22	0.23	0.26	0.24

TABLE VII

Physical properties of 10-triptoic acids and esters

9-Substituent	Acid		Methyl ester	
	m.p. (°C)	Lit. m.p. (°C)	m.p. (°C)	Lit. m.p. (°C)
H	356–358	356–358*	205	204–205*
Me	374	(*a*)	282	(*e*)
Cl	366	(*b*)	218	(*f*)
Br	358	(*c*)	227–228	(*g*)
NO_2	368	(*d*)	224–225	(*h*)

*See ref. 22.
(*a*) Anal. Calcd. for $C_{22}H_{16}O_2$: C, 84.6; H, 5.13. Found: C, 84.5; H, 5.20.
(*b*) Anal. Calcd. for $C_{21}H_{13}O_2Cl$: C, 75.8; H, 3.91; Cl, 10.7. Found: C, 75.7; H, 3.89; Cl, 10.7.
(*c*) Anal. Calcd. for $C_{21}H_{13}O_2Br$: C, 66.8; H, 3.45; Br, 21.2. Found: C, 67.0; H, 3.56; Br, 21.3.
(*d*) Anal. Calcd. for $C_{21}H_{13}O_4N$: C, 73.4; H, 3.82; N, 4.08. Found: C, 73.8; H, 3.88; N, 4.03.
(*e*) Anal. Calcd. for $C_{23}H_{18}O_2$: C, 84.7; H, 5.52. Found: C, 84.9; H, 5.60.
(*f*) Anal. Calcd. for $C_{22}H_{15}O_2Cl$: C, 76.2; H, 4.33; Cl, 10.2. Found: C, 76.4; H, 4.50; Cl, 10.1.
(*g*) Anal. Calcd. for $C_{22}H_{15}O_2Br$: C, 67.5; H, 3.84; Br, 20.5. Found: C, 67.7; H, 3.95; Br, 20.5.
(*h*) Anal. Calcd. for $C_{22}H_{15}O_4N$: C, 73.9; H, 4.23; N, 3.92. Found: C, 74.3; H, 4.28; N, 3.88.

esterification of the triptoic acids with the solvent closely parallels that for the acetic acids (13*b*). The solvents in the present study are all alcohols. However, the reaction constants do increase, as found before for the acetic acid system (13*b*), with decreasing dielectric constant of the alcohol. In the acetic acid system, the relation between the reaction constant and the solvent has been interpreted as being due, in the main, to solvent dependence of the reaction rather than field effect transmission through the medium. The reaction constants for the meta/para-substituted benzoic acid system shows solvent dependence which is more distinct (19). This probably results from both solvent dependence of the reaction and medium transmission of the substituent polar effect from these less proximate substituents. For triptoic acids, it seems very possible that the bulky aromatic groups would largely exclude the solvent from the "wings" of the cavity transmitting the field effect. The solvent dependence of the ionization of 4-substituted bicyclo(2,2,2)-octane-1-carboxylic acids has been investigated (20), but the results are unfortunately not well correlated by linear free energy relations and are not very certain. Their solvent dependence could be interpreted as solvent dependence of the reaction and transmission by the medium, as for meta/para-substituted benzoic acids (21).

It may be concluded, from this study, that the π-inductive effect has no major role in transmission through π-electron systems such as found in the 9-substituted 10-triptoic acids. Furthermore, a field effect will account for transmission of the polar substituent effect, mainly through the low dielectric cavity of the molecule.

Experimental

Materials

The 9-substituted 10-triptoic acids were prepared from the corresponding methyl esters by hydrolysis with potassium hydroxide in diethyleneglycol (22). The methyl esters had been synthesized by an adaption of the method of Friedman and Logullo (23). Anthranilic acid (3.05 g, 0.022 mole) dissolved in acetone (20 ml) was added to a refluxing solution of the appropriate methyl 9-substituted 10-anthroate (0.02 mole) in methylene chloride (60 ml) containing isoamyl nitrite (2.98 g, 0.025 mole) over a period of 4 h. After removal of the solvent under reduced pressure, the resulting pasty solid was dissolved in benzene and subjected to column chromatography on alumina using benzene as the eluent. The first eluate contained the methyl 9-substituted 10-triptoate and the successive eluate contained the unreacted methyl 9-substituted 10-anthroate which was recovered for recycling. The crude triptoic ester was refluxed with an equal weight of N-ethylmaleimide for 2 h in chloroform solution. After removing the chloroform under reduced pressure, the residue was dissolved in benzene and again subjected to column chromatography on alumina using benzene as the eluent. After removing the benzene, the methyl 9-substituted 10-triptoate was recrystallized from methylcyclohexane to give colorless or almost colorless crystalline solids. The conversion to the triptoate esters was between 40–60%, but this only amounted to 5–10% for the nitro-ester. The recovered anthroate esters amounted to 50–30%, but this again only amounted to 5–10% for the nitro-ester. The melting points of the 9-substituted 10-triptoic acids and methyl esters are given in Table VII, together with the required elemental analyses. The methyl 9-substituted 10-anthroates were prepared by methylation of the corresponding 9-substituted 10-anthroic acids (24) with trifluoroacetic anhydride and methanol in benzene (25), except for the nitro-ester which was prepared by direct nitration (24).

Can. J. Chem. Downloaded from www.nrcresearchpress.com by 210.87.254.6 on 09/05/12
For personal use only.

Other materials for the kinetic and equilibria measurements were prepared as described previously and had similar physical constants (13*b*).

Measurements

Rate Coefficients for Diazodiphenylmethane Reaction

These were determined at 30° (±0.05), in the manner described previously (13*b*, 26), using equal acid and DDM concentrations (0.006 *M*).

pK_a Values

The pK_a values were determined, at 25° (±0.1), as described previously (13*b*).

1. J. D. Roberts and W. T. Moreland. J. Am. Chem. Soc. **75**, 2167 (1953).
2. S. Siegel and J. M. Komarmy. J. Am. Chem. Soc. **82**, 2547 (1960).
3. M. J. S. Dewar and P. J. Grisdale. J. Am. Chem. Soc. **84**, 3539 (1962); **84**, 3548 (1962).
4. K. Bowden. Can. J. Chem. **41**, 2781 (1963).
5. R. Golden and L. M. Stock. J. Am. Chem. Soc. **88**, 5928 (1966).
6. K. Bowden and D. C. Parkin. Can. J. Chem. **46**, 3909 (1968).
7. J. G. Kirkwood and F. H. Westheimer. J. Chem. Phys. **6**, 506 (1938).
8. J. C. McGowan. J. Appl. Chem. London, **10**, 312 (1960).
9. O. Exner and J. Jonas. Collection Czech. Chem. Commun. **27**, 2296 (1962). O. Exner. Tetrahedron Letters, 815 (1963). O. Exner. Collection Czech. Chem. Commun. **31**, 2016 (1966).
10. H. D. Holtz and L. M. Stock. J. Am. Chem. Soc. **86**, 5188 (1964).
11. C. F. Wilcox and J. S. McIntyre. J. Org. Chem. **30**, 777 (1965).
12. F. W. Baker, R. C. Parish, and L. M. Stock. J. Am. Chem. Soc. **89**, 5677 (1967).
13. *a*. M. Charton. J. Org. Chem. **29**, 1222 (1964); *b*. K. Bowden, M. Hardy, and D. C. Parkin. Can. J. Chem. **46**, 2929 (1968).
14. K. Bowden. Unpublished studies.
15. G. Kortum, W. Vogel, and K. Andrussow. Pure Appl. Chem. **1**, 190 (1960).
16. S. Ehrenson. Progr. Phys. Org. Chem. **2**, 195 (1964).
17. K. Bowden. Can. J. Chem. **43**, 3354 (1965).
18. C. Tanford. J. Am. Chem. Soc. **79**, 5348 (1957).
19. A. Buckley, N. B. Chapman, M. R. J. Dack, J. Shorter, and H. M. Wall. J. Chem. Soc. B, 631 (1968).
20. C. D. Ritchie and E. S. Lewis. J. Am. Chem. Soc. **84**, 591 (1962).
21. K. Bowden and G. E. Manser. Can. J. Chem. **46**, 2941 (1968).
22. P. D. Bartlett and F. D. Greene. J. Am. Chem. Soc. **76**, 1094 (1954).
23. L. Friedman and F. M. Logullo. J. Am. Chem. Soc. **85**, 1549 (1963).
24. R. O. C. Norman and P. D. Ralph. J. Chem. Soc. 2221 (1961).
25. R. C. Parish and L. M. Stock. J. Org. Chem. **30**, 927 (1965).
26. K. Bowden and D. C. Parkin. Can. J. Chem. **44**, 1493 (1966).

Can. J. Chem. Downloaded from www.nrcresearchpress.com by 210.87.254.6 on 09/05/12
For personal use only.

The transmission of polar effects. Part X.[1] The esterification with diazodiphenylmethane and the ionization of 9-substituted 10-anthroic and 8-substituted 1-naphthoic acids

KEITH BOWDEN AND D. C. PARKIN
Department of Chemistry, The University of Essex, Wivenhoe Park, Colchester, Essex, England
Received February 16, 1968

The rate coefficients for the reaction with diazodiphenylmethane in methanol, ethanol, isopropyl alcohol, *t*-butyl alcohol, 2-methoxyethanol, 2-*n*-butoxyethanol, and ethyl acetate at 30° and the pK_a values in 80% 2-*n*-butoxyethanol–water of a series of 9-substituted 10-anthroic and 8-substituted 1-naphthoic acids have been determined. The effect of substitution has been analyzed by linear free energy relations. The variation in the susceptibilities of the systems to polar substituent effects with the medium are examined. The occurrence of reversed dipolar substituent effects in the reactions of the 1,8-naphthoic acids is detected. The implications of the results for the inductive and field effect models for the transmission of polar effects are discussed.

Canadian Journal of Chemistry, **47**, 185 (1969)

Introduction

The transmission of substituent polar effects by a field effect has an implicit role for the medium. The transmissive cavity, lying between and around the substituent and the reaction site, can be composed of the low dielectric molecular cavity and the medium (1). The extent of their contributions will be determined by the molecular structure. The inductive model for transmission has no implicit role for the medium. However, polar reactions demand solvation. A lack of solvation can increase the susceptibility of the reaction to polar effects (2, 3).

It should be possible to construct and study model systems which can indicate the role of the medium. The models chosen for the present study are the 9-substituted 10-anthroic (**1**) and 8-substituted 1-naphthoic acids (**2**). These systems can be compared with meta/para-substituted benzoic acids. The anthroic system has a much more massive low dielectric molecular cavity than the benzoic system and this cavity will replace solvent in these "wing" areas. The naphthoic system has a minimal substituent–reaction site distance which should allow direct interactions at very close proximity. Both model systems have disadvantages. The anthroic acids have a highly sterically shielded reaction-site and the naphthoic acids have steric and proximity effects from the substituent on the reaction site.

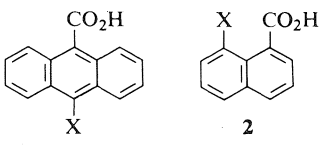

1 **2**

In this study, the reactivity of a number of 8-substituted 1-naphthoic and 9-substituted 10-anthroic acids have been measured in their esterification with diazodiphenylmethane (DDM) in a series of solvents and in their ionization in 80% w/w 2-methoxyethanol–water (80% MCS). Comprehensive studies have been made on the ionization of substituted 1- and 2-naphthoic acids (4, 5), with the exception of 8-substituted 1-naphthoic acids. Reported measurements on the latter are restricted to two single measurements (6, 7). The ionization (8) and esterification with DDM in ethanol (9) of 9-substituted 10-anthroic acids have been previously investigated. In this study, the effect of substitution has been assessed by linear free energy relations and the reaction constants obtained are discussed.

Results and Discussion

In Table I the rate coefficients for the esterification of the acids with diazodiphenylmethane in the various solvents are shown. Table II shows the pK_a values of the acids in 80% w/w 2-methoxyethanol–water.

A comprehensive study of the reaction of meta/para-substituted benzoic acids with diazodiphenylmethane in a number of solvents has been made by Chapman, Shorter, and their

[1]For Part IX; see preceding paper. A preliminary account of certain aspects of these studies has appeared in Chem. Commun. 75 (1968).

TABLE I

Rate coefficients for the esterification of the 8-substituted 1-naphthoic and 9-substituted 10-anthroic acids with diazodiphenylmethane at 30.0°

	k*						
Substituents	Methanol	Ethanol	Isopropyl alcohol	*t*-Butyl alcohol	2-Methoxy-ethanol	2-*n*-Butoxy-ethanol	Ethyl acetate
8-Substituted 1-naphthoic acid							
H	4.08	1.58	1.08	0.376	0.802	0.375	0.208
Me	12.9	5.00	3.18	1.18	2.14	1.16	0.381
Cl	16.2	6.81	4.32	1.72	2.65	1.37	0.428
Br	16.3	6.84	4.62	1.71	2.51	1.36	0.422
NO_2	21.4	11.5	9.68	4.48	9.94	2.98	2.21
9-Substituted 10-anthroic acid							
H	29.3	11.3	9.06	2.60	4.82	0.247	1.45
Me	28.7	10.1	6.25	2.16	4.21	0.222	1.03
Cl	41.3	16.9	10.7	4.43	8.77	0.506	3.86
Br	52.6	18.3	13.4	4.68	10.8	0.564	6.38
NO_2	94.0	34.8	26.5	8.95	20.8	1.30	17.0

*The rate coefficients, k (l mole^{-1} min^{-1}), are reproducible to ± 3% or better, and are the mean of at least two determinations. Previous workers (9–11) have found k for 1-naphthoic to be: 1.53, in ethanol; 0.356, in 2-*n*-butoxyethanol; and for 9-substituted 10-anthroic acids: 8.49, H; 8.22, Me; 12.9, Cl; 15.8, Br; in ethanol.

co-workers (13). However, measurements were required for one solvent, 2-*n*-butoxymethanol, to complete the comparison and these are reported in Table III.

A means of analyzing the results must be considered. Previously, it had been found possible to correlate the reactivity of 9-substituted 10-anthroic acids using σ^n values, excluding substituents, such as the nitro group, which were deconjugated by peri steric interactions (2, 8, 9). This type of treatment was impossible for the 8-substituted 1-naphthoic acids. It was therefore decided to take the esterification of the acids in ethanol with diazodiphenylmethane at 30° as standard *for each reaction series.* Thus, the reaction constant is arbitrarily set at a value of 0.944, i.e. the ρ for meta/para-substituted benzoic acids (13), for all systems. Then, "effective" substituent constants are calculated for each

TABLE II

pK_a values of the acids in 80% w/w 2-methoxyethanol–water at 25°

Substituents	pK_a*
8-Substituted 1-naphthoic	
H	6.40†
Me	5.99
Cl	6.04
Br	6.16
NO_2	6.00
10-Substituted 9-anthroic	
H	5.59‡
Me	5.71‡
Cl	5.03‡
Br	5.03‡
NO_2	4.40‡

*The pK_a values are the mean of at least two determinations and reproducible to ± 0.03 unit.
†Previous workers (12) found the pK_a value of 1-naphthoic acid to be 6.45.
‡Literature values (8).

TABLE III

Rate coefficients for the esterification of substituted benzoic acids with diazodiphenylmethane in 2-*n*-butoxyethanol at 30.0°

Substituent	k*
H	0.328†
m-Me	0.268
m-Cl	0.989
m-NO_2	2.36

*See footnote of Table I.
†Other workers (12) have found k for benzoic acid to be 0.331.

TABLE IV

Effective substituent constants for 1,8-naphthoic and 9,10-anthroic acids

	Effective substituent constants	
Substituent	1,8-Naphthoic	9,10-Anthroic
H	0.0	0.0
Me	0.530	−0.053
Cl	0.672	0.184
Br	0.674	0.222
NO_2	0.911	0.517

TABLE V

Reaction constants, "ρ"

System	Reaction	Solvent	Reaction constant	log k_0	r*	n†
1,8-Naphthoic	Esterification with DDM at 30°	Methanol	0.819	0.638	0.990	5
1,8-Naphthoic	Esterification with DDM at 30°	Ethanol	0.944	0.199	—	5
1,8-Naphthoic	Esterification with DDM at 30°	Isopropyl alcohol	1.008	0.003	0.991	5
1,8-Naphthoic	Esterification with DDM at 30°	*t*-Butyl alcohol	0.938	−0.446	0.988	5
1,8-Naphthoic	Esterification with DDM at 30°	2-Methoxyethanol	1.062	−0.181	0.928	5
1,8-Naphthoic	Esterification with DDM at 30°	2-*n*-Butoxyethanol	0.938	−0.446	0.988	5
1,8-Naphthoic	Esterification with DDM at 30°	Ethyl acetate	0.922	−0.814	0.821	5
1,8-Naphthoic	Ionization at 25°	80% MCS	0.431	6.36	0.854	5
9,10-Anthroic	Esterification with DDM at 30°	Methanol	0.938	1.484	0.991	5
9,10-Anthroic	Esterification with DDM at 30°	Ethanol	0.944	1.053	—	5
9,10-Anthroic	Esterification with DDM at 30°	Isopropyl alcohol	1.017	0.890	0.980	5
9,10-Anthroic	Esterification with DDM at 30°	*t*-Butyl alcohol	1.075	0.417	0.995	5
9,10-Anthroic	Esterification with DDM at 30°	2-Methoxyethanol	1.242	0.704	0.993	5
9,10-Anthroic	Esterification with DDM at 30°	2-*n*-Butoxyethanol	1.380	−0.577	0.996	5
9,10-Anthroic	Esterification with DDM at 30°	Ethyl acetate	2.157	0.184	0.985	5
9,10-Anthroic	Ionization at 25°	80% MCS	2.318	5.56	0.994	5
m/*p*-Benzoic	Esterification with DDM at 30°	2-*n*-Butoxyethanol	1.327	−0.488	1.000	4

*r is the correlation coefficient.
†n is the number of substituents studied.

substituent in each system, as shown in Table IV. The results for the esterification and ionization reactions are then correlated with these values. The correlations are shown in Table V. The correlations are all very good for the anthroic acids, whereas for the naphthoic acids they are particularly poor for the esterification in ethyl acetate and the ionization reaction. However, it is apparent that the 1,8-naphthoic system shows little variation in reactivity with change in the medium for the esterification reaction. The reaction constants are contrasted with those for other systems in Table VI. A somewhat tentative interpretation of the variation of the reaction constants with the medium follows. Caution appears to be indicated as the variations are small and, sometimes, rather uncertain. The 9,10-anthroic system appears to have a medium dependence closely comparable with that shown by meta/para-substituted benzoic acids. The factors, which determine this variation, are probably the extent of transmission through the medium and the solvating power of the medium (3, 13, 16). This study suggests that, for very proximate substituent-reaction site systems, e.g. the 1,8-naphthoic, the medium dependence of the reaction constants is greatly reduced. This would agree with a field effect model for transmission. The latter system would have a transmissive cavity which is largely composed of the molecule. The occurrence of low-dielectric "wings", as in the 9,10-anthroic acids, does not greatly affect this transmission. A field effect would thus be transmitted mainly by the "core" of the molecule.

A comparison of the rate coefficients for the

TABLE VI

Comparison of reaction constants for various systems

System	Solvents							Reference
	Methanol	Ethanol	Isopropyl alcohol	*t*-Butyl alcohol	2-Methoxy-ethanol	2-*n*-Butoxy-ethanol	Ethyl acetate	
m/*p*-Benzoic, ρ	0.88	0.94	1.06	1.28	1.19	1.33	2.10	13 and this study
9,10-Anthroic, "ρ"	0.94	0.94	1.02	1.07_5	1.24	1.38	2.16	This study
1,8-Naphthoic, "ρ"	0.82	0.94	1.01	0.94	1.06	0.94	0.92	This study
trans-3-Acrylic, ρ	—	1.68	—	2.07	—	—	2.96	14
Acetic, ρ_I	0.59	0.62	0.65	0.74	0.74	0.76	0.95	3
9,10-Triptoic, ρ_I	0.13	0.15	0.15	—	0.18	0.18	—	15

parent unsubstituted acids with those for benzoic acid (13) in the same solvents is interesting. The relation between the three acids is almost linear for all the four simple alcohols and ethyl acetate. The rate coefficients for the alkoxyethanols seem to be reduced for the naphthoic and anthroic acids relative to those of benzoic acid. A similar observation has been made previously in comparing the esterification of the two naphthoic acids and benzoic acid in ethanol and in 2-*n*-butoxyethanol (11). As the effect is very much more severe for 9-anthroic acid and 2-*n*-butoxyethanol, it appears to be an effect associated with hindered solvation of a sterically shielded carboxylic acid group by a long chain alcohol. This is probably the reason for the less satisfactory correlations observed for the naphthoic acids, where the steric environment of the site is varied.

Substituent Effects

The effects of 9-substituents on the reactivity of 10-anthroic acid have been discussed previously (2, 9). The same considerations apply to this study. The deconjugation of the carboxylic acid group by the peri-positions results in a strong acid-strengthening effect (17). The effects of 8-substituents on the reactivity of 1-naphthoic acid is more interesting. In the ionization reaction, all the 8-substituted 1-naphthoic acids are stronger than the unsubstituted acid. All these substituents cause the carboxylic acid group to be completely or very extensively deconjugated with the aromatic ring. This steric effect results in a twist of at least 60° for the carboxylic group caused by the nitro-group and in even greater twists for other substituents (18). This is confirmed by a study of Catalin models. The 8-substituents employed in this study do not appear to lead to severe steric interactions that could cause distortion of the aromatic rings (19). The deconjugation results in acid-strengthening by preferentially destabilizing the acid compared to the carboxylate anion (17). The resonance stabilization will be decreased by at least 75% for the nitro-group and more for the other substituents[2] (20). Thus, this steric effect can be considered to be constant for all the 8-substituents studied. For the 8-methyl acid, the latter effect easily overcomes the small polar acid-weakening effect of the methyl group. All the strongly dipolar and *normally* strongly acid-strengthening substituents are now no longer effective. This results from the disproportionately strong influence of the "negative" end of the dipolar substituent which is extremely close to the

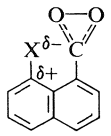

3

carboxylate group (**3**). This results in a reversal of the normal substituent effect which is characterized by that end of the dipole embedded in the molecule. The reversal is small due to the fine balance between the effects of each end of the substituent dipole. This reversed dipolar substituent effect has been observed in other systems (21–23). A reduced effect of the 8-nitro group, relative to the unsubstituted acid, has been noted previously in the ionization of 8-nitro-1-naphthoic (6) and 8-nitro-2-naphthoic (5) acids. An alternative explanation has been offered for the very small acid-strengthening effect of the 8-chloro substituent on 1-naphthoic acid (7), that is, steric inhibition of solvation of the carboxylate anion occurs. However, the effect of the more bulky 8-methyl group found in this study shows that cannot be the case[3]. These reversed dipolar substituent effects are shown to a lesser degree in the esterification reaction. Secondary steric

[2]The reported pK_a values in 80% MCS (12) for 1-naphthoic (6.45), 2-naphthoic (6.54), and benzoic (6.63) acids, as well as those in water, confirm that this steric effect is small for 1-naphthoic acid itself.

[3]At the same time as our preliminary account of some of these results (22), an independent investigation of 8-substituted 1-naphthoic acids was published by Hojo and co-workers (31). These workers give experimental data and discussion which agrees with and is closely related to those presented by us. However, Dewar (32) has put forward a different interpretation in a comment on our study. His interpretation involves hydrogen-bonding of the carboxylic acid hydrogens to the 8-substituents causing acid-weakening. *No* relevant *experimental evidence* is provided. What is more Dewar has apparently overlooked both Hojo's study (31) and recent studies of hydrogen-bonding in closely related carboxylic acids in carbon tetrachloride (33). Intramolecular hydrogen-bonding is *not* indicated either for *ortho*- halogeno or nitro benzoic acids or for 8-methoxy-1-naphthoic acid. The reported OH-stretching frequencies for the 8-substituted 1-naphthoic acids (31) *all* lie within the accepted limits for unbonded OH-stretching frequencies (33). Moreover, the measurements reported in this

effects have been shown to be less important in this reaction than in the ionization reaction (10, 11). However, the order of reactivity, i.e. $NO_2 > Br \approx Cl \approx Me > H$, indicates the reduced effect of the dipolar substituents. The transition state for the DDM reaction involves only partial transfer of the proton to the DDM molecule, forming an incipient ion-pair (10, 24). The ionization reaction gives the carboxylate anion and appears to demonstrate more conclusively the reversed dipolar substituent effect.

It seems very probable that a reversed dipolar substituent effect intervenes in the ionization of 2′-substituted biphenyl-4-carboxylic acids (**4**) (25). The usually strongly acid-strengthening

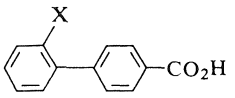

4

dipolar substituents have either very small acid-weakening, e.g. the halogeno and cyano groups, or acid-strengthening, e.g. the nitro group, effects. These substituents all cause significant twisting of the phenyl groups. The end of the substituent dipole embedded in the molecule no longer has a favorably positioned low dielectric cavity for transmission and is effectively opposed by the "negative" end of the dipole.

The evidence provided in this study demonstrates the variation in the solvent dependence of reactivity with the type of system. Further examples of reversed dipolar substituent effects have been noted. The field theory for the transmission of substituent polar effects appears to account for these observations.

Experimental

Materials

The 9-bromo-, chloro-, and methyl-10-anthroic acids were prepared by treatment of the 10-substituted 9-bromoanthracene with phenyl lithium, followed by carboxylation (26). 9-Nitro-10-anthroic acid was prepared by nitration of methyl 9-anthroate, followed by hydrolysis (8). Nitration of 1-naphthoic acid and separation from the 5-substituted isomer gave 8-nitro-1-naphthoic acid (27). The halogenation of the mercurated complex of 1-naphthoic acid was used to prepare 8-bromo- and chloro-1-naphthoic acids (28). 8-Methyl-1-naphthoic acid was synthesized by reduction of 1,8-naphthaldehydic acid using a modified Clemmensen reduction (29). 1-Naphthoic and 9-anthroic acids were obtained commercially. The acids were recrystallized to constant melting points which were identical or very close to those in the literature. Neutralization equivalents were determined and were within 1% of the theoretical values.

Other materials for the kinetic and equilibria measurements were prepared as described previously and had similar physical constants (3).

Measurements

Rate Coefficients for Diazodiphenylmethane Reaction

These were determined, at 30° (±0.05), in the manner described previously (3, 30) using equal acid and diazodiphenylmethane concentrations (0.006 *M*) for the anthroic acids because of their low solubility and a 10-fold excess of acid (0.06 *M*) for the naphthoic acids.

pK_a Values

Due to the low solubility of the acids in water, the pK_a values were determined in 80% w/w 2-methoxyethanol–water at 25° (±0.1), as described previously (3).

study are in media very much less likely to allow intramolecular hydrogen-bonding, and it seems extremely unlikely that Dewar's explanation is valid. The fact that we did not consider Dewar's and related studies (4, 5) on naphthoic acids to be most relevant to our preliminary communication should not detract from our interpretation. Dewar's results and analysis (4) did not provide a "clear distinction between field and inductive effects" (32), unlike those of Golden and Stock (21). The former studies do provide a useful guide which suggests the relative importance of the field and various inductive effects in similar ways to our previous studies (2, 14). We consider that the understanding of the factors governing reactivity in peri-substituted and similar systems will considerably advance the full comprehension of substituent effects in general and we are therefore pursuing these studies.

1. J. G. Kirkwood and F. H. Westheimer. J. Chem. Phys. **6**, 506 (1938).
2. K. Bowden. Can. J. Chem. **41**, 2781 (1963).
3. K. Bowden, M. Hardy, and D. C. Parkin. Can. J. Chem. **46**, 2929 (1968).
4. M. J. S. Dewar and P. J. Grisdale. J. Am. Chem. Soc. **84**, 3539 (1962); **84**, 3548 (1962).
5. P. R. Wells and W. Adcock. Australian J. Chem. **18**, 1365 (1965).
6. E. Berliner and E. H. Winicov. J. Am. Chem. Soc. **81**, 1630 (1959).
7. A. Fischer, R. E. J. Hutchinson, and R. D. Topsom. J. Chem. Soc. 5781 (1965).
8. R. O. C. Norman and P. D. Ralph. J. Chem. Soc. 2221 (1961).
9. K. Bowden, N. B. Chapman, and J. Shorter. Can. J. Chem. **42**, 1979 (1964).
10. K. Bowden, A. Buckley, N. B. Chapman, and J. Shorter. J. Chem. Soc. 3380 (1964).
11. A. Buckley, N. B. Chapman, and J. Shorter. J. Chem. Soc. 6310 (1965).
12. W. Simon *et al.* Zusammenstellung von scheinbaren Dissoziation-konstanten im Losungsmittelsystem Methylcellosolve/Wasser. Vol. 1. Juris–Verlag, Zurich. 1959.
13. A. Buckley, N. B. Chapman, M. R. J. Dack, J. Shorter, and H. M. Wall. J. Chem. Soc. B, 631 (1968).
14. K. Bowden. Can. J. Chem. **43**, 3354 (1965).
15. K. Bowden and D. C. Parkin. Can. J. Chem. Part IX, preceding paper.

16. K. BOWDEN and G. E. MANSER. Can. J. Chem. **46**, 2941 (1968).
17. G. S. HAMMOND. *In* Steric effects in organic chemistry. *Edited by* M. S. Newman. John Wiley and Sons Inc., New York. 1956. Chap. 9.
18. T. FUJITA, K. KOSHIMIZU, and T. MITSUI. Tetrahedron, **22**, 1587 (1966); **23**, 2633 (1967).
19. G. M. HOOP and J. M. TEDDER. J. Chem. Soc. 4853 (1962).
20. M. J. S. DEWAR. J. Am. Chem. Soc. **74**, 3341 (1952).
21. R. GOLDEN and L. M. STOCK. J. Am. Chem. Soc. **88**, 5928 (1966).
22. K. BOWDEN and D. C. PARKIN. Chem. Commun. 75 (1968).
23. K. BOWDEN and D. C. PARKIN. Can. J. Chem. **46**, 3909 (1968).
24. R. A. MORE O'FERRALL, W. K. KWOK, and S. I. MILLER. J. Am. Chem. Soc. **86**, 5553 (1964).
25. D. J. BYRON, G. W. GRAY, and R. C. WILSON. J. Chem. Soc. C, 837 (1966).
26. B. M. MIKHAILOV and V. P. BRONOVITSKAYA. J. Gen. Chem. USSR, Eng. Transl. **22**, 195 (1952).
27. C. F. KOELSCH and D. O. HOFFMAN. J. Am. Chem. Soc. **65**, 989 (1943).
28. H. G. RULE and A. J. G. BARRETT. J. Chem. Soc. 177 (1932). G. J. LEUCK, R. P. PERKINS, and F. C. WHITMORE. J. Am. Chem. Soc. **51**, 1831 (1929). F. C. WHITMORE and A. L. FOX. J. Am. Chem. Soc. **51**, 3366 (1950).
29. F. C. FUSON and G. MUNN. J. Am. Chem. Soc. **71**, 1870 (1949).
30. K. BOWDEN and D. C. PARKIN. Can. J. Chem. **44**, 1493 (1966).
31. M. HOJO, K. KATSURAKAWA, and Z. YOSHIDA. Tetrahedron Letters, 1497 (1968).
32. M. J. S. DEWAR. Chem. Commun. 547 (1968).
33. C. J. W. BROOKS, G. EGLINTON, and J. F. MORMAN. J. Chem. Soc. 106 (1961). H. A. LLOYD, K. S. WARREN, and H. M. FALES. J. Am. Chem. Soc. **88**, 5544 (1966).

Effect of temperature on "saturation currents" in gas phase radiolysis cells: the conductance of Pyrex and other cell materials

R. M. Byrtus and G. R. Freeman
Department of Chemistry, University of Alberta, Edmonton, Alberta

Received July 8, 1968

When gas-filled Pyrex cells were heated above about 50°, the saturation currents obtained in a gamma radiation field apparently decreased. At temperatures above 100° good saturation currents were not obtained. At temperatures below 50° the conductance of Pyrex was negligible, and "true" saturation currents were measured. At temperatures greater than 50° the Pyrex conducted appreciably, so the total current flowing in the circuit was appreciably greater than the gas phase saturation current (absorbed dose rate 10^{10}–10^{13} eV/ml s). If the outer surface of the cell was grounded, for example by ionized air, part of the current by-passed the measuring ammeter, thereby decreasing the "apparent" saturation current. The magnitude of the temperature effect was greatly decreased by wrapping the cell with teflon tape, thereby insulating it from the ionized air.

The effect of temperature on apparent saturation currents measured in quartz cells was much smaller than that in Pyrex cells, because the conductance of quartz was much less than that of Pyrex at temperatures above 50°.

When a metal cell that contains a Pyrex insulator between the electrodes is used, the temperature of the Pyrex should be kept below about 50°.

Canadian Journal of Chemistry, **47**, 191 (1969)

Can. J. Chem. Downloaded from www.nrcresearchpress.com by 210.87.254.5 on 09/05/12
For personal use only.

Introduction

Saturation current measurement in gas phase radiolysis cells is a useful and convenient form of dosimetry (1). However, it has been observed that "saturation currents" are temperature dependent when radiolysis cells are heated to 100 °C or more (2, 3). This dependence is not due to a temperature effect on the formation of ions, because in the temperature (up to 200°) and pressure ($\sim 10^2$–10^3 Torr) range studied the temperature coefficient of ionization is negligible (4–6). Furthermore, ion recombination coefficients and space charges at the electrodes, although they might be temperature dependent, should not appreciably influence the saturation currents (7). The observed effects are too large to be explained by the diffusion of ions to the vessel walls (8–13) and the photoelectric effect should be independent of temperature in the range studied (14).

The most likely explanation of the temperature dependence of the "saturation currents" was that it was an experimental artifact, and it was necessary to trace it.

Experimental

Argon, helium, and hydrogen, all of 99.9% minimum purity, and air were used. The gases were dried by passing them through a cold trap filled with 14–20 mesh Silica Gel and immersed in a 95% ethanol slush (−110°).

Most of the cells contained parallel plate electrodes 5 cm in diameter, spaced 2.5 cm apart. The electrodes were of aluminium, stainless steel, platinum, or Aquadag. The cell envelopes were made of Pyrex or quartz. Attempts to make vacuum-tight ceramic cells that were cleanable and that could withstand the temperature changes were unsuccessful (15). Furthermore, most of the ceramics conducted electricity to an appreciable extent in the presence of the radiation field.

Several 250 ml spherical cells were constructed of Pyrex, quartz, or stainless steel. The central electrode in each cell was a 1 cm diameter sphere of either stainless steel or aluminium. The inner surface of a Pyrex or quartz spherical cell was coated with Aquadag to serve as the outer electrode (15).

Prior to filling, the cells were evacuated and baked at 360–400° for about 4 h. They were then cooled to room temperature, flushed out several times with the gas to be irradiated, filled to the desired pressure, and sealed off.

The outside surfaces of the Pyrex and quartz cells were thoroughly washed with ethanol to remove fingerprints, which appear to be moderately good semiconductors.

The filled and cleaned cells were enclosed in a heating mantle and were irradiated with ^{60}Co gamma rays (10 000 Ci Gammacell-220 or 5 000 Ci irradiation cave). When current measurements were being taken, the power supply to the heating mantle was turned off to avoid inducing extraneous currents in the measuring circuit.

The currents were in the range 10^{-13}–10^{-4} A and were measured with a calibrated E-H Model 240 micro-microammeter.

Results and Discussion

Pyrex Cells with Parallel Plate Electrodes

It should be mentioned before proceeding that temperature effects were first observed with cylindrical cells of the design (1–3) most frequently used by radiation chemists, and that the

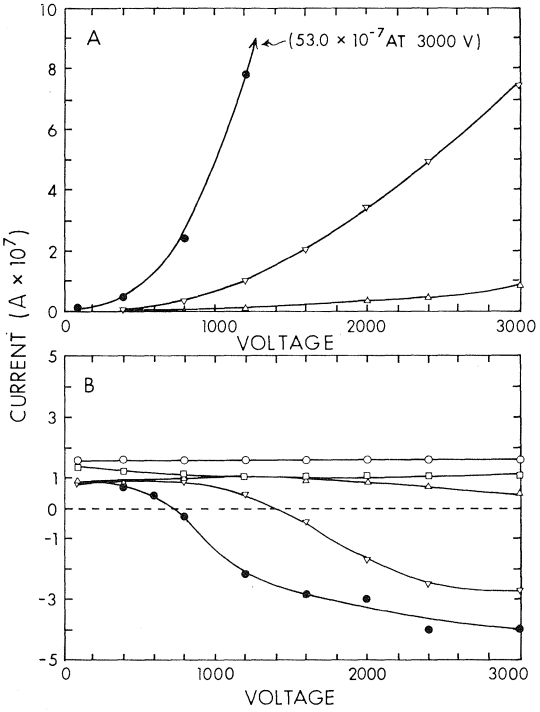

FIG. 1. Currents measured in hydrogen in Pyrex cell with aluminium electrodes (5.0 cm diameter, 2.5 cm apart); hydrogen pressure at 25° = 299 Torr; density = 3.24×10^{-5} g/cm³.

A. Background current: △, 110°; ▽, 140°; ●, 170°. In addition, the following background currents were measured: 25°, 1×10^{-11} A at 3000 V; 80°, 4×10^{-9} A at 3000 V.

B. Net positive current: ○, 25°; □, 80°; △, 110°; ▽, 140°; ●, 170°.

effects were similar to those obtained with the present parallel plate cells.

Background currents were measured in the absence of the radiation field. Typical background currents at different voltages and temperatures are shown in Fig. 1A. Net currents in the presence of the radiation field were obtained by taking the difference between the ammeter readings in the presence and absence of the radiation field. Typical net currents at different voltages and temperatures are shown in Fig. 1B. These results were obtained with a cell filled with hydrogen, but similar results were obtained with the other gases.

When the gas-filled Pyrex cells with parallel plate electrodes were heated above about 50°, the saturation currents apparently decreased. In a typical case the current at 80° was 20% smaller than at 25°, and at temperatures above 100° good saturation currents were not obtained (Fig. 1B).

The amount of decrease at a given temperature could be increased in two ways: (1) decreasing the ratio of the electrode diameter to the distance between the electrodes; (2) painting the outer surface of the cell with Aquadag and grounding it with a wire. The amount of temperature dependence could be decreased by insulating the exterior of the cell from the ionized air by wrapping the cell with teflon tape.

Saturation currents were unaffected by reducing the cell temperature from 25 to −196°, although higher voltages were required to attain them.

At the elevated temperatures, the saturation currents measured by collecting positive ions decreased more than did those measured by collecting negative ions.

The temperature effects were independent of gas pressure over the range 50–600 Torr.

The dose rate was varied in the region 10^{10}–10^{13} eV/ml s. The temperature effect increased somewhat with decreasing dose rate.

Interpretation of the Temperature Effects

At room temperature the conductance of Pyrex is negligible, and essentially all the gaseous ions of the appropriate sign are collected on the collecting electrode. The ammeter (Am in Fig. 2A) therefore registers the true saturation current. At temperatures greater than 50° the Pyrex conducts appreciably, so the total current flowing in the circuit is greater than the gas phase saturation current. Furthermore, when the Pyrex becomes a conductor the walls of the cell also act as collecting electrodes, so all the ions are not collected on the metal electrodes. If the outer surface of the cell is insulated, the total current in the circuit passes through the meter. However, if the outer surface of the cell is grounded, for example by ionized air, part of the current by-passes the meter (Fig. 2B). The fraction of the total current that by-passes the meter depends on the relative resistances of the two grounding paths (Fig. 2B). This fraction was increased by painting part of the outer surface of the Pyrex cell with Aquadag and grounding it with a wire, and was decreased by insulating the exterior of the cell from the ionized air by wrapping the cell with teflon tape.

Can. J. Chem. Downloaded from www.nrcresearchpress.com by 210.87.254.5 on 09/05/12
For personal use only.

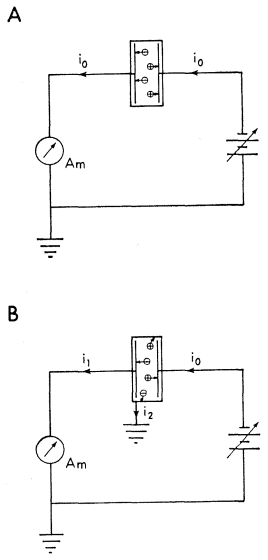

FIG. 2. Interpretation of temperature effects in Pyrex cells.

A. Current measurements when Pyrex cell wall does not conduct; $i_0 = i_s$; i_0 = total current in circuit; i_s = saturation current.

B. Current measurements when Pyrex cell wall conducts; $i_0 = i_1 + i_2 > i_s$; i_1 and i_2 each contain components due to collection of gaseous ions in the cell and to conductance of the glass.

At temperatures greater than 110° the conductance of Pyrex at high voltages was so large that, when the unwrapped cell was in the radiation field, the amount of current shunted through the ionized air was greater than the current due to the collection of gaseous ions in the cell. The net current was therefore negative under these conditions (140 and 170° curves in Fig. 1B).

At elevated temperatures the net currents measured by collecting positive ions decreased more than did those measured by collecting negative ions because Pyrex is a better conductor of positive than of negative charge (16).

The small increase of the temperature effect with decreasing dose rate indicates that space or surface charges along the cell walls tend to prevent ions from collecting on the walls. At the higher dose rates the surface charges are apparently greater, so a smaller fraction of the ions is collected on the walls.

Spherical Pyrex Cell

In the spherical Pyrex cell, the apparent saturation current increased with increasing temperature. The measured current was collected on an Aquadag coating on the inside of the Pyrex sphere. The increase in current was caused by ions from the surrounding ionized air being collected on the outer surface of the cell and being conducted through the glass. Since Pyrex conducts positive charge better than negative charge, the apparent increase in the positive saturation current was greater than that of the negative saturation current.

When the spherical cell was wrapped with teflon tape, the net current was less temperature dependent, as expected.

Conductance of Solid Plugs of Pyrex or Quartz

The preceding interpretation of the temperature effects observed with Pyrex cells is supported by measurements made with solid plugs of Pyrex and of quartz.

A 1 cm long solid plug of Pyrex or quartz was made in the center of a piece of the respective tubing (10 cm long × 1 cm diameter) by collapsing the center of the tubing with a flame. A tungsten lead was imbedded in each side of the plug, inside the tubing. The ends of the tungsten wires were separated by 2–3 mm of the glass. The surface of the plug and tubing was cleaned with ethanol to reduce surface conduction.

Currents in the range 10^{-12}–10^{-9} A were generated by the tungsten–Pyrex seals, in the absence of applied voltage. The currents were larger at the higher temperatures and also in the presence rather than in the absence of radiation. The currents generated by the tungsten–quartz seals in the absence of applied voltage were about 10^{-12} A in the absence, and 10^{-10} A in the presence of radiation (Gammacell) at all temperatures (25–170°). These currents were not reproducible and depended on the previous history of the sample (tungsten–glass seal).

At 170° and 3000 V the current passing through one Pyrex plug in the absence of a radiation field was 2.2×10^{-6} A. When the plug was lowered into the Gammacell, the current passing through the ammeter decreased to 1.9×10^{-6} A. The current through the ammeter was reduced because the ionized air in the radiation field partially grounded the plug and diverted some of the current from the meter, similar to the situation in Fig. 2B.

Insulation of a Pyrex plug from the ionized

Can. J. Chem. Downloaded from www.nrcresearchpress.com by 210.87.254.5 on 09/05/12
For personal use only.

air, by wrapping the plug with teflon tape, forced all the current to pass through the ammeter. Under these conditions the current was larger in the presence (e.g. 5.6×10^{-6} A at 170°, 3000 V) than in the absence (3.9×10^{-6} A at 170°, 3000 V, in the same plug) of the radiation field.

The current passing through the quartz plug was 10^{-12}–10^{-11} A in the absence and $\sim 10^{-10}$ A in the presence of a radiation field (Gammacell) at all temperatures (25–170°) and applied voltages (0–3000 V). The conductance of quartz is therefore much smaller than that of Pyrex at temperatures greater than about 50°.

Quartz Cells

Since the conductivity of a quartz plug at 110 and 170° was much smaller than that of a Pyrex plug, it was expected that the apparent saturation currents would be less temperature dependent in quartz cells than in Pyrex cells. Such was the case. In fact, the apparent saturation current in a parallel plate cell decreased by only 3% when the temperature increased from 25 to 170°.

Spherical Stainless Steel Cell

The central electrode in this cell was a 1 cm diameter stainless steel ball attached to a tungsten stem. The tungsten stem was passed through a Pyrex seal, which was attached to the outside of the stainless steel vessel through a Kovar seal. The exterior of the steel vessel was insulated with a baked coating of stove cement (Sairset High Temperature Bonding Mortar, manufactured by A. P. Green, Edmonton). During experiments, the Pyrex–tungsten seal protruded outside the heating mantle, so the Pyrex remained relatively cool. The insulation between the tungsten and steel electrodes was therefore relatively good even when the cell was heated. The apparent saturation currents increased by only 4% when the cell temperature was increased from 25 to 170°.

Conclusion

Pyrex cells with no exterior insulation should only be used for gas phase ion current measurements at temperatures below 50°. For higher temperatures the exterior of the cell should be insulated from the ionized gas in the radiation field. The glass–metal seal for the collecting electrode connection should be kept at a temperature below 100°, and preferably below 50°.

Similar but less stringent precautions should be taken with quartz cells.

When metal cells are used, the insulator between the electrodes should be adequate. Since the insulator used is frequently Pyrex, its temperature should be kept below 50°.

Acknowledgment

This work received financial assistance from the National Research Council of Canada.

1. R. A. Back, T. W. Woodward, and K. A. McLauchlan. Can. J. Chem. **40**, 1380 (1962).
2. F. T. Jones and T. J. Sworski. J. Phys. Chem. **70**, 1546 (1966).
3. W. J. Holtslander. Ph.D. Thesis, University of Alberta. Edmonton, Alberta. 1966.
4. R. K. McClung. Phil. Mag. **7**, 81 (1904).
5. J. A. Crowther. Proc. Roy. Soc. London, **82**, 351 (1909).
6. A. H. Compton, R. D. Bennett, and J. C. Stearns. Phys. Rev. **39**, 873 (1932).
7. A. von Engel. Ionized gases. 2nd ed. The Clarendon Press, Oxford. 1965.
8. T. W. Woodward and R. A. Back. Can. J. Chem. **41**, 1463 (1963).
9. C. E. Klots and V. E. Anderson. J. Phys. Chem. **71**, 265 (1967).
10. C. J. Wood, R. A. Back, and D. H. Dower. Can. J. Chem. **45**, 3071 (1967).
11. D. A. Armstrong and R. A. Back. Can. J. Chem. **45**, 3079 (1967).
12. S. McGowan. Can. J. Phys. **45**, 429 (1967).
13. G. R. Freeman. Radiation Res. Rev. **1**, 1 (1968).
14. R. A. Millikan and G. Winchester. Phil. Mag. **14**, 188 (1907).
15. R. M. Byrtus. M.Sc. Thesis, University of Alberta. Edmonton, Alberta. 1968.
16. O. V. Mazurin. Electrical properties and structure of glass. Consultants Bureau, New York. 1965.

Can. J. Chem. Downloaded from www.nrcresearchpress.com by 210.87.254.5 on 09/05/12
For personal use only.

Can. J. Chem. Downloaded from www.nrcresearchpress.com by 210.87.254.5 on 09/05/12
For personal use only.

A thermochemical study of addition complexes of zirconium and hafnium tetrahalides

FINE MAN CHUNG AND ALAN D. WESTLAND
Department of Chemistry, University of Ottawa, Ottawa 2, Canada

Received July 15, 1968

Enthalpies of addition were determined calorimetrically for the crystalline complexes $MX_4 \cdot 2L$ where M = Zr or Hf, X = Cl or Br, and L = tetrahydrofuran or tetrahydrothiophene. With oxygen as the donor atom of L, the two metal halides exhibited nearly identical acceptor power but with sulfur as donor, $HfCl_4$ proved to be the better acceptor. Hafnium(IV) shows more class *b* character than zirconium(IV).

Canadian Journal of Chemistry, **47**, 195 (1969)

There are several features of interest in connection with the elements zirconium and hafnium. The foremost amongst these is the fact that these two elements are very nearly alike in behavior. A quantitative comparison of the relative acceptor ability of the anhydrous halides would be interesting especially in comparison to similar pairs of elements, e.g. Mo and W or Pd and Pt. It has been shown (1) that $TiCl_4$ exhibits class *b* character in the terminology of Ahrland *et al.* (2). The larger size of the Zr and Hf atoms should effect a diminution in class *b* character. However, little is known as yet in this connection concerning the elements at the extreme left end of the transition series.

Some heats of reaction were determined by Hummers *et al.* for the complexing of $ZrCl_4$ and $HfCl_4$ with esters (3). Very little difference between the two acceptors was observed. We feel that this is to be expected in cases where the donor atom has a low polarizability, e.g. N, O, and F. It follows that nearly all of the aqueous chemistry of zirconium and hafnium will show little difference between the two elements. In order to test the effect of using donor atoms of higher polarizability, we have employed a thioether as well as an ether as a donor molecule in a nonaqueous system.

Anhydrous zirconium and hafnium halides react with tetrahydrofuran and tetrahydrothiophene to give 1:2 complexes. The compounds are soluble in excess of the respective ligands. Therefore, by measuring the heat of solution of the anhydrous halides in the liquid ligands and subtracting the heats of solution of the complexes, one may obtain the heats of addition. Similar studies have been carried out by Richards and Thompson using aluminium and gallium halides as acceptor molecules (4).

Results

Addition of the calculated amount of tetrahydrofuran (THF) or tetrahydrothiophene (THT) to $ZrCl_4$, $ZrBr_4$, or $HfCl_4$ suspended in benzene resulted in the formation of complexes $MX_4 \cdot 2THF$ and $MX_4 \cdot 2THT$. The analyses of the complexes are given in Table I.

The heats of addition were determined in each case. The heat quantities referred to in the following sections are defined as follows where A is the acceptor and L is the donor ligand

$$A(c) + (x + 2)L(l) \rightarrow AL_2(soln.) - \Delta H_1$$

$$AL_2(c) + xL(l) \rightarrow AL_2(soln.) - \Delta H_2$$

$$A(c) + 2L(l) \rightarrow AL_2(c) - \Delta H_c$$

$$\text{and} \quad \Delta H_c = \Delta H_1 - \Delta H_2$$

The letters c, l, and g refer to the crystalline, liquid, and gaseous states respectively.

Heats of solution, ΔH_1, are listed in Table II. Duplicate determinations are shown in each case. It can be seen that there is very little difference in the behavior of $ZrCl_4$ and $HfCl_4$ towards both THF and THT. The degree of dilution of the complex in the solutions of THF and THT is quite great with mole ratios of solute:solvent of one to several hundred. Varying the mole ratio had no observable effect upon the molar heat evolved. This can be seen from the weights of chloride which in some duplicate determinations differ by a large amount while the weight of solvent is nearly constant in all cases. The measured values are thus very close to integral heats of solution. The heats of solution of the complexes, ΔH_2, are listed in Table III.

Values of ΔH_c, listed in Table IV, refer to the mean values for the complexing process when all the participants in the reaction are in the condensed state. The process in this case entails

Can. J. Chem. Downloaded from www.nrcresearchpress.com by 210.87.254.5 on 09/05/12
For personal use only.

TABLE I

Analyses of zirconium and hafnium complexes

Compound	Anal. Calcd. (%)			Found (%)		
	Metal	Halogen	Sulfur	Metal	Halogen	Sulfur
$ZrCl_4 \cdot 2THF$	24.18	37.59		25.90	36.32	
$ZrCl_4 \cdot 2THT$	22.28	34.65	15.67	23.40	35.58	14.48
$ZrBr_4 \cdot 2THF$	16.43	57.59		17.49	57.96	
$ZrBr_4 \cdot 2THT$	15.54	54.43	10.92	14.98	54.32	9.71
$HfCl_4 \cdot 2THF$	38.42	30.53		39.47	29.61	
$HfCl_4 \cdot 2THT$	35.94	28.56	12.91	35.65	28.45	12.02

TABLE II

Molar heats of solution, ΔH_1, for the process MX_4 + excess ligand → complex in solution

MX_4	Solvent	Weight of solute (g)	$-\Delta H_1$ (kcal mole^{-1})
$ZrCl_4$	THF	0.4508	39.8
		0.3141	40.6
$ZrCl_4$	THT	0.4589	42.9
		0.2983	41.1
$ZrBr_4$	THF	0.7475	51.8
		0.1995	52.4
$ZrBr_4$	THT	2.2386	29.4
		0.2834	30.1
$HfCl_4$	THF	0.4799	41.0
		0.4233	41.0
$HfCl_4$	THT	0.4601	40.3
		0.2239	40.1

TABLE III

Molar heats of solution, ΔH_2, for the complexes $MX_4 \cdot 2THF$ and $MX_4 \cdot 2THT$

Complex	Solvent	Weight of solute (g)	$-\Delta H_2$ kcal mole^{-1}
$ZrCl_4 \cdot 2THF$	THF	0.1553	6.7
		0.2046	6.5
$ZrCl_4 \cdot 2THT$	THT	0.1524	12.2
		0.1602	12.2
$ZrBr_4 \cdot 2THF$	THF	0.4461	16.4
		0.1141	15.5
$ZrBr_4 \cdot 2THT$	THT	0.2577	21.1
		0.2235	21.1
$HfCl_4 \cdot 2THF$	THF	0.2134	6.2
		0.1486	6.5
$HfCl_4 \cdot 2THT$	THT	0.1608	6.9
		0.0678	7.2

vaporization of the reactants, reorganization of the acceptor molecule from tetrahedral to quasi-octahedral geometry, and condensation of the product to form a lattice. It is clear that the gas phase process $A(g) + 2L(g) \rightarrow AL_2(g) - \Delta H_g$ is more amenable to interpretation. In this case it is necessary to account only for possible differences in reorganization energies for various acceptor molecules.

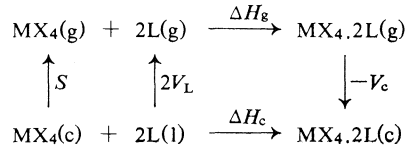

FIG. 1. Thermochemical cycle. Legend: S = heat of sublimation of metal halide. V_L = heat of vaporization of ligand (the value for tetrahydrothiophene (9.4 kcal mole^{-1}) was obtained from ref. 8. The value for tetrahydrofuran (7.1 kcal mole^{-1}) was estimated from Trouton's rule). V_c = heat of vaporization of complex.

The heat quantities involved in converting the results to those for the gaseous state are defined in Fig. 1 which shows the enthalpy cycle. The heats of sublimation of the tetrahalides are experimental values (5, 6). These are somewhat lower than the values which may be obtained from the calculated enthalpies of formation for the ideal monomeric gases (7). The discrepancy may be due to association of molecules in the form of dimers in the real vapor. The discrepancy is nearly the same for each of the tetrahalides and so may be safely neglected for the purpose of comparing the various systems.

TABLE IV

Mean heats of complexing for the formation of crystalline complexes*

Complex	$-\Delta H_c$ kcal mole^{-1}	$-\Delta H_g + V_c$ kcal mole^{-1}
$ZrCl_4 \cdot 2THF$	33.6±0.5	72.5±0.5
$ZrCl_4 \cdot 2THT$	29.8±0.9	73.3±0.9
$ZrBr_4 \cdot 2THF$	36.2±0.4	77.5±2.2
$ZrBr_4 \cdot 2THT$	8.7±0.4	54.6±2.2
$HfCl_4 \cdot 2THF$	34.6±0.2	72.6±0.3
$HfCl_4 \cdot 2THT$	33.1±0.2	75.7±0.3

*From reactants in their standard states (ΔH_c) and from reactants in the gaseous state ($\Delta H_g - V_c$).

TABLE V

Comparison of n.m.r. internal shifts with heats of adduct formation in solution

Compound	Chemical shift relative to TMS(τ) α-CH_2	β-CH_2	Internal shift (τ)	$-\Delta H_1$	$-\Delta H_g + V_c$
THF	6.72	8.78	2.06		
$ZrCl_4 \cdot 2THF$	6.24	9.14	2.90	40.2	72.5
$ZrBr_4 \cdot 2THF$	5.96	9.31	3.35	52.1	77.5
$HfCl_4 \cdot 2THF$	5.76	8.83	3.07	41.0	72.6
THT	7.47	8.45	0.98		
$ZrCl_4 \cdot 2THT$	7.44	9.01	1.57	42.0	73.3
$ZrBr_4 \cdot 2THT$	7.84	9.27	1.43	29.8	54.6
$HfCl_4 \cdot 2THT$	7.22	8.77	1.55	40.2	75.7

The heats of sublimation of the complexes are of course unknown so that we are able at best to deal with the process $A(g) + 2L(g) \rightarrow AL_2(c) - (\Delta H_g - V_c)$. Values of the heat for the reaction, $\Delta H_g - V_c$, are also listed in Table IV.

Upon complex formation, there was a change in the chemical shifts of the protons in the α and β positions in the ligand rings. The differences between the α and β chemical shifts, known as the internal shifts, are listed in Table V.

Discussion

The heats of adduct formation with THF do not vary greatly. The close agreement between the values for $ZrCl_4 \cdot 2THF$ and $HfCl_4 \cdot 2THF$ is not unexpected in the light of our knowledge of the behavior of zirconium and hafnium generally. The values which refer to gaseous reactants are in especially close agreement. The metal–oxygen bond is probably of a largely electrostatic nature so that the nearly identical sizes and charges of the Zr^{4+} and Hf^{4+} ions make the two bonds of very nearly the same strength. The heats of sublimation, V_c, for the two chloro complexes are presumably very nearly equal so that the values of $\Delta H_g - V_c$ probably parallel ΔH_g fairly closely.

The THF adduct with $ZrBr_4$ is somewhat more stable than the corresponding chloride. This is contrary to what would be expected on the basis of the relative electronegativities of the halogens as, for example, in the affinity toward N, O, and S of the gallium halides which is in the order $GaCl_3 > GaBr_3 > GaI_3$ (9, 10). Instead, the situation is similar to that encountered with the boron and aluminium halides where the usual order of acceptor strength is $MF_3 < MCl_3 < MBr_3$ (11–13). In the case of boron, the order is apparently the consequence of two factors: (*i*) the relative reorganization energies and (*ii*) the effect of π-character in the B—X bond on electronegativity of the boron atom (9, 14). It is claimed that the π-bonding ability of the halogens decreases in the order F > Cl > Br > I (11). It is reasonable to consider that these same factors are operative in our case. Of course, only one of the factors may in fact be important. The reorganization energy is probably nearly constant for the halides of an element in the fifth period for there is a decrease in the difference between the fluoride and the chloride when passing down the elements of Group IIIA, for example. The differences in the values are BX_3, 13–18; AlX_3, 3.7; GaX_3, 0.2 kcal $mole^{-1}$ (9, 15, 16). It appears that π-bonding is involved to some extent if only to cancel the effect of halogen electronegativity.

There is greater variation in the heats of complexing with THT. The bromide complex is less stable presumably because of steric hindrance which is evident from a model. This is seen also in the complexes $GaX_3 \cdot 2py$ but not in $GaX_3 \cdot py$ (17). The large values of ΔH_2 for $ZrBr_4$ complexes are probably the result of large solvation interactions between the highly polarizable bromine atoms and the outer coordination sphere. The most interesting result is the observation that the heat of formation of the hafnium complex is significantly greater than that of the others. This indicates that hafnium has more class *b* character than zirconium or, in Pearson's sense, it is a "softer acid". We conclude that the use of more polarizable ligands in association with the second and third row transition elements has the effect of enhancing differences in the behavior of related elements.

Can. J. Chem. Downloaded from www.nrcresearchpress.com by 210.87.254.5 on 09/05/12
For personal use only.

Can. J. Chem. Downloaded from www.nrcresearchpress.com by 210.87.254.5 on 09/05/12
For personal use only.

The origin of these chemical differences is to be found in the non-electrovalent features of the bonding. In particular, we note that the valence orbitals of the third row elements are more diffuse than those of the second row. Further, the effective nuclear charge of the hafnium atom should be somewhat greater than that of zirconium owing to the presence of the 4f subshell in the former atom. The hafnium nucleus would consequently have a greater polarizing ability. The difference in behavior between zirconium and hafnium is much less than the difference between aluminium and gallium. The contrast between the two pairs is understandable in terms of the relative shielding coefficients for 3d and 4f electrons respectively. Slater's rules provide for total shielding by a 4f electron but a fraction of only 0.85 for a 3d electron. These rules appear to overestimate somewhat the shielding by f-electrons.

The nuclear magnetic resonance (n.m.r.) internal shifts correlate fairly well with the thermal data as shown in Table V. Richards and Thompson observed such a correlation for complexes of Group III halides and discussed the implications and limitations of this type of experiment (4). The correlation is slightly better with $-\Delta H_l$ than with $-\Delta H_g + V_c$. If there is any significance to this, it implies that the condition of the complex in the dissolved state is important in determining both the internal shift and the heat of solution. The dissolved species may be an equilibrium mixture involving $MX_4 \cdot L$, $MX_4 \cdot 2L$, and $MX_4 \cdot 3L$, for example.

Experimental

Preparations

Zirconium(IV) chloride and hafnium(IV) chloride (nuclear grade) supplied by A. D. Mackay Inc., were purified by sublimation at 280° in a sealed tube containing nitrogen.

Anal. Calcd. for $ZrCl_4$: Zr, 39.14; Cl, 60.86. Found: Zr, 38.83; Cl, 60.95.

Anal. Calcd. for $HfCl_4$: Hf, 55.73; Cl, 44.27. Found: Hf, 54.48; Cl, 44.88.

Zirconium(IV) bromide was prepared in a sealed tube from nuclear grade zirconium sponge by allowing it to react with bromine vapor. One end of the tube containing the liquid bromine was maintained at room temperature so that the compound sublimed from the hot reaction zone into a cooler region. Excess bromine present at the end of the reaction period was removed by pumping.

Anal. Calcd. for $ZrBr_4$: Zr, 22.20; Br, 77.80. Found: Zr, 22.22; Br, 77.04.

Tetrahydrofuran (Fisher Certified Reagent) and tetrahydrothiophene (Aldrich) were purified by distillation, the middle fraction only being used.

Complexes were purified as follows:

Carefully dried, sulfur-free benzene was distilled at reduced pressure from sodium metal into a Schlenk tube immersed in liquid nitrogen. The distillate (50 ml) was allowed to attain room temperature, and dry nitrogen was then admitted. The content of an ampul of metal halide (1.5 g) was introduced into the tube and to this suspension was added ligand (1.05 molecular equivalent) dissolved in benzene (5 ml). Vigorous stirring for a few hours produced a heavy precipitate. Stirring was continued for a further 1 to 2 days to ensure complete reaction. The solvent was then reduced to $\frac{1}{3}$ the original volume by pumping, before the solid material was separated in a filtering apparatus similar to that described by Fritz *et al.* (18). The product was washed with two volumes of benzene before drying under vacuum at room temperature. As these complexes were hygroscopic they were stored in ampuls under nitrogen.

Calorimetric Measurements

A solution calorimeter similar to that described by Greenwood and Perkins (19) was used. The calibration of the associated equipment was checked by hydrolyzing $POCl_3$ in the calorimeter. In two determinations, molar heats of hydrolysis of 80.0 and 80.2 kcal $mole^{-1}$ were obtained. This is in good agreement with a published value of 79.9 ± 0.3 kcal $mole^{-1}$ (20).

The volume of THF or THT employed in the calorimeter was 100 cc. Measurements were carried out in duplicate. The calorimeter temperature was in all cases within 2° of that of the water bath which was maintained at 25 °C.

Nuclear Magnetic Resonance Spectra

The n.m.r. spectra were obtained with a Varian Associates 60 Mc/sec high resolution spectrometer. Spectra were calibrated with respect to tetramethylsilane as internal standard. The samples were dissolved in benzene to form saturated solutions.

Acknowledgment

The authors wish to express their appreciation to the National Research Council of Canada for financial assistance.

1. K. Baker and G. W. A. Fowles. Proc. Chem. Soc. 362 (1964).
2. S. Ahrland, J. Chatt, and N. R. Davies. Quart. Rev. London, **12**, 265 (1958).
3. W. S. Hummers, S. Y. Tyree Jr., and S. Yolles. J. Am. Chem. Soc. **74**, 139 (1952).
4. R. L. Richards and A. Thompson. J. Chem. Soc. A, 1244, 1248 (1967).
5. A. A. Palko, A. D. Ryon, and D. W. Kuhn. J. Phys. Chem. **62**, 319 (1958).
6. H. L. Schläfer and H. Skoludek. Z. Electrochem. **66**, 367 (1962).
7. JANAF Interim Thermochemical Tables. Dow Chemical Company, Midland, Mich. 1960.
8. J. V. Davies and S. Sunner. Acta Chem. Scand. **16**, 1870 (1962).
9. N. N. Greenwood and T. S. Srivastava. J. Chem. Soc. A, 270 (1966).

10. N. N. GREENWOOD and P. G. PERKINS. J. Chem. Soc. 1145 (1960).
11. H. C. BROWN and R. R. HOLMES. J. Am. Chem. Soc. **78**, 2173 (1956).
12. N. N. GREENWOOD and P. G. PERKINS. J. Chem. Soc. 1141 (1960).
13. N. N. GREENWOOD and K. WADE. Friedel–Crafts and related reactions. Vol. 1. *Edited by* G. A. Olah. Interscience Publishers, Inc., New York. 1963. Chap. VII.
14. C. M. BAX, A. R. KATRITZKY, and L. E. SUTTON. J. Chem. Soc. 1258 (1958).
15. F. A. COTTON and J. R. LETO. J. Chem. Phys. **30**, 993 (1959).
16. D. D. ELEY and H. WATTS. J. Chem. Soc. 1319 (1954).
17. N. N. GREENWOOD and T. S. SRIVASTAVA. J. Chem. Soc. A, 267 (1966).
18. G. FRITZ, D. HAVEL, D. KUMMER, and G. TEICHMAN. Z. Anorg. Allgem. Chem. **302**, 60 (1959).
19. N. N. GREENWOOD and P. G. PERKINS. J. Inorg. Nucl. Chem. **4**, 291 (1957).
20. E. NEALE and L. T. D. WILLIAMS. J. Chem. Soc. 4535 (1952).

Can. J. Chem. Downloaded from www.nrcresearchpress.com by 210.87.254.5 on 09/05/12
For personal use only.

Can. J. Chem. Downloaded from www.nrcresearchpress.com by 210.87.254.40 on 09/05/12
For personal use only.

Spectres Raman de N_2H_4 et N_2D_4 à l'état cristallin

M. GUAY[1] ET R. SAVOIE
Département de Chimie, Université Laval, Québec 10, Québec

Reçu le 21 juin 1968

Les spectres Raman de N_2H_4 et N_2D_4 cristallins ont été enregistrés à diverses températures entre -70 et -195 °C. Les dédoublements des fondamentales, le grand nombre de modes de réseau observés et la non-coïncidence probable des fréquences Raman et infrarouges sont en désaccord avec les structures cristallines obtenues par diffraction des rayons-X et des neutrons. Les résultats infrarouges et Raman suggèrent une structure à quatre molécules dans des positions générales d'une maille monoclinique de classe C_{2h}.

Raman spectra of crystalline N_2H_4 and N_2D_4 have been recorded at various temperatures between -70 and -195 °C. The splitting of the internal modes, the large number of active lattice vibrations, and the apparent non-coincidence of infrared and Raman bands cannot be explained on the basis of the crystal structures obtained from X-ray and neutron-diffraction studies. The results suggest instead a monoclinic unit cell described by one of the C_{2h} space groups and containing four molecules located in general positions.

Canadian Journal of Chemistry, 47, 201 (1969)

Introduction

La molécule d'hydrazine est d'un intérêt tout particulier du fait que sa symétrie est déterminée par l'orientation relative des groupements NH_2. La structure *gauche* (symétrie C_2) déduite par Penney et Sutherland (1) n'a pu être confirmée par diffraction des électrons (2, 3). Cependant, une analyse détaillée du spectre infrarouge de la vapeur dans la région du mode de torsion interne, centré à 376.74 cm^{-1}, a indiqué que l'angle azimuthal est voisin de 90° (4). Ce résultat a été confirmé par le spectre micro-onde (5), qui a de plus permis d'évaluer les barrières de potentiel empêchant l'inversion et la torsion interne (*trans*) à 990 et 1100 cm^{-1} respectivement. La structure *gauche* est également en accord avec le moment dipolaire de 1.75 D calculé à partir du spectre micro-onde (5, 6). Une valeur de 1.83 D avait été obtenue à partir du liquide (7). Il n'est pas impossible cependant qu'une petite fraction des molécules existent sous une autre conformation. Les nombreux spectres infrarouges (4, 8–14) et Raman (13–20) déjà publiés ne permettent pas d'éliminer cette possibilité.

Il existe une certaine confusion quant à la structure cristalline du solide. La mesure des chaleurs spécifiques et le calcul des fonctions thermodynamiques à partir des données spectroscopiques a conduit à une entropie résiduelle de 0.44 u.e. au zéro degré absolu (21). Cette valeur ne permet cependant pas de conclure à une structure désordonnée du solide puisqu'elle est moindre que l'imprécision sur la valeur calculée et celle obtenue expérimentalement. Une étude du cristal par diffraction des rayons-X, par Collin et Lipscomb (22), suggère une maille élémentaire à deux molécules et définie par le groupe spatial $C^2{}_{2h}$–$P2_1/m$. Dans cette structure, les molécules occupent des sites de symétrie C_s et doivent par conséquent exister sous la forme *cis* (éclipsée, symétrie C_{2v}) ou *trans* (symétrie C_{2h}). Cela n'implique pas que l'une de ces configurations est la plus stable dans la molécule libre puisque, dans le cristal, d'autres facteurs (liaisons hydrogène, . . . *etc.*) entrent en jeu. Une étude par diffraction des neutrons (23) a conduit à une structure légèrement différente de celle obtenue par diffraction des rayons-X. Le groupe spatial $C^2{}_2$–$P2_1$ est suggéré, avec deux molécules par maille élémentaire. Il est à noter que les seuls sites possibles dans ce groupe sont de symétrie C_1. Baglin, Bush et Durig (24) ont récemment étudié les spectres de N_2H_4 et N_2D_4 cristallins dans l'infrarouge lointain en vue de choisir entre les deux structures cristallines proposées. En se basant sur le nombre de bandes observées, ils concluent que la structure obtenue à partir de la diffraction des neutrons est la bonne. Afin de vérifier cette déduction, nous avons étudié les spectres Raman de l'hydrazine et de son analogue deutérié à diverses températures entre -70 et -195 °C.

Partie expérimentale

L'hydrazine (N_2H_4) utilisé a été obtenu à partir du produit commercial (Matheson, Coleman, and Bell, à

[1]Boursier du Conseil National de Recherches du Canada.

TABLEAU I

Corrélations entre les symétries des vibrations pour diverses structures possibles de N_2H_4 cristallin

Molécule		Site	Cristal	Site	Cristal
C_{2v}	C_{2h}	C_s	C_{2h}	C_1	C_2
A_1	A_g	A'	A_g (Raman)	A	A (Raman, i.r.)
B_2	B_u		B_u (i.r.)		
A_2	A_u	A''	A_u (i.r.)		B (Raman, i.r.)
B_1	B_g		B_g (Raman)		

97% anhydre), par séchage sur CaH_2 et distillation sous vide, suivant la méthode de Lucien (25). Un dosage de l'échantillon par une solution aqueuse d'iodate (26, 27) a révélé une pureté de 100%, à 0.2% près. Le composé deutérié a été obtenu de Merck, Sharpe, and Dohme (concentration en deutérium 97%, < 1% D_2O) et utilisé sans aucune purification.

Les échantillons ont été cristallisés dans des cellules cylindriques en Pyrex de 19 mm de diamètre qu'on laissait descendre lentement (~ 24 h) dans un bain thermostatisé maintenu à quelques degrés au-dessous du point de fusion (1.4 °C). La cristallisation a dû être amorcée dans la plupart des cas car l'hydrazine montre une tendance marquée à la surfusion. De plus, nous avons placé un anneau chauffant autour des cellules, de façon à éviter que la cristallisation ne se produise d'abord sur les parois. Pour l'enregistrement des spectres, les cellules étaient placées à l'intérieur d'un Dewar de Pyrex et refroidies par un courant d'azote gazeux, tel que décrit précédemment (28).

Les spectres ont été enregistrés avec un spectromètre Cary, modèle 81, muni d'une lampe Toronto conventionnelle. Les fentes du monochromateur étaient ajustées de 0.5 à 4 cm^{-1}, suivant l'intensité des bandes. Les fréquences rapportées plus loin sont précises à ± 2 cm^{-1} dans le cas des bandes fines.

Résultats et Discussion

Structures cristallines et spectres vibrationnels

L'analyse des spectres vibrationnels de l'hydrazine à l'état cristallin, à la lumière de la théorie des groupes (29, 30), devrait permettre de distinguer entre la structure proposée d'après la diffraction des rayons-X ($C^2{}_{2h}$) et celle obtenue par diffraction des neutrons ($C^2{}_2$). Dans le premier cas, la symétrie locale dans le cristal (C_s) implique une symétrie moléculaire C_{2v} (forme éclipsée, *cis*) ou C_{2h} (forme *trans*). Dans les deux cas, les modes vibrationnels de la molécule se transforment en espèces A' ou A'' dans l'approximation du site; celles-ci se scindent ensuite en deux composantes, l'une active en Raman et l'autre en infrarouge, par suite de l'effet de couplage dans le cristal (voir Tableau I). D'après ce modèle, chacune des vibrations internes devrait donner une seule composante tant en diffusion qu'en absorption, les bandes ayant des fréquences différentes dans les deux types de spectres puisqu'elles correspondent à des modes différents. Les trois modes de libration devraient également se comporter de cette façon, tandis que les modes de translation gênée ne devraient être actifs qu'en Raman seulement, les composantes infrarouges correspondant aux modes acoustiques, de fréquence zéro à la limite ($k = 0$). La présence de quelque neuf bandes observées par Baglin, Bush et Durig (24) dans le spectre infrarouge entre 100 et 400 cm^{-1}, au lieu des trois prévues, les a conduit à rejeter cette structure cristalline.

Si le cristal était du groupe $C^2{}_2$–$P2_1$, tel qu'indiqué par la diffraction des neutrons (23), les deux molécules de la maille cristalline devraient se situer dans les positions générales (sites de symétrie C_1). Les espèces vibrationnelles de la molécule isolée, de même que les rotations et translations, se transformeraient alors en espèces A dans la symétrie du site, pour ensuite se dédoubler en composantes de symétrie A et B dans le groupe factoriel $C^2{}_2$ (voir Tableau I). Cette structure se caractérise donc par un dédoublement de toutes les bandes, sauf celles correspondant aux modes de translation, et par la coïncidence des fréquences Raman et infrarouges. Le spectre infrarouge lointain de l'hydrazine cristallin (24) a clairement indiqué que cette structure cristalline était plus probable que celle obtenue par diffraction des rayons-X.

Région des basses fréquences

On observe dans la région des basses fréquences du spectre Raman de N_2H_4 cristallin une douzaine de bandes qui se retrouvent, décalées d'un

Can. J. Chem. Downloaded from www.nrcresearchpress.com by 210.87.254.40 on 09/05/12
For personal use only.

TABLEAU II

Fréquences en cm^{-1} des bandes infrarouges et Raman de N_2H_4 et N_2D_4 cristallins ($\nu < 700\ cm^{-1}$)

Infrarouge*		Raman					
N_2H_4 (< -130 °C)	N_2D_4 (< -130 °C)	N_2H_4 (-70 °C)	N_2H_4 (-195 °C)	N_2D_4 (-70 °C)	N_2D_4 (-195 °C)	ν_D/ν_H†	Attribution
650	492					0.757	Libration ou
		524	533		394	0.739	torsion interne
		496	508		375	0.738	
405	298					0.736	" "
405	277					0.684	
		278	289	254	264	0.913	Libration
274.9	243					0.884	Libration
			~260		~245	0.942	2×132.5?
		212	226	209	217.5	0.962	Translation
			226		197.5	0.874	Libration
			198	181	182	0.919	Libration
180.5	169.5					0.939	Translation
		166	172	156.5	162.5	0.945	Translation
172.5	156.5					0.907	Libration
154	142.3					0.924	Translation
154	136.9					0.889	Libration
136.3	123					0.902	Libration
		126	132.5	117	123	0.928	Libration
			122		116.5	0.955	Translation
			112.5	107	108	0.960	Translation
		~109	109	~101	101	0.927	Translation
106.7	101.5					0.951	Translation
		94	97	87	90	0.928	Translation

*Référence 24.
†Rapport isotopique des fréquences (à -195 °C en Raman).

facteur variant de 0.73 à 0.96, dans le spectre du composé deutérié (Fig. 1 et Tableau II). De plus, la plupart des bandes infrarouges n'ont pas d'équivalent en Raman. La variation des fréquences avec la température (Tableau II) n'est pas responsable de cette disparité. Nous avons pensé que celle-ci pouvait provenir d'une mauvaise cristallisation des échantillons étudiés en infrarouge sur des films de polyéthylène (24). Afin d'éliminer cette possibilité, nous avons réexaminé le spectre infrarouge de N_2H_4, cristallisé lentement à partir du liquide entre deux fenêtres de quartz cristallin, dans la région de 40 à 200 cm^{-1}. Le spectre, obtenu avec un interféromètre (RIIC, modèle FS-720), était presque identique à celui déjà publié (24), sauf que les deux bandes de plus basses fréquences sont apparues à 108.5 et 138 cm^{-1} (comparativement à 106.7 et 136.3 cm^{-1}) et que la bande à 172 cm^{-1} était plus intense relativement à celle de 154 cm^{-1}.

En se basant sur le grand nombre de bandes dans la région de 90 à 300 cm^{-1} du spectre Raman, de même que sur la non-coincidence de leurs fréquences avec celles des bandes en infrarouge, il semble bien que nos résultats ne soient en accord avec aucune des deux structures cristallines obtenues par diffraction. De plus, compte tenu des quelque douze bandes observées en Raman, en plus de celles à d'autres fréquences en infrarouge, nos résultats indiquent que la maille primitive du cristal contient plus de deux molécules. Dans ce cas le nombre maximum de modes de réseau serait de neuf. Il se peut également que la structure du cristal soit désordonnée par suite de la présence dans le solide d'isomères de structure, comme dans le cas de N_2F_4 (31). Cette possibilité ne peut être écartée, quoiqu'elle semble assez improbable, vu la barrière de potentiel relativement élevée à la position *trans* ($\sim$ 3 kcal) (5). De plus, la finesse des bandes dans le spectre Raman suggère une structure cristalline bien ordonnée. Par conséquent, si la structure cristalline est bien monoclinique tel qu'établi par la diffraction des rayons-X et des neutrons, elle doit se situer dans un des groupes de la classe C_{2h}, avec quatre molécules dans des positions générales (site de symétrie C_1) de la maille primitive. Il est à noter que cette conclusion, basée sur la liste des positions générales et spéciales des groupes du système monoclinique (32), n'est valable que si

Can. J. Chem. Downloaded from www.nrcresearchpress.com by 210.87.254.40 on 09/05/12
For personal use only.

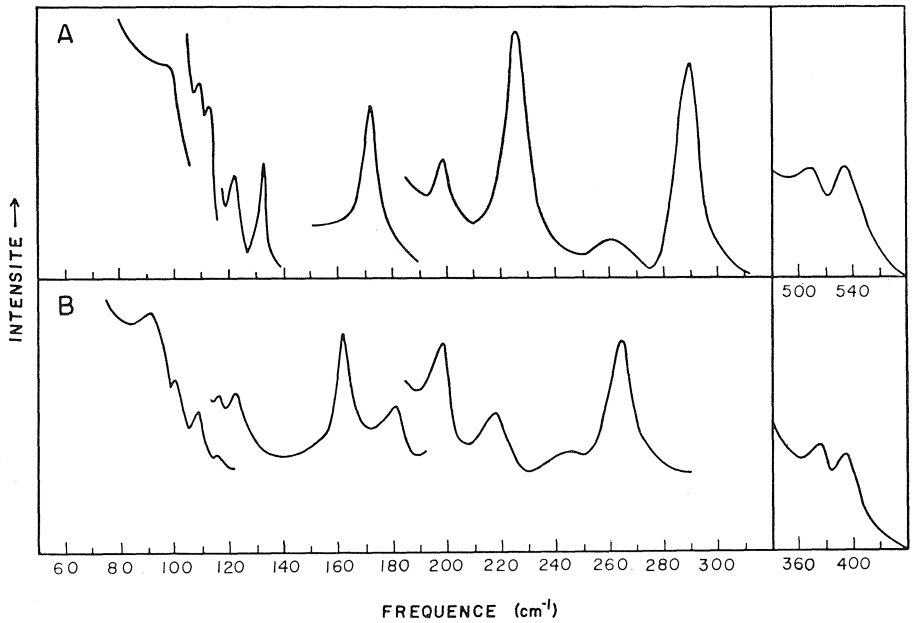

FIG. 1. Spectres Raman de N_2H_4 (A) et N_2D_4 (B) cristallins à -195 °C dans la région des basses fréquences. Fente spectrale $\leq 3\ cm^{-1}$.

les molécules n'occupent qu'un seul ensemble de sites dans la maille cristalline (le contraire serait exceptionnel pour un cristal moléculaire).

L'attribution des modes de réseau de N_2H_4 et N_2D_4 cristallins (Tableau II) s'explique assez bien dans l'hypothèse d'une maille primitive de symétrie C_{2h} et contenant quatre molécules. En se référant au tableau de corrélation (Tableau I), ce modèle prédit que chacun des degrés de liberté de translation et rotation d'une molécule isolée devrait donner naissance à quatre modes vibrationnels dans le cristal, les espèces A_g et B_g n'étant actives qu'en Raman et les deux autres (A_u et B_u) en infrarouge seulement. Après avoir éliminé les trois modes acoustiques ($A_u + 2B_u$), qui correspondent aux déplacements de l'ensemble de la maille primitive suivant chacun des axes, on prédit 12 bandes en Raman (6 librations et 6 translations) et 9 en infrarouge (6 librations et 3 translations).

L'attribution des modes de réseau de N_2H_4 cristallin est facilitée par les résultats obtenus à partir du composé deutérié. En première approximation, le décalage isotopique des fréquences devrait être proportionnel à la racine carrée du rapport des masses moléculaires (0.94) ou des moments d'inertie, suivant qu'il s'agit de translation ou de libration. D'après les paramètres de structure de la molécule libre (2, 3), le rapport isotopique des fréquences devrait être de 0.72 pour les librations autour de l'axe mineur et de 0.87 pour celles autour des deux axes majeurs.

Par analogie avec le cas de H_2O_2 solide (33), on devrait retrouver dans la région de 400 à 800 cm^{-1} des spectres de l'hydrazine deux séries de bandes, correspondant aux modes de torsion interne et à ceux de libration autour de l'axe mineur de la molécule. Les deux doublets prévus en infrarouge se situent probablement à 650 cm^{-1} (492 cm^{-1} dans N_2D_4) et à 405 cm^{-1} (277/298 cm^{-1} dans N_2D_4). Les derniers ont été attribués par Baglin, Bush et Durig (24) au mode de torsion interne, à la suite d'une analyse vibrationnelle du solide. Ces auteurs ont également expliqué la bande forte à 650 cm^{-1} par une combinaison de celle à 405 cm^{-1} avec un mode de réseau. Il semble plus probable que les deux bandes fortes observées en infrarouge soient toutes deux des fondamentales, bien qu'il soit difficile de prévoir laquelle provient de la torsion interne. Dans le spectre Raman du solide, un des doublets prévus apparaît faiblement à 533/508 cm^{-1} (394/375 cm^{-1} dans N_2D_4), et l'autre n'a pas été localisé.

Les bandes de fréquences inférieures à 300 cm^{-1},

Can. J. Chem. Downloaded from www.nrcresearchpress.com by 210.87.254.40 on 09/05/12
For personal use only.

TABLEAU III

Fréquences en cm^{-1} des bandes infrarouges et Raman de N_2H_4 ($\nu > 700\ cm^{-1}$)

Vapeur*	Liquide*		Solide				
i.r.	i.r.	Raman	i.r.*	Raman (−70 °C)	Raman (−195 °C)	Intensité†	Attribution
3350	3332	3333	3310	3300	3299	428	
3325		3264					
3314		3248					Valence N—H
3280	3189	3186	3200	3195	3194	64	
		3139			3188	58	
		3085		3174	3168	796	
				1661	1663	21	
			1655		~1658	11	Déformation H—N—H
1628				1639	1637	14	
1587	1608	1614	1603	1610	1609	6	
			1350	1345	1347	1	
	1324			1329	1333	7	Déformation N—N—H
				1316	1319	3	
1275	1283		1304	1305	1304	1	
				1133	1144	9	
			1126	1130	1133	18	
		1100		1111	1113	237	Valence N—N
1098	1098			~1100	~1106	15	et déformation N—N—H
966	1042	988	1066				
933		936					
				901	905	3	Déformation N—N—H
780	871	872	884	883	883	82	

*Référence 14.
†Intensité approximative basée sur la hauteur relative des pics dans le spectre Raman à −195 °C.

qui montrent un décalage isotopique variant entre 0.87 et 0.96, peuvent s'expliquer par des modes de translation et de libration autour des deux axes majeurs des molécules. Le spectre infrarouge s'explique assez bien selon le modèle favorisé ici (voir Tableau II). Les spectres Raman sont plus compliqués du fait que 6 modes de translation sont prévus (par comparaison avec trois seulement en infrarouge), en plus de quatre librations. On observe bien une dizaine de pics au-dessous de 300 cm^{-1}, mais les différences entre les rapports isotopiques observés et calculés indiquent que le couplage entre les divers modes de réseau est appréciable. La distinction entre modes de translation et libration, telle qu'établie dans le Tableau II, est donc très approximative.

Région des hautes fréquences

Le nombre de bandes observées dans la région de 700 à 3500 cm^{-1} des spectres Raman de N_2H_4 et N_2D_4 cristallins (Fig. 2) est de beaucoup supérieur à celui obtenu en infrarouge. Notre interprétation des spectres (Tableaux III et IV) est par ailleurs en bon accord avec celle des bandes infrarouges par Durig et ses collaborateurs (14). Cependant, l'attribution des bandes provenant des quatre modes faisant intervenir des déformations N—N—H est quelque peu incertaine à cause du couplage de certaines de ces vibrations avec celle de valence N—N. Cet effet, différent dans N_2H_4 et N_2D_4, explique certains décalages isotopiques différents de ceux prévus. Les rapports isotopiques des fréquences devraient être de l'ordre de 0.7 pour les vibrations de déformation N—N—H et de 0.9 environ pour la vibration de valence N—N. Expérimentalement, on trouve des valeurs de 0.63 à 0.85 dans le premier cas, alors que le décalage de la vibration de valence donne un rapport de 0.85. Le spectre de N_2D_4 est de plus compliqué par des bandes provenant de l'espèce isotopique N_2D_3H. Compte tenu de la teneur en hydrogène de l'échantillon (~3%), on peut estimer la concentration de cette impureté à environ 11%.

La région des hautes fréquences du spectre Raman de N_2H_4 cristallin est plus caractéristique que la région correspondante du spectre infrarouge en ce qui concerne la structure du solide.

Can. J. Chem. Downloaded from www.nrcresearchpress.com by 210.87.254.40 on 09/05/12
For personal use only.

TABLEAU IV

Fréquences en cm^{-1} des bandes infrarouges et Raman de N_2D_4 ($\nu > 700\ cm^{-1}$)

Vapeur*	Liquide*		Solide				
i.r.	i.r.	Raman	i.r.*	Raman (−70 °C)	Raman (−195 °C)	Intensité†	Attribution
				3283	3284	7	
				3278	3275	10	Valence N—H (N_2D_3H)
				3263	3256	8	
				3254	3244	4	
	2493	2487	2479	2467	2463	460	Valence N—D
2431			2469	2430	2435	4	
	2415	2411	2407	2409	2399	12	Valence N—D (N_2D_3H)
				2392	2386	5	
				2358	2355	19	
	2353	2348	2347	2348	2342	72	Valence N—D
				2338	2333	540	
				1226	1225	7	
			1213	1221	1221	6	
1197	1194	1198		1202	1200	8	Déformation D—N—D
1140			1184	1192	1190	2	
	1032	1030	1041	1031	1035	91	Valence N—N (N_2D_3H)
985	987		1004	1015	1016	7	
				962	962	5	Déformation N—N—D
				956	956	9	Valence N—N
	936	938	938	940	939	530	
				890	891	3	Valence $^{15}ND_2$–$^{14}ND_2$
				860	862	3	Déformation N—N—D (N_2D_3H)
				827	834	11	Déformation N—N—D
	787	806	814	822	821	2	
				785	791	1	Déformation N—N—D (N_2D_3H)?
722				766	769	7	Déformation N—N—D
688	727	733	744	748	749	11	

*Référence 14.
†Intensité approximative basée sur la hauteur relative des pics dans le spectre Raman à −195 °C.

On observe en effet un dédoublement de la plupart des fondamentales, phénomène qui est particulièrement évident dans la région des modes de déformation H—N—H, où deux doublets sont présents, tant dans le spectre de N_2H_4 que dans celui de N_2D_4. Ce dédoublement des fondamentales est incompatible avec la structure déduite de l'étude par diffraction des rayons-X, pour laquelle une seule composante Raman est prédite pour chacune des fondamentales (Tableau I). La distinction entre la structure proposée à partir de la diffraction des neutrons et celle à quatre molécules par maille primitive proposée plus haut est cependant plus difficile. Dans le premier cas, et au contraire du second, il devrait y avoir coïncidence des fréquences des doublets prévus en infrarouge et observés en Raman. Une comparaison entre les fréquences des bandes infrarouges et celles des composantes Raman les plus proches (Tableaux III et IV) montre dans plusieurs cas des différences d'environ 6 cm^{-1}. Ces différences assez faibles, qui peuvent s'expliquer en partie par les imprécisions dans la mesure des fréquences, favorisent légèrement la structure à quatre molécules par maille, de préférence à celle obtenue par la diffraction des neutrons.

Dans le spectre de N_2D_4 cristallin, les vibrations de valence N—H des impuretés isotopiques N_2D_3H, pour la plupart isolées dans la matrice solide de N_2D_4, sont d'un intérêt tout particulier. On observe en effet quatre bandes (Fig. 2), situées entre 3244 et 3284 cm^{-1}. Le même phénomène se produit lorsqu'une petite quantité de N_2H_3D ($\sim 4\%$) est présente dans N_2H_4, alors que quatre bandes de valence N—D (à 2396, 2402, 2428 et 2431 cm^{-1}) apparaissent dans le

Can. J. Chem. Downloaded from www.nrcresearchpress.com by 210.87.254.40 on 09/05/12
For personal use only.

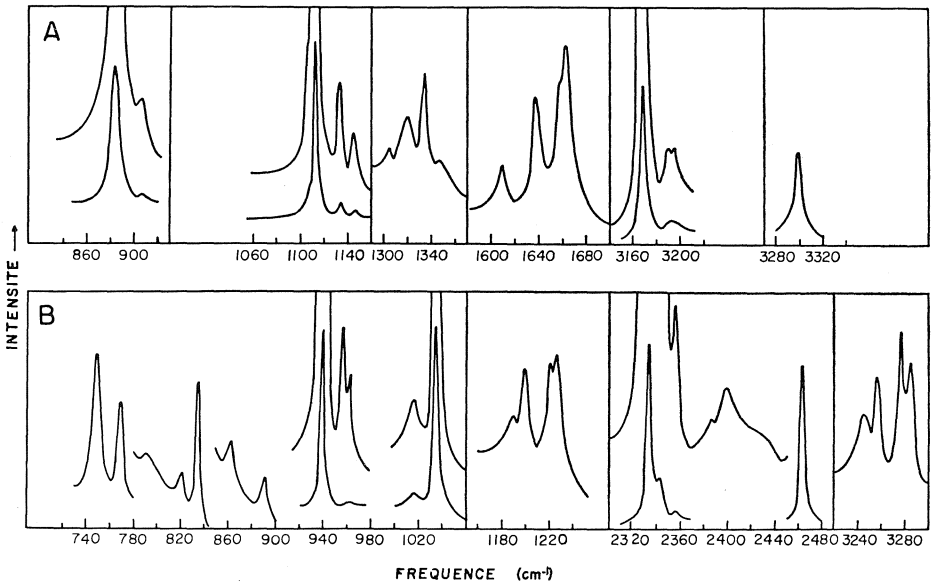

FIG. 2. Spectres Raman de N_2H_4 (A) et N_2D_4 (B) cristallins à -195 °C. Fente spectrale ≤ 3 cm^{-1}.

spectre Raman du solide. Ces pics ne sont donc pas dus à des harmoniques ou combinaisons, ou encore à un effet de couplage entre paires de molécules de l'impureté dans le cristal. On peut donc conclure que les quatre liaisons N—H (ou N—D) ne sont pas équivalentes dans le cristal, ce qui nécessite des sites de symétrie C_1. Cette observation est en contradiction avec la structure obtenue par diffraction des rayons-X (sites de symétrie C_s), mais elle ne permet pas de distinguer entre celle obtenue par diffraction des neutrons et celle que nous avons proposée plus haut. Dans l'hypothèse d'une structure où deux types d'isomères structuraux (présumément dans les configurations *gauche* et *trans*) seraient présents, on devrait attribuer deux des quatre bandes observées à chacun des isomères. Etant donné que les quatre composantes Raman ont des intensités assez semblables, il faudrait que les deux isomères existent dans des concentrations à peu près égales. Cela est assez improbable du point de vue énergétique et devrait conduire à une entropie résiduelle appréciable au zéro degré absolu ($\simeq R \ln 2 = 1.38$ u.e.).

Conclusion

L'analyse des spectres Raman de N_2H_4 et N_2D_4 cristallins, compte tenu des résultats précédemment obtenus en infrarouge, est incompatible avec les structures cristallines déduites des études par diffraction sur N_2H_4 solide. Il est cependant probable que les positions des atomes d'azote dans la maille cristalline, telles que déterminées par diffraction, sont essentiellement correctes. L'incompatibilité avec les résultats spectroscopiques est sans doute reliée à la configuration et à l'orientation des molécules dans le cristal. Une étude de la diffraction des neutrons sur N_2D_4 cristallin semble particulièrement indiquée en vue de résoudre ce problème.

Remerciements

Nous remercions le Conseil National de Recherches du Canada qui a rendu cette étude financièrement réalisable par un octroi de recherches (R.S.) et une bourse d'études (M.G.).

1. W. G. PENNEY et G. B. B. M. SUTHERLAND. J. Chem. Phys. **2**, 492 (1934).
2. P. A. GIGUÈRE et V. SCHOMAKER. J. Am. Chem. Soc. **65**, 2025 (1943).
3. Y. MORINO, T. IIJIMA, et Y. MURATA. Bull. Chem. Soc. Japan, **33**, 46 (1960).
4. A. YAMAGUCHI, I. ICHISHIMA, T. SHIMANOUCHI, et S. MIZUSHIMA. Spectrochim. Acta, **16**, 1471 (1960).
5. T. KASUYA. Papers Inst. Phys. Chem. Res. Tokyo, **56**, 1 (1962).
6. T. KOJIMA, H. HIRAKAWA et T. OKA. J. Phys. Soc. Japan, **13**, 321 (1958).
7. L. F. AUDRIETH, W. NESPITAL et H. ULICH. J. Am. Chem. Soc. **55**, 673 (1933).

Can. J. Chem. Downloaded from www.nrcresearchpress.com by 210.87.254.40 on 09/05/12
For personal use only.

8. M. FREYMANN et R. FREYMANN. Compt. Rend. **200**, 1043 (1935); Compt. Rend. **205**, 852 (1937); Ann. chim. et phys. **11**, 11 (1939).
9. S. S. KRIVICH. Compt. rend. acad. sci. U.R.S.S., **23**, 36 (1939); J. Phys. Chem. USSR, English Transl. **15**, 739 (1941).
10. W. FRESENIUS et J. KARWEIL. Z. Physik. Chem. Leipzig, B, **44**, 1 (1939).
11. P. A. GIGUÈRE et I. D. LIU. J. Chem. Phys. **20**, 136 (1952).
12. E. CATALANO, R. H. SANBORN, et J. W. FRAZER. J. Chem. Phys. **38**, 2265 (1963).
13. YU I. KOTOV et V. M. TATEVSKII. Opt. Spectry. USSR, English Transl. **13**, 487 (1962); Opt. Spectry. USSR, English Transl. **15**, 65 (1963). YU I. KOTOV, G. S. GOPTOV, YU A. PENTIN et V. M. TATEVSKII. Opt. Spectry. USSR, English Transl. **15**, 303 (1963).
14. J. R. DURIG, S. F. BUSH, et E. E. MERCER. J. Chem. Phys. **44**, 4238 (1966).
15. G. B. B. M. SUTHERLAND. Nature, **126**, 196 (1930).
16. S. IMANISHI. Nature, **127**, 782 (1931).
17. L. KAHOVEC et K. N. F. KOHLRAUSCH. Z. Physik. Chem. Leipzig, B, **38**, 96 (1939).
18. J. GOUBEAU. Z. Physik. Chem. Leipzig, B, **45**, 237 (1940).
19. G. SCHWAB, K. KOLLER, et K. LORENZEN. Angew. Chem. **73**, 219 (1961).
20. J. S. ZIOMEK et M. D. ZEIDLER. J. Mol. Spectry. **11**, 163 (1963).
21. D. W. SCOTT, G. D. OLIVER, M. E. GROSS, W. N. HUBBARD et H. M. HUFFMAN. J. Am. Chem. Soc. **71**, 2293 (1949).
22. R. L. COLLIN et W. N. LIPSCOMB. J. Chem. Phys. **18**, 566 (1950); Acta Cryst. **4**, 10 (1951).
23. W. R. BUSING, M. ZOCCHI et H. A. LEVY. Program of the Annual Meeting of the American Crystallographic Association. Paper N-3, August 1961.
24. F. G. BAGLIN, S. F. BUSH et J. R. DURIG. J. Chem. Phys. **47**, 2104 (1967).
25. H. W. LUCIEN. J. Chem. Eng. Data, **7**, 541 (1962).
26. R. A. PENNEMAN et L. F. AUDRIETH. Anal. Chem. **20**, 1058 (1948).
27. I. M. KOLTHOFF. J. Am. Chem. Soc. **46**, 2009 (1924).
28. R. SAVOIE et M. PÉZOLET. Can. J. Chem. **45**, 1677 (1967).
29. H. WINSTON et R. S. HALFORD. J. Chem. Phys. **17**, 607 (1949).
30. D. F. HORNIG. J. Chem. Phys. **16**, 1063 (1948).
31. J. R. DURIG et J. W. CLARK. J. Chem. Phys. **48**, 3216 (1968).
32. H. F. M. HENRY et K. LONSDALE (*Editeurs*). International tables for X-ray crystallography. Vol. I. Kynoch Press, Birmingham, England. 1952.
33. P. A. GIGUÈRE et C. CHAPADOS. Spectrochim. Acta, **22**, 1131 (1966).

Can. J. Chem. Downloaded from www.nrcresearchpress.com by 210.87.254.40 on 09/05/12
For personal use only.

Can. J. Chem. Downloaded from www.nrcresearchpress.com by 210.87.254.42 on 09/05/12
For personal use only.

Substituent effects on H—F couplings and additivity of these effects in a series of fluorobenzene derivatives

J. E. LOEMKER[1], K. M. PRYSE, J. M. READ, JR.[2], AND J. H. GOLDSTEIN
Chemistry Department, Emory University, Atlanta, Georgia

Received June 19, 1968

The nuclear magnetic resonance spectra of a series of monosubstituted fluorobenzenes have been recorded and analyzed, and the substituent effects on the H—F couplings have been determined by comparison with the corresponding H—F couplings in fluorobenzene. These substituent effects have then been successfully employed in calculating the H—F couplings for a series of di- and tri-substituted fluorobenzenes.

Canadian Journal of Chemistry, **47**, 209 (1969)

Introduction

The determination of substituent effects on the H—H couplings in benzene derivatives has recently been made possible as a result of accurate analyses of the nuclear magnetic resonance (n.m.r.) spectra of a series of monosubstituted benzenes (1) and of the ^{13}C—H satellite spectra of benzene itself (2). The additivity of these substituent effects has also been established in a series of 32 disubstituted benzenes (3–5). Other studies of the additivity of substituent effects have been reported for the meta H—H couplings in a series of unsymmetrical para-disubstituted benzenes (6) and for the H—H couplings in a series of ortho-substituted benzenes (7).

This paper describes an extension of the above studies to the H—F couplings in a series of fluorobenzene derivatives. The substituent effects have been determined here by analyzing the n.m.r. spectra of 12 monosubstituted fluorobenzenes (C_6H_4FX with X = F, Cl, Br, and NO_2) and comparing the H—F couplings obtained with the corresponding values in fluorobenzene itself (8).

Finally, the spectra of a series of 9 di- and tri-substituted fluorobenzenes were analyzed and it was found that the H—F couplings in these compounds could be estimated approximately from the previous substituent effects and the assumption of additivity.

Experimental and Calculations

All of the compounds studied were the commercially available materials, of sufficient purity as indicated by their n.m.r. spectra. In order to insure maximum reliability, all compounds were examined in the same solvent, acetone, at approximately the same concentration, 10 mole %. For the monosubstituted fluorobenzenes, the proton spectra, with one exception, were obtained at 60 MHz on a Varian A60-A spectrometer. For *p*-difluorobenzene, the proton spectrum was examined at 100 MHz and the fluorine spectrum at 94.077 MHz using a Varian HA-100. For the di- and tri-substituted fluorobenzenes, the majority of the proton spectra were obtained at 60 MHz, but in some instances, the proton spectra were obtained at 100 MHz, and the fluorine spectra at 94.077 MHz.

The calibrated frequencies were the averages of at least four spectra (two forward and two reverse sweeps) in each case, and the average deviations of the measured frequencies were approximately 0.05 Hz. All of the analyses were carried out by an iterative least-squares computer routine. The agreement between the calculated and observed spectra was 0.04 Hz or better in all cases, and the estimated reliability of the coupling parameters was within 0.05 Hz. The coupling parameters obtained are summarized in Table I (the chemical shift data have been omitted to conserve space), with the substituent effects on the H—F couplings shown in parentheses. These substituent effects are calculated using the fluorobenzene values $J_o^{HF} = 9.31$, $J_m^{HF} = 5.79$, and $J_p^{HF} = 0.34$ Hz, obtained from the 10 mole % solution of fluorobenzene in acetone. It should be noted that the para H—F couplings, unlike those of the protons, have previously been observed to have either sign relative to the ortho and meta couplings. The latter two have been shown to be of the same sign (9–13).

Table II contains the H—H, H—F, and F—F coupling parameters obtained from the analyses of the spectra for the di- and tri-substituted fluorobenzenes (again the chemical shifts have been omitted to conserve space). The corresponding additivity calculated H—F couplings are shown in parentheses, and the corresponding meta and para F—F couplings calculated from the substituent effects of Abraham *et al.* (14) are shown in square brackets.

As an example of the quality of these analyses, the observed and calculated proton spectra for 1,2,4-trifluorobenzene at 100 MHz are shown in Fig. 1.

---

[1]NASA Predoctoral Trainee, 1966–1969.

[2]Present address: E.I. DuPont de Nemours and Co., Experiment Station, Plastics Department, Wilmington, Del., U.S.A.

Can. J. Chem. Downloaded from www.nrcresearchpress.com by 210.87.254.42 on 09/05/12
For personal use only.

TABLE I

Substituent effects on H—F couplings[a]

Compound	J_{12}	J_{13}	J_{14}	J_{15}	J_{16}	J_{23}	J_{24}	J_{25}	J_{26}	J_{34}	J_{35}	J_{36}	J_{45}	J_{46}	J_{56}
Fϕ[b]	9.31	5.79	0.34	5.79	9.31	8.37	1.04	0.43	2.75	7.46	1.84	0.43	7.46	1.04	8.37
1,2-diF	−20.53	8.17	−1.31	4.51	10.93	10.93	4.51	−1.31	8.17	8.34	1.61	0.27	7.45	1.61	8.34
benzene		(+2.38)	(−1.65)	(−1.28)	(+1.62)										
1,2-BrF						9.10	4.97	−0.52	7.10	8.33	1.47	0.26	7.49	1.63	8.02
benzene						(−0.21)	(−0.82)	(−0.86)	(+1.31)						
1,2-ClF						9.64	5.01	−0.85	7.62	8.30	1.48	0.30	7.55	1.68	8.06
benzene						(+0.33)	(−0.78)	(−1.19)	(+1.83)						
1,2-NO_2F						11.40	4.61	−0.86	7.46	8.42	1.23	0.24	7.49	1.79	8.24
benzene						(+2.09)	(−1.18)	(−1.20)	(+1.67)						
1,3-diF	9.60	6.30	−0.88	6.69	8.70	9.60	2.53	0.32	2.53	8.70	6.69	−0.88	8.14	0.88	8.41
benzene	(+0.29)		(−1.22)	(+0.90)	(−0.61)	(+0.29)				(−0.61)	(+0.90)	(−1.22)			
1,3-BrF						8.61	2.48	0.24	1.89	8.69	6.45	−0.63	8.34	1.13	8.01
benzene						(−0.70)				(−0.62)	(+0.66)	(−0.97)			
1,3-ClF						9.02	2.48	0.37	1.92	8.63	6.30	−0.47	8.46	0.90	8.08
benzene						(−0.29)				(−0.68)	(+0.51)	(−0.81)			
1,3-NO_2F						8.82	2.58	0.41	2.10	8.28	5.60	−0.53	8.36	0.97	8.14
benzene						(−0.49)				(−1.03)	(−0.19)	(−0.87)			
1,4-diF	8.19	4.16	17.79	4.16	8.19	9.00	4.16	0.28	3.37	8.19	3.37	0.28	8.19	4.16	9.00
benzene	(−1.12)	(−1.63)		(−1.63)	(−1.12)		(−1.63)			(−1.12)			(−1.12)	(−1.63)	
1,4-BrF						8.75	4.90	0.20	2.61	8.62	3.25	0.20	8.62	4.90	8.75
benzene							(−0.89)			(−0.69)			(−0.69)	(−0.89)	
1,4-ClF						8.87	4.79	0.31	2.80	8.48	3.21	0.31	8.48	4.79	8.87
benzene							(−1.00)			(−0.83)			(−0.83)	(−1.00)	
1,4-NO_2F						9.13	4.71	0.28	2.93	8.13	2.91	0.28	8.13	4.71	9.13
benzene							(−1.08)			(−1.18)			(−1.18)	(−1.08)	

[a]In Hz. The values in parentheses are the substituent effects on the H—F couplings. See text for further details.
[b]Fϕ = fluorobenzene. Numbering begins with fluorine in fluorobenzene and the difluorobenzenes. In all other cases, numbering begins with the nonfluorine substituent.

Can. J. Chem. Downloaded from www.nrcresearchpress.com by 210.87.254.42 on 09/05/12
For personal use only.

TABLE II

Additivity of H—F couplings[a]

Compound	J_{12}	J_{13}	J_{14}	J_{15}	J_{16}	J_{23}	J_{24}	J_{25}	J_{26}	J_{34}	J_{35}	J_{36}	J_{45}	J_{46}	J_{56}
3,4-diCl	8.35			5.41	7.93			0.32	2.92						8.93
Fϕ	(8.19)			(5.30)	(7.80)										
2,4-diNO_2		6.49		3.72	10.19						2.87	0.26			9.19
Fϕ		(6.38)		(3.53)	(10.22)										
2,4-diBr		6.13		4.33	8.54						2.44	0.18			8.80
Fϕ		(6.21)		(4.08)	(8.41)										
3-Cl-4-F-NO_2ϕ							6.36	0.32	2.86				8.43	4.11	9.10
							(6.54)						(8.46)	(3.93)	
1-Br-2,5-diFϕ						8.23	3.72	15.62	5.40	9.23	4.68	0.29	7.91	3.11	7.81
						(7.98)	(3.34)	[16.0]	(5.47)		(4.82)		(7.57)		(7.49)
1-NO_2-2,5-diFϕ						10.59	3.49	17.19	5.80	9.25	4.34	0.36	7.48	3.19	7.91
						(10.28)	(2.98)	[17.5]	(5.83)		(3.97)		(7.16)		(7.70)
1-NO_2-2,4-diFϕ						11.26	13.36	−1.58	8.64	8.68	2.68	0.29	7.70	5.73	9.27
						(11.69)	[11.4]	(−2.08)	(8.36)	(8.42)			(7.52)	(5.61)	
1,5-diNO_2-2,4-diFϕ						10.56			7.62	10.56		0.53		7.62	
						(10.51)			(7.28)	(10.51)				(7.28)	
1,2,4-triFϕ	−20.46	6.39	15.15	3.33	10.25	10.77	3.24	−2.02	9.10	8.45	3.08	0.33	8.01	5.12	9.29
		(6.54)	[14.9]	(2.88)	(9.81)	(11.22)	[2.0]	(−2.53)	(9.07)	(8.48)			(7.58)	(5.06)	

[a]In Hz. The values in parentheses are the additivity calculated H—F couplings; those in square brackets are the additivity calculated F—F couplings from ref. 14.

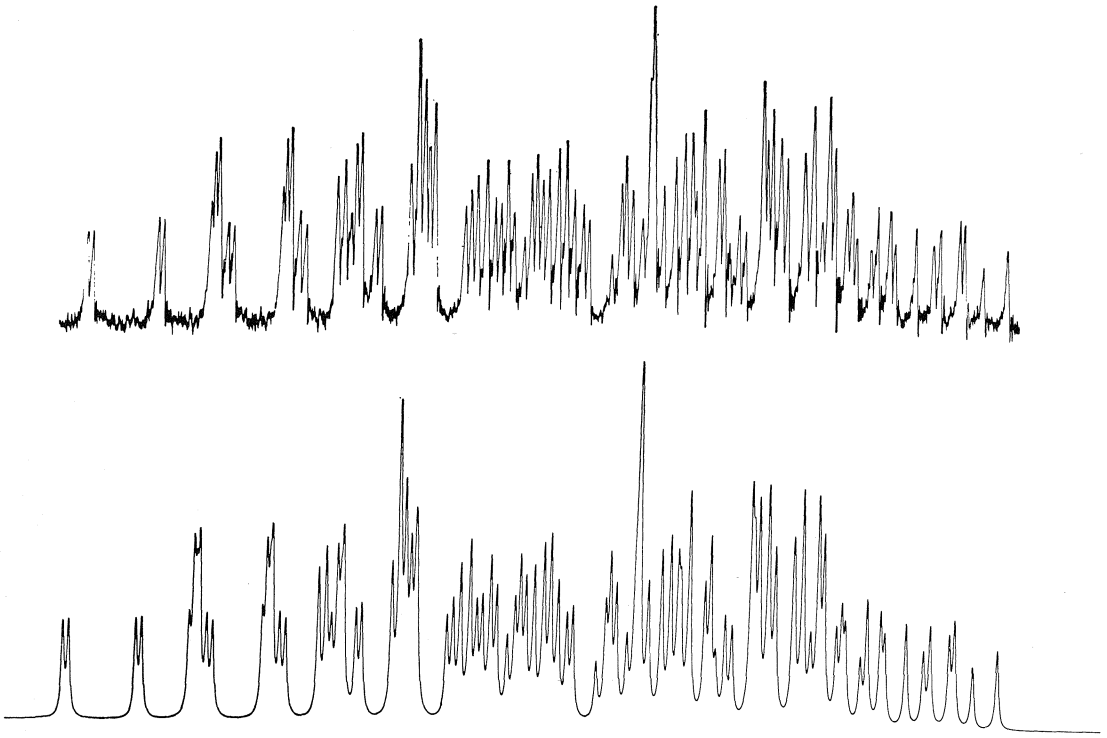

FIG. 1. Experimental (top) and theoretical (bottom) proton spectra of 1,2,4-trifluorobenzene at 100 MHz.

Discussion

It is interesting to note that the ranges of the H—F couplings for the compounds studied are significantly greater than those for the H—H couplings, especially those for which long-range effects are observed. For example, the substituent effects on the para H—H couplings in the monosubstituted benzenes are all approximately −0.20 Hz (3), while those on the para H—F couplings range from −0.81 to −1.65 Hz.

Additivity of substituent effects has previously been noted for H—H couplings (3, 6, 7) and the meta and para F—F couplings (14). Hence it is worthwhile to consider whether the substituent effects on H—F couplings obtained in this study (shown in Table I) are additive in aromatic systems. These additivity calculated H—F couplings are collected in Table II.

For the H—H couplings, the largest deviation between the observed and calculated couplings was approximately 0.25 Hz, the greatest range in the observed couplings being approximately 1.3 Hz (3). For the H—F couplings given in Table II, the largest deviation between observed and calculated values is 0.50 Hz, but in most cases the deviation is considerably smaller. Since the range of substituent effects for H—F couplings is 2.4 Hz, it is apparent that the assumption of additivity is approximately as valid, on a relative basis, for the H—F couplings as for the H—H couplings. It should be mentioned that the availability of initial predicted values of the couplings based on the assumption of additivity was found to be a considerable aid in the analyses of these spectra.

The analyses of two of these compounds have been described previously, 1,5-dinitro-2,4-difluorobenzene (15, 16) and 2,4-dinitrofluorobenzene (16–18). However, the coupling values in the former studies were only reported to 0.1 Hz, at best, and are of insufficient precision for our purposes.

As has been previously noted, the H—F couplings may be subject to significant solvent effects (8, 19). An effort has been made here to minimize this source of error by the use of a uniform and relatively dilute concentration in the single solvent, acetone, chosen because some of the compounds were not sufficiently soluble in

Can. J. Chem. Downloaded from www.nrcresearchpress.com by 210.87.254.42 on 09/05/12
For personal use only.

the more inert solvents. However, some small residual uncertainty from this source may still remain.

It is felt that the regularities which have been observed here merit further study, both as a practical aid in spectral analysis and as a possible source of further insight into the mechanism whereby substituent effects operate. A linear correlation of H—F couplings with the Pauling electronegativity of the substituent in a series of monohalosubstituted fluorobenzenes has recently been observed (5). There appears to be a similar qualitative trend in the results presented here, but, in spite of the considerable amount of data obtained, the series is too limited to justify efforts toward either empirical correlations or theoretical interpretations of the substituent effects. Further studies of related compounds, however, should provide a basis for investigating these interesting questions.

Acknowledgment

This research was supported in part by a grant from the National Institutes of Health.

1. J. M. READ, JR. and J. H. GOLDSTEIN. J. Mol. Spectry. **23**, 179 (1967).
2. J. M. READ, JR., R. E. MAYO, and J. H. GOLDSTEIN. J. Mol. Spectry. **22**, 419 (1967).
3. J. M. READ, JR., R. W. CRECELY, R. S. BUTLER, J. E. LOEMKER, and J. H. GOLDSTEIN. Tetrahedron Letters, No. 10, 1215 (1968).
4. R. W. CRECELY, R. S. BUTLER, J. M. READ, JR., and J. H. GOLDSTEIN. Spectrochim. Acta. In press.
5. J. E. LOEMKER, J. M. READ, JR., and J. H. GOLDSTEIN. J. Phys. Chem. **72**, 991 (1968).
6. B. DISCHLER. Z. Naturforsch. **20a**, 888 (1965).
7. S. CASTELLANO and R. KOSTELNIK. Tetrahedron Letters, No. 51, 5211 (1967).
8. J. E. LOEMKER, J. M. READ, JR., and J. H. GOLDSTEIN. Mol. Phys. **13**, 433 (1967).
9. H. S. GUTOWSKY, C. H. HOLM, A. SAIKA, and G. A. WILLIAMS. J. Am. Chem. Soc. **79**, 4596 (1957).
10. W. G. PATTERSON and H. SPEDDING. Can. J. Chem. **41**, 2706 (1963).
11. D. F. EVANS. Mol. Phys. **6**, 179 (1963).
12. E. LUSTIG and P. DIEHL. J. Chem. Phys. **44**, 2974 (1966).
13. C. BARBIER, H. FAUCHER, D. GAGNAIRE, and A. ROUSSEAU. J. Chim. Phys. **63**, 283 (1966).
14. R. J. ABRAHAM, D. B. MACDONALD, and E. S. PEPPER. J. Am. Chem. Soc. **90**, 147 (1968).
15. A. KUMAR. Mol. Phys. **12**, 593 (1967).
16. T. P. SCHAEFER. Can. J. Chem. **40**, 431 (1962).
17. B. D. NAGESWARO RAO and P. VENKATESWARLU. Proc. Indian Acad. Sci. Sect. A, **52**, 109 (1960).
18. B. D. NAGESWARO RAO. Mol. Phys. **7**, 307 (1963).
19. J. E. LOEMKER and J. H. GOLDSTEIN. Spectr. Letters, **1**, 153 (1968).

Can. J. Chem. Downloaded from www.nrcresearchpress.com by 210.87.254.42 on 09/05/12
For personal use only.

Can. J. Chem. Downloaded from www.nrcresearchpress.com by 210.87.254.105 on 09/05/12
For personal use only.

Hydrogenation of methylacetylene. IV. The reaction of methylacetylene with hydrogen catalyzed by palladium, platinum, iridium, rhodium, and ruthenium catalysts[1]

R. S. Mann and K. C. Khulbe
Department of Chemical Engineering, University of Ottawa, Ottawa 2, Canada

Received June 18, 1968

The reaction between methylacetylene and hydrogen over pumice supported and unsupported palladium, platinum, iridium, rhodium, and ruthenium catalysts has been investigated between 12 and 160 °C for a wide range of reactant ratios. The order of reaction with respect to hydrogen was one and with respect to methylacetylene was zero to slightly negative. The overall apparent activation energies for supported and unsupported palladium, platinum, iridium, and rhodium were 10.5, 9.5, 12.4, 14.7, 8.6, 6.2, 10.7, and 11.7 kcal/mole respectively.

Canadian Journal of Chemistry, **47**, 215 (1969)

Introduction

In Parts I, II, and III of this series, we have reported the kinetics and products obtained from the reaction of methylacetylene with hydrogen catalyzed by pumice supported nickel (1), unsupported nickel, cobalt, and iron (2), and nickel, copper, and their alloys (3). In this concluding paper of the series, we report the reaction of methylacetylene with hydrogen catalyzed by palladium, platinum, iridium, rhodium, ruthenium, and osmium.

Experimental

The apparatus, materials, experimental procedure, and method of analysis of the products have been described previously (2). The catalysts were prepared by impregnating and evaporating the solution containing the calculated weight of Analar grade chemicals in the presence of pumice. The unsupported catalysts were prepared by evaporating the solutions. The palladium, platinum, iridium, rhodium, ruthenium, and osmium metal catalysts were prepared from $(NH_4)_2PdCl_6$, $PtCl_4$, $(NH_4)_2IrCl_6$, $RhCl_3.3H_2O$, $(NH_4)_2RuCl_6$, and $(NH_4)_2OsCl_6$, respectively.

Results

Supported and unsupported platinum, palladium, iridium, and rhodium catalysts were found to be quite active and did not get poisoned when methylacetylene or hydrogen was admitted first into the reactor. The activity remained fairly constant for several days. Ruthenium was found to be active at the beginning, and lost its activity after a few runs. Osmium catalysts showed no noticeable activity up to 200 °C.

[1]Based on the paper presented at the 51st Annual Meeting, Chemical Institute of Canada, Physical Chemistry Division, Vancouver, B.C., June 2–5, 1968.

(a) Reaction Rates

The pressure time curves obtained during methylacetylene hydrogenation (Fig. 1) over pumice supported and unsupported palladium, platinum, rhodium, and iridium catalysts, consisted of two nearly linear portions (curve AFG, Type I, Fig. 1) of different slopes for hydrogen/methylacetylene ratios ($\bar{R}$) of less than 2 at all temperatures. For hydrogen/methylacetylene ratios of 2 or more, pressure–time curve AMN (Type III, Fig. 1) was obtained for unsupported

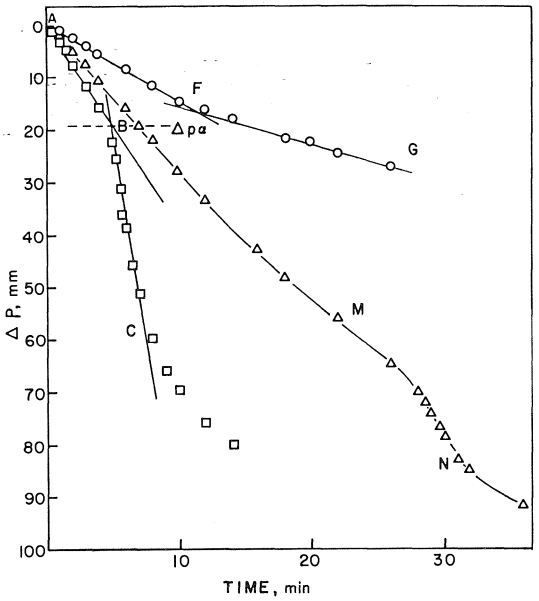

FIG. 1. Pressure–time curves. Curve ABC: Pd–pumice, $P_{C_3H_4} = 50$ mm, $P_{H_2} = 104$ mm. Curve AFG: Ir–pumice, $P_{C_3H_4} = P_{H_2} = 50$ mm, $T = 24$ °C. Curve AMN: Ir–pumice, $P_{C_3H_4} = P_{H_2} = 50$ mm, $T = 55$ °C.

TABLE I

Order of reaction and activation energies

Catalyst	Weight of catalyst (g)	Temperature range (°C)	Order with respect to hydrogen	Order with respect to methylacetylene	k, specific rate at 60 °C (min^{-1} g^{-1})	Energy of activation (kcal/mole)
Platinum	0.025	95–135	1.01±0.01	−0.3 ±0.3	0.06	14.7±0.2
Platinum–pumice	0.025	72–135	1.01±0.01	−0.4 ±0.3	0.20	12.4±0.2
Iridium	0.025	40–70	1.03±0.03	0.00	2.48	6.2±0.2
Iridium–pumice	0.025	85–121	1.03±0.01	−0.2 ±0.1	0.80	8.6±0.2
Palladium	0.011	12–45	1.25±0.05	−0.24±0.13	9.10*	9.5±0.2
Palladium–pumice	0.025	16–41	1.25±0.05	−0.52±0.11	5.00*	10.5±0.2
Rhodium	0.025	73–111	1.00±0.11	0.00	0.04	11.7±0.2
Rhodium–pumice	0.025	47–76	1.00±0.11	0.00	0.21	10.7±0.2
Ruthenium	0.1	70–200	Catalyst deactivated after few runs			
Ruthenium–pumice	0.075	85–180				
Osmium						
Osmium–pumice						

*k at 40 °C.

platinum, palladium, and supported and unsupported iridium and rhodium. In the case of platinum–pumice, while for a hydrogen/methylacetylene ratio of 2, the rate of pressure fall during the course of reaction was nearly constant till nearly all the methylacetylene had reacted (curve AB), a different type of curve (curve ABC, Type II, Fig. 1) was obtained for a hydrogen/methylacetylene ratio greater than 2. Similar results were obtained for palladium–pumice catalysts, except that the acceleration was observed for all hydrogen/methylacetylene ratios greater than 1.5. Similar curves were observed by Bond and Wells (4) for acetylene hydrogenation over platinum and by Tamaru (5). In the region AB, the reaction was first order with respect to hydrogen and the main product was propylene, whereas after the rapid acceleration (BC region) the main process was the further hydrogenation of propylene to propane.

The acceleration point ($-\Delta p_\alpha$), defined as the pressure obtained by the intersection of the linear portions of the first and second stages of the reaction (Fig. 1) was observed while hydrogenating methylacetylene over pumice supported platinum ($\bar{R} > 2$) and palladium–pumice ($\bar{R} > 1.5$). No such acceleration was observed over other catalysts. The acceleration point was dependent on temperature and initial hydrogen pressure. It decreased fairly linearly with increasing temperatures and hydrogen pressures.

Since methylacetylene is more strongly adsorbed than propylene or hydrogen, an increase in the initial pressure of propylene or hydrogen would facilitate the entry of propylene into the reactive layer and further the hydrogenation of propylene to propane. This would result in an acceleration of the reaction.

Orders in hydrogen were determined from the initial rates at a fixed methylacetylene pressure of 30 mm and a wide range of hydrogen pressures (25–200 mm). Orders in methylacetylene were obtained similarly at a fixed hydrogen pressure of 60 mm and a wide range of methylacetylene pressures, 30–150 mm. The results are given in Table I. The order with respect to hydrogen was always about 1, and did not depend on temperature for all catalysts, except palladium, for which it was greater than 1. The order of reaction with respect to methylacetylene for iridium powder, and supported and unsupported rhodium was zero and temperature independent. In other cases, it varied between zero and slightly negative values (specially at $P_{C_3H_4} > 100$ mm) and was temperature dependent.

Rate coefficients, k, per gram of the metal were obtained from initial rate measurement for reactions of 30 mm methylacetylene with 25–200 mm of hydrogen between 12 and 150 °C. Plots of $\log_{10}$ (rate coefficients) against absolute temperature were very good straight lines over a wide range of temperatures. The derived apparent activation energy for the catalyst investigated is given in Table I.

(b) Selectivity

The course of reaction (50 mm methylacetylene and 50 mm hydrogen) was followed by analyzing

Can. J. Chem. Downloaded from www.nrcresearchpress.com by 210.87.254.105 on 09/05/12
For personal use only.

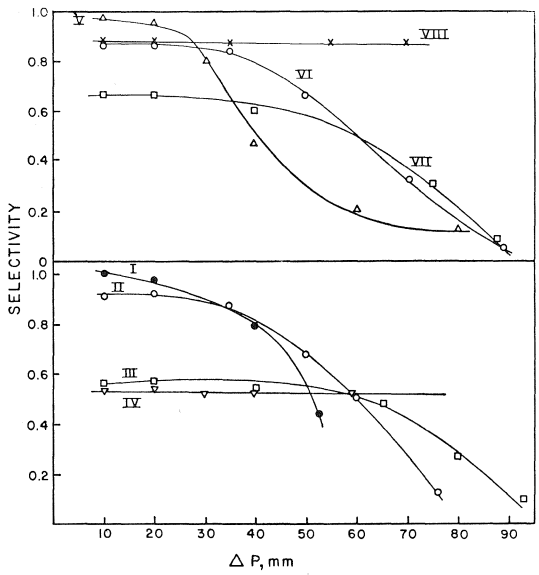

FIG. 2. Dependence of selectivity on pressure fall: $P_{C_3H_4}$ = 50 mm, P_{H_2} = 150 mm. I, Pd powder, T = 110 °C; II, Pt powder, T = 110 °C; III, Ir powder, T = 55 °C; IV, Rh powder, T = 93 °C; V, Pd–pumice, P_{H_2} = 104 mm, T = 24 °C; VI, Pt–pumice, T = 85 °C; VII, Ir–pumice, T = 115 °C; VIII, Rh–pumice, P_{H_2} = 155 mm, T = 55 °C.

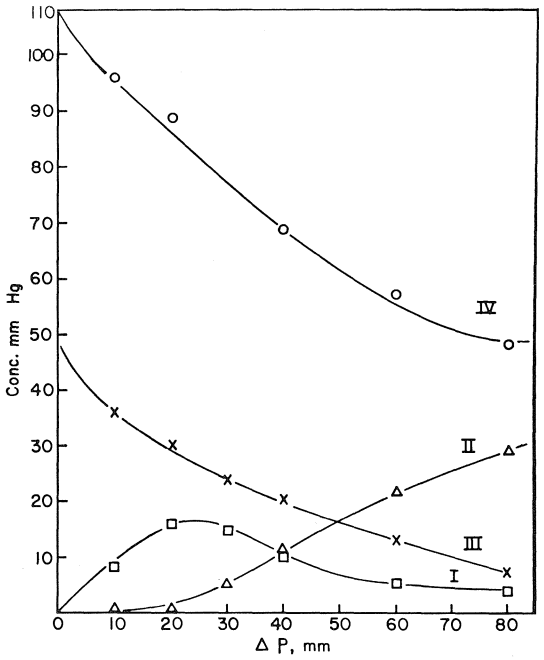

FIG. 3. Course of reaction over Pd–pumice: $P_{C_3H_4}$ = 50 mm, P_{H_2} = 104.5 mm, T = 24 °C.

the reaction products after various falls in pressure, and the selectivity, S, defined as the ratio of propylene to propylene plus propane, was determined. The selectivity was independent of pressure fall for all catalysts, except iridium, in which case it decreased with increasing pressure falls. A similar effect was observed in iron powder catalyst.

The selectivity decreased with increasing pressure falls for hydrogen/methylacetylene ratios greater than 2 for all catalysts except palladium ($\bar{R} > 1.5$). Figure 2 shows the dependence of selectivity on pressure fall. The distribution of products and unreacted hydrogen and methylacetylene at different pressure falls during the course of reaction for palladium–pumice catalyst is shown in Fig. 3. Similar results were obtained for all catalysts at hydrogen/methylacetylene ratios greater than 2.

Measurements were made of selectivity of the catalyst as a function of initial hydrogen pressure at several temperatures by using a fixed methylacetylene pressure of 50 mm and varying the hydrogen pressure. Products were analyzed when the total pressure fall was equal to 20 mm. The results are shown in Figs. 4 *a* and *b*. The selectivity of rhodium was nearly independent of initial hydrogen pressure. Similar results were observed earlier (2) for unsupported nickel and iron. For other catalysts, the selectivity was nearly constant up to a certain hydrogen/methylacetylene ratio, whereafter it decreased rapidly with increased initial hydrogen pressures. The decrease in selectivity with increased hydrogen pressures was fairly linear for supported iridium.

No significant variation in selectivity was observed with initial methylacetylene pressures (45–150 mm) for a fixed initial hydrogen pressure (60 mm).

The temperature dependence of selectivity was studied for an equimolal mixture of reactants (50 mm each). The products were analyzed at several temperatures for a total pressure fall of 20 mm. The results are summarized in Fig. 5. Selectivity was independent of temperature for all catalysts except unsupported iridium and supported platinum for which it increased with increasing temperatures. Polymerization was maximum over ruthenium and palladium and least over platinum catalysts (Table II).

Can. J. Chem. Downloaded from www.nrcresearchpress.com by 210.87.254.105 on 09/05/12
For personal use only.

TABLE II

Selectivity and % polymerization

Catalyst	Temperature (°C)	Selectivity	Polymerization (%)
Platinum–pumice	95	0.915	2.85
Platinum	95	0.935	2.85
Iridium–pumice	95	0.787	4.50
Iridium	95	0.712	10.00
Palladium–pumice	40	0.967	19.00
Palladium	37	1.00	8.00
Rhodium–pumice	72	0.93	7.70
Rhodium	106	0.522	6.30
Ruthenium–pumice	154	0.882	11.00
Ruthenium	140	0.851	28.00

Initial hydrogen pressure = initial methylacetylene pressure = 60 mm Hg; pressure fall = 20 mm.

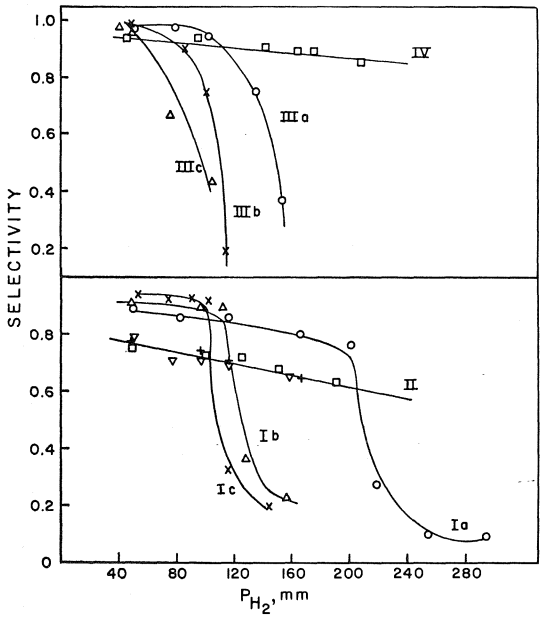

FIG. 4*a*. Dependence of selectivity on initial hydrogen pressure: $P_{C_3H_4}$ = 50 mm.
Pt–pumice: I*a*, T = 84°; I*b*, T = 110°; I*c*, T = 116°.
Ir–pumice: II, ▽, T = −95°; □, T = −115°; +, T = −125 °C.
Pd–pumice: III*a*, T = 24°; III*b*, T = 35°; III*c*, T = 40°.
Rh–pumice: IV, T = 55°.

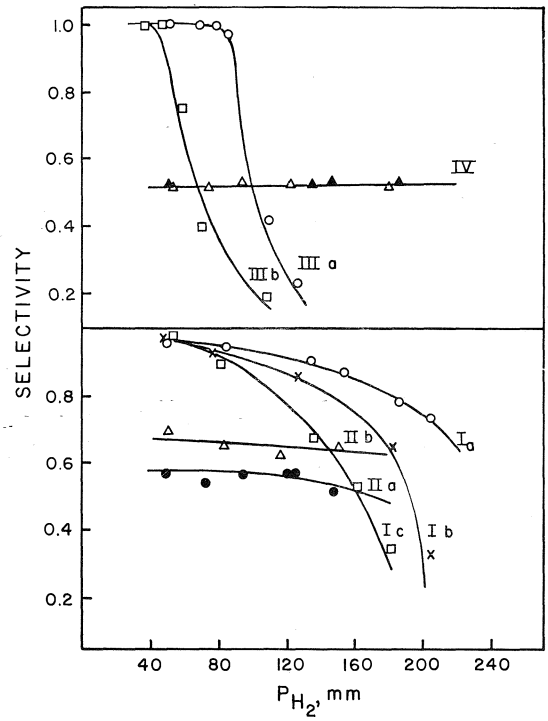

FIG. 4*b*. Dependence of selectivity on initial hydrogen pressure: $P_{C_3H_4}$ = 50 mm.
Pt powder: I*a*, T = 110°; I*b*, T = 120°; I*c*, T = 140°.
Ir powder: II*a*, T = 55°; II*b*, T = 115°.
Pd powder: III*a*, T = 24°; III*b*, T = 45°.
Rh powder: IV, ▲, T = −93°; △, T = −111°.

Discussion

Bond and Sheridan (7) studied the kinetics of methylacetylene hydrogenation over pumice supported platinum, nickel, and palladium catalysts. A comparison of our results for platinum and palladium catalysts with those of Bond and Sheridan is given in Table III.

In the present investigations, for hydrogen/methylacetylene ratios of 2 or less, a Type I curve (curve AFG, Fig. 1) was always observed for all catalysts that were investigated. However, for hydrogen/methylacetylene ratios greater than

Can. J. Chem. Downloaded from www.nrcresearchpress.com by 210.87.254.105 on 09/05/12
For personal use only.

TABLE III

Comparison of the results of present investigations with those of Bond and Sheridan*

Catalyst	Type of P–t curve	Temperature range (°C)	Order with respect to hydrogen	Order with respect to methylacetylene	Activation energy (kcal/mole)
Platinum–pumice	I and III	72–118	1.01 ± 0.01	$-0.3\ \pm0.3$	12.4 ± 0.2
		(65–181)	(1)	(0)	(17.3 ± 0.5)
Platinum	I and III	95–135	1.01 ± 0.01	$-0.4\ \pm0.3$	14.7 ± 0.2
Palladium–pumice	I and II	16–41	1.25 ± 0.05	-0.52 ± 0.11	10.5 ± 0.2
		(78–198)	(1)	(0)	(16.5 ± 0.5)
Palladium	I and III	12–45	1.25 ± 0.05	-0.24 ± 0.13	9.5 ± 0.2

*Values in parentheses are those of Bond and Sheridan (7).

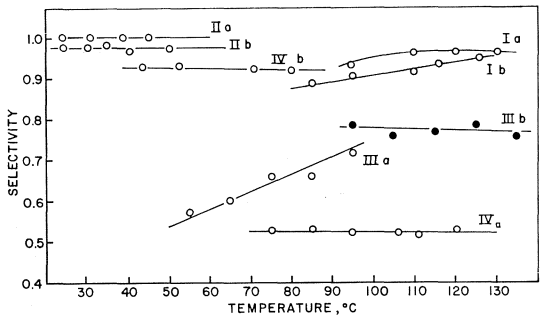

FIG. 5. Dependence of selectivity on temperature: $P_{C_3H_4} = P_{H_2} = 50 \pm 1$ mm. Pt powder, I*a*; Pt–pumice, I*b*; Pd powder, II*a*; Pt–pumice, II*b*; Ir powder, III*a*; Ir–pumice, III*b*; Rh powder, IV*a*; Rh–pumice, IV*b*.

2, a Type III (curve AMN) was obtained for all catalysts, except pumice supported platinum and palladium. There was a slight acceleration at the end of the reaction in all cases. These curves were similar to those obtained by Bond (8) in acetylene hydrogenation over nickel for hydrogen/acetylene ratios greater than 2. In the case of pumice supported platinum and palladium, for hydrogen/methylacetylene ratios greater than 2, a different curve (curve ABC, Fig. 1) was obtained. This was similar to those observed by Bond and Wells (4, 6) for acetylene hydrogenation over alumina supported platinum and palladium, by Tamaru (5) over palladium–alumina, by Farkas and Farkas (10) over platinum, and by Cremer, Knorr, and Plieninger (11) over palladium; Mann and Khulbe (3) observed such curves in methylacetylene hydrogenation over nickel–copper alloys.

In the first stage of the reaction, the main product was propylene, whereas in the rapid acceleration (BC region) period, the main process occurring was the further hydrogenation of propylene to propane.

The differences in the shape of pressure–time curves observed by Bond (8) for acetylene hydrogenation over nickel, and by us for methylacetylene hydrogenation at hydrogen/methylacetylene ratios less than 2 may be due to (*a*) difference in the method of preparation and subsequent activation of catalyst, (*b*) use of methylacetylene pretreated catalysts, and (*c*) different comparative surface coverage by the reactants.

The metals can be placed in the following sequence of decreasing selectivity (Table II).

[*i*] supported Pd > Rh > Pt > Ru > Ir ≫ Os

[*ii*] unsupported Pd > Pt > Ru > Ir > Rh ≫ Os

The order of sequence [*i*] confirms the order of selectivities derived from the literature. It is important to note that the selectivity exhibited is primarily a function of the metal and is substantially independent of the hydrocarbon undergoing reaction and of the condition under which the reaction was carried out. In sequence [*ii*] only rhodium shows dissimilarity with [*i*]. It is pertinent to note that in the case of rhodium no significant change in the selectivity with the increase of initial hydrogen pressure was observed (Figs. 4 *a* and *b*). Rhodium has a different electronic structure to platinum, palladium, or nickel. It has 9 electrons ($4d^85s^1$) outside a closed krypton core, whereas platinum, palladium, and nickel have 10 outer electrons. The effect of support on the selectivity is very large (90%) in the case of rhodium as compared to other transition metals investigated (Table II).

The observed activity pattern per g of metal (Table I) is

[*iii*] supported metals
Pd > Ir > Rh > Pt > Ru > Os

Can. J. Chem. Downloaded from www.nrcresearchpress.com by 210.87.254.105 on 09/05/12
For personal use only.

[*iv*] unsupported metals
Pd > Ir > Pt > Rh > Ru > Os

Thus if the activity for methylacetylene hydrogenation was the only factor governing selectivity, the observed order of selectivity would be

[*v*] supported metals
Ru > Pt > Rh > Ir > Pd

[*vi*] unsupported metals
Ru > Pt > Rh > Ir > Pd

The differences in the selectivity sequence of the metals, based primarily on the analysis of products [*i*] and [*ii*], and based on the activity [*v*] and [*vi*] is due to the strong adsorption of methylacetylene on the surface of the metals, as compared to propylene, which is formed as a reaction product. The surface of the catalyst is almost covered with methylacetylene and propylene formed in the reaction is displaced from the surface.

Under these conditions, readsorption of propylene from the gas phase cannot occur (shown by the independence of selectivity during the course of reaction at equimolal amounts of reactants); hence the reduction in the rate of formation of propane. In the early stages of the reaction, the formation of propane is due to the hydrogenation of the adsorbed propylene formed on the surface from methylacetylene and not by readsorption of propylene from the gaseous phase. It is considered that the selective hydrogenation may be due to the difference in the adsorbability of methylacetylene and propylene on the catalyst surface and not to the differences in the velocity of the hydrogenation reaction.

Bond and Sheridan (7) did not study the effect of temperature on the yields of propylene to propane. Selectivity was found to be independent of temperature for all catalysts except unsupported iridium and supported platinum. In the present investigation, the general characteristic and the products were found to be similar to those of Bond and Sheridan. However, the extent of polymerization in our case was much less. The small amount of polymerization and much lower activation energy is attributed to the method of preparation and activation of the catalyst.

The reaction of methylacetylene and hydrogen over the catalysts investigated were all pseudo first order reactions, A→B→C (Fig. 3). The negative or zero order in methylacetylene and positive order in hydrogen shows that the former was the more strongly adsorbed reactant, and that the surface coverage was high, whereas hydrogen was weakly adsorbed by comparison and its surface coverage was correspondingly low.

Since the general characteristics of the hydrogen–methylacetylene reaction over the metal catalysts investigated is the same, the mechanism of the reaction over these metals could be assumed to be the same. The following mechanism is postulated for the hydrogenation of methylacetylene, based on the mechanism of ethylacetylene hydrogenation (12)

[1] $H_3C-C\equiv CH + 2(*) \underset{k_{-1}}{\overset{k_1}{\rightleftharpoons}} H_3C-\underset{*}{C}=\underset{*}{CH}$

[2] $H_2 + 2(*) \underset{k_{-2}}{\overset{k_2}{\rightleftharpoons}} \underset{*}{H} + \underset{*}{H}$

[3] $H_3C-\underset{*}{C}=\underset{*}{CH} + \underset{*}{H} \underset{k_{-3}}{\overset{k_3}{\rightleftharpoons}} H_3C-\underset{*}{C}=CH_2 + 2(*)$

and

[4] $H_3C-\underset{*}{C}=CH_2 + \underset{*}{H} \xrightarrow{k_4} H_3C-CH=CH_2 + 2(*)$

Step [4] is not considered as reversible, since propylene produced in the gas phase did not readsorb due to the presence of strongly adsorbed methylacetylene, usually in much excess. Any adsorbed propylene so formed would be rapidly displaced from the surface by adsorbing methylacetylene or form a radical with active site

$$(CH_3-\dot{\underset{*}{C}}-\underset{*}{CH_2})$$

for further hydrogenation. Consequently, equating the rates of formation and removal of half hydrogenated state (C_3H_5) the rate of propylene formation is

$$\frac{dP_{C_3H_6}}{dt} = \frac{(k_4\theta_H)(k_3\theta_H)(\theta_{C_3H_4})}{k_4\theta_H + k_{-3}[*]^2}$$

The value of $\theta_{C_3H_4}$ (fractional surface covered by C_3H_4) is generally very high and approaches 1. Now if $k_4\theta_H \gg k_{-3}[*]^2$, then the reaction would be first order in hydrogen pressure. Hence, the observed order of 1 with respect to hydrogen is understandable. A slightly different mechanism may be possible in the case of palladium, where

Can. J. Chem. Downloaded from www.nrcresearchpress.com by 210.87.254.105 on 09/05/12
For personal use only.

the order with respect to hydrogen was slightly greater than 1.

A negative order with respect to hydrocarbons has been reported by Farkas and Farkas (10), and by Bond and Sheridan (7) for platinum catalysts in the hydrogenation of acetylene and methylacetylene respectively. Bond and Wells (4, 6) also observed a negative value of the order with respect to acetylene over alumina supported platinum and palladium. The observed negative order in methylacetylene may be due to the fact that at higher pressures, the molecules form a more ordered array on the surface, thus reducing the number of vacant sites, and therefore reduce hydrogen adsorption by eq. [3]. Alternately, an increase in methylacetylene pressure may enable it to compete more effectively with hydrogen for the surface.

The order with respect to methylacetylene was temperature dependent in the case of supported and unsupported platinum, palladium, and supported iridium. Similar results were obtained by Bond and Wells in acetylene hydrogenation over alumina supported palladium. An increase in temperature would decrease the amounts of reactants on the surface. Since methylacetylene is generally more strongly adsorbed on the surface than hydrogen, it is possible that with increasing temperature, the desorption of methylacetylene would be less than hydrogen, resulting in decreased hydrogen/methylacetylene ratios on the surface. Hence, the order of the reaction with respect to methylacetylene becomes more negative with increased temperature.

Acknowledgment

The authors are grateful to National Research Council of Canada for the award of a research grant A-1125.

1. R. S. MANN and S. C. NAIK. Can. J. Chem. **45**, 1023 (1967).
2. R. S. MANN and K. C. KHULBE. Can. J. Chem. **45**, 2755 (1967).
3. R. S. MANN and K. C. KHULBE. Can. J. Chem. **46**, 623 (1968).
4. G. C. BOND and P. B. WELLS. J. Catalysis, **4**, 211 (1965).
5. K. TAMARU. Bull. Chem. Soc. Japan, **23**, 64 (1950).
6. G. C. BOND and P. B. WELLS. J. Catalysis, **5**, 65 (1965).
7. G. C. BOND and J. SHERIDAN. Trans. Faraday Soc. **48**, 651 (1952).
8. G. C. BOND. J. Chem. Soc. 2705 (1958).
9. J. SHERIDAN. J. Chem. Soc. 133 (1945).
10. A. FARKAS and A. FARKAS. J. Am. Chem. Soc. **61**, 3396 (1939).
11. E. CREMER, C. A. KNORR, and H. PLIENINGER. Z. Electrochem. **49**, 737 (1941).
12. R. S. MANN and K. C. KHULBE. J. Catalysis, **10**, 408 (1968).

Can. J. Chem. Downloaded from www.nrcresearchpress.com by 210.87.254.105 on 09/05/12
For personal use only.

Application of interferometry to reaction kinetics: hydrolysis of ethyl acetate

R. N. O'Brien and A. Glasel
Department of Chemistry, University of Victoria, Victoria, British Columbia
Received June 5, 1968

The use of multiple-beam interferometry has been extended to the study of the kinetics of the hydrolysis of ethyl acetate in acid solution. The rate of change of refractive index in the reacting solution is shown to be directly proportional to the disappearance of the reactants and the appearance of products. The rate of movement of fringes on a wedge interferometer was measured with a photomultiplier tube by recording the response of the tube on passage of a bright fringe. A continuous uniphase output gas laser was used as a light source. Extremely small refractive index changes, hence very small concentration changes, can be detected. Design characteristics of the cell are discussed.

Canadian Journal of Chemistry, **47**, 223 (1969)

Can. J. Chem. Downloaded from www.nrcresearchpress.com by 210.87.254.105 on 09/05/12
For personal use only.

Recently, multiple-beam interferometry has been applied by O'Brien and co-authors to the investigation of single-ion diffusion constants (1), concentration gradients at working electrodes (2), gases diffusing into liquids, and thermal conductivity (3). The hydrodynamic shear zone and diffusion layer at the rotating disc electrode (4), as well as the electrodialysis of sea water (5), have been studied interferometrically. The availability of the single mode output, continuous gas laser permits long path, wedge interferometers to be designed with the possibility of both great accuracy and great precision in measuring refractive index changes during chemical reactions. Reaction streams in commercial chemical processes have been monitored by refractometers placed in side-streams, but it is believed that this is the first time the whole reaction vessel has been used as an interferometer to measure reaction rates.

The reaction studied was the hydrolysis of ethyl acetate in HCl solution. A simple rugged optical system is presented requiring negligible optical manipulative skill and using only readily available components.

Since refractive index changes which are directly proportional to reaction progress are instantaneously recorded and very small changes can be detected, the system should be applicable to fast reactions, reactions better studied in dilute solutions, and those where spectrophotometry gives ambiguous results.

Experimental Arrangements and Theory

The reaction vessel, which also serves the dual purpose of an interferometer, consists of a teflon cyclinder bounded on each side by $1\frac{1}{2}$ in. diameter and $\frac{1}{4}$ in. thick $\lambda/4$ flat glass discs with high efficiency dichroic coating mirrors[1] on the solution side. These partially reflecting mirrors were pressed tightly against the teflon cylinder by a set of three knurled knobs on threaded pins to seal the cell and to generate a wedge for the formation of the fringe system. The teflon cylinder wall had two openings. Into one a sleeve was fitted for a vibrationless mechanical stirrer which consisted of a $\frac{1}{8}$ in. diameter teflon screw. Here the stirrer is considered vibrationless when the vibrations are sufficiently small that the wedge is not distorted, and ensure that the fringe system is not susceptible to random movement. This was readily accomplished by isolating the motor from the cell, securing the sleeve of the stirrer in a rigid brass cell holder, and by mounting a vibration absorbing spring, maintaining a slight pressure on the stirrer shaft (Fig. 1) on the cell holder. The efficiency of the stirrer was determined from the time (5 s) at which fringe perturbations were eliminated after additions to the cell. The other opening was fitted with a teflon tube for injecting solution into the cell. The volume of the cell was about 8.0 ml. The cell body was securely mounted in a heavy brass support resting on a tripod, which could be moved to adjust the angular relationships between the laser beam and the mirror plane. Figure 2 shows the cell details.

A He–Ne C. W. model 130 B Spectra–Physics gas laser[2] having an output of 1 mW in the T_{00} mode was used to provide a monochromatic and collimated beam. The laser beam

[1]These flats were obtained from the Libby-Owens-Ford Export Company.
[2]This laser may be obtained from Allan Crawford Associates Ltd.

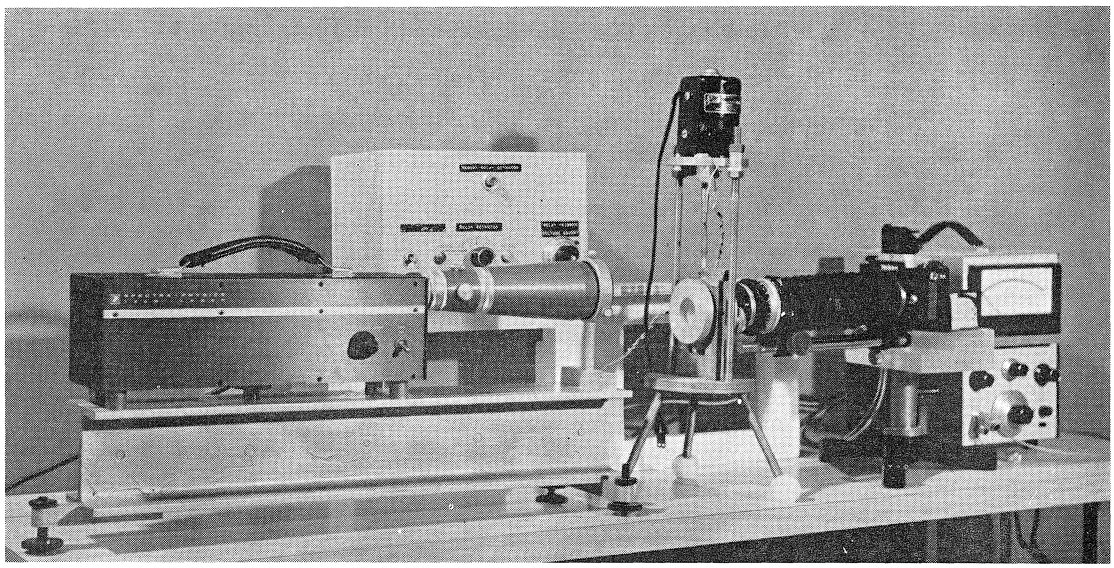

FIG. 1. Photograph showing apparatus arrangement.

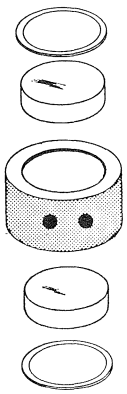

FIG. 2. An exploded view of the interferometric cell.

was passed through a Spectra–Physics spatial filter (model 332) and beam expanding telescope (model 331). The resulting beam was 50 mm in diameter with a smooth Gaussian intensity distribution. The laser system was aligned so that the beam struck the mirror plane at an angle closely approximating 90°. The two mirrors in the interferometer were both 70% reflecting in air at 6328 Å. The ratio of intensity between the bright transmission fringes and dark regions, I_{max}/I_{min}, was about 32/1, and intensity at half fringe width was about 1/9. The cell thickness was 9.57 mm. The wedge thickness, which is a distortion of the thickness of the teflon cylinder, is negligible compared to the thickness of the cell, and of the order of 0.01 mm to give about 2 fringes/mm.

A Nikon F camera (F/1.4, 50 mm) with a bellows focussing attachment provided a magnification of up to 3.5 of the interference cell. The camera was fitted with a viewfinder to allow visual examination of the fringe system for adjustment. The camera back was removed and an $RCAI_p$ 28 photomultiplier tube mounted in a box was placed behind the camera. The opening toward the photocell consisted of a pinhole in a cone having a diameter of 1.0 mm at the apex. A diffusing element consisting of a 1 cm square piece of glass frosted on one side was placed behind the pinhole facing the photomultiplier tube. After magnification of the cell by the camera, the size of the pinhole was about 1/3 to 1/5 of the fringe separation. To prevent stray light from entering the photocell compartment, a No. 24 Wratten filter (pass band 5900 $\rightarrow$; dominant λ = 6106) was placed in front of the camera. Figure 3 shows the optical path.

The electrical circuit consists of a power supply for the photomultiplier tube, a 610 A Keithly Electrometer, and a 1508 Honeywell visicorder.

The position of maxima for localized Fizeau

Can. J. Chem. Downloaded from www.nrcresearchpress.com by 210.87.254.105 on 09/05/12
For personal use only.

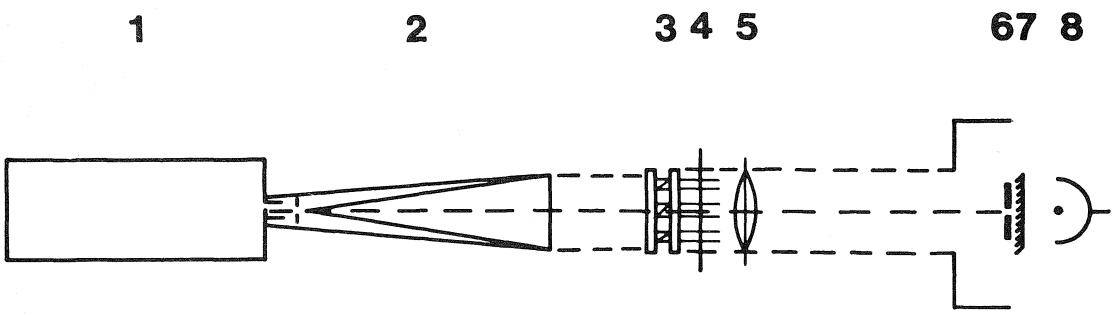

FIG. 3. Schematic diagram of light path showing: 1, He–Ne C. W. laser; 2, spatial filter and beam expanding telescope; 3, interferometer; 4, filter; 5, camera with bellows; 6, pinhole; 7, diffusing element; and 8, photomultiplier cell.

fringes when the wavefront falls on the interferometer at an angle of incidence very close to zero is given by

$$n\lambda = 2\mu d$$

where n = order of interference, λ = wavelength of light (cm), μ = refractive index, and d = thickness of cell (cm).

The relationship between refractive index change and fringe movement can be determined by noting that since d = constant for any fringe, a change in d, Δd, causes a corresponding movement of the fringe along the wedge, i.e. a change in d, Δd. The analytical expression for a movement equal to the fringe spacing is

$$\Delta d\mu + \Delta\mu d + \Delta\mu\Delta d = \frac{\lambda}{2}$$

This relationship can also be obtained by noting that the optical path length difference between successive bright fringes — or between two positions, separated by a fringe spacing, which the fringe may occupy as it moves along the wedge — is $\lambda/2$, i.e.

$$(\mu + \Delta\mu)(d + \Delta d) - \mu d = \frac{\lambda}{2}$$

This expression can be rearranged to:

$$\Delta\mu(d + \Delta d) + \Delta d\mu = \frac{\lambda}{2}$$

Since $\frac{\Delta d}{d}$ can be considered negligible for the interferometer under consideration,

$$\Delta\mu = \pm\frac{\lambda}{2d}$$

For the general case, the fringe is displaced from its reference position by the optical path length difference $F\lambda/2$ where F is the fraction of an order of displacement and may have any value, $|F| \geq 0$, giving

$$\Delta\mu = \pm F\frac{\lambda}{2d}$$

For each successive integral value of F ($F = 1, 2, 3, \cdots, N$) a refractive index change of $\lambda/2d$ displaces the fringe pattern by the fringe spacing distance. The photomultiplier tube reacting to the intensity distribution between the light and dark fringes produces a variation in voltage output with the movement of the fringe system. As a bright fringe goes past the tube, the output reaches a sharp maximum, then declines; the output is recorded on a fast recorder.

The change in refractive index occurring during the reaction is related to the change in concentration of chemical species present, the reaction being

$$\mathrm{EtAc} + \mathrm{H_2O} \xrightarrow{\mathrm{H^+}} \mathrm{HAc} + \mathrm{EtOH}$$

If the bulk refractive index at a time t_1 is given by μ_1 and the reaction is allowed to progress to time t_2, described by a bulk refractive index of μ_2, then

$$\mu_2 - \mu_1 = \Delta\mu = \sum_i \Delta\mu_i$$

where $\Delta\mu_i$ is the refractive index change for one of the participating species.

During the reaction, the refractive index change for the ethyl acetate is negative, and for HAc and EtOH positive. The refractive index change for water is assumed to be zero.

The $\Delta\mu$ (EtAc), $\Delta\mu$ (HAc), $\Delta\mu$ (EtOH) are obtained by plotting μ vs. concentration of

Can. J. Chem. Downloaded from www.nrcresearchpress.com by 210.87.254.105 on 09/05/12
For personal use only.

ethyl acetate, and vs. concentration of EtAc in HCl solutions with the reaction having gone to completion.

Since the refractive index plots of both reactants and products are linear with concentration and follow the general pattern $\mu = \mu^0 + mc$

$$\Delta\mu = \Delta m_i \Delta c_i$$

where m_i is the slope of the plot of μ vs. concentration for one species, and Δc_i the corresponding concentration change. The value μ^0 corresponds to the acid solution and is constant.

For the ethyl acetate reaction, the change of refractive index is then

$$\Delta\mu = (m_2 - m_1)\,\Delta c$$

where m_2 is the slope of products' refractive index plot, m_1 is the slope of reactants' refractive index plot, and Δc, the concentration change per fringe shift, given by

$$\Delta c = \frac{1}{(m_2 - m_1)} \frac{\lambda}{2d}$$

For every concentration change corresponding to Δc, a peak will be recorded, and the distance between the peaks gives a direct display of the rate of disappearance of reactants and formation of products.

Results

Plots of refractive index for ethyl acetate and the products of EtAc vs. concentration are given in Fig. 4 and the values of the slopes in Table I. The last column gives the corresponding calculated concentration change of EtAc per fringe shift. The product slope was obtained by addition of the EtOH and HAc slopes.

Since the rate of change of concentration for reactants and products is given by

$$\Delta c_1 \approx \frac{\Delta\mu_1}{m_1} = -ake^{-kt}\Delta t$$

and

$$\Delta c_2 \approx \frac{\Delta\mu_2}{m_2} = -ake^{-kt}\Delta t$$

the relationship for the total refractive index change is then

$$\frac{\Delta\mu_{\text{total}}}{\Delta t} = ak(m_1 - m_2)e^{-kt}$$

or

$$\log t = -\log\left[\frac{ak(m_1 - m_2)}{\Delta\mu}\right] + \frac{kt}{2.303}$$

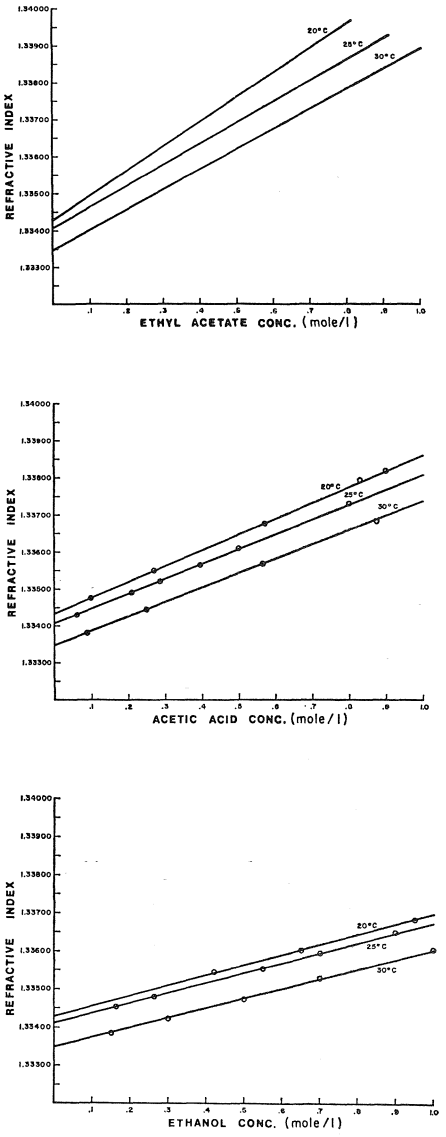

FIG. 4. Plots of refractive index versus concentration for several temperatures.

Since $\Delta\mu = \dfrac{\lambda}{2d}$

$$\log \Delta t = -\log\left[\frac{ak(m_1 - m_2)2d}{\lambda}\right] + \frac{kt}{2.303}$$

The slope of the plot of $\log \Delta t$ vs. time gives the value $k/2.303$.

Reactions were carried out at various HCl concentrations. Table II gives the results of

Can. J. Chem. Downloaded from www.nrcresearchpress.com by 210.87.254.105 on 09/05/12
For personal use only.

TABLE I

Refractive index slopes

Temperature (°C)	m_1 (EtAc slope)	m_2 (products)	Δc EtAc/fringe shift
20	6.70×10^{-3}	7.01×10^{-3}	10.68×10^{-2}
25	5.71×10^{-3}	6.67×10^{-3}	3.62×10^{-2}
30	5.50×10^{-3}	6.70×10^{-3}	2.77×10^{-2}

some of these runs. A comparative literature value is given in the last column.

The variations in the rate constants are thought to be due to experimental errors such as the uncertainty of volume injected and thermostating, rather than in the interferometric method. The temperature was checked with a thermocouple inserted into the interferometric cell and the temperature variation was found to be less than 0.5 °C throughout the run (i.e. a variation of less than 4% in rate). It should, however, be readily possible to incorporate thermostating features into the interferometric cell permitting precise temperature control. Other design features, such as volume of cell, wedge angle, etc., will require alteration depending upon the system to be studied.

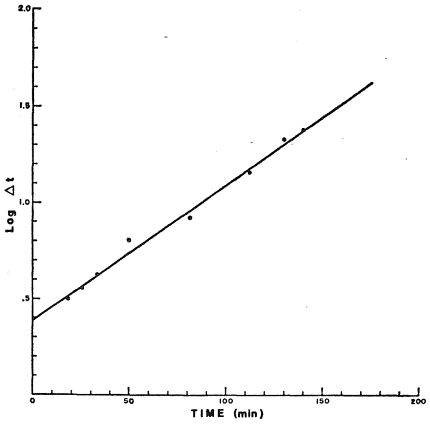

FIG. 5. Plot of log Δt versus time for $a = 0.1157$ moles/l, HCl concentration = 2.435 N, $T = 24$ °C.

From the intercept, Δc may be calculated. These values were found to differ somewhat from the independently determined value of Δc from refractive index measurements. In Fig. 5 ($k = 1660 \times 10^{-5}$ min^{-1}, $a = 0.1157$ moles/l, $T = 24$ °C) from the intercept value of 0.38

$$m_2 - m_1 = \frac{\lambda}{2dak} e^{-2.303(38)}$$
$$= 0.714 \times 10^{-3} \text{ mole}^{-1}$$

or $\Delta c = 4.64 \times 10^{-2}$ moles per fringe shift, which is comparable to the interpolated value of 4.41×10^{-2} from Table I. The refractive index data primarily serves to determine the range of concentrations to be used for the interferometer employed.

Discussion

The results show that interferometry can be used successfully in the study of reaction kinetics. The accuracy of the monitored refractive index data obtained from multiple beam interferometry is comparable to or better than refractive index readings obtained with the Precision refractometer. The change of refractive index detectable with the method described is $\lambda/2d = 3.306 \times 10^{-5}$. Long path interferometers have been designed with a cell thickness of over 2 cm. For a 3 cm cell, it would have been possible to record consecutive refractive index differences corresponding to 1 part in 10^5 during the progress of the reaction. For the hydrolysis of ethyl

TABLE II

Reaction rate constants

Temperature (°C)	Initial concentration (moles/l)	HCl concentration (moles/l)	Rate constant (min^{-1})	Literature value (8) (min^{-1})
24	0.1157	2.435	1660×10^{-5}	1570×10^{-5}
24	0.1157	2.435	1670×10^{-5}	1570×10^{-5}
24	0.3629	1.714	1170×10^{-5}	1120×10^{-5}

Can. J. Chem. Downloaded from www.nrcresearchpress.com by 210.87.254.105 on 09/05/12
For personal use only.

acetate, this would be recording 1 mmole/l per recorded peak.

The application of real-time holographic interferometry (6, 7) toward the study of reaction kinetics has also been considered. While holographic interferometry differs markedly in design and technique, a fringe system is created using a spectroscopic plate in two steps, each step forming one arm of a Mach–Zehnder interferometer. The movement of the fringe system is monitored with the use of a photomultiplier tube in the same manner as with the described multiple beam interferometer.

One advantage of the holographic system is a greater freedom in the design characteristics of the reaction vessel, while one disadvantage is the increased fringe width and usually there is decreased fringe contrast.

1. R. N. O'Brien and C. Rosenfield. J. Phys. Chem. **67**, 643 (1963). R. N. O'Brien, R. Darsi, and D. Quon. J. Electrochem. Soc. In press.
2. R. N. O'Brien. J. Electrochem. Soc. **113**, 299 (1966).
3. R. N. O'Brien, E. A. Beer, K. Beach, J. Leja, S. Weiner, and K. S. Spiegler. Rev. Sci. Instr. In press.
4. R. N. O'Brien. J. Electrochem. Soc. **114**, 710 (1967).
5. K. S. Spiegler, R. N. O'Brien, and K. Beach. To be published in Proc. 17th Meeting C.I.T.C.E. Intern. Comm.
6. K. A. Stetson. J. Opt. Soc. Am. **56**, 1161 (1966).
7. B. J. Thompson and W. R. Zinky. Research/Development. July 1967. Holography: A Status Report.
8. H. S. Harned and R. Pfanstiel. J. Am. Chem. Soc. **44**, 2193, 1922.

Can. J. Chem. Downloaded from www.nrcresearchpress.com by 210.87.254.105 on 09/05/12
For personal use only.

Gallium(III) isothiocyanate and its addition compounds

S. J. Patel and D. G. Tuck
Department of Chemistry, Simon Fraser University, Burnaby 2, British Columbia
Received July 8, 1968

Gallium(III) tris-isothiocyanate trihydrate has been prepared, together with a series of compounds with monodentate ligands of the type $Ga(NCS)_3L_3$. Bidentate donors gave either $Ga(NCS)_3L_3$ or $Ga(NCS)_3L_{1.5}$. The structure and properties of these species are compared with those of other gallium(III) addition compounds, and of the corresponding indium(III) complexes.

Canadian Journal of Chemistry, 47, 229 (1969)

Can. J. Chem. Downloaded from www.nrcresearchpress.com by 210.87.254.6 on 09/05/12
For personal use only.

In the course of preparative and structural studies of indium(III) compounds and their adducts (1), indium(III) thiocyanate was isolated, and shown to be a thiocyanate-bridged polymer in the solid state (2). The addition compounds obtained with monodentate ligands were all of the type $In(NCS)_3L_3$, contrasting with the range of stoichiometries from InX_3L_3 to InX_3L (X = Cl, Br, or I) found in the indium(III) halide series (3). We have now extended the work on thiocyanates by preparing gallium(III) tris-isothiocyanate trihydrate, together with a series of compounds of $Ga(NCS)_3$ and various donor ligands. The properties of these species compare interestingly with those of related indium and gallium complexes.

Results and Discussion

Gallium(III) Tris-isothiocyanate Trihydrate

There appears to be no report of the preparation of any gallium(III) pseudohalides in the literature (4, 5). Following earlier work on indium(III) thiocyanate, gallium(III) sulfate was treated with the stoichiometric quantity of barium thiocyanate in aqueous solution; evaporation of the resultant solution yielded $Ga(NCS)_3.3H_2O$ as a stable pale-yellow solid. The anhydrous compound could not be obtained by heating to 100° in vacuo, since at about 85° the material swelled, turned yellow, and lost weight (~ 24%). The infrared spectrum of this new material showed absorption bands due to C≡N and OH, but the analytical data did not correspond to any simple stoichiometry, and the material was not investigated further.

The infrared spectrum of gallium tris-isothiocyanate trihydrate shows absorptions at 3360 s, 2076 s, 1655 sh + 1642 + 1614 m, 1425 sh + 1400 m, 1070 m, 960 w, 895 w, 580 w, 475 m, and 360 m, cm^{-1}; the compound mulled poorly and all the bands are broader than in the spectra of the adducts. We assign the strong 2076 cm^{-1} band to the C≡N stretch of the thiocyanate group, and that at 475 cm^{-1} to the N—C—S bending mode. These assignments are both consistent with Ga—NCS bonding, which suggests that the absorption at 895 cm^{-1} may be the C≡S stretch, lying slightly above the frequency region in which this mode is usually found in isothiocyanate compounds (6). The C≡N stretch is typical of that reported for N-bonded thiocyanate groups, and is significantly lower than in the anhydrous indium thiocyanate, for which a polymeric thiocyanate-bridged structure is consistent with both spectroscopic and chemical evidence (2). The broad band at 3360, and the 1655 + 1642 + 1614 cm^{-1} multiplet are presumably O—H stretching and bending modes of H_2O.

There are no bands that can be assigned to pure ν(Ga—N) or ν(Ga—O) modes. In the adducts of gallium isothiocyanate (see below), the ν(Ga—N) vibrations are in the 250–320 cm^{-1} region, in agreement with earlier work. Data on ν(Ga—O) frequencies are sparse. The totally symmetric Raman active vibration observed with an aqueous (sulfate) solution of $[Ga(H_2O)_n]^{3+}$ is at 475 cm^{-1}; the general range for this mode in aquated trivalent metal ions is 540–488 cm^{-1} (7). Hester and Plane (8), and Djordjevic (9), have reported ν_s and ν_{as} of Ga—O in $[Ga(acac)_3]$ at 460 and 525 cm^{-1} respectively. Lewis *et al.* (10) were unable to identify any unique M—O vibrations in gallium(III) halide – ether adducts, and it is very probable that there will be extensive mixing of the ν(Ga—O) and ν(Ga—N) vibrations in a monomeric $Ga(NCS)_3(H_2O)_3$ species. We therefore suggest that the band at 360 cm^{-1} is such a mode involving both ν(Ga—NCS) and ν(Ga—OH_2).

This discussion leaves unassigned the bands at 1425 + 1400, 1070, 965, and 580 cm^{-1}, of which

Can. J. Chem. Downloaded from www.nrcresearchpress.com by 210.87.254.6 on 09/05/12
For personal use only.

the last three may possibly be related to wagging and rocking modes of the Ga—OH_2 group (see for example, ref. 11).

With the preparation of gallium isothiocyanate trihydrate, for which the infrared data indicate a monomeric structure in the solid state, information is now available on the thiocyanates of all the Group IIIB elements. Boron tris-isothiocyanate (12) is a liquid (boiling point 92°/0.1 mm) soluble in benzene, chloroform, and *n*-heptane, but with a tendency to polymerize in these solvents. Aluminium thiocyanate has been known for many years (13), and the preparative method is similar to that used for the gallium and indium compounds, but no structural information is available. Gallium thiocyanate is described above, and indium thiocyanate is a thiocyanate bridged polymer (2). Thallium(III) thiocyanate has not been reported, and may in fact be unstable as a result of the redox properties of Tl(III) and CNS^-; the compounds R_2TlNCS (R = Me, Et) (14, 15) and $PhTl(NCS)_2$ (16) are, however, known.

It is worth noting that, with one exception, the Group IIIB thiocyanate species and all the adducts with donor ligands involve N-bonded thiocyanate; indium(III) thiocyanate is unique in this group in that the thiocyanate group bridges two metal atoms (2).

Adducts of Gallium(III) Isothiocyanate

A series of simple reactions between gallium(III) isothiocyanate and donor ligands in various nonaqueous media (see Experimental section) gave rise to a group of addition compounds.

The infrared spectra of the donor groups in the sodium chloride region showed that these complexes involve Ga—N bonding in the case of pyridine, γ-picoline, 2,6-lutidine, quinoline, ethylenediamine, 2,2′-bipyridyl and 1,10-phenanthroline, and Ga—O bonding in the case of dimethylsulfoxide and triphenylphosphine oxide. In general, the spectral changes establishing this bonding were within the experimental accuracy identical to those reported previously for the analogous indium(III) halide and pseudohalide adducts (2, 3). For the γ-picoline complex, not discussed previously, bands at 1606, 1224, 997, 800, and 515 cm^{-1} in the free ligand move to 1630, 1236, 1026, 810, and 552 cm^{-1} in the complex, in agreement with results reported by Goodgame and Hayward (17). For the 2,6-lutidine adduct, the principal changes are *(a)* the two bands at 1597 s and 1585 s in the free ligand move to higher energy and split to a quartet at 1659, 1644, 1635, and 1625 (all s) cm^{-1}, and *(b)*, the band at 775 cm^{-1} is replaced by new absorptions at 796 s, 787 s, and 770 w cm^{-1}. Similar changes have been reported (18) on coordination of 2,6-lutidine with copper(II) chloride and bromide. In the $Ga(NCS)_3$–quinoline complex, bands were observed at 1643 m and 1603 m, compared with 1620 and 1592 cm^{-1} in the free ligand.

TABLE I

Molar conductivities of gallium(III) tris-isothiocyanate adducts[a]

Compound[b]	Conductivity (Ω^{-1} cm^2) Nitromethane	Acetonitrile
$Ga(NCS)_3py_3$	92	137
$Ga(NCS)_3pic_3$	88	119
$Ga(NCS)_3lut_3$	128	260
$Ga(NCS)_3quin_3$	(c)	(c)
$Ga(NCS)_3(dmso)_3$	38	55
$Ga(NCS)_3(Ph_3PO)_3$	34	29
$Ga(NCS)_3bipy_{1.5}$	40	52
$Ga(NCS)_3phen_{1.5}$	35	55
$Ga(NCS)_3en_3$	(c)	(c)

[a]Concentration = 10^{-3} *M*; temperature = 25°.
[b]py = pyridine; pic = 4-methylpyridine; lut = 2,6-lutidine; quin = quinoline; dmso = dimethylsulfoxide; bipy = 2,2′-bipyridyl; phen = 1,10-phenanthroline; en = ethylenediamine.
[c]Compound insufficiently soluble.

The molar conductivities of the adducts were measured in nitromethane and acetonitrile solution, with the results shown in Table I.

The values reported for 1:1 electrolytes under these conditions are in the range 70–90 and 120–130 Ω^{-1} cm^2 in nitromethane (19) and 130–170 Ω^{-1} cm^2 in acetonitrile (20). For 1:2 electrolytes, the values are 150–200 and approximately 300 Ω^{-1} cm^2, respectively (19, 20). The values reported in Table I, therefore, imply appreciable dissociation in nonaqueous solution. As in the indium case, however, it does not follow that the compounds are to be formulated as electrolytes in the solid state (2). Following the dissociative mechanism proposed to explain the conductivity in melts of $GaCl_3L_2$ complexes (4), the dissociation is rather attributed to equilibria such as

$$Ga(CNS)_3L_3 \rightleftarrows [Ga(CNS)_2L_3]^+ + CNS^-$$

$$[Ga(CNS)_2L_3]^+ \rightleftarrows [Ga(CNS)L_3]^{2+} + CNS^- \text{ etc.}$$

in which species with coordination numbers less

TABLE II

Infrared absorption spectra of gallium(III) isothiocyanate adducts

Compound	ν(C≡N)	δ(NCS)	ν(M—N)
$Ga(NCS)_3py_3$	2095 br	483	220, 247, 285 br, 305 sh
$Ga(NCS)_3pic_3$	2090	455	253, 278
$Ga(NCS)_3lut_3$	2040, 2095	480	238(*b*)
$Ga(NCS)_3quin_3$	2095	~475 br	(*b*) (*c*)
$Ga(NCS)_3dmso_3$	2100	473	235, 280
$Ga(NCS)_3(Ph_3PO)_3$	2085, 2110	475	(*b*)
$Ga(NCS)_3bipy_{1.5}$	2075	478, 495	220, 252, 268, 290
$Ga(NCS)_3phen_{1.5}$	2075	480	260, 280, 315(*b*)
$Ga(NCS)_3en_3$	2070	(*a*)	(*a*)

[a]See text.
[b]Ligand vibrations also present in this region.
[c]All bands very broad in this region.

than 6 are formed. The conductivities are significantly higher than for the corresponding indium(III) thiocyanate adducts, presumably because the 6-coordinate state in gallium(III) involves higher steric interference and hence weaker metal ligand bonding than in the indium case, leading to easier dissociation. This steric factor may also explain the order of conductivities for the monodentate nitrogen donor adducts, for which the order 2,6-lutidine > γ-picoline ≈ pyridine is found.

Complexes with triphenylphosphine, urea, and thiourea could not be obtained by methods identical to those used successfully for the preparation of indium(III) thiocyanate adducts of these ligands.

Infrared Structural Studies

As in the earlier work (2), an important point is the mode of bonding of the thiocyanate ligand. Inspection of the solid state infrared spectra show that for all the addition compounds, as for gallium isothiocyanate hydrate itself, the intense C≡N stretching frequency is in the region 2116–2038 cm^{-1}, implying *N*-bonding of the thiocyanate group. The evidence from the frequency of the NCS bending mode (see Table II) is in agreement with this conclusion. The only compound for which this conclusion is at all in doubt is in the interesting case of the γ-picoline adduct, for which the δ(NCS) mode is some 20 cm^{-1} below the average value in these complexes. There has been considerable discussion as to the structure of the palladium(II) thiocyanate – pyridine and γ-picoline compounds, and despite earlier views, it now appears that the mode of bonding of the thiocyanate group is the same in both cases (i.e. Pd—SCN) (see ref. 6 for details). The present result for $Ga(NCS)_3pic_3$ therefore is taken as showing some weakening of the δ(NCS) force constant due to methyl substitution at the 4-position, but not to an extent compatible with *S*-bonding of thiocyanate. The weak C≡S stretching mode could not be identified in most of the complexes because of overlying ligand vibrations.

As noted above, it is the smaller and more electronegative atom, rather than sulfur, which is bonded to the metal in gallium thiocyanate and its adducts, so that as with indium(III) (1–3), *N*-bonded thiocyanate favors high coordination numbers, even in the presence of a ligand such as triphenylphosphine oxide. This is especially striking since with gallium(III) chloride and bromide, only GaX_3L and GaX_3L_2 neutral adducts appear to have been isolated (4). A more meaningful comparison would probably be with gallium(III) fluoride, for which the only known adducts are $GaF_3.3H_2O$ and $GaF_3.3NH_3$, suggesting a coordination number of 6, which is also found in certain GaF_6^{3-} salts.

Table II also lists the absorption bands detected in the 220–320 cm^{-1} region, where ν(Ga—N) vibrations would be expected (21). Two factors prevent any detailed analysis of these absorptions in terms of the symmetry of the complexes; the unknown extent of ν(Ga—NCS) and ν(Ga–donor) coupling, and the presence of ligand absorption bands in this region in some of the compounds. It is, however, clear that the presence of ν(M—N) absorptions in the spectra are compatible with the Ga—NCS bonding discussed above.

No identification of ν(Ga—O) could be made,

Can. J. Chem. Downloaded from www.nrcresearchpress.com by 210.87.254.6 on 09/05/12
For personal use only.

since ligand absorptions occur in the region of interest in both $Ga(NCS)_3(dmso)_3$ and $Ga(NCS)_3(Ph_3PO)_3$.

Bidentate Nitrogen Donors

As with the adducts of indium thiocyanate with 2,2′-bipyridyl and 1,10-phenanthroline, the infrared evidence for $Ga(NCS)_3bipy_{1.5}$ and $Ga(NCS)_3phen_{1.5}$ shows that the thiocyanate groups are monodentate rather than bridging. The far-infrared spectra of $In(NCS)_3bipy_{1.5}$ and $Ga(NCS)_3bipy_{1.5}$ are analogous, suggesting that the gallium and indium compounds may be isostructural. Work is still proceeding on the structure of these species (22).

The far-infrared spectrum of $Ga(NCS)_3en_3$ is completely different from that of all the other compounds prepared, and closely resembles the spectrum of $[Ni(en)_3][PtCl_4]$ (23), so that the compound is formulated as $[Ga(en)_3](CNS)_3$. As with the corresponding indium compound, insolubility in the appropriate solvents hinders any conductivity investigation of this aspect of the problem. The ethylenediamine compound is unique in this series in that it is hygroscopic; the compound as prepared (from ethylenediamine hydrate) contained about 1.5 moles of water, which could be removed by heating to 110°.

Experimental

General

Infrared spectra were obtained on both Unicam SP 200 and Beckman IR-12 instruments. Other instrumental techniques were as described earlier (2, 3).

Gallium was analyzed either gravimetrically as the oxide, or volumetrically by titration against potassium ferrocyanide in dilute acid, using 3,3′-dimethylnaphthidine as indicator (24). Thiocyanate was determined gravimetrically as silver thiocyanate, precipitated from aqueous ethanol or nitromethane solutions to avoid interference from organic ligands present.

Gallium metal was Fisher Certified material (99.99% pure). Ligands were as in previous work; γ-picoline, 2,6-lutidine, and quinoline were recrystallized before use.

Gallium(III) Isothiocyanate Trihydrate

Gallium metal was dissolved in hot conc. sulfuric acid, the resultant solution evaporated to dryness, and the residue finally heated to 250° for some hours to give anhydrous gallium(III) sulfate.

Found: Ga, 32.4; SO_4^{2-}, 67.1; $Ga_2(SO_4)_3$ requires Ga, 32.6; SO_4^{2-}, 67.4.

Stoichiometric quantities of this material were treated with barium thiocyanate (1:3) in water, barium sulfate filtered off, and the filtrate evaporated in vacuo to give a pale-yellow solid.

Found: Ga, 23.3; CNS, 58.1; $Ga(NCS)_3.3H_2O$ requires Ga, 23.4; CNS, 58.5.

Attempted recrystallization of this material led to apparent decomposition and loss of thiocyanic acid.

Found: C, 3.5; H, 3.2; N, 3.6; S, 16.9; $Ga(NCS)_3.3H_2O$ requires C, 12.1; H, 2.1; N, 14.1; S, 32.4.

Gallium(III) isothiocyanate hydrate is deliquescent, and readily soluble in water; on standing at room temperature the solution deposits a white precipitate (gallium hydroxide?) within a few hours. The compound is soluble in ethanol, methanol, acetone, acetonitrile, ethyl acetate, chloroform, nitrobenzene, and ethyl ether, but is insoluble in methylene dichloride, cyclohexane, and chloroform. As noted above, decomposition and loss of weight occurred on heating to 100°.

Trispyridine Gallium(III) Isothiocyanate

Gallium(III) isothiocyanate trihydrate in the minimum volume of methanol was treated with excess pyridine at approximately 75° for 1 h. After filtration, the filtrate was evaporated in vacuo to give a white product which was washed with ether and recrystallized from methanol. The compound is soluble in acetone, lower alcohols, nitromethane, and acetonitrile, but is insoluble in water, ether, methylene dichloride, benzene, chloroform, and cyclohexane. Melting occurred over a range of temperatures above 95°; pyridine was released on heating to 110° in vacuo. The analytical data for this, and the other adducts, are given in Table III. Tris-(4-methyl-pyridine) gallium(III) isothiocyanate (melting point (m.p.) 127°), tris-(2,6-lutidine) gallium(III) isothiocyanate (m.p. 80°), and trisquinoline gallium(III) isothiocyanate (decomposes at approximately 200°) were prepared by reactions similar to those used for the pyridine compound. The solubilities are identical with those of the latter, with the exception that the quinoline adduct is insoluble in both nitromethane and acetonitrile.

Tris(dimethylsulfoxide) Gallium(III) Isothiocyanate

A mixture of dimethylsulfoxide and gallium(III) isothiocyanate trihydrate in ethanol was heated to 60° for 1 h, after which the solution was filtered and pumped to dryness. The product, which was recrystallized from methanol, is soluble in most of the organic solvents listed above except ether, benzene, and cyclohexane. Decomposition occurs above ~ 95°.

Tris(triphenylphosphine oxide) Gallium(III) Isothiocyanate

A mixture of triphenylphosphine oxide and gallium(III) isothiocyanate trihydrate in the minimum volume of ethanol was refluxed for 17 h, filtered hot, and set aside at room temperature for one week, when pink crystals (m.p. 139°) were obtained. The color is probably due to iron impurity. Other than water and cyclohexane, the compound is soluble in all the solvents examined (see above).

Gallium(III) Isothiocyanate – 2,2′-Bipyridyl Adduct

Solutions of 2,2′-bipyridyl and gallium(III) isothiocyanate trihydrate (3:1) in ethanol gave a pale pink precipitate on mixing; this was eventually recrystallized from nitromethane (m.p. above 300°). Apart from nitrobenzene, nitromethane, and acetonitrile, the compound is insoluble in the solvents examined. The preparation and properties of the *1,10-phenanthroline adduct* were essentially identical.

Can. J. Chem. Downloaded from www.nrcresearchpress.com by 210.87.254.6 on 09/05/12
For personal use only.

TABLE III

Analytical results for gallium(III) isothiocyanate adducts

Compound	Found (%)						Theoretical (%)					
	Ga	CNS	C	H	N	S	Ga	CNS	C	H	N	S
$Ga(NCS)_3py_3$	14.5	36.0	44.8	3.0	17.6	—	14.5	36.2	44.9	3.1	17.5	—
$Ga(NCS)_3pic_3$	13.2	33.3	—	—	—	—	13.3	33.3	—	—	—	—
$Ga(NCS)_3lut_3$	12.3	30.6	—	—	—	—	12.3	30.8	—	—	—	—
$Ga(NCS)_3quin_3$	11.0	28.0	—	—	—	—	11.0	27.6	—	—	—	—
$Ga(NCS)_3(dmso)_3$	14.6	36.2	22.5	3.8	8.9	—	14.6	36.4	22.6	3.8	8.8	—
$Ga(NCS)_3(Ph_3PO)_3$	6.4	16.2	63.3	4.0	4.0	—	6.5	16.2	63.5	4.2	3.9	—
$Ga(NCS)_3bipy_{1.5}$	14.4	36.2	45.0	2.4	17.6	20.0	14.6	36.4	45.2	2.5	17.6	20.1
$Ga(NCS)_3phen_{1.5}$	13.4	33.6	49.0	2.4	16.0	18.8	13.6	33.9	49.1	2.4	16.3	18.7
$Ga(NCS)_3en_3$	16.5	41.0	24.6	5.4	28.4	—	16.4	41.1	25.5	5.7	29.7	—

Tris(ethylenediamine) Gallium(III) Thiocyanate

Addition of ethylenediamine hydrate to a solution of gallium(III) isothiocyanate hydrate in methanol gave an immediate white precipitate, soluble in excess ethylenediamine. Treatment of this solution with several volumes of dry ether yielded a resinous mass which on addition of absolute ethanol gave a white solid; this was washed with ethanol and ether, and recrystallized from ethanol. From the analytical and infrared evidence, this material is a hydrate.

Found: C, 23.8; H, 5.9; N, 27.6; Ga, 15.5; CNS, 38.4 (see Table III for values for $Ga(en)_3(CNS)_3$). This hydrate lost ~6% by weight on heating to 110° for 2–3 days. The final product had no infrared absorptions at 3450 or 1650 cm^{-1}; the slight yellow of the material suggests that some slight decomposition may have occurred in the final stages of heating and the low C and N analyses (see Table III) probably arise from this. The hydrated material, m.p. 260°, is soluble only in methanol amongst the solvents examined.

Acknowledgment

This work was supported in part by Operating Grants from the National Research Council of Canada.

1. D. G. Tuck. Coord. Chem. Rev. **1**, 286 (1966).
2. D. B. Sowerby, S. J. Patel, and D. G. Tuck. J. Chem. Soc. A, 1187 (1967). P. L. Goggin, I. J. McColm, and R. Shore. J. Chem. Soc. A, 1314 (1966).
3. A. J. Carty and D. G. Tuck. J. Chem. Soc. A, 1081 (1966).
4. N. N. Greenwood. Advan. Inorg. Chem. Radiochem. **5**, 91 (1963).
5. M. F. Lappert and H. Pyszora. Advan. Inorg. Chem. Radiochem. **9**, 133 (1966).
6. J. L. Burmeister. Coord. Chem. Rev. **1**, 205 (1966), and references therein.
7. R. E. Hester and R. A. Plane. Inorg. Chem. **3**, 768 (1964).
8. R. E. Hester and R. A. Plane. Inorg. Chem. **3**, 513 (1964).
9. C. Djordjevic. Spectrochim. Acta, **17**, 448 (1961).
10. J. Lewis, J. R. Miller, R. L. Richards, and H. Thompson. J. Chem. Soc. 5850 (1965).
11. K. Nakamoto. Infrared spectra of inorganic and coordination compounds. John Wiley and Sons, Inc., New York. 1963. p. 156.
12. D. B. Sowerby. J. Am. Chem. Soc. **84**, 1831 (1962).
13. P. Pascal. (*Editor*) Nouveau traité de chimie minèrale. Vol. VI. Masson et Cie, Paris. 1961. p. 652.
14. A. E. Goddard. J. Chem. Soc. **119**, 672 (1921).
15. J. V. Haffon. J. Chem. Phys. **40**, 933 (1964).
16. F. Challenger and O. V. Richards. J. Chem. Soc. 405 (1934).
17. M. Goodgame and P. J. Hayward. J. Chem. Soc. A, 632 (1966).
18. M. Goldstein, E. F. Mooney, A. Anderson, and H. A. Giebble. Spectrochim. Acta, **21**, 105 (1965).
19. R. S. Nyholm and R. V. Parish. Chem. Ind. London, 470 (1956). J. E. Fergusson and R. S. Nyholm. Nature, **183**, 1039 (1959). F. A. Cotton and J. A. McCleverty. Inorg. Chem. **6**, 229 (1967).
20. F. A. Cotton, B. F. G. Johnson, and R. M. Wing. Inorg. Chem. **4**, 502 (1965).
21. D. M. Adams. Metal-ligand and related vibrations. Edward Arnold and Co., London. 1967. p. 284.
22. A. J. Carty, S. J. Patel, and D. G. Tuck. Unpublished results.
23. D. B. Powell and N. Sheppard. Spectrochim. Acta, **17**, 68 (1961).
24. R. Belcher, A. J. Nutten, and W. I. Steppen. J. Chem. Soc. 2438 (1952).

Can. J. Chem. Downloaded from www.nrcresearchpress.com by 210.87.254.6 on 09/05/12
For personal use only.

Can. J. Chem. Downloaded from www.nrcresearchpress.com by 210.87.254.5 on 09/05/12
For personal use only.

Infrared spectra of diphenylethine and diphenylethine-d_{10}[1]

CESARE PECILE AND BRUNO LUNELLI
Institute of Physical Chemistry, The University, Padua, Italy

Received April 26, 1968

The infrared spectra of diphenylethine and diphenylethine-d_{10} have been measured in the 4000–33 cm^{-1} region both for solution and solid samples. Polarized spectra of oriented crystals, (001) crystal plane, allow segregation of most bands into their respective symmetry classes. The slightness of correlation crystal field effects suggested by the comparison between crystal and solution spectra is confirmed by measurements on dilute isotopic solutions. The oriented gas model predictions are a useful guide despite some well-identified deviations.

The assignment of the infrared active fundamentals is proposed on the basis of the dichroic indications and the isotopic shifts. Most of the relevant absorption frequencies of diphenylethine and diphenylethine-d_{10} are recognized as characteristic of a monosubstituted benzene and the spectra are interpretable on the basis of two phenyl groups weakly interacting through the acetylenic bridge.

Canadian Journal of Chemistry, 47, 235 (1969)

Introduction

The interests in the spectroscopic studies of noncondensed aromatic hydrocarbons with chain structure (1) leads to the investigation of the vibrational behavior of diphenylethine (tolane) and *trans*.-1,2-diphenylethylene (stilbene), the simplest members of this class of compounds. The vibrational spectrum of tolane is far from being satisfactorily interpreted; this is because experimental information is limited (2–4) and because, as for biphenyl (5), a complete vibrational assignment is intrinsically difficult.

In this paper we present and analyze the experimental data obtained by measuring the spectra of solutions and of a well-known crystal plane of tolane and tolane-d_{10}. The vibrational assignment proposed together with the critical examination of the dichroic behavior will provide a basis for the analogous study of stilbene which is the object of the following paper.

Experimental

The tolane used (m.p. 61 °C, corr.) was a reagent grade product, purified by repeated sublimation and finally by two crystallizations from light petrol. The preparation of tolane-d_{10} was first attempted by exchange (48 h at 300 °C) with $Ca(OD)_2$ and with NaOD (4%) supported on $Ca(OD)_2$ (6). In spite of the encouraging reports on the thermal stability of tolane (7), we obtained only tars from which no more than 2% of pure compound could be recovered[2]. Tolane-d_{10} was prepared by starting with *trans*-1,2-diphenylethylene-d_{12}[3] and using a method similar to that reported for the preparation of tolane (8). The product was purified as reported above for the light compound.

The pure product has m.p. 61 °C (corr.) and displays the same very weak infrared absorption in the CH stretching region as the starting *trans*-1,2-diphenylethylene-d_{12} so that a corresponding isotopic composition can be assumed.

Single crystals of tolane and tolane-d_{10} were prepared by sublimation at about 45 °C under atmospheric pressure. X-ray analysis showed that the thin sheets always contained the *a* and *b* crystal axes. Polycrystalline oriented samples, obtained by slow cooling of the melt between KBr plates, were found to contain the same crystal plane. The direction of the *b* crystal axis in different samples was determined by optical methods.

The spectra were recorded on Beckman model IR9 and IR11 spectrometers. The crystal samples were mounted in a beam condenser unit and a silver chloride polarizer was inserted in front of the entrance slit. The crystals were rotated so that the *b* axis was first parallel and then perpendicular to the direction of the electric vector of the incident radiation.

In the 400–33 cm^{-1} spectral region no absorption was detected by using Nujol mulls; however, saturated benzene and cyclohexane solutions in a cesium iodide cell (1 mm thick) revealed some weak bands in the 400–200 cm^{-1} frequency region.

The accuracy of most of the wavenumbers is estimated to be ± 1 cm^{-1}.

Selection Rules

The schematic drawing of the tolane molecule is shown in Fig. 1; the molecular axes have been chosen according to Mulliken's convention (9).

Tolane crystallizes in the monoclinic system,

[1]This work was supported in part by the Chemistry Committee, National Research Council of Italy.

[2]Pure tolane heated in an evacuated pyrex bulb also gave (at 300 °C for 48 h) a tar from which no more than 2% of pure compound could be recovered.

[3]Source: Merck, Sharp and Dohme of Canada Ltd.; mass spectral analysis: *trans*-1,2-diphenylethylene-d_{12}, 76.09%; -d_{11}, 18.77%; -d_{10}, 4.73%; -d_9, 0.38%; -d_8, 0.03%; overall deuterium percentage, 97.2%.

TABLE I

Symmetry classes and selection rules for diphenylethine as a free molecule and in the crystalline state

Molecular symmetry D_{2h}		Site symmetry C_i	Factor group symmetry C_{2h}	
Species and activity*	Degrees of freedom		Species and activity*	Degrees of freedom
a_g (R, p)	$12(\nu_1-\nu_{12})$	a_g (R, p)	a_g (R, p)	72
b_{1g} (R, dp)	$3(\nu_{17}-\nu_{19})+R_Z$			(6 torsional)
b_{2g} (R, dp)	$7(\nu_{31}-\nu_{37})+R_Y$		b_g (R, dp)	72
b_{3g} (R, dp)	$11(\nu_{49}-\nu_{59})+R_X$			(6 torsional)
a_u	$4(\nu_{13}-\nu_{16})$	a_u (i.r.)	a_u (i.r.)	72
b_{1u} (i.r.)	$11(\nu_{20}-\nu_{30})+T_Z$			(5 translational)$+T_b$
b_{2u} (i.r.)	$11(\nu_{38}-\nu_{48})+T_Y$		b_u (i.r.)	72
b_{3u} (i.r.)	$7(\nu_{60}-\nu_{66})+T_X$			(4 translational)$+T_{a,c}$

*R = Raman, i.r. = infrared, p = polarized, dp = depolarized.

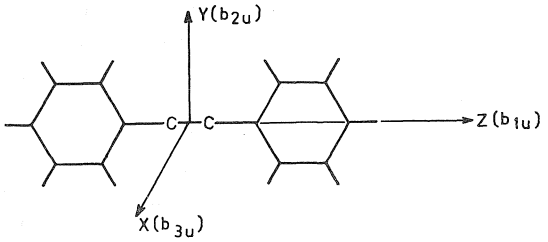

FIG. 1. Molecular structure and choice of molecular axes for diphenylethine, $C_{14}H_{10}$.

space group C_{2h}^5 ($P2_1/a$), with four molecules in the unit cell (10). Its structure consists of two layers with no symmetry relation between them and an equal number of molecules in each layer. Each molecule is planar and located on a C_i symmetry site. The projection of the crystal structure on (001) is shown in Fig. 2.

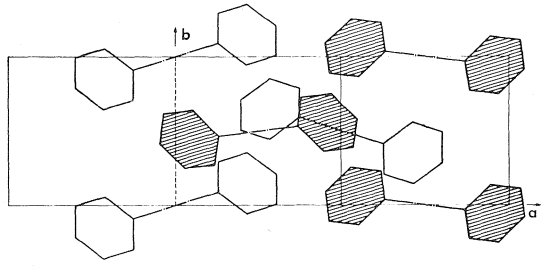

FIG. 2. Projection of the crystal structure of diphenylethine on (001). Shaded molecules belong to one of the two crystallographically independent sets.

The selection rules for the molecular point group D_{2h}, the site group C_i, and the factor group C_{2h} are reported in Table I. For the isolated molecule the normal modes of b_{1u}, b_{2u}, and b_{3u} species are infrared active; the direction of the b_{1u} transition moments is that of the "long molecular axis" Z, the b_{2u} have the "short axis" Y direction, and the b_{3u} have the "normal axis" X direction.

In the crystal, the vibrations of the molecular unit, which lies on a site of C_i symmetry, are distributed between a_g and a_u species; the modes of the a_u species of the free molecule become infrared active. The effect of dynamic interaction of the molecules set by set in the unit cell can be accounted for by factor group analysis: each u fundamental of the isolated molecule gives rise to two b_u modes with the transition moment in the ac crystal plane, and two a_u modes with the transition moment along the b axis. The g fundamentals of both the molecule and the unit cell are infrared inactive.

Table II lists the squared values of the direction cosines of the molecular axes with respect to the crystal axes a, b, and c^* calculated using the known crystal structure (10). The orientation of the molecules is such that the values in Table II are almost equal for both sets; therefore separate consideration is unnecessary for the two sets. Once we assume the oriented gas model using the data in Table II, we can predict the dichroic behavior of the absorption bands in the crystal spectrum. With plane-polarized radiation incident normally on the (001) plane, the vibrations of the b_{1u} species should display strong absorption when the electric vector is perpendicular to the b crystal axis and weak absorption when it is parallel (perpendicular bands). The b_{2u} vibrations should exhibit a reverse behavior (parallel

Can. J. Chem. Downloaded from www.nrcresearchpress.com by 210.87.254.5 on 09/05/12
For personal use only.

TABLE II
Proportionality factors for band intensity

	Set I molecules			Set II molecules		
Crystal axis	$b_{1u}(Z)$	$b_{2u}(Y)$	$b_{3u}(X)$	$b_{1u}(Z)$	$b_{2u}(Y)$	$b_{3u}(X)$
a	0.66	0.21	0.13	0.68	0.12	0.20
b	0.06	0.69	0.25	0.01	0.75	0.24
c^* ($\perp ab$)	0.28	0.10	0.62	0.31	0.13	0.56

bands) and the b_{3u} modes should be slightly parallel.

Results and Vibrational Assignment

The polarized infrared spectra of tolane and tolane-d_{10}, *ab* crystal plane, are shown in Figs. 3 and 4. The absorption frequencies, the relative intensities, and the type of polarization are given in Tables III and IV.

The well-settled assignment of numerous monosubstituted benzenes (11–14) gives a clear indication of the number of modes insensitive to the nature of the substituent (X-insensitive) and of their location in the spectrum. These modes, excluding the CH stretching fundamentals, are $5a_1$, $7b_1$, $3a_2$, and $4b_2$ under the local C_{2v} symmetry of the phenyl ring. Such a spectral feature is also found in quite a number of molecular structures where the phenyl group is present. It is then reasonable to suppose that in the tolane molecule the spectroscopic behavior of the phenyl fragment follows the same pattern, if a strong vibrational coupling of the two phenyl rings is absent. The same regularity has been observed also for the fully deuterated monosubstituted benzenes whose infrared spectra have been reported (12–14, 16). A first inspection of solution and powder spectra of tolane and tolane-d_{10} reveals a clear fit with the above-mentioned correlative scheme.

In the whole tolane molecule the transition moments of the vibrations of the b_{1u}, b_{2u}, and b_{3u} species have the same direction as the transition moments of the phenyl fragment vibrations of the a_1, b_1, and b_2 species respectively under the local C_{2v} symmetry. Consequently, both overall and local symmetry, together with assumption of the oriented gas model, allow us to predict that the corresponding absorptions should display perpendicular, parallel, and slightly parallel polarization in the order, when the *ab* crystal plane is examined. The assumption of the oriented gas model is justified by the similarity of the crystal and solution spectra, and by the values of the correlation crystal field splittings observed, none of which exceeds 4 cm^{-1}. Dilute isotopic solutions were used to prove, where possible, that the splittings had a factor group origin. The lack of significant differences between solution and crystal spectra might also suggest an identical planar structure in the two phases; the same indication was also given by electronic spectra (17).

The presence of an inversion center (Table I) makes it impossible to know all the g modes in the lack of a complete and satisfactory Raman spectrum (4); as a consequence no attempt will be made to identify combination tones.

The frequency values used in the following discussion are those of the crystal spectra.

Vibrations of b_{1u} Species

Since the tolane and tolane-d_{10} spectra conform well to the interpretative scheme suggested by the monosubstituted benzenes, the first step in the assignment of the eleven b_{1u} infrared active fundamentals is to consider the frequencies of the modes similar to the five X-insensitive phenyl ring modes of the a_1 species.

The assignment of the bands at 1600, 1502, 1158, 1027, and 998 cm^{-1} of tolane and at 1570, 1414, 958, and 850 cm^{-1} of tolane-d_{10} to fundamentals of the b_{1u} species is almost direct. The clearly perpendicular character of the corresponding absorptions in the crystal spectra supports their segregation as b_{1u} modes. The lowest frequency X-insensitive a_1 vibration of fully deuterated monosubstituted benzenes is located in the 815–820 cm^{-1} region (5, 12–14). The corresponding mode in tolane-d_{10} is assigned at 820 cm^{-1}, overlapped by the stronger parallel band of the b_{2u} species.

The highest X-sensitive frequency in the a_1 class of monosubstituted benzenes, which in

Can. J. Chem. Downloaded from www.nrcresearchpress.com by 210.87.254.5 on 09/05/12
For personal use only.

Can. J. Chem. Downloaded from www.nrcresearchpress.com by 210.87.254.5 on 09/05/12
For personal use only.

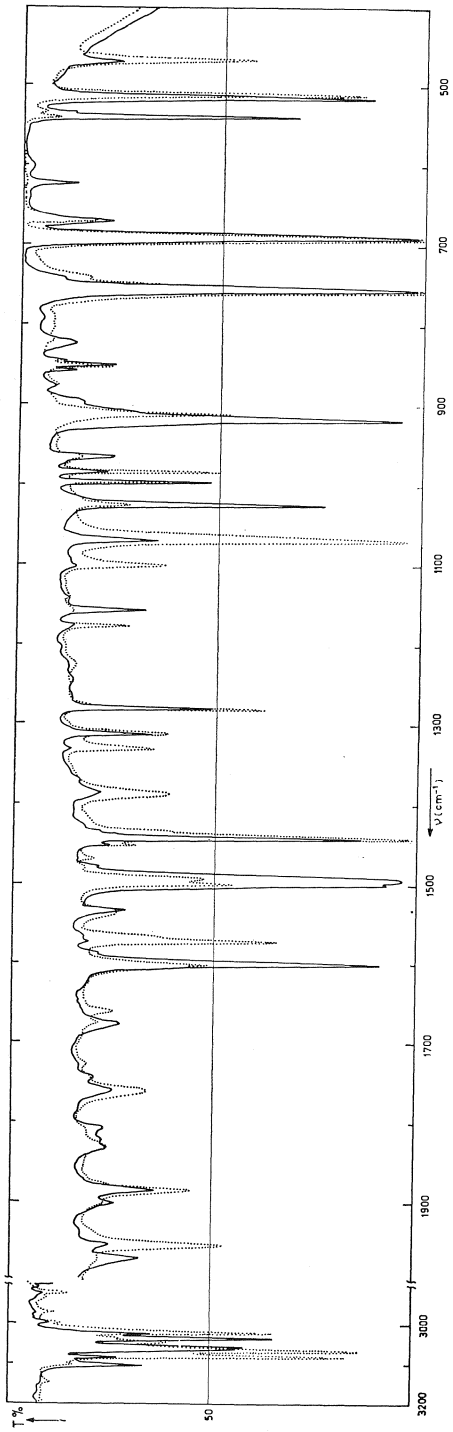

FIG. 3. Polarized infrared spectra of diphenylethine, *ab* crystal plane. Solid line, electric vector perpendicular to *b* axis; dotted line, electric vector parallel to *b* axis.

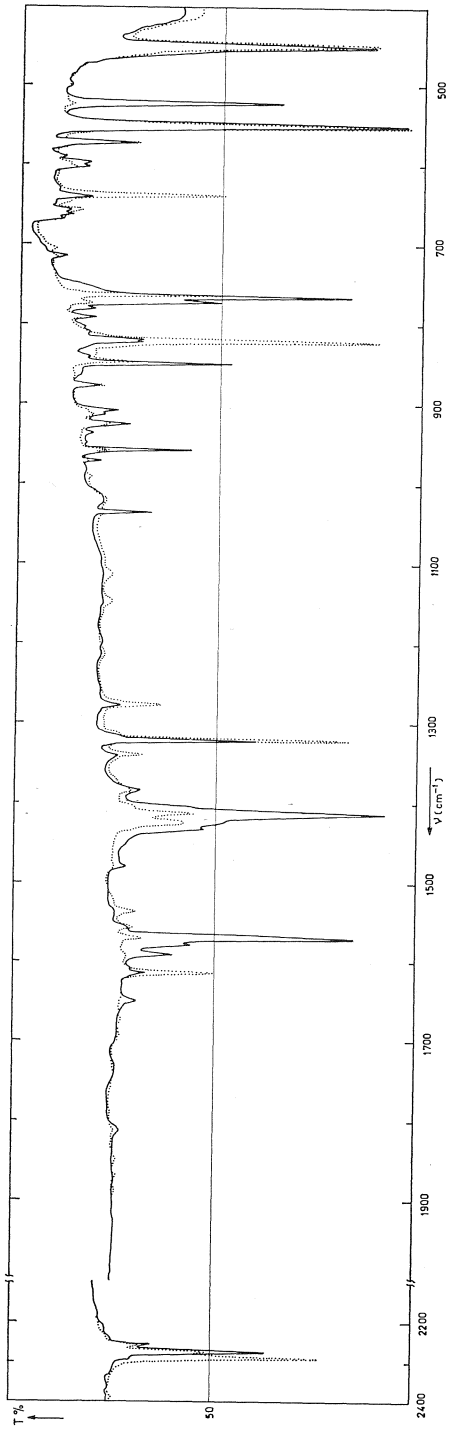

FIG. 4. Polarized infrared spectra of diphenylethine-d_{10}, *ab* crystal plane. Solid line, electric vector perpendicular to *b* axis; dotted line, electric vector parallel to *b* axis.

TABLE III
Infrared spectrum of diphenylethine

Crystal			Solution		Crystal			Solution	
	Intensity[b,c]					Intensity[b,c]			
Frequency[a] (cm^{-1})	⊥ to b	∥ to b	Frequency (cm^{-1})	Intensity[b,d]	Frequency[a] (cm^{-1})	⊥ to b	∥ to b	Frequency (cm^{-1})	Intensity[b,d]
			292	w	1386	5	15	1380	5
			340	v bd	1435 sh			1422 sh	
			403	w	1442		225	1443	115
467	10	35	473[e]	5	1444	75			
509		85	509	55	1453		5	1452 sh	
512	90				1494	(155)	(20)	1492 sh	
536	50		538	100	1502	(95)	(25)	1499	300
620	15	0	625		1533	7	5		
668	10	10	670	5	1567 sh				
690	260	220	690	665	1572		40	1575	20
756	275		754	1210	1600	100		1601 sh	
759		395			1603		25	1604	100
824	+	0	826[f] sh		1660	0	5	1667	10
845	−	+	838 sh		1675	5	0		
850	10		844	(10)	1743	+	0	1734 sh	
854		10			1760	5	10	1750	10
857	+	0			1807	5	0	1802	10
909 sh			909 sh		1832	≃	≃	1822	5
914		30	914[e]	60	1884	10	20	1876	10
918	130				1900	+	−	1893	10
965	10		958[f]	10	1952		25	1945	15
986	5	25	981	5	1970	10	0	1964	10
998	25	20	999	5	3020		40	3023	(35)
1027	60	10	1028	50	3022	(15)			
1071	15	130	1070	50	3034	(40)	0	3037	(40)
1103		15	1098	10	3044	0	15		
1158	10		1157		3055	(30)	0	3062 sh	
1179		10	1176		3060	(30)		3066	(60)
1281	25	35	1278	10	3065		(85)		
1311	10		1309[e]	20	3080	7	(75)	3085	(60)
1313		15			3100	12	0	3104	10
1332	0	10	1327						

[a]Bracketed frequency doublets have correlation crystal field origin.
[b]Intensity values were not corrected for band overlap. Values in parentheses refer to cases in which the overlapping is quite strong.
[c]Intensity expressed as peak absorbance, relative to a value of 100 assumed for the perpendicular component at 1600 cm^{-1}. The resulting values are rounded off to the next multiple of five. The marks +, −, 0, ≃ indicate the intensity of the parallel and perpendicular component of the weak bands; sh, shoulder.
[d]Intensity expressed as peak extinction coefficient ($mole^{-1}$ l cm^{-1}) relative to a value of 100 assumed for the band at 1604 cm^{-1}. The resulting values are rounded off to the next multiple of five; bd, broad; sh, shoulder; w, weak.
[e]Solution in carbon tetrachloride.
[f]Solution in carbon disulfide.

tolane may be approximately considered an inter-ring stretching, should be localized in the region of 1200 cm^{-1}, as suggested by the assignments of benzonitrile (14), ethynylbenzene (15), and toluene (13). The spectral features of tolane at about 1200 cm^{-1} do not allow us to locate this mode. The difficulty may be due to the low intensity of this absorption, as observed in the case of ethynylbenzene where the assignment had to be based on the strong polarized Raman line. No help is offered by the spectra of tolane-d_{10}.

For the location of the two remaining X-sensitive modes the examination of C_6H_5X and C_6D_5X (X = CH_3, CN) (13, 14, 18) assignments justifies the choice of the bands at 536 and 824 cm^{-1} for tolane and at 523 and 755 cm^{-1} for tolane-d_{10}. The perpendicular polarization in the crystal spectra supports this assignment.

In the CH and CD stretching regions the isotopic shifts and the polarization, perpendicular for b_{1u} and parallel for b_{2u} modes, lead to the assignment summarized in Table V.

Vibrations of b_{2u} Species

Six out of the seven vibrations corresponding to phenyl ring X-insensitive modes of the b_1 class are found directly in the spectra of tolane (at 1572, 1443, 1332, 1281, 1179, and 1071 cm^{-1}).

Can. J. Chem. Downloaded from www.nrcresearchpress.com by 210.87.254.5 on 09/05/12
For personal use only.

TABLE IV

Infrared spectrum of diphenylethine-d_{10}

Crystal			Solution		Crystal			Solution	
	Intensity[b,c]					Intensity[b,c]			
Frequency[a] (cm^{-1})	⊥ to b	∥ to b	Frequency (cm^{-1})	Intensity[b,d]	Frequency[a] (cm^{-1})	⊥ to b	∥ to b	Frequency (cm^{-1})	Intensity[b,d]
451		125	449[e]	165	958	25	(5)	960	5
454	125				973	+	−		
523	60		523	80				1003	
549	205		549	270	1036	15	10	1034	10
552		215			1115	−	+	1102	5
573	15	15	568	30	1277	5	15	1275	5
597	(5)		585		1322	45	100	1321	25
603	(5)		599	10	1340		10	1340	
639	10	40	635	65	1382	10		1383[f]	5
656	−	+	655	15				1400	
665	+	−	665 sh		1414	145		1412	135
705	0	+	701		1425		10	1425	
715	15		710	5	1434 sh			1432	
755	+	0			1480	+	0		
765		35	763	(80)	1538	0	5		
768	(105)				1556	0	+		
774	(40)		771	(40)	1570	100	5	1569	100
782	+	−	780		1578	15	0	1575 sh	
793	≃	≃			1590	10	0	1586	
822	(15)	135	819	55	1613	5	20	1609	10
824	(15)	0			1649	+	0	1640	5
847		10	843	(20)	2235	+	0		
850	(40)		849	(55)	2258	5	5	2256	(10)
878	5	5			2275	35	(20)	2278	(40)
909	(10)		909	15	2289	0	65	2291	(55)
915	≃	≃			2370				
925	10	5	922						

[a]Bracketed frequency doublets have correlation crystal field origin.
[b]Intensity values were not corrected for band overlap. Values in parentheses refer to cases in which the overlapping is quite strong.
[c]Intensity expressed as peak absorbance, relative to a value of 100 assumed for the perpendicular component at 1570 cm^{-1}. The resulting values are rounded off to the next multiple of five. The marks +, −, 0, ≃ indicate the intensity of the parallel and perpendicular component of the weak bands; sh, shoulder.
[d]Intensity expressed as peak extinction coefficient ($mole^{-1}$ l cm^{-1}) relative to a value of 100 assumed for the band at 1569 cm^{-1}. The resulting values are rounded off to the next multiple of five; sh, shoulder; w, weak.
[e]Solution in carbon tetrachloride.
[f]Solution in carbon disulfide.

The last X-insensitive vibration, expected at about 620 cm^{-1} (11), is associated with the perpendicular absorption at 620 cm^{-1}. The perpendicular polarization is inconsistent with that predicted for a b_{2u} mode; however, in this case correlations are more dependable than dichroism, which consequently has to be considered anomalous. In tolane-d_{10} the parallel bands at 1538, 1277, and 822 cm^{-1} are directly recognized as belonging to this class and corresponding to X-insensitive b_1 modes of the phenyl fragment. The remaining three X-insensitive modes of tolane-d_{10} can be located by taking into account the frequency ranges (1040–990, 870–840, 600–590) in which they are assigned in C_6D_5X (X = F, Cl, CN, CH_3). Along these lines we propose the bands at 1036, 597, and 847 cm^{-1} despite the perpendicular polarization of the first two bands. The parallel absorption at the latter frequency is a component of the doublet 850–847 cm^{-1} which does not have a factor group origin owing to its persistence in solution.

Two more fundamentals are to be assigned in this class. One is similar to the lowest frequency X-sensitive mode and is discussed afterwards, since it is presumably located below 400 cm^{-1}; the other is found only in the light compound, and associated with the parallel peak at 467 cm^{-1}, in a spectral region suggested by the b_1 skeletal bending of ethynylbenzene (15), located at 467 cm^{-1}.

Vibration of b_{3u} Species

The four out-of-plane X-insensitive modes of the light as well as of the heavy tolane are found in the very narrow frequency ranges indicated by correlations. Although the strong b_{2u} band at 822 cm^{-1} hinders the observation of the b_{3u}

Can. J. Chem. Downloaded from www.nrcresearchpress.com by 210.87.254.5 on 09/05/12
For personal use only.

Can. J. Chem. Downloaded from www.nrcresearchpress.com by 210.87.254.5 on 09/05/12
For personal use only.

TABLE V

Vibrational assignment of infrared active fundamentals[a] of diphenylethine and diphenylethine-d_{10}

Symmetry species	$C_{14}H_{10}$	$C_{14}D_{10}$	Approximate description[b]
b_{1u}	3080	2275	CH stretch.
	3055	2275	CH stretch.
	3034	2258	CH stretch.
	1600	1570	Ring stretch.
	1502	1414	Ring stretch.
	....	....	Skeletal stretch.
	1158	850	CH bend.
	1027	(820)	CH bend.
	998	958	Ring breathing
	824	755	Skeletal def.
	536	523	Skeletal def.
b_{2u}	3080	2289	CH stretch.
	3065	2275	CH stretch.
	1572	1538	Ring stretch.
	1443	1322	Ring stretch.
	1332	1036	CH bend.
	1281	1277	Ring stretch.
	1179	847	CH bend.
	1071	822	CH bend.
	620	597	Ring def.
	467	...	Skeletal def.
	292	...	Skeletal def.
b_{3u}	998	(820)	CH bend.
	916	766	CH bend.
	758	550	CH bend.
	690	639	Ring def.
	511	452	Skeletal def.
	...	...	Skeletal def.
	...	...	Skeletal def.

[a]Frequency values (cm^{-1}) observed in the spectra of oriented crystals. Bracketed values correspond to bands assumed to be strongly overlapped by other absorptions.

[b]As a consequence of the correspondence, used throughout the discussion, between tolane and monosubstituted benzenes vibrations, the approximate descriptions given are inferred from the results of calculations reported for C_6H_5Cl. The alignment of the frequencies of $C_{14}H_{10}$ and $C_{14}D_{10}$ has been guided by the inspection of the atomic displacements in C_6H_5Cl and C_6D_5Cl normal vibrations. For the correct description of normal vibrations of both C_6H_5Cl and C_6D_5Cl in terms of potential energy distribution, the original literature should be consulted (16).

[c]Average value of the frequencies observed in the crystal spectra for bands presenting correlation field splitting.

absorption in this position, its location cannot be questioned.

The slightly parallel dichroism predicted for b_{3u} bands is observed only for the absorptions at 758 and 690 cm^{-1} of tolane and at 550 cm^{-1} of tolane-d_{10}. In the other cases, the polarization is anomalous, and the results are of a perpendicular or parallel type.

Correlations offer a guide to assignment only for two out of the three skeletal deformations of b_{3u} species, that is for those which correspond to phenyl ring b_2 X-sensitive vibrations. One of these is located below 400 cm^{-1} and is discussed in the next section; the other is associated with the slightly parallel bands at 511 cm^{-1} in tolane and at 452 cm^{-1} in tolane-d_{10}. These frequency values compare well with the assignment at 529 in ethynylbenzene (15) and at 548 and 488 cm^{-1} in benzonitrile and benzonitrile-d_5 respectively (14). The location of the last skeletal deformation of the b_{3u} species cannot be inferred from correlative data and is left unassigned.

Vibrational Modes below 400 cm^{-1}

As reported in the experimental section, the powder spectra of both tolane and tolane-d_{10} in the region 400–33 cm^{-1} do not reveal any absorption. The only experimental data obtained in the low frequency region are the spectra of tolane in benzene and cyclohexane solutions from 400 to 200 cm^{-1} (Table III). The infrared active fundamentals still unassigned are one b_{2u} and one b_{3u} skeletal deformation. The first can be regarded as an asymmetric vibration of the tolane skeleton whose corresponding totally symmetric mode may well be identified with the frequency at 260 cm^{-1} observed in the fluorescence spectrum (1). In the infrared spectrum of tolane, it can be associated with the band at 292 cm^{-1}.

The absorption pattern between 290 and 400 cm^{-1} in the solution spectrum of tolane is not satisfactorily interpretable by using the available data. This spectral feature might be originated by accidental superposition of combination tones or by the activation in the infrared of Raman active modes, due to the existence of a twisted molecule in solution. The similarity of the solution and crystal spectra in the 4000–400 cm^{-1} region does not exclude this possibility since the extensive coincidence of the reported Raman frequencies (4) with those of the observed infrared active modes in this region makes it difficult to reveal any possible activation of the former in the infrared spectra. Clarification of this rather unusual coincidence will require more satisfactory Raman spectra than are now available.

The b_{3u} skeletal bending, which corresponds to the lowest frequency X-sensitive phenyl ring skeletal bending, was found at 170 cm^{-1} in benzonitrile (14) and at 165 cm^{-1} in ethynylbenzene (15). In the tolane spectrum, as well, it is presumably located in the same region, for which solution spectra were not obtained.

Conclusions

Most of the relevant absorption frequencies of tolane and tolane-d_{10} spectra are recognized as characteristic of a monosubstituted benzene and the spectra are interpretable on the basis of two

phenyl groups weakly interacting through the acetylenic bridge. However, more extensive investigations are required if the vibrational assignment has to be considered complete or is to be used to provide information on the degree of coupling of the phenyl ring fundamentals and on the problem of the molecular planarity in solution (5). The assignment of tolane, summarized in Table V, generally agrees with the previously reported ones (2) and is significantly supported by the parallel assignment of tolane-d_{10}.

The degree of reliability of fundamentals assignment, mainly for modes corresponding to X-insensitive phenyl ring vibrations, gives sufficient confidence to allow a critical evaluation of the observed dichroism. The experimental dichroic behavior generally agrees with the predicted one for the bands due to planar vibrations, while the anomaly is more the rule than the exception for the out-of-plane vibrations. Anomalies like these, not unusual in crystal spectra of aromatic compounds (19) and explained in an unsatisfactory way (20), must be clearly identified to know the limits of validity of dichroic indications and to study the empirical polarization specificity of phenyl ring vibrations in those cases, like stilbene, where the local symmetry of the phenyl ring and the whole molecular symmetry do not fix the same direction of the transition moments.

1. G. V. GOBOV. Opt. Spectry. USSR, English Transl. **15**, 194 (1963).
2. R. MECKE and E. GREINACHER. Z. Elektrochem. **61**, 530 (1957). J. MANN and H. W. THOMPSON. Proc. Roy. Soc. London, Ser. A, **192**, 489 (1947); **211**, 168 (1952).
3. I. N. KHALIMONOVA. Opt. Spectry. USSR, English Transl. **14**, 339 (1963).
4. A. DADIEU, A. PONGRATZ, and K. W. F. KOHLRAUSCH. Monatsh. Chem. **60**, 221 (1932).
5. D. STEELE and E. R. LIPPINCOTT. J. Mol. Spectry. **6**, 238 (1961). J. E. KATON and N. T. MCDEVITT. J. Mol. Spectry. **14**, 308 (1964). G. V. PEREGUDOV. Opt. Spectry. USSR, English Transl. **9**, 155 (1960). G. ZERBI and S. SANDRONI. Spectrochim. Acta, **24A**, 483, 511 (1968).
6. B. LUNELLI and C. PECILE. Can. J. Chem. **46**, 391 (1968).
7. I. B. JOHNS, E. A. MCELHILL, and J. O. SMITH. J. Chem. Eng. Data, **7**, 277 (1962).
8. L. F. FIESER. J. Chem. Educ. **31**, 291 (1954).
9. R. MULLIKEN. J. Chem. Phys. **23**, 1997 (1955).
10. J. M. ROBERTSON and I. WOODWARD. Proc. Roy. Soc. London, Ser. A, **164**, 436 (1938).
11. W. S. WILCOX, C. V. STEPHENSON, and W. C. COBURN. Wright Air Development Division (U.S.A.), Tech. Rept. 60-333, May, 1960.
12. D. STEELE, E. R. LIPPINCOTT, and J. XAVIER. J. Chem. Phys. **33**, 1242 (1960). T. R. NANNEY, R. T. BAILEY, and E. R. LIPPINCOTT. Spectrochim. Acta, **21**, 1495 (1965). T. R. NANNEY, E. R. LIPPINCOTT, and J. C. HAMER. Spectrochim. Acta, **22**, 737 (1966).
13. N. FUSON, C. GARRISON-LAGRANGE, and M. L. JOSIEN. Spectrochim. Acta, **16**, 106 (1960).
14. R. J. JAKOBSEN. Spectrochim. Acta, **21**, 127 (1965).
15. J. C. EVANS and R. A. NYQUIST. Spectrochim. Acta, **16**, 918 (1960).
16. J. R. SCHERER. Spectrochim. Acta, **20**, 345 (1964); **21**, 321 (1965); **24A**, 747 (1968).
17. H. SUZUKI. Bull. Chem. Soc. Japan, **33**, 389, 944 (1960).
18. P. R. GRIFFITH and H. W. THOMPSON. Proc. Roy. Soc. London, Ser. A, **298**, 51 (1967).
19. D. A. DOWS. Physics and chemistry of the organic solid state. *Edited by* D. Fox, M. M. Labes, and A. Weissberger. John Wiley and Sons, Inc., New York. 1963 and 1965. Vol. 1, Chap. 11 and Vol. 2, p. 881.
20. A. KIMOTO and H. YAMADA. Bull. Chem. Soc. Japan, **40**, 243 (1967). T. L. BROWN. J. Chem. Phys. **43**, 2780 (1965).

Can. J. Chem. Downloaded from www.nrcresearchpress.com by 210.87.254.5 on 09/05/12
For personal use only.

Infrared spectra of *trans*-1,2-diphenylethylene and *trans*-1,2-diphenylethylene-d_{12}[1]

CESARE PECILE AND BRUNO LUNELLI
Institute of Physical Chemistry, The University, Padua, Italy

Received April 26, 1968

The location of the infrared active fundamentals of *trans*-1,2-diphenylethylene and *trans*-1,2-diphenylethylene-d_{12} are discussed on the evidence given by the absorption spectra measured in the 4000–33 cm^{-1} region for solid and solution samples. This assignment is consistent with that reported in the preceding article for diphenylethine and fits the correlative scheme offered by the monosubstituted benzenes in the case of the light as well as of the heavy compound.

The polarized spectra of single crystals, (001) crystal plane, allowed examination of the dichroic behavior of the bands corresponding to planar vibrations for which no prediction is possible on the basis of the overall C_{2h} symmetry. The local symmetry C_{2v} of the aromatic fragment is not observed to prevail in such a complete and satisfactory way as to indicate the presence of an empirical polarization specificity, even though to some extent, particularly in the case of the a_1 modes of the phenyl ring, there is coincidence between the polarization observed and that predicted on the basis of the local symmetry.

Canadian Journal of Chemistry, 47, 243 (1969)

Can. J. Chem. Downloaded from www.nrcresearchpress.com by 210.87.254.42 on 09/05/12
For personal use only.

Introduction

The use of polarization specificity greatly increases the amount of structural information which can be obtained from vibrational spectra of molecular crystals. The vibrational modes of isolated polyatomic molecules have the property of polarization specificity if they satisfy some basic conditions recently stated by Sverdlov (1). To exploit this property most readily, single crystals in which the molecules are ordinately oriented should be used, allowing measurement of the dichroic ratios.

However, the intensity changes which are observed to occur upon condensation and the deviations of the dichroism from the oriented gas model predictions (2) clearly indicate that the crystal field can strongly affect infrared band intensity and dichroism of the free molecule.

These still obscure facts (2) make it difficult to exploit the potential polarization specificity; therefore, a collection of empirical evidence of the existence of the specificity for molecular fragments characterized by group frequencies can offer a basis for theoretical progress and wider practical utilization of dichroic ratios. Molecules containing the phenyl group appear suitable for this empirical test.

The reported study of diphenylethine (3) has indicated that the phenyl group vibrations display frequency specificity both in the light and heavy compound, but several well-identified deviations from the predicted dichroism occur, specially in the case of the out-of-plane modes. Crystalline *trans*-1,2-diphenylethylene (stilbene) (4) is isostructural with diphenylethine (tolane) (5), a fact which allows the prediction of similar crystal field effects in the crystal spectra. The molecular symmetry of stilbene (C_{2h}) being different from that of tolane (D_{2h}), the direction of stilbene transition moments in the molecular plane is not fixed by symmetry.

In this paper we examine the infrared spectra of stilbene and stilbene-d_{12} in order to get an improved assignment which allows us to ascertain whether the empirical dichroic behavior of phenyl ring group vibrations in the spectra is determined by its local symmetry C_{2v} or by the C_{2h} symmetry of the whole molecule.

Infrared spectra (6, 7) and a partial Raman spectrum (8) of light stilbene have been reported previously.

Experimental

The stilbene used (m.p. 124 °C, corr.) was a reagent-grade product, purified by repeated crystallization from ethanol. The stilbene-d_{12} was obtained by allowing stilbene (1 g) to exchange (48 h at 300 °C) with calcium deuteroxide (10 g) in a Carius tube and repeating this procedure six times (9). The final product, purified by crystallization, gave an infrared spectrum which appeared to be identical with that of commercial stilbene-d_{12} of well-known isotopic composition[2]. Later, we exchanged stilbene with NaOD supported on $Ca(OD)_2$. We started with stilbene (300 mg), sodium (230 mg), calcium oxide (7 g), and deuterium oxide (2.4 ml) and used the method

[1]This work was supported in part by the Chemistry Committee, National Research Council of Italy.

[2]Source: Merck, Sharp and Dohme of Canada, Ltd.; mass spectral analysis: stilbene-d_{12}, 76.09%; -d_{11}, 18.77%; -d_{10}, 4.73%; -d_9, 0.38%; -d_8, 0.03%; overall deuterium percentage, 97.2%.

TABLE I

Symmetry classes and selection rules for *trans*-1,2-diphenylethylene as a free molecule and in the crystalline state

Molecular symmetry C_{2h}		Site symmetry C_i	Factor group symmetry C_{2h}	
Species and activity*	Degrees of freedom		Species and activity*	Degrees of freedom
a_g (R, p)	$25(\nu_1-\nu_{25})$	a_g (R, p)	a_g (R, p)	78 (6 torsional)
b_g (R, dp)	$11(\nu_{38}-\nu_{48})$		b_g (R, dp)	78 (6 torsional)
a_u (i.r.)	$12(\nu_{26}-\nu_{37})$	a_u (i.r.)	a_u (i.r.)	78 (5 translational)+T_b
b_u (i.r.)	$24(\nu_{49}-\nu_{72})$		b_u (i.r.)	78 (4 translational)+$T_{a,c}$

*R = Raman, i.r. = infrared, p = polarized, dp = depolarized.

reported for the preparation of biphenylene-d_8 (10). Four exchanges under the same conditions gave 110 mg of pure stilbene (m.p. 124 °C, corr.). Its isotopic purity was estimated to be better than that of the sample obtained with the first method, as shown by the much weaker infrared absorptions in the CH stretching region. The series of spectra of the products of successive exchanges allowed the identification, in the spectrum of the final deuterated compound, of some weak bands which can be attributed to partially deuterated stilbenes.

Single crystals of stilbene and stilbene-d_{12}, in the form of thin sheets, were prepared by slow sublimation at about 110 °C, under atmospheric pressure. The sheet plane was shown by X-ray analysis to contain the *a* and *b* crystal axes. In the polycrystalline oriented films, obtained by slow cooling of the melt between KBr plates, the same crystal plane is developed.

The methods used to measure the standard and polarized spectra are the same as reported in the preceding work (3).

Selection Rules

Stilbene (Fig. 1) crystallizes in the monoclinic system (4), space group $C_{2h}{}^5$–$P2_1/a$. In the unit cell there are four molecules distributed into two crystallographically independent sets. Each set consists of two molecules, which lie on inversion centers. The projection of the crystal structure on (001) is shown in Fig. 2. In the crystal the molecules are planar[3] and belong to the C_{2h} point group. Molecular axes have been chosen (Fig. 1) as in the previous study of tolane (3) in order to keep the same reference system for the phenyl group vibrations.

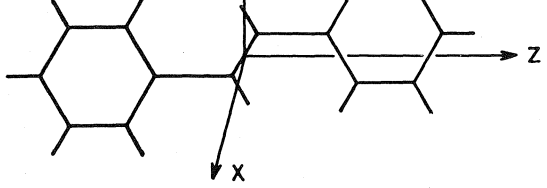

FIG. 1. Molecular structure and choice of molecular axes for *trans*-1,2-diphenylethylene, $C_{14}H_{12}$.

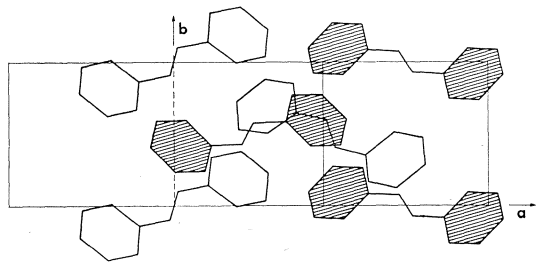

FIG. 2. Projection of the crystal structure of *trans*-1,2-diphenylethylene on (001). Shaded molecules belong to one of the two crystallographically independent sets.

The selection rules for the molecular point group C_{2h}, the site symmetry C_i, and the factor group C_{2h} are reported in Table I. The normal modes of the isolated molecule of a_u and b_u species are infrared active, while those of a_g and b_g species are Raman active. For the isolated molecule the transition moments of the a_u vibrations have the direction of the normal molecular axis *X* and those of the b_u vibrations are localized in the *YZ* molecular plane.

By using the X-ray data (4) we calculated the direction cosines of molecular axes with respect to crystal axes. Their squared values are reported

[3]A slight deviation from planarity was observed (4) for molecules belonging to one of the two independent sets.

Can. J. Chem. Downloaded from www.nrcresearchpress.com by 210.87.254.42 on 09/05/12
For personal use only.

Can. J. Chem. Downloaded from www.nrcresearchpress.com by 210.87.254.42 on 09/05/12
For personal use only.

in Table II. Since here, as in the case of tolane (3), the orientation of the molecules is such that the figures in Table II are almost equal for both sets, the two sets need no separate consideration. In the oriented gas approximation the figures in Table II (first column) represent the proportionality factors for absorption intensity of a_u molecular vibrations. The corresponding bands in the spectra of the (001) crystal plane should prove almost unpolarized. The b_u transition moments lie on the molecular YZ plane, but since their direction is not further fixed by symmetry no prediction can be made of their dichroic behavior and consequently the polarized spectra may be extremely difficult to interpret.

TABLE II

Squared values of direction cosines of molecular axes X, Y, Z, with respect to the crystal axes a, b, c^*

Crystal axis	Set I molecules			Set II molecules		
	X	Y	Z	X	Y	Z
a	0.13	0.18	0.70	0.18	0.09	0.72
b	0.30	0.67	0.03	0.30	0.70	0.00
c^* ($\perp ab$)	0.57	0.15	0.27	0.52	0.21	0.28

By assuming the local symmetry C_{2v} for the phenyl groups the polarization of the corresponding group modes can be predicted. The vibrations with transition moment along the X molecular axis (Fig. 1) are thus of b_2 type and should have the same dichroic ratio as the a_u modes of the whole molecule, being almost unpolarized upon examination of the (001) crystal plane. The vibrations of local symmetry a_1 have a transition moment directed along the Z molecular axis and the corresponding bands should display strong absorption when the electric vector is perpendicular and weak when it is parallel to the b crystal axis (perpendicular bands). The transition moment of the vibrations of local symmetry b_1 is directed along the Y molecular axis; therefore, the corresponding bands should display the reverse pattern (parallel bands).

Results and Vibrational Assignment

Figures 3 and 4 show the polarized spectra of single crystals, (001) plane, of stilbene and stilbene-d_{12}. The absorption frequencies, relative intensities, and type of polarization are reported in Tables III and IV.

For stilbene as for tolane (3), examination of the spectra reveals that most frequencies are in the positions indicated by phenyl ring assignments; therefore, the interpretative scheme is mainly based on phenyl group vibrations (11, 12). Two experimental features must be pointed out: the close resemblance between solution and crystal spectra, which might suggest planar structure in solution[4], and the slightness of correlation crystal field splittings.

The Raman spectra which we have found in the literature (8) are not extensive enough to allow a more complete and conclusive interpretation of the infrared spectra. As in the case of tolane, the Raman and infrared frequencies coincide to a great extent.

Vibrations of a_u Species

As we noted above, the phenyl ring frequencies coincide closely with the spectral pattern of stilbene and stilbene-d_{12}. Thus, application of a correlative scheme based on the assignments of monosubstituted benzenes allows ample interpretation of the spectra by using the parallelism with the modes of the phenyl ring in terms of its local symmetry C_{2v}. In this way the modes corresponding to the four b_2 X-insensitive and to one b_2 X-sensitive fundamentals can be rather safely assigned in the spectra of both stilbene and stilbene-d_{12} and need no further comments than those given on the analogous vibrations of tolane (3). The lowest frequency b_2 X-sensitive mode is left unassigned because we did not examine in solution (see Experimental) the spectral region below 200 cm^{-1} where it is presumably located (11). The three vibrations corresponding to the a_2 phenyl ring modes are easily sorted out from the spectra by comparison with the assignments of the a_2 Raman active modes of monosubstituted benzenes (11).

The very strong bands at 966 cm^{-1} in stilbene and 715 cm^{-1} in stilbene-d_{12} are characteristic of the *trans*-1,2-disubstituted ethylene structure of stilbene. Their frequency values are in close agreement with the well-known data on the CH/CD out-of-plane bending of *trans*-1,2-disubstituted ethylenes (14). The remaining two modes, which can be approximately described as skeletal deformations, can be only tentatively associated with the absorptions at 419 and 275

[4]Electronic spectra give the same indication (13).

Can. J. Chem. Downloaded from www.nrcresearchpress.com by 210.87.254.42 on 09/05/12
For personal use only.

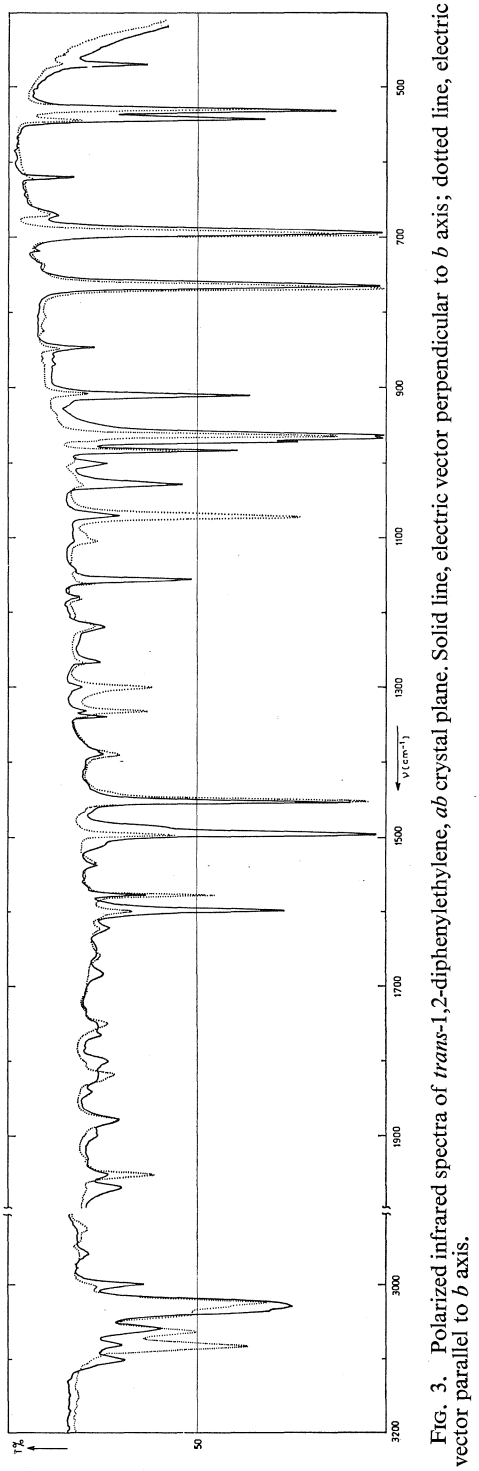

FIG. 3. Polarized infrared spectra of *trans*-1,2-diphenylethylene, *ab* crystal plane. Solid line, electric vector perpendicular to *b* axis; dotted line, electric vector parallel to *b* axis.

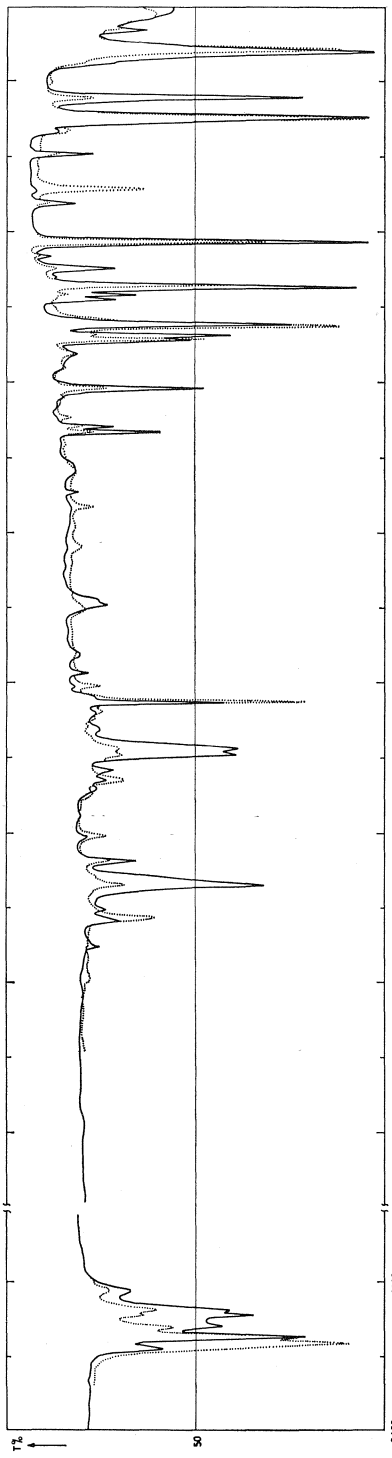

FIG. 4. Polarized infrared spectra of *trans*-1,2-diphenylethylene-d_{12}, *ab* crystal plane. Solid line, electric vector perpendicular to *b* axis; dotted line, electric vector parallel to *b* axis.

TABLE III

Infrared spectrum of *trans*-1,2-diphenylethylene

Crystal			Solution		Crystal			Solution	
	Intensity[b,c]					Intensity[b,c]			
Frequency[a] (cm^{-1})	⊥ to *b*	∥ to *b*	Frequency (cm^{-1})	Intensity[b,d]	Frequency[a] (cm^{-1})	⊥ to *b*	∥ to *b*	Frequency (cm^{-1})	Intensity[b,d]
			233	w	1300		25	1303[e]	
			275	w	1332		25	1328	5
			403	w	1339	10	0	1337	5
			419	w	1390	10	15	1382	
469	35		495[e]		{1451		370	1452	170
{527		110	526		{1453	220			
{529	(185)				1485 sh			1488 sh	
541	(105)	15	539		1496	360	35	1497	225
620	15		622		1510 sh			1506 sh	
			628		1535	0	+		
{692	560		691[f]	750	1539	+	0		
{694		570			1577	20	50	1580	25
738	≃	≃	734	20	1599	100	15	1601	100
{763	475		760	730	1622	+	−		
{766		620			1655	+	0		
824	−	+	834	5	1660	0	+		
848	15		848		1684	+	0	1673	
{908		10	909[e]	10	1700	−	+	1693	
{910	85				1750		10	1742	5
962	440		961	375				1754 sh	
963		180			1766	+	0		
966	570	0			1800	5	0	1796	(10)
972	+	−			1817		10	1808	(10)
985	65	50	982	50	1842	+	0	1830	
1002	10	0	1000 sh		1878	10	15	1873	(10)
1030	40		1031	45	1897	+	0	1887	(5)
1073	15	120	1072	60	1950	5	30	1942	15
1099 sh					1968	10	0	1960	10
1106	0	5	1102		2960	+	0	2956[e]	
1156	45		1156	5	2998	20		3004 sh	
1163		10			3022		(85)		
{1180	+	0	1181		3028	(105)		3030	155
{1183	0	+			3034 sh				
1220	10	5	1215	5	3057	20			
			1234[f]		3062		30	3063	(60)
			1259		3080	10	60	3084	(55)
{1266	10	0	1266	(5)	3100	0	0	3100 sh	
{1268	0	+							

[a]Bracketed frequency doublets have correlation crystal field origin.
[b]Intensity values were not corrected for band overlap. Values in parentheses refer to cases in which the overlapping is quite strong.
[c]Intensity expressed as peak absorbance, relative to a value of 100 assumed for the perpendicular component at 1599 cm^{-1}. The resulting values are rounded off to the next multiple of five. The marks +, −, 0, ≃ indicate the intensity of the parallel and perpendicular component of the weak bands; sh, shoulder.
[d]Intensity expressed as peak extinction coefficient ($mole^{-1}$ l cm^{-1}) relative to a value of 100 assumed for the band at 1601 cm^{-1}. The resulting values are rounded off to the next multiple of five; sh, shoulder; w, weak.
[e]Solution in carbon tetrachloride.
[f]Solution in carbon disulfide.

cm^{-1} in stilbene and with the absorption at 410 cm^{-1} in stilbene-d_{12} spectra. The dichroic pattern observed for the bands (above 400 cm^{-1}) due to the a_u fundamentals is in many cases rather different from the slightly parallel character predicted for the modes of this class. The polarization of the absorptions, similar to the phenyl ring b_2 vibrations and comparable to the b_{3u} out-of-plane modes of tolane, shows the same trend and the same deviations already discussed in that case (3).

Vibrations of b_u Species

Regarding the phenyl ring frequency location, we adopted the same criteria used for tolane (3) and the results, listed in Table V, do not require further detailed comment.

The structure of *trans*-1,2-disubstituted ethylene of stilbene justifies the assignment at 1300 and at 1068 cm^{-1} of the ethylenic CH and CD bending vibrations respectively (14). The last fundamental to be considered is a skeletal deformation involving the ethylenic bridge.

Can. J. Chem. Downloaded from www.nrcresearchpress.com by 210.87.254.42 on 09/05/12
For personal use only.

TABLE IV

Infrared spectrum of *trans*-1,2-diphenylethylene-d_{12}

Crystal			Solution		Crystal			Solution	
	Intensity[b,c]					Intensity[b,c]			
Frequency[a] (cm^{-1})	⊥ to b	∥ to b	Frequency (cm^{-1})	Intensity[b,d]	Frequency[a] (cm^{-1})	⊥ to b	∥ to b	Frequency (cm^{-1})	Intensity[b,d]
			353	w	1068	0	10	1063	
			410	w	1120	−	+		
433	15	0	435 sh		1190	+	−		
{459		215	458	750	1198	15	5	1196	10
{462	390				1264	+	−	1257	5
521	160	15	519	140	1287	+	−	1285	10
{546	355		545	770	1305 P	0	10	1303	
{549		320			1327	70	150	1326	40
595	20	10	596	10	1388	(50)	(10)	1385 sh	
644	0	40	642	55	1396	(50)	(10)	1395	140
661	15		650 sh		1416	10	0	1419 sh	
715	350	115	710	335	1432	5	15	1422	25
733	+	−	723		1443	≃	≃	1438	5
749	30	5	748		1506		10	1499	10
{773		85	774		1537	20	10	1537	
{775	280				1559 sh				
784 P	25	3	785		1565 sh				
791	20	0			1570	100	15	1568	100
824	140		824	140	1602	+	0	1574 sh	
827		215			1613		30	1610	25
838	(80)	0			1617	10			
844	(60)	60	841	130	2209	10	5	2210	10
863	≃	≃			2232	(40)	(20)		
882 sh			885 sh		2240	(55)	(10)	2238	65
908 P	60	15	904	30	2255	(30)			
959	15	10	944		2257		10	2256	
966 P	35	10	960	25	2270	90	(90)		
			1003		2278	0	155	2280	(165)
1015	5		1020	5	2287	15		2290	(120)
1048	+	−	1048	5					

[a]Bracketed frequency doublets have correlation crystal field origin; P indicates bands probably due to partially deuterated stilbenes (see text).
[b]Intensity values were not corrected for band overlap. Values in parentheses refer to cases in which the overlapping is quite strong.
[c]Intensity expressed as peak absorbance, relative to a value of 100 assumed for the perpendicular component at 1570 cm^{-1}. The resulting values are rounded off to the next multiple of five. The marks +, −, 0, ≃ indicate the intensity of the parallel and perpendicular component of the weak bands; sh, shoulder.
[d]Intensity expressed as peak extinction coefficient ($mole^{-1}$ l cm^{-1}) relative to a value of 100 assumed for the band at 1568 cm^{-1}. The resulting values are rounded off to the next multiple of five; sh, shoulder; w, weak.
[e]Solution in carbon tetrachloride.
[f]Solution in carbon disulfide.

Taking into account fluorescence studies (15), which indicate the presence of a symmetric planar skeletal bending mode at 212 cm^{-1}, we propose the assignment of the band observed at 233 cm^{-1} in light stilbene to the infrared active asymmetric analogue of this vibration.

The unpredictable dichroism of b_u modes has been discussed above, together with the behavior which can be inferred for X-insensitive phenyl ring fundamentals by using the local symmetry of the aromatic fragment. If there is polarization specificity, the local symmetry will prevail and the modes corresponding to the vibrations of a_1 species of the phenyl fragment should display perpendicular polarization, while those corresponding to b_1 species should be parallel. Careful inspection of the spectra shows that all a_1 fundamentals, both in the light and heavy compounds, fit the expected dichroic behavior. On the other hand, the dichroism of the bands due to vibrations of the b_1 class is often anomalous (see Tables III and IV).

Conclusion

The proposed assignment for infrared active fundamentals of stilbene and stilbene-d_{12} is summarized in Table V. This assignment is supported by the new experimental information obtained from the spectra of stilbene-d_{12} and from the polarized light spectra of well-identified crystal planes of both the light and heavy compounds. The frequency values of the fundamentals

Can. J. Chem. Downloaded from www.nrcresearchpress.com by 210.87.254.42 on 09/05/12
For personal use only.

Can. J. Chem. Downloaded from www.nrcresearchpress.com by 210.87.254.42 on 09/05/12
For personal use only.

TABLE V

Vibrational assignment of infrared active fundamentals[a] of *trans*-1,2-diphenylethylene and *trans*-1,2-diphenylethylene-d_{12}

Symmetry species	$C_{14}H_{12}$	$C_{14}D_{12}$	Approximate description[b,c]	
a_u	985	(820)	CH bend.	b_2
	972	791	CH bend.	a_2
	966	715	CH_e bend.	
	909[d]	774[d]	CH bend.	b_2
	848	661	CH bend.	a_2
	764[d]	547[d]	CH bend.	b_2
	693[d]	644	Ring def.	b_2
	529[d]	461[d]	Skeletal def.	b_2Xs
	419	410	Skeletal def.	
	403	353	Skeletal def.	a_2
	275	...	Skeletal def.	
	...	...	Skeletal def.	b_2Xs
b_u	3100	2287	CH stretch.	a_1
	3080	2278	CH stretch.	b_1
	3062	(2260)	CH stretch.	b_1
	3057	2255	CH stretch.	a_1
	3034	2240	CH stretch.	a_1
	3022	2270	CH_e stretch.	
	1599	1570	Ring stretch.	a_1
	1577	1537	Ring stretch.	b_1
	1496	1396	Ring stretch.	a_1
	1452[d]	1327	Ring stretch.	b_1
	1332	1048	CH bend.	b_1
	1300	1068	CH_e bend.	
	1267[d]	1264	Ring stretch.	b_1
	1220	1120	Skeletal stretch.	a_1Xs
	1181[d]	844	CH bend.	b_1
	1156	838	CH bend.	a_1
	1073	826[d]	CH bend.	b_1
	1030	(820)	CH bend.	a_1
	1002	959	Ring breathing	a_1
	(848)	749	Skeletal def.	a_1Xs
	620	595	Ring def.	b_1
	541	521	Skeletal def.	a_1Xs
	469	433	Skeletal def.	b_1Xs
	233	...	Skeletal def.	

[a]Frequency values (cm^{-1}) observed in the spectra of oriented crystals. Bracketed values correspond to bands assumed to be strongly overlapped by other absorptions.

[b]As a consequence of the correspondence, used throughout the discussion, between stilbene and monosubstituted benzenes vibrations, the approximate descriptions given are inferred from the results of calculations reported for C_6H_5Cl. The assignment of the frequencies of $C_{14}H_{12}$ and $C_{14}D_{12}$ has been guided by the inspection of the atomic displacements in C_6H_5Cl and C_6D_5Cl normal vibrations. For the correct descriptions of normal vibrations of both C_6H_5Cl and C_6D_5Cl in terms of potential energy distribution, the original literature should be consulted (12).

[c]a_1, b_1, and b_2 are the symmetry species of the group vibrations of the phenyl rings under the local symmetry C_{2v}; Xs, substituent sensitive modes.

[d]Average value of the frequencies observed in the crystal spectra for bands presenting correlation field splitting.

which can be related to group vibrational modes of the monosubstituted benzenes have been localized without difficulty in nearly all the cases according to (and within the same limits of) the reported assignments of monohalogenobenzenes and their fully deuterated analogues.

The principal aim of the present study, as emphasized in the Introduction, is the ascertainment of empirical polarization specificity for those fundamentals which display frequency specificity and whose transition moment direction can be known only when the C_{2v} local symmetry of the phenyl fragment is used. The results show that, though all a_1 and a few b_1 band polarizations match the requirements for polarization specificity, the general dichroic trend is not sufficiently uniform to indicate the existence of reliable polarization specificity. This partially erratic dichroism goes beyond the anomalies observed in the case of tolane, anomalies which would not alone affect the exploitation of an existing polarization specificity.

The qualitative dichroic trend in stilbene is very similar to that reported by Daasch (16) for *trans*-azobenzene. However, we consider it untimely to draw analogous conclusions, since, even if the experimental polarization specificity were sufficiently established, the quantitative dichroic ratios are to some extent unreliable because of the instrumental errors and the influence of the solid state on the band intensity.

Acknowledgments

The authors wish to express their appreciation to Professor S. Califano for originally suggesting the present study, and to thank Dr. A. Dal Pra' for the X-ray analysis of the crystals.

1. L. M. SVERDLOV. Opt. Spectry. USSR, English Transl. **9**, 353 (1960).
2. D. A. DOWS. *In* Physics and chemistry of the organic solid state. *Edited by* D. FOX, M. M. Labes, and A. Weissberger. John Wiley and Sons, Inc., New York. 1963 and 1965. Vol. 1. Chap. 11 and Vol. 2, p. 881. A. KIMOTO and H. YAMADA. Bull. Chem. Soc. Japan, **40**, 243 (1967).
3. C. PECILE and B. LUNELLI. Can. J. Chem. This Issue.
4. J. M. ROBERTSON and I. WOODWARD. Proc. Roy. Soc. London, Ser. A, **162**, 568 (1937).
5. J. M. ROBERTSON and I. WOODWARD. Proc. Roy. Soc. London, Ser. A, **164**, 436 (1938).
6. R. MECKE and E. GREINACHER. Z. Elektrochem. **61**, 530 (1957).
7. M. P. LISITSA, I. N. KHALIMONOVA, and N. P. KHARCHENKO. Ukr. Fiz. Zh. **9**, 53 (1964).
8. A. DADIEU and K. V. F. KOHLRAUSCH. Monatsh. Chem. **60**, 221 (1932). R. GASE, W. LOHMANN, and M. SCHUBERT. Z. Physik. Chem. Leipzig, **223**, 43 (1963).
9. L. H. P. WELDON and C. L. WILSON. J. Chem. Soc. 244 (1946). E. R. LIPPINCOTT and R. D. NELSON. Spectrochim. Acta, **10**, 307 (1958).
10. B. LUNELLI and C. PECILE. Can. J. Chem. **46**, 391 (1968).

11. D. STEELE, E. R. LIPPINCOTT, and J. XAVIER. J. Chem. Phys. **33**, 1242 (1960). R. J. JACOBSEN. Spectrochim. Acta, **21**, 127 (1965). T. R. NANNEY, R. T. BAYLEY, and E. R. LIPPINCOTT. Spectrochim. Acta, **21**, 1495 (1965). T. R. NANNEY, E. R. LIPPINCOTT, and J. C. HAMER. Spectrochim. Acta, **22**, 737 (1966). N. FUSON, C. GARRIGOU-LAGRANGE, and M. L. JOSIEN. Spectrochim. Acta, **16**, 106 (1960).
12. J. R. SCHERER. Spectrochim. Acta, **20**, 345 (1964); **21**, 321 (1965); **24A**, 167 (1968).
13. H. SUZUKI. Bull. Chem. Soc. Japan, **33**, 379 (1960).
14. J. T. SHIMOZAWA and M. K. WILSON. Spectrochim. Acta, **22**, 1599 (1966), and references therein.
15. R. H. DUCK and D. S. MCCLURE. J. Chem. Phys. **36**, 2333 (1962).
16. L. W. DAASCH. J. Mol. Spectry. **8**, 86 (1962).

Downloaded from www.nrcresearchpress.com by 210.87.254.42 on 09/05/12
For personal use only.

Kinetics of the thermal reactions of ethylene

M. Simon and M. H. Back
Department of Chemistry, University of Ottawa, Ottawa, Canada
Received June 20, 1968

Measurements of the yields of products and the decrease in pressure as a function of time have shown the relation between the mechanisms for the thermal reactions of ethylene proposed in two separate studies, which jointly cover the range 776–924 °K and 10–600 Torr. Specifically, the measurements relate the polymerization and decomposition processes and show the dependence on temperature and pressure of the reactions proposed.

Canadian Journal of Chemistry, 47, 251 (1969)

Can. J. Chem. Downloaded from www.nrcresearchpress.com by 210.87.254.6 on 09/05/12
For personal use only.

Introduction

In two recent studies of the pyrolysis of ethylene (1, 2) a similar range and distribution of products was reported but different behavior was observed on two important aspects. As a result, two somewhat different interpretations of the mechanism of the reaction were proposed. The first study, which covered the range 798–923 °K and 10–270 Torr, reported that all products showed self-acceleration and none appeared to be formed with a non-zero initial rate. Furthermore, no changes in total pressure were observed. It was suggested that the mechanism was a degenerately branched chain reaction initiated by the breakdown of butene, one of the major products. The second study, which covered the range 776–873 °K and 150–600 Torr, reported induction periods for all products except ethane, whose yield was observed to rise linearly with time from the origin. In addition a pressure decrease was observed which was considerably in excess of that calculated from the yields of measured products. The decrease in pressure with time was an S-shaped curve. An initial rapid rate decreased to a minimum value, then increased again to a constant value, less rapid than the initial. The period of minimum rate corresponded roughly with the induction period observed for the major products. This pressure decrease was interpreted as due to a rapid radical chain polymerization and it was suggested that ethane was the only low molecular weight product of this process. The other products were suggested to arise from a slow thermal breakdown of the polymer.

The main difference in conditions between the two studies was in the range of pressure. The free radical polymerization process and the concurrent rate of formation of ethane were second order in ethylene and might therefore be expected to become less important relative to other processes as the pressure was lowered. Indeed it appeared from the results of Halstead and Quinn (1) that the decrease in pressure probably became insignificant in the neighborhood of 100 Torr and that these authors observed only the main products arising from the branched chain reaction initiated by butene. To clarify this aspect measurements of the pressure decrease have been extended to cover the range of pressures studied by Halstead and Quinn (1). At the same time some measurements of the principal products were made in the early stages of the reaction in an attempt to clarify the conditions under which an induction period is observed for the formation of ethane.

Experimental

The apparatus and analytical techniques were those described in ref. 2. Several minor improvements gave an increased precision to the results. The fluctuation in the furnace temperature was reduced to less than $\pm 0.5°$. Using a new, slightly longer (36 in.) column of the same materials, which gave somewhat better resolution, reproducibility of the product analyses was usually better than $\pm 5\%$. The purification technique for the ethylene was as described previously. For the lower pressures used in this work the yields of ethane were corrected for the ethane impurity in the ethylene (approximately 0.01 mole %). The pressure measurements were made with a Texas Instrument fused quartz spiral gauge, model 145. The gauge was provided with a digital counter. One unit in the final digit corresponded to a pressure of 0.002 Torr. This gauge was a later model than the one used in ref. 2 and also gave some improvement in precision. The temperature of the furnace was monitored during the experiments in which the pressure was measured and corrections to the pressure were made for the periodic fluctuation of the temperature. These corrections were sometimes as large as 20% of the measured ΔP. The volume of the tubing connecting the reaction vessel to the pressure gauge amounted to 4% of the volume of the reaction vessel. The correction for this dead space, which was at room temperature, was therefore 10% of ΔP at 823 °K.

Can. J. Chem. Downloaded from www.nrcresearchpress.com by 210.87.254.6 on 09/05/12
For personal use only.

Results

The pressure in the reaction vessel as a function of time is shown in Fig. 1 for three pressures at 823 °K. At 10 Torr the change in pressure was scarcely above the limit of detection of the gauge. Duplicate experiments, after correction for temperature fluctuation, showed a variation from the average of up to 5% in ΔP. All curves except those at 30 Torr (where the time taken was not sufficient) showed the S-shaped behavior which had characterized the measurements at higher pressures (2). As had been observed previously, the minimum rate occurred at longer times as the pressure was lowered.

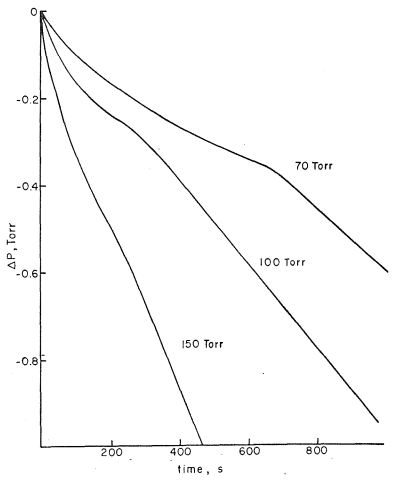

FIG. 1. Pressure as a function of time at 823 °K.

The pressure measurements are compared to the product yields in Figs. 2, 3, and 4 for three temperatures at a pressure of 100 Torr. Only the three main products, ethane, propylene, and butene are shown. The pressure decrease calculated from the yields of propylene and butene is shown for comparison with the measured ΔP. The only other product of significance at these small conversions is butadiene, inclusion of which would lower slightly the calculated ΔP curve.

In ref. 2 the rate of pressure decrease was too fast to allow a reliable measure of the initial rate. At the lower pressures studied here, however, better values could be obtained. At 823 °K and over the pressure range 30–150 Torr the order of the initial rate was 1.8. This is added support for the mechanism for the polymerization suggested in ref. 2, which predicted an order of 2.

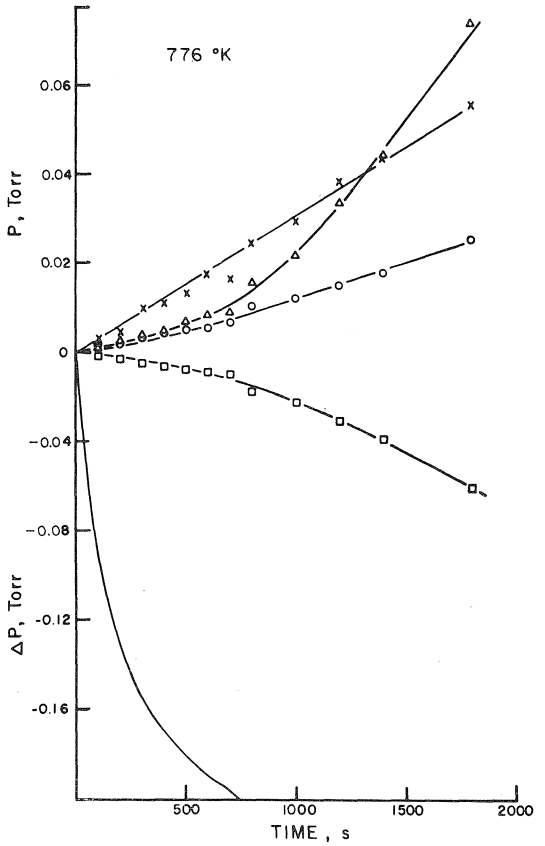

FIG. 2. Product yields and pressure as a function of time at 100 Torr: ×, ethane; △, propylene; ○, butene; □, calculated pressure decrease; and smooth curve, measured pressure decrease.

Discussion

Two points of significance are apparent from these measurements.

(1) A rapid decrease in the pressure of ethylene occurs in the initial stages of the pyrolysis without the induction period observed for most of the low molecular weight products. This decrease is readily measurable with the present techniques at pressures as low as 30 Torr, over the range of temperatures studied. Since the decrease is considerably greater than that calculated from the products measured, products of higher molecular weight than those analyzed must be formed. In ref. 2, where more extensive analysis was reported, it was estimated that these products must be of a composition corresponding to C_8 or greater.

(2) The product ethane is formed without an induction period under conditions of high

Can. J. Chem. Downloaded from www.nrcresearchpress.com by 210.87.254.6 on 09/05/12
For personal use only.

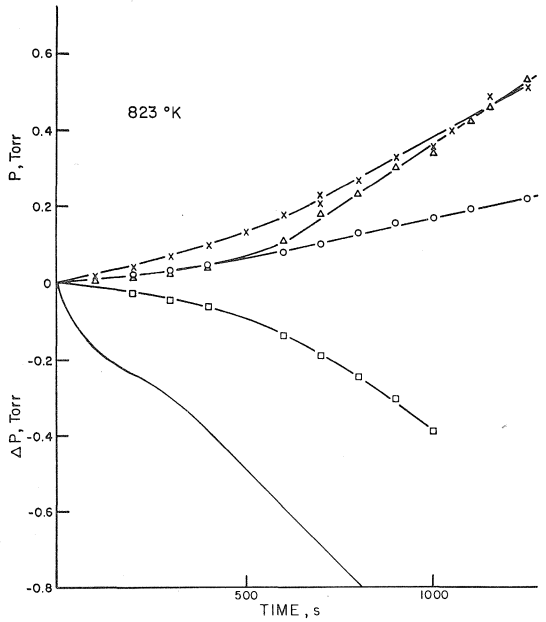

FIG. 3. Product yields and pressure as a function of time at 100 Torr: ×, ethane; △, propylene; ○, butene; □, calculated pressure decrease; and smooth curve, measured pressure decrease.

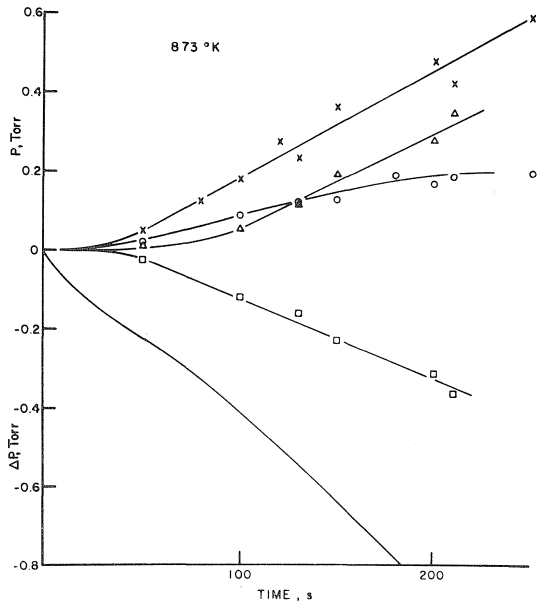

FIG. 4. Product yields and pressure as a function of time at 100 Torr: ×, ethane; △, propylene; ○, butene; □, calculated pressure decrease; and smooth curve, measured pressure decrease.

pressure and low temperature, but gradually assumes an induction period as the pressure is lowered or the temperature increased. This change in behavior is linked with the relative importance of the polymerization process. Where the polymerization is a major process the ethane yield does not show an induction period, but as the polymerization becomes relatively less important the yield of ethane also becomes very small in the initial stages. Thus the conditions of the pyrolysis in ref. 1 would give an induction period for ethane, while those of ref. 2 would tend to give a linear yield–time curve.

The general conclusion reached from these results is that the mechanisms proposed in refs. 1 and 2 are essentially complementary and one or the other becomes predominant under certain conditions of temperature and pressure. On the other hand, the measurement of the pressure decrease shows that the high molecular weight product is formed initially even at low pressures and the persistence of the S-shaped curves suggests that this polymer subsequently decomposes, possibly yielding some of the low molecular weight products.

Taking into account all the results, the following general mechanism is proposed. In the initial stages of the reaction a radical chain polymerization, initiated by the bimolecular reaction of two ethylene molecules to give a vinyl and an ethyl radical, yields a high molecular weight product and, at high pressures, measurable amounts of ethane.

$$[1] \quad C_2H_4 + C_2H_4 \rightarrow C_2H_3 + C_2H_5$$

$$[2a] \quad C_2H_5 + C_2H_4 \rightarrow C_2H_6 + C_2H_3$$

$$[2b] \quad \rightarrow C_4H_9$$

$$[3] \quad C_2H_3 + C_2H_4 \rightarrow C_4H_7$$

$$[4] \quad C_4H_7 + C_2H_4 \rightarrow C_6H_{11}$$

$$[5] \quad C_nH_{2n-1} + C_2H_4 \rightarrow C_2H_5 + C_nH_{2n-2}$$

$$[6] \quad C_nH_{2n+1} + C_2H_4 \rightarrow C_2H_5 + C_nH_{2n}$$

$$[t] \quad C_2H_5 + C_2H_5 \rightarrow C_4H_{10}$$

The assumptions underlying this type of polymerization and the kinetic parameters to be expected for the products were outlined in ref. 2. At high pressures the two primary products are a polymer and ethane. If termination occurs by the combination of ethyl radicals then butane will also be a primary product, although a minor one. Amounts of butane observed were too small to be

Can. J. Chem. Downloaded from www.nrcresearchpress.com by 210.87.254.6 on 09/05/12
For personal use only.

certain of the distinction between a primary and a secondary product.

As the pressure is lowered, reversal of the addition steps will become increasingly important, the molecular weight of the polymer will decrease, and the yield of ethane in the initial stages will also decrease. In ref. 2 it was suggested that the polymer itself decomposed giving rise to those products which were observed to have an induction period, the main ones being propylene, butene, and butadiene. The mechanism for this breakdown and formation of the products was not specified. In ref. 1 where a decrease in pressure was not observed, it was suggested that the decomposition of butene-1 initiated the branching chain reaction which produced the main products. This would be expected to occur under conditions where dissociation of radicals could compete favorably with the addition to ethylene.

The difference between the two mechanisms depends on the extent of polymerization that occurs before the dissociation of the radicals or unsaturated compounds creates an important source of radicals which in turn gives rise to the lower molecular weight products. At low temperatures and high pressures polymerization is favored and the high molecular weight unsaturated compounds would be expected to be the major source of secondary initiation. At high temperatures and low pressures, on the other hand, where higher compounds may not be formed, dissociation of butene-1 will probably be the main initiation process. It should be pointed out that although in this region the rate of formation of butene from the dissociation reaction is second order, the rate will become first order in ethylene as addition begins to compete with dissociation. Thus as the pressure is increased the polymerization process, which is second order in ethylene, will be favored.

The extent of polymerization depends not only on the relative rates of the propagation reactions—addition and decomposition—but on the relative rates of the initiation processes—the bimolecular reaction of two ethylene molecules and the dissociation of butene or higher molecular weight olefins. Using the values of Halstead and Quinn (1) for the rate constants for these initiation steps the rates of initiation were calculated at various pressures of ethylene and different extents of reaction. As the yield of butene increases during the course of the reaction, these initiation rates will eventually become equal and beyond this point the dissociation of butene will become the most important initiation step. Generally these initiation rates became equal at approximately the point in the reaction where the yield of ethane showed a rapid secondary increase in rate beyond the initial linear rise from the origin. The dissociation of butene may be the source of additional initiation which causes this increase in the rate of production of ethane. Under the conditions of the pyrolysis in ref. 2 this point in the reaction was usually well beyond the initial stages at which products were measured. Dissociation of butene may also cause the increased rate of polymerization which was observed at about the end of the induction period and it may not be necessary to suggest the formation of two types of polymers as was done in ref. 2.

The two sets of data are not in complete agreement on the conditions of temperature and pressure where the polymerization may be regarded as an important process in the initial stages of the reaction. The present data show that the decrease in pressure observed is in excess of that calculated from the products measured at a pressure as low as 30 Torr at 823 °K. Such a difference should have been observed by Halstead and Quinn (1) at least by about 70 Torr, although they did not observe a decrease in pressure even at 127 Torr. The decrease in pressure in the pyrolysis of ethylene has been measured many times and the present results are in reasonable agreement with previous measurements (3, 4), except in the shape of the initial portion of the pressure–time curve, which previous techniques were not sufficiently sensitive to detect.

Halstead and Quinn (1) also did not observe a finite initial rate of production of ethane even at 127 Torr at 823 °K, although this was observed in the present results at 100 Torr at the same temperature (Fig. 3). The cause of this discrepancy is not obvious, although we believe it is linked with the failure to observe a decrease in pressure. The rate of polymerization was independent of surface/volume ratio down to 150 Torr of ethylene (2). With good vacuum techniques the level of oxygen impurity can be kept below 1 p.p.m. and was probably not significantly different in the two systems.

An apparent disagreement between refs. 1 and 2 is the activation energy for the formation of ethane, which was 54.1 kcal/mole in ref. 1 but

42 kcal/mole in ref. 2. The difference is explained by the fact that the measurements refer to different stages of the reaction. Those of ref. 2 were the measurements of the ethane formed without an induction period, while in ref. 1 the measurements were made where the rate of formation increased with time. The activation energy for the rate of formation of butane was reported as 69.5 kcal/mole in ref. 1 and 70 kcal/mole in ref. 2. In each case butane was suggested to be formed from the termination step in the chain reaction so that the activation energy for formation of butane should equal that of the initiation. In ref. 1 the initiation was suggested to be the dissociation of butene, while in ref. 2 initiation by reaction [1] was postulated. The endothermicities of these steps are not sufficiently different that the measured activation energy would favor the occurrence of one over the other. In any case as already discussed there is probably a change from one initiation step to the other as the pressure is lowered.

Acknowledgment

The authors thank the National Research Council of Canada for continued financial assistance.

1. M. P. HALSTEAD and C. P. QUINN. Trans. Faraday Soc. **64**, 103 (1968).
2. M. L. BOYD, T. M. WU, and M. H. BACK. Can. J. Chem. **46**, 2415 (1968).
3. M. J. MOLERA and F. J. STUBBS. J. Chem. Soc. 381 (1965).
4. M. TANIEWSKI. Proc. Roy. Soc. London, Ser. A, **265**, 519 (1962).

Can. J. Chem. Downloaded from www.nrcresearchpress.com by 210.87.254.6 on 09/05/12
For personal use only.

Infrared spectra of photodimers of anthracene, benzo[*a*]anthracene, and tetracene

SURJIT SINGH AND C. SANDORFY
Department of Chemistry, University of Montreal, Montreal, Quebec
Received June 11, 1968

Infrared spectra of the photodimers of anthracene, anthracene-d_{10}, tetracene, and benzo[*a*]anthracene are reported in the region 4000–200 cm^{-1}. An attempt is made to correlate the observed bands with the proposed structure of the anthracene dimer. The infrared spectra indicate that the dimers of benzo[*a*]anthracene and tetracene have similar structures.

Canadian Journal of Chemistry, 47, 257 (1969)

Can. J. Chem. Downloaded from www.nrcresearchpress.com by 210.87.254.105 on 09/05/12
For personal use only.

Introduction

Anthracene is known (1, 2) to form a photodimer when its deaerated solution in cyclohexane or in benzene is exposed to ultraviolet radiation. X-Ray (3) and electronic spectral (2) data show that in dianthracene the two anthracene molecules are joined at their meso positions. The top and bottom of the central rings are bent forwards and the outer rings backwards as a result of electrostatic repulsion. Mustafa and co-workers (4) prepared the dimer of benzo[*a*]anthracene and more recently Birks (5), Livingston (6), and their co-workers have reported the formation of ditetracene under similar experimental conditions. It was thought of interest to study the infrared spectra of these dimers and correlate the spectral results with the proposed structures. The infrared spectra of anthracene, benzo[*a*]anthracene, tetracene, and many other polynuclear aromatic hydrocarbons were studied by Cannon and Sutherland (7). Attempts have also been made to assign the infrared and Raman spectra of anthracene by carrying out a normal coordinate analysis (8) and polarized radiation (9) studies.

We have now prepared the photodimers of anthracene, anthracene-d_{10}, benzo[*a*]anthracene, and tetracene. The infrared spectra of these dimers are discussed using the available (7–9) assignments of monomers.

Experimental

Zone refined anthracene and anthracene-d_{10} were obtained from Dr. W. G. Schneider of the National Research Council of Canada and recrystallized pure tetracene was obtained from Professor M. S. Newman of Ohio State University, to whom our sincere thanks are due. Benzo[*a*]anthracene was purchased from Eastman Organic Chemicals. The anthracenes and tetracene were used without further purification. Benzo[*a*]anthracene was recrystallized from alcohol before use. Spectrograde benzene and cyclohexane were used without further purification. The dianthracenes were prepared by irradiating saturated cyclohexane solutions (1 g/l) of anthracene for 7 to 8 h by a Hanovia high pressure mercury–xenon arc type 6-B-1. Dimers of benzo[*a*]-anthracene and tetracene were prepared by irradiating their saturated solutions in benzene using a 1 kW tungsten lamp for 3 to 4 days. The solutions were flushed with dry nitrogen for 20–30 min before irradiating. The reactions were carried out in quartz tubes kept in Pyrex water jackets to avoid unnecessary heating of the samples. The crystalline precipitates were washed 10 to 12 times with the solvents which were used and dried in a vacuum desiccator. The ultraviolet spectra of the dimers show that di(benzo[*a*]anthracene) and ditetracene have monomer impurities which may not be more than 1%. The infrared spectra were recorded on a Perkin–Elmer 621 spectrophotometer. The samples were handled in the form of potassium bromide pellets, Nujol mulls, or solutions in 2.5 cm long cells with sodium chloride windows.

Results and Discussion

The infrared spectra of dianthracene and dianthracene-d_{20} are shown in Figs. 1 and 2. The band positions of the anthracene monomer and dimer and dianthracene-d_{20} are listed in Table I. Results from spectra taken in both KBr pellets and Nujol mulls are listed. The spectra in the C—H region were taken in saturated carbon tetrachloride and carbon disulfide solutions too.

The infrared spectrum of dianthracene shows 7 to 8 well defined bands in the C—H region (Table I). The bands are of medium or weak intensity and are observed almost at the same positions in KBr pellets and in the solution spectra. Two of the bands are considerably below the aromatic C—H stretching region (2945 and 2921 cm^{-1}). The spectra in carbon tetrachloride and carbon disulfide solutions in this region are ill defined due to strong solvent absorption.

According to the available X-ray (3) and

Can. J. Chem. Downloaded from www.nrcresearchpress.com by 210.87.254.105 on 09/05/12
For personal use only.

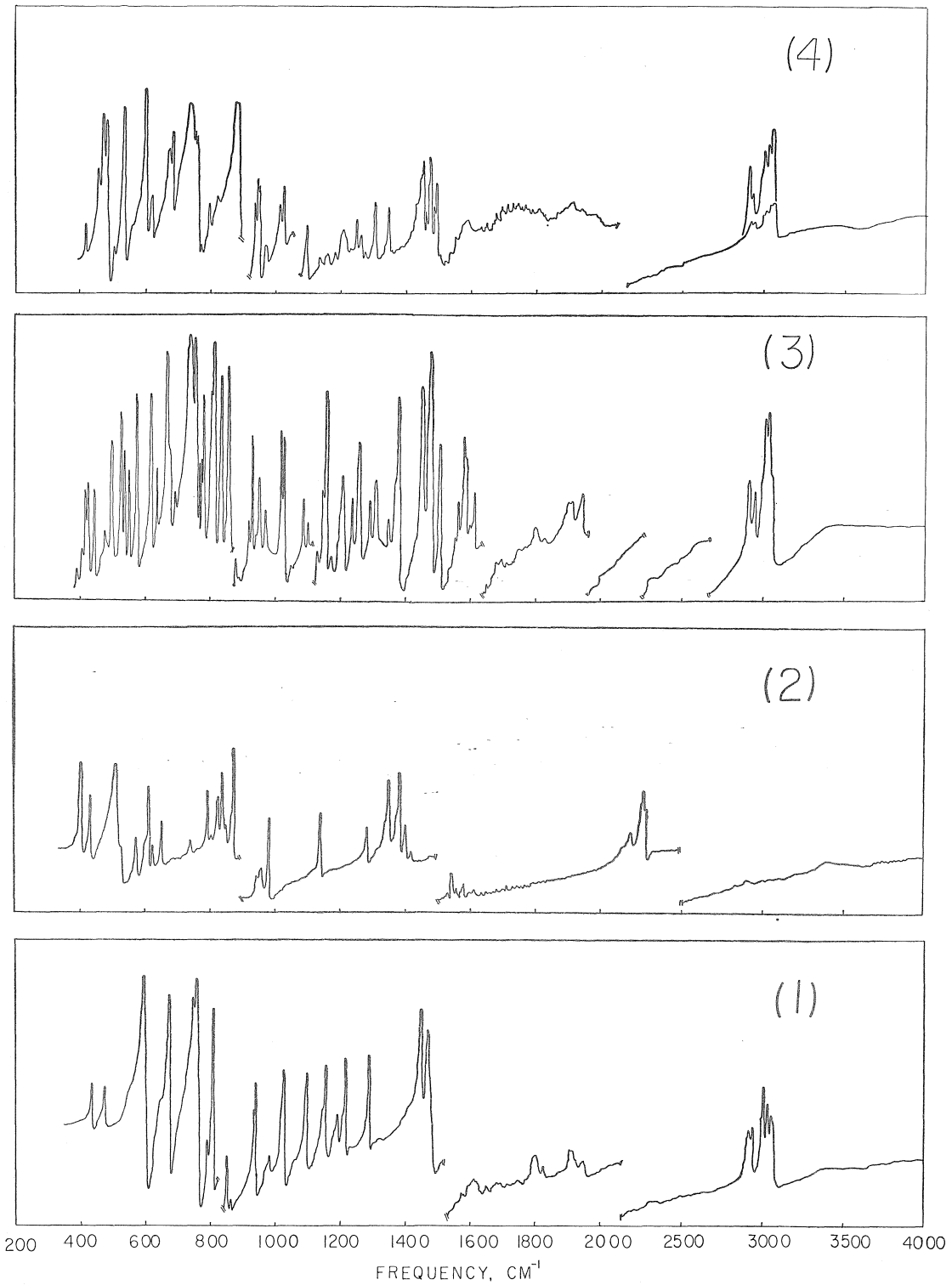

FIGS. 1–4. Infrared spectra of photodimers of (1) anthracene, (2) anthracene-d_{10}, (3) benzo[*a*]anthracene, and (4) tetracene in KBr pellet.

Can. J. Chem. Downloaded from www.nrcresearchpress.com by 210.87.254.105 on 09/05/12
For personal use only.

TABLE I

Infrared absorption bands of dianthracene and dianthracene-d_{20}*

Band positions of				
anthracene in KBr pellet	dianthracene in		dianthracene-d_{20} in	
	KBr pellet	Nujol mull†	KBr pellet	Nujol mull
		3090 vw	2290 msh	2282 msh
3100 w	3070 msh	3070 wsh	2267 m	2275 msh
3080 wsh	3059 m	3060 m	2260 msh	2265 m
	3035 m	3035 m	2255 msh	2255 msh
3045 s	3012 m	3015 m		2235 vwsh
3020 ssh	3000 msh	3000 wsh	2190 w	2190 w
	2945 m			2145 w,b
3000 msh	2921 m	2905–2940 vb,w		
	2905 wsh			
1923 m,b	1948 w	1950 vw		
	1908 w	1915 vvw,b		
	1830 vw	1830 vvw		
1800 mb	1800 w	1800 vvw		
1700 w,b		1680 vvw		
		1650 vvw	1575 vw	1572 vw
1613 w	1620 vw	1620 vvw	1545 vw	1545 vw
1560 w			1420 vw	
1520 wb	1575 vw		1402 w	1400 w
1444 m	1471 m		1385 m	1385 m
1440 msh	1465 msb		1375 msh	1365 msh
1390 w	1453 m		1351 m	1350 m
1340 w	1445 msh		1340 w,sh	1340 wsh
1310 mb			1283 m	1287 m
1265 w	1292 m	1290 m	1270 wsh	1270 wsh
1260 m	1220 m	1215 m		
1255 w	1205 wsh	1205 vw		
			1141 m	1140 m
	1195 w	1190 w	984 m	980 m
1164 m	1180 wsh	1180 vw	959 w	960 w
1144 w	1160 m	1165 msh	945 vw	945 vw
		1162 m	876 m	873 m
1122 m	1150 msh			
		1145 wsh	865 wsh	865 wsh
			850 vw	850 w
	1102 m	1100 m	845 w	840 wsh
	1095 msh	1095 wsh	838 m	837 m
995 m	1030 m	1025 m	827 w	825 w
975 w	1020 msh	1020 wsh	805 vw	805 vw
970 w	985 w	950 vw	794 m	793 m
		965 vw	739 w	740 w
950 s				
925 w	944 m	945 m		690 vw
900 m	939 m	940 w	653 m	652 m
884 s	868 w	865 w	622 w	620 w
850 m	856 w	855 wsh	611 m	608 m
		850 w	600 wsh	595 vw
	815 s	810 s	575 m	570 m
			530 wsh	
	797 w	790 w	508 s	515 vs
				490 wsh
		770 wsh		
765 vw		760 vs		
750 vw	762 vs	750 s	431 m	425 m
740 m	753 s	745 s	402 s	400 s
730 s	745 msh	735 wsh		
725 vs		675 s		
645 vw	677 s			
	665 msh			
600 m	650 msh	650 w		
560 vw	599 s	600 m		
		595 vs		
465 s	474 m	470 m		
455 s	435 m	430 m		
		340 w		
		312 w		

*v = very; w = weak; m = medium; s = strong; sh = shoulder; b = broad.
†The 3090–2905 cm^{-1} range reported is from the spectra in carbon disulfide and carbon tetrachloride solutions.

Can. J. Chem. Downloaded from www.nrcresearchpress.com by 210.87.254.105 on 09/05/12
For personal use only.

electronic spectral (2) results, the highest symmetry dianthracene can have is D_{2h}. By simple group theoretical considerations (10) using internal coordinates, the 20 C—H stretching vibrations can be shown to belong to the following symmetry species

$$\Gamma_D\nu(\text{C—H}) = 3A_g + 2B_{1g} + 2B_{2g} + 3B_{3g} + 2A_u + \underline{3B_{1u}} + \underline{3B_{2u}} + \underline{2B_{3u}}$$

B_{1u}, B_{2u}, and B_{3u} are the only infrared active species and are underlined. In the proposed structure of dianthracene (2) not all 20 protons are aromatic. Four protons in the meso positions of the monomer anthracene units become tertiary aliphatic protons. The normal vibrations due to these 4 C—H bonds can be shown to belong to the A_g, B_{3g}, $\underline{B_{1u}}$, and $\underline{B_{2u}}$ species. Thus 2 out of 4 aliphatic C—H vibrations are expected to be infrared active. The 10 C—H stretching vibrations in the anthracene monomer have similarly been shown to belong to the A_g, B_{1g}, B_{2u}, and B_{3u} species as follows:

$$\Gamma_M\nu(\text{C—H}) = 3A_g + 2B_{1g} + \underline{3B_{2u}} + \underline{2B_{3u}}$$

The 5 infrared active vibrations ($3B_{2u}$ and $2B_{3u}$) have been (8) assigned to the 5 bands appearing in the range 3100–2990 cm^{-1} in the anthracene spectrum. Based on the above arguments we assign the 2 low lying bands at 2945 and 2921 cm^{-1} to the aliphatic C—H stretching vibrations. The remaining 5 bands at 3070, 3059, 3035, 3012, and 3000 cm^{-1} can thus be assigned to the aromatic, =C—H stretching vibrations. It can be seen that in the spectrum of dianthracene-d_{20} also, though the bands are not as well resolved, the 2 groups of bands are present in the C—D stretching region. This gives additional support to the proposed structure of dianthracene.

The C—C stretching vibrations are quite weak as usual, and a detailed discussion of them is not warranted. About 10–15 bands of very weak to medium intensity are found in the region 2000 to 1300 cm^{-1}. Weak bands from 1700 to 2500 cm^{-1} are usually assigned to overtones and combinations (11).

The lower frequency region is more interesting. There are 4 very strong bands and about 10 medium strong bands in the spectrum of dianthracene in the region 1300–200 cm^{-1}. Dianthracene-d_{20} has a similar spectrum. While surveying the bands in Table I it appears that the bands at 1215, 1100, 1025, 810, and the broad band at 760 cm^{-1} with shoulders at 750 and 745 cm^{-1} in dianthracene experience an isotopic shift when compared to the spectrum of dianthracene-d_{20}. The ν(H)/ν(D) ratio varies between 1.2 and 1.4. All other bands undergo only a very slight shift, the ν(H)/ν(D) being 1.1 for the most shifted and 1.01 for the least shifted band. It can therefore be concluded that the bands with a shift of the order of 1.2 to 1.4 might belong to the C—H in-plane or out-of-plane bending vibrations and the other bands to the C—C bending motions or skeletal distortions. As can be seen from Fig. 1 the bands at 810 and 760 cm^{-1} are very strong, a characteristic of the C—H out-of-plane bending vibrations. The in-plane bendings are usually weaker. Anthracene shows 3 C—H out-of-plane bending vibrations

$$\Gamma_M\nu(\text{C—H}) = 2B_{2g} + 3B_{3g} + 2A_u + \underline{3B_{1u}}$$

at 954, 884, and 727 cm^{-1} in solutions (9). Another band at 870 cm^{-1} has been reported in the crystal spectrum (9). This is assumed to be due to an infrared inactive vibration, A_u, which is allowed by site symmetry. The dimer should have 6 infrared active vibrations due to out-of-plane aromatic C—H deformations and 2 infrared active out-of-plane aliphatic C—H deformation vibrations

$$\Gamma_D\nu(\text{C—H)Ar} = 2A_g + 2B_{1g} + 2B_{2g} + 2B_{3g} + 2A_u + \underline{2B_{1u}} + \underline{2B_{2u}} + \underline{2B_{3u}}$$

$$\Gamma_D\nu(\text{C—H)Al} = A_g + B_{3g} + \underline{B_{1u}} + \underline{B_{2u}}$$

The bands which we assign to the out-of-plane C—H deformations are quite broad and therefore too much emphasis cannot be laid on the number of bands expected and observed. The spectra can be further discussed on the basis of the conclusions reached by Cannon and Sutherland (7).

Cannon and Sutherland (7) suggested that for condensed ring systems containing 3 or more rings, bands near 750 cm^{-1} arise from C—H bonds that are approximately parallel to the longer axis of the molecule, and bands near 900 cm^{-1} arise from C—H bonds approximately perpendicular to the longer axis of the molecule. 9,10-Substitution has been found (7, 11) to remove the band at 884 cm^{-1} in anthracene. Therefore the band at 884 cm^{-1} has been attributed to the deformation vibration of the C—H bonds in the 9 and 10 positions.

Can. J. Chem. Downloaded from www.nrcresearchpress.com by 210.87.254.105 on 09/05/12
For personal use only.

In the dianthracene spectrum we do not find any band near 900 cm^{-1}. This is in line with the fact that the C—H bonds at 9,10 positions are no more aromatic. On the other hand we see a new band at 810 cm^{-1}. The 727 cm^{-1} band of anthracene also shifts to higher frequencies. The band at ~810 cm^{-1} is probably due to the aliphatic C—H out-of-plane bending vibrations. The aromatic C—H bonds of dianthracene resemble ortho disubstituted benzene C—H bonds. It is interesting to note that the C—H out-of-plane bending vibrations in ortho disubstituted benzenes have been found (11) to lie in the range 740 to 760 cm^{-1} which is certainly higher than the anthracene C—H out-of-plane deformation vibration under consideration; this explains the shift of the 727 cm^{-1} band of anthracene to higher frequencies on dimerization.

TABLE II

Infrared spectra of benzo[*a*]anthracene, monomer and dimer

Position of bands	
Monomer	Dimer
3045 m	3044 s
3030 msh	3024 s
3000 w	2958 m
	2923 m
	1949 w
1910 w	1919 w
	1905 w
	1830 vw
	1800 vw
1770 wb	
1617 w	1618 m
1604 wsh	1600 vw
1580 vw	1590 msh
1560 vw	1587 m
1540 vw	1570 m
	1513 m
1447 m	1485 s
1474 m	1457 s
1450 vw	
1420 w	
1410 w	
	1385 s
1337	1370 msh
	1353 m
	1317 m
1299 m	1298 m
1290 msh	1265 m
1276 w	1243 m
1255 vw	1215 m
1238 m	1200 msh
1224 m	
1215 wsh	
1170 w	1177 w
1150 w	1165 s
1135 w	1153 m
1127 w	1137 w
	1108 w
1090 w	1094 m
1037 m	1050 vw
1004 m	1034 m
	1025 m
954 m	976 m
944 m	958 m
	940 w
	936 m
	920 w
899 s	885 vw
884 vs	863 s
	842 s
844 m	830 s
811 vs	812 ssh
782 s	787 s
742 b,vs	780 m
	773 m
	760 vs
	744 vs,b
687 s	698 msh
646 w	680 msh
618 w	674 s
	644 m
	625 s
586 m	580 s
546 m	558 m
530 w	543 m
513 m	532 m
	503 m
472 s	477 w
423 m	449 m
	431 m
	422 m
	405 w

Infrared spectra of di(benzo[*a*]anthracene) and ditetracene are shown in Figs. 3 and 4 and the positions and relative intensities of the bands observed for the monomers and dimers have been listed in Tables II and III. Both di(benzo[*a*]-anthracene) and ditetracene are found to have bands below 3000 cm^{-1} due to the above discussed aliphatic C—H stretching vibrations. This shows that the mode of linkage in the three dimers under investigation is similar. The formation of aliphatic C—H bonds is a result of dimerization. Anthracene and benzo[*a*]anthracene on dimerization can have only 4 aliphatic C—H bonds (Fig. 5*a*, 5*b*). Ditetracene can have 4 or 8 depending on whether covalent linkage takes place at 2 centers of each tetracene molecule (Fig. 5*c*(*i*)) or 4 (Fig. 5*c*(*ii*)).

Can. J. Chem. Downloaded from www.nrcresearchpress.com by 210.87.254.105 on 09/05/12
For personal use only.

TABLE III

Infrared spectra of tetracene monomer and dimer

Position of bands	
Monomer	Dimer
3042 m	3060 m
3020 msh	3036 m,sh
	3010 m,sh
	2996 m,sh
	2936 w
	2915 m
1803 m	1900 wb
1737 w	1730 wb
1670 m	1580 wb
1624 m	
1534 m	
	1498 m,sh
	1496 m
	1490 w
1462 m	1477 m
	1470 m,sh
	1465 w
	1457 m
	1450 m,sh
	1430 m,sh
1386 m	1351 m
	1310 m
1295 s	
1289 s	1280 w
1270 m,sh	1266 w
	1253 w
	1212 wb
	1180 vw
1162 m	1160 vw
1122 m	1135 vw
	1100 w
	1031 m
	1018 m
995 m	976 w,b
957 s	955 m
929 w	950 m
900 vs	942 m
	888 sb
870 msh	826 w
792 vw	802 w
750 s	764 m,sh
738 vs	757 m,sh
	740 sb
	690 s
	680 m
625 m	625 w
607 m	606 s
575 w	540 s
558 w	508 w
	486 s
470 s	474 s
455 s	459 m
	419 w

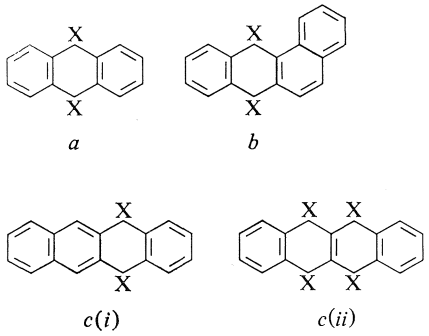

FIG. 5. Possible centers of covalent linkage in (*a*) anthracene, (*b*) benzo[*a*]anthracene, (*c*) tetracene for photodimerization.

Group theory demands 3 bands in the infrared due to aliphatic C—H stretching vibrations

$$\Gamma\nu(\text{C—H})\text{Al} = A_g + B_{1g} + B_{2g} + B_{3g} + A_u + \underline{B_{1u}} + \underline{B_{2u}} + \underline{B_{3u}}$$

if the dimer formation is through covalent linkages at 4 centers of each tetracene molecule and D_{2h} symmetry is assumed for the dimer. On the other hand if the dimerization takes place through linkages at 2 centers only, it can have either *cis* (C_{2v}) or *trans* (C_{2h}) configuration. Three out of 4 aliphatic C—H stretching vibrations are expected to be infrared active in the *cis* form ($\underline{A_1} + A_2 + \underline{B_1} + \underline{B_2}$) and 2 aliphatic stretching vibrations are expected to be infrared active in the *trans* form ($A_g + B_g + \underline{A_u} + \underline{B_u}$). Two bands appearing at 2936 and 2915 cm^{-1} can be assigned to the aliphatic C—H stretching vibrations; this makes the *trans* (C_{2h}) structure more probable than the other two structures of ditetracene.

The lower frequency part of the spectrum of di(benzo[*a*]anthracene) is quite complicated whereas that of ditetracene is comparatively simple. Tetracene has 2 strong bands at ~900 and 750 cm^{-1} which have been assigned to C—H deformation vibrations by Cannon and Sutherland (7). A strong broad band has been found in the spectrum of ditetracene at 888 cm^{-1}. Another strong band appears at 740 cm^{-1} with shoulders at 757 and 764 cm^{-1}. Two weak bands are observed at 802 and 826 cm^{-1}. It is not possible to draw any conclusion concerning the structure of ditetracene from this part of the spectrum, but the appearance of a band at 888 cm^{-1} seems to

suggest that there are aromatic C—H bonds at axes perpendicular to the longer axis of tetracene. This is in favor of the view that covalent links are formed at 2 centers of the tetracene monomers and not 4 as suggested in Fig. 5*c*(*ii*). We cannot go further without an X-ray analysis. All the spectral conclusions are confined to the spectra in solid phase because the compounds are not soluble in solvents commonly used for recording the infrared spectra in solution. But this is expected to have only a slight influence on the spectra. Raman spectra might give additional credence to the arguments.

Acknowledgment

We acknowledge financial support from the National Research Council of Canada.

1. (*a*) J. FRITZSCHE. J. Prakt. Chem. **101**, 337 (1867). (*b*) C. J. BOWEN and D. W. TANNER. Trans. Faraday Soc. **51**, 475 (1955).
2. C. A. COULSON, L. E. ORGEL, W. TAYLOR and J. WEISS. J. Chem. Soc. 2961 (1955).
3. J. HENGSTENBERG and J. PALACIOS. Anales soc. españ. fis. y quím. **30**, 5 (1932).
4. A. SCHÖNBERG, A. MUSTAFA, M. Z. BARAKAT, N. LATIF, R. MOUBASHER, and A. MUSTAFA-SAID. J. Chem. Soc. 2126 (1948).
5. J. B. BIRKS, J. H. APPLEYARD, and R. POPE. Photochem. Photobiol. **2**, 492 (1963).
6. KEI SIN WEI and R. LIVINGSTON. Photochem. Photobiol. **6**, 229 (1967).
7. C. G. CANNON and G. B. B. M. SUTHERLAND. Spectrochim. Acta, **4**, 373 (1951).
8. E. P. KRAINOV. Opt. Spectr. USSR, English Transl. **16**, 532 (1964).
9. L. COLOMBO. Spectrochim. Acta, **20**, 547 (1964).
10. F. A. COTTON. Chemical applications of group theory. Interscience Publishers, Inc., New York. 1964. p. 249.
11. R. N. JONES and C. SANDORFY. *In* Chemical applications of spectroscopy. Techniques of organic chemistry. Vol. IX. Interscience Publishers, Inc., New York. 1956.

Can. J. Chem. Downloaded from www.nrcresearchpress.com by 210.87.254.105 on 09/05/12
For personal use only.

Can. J. Chem. Downloaded from www.nrcresearchpress.com by 210.87.254.6 on 09/05/12
For personal use only.

Effect of pH and phosphate ions on the polarographic behavior of D-glucuronolactone

R. J. THIBERT AND J. R. JOHNSTON
Department of Chemistry, University of Windsor, Windsor, Ontario

Received August 12, 1968

The polarographic determination of D-glucuronolactone in aqueous solution was shown to be feasible up to a concentration of 6 mg per ml in KCl, NaCl, and LiCl with gelatin as the maximum suppressor. The effect of pH and phosphate ions on the polarographic wave of D-glucuronolactone is discussed and compared to the reaction of dialkyl hydrogen phosphites and trialkyl phosphites with β-propiolactones. The effect of pH and phosphate ions on the polarographic wave of D-glucuronic acid was also investigated.

Canadian Journal of Chemistry 47, 265 (1969)

Introduction

The polarographic determination of D-glucuronolactone has not been widely investigated. Ishidate and Shimozawa (1) attempted a polarographic study of D-glucuronic acid and D-glucuronolactone, but were unable to obtain reproducible waves for either species. Thibert and Boyle (2) were able to obtain reproducible waves with D-glucuronolactone in an unbuffered medium. The concentration range studied by them was that usually encountered in biological fluids: 0–100 μg per ml. They noted, however, that any of the standard buffers completely suppressed the wave. In particular, phosphate annihilated the wave.

It is generally assumed (3, 4) that the waves produced by lactones are caused by their reduction to the corresponding sugars

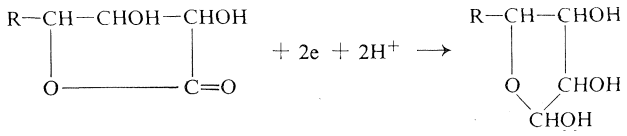

Also, polyhydroxy acids give only a hydrogen wave (4).

The study of D-glucuronolactone in aqueous medium is complicated by the lactone–acid equilibrium. A fairly concentrated solution of D-glucuronolactone took 8 weeks to reach equilibrium (20% lactone, 80% acid) at room temperature (5). In the much more dilute range in which Thibert and Boyle (2) worked, it is probable that the large excess of water causes the equilibrium to be more on the acid side, and for this equilibrium to be attained more rapidly.

Dowben (6), using 0.02 *M* D-glucuronolactone solutions (i.e., about 3.52 mg lactone per ml) and at 37 °C, observed only a slight hydrolysis (about 5%) in distilled water after 24 h; about 50% hydrolysis in 0.2 *M* Tris buffer, pH 7.2, after 24 h; but 90% hydrolysis in potassium phosphate buffer, pH 7.2, after 24 h. Thus, D-glucuronolactone was hydrolyzed about 8 times more rapidly in the Tris buffer than in distilled water, and about 40 times more rapidly in the phosphate buffer than in distilled water.

This paper presents a detailed study of pH of D-glucuronolactone solutions over a wide range of concentration, and the relationship of pH to the polarographic wave. The concentration range has been extended 60-fold relative to the results reported by Thibert and Boyle (2). The effect of changing supporting electrolytes, maximum suppressor concentration, and ionic strength is reported. Detailed experiments have been made, examining the effect of adding phosphate as $H_2PO_4^-$, HPO_4^{2-}, and PO_4^{3-}. A preliminary study has also been made with D-glucuronic acid.

Experimental

Materials

Gelatin (purified, calfskin), D-glucuronolactone, both from Eastman Organic Chemicals; D-glucuronic acid, 99% from Sigma Chemical Co.; mercury (triple-distilled) from Engelhard Industries of Canada, Ltd.; LiCl, KCl, NaCl, KH_2PO_4, K_2HPO_4, K_3PO_4, NaH_2PO_4, Na_2HPO_4,

Can. J. Chem. Downloaded from www.nrcresearchpress.com by 210.87.254.6 on 09/05/12
For personal use only.

Na_3PO_4, from Fisher Scientific Co., Ltd., were all Fisher certified reagents.

All reagents were used as received from the suppliers. Solutions were prepared using deionized distilled water in all cases. This water was obtained by passing distilled water through a column containing Rexyn I-300, Research Grade resin (a mixed bed resin).

Preparation and Storage of Stock Solutions

Stock solutions of 1 mg D-glucurono-γ-lactone per ml were prepared fresh daily and were found to be stable for at least 5 h. Stock solutions of D-glucuronic acid were prepared in a similar manner.

Gelatin was generally prepared fresh daily, although on occasion a solution was stored overnight in a refrigerator. At no time was a gelatin solution used that was more than 36 h old.

The various supporting electrolytes were prepared as 1 *M* solutions and were stored in flint bottles. It was found that upon aging, the pH of these solutions increased, affecting the unbuffered solutions which were polarographed. Therefore, the solutions were prepared in 500-ml batches, and the residue (if any) was discarded after 2 weeks.

Methods

(1) Polarographic Determination of D-*Glucuronolactone*

(a) Calibration for the range 0–100 μg D-*glucuronolactone per ml*—Ten milliliters of a 1 *M* stock solution of the supporting electrolyte (KCl, NaCl, or LiCl) were added to a 50-ml volumetric flask via a burette or pipette. Two and a half milliliters of 0.1% gelatin solution (maximum suppressor) were added via a Mohr pipette (giving a final gelatin concentration of 0.005%).

The desired amount of D-glucuronolactone was then pipetted from a stock solution of 1 mg D-glucurono-γ-lactone per ml. The solution was then diluted to volume, mixed, and a small amount was quickly transferred to the polarographic cell (an H-cell). (*NOTE*: For reproducibility, the solution to be polarographed must be prepared from the stock solution of D-glucuronolactone *just* before it is to be placed in the H-cell and deaerated, because dilute solutions tend to age rapidly at lower concentrations, and even a minute or two difference in time from one run to another can cause discrepancies.)

Nitrogen was bubbled through the solution for 5 min. During this time, the H-cell was being brought to 25 °C in a thermostat. The temperature of the thermostat was maintained at 25 ± 0.1 °C by means of a Haake thermostated circulating pump.

The nitrogen was purified by passing the gas through a gas-washing bottle containing a 1:1 ammonium hydroxide solution saturated with ammonium chloride, and containing some copper turnings. Ammonia was removed by subsequent passage through a second gas-washing bottle containing a 1 *M* sulfuric acid solution. The nitrogen was then saturated with water vapor by bubbling through two more gas-washing bottles, the first at room temperature, the second at 25 °C.

Immediately after deaeration the cell was sealed and a polarogram was then run over the voltage range −1.0 to −2.0 V, with the appropriate sensitivity setting. For this purpose the Sargent (E. H. Sargent and Co.) model XXI polarograph was used. The polarographic cell was an H-cell with a saturated calomel electrode (s.c.e.) as the reference electrode. All $E_{1/2}$ values reported are with respect to the s.c.e. The characteristics of the capillary were $m = 1.785$ mg s^{-1}, $t = 3.53$ s, $m^{2/3}t^{1/6} = 1.816$ $mg^{2/3}$ $s^{-1/2}$ at −1.48 V. All polarograms were run at 50 cm mercury. No damping was used at any time.

(b) Calibration for the range 0–1000 μg D-*glucuronolactone per ml*—The procedure was the same as (*a*), except that 3.75 ml of a 0.1% gelatin solution were added to the 50-ml flask (giving a final gelatin concentration of 0.0075%). Due to the higher range of lactone concentrations, a stock solution was not prepared. Rather, the desired amount of the lactone was weighed into a small beaker and then was transferred quantitatively to the 50-ml flask. For reproducibility, the solution to be polarographed must be prepared just before it is to be placed in the H-cell and deaerated.

Other maximum suppressors were tried using method (*b*): methyl red (0.004%), methyl orange (0.001%), methylene blue (0.001%), bromophenol blue (0.001%), Triton X-100, agar, gum tregacanth, and peptone all at 0.0075%. Gelatin was by far the most successful in suppressing the maximum.

(c) Calibration for the range of concentration ⩾1 mg D-*glucuronolactone per ml*—The procedure used was the same as procedure (*b*), except that 5.0 ml of 0.1% gelatin solution were added to the 50-ml flask (giving a final gelatin concentration of 0.01%). The solution was deaerated in the H-cell for 7 min.

(2) Polarographic Determination of D-*Glucuronic Acid*

The procedure used was exactly the same as procedure (*a*) for D-glucuronolactone. Solutions of D-glucuronic acid appear to be quite stable relative to comparable solutions of D-glucuronolactone, and thus can be prepared several minutes in advance of being placed in the H-cell.

(3) pH Measurements of D-*Glucuronolactone and* D-*Glucuronic Acid*

The desired amounts of D-glucuronolactone or D-glucuronic acid, supporting electrolyte, and gelatin were placed in a 50-ml volumetric flask as described in (*1*) and (*2*), and the appropriate type of water (deionized or boiled deionized) was used to dilute the solution to volume. Approximately 15 ml of the solution were placed in a 50-ml beaker. The beaker was put into the thermostat at 25 °C and nitrogen was bubbled through the solution via a fritted glass bubbling tube for the proper length of time as in procedure (*1*) and (*2*), depending on the concentration. At a D-glucuronolactone concentration of 80 μg per ml, the pH was adjusted with 0.01 *N* HCl or 0.01 *N* KOH; at a D-glucuronolactone concentration of 1 mg per ml, pH adjustment was made with 0.1 *N* KOH or 0.1 *N* HCl.

pH measurements were made with a Radiometer type TTT1c titrator (used as a pH meter) and a Radiometer model PHA630T scale expander. The meter was standardized with buffers of pH 4.01 (0.05 *M* potassium acid phthalate) and 6.48 (Radiometer buffer solution S1001).

(4) Addition of Phosphate

$H_2PO_4^-$, HPO_4^{2-}, and PO_4^{3-} solutions were prepared as 1 mg PO_4^{3-} per ml, or 10 mg PO_4^{3-} per ml, regardless of the cation. The desired amount of phosphate was pipetted into a 50-ml volumetric flask containing gelatin,

Can. J. Chem. Downloaded from www.nrcresearchpress.com by 210.87.254.6 on 09/05/12
For personal use only.

supporting electrolyte, and the appropriate amount of D-glucuronolactone or D-glucuronic acid. The solution was diluted to volume, mixed, and treated as detailed in methods (*1*) and (*2*). The pH of the solution was determined as detailed in method (*3*).

Results

A typical polarogram is shown in Fig. 1. There is a linear relationship between diffusion current and concentration of D-glucuronolactone, from 20 μg lactone per ml to 6000 μg lactone per ml, as is reported in Table I. From 0 to 20 μg D-glucuronolactone per ml, the relationship is not linear, but is reproducible. Above a concentration of 6000 μg per ml, the wave heights could not be reproduced. Where KCl is the supporting electrolyte, the values given are the average of triplicate determinations. When NaCl or LiCl is the supporting electrolyte, the values are the average of duplicate determinations.

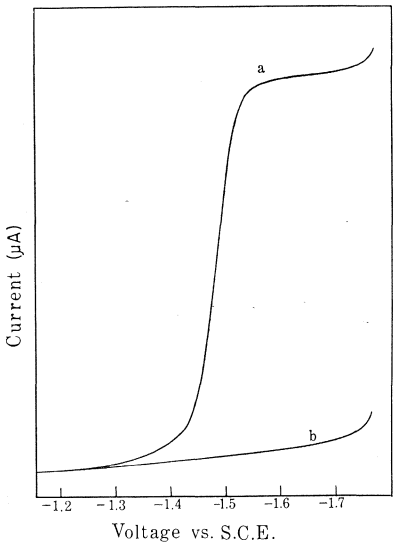

FIG. 1. A typical polarogram and a normal blank; *a*, polarogram of D-glucuronolactone; *b*, blank.

The gelatin concentration was kept as low as possible to obtain maximum sensitivity, but it was found that maxima appeared in the upper 30% of the lower and middle ranges. Therefore, when proceeding to the next highest range, the gelatin concentration was increased. Such an increase had only a small effect on the half-wave potential, but reduced the sensitivity. For example, when the D-glucuronolactone concentration was 20 μg per ml, the wave was well defined in the presence of 0.005% gelatin, but was virtually eliminated in the presence of 0.0075% gelatin. The effect of gelatin concentration on the diffusion current may be seen in Table I at the 100 and 1000 μg per ml concentrations of D-glucuronolactone.

TABLE I

Effect of supporting electrolyte on diffusion current of D-glucuronolactone

Lactone (μg/ml)	i_D (μA) in supporting electrolyte*		
	KCl	NaCl	LiCl
10	0.048		
20	0.099	0.102	0.086
30	0.243		
40	0.453	0.354	0.348
50	0.639		
60	0.852		
70	1.08		
80	1.25	1.15	0.977
90	1.48		
100†	1.66	1.50	1.33
100	1.60	1.42	1.23
200	3.92	3.58	3.12
400	8.52	7.60	6.37
600	12.2		
800	16.6	15.3	13.0
1000‡	21.0	19.0	16.4
1000§	17.4	13.9	13.1
2000	34.0	27.5	25.6
4000	69.5	57.0	49.6
6000	95.8	82.2	78.0

*Electrolytes are 0.2 *M*. KCl values are the average of triplicate determinations, NaCl and LiCl values are the average of duplicate determinations.
†0.005% gelatin.
‡0.0075% gelatin.
§0.01% gelatin.

Attempts to determine the concentration of D-glucuronic acid failed due to the wide variation of diffusion currents (±10%) at identical concentrations of the acid.

An attempt was made to determine accurately the half-wave potentials of the lactone, but due to the instability of the lactone in aqueous solution the results were not reliable. The approximate half-wave potential for D-glucuronolactone was found to be −1.48 V vs. s.c.e. for the range 0–100 μg per ml, −1.53 V vs. s.c.e. for the range 0–1000 μg per ml, and −1.60 V vs. s.c.e. for the range 0–6000 μg per ml.

The pH study of D-glucurono-γ-lactone in boiled deionized water showed that as the concentration was increased from 20 μg per ml to 20 000 μg per ml, the pH fell fairly steadily from 5.85 to 4.00 for solutions which were not deaerated, and from 6.53 to 4.07 for deaerated

TABLE II

pH study of D-glucuronolactone in 0.2 *M* KCl

Lactone (μg/ml)	pH*			
	A	B	C	D
0	5.76	6.49	5.09	5.20
20	5.67	6.02	5.16	5.18
40	5.75	6.35	5.19	5.23
60	5.63	6.00	5.27	5.20
80	5.59	6.11	5.08	5.18
100	5.86	6.23	5.14	5.21
0	5.85	6.53	5.23	5.30
200	6.02	6.28	5.26	5.28
400	5.85	6.05	5.17	5.25
600	5.76	5.99	5.23	5.31
800	5.74	5.89	5.15	5.30
1000	5.74	5.81	5.18	5.14
0	5.85	6.53	5.07	5.38
2000	5.36	5.46	4.96	5.00
3000	5.13	5.48	4.92	4.94
4000	5.13	5.37	4.90	4.88
5000	4.94	5.01	4.77	4.79
6000	4.88	4.88	4.77	4.81
7000	4.75	4.78	4.78	4.72
8000	4.72	4.79	4.69	4.61
9000	4.60	4.63	4.63	4.55
10000	4.62	4.58	4.62	4.58

*pH study of D-glucuronolactone in 0.2 *M* KCl, showing typical values. A: boiled deionized water, no gelatin; B: boiled deionized water, no gelatin, deaerated solution; C: deionized water, gelatin, deaerated solution; D: boiled deionized water, gelatin, deaerated solution.

solutions. It was found that the greater the concentration of the lactone, the more reproducible were the pH values. In the dilute range, the reproducibility is about ±0.15 pH. The pH study of D-glucuronolactone in 0.2 *M* KCl is shown in Table II. Similar results were obtained using 0.2 *M* NaCl and 0.2 *M* LiCl. The trend from one electrolyte to another was: pH KCl solutions < pH NaCl solutions < pH LiCl solutions. The reproducibility was much better than with pure aqueous solutions of D-glucuronolactone, particularly when gelatin was present; e.g., in the dilute range, the reproducibility was ±0.05 pH.

In marked contrast to this was the pH study of D-glucuronic acid in 0.2 *M* KCl – 0.005% gelatin solutions. The pH of a solution containing 10 μg D-glucuronic acid per ml was 4.59, while that of a solution containing 100 μg acid per ml was 3.59. The reproducibility of these values was similar to comparable solutions of D-glucuronolactone.

Changing the concentration of the supporting electrolyte through the range 0.1 to 0.4 *M* caused no change in pH and only a slight change in diffusion current for D-glucuronolactone; no

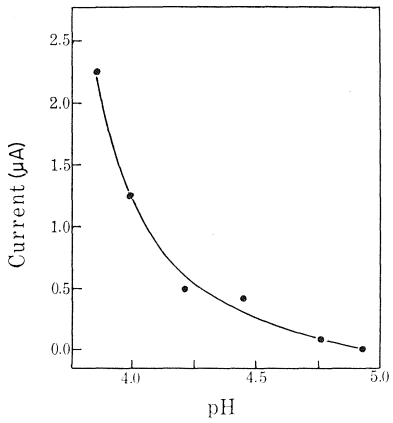

FIG. 2. The effect of pH on the diffusion current of 50 μg D-glucuronic acid per ml.

study was made with D-glucuronic acid because of the lack of reproducibility of the diffusion current.

Figure 2 shows the effect of pH on the diffusion current of D-glucuronic acid, while Figs. 3 and 4

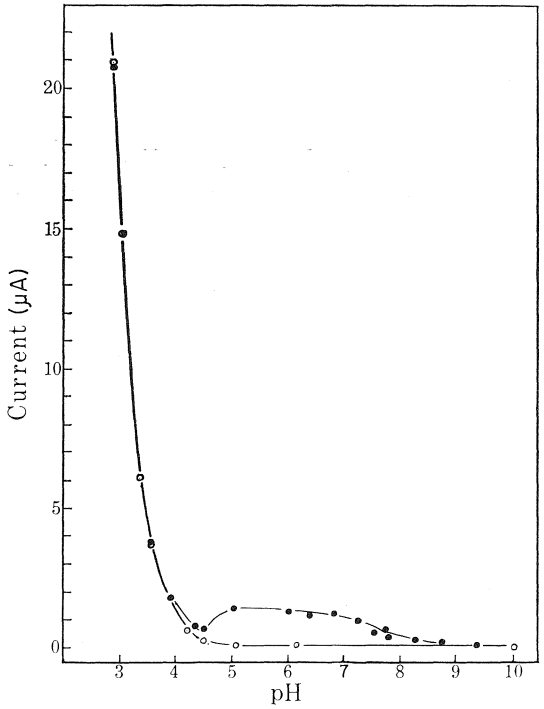

FIG. 3. The effect of pH on the diffusion current of 80 μg D-glucuronolactone per ml; ●, D-glucuronolactone; ○, blank.

Can. J. Chem. Downloaded from www.nrcresearchpress.com by 210.87.254.6 on 09/05/12
For personal use only.

TABLE III

Effect of $H_2PO_4^-$ on the D-glucuronolactone wave

PO_4^{3-} added* (μg/ml)	i_D (μA)	pH	Comment
		KCl, KH_2PO_4	
1	21.1	5.06	No difference from pure D-glucuronolactone wave
10	21.2	5.01	Slight irregularity along the plateau, slight pre-wave
20	21.7	5.00	Maximum enhanced
40	21.4	4.98	Good wave
60	20.2	4.84	Current increased rapidly at the decomposition potential, then increased at usual rate, plateau irregular
80	?	4.90	Plateau highly irregular, not reproducible
90	?	4.91	Plateau highly irregular, not reproducible
100	?	4.92	Two step reduction wave appears, $E_{1/2}$ first wave ≈ -1.48 V, $E_{1/2}$ second wave ≈ -1.82 V, not reproducible, a pre-wave was present, and the current increased rapidly with voltage at the decomposition potential
200	4.10	4.83	Smooth wave, $E_{1/2} \approx -1.63$ V
400	11.0	4.72	Smooth wave, $E_{1/2} \approx -1.70$ V
1000	25.7	4.59	No D-glucuronolactone wave, resembled wave for blank, 1000 μg PO_4^{3-} per ml
		NaCl, NaH_2PO_4	
10	19.4	4.94	Resembled pure D-glucuronolactone
50	19.0	4.86	Slight irregularities on the wave
80	?	4.82	More than one wave, first wave highly irregular
100	?	4.80	Similar to 80 μg, PO_4^{3-} per ml, but worse
200	6.20	4.70	Ill-defined wave, $E_{1/2} \approx -1.68$ V, no D-glucuronolactone wave
400	12.7	4.59	$E_{1/2} \approx -1.71$ V
1000	27.3	4.45	Ill-defined wave, $E_{1/2} \approx -1.74$ V

*All solutions contain 1 mg D-glucuronolactone per ml, are 0.2 *M* in supporting electrolyte, and are 0.0075% with respect to gelatin.

show the effect of pH on the diffusion current of D-glucuronolactone (Fig. 4 is an expanded version of Fig. 3).

In an attempt to determine the type of wave, the height of the mercury column was varied from 30 to 50 cm. For a concentration of 80 μg D-glucuronolactone per ml, there was no change in diffusion current with change in the height of the mercury column (within experimental error), indicating that the wave is either kinetic or catalytic. For a concentration of 800 μg D-glucuronolactone per ml, there was a non-linear variation of diffusion current with the height of the mercury column. On plotting the diffusion current versus the square root of the height of the mercury column, the variation was still not linear. For a concentration of 4000 μg D-glucuronolactone per ml, the variation of diffusion current with the height of the mercury column was almost linear. The plot of diffusion current versus the square root of the height of mercury column was more linear.

As far as D-glucuronic acid is concerned, all that can be said is that the diffusion current increases with an increase in the height of the mercury reservoir.

When phosphate was added as $H_2PO_4^-$, two distinct phenomena were observed, depending on the concentration of D-glucuronolactone. At 100 μg D-glucuronolactone per ml, the wave height was considerably depressed on the addition of phosphate, even 2.5 μg PO_4^{3-} per ml had a noticeable effect on the wave height. As little as 7.5 μg PO_4^{3-} per ml reduced the wave to the residual current. The effect of adding $H_2PO_4^-$ at a D-glucuronolactone concentration of 1 mg per ml is shown in Table III. A blank made in the presence of 10 μg PO_4^{3-} per ml showed an

Can. J. Chem. Downloaded from www.nrcresearchpress.com by 210.87.254.6 on 09/05/12
For personal use only.

Can. J. Chem. Downloaded from www.nrcresearchpress.com by 210.87.254.6 on 09/05/12
For personal use only.

TABLE IV

Effect of HPO_4^{2-} on the D-glucuronolactone wave

PO_4^{3-} added* (μg/ml)	i_D μA	pH	Comment
		KCl, K_2HPO_4	
1	21.4	4.97	Identical to polarograms with pure D-glucuronolactone
10	21.3	6.54	Maximum enhanced
100	20.8	7.20	Maximum enhanced
200	22.0	7.54	Maximum enhanced
400	19.7	7.82	Maximum slightly enhanced
800	17.3	7.91	Maximum greatly enhanced, wave height depressed
1000	15.0	7.97	Maximum greatly enhanced, wave height depressed
		NaCl, Na_2HPO_4	
1	18.7	5.48	Resembled normal polarograms. As the concentration of phosphate was increased the wave height gradually decreased
10	18.8	6.42	
100	18.4	7.14	
200	18.1	7.29	
400	17.0	7.52	Plateau irregular
800	14.2	7.64	Plateau irregular, maximum greatly enhanced
1000	13.2	7.72	Plateau irregular, maximum enhanced

*All solutions contain 1 mg D-glucuronolactone per ml, are 0.2 *M* in supporting electrolyte, and are 0.0075% with respect to gelatin.

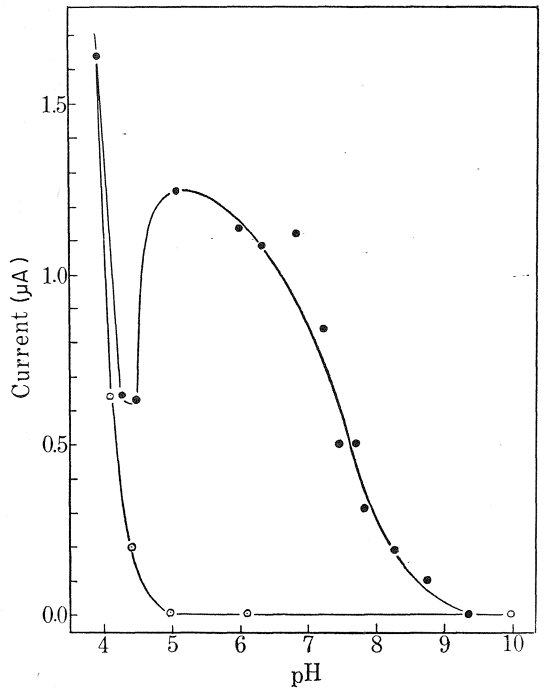

FIG. 4. The effect of pH on the diffusion current of 80 μg D-glucuronolactone per ml (an expanded version of Fig. 3); ●, D-glucuronolactone; ○, blank.

indistinct wave, and a blank containing 100 μg PO_4^{3-} per ml showed a distinct wave whose $E_{1/2}$ was −1.70 V.

The highly irregular waves mentioned in Table III resembled those made with a contaminated capillary.

When phosphate was added as HPO_4^{2-} or PO_4^{3-}, blanks with phosphate resembled normal blanks. The effect on the wave height of D-glucuronolactone solutions appeared to be a pH effect only, when the results were compared to Figs. 3 and 4. Table IV shows the effect of adding HPO_4^{2-} to solutions containing 1 mg D-glucuronolactone per ml.

Discussion

Effect of pH

Ishidate and Shimozawa (1) could not obtain reproducible waves with D-glucuronolactone or D-glucuronic acid. It is evident from Fig. 2 that the diffusion current is extremely pH sensitive when the D-glucuronic acid concentration is kept constant. Further, the pH of D-glucuronic acid solutions decreases rapidly as the concentration is increased. This is reasonable, because the acid is free and uncombined. (The pK_a of D-glucuronic acid is 3.20.) The considerable variance of the diffusion current with pH for D-glucuronic acid may account for the difficulties met by the previous investigators.

The pH of D-glucuronolactone solutions does not change nearly as much with concentration, although the trend is to lower pH values as the

Can. J. Chem. Downloaded from www.nrcresearchpress.com by 210.87.254.6 on 09/05/12
For personal use only.

concentration increases. This is due to the lactone–acid equilibrium. As the concentration of the lactone increases, so does the concentration of the free acid, and the pH decreases. The presence of supporting electrolyte and gelatin appeared to help stabilize the pH, indicating that they are functioning to some extent as weak buffering agents. This is supported by the observation that the reproducibility of pH measurement is increased in these solutions compared to solutions of D-glucuronolactone alone. In fact it was noted that the greater the overall concentration of the solutes, the better was the reproducibility of the pH.

Below pH 5, the buffering effect of supporting electrolyte and gelatin is poor, as illustrated by the D-glucuronic acid solutions. This was also observed when HCl was added to D-glucuronolactone solutions.

Above pH 5, however, the buffering effect is assisted greatly by the lactone itself. (A blank and a D-glucuronolactone solution, treated identically, gave pH values 9.18 and 6.52, respectively.) The lactone hydrolyzes, removing OH^- ions from solution and decreasing the pH

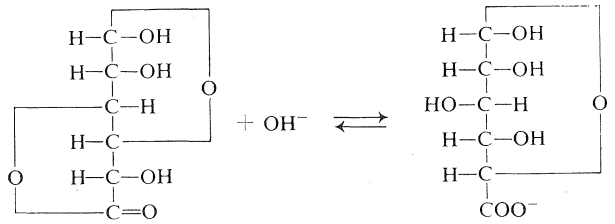

This effect is not instantaneous, but proceeds slowly. This could be seen on the pH meter as the pH dropped slowly for several minutes before stabilizing.

Below a pH of 4, the polarographic waves of D-glucuronolactone solutions could not be distinguished from blanks at similar pH values, indicating that here the wave merely represents the reduction of hydrogen ions. The half-wave potentials of waves made with solutions containing hydrogen ion, D-glucuronolactone, or D-glucuronic acid are too close together to distinguish the species present.

The decrease in diffusion current of D-glucuronolactone as the pH was increased with KOH, as shown in Fig. 4, is no doubt due to the base hydrolysis of the lactone to the glucuronate. A similar study was made with a lactone concentration of 1 mg per ml. Here 0.1 *N* KOH was used to adjust the pH. When the base was added, the large local excess caused a partial decomposition of the lactone molecule, as indicated by the appearance of a greenish-yellow color which was first noticed at a pH of about 7 (the Lobry de Bruyn – van Ekenstein transformation of carbohydrates).

Varying the height of the mercury column in an attempt to determine the type of wave produced different results at different concentrations. It appears that at 80 μg D-glucuronolactone per ml, the wave is kinetic or catalytic; at 800 μg lactone per ml the wave is neither kinetic or catalytic, nor diffusion controlled; while at 4 mg lactone per ml, the process appears to be diffusion controlled, probably due to the large amount of reducible species being produced by the kinetic or catalytic reaction which was observed in the lowest concentration range. This would suggest that the results at the intermediate concentration (800 μg per ml) reflect a transition from a predominantly kinetic or catalytic controlled process to a predominantly diffusion controlled process. Nothing precise can be said about D-glucuronic acid other than the process is not kinetic or catalytic (the diffusion current varies with the height of the mercury column).

Addition of Phosphate

(1) As $H_2PO_4^-$

The pH studies indicate that approximately 99% of the phosphate is present as $H_2PO_4^-$, with approximately 1% present as H_3PO_4, regardless of the amount of D-glucuronolactone present.

Blank solutions exhibited a wave at high phosphate concentrations, but the half-wave potential was about 0.2 V more negative than that of D-glucuronolactone.

With a lactone concentration of 100 μg per ml, the addition of as little as 2.5 μg $H_2PO_4^-$ per ml considerably reduced the wave height, and approximately 7.5 μg $H_2PO_4^-$ per ml annihilated the lactone wave. Since the pH of these solutions

Can. J. Chem. Downloaded from www.nrcresearchpress.com by 210.87.254.6 on 09/05/12
For personal use only.

remained fairly constant, and since the phenomenon was observed with KH_2PO_4 and NaH_2PO_4, the phosphate ion must be responsible for the change of wave height. A preliminary study with D-glucuronic acid indicated that this suppression of the wave height was not accomplished until approximately 1000 μg $H_2PO_4^-$ per ml had been added. A preliminary kinetic study indicated that the reaction between $H_2PO_4^-$ and the lactone reaches equilibrium fairly rapidly (within the mixing and deaeration time). The reaction between D-glucuronolactone and $H_2PO_4^-$ is not clear but may involve the oxygen of the lactone ring, since this is the major difference between D-glucuronic acid and its lactone.

When the D-glucuronolactone concentration was 1 mg per ml, $H_2PO_4^-$ had very little effect up to a concentration of 60 μg per ml. Above an $H_2PO_4^-$ concentration of 60 μg per ml, the highly irregular plateaux on the polarograms, resembling those made with a contaminated capillary, suggest that over an $H_2PO_4^-$ concentration range of 60 to between 100 and 200 μg per ml, and in the presence of 1 mg D-glucuronolactone per ml, the surface tension of the mercury drop becomes irregular, resulting in a non-uniform drop rate. (More work needs to be done in this regard.)

Approximately 200 μg PO_4^{3-} (as $H_2PO_4^-$) was required to completely react with the lactone. On a proportional basis, this is about twice the amount required to react with 100 μg D-glucuronolactone per ml, indicating that a greater excess of $H_2PO_4^-$ is required to cause the reaction to go to completion at the higher lactone concentration.

(2) Adding Phosphate as HPO_4^{2-} or PO_4^{3-}

At low phosphate concentrations (up to about 10 μg PO_4^{3-} per ml as HPO_4^{2-}), the pH studies indicate that the predominant species in solution is $H_2PO_4^-$. Above this level, the concentration of HPO_4^{2-} increases until at 100 μg PO_4^{3-} (as HPO_4^{2-}), the ratio $H_2PO_4^-$: HPO_4^{2-} is about 1:1, (with Na_2HPO_4, about 200 μg phosphate is required). This ratio gradually shifts in favor of HPO_4^{2-} as the phosphate concentration is increased. (At 1000 μg per ml, the ratio $H_2PO_4^-$: HPO_4^- is about 1:6 when added as K_2HPO_4, and about 1:3 when added as Na_2HPO_4.) When phosphate is added as PO_4^{3-}, the predominant species in solution is HPO_4^{2-}.

At a D-glucuronolactone concentration of 100 μg per ml, the effect of phosphate on the wave height resembled the pH effect shown in Fig. 4. This indicates that the reacting species is OH^-, and not phosphate. Similar results were observed with a lactone concentration of 1 mg per ml.

The difference in the amount of phosphate added, comparing $H_2PO_4^-$ to HPO_4^{2-} or PO_4^{3-} is extreme. For example, at a lactone concentration of 100 μg per ml, 7.5 μg PO_4^{3-} (as $H_2PO_4^-$) sufficed to obliterate the D-glucuronolactone wave but with HPO_4^{2-}, even 300 μg PO_4^{3-} could not suppress the wave to the residual current. This indicates that $H_2PO_4^-$ is an extremely reactive species.

An analogy can be made with the work of McConnell and Coover (7, 8) who reacted β-propiolactones with dialkylhydrogen phosphites and trialkyl phosphites. The latter cleaved the lactone ring at the β-carbon, but the former, having a replaceable hydrogen, cleaved the ring at the carbonyl group (the hydrogen bonds to the oxygen of the lactone ring). It is possible that $H_2PO_4^-$ (having a hydrogen which is about 10^5 more easily removed than HPO_4^{2-}) reacts with lactones in a similar manner to dialkyl hydrogen phosphites. HPO_4^{2-} (or PO_4^{3-}), like trialkyl phosphites, probably does not react at the carbonyl group due to the difficulty of hydrogen bonding with the oxygen of the lactone ring. In nonaqueous media, HPO_4^- (or PO_4^{3-}) may possibly cleave the lactone ring at the γ-carbon, but in aqueous medium, the reaction appears to be merely hydrolysis by OH^- to give the glucuronate.

Acknowledgment

The authors gratefully acknowledge the financial assistance of the National Research Council of Canada.

1. M. Ishidate and T. Shimozawa. J. Pharm. Soc. Japan, **64**, 53 (1944).
2. R. J. Thibert and A. J. Boyle. Talanta, **7**, 175 (1961).
3. I. M. Kolthoff and J. J. Lingane. Polarography. Vol. II. Interscience Publishers, Inc., New York. 1952. p. 720.
4. H. Matheson, H. S. Isbell, and E. R. Smith. J. Res. Natl. Bur. Std. **28**, 95 (1942).
5. Corn Products Sales Company. Tech. Bull. JN-2.
6. R. M. Dowben. Biochim. Biophys. Acta, **31**, 454 (1959).
7. R. L. McConnell and H. W. Coover, Jr. J. Am. Chem. Soc. **78**, 4450 (1956).
8. R. L. McConnell and H. W. Coover, Jr. J. Am. Chem. Soc. **78**, 4453 (1956).

Electron spin resonance study of tert-butyl halides and carbon tetrachloride, neopentane and carbon tetrachloride binary mixtures irradiated at 77 °K

F. C. THYRION[1]

Chemistry Department, Laval University, Quebec 10, Quebec

Received March 27, 1968

Tert-butyl halides and carbon tetrachloride, neopentane and carbon tetrachloride binary mixtures were irradiated at 77 °K and electron spin resonance spectra were recorded at increasing temperatures until the radicals disappeared.

Even at high concentrations of tert-butyl halides, the radicals obtained from CCl_4 predominate, indicating that CCl_4 has a high efficiency for electron capture. Maximum radical yields and the appearance of a narrow line spectrum with rising temperature were observed in $(CH_3)_3C—X - CCl_4$ mixtures (X = Cl, Br, I) in concentration ranges where only a single phase exists. This spectrum consists of 17 lines which appear to belong to one odd-numbered spectrum (7 lines due to $(CH_3)_2\dot{C}—X$ radical) and two even-numbered spectra (4 and 10 lines, the last being due to $(CH_3)_3\dot{C}$ radical). The disappearance of the CCl_4 broad band and the appearance of these radicals with increasing temperature can be interpreted as due to charge transfer from carbon tetrachloride cation to tert-butyl halide, facilitated by greater freedom of movement in the solid solutions. In contrast, neopentane and carbon tetrachloride mixtures do not display these features.

Des mélanges binaires d'halogénures de tertiobutyl et neopentane dans le CCl_4 ont été irradiés à 77 °K. Les spectres de résonance paramagnétique indiquent que la concentration des radicaux issus du tétrachlorure de carbone est prépondérante, même aux fortes concentrations en halogénures de tertiobutyl, ce qui fait ressortir la haute efficacité de capture d'électrons thermiques par les molécules de CCl_4. Lorsque les deux substances forment une solution solide à basse température, on constate un maximum dans les valeurs des rendements radicalaires et l'apparition d'un très beau spectre par élévation de température. Ce dernier comprend 17 raies appartenant à 3 espèces radicalaires différentes. La disparition de la bande attribuée à l'ion-radical CCl_4^+ et l'apparition de nouvelles espèces radicalaires par élévation de température peuvent être interprétées par le transfert de charge de CCl_4^+ sur l'halogénure de tertiobutyl. Celui-ci est favorisé par la libération progressive des mouvements moléculaires dans les solutions solides étudiées. Par contre, les mélanges de neopentane et tétrachlorure de carbone ne présentent pas ces particularités.

Canadian Journal of Chemistry, 47, 273 (1969)

Introduction

In earlier work (1), ethyl iodide and carbon tetrachloride mixtures were irradiated; radiochemical yields obtained by electron spin resonance (e.s.r.) and analysis of reaction products enabled us to show that electron capture was very efficient in alkyl halides and in carbon tetrachloride. Hamill and his co-workers (2) have also reached this conclusion in work describing the relative efficiency of electron capture for a series of solutes dissolved in suitable solvents.

It ought to be interesting to study the effects of irradiation on solutions of globular or near-globular (3) alkyl halides and carbon tetrachloride, since Powles and Gutowsky have shown that molecular motions occur even at low temperatures (4). The spectra, G values and disappearance temperatures of radicals in $(CH_3)_3C—X$ or neopentane – carbon tetrachloride solid solutions are compared with those of ethyl iodide – carbon tetrachloride mixtures (X = Cl, Br, I).

Experimental

Carbon tetrachloride (Baker Company, spectroscopic grade) was purified as previously described (1). Tert-butyl iodide (Eastman) was purified through fractional distillation under reduced pressure. Tert-butyl bromide and chloride (Eastman) and neopentane (Matheson Company) were trap to trap distilled at liquid nitrogen temperature. The solutions were prepared under vacuum by mixing known volumes of the components (total of 0.2 ml) in Suprasil tubes. Before sealing, samples were evacuated to 10^{-4} Torr. They were then rapidly cooled, and afterwards irradiated in a Gammacell 220 irradiator (A.E.C.L.) at a dose of 2.92×10^{19} eV g^{-1}. Yields are reported relative to $G = 15.6$ for the Fricke dosimeter but corrections were made in the case of $(CH_3)_3C—I$ to take into account the increase in energy absorbed by iodine atoms.

Radical or radical-ion spectra were obtained with a Varian electron paramagnetic resonance (Model

[1]Present address: Laboratoire de Chimie-Physique III, 39, Schapenstr., Louvain, Belgium.

Can. J. Chem. Downloaded from www.nrcresearchpress.com by 210.87.254.5 on 09/05/12
For personal use only.

4500.10A, X-band) spectrometer equipped with a variable temperature dual-cavity and cooling system. Spectra were observed at temperatures (maintained to within 0.5 °C) of 77 °K or higher. The first derivative spectra were obtained with a X–Y recorder. The radical concentrations were determined by calibration with DPPH in CCl_4. The overall sensitivity after corrections was estimated to be ±20%.

Results

Spectra in Pure CCl_4

Pure carbon tetrachloride spectrum at 77 °K consists of a very broad asymmetric band centered at $G = 2.014$, which decreases and begins to show structure at 120 °K, and is resolved better at 175 °K (Fig. 1). At this temperature, the pattern indicates a superposition of spectra. This has been ascribed to CCl_3 and CCl radicals (10 and 4 lines) by Leray (5).

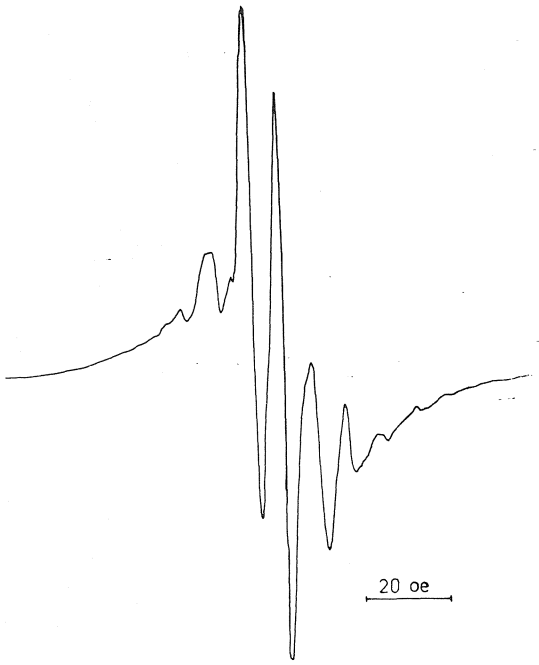

FIG. 1. Spectrum of pure CCl_4 at 192 °K.

Spectra in Tert-butyl Halides – Carbon Tetrachloride Mixtures

The spectra observed at 77 °K for solutions of tert-butyl halides and carbon tetrachloride are similar to that of pure CCl_4. However, we already observe some shoulders, at low and medium concentrations in halides which are due to a 17-line spectrum described later (Fig. 2).

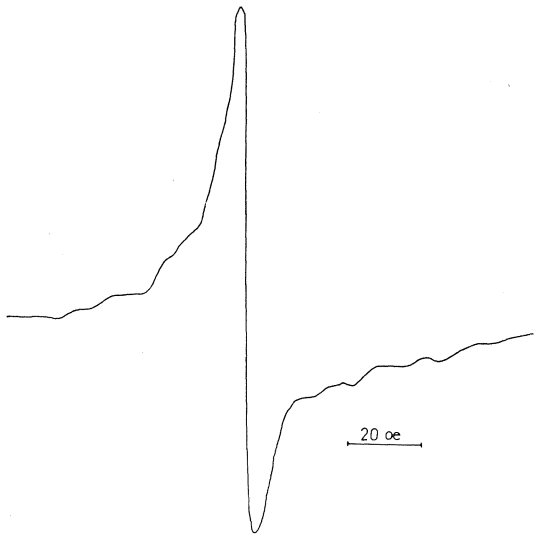

FIG. 2. Typical spectrum of tert-butyl halide – carbon tetrachloride mixtures at 77 °K.

Three cases can be considered depending on the tert-butyl halide concentration.

(*a*) In solutions with less than 35 mole % of tert-butyl halides, the spectra are similar to that of pure CCl_4. The disappearance temperatures are between 190 and 215 °K.

(*b*) In the range of 35–75 mole % tert-butyl halides (45–75% for iodide) a more resolved spectrum begins to appear at 125–130 °K. When the temperature is alternately lowered and raised, one obtains a highly symmetrical spectrum with 17 regularly spaced lines (11.6 Oe) and a 4.7 Oe line width (Fig. 3). In the case of $(CH_3)_3C—I$ mixtures, however, no symmetrical spectrum was observed. The 17-line spectrum can be resolved into two spectra with odd and even number of lines, since with increasing temperature, the former spectrum disappears faster. The peaks of the last spectrum have a relative intensity ratio of 1:6:15:20:16:6:1.2, very close to the ratio expected for the interaction of an unpaired electron with six equivalent protons. Moreover, the spectrum is quite similar to that obtained by Roncin (6) from irradiation of $(CH_3)_2CCl_2$. He assigned this to $(CH_3)_2\dot{C}—Cl$. In the even line spectrum, 8 lines with relative intensities x:2.2:7.4:15:15.2:7.8:2.3:x are observed. This spectrum should result from the superimposition of a 10-line spectrum due to the well known tert-butyl radical, and a 4-line spectrum with relative intensi-

Can. J. Chem. Downloaded from www.nrcresearchpress.com by 210.87.254.5 on 09/05/12
For personal use only.

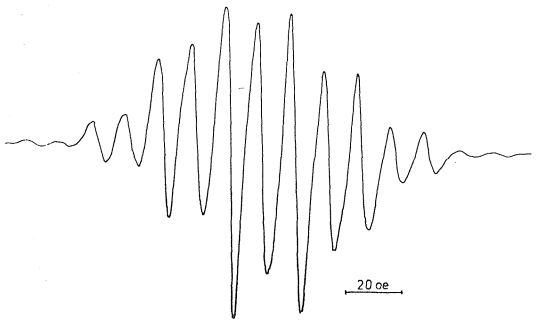

FIG. 3. Typical spectrum obtained for medium concentration $(CH_3)_3C—X - CCl_4$ mixtures, at 130 °K, (X = Cl, Br, I): spectrum of a 65 mole % $(CH_3)_3C—Cl$ mixture.

ties 1:3:3:1, which could be attributed to the CH_3 radical. Waugh (7) found that self-diffusion in solid methane was very rapid at about 60 °K. In other matrices, however, the CH_3 radical has been observed at 77 °K by several investigators (8, 9), but it seems unlikely that this radical exists up to 140 °K. If we take into account the spacing between lines and the line width observed (11.6 and 4.7 Oe), we get a nearly superimposable theoretical spectrum by assigning the following weight relationships to the three radicals: 25.6% to the 4-, 32.4% to the 10-, and 42% to the 7-line spectrum. The spectrum disappears at 140–145 °K. It is important to note that the intensity of the 17-line spectrum increases by a factor of ~ 5 on increasing the temperature from 77 to 125 °K. A comparison of the line widths at these temperatures cannot explain this enhancement.

(*c*) At higher concentrations of tert-butyl halide, a superimposition of two spectra was observed, one being the tert-butyl radical spectrum and the other being the broad band of CCl_4. At increasing temperature, the tert-butyl radical spectrum shows better resolution. The spectra disappear below the disappearance temperature observed in pure tert-butyl chloride (190 °K) and tert-butyl bromide (215 °K). Finally, a nearly equimolecular mixture of tert-butyl chloride and bromide gives the typical spectrum of the tert-butyl radical.

Annealed solid solutions of tert-butyl halides in carbon tetrachloride were also checked. The spectra of bromide and chloride did not differ from the spectra reported above. The tert-butyl iodide showed quite a different spectrum consisting of 8 broad lines with a 5.5 Oe spacing superimposed on the CCl_4 broad band. It disappears at temperatures well above those which give in destruction of radicals in a rapidly cooled mixture (Fig. 4). Complex spectra have been previously observed in polycrystalline alkyl iodides, but interpretation was difficult (10, 11).

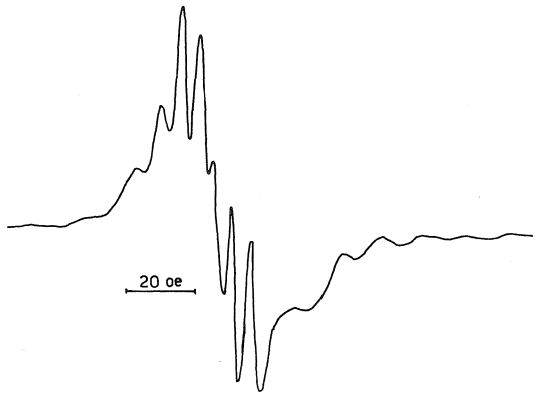

FIG. 4. Spectrum of a 36 mole % $(CH_3)_3C—I$ mixture at 130 °K, annealed before irradiation.

Spectra in Neopentane – Carbon Tetrachloride Mixtures

In all cases, the spectra appear to be a superimposition of the broad band of CCl_4 and the complex spectrum of neopentane. The latter spectrum consists of a prevailing triplet (neopentyl radical (12)) with superimposed sets of lines, and is detected even at low concentrations of neopentane.

Disappearance of Radicals

Figure 5 is a plot of the disappearance temperatures of radicals vs. mole % of solute in CCl_4. It can be noted that the curves are very similar in shape for the tert-butyl halides, but are quite different in the C_2H_5I mixtures. Neopentane is intermediate in behavior.

Yields of the Trapped Radicals

Figure 6 is a plot of $G(R)$ vs. electron % of tert-butyl halides and neopentane in carbon tetrachloride. For comparison, results previously obtained in the $C_2H_5I - CCl_4$ mixtures (1) are also indicated. A higher yield is obtained in a nearly equimolecular mixture in $(CH_3)_3—Cl$ and $(CH_3)_3C—Br$ where $G(R) = 3$. The radical yields for pure compounds are: CCl_4, 0.36; $(CH_3)_4C$, 1.42; $(CH_3)_3C—Cl$, 1.3; $(CH_3)_3C—Br$, 0.75;

Can. J. Chem. Downloaded from www.nrcresearchpress.com by 210.87.254.5 on 09/05/12
For personal use only.

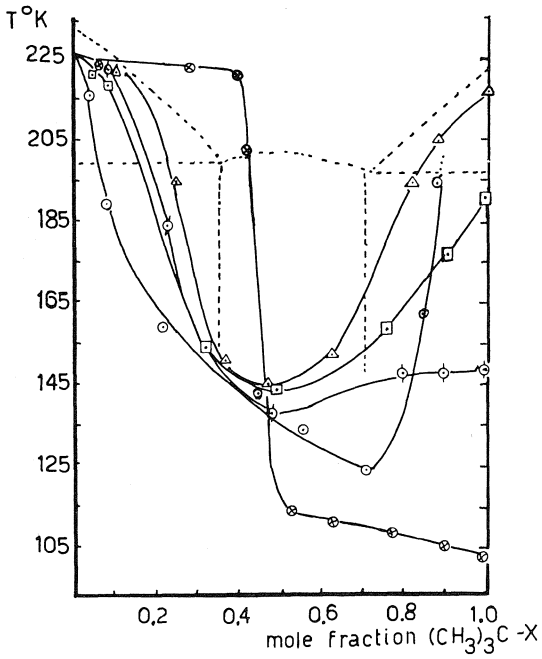

FIG. 5. Disappearance temperatures of radicals, in binary mixtures of CCl_4 with $(CH_3)_3C$—Br (△), $(CH_3)_3$-C—Cl (⊡), $(CH_3)_3C$—I (⊙), $(CH_3)_4C$ (⊙), C_2H_5I (⊗).
The dotted lines indicate the equilibrium phase diagram proposed by Conner and Smyth for the $(CH_3)_3C$—Cl – CCl_4 system (22).

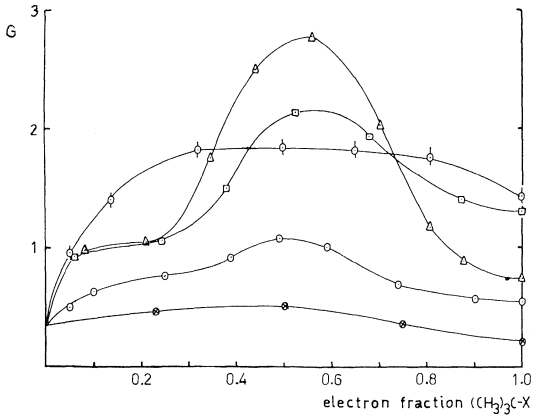

FIG. 6. Total radical yields at 77 °K in binary mixtures of CCl_4 with $(CH_3)_3C$—Br (△), $(CH_3)_3C$—Cl (⊡), $(CH_3)_3C$—I (⊙), and $(CH_3)_4C$ (⊙). Radical yields in C_2H_5I–CCl_4 mixtures are given for comparison (⊗).

and $(CH_3)_3C$—I, 0.57. The relative concentrations of radicals found in tert-butyl halides, or ethyl iodide and carbon tetrachloride systems, are similar. For instance, in 82 and 90 mole % tert-butyl bromide, the CCl_4 radical species concentrations are respectively 90 and 61% of the total concentration.

Discussion

The pure carbon tetrachloride e.s.r. spectrum at 77 °K has been reported by many investigators (13–15). It consists of a broad band which can be assigned to CCl_3 radical, CCl_4^+ or CCl_4^- radical–ions. Bennett and Thomas observed the same spectrum when CCl_3 was prepared by a chemical method (16). More recently, Shida and Hamill (17) observed, in γ-irradiated polycrystalline CCl_4 at 77 °K, a band centered at 4000 Å, which they attributed to trapped positive holes in the CCl_4 matrix. This band disappeared rapidly when the sample was warmed from 77 to 143 °K. The disappearance of this band agrees with the fact of the decay of the broad asymmetric band observed in e.s.r. spectrum. It will be assumed that CCl_4^+ is mainly responsible for it, even though Leray (5) attributed it to CCl_4^-. Indeed, Van Dunsen and Hamill (18) have indicated that it is unlikely that CCl_4^- ion can exist in polar media.

Efficient production of CCl_4^+ derives from the effective scavenging of electrons by CCl_4 itself or by tert-butyl halide, otherwise the electrons would recombine with CCl_4^+. The following set of reactions may be postulated if the positive hole migrates (17), and the electrons ejected by ionization are scavenged by the matrix:

$$[1] \qquad CCl_4 \text{—}\sim\!\!\rightarrow CCl_4^+ + e^-$$

$$[2] \qquad e^- + CCl_4 \rightarrow CCl_3 + Cl^-$$

$$[3] \qquad e^- + RX \rightarrow R + X^-$$

$$[4] \qquad CCl_4^+ + CCl_4 \rightarrow CCl_4 + CCl_4^+$$

$$[5] \qquad CCl_4^+ + RX \rightarrow CCl_4 + RX^+$$

$$[6] \qquad CCl_4^+ + X^- \rightarrow CCl_4 + X$$

$$[7] \qquad RX^+ + X^- \rightarrow R + X_2$$

$$[8] \qquad \rightarrow \dot{R}'X + Y$$

where RX represents tert-butyl halide molecule, and X^- is halide ion formed in reaction [2] or [3].

Dissociative attachment of thermal electrons by CCl_4 (reaction [2]) has been shown by several authors to be a very efficient process, more favorable than for other alkyl halides (reaction

Can. J. Chem. Downloaded from www.nrcresearchpress.com by 210.87.254.5 on 09/05/12
For personal use only.

Can. J. Chem. Downloaded from www.nrcresearchpress.com by 210.87.254.5 on 09/05/12
For personal use only.

[3]) (2). Minor contributions of tert-butyl radical are observable at high concentrations in halides at 77 °K. The same was observed in C_2H_5I–CCl_4 mixtures when the competition was effective (at about 90 mole % in C_2H_5I). Positive charge exchange between a molecule and an ion (reaction [4]) has been postulated by Shida and Hamill (17). Thermal activation restores the stabilized hole to a conducting configuration, and this migrating positive hole is assumed to interact with a tert-butyl halide molecule (reaction [5]) by simple electron transfer, since the ionization potential (i.p.) of CCl_4 (taken as 11.47 eV) (19) is somewhat higher than that of $(CH_3)_3C$—X (i.p. of $(CH_3)_3C$—Cl = 10.2 eV) (20). Further reactions [7] and [8] should produce radical species such as $(CH_3)_3\dot{C}$ and $(CH_3)_2\dot{C}$—X. If one attempts to explain the 4-line spectrum observed at 130–140 °K, it is necessary to postulate a $(CH_3)_3C$—X^+ radical–ion with an electron vacancy being well shielded in the C—C bonds. However, some authors (21) have assumed that the halogen-containing radicals give low- and high-field spectra. The existence of this ion in CCl_4 matrix should be favored by the great efficiency of CCl_4 in stabilizing ejected electrons.

The differences observed in spectra of tert-butyl halide – CCl_4 and ethyl iodide – CCl_4 mixtures with rising temperature are due to their different phase state. The onset of reorientations or rotations occurs gradually with increasing temperature in plastic crystals. Charge migration is allowed without displacement of molecules and radical recombination. In the C_2H_5I mixtures, on the contrary, the onset of these motions is abrupt, and radicals rapidly recombine. To explain the narrow line spectrum in intermediate concentration mixtures of halides with increasing temperature, it would be interesting to compare our results with those obtained by different methods, such as proton magnetic resonance studies and dielectric constant studies (4, 22). Powles and Gutowsky (4) have concluded that there is only one phase at all temperatures for tert-butyl chloride in carbon tetrachloride, at concentrations between 34.9 and 70.6 mole %. Furthermore, there are motions in the solution which do not occur at the same temperature in pure tert-butyl chloride. In this compound, the —CH_3 groups rotate even at very low temperature, and, as shown by dielectric measurements (23), the C—Cl axis is fixed at temperatures up to 220 °K. The proton magnetic resonance narrowing observed at about 100 °K (24) reveals reorientation about this axis; but below the transition at 183 °K, the three possible orientations are indistinguishable. Above 190 °K, movement is sufficient to permit diffusion and recombination of radicals. In contrast, there exists in solid solutions an effective C_3 rotation of the whole molecule, and also rotation of the three —CH_3 groups, well below 183 °K. The appearance temperature of the 17-line spectrum agrees with that corresponding to the reduction in second moment of the proton magnetic resonance spectra observed by Powles and Gutowsky in $(CH_3)_3C$—Cl – CCl_4 solid solutions (4). Furthermore, the concentration range, where the 17-line spectrum appears, corresponds exactly to the single phase limits observed by these authors. From the results reported here, tert-butyl bromide mixtures are expected to have similar properties. Tert-butyl iodide mixtures, however, do not display similar features. Some results (21) have indicated the absence of a solid solution at low temperature. When annealed samples of tert-butyl iodide – carbon tetrachloride mixtures are irradiated, their e.s.r. spectra are different from those obtained in rapidly cooled solutions. In the first case, the solid separates out in two phases below 203 °K (25), and the influence of one compound on the other is very weak. In rapidly cooled solutions, the typical spectrum of a single phase was obtained, at intermediate concentrations. This indicates a homogeneous mixture of two substances where molecular motions occur at 125 °K. This probably arises with difficulty since $(CH_3)_3C$—I molecules possess a less spherical shape than the other tert-butyl halides.

In neopentane mixtures, no definite spectral changes occur with temperature. The perfectly spherical neopentane molecule is known to rotate even at low temperatures (24), and this seems to occur in its solid solutions with CCl_4, from the narrow line width of e.s.r. spectra. Westrum and Chang pointed out, from studies of heat capacities and enthalpies of mixing, that an apparently first order transition associated with a molecular freedom of the $(CH_3)_4C$ molecules occurs in 50 and 66.5 mole % mixtures of neopentane in carbon tetrachloride at 142.5 °K (26). The persistent broad band of CCl_4 with increasing temperature suggests that positive

charge transfer between CCl_4^+ and neopentane should be less efficient.

Radical Yields

The yield of trapped radicals in pure tert-butyl halides decreases in the order: chloride > bromide > iodide. This order has already been established by several investigators (13, 27), while Shirom and Willard (28) found no difference in radical yields observed in halide containing glasses at 77 °K. The deviations relative to the mixture law observed in all the mixtures indicates a sensitization by carbon tetrachloride which is particularly effective at intermediate concentrations of bromide and chloride in carbon tetrachloride. This observation and other effects described above (appearance of the 17-line spectrum, temperature of radicals disappearance) outline the importance of phase state and molecular motions on G values. A significant argument arises from the high G value obtained in the tert-butyl bromide and chloride mixture, where a narrow line spectrum is observed, even at 77 °K, due to less restriction of molecular motions than in pure compounds. In neopentane mixtures, $G(R)$ is high for all concentration ranges. This is in good agreement with the conclusions about molecular motions described previously.

Acknowledgments

The author thanks the National Research Council of Canada for a postdoctoral fellowship. The major part of this work was done in the Chemistry Department, Laval University, Quebec. It is a pleasure to acknowledge the assistance of Dr. J. A. Herman of this department and of Dr. J. Savard of the Solid State Research Center.

1. R. M. Leblanc, F. C. Thyrion, and J. A. Herman. Can. J. Chem. **46**, 1625 (1968).
2. J. P. Guarino, M. R. Ronayne, and W. H. Hamill. Radiation Res. **17**, 379 (1962).
3. J. Timmermans. Phys. Chem. Solids, **18**, 1 (1961).
4. J. G. Powles and H. S. Gutowsky. J. Chem. Phys. **21**, 1704 (1953).
5. N. Leray. Thesis, Paris, 1966.
6. J. Roncin. Mol. Cryst. **3**, 117 (1967).
7. J. S. Waugh. J. Chem. Phys. **26**, 966 (1957).
8. B. Smaller and M. S. Matheson. J. Chem. Phys. **28**, 1169 (1958).
9. D. W. Skelly, R. G. Hayes, and W. H. Hamill. J. Chem. Phys. **43**, 2795 (1965).
10. H. W. Fenrick, S. V. Filseth, A. L. Hanson, and J. E. Willard. J. Am. Chem. Soc. **85**, 3731 (1963).
11. H. W. Fenrick and J. E. Willard. J. Am. Chem. Soc. **88**, 412 (1966).
12. F. C. Thyrion, J. P. Dodelet, C. Fauquenoit, and P. Claes. J. Chim. Phys. **65**, 227 (1968).
13. R. F. C. Claridge and J. E. Willard. J. Am. Chem. Soc. **87**, 4992 (1965).
14. J. B. Gallivan and W. H. Hamill. J. Chem. Phys. **44**, 2378 (1966).
15. V. A. Roginskii, A. G. Kotov, and S. Ya Pshezhetskii. Russ. J. Phys. Chem. English Transl. **39**, 1544 (1965).
16. J. E. Bennett and A. Thomas. Intern. Symp. Free Radicals 6th. Cambridge, England. 1963.
17. T. Shida and W. H. Hamill. J. Chem. Phys. **44**, 2369 (1966).
18. W. Van Dunsen and W. H. Hamill. J. Am. Chem. Soc. **84**, 67 (1962).
19. K. Watanabe, T. Nekayama, and J. Mottl. J. Quant. Spectry. Radiative Transfer, **2**, 369 (1962).
20. W. C. Price. Chem. Rev. **41**, 257 (1947).
21. R. J. Egland and J. E. Willard. J. Phys. Chem. **71**, 4158 (1967).
22. W. P. Conner and C. P. Smyth. J. Am. Chem. Soc. **63**, 3424 (1941).
23. L. M. Kushner, R. W. Crowe, and C. P. Smyth. J. Am. Chem. Soc. **72**, 1091 (1950).
24. J. G. Powles and H. S. Gutowsky. J. Chem. Phys. **21**, 1695 (1953).
25. H. Chihara, M. Otsuru, and S. Seki. Bull. Chem. Soc. Japan, **39**, 2145 (1966).
26. E. F. Westrum and E. Chang. Progr. Intern. Res. Thermodyn. Transport Properties, Papers Symp. Thermophys. Properties 2nd. Princeton, New Jersey. 1962. p. 172–177.
27. P. B. Ayscough and C. Thomson. Trans. Faraday Soc. **58**, 1477 (1962).
28. M. Shirom and J. E. Willard. J. Phys. Chem. **72**, 1702 (1968).

Can. J. Chem. Downloaded from www.nrcresearchpress.com by 210.87.254.5 on 09/05/12
For personal use only.

Basic dissociation constant for ethylamine by a convenient conductance method[1]

W. VAN DER LINDE[2], D. NORTHCOTT, W. REDMOND[3], AND R. E. ROBERTSON
Division of Pure Chemistry, National Research Council of Canada, Ottawa, Canada

Received April 24, 1968

A dilution technique is described which permits a determination of the ionization constant of amines by a conductance method, in a closed system. Small amounts (5–6 g) of the amine salt are required, making the method useful in studying isotope effects. Values of K_i for ethylamine over the temperature range 1.5–45.3 °C led to calculated values at 25 °C of $\Delta G = 4528.3 \pm 0.8$ cal/mole, $\Delta H = -266 \pm 12$ cal/mole, $\Delta S = -16.08 \pm 0.04$ cal/mole deg, $\Delta C_p = -62.2 \pm 1.8$ cal/mole deg.

Canadian Journal of Chemistry, 47, 279 (1969)

Can. J. Chem. Downloaded from www.nrcresearchpress.com by 210.87.254.105 on 09/05/12
For personal use only.

Problems arising in connection with the interpretation of certain deuterium isotope effects (1–3) created the need of a method for determining the ionization constant for weak electrolytes which was at once capable of the required accuracy and economical with respect to quantitative requirements of deuterated materials. The system developed to meet these requirements is described here and its capabilities are illustrated by a study of the temperature dependence of the basic dissociation constant of ethylamine over the range 1.5–45 °C. The choice of this amine was determined in part by its utility in isotopic studies and partially by the fact that no such careful study had been made previously.

In the initial stages of the work (4), attempts were made to achieve the above goals by combining a precision syringe (5) with a mixing chamber and the double conductance cell of Ives and Pryor (6), calculation of Λ_0 and K_i being made from a single set of concentration–resistance data according to the extrapolation method of Ives (7). This system proved adequate for the determination of K_b^H/K_b^D (4) but failed to give that degree of reproducibility and accuracy required for defining the temperature coefficients of the equilibrium. Minor modifications of the system did not give the required improvement (8).

Part of the difficulty may be attributed to the use of the extrapolation method for determining K_b since the value lies in the borderline region where this method becomes unreliable (9–11). In this instance, errors of about 1% between successive runs were found. Kilpatrick (11) in a detailed analysis of the factors contributing to error in the use of the extrapolation method in calculating the ionization constant of weak acids seems to suggest a lower limit of $K_i = 10^{-5}$, hence the sources of the above error may not have been due entirely to the method of calculation. This question was not explored since important changes in the design of the cell were introduced concurrently with a change to the additive method of calculating Λ_0. Fortunately, the system provides a convenient experimental approach for determining the required value of Λ_0 for the ethyl amonium chloride with a minimum of labor.

Experimental

The main features of the conductance cell will be apparent from Fig. 1. This consists of a mixing chamber bearing a fine inlet joined to the precision syringe, and two opposed conductance cells. Stirring and circulation of the stirred solution through the cells is accomplished with a glass-enclosed magnet at the bottom of the central shaft bearing stirrers and impeller blades. This is set in a frame above a rotating magnet fixed centrally below the cell. The essential feature of the cells would appear to be the constriction of the central portion such that the platinum electrodes in the foreshortened dumb-bell shaped cell were much larger than the connecting tube. Such an arrangement was found to be essentially frequency independent (500–10 000 Hz) when used in an oil bath. Grounding the unused cell through the bridge ground when making a measurement eliminated a source of interference. It is recognized that this design merely represented a return to the inherent feature of the classical dumb-bell shape of the Kohlrausch cell, which had been omitted in the Ives–Pryor design (6). The attachment of the electrodes was accomplished by mounting on glass studs and electrical connection established by sealing on a very thin platinum sheet (0.0005 in.), through

[1]Issued as NRCC No. 10 342.
[2]Postdoctoral Fellow, 1961–63. Present address: E. I. Dupont de Nemours, Marshall Laboratories, Philadelphia, Pa.
[3]Postdoctoral Fellow, 1965–67. Present address: Abitibi Paper Co., Research and Development Center, Sheridan Park, Ontario.

Can. J. Chem. Downloaded from www.nrcresearchpress.com by 210.87.254.105 on 09/05/12
For personal use only.

a pinched joint terminating by electrowelding to a copper wire. This was welded in turn to a tungsten terminal, the latter being topped with a nickel sleeve. The glass arms bearing the terminals were placed under vacuum, hence any leakage past the platinum pinch-joint was readily detected.

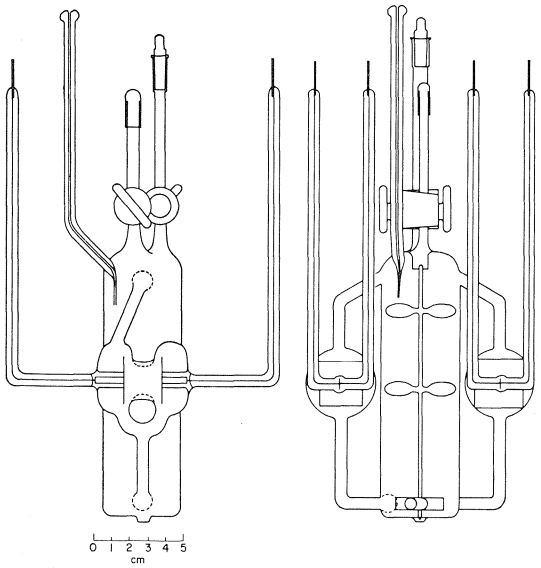

FIG. 1. Double conductance cell with mixing chamber.

One of the problems, indeed one of the major sources of error inherent in the conductance method is the property of glass walls to absorb ions from the solution. This will be most apparent in dilute solutions. Where there is no restriction on the amount of solution, repeated flushing will bring the walls into equilibrium with the solution but this possibility was inadmissible here. To minimize wall effects pretreatment of the cells was carefully standardized between runs. This consisted of leaving the cell stand with the solution of the amine overnight, rinsing and throughly steaming out for 10 min followed by pumping to dryness and filling with purified nitrogen. At this stage the cell was weighed to 1 mg on a balance sensitive to 0.5 mg/1 kg load, and filled to a point above the sidearms with distilled water under a positive pressure of purified nitrogen, in order to prevent the entrance of CO_2. Unless the water had a nominal value of 5×10^{-8} ohm^{-1} cm^{-1} (10 °C), experience showed that useful results could not be obtained.

Using the same procedures, values of the cell constant for the "hypothetical" cell (i.e. the difference of the two measured cells) were found to be $0.27905 \pm 0.0^{4}2$ for four determinations and after 8 weeks $0.27906 \pm 0.0^{4}3$ on two determinations (12).

[4]We are grateful for the skilled workmanship and practical advice available to us through our glass-blower, Mr. Jack van den Hoff.

The titrimeter was a more compact form of an earlier model previously described and was capable of delivering up to 10 ml in small increments, with high accurancy (5).

KCl

Analytical grade KCl was recrystallized from conductivity water twice and fused in a platinum boat in an electric furnace (13).

NaCl

NaCl (analytical grade) was precipitated from a saturated solution in conductivity water by bubbling in HCl, and the resulting crystals were filtered off, dried in an electric oven, and fused as above.

Ethylammonium Chloride

The amine-hydrochloride was prepared by bubbling dry HCl gas through an ethereal solution of the pure amine and filtering under dry nitrogen. Recrystallization from dry *n*-butanol and drying under vacuum gave a white fluffy crystalline hydrochloride. This was kept in a desiccator and either used directly (Λ_0) or as a source of amine (K_i). To get amine solutions (0.2 molar) the requisite amount of hydrochloride and KOH were added to a reaction vessel on a vacuum-line and the system repeatedly evacuated and flushed with dry, purified nitrogen. The addition of conductivity water to the reaction cell led to the regeneration of the amine which was swept into a trap cooled with liquid N_2. The amine was distilled from bulb-to-bulb, the middle fraction being stored for use. The purity was checked by mass spectral analysis and showed no significant amounts of other amines. The amine solution was made up in a special flask (Fig. 2*b*) containing 125 cc conductivity water, and the flask was thoroughly degassed. The required approximate amount of amine was transferred to the flask, air being excluded at all times. Transfer of the amine solution from the make-up flask to the titrimeter and guard-bubblers is done after flushing the system repeatedly with N_2 through loosely clamped joints during the successive filling of the bubblers C, B, and the reservoir A (Fig. 2*a*). The concentration of the amine was determined by titration from the precision titrimeter against standard HCl solution using a glass electrode and pH meter to detect the end point.

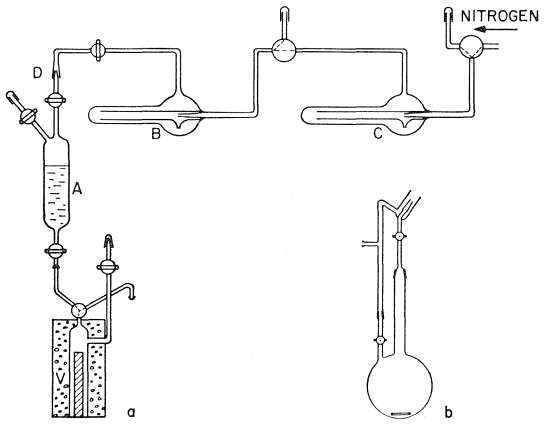

FIG. 2. Titrimeter filling train.

Can. J. Chem. Downloaded from www.nrcresearchpress.com by 210.87.254.105 on 09/05/12
For personal use only.

Conductance water was obtained from a still of the Stuart–Wormwell type, (14), the initial distillation being from $KOH/KMnO_4$ (3–4 g each in 5 l), the output being condensed into the final still where distillation takes place from $NaHSO_4$ (0.1 g/3 l). The vapors from the latter pass through an all-glass spray-suppressor of the same general design as in the original system whence partial condensation takes place in a stream of purified nitrogen on a silica condenser. Water was discarded until a nominal value of specific conductance of less than 5×10^8 ohm^{-1} cm^{-1} at 10 °C was established as determined by a cell forming part of the collection system. It was found that this value could be maintained by storage overnight in a polypropylene container, an integral part of the closed system.

In order to eliminate the error[5] introduced through the simultaneous determination of Λ_0 and of K_b (10, 11), a preliminary determination of the Λ_0 values for ethylammonium chloride was made over the experimental range of interest. While the reproducibility of Λ_0 by our method falls short of what can be obtained by the most careful workers (12), the minor variations in Λ_0 were not judged important for our purpose. The inherent convenience of being able to determine Λ/c for 20–30 different concentrations in a closed system in 1–2 h is self-evident.

Conductance–concentration data for determination of Λ_0 and K_b were obtained by adding increments of the stock solution of the salt, in this case $C_2H_5NH_3Cl$ (for Λ_0) or of the amine $C_2H_5NH_2$ from the titrimeter into a weighed amount of conductance water in the cell. The cumulated concentration of solute in the cell for each incremental addition could be calculated using the equation

$$[1] \qquad M_s = \frac{f \times d_s \times 1000 d_0 \left(\frac{M_0}{1000 d_s}\right) c}{\text{mol. wt.} \times (W_0 + f \times d_s \times c)}$$

where

f = titrimeter factor in ml/1000 counts,
d_s = density of titrant solution,
d_0 = density of conductivity water,
M_0 = concentration of titrant in moles/l,
W_0 = weight of conductivity water originally in cell,
c = number of counts on the titrimeter,
M_s = concentration of substrate in moles/l in the conductivity cell, and
mol. wt. = molecular weight of solute.

It will be apparent that in such a system precautions will have to be taken to minimize zero-point errors and the effects of unavoidable diffusion from the titrimeter capillary. The first was reduced by carefully calibrating the "syringe-units" required to fill the delivery tip from an arbitrary calibration line on the delivery capillary leading to the cell. This could be further corrected by adding small increments, noting the incremental changes in resistance and extrapolating back to "zero-reading". Either method was adequate under optimum conditions, the correction method being preferred when there was some doubt about the reading at the calibration line. At higher temperatures and with volatile amines, only the calibration method was useful. Diffusion between points could be effectively eliminated by "backing-off" a few counts after each addition, thus filling the fine tip of the capillary with the same solution as in the bulk. Such precautions as allowing for steady resistance reading before further additions are obvious. In practice this occurred in less than 1 min.

Temperature Control

Temperature control of about 0.001 °C was achieved by surrounding a small stirred oil bath by a large grounded water bath of conventional design and control to 0.002 °C.

Conductance Bridge

A Dekatron, D272A decade transformer with a norminal accuracy of 0.5 p.p.m. provided the measuring arm of a bridge against standard resistances of known values and capacitances. The frequency source was a GR.1311-A Audio oscillator with a GR.1231-P5 filter. The detector system was a GR.1232-A tuned amplifier and null detector, the final balance being determined on an oscilloscope.

Λ_0 of NaCl and KCl

As a test of the system, Λ_0 for NaCl and KCl was determined by loading the syringe with the respective solutions (0.2 M) and determining concentration–resistance relationships at 25 °C for two series on two successive days for NaCl and over a wider period for KCl. The individual Λ_0 values were found for NaCl from a LMS fit to the Onsager equation [2]

$$[2] \qquad \frac{1000 K_x \left(\frac{1}{R_i} - \frac{1}{R_0}\right)}{(C_i - C_0)} = \Lambda_0 + A \frac{(C_i^{3/2} - C_0^{3/2})}{(C_i - C_0)}$$

where R_i and R_0 are the measured resistance at concentrations C_i and C_0. A is the limiting Λ/c slope, K_x is the cell constant, and Λ_0 is the intercept.

A modification is included to correct for any errors in zeroing the titrimeter, possible adsorption at the walls of the cell at lowest concentrations (the assumption being the major part of such adsorption in so far as it exists, will be established quickly), and as a check on the water correction. Thus Λ_0 was calculated first setting $C_0 = 0.0$ and taking the resistance of water as R_0, then the calculation was repeated using low initial readings of C and R in eq. [2]. The values of Λ_0 so determined were usually within experimental error of the original value but if an error from the above sources was present it would be detected by a change in Λ_0. An illustration of the operation of this procedure is given in Table I.

Values of Λ_0 so determined for NaCl were 126.57, 126.29, 126.47, and 126.89 giving an average value of 126.57 ± 0.17. Shedlovsky (15) gives a value of 126.45 later confirmed by Benson and Gordon (16). The experimental error in the above method is somewhat larger but there is the compensation of economy in time, 2 h being

[5]Professor J. M. W. Scott of Memorial University, St. John's, first drew this possibility to our attention.

TABLE I

Data to illustrate zero point correction

C/1000*	Concentration (mole/l)	Λ_0†
0.0	0.0	126.47
0.1	0.2157×10^{-4}	126.48
0.31	0.6681×10^{-4}	126.40
0.50	1.076×10^{-4}	126.50

*C = titrimeter units.
†Units of Λ_0 throughout the paper are $cm^2\ ohm^{-1}\ equivalent^{-1}$.

sufficient to determine Λ_0 after temperature equilibrium is established.

The values of Λ_0 for KCl were found over a period of 3 months to be 149.94, 149.88, 149.72, and 150.23 giving an average value of 149.94 ± 0.12 compared to the literature value of 149.93 (149.87–149.98 depending on the author (12)).

Determination of Λ_0 for Ethylammonium Chloride

Following the procedures outlined above, the resistance of 30 solutions of increasing ethylammonium chloride concentration were determined. The value of Λ_0 calculated as above from the data in Table II at 25.005 °C is 245.6 with a standard deviation of 0.076%. This is typical of what was obtained through the series though we do not believe that it represents the ultimate precision inherent in the method. Corresponding values for other temperatures are recorded in Table IV.

TABLE II

Concentration–equivalent conductance data* for ethylammonium chloride at 25.005 °C

Concentration (moles/l × 10^{-3})	Conductance	
	Observed†	Calculated
0.13944	121.51	121.28
0.21747	120.90	120.91
0.29522	120.54	120.61
0.38126	120.24	120.32
0.46696	120.02	120.06
0.54379	119.83	119.85
0.62033	119.64	119.65
0.69659	119.51	119.47
0.77258	119.36	119.30

*These data represent about ⅓ of the actual data.
†Left hand side of eq. [2].

By applying the Kohlrausch equation

$$[3]\quad \Lambda_0 R_0NH_3{}^+OH^- = \Lambda_0 R_0NH_3{}^+Cl^- + \Lambda_{0\,OH^-} - \Lambda_{0\,Cl^-}$$

and determining the values of $\Lambda_{0_{OH^-}}$ and $\Lambda_{0_{Cl^-}}$ from the equation

$$[4]\quad \Lambda_{0_t} = \Lambda_{0_{(25°)}} + A(t-25) + B(t-25)^2 + C(t-25)^3$$

the corresponding values of A, B, C, and $\Lambda_0{}^{25}$ are obtained and are given in Table III (17).

TABLE III

Constants for temperature dependence of Λ_0

	$\Lambda_0{}^{25}$	A	$B \times 10^2$	$C \times 10^4$
Cl^-	76.35	1.54037	0.465	−0.1285
OH^-	199.18	3.3604	0.306	−0.4828

The corresponding values of Λ_0 for ethylammonium hydroxide can be determined for each temperature for which K_b is to be determined. The resulting Λ_0 values were fitted to a Λ_0 vs. $(t-25)$ relationship of the conventional form to give the equations: Λ_0–temperature relation for ethylammonium hydrochloride, [5], and Λ_0–temperature relation for ethylammonium hydroxide [6].

$$[5]\quad \Lambda_0 = 122.772 + 2.5822\,(t-25) + 0.0071757\,(t-25)^2 - 0.00015079\,(t-25)^3$$

$$[6]\quad \Lambda_0 = 245.777 + 4.3945\,(t-25) + 0.004948\,(t-25)^2 - 0.00018098\,(t-25)^3$$

Determination of K_b

After the necessary values of Λ_0 for ethylammonium chloride were obtained, the syringe was loaded with an amine solution taking particular precaution to exclude CO_2, and a new series of concentration–resistance readings determined. These data were then fitted to the Shedlovsky–Kay equation (19),

$$[7]\quad \frac{1}{\Lambda S(z)} = \frac{1}{\Lambda_0} + \frac{C\Lambda S(z) f^2}{K{\Lambda_0}^2}$$

where

$$S(z) = 1 + z + \frac{z^2}{2} + \cdots$$

and

$$z = \left(\frac{\alpha\Lambda_0 + \beta}{\Lambda_0{}^{3/2}}\right)\sqrt{(\Lambda C)}$$

$$-\log f^2 = a\sqrt{(cx)}$$

$$a = \frac{3.649 \times 10^6}{(DT)^{3/2}}$$

and

$$x = \frac{\Lambda S(z)}{\Lambda_0}$$

A linear least squares analysis of these data gives a straight line, the slope of which is $1/K_i{\Lambda_0}^2$ and the intercept $1/\Lambda_0$, the value of Λ_0 being that determined in the previous experiments. Values of K_b so determined for a series of temperatures are given in Table V.

Values of the corresponding acid dissociation constant (K_{bh}) for the dissociation

$$EtNH_3{}^+ \rightleftharpoons EtNH_2 + H^+$$

Can. J. Chem. Downloaded from www.nrcresearchpress.com by 210.87.254.105 on 09/05/12
For personal use only.

Can. J. Chem. Downloaded from www.nrcresearchpress.com by 210.87.254.105 on 09/05/12
For personal use only.

TABLE IV

Concentration – equivalent conductance data for ethylamine at 24.947 °C

Concentration (moles/l × 10^{-3})	Conductance (observed)
0.44812	142.09
0.53752	162.11
0.67149	189.92
0.73395	202.11
0.80529	215.43
0.89440	231.42
0.98343	246.74
1.0813	262.85
1.1968	281.11
1.2501	289.27
1.3389	302.51
1.4275	315.34
1.5161	327.83
1.6047	339.93
1.7019	352.91
1.7815	363.29
1.8698	374.51
1.9580	385.57
2.0462	396.28
2.1343	406.88
2.2223	417.26
2.3103	427.36
2.3982	437.33
2.4860	447.15
2.5737	456.70
2.6614	466.14
2.7577	476.40
2.8365	484.59
2.9239	493.67

TABLE V

Temperature – ionization constants for ethylamine

T (°C)	K_b (observed) × 10^6	% Difference*	Λ_0
1.497	445.0	−0.17	147.3
1.837	447.8	+0.19	148.8
5.121	455.7	−0.38	162.0
5.137	455.7	+0.38	162.0
10.137	470.1	+0.12	181.9
10.125	470.0	+0.11	181.9
15.250	479.3	+0.49	203.5
15.244	479.1	+0.45	203.5
20.051	482.4	+0.58	223.9
20.065	479.8	+0.04	223.9
24.934	478.8	−0.02	245.2
24.947	478.0	+0.15	245.2
30.003	469.8	−0.57	268.0
30.004	469.6	−0.61	268.0
34.927	461.5	−0.42	289.9
34.933	461.6	−0.39	289.9
39.951	451.8	+0.18	312.5
39.957	451.4	+0.10	312.5
45.308	436.3	+0.38	335.8
45.318	435.3	+0.15	335.8

*{[K_b (observed) − K_b (calculated)]/K_b (observed)} × 100.

can be readily calculated from the relation $K_b = K_w/K_{bh}$. A series of values of $-\log K_{bh}$ using values of K_w determined by Harned and Robinson (20) are given in Table VI.

TABLE VI

Summary of dissociation constants for ethylamine K_b and ethylammonium ion K_{bh} from 0 to 40 °C

T (°C)	$-\log K_b$	$-\log K_{bh}$
0	3.354_9	11.5886
10	3.327_4	11.2074
20	3.318_0	10.8486
25	3.319_3	10.6772
30	3.324_4	10.5086
40	3.344_8	10.1900

The data in Table VI permit the temperature dependence of the ionization constant K_b for the equilibrium

$$C_2H_5NH_2 + H_2O \rightleftharpoons C_2H_5\overset{+}{N}H_3 + \overset{-}{O}H$$

to be fitted to an equation of the type

$$R \ln K_b = A + B/T + C \ln T + DT + \cdots\cdots$$

using the method of Clarke and Glew (21). The accuracy of these data warrant fit to 3 terms only, i.e. equivalent to setting $d\Delta C_p/dT = 0$, contrary to reasonable theoretical expectations. The thermodynamic constants for a series of temperatures together with standard errors are given in Table VII for a series of temperatures. Values of K_b at intermediate temperatures can be interpolated from the equation

$$[8] \quad \log K_b = 87.52367 - 3994.444/T - 31.29822 \log T$$

with an error comparable to those given in Table VI provided sufficiently accurate log-tables are used.

Discussion

In Table VIII values of K_b obtained in this work are compared with those of previous workers. Everett and Wynne-Jones have commented that potentiometric methods tend to be low. However, their suggestion that conductivity methods may yield correspondingly high results because of the failure to extrapolate to infinite dilution does not apply here.

The calculated standard error is given below each constant and illustrates the change in error across the experimental temperature range, or alternately the inadequacy of the three constant equation.

A better indication of the capability of the system may be made by a comparison of the

Can. J. Chem. Downloaded from www.nrcresearchpress.com by 210.87.254.105 on 09/05/12
For personal use only.

TABLE VII

Thermodynamic constants for the basic dissociation of ethylamine

T (°C)	ΔG (cal/mole)	ΔH (cal/mole)	ΔS (cal/mole deg)	ΔC_p (cal/mole deg)
0.0	4193.1	1288	−10.63	−62.2
	1.3	40	.14	1.8
10.0	4311.04	667	−12.87	−62.2
	.67	24	.08	1.8
20.0	4450.6	45	−15.03	−62.2
	.7	11	.03	1.8
25.0	4528.3	−266	−16.08	−62.2
	.8	12	.04	1.8
30.0	4611.4	−577	−17.11	−62.2
	.7	17	.06	1.8
40.0	4792.7	−1199	−19.1	−62.2
	.9	33	.1	1.8

*Concentration units: moles/l; 1 cal = 4.185 joules.

TABLE VIII

A comparison of K_b values for ethylamine

Temperature (°C)	$K_b \times 10^4$ This work	Literature	Reference
0	4.40_5	4.29	22
20	4.80	4.32	23
25	4.78	4.72	24
		4.65	22
40	4 51	4.19	23

errors in the derived constants given in Table VII with the corresponding values obtained by treating the data of Everett and Wynne-Jones (25) by the same analysis (Table IX). There it is seen that the indeterminacy in the values is approximately the same. It may also be noted that the difference between the values for monomethylamine and monoethylamine are not very different, in agreement with normal expectations.

Since it is the intent of this paper to illustrate the experimental potential and convenience of our conductance system for determining Λ_0 and K_i, no comment will be made at this time on the possible theoretical implications of the results reported.

TABLE IX

A comparison of errors in derived constants at 25 °C from the temperature dependence of K_i determined by conductance and potentiometric methods

Amine	Method*	ΔG_b (cal/mole)	ΔH_b (cal/mole)	ΔS_b (cal/mole deg)	$\Delta C_{p,b}$ (cal/mole deg)
Monomethylamine	P[a]	4598.0±0.8	435 ±9	−13.96±0.04	−56.1±1.2
	C[b]	4562.8±0.5	105.4±8	−14.95±0.02	−59.8±1.1
Dimethylamine	P[a]	4394.1±0.9	1655 ±10	− 9.18±0.04	−68.1±1.4
Trimethylamine	P[a]	4361.3±1.9	4701 ±22	1.14±0.07	−89 ±3
Monoethylamine	C[c]	4528.3±0.8	−266 ±12	−16.08±0.04	−62.2±1.8

*P = potentiometric, C = conductance.
[a]Reference 24.
[b]Reference 25.
[c]This work.

1. K. T. Leffek, R. E. Robertson, and S. E. Sugamori. Chem. Ind. London, 259 (1961).
2. L. Hakka, A. Queen, and R. E. Robertson. J. Am. Chem. Soc. **87**, 161 (1965).
3. M. Wolfsberg and M. J. Stern. Symposium on isotope mass effects in chemistry and biology. Butterworths, London. 1964. p. 325.
4. W. van der Linde and R. E. Robertson. J. Am. Chem. Soc. **86**, 4505 (1964).
5. S. Martin, R. E. Robertson, and G. C. Benson. J. Sci. Instr. **41**, 237 (1964).
6. D. J. G. Ives and J. H. Pryor. J. Chem. Soc. 2104 (1955).
7. D. J. G. Ives. J. Chem. Soc. 731 (1933).
8. I. Ross and R. E. Robertson. Unpublished results.
9. T. Shedlovsky. J. Franklin Inst. **225**, 739 (1938).
10. D. Belcher. J. Am. Chem. Soc. **60**, 2744 (1938).
11. M. L. Kilpatrick. J. Chem. Phys. **8**, 306 (1940).

12. J. E. LIND, JR., J. J. ZWOLENIK, and R. M. FUOSS. J. Am. Chem. Soc. **81**, 1557 (1959).
13. T. SHEDLOVSKY. J. Am. Chem. Soc. **54**, 1411 (1932).
14. J. M. STUART and F. WORMWELL. J. Chem. Soc. 85 (1930).
15. T. SHEDLOVSKY, A. S. BROWN, and D. A. MCINNES. Trans. Electrochem. Soc. **66**, 165 (1934).
16. G. C. BENSON and A. R. GORDON. J. Chem. Phys. **13**, 473 (1945).
17. H. S. HARNED and B. B. OWEN. The physical chemistry of electrolytic solutions. 3rd ed. Reinhold Publishing Co., New York. p. 233.
18. K. N. MARSH and R. H. STOKES. Australian J. Chem. **17**, 740 (1964).
19. T. SHEDLOVSKY and R. L. KAY. J. Phys. Chem. **60**, 151 (1956).
20. E. C. W. CLARKE and D. N. GLEW. Trans. Faraday Soc. **62**, 539 (1966).
21. W. C. SOMMERVILLE. J. Phys. Chem. **35**, 2412 (1931).
22. A. G. EVANS and S. D. HAMANN. Trans. Faraday Soc. **47**, 25 (1951).
23. N. F. HALL and M. R. SPRINKLE. J. Am. Chem. Soc. **54**, 3469 (1932).
24. D. H. EVERETT and W. F. K. WYNNE-JONES. Proc. Roy. Soc. London, Ser. A, **177**, 499 (1941).
25. D. NORTHCOTT. Unpublished results.

Can. J. Chem. Downloaded from www.nrcresearchpress.com by 210.87.254.105 on 09/05/12
For personal use only.

Can. J. Chem. Downloaded from www.nrcresearchpress.com by 210.87.254.105 on 09/05/12
For personal use only.

Formation of diphenyl nitroxide in diphenylamine inhibited autoxidations[1]

K. ADAMIC[2], M. DUNN[3], AND K. U. INGOLD
Division of Applied Chemistry, National Research Council of Canada, Ottawa, Canada

Received July 23, 1968

The formation of diphenyl nitroxide in diphenylamine inhibited, α,α′-azo-bis-isobutyronitrile initiated, autoxidations at 65° has been studied by electron spin resonance. Diphenylamine is oxidized to a diphenylamino radical which is then converted to the nitroxide by an oxygen atom transfer from a peroxy radical. The initial rates of conversion of diphenylamine to diphenyl nitroxide and the maximum nitroxide concentrations attained are generally greater for oxidations with tertiary peroxy radicals than for oxidations with primary or secondary peroxy radicals. The lower efficiency of nitroxide formation by primary and secondary peroxy radicals is attributed to a cage disproportionation between alkoxy radical and nitroxide which leads to the formation of a carbonyl compound and diphenyl hydroxylamine. This reaction cannot occur with tertiary radicals. The rate of formation of diphenyl nitroxide is greater for tertiary peroxy radicals which give stable tertiary alkoxy radicals. Nitroxide formation is inhibited by secondary, but not by tertiary, hydroperoxides.

Canadian Journal of Chemistry, **47**, 287 (1969)

One of the most important developments in our understanding of the inhibition of oxidation by amines was the discovery by Thomas and coworkers (refs. 1–4, see also refs. 5–7) that relatively stable diaryl nitric oxide radicals (nitroxides) are produced in fairly high concentrations during inhibition with diarylamines. They are believed to be formed by the reaction sequence

$$ROO^{\cdot} + Ar_2NH \rightarrow ROOH + Ar_2N^{\cdot}$$

$$ROO^{\cdot} + Ar_2N^{\cdot} \rightarrow RO^{\cdot} + Ar_2NO^{\cdot}$$

A similar reaction sequence with dialkyl amines leads to the production of dialkyl nitroxides (3, 8).

Although there have been many studies of the kinetics of the inhibition of autoxidation by amines[4] (cf. 9, 10 and references cited therein) the kinetics of nitroxide formation in these systems has been the subject of only one serious investigation. In 1962 Thomas and Tolman (4) used electron spin resonance (e.s.r.) spectroscopy to follow the formation of diphenyl nitroxide in the diphenylamine inhibited oxidation of cumene at 68.5°. Unfortunately, the importance of chain transfer reactions between inhibitor radicals and hydroperoxide products was not appreciated at that time and some of the results were incorrectly interpreted in terms of complex formation between peroxy radicals and inhibitors. The overall process of inhibition is now so much better understood that we decided to re-investigate the formation of diphenyl nitroxide in diphenylamine inhibited oxidations. Cumene and a number of other hydrocarbons were used as oxidizing substrates.

Experimental

Apparatus

In order to obtain an essentially continuous record of the free radical concentration the reagents were circulated through the cavity of a Varian E-3 e.s.r. spectrometer. The apparatus is shown schematically in Fig. 1. It is built of Pyrex except for a 3 mm i.d. quartz tube running through the spectrometer cavity. The reagents (55–60 ml) are normally saturated with oxygen[5] and circulated at a rate of ~ 10 ml/s by a reciprocating 10 ml

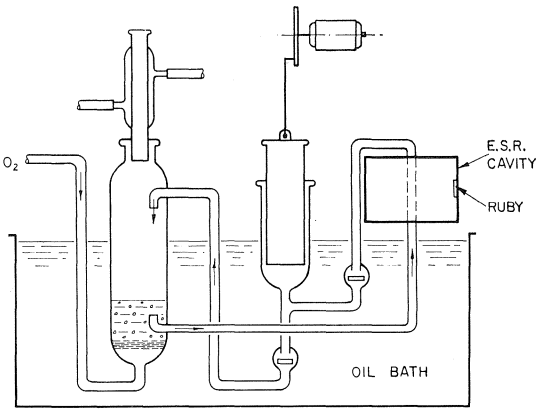

FIG. 1. Diagram of experimental apparatus.

[1]Issued as NRCC No. 10 412.
[2]NRCC Postdoctorate Fellow, 1967–1968.
[3]NRCC Summer Student 1967.
[4]Inhibition by stable nitroxide radicals has also been extensively investigated (cf. 11, 12 and cited references).
[5]Electron spin resonance signals of about the same intensity are usually formed in systems saturated with air.

Can. J. Chem. Downloaded from www.nrcresearchpress.com by 210.87.254.105 on 09/05/12
For personal use only.

hypodermic syringe associated with two glass float valves. The apparatus is immersed in an oil bath thermostated at 69° which ensures that the circulating reactants are held at 65 °C.

Procedure

A 55 ml aliquot of the hydrocarbon to be oxidized was poured into the main reservoir. A chlorobenzene solution of diphenylamine, Ph_2NH, (typically 0.5 ml of a 0.1 *M* solution) was immediately added and the circulating pump started. The e.s.r. spectrometer was tuned and a background spectrum obtained. A chlorobenzene solution of α,α′-azo-bis-isobutyronitrile, AIBN, (typically 5 ml of a 0.3 *M* solution) was then pipetted into the reservoir, the completion of its addition being considered to represent the start of the reaction (time zero). The radical concentration was monitored at frequent intervals, the minimum time between readings being 30 s. Not less than 5 ml of chlorobenzene were used in all the experiments. In some runs no hydrocarbon was present, the reactants being 50–55 ml of chlorobenzene, Ph_2NH, 0.05–5 ml of a hydroperoxide, and AIBN, added in that order.

To obtain reproducible results it was necessary to add the Ph_2NH before the AIBN. Two complications can arise if the reverse mode of addition is employed. In the first place, some hydrocarbons which oxidize by way of tertiary peroxy radicals (e.g. cumene) quickly develop a steady e.s.r. signal due to these peroxy radicals. Although this signal disappears as soon as the Ph_2NH is added and although it is reasonably well distinguishable from the diphenyl nitroxide signal[6], it can interfere with the integration of the first derivative. The second complication arises with hydrocarbons which oxidize to give primary or secondary peroxy radicals. Although these hydrocarbons give a very small steady-state peroxy radical signal[7], the hydroperoxides formed in these oxidations appear to react quite rapidly with nitroxide radicals. The formation of these hydroperoxides in the system prior to the introduction of the Ph_2NH leads to lower rates of formation and much smaller maximum concentrations of nitroxide radicals than for systems which are initially free from hydroperoxide. This difficulty does not arise with hydrocarbons forming tertiary hydroperoxides, as these do not seem to react with nitroxides nearly so rapidly as secondary hydroperoxides.

Calibration of the Radical Concentration

In place calibration of the system was done with freshly prepared 2,2-diphenyl-1-picrylhydrazyl (DPPH) solutions in chlorobenzene (10^{-4} *M* at 65 °C). The radical concentrations were determined by double integration of the first derivative e.s.r. signal using a Honeywell GPI-10 general purpose integrator. A small single crystal of synthetic ruby was attached to the inside of the cavity with a dab of Apiezon grease and its signal at ~ 2 kG was used to correct for variations in spectrometer sensitivity due to solvent induced variations in cavity Q (17).

Determination of the Rate of Chain Initiation (R_i)

The rate of free radical formation by the AIBN was determined by allowing it to react with known concentrations of stable nitroxide radicals in chlorobenzene. The reaction was carried out in the absence of oxygen by flushing the system continuously with helium. The radicals 4,4′-dimethoxydiphenyl nitroxide and 2,2,6,6-tetramethyl-4-pyridone nitroxide were stable for several thousand seconds at 65° in the absence of AIBN. 4,4′-Dinitrodiphenyl nitroxide was not stable under these conditions. Upon the addition of AIBN the e.s.r. signal due to the stable nitroxides declined linearly with time (i.e. the destruction of nitroxide is zero order in nitroxide). With 2.5×10^{-2} *M* [AIBN] the rate of chain initiation was found to be 5.2×10^{-7} *M* s^{-1} which, when combined with the known rate constant for the decomposition of AIBN at this temperature (1.8×10^{-5} s^{-1} (9)), gives a value of 58% for the efficiency of chain initiation.

Materials

Commercial diphenylamine was purified by zone refining. Ethylbenzene, cumene, and *sec*-butylbenzene were Phillips Research grade materials. The other hydrocarbons were of C.P. grade and were further purified by distillation under vacuum. Fisher certified chlorobenzene was used as an "inert" diluent. The hydrocarbons and chlorobenzene were passed through alumina immediately before use in order to remove any trace of hydroperoxide (14). The preparation and purification of the hydroperoxides has been described in previous publications from this laboratory (18).

Results

A typical set of nitroxide accumulation curves are shown in Fig. 2. The substrate is α-methylstyrene and the AIBN concentration is 2.5×10^{-2} *M*. It can be seen that as the Ph_2NH concentration is reduced the maximum concentration of diphenyl nitroxide decreases, but the initial rate of nitroxide formation increases and appears to approach a limiting value at the lowest Ph_2NH concentrations. The initial rate of nitroxide formation can also be increased at constant Ph_2NH concentration by increasing the AIBN concentration.

A measure of the efficiency of nitroxide formation can be obtained by dividing the measured rate of nitroxide formation, ρ, by the known rate of chain initiation, R_i. Values of ρ/R_i at an AIBN concentration of 2.5×10^{-2} *M* are summarized in Tables I and II. These tables also include the maximum nitroxide concentration $[Ph_2NO^{\cdot}]_{max}$ and the time taken to reach the maxima for the reactions with 8.3×10^{-4} *M* $[Ph_2NH]$. The initial chain lengths, ν, (Table I) were calculated

[6]The *g* values for peroxy radicals are in the range 2.014–2.016 (13, 14) while the *g* values for nitroxide radicals are below 2.010 and are generally in the range 2.003–2.008 (see, for example, ref. 15).

[7]Because of the rapid self-reaction of these peroxy radicals compared with the rate for the self-reaction of tertiary peroxy radicals (16).

Can. J. Chem. Downloaded from www.nrcresearchpress.com by 210.87.254.105 on 09/05/12
For personal use only.

TABLE I

The formation of diphenyl nitroxide in diphenylamine inhibited autoxidations*

Substrate‡	$\rho/R_i \times 10^3$ at $[Ph_2NH] \times 10^{-4}$ of 83 *M*	17 *M*	8.3 *M*	3.3 *M*	1.7 *M*	$[Ph_2NO^{\cdot}]_{max} \times 10^6$ (*M*)	Time† (s)	Initial chain lengths (ν)
Allylbenzene (*p*)	76	105	110	110	105	13	400	11
Tetralin (*s*)	115	120	110	80	65	30	950	7
Ethylbenzene (*s*)	45	115	165	190	180	140	2900	1.5
Styrene (*s*)	47	90	90	110	78	26	1050	49
Chlorobenzene (*t*)	30	66	105	135	165	96	2300	0
t-Butylbenzene (*t*)	23	58	90	130	135	100	3200	0
α-Methylstyrene (*t*)	60	135	155	190	195	69	1250	11
sec-Butylbenzene (*t*)	33	94	135	190	225	130	3200	0.07
Cumene§ (*t*)	46	140	225	310	330	185	2400	0.18

*At 65 °C ([AIBN] = 2.5×10^{-2} *M*. Substrate 90% by volume, chlorobenzene 10%).
†Time taken to reach maximum nitroxide concentration, $[Ph_2NO^{\cdot}]_{max}$. The $[Ph_2NH]$ was 8.3×10^{-4} *M*.
‡The type of peroxy radical nominally present in the oxidation is denoted by *p* (primary), *s* (secondary), and *t* (tertiary).
§The results of Thomas and Tolman (4) at 68.5 °C using 4 *M* cumene in chlorobenzene as the substrate and with $[Ph_2NH] = 1 \times 10^{-4}$ *M* and $[AIBN] = 1 \times 10^{-3}$ *M* ($R_i = 2.36 \times 10^{-5}$ *M* s^{-1}) give $\rho/R_i = 0.30$, $[Ph_2NO^{\cdot}]_{max} = 1.8 \times 10^{-5}$ *M* at ~ 4200 s.

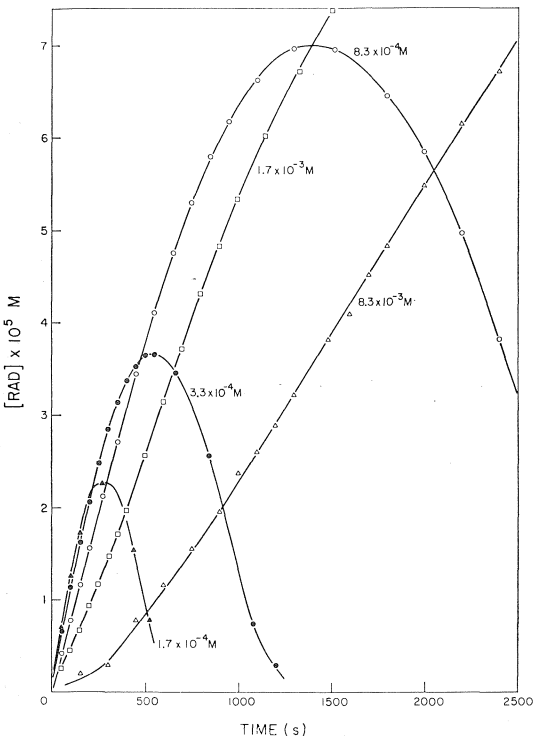

FIG. 2. The formation of diphenylnitroxide in the diphenylamine inhibited oxidation of α-methylstyrene at 65°. The AIBN concentration is 2.5×10^{-2} *M*. The numbers on the curves refer to the Ph_2NH concentration.

from the relation $\nu = k_2[RH]/k_3[Ph_2NH]$, where k_2 and k_3 are the rate constants for the reactions,

[2] $ROO^{\cdot} + RH \rightarrow ROOH + R^{\cdot}$ (or $ROO\dot{R}H$)

[3] $ROO^{\cdot} + Ph_2NH \rightarrow ROOH + Ph_2N^{\cdot}$

TABLE II

The formation of diphenyl nitroxide in diphenylamine inhibited autoxidations*

Substrate	$\frac{\rho}{R_i} \times 10^3$	$[Ph_2NO^{\cdot}]_{max} \times 10^6$ (*M*)	Time† (s)
Allylbenzene	130	39	1100
Tetralin	200	140	2200
Ethylbenzene	130	115	2700
Styrene	135	75	2000
t-Butylbenzene	100	97	2500
α-Methylstyrene	185	145	2300
sec-Butylbenzene	125	125	2400
Cumene	145	135	2500

*At 65 °C ([AIBN] = 2.5×10^{-2} *M*, $[PH_2NH] = 8.3 \times 10^{-4}$ *M*. Substrate 16% by volume, chlorobenzene 84%).
†Time taken to reach maximum nitroxide concentration, $[Ph_2NO^{\cdot}]_{max}$.

Values of k_2 at 65° were assumed to be 5 times as great as the values measured at 30° in this laboratory by the rotating sector method (16). The rate constant for reaction 3 with poly-(peroxystyryl)peroxy radicals is about 4×10^4 M^{-1} s^{-1} (10).

Peroxy radicals can be produced not only by the oxidation of hydrocarbons but also by the free-radical induced decomposition of hydroperoxides, i.e.

$$ROOH + X^{\cdot} \rightarrow ROO^{\cdot} + XH$$

The hydroperoxide was added to chlorobenzene containing the amine and this was followed by the addition of AIBN. The results obtained by this procedure using 1.0–0.01 *M* [hydroperoxide], 8.3×10^{-4} *M* $[Ph_2NH]$, and 2.5×10^{-2} *M* [AIBN] are summarized in Table III. Similar results were obtained in *t*-butylbenzene and in

TABLE III

The formation of diphenyl nitroxide during diphenylamine inhibited decomposition of hydroperoxides in chlorobenzene*

Hydroperoxide	$\rho/R_i \times 10^3$ at [hydroperoxide] of						$[Ph_2NO^\cdot]_{max}$† $\times 10^5$ (M)	Time‡ (s)
	1.0 M	0.2 M	0.1 M	0.04 M	0.02 M	0.01 M		
9,10-Dihydroanthracyl-9-(*s*)	—	—	0§	—	0§	—	0	—
Tetralyl (*s*)	—	—	50	—	150	—	10	900
1,1-Diphenylethyl (*t*)	—	—	140	—	195	—	14	600
2-Phenylbutyl-2-(*t*)	—	—	340	—	400	—	78	1300
Cumyl (*t*)	—	410	375	—	415	—	100	900
t-Butyl (*t*)	190	410	460	550	580	580	110	1300

*At 65 °C ([AIBN] = 2.5×10^{-2} M, $[Ph_2NH] = 8.3 \times 10^{-4}$ M).
†At 0.1 M [hydroperoxide].
‡Time taken to reach maximum nitroxide concentration, at 0.1 M [hydroperoxide].
§No nitroxide detectable.

chlorobenzene – *t*-butylbenzene mixtures. It is obvious from the data in this table that secondary hydroperoxides strongly inhibit the formation of nitroxide. None is detected in the presence of as little as 0.02 M [9,10-dihydroanthracyl-9-hydroperoxide]. Tetralin hydroperoxide at 0.1 M depresses ρ/R_i and the maximum radical concentration compared with the values found for these quantities in tetralin or chlorobenzene (cf. Table I). After the maximum nitroxide concentration is attained the radical concentration remains virtually constant for a prolonged period. This steady nitroxide concentration is roughly inversely proportional to the concentration of the added tetralin hydroperoxide. The addition of tetralin hydroperoxide to oxidizing tetralin during the reaction but before the attainment of the maximum radical concentration produces a sharp decrease in the nitroxide concentration. After about 300–600 s the nitroxide concentration steadies at a relatively low value.

In contrast to these results with secondary hydroperoxides, the tertiary hydroperoxides produce high ρ/R_i values and the curves for nitroxide formation resemble those obtained in oxidizing hydrocarbons. The values of ρ/R_i for cumene hydroperoxide are larger than for cumene and, in fact, if the AIBN is added to cumene before the amine, a higher value of ρ/R_i is obtained than when the usual procedure is followed. Thus, at $[Ph_2NH] = 8.3 \times 10^{-4}$ M, $\rho/R_i = 0.37$ if the AIBN is added 2–3 min before the Ph_2NH, whereas a value of 0.22 is obtained (Table I) when the amine is added first. This difference is clearly due to the formation of cumene hydroperoxide (probably $\sim 5 \times 10^{-3} - 1 \times 10^{-2}$ M) before the amine is added.

Discussion

Diphenylamine stops slightly more than two reaction chains per molecule in oxidizing cumene (4, 19). The changes in nitroxide concentration with time shown in Fig. 2 indicate that the nitroxide is essentially all consumed by the end of the induction period, as has been previously reported (4). That is, the induction period is approximately given by $2[Ph_2NH]/R_i$ which, for $R_i = 5.2 \times 10^{-7}$ $M\,s^{-1}$, is 650, 1270, and 3200 s at $[Ph_2NH] = 1.7$, 3.3, and 8.3×10^{-4} M, respectively.

Although secondary and, presumably, primary hydroperoxides tend to inhibit the formation of nitroxide this should not affect the measured values of ρ/R_i which are given in Table I. This is because the normal experimental procedure ensures that no hydroperoxide is present at the beginning of the reaction. On the other hand, the maximum concentration of nitroxide which is obtained may be influenced by the substrate because of the nature of the hydroperoxide it forms in reactions [2] and [3]. That is, we might expect to get lower maximum nitroxide concentrations for substrates giving primary or secondary hydroperoxides than for those giving tertiary hydroperoxides. With the exception of ethylbenzene, this generally seems to be the case (cf. Table I). The exception may perhaps be attributable to the short chain length in ethylbenzene which implies that a large fraction of the hydroperoxide formed during reaction will be the

Can. J. Chem. Downloaded from www.nrcresearchpress.com by 210.87.254.105 on 09/05/12
For personal use only.

tertiary hydroperoxide formed from the initiator rather than the secondary 1-phenylethyl hydroperoxide.

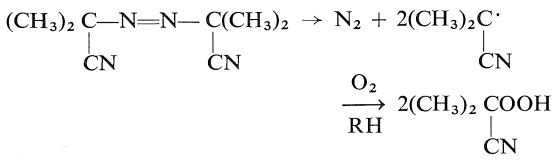

The following scheme represents the simplest sequence of reactions that is consistent with our results:

[1] $\text{AIBN} \xrightarrow{O_2} 2e\text{IOO}^{\cdot}$ (Rate R_i)

[2] $\text{ROO}^{\cdot} + \text{RH} \xrightarrow{O_2} \text{ROOH} + \text{ROO}^{\cdot}$

[2a] $\text{RO}^{\cdot} + \text{RH} \xrightarrow{O_2} \text{ROH} + \text{ROO}^{\cdot}$

[3] $\text{ROO}^{\cdot} + \text{Ph}_2\text{NH} \rightleftarrows \text{ROOH} + \text{Ph}_2\text{N}^{\cdot}$

[4] $\text{ROO}^{\cdot} + \text{Ph}_2\text{N}^{\cdot} \rightarrow \text{RO}^{\cdot} + \text{Ph}_2\text{NO}^{\cdot}$

[4a] $\text{ROO}^{\cdot} + \text{Ph}_2\text{N}^{\cdot} \rightarrow$ Molecular products

[5] $\text{ROO}^{\cdot} + \text{ROO}^{\cdot} \rightarrow$ Molecular products

[6] $\text{ROO}^{\cdot} + \text{Ph}_2\text{NO}^{\cdot} \rightarrow$ Molecular products

[7] $\text{R}^{\cdot} + \text{Ph}_2\text{NO}^{\cdot} \rightarrow$ Molecular products

[8] $\text{Ph}_2\text{N}^{\cdot} \rightarrow ?$

[9] $\text{ROOH} + \text{Ph}_2\text{NO}^{\cdot} \rightleftarrows \text{ROO}^{\cdot} + \text{Ph}_2\text{NOH}$

The AIBN decomposes to give *iso*-butyronitrile radicals with an efficiency e, and these react with oxygen to give $\text{IOO}^{\cdot}$ radicals which attack the substrate RH or the amine. In this scheme it is understood that all reactions involving $\text{ROO}^{\cdot}$ and $\text{RO}^{\cdot}$ radicals may equally well involve $\text{IOO}^{\cdot}$ or $\text{IO}^{\cdot}$ radicals and must, of course, involve only these radicals in the non-oxidizable substrates, chlorobenzene and *t*-butylbenzene. The relative importance of the radicals from the initiator will increase as the chain length decreases, as occurs when an oxidizable substrate is diluted with chlorobenzene (see Table II).

At high diphenylamine concentrations the initial rate of nitroxide formation is low because most of the $\text{ROO}^{\cdot}$ radicals are trapped by the amine in reaction [3] and they are therefore not available to take part in reaction [4]. Since the $\text{Ph}_2\text{N}^{\cdot}$ radical does not accumulate under these conditions it must be able to react in some way other than reactions [4] or [4*a*]. The unknown mode or modes of reaction are represented by reaction [8].

At very low diphenylamine concentrations the initial rate of nitroxide formation is low because some peroxy radicals are destroyed in the normal termination process, reaction [5]. Maximum rates of nitroxide formation occur at intermediate amine concentrations which are primarily determined by the rate constant of reaction [5]. That is, the rate constant of reaction [5] is generally considerably greater for primary and secondary than for tertiary peroxy radicals (16). In agreement with this, the ρ/R_i values pass through maxima at $[\text{Ph}_2\text{NH}] \geqslant 3 \times 10^{-4}\ M$ for the substrates giving primary and secondary peroxy radicals whereas the substrates giving tertiary peroxy radicals and the non-oxidizing substrates all have maximum ρ/R_i values at amine concentrations below $1.7 \times 10^{-4}\ M$.

In the diphenylamine inhibited decomposition of the hydroperoxides the value of ρ/R_i decreases as the hydroperoxide concentration is increased (Table III). This suggests the occurrence of a direct reaction between the hydroperoxide and the amino radical (reaction [−3]) and/or the occurrence of a direct reaction between the hydroperoxide and the nitroxide (reaction [9]). Reaction [−3] was previously proposed by Thomas to explain the fact that the rate of the diphenylamine (or phenol) inhibited oxidation of cumene increased with increasing concentration of cumene hydroperoxide (20). However, in amine inhibited oxidations, reaction [−3] is not kinetically distinguishable from reaction [9], the analogous reaction with nitroxide (see ref. 9, footnote 4). Although our present measurements on the formation of nitroxide cannot determine the relative importance of reactions [−3] and [9] some reasonably direct evidence for the occurrence of the latter reaction has been obtained in experiments with the free radical 4,4′-dimethoxydiphenyl nitroxide. This radical is stable in chlorobenzene at 65°. Hydroperoxide was added to a $1.8 \times 10^{-3}\ M$ solution of the nitroxide in the absence of AIBN and oxygen. The secondary hydroperoxides (0.1 M) produced an immediate rapid decrease in the nitroxide concentration (50% consumption in 500 s with 9,10-dihydroanthracyl-9-hydroperoxide and in 2000 s with tetralin hydroperoxide). In contrast, the addition of the tertiary hydroperoxides, *t*-butyl, cumyl,

Can. J. Chem. Downloaded from www.nrcresearchpress.com by 210.87.254.105 on 09/05/12
For personal use only.

Can. J. Chem. Downloaded from www.nrcresearchpress.com by 210.87.254.105 on 09/05/12
For personal use only.

2-phenylbutyl-2, and 1,1-diphenylethyl, at the same concentration caused little or no loss of nitroxide for a period of 1000–3000 s or more. Thereafter, the nitroxide concentration started to decrease but it decreased at a lower rate than with either of the secondary hydroperoxides. The most probable reaction between a nitroxide and a secondary hydroperoxide would seem to be a hydrogen atom transfer to give a hydroxylamine and a peroxy radical (i.e. reaction [9]). However, there is no very obvious reason why such a reaction should not also occur with tertiary hydroperoxides. The difference between the two classes of hydroperoxides may perhaps be attributed to differences in the importance of reaction [−9] which result from differences in the rate constants for the self-reactions of the secondary or tertiary peroxy radicals produced in reaction [9]. That is, since reaction [−9] is extremely rapid (11) the dimethoxydiphenyl nitroxide concentration must be determined to some extent by the amount of hydroxylamine which has been formed in reaction [9] and by the peroxy radical concentration. In the presence of a secondary hydroperoxide the concentration of the peroxy radicals produced in reaction [9] will be small because of their rapid disappearance by reaction [5]. Reaction [−9] will therefore be relatively unimportant and the rate of loss of dimethoxydiphenyl nitroxide will be large. On the other hand, the slow self-reaction of tertiary peroxy radicals means that in the presence of a tertiary hydroperoxide the nitroxide will be lost slowly since it is being reformed by reaction [−9].

Differences in the rate constants of the self-reactions of secondary and tertiary peroxy radicals may also be partly responsible for the difference in the rates of formation and maximum concentrations of diphenyl nitroxide in the presence of secondary and tertiary hydroperoxides.

In a system saturated with oxygen at 1 atm pressure the steady-state concentration of R· radicals is so much less than the concentration of ROO· radicals that it might be supposed that reaction [7] could play no part in the overall process. However, it is known that the autoxidation of hydrocarbons can be inhibited by aliphatic nitroxide radicals such as 2,2,6,6-tetramethyl-4-pyridone nitroxide under conditions similar to those used in the present work (11). This nitroxide reacts rapidly with R· radicals ($k_7 \geqslant 1 \times 10^7\ M^{-1}\ s^{-1}$ (11)) but slowly, or not at all, with ROO· radicals (11, 21–23). When this nitroxide was added ($10^{-4}\ M$) to oxygen saturated chlorobenzene containing AIBN ($2.5 \times 10^{-2}\ M$) in the present apparatus it was consumed at about $\frac{1}{5}$ of the rate of chain initiation. Since aromatic nitroxides react equally rapidly with R· radicals (2, 4, 11, 21–23) it seems likely that reaction [7] represents an important route for the destruction of diphenyl nitroxide[8]. However, it is not the only route since aromatic nitroxides do react with peroxy radicals. For example, k_6 is about $5 \times 10^4\ M^{-1}\ s^{-1}$ at 65° for 4,4′-dimethoxydiphenyl nitroxide (11) and probably has a similar value for diphenyl nitroxide (cf. footnote 4 in ref. 11). The rate constant for the reaction of Ph_2NO· with peroxy radicals is of comparable magnitude to that for the reaction of Ph_2NH with peroxy radicals ($4 \times 10^4\ M^{-1}\ s^{-1}$ (10)). It is therefore easy to understand why quite high concentrations of nitroxide can accumulate in oxygen saturated systems.

According to the reaction scheme given above, the maximum value of ρ/R_i is 1.0. This assumes that reactions [4*a*] and [5] do not occur and that all the RO· radicals formed in reaction [4] regenerate ROO· radicals *via* reaction [2*a*] or the analogous reaction [2*b*]

$$[2b] \qquad RO\cdot + ROOH \rightarrow ROH + ROO\cdot$$

That is, $\rho/R_i = 1.0$ if all Ph_2N· radicals are converted to Ph_2NO· and all RO· regenerate ROO·. Experimentally, with diphenylamine at 65°, we have never found a value of $\rho/R_i > 0.58$ which suggests that not all ROO· + Ph_2N· reactions lead to the formation of a nitroxide radical. It is for this reason that reaction [4*a*] is included in the reaction scheme.

From the results in Table I it can be seen that the maximum values of ρ/R_i are in the range 0.11–0.19 for hydrocarbons giving primary and secondary peroxy radicals. The hydrocarbons oxidizing to give tertiary peroxy radicals have maximum ρ/R_i values greater than the largest measured values (0.20 for α-methylstyrene, 0.23

[8]Reaction [7] should be much less important in the diphenylamine inhibited decomposition of hydroperoxides than in diphenylamine inhibited oxidations since R· radicals are not formally involved in the induced decomposition of hydroperoxides. The higher ρ/R_i values obtained in *t*-hydroperoxides compared with those obtained in *t*-hydrocarbons are consistent with this idea.

for *sec*-butylbenzene, and 0.33 for cumene). For the inert substrates, in which the tertiary 2-cyanopropyl-2-peroxy radical may be expected to predominate, the ρ/R_i values are greater than 0.14 (*t*-butylbenzene) and 0.17 (chlorobenzene). The ρ/R_i values in Table III are greater for tertiary than for secondary hydroperoxides, rising to a maximum of 0.58 with *t*-butyl hydroperoxide. A plausible explanation for the higher ρ/R_i ratios obtained with tertiary peroxy radicals is that the primary and secondary peroxy radicals undergo a hydrogen atom exchange in the cage to give a carbonyl compound and a hydroxylamine. That is,

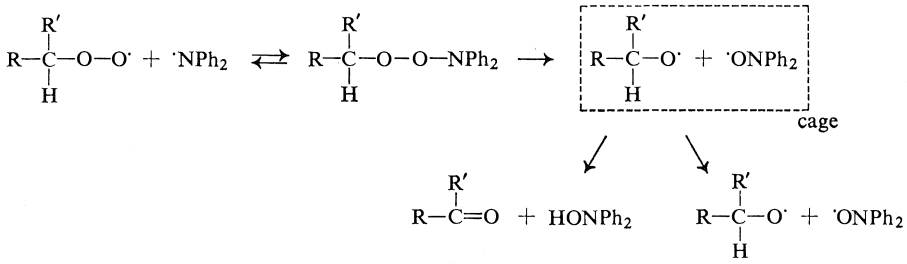

Such a hydrogen atom transfer is obviously impossible for a tertiary peroxy radical and they are, therefore, more efficient than primary or secondary peroxy radicals at converting diphenylamine into diphenyl nitroxide.

Under standard conditions, the variations in ρ/R_i appear to be greater among the different tertiary peroxy radicals than among the secondary peroxy radicals. Some of the differences in the ρ/R_i values can probably be attributed to differences in the stabilities of the alkoxy radical which is formed in conjunction with the nitroxide in reaction [4]. That is, a stable alkoxy radical will tend to regenerate its parent peroxy radical directly by reaction [2*a*] or [2*b*], whereas an unstable alkoxy radical will be more likely to undergo β-scission to form a carbonyl compound and a carbon centered radical,

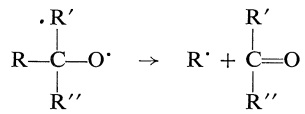

It is possible that some alkoxy radicals are actually so unstable that they undergo scission while still in the solvent cage with the nitroxide. For primary and secondary alkoxy radicals (which are generally less stable than most tertiary alkoxy radicals), β-scission will usually lead to the formation of a primary peroxy radical. The types of peroxy radicals present in the amine inhibited reaction will therefore not be greatly changed from the types present in the uninhibited oxidation. However, the β-scission of many tertiary alkoxy radicals also gives primary peroxy radicals, e.g.

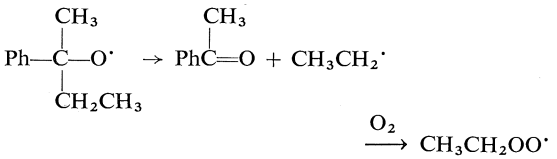

and these presumably will tend to decrease the value of ρ/R_i. The results in Tables I, II, and III support the idea that decreased β-scission tends to increase ρ/R_i. For example, the series 1,1-diphenylethyl, 2-phenylbutyl-2, cumyl, *t*-butyl, corresponds to decreasing rates of alkoxy radical β-scission and to increasing values of ρ/R_i. The rate of β-scission must also be high for the 2-cyano-2-propoxy radical (IO$^{\cdot}$) and the alkoxy radical from the α-methylstyrene–oxygen copolymer. In this last case (and also with styrene), the formation of a polymeric alkoxy radical normally leads to its rapid and complete depolymerization to acetophenone (or benzaldehyde), formaldehyde, and the radical that initiated the polymerization.

In summary, the initial rates of conversion of diphenylamine to diphenyl nitroxide and the maximum nitroxide concentrations attained are generally greater for oxidations with tertiary peroxy radicals than for oxidations with primary or secondary peroxy radicals. The more efficient tertiary peroxy radicals are those giving the more stable tertiary alkoxy radicals. The formation of the nitroxide is inhibited by secondary, but not by tertiary, hydroperoxides.

Can. J. Chem. Downloaded from www.nrcresearchpress.com by 210.87.254.105 on 09/05/12
For personal use only.

1. O. L. HARLE and J. R. THOMAS. J. Am. Chem. Soc. **79**, 2973 (1957).
2. J. R. THOMAS. J. Am. Chem. Soc. **82**, 5955 (1960).
3. J. C. BAIRD and J. R. THOMAS. J. Chem. Phys. **35**, 1507 (1961).
4. J. R. THOMAS and C. A. TOLMAN. J. Am. Chem. Soc. **84**, 2930 (1962).
5. R. H. HOSKINS. J. Chem. Phys. **25**, 788 (1956).
6. A. T. KORITSKII and A. F. LUKOVNIKOV. Dokl. Akad. Nauk SSSR, **147**, 1126 (1962).
7. A. L. BUCHACHENKO. Opt. i Spektroskopiya, **13**, 795 (1962).
8. J. Q. ADAMS, S. W. NICKSIC, and J. R. THOMAS. J. Chem. Phys. **45**, 654 (1966).
9. I. T. BROWNLIE and K. U. INGOLD. Can. J. Chem. **44**, 861 (1966).
10. I. T. BROWNLIE and K. U. INGOLD. Can. J. Chem. **45**, 2419 (1967).
11. I. T. BROWNLIE and K. U. INGOLD. Can. J. Chem. **45**, 2427 (1967).
12. M. B. NEIMAN (*Editor*). Aging and stabilization of polymers. Consultants Bureau. New York. 1965. Chaps. 1, 2, and 5.
13. M. BERSOHN and J. R. THOMAS. J. Am. Chem. Soc. **86**, 959 (1964).
14. K. U. INGOLD and J. R. MORTON. J. Am. Chem. Soc. **86**, 3400 (1964).
15. A. L. BUCHACHENKO. Stable radicals. Consultants Bureau. New York. 1965. Chap. 4.
16. J. A. HOWARD and K. U. INGOLD. Can. J. Chem. **45**, 793 (1967).
17. L. S. SINGER. J. Chem. Phys. **30**, 1463 (1959).
18. J. A. HOWARD and K. U. INGOLD. Can. J. Chem. **46**, 2655 (1968); **46**, 2661 (1968).
19. C. E. BOOZER, G. S. HAMMOND, C. E. HAMILTON, and J. N. SEN. J. Am. Chem. Soc. **77**, 3233 (1955).
20. J. R. THOMAS. J. Am. Chem. Soc. **85**, 2166 (1963).
21. M. B. NEIMAN and E. G. ROZANTSEV. Izv. Akad. Nauk SSSR, Ser. Khim. 1178 (1964).
22. M. S. KHLOPLYANKINA, A. L. BUCHACHENKO, M. B. NEIMAN, and A. G. VASIL'EVA. Kinetika i Kataliz, **6**, 394 (1965).
23. L. L. YASINA, V. B. MILLER, YU. A. SHLYAPNIKOV, and L. A. SKRIPKO. Izv. Akad. Nauk SSSR, Ser. Khim. 1481 (1965).

Can. J. Chem. Downloaded from www.nrcresearchpress.com by 210.87.254.105 on 09/05/12
For personal use only.

Can. J. Chem. Downloaded from www.nrcresearchpress.com by 210.87.254.105 on 09/05/12
For personal use only.

Formation of radicals in the amine inhibited decomposition of *t*-butyl hydroperoxide[1]

K. ADAMIC[2] AND K. U. INGOLD

Division of Applied Chemistry, National Research Council of Canada, Ottawa, Canada

Received July 23, 1968

The radicals formed in the amine inhibited, α,α′-azo-bis-isobutyronitrile initiated, decomposition of *t*-butyl hydroperoxide at 65° have been examined by electron spin resonance. In the absence of amine a strong peroxy radical signal is obtained. Amines with structures that do not correspond to those of conventional antioxidants (i.e. primary and secondary aliphatic amines and tertiary amines) generally have little or no effect on this signal. Nitroxide radicals are generated from secondary aromatic (diaryl and alkaryl) amines. The rate of conversion of these amines to nitroxides reached a maximum of 50–60% of the rate of chain initiation for some diphenylamines. A maximum concentration of nitroxide of about half the initial amine concentration was obtained with 4,4′-dimethyldiphenylamine.

N,N,N′,N′-Tetramethyl-*p*-phenylenediamine is very rapidly oxidized by *t*-butyl hydroperoxide to give Wurster's Blue cation and, presumably, a *t*-butoxy radical. This amine is therefore an initiator of oxidation rather than an inhibitor as has commonly been supposed.

Primary aromatic amines do not appear to form simple aryl nitroxides. It is proposed that arylamino radicals (ArNH) are directly oxidized to nitroso compounds by peroxy radicals.

Canadian Journal of Chemistry, 47, 295 (1969)

Quite a large number of aromatic and aliphatic nitroxide radicals have been prepared by oxidizing amines with peroxy radicals (see e.g. 1–5) and hydroperoxides (see e.g. 6, 7). However, there have been no attempts to compare the rates of formation of the various nitroxides under standard conditions although this information has an obvious bearing on the mechanism of the inhibition of autoxidation by amines. The preceding paper (8) describes a quantitative study of the oxidation of diphenylamine to diphenyl nitroxide by a number of peroxy radicals. The present paper extends this work to a variety of amines. The *t*-butylperoxy radical was generally used as the oxidizing species since it proved to be most efficient at converting diphenylamine to diphenyl nitroxide.

Experimental

The experimental apparatus and general procedure were described in the preceding paper (8). The amines used in this work were reagent grade materials which were purified by standard methods. The *t*-butylperoxy radicals were produced by the α,α′-azo-bis-isobutyronitrile, AIBN, induced decomposition of *t*-butyl hydroperoxide (8). The conditions used for most of this work were: [amine] = 8.3×10^{-4} *M*, [$(CH_3)_3COOH$] = 0.02 *M*, [AIBN] = 2.5×10^{-2} *M*, in oxygen saturated chlorobenzene at 65 °C. The reagents were added to the chlorobenzene in the order, amine, hydroperoxide, AIBN, the beginning of the reaction being considered to be the moment of completion of the AIBN addition.

Results

An electron spin resonance (e.s.r.) signal due to *t*-butylperoxy radicals is observed in the absence of amine. The peroxy radical concentration reaches a maximum[3] of $\sim 2 \times 10^{-5}$ *M* at about 200 s and then decreases rather slowly as the hydroperoxide is consumed ([ROO·] = 1×10^{-5} *M* at ~4000 s).

An amine that terminates all oxidation chains and reacts with two peroxy radicals per molecule will be consumed in about 3200 s under the standard experimental conditions (8). It is, therefore, not surprising to find that a peroxy radical signal appears after about 3200 s in oxidations containing amines known to be inhibitors or with structures similar to those of known inhibitors (i.e., principally primary and secondary aromatic amines). The peroxy radical signal appears at about this time whether or not a nitroxide signal was visible earlier[4]. A maximum peroxy radical concentration of ~ 0.9–1.1×10^{-5} *M* was generally attained at ~3000–5000 s. However, *N,N′*-dimethyl-*p*-phenylenediamine,

[1]Issued as NRCC No. 10413.

[2]NRCC Postdoctorate Fellow, 1967–1968.

[3]Since $R_i = 5.2 \times 10^{-7}$ *M* s^{-1} (8) this concentration corresponds to a rate constant for the self-reaction of *t*-butylperoxy radicals of $5.2 \times 10^{-7}/(2 \times 10^{-5})^2 = 1.3 \times 10^3$ M^{-1} s^{-1}.

[4]Similarly, a peroxy radical signal appears after about 3000 s if the reaction is inhibited with the same concentration of phenol or 2,4,6-tri-*t*-butylphenol, or half the standard concentration of 4,4′-methylene-bis-2,6-di-*t*-butylphenol. With these phenols no e.s.r. signal was detected in the first 3000 s of reaction.

Can. J. Chem. Downloaded from www.nrcresearchpress.com by 210.87.254.105 on 09/05/12
For personal use only.

N,N,N'-trimethyl-*p*-phenylenediamine, and *N,N,N',N'*-tetramethyl-*p*-phenylenediamine develop peroxy radical signals at 2500–4000 s which do not build up to their maxima ($\sim 8 \times 10^{-6}$ *M*) until 8000–10 000 s (see Fig. 1). Presumably these *p*-phenylenediamines (or their oxidation products, see below) react readily with about two peroxy radicals per molecule to form products that are not very reactive but are still able to trap about two additional peroxy radicals. In contrast to the *N*-methyl derivatives, the peroxy radical signals in the presence of *p*-phenylenediamine itself and the *N,N'*-diphenyl derivative appear at $\sim$ 3000 s and rise very rapidly to their maximum values ($\sim 1.1 \times 10^{-5}$ *M*). This behavior was expected of the diphenyl derivative which is a very efficient antioxidant and is known to react with two peroxy radicals per molecule (9).

A number of amines show a peroxy radical signal from the beginning of the reaction. Essentially identical curves for the build up and decay of peroxy radicals were obtained in the absence of amine and in the presence of triphenylamine, piperidine, quinoline (see Fig. 1), *N*-methyl diphenylamine, 2-anilino-1,4-naphthoquinone[5], or *t*-butylamine. As we might expect from their structures, these six amines do not appear to react with peroxy radicals under the present experimental conditions. With 1,6-hexanediamine and tribenzylamine the curves of peroxy radical concentration against time are of the same general shape as in the absence of amine, but the maximum radical concentration was only about half as great. With 2-anilino-1,4-naphthoquinone-4-anil[5] the maximum concentration of peroxy radicals (9×10^{-6} *M*) was reacted after $\sim$1500 s. Presumably, these last three amines react rather slowly with peroxy radicals. The changes in peroxy radical concentrations with time suggest that they are not consumed in the usual 3000–5000 s period and, therefore, most peroxy radicals must be destroyed by the normal bimolecular reaction.

Peroxy radicals were also formed from the beginning of the reaction with aniline, *p*-toluidine, and dibenzylamine. The radical concentrations rise rapidly in the first 200 s and then level off for about 1000–1500 s before increasing again and passing through maxima at 4000–5500 s (see Fig. 1).

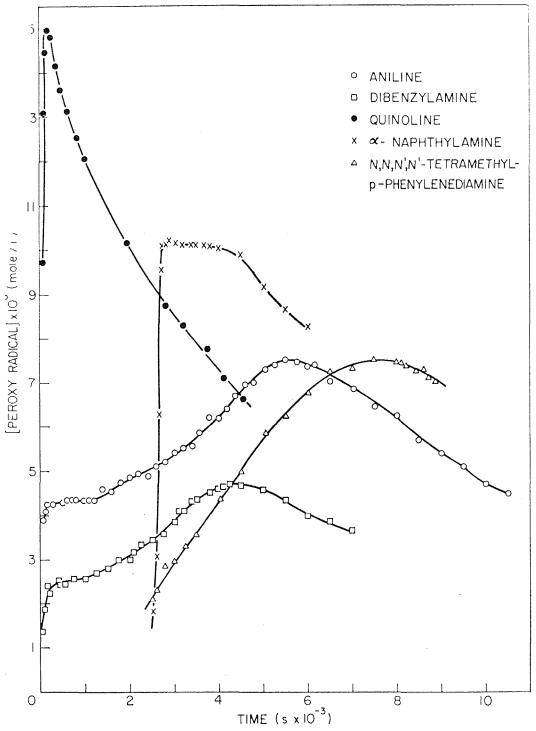

FIG. 1. The formation of peroxy radicals in amine (8.3×10^{-4} *M*) inhibited, AIBN (2.5×10^{-2} *M*) induced, decomposition of *t*-butyl hydroperoxide (1.7×10^{-3} *M*) in chlorobenzene at 65°.

Those amines which gave significant concentrations of nitroxide radicals[6] are listed in Table I. The initial rate of production of nitroxide, ρ/R_i (8), and the maximum concentration are given in this Table.

No radical signal was detected under the standard conditions for the first 3000 s with *p*-anisidine, *p*-phenylenediamine, *N,N'*-diphenyl-*p*-phenylenediamine, or α-naphthylamine (see Fig. 1). The usual peroxy radical signal develops after 3000 s.

Very small concentrations of radicals (maximum concentration $< 1 \times 10^{-6}$ *M*) were detected in reactions with *N,N'*-dimethyl-*p*-phenylenediamine, *N,N,N'*-trimethyl-*p*-phenylenediamine, and *N,N,N',N'*-tetramethyl-*p*-phenylenediamine. These radicals did not seem to be nitroxides as they appeared at slightly higher magnetic fields (lower *g* values) than the nitroxides. The radical from the tetramethyl-*p*-

[5]A product of the oxidation of *N*-phenyl-2-naphthylamine with peroxy radicals (10).

[6]A radical concentration of about 1×10^{-6} *M* was close to the limit of detection in the present system.

TABLE I

The formation of nitroxide radicals in amine inhibited decomposition of *t*-butyl hydroperoxide*

Amine	$\rho/R_i \times 100$	$[\text{Nitroxide}]_{max} \times 10^5$ (M)
Diphenylamine	56	19
4-Nitrodiphenylamine	54	11
4,4′-Dinitrodiphenylamine	64	15
4,4′-Dimethyldiphenylamine	55	40
4-Methoxydiphenylamine	32	25
4,4′-Dimethoxydiphenylamine	41	28
N-Phenyl-1-naphthylamine	1.0	0.4
N-Phenyl-2-naphthylamine	1.5	0.4
1,1′-Bis(*N*-phenyl-2-naphthylamine)	12	4.5
N-Methylaniline	$\lesssim$10	0.3
N-Methyl-*p*-toluidine	$\lesssim$10	0.4
N-Methyl-*m*-toluidine	$\lesssim$10	0.3

*At 65° ($[(CH_3)_3COOH] = 0.02\ M$, $[AIBN] = 0.25\ M$, $[amine] = 8.3 \times 10^{-4}\ M$, in chlorobenzene).

phenylenediamine was identified as Wurster's Blue cation $(CH_3)_2NC_6H_4N(CH_3)_2^{\cdot +}$ in experiments at relatively high reactant concentrations. With 10 times the usual amine concentration (i.e., $8.3 \times 10^{-3}\ M$) the addition of 50 times the usual amount of *t*-butyl hydroperoxide (i.e., 1.0 M) resulted in the immediate development of a deep blue solution with an e.s.r. spectrum which, though rather poorly resolved, was consistent with that of Wurster's Blue cation (11, 12). No AIBN was required to develop the signal and, in fact, the addition of AIBN had little or no effect on the formation and decay of the cation radical. The maximum radical concentration ($6–7 \times 10^{-5}\ M$) was reached within 100 s; it decayed rather slowly reaching half its maximum concentration after about 3000 s. Under similar conditions, more transitory blue colors, which are assumed to be due to similar cation radicals, appeared with dimethyl- and trimethyl-*p*-phenylenediamine. The maximum radical concentrations ($2 \times 10^{-5}\ M$ for dimethyl- and $4 \times 10^{-5}\ M$ for trimethyl-*p*-phenylenediamine) were recorded on the first measurement 30 s after the start of the reaction. The concentrations of both radicals fell to $\sim 1 \times 10^{-5}\ M$ at 200 s and $\sim 3 \times 10^{-6}\ M$ at 800 s. Similar experiments with *p*-phenylenediamine and *N*,*N*′-diphenyl-*p*-phenylenediamine generated neither a blue color nor an e.s.r. signal.

Discussion

Amines with structures which do not correspond to conventional antioxidants, i.e., tertiary amines and primary and secondary aliphatic amines, generally show a peroxy radical signal whose behavior is similar to that observed in the absence of amine. Clearly such amines do not react with peroxy radicals at an appreciable rate under the present experimental conditions.

The behavior of the peroxy radical signals found in the presence of aniline, *p*-toluidine, and dibenzylamine (Fig. 1) suggests that these amines are consumed in the same length of time as the more efficient antioxidants. Since these amines probably react with two peroxy radicals per molecule they must stop essentially all the reaction chains and completely suppress bimolecular termination between *t*-butylperoxy radicals. However, these amine-peroxy radical reactions must either be reversible or be slow compared with the rate for more powerful antioxidants. Aniline and *p*-toluidine can presumably give amino radicals. Benzylamine may form either an amino radical (2) or a benzylic radical. The latter would yield a secondary peroxy radical which could trap *t*-butylperoxy radicals quite efficiently (13–15).

The rate of nitroxide formation and the maximum concentration of nitroxide are, quite understandably, greatest for those amines which give particularly stable nitroxides—specifically, diphenylamine and its ring substituted derivatives[7], i.e.

[4] $\quad ROO^{\cdot} + Ph_2N^{\cdot} \rightarrow RO^{\cdot} + Ph_2NO^{\bullet}$

However, in no case does the rate of nitroxide formation equal the rate of chain initiation which is its theoretical limiting value (8), i.e., in no case is $\rho/R_i = 1.0$. Although this feature of the reaction might be due to a number of causes, our studies on the oxidation of *N*-phenyl-2-naphthyl-

[7]The reactions are numbered in the same way as in the preceding paper (8).

Can. J. Chem. Downloaded from www.nrcresearchpress.com by 210.87.254.105 on 09/05/12
For personal use only.

amine with peroxy radicals suggest that the reaction of peroxy radicals with aromatic amino radicals may involve attack on the ring as well as on the nitrogen atom (10). That is, the reaction

[4*a*] $ROO^{\cdot} + Ph_2N^{\cdot} \rightarrow$ Molecular products

may take the following course,

[4*b*] $ROO^{\cdot} + Ph_2N^{\cdot} \longrightarrow$ 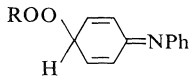

$\longrightarrow ROH +$ 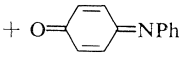

The rates of nitroxide formation from methyl and methoxy substituted diphenylamines are somewhat lower than from diphenylamine itself which suggests that reaction [4*a*] is accelerated relative to reaction [4] by electron donating *para*-substituents. Since peroxy radicals are electrophilic, it is not unreasonable to suppose that their rate of attack on the ring will be accelerated by electron donating substituents on the ring. The low ρ/R_i values for *N*-phenyl-1- and -2-naphthylamines suggest that the attack of peroxy radicals on naphthyl rings is considerably faster than their attack on phenyl rings.

With the three *N*-methyl anilines the maximum concentration of nitroxides is low but the initial rate of formation is high: too high, in fact, to measure accurately during the very short time that the rate of nitroxide formation is presumably constant. In all three cases the nitroxide concentration reaches 50% of its maximum value by the time the first measurement is made 30 s after the (arbitrarily defined) start of the reaction, and reaches 80–90% of its maximum value after 100 s. The initial rate of nitroxide formation may actually be as high as for the diphenylamines. The low maximum concentrations of phenyl methyl nitroxides must be due to their high reactivity in the present reaction system.

The absence of nitroxides from tertiary amines and from other amines which are unlikely to react with peroxy radicals is readily understood. The absence of a nitroxide from *N*,*N*′-diphenyl-*p*-phenylenediamine can be explained by its known oxidation by peroxy radicals to *N*,*N*′-diphenyl-*p*-quinonediimine (9)

[4*c*] $ROO^{\cdot} +$ 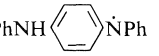

$\longrightarrow ROOH +$ 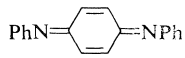

The tertiary amine *N*,*N*,*N*′,*N*′-tetramethyl-*p*-phenylenediamine is an interesting compound as its structure suggests that it should have little or no antioxidant activity. This compound was first reported to be an inhibitor by Boozer and Hammond (16) and its inhibitory activity has subsequently been confirmed by Yates and Ihrig (17). Our own rather limited conventional inhibition studies (18) have shown that this phenylenediamine behaves completely differently to other amine inhibitors. When it is used to inhibit the AIBN initiated oxidation of hydrocarbons such as styrene or tetralin there is a rather short induction period which is followed by an *extremely* rapid absorption of a relatively small amount of oxygen. This reaction ceases abruptly and further oxygen is only absorbed slowly. The rapid absorption of oxygen appears to be due to a chain initiating reaction involving the phenylenediamine and peroxide, presumably,

$$(CH_3)_2NC_6H_4N(CH_3)_2 + ROOH \rightarrow [(CH_3)_2NC_6H_4N(CH_3)_2]^+ OH^- + RO^{\cdot}$$

The short induction period may be due to traces of impurities in the diamine which have conventional antioxidant properties. The abrupt cessation of oxygen absorption occurs when all the diamine has been oxidized to the Wurster cation. Subsequent reactions of the cation must yield products with antioxidant activity, perhaps by the loss of a methyl group.

Dimethyl- and trimethyl-*p*-phenylenediamine behave quite normally in conventional inhibition studies (19) presumably because they can inhibit oxidation by the usual transfer of an amino hydrogen to a peroxy radical. This transfer is extremely fast with these two amines (19) and the hydroperoxide concentration will therefore be prevented from reaching a level where direct reaction with the phenylenediamines becomes important.

The most interesting group of amines that failed to give nitroxides in significant yields are the primary aromatic amines (*p*-anisidine, α-naphthylamine, and *p*-phenylenediamine). The absence of nitroxides cannot be due to the low reactivity of these amines towards peroxy radicals

[3*a*] $ROO^{\cdot} + ArNH_2 \rightarrow ROOH + Ar\dot{N}H$

since they are all known to be powerful oxidation inhibitors and, furthermore, since they do not show a peroxy radical signal at the beginning of

Can. J. Chem. Downloaded from www.nrcresearchpress.com by 210.87.254.105 on 09/05/12
For personal use only.

Can. J. Chem. Downloaded from www.nrcresearchpress.com by 210.87.254.105 on 09/05/12
For personal use only.

the reaction (cf. aniline and *p*-toluidine). Although the absence of nitroxides cannot be due to any inherent lack of stability of the ArN(H)O· radical[8] the possibility remained that these radicals would be unstable under our experimental conditions[9]. However, under the usual conditions, phenylhydroxylamine (8.3×10^{-4} *M*) gave readily detectable amounts of nitroxide, the concentration reaching a maximum of 1.6×10^{-6} *M* and being fairly constant from 150–1500 s. α-Naphthylhydroxylamine did not give a detectable signal under the usual conditions but 8.3×10^{-3} *M* was rapidly oxidized by 1.0 *M* [*t*-butylhydroperoxide] to give a radical (maximum concentration 6×10^{-6} *M*) which is presumably α-naphthyl nitroxide[10]. This radical decayed rather slowly (concentration $\sim 2 \times 10^{-6}$ *M* at 1500 s). No e.s.r. signal was detected from α-naphthylamine under similar conditions even after the addition of the usual quantity of AIBN. These results all suggest that the conversion of ArṄH radicals to ArN(H)O· radicals by reaction with peroxy radicals has a very low efficiency. We would like to suggest that oxidation occurs by the alternate pathway,

$$[4d] \quad \mathrm{ArṄH} + \mathrm{ROO}\cdot \rightarrow [\mathrm{ArN}\overset{\mathrm{H}}{\mathrm{O}}\mathrm{OR}] \rightarrow \mathrm{ArNO} + \mathrm{ROH}$$

The analogous reaction,

$$[4e] \quad \mathrm{PhNO}\overset{\mathrm{H}}{\mathrm{O}}\mathrm{H} \rightarrow \mathrm{PhNO} + \mathrm{H_2O}$$

is probably important in the base catalyzed oxidation of aniline to azobenzene (25). The direct formation of aromatic nitroso compounds by reaction [4*d*] provides an attractively simple explanation for the absence of aryl nitroxides in primary aromatic amine inhibited oxidations.

Acknowledgment

We should like to thank Dr. D. F. Bowman for the preparation of the phenylhydroxylamine and α-naphthylhydroxylamine.

1. O. L. Harle and J. R. Thomas. J. Am. Chem. Soc. **79**, 2973 (1957).
2. J. C. Baird and J. R. Thomas. J. Chem. Phys. **35**, 1507 (1961).
3. A. L. Buchachenko. Opt. i Spektroskopiya, **13**, 795 (1962).
4. A. T. Koritskii and A. F. Lukovnikov. Dokl. Akad. Nauk SSSR, **147**, 1126 (1962).
5. J. Q. Adams, S. W. Nicksic, and J. R. Thomas. J. Chem. Phys. **45**, 654 (1966).
6. G. M. Coppinger and J. D. Swalen. J. Am. Chem. Soc. **83**, 4900 (1961).
7. C. Jackson and N. K. D. Patel. Tetrahedron Letters, 2255 (1967).
8. K. Adamic, M. Dunn, and K. U. Ingold. Can. J. Chem. This issue.
9. C. E. Boozer, G. S. Hammond, C. E. Hamilton, and J. N. Sen. J. Am. Chem. Soc. **77**, 3233 (1955).
10. D. F. Bowman and B. S. Middleton. Unpublished results from this laboratory.
11. T. R. Tuttle, Jr. J. Chem. Phys. **30**, 331 (1959).
12. J. R. Bolton, A. Carrington, and J. dos Santos-Veiga. J. Mol. Phys. **5**, 615 (1962).
13. G. A. Russell. J. Am. Chem. Soc. **77**, 4583 (1955); **78**, 1047 (1956).
14. J. A. Howard, W. J. Schwalm, and K. U. Ingold. Advan. Chem. Ser. **75**, 6 (1968).
15. J. A. Howard and K. U. Ingold. Can. J. Chem. **46**, 2655 (1968); **46**, 2661 (1968).
16. C. E. Boozer and G. S. Hammond. J. Am. Chem. Soc. **76**, 3861 (1954).
17. W. R. Yates and J. L. Ihrig. J. Am. Chem. Soc. **87**, 710 (1965).
18. I. T. Brownlie. Unpublished results from this laboratory.
19. I. T. Brownlie and K. U. Ingold. Can. J. Chem. **45**, 2419 (1967).
20. A. L. Buchachenko. Izv. Akad. Nauk SSSR, Otd. Khim. Nauk, 1120 (1963).
21. C. J. W. Gutch and W. A. Waters. Proc. Chem. Soc. 230 (1964).
22. E. J. Geels, R. Konaka, and G. A. Russell. Chem. Commun. 13 (1965).
23. T. A. J. W. Wajer, A. Mackor, T. J. de Boer, and J. D. W. van Voorst. Tetrahedron Letters, 1941 (1967).
24. G. A. Russell, E. J. Geels, F. J. Smentowski, K. Y. Chang, J. Reynolds, and G. Kaupp. J. Am. Chem. Soc. **89**, 3821 (1967).
25. R. Konaka, K. Kuruma, and S. Terabe. J. Am. Chem. Soc. **90**, 1801 (1968).

[8]Phenyl nitroxide can readily be prepared by the action of various inorganic oxidizing agents on phenylhydroxylamine (20) and by a number of other methods (see e.g., 21–23).

[9]An early report by Baird and Thomas (2) suggested that the nitrogen containing radical formed by the oxidation of aniline with peroxy radicals was phenyl nitroxide or, rather, a time average between PhṄOH and PhN(H)O·. The e.s.r. spectrum has since been assigned to a radical with the probable structure PhN(O·)ON(H)Ph which is formed by the coupling of two oxidized aniline species (24). In our apparatus we could not detect a nitroxide signal from aniline under the standard experimental conditions. However, a very weak signal, probably due to PhN(O·)ON(H)Ph, was obtained by increasing the aniline concentration to 1.0 *M* and the AIBN concentration to 0.1 *M*. A similar type of radical was detected with 0.01 *M* [*p*-anisidine], 1.0 *M* [*t*-butylhydroperoxide], and 0.05 *M* [AIBN].

[10]A 10 line spectrum was obtained with 1.25 G modulation. This may be derived as a partially resolved 18 line spectrum assuming hyperfine splittings $A_{H-N} \approx 13$ G, $A_N \approx 9$ G, and a further 1:2:1 splitting of ~ 3 G from the equivalent 2- and 4- aromatic protons (23).

Can. J. Chem. Downloaded from www.nrcresearchpress.com by 210.87.254.105 on 09/05/12
For personal use only.

Nuclear charge dispersion in the fission of ^{232}Th by protons of energy 20–85 MeV[1,2]

P. P. BENJAMIN[3], D. A. MARSDEN[4], N. T. PORILE[5], AND L. YAFFE
Radiochemistry Laboratory, Department of Chemistry, McGill University, Montreal, Quebec

Received July 29, 1968

^{232}Th was irradiated with protons of energy 20–85 MeV and the independent yields of ^{130}Cs, ^{132}Cs, ^{134}Cs^{m}, ^{134}Cs^{g}, ^{136}Cs, ^{138}Cs, ^{86}Rb, and the cumulative yields of ^{137}Cs and ^{138}Xe were measured radiochemically. Charge dispersion curves were constructed at various energies and, as in previous studies, the broadening with increasing energy and shift of the most probable charge towards stability were observed. The most probable charge of a fission fragment of a given mass number lies closer to the line of β-stability in the case of thorium fission than in uranium. Detailed calculations in an attempt to correlate the experimental data with equal charge displacement (e.c.d.) and unchanged charge displacement (u.c.d.) charge distribution postulates were attempted. The results are not conclusive, lying in between the two, but favoring u.c.d. at the higher energies.

Canadian Journal of Chemistry, **47**, 301 (1969)

Introduction

Very few independent yields have been determined in the proton-induced fission of ^{232}Th. Pate, Foster, and Yaffe (1) obtained independent yields for various isotopes of iodine and tellurium for the fission of thorium induced by protons of energy 8–87 MeV. They were able to obtain charge dispersion curves, studied the behavior of these with energy, and attempted to draw conclusions about the mechanism of the charge distribution in fission. The work was extended by Kjelberg, Taniguchi, and Yaffe (2) who obtained fractional yields of ^{72}Ga, ^{82}Br, ^{112}Ag, and ^{140}La at the same bombarding energies.

Other workers (3–5), have obtained independent yields from the proton fission of uranium and drawn conclusions regarding the mechanism of the charge distribution, particularly the role of the neutron-to-proton ratio in the target and the resulting fission product.

It was of interest to determine independent yields in the same mass region as these previous workers, but with thorium as a target, and to compare the results as a function of the neutron-to-proton ratios of the two targets.

[1]With financial assistance from the Directorate of Chemical Sciences, U.S. Air Force Office of Scientific Research, Grant Nos. AF-AFOSR 62-64 and 489-64.

[2]Based on a thesis submitted by P. P. Benjamin in partial fulfilment of the requirements for the degree of Doctor of Philosophy at McGill University.

[3]Present address: Ewing Christian College, Allahabad, Keralla, India.

[4]Present address: Chalk River Nuclear Laboratory, Atomic Energy of Canada Ltd., Chalk River, Ontario.

[5]Also at Department of Chemistry, Purdue University, Lafayette, Indiana.

Experimental

(a) Irradiations

All irradiations were performed in the internal circulating beam of the McGill synchrocyclotron. The energy spread of the beam was known to ±2 MeV. Thorium metal foil (~ 80 mg/cm^2) was used as the target material. In all experiments, but the one at 20 MeV, foils were in stacks of three to compensate for recoil. A monitor foil, again with a guard foil on each side except for the 20-MeV experiment, was sandwiched to and placed upstream from the target. The leading edges of all foils were carefully aligned. The proton beam was monitored by the reaction ^{65}Cu(p,pn)^{64}Cu for all energies and also by the reaction ^{27}Al(p,3pn)^{24}Na at energies above 60 MeV. The values used were those of Meghir (6) and are given in Table I. Where single foils were used the results were corrected for recoil losses by means of the data of Noshkin and Sugihara (7). Recoil loss of ^{86}Rb was assumed to be the same as that of ^{83}Br (8%) and a value of 5% was estimated for the Cs isotopes.

The length of irradiations varied from 5 to 30 min and the energy range covered was 20 to 85 MeV.

TABLE I

Monitor cross sections

Energy (MeV)	Cross section (mb)	
	^{65}Cu(p,pn)^{64}Cu	^{27}Al(p,3pn)^{24}Na
20	240	
30	400	
40	260	
45	240	
50	210	
57	190	
65	170	13.8
70		13.8
73		13.8
75	150	
80	140	
85	140	12.4

TABLE II

Methods of measurement and relevant properties of nuclides

Nuclide	Half-life*	Radiation measured	Branch abundance	Instrument used
^{130}Cs	30 min	β^+	0.46	511–511 coincidence
^{132}Cs	6.5 d	673-keV γ	0.99	Scintillation spectrometer
$^{134}Cs^g$	2.1 y	797-keV γ / 801-keV γ	0.83	,,
$^{134}Cs^m$	2.9 h	e^-, β^-	1	$4\pi\beta$ and end-window proportional counters
^{136}Cs	12.9 d	β^-	1	,,
^{137}Cs	30 y	661-keV γ	0.84	Scintillation spectrometer
^{138}Cs	32.2 min	β^-	1	End-window proportional counter
^{86}Rb	18.6 d	β^-	1	,,

*The abbreviations used are: min for minutes, h for hours, d for days, and y for years.

(b) Chemical Separation

(i) Cesium

The procedure used was essentially that of Evans (8). The thorium foil was dissolved in concentrated hydrochloric acid and a few drops of ammonium silicofluoride were added to dissolve the last traces of residue. Carriers were added (Cs, 20 mg; Rb, 20 mg; Ba, 5 mg; 2 mg each of Sr, La, Ce, Y, and Zr) and the insoluble hydroxides and carbonates precipitated with 12 *N* sodium hydroxide and 2 *N* sodium carbonate solutions. The supernate was scavenged with lanthanum hydroxide, acidified with hydrochloric acid, cooled, and $Cs_3Bi_2I_9$ precipitated by the addition of BiI_3–HI reagent. The supernate was used for the subsequent rubidium separation. The Cs activity was purified by repeated precipitations as the bismuth iodide and finally either left as a precipitate or dissolved and made up to standard volume for activity measurement. The chemical yield determination was as the chloroplatinate.

(ii) Rubidium

The solution containing the Rb fraction was scavenged by $Cs_3Bi_2I_9$ precipitations. The excess reagent was removed by boiling with nitric acid to drive off the iodine and precipitation of bismuth as the oxynitrate. Rubidium was precipitated as Rb_2PtCl_6, washed with ethanol, the complex reduced to platinum with formic acid, and the excess formic acid destroyed by boiling with hydrochloric acid. Cesium bismuth iodide was precipitated and repeated until it showed no cesium activity. The rubidium was finally reprecipitated as the chloroplatinate, weighed for chemical yield determination, and the activity measured.

(iii) Aluminium

No chemical separation of sodium from aluminium was necessary. The aluminium foil was dissolved in the minimum amount of hydrochloric acid, made to volume, and aliquots taken for $4\pi\beta$ activity measurements. The samples were placed on VYNS films, dried, and covered with similar thin VYNS films to prevent absorption of moisture by the aluminium chloride.

(iv) Copper

The copper was separated from other activities by the ion-exchange method of Kraus and Moore (9). The chemical yield of copper was determined by direct titration with ethylenediamine tetraacetic acid with murexide as indicator (10).

(c) Activity Measurements

The methods of measurement of the various isotopes of cesium and ^{86}Rb are given in Table II. Unless otherwise stated, the data given were taken from Nuclear Data Sheets (11). Corrections, where applicable, were made for counter efficiency, self-absorption, external absorption, and resolution losses in the usual manner. The errors associated with these corrections are reflected in the general error associated with the cross section value quoted. The correction for the self-absorption of the conversion electrons from $^{134}Cs^m$ was arrived at by use of the decay scheme calculations of Baerg *et al.* (12).

(d) Decay Curve Analysis

The data obtained from the proportional counters were easily resolved into three components due to ^{138}Cs (32 min), ^{134}Cs (2.9 h), and ^{136}Cs (13 days) and a long-lived tail which by gamma analysis was found to consist of $^{134}Cs^g$ and ^{137}Cs. The radiations of ^{132}Cs, $^{134}Cs^g$, and ^{137}Cs were measured by γ-scintillation spectrometry. The area under the 670-keV photopeak of ^{132}Cs was obtained after the ^{136}Cs contribution had been subtracted from the entire spectrum. The contributions due to $^{134}Cs^g$ and ^{137}Cs were obtained from γ-ray measurements made about 1 year after irradiation.

The ^{24}Na and ^{64}Cu activities were determined by $4\pi\beta$ and γ-scintillation spectrometry respectively and gave pure single-component curves.

(e) Calculations

Formation cross-sections, σ, were obtained by application of equations readily available (3). Thorium and aluminium are monoisotopic so no corrections for isotopic abundance had to be introduced, but in the case of copper the isotopic abundance of copper was taken as 31%.

In the case of ^{138}Cs, a correction for its formation from its parent ^{138}Xe during irradiation and prior to separation has to be applied to obtain the independent yield of ^{138}Cs. The separation time was taken as that of foil dissolution since the xenon was removed by bubbling.

Can. J. Chem. Downloaded from www.nrcresearchpress.com by 210.87.254.105 on 09/05/12
For personal use only.

Can. J. Chem. Downloaded from www.nrcresearchpress.com by 210.87.254.105 on 09/05/12
For personal use only.

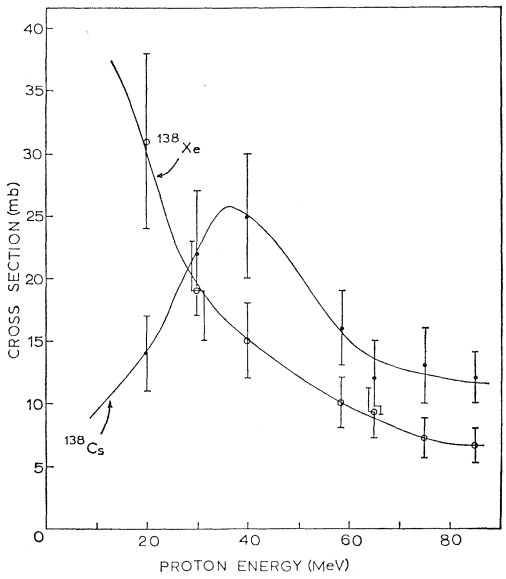

FIG. 1. Excitation functions for ^{138}Cs and ^{138}Xe: ○, cumulative yields of ^{138}Xe; ●, independent yields of ^{138}Cs.

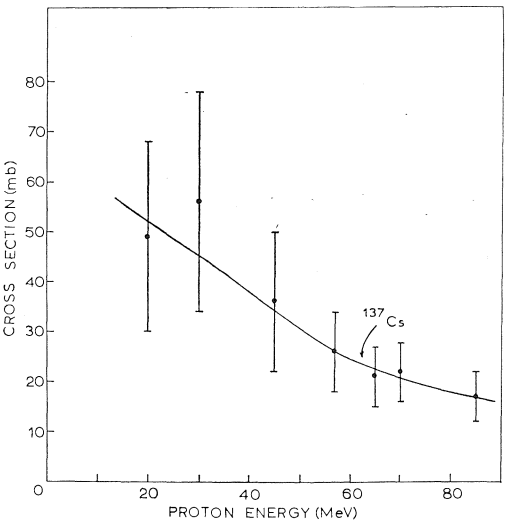

FIG. 2. Excitation function for ^{137}Cs (cumulative).

In all the other cases where the independent yield was obtained the nuclides were "shielded" by stable isobars. In the case of ^{138}Cs two short irradiations were performed at each energy. In one, the target was dissolved as quickly as possible at the end of bombardment while the other was processed about 1 h after irradiation. The data yielded two equations which were solved simultaneously to obtain the independent and cumulative cross-sections of ^{138}Cs and ^{138}Xe respectively.

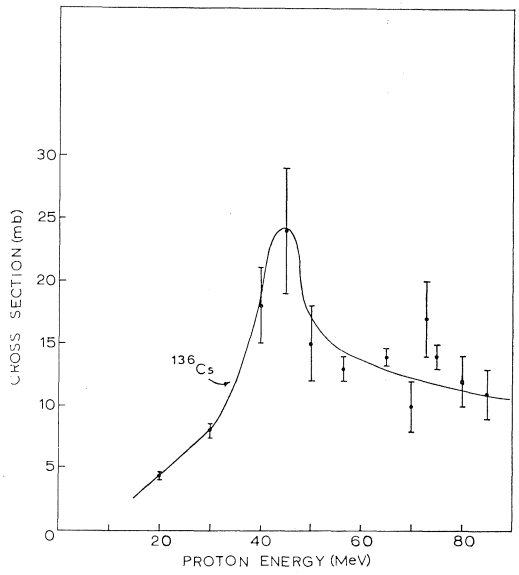

FIG. 3. Excitation function for ^{136}Cs (independent).

Uncertainties in determination of disintegration rates, chemical yields, pipetting, superficial densities, and decay curve analyses were obtained with a resulting probable error of ±20% in the case of ^{138}Cs, ^{138}Xe, ^{136}Cs, ^{134}Cs^{m}, ^{86}Rb; ±25% for ^{130}Cs and ^{132}Cs; and ±30% for ^{134}Cs^{g} and ^{137}Cs. Uncertainties in decay schemes and branching ratios were not included in the estimate. Where more than one determination at any energy was made the standard deviation from the mean value is given. The deviations were quite comparable to the estimated errors for the individual determination.

Results and Discussion

(a) Cross Sections and Excitation Functions

The cross sections obtained are shown in Table III and are plotted as a function of energy in Figs. 1–6 inclusive. As observed by other workers (3, 4) the excitation functions of the neutron-excess isotopes normally associated with low-energy fission reach a peak at relatively low energies, e.g. ^{136}Cs at 45 MeV, while the excitation functions of the more neutron-deficient isotopes increase in the energy range studied. As done by previous workers (3, 4) for uranium fission, the energies at which the excitation functions reach their maxima are plotted against the neutron-to-proton (N/Z) ratio of the nuclide and shown in Fig. 7. The data in the present paper alone are too sparse for a meaningful plot. They have been reinforced with data obtained by Forster *et al.* (13) for ^{133}Xe and ^{135}Xe in the

Can. J. Chem. Downloaded from www.nrcresearchpress.com by 210.87.254.105 on 09/05/12
For personal use only.

TABLE III

Formation cross sections at various energies

Product	Type of yield	Cross section* (mb) at energy											
		20 MeV	30 MeV	40 MeV	45 MeV	50 MeV	57 MeV	65 MeV	70 MeV	73 MeV	75 MeV	80 MeV	85 MeV
^{138}Cs	Independent	14±3	22±4	25±5			16±3	12±2			13±3		12±2
^{138}Xe	Cumulative	31±6	19±4	15±3			10±2	9.2±1.8			7.2±1.4		6.6±1.4
^{137}Cs	Cumulative	49±19	56±22		36±14		26±8 (2)	21±6	22±6				17±5
^{136}Cs	Independent	4.4 ±0.3	8.0 ±0.6 (2)	18±3 (3)	24±5 (3)	15±3	13±1 (4)	14±0.7 (5)	10±2	17±3	14±1 (3)	12±2	11±2 (4)
^{134}Cs^{m}	Independent	0.24±0.02	0.81±0.2 (2)	3.0±0.5 (3)	3.5±0.8 (2)	2.0±0.4	4.4±0.6 (3)	5.0±1.0 (4)	4.9±1.1	7.3±1.5	6.1±0.1 (3)	5.6±1.3	6.6±0.2 (4)
^{134}Cs^{m+g}	Independent	0.50±0.21	1.5 ±0.6		6.0±2.7		6.6±0.7 (2)	6.0±2.7	6.8±2.6				8.8±2.0
^{132}Cs	Independent							1.4±0.06 (4)	1.2±0.3		2.4±0.6 (2)		2.9±0.7 (3)
^{130}Cs	Independent											<0.3±0.1	<0.4±0.1
^{86}Rb	Independent	0.04±0.1	0.3 ±0.1	0.4±0.1		0.3±0.1	0.2±0.1	0.7±0.2	0.8±0.2		0.6±0.1		1.1±0.2

*Numbers in parentheses show the numbers of experiments; if no number is shown only one experiment was performed.

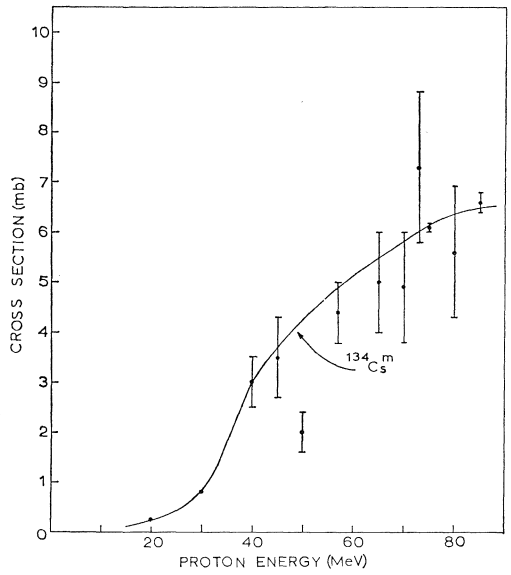

FIG. 4. Excitation function for ^{134}Cs^{m} (independent).

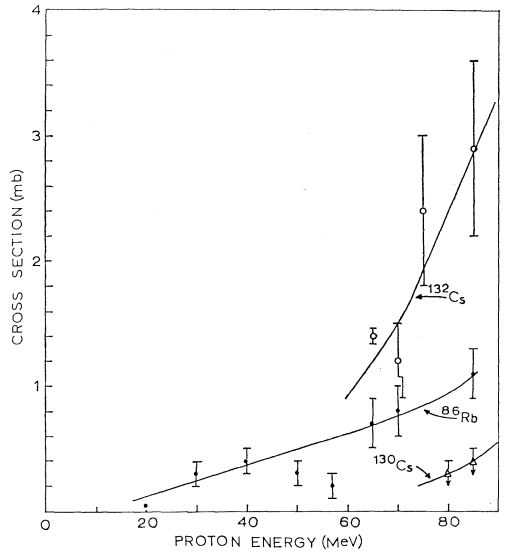

FIG. 6. Excitation functions for ^{130}Cs, ^{132}Cs, and ^{86}Rb (independent).

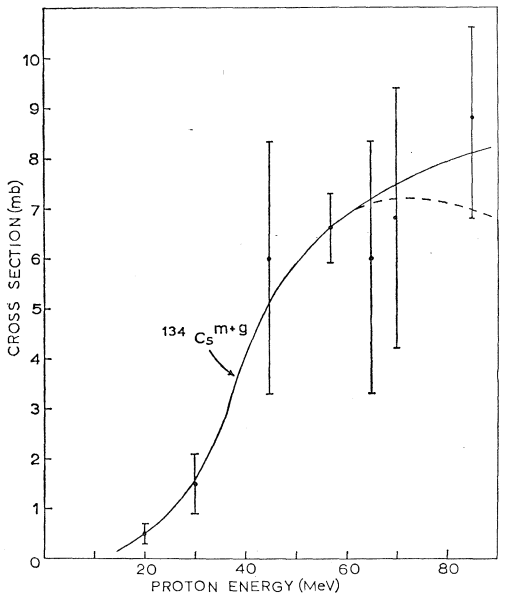

FIG. 5. Excitation function for ^{134}Cs^{m+g} (independent).

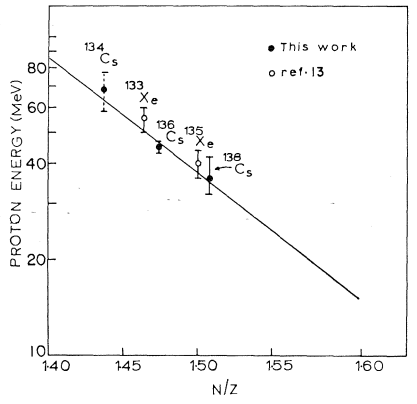

FIG. 7. Energies at which excitation functions reach their maxima.

fission of ^{232}Th. The limits on the data shown in Fig. 5 for ^{134}Cs are too great to allow the excitation function to be very closely defined. The dotted curve shows where the curve would be expected to reach its maximum (as obtained from Fig. 7) and this is not inconsistent with the data.

The curve in Fig. 7 for the fission of ^{232}Th is not as steep as that obtained in the same energy range (4) for ^{238}U fission, the slope of the latter being approximately twice as great. However, more data are needed before more meaningful conclusions can be drawn. It is apparent though that the energy at which ^{138}Cs has its greatest probability of formation is roughly the same (30 and 36 MeV) for ^{238}U and ^{232}Th respectively. However, ^{134}Cs has its greatest probability of formation at 100 MeV and 68 MeV for ^{238}U and ^{232}Th, respectively.

Can. J. Chem. Downloaded from www.nrcresearchpress.com by 210.87.254.105 on 09/05/12
For personal use only.

Can. J. Chem. Downloaded from www.nrcresearchpress.com by 210.87.254.105 on 09/05/12
For personal use only.

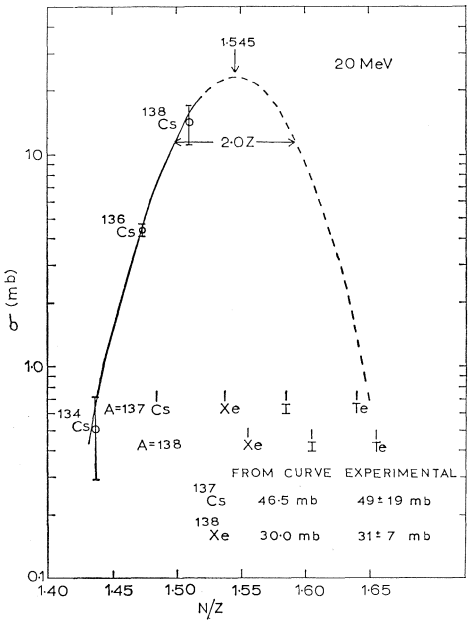

FIG. 8. Charge dispersion curve at 20 MeV.

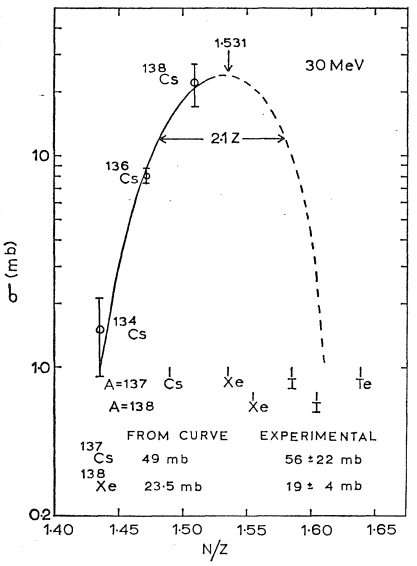

FIG. 9. Charge dispersion curve at 30 MeV.

Once again it is apparent that the N/Z value is an extremely useful parameter. From previous considerations (3) and the data in Fig. 7 one would expect the excitation function for ^{86}Rb to reach a maximum at energies far beyond those investigated here.

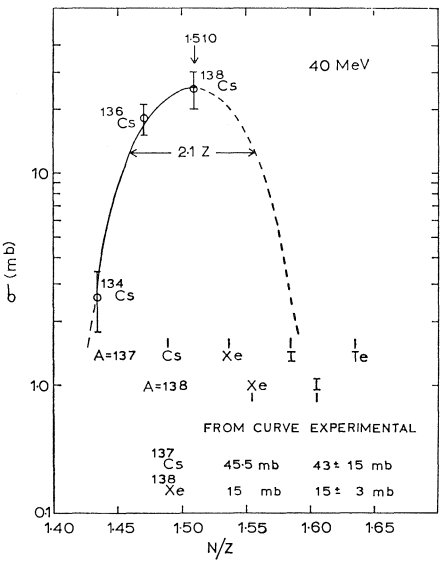

FIG. 10. Charge dispersion curve at 40 MeV.

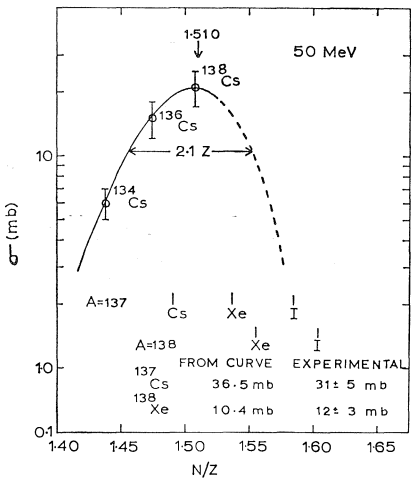

FIG. 11. Charge dispersion curve at 50 MeV.

(b) Charge Dispersion

Charge dispersion curves were constructed for bombarding energies of 20, 30, 40, 50, 57, 65, 75, and 85 MeV and are shown in Figs. 8–15 inclusive. The data consisted of the independent yields experimentally determined. The right-hand portion of the curve was fitted so that the independent yields read off the curve totalled to the cumulative yields for ^{137}Cs and ^{138}Xe experimentally determined. It has been shown (1, 3) that this constraint uniquely defines this

Can. J. Chem. Downloaded from www.nrcresearchpress.com by 210.87.254.105 on 09/05/12
For personal use only.

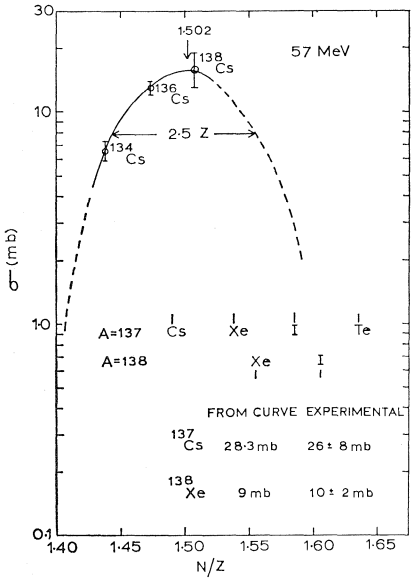

FIG. 12. Charge dispersion curve at 57 MeV.

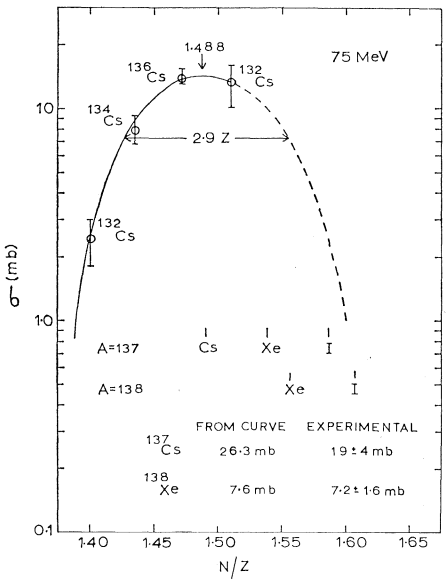

FIG. 14. Charge dispersion curve at 75 MeV.

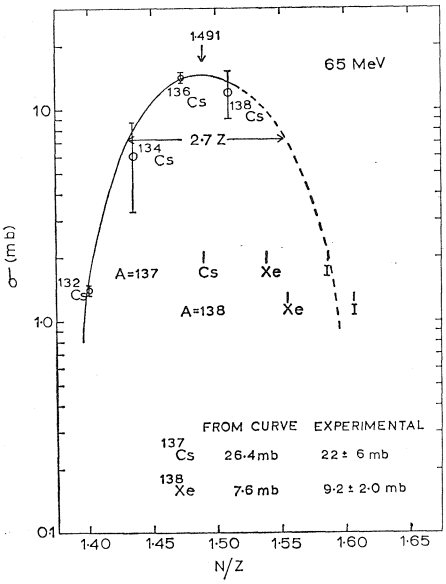

FIG. 13. Charge dispersion curve at 65 MeV.

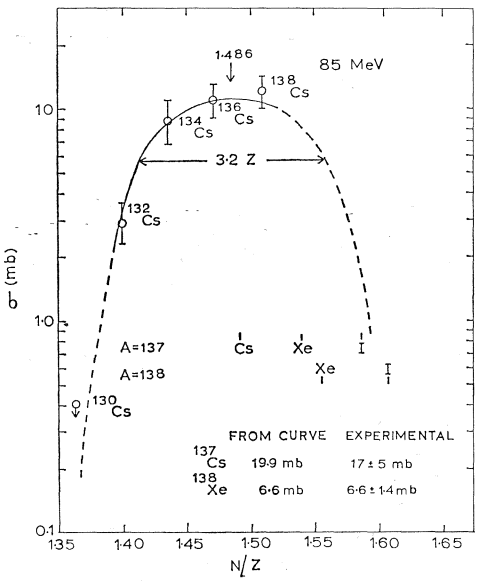

FIG. 15. Charge dispersion curve at 85 MeV.

portion of the curve. A basic assumption in plotting such a curve is that the mass-yield curve is sensibly flat at the appropriate energy for the narrow mass region under consideration.

In Fig. 16 and Table IV are shown the variation of the full-width at half-maximum (f.w.h.m.) with bombarding energy. As in previous work, both with Th (1) and U (4, 13) initially (up to around 50 MeV) the f.w.h.m. remains essentially constant and then increases with bombarding energy. This would seem to indicate two separate reaction mechanisms occurring, e.g. compound nucleus formation at the lower energies, and direct interaction at the higher.

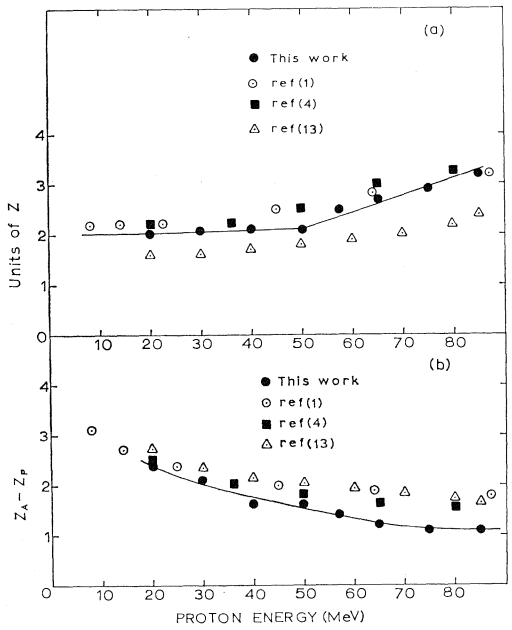

FIG. 16. (*a*) Variation of full-width at half-maximum of charge dispersion curves with bombarding energy. (*b*) Displacement of most probable charge, Z_p, towards beta stability, Z_A, with increase in bombarding energy.

In Fig. 16 is also given the plot of $Z_A - Z_p$ with increase in bombarding energy, where Z_A is the most stable charge for mass number A (14) and Z_p the most probable charge formed in fission. The movement of Z_p towards stability with increase in energy, as also shown by others, is clearly evident.

An attempt has been made to calculate the most probable charge of a fission fragment in the mass region of interest on the basis of the equal charge displacement (e.c.d.) (15) and unchanged charge displacement (u.c.d.) (16) postulates. These values are then compared with the experimentally determined Z_p values for $A = 136$.

Compound nucleus formation is assumed at proton bombarding energies of 20, 50, and 57 MeV and the results of published calculations on the prompt nuclear cascade (17, 18) were used as well as the data of Vandenbosch and Huizenga (19) on fission–spallation competition for proton energies of 80 and 85 MeV. The experimental results of Davies and Yaffe (4) on the proton-induced fission of uranium over a similar energy range were included in the present analysis for purposes of comparison.

TABLE IV

Parameters of charge dispersion curves

Proton energy (MeV)	Full-width at half-maximum ΔZ	Displacement from stability ($Z_A - Z_p$)
20	2.0	2.4
30	2.1	2.1
40	2.1	1.6
50	2.1	1.6
57	2.5	1.4
65	2.7	1.2
75	2.9	1.1
85	3.2	1.1

According to the e.c.d. postulate, the most probable charge $(Z_p)_i$ of a fission fragment of initial mass number A_i is given by

$$[1] \quad (Z_p)_i = Z_{A_i} - \tfrac{1}{2}[Z_{A_i} + Z_{(A_F - A_i)} - Z_F]$$

where A_F and Z_F denote the mass number and nuclear charge of the fissioning nucleus; $Z_{(A_F - A_i)}$ and Z_{A_i} are the most stable charges of the two complementary fission fragments with mass numbers A_i and $(A_F - A_i)$, respectively. Values of Z_{A_i} are those of Coryell (14).

According to the u.c.d. postulate, the most probable charge is given by

$$[2] \quad Z_{p_i} = \left(\frac{Z_F}{A_F}\right) A_i$$

Calculations were performed for a variety of fissioning nuclei to allow for prefission neutron emission and the Z_p values arrived at in this fashion refer to the primary fragments which may subsequently evaporate neutrons to lead to the observed fission products. If the fragments emit n neutrons after fission to give the final mass number A_f (experimentally studied), then Z_p for A_f is calculated from eqs. [1] and [2] with $A_i = A_f + n$.

To obtain n, the following assumptions were made:

(*i*) On the average 2 fission neutrons are emitted promptly regardless of excitation energy or the fission mode (20). These are equally divided between the two fragments and originate from the deformation energy of the fissioning nucleus.

(*ii*) The excitation energy of the fissioning nucleus is divided between the fragments in the ratio of their masses.

Can. J. Chem. Downloaded from www.nrcresearchpress.com by 210.87.254.105 on 09/05/12
For personal use only.

(*iii*) The average number of neutrons evaporated from the primary fragments is obtained using an average neutron binding energy of 7 MeV (21) plus an estimated average neutron kinetic energy of 2 MeV (22).

On these assumptions the fissioning nucleus divides into two fragments such that one has a mass number

$$[3] \qquad A_H = 136 + 1 + \left(\frac{E_F^*}{9} \times \frac{A_H}{A_F}\right)$$

where A_F is the mass number of the fissioning nucleus and E_F^* is its excitation energy in MeV. The equation can be rearranged to give

$$[4] \qquad A_H = \frac{137}{\left(1 - \frac{E_F^*}{9A_F}\right)}$$

The excitation energy E_C of the compound nucleus is given by the sum of the kinetic and binding energy of the impinging proton. The residual excitation energy, E_r, after emission of a neutron is given by

$$[5] \qquad E_r = E_C - (B_n + \bar{E}_k)$$

where B_n is the neutron binding energy, $\bar{E}_k = 2\tau$ is the average kinetic energy of the neutron, τ being the nuclear temperature. The proton and neutron binding energies are taken from Levy (21) and the calculation is carried through until the excitation value reaches an energy below the neutron binding energy. The excitation energies of the various nuclei formed from the compound nuclei by successive evaporation of neutrons and the estimated initial fragment masses are given elsewhere (23).

The probability G for fission of a given nucleus at these energies is given by

$$[6] \qquad G = \Gamma_F/(\Gamma_n + \Gamma_F)$$

where Γ_F and Γ_n are fission and neutron evaporation widths (charged particle evaporation is considered unlikely at these energies (17)). The dependence of G on the fissioning nucleus is quite pronounced and the data used are those of Vandenbosch and Huizenga (19) in order to get the fission probability of each fissioning nucleus. It was assumed that the formation probability of the compound nucleus (^{233}Pa) was 1, and Z_p values, calculated on the basis of e.c.d. and u.c.d., were weighted by the fission probability of each fissioning nucleus and the average $\bar{Z}_p$ determined for bombarding energies of 20, 50, and 57 MeV for thorium, and 20 and 50 MeV for uranium.

For ^{232}Th and ^{238}U, bombarded with protons of energies 85 and 80 MeV respectively, the experimental data were compared with an analysis starting with the results of the prompt cascade for 82-MeV protons incident on ^{238}U (17). The difference in energy of bombardment was neglected and appropriate shifts in charges and masses of the reaction products made to allow for the difference in mass and charge of the targets.

A total of 1258 cascades was followed in the prompt interaction calculation in addition to 78 events in which nuclear transparency is indicated. The excitation spectrum was also obtained from ref. (17). The cascade products, relative frequencies and their average excitation energies are given in ref. (23). Charged particle evaporation was neglected (18). For each cascade product the spectrum of residual excitation energies was divided into a number of bins and an average excitation energy taken for each bin. This procedure simplified the calculation without introducing any significant distortion of the results. The evaporation reaction, as in the low-energy cases, was allowed to proceed until a value below the neutron binding energy was reached.

Fission was assumed to compete with neutron evaporation in these cascade products as in the low-energy reactions. The average Z_p value of the fission fragment (final mass number $A = 136$), calculated for each cascade product, was weighted with the relative frequencies of each cascade reaction and the final weighted average of Z_p was compared with the experimental values.

The results for both the low and higher energy calculations are given in Table V. The maximum

TABLE V

Comparison of calculated and experimental Z_p values for $A = 136$

Target	Proton energy (MeV)	Z_p e.c.d.	Z_p u.c.d.	Z_p Experimental
^{232}Th	20	52.8	53.9	53.5
	50	53.4	54.7	54.2
	57	53.5	54.8	54.4
	85	53.8	54.8	54.6
^{238}U	20	52.4	53.7	53.3
	50	53.2	54.5	54.2
	80	53.4	54.6	54.4

Can. J. Chem. Downloaded from www.nrcresearchpress.com by 210.87.254.105 on 09/05/12
For personal use only.

Can. J. Chem. Downloaded from www.nrcresearchpress.com by 210.87.254.105 on 09/05/12
For personal use only.

uncertainty in the estimation of the primary fragment mass number is estimated to be ± 1 mass unit. This would introduce an uncertainty of ± 0.4 charge units in both the e.c.d. and u.c.d. calculations. In addition, in the case of the e.c.d. calculations, an uncertainty of about $\pm 0.5\,Z$ units in the Z_A values would make the e.c.d. values have a total uncertainty of ± 0.63 charge units. For the experimental Z_p values an uncertainty of $\pm 0.25\,Z$ units is estimated for $E \leqslant 50$ MeV and $\pm 0.5\,Z$ for $E \geqslant 50$ MeV.

Because of these limits, it is difficult to draw any definite conclusions. However, some general trends can be noted. The experimental values of Z_p lie between the e.c.d. and u.c.d. predictions for both uranium and thorium up to about 57 MeV, although they are somewhat closer to the u.c.d. predictions. At 80 and 85 MeV the values are much closer to those predicted by u.c.d. than e.c.d. However, it should be borne in mind that at these energies the charge dispersion curves are becoming much broader and the uncertainty in defining Z_p experimentally becomes greater. As the excitation energy increases both the e.c.d. and u.c.d. values of Z_p increase, showing slightly greater values of Z_p for thorium than uranium fission at comparable energies. The experimental data conform with these trends.

Aagard *et al.* (24) found, in a study of mass numbers about 130 formed in the fission of uranium by 170-MeV protons, that their data fell between the u.c.d. and e.c.d. values calculated by Rudstam and Pappas (25). Colby and Cobble (26) found that their data on the α-induced fission (20–40 MeV) of ^{233}U, ^{235}U, and ^{238}U correlated better with u.c.d. than e.c.d. Pate (27), with data obtained (1) in ^{232}Th fission by protons, concluded that fission up to energies as high as 480 MeV proceeds predominantly by a process consistent with the e.c.d. postulate.

The present analysis differs from that of Pate. He assumed that $\Gamma_F/(\Gamma_n + \Gamma_F)$ was energy-dependent. The present treatment assumes energy independence and incorporates published values of $\Gamma_F/(\Gamma_n + \Gamma_F)$ at every stage of neutron evaporation after the prompt interaction.

(c) $^{134}Cs^m/^{134}Cs^g$ Isomer Ratio

The cross section for the independent formation of ^{134}Cs includes contributions from metastable ^{134}Cs^m (spin and parity 8−, $t_{1/2} = 2.9$ h) as well as ^{134}Cs^g (spin and parity 4+, $t_{1/2} = 2.05$ years). Independent cross sections have been determined for the formation of both states and thus the isomer ratio can be calculated as a function of energy. The results are shown in Fig. 17. It is seen that the isomer ratio increases from approximately unity at the lowest energy to nearly three at the highest. It should be pointed out, however, that the experimental values are subject to an uncertainty of nearly a factor-of-two due primarily to the large error in the determination of the disintegration rates of ^{134}Cs[8].

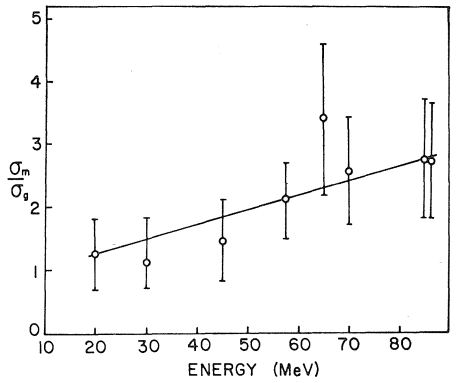

FIG. 17. Ratio of formation cross sections of the metastable and ground states of ^{134}Cs as a function of proton bombarding energy.

The isomer ratio of independently-formed fission products may be used to determine the intrinsic angular momentum of the primary fragments. A number of such determinations have been reported recently for low- or intermediate-energy fission (28–32). In common with these previous calculations we assume that the angular momentum distribution of a primary fragment, $P(J)$, is proportional to $(2J + 1)$ $\exp - J(J \pm 1)/\langle J^2 \rangle$ where $\langle J^2 \rangle$ is the mean square angular momentum. This functional form has been postulated by Nix and Swiatecki (33) on the basis of the liquid drop model. The calculation of the isomer ratio of the final products then follows the method of Vandenbosch and Huizenga (34). It is assumed that the primary fragment emits either 1 or 2 neutrons, having an average kinetic energy of 2 MeV (22). Following neutron emission the excited product is allowed to emit either 3 or 4 dipole photons (34). The last γ-ray populates either the metastable or ground state of ^{134}Cs, depending on which transition involves the smallest spin change. The calculation was performed with a value of the spin cutoff

TABLE VI

Isomer ratio, $^{134}Cs^m/^{134}Cs^g$

N_n*	N_γ†	σ‡ 3	σ‡ 4	σ‡ 5	Experimental value
Trial 1 $\langle J^2\rangle^{1/2} = 2.64$					
1	3	0.012	0.016	0.053	
1	4	0.013	0.017	0.066	
2	3	—	0.033	0.094	
2	4	—	0.041	0.108	~1.2
Trial 2 $\langle J^2\rangle^{1/2} = 7$					
1	3	0.278	0.513	0.677	
1	4	0.239	0.488	0.669	
2	3	0.204	0.470	0.672	
2	4	—	0.447	0.666	~1.2
Trial 3 $\langle J^2\rangle^{1/2} = 9$					
1	3	0.579	0.968	1.24	
1	4	0.479	0.908	1.21	
2	3	0.430	0.848	1.18	
2	4	0.354	0.798	1.15	~1.2
Trial 4 $\langle J^2\rangle^{1/2} = 10$					
1	3	0.773	1.25	1.59	
1	4	0.666	1.17	1.54	
2	3	0.550	1.08	1.46	
2	4	0.472	1.02	1.42	~1.2

*N_n, number of prompt neutrons emitted from primary fragment.
†N_γ, number of prompt gammas.
‡σ, spin cut-off factor.

parameter, σ, of 3–5 (34). The neutron transmission coefficients were obtained from the compilation by Feld *et al.* (35).

The results of the calculation are summarized in Table VI. It is seen that the value of $\langle J^2\rangle^{1/2}$ required to fit the experimental value of σ_m/σ_g obtained at incident energies of 20–25 MeV is approximately 9–10. The angular momentum of the primary fragments arises, at least in part, from the angular momentum of the compound nucleus as modified by the emission of pre-fission neutrons. In addition, previous comparisons of experimental and calculated isomer ratios (28–32) indicate that substantial amounts of intrinsic angular momentum can be generated in the fission act, in agreement with a prediction by Strutinskii (36).

We have assessed the relative importance of these two factors by calculating the angular momentum of the fissioning nucleus and then determining the isomer ratio expected on the assumption that the primary fission fragment has the same angular momentum as the fissioning nucleus. The calculation was performed for protons of 19- and 24-MeV incident energy. The proton transmission coefficients were taken from the tabulation by Feshbach *et al.* (37). It was expected, on the basis of the available excitation energy, that up to 3 neutrons could be emitted from the compound nucleus if fission followed neutron emission, or that up to 2 neutrons could be emitted by the primary fragment if fission preceded evaporation. The calculation was performed for both these extreme assumptions using the above mentioned parameters. Typical results for bombardment by 19-MeV protons are summarized in Table VII. It is seen that the value of $\langle J^2\rangle^{1/2}$ of the fissioning nucleus is approximately 4.5, regardless of whether fission occurs prior to or after neutron emission. This value is much smaller than the value $\langle J^2\rangle^{1/2} = 10$ required to fit the experimental isomer ratio and, as expected, the ratio calculated on the basis of the angular momentum of the fissioning nucleus is much too small. The same conclusion also follows from the calculation for 24-MeV protons. The present results thus bear out Strutinskii's prediction (36).

Although the angular momentum of the compound nucleus does not appear to be the primary factor determining the isomer ratio in fission, it does nonetheless play an important role. This can be seen by comparing a particular isomer ratio obtained in fission induced by different projectiles with varying bombarding energies. The angular momentum generated in fission should be the same in all these cases and the variation in the number of emitted neutrons

TABLE VII

Isomer ratio $^{134}Cs^m/^{134}Cs^g$

Fission before de-excitation. Energy = 19 MeV, $\langle J^2\rangle^{1/2} = 4.47$, σ = 4			Fission after de-excitation by emission of 2 neutrons. Energy = 19 MeV, $\langle J^2\rangle^{1/2} = 4.45$, σ = 4		
N_n*	N_γ†		N_n	N_γ	
2	3	4	1	3	4
	0.19	0.21		0.20	—
	1.2	1.2		1.2	1.2

*N_n, number of prompt neutrons emitted from primary fragment.
†N_γ, number of prompt gammas.

Can. J. Chem. Downloaded from www.nrcresearchpress.com by 210.87.254.105 on 09/05/12
For personal use only.

TABLE VIII

Correlation of experimental ^{134}Cs isomer ratio with root-mean-square angular momentum of $\langle J^2 \rangle^{1/2}$ of different compound nuclei

Compound nuclei	Energy (MeV)	$\langle J_c^2 \rangle^{1/2}$	$\sigma_{^{134}Cs^m}/\sigma_{^{134}Cs^g}$ isomer ratio	Reference number
$^{233}U + \gamma$	16	1	0.75	29
$^{238}U + P$	20	4	20	38
$^{232}Th + P$	20	4.2	1.2	Present work
$^{237}Np + d$	21	6	1.6	29
$^{238}U + P$	45	8.6	6	38
$^{232}Th + P$	45	8.7	1.4	Present work
$^{232}Th + P$	65	11	3.4	Present work
$^{238}U + P$	65	11	4	38
$^{237}Np + {}^4He$	42	11	4.7	29
$^{235}U + {}^4He$	42	11	3.3	29

should only lead to a minor effect on the isomer ratio. If the differences in the spins of the various targets and projectiles are neglected, one should then see a correlation between the isomer ratio and the orbital angular momentum brought into the compound nucleus by the bombarding particle.

The $^{134}Cs^m/^{134}Cs^g$ ratio constitutes a good case in point since it has been determined in a variety of fission reactions (28, 38). The results of this comparison are summarized in Table VIII. The root-mean-square value of the angular momentum of the compound nucleus was obtained by use of the sharp cutoff approximation (39). It is seen that, except for the surprisingly large values of σ_m/σ_g reported by Davies and Yaffe (38) at low energies, a reasonably good correlation between $\langle J^2 \rangle^{1/2}$ and the isomer ratio is found.

Acknowledgments

The authors wish to express their appreciation to Professor R. E. Bell, Director, Foster Radiation Laboratory, McGill University for his ready permission to use the cyclotron and to Mr. R. H. Mills who cheerfully performed the irradiations.

1. B. D. Pate, J. S. Foster, and L. Yaffe. Can. J. Chem. **36**, 1691 (1958).
2. A. Kjelberg, H. Taniguchi, and L. Yaffe. Can. J. Chem. **39**, 635 (1961).
3. G. Friedlander, L. Friedman, B. Gordon, and L. Yaffe. Phys. Rev. **129**, 1809 (1963).
4. J. H. Davies and L. Yaffe. Can. J. Phys. **41**, 762 (1963).
5. S. S. Parikh, D. A. Marsden, N. T. Porile, and L. Yaffe. Can. J. Chem. **45**, 1863 (1967).
6. S. Meghir. Ph.D. Thesis, McGill University, Montreal, Quebec. 1962.
7. V. E. Noshkin and T. T. Sugihara. J. Inorg. Nucl. Chem. **27**, 943 (1965).
8. H. B. Evans. Natl. Nuclear Energy Ser. Vol. 9, Div. IV, Paper 284, Book 3. McGraw-Hill Book Co., Inc., New York. 1951.
9. K. A. Kraus and G. E. Moore. J. Am. Chem. Soc. **75**, 1460 (1953).
10. F. J. Welcher. The analytical use of ethylenediamine tetraacetic acid. D. Van Nostrand Co., Inc., Princeton. 1967. p. 240.
11. Nucl. Data Sheets. Natl. Acad. Sci. Natl. Res. Council. U.S. Government Printing Office, Washington, D.C. 1961 *et seq.*
12. A. P. Baerg, R. M. Bartholomew, and R. H. Betts. Can. J. Chem. **38**, 2147 (1960).
13. J. H. Forster, N. T. Porile, and L. Yaffe. Can. J. Chem. **44**, 2951 (1966).
14. C. D. Coryell. Ann. Rev. Nucl. Sci. **2**, 305 (1953).
15. L. E. Glendenin, C. D. Coryell, and R. R. Edwards. Phys. Rev. **75**, 337 (1949). National nuclear energy series. Div. IV. Paper 52. McGraw-Hill Book Co., Inc., New York. 1951. p. 9.
16. R. H. Goeckermann and I. Perlman. Phys. Rev. **73**, 1127 (1948).
17. N. Metropolis, R. Bivins, M. Storm, A. Turkevich, J. M. Miller, and G. Friedlander. Phys. Rev. **110**, 185 (1958).
18. I. Dostrovsky, P. Rabinowitz, and R. Bivins. Phys. Rev. **111**, 1659 (1958).
19. R. Vandenbosch and J. Huizenga. Proc. 2nd Intern. Conf. Peaceful Uses At. Energy. Vol. 15. Paper P/68 U.N. Geneva. p. 284. 1958.
20. G. N. Harding and F. J. M. Farley. Proc. Phys. Soc. London, A, **69**, 853 (1956).
21. H. B. Levy. Phys. Rev. **106**, 1265 (1957).
22. I. Halpern. Ann. Rev. Nucl. Sci. **9**, 321 (1959).
23. P. P. Benjamin. Ph.D. Thesis, McGill University, Montreal, Quebec. 1965.
24. P. Aagard, G. Andersson, J. O. Burgman, and A. C. Pappas. J. Inorg. Nucl. Chem. **5**, 105 (1957).
25. G. Rudstam and A. C. Pappas. Nucl. Phys. **22**, 468 (1961).
26. J. Colby and J. W. Cobble. Phys. Rev. **121**, 1410 (1961).
27. B. D. Pate. Can. J. Chem. **36**, 1707 (1958).
28. H. Warhanek and R. Vandenbosch. J. Inorg. Nucl. Chem. **26**, 669 (1964).
29. E. Hagebo. J. Inorg. Nucl. Chem. **25**, 1201 (1963).
30. E. Hagebo. J. Inorg. Nucl. Chem. **27**, 927 (1965).
31. D. G. Sarantites, C. D. Coryell, and G. E. Gordon. Phys. Rev. **138**, B353 (1965).
32. C. Rudy, R. Vandenbosch, and C. T. Ratcliffe. J. Inorg. Nucl. Chem. **30**, 365 (1968).
33. J. R. Nix and W. J. Swiatecki. Nucl. Phys. **71**, 1 (1965).
34. R. Vandenbosch and J. R. Huizenga. Phys. Rev. **120**, 1313 (1960).
35. B. T. Feld, H. Feshbach, M. L. Goldberger, H. Goldstein, and V. F. Weisskopf. U.S. At. Energy Comm. Report NYO-636. 1951.
36. V. M. Strutinskii. Zh. Eksperim. Teor. Fiz. **37**, 861 (1959). See Soviet Phys. JETP, **10**, 613 (1960) for a translation.
37. H. Feshbach, M. M. Shapiro, and V. F. Weisskopf. U.S. At. Energy Comm. Report NYO-3077. 1953.
38. J. H. Davies and L. Yaffe. Can. J. Chem. **41**, 1836 (1963).
39. N. T. Porile. Nuclear chemistry. *Edited by* L. Yaffe. Academic Press, Inc., New York. 1968. Chap. II.

Can. J. Chem. Downloaded from www.nrcresearchpress.com by 210.87.254.105 on 09/05/12
For personal use only.

Kinetics and mechanisms of the reaction between carbon monoxide and copper(II) in aqueous solution

J. J. BYERLEY
Department of Chemical Engineering, University of Waterloo, Waterloo, Ontario

AND

E. PETERS
Department of Metallurgy, University of British Columbia, Vancouver 8, British Columbia

Received June 24, 1968

The kinetics of the reduction of copper(II) to copper(I) by carbon monoxide in aqueous solutions have been investigated at 120 °C and carbon monoxide pressures up to 1360 atm. The reaction is homogeneous and proceeds by two paths, one of which is virtually independent of carbon monoxide pressure due to the formation of a stable cuprous carbonyl complex $Cu(CO)^+$. The second reaction path contains both a pH-dependent and pH-independent component. The rate-determining step in both paths appears to be the decomposition of a carbon monoxide insertion complex by a cupric ion. Complexing ligands such as acetate were observed to have a minor inhibiting effect on the overall reaction.

Canadian Journal of Chemistry, **47**, 313 (1969)

Can. J. Chem. Downloaded from www.nrcresearchpress.com by 210.87.254.42 on 09/05/12
For personal use only.

Introduction

Carbon monoxide reduces a number of metal ions under pressurized conditions and elevated temperatures. The kinetics and mechanisms of many of these reactions, for example, silver(I) (1–3), nickel(II) (4), cobalt(II) (5), and mercury(II) (6), are described in the literature.

The reaction of copper(II) with carbon monoxide was first studied by Bauch, Pawlek, and Plieth (1) who reported a first-order dependence on carbon monoxide and a second-order dependence on dissolved copper. McAndrew and Peters (7) using a pressure drop technique (8–10) reported that the overall reaction takes place in 2 stages; the first stage which may be represented by the stoichiometry

$$[1] \quad 2Cu(II) + 3CO + H_2O \rightleftarrows 2Cu(CO)^+ + CO_2 + 2H^+$$

is followed by a second stage described as a further reduction to metallic copper, hydrolysis or disproportionation depending on prevailing chemical conditions.

In a previous paper the present authors (11) indicated that at low initial copper levels the process would proceed only through the first stage providing the carbon monoxide pressure was maintained at a sufficiently high value to stabilize the cuprous ion. Under these conditions it was found that the kinetics of the homogeneous reactions described by reaction [1] were expressible by a 2 term rate law

$$[2] \quad \frac{-d[Cu(II)]}{dt} = k_1 \frac{[Cu(II)][Cu(I)]}{[H^+]} + k_2 \frac{[Cu(II)]^2}{[H^+]} P_{CO}$$

The reaction mechanism postulated from the kinetic evidence centered on the formation of carbon monoxide insertion complexes such as

$$(Cu—\overset{\overset{O}{\|}}{C}—OH)^+$$

It is now possible, through a combination of the earlier information and new data, especially that obtained at high carbon monoxide pressures, to provide a much more comprehensive understanding of the reaction.

Experimental

All chemicals were reagent grade and used without further purification. Carbon monoxide (99.5% minimum) was supplied by the Matheson Company. The copper(II) solutions employed in the kinetic study were prepared by diluting standardized stock solutions. Most experiments were carried out in acetate buffered solutions.

The progress of the reaction of copper(II) with carbon monoxide was followed spectrophotometrically using a titanium alloy cell which fitted directly into the sample compartment of a DK-2 ratio-recording spectrophotometer. This cell has been described in detail in the literature (12). The spectrophotometer was modified somewhat to permit the recorder pen carriage to be driven at constant speed while the wavelength scroll remained fixed at a desired wavelength (approximately

Can. J. Chem. Downloaded from www.nrcresearchpress.com by 210.87.254.42 on 09/05/12
For personal use only.

750 mμ for cupric acetate; the absorption peaks are temperature dependent). This arrangement produced a continuous record of optical density change as the copper(II) species was reduced.

The experimental procedure consisted of filling the reaction cell (total liquid volume 1 cc) with copper(II) solution using a hypodermic syringe. The remaining volume in the cell was flushed with nitrogen and carbon monoxide through the exhaust valve on the side of the vessel. With the cell placed in the sample compartment of the spectrophotometer, the temperature was raised to 120 °C under a pressure of about 20 atm of carbon monoxide. A thermistor temperature controller provided temperature regulation to within ±0.3 °C. When the reaction temperature was reached, the desired carbon monoxide pressure was applied, and the solution was immediately agitated for 2 min by a magnetic plunger. The reaction thus being initiated was allowed to proceed without further agitation[1] since the solubility of carbon monoxide at the applied pressures (68 to 1360 atm) was at least 5 times that required for complete reduction of the dissolved cupric salt.

Experimental Results

The General Form of the Rate Law

Three typical experimental curves with optical density replaced by copper(II) concentration showing the reduction of cupric acetate by carbon monoxide are given in Fig. 1. This characteristic "S" shape was observed for all experiments in the acetate buffered system except when certain extreme chemical conditions were applied. Under these conditions (discussed later) it was possible to virtually eliminate the initial downward curvature. Curves of the type shown in Fig. 1 were consistently found to yield maximum slopes at the point where 50% of the copper(II) had been reduced regardless of the initial copper(II) concentration. The rate at this mid-point was found to be the most reproducible stage of the experiment (normally within 5%) and thus was selected as the reaction parameter for most experiments.

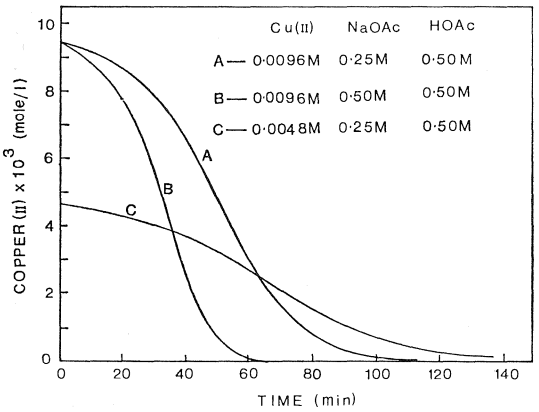

FIG. 1. Typical experimental curves for the reduction of copper(II) by carbon monoxide: P_{CO} = 68 atm; temperature = 119.4 °C.

[1]Agitation during the course of the reaction did not produce any detectable change in the rate of the reaction.

Examination of the experimental curves shown in Fig. 1 indicates a definite dependence of reaction rate on copper(II) and acid concentrations. Although a consideration of these variables (along with the carbon monoxide dependence) has resulted in a preliminary rate law formulation, given in the paper cited earlier, it is appropriate to repeat briefly this discussion to facilitate a clear understanding of the final rate law.

Figure 2 shows the results of graphically differentiating curves of the type shown in Fig. 1. These curves which are nearly symmetrical about the 50% reduction point, indicate a rate law of the form

$$[3] \qquad -\frac{d[Cu(II)]}{dt} = A[Cu(II)][Cu(I)] + B[Cu(II)]^n$$

In this expression the product of the concentrations of 2 copper species is the dominant term

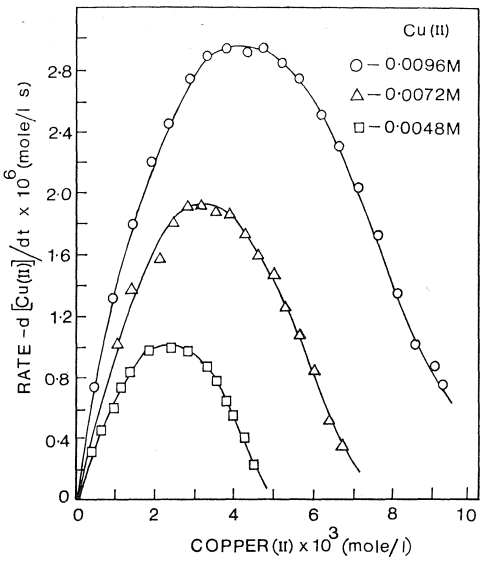

FIG. 2. Differential plot showing $-d[Cu(II)]/dt$ vs. [Cu(II)] for 3 initial copper(II) concentrations: 0.25 *M* NaOAc; 0.50 *M* HOAc; P_{CO} = 68 atm; temperature = 119.4 °C.

whereas the second term is added to account for the initiation of the reaction which must be dependent on copper(II) alone.

Further evidence to support the form of eq. [3] is found through maximum rate measurements. The maximum rate still retains some contribution from the rate due to the second term but this may be neglected. Figure 3 shows a plot of maximum rate for a series of experiments using different initial copper concentrations. A linear dependence on [Cu(II)][Cu(I)] is apparent. The zero intercept arises because at the point of measurement the concentration of copper(II) is about equal to the concentration of copper(I).

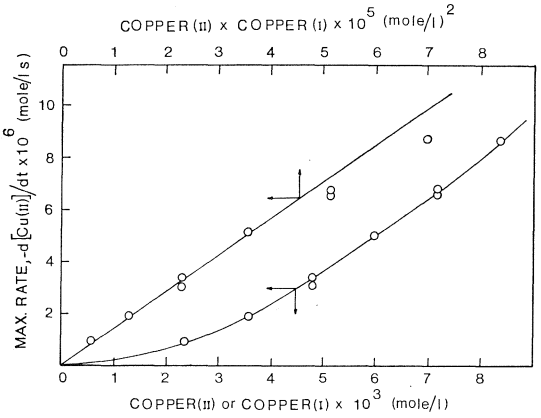

FIG. 3. Dependence of maximum rate on [Cu(II)] and [Cu(II)][Cu(I)] at 50% reduction: 0.25 *M* NaOAc; 0.50 *M* HOAc; P_{CO} = 68 atm; temperature = 119.4 °C.

The dependence of maximum rate on the reciprocal of acetic acid concentration is shown in Fig. 4. In view of this result, eq. [3] may be rewritten in the following form

$$[4] \quad -\frac{d[Cu(II)]}{dt} = A'\frac{[Cu(II)][Cu(I)][OAc^-]}{[HOAc]} + B'\frac{[Cu(II)]^n[OAc^-]}{[HOAc]}$$

Under the conditions prevailing in this series of experiments only the form of the dominant first term appears justified although it does not seem unreasonable to expect the same acid behavior to be reflected in the second term. Further discussion of this point will be given later. By using the expression for the ionization constant of acetic acid, eq. [4] may be rewritten in terms of a new set of rate constants

$$[5] \quad -\frac{d[Cu(II)]}{dt} = k_1'\frac{[Cu(II)][Cu(I)]}{[H^+]} + k_2'\frac{[Cu(II)]^n}{[H^+]}$$

where $k_1' = A'K_i$, $k_2' = B'K_i$, and K_i is the ionization of acetic acid.

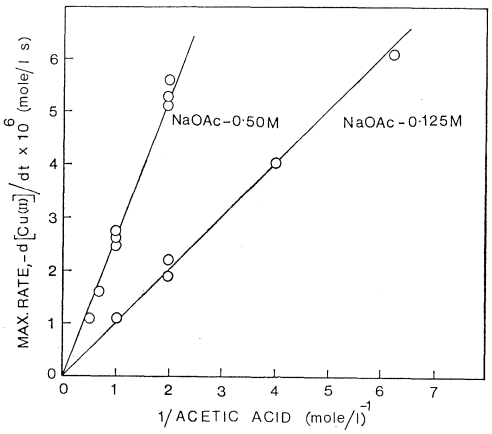

FIG. 4. Dependence of maximum rate on 1/[HOAc]: 0.0096 *M* initial Cu(II); P_{CO} = 68 atm; temperature = 119.4 °C.

The composition of the solution used in these experiments is such that free cupric ions would form a negligible part of the total copper(II) concentration while the concentrations of $Cu(OAc)^+$ and $Cu(OAc)_2$ are present in significant concentrations. Figure 4 may be used to illustrate the inhibiting effect of increasing acetate complexing on the reaction rate by simply selecting a point on each curve of equivalent [NaOAc]/[HOAc] ratio. This result indicates that the diacetate complex which increases in concentration on addition of sodium acetate apparently has a somewhat lower reactivity than the monocetate. A portion of the decrease in rate at constant [NaOAc]/[HOAc] is probably due to a salt effect which would cause an increase in the ionization constant of acetic acid and thus an increase in hydrogen ion concentration. No attempt was made to resolve the complexing effect from the rate constants although experiments carried out in perchlorate media, which is considered a very weak complexing ligand, correlated quite well with rates obtained by extrapolating acetate data to "zero" complexing.

Can. J. Chem. Downloaded from www.nrcresearchpress.com by 210.87.254.42 on 09/05/12
For personal use only.

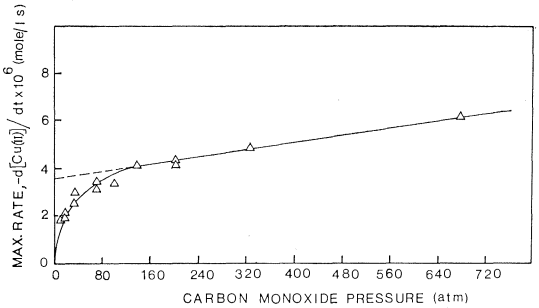

FIG. 5. Effect of carbon monoxide pressure on maximum rate: 0.0096 *M* initial Cu(II), 0.25 *M* NaOAc; 0.50 *M* HOAc; temperature = 119.4 °C.

Effect of Carbon Monoxide Pressure

The effect of carbon monoxide pressure on the reaction rate is recorded in Fig. 5. This plot indicates that the rate of reaction increases very little over the pressure range of about 60 to 680 atm. In view of the fact that the maximum rate is rather insensitive to large carbon monoxide pressure variation, it is reasonable to assume that the pressure-dependence is primarily related to the second term of the rate law. This can be interpreted in terms of a stable cuprous carbonyl (10) complex given by the equilibrium

$$[6] \qquad Cu^+ + CO \overset{K}{\rightleftharpoons} Cu(CO)^+$$

The concentration of $Cu(CO)^+$ can be written as

$$[7] \qquad [Cu(CO)^+] = \frac{K[Cu^+_t][CO]}{1 + K[CO]}$$

where $[Cu^+_t]$ is the total monovalent copper. Since K is known to be large, eq. [7] loses the pressure-dependence and $[Cu(CO)^+] \simeq [Cu^+_t]$. Thus, with the equilibrium of eq. [6] shifted far to the right, the pressure effect would pertain only to the term not involving Cu(I). The effect of pressure on the first term would only become significant when the CO pressure is so low as to shift the $Cu^+ - CO$ equilibrium to the left. The form of Fig. 5 implies that when the CO pressure is above $\sim$ 60 atm a linear dependence on CO pressure can be assigned to the second term of the rate expression. Equation [5] can be written as

$$[8] \qquad -\frac{d[Cu(II)]}{dt} = k_1' \frac{[Cu(II)][Cu(I)]}{[H^+]} + k_2'' \frac{[Cu(II)]^n}{[H^+]} P_{CO}$$

The form of eq. [8] suggests a method of resolving the rates due to the first and second terms. The intercept of Fig. 5 is an estimate of the rate due to the first term. The additional rate at a particular carbon monoxide pressure is the contribution from the second term. Thus a closer inspection of the 2 individual terms in the rate expression and a resolution of their rate constants is possible under high pressure conditions.

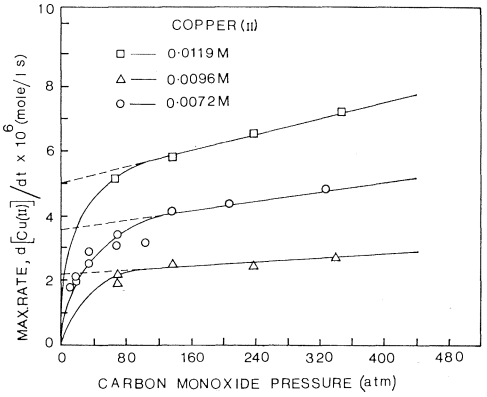

FIG. 6. Resolution of pressure-dependent and pressure-independent terms using [Cu(II)] as the variable: 0.25 *M* NaOAc; 0.50 *M* HOAc; temperature = 119.4 °C.

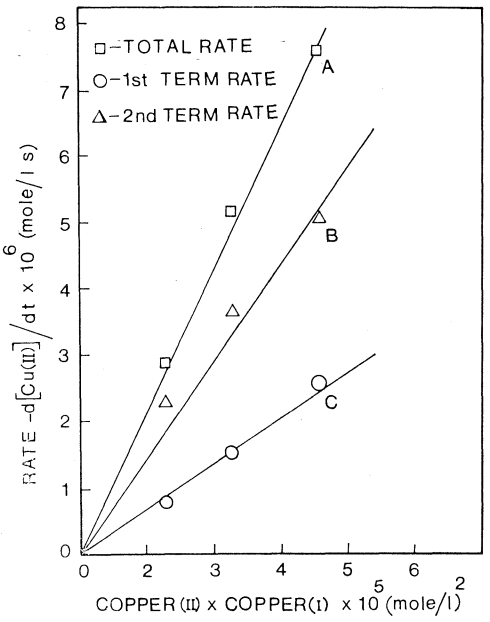

FIG. 7. Dependence of total rate, first term rate and second term rate on [Cu(II)][Cu(I)] or $[Cu(II)]^2$, total rate and second term rate measured at 400 atm (Fig. 6): 0.25 *M* NaOAc; 0.50 *M* HOAc; temperature = 119.4 °C.

Can. J. Chem. Downloaded from www.nrcresearchpress.com by 210.87.254.42 on 09/05/12
For personal use only.

Can. J. Chem. Downloaded from www.nrcresearchpress.com by 210.87.254.42 on 09/05/12
For personal use only.

Recorded in Fig. 6 is a series of experiments similar to those shown in Fig. 5 except that 3 different initial copper concentrations were investigated. Figure 7 presents the graphical data taken from Fig. 6. Curves A and B are plots of the total rate at 400 atm and the first term rate vs. [Cu(II)][Cu(I)] and give the expected linear relationships and zero intercepts. Curve C is a plot of the rate due to the second term and is also linear in [Cu(II)][Cu(I)] which is equivalent to $[Cu(II)]^2$ at 50% reduction. Equation 8 may thus be rewritten in the form

$$[9] \quad -\frac{d[Cu(II)]}{dt} = k_1' \frac{[Cu(II)][Cu(I)]}{[H^+]} + k_2'' \frac{[Cu(II)]^2}{[H^+]} P_{CO}$$

where $k_1' = 5.43 \times 10^{-6}$ s^{-1} ($\pm 10\%$) and $k_2'' = 5.70 \times 10^{-9}$ s^{-1} atm^{-1} ($\pm 20\%$), concentration of NaOAc = 0.25 *M*, temperature = 119.4 °C.

Another series of experiments was carried out in which the $[H^+]$ was varied instead of the [Cu(II)]. These results are shown in Fig. 8. Curve A of Fig. 9 is a plot of the total rate of the reaction at a CO pressure of 400 atm. The curve does not pass through the origin which suggests a pH-independent component of the reaction. This result was not evident in the data obtained from the acid series at 68 atm of carbon monoxide. Thus the pH-independent component must be contained only in the second term of the rate law. Curve B shows the expected inverse linearity of the first term along with a zero intercept. In view of these results the kinetics may be described by a 3 term rate expression

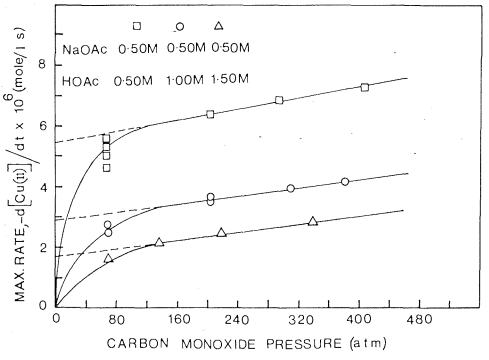

FIG. 8. Resolution of pH-dependent and pH-independent terms: 0.0096 *M* initial Cu(II); temperature = 119.4 °C.

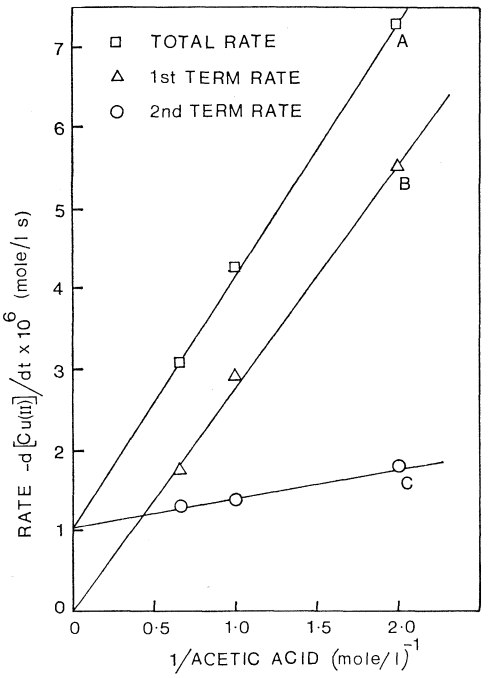

FIG. 9. Dependence of total rate, first term rate, and second term rate on 1/[HOAc], total rate and second term rate measured at 400 atm (Fig. 8): 0.0096 *M* initial Cu(II), 0.50 *M* NaOAc; temperature = 119.4 °C.

$$[10] \quad -\frac{d[Cu(II)]}{dt} = k_1 \frac{[Cu(II)][Cu(I)]}{[H^+]} + k_2 \frac{[Cu(II)]^2}{[H^+]} P_{CO} + k_3 [Cu(II)]^2 P_{CO}$$

where the rate constants as obtained from the data in Fig. 9 are given as follows: $k_1 = 4.24 \times 10^{-6}$ s^{-1} ($\pm 10\%$), $k_2 = 1.40 \times 10^{-9}$ s^{-1} atm^{-1} ($\pm 20\%$), $k_3 = 1.15 \times 10^{-4}$ s^{-1} M^{-1} atm^{-1} ($\pm 15\%$), concentration of NaOAc = 0.50 *M*, temperature = 119.4 °C.

Through the use of the pressure variable it is possible to enhance the contribution of the pressure-dependent terms which at modest pressure account for less than 10% of the maximum reaction rate. Estimation of the second term rate constant k_2'' has, up to now, been made on the

Can. J. Chem. Downloaded from www.nrcresearchpress.com by 210.87.254.42 on 09/05/12
For personal use only.

basis of maximum rates which can produce large errors. Initial rate measurements at low pressure were also found to suffer from large errors not only because of the inherent difficulty associated with initial rate measurement but also because the reaction is changing very rapidly from a pure cupric dependence to a cupric–cuprous dependence. A series of experiments were performed at carbon monoxide pressures from 68 to 1360 atm. The experimental curves are reproduced in Fig. 10. The gradual elimination of the characteristic "S" shape can be explained in terms of a superposition of curves, a convex curve due to the second-order dependence of copper(II) in the second term and an "S" curve with a very slow initial downward curvature increasing only when the copper(I) level becomes significant. As the second term contribution becomes large with increasing carbon monoxide pressure the initial downward curvature disappears.

Using a one term approximation of eq. [9], that is

$$[11] \quad -\frac{d[Cu(II)]}{dt} = k_2'' \frac{[Cu(II)]^2}{[H^+]} P_{CO}$$

the average value of k_2'' was found to be 5.02×10^{-9} s^{-1} atm^{-1}. This average does not include the evaluation of k_2'' taken from the experiment at 68 atm. It should be noted that the value of the ionization constant of acetic acid is affected by hydrostatic pressure. This pressure dependence which has been reported by Hamann and Strauss (13) shows that the ionization constant varies from 1.75×10^{-5} to 5.4×10^{-5} at 25 °C in the pressure range 1 to 3000 atm. This factor has been taken into account when calculating k_2''.

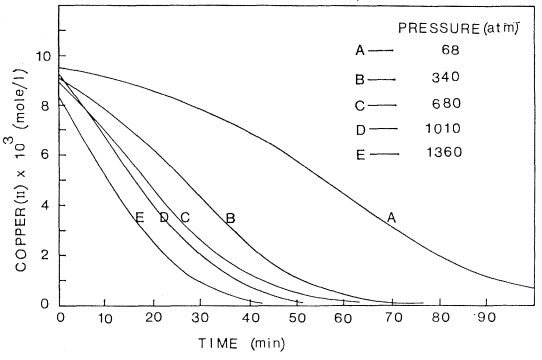

FIG. 10. Alteration of experimental curves by increasing carbon monoxide pressure: 0.0096 *M* initial Cu(II), 0.125 *M* NaOAc; 0.50 *M* HOAc; temperature = 119.4 °C.

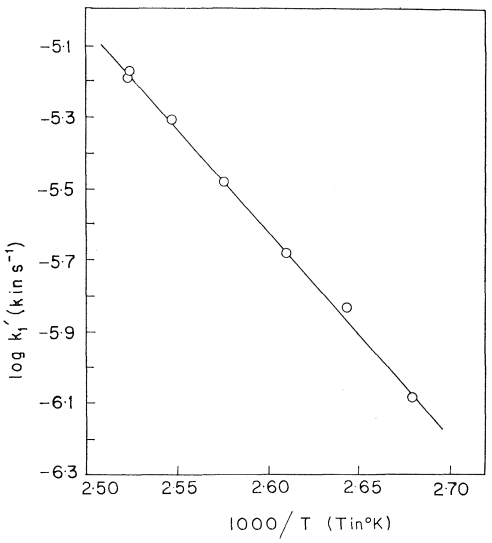

FIG. 11. Arrhenius plot for the reduction of Cu(II) by carbon monoxide: 0.0096 *M* initial Cu(II), 0.25 *M* NaOAc; 0.25 *M* HOAc; P_{CO} = 68 atm.

The Temperature Dependence

The effect of temperature on the reduction of copper(II) was investigated over the temperature range 100 to 123 °C. The rate constants plotted in Fig. 11 are those which pertain to the dominant term since they were obtained from maximum rate measurements. No attempt was made to separate the temperature dependence of the smaller terms. From the slope of this Arrhenius plot, an experimental activation of 25.8 ± 1.0 kcal/mole was calculated.

Reaction Mechanism

A reaction mechanism may be postulated which is compatible with the kinetic evidence summarized in the 3 term rate law given by eq. [10]. This mechanism which defines 2 reaction paths may be represented as follows

PATH A

$$[12a] \quad Cu(II) + CO + H_2O \underset{\text{rapid equilibrium}}{\overset{K_a}{\rightleftharpoons}} (Cu{-}\overset{OH}{\overset{|}{C}}{=}OH)^{2+}$$

[12*b*] $$(\mathrm{Cu{-}C(OH){=}OH})^{2+} + \mathrm{Cu(II)} \xrightarrow{k_a} \mathrm{CO_2} + 2\mathrm{Cu(I)} + 2\mathrm{H^+}$$

[12*c*] $$\mathrm{Cu(II)} + \mathrm{CO} + \mathrm{H_2O} \underset{\text{rapid equilibrium}}{\overset{K_b}{\rightleftharpoons}} (\mathrm{Cu{-}C(=O){-}OH})^{+} + \mathrm{H^+}$$

[12*d*] $$(\mathrm{Cu{-}C(=O){-}OH})^{+} + \mathrm{Cu(II)} \xrightarrow{k_b} \mathrm{CO_2} + 2\mathrm{Cu(I)} + \mathrm{H^+}$$

PATH B

[12*e*] $$\mathrm{Cu^+} + \mathrm{CO} \xrightarrow[\text{fast}]{} \mathrm{Cu(CO)^+}$$

[12*f*] $$\mathrm{Cu(CO)^+} + \mathrm{H_2O} \underset{\text{rapid equilibrium}}{\overset{K_c}{\rightleftharpoons}} (\mathrm{Cu{-}C(=O){-}OH}) + \mathrm{H^+}$$

[12*g*] $$(\mathrm{Cu{-}C(=O){-}OH}) + \mathrm{Cu(II)} \xrightarrow{k_c} \mathrm{CO_2} + \mathrm{CuH^+} + \mathrm{Cu(I)}$$

[12*h*] $$\mathrm{CuH^+} + \mathrm{Cu(II)} \xrightarrow[\text{fast}]{} 2\mathrm{Cu(I)} + \mathrm{H^+}$$

The rate law derived from this reaction sequence corresponds to

$$[13] \quad -\frac{\mathrm{d[Cu(II)]}}{2\mathrm{d}t} = k_c K_c \frac{[\mathrm{Cu(II)}][\mathrm{Cu(CO)^+}]}{[\mathrm{H^+}]} + k_b K_b \frac{[\mathrm{Cu(II)}]^2}{[\mathrm{H^+}]} P_{\mathrm{CO}} + k_a K_a [\mathrm{Cu(II)}]^2 P_{\mathrm{CO}}$$

Equation [13] is identical to eq. [10] if $k_c K_c = k_1$, $k_b K_b = k_2$, $k_a K_a = k_3$, $[\mathrm{Cu(CO)^+}] = [\mathrm{Cu(I)}]$, and the stoichiometry is taken into account.

The first term does not appear to have a pH-independent component. According to the proposed mechanism the observed pH-independent reaction results from the doubly charged intermediate

$$(\mathrm{Cu{-}C(OH){=}OH})^{2+}$$

where the carbon co-ordinates 2 hydroxyl groups. An analogous equilibrium to reaction [12*a*] could exist

[14] $$\mathrm{Cu(CO)^+} + \mathrm{H_2O} \overset{K}{\rightleftarrows} (\mathrm{Cu{-}C(OH){=}OH})^{+}$$

resulting in a singly charged intermediate. The absence of the pH-independent contribution suggests that either this structure is extremely labile and does not exist long enough to react with copper(II), or the attack of the intermediate by copper(II) is too slow to contribute an observable effect.

There are 2 important features evident in the proposed mechanism, the insertion of a carbon monoxide molecule between a metal ion and co-ordinated water molecule, and the decomposition of the insertion complex by another metal ion.

The postulation of a carbon monoxide insertion intermediate is not new. The reduction of silver(I) (2, 3, 9) in both acidic and basic solutions incorporate carbon monoxide insertion complexes into the mechanisms which subsequently undergo decomposition by a metal ion. In the reduction of mercury(II) (6, 14) and nickel(II) (4) by carbon monoxide and the metal ion-catalyzed reduction of MnO_4^- (6, 14), similar intermediates have been postulated. There is no kinetic evidence for the attack of these intermediates by metal ions to facilitate their decomposition as in the case of silver(I) and copper(II) reductions.

In the development of the reaction mechanism

Can. J. Chem. Downloaded from www.nrcresearchpress.com by 210.87.254.42 on 09/05/12
For personal use only.

Can. J. Chem. Downloaded from www.nrcresearchpress.com by 210.87.254.42 on 09/05/12
For personal use only.

not only have insertion complexes been suggested, but also the carbonyl complex (10) $Cu(CO)^+$. In order to account for the pressure-independent character of the first term of the rate law, a fast reaction involving the complexing of Cu^+ with carbon monoxide has been proposed. This is in contrast to the pressure-dependency of the second term, where carbon monoxide participates in a pre-equilibrium. The Cu^+ ion does possess the characteristics necessary for carbonyl formation and indeed shows a great affinity for carbon monoxide. The existence of a stable carbonyl clearly distinguishes the Cu(II)–CO reduction mechanism from the earlier mechanisms proposed for silver(I), mercury(II), and the catalyzed reduction of MnO_4^-.

The explanation of the pH-independent term of the rate law appears in the mechanisms in the form of an intermediate exhibiting a protonated carboxyl group. Although the attachment of 2 OH^- groups to the same carbon atom lacks stability, the presence of a species such as Cu^{2+} could have sufficient electrophilic character to promote stabilization. Further stability of this intermediate may also be gained by admitting resonance structures such as

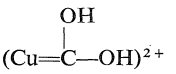

The slow step in both reaction paths is the attack of the insertion complexes by copper(II). In path B the slow step implies the transfer of an H atom or hydride ion H^-. It seems reasonable to assume that the copper ion forming the CuH^+ intermediate comes from the insertion complex whereas the attacking copper(II) acts as the electron acceptor[2]. Removal of a hydride ion from H_2 to form CuH^+ has already been postulated for the mechanism of hydrogen reduction of copper(II) and thus is not without support (15). The postulation of CuH^+ permits the use of one Cu^{2+} ion in the rate-determining step as allowed by the rate law whereas the overall stoichiometry would require two Cu^{2+} ions.

The alternate products to CuH^+ are copper atoms and a proton. The available thermodynamic data indicates that the formation of such species is energetically inconsistent (81.5 kcal/mole) with the activation energy of 26 kcal/mole observed for the reduction of copper(II) by molecular hydrogen in which CuH^+ is the proposed intermediate (16, 17).

The final decomposition of CuH^+ by reaction with another copper(II) species is regarded as fast and does not affect the kinetics. In strong acid solutions it would be expected to compete with another reaction between CuH^+ and hydrogen ions which would yield molecular hydrogen, i.e.

[15]

This reaction was never observed in acetate solutions and would be difficult to obtain because of the slow nature of the overall reaction in strongly acid solutions due to the reciprocal dependence of the rate on hydrogen ion concentration.

The principle difference in the rate-determining step of path A is that the intermediate species

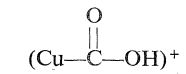

(or the protonated form) has a net positive charge. The charged intermediate would be a stronger acid than the neutral species

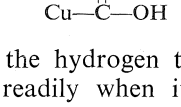

thus allowing the hydrogen to come off as a proton more readily when it is attacked by copper(II). The result is a simple oxidation–reduction reaction. In contrast to the reduction of silver(I) by carbon monoxide in acetate solution the present reaction exhibited only minor sensitivity to the acetate ligand. No attempt was made to resolve this variable nor is it considered in the reaction mechanism.

Acknowledgment

The authors gratefully acknowledge the financial support from the National Research Council of Canada.

[2]At first glance the species

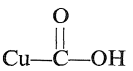

appears to be an acid and upon dissociation a proton would be produced. However, the intermediate is sufficiently electron rich so that in the presence of a suitable recipient 1 or even 2 electrons may accompany the proton in which case the result is either hydrogen atom or hydride ion transfer.

1. G. BAUCH, F. VON PAWLEK, and K. PLIETH. Z. Erzbergbau Metallhuttenew, **11**, 1 (1958).
2. R. T. MCANDREW and E. PETERS. Can. Met. Quart. **3**, 153 (1964).
3. S. NAKAMURA and J. HALPERN. J. Am. Chem. Soc. **83**, 4102 (1961).
4. E. HIRSCH and E. PETERS. Can. Met. Quart. **3**, 137 (1964).
5. H. N. HALVERSON. Ph. D. Thesis, University of British Columbia, Vancouver, British Columbia. 1966.
6. A. C. HARKNESS and J. HALPERN. J. Am. Chem. Soc. **83**, 1258 (1961).
7. R. T. MCANDREW and E. PETERS. Unpublished observations.
8. R. T. MCANDREW. Ph.D. Thesis, University of British Columbia, Vancouver, British Columbia. 1962.
9. R. T. MCANDREW and E. PETERS. Can. Met. Quart. **3**, 153 (1964).
10. J. J. BYERLEY and J. Y. H. LEE. Can. J. Chem. **45**, 3025 (1967).
11. J. J. BYERLEY and E. PETERS. Symp. Unit Processes Hydromet. Met. Soc. Conf. Vol. 24. Gordon and Breach, New York. 1964.
12. J. J. BYERLEY and E. PETERS. Rev. Sci. Instr. **34**, 819 (1963).
13. S. D. HAMANN and W. STRAUSS. Trans. Faraday Soc. **51**, 1684 (1955).
14. A. C. HARKNESS. Ph.D. Thesis, University of British Columbia, Vancouver, British Columbia. 1963.
15. J. HALPERN. Quart. Rev. London, **10**, 463 (1956).
16. R. G. DAKERS and J. HALPERN. Can. J. Chem. **32**, 969 (1954).
17. J. HALPERN, E. R. MACGREGOR, and E. PETERS. J. Phys. Chem. **60**, 1455 (1956).

Can. J. Chem. Downloaded from www.nrcresearchpress.com by 210.87.254.42 on 09/05/12
For personal use only.

Isomerization of butene over a chromia–alumina catalyst

H. C. CHEN[1], R. R. HUDGINS, AND P. L. SILVESTON
Department of Chemical Engineering, University of Waterloo, Waterloo, Ontario

Received May 15, 1968

Isomerization runs were performed in a micro-reactor at 325 °C over a range of butene partial pressure of 84 to 763 mm Hg and at a total pressure of approximately 1 atm. The isomerization rate of 1-butene passed through a maximum with increasing 1-butene partial pressure; the isomerization rate of *cis*- and *trans*-2-butene increased asymptotically with increasing *cis*- and *trans*-2-butene partial pressures respectively. Stereoselectivity was observed in the isomerization of each butene, and was found to be independent of pressure. Catalyst deactivation resulted in loss in stereoselectivity. Results suggest that surface reactions control isomerization and proceed simultaneously on different active sites.

Canadian Journal of Chemistry, 47, 323 (1969)

Can. J. Chem. Downloaded from www.nrcresearchpress.com by 210.87.254.105 on 09/05/12
For personal use only.

Despite the commercial importance of chromia–alumina catalysts for dehydrogenation–isomerization reactions, our understanding of the reaction mechanism on the catalyst and the transport-kinetic rate-controlling steps is incomplete. This paper furnishes new kinetic data on the isomerization of butenes over a commercial chromia–alumina catalyst taken with the intent of establishing rate-controlling steps and helping to elucidate the catalytic mechanism. This study extends earlier work (1) on butane dehydrogenation using the same catalyst, and supplements the work of Amenomiya and Cvetanović (2), the latter being the only account of butene isomerization on chromia–alumina reported to date.

Under the conditions employed, *cis–trans* isomerization of 2-butene and a double bond shift occur. Isobutylene is not found normally, and was not found in this study.

Catalytic isomerization of butenes exhibits a high degree of stereoselectivity which is dependent upon the catalyst (2–9), temperature, and conversion (6, 11). Foster and Cvetanović (6) show that alkaline catalysts favor double bond migration, whereas typically acidic catalysts favor *cis–trans* isomerization. Neutral and metal catalysts exhibit less stereoselectivity. Higher temperatures also reduce stereoselectivity. Selectivity observations have led to the view that isomerization proceeds via a carbanion radical on alkaline catalysts, whereby the stereoselectivity is due to lack of rotation of the allylic carbanion (6, 8, 10). A carbonium ion mechanism has been proposed for the acidic catalysts by Lucchesi *et al.* (7) and is given support by other investigators (9–11). In particular, Hall and co-workers using isotope and tracer techniques (9) provide considerable evidence for a carbonium ion intermediate on silica–alumina. Their studies (9) on activated γ-alumina lead them to suggest that more than one mechanism is operative. Brouwer (5) attributes olefin isomerization on γ-alumina to a carbonium ion mechanism for *cis–trans* isomerization and a hydrogen switch mechanism for a double bond shift. The interpretation of a carbonium ion mechanism for the steric isomerization and an allylic intermediate (though not necessarily ionic) for the double bond shift is suggested by Ogasawara and Cvetanović (8) for Na_2CO_3 impregnated alumina. It is offered, as well, as an interpretation for the chromia–alumina system by Amenomiya and Cvetanović (2).

Chromia is believed to occur in co-precipitated or impregnated catalysts as 10 to 150 Å semicrystalline nodules (12, 13). Foster and Cvetanović (6) find both unsupported chromia and K_2CrO_4 catalyze butene isomerization and are stereoselective. Burwell *et al.* (14) also report olefin isomerization on chromia. According to Harnsberger *et al.* (12), the alumina support is inactive for dehydrogenation at 500 °C. However, Carra and Ragaini (23) in their study of butene isomerization over alumina supported palladium, report some isomerization activity above 240 °C. Nonetheless, it is reasonable to assume that the bulk of the isomerization occurs on the chromia nodules.

Experimental

Apparatus

Details of the apparatus, calibration of rotameters, thermocouples, gas chromatograph, and analysis of products are described elsewhere (1), except for slight

[1]Present address: Department of Chemical Engineering, McMaster University, Hamilton, Ontario.

Can. J. Chem. Downloaded from www.nrcresearchpress.com by 210.87.254.105 on 09/05/12
For personal use only.

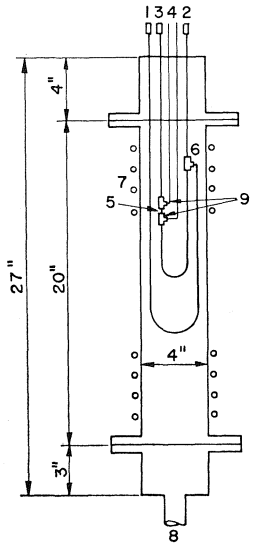

FIG. 1. Micro-reactor and sand bath assembly. 1, Nitrogen inlet; 2, butene inlet; 3, product gas outlet; 4, thermocouples; 5, micro-reactor; 6, mixing tee; 7, nichrome wire heaters; 8, fluidizing air inlet; 9, thermocouple inserted tee.

modifications to the micro-reactor. The micro-reactor employed is shown in Fig. 1.

Calibration of the gas chromatograph was done with standard hydrocarbon mixture No. 37 (Lot 14) from Phillips Petroleum Company, Texas, U.S.A. Propylene carbonate (30% by weight) on 60–80 mesh chromosorb was used for the column.

A commercial chromia–alumina catalyst (approximately 21% Cr_2O_3, 0.46% Na_2O) supplied by Davison Division of W. R. Grace and Co., Baltimore, Md., U.S.A., was used after crushing to provide 40–50 mesh catalyst grains. Properties of this catalyst are detailed elsewhere (1). Compressed nitrogen (prepurified grade) and butene gases of C.P. grade purity (99% minimum) were obtained from Matheson of Canada, Ltd. Analyses by gas chromatography revealed no detectable impurities.

Procedures

Deactivation made it necessary to regenerate the catalyst periodically. It was also necessary to activate the ground fresh catalyst before use. Activation was accomplished by passing pure butene over the fresh catalyst at reaction temperature. On regeneration, the catalyst activity increased. Subsequent regenerations did not alter the activity; as a result, the same batch of catalyst was used for all measurements. Regeneration was carried out by first purging the reactor with pure nitrogen, treating with air for 2 h at 325 °C, and then flushing the reactor again with nitrogen.

The experimental objective was to obtain rate and selectiveness ratios (defined as the ratio of rates of formation of any two butene isomers from the third) for various butenes as a function of butene partial pressure and time of deactivation. Thus, the partial pressure of butene was varied by changing the relative flows of nitrogen and butene while keeping the total flow constant. Butene flow was controlled by a $\frac{1}{4}$-in. toggle valve located upstream from the tee where butene and nitrogen were mixed. In a typical run, this toggle valve was opened for several minutes to allow for flushing and for a quasi steady-state to be reached on the catalyst surface. After several minutes, a gas sample was collected and analyzed immediately by an on-line gas chromatograph. During analysis, only nitrogen passed over the catalyst. The time on stream (with butene in the feed) was accumulated for each series of readings to give conversion as a function of the time butene passed over the catalyst. Initial rates and selectiveness ratios were obtained by extrapolating to zero time on stream.

Results

Butene isomerization rates and selectiveness ratios were obtained for a range of partial pressures from 84–763 mm Hg at approximately 1 atm total pressure and 325 ± 2 °C. Nitrogen was the diluent. Results reported are extrapolations to zero time on stream. Figures 2, 3, and 4 for *trans*-2-butene, *cis*-2-butene, and 1-butene respectively, show the rate of disappearance of the isomer as a function of isomer partial pressure. The selectiveness ratios for different reactant partial pressures are shown as a function of time on stream in Figs. 5, 6, and 7, for *trans*-2-butene, *cis*-2-butene, and 1-butene respectively. It is seen that selectivity is affected by catalyst deactivation but not by butene partial pressures.

Reproducibility and Sources of Error

At the same reactant partial pressure, 2 or 3 series of experiments were performed to test reproducibility. A series is a set of reaction rates measured at different times on stream after a regeneration of the catalyst. Reproducibility was good in almost all cases. Figure 8, a typical plot

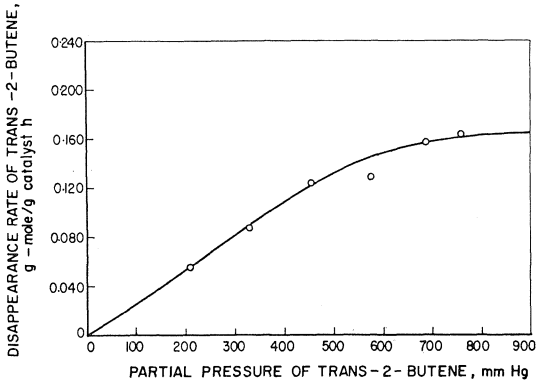

FIG. 2. Rate of disappearance of *trans*-2-butene.

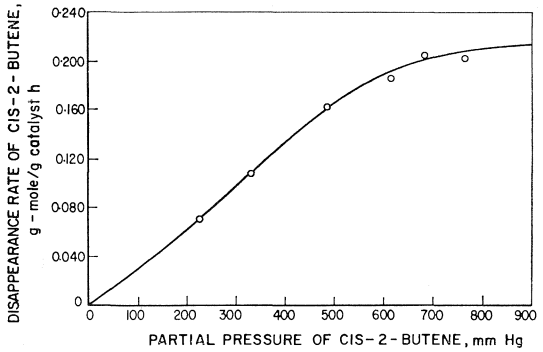

FIG. 3. Rate of disappearance of *cis*-2-butene.

of conversion data vs. time on stream, shows a slight spread of points for different series. If the spread was greater than shown, extrapolation was carried out using the points of highest activity. Occasionally a series would show a significantly lower activity than the others, probably owing to incomplete regeneration. Such a series was disregarded and extrapolation was based on data points with high activity. In the worst case, use of the low activity data would have resulted in a rate only 11% less than that obtained with the high activity data.

The standard deviation in conversion at various times on stream, and of replicate data points, rarely exceeded 15% and averaged about 10%. Thus, reproducibility was deemed satisfactory.

Isomerization was treated as irreversible and conversion was considered differential. Thus, rates could be calculated directly from conversion and mass flow rate of the reactant. Conversion in the reactor averaged about 8%, which is well below equilibrium conversion corresponding to an equilibrium distribution at 325 °C of 20.0, 33.5, and 46.5% for 1-butene, *cis*-2-butene, and *trans*-2-butene respectively (3). It is shown elsewhere (15) that the irreversible and differential assumption introduced a negligible error.

To test the contribution of homogeneous thermal isomerization, a series of runs was made at a low flow rate with about 50% butene mixture using a roll of stainless steel screen to replace the catalyst in the micro-reactor. No perceptible conversion was detected by gas chromatography. This result agrees with the literature

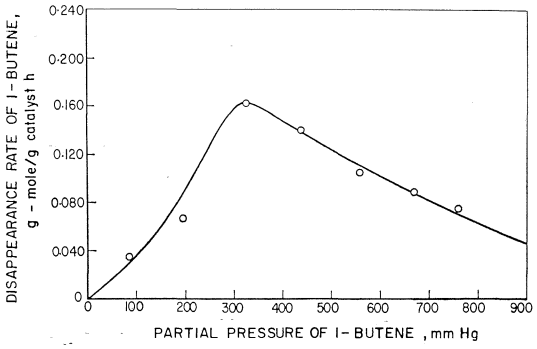

FIG. 4. Rate of disappearance of 1-butene.

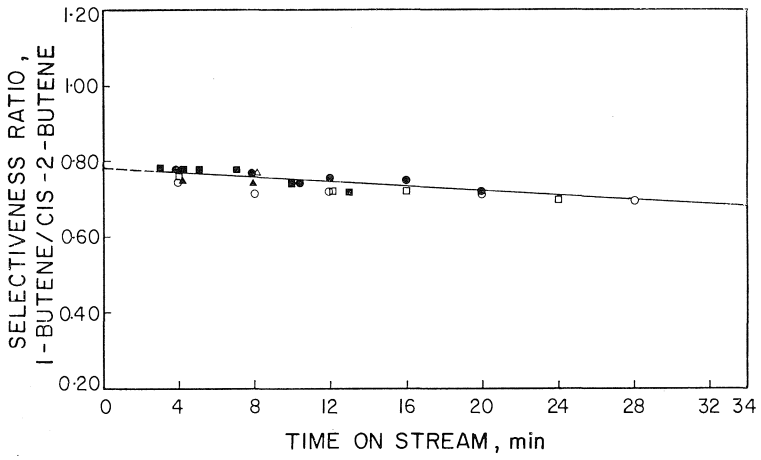

FIG. 5. Selectiveness ratio of 1-butene to *cis*-2-butene from *trans*-2-butene as catalyst decays. ○, 208 mm Hg of *trans*-2-butene; ●, 330 mm Hg of *trans*-2-butene; △, 452 mm Hg of *trans*-2-butene; ▲, 573 mm Hg of *trans*-2-butene; □, 682 mm Hg of *trans*-2-butene; ■, 756 mm Hg of *trans*-2-butene.

Can. J. Chem. Downloaded from www.nrcresearchpress.com by 210.87.254.105 on 09/05/12
For personal use only.

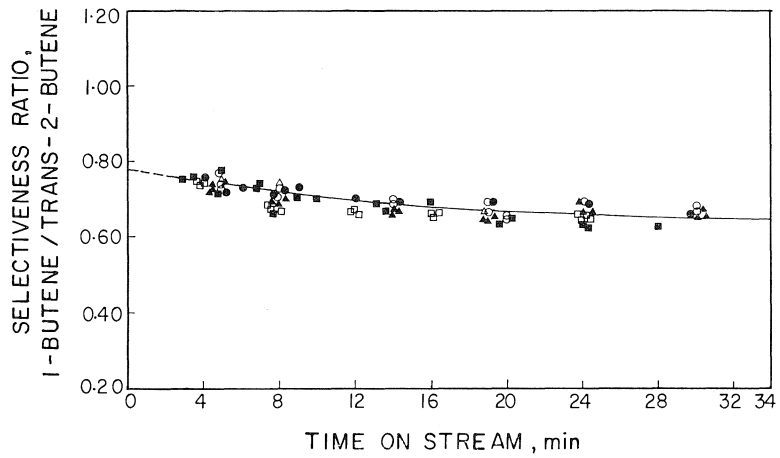

FIG. 6. Selectiveness ratio of 1-butene to *trans*-2-butene from *cis*-2-butene as catalyst decays. ○, 224 mm Hg of *cis*-2-butene; ●, 330 mm Hg of *cis*-2-butene; △, 482 mm Hg of *cis*-2-butene; ▲, 612 mm Hg of *cis*-2-butene; □, 680 mm Hg of *cis*-2-butene; ■, 763 mm Hg of *cis*-2-butene.

(16, 17), which reports that homogeneous thermal reactions are negligible for the experimental conditions used in the study.

Catalytic cracking of butenes was also negligible as shown by the presence of only trace amounts of cracking products in the chromatographic analyses, and a satisfactory carbon balance considering only butenes.

The results reported in Figs. 2–7 were obtained using a 40–50 mesh catalyst. The average diameter based on mesh opening was 0.35 mm. As a check for the influence of pore diffusion, a series of runs was made for *cis*-2-butene using a 60–70 mesh catalyst (average diameter 0.22 mm). A comparison of rates obtained by extrapolating differential conversions versus time on stream to zero time gave the results summarized in Table I. If pore diffusion played a significant role, a 59% increase in rate should have been detected for this size change. The rate difference is negligible; therefore, pore diffusion is not important in this study.

According to Petersen (18), if intraparticle resistance to mass transfer is unimportant, so too is

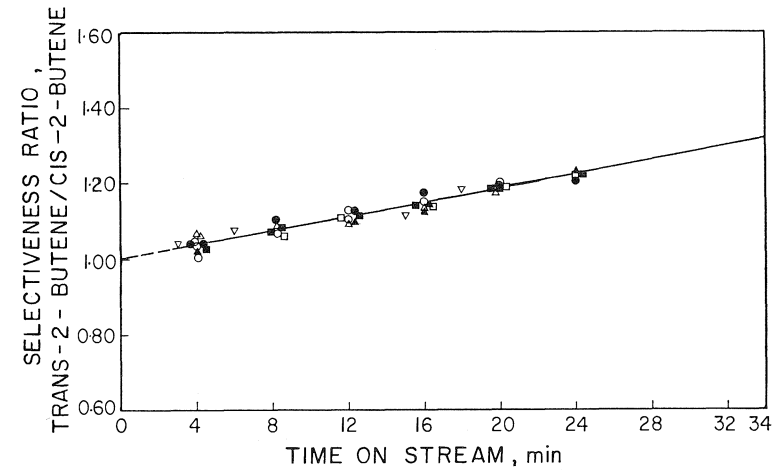

FIG. 7. Selectiveness ratio of *trans*-2-butene to *cis*-2-butene from 1-butene as catalyst decays. ○, 84 mm Hg of 1-butene; ●, 196 mm Hg of 1-butene; △, 320 mm Hg of 1-butene; ▲, 438 mm Hg of 1-butene; □, 556 mm Hg of 1-butene; ■, 670 mm Hg of 1-butene; ▽, 760 mm Hg of 1-butene.

Can. J. Chem. Downloaded from www.nrcresearchpress.com by 210.87.254.105 on 09/05/12
For personal use only.

TABLE I

Comparison of isomerization rates of *cis*-2-butene at two different catalyst particle diameters

Catalyst mesh size	Mole fraction butene in feed	Space velocity (h^{-1})	Rate at zero time g-mole/g catalyst min
40–50	0.43	26 100	0.110
60–70	0.41	26 200	0.107

external resistance to mass transfer. Furthermore, the sharp reduction in conversion with catalyst deactivation, shown in Fig. 8, suggests that reaction or adsorption rates and not mass transfer rates were measured in this study. A calculation of the partial pressure difference between the gas and catalyst surface indicated a difference of the order of 10^{-2} atm which confirms that mass transfer can be neglected in interpreting the kinetic measurements.

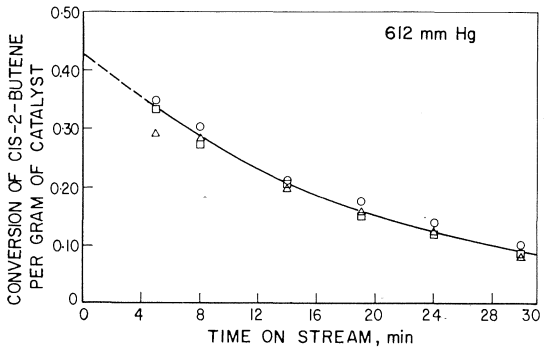

FIG. 8. Conversion data for *cis*-2-butene and extrapolation to zero time on stream, using 612 mm Hg of *cis*-2-butene. ○, Reading numbers 300–305 (series 1); □, reading numbers 306–311 (series 2); △, reading numbers 312–317 (series 3).

Modelling and Interpretation of Results

The salient features of the experimental results are:

(*1*) The apparent asymptotic behavior of the rate of disappearance of *cis*- and *trans*-2-butene as the isomer partial pressure increases (Figs. 2 and 3).

(*2*) The maximum found in the rate of disappearance of 1-butene over the same range of partial pressures (Fig. 4).

(*3*) Stereoselectivity showing *cis*- and *trans*- equally favored in the double bond shift, and *cis–trans* isomerization favored over a double bond shift (Figs. 5–7).

(*4*) Lack of a pressure effect on selectivity (Figs. 5–7).

(*5*) A trend towards equilibrium distributions of isomers as the catalyst deactivates.

Any rate-controlling step or kinetic mechanism proposed for the system must be consistent with these observations.

Amenomiya and Cvetanović (2) postulate that isomerization over chromia–alumina follows a reaction scheme:

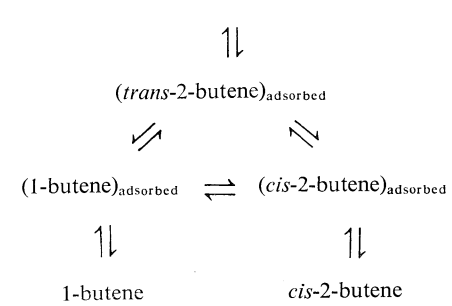

and assume that the rate is described by $kKp/(1+Kp)$, where k is a rate constant, K, an adsorption equilibrium constant, and p, the partial pressure of the butene reactant. This model is adequate for the description of 2-butene isomerization, but will not yield a maximum in rate. This maximum was found for 1-butene (Fig. 4).

The model proposed by Amenomiya and Cvetanović corresponds to a Langmuir–Hinshelwood model for rate-controlling surface reaction occurring at a single active site or desorption of a product. The highly idealized Langmuir–Hinshelwood models (19, 20) should, according to Boudart (21), adequately describe reaction rates measured at one temperature for moderate ranges of pressure and concentration. These conditions are met in this study and models for various rate-controlling steps have been compared to the data as a means of indicating the controlling step. Details are given by Chen (15). Isomerization can be treated as irreversible and interconversion between products neglected for the conversion range used. The Langmuir–Hinshelwood models for different rate-controlling steps are:

(*a*) desorption of product or surface reaction involving a single active site

$$[1] \qquad r = \frac{Ap}{1 + Bp}$$

Can. J. Chem. Downloaded from www.nrcresearchpress.com by 210.87.254.105 on 09/05/12
For personal use only.

(*b*) adsorption of reactant on a single active site

$$[2] \qquad r = Cp$$

(*c*) surface reaction involving dual sites or dissociative adsorption involving dual sites

$$[3] \qquad r = \frac{Dp}{(1 + Ep)^2}$$

An expansion of eq. [3], gives

$$[4] \qquad r = \frac{Dp}{1 + Fp + Gp^2}$$

In the above equations, p is the reactant partial pressure, and A to G are constants representing collections of equilibrium constants and rate coefficients. The contributions of adsorption terms for reaction products were neglected, because adsorption equilibrium constants were believed to be all about the same size while experimental conversions were low. Also the contributions of adsorption terms for the nitrogen diluent were neglected; this is common practice. This assumption is supported by measurement by Uesugi (22) of the adsorption of N_2 on the catalyst at 325 °C. His measurements indicate that N_2 accounts for less than 0.5% of monolayer coverage for the highest diluent partial pressures used.

Equations [1]–[4] were rearranged to give linear forms and fitted to the data by the method of linear least squares. The variance of the fit was compared to an estimate of experimental error of 11% (see discussion of reproducibility above) to test the adequacy of the models. Another test was provided by the fact that all constants of the models should be positive.

This fitting procedure found that eq. [1] gave an adequate fit of the 2-butene data with both A and B positive. Equations [1] and [2] failed to give an adequate fit of the 1-butene data as might be expected; eq. [3], although allowing for the shape of Fig. 4, also failed to give a good fit and; for eq. [4], one of the constants in the denominator was found to be negative in the region between confidence limits. The inconclusiveness of the statistical test may be due to insufficient data, but could also result from the assumption that isomerization occurs via a single mechanism. Carra and Ragaini (23) propose parallel mechanisms for the isomerization of 1-butene.

The model results suggest that surface reaction of chemisorbed intermediates controls butene isomerization. This is in accord with the findings of other investigators (5, 9, 8, 11), albeit for other catalysts. Desorption control is normally dismissed if isomerization is stereoselective (8). However, if the reaction proceeds through a geometrically stable allylic intermediate, stereoselectivity is possible for desorption control. In this case, desorption control may be rejected because it is unlikely that 2-butene isomerization is desorption controlled while 1-butene is surface-reaction controlled.

Figures 5–7 show selectiveness ratios of (1-butene)/(*trans*-2-butene) = 0.77, (1-butene)/(*cis*-2-butene) = 0.77, (*trans*-2-butene)/(*cis*-2-butene) = 1.00, at zero time on stream. The equilibrium distribution at 325 °C corresponds to ratios of 0.43, 0.60, and 1.42, respectively. Chromia–alumina is thus stereoselective and favors double bond migration over a *cis–trans* shift for 2-butene, and the formation of *cis*-2-butene from 1-butene. Amenomiya and Cvetanović (2) found a similar stereoselectivity for unpromoted chromia–alumina between 210 to 260 °C. A difference in catalyst prevents a quantitative comparison of selectivity. Foster and Cvetanović (6) report that *cis* is favored over *trans* for isomerization of 1-butene, and that 1-butene is favored over *cis–trans* for 2-butene isomerization on unsupported chromia at 250 °C. Chromia on alumina and unsupported chromia exhibit a selectivity in between those found by Foster and Cvetanović to characterize acidic and basic catalysts. Their stereoselectivity is similar to that found for activated carbon. Chromia is not considered to be a strong acid catalyst. A carbonium ion mechanism, however, is invoked by Habeshaw and Hill (24) for polymerization of ethylene on chromia supported on silica or silica–alumina gels. A number of mechanisms are proposed to account for the transfer of hydroxyl protons from the support to the chromia surface. This transfer may also occur with an alumina support. Acid sites have been measured on potassium promoted chromia–alumina by Voltz *et al.* (25). The marked decrease in site density when the catalyst is reduced clearly associates the majority of sites with the chromia. Burwell and co-workers (14) find *cis–trans* and double bond isomerization of hexenes occurs readily at 200 °C on unsupported chromia and suggest an allylic carbanion intermediate.

Activated alumina (6, 9) is acidic and favors

Can. J. Chem. Downloaded from www.nrcresearchpress.com by 210.87.254.105 on 09/05/12
For personal use only.

Can. J. Chem. Downloaded from www.nrcresearchpress.com by 210.87.254.105 on 09/05/12
For personal use only.

cis–trans isomerization of 2-butene over double bond migration. This is not observed for this catalyst, confirming the assumption that the support is inactive.

The product distribution obtained here is identical to that predicted by the isomerization model of Hightower and Hall (9), which invoked a common 2-butyl carbonium ion for both *cis–trans* and double bond migration. However, agreement seems fortuitous since their (1-butene)/(*cis*-2-butene) = (1-butene)/(*trans*-2-butene) = 0.75 ratios are for room temperature only. The major failing of the 2-butyl carbonium ion intermediate model is that it does not predict a change in selectivity on deactivation.

Leftin and Hermana (11) propose configurationally different allylic carbonium ion intermediates for double bond migration to yield *cis* and *trans*-2-butene. This model also fails to predict the deactivation effect unless some complex and unlikely assumptions are made. If, for example, preferentially deactivated sites favor the *cis* precursor, intraconversion of the allylic configurations will occur readily, and is less affected by deactivation than the double bond migration.

Ogasawara and Cvetanović (8) suggest that geometric and double bond isomerization occur by simultaneous mechanisms. A carbonium ion mechanism is responsible for *cis–trans* isomerization, and either an allylic radical or ion, or the concerted hydrogen switch mechanism, is responsible for the double bond shift. This is more satisfactory than Brouwer's postulate of either carbonium or hydrogen switch occurring at the same site. The Brouwer model also fails to predict the observed decrease in *cis–trans* selectivity on deactivation. If one assumes separate sites for the simultaneous mechanisms with an activity hierarchy

$$\text{1-butene} \rightleftharpoons \textit{cis}\text{-2-butene} > \text{1-butene}$$

$$\textit{trans}\text{-2-butene} > \textit{cis} \rightleftharpoons \textit{trans}$$

and preferential deactivation of the most active sites, the observed behavior would result.

The proposal of Carra and Ragaini of parallel mechanisms for 1-butene isomerization is particularly attractive event though it was originally put forward to explain isomerization over metal catalyst (23). The first mechanism involves π-adsorbed butene forming a carbonium ion, interacting with another site to shift a hydrogen atom, and give σ-bonding on two metal sites. Desorption yields only *cis*-2-butene. The parallel mechanism involves a single site and the formation of an allyl radical, and, according to Carra and Ragaini, is not stereoselective. If one assumes that intraconversion of the intermediates or a separate *cis–trans* isomerization is possible to account for the 2-butene results, and that the stereoselective sites for 1-butene are preferentially deactivated, the proposal is fully in accord with the selectivity, deactivation, and rate model results.

1. S. Noda, R. R. Hudgins, and P. L. Silveston. Can. J. Chem. Eng. **45**, 294 (1967).
2. Y. Amenomiya and R. J. Cvetanović. Can. J. Chem. **40**, 2130 (1962).
3. H. H. Voge and N. C. May. J. Am. Chem. Soc. **68**, 550 (1946).
4. W. O. Haag and H. Pines. J. Am. Chem. Soc. **82**, 387 (1960).
5. D. M. Brouwer. J. Catalysis, **1**, 22 (1962).
6. N. F. Foster and R. J. Cvetanović. J. Am. Chem. Soc. **82**, 4274 (1960).
7. P. J. Lucchesi, D. L. Baeder, and J. P. Longwell. J. Am. Chem. Soc. **81**, 3235 (1959).
8. S. Ogasawara and R. J. Cvetanović. J. Catalysis, **2**, 45 (1963).
9. J. W. Hightower and W. K. Hall. Chem. Eng. Progr. Symp. Ser. **63**, No. 73, 122 (1967).
10. W. O. Haag and H. Pines. J. Am. Chem. Soc. **82**, 2488 (1960).
11. H. P. Leftin and E. Hermana. 3rd Int. Congr. Catalysis. Vol. 2. North Holland Publ. Co., Amsterdam. 1964. p. 1064.
12. H. F. Harnsberger. Private communication.
13. J. Deren, J. Haber, and J. Siechowski. 3rd Int. Congr. Catalysis. Vol. 2. North Holland Publ. Co., Amsterdam. 1964. p. 993.
14. R. L. Burwell, Jr., A. B. Littlewood, M. Cardew, G. Pass, and C. T. H. Stoddard. J. Am. Chem. Soc. **82**, 6272 (1960).
15. H. C. Chen. M.A.Sc. Thesis. University of Waterloo, Waterloo, Ontario. 1968.
16. G. B. Kistiakowsky and W. R. Smith. J. Am. Chem. Soc. **58**, 766 (1936).
17. W. F. Anderson, J. A. Bell, J. M. Diamond, and K. R. Wilson J. Am. Chem. Soc. **80**, 2384 (1957).
18. E. E. Petersen. Chemical reaction analysis. Prentice-Hall, Inc., New York. 1965.
19. K. J. Laidler. *In* Catalysis. *Edited by* P. H. Emmett. Vol. 1. Reinhold Publishing Corp., New York. 1952.
20. J. M. Thomas and W. J. Thomas. Introduction to the principles of heterogeneous catalysis. Academic Press, Inc., New York. 1967.
21. M. Boudart. A.I.Ch.E. J. **2**, 62 (1956).
22. S. Uesugi. Private communication.
23. S. Carra and V. Ragaini. J. Catalysis, **10**, 230 (1968).
24. J. Habeshaw and T. Hill. 3rd Int. Congr. Catalysis. Vol. 2. North Holland Publ. Co., Amsterdam. 1964. p. 975.
25. S. E. Voltz, A. E. Hirschler, and A. Smith. J. Phys. Chem. **64**, 1594 (1960).

Analysis of line-width effects in the electron spin resonance spectra of monoprotonated semiquinones

T. E. GOUGH
Department of Chemistry, University of Waterloo, Waterloo, Ontario
Received April 17, 1968

Electron spin resonance spectra of monoprotonated *p*-benzosemiquinone, 2:6-dimethyl-*p*-benzosemiquinone, and durosemiquinone dissolved in tetrahydrofuran at −70 °C are reported. Under such conditions restricted rotation of the hydroxyl group causes the ring positions meta to the site of protonation to appear as non-equivalent, though this effect is not observed for monoprotonated durosemiquinone. The spectra of monoprotonated *p*-benzosemiquinone in tetrahydrofuran exhibit both anisotropic and alternating line-width trends; equations are presented which allow the separation of these two effects and the determination of the energy of activation for the rotation of the hydroxyl group as between 31 and 40 kJ/mole. Spectra of monoprotonated 2:3- and 2:5-dimethyl-*p*-benzosemiquinones in 1:2 dimethoxyethane at 20 °C are also reported.

Canadian Journal of Chemistry, **47**, 331 (1969)

Can. J. Chem. Downloaded from www.nrcresearchpress.com by 210.87.254.42 on 09/05/12
For personal use only.

Introduction

Ultraviolet irradiation of neutral solutions of quinones results in the formation of monoprotonated semiquinone radicals of general formula HO—Ar—O·, which have been characterized by their electronic (1, 2) and electron spin resonance (3–5) spectra. The latter show that protonation of the semiquinone causes a redistribution in unpaired electron density; positions ortho to the hydroxyl group carry a small negative spin density (of the order of −0.02) while the meta positions carry an appreciable positive spin density (of the order of +0.2). The signs of these spin densities have been inferred from valence-bond calculations (3) and from the fact that, when due consideration is given to their signs, the mean of the ortho and meta splitting constants closely approximates the splitting constant of the semiquinone anion. The magnitude of the perturbation produced by protonation depends upon the polarity of the solvent (as defined by Kosower (6)), less polar solvents giving larger perturbations of the semiquinone's spin density distribution. The hydroxylic proton's hyperfine splitting pattern is broadened to high field, indicating (7) a negative splitting constant for this proton. To date, all electron spin resonance studies have been performed at room temperature, when the hydroxyl group is rotating sufficiently rapidly to give the radicals an effective C_{2v} symmetry.

Studies performed on several other hydroxy-substituted radicals (8–11) have shown the possibility of observing the effects of the restricted rotation of hydroxyl groups upon the resonance spectra. Under suitable conditions, rotation of the hydroxyl group modulates the hyperfine splitting constants of the radical and gives rise to an alternating line-width effect which may be used to determine the frequency factor and energy of activation of the rotational process. Quantitatively, the method of Carrington (12) has been most widely used for this purpose; the Bloch equations, modified to include the effects of exchange (13), are solved for a series of trial values of the rotational correlation time. The results are then used to simulate theoretical spectra which are compared with the experimental spectrum. However, the rotational correlation time is not the only variable to be assigned; in addition, it is necessary to determine a value for the transverse relaxation time, and, when these two quantities are comparable, considerable errors in the evaluation of the rotational correlation time can be encountered.

An alternative approach to the evaluation of kinetic data is to use, not the complete solution of the modified Bloch equations, but the approximate solutions for slow and rapid exchange rates. Within these approximations, the excess width of a line may be related to the correlation time of the process causing the broadening. The peak to peak amplitude of the first derivative of a Lorentzian line is inversely proportional to the square of the line-width: this amplitude is, therefore, sensitive to line-broadening and so it is the experimental quantity most often used to evaluate the exchange rate. However, to do this, the proportionality constant linking the amplitude and the width must be eliminated. This has been done

Can. J. Chem. Downloaded from www.nrcresearchpress.com by 210.87.254.42 on 09/05/12
For personal use only.

by using amplitude ratios, either of the same line in the presence and absence of the broadening mechanism (14), or of two lines in the spectrum affected to different extents by the broadening mechanism (15). The results obtained using the approximate methods are in good agreement with those from the complete solution of the Bloch equations (15).

If the experimental spectra are recorded under conditions when their anisotropic components are incompletely averaged, additional broadening, varying from line to line, will be superimposed on the effects of the exchange process. Freed and Fraenkel (16, 17) have shown that such anisotropic effects can be described by equations involving the spectral indices characterizing each line; the peak to peak amplitudes of the lines were used to determine their widths, the proportionality factor being eliminated by defining the widths relative to a standard line.

In the present work, the results of the approximate solutions of the Bloch equations modified to include two-site exchange are combined with Freed and Fraenkel's description of anisotropic broadening to give equations applicable to spectra showing considerable anisotropic and alternating line-width effects.

Experimental

Quinones were purified by vacuum sublimation, and solvents were fractionated and dried by standard methods. Solutions were prepared in the open laboratory, not in a vacuum apparatus. This procedure is not recommended when the accurate measurement of splitting constants and their dependence upon temperature is required (18). However, the present paper deals primarily with the measurement of amplitudes. The stationary concentration of radicals attained was rather low, and so slow sweeps, and hence frequent replacement of the sample, were necessary. For this reason, preparation of the solutions was performed in the open laboratory. The sample was irradiated using a Westinghouse H38-4GS 100 W lamp. Electron spin resonance (e.s.r.) spectra were recorded on a Varian E-3 spectrometer equipped with a variable temperature accessory. Temperatures were measured using a copper–constantan thermocouple inserted into the sample immediately before and after each scan. The temperature was found to vary by less than 1 °C during each scan, after which the sample was replaced by a fresh solution.

Results

The general structural formula of the radicals under investigation, and the numbering system used is given in Fig. 1.

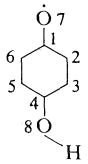

FIG. 1. General structural formula of monoprotonated semiquinones and the numbering system used. For the dimethyl-substituted radicals, the numbering system corresponds to the numbering system of the parent quinone.

The most suitable solvent for the observation of monoprotonated semiquinones at reduced temperatures was tetrahydrofuran; however, results similar to those described have been obtained for solutions in acetone, 1:2-dimethoxyethane and methanol.

Spectra of monoprotonated *p*-benzo- , duro- , and 2:6-dimethyl-*p*-benzosemiquinones at −70 °C were analyzed in terms of the splitting constants given in Table I. Spectra were recorded for sample temperatures as low as −110 °C, but no evidence was found for inequivalence of the positions ortho to the hydroxyl group for any of these radicals. Further, for monoprotonated durosemiquinone no evidence was found for inequivalence of the protons meta to the hydroxyl group.

Increasing the temperature to +20 °C caused the differences in the meta splitting constants of monoprotonated *p*-benzo- and 2:6-dimethyl-*p*-benzosemiquinones to be removed by rapid rotation of the hydroxyl group. At intermediate temperatures line-width alternation caused by incomplete averaging of the meta splitting constants was observed: for monoprotonated *p*-benzosemiquinone, spectra obtained between −18 and −65 °C were used to estimate the activation energy of the rotation of the hydroxyl group (see below). Above −18 °C the radical concentration diminished appreciably during the course of a 30 min scan, while below −65 °C line-width effects due to incomplete averaging of the anisotropic hyperfine and *g*-tensor interactions (16, 17) obscured the line-width alternation.

The incomplete averaging of these anisotropic interactions resulted in the following line-width trends; patterns associated with hydroxylic protons broadened to high field, patterns associated with ring protons broadened to low field, and patterns associated with methyl groups did not broaden asymmetrically to any appreciable extent. The line-width trends for the hydroxylic

TABLE I

Proton hyperfine splitting constants observed for monoprotonated semiquinone radicals

Parent quinone	Solvent	Temperature (°C)	Hyperfine splitting constants* (G)				
			a_2	a_3	a_5	a_6	a_{OH}
p-Benzoquinone	Tetrahydrofuran	−70	−5.69	0.57	0.57	−5.34	−1.90
p-Benzoquinone (calculated)†			−5.71	0.57	0.48	−5.37	
Duroquinone	Tetrahydrofuran	−70	5.08	−0.94	−0.94	5.08	−0.80
2:6-Dimethyl-*p*-benzoquinone	Tetrahydrofuran	−70	5.17	0.61	0.61	4.78	−1.70
2:3-Dimethyl-*p*-benzoquinone	1:2 Dimethoxyethane	20	4.95	−1.10	0.48	−5.68	−1.60
2:5-Dimethyl-*p*-benzoquinone	1:2 Dimethoxyethane	20	5.90	1.10	−0.70	−4.93	−1.37

*Values tabulated are ±0.02 G. Numerical subscripts correspond to the numbering system of Fig. 1. Underlined values are methyl groups splitting constants.

†Parameters used: $Q_{CH} = -24.0$ G, $\lambda = 1.20$, $h_{C_3} = 0.05$, $h_{O_7} = h_{O_8} = 1.17$, $k_{C_1O_7} = 1.91$, $k_{C_4O_8} = 1.01$; for definitions of h and k, see ref. (27).

protons are in the same direction as the corresponding trends observed for diprotonated semiquinone cations (11) whereas the trends for the ring protons are in the opposite sense. This discrepancy underlines the dangers inherent in the evaluation of signs of splitting constants from line-width trends, especially those of aromatic CH fragments (7).

A typical spectrum of monoprotonated *p*-benzosemiquinone, recorded under slow-rotation conditions, is shown in Fig. 2; all 24 components of the spectrum are readily distinguishable, and both the alternation and the trends in line-width can be seen. The sharpest line in the spectrum has a peak-to-peak line width of 110 mg and is thus almost as narrow a line as can be obtained with the 4 in. magnet of the E-3 spectrometer.

Table I also contains the experimental splitting constants of monoprotonated 2:3- and 2:5-dimethyl-*p*-benzosemiquinones, which have not been hitherto reported. The dependence of these spectra upon solvent parallels that for other similar radicals (3–5), less polar solvents leading to greater perturbation of the semiquinone's spin density distribution. The results obtained using 1:2-dimethoxyethane as solvent are given in Table I, since these spectra showed a minimum of overlapping lines, thereby allowing a more accurate determination of the hyperfine splitting constants. No evidence was obtained for two isomers of either of these radicals, suggesting that the hydroxyl group does not rotate freely but tends to point away from the adjacent methyl group (cf. ref. 11).

Discussion

In order to evaluate the activation energy for the rotation of the hydroxyl group of monoprotonated *p*-benzosemiquinone from the spectra the following procedure was adopted. For each line a quantity A, equal to the peak-to-peak amplitude of the first derivative curve divided by the degeneracy of the line, was recorded. Assuming a Lorentzian line-shape, A is related to W, the half-width at half-height, by eq. [1]

$$[1] \qquad A^{-\frac{1}{2}} = S \cdot W$$

where S is a proportionality constant determined by radical concentration and spectrometer sensitivity. Previous workers (14, 15, 17) have eliminated S through the use of relative values of A referred to some standard line. However, in the present studies, the signal-to-noise ratio was often so low that, for a series of spectra run under identical conditions, the results were strongly dependent on the choice of reference line. Accordingly, a more statistically valid approach was employed.

Three major contributions to the line-width were considered. These were broadening from mechanisms independent of the spectral indices, $\tilde{M}$, characterizing a line, broadening from anisotropic dipolar and g-tensor interactions, and broadening from the modulation of isotropic hyperfine splitting constants due to rotation of the hydroxyl group. The most important broadening independent of spectral indices was, under the experimental conditions employed, caused

Can. J. Chem. Downloaded from www.nrcresearchpress.com by 210.87.254.42 on 09/05/12
For personal use only.

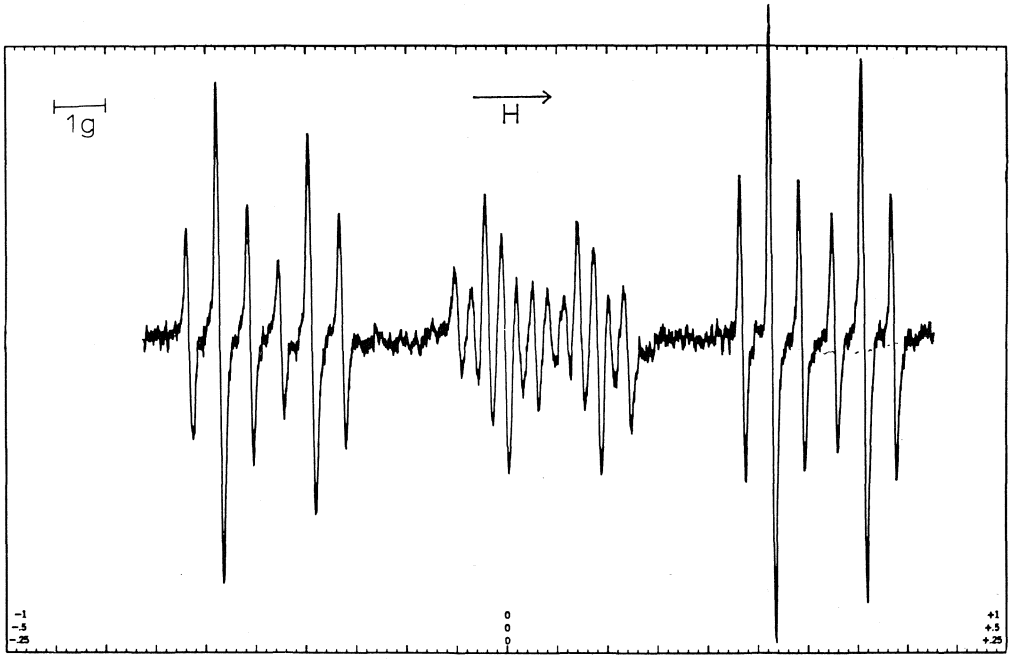

FIG. 2. Electron spin resonance spectrum of monoprotonated *p*-benzosemiquinone in tetrahydrofuran at −60 °C, when rotation of the hydroxyl group is slow. Magnetic field increases from left to right.

by inhomogeneity of the applied magnetic field. Therefore, for each line of a spectrum there will be a constant contribution, denoted by $S \cdot B$, to $A^{-\frac{1}{2}}$; further $S \cdot B$ will be a constant from scan to scan, even though the individual values of S and B may vary with changes in radical concentration and instrument settings.

Contributions to the width of a line from anisotropic dipolar and *g*-tensor interactions may be expressed as functions of the spectral indices[1] characterizing that line (16, 17). For the spectra under consideration, anisotropic effects were described satisfactorily by terms linear in the spectral indices. Since all protons in the radical are nonequivalent (in the terminology of Fraenkel (19)) the spectral indices describing the lines can only take values of $\pm\frac{1}{2}$. Therefore, terms involving the squares of the spectral indices, being independent of spectral indices, contribute to $S \cdot B$ and are not capable of independent evaluation. Terms involving the products of the spectral indices were found to be statistically insignificant, except at sample temperatures below −70 °C when line-width alternation was unimportant. The anisotropic effects, therefore, make contributions to $A_i^{-\frac{1}{2}}$ of the form $S \sum_j C_j \tilde{M}_{i,j}$ where the subscript i denotes the ith line of the spectrum, and the subscript j denotes the jth proton of the molecule. Using the numbering system of Fig. 1, C_3 was always set equal to C_5 and, when the rotation of the hydroxyl group was fast, C_2 was set equal to C_6.

Rotation of the hydroxyl group modulates the splitting of protons 2 and 6 and so gives finite contributions to $A_i^{-\frac{1}{2}}$ for all lines having $\tilde{M}_{i,2}$ not equal to $\tilde{M}_{i,6}$. These contributions may therefore be described by a term of the form $S \cdot P \cdot (\tilde{M}_{i,2} - \tilde{M}_{i,6})^2$ where P is determined by the rate of rotation.

Combining all three contributions to $A_i^{-\frac{1}{2}}$ by assuming their effects to be additive, forms eq. [2]

$$[2] \quad A_i^{-\frac{1}{2}} = S \cdot B + S \sum_j C_j \tilde{M}_{i,j} + S \cdot P \cdot (\tilde{M}_{i,2} - \tilde{M}_{i,6})^2$$

(a) Slow Rotation Approximation

Twenty four lines, giving 24 values of $A_i^{-\frac{1}{2}}$, were obtained and from these values and eq. [2] standard statistical methods were used to evaluate B, C_2, C_3, C_6, C_8, and P (subscript 8 refers

[1] $\tilde{M}_{i,j}$, the spectral index, is equal to $M_{i,j}$, the spin quantum number, after any necessary sign changes have been made to place positive $\tilde{M}_{i,j}$ to high field.

Can. J. Chem. Downloaded from www.nrcresearchpress.com by 210.87.254.42 on 09/05/12
For personal use only.

TABLE II

Results of line-width analysis for spectra of monoprotonated *p*-benzosemiquinone in tetrahydrofuran*

	Temperature (°K)	B	C_2	C_3	C_6	C_8	P	F†
								$F(5, 18)$
Slow rotation	208	0.417	−0.072	−0.054	−0.022	0.073	0.078	15.1
	216	0.357	−0.048	−0.044	−0.022	0.065	0.112	16.8
	223	0.372	−0.046	−0.029	−0.005	0.041	0.233	42.8
								$F(4, 13)$
Rapid rotation	232	0.331	−0.018	−0.018		0.024	0.493	141.0
	240	0.410	−0.014	−0.020		0.038	0.367	121.2
	248	0.424	−0.002	−0.013		0.017	0.214	299.8
	255	0.413	0.001	−0.003		0.023	0.127	59.3

*B, C, and P are defined in the text.
†Ratio test for the significance of fit; all F ratios indicate that the fit is significant at the 99% confidence level.

to the hydroxylic proton). By these means, the broadening due to line-width alternation was separated from the other two broadening mechanisms.

For lines broadened by the modulation of hyperfine splitting constants, the effective transverse relaxation time, T_2', is, within the slow rotation approximation (20), given by

$$[3] \qquad (T_2')^{-1} = T_2^{-1} + \tau^{-1} = W$$

where τ is the rotational correlation time. Comparing eqs. [2] and [3]

$$[4] \quad \tau^{-1} = S \cdot P \cdot (\tilde{M}_{i,2} - \tilde{M}_{i,6})^2 = S \cdot P = k$$

where k is the rate constant for the rotation. S may vary from scan to scan, but since $S \cdot B$ is a constant we may write

$$[5] \qquad k = S \cdot B \cdot \frac{P}{B}$$

Expressing k in terms of the Arrhenius equation, we have

$$[6] \qquad Z \exp(-E_a/RT) = S \cdot B \cdot \frac{P}{B}$$

where Z is the frequency factor and E_a the energy of activation. Taking natural logarithms

$$[7] \qquad \ln \frac{P}{B} = \ln \frac{Z}{SB} - \frac{E_a}{RT}$$

and so a plot of $\ln P/B$ versus $1/T$ should afford a straight line with slope $-E_a/R$.

(b) Fast Rotation Approximation

Eighteen lines were obtained from which the five constants B, C_2, C_3, C_8, and P were determined as above. Using a derivation analogous to that of [7] but imposing the rapid rotation approximation (20)

$$[8] \qquad \ln \frac{B}{P} = \ln \frac{8ZSB}{(\Delta a)^2} - \frac{E_a}{RT}$$

where Δa is the difference in splitting constants between positions 2 and 6. In this approximation therefore, a plot of $\ln B/P$ against $1/T$ should be a straight line of slope $-E_a/R$.

Values of B, C_j, and P are given in Table II. These values have, of course, no absolute significance, but indicate the relative importance of the anisotropic and the alternating line-width effects at the various temperatures.

The appropriate graphs corresponding to eqs. [7] and [8] are shown in Fig. 3. Values for E_a of 31.4 and 33.2 kJ/mole were obtained from the slow and rapid approximations, respectively. Estimates of the accuracy of these energies are difficult to make; the internal consistency of the method appears to be good, the root mean square error in fitting the rapid rotation values of $\ln B/P$ to the line drawn being only 0.024 units. In order to check on the value of E_a, an independent determination was made using the complete solution of the Bloch equations modified (13) to include a two-jump exchange process. Spectra were calculated for trial values of the rotational exchange rate and compared with the experimental traces: anisotropic effects were allowed for by averaging corresponding experimental intensity ratios in the high and low field halves of the spectrum before comparison with the simulated plots. By this method the comparable value of $E_a = 40.2$ kJ/mole was obtained. The simulation

Can. J. Chem. Downloaded from www.nrcresearchpress.com by 210.87.254.42 on 09/05/12
For personal use only.

Can. J. Chem. Downloaded from www.nrcresearchpress.com by 210.87.254.42 on 09/05/12
For personal use only.

method required considerably more computer time, however, each trial spectrum taking approximately 10 s execution and 90 s plotting time. Further, it was usually necessary to compute four trial spectra for each experimental one. In contrast, the total execution time to generate all points in Fig. 3 was less than 4 s.

An additional advantage of eq. [8] is that it allows evaluation of E_a without any knowledge of Δa. The assumption is made that Δa is a constant, but this assumption is also made when employing the complete solution of the modified Bloch equations. Equation [8] is, therefore, suitable for determining the energy of activation when it is not possible to obtain slow-exchange spectra; e.g. the dinitro-durene anion in dimethylformamide (21), thereby eliminating the necessity of estimating Δa as, in this case, 20 G (22).

The values obtained for E_a for the rotation of the hydroxyl group of monoprotonated *p*-benzosemiquinone are in agreement with the value of 42 ± 12 kJ/mole previously observed for the hydroquinone cation (9). It is, therefore, somewhat surprising that it was not possible to observe the effects of the rotation of the hydroxyl group of monoprotonated durosemiquinone since comparable experiments have been successful for the duroquinol cation (10).

Molecular Orbital Calculations

Spin densities were calculated according to McLachlan's self-consistent field theory (23) using a program written by Fritsch, Layloff, and Adams (24). The parameters used to include the oxygen hetero-atoms were obtained as described for similar calculations performed to simulate the spin density distributions in semiquinone–alkali metal ion-pairs (25). The inequivalence between positions 2 and 6 was satisfactorily reproduced by increasing empirically the Coulomb integral of carbon atom 3 (9–11): the calculated inequivalence between positions 3 and 5, while small should have been detectable, at least as a line-width alternation phenomenon; such was not the case. The inequivalence between positions 2 and 6 may also be reproduced by introducing a finite resonance integral between oxygen atom 8 and carbon atom 5 (26). Such a procedure predicts a greater difference between positions 3 and 5 than does increasing the Coulomb integral of carbon atom 3 and is, therefore, even less satisfactory. Until carbon-13 hyperfine splitting constants are determined for such systems, the evaluation of a unique set of parameters best describing the molecule does not seem feasible.

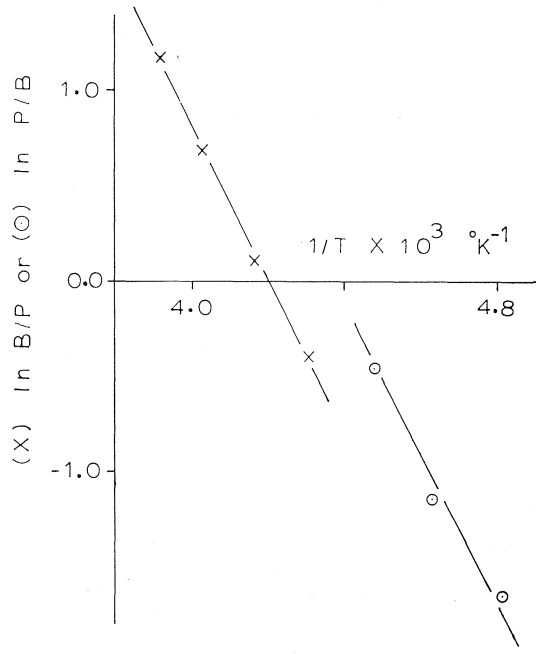

FIG. 3. Plot used to determine the energy of activation of the rotation of the hydroxyl group of monoprotonated *p*-benzosemiquinone in tetrahydrofuran (⊙ = slow rotation approximation; × = rapid rotation approximation).

Acknowledgments

This work received financial support from the National Research Council of Canada and the Ontario Department of University Affairs. The author thanks Drs. Bolton and Sullivan for the manuscript of their paper prior to publication.

1. N. K. BRIDGE and G. PORTER. Proc. Roy. Soc. London, Ser. A, **244**, 259 (1958).
2. N. K. BRIDGE and G. PORTER. Proc. Roy. Soc. London, Ser. A, **244**, 276 (1958).
3. T. A. CLAXTON, T. E. GOUGH, and M. C. R. SYMONS. Trans. Faraday Soc. **62**, 279 (1966).
4. T. E. GOUGH. Trans. Faraday Soc. **62**, 2321 (1966).
5. T. A. CLAXTON, J. OAKES, and M. C. R. SYMONS. Trans. Faraday Soc. **63**, 2125 (1967).
6. E. M. KOSOWER. J. Am. Chem. Soc. **80**, 3353 (1958).
7. A. CARRINGTON and H. C. LONGUET-HIGGINS. Mol. Phys. **5**, 224 (1962).
8. J. R. BOLTON and A. CARRINGTON. Mol. Phys. **5**, 161 (1962).
9. A. B. BARABAS, W. F. FORBES, and P. D. SULLIVAN. Can. J. Chem. **45**, 267 (1967).
10. P. D. SULLIVAN. J. Am. Chem. Soc. **89**, 4294 (1967).

11. P. D. SULLIVAN and J. R. BOLTON. J. Am. Chem. Soc. In press.
12. A. CARRINGTON. Mol. Phys. **5**, 425 (1962).
13. H. S. GUTOWSKY, D. W. MCCALL, and C. P. SLICHTER. J. Chem. Phys. **21**, 279 (1953).
14. R. L. WARD and S. I. WEISSMAN. J. Am. Chem. Soc. **79**, 2086 (1957).
15. N. M. ATHERTON and A. E. GOGGINS. Trans. Faraday Soc. **61**, 1399 (1965).
16. J. H. FREED and G. K. FRAENKEL. J. Chem. Phys. **39**, 326 (1963).
17. J. H. FREED and G. K. FRAENKEL. J. Chem. Phys. **40**, 1815 (1964).
18. T. E. GOUGH and G. A. TAYLOR. Unpublished results.
19. G. K. FRAENKEL. J. Phys. Chem. **71**, 139 (1967).
20. J. A. POPLE, W. G. SCHNEIDER, and H. J. BERNSTEIN. High-resolution nuclear magnetic resonance. McGraw-Hill Book Co., Inc., New York. 1959.Chap. 10.
21. J. H. FREED and G. K. FRAENKEL. J. Chem. Phys. **37**, 1156 (1962).
22. J. H. FREED and G. K. FRAENKEL. J. Chem. Phys. **41**, 699 (1964).
23. A. D. MCLACHLAN. Mol. Phys. **3**, 233 (1960).
24. J. M. FRITSCH, T. P. LAYLOFF, and R. N. ADAMS. J. Am. Chem. Soc. **87**, 1724 (1965).
25. P. S. GILL and T. E. GOUGH. Trans. Faraday Soc. **64**, 1997 (1968).
26. E. W. STONE and A. H. MAKI. J. Chem. Phys. **38**, 1999 (1963).
27. A. STREITWEISER. Molecular orbital theory for organic chemists. John Wiley & Sons, Inc., New York. 1961. Chap. 5.

Can. J. Chem. Downloaded from www.nrcresearchpress.com by 210.87.254.42 on 09/05/12
For personal use only.

Arsinohydrazines: reactions of hydrazine and substituted hydrazines with organo-arsine derivatives

L. K. PETERSON AND K. I. THÉ
Department of Chemistry, Simon Fraser University, Burnaby 2, British Columbia
Received September 16, 1968

Reactions between organo-arsine derivatives $(CF_3)_2AsX$ and $(CF_3)_3As$ and hydrazine or substituted hydrazines are discussed as synthetic routes to a new class of hydrazinoarsine compounds. The systems $[(CF_3)_2As]_x\ N_2H_{4-x}$ are unstable with respect to elimination of CF_3H and N_2, but stability increases with increased methylation of the nitrogen atoms. The new compounds described are: N-methyl,N′-bis-(trifluoromethyl)arsinohydrazine, $MeNHNHAs(CF_3)_2$, (**1**) (highly unstable at room temperature); N,N-dimethyl,N′-bis(trifluoromethyl)arsinohydrazine, $Me_2NNHAs(CF_3)_2$, (**2**) (m.p. 3.00° ± 0.15°, b.p. 20°/14.6 mm); and trimethylhydrazino-bis(trifluoromethyl)arsine, $Me_2NNMeAs(CF_3)_2$, (**3**) (m.p. −41.5° ± 0.5°, b.p. 15°/6.30 mm). The observed order of stability was **2** > **3** ≫ **1**.

Canadian Journal of Chemistry, **47**, 339 (1969)

Can. J. Chem. Downloaded from www.nrcresearchpress.com by 210.87.254.6 on 09/05/12
For personal use only.

Discussion

In an effort to increase the number of available compounds based on a N—N—As skeleton, with varying electronic and steric or structural characteristics, we have investigated synthetic routes involving reaction between hydrazine and substituted hydrazines and organo-arsine derivatives. The N—N—As system is of interest as a Lewis base and potential chelating agent toward acceptor species (1, 2). The N—N hydrazine moiety is in itself of interest from the point of view of bonding, structure, and potential bidentate character (3–7). The modification of these characteristics, and the variation in the N—N bond energy and stability with differing metalloidal substituents, has not been widely studied.

This paper is concerned with the family of perfluoroalkyl-arsinohydrazines $(CF_3)_xAs(NRNR'R'')_{3-x}$ with R, R′, and R″ = H or Me, and $x = 0-3$. Studies of analogous alkyl-arsinohydrazines are in progress. The N atoms may be expected to function as differential Lewis bases, while the As atom may exhibit both σ donor and π acceptor behavior, both strongly influenced by the electronegative CF_3 groups. The hydrazine unit, with lone pairs of electrons on adjacent N atoms, is relatively unstable with respect to oxidation processes which result ultimately in the production of the stable N_2 molecule. One might expect enhanced stability with substituents that permit intramolecular dative π bonding, as discussed for phosphinohydrazines, for example (2).

Our studies show that bis(trifluoromethyl)arsinohydrazines are sensitive to the replacement of H on nitrogen by methyl groups. Reaction between hydrazine and $(CF_3)_3As$ or $(CF_3)_2AsCl$ yielded large quantities of fluoroform, nitrogen, and colored (brown, black) residues, as well as oily, low volatile liquids. During handling on the vacuum line, the latter decomposed into colored residues and CF_3H and N_2. While it seems that all of the CF_3—As bonds are ultimately cleaved, only partial elimination of the hydrazine moiety, as N_2, occurs; the fate of the remaining hydrazine linkages cannot easily be established. We may infer, however, that an intermediate, such as **4**, is highly unstable.

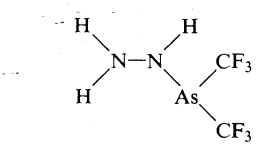

4

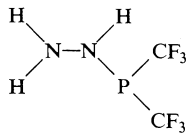

5

The corresponding studies with mixtures of $(CF_3)_3P$ or $(CF_3)_2PI$ and hydrazine indicated that reaction does not occur unless a basic medium, such as trimethylamine, is present (2). The intermediate phosphinohydrazines, such as **5**, suffer loss of CF_3H, condensing to form waxy, intractable materials, but elimination of N_2 was not found. These observations are in keeping with the fact that simple covalent compounds of arsenic have lower thermal stability than those of phosphorus (8). In addition, N→P π bonding (9) in the N—N—P system should modify the electron density about the skeleton of the molecule, reducing repulsion energies in a way such as to improve its stability against the

Can. J. Chem. Downloaded from www.nrcresearchpress.com by 210.87.254.6 on 09/05/12
For personal use only.

elimination of the N≡N unit. This stabilizing effect was shown to be less significant for the nitrogen–arsenic bond, in the systems $(CF_3)_2$-AsNRP$(CF_3)_2$, (R = H, Me), where bond cleavage, with HCl or NH_3, occurred preferentially at the N—As, rather than at the N—P, bond (10).

Methylhydrazine reacts with $(CF_3)_3As$ and $(CF_3)_2AsCl$ in much the same way as hydrazine itself, yielding, at room temperature, highly colored decomposition products together with CF_3H, N_2, and involatile oily liquids. Trifluoroethane was not observed.

Under carefully controlled conditions, however, the unstable compound N-methyl,N′-bis(trifluoromethyl)arsinohydrazine MeNHNHAs$(CF_3)_2$, **1**, was isolated. The vapor phase molecular weight (M_{obsd}, 259; M_{calcd}, 258) and the ^1H nuclear magnetic resonance (n.m.r.) spectrum established this formulation. The latter consisted of three absorptions in a 1:3:1 ratio, corresponding to the protons H—NAs (at τ 7.30, reference internal $SiMe_4$), H_3C—NN (τ 6.76), and H—NN (τ 4.95). The assignments were based upon comparisons with the spectra of methylhydrazine and NN-dimethyl-N′-bis-(trifluoromethyl)arsinohydrazine (1). Significantly, there was no evidence suggesting the formation of the isomeric compound, $(CF_3)_2$-AsNMeNH_2, a result contrary to the observation that alkylation of hydrazines occurs at the most highly substituted nitrogen atom (11). For the alkylation process, a preference for the transition state **6** rather than **7** has been postulated (9):

6 **7**

In a somewhat similar situation, however, alkylalanes react at the least substituted nitrogen atom of dimethylhydrazine, suggesting that steric factors prohibit attack at the alternative, substituted site (12). It seems likely that similar factors would operate with $(CF_3)_2AsCl$, giving rise to MeNHNHAs$(CF_3)_2$, rather than its isomer.

The effect of the next methyl group is dramatic; thus NN-dimethylhydrazine with the appropriate haloarsine reacts smoothly to give a high yield of NN-dimethyl-N′-bis(trifluoromethyl)-arsinohydrazine, $Me_2NNHAs(CF_3)_2$, **2**, a compound which decomposes quite slowly at room temperature (1). The solvolysis of $(CF_3)_3As$ with Me_2NNH_2 was not a feasible synthetic route to compound **2**. The trimethylamine needed to promote CF_3H elimination also facilitated the decomposition of the desired product.

The next member of the series, the new compound trimethylhydrazino-bis(trifluoromethyl)-arsine, $(CF_3)_2AsNMeNMe_2$, **3**, was obtained in high yield from a low temperature reaction between trimethylhydrazine and $(CF_3)_2AsCl$ in ether (or cyclohexane) as solvent. The p.m.r. spectrum consisted of two resonance absorptions in a 2:1 ratio, corresponding to two equivalent CH_3 groups (at τ 7.80, reference internal $SiMe_4$), and one distinct CH_3 group (τ 7.35). The ^{19}F resonance consisted of a quartet indicative of long range proton–fluorine coupling involving the N—CH_3 group (δ, midpoint, 53.2 p.p.m.; J_{H-F}, 0.8 c.p.s., reference internal $CFCl_3$). Compound **3** is reasonably stable at room temperature, but decomposes more rapidly than $Me_2NNHAs(CF_3)_2$.

Experimental

Votatile materials were handled in a vacuum system, while involatile, air-sensitive substances were manipulated in a nitrogen-filled dry box. Reactions were carried out in sealed Pyrex tubes, fitted, where necessary, with *in situ* filtration facilities. Appropriate spectra were determined with Varian A56/60 (n.m.r.), Beckman I.R. 12 (infrared), and Hitachi Perkin–Elmer RMU-6E (mass spectra) spectrometers.

Tris(trifluoromethyl)arsine and bis(trifluoromethyl)-iodoarsine were prepared by the method of Brandt *et al.* (13). Conversion of the iodoarsine to the chloro compound was effected by reaction with mercuric chloride. Final purifications were achieved by means of low temperature fractional distillation, under vacuum, using a 36 in. vacuum-jacketed, all-glass column. Dimethylhydrazine and hydrazine were dried over anhydrous barium hydroxide, and were distilled under nitrogen, the latter at reduced pressure. Trimethylhydrazine was prepared by the method of Class *et al.* (14), and freed from dimethylhydrazine by low temperature column distillation, under vacuum. Solvents were rigorously dried, and distilled, before use.

Reactions of Hydrazine with $(CF_3)_3As$ and $(CF_3)_2AsCl$

A mixture of equal molar proportions of hydrazine and $(CF_3)_3As$, allowed to warm from −196° to room temperature, reacted to give a proportionate amount of CF_3H, corresponding to all of the available CF_3 groups, and N_2, representing about half of the original proportion of hydrazine, together with an intractable black residue

Can. J. Chem. Downloaded from www.nrcresearchpress.com by 210.87.254.6 on 09/05/12
For personal use only.

with the approximate composition $As_2N_2H_3$. Reactions with $(CF_3)_2AsCl$ were carried out at low temperatures (−78 to −33°), in dilute ethereal solution. Initial precipitates of N_2H_5Cl were contaminated with black residues, while other decomposition products included N_2 and CF_3H. Materials of low volatility were obtained in our fractionation trains, but these rapidly decomposed into involatile, black residues, with elimination of N_2 and CF_3H.

Reactions of Methylhydrazine with $(CF_3)_3As$ and $(CF_3)_2AsCl$

A mixture of methylhydrazine and a threefold excess of $(CF_3)_3As$ reacted readily at room temperature, giving an amount of CF_3H corresponding to the cleavage of one CF_3 group from $(CF_3)_3As$. Unstable yellow liquids were also found. Reactions with $(CF_3)_2AsCl$ were carried out under carefully controlled conditions, using dilute ethereal solutions and low temperatures (−78 to −33°). The hydrazine hydrochloride salt was filtered off, and fractionation revealed a pale yellow liquid, held at −33°, with an n.m.r. spectrum and a vapor phase molecular weight (M_{obsd}, 259; M_{calcd}, 258) corresponding to $MeNHNHAs(CF_3)_2$, **1**. The infrared spectrum of compound **1** is given in Table I. At room temperature, compound **1** rapidly turned black, eliminating N_2 and CF_3H.

Reactions of N,N-Dimethylhydrazine with $(CF_3)_3As$ and $(CF_3)_2AsCl$

A mixture of dimethylhydrazine and $(CF_3)_3As$ showed no evidence of reaction after 48 h at room temperature, but at 80°, both CF_3H and N_2 were readily formed. Attempts to promote solvolysis (hydrazinolysis) of the As—CF_3 bond at room temperature by means of added trimethylamine were unsuccessful, but at 80°, both CF_3H and N_2 were again formed. In neither case could the desired arsinohydrazine be detected; in both cases of reaction, colored residues (yellow to black) indicated the ultimate thermal decomposition of intermediate species.

TABLE I

Infrared spectrum of $MeNHNHAs(CF_3)_2$

Frequency*	Intensity†	Frequency*	Intensity†
730	20	1350	3
810	7	1445	4
956	3	2225	3
1110	87	2800	5
1125	87	2850	6
1155	94	2900	5
1180	100	2970	7
1260	5	3000	4

*Frequency in cm^{-1}.
†Intensities are quoted relative to the strongest band, at 1180 cm^{-1}, with a value of 100 arbitrary units.

With $(CF_3)_2AsCl$ and dimethylhydrazine, in ether solution, reaction proceeded smoothly to give $Me_2NNHAs(CF_3)_2$, **2**, in good yield (1). The melting point of samples sealed into capillary tubes was 3.00 ± 0.15°, while vapor pressure measurement with a mercury tensimeter indicated the volatility b.p. 20°/14.6 mm. Infrared data are given in Table II.

Reaction of Trimethylhydrazine with $(CF_3)_2AsCl$

A mixture of trimethylhydrazine (0.1798 g) and $(CF_3)_2AsCl$ (0.3345 g) in ether solution (1.8656 g) was allowed to react at −78° for 14 h and at −33° for 2 h. Separation procedures yielded an "ether fraction"

TABLE II

Infrared spectrum of $Me_2NNHAs(CF_3)_2$

Frequency*	Intensity†	Frequency*	Intensity†	Frequency*	Intensity†	Frequency*	Intensity†
530	9	1125	93	1470	20	2940	7
730	18	1160	100	1525	3	2970	33
795	9	1180	100	2220	6	3000	24
850	31	1260	shoulder	2780	29	3270	5
1015	12	1365	12	2830	29		
1055	shoulder	1440	shoulder	2870	21		
1110	96	1460	21	2910	13		

*Frequency in cm^{-1}.
†Intensities are quoted relative to the strongest band, at 1160 cm^{-1}, with a value of 100 arbitrary units.

TABLE III

Infrared spectrum of $Me_2NNMeAs(CF_3)_2$

Frequency*	Intensity†	Frequency*	Intensity†	Frequency*	Intensity†	Frequency*	Intensity†
530	3	1060	shoulder	1460	20	2850	23
610	3	1110	97	1520	9	2870	22
760	20	1150	100	2210	9	2910	22
820	17	1180	99	2780	19	2960	34
1040	shoulder	1250	shoulder	2830	20	3000	16

*Frequency in cm^{-1}.
†Intensities are quoted relative to the strongest band, at 1150 cm^{-1}, with a value of 100 arbitrary units.

(1.9090 g) and the new compound $(CF_3)_2AsNMeNMe_2$, **3**, (0.3125 g, 90% yield) held at −33°. Compound **3** was identified by its molecular weight (M_{obsd}, 284; M_{calcd}, 286), and by infrared (Table III) and n.m.r. spectra. The observed melting point and volatility were −41.5 ± 0.5°, and b.p. 15°/6.30 mm, respectively.

Acknowledgments

The authors gratefully acknowledge financial support from the National Research Council of Canada and from the President's Research Fund of Simon Fraser University. The assistance of Mrs. M. Tracey and Dr. J. Hallett, in expediting the n.m.r. studies of our least stable compounds, was of considerable value.

1. L. K. PETERSON and K. I. THÉ. Chem. Commun. 1056 (1967).
2. L. K. PETERSON and G. L. WILSON. Can. J. Chem. **46**, 685 (1968).
3. L. S. BARTELL and H. K. HIGGINBOTHAM. Inorg. Chem. **4**, 1346 (1965).
4. K. A. JENSEN, A. HOLM, B. KÄGI, and C. T. PEDERSEN. Acta Chem. Scand. **19**, 772 (1965).
5. W. G. PATERSON and M. ONYSZCHUK. Can. J. Chem. **41**, 1872 (1963).
6. D. F. CLEMENS, W. S. BREY, and H. H. SISLER. Inorg. Chem. **2**, 1251 (1963).
7. N. R. FETTER, B. BARTOCHA, F. E. BRINCKMAN, and D. W. MOORE. Can. J. Chem. **41**, 1359 (1963).
8. F. A. COTTON and G. WILKINSON. Advanced inorganic chemistry. Interscience Publishers Inc., New York. 1962. Chap. 20.
9. A. B. BURG and J. HENERS. J. Am. Chem. Soc. **87**, 3092 (1965).
10. J. SINGH and A. B. BURG. J. Am. Chem. Soc. **88**, 718 (1966).
11. R. L. HINMAN. J. Org. Chem. **23**, 1587 (1959).
12. N. R. FETTER and B. BARTOCHA. Can. J. Chem. **39**, 2001 (1961).
13. G. R. A. BRANDT, H. J. EMELÉUS, and R. N. HASZELDINE. J. Chem. Soc. 2552 (1952).
14. J. B. CLASS, J. G. ASTON, and T. S. OAKWOOD. J. Am. Chem. Soc. **75**, 2937 (1953).

Can. J. Chem. Downloaded from www.nrcresearchpress.com by 210.87.254.6 on 09/05/12
For personal use only.

Can. J. Chem. Downloaded from www.nrcresearchpress.com by 210.87.254.40 on 09/05/12
For personal use only.

Electric moments, sulfur bonding, and conformations of substituted thiochloroformate esters in benzene solutions

A. QUEEN, T. A. NOUR[1], AND E. BOCK
Parker Chemistry Laboratory, University of Manitoba, Winnipeg, Manitoba

Received July 18, 1968

The dipole moments of a series of aryl and alkyl thiochloroformate esters have been determined in benzene solution at 25 °C and compared with the corresponding values for chloroformate and fluoroformate esters. The results have been interpreted in terms of conjugative and hyperconjugative electron release by the hydrocarbon group to the d-orbitals of the sulfur atom in the thio compounds. Vector model, bond moment calculations indicate that, as in the cases of the chloroformate and fluoroformate esters, the preferred conformations of the thiochloroformates are those in which the hydrocarbon group and the halogen atom are *cis* to each other.

Canadian Journal of Chemistry, **47**, 343 (1969)

Introduction

Dipole moment measurements made in this laboratory have led us to conclude (1), in agreement with other workers (2–4), that the most favorable configuration of alkyl formates is that in which the alkyl group and carbonyl oxygen are *cis* to each other (**1**). In contrast, the corresponding chloroformate and fluoroformate esters seem to prefer the arrangement that brings the halogen atom into the *cis* position with respect to the alkyl group (**2**; X = Cl or F) (5, 6). This surprising difference, brought about by the replacement of a hydrogen atom in (**1**) by a halogen atom, has led us to extend our studies to the analogous thiochloroformate esters (**3**).

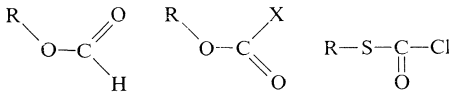

(**1**) (**2**) (**3**)

One of the present authors has previously commented (7) on the fact that the dipole moments of thioethers are larger than those of the corresponding oxygen compounds, although the opposite is true for hydrogen sulfide and water and for thiols and alcohols (Table I). It was suggested that the difference could be explained in terms of conjugative or hyperconjugative electron release to the sulfur atom, which uses its d-orbitals to accept these electrons. The data in Table I show that there is insufficient information available for ethers and thioethers containing secondary and tertiary alkyl groups to allow any conclusion to be reached regarding the importance of hyperconjugation in these compounds. Although this does not apply to alcohols and thiols, it is difficult to interpret the data in terms of hyperconjugation, despite the obvious dependence of the dipole moments of the thiols on the branched natures of the alkyl groups. For example, the changes in the values of $\Delta\mu$(S—O) seem to be in the wrong direction. It is possible that hydrogen bonding effects complicate the situation for alcohols.

Thiochloroformate esters possess several features likely to enhance electron-pair acceptance by sulfur. Hydrogen bonding is small and the chlorocarbonyl group withdraws electrons both inductively and conjugatively. In agreement with this argument, it was previously noted (7) that the dipole moment of phenyl thiochloroformate is significantly greater than that of phenyl chloroformate, consistent with conjugative electron release from the aromatic ring to the sulfur atom.

In order to test the importance of electron-pair acceptance by sulfur, we have measured the dipole moments of methyl, ethyl, propyl, isopropyl, butyl, and tertiary butyl thiochloroformates in benzene solution. The dipole moment of the phenyl ester has been redetermined with a carefully purified sample of the compound and, for purposes of comparison, we have also measured the corresponding values for isopropyl chloroformate, isopropyl fluoroformate, and *p*-chlorophenyl thiochloroformate.

Experimental

Solvent

Fisher certified reagent benzene was used as solvent.

[1]University of Manitoba Postdoctorate Fellow, 1967–1968.

TABLE I

Dipole moments in benzene solution at 20 °C*

R	μ R—O—R	μ R—S—R	Δμ(S—O)†	μ R—O—H	μ R—S—H	Δμ(S—O)†
H	1.85	0.97	−0.88	1.85	0.97	−0.88
CH_3	1.25	1.45	+0.20	1.69‡	1.26‡	−0.43‡
C_2H_5	1.30	1.58	+0.28	1.72	1.44	−0.28
n-C_3H_7	1.31	1.56	+0.29	1.68	1.44	−0.24
n-C_4H_9	1.26	1.58	+0.32	1.66	1.43	−0.23
i-C_3H_7	1.26			1.69	1.55	−0.14
t-C_4H_9				1.74	1.57	−0.17
C_6H_5	1.11	1.55	+0.44	1.5–1.8	1.2–1.3	(−0.8)

*Given in Debye units, D; see ref. 8.
†Δμ(S—O) = μ(R—S—R) − μ(R—O—R).
‡From values measured in the vapor phase. The value for methanol in benzene solution is 1.65 D.

TABLE II

Boiling points of chloroformate, fluoroformate, and thiochloroformate esters*

R	X	Y	Present work Boiling point (°C)	Present work Pressure (mm)	Literature Boiling point (°C)	Literature Pressure (mm)	Literature Reference
CH_3	S	Cl	110		110		12
C_2H_5	S	Cl	136		136		10
n-C_3H_7	S	Cl	62	30	59–60	26	10
i-C_3H_7	S	Cl	144		133–135		13
n-C_4H_9	S	Cl	177		179		10
t-C_4H_9	S	Cl	37	7	30–32	1	14
C_6H_5	S	Cl	92	10	104	13	10
p-ClC_6H_5	S	Cl	89–90	1	126	10	15
i-C_3H_7	O	Cl	104		104		9
i-C_3H_7	O	F	81–82		81–82		11

*General formula R—X—(CO)—Y.

It was dried by repeated shaking with Linde molecular sieves, type 4A.

Solutes

Isopropyl chloroformate and methyl thiochloroformate were prepared by reacting isopropanol and methanethiol, respectively, with a large excess of phosgene (9, 10). Isopropyl fluoroformate was obtained from the corresponding chloroformate by reacting it with an equivalent amount of thallous fluoride (11). The other compounds were commercial samples[2]. All the compounds were fractionally distilled through a short column packed with glass helices and their purities then checked by means of vapor phase chromatography. Isopropyl fluoroformate was further purified by vapor phase chromatography. Experimental data are recorded in Table II.

Procedure

The dipole moment apparatus and experimental procedure have been previously described (16).

[2]Obtained from K. and K. Laboratories, Inc., Plainview, New York.

Results and Discussion

The experimental data are summarized in Table III, and Table IV lists the solution dipole moments calculated by Smith's method (17), using eq. [1].

$$[1] \qquad \mu = \frac{27kT}{4N} \cdot \frac{M_2}{d_1(\varepsilon_1 + 2)^2} \cdot (\alpha - \nu)$$

where the symbols have the same meanings as those used in our earlier papers (6). In order to facilitate comparisons, this table also includes previously determined values of the dipole moments of the corresponding chloroformate and fluoroformate esters.

The results in Table IV show that both the fluoroformate and thiochloroformate esters have larger dipole moments than the chloroformates. However, it can be seen that while the values for the fluoro compounds are quite uniformly

Can. J. Chem. Downloaded from www.nrcresearchpress.com by 210.87.254.40 on 09/05/12
For personal use only.

Can. J. Chem. Downloaded from www.nrcresearchpress.com by 210.87.254.40 on 09/05/12
For personal use only.

TABLE III

Weight fraction, w, dielectric constant, ε, refractive index, n, and density, d, of benzene solutions at 25 °C

$w \times 10^3$	ε	n	d
Methyl thiochloroformate ($\alpha = 6.78$, $\nu = -0.32$)			
1.6595	2.2840	1.49770	0.87444
2.9822	2.2930	1.49760	0.87489
4.5978	2.3042	1.49750	0.87574
6.4664	2.3165	1.49735	0.87591
8.0380	2.3274	1.49730	0.87662
Ethyl thiochloroformate ($\alpha = 6.83$, $\nu = -0.24$)			
1.1897	2.2806	1.49787	0.87406
2.3748	2.2885	1.49780	0.87429
4.7488	2.3052	1.49764	0.87494
6.3872	2.3164	1.49749	0.87539
7.4905	2.3235	1.49740	0.87538
n-Propyl thiochloroformate ($\alpha = 6.35$, $\nu = -0.14$)			
1.2068	2.2802	1.49795	0.87425
2.5524	2.2889	1.49788	0.87448
5.1992	2.3059	1.49775	0.87481
6.3882	2.3151	1.49770	0.87499
7.7056	2.3215	1.49763	0.87558
i-Propyl thiochloroformate ($\alpha = 6.64$, $\nu = -0.23$)			
1.2894	2.2812	1.49787	0.87404
2.3270	2.2880	1.49780	0.87468
4.5468	2.3029	1.49767	0.87528
6.2053	2.3133	1.49749	0.87546
7.8222	2.3245	1.49740	0.87575
n-Butyl thiochloroformate ($\alpha = 5.90$, $\nu = -0.21$)			
1.1728	2.2796	1.49788	0.87414
2.7670	2.2888	1.49780	0.87463
4.9756	2.3021	1.49767	0.87486
6.2050	2.3093	1.49749	0.87538
7.8953	2.3191	1.49743	0.87545
t-Butyl thiochloroformate ($\alpha = 7.02$, $\nu = -0.31$)			
1.5003	2.2839	1.49780	0.87425
2.8566	2.2933	1.49770	0.87501
4.4401	2.3046	1.49750	0 87525
6.5413	2.3193	1.49740	0.87550
7.9972	2.3303	1.49720	0.87559
Phenyl thiochloroformate ($\alpha = 5.31$, $\nu = +0.15$)			
1.5963	2.2826	1.49807	0.87437
2.5379	2.2861	1.49812	0.87466
4.2106	2.2947	1.49820	0.87520
5.9219	2.3039	1.49828	0.87543
8.1524	2.3154	1.49840	0.87567
p-Chlorophenyl thiochloroformate ($\alpha = 2.16$, $\nu = +0.20$)			
1.7806	2.2762	1.49815	0.87460
2.7864	2.2784	1.49822	0.87503
4.7743	2.2827	1.49837	0.87588
6.3034	2.2860	1.49842	0.87627
8.5472	2.2909	1.49852	0.87656
i-Propyl chloroformate ($\alpha = 6.88$, $\nu = -0.37$)			
1.3476	2.2821	1.49775	0.87381
2.5335	2.2903	1.49760	0.87416
4.6890	2.3051	1.49742	0.87495
6.4941	2.3171	1.49730	0.87535
8.0546	2.3278	1.49700	0.87558
i-Propyl fluoroformate ($\alpha = 9.03$, $\nu = -0.63$)			
1.4070	2.2865	1.49780	0.87399
2.5815	2.2955	1.49760	0.87432
4.8191	2.3139	1.49730	0.87480
6.2795	2.3270	1.49700	0.87504
8.8332	2.3478	1.49680	0.87521

TABLE IV

Dipole moments for chloroformate, fluoroformate, and thiochloroformate esters in benzene solution at 25 °C*

R	μD			Δμ(F—Cl)†	Δμ(S—O)‡
	RO—(CO)—Cl	RO—(CO)—F	RS—(CO)—Cl		
p-ClC_6H_4			1.93§		
C_6H_5	2.39‖	2.65¶	2.86§	+0.26	+0.47
CH_3	2.38‖	2.61¶	2.69§	+0.23	+0.31
C_2H_5	2.66‖	2.85¶	2.84§	+0.19	+0.18
C_3H_7	2.70‖	2.91¶	2.88§	+0.21	+0.18
n-C_4H_9	2.71‖	2.92¶	2.93§	+0.21	+0.22
n-C_5H_{11}	2.71‖	2.93¶		+0.22	
i-C_3H_7	2.86§	3.07§	2.96§	+0.21	+0.10
t-C_4H_9			3.20§		

*Given in Debye units, D.
†$\Delta\mu(F—Cl) = \mu(RO—CO—F) - \mu(RO—CO—Cl)$.
‡$\Delta\mu(S—O) = \mu(RS—CO—Cl) - \mu(RO—CO—Cl)$.
§Values obtained in this work.
‖Ref. 5.
¶Ref. 6.

greater than those of the chloroformates by about 0.2 D, this parallelism does not hold for the oxygen and sulfur compounds. In the alkyl series, the differences in the dipole moments of these latter compounds appear to depend on the number of hydrogen atoms bonded to the α-carbon atom of the alkyl group. The magnitude of the difference, Δμ(S—O), progressively decreases as the number of such hydrogens decreases, strongly suggesting that hyperconjugative electron release to the sulfur atom occurs in the thiochloroformates (**4**, **5**, **6**).

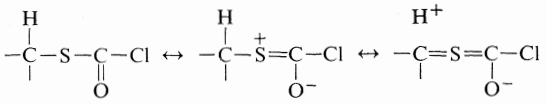

(**4**) (**5**) (**6**)

The much greater effect of conjugative electron release can be deduced from the fact that phenyl thiochloroformate has a dipole moment that is 0.47 D greater than that of the corresponding oxygen compound. It is furthermore significant that phenyl thiochloroformate has a higher dipole moment than methyl thiochloroformate, while the corresponding two oxygen analogues have practically the same moment. In the latter case, resonance effects similar to that represented by structure (**6**) do not exist.

These results are interesting in the light of the conclusion of Bordwell and Boutan (18) that divalent sulfur in certain substituted phenols and carboxylic acids (**7**; R = OH or COOH, R′ = CH_3—(CO)—S, —SCN) shows little tendency to act as an electron-pair acceptor. Similar conclusions were reached (19) from a study of the rates of hydrolysis of substituted aryl chloromethyl sulfides. On the other hand, Campbell and Rogers (20) have concluded, on the basis of dipole moment measurements, that electron-pair acceptance by sulfur does occur in the para-substituted phenylthiocyanates (**7**; R = —SCN, R′ = NH_2, $N(CH_3)_2$, OCH_3).

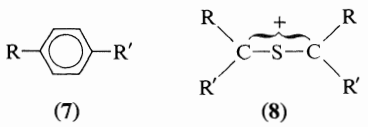

(**7**) (**8**)

Caserio, Pratt, and Holland (21) have recently obtained evidence from their studies of the nuclear magnetic resonance (n.m.r.) spectra of α,β-unsaturated alkylsulfides for electron acceptance by sulfur. Undoubtedly, the same effect accounts for the remarkable stabilities of the sulfonium methylides (**8**; R and R′ = CH_3 and C_2H_5) (22). Variations in the rates of hydrolysis of alkyl-2-chloroethyl sulfides have been explained (23) in terms of hyperconjugative stabilization of the cyclic intermediates (**9**, **10**) and our studies of the rates of hydrolysis of the present thiochloroformate esters in water (24) support the conclusions we have reached from dipole moment measurements. Other examples of d-orbital bonding by sulfur are known (25–28).

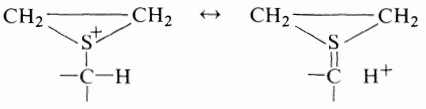

(**9**) (**10**)

A vector model, bond moment calculation, similar to those previously carried out for methyl chloroformate (5) and methyl fluoroformate (6), indicates that the preferred conformation of methyl thiochloroformate is that in which the chlorine atom and the alkyl group are *cis* to each other. The bond moments H—C = 0.4 D, C=O = 2.4 D, C—Cl = 1.5 D are those given by Smith (29). In view of the possibility of hyperconjugative electron release to the sulfur atom, the group moment CH_3—S = 1.2 D was calculated from dipole moment (30) and bond angle (31) data for dimethyl sulfide; viz. 1.45 D and 99°, respectively. It was assumed that the H—C and CH_3 moments were equal and, hence, that the C—S bond moment could be obtained by subtracting the C—H bond moment from the value calculated for CH_3—S. While the value so obtained for the C—S bond moment is probably too small, it can easily be shown that a larger value would reduce the calculated dipole moment of methyl thiochloroformate, a conclusion that reinforces our arguments. In the absence of appropriate data for methyl thiochloroformate itself, the bond angles used in Fig. 1 are based on values obtained for thiolacetic acid (32). It can be seen that, irrespective of the value assumed for the angle ψ, the dipole moment decreases as the angle θ increases from 0 to 180°. If the contribution from the CH_3—S bond to the vector *A* is ignored, the group moment of S—(CO)—Cl may be calculated to be 1.22 D, centered on the carbonyl carbon atom at an angle of 152° 49′ to the

Can. J. Chem. Downloaded from www.nrcresearchpress.com by 210.87.254.40 on 09/05/12
For personal use only.

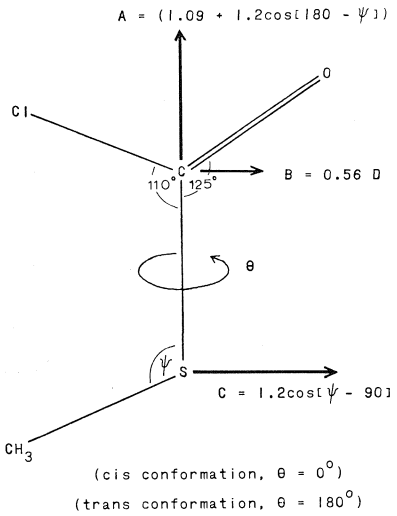

FIG. 1. Vector model for methyl thiochloroformate.

direction of the S—C bond. This is shown as a dotted line in Fig. 1. The maximum value of the dipole moment of methyl thiochloroformate will correspond to the situation where $\theta = 0°$ and $\psi = 152° 49'$. The calculated value for this situation is 2.4 D. It is unlikely that ψ is as large as $152° 49'$ since the corresponding angle in methyl formate is only $114° 47'$ (4) and the bond angles are usually smaller in thioethers than in ethers (28, 31, 33). Assuming a more reasonable value of 110° for the angle ψ, the calculated dipole moments for the *cis* and *trans* conformations are 2.3 D and 1.6 D, respectively[3]. While both values are smaller than the experimental value of 2.69 D, these figures would seem to indicate a preference for the *cis* conformation. As already pointed out, the use of dimethyl sulfide as a model for calculating the CH_3—S group moment is likely to give too small a value; furthermore, this value does not take into account the fact that hyperconjugation is probably more important in methyl thiochloroformate than in dimethyl sulfide. However, an improbably large moment of about 2.5 D would have to be assumed for the CH_3—S group in order to raise the calculated dipole moment of the *trans* conformer to the experimental value of 2.69 D.

We have carried out another calculation using our data for phenyl thiochloroformate and its *p*-chlorophenyl analogue. Making the reasonable assumption tha the chlorine atom attached to the aromatic ring affects the dipole moment of the molecule mainly by virtue of its electron withdrawing properties and using the accepted value of 1.58 D for the aryl–Cl bond moment (29), we have calculated the angle between the aryl–S bond and the dipole moment vector of the phenyl—S—(CO)—Cl unit to be 140°. The two extreme *cis* and *trans* conformations are shown in Fig. 2. It can be seen that the *trans* arrangement requires the phenyl—S—C bond to be at least 140° which is unlikely and the *cis* arrangement is, therefore, preferred.

The proton magnetic resonance spectra of the chloroformate and thiochloroformate esters in carbon tetrachloride solutions have been compared by Hutton and Schaefer[4]. Although the

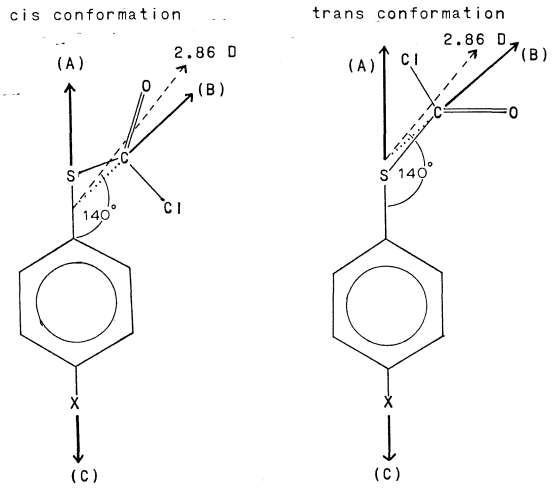

FIG. 2. Vector models for phenyl thiochloroformate (X = H, $C = 0$ D) and *p*-chlorophenyl thiochloroformate (X = Cl, $C = 1.58$ D). ***A*** is the group moment for C_6H_5—S, ***B***, that for S—(CO)—Cl, and ***C***, that for C_6H_5—X.

[3]A referee has objected to the use of bond moments based on the value of 0.4 D for the carbon–hydrogen bond in the sense $\overset{+}{H}$—$\overset{-}{C}$. Some doubt exists not only as to the magnitude of this moment but also to its direction and there is some theoretical evidence that, in many aliphatic compounds, the value 0.3 D in the sense $\overset{-}{H}$—$\overset{+}{C}$ may be more appropriate. Smith (29) has discussed the situation in detail and listed other bond moments based on this latter value. The calculated dipole moments are not greatly changed by using these alternative bond moments, the values for the *cis* and *trans* conformations, assuming that the angle $\psi = 110°$, being 2.15 and 1.58 D, respectively.

[4]H. Hutton and T. Schaefer, unpublished data.

Can. J. Chem. Downloaded from www.nrcresearchpress.com by 210.87.254.40 on 09/05/12
For personal use only.

chemical shifts of the protons on the β, γ, and δ carbon atoms of the alkyl groups are very similar in both series of compounds, the same is not true for the protons attached to the α carbon atoms. These protons of the thioesters resonate about 80 cycles to higher field than the corresponding protons in alkyl chloroformates. Much smaller differences are found when the n.m.r. spectra of thiols and alcohols are compared. These observations are consistent with hyperconjugation in the alkyl thiochloroformates but the detailed interpretation of the n.m.r. spectra is not straightforward. Further work is in progress to determine the coupling constants for the present compounds and their fluoro analogues.

Acknowledgments

We thank Drs. T. Schaefer and H. Hutton for helpful discussion of our results and the National Research Council of Canada for financial assistance.

1. E. Bock. Can. J. Chem. **45**, 2761 (1967).
2. S. Mizushima and M. Kubo. Bull. Chem. Soc. Japan, **13**, 174 (1938).
3. J. M. O'Gorman, W. Shand, Jr., and V. Schomaker. J. Am. Chem. Soc. **72**, 4222 (1950).
4. R. F. Curl, Jr. J. Chem. Phys. **30**, 1529 (1959).
5. E. Bock and D. Iwacha. Can. J. Chem. **45**, 3177 (1967).
6. E. Bock, D. Iwacha, H. Hutton, and A. Queen. Can. J. Chem. **46**, 1645 (1968).
7. E. Bock and D. Iwacha. Can. J. Chem. **46**, 523 (1968).
8. A. L. McClellan. Tables of experimental dipole moments. W. H. Freeman and Co., San Francisco. 1963.
9. C. S. Hamilton and C. Sly. J. Am. Chem. Soc. **47**, 437 (1925).
10. R. Riemschneider and O. Lorenz. Monatsh. Chem. **84**, 518 (1953).
11. S. Nakanishi, T. C. Myers, and E. V. Jensen. J. Am. Chem. Soc. **77**, 3099 (1955).
12. F. Arndt, E. Milde, and G. Eckert. Chem. Ber. **56**, 1976 (1923).
13. H. Bretschneider and H. Haas. Monatsh. Chem. **81**, 939 (1950).
14. D. S. Tarbell and T. Parasaran. J. Org. Chem. **29**, 2471 (1964).
15. Stauffer Chemical Company. British Patent No. 948, 831. Feb. 5, 1964.
16. E. Bock and E. F. Dojack. Can. J. Chem. **45**, 1097 (1967).
17. J. W. Smith. Trans. Faraday Soc. **46**, 394 (1950).
18. F. G. Bordwell and P. J. Boutan. J. Am. Chem. Soc. **78**, 854 (1956).
19. F. G. Bordwell, G. D. Cooper, and H. Morita. J. Am. Chem. Soc. **79**, 376 (1957).
20. T. W. Campbell and M. T. Rogers. J. Am. Chem. Soc. **70**, 1029 (1948).
21. M. C. Caserio, R. E. Pratt, and R. J. Holland. J. Am. Chem. Soc. **88**, 5747 (1966).
22. C. P. Lillya and P. Miller. J. Am. Chem. Soc. **88**, 1560 (1966).
23. C. E. Williamson, J. I. Miller, S. Sass, and B. Witten. U.S. Dept. Com., Office Tech. Serv., A.D. 611,869, **2**, 493 (1965).
24. A. Queen, T. A. Nour, and K. Preston. To be published.
25. W. von E. Doering and K. C. Schreiber. J. Am. Chem. Soc. **77**, 514 (1955).
26. W. von E. Doering and A. K. Hoffmann. J. Am. Chem. Soc. **77**, 52 (1955).
27. S. Oae, W. Tagaki, and A. Ohno. J. Am. Chem. Soc. **83**, 5036 (1961).
28. C. C. Price and S. Oae. Sulphur bonding. The Roland Press Company, New York. 1962.
29. J. W. Smith. Electric dipole moments. Butterworths Scientific Publications, London. 1955.
30. C. W. N. Cumper, J. F. Read, and A. I. Vogel. J. Chem. Soc. 5323 (1965).
31. L. Pierre and M. Hayashi. J. Phys. Chem. **35**, 479 (1961).
32. W. Gordy. J. Chem. Phys. **14**, 560 (1946).
33. U. Bulkis, P. H. Kasai, and R. J. Meyers. J. Chem. Phys. **38**, 2753 (1963).

Can. J. Chem. Downloaded from www.nrcresearchpress.com by 210.87.254.40 on 09/05/12
For personal use only.

Can. J. Chem. Downloaded from www.nrcresearchpress.com by 210.87.254.42 on 09/05/12
For personal use only.

Reactions of ethylene with rhodium(III) chloride. Part II.[1] Catalyzed substitution at rhodium(III)

B. R. JAMES, M. KASTNER, AND G. L. REMPEL
Department of Chemistry, University of British Columbia, Vancouver 8, British Columbia

Received June 26, 1968

Ethylene has been found to catalyze at ambient temperatures the production of $RhCl_2(H_2O)_4^+$ species from freshly made solutions of $RhCl_3.3H_2O$ in water. A mechanism involving trace amounts of chlororhodate(I) species is indicated.

Canadian Journal of Chemistry, **47**, 349 (1969)

We have been studying the reaction of rhodium(III) chloride trihydrate with ethylene in both aqueous and non-aqueous solvents (1) and have found that the rhodium products may be derivatives of the tri-, uni-, or zero-oxidation state depending on the conditions.

A fresh solution of $RhCl_3.3H_2O$ in water or perchloric acid is a complex mixture containing both monomeric and polymeric species (2). The initial electronic spectrum slowly changes, showing decreasing absorption over the whole range from 350–600 mμ. After several weeks at 80° the spectrum becomes steady (λ_{max} = 355 mμ, ε = 70; and λ_{max} = 464 mμ, ε = 65) which, according to the data reported for the various rhodium(III) chloride complexes (3), indicates a mixture of mainly the $RhCl_2(H_2O)_4^+$ and $RhCl_3(H_2O)_3$ species. If ethylene, however, is bubbled through the fresh Rh(III) solution at room temperature, the initial spectrum changes rapidly to a steady one showing peaks at 350 mμ (ε = 60) and 455 mμ (ε = 75) which is close to that of the $RhCl_2(H_2O)_4^+$ species (3). Wilkinson and co-workers (4) have reported a similar observation using molecular hydrogen and suggested a catalytic substitution process via intermediate hydride species; we have found that rhodium metal usually appears when H_2 is used.

Attempts to investigate the kinetics and mechanism of the ethylene reaction were made by following continuously as a function of time the decrease in absorption at 550 mμ, where the molar absorptivity for the fresh solution was about 115 and for either the 2:1 or 3:1 chloro complexes is about 10. Figure 1 shows such an investigation at 7° for a 7×10^{-3} *M* solution of $RhCl_3.3H_2O$. The "noise" appearance of the plot is due to interference on the absorption by the continuous stream of gas bubbles. The plots were rather irreproducible, the sharp decrease in optical density occurring anywhere between about 200 and 500 s for repeated experiments, but all exhibited the autocatalytic character. The irreproducibility may be due to diffusion problems with ethylene saturation and/or the presence of traces of O_2 (see later); mixing of the Rh(III) and presaturated ethylene solutions gave similar plots. The autocatalytic character was not due to any reaction involving the observed product $RhCl_2(H_2O)_4^+$, or $RhCl_3(H_2O)_3$. Separate experiments using fresh 5×10^{-2} *M* Rh(III) solutions showed that no measurable amount ($< 5 \times 10^{-4}$ *M*) of ethylene was consumed in the process. No such catalyzed substitution reactions were observed when starting with (*a*) a fresh

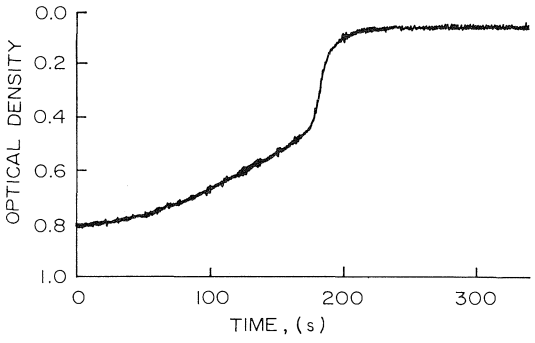

FIG. 1. Optical density at 550 mμ as a function of time, on bubbling C_2H_4 through a 7×10^{-3} *M* aqueous solution of $RhCl_3.3H_2O$ at 7°; 1 cm cell.

[1]For Part I, see ref. 1.

solution of 10^{-2} *M* $Na_3RhCl_6.12H_2O$, which initially gives the spectrum (3) of $RhCl_6^{3-}$ and changes to a mixture of the 2:1 and 3:1 chloro complexes over a few hours at room temperature; (*b*) a thermal equilibrated solution of the 2:1 and 3:1 chloro complexes; (*c*) any other thermal equilibrated solution containing the complexes (3) $RhCl_n(H_2O)_{6-n}^{(n-3)-}$.

Investigations involving pH measurements have proved to be complex, which is not too surprising in view of the complex nature of such solutions (2). However, the initial pH of a 10^{-2} *M* solution of $RhCl_6^{3-}$ is about 4.0 indicating little hydrolysis, whereas that of $RhCl_3.3H_2O$ is about 2.7. We suggest that compared with solutions (*a*), (*b*), and (*c*), the fresh $RhCl_3.3H_2O$ solution contains more appreciable amounts of Rh(III) species with coordinated hydroxy groups either as such or as bridging ligands in polymeric species, and it is thought that the presence of these aids the production of small amounts of Rh(I) species through the mechanism previously postulated for the ethylene reduction of metal ions (1, 5)

$$[1]\quad \overset{OH}{\underset{|}{Rh(III)}} + C_2H_4 \rightarrow \overset{OH}{\underset{|}{Rh}}\!\!-\!\!\underset{CH_2}{\overset{CH_2}{\|}} \rightarrow -RhCH_2CH_2OH \quad (\sigma\text{-complex})$$

$$\rightarrow Rh(I) + CH_3CHO + H^+$$

The reduction occurs via a 2 electron transfer in the σ intermediate produced by migration of the coordinated hydroxide. Rh(I) species are labile while the Rh(III) species here are substitution inert, and the catalyzed substitution process forming $RhCl_2(H_2O)_4^+$ could result through formation of a chloride bridged intermediate with a subsequent 2 electron transfer

$$[2]\quad Cl\text{—}Rh(I)\text{—}Cl\text{—}Rh(III)Cl_2 \rightarrow Cl\text{—}Rh(III)\text{—}Cl\overset{\diagup\diagdown}{\underset{\diagdown\diagup}{}}Rh(I)Cl_2$$

Such bridged intermediates seem well established for Rh(III)–Rh(I) systems (6–8). Breakage of the labile bond yields $Cl_2Rh(III)$ and $Rh(I)Cl_2$; this Rh(I) species can then react further with more Rh(III). The Rh(III) species formed will depend on the number of chlorides attached to Rh(I) in the bridged intermediate and this would seem to be 2.

The autocatalytic nature of the reaction is explained by the build up of concentration of the Rh(I) species, which, however, must remain quite small since none could be detected according to the stoichiometry of reaction [1], and also no metallic rhodium was formed. The disproportionation reaction,

$$[3]\quad 2Rh(I) \rightleftharpoons Rh(0) + Rh(II)$$

is probably important but no quantitative data are available for this process. Rh(I) intermediates are appealing since C_2H_4 is known to reduce Rh(III) to Rh(I) species in non-aqueous solvents (1, 9) and at higher temperatures ($\sim 50°$) in aqueous solution, metal production occurs, presumably through reaction [3]. These findings are in agreement with those of Rund (8) who reports that concentrations of Rh(I) complexes as low as 10^{-6} *M* are sufficient to catalyze substitution reactions of Rh(III). These systems are probably very sensitive to the presence of traces of oxygen, which would oxidize any chlororhodate(I) species present, and this could account for the inconsistency of the kinetic data. The presence of an oxidizing agent, such as quinone, in solution completely inhibited the catalytic substitution reactions; quinone is also known to be reduced by weak field rhodium(III) hydrides in aqueous solution (10), but a hydridic mechanism seems less likely.

Quantitative kinetic data for this catalyzed substitution process will be difficult to obtain, although on comparison with the ethylene reduction of Rh(III) in dimethylacetamide solution (1), the step involving ethylene coordination in [1] is likely to be rate determining.

Acknowledgment

Grateful acknowledgment is made to the National Research Council of Canada for support of this research.

1. B. R. James and G. L. Rempel. Can. J. Chem. **46**, 571 (1968).
2. W. P. Griffith. The chemistry of the rarer platinum metals. Interscience Publishers, Inc., London. 1967. p. 319.
3. W. C. Wolsey, C. A. Reynolds, and J. Kleinberg. Inorg. Chem. **2**, 463 (1963).
4. R. D. Gillard, J. A. Osborn, P. B. Stockwell, and G. Wilkinson. Proc. Chem. Soc. 284 (1964).
5. P. M. Henry. J. Am. Chem. Soc. **86**, 3246 (1964).
6. B. R. James and G. L. Rempel. Chem. Commun. 158 (1967).
7. D. J. Baker and R. D. Gillard. Chem. Commun. 520 (1967).
8. J. V. Rund. Inorg. Chem. **7**, 24 (1968).
9. R. Cramer. Inorg. Chem. **1**, 722 (1962).
10. M. Iguti. J. Chem. Soc. Japan, **60**, 1787 (1939).

Can. J. Chem. Downloaded from www.nrcresearchpress.com by 210.87.254.42 on 09/05/12
For personal use only.

Effect of temperature on yields in the radiolysis of nitrous oxide with high intensity electron pulses[1]

A. W. Boyd, C. Willis, and O. A. Miller
Research Chemistry Branch, Chalk River Nuclear Laboratories, Atomic Energy of Canada Limited, Chalk River, Ontario

Received July 23, 1968

Nitrous oxide has been irradiated with single electron pulses at a dose rate of 0.8×10^{27} eV/g s at temperatures between 24 and 500 °C. The gas yields showed no dependence on temperature below 200 °C but above this $G(N_2)$ increased and $G(O_2)$ decreased. The yields were found to be independent of dose up to 4×10^{20} eV/g.

Canadian Journal of Chemistry, **47**, 351 (1969)

Can. J. Chem. Downloaded from www.nrcresearchpress.com by 210.87.254.5 on 09/05/12
For personal use only.

A disadvantage of nitrous oxide as a gas phase dosimeter is the dependence of the nitrogen yield on temperature. Jones and Sworski (1) using Van de Graaff electrons and a dose rate of $\sim 10^{18}$ eV/g s found that the yield of nitrogen increased from $G(N_2) = 10$ to $G(N_2) = 20$ between 24 and 200 °C. Gorden and Ausloos (2) using γ-rays at 1.3×10^{17} eV/g s and isotopically substituted N_2O found that $G(N_2)$ increased by a factor of nearly 8 between 40 and 376 °C.

In a previous publication (3) we reported a nitrogen yield of $G(N_2) = 12.4$ in the radiolysis of N_2O at 24 °C using electron pulses from a Febetron 705. In this work the gas was irradiated in a metal cell with a 0.0127 cm stainless steel window. With this cell the dose per pulse was 2.3 Mrads at 2 cm from the Febetron tube window. This dose was measured using calorimeters consisting of thin aluminium disks. The yield of nitrogen with these pulses, which give an average dose rate of 1.8×10^{27} eV/g s, was independent of pressure within 5% from 0.5 to 5.0 atm.

In these irradiations (3) the temperature of the N_2O might have been raised as much as 25° by one of these pulses so that the effective temperature of the N_2O during irradiation was uncertain. Because of this uncertainty we have determined the effect of temperature in N_2O radiolysis with the Febetron.

In the present work the N_2O was contained at 1 atm in a 100 ml cylindrical quartz cell of 4.2 cm diameter and 7.5 cm long. One end of the cell was flattened to form a thin (0.05 cm) window for electrons, the other was fitted with a breakseal. With the cell placed so that the window was 2 cm from the Febetron tube window the dose in the N_2O was 1 Mrad per pulse (taking $G(N_2) = 12.4$ (3)) giving a dose rate of 0.8×10^{27} eV/g s. The cell was contained in an annular furnace. The temperature was measured using thermocouples embedded in the inner wall of the furnace. Medical grade nitrous oxide (Liquid Air Company Ltd.) was used directly from the bottle after several freeze–pump–thaw cycles to remove any non-condensable impurities. The irradiation products were measured by freezing out with a liquid nitrogen cold trap and pumping the non-condensable gases into a standard volume (3). The measured volume of gas was analyzed by mass spectrometry.

The N_2 and O_2 yields as a function of temperature are shown in Fig. 1. As can be seen, both yields are constant from 24 to 200 °C.

Pyrolysis was negligible below 375°. Above this temperature corrections for pyrolysis were

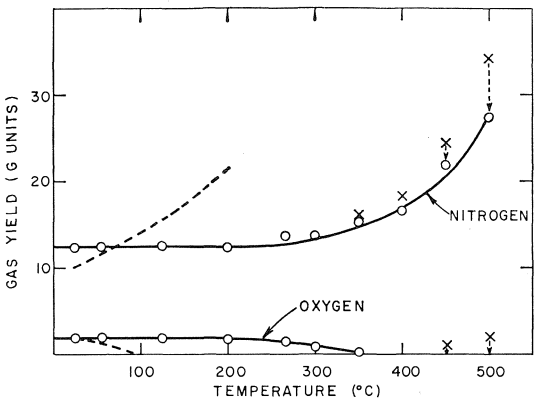

FIG. 1. Temperature dependence of product yields from N_2O radiolysis at high dose rates.
Circles are yields corrected for pyrolysis at 0.8×10^{27} eV/g s; crosses are uncorrected yields at 0.8×10^{27} eV/g s; and dashed lines denote yields at 10^{18} eV/g s taken from ref. (1).

[1]Issued as A.E.C.L. No. 3179.

made by subtracting from the irradiated samples the amounts of N_2 and O_2 formed in identical unirradiated samples which had been heated for the same time.

The dose dependence of the N_2 and O_2 yields was determined by varying the number of pulses. Between 6×10^{19} eV/g (1 pulse) and 4×10^{20} eV/g (7 pulses) there was no change in yields.

The temperature dependence shown in Fig. 1 is markedly different from the results obtained at low dose rates (1, 2). The energy of activation corresponding to the increase in the nitrogen yield (corrected for pyrolysis) with temperature between 200 and 500 °C is $\sim$ 13 kcal/mole.

At room temperature there is no apparent effect of dose rate on the yields of nitrogen and oxygen (within 20%) between 10^{16} eV/g s (1) and 10^{27} eV/g s (3). This, and the independence of the nitrogen yields at 10^{27} eV/g s over the wide range of temperature, 20–200 °C, make nitrous oxide a satisfactory dosimeter at very high dose rates.

1. F. T. Jones and T. J. Sworski. J. Phys. Chem. **70**, 1546 (1966).
2. R. Gorden, Jr. and P. Ausloos. J. Res. Natl. Bur. Std. A, **69**, 79 (1965).
3. C. Willis, O. A. Miller, A. E. Rothwell, and A. W. Boyd. Advan. Chem. Ser. **81**, 539 (1968).

Can. J. Chem. Downloaded from www.nrcresearchpress.com by 210.87.254.5 on 09/05/12
For personal use only.

Catalytic hydrodesulfurization of thiophene. VII. Comparison between thiophene, tetrahydrothiophene, and *n*-butanethiol[1]

S. Kolboe[2]
Division of Applied Chemistry, National Research Council of Canada, Ottawa, Canada

Received December 13, 1967

The desulfurization rates in hydrogen of thiophene, tetrahydrothiophene, and *n*-butanethiol over molybdenum disulfide, an alumina supported cobalt molybdate, and a chromia catalyst have been measured.

Measurements of the interconversion rates of the three sulfur compounds were also carried out.

Canadian Journal of Chemistry, 47, 352 (1969)

Refinements introduced in the previous paper of this series (1) strongly suggested a more detailed evaluation and comparison of the catalytic reactions of thiophene, tetrahydrothiophene, and *n*-butanethiol over different catalysts.

Experimental

Apparatus and Experimental Technique

The apparatus and experimental technique employed were the same as in the previous paper (1).

Materials

The additional materials used were tetrahydrothiophene and *n*-butanethiol (both from Eastman, used as received). The tetrahydrothiophene contained 0.14% thiophene and 0.002% of a compound which may have been butanethiol. The butanethiol was identical with the sample used in Part V of this series (2). The catalysts used were pure MoS_2 heat treated to 650 °C, a commercial alumina-supported cobalt molybdate (Girdler, G.35A), and chromia, designated as catalysts V, VII, and VIII in the previous publication (1) and characterized there in more detail.

Results and Discussion

Generally speaking the desulfurization rate of thiophene and tetrahydrothiophene was about the same on all catalysts in contrast to the desulfurization of butanethiol which was 15–40 times faster under the chosen conditions (see Table I). Results on the product distribution are given in Table II.

It was shown previously that the hydrogenation of gas phase butenes was negligible under the prevailing desulfurization conditions and that the isomerization rate was very small, but the hydrogenation of butadiene to butenes was quite important (1). Similar tests carried out for tetrahydrothiophene and butanethiol led to the same results. The numbers given in Table II therefore reflect the primary product distribution when it is taken into account that the amount of butadiene is too low and that the amount of the

[1]Issued as NRCC No. 10 344.
[2]NRCC Postdoctoral Fellow 1963–64. Present address: Central Institute for Industrial Research, Oslo 3, Norway.

made by subtracting from the irradiated samples the amounts of N_2 and O_2 formed in identical unirradiated samples which had been heated for the same time.

The dose dependence of the N_2 and O_2 yields was determined by varying the number of pulses. Between 6×10^{19} eV/g (1 pulse) and 4×10^{20} eV/g (7 pulses) there was no change in yields.

The temperature dependence shown in Fig. 1 is markedly different from the results obtained at low dose rates (1, 2). The energy of activation corresponding to the increase in the nitrogen yield (corrected for pyrolysis) with temperature between 200 and 500 °C is $\sim$ 13 kcal/mole.

At room temperature there is no apparent effect of dose rate on the yields of nitrogen and oxygen (within 20%) between 10^{16} eV/g s (1) and 10^{27} eV/g s (3). This, and the independence of the nitrogen yields at 10^{27} eV/g s over the wide range of temperature, 20–200 °C, make nitrous oxide a satisfactory dosimeter at very high dose rates.

1. F. T. Jones and T. J. Sworski. J. Phys. Chem. **70**, 1546 (1966).
2. R. Gorden, Jr. and P. Ausloos. J. Res. Natl. Bur. Std. A, **69**, 79 (1965).
3. C. Willis, O. A. Miller, A. E. Rothwell, and A. W. Boyd. Advan. Chem. Ser. **81**, 539 (1968).

Can. J. Chem. Downloaded from www.nrcresearchpress.com by 210.87.254.42 on 09/05/12
For personal use only.

Catalytic hydrodesulfurization of thiophene. VII. Comparison between thiophene, tetrahydrothiophene, and *n*-butanethiol[1]

S. Kolboe[2]
Division of Applied Chemistry, National Research Council of Canada, Ottawa, Canada

Received December 13, 1967

The desulfurization rates in hydrogen of thiophene, tetrahydrothiophene, and *n*-butanethiol over molybdenum disulfide, an alumina supported cobalt molybdate, and a chromia catalyst have been measured.

Measurements of the interconversion rates of the three sulfur compounds were also carried out.

Canadian Journal of Chemistry, 47, 352 (1969)

Refinements introduced in the previous paper of this series (1) strongly suggested a more detailed evaluation and comparison of the catalytic reactions of thiophene, tetrahydrothiophene, and *n*-butanethiol over different catalysts.

Experimental

Apparatus and Experimental Technique

The apparatus and experimental technique employed were the same as in the previous paper (1).

Materials

The additional materials used were tetrahydrothiophene and *n*-butanethiol (both from Eastman, used as received). The tetrahydrothiophene contained 0.14% thiophene and 0.002% of a compound which may have been butanethiol. The butanethiol was identical with the sample used in Part V of this series (2). The catalysts used were pure MoS_2 heat treated to 650 °C, a commercial alumina-supported cobalt molybdate (Girdler, G.35A), and chromia, designated as catalysts V, VII, and VIII in the previous publication (1) and characterized there in more detail.

Results and Discussion

Generally speaking the desulfurization rate of thiophene and tetrahydrothiophene was about the same on all catalysts in contrast to the desulfurization of butanethiol which was 15–40 times faster under the chosen conditions (see Table I). Results on the product distribution are given in Table II.

It was shown previously that the hydrogenation of gas phase butenes was negligible under the prevailing desulfurization conditions and that the isomerization rate was very small, but the hydrogenation of butadiene to butenes was quite important (1). Similar tests carried out for tetrahydrothiophene and butanethiol led to the same results. The numbers given in Table II therefore reflect the primary product distribution when it is taken into account that the amount of butadiene is too low and that the amount of the

[1]Issued as NRCC No. 10 344.
[2]NRCC Postdoctoral Fellow 1963–64. Present address: Central Institute for Industrial Research, Oslo 3, Norway.

TABLE I

Desulfurization rates* of thiophene, tetrahydrothiophene, and *n*-butanethiol

Catalyst	Thiophene		Tetrahydrothiophene		Butanethiol	
	Rate (mole $s^{-1}m^{-2}$)	Conversion (%)	Rate (mole $s^{-1}m^{-2}$)	Conversion (%)	Rate (mole $s^{-1}m^{-2}$)	Conversion (%)
V	2.25×10^{-9}	0.7	4.75×10^{-9}	1.4	82×10^{-9}	24
VII	1.7×10^{-9}	0.5	2.1×10^{-9}	0.6	40×10^{-9}	11
VIII	2.0×10^{-9}	0.7	1.5×10^{-9}	0.5	32×10^{-9}	11

*Temperature = 288 °C, in hydrogen at atmospheric pressure. Flow rate = 96.5–125 ml/min; partial pressure of reactants = 4.5 Torr; weight of catalyst = 6–20 mg.

TABLE II

Product distribution* over three catalysts

Catalyst	Product	Distribution (mole %)		
		Thiophene	Tetrahydrothiophene	Butanethiol
V, MoS_2	Butadiene	6.3	14.6	0
	cis-2-Butene	17.8	11.2	2.75
	trans-2-Butene	22.8	20.6	2.45
	1-Butene	41.7	43.3	78.2
	n-Butane	11.5	9.3	16.7
VII, alumina-supported $CoMoO_4$	Butadiene	3.8	21.1	0
	cis-2-Butene	18.2	8.5	1.3
	trans-2-Butene	18.7	11.8	1.2
	1-Butene	53.3	53.5	86.3
	n-Butane	5.7	5.1	11.3
VIII, Cr_2O_3	Butadiene	8.7	13.0	0
	cis-2-Butene	12.7	2.0	1.1
	trans-2-Butene	10.8	2.5	1.0
	1-Butene	31.8	23.8	13.1
	n-Butane	36.0	59.0	85.0

*Conditions same as in Table I, except thiophene partial pressure equals 20 Torr. The product distribution from thiophene is essentially independent of the thiophene pressure from 4 to 20 Torr.

butenes therefore is slightly high. The product distribution varies with the catalyst as well as the sulfur compound. Chromia gives much more butane than the other catalysts. Thiophene and tetrahydrothiophene yield product distributions which are qualitatively similar. Surprisingly, the saturated compound tetrahydrothiophene yields more butadiene than the unsaturated thiophene over all catalysts. It also yields more 1-butene and the *trans* to *cis* ratio is higher. *n*-Butanethiol yields mainly 1-butene and *n*-butane.

Some experiments were carried out in order to obtain information on the possible interconversions and their rates. It has previously been established that tetrahydrothiophene under conditions similar to the ones used here can be transformed into thiophene (2). The transformation of *n*-butanethiol to thiophene and tetrahydrothiophene was not investigated as these reactions are thermodynamically unfavorable (3). Also the fact that the butanethiol is desulfurized much faster than the two other compounds makes these reactions less interesting. The results are given in Table III. An interesting parallel is seen between the activity of a catalyst for hydrogenating thiophene to tetrahydrothiophene and the relative amounts of butane formed over the catalyst (Table II). The hydrogenation of thiophene to tetrahydrothiophene did not show such a marked dependence upon conversion as the desulfurization reactions (1).

One may conclude that no organo-sulfur compounds are gas phase intermediates when thiophene, tetrahydrothiophene, or butanethiol are reacting under steady state conditions, low conversions, and a fairly low hydrogen pressure. (For pertinent literature references see paper I of this series (4).) It also seems unlikely that thiophene or tetrahydrothiophene reacts via a ring hydrogenation or dehydrogenation and then

Can. J. Chem. Downloaded from www.nrcresearchpress.com by 210.87.254.42 on 09/05/12
For personal use only.

TABLE III

Rate of interconversion of thiophene, tetrahydrothiophene, and butanethiol*

Reactant	Rate of conversion		
	Thiophene	Tetrahydrothiophene	Butanethiol
Thiophene (20 Torr)	—	0.1 (V) 0.05 (VII) 0.2 (VIII)	0.01 (V) 0.01 (VII)
Tetrahydrothiophene (4 Torr)	0.005 (VII)†	—	0.005 (VII)‡

*Temperature = 288 °C; reaction in hydrogen at atmospheric pressure. The conversion rates are given relative to the desulfurization rate at the same conditions. The catalysts over which the results were obtained are shown with a roman numeral to the right of the numbers.

†Measured at 400 °C, not accurately measurable at 288 °C because of thiophene impurity, but it is less than 0.02 at 288 °C.

‡Not definitely identified as butanethiol but having the correct retention time.

reacts further without leaving the surface because the product distribution from thiophene and tetrahydrothiophene are not equal.

The available data do not permit positive conclusions regarding the mechanism of the desulfurization reaction or detailed deductions about the reaction route. A rough scheme can be proposed, however, which is believed to be consistent with the observations. According to this scheme the desulfurization reaction is a dehydrosulfurization reaction rather than a hydrodesulfurization reaction. That is, it is proposed that the desulfurization step consists of the splitting off of an H_2S entity, analogous to the dehydration of an alcohol. More specifically, it is proposed that when the C—S bond in a group $(R \cdot (CH_n) \cdot (CH_n)—S—)_{ads}$ is ruptured, the following group results $[R \cdot (CH_{n-1}) \cdot (CH_n)]_{ads}$.

The resulting C_4-containing molecule is 1-butene when butanethiol reacts, 3-butenethiol when tetrahydrothiophene reacts, and 1-butene-3-yne-1-thiol when thiophene reacts. When the reactants are thiophene or tetrahydrothiophene the above reaction can proceed once more, splitting the second C—S bond whereby thiophene produces an adsorbed diacetylene and tetrahydrothiophene an adsorbed butadiene. Parallel with the second C—S splitting a hydrogenation of the unsaturated C_4-residue may go on. The residues produced in the above way will then probably be bonded to the catalyst surface with each of the free valencies. The last assumption is consistent with the fact that the C_4-compounds formed from the desulfurization reaction are not bonded to the surface in the same way as the corresponding C_4-compound when adsorbed from gas phase. This was shown in the previous publication (1). The products to be expected from the various C_4-compounds are:

Butanethiol

Butane, if the butene is hydrogenated before it is desorbed, otherwise butene. The butene is most likely to be 1-butene, but it may well be expected to show some isomerization before desorption.

Tetrahydrothiophene

The primary adsorbate may desorb as such or it may be hydrogenated once or twice during its stay on the surface, thus producing butadiene, butenes, and *n*-butane. Desorption of a molecule after rupture of the first C—S bond, but prior to rupture of the second C—S bond, may lead to small amounts of *n*-butanethiol or *n*-butenethiol.

Thiophene

The primary adsorbate (acetylenic residue) is not likely to desorb as such, because acetylene is known to be very strongly adsorbed. One may therefore expect that no (measurable) desorption will take place until it has been partially hydrogenated so that there are no acetylenic bonds left. Thiophene should therefore yield the same products as tetrahydrothiophene.

It was shown in Table II that a higher yield of butadiene was obtained from tetrahydrothiophene than from thiophene. This appears surprising at first sight, but may not really be so. If the probability is about the same for an olefinic bond being hydrogenated as for an acetylenic bond, a substantial part of the C_4-molecules from thiophene will never exist as adsorbed butadiene

Can. J. Chem. Downloaded from www.nrcresearchpress.com by 210.87.254.42 on 09/05/12
For personal use only.

molecules. The well-known fact that acetylene usually is selectively hydrogenated before an olefin when both are present does not invalidate this argument because the acetylene is much more strongly adsorbed, and displaces the olefin from the catalyst surface (5).

It is a well-known fact that the desulfurization reaction of thiophene can only be made to proceed in the presence of hydrogen. The proposed scheme is consistent with this observation, as the surface would soon be covered by acetylenic residues in the absence of hydrogen.

Acknowledgment

Helpful discussions with Dr. C. H. Amberg are acknowledged.

1. S. Kolboe and C. H. Amberg. Can. J. Chem. **44**, 2623 (1966).
2. P. Desikan and C. H. Amberg. Can. J. Chem. **42**, 843 (1964).
3. A. Girelli and L. Burlamacchi. La Rivista dei Combustibili, **15**, 121 (1961).
4. P. J. Owens and C. H. Amberg. Advan. Chem. Ser. **33**, 182 (1961).
5. G. C. Bond and P. B. Wells. Advan. Catalysis, **15**, 91 (1964).

Erratum: Octacyanomolybdate(IV) ion, scavenger for hydroxyl radical

B. K. Sharma
Department of Chemistry, University of Delhi, Delhi, India

Received November 11, 1968

(Ref.: Can. J. Chem. **46**, 2757 (1968))

Canadian Journal of Chemistry, **47**, 355 (1969)

The vertical scale in Fig. 1 is in error and should be multiplied by a factor of 2.

Can. J. Chem. Downloaded from www.nrcresearchpress.com by 210.87.254.42 on 09/05/12
For personal use only.

Photochemical decomposition of methanethiol. II. The wavelength dependence of the hydrogen atom energy[1]

JOHN M. WHITE AND G. P. STURM, JR.[2]
The University of Texas at Austin, Austin, Texas 78712

Received November 5, 1968

Data are presented which indicate that the energy distribution of the hydrogen atom produced in the photolysis of methanethiol varies with wavelength in the region 2288 to 2537 Å.

Canadian Journal of Chemistry, 47, 357 (1969)

Introduction

Recently several papers have appeared which deal with the photolysis of methanethiol in the presence of various substrates (1–5). Two, in particular, provide evidence for important effects of translationally excited hydrogen atoms in the $CH_3SH - C_2H_4$ systems (2) and the $CH_3SH - D_2$ systems (4) respectively. We wish to report here an extension of the $CH_3SH - D_2$ experiments from which it is concluded that the energy distributions of hydrogen atoms produced in photolyses of CH_3SH at 2537 and 2288 Å differ significantly. This conclusion is in disagreement with that of Steer and Knight (2), who conclude, from $CH_3SH - C_2H_4$ photolyses, that 2537 and 2288 Å radiation give rise to essentially the same hydrogen atom energy distribution.

Experimental Procedure and Results

We have photolyzed $CH_3SH - D_2$ mixtures at room temperature and wavelengths 2537 or 2288 Å, and measured the $2H_2/HD$ ratio in the products by mass spectrometry. No variation of $2H_2/HD$ with fractional decomposition of CH_3SH over the range 0.04 to 0.2 was noted. At 2537 Å, the CH_3SH pressure ranged from 45 to 54 Torr while the D_2 pressure varied from 13 to 442 Torr. In most photolyses at 2288 Å the CH_3SH pressure was in the range 18 to 24 Torr and the D_2 pressure varied from 9 to 180 Torr. In a few experiments at 2288 Å, the CH_3SH pressure was varied over the range 10 to 40 Torr. Other experimental details have been given previously (4).

Figure 1 shows the product ratio $2H_2/HD$ as a function of the CH_3SH/D_2 reactant ratio. Fitting the data to a linear function by least squares furnishes an intercept of 5.30 ± 0.47 and a slope of 6.90 ± 0.23 at 2537 Å. At 2288 Å the slope is 4.88 ± 0.13 and the intercept is 1.96 ± 0.12. The uncertainties quoted are the standard deviations. Experiments in which the CH_3SH pressure was varied as described above are included in Fig. 1; clearly the product ratio depends only on the reactant ratio with no additional dependence on CH_3SH pressure.

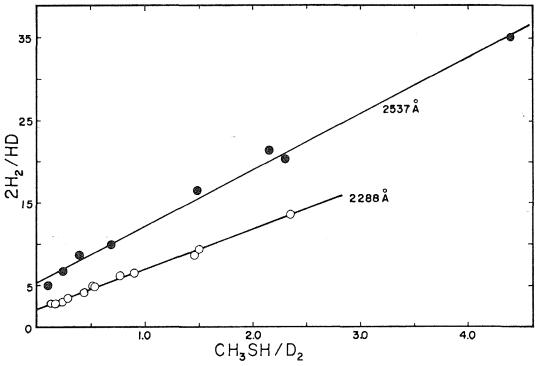

FIG. 1. Variation of the $2H_2/HD$ product ratio with the CH_3SH/D_2 reactant ratio in photolyses of methanethiol–deuterium mixtures at 2537 Å (●), and 2288 Å (○).

Discussion

The following mechanism satisfactorily accounts for the observed results:

[1] $CH_3SH + h\nu \rightarrow CH_3S + H^*$

[2] $H^* + CH_3SH \rightarrow H_2 + CH_3S$

[3] $H^* + D_2 \rightarrow HD + D$

[4] $H^* + CH_3SH \rightarrow H + CH_3SH$

[5] $H^* + D_2 \rightarrow H + D_2$

[6] $H^* + M \rightarrow H + M$

[7] $H + CH_3SH \rightarrow H_2 + CH_3S$

[1]Supported in part by the Petroleum Research Fund of the American Chemical Society and The Robert A. Welch Foundation.

[2]N.A.S.A. Trainee.

[8] $D + CH_3SH \rightarrow HD + CH_3S$

[9] $CH_3S + CH_3S \rightarrow CH_3SSCH_3$

In this mechanism H* denotes translationally excited hydrogen atoms whose energy distribution may be a function of the photolysis wavelength and the cross sections for reactions [2] through [6]. H denotes thermal hydrogen atoms whose energy distribution is a function only of the macroscopic reaction vessel temperature. Steady-state analysis of the mechanism[3] furnishes

$$\frac{2[H_2]}{[HD]} = \frac{(k_2 + k_4)}{k_3}\frac{[CH_3SH]}{[D_2]} + \frac{k_5}{k_3} + \frac{k_6}{k_3}\frac{[M]}{[D_2]}$$

In the present experiments, the last term may be neglected, since the pressures are sufficiently high to preclude wall thermalization, and no gaseous thermalizing species are present other than CH_3SH and D_2 which are accounted for by [4] and [5]. We therefore interpret the slopes in Fig. 1 as being equal to $(k_2 + k_4)/k_3$ and the intercepts as k_5/k_3.

It should be pointed out that, as discussed previously (4), the reaction of thermal hydrogen atoms with D_2 is negligible under the conditions of these experiments. A significant variation with wavelength of the energy distribution of the hydrogen atoms is suggested by the observed increase in the intercept with increasing photolysis wavelength. Since k_5 decreases while k_3 increases with the average hydrogen atom energy (6), the hydrogen atoms reacting at 2288 Å appear to have on the average significantly more energy than those produced at 2537 Å. The variation of the slopes may also be accounted for by similar qualitative arguments. Since the thermal activation energy for abstraction of D from D_2 is larger than for abstraction of H from CH_3SH (7, 5), the rate coefficient for the hot atom reaction [3] is expected to show a stronger energy dependence than reaction [2] in the range of energies being dealt with here ($\lesssim 2$ eV). Therefore it is concluded that $(k_2 + k_4)/k_3$ should decrease as the energy of the hydrogen atoms increases. This is consistent with the above interpretation of the intercepts and the observed slopes.

The apparent discrepancy in these results and those of Steer and Knight may be accounted for in the following way. Photolyses using D_2 as a detector molecule for hot hydrogen atoms may be expected to provide a more sensitive test for differences in translational excitation than photolyses using C_2H_4 or CH_3SH as a detector. Steer and Knight (2) found that in thermalized systems $k_7/k_{10} = 1.15 \pm 0.10$. The hot atom counterpart of this ratio is 2.32 ± 0.11 (2).

[10] $H + C_2H_4 \rightarrow C_2H_5$

The corresponding ratios in the $CH_3SH - D_2$ systems are k_7/k_{11} and k_2/k_3. The ratio k_7/k_{11} is estimated to be greater than 10^{+3} near 300 °K (4).

[11] $H + D_2 \rightarrow DH + H$

Furthermore, the cross section for [11] or [3] is expected to be a sensitive function of the hydrogen atom energy in the region of interest here (6, 9). The data shown in Fig. 1 confirm this statement; the small magnitude of the slopes arises because k_2/k_3 is more than 100 times smaller than its thermal counterpart k_7/k_{11}. Because of this strong variation, we conclude that D_2 is significantly more sensitive to changes in the hydrogen atom energy distribution than is either CH_3SH or C_2H_4.

[3]It should be noted that it is not necessary to require $k_7 = k_8$. The important assumption is that the only detectable reaction of thermal D and H atoms is with CH_3SH.

1. R. P. Steer and A. R. Knight. J. Phys. Chem. **72**, 2145 (1968).
2. R. P. Steer and A. R. Knight. Can. J. Chem. **46**, 2880 (1968).
3. R. R. Kuntz. J. Phys. Chem. **71**, 3343 (1967).
4. G. P. Sturm, Jr. and J. M. White. J. Phys. Chem. **72**, 3679 (1968).
5. T. Inaba and B. deB. Darwent. J. Phys. Chem. **64**, 1431 (1960).
6. Aron Kuppermann and J. M. White. J. Chem. Phys. **44**, 4352 (1966).
7. (*a*) W. R. Schultz and D. J. LeRoy. Can. J. Chem. **42**, 2480 (1964). (*b*) A. A. Westenberg and N. deHaas. J. Chem. Phys. **47**, 1393 (1967).
8. B. G. Dzantiev, A. P. Shvedchikov, and B. V. Borshagovskii. Dokl. Akad. Nauk SSSR, **157**, 653 (1964).
9. M. Karplus, R. N. Porter, and R. D. Sharma. J. Chem. Phys. **43**, 3259 (1965).

Tris(ethylenediamine)ruthenium(III) iodide

GEORGE W. WATT AND C. V. SENOFF[1]
Department of Chemistry, The University of Texas at Austin, Austin, Texas 78712
Received October 10, 1968

The synthesis and electronic spectrum of $[Ru(en)_3]^{3+}$ have been described.

Canadian Journal of Chemistry, 47, 359 (1969)

Can. J. Chem. Downloaded from www.nrcresearchpress.com by 210.87.254.6 on 09/05/12
For personal use only.

The preparation and properties of $[Ru(en)_3]^{3+}$ have been described (1–3) and salts of *cis*-$[Ru(en)_2X_2]^{2+}$ (X = Cl, Br) have been reported recently (4). We now wish to report a facile synthesis of $[Ru(en)_3]^{3+}$ *via* the oxidation of $[Ru(en)_3]^{2+}$ with concentrated nitric acid[2].

A small amount of concentrated nitric acid was added to a suspension of $[Ru(en)_3][ZnCl_4]$ in concentrated aqueous en.2HNO$_3$ to form $[Ru(en)_3]^{3+}$ in solution. The oxidation is quite rapid and is complete within 5 min at room temperature. The hydrated bromide salt[3], $Ru(en)_3Br_3.5H_2O$, may be precipitated from the solution by the addition of aqueous sodium bromide. This salt may then be converted to $[Ru(en)_3]I_3$ by the addition of sodium iodide (saturated solution) to a concentrated aqueous solution of the bromide salt. It should be pointed out that the colors of these salts are dependent on the anion present; the bromide salt is yellow while the iodide salt is dark purple. A similar effect of the counter anion has been observed with various hexaaminеruthenium(III) salts (6). The iodide salt is paramagnetic with μ_{eff} = 2.2 B.M. at 297 °K confirming the presence of ruthenium (III) (7).

The electronic spectrum of $[Ru(en)_3]I_3$ in aqueous solution has been investigated; surprisingly, the spectrum is not stable and changes with time. Despite this behavior, a very good estimate of the spectral parameters may be obtained by *quickly* recording the spectrum of a freshly prepared sample. The spectral data are presented in Table I together with assignments for the observed absorption bands. A value of 29 000 cm^{-1} for the crystal field splitting parameter, $10Dq$, has been calculated from these data using the energy level data of Tanabe and Sugano for d^5 ions (8). This value of the crystal field splitting parameter is consistent with $10Dq$ = 19 500 cm^{-1} reported for the isoelectronic, low-spin, $[Fe(en)_3]^{3+}$ (9). It may be noted that $10Dq$ for $[Ru(en)_3]^{3+}$ is only slightly larger than that reported for $[Ru(en)_3]^{2+}$ (3, 10). Further aspects of the chemistry of these and related complexes are being investigated.

TABLE I
Electronic spectral data for $[Ru(en)_3]^{3+}$

$\bar{\nu}$ (cm^{-1})	ε	Transition
32 100	~370	$^2T_2 \rightarrow {}^2E$
26 700	~105	$^2T_2 \rightarrow {}^2T_2$
22 500	~100	$^2T_2 \rightarrow ({}^2T_1, {}^2A_2)$
(17 400)	~25	$^2T_2 \rightarrow {}^4T_2$

Acknowledgments

The authors wish to thank the U.S. Atomic Energy Commission and the Robert A. Welch Foundation for financial support.

1. F. M. LEVER and R. BRADFORD. Platinum Metals Rev. **8**, 106 (1964).
2. A. D. ALLEN and C. V. SENOFF. Can. J. Chem. **43**, 888 (1965).
3. H. H. SCHMIDKE and D. GARTHOFF. Helv. Chim. Acta, **49**, 2039 (1966).
4. J. A. BROOMHEAD and L. A. P. K. MAGUIRE. J. Chem. Soc. 546 (1967).
5. T. J. MEYER. Dissertation Abstr. **27B**, 4294 (1967).
6. A. D. ALLEN and C. V. SENOFF. Can. J. Chem. **45**, 1137 (1967).
7. H. HARTMANN and C. BUSHBACK. Z. Phys. Chem. Frankfurt am Main, **11**, 120 (1967).
8. Y. TANABE and S. SUGANO. J. Phys. Soc. Japan, **9**, 753 (1954).
9. G. A. RENOVITCH and W. A. BAKER, JR. J. Am. Chem. Soc. **90**, 3585 (1968).
10. C. V. SENOFF. Ph.D. Thesis, University of Toronto, Toronto. 1965.

[1]Present address: Department of Chemistry, University of Guelph, Guelph, Ontario. Author to whom enquires should be addressed.

[2]While the present work was in progress it was reported that iodine could also be used as the oxidizing agent (5).

[3]Anal. Calcd. for $C_6H_{26}Br_3N_6ORu$: C, 11.78; H, 4.24; N, 13.75; Ru, 16.53. Found: C, 11.57; H, 4.36; N, 14.02; Ru, 15.9.

Anal. Calcd. for $C_6H_{24}I_3N_6Ru$: C, 10.88; H, 3.63; N, 12.68; Ru, 15.26. Found: C, 10.78; H, 3.77; N, 12.56; Ru, 15.5.

FOR ERRATA SEE
v.47#8 1969 p.1443

Can. J. Chem. Downloaded from www.nrcresearchpress.com by 210.87.254.5 on 09/05/12
For personal use only.

Canadian Journal of Chemistry

Published by THE NATIONAL RESEARCH COUNCIL OF CANADA

VOLUME 47 FEBRUARY 1, 1969 NUMBER 3

Studies of specifically fluorinated carbohydrates. Part III. A new method for the addition of the elements of "BrF" and of "IF" to unsaturated carbohydrate derivatives

L. D. HALL[1] AND J. F. MANVILLE[2]

Department of Chemistry, The University of British Columbia, Vancouver 8, British Columbia

Received June 3, 1968

A smooth addition of the elements of "BrF", to D-glucal triacetate (**1**), occurs when bromine is reacted with **1** in the presence of silver monofluoride and a suitable solvent. This reaction affords a major product 2-bromo-2-deoxy-α-D-mannopyranosyl fluoride triacetate, together with smaller quantities of 2-bromo-2-deoxy-α-D-glucopyranosyl fluoride triacetate and the corresponding β-D-anomer. The structures of these products have been elucidated by fluorine and proton magnetic resonance studies, and confirmed by several independent syntheses. The same three products are obtained when "BrF" is generated *in situ* from *N*-bromosuccinimide and HF; however, under these conditions 2-deoxy-α-D-*arabino*-hexopyranosyl fluoride triacetate is also formed in ca. 7% yield. The Br_2/AgF reagent has also been reacted with several 3,4-dihydro-2*H*-pyran derivatives and with other glycals. In all cases the major product(s) corresponds to the *trans* addition of "BrF". Similar results are obtained for the addition of the elements of "IF" to all of the above derivatives.

Canadian Journal of Chemistry, **47**, 361 (1969)

Introduction

In the two previous papers (1) of this series, we described studies of glycopyranosyl fluorides which gave us some insight as to the stereospecific dependencies of the ^{19}F nuclear magnetic resonance (^{19}F n.m.r.) parameters of fluorine attached to the anomeric center of a pyranose sugar. We also indicated the potential which ^{19}F n.m.r. spectroscopy has, as a "stereospecific probe", for studying the conformational symmetries of carbohydrate derivatives. In view of the proven sensitivity of ^{19}F chemical shifts with respect to the environment of a fluorine substituent, it occurred to us that ^{19}F n.m.r. spectroscopy might have a unique potential for studying the course of certain electrophilic addition reactions of unsaturated carbohydrate derivatives. The present study is concerned, in part, with the development of this hypothesis and, in part, with an investigation of the potential of unsaturated carbohydrate derivatives as precursors for specifically fluorinated carbohydrates.[3]

Bowers and co-workers (3) described the *in situ* generation, and addition to alkenes, of the elements of "XF" (where X = Cl, Br, or I) by reaction of the appropriate *N*-haloamide with HF in the presence of the alkene. Pattison and co-workers (4) subsequently applied this procedure to a variety of unsaturated systems and Kent and co-workers (5) also described its application to several glycal derivatives. In spite of the evident success of these studies we felt that the use of anhydrous HF would preclude the general application of the Bowers reagent to unsaturated carbohydrate derivatives and as a result, developed the reaction sequence outlined below. The sequence is basically an extension of the concept developed originally for the addition of "BrOMe" to alkenes (6) and subsequently applied to carbohydrate derivatives by Lemieux and co-workers (7).

[1]All correspondence should be addressed to this author.

[2]Recipient of a British Columbia Sugar Refining Co. Scholarship, 1964–1965 and a NRCC Studentship, 1966–1967. Present address: Forest Products Laboratory, N.W. Marine Drive, Vancouver 8, British Columbia.

[3]See ref. 2 for a preliminary communication of these studies.

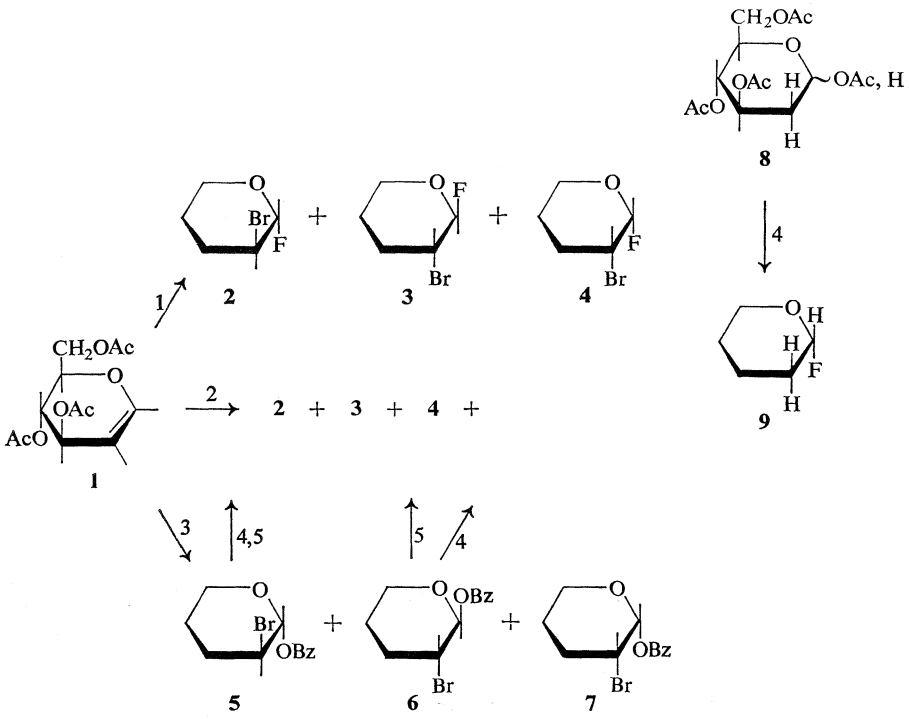

1, Br_2 in C_6H_6, AgF in CH_3CN
2, *N*-bromosuccinimide and anhydrous liquid HF in Et_2O
3, Br_2 in C_6H_6, AgOBz in C_6H_6
4, HF
5, *a*, HBr in HOAc; *b*, AgF in CH_3CN

Flow Sheet 1

Following the usual procedure for electrophilic addition reactions (8) we anticipated reaction of the alkene with bromine to give the appropriate bromonium (or carbonium) ion, plus the bromide anion. Our variant required the immediate removal of this bromide anion, as silver bromide, by reaction with silver monofluoride. Reaction of the concomitantly-formed fluoride anion with the bromonium intermediate, which had been generated in the initial stage of the reaction, should then afford the desired "BrF" adduct. As will be shown below, this hypothetical sequence proved to be successful for "XF" additions (where X = Br, I) to a variety of α,β-unsaturated cyclic ethers.

Subsequent to our studies, a detailed literature search showed that the utilization of the above sequence for effecting the addition of "IF" to cyclohexene had previously been the subject of some controversy. Bergmann and Shahak (9) used an excess of cyclohexene as the reaction solvent and characterized the product as 3-iodocyclohex-1-ene. Schmidt and Meinert (10) used acetonitrile as solvent and reported the isolation of *trans*-2-iodo-cyclohexylfluoride. However, an unsuccessful attempt to repeat this work (11) resulted in the isolation of *N*-acetyl-2-iodo-cyclohexylamine. We have recently shown (12) that when a mixture of acetonitrile and/or benzene is used as solvent, the "IF" adduct of cyclohexene can be obtained in high yield; the reaction follows an exclusively *trans* addition.

Results and Discussion

When an acetonitrile solution of D-glucal triacetate (**1**) was stirred with silver monofluoride, and a solution of bromine (10%, in benzene) was added dropwise, an immediate precipitation occurred. Subsequent work-up of the reaction mixture afforded a syrup, a solution of which showed *three* separate fluorine resonances (Fig. 1) whose shifts were characteristic of pyranosyl

Can. J. Chem. Downloaded from www.nrcresearchpress.com by 210.87.254.5 on 09/05/12
For personal use only.

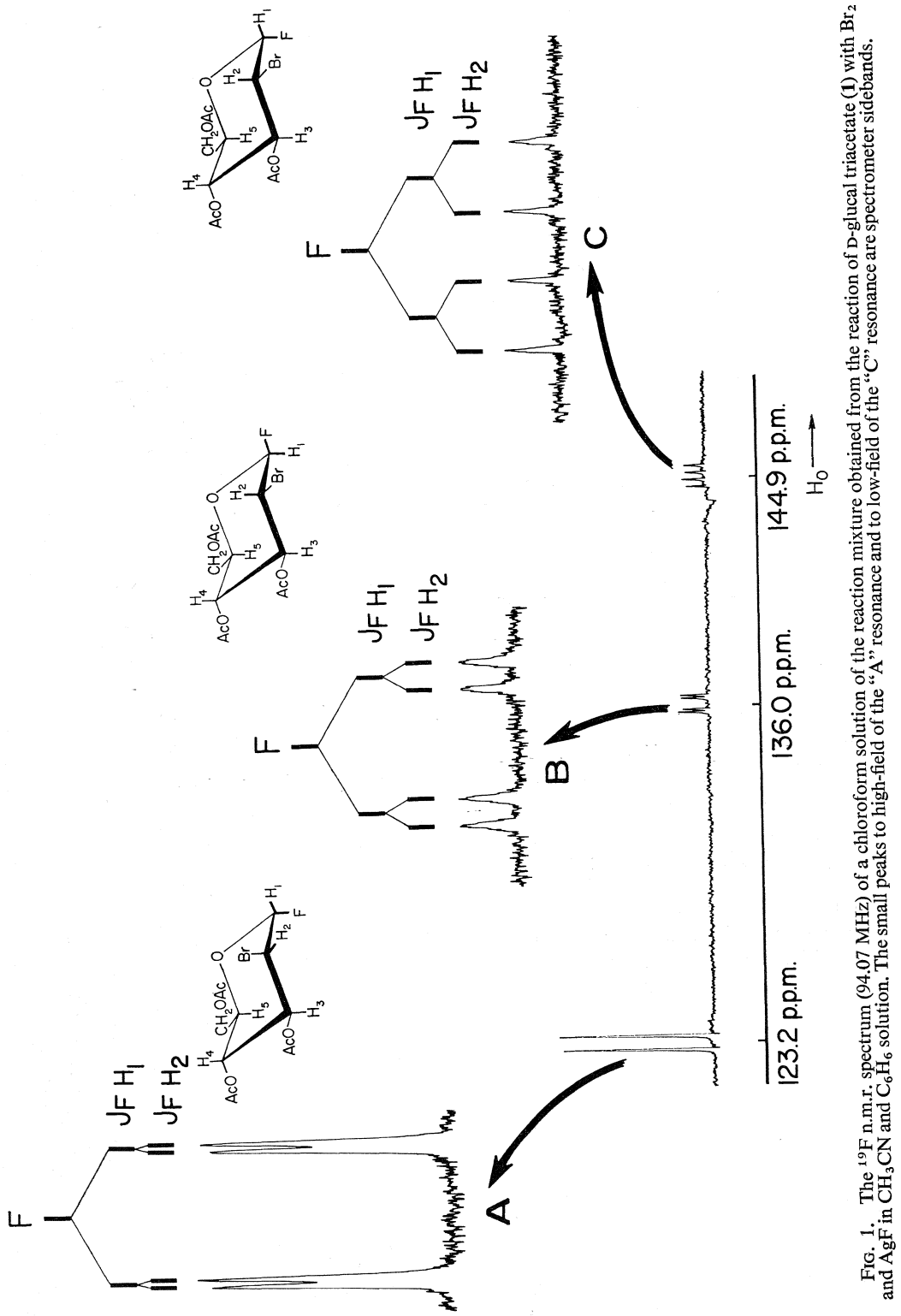

FIG. 1. The ^{19}F n.m.r. spectrum (94.07 MHz) of a chloroform solution of the reaction mixture obtained from the reaction of D-glucal triacetate (**1**) with Br_2 and AgF in CH_3CN and C_6H_6 solution. The small peaks to high-field of the "A" resonance and to low-field of the "C" resonance are spectrometer sidebands.

Can. J. Chem. Downloaded from www.nrcresearchpress.com by 210.87.254.5 on 09/05/12
For personal use only.

Can. J. Chem. Downloaded from www.nrcresearchpress.com by 210.87.254.5 on 09/05/12
For personal use only.

fluorides; there was no evidence for any products having fluorine attached to a secondary carbon (13, 14). The major component (**A**) of this mixture readily crystallized and, as will be shown below, it has the structure 2-bromo-2-deoxy-α-D-mannopyranosyl fluoride triacetate (**2**). A second derivative (**C**), found to be 2-bromo-2-deoxy-α-D-glucopyranosyl fluoride triacetate (**4**), crystallized out more slowly. The third component (**B**) has not to date, been obtained in crystalline form, but it has been shown to be 2-bromo-2-deoxy-β-D-glucopyranosyl fluoride triacetate (**3**). Evidence leading to the structural elucidation of these compounds will now be discussed.

The ^{19}F resonance ($\phi_c = +144.9$) of compound **C**, Fig. 1*c*, showed in addition to the characteristic *geminal* ^{19}F–^{1}H coupling (51.7 Hz) a large (25.1 Hz) *vicinal* ^{19}F–^{1}H coupling, which immediately indicated that this fluorine was *trans-diaxial* with respect to the proton at C-2; therefore, this compound must have the α-D-configuration. Analysis of the proton magnetic resonance (p.m.r.) spectrum, Fig. 2*b*, confirmed that this compound had the D-*gluco* configuration (large *vicinal* couplings of ca. 9 Hz between H-2, H-3; H-3, H-4; and H-4, H-5) and confirmed the α-configuration at C-1 ($J_{1,2} = 2.5$ Hz). On this basis, **C** has the structure 2-bromo-2-deoxy-α-D-glucopyranosyl fluoride triacetate.

The impure sample of derivative **B**, gave a p.m.r. spectrum consistent with the D-*gluco* configuration ($J_{2,3} = 9.0$ Hz) and with the β-configuration at C-1 ($J_{1,2} = 8.0$ Hz). The fact that the ^{19}F chemical shift of this derivative was to low field ($\phi_c = +136.0$) of that of the corresponding α-anomer ($\phi_c = +144.9$) is also consistent (1) with their respective anomeric configurations. The ^{19}F–^{1}H couplings observed in the ^{19}F spectrum (Fig. 1*b*) of this compound are again consistent with the above assignment (*geminal* coupling, 50.3 Hz; *vicinal*, 10.0 Hz). Thus, **B** has the structure, 2-bromo-2-deoxy-β-D-glucopyranosyl fluoride triacetate.

The ^{19}F n.m.r. spectrum of compound **A**, (Fig. 1*a*) exhibited a resonance at ϕ_c +123.1 which had a *vicinal* ^{19}F–^{1}H coupling of 2.9 Hz, which indicated a *gauche* relationship between these substituents. Although the p.m.r. spectrum indicated that this derivative has the D-*manno* configuration ($J_{2,3} = 3.95$ Hz), the *vicinal* H_1–H_2 coupling (1.5 Hz) offered no unequivocal evidence concerning the anomeric configuration. However, the observation that the ^{19}F shift was essentially temperature invariant ($\Delta\phi_c = 0.16$ p.p.m. between $+30°$ and $-80°$), indicated that this derivative has the α-configuration. We had previously observed (1) that the ^{19}F shift of β-D-hexopyranosyl fluorides are temperature dependent whereas those of the α-anomers are essentially invariant. Evidently the replacement of the oxygen substituent at C-2 by a bromine atom does not significantly alter this behavior: thus the ^{19}F shift of **3**, which is assigned the β-D-gluco configuration, changed by 3.2 p.p.m., whilst that of **4**, which is the corresponding α-anomer, changed by only 0.1 p.p.m. over the same temperature range. Thus, a straightforward application of the ^{19}F n.m.r. and p.m.r. methods afforded a facile identification of the three reaction products (**2**, **3**, **4**).

Since this was our first application in the carbohydrate area of this new method of generating "BrF", and also of ^{19}F n.m.r. as a method of structural elucidation in the carbohydrate area, it was felt desirable to confirm the above structural assignments by independent syntheses. The first of these started with the syntheses of 1-*O*-benzoyl-2-bromo-2-deoxy-α-D-mannopyranose triacetate (**5**) and the corresponding β-D-*gluco* isomer **6**. The proof of structure of these two derivatives follows from the known (15) stereochemistry of the Prevost reaction and from consideration of their p.m.r. spectra. These two derivatives were then reacted separately with anhydrous liquid HF, under conditions which are known (16, 17) to afford the most thermodynamically stable glycopyranosyl fluoride, which in the present series is the α-anomer. Reaction of the D-*manno* derivative **5** afforded as the sole product a crystalline material identical in all respects with the derivative previously assigned the α-D-*manno* configuration (**2**). Under identical reaction conditions, the D-*gluco* derivative **6** gave material which was the same in all respects with the compound previously assigned the α-D-*gluco* configuration (**4**). In one such reaction a second, minor component was detected by ^{19}F n.m.r. spectroscopy which gave an identical spectrum with that of the material tentatively assigned the β-D-*gluco* configuration (**3**). Since this derivative isomerized readily to the α-anomer (**4**), this provided further evidence (17) that **3** is the β-D-*gluco* derivative.

Although the above reactions provided reasonable proof for the structures of the two α-anomers, it was desirable to obtain a more satisfactory

Can. J. Chem. Downloaded from www.nrcresearchpress.com by 210.87.254.5 on 09/05/12
For personal use only.

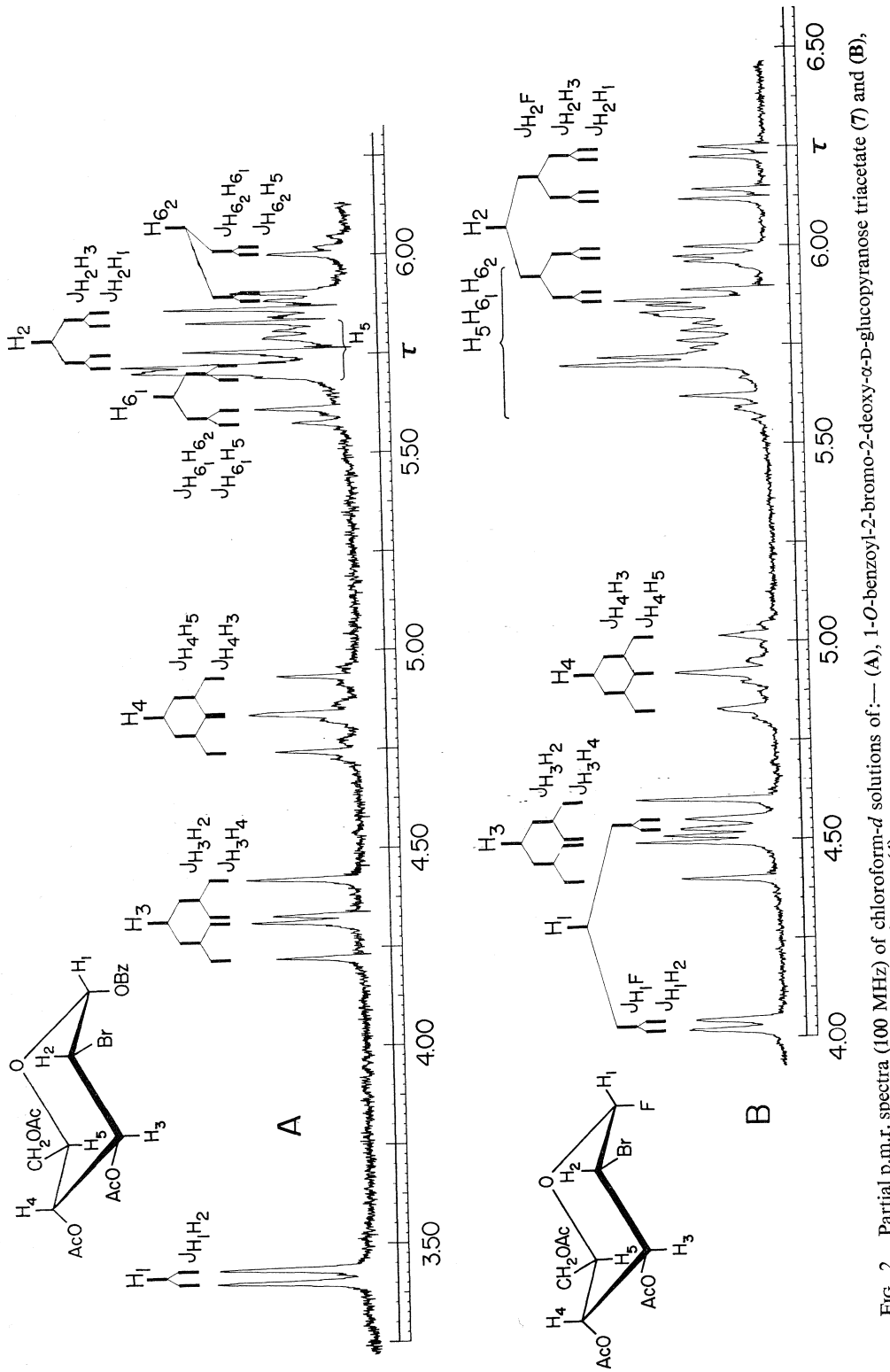

FIG. 2. Partial p.m.r. spectra (100 MHz) of chloroform-*d* solutions of:— (**A**), 1-*O*-benzoyl-2-bromo-2-deoxy-α-D-glucopyranose triacetate (**7**) and (**B**), 2-bromo-2-deoxy-α-D-glucopyranosyl fluoride triacetate (**4**).

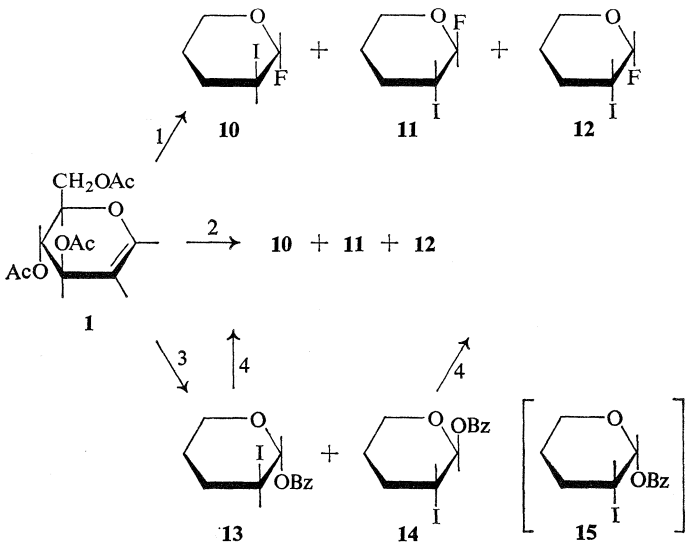

1, I_2 in C_6H_6, AgF in CH_3CN
2, *N*-iodosuccinimide and anhydrous liquid HF in Et_2O
3, I_2 in C_6H_6, AgOBz in C_6H_6
4, HF

Flow Sheet 2

synthesis for the β-D-*gluco* derivative (**3**). Partial success of this objective was attained as follows. Reaction of the β-D-*gluco*-bromo-benzoate (**6**) with HBr in glacial acetic acid afforded the corresponding glucopyranosyl bromide (18). The p.m.r. spectrum of this crude product showed that no starting material remained and that the bromide had the α-D-*gluco* configuration. This bromide was then reacted, without purification, with silver monofluoride in acetonitrile solution. This reaction afforded in high yield, as the sole glycosyl fluoride {^{19}F n.m.r. showed that none of the *cis* product (α-anomer) was formed}, material having spectral properties identical with those of the β-D-glucosyl fluoride (**3**). Initially, this syrupy material was contaminated with some of the bromo-benzoate (**6**) which was partially removed by crystallization. However, all attempts to crystallize **3** have failed, even though it contains less than 5% of impurities (p.m.r.); thin-layer chromatography (t.l.c.) shows only one spot. A similar reaction sequence, starting with the D-*manno* bromo-benzoate (**5**) gave as the sole glycosyl fluoride (^{19}F n.m.r.) the α-D-mannosyl fluoride (**2**). This reaction demonstrates that the bromine at C-2 participates during these exchange reactions. Again the fluoride was contaminated with its bromo-benzoate precursor; however, since the crude bromide did not contain any starting material (p.m.r.), the bromo-benzoate (**5**) must have been formed during the exchange reaction itself (see later). The mannosyl fluoride (**2**) was obtained pure after fractional crystallization.

To characterize further the α-D-*manno* derivative (**2**) attempts were made to remove the bromine substituent from C-2 by hydrogenolysis, which should afford the known (19) 2-deoxy-α-D-*arabino*-hexopyranosyl fluoride triacetate (**9**). Although a pure specimen could not be isolated from an atmospheric hydrogenolysis (palladium catalyst), it was present in the reaction product to the extent of ca. 40% as evidenced by both ^{19}F n.m.r. and p.m.r. spectroscopy. The ^{19}F n.m.r. spectrum showed, apart from a small amount of the starting material remaining, and the desired product **9**, *no other glycosyl fluoride resonances*. Interestingly the p.m.r. spectrum showed that the major by-product of the hydrogenolysis was D-glucal triacetate (**1**). Since the bromo-fluoro derivative (**2**) could be recovered in high yield after stirring with diethylamine and palladium–charcoal at 100° for 2 h, this by-product could not have come directly from **2**.

Can. J. Chem. Downloaded from www.nrcresearchpress.com by 210.87.254.5 on 09/05/12
For personal use only.

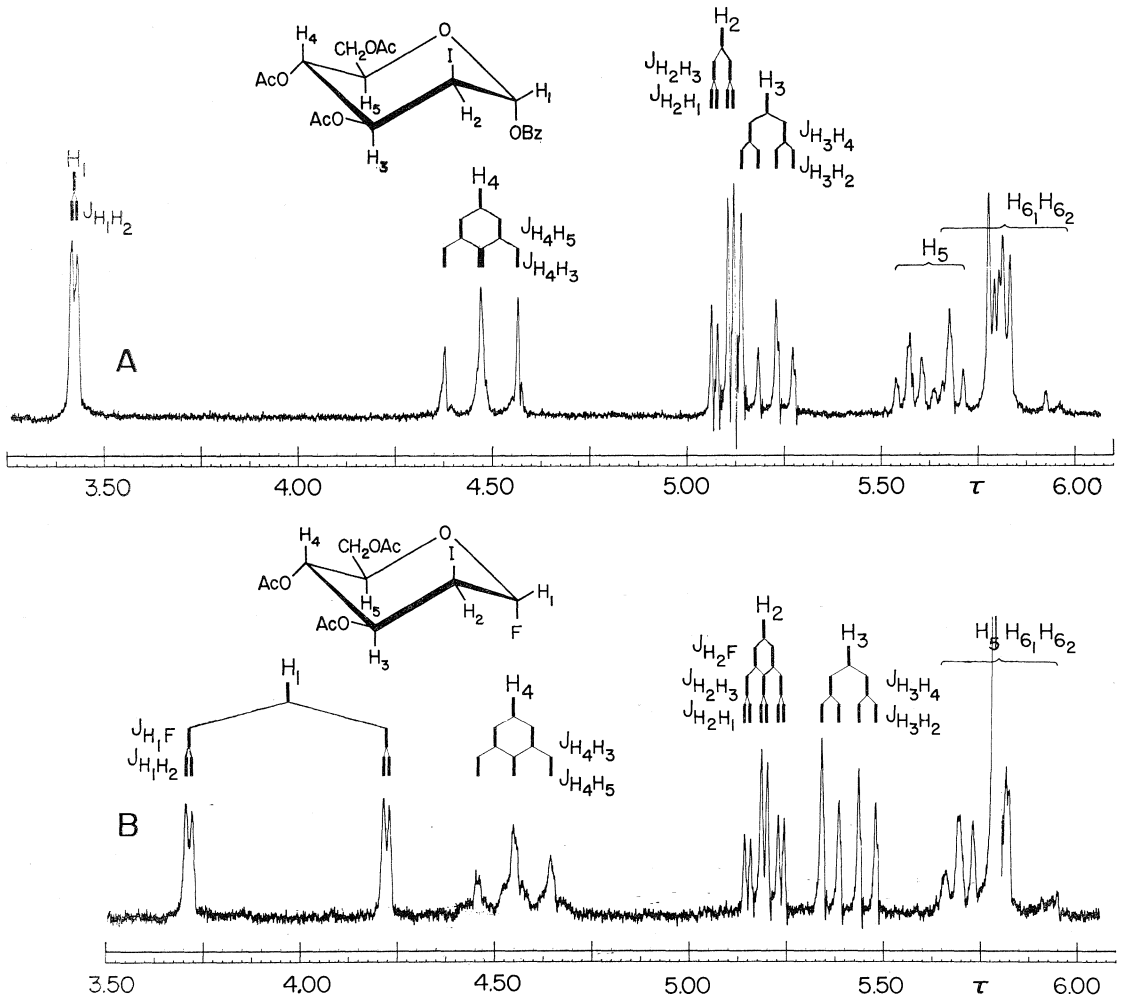

FIG. 3. Partial p.m.r. spectra (100 MHz) of acetone-d_6 solutions of:— (**A**), 1-*O*-benzoyl-2-deoxy-2-iodo-α-D-mannopyranose triacetate (**13**) and (**B**), 2-deoxy-2-iodo-α-D-mannopyranosyl fluoride triacetate (**10**).

The demonstrated success of the Br_2/AgF reagent for effecting the addition of "BrF" to D-glucal triacetate (**1**), prompted us to extend this approach to the addition of "IF" to **1**. Flow Sheet 2 outlines the reactions which were studied and the products which were isolated. Since the basic format of this part of the work parallels that described above for the addition of "BrF", a detailed discussion will not be given. The details are outlined in the Experimental section and the product ratios are given in Table I. It is sufficient to state here that the products isolated in crystalline form were shown to be 2-deoxy-2-iodo-α-D-mannopyranosyl fluoride triacetate (**10**), 2-deoxy-2-iodo-α-D-glucopyranosyl fluoride triacetate (**12**); an impure sample of syrupy 2-deoxy-2-iodo-β-D-glucopyranosyl fluoride triacetate (**11**) was also isolated. The ^1H spectrum of the α-D-*manno* derivative (**10**) is shown in Fig. 3*b*, together with that of the corresponding 1-*O*-benzoate (**13**) (Fig. 3*a*) for comparison.

At this point, a comparison will be made of the procedure for adding the elements of "XF" outlined above and the Bowers method (3) together with a discussion of points of mechanistic interest.

Kent and co-workers (5) have studied the Bowers addition of "BrF" and "IF" to D-glucal

Can. J. Chem. Downloaded from www.nrcresearchpress.com by 210.87.254.5 on 09/05/12
For personal use only.

TABLE I

Product ratios for the addition of the elements of "XF" and of "XOBz" to D-glucal triacetate (**1**)

		Products*			
		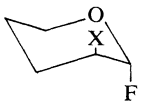	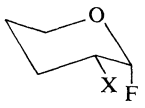	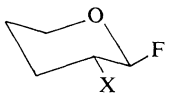	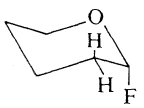
$AgF+X_2$	X=Br	70%	9%	21%	—
	X=I	60%	6%	34%	—
HF+NXS†	X=Br	55%	9%	30%	7%
	X=I	71%	23%	3%	0%
$AgOBz+X_2$	X=Br	31%	26%	42%	—
	X=I	64%	8%	28%	—

*Ratios determined by integration of the ^{19}F n.m.r. and/or p.m.r. spectra.
†NXS = *N*-halosuccinimide.

triacetate. This reaction has been repeated during the present study and with the aid of ^{19}F n.m.r. spectroscopy, the products (shown in Table I), together with their ratios, have been found. The major components, which Kent reported as the β-D-*manno* derivatives were found to be identical with the α-D-mannopyranosyl fluorides (**2** and **10**) described in this paper. It is evident that the published (5) description of these derivatives as possessing the β-D-manno configuration, will have to be corrected; as a direct result it is necessary for Kent's proof of a "*cis*" mechanism to withstand closer examination. It is noteworthy that in the Bowers addition of "BrF" to D-glucal triacetate (**1**) a product arising from the addition of HF across the double bond is formed, namely, 2-deoxy-α-D-*arabino*-hexopyranosyl fluoride triacetate (**9**). The formation of this product was not anticipated since Pedersen (20) had shown that treatment of **1** with anhydrous HF affords 4,6-di-*O*-acetyl-2,3-dideoxy-D-*erythro*-hexosyl fluoride. However, neglecting the above "by-product", the product ratios, resulting from these two different methods for generating "XF", are extremely close; thus for **1**, the two methods may follow a similar mechanism.

Before discussing any details of this mechanism it is necessary to consider the stereospecificity of some of the reactions encountered during the proof of structure of the "BrF" adducts. The most important of these concerns the fluorine exchange reactions of the glycosyl bromides involved in the conversion of **5** to **2** and of **6** to **3**. In both instances this reaction proceeds to give exclusively that glycosyl fluoride having the fluorine *trans* to the C_2-halogen substituent. It is particularly significant that the conversion of **6** to **3** *does not* lead to the formation of any of the α-anomer, which is formed, in ca. 9% yield, during the "XF" addition reaction itself. This finding immediately excludes the possibility, which we have thus far ignored, that the "XF" addition itself merely involves the formation of the 1,2-dibromide(s) (18) which subsequently react(s) with the silver fluoride to give the glycosyl fluoride(s).

The conversion of **5** exclusively to **2** demonstrates conclusively that a halogen atom (bromine) at C-2 of a pyranose carbohydrate controls the course of the exchange reaction at C-1, when silver fluoride is used to effect this exchange. This exchange proceeds with 100% retention of configuration at C-1, possibly via an S_Ni mechanism, in which the bromine at C-2 participates in the ejection of the halide from C-1, forming a halonium type intermediate, which subsequently reacts with the incoming nucleophile, F^-.

This observed participation of halogen (bromine) at C-2 in exchange reactions at C-1 has an important significance as to the proposed mechanism (5, 21) for electrophilic addition reactions of glycals. Lemieux and Fraser-Reid (7) proposed for such reactions that the initiating step is the formation of a cyclic halonium ion and that the actual transition state ". . . . can be expected to be a resonance hybrid of the following canonical structures" (for example)

Can. J. Chem. Downloaded from www.nrcresearchpress.com by 210.87.254.5 on 09/05/12
For personal use only.

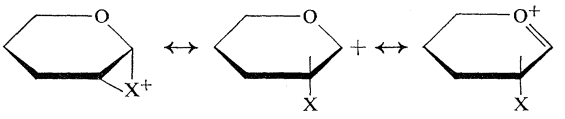

A B C

This statement is acceptable insofar that **A** could clearly afford a *trans* product, whilst both **B** and **C** could lead to either *trans* or (more importantly) *cis* products. However, it is difficult to see why a cyclic halonium ion (**A**) formed during a direct "XF" addition should be in resonance with **B** and **C**, whereas the cyclic halonium ion postulated for the halogen exchange reaction is apparently (by lack of formation of *cis* products) not in resonance with either **B** or **C**. Several possible rationales can be offered for this apparent dilemma, although it must be emphasized that no definitive experimental evidence is presently available. One is that it is totally inappropriate to compare the "XF" addition reaction with the exchange reaction. However, since particular attempts were made during this work to keep the reaction conditions of these two sequences as near identical as possible, this seems to beg the issue. A second rationale is that in the case of electrophilic additions, the initially formed ion has the form (**C**); its formation could result from anchimeric assistance from the ring oxygen as indicated below. This ion could then react directly with F^- to give either *cis* or *trans*

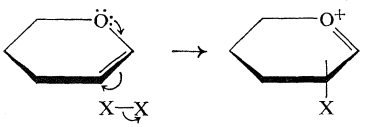

C

products. Alternatively, it could change to, or be in resonance with, the carbonium ion (**B**) which would also lead to *cis* or *trans* products; or it could change to **A** which, by analogy with the AgF exchange reactions, would necessarily lead exclusively to the *trans* product. To account for the exclusive formation of *trans* products during AgF exchange reactions, it would be necessary to postulate that reaction of a halonium ion such as **A** with F^- be very fast compared with the possible equilibrium between **A** and **B** or **C**.

In view of the paucity of really definite data it is not worthwhile pursuing this discussion further at this time. It is, however, interesting to note the similarity between the product ratios for the "XF" additions described in this study and those previously reported by Lemieux and Fraser-Reid (7) for "XOR" additions; in many instances the basic characteristics of the "XF" and "XOR" reactions would appear to be similar. If this is generally the case, it seems reasonable to suggest that studies of "XF" addition reactions may serve as convenient models for gaining insight as to the nature of the more general "XOR" additions. Thus, advantage can be taken of the wide dispersion of ^{19}F chemical shifts to monitor the product ratios and to determine in a facile and unequivocal fashion the configurations of the products arising from these reactions.

Already one situation has been encountered where such a "model" study proved to be useful. During the course of reactions leading to the stereoselective syntheses of the "XF" adducts, it was necessary to effect the addition of "XOBz" to D-glucal triacetate (**1**). Following closely the method of Lemieux and Levine (15) the two products arising from *trans* addition of "IOBz" were isolated. However, the observation, by ^{19}F n.m.r. spectroscopy, of ca. 9% of the α-D-*gluco* adduct from an "IF" addition to **1**, prompted the reinvestigation of the original "IOBz" addition. Inspection of the crude reaction mixture by p.m.r. spectroscopy revealed the presence (ca. 8%) of an anomeric resonance corresponding to the α-D-*gluco* derivative. Following a similar reaction sequence, "BrOBz" addition to **1** resulted in significant amounts (ca. 26%) of the *cis*, or α-D-*gluco*, adduct (**7**).

It is, therefore, clearly established that electrophilic addition reactions can result in *cis* addition to the double bond of acetylated glycals, although the *cis* product is usually a minor component. This result should be compared with those found for electrophilic addition reactions to cycloalkenes, in which *trans* additions are generally (though not exclusively) observed (8, 12) for those reactions proceeding via an ionic mechanism. It follows that the ring oxygen of the glycals must significantly alter the nature of the reaction, thus allowing the formation of *cis* products.

It is convenient at this time to discuss the use of ^{19}F n.m.r. for determining the nature and ratio of the products arising from "XF" addition reactions to other α,β-unsaturated cyclic ethers. Since most of these products were not in an analytically pure state and were identified mainly

Can. J. Chem. Downloaded from www.nrcresearchpress.com by 210.87.254.5 on 09/05/12
For personal use only.

TABLE II

Product ratios for the addition of the elements of "XF" to some 3,4-dihydro-2*H*-pyrans

Reactant	Reaction	% yield and configuration of products		
		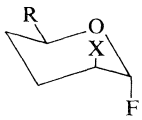	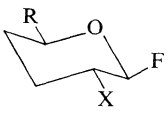	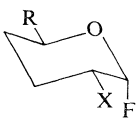
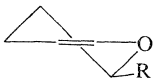 **(16)** R = H	BrF*	84 (**19**)	—	16 (**20**)
	BrF†	55–60 (**19**)	—	40–45 (**20**)
	IF*	95 (**21**)	—	ca. 5 (**22**)
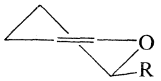 **(17)** R = CH_2OAc	BrF*	57 (**23**)	20 (**24**)	18 (**25**)
	IF*	78 (**26**)	17 (**27**)	ca. 5 (**28**)
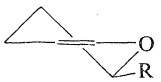 **(18)** R = CH_2OTs	BrF*	66 (**29**)	25 (**30**)	6 (**31**)
	BrF†	55 (**29**)	— (**30**)	45 (**31**)
	IF*	76 (**32**)	18 (**33**)	5 (**34**)

*"XF" generated from AgF and X_2.
†"BrF" generated from anhydrous liquid HF and *N*-bromosuccinimide.

on the basis of their ^{19}F n.m.r. parameters, these results have not been used during the discussion of possible mechanisms for the "XF" addition reaction. The results arising from these reactions are summarized in Table II. The ^{19}F n.m.r. parameters for these reaction products will be found in the Experimental section.

The "XF" addition reactions of dihydropyran (**16**) resulted in the formation of *two* products; these are the trans-diaxial (α-*manno*)[4] and *cis* (α-*gluco*)[4] isomers. Their identification is straightforward since the *cis* isomers (**20, 22**) displayed large (ca. 25 Hz) *vicinal* ^{19}F–^{1}H couplings, indicative of a *trans-diaxial* arrangement, whereas, the *trans* isomers (**19, 21**) showed small (ca. 1.5 Hz) couplings. The product ratios found for the "XF" reactions (AgF + X_2) are as expected, 80% *trans*. The unusually large percentage of *cis* (**20**) formation found for the Bowers reaction may reflect the fact that there is now equilibrium control over the product ratio.

The "XF" additions (X_2 + AgF) to the "C-5" substituted dihydropyrans[4] **17** and **18** resulted in formation of *two trans* isomers and a smaller percentage of the *cis* isomer (α-*gluco*). These results are qualitatively the same as those found previously for D-glucal triacetate (**1**). The high percentage of *cis* product (**31**) arising from the "BrF" (Bowers) reaction to **18** could be a result of isomerization of the *trans-diequatorial* isomer (β-*gluco*) to the more stable *cis* isomer (α-*gluco*) as the former could not be detected.

Results of "XF" (X_2 + AgF) addition to three other glycals are summarized in Table III. Tentative identification of these reaction products followed from comparison with the results found for D-glucal triacetate **1** and their ^{19}F n.m.r. parameters which can be found in the Experimental section. The product ratios arising from "XF" addition to D-galactal triacetate (**35**) appear to reflect the fact that there is now an axially oriented acetoxy substituent at C-4 {low percentage of the α-D-*talo* isomers **38** and **41**} and

[4]We have used the expressions "α-*gluco*" and "α-*manno*" in order to facilitate comparison of these results with those described earlier. Strictly, this nomenclature is incorrect, as also is the reference to "C-5 substituted dihydropyrans".

Can. J. Chem. Downloaded from www.nrcresearchpress.com by 210.87.254.5 on 09/05/12
For personal use only.

TABLE III

Product ratios for the addition of the elements of "XF" to glycals*

Reactant	Reaction	% yield and configuration of products			
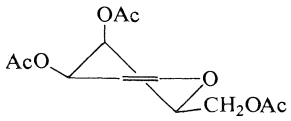 (35)	BrF	34 (**38**)	43 (**39**)	24 (**40**)	—
	IF	25 (**41**)	41 (**42**)	34 (**43**)	—
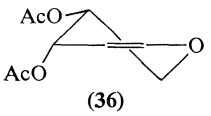 (36)	BrF	62 (**44**)	20 (**45**)	18 (**46**)	—
	IF	49 (**47**)	38 (**48**)	13 (**49**)	—
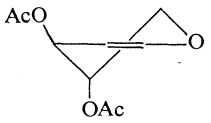 (37)	BrF	55 (**51**)	32 (**52**)	5 (**53**)†	8 (**54**)†
	IF	46 (**55**)	43 (**56**)	8 (**57**)†	3 (**58**)†

*"XF" addition reactions using X_2 and AgF.
†Identification *tentative*, see Experimental.

these results are in agreement with those reported by Lemieux and Fraser-Reid (7) for "XOR" addition reactions.

Identification of the reaction products arising from "XF" addition to the pentals (**36**) and (**37**) are tentative. They were identified on the basis of their *vicinal* ^{19}F–^{1}H couplings and the fact that the *trans-diaxial* isomers are expected to be the preferred ones. Nevertheless, there is one very interesting result that does not depend on the precise identification of the individual products. It was noted that "XF" (X = Br,I) additions to D-xylal diacetate **37** results in the formation of all *four* diastereoisomers, whereas, only three are formed in the case of D-arabinal diacetate **36**. This result may reflect the difference in the ground state conformations of these two molecules, which are shown in Table III, (these conformations were deduced from detailed analysis of their p.m.r. spectra). The conformation of D-arabinal diacetate is such that both acetate substituents are in stereo-electronically favorable orientations; the one at C-3 is *pseudo-axial* {allylic effect (22)} and the acetate at C-4 is *equatorial*. In contrast, D-xylal diacetate has the acetate at C-4, *axially* oriented, in the ground state conformation. As soon as either of these glycals react with halogen, the allylic effect of the double bond will be removed: for D-arabinal diacetate the resulting (carbonium?) ion will be in an energetically stable ground state; however, for D-xylal diacetate, the ion will have at least two substituents axially oriented and will therefore be energetically metastable with respect to the inverted ($^{4}C_{1}$-D) conformer. In the event that the rate of conformational inversion exceeds the rate of attack by F^{-}, it is clearly possible for the intermediate ion to form products from either of its

Can. J. Chem. Downloaded from www.nrcresearchpress.com by 210.87.254.5 on 09/05/12
For personal use only.

Can. J. Chem. Downloaded from www.nrcresearchpress.com by 210.87.254.5 on 09/05/12
For personal use only.

two possible conformers and hence to form four, rather than three, adducts.

The addition of "IOBz" to D-arabinal diacetate and to D-xylal diacetate resulted in syrupy mixtures of three and four products, respectively. Only one component, from the D-arabinal addition reaction was obtained crystalline. It proved to be 1-*O*-benzoyl-2-deoxy-2-iodo-β-D-ribopyranose diacetate (**50**) (p.m.r. evidence; see Experimental section). Since further attempts to obtain these materials in crystalline form are to be made, we shall not discuss them further at this time. It is unfortunate that the isomeric sets of derivatives have similar mobilities on t.l.c. plates.

In conclusion, we have shown that ^{19}F n.m.r. spectroscopy provides a facile method for identifying the products arising from the addition of the elements of "XF" to unsaturated carbohydrate systems. We further suggest that advantage can be taken of the considerable steric sensitivity of ^{19}F chemical shifts to use "IF" additions as models for other "IOR" addition reactions; we are continuing to develop this approach and to study the effect of solvent changes on the product ratios. It is regrettable that the concept of *cis* addition of the elements of "XF" to glycals should have as its foundation the incorrect assignment of a structure (the α-D-*manno* derivatives (**2**) and (**10**)), since the result is evidently quite general and of some importance as far as electrophilic addition reactions to α,β-unsaturated cyclic ethers are concerned. Since the acceptance of a preliminary communication of these results (2), Dr. Kent has informed us[5] that he has independently revised the structure for "BrF" adduct (**2**) derived from D-glucal triacetate (**1**), and now concurs with the α-D-*manno* configuration.

A detailed discussion of the n.m.r. parameters of the derivatives whose syntheses have been described in this paper will be given later in this series.

Experimental

The general methods and nuclear magnetic resonance (n.m.r.) measurements followed the format outlined previously (1).

Electrophilic Addition Reactions of D-*Glucal Triacetate (**1**) Addition of the Elements of "BrF"*

(a) Generated from Br_2 and AgF—D-Glucal triacetate (**1**)[6] (1.36 g) in dry acetonitrile (ca. 25 ml) was stirred vigorously with powdered silver monofluoride[7] (4 g). A solution of bromine (0.85 g, 10% w/v in benzene) was then added dropwise. After completion of the bromine addition (ca. 10 min), the solution was stirred for a further 20 min and then filtered from the copious precipitate of silver halide. To this solution were added 5 ml of saturated aqueous sodium chloride, the precipitated silver chloride was removed, the filtrate was concentrated to ca. 10 ml and chloroform (30 ml) was added. The chloroform solution was extracted successively with aqueous sodium thiosulfate, aqueous sodium bicarbonate and water. After drying (Na_2SO_4), evaporation produced a clear syrup (1.8 g, 97%). Inspection (by proton magnetic resonance (p.m.r.)) of the crude reaction product showed that no starting material remained and ^{19}F n.m.r. showed the presence of *three* glycopyranosyl fluorides which were subsequently identified as:—2-bromo-2-deoxy-α-D-mannopyranosyl fluoride triacetate (**2**) 70%, ϕ_c +123.2, $J_{1,F}$ 50.2 Hz; $J_{2,F}$ 2.85 Hz; 2-bromo-2-deoxy-β-D-glucopyranosyl fluoride triacetate (**3**) 21%, ϕ_c +136.0, $J_{1,F}$ 50.3 Hz; $J_{2,F}$ 10.0 Hz and 2-bromo-2-deoxy-α-D-glucopyranosyl fluoride triacetate (**4**) 9%, ϕ_c +144.9, $J_{1,F}$ 51.5 Hz; $J_{2,F}$ 25.2 Hz.

After work-up, the reaction mixture was dissolved in boiling diethyl ether and on cooling the solution deposited crystals (0.98 g), m.p. 137–142°; addition of light petroleum afforded a second crop of the same material (0.13 g), total yield 1.11 g; 56%. Recrystallization from ethanol afforded pure **2** as prismatic crystals m.p. 138–140°, $[\alpha]_D^{22}$ −32.0° (*c*, 2.06).

Anal. Calcd. for $C_{12}H_{16}O_7BrF$: C, 38.8; H, 4.3; F, 5.1. Found: C, 39.0; H, 4.5; F, 5.0.

The mother liquors remaining after isolation of **2** were evaporated and the resulting syrup dissolved in ethanol and cooled to −5°; after several weeks an impure sample of **4** was obtained (0.12 g, 6%). Recrystallization, twice from aqueous ethanol afforded pure **4** as fine needles; m.p. 120–121°, $[\alpha]_D^{22}$ +134.5° (*c*, 1.80).

Anal. Calcd. for $C_{12}H_{16}O_7BrF$: C, 38.8; H, 4.3; F, 5.1. Found: C, 39.0; H, 4.45; F, 4.95.

The residual syrup from above was shown (by n.m.r.) to contain mainly the β-D-*gluco* isomer (**3**) together with smaller quantities of the other isomers (**2**) and (**4**). Fortunately this syrup was sufficiently pure for detailed n.m.r. analysis; it has so far failed to crystallize.

Reinvestigation of the above reaction, using only benzene as solvent, yielded the same three isomers, but in quite different ratios and the overall yield of adducts was only 83%; the α-D-*manno* isomer (**2**), 42%, the β-D-*gluco* isomer (**3**), 42% and the α-D-*gluco* isomer (**4**) 16%.

(b) Generated from N-bromosuccinimide and anhydrous liquid HF—Following the procedure outlined by Kent *et al.* (5*a*), this reaction was repeated several times, using slightly different reaction times. The yields reported are

[5]P. W. Kent. Private communication, December 27, 1967.

[6]**1** was a commercial sample from the Aldrich Chemical Co., Milwaukee, Wisconsin, which was purified by recrystallization from aqueous ethanol.

[7]The silver monofluoride was a commercial sample from Harshaw Chemical Co. Cleveland, Ohio, and was ground to a fine powder before use.

Can. J. Chem. Downloaded from www.nrcresearchpress.com by 210.87.254.5 on 09/05/12
For personal use only.

average results. Anhydrous hydrogen fluoride (10 g) was added to anhydrous diethyl ether (18 g) in a polythene bottle cooled to ca. −78° (solid-CO_2/acetone). *N*-Bromosuccinimide (4.0 g) and D-glucal triacetate (**1**) (5.0 g) were added, portionwise, to the stirred solution, over the course of ca. 10 min. After 0.5–2 h at −78°, the temperature was raised to 0° for a further 0.5–2 h. After dilution with anhydrous diethyl ether, the solution was decomposed by pouring directly into an ice-cold, saturated aqueous solution of sodium bicarbonate. The ethereal layer was subsequently extracted with water, dried (Na_2SO_4), and evaporated. Investigation (p.m.r.) of the crude reaction product showed that no starting material remained and ^{19}F n.m.r. showed the presence of *four* glycopyranosyl fluorides which were identified on the basis of their ^{19}F chemical shifts and ^{19}F–^1H coupling constants, as the α-D-*manno* isomer (**2**) ca. 55%, the β-D-*gluco* isomer (**3**) ca. 30% and the α-D-*gluco* isomer (**4**) ca. 9%; the fourth resonance has been identified (19) as 2-deoxy-α-D-*arabino*-hexopyranosyl fluoride triacetate (**9**) ca. 8%, ϕ_c +131.1, $J_{1,F}$ 51.2 Hz; $J_{2e,F}$ 5.0 Hz; $J_{2a,F}$ 38.0 Hz.

The syrupy mixture was dissolved in diethyl ether and on cooling, the solution deposited **2** (1.85 g, 32%). Recrystallization from 1:5 v/v chloroform – light petroleum afforded pure **2** m.p. and mixture m.p. 139–140°, with the compound obtained above. The remaining compounds from this reaction were not isolated as they had been previously characterized in this study.

The α-D-*manno* isomer **2** was heated under reflux for 24 h in acetonitrile containing a molar excess of silver monofluoride and was recovered unchanged. It was also unaffected when resubjected to treatment with *N*-bromosuccinimide and anhydrous HF as described above.

Partial hydrogenolysis of **2**, at atmospheric pressure (10% palladium–charcoal catalyst, diethylamine as acid acceptor) in methanol solution gave (n.m.r. evidence) the 2-deoxy fluoride (**9**) together with unreacted starting material (**2**) and D-glucal triacetate (**1**). The α-D-*manno* derivative (**2**) was unaltered when heated under reflux in methanol solution containing diethylamine and palladium–charcoal catalyst.

Addition of the Elements of "IF"

(a) Generated from I_2 and AgF—Following the same procedure (as described above for the generation of "BrF" from Br_2 and AgF), D-glucal triacetate (**1**) (1.36 g) was reacted with I_2 (1.25 g) and AgF (2 g) to form a clear syrup in 98% yield. This syrup contained (^{19}F n.m.r.) *three* glycopyranosyl fluorides: 2-deoxy-2-iodo-α-D-mannopyranosyl fluoride triacetate (**10**) 60%, ϕ_c + 116.9, $J_{1,F}$ 51.7 Hz; $J_{2,F}$ 3.9 Hz; 2-deoxy-2-iodo-β-D-glucopyranosyl fluoride triacetate (**11**) 34%, ϕ_c +132.3, $J_{1,F}$ 49.9 Hz; $J_{2,F}$ 9.3 Hz and 2-deoxy-2-iodo-α-D-glucopyranosyl fluoride triacetate (**12**) 6%, ϕ_c + 139.8, $J_{1,F}$ 50.5 Hz; $J_{2,F}$ 27.8 Hz.

The α-D-*manno* isomer (**10**) was obtained crystalline from an ether solution of the reaction mixture and was crystallized from ethanol to give pure **10** as prismatic crystals (yield 1.0 g, 47%); m.p. 155–156°, $[\alpha]_D^{22}$ −46.1° (*c*, 2.54).

Anal. Calcd. for $C_{12}H_{16}O_7FI$: C, 34.45; H, 3.85; F, 4.55. Found: C, 34.7; H, 4.0; F, 4.65.

The mother liquors remaining from crystallization of **10** were concentrated to a syrup which was dissolved in ethanol. The α-D-*gluco* isomer (**13**) was obtained from this solution after several weeks of standing at 0°. Recrystallization from aqueous ethanol afforded fine needles (yield 0.10 g, 4.8%); m.p. 143–144°, $[\alpha]_D^{22}$ +180.5° (*c*, 2.72).

Anal. Calcd. for $C_{12}H_{16}O_7FI$: C, 34.45; H, 3.85; F, 4.55. Found: C, 34.6; H, 4.0; F, 4.65.

The mother liquors were found (n.m.r.) to contain mainly the β-D-*gluco* isomer (**11**). Column chromatography (silica gel, 1% MeOH in CH_2Cl_2 as eluant) yielded a clear syrup which was sufficiently pure for detailed n.m.r. analysis. To date, this compound has not been obtained crystalline.

Upon reinvestigation of this reaction, using only benzene for solvent, the same three isomers were obtained (yield 79%) in the following ratio: the α-D-*manno* isomer (**10**) 33%, the β-D-*gluco* isomer (**11**) 45%, and the α-D-*gluco* isomer (**12**) 22%.

(b) Generated from N-iodosuccinimide and anhydrous liquid HF—Following the procedure of Wood *et al.* (5*b*), a partially crystalline mass was obtained which contained (^{19}F n.m.r.) the same *three* glycopyranosyl fluorides in the following ratios: the α-D-*manno* isomer (**10**) 71%, the β-D-*gluco* isomer (**11**) 3%, and the α-*gluco* isomer (**12**) 23% together with a small (3%) unidentifiable resonance at ϕ_c +125.3. None of the deoxy isomer (**9**) could be detected.

Addition of the Elements of "BrOBz"

D-Glucal triacetate (**1**) (1.36 g) was dissolved in benzene (25 ml) to which was added silver benzoate[8] (2.5 g); 8.5 ml of a bromine solution (10% w/v in benzene) were added dropwise to the stirred suspension. After a further 20 min, the suspension was filtered and the filtrate was then extracted successively with aqueous sodium bicarbonate and water. The benzene solution was dried (Na_2SO_4) and evaporated to a clear syrup (2.23 g).

Inspection (by p.m.r.) of this crude reaction product indicated four anomeric resonances, which were attributed to the four isomeric "BrOBz" adducts. They were formed in the following yields: the α-D-*manno* isomer (**5**) 31%, τ H_1 = 3.44, $J_{1,2}$ 1.8 Hz; α-D-*gluco* isomer (**7**) 26%, τ H_1 = 3.43, $J_{1,2}$ 3.5 Hz; β-D-*gluco* isomer (**6**) 42%, τ H_1 = 3.94, $J_{1,2}$ 9.1 Hz; and β-D-*manno* isomer 2%, τ H_1 = 3.56, $J_{1,2}$ 3.5 Hz.

This crude reaction product was dissolved in a minimum of boiling ethanol and left at room temperature overnight, during which time crystals (1.61 g, 68%) were deposited. These were shown (by p.m.r.) to be an almost equal mixture of the two *trans* isomers (**5**) and (**6**).

The mother liquors were cooled to ca. 0° and after several weeks fine needle shaped crystals were deposited (0.55 g, 23%); recrystallization from aqueous ethanol afforded pure 1-*O*-benzoyl-2-bromo-2-deoxy-α-D-glucopyranose triacetate (**7**) m.p. 112–113°, $[\alpha]_D^{25}$ +213° (*c*, 0.89).

Anal. Calcd. for $C_{19}H_{21}O_9Br$: C, 48.2; H, 4.45; Br, 17.0. Found: C, 48.0; H, 4.5; Br, 17.0.

---

[8]Silver benzoate was formed by reacting equimolar aqueous solutions of silver nitrate and sodium benzoate; the crude precipitate was washed with copious amounts of water, filtered (suction), and dried at 120° for 8 h.

Can. J. Chem. Downloaded from www.nrcresearchpress.com by 210.87.254.5 on 09/05/12
For personal use only.

The mixture of **5** and **6** was separated in the manner of Lemieux and Levine (15) and was each recrystallized from aqueous ethanol. 1-*O*-Benzoyl-2-bromo-2-deoxy-α-D-mannopyranose triacetate (**5**) had m.p. 168–169°, $[\alpha]_D^{28}$ +62.3° (*c*, 1.54).

Anal. Calcd. for $C_{19}H_{21}O_9Br$: C, 48.2; H, 4.45; Br, 17.0. Found: C, 48.0; H, 4.5; Br, 17.1.

1-*O*-Benzoyl-2-bromo-2-deoxy-β-D-glucopyranose triacetate (**6**) had m.p. 161–162°, $[\alpha]_D^{28}$ +15.3° (*c*, 0.72).

Anal. Calcd. for $C_{19}H_{21}O_9Br$: C, 48.2; H, 4.45; Br, 17.0. Found: C, 48.05; H, 4.6; Br, 17.1.

When the above reaction was repeated using acetonitrile to dissolve the D-glucal triacetate (**1**), the same four products were observed (by n.m.r.) in the following ratios; the α-D-*manno* isomer (**5**) 20%, the β-D-*gluco* isomer (**6**) 35%, the α-D-*gluco* isomer (**7**) 40% and the β-D-*manno* isomer 6%.

Addition of the Elements of "IOBz"

The two isomeric *trans* 1-*O*-benzoyl-2-deoxy-2-iodo-D-pyranose triacetates, **13** and **14**, were obtained by a variant of the method described by Lemieux and Levine (15). 1.36 g of **1** in benzene solution, was used and the iodine (1.35 g) was dissolved in benzene (10% w/v) and added dropwise to the stirred solution.

Investigation (by n.m.r.) of the crude reaction product showed the presence of a third product, not reported by Lemieux and Levine. It was assigned to 1-*O*-benzoyl-2-deoxy-2-iodo-α-D-glucopyranose triacetate (**15**) (τ H-1 = 3.42; $J_{1,2}$ 3.0 Hz). The product ratios as determined by p.m.r. were:— α-D-*manno* isomer (**13**) 46%, the α-D-*gluco* isomer (**15**) 8%, and the β-D-*gluco* isomer (**14**) 46%.

This reaction was repeated, using an acetonitrile solution of D-glucal triacetate (**1**). The same products were observed in the following ratios: the α-D-*manno* isomer (**13**), 64%; the β-D-*gluco* isomer, (**14**) 28%; and the α-D-*gluco* isomer (**15**) 8%.

The α-D-*gluco* isomer (**15**) was not isolated from the mother liquors. The α-D-*manno* isomer (**13**) had m.p. 160–161°, lit. (15) m.p. 159.5–160°, $[\alpha]_D$ +45.3° and the β-D-*gluco* isomer (**14**) had m.p. 150–151°, lit. (15) m.p. 150–151.5°, $[\alpha]_D$ +2.2°.

Stereoselective Syntheses of Products Formed during the Addition Reactions of D-*Glucal Triacetate*

2-Bromo-2-deoxy-α-D-mannopyranosyl fluoride triacetate (2)—1-*O*-Benzoyl-2-bromo-2-deoxy-α-D-mannopyranose triacetate (**5**) (0.25 g) was converted to the 2-bromo-2-deoxy-α-D-mannopyranosyl bromide triacetate (18) which was immediately dissolved in acetonitrile (20 ml) containing silver monofluoride (1 g). The solution was then shaken for ca. 20 min (no more precipitate was formed after ca. 15 min). Work-up, following the procedure described previously (1) for halogen exchange reactions, produced a clear syrup which contained (^{19}F n.m.r.) only *one* fluoride (**2**); however, p.m.r. showed the presence of ca. 20% of the starting material (**5**).

This syrup was dissolved in ethanol and the benzoate (**5**) was precipitated (0.050 g, m.p. 171–174°) leaving a colorless solution which contained mainly the desired fluoride. This solution was evaporated, dissolved in 3 ml of chloroform, petroleum ether (20 ml) was added and the solution cooled to ca. 5°. Crystals of **2** m.p. 137–142° were deposited which were recrystallized from aqueous ethanol (0.102 g, 51%) m.p. 138–140°.

The fluoride (**2**) was also prepared, as described (1) for the formation of α-D-glucopyranosyl fluoride tetraacetate, from the benzoate (**5**) (0.05 g) by action of anhydrous liquid HF. The desired compound (**2**) was obtained in 63% yield; m.p. and mixture m.p. with samples obtained previously, 139–140°.

This compound was identical in every respect with the product obtained in the bromofluorination reactions described above.

2-Bromo-2-deoxy-β-D-glucopyranosyl fluoride triacetate (3)—1-*O*-Benzoyl-2-bromo-2-deoxy-β-D-glucopyranose triacetate (**6**) (0.25 g) was converted as described above to the 2-bromo-2-deoxy-α-D-glucopyranosyl bromide triacetate, which was immediately dissolved in acetonitrile (20 ml) containing silver monofluoride (1 g). Starting material (0.053 g, 21%) was isolated from this reaction leaving the desired fluoride (**3**) (0.095 g, 62%). This product, however, has not been obtained either pure or crystalline. ^{19}F n.m.r. showed only the desired fluoride, none of the corresponding *cis* isomer (**4**) could be detected

2-Bromo-2-deoxy-α-D-glucopyranosyl fluoride triacetate (4)—1-*O*-Benzoyl-2-bromo-2-deoxy-β-D-glucopyranose triacetate (**6**) (0.25 g) was converted, in the manner described (1) for the formation of α-D-glucopyranosyl fluoride tetraacetate, with anhydrous hydrogen fluoride, into the desired fluoride (**4**) (0.11 g, 58%) with m.p. and mixture m.p. with sample obtained previously, 120–121°.

2-Deoxy-2-iodo-α-D-mannopyranosyl fluoride triacetate (10)—1-*O*-Benzoyl-2-deoxy-2-iodo-α-D-mannopyranose triacetate (**13**) (0.25 g) was reacted in the usual manner with anhydrous hydrogen fluoride to give the desired fluoride (**10**), (0.10 g, 50%) with m.p. and mixture m.p. with a sample previously obtained, 153–155°.

2-Deoxy-2-iodo-α-D-glucopyranosyl fluoride triacetate (12)—1-*O*-Benzoyl-2-deoxy-2-iodo-β-D-glucopyranose triacetate (**14**) (0.25 g) was subjected, in the usual manner, to react with hydrogen fluoride. The desired fluoride (**12**) was formed in a yield of 60%; m.p. and mixture m.p. with a sample obtained previously, 142–144°.

The above halogenofluorinations (bromine and iodine) were also performed on the following model compounds; vinyl acetate, 3,4-dihydro-2*H*-pyran (**16**), the acetate of 3,4-dihydro-2*H*-pyran-2-methanol (**17**), and the *p*-toluenesulfonate of 3,4-dihydro-2*H*-pyran-2-methanol (**18**). In each case, the product had halogen at C-2 and fluorine at C-1[9]: with the exception of those from the tosylate (**18**), the products were unstable liquids or oils which could not be isolated in a pure state. However, it was possible to determine their product ratios by ^{19}F n.m.r.

Reactions of Vinyl Acetate[10]

(a) Bromofluorination, "BrF" generated from Br_2 and AgF—This bromofluorination afforded only *one* fluorine

[9]These reaction products are given trivial names. It is felt that these trivial names adequately describe the reaction products and facilitate greatly the comparison between these reaction products and those described previously for the D-glucal triacetate adducts. See also footnote[4] given in the discussion.

[10]Vinyl acetate was a commercial sample from the Aldrich Chemical Co., Inc., Milwaukee, Wisconsin.

Can. J. Chem. Downloaded from www.nrcresearchpress.com by 210.87.254.5 on 09/05/12
For personal use only.

containing product; ϕ_c +121.9, (doubletted triplet) J_{gem} ca. 50 Hz, J_{vic} ca. 15 Hz. Solely on the basis of the ^{19}F n.m.r. data, it was concluded that the product had the structure $CH_2BrCHFOAc$.

*Reactions of 3,4-Dihydro-2H-Pyran (**16**)*[11]

(a) Bromofluorination, "BrF" generated from Br_2 and AgF—This bromofluorination of **16** afforded *two* fluorine containing products: the *trans* isomer (**19**) 84%, ϕ_c +122.8, $J_{1,F}$ 51.3 Hz, $J_{2,F}$ 4.6 Hz and the *cis* isomer (**20**) 16%, ϕ_c +149.4, $J_{1,F}$ 52.2 Hz, $J_{2,F}$ 26.3 Hz.

(b) Bromofluorination, "BrF" generated from N-bromosuccinimide and anhydrous liquid HF—Following the general procedure as outlined for the reaction of D-glucal triacetate (**16**) afforded a yellow syrup which contained (^{19}F n.m.r.) the same *two* fluorine resonances: these were assigned to the *trans* isomer (**19**) 55–60% and *cis* isomer (**20**) 40–45%.

(c) Iodofluorination, "IF" generated from I_2 and AgF—The iodofluorination of **16** also yielded *two* compounds; the *trans* isomer (**21**) ca. 95%, ϕ_c +117.5, $J_{1,F}$ 51.3 Hz, $J_{2,F}$ 5.2 Hz and the *cis* isomer ca. 5%, ϕ_c +143.5, $J_{1,F}$ 51.1 Hz, $J_{2,F}$ 27.2 Hz.

(d) Iodofluorination, "IF" generated from N-iodosuccinimide and anhydrous liquid HF—When this iodofluorination reaction was attempted, a black tar was obtained, which did not contain any fluorine organic products.

*Reactions of the Acetate of 3,4-Dihydro-2H-Pyran-2-Methanol (**17**)*[12]

(a) Bromofluorination, "BrF" generated from Br_2 and AgF—The bromofluorination of the acetate (**17**), b.p. 104–106°, 15 mm led to the formation of the *trans-diaxial* (α-*manno*) isomer (**23**) 57%, ϕ_c +119.7, $J_{1,F}$ 51.1 Hz, $J_{2,F}$ 4.0 Hz; the *trans-diequatorial* (β-*gluco*) isomer (**24**) 20%, ϕ_c +126.9, $J_{1,F}$ ca. 52 Hz and the *cis* (α-*gluco*) isomer (**25**) 18%, ϕ_c +147.1, $J_{1,F}$ 51.6 Hz, $J_{2,F}$ 26.0 Hz. (A minor unidentified resonance at ϕ_c +121.9 was also detected.)

(b) Iodofluorination, "IF" generated from I_2 and AgF—The iodofluorination of **27** resulted in the formation of the *trans-diaxial* (α-*manno*) isomer (**26**) 78%, ϕ_c +114.5, $J_{1,F}$ 51.4 Hz, $J_{2,F}$ 5.0 Hz; the *trans-diequatorial* (β-*gluco*) isomer (**27**) 17%, ϕ_c +122.3 $J_{1,F}$ ca. 50 Hz and the *cis* (α-*gluco*) isomer (**28**) ca. 5%, ϕ_c ca. +141. (This resonance was too weak for an accurate determination of ϕ_c or of the coupling constants.) No other ^{19}F resonances were discernible.

*Reactions of the p-Toluenesulfonate of 3,4-Dihydro-2H-Pyran-2-Methanol (**18**)*

(a) Bromofluorination, "BrF" generated from Br_2 and AgF—The bromofluorination of **18**, (m.p. 46.5–47.5°) afforded the *trans-diaxial* (α-*manno*) isomer (**29**) 66%, ϕ_c +120.1, $J_{1,F}$ 50.5 Hz, $J_{2,F}$ 3.7 Hz; the *trans-diequatorial* (β-*gluco*) isomer (**30**) 25%, ϕ_c +125.8 $J_{1,F}$ ca. 51 Hz and the *cis* (α-*gluco*) isomer (**31**) 6%, ϕ_c +147.5, $J_{1,F}$ 52.0 Hz, $J_{2,F}$ 26.0 Hz, together with two other very minor, unidentified resonances.

(b) Bromofluorination, "BrF" generated from N-bromosuccinimide and anhydrous liquid HF—The bromofluorination of **18** (5 g) afforded a crystalline mass (1.4 g, 20%): m.p. 106–110°. ^{19}F n.m.r. showed this reaction product to consist of almost equal portions of the *trans-diaxial* (α-*manno*) isomer (**29**) ca. 55%, and the *cis* (α-*gluco*) isomer (**31**) ca. 45%. Successive recrystallizations (7 times) failed to separate these two isomers; m.p. 121–122.5°.

Anal. Calcd. for $C_{13}H_{16}O_4BrFS$: C, 42.5; H, 4.35; F, 5.2. Found: C, 42.4; H, 4.4; F, 5.25.

(c) Iodofluorination, "IF" generated from I_2 and AgF—The iodofluorination of **18** afforded three products. They were identified (by ^{19}F n.m.r.) as the *trans-diaxial* (α-*manno*) isomer (**32**) 76%, ϕ_c +114.8, $J_{1,F}$ 51.5 Hz, $J_{2,F}$ 5.1 Hz; the *trans-diequatorial* (β-*gluco*) isomer (**33**) 18%, ϕ_c +121.0, $J_{1,F}$ ca. 50 Hz and the *cis* (α-*gluco*) isomer (**34**) 5%, ϕ_c ca. +141.

*Reactions of D-Galactal Triacetate (**35**)*

(a) Bromofluorination, "BrF" generated from Br_2 and AgF—In the manner described for "BrF" addition to **1**, D-galactal triacetate[13] (**35**) (1.36 g) was reacted in acetonitrile solution with bromine and silver monofluoride. A 98% yield of a light amber syrup was obtained, which so far has failed to crystallize; ^{19}F n.m.r. showed that *three* glycopyranosyl fluorides were formed. Their structures were tentatively assigned, on the basis of their ϕ_c values and first order ^{19}F–^{1}H coupling constants, and by analogy with the products obtained from D-glucal triacetate as: 2-bromo-2-deoxy-α-D-talopyranosyl fluoride triacetate (**38**) 34%, ϕ_c +121.4, $J_{1,F}$ 49.8 Hz, $J_{2,F}$ 4.6 Hz, 2-bromo-2-deoxy-β-D-galactopyranosyl fluoride triacetate (**39**) 43%, ϕ_c +135.6, $J_{1,F}$ 49.7 Hz, $J_{2,F}$ 10.0 Hz and 2-bromo-2-deoxy-α-D-galactopyranosyl fluoride triacetate (**40**), 24%, ϕ_c +145.0, $J_{1,F}$ 50.5 Hz, $J_{2,F}$ 25.1 Hz. {Compare with those results reported by Kent *et al.* (21*b*).}

(b) Iodofluorination, "IF" generated from I_2 and AgF—A 96% yield of a clear syrup was obtained, which has failed to crystallize. Again ^{19}F n.m.r. showed that *three* glycopyranosyl fluorides had been formed. Tentatively, these have the structures 2-deoxy-2-iodo-α-D-talopyranosyl fluoride triacetate (**41**), 25%, ϕ_c +114.6, $J_{1,F}$ 50.5 Hz, $J_{2,F}$ 6.3 Hz; 2-deoxy-2-iodo-β-D-galactopyranosyl fluoride triacetate (**42**) 41%, ϕ_c +130.8, $J_{1,F}$ 49.8 Hz, $J_{2,F}$ 10.2 Hz and 2-deoxy-2-iodo-α-D-galactopyranosyl fluoride triacetate (**43**) 34%, ϕ_c +139.4, $J_{1,F}$ 50.0 Hz, $J_{2,F}$ 27.6 Hz.

*Reactions of D-Arabinal Diacetate (**36**)*[14]

(a) Bromofluorination, "BrF" generated from Br_2 and AgF—Following the established procedure a syrup was obtained from **36** (1.0 g) in 93% yield, which has not crystallized. ^{19}F n.m.r. showed only *three* anomeric fluorine resonances. They were tentatively assigned as: 2-bromo-2-deoxy-α-D-arabinopyranosyl fluoride diacetate (**44**) 62%, ϕ_c +126.4, $J_{1,F}$ 50.5 Hz, $J_{2,F}$ 3.5 Hz; 2-bromo-2-deoxy-β-D-ribopyranosyl fluoride diacetate

[11]3,4-Dihydro-2*H*-pyran, was a commercial sample from Eastman Organic Chemicals, Rochester, New York.

[12]3,4-Dihydro-2*H*-pyran-2-methanol was a gift from Shell Chemical Co., New York.

[13]D-Galactal triacetate (**35**), was a commercial sample from Koch Light Laboratories Ltd., England and was used as received.

[14]D-Arabinal diacetate (**36**), was prepared by Miss Zinat Mia, according to the procedure of Humoller (23); had b.p. (1 mm) 90°; lit. (23) b.p. 0.3 mm) 79°; $[\alpha]_D$ +266°.

(**45**), 20%, ϕ_c +127.9, $J_{1,F}$ 50.4 Hz, $J_{2,F}$ 3.4 Hz and 2-bromo-2-deoxy-α-D-ribopyranosyl fluoride diacetate (**46**), 18%, ϕ_c +147.6, $J_{1,F}$ 51.3 Hz, $J_{2,F}$ 25.1 Hz. {Compare with the results of Kent *et al.* (21*a*).}

(b) Iodofluorination, "IF" generated from I_2 and AgF—An 82% yield of a clear syrup was obtained from **36** (1.0 g) which so far has failed to crystallize. ^{19}F n.m.r. showed only three anomeric resonances. These resonances were tentatively assigned as: 2-deoxy-2-iodo-α-D-arabino-pyranosyl fluoride diacetate (**47**) 49%, ϕ_c +121.6, $J_{1,F}$ ca. 50 Hz, $J_{2,F}$ ca. 5 Hz; 2-deoxy-2-iodo-β-D-ribopyranosyl fluoride diacetate (**48**) 38%, ϕ_c +123.9, $J_{1,F}$ 51.0 Hz, $J_{2,F}$ 6.5 Hz and 2-deoxy-2-iodo-α-D-ribopyranosyl fluoride diacetate (**49**) 13%, ϕ_c +141.9 $J_{1,F}$ 50.7 Hz, $J_{2,F}$ 27.6 Hz.

(c) Iodobenzoylation—Following the same procedure as described for D-glucal triacetate (**1**), Miss Zinat Mia effected the addition "IOBz" to **36** in benzene solution and obtained a semi-crystalline syrup which was found (by p.m.r.) to contain three anomeric resonances.

One isomer was obtained crystalline, from an ethanol solution and was recrystallized twice from aqueous ethanol to afford hard needles of 1-*O*-benzoyl-2-deoxy-2-iodo-β-D-ribopyranose diacetate (**50**), m.p. 129–130° $[\alpha]_D^{27}$ −26.5° (*c*, 1.46).

Anal. Calcd. for $C_{16}H_{17}O_7I$: C, 42.85; H, 3.8; I, 28.3. Found: C, 42.6; H, 3.9; I, 28.1.

This component (**50**) accounted for 45% of the reaction product.

Reactions of D-*Xylal Diacetate (**37**)*[15]

(a) Bromofluorination, "BrF" generated from Br_2 and AgF—Following the established procedure a clear syrup was obtained from **37** in 91% yield which has to date failed to crystallize. ^{19}F n.m.r. showed that all *four* isomeric "BrF" adducts were formed. They are (the structures are tentative):— 2-bromo-2-deoxy-α-D-lyxo-pyranosyl fluoride diacetate (**51**) 55%, ϕ_c +126.7, $J_{1,F}$ 50.1 Hz, $J_{2,F}$ 3.5 Hz; 2-bromo-2-deoxy-β-D-xylopyranosyl fluoride diacetate (**52**) 32%, ϕ_c +128.0, $J_{1,F}$ 51.0 Hz, $J_{2,F}$ 9.0 Hz; the β-D-*lyxo* or the α-D-*xylo* isomer (**53**) 5%, ϕ_c +144.1, $J_{1,F}$ 50.8 Hz, $J_{2,F}$ 26.8 Hz and the α-D-*xylo* or the β-D-*lyxo* isomer (**54**) 8%, ϕ_c +146.5, $J_{1,F}$ 50.3 Hz, $J_{2,F}$ 25.1 Hz.

(b) Iodofluorination, "IF" generated from I_2 and AgF—Following the established procedure a colorless syrup was obtained, which has failed to crystallize. ^{19}F n.m.r. again showed that all *four* isomeric "IF" adducts were formed.

The resonances were tentatively assigned as: 2-deoxy-2-iodo-α-D-lyxopyranosyl fluoride diacetate (**55**) 46%, ϕ_c +120.4, $J_{1,F}$ 50.0 Hz, $J_{2,F}$ 3.5 Hz; 2-deoxy-2-iodo-β-D-xylopyranosyl fluoride diacetate (**56**) 43%, ϕ_c +122.5, $J_{1,F}$ 51.1 Hz, $J_{2,F}$ 9.2 Hz; the α-D-*xylo* or β-D-*lyxo* isomer (**57**) 8%, ϕ_c +138.0, $J_{1,F}$ 50.8 Hz, $J_{2,F}$ 29 Hz and the β-D-*lyxo* or α-D-*xylo* isomer (**58**) 3%, ϕ_c +141.1, $J_{1,F}$ 50.8 Hz, $J_{2,F}$ 29 Hz.

(c) Iodobenzoylation—When "IOBz" was reacted with **37** (1.0 g) in the manner described above for the reaction with D-glucal triacetate in acetonitrile solution, a light-yellow syrup was obtained (2.1 g, 94%). It was not possible to obtain any crystalline products from this reaction and although p.m.r. showed the presence of four anomeric resonances, they could not be assigned.

[15]D-Xylal diacetate (**37**), was prepared, with the assistance of Mrs. Liane Evelyn following the procedure of Weygand (24); had m.p. 37–39°, lit. m.p. 40°, $[\alpha]_D$ −314.7°.

Note added in proof: Since the preparation of this manuscript Campbell *et al.* (25) have reported an X-ray study of the major product from their addition of "BrF" to D-glucal triacetate. On this basis they have revised their original assignment of the β-D-*manno* configuration to the, correct, α-D-*manno* configuration. Their structure of the corresponding "IF" adduct must be similarly corrected.

Acknowledgments

This work was supported by grants from the National Research Council of Canada and the National Cancer Institute of Canada. This paper was written during the tenure (by L. D. H.) of a Royal Society and Nuffield Foundation Commonwealth Bursary at the University of New South Wales, Australia; it is a pleasure to thank Professor S. J. Angyal for his generous hospitality during this period.

1. L. D. HALL, J. F. MANVILLE, and N. S. BHACCA. Can. J. Chem. **47**, 1 (1969); L. D. HALL and J. F. MANVILLE. Can. J. Chem. **47**, 19 (1969).
2. L. D. HALL and J. F. MANVILLE. Chem. Commun. 35 (1968).
3. (*a*) A. BOWERS, E. DENOT, L. C. IBANES, and R. BECERRA. J. Am. Chem. Soc. **82**, 4001 (1960); (*b*) A. BOWERS, E. DENOT, and R. BECERRA. J. Am. Chem. Soc. **82**, 4007 (1960); (*c*) A. BOWERS. J. Am. Chem. Soc. **81**, 4107 (1959).
4. F. H. DEAN, D. R. MARSHALL, E. W. WARNHOFF, and F. L. M. PATTISON. Can. J. Chem. **45**, 2279 (1967), and references therein to previous papers by F. L. M. Pattison and co-workers.
5. (*a*) P. W. KENT, F. O. ROBSON, and V. A. WELCH. J. Chem. Soc. 3273 (1963); (*b*) K. R. WOOD, P. W. KENT, and D. FISHER. J. Chem. Soc. C 912 (1966).
6. D. S. TARBELL and P. D. BARTLETT. J. Am. Chem. Soc. **58**, 466 (1936).
7. R. U. LEMIEUX and B. FRASER-REID. Can. J. Chem. **42**, 532 (1964); R. U. LEMIEUX and B. FRASER-REID. Can. J. Chem. **43**, 1460 (1965), and references therein.
8. P. B. D. DE LA MARE and R. BOLTON. Electrophilic additions to unsaturated systems. *Edited by* C. Eaborn. Elsevier Publishing Co. New York. 1966.
9. E. D. BERGMANN and I. SHAHAK. J. Chem. Soc. 1418 (1959).
10. H. SCHMIDT and H. MEINERT. Angew. Chem. **71**, 126 (1959); H. SCHMIDT and H. MEINERT. Angew. Chem. **72**, 109, 493 (1960).
11. R. H. ANDREATTA and A. V. ROBERTSON. Australian J. Chem. **19**, 161 (1966).
12. L. D. HALL, D. L. JONES, and J. F. MANVILLE. Chem. Ind. London. 1787 (1967).
13. L. D. HALL, I. JOHANSSON, and B. LINDBERG. To be published.
14. A. B. FOSTER, L. D. HALL, and R. HEMS. To be published.

Can. J. Chem. Downloaded from www.nrcresearchpress.com by 210.87.254.5 on 09/05/12
For personal use only.

15. R. U. LEMIEUX and S. LEVINE. Can. J. Chem. **40**, 1926 (1962).
16. F. MICHEEL and A. KLEMER. Advan. Carbohydrate Chem. **16**, 85 (1961), and references therein.
17. C. PEDERSEN. Acta Chem. Scand. **20**, 963 (1966), and references therein.
18. H. NAKAMURA, S. TEHIMA, and M. AKAGI. Chem. Pharm. Bull. **12**, 1302 (1964).
19. L. D. HALL and J. F. MANVILLE. Can. J. Chem. **45**, 1299 (1967).
20. C. PEDERSEN. Acta Chem. Scand. **20**, 1369 (1966).
21. (*a*) P. W. KENT and J. E. G. BARNETT. J. Chem. Soc. Supplement **2**, 6196 (1964); (*b*) P. W. KENT and M. R. FREEMAN. J. Chem. Soc. C, 910 (1966).
22. R. U. LEMIEUX. Hudson Award Address. 152nd Meeting of the American Chemical Society. New York. (1966).
23. F. L. HUMOLLER. Methods in Carbohydrate Chem. **1**, 83 (1962).
24. F. WEYGAND. Methods in Carbohydrate Chem. **1**, 182 (1962).
25. J. C. CAMPBELL, R. A. DWEK, P. W. KENT, and C. K. PROUT. Chem. Commun. 34 (1968).

Can. J. Chem. Downloaded from www.nrcresearchpress.com by 210.87.254.5 on 09/05/12
For personal use only.

Studies of specifically fluorinated carbohydrates. Part IV. Addition of the elements of "ClF" to D-glucal triacetate[1]

L. D. HALL[2] AND J. F. MANVILLE[3]

Department of Chemistry, The University of British Columbia, Vancouver 8, British Columbia

Received June 3, 1968

Reaction of chlorine with a suspension of D-glucal triacetate and silver monofluoride in an acetonitrile/benzene solution, affords a mixture of the four possible 2-chloro-2-deoxy-D-glycopyranosyl fluoride triacetates. The structures of these derivatives have been established by nuclear magnetic resonance studies and confirmed by independent syntheses. The major product is 2-chloro-2-deoxy-β-D-glucopyranosyl fluoride triacetate. These results are compared with those from the related "BrF" and "IF" additions.

Canadian Journal of Chemistry, 47, 379 (1969)

Can. J. Chem. Downloaded from www.nrcresearchpress.com by 210.87.254.42 on 09/05/12
For personal use only.

Introduction

In the previous paper of this series (2) we described the synthesis of the "BrF" and "IF" adducts of D-glucal triacetate (**1**) by several independent routes, all of which located the halogen (Br or I) at C-2 and the fluorine at C-1. We shall now discuss, as an extension of that study, the addition of the elements of "ClF" to **1**. It will be shown that the addition of this electrophile to **1** differs from that of either "BrF" or "IF" in several important details.

Results and Discussion

Reaction of D-glucal triacetate (**1**) with halogen (Br_2 or I_2) in the presence of silver fluoride resulted (2) in the formation of three of the four possible stereoisomers of the 2-deoxy-2-halo-D-glycosyl fluoride system: none of the β-D-*manno* isomer could be detected. When an acetonitrile/benzene solution of D-glucal triacetate (**1**) was stirred vigorously with silver monofluoride and chlorine gas was bubbled into the suspension, an immediate precipitation occurred. Subsequent work up of the reaction mixture afforded a syrup, which gave (^{19}F nuclear magnetic resonance-^{19}F n.m.r.) *four* separate "glycosyl fluoride" resonances; no secondary fluorine resonances (3) were discernable. This was the first time in our experience that an "XF" reaction to D-glucal triacetate (**1**) has resulted in the formation of all four diastereoisomers, the fourth being (presumably) the β-D-mannopyranosyl fluoride (**5**).

A minor component from the syrupy reaction product crystallized after several days at ca. 0°; it proved to be the α-D-mannosyl fluoride (**2**). The major component, the β-D-glucosyl fluoride (**3**) was obtained crystalline after seeding with an authentic sample made by the AgF exchange method (*vide infra*). Remaining in the mother liquors were the α-D-*gluco* (**4**) and β-D-*manno* (**5**) isomers. These were not separated, although the α-D-glucosyl fluoride (**6**) was subsequently obtained *via* the reaction of HF on the α-D-*gluco* chloro-benzoate (**7**).

The proof of structure for the three crystalline fluorides followed the general format previously described (2) for the "BrF" derivatives. Since the α-D-*mannosyl* fluoride (**2**) was not characterized by independent syntheses the n.m.r. evidence leading to its structural elucidation will be presented in some detail.

The ^{19}F resonance (ϕ_c +127.8) of this compound exhibited a *vicinal* ^{19}F–^{1}H coupling of ca. 2 Hz, which indicated a *gauche* relationship between these substituents. Also, the proton magnetic resonance (p.m.r.) spectrum (Fig. 1) indicated that this compound had the D-*manno* configuration ($J_{2,3}$ = 3.6 Hz); however, the anomeric configuration could not be determined with absolute certainty since there would necessarily be a *gauche* relationship between H-2 and both H-1 and F-1 for either the α- or β-anomers. The close similarity between the spectrum of this derivative and that obtained previously (2) for 2-bromo-2-deoxy-α-D-mannopyranosyl fluoride triacetate supported the α-configuration and consideration of the chemical shift of H-5 (τ 6.08,

[1]For a preliminary communication, see ref. (1).

[2]All correspondence should be addressed to this author.

[3]Recipient of a British Columbia Sugar Refining Co. Scholarship, 1965–1966 and a NRCC Studentship, 1966–1967. Present address: Forest Products Laboratory, N.W. Marine Drive, Vancouver 8, British Columbia.

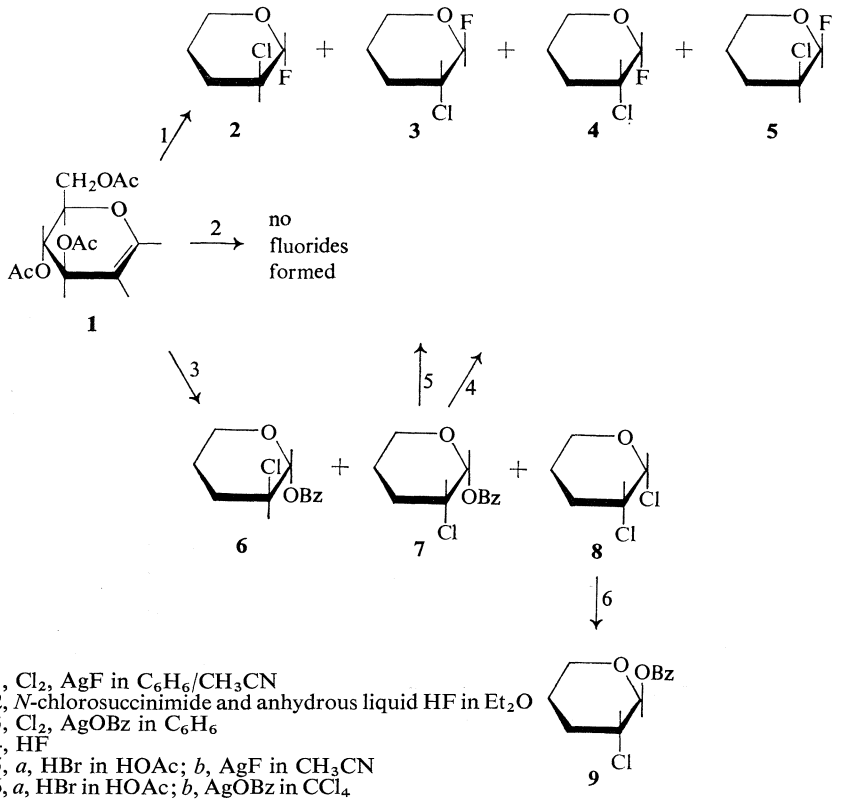

benzene-d_6) further supported the assigned α-configuration at C-1. (The shift of H-5 for the β-D-*gluco* derivative (**3**) is τ 6.53, benzene-d_6, whilst that of the α-D-*gluco* isomer (**4**) is τ 6.06, benzene-d_6.)

The p.m.r. spectrum of the α-D-*gluco* derivative (**4**) was essentially the same as that found (2) for the bromo-analogue and the observation of a large (24 Hz) *vicinal* ^{19}F–^{1}H coupling left no doubt as to its structure. Since the β-D-*gluco* derivative (**3**) is the only "XF" adduct of **1** which has this configuration and which we have obtained crystalline thus far, its p.m.r. spectrum has been included in this paper; that of the corresponding 1-benzoate (**9**) is included for comparison purposes.

The independent syntheses of some of these "ClF" adducts were planned to follow the addition of the elements of "ClOBz" to **1** with subsequent conversion of the 1-*O*-benzoyl derivatives to the corresponding glycosyl fluorides. It has previously been observed that, in contrast to either bromine or iodine, the chlorine cation adds to D-glucal triacetate to give preferentially D-*gluco* adducts; chlorine itself is reported (4, 5) to lead to greater than 80% formation of the α-D-glucosyl chloride. In accord with this generalization, the major product from the attempted addition of "ClOBz" to **1** was the α-D-*gluco* chloro-benzoate (**7**) together with, somewhat unexpectedly, the α-D-glucosyl chloride (**8**). Although small quantities of the α-D-*manno* chloro-benzoate (**6**) could be isolated, none of the *trans* β-D-*gluco* isomer (**9**) could be recovered; however, the p.m.r. spectrum of the reaction product indicated that ca. 5% of this isomer was formed. The dichloride (**8**) was found to be extremely stable with respect to reaction with AgOBz, with which it could be treated under reflux in CCl_4 solution, and recovered unchanged. In fact, it was necessary to convert **8** to the corresponding glucosyl bromide, by reaction with HBr in acetic acid, before successful conversion to the β-D-*gluco* chloro-benzoate (**9**) could be effected.

In accord with the above result from the

Can. J. Chem. Downloaded from www.nrcresearchpress.com by 210.87.254.42 on 09/05/12
For personal use only.

Can. J. Chem. Downloaded from www.nrcresearchpress.com by 210.87.254.42 on 09/05/12
For personal use only.

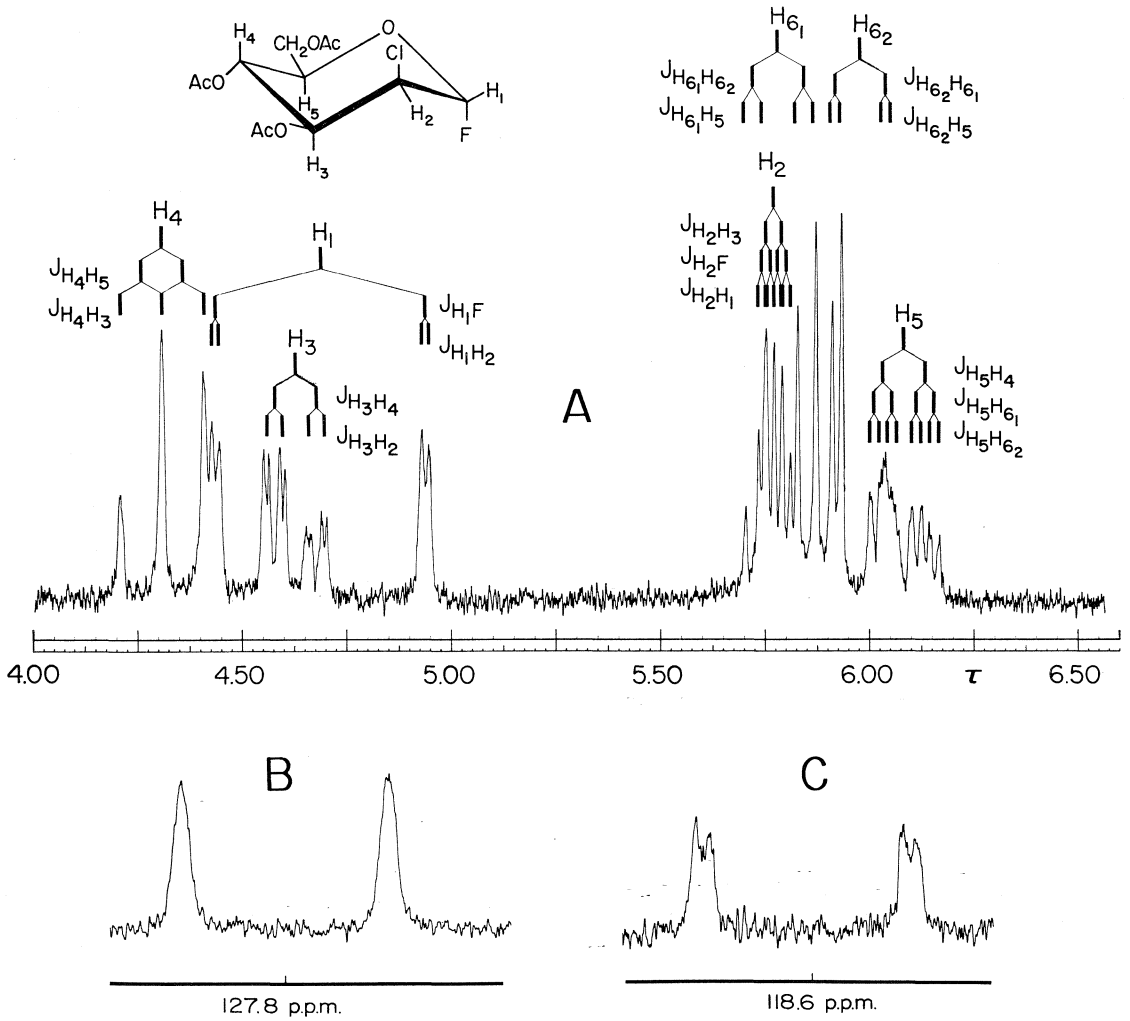

FIG. 1. (*a*) Partial 100 MHz proton magnetic resonance spectrum of 2-chloro-2-deoxy-α-D-mannopyranosyl fluoride triacetate (**2**) in benzene-d_6 solution; (*b*) ^{19}F n.m.r. spectrum of **2** in chloroform-*d* solution; (*c*) ^{19}F n.m.r. spectrum of 2-chloro-2-deoxy-β-D-mannopyranosyl fluoride triacetate (**5**) in chloroform-*d* solution.

"ClOBz" addition, reaction of **1** with "ClF" affords mainly the D-*gluco* isomers (**3**) and (**4**), and in contrast with previous experience, the major product has the β-D-*gluco* configuration. The β-D-anomer (**3**) is in fact the one expected for the *gluco*-series since *trans* addition would be expected to predominate over *cis* addition and anomerization is not generally observed for "XF" addition reactions (2). It is, therefore, most likely that the formation of the α-D-*gluco*-dichloride (**8**) (*cis* product) during reaction of **1** with Cl_2, reflects the instability of the *trans* isomer (equatorial chlorine), which anomerizes to the more stable α-anomer (axial chlorine) during the course of the chlorination reaction.

Reaction of the α-D-*gluco* chloro-benzoate (**7**) with anhydrous HF afforded as sole product material identical to that to which the α-D-glucosyl fluoride structure (**4**) had been assigned. The same chloro-benzoate (**7**) afforded the β-D-glucosyl fluoride (**3**) when reacted with HBr in acetic acid, followed by halogen exchange with silver monofluoride. This particular conversion was important since it demonstrated that a chlorine substituent at C-2 was capable of participating in C-1 halogen exchange reaction in an

Can. J. Chem. Downloaded from www.nrcresearchpress.com by 210.87.254.42 on 09/05/12
For personal use only.

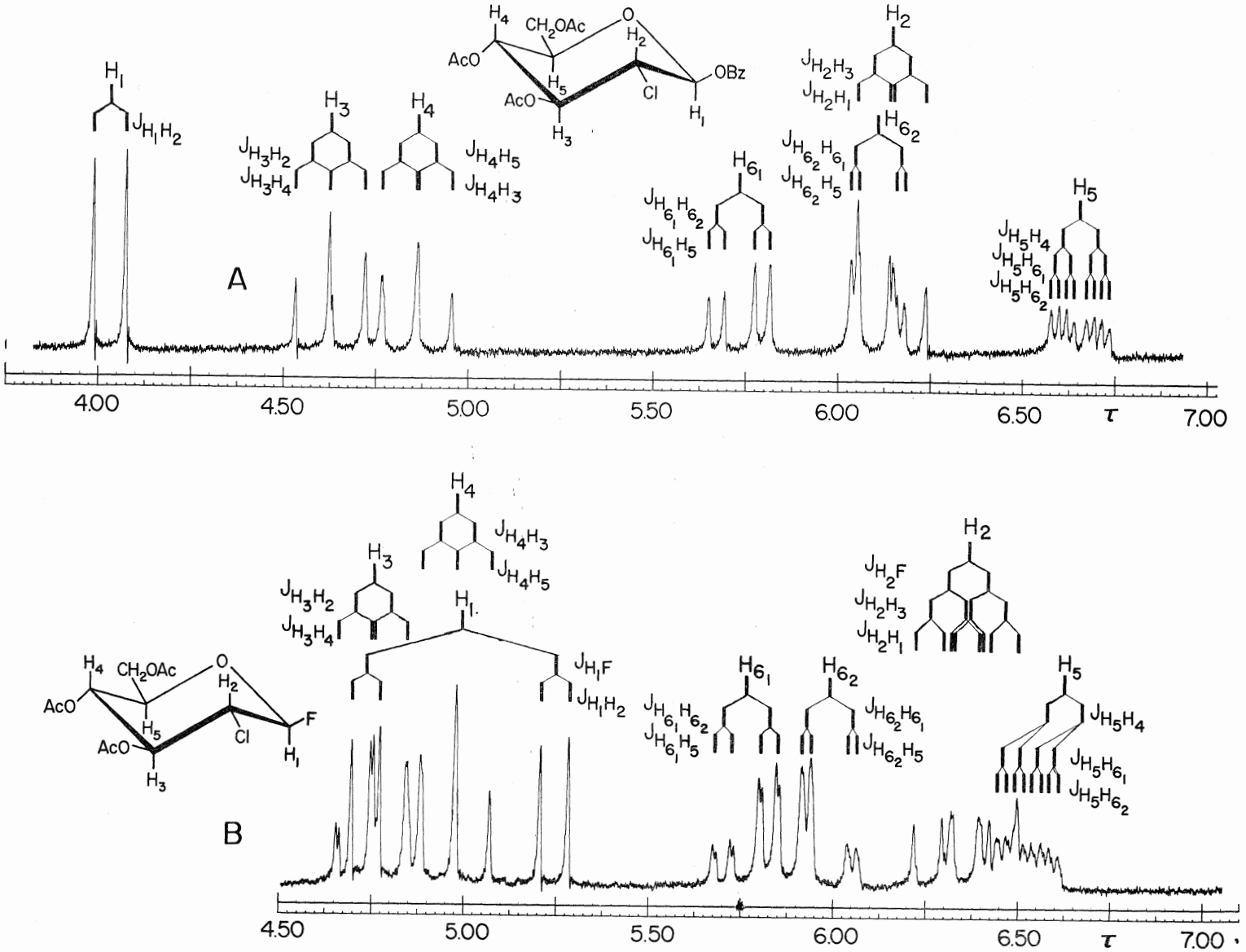

FIG. 2. Partial 100 MHz proton magnetic resonance spectra of — (*a*) 1-*O*-benzoyl-2-chloro-2-deoxy-β-D-glucopyranose triacetate (**9**) in benzene-d_6 solution; (*b*) 2-chloro-2-deoxy-β-D-glucopyranosyl fluoride triacetate (**3**) in benzene-d_6 solution.

Can. J. Chem. Downloaded from www.nrcresearchpress.com by 210.87.254.42 on 09/05/12
For personal use only.

analogous fashion to that previously established for bromine (2).

Attempts to utilize the same set of reaction sequences for the stereospecific syntheses of either of the mannosyl fluorides (**2**) or (**5**) were hindered by lack of sufficient quantities of the α-D-*manno* chloro-benzoate derivative (**6**). Nevertheless some results were obtained as follows. The mixture of products obtained from direct chlorination of **1** was dissolved in benzene: acetonitrile (2:1 v/v) and this solution shaken at room temperature with silver monofluoride. The halogen exchange reaction was observed (by ^{19}F n.m.r.) to be very slow and after 30 h at room temperature only ca. 5% of the dichlorides had been converted to the *trans* chloro-fluorides (**2**) and (**3**). Interestingly, the α-D-*manno* isomer (**2**) was formed at a much faster rate than the corresponding β-D-*gluco* isomer (**3**), in spite of the predominance of the α-D-glucosyl chloride in the original starting material. Presumably this enhanced reactivity of the mannosyl chloride reflects the fact that the C_2-halogen substituent of this derivative is *trans-diaxial* with respect to the C_1-chlorine substituent and is hence able to participate more readily in the halogen exchange reaction. Nevertheless, the overall slow rate of halogen exchange for these dichloride derivatives confirms their high chemical stability.

It is unfortunate that it was not possible to isolate a pure sample of the β-D-*manno* chloro-fluoride (**5**) since the formation of a product having this configuration, from D-glucal triacetate, has not previously been reported (4). Nevertheless we believe that the ^{19}F n.m.r. data are uniquely consistent with this configurational assignment. The small (3.6 Hz) *vicinal* ^{19}F–^{1}H coupling indicates not only that the F-1 and H-2 substituents have a *gauche* relationship but also, that either F-1 or H-2 are antiparallel to an electronegative substituent (7). This requirement could only be satisfied by a derivative having the D-*manno* configuration. The *geminal* ^{19}F–^{1}H coupling (49.4 Hz) accords with this conclusion; both the D-*gluco* isomers have geminal couplings of ca. 51 Hz.

Several interesting points were revealed during the stereospecific syntheses of the β-D-*gluco* chloro-fluoride (**3**) and chloro-benzoate (**9**). The stereospecific reaction sequence designed to produce only the β-D-glucosyl fluoride **3** from **7** resulted in a mixture consisting of three components; these were, starting material (**7**) which had not been converted into the intermediate bromide, the β-D-*gluco*-benzoate (**9**) and the anticipated β-D-*gluco*-fluoride (**3**) which was the *only glycosyl fluoride* formed. Fractional crystallization successfully separated all three components. The formation of the β-D-*gluco*-chloro-benzoate (**9**) demonstrates that the "starting" material found in the previous (2) exchanges, (X = Br) had been formed during the exchange reaction itself and was not unreacted starting material. The participation of chlorine in an AgF exchange reaction is clearly confirmed by this reaction sequence since only *trans* products were formed. It is interesting to note that Olah and co-workers have recently (6) obtained evidence for the ability of chlorine to participate in the formation of cyclic "chloronium" ions.

Attempts were made during this study to effect the addition of the elements of "ClF" to **1** using *N*-chlorosuccinimide with anhydrous liquid HF. Surprisingly, no fluorinated products could be detected (by ^{19}F n.m.r.).

The syntheses described in this paper complete the sequence of "XF" additions to **1**, for X = Cl, Br, I. The n.m.r. parameters of the derivatives synthesized in this and the previous (2) paper will be discussed in the next paper of this series.

Experimental

The general methods and nuclear magnetic resonance measurements followed the format previously described (7).

Addition of the Elements of "ClF" to ***1***

(a) Generated from Cl_2/AgF—Following closely[4] the procedure outlined previously for the addition of "BrF" from Br_2/AgF (2), an amber syrup was obtained in 91% yield which contained (^{19}F n.m.r.) all *four* isomeric "ClF" adducts. These were shown to be: 2-chloro-2-deoxy-α-D-mannopyranosyl fluoride triacetate (**2**) 16%, ϕ_c +127.8, $J_{1,F}$ 49.5 Hz; $J_{2,F}$ ca. 2 Hz; 2-chloro-2-deoxy-β-D-mannopyranosyl fluoride triacetate (**5**) 16%, ϕ_c +118.6, $J_{1,F}$ 49.4 Hz; $J_{2,F}$ 3.6 Hz; 2-chloro-2-deoxy-α-D-glucopyranosyl fluoride triacetate (**4**), 6%, ϕ_c +147.6, $J_{1,F}$ 51.2 Hz; $J_{2,F}$ 24.0 Hz; and 2-chloro-2-deoxy-β-D-glucopyranosyl fluoride triacetate (**3**) 62%, ϕ_c +138.9, $J_{1,F}$ 51.0 Hz; $J_{2,F}$ 10.6 Hz.

Over the course of several days at ca. 0°, an ethanolic solution of the reaction product precipitated the α-D-*manno* isomer (**2**) (0.17 g, 10%). Recrystallization from

[4]The only modification required was that benzene (20 ml) was added to the acetonitrile solution and the chlorine gas was bubbled into the stirred solution. Excess chlorine was subsequently removed with a stream of dry air.

aqueous ethanol afforded pure **2**; m.p. 120–121°, $[\alpha]_D^{25}$ −23.4° (*c*, 0.96, $CHCl_3$).

Anal. Calcd. for $C_{12}H_{16}O_7ClF$: C, 44.1; H, 4.9; F, 5.9. Found: C, 44.3; H, 5.1; F, 5.6.

The mother liquors, when seeded with an authentic sample of **3** yielded 0.83 g (51%) of the β-D-*gluco* isomer which when recrystallized from aqueous ethanol afforded crystalline plates; m.p. 77–78°, $[\alpha]_D^{25}$ +124° (*c*, 1.13, $CHCl_3$).

Anal. Calcd. for $C_{12}H_{16}O_7ClF$: C, 44.1; H, 4.9; F, 5.9. Found: C, 44.15; H, 5.1; F, 5.8.

The remaining compounds (**4**) and (**5**) were not obtained crystalline from this reaction.

(b) Generation from N-chlorosuccinimide and anhydrous liquid HF—The reaction of D-glucal triacetate (**1**) with anhydrous liquid HF and *N*-chlorosuccinimide did not lead to any fluorine containing material (^{19}F n.m.r.).

Addition of the Elements of "ClOBz" to 1

D-Glucal triacetate (**1**) (5.6 g) was dissolved in dry benzene (70 ml) containing silver benzoate (5.6 g) and chlorine gas was bubbled in until an excess was present as evidenced by the color of the solution. After 20 min the excess chlorine was removed by a stream of dry air. The resulting solution was filtered and successively extracted with aqueous sodium thiosulfate, aqueous sodium bicarbonate and water. The benzene solution was dried (Na_2SO_4) and evaporated to a clear syrup (8.9 g, 105%).

The reaction product was dissolved in ethanol and after standing at −5° overnight, deposited crystals (1.3 g, 15%) m.p. 150–153°. Recrystallization twice from ethanol afforded 1-*O*-benzoyl-2-chloro-2-deoxy-α-D-glucopyranose triacetate (**7**) as needles, m.p. 153–154°, $[\alpha]_D^{28}$ +195.0° (*c*, 0.50, $CHCl_3$).

Anal. Calcd. for $C_{19}H_{21}O_9Cl$: C, 53.2; H, 4.9; Cl, 8.3. Found: C, 53.3; H, 5.05; Cl, 8.25.

The mother liquors remaining after isolation of **7**, deposited light needles (0.37 g, 4.2%) of 1-*O*-benzoyl-2-chloro-2-deoxy-α-D-mannopyranose triacetate (**6**). Recrystallized from ethanol afforded pure **6**, m.p. 169–170°, $[\alpha]_D^{28}$ +79.3° (*c*, 0.52, $CHCl_3$).

Anal. Calcd. for $C_{19}H_{21}O_9Cl$: C, 53.2; H, 4.9; Cl, 8.3. Found: C, 53.0; H, 4.95; Cl, 8.4.

Proton magnetic resonance (p.m.r.) analysis showed that a major component remaining in solution was 2-chloro-2-deoxy-α-D-glucopyranosyl chloride triacetate (**8**). It was identified from comparison of its p.m.r. spectrum with that published by Lemieux and Fraser-Reid (4). No attempt was made to purify further this compound.

Stereoselective Syntheses

2-Chloro-2-Deoxy-α-D-Glucopyranosyl Fluoride Triacetate (4)

1-*O*-Benzoyl-2-chloro-2-deoxy-α-D-glucopyranose triacetate (**7**) (0.50 g) was converted to the desired fluoride (**4**) by the action of anhydrous hydrogen fluoride, (yield 0.23 g, 60%) m.p. 87–95°. Three recrystallizations from aqueous ethanol afforded needle-like crystals of the fluoride (**4**); m.p. 95–97°, $[\alpha]_D^{25}$ +203° (*c*, 1.13, $CHCl_3$).

Anal. Calcd. for $C_{12}H_{16}O_7ClF$: C, 44.1; H, 4.9; F, 5.9. Found: C, 44.05; H, 5.1; F, 5.65.

2-Chloro-2-Deoxy-β-D-Glucopyranosyl Fluoride Triacetate (3)

1-*O*-Benzoyl-2-chloro-2-deoxy-α-D-glucopyranose triacetate (**7**) (0.50 g) was converted to the corresponding bromide. Proton magnetic resonance showed that the desired bromide had formed in ca. 86% yield, and that the remainder was unreacted starting material. The crude bromide was dissolved in acetonitrile (25 ml) and silver monofluoride (1 g) was added. This mixture was shaken for ca. 20 min (until no more silver halide was precipitated). Standard work-up produced a partially crystalline product (0.38 g), which was found (by p.m.r.) to consist of three components. They were identified as starting material (**7**), the corresponding β-D-benzoate (**9**), and the desired β-D-fluoride (**3**). ^{19}F Nuclear magnetic resonance showed that only one fluoride (**3**) had formed, none of the corresponding *cis* fluoride (**4**) could be detected.

This syrupy material was dissolved in ethanol (20 ml) and cooled to ca. 5°; after 12 h the 1-*O*-benzoyl-2-chloro-2-deoxy-β-D-glucopyranose triacetate (**9**) crystallized, and was removed from solution. Recrystallization from ethanol afforded fine needles, m.p. 160–161°, $[\alpha]_D^{25}$ +35.5 (*c*, 1.46, $CHCl_3$).

Anal. Calcd. for $C_{19}H_{21}O_9Cl$: C, 53.2; H, 4.9; Cl, 8.3. Found: C, 53.1; H, 5.1; Cl, 8.1.

The mother liquors, after removal of **9**, were left a further 24 h at ca. 5°, during which time the chloro-benzoate (**7**) was precipitated. This filtrate was then diluted with petroleum ether (15 ml) and cooled to ca. −5° and after several days impure crystals of the fluoride (**4**) were obtained. These crystals were recrystallized from aqueous ethanol three times but were not obtained pure (m.p. 75–82°); p.m.r. showed that they were contaminated with chloro-benzoate (**7**). These crystals were nevertheless suitable for seeding the solution obtained from the chloro-fluorination reaction described previously.

1-O-Benzoyl-2-Chloro-2-Deoxy-β-D-Glucopyranose Triacetate (9)

D-Glucal triacetate (**1**) (1.36 g) was dissolved in 25 ml CCl_4 and cooled to 0°. Chlorine was bubbled into the solution until an excess was present; after 25 min air was passed through the solution to remove the excess chlorine. This solution was then heated under reflux for 45 min with silver benzoate (2 g). Only the dichloride starting material was observed (p.m.r. evidence).

This dichloride was then dissolved in hydrogen bromide/acetic acid (35% w/w) and left for 4 h at room temperature. Standard work-up yielded a syrup which was heated under reflux with AgOBz in CCl_4 for 1 h. The solution was filtered and concentrated. Crystals (1.50 g, 70%) were obtained which were recrystallized from aqueous ethanol. These light needles proved to be the desired benzoate (**9**); the m.p. and mixture m.p., with a sample previously obtained, were 160–161°.

The high stability of the chlorine adducts of D-glucal triacetate was further demonstrated with the following reaction. The material obtained from the chlorination of **1** was dissolved in a solution of benzene and acetonitrile (2:1 v/v) containing silver monofluoride. This chlorine exchange reaction was observed to be very slow, after 30 h at room temperature ca. 5% of the dichlorides had been converted into the *trans* chloro-fluorides (**2**) and (**3**).

Can. J. Chem. Downloaded from www.nrcresearchpress.com by 210.87.254.42 on 09/05/12
For personal use only.

Interestingly it was observed that the D-*manno* isomer(s) exchanged preferentially.

Note Added in Proof:—Since the preparation of this manuscript Igarashi *et al.* (8) have re-investigated the addition of chlorine to D-glucal triacetate (1) and have been able to obtain all four diastereoisomers. They noted that the two *cis* isomers were predominant from the chlorination of **1** in CCl_4. It was concluded, therefore, that this reaction "mainly proceeds by way of a four-centered transition state or a concerted mechanism". It is interesting to note that the major product from this reaction is the α-D-gluco isomer, whereas that from the "ClF" addition is the β-D-gluco isomer. Possibly this reflects the different nature of the intermediates in these two reactions and/or the important role played by the solvent during addition reactions of glycols.

Acknowledgments

This work was supported by grants from the National Research Council of Canada and the National Cancer Institute of Canada. This paper was written during the tenure by one of us (L. D. H.) of a Royal Society and Nuffield Foundation Commonwealth Bursary at the University of New South Wales, Australia; it is a pleasure to thank Professor Angyal for his hospitality during this period.

1. L. D. HALL and J. F. MANVILLE. Chem. Commun., 35 (1968).
2. L. D. HALL and J. F. MANVILLE. Can. J. Chem. This issue.
3. L. D. HALL, I. JOHANSSON, and B. LINBERG. To be published; A. B. FOSTER, L. D. HALL, and R. HEMS. To be published.
4. R. U. LEMIEUX and B. FRASER-REID. Can. J. Chem. **43**, 1460 (1965).
5. M. S. LEFAR and C. E. WEILL. J. Org. Chem. **30**, 954 (1965).
6. G. A. OLAH and J. M. BOLLINGER. J. Am. Chem. Soc., **89**, 4744 (1967).
7. L. D. HALL and J. F. MANVILLE. Can. J. Chem. submitted.
8. K. IGARASHI, T. HONMA, and T. IMAGAWA. Tetrahedron Letters, 755 (1968).

Can. J. Chem. Downloaded from www.nrcresearchpress.com by 210.87.254.42 on 09/05/12
For personal use only.

Aromatic oxidation by cobaltic acetate in acetic acid

KOICHIRO SAKOTA,[1] YOSHIO KAMIYA,[2] AND NOBUTO OHTA[2]
Department of Fuel Technology, Faculty of Engineering, Tokyo University, Bunkyo-ku, Tokyo, Japan
Received May 9, 1968

A detailed kinetic study of oxidation of toluene and its derivatives by cobaltic acetate in 95 vol% acetic acid is reported. The reaction was found to be profoundly affected by a steric factor and rather insensitive to the C—H bond energy. The order of reactivities of various alkylbenzenes is quite reversal to that of hydrogen abstraction reactions. The reaction was of first-order with respect to toluene, of second-order with respect to cobaltic ion and of inverse first-order with respect to cobaltous ion. The oxidation by cobaltic ion seems to proceed via an initial reversible electron transfer from toluene to cobaltic ion, yielding $(\phi CH_3)^+$ which is oxidized into benzyl acetate by another cobaltic ion. The apparent activation energy for toluene was found to be 25.3 kcal mole^{-1}, and the same activation energy was found for ethylbenzene, cumene, diphenylmethane, and triphenylmethane.

Canadian Journal of Chemistry, 47, 387 (1969)

Can. J. Chem. Downloaded from www.nrcresearchpress.com by 210.87.254.105 on 09/05/12
For personal use only.

There have been many papers discussing the mechanism of an initiation step in autoxidation. But the detailed explanation of the roles played by the transition metal ions as catalyst has not been fully given. The main role established in autoxidation is to decompose hydroperoxide (1) into radicals which can abstract hydrogen from reactants, namely via the Harber–Weiss mechanism. Recently the other roles of transition

$$M^{n+} + ROOH \rightarrow RO\cdot + OH^- + M^{n+1}$$

$$M^{n+1} + ROOH \rightarrow ROO\cdot + H^+ + M^{n+}$$

metal ions have been studied. One of them is the oxidation by higher valence state ion itself involving hydrogen abstraction.

$$M^{n+1} + RH \rightarrow M^{n+} + R\cdot + H^+$$

Bawn and Sharp explained their kinetic results on the autoxidation of benzaldehyde and acetaldehyde in terms of this hydrogen-abstraction mechanism. The overall oxidation could be appreciably accelerated by this reaction only if the reoxidation of cobaltous ion were fast. The reactions where a ligand undergoes oxidation by the central ion via electron transfer have been reported and are of much interest. The acceleration effect of methyl ethyl ketone (2) and acetaldehyde (3) on the autoxidation of *p*-toluic acid could be explained on the basis of oxidation of *p*-toluic acid by cobaltic ion. Oxidation of toluene in 50% aqueous methyl cyanide by cobaltic perchlorate (4) is reported to follow the kinetic scheme below.

$$\phi CH_3 + Co^{3+}{}_{aq} \rightarrow \phi CH_2\cdot + Co^{2+}{}_{aq} + H_3O^+$$

$$\phi CH_2\cdot + Co^{3+}{}_{aq} \rightarrow \phi CH_2OH + Co^{2+}{}_{aq} + H_3O^+$$

Here it should be mentioned that cobaltic acetate is a weak oxidant for the hydrocarbons as compared with cobaltic sulfate and cobaltic perchlorate. Oxidation of *p*-methoxy toluene by manganic acetate in glacial acetic acid (5) is reported to proceed via an electron transfer as follows.

$$ArCH_3 + Mn(OAc)_3 \rightleftarrows [(ArCH_3)^+, AcO^-] + Mn(OAc)_2$$

$$[(ArCH_3)^+, AcO^-] \rightarrow ArCH_2\cdot + AcOH$$

$$ArCH_2\cdot + Mn^{3+} \rightarrow ArCH_2{}^+ + Mn^{2+}$$

$$ArCH_2{}^+ + AcOH \rightarrow ArCH_2OAc + H^+$$

Oxidation of toluene by cobaltic acetate in acetic acid is supposed to follow the similar mechanism to that by manganic acetate. But some changes in the mechanism are expected when manganic ion is replaced with cobaltic ion because of the differences in redox potentials and so on.

It is of interest to obtain the value of the rate constant of oxidation by cobaltic acetate in acetic acid in the absence of molecular oxygen and to clarify the mechanism, because cobalt ions exhibit a strong catalysis in the autoxidation of many hydrocarbons in acetic acid.

Results and Discussion

Kinetic studies were carried out on toluene and its derivatives mainly at 40 °C in 95% acetic

[1]Present address: Products Development Institute, Teijin Limited, 2-1-Hinode-cho, Iwakuni-City, Yamaguchi-Pref., Japan.
[2]Authors to whom inquiries should be addressed.

Can. J. Chem. Downloaded from www.nrcresearchpress.com by 210.87.254.105 on 09/05/12
For personal use only.

acid solution. Oxygen was carefully excluded and every run was made under purified argon atmosphere, because hydrocarbons are easily autoxidized under the conditions employed here. The reactions were followed by potentiometric titration of cobaltic acetate and cobaltous acetate separately. The reactions were carried out under conditions where the concentration change of hydrocarbons is substantially small in comparison with the initial concentration. The plots of concentration of cobaltic ion against reaction time gave no simple relations. However, a function was found which established a satisfactory linear relation against reaction time. It is convenient at this point to introduce the symbols used here. They are as follows: x, a, y, Θ and t are the concentrations of cobaltic acetate, of cobaltic acetate plus cobaltous acetate, of hydrocarbon to be oxidized (in M), the portion of cobaltic acetate to the total concentration of cobalt ions, and reaction time (in min), respectively. A typical plot of Θ vs. t as well as the plot of $1/\Theta + \log \Theta$ vs. t are shown in Fig. 1. The latter plot of $1/\Theta + \log \Theta$ gave a satisfactory straight line. Therefore,

$$[1] \qquad 1/\Theta + \log \Theta = kt + \text{constant},$$

where k is the slope of the line.

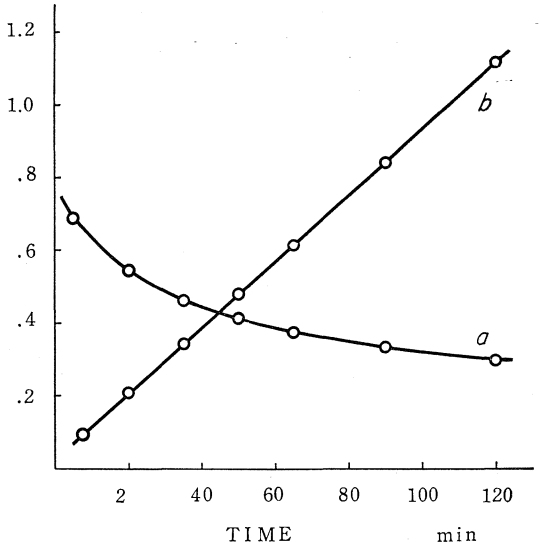

FIG. 1. A typical kinetic run, plots of Θ and $1/\Theta + \log \Theta$ vs. t at 40 °C, $[\phi CH_3] = 1.88$ mole l^{-1}, [cobalt] = $2 \cdot 10^{-2}$ mole l^{-1}; $a : \Theta$; $b : 1/\Theta + \log \Theta$.

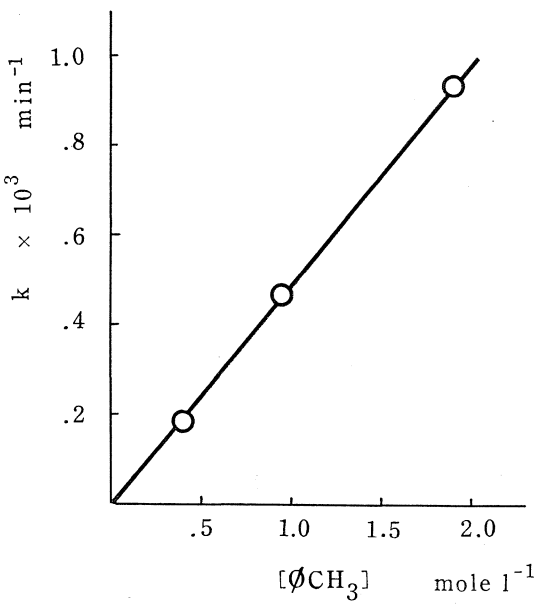

FIG. 2. Plots of k vs. initial concentrations of toluene.

Taking the derivative of both sides of eq. [1], we get

$$[2] \qquad -d\Theta/dt = k \cdot \Theta^2 \cdot (1-\Theta)^{-1}$$

Since $x = a \cdot \Theta$,

$$[3] \qquad -dx/dt = k \cdot x^2 \cdot (a-x)^{-1}$$

In other words, the oxidation by cobaltic acetate was found to follow the kinetic law below.

$$[4] \quad -d[Co^{3+}]/dt = k \cdot [Co^{3+}]^2 \cdot [Co^{2+}]^{-1}$$

k which was established as the slope of the line was found to be proportional to the initial concentration of toluene as shown in Fig. 2. Using these results, we get

$$[5] \quad -d[Co^{3+}]/dt = k_{obs} \cdot [\phi CH_3] \cdot [Co^{3+}]^2 \cdot [Co^{2+}]^{-1},$$

where $k = k_{obs} \cdot [\phi CH_3]$.

The stoichiometry of this reaction was found as follows.

$$\phi CH_3 + 2\ Co^{3+} \rightarrow \phi CH_2OAc + 2\ Co^{2+} + AcOH$$

The integral of both sides of eq. [5] with the value of two for dx/dy $(= d[Co^{3+}]/d[\phi CH_3])$ gives,

Can. J. Chem. Downloaded from www.nrcresearchpress.com by 210.87.254.105 on 09/05/12
For personal use only.

[6] $a/((2b - a)x) + 2b/(2b - a)^2 \cdot \log x/(x - a + 2b) = k_{obs} \cdot t/2 + \text{constant}$,

where b is equal to y at time $t = 0$.

When the assumption $b \gg a$ and $b \gg x$, is satisfied, eq. [6] can be simply expressed as eq. [7].

[7] $a/x + \log x = b \cdot k_{obs} \cdot t + \text{constant}$

Since $x = a \cdot \Theta$, eq. [7] is equivalent to eq. [1]. Under the conditions where the assumption $b \gg a$ and $b \gg x$ is not satisfied, k_{obs}'s was established from eq. [6] using an Okitac computer. The oxidation of *p*-methoxytoluene by manganic acetate in acetic acid has been reported (5) to follow the kinetic law [8],

[8] $-\mathrm{d}[Mn^{3+}]/\mathrm{d}t = k' \cdot [CH_3O—C_6H_4CH_3] \cdot [Mn^{3+}] \cdot [Mn^{2+}]^{-1}$

By using Θ and with the assumption of $b \gg a$ and $b \gg x$, eq. [8] is rewritten as follows:

[9] $\Theta + \log 1/\Theta = (b \cdot k'/a) \cdot t + \text{constant}$

If this reaction does follow the kinetic law [8], the slope of the line, k $(=b \cdot k'/a)$ established by the plot of $(\Theta + \log 1/\Theta)$ vs. t must be inversely proportional to the total concentration of cobalt ions. And k_{obs} $(=k/b)$ must also be of the same dependence as k. If the reaction follows the kinetic law [5], the slope of the line, k and k_{obs} $(=k/b)$ must be independent of the total concentration of cobalt ions. It is convenient to mention at this point that the functions $(1/\Theta + \log \Theta)$ and $(\Theta + \log 1/\Theta)$ behave similarly to each other according to the change of Θ. The expansions of both functions in terms of α are:

$$1/\Theta + \log \Theta = 1 + 1/2\,\alpha^2 + 2/3\,\alpha^3$$

$$\Theta + \log 1/\Theta = 1 + 1/2\,\alpha^2 + 1/3\,\alpha^3,$$

where $\alpha = 1 - \Theta$.

These expansions suggest that it is not only necessary to carry out the runs to the extent where the decrease in Θ is large enough, but also to examine the dependence of k_{obs} (or k) on the total concentration of cobalt ions in order to determine which law is obeyed in this reaction, eq. [1] or eq. [9]. Figure 3 shows a plot of k_{obs} against the total concentration of cobalt ions (line *a*). Here again a linear plot was obtained, implying that the kinetic law [1] is operative. But the line had a small negative slope and was not completely independent of the total concentration of cobalt ions. This may be easily explained in terms of a cobalt monomer–dimer equilibrium (6), i.e., $2\,M \overset{K}{\rightleftarrows} D$, where only the monomeric species being active (7) in this reaction. It is also known that cobaltous ion has little tendency to form polymeric species contrary to cobaltic ion. The concentration of monomeric cobaltic ion is equal to $(\sqrt{1 + 8Kx} - 1)/4K$, where K is the equilibrium constant. Substitution of this term into eq. [5] and taking the integral of the equation result in eq. [10].

[10] $(1 + 8Kx)/4 + (1 + 8kx)^{1/2} + (1 - 4Kx)((1 + 8Kx)^{1/2} - 1) = k_{obs} \cdot b \cdot t$

The rate constants corrected in terms of a monomer–dimer equilibrium are obtained using eq. [10] with the aid of a computer using a method of least squares. The employed value of K was 0.3 M^{-1}. The plot of these corrected constants gives a linear line parallel to an abscissa, in Fig. 3 (line *b*). When hydrocarbons are absent, the decrease of the concentration of cobaltic ion in acetic acid solution was not observed under the reaction conditions employed here. Then the reactions where water or acetic acid is oxidized to yield hydroxy or alkyl radicals need not be considered. The outstanding point is that rates are inversely proportional to the concentration of cobaltous ion as was shown in eq. [5]. This inverse dependence is easily explained when a reversible step is assumed. Only the electron transfer below can readily explain a reversible step.

[11] $\phi CH_3 + Co^{3+} \rightleftarrows (\phi CH_3)^+ + Co^{2+}$

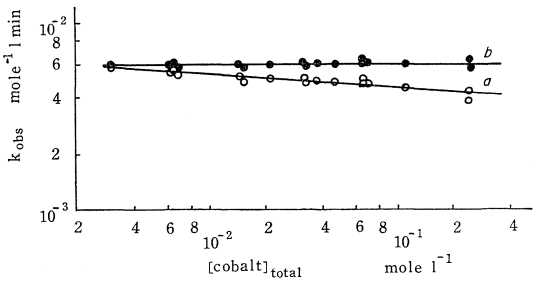

FIG. 3. Dependence of rate constant on the total concentration of cobalt ions.

Can. J. Chem. Downloaded from www.nrcresearchpress.com by 210.87.254.105 on 09/05/12
For personal use only.

The further fate of the incipient ion, ϕCH_3^+ is the next question. The incipient ion may either undergo self-decomposition into a benzyl radical and a proton or react with cobaltic ion when the life time of toluene ion is long enough. It is determined by the degree of the stability of toluene ion and the oxidizing power of cobaltic ion in acetic acid. The second-order dependence on the concentration of cobaltic acetate supports the reaction path below. A disproportionation step is not

$$[12]\quad \phi CH_3^+ + Co^{3+} \rightarrow \phi CH_2OAc + Co^{2+}$$

probable, since the existence of Co^{4+} ion in this reaction is vague and its participation is still more unlikely.

Kinetic studies led to the formulation of the reaction as initial electron transfer from toluene to cobaltic ion to give the toluene cation. Toluene cations then react with cobaltic ion to give benzyl acetate. The tentative mechanism which is consistent with the experimental results is as follows:

$$[13]\quad Co^{3+}(AcO)_3 + \phi CH_3 \rightleftarrows Co^{2+}(AcO)_2 + [(\phi CH_3)^+, AcO^-]$$

$$[14]\quad [(\phi CH_3)^+, AcO^-] + Co^{3+}(AcO)_3 \xrightarrow{k_2} \phi CH_2OAc + Co^{2+}(AcO)_2 + AcOH$$

This will lead to the kinetic expression below.

$$[15]\quad -d[Co^{3+}]/dt = 2k_1k_2[\phi CH_3] \cdot [Co^{3+}]^2/(k_{-1}[Co^{2+}] + k_2[Co^{3+}])$$

When the electron transfer step is rate-determining, $k_1[Co^{3+}]\cdot[\phi CH_3]$ is smaller than $k_2[(\phi CH_3)^+, AcO^-]\cdot[Co^{3+}]$. When $k_2[(\phi CH_3)^+, AcO^-]\cdot[Co^{3+}]$ is much smaller than $k_{-1}[(\phi CH_3)^+]\cdot[Co^{2+}]$, then we obtain eq. [16] from eq. [15],

$$[16]\quad -d[Co^{3+}]/dt = 2k_1k_2k_{-1}^{-1}[\phi CH_3]\cdot[Co^{3+}]^2\cdot[Co^{2+}]^{-1},$$

which is identical with eq. [5].

Rate constants were estimated by means of the Hammett relationship (Fig. 4). The ρ value obtained vs. σ^+ was −0.7. Negative value of ρ shows that electron withdrawing substituents retard the reaction in agreement with the oxidation of substituted toluenes by organic and halogen radicals. The ρ values for abstraction of benzylic hydrogen atoms by trichloromethyl (8), *t*-butoxy (9), *p*-chlorobenzoylperoxy (10), and bromine (11) radicals are reported to be −1.46, −0.68, −1.668, and −1.38, respectively. Although the ρ of −0.7 does not exclude the possibility that the C—H bond rupture (hydrogen or hydride abstraction) is rate-determining (k_2), it is very easily explained when the electron transfer step (k_1) is rate-determining. When the C—H bond rupture process is the rate-determining step, the reaction has a large negative value of ρ and depends strongly on the C—H bond energy. And the order of the rate constants also holds as tertiary hydrogen > secondary hydrogen > primary hydrogen. The Arrhenius plot for oxidation by cobaltic ion is shown in Fig. 5. The same apparent activation energies (25.3 kcal/mole) were found for toluene, ethylbenzene, cumene, diphenylmethane, and triphenylmethane. The effect of the strength of the bond being broken on the rate is summarized in Table I. The order of relative reactivities per active hydrogen was found to be reversal to that of the C—H bond energy. The replacement of hydrogen atoms in a side chain of toluene with a methyl or a phenyl group did not change the apparent activation energy. But the rate constant was profoundly affected in an inverse way to the cases of oxidation by radicals. These results are not explicable in terms of the C—H bond rupture process, but support that the electron transfer process is rate-determining. The C—H bond is considered to be scarcely elongated in the rate-

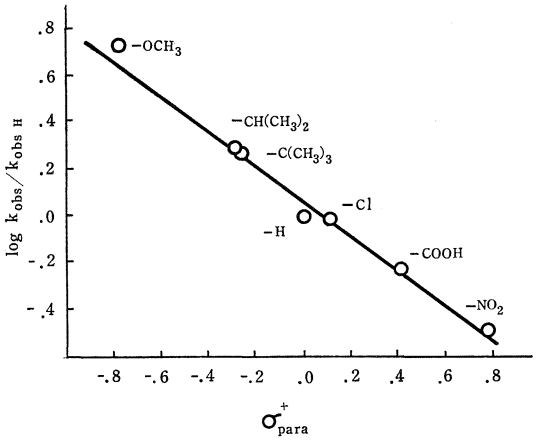

FIG. 4. Substituent effect in oxidation of toluene by cobaltic acetate at 40 °C.

TABLE I

Relative reactivities (per active hydrogen) of aromatics toward cobaltic acetate at 40 °C and some radicals

Hydrocarbons	Co^{3+}	$\phi(CH_3)_2COO\cdot$(12)	t-BuO·(13)	$CCl_3\cdot$(14)	Br·(14)
ϕ-CH_3	1.0	1.0	1.0	1.0	1.0
$\phi(CH_3)CH_2$	1.2	18	3.2	29	11
$\phi(CH_3)_2CH$	0.20	30	6.8	72	12
ϕ_2-CH_2	0.80		4.7		7
ϕ_3-CH	0.70*		9.6		5.5

*Solvent: AcOH/ϕH = 1 (v/v).
NOTE: Only benzylic hydrogens are considered labile.

determining step. And the distortion which reduces the internal rotations of hydrocarbon is a main factor in that step. The difference in reactivities toward cobaltic acetate may be ascribed to that of the entropy decrease of the hydrocarbon in the transition state. If hydrogen atom in methyl group of toluene is replaced by a group with many more internal degrees of freedom, the activation process will also be accompanied by a greater loss of internal motions. This results in unfavorable decrease of activation entropy, which explains, for example, fivefold decrease in the rate of cumene relative to toluene. Hydrogen abstraction from cumene by cumylperoxy radical proceeds thirty times faster than that from toluene in contrast to this oxidation by cobaltic ion. The reaction [12] may be expressed more adequately as follows:

$$[(\phi CH_3)^+, AcO^-] + Co^{3+}(AcO)_3$$
$$\rightarrow [[(\phi CH_3)^+ + OAc^-] \leftrightarrow$$
$$[(\phi CH_2\cdot) + HOAc]] + Co^{3+}(AcO)_3$$
$$\rightarrow [(\phi CH_2\cdot) + Co^{3+} + HOAc]$$
$$\rightarrow \phi CH_2OAc + Co^{2+}(OAc)_2 + AcOH$$

If the above is accepted as a proper interpretation of the course of the reaction [12], let us turn to the problem concerning the initiation mechanism of autoxidation tentatively proposed as follows:

$$RH + Co^{3+} \rightarrow R\cdot + Co^{2+} + H^+$$

When a sufficient amount of molecular oxygen is present, benzylperoxy radical which can initiate the chain of autoxidation can possibly be expected to be produced instead of (or together with) benzyl acetate in this reaction.

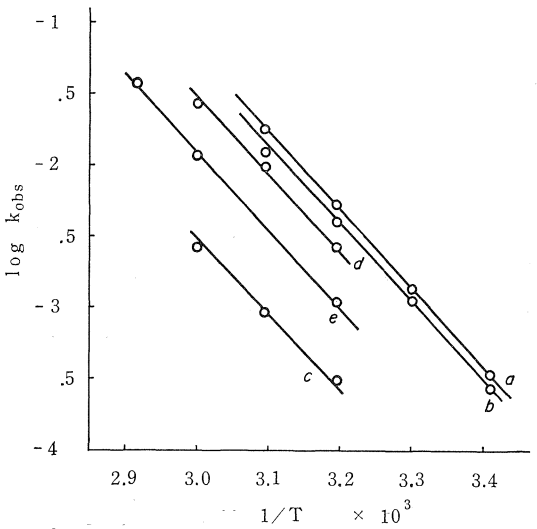

FIG. 5. Effect of temperature on rate of consumption of cobaltic acetate; *A* : toluene; *b* : ethylbenzene; *c* : cumene; *d* : diphenylmethane; *e* : triphenylmethane (solvent : AcOH/ϕH = 1 (v/v)).

Experimental

Analytical Method

The concentration of cobaltic acetate was determined by potentiometric titration (7). A known volume of the solution was added to a 1 *M* sulfuric acid solution containing a known excess of standard ferrous ammonium sulfate. After standing until the initial green color disappeared (ca. 5 min), the solution was back-titrated with standard ceric sulfate solution. Titration curves were obtained with the aid of a Yokogawa "PKH-11A" pH meter. A procedure for cobaltous acetate (15) was also a potentiometric one. Cobaltous acetate was oxidized in an ammoniacal solution containing ammonium citrate with potassium ferricyanide. The excess potassium ferricyanide was back-titrated with standard cobaltous acetate solution. Other methods, such as polarography and potentiometric titration with EDTA did not give satisfactory results.

Materials

The preparations of cobaltic acetate and perchlorate

Can. J. Chem. Downloaded from www.nrcresearchpress.com by 210.87.254.105 on 09/05/12
For personal use only.

have been reported by many authors. In the case of acetic acid solution there are two ways to avoid the difficulties caused by low electric conductivity. One is to add electrolyte, such as sodium acetate and the other is to use acetic acid – water solution as solvent. We adopted 95 vol% acetic acid solution. This amount of water did not disturb elucidation of the mechanism of oxidation by cobaltic acetate. And cobaltic acetate was found to be stable enough to carry out the reaction in this solution. Anodic oxidation was used for the preparation of the cobaltic acetate at room temperature at ca. 10 V. The electrolysis cell was made of polyethylene and separated into two rooms with an ion exchange film "Selemion CMV" made by Asahi Glass Co., one with a platinum electrode and another with a stainless steel electrode.

Procedure

The reaction vessel is a ca. 60 ml glass flask with two necks, one at the top and another at the side of the flask. The vessel was connected through a Tygon tube to a vacuum line and an argon reservoir. The solution was de-gassed as usual and the vessel was filled with purified argon. After thermal equilibrium had been attained, samples of the solution were withdrawn through a side neck at appropriate intervals with a current of purified argon. The volume of each sample was 5 ml. Determination of cobaltic and cobaltous acetate was carried out by potentiometric titration.

1. R. B. MESROBIAN. J. Am. Chem. Soc. **75**, 6189 (1953); A. S. HAY, and H. S. BLANCHARD. Can. J. Chem. **43**, 1306 (1953); Y. KAMIYA, S. BEATON, A. LAFORTUNE, and K. U. INGOLD. Can. J. Chem. **41**, 2020, 2034 (1963); Y. KAMIYA, and K. U. INGOLD. Can. J. Chem. **43**, 1306 (1965).
2. E. F. BRILL. Ind. Eng. Chem. **52**, 837 (1960).
3. U.S. Patent No. 2,673,217 to Eastman Kodak Company (March 23, 1954).
4. T. A. COOPER, A. A. CLIFFORD, D. J. MILLS, and W. A. WATERS. J. Chem. Soc. 793, 1966.
5. P. J. ANDRULIS, M. J. S. DEWAR, R. DIETS, and R. L. HUNT. J. Am. Chem. Soc. **88**, 5473 (1966).
6. J. H. BAXENDALE and C. F. WELLS. Trans. Faraday Soc. **53**, 800 (1957).
7. MICHAEL ANBAR and ISRAEL PECHT. J. Am. Chem. Soc. **89**, 2553 (1967); E. KOUBEK and J. O. EDWARDS. J. Inorg. Nucl. Chem. **25**, 1401 (1963).
8. E. S. HUYSER. J. Am. Chem. Soc. **82**, 291 (1960).
9. B. R. KENNEDY, and K. U. INGOLD. Can. J. Chem. **44**, 2381 (1966).
10. C. WALLING, and E. A. MCELHILL. J. Am. Chem. Soc. **73**, 2927 (1951).
11. C. WALLING, A. L. RIEGER, and D. TANNER. J. Am. Chem. Soc. **85**, 3129 (1963).
12. J. A. HOWARD, W. J. SCHWALM, and K. U. INGOLD. International Oxidation Symposium, San Francisco, California. August, 1967
13. C. WALLING and V. STANNETT. J. Am. Chem. Soc. **82**, 6108 (1960).
14. G. A. RUSSELL, C. DEBOER, and K. M. DESMOND. J. Am. Chem. Soc. **85**, 365 (1963).
15. W. W. SCOTT. Standard methods of analysis. D. van Nostrand, Co., Inc., New York. (1962).

Can. J. Chem. Downloaded from www.nrcresearchpress.com by 210.87.254.105 on 09/05/12
For personal use only.

Some aspects of the formation of hex-2-enopyranosides from methyl 2,3-di-*O*-methanesulfonyl-α-D-glucopyranosides

BERT FRASER-REID[1] AND (MRS.) BAHYA BOCTOR
Chemistry Department, University of Waterloo, Waterloo, Ontario
Received August 6, 1968

The elimination of vicinal sulfonyloxy groups from methyl 2,3-di-*O*-methanesulfonyl-α-D-glucopyranosides with the formation of hex-2-enopyranosides using potassium iodide, and zinc in refluxing dry dimethyl formamide has been investigated. The specific use of a zinc–copper couple has been found to be highly advantageous to the yield and reproducibility of the reaction, and the elimination proceeds successfully whether acid or base labile groups are present at carbon-4 or -6. Both the 4,6-di-*O*-benzoyl (**3***b*) and the 6-*O*-benzoyl (**3***d*) precursors give methyl 6-*O*-benzoyl-α-D-*erythro*-hex-2-enopyranoside (**4***d*) as the major product, the latter also being obtainable by selective benzoylation of methyl α-D-*erythro*-hex-2-enopyranoside (**4***c*). The reaction of the dibenzoate therefore occurs with some deacylation at carbon-4, but it is noteworthy that this is not accompanied by any epimerization. A similar pattern of reaction apparently occurs with the 4,6-di-*O*-acetyl derivative (**3***a*). The conformations of the starting di-*O*-methanesulfonyl esters are discussed and suggestions for the n.m.r. assignments of the groups are made.

Canadian Journal of Chemistry, 47, 393 (1969)

Can. J. Chem. Downloaded from www.nrcresearchpress.com by 210.87.254.6 on 09/05/12
For personal use only.

For certain projects underway in this laboratory it is necessary to have available in fairly large quantities various substituted methyl hex-2- or hex-3-enopyranosides. These compounds are of interest because of their possible biological significance (1), and because of their projected utility for the synthesis of "rare and modified" sugars (2) as well as higher saccharides (3). Of the two classes of olefins, the hex-2-enopyranosides such as **4** are better known, having been first prepared over 30 years ago (4).

At the time this work was undertaken the main routes to the hex-2-enopyranosides were (*a*) the high temperature reaction of alcohols with acylated glycals which proceeds with concomitant rearrangement of the double bond and displacement of the carbon-3 function (5, 6) and (*b*) the elimination of vicinal sulfonyloxy groups by potassium ethyl xanthate (7). We considered it desirable to have a method of preparation applicable to a wide variety of substrates. The elimination method (*b*) cannot be utilized for the preparation of **4***a*, for example, because when the compound **3***a* was treated for 1 h with xanthate, the recovered material had undergone extensive decomposition including the loss of the glucosidic methoxyl group, and contained none of the desired olefin. On the other hand the high temperature rearrangement (5, 6) gives mixtures of anomers,[2] and since acid is liberated during the reaction, the method might prove inapplicable in the presence of acid sensitive groups. Moreover, this method may not be adaptable to the synthesis of the hex-3-enopyranosides of interest to us. Recently Lemieux, Fraga, and Watanabe (1) developed a third synthetic route to compounds such as **2** which involves the conversion of an epoxide to the iodohydrin, and treatment of the latter with a sulfonyl chloride, whereupon rapid elimination of the iodo- and sulfonyloxy-groups occurs. Since this sequence begins with an epoxide, this method would not be applicable to the formation of olefins such as **4***a* or **4***b*, in which the possibility of oxide ring migration could occur in the precursor (8, 9).

The olefin-forming reaction of Corey and Winter (10) which has been successfully used for the formation of **2** from methyl 4,6-*O*-benzylidene-α-D-mannopyranoside-2,3-thionocarbonate appears promising, but the prohibitive cost[3] of methyl α-D-mannopyranoside places this procedure beyond our economic resources for large

[1]All correspondence should be addressed to this author.

[2]A recent communication (3) indicates that conditions have been found for enhancing the stereospecificity and yield of these reactions for the preparation of compounds such as **4***a*.

[3]Rare Chemicals, K & K Laboratories, Plainview, New York.

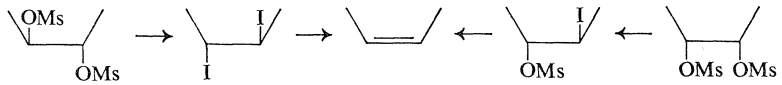

SCHEME 1

scale preparations. The related 2,3-*trans* thionocarbonate has recently been synthesized (11)[4] from less expensive α-D-glucoside precursors, but the stereospecificity of the Corey reaction makes it impossible for such a compound to furnish the olefin **2**.

The elimination of vicinal sulfonyloxy groups first reported by Tipson and Cohen (12) seemed to have none of the disadvantages cited above. This reaction, employing zinc dust and sodium iodide in refluxing dimethyl formamide, was used successfully with 3,4-disulfonate esters of 1,2:5,6-di-*O*-isopropylidene-D-mannitol. Furthermore, results on *cis* and *trans* 1,2-ditosyloxycyclohexane (13) suggested that this method might apply whether the vicinal sulfonyloxy groups existed in a *cis* or *trans* relationship. If *trans*, both groups might be replaced to give the *trans* diiodide which would rapidly form olefin (14). If *cis*, replacement of one group would give a *trans* iodomesylate which according to Cristol *et al.* (15), Newth (16), and Lemieux *et al.* (1), should also readily undergo elimination to the olefin. Of additional importance is the observation of Kochi and Singleton (17) that the solvent used in this reaction, dimethyl formamide, is particularly effective for promoting certain reductive eliminations. We now report on the use of this method for the synthesis of some hex-2-enopyranosides.

The conversion of **1** to **2** was chosen for preliminary investigation since **1** is readily available (18) and **2** has been well characterized (7, 19). A cursory study of this transformation has been reported (7) but in view of our desire to develop a method capable of relatively large scale operation[5] we pursued the investigation further. The reaction could be monitored conveniently by observing the nuclear magnetic resonance (n.m.r.) changes for the glycosidic methoxyl and the methanesulfonyl groups.

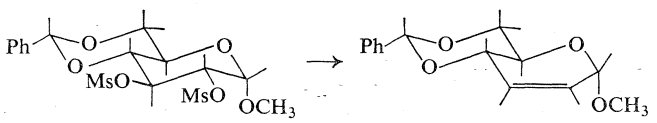

1 **2**

Since a product of the reaction is the Lewis acid zinc iodide, it is desirable to exclude water which would otherwise hydrolyze the reactive glycosidic group. Use of potassium iodide tended to improve the rate and yield of the reaction, in spite of the greater solubility (20) in organic solvents of the generally used sodium salt (7, 12, 21). Of additional significance to us is the fact that the potassium salt is less expensive (22).

In our early work, the results were very dependent upon the zinc used, and were generally erratic and unreproducible. Use of zinc–copper couple caused a remarkable improvement, and also enhanced the yield and rate of reaction. Initially the compound, **1**, potassium iodide and zinc–copper couple were used in the mole ratio 1:10:10 and the reaction proceeded to completion in 10 h, but reduction of the ratio to 1:10:5 and then to 1:5:5 did not alter the rate or the yield of the reaction. However, a further reduction to 1:2.5:5 did diminish the rate, and hence a ratio of 1:5:5 was adopted. Reasonably pure material (**2**) was isolated in about 30% yield from these large scale preparations without resorting to chromatographic fractionations (cf. 7).

[4]We are grateful to Dr. Stout for providing us with a sample of this material and for making this information available prior to its publication.

[5]If the published reaction conditions (7) were adopted, the "large scale preparation" reported below would require 3000 g of sodium iodide, 1400 g of zinc, and 5000 ml of dimethyl formamide.

Can. J. Chem. Downloaded from www.nrcresearchpress.com by 210.87.254.6 on 09/05/12
For personal use only.

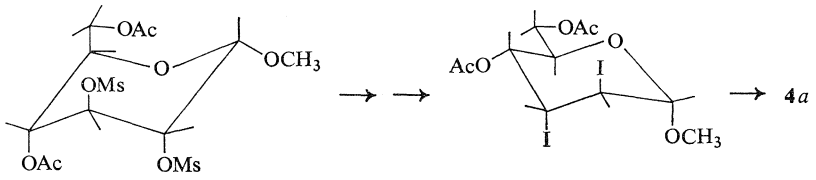

SCHEME 2

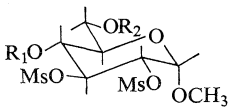

3

a, $R_1 = R_2 = CH_3CO$
b, $R_1 = R_2 = C_6H_5CO$
c, $R_1 = R_2 = H$
d, $R_1 = H$ $R_2 = C_6H_5CO$

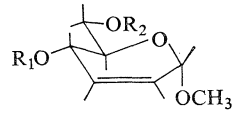

4

a, $R_1 = R_2 = CH_3CO$
b, $R_1 = R_2 = C_6H_5CO$
c, $R_1 = R_2 = H$
d, $R_1 = H$ $R_2 = C_6H_5CO$
e, $R_1 = H$ $R_2 = CH_3CO$

Having established the general experimental procedure, we turned our attention to the diacyl derivatives **3***a* and **3***b*, readily available from **1** *via* **3***c* by conventional methods. The diacetate **3***a* underwent elimination in one-seventh the time required by **1**, presumably because the *trans*-fused benzylidene ring of **1** restricts the facility with which the equatorial sulfonyloxy groups are displaced. This constraint is absent in **3***a* and the compound may react from the unfavorable 1C conformation (Scheme 2), in which the sulfonyloxy groups, now diaxially oriented, are well disposed for displacement by iodide ion. This effect is also in evidence in eliminations of the dibenzoate, **3***b*, and monobenzoate, **3***d*, which require reaction periods of $2\frac{1}{2}$ h and 1 h, respectively. Judging from the color change in the reaction, the diol **3***c* seems to achieve elimination within 10 min.

Elimination from the diacetyl derivative **3***a* gave a product containing two hex-2-enopyranosides of R_f 0.50 ("**A**") and 0.43 ("**B**") on thin-layer chromatograms. The adverse n.m.r. ratio of methoxyl to acetoxyl protons (1:1.6), the presence of a n.m.r. signal removable by exchange with D_2O, and infrared evidence, indicated that some deacetylation had occurred. Reacetylation converted the slower moving component, "**B**", into the faster "**A**", while deacetylation gave a new hex-2-enopyranoside, "**C**". "**A**" was identified as the olefinic diacetate **4***a* (5) and "**C**" as the corresponding diol **4***c*. Prolonged reaction resulted in complete deacetylation, but the diol **4***c* accumulated in the aqueous phase during work-up and could not be conveniently recovered therefrom. Thus, the preferred route to **4***c* is *via* deacylation of **4***a* or **4***b* and not by elimination from **3***c* (see Experimental).

It was of interest to determine whether the acyl group was being lost from carbon-4 or carbon-6, assuming that deacetylation was initiated by dimethylamine produced upon thermal decomposition of dimethyl formamide (23). Because debenzoylation is a slower process than deacetylation[6] the dibenzoate was subjected to elimination for $2\frac{1}{2}$ h. The major product was a non-crystalline monobenzoyl olefin, which could also be derived by selective benzoylation of the diol **4***c*. Partial acylation customarily occurs at the primary hydroxyl group (24) in pyranosides such as **3***c*, but it was feared that the allylic hydroxyl group of **4***c* might possess abnormally high reactivity towards benzoyl chloride. Conclusive evidence that this was not the case was obtained since the 6-*O*-monobenzoyl derivative **3***d* underwent elimination to give the same olefin as that obtained in the two processes detailed above. It is to be noted that acyl groups preferentially migrate from a secondary to a primary hydroxyl group (8), and although the secondary hydroxyl group involved here is allylic, it was hoped that the

[6]Using the triethylamine – methanol – water system, de-esterification of **4***a* is complete in 1 h, while **4***b* requires upwards of 7 h (see Experimental).

Can. J. Chem. Downloaded from www.nrcresearchpress.com by 210.87.254.6 on 09/05/12
For personal use only.

Can. J. Chem. Downloaded from www.nrcresearchpress.com by 210.87.254.6 on 09/05/12
For personal use only.

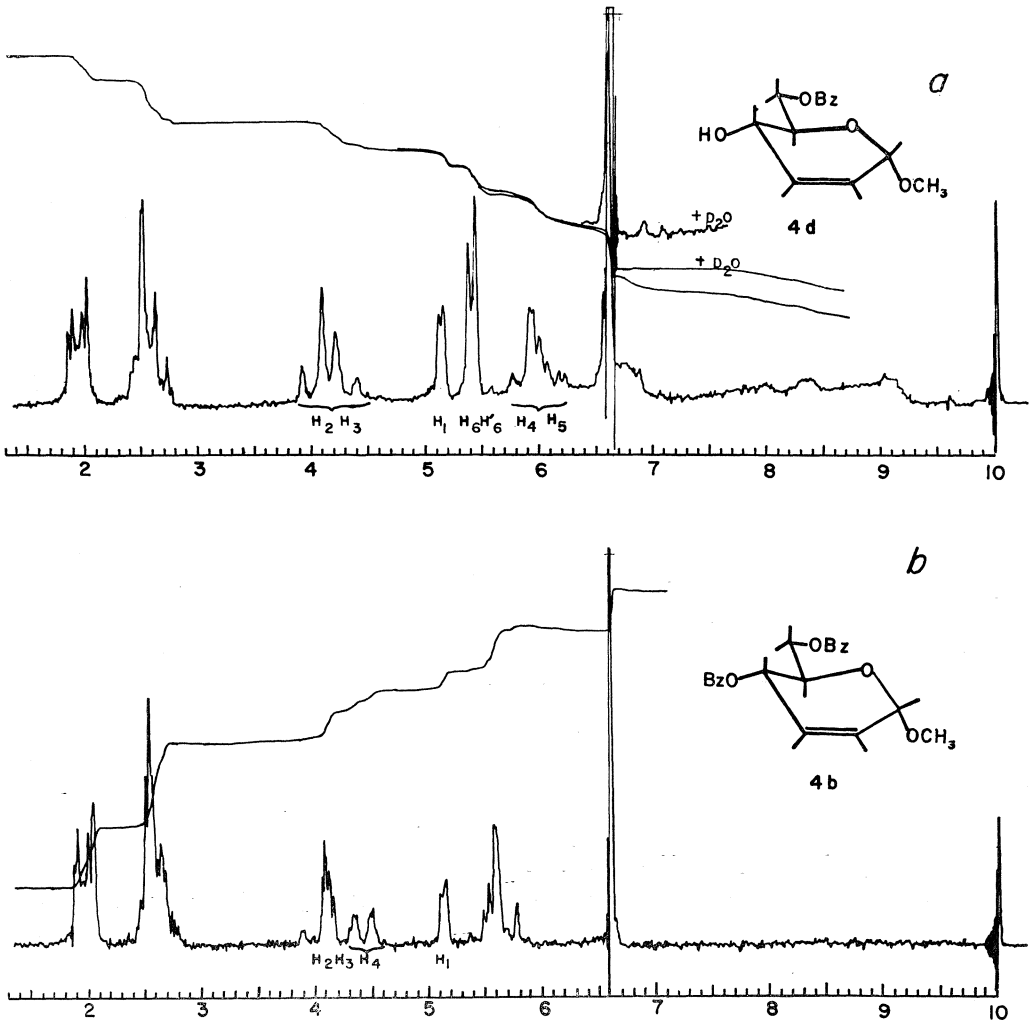

FIG. 1*a*. The nuclear magnetic resonance spectrum (60 Mc.p.s.) of methyl 6-*O*-benzoyl-α-D-erythro-hex-2-enopyranoside (**4***d*) in $CDCl_3$. *b*. The nuclear magnetic resonance spectrum (60 Mc.p.s.) of methyl 4,6-di-*O*-benzoyl-α-D-erythro-hex-2-enopyranoside (**4***b*) in $CDCl_3$.

established pattern would prevail and preclude migration of the 6-*O*-benzoyl group to the 4-position. This appears to have been the case.

The n.m.r. spectrum, Fig. 1*a*, provides independent evidence for the structure of **4***d*. The signal in the vicinity of τ 6 is acceptably located for an allylic proton (cf. 25), and in the dibenzoate, **4***b* (Fig. 1*b*), this signal is shifted 1.47 p.p.m. to lower field as is to be expected for the geminal proton upon benzoylation of a secondary hydroxyl group (26). The two benzyloxymethyl protons (H_6, H_6') of **4***d* are conveniently assigned as shown (26). Migration of the 6-*O*-benzoyl group to carbon-4 would produce a molecule in which the 4-hydrogen would resonate around τ 4.5 (cf **4***b*), and possessing a complex pattern for the hydroxy methyl function. Neither of these features is present in Fig. 1*a*. The structure of **4***d* is therefore secure. By analogy, the major product derived from the diacetate **3***a*, is therefore presumed to be **4***e*.

The foregoing discussion confirms the presence but not the *configuration* of the free hydroxyl group at carbon-4. If instead of the presumed

Can. J. Chem. Downloaded from www.nrcresearchpress.com by 210.87.254.6 on 09/05/12
For personal use only.

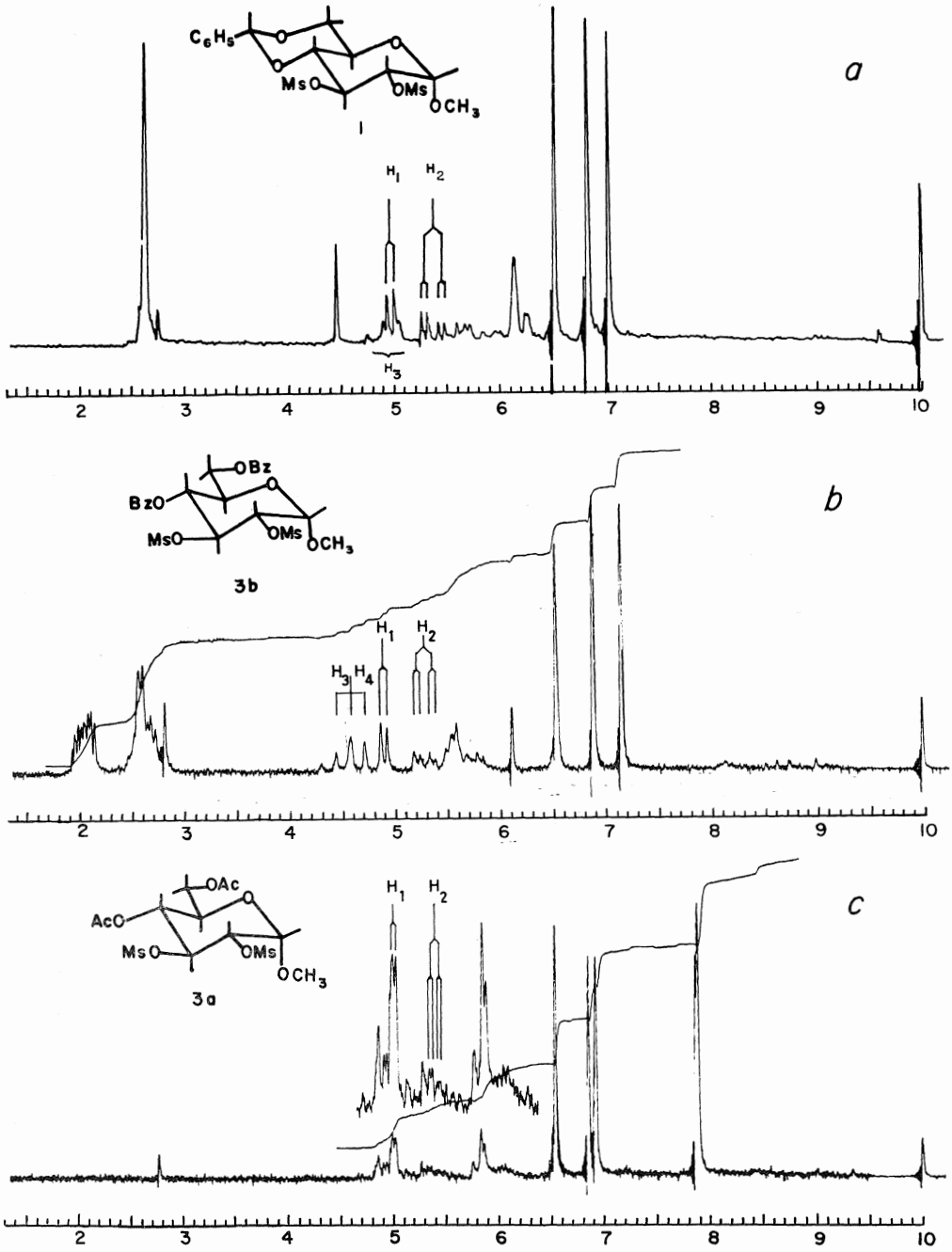

FIG. 2*a*. The nuclear magnetic resonance spectrum (60 Mc.p.s.) of 4,6-*O*-benzylidene-2,3-di-*O*-methanesulfonyl-α-D-glucopyranoside (**1**) in $CDCl_3$. *b*. The nuclear magnetic resonance spectrum (60 Mc.p.s.) of 4,6-di-*O*-benzoyl-2,3-di-*O*-methanesulfonyl-α-D-glucopyranoside (**3***b*) in $CDCl_3$. *c*. The nuclear magnetic resonance spectrum (60 Mc.p.s.) of 4,6-di-*O*-acetyl-2,3-di-*O*-methanesulfonyl-α-D-glucopyranoside (**3***a*) in $CDCl_3$.

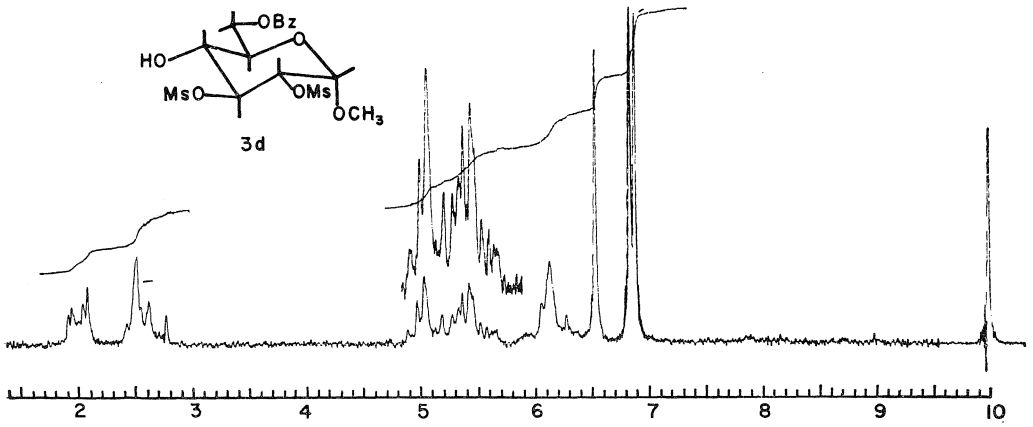

FIG. 3. The nuclear magnetic resonance spectrum of methyl 6-*O*-benzoyl-2,3-di-*O*-methanesulfonyl-α-D-gluco-pyranoside (**3***d*) in $CDCl_3$.

deacylation, an inversive displacement of the allylic acyl group occurred, the olefin obtained would be the *threo* rather than the *erythro* hexenopyranoside. Such an event warranted particular attention in view of the facility with which epimerization was found to occur at the allylic center of certain related hexenopyranosides (27). Fortunately inversion of configuration at carbon-4 of these systems is accompanied by dramatic changes in optical rotation. Thus the diacetate (**4***a*) derived by acetylation of **4***e* had an optical rotation of $+143.5°$ in full agreement with the reported value (4, 5), and vastly different from that ($-174°$) for the corresponding *threo* hex-2-enopyranoside (6).

Treatment of the monobenzoyl olefin **4***d* with benzoyl chloride in pyridine gave the dibenzoate **4***b* as a crystalline material.

Of some interest are the n.m.r. spectra shown in Fig. 2. The most striking feature in the spectra is the difference in the OSO_2CH_3 resonances of the various compounds. For the diacetate, **3***a* (Fig. 2*c*), these are separated by about 4.5 c.p.s. while in the dibenzoate **3***b* (Fig. 2*b*), the separation is about 17 c.p.s. The latter value is close to that (14 c.p.s.) found for **1** (Fig. 2*a*). These effects are presumably due to interactions introduced in the pyranose ring by the different substituents at carbons-4 and -6. The resonances for the annular protons would also be expected to reflect any changes. The assignments shown in Fig. 2 follow patterns now well entrenched for n.m.r. analysis of carbohydrate derivatives (28–31). The pronounced doublet at τ 4.96 ($J = 3.8$ c.p.s.) in Fig. **2***a* is ascribable to the anomeric proton of compound **1**, and the quartet centered at τ 5.37 with spacings of 3.8 and 9.8 c.p.s. can therefore be assigned to the 2-hydrogen. The broad multiplet around τ 4.8, partly obscured by the signal for the anomeric hydrogen, arises from a deshielded proton, strongly coupled to its neighbors. This is to be expected for the 3-hydrogen. Comparable analysis of compounds **3***a* and **3***b* results in the assignments shown in Fig. 2.

The constant chemical shift of the 2-hydrogens in compounds **1**, **3***a*, and **3***b* (Fig. 2) suggests that the geminal methanesulfonyl groups might also resonate at a relatively constant frequency. For this reason the lower-field OSO_2CH_3 signals occurring in these compounds at τ 6.85, 6.81, and 6.88, respectively, may be presumed to arise from the group attached at carbon-2. It is not surprising that the resonance of the group at carbon-3 should show greater perturbation than that at carbon-2 upon varying the substituents at carbon-4 (32). These effects are again observed for the related 6-*O*-monobenzoate, **3***d* (Fig. 3), obtained by selective benzoylation of **3***c*. The multiplet around τ 6.1 is to be expected for a proton geminal to a free secondary hydroxyl group (26). Upon benzoylation of such a hydroxyl group, the geminal proton should be shifted downfield by about 1.5 p.p.m. (26). This is seen to be correct by comparison with the dibenzoate **3***b* (Fig. 2*b*). Following the reasoning

Can. J. Chem. Downloaded from www.nrcresearchpress.com by 210.87.254.6 on 09/05/12
For personal use only.

Can. J. Chem. Downloaded from www.nrcresearchpress.com by 210.87.254.6 on 09/05/12
For personal use only.

above, the signal at τ 6.83 in compound **3***d* (Fig. 3) is probably assignable to the OSO_2CH_3 group at carbon-2 while the carbon-3 group, now not as shielded as in its counterpart **3***b*, would resonate at τ 6.88. Further study of these shielding and conformational effects is warranted but is outside the scope of the present communication.

The elimination of vicinal methanesulfonyloxy groups using zinc–copper couple and potassium iodide in refluxing dimethyl formamide can therefore be utilized whether or not acid or base sensitive groups are present in the molecule. The deacylation which occurs predominantly at carbon-4 may prove valuable, and it is reassuring to note that this reaction takes place without isomerization. Further work is underway to explore the applicability of the reaction for the preparation of other hexenopyranosides, and polyhydroxylated olefins in general.

Experimental

Melting points were determined on a Kofler block and are uncorrected. Nuclear magnetic resonance (n.m.r.) spectra were recorded using a JEOLCO C-60-H spectrometer with tetramethylsilane as internal standard. For analytical thin-layer chromatography Merck, Silica Gel HF_{254} was used and for preparative work the GF_{254} variety was employed. Solvent systems used for development were (*a*) benzene–chloroform (1:1), (*b*) ethyl acetate – petroleum ether (35–60 °C) (2:3) and ethyl acetate – petroleum ether (35–60 °C) (1:1). *N,N*-Dimethyl formamide was dried by refluxing over, followed by distillation from, calcium hydride. Zinc–copper couple was prepared as that used in the Simmonds–Smith reaction (33). Microanalyses were performed by Mr. A. B. Gygli, 329 St. George Street, Toronto, Ontario.

Methyl 4,6-O-Benzylidene-α-D-erythro-hexenopyranoside (2)

(i) Preliminary Experiments

(a) In a typical experiment, methyl 4,6-*O*-benzylidene-2,3-di-*O*-methanesulfonyl-α-D-glucopyranoside, **1**, (9 g, 0.02 mole) (18) was added to an efficiently stirred mixture of potassium iodide (17 g, 0.1 mole) and zinc–copper couple[7] (6.5 g, 0.1 g-atom) in 50 ml of dimethyl formamide. The solution was refluxed and at the intervals indicated, samples of the refluxing mixture were removed with a sawn-off pipette and poured into ice water. The slurry was washed with chloroform[8] filtered through a bed of Celite and the filter cake washed with a mixture of chloroform and water. The chloroform phase was washed with sodium thiosulfate solution, with water, then dried with calcium chloride and evaporated to dryness using a rotary evaporator. Most of the dimethyl formamide accumulated in the aqueous phase, but traces were removed by attaching the evaporator to a high vacuum pump. The degree of conversion of **1** to **2** was determined by comparison of the n.m.r. signal for the methoxyl groups at τ 6.52 with the OSO_2CH_3 groups at τ 6.85 and τ 7.02. This was determined to be as follows: 1 h, 43%; 3 h, 60%; 6 h, 73%; 8 h, 89%; 10 h, 100%.

(b) When the molar ratio of the di-*O*-methanesulfonate, potassium iodide and zinc–copper couple was changed from those used in part (*a*) to 1:10:5 or to 1:10:10 the reactions were also complete in 10 h.

(c) When the ratio of the reactants was reduced from that used in part (*a*) to 1:2.5:5 respectively, there was 73% conversion after 10 h.

(d) When previously dried sodium iodide (15 g, 0.1 mole) was substituted for potassium iodide under the conditions used in part (*a*), the observed conversion was as follows: 1 h, 23.5%; 3 h, 42.4%; 6 h, 67.5%; 8 h, 76.4%; 10 h, 92%; 12 h, 100%.

(ii) Large Scale Preparation

Compound **1** (180 g, 0.41 mole) was added to a mixture of potassium iodide (360 g, 2.2 moles) and zinc–copper couple (132 g, 2.0 g-atom) in dry dimethyl formamide (1 l). After refluxing with rapid stirring for 10 h, the hot solution was poured into 3500 ml ice-water mixture, chloroform (1 l) added, and the mixture stirred for 15 min. The insoluble material was removed by filtration and the filter cake was stirred with an equal mixture of chloroform and water. After repeating the latter process twice, the chloroform phases were combined and treated in a manner similar to that described above. The dried (calcium chloride) solution on evaporation afforded a brown residue which was dissolved in ethanol and boiled with charcoal for 30 min. The filtrate was concentrated and upon cooling deposited 30.5 g (29% yield) of material. After two recrystallizations from ethanol it melted at 121–122° and did not depress the melting point of an authentic sample (7). The syrup obtained from the mother liquors was eluted through a column of deactivated alumina (7) with petroleum ether (35–60 °C). Evaporation and crystallization from methanol gave an additional 2.3 g of material raising the overall yield to 32%.

Methyl 2,3-Di-O-methanesulfonyl-α-D-glucopyranoside, 3c

Methyl 4,6-*O*-benzylidene-2,3-di-*O*-methanesulfonyl-α-D-glucopyranoside, **1**, (30 g, 0.067 mole) was refluxed for 3 h with 360 ml of dioxane–water mixture (2:1) containing 10 ml of 10% sulfuric acid. The cooled solution was neutralized with sodium bicarbonate, and then extracted twice with petroleum ether to remove benzaldehyde. The aqueous layer was evaporated to dryness and traces of water removed by co-distillation with ethanol. Finally, the residue was boiled with ethanol and the inorganic salts collected by filtration. On concentration of the filtrate and cooling, **3***c* (22 g, 92%) crystallized from solution. Recrystallization from ethanol gave material (**3***c*) of melting point 150–151° $[\alpha]_D^{25}$ +82.4° (*c*, 1.06 in methanol).

Anal. Calcd. for $C_9H_{18}O_{10}S_2$: C, 30.86; H, 5.14. Found: C, 30.78; H, 5.19.

[7]Use of unactivated zinc gave a slower reaction (e.g. 21% after 1 h) and the results were also found to be unreproducible.

[8]It is to be noted that **2** unlike **1** is very insoluble in ether. Use of this solvent for extraction therefore led to erroneous estimates of the degree of conversion.

Can. J. Chem. Downloaded from www.nrcresearchpress.com by 210.87.254.6 on 09/05/12
For personal use only.

Methyl 4,6-Di-O-acetyl-2,3-di-O-methanesulfonyl-α-D-glucopyranoside, 3a

Compound **3***c* (24 g, 0.07 mole) was dissolved in pyridine (100 ml) and treated overnight with 60 ml of acetic anhydride. The excess anhydride was destroyed by addition of methanol to the ice-cold solution. The residue obtained upon evaporation was freed of pyridine by azeotropic distillation with toluene, and the resulting syrup was set to crystallize from methanol. The material obtained melted over a wide range, and n.m.r. analysis indicated that it contained methanol of crystallization. As an alternative work-up procedure, the acetylation mixture was poured into ice water, whereupon **3***a* crystallized out in an analytically pure condition; m.p. 79.5–80.5° $[\alpha]_D^{25}$ +91.7° (*c*, 1.04 in chloroform).

Anal. Calcd. for $C_{13}H_{22}O_{12}S_2$: C, 35.94; H, 5.07. Found: C, 35.71; H, 5.06.

Methyl 6-O-Benzoyl-2,3-di-O-methanesulfonyl-α-D-glucopyranoside, 3d

To a solution of compound **3***c* (20 g, 0.057 mole) in pyridine (100 ml) which had been cooled in an ice-salt bath, benzoyl chloride (6 ml, 7.17 g, 0.051 mole) was added slowly. The mixture was allowed to warm up to and stand at room temperature overnight. The benzoylated material, **3***d*, obtained in a manner analogous to that described for **3***b*, was a crystalline material of melting point 122–123° $[\alpha]_D^{25}$ = +63.2° (*c*, 0.79 in chloroform).

Anal. Calcd. for $C_{23}H_{22}O_{11}S_2$: C, 42.30; H, 4.89. Found: C, 42.61; H, 5.20.

Reductive Elimination of Methyl 4,6-Di-O-acetyl-2,3-di-O-methanesulfonyl-α-D-glucopyranoside, 3a. Methyl α-D-Erythro-hex-enopyranoside, 4c, and its 4,6-Di-O-acetate, 4a

Compound **3***a* (36 g, 0.083 mole) was refluxed in dimethyl formamide (200 ml) with zinc–copper couple (26.4 g, 0.42 g-atom) and potassium iodide (72 g, 0.43 mole). The reaction monitored previously by n.m.r. had been shown to progress as shown in Table I.

TABLE I

Reductive elimination of **3***a*

	Ratio of groups*		
Time (min)	OSO_2CH_3	OCH_3	$OCOCH_3$
20	1	2.6	5.7
40	1	4.7	9.0
60	1	5.0	9.3
75	1	7.3	12.0

*Nuclear magnetic resonance determination.

Beyond this time secondary reactions set in which resulted in deacetylation of the product. The residue obtained upon evaporation of the aqueous layer from work-up showed the presence (t.l.c.) of considerable olefinic diol, **4***c*. A reaction period of 1½ h was selected as optimal.

The product isolated in the same manner as **2** afforded 9.3 g of material which on thin-layer chromatograms (solvent system *b*) revealed two components of R_f 0.5 ("**A**") and 0.43 ("**B**"). The latter was the major component. Treatment of a 4.3 g portion of the reaction product with acetic anhydride and pyridine in the usual way gave "**A**" as the sole component. Distillation of the re-acetylated product at 110° and 0.5 mm afforded 2.15 g (ca. 25% from **3***a*) of material having identical spectral characteristics as an authentic sample of **4***a*.[9] Its optical rotation $[\alpha]_D^{25}$, was +143.5° (*c*, 0.87 in benzene) in good agreement with the literature values of +143° (34) and +139 (5) for **4***a*.

The mixture of "**A**" and "**B**" (1.0 g) was stirred with methanol – water – triethylamine (5:4:1) mixture for 1 h, after which time the liquids were removed on a rotary evaporator. Water–methanol mixture (1:1) was twice evaporated from the residue to ensure hydrolysis of any quaternary amides. A different hex-2-enopyranoside "**C**" (0.61 g) of R_f 0.36 in ethyl acetate was obtained. The non-crystalline material had an optical rotation of $[\alpha]_D^{20}$ +127.8° (*c*, 1.01 in methanol). "**C**" could be acetylated to **4***a*, selectively benzoylated to **4***d*, or fully benzoylated to **4***b*. "**C**" is therefore **4***c*.

Methyl 6-O-Benzoyl-α-D-erythro-hex-2-enopyranoside, 4d

(a) By Reductive Elimination of Compound 3b

Compound **3***b* (30 g, 0.054 mole) along with potassium iodide (42 g, 0.25 mole) and zinc–copper couple (16 g, 0.25 g-atom) was refluxed in 120 ml dimethyl formamide for 2½ h, this period of time having been previously determined in the manner already described, as being optimal for the conversion. The product (5.71 g) contained one major hexenopyranoside of R_f 0.54 (solvent system *c*) on thin-layer chromatograms. A portion of the product (0.307 g) was applied to a preparative chromatogram for development in solvent system *c*, and the appropriate zone was located by exposure to ultraviolet light. The band was separated and eluted with ethyl acetate to afford 0.121 g of non-crystalline material.

(b) By Reductive Elimination of Compound 3d

Methyl 6-*O*-benzoyl-2,3-di-*O*-methanesulfonyl-α-D-glucopyranoside, **3***d*, (9.5 g, 0.021 mole) in 45 ml of dimethyl formamide was treated with potassium iodide (16 g, 0.95 mole) and zinc–copper couple (6.0 g, 0.95 g-atom) under reflux, and the reaction followed in the usual way. The percent completion was: 30 min, 30%; 40 min, 45%; 1 h, 83%. The ratio of methoxyl to aromatic protons at these times was respectively as follows: 1:1.8; 1:1.7, and 1:2.1. At 1½ and 2 h the ratios were 1:2.7, and 1:2.6. A reaction time of 1 h was adopted, since it was evident that the methoxyl group was being lost during the reaction.

The product obtained by the customary work-up procedure weighed 1.07 g. Of this, 0.430 g was fractionated by preparative layer chromatography as described in part (*a*) above to give 0.140 g of the material of interest.

(c) From Selective Benzoylation of 4c

A pyridine (15 ml) solution of methyl α-D-erythro-hex-2-enopyranoside, **4***c*, (0.65g, 0.004 mole) was treated at ice-salt temperature with benzoyl chloride (0.44 ml,

[9]We are grateful to Dr. R. J. Ferrier for providing us with the authentic sample.

Can. J. Chem. Downloaded from www.nrcresearchpress.com by 210.87.254.6 on 09/05/12
For personal use only.

0.525 g, 0.0037 mole). After being allowed to warm up gradually to room temperature and stand there overnight, the reaction mixture was subjected to the customary work-up procedure. The reaction product (0.492 g) contained one major component which was isolated by preparative layer chromatography as in part (*a*) above. Thereby 0.202 g of material of R_f 0.54 (solvent system *c*) was recovered.

The substance obtained by the different routes described in parts (*a*), (*b*), and (*c*) had identical R_f (0.54) in solvent system *c*, and identical infrared and n.m.r. (Fig. 1*a*) spectra. It was a non-crystalline material of optical rotation $[\alpha]_D^{25}$ +58.1° (*c*, 0.74 in chloroform) which was judged to be the title compound, **4***d*.

*Methyl 4,6-Di-O-benzoyl-α-*D*-erythro-hex-2-enopyranoside*, **4***b*

In one experiment, the product derived from the reductive elimination of compound **3***b* (see part (*a*) immediately above) was dissolved in pyridine and treated with excess benzoyl chloride. Work-up in the manner described above gave 6.5 g of a syrup essentially homogeneous by t.l.c. Prolonged cooling of a methanolic solution caused the deposition of 5.44 g (27%) of the olefinic dibenzoate **4***b*. Its melting point was 72–73°, $[\alpha]_D^{25}$ +189.5° (*c*, 1.0 in chloroform).

Anal. Calcd. for $C_{21}H_{20}O_6$: C, 49.48; H, 4.66. Found: C, 49.27; H, 4.87.

Treatment of a sample of **4***b* with methanol – water – triethylamine (5:4:1) required 7 h for conversion to the diol **4***c*.

Acknowledgments

The authors are grateful to the National Research Council of Canada and the University of Waterloo for providing generous financial support for this work.

1. R. U. Lemieux, E. Fraga, and K. A. Watanabe. Can. J. Chem. **46**, 61 (1968), and references cited therein.
2. E. L. Albano, D. Horton, and J. H. Lauterbach. Chem. Commun. **7**, 357 (1968).
3. R. J. Ferrier and N. Prasad. Chem. Commun. **8**, 476 (1968).
4. M. Bergmann. Ann. **434**, 81 (1923).
5. R. J. Ferrier. J. Chem. Soc. 5443 (1964).
6. R. J. Ferrier. J. Chem. Soc. 441 (1966).
7. E. Albano, D. Horton, and T. Tsuchiya. Carbohydrate Res. **2**, 349 (1966).
8. R. U. Lemieux. *In* Molecular rearrangements. Vol. 2. *Edited by* P. de Mayo. John Wiley and Sons, Inc., New York. 1963.
9. R. U. Lemieux and B. Fraser-Reid. Can. J. Chem. **42**, 539 (1964).
10. E. J. Corey and R. A. Winter. J. Am. Chem. Soc. **88**, 2677 (1963).
11. E. I. Stout, W. M. Doane, B. S. Shasha, C. R. Russell, and C. E. Rist. Carbohydrate Res. **3**, 354 (1967).
12. R. S. Tipson and A. Cohen. Carbohydrate Res., **1**, 338 (1965).
13. S. J. Angyal and R. J. Young. Australian J. Chem. **14**, 8 (1961).
14. D. V. Banthorpe. Reaction mechanisms in organic chemistry. Vol. 2. Elsevier Publishing Co., Inc., New York. 1963. p. 140.
15. S. J. Cristol, J. R. Weber, and M. C. Brindell. J. Am. Chem. Soc. **78**, 598 (1956).
16. F. H. Newth. J. Chem. Soc. 471 (1956).
17. J. K. Kochi and D. M. Singleton. J. Am. Chem. Soc. **90**, 1582 (1968).
18. J. Honeyman and J. W. W. Morgan. J. Chem. Soc. 3660 (1955).
19. R. J. Ferrier. Advan. Carbohydrate Chem. **20**, 101 (1965).
20. Handbook of chemistry and physics. The Chemical Rubber Co., Ohio. (1966).
21. J. Defaye and J. Hildescheim. Bull. Soc. Chim. France, **3**, 940 (1967).
22. Fischer Chemical Index 68–6, Fischer Scientific Co., Ltd. (1967).
23. DuPont Dimethyl Formamide Product Information. E. I. DuPont de Nemours and Co. (Inc.), Wilmington, Delaware. A-55617. (1967).
24. F. D. Cramer. Methods Carbohydrate Chem. **2**, 244 (1963).
25. High resolution n.m.r. spectra catalogue. Varian Associates. Spectrum No. 34. (1962).
26. L. M. Jackman. Nuclear magnetic resonance spectroscopy. The Pergamon Press Ltd., New York. 1959. p. 55.
27. D. M. Ciment, R. J. Ferrier, and W. G. Overend. J. Chem. Soc. 446 (1966).
28. R. U. Lemieux, R. K. Kullnig, H. J. Bernstein, and W. G. Schneider. J. Am. Chem. Soc. **81**, 6098 (1958).
29. R. U. Lemieux and B. Fraser-Reid. Can. J. Chem. **42**, 532 (1964).
30. L. D. Hall. Advan. Carbohydrate Chem. **19**, 51 (1964).
31. N. S. Bhacca, D. Horton, and H. Paulsen. J. Org. Chem. **33**, 2484 (1968).
32. M. Karplus. J. Am. Chem. Soc. **85**, 2870 (1963), and references cited therein.
33. Organic Syntheses, John Wiley and Sons, Inc. **41**, 72 (1961).
34. M. Bergmann and K. Freidenberg. Ber. **64**, 158 (1931).

Stereochemical dependence of vicinal H—C—O—H coupling constants

ROBERT R. FRASER, M. KAUFMAN, AND PETER MORAND
Department of Chemistry, University of Ottawa, Ottawa, Canada

AND

G. GOVIL[1]
Division of Pure Chemistry, National Research Council of Canada, Ottawa, Canada

Received August 15, 1968

The exact analysis of the ABC type absorption due to the —CH_2OH group of 3β-acetoxy-5β,6β-oxidocholestan-19-ol provides two vicinal HCOH coupling constants for dihedral angles of 80° and 160°. A least squares fit of these and previous data in the literature to a "Karplus" relation provides values for the coefficients in such an equation. The theoretical justification for such a relation has been obtained by extended Hückel molecular orbital calculations for methanol with different dihedral angles. The practical limitations in, and applications of the relation are discussed. An effect of solvent on the vicinal coupling constants is also noted and discussed.

Canadian Journal of Chemistry, **47**, 403 (1969)

Can. J. Chem. Downloaded from www.nrcresearchpress.com by 210.87.254.5 on 09/05/12
For personal use only.

Introduction

The Karplus relation between the magnitude of the vicinal proton–proton coupling constant for the H—C—C—H fragment (J_{HCCH}) and the dihedral angle (ϕ) between the planes passing through H—C—C and C—C—H has been of invaluable aid in the solution of stereochemical problems (1). In its most general form, such a relation can be written as a power series limited to the second power in cos ϕ

[1] $$J_{HCCH} = A\cos^2\phi + B\cos\phi + C$$

with $A \sim 13.0$, $B \sim -1.5$ and $C \sim -0.3$ Hz. A similar angular dependence of the proton–proton coupling (J_{HCOH}) for the H—C—O—H fragment has been proposed by a number of authors (2–5) and in several papers the relation between J_{HCOH} and ϕ has been discussed on empirical grounds (6–8). However, while a functional behavior of the type given by eq. [1] for J_{HCCH} has been predicted on the basis of valence bond and molecular orbital (MO) theories and confirmed experimentally,[2] the basis for postulating the same functional form for J_{HCOH} is purely intuitive, requiring the assumption that replacement of one of the carbons by oxygen does little to disturb such a relation. Thus Bauld and Rim (4) believe that $J_{HCCH}(\phi)$ and $J_{HCOH}(\phi)$ are quantitatively comparable. Stolow and Gallo (5) on the other hand assume that $C = 0$ and solve for A and B from values of J_{HCOH} in two molecules with known stereochemistry. The experimental measurements available prior to the present paper (4, 5) were just sufficient to solve for A, B, and C and allowed no test of applicability of eq. [1] for J_{HCOH}. In this paper we wish to report our observations on the spectrum produced by the CH_2OH group of a steroidal epoxyalcohol. The coupling constants obtained from an exact analysis of this ABC system add two more measurements for testing of the Karplus relation for J_{HCOH}. The functional dependence of J_{HCOH} on cos ϕ has also been examined using calculations based on molecular orbital theory.

Molecular Orbital Calculation of J_{HCOH}

A survey (9) of the various theoretical methods employed in calculations of *vicinal* and *geminal* proton–proton coupling constants in ethane as a function of ϕ, indicates that the method employed by Fahey *et al.* (10) using extended Hückel theory (EHT) is more satisfactory than other methods. We therefore decided to perform similar calculations on methanol. Since the basic theory and details of calculation are the same as given in (10) we will not discuss them here. The 1s orbitals on the four hydrogens and the 2s and 2p orbitals on carbon and oxygen were chosen as the basis set and Slater exponents of 1.2, 1.625, and 2.275 for hydrogen, carbon and oxygen, respectively, were used. The chosen Coulomb integrals of various atomic orbitals [H (1s) = −13.60, C (2s)

[1]NRCC Postdoctorate Fellow 1967–1968.

[2]It might be mentioned that the theoretical results for J_{HCCH} are generally lower than the experimental values and therefore the theoretically estimated, A, B, and C are different from those obtained by a least squares fitting of the experimental data [see for example reference (9)].

TABLE I

Calculated values of J_{HCOH} as a function of ϕ

ϕ	J in Hz
0	1.64
30°	1.46
60°	1.12
90°	0.92
120°	0.95
150°	1.13
180°	1.24

$= -21.43$, C (2p) $= -11.42$, O (2s) $= -35.30$, O (2p) $= -17.28$ eV] are the same as used by other workers (11, 12). The calculated values of the contribution of the contact term to the coupling constant J_{HCOH} as a function of ϕ are given in Table I. It can be seen that a functional form of the type given by eq. [1] is predicted by theory, but the calculated values are in general much lower than the observed ones. Thus for methanol in its equilibrium conformation, J is predicted to be 1.16 Hz as compared to the observed value of 5.3 Hz (22). Although a similar behavior is found for ethane (10) [$J_{calculated} = 5.2$ Hz, $J_{observed} = 8.0$ Hz] the discrepancy between the calculated and observed values is much larger for CH_3OH. Several factors might be responsible for this, among them the choice of wrong Coulomb integrals for oxygen, the neglect of the contributions of spin-dipolar and spin-orbital interactions to J_{HCOH} and the neglect of all but the one and certain two electron terms in the calculation of the contact term. For these reasons it is felt that attempts at further refinement of the calculations are unwarranted.

3β-Acetoxy-5β,6β-oxidocholestan-19-ol(2)

During an investigation of synthetic routes to the A/B ring of strophanthidin, the intermediate 3β-acetoxy-5β,6β-oxidocholestan-19-ol, **2** was prepared by the peracid oxidation of 3β-acetoxycholest-5-en-19-ol, **1**. As expected (13, 14), **2** was the major product (72%) of this reaction. In addition the isomeric 5α,6α-epoxide, **3** was formed in 14% yield. Epoxides **2** and **3** were isolated separately by chromatography on silica gel. The configurations of **2** and **3** can be ascertained from their nuclear magnetic resonance (n.m.r.) spectra. The spectrum of **3** in deuteriochloroform showed a broad multiplet for the axial proton at C-3. It appeared at τ 5.08, a chemical shift at lower field than was observed for the proton at C-3 in either **1** (τ 5.38) or **2** (τ 5.18). This deshielding effect in **3** is indicative of an alpha orientation for the epoxide (15, 16). In addition the absorption at τ 7.02 in the spectrum of **3** appears as a doublet of spacing 3.5 Hz and is consistent only with an α epoxide ring (16). The n.m.r. spectrum of **2**, which we will describe in detail shortly, offers strong evidence for the β-orientation of the epoxide ring. Chemical proof of

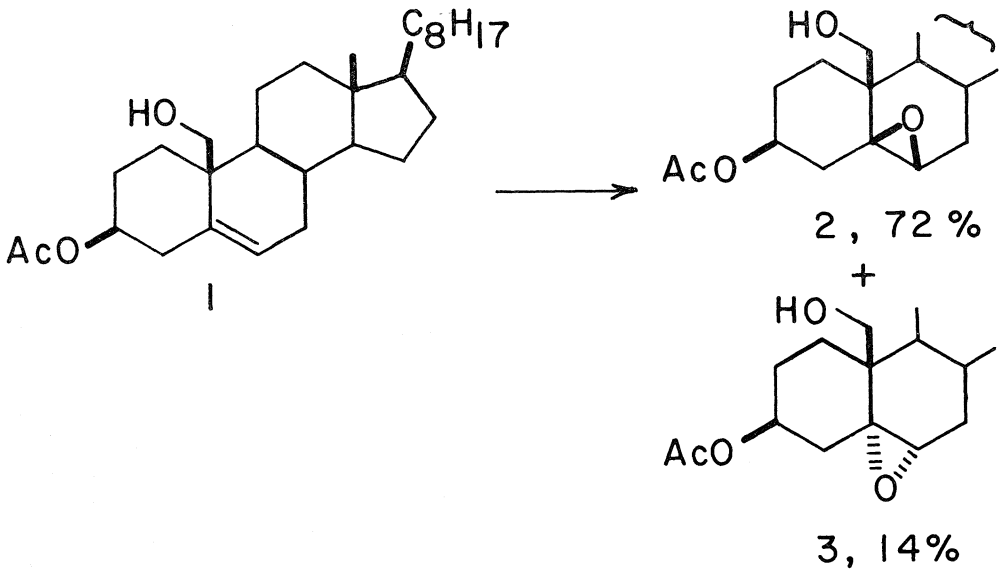

Can. J. Chem. Downloaded from www.nrcresearchpress.com by 210.87.254.5 on 09/05/12
For personal use only.

TABLE II

Parameters obtained from the ABC analysis of the CH_2OH group of **2**

ν_A	ν_B	ν_C	J_{AB}	J_{AC}	J_{BC}	Solvent
240.8	217.0	193.4	−11.5	2.5	9.2	Acetone–$CDCl_3$ (2:1)
244.3	209.5	182.9	−11.8	0.3	10.4	Benzene
250.3	217.8	182.4	−11.5	0.1	10.5	$CDCl_3$

structure for **2** and **3** has also been obtained and will be described in detail in a separate paper (17).

Analysis of Spectra of 2

The n.m.r. spectrum of **2** in deuteriochloroform showed a typical ABC pattern in the region of τ 5.8–7.0 which is attributed to the CH_2OH group at C-19. All peaks had a half-band width of about 1 Hz which did not change on cooling the sample to −40°. The two peaks at highest field (spacing of 10.3 Hz) disappeared when a drop of D_2O was added to the solution and therefore represent the OH proton. The spectrum of **2** measured in benzene was very similar to that in deuteriochloroform. When a 2:1 mixture of acetone and deuteriochloroform was used as solvent the pattern changed to the extent that the OH absorption appeared as a quartet. The region of interest in this spectrum, τ 5.9–7.3 is shown in Fig. 1. Twelve peaks due to the ABC pattern are observed, the thirteenth transition of observable intensity being obscured by the doublet due to the proton at C-6. The strong close-spaced quartet is the signal for the $^{13}CH_3$ side band of acetone solvent.

The spectra in each of these three solvents were subjected to computer analysis using the LAOCOON II program (18) on an IBM 360–65 computer. The results of these analyses are given in Table II. Because of the line widths encountered in all spectra, the parameters obtained from the analysis are only accurate to 0.2 Hz or better, although the average agreement between observed and calculated transitions was 0.06 Hz. In general in a solution of an ABC spectrum more than one set of parameters can give agreement with the observed line positions and intensities (19), within experimental accuracies. To make a proper choice from such solutions and establish the relative signs of the three coupling constants, spin-tickling experiments (20) were performed to show that the relative signs given in Table I are indeed correct.

It was observed for example, that spin-tickling of C2 splits B1 and A4 into sharp doublets. Similarly irradiation of A4 showed that it is connected 'regressively' with the transitions B4 and C2. These experiments show that J_{AB} has opposite sign as compared to the two J_{HCOH} couplings, J_{AC} and J_{BC}. Further, in view of the absolute negative sign of the geminal proton–proton coupling constants in related compounds [see for example reference (10)] both the J_{HCOH} couplings can be assigned positive values. These results are in agreement with the observations of Hruska *et al.* (21) on 2-methyl-2-nitro-1,3-propanediol where the sign of the geminal versus the vicinal J's averaged over all the rotational isomers, has been determined.

The spectral characteristics of the CH_2OH group are unusual in the sense that the H—C—O—H splittings can be observed in a variety of solvents. Normally either scrupulously purified solvent and solute (22) or dry dimethyl sulfoxide (23, 24) must be used in order to retard the rate of exchange of the OH proton sufficiently to allow observation of vicinal coupling. The particularly slow OH exchange in **2** can be attributed to the presence of an intramolecular hydrogen bond to the β-epoxide group.[3] In contrast epoxide **3** lacks the proper orientation and shows no H—C—O—H coupling in its n.m.r. spectrum in deuteriochloroform.

Angular Dependence of Observed J_{HCOH}

The measurement of two vicinal H—C—O—H coupling constants involving the same OH proton provides us with the opportunity to examine their stereochemical dependence with greater precision than was previously possible since the two diastereotopic protons at C-19 have interdependent dihedral angles with respect to the OH proton.

[3]A 1% (w/v) solution of **2** in carbon tetrachloride showed only one band at 3560 cm^{-1} in the hydroxyl region. This band is in the region of intramolecularly hydrogen-bonded O—H vibrations.

Can. J. Chem. Downloaded from www.nrcresearchpress.com by 210.87.254.5 on 05/05/12
For personal use only.

FIG. 1. Partial nuclear magnetic resonance spectrum of 3β-acetoxy-5β,6β-oxidocholestan-19-ol taken in deuteriochloroform.

Can. J. Chem. Downloaded from www.nrcresearchpress.com by 210.87.254.5 on 09/05/12
For personal use only.

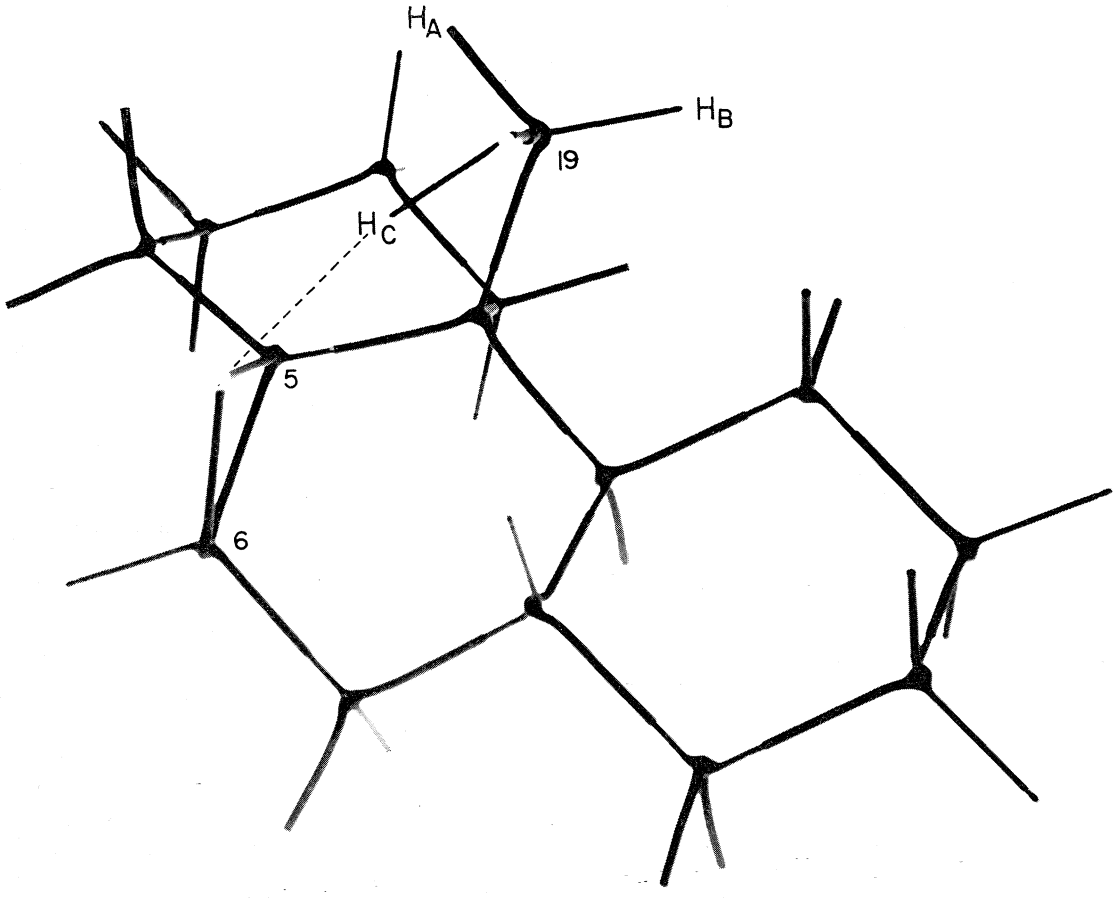

FIG. 2. The Dreiding molecular model of 3β-acetoxy-5β,6β-oxidocholestan-19-ol which indicates the most likely conformation for the CH_2OH group.

Dreiding models of **2** indicate the most likely conformation for the CH_2OH group to be that shown in Fig. 2. In this conformation the dihedral angles between the OH and the two C—H protons are estimated (±10°) to be 160° and 80°. The values of J_{HCOH} for **2** in deuteriochloroform have been combined with all the previous known values of $J_{HCOH}(\phi)$ in Table III. A least squares fitting of eq. [1] with the observed data gives

$$[2] \quad J_{HCOH} = 10.4 \cos^2 \phi - 1.5 \cos \phi + 0.2$$

The fit of the observed values with eq. [2] is also given in Table III. It appears that a Karplus type of behavior does account for the variations of J_{HCOH}.

In applying eq. [2] to any conformational problem, one must remember its limitations, which more or less are the same as that for J_{HCCH} (25). No account for changes of hybridization and electronegativity due to substitution effects in solving eq. [2] have been made, and like in J_{HCCH} such effects might be appreciable (22, 26, 27). An extreme example of the effect of hybridization on the observed J values is provided by protonated formaldehyde where *cis* and *trans* coupling constants of 8.5 and 18.5 (26), and 8.7 and 21.1 (27) Hz have been reported by two groups of workers. Although the substitution effects on J_{HCOH} couplings in tetrahedral systems are likely to be much smaller than the extreme case of protonated formaldehyde, the knowledge of similar effects on J_{HCCH} indicates that eq. [2] can probably predict J_{HCOH} to no better than 1 or 2 Hz.

Can. J. Chem. Downloaded from www.nrcresearchpress.com by 210.87.254.5 on 09/05/12
For personal use only.

TABLE III

Values of J_{HCOH} as a function of ϕ

Reference	ϕ	$J_{observed}$ in Hz	$J_{calculated}$ from eq. [2] in Hz
Present work	80	0.3	0.2
Present work	160	10.5	10.8
Stolow and Gallo (5)	167	11.4	11.5
Bauld and Rim (4)	180	12.5	12.1
Value for Methanol (22)	$\frac{1}{3}[2J(60°)+J(180°)]$	5.3	5.4

Solvent Effect on J_{HCOH}

There is one more point which deserves mention, namely the solvent effect on J_{HCOH}. It is seen from Table II that the values of J_{HCOH} in going from deuteriochloroform to acetone/deuteriochloroform change significantly. Thus J_{AC} increases by 2.2 Hz while J_{BC} decreases by 1.2 Hz. It is possible that when a fixed dihedral angle is maintained, J_{HCOH} might change with solvent. Such effects in sp^3 hybridized systems are usually small. For example, the difference between the coupling constant of methanol in carbon tetrachloride and dimethyl sulfoxide is only 0.1 Hz (22). An alternative explanation for the solvent effect on the coupling constants should also be considered. This explanation involves a change in the population of rotamers.

In order to examine this possibility we refer back to Fig. 2. As one rotates the O—H_C bond about the C—O axis the potential energy of the whole molecular system goes through three minima. These occur at $\phi_{AC} \sim 80$, 180, and 300°[4] where ϕ_{AC} is the dihedral angle between the planes containing H_COC and H_ACO. In nonpolar solvents like $CDCl_3$ and C_6H_6 the possibility of intramolecular hydrogen bonding leads to a very stable configuration at $\phi_{AC} = 80°$. Thus, almost no molecules exist in the form for which $\phi_{AC} = 180$ or 300°. In the presence of acetone however, the O—H_C group can also form hydrogen bonds with the solvent. Such bonds are favored in conformations corresponding to $\phi_{AC} = 180$ and 300° for steric reasons. Thus the concentration of such structures might change significantly with a change in solvent. Calling the conformations with $\phi_{AC} = 80$, 180, and 300° I, II, and III respectively, one calculates using eq. [2]

$$J_{AC}^{I} = 0.2 \quad J_{AC}^{II} = 12.1 \quad J_{AC}^{III} = 2.0$$

$$J_{BC}^{I} = 10.2 \quad J_{BC}^{II} = 2.0 \quad J_{BC}^{III} = 2.0$$

If the interconversion between I, II, and III is rapid then one would observe only an average coupling constant

$$[3] \qquad J_{\alpha\beta} = \sum_{i=I,II,III} p^i \, j^i \alpha\beta / \sum_i p^i$$

where p^i is the population of the structures I, II, and III. (Since no bond cleavage takes place during internal rotation, such a process need not lead to 'washing' of spin-multiplets.) We have calculated values for J_{AC} and J_{BC} assuming a decrease in the proportion of conformer I along with equal increments in II and III. We find the best agreement with the experimental values for an 8:1:1 mixture of conformers I, II, and III. The calculated values for J_{AC} and J_{BC} in this case are 1.6 and 8.5 Hz compared with the experimental values in acetone–deuteriochloroform of 2.5 and 9.2 Hz. This agreement does not appear to be sufficient to rule out the aforementioned possibility of a solvent effect on J in conformer I alone. Both effects may be operative. In any event careful consideration must be given to solvent effects when employing a Karplus-type relation between J_{HCOH} and ϕ.

Experimental

Microanalyses were done by A. Bernhardt, Mülheim, Germany. Melting points were determined in capillary tubes on a Hoover Uni-Melt apparatus and are uncorrected. A Perkin–Elmer model 141 polarimeter was used to determine the optical rotation of the compounds in chloroform solution at room temperature. Petroleum ether refers to that fraction with b.p. 30–60°.

Florisil (60–100 mesh, Floridin Co.) and silica gel ("SilicAR" CC–7, 200–325 mesh) were used for column

[4]Stolow and Gallo (5) have pointed out that an asymmetry in the curve is expected due to hydrogen bonding. Consequently, the minimum in potential energy for the bonded conformer does not occur at the expected interval of 120° for ϕ but instead assumes a conformation most favorable for hydrogen bonding.

Can. J. Chem. Downloaded from www.nrcresearchpress.com by 210.87.254.5 on 09/05/12
For personal use only.

chromatography. Silica gel G (according to Stahl, E. Merck Co., Germany) was used for thin-layer chromatography.

The n.m.r. spectra were recorded on a Varian HA-60-IL nuclear magnetic resonance spectrometer.

Epoxidation of 3β-Acetoxycholest-5-en-19-ol(1)

A solution of 3.20 g of 3β-acetoxycholest-5-en-19-ol (28) in ether was treated with an excess of monoperphthalic acid in ether for 2 h at room temperature. The reaction solution was washed with a 20% aqueous solution of sodium sulfite and dried over magnesium sulfate. The ethereal solution was then eluted on a Florisil (500 g) column to remove completely the phthalic acid. A crude product was obtained in this manner in which three components were detected by thin-layer chromatography.

This mixture was separated by column chromatography using silica gel as the adsorbant and benzene as eluent. The first substance (0.15 g) collected from the column has the same R_f value as the starting material by thin-layer chromatography and was not characterized further. The second fraction (2.27 g) was identified as *3β-acetoxy-5β,6β-oxido-cholestan-19-ol*, **2**. An analytical sample obtained by crystallization from petroleum ether – ether had m.p. 129–130.5°, $[M]_D = -30°$ (*c*, 2.3 mg/ml).

Anal. Calcd. for $C_{29}H_{48}O_4$: C, 75.60; H, 10.50. Found: C, 75.42; H, 10.51.

The third solid material (0.45 h) to be eluted from the column was identified as 3β-acetoxy-5α,6α-oxidocholestan-19-ol, **3**. Crystallization from methanol gave an analytical sample, m.p. 184–186°, $[M]_D = -267°$ (*c*, 2.5 mg/ml). The n.m.r. spectrum in $CDCl_3$ showed a singlet at τ 5.0 (3α-H; $w/2 = 20$ Hz), a singlet at τ 6.05 (C-19 methylene group), a doublet centered at τ 6.99 (6β-H; $J_{a,a} = 3.4$ Hz), and a singlet at τ 8.0 (3—OAc).

Anal. Calcd. for $C_{29}H_{48}O_4$: C, 75.60; H, 10.50. Found: C, 75.77; H, 10.50.

Acknowledgment

The authors wish to thank the National Research Council of Canada for generous financial support.

1. A. A. Bothner-By. *In* Advances in magnetic resonance. *Edited by* J. S. Waugh. Academic Press, Inc., New York. 1965.
2. R. J. Ouellette. J. Am. Chem. Soc. **86**, 4378 (1964).
3. C. P. Rader. J. Am. Chem. Soc. **88**, 1713 (1966).
4. N. L. Bauld and Y. S. Rim. J. Org. Chem. **33**, 1303 (1968).
5. R. D. Stolow and A. A. Gallo. Tetrahedron Letters, 3331, 1968.
6. W. Mackie and A. S. Perlin. Can. J. Chem. **44**, 2039 (1966).
7. B. Casu, M. Reggiani, G. G. Gallo, and A. Vigevani. Tetrahedron, **22**, 3061 (1966).
8. J. J. Uebel and H. W. Goodwin. J. Org. Chem. **31**, 2040 (1966).
9. G. Govil and H. J. Bernstein. J. Chem. Phys. **49**, 911 (1968) and references contained therein.
10. R. C. Fahey, C. G. Graham, and R. L. Piccioni. J. Am. Chem. Soc. **88**, 193 (1966).
11. T. Yonezawa, I. Moroshima, and M. Fujii. Bull. Chem. Soc. Japan, **39**, 2110 (1966).
12. B. P. van Eijck. Rec. Trav. Chim. **85**, 1129 (1966).
13. H. B. Henbest and R. A. L. Wilson. J. Chem. Soc. 1958 (1957).
14. M. Mousseron-Canet, B. Labeeuw, and J. C. Lanet. Compt. Rend. **262**, 1438 (1966).
15. N. S. Bhacca and D. H. Williams. Applications of n.m.r. spectroscopy in organic chemistry. Holden-Day, Inc., San Francisco. 1964, p. 187.
16. A. D. Cross. J. Am. Chem. Soc. **84**, 3206 (1962).
17. P. Morand and M. Kaufman. Unpublished results.
18. S. Castellano and A. A. Bothner-By. J. Chem. Phys. **41**, 3863 (1964).
19. R. R. Fraser. Can. J. Chem. **40**, 1483 (1962).
20. R. Freeman and W. A. Anderson. J. Chem. Phys. **37**, 2053 (1962); W. A. Anderson, R. Freeman, and C. A. Reilly. J. Chem. Phys. **39**, 518 (1963).
21. F. Hruska, T. Schaefer, and C. A. Reilly. Can. J. Chem. **72**, 697 (1964).
22. W. B. Moniz, C. F. Poranski, Jr., and T. N. Hall. J. Am. Chem. Soc. **88**, 190 (1966).
23. D. E. McGreer and M. M. Mocek. J. Chem. Educ. **40**, 358 (1963).
24. O. L. Chapman and R. W. King. J. Am. Chem. Soc. **86**, 1256 (1964).
25. M. Karplus. J. Am. Chem. Soc. **85**, 2870 (1963).
26. M. Brookhart, G. C. Levi, and S. Winstein. J. Am. Chem. Soc. **89**, 1735 (1967).
27. G. A. Olah, D. M. O'Brien, and M. Calin. J. Am. Chem. Soc. **89**, 3582 (1967).
28. R. M. Moriarty and T. D. J. D'Silva. Tetrahedron, **21**, 547 (1965).

Can. J. Chem. Downloaded from www.nrcresearchpress.com by 210.87.254.5 on 09/05/12
For personal use only.

Some enzymic syntheses of ^{15}N-L-aspartic acid and ^{15}N-L-glutamic acid

J. A. ZINTEL, A. J. WILLIAMS, AND R. S. STUART
Biosynthetic Isotopic Research Laboratories, Merck, Sharp and Dohme of Canada Limited, Montreal, Quebec
Received September 10, 1968

Some methods for the preparation of ^{15}N-L-aspartic acid and ^{15}N-L-glutamic acid using enzyme catalyzed reactions are described. ^{15}N-L-Aspartic acid is prepared by the addition of ammonia to fumaric acid, catalyzing the reaction with aspartase which was partially purified from *E. coli*. ^{15}N-L-Glutamic acid with a high $^{15}N/^{14}N$ ratio is prepared by transamination with ^{15}N-L-aspartic acid catalyzed by aspartate aminotransferase. ^{15}N-L-Glutamic acid with a low $^{15}N/^{14}N$ ratio is prepared by a glutamic acid dehydrogenase catalyzed exchange of L-glutamic acid with ^{15}N-ammonia. These enzymes are commercially available. Since efficient utilization of ^{15}N is obtained, aspartic acid or glutamic acid may be prepared with any desired $^{15}N/^{14}N$ ratio.

Canadian Journal of Chemistry, **47**, 411 (1969)

Can. J. Chem. Downloaded from www.nrcresearchpress.com by 210.87.254.105 on 09/05/12
For personal use only.

Introduction

During the last few years new methods for the detection and analysis of stable isotopes have greatly increased their utility as tracers in biological sciences. For example, Tanabe and Detre (1) verified the biosynthetic pathway of griseofulvin by growing *Penicillium urticae* on ^{13}C-labeled acetate, isolating griseofulvin, and determining the position and abundance of each labeled carbon by nuclear magnetic resonance spectroscopy. This process eliminated the degradative work which would have been required with radioactive carbon. Using mass spectrometry, Bose *et al.* (2) identified the nitrogen precursors of gliotoxin isolated from an organism grown on ^{15}N-glycine or ^{15}N-phenylalanine. Since continuing research into nitrogen metabolism would be aided by making readily available some nitrogen labeled substrates, we have initiated a program to synthesize ^{15}N-L-amino acids.

Two of the best procedures for the synthesis of amino acids are the direct amination of α-halogen carboxylic acids and the Gabriel synthesis with potassium phthalimide. Neither of these syntheses is satisfactory for preparing amino acids with a high $^{15}N/^{14}N$ ratio, as the former requires a large excess of ammonia and the latter requires the preparation of ^{15}N-potassium phthalimide. In addition, chemical syntheses yield racemic mixtures which must be resolved if the L-isomer is to be used in biological studies (it has been pointed out that use of D,L mixtures has sometimes led to misleading results (3)). In any case, use of D,L mixtures wastes half of the isotope since, in general, only the L form is metabolized. These difficulties encountered in chemical syntheses of amino acids have been obviated by using enzyme catalyzed reactions. Aspartase has absolute stereochemical specificity for L-aspartic acid (4) and aspartate aminotransferase has absolute stereochemical specificity for both L-aspartic acid and L-glutamic acid (5). In this report, we describe syntheses of ^{15}N-L-glutamic acid and ^{15}N-L-aspartic acid with good yields and low isotopic loss.

Experimental

Chemicals

Aspartate aminotransferase (E.C. 2.6.1.1) and β-nicotinamide adenine dinucleotide (NAD) were obtained from Sigma Chemical Co., St. Louis, Missouri; glutamate dehydrogenase (GDH) (E.C. 1.4.1.2) from Boehringer Mannheim, New York; pyridoxal phosphate from Nutritional Biochemicals, Cleveland, Ohio; ^{15}N-ammonium chloride from Merck, Sharp & Dohme of Canada Limited, Montreal, Quebec; bacteriological grade alumina (A-305) from Canada Colors and Chemicals, Montreal, Quebec; and Whatman glass filter paper from Reeve Angel, Clifton, New Jersey. α-Ketoglutaric acid was a product of Matheson, Coleman and Bell. All other chemicals were standard reagent grade.

Thin-layer Chromatography

All thin-layer chromatography (t.l.c.) of amino acids was done on silica gel (K301R) chromogram sheets manufactured by Eastman Kodak. The sheets were developed with butanol/glacial acetic acid/water solvent (80:20:20 v/v) and the amino acids were visualized by spraying with 0.2% ninhydrin in butanol. Amino acids were estimated by comparing the spot size to standards.

Purification of Amino Acids

A single procedure was used for purifying glutamic and aspartic acids from any reaction mixture. The boiled, charcoal-treated amino acid reaction mixture was absorbed on a column (3.8 × 28.5 cm) of Dowex 50W × 8, 50–100 mesh, charged in the hydrogen form. The column was washed with at least 300 ml of distilled water and then

Can. J. Chem. Downloaded from www.nrcresearchpress.com by 210.87.254.105 on 09/05/12
For personal use only.

amino acids were eluted with 0.75 *N* ammonium hydroxide solution. Fractions containing amino acids were combined, flash evaporated to dryness, dissolved in 300 ml of water, and absorbed on a column (4.5 × 38.0 cm) of Amberlite CG-45 type II in the acetate form. After washing the column with 500 ml or more of 0.05 *M* acetic acid, glutamic acid was eluted with 0.15 *M* acetic acid and then aspartic acid was eluted with 0.25 *M* acetic acid (6). The amino acid solutions were flash evaporated to dryness (40°), dissolved in a minimum volume of hot water, and crystallized from solution by adding 0.5 volumes of absolute ethanol. The product was collected by filtration, dried, and weighed. Mass spectrometric isotopic analyses were done on a Hitachi RMU-6D with an M/G-150 direct introduction system.

Isolation of Aspartase

Escherichia coli cells (N.T.C. 9001) were grown on agar in standard Roux culture bottles as described by Wu and Rittenberg (7). In a typical isolation, cells from 19 Roux bottles were used. All steps in the isolation were done at 0–5°. The cells from each Roux bottle were suspended in 10 ml of 0.001 *M* sodium phosphate buffer solution, pH 7.4, combined, and the suspension was centrifuged at 10 000 × g for 10 min. The supernatant was discarded, the cells were suspended in 20 ml of the same buffer, and ground in a mortar with two volumes of alumina. The ground cell paste was diluted with 100 ml of buffer and centrifuged as before. Streptomycin was added (in the form of a 5% solution of streptomycin sulfate) to the supernatant to a final concentration of 1%. After 30 min, the suspension was centrifuged at 10 000 × g for 10 min, the precipitated nucleic acids were discarded, and the supernatant was dialyzed for 18 h against 3 l of tap water. The dialyzate was acidified to pH 4.4 with 10% acetic acid and stored overnight. The suspension was centrifuged as before, the supernatant was discarded, and the pellet dissolved in 45 ml of 0.001 *M* sodium phosphate buffer, pH 7.4; it was necessary to readjust the pH of the solution to 7.4 by adding 0.1 *N* sodium hydroxide solution. Insoluble material was removed by centrifugation at 10 000 × g for 10 min. The clear supernatant constituted the aspartase preparation used in syntheses. When stored at 4°, the aspartase preparation was found to be stable for at least one month.

Synthesis of ^{15}N-L-Aspartic Acid

To 63 ml of 0.05 *M* sodium phosphate buffer, pH 7.4, was added 10.5 g of sodium fumarate, 2.8 g of ammonium chloride (96.5 atom % ^{15}N), and 24.5 ml of aspartase preparation. The mixture was incubated at 37° for the required time, usually 72 h, and then boiled for a few minutes to inactivate the enzymes. ^{15}N-L-Aspartic acid was purified by column chromatography. After crystallization from water–ethanol, 5.4 g of L-aspartic acid were obtained, a yield of 78% based on ^{15}N-ammonium chloride. The product was determined by mass spectrometry to have the same isotopic composition (96.5 atom % ^{15}N) as the ammonium chloride used: $[\alpha]_D^{22}$ +42.5 (*c*, 2.00 in 2 *N* HCl). Non-labeled L-aspartic acid standard: $[\alpha]_D^{22}$ +46.6 (*c*, 2.00 in 2 *N* HCl).

Synthesis of ^{15}N-L-Glutamic Acid by ^{15}N Exchange

Five grams (0.034 moles) of L-glutamic acid and 1.92 g (0.034 moles) of ammonium chloride (96.7 atom % ^{15}N) were dissolved in 500 ml of distilled water. The pH of the solution was adjusted to 8.3 by dropwise addition of 4 *M* sodium hydroxide solution, chilled, and 150 mg NAD and 1 mg GDH (specific activity 2.9 EU/mg protein) were added. This mixture was incubated at 37° for 48 h after which time it was adjusted to pH 3.2 with 85% lactic acid and shaken for 45 min with 200 mg of Darco X charcoal. The suspension was filtered on glass filter paper and the filtrate was flash evaporated (40°) to dryness. The residue was dissolved in a minimum volume of hot water, 0.5 volumes of absolute ethanol added, and L-glutamic acid was allowed to stand at 5° for two days. The crystals were collected by suction filtration, washed with 20 ml of hot absolute ethanol, and dried at reduced pressure over P_2O_5. A 91% (4.8 g) recovery of L-glutamic acid was obtained which had an isotopic content of 50 ± 1 atom % ^{15}N; $[\alpha]_D^{22}$ +46.9 (*c*, 2.00 in 2 *N* HCl). Non-labeled L-glutamic acid standard: $[\alpha]_D^{22}$ +45.9 (*c*, 2.00 in 2 *N* HCl).

Synthesis of ^{15}N-L-Glutamic Acid from α-Ketoglutaric Acid

Glucose dehydrogenase was obtained from beef liver using the procedure of Strecker (8) up to and including the acid precipitation step.

To 250 ml of 0.05 *M* sodium phosphate buffer, pH 7.6, were added 50 ml of glucose dehydrogenase preparation, 200 mg of NAD, 5.0 g of glucose, 100 mg of ammonium chloride (96.5 atom % ^{15}N), 50 mg of monosodium α-ketoglutarate, and about 3 mg of glutamic acid dehydrogenase (specific activity 2.9 EU/mg protein). The reaction was followed by measuring the change in absorbance of the mixture (usually at 280 mμ) due to formation or disappearance of $NADH_2$. After 2 h, when the absorbance of the reaction mixture was constant, an additional 50 mg of monosodium α-ketoglutarate were added and the pH was readjusted to 7.6 with 1 *M* sodium hydroxide solution. Over the next 90 min, three 50 mg portions of α-ketoglutarate were added. Then 100 mg of ^{15}N-ammonium chloride and 300 mg of α-ketoglutarate were added, the pH was adjusted to 7.6, and the reaction mixture was stirred slowly overnight at room temperature. A final lot of 150 mg of ^{15}N-ammonium chloride and 200 mg of monosodium α-ketoglutarate were added and the pH was adjusted as before. After 6 h, the solution was boiled for a few min and then stored at 0° until glutamic acid was purified by chromatography. The yield was 450 mg or 47% based on ^{15}N-ammonium chloride. However, considerable isotopic dilution occurred and the product was only 30.0 ± 1 atom % ^{15}N.

Synthesis of ^{15}N-L-Glutamic Acid Using Aspartate Aminotransferase

To 75 ml of distilled water was added 1.5 g of ^{15}N-L-aspartic acid (96.5 atom % ^{15}N) and 2.1 g of α-ketoglutaric acid. The suspension was stirred slowly and the reactants were dissolved by adding 4 *M* sodium hydroxide solution until the pH was 7.6. A few mg of pyridoxal phosphate, 50 mg of CG-45 (in acetate form), and 2 mg of aspartate aminotransferase were added. The mixture was incubated at 25°; the pH was checked hourly and adjusted to 7.6 with 1 *M* hydrochloric acid solution. After 6 h the solutions was acidified to pH 6.5 with 10% acetic acid solution

and the reaction mixture was stirred slowly overnight. After 18 h, the pH was again made 7.6 with 4 *M* sodium hydroxide solution and maintained at this value for 6 h. After the solution was acidified to pH 5.0 with 10% acetic acid solution, the reaction mixture was stirred for 30 min with 200 mg of Darco X charcoal and filtered on glass paper. Glutamic and aspartic acids were purified by chromatography. The yield was 700 mg or 42% based on aspartic acid and the isotopic content of L-glutamic acid was 96.5 atom % ^{15}N, $[\alpha]_D^{22}$ +49.2 (*c*, 2.00 in 2 *N* HCl). Non-labeled L-glutamic acid standard: $[\alpha]_D^{22}$ +45.9 (*c*, 2.00 in 2 *N* HCl).

Results and Discussion

A procedure for synthesizing ^{15}N-L-aspartic acid was reported by Wu and Rittenberg (7) using a resting cell suspension of *E. coli* as a source of aspartase to catalyze the addition of ammonia to fumaric acid as is shown below:

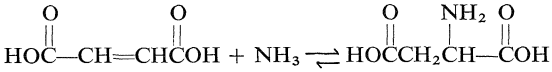

They reported a 60% yield of ^{15}N-L-aspartic acid based on ^{15}N-ammonia as ammonium chloride and very little isotopic dilution; we have found that this procedure gave highly variable yields and often gave considerable isotopic dilution. However, these difficulties were overcome by catalyzing the reaction with partially purified *E. coli* aspartase. In several experiments run with different batches of aspartase, the lowest yield was 70% in a reaction starting with 0.4 g of ammonium chloride (a more typical yield was 78% which was obtained in a larger reaction using 2.8 g of ammonium chloride). In no case did isotopic dilution occur, thus, this procedure is very suitable for preparing L-aspartic acid with any desired $^{15}N/^{14}N$ ratio.

Since the utility of this synthesis of ^{15}N-L-aspartic acid is dependent on a partial purification of aspartase from *E. coli*, each step in the purification was chosen so that it could be duplicated easily. Each batch of aspartase was checked by running a small scale synthesis and estimating by t.l.c. on silica gel the amount of aspartic acid synthesized. For a synthesis on the scale described, volumes from 20 to 30 ml of aspartase preparation were used and a convenient reaction rate was always obtained.

A direct synthesis of ^{15}N-L-glutamic acid was also devised. In the reaction illustrated below, glutamic acid dehydrogenase (GDH) catalyzed the addition of ammonia to α-ketoglutaric acid with a concomitant oxidation of $NADH_2$ to NAD. To eliminate the requirement for a large amount of $NADH_2$, $NADH_2$ was regenerated *in situ* from NAD by an alcohol dehydrogenase (ADH) catalyzed oxidation of ethanol to acetaldehyde. An advantage of this system is that both enzymes are available commercially from biochemical supply houses in highly purified form. However, the yields from this reaction were very low as the large excess of ethanol that was required to drive the reaction in the direction shown, brought about rapid denaturation of the enzymes. Greater success was attained when $NADH_2$ was regenerated by using glucose dehydrogenase to catalyze the oxidation of glucose to gluconic acid. Using this latter system a typical yield was 50% based on ammonium chloride; but in a reaction using 96.5 atom % ^{15}N-ammonium chloride, the L-glutamic acid synthesized was found to contain only 30 atom % ^{15}N. This dilution could be eliminated by dialyzing both enzyme preparations prior to use. However, glucose dehydrogenase must be isolated from beef liver and great care is required in carrying out the reaction; hence this procedure for the preparation of ^{15}N-L-glutamic acid was inferior to others that were developed.

The preparation of ^{15}N-L-glutamic acid with an isotopic content of 50 atom % ^{15}N or less was best achieved through a very simple exchange reaction with ^{15}N-ammonia and L-glutamic acid catalyzed by GDH and NAD. L-Glutamic acid and ^{15}N-ammonium chloride were dissolved in a buffer solution, GDH and a trace of NAD were added, and the mixture was incubated at 37°

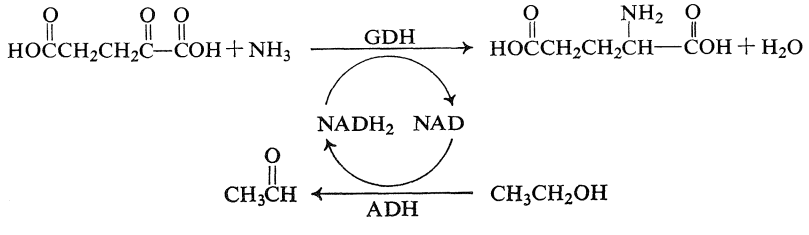

Can. J. Chem. Downloaded from www.nrcresearchpress.com by 210.87.254.105 on 09/05/12
For personal use only.

two days, after which over 90% of the L-glutamic acid was recovered in pure form, having an isotopic content equal to the theoretical value calculated by assuming complete equilibration of nitrogen.

Transamination reactions in which the enzyme source was either a whole cell suspension or a cell homogenate have been used to synthesize non-labeled amino acids (9–14). Our experience has shown that such syntheses are more reproducible and result in no detectable isotopic dilution if the enzyme is at least partially purified from proteins and metabolites. As pure aspartate aminotransferase may be obtained from biochemical supply houses, a transamination synthesis of L-glutamic acid was developed, which is shown by the following reaction:

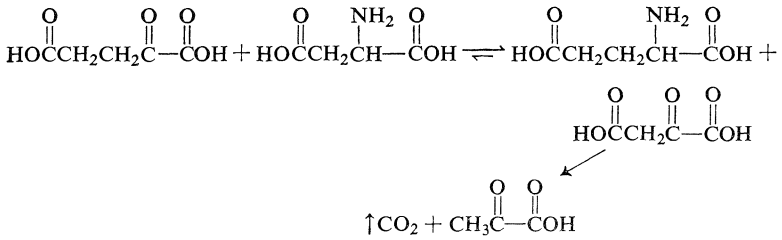

The synthesis requires ^{15}N-L-aspartic acid, but as mentioned earlier, this was prepared in good yield by the aspartase catalyzed addition of ^{15}N-ammonia to fumaric acid; in addition, almost quantitative transfer of amino nitrogen was achieved by decarboxylating oxalacetic acid during transamination.

To ensure decarboxylation of oxalacetic acid, the reaction was run in a dilute buffer solution which was initially adjusted to pH 7.6, but as transamination proceeded the pH decreased to about 6 and a slow acid-catalyzed decarboxylation occurred. Also, a primary amine resin, CG-45, was added to the reaction as primary amines are specific catalysts for decarboxylating β-keto acids. Although at pH 6 the contribution of CG-45 to the net decarboxylation was low, its use was warranted as it was removed easily by filtration at the end of the reaction period. In the example given of this reaction, a preparation with ^{15}N, a 42% yield was obtained. A 77% yield was obtained from the same scale reaction using non-labeled L-aspartic acid. Since, at the end of the ^{15}N reaction period, very little aspartic acid was detected by t.l.c., the low yield was probably due to mechanical loss during isolation and not due to an isotope effect. A yield of 75% can be expected.

Each of these enzyme catalyzed syntheses of ^{15}N-L-amino acids was reproducible, gave the L-isomer in good yield, and was superior to conventional chemical syntheses. We think that ^{15}N-L-aspartic acid is best prepared from the aspartase reaction, ^{15}N-L-glutamic acid with a low $^{15}N/^{14}N$ ratio is best prepared by the glutamic acid dehydrogenase catalyzed exchange reaction, and ^{15}N-L-glutamic acid with a high $^{15}N/^{14}N$ ratio is best prepared by transamination with ^{15}N-L-aspartic acid. It is possible that ^{15}N-L-glutamic acid could also be prepared by combining the aspartase synthesis with the aspartate aminotransferase reaction so that it would not be necessary to isolate ^{15}N-L-aspartic acid as an intermediate. One approach, which would minimize the chances of forming L-alanine by transamination with pyruvic acid, would be to add α-ketoglutarate and aspartate aminotransferase to an aspartase synthesis reaction that was nearing completion. These enzyme reactions also have potential for a very large scale production of amino acids if the enzymes are stabilized by attaching them to an insoluble inert support, such as beads of Sephadex G-200; Axén and Porath (15) have published a procedure for attaching enzymes to Sephadex G-200. By attaching aspartase to Sephadex beads, a continuous synthesis of L-aspartic acid could be made by simply percolating a solution of fumaric acid and ammonium chloride through a column of aspartase beads held at 37°. Similarly, L-glutamic acid could be synthesized by using a mixed bed column of aspartase beads and aspartate aminotransferase beads.

Acknowledgments

We thank Professor D. R. McCalla at

Can. J. Chem. Downloaded from www.nrcresearchpress.com by 210.87.254.105 on 09/05/12
For personal use only.

McMaster University for helpful suggestions in preparing this manuscript, Professor Y. Rousseau at the Université de Montréal for doing mass spectrometric analyses, and D. B. Weadon and R. White for technical assistance. We also thank the National Research Council of Canada for their support with an Industrial Research Grant.

1. M. TANABE and G. DETRE. J. Am. Chem. Soc. **88**, 4515 (1966).
2. A. K. BOSE, K. G. DAS, P. T. FUNKE, I. KUGAJEVSKY, O. P. SHUKLA, K. S. KHANCHANDANI, and R. J. SUHADOLNIK. J. Am. Chem. Soc. **90**, 1038 (1968).
3. J. P. GREENSTEIN and M. WINITZ. *In* Chemistry of the amino acids. Vol. 2. John Wiley & Sons, Inc., New York. p. 1748.
4. A. I. VIRTANEN and N. ELLFOLK. *In* Methods in enzymology. Vol. 2. *Edited by* S. P. Colowick and N. O. Kaplan. Academic Press, Inc., New York. 1955. p. 386.
5. W. T. JENKINS, D. A. YPHANTIS, and I. W. SIZER. J. Biol. Chem. **234**, 51 (1959).
6. K. KURAHASI. J. Chromatog. **13**, 278 (1964).
7. H. WU and D. RITTENBERG. J. Biol. Chem. **179**, 847 (1949).
8. H. J. STRECKER. *In* Methods in enzymology. Vol. 1. *Edited by* S. P. Colowick and N. O. Kaplan. Academic Press, Inc., New York. 1955. p. 335.
9. S. AKABORI and I. OSHIO. Japan Patent 2014 (1959).
10. S. SAKURAI and S. AKABORI. Japan Patent 3768 (1956).
11. S. YAMADA and S. SAKURAI. J. Biochem. Tokyo, **44**, 557 (1957).
12. S. SAKURAI. J. Biochem. Tokyo, **45**, 379 (1958).
13. S. SAKURAI. J. Biochem. Tokyo, **44**, 47 (1957).
14. S. SAKURAI. J. Biochem. Tokyo, **43**, 851 (1956).
15. R. AXÉN and J. PORATH. Nature, **210**, 367 (1966).

Can. J. Chem. Downloaded from www.nrcresearchpress.com by 210.87.254.105 on 09/05/12
For personal use only.

Can. J. Chem. Downloaded from www.nrcresearchpress.com by 210.87.254.6 on 09/05/12
For personal use only.

Electrolysis of low molecular weight carbohydrates in non-aqueous media.[1] I. The products of electrolysis of monosaccharides

G. W. HAY[2,3,4]

Department of Chemistry, Queen's University, Kingston, Ontario

AND

F. SMITH[5]

Department of Biochemistry, College of Biological Sciences, University of Minnesota, St. Paul, Minnesota 55101

Received September 6, 1968

The electrolysis of monosaccharides in alkaline, non-aqueous media caused a sequential descent of the series as a result of the elimination of one-carbon units from the reducing end of the molecule, without the formation of chromatographically detectable quantities of oxidized derivatives.

Canadian Journal of Chemistry, 47, 417 (1969)

Introduction

Since the initial detection of acids from the electrolysis of sucrose (1) and glucose (2) relatively few studies of electrochemical reactions of carbohydrates have been published. The synthetic applications other than the electrochemical synthesis of D-gluconic (3–6) and other aldonic acids (7–10), D-glucitol and D-mannitol (11, 12), and periodate oxystarch (13) remain largely unexploited.

The electrolysis of carbohydrates in aqueous solution usually involves both hydrolytic and oxidative reactions in which carbonyl (4, 14, 15) and/or carboxyl (1, 3–9, 16) groups are introduced into the parent compound. Thus, polysaccharides and proteins may be depolymerized, and the monomers degraded to lower molecular weight products (1, 14, 17–23).

Occasionally the literature has reported the electrochemical reduction of aldoses (16, 24) and other carbohydrates (25), and of aliphatic and aromatic aldehydes (26–28). The mechanism of such a reduction of glucose, which produced as side-products small amounts of mannitol and 2-deoxyglucitol, was elucidated by Wolfrom *et al.* (29, 30).

The qualitative and quantitative study reported herein was instigated to determine the effect on simple carbohydrates of electrolysis in a system in which the generation of a significant concentration of methoxyl free radicals could be anticipated (31).

Discussion

Paper chromatographic analysis of the products of electrolysis revealed the stepwise degradation of the parent compound to a mixture of lower aldoses (Table I). In accord with earlier studies (14), these reactions exhibited a high initial rate. In one typical experiment, a detectable amount of the secondary reaction, arabinose → erythrose, was obtained after 10 min electrolysis of D-glucose. D-Galactose underwent a more efficient degradation than D-glucose and gave a higher yield of pentose (cf. ref. 20).

A large volume of gas containing both H_2 and CO_2 was evolved during the reaction, principally from the cathode. Whereas it is likely that the H_2, and much of the CO_2, came from the electrolysis of methanol (31), the lack of quantitative recovery of carbohydrate suggested that some of the parent compound was completely oxidized to CO_2 (18).

Experiments in which maltose, because of its low solubility in methanol, was electrolyzed in water to which sodium methoxide was added, disclosed rapid and extensive cleavage of the glycosidic bond. Paper chromatographic analysis revealed no identifiable oxidation product of maltose; glucose and arabinose were the earliest degradation products detected (see Table I). These observations are consistent with an initial

---

[1]Issued as Paper No. 6619, Scientific Journal Series, Minnesota Agricultural Experiment Station.

[2]Part of this paper was abstracted from Part II of a thesis submitted by G. W. Hay in partial fulfillment of the requirements for the Ph.D. degree, University of Minnesota, 1959.

[3]To whom enquiries should be addressed.

[4]Supported by grants from Brewing Industries Research Institute, and the Ontario Department of University Affairs.

[5]Deceased.

Can. J. Chem. Downloaded from www.nrcresearchpress.com by 210.87.254.6 on 09/05/12
For personal use only.

TABLE I

Results obtained from the electrolysis of various carbohydrates under a variety of conditions

Experiment number	Compound (amount used in g)	Solvent (amount used in ml)	Electrolyte (amount used in mg)	Current (max. V, max. A, type*)	Time (h)	Chromatographic analysis	
						Products†	Solvents
1	D-Glucose (10)	EtOH (200)	Na (80)	—,—,*d*	7	G;Ara;Ery	*a,b,c*
2	D-Glucose (10)	MeOH (200)	KOH (80)	—,—,*d*	24	G;Ara;Ery	*a,b,c*
3	D-Glucose (15)	MeOH (200)	Na (50)	40,—,*a*	21	G;Ara;Ery	*a,b,c*
4	D-Glucose (10)	MeOH (230)	Na (30) V_2O_5 (1)	40, 0.3,*d*	22	G;Ara;Ery	*a,c*
5	D-Glucono-1,5-lactone (10.5)	MeOH (200)	Na (55)	40,—,*a*	24	GA;Ara;Ery	*b,c*
6	Methyl-α-D-glucopyranoside (2)	MeOH (200)	Na (40)	50, 0.3,*d*	36	Unk;G;MeG	*f*
7	D-Galactose (9)	MeOH (200)	NaOH (70)	46, 0.7,*d*	21	Gal;Lyx;Thr‡	*b,c,d*
8	D-Galacturonic acid (5)	MeOH (200)	Na (50)	60,—,*a*	44	Gal A;Ara	*d*
9	D-Mannose (3)	MeOH (100)	Na (30)	47, 0.2,*d*	24	Man;Ara;Ery	*a,c,d*
10	Maltose (10)	H_2O (250)	Na (60) in MeOH (3 ml)	47, 0.45,*d*	24	Mal;G;Ara;Ery	*b,c*

d, direct current; *a*, alternating (60 Hz) current.

†The abbreviations used are: Ara, arabinose; Ery, erythrose; Gal, galactose; Gal A, galacturonic acid; G, glucose; GA, gluconic acid; Lyx, lyxose; Mal, maltose; Man, mannose; MeG, methyl glucoside; Thr, threose; Unk, unidentified. Products are listed in order of increasing R_f.

‡Identified as threitol after reduction with $NaBH_4$.

Can. J. Chem. Downloaded from www.nrcresearchpress.com by 210.87.254.6 on 09/05/12
For personal use only.

hydrolysis of the glycosidic bond followed by the usual electrolytic degradation of glucose, and with the synthesis of 3-*O*-α-D-glucopyranosyl-D-arabinose (32) followed instantly by hydrolysis to D-glucose and D-arabinose. The elucidation of the route(s) is under investigation.

As adduced from qualitative paper chromatographic analysis, the same products were obtained by electrolysis with each of sodium methoxide, sodium ethoxide, sodium hydroxide, and potassium hydroxide (see Table I).

In this study an amperage lag of 0.1–0.5 min occurred at the start of electrolysis before the amperage rose to a maximum value (usually after 0.1–0.5 h) and thereafter slowly declined. The porosity of the graphite electrodes and/or the formation of an insulating residue on the cathode surface may explain in part this decline. However, the reversal of polarity, which caused the residue to flake off of the new anode, and/or the cleaning of the electrode surface, failed to restore maximum current. Some current-conducting component appeared to have been consumed or otherwise irreversibly removed from the system.

The non-aqueous system was peculiar in that it formed aldoses in the absence of chromatographically detectable quantities of aldonic acids (3–9, 14, 16) and other oxidized derivatives (4, 14, 15). Nevertheless the most probable mechanism of sequential degradation would involve the formation of an aldonic acid as the first, or an early, step in the electrolysis, since these are known to form from (16, 17), and to degrade to (14, 20, 33), aldoses during electrolysis. Neuberg's (14) discovery of ozones in the electrolysis of aldoses may mean that an α-keto compound is formed (34) either prior to, or after, the carboxyl group, thus giving an α-ketoaldonic acid which can decarboxylate to an aldose having one less carbon atom (35). Consistent with such a theory are the alkaline oxidative degradation of D-glucose to D-arabonic acid (36) and L-arabinose to L-erythronic acid (37), the formation in alkali of carbonyl derivatives of carboxylic acids (31), and the detection of a keto acid from the electrolysis of erythronic acid (21). If such acidic intermediates participate in these reactions the aldoses must be strongly favored in any equilibria involving the oxidized compounds, and/or the oxidation must be very slow relative to decarboxylation so that at any instant the concentration of the intermediate is below present levels of detection.

Electrolysis offers a facile, and potentially useful method for the sequential degradation of sugars, and sugar derivatives (14, 33) to lower homologues. The method is of broad application (Table I, see ref. 33) and avoids the necessity of synthesizing special derivatives (38) for subsequent chemical degradation. Both the mechanism of the process, and conditions whereby higher yields of a desired product can be obtained, remain to be established, however, even in its present state of development it is a practical means of obtaining certain unusual sugars such as D-arabinose and D-threose in semi-micro amounts, as has been clearly established by the isolation of milligram quantities of the pure products by preparative paper partition chromatography. There seems to be no reason to question the ability of still more recent separatory techniques to provide equal or superior resolution and recovery of the individual components on a macro scale.

Experimental

General Methods

All evaporations were carried out at 35–45 °C under reduced pressure, unless stated otherwise. Melting points were determined with a Fisher–Johns Melting Point Block (Fisher Scientific Co.) and are uncorrected. The water used for optical rotation studies of free sugars contained a trace of ammonium hydroxide to catalyze the formation of an equilibrium mixture of anomers.

Paper chromatography by the descending technique, using Whatman no. 1 and 3MM paper, was effected with one or more of the following solvent systems (39): (*a*) 1-butanol:ethanol:water, 4:1:5; (*b*) 1-butanol:pyridine:water, 6:4:3; (*c*) pyridine:ethyl acetate:water, 2:5:7; (*d*) 1-butanol:acetic acid:water, 2:1:1; (*e*) 2-butanone–water azeotrope; (*f*) ethyl acetate:acetic acid:formic acid:water, 18:3:1:4. Chromatograms were visualized (39) with ammoniacal silver nitrate, or with *p*-anisidine–trichloroacetate.

Electrolysis Cell and Power Supplies

The cell was a standard 800 ml (13 × 9.5 cm) beaker which was slightly reshaped to remove the pouring lip. Two holes were drilled in a stopper (size 15) to accommodate 4.0 cm diameter graphite electrodes approximately 0.5 cm apart. Each electrode was fitted with a brass terminal at the exterior end. A third hole was drilled in the stopper in which was inserted a 19/38 to 24/40 standard taper adapter which received a reflux condensor.

A power supply from a Reco Electric Desalter (Research Equipment Corp.) with a maximum output of 3.0 A at 50 V, or a transistorized rectifier module (fused at 2 A) attached to a Powerstat variable resistance (The Superior Electric Co.), supplied direct current for the experiments. The Powerstat control without rectifier was used to supply alternating current (60 Hz).

Can. J. Chem. Downloaded from www.nrcresearchpress.com by 210.87.254.6 on 09/05/12
For personal use only.

General Electrolytic Method

In almost all experiments, the sugar sample and the solvent were introduced into the dry, sealed electrolysis cell. The electrodes extended 3.5–4.5 cm below the surface of the reaction mixture. The electrolyte (Na, NaOH, KOH, or $NaOCH_3$) was dissolved whereupon the voltage was applied to give maximum current. Electrolysis was continued for widely variable lengths of time.

Miscellaneous Electrolyses

A relatively large number of experiments were investigated only by qualitative paper partition chromatographic analysis. The results of a series of typical experiments are recorded in Table I.

Electrolysis of D-*Glucose*

A sample (15.0 g) of D-glucose (anhydrous powder) was suspended in 200 ml methanol to which 0.05 g freshly cut sodium then was added. The solution was electrolyzed for 44 h using direct current (d.c.). The current rose to a maximum of 1.1 A at 45 V after 0.5 h and then declined slowly to a terminal value of 0.15 A at 47 V. Aliquots were removed 3, 5, 15, 24, and 44 h after the start of the experiment and were found by paper partition chromatography in solvents *a*, *b*, and *c* to contain glucose, arabinose, erythrose, and some unidentified material. Evaporation of the solvent gave 8.2 g of heavy, amber syrup.

A sample (0.3587 g) was resolved quantitatively by preparative paper chromatography in solvents *a* and *b*. The components having R_f values greater than that of erythrose were reduced with sodium borohydride whereupon glycerol was detected. The individual components were isolated and identified in the following manner.

D-Glucose: glucose (0.2208 g, yield: 51.0%) $[\alpha]_D^{24}$ +54.0° (*c*, 1 in H_2O) (40), was converted to the characteristic *N*-*p*-nitrophenyl-β-D-glucosylamine, m.p., and mixture m.p. 184.5–186 °C (41).

D-Arabinose: this component (0.0528 g, yield: 12.4%) $[\alpha]_D^{25}$ −101° (*c*, 0.8 in H_2O) (42), afforded D-arabinose benzoylhydrazone, m.p. and mixture m.p. 189–190 °C (hot, 95% ethanol) (43).

D-Erythrose: this fraction (0.0430 g, yield: 9.9%) $[\alpha]_D^{24}$ −15.5° (*c*, 1 in H_2O) (44–46), was reduced in aqueous solution $NaBH_4$. Erythritol was characterized as the tetra-*p*-nitrobenzoate, m.p., and mixture m.p. 249–251 °C. An authentic sample had the same m.p.

Glyceraldehyde: the components migrating faster than erythrose on the paper chromatograms were eluted with water, reduced with $NaBH_4$, and rechromatographed after removal of borate (47). Glycerol (0.0181 g, yield: 4.2%) was identified as the tri-*p*-nitrobenzoate, m.p., and mixture m.p. 191–192.5 °C (48).

The remaining eluates were combined and evaporated to a light-amber syrup (0.0161 g, yield: 3.7%).

Control Experiment

A duplicate solution of D-glucose in sodium methoxide–methanol was refluxed for the period during which electric current was allowed to flow.

Chromatographic analysis of the reaction product in solvents *a* and *d*, revealed the presence of glucose with traces of mannose and arabinose.

Electrolysis of D-*Galactose*

D-Galactose (9.1 g) was electrolyzed in 200 ml methanol to which was added 0.04 g sodium. A direct current was passed through the solution for 20 h using graphite electrodes. The current rose to a maximum of 0.9 A at 44 V after 0.25 h and thereafter declined to the terminal value of 0.55 A at 46 V. Evaporation of the reaction mixture gave 8.6 g of viscous syrup.

A sample (0.1631 g) was resolved by paper chromatography in the manner described for glucose, except that the components migrating ahead of lyxose were eluted, combined, reduced, and rechromatographed. The individual components were identified on the basis of the following data:

D-Galactose: galactose (0.0466 g, yield: 27.0%), $[\alpha]_D^{25.5}$ +78.4° (*c*, 1.2 in H_2O) (40), was converted in the usual manner to D-galactose *unsym.*-methylphenylhydrazone, m.p. and mixture m.p. 186–187 °C (43).

D-Lyxose: this component (0.0413 g, yield: 24.0%) $[\alpha]_D^{24.2}$ −12.6° (*c*, 1 in H_2O) (42), afforded the 2,5-dichlorophenylhydrazone of D-lyxose, m.p. and mixture m.p. 140–142.5 °C (hot aqueous ethanol) (49).

D-Threitol: threitol (0.0293 g, yield: 17.0%) $[\alpha]_D^{25.2}$ +4.5° (*c*, 4.75 in H_2O) (50–51), was converted in the usual manner to di-*O*-benzylidene-D-threitol, m.p. 222–223.5 °C, mixture m.p. 224–225 °C (52).

Glycerol: this component (0.0094 g, yield: 5.4%) was identified as described above (48).

The unidentified residue weighed 0.0329 g, yield: 19.1%. A control experiment was performed in the usual manner.

Analysis of Electrode Gases

The electrolysis of 10 g D-glucose in 200 ml methanol in which 0.05 g sodium had been dissolved, was allowed to proceed for 6 h to displace air initially present in the cell. The evolved gas was passed into a clear solution of $Ba(OH)_2$. The formation of a white precipitate was accepted as a presumptive test for CO_2.

A similar experiment was performed on a smaller scale using an "H" tube to separate the anode and cathode. Cathodic gases were collected under water. The water vapor was frozen out with Dry Ice – acetone and the gases analyzed in a mass spectrometer.[6] Hydrogen was identified as a major component of the mixture.

1. M. A. BRESTER. Bull. Soc. Chim. France, [2], **8**, 23 (1866).
2. H. T. BROWN. J. Chem. Soc. **24**, 578 (1872).
3. H. J. ISBELL and H. L. FRUSH. J. Res. Natl. Bur. Std. **6**, 1145 (1931); **14**, 359 (1935).
4. C. G. FINK and D. B. SUMMERS. Trans. Am. Electrochem. Soc. **74**, 325 (1938).
5. A. N. KAPPARA and K. M. JOSHI. J. Indian Chem. Soc. **29**, 69 (1952).
6. S. SATHYANARAYANA and H. V. K. UDUPA. Bull. Acad. Polon. Sci. Ser. Sci. Chim. **6**, 493 (1958).
7. H. KILIANI. Ber. **66B**, 117 (1933).
8. M. STEIGER. Helv. Chim. Acta, **19**, 189 (1936).
9. O. T. SCHMIDT and A. SIMON. J. prakt. Chem. **152**, 19 (1939).

[6]The mass spectrometric analyses were obtained through the courtesy of Dr. J. A. Stone, Department of Chemistry, Queen's University.

10. M. L. SEN GUPTA, N. BHATTACHARYA, and U. P. BASU. Indian J. Technol. **5**, 152 (1967).
11. H. G. CREIGHTON. Trans. Am. Electrochem. Soc. **75**, 289 (1939); **90**, 15 (1946).
12. C. L. FAUST and L. D. MCGRAW. Ind. Eng. Chem. **50**, 46A (1958).
13. C. L. MEHLTRETTER, J. C. RANKIN, and P. R. WATSON. Ind. Eng. Chem. **49**, 350 (1957).
14. C. NEUBERG. Biochem. Z. **17**, 27 (1909).
15. F. H. CHOUDHURY and M. H. KHUNDKAR. Pakistan J. Sci. Research, **5**, 77 (1953).
16. A. RENARD. Ann. Chim. et Phys. [5], **17**, 289 (1879).
17. A. FINDLAY and V. H. WILLIAMS. Trans. Faraday Soc. **17**, 453 (1932).
18. J. O'M. BOKRIS, B. J. PIERSMA, and E. GILEADI. Electrochim. Acta, **9**, 1329 (1964).
19. W. LÖB. Z. Elektrochem. **16**, 1 (1910).
20. C. NEUBERG, L. SCOTT, and S. LACHMANN. Biochem. Z. **24**, 152 (1910).
21. C. NEUBERG and E. HIRSCHBERG. Biochem. Z. **27**, 327 (1910).
22. K. ULSCH. Z. Elektrochem. **5**, 539 (1899).
23. F. H. CHOUDHURY and M. H. KHUNDKAR. Pakistan J. Sci. Research, **4**, 103 (1952).
24. M. BERTHELOT. Compt. Rend. **87**, 494 (1881).
25. J. TAFEL and B. EMMERT. Z. Elektrochem. **17**, 569 (1911).
26. H. J. CREIGHTON. Trans. Am. Electrochem. Soc. **75**, 289 (1939).
27. W. SCHEPPS. Ber. **46B**, 2564 (1914).
28. J. O'B. GUNN. German Patent 140,318 (1900); Chem. Zentralblatt, 914 (1903).
29. M. L. WOLFROM, M. KONIGSBERG, F. B. MOODY, and R. M. GEOPP, JR. J. Am. Chem. Soc. **68**, 122 (1946).
30. M. L. WOLFROM, F. B. MOODY, M. KONIGSBERG, and R. M. GEOPP, JR. J. Am. Chem. Soc. **68**, 578 (1946).
31. K. SASAKI, C. HAMAGUCHI, and S. NAGAURA. Bull. Chem. Soc. Japan, **37**, 1086 (1964).
32. A. M. GAKHOKIDZE. Zh. Obshch. Khim. **18**, 60 (1948); Chem. Abstr. **42**, 4948 (1948).
33. D. J. MACGREGOR. M.Sc. Thesis. Queen's University, Kingston, Ontario. 1961.
34. R. D. BROOKS and N. S. THOMPSON. Tappi, **49**, 362 (1966).
35. C. E. DALGLIESH, A. W. JOHNSON, and L. J. HAYNES. *In* Chemistry of carbon compounds. Vol. I. 1st ed. *Edited by* E. H. Rodd. Elsevier Publ. Co., Inc., Amsterdam. 1942. pp. 782–783.
36. O. SPENGLER and A. PFANNENSTIEL. Z. Wirtschaftsgruppe Zuckerind. Allgem. Tl. Tech. Tl. **85**, 546 (1935).
37. J. U. NEF, O. F. HEDENBURG, and J. W. E. GLATTFELD. J. Am. Chem. Soc. **38**, 1638 (1917).
38. O. KJØLBERG. Acta Chem. Scand. **14**, 1118 (1960).
39. J. STANĚK, M. ČERNÝ, J. KOCOUREK, and J. PACÁK. The monosaccharides. Academic Press, Inc., New York. 1963. pp. 927–943.
40. F. J. BATES and associates. Polarimetry, saccharimetry, and the sugars. Natl. Bur. Stds. Circ. C440, U.S. Gov't. Printing Office, Washington. 1942. pp. 153–212.
41. F. WEYGAND, W. PERKOW, and P. KUHNER. Chem. Ber. **84**, 594 (1951).
42. C. S. HUDSON and E. YANOVSKY. J. Am. Chem. Soc. **39**, 1013 (1917).
43. E. L. HIRST, J. K. N. JONES, and E. A. WOOD. J. Chem. Soc. 1048 (1947).
44. W. G. OVEREND, M. STACEY, and L. F. WIGGINS. J. Chem. Soc. 1358 (1949).
45. O. RUFF. Ber. **32**, 3672 (1899).
46. R. A. WEERMAN. Rec. Trav. Chim. **37**, 16 (1917).
47. F. SMITH and R. MONTGOMERY. *In* Methods of biochemical analysis. Vol. III. *Edited by* D. Glick. Interscience Publishers, Inc., New York. 1956. pp. 153–212.
48. Dictionary of organic compounds. 4th ed. Vol. 3. Eyre and Spottiswood, Ltd., London. 1965. p. 1534.
49. I. MANDL and C. NEUBERG. Arch. Biochem. Biophys. **35**, 326 (1952).
50. L. MAQUENNE. Bull. Soc. Chim. France, [3], **23**, 587 (1900).
51. L. MAQUENNE. Compt. Rend. **130**, 1402 (1900).
52. H. KLOSTERMAN and F. SMITH. J. Am. Chem. Soc. **74**, 5336 (1952).

Can. J. Chem. Downloaded from www.nrcresearchpress.com by 210.87.254.6 on 09/05/12
For personal use only.

Studies of stereochemical influences upon anti-histaminic activity. The synthesis, configuration, and anti-histaminic properties of some isomeric aminobutenes[1]

A. F. CASY AND A. P. PARULKAR
Faculty of Pharmacy, University of Alberta, Edmonton, Alberta

Received August 23, 1968

The acid-catalyzed dehydration of 4-dimethylamino-2-*p*-methoxyphenyl-1-phenylbutan-2-ol yields all four possible 4-amino-1,2-diarylbutenes. Pure samples of each isomer have been isolated, double bond positions and configurations being established from proton magnetic resonance and ultraviolet spectroscopic data. A stereoselective route to *cis* aminobut-1-enes has been further investigated. The anti-histaminic properties of the reported butenes together with some related compounds are given and structural influences upon activity discussed.

Canadian Journal of Chemistry, 47, 423 (1969)

In 1950 Stoll and co-workers reported the anti-histaminic properties of some 4-amino-1,2-diarylbutenes formed by dehydration of 1,2-diaryl-4-*t*-aminobutan-2-ols (**1**), certain members having activities approaching that of Antergan (1). Since the aminobutenes were not characterized satisfactorily, the elimination of water from the butanols **1** has been further investigated and the double bond position and configuration of a series of so-derived isomeric aminobutenes established by spectroscopic means and the most active product of the Geigy workers shown to be a ternary mixture (2–4). In this paper further pharmacological data upon this mixture and upon a number of isomerically pure 4-aminobut-1-enes and -but-2-enes are given and tentative structure activity relationships drawn from the results.

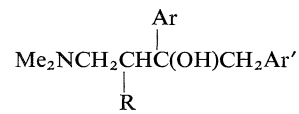

1 R = (*a*), H; (*b*), Me.

$Me_2NCH_2CHMeCAr{=}CHAr^1$

2

$Me_2NCH_2CH{=}CArCH_2Ph$ $Me_2N(CH_2)_2CAr{=}CHPh$

Ar and H reference groups Ar and Ph reference groups

3 **4**

Ar = (*a*), Ph; (*b*), *p*-MeO·C_6H_4.

Chemistry

All the compounds tested (Tables II and III) were obtained by fractional crystallization of 4-aminobutene hydrochloride mixtures derived by acid-catalyzed elimination of the corresponding *t*-alcohols **1**. Those alcohols with 3-methyl substituents (**1***b*) gave but-1-enes exclusively (**2**) while the nor-analogues (**1***a*) gave all four possible isomers, namely *cis* and *trans* **3** and **4** (2, 3). An additional series of 2-*p*-methoxyphenylbutenes was synthesized by the sequence **5** through **8** and the four aminobutenes separated by fractional crystallization of their hydrochloride salts. Amongst these isomers, but-1-enes were differentiated from but-2-enes by the multiplicities of their vinylic proton magnetic resonance (p.m.r.) signals (but-1-ene signals were singlets and but-2-ene signals were triplets, $J = 7$ Hz), whilst configurational assignments rested upon association of the lower field vinylic chemical shift with the more planar of the two isomers (in both but-1-enes and but-2-enes the vinylic proton is subject to a greater degree of aromatic deshielding in the more planar isomer) (3, 4) (Table I). Models show the *trans* (Ph/Ar) but-1-ene **4***b* and the *cis* (Ar/H) but-2-ene **3***b* to be more planar forms. Ultraviolet (u.v.) data

TABLE I

Spectral data of 4-dimethylamino-2-*p*-methoxyphenyl-1-phenylbutenes

Butene	Chemical shift* vinylic signal	λ(ε)†
trans Ph/Ar **4***b*	411 Singlet	278 (18 300)
cis Ph/Ar **4***b*	397 Singlet	228 (21 200)
		276 (13 130)
trans Ar/H **3***b*	353 Triplet, $J = 7$ Hz	239 (8 400)
cis Ar/H **3***b*	370 Triplet, $J = 7$ Hz	263 (14 600)

*Chemical shifts in Hz from tetramethylsilane (60 MHz operating frequency, Varian A-60 spectrometer), solvent $CDCl_3$.
†Solvent ethanol. λ is wavelength in mμ; extinction coefficient ε shown in parentheses.

[1]Presented in part at the 11th National Medicinal Chemistry Symposium, Quebec City, June 1968.

$$\mathrm{ArCOMe} \xrightarrow[\mathrm{CH_2O}]{\mathrm{NHMe_2}} \mathrm{ArCO(CH_2)_2NMe_2}$$
5 **6**

$$\xrightarrow{\mathrm{PhCH_2MgCl}} \mathrm{Me_2N(CH_2)_2C(Ar)(OH)CH_2Ph} \xrightarrow{\mathrm{HCl—HAc}} \text{butene mixture}$$
7 **8**

Ar = *p*-MeO·C_6H_4

supports these assignments, the absorption maxima and extinction coefficients of *trans* **4***b* and *cis* **3***b* being at longer wavelengths and more intense respectively than those of the corresponding *cis* and *trans* isomers (Table I). These spectral results are in accord with data obtained for related isomers (3). The *cis* but-1-ene **4***b* showed an additional wavelength band (peak at 228 mμ) apparent only as a shoulder near 227 mμ in the *trans* isomer, the more complex *cis* spectrum resembling those of the 3-methyl congeners **9** (*trans*, maxima at 232 mμ, ε 17 200 and 256 mμ, ε 12 130; *cis* broad band between 222 mμ, ε

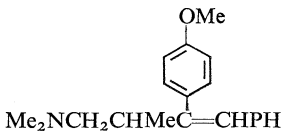

9

14 600 and 263 mμ, ε 10 990) (4). The butenes *cis* **4***b* and *cis* and *trans* **9** are all highly crowded molecules in which no single chromophore is likely to be favored and this may be the reason why they give u.v. spectra that are more complex than those of the *trans* but-1-ene **4***b* and the but-2-enes **3** where favored planar conformations are clear upon inspection of models.

An alternative route to but-1-enes, exemplified by the sequence **10** through **13**, has previously been shown to lead to a *cis* isomer (3). Further study shows these reactions to be stereoselective respecting:

$$\mathrm{PhCH_2COPh} \xrightarrow[\mathrm{NaNH_2}]{\mathrm{RCl}} \mathrm{PhCH(R)COPh} \xrightarrow{\mathrm{LAlH_4}} \mathrm{PhCH(R)CHOHPh}$$
10 **11** **12**

$$\xrightarrow{\mathrm{KHSO_4}} \mathrm{RCPh{=}CHPh} \qquad \mathrm{PhCH{=}C(OR)Ph}$$
13 **14**

R = $Me_2N(CH_2)_2$

(*a*) reduction of the ketone **11**. The p.m.r. spectrum of the total alcoholic product in $CDCl_3$ displayed sharp signals for the 1-methine, 2-methine, and NMe_2 protons (doublet $J = 7$, quartet $J = 7$, and singlet at 283, 177, and 121 Hz from TMS respectively) indicative of the preponderance of one diastereoisomer, and

(*b*) the dehydration step **12** to **13**. The p.m.r. spectrum of the total product of elimination showed vinylic signals at 390 and 407 Hz (from TMS) characteristic of *cis* and *trans* **13** respectively (3), present in the ratio of approximately 2 to 1 (cf. the same elimination of the α-ethyl analogue of **11** which led chiefly to *trans* α-ethylstilbene) (4).

Both *C*- and *O*-alkylated products were isolated upon alkylation of desoxybenzoin with 2-dimethylaminoethyl chloride in benzene, the enol ether **14** being characterized by its vinylic p.m.r. signal (a sharp singlet near 350 Hz) and infrared (i.r.) (doublet, 1670 and 1635 cm^{-1}) and u.v. (λ_{max} 287 mμ; ε 27 540; hydrochloride in ethanol) features typical of conjugated enol ethers (5, 6). The ratio of *O*- to *C*-alkyl product was about 7 to 1.5, a result in contrast with alkylation experiments upon desoxybenzoin using simple alkyl halides in which only minor amounts of *O*-alkylated products were detected (4). The proportion of the *C*-alkyl derivative **11** was raised when the reaction was repeated using dimethylsulfoxide as solvent, the total alkylation product consisting of about 40% **11**, 50% **14**, and 10% starting material as assessed from p.m.r.

TABLE II

Inhibition of histamine-induced contractions of isolated guinea-pig ileum by some aminobutenes (series 1)

Number	Structure	Ar	Ar′	Dose µg/ml	Percentage inhibition
1	*trans* **4***a*	Ph	Ph	1.0	62
2	*trans* **3***a*	Ph	Ph	1.0	49
				5.0	74
3	Ternary mixture (*cis* **3***a*, *cis* and *trans* **4***a*)	Ph	Ph	1.0	100
4	*trans* **2**	Ph	Ph	1.0	45
				5.0	71
5	*trans* **2**	Ph	*p*-MeC_6H_4	1.0	52
6	*trans* **2**	Ph	2-pyridyl	1.0	24
7	*trans* **2**	Ph	*o*-MeC_6H_4	1.0	5
				10.0	32
8	*cis* **2**	Ph	*o*-MeC_6H_4	1.0	11
				10.0	59
9	*trans* **2**	2-Thienyl	Ph	1.0	65
10	*trans* **2**	*p*-$MeOC_6H_4$	Ph	1.0	2.5
				10.0	68
11	*cis* **2**	*p*-$MeOC_6H_4$	Ph	1.0	43

TABLE III

Inhibition of histamine induced contractions of isolated guinea-pig ileum by some aminobutenes (series 2)

Number	Structure	Dose µg/ml	Percentage inhibition at time (in min)								
			3	6	9	12	15	18	21	24	27
1	*trans* **2** (Ar = Ar′ = Ph)	0.1	95	47	14	0					
2	*trans* **2** (Ar′ = *o*-F·C_6H_4, Ar = Ph)	0.1	53	24	7	0					
3	*trans* **2** (Ar′ = *o*-Cl·C_6H_4, Ar = Ph)	0.1	7	0	0						
4	*trans* **4***b*	0.1	100	95	64	58	30	20	13	8	2
5	*cis* **4***b*	0.1	16	10	0						
6	*trans* **3***b*	0.1	0	0							
7	*cis* **3***b*	0.1	100	95	90	78	52	60	38	40	36
8	Mepyramine	0.001	99	97	91	82	71	70	38	19	23

integrals of characteristic signals. The configuration of the *O*-alkyl derivative **14** is unknown but is probably *trans* Ph/Ph on the grounds of its very intense u.v. absorption band.

Preliminary Pharmacological Results and Discussion

The anti-histaminic potencies of a series of aminobutenes, as measured by their ability to antagonize the histamine-induced contraction of the guinea-pig ileum, are given in Tables II and III. Thanks are due to Drs. R. T. Brittain and R. G. W. Spickett of Allen and Hanburys, Ware, U.K. for arranging these tests. Tentative structure–activity relationships drawn from results of the initial series (Table II) are as follows:

First, amongst the diphenylbutene samples (Table II, Nos. 1–3) the ternary mixture is by far the most active; it has a pA_2 value of 9.4 comparable with those of highly active anti-histaminic agents (7). This mixture is composed of the *cis* and *trans* but-1-enes **4***a* and the *cis* but-2-ene **3***a*, and since the but-1-enes are much less active than the mixture [the *cis* isomer **4***a*, not included in these tests, has previously been shown to have a low order of activity (8)], it may be deduced (assuming

synergism is not operative in the mixture) that the *cis* but-2-ene **3***a* is the most active of the four isomers derived from the butanol **1***a* (Ar = Ar′ = Ph). Pure *cis* **3***a*, unavailable at the time of these tests, has now been isolated and a study of its anti-histaminic properties is in hand.

Secondly, a 3-methyl substituent reduced activity in *trans* but-1-enes (Table I, Nos. 1 and 4). In the same series the 1, 2-diphenyl and 1-*p*-tolyl, 2-phenyl members have comparable activities (Nos. 4 and 5) while the 1-2(2-pyridyl) and 1-(*o*-tolyl) analogues are of significantly reduced potency (Nos. 6 and 7). Replacement of 2-phenyl in No. 4 by 2-thienyl is advantageous (No. 9) but substitution of 2-phenyl by *p*-methoxyphenyl gives a less potent compound (No. 10).

Thirdly, among the two but-1-ene pairs Nos. 7/8, and 10/11, the *cis* member is more potent than the *trans* isomer.

These initial results indicative of the antagonism of histamine by aminobutene derivatives being stereoselective in nature, encouraged us to examine a second series, data for which (Table III) is summarized below:

First, *o*-fluoro and particularly *o*-chloro substituents in the phenyl group at C-1 of *trans* **2** (Ar = Ar′ = Ph) reduce activity (Table III, No. 1–3); cf. similar influence of *o*-methyl in previous series (Table II, Nos. 4 and 7).

Secondly, amongst the *p*-methoxyphenyl derivatives (Table III, Nos. 4–7), the *trans* but-1-ene **4***b* and the *cis* but-2-ene **3***b* are far more active than corresponding geometrical isomers, the duration of action of *cis* **3***b* being particularly prolonged. *Cis* **3***b* (pA_2 6.94) is substantially less potent than the standard drug mepyramine (pA_2 8.67).

These results further emphasize the influence of steric factors upon activity among anti-histaminic aminobutenes and confirm that the disposition of functions about the double bond in a *cis* (Ar/H) 1,2 diarylbut-2-ene appear to be optimal for activity. It is significant that pyrrobutamine, an aminobut-2-ene already marketed as an anti-histaminic agent (9), has the same *cis* configuration **15** (unpublished p.m.r. results).

Differences in the anti-histaminic properties of geometrical isomers have previously been reported for Triprolidine **16** and its *trans* (2-pyridyl/H) analogue (10). The former compound and the *cis* but-2-enes **3***a*, **3***b*, and **15** possess the common structural feature **17** rigidly orientated in the same manner and it is attractive to postulate that their histamine-blocking actions are of like nature involving similar drug-receptor association modes.

Kier (11) has recently proposed favored *anti* and gauche $\overset{+}{N}H_3$/Ar conformations for histamine based on molecular orbital calculations, and has suggested that the similar N to N interatomic distances of the *anti* conformer and triprolidine may be of significance regarding the latter compound's antagonistic properties. The present demonstration of stereospecific action among anti-histaminic agents which lack a pyridine substituent, suggests that the distance between the side chain nitrogen atom and the center of the aromatic ring attached to C-1 more truly represents the critical parameter for activity in these compounds. The problem of explaining the activity difference between triprolidine and its *trans* Ph/H isomer remains (since both forms may satisfy the aryl–nitrogen distance requirement), and further structure–activity data upon triprolidine analogues and related aminobutenes are being sought to provide more evidence upon this question.

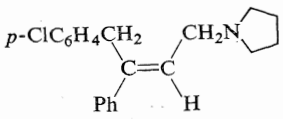

15

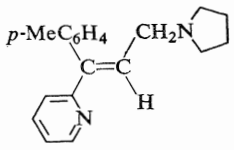

16

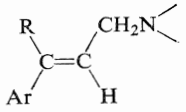

17

Experimental

The proton magnetic resonance (p.m.r.) spectra were recorded on a Varian A-60 spectrometer using $CDCl_3$, CCl_4, or D_2O as solvent. Chemical shifts are expressed in Hz from the TMS standard.

β-*Dimethylamino-p-methoxypropiophenone*

A mixture of *p*-methoxyacetophenone (22.5 g), dimethylamine hydrochloride (15.75 g), paraformaldehyde (5.8 g), concentrated hydrochloric acid (0.4 ml), and ethanol (38 ml) was heated under reflux for 20 h. The cooled product was diluted with acetone (150 ml) when the *hydrochloride* of the β-*aminoketone* **6** (36 g), m.p. 186–186.5° separated.

Anal. Calcd. for $C_{12}H_{18}ClNO_2$: C, 59.1; H, 7.45; N, 5.7. Found: C, 58.7; H, 7.2; N, 5.3.

4-Dimethylamino-2-p-methoxyphenyl-1-phenylbutan-2-ol and its Elimination

The β-aminoketone **6** (24.5 g) in ether (50 ml) was added to benzylmagnesium chloride in ether (125 ml) prepared from benzyl chloride (29.7 g) and magnesium (6.7 g), the mixture heated under reflux for 3 h, and then decomposed with NH_4Cl–ice. The organic layer was dried (Na_2SO_4) and evaporated to give the impure butanol **7** (29 g), characterized as the *hydrochloride*, m.p. 195–196° from ethanol–ether.

Anal. Calcd. for $C_{19}H_{26}ClNO_2$: C, 67.9; H, 7.8; N, 4.2. Found: C, 67.6; H, 7.7; N, 4.0.

A mixture of the butanol **7** hydrochloride (9.5 g), concentrated hydrochloric acid (25 ml), and glacial acetic acid (70 ml) was heated under reflux for 4 h. The product was concentrated under reduced pressure and the free base recovered as usual. The p.m.r. spectrum of the total butene mixture in $CDCl_3$ displayed 4 vinylic signals (2 broad singlets and 2 triplets) and 4 closely placed OMe and NMe_2 singlets near 225 and 183 Hz from TMS respectively. Fractional crystallization of the base hydrochloride from ethanol–ether gave the following isomers (listed in order of separation):

The *trans but-1-ene* **4***b hydrochloride* (800 mg), m.p. 227–228°.

Anal. Calcd. for $C_{19}H_{24}ClNO$: C, 71.8; H, 7.6; N, 4.5. Found: C, 72.2; H, 7.8; N, 4.2.

The *trans but-2-ene* **3***b hydrochloride* (290 mg), m.p. 186.5–187.5°. Found: C, 72.05; H, 8.1.

The *cis but-2-ene* **3***b hydrochloride* (320 mg), m.p. 203–204°. Found: C, 71.9; H, 7.4.

The *cis but-1-ene* **4***b hydrochloride* (400 mg), m.p. 178.5–179.5°. Found: C, 71.9; H, 7.8.

Alkylation of Desoxybenzoin with 2-Dimethylaminoethyl Chloride

Sodamide (2.5 g) was added to desoxybenzoin (10.8 g) in benzene (20 ml) and the mixture heated under reflux for 3 h, cooled, and treated with 2-dimethylaminoethyl chloride (6.75 g), freshly liberated from the hydrochloride. After a further reflux period of 16 h, the reaction mixture was cooled, filtered, and concentrated *in vacuo*. The residue gave a distillate (13.1 g), b.p. 145–172°/1.2 mm and its p.m.r. spectrum in CCl_4 showed it to consist of about 70% of the *O*-alkyl-derivative **14** (integral of the vinylic singlet at 361 Hz), 15% of the *C*-alkyl isomer **11** (integral of the methine triplet at 283 Hz), and 15% desoxybenzoin (integral of the methylene singlet at 244 Hz). The total product in cold ether was acidified with ethereal HCl, and the precipitated salt collected, washed with ether, and fractionally crystallized from ethanol to give the *C-alkylamine* **11** *hydrochloride* (1 g), m.p. 250–253°.

Anal. Calcd. for $C_{18}H_{22}ClNO$: C, 71.2; H, 7.25; N, 4.6. Found: C, 70.8; H, 7.15; N, 4.3.

The *O-alkylisomer* **14** *hydrochloride* (7.2 g), m.p. 185–185.5°. Found: C, 71.2; H, 7.2; N, 4.4. Characteristic p.m.r. signals in D_2O: singlet 345 Hz (vinylic proton) and deformed, object–mirror image, triplets centered at 214 Hz (OCH_2) and 190 Hz (NCH_2) (in the base, CCl_4 solvent, these methylene signals are approximate first order triplets, $J = 7$ Hz). Repetition of the alkylation reaction with dimethyl sulfoxide as solvent (sodio derivative of desoxybenzoin formed as before then solvent benzene replaced by DMSO) and a heating period of 16 h at 80°, gave the *C*- and *O*-alkyl isomers in a ratio of 4:5.

Acknowledgment

The authors thank the Medical Research Council of Canada for financial support.

1. W. G. Stoll, Ch. J. Morel, and Ch. Frey. Helv. Chim. Acta, **33**, 1194 (1950).
2. A. F. Casy, J. L. Myers, and P. Pocha. Tetrahedron, **22**, 1001 (1966).
3. A. F. Casy and P. Pocha. Tetrahedron, **23**, 633 (1967).
4. A. F. Casy, A. Parulkar, and P. Pocha. Tetrahedron, **24**, 3031 (1968).
5. A. L. Nussbaum, E. Yuan, D. Dincer, and E. P. Oliveto. J. Org. Chem. **26**, 3925 (1961).
6. H. Rosenkrautz and M. Gut. Helv. Chim. Acta, **36**, 1000 1953.
7. R. B. Barlow. Introduction to chemical pharmacology. 2nd ed. Methuen and Co., Ltd., London. 1964. p. 357.
8. W. G. Stoll, Ch. Frey, and Ch. J. Morel. Helv. Chim. Acta, **33**, 1208 (1950).
9. U.S. Patent No. 2,655,509 (1953); Chem. Abstr. **48**, 13726*c* (1953).
10. D. W. Adamson, P. A. Barrett, J. W. Billinghurst, and T. S. G. Jones. J. Chem. Soc. 2315 (1957).
11. L. B. Kier. J. Med. Chem. **11**, 441 (1968).

Can. J. Chem. Downloaded from www.nrcresearchpress.com by 210.87.254.105 on 09/05/12
For personal use only.

Conformational analysis of 1,4-disubstituted cyclohexanes. III. *trans*-1,4-Di(trifluoroacetoxy)cyclohexane[1]

GORDON WOOD, E. P. WOO,[2] AND M. H. MISKOW[3]
Department of Chemistry, University of Windsor, Windsor, Ontario

Received September 13, 1968

By the low temperature nuclear magnetic resonance integration method the standard free energy difference between the diequatorial and the diaxial forms of *1-H,4-H-trans*-1,4-di(trifluoroacetoxy)-cyclohexane-d_8 was found to be 77 ± 5 cal/mole. The conformational free energy ($-\Delta G°$) of the trifluoroacetoxy group in the monosubstituted cyclohexane was 485 ± 4 cal/ mole at the same temperature. The non-additivity of the $-\Delta G°$ values is discussed in terms of transannular electrostatic interaction.

Canadian Journal of Chemistry, 47, 429 (1969)

Introduction

Studies on the additivity of conformational energies of 1,4-substituents on cyclohexanes are quite uncommon. Generally, when one of the substituents is an alkyl group, it is assumed that additivity holds (1). However, recent work from our laboratory (2, 3) has shown that if two polar groups are *trans* to each other, marked deviations from additivity are observed. Thus, the relative proportion of the two conformers of *cis*-1,4-bromochlorocyclohexane present at low temperature was shown to be nearly equal as expected from additivity of conformational energies. However, the conformational composition of a series of *trans*-1,4-dihalocyclohexanes was shown to differ considerably from the predicted values; indeed, the experimental preference for the diequatorial form was only one-fifth of the expected values.

One plausible explanation of non-additivity involves electrostatic interactions. Polarization of the C—X bonds results in partial charges on these atoms. The attractive interaction between C-1 and 4-X and between C-4 and 1-X is greater in the diaxial form than in the diequatorial form

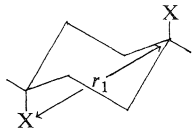

1

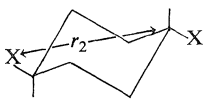

2

(**1** vs. **2**);[4] for example, if X = Cl, r_1 = 3.9 Å, and r_2 = 4.8 Å. This postulate accommodates our results as well as some observations in the literature.[5] We report here some further results which are in agreement with the proposal.[6]

We have studied the conformational equilibrium of *1-H,4-H-trans*-1,4-di(trifluoroacetoxy)-cyclohexane-d_8 (**3**) at low temperature by integration of the separate axial and equatorial proton signals. The trifluoroacetoxy group was chosen for its high electronegativity (3.77 vs. 3.25 for chlorine and 2.96 for bromine according to the scale of Cavanaugh and Dailey (5)). Higher electronegativity in the group X should favor the diaxial form and thus result in an increase in the deviation from additivity.[7]

Results and Discussion

The nuclear magnetic resonance (n.m.r.) spectrum of **3** followed the usual pattern of cyclohexyl compounds on cooling. The coalescence

[1]See refs. 2 and 3 for the previous papers in this series.
[2]Present address: Department of Chemistry, University College, London, England.
[3]Holder of NRCC Studentships, 1966–1968.

[4]The repulsive interaction between 1-X and 4-X favors the diequatorial form, but because the potential energy varies as $1/r^2$ this interaction will not be as large as the attractive one.
[5]Note that *trans*-1,2-dihalocyclohexanes also exist in approximately equal mixtures of diaxial and diequatorial forms (4). While this result may be caused by electrostatic interactions, it is by no means clear what role steric effects play here.
[6]While this work was in progress, a similar proposal was put forward by Prof. R. Stolow to explain anomalous results in 4-hydroxycyclohexanones (see later discussion).
[7]Determination of the position of conformation equilibrium in 1,4-disubstituted cyclohexanes where only one group is polar would constitute an interesting test for this postulate. We have prepared *cis*-4-methylcyclohexyl chloride for this purpose, but so far have not been able to detect the signal from the axial C-1 proton. Results on *cis*-4-methylcyclohexylamine suggest that additivity is followed at least approximately in this compound (6).

Can. J. Chem. Downloaded from www.nrcresearchpress.com by 210.87.254.105 on 09/05/12
For personal use only.

temperature was ca. −90°. Upon further cooling to −103°, two separate signals were obtained (peak widths at half-height were 3.5 Hz). Integration of the peak areas allowed calculation of the free energy difference between the diequatorial and diaxial form. A value of 77±5 cal/mole in favor of the former was found. At the same temperature this method gave a value for $-\Delta G°$ of 485±4 cal/mole for trifluoroacetoxycyclohexane-2,2,6,6-d_4. Assuming additivity, the free energy difference between the two conformers of **3** should be 970 cal/mole. The importance of this deviation can be appreciated if one remembers that the predicted value corresponds to a 95:5 ratio of conformers and the actual value corresponds to a 55:45 ratio at the temperature studied.

Several results in the recent literature may involve an electrostatic interaction of the kind proposed here. Notable among these is the report that the conformational equilibrium constant for 4-hydroxycyclohexanone is very nearly unity (7). Thus the apparent $-\Delta G°$ value for hydroxyl is reduced from its usual value of 0.7 kcal/mole or higher (8) to zero. Similar results were reported by Stolow *et al.* (9) from equilibration of *cis*- and *trans*-2-*t*-butyl-4-hydroxycyclohexanone.

Equilibration of 4-chlorocyclohexanol resulted in a slight preponderance (54.5%) of the *cis* isomer (10). Although further study is required to establish the cause of this result, it is clear that application of the $-\Delta G°$ values for the individual groups fails to predict it. The protonation of cyclohexane-1,4-bisnitronate ion also gave 55% of the *cis* isomer. Although this result was originally attributed to steric hindrance to axial protonation of the half-protonated form (11), some doubt has recently been cast on this explanation (12). It seems likely to us that electrostatic interaction across the ring is responsible for both of these results, although in the latter case the interaction would have to be operative in the transition state if this reaction is kinetically controlled.

Our conclusion is that interaction between polar groups across a cyclohexane ring is a general phenomenon which frequently determines the position of conformation equilibrium and the stereochemical outcome of reactions for such compounds.

Experimental

Nuclear magnetic resonance spectra were recorded with a JEOL 60 MHz instrument in 10–15% acetone-d_6 solutions. Tetramethylsilane was used as the internal standard. Twelve integrations were performed on the diester and fourteen on the monoester. A computer program was used for all the calculations. The relative peak areas of each integration were converted to the corresponding equilibrium constant. A standard deviation was obtained for each set of data, from which the reported errors were computed.

Preparative gas–liquid chromatography (g.l.c.) was carried out with an F and M 720 instrument. The column (8 ft × 0.5 in.) was packed with Lac 728. Melting points were determined on a Fisher–Johns apparatus and are uncorrected. All samples were purified by preparative g.l.c immediately before use.

Cyclohexane-1,4-dione-d_8[8]

To a solution of 0.5 g of PCl_5 and 25 ml of D_2O (99.7%) was added 5.0 g of cyclohexane-1,4-dione. After standing at room temperature for 5 days, the solution was extracted with four 10 ml portions of methylene chloride. The combined organic phase was dried with anhydrous Na_2SO_4 and filtered. Removal of the solvent afforded 4.7 g of white solid which was dissolved in a solution of 35 ml of D_2O containing 1 g of PCl_5. Four days standing at room temperature followed by the usual isolation procedure yielded 3.3 g of white crystalline solid, m.p. 78–80° (lit. m.p. 78° for the hydrogen analogue (14)). Integration of the relative peak areas of the residual hydrogen and a known amount of dioxane showed 94% isotopic purity.

Cyclohexane-1,4-diol-2,2,3,3,5,5,6,6-d_8

The procedure of Lemieux and Lown (15) for the reduction of the dione was followed, and gave 2.6 g of viscous brown oil which was used in the next step without purification.

1-H,4-H-trans-1,4-Di(trifluoroacetoxy)cyclohexane-d_8

The brown oil obtained above was dissolved in 10 ml of tetrahydrofuran and cooled in an ice-bath. Trifluoroacetic anhydride (4 ml) was added dropwise with stirring. After standing at 0° for 1 h, the solution was poured onto ice and saturated with potassium carbonate. The organic layer was separated and the aqueous layer extracted with 10 ml of ether. After drying and removal of the solvent, a viscous brown oil was obtained which was shown by g.l.c. (110°) to consist of two main components in the ratio 70:30. Collection of the larger peak (retention time, 18 min) gave a white crystalline solid, m.p. 57.5–58°, and the second (retention time, 27 min) yielded a colorless liquid. The retention times were identical to those of the hydrogen analogues prepared in the same manner. The structure of the *trans* isomer was confirmed by saponification of the hydrogen analogue (m.p. 57–58°), according to the method of Owen and Robins (16), to the *trans*-diol, m.p. 140–142° (lit. m.p. 141° (16)).

Trifluoroacetoxycyclohexane-2,2,6,6-d_4

Deuteration and subsequent reduction of cyclohexanone was performed according to the method of Premuzic

[8]The potassium carbonate-catalyzed exchange procedure reported by Bhatt *et al.* (13) consistently gave a dark brown gum.

and Reeves (17). The trifluoroacetate was prepared by essentially the same method as above except that ether was used as solvent.

Acknowledgments

The authors thank the National Research Council of Canada for generous financial support as well as a grant towards the purchase of the spectrometer. A helpful discussion with Prof. R. Stolow, Tufts University is gratefully acknowledged. We are also indebted to Mr. Gary Small for writing the computer program and Miss Dolores Sjostrom for able technical assistance.

1. E. W. DELLA. J. Am. Chem. Soc. **89**, 5221 (1967).
2. G. WOOD and E. P. WOO. Can. J. Chem. **45**, 1293 (1967).
3. G. WOOD and E. P. WOO. Can. J. Chem. **45**, 2477 (1967).
4. M. HANACH. Conformational theory. Academic Press, Inc., New York. 1965. p. 121.
5. J. R. CAVANAUGH and B. P. DAILEY. J. Chem. Phys. **34**, 1099 (1961).
6. G. RANSBOTYN, J. C. CELOTTI, R. OTTINGER, and G. CHIURDOGLU. Tetrahedron, **24**, 3647 (1968).
7. W. F. TRAGER, B. J. NIST, and A. C. HUITRIC. J. Pharm. Sci. **56**, 698 (1967).
8. E. ELIEL, N. ALLINGER, S. ANGYAL, and G. MORRISON. Conformational analysis. Interscience Publishers, Inc., New York. 1965. p. 437.
9. R. D. STOLOW and T. GROOM. Tetrahedron Letters, 4069 (1968).
10. E. L. ELIEL and T. J. BRETT. J. Am. Chem. Soc. **87**, 5039 (1965).
11. A. T. NIELSON. J. Org. Chem. **27**, 2001 (1962).
12. F. G. BORDWELL and M. M. VESTLING. J. Am. Chem. Soc. **89**, 3906 (1967).
13. M. V. BHATT, G. SRINIVASAN, and P. NEELAKANTAN. Tetrahedron, **21**, 291 (1965).
14. A. J. BIRCH. J. Chem. Soc. 102 (1947).
15. R. U. LEMIEUX and J. W. LOWN. Can. J. Chem. **42**, 893 (1964).
16. L. N. OWEN and P. A. ROBINS. J. Chem. Soc. 320 (1949).
17. E. PREMUZIC and L. W. REEVES. Can. J. Chem. **40**, 1870 (1962).

Can. J. Chem. Downloaded from www.nrcresearchpress.com by 210.87.254.105 on 09/05/12
For personal use only.

The total synthesis of optically active annotinine

K. Wiesner, Lizzie Poon, I. Jirkovský, and M. Fishman
Natural Product Research Center, University of New Brunswick, Fredericton, New Brunswick
Received October 21, 1968

The total synthesis of the first *Lycopodium* alkaloid annotinine in the optically active form is described. The key step in this synthesis was the photochemical addition of allene to the tricyclic vinylogous imide (**3**) which yielded the photoadduct (**6**).

Canadian Journal of Chemistry, **47**, 433 (1969)

Can. J. Chem. Downloaded from www.nrcresearchpress.com by 210.87.254.105 on 09/05/12
For personal use only.

In the years 1956–1957 we have deduced the structure of the first *Lycopodium* alkaloid annotinine (**1**) (1). The only feature of the formula (**1**) which did not follow from the chemical evidence was the configuration of the methyl group. The complete stereochemistry of annotinine was later revealed by an X-ray crystallographic structure determination of annotinine bromohydrin (2). It seemed to us that the *Lycopodium* alkaloids in general and annotinine in particular offer an interesting synthetic challenge. A simple and successful solution of the problems involved would require the design of new synthetic methods and these would presumably be capable of a wider application.

A stereospecific synthesis would also provide chemical evidence for the configuration of the annotinine methyl group and we felt that we owe to this classical structural problem a rigorous and complete chemical solution.

At the outset of our synthetic studies one of us (K.W.) proposed two general approaches to the various *Lycopodium* systems: (1) The reaction of Grignard reagents with properly constituted vinylogous amides and (2) The photo-addition of allene to properly constituted vinylogous imides. It was the second approach which seemed promising for a very simple tailor-made annotinine synthesis and after a verification of the novel photo-reaction on model compounds (3) we indeed succeeded in synthesizing racemic annotinine in 1967 (4). In the following year we have made considerable improvements in the later stages of the synthesis and also achieved a resolution of a suitable intermediate into optical antipodes. Consequently, we wish to give in the present communication a full account of the preferred synthetic route to optically active annotinine.

Our starting material was the bicyclic vinylogous amide (**2**), which may be easily prepared from acrylonitrile and methyl acrylate (5). This compound is destined to form rings B and C of annotinine. The first task in our synthesis was now to fuse ring A to the system and to obtain the tricyclic vinylogous imide (**3**). We have envisaged that this objective might be accomplished by the treatment of (**2**) with acrylonitrile or methyl acrylate in the presence of various basic catalysts. However, only small amounts of the product (**3**) were produced under these conditions. Finally it was found that heating of the bicyclic starting material (**2**) with a small excess of acrylic acid to 135 °C gives an excellent yield of the desired tricyclic product (**3**). Compound (**3**) was crystalline and showed characteristic ultraviolet and infrared spectra.[1] (Ultraviolet: $\lambda_{max} = 298$ mμ; $\log \varepsilon = 4.1$; Infrared ($CHCl_3$): maxima at 1695, 1645, 1610 cm^{-1}). A possible rationalization of the process leading to (**3**) is the initial formation of the vinylogous imide (**4**) which may protonate on the amidic oxygen and undergo a thermal cyclization as portrayed in the formula (**5**).

The next step (**3**) → (**6**) was of crucial importance, since on its outcome depended the success of the entire synthesis. We have hoped to accomplish it by a photochemical addition of allene to (**3**) at low temperature. *A priori* it was not at all certain that only one compound would result in this process. Isomers with the exocyclic double bond located at the asterisked carbon and diastereoisomers at the carbon marked with the arrow were clearly possible products of the novel photo-addition. In fact, a single compound was formed in high yield and it was shown to possess the structure (**6**) (*vide infra*). The photoadduct was homogeneous, crystalline, and yielded analytical

[1]Only specially relevant spectral data are mentioned in the theoretical part; for more spectral data and full characterization of compounds see Experimental.

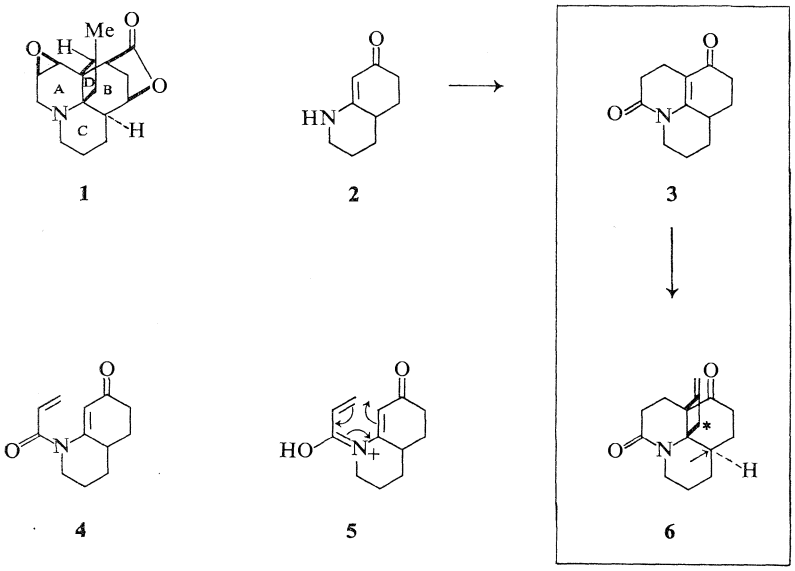

1 2 3 4 5 6

and spectroscopic data consistent with the formula (**6**). (Infrared ($CHCl_3$): 1700 (ketone), 1640 (lactam), 908 cm^{-1} (exocyclic methylene); Nuclear magnetic resonance (n.m.r.): narrow doublet (2 H) $\tau = 5$ p.p.m. (vinylic hydrogen).

The next compound required, both for the purpose of the structure proof of (**6**) and to carry on the synthesis, was the ketal (**7**). It was prepared in a quantitative yield by ketalization of (**6**) in benzene with *p*-toluenesulfonic acid and ethylene glycol. The ketal (**7**) was crystalline and it was fully characterized. The transformation of the ketal (**7**) to the diketone (**10**) was carried out in our laboratories by H. Dugas in connection with another problem.[2] The process involved an epoxidation of (**7**) to (**8**), reduction of the epoxide with lithium borohydride to the tertiary alcohol (**9**), and finally the treatment of compound (**9**) with aqueous acid, which yielded by deketalization and simultaneous retroaldol reaction the diketone (**10**). The sequence (**7**) → (**10**) proves unambiguously the relative position of the keto group and the exocyclic methylenic group in the photoadduct (**6**) and thus it proves the structure of this compound.

The only point which is still in question is the configuration of the asymmetric center marked with the arrow in formula (**6**). For the purposes of the annotinine synthesis this configuration is unimportant, since the asymmetric center involved becomes epimerizable and equilibrates in one of the subsequent steps.

Nevertheless, we believe that the configuration of our photoadduct is in fact as shown in the formula. Several cases of related stereospecific photo-additions to α,β-unsaturated carbonyl compounds studied in our laboratories can be rationalized without exception by the hypothesis (7) that the stereochemistry of the photo-addition is not controlled by the stability of the product, but by the tendency of the excited state to exist preferentially in the most stable configuration. If the excited state is assumed to have carbonium character in the position α to the carbonyl group and an orbital with an electron pair in the β position, then its most stable configuration in the present case would be the one shown in formula (**13**), in which the orbital and the adjacent hydrogen (indicated by arrows) are axial *trans*. The addition of allene to this species would then yield an adduct with the configuration as in (**6**). Experimental evidence which supports this configuration and which is based on infrared spectroscopy of various transformation products of compound (**10**) may be found in H. Dugas' thesis (6).

With all the important structural features of the photoadduct established, we may now return to the description of our main synthetic pathway. At this point it is advantageous to effect a stereo-

[2]This transformation is described in the Ph.D. Thesis of H. Dugas and it will be published separately.

Can. J. Chem. Downloaded from www.nrcresearchpress.com by 210.87.254.105 on 09/05/12
For personal use only.

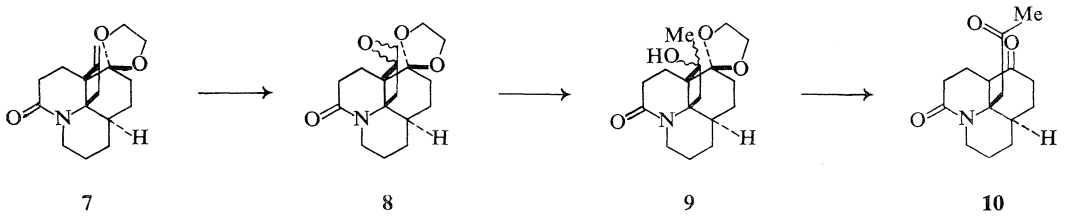

7 8 9 10

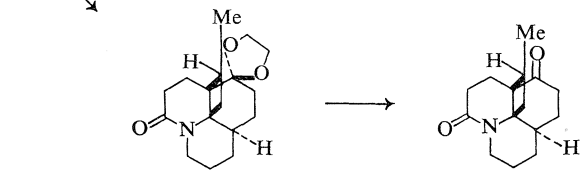

11 12

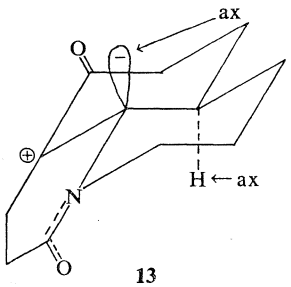

13

specific hydrogenation of the exocyclic methylenic double bond in the photoadduct. A derivative particularly suitable for this purpose is the ketal (**7**). In this compound the double bond is shielded by the plane of the dioxolane ring and consequently it hydrogenates stereospecifically from the opposite direction to yield exclusively the dihydro derivative (**11**). Compound (**11**) was crystalline and homogeneous and it was fully characterized. By deketalization it yielded the crystalline and homogeneous ketolactam (**12**).

This last compound (**12**) was now reduced with sodium borohydride in aqueous tetrahydrofuran to the alcohol (**14**) in a quantitative yield. Compound (**14**) was crystalline and it was fully characterized. The configuration of the hydroxyl in this product is assumed to be *cis* to the cyclobutane ring. The keto group of compound (**12**) is strongly hindered from the side of the cyclobutane ring and it is assumed that in the reduction process the borohydride approaches from the less

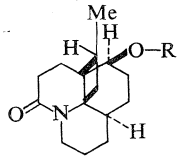

14 R = H
15 R = mesyl

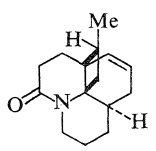

16

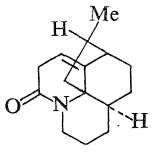

17

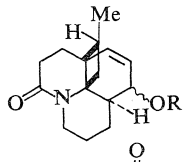

18 R = Me—C(=O)—
19 R = H

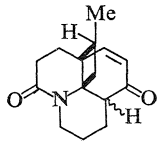

20

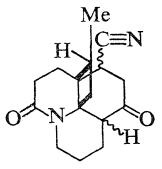

21

hindered side. The alcohol (**14**) was converted into the mesylate (**15**) with methane sulfonyl chloride in pyridine in a 92% yield. The mesylate

Can. J. Chem. Downloaded from www.nrcresearchpress.com by 210.87.254.105 on 09/05/12
For personal use only.

Can. J. Chem. Downloaded from www.nrcresearchpress.com by 210.87.254.105 on 09/05/12
For personal use only.

crystallized from benzene and was fully characterized. Attempts to achieve an elimination of the mesyl group under various basic conditions gave only modest yields of the desired olefin (**16**) accompanied by equal quantities of the rearrangement product (**17**). Finally it was found that treatment of the mesylate (**15**) with potassium tertiary butoxide in absolutely anhydrous dimethyl sulfoxide yielded the desired compound (**16**) as a crystalline single product in a yield of 83%. The n.m.r. spectrum of (**16**) showed a multiplet (2 H) centered at $\tau = 4.45$ p.p.m. for the two olefinic protons. The shift of the methyl group doublet (3 H) from $\tau = 8.66$, 8.76 p.p.m. in the n.m.r. spectrum of the mesylate (**15**) to $\tau = 9.06$, 9.18 p.p.m. in the n.m.r. spectrum of the olefin (**16**) constitutes independent evidence for the configuration of the methyl group, which in compound (**16**) is located in the shielding region of the double bond.

We believe that there may be some theoretical significance in the fact that we have not succeeded in finding any other basic conditions which would yield only elimination unaccompanied by rearrangement besides the conditions given above. It is well known that Hofmann eliminations are not prone to rearrangement. In a recent summarizing article it was pointed out that eliminations of halides and sulfonates with potassium tertiary butoxide in DMSO follow (in cases unlike ours, where there is a choice) the Hofmann rule rather than the Zajcev rule and thus, in this respect, resemble Hofmann eliminations (8). The lack of rearrangement found by us and the special directional behavior of this type of sulfonate eliminations might well have a common cause and be due to the nature of the transition state of this reaction.

Oxidation of the olefin (**16**) with selenium dioxide in glacial acetic acid yielded the oily acetate (**18**) in a 67% yield. It was characterized by spectroscopy and was homogeneous in t.l.c. Basic hydrolysis of the acetate proceeded in quantitative yield and the alcohol (**19**) was oxidized to the α,β-unsaturated ketone (**20**) with chromium trioxide in pyridine. Compound (**20**) was crystalline and showed an infrared and an ultraviolet spectrum in agreement with the structure assigned to it. [Infrared ($CHCl_3$): 1690, 1660, 1620 cm^{-1} (conjugated ketone, double bond, and lactam); ultraviolet: $\lambda_{max} = 230$ mμ, $\log \varepsilon = 4.0$]. In the n.m.r. spectrum of (**20**) a quadruplet (2 H) centered at $\tau = 3.58$ p.p.m. was assigned to the two vinylic protons. The configuration of the hydrogen next to the ketone in formula (**20**) is left unassigned, since we have not investigated whether this configuration has undergone epimerization on work-up and chromatography of the reaction mixture. The optically active form of (**20**) is known, since many years ago we prepared it by degradation of annotinine (1*b*). We did not possess a reference sample, but it was a matter of some satisfaction that the infrared spectra of the "natural" and synthetic materials were identical in every detail.

With an efficient method for the preparation of the α,β-unsaturated ketone (**20**) in hand, the stage is set for the introduction of the annotinine carboxyl. The ketone (**20**) was subjected to a hydrocyanation reaction in dimethyl formamide (9), which gave two diastereoisomers of compound (**21**) in a total yield of 82%. The two compounds were purified by chromatography, but not separated from each other. The mixture was characterized by the mass spectrum, which displayed a correct molecular ion and by its infrared spectrum. (Infrared ($CHCl_3$): 2230, 1720, 1650 cm^{-1} [nitrile, ketone, lactam]). It gave two spots of equal intensity on a thin-layer chromatogram.

The nitrile mixture (**21**) was now converted by refluxing with methanol and sulfuric acid into the crystalline methyl ester (**22**). After chromatography and crystallization the yield of this material was 46%. We have described (1*b*) the optically active form of this compound 10 years ago and it is readily available from annotinine.

The synthetic racemate (**22**) was found to be identical with the "natural" optically active compound (**22**) by t.l.c., i.r. spectrum in potassium bromide and carbon tetrachloride and by mass spectrometry. The configuration of the synthetic compound (**22**) follows from this identity, since for the "natural" material the stereochemistry portrayed in formula (**22**) was rigorously proved (1*b*). It clearly corresponds to the most stable configuration and the proof cited above is independent of the fact that the conformational analysis of the system is difficult and unconvincing.

The synthetic racemic ester (**22**) was now hydrolyzed to the crystalline racemic acid (**23**) and this last material was converted into the diastereoisomeric brucine salts by treatment with one equivalent of brucine. The less soluble di-

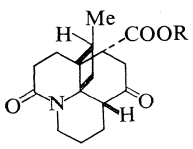

22 R=Me
23 R=H

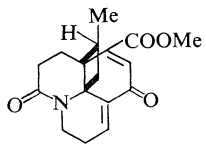

24

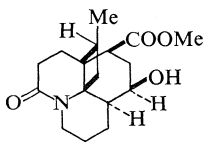

25

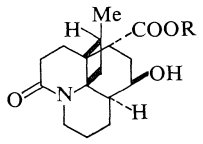

26 R=H
29 R=Me

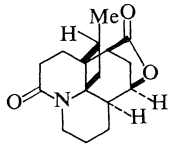

27

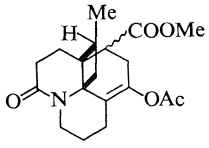

28

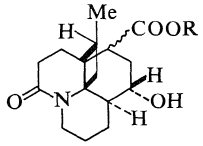

30 R=Me
31 R=H

astereoisomer was obtained pure by crystallization from acetone–methanol mixtures and melted constantly at 158–160 °C. Decomposition of this salt yielded the crystalline optically active acid (**23**), which was esterified with diazomethane to the totally synthetic optically active ester (**22**). After recrystallization this compound melted at 198–200 °C, and did not depress the identical melting point of the "natural" ester (**22**). Both materials showed also practically superimposable rotatory dispersion curves, a clear proof of the complete optical purity of the synthetic compound (Fig. 1). Infrared (CCl_4 and KBr) and mass spectra of both materials were also identical in every detail.

The next problem which had to be solved was the conversion of the optically active ester (**22**) to the lactam-lactone (**27**). This task involved the inversion of two asymmetric centers and the creation of a third one. In our preliminary communication (4*b*) we have described a route via the selenium dioxide dehydrogenation of (**22**) to (**24**), a step which proceeded in a very low yield and was known already from the time of our structural studies (1*a*, *b*). Hydrogenation of (**24**) proceeded stereospecifically and yielded the ester (**25**). Basic hydrolysis of (**25**) accompanied by epimerization of the carboxyl gave the acid (**26**). This compound finally yielded the lactam-lactone (**27**) by lactonization in benzene – dimethyl formamide with *p*-toluenesulfonic acid with a new epimerization of the carboxyl.

We have now succeeded in elaborating a more efficient method, which completely avoids the low yield step (**22**) → (**24**). The ester (**22**) was converted into the crystalline enol-acetate (**28**) in a yield of 91% after recrystallization. The n.m.r. and i.r. spectra of this material defined the structure as given in the formula. (Nuclear magnetic resonance: singlets (3 H) each τ = 6.29 and 7.84 p.p.m. (ester and acetate methyls), no vinylic hydrogen; Infrared ($CHCl_3$): 1750, 1640 cm^{-1} (esters and lactam)). The enol-acetate (**28**) was now subjected to a reduction with sodium borohydride in absolute tetrahydrofuran and methanol. The result of this reduction was a mixture of the hydroxyester (**29**) and an isomeric hydroxyester presumably (**30**). The two compounds were purified by chromatography, but not separated from each other. They were characterized by the correct molecular ion in mass spectrometry, and by the infrared spectrum. The reason for the

Can. J. Chem. Downloaded from www.nrcresearchpress.com by 210.87.254.105 on 09/05/12
For personal use only.

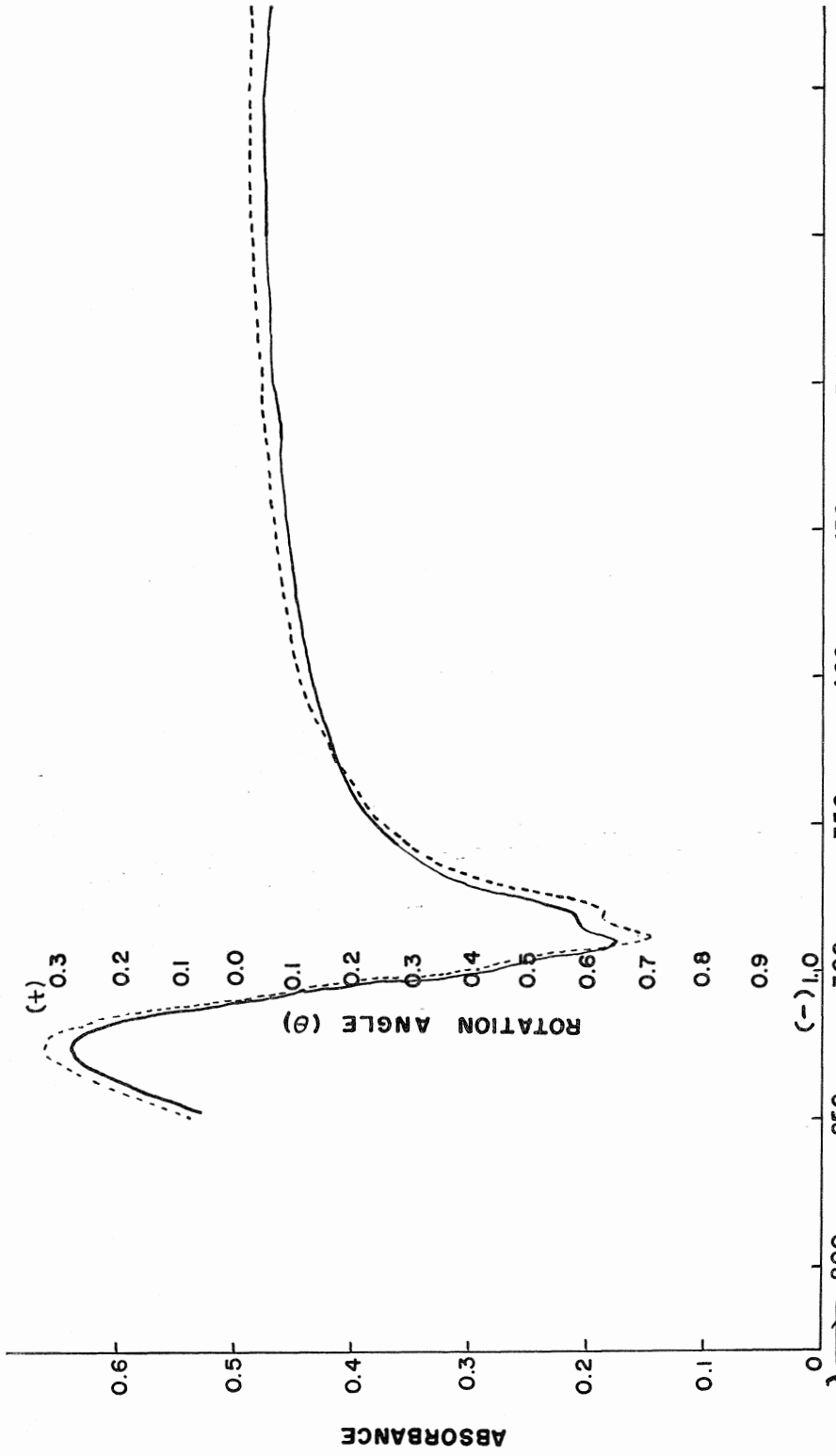

FIG. 1. Optical rotatory dispersion curve of the "natural" ester (**22**) (solid line). Optical rotatory dispersion curve of the synthetic ester (**22**) (dotted line).

Can. J. Chem. Downloaded from www.nrcresearchpress.com by 210.87.254.105 on 09/05/12
For personal use only.

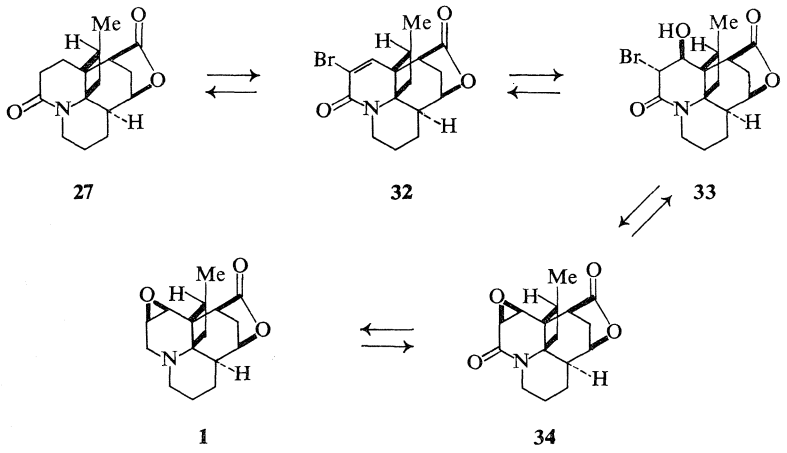

assumption, that the second isomer may be represented by the formula (**30**) is the fact that both the reduction products of compound (**28**) were distinctly different (t.l.c.) from the analogous borohydride reduction product of the keto-ester (**22**).

The mixture of the esters (**29**) and (**30**) was hydrolyzed to the corresponding carboxylic acids (**26**) and (**31**) and these materials were, without separation, subjected to lactonization in dry benzene with *p*-toluenesulfonic acid. Work-up and chromatography gave the crystalline lactone (**27**) in a yield of 38%. It was proved to be identical with the product of the same structure which may be simply prepared directly from annotinine (10) by mixed melting point, infrared spectrum in chloroform, mass spectrum, and thin-layer chromatography.

Under the lactonization conditions used, the hydroxy acid (**31**) remained unchanged and was isolated in approximately the same yield as the lactone. Since the acid (**31**) could be presumably esterified and oxidized back to the keto-ester (**22**), the presently described process for the conversion of (**22**) to (**27**) could be made reasonably efficient. As it is, even without the reconversion of (**31**) to (**22**), the overall yield from the enol-acetate (**28**) to the lactam-lactone (**27**) was 25%.

The formulae (**28**), (**30**), and (**31**) leave the configuration of the carboxyl unassigned, because it is unproved. The remaining structures represent compounds known from our degradative work and their complete configurations have been fully documented, cf. (1*c*). We believe that the reduction process of (**28**) to the mixture (**29**) and (**30**) proceeds as follows: (1) Alcoholysis of the enol-acetate (**28**) to the corresponding enolate ion. (2) Kinetically controlled protonation of the enolate ion to a keto-ester epimeric with the ester (**22**) on the asymmetric carbon α to the keto group. (3) Non-stereospecific reduction of the keto group in this hypothetical intermediate, before it can isomerize to the more stable ester (**22**).

The final task which we face at this point is the conversion of the lactam-lactone (**27**) to annotinine (**1**). The reaction sequence, which we worked out to this end, is portrayed in the formula Scheme V. All the intermediates in this sequence may be reached also in the opposite direction, i.e. by unexceptional degradation reactions of annotinine. Since some of these compounds have not been described in the literature, it is convenient to discuss the degradation series first.

The potassium permanganate oxidation of annotinine to oxoannotinine (**34**) is well known (cf. 1*c*). It is also well known that the treatment of (**34**) with hydrochloric acid yields oxoannotinine chlorohydrin, which may be dehydrated to oxoanhydroannotinine chlorohydrin by phosphorus oxychloride. These two chlorine containing derivatives have well established structures (cf. 1*c*), and are chlorine analogues of the two bromo compounds (**33**) and (**32**). The heating of oxoannotinine (**34**) with aqueous hydrobromic acid (19%) gave a good yield of the bromohydrin (**33**), which crystallized directly from the reaction mixture on cooling and was fully characterized.

Compound (**33**) was then subjected to dehydration with phosphorus oxychloride to the anhydro derivative (**32**). Also this material was crystalline

Can. J. Chem. Downloaded from www.nrcresearchpress.com by 210.87.254.105 on 09/05/12
For personal use only.

Can. J. Chem. Downloaded from www.nrcresearchpress.com by 210.87.254.105 on 09/05/12
For personal use only.

and fully characterized and analyzed. It is interesting that the infrared spectrum of (**32**) was superimposable on the spectrum of the previously known chloro analogue. The mass spectra of both materials were identical except for the shift due to the difference in the atomic weight of bromine and chlorine.

With all the intermediates characterized, we may now discuss the reverse process, i.e. the conversion of the lactam-lactone (**27**) to annotinine (**1**). Compound (**27**) was dissolved in carbon tetrachloride and brominated with *N*-bromosuccinimide under irradiation with visible light and reflux. Chromatography on silica gel followed by crystallization allowed the isolation of compound (**32**) in a yield of 16%. Identity of the totally synthetic compound (**32**) and the same product prepared from annotinine (*vide supra*) was established by mixed melting point, infrared spectrum (KBr), mass spectrum, and thin-layer chromatography. The conversion of compound (**32**) to the bromohydrin (**33**) was accomplished by an acid-catalyzed hydration in hot aqueous hydrobromic acid. An equilibrium between various possible compounds was probably established under these conditions, and it was our good fortune that the desired product (**33**) crystallized gradually from the reaction mixture thus shifting the equilibrium in its favor. The synthetic compound (**33**) was purified by recrystallization and rigorously identified with the material prepared from oxoannotinine (**34**) by mixed melting point, t.l.c., mass, and infrared (KBr) spectroscopy.

With the successful preparation of the bromohydrin (**33**) the last serious obstacle in the total synthesis of annotinine was removed. The bromohydrin (**33**) yielded predictably oxoannotinine (**34**) (for the analogous reaction in the chloro series cf. 1*c*) on refluxing with sodium bicarbonate in aqueous acetone. Also in this step the product crystallized directly from the reaction mixture and was purified by recrystallization. Identity of the synthetic compound (**34**) and the material obtained by oxidation of annotinine was rigorously established (mixed m.p., t.l.c., i.r. (KBr), mass spectrum). Having synthesized oxoannotinine, we have formally completed the total synthesis of the natural alkaloid annotinine itself. The conversion of oxoannotinine to annotinine by an unusual hydrogenolysis with platinum oxide in methanolic hydrochloric acid has already been described by Betts and MacLean (11). Because we wished to actually perform the entire synthesis and also because of the unusual nature of the reported last step, we have repeated the hydrogenation of oxoannotinine according to the directions of the above authors. Annotinine was indeed obtained in a yield of 56% and rigorously identified. Besides annotinine we isolated some starting material and oxoannotinine chlorohydrin. Since this last compound is convertible to oxoannotinine by bicarbonate (*vide supra*) the yield obtainable in MacLean's hydrogenolysis is actually very high. Thus the total synthesis of the first natural *Lycopodium* alkaloid is complete.

Experimental

Preparation of the Tricyclic Vinylogous Imide (3)

The bicyclic compound (**2**) (1.4 g) and acrylic acid (0.67 g) were heated to 135 °C for 2 h. After this the mixture was cooled to 50 °C and chloroform (100 ml) was added to it. The chloroform solution was then washed five times with 5% hydrochloric acid (30 ml), dried, and evaporated to dryness. It yielded 1.2 g (63%) of compound (**3**), m.p. 81–83 °C, homogeneous in t.l.c.

Anal. Calcd. for $C_{12}H_{15}NO_2$ (mol. wt., 205): C, 70.24; H, 7.32. Found (mass spectroscopy, 205): C, 70.35; H, 7.23.

Infrared ($CHCl_3$): 1695, 1645, 1610 cm^{-1}. Ultraviolet: $\lambda_{max} = 298$ mμ ($\log \varepsilon = 4.1$.).

Preparation of the Photoadduct (6)

The tricyclic compound (**3**) (102 g) was dissolved in distilled tetrahydrofuran (4 l) and cooled to −70 °C. Allene was added in great excess (about 500 ml) and the mixture was irradiated by a mercury lamp with a Pyrex glass jacket, through which methanol cooled to −70 °C was circulated. The irradiation was continued for 20 h. After evaporation of the solvent the photoadduct (**6**) was purified by crystallization from ethyl acetate. After several crystallizations the yield was 66 g (54%), m.p. 155–157 °C.

Anal. Calcd. for $C_{15}H_{19}NO_2$ (mol. wt., 245): C, 73.47; H, 7.76. Found (mass spectroscopy, 245): C, 73.35; H, 7.78.

Infrared ($CHCl_3$): 1700 (ketone), 1640 (lactam), 908 cm^{-1} (exocyclic methylene). Nuclear magnetic resonance: narrow doublet (2 H), $\tau = 5$ p.p.m. (vinylic hydrogen).

Preparation of the Ketal (7)

The photoadduct (**6**) (10 g) was dissolved in dry benzene (500 ml) to which ethylene glycol (54 g) and *p*-toluenesulfonic acid (3.8 g) were added. The solution was refluxed overnight with a water separator. After this the solution was cooled, washed with water, dried, and evaporated to dryness. The ketal (**7**) was recrystallized from ether to a m.p. of 95–97 °C. The yield was 11.5 g (97%).

Anal. Calcd. for $C_{17}H_{23}NO_3$: mol. wt. 289. Found (mass spectroscopy/mol. wt.): 289.

Infrared ($CHCl_3$): 1630 (lactam), 910 cm^{-1} (exocyclic

Can. J. Chem. Downloaded from www.nrcresearchpress.com by 210.87.254.105 on 09/05/12
For personal use only.

methylene). Nuclear magnetic resonance: quadruplet (2 H) τ = 4.80, 5.04 p.p.m. (vinylic hydrogen), singlet (4 H) τ = 6.05 p.p.m. (dioxolane hydrogen).

Hydrogenation of (7) to (11)

The ketal (**7**) (11.5 g) was hydrogenated in 400 ml of ethanol with 2 g of prehydrogenated platinum oxide for 2 h. The product (**11**) was recrystallized from ether to a m.p. of 162–164 °C. The yield was 11.2 g (96%).

Anal. Calcd. for $C_{17}H_{25}NO_3$: mol. wt., 291. Found (mass spectroscopy): mol. wt. 291.

Infrared ($CHCl_3$): 1615 cm^{-1} (lactam). Nuclear magnetic resonance: singlet (4 H) τ = 6.03 p.p.m. (dioxolane hydrogen), doublet (3 H) τ = 8.69, 8.83 p.p.m. (*C*-methyl).

Deketalization of (11) to (12)

Compound (**11**) (11.2 g) was dissolved in acetone (500 ml) and *p*-toluenesulfonic acid (2.6 g) was added to the solution. The mixture was then heated under reflux overnight. The acetone was evaporated *in vacuo*, chloroform (200 ml) was added and the solution was washed, dried, and evaporated to dryness. The product (**12**) was recrystallized from ethyl acetate to a m.p. of 165–167 °C. The yield was 9 g (95%).

Anal. Calcd. for $C_{15}H_{21}NO_2$ (mol. wt., 247): C, 72.85; H, 8.56; N, 5.66. Found (mol. wt., mass spectroscopy, 247): C, 72.37; H, 8.63; N, 5.68.

Infrared (CCl_4): 1700 (ketone), 1660 cm^{-1} (lactam). Nuclear magnetic resonance: doublet (3 H) τ = 8.94, 9.05 p.p.m. (*C*-methyl).

Reduction of (12) to (14)

The keto lactam (**12**) (9 g) was dissolved in tetrahydrofuran (400 ml) and sodium borohydride in water (40 ml) was added. The reaction mixture was stirred for 2 h, after which the tetrahydrofuran was evaporated *in vacuo* and chloroform (200 ml) was added. The solution was washed, dried, and evaporated to dryness. The product (**14**) was recrystallized to a m.p. 182–183 °C from benzene. The yield was 8.6 g (96%).

Anal. Calcd. for $C_{15}H_{23}NO_2$ (mol. wt., 249): C, 72.37; H, 9.29; N, 5.62. Found (mol. wt., mass spectroscopy, 249): C, 72.48; H, 9.52; N, 5.76.

Infrared ($CHCl_3$): 3600 (hydroxyl), 1620 cm^{-1} (lactam). Nuclear magnetic resonance: doublet (3 H) τ = 8.71, 8.83 p.p.m. (*C*-methyl).

Preparation of the Mesylate (15)

The alcohol (**14**) (1 g) was dissolved in pyridine (10 ml) and methane sulfonyl chloride (0.65 g) was added. The reaction mixture was stirred for 15 h at room temperature and worked up in the usual manner. The product (**15**) was recrystallized from benzene to a m.p. of 162–164 °C. The yield was 1.23 g (92%).

Anal. Calcd. for $C_{16}H_{25}NO_4S$: C, 58.76; H, 7.65; N, 4.28. Found: C, 59.61; H, 7.60; N, 4.23.

Infrared ($CHCl_3$): 1620 (lactam), 1375, 1175 cm^{-1} (OSO_2). Nuclear magnetic resonance: singlet (3 H) τ = 6.92 p.p.m. (—O_3S—CH_3), doublet (3 H) τ = 8.66, 8.76 p.p.m. (C—CH_3).

Preparation of the Olefin (16)

The mesylate (**15**) (100 mg) was dissolved in absolutely dry dimethyl sulfoxide and freshly sublimed potassium tertiary butoxide (42 mg) was added. The mixture was heated for 15 h to 70 °C with *absolute* exclusion of moisture. The reaction mixture was then poured into ice-water and extracted with cloroform. After washing and drying the chloroform was evaporated to dryness and the residue chromatographed on a column of silica gel (10 g). Elution with chloroform yielded the olefin (**16**). It was recrystallized from benzene–ether to a m.p. of 76–77 °C. The yield was 83%. Elution of the column with 1% methanol in chloroform yielded 15 mg of the starting material (**15**).

A large amount of the mesylate (**15**) was transformed to (**16**) in a series of small runs not exceeding 200 mg, since the yields in larger runs were lower for reasons unknown.

Anal. Calcd. for $C_{15}H_{21}NO$ (mol. wt., 231): C, 77.89; H, 9.15; N, 6.06. Found (mol. wt., mass spectroscopy, 231): C, 78.16; H, 9.24; N, 5.94.

Infrared ($CHCl_3$): 1615 cm^{-1} (lactam). Nuclear magnetic resonance: multiplet (2 H) τ = 4.45 p.p.m. (vinylic hydrogen), doublet (3 H) τ = 9.06, 9.18 p.p.m. (C—CH_3).

Oxidation of (16) to (18)

The olefin (**16**) (100 mg) was dissolved in glacial acetic acid (5 ml) and a solution of freshly sublimed selenium dioxide (100 mg) in water (1 ml) was added. The mixture was heated under reflux overnight, filtered, and evaporated to dryness. The residue was taken up in chloroform, washed, dried, and evaporated to dryness again to yield the crude mixture of the epimeric acetates (**18**). It was purified for spectroscopic examination by chromatography (yield 67%), but was used in the crude form for further work.

Anal. Calcd. for $C_{17}H_{23}NO_3$: mol. wt., 289. Found (mass spectroscopy): mol. wt., 289.

Infrared ($CHCl_3$): 1745 (acetate), 1630 cm^{-1} (lactam). Nuclear magnetic resonance: multiplet (2 H) τ = 4.45 p.p.m. (vinylic hydrogen); singlet (3 H) τ = 7.89 p.p.m. (acetate methyl), doublet (3 H) τ = 9.00, 9.15 p.p.m. (*C*-methyl).

Hydrolysis of (18) to (19)

The acetate (**18**) was hydrolyzed by heating under reflux with a large excess of 1% methanolic potassium hydroxide for 5 h. After work-up in the usual manner the crude alcohol (**19**) was obtained in a yield of 90%. It was immediately oxidized to the ketone (**20**).

Preparation of the α,β-Unsaturated Ketone (20)

To an ice-cold solution of the crude alcohol (**19**) (100 mg) in pyridine (7 ml), chromium trioxide (100 mg) in pyridine (7 ml) was added. The ice bath was removed and the mixture was stirred at room temperature for 15 h. The reaction mixture was worked up as usual and the crude material chromatographed on a column of silica gel (10 g). The product (**20**) was eluted by chloroform and recrystallized to a m.p. of 150–152 °C from benzene–ether. The yield was 50 mg (50%).

Anal. Calcd. for $C_{15}H_{19}NO_2$ (mol. wt., 245): C, 73.43; H, 7.81; N, 5.72. Found (mol. wt., mass spectroscopy, 245): C, 73.40; H, 7.96; N, 5.65.

Infrared ($CHCl_3$): 1690 (ketone), 1660 (double bond), 1620 cm^{-1} (lactam). Ultraviolet: λ_{max} = 230 mμ (log ε = 4). Nuclear magnetic resonance: quadruplet (2 H)

centered at τ = 3.58 p.p.m. (vinylic hydrogen), doublet (3 H) τ = 8.97, 9.10 p.p.m. (*C*-methyl).

*Preparation of the Nitrile (**21**)*

The α,β-unsaturated ketone (**20**) (150 mg) was dissolved in dimethyl formamide (50 ml) and potassium cyanide (80 mg) and ammonium chloride (50 mg) in water (5 ml) was added. The mixture was heated for 48 h to 140–150 °C. After this time the solvent was removed *in vacuo* and the residue was dissolved in chloroform. After washing and drying the chloroform soluble material was chromatographed on a column of neutral alumina (20 g). Chloroform eluted 135 mg (82%) of the nitriles (**21**). The material gave two spots in t.l.c. and no attempt was made to separate the two diastereoisomers.

Anal. Calcd. for $C_{16}H_{20}N_2O_2$: mol. wt., 272. Found mol. wt. (mass spectroscopy): 272.

Infrared ($CHCl_3$): 2230 (nitriles), 1720 (ketone), 1645 cm^{-1} (lactam).

*Preparation of the Racemic Ester (**22**)*

The nitriles (**21**) (135 mg) was heated under reflux with methanol (8 ml) and concentrated sulfuric acid (2 ml) for 48 h. The mixture was then poured on ice and extracted with chloroform. After washing and drying the chloroform soluble material was chromatographed on silica gel (8 g). Elution with 20% ether in benzene gave the racemic ester (**22**). It was recrystallized from benzene–ether to a m.p. of 190–192 °C. The yield was 70 mg (46%).

Anal. Calcd. for $C_{17}H_{23}NO_4$: mol. wt., 305. Found mol. wt. (mass spectroscopy): 305.

Infrared (CCl_4): 1740 (ester), 1730 (ketone), 1650 cm^{-1} (lactam). Nuclear magnetic resonance: singlet (3 H) τ = 6.23 p.p.m. (—O—CH_3), doublet (3 H) τ = 8.53, 8.65 p.p.m. (C—CH_3). For comparison with the optically active "natural" compound (22) see theoretical part.

*Preparation of the Racemic Acid (**23**)*

The racemic ester (**22**) was saponified by heating under reflux with 5% methanolic potassium hydroxide overnight. After work-up in the usual manner the racemic acid (**23**) was recrystallized from methanol to a m.p. of 224–226 °C.

Anal. Calcd. for $C_{16}H_{21}NO_4$ (mol. wt., 291): C, 65.74; H, 7.24; N, 4.79. Found mol. wt. (mass spectroscopy): 291: C, 64.70; H, 7.07; N, 4.62.

Infrared (KBr): 1740 (carboxyl), 1730 (ketone), 1610 cm^{-1} (lactam).

*Preparation of the Synthetic Optically Active Acid (**23**)*

The racemic acid (**23**) (145 mg) was dissolved in acetone (10 ml) and a few drops of methanol were added. To this solution brucine (200 mg) in acetone (10 ml) was added and the volume of the solvent was reduced to 5 ml. Crystals appeared after standing for 2 h and they were recrystallized several times from methanol–acetone until the constant m.p. of 158–160 °C was reached. The yield of the pure constant melting brucine salt was 100 mg. This material was dissolved in a small volume of methanol and 10% sulfuric acid (30 ml) was added to the solution. Continuous extraction of the mixture with ether yielded 45 mg of the optically active acid (**23**). It was recrystallized from methanol to a m.p. of 240–242 °C. Its mass and infrared (KBr) spectra were identical with the spectra of the racemic acid (**23**).

*Preparation of the Synthetic Optically Active Ester (**22**)*

The pure synthetic optically active acid (**23**) (70 mg) was esterified with diazomethane and the optically active ester (**22**) was obtained in quantitative yield. It was recrystallized from benzene–ether to a constant m.p. of 198–200 °C.

Anal. Calcd. for $C_{17}H_{23}NO_4$: C, 66.95; H, 7.59; N, 4.59. Found: C, 66.54; H, 7.54; N, 5.17.

All the spectral data for the optically active ester (**22**) and the racemic ester (**22**) were identical. The synthetic optically active ester (**22**) was found to be identical with the material of the same structure prepared from annotinine by melting point, mixed melting point, t.l.c., i.r. spectrum in KBr and CCl_4, mass spectrum, and rotatory dispersion curve (see Fig. 1).

*Preparation of the Enol-acetate (**28**)*

The optically active keto-ester (**22**) (160 mg) and *p*-toluenesulfonic acid (30 mg) were dissolved in acetic anhydride (10 ml) and heated under reflux for 6 h. The acetic anhydride was then distilled off *in vacuo* and the residue was taken up in chloroform. The chloroform solution was washed, dried, and evaporated to dryness. The pure compound (**28**) was obtained by recrystallization from benzene. It melted at 162–163 °C. The yield was 165 mg (91%).

Anal. Calcd. for $C_{19}H_{25}NO_5$ (mol. wt., 347): C, 65.69; H, 7.25; N, 4.01. Found mol. wt. (mass spectroscopy): 347: C, 65.75; H, 7.39; N, 3.99.

Infrared ($CHCl_3$): 1750 (esters), 1640 cm^{-1} (lactam); Nuclear magnetic resonance: singlet (3 H) τ = 6.29 p.p.m. (—O—CH_3), singlet (3 H) τ = 7.84 p.p.m. (—O—C—CH_3), doublet (3 H), τ = 8.87, 9.00 p.p.m. (C—CH_3).

*Preparation of the Lactam–Lactone (**27**)*

The enol-acetate (**28**) (200 mg) was dissolved in dry tetrahydrofuran (20 ml) and a solution of sodium borohydride (200 mg) in absolute methanol (4 ml) was added. The crude reduction product obtained by working up in the usual manner was chromatographed on silica gel (20 g). Elution with 5% methanol in chloroform gave 140 mg (78%) of the mixture of the isomeric hydroxy esters (**29**) and (**30**).

Anal. Calcd. for $C_{17}H_{25}NO_4$: mol. wt., 307. Found: mol. wt. (mass spectroscopy), 307.

The above material was hydrolyzed by heating under reflux with 5% methanolic potassium hydroxide (40 ml) for 24 h. The acids (**26**) and (**31**) were isolated in the usual manner. The yield was 110 mg (90%). This material (200 mg) was subjected without purification to the lactonization reaction. It was dissolved in dry benzene (200 ml) and *p*-toluenesulfonic acid (60 mg) was added. The solution was refluxed for 3 days with a water separator. After this time the benzene was distilled off, the residue was taken up in chloroform and washed with 1% aqueous potassium hydroxide and with water. The chloroform layer was then dried and evaporated to dryness. The pure lactone (**27**) was eluted from a column of silica gel (10 g) with ether and it was crystallized from ether and methanol to a m.p. of 179–180 °C. The yield was 72 mg (38%).

Can. J. Chem. Downloaded from www.nrcresearchpress.com by 210.87.254.105 on 09/05/12
For personal use only.

Can. J. Chem. Downloaded from www.nrcresearchpress.com by 210.87.254.105 on 09/05/12
For personal use only.

Anal. Calcd. for $C_{16}H_{21}NO_3$ (mol. wt., 275): C, 69.80; H, 7.69; N, 5.09. Found (mol. wt. (mass spectroscopy) 275): C, 69.37; H, 7.64; N, 4.69.

Infrared ($CHCl_3$): 1770 (lactone), 1620 cm^{-1} (lactam); nuclear magnetic resonance: doublet (3 H) $\tau = 8.73$, 8.84 p.p.m. (C—CH_3). The synthetic compound (**27**) was identical with the material of the same structure prepared from annotinine by melting point, mixed melting point, t.l.c., i.r. spectrum (KBr) and ($CHCl_3$), and mass spectrum.

*Preparation of Compound (**32**) by Total Synthesis*

The lactone (**27**) (500 mg) was dissolved in carbon tetrachloride (300 ml) and *N*-bromosuccinimide (540 mg) was added to the solution. The reaction mixture was irradiated with a strong visible light source and refluxed for 30 min. The solution was then washed extensively with water, dried, and evaporated to dryness. The residue was chromatographed on a column (60 g) of silica gel. The product (**32**) was eluted by 30% chloroform in benzene and recrystallized from methanol to a constant m.p. of 212 °C. The yield of the pure compound (**32**) was 100 mg. (16%).

Anal. Calcd. for $C_{16}H_{18}NO_3Br$: C, 54.78; H, 5.15; Br, 22.71. Found: C, 55.54; H, 5.14; Br, 23.27.

Mass spectrum: *m/e* 309, 311 (M-42). Infrared (KBr): 1785 (lactone), 1655, 1630 cm^{-1} (lactam and double bond); nuclear magnetic resonance: doublet (3H) $\tau =$ 8.62, 8.74 p.p.m. (C—CH_3), singlet (1 H) $\tau = 3.31$ p.p.m. (vinylic hydrogen). The synthetic compound (**32**) was identical with the material of the same structure obtained by degradation of annotinine (*vide infra*) by melting point, mixed melting point, t.l.c., i.r. (KBr), and mass spectrum.

*Preparation of Compound (**33**) by Total Synthesis*

The synthetic compound (**32**) (300 mg) was dissolved in 10% hydrobromic acid (200 ml) and heated to 100 °C overnight. The crystalline precipitate of compound (**33**) which was gradually formed during the night was filtered off and recrystallized from methanol to a constant m.p. of 260–262 °C. The yield of the pure product was 30%.

Anal. Calcd. for $C_{16}H_{20}NO_4Br$: C, 51.91; H, 5.45; Br, 21.57. Found: C, 52.01; H, 5.42; Br, 20.31.

Infrared (KBr): 1765 (lactone), 1630 cm^{-1} (lactam). The synthetic compound (**33**) was identical with the material of the same structure prepared from annotinine (*vide infra*) by melting point, mixed melting point, t.l.c., i.r. spectrum (KBr), and mass spectrum.

*Preparation of Oxoannotinine (**34**) by Total Synthesis*

The bromohydrin (**33**) (200 mg) was dissolved in acetone (25 ml) and a solution of sodium bicarbonate (75 mg) in water (2 ml) was added. The reaction mixture was heated under reflux for 4 h. After this time the acetone was removed by distillation and water was added. The crystalline product (34) was filtered off and purified by crystallization from methanol to a constant m.p. of 233–234 °C. The yield was 156 mg (78%).

Anal. Calcd. for $C_{16}H_{19}NO_4$: C, 66.42; H, 6.62; N, 4.84. Found: C, 66.51; H, 6.69; N, 4.82.

The synthetic compound (**34**) was identified with the known oxoannotinine (10) by melting point, mixed melting point, t.l.c., i.r. (KBr and $CHCl_3$), and mass spectrum.

*Hydrogenolysis of Oxoannotinine (**34**) to Annotinine (**1**)*

This experiment is a repetition of the reaction described by Betts and MacLean (11). To a solution of oxoannotinine (**34**) (600 mg) in methanol (100 ml) six drops of concentrated hydrochloric acid were added. The solution was hydrogenated at room temperature for 20 h with prehydrogenated platinum oxide (200 mg) at a pressure of 60 p.s.i. The catalyst was filtered off and the solution was evaporated to dryness. Water was then added and the insoluble crystalline material (165 mg) filtered off. It was identified after recrystallization from methanol by melting point (286 °C) and i.r. spectrum (KBr) as the known oxoannotinine chlorohydrin. The aqueous filtrate was basified with ammonia and extracted with chloroform. After washing and drying the chloroform extract was chromatographed on silica gel (30 g). Elution with chloroform yielded annotinine, which was recrystallized from methanol to a melting point of 234–235 °C. The yield was 250 mg (56%). The material was identified with an authentic sample of annotinine by melting point, mixed melting point, t.l.c., and i.r. spectrum (KBr). Later fractions of the chromatogram yielded a small amount of oxoannotinine (20 mg). It was identified by mixed melting point (233–234 °C) and i.r. spectrum (KBr) with an authentic sample.

*Preparation of the Bromohydrin (**33**) from Oxoannotinine (**34**)*

A solution of oxoannotinine (**34**) (2 g, prepared by oxidation of annotinine (10)) in 19% hydrobromic acid (260 ml) was heated for 2 h to 100 °C. The product (**33**) crystallized directly from the reaction mixture and was purified by recrystallization from methanol to a melting point of 260–262 °C. The yield was 1.8 g (72%).

Anal. Calcd. for $C_{16}H_{20}NO_4Br$: C, 51.91; H, 5.45; Br, 21.57. Found: C, 51.98; H, 5.41; Br, 21.49.

The i.r. and mass spectra of compound (**33**) prepared in this manner were identical with the corresponding spectra of the synthetic material (*vide supra*).

*Dehydration of (**33**) to (**32**)*

The bromohydrin (**33**) (500 mg) was heated under reflux with phosphorus oxychloride (30 ml) for 2 h. The oxychloride was distilled off *in vacuo* and the residue was dissolved in chloroform, washed with water, dried and evaporated to dryness. Chromatography on a column of neutral alumina (10 g) with chloroform as eluant gave the product (**32**). It was recrystallized from methanol to a constant melting point of 212–214 °C. The yield was 122 mg (26%).

Anal. Calcd. for $C_{16}H_{18}NO_3Br$: C, 54.78; H, 5.15; Br, 22.71. Found: C, 55.55; H, 5.30; Br, 23.20.

The i.r. and mass spectra of compound (**32**) prepared in this manner were identical with the corresponding spectra of the synthetic material (*vide supra*).

Acknowledgments

We wish to thank the National Research Council of Canada, the Research Corporation, New York, the Ciba Company Limited, Dorval, Quebec, and the Hoffmann–La Roche Company, Nutley, New Jersey, for supporting the various

fundamental studies which eventually led to the present synthesis as well as the synthesis proper. We also wish to thank Dr. J. G. McCluskey for his participation in various unpublished model studies. We wish to thank also Dr. W. A. Ayer, University of Alberta, Edmonton, for recording the optical rotatory dispersion curves.

1. *a*. K. WIESNER, Z. VALENTA, W. A. AYER, and C. BANKIEWICZ. Chem. and Ind. 1019 (1956); K. WIESNER, W. A. AYER, L. R. FOWLER, and Z. VALENTA. Chem. and Ind. 564 (1957).
b. K. WIESNER, Z. VALENTA, W. A. AYER, L. R. FOWLER, and J. E. FRANCIS. Tetrahedron, **4**, 87 (1958).
c. K. WIESNER. Progress in the chemistry of organic natural products. Vol. XX. *Edited by* L. Zechmeister. Springer–Verlag, Wien. 1962. p. 271.
2. M. PRZYBYLSKA and L. MARION. Can. J. Chem. **35**, 1075 (1957).
3. E. H. W. BÖHME, Z. VALENTA, and K. WIESNER. Tetrahedron Letters, No. 29, 2441 (1965).
4. *a*. K. WIESNER, I. JIRKOVSKÝ, M. FISHMAN, and C. A. J. WILLIAMS. Tetrahedron Letters, No. 16, 1523 (1967).
b. K. WIESNER and I. JIRKOVSKÝ. Tetrahedron Letters, No. 22, 2077 (1967).
c. K. WIESNER and LIZZIE POON. Tetrahedron Letters, No. 49, 4937 (1967).
5. C. A. GROB and J. H. WILKENS. Helv. Chim. Acta, **48**, 808 (1965).
6. H. DUGAS. Ph.D. Thesis, University of New Brunswick. Fredericton, New Brunswick. (1967).
7. To be published.
8. D. MARTIN, A. WEISE, and H. J. NICLAS. Angew. Chem. **79**, 340 (1967).
9. W. NAGATA, S. HIRAI, H. ITAZAKI, and K. TAKEDA. J. Org. Chem. **26**, 2413 (1961).
10. D. B. MACLEAN and H. C. PRIME. Can. J. Chem. **31**, 543 (1953).
11. E. E. BETTS and D. B. MACLEAN. Can. J. Chem. **35**, 211 (1957).

Can. J. Chem. Downloaded from www.nrcresearchpress.com by 210.87.254.105 on 09/05/12
For personal use only.

Can. J. Chem. Downloaded from www.nrcresearchpress.com by 210.87.254.105 on 09/05/12
For personal use only.

Specifically ring-labelled (±)-pelletierine

R. N. Gupta and Ian D. Spenser
Department of Chemistry, McMaster University, Hamilton, Ontario

Received September 9, 1968

A synthesis of 2-^{14}C- and of 6-^{14}C-(±)-pelletierine and (±)-α-phenacylpiperidine is described, starting from 2-^{14}C- and 6-^{14}C-(±)-lysine, respectively.

Canadian Journal of Chemistry, **47**, 445 (1969)

It has been suggested that pelletierine (**1**)[1] is the biogenetic precursor of the *Lycopodium* (2) and the *Lythraceae* (3) alkaloids, and that the *Lobelia* alkaloid lobinaline is derived from α-phenacylpiperidine (**2**) (4). For investigations of the biosynthesis of these alkaloids we required samples of the postulated precursors, specifically labelled either at C-2 or at C-6 of the piperidine nucleus.

A number of syntheses of (±)-pelletierine and its phenyl analogue have been described, but none of these lend themselves to the preparation of the desired radiomers. In several of the syntheses (5–10) the piperidine nucleus of the products is generated by reduction of a pyridine nucleus. Suitably labelled samples of the required pyridine derivatives which serve as starting materials are not readily accessible.

In another, biogenetically modelled (11), synthetic approach (12–19), the piperidine ring of the products is supplied by Δ^1-piperideine, which, in turn, may be readily prepared from piperidine (20) or from cadaverine (1,5-diaminopentane) (16, 21, 22). Since piperidine and cadaverine are symmetrical molecules, a radiochemical synthesis starting with 2-^{14}C-piperidine or 1-^{14}C-cadaverine would yield an equimolar mixture of 2-^{14}C- and 6-^{14}C-Δ^1-piperideine and hence of 2-^{14}C- and 6-^{14}C-(±)-pelletierine or its phenyl analogue. Other attempts to prepare Δ^1-piperideine failed (23) or gave the product in very poor yield (13, 24, 25).

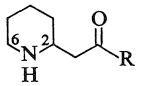

1 R = CH_3 Pelletierine
2 R = C_6H_5 α-Phenacylpiperidine

We have now obtained the desired singly labelled radiomers of (±)-pelletierine and of (±)-α-phenacylpiperidine in 45–50% overall yield, starting from 2-^{14}C- or from 6-^{14}C-(±)-lysine (cf. ref. 25). Lysine was oxidized with *N*-bromosuccinimide (26), and the product of this reaction, presumably Δ^1-piperideine, was condensed, without isolation, with acetoacetic acid or benzoylacetic acid (14, 19). The products, (±)-pelletierine and (±)-α-phenacylpiperidine, respectively, were purified and isolated as hydrochlorides.

Radioactive (±)-pelletierine, obtained from 6-^{14}C-(±)-lysine, was degraded by conventional methods to establish the site of labelling.

All activity of the compound was recovered in the formaldehyde (isolated as the dimedone derivative), obtained from C-6 of the piperidine ring of the labelled (±)-pelletierine. The (±)-pelletierine from 6-^{14}C-(±)-lysine is thus 6-^{14}C-(±)-pelletierine.

In an analogous manner 2-^{14}C-(±)-pelletierine was prepared from 2-^{14}C-(±)-lysine, 4,5-$^3H_2$-(±)-pelletierine from 4,5-$^3H_2$-(±)-lysine, and 6-^{14}C-(±)-α-phenacylpiperidine from 6-^{14}C-(±)-lysine.

Evidently no randomization of activity occurs between C-6 and C-2 of Δ^1-piperideine, the intermediate in the synthesis.

Experimental

Starting Materials

Solutions of the sodium salts of acetoacetic acid and benzoylacetic acid were prepared by hydrolysis, at room temperature, of the corresponding ethyl esters with the calculated volume of 0.5 *N* sodium hydroxide (19). The labelled samples of (±)-lysine (2-^{14}C-(±)-lysine monohydrochloride, nominal specific activity 3.3 mC/mmole, New England Nuclear Corporation; 6-^{14}C-(±)-lysine, nominal specific activity 9.2 mC/mmole, Commissariat à L'Energie Atomique, France; 4,5-$^3H_2$-(±)-lysine monohydrochloride, nominal specific activity 0.25 C/mmole, Radiochemical Center were commercial products.

(±)-Pelletierine (cf. ref. 14, 26)

N-Bromosuccinimide (178 mg, 1 mmole) was added to a solution of lysine monohydrochloride (92 mg, 0.5 mmole in 10 ml water) in a small flask. The flask was

[1] 2-Piperidylpropanone (**1**), known for many years as isopelletierine, is now referred to as pelletierine, following the suggestion of Gilman and Marion (1).

Can. J. Chem. Downloaded from www.nrcresearchpress.com by 210.87.254.105 on 09/05/12
For personal use only.

rotated by means of a rotary evaporator, under mild suction, while immersed in a water bath at 40°. When the solution had become colorless (20 min) it was transferred quantitatively, with repeated washing (2 × 1 ml water), by means of a Pasteur pipette into a dropping funnel which had been calibrated to deliver approximately 0.5 ml/h. The solution was added at room temperature over a period of 24 h to a solution of sodium acetoacetate (2 mmoles) (*vide supra*) in citrate buffer, pH 6.9 (5 ml), which was continuously stirred under nitrogen. The dropping funnel was washed (1 ml water), and the washings were allowed to drop into the reaction mixture. When addition was complete, the reaction mixture was cooled (5°), basified with cold aqueous potassium hydroxide (10% w/v), and the product was extracted into chloroform (5 × 1 ml). The chloroform extract was dried (Na_2SO_4), the solution was removed from the desiccant by means of a Pasteur pipette, a drop of concentrated hydrochloric acid was added, and the mixture was evaporated to dryness. The residue was dissolved in chloroform (0.5 ml) and applied to a column (10 × 1 cm) of neutral alumina (activity I). The column was eluted with ethyl acetate (10 ml) and the eluate discarded. Ethyl acetate containing 5% methanol (200 ml) then eluted the product (27). The eluate was evaporated and the residue dissolved in a little methanol. Addition of ether yielded (±)-pelletierine hydrochloride (42 mg, 47% based on lysine), m.p. 144–145° (reported m.p. 141–143° (15), 144–145° (5, 18)), identical (mass spectrum,[2] m.p., mixture m.p.) with an authentic sample, prepared from 1-[2-pyridyl]-propan-2-one (9).

The labelled samples of (±)-pelletierine hydrochloride were synthesized in the manner outlined above from labelled lysine (2-^{14}C-(±)-lysine, 0.5 mC; 6-^{14}C-(±)-lysine, 0.5 mC; 4,5-$^{3}H_2$-(±)-lysine, 5 mC). So that the active runs could be carried out on the same scale as the pilot run, unlabelled (±)-lysine was added to the labelled lysine samples to yield ^{14}C-labelled lysine of specific activity 1 mC/mmole, and ^{3}H-labelled lysine of specific activity 10 mC/mmole. The resulting labelled samples of (±)-pelletierine hydrochloride were of corresponding specific activity. Products of higher specific activity would be obtainable by scaling down the preparation, or by starting with higher total activities.

The radiochemical purity of the products was established by paper chromatography (1-butanol – acetic acid – water, 2:1:1) and radioscanning. The products showed a single radioactive component, R_f 0.76.

(±)-α-Phenacylpiperidine (cf. ref. 14)

The scale and method of preparation were analogous to those described for (±)-pelletierine, except that benzoylacetic acid was used in place of acetoacetic acid. (±)-α-Phenacylpiperidine hydrochloride, R_f 0.87 (1-butanol – acetic acid – water, 2:1:1), m.p. 165–167° (reported melting point 170–172° (18)) was obtained in 51% yield. The mass spectrum of the salt, introduced into the mass spectrometer by the direct inlet system, showed a signal *m/e* 203. The free base did not show this signal of the molecular ion.

Degradation of Labelled (±)-Pelletierine, Obtained from 6-^{14}C-(±)-Lysine

A small sample (total activity approximately 3×10^5 counts min^{-1}) of the (±)-pelletierine hydrochloride, obtained from 6-^{14}C-(±)-lysine, was dissolved in methanol and was added to a solution of unlabelled (±)-pelletierine hydrochloride (350 mg) in methanol. The solution was concentrated, ether was added, and (±)-pelletierine hydrochloride crystallized. This was recrystallized to constant activity (Found: $(13.0 \pm 0.3) \times 10^4$ counts min^{-1} mmole^{-1}).

This sample of (±)-pelletierine hydrochloride (300 mg) was dissolved in methanol (10 ml), the solution was cooled to 0°, and excess sodium borohydride (0.6 g) was added in portions. The mixture was kept for 12 h at room temperature, methanol was evaporated, and ice cold 10% hydrochloric acid was added to the residue until the solution was acidic. Aqueous potassium hydroxide solution (10%) was added and the alkaline solution was extracted with chloroform. The chloroform extract was dried (Na_2SO_4) and evaporated, and the residue was sublimed at 0.5 mm and 70–90°, to yield 1-(2-piperidyl)-propan-2-ol (240 mg, 80% yield), m.p. 50–55° (reported m.p. for the diastereoisomeric mixture ((±)-sedridine plus (±)-allosedridine) approximately 50° (7); 60–64° (9)).

The product was dissolved in methanol (10 ml); methyl iodide (2 ml) and anhydrous sodium bicarbonate were added and the mixture was stirred at room temperature. After 24 h more methyl iodide (2 ml) was added and stirring continued for 24 h. The solid was filtered off and washed with methanol, and the filtrate evaporated to dryness. The residue was redissolved in dry methanol (10 ml) and filtered. An equal volume of water was added to the filtrate, the solution was warmed on the steam bath, freshly precipitated silver oxide (300 mg) was added, and the mixture was kept for 4 h in the dark with occasional stirring. It was then filtered, the solvents were evaporated, the oily basic residue was distilled at 0.5 mm and 110–140°, and the distillate collected in a trap which was cooled in ice.

Ozonolysis of a portion of the distillate failed to yield formaldehyde, indicating that Hofmann degradation yields only 8-dimethylaminooct-3- or -4-en-2-ol, and no 4-dimethylaminooct-7-en-2-ol. This mode of reaction is similar to that of sedamine (28).

The major portion of the Hofmann base was dissolved in methanol, palladium on charcoal (5%, 100 mg) was added, and the mixture was stirred under hydrogen at atmospheric pressure until there was no further uptake of hydrogen. The mixture was filtered, methanol was evaporated, and the oily residue distilled at 0.5 mm and 100–120°, yielding the product, 8-dimethylaminooctan-2-ol (mass spectrum : molecular ion *m/e* 173), as an oil.

The oily product was dissolved in a mixture of equal volumes of methanol and ether (10 ml); methyl iodide (1 ml) was added, the mixture was allowed to stand 12 h, and was then evaporated to dryness. The residue was washed with dry ether, and was dissolved in 50% aqueous methanol (5 ml). The solution was heated, freshly precipitated silver oxide (200 mg) was added, and the mixture was kept for 4 h in the dark. It was filtered, solvents were

[2]The signal *m/e* 141 (molecular ion of the free base) was observed when isopelletierine hydrochloride was introduced into the direct inlet system of the mass spectrometer.

evaporated, the oily residue was distilled at 0.5 mm and 120–150°, and the distillate was collected in a trap which was cooled in solid carbon dioxide/acetone. The distillate was dissolved in ethyl acetate (3 ml), and the solution was washed with dilute hydrochloric acid to remove basic components. Glacial acetic acid (2 ml) was added to the organic layer, the solution was cooled in an ice–salt mixture and a slow current of ozonized oxygen was passed through it for 15 min. Water (50 ml) and zinc dust (100 mg) were then added, and the mixture was distilled until 40 ml distillate had been collected. 5,5-Dimethyl-1,3-cyclohexanedione (dimedone) (50 mg) was added to the distillate, the mixture was warmed to evaporate ethyl acetate, and was then kept for 6 h at 0°, when crystallization of formaldehyde dimethone (10 mg) was complete. The product was recrystallized from aqueous methanol to constant activity (Found: $(13.8 \pm 0.3) \times 10^4$ counts min^{-1} $mmole^{-1}$).

Determination of Radioactivity

Radioactivity was assayed on samples of finite thickness on aluminium planchets, using a Nuclear Chicago Corp. gas flow system. The usual corrections for background and self-absorption were applied. For plating, a 1% solution of collodion in dimethyl formamide was used as the solvent.

Acknowledgment

This investigation was supported by a grant from the National Research Council of Canada.

1. R. E. Gilman and L. Marion. Bull. Soc. Chim. France, 1993 (1961).
2. R. N. Gupta, M. Castillo, D. B. MacLean, I. D. Spenser, and J. T. Wróbel. J. Am. Chem. Soc. **90**, 1360 (1968).
3. J. P. Ferris, C. B. Boyce, and R. C. Briner. Tetrahedron Letters, 5129 (1966).
4. R. N. Gupta and I. D. Spenser. Chem. Commun. 893 (1966).
5. J. Meisenheimer and E. Mahler. Ann. Chem. **462**, 301 (1928).
6. J. P. Wibaut, C. C. Kloppenburg, and M. G. J. Beets. Rec. Trav. Chim. **63**, 134 (1944).
7. H. C. Beyerman and Y. M. F. Muller. Rec. Trav. Chim. **74**, 1568 (1955).
8. H. C. Beyerman, J. Eenshuistra, W. Eveleens, and A. Zweistra. Rec. Trav. Chim. **78**, 43 (1959).
9. J. Büchi, F. Kracher, and G. Schmidt. Helv. Chim. Acta, **45**, 729 (1962).
10. G. A. Cooke and G. Fodor. Can. J. Chem. **46**, 1105 (1968).
11. R. Robinson. J. Chem. Soc. **111**, 876 (1917).
12. C. Schöpf. Angew. Chem. **61**, 31 (1949).
13. E. F. L. J. Anet, G. K. Hughes, and E. Ritchie. Nature, **164**, 501 (1949); Australian J. Sci. Research, Series A, **3**, 336 (1950).
14. C. Schöpf, F. Braun, K. Burkhardt, G. Dummer, and H. Müller. Ann. Chem. **626**, 123 (1959).
15. A. J. Clarke and P. J. G. Mann. Biochem. J. **71**, 596 (1959).
16. H. Tuppy and M. S. Faltaous. Monatsh. Chem. **91**, 167 (1960).
17. K. Hasse and G. Schmid. Biochem. Z. **337**, 480 (1963).
18. J. Van Noordwijk, J. J. Mellink, B. J. Visser, and J. H. Wisse. Rec. Trav. Chim. **82**, 763 (1963).
19. J. H. Wisse, H. de Klonia, and B. J. Visser. Rec. Trav. Chim. **83**, 1265 (1964).
20. C. Schöpf, A. Komzak, F. Braun, and E. Jacobi. Ann. Chem. **559**, 1 (1947).
21. P. J. G. Mann and W. R. Smithies. Biochem. J. **61**, 89 (1955).
22. K. Hasse and H. Maisack. Biochem. Z. **327**, 296 (1955).
23. F. Galinowsky, A. Wagner, and R. Weiser. Monatsh. Chem. **82**, 551 (1951).
24. R. Lukeš and J. Kovař. Coll. Czechoslov. Chem. Commun. **21**, 1317 (1956).
25. B. Franck and D. Randau. Angew. Chem. Intern. Ed. **5**, 131 (1966).
26. N. Konigsberg, G. Stevenson, and J. M. Luck. J. Biol. Chem. **235**, 1341 (1960).
27. M. M. El Olemy, A. E. Schwarting, and W. J. Kelleher. Lloydia, **29**, 58 (1966).
28. C. Schöpf, G. Dummer, and W. Wüst. Ann. Chem. **626**, 134 (1959).

Can. J. Chem. Downloaded from www.nrcresearchpress.com by 210.87.254.105 on 09/05/12
For personal use only.

Alkaloids of *Lycopodium lucidulum* Michx. Structure and properties of alkaloid L.23

W. A. AYER AND B. ALTENKIRK
Department of Chemistry, University of Alberta, Edmonton, Alberta

AND

R. H. BURNELL AND M. MOINAS
Department of Chemistry, Laval University, Quebec City, Quebec

Received September 9, 1968

The minor alkaloids present among the strong bases of *Lycopodium lucidulum* have been reinvestigated. Manske and Marion's alkaloid L.23 has been shown to be epimeric with lycodoline at C-12 and the nitrogen. A correlation between the two alkaloids has been achieved. The presence of a σ-coupled p interaction in the ultraviolet spectrum of lycopodine, lycodoline, and related compounds is described. A Cotton effect due to this chromophore has been detected by means of circular dichroism. The optical rotatory dispersion and circular dichroic properties of lycopodine, 12-epilycopodine, lycodoline, and alkaloid L.23 are discussed in terms of the absolute configuration assigned to these alkaloids.

Canadian Journal of Chemistry, **47**, 449 (1969)

Can. J. Chem. Downloaded from www.nrcresearchpress.com by 210.87.254.42 on 09/05/12
For personal use only.

The alkaloids of *Lycopodium lucidulum* Michx. were first investigated by Manske and Marion in 1946 (1). They reported the isolation of nicotine, lycopodine (**1**), alkaloid L.13,[1] and six other bases which were designated alkaloids L.20, L.21, L.22, L.23, L.24, and L.25. In previous papers dealing with this species we have reported on the structures of alkaloids L.20 (**2**) (2) and L.21 (**3**) (3) and have noted the occurrence of lycodoline (alkaloid L.8) (**4**) (2) in *L. lucidulum*. Further examination of the strong bases (2) has led to the isolation of lycodine (**5**), flabelliformine (**6**), alkaloid L.23,[2] and a compound $C_{16}H_{25}O_2N$, m.p. 230–233°, previously isolated from *L. clavatum* var. *megastachyon* (4). The molecular formula of this alkaloid corresponds to that assigned to alkaloid L.25 which was isolated and characterized as its perchlorate, m.p. 297°. The perchlorate of the compound we have isolated melts at 238–240°. In this paper we report on the structure of alkaloid L.23 and discuss the ultraviolet, optical rotatory dispersion, and circular dichroism spectra of this and related compounds.

Alkaloid L.23, which has also been isolated from *L. selago* (5) and which is probably identical with the pseudoselagine of Achmatowicz and Rodewald (6), has structure **7** and thus is epimeric with lycodoline (**4**) at C-12 (and consequently also at the nitrogen). The structure was established in the following manner. The infrared spectrum ($CHCl_3$) shows carbonyl absorption at 1690 cm^{-1}, a concentration independent band at 3510 cm^{-1} indicative of an intramolecularly hydrogen bonded hydroxyl, and intense "Bohlmann bands" at 2810, 2760, and 2680 cm^{-1} indicative of a *trans*-quinolizidine system (7). The nuclear magnetic resonance spectrum revealed the presence of the secondary *C*-methyl group (poorly resolved doublet at τ 9.04) and suggested that the hydroxyl group was tertiary (no signal other than that for OH (τ 6.4, readily exchanged for deuterium) below τ 6.7. The finding that the alkaloid is resistant to acetylation is consistent with this observation.

The mass spectrum of alkaloid L.23 (Fig. 1*a*) confirms the molecular formula assigned earlier (1) and is strikingly similar (see Fig. 1) to that of lycodoline (**4**, Fig. 1*b*). The mass spectral fragmentation pattern for lycodoline has previously been discussed (8). The similarity of the two spectra suggests that the compounds are stereoisomers and since alkaloid L.23 appears to contain a *trans*-quinolizidine system (Bohlmann bands) it appeared likely that the two were stereoisomeric at least at C-12 and nitrogen. The ultraviolet spectrum of lycodoline (**4**) (Table I) shows a maximum at 221 mμ (ε 1500). This absorption band is not present in the spectra of salts of lycodoline and is also absent in the ultraviolet spectrum of alkaloid L.23, which shows only end absorption in this region. It has

[1]A sample of the perchlorate of alkaloid L.13, provided by Dr. Marion, proved to be identical with lycopodine perchlorate.

[2]Identical with an authentic sample kindly provided by Dr. L. Marion.

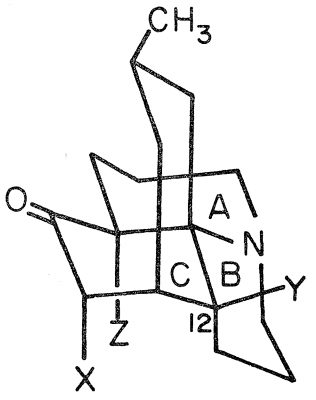

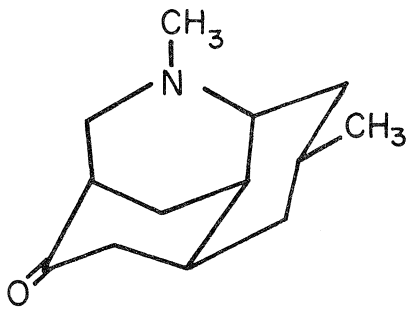

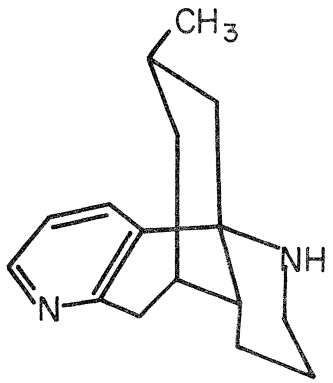

1 X = Y = Z = H

2 X = OH, Y = Z = H

4 X = Z = H, Y = OH

6 X = Y = H, Z = OH

3

5

TABLE I

Ultraviolet spectra of lycopodine type alkaloids in the region 215–230 mμ

Compound	Solvent	λ_{max} (ε value)
Lycopodine (**1**)	MeOH	217 mμ (2400)*
Lycopodine (**1**)	Octane	217 mμ (2400)*
Alkaloid L.20 (**2**)	MeOH	220 mμ (2500)*
Lycodoline (**4**)	MeOH	221 mμ (1500)*
Clavolonine (ref. 14)	MeOH	218 mμ (1670)*
Flabelliformine (**6**)	MeOH	228 mμ (inf) (≃500)*
Epilycopodine (**9**)	MeOH	No maximum
Lycopodine lactam	MeOH	No maximum
Alkaloid L.23 (**7**)	MeOH	No maximum
Epiallolycopodine†	MeOH	No maximum
Dihydrolycopodine (**14**)	MeOH	No maximum

*Disappears on acidification of solution.
†C-15 Epimer of **9**.

been shown (9) that β-aminoketones in which the unshared pair on nitrogen, the α,β σ-bond and the π orbital of the carbonyl are parallel (**8** illustrates the present case) give rise to a non-classical E. T. band in the 220–260 mμ region of the ultraviolet. As may be seen in Table I, all of the lycopodine-like alkaloids with a carbonyl group at C-5 and in which the nitrogen lone pair is equatorial to ring A show an absorption band in this region whereas 12-epilycopodine (**9**) and alkaloid L.23 do not. Ultraviolet spectroscopy may therefore be used as an adjunct to infrared spectroscopy (Bohlmann bands) in assigning the configuration at the nitrogen in these alkaloids. As is discussed later, optical rotatory dispersion and/or circular dichroism may be used to the same end.

In order to establish that alkaloid L.23 differed from lycodoline (**4**) only in the stereochemistry at C-12 and the nitrogen, it was necessary to establish a direct correlation between the two. Dehydration of alkaloid L.23 with either phenyl-

Can. J. Chem. Downloaded from www.nrcresearchpress.com by 210.87.254.42 on 09/05/12
For personal use only.

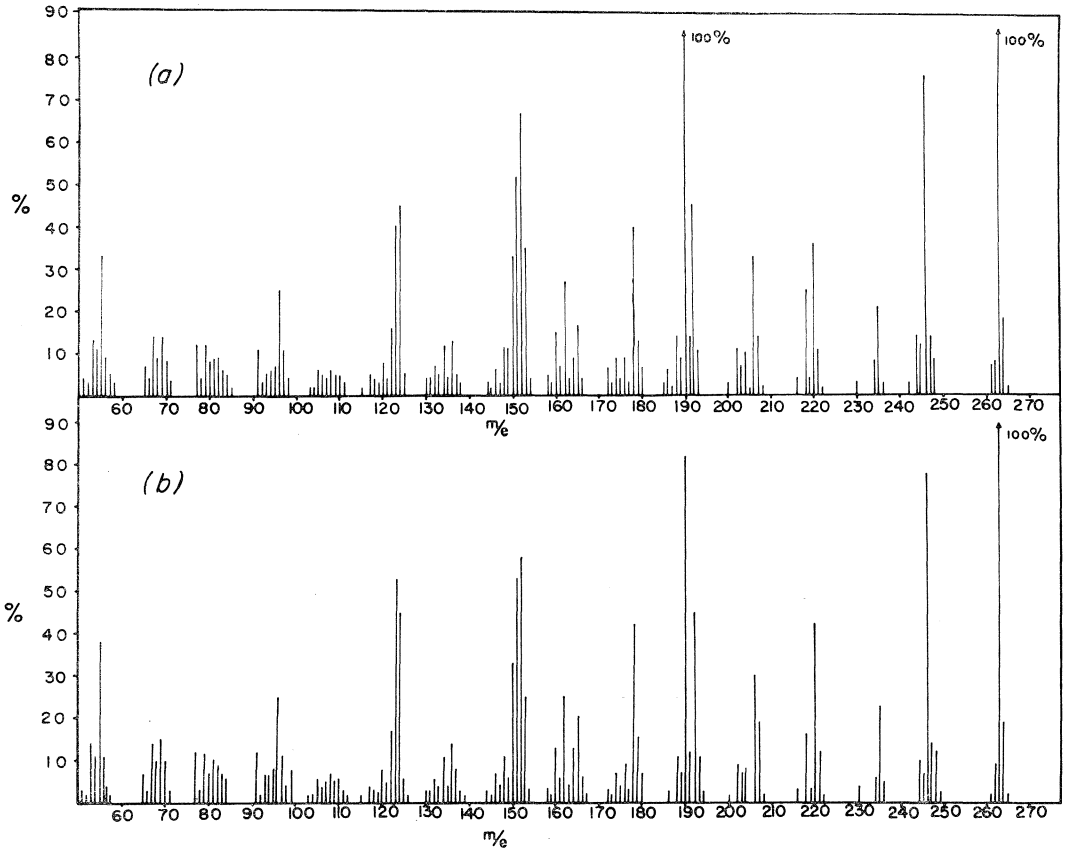

FIG. 1. Mass spectrum of (*a*) alkaloid L.23, (*b*) lycodoline.

phosphonic dichloride in pyridine or with phosphorus pentoxide in toluene gave, albeit in low yield, anhydrolycodoline (**10**) (10, 11), isolated as its hydrochloride. Alkaloid L.23 is the second naturally occurring alkaloid of this group to possess the "epi" configuration at C-12, the other being sauroxine (**11**) (12).

Anhydrolycodoline has been transformed into lycopodine (10) and thus alkaloid L.23 belongs to the same enantiomeric series as lycopodine (**1**) and lycodoline (**4**). The absolute configuration of lycopodine was assigned by application (13, 14) of the octant rule (15) and of the axial haloketone rule (2). As is predicted by the octant rule, both lycopodine and lycodoline (octant diagrams **12***a* and **12***b*, respectively) show positive Cotton effects (Table II) associated with the $n\rightarrow\pi^*$ transition of the keto group. As may be seen in the octant diagram **13***a* for alkaloid L.23, the octant rule predicts a positive Cotton effect in this case as well. *Alkaloid L.23 however shows a negative Cotton effect* (Table II). The salts of alkaloid L.23 also show a negative Cotton effect, although of lesser magnitude than that of the free base. In the case of lycopodine and lycodoline, salt formation causes a reversal of the sign of the Cotton effect (2, 16). Epilycopodine (octant diagram **13***b*), like alkaloid L.23 shows a negative Cotton effect for both the salt and the free base. It appears, therefore, that the sign of the Cotton effect depends on the configuration at C-12 and nitrogen and only in the case of the free bases with the lycopodine configuration does the octant rule correctly predict the sign of the Cotton effect. Circular dichroism (c.d.) measurements (Table II) show that lycopodine displays two Cotton effects above 200 mμ, a positive centered at 288 mμ and associated with the $n\rightarrow\pi^*$ transition and a negative centered at 223 mμ associated with the σ-coupled p interaction discussed above. The

Can. J. Chem. Downloaded from www.nrcresearchpress.com by 210.87.254.42 on 09/05/12
For personal use only.

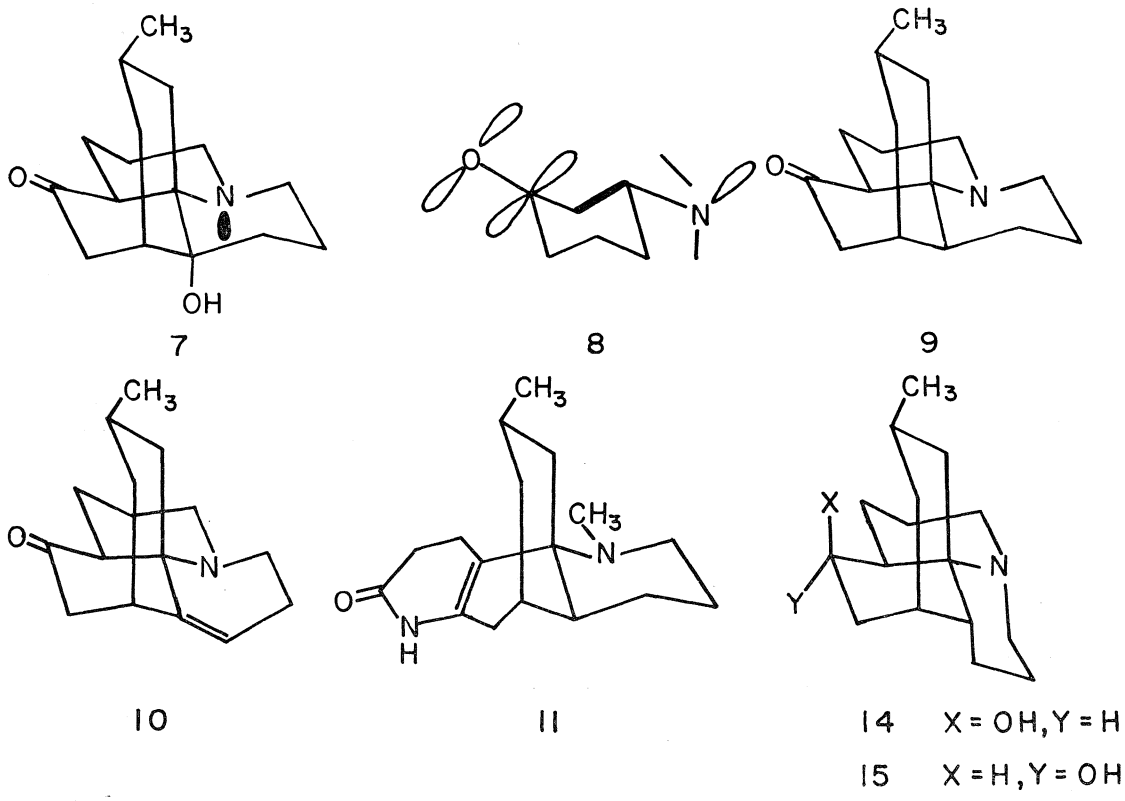

TABLE II

Cotton effects for some lycopodium alkaloids

Compound	Rotatory dispersion molecular amplitude*	Circular dichroism molecular ellipticity (wavelength)
Lycopodine	+203	+11 700 (288 mμ) −16 200 (223 mμ)
Lycopodine·HCl	−28!	−2 050 (290 mμ)
Lycodoline	+198	+10 900 (292 mμ) −16 350 (230 mμ)
Lycodoline·HCl	−39	−2 580 (288 mμ)
Epilycopodine†	−51!	
Epilycopodine·HCl	−36!	
Alkaloid L.23	−68	−4 230 (287 mμ)
Alkaloid L.23·HCl	−32	−2 470 (292 mμ)

*The symbol ! indicates that the extremum of shorter wavelength was not accurately measured.
†Values taken from ref. 10.

large negative rotation at 250 mμ (−15 000°) in the optical rotatory dispersion (o.r.d.) curve is thus the result of the overlapping of the troughs of the two Cotton curves. Protonation of the nitrogen removes the shorter wavelength Cotton effect in the c.d. curve and the one at longer wavelength becomes negative. The c.d. curve for alkaloid L.23 shows a single, negative, Cotton effect. It is thus obvious that the octant rule cannot be safely applied in these cases at least until the effect of nitrogen, charged and uncharged, is fully understood. The argument used previously in the case of lycopodine (2), i.e., that charged nitrogen makes an anti-octant contribu-

Can. J. Chem. Downloaded from www.nrcresearchpress.com by 210.87.254.42 on 09/05/12
For personal use only.

Can. J. Chem. Downloaded from www.nrcresearchpress.com by 210.87.254.42 on 09/05/12
For personal use only.

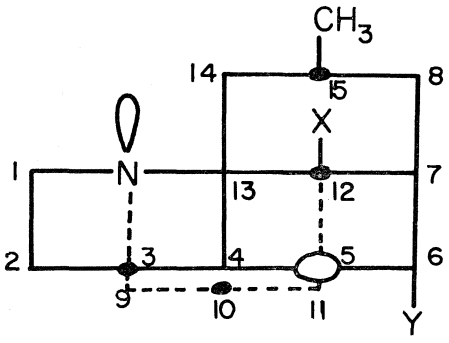

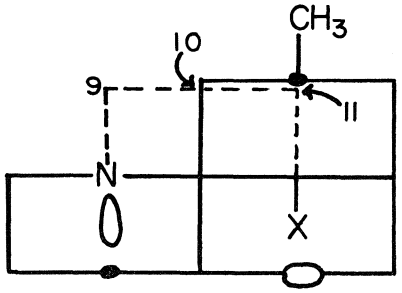

12*a* X = Y = H

12*b* X = OH, Y = H

12*c* X = H, Y = Br

13*a* X = OH

13*b* X = H

tion, does not explain the negative Cotton effect observed for L.23 and epilycopodine.

It is now necessary to consider the possibility that lycopodine is the anomalous case, that this is the system which shows the unusual charge transfer band, and that the absolute configurational assignment should be reversed. The following observations lead us to believe that the originally assigned (13, 14) configuration is probably correct. Both 6-α-bromolycopodine (**12***c*) and its hydrobromide show Cotton effects which are much more positive than those of the corresponding unbrominated compounds (2). Application of the axial halo ketone rule should be independent of the effect of the nitrogen. Application of the Horeau method (17) to dihydrolycopodine (**14**) and α-dihydrolycopodine (**15**) gives results in agreement with the absolute configuration portrayed (18). The absolute configurations of annotinine (**16**) (13), annopodine (**17**), (19), and alopecurine (**18**) (22) have been determined, the latter two by the X-ray method, and although they have different skeletons they belong to the same absolute stereochemical series as that

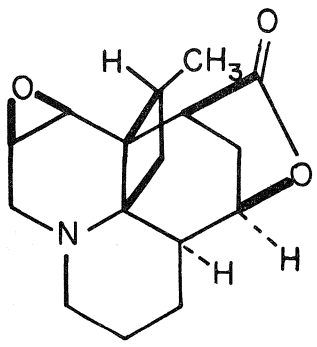

16

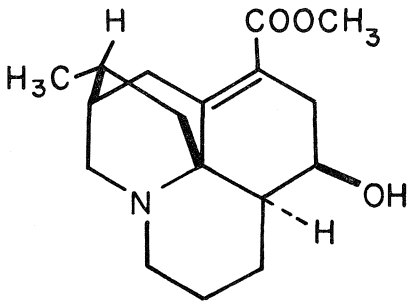

17

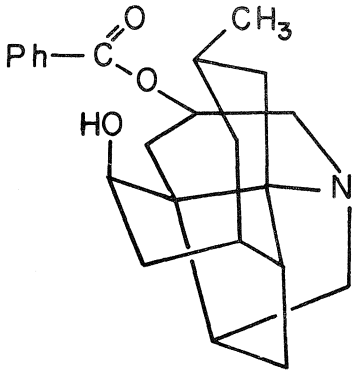

18

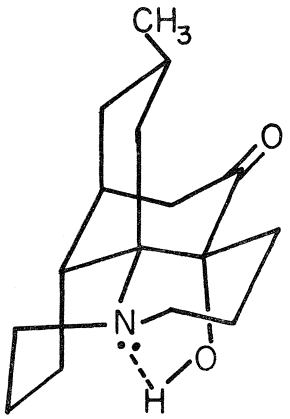

19

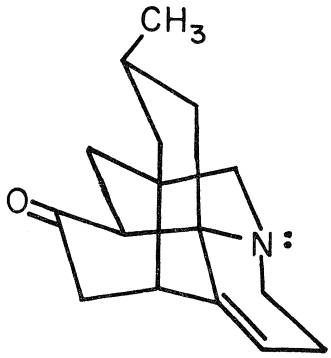

20

assigned to lycopodine. Because of the uncertainties created by the o.r.d. and c.d. studies, the determination of the absolute configuration of a lycopodine derivative by the X-ray method is in progress.

It has been suggested (20) that flabelliformine exists in conformation **19** rather than **6** since the hydroxyl group is intramolecularly hydrogen bonded (infrared evidence) and it is inferred that this hydrogen bonding involves the nitrogen as receptor rather than the carbonyl. Since o.r.d., c.d., and u.v. measurements appear to offer a means of determining the orientation of the lone pair on the nitrogen in this system, we have examined the spectra of flabelliformine. The ultraviolet spectrum (Table I) shows an inflexion at 228 mμ. A much clearer indication of the presence of this chromophore is obtained from the c.d. spectrum (MeOH) which shows a strong ($\Theta = -18\,000$) negative Cotton effect at 225 mμ in addition to a positive Cotton effect ($\Theta = -8\,600$) at 293 mμ. The c. d. spectrum is very similar to that of lycopodine and lycodoline (Table II). The o.r.d. spectrum (extrema 316 mμ (+2250°) and 257 mμ (−13 500°)) is also similar to that of lycopodine. Flabelliformine hydrochloride shows a negative Cotton effect. We feel therefore that flabelliformine exists mainly in conformation **6**, at least in methanol. As noted previously, anhydrolycodoline also shows a strong positive Cotton effect ($a = +13\,300°$ (10)). This suggests that conformation **20** makes an important contribution to the description of the stereochemistry of anhydrolycodoline. Conformation **10** was previously assigned (10) on the basis of the "Bohlmann bands" present in the infrared spectrum. As with flabelliformine, the infrared assignments were made on spectra determined in aprotic solvents and the o.r.d. and c.d. measurements were made in protic solvents.

Experimental

Optical rotatory dispersion, circular dichroism and ultraviolet spectra were recorded on a Durrum–Jasco Recording Spectropolarimeter, model 5. Most of the spectra were recorded in methanol in 1 cm and 1 mm cells. The concentrations used for the o.r.d. and c.d. measurements were about 0.01 *M*. The mass spectra shown in Fig. 1 were recorded on an AEI MS-2H mass spectrometer using a heated inlet system at 185°. The high resolution mass spectra were determined on an AEI MS-9 mass spectrometer.

Isolation Procedure

The "strong bases" of *Lycopodium lucidulum* Michx. (35 g) obtained as previously described (3), were subjected to seven funnel countercurrent distribution between chloroform (400 ml fractions, moving phase) and potassium hydrogen phthalate buffer (pH 5). After completion of the distribution, each fraction was made strongly basic and extracted into chloroform: fraction 1, 4.3 g; fraction 2, 4.1 g; fraction 3, 5.6 g; fraction 4, 2.6 g; fraction 5, 1.6 g; fraction 6, 3.0 g; fraction 7, 13 g. Fraction 7, containing the weak bases was combined with the "weak base" fraction from the original separation (3).

Fraction 3 was subjected to chromatography over alumina (activity II–III, 170 g). Elution with benzene (200 ml) and benzene–ether (1:1, 500 ml) gave lycopodine

Can. J. Chem. Downloaded from www.nrcresearchpress.com by 210.87.254.42 on 09/05/12
For personal use only.

Can. J. Chem. Downloaded from www.nrcresearchpress.com by 210.87.254.42 on 09/05/12
For personal use only.

(0.4 g). Elution with ether (500 ml) gave a mixture (0.23 g) of lycodoline and flabelliformine. The components were separated by preparative t.l.c. and identified by comparison with authentic samples. Elution with ether–chloroform (500 ml) and chloroform (500 ml) gave, after evaporation of the solvents, mixed crystals of lycodoline and alkaloid L.23. These were separated by fractional crystallization from acetone. Lycodoline crystallized first leaving alkaloid L.23 in the mother liquor. Alkaloid L.23 was recrystallized from a small volume of acetone, m.p. 163–164° both alone and when admixed with an authentic sample of alkaloid L.23 provided by Manske and Marion (1). $[\alpha]_D^{26} - 43°$ (*c*, 0.13, EtOH). Pertinent details of the infrared, nuclear magnetic resonance, and ultraviolet spectra are discussed in the text. The mass spectrum is shown in Fig. 1*a*.

Anal. Calcd. for $C_{16}H_{25}O_2N$: mol. wt., 263.1885. Found: mol. wt., 263.1888 (mass spectrometry).

Fractions 2 and 4 gave further quantities of alkaloid L.23.

Chromatography of fraction 6 over alumina and elution with benzene–ether gave a mixture of lycopodine and lycodine. Separation was achieved by reducing the mixture with sodium borohydride and then separating the lycodine from the dihydrolycopodine by chromatography over alumina. Further elution of fraction 6 with chloroform–methanol gave a compound,[3] m.p. 230–233°, identical (melting point, mixture melting point, infrared spectrum) with that previously isolated (4) from *L. clavatum* var. *megastachyon*. High resolution mass spectrometry showed that this compound has the molecular formula $C_{16}H_{25}O_2N$ (Calcd. mol. wt., 263.1885; Found 263.1885). The infrared spectrum of this compound shows OH absorption but no carbonyl absorption. The perchlorate melts at 238–240° (decomp.).

Anhydrolycodoline from Alkaloid L.23

Alkaloid L.23 (60 mg) was dissolved in pyridine (4 ml) containing phenylphosphonic dichloride (4 ml) and the solution was heated to 60° for 17 h. The reaction mixture was cooled and poured onto ice. The resulting solution was made basic by the addition of sodium hydroxide pellets and then extracted several times with chloroform. Evaporation of the chloroform left an oil (40 mg) which showed two spots on t.l.c., one corresponding to starting material and the other to anhydrolycodoline. Chromatography over alumina and elution with benzene gave an oil (ca. 2 mg) which with hydrogen chloride in methanol gave crystals of anhydrolycodoline hydrochloride, m.p. 273–275° (decomp.). The infrared spectrum was identical with that of an authentic sample. The o.r.d. spectrum of the free base was virtually identical with that of anhydrolycodoline prepared by dehydration of lycodoline (10).

Further elution of the chromatogram with benzene–ether and ether gave first a mixture of anhydrolycodoline and alkaloid L.23 (ca. 10 mg) and then alkaloid L.23 (20 mg).

The dehydration was also accomplished by heating alkaloid L.23 in toluene in the presence of phosphorus pentoxide. In this case, the yield of anhydrolycodoline was again poor and very little starting material was recovered.[4]

[3]We previously reported a melting point of 261–263° for this compound.

Acknowledgments

We wish to thank Dr. L. Marion of the University of Ottawa for samples of several alkaloids, A. N. Hogg and A. Budd for determining the mass spectra, R. N. Swindlehurst for the infrared and nuclear magnetic resonance spectra, and J. Hoyle for the optical rotatory dispersion and circular dichroism measurements. The financial support of the National Research Council of Canada is gratefully acknowledged.

1. R. H. F. Manske and L. Marion. Can. J. Res. B, **24**, 57 (1946).
2. W. A. Ayer, J. A. Berezowsky, and D. A. Law. Can. J. Chem. **41**, 649 (1963).
3. W. A. Ayer, N. Masaki, and D. S. Nkunika. Can. J. Chem. To be published.
4. W. A. Ayer and D. A. Law. Can. J. Chem. **40**, 2088 (1962).
5. I. G. Schrager and P. E. Rosentsveig. Farmatsevt Zh. Kiev, **19**, 49 (1964); Chem. Abstr. **61**, 5450 (1964).
6. O. Achmatowicz and W. Rodewald. Roczniki Chem. **30**, 233 (1956).
7. F. Bohlmann. Chem. Ber. **91**, 2157 (1958).
8. D. B. MacLean. Can. J. Chem. **41**, 2654 (1963).
9. R. C. Cookson, J. Henstock, and J. Hudec. J. Am. Chem. Soc. **88**, 1060 (1966).
10. W. A. Ayer and G. G. Iverach. Can. J. Chem. **42**, 2514 (1964).
11. W. A. Ayer, B. Altenkirk, S. Valverde-Lopez, B. Douglas, R. F. Raffauf, and J. A. Weisbach. Can. J. Chem. **46**, 15 (1968).
12. W. A. Ayer, T. E. Habgood, V. Deulofeu, and H. R. Juliani. Tetrahedron, **21**, 2169 (1965).
13. K. Wiesner, J. E. Francis, J. A. Findlay, and Z. Valenta. Tetrahedron Letters, No. 5, 187 (1961).
14. R. H. Burnell and D. R. Taylor. Tetrahedron, **15**, 173 (1961).
15. W. Moffitt, R. B. Woodward, A. Moscowitz, W. Klyne, and C. Djerassi. J. Am. Chem. Soc. **83**, 4013 (1961).
16. E. G. Höhn and O. E. Wiegang, Jr. J. Chem. Phys. **48**, 1127 (1968).
17. A. Horeau and H. B. Kagan. Tetrahedron, **20**, 2431 (1964), and references therein.
18. S. Valverde-Lopez. Ph.D. Thesis. University of Alberta, Edmonton, Alberta. 1966. p. 131.
19. W. A. Ayer, G. G. Iverach, J. K. Jenkins, and N. Masaki. Tetrahedron Letters. 4597 (1968).
20. M. Curcumelli-Rodostamo and D. B. MacLean. Can. J. Chem. **40**, 1068 (1962).
21. W. Rodewald and G. Grynkiewicz. Roczniki Chem. **42**, 465 (1968).
22. W. A. Ayer, B. Altenkirk, and N. Masaki. To be published.

[4]After the completion of this manuscript a paper by Rodewald and Grynkiewicz (21) came to our attention. These authors assign structure **7** to pseudoselagine (alkaloid L.23), mainly on the similarity of its mass spectrum to that of lycodoline. No direct correlation of the two compounds was reported.

Can. J. Chem. Downloaded from www.nrcresearchpress.com by 210.87.254.40 on 09/05/12
For personal use only.

Lignans of Western Red Cedar (*Thuja plicata* Donn). VIII. Plicatinaphthol

HAROLD MACLEAN AND B. F. MACDONALD

Forest Products Laboratory, Department of Forestry and Rural Development of Canada, 6620 N.W. Marine Drive, Vancouver 8, British Columbia

Received August 21, 1968

The isolation and structure of a new lignan, 1,6-dihydroxy-2-(hydroxymethyl)-7-methoxy-4-(3′,4′-dihydroxy-5′-methoxyphenyl)-3-naphthoic acid lactone (plicatinaphthol, **2**), in which the 4-aryltetrahydronaphthalene structure of plicatin (**1**) has been aromatized to a 4-arylnaphthol nucleus are described. Proof of structure of the parent compound and its tetramethyl, tetraacetyl, and tetraethyl derivatives is presented both by analytical and spectral techniques, in addition to the synthesis of the tetramethyl derivative starting from podophyllotoxin.

Canadian Journal of Chemistry, **47**, 457 (1969)

The lignans of Western Red Cedar (*Thuja plicata* Donn) fall into two classes, the five dibenzyl butyrolactones of the thujaplicatin series (1–4) and plicatic acid and plicatin (**1**), the 4-aryltetrahydronaphthalene derivatives (5, 6). These lignans are novel in that they all contain a guaiacyl ring in conjunction with either a monomethylated pyrogallol or a syringyl group. A new 4-arylnaphthol derivative, 1,6-dihydroxy-2-(hydroxymethyl)-7-methoxy-4-(3′,4′-dihydroxy-5′-methoxyphenyl)-3-naphthoic acid lactone, which has been given the trivial name plicatinaphthol (**2**), is now reported.

Other 4-arylnaphthols previously reported are diphyllin (7), justicidin A (8), dehydropodophyllotoxin (**6**) (9), and taiwanin E (10), the latter two suspected as being produced by acetone photolysis oxidation in the separation procedure (10). Plicatinaphthol is not an artifact, as it can be obtained directly from the wood meal by neutral solvent extraction in the dark, although in small amounts.

Separation was accomplished in two ways. After the hot-water extract of cedar heartwood meal had been chloroform extracted, the residual water solution was extracted with ethyl acetate. The ethyl acetate solubles were column chromatographed, either on cellulose or first on polyamide followed by cellulose. Plicatinaphthol is strongly absorbed by silica gel from which it cannot be totally reclaimed.

Plicatinaphthol (**2**) is an optically inactive crystalline compound having strong blue fluorescence under long (365 mμ) and weak blue fluorescence under short (254 mμ) ultraviolet light. The broad melting-point range of 260–270 °C with decomposition for plicatinaphthol has been previously noted for dehydropodophyllotoxin (**6**) (11). Carbon–hydrogen and methoxyl analyses indicated $C_{20}H_{16}O_8$. A double-focusing, high-resolution mass spectrum showed the parent ion to be the base peak at M^+ 384.0835 confirming the analytical results. A low-resolution mass spectrum showed, in addition to the large parent-ion

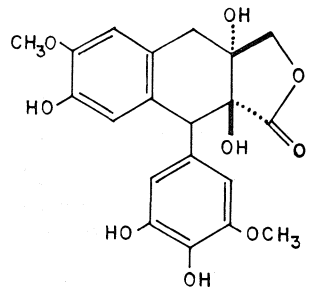

1

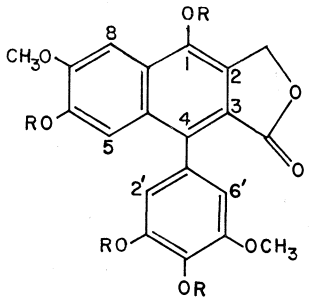

2 R=H 4 R=C_2H_5
3 R=CH_3 5 R=Ac

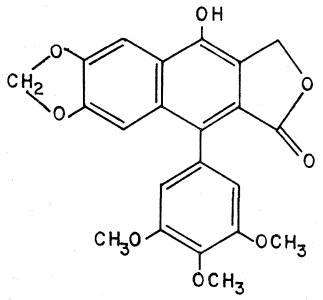

6

Can. J. Chem. Downloaded from www.nrcresearchpress.com by 210.87.254.40 on 09/05/12
For personal use only.

base peak, major fragmentation peaks at M − 16 (loss of oxygen), M − 58 (loss of lactone), M − 75 (loss of lactone and phenolic hydroxyl), M − 89 (loss of lactone and methoxyl group), followed by a series of small peaks indicative of a peeling of the hydroxyl and methoxyl groups (12) resulting in a complex pattern. Other major peaks, the M^{++} peak at 192, an unexplained peak at 176, and the pendant-ring split-off peaks, are clearly visible at 139–140. Since oxidation with alkaline nitrobenzene (13) produced only a small yield of vanillin and no syringaldehyde, the possibility of a syringyl group in the pendant ring was eliminated. Chromatography on molybdic acid – treated paper with butanol – acetic acid – water shows a considerably reduced R_f value (0.62) as found previously for other lignans containing pyrocatechol groups, when compared to untreated paper (0.74).

Plicatinaphthol is insoluble in deuteriochloroform and sparingly soluble in deuterioacetone. Positive identification of its four phenolic peaks by nuclear magnetic resonance (n.m.r.) was made more difficult owing to rapid exchange with the deuterioacetone solvent. However, n.m.r. spectra of the tetramethyl (**3**), tetraacetyl (**5**), and tetraethyl derivative (**4**) all indicated four hydroxyl groups and were confirmatory both as to species and number of protons, the aromatic protons appearing as two one-proton singlets for C-5 and C-8 and a two-proton singlet for C-2′ and C-6′ similar to plicatic acid (5), since no additional aromatic protons were introduced by the aromatization to plicatinaphthol. These n.m.r. data are in agreement with the substitution pattern shown for plicatinaphthol (**2**). Ultraviolet (u.v.) spectra were typical for a naphthalene nucleus (14) in all compounds. Infrared (i.r.) spectra were as expected for both the parent compound and the three derivatives, although the lactone band in plicatinaphthol is very broad and shifted to longer wavelengths when compared to dehydropodophyllotoxin (**6**) owing, probably, to intermolecular hydrogen bonding effects of the four phenolic groups. Diphyllin, which has the naphthol–lactone structure with the lactone carbonyl in the inverted position, i.e., in association with the naphthol group (7, 8), shows a hindered carbonyl absorbing at much lower wavelength still, 1705 cm^{-1}, compared to 1724 cm^{-1} for plicatinaphthol.

Similar to dehydropodophyllotoxin, the lactone ring of the tetramethyl plicatinaphthol could not be opened by 10% sodium hydroxide solution on a steam bath (17).

The tetraethyl derivative (**4**) was oxidized in alkaline permanganate as outlined in a previous paper (4) and 3,4-diethoxy-5-methoxybenzoic acid detected by both paper and thin-layer chromatography (t.l.c.) in conjunction with a known sample establishing the phenol substitution pattern of the pendant ring.

These data leave in doubt the position of an hydroxyl at C-1 or C-8 (as in the peltatins (15)) and the placement of the carbonyl of the lactone ring at either C-2 or C-3. A synthesis of the tetramethyl derivative of plicatinaphthol was successfully undertaken by preparing dehydropodophyllotoxin (**6**) from podophyllin resin (16, 17), opening the methylenedioxy ring with boron trichloride (18), and remethylating. Earlier attempts to cleave the methylenedioxy grouping were unsuccessful. A Birch reaction (19) failed apparently due to solubility considerations and a boron trifluoride reaction (20) resulted in excessive decomposition. After the boron trichloride treatment, t.l.c. showed five more products than the compound expected from cleaving the methylenedioxy ring, none of which were the original dehydropodophyllotoxin. As remethylation produced only the one major product, the boron trichloride reagent apparently cleaved additional methoxyl groups. The resultant product after remethylation was identical with the tetramethyl derivative (**3**) of plicatinaphthol by mixture melting point and quantitative i.r. spectral comparison.

In conclusion, the structure of plicatinaphthol (**2**) is therefore 1,6-dihydroxy-2-(hydroxymethyl)-7-methoxy-4-(3′,4′-dihydroxy-5′-methoxyphenyl)-3-naphthoic acid lactone.

Experimental

The following equipment was used: melting points, Fisher–Johns heated block (uncorrected); infrared (i.r.) spectra, Perkin–Elmer 521 grating spectrometer (KBr disks); ultraviolet spectra, Beckman DK-2 spectrophotometer (ethanol); nuclear magnetic resonance (n.m.r.) spectra, Varian HA-100 (tetramethylsilane, $\delta = 0$ as internal standard in the solvents shown). The following services were used: analyses, Clark Microanalytical Laboratories, Urbana, Illinois; mass spectrum, Morgan–Schaffer Laboratory, Montreal; high-resolution mass spectrum (parent ion), University of British Columbia. Thin-layer chromatography (t.l.c.) values were obtained with silica gel G

Can. J. Chem. Downloaded from www.nrcresearchpress.com by 210.87.254.40 on 09/05/12
For personal use only.

(Merck) as adsorbent, benzene – ethanol – acetic acid (90:10:1) as developer with ultraviolet light followed by nitric acid – sulfuric acid (1:1) spray and heat as detector. Paper chromatograms were developed with butanol – acetic acid – water (60:15:25) or with 2% aqueous acetic and detected with potassium ferricyanide – ferric chloride reagent (mixed 1% solutions).

Plicatinaphthol (2)

The reserved aqueous layer from the hot-water extract of Western Red Cedar heartwood (1 kg moisture-free basis), which had been extracted with chloroform as outlined in a previous paper (4), was extracted with ethyl acetate (3 × 500 ml). After evaporation of the ethyl acetate solvent (yield 10.2 g), part of the residue (2 g) was dissolved in ethanol (20 ml) and added to a cellulose column (60 cm × 5 cm) using water as eluting solvent. Fractions were monitored by paper chromatography (2% acetic acid). After approximately 3 l elution, the following 1.5 l contained plicatinaphthol (R_f 0.09). After evaporation, fractions containing contaminant R_f 0.20 were purified by triturating with chloroform. After crystallization from ethanol, plicatinaphthol (150 mg) was obtained, m.p. 260–270 °C decomp.

An alternate method made a gross separation of the ethyl acetate residue on a polyamide (Woelm) column with *n*-butanol – formic acid (9:1) as eluting solvent. The fractions were monitored by paper chromatography (2% acetic acid) (R_f 0.09) or t.l.c. (R_f 0.10). The fractions containing plicatinaphthol were further purified on a cellulose column. Nitrobenzene oxidation (13) yielded vanillin only (4%).

Spectra: λ_{max} in mμ (log ε), 263.5 (4.59) (shifting to 275 in alkaline media), 312 (3.89), 323 (3.88), 365 (3.68): ν_{max} 3400 (broad hydroxyl), 1724 (lactone), 780 (tri-substituted phenyl) cm^{-1}; n.m.r. (deuterioacetone), 9.05, 8.28, 7.61, 7.44 (1H each, broad singlets, phenols), 7.70, 7.10 (1H each, singlets, C-5 and C-8), 6.44 (2H, singlet (width at half height 1.5 Hz), C-2′ and C-6′), 5.33 (2H, singlet, lactone methylene), δ 3.79 and 4.02 (3H each, singlets, methoxyls) (all phenol peaks were shifted to higher field by warming to 50 °C); mass (high resolution), M^+ 384.0835 (Calcd. for $C_{20}H_{16}O_8$: 384.0845), mass (low resolution), parent ion = base peak 384, M − 16 (18%), M − 58 (6%), M − 75 (5%), M − 89 (12%), M^{++} peak at 192 (4%), 176 (4%), 139 (6%), and 140 (6%).

Tetramethyl Plicatinaphthol (3)

Plicatinaphthol (100 mg) was dissolved in methanol (40 ml) with warming. On cooling, diazomethane in ether (5 ml) was added each hour for 5 h at room temperature with stirring and allowed to stand overnight. The product (t.l.c. R_f 0.46) was evaporated to dryness, crystallized from methanol to yield 2-(hydroxymethyl)-1,6,7-trimethoxy-4-(3′,4′,5′-trimethoxyphenyl)-3-naphthoic acid lactone (**3**) (60 mg), m.p. 259–260 °C.

Anal. Calcd. for $C_{24}H_{24}O_8$ (mol. wt., 440): C, 65.22; H, 5.46; OCH_3, 42.2. Found (mol. wt., 440; mass spectrum): C, 65.05; H, 5.49; OCH_3, 40.05.

Spectra: λ_{max} in mμ (log ε), 261 (4.66), 310 shoulder (3.90), 320 (3.93), 351 (3.58); ν_{max}, no hydroxyl band, 1760 (lactone) cm^{-1}; n.m.r. (deuteriochloroform) (all peaks are sharp singlets), 7.56 and 7.11 (1H each, C-5 and C-8), 6.58 (2H, C-2′ and C-6′), 5.54 (2H, lactone methylene), 4.13, 4.06, 3.97, and 3.78 (3H each, methoxyl), and δ 3.84 (6H, methoxyl C-3′ and C-5′).

Tetraacetyl Plicatinaphthol (5)

Plicatinaphthol (195 mg) was dissolved with warming in acetic anhydride (25 ml) and left standing for 3 h. The reaction mixture was heated on a steam bath for 1 h, *p*-toluenesulfonic acid (75 mg) added, and the mixture heated for an additional hour. It was cooled overnight and added slowly to ice water (400 ml) with stirring. After filtering, the crude acetate (110 mg) was purified by alumina chromatography using gradient elution with benzene–ethanol solvent. The column was monitored by t.l.c. (R_f 0.38) and the product crystallized from ethanol – ethyl acetate (40:15) by addition of water (7 ml) to yield 1,6-diacetoxy-2-(hydroxymethyl)-7-methoxy-4-(3′,4′-diacetoxy-5′-methoxyphenyl)-3-naphthoic acid lactone (**5**) (68 mg), m.p. 234–235 °C.

Spectra: ν_{max}, no hydroxyl band, 1765 (lactone), shoulders at 1750, 1740, 1730, and 1710 (acetyl) cm^{-1}; n.m.r. (deuteriochloroform), all peaks sharp singlets, 7.61 and 7.27 (1H each, C-5 and C-8), 6.86 (2H, width at half height 1.5 Hz, C-2′ and C-6′), 5.25 (2H, lactone methylene), 3.96 and 3.83 (3H each, methoxyls), 2.54 and 2.29 (3H each, acetyls), and δ 2.36 (6H-acetyl).

Tetraethyl Plicatinaphthol (4)

Plicatinaphthol (50 mg) in acetone (30 ml) containing anhydrous potassium carbonate (5 g) was treated with diethyl sulfate (1 ml per hour) for 5 h. After filtration and solvent removal the reaction product was purified by column chromatography on alumina by benzene–ethanol gradient elution to yield, after crystallization from ether, 1,6-diethoxy-2-(hydroxymethyl)-7-methoxy-4-(3′,4′-diethoxy-5′-methoxyphenyl)-3-naphthoic acid lactone (**4**) (23 mg), m.p. 156–157 °C; t.l.c. R_f 0.60.

Spectra: ν_{max}, no hydroxyl band, 1760 (lactone) cm^{-1}; n.m.r. (deuteriochloroform), 7.52 and 7.05 (1H each, singlets, C-5 and C-8), 6.56 (2H, singlet, C-2′ and C-6′), 5.48 (2H, singlet, lactone methylene), 4.48–3.76 (8H, multiplet centered at 4.12 partially obscured by methoxyl, ethoxyl methylenes), 4.06 and 3.83 (3H each, singlets, methoxyl), δ 1.67–1.32 (12H, unsymmetrical quartet centered at 1.49, ethoxyl methyls).

Synthesis of Tetramethyl Plicatinaphthol (3) from Podophyllin Resin

Podophyllotoxin was extracted from crude podophyllin resin by the method of Hartwell and Detty (16). Dehydropodophyllotoxin (**6**) was prepared from podophyllotoxin by the method of Gensler and Johnson (17). Dehydropodophyllotoxin (150 mg) in dichloromethane (30 ml) was cooled in a dry ice–acetone mixture and freshly distilled boron trichloride (30 ml) was added (18). The reaction mixture was allowed to come to room temperature overnight after which it was heated gently to expel boron trichloride. The solvents were evaporated at reduced pressure to yield an amorphous solid. Methanol containing ca. 1% water was added and then evaporated to remove final traces of boron trichloride. The residue was triturated with water containing a few drops of dilute hydrochloric acid with warming and the solution evaporated to dryness. Thin-layer chromatography showed six reaction products (70 mg), none of which were the original

dehydropodophyllotoxin. On methylation with diazomethane in methanol in the usual manner a single product, crystallizing from the reaction mixture, was obtained, which on recrystallization from methanol, yielded 2-(hydroxymethyl)-1,6,7-trimethoxy-4-(3′,4′,5′-trimethoxyphenyl)-3-naphthoic acid lactone (**3**) (30 mg) identical by quantitative i.r. spectrum and mixture melting point with tetramethyl plicatinaphthol.

1. H. MacLean and K. Murakami. Can. J. Chem. **44**, 1541 (1966).
2. H. MacLean and K. Murakami. Can. J. Chem. **44**, 1827 (1966).
3. H. MacLean and K. Murakami. Can. J. Chem. **45**, 305 (1967).
4. H. MacLean and B. F. MacDonald. Can. J. Chem. **45**, 739 (1967).
5. J. A. F. Gardner, E. P. Swan, S. A. Sutherland, and H. MacLean. Can. J. Chem. **44**, 52 (1966).
6. R. J. Swan, W. Klyne, and H. MacLean. Can. J. Chem. **45**, 319 (1966).
7. T. Murakami and A. Matsushima. J. Pharm. Soc. Japan, **81**, 1596 (1961).
8. K. Munakata, S. Marumo, K. Ohta, and Y-L. Chen. Tetrahedron Letters, **47**, 4167 (1965).
9. H. Kofod and C. Jørgensen. Acta Chem. Scand. **8**, 1296 (1954).
10. Y-T. Lin, T-B. Lo, K-T. Wang, and B. Weinstein. Tetrahedron Letters, **9**, 849 (1967).
11. W. J. Gensler, F. Johnson, and A. D. B. Sloan. J. Am. Chem. Soc. **82**, 6079 (1960).
12. H. Budzikiewicz, C. Djerassi, and D. H. Williams. Interpretation of mass spectra of organic compounds. Holden-Day Inc., San Francisco. 1964. p. 181.
13. J. M. Pepper and M. Siddiqueullah. Can. J. Chem. **39**, 390 (1961).
14. A. I. Scott. Interpretation of the ultraviolet spectra of natural products. The Macmillan Co., New York. 1964. p. 126.
15. A. W. Shrecker and J. L. Hartwell. J. Am. Chem. Soc. **75**, 5924 (1953).
16. J. L. Hartwell and W. E. Detty. J. Am. Chem. Soc. **72**, 246 (1950).
17. W. J. Gensler and F. Johnson. J. Am. Chem. Soc. **77**, 3674 (1955).
18. T. G. Bonner and N. M. Saville. J. Chem. Soc. 2851 (1960).
19. G. K. Hughes and E. Ritchie. Australian J. Chem. **7**, 104 (1954).
20. C. R. Narayanan and K. N. Iyer. J. Org. Chem. **30**, 1734 (1965).

Can. J. Chem. Downloaded from www.nrcresearchpress.com by 210.87.254.40 on 09/05/12
For personal use only.

Can. J. Chem. Downloaded from www.nrcresearchpress.com by 210.87.254.5 on 09/05/12
For personal use only.

Evidence for the formation of *exo* and *endo* aziridines in the reaction of *cis–endo* and *cis–exo*-bicyclo[2·2·1]-5-heptene-2,3-dicarboxylic anhydride and benzenesulfonyl azide[1,2]

A. C. Oehlschlager[3] and L. H. Zalkow

School of Chemistry, Georgia Institute of Technology, Atlanta, Georgia 30332, and Department of Chemistry, Oklahoma State University, Stillwater, Oklahoma 74075

Received August 16, 1968

Benzenesulfonyl azide has been found to react with *cis–endo* and *cis–exo* bicyclo[2·2·1]-5-heptene-2,3-dicarboxylic anhydride to give in both cases, predominantly the more hindered *endo* aziridine in addition to the *exo* aziridine in apparent violation of the "*exo*-addition rule" (3). The stereochemistry of the aziridine rings were determined by nuclear magnetic resonance analysis and by conversion of the *endo*-aziridine-*exo*-anhydride to 2-*endo*-benzenesulfonamidobicyclo[2·2·1]heptane. The *endo*-aziridine-*endo*-anhydride has been previously (4) converted into a lactone-*N*-benzenesulfonyl-lactam.

Canadian Journal of Chemistry, 47, 461 (1969)

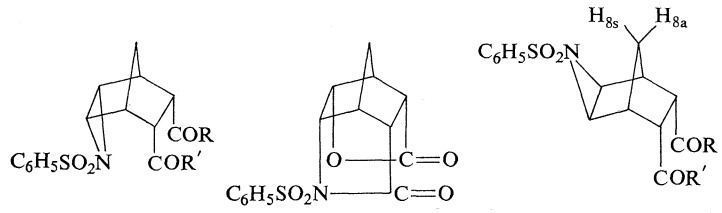

1 R = R′ = O
3 R = R′ = OCH_3

2

4 R = R′ = OCH_3

We have previously reported (4) that benzenesulfonyl azide reacts with bicyclo[2·2·1]-5-heptene-*endo*-cis-2,3-dicarboxylic anhydride in refluxing carbon tetrachloride to give the *endo* aziridine **1**, which was converted in two steps into **2**. After removal of crystalline **1**, the mother liquors were esterified with diazomethane in methanol–ether and then chromatographed on alumina. In addition to **3**, the dimethyl ester derived from **1**, there was thus obtained the previously unreported *exo* aziridine **4** in about 20% yield.

The infrared spectrum of **4** showed the presence of ester (1740 cm^{-1}) and benzenesulfonamido (1325, 1200, 1160 cm^{-1}) groups but the absence of N—H and C=N absorptions. The nuclear magnetic resonance (n.m.r.) spectrum of **4** showed two protons, by integration, at low field (δ 3.13) which could be assigned to carbons bearing nitrogen. Since this signal was much sharper (width at half-height, $w_{1/2h}$ = 2 c.p.s.), then the corresponding signal (δ 2.63, $w_{1/2h}$ = 6.5 c.p.s.) in **3** the *exo* aziridine structure was suggested. Additional support for the assignment of an *exo* aziridine structure to **4** was found in the positions of the C-8 protons in the n.m.r. Thus one proton (C-8*a*) appeared as a doublet: $J_{8a,8s}$ = 10.5 c.p.s.) at δ 0.90 whereas the other (C-8s) appeared at δ 1.70. By contrast, in **3** the C-8 protons gave similar doublets but centered at δ 1.54 and δ 1.98. Tori *et al.* (5) have shown that an *exo* aziridine ring produces an anisotropic shielding effect on the 8-*anti* proton. Additional support for structure **4** has been provided (6) by the conversion of **4** to the lactone **5**, which differs from the previously reported (6) **6** in not being readily converted into **2**. Finally, the carbomethoxy groups and the bridgehead protons in **4** are each magnetically equivalent, indicating that no epimerization of the carbomethoxy groups occurred in the reaction.

The reaction of benzenesulfonyl azide with bicyclo[2·2·1]-5-heptene-*exo–cis*-dicarboxylic anhydride in refluxing carbon tetrachloride also led to the formation of two isomeric products

[1]For a preliminary account of this work see ref. 1.
[2]Bridged ring compounds. XIV. For Part XIII, see ref. 2.
[3]Present address: Department of Chemistry, Simon Fraser University, Burnaby 2, British Columbia.

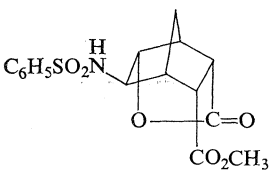

5

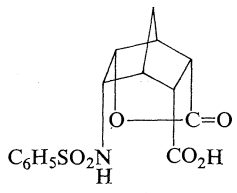

6

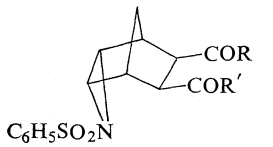

7*a* R=R′=O
7*b* R=R′=OCH_3

which could be separated in a manner similar to that described above. The predominant product (≃74%), which crystallized from the reaction mixture in benzene, was originally assigned (4) the *exo* aziridine structure. This product is now known to be the *endo* aziridine **7***a*. Thus the n.m.r. spectrum of **7***b*, the dimethyl ester derived from **7***a*, showed a broad signal ($w_{1/2h}$ = 6.5 c.p.s.) for the C-6, C-7 protons centered at δ 3.50. However, a more definitive proof of the stereochemistry of the aziridine ring in **7** was sought and provided as follows.

Anhydride **7***a* was converted into the corresponding *exo–cis* dicarboxylic acid in boiling water. That no epimerization occurred under these conditions was shown by conversion of a small amount of the diacid into **7***b* with methanolic diazomethane. On treatment with lead tetraacetate in pyridine the diacid gave **8**. The unsaturated aziridine **8** was found to differ from the previously reported (7) **9**, the latter being very unstable and readily rearranging to **10**. Hydrogenation of **8**

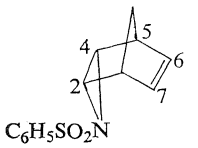

8
11 6,7-dihydro

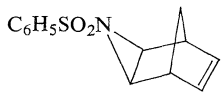

9
12 6,7-dihydro

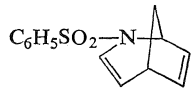

10

gave **11** which again differed from the previously reported (8) *exo* aziridine **12**. In particular, the C-2 and C-4 protons in **11** appeared as a broad signal ($w_{1/2h}$ = 6 c.p.s.) whereas in **12** they appear as a sharper singlet ($w_{1/2h}$ ~2 c.p.s.). Finally, treatment of **11** with potassium thiophenoxide gave **13** which on reductive removal of the thiophenoxy group gave the known (9) 2-*endo*-benzenesulfonamidobicyclo[2·2·1]heptane, **14**. The preparation of **14** from **7** shows that

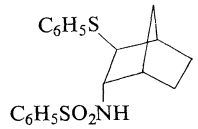

13

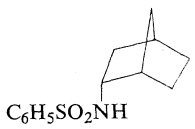

14

the aziridine ring in **7** is *endo* if no skeletal rearrangement has occurred. However, it is not unreasonable that during decarboxylation skeleton rearrangement did occur and that **7** therefore possesses an *exo* aziridine ring as illustrated in Scheme I. It is well known (10) that cationic intermediates are generated during oxidative decarboxylations using lead tetraacetate and the bicyclo[2·2·1]heptane ring system is particularly prone to rearrangment in reactions in which a nuclear cationic charge is generated (11). In such a rearrangement (illustrated in Scheme I), the original carbon atoms C-6 and C-7 end up at positions C-1 and C-8. To determine if rearrangement occurred carbon atoms C-6 and C-7 were labeled with deuterium as follows. Maleic anhydride-d_2 and cyclopentadiene were condensed in a Diels–Alder reaction to give 2,3-*exo*-dideuterio-2,3-*endo*-dicarboxybicyclo[2·2·1]-5-heptene anhydride, which was partially converted into 2,3-*endo*-dideuterio-2,3-*exo*-dicarboxybicyclo-[2·2·1]-5-heptene anhydride on heating at 200°. The latter, on treatment with benzenesulfonyl azide in refluxing carbon tetrachloride, gave 2,3-dideuterio-**7** which contained 71±2% deuterium at C-6 and C-7. Hydrolysis in D_2O gave the corresponding acid, which on oxidative decarboxylation with lead tetraacetate gave **8** which contained 72±2% deuterium at C-6 and C-7. Thus no skeletal rearrangement occurred during the decarboxylation.

The n.m.r. spectrum of the dimethyl ester of the minor product (~22%) from the reaction of benzenesulfonyl azide and bicyclo[2·2·1]-5-heptene-*exo–cis*-2,3-dicarboxylic anhydride has

Can. J. Chem. Downloaded from www.nrcresearchpress.com by 210.87.254.5 on 09/05/12
For personal use only.

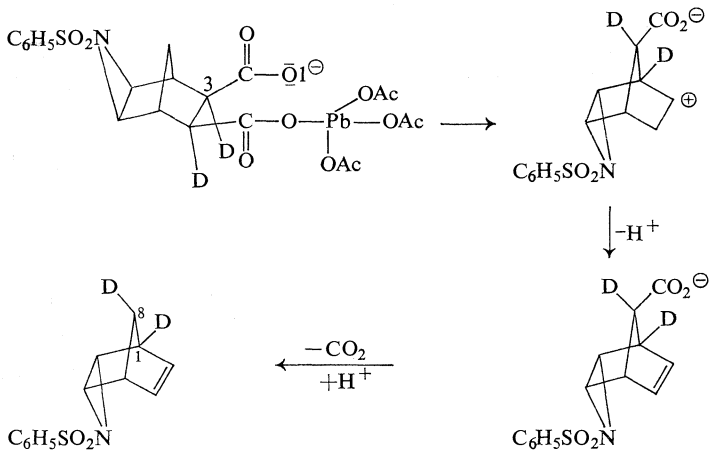

SCHEME I

been assigned structure **16** on the basis of the following evidence. The protons at C-6 and C-7 appeared as a sharp singlet ($w_{1/2h}$ = 2.5 c.p.s.) at δ 3.03, characteristic of *endo* protons and therefore an *exo* aziridine ring. Because of the presence of *exo*-carbomethoxy groups in **16**, the deshielding of the 8-*anti* proton by the *exo* aziridine ring is not so apparent in this case. The n.m.r. spectrum of **16** was very similar to that of

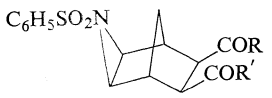

15 R = R′ = O
16 R = R′ = OCH_3

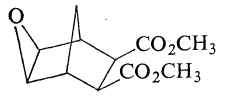

17

17. Thus in **16** the protons at C-1, C-2, C-4, and C-5 appeared as a narrow signal at δ 2.82, while in **17** these protons gave a similar signal at δ 2.80. In **16** the C-8 protons showed an AB quartet (J = 11 c.p.s.) with the two doublets centered at δ 1.47 and 1.75 while in **17** the two doublets (J = 10.5 c.p.s.) appeared at δ 1.33 and 1.64.

Detailed studies of the reactions of aryl and aryl-sulfonyl azides with bicyclo[2·2·1]heptene derivatives have provided an insight into the mechanism by which bicyclo[2·2·1]-5-heptene *endo* and *exo–cis*-2,3-dicarboxylic anhydrides react with benzene sulfonyl azide to give both *exo* and *endo* aziridine products (6). These investigations indicate the reaction involves the conversion of an initially formed, unstable *exo*-1,2,3-Δ^2 triazoline adduct **18** to a diazoimine intermediate **19** which rearranges with loss of nitrogen (via **20**) to the observed *exo* and *endo* aziridine products.

Experimental

Melting points were taken on a Fisher–Johns apparatus and are uncorrected. Infrared (i.r.) spectra were recorded with a Beckman IR-5 spectrophotometer, n.m.r. spectra were obtained with the Varian A-60 spectrometer, using tetramethylsilane (TMS) as an internal standard (δ = 0) and using deuteriochloroform, carbon tetrachloride, or carbon disulfide as a solvent. Carbon and hydrogen analyses were performed by Midwest Microlabs, Inc., Indianapolis, Indiana.

Reaction of Benzenesulfonyl Azide with Bicyclo[2·2·1]-5-heptene-endo–cis-2,3-dicarboxylic Anhydride

A solution of bicyclo[2·2·1]-5-heptene-2,3-*endo–cis*-dicarboxylic anhydride (4.4 g, 26.8 mmole) and benzenesulfonyl azide (6.0 g, 32.8 mmole) in 65 cm^3 carbon tetrachloride was refluxed for 48 h. The solvent was removed *in vacuo* and **1** (4.13 g, 13.0 mmole) crystallized from benzene–acetone to give m.p. 206–210°. The crystalline product had m.p. 215–216° (lit. (4), m.p. 215–216.5°)

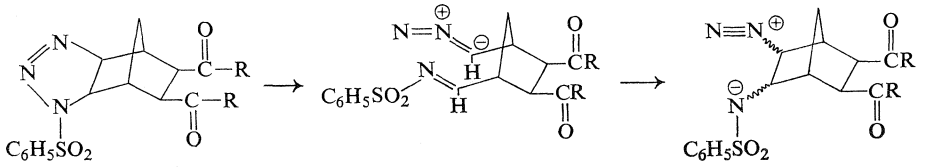

18 **19** **20**

Can. J. Chem. Downloaded from www.nrcresearchpress.com by 210.87.254.5 on 09/05/12
For personal use only.

Can. J. Chem. Downloaded from www.nrcresearchpress.com by 210.87.254.5 on 09/05/12
For personal use only.

after recrystallization from acetone. The mother liquors were combined and concentrated. The concentrate was treated with excess diazomethane in ether–methanol. The esterified mixture was concentrated and chromatographed directly on 250 g of Merck acid-washed alumina. Elution with 0.5 l of benzene gave 0.71 g of benzenesulfonyl azide. Elution with 1 l of benzene–chloroform (9:1) gave dimethyl bicyclo[2·2·1]-5-heptene-2,3-*endo–cis*-dicarboxylate (0.252 g, 1.2 mmole). Elution with 1 l (8:2), 0.5 l (7:3), and 0.7 l benzene–chloroform (6:4) gave **4** (1.76 g, 4.8 mmole). The analytical sample, prepared by crystallization from methanol, had m.p. 113–114°; ν_{max}(KBr) 1740, 1325, 1200, 1160, and 880 cm^{-1}; n.m.r. (in $CDCl_3$) δ 0.90 (*anti* C-8 proton, doublet, J = 10.5 c.p.s.), 1.70 (*syn* C-8 proton, doublet, J = 10.5 c.p.s.), 2.83 (protons at C-1 and C-5), 3.13 (protons at C-2 and C-4), 3.53 (protons at C-6 and C-7), 3.67 (6 protons of dimethyl ester), and 7.5–8.1 (5 aromatic protons).

Anal. Calcd. for $C_{17}H_{19}O_6NS$: C, 55.88; H, 5.24. Found: C, 56.22; H, 5.45.

Continued elution with 0.4 l of benzene–chloroform (6:4) gave **3** (0.86 g, 2.4 mmole) which had m.p. 129–130° after recrystallization from ether (lit. (4), m.p. 130–131°). Elution with 2 l of chloroform gave 0.77 g of an unidentified oil containing N—H absorption in the i.r. and whose n.m.r. spectrum showed several methoxyl signals. Thin-layer chromatographic analysis showed this material to be a mixture of several very polar components.

Reaction of Benzenesulfonyl Azide with Bicyclo-[2·2·1]-5-heptene-exo–cis 2,3-dicarboxylic Anhydride

A solution of bicyclo[2·2·1]-5-heptene-*exo–cis*-2,3-dicarboxylic anhydride (4.77 g, 29 mmole) and benzenesulfonyl azide (5.95 g) in 62 cm^3 of carbon tetrachloride was refluxed for 48 h during which time a gummy solid precipitated. The solvent was stripped *in vacuo* and the precipitate partially crystallized from benzene to give **7** (4.18 g, 13.1 mmole), m.p. 167–168°, (lit. (4), 168–168.5°). The mother liquors were concentrated and treated with excess diazomethane in ether–methanol. The esterified mixture was chromatographed on 500 g of Merck acid-washed alumina. Elution with 0.5 l benzene gave 0.69 g of benzenesulfonyl azide. Continued elution with 1.5 l of benzene gave 0.65 g (3.1 mmole) of dimethylbicyclo-[2·2·1]-5-heptene-*exo–cis*-dicarboxylate. Elution with 1 l (9:1), 1 l (8:2), and 1 l (7:3) benzene–chloroform gave 0.245 g of a mixture which was shown by n.m.r. analysis to contain 1.5 1 mmole of dimethylbicyclo[2·2·1]-5-heptene-*exo–cis*-dicarboxylate and 0.6 mmole of **8**. Elution with 1 l (6:4) benzene–chloroform gave 2.94 g of a mixture of 4.3 mmole of **8** and 3.7 mmole of **16**. Elution with 1 l (1:1) benzene–chloroform gave 1.12 g of a mixture of 1.05 mmole **8** and 2.05 mmole **16**. Crystallization of the last mentioned eluate from ether gave 0.35 g of **16**, m.p. 149–149°; ν_{max}(KBr) 1740, 1365, 1322, 1220, and 1160 cm^{-1}; n.m.r. (in $CDCl_3$) δ 1.47 (*anti* C-8 proton, doublet, J = 11 c.p.s.), 1.75 (*syn* C-8 proton, doublet, J = 11 c.p.s.), 2.82 (protons at C-1, C-2, C-4, and C-5), 3.03 (protons at C-6 and C-7), 3.68 (6 protons of dimethyl ester), and 7.5–8.0 (5 aromatic protons).

Anal. Calcd. for $C_{17}H_{19}O_6NS$: C, 55.88; H, 5.24. Found: C, 56.11; H, 5.07.

Elution with 1 l (1:9) benzene–chloroform gave 0.35 g of an unidentified oil which showed N—H absorption in the i.r. and several methoxyl signals in the n.m.r. spectrum. Thin-layer chromatographic analysis showed this to be a mixture of several polar components.

*Decarboxylation of 7: Preparation of N-Benzenesulfonyl-3-azatricyclo[3·2·1·$0^{2,4\ endo}$]-5-octene (**8**)*

Aziridine **7** (2.37 g) was dissolved in 100 cm^3 of hot water over a period of 20 min. Upon cooling 2.08 g of aziridine diacid precipitated and had m.p. 180–182°. The dimethyl ester was prepared using diazomethane and after recrystallization from petroleum ether had m.p. 102–103° (lit. (4), m.p. 102–103)°.

The aziridine diacid (1.49 g) was dissolved in 50 cm^3 dry pyridine at 50° under nitrogen. Lead tetraacetate (4.33 g) was added and the temperature was raised to 80° over a period of 20 min. The reaction mixture was cooled and the pyridine evaporated under vacuum. The residue remaining was taken up in 50 cm^3 of chloroform which was washed with 30 cm^3 of dilute hydrochloric acid and filtered. The chloroform portion was decanted, dried over anhydrous magnesium sulfate, and evaporated to give ca. 0.9 g of a dark oil. Thin-layer chromatography on Silica Gel-G (15 cm) in chloroform gave three small spots below R_f 0.25 and one large spot at R_f 0.60. Chromatography of this residue on 29 g of Merck acid-washed alumina gave 0.67 g (58%) of **8** m.p. 90–92°, eluted in benzene. The analytical sample of **8** was prepared by recrystallization from ethanol and had m.p. 92–93.5°; ν_{max}(KBr) 1305, 1155, 715 cm^{-1}; n.m.r. (in $CDCl_3$) δ 1.76 (2 protons at C-8), 2.87 (protons at C-1 and C-5), 3.55 (protons at C-2 and C-4, triplet, J = 1.8 c.p.s.), 5.86 (protons at C-6 and C-7, triplet, J = 1.5 c.p.s.), and 7.3–8.1 (5 aromatic protons).

Anal. Calcd. for $C_{13}H_{13}NO_2S$: C, 63.13; H, 5.30. Found: C, 63.04; H, 5.29.

*Preparation of N-Benzenesulfonyl-3-azatricyclo-[3·2·1·$0^{2,4\ endo}$]-octane (**11**)*

The unsaturated aziridine **8** (0.24 g) was hydrogenated in the presence of 0.2 g of 10% palladium-on-charcoal catalyst in 50 cm^3 of methanol under hydrogen at atmospheric pressure. The theoretical volume of hydrogen was absorbed in 15 min. Removal of the catalyst by filtration followed by evaporation of the methanol gave 0.21 g of **9**, b.p. (0.03 mm) 150±5°; ν_{max}(film) 1310, 1160, and 910 cm^{-1}; n.m.r. (in CS_2) δ 1.2–1.5 (5 protons), 1.83 (1 proton, doublet, J = 9.5 c.p.s.), 2.31 (protons at C-1 and C-5), 3.29 (protons at C-2 and C-4, triplet, J = 2 c.p.s.), and 7.4–8.0 (5 aromatic protons).

*Preparation of 2-exo-Thiphenoxy-3-endo-benzenesulfonamidobicyclo[2·2·1]heptane (**8**)*

A solution of 0.83 g of **11** and thiophenol (0.70 g) in 7 cm^3 of 0.1 *N* potassium *tert*-butoxide in *t*-butyl alcohol was refluxed overnight. The reaction mixture was poured onto water and neutralized with 5% hydrochloric acid. The aqueous solution was extracted with ether which was then dried over anhydrous magnesium sulfate. Evaporation of the ether extract gave 1.15 g of **13** which, after washing with petroleum ether, had m.p. 114–115°; n.m.r. (in nitrobenzene containing CF_3COOH); δ 1.1–1.9 (6 protons), 2.08 (proton at C-1, broad multiplet), 2.25 (proton at C-4, broad multiplet), 2.98 (proton at C-2, quartet, $J_{2,3}$ = 4 c.p.s., $J_{2,7\text{-}anti}$ = 2 c.p.s.), and 3.54 (proton at C-3, triplet, $J_{2,3} = J_{3,4}$ = 4 c.p.s.).

Can. J. Chem. Downloaded from www.nrcresearchpress.com by 210.87.254.5 on 09/05/12
For personal use only.

Anal. Calcd. for $C_{19}H_{21}NO_2S_2$: C, 63.48; H, 5.89. Found: C, 63.37; H, 6.05.

Conversion of ***13*** *to 2-endo-Benzenesulfonamidobicyclo-[2·2·1]heptane (****14****)*

The thiophenol addition product **13** (0.71 g) was refluxed for 15 h with a slurry of 6 g of Raney nickel (W-2) in 15 cm³ of isopropyl alcohol. The solution was filtered and the catalyst was washed several times with ethanol. Evaporation of the alcohol filtrate gave 0.18 g of **14**, m.p. 104–105°. The mixture melting point with authentic **14** which had m.p. 104–105°, prepared as described previously (9), was undepressed. Mixture melting point with 7-benzenesulfonamidobicyclo[2·2·1] heptane, m.p. 103–104°, prepared as described earlier (9), gave m.p. 90–93°. Authentic 2-*exo*-benzenesulfonamidobicyclo[2·2·1]heptane gave m.p. 89–91°, well below that of **14**.

Preparation of N-Benzenesulfonyl-3-azatricycolo [3·2·1·$0^{2,4\ endo}$]-octane-6,7-endo-dideuterio-6,7-exo-dicarboxylic Anhydride

A mixture (3.9 g) of 2,3-*exo*-dideuterio-2,3-*endo*-dicarboxybicyclo[2·2·1]-5-heptene anhydride and the protio species were prepared by the reaction of maleic anhydride-d_2 and cyclopentadiene according to the procedure of Van Sickle and Rodin (12). Analysis of the mixture by n.m.r. showed 70 ± 5% deuterium in the 2,3 positions.

Heating 3.3 g of the *endo* anhydride in an open flask at 200° for 2 h gave a mixture of *endo* and *exo* anhydrides from which 0.72 g of the *exo* anhydride crystallized in benzene (13). Gas–liquid chromatography using a 0.25 in. × 10 ft column of 5% SE-30 on acid-washed Chromosorb at 180° with helium flow rate of 80 cm³ per min showed the *exo* anhydride to be uncontaminated with the *endo* anhydride. Analysis by n.m.r. showed the *exo* anhydride to contain 71 ± 2% deuterium in the 2,3-positions.

A solution of 0.65 g deuterated *exo* anhydride and 0.59 g benzenesulfonyl azide in 10 cm³ of carbon tetrachloride was refluxed for 36 h. The carbon tetrachloride was decanted and the residue was crystallized thrice from benzene to give 0.4 g of **7**-6,7-$d_{1,4}$, m.p. 167–168°. Analysis by n.m.r. showed 71 ± 2% deuterium at C-6 and C-7.

Preparation of N-Benzenesulfonyl-3-azatricyclo-[3·2·1·$0^{2,4\ endo}$]-6,7-dideuterio-5-octene

Aziridine **7**-6,7-$d_{1,4}$ (0.4 g) was dissolved in 15 cm³ of hot 80% D_2O over a period of 30 min. Evaporation of the aqueous portion *in vacuo* gave 0.41 g of the corresponding diacid which after drying over phosphorus pentoxide for 12 h had m.p. 181–183°; ν_{max}(KBr) 1750 cm^{-1}.

The aziridine diacid (0.41 g) was dissolved in 13 cm³ dry pyridine under nitrogen at 50° and 1.19 g of lead tetraacetate was added. The reaction mixture was stirred at 75° for 20 min and then worked up by the usual procedure. Chromatography of the reaction mixture directly on Merck acid-washed alumina gave 35 mg of **8**-6,7-$d_{1,4}$, m.p. 90–91°, eluted in benzene. Analysis of **8**-6,7-$d_{1,4}$ by n.m.r. showed 72 ± 2% deuterium at C-6 and C-7.

1. A. C. Oehlschlager and L. H. Zalkow. Chem. Commun. 5, 1 (1966).
2. A. C. Oehlschlager and L. H. Zalkow. J. Org. Chem. **31**, 1682 (1966).
3. K. Alder and G. Stein. Ann. **515**, 185 (1935); Ann. **525**, 183 (1936).
4. L. H. Zalkow and C. D. Kennedy. J. Org. Chem. **28**, 3309 (1963).
5. K. Tori, K. Kitahonoki, Y. Takano, H. Tanida, and T. Tsuji. Tetrahedron Letters, 869 (1965).
6. R. L. Hale and L. H. Zalkow. Tetrahedron. To be published.
7. A. C. Oehlschlager and L. H. Zalkow. Chem. Commun. 70 (1965).
8. L. H. Zalkow, A. C. Oehlschlager, G. A. Cabat, and R. L. Hale. Chem. Ind. London, 1556 (1964). J. E. Franz, C. Osuch, and M. W. Dietrich. J. Org. Chem. **29**, 2933 (1964).
9. L. H. Zalkow and A. C. Oehlschlager. J. Org. Chem. **28**, 3303 (1963).
10. J. K. Kochi, J. D. Bacha, and T. W. Bethea, III. J. Am. Chem. Soc. **89**, 6538 (1967), and references therein.
11. J. A. Berson. Carbonium ion rearrangements in bridged bicyclic systems. *In* Molecular rearrangements. Part I. *Edited by* P. de Mayo. Interscience Publishers, Inc., New York. 1963. Chap. 3.
12. D. E. Van Sickel and J. O. Rodin. J. Am. Chem. Soc. **86**, 3091 (1964).
13. D. Craig. J. Am. Chem. Soc. **73**, 4889 (1951).

Can. J. Chem. Downloaded from www.nrcresearchpress.com by 210.87.254.5 on 09/05/12
For personal use only.

Chemistry of the aminochromes. Part X. Some further observations on the reactions of aminochromes with thiols[1,2,3]

W. POWELL[4,5] AND R. A. HEACOCK[6]
Atlantic Regional Laboratory, National Research Council of Canada, Halifax, Nova Scotia

AND

G. L. MATTOK[6,7] AND D. L. WILSON
Psychiatric Research Unit, University Hospital, Saskatoon, Saskatchewan

Received May 21, 1968

The reactions between aminochromes and thiols have been reinvestigated. In general aminochromes react with thiols to give mixtures of products including: 5,6-dihydroxyindoles; thio-substituted 5,6-dihydroxyindoles (the mercapto residue is now considered to be in the 4-position of the indole nucleus and not the 7-position as previously reported); and relatively unstable addition products formed between the aminochrome and the thiol. The mechanisms by which these compounds are formed are discussed. The characterization of three thio-substituted 5,6-dihydroxyindoles by nuclear magnetic resonance spectroscopy is described. The nuclear magnetic resonance spectra of a number of 5,6-diacetoxyindole derivatives are reported.

Canadian Journal of Chemistry, **47**, 467 (1969)

Solutions of adrenochrome (**1**) are readily decolorized by a wide variety of thiols (1–9). The nature of the products obtained from aminochromes in reactions of this type and the mechanisms by which they were formed have been the subjects of several recent investigations (6–13). As a result of these studies it was concluded that (6–9) aminochromes react with thiols to form three different types of product: (**A**) 5,6-dihydroxyindoles; (**B**) thio-substituted 5,6-dihydroxyindoles; and (**C**) addition products of the aminochrome with the thiol which appear to be structurally similar to the adrenochrome–sodium bisulfite addition product (cf. 14). It has been reported that in the case of the reaction between adrenochrome (**1**) and glutathione the type **A**, **B**, and **C** products are respectively: (**A**) 5,6-dihydroxy-1-methylindole (**2**); (**B**) 7-*S*-glutathionyl-5,6-dihydroxy-1-methylindole (**3**); and (**C**) 9-*S*-glutathionyl-2,3,6,9-tetrahydro-3,5-dihydroxy-1-methyl-6-oxoindole (**4**).

Reactions of this type may be of biological importance since the attachment of melanin pigment molecules to proteins could involve interaction of the thiol groups of the protein molecule with aminochrome units, which were either formed as intermediates in the melanization process or were present as integral parts of the melanin macromolecule. The presence of sulfide linkages in melanoproteins was first suggested in 1950 (15), however the manner by which such linkages could form has only recently been systematically investigated (cf. 10–12, 16, 17). Bouchilloux and Kodja studied the reactions that occurred between several oxidized catechol derivatives and the thiol-substituted aminoacids glutathione and cystein (10–12), and observed that a number of products were formed when glutathione reacts with dopachrome (**5**) including 5,6-dihydroxyindole-2-carboxylic acid (**6**), 5,6-dihydroxyindole (**7**), and a compound described as 4-*S*-glutathionyl-5,6-dihydroxyindole (**8**) (12). Mason and Peterson also reported the formation of thio-substituted 5,6-dihydroxyindoles by the interaction of suitable thiols with oxidized 5,6-dihydroxyindole (or 3,4-dihydroxyphenylalanine), (16).

The possibility that aminochrome–thiol addition products (cf. 4) may play a different significant physiological role has been considered. Inchiosa suggested that the inhibition of cardiac actomyosin ATPase by an adrenaline derivative involves the formation of a specific addition product between an oxidation product of adrenaline,

---

[1]Issued as NRCC No. 10374.
[2]Part IX. Can. J. Chem. **44**, 565 (1966).
[3]Presented in part at the 50th Annual Conference of the Chemical Institute of Canada (Toronto, Ontario, June, 1967).
[4]NRCC Summer Student 1966 and 1967.
[5]Graduate Student, Department of Chemistry, Dalhousie University, Halifax, Nova Scotia.
[6]Reprint requests and general correspondence concerning this paper should be addressed to either of these authors.
[7]Present address: Research Laboratories, Food and Drug Directorate, Department of National Health and Welfare, Ottawa, Canada.

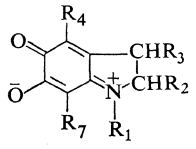

1 : $R_1 = CH_3$; $R_2 = R_4 = R_7 = H$; $R_3 = OH$
5 : $R_1 = R_3 = R_4 = R_7 = H$; $R_2 = COOH$
9 : $R_1 = R_2 = R_7 = H$; $R_3 = OH$; $R_4 = CH_3$
10 : $R_1 = R_2 = R_4 = H$; $R_3 = OH$; $R_7 = CH_3$
16 : $R_1 = R_2 = R_4 = H$; $R_3 = OH$; $R_7 = I$
23 : $R_1 = C_2H_5$; $R_2 = R_4 = R_7 = H$; $R_3 = OH$
24 : $R_1 = i\text{-}C_3H_7$; $R_2 = R_4 = R_7 = H$; $R_3 = OH$

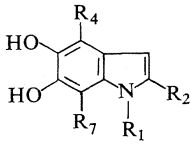

2 : $R_1 = CH_3$; $R_2 = R_4 = R_7 = H$
6 : $R_1 = R_4 = R_7 = H$; $R_2 = COOH$
7 : $R_1 = R_2 = R_4 = R_7 = H$
11 : $R_1 = R_4 = CH_3$; $R_2 = R_7 = H$
12 : $R_1 = R_7 = CH_3$; $R_2 = R_4 = H$

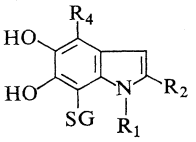

3 : $R_1 = CH_3$; $R_2 = R_4 = H$
14 : $R_1 = R_4 = CH_3$; $R_2 = H$

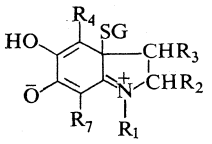

4 : $R_1 = CH_3$; $R_2 = R_4 = R_7 = H$; $R_3 = OH$
17 : $R_1 = R_7 = CH_3$; $R_2 = R_4 = H$; $R_3 = OH$

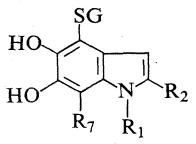

8 : $R_1 = R_2 = R_7 = H$
13 : $R_1 = CH_3$; $R_2 = R_7 = H$
15 : $R_1 = CH_3$; $R_2 = H$; $R_7 = I$

SG = glutathione residue

(isomeric with adrenochrome) and the thiol groups in the myosin molecules (13). Mattok and Heacock had previously suggested that the formation of adrenochrome–thiol adducts (such as **4**) offered the possibility that suitable thiols could act as "carriers" for the highly reactive aminochromes in physiological systems (6, 7).

The structures of the thio-substituted 5,6-dihydroxyindole derivatives (cf. **3** or **8**) were proposed on the basis of chromatographic and spectroscopic evidence (cf. 6–12) and on mechanistic considerations (6–8). Whilst structures of the type **3** or **8** were not incompatible with the evidence available, the question of the precise position of the thiol residue was not satisfactorily resolved. It was therefore decided, firstly to investigate the influence of substituents in the 4- and 7-positions of the aminochrome nucleus on their reactions with thiols in general, and secondly to attempt the isolation and unambiguous characterization of one of the thio-substituted 5,6-dihydroxyindole derivatives.

Aqueous solutions of adrenochrome (**1**); 4-methyladrenochrome (**9**); and 7-methyladrenochrome (**10**) were treated, in turn, with a slight excess of each of several different thiols. After filtration the reaction mixtures were examined spectroscopically and paper chromatographically (cf. 5–9). 4-Methyladrenochrome (**9**) reacts with these thiols to give essentially two products. The main product (R_f, 0.34)[8] appeared to be 5,6-dihydroxy-1,4-dimethylindole (**11**). A second, minor, product (R_f, ca. 0.49–0.55) was also detected in most cases. However, no products

[8]Unless otherwise stated the R_f values quoted in this paper were obtained by means of descending paper chromatography, using 2% acetic acid in water as the running solvent, and Ehrlich's reagent for visualization.

Can. J. Chem. Downloaded from www.nrcresearchpress.com by 210.87.254.5 on 09/05/12
For personal use only.

Can. J. Chem. Downloaded from www.nrcresearchpress.com by 210.87.254.5 on 09/05/12
For personal use only.

with R_f values > 0.8 were observed in any of the reaction mixtures derived from **9**. The chromatographic pictures obtained from the reaction mixtures derived from 7-methyladrenochrome (**10**) were somewhat different. Two main products were observed in most cases, neither of which appeared to be 5,6-dihydroxy-1,7-dimethylindole (**12**); one had an R_f value of ca. 0.55 whilst a second product (R_f, ca. 0.8), which reacted quite slowly with Ehrlich's reagent, was detected.

All the reaction mixtures absorbed maximally in the 275–300 mμ region. The reaction mixtures prepared from **1** or **10** had absorption maxima at 300 mμ, whilst those from **9** absorbed maximally at 276 mμ (shoulder at 290 mμ). The adrenochrome (**1**) reaction mixtures also showed absorption maxima at 350 mμ, whilst those from its 7-methyl derivative (**10**) absorbed at 380 mμ; however, no significant absorption was detected in the 300–400 mμ region in the products derived from 4-methyladrenochrome (**9**). For comparison purposes solutions of 5,6-dihydroxy-1-methylindole (**2**), 5,6-dihydroxy-1,4-dimethylindole (**11**), and 5,6-dihydroxy-1,7-dimethylindole (**12**) were prepared by the reduction of **1**, **9**, and **10** respectively by sodium hydrosulfite. The R_f values of authentic samples of **11** and **12** were 0.36 and 0.31 respectively.

The above-mentioned results suggest that the type and distribution of products obtained by the action of thiols on the aminochromes **9** and **10** are different both from each other and from the corresponding products obtained from **1**. Only traces of 5,6-dihydroxy-1,7-dimethylindole (**12**) were formed by the action of glutathione on **10**. The major product (R_f, 0.56) which contained the thiol residue could not, in view of the substituent originally present in the 7-position, be a 7-thio derivative; this fact alone indicated that the previous formulation of this type of product as a 7-thio derivative (cf. **3**) (cf. 6–9) was incorrect. An examination of the products obtained by the action of glutathione on 4-methyladrenochrome (**9**) tended to confirm this thesis. 5,6-Dihydroxy-1,4-dimethylindole (**11**) (R_f, 0.33) was the major product formed in this case and only traces of a second product (R_f, 0.50) were detected. Substituents in the 4-position of the aminochrome nucleus therefore prevent the formation of thio-substituted 5,6-dihydroxyindoles, similar to those which can be obtained from **1** and **10** (cf. **3** or **8**). These facts suggest that the thiol residue is attached to position-4 of the indole nucleus in the type **B** products and that the product obtained from adrenochrome (**1**) by the action of glutathione, previously described as 7-*S*-glutathionyl-5,6-dihydroxy-1-methylindole (**3**) (cf. 6, 7), is actually the isomeric product 4-*S*-glutathionyl-5,6-dihydroxy-1-methylindole (**13**). The minor product (R_f, 0.50) obtained from **9** may be the 7-*S*-glutathionyl-5,6-dihydroxyindole derivative **14**.

4-*S*-Glutathionyl-5,6-dihydroxy-7-iodo-1-methylindole (**15**) was reported to be one of the major products obtained by the action of glutathione on 7-iodoadrenochrome (**16**) (8); the current results suggest that this structure is the correct one for this compound. Reaction mixtures derived from **1** by the action of thiols always showed strong absorption at ca. 350 mμ; however, this absorption was observed at ca. 380 mμ in the case of the products derived from **10**. This latter value is close to that previously reported for one of the 7-iodoadrenochrome–glutathione reaction products (8). In general 7-substituted aminochromes exhibit absorption maxima at longer wavelengths than the parent compounds [e.g. **1**: λ_{max}, 487 mμ; **16**, λ_{max}, 535 mμ; **10**: λ_{max}, 534 mμ (cf. 18, 19)]. An absorption maximum of ca. 380 mμ would therefore be expected for the 7-methyladrenochrome-glutathione addition product (**17**). However, this type of compound is not formed from 4-methyladrenochrome (**9**), since reaction mixtures derived from **9** by the action of thiols show no absorption at ca. 350 mμ. The fact that this type of compound is not formed in this case may be due to steric hindrance by the 4-methyl substituent to reaction by the thiol at the bridgehead 9-position.

Preliminary attempts to isolate one of the thio-substituted 5,6-dihydroxyindole derivatives, obtained from **1** by the action of thiol-containing aminoacids, were not successful. However, a derivative of a compound of this type has been isolated from the products obtained by the action of thioglycollic acid on adrenochrome (**1**). The reduction of adrenochrome by thioglycollic acid was first described in 1945 (2), and the nature of the products formed was subsequently investigated by Heacock and Scott (5). It appeared that two major products (R_f values: 0.42 and 0.48) and one minor product (R_f, 0.18) were formed. One of the major products (R_f, 0.42) was 5,6-dihydroxy-1-methylindole (**2**) and could be

Can. J. Chem. Downloaded from www.nrcresearchpress.com by 210.87.254.5 on 09/05/12
For personal use only.

separated from the other major product (R_f, 0.48) since the latter was soluble in aqueous sodium bicarbonate, whilst **2** was not. The product (R_f, 0.48) exhibited color reactions expected for the indole ring system, the *o*-diphenol group, the carboxy group, and divalent sulfur [alkaline sodium nitroprusside spray reagent (20)]. This substance, presumably **18** or **19**, and in view of some of the evidence presented above, probably the latter, could only be obtained as a yellow oil. A crystalline acetyl derivative was obtained on treatment of the crude product with acetic anhydride and pyridine. The acetyl derivative was not acidic and its infrared spectrum showed no absorption in the NH/OH stretching region, but did show absorption in the carbonyl region at 1765 and 1775 cm^{-1}. The ultraviolet spectrum confirmed that the indole ring system was still intact. Microanalytical data and mass spectrometry indicated an empirical formula of $C_{13}H_{11}NO_4S$. These facts suggested that an intramolecular cyclization reaction had occurred at the same time as the acetylation, to give a structure such as **20** or **21**. An analogous internal cyclization reaction had been observed earlier when the corresponding product obtained by the action of thioglycollic acid on *p*-benzoquinone (21, 22) was allowed to stand in a vacuum desiccator in the presence of phosphorus pentoxide (21).

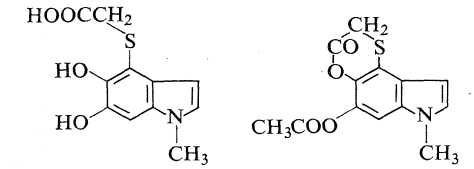

19

21

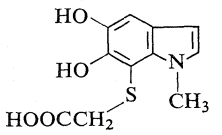

18

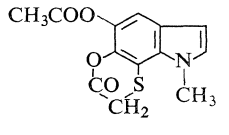

20

Nuclear magnetic resonance (n.m.r.) spectroscopy has been widely used for the elucidation of structural problems in the indole series and it appeared that this technique should provide a convenient method for determining which of the structures **20** or **21** was correct for the acetyl derivative, since the problem was essentially one of distinguishing between the presence or absence of the 4- and 7-protons in the indole ring system. The signals due to the protons in the 2- and 3-positions of the indole nucleus are easily recognized (cf. 23–25). Recently, long range coupling has been observed between the protons in the 3- and 7-positions in the indole nucleus (26–31); this coupling (ca. 0.8–1.0 Hz) is of greater magnitude than any of the other possible long range couplings, ignoring couplings involving the proton at position-1, which are not relevant in the present case. The majority of the other couplings are $\leqslant$ 0.3 Hz and are scarcely detectable (30). The exceptions [$J_{2,6} \sim$ 0.4–0.5 Hz and $J_{4,7} \sim$ 0.5–0.8 Hz (30)] would not be observable in compounds such as **20** and **21**.

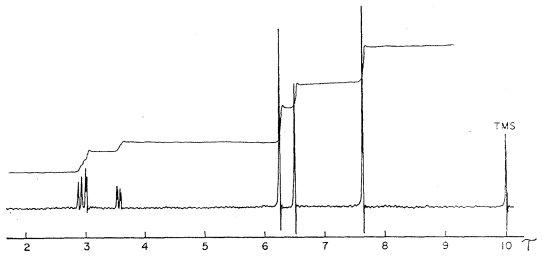

FIG. 1. The nuclear magnetic resonance spectrum of 6-acetoxy-4-*S*-carboxymethylthio-5-hydroxy-1-methylindole lactone (**21**) in $CDCl_3$ with tetramethylsilane as an internal standard.

The n.m.r. spectrum of the acetyl derivative which is shown in Fig. 1 shows that formula **21** is the correct structure for this compound. The signals due to the *C*—CH_3 (τ, 7.65), *N*—CH_3 (τ, 6.5), and *S*—CH_2— (τ, 6.25) (cf. 32) can clearly be seen in the spectrum. In the aromatic proton region the signal due to the 3-proton appears as a doublet of doublets centered at τ, 3.55 with splittings of 3.0 Hz ($J_{2,3}$) and 0.8 Hz ($J_{3,7}$). The 2-proton is observed as a doublet centered at τ, 2.9 ($J_{2,3}$ = 3.0 Hz) whilst the 7-proton appears as a doublet centered at τ, 3.0 ($J_{3,7}$ = 0.8 Hz).

The n.m.r. spectra of a number of related indole compounds with two or more substituents in the benzene ring have been recorded and the relevant τ values and coupling constants for the protons in the 2-, 3-, 4-, and 7-positions are given in Table I. The aromatic proton regions of the n.m.r. spectra of four of these compounds are shown in Fig. 2 and it can clearly be seen that the assignments made for compound **21** are probably correct. In general the signal due to the 4-proton in the

TABLE I

Nuclear magnetic resonance spectral* data for some 5,6-diacetoxyindole derivatives

Indole compound	τ-Values†				Coupling constants (Hz)	
	2-H	3-H	4-H	7-H	$J_{2,3}$	$J_{3,7}$
5,6-Diacetoxy-1-methylindole	3.01 (d)‡	3.61 (dd)‡	2.63 (s)‡	2.9 (d)	3.1	1.0
5,6-Diacetoxy-1,4-dimethylindole	3.02 (d)	3.55 (dd)	—	3.05 (d)	3.0	0.8
5,6-Diacetoxy-1,7-dimethylindole	3.05 (d)	3.61 (d)	2.78 (s)	—	3.0	—
5,6-Diacetoxy-7-iodo-1-methylindole	3.05 (d)	3.69 (d)	2.67 (s)	—	3.1	—
5,6-Diacetoxy-7-iodo-1,4-dimethylindole	3.03 (d)	3.65 (d)	—	—	3.0	—
3,5,6-Triacetoxy-7-iodo-1-methylindole	2.73 (s)	—	2.67 (s)	—	—	—
5,6-Diacetoxy-1-isopropylindole§	2.79 (d)	3.55 (dd)	2.63 (s)	2.82 (d)	3.2	1.0
5,6-Diacetoxy-7-iodo-1-isopropylindole§	2.67 (d)	3.58 (d)	2.63 (s)	—	3.3	—
6-Acetoxy-4-carboxymethylthio-5-hydroxy-1-methylindole lactone	2.9 (d)	3.55 (dd)	—	3.0 (d)	3.0	0.8
6-Acetoxy-4-(β-carboxyethyl)thio-5-hydroxy-1-methylindole lactone	2.85 (d)	3.32 (dd)	—	2.88 (d)	3.2	0.9
6-Acetoxy-4-carboxymethylthio-5-hydroxy-1-isopropylindole lactone§	2.73 (d)	3.53 (dd)	—	2.94 (d)	3.0	0.9

*The spectra were recorded in $CDCl_3$ with tetramethylsilane as an internal reference.
†The N-CH_3 signal was always observed as a well defined singlet at τ, 5.8–6.4.
‡(d) = doublet; (dd) = doublet of doublets; (s) = singlet.
§The methine proton was observed as a complex multiplet centered at τ, 5.4 and 5.5 respectively in the cases of 5,6-diacetoxy-1-isopropylindole and 6-acetoxy-4-carboxymethylthio-5-hydroxy-1-isopropylindole lactone, whereas in the case of the 7-iodo compound, 5,6-diacetoxy-7-iodo-1-isopropylindole the methine proton was observed as a complex multiplet centered at τ, 4.00, presumably due to the deshielding effect of the 7-iodo substituent.

spectra of 5,6-disubstituted indole derivatives is observed as a well defined singlet downfield from the other aromatic proton signals (see Fig. 2, spectra of 5,6-diacetoxy-1,7-dimethylindole and 5,6-diacetoxy-7-iodo-1-methylindole), whereas the signal due to the 7-proton is usually seen as a doublet (provided the 3-position is free) with a splitting ($J_{3,7}$) of ca. 0.8–1.0 Hz (see Fig. 2, spectra of 5,6-diacetoxy-1-methylindole and 5,6-diacetoxy-1,4-dimethylindole).

The ultraviolet absorption patterns of solutions of **21** change on alkalinization in the manner that would be expected if the lactone ring opened (see Fig. 3). The long wavelength absorption maximum shifts from 298 mμ (shoulder at 307 mμ) in neutral solution to 337 mμ in alkaline solution; on acidification of the alkaline solution the peak is observed at 320 mμ, suggesting that the lactone ring does not reform. This latter shift (i.e. 337 mμ → 320 mμ) is probably due to the change in absorption associated with the ArO^- → ArOH change. The ultraviolet spectrum of **21** did not change appreciably with time, in alkaline solution (see Fig. 3). In view of the known instability of 6-hydroxyindoles, relative to the corresponding 5-hydroxy isomers, in alkaline solution, this observation tends to confirm that the unacetylated phenolic group is in the 5-position, (after the lactone ring has been opened), rather than in the 6-position, of the indole nucleus.

β-Mercaptopropionic acid readily reduces adrenochrome (**1**) in solution; in this case the major products are 5,6-dihydroxy-1-methylindole (**2**) and 4-*S*-(β-carboxyethylthio)-5,6-dihydroxy-1-methylindole. On treatment with an acetic anhydride – pyridine mixture the latter compound also undergoes an intramolecular cyclization to form a cyclic lactone (i.e. **22**), analogous to **21**, which in this case, contains a seven-membered ring. The structure of this lactone was confirmed by the micronalytical data and by n.m.r. and mass spectroscopy.

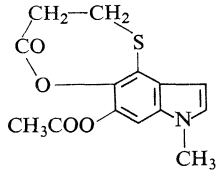

22

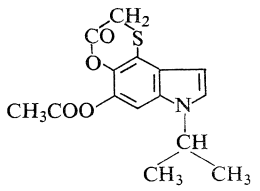

25

Preliminary paper chromatographic studies indicated that *N*-ethylnoradrenochrome (**23**) and *N*-isopropylnoradrenochrome (**24**) react analogously to adrenochrome (**1**) with thioglycollic

Can. J. Chem. Downloaded from www.nrcresearchpress.com by 210.87.254.5 on 09/05/12
For personal use only.

Can. J. Chem. Downloaded from www.nrcresearchpress.com by 210.87.254.5 on 09/05/12
For personal use only.

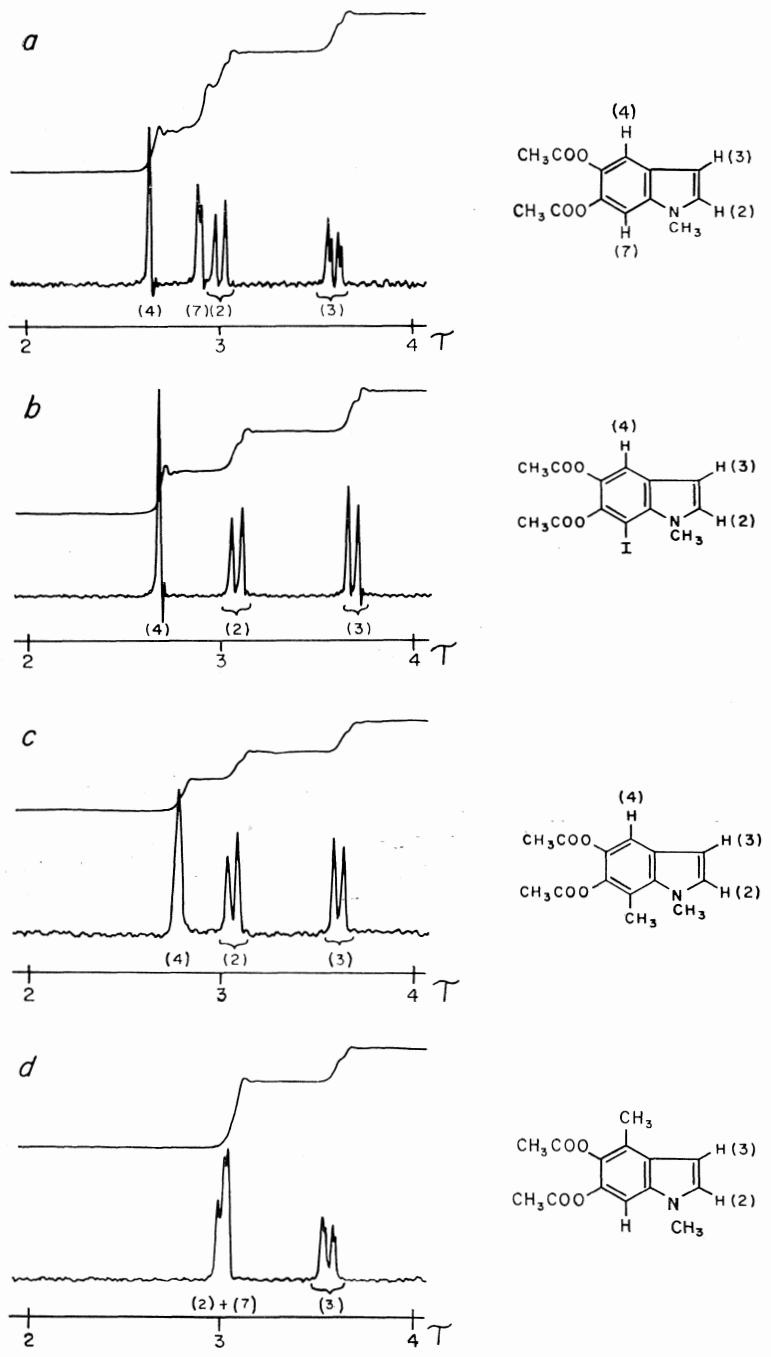

FIG. 2. The nuclear magnetic resonance spectra (in the region τ, 2.00 to τ, 4.00) of: 5,6-diacetoxy-1-methylindole (*a*); 5,6-diacetoxy-7-iodo-1-methylindole (*b*); 5,6-diacetoxy-1,7-dimethylindole (*c*); 5,6-diacetoxy-1,4-dimethylindole (*d*). The spectra were recorded in $CDCl_3$ with tetramethylsilane as an internal standard.

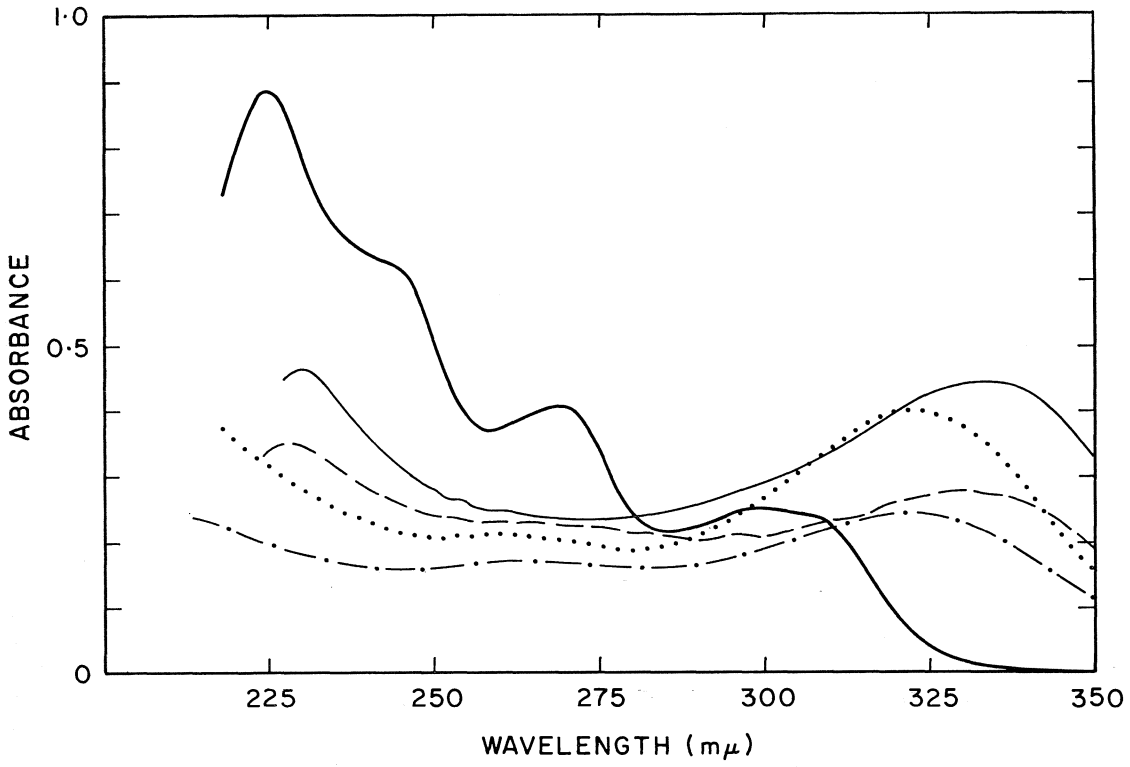

FIG. 3. Absorption spectra of: (*a*) **21** in ethanol (———); (*b*) **21** in ethanol directly after the addition of a few drops of aqueous NaOH (———); (*c*) **21** in ethanol 18 h after addition of the alkali (— — —); (*d*) solution (*b*) acidified (. . . . .); (*e*) solution (*c*) acidified (—·—·—).

acid to form the appropriate 1-alkyl-5,6-dihydroxyindole; 1-alkyl-4-*S*-carboxymethylthio-5,6-dihydroxyindole; and an unknown product, in each case. In the latter case the lactone analogous to **21** (i.e. **25**) was isolated and characterized unambiguously.

It was suggested that the main products obtained by the interaction of thiols with aminochromes were formed either by direct reduction, or by 1,4-addition of the thiol to the two α,β-unsaturated carbonyl systems apparently present in the aminochrome molecule. These were the systems involving the C-5 carbonyl group and either the C_6—C_7 or the C_4—C_9 double bond (6–8) and gave, in the case of the adrenochrome–glutathione reaction, the products **3** and **4** respectively. It would now appear that whilst the second of these alternatives satisfactorily accounts for the formation of **4**, the former reaction probably does not occur. A reaction sequence involving an initial nucleophilic attack at the adrenochrome C-4 carbon by the mercaptide anion, as shown below (i.e. **26** → **27** → **28** → **29**) would, however, satisfactorily account for the formation of 4-thio-substituted 5,6-dihydroxyindole derivatives such as **8** or **13**. The formation of quinone thioethers by nucleophilic substitution reactions has

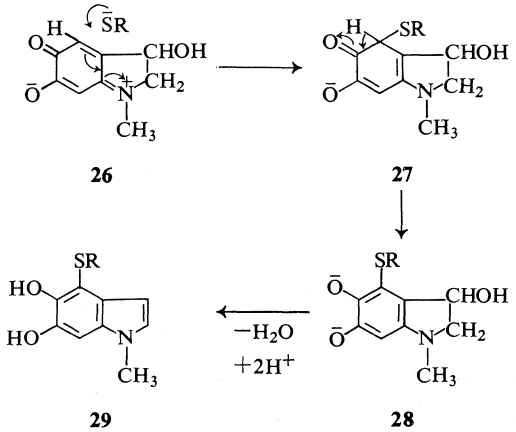

Can. J. Chem. Downloaded from www.nrcresearchpress.com by 210.87.254.5 on 09/05/12
For personal use only.

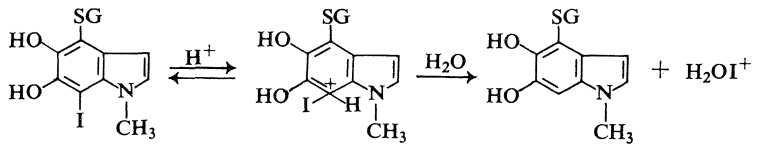

15 **30** **13**

previously been described (34). It has also been shown that, like glutathione (cf. 7), thioglycollic acid does not react with 5,6-dihydroxy-1-methylindole (**2**) under the conditions employed in this investigation; thus the initial nucleophilic attack by the mercaptide anion must be on the aminochrome molecule.

It would now appear that some of the mechanisms previously proposed for the formation of the products that are observed in 7-iodoadrenochrome–glutathione reaction mixtures (8) require revision. 4-*S*-Glutathionyl-5,6-dihydroxy-7-iodo-1-methylindole (**15**), one of the major products, could be formed from 7-iodoadrenochrome (**16**) by a mechanism analogous to that described above (cf. Scheme 4). The product previously described (8) as 7-*S*-glutathionyl-5,6-dihydroxy-1-methylindole (**3**) is in all probability the isomeric 4-*S*-glutathionyl derivative (i.e. **13**), formed by the acid-catalyzed deiodination of **15** [cf. acid-catalyzed deiodination of some aromatic iodo compounds by the mechanism suggested by Batts and Gold (35)]. Such a mechanism (i.e. **15** → **30** → **13**), would account for the preponderance of deiodinated products observed among the products obtained from 7-iodoadrenochrome (**16**) by the action of glutathione as the free acid as compared to those produced by glutathione as the monosodium salt (8).

Experimental

The infrared spectra were recorded on a Perkin–Elmer model 237 recording spectrophotometer; the ultraviolet (u.v.) absorption spectra were obtained on either a Beckman DK-2 or a Bausch and Lomb "Spectronic 505" recording spectrophotometer and the nuclear magnetic resonance spectra were recorded on a Varian A-60-A instrument.

*Reactions of Adrenochrome (**1**), 4-Methyladrenochrome (**9**), and 7-Methyladrenochrome (**10**) with Some Thiols*

Materials

Adrenochrome (36), 4- and 7-methyladrenochrome (19), *N*-ethylnoradrenochrome (33), *N*-isopropylnoradrenochrome (33), and adrenochrome methyl ether (33) were prepared by methods described in the literature. Glutathione, its monosodium salt, and homocysteine were obtained from the Nutritional Biochemicals Corporation; thioglycollic acid and β-mercaptopropionic acid from the Eastman Kodak Company.

Reaction Mixtures

The reactions were all carried out at room temperature. Aqueous solutions (1 ml) of each of the aminochromes (2 mg/ml) were treated, in turn, with a slight excess (i.e. until the red color of the solution was permanently discharged) of some of the thiols mentioned above. The reaction mixtures were filtered and examined by paper chromatography and by ultraviolet–visible spectroscopy.

Paper Chromatography

Descending chromatography was carried out on Whatman No. 1 paper with 2% acetic acid in water as the running solvent. In all cases the solvent was allowed to descend ca. 35–40 cm, which required 2.5–3.0 h. The developed chromatograms were allowed to dry in air at room temperature; they were then examined for fluorescence in u.v. light and then sprayed with one of the following chromogenic reagents:[9] Ehrlich's reagent, cinnamaldehyde, *p*-dimethylaminocinnamaldehyde, ninhydrin, and Gibb's reagent.

Spectroscopy

Spectra were obtained from suitably diluted solutions of the reaction mixtures or ether extracts, and were recorded on a Beckman DK-2 spectrophotometer.

The results of the chromatographic and spectroscopic examination of the reaction mixtures are shown in Tables II and III.

*6-Acetoxy-4-S-carboxymethylthio-5-hydroxy-1-methylindole Lactone (**21**)*

Freshly prepared silver oxide (30 g) was added portionwise, during a period of about 3–4 min to a stirred solution of adrenaline bitartrate (7.0 g) in water (150 ml). The temperature of the reaction mixture was not allowed to exceed 30° during the addition of the oxidant. The resulting deep red suspension was filtered through a Dowex-1 (×10) (Cl^-) resin bed[10] (diameter = 4.5 cm; height = 2.5 cm) and thioglycollic acid (4 ml) added dropwise, with stirring, to the filtrate. The resulting opaque and brownish-green solution was acidified with conc. hydrochloric acid (3 ml) and extracted with ether[11] (6 × 100 ml). The combined ether extracts, which contained both 5,6-dihydroxy-1-methylindole and 4-*S*-car-

[9]The chromogenic reagents were prepared by the usual methods described in the literature (cf. ref. 37).

[10]The resin was prepared by extensive washing with: (*1*) 3 *N* hydrochloric acid and (*2*) water, until neutral to litmus.

[11]Peroxide-free ether was used throughout this investigation.

Can. J. Chem. Downloaded from www.nrcresearchpress.com by 210.87.254.5 on 09/05/12
For personal use only.

TABLE II

Paper chromatography* and ultraviolet absorption characteristics of some aminochrome–glutathione reaction mixtures

Aminochrome	λ_{max} (mμ)	R_f values and colors †of products§ with Ehrlich's reagent		
Adrenochrome	350^m‡; 300^m	0.42 (b.v.)^m	0.65 (b.v.)^m	0.85 (b)^m
4-Methyladrenochrome	290^m; 276^m	0.35 (r.b.)^s	0.49 (b)^{vw}	
7-Methyladrenochrome	295^s		0.56 (r.b.)^s	

*Descending development with 2% acetic acid in water on Whatman No. 1 paper.
†Colors: b = blue; b.v. = blue-violet; r.b. = royal blue. Spots due to excess glutathione and oxidized glutathione are not reported.
‡Intensities of spots and absorptions: ^{s} = strong; ^{m} = medium; ^{vw} = very weak.
§The R_f values of authentic samples of 5,6-dihydroxy-1-methylindole, 5,6-dihydroxy-1,4-dimethylindole, and 5,6-dihydroxy-1,7-dimethylindole under these conditions are 0.41, 0.36, and 0.31 respectively.

TABLE III

Paper chromatography* of the products obtained by the action of thioglycollic acid on some aminochromes

Aminochrome	R_f values† and intensities of main spots	Colors with chromogenic reagents‡			
		Ehr.	Cinn.	DMAC	NaNP
Adrenochrome	0.18 (m)§	B	P→GyV	B→BGy	G→Gy
	0.44 (s)	BV	OrBr→VBr	BG→B	—
	0.51 (s)	BV	OrR→GyV	BG→BGy	BG→Bg
	0.80 (m)‖				
N-Ethylnoradrenochrome	0.24 (m)	B	P→GyV	B→BGy	G→Gy
	0.52 (s)	BV	OrBr→VBr	BG→B	—
	0.55 (s)	BV	OrR→GyV	BG→BGy	BG→Bg
	0.80 (m)‖				
N-Isopropylnoradrenochrome	0.28 (m)	B	P→GyV	B→BGy	G→Gy
	0.57 (s)	BV→V	OrBr→VBr	BG→BGy	—
	0.60 (s)	V→BV	OrR→GyV	BG→BGy	BG→Bg
	0.80 (m)‖				
Adrenochrome methyl ether	0.16 (m)	B	P→GyV	B→BGy	G→Gy
	0.44 (s)	BV	OrBr→VBr	BG→B	—
	0.48 (s)	BV	OrR→GyV	BG→BGy	BG→Bg
	0.80 (m)‖				

*Descending development with 2% acetic acid in water on Whatman No. 1 paper.
†The R_f values of the first three spots using radial development are 0.27, 0.56, and 0.61 respectively.
‡Reagents: Ehr. = Ehrlich's reagent; Cinn. = cinnamaldehyde; DMAC = *p*-dimethylaminocinnamaldehyde; NaNP = sodium nitroprusside. Colors: B = blue; BV = blue–violet; BG = blue–green; BGy = blue–grey; V = violet; VBr = violet–brown; GyV = grey–violet; OrBr = orange–brown; OrR = orange–red; Gy = grey; Bg = beige.
§s = strong; m = medium; w = weak.
‖Excess thioglycollic acid (no color reactions given).

boxymethylthio-5,6-dihydroxy-1-methylindole, were extracted with saturated aqueous sodium bicarbonate (6 × 100 ml). Concentrated hydrochloric acid (50 ml) was added slowly with stirring to a two-phase system composed of the combined sodium bicarbonate extracts and ether (100 ml). Small quantities of ether were added from time to time to replace losses due to evaporation. After addition of the acid was complete, the ether layer was separated and the aqueous mother liquors further extracted with ether (5 × 100 ml). The original ether layer and extracts were combined, dried (Na_2SO_4), and filtered. A mixture of acetic anhydride (7.5 ml) and dry pyridine (7.5 ml) was added to the filtrate and the reaction mixture allowed to stand overnight at room temperature, after which time the ether was removed *in vacuo*, below 30°, and the resulting solution added, dropwise, with stirring to an ice–water mixture (500 ml). The crude acetyl derivative, which was obtained as a pale-yellow gummy solid, was dissolved in a benzene–light petroleum[12] mixture (3:1), and adsorbed on a silica gel[13] column (diameter = 2 cm; height = 15 cm). The column was eluted with the same solvent and a series of fractions (50 ml) collected until the eluant gave a positive reaction with Ehrlich's reagent. Concentration, *in vacuo*, below 30°, of the first four Ehrlich negative fractions merely gave traces of unidentifiable gummy products which were discarded. Further elution of the column with the same solvent (300 ml) and (700 ml) gave crude **21** as white crystalline solids (137 mg;

[12]British Drug Houses Analar grade (b.p, 60–80°).
[13]Obtained from the Koch–Light laboratories (200/300 mesh size).

Can. J. Chem. Downloaded from www.nrcresearchpress.com by 210.87.254.5 on 09/05/12
For personal use only.

m.p. 159–161°) and (119 mg; m.p. 136–157°). The latter product was a somewhat impure version of the former. The presence of **21** in the eluant was determined by radial chromatography on formamide treated paper using benzene – light petroleum mixtures [either (1:1) or (1:2)] as running solvent. The R_f values of **21** in these systems are 0.86 and 0.65 respectively. The compound **21** could easily be located on the developed chromatograms by spraying with the modified Ehrlich's reagent (*p-N,N*-bis(2-chloroethyl)aminobenzaldehyde) (mauve color) or the sodium nitroprusside reagent (blue–green color) (see Table II).

Pure 6-acetoxy-4-*S*-carboxymethylthio-5-hydroxy-1-methylindole lactone (**21**) (53.6 mg; m.p. 161–163°) was obtained as colorless needles on repeated careful recrystallization of the solid product obtained from the column from light petroleum (b.p. 80–100°): λ_{max} (cyclohexane): 225, 244 (sh), 268, 300, 310 mμ; λ_{max} (EtOH)[14]: 225, 245 (sh), 268, 299, 308 (sh) mμ; ν_{max} (Nujol): 1765, 1775 (sh) cm^{-1}.

Anal. Calcd. for $C_{13}H_{11}NO_4S$ (mol. wt., 277): C, 56.30; H, 4.00; N, 5.05; S, 11.57. Found (mol. wt., 277): C, 56.06; H, 4.02; N, 5.12; S, 11.73.

6-Acetoxy-4-S-(β-carboxyethyl)thio-5-hydroxy-1-methylindole Lactone (*22*)

This was prepared from adrenaline by essentially the procedure described above, using β-mercaptopropionic acid in place of thioglycollic acid and gave colorless plates, m.p. 165–168°.

Anal. Calcd. for $C_{14}H_{13}NO_4S$: C, 57.73; H, 4.50; N, 4.82; S, 11.01. Found: C, 57.45; H, 4.25; N, 4.81; S, 11.28.

6-Acetoxy-4-S-carboxymethylthio-5-hydroxy-1-isopropylindole Lactone (*25*)

This was prepared in an analogous manner from *N*-isopropylnoradrenaline hydrochloride and thioglycollic acid and gave colorless plates, m.p. 154–157°.

Anal. Calcd. for $C_{15}H_{15}NO_4S$: C, 58.98; H, 4.95; N, 4.59; S, 10.51. Found: C, 58.85; H, 4.62; N, 4.73, S, 10.17.

Acknowledgments

The assistance of Mrs. B. D. Scott (Psychiatric Research Unit) with some of the preliminary paper chromatographic work is gratefully acknowledged. The authors also wish to express their thanks to Mr. D. G. Smith and Mr. J. van Ingen (Atlantic Regional Laboratory) for recording the nuclear magnetic resonance spectra.

1. D. E. Green and D. Richter. Biochem. J. **31**, 596 (1937).
2. G. N. Cohen. Compt. Rend. **220**, 796 (1945).
3. E. M. Trautner and T. R. Bradley. Australian J. Sci. B, **4**, 303 (1951).
4. R. A. Heacock and B. D. Laidlaw. Chem. Ind. London, 1510 (1958).
5. R. A. Heacock and B. D. Scott. Can. J. Biochem. Physiol. **37**, 1087 (1959).
6. R. A. Heacock and G. L. Mattok. Arch. Biochem. Biophys. **107**, 352 (1964).
7. G. L. Mattok and R. A. Heacock. Can. J. Chem. **43**, 119 (1965).
8. G. L. Mattok and R. A. Heacock. Can. J. Chem. **44**, 565 (1966).
9. G. L. Mattok. Arch. Biochem. Biophys. **120**, 170 (1967).
10. S. Bouchilloux and A. Kodja. Compt. Rend. **251**, 1920 (1960).
11. A. Kodja and S. Bouchilloux. Compt. Rend. Soc. Biol. **154**, 737 (1960).
12. S. Bouchilloux and A. Kodja. Bull. Soc. Chim. Biol. **42**, 1045 (1960).
13. M. A. Inchiosa. Biochem. Pharmacol. **16**, 329 (1967).
14. R. L. Tse and M. J. Oesterling. Clin. Chim. Acta, **8**, 393 (1963).
15. H. Burton and J. L. Stoves. J. Soc. Dyers Colourists, **66**, 474 (1950).
16. H. S. Mason and E. W. Peterson. Biochim. Biophys. Acta, **111**, 134 (1965).
17. G. Prota and R. A. Nicolaus. Gazz. Chim. Ital. **97**, 665 (1967).
18. R. A. Heacock. Advan. Heterocyclic Chem. **5**, 205 (1965).
19. R. A. Heacock and O. Hutzinger. Can. J. Chem. **43**, 2535 (1965).
20. D. K. Black. J. Chem. Soc. 1123 (1966).
21. J. M. Snell and A. Weissberger. J. Am. Chem. Soc. **61**, 450 (1939).
22. M. Schubert. J. Am. Chem. Soc. **69**, 712 (1947).
23. L. A. Cohen, J. W. Daly, H. Kny, and B. Witkop. J. Am. Chem. Soc. **82**, 2184 (1960).
24. R. V. Jardine and R. K. Brown. Can. J. Chem. **41**, 2067 (1963).
25. R. A. Heacock, O. Hutzinger, B. D. Scott, J. W. Daly, and B. Witkop. J. Am. Chem. Soc. **85**, 1825 (1963).
26. J. A. Elvidge and R. G. Foster. J. Chem. Soc. 981 (1964).
27. S. Sternhell. Rev. Pure Appl. Chem. **14**, 15 (1964).
28. P. J. Black and M. L. Heffernan. Australian J. Chem. **18**, 353 (1965).
29. M. Martin-Smith, S. T. Reid, and S. Sternhell. Tetrahedron Letters, 2393 (1965).
30. S. Sternhell. Private communication. 1967.
31. S. Kašpárek and R. A. Heacock. Can. J. Chem. **44**, 2805 (1966).
32. M. Brink. Acta Chem. Scand. **20**, 1432 (1966).
33. R. A. Heacock and B. D. Scott. Can. J. Chem. **38**, 516 (1960).
34. W. J. Nickerson, G. Falcone, and G. Strauss. Biochemistry, **2**, 537 (1963).
35. B. D. Batts and V. Gold. J. Chem. Soc. 5753 (1964).
36. R. A. Heacock, C. Nerenberg, and A. N. Payza. Can. J. Chem. **36**, 853 (1958).
37. R. A. Heacock, M. E. Mahon, and B. D. Scott. Can. J. Chem. **39**, 231 (1961).

[14]The u.v. spectrum of **21** in methanol solution is initially similar to those obtained in ethanol or cyclohexane; however, within 30 min at room temperature the above maxima disappear and, are replaced by new maxima at 312 and 240 mμ.

Can. J. Chem. Downloaded from www.nrcresearchpress.com by 210.87.254.5 on 09/05/12
For personal use only.

Can. J. Chem. Downloaded from www.nrcresearchpress.com by 210.87.254.40 on 09/05/12
For personal use only.

New synthesis of formaldehyde-d_2[1,2]

J. G. Atkinson, D. W. Cillis, and R. S. Stuart
Isotopic Laboratories, Merck Sharp and Dohme of Canada, Ltd., Montreal, Quebec

Received August 6, 1968

A new and improved synthesis of formaldehyde-d_2 on a molar scale has been developed *via* the reactions:

$$CH_2Br_2 + D_2O \rightarrow CD_2Br_2 \rightarrow CD_2(OAc)_2 \rightarrow CD_2O$$

The yield from deuterated methylene bromide is 50%, and the deuterium content is over 98%.

Une nouvelle synthèse, à l'échelle molaire, du formaldéhyde-d_2, fondée sur les réactions suivantes, est rapportée:

$$CH_2Br_2 + D_2O \rightarrow CD_2Br_2 \rightarrow CD_2(OAc)_2 \rightarrow CD_2O$$

Le rendement à partir du bromure de méthylène deuterié est 50%, et le taux de deutérium dépasse 98%.

Canadian Journal of Chemistry, **47**, 477 (1969)

Introduction

Formaldehyde-d_2 is a reagent of considerable utility as the starting point for further syntheses of deuterium labelled compounds (2) and for the study of reaction mechanisms (ref. 3 p. 213). The need for this material has grown considerably, and as part of a program to develop improved syntheses of labelled compounds, we have investigated and developed a new synthetic approach by which we have prepared up to 15 moles of formaldehyde-d_2.

The most satisfactory previous synthesis of formaldehyde-d_2 was that of Bannard, Morse, and Leitch (4) which consists of the lead tetraacetate cleavage of ethylene-d_4 glycol to yield pure, polymeric formaldehyde-d_2 in 75% yield. This procedure has the major disadvantage that the deuterated precursor is itself rather expensive, and, in addition, it is operationally difficult to carry out on a molar scale or larger. Elwyn *et al.* (5) have also described a synthesis in 33% yield by decarboxylation of dihydroxymaleic acid in heavy water followed by periodate cleavage of the resulting glycolaldehyde-d_4. Very recently, Olofson and Zimmerman (6) have reported a new synthesis of benzaldehyde-d_1 and formaldehyde-d_2 by exchange of a bisiminium cation with deuterium oxide, although the formaldehyde-d_2 was isolated only as a derivative. These latter preparations have the disadvantage that the product is obtained initially as a relatively dilute aqueous solution containing large amounts of inorganic salts so that a lengthy steam distillation is required in order to obtain pure material. Renaud and Leitch (7) have also recently described a novel preparation based on the Polonovsky reaction of trimethyl-d_9-amine oxide.

Results

The first step in the present synthesis was based on the discovery by Blanchard and Simmons (8) that methylene iodide could be exchanged in a basic solution of ethanol-OD and deuterium oxide. We have re-investigated this system extensively and have found that both methylene bromide and methylene iodide undergo ready exchange with refluxing, basic heavy water without the need of a co-solvent. By repeated exchange the deuterium content can be brought up to 99 atom % D and the partially depleted heavy water can be re-used in subsequent preparations.

$$CH_2Br_2 \xrightarrow{D_2O/OD^-} CD_2Br_2$$

$$CH_2I_2 \xrightarrow{D_2O/OD^-} CD_2I_2$$

Hydrolysis is very slow under these conditions and after 6–8 exchanges, 65–75% yields of fully deuterated halide were obtained. The exchange presumably proceeds through the dihalomethyl anion which reacts with D_2O much more rapidly

[1]Synthetic aspects of stable isotope chemistry. V. For Part IV, see ref. 1.

[2]Presented in part at the Second International Conference on Methods of Preparing and Storing Labelled Molecules, Brussels, Belgium. November 28–December 3, 1966.

Can. J. Chem. Downloaded from www.nrcresearchpress.com by 210.87.254.40 on 09/05/12
For personal use only.

than it decomposes to a halocarbene, thus accounting for the relatively high recovery even after a number of exchanges. By analogy with the addition of the trichloromethyl anion to aldehydes (9) and acid anhydrides (10), it might be expected that the dihalomethyl anion could be trapped by electrophilic species other than D^+, and such experiments would be of potential synthetic interest.[3]

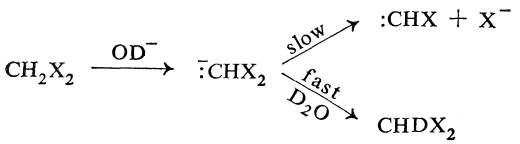

Many attempts at the direct conversion of the methylene halides to formaldehyde confirmed their resistance to hydrolysis. This is a "textbook" reaction, but upon heating methylene iodide with water at 180° only carbon and iodine were obtained. Heating in a glass bomb with water and $Ba(OH)_2$, PbO, or Ag_2O caused the bomb to explode in each case. Heating with concentrated H_2SO_4 at 100° resulted in the liberation of iodine, and no reaction was observed with refluxing aqueous mixtures of silver oxide, silver carbonate, or silver acetate with either halide.

A two-step conversion to formaldehyde-d_2 was then developed when it was found that the methylene-d_2 halides would react with silver acetate or potassium acetate under anhydrous conditions to yield methylene-d_2 diacetate in 60-65% yields. The optimum conditions involved the reaction of 3–4 moles of potassium acetate with one mole of halide in refluxing acetic acid containing 5% of acetic anhydride. Methylene-d_2 bromide is preferred over the iodide because if any of the latter is left unreacted it is difficult to separate from methylene-d_2 diacetate. Methylene-d_2 diacetate is easily and rapidly hydrolyzed to formaldehyde-d_2 in over 80% yield. The formaldehyde solution thus obtained is very concentrated and contains only volatile materials, so that upon evaporation to dryness, pure polymeric formaldehyde-d_2 is readily obtained.

A very careful check on the deuterium content of the intermediate methylene-d_2 diacetate and

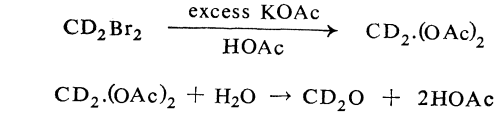

the formaldehyde-d_2 showed that the latter had the same isotopic purity as the starting deuterated methylene halide. Thus, no back-exchange occurs in either of the hydrolytic steps.

Appendix

Several other much less successful approaches to the preparation of deuterated formaldehyde were investigated at some length and are included for the sake of completeness.

Leitch (11) has prepared acetaldehyde-1-d_1 from nitroethane-1,1-d_2 by hydrolysis of the sodium salt. When this reaction, or the modification introduced by Schechter and Williams (12) was applied to nitromethane, little if any formaldehyde was produced. Since this reaction would have led to an aqueous solution of formaldehyde-d_2 containing large amounts of inorganic salts, it was not investigated further.

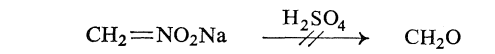

Dimethyl sulfoxide is known to react with electrophilic reagents to yield derivatives which can be hydrolyzed to formaldehyde (13). We have investigated the reaction of dimethyl-d_6-sulfoxide with hydrogen chloride gas in a hot benzene solution. With the protio compound, formaldehyde sublimed out of the reaction mixture in 45% yield, but from dimethyl-d_6-sulfoxide less than 10% yield of formaldehyde-d_2 resulted, the major product being dimethyl-d_6 sulfide.

The nature of the reduction reaction was not further investigated,[4] but it provides an interesting example of how an isotope effect may influence a multi-directional reaction when a C—H or C—D bond must be broken in one of the reaction paths.

A Polonovsky-type reaction between acetic anhydride and dimethyl-d_6-sulfoxide led to α-acetoxy dimethylsulfide-d_5 in 80% yield, hydrolysis of which led to formaldehyde-d_2 in less than 25% yield. The low yield was found to be due to the formation of the very stable dimethyl-d_6-

[3]*Note added in proof*: The trapping of dihalomethyl lithium species with carbonyl compounds has recently been reported (15).

[4]The reduction of sulfoxides to sulfides by iodide ion is a well-known reaction, see ref. 14.

Can. J. Chem. Downloaded from www.nrcresearchpress.com by 210.87.254.40 on 09/05/12
For personal use only.

thioacetal of the aldehyde. This approach was abandoned because of the low yield and the presence of sulfur impurities in the formaldehyde-d_2 which were difficult to remove.

$$CD_3 \cdot SO \cdot CD_3 + Ac_2O \rightarrow CD_3 \cdot S \cdot CD_2 \cdot OAc + DOAc$$

$$2CD_3 \cdot S \cdot CD_2 \cdot OAc + H_2O \rightarrow CD_2O + (CD_3 \cdot S)_2 \cdot CD_2 + 2HOAc$$

Experimental

Nuclear magnetic resonance (n.m.r.) spectra were run on a Varian A60-A instrument and mass spectra were performed by the Morgan-Schaeffer Corporation, Montreal, Quebec.

Methylene-d_2 Bromide

A heterogeneous mixture of 500 g of methylene bromide and 210 g of a 10% solution of sodium deuteroxide in deuterium oxide was stirred and refluxed for 24 h. The organic layer was separated and further exchanged with successively decreasing amounts of 10% sodium deuteroxide (160, 150, 130, 100, 100, and 100 g). The organic layer was finally distilled through a short Vigreux column. A water–methylene-d_2 bromide azeotrope was first collected, followed by the bulk of the dry methylene-d_2 bromide. The azeotropic mixture was dried by passage over phosphorous pentoxide on a vacuum line and combined with the dry material from the distillation, to give a yield of 319 g (63%). Nuclear magnetic resonance and mass spectral analyses showed the methylene-d_2 bromide to contain 99 atom % D.

Methylene-d_2 Diacetate

To a mechanically stirred solution of methylene-d_2 bromide (176 g, 1.0 moles) in 600 ml glacial acetic acid containing 30 g of acetic anhydride was added potassium acetate (294 g, 3.0 moles) at such a rate as not to prevent stirring. On heating the mixture to reflux, all of the potassium acetate dissolved and after 1 h potassium bromide began to crystallize from the solution. Stirring and refluxing was continued for 24 h, after which time the solution was allowed to cool with continued stirring in order to avoid cake formation. To the cooled reaction mixture was added 1500 ml of ether, and the precipitate was filtered off and washed with ether until no odor of acetic acid remained.[5]

The filtrate and washings were combined and distilled at atmospheric pressure to remove the ether and the bulk of the acetic acid. If more solid was seen to crystallize at this point, the dilution with ether and filtration were repeated. If not, the distillation was continued at 12 mm pressure and, after removal of acetic acid and acetic anhydride, a fraction was collected at 61–63 °C to yield 83 g (0.62 moles, 62%) of methylene-d_2 diacetate. The deuterium content of the methylene group was found by n.m.r. analysis to be 99%.

Formaldehyde-d_2

A mixture of methylene-d_2 diacetate (240 g, 1.79 moles), 45 ml of water, and 5 ml of concentrated hydrochloric acid was refluxed for 17 h. Upon cooling of the solution, some polymeric formaldehyde-d_2 crystallized out and was filtered off. The filtrate was taken to dryness in vacuum to leave the bulk of the product as a white solid. A second distillation of the solvent mixture was necessary to recover all of the product. The combined crops of formaldehyde-d_2 were dried at 0.5 mm and 100 °C in order to remove the last traces of acetic acid and gave a yield of 49.4 g (1.54 moles, 86%); m.p. 172–174 °C, which corresponds to that of α-polyoxymethylene (ref. 3 p. 158).

The dimedone derivative had a m.p. 188–190 °C and mixture m.p. of 188–189 °C.

Analysis of Formaldehyde-d_2

A mixture of polymeric formaldehyde-d_2 (0.50 g, 15.6 mmoles), methanethiol (10 g, 208 mmoles), and ether (15 ml) was stirred for 18 h in a stoppered flask. After removal of the volatile materials, formaldehyde-d_2 dimethylthioacetal was distilled at 38–40 °C/5 mm in a yield of 1.2 g (10.9 mmoles, 70%). Nuclear magnetic resonance analysis showed the methylene group to contain 98.5 atom % D.

[5]This operation must be carried out as quickly as possible to minimize exposure since methylene diacetate reacts very rapidly with atmospheric moisture with a resulting lowering of yield.

Acknowledgments

We thank Mr. S. C. Ho of our Analytical Department and Professor Jean-Claude Richer of the University of Montreal for the nuclear magnetic resonance spectra. This work was supported by an Industrial Research Grant from the National Research Council of Canada.

1. J. G. Atkinson, J. J. Csakvary, G. T. Herbert, and R. S. Stuart. J. Am. Chem. Soc. **90**, 498 (1968).
2. T. C. Jones and E. R. Thornton. J. Am. Chem. Soc. **89**, 4863 (1967); J. G. Atkinson, M. H. Fisher, D. Horley, A. T. Morse, R. S. Stuart, and E. Synnes. Can. J. Chem. **43**, 1614 (1965).
3. J. F. Walker. Formaldehyde. 3rd ed. Reinhold Publishing Corp., New York. 1964.
4. R. A. B. Bannard, A. T. Morse, and L. C. Leitch. Can. J. Chem. **31**, 351 (1953).
5. D. Elwyn, A. Weissbach, S. S. Henry, and D. B. Sprinson. J. Biol. Chem. **213**, 281 (1955).
6. R. A. Olofson and D. M. Zimmerman. J. Am. Chem. Soc. **89**, 5057 (1967).
7. R. N. Renaud and L. C. Leitch. Can. J. Chem. **46**, 385 (1968).
8. E. P. Blanchard and H. E. Simmons. J. Am. Chem. Soc. **86**, 1337 (1964).
9. W. Reeve and C. W. Woods. J. Am. Chem. Soc. **82**, 4062 (1960).
10. A. Winston, R. E. Thomas, and D. E. Battin. J. Org. Chem. **33**, 1011 (1968).
11. L. C. Leitch. Can. J. Chem. **33**, 400 (1955).
12. H. Shechter and F. Williams. J. Org. Chem. **27**, 3699 (1962).
13. C. Agami. Bull. Soc. Chim. France, 1021 (1965); R. Michelot and B. Tchoubar. Bull. Soc. Chim. France, 3039 (1966).
14. R. A. Strecker and K. K. Andersen. J. Org. Chem. **33**, 2234 (1968).
15. G. Köbrich and R. H. Fischer. Chem. Ber. **101**, 3208 (1968).

Can. J. Chem. Downloaded from www.nrcresearchpress.com by 210.87.254.105 on 09/05/12
For personal use only.

Biosynthesis of aristolochic acid[1]

F. Comer, H. P. Tiwari, and I. D. Spenser
Department of Chemistry, McMaster University, Hamilton, Ontario

Received August 12, 1968

The biosynthesis of aristolochic acid-**1** (**1**) was studied in *Aristolochia sipho*. Tyrosine, dopa, dopamine, and noradrenaline serve as specific precursors. The nitro group of aristolochic acid is derived from the amino group of tyrosine. The aristolochic acids are yet another group of natural products related to norlaudanosoline.

Canadian Journal of Chemistry, **47**, 481 (1969)

The aristolochic acids (e.g. **1**), a group of substituted 10-nitro-1-phenanthroic acids, have been found to occur in many species of the genus *Aristolochia* (2–5), as well as in other members of the family Aristolochiaceae (6). A biogenetic relationship between these compounds and the aporphine alkaloids has been suspected on structural grounds (2, 3, 7). An aporphine alkaloid, magnoflorine, does indeed accompany aristolochic acids in various *Aristolochia* species (5, 7).

The biosynthetic derivation of the aporphine skeleton from norlaudanosoline or related benzylisoquinoline precursors is now well established (8–10). The benzylisoquinoline precursors, in turn, originate from tyrosine (e.g. ref. 11).

We have examined the incorporation of tyrosine and of a number of its biochemical relatives into aristolochic acid-**1** (**1**). Our results are consistent with the view that the aristolochic acids arise from aporphines by oxidative cleavage of the hetero ring.

In a series of experiments [β-^{14}C]-DL-tyrosine, [β-^{14}C,^{15}N]-tyrosine, [α-^{14}C]-DL-dihydroxyphenylalanine (dopa), [2-^{14}C]-dihydroxyphenylethylamine (dopamine), and [2-^{14}C]-DL-noradrenaline were administered to plants of *Aristolochia sipho* (Dutchman's pipe) by the wick technique (12). In each experiment aristolochic acid-**1** was extracted from roots and rhizomes of the plants, and was purified to constant activity. The details of these experiments are summarized in Table I. Little, if any, of the desired product was detected in the green parts of the plant.

The labelled samples of aristolochic acid-**1** were diluted with carrier and degraded to locate the sites of activity, by reaction sequences shown in Scheme 1. The specific activities of the degradation products are recorded in Table II.

All activity of the samples of aristolochic acid-**1**, derived from the experiments with [2-^{14}C]-dopamine (Expt. 4) and with [2-^{14}C]-DL-noradrenaline (Expt. 5) was confined to the carboxyl group (**1** minus **2**).

All activity of the aristolochic acid obtained from the plants which had been fed with [α-^{14}C]-dopa (Expt. 3) was located at C-10 (**3** minus **4** minus C_1 units).[2] Attempts to isolate C-10 directly, in the form of bromopicrin, failed. Treatment of aristolochic acid-**1** with bromine, under conditions which give good yields of bromopicrin from simple nitrophenols (13), gave only traces of the desired degradation product.

The samples of aristolochic acid-**1**, derived from the experiments with [β-^{14}C]-tyrosine (Expts. 1 and 2) contained label at more than one site. In each case approximately 70% of the activity was located at the carboxyl group (**1** minus **2**). Since the specific activity of the lactone (**4**) was identical with that of the nitrophenanthrene (**2**), none of the activity was present at C-10, or at the peripheral C_1 units of the aristolochic acid-**1**. Lack of material precluded completion of the final step in the degradation, hydrolysis, and decarboxylation of the lactone, after protection of the phenolic groups. Even so, it can be assumed that the remaining 30% of the activity was located at the carboxyl group, the one remaining extranuclear carbon atom of the lactone, and hence at C-9 of aristolochic acid-**1**,

[1]A preliminary account of part of this work has been published (1).

[2]In many natural products C_1 units in general, and *O*-methyl and methylenedioxy groups in particular, have been shown to be derived from one and the same source, the *S*-methyl group of methionine (11). Since the methylenedioxy carbon was devoid of activity (formaldehyde), it can be inferred that the *O*-methyl group was also inactive.

Can. J. Chem. Downloaded from www.nrcresearchpress.com by 210.87.254.105 on 09/05/12
For personal use only.

TABLE I

Incorporation of labelled compounds into aristolochic acid-**1**

Experiment	Precursor	Specific activity (counts min^{-1} $mmole^{-1}$) ($\times 10^{-9}$)	Total activity fed (counts min^{-1}) ($\times 10^{-7}$)	Product: Weight of dry plant material (g)	Product: Aristolochic acid-**1** Weight (mg)	Product: Aristolochic acid-**1** Specific activity (counts min^{-1} $mmole^{-1}$) ($\times 10^{-4}$)	SRY‡ $\times 10^4$
1	[β-^{14}C]-DL-Tyrosine*	3.08±0.04	4.59±0.06	28	39	2.78±0.04	9.0
2	[β-^{14}C]-DL-Tyrosine*	0.102±0.002	5.11±0.07	76	45	8.17±0.30	800
3	[α-^{14}C]-DL-Dihydroxy-phenylalanine (dopa)†	16.57±0.14	2.65±0.02	30	38	3.21±0.09	1.9
4	[2-^{14}C]-Dihydroxyphenyl-ethylamine (dopamine) hydrochloride†	13.82±0.17	6.34±0.08	38	58	8.55±0.27	6.2
5	[2-^{14}C]-DL-Noradrenaline DL-bitartrate†	4.60±0.07	5.37±0.08	24	40	3.44±0.01	7.5

*Nuclear Chicago Corporation.
†Radiochemical Center.
‡Specific radiochemical yield = 100 (specific activity of product)/(specific activity of precursor).

TABLE II

Degradation of aristolochic acid-**1** derived from labelled precursors

	Precursor: [β-^{14}C]-Tyrosine Expt. 1 SA* counts min^{-1} $mmole^{-1}$ $\times 10^{-3}$	Expt. 1 RSA† %	Expt. 2 SA counts min^{-1} $mmole^{-1}$ $\times 10^{-4}$	Expt. 2 RSA %	[α-^{14}C]-Dopa Expt. 3 SA counts min^{-1} $mmole^{-1}$ $\times 10^{-3}$	Expt. 3 RSA %	[2-^{14}C]-Dopamine Expt. 4 SA counts min^{-1} $mmole^{-1}$ $\times 10^{-3}$	Expt. 4 RSA %	[2-^{14}C]-Noradrenaline Expt. 5 SA counts min^{-1} $mmole^{-1}$ $\times 10^{-3}$	Expt. 5 RSA %
Aristolochic acid-**1** (diluted) (**1**)	3.37±0.09	100±3	2.79±0.06	100±2	3.09±0.09	100±3	6.50±0.17	100±3	9.35±0.32	100±3
Methyl aristolochate-**1**	—		—		—		—		8.80±0.32	94±5
Nitrophenanthrene (**2**)	1.07±0.02	32±1	0.76±0.03	27±1	3.02±0.22	98±8	0.10±0.01	2±0.1	0.17±0.05	2±1
Dicarboxylic acid (**3**)	1.07±0.02	32±1	—		2.73±0.12	88±5	—		—	
Lactone (**4**)	1.07±0.02	32±1	—		0.04±0.17	1±5	—		—	
Formaldehyde (dimedone deriv.)	—		—		Inactive	0	—		—	

*SA = Specific activity.
†RSA = Relative specific activity (diluted aristolochic acid-**1** = 100).

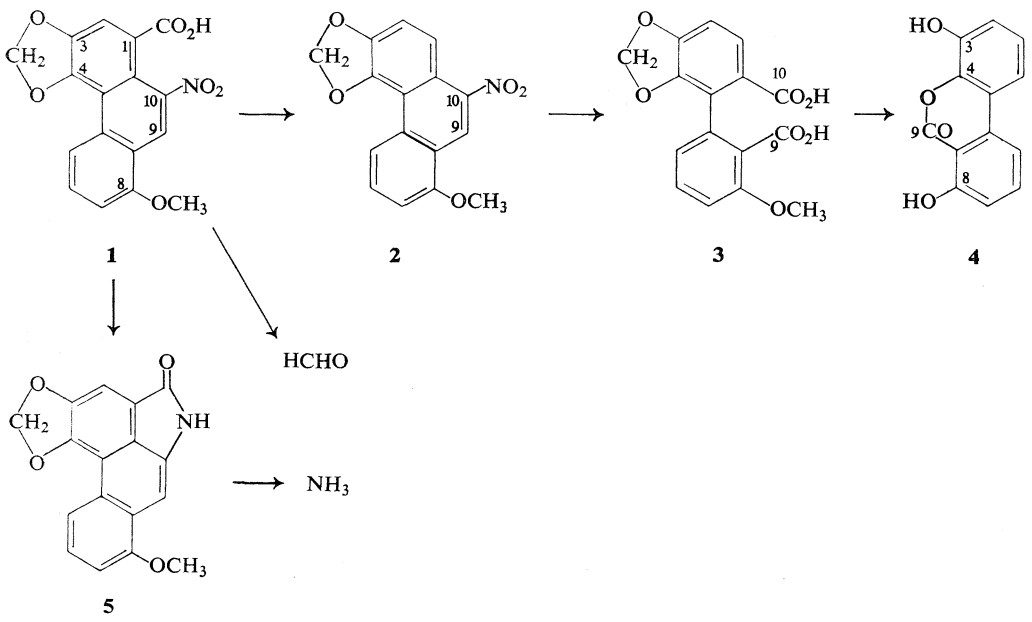

SCHEME 1
Degradation of aristolochic acid–**1**

the predicted site. The absence of activity in the lactone, obtained by degradation of the aristolochic acid-**1** derived from [α-^{14}C]-dopa (Expt. 3), strengthens this inference.

The observed pattern of incorporation of radiocarbon from the labelled samples of tyrosine (**6**), dopa (**7**), and dopamine (**8**) into aristolochic acid-**1** (**1**) corresponds to the distribution which would be predicted if norlaudanosoline (**10**) were an intermediate on the pathway from the administered precursors to the product (cf. Scheme 2). In an independent, concurrent, investigation Schütte, Orban, and Mothes (5) demonstrated that norlaudanosoline (**10**) does indeed serve as a specific precursor of aristolochic acid-**1**.

The evidence is strong that tyrosine supplies both C_6–C_2 units in the skeletons of the many structural variants amongst the alkaloids related to norlaudanosoline (11). It is also well-documented that dopamine supplies only one of these units (11). Dopa has long been regarded as a stage of the pathway. Specific incorporation of dopa into a natural product related to norlaudanosoline is now demonstrated for the first time. A biogenetic sequence from tyrosine to aristolochic acid-**1**, consistent with the results of the tracer experiments, is shown in Scheme 2. Orientaline (**11**), orientalinone (**12**), orientalinol (**13**), and an aporphine (**14**) are shown as hypothetical stages of the postulated pathway, which involves a phenol-oxidation step and a dienol–benzene rearrangement (8, 9).

On the basis of this sequence it would be predicted that the nitro group of aristolochic acid originates from the amino group of tyrosine. The result of a feeding experiment with [β-^{14}C,^{15}N]-tyrosine (Expt. 2) (Tables II and III) provides evidence in support of this view. Aristolochic acid-**1** obtained from this experiment was specifically labelled with ^{14}C (Table II, Expt. 2) and enriched in ^{15}N (Table III).

If an intact C_6–C_2–N unit derived from tyrosine had been incorporated, the ^{15}N/carboxyl-^{14}C ratio of the isolated aristolochic acid (found $(0.69 \pm 0.08) \times 10^{-6}$) should have been identical with the ^{15}N/^{14}C ratio of the L-tyrosine pool of the plant (found $(1.05 \pm 0.04) \times 10^{-6}$) (represented by the re-isolated protein-bound tyrosine). In fact ca. 30% of the ^{15}N relative to ^{14}C had been lost in the course of conversion of tyrosine into aristolochic acid-**1** (Table III). Since the route from tyrosine to the product runs via dopa, an amino acid which is known to undergo reversible transamination in plants (14), this

Can. J. Chem. Downloaded from www.nrcresearchpress.com by 210.87.254.105 on 09/05/12
For personal use only.

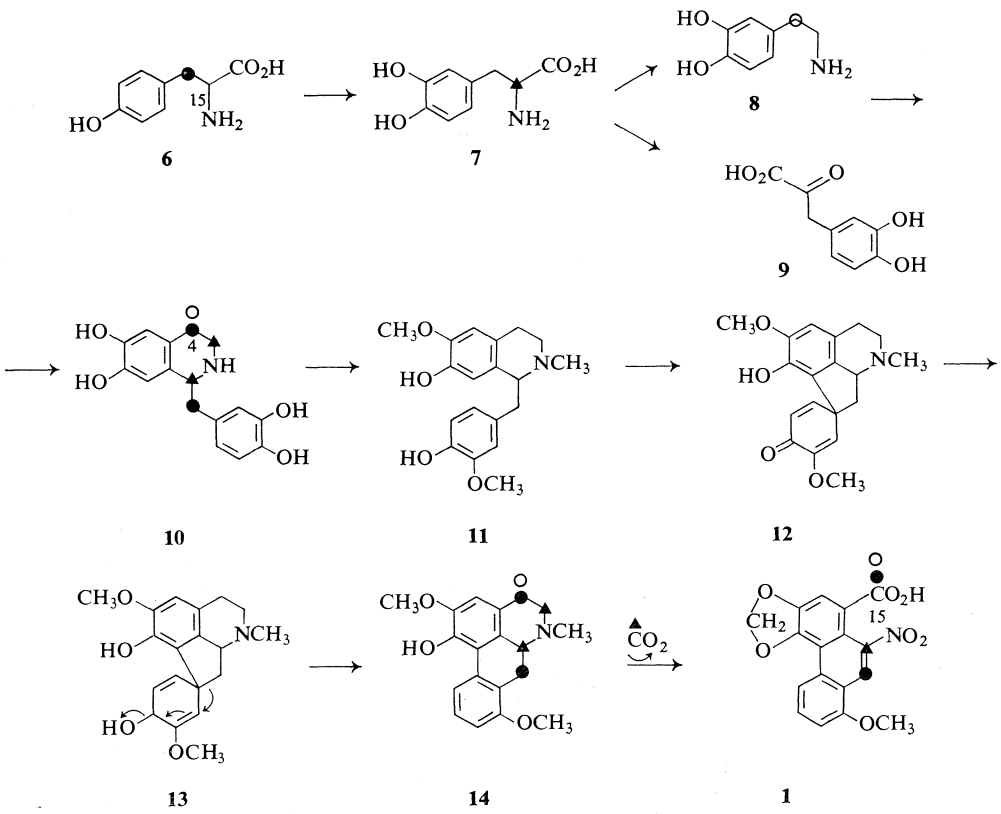

SCHEME 2
Origin of aristolochic acid-**1**

loss is not surprising.[3] It is significant that the ^{15}N enrichment of the amino acids, other than tyrosine, which were isolated from the experimental plants (found 0.011 ± 0.002 atom % excess) was markedly lower than the ^{15}N enrichment of the aristolochic acid (found 0.041 ± 0.005 atom % excess) (Table III).

The outcome of a further experiment is difficult to reconcile with the sequence shown in Scheme 2.

Administration of [2-^{14}C]-noradrenaline to *A. sipho* yielded aristolochic acid-**1**, specifically labelled in the carboxyl group (Expt. 5). If noradrenaline were an obligatory precursor of the acid, Scheme 2 would have to be modified to include 4-hydroxynorlaudanosoline and the correspondingly hydroxylated derivatives of orientaline (**11**) and of the later intermediates (**12–14**). It would be enticing to speculate that it is the presence of a benzylic hydroxyl group which predisposes an aporphine intermediate to oxidative conversion into an aristolochic acid.[4] Since noradrenaline is derived from tyrosine by way of dopa (**7**) and dopamine (**8**), the observed incorporation pattern of these compounds is consistent with this alternative; however, the incorporation of norlaudanosoline is not.

It is tempting to regard the specific incorporation of noradrenaline into aristolochic acid-**1** as evidence for a normal biosynthetic pathway. But incorporation, even though specific, does not constitute proof of an obligatory precursor–product relationship. The specific incorporation (5) of norlaudanosoline into aristolochic acid-**1** lends weight to the possibility that entry of nor-

[3]Comparison of the $^{15}N/^{14}C$ ratios of the administered $((1.66 \pm 0.07) \times 10^{-6}$, see Experimental) and protein-bound $((1.05 \pm 0.04) \times 10^{-6}$, see Table III) L-tyrosine indicates that this amino acid also undergoes transamination within the plant.

[4]Attempts to convert 4-hydroxyanonaine into aristolochic acid-**2** by chemical oxidation have so far been unsuccessful however (15).

Can. J. Chem. Downloaded from www.nrcresearchpress.com by 210.87.254.105 on 09/05/12
For personal use only.

TABLE III

Conversion of [β-^{14}C,^{15}N]-tyrosine into aristolochic acid-**1**

Compounds isolated from experimental plants	Atom % excess ^{15}N above natural abundance	Specific activity (counts $min^{-1}mmole^{-1}$) ($\times 10^{-4}$)	Atom % excess ^{15}N above natural abundance	$^{15}N/^{14}C$ ($\times 10^{6}$)
		After dilution with carrier		
L-Tyrosine (isolated from plant protein)	0.29±0.01	4.46±0.08	0.047±0.002	1.05±0.04
Aristolochic acid-**1**	0.041±0.005	2.03±0.07*	0.014±0.002	0.69±0.08
Amino acids other than tyrosine	0.011±0.002			

*The specific activity shown is that at the carboxyl carbon atom. This was determined as the difference of the specific activities of aristolochic acid-**1** (**1**) (2.79±0.06) × 10^4 counts $min^{-1}mmole^{-1}$ and of the nitrophenanthrene (**2**) (0.76±0.03) × 10^4 counts $min^{-1}mmole^{-1}$ (c.f. Table II, Expt. 2).

adrenaline constitutes an aberrant pathway to a normal tissue component. Noradrenaline has not hitherto been detected in *A. sipho*. If the enzyme which normally catalyzes the condensation of dopamine with the α-keto acid (**9**) lacked absolute specificity, a dopamine analogue not normally present in the plant might be used as a substrate, if forced upon the system, to yield an abnormal intermediate which, in subsequent enzymatic steps of similar non-specificity, might be converted to a normal component.

Further evidence is required to decide whether the observed specific incorporation of noradrenaline into aristolochic acid-**1** in *A. sipho* represents the norm or whether this result was obtained as a consequence of a biochemical uncertainty principle.

Experimental

*Isolation of Aristolochic Acid-**1** (**1**) (16)*

Dried and finely powdered roots and rhizomes of *Aristolochia sipho* (28 g) were wetted with aqueous sulfuric acid (0.5%) and extracted first with petroleum ether and then with dichloromethane. The petroleum ether extract was discarded. The dichloromethane extract was evaporated to dryness and the residue digested with a saturated solution of sodium bicarbonate (10 ml). The mixture was filtered, the filtrate was freed from non-acidic material by extraction with ether, and was then acidified with hydrochloric acid (5%). Aristolochic acid-**1** which precipitated was washed with water, dried, and recrystallized from ethanol. Thin-layer chromatography (t.l.c.) of a sample of this product on alkaline cellulose revealed the presence of a red impurity near the origin of the developed plate. The product was, therefore, further purified by preparative t.l.c. (6) using cellulose plates which had been sprayed with a buffer solution (pH 9.2) consisting of sodium carbonate (0.05 *M*) and sodium bicarbonate (0.05 *M*), and had then been dried at room temperature. Aristolochic acid-**1** was applied in ethanol solution and the plates were developed with water-saturated butanol:dimethylformamide (5:1). Sodium aristolochate was extracted from the cellulose with ethanol. The solvent was evaporated, the residue was suspended in chloroform, and aristolochic acid regenerated by addition of dilute hydrochloric acid. The product was recrystallized from ethanol; yield 48 mg, m.p. 280° (decomp.) (reported m.p. 281–286° (decomp.) (17), 274–278° (decomp.) (18)).

The infrared (17) and ultraviolet (19) spectra of this product agreed with those reported. Decarboxylation of this product (*vide infra*) gave a nitrophenanthrene derivative whose behavior on t.l.c. on alumina (benzene:petroleum ether (30–60°), 1:1) matched that of an authentic sample of 1-methoxy-5,6-methylenedioxy-9-nitrophenanthrene, obtained by decarboxylation of a sample of aristolochic acid-**1**, isolated from *Aristolochia indica* (20).

*Methyl Aristolochate-**1** (17, 18)*

Aristolochic acid-**1** (15 mg) was dissolved in warm dioxane (1 ml). After cooling, diazomethane in ether was added and the mixture allowed to stand 2 h. Solvent was evaporated, the residue dissolved in chloroform (15 ml), and unchanged acid extracted into saturated sodium bicarbonate solution. The chloroform layer was washed with water (5 ml), dried (Na_2SO_4), and concentrated. On addition of hot methanol the ester crystallized as yellow needles (12 mg); m.p. 282° (reported m.p. 281° (17) 280–282° (18)); mass spectrum, molecular ion *m/e* 355. The ester was very sparingly soluble in most solvents. Several attempts to hydrolyze the ester failed to regenerate aristolochic acid-**1** (cf. 17).

*Aristolactam-**1** (5) (20)*

A mixture of aristolochic acid-**1** (95 mg) and zinc dust (300 mg, activated by brief treatment with 2 *N* hydrochloric acid, washed with water, ethanol and ether, and dried at 70° for 2 h) in glacial acetic acid (10 ml) was refluxed gently for 20 min. The solution was filtered and diluted with water to yield the product (80 mg, m.p. 310–315°) as a yellow precipitate. Sublimation at 10^{-3} mm and 240–250° raised the m.p. to 317–318°; reported m.p. 319° (17).

Can. J. Chem. Downloaded from www.nrcresearchpress.com by 210.87.254.105 on 09/05/12
For personal use only.

Can. J. Chem. Downloaded from www.nrcresearchpress.com by 210.87.254.105 on 09/05/12
For personal use only.

1-Methoxy-5,6-methylenedioxy-9-nitrophenanthrene (2) (17, 18)

Aristolochic acid-**1** (**1**) (120 mg) was heated 10 min with copper powder (40 mg) in freshly distilled quinoline (5 ml). After cooling, ether (25 ml) was added and copper was filtered off. The filtrate was washed repeatedly with hydrochloric acid (6 *M*), until the acid extract was no longer colored, and then with aqueous sodium hydroxide (1%), until the alkaline extract was no longer colored. The ether solution was washed with water, dried (Na_2SO_4), and concentrated. The residue was dissolved in chloroform and applied to a column of alumina (grade I) which had been slurried in petroleum ether (30–60°). Elution of the column with petroleum ether (30–60°) – benzene (95:5 v/v) gave a small amount of a low melting impurity. Benzene then eluted a broad yellow band of the desired product. Benzene was evaporated and the residue crystallized from chloroform/ethanol, to yield orange needles of 1-methoxy-5,6-methylenedioxy-9-nitrophenanthrene (65 mg), melting at 212° (reported m.p. 212 (17) 206–212° (18)).

3-Methoxy-5′,6′-methylenedioxybiphenyl-2,2′-dicarboxylic Acid (3) (17)

A mixture consisting of the nitrophenanthrene (**2**) (60 mg) in tetrahydrofuran (15 ml) and aqueous sodium hydroxide (10% w/v, 5 ml) was refluxed very gently with continuous stirring. Hydrogen peroxide (30%, 100 ml) was added dropwise over a period of 6 h, at which time the solution had become colorless. Tetrahydrofuran was distilled off *in vacuo*, the alkaline solution was then boiled 10 min, cooled, washed with ether, acidified with hydrochloric acid, and the product extracted into ether (5 × 10 ml). The combined ether extracts were washed with water, dried (Na_2SO_4), and concentrated. The residue crystallized on addition of chloroform, and was recrystallized from ethanol/chloroform, when the dicarboxylic acid (16 mg) was obtained as colorless plates, m.p. 242° (reported m.p. 243° (17)). A small sample of the product was converted to the dimethyl ester, m.p. 115° (reported m.p. 114° (17)), mass spectrum: molecular ion *m/e* 344.

3,2′,3′-Trihydroxybiphenyl-2-carboxylic Acid Lactone (4) (17)

A mixture of the dicarboxylic acid (**3**) (12 mg) and resorcinol (30 mg) in concentrated hydrochloric acid (1 ml) was heated for 4 h at 130° in a sealed tube. The solution was evaporated to dryness and the residue sublimed at 3×10^{-3} mm. Resorcinol sublimed at 80–90°. The product, which sublimed at 120–125°, was recrystallized from ethanol; yield 3 mg, m.p. 205° (reported m.p. 204° (17)); mass spectrum: molecular ion *m/e* 228.

Hydrolytic Cleavage of the Methylenedioxy Group of Aristolochic Acid-1

A solution of aristolochic acid-**1** (**1**) (15 mg) and dimedone (5,5-dimethyl-1,3-cyclohexanedione) (50 mg) in concentrated hydrochloric acid (1 ml) was heated in a sealed tube at 120–130° for 18 h. The cooled reaction mixture was diluted with water (10 ml) and extracted with ether. The ether extract was washed with sodium bicarbonate solution and with water, and was then dried over sodium sulfate and evaporated. The residue was purified by preparative t.l.c. on silica gel GF_{254} using benzene:ethyl acetate 9:1. The dimedone derivative of formaldehyde was crystallized from aqueous methanol and obtained as white silky needles, melting at 189–190°; yield 4 mg.

Administration of ^{14}C-Labelled Compounds to Aristolochia sipho, and Isolation and Degradation of Radioactive Aristolochic Acid-1

Six two-year-old plants of *A. sipho* were used in each feeding experiment. The labelled tyrosine was dissolved in dilute hydrochloric acid (0.01 *M*, 10 ml), and the labelled samples of dopa, dopamine, and noradrenaline were dissolved in dilute hydrochloric acid (0.01 *M*, 10 ml) containing ascorbic acid (5 mg). In each experiment equal portions of the tracer solution were administered to individual plants by aspiration into the stem through a cotton wick (12). The plants were left in contact with tracer for 3 days. The labelled compounds which were administered to the plants in separate experiments are listed in Table I. In each case aristolochic acid-**1** was isolated from the dried roots and rhizomes of the plants and the samples so obtained were recrystallized to constant activity from ethanol. Chemical and radiochemical yields are shown in Table I.

Each labelled sample of aristolochic acid-**1** was diluted with carrier, and the diluted samples were degraded by the reactions described above. The products were purified to constant activity. The specific activities of the degradation products are recorded in Table II.

Radioactivity was assayed on samples of finite thickness on aluminium planchettes, using a Nuclear Chicago Corp. gas flow counter (model 1052) in a low background sample changer (C115). Counts were recorded on a printing timer (C111B) in association with a scaler (181B). For plating of the samples a 1% solution of collodion in dimethylformamide was used as the solvent. The usual corrections for background and self-absorption were applied. Limits shown in the Tables are the standard deviation of the mean.

Experiment with [β-^{14}C,^{15}N]-Tyrosine

The doubly-labelled tyrosine used in this experiment was a mixture of [β-^{14}C]-DL-tyrosine (2.7 mg, specific activity $(3.43 \pm 0.05) \times 10^9$ counts min^{-1} $mmole^{-1}$, Nuclear Chicago Corporation) and [^{15}N]-L-tyrosine (87.9 mg, 89.7 ± 0.4 atom % excess ^{15}N above natural abundance, Schwarz BioResearch Inc.). This yielded a product with a specific activity of $(1.02 \pm 0.02) \times 10^8$ counts min^{-1} $mmole^{-1}$ and an ^{15}N content of 86.7 ± 0.4 atom % excess ^{15}N above natural abundance, i.e. with an $^{15}N/^{14}C$ ratio $(0.85 \pm 0.01) \times 10^{-6}$.

The mixture was dissolved in 0.01 *M* hydrochloric acid (25 ml). A small sample of this solution (20 μl) was added to a solution of unlabelled L-tyrosine (181 mg) in 0.01 *M* hydrochloric acid. Neutralization gave a precipitate which was recrystallized from water. The specific activity of this diluted tyrosine was $(2.36 \pm 0.05) \times 10^4$ counts min^{-1} $mmole^{-1}$ and the ^{15}N content was 0.0391 ± 0.0016 atom % excess ^{15}N above natural abundance. The specific activity and the $^{15}N/^{14}C$ ratio $(1.66 \pm 0.07) \times 10^{-6}$ of this sample are consistent with the complete loss of [β-^{14}C]-D-tyrosine in the course of dilution and recrystallization of the original sample.

The tracer solution was administered by wick to eleven *A. sipho* plants. The plants were kept in contact with

Can. J. Chem. Downloaded from www.nrcresearchpress.com by 210.87.254.105 on 09/05/12
For personal use only.

tracer for 3 days. The dried roots and rhizomes of the plants (76 g) were extracted with petroleum ether and then with dichloromethane. Aristolochic acid (45 mg) was obtained from the dichloromethane extract, in the manner described above.

The plant material was freed from non-protein amino acids by extraction, first with cold aqueous ethanol (70% v/v) and then with boiling water. Protein-bound tyrosine was then isolated as follows. The plant material was digested by refluxing with 6 *N* hydrochloric acid (500 ml) for 20 h. The solution was filtered and the filtrate neutralized by addition of saturated sodium hydroxide solution. The amino acids were collected on Dowex 50W-X4 (100 g, H^+ form) by keeping the resin, tied in a bag of dialysis tubing ($1\frac{1}{8}$ in. diameter), suspended in the aqueous solution for 2 days. The resin was then transferred into a column, was washed with water, and the amino acids were eluted with 2 *N* ammonia. The eluate was evaporated to dryness *in vacuo*. Quantitative amino acid analysis of this residue showed that it contained 25 mg of tyrosine. L-Tyrosine (50 mg) was added to the residue as carrier, the mixture was dissolved in *N* hydrochloric acid (4 ml), and the solution was filtered and neutralized with *N* sodium hydroxide. Tyrosine (65 mg), which crystallized, was mixed further with carrier L-tyrosine (70 mg), and the sample was redissolved in *N* hydrochloric acid. The solution was lightly charcoaled, filtered, and neutralized, and the product was recrystallized from hot water. The L-tyrosine (87 mg) so obtained was analyzed for ^{15}N and ^{14}C (Table III).

A sample of amino acids other than tyrosine was obtained as follows. The mixture of amino acids from which radioactive tyrosine had been precipitated with carrier L-tyrosine was hydrolyzed further with 6 *N* hydrochloric acid for 20 h. The solution was neutralized by addition of a saturated solution of sodium hydroxide. The amino acids were collected on a Dowex 50W-X4 column (55 g, H^+ form) and eluted with 2 *N* ammonium hydroxide. The eluate was evaporated to dryness and a solution of barium hydroxide was then added. The solution was distilled to remove any ammonia, and barium ions were then removed by precipitation of barium carbonate with carbon dioxide. The solution was filtered and charcoaled three times to remove any tyrosine. The solution was evaporated to dryness to give a residue shown to be devoid of tyrosine by amino acid analysis. This mixture of amino acids was analyzed for ^{15}N.

Assay of [^{15}N]-Labelled Compounds

The ^{15}N content of the [^{15}N]-labelled compounds was determined mass spectrometrically on nitrogen gas samples prepared by oxidation of the ammonia formed by Kjeldahl digestion (21, 22). The sample of aristolochic acid-**1**, obtained from plants to which [β-^{14}C,^{15}N]-labelled tyrosine had been administered, was reduced to aristolactam-**1** (**5**) (*vide supra*) prior to digestion. The ^{15}N-content of the nitrogen gas samples obtained from aristolactam-**1**, from the doubly-labelled tyrosine and the sample of amino acids other than tyrosine, isolated from the plants to which [β-^{14}C,^{15}N]-tyrosine had been administered, and from the doubly-labelled L-tyrosine, obtained from the original tracer solution by carrier dilution and recrystallization, was measured by double collection and balancing of the signals from the ions of mass 28 and 29 by the null method (23). The ^{15}N-content of the nitrogen gas samples derived from the precursor ^{15}N-L-tyrosine was measured, conventionally, by repeated scanning of the signals from mass 28 and 29 and normalization to the line standard. In every case ^{15}N analysis was carried out on duplicate samples and sufficient material was digested to yield 1–2 ml nitrogen gas (at N.T.P.) from each sample.

Acknowledgments

Mass spectrometric measurements were carried out by Mr. J. Monster, Department of Chemistry, and amino acid analyses by Mr. M. Abdulla, Department of Biochemistry, McMaster University. This work was supported by a grant from the National Research Council of Canada.

1. I. D. Spenser and H. P. Tiwari. Chem. Commun. 55 (1966).
2. M. Pailer. Fortschr. Chem. Org. Naturstoffe, **18**, 66 (1960).
3. H.-G. Boit. Ergebnisse der Alkaloid-Chemie bis 1960. Akademie-Verlag, Berlin. 1961. p. 270.
4. M. Pailer, P. Bergthaller, and G. Schaden. Monatsh. Chem. **96**, 863 (1965).
5. H. R. Schütte, U. Orban, and K. Mothes. European J. Biochem. **1**, 70 (1967).
6. R. W. Doskotch and P. W. Vanevenhoven. Lloydia, **30**, 141 (1967).
7. M. Pailer and G. Pruckmayr. Monatsh. Chem. **90**, 145 (1959).
8. A. R. Battersby, R. T. Brown, J. H. Clements, and G. G. Iverach. Chem. Commun. 230 (1965).
9. A. R. Battersby and T. H. Brown. Chem. Commun. 170 (1966).
10. D. H. R. Barton, D. S. Bhakuni, G. M. Chapman, and G. W. Kirby. Chem. Commun. 259 (1966); J. Chem. Soc. C, 2134 (1967).
11. I. D. Spenser. Lloydia, **29**, 71 (1966).
12. J. R. Gear and I. D. Spenser. Can. J. Chem. **41**, 783 (1963).
13. A. J. Birch, C. J. Moye, R. W. Rickards, and Z. Vanek. J. Chem. Soc. 3586 (1962).
14. A. Jindra, P. Kovács, Z. Pitnerová, and M. Pšenák. Phytochemistry, **5**, 1303 (1966).
15. D. R. Dalton, S. I. Miller, and C. K. Crelling. 5th Intern. Symp. Chem. Nat. Prod. London. 1968. Abstracts G21. p. 422.
16. W. Schunack, E. Mutschler, and H. Rochelmeyer. Pharmazie, **20**, 685 (1965).
17. M. Pailer, L. Belohlav, and E. Simonitsch. Monatsh. Chem. **87**, 249 (1956).
18. H. Rosenmund and T. Reichstein. Pharm. Acta Helv. **18**, 243 (1943).
19. M. Pailer and A. Schleppnik. Monatsh. Chem. **88**, 367 (1957).
20. S. M. Kupchan and R. W. Doskotch. J. Med. Pharm. Chem. **5**, 657 (1962).
21. D. Rittenberg. *In* Preparation and measurement of isotopic tracers. J. W. Edwards. Ann Arbor, Michigan. 1946. p. 31.
22. G. Ayrey, A. N. Bourns, and V. A. Vyas. Can. J. Chem. **41**, 1759 (1963).
23. R. K. Wanless and H. G. Thode. J. Sci. Instr. **30**, 395 (1953).

Can. J. Chem. Downloaded from www.nrcresearchpress.com by 210.87.254.40 on 09/05/12
For personal use only.

Diethyl malonate as leaving group: Facile synthesis of some 1,3,4-benzotriazepines and benzotriazepinones

C. Podesva, G. Kohan, and K. Vagi
Delmar Chemicals Limited, Lasalle, Quebec

Received August 16, 1968

Reaction between 2-(2′,2′-bis-carboethoxyvinylamino)-benzophenones, resulting from the condensation of 2-aminobenzophenones with diethyl ethoxymethylenemalonate, and hydrazine hydrate yields 5-hydroxy-5-phenyl-1,3,4-3*H*-4,5-dihydrobenzotriazepines or their double bond isomers. These products on acetylation afford *O*,*N*,*N*-triacetates, which on treatment with ammonia are transformed into 4-phenylquinazolines. Structure proof of these substances is reported.

Canadian Journal of Chemistry, **47**, 489 (1969)

When diethyl ethoxymethylenemalonate was heated together with 2-amino-5-chlorobenzophenone, the expected 2-(2′,2′-bis-carboethoxyvinylamino)-5-chlorobenzophenone (**1**) was readily formed. Other 2-aminobenzophenones as well as methyl anthranilate and methyl 5-chloroanthranilate reacted in the same manner. The infrared (i.r.) spectra of these substances were in good agreement with the assigned structures, exhibiting α,β-unsaturated ester absorptions at 1680 cm^{-1} together with the benzophenone carbonyl absorption at 1640 cm^{-1}. The reaction products are summarized in Table I.

When **1** was allowed to react with hydrazine hydrate in methanolic solution at room temperature, a high yield of a crystalline material could be isolated whose elemental analysis corresponded to a formula of $C_{14}H_{12}ClN_3O$. Obviously, this substance must have been formed from the starting material by the elimination of the diethyl malonate moiety and by the addition of one molecule of hydrazine. Its i.r. spectra (KBr) exhibited a sharp peak at 3325 cm^{-1}, a peak of medium intensity at 2780 cm^{-1} together with a weaker peak at 2600 cm^{-1}, thus disclosing very strong hydrogen bonding (1, 2), plus a strong peak at 1640 cm^{-1}. On acetylation of this product with acetic anhydride in pyridine an *O*,*N*,*N*-triacetate was formed (ν_{max} (KBr) 1730, 1665, and 1645 cm^{-1}), which on controlled alkaline hydrolysis afforded an *N*,*N*-diacetate having a free hydroxyl (ν_{max} (KBr) 3230, 1670, and 1620 cm^{-1}). In the light of this, the i.r. absorption at 1640 cm^{-1} in the original product must be assigned to a C=N grouping rather than a C=O.

From the presence of the C=N and OH together with three N atoms in the molecule and in view of the nature of starting material it was concluded that the initial product had to possess a 1,3,4-benzotriazepine skeleton. The hydroxyl group could be attached either to C-5 and the position of the double bond then would be as shown in structure **7** or between C-2 and N-3, or to C-2 with the double bond between N-4 and C-5.

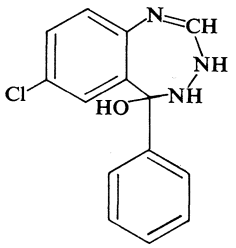

7

The position of attachment of the hydroxyl was established in a somewhat unexpected way. On attempted selective saponification of the ester function in the above mentioned *O*,*N*,*N*-triacetate with aqueous methanolic ammonia, a high yield of a crystalline substance was isolated which was identified as 4-phenyl-6-chloroquinazoline (**8**) by comparison of physical properties and i.r. spectra

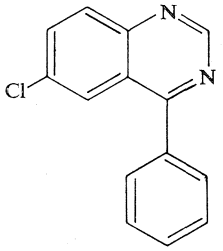

8

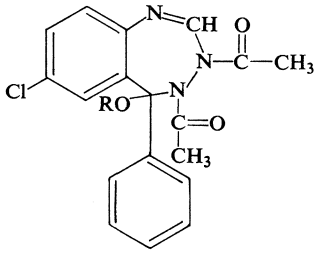

9, R = Ac
10, R = H

Can. J. Chem. Downloaded from www.nrcresearchpress.com by 210.87.254.40 on 09/05/12
For personal use only.

TABLE I

Compound*	R_1	R_2	Yield, %	Melting point (°C)	Solvent†	Formula	C (%) Calcd.	C (%) Found	H (%) Calcd.	H (%) Found	N (%) Calcd.	N (%) Found
1	Cl	Ph	77	135–137	*a*	$C_{21}H_{20}ClNO_5$‡	62.76	62.72	5.01	4.75	3.48	3.82
2	H	Ph	72	105–107	*b*	$C_{21}H_{21}NO_5$	68.65	68.75	5.76	5.67	3.81	4.03
3	Cl	2-Cl Ph	50	180–182	*a*	$C_{21}H_{19}Cl_2NO_5$§	57.81	58.03	4.38	4.53	3.20	3.43
4	NO_2	Ph	92	172–174	*a*	$C_{21}H_{20}N_2O_7$	61.15	61.07	4.88	4.87	6.79	7.05
5	H	OCH_3	78	71–72	*c*	$C_{16}H_{19}NO_6$	59.80	59.70	5.96	6.30	4.36	4.11
6	Cl	OCH_3	83	95	*d*	$C_{16}H_{18}ClNO_6$‖	54.01	54.26	5.10	5.22	3.94	3.82

*General formula:

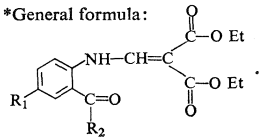

†Solvents: *a*, methanol; *b*, ethanol; *c*, hexane; *d*, aqueous methanol.
‡Anal. Calcd.: Cl, 8.82; Found: Cl, 8.79.
§Anal. Calcd.: Cl, 16.25; Found: Cl, 16.37.
‖Anal. Calcd.: Cl, 9.97; Found: Cl, 10.17.

TABLE II

5-Hydroxy-5-phenyl-1,3,4-3*H*-4,5-dihydrobenzotriazepines*

Compound	R_1	R_2	Yield, %	Melting point (°C)	Solvent†	Formula	C (%) Calcd.	C (%) Found	H (%) Calcd.	H (%) Found	N (%) Calcd.	N (%) Found
7	Cl	Ph	90	198–200‖	*a*	$C_{14}H_{12}ClN_3O$‡	61.43	61.59	4.42	4.73	15.34	15.24
11	H	Ph	88	179–181	*b*	$C_{14}H_{13}N_3O$	70.27	69.99	5.47	5.60	17.50	17.82
12	Cl	2-Cl Ph	75	200	*a*	$C_{14}H_{11}Cl_2N_3O$§	54.56	54.94	3.59	3.88	13.63	13.88
13	NO_2	Ph	86	190–191	*b*	$C_{14}H_{12}N_4O_3$	59.14	59.29	4.25	4.40	19.71	19.96

*General formula:

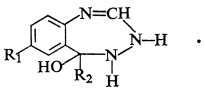

†Solvents: *a*, dimethyl formamide – water; *b*, methanol.
‡Anal. Calcd.: Cl, 12.95; Found: Cl, 13.16.
§Anal. Calcd.: Cl, 23.03; Found: Cl, 23.33.
‖Sometimes a different crystalline form having a m.p. of 185–187°, but having the same i.r. spectrum was obtained.

with a sample prepared by an independent synthesis.

The same product was also obtained when the diester **1** was subjected to a similar treatment using methanolic ammonia, and also when the *N,N*-diacetate was kept for some time in aqueous methanolic ammonia solution in presence of catalytic amount of triethylamine. (It is noteworthy, that whereas in the case of the triacetate the reaction was completed in about 30 min, the uncatalyzed reaction with the *N,N*-diacetate proceeded very slowly. A likely explanation is, that in the first case the liberated electron pair on the alcoholic oxygen immediately became involved in the transfer shown in the postulated mechanism (*vide infra*), whereas once protonated a stronger base than ammonia was needed to produce the necessary anion). On the other hand, when the non-acetylated material was treated with aqueous methanolic ammonia under the same conditions, the starting material was recovered unchanged, thus showing that in order for elimination to occur the hydrazine portion had to be acetylated. A plausible mechanism for the formation of **8** from the triacetate formulated as **9** can be represented as follows:

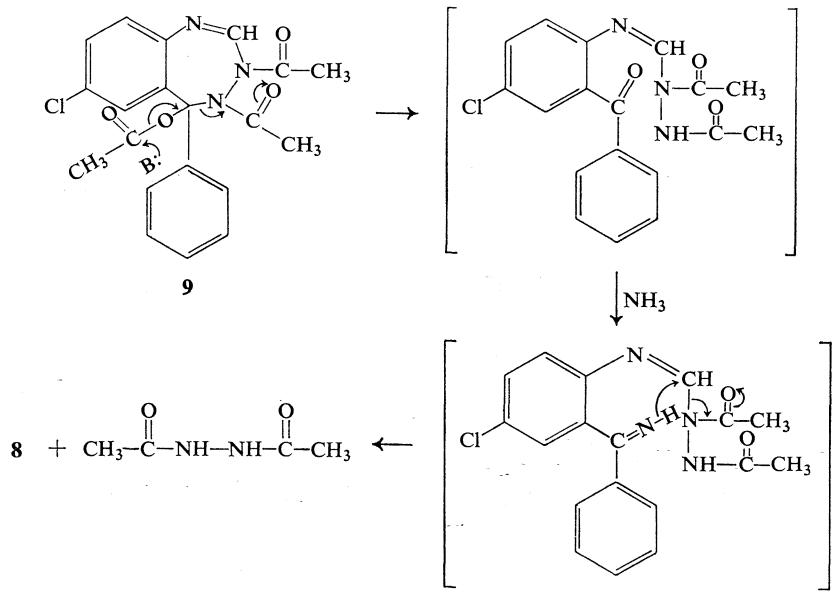

9

It can be seen, that the above mechanism postulates elimination of hydrazine in the form of a symmetrical diacetate. On the other hand, if a similar elimination is considered for the diacetylated 2-hydroxy isomer, an unlikely ammonolysis of an *N*-acetyl would be anticipated and hydrazine would have to be eliminated in the form of a monoacetate. As we were able, however, to isolate from the reaction mother liquors a high yield of 1,2-diacetylhydrazine, identified by comparison of its physical properties and i.r. spectra with a sample prepared by an independent synthesis, the correctness of the above mechanism is rigorously proved and at the same time the sites of the acetylation as well as the position of the double bond in the acetates clearly established, as shown in structures **9** and **10**. Consequently, for the nonacetylated product, structure **7** would appear to be the most likely one. As, however, a double bond migration might have taken place during the acetylation, a double bond isomer of **7** cannot be excluded. Attempts to solve this question by nuclear magnetic resonance (n.m.r.) spectra were frustrated by insufficient solubility of this substance in deuterated solvents.

When compounds **2**–**4** listed in Table I, were brought in contact with hydrazine hydrate under the same conditions as **1**, they afforded readily the corresponding 1,3,4-benzotriazepines listed in Table II. Similarly compounds **5** and **6**, when allowed to react with hydrazine hydrate, yielded the corresponding 1,3,4-benzotriazepine-5-ones

Can. J. Chem. Downloaded from www.nrcresearchpress.com by 210.87.254.40 on 09/05/12
For personal use only.

14 and **15**. (We placed the double bonds in **14** and **15** between N-1 and C-2 by analogy with the benzotriazepines listed in Table II, nevertheless, we do not have any rigorous proof for this assignment. Ultraviolet spectra proved to be of little value due to the lack of appropriate models).

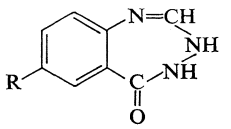

14, R = H
15, R = Cl

The reaction mechanism by which 1,3,4-3*H*-4,5-dihydrobenzotriazepines are formed from the appropriate 2-(2′,2′-bis-carbethoxyvinylamino)-benzophenones and hydrazine hydrate is readily conceivable and can be represented as follows:

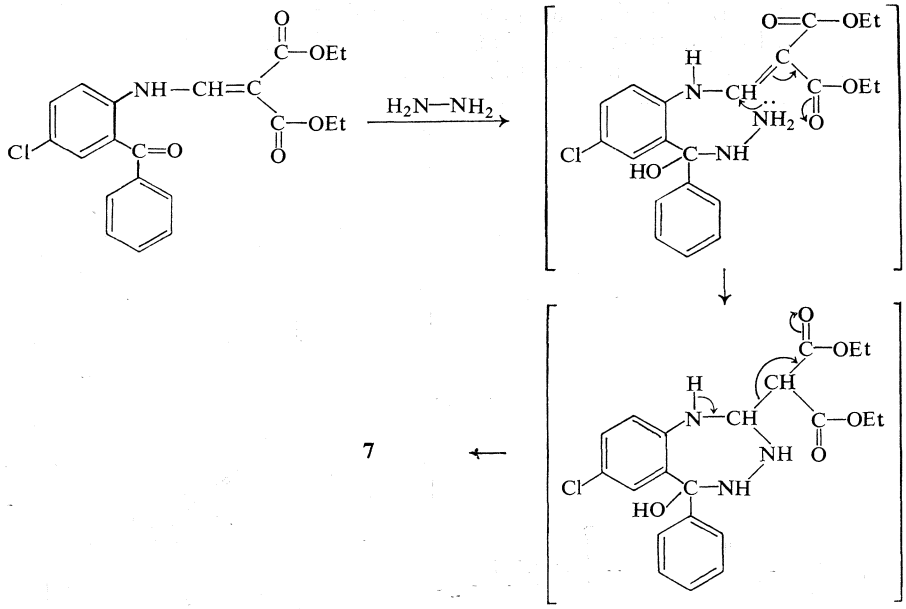

7

Because the above reactions were carried out using an excess of hydrazine hydrate, the question arose as to whether the leaving group is indeed diethyl malonate or rather pyrazolidine-3,5-dione resulting from the hydrazinolysis of the diester. For that reason the reaction was repeated using only one mole equivalent of hydrazine hydrate. Isolation of about the same yield of the benzotriazepine as in the previous experiments clearly showed that the leaving group is indeed the diethyl malonate.

The general applicability of the above described method for introduction of a =CH— group between two nitrogens was further tested by treating 1-amino-3-chlorobenzene-4,6-disulfonamide **16** with diethylethoxymethylenemalonate. The expected 6-chloro-7-sulfamyl-1,2,4-benzothiadiazine-1,1-dioxide **17**, identified by comparison of physical properties and i.r. spectra with an authentic sample prepared by independent synthesis was obtained in high yield. The above described method has therefore a wide applicability and constitutes a method of choice whenever the use of formic acid, ethyl orthoformate etc. is excluded for one reason or other.

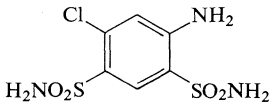

16

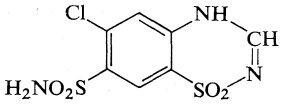

17

Experimental

The i.r. spectra were taken on Perkin–Elmer 237 and 237B instruments. The melting points were determined in capillaries on a Mel-Temp apparatus and are uncorrected. Microanalyses were performed by Dr. C. Daessle, Organic Microanalysis, Montreal.

Can. J. Chem. Downloaded from www.nrcresearchpress.com by 210.87.254.40 on 09/05/12
For personal use only.

Can. J. Chem. Downloaded from www.nrcresearchpress.com by 210.87.254.40 on 09/05/12
For personal use only.

Condensation of Diethyl Ethoxymethylenemalonate with 2-Aminobenzophenones and Anthranilic Esters

General Procedure

A mixture of approximately equal weights of the appropriate amine and diethyl ethoxymethylenemalonate was kept at a temperature of about 110° (140° in case of anthranilic esters) for 30 min. After cooling to about 80° the reaction mixture was diluted with some ethanol and the reaction product was allowed to crystallize in an ice box overnight. The crystalline material was collected by filtration and recrystallized from the appropriate solvent.

Synthesis of 5-Hydroxy-5-phenyl-1,3,4-3H-4,5-dihydrobenzotriazepines

General Procedure

An approximately 10% ethanolic solution of the diester was stirred at room temperature overnight in presence of 1–3 mole equivalents of hydrazine hydrate. The crystalline reaction product was collected by filtration, washed with water, and recrystallized from the appropriate solvent.

*1,3,4-3H-4,5-Dihydrobenzotriazepine-5-one (**14**)*

A solution of **5** (2 g) in ethanol (10 ml) was left standing at room temperature for 4 days in presence of 100% hydrazine hydrate (1 g). The crystalline precipitate was collected by filtration, washed with some ethanol (0.94 g, 94%), and recrystallized for analysis from isopropanol, m.p. 214–215°.

Anal. Calcd. for $C_8H_7N_3O$: C, 59.61; H, 4.38; N, 26.07. Found: C, 59.74; H, 4.51; N, 25.84.

*7-Chloro-1,3,4-3H-4,5-dihydrobenzotriazepine-5-one (**15**)*

A solution of **6** (7.1 g) in ethanol (50 ml) containing 100% hydrazine hydrate (3 g) was allowed to stand at room temperature for overnight. The crystalline precipitate was collected by filtration (3 g, 77%), washed with some ethanol, and recrystallized for analysis from chloroform – methanol mixture, m.p. 230–232°.

Anal. Calcd. for $C_8H_6Cl\ N_3O$: C, 49.11; H, 3.09; Cl, 18.13; N, 21.48. Found: C, 49.00; H, 2.84; Cl, 18.31; N, 21.43.

Acetylation of 7

A mixture of **7** (54.7 g, 0.2 mole), acetic anhydride (122.4 g, 1.2 mole), and dry pyridine (170 ml) was allowed to stand at room temperature for 48 h. The reaction mixture was evaporated to dryness *in vacuo* and water was added to the residue. The reaction product was extracted into 2 × 150 ml of chloroform and the solution washed first with 5% HCl, then with 15% aqueous solution of $NaHCO_3$, and eventually with water. The solvent was removed *in vacuo* and the residue crystallized first from ethanol, then from methanol. The yield of **9** was 42 g (52.5%), m.p. 103–104°.

Anal. Calcd. for $C_{20}H_{18}Cl\ N_3O_4$: C, 60.07; H, 4.53; Cl, 8.86; N, 10.50. Found: C, 60.15; H, 4.72; Cl, 9.05; N, 10.68.

Saponification of 9

To a solution of **9** (8 g, 0.02 mole) in methanol (20 ml), previously warmed to about 45°, was added alcoholic KOH till a pH of about 10 was reached. After allowing the warm solution to stand for about 30 min, cold water (300 ml) was added; the precipitated solid was collected by filtration, washed with water, and dried at 60° (6 g, 85.7%). The analytically pure **10**, m.p. 170–172°, was prepared by crystallization from tetrahydrofuran – ether mixture.

Anal. Calcd. for $C_{18}H_{16}Cl\ N_3O_3$: C, 60.42; H, 4.51; Cl, 9.91; N, 11.74. Found: C, 60.61; H, 4.55; Cl, 10.07; N, 11.91.

*4-Phenyl-6-chloroquinazoline (**8**)*

Method a

To a solution of **9** (18 g, 0.0045 mole) in methanol (50 ml) was added aqueous NH_3 till a pH of 9.5 was reached. After standing for 30 min at a temperature of about 30°, the reaction mixture was cooled to 0° and the precipitated **8** (9.72 g, 90%) was collected by filtration and purified by crystallization from methanol, m.p. 137–139°.

Anal. Calcd. for $C_{14}H_9Cl\ N_2$: C, 69.89; H, 3.77; Cl, 14.74; N, 11.64. Found: C, 70.10; H, 3.94; Cl, 15.04; N, 11.59.

This product was found identical by comparison of physical properties and i.r. spectra with the product obtained by a method described by Palazzo for the preparation of 4-phenylquinazoline (3), using 2-amino-5-chlorobenzophenone instead of 2-aminobenzophenone. The filtrate from the above experiment was evaporated to dryness *in vacuo* and the residue (4 g, 80%) was recrystallized from methanol, m.p. 138–139°. It was found identical with 1,2-diacetylhydrazine prepared by the method of Stollé (4), by comparison of physical properties and i.r. spectra.

Method b

A solution of **1** (2 g, 0.005 mole) in anhydrous methanol (150 ml) previously cooled in an ice bath was saturated with NH_3 gas. After standing at room temperature over the weekend, the reaction mixture was concentrated to a small volume under reduced pressure and the crystalline precipitate was collected by filtration (0.6 g, 50%) and recrystallized from methanol, m.p. 137–139°, undepressed on admixture of the product obtained by Method *a*. Infrared spectra of these two products were superimposable.

Method c

A solution of **10** (0.7 g, 0.00195 mole) in a mixture of methanol (70 ml) and water (20 ml) containing a few drops of triethylamine was saturated with HN_3 gas and allowed to stand at room temperature overnight. The reaction mixture was concentrated to a small volume under reduced pressure, diluted with water, and the reaction product was extracted into chloroform. The solution was evaporated to dryness *in vacuo* and the residue treated with a small amount of methanol. The crystalline reaction product was collected by filtration (0.15 g, 31%) and identified as **8** by m.p., mixture m.p., and by comparison of i.r. spectra.

When the above experiment was carried out in absence of triethylamine, most of the starting material was recovered even after 48 h standing.

*6-Chloro-7-sulfamyl-1,2,4-benzothiadiazine-1,1-dioxide (**17**)*

A mixture of **16** (5.4 g, 0.02 mole) and diethyl ethoxymethylenemalonate (4.32 g, 0.02 mole) was heated to 210° for 10 min. After cooling the solid product was triturated with methanol, collected by filtration, and purified by recrystallization from methanol – ethyl acetate mixture. The yield was 3 g (51%), m.p. 343°, undepressed

on admixture of a sample prepared by a previously described method (5). The i.r. spectra of these two products were superimposable.

Acknowledgments

Skillful technical assistance was provided by Miss Anna Nagy and Mr. Peter Pipasts.

1. A. FOLDES and C. SANDORFY. J. Mol. Spectry. **20**, 262 (1966).
2. H. ZIMMERMAN. Z. Elektrochem. **65**, 821 (1961).
3. S. PALAZZO. Boll. sedute accad. Gioenia sci. nat. Catania, **71**, No. 227, 75 (1959); Chem. Abstr. **55**, 12412*i* (1961).
4. R. STOLLÉ. Ber. **32**, 796 (1899).
5. F. C. NOVELLO. U. S. Patent No. 2,809,194 to Merck and Co., Inc., Rahway, New Jersey. (1957).

Can. J. Chem. Downloaded from www.nrcresearchpress.com by 210.87.254.40 on 09/05/12
For personal use only.

Can. J. Chem. Downloaded from www.nrcresearchpress.com by 210.87.254.42 on 09/05/12
For personal use only.

Conversion of uridine 2′,3′-carbonates to anhydrouridines

K. K. OGILVIE AND D. IWACHA[1]
Department of Chemistry, University of Manitoba, Winnipeg, Manitoba

Received September 25, 1968

Uridine 2′,3′-carbonates are readily converted to 2,2′-anhydrouridines in hot dimethyl formamide with base catalysis. 3′,5′-Di-*O*-trityluridine is converted to 3′,5′-di-*O*-trityl-2,2′-anyhdro-1-β-D-arabinofuranosyluracil with diphenyl carbonate in the presence of sodium bicarbonate in hot dimethyl formamide.

Canadian Journal of Chemistry, **47**, 495 (1969)

In a recent publication, Hampton and Nichol (1) reported the formation of 2,2′-anhydro-1-β-D-arabinofuranosyluracil (**2***a*) when uridine (**1***a*) was treated with diphenyl carbonate and sodium bicarbonate in hot *N*,*N*-dimethyl formamide (DMF). Replacement of uridine by other ribonucleosides in this reaction yielded 2′,3′-cyclic carbonates. These authors suggested that either uridine 2′,3′-carbonate (**3***a*) or 2′-phenoxycarbonyluridine (**4***a*) was probably the intermediate in the reaction (1). In an analogous case Ruyle *et al.* (2) found that 5′-*O*-trityluridine 2′,3′-thionocarbonate was readily converted to 5′-*O*-trityl-2,2′-anhydro-1-β-D-arabinofuranosyluracil when heated with imadazole in toluene. Since uridine 2′,3′-carbonates (**3***a*, *b*) were readily available as a result of another study (3) it was of interest to us to test them under the reaction conditions used by Hampton and Nichol.

As expected we found that both uridine 2′,3′-carbonate (**3***a*) and 5′-*O*-trityluridine 2′,3′-carbonate were readily converted to the anhydrouridines **2***a* and **2***b* respectively when heated in DMF with sodium bicarbonate or sodium carbonate. The cyclic carbonates were not converted to their anhydroforms when heated alone in DMF or in DMF containing phenol.

For comparison we obtained 3′,5′-di-*O*-trityluridine (**1***c*) and 2′,5′-di-*O*-trityluridine by a variation of the procedure of Yung and Fox (4) and subjected them to the diphenyl carbonate reaction of Hampton and Nichol. The 3′,5′-di-*O*-trityluridine was smoothly converted to 3′,5′-di-*O*-trityl-2,2′-anhydro-1-β-D-arabinofuranosyluracil (**2***c*) when heated with diphenylcarbonate and sodium bicarbonate in DMF. However 2′,5′-di-*O*-trityluridine was not converted to the 2,3′-anhydrouridine analogue under these conditions, but gave instead a good yield of 2′,5′-di-*O*-trityl-3′-*O*-phenoxycarbonyluridine. This result was not unexpected in view of previous observations (5) that 2,2′-anhydrouridines form much more readily than 2,3′-anhydrouridines.

These results confirm that uridine 2′,3′-carbonates **3***a* and **3***b* are probable intermediates in the conversion of uridine derivatives **1***a* and **1***b* to their anhydroforms using diphenyl carbonate in dimethyl formamide with base catalysis. However, when the 3′-position is blocked (**1***c*) other intermediates, most likely **4***c*, must occur.

Experimental

Materials

Thin-layer chromatography was carried out on Eastman Chromagram Sheets 6060 by the ascending technique. Thick-layer chromatography was carried out on glass plates (15 × 20 cm) coated with a 2 mm thick layer of silica gel DSF-5 (Mondray Chemicals Ltd.). Elemental analysis were performed by MicroTech Laboratories, Skokie, Illinois.

Melting points were obtained on a Fisher–Johns melting point apparatus and are reported uncorrected.

Uridine 2′,3′-carbonate (m.p. 122–126 °C) and 5′-*O*-trityluridine 2′,3′-carbonate (m.p. 134–135 °C) were prepared as previously described (3).

3′,5′-Di-*O*-trityluridine was prepared from uridine by the method of Yung and Fox (4). The isolation procedure was modified in that the 3′,5′- and 2′,5′-ditrityl mixture produced was separated by thick-layer chromatography using ether as developing agent. 2′,5′-Di-*O*-trityluridine (m.p. 216–218 °C) traveled fastest (R_f 0.76) while the 3′,5′-di-*O*-trityluridine (m.p. 134–138 °C) had an R_f value of 0.63 in ether.

5′-*O*-Trityluridine (m.p. 115–117 °C) was prepared by the procedure of Lohrman and Khorana (6).

2,2′-Anhydro-β-D-arabinofuranosyluracil (anhydrouridine m.p. 245–247 °C) was obtained from uridine by the

[1]NRCC Scholarship Recipient, 1968–1969.

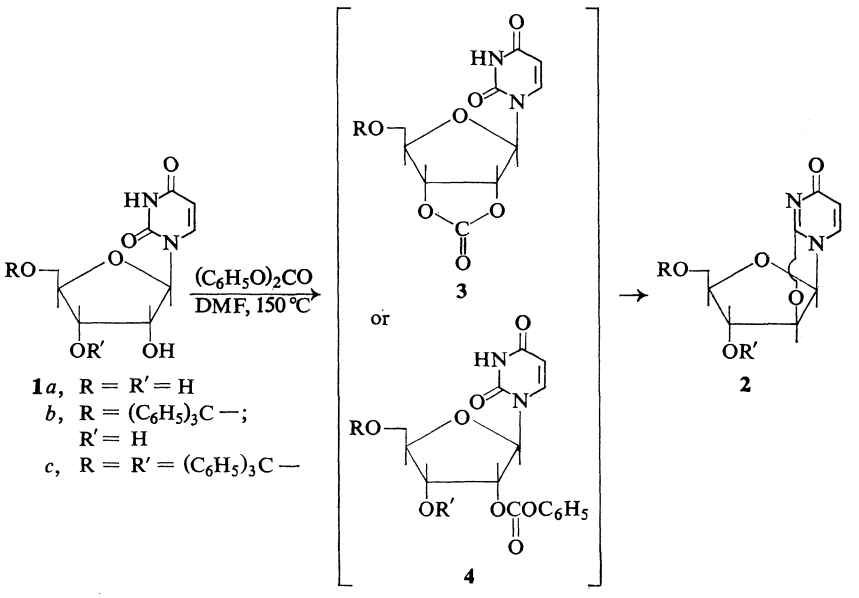

1*a*, R = R′ = H
b, R = $(C_6H_5)_3C-$; R′ = H
c, R = R′ = $(C_6H_5)_3C-$

3

4

2

method of Hampton and Nichol (1); the ultraviolet spectrum in 95% ethanol had λ_{max} 248 mμ (ε 8680), and λ_{max} 224 mμ (ε 10 600) and λ_{min} 236.5 mμ (ε 7560) and λ_{min} 210 mμ (ε 7130).

5′-O-Trityl-2,2′-anhydro-1-β-D-arabinofuranosyluracil (2b) from 5′-O-Trityluridine

5′-*O*-Trityluridine (0.67 g, 1.37 mmole) and diphenyl carbonate (0.39 g, 1.8 mmole) were dissolved in dimethyl formamide (1.5 ml). Sodium bicarbonate (0.01 g) was added and the mixture was heated at 150 °C for 30 min, cooled to room temperature and poured onto ether. A gummy precipitate formed and was collected and recrystallized from ethanol to yield 0.40 g (62%) of **2***b*, m.p. 218–220 °C (7), infrared spectrum (KBr disk): 6.15, 6.6, 6.8, and 14.2 μ; ultraviolet spectrum (95% ethanol): λ_{max} 249 mμ (ε 6630) and 224 mμ (sh); thin-layer R_f values were 0.70 (ethanol) and 0.55 (tetrahydrofuran). The product was identical to a sample prepared by the reaction of anhydrouridine (**2***a*) with trityl chloride in pyridine at room temperature.

Reactions of Uridine 2′,3′-carbonates in Dimethyl Formamide at 150 °C

(a) 5′-*O*-Trityluridine 2′,3′-carbonate (**3***b*, 204 mg, 0.4 mmole) was heated with diphenyl carbonate (114 mg, 0.64 mmole) and sodium bicarbonate (25 mg) in dimethyl formamide (0.2 ml) at 150 °C for 30 min. The solution was cooled and upon addition of ether a gummy precipitate formed which was collected and crystallized from ethanol to yield 110 mg (59%) of 5′-*O*-tritylanhydrouridine (**2***b*) m.p. 218–220 °C (mixed melting point 218–220 °C). Thin-layer R_f values were 0.55 (tetrahydrofuran) and 0.70 (ethanol). Spectral properties were identical to those of the sample prepared above.

(b) **3***b* (51 mg, 0.1 mmole) and sodium bicarbonate (3 mg) were heated in dimethyl formamide (0.05 ml) at 150 °C for 30 min. The reaction mixture was worked up as in *a* to yield 40 mg of **2***b* (85%) m.p. 219–220 °C.

(c) Reaction *b* was repeated except that sodium carbonate (2 mg) was used in place of sodium bicarbonate. A yield of 38 mg (81%) of **2***b* was obtained, m.p. 218–220 °C.

(d) Reaction *c* was repeated except that **3***a* (30 mg) was used in place of **3***b* and a yield of 18 mg (72%) of **2***a* was obtained, m.p. 245–247 °C, mixed melting point 246–248 °C; Spectral properties were identical to those of the sample prepared above.

(e) **3***b* (51 mg) was dissolved in dimethyl formamide (0.05 ml) and after 30 min heating at 150 °C the products were separated by thick-layer chromatography using ethyl acetate. Two compounds appeared (R_f 0.42 and 0.84) and these were eluted to yield 5′-*O*-trityluridine 2′,3′-carbonate 25 mg, 48%; R_f 0.84 (ethyl acetate) and R_f 0.25 (ether (1); m.p. 133–135 °C; infrared spectrum (KBr disk) showed major bands at 5.57, 6.0, and 14.2 μ) and uridine 2′,3′-carbonate (10 mg, 37%; m.p. 122–126 °C; thin-layer R_f values of 0.42 (ethyl acetate) and 0.00 (ether); the infrared spectrum (KBr disk) showed prominent peaks at 5.56 and 5.95 μ).

(f) Reaction *e* was repeated except that phenol (3 mg) was added and heating was continued for 3 h. After 30 min thin-layer chromatography in ethyl acetate showed two separate spots of nearly equal intensity at R_f 0.79 (**3***b*) and 0.38 (**3***a*). After 3 h the reaction was worked up by thick-layer chromatography to yield 25 mg (92%) of uridine 2′,3′-carbonate (**3***a*), m.p. 120–125 °C.

3′,5′-Di-O-trityl-2,2′-anhydro-1-β-D-arabinofuranosyluracil (2c)

3′,5′-Di-*O*-trityluridine (40 mg, 0.055 mmole) and diphenyl carbonate (19 mg, 0.086 mmole) were heated with sodium bicarbonate (2 mg) in dimethyl formamide (0.05 ml) at 150 °C for 30 min. On cooling to room

Can. J. Chem. Downloaded from www.nrcresearchpress.com by 210.87.254.42 on 09/05/12
For personal use only.

temperature ether (2 ml) was added and the solution was applied to two thick layers plates which were developed in ethyl acetate. A band appeared at R_f 0.35 and was eluted to yield 27 mg (67%) of **2***c*, m.p. 141–143 °C; in 95% ethanol the compound showed two shoulders at 249 mμ (ε 6740) and 223 mμ; the infrared spectrum (KBr disk) displayed prominent peaks at 6.06, 6.82, and 14.3 μ.

Anal. Calcd. for $C_{47}H_{32}N_2O_6$: C, 77.35; H, 5.25; N, 3.84; Found: C, 77.33; H, 5.12; N, 3.99.

2′,5′-Di-O-trityl-3′-O-phenoxycarbonyluridine

2′,5′-Di-*O*-trityluridine (200 mg, 0.27 mmole) was heated with diphenyl carbonate (95 mg, 0.43 mmole) and sodium bicarbonate (10 mg) in dimethyl formamide (0.25 ml) at 150 °C for 30 min. The solution was cooled to room temperature, diluted with ether, and separated from a small amount of insoluble material. On addition of hexane a precipitate formed which was collected by filtration and recrystallized from ether–hexane to yield 175 mg (77%) of 2′,5′-di-*O*-trityl-3′-*O*-phenoxycarbonyluridine as a white solid, m.p. 156–159 °C. The infrared spectrum (KBr disk) displayed major peaks at 5.63, 5.85, and 14.2 μ.

Anal. Calcd. for $C_{54}H_{44}N_2O_8$: C, 76.40; H, 5.22; N, 3.30. Found: C, 76.41; H, 5.31; N, 3.20.

Acknowledgments

Financial assistance from the National Research Council of Canada and the Faculty of Graduate Studies of the University of Manitoba is gratefully acknowledged.

1. A. Hampton and A. W. Nichol. Biochemistry, **5**, 2076 (1966).
2. W. V. Ruyle, T. V. Shen, and A. A. Patchette. J. Org. Chem. **30**, 4353 (1965).
3. R. L. Letsinger and K. K. Ogilvie. J. Org. Chem. **32**, 296 (1967).
4. N. C. Yung and J. J. Fox. J. Am. Chem. Soc. **83**, 3060 (1961).
5. D. M. Brown, D. B. Parihar, Sir A. R. Todd, and S. Varadarajan. J. Chem. Soc. 3028 (1958).
6. R. Lohrman and H. G. Khorana. J. Am. Chem. Soc. **86**, 4188 (1966).
7. J. J. Fox and I. Wempen. Tehrahedron Letters, 643 (1965).

Can. J. Chem. Downloaded from www.nrcresearchpress.com by 210.87.254.42 on 09/05/12
For personal use only.

Photolysis of a diterpene nitrosamine

W. B. Watkins[1]
Department of Pharmacology, South Parks Road, Oxford, England

AND

R. N. Seelye
Cancer Laboratories, Cornwall Hospital, Auckland, New Zealand

Received August 16, 1968

Photolysis of the diterpene nitrosamine, 4-*N*-nitroso-4-*N*-methyl-12-methoxy-16-norpodocarpa-8,11,-13-trien-4-amine in cyclohexane solvent gave the corresponding amine as the major product.

Canadian Journal of Chemistry, **46**, 497 (1968)

The photolysis of nitrites has now become an established method, in the steroid field, for the functionalization of suitably placed saturated carbon atoms (1). In recent years work has been carried out to investigate the products resulting from the photolytic decomposition of the spectroscopically similar nitrosamines (2). In Chow's latest work (3) he has further established that simple acyclic and alicyclic *N*-nitrosodialkylamines undergo photolysis in the presence of acid to give amidoximes and the parent secondary amine.

In this present paper we have further investigated the scope of the latter reaction by studying the photolysis of the polycyclic nitrosamine, 4-*N*-nitroso-4-*N*-methyl-12-methoxy-16-norpodocarpa-8,11,13-trien-4-amine (**8**). The stereochemistry of podocarpic acid **1** is such that the axial carboxyl group at C-4 is *cis* to the C_{10}-angular methyl, the latter being forced close to the former by the steric compression offered by ring C. In this system, a nitrosamine group at C-4 might thus be expected to oxygenate the methyl at C-10.

Treatment of the acid chloride of 12-methoxypodocarpa-8,11,13-trien-16-oic acid **2** (4) with sodium azide gave the isocyanate **4** which on reduction with excess lithium aluminium hydride

[1]To whom all correspondence should be addressed.

temperature ether (2 ml) was added and the solution was applied to two thick layers plates which were developed in ethyl acetate. A band appeared at R_f 0.35 and was eluted to yield 27 mg (67%) of **2***c*, m.p. 141–143 °C; in 95% ethanol the compound showed two shoulders at 249 mμ (ε 6740) and 223 mμ; the infrared spectrum (KBr disk) displayed prominent peaks at 6.06, 6.82, and 14.3 μ.

Anal. Calcd. for $C_{47}H_{32}N_2O_6$: C, 77.35; H, 5.25; N, 3.84; Found: C, 77.33; H, 5.12; N, 3.99.

2′,5′-Di-O-trityl-3′-O-phenoxycarbonyluridine

2′,5′-Di-*O*-trityluridine (200 mg, 0.27 mmole) was heated with diphenyl carbonate (95 mg, 0.43 mmole) and sodium bicarbonate (10 mg) in dimethyl formamide (0.25 ml) at 150 °C for 30 min. The solution was cooled to room temperature, diluted with ether, and separated from a small amount of insoluble material. On addition of hexane a precipitate formed which was collected by filtration and recrystallized from ether–hexane to yield 175 mg (77%) of 2′,5′-di-*O*-trityl-3′-*O*-phenoxycarbonyluridine as a white solid, m.p. 156–159 °C. The infrared spectrum (KBr disk) displayed major peaks at 5.63, 5.85, and 14.2 μ.

Anal. Calcd. for $C_{54}H_{44}N_2O_8$: C, 76.40; H, 5.22; N, 3.30. Found: C, 76.41; H, 5.31; N, 3.20.

Acknowledgments

Financial assistance from the National Research Council of Canada and the Faculty of Graduate Studies of the University of Manitoba is gratefully acknowledged.

1. A. Hampton and A. W. Nichol. Biochemistry, **5**, 2076 (1966).
2. W. V. Ruyle, T. V. Shen, and A. A. Patchette. J. Org. Chem. **30**, 4353 (1965).
3. R. L. Letsinger and K. K. Ogilvie. J. Org. Chem. **32**, 296 (1967).
4. N. C. Yung and J. J. Fox. J. Am. Chem. Soc. **83**, 3060 (1961).
5. D. M. Brown, D. B. Parihar, Sir A. R. Todd, and S. Varadarajan. J. Chem. Soc. 3028 (1958).
6. R. Lohrman and H. G. Khorana. J. Am. Chem. Soc. **86**, 4188 (1966).
7. J. J. Fox and I. Wempen. Tehrahedron Letters, 643 (1965).

Can. J. Chem. Downloaded from www.nrcresearchpress.com by 210.87.254.6 on 09/05/12
For personal use only.

Photolysis of a diterpene nitrosamine

W. B. Watkins[1]
Department of Pharmacology, South Parks Road, Oxford, England

AND

R. N. Seelye
Cancer Laboratories, Cornwall Hospital, Auckland, New Zealand

Received August 16, 1968

Photolysis of the diterpene nitrosamine, 4-*N*-nitroso-4-*N*-methyl-12-methoxy-16-norpodocarpa-8,11,-13-trien-4-amine in cyclohexane solvent gave the corresponding amine as the major product.

Canadian Journal of Chemistry, **46**, 497 (1968)

The photolysis of nitrites has now become an established method, in the steroid field, for the functionalization of suitably placed saturated carbon atoms (1). In recent years work has been carried out to investigate the products resulting from the photolytic decomposition of the spectroscopically similar nitrosamines (2). In Chow's latest work (3) he has further established that simple acyclic and alicyclic *N*-nitrosodialkylamines undergo photolysis in the presence of acid to give amidoximes and the parent secondary amine.

In this present paper we have further investigated the scope of the latter reaction by studying the photolysis of the polycyclic nitrosamine, 4-*N*-nitroso-4-*N*-methyl-12-methoxy-16-norpodocarpa-8,11,13-trien-4-amine (**8**). The stereochemistry of podocarpic acid **1** is such that the axial carboxyl group at C-4 is *cis* to the C_{10}-angular methyl, the latter being forced close to the former by the steric compression offered by ring C. In this system, a nitrosamine group at C-4 might thus be expected to oxygenate the methyl at C-10.

Treatment of the acid chloride of 12-methoxypodocarpa-8,11,13-trien-16-oic acid **2** (4) with sodium azide gave the isocyanate **4** which on reduction with excess lithium aluminium hydride

[1]To whom all correspondence should be addressed.

in ether afforded the *N*-methyl amine **5**. Nitrosation of **5** in aqueous acetic acid gave the nitrosamine **8** in yields up to 61%. On irradiation of the *N*-nitrosamine **8** in the absence of acid, the absorption of the NNO at 352 mμ rapidly disappeared with the formation of the secondary

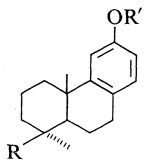

	R'	*R*
1	H	COOH
2	Me	COOH
3	Me	COCl
4	Me	NCO
5	Me	NHMe
6	Me	NHMe.HCl
7	Me	N(OAc)Me
8	Me	N(NO)Me
9	Me	·NMe

amine **5** together with polymeric material. This reaction is yet another example in which homolysis of **8** to the radical **9** and subsequent disproportionation to **5** appears to occur in preference to hydrogen abstraction from the C-10 methyl. Chow (3) has similarly found that photolysis of *N*-nitroso-*trans*-decahydroquinoline gave the parent amine as the only product.

Experimental

Infrared spectra were measured on a Perkin–Elmer Infracord model 237 spectrophotometer and the ultraviolet spectra were measured on a Perkin–Elmer model 137-UV spectrophotometer. Nuclear magnetic resonance spectra were recorded on a Varian A60 spectrophotometer with tetramethylsilane as an internal reference. Photolyses were carried out in an atmosphere of nitrogen using a Hanovia lamp (450–500 W). Melting points were taken on a Köfler block and are uncorrected. Microanalyses are by Dr. A. D. Campbell and associates, University of Otago, New Zealand.

12-Methoxypodocarpa-8,11,13-trien-16-oyl Chloride (3)

Phosphorus pentachloride (10 g) was slowly added to powdered 12-methoxypodocarpa-8,11,13-trien-16-oic acid **2** (10 g) (4) and the mixture heated for 1 h at 80°. The resultant oil was washed until neutral to give the acid chloride **3** (9.9 g, 90%) as a yellow gum, b.p. 179–183°/0.3 mm; ν_{max} (film) 1802 cm^{-1} (C=O).

4-N-Methyl-12-methoxy-16-norpodocarpa-8,11,13-trien-4-amine (5)

A cold (ca. 15°) solution of sodium azide (2.8 g) in water (11 ml) was added to a stirred solution of **3** (10.7 g) in acetone (50 ml) and stirring continued for 1 h. The mixture was diluted with water, extracted with benzene and the benzene extract refluxed for 2 h to give the isocyanate **4** (9.1 g, 91%) as an oil; ν_{max} (CCl_4) 2270 cm^{-1} (N=C=O).

A solution of **4** (7.4 g) in dry ether (100 ml) was added in portions to a stirred suspension of lithium aluminium hydride (5.8 g) in ether (100 ml) and then refluxed for 1 h. The excess hydride was decomposed with ethyl acetate and the ethereal layer washed to give **5** (5.7 g, 80%) as rods, m.p. 48–50°, b.p. 146°/0.4 mm; ν_{max} (film) 3400 (N—H), 2800 cm^{-1} (N—Me); δ ($CDCl_3$) 0.98 (N*H*Me), 1.10 (C_{15}—Me), 1.34 (C_{17}—Me), 2.28 (N—Me), 3.78 (ArOMe), 6.50–7.10 (C-11,13,14-aromatics).

Anal. Calcd. for $C_{18}H_{27}NO$: C, 79.07; H, 9.95; N, 5.12; O, 5.85. Found: C, 79.13; H, 9.95; N, 5.00; O, 6.10.

Hydrochloride **6** had m.p. (sealed tube) 290–295° (decomp.).

Anal. Calcd. for $C_{18}H_{28}NOCl$: C, 69.76; H, 9.10; N, 4.52. Found: C, 70.06; H, 9.02; N, 4.57.

Acetyl derivative **7**, needles from ethanol–water m.p. 108–109°; ν_{max} (CCl_4) 1681 cm^{-1} (C=O); δ (CCl_4) 1.29 (C_{15}—Me), 1.34 (C_{17}—Me), 1.99 (acetyl methyl), 2.89 (N—Me), 3.70 (ArOMe), 6.46–6.90 (C-11,13,14-aromatics).

Anal. Calcd. for $C_{20}H_{29}NO_2$: C, 76.15; H, 9.27; N, 4.44. Found: C, 76.30; H, 9.44; N, 4.23.

4-N-Nitroso-4-N-methyl-12-methoxy-16-norpodocarpa-8,11,13-trien-4-amine (8)

The amine **5** (21.9 g) was dissolved in 25% (v/v) aqueous acetic acid (400 ml), glacial acetic acid (10 ml), and ether (200 ml). A saturated aqueous solution of sodium nitrite (6.9 g) was added over a period of 30 min and stirring continued for 2½ h. The solid product was filtered off and after recrystallization from ethanol gave **8** (14.8 g, 61%), as needles m.p. 131–131.5°; λ_{max} (EtOH) 279, 287, 352 mμ (ε = 3240, 2900, 72); δ ($CDCl_3$) 0.94 (C_{15}—Me), 1.49 (C_{17}—Me), 3.05 (N—Me), 3.79 (ArOMe), 6.60–7.10 (C-11,13,14-aromatics).

Anal. Calcd. for $C_{18}H_{26}N_2O_2$: C, 71.49; H, 8.67; N, 9.26; O, 10.58. Found: C, 71.61; H, 8.83; N, 9.40; O, 10.85.

Photolysis of Nitrosamine 8

The nitrosamine **8** (4.9 g) was photolyzed in cyclohexane (9 L) at 80° for 1½ h to give a pale-yellow reaction mixture. The ethereal extract of the photolyzate was acidified with dilute hydrochloric acid and the aqueous phase then made basic to yield the secondary amine **5** (3 g) which was identified by comparison of its infrared and nuclear magnetic resonance spectra with those of an authentic sample. Concentration of the remaining ethereal extract gave the nitrosamine **8** (230 mg), while the residual photolyzate consisted of polymeric material.

Acknowledgments

W. B. Watkins thanks the University of Auckland, New Zealand, for the award of a Senior Scholarship and the Grace Phillips Memorial Fellowship.

1. K. Schaffner, D. Arigoni, and O. Jeger. Experientia, **16**, 169 (1960); A. L. Nussbaum, F. E. Carlon, E. P. Oliveto, E. Townley, P. Kabasakalian, and D. H. R. Barton. J. Am. Chem. Soc. **82**, 2973 (1960).
2. E. M. Burgess and J. M. Lavanish. Tetrahedron Letters, No. **20**, 1221 (1964); Y-L Chow. Tetrahedron Letters, No. **34**, 2333 (1964).
3. Y-L Chow. Can. J. Chem. **45**, 53 (1967).
4. C. R. Bennett and R. C. Cambie. Tetrahedron, **23**, 927 (1967).

Can. J. Chem. Downloaded from www.nrcresearchpress.com by 210.87.254.6 on 09/05/12
For personal use only.

Structure of lucidioline. An alkaloid of *Lycopodium lucidulum*

W. A. AYER AND B. ALTENKIRK
Department of Chemistry, University of Alberta, Edmonton, Alberta

Received October 21, 1968

The alkaloid lucidioline is shown to have structure **1**. The transformation of lucidioline into desacetyllycoclavine (**8**) is described.

Canadian Journal of Chemistry, 47, 499 (1969)

Can. J. Chem. Downloaded from www.nrcresearchpress.com by 210.87.254.42 on 09/05/12
For personal use only.

Recently we described the isolation of an alkaloid $C_{16}H_{25}O_2N$ from *Lycopodium lucidulum* (1). This compound had previously been isolated from *L. clavatum* var. *megastachyon* (2). We now wish to report that this alkaloid, for which we suggest the trivial name lucidioline, possesses structure **1**.

Inspection of the infrared and nuclear magnetic resonance (n.m.r.) spectra of lucidioline and its simple derivatives (see Experimental) revealed that the oxygens are present as hydroxyl groups, the nitrogen is tertiary, and the molecule contains a trisubstituted double bond. The presence of a secondary *C*-methyl group was obvious from the n.m.r. spectra. With these as the functional groups, the molecule is tetracyclic.

The mass spectrum of lucidioline (Fig. 1) proved to be very informative. The base peak in the spectrum is at *m/e* 203 and corresponds to the ion $C_{14}H_{21}N^+$, as shown by high resolution measurements. An intense metastable peak centered at 156.8 indicates that the ion *m/e* 203 is formed directly from the molecular ion (calculated for 263 → 203, 156.5). This corresponds to the loss of $C_2H_4O_2$ and indicates that *the two hydroxyl groups are on adjacent carbon atoms.* The base peak in the mass spectra of Lycopodium alkaloids containing the skeleton **2** is usually derived by loss of the "bridging" ring (carbons 8, 14, 15, and 16) and the hydrogen from C-12 to form a stabilized ion of type **3** (3), except in cases where there is no hydrogen at C-12 (1, 3). We felt that structure **4** offered a good explanation for the observed mass spectral fragmentation pattern, a possible origin of the ion *m/e* 203 being illustrated in the sequence 4 → 5 → 6 → 7. Accordingly we set about to correlate lucidioline with a compound of known structure.

Hydrogenation of lucidioline over platinum in methanol resulted in the uptake of one molar equivalent of hydrogen and gave a product which consisted of two components in the ratio of about 19:1. The minor component could not be isolated in pure form; however, on thin-layer chromatoplates it was indistinguishable from desacetyllycoclavine (**8**) (2). When the hydrogenation was carried out in the presence of perchloric acid, the same two components were

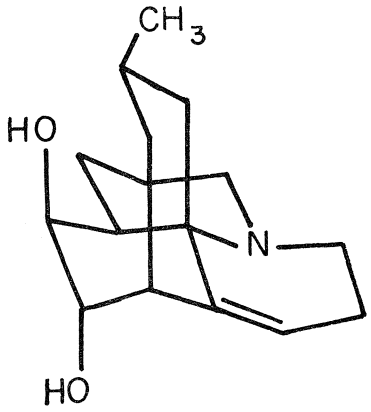

1

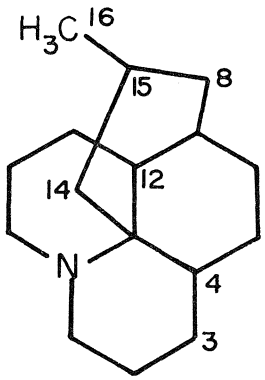

2

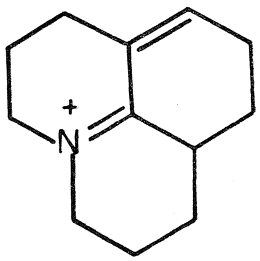

3

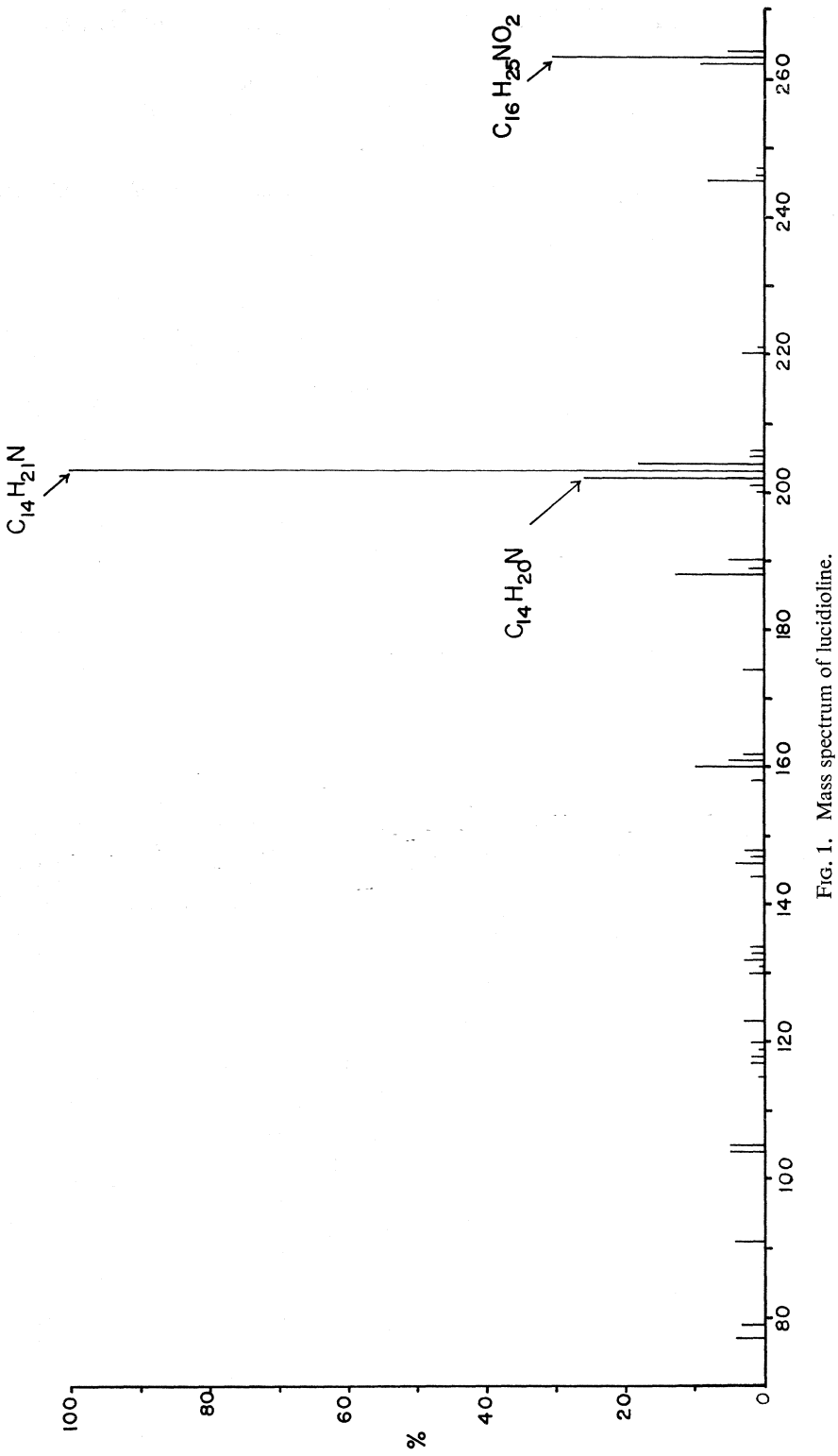

FIG. 1. Mass spectrum of lucidioline.

Can. J. Chem. Downloaded from www.nrcresearchpress.com by 210.87.254.42 on 09/05/12
For personal use only.

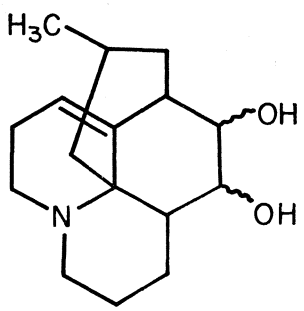

4

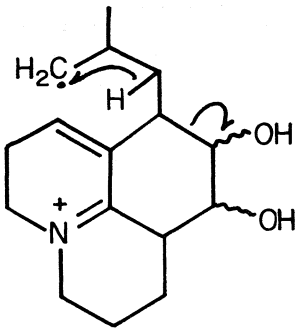

5

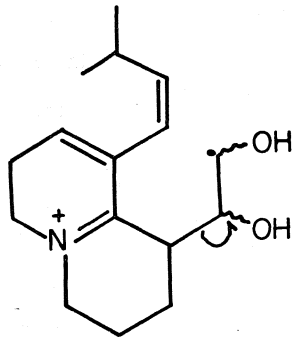

6

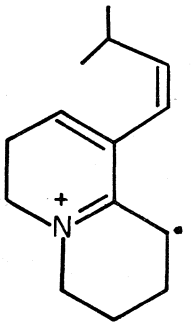

7

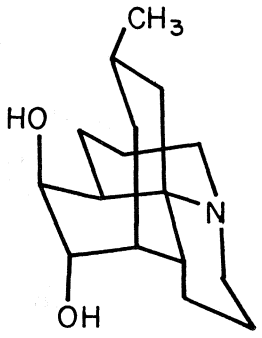

8

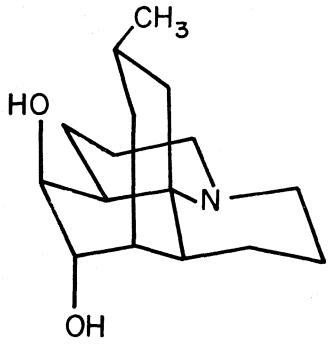

9

obtained but now in approximately equal amounts. The two were separated by chromatography. The component of higher R_f value proved to be identical with desacetyllycoclavine (**8**), establishing that lucidioline is a *dehydro* desacetyllycoclavine. Since the double bond in lucidioline is trisubstituted and since the methyl group is not located on the double bond, only the 11, 12-, or

Can. J. Chem. Downloaded from www.nrcresearchpress.com by 210.87.254.42 on 09/05/12
For personal use only.

the 3,4-position are possible for the double bond. The second product formed in the hydrogenation was isomeric with desacetyllycoclavine. Acetylation gave a di-*O*-acetyl derivative which shows prominent "Bohlmann bands" in the infrared, indicative of the presence of a *trans*-quinolizidine system (4) in this compound. This indicated that the dihydro compounds are epimeric at C-12 (and at nitrogen) and identifies this carbon as one terminus of the double bond. Lucidioline thus has structure **1** and the second hydrogenation product is **9**.

Oxidation of lucidioline with Jones' reagent gave an oily unstable product which from its ultraviolet spectrum appeared to be a diosphenol.

Experimental

Isolation of Lucidioline

Lucidioline was isolated as previously described (1), m.p. 230–233°. The mass spectrum is shown in Fig. 1. Exact mass measurements: *m/e* 203. Calcd. for $C_{14}H_{21}N$: 203.1674. Found: 203.1672. *m/e* 202. Calcd. for $C_{14}H_{20}N$: 202.1596. Found: 202.1595. Infrared spectrum: ν_{max}(Nujol) 3400, 2600–3300 (intermolecularly H-bonded OH), 1678 (C=C). Nuclear magnetic resonance spectrum (CD_3COOD): τ 4.38 (1H, doublet, $J \simeq 5$ c.p.s., olefinic proton), 9.08 (3H, doublet, splitting 6 c.p.s., $CHCH_3$).

The *hydroperchlorate* was formed in methanol and recrystallized from methanol, m.p. 238–240° (decomp.).

Hydrogenation of Lucidioline

(a) In Methanol

Lucidioline (50 mg) in methanol (50 ml) was hydrogenated over Adams' catalyst (25 mg) at 50 p.s.i. for 3 h. After the catalyst and solvent were removed the product (50 mg) solidified. Thin-layer chromatography (t.l.c.) indicated the presence of a major and a very minor component. The major component was isolated by crystallization from acetone–methanol and after sublimation melted at 247–251°. Calculated molecular weight for $C_{16}H_{27}O_2N$, 265. Found, 265 (mass spectroscopy). The base peak in the mass spectrum appeared at *m/e* 208. This compound, **9**, was further characterized as its diacetyl derivative (below).

The mother liquors from the crystallization were separated by preparative t.l.c. The minor component could not be obtained in crystalline form. Its t.l.c. behavior was identical with that of desacetyllycoclavine.

(b) In the Presence of Perchloric Acid

Lucidioline (47 mg) in methanol (50 ml) containing 70% perchloric acid (2 drops) was hydrogenated over Adams' catalyst (25 mg) as above. After the catalyst was removed and the solution concentrated, aqueous ammonia was added, and the solution was extracted with chloroform. Evaporation of the chloroform gave a semicrystalline solid (45 mg) comprising two components (determined by t.l.c.) in approximate equal amounts. Separation was achieved by chromatography over basic alumina (2 g, activity II–III) using ethyl acetate (20 ml fractions) as the eluting solvent. Fractions 3 to 5 were homogeneous (t.l.c.) and crystallized to give desacetyllycoclavine (**8**, 8 mg), identical (m.p., infrared spectrum, mass spectrum, t.l.c. behavior) with an authentic sample (2). Fractions 6 and 7 (15 mg) contained both components. Fractions 8 to 20 yielded 19 mg of the 12-*epi*-desacetyllycoclavine (**9**).

Acetylation of 9

12-*Epi*-desacetyllycoclavine (**9**) was kept in a mixture of pyridine (2 ml) and acetic anhydride (2 ml) at room temperature for 3 days. After work-up an oil (44 mg) was obtained. This was purified by chromatography over alumina. The material (38 mg) thus obtained was homogeneous as determined by t.l.c. but could not be induced to crystallize. The analytical sample was purified by evaporative distillation.

Calculated molecular weight for $C_{20}H_{31}O_4N$: 349.2253. Found: 349.2253 (high resolution mass spectroscopy).

The base peak in the mass spectrum appeared at *m/e* 230. Infrared spectrum (CCl_4): no OH or NH absorption, 2750 and 2800 (Bohlmann bands), 1735 cm^{-1} (OAc). Nuclear magnetic resonance spectrum (CCl_4): τ 5.07 (1H, doublet, $J \simeq 7$ c.p.s., C*H*OAc), 5.45 (1H, singlet, $W_{1/2}$, 3 c.p.s., C*H*OAc), 7.98 and 8.02 (two 3-proton singlets, $OCOCH_3$), 9.08 (3H, doublet, splitting 6 c.p.s., $CHCH_3$).

Oxidation of Lucidioline

Lucidioline (14 mg) was dissolved in acetone (15 ml) and Jones' reagent (0.5 ml) added dropwise. After a few minutes methanol (10 drops) was added and then most of the solvent removed under reduced pressure. The residue was dissolved in water, aqueous ammonia added, and the solution was extracted with chloroform. Evaporation of the chloroform left an oil (5 mg) which could not be induced to crystallize. Ultraviolet spectrum: λ_{max}(EtOH) 280 mμ (ε 8000); λ_{max}(EtOH, $^-$OH) 323 mμ (ε 7000). Infrared spectrum: ν_{max}($CHCl_3$) 1670 and 1635 cm^{-1}.

Acknowledgment

We wish to thank the National Research Council of Canada for financial support of this work.

1. W. A. Ayer, B. Altenkirk, R. H. Burnell, and M. Moinas. Can. J. Chem. This issue.
2. W. A. Ayer and D. A. Law. Can. J. Chem. **40**, 2088 (1962).
3. D. B. MacLean. Can. J. Chem. **41**, 2654 (1963).
4. F. Bohlmann. Chem. Ber. **91**, 2157 (1958).

Can. J. Chem. Downloaded from www.nrcresearchpress.com by 210.87.254.42 on 09/05/12
For personal use only.

Preparation of diphenylamines via the Chapman rearrangement

OWEN H. WHEELER, FERNANDA ROMAN, MARCELINA V. SANTIAGO, AND FRANCISCO QUILES
Department of Chemistry and Puerto Rico Nuclear Center, University of Puerto Rico, Mayaguez, Puerto Rico

Received August 16, 1968

The optimum conditions have been determined for preparing substituted diphenylamines using the Chapman rearrangement. The rearrangement was best carried out in boiling tetraglyme. Phenyl *N*-phenylcinnamidate rearranged at a lower temperature than the corresponding benzimidate.

Canadian Journal of Chemistry, 47, 503 (1969)

Can. J. Chem. Downloaded from www.nrcresearchpress.com by 210.87.254.105 on 09/05/12
For personal use only.

The Chapman rearrangement (1, 2) of phenylbenzimidates (**1**) to benzoyldiphenylamines (**2**) affords a general method (3) for the synthesis of substituted diphenylamines, and is often the only method available (4). The rearrangement is usually carried out by heating the fused imidate to an elevated temperature (280–300°), although this gives a low yield in some cases. Nitrobenzene, diphenyl (5), or diphenyl ether (6) have been used as solvent, but are inconvenient for isolating the product.

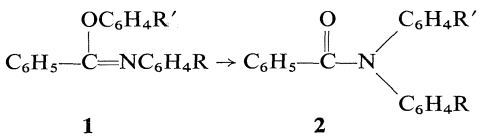

1 **2**

It has now been found that the rearrangement can be carried out in nearly quantitative yield by refluxing the benzimidate in tetraethylene glycol dimethyl ether (tetraglyme) (b.p. 276°). The benzoyldiphenylamines were readily isolated by adding water. The reaction could also be carried out in triethylene glycol (b.p. 285°), although with charring and in a lower yield (75–80%). The rearrangement was incomplete in triglyme (b.p. 225°).

The benzimidates (**1**) were prepared by the reaction of a benziminyl chloride with a sodium phenoxide. These chlorides were most conveniently prepared from the benzoylaniline, using a small excess of thionyl chloride (8, 9). The use of phosphorus pentachloride (10, 11) resulted in considerable polymerization on distilling the chloride. The benziminyl chloride in ether was then condensed with the phenol in methanol containing an equivalent of sodium methoxide (1, 4, 12). Dioxane and pyridine have also been used (5, 7) as solvents. It was found that there was no advantage in using sodium methoxide in dimethyl formamide and benzene. Lower yields were obtained with sodium methoxide in tetraglyme, triglyme, or in triethylene glycol. The condensation of the benziminyl chloride in tetraglyme and the rearrangement of the resulting benzimidate without isolation gave only a low yield of product.

A number of substituted benzimidate and benzoyldiphenylamines were prepared (see Table I) in good yield. *N*-Phenylcinnamamide was also prepared by the direct condensation of cinnamic acid and aniline in high yield (91%). The amide was easily converted to the corresponding iminyl chloride by reacting with thionyl chloride. The iminyl chloride reacted smoothly with sodium phenoxide in methanol to give phenyl *N*-phenylcinnamimidate which was rearranged in triglyme in 85% yield, at a lower temperature (225°) than that utilized for the rearrangement of the other compounds studied. Presumably the additional resonance contribution of the cinnamyl group facilitated the rearrangement.

Experimental

Phenylbenziminyl Chloride

Recrystallized benzanilide (19.7 g) was gently heated to reflux with thionyl chloride (15.5 g) for 1 h. The excess thionyl chloride was removed by evacuating at the water pump and the product (28 g, 91%) was distilled, b.p. 115°/6 mm, m.p. 40–41° (lit. (8), m.p. 40°).

Benzo-*p*-toluide (21 g) gave in the same manner *N*-*p*-tolylbenziminyl chloride (32 g, 97%), b.p. 141–144°/10 mm, m.p. 51–52° (lit. (13), b.p. 186°/10 mm).

4-Chlorophenyl-N-phenylbenzimidate
*(**1**; $R = H_1R^1 = pCl$)*

p-Chlorophenol (2.32 g) was added to anhydrous methanol (25 ml) containing sodium (0.42 g). Phenylbenziminyl chloride (3.96 g) in ether (15 ml) was added with stirring. The solution was stirred at room temperature overnight, diluted with water, and extracted with ether. The ether solution was washed with 10% sodium hydroxide and water. The product (3.93 g, 80%), m.p. 91–92° (lit. (2), m.p. 92–93°) was recrystallized from methanol.

The other benzimidates (see Table I) were prepared in the same manner.

TABLE I

Physical constants of compounds

Substituents	Benzimidates (1) Yield (%)	Melting point (°C)	Lit. melting point (°C)	Reference	Benzoyldiphenylamines (2) Yield (%)	Melting point (°C)	Lit. melting point (°C)	Reference
R = R¹ = H	81	104–105	105	6	96	180–181	180	1
R = Me, R¹ = H	82	116–118	117–119	14	96	89–90*	—	—
R = H, R¹ = *p*Br	75	89–90	83–84	6	80	178–180†	—	—
R = Me, R¹ = *p*Br	65	136–138‡	—	—	85	117–180§	—	—
R = H, R¹ = *m*Br	80	84–85‖	—	—	75	132–134¶	—	—
R = H, R¹ = *m*MeO	83	77–78	79–80	2	86	123	121	2
R = H, R¹ = *p*Cl	80	91–92	92–93	2	87	110	110	2
R = H, R¹ = *o*Cl	77	89–90	88	1	91	95	95–96	1

*Anal. Calcd. for $C_{20}H_{17}NO$: C, 83.59; H, 5.92. Found: C, 84.16; H, 5.74.
†Anal. Calcd. for $C_{19}H_{14}BrNO$: C, 64.79; H, 4.00. Found: C, 64.65; H, 4.13.
‡Anal. Calcd. for $C_{20}H_{16}BrNO$: C, 65.58; H, 3.85. Found: C, 65.87; H, 4.03.
§Found: C, 65.5; H, 3.92.
‖Anal. Calcd. for $C_{19}H_{14}BrNO$: C, 64.79; H, 4.00. Found: C, 64.45; H, 3.84.
¶Found: C, 64.52; H, 4.21.

N-Benzoyl-4-chlorodiphenylamine
(2; R = H, R¹ = pCl)

4-Chlorophenyl-*N*-phenylbenzimidate (1.5 g) in tetraglyme (15 ml) was heated under reflux for 4 h. The cooled solution was then poured into water, and the solid recrystallized from ethanol (1.3 g, 87%), m.p. 110° (lit. (2), m.p. 110°).

The other diphenylamines (see Table I) were prepared similarly.

N-Phenyl-N-phenylcinnamimidate

A mixture of cinnamic acid (15 g) and aniline (12 g) was heated under reflux at 180° for 2 h. The excess aniline was distilled off *in vacuo*, and the residue of *N*-phenylcinnamamide (22.1 g, 91%) was washed with water and dried, m.p. 149–150° (lit. (14), m.p. 151–152°).

A mixture of *N*-phenylcinnamamide (22 g) and thionyl chloride (12 g) was submitted to the same procedure as before. Distillation of the product gave a light-brown liquid, b.p. 170–175°, 5 mm. On cooling a solid was obtained (25 g, 80%), m.p. 60–61°.

N-Phenylcinnaminyl chloride (2.8 g) was reacted with phenol (1.1 g) in the presence of sodium methoxide (0.6 g) as before to give an oily product. This was chromatographed on alumina and the product eluted with hexane and benzene giving crystals (1.7 g, 48%), m.p. 65–66°, from benzene–hexane. Infrared: 1600 cm^{-1} (CON), 1480 cm^{-1} (C=N), and 1250 cm^{-1} (C—O—Ar).

Anal. Calcd. for $C_{21}H_{17}NO$: C, 84.25; H, 5.72; N, 4.69. Found: C, 84.36; H, 5.66; N, 4.75.

N-Cinnamoyldiphenylamine

Phenyl-*N*-phenylcinnamimidate (1.2 g) was heated under reflux in triglyme (15 ml) for 3 h. The product (1.0 g, 84%) was recrystallized from ethanol, m.p. 153–155° (lit. (13), m.p. 154–156°).

Acknowledgments

This work was supported in part by an Undergraduate Research Participation grant from the National Science Foundation. One of the authors (F.R.) was on leave of absence from the Economic Development Administration Laboratory, Commonwealth of Puerto Rico. The Puerto Rico Nuclear Center is operated by the University of Puerto Rico for the United States Atomic Energy Commission.

1. A. W. CHAPMAN. J. Chem. Soc. **127**, 1992 (1925).
2. A. W. CHAPMAN. J. Chem. Soc. 1743 (1927).
3. J. W. SCHULENBERG and S. ARCHER. Organic reactions, Vol. 14. John Wiley and Sons, Inc., New York. 1965. p. 1.
4. E. R. H. JONES and F. G. MANN. J. Chem. Soc. 786 (1956).
5. R. C. COOKSON. J. Chem. Soc. 643 (1953).
6. K. B. WIBERG and B. I. ROWLAND. J. Am. Chem. Soc. **77**, 2205 (1955).
7. A. P. T. EASSON. J. Chem. Soc. 1029 (1961).
8. J. VAN BRAUN and W. PINKERNELLE. Ber. **67**, 1218 (1934).
9. W. M. LAUER and R. G. LOCKWOOD. J. Am. Chem. Soc. **76**, 3974 (1954).
10. O. WALLACH. Ann. **184**, 79 (1877).
11. R. C. ELDERFIELD, W. J. GENSLER, T. H. BEMBRY, C. B. KREMER, J. D. HEAD, F. BRODY, and R. FROHARDT. J. Am. Chem. Soc. **68**, 1272 (1946).
12. J. W. SCHULENBERG and S. ARCHER. J. Am. Chem. Soc. **82**, 2035 (1960).
13. C. S. GIBSON and J. D. A. JOHNSON. J. Chem. Soc. 2743 (1929).
14. D. H. HEY and T. M. MOYNEHAN. J. Chem. Soc. 1563 (1959).

Can. J. Chem. Downloaded from www.nrcresearchpress.com by 210.87.254.105 on 09/05/12
For personal use only.

Synthesis of some para-substituted 3,3,3-triarylpropionic acid derivatives

T. J. ADLEY AND D. R. CLARKE
Department of Chemistry, Sir George Williams University, Montreal, Quebec

Received June 26, 1968

The syntheses of representative compounds of the type $4\text{-}XC_6H_4(4'\text{-}YC_6H_4)C_6H_5CCH_2CO_2R$ are described.

Canadian Journal of Chemistry, 47, 505 (1969)

Can. J. Chem. Downloaded from www.nrcresearchpress.com by 210.87.254.5 on 09/05/12
For personal use only.

Introduction

We wish to report the synthesis of a number of new substituted triphenylpropionic acid derivatives of the type $4\text{-}XC_6H_4(4'\text{-}YC_6H_4)C_6H_5CCH_2CO_2R$. In a recent publication Snyder (1) has pointed out that the ^1H nuclear magnetic resonance (n.m.r.) spectra of compounds of this class might be of interest, since any magnetic non-equivalence observed for the methylene protons could be attributed to an "asymmetry effect".[1]

Examples of substituted triarylpropionic acid derivatives of the series $4\text{-}XC_6H_4(4'\text{-}XC_6H_4)\text{-}C_6H_5CCH_2CO_2R$ have been reported (4), but the aryl substituents have generally been of a type which did not readily permit their selective conversion to the required class of compounds.

Results and Discussion

The sequence of reactions employed in the synthesis of (±)methyl 3-[4-anilino-4′-nitrophenyl-phenyl]-propionate (**4***b*) is outlined in Reaction Scheme 1.

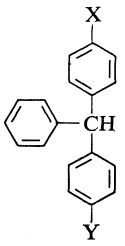

1 (*a*) X = Y = NH_2
1 (*b*) X = Y = NO_2

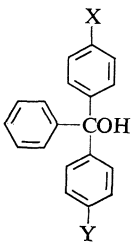

2 (*a*) X = Y = NO_2
2 (*b*) X = NH_2, Y = NO_2
2 (*c*) X = $NHCOCH_3$, Y = NO_2

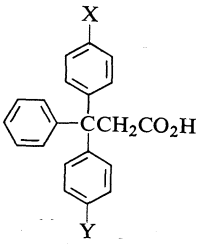

3 (*a*) X = $NHCOCH_3$, Y = NO_2
3 (*b*) X = NH_2, Y = NO_2

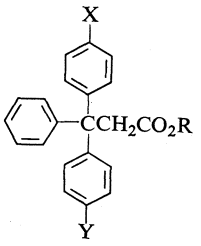

4 (*a*) X = NH_2, Y = NO_2, R = CH_2CH_3
4 (*b*) X = NH_2, Y = NO_2, R = CH_3

REACTION SCHEME 1

4,4′-Diaminotriphenylmethane (**1***a*) (5) could be selectively oxidized with hydrogen peroxide to the corresponding 4,4′-dinitro compound (**1***b*) (6). Treatment of **1***b* with chromium trioxide

[1]Snyder (1) also suggested that since the barrier to free rotation of the methyl group in methyl acetylene is extremely low (less than 0.1 kcal $mole^{-1}$) (2), the contribution of an "asymmetry effect" to magnetic non-equivalence could be unambiguously assessed by an examination of the n.m.r. spectra of compounds of the series $ACH_2C{\equiv}CCXYZ$. We have synthesized two compounds of this class (3) but their n.m.r. spectra reveal no multiplicity for the methylene protons attributable to magnetic non-equivalence.

Can. J. Chem. Downloaded from www.nrcresearchpress.com by 210.87.254.5 on 09/05/12
For personal use only.

gave the alcohol 4,4′-dinitrotriphenylmethanol[2] (**2***a*) (8). The partial reduction of **2***a* → **2***b* was carried out in 64% yield by addition of sodium polysulfide and sulfur to a refluxing solution of the dinitro compound in aqueous ethanol. The n.m.r. spectrum of **2***b* clearly indicated the presence of two AA′BB′ systems centered at δ 6.91 and 8.0. The only analogous examples of reductions of this type were carried out by Litvinenko and Levchenko, who successfully reduced 4,4′-dinitrodiphenylmethane (9*a*) and 4,4′-dinitrobenzophenone (9*b*) to the corresponding monoamino derivatives in yields of the order of 50%, using phenylhydrazine and sodium disulfide, respectively. Treatment of **2***b* with acetic anhydride gave the amide **2***c* which failed to crystallize, but was readily identified by its infrared (i.r.) and n.m.r. spectra.

Patai and Dayagi reported (4) that the tendency of substituted triarylmethanols to undergo condensation with malonic acid depended on the nature of the aryl substituents. They found that nitro substituted triarylmethanols have little tendency to give carbonium ions and fail to react, whereas carbonium ions formed from more active alcohols (i.e., those containing electron donating substituents), may undergo intramolecular cyclization to form fluorene derivatives (10). Patai and co-workers (11) found that much milder conditions were required for the condensation of triphenylmethyl chloride with active methylene compounds and the extent of side reactions and the amount of by-products were reduced considerably. Our attempt to synthesize 4,4′-dinitrotriphenylmethyl chloride[3] by the reaction of acetyl chloride with the corresponding triarylmethanol derivative (13) gave 4,4′-dinitrobenzophenone in high yield. A precedent for this unusual rearrangement has recently been reported by Starnes (14*a*, 14*b*) who observed a similar rearrangement when certain triarylmethanols were treated with lead tetraacetate.

Despite the difficulties reported for condensation reactions of nitro substituted triarylmethanols (4) we found that fusion of **2***c* with malonic acid at 170° readily furnished the acid **3***a* in 76% yield. The n.m.r. spectrum of this compound indicated the presence of a singlet (CO_2H) at δ 9.84 and a singlet (CH_2) at δ 4.22. The i.r. absorption band at 1715 cm^{-1} substantiated the presence of the acid. Of the methods attempted, hydrolysis of **3***a* to the amino acid **3***b* was found to proceed most smoothly with a solution of 10% aqueous hydrochloric acid in ethanol, although some of the ethyl ester **4***a* was formed in the process. Esterification of the amino acid **3***b* with dimethyl sulfite after the method of Cruickshank and Sheehan (15) produced the methyl ester (**4***b*) in nearly quantitative yield. The n.m.r. spectrum of **4***b* showed a singlet (CH_2) at δ 3.80 and a singlet (CH_3) at δ 3.46.

Experimental

Melting points were determined on a Mettler FP1 Melting and Boiling Point Apparatus and are uncorrected. Elemental analyses were performed using an F and M model 185 CHN analyzer.

Thin-layer chromatographic (t.l.c.) determinations were on Eastman Chromatogram Sheets 6060 coated with silica gel containing fluorescent indicator.

Infrared (i.r.) spectra were recorded on a Perkin–Elmer 225 Grating Spectrophotometer and Beckman IR-8 Spectrophotometer.

Mass spectra were determined on a Hitachi RMU-6E single-focus mass spectrometer using an ionizing voltage of 70 eV and a source temperature of 250°.

The ^1H nuclear magnetic resonance (n.m.r.) spectra were recorded on Varian A-60A and HA-100 spectrometers operating at 60 and 100 MHz respectively. The chemical shifts are in parts per million from tetramethylsilane as internal reference and are recorded on the δ scale.

*4,4′-Diaminotriphenylmethane (**1***a*)*

This compound was prepared in 45% yield according to the procedure of Baeyer and Villeger (5). The solid obtained had a m.p. of 110° in agreement with the value quoted when benzene of crystallization is present.

*4,4′-Dinitrotriphenylmethane (**1***b*)*

4,4′-Diaminotriphenylmethane (**1***a*) (15 g, 0.055 mole) was added to a mixture of 180 ml H_2O_2 (30%), concentrated H_2SO_4 (12 ml), and acetic acid (400 ml) (6). The reaction mixture which immediately turned light-brown was slowly heated to 70° at which point heating was discontinued. After approximately 30 min a solid precipitated from solution and heat was reapplied. The reaction mixture was then maintained between 70–80° overnight. After cooling a yellow-brown product was removed by filtration, washed with water, and dried. A small additional quantity of crude material could also be obtained by the addition of water to the filtrate. Recrystallization from *n*-propyl alcohol – benzene (1:1) gave the required product, m.p. 169–170° (9.3 g, 51%). An analytical sample was prepared by sublimation at 3 mm, 160° (bath) to give yellow prisms, m.p. 169–170°; ν_{max} (KBr) 1605, 1595, 1515

[2]This compound has been previously reported by Deno *et al.* (7). No experimental details on its preparation or physical properties were given.

[3]4,4′-Dinitrotriphenylmethyl chloride has been synthesized by Ziegler and Mathes (12), in a six-step synthesis from *p*-nitrobenzyl chloride.

Can. J. Chem. Downloaded from www.nrcresearchpress.com by 210.87.254.5 on 09/05/12
For personal use only.

(C—NO_2), and 1347 cm^{-1} (C—NO_2); δ ($CDCl_3$) 7.2–8.6 (13 proton multiplet in which an AA′BB′ pattern was observed), 5.9 (one proton singlet, CH); mass spectrometry indicated the presence of a molecular ion at *m/e* 334.

Anal. Calcd. for $C_{19}H_{14}N_2O_4$: C, 68.26; H, 4.22; N, 8.38. Found for **1***b*: C, 68.57; H, 3.97; N, 8.56.

4,4′-Dinitrotriphenylmethanol (2a)

4,4′-Dinitrotriphenylmethane (**1***b*), (10 g, 0.03 mole) was added to a previously cooled solution (0°) of chromium trioxide (6 g, 0.06 mole) and water (6 ml) in acetic acid (40 ml) (8). The reaction mixture was slowly brought to reflux temperature and the disappearance of the methine proton was monitored by removing 5 ml aliquots and examining the n.m.r. spectrum of the product after work-up. The reaction was generally complete after 12 h. Upon cooling a solid precipitated which was removed by filtration, washed with water, and dried. The solid could be recrystallized from $CCl_4 - C_6H_6$ (1:1). Subsequent recrystallization from *n*-propanol gave white crystals of **2***a*, m.p. 133°, (7.96 g, 76%); ν_{max} (KBr) 3565 cm^{-1} (O—H); δ ($CDCl_3$) 7.1–8.6 (13 proton multiplet, benzenoid protons), 3.68 (1 proton singlet, O—H).

Anal. Calcd. for $C_{19}H_{14}N_2O_5$: C, 65.14; H, 4.03; N, 8.00. Found for **2***a*: C, 65.26; H, 4.33; N, 7.86.

(±)-4-Amino-4′-nitrotriphenylmethanol (2b)

4,4′-Dinitrotriphenylmethanol (**2***a*) (5.0 g, 0.14 mole) was dissolved in 5 ml of ethanol and heated to reflux. To this was added dropwise a solution of sodium polysulfide (2.5 g) and sulfur (0.7 g) in aqueous ethanol. Refluxing was continued for 15 min. The reaction solution was then cooled and poured into ten times its volume of ice-water. The yellow solid obtained was removed by filtration and dried *in vacuo*. Recrystallization from *n*-propanol gave a yellow solid which was sufficiently pure to use in subsequent reactions, (2.92 g, 64%). In order to prepare an analytical sample the product was purified by chromatography on neutral alumina (Brockman Activity 1, 80–200 mesh) eluting with benzene followed by benzene–chloroform (1:1). The syrupy product was crystallized from *n*-propanol. Repeated recrystallization from the same solvent gave crystals of **2***b* m.p. 122.5–123°; ν_{max} (KBr) 3458 (OH), 3380 and 3306 (NH), 1615 (NH bending), 1503 and 1340 cm^{-1} (C—NO_2); δ ($CDCl_3$) 6.56–8.42 (13 proton multiplet, benzenoid; two AA′BB′ systems, centered at 6.91 and 8.0 p.p.m. were clearly observed, 3.6 (singlet 3 protons, OH and NH_2 overlapping). Mass spectrometry showed the presence of a molecular ion at *m/e* 320.

Anal. Calcd. for $C_{19}H_{16}N_2O_3$: C, 71.24; H, 5.03; N, 8.75. Found for **2***b*: C, 71.16; H, 4.98; N, 8.59.

(±)-4-Acetanilidyl-4′-nitrophenyl-phenyl-methanol (2c)

(±)-4-Amino-4′-nitrotriphenylmethanol (**2***b*) (20 g, 0.063 mole) was acetylated at room temperature with acetic anhydride (19.1 g, 0.12 mole) in the presence of a few drops of pyridine. After pouring the reaction mixture into water, the product was extracted with chloroform. The solution was washed first with a saturated aqueous $NaHCO_3$ solution, then with water, and dried over anhydrous sodium sulfate. Concentration under reduced pressure yielded a glass which when heated with ligroin gave an amorphous solid. Chromatography of **2***c* on neutral alumina (Brockman Activity 1, 80–200 mesh) eluting with benzene–diethyl ether (3:1) gave a brown glass which could not be induced to crystallize (18.8 g, 83%); ν_{max} (KBr) 1670 cm^{-1} (C=O); δ ($CDCl_3$) 8.2 (1 proton singlet NH), 6.8–8.0 (13 proton multiplet, benzenoid protons), 4.02 (1 proton singlet, OH), and 1.88 (3 proton singlet, CH_3); mass spectrometry indicated the presence of a molecular ion at *m/e* 362.

(±)-3-[4-Acetanilidyl-4′-nitrophenyl-phenyl]-propionic Acid (3a)

To (±)-4-acetanilidyl-4′-nitrophenyl-phenyl-methanol (**2***c*) (2 g, 0.006 mole) was added malonic acid (8 g, 0.08 mole) (4). The solids were fused at 170° for 36 min. After cooling, the product was extracted with a saturated aqueous solution of $NaHCO_3$ and precipitated by the addition of dilute HCl. After filtration the product was dried and recrystallized from benzene. Subsequent recrystallization from ethanol–benzene (1:1) and ethanol, gave a white amorphous solid **3***a*, m.p. 174°, 1.7 g (76%); ν_{max} (KBr) 1715 (C=O, acid), 1665 cm^{-1} (C=O, amide); δ (CF_3CO_2H) 9.84 (1 proton singlet, acid proton), 8.80–7.40 (14 proton multiplet, benzenoid protons overlapping with N—H), 4.22 (2 proton singlet, CH_2), 2.70 (3 proton singlet, CH_3). Mass spectrometry indicated the presence of a molecular ion at *m/e* 404.

Anal. Calcd. for $C_{23}H_{20}N_2O_5$: C, 68.31; H, 4.99; N, 6.93. Found for **3***a*: C, 68.45; H, 5.17; N, 7.01.

Hydrolysis of the Amide 3a and Esterification of the Product to (±)Methyl 3-[4-anilino-4′-nitrophenyl-phenyl]-propionate (4b)

(±)-3-[4-Acetanilidyl-4′-nitrophenyl-phenyl]-propionic acid (**3***a*) (4 g, 0.01 mole) was dissolved in 100 ml of hot aqueous ethanol. An aqueous solution of 10% HCl (40 ml) was then added dropwise. Refluxing was continued until t.l.c. showed complete disappearance of **3***a*. After cooling, ammonium hydroxide (Sp. G.0.90) was added until pH 5.9, whereupon a yellow solid precipitated. Chromatography of the product on partially deactivated alumina (Brockman, Neutral Activity 1 (100 g) to which had been added 5 g water) yielded upon elution with chloroform (±)ethyl 3-[4-anilino-4′-nitrophenyl-phenyl]-propionate (**4***a*), identified by its ^1H n.m.r. and i.r. spectra. The amino acid could be removed from the column by the addition of ammonium hydroxide (Sp. G.0.90). Careful addition of HCl (36.5%) to the ammoniacal solution caused precipitation of the amino acid at pH 5.9. After drying *in vacuo* the solid had a m.p. 120–125°. It was identified as (±)-3-[4-anilino-4′-nitrophenyl-phenyl]-propionic acid (**3***b*) from its i.r. and n.m.r. spectra. The hydrochloride of **3***b* (2 g, 0.005 mole) was esterified with dimethyl sulfite (5 g, 0.045 mole) (15) to give the methyl ester hydrochloride as a glass in quantitative yield. The free amine **4***b* was obtained by treatment of an aqueous ethanolic solution of the hydrochloride of **4***b* with ammonium hydroxide (Sp. G.0.90). The compound failed to recrystallize from any of the usual solvents. Chromatography of **4***b* on neutral alumina (Brockman Activity 1, 80–200 mesh) gave after elution with carbon tetrachloride followed by benzene a yellow glass, which could not be induced to crystallize. Its i.r. spectrum showed ν_{max} 3490 (N—H), 3395 (N—H), 1735 (C=O), 1620 (N—H bending), 1512 (C—NO_2),

1348 cm^{-1} (C—NO_2); δ ($CDCl_3$) 6.50–8.38 (13 proton multiplet, benzenoid; two AA′BB′ systems were clearly discernible), 3.80 (4 protons, a sharp spike for CH_2 superimposed on a broad peak, NH_2), 3.46 (3 proton singlet, CH_3). The 100 MHz n.m.r. spectrum failed to reveal any multiplicity in the signal for the methylene group. A mass spectrum indicated the presence of a molecular ion at *m/e* 376.

Anal. Calcd. for $C_{22}H_{20}N_2O_4$: C, 70.20; H, 5.36; N, 7.44. Found for **4***b*: C, 70.14; H, 5.64; N, 7.58.

Acknowledgments

The authors are pleased to acknowledge the financial support of the National Research Council of Canada. We are also indebted to Dr. R. T. B. Rye for CHN analyses.

1. E. I. Snyder. J. Am. Chem. Soc. **88**, 1165 (1966).
2. V. W. Laurie and D. R. Lide. J. Chem. Phys. **31**, 939 (1959).
3. C. B. Clarke and A. R. Pinder. J. Chem. Soc. 1967 (1958).
4. S. Patai and S. Dayagi. J. Chem. Soc. 716 (1962).
5. A. Baeyer and V. Villeger. Ber. **37**, 2848 (1904).
6. R. R. Holmes and R. P. Bayer. J. Am. Chem. Soc. **82**, 3454 (1960).
7. N. C. Deno, J. J. Jaruzelski, and A. Schriesheim. J. Am. Chem. Soc. **77**, 3044 (1955).
8. K. B. Wiberg and R. J. Evans. Tetrahedron, **8**, 313 (1960).
9. (*a*) L. M. Litvinenko and N. F. Levchenko. Zh. Obsch. Khim. **29**, 3079 (1959). (*b*) L. M. Litvinenko and N. F. Levchenko. Zh. Obsch. Khim. **31**, 562 (1961).
10. R. A. Benkeser and W. Schroeder. J. Org. Chem. **23**, 1059 (1958).
11. S. Patai, S. Dayagi, and R. Friedlander. J. Chem. Soc. 723 (1962).
12. K. Ziegler and W. Mathes. Ann. **479**, 111 (1930).
13. W. E. Bachmann. Org. Syn. Coll. Vol. III. John Wiley and Sons, Inc. New York. 1955. p. 841.
14. (*a*) W. H. Starnes, Jr. J. Am. Chem. Soc. **90**, 1807 (1968). (*b*) W. H. Starnes, Jr. J. Am. Chem. Soc. **89**, 3368 (1967).
15. P. A. Cruickshank and J. C. Sheehan. Anal. Chem. **36**, 1191 (1964).

Can. J. Chem. Downloaded from www.nrcresearchpress.com by 210.87.254.5 on 09/05/12
For personal use only.

Can. J. Chem. Downloaded from www.nrcresearchpress.com by 210.87.254.42 on 09/05/12
For personal use only.

Total synthesis of the *Ormosia* alkaloid skeleton

H. J. LIU, Z. VALENTA, J. S. WILSON, AND T. T. J. YU
Department of Chemistry, University of New Brunswick, Fredericton, New Brunswick

Received November 29, 1968

A total synthesis of dilactam (**3**) possessing the complete pentacyclic skeleton of the *Ormosia* alkaloids has been completed.

Canadian Journal of Chemistry, **47**, 509 (1969)

The determination of the structure of the *Ormosia* alkaloid jamine by X-ray crystallography (1) led directly to the structure of ormosanine and, through a study of the reduction of the dehydrogenation product (**1**) (2, 3), to the structure and stereochemistry of additional alkaloids of this type (4). Since the alkaloid piptanthine (**2**) together with four isomeric bases has already been prepared by a controlled reduction of **1** (4) and since most of the stereochemical and functional variation in compounds of this class occurs in rings A, B, and E, it was deemed desirable to develop a synthetic approach in which ring E would be aromatic to the penultimate stage and in which ring A would be added last. The following total synthesis of the crystalline racemic dilactam (**3**) satisfies these requirements.

The known compound (**4**) (5), m.p. 126–127°, was reduced with Pd–C in ethanol to give an 80% yield of the oily lactam ester (**5**), a mixture of at least two isomers.[1] Treatment of crude **5** with sodium hydride and ethyl acrylate in dimethyl formamide at 110° for 12 h gave the keto-ester (**6**), m.p. 155–156°, in 53% yield. In order to establish its stereochemistry, **6** was hydrolyzed with 10% aqueous sulfuric acid to give **7**, m.p. 173–176°. Vigorous reduction of **7** with lithium aluminium hydride gave the corresponding hydroxyamine which showed strong Bohlmann bands (6) in the 2800 cm^{-1} region of the i.r. spectrum ($CHCl_3$). Based on previous study (4), this clearly establishes that the C_6—H is *cis* to the C_7—C_9 bridge. Treatment of **6** with selenium dioxide and acetic acid in boiling *tert*-butyl alcohol gave the unsaturated keto-ester (**8**), m.p. 200–201°, in 78% yield; this was then converted to ketone (**9**), m.p. 193–194°, in 71% yield on boiling with 10% aqueous sulfuric acid.

Since standard methods applied for construction of ring A using **7**, **8**, and **9** proved unpromising, the following novel synthetic application of the versatile photo-addition of olefins to α,β-unsaturated ketones[2] was developed. Irradiation of **9** in vinyl acetate and tetrahydrofuran (Hanovia 100 W High-Pressure Hg vapor lamp, Pyrex filter) at 25° for 2 h gave a 60% yield of a mixture composed of four isomers of acetate (**10**). Bromination of crude **10** with pyridinium bromide perbromide in glacial acetic acid gave a mixture of four bromo-ketones (**11**) in 78% yield. Treatment of crude **11** with sodium carbonate in aqueous methanol followed by chromatography on silica gel gave a 76% yield of pure keto-aldehyde (**12**), i.r. maxima at 2730, 1730, 1680, 1640, 1585, and 1575 cm^{-1}, nuclear magnetic resonance signals at 0.32 and 2.25 τ (singlet). Although a fragmentation reaction (8) in compound (**11**) could in principle take place in two different ways, fragmentation in the sense of the dotted arrow in formula (**11**) was in fact not observed.

Reduction of **12** with lithium aluminium tri-*tert*-butoxy hydride in tetrahydrofuran to alcohol (**13**) (89% yield) was followed by conversion with methanesulfonyl chloride in pyridine to **14** (97%) and by a treatment of the mesylate with lithium

[1]All reported compounds showed satisfactory spectral properties, including correct molecular ions in mass spectrometry. For brevity, only spectral data of special significance are given. All crystalline compounds gave correct elemental analysis. Unless otherwise stated, all oily compounds were purified by column chromatography on silica gel and were homogeneous in thin-layer chromatography.

[2]See reference (7) for a recent summary of relevant literature.

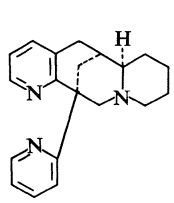

1

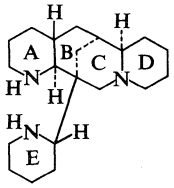

2

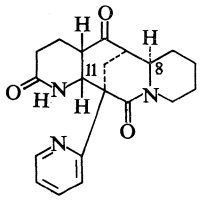

3

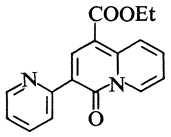

4

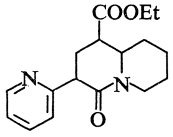

5

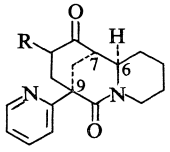

6 R = COOEt
7 R = H

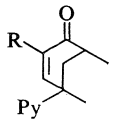

8 R = COOEt
9 R = H

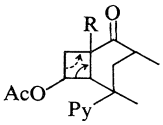

10 R = H
11 R = Br

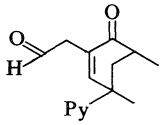

12

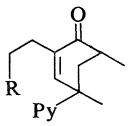

13 R = OH
14 R = OMs
15 R = Cl
18 R = CN
19 R = COOEt

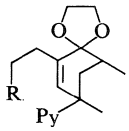

16 R = Cl
17 R = CN

chloride in boiling acetone to give the chloride (**15**) in 84% yield. Spectroscopic and analytical evidence has indicated that treatment of **15** with sodium cyanide does not give the desired nitrile (**18**), but in fact involves the addition of the cyanide ion to the β-position of the α,β-unsaturated ketone with the concomitant formation of a cyclopropane ring. In order to prevent this interesting reaction, **15** was first converted to the ketal **16** with ethylene glycol and *p*-toluenesulfonic acid in boiling benzene in 98% yield. As expected, **16** underwent normal displacement with sodium cyanide in dimethyl sulfoxide at 125° to give nitrile (**17**) in 98% yield. Deketalization of **17** with 10% sulfuric acid in tetrahydrofuran gave **18** (95% yield), which was converted to the keto-ester (**19**) in 85% yield on treatment with alcoholic hydrogen chloride followed by hydrolysis of the resulting imino-ester on a column of silica gel.

Finally, prolonged treatment of **19** with ammonia in ethanol gave the desired dilactam (**3**), m.p. 245–247°, in 65% yield (*m/e* 353, i.r. maxima at 3310, 1715, 1638, 1590 and 1575 cm^{-1}). The stereochemistry of the A/B ring-juncture in **3** follows from the fact that the addition of ammonia to the unsaturated ketone in **19** can be expected to take place from the side opposite to the bulky tertiary lactam grouping and from the coupling constant of the C_{11}-H atom (J_{AB} = 4 c.p.s.; 5.2 τ) which is in agreement with a *cis*-juncture.

The totally synthetic dilactam (**3**) has the correct stereochemistry at C-6 for the synthesis of the dipyridine (**1**) and at C-6 and C-11 for the synthesis of the alkaloid ormojanine (3). The efficient conversion of **3** to compounds of natural origin and the general scope of the fragmentation reaction **11** → **12** are under active study.

Acknowledgments

The financial assistance of the National Re-

Can. J. Chem. Downloaded from www.nrcresearchpress.com by 210.87.254.42 on 09/05/12
For personal use only.

search Council of Canada and National Research Council of Canada Fellowships to H. J. Liu and J. S. Wilson are gratefully acknowledged.

1. T. L. KARLE and J. KARLE. Tetrahedron Letters, 2065 (1963).
2. P. NAEGELI, R. NAEGELI, W. C. WILDMAN, and R. J. HIGHET. Tetrahedron Letters, 2075 (1963).
3. Z. VALENTA, P. DESLONGCHAMPS, M. H. RASHID, R. H. WIGHTMAN, and J. S. WILSON. Can. J. Chem. **44**, 2525 (1966).
4. P. DESLONGCHAMPS, Z. VALENTA, and J. S. WILSON. Can. J. Chem. **44**, 2539 (1966).
5. G. CLEMO, W. MORGAN, and R. RAPER. J. Chem. Soc. 1025 (1936).
6. F. BOHLMANN. Chem. Ber. **91**, 2157 (1958).
7. P. DE MAYO, J-P. PETE, and M. TCHIR. Can. J. Chem. **46**, 2535 (1968).
8. C. A. GROB and P. W. SCHIESS. Angew. Chem. **79**, 1 (1967).

Facile elimination accompanying some methyl sulfoxide oxidations. Formation of unsaturated carbohydrates

G. M. CREE,[1] D. W. MACKIE, AND A. S. PERLIN
Department of Chemistry, McGill University, Montreal, Quebec

Received October 16, 1968

Oxidation of some partially-acetylated carbohydrates with methyl sulfoxide, activated by sulfur trioxide – pyridine and triethylamine, leads to facile elimination of the elements of acetic acid and the formation of novel, unsaturated, derivatives.

Canadian Journal of Chemistry, **47**, 511 (1969)

Can. J. Chem. Downloaded from www.nrcresearchpress.com by 210.87.254.42 on 09/05/12
For personal use only.

Pfitzner and Moffatt (1) found that the treatment of various nucleotides and nucleoside derivatives with a mixture of methyl sulfoxide (DMSO), dicyclohexylcarbodiimide, and orthophosphoric acid, results in rapid oxidation of unprotected hydroxyl groups of the sugar moieties and, in some instances, in extensive elimination of substituents. Thymidine, for example, yielded the free base and inorganic phosphate, probably because DMSO oxidation of the 3^1- hydroxyl group was followed by acid-catalyzed β-elimination (1). Other compounds, however, were oxidized smoothly without decomposition. Originating in these observations, DMSO oxidation now finds wide use for the preparation of carbonyl compounds from alcohols (2), although accompanying elimination reactions appear to be rarely encountered.

In examining the reaction of various carbohydrate derivatives with a modified oxidant developed by Parikh and Doering (3)—which consists of DMSO, sulfur trioxide, pyridine, and triethylamine—we have found that some compounds undergo both oxidation and elimination rapidly and efficiently. In such instances the reaction provides a high-yield route to novel types of unsaturated carbohydrates.

For example, methyl 2,3,4-tri-*O*-acetyl-α-D-mannopyranoside (**1**) was treated with the oxidant (3) for 15 min. The reaction mixture was diluted with chloroform, washed successively with cold, saturated tartaric acid and sodium bicarbonate, and concentrated, affording a crystalline solid (**2**) in 75% yield; m.p. 57 °C.

Anal. Calcd. for $C_{11}H_{14}O_7$ (mol. wt., 258): C, 51.16; H, 5.47. Found (M^+, 258): C, 51.1; H, 5.4.

The proton magnetic resonance spectrum of **2** ($CDCl_3$) indicates that it is an aldehyde (δ 9.2, one H, singlet), and that it contains two *O*-acetyl groups, one *O*-methyl group, and one H on each of C-1 to C-4. Together with other spectral data λ_{max} 250nm,ε 3600 (CH_3OH); 1720 cm^{-1} (HC=O), 1660 cm^{-1} (C=C) and chemical tests (reaction with semicarbazide; bromine uptake following borohydride reduction), this evidence shows that **2** is a 6-*aldehydo* derivative containing a 4,5-double bond, i.e., methyl 2,3-di-*O*-acetyl-6-*aldo*-4-deoxy-β-L-*erythro*-hex-4-enopyranoside. Its formation from **1** is attributed to DMSO oxidation of the primary carbinol group followed by elimination of H-5 and the 4-acetoxyl group, the latter step perhaps being catalyzed by the triethylamine present.[2]

[1]Harold Hibbert Memorial Postdoctorate Fellow, 1967–1968.

[2]Although this may involve a *cis*-elimination, a referee has pointed out that prior epimerization at C-5 could result in a *trans*-elimination. As shown herein, however, a compound in which the H and OAc eliminated are *trans* originally is less reactive than its epimer.

search Council of Canada and National Research Council of Canada Fellowships to H. J. Liu and J. S. Wilson are gratefully acknowledged.

1. T. L. KARLE and J. KARLE. Tetrahedron Letters, 2065 (1963).
2. P. NAEGELI, R. NAEGELI, W. C. WILDMAN, and R. J. HIGHET. Tetrahedron Letters, 2075 (1963).
3. Z. VALENTA, P. DESLONGCHAMPS, M. H. RASHID, R. H. WIGHTMAN, and J. S. WILSON. Can. J. Chem. **44**, 2525 (1966).
4. P. DESLONGCHAMPS, Z. VALENTA, and J. S. WILSON. Can. J. Chem. **44**, 2539 (1966).
5. G. CLEMO, W. MORGAN, and R. RAPER. J. Chem. Soc. 1025 (1936).
6. F. BOHLMANN. Chem. Ber. **91**, 2157 (1958).
7. P. DE MAYO, J-P. PETE, and M. TCHIR. Can. J. Chem. **46**, 2535 (1968).
8. C. A. GROB and P. W. SCHIESS. Angew. Chem. **79**, 1 (1967).

Facile elimination accompanying some methyl sulfoxide oxidations. Formation of unsaturated carbohydrates

G. M. CREE,[1] D. W. MACKIE, AND A. S. PERLIN
Department of Chemistry, McGill University, Montreal, Quebec

Received October 16, 1968

Oxidation of some partially-acetylated carbohydrates with methyl sulfoxide, activated by sulfur trioxide – pyridine and triethylamine, leads to facile elimination of the elements of acetic acid and the formation of novel, unsaturated, derivatives.

Canadian Journal of Chemistry, **47**, 511 (1969)

Can. J. Chem. Downloaded from www.nrcresearchpress.com by 210.87.254.105 on 09/05/12
For personal use only.

Pfitzner and Moffatt (1) found that the treatment of various nucleotides and nucleoside derivatives with a mixture of methyl sulfoxide (DMSO), dicyclohexylcarbodiimide, and orthophosphoric acid, results in rapid oxidation of unprotected hydroxyl groups of the sugar moieties and, in some instances, in extensive elimination of substituents. Thymidine, for example, yielded the free base and inorganic phosphate, probably because DMSO oxidation of the 3^1- hydroxyl group was followed by acid-catalyzed β-elimination (1). Other compounds, however, were oxidized smoothly without decomposition. Originating in these observations, DMSO oxidation now finds wide use for the preparation of carbonyl compounds from alcohols (2), although accompanying elimination reactions appear to be rarely encountered.

In examining the reaction of various carbohydrate derivatives with a modified oxidant developed by Parikh and Doering (3)—which consists of DMSO, sulfur trioxide, pyridine, and triethylamine—we have found that some compounds undergo both oxidation and elimination rapidly and efficiently. In such instances the reaction provides a high-yield route to novel types of unsaturated carbohydrates.

For example, methyl 2,3,4-tri-*O*-acetyl-α-D-mannopyranoside (**1**) was treated with the oxidant (3) for 15 min. The reaction mixture was diluted with chloroform, washed successively with cold, saturated tartaric acid and sodium bicarbonate, and concentrated, affording a crystalline solid (**2**) in 75% yield; m.p. 57 °C.

Anal. Calcd. for $C_{11}H_{14}O_7$ (mol. wt., 258): C, 51.16; H, 5.47. Found (M^+, 258): C, 51.1; H, 5.4.

The proton magnetic resonance spectrum of **2** ($CDCl_3$) indicates that it is an aldehyde (δ 9.2, one H, singlet), and that it contains two *O*-acetyl groups, one *O*-methyl group, and one H on each of C-1 to C-4. Together with other spectral data λ_{max} 250nm,ε 3600 (CH_3OH); 1720 cm^{-1} (HC=O), 1660 cm^{-1} (C=C) and chemical tests (reaction with semicarbazide; bromine uptake following borohydride reduction), this evidence shows that **2** is a 6-*aldehydo* derivative containing a 4,5-double bond, i.e., methyl 2,3-di-*O*-acetyl-6-*aldo*-4-deoxy-β-L-*erythro*-hex-4-enopyranoside. Its formation from **1** is attributed to DMSO oxidation of the primary carbinol group followed by elimination of H-5 and the 4-acetoxyl group, the latter step perhaps being catalyzed by the triethylamine present.[2]

[1]Harold Hibbert Memorial Postdoctorate Fellow, 1967–1968.

[2]Although this may involve a *cis*-elimination, a referee has pointed out that prior epimerization at C-5 could result in a *trans*-elimination. As shown herein, however, a compound in which the H and OAc eliminated are *trans* originally is less reactive than its epimer.

Can. J. Chem. Downloaded from www.nrcresearchpress.com by 210.87.254.105 on 09/05/12
For personal use only.

Elimination also accompanied the oxidation of 1,2,3,4-tetra-*O*-acetyl-β-D-glucopyranose. Under the same reaction conditions, the latter afforded an 83% yield of a chromatographically-pure syrup[3] (**3**); δ, 9.2 (one H, singlet), three *O*-acetyl singlets, and one H signal for each of C-1 to C-4 ($CDCl_3$); λ_{max} 245 nm, ε 2750 (CH_3OH); 1725 cm^{-1} (HC=O), 1662 cm^{-1} (C=C); semicarbazone, m.p. 205–207 °C.

Anal. Calcd. for $C_{13}H_{17}N_3O_8$ (mol. wt., 343): N, 12.24. Found (M^+, 343): N, 12.38.

Similarly, methyl 2,3,4-tri-*O*-acetyl-α-D-glucopyranoside gave syrupy **4** in 82% yield. The overall spectral characteristics of **4** paralleled those of **2** and **3** sufficiently closely to indicate that this product also is an α,β-unsaturated 6-aldehyde, i.e., the expected L-*threo* isomer corresponding to **2**.

Facile elimination has been found also with partially-acetylated derivatives in which the free hydroxyl group is secondary or an anomeric hydroxyl. Thus, 2,3,4,6-tetra-*O*-acetyl-α-D-glucopyranose yielded 81% of a syrupy product (**5**); 1755 cm^{-1} (broad multiplet, C=O), 1670 cm^{-1} (C=C); one H signal for each of C-3 to C-5, two H signals for C-6, δ 2.10–2.15 (two *O*-acetyl singlets), δ 2.3 (enol acetate singlet)($CDCl_3$); *m/e* 244 ($M - COCH_2$), *m/e* 226 ($M - CH_3COOH$), *m/e* 184 ($M - CH_2CO - CH_3COOH$), etc. Since 2,3,4,6-tetra-*O*-acetyl-α-D-mannopyranose also yielded the same product, although at only about one-third the rate of the D-*gluco*-epimer, **5** undoubtedly is an α,β-unsaturated lactone (i.e., 2,4,6-tri-*O*-acetyl-3-deoxy-D-*erythro*-hex-2-en-2-ol-1 → 5 lactone) the formation of which must involve elimination of H-2 and the 3-acetoxyl group. *Two* elimination reactions accompanied the oxidation of 1,3,4,6-tetra-*O*-acetyl-α-D-glucopyranose, which afforded an unsaturated diacetate (**6**) in 61% yield; m.p. 95 °C, $[\alpha]_D$ 0° (5, CH_3OH).

Anal. Calcd. for $C_{10}H_{10}O_6$ (mol. wt., 226): C, 53.10; H, 4.46. Found (M^+, 226): C, 53.5; H, 4.4.

[3]All syrupy products were contaminated with small quantities of odorous by-products which were difficult to remove by distillation.

λ_{max} 252 nm, ε 1060 (CH_3OH); 3082 cm^{-1}, 980 cm^{-1} ($C=CH_2$); 1781 cm^{-1} (enol Ac), 1760 cm^{-1} (OAc), 1678 cm^{-1} (doublet C=O, C=C); δ 7.85 (1H, singlet), 7.05 (1H, singlet), 4.90 (2H, singlet), 2.30 (enol Ac, singlet), 2.15 (OAc, singlet) ($CDCl_3$). Tentatively, **6** is formulated as the conjugated 3,5-diene-2-one that would be derived by successive α,β- and γ,δ-eliminations.

1,2:3,4-Di-*O*-isopropylidene-α-D-galactopyranose, when oxidized under the same conditions, did not undergo elimination but readily yielded the 6-*aldehydo* diketal (4) in 85% yield. Similarly, 1,2:4,5-di-*O*-isopropylidene-D-*erythro*-hexopyranos-2,3-diulose (5–7) was prepared in 65% yield by oxidation of 1,2:4,5-di-*O*-isopropylidene-D-fructopyranose. In both reactions, only a trace of the contaminating methyl thiomethyl ether was produced, and the work-up of the reaction mixtures appeared to be more satisfactory than in parallel experiments (4–7) with other modifications of the DMSO oxidant. Also, in preliminary experiments with partially-substituted *O*-benzyl and *O*-trimethylsilyl ethers satisfactory oxidation without elimination has been observed, but 1,2:3,5-di-*O*-methylene-α-D-glucofuranose suffered extensive decomposition to unidentified products. Since the methylene groups themselves are not attacked by the reagent, this breakdown probably was initiated by formation of the 6-aldehydo compound.

Acknowledgment

The authors gratefully acknowledge financial support by the National Research Council of Canada, and technical assistance by N. Ness.

1. K. E. PFITZNER and J. G. MOFFATT. J. Am. Chem. Soc. **85**, 3027 (1963); K. E. PFITZNER and J. G. MOFFATT. J. Am. Chem. Soc. **87**, 5661 (1965).
2. W. W. EPSTEIN and F. W. SWEAT. Chem. Rev. **67**, 247 (1967).
3. J. R. PARIKH and W. VON E. DOERING. J. Am. Chem. Soc. **89**, 5505 (1967).
4. D. HORTON, M. NAKADATE, and J. M. J. TRONCHET. Carbohyd. Res. **7**, 56 (1968).
5. E. J. MCDONALD. Carbohyd. Res. **5**, 106 (1967).
6. K. JAMES, A. R. TATCHELL, and P. K. RAY. J. Chem. Soc. (C) 2681 (1967).
7. G. M. CREE and A. S. PERLIN. Can. J. Biochem. **46**, 765 (1968).

A nuclear magnetic resonance study of the conformations of triribonucleoside diphosphates, diribonucleoside phosphates, 5′-ribonucleoside phosphates, and ribonucleosides of uracil and cytosine; temperature dependence of the base proton chemical shifts[1]

IAN C. P. SMITH[2] AND B. J. BLACKBURN[3]
Division of Biochemistry and Molecular Biology, National Research Council of Canada, Ottawa 7, Canada

AND

TETSUO YAMANE
Bell Telephone Laboratories, Murray Hill, New Jersey 07974

Received November 28, 1968

The temperature dependence of the nuclear magnetic resonance spectra of U, C, 5′-UMP, 5′-CMP, UpU, and CpU indicates a specific deshielding of the base proton at position-6 by an hydroxyl, phosphodiester, or phosphate group at position-5′, and demonstrates that in these compounds the bases exist in the *anti* conformation. Similar experiments on the wobble pair UpUpU and UpUpC suggest that the spatial arrangements of both trinucleoside diphosphates are identical, and that in these arrangements the bases are predominantly in the *anti* conformation.

La variation avec la température de spectres de résonance magnétique nucléaire de U, C, 5′-UMP, 5′-CMP, UpU, et CpU indique un effet spécifique de déblindage des protons des bases à la position-6 par des groupements-5′ hydroxyls, phosphodiesters, ou phosphates, et démontre que dans ces composés les bases ont la conformation *anti*. Des expériences semblables sur le couple de "wobble" UpUpU et UpUpC suggèrent que les structures des deux composés soient identiques, et que dans ces structures les bases aient surtout la conformation *anti*.

Canadian Journal of Chemistry, **47**, 513 (1969)

The fundamental unit of genetic information in messenger RNA is a trinucleotide sequence (1). In the genetic code more than one such sequence can represent a particular amino acid, i.e. for phenylalanine the codons are UpUpU and UpUpC.[4] In order to account for the recognition of degenerate codons by the trinucleotide in the anticodon position of transfer RNA, Crick proposed that the conditions for binding of the third base are less stringent than those for the first two, i.e. the third base is allowed to "wobble" (2). As part of a study of trinucleotide-transfer RNA interactions we have investigated the 220 MHz nuclear magnetic resonance spectra of UpUpU and UpUpC, and related nucleotides, nucleosides, and dinucleoside phosphates. We present here evidence that the environments of the corresponding bases in UpUpU and UpUpC are identical, and that the bases are present in the *anti* conformation relative to the 5′-position.

In Fig. 1 we show the 220 MHz spectra due to the protons at position-6 in the uracil and cytosine moieties of UpUpU and UpUpC at 15 and 53 °C. The individual U and C resonances can be identified by means of the spin–spin splitting due to the protons at position-5 (8.0 Hz for U, 7.5 Hz for C). In the 15 °C spectrum of UpUpU it is apparent that the magnetic environments of two of the uracil bases are equivalent; in the corresponding spectrum for UpUpC the two uracil bases are magnetically equivalent to one another, as well as to the two equivalent uracil bases in UpUpU. Similarly, in the 53 °C spectra of UpUpU and UpUpC, the uracil resonances of both codons fall in almost identical positions. This suggests strongly that the orientations of the bases in UpUpU and UpUpC are identical. Further evidence for this comes from the temperature dependence of the chemical shifts of the protons at position-6, illustrated in Fig. 2. The resonances due to the two U bases of UpUpU and UpUpC, which were equivalent at 15 °C,

[1]NRCC No. 10539. Presented at the International Symposium on Macromolecular Chemistry, Toronto, Ontario. September 1968.
[2]To whom all correspondence should be addressed.
[3]NRCC Postdoctorate Fellow, 1968–1969.
[4]Abbreviations used: UpUpU, uridylyl-(3′,5′)-uridylyl-(3′,5′)-uridine; UpUpC, uridylyl-(3′,5′)-uridylyl-(3′,5′)-cytidine; U, uridine; C, cytidine; 5′-UMP, uridine-5′-phosphate; 5′-CMP, cytidine-5′-phosphate.

Can. J. Chem. Downloaded from www.nrcresearchpress.com by 210.87.254.42 on 09/05/12
For personal use only.

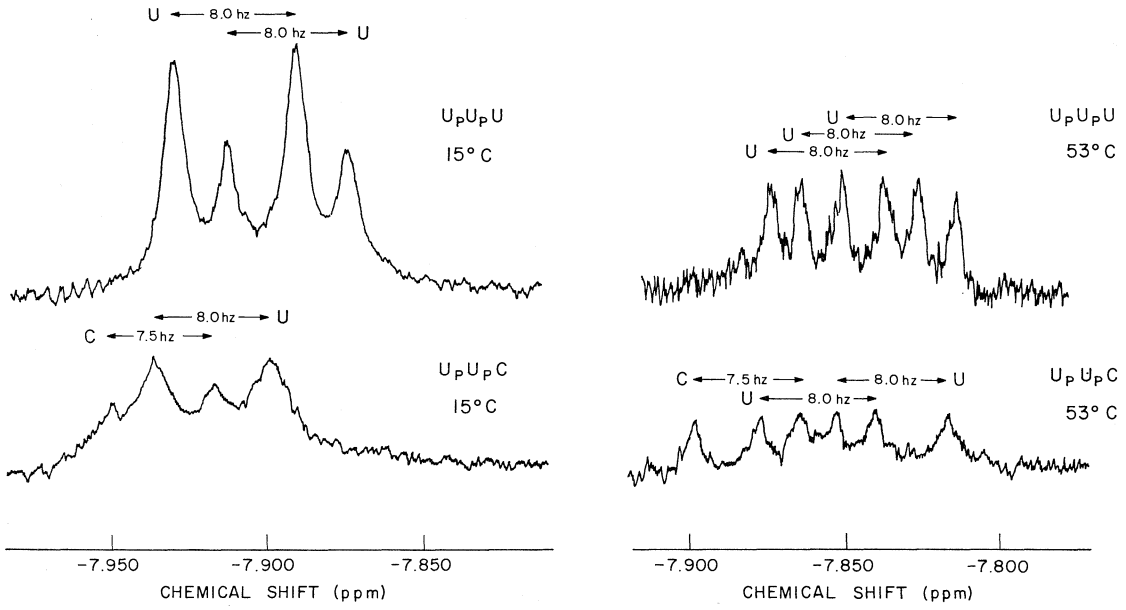

FIG. 1. 220 MHz nuclear magnetic resonance spectra (region due to the protons at position-6 only) of 0.02 *M* solutions of UpUpU and UpUpC in D_2O, pD 7.0, 0.1 *M* NaCl, 0.04 *M* $MgCl_2$. Chemical shifts are measured relative to internal 3-(trimethylsilyl)-propanesulfonic acid.

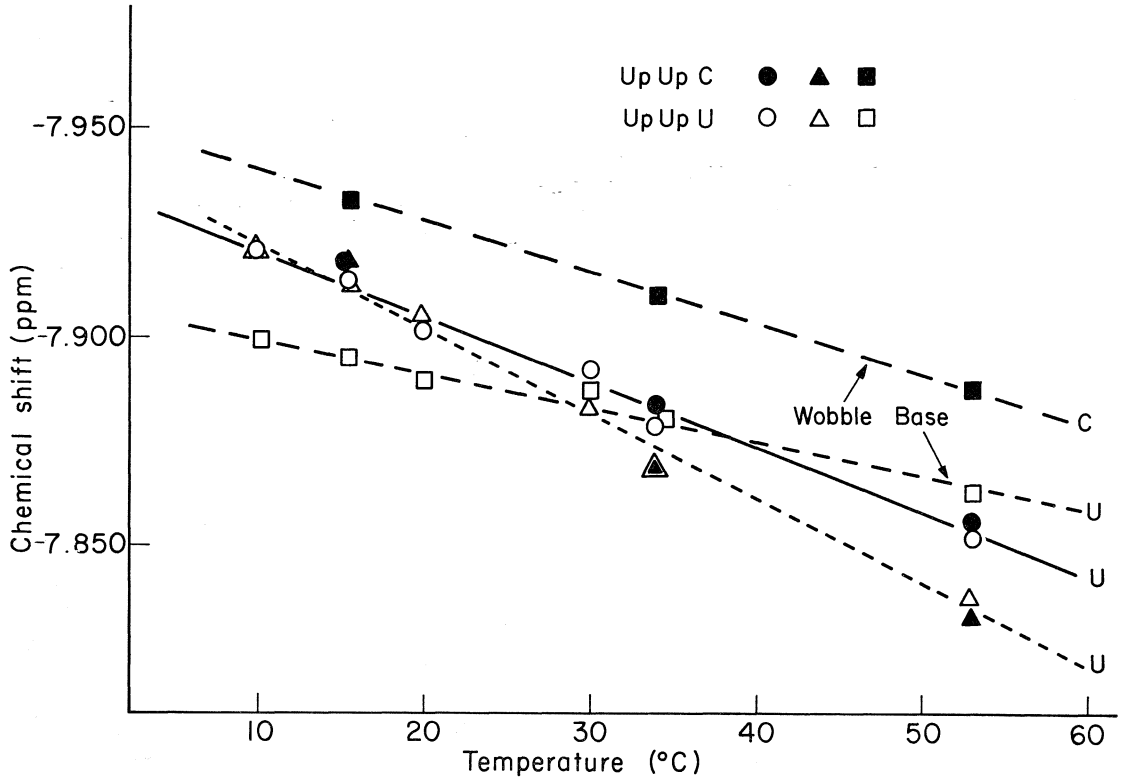

FIG. 2. Temperature dependence of the chemical shifts of the protons at position-6 in the bases of UpUpU (open symbols) and UpUpC (filled symbols). Other conditions were the same as for Fig. 1.

Can. J. Chem. Downloaded from www.nrcresearchpress.com by 210.87.254.42 on 09/05/12
For personal use only.

show identical temperature dependences (indicated by circle and triangles in Fig. 2, open for UpUpU, filled for UpUpC). The third U resonance of UpUpU has a temperature dependence very similar to that of the C resonance in UpUpC; we assign this third U resonance (indicated by open squares in Fig. 2) to the uracil at the 3′ wobble end of UpUpU. This assignment is valuable for a study of the relative binding constants of the three bases of UpUpU and UpUpC to the anticodon region of $tRNA^{Phe}$.

In order to elucidate the source of these temperature-dependent chemical shifts in terms of molecular structure, we have examined the n.m.r. spectra of the relevant 5′-nucleotides, nucleosides, and dinucleoside phosphates under the same conditions. For each of U, C, 5′-UMP, and 5′-CMP the resonances due to the protons at position-6 moved to higher magnetic field (lower chemical shift) with increasing temperature, at rates comparable to those shown in Fig. 2, whereas the resonances due to the protons at position-5 did not vary appreciably with temperature. Similar behavior was observed for both bases of each of UpU and CpU. Schweizer *et al.* have demonstrated that substitution of a charged phosphate group at position-5′ in U or C causes a specific downfield shift (deshielding) of the resonance due to the proton at position-6, while causing no appreciable change in the resonance due to the proton at position-5 (3). They presented strong evidence that this was due to the bases being in the *anti* conformation relative to the 5′-position—that is, with the base rotated about the glycosyl bond so that the 5,6 side of the pyrimidine ring is directed towards the 5′-position. In this conformation the proton at position-6 of the pyrimidine ring is much nearer the 5′-position than is the proton at position-5 of the pyrimidine ring. A comparison of earlier 30 °C nuclear magnetic resonance spectra of pUpU and UpU (4) suggests that the effect of a monocharged 5′-phosphodiester linkage is similar to that of a 5′-hydroxyl group. The observed temperature dependences reported here for 5′-UMP and 5′-CMP are consistent with the removal of a specific deshielding effect by a gradual conversion of the conformations from *anti* to *syn*. Our observation that U, C, UpU, and CpU all exhibit behavior similar to that of 5′-UMP and 5′-CMP indicates that the 5′-hydroxyl group also has a specific deshielding effect on the protons at position-6, which is considerably weaker than that due to a doubly-charged 5′-phosphate but comparable to that due to a singly-charged 5′-phosphodiester group. Thus, the temperature dependences of the resonances due to the U and C moieties of UpUpU and UpUpC suggest that in the trinucleoside diphosphates at physiological temperatures all the bases are predominantly in the *anti* conformation.

Acknowledgment

We are indebted to Dr. R. G. Shulman and Dr. M. P. Schweizer for helpful discussions.

1. Cold Spring Harbour Symposia on Quantitative Biology, **31** (1966).
2. F. H. C. Crick. J. Mol. Biol. **19**, 548 (1966).
3. M. P. Schweizer, A. D. Broom, P. O. P. Ts'O, and D. P. Hollis. J. Am. Chem. Soc. **90**, 1042 (1968).
4. M. P. Schweizer. Ph.D. Dissertation. The Johns Hopkins University, Baltimore, Maryland. 1968.

Synthetic approach to ryanodine; the use of *O*-spirodienone lactone in organic synthesis

Daniel Berney and Pierre Deslongchamps[1]
Département de Chimie, Université de Sherbrooke, Sherbrooke, Québec

Received November 19, 1968

The key steps for this synthetic approach are the preparation of *o*-spirodienone lactone **15**, its reaction with methylvinyl ketone which gave **16** and **17**, and the conversion of **16** and **17** into compound **19** by base. Finally ozonolysis of **26** followed by internal condensation gave compound **28**.

Canadian Journal of Chemistry, **47**, 515 (1969)

The insecticide ryanodine **1** isolated from *Ryana speciosa* Vahl is the ester of pyrrole-α-carboxylic acid with ryanodol **2**. The structure elucidation of this complex insecticide and one of its key degradation products, anhydroryanodol **3** was solved by Valenta and Wiesner and their

[1]To whom inquiries should be addressed.

Can. J. Chem. Downloaded from www.nrcresearchpress.com by 210.87.254.42 on 09/05/12
For personal use only.

Can. J. Chem. Downloaded from www.nrcresearchpress.com by 210.87.254.40 on 09/05/12
For personal use only.

show identical temperature dependences (indicated by circle and triangles in Fig. 2, open for UpUpU, filled for UpUpC). The third U resonance of UpUpU has a temperature dependence very similar to that of the C resonance in UpUpC; we assign this third U resonance (indicated by open squares in Fig. 2) to the uracil at the 3′ wobble end of UpUpU. This assignment is valuable for a study of the relative binding constants of the three bases of UpUpU and UpUpC to the anticodon region of $tRNA^{Phe}$.

In order to elucidate the source of these temperature-dependent chemical shifts in terms of molecular structure, we have examined the n.m.r. spectra of the relevant 5′-nucleotides, nucleosides, and dinucleoside phosphates under the same conditions. For each of U, C, 5′-UMP, and 5′-CMP the resonances due to the protons at position-6 moved to higher magnetic field (lower chemical shift) with increasing temperature, at rates comparable to those shown in Fig. 2, whereas the resonances due to the protons at position-5 did not vary appreciably with temperature. Similar behavior was observed for both bases of each of UpU and CpU. Schweizer *et al.* have demonstrated that substitution of a charged phosphate group at position-5′ in U or C causes a specific downfield shift (deshielding) of the resonance due to the proton at position-6, while causing no appreciable change in the resonance due to the proton at position-5 (3). They presented strong evidence that this was due to the bases being in the *anti* conformation relative to the 5′-position—that is, with the base rotated about the glycosyl bond so that the 5,6 side of the pyrimidine ring is directed towards the 5′-position. In this conformation the proton at position-6 of the pyrimidine ring is much nearer the 5′-position than is the proton at position-5 of the pyrimidine ring. A comparison of earlier 30 °C nuclear magnetic resonance spectra of pUpU and UpU (4) suggests that the effect of a monocharged 5′-phosphodiester linkage is similar to that of a 5′-hydroxyl group. The observed temperature dependences reported here for 5′-UMP and 5′-CMP are consistent with the removal of a specific deshielding effect by a gradual conversion of the conformations from *anti* to *syn*. Our observation that U, C, UpU, and CpU all exhibit behavior similar to that of 5′-UMP and 5′-CMP indicates that the 5′-hydroxyl group also has a specific deshielding effect on the protons at position-6, which is considerably weaker than that due to a doubly-charged 5′-phosphate but comparable to that due to a singly-charged 5′-phosphodiester group. Thus, the temperature dependences of the resonances due to the U and C moieties of UpUpU and UpUpC suggest that in the trinucleoside diphosphates at physiological temperatures all the bases are predominantly in the *anti* conformation.

Acknowledgment

We are indebted to Dr. R. G. Shulman and Dr. M. P. Schweizer for helpful discussions.

1. Cold Spring Harbour Symposia on Quantitative Biology, **31** (1966).
2. F. H. C. Crick. J. Mol. Biol. **19**, 548 (1966).
3. M. P. Schweizer, A. D. Broom, P. O. P. Ts'O, and D. P. Hollis. J. Am. Chem. Soc. **90**, 1042 (1968).
4. M. P. Schweizer. Ph.D. Dissertation. The Johns Hopkins University, Baltimore, Maryland. 1968.

Synthetic approach to ryanodine; the use of *O*-spirodienone lactone in organic synthesis

Daniel Berney and Pierre Deslongchamps[1]
Département de Chimie, Université de Sherbrooke, Sherbrooke, Québec

Received November 19, 1968

The key steps for this synthetic approach are the preparation of *o*-spirodienone lactone **15**, its reaction with methylvinyl ketone which gave **16** and **17**, and the conversion of **16** and **17** into compound **19** by base. Finally ozonolysis of **26** followed by internal condensation gave compound **28**.

Canadian Journal of Chemistry, **47**, 515 (1969)

The insecticide ryanodine **1** isolated from *Ryana speciosa* Vahl is the ester of pyrrole-α-carboxylic acid with ryanodol **2**. The structure elucidation of this complex insecticide and one of its key degradation products, anhydroryanodol **3** was solved by Valenta and Wiesner and their

[1]To whom inquiries should be addressed.

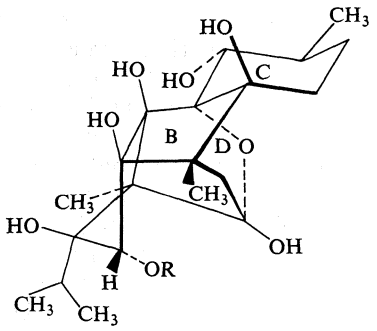

2 R = H

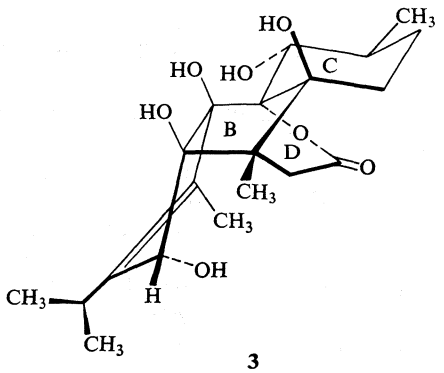

3

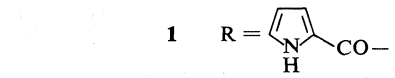

1

co-workers (1). Recently, an X-ray analysis on ryanodol-*p*-bromo benzyl ether achieved by Srivastava and Przybylska (2) has confirmed the proposed structure for ryanodine except that the configuration of the isopropyl side chain was found to be the opposite.

In this communication, we wish to describe a synthetic approach which appears to be an attractive scheme for the syntheses of ryanodine and its closely related degradation product **3**.

5,6-Dimethoxyindane **4** which is readily available from veratraldehyde (3) was treated with bromine in carbon tetrachloride at room temperature and gave bromoindane **5**. Reaction of **5** with magnesium in ether in presence of methyl iodide gave the expected Grignard derivative of **5** which by reaction with triethyl orthoformate followed by acid hydrolysis gave methoxyphenolaldehyde **6**[2,3,4] (m.p. 118–119 °C, 75% yield from 4).

Reaction of **6** with boron tribromide in dichloromethane (4) gave the *o*-phenol **9** (m.p. 178 °C, 80% yield). Treatment of **9** with bromoacetyl bromide in benzene and pyridine gave bromoacetate **10** (m.p. 110 °C, 70% yield) which was transformed into lactone aldehyde **11** (m.p. 131–132 °C, 75% yield) in boiling tetrahydrofuran containing potassium carbonate.[5]

Wolff–Kischener reduction of lactone aldehyde **11** gave lactone **14** (m.p. 74–75 °C; 80% yield). Treatment of lactone **14** with one mole of sodium hydroxyde in acetonitrile–water followed by the addition of one mole of *N*-bromosuccinimide yielded the stable *o*-spirodienone lactone **15** (m.p. 97–98 °C; 90% yield; mol. wt. (mass spectroscopy) 220; ν_{max} 1790, 1665, 1640, and 1600 cm^{-1}; λ_{max} (EtOH) 355 mμ (3100); τ 3.97 (1H, singlet, H-1), 5.25 and 5.60 (2H, double doublet, J = 15 c.p.s., H-2 and H-3) and 8.10 (3H, singlet, CH_3)).

Compound **15** was refluxed for 5 min in methylvinyl ketone and gave the tricyclic compounds **16** and **17** (ratio 1 ~ 1) which could be separated by preparative thin-layer chromatography. **16** (oil; mol. wt. (mass spectroscopy) 290; ν_{max} 1810, 1740, and 1720 cm^{-1}; τ 5.34 and 5.74 (2H, double doublet, J = 14 c.p.s., H-3 and H-4), 6.44 (1H, doublet, J = 2 c.p.s., H-1), 6.93 (1H, octuplet, J = 2, 6, and 9 c.p.s., H-2), 7.87 (3H,

[2]All new crystalline compounds gave satisfactory analytical and mass spectral (mol. wt.) data. Infrared (dichloromethane), ultraviolet, and nuclear magnetic resonance (deuteriochloroform with tetramethylsilane as internal standard) spectra are consistent with the structures proposed. All yields reported have been calculated after purification by crystallization.

[3]A specific cleavage of one methoxyl group has occurred during the Grignard reaction. Discussion concerning this unexpected result will be included in our article.

[4]Reduction of **6** with lithium aluminium hydride gave phenol alcool **7** (m.p. 100 °C) which was transformed into the carbonate **8** (m.p. 146 °C) by reaction with phosgene in benzene containing pyridine. This result shows that the methoxyl group remaining in **6** is at C-6.

[5]A rigorous chemical proof for lactone aldehyde **11** was obtained in the following way. Lactone aldehyde **11** was transformed into compound **12** (m.p. 99–100 °C) by methylation with dimethyl sulfate in aqueous base followed by esterification with diazomethane. Alkylation of the known methoxy phenol aldehyde **6** with ethyl bromoacetate in tetrahydrofuran containing potassium carbonate gave compound **13** (m.p. 83–84 °C) which by hydrolysis in aqueous base followed by diazomethane esterification gave a compound which was found identical with compound **12**.

Can. J. Chem. Downloaded from www.nrcresearchpress.com by 210.87.254.40 on 09/05/12
For personal use only.

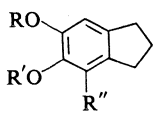

4 R = CH_3, R′ = CH_3, R″ = H
5 R = CH_3, R′ = CH_3, R″ = Br
6 R = CH_3, R′ = H, R″ = CHO
7 R = CH_3, R′ = H, R″ = CH_2OH
9 R = H, R′ = H, R″ = CHO
10 R = $BrCH_2CO$, R′ = H, R″ = CHO
12 R = CH_3, R′ = CH_3OOCCH_2, R″ = CHO
13 R = CH_3, R′ = $C_2H_5OOCCH_2$, R″ = CHO

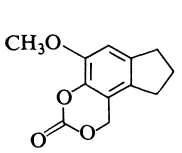

8

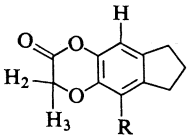

11 R = CHO
14 R = CH_3

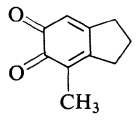

20

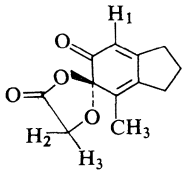

15

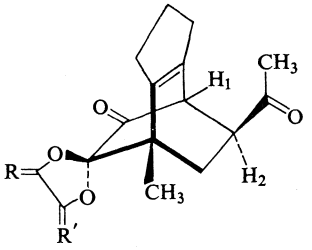

16 R = H_3, H_4, R′ = O
17 R = O, R′ = H_3, H_4

singlet, CH_3CO) and 8.75 (3H, singlet, CH_3)), and **17** (m.p. 113–115 °C; mol. wt. (mass spectroscopy) 290; ν_{max} 1810, 1740, and 1720 cm^{-1}; τ 5.34 and 5.68 (2H, double doublet, J = 14 c.p.s., H-3 and H-4), 6.36 (1H, doublet, J = 2 c.p.s., H-1), 6.83 (1H, octuplet, J = 2, 6, and 9 c.p.s., H-2), 7.83 (3H, singlet, CH_3CO) and 8.74 (3H, singlet, CH_3)).

Treatment of an ethereal solution of the mixture **16** and **17** with aqueous base gave the liquid triketone **18**.[6] Treatment of compound **18** with aqueous tetrahydrofuran containing sodium hydroxide at room temperature gave the tetracyclic hydroxydiketone **19** (m.p. 69–70 °C; mol. wt. (mass spectroscopy) 232; ν_{max} 3520, 1745, and 1720 cm^{-1}; τ 6.66 (1H, doublet, J = 4 c.p.s., H-1), 7.50 (2H, singlet, H-2, and H-3)[7] and 8.73 (3H, singlet, CH_3)). Compound **19** was best prepared in 70% overall yield by treating directly the crude mixture **16** and **17** with the basic treatment described above. Consequently, by a simple three-step procedure (**14** → **15** → **16** and **17** → **19**), a high yield of the complex tetracyclic hydroxydiketone **19** can be obtained from the simple aromatic compound **14**.[8] Compound **19** was transformed into the keto-acetate **21** (m.p. 128–130 °C, 90% yield) by a 15 min reflux in pyridine – acetic anhydride and was selectively ketalized with ethylene glycol, benzene, and *p*-toluenesulfonic acid to give ketal acetate **22** (m.p. 149–152 °C; 90% yield). Reaction of ketal acetate **22** with lithium borohydride in tetrahydrofuran at room temperature followed by addition of lithium aluminium hydride and reflux gave the *trans*-diol **23**[9] (m.p. 145–147 °C; 80% yield). Reaction of *trans*-diol **23** with pyridine in acetic anhydride at room temperature for 3 h gave the liquid acetate **26**.

[6]The formation of **18** from **16** and **17** combined with the spectral data confirms the position of the methyl ketone side chain in **16** and **17** as shown but does not determine the configuration of this side chain. The methyl ketone side chain has been shown to be *syn* to the double bond by several deuterium exchange experiments. Those results will be included in our article.

[7]The singlet at 7.50 τ was shown to correspond to H-2 and H-3 by deuterium exchange experiments.

[8]Compound **15** is crystalline and stable at room temperature; consequently, the *o*-spiro lactone ketal blocking group has a high stabilizing effect since the corresponding *o*-quinone **20** is unstable at room temperature. Furthermore, such blocking group on the *o*-quinone permits a very stereospecific Diels–Alder reaction with an unsymmetrical dienophile. The preparation of compound **20** will be reported in our article.

[9]A chemical reduction of ketal acetate **22** with sodium in liquid ammonia containing ethanol gave two compounds which were separated by column chromatography. The minor product was the *trans*-diol **23** and the major product, the *cis*-diol **24** (m.p. 115–117 °C). The diol **24** was shown to be the *cis* isomer in the following way: reaction of **24** with phosgene in benzene containing pyridine gave the carbonate **25** (m.p. 102–103 °C; 85% yield).

Can. J. Chem. Downloaded from www.nrcresearchpress.com by 210.87.254.40 on 09/05/12
For personal use only.

Can. J. Chem. Downloaded from www.nrcresearchpress.com by 210.87.254.40 on 09/05/12
For personal use only.

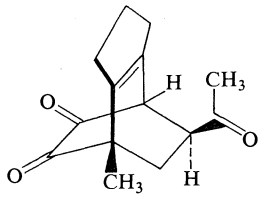

18

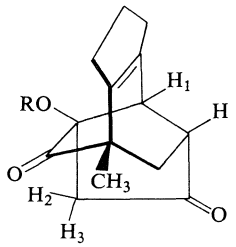

19 R = H
21 R = CH_3CO

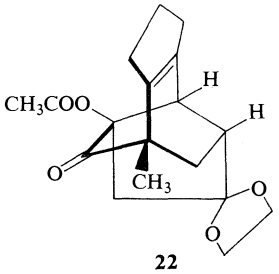

22

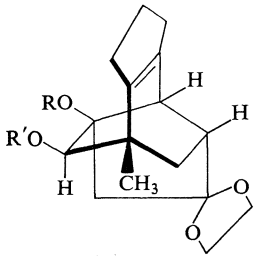

24 R = H, R′ = H
25 R, R′ = C = O

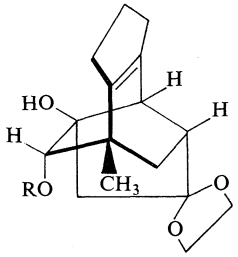

23 R = H
26 R = CH_3CO

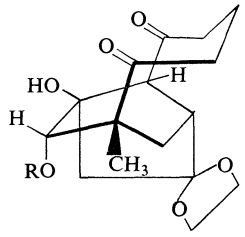

27 R = CH_3CO

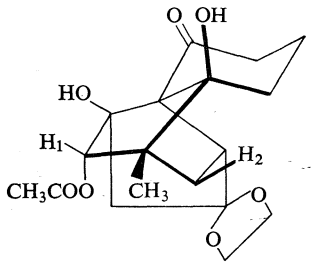

28

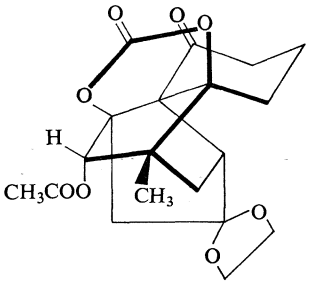

29

The entry into a ring skeleton related to ryanodine and its degradation product **3** was achieved in the following way: ozonolysis of **26** in methanol at room temperature followed by catalytic reduction with palladium-on-charcoal gave crude diketone **27** which underwent internal aldol condensation by filtration through silica gel to give dihydroxyketo acetate **28** (m.p. 176–177 °C; 55% yield from **23**; ν_{max} 3450, 1735, and 1700 cm^{-1}; τ 4.75 (1H, doublet, J = 2 c.p.s., H-1)[10], 6.10 (4H, multiplet, OCH_2CH_2O), 7.78 (3H, singlet, CH_3CO) and 9.00 (3H, singlet, CH_3)).

[10]H-1 appears as a doublet due to W coupling (5) with H-2. By irradiation at 8.2–8.4 τ, the doublet at 4.75 τ collapsed into a singlet.

Compound **28** gave the six-membered carbonate **29** by reaction with phosgene in benzene containing pyridine (m.p. 204–205 °C; 85% yield; ν_{max} 1755, 1740, and 1715 cm^{-1}).

Compound **28** contains in principle all the necessary functional groups for the complete elaboration of rings A, B, C, D, and E of ryanodine and its degradation product **3**. Work in this direction and in the synthesis of new polycyclic systems of the type **19** by using different dienophiles with **15** is now in progress.

Acknowledgment

Financial support by the National Research Council of Canada is gratefully acknowledged.

1. K. WIESNER, Z. VALENTA and J. A. FINDLAY. Tetrahedron Letters, **221** (1967), and references quoted therein.
2. S. N. SRIVASTAVA and M. PRZYBYLSKA. Can. J. Chem. **46**, 795 (1968).
3. R. GRANGER, P. F. G. NAU, J. NAU, and C. FRANÇOIS. Bull. Soc. Chim. France, **496** (1958).
4. F. L. BENTON and T. E. DILLON. J. Am. Chem. Soc. **64**, 1128 (1942).
5. I. FLEMING and R. B. WOODWARD. J. Chem. Soc. (C) 1289 (1968), and references quoted therein.

Can. J. Chem. Downloaded from www.nrcresearchpress.com by 210.87.254.40 on 09/05/12
For personal use only.

Can. J. Chem. Downloaded from www.nrcresearchpress.com by 210.87.254.5 on 09/05/12
For personal use only.

Canadian Journal of Chemistry

Published by THE NATIONAL RESEARCH COUNCIL OF CANADA

VOLUME 47 FEBRUARY 15, 1969 NUMBER 4

Mass spectrometric studies of chemical reactions in shock waves: the thermal decomposition of nitrous oxide

S. C. BARTON[1] AND J. E. DOVE

Department of Chemistry, University of Toronto, Toronto 5, Ontario

Received June 19, 1968

Apparatus for the mass spectrometric study of rapid gas reactions in reflected shock waves is described. This apparatus has been applied to the thermal decomposition of 2% N_2O in Kr at total gas concentrations of about 1.6×10^{-6} mole cm^{-3}, in the temperature range 1800 to 2800 °K. The principal products of the reaction were found to be N_2, O_2, NO, and O. The rate coefficient for the unimolecular decomposition of N_2O was calculated from the experimental data, and the rates of the secondary reactions between O and N_2O were estimated. The possibility of the occurrence of a "weak collision" mechanism in the unimolecular reaction of N_2O is discussed.

Canadian Journal of Chemistry, **47**, 521 (1969)

Introduction

It is now well established that the primary reaction of the thermal decomposition of nitrous oxide is

$$N_2O \rightarrow N_2 + O$$

This is a unimolecular reaction of a simple molecule whose structural parameters are relatively well known. This system, therefore, appears very suitable for testing theories of unimolecular reaction, and a number of theoretical studies have, indeed, already been made (1–8). However, a complication is the fact that the direct decomposition to ground state products is spin-forbidden:

$$N_2O(^1\Sigma) \rightarrow N_2(^1\Sigma) + O(^3P)$$
$$\Delta H_0^0 = +38.68 \text{ kcal}$$

The spin-allowed process is considerably more endothermic (9–11):

$$N_2O(^1\Sigma) \rightarrow N_2(^1\Sigma) + O(^1D)$$
$$\Delta H_0^0 = +84.05 \text{ kcal}$$

It is therefore generally considered that the decomposition involves crossing from the potential surface of the singlet ground state molecule to the potential surface of a triplet intermediate which then decomposes to ground state products (12, 13). The minimum energy required for this process is likely to be appreciably less than the 84 kcal $mole^{-1}$ needed for the spin-allowed decomposition. However, in the absence of detailed information about the potential surfaces, the actual value cannot be accurately predicted. This is in contrast to very many other decomposition reactions, where the minimum energy required for reaction can often be assumed without serious error to be equal to the dissociation energy of the bond which is broken. It is, therefore, particularly of interest in the case of N_2O to measure the energy of activation experimentally. To help in the theoretical interpretation of the results, it is also desirable to look for a possible dependence of the Arrhenius activation energy on concentration and temperature.

Accurate experimental study of the primary unimolecular process is made difficult by the occurrence of a number of secondary reactions, some of which also consume nitrous oxide. Johnston (14) has made a careful analysis of the results obtained below 1050 °K by a number of previous workers, and has concluded that the

[1]Present address: Ontario Research Foundation, Sheridan Park, Ontario.

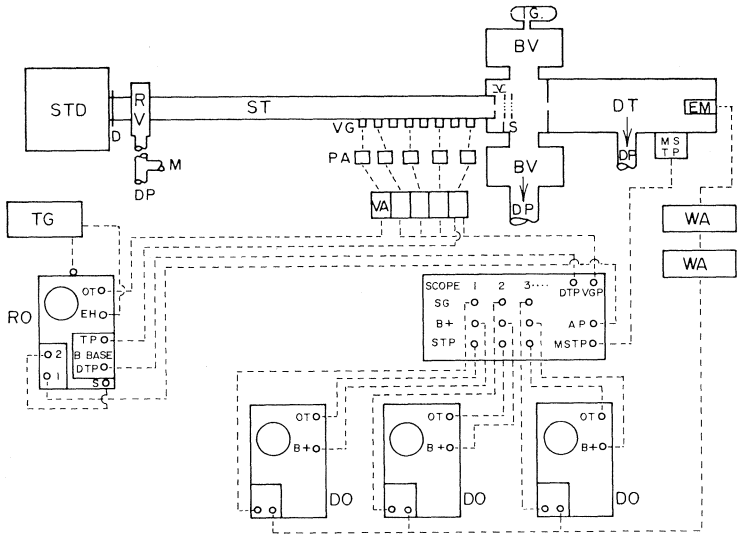

FIG. 1. Schematic diagram of apparatus.

AP, common output of velocity gauge pulses and display oscilloscope timing pulses; B+, "+ gate B" output; BV, buffer volume; D, diaphragm; DO, mass spectrum display oscilloscope (Tektronix 543B); DP, diffusion pump; DT, mass spectrometer drift tube; DTP, delayed trigger pulse output or input; EH, external drive for oscilloscope horizontal amplifier; EM, electron multiplier; IG, ion accelerating grids; IS, ion source; M, gas manifold; MSTP, mass spectrometer trigger pulse output or input; OT, external trigger pulse input; PA, preamplifiers for shock velocity gauge signals; RO, raster oscilloscope (Tektronix 535A); S, sawtooth waveform output; SG, output from staircase waveform generator; ST, shock tube (driven section); STD, shock tube (driver section); STP, display oscilloscope trigger pulse output; TG, timing marker generator (Radionics TWM2-A); TP, trigger pulse input; VA, main amplifiers for shock velocity gauge signals; VG, shock velocity gauge; VGP, shock velocity signal input; WA, wideband amplifier.

minimum critical energy for the primary process is about 60 kcal mole^{-1}. This figure, and the rate coefficients which he obtained, are now widely accepted and have been used in most of the subsequent work on the reaction. Some objections have, however, been raised to Johnston's analysis (12). Moreover, in a later paper, Johnston and White (15) found that the available data on N_2O decomposition did not meet consistency tests which they applied. They concluded that the rate constants were still in doubt and that the data then available should not be used for a close test of reaction rate theories.

We have measured the rate and Arrhenius activation energy of the unimolecular reaction at low total concentration over a large range of temperatures, using shock tube techniques. At the time that our work was begun, only one study had been made in a higher temperature range (16), and there appeared to be doubts about the quantitative nature of the results. Since then, several other high temperature studies have appeared (7, 17–21). However, there is still conflict about some of the main experimental findings, and the theoretical interpretation of the results is in considerable doubt.

Experimental

The apparatus, shown schematically in Fig. 1, consisted of a shock tube coupled to a time-of-flight mass spectrometer. Gas was sampled directly from the reflected shock region into the ion source of the mass spectrometer. The changes in gas concentration during the reaction period were monitored by recording the mass spectra from cathode ray oscilloscopes. This type of experimental arrangement, in which the time-of-flight mass spectrometer is used to follow very rapid reactions, was pioneered in the laboratory of Professor G. B. Kistiakowsky at Harvard (22, 16, 23); important developments have also been made in other laboratories (19, 20, 24–26).

Shock Tube

The stainless steel shock tube was of 2.54 cm inside diameter and 570 cm in length, with a driver section of 25 cm diameter and 35 cm in length. This configuration of driver almost completely eliminates the effects of the rarefaction wave from the driver gas, which might otherwise affect the gas in the reflected shock region during the observation period (27, 28). The main section of the

Can. J. Chem. Downloaded from www.nrcresearchpress.com by 210.87.254.5 on 09/05/12
For personal use only.

Can. J. Chem. Downloaded from www.nrcresearchpress.com by 210.87.254.5 on 09/05/12
For personal use only.

shock tube, which contained the experimental gas at an initial pressure of typically 5 Torr, was separated from the driver (containing, e.g., 400 Torr of helium) by a thin aluminium diaphragm. To initiate the shock wave, this diaphragm was cut by a spring-driven four-bladed knife. Metal diaphragms broken in this manner generally "petal" without losing any fragments. This avoids the necessity for dismantling the shock tube after each experiment to remove pieces of diaphragm material; the mass spectrometer vacuum would have to be broken at the same time.

Because of the possibility of serious deviations from ideal shock tube behavior, we have made careful experiments in which the shock wave pressure was monitored by a Kistler Model 603 pressure transducer[2] mounted in the end plate of the shock tube. For shock waves in argon or krypton, we found that the pressure remained steady for 380 to 1100 μs after shock reflection, depending on the gas used and the Mach number of the shock wave. The steady pressure regime was terminated by the arrival of a disturbance which we believe to be a wave reflected from the contact surface. The arrival of this wave always occurred well after the longest time for which kinetic data were taken by us under those conditions. However, the time of arrival was much earlier than would be calculated on the assumption of ideal behavior of the driver, as has been found by some other workers (28).

Shock Velocity Measurement

The velocity of the shock waves was measured by using 5 gold thin-film resistance thermometers at accurately known positions along the shock tube. The signals from these, after being amplified by circuits having a gain of 100 000 and a rise time of 0.5 μs, were used to trigger bistable multivibrators. The outputs of the multivibrators were combined in an "or" gate circuit and displayed on a raster trace (Fig. 2) produced by a Radionics Model TWM2-A waveform generator[3] and a Tektronix type 535A oscilloscope. In this way, the shock velocity between any pair of stations could be measured to within 0.5%. The shock attenuation was then calculated and was used to determine, by a short extrapolation, the velocity and arrival time of the shock wave at the end plate of the shock tube.

Gas Sampling

Gas was sampled continuously from the end of the shock tube directly into the ion source of the mass spectrometer. The sampling orifice was a round hole or a short re-entrant nozzle in a disc of gold or stainless steel foil of 0.0025 to 0.005 cm thickness, mounted on the end plate of the shock tube. The diameter of the hole used was 0.010 to 0.013 cm. The end plate of the shock tube also acted as the base of the ion source, and the ionizing electron beam was about 0.2 cm beyond the sampling hole.

Mass Spectrometer

The time-of-flight mass spectrometer (29, 30) was a Bendix Model 12 with type 14-101 "fast reaction" ion source; it had been specially modified to produce mass spectra at any chosen repetition frequency in the range 10 to 100 kHz. The ion currents, after amplification in the electron multiplier of the mass spectrometer, were further amplified in 2 Hewlett–Packard 460A wideband amplifiers and recorded photographically from oscilloscopes.

In order to obtain a representative sample of the reacting gas, it is necessary to use an orifice whose diameter is large compared with the mean free path in the shock-heated gas (31, 23). The large inflow of gas from such an orifice demands a fairly big pumping system for the mass spectrometer. The ion source was pumped by an Edwards F603 6-in. oil diffusion pump with cold cap and water-cooled CB06 baffle. With about 5 Torr of gas in the shock tube, the steady reading of a Bayard–Alpert ionization gauge attached to the ion source was about 4×10^{-5} Torr. The flow of gas into the ion source increased sharply on arrival of the shock wave. In order to keep the rate of pressure rise within reasonable bounds, 2 ballast volumes of 15 l each were added to the ion source. The openings to these 2 ballast volumes were 9 cm in diameter and were respectively 4.5 cm above and below the sampling orifice. Since our experiments were completed within at most a few hundred μs after shock arrival, these ballast volumes reduced the rate of pressure rise just as effectively as the addition of extra pumps. The flight tube, 1 m in length, was separated from the ion source by a baffle containing an opening of 0.5 cm × 1.2 cm (situated 13 cm from the sampling orifice), and was differentially pumped by a 4-in. mercury diffusion pump with refrigerated baffle and liquid nitrogen trap. When

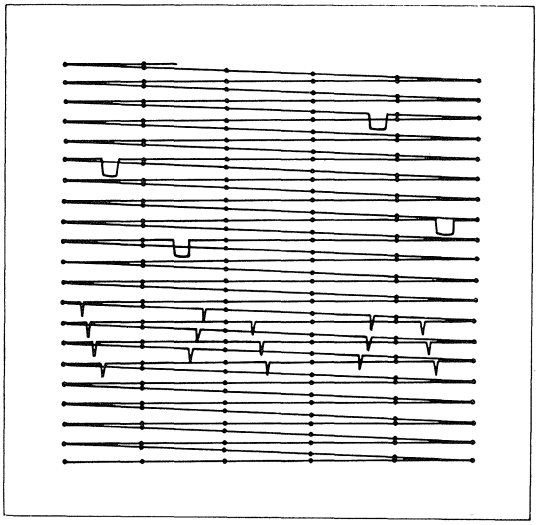

FIG. 2. Trace from raster oscilloscope display.

Zero time is at the top left. The approximately rectangular pulses are from the shock velocity gauges. The sharp narrow pulses near the bottom of the trace indicate the times at which the oscilloscopes were triggered to record the mass spectra. The bright dots are crystal-controlled timing markers.

[2]Kistler Instrument Corp., North Tonawanda, N.Y.
[3]Radionics Inc., 76 Cambridge St., Burlington, Mass.

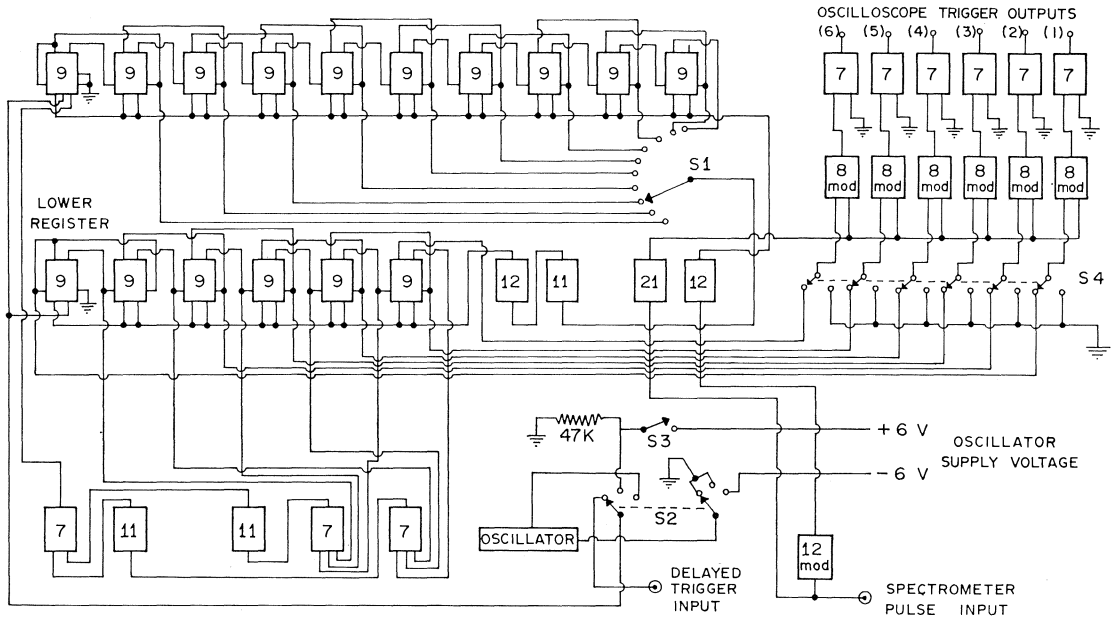

FIG. 3. Block schematic diagram of the control electronics for recording the mass spectrometric data. The figures on the circuit blocks are "PSC" numbers from ref. 33; where the circuit has been slightly modified, "mod" is added below the PSC number.

the shock tube was filled to pre-shock pressure, this pumping system kept the pressure in the flight tube at least an order of magnitude less than in the ion source. Between experiments, the mass spectrometer was pumped down to about 10^{-7} Torr.

Data Recording

A major problem is the accurate recording of the great amount of data which is produced in a very short time by the mass spectrometer. The ideal system would record the data directly in digital form, ready to be fed into the computer. Unfortunately this is at present prohibitively expensive, since it needs a recording system with a bandwidth of at least 30 MHz. We therefore record our mass spectra by photographing them from the screens of several oscilloscopes. The special electronic circuitry (32), which we have devised for this purpose, is shown schematically in Fig. 3. It has proved very successful and reliable.

The principle of operation is as follows. The mass spectrometer operates continuously at the chosen frequency. The external circuitry selects, at the appropriate time, a group of successive mass spectra to be recorded in time-resolved fashion. This is accomplished by gating and counting the trigger pulses which are being produced automatically by the mass spectrometer, and feeding them in a predetermined manner to the "external trigger" inputs of the oscilloscopes.

The heart of the recording electronics in Fig. 3 is the combination of 2 counting registers. These consist of binaries arranged in modified T connection (33, 34). In operation, the sequence of events is started by a pulse from one of the velocity gauges, suitably delayed by an accurate electronic delay circuit. The upper register then counts mass spectrometer trigger pulses until a certain number, preset by switch S1, has been reached. The registers are interconnected in such a manner that the first binary of the lower register is turned to state "0" by the initial trigger pulse and is returned to state "1" when the preset count is reached. The second lower binary then switches to state "0", and the upper register again counts the preset number of mass spectrometer pulses; the second lower binary then returns to "1". This continues until each of the binaries of the lower register has operated, after which the circuit stops automatically.

The waveform from the first binary of the lower register is used to gate the oscilloscope trigger pulses so that they can trigger the first recording oscilloscope for the required number of traces. The second binary acts similarly for the second oscilloscope, and so on. Our system can use up to 6 oscilloscopes with 1 to 10 spectra displayed on each. Typically, we record 4 to 6 mass spectra on each of 3 or 4 oscilloscopes. Tektronix 543B oscilloscopes are used since they have good bandwidth and a 6 cm high display area. Spectra are photographed onto Polaroid 10 000 ASA film.

The main remaining requirement is a staircase (step waveform) generator which displaces the oscilloscope trace vertically upwards between each triggering. The type of display which is obtained is shown in Fig. 4.

An additional feature which is extremely useful is that pulses showing the times of triggering of each oscilloscope are combined with the velocity gauge signals and recorded on the raster trace (Fig. 2). Since the time

Can. J. Chem. Downloaded from www.nrcresearchpress.com by 210.87.254.5 on 09/05/12
For personal use only.

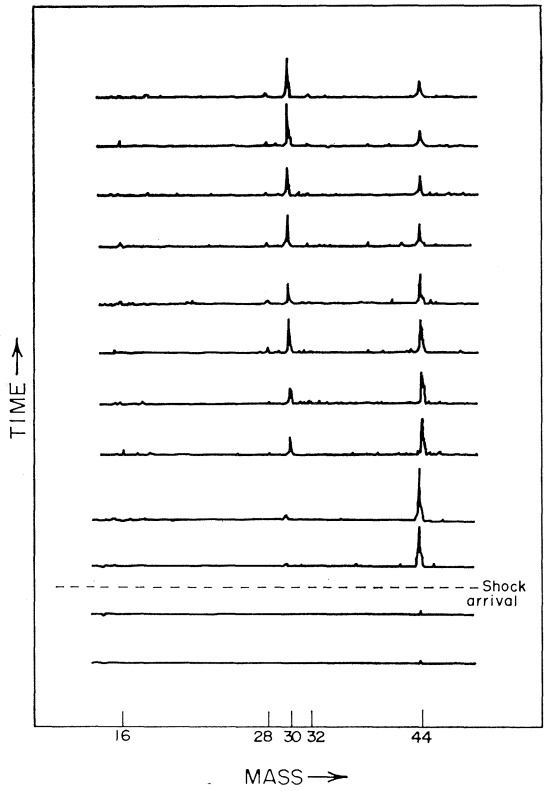

FIG. 4. Oscilloscope records of mass spectrum showing arrival of shock wave and subsequent reaction, with decrease of reactant N_2O (m/e = 44) and increase of N_2, NO, and O_2 (m/e = 28, 30, 32).

interval between the mass spectrometer electron beam pulse and the oscilloscope trigger pulse is known from calibration experiments, the raster records enable the times at which the mass spectrometric concentration measurements were made to be precisely established with respect to the start of chemical reaction (arrival of the shock wave). Strictly, a small additional correction is also required for the time that the gas takes to travel from the sampling orifice to the electron beam.

The system also includes a low-frequency internal oscillator, to trigger the electronics repetitively for setting-up purposes.

A definite problem with any system which uses oscilloscopes for data recording is the limited dynamic range available in any one trace. This difficulty is accentuated in the present application, by the characteristics of the mass spectral traces, which consist of very narrow pulses rising from a relatively slow-moving horizontal scan. The rise time of the pulses is so short that almost the maximum beam intensity of the cathode ray tube (c.r.t.) is required to make the pulses visible on the film at all. At this intensity, the base line is heavily over-exposed and thickened, and very small mass peaks are completely obscured. To minimize this problem, we feed a portion of the mass spectrum signal, suitably amplified and synchronized, as a "bright-up" signal to the c.r.t. cathodes. The c.r.t. beam can then be used well below maximum intensity and is automatically turned up to full brightness for the duration of any large mass spectrum peak.

Gas Mixtures

Gas mixtures were prepared in a conventional glass high vacuum system by manometric measurement of partial pressures, and were stirred before use. The purity of all the gases was checked by mass spectrometric analysis.

Krypton of Matheson "research" grade was used without further purification; the main impurities were Xe and N_2, each 25 p.p.m. Nitrous oxide of Matheson "regular" grade (98%, the main impurity being air) was purified by repeated fractional distillation after condensation with liquid nitrogen, only the middle fraction being retained each time. Oxygen, required for calibration experiments, was prepared by heating "research" grade potassium permanganate, and was then dried and purified by fractional distillation. Nitrogen, used for calibration experiments only, was Matheson "high purity" grade (99.9% minimum purity), and was dried by passing through a liquid nitrogen trap before use. Nitric oxide, also used only for calibration, was Matheson "C.P." grade (99.8% minimum) and was condensed in liquid nitrogen, degassed, and distilled once.

Shock Parameter Calculations

The temperature, pressure, and density of the unreacted gas mixture behind the reflected shock wave were calculated from the extrapolated incident velocity. The standard conservation equations (35) were solved by an iterative procedure, using a Fortran program on an IBM 7094 computer. Enthalpies were obtained from ref. 9 and were fitted to fifth order polynomials in T. Ideal shock reflection was assumed.

After the chemical reaction has begun, the temperature of the gas may change as a result of endothermicity or exothermicity. In order to calculate this change, a detailed knowledge of the reaction mechanism is needed, as discussed below.

Results

Experiments were carried out at temperatures between 1780 and 2790 °K with total gas concentrations of 1.4×10^{-6} to 1.8×10^{-6} mole cm^{-3}. The reactant mixtures contained 2.1% N_2O. Krypton was chosen as the diluent, rather than argon, mainly because its mass spectral peaks are well outside the region of main interest and therefore do not interfere. The predominant peaks of the reacting gas were determined to be of mass 44, 32, 30, and 28, corresponding to N_2O, O_2, NO, and N_2 respectively. No peak was found at mass 46 (NO_2).

Mass Spectrometric Data

The full sensitivity of the mass spectrometer could not be used with the large gas influx of

Can. J. Chem. Downloaded from www.nrcresearchpress.com by 210.87.254.5 on 09/05/12
For personal use only.

Can. J. Chem. Downloaded from www.nrcresearchpress.com by 210.87.254.5 on 09/05/12
For personal use only.

these experiments, otherwise the electron multiplier which was used as a detector would have been overloaded and driven beyond its range of linear response. The overall sensitivity was therefore reduced by operating the ionizing electron beam at an energy of 18 V (rather than the more conventional 50 to 70 V). The use of such a relatively low voltage had two major advantages. The formation of fragment ions or doubly-charged ions was almost completely eliminated, thus simplifying the interpretation of the mass spectra. Also, the ionization of the inert diluent, which has a relatively high ionization potential, was reduced much more than that of most of the gases of kinetic interest.

Because any mass peak on a given trace results from a finite, and sometimes small, number of detected ions, statistical fluctuations of peak height occur. These fluctuations are superimposed on any change of concentration due to chemical reaction, and are one of the factors limiting the accuracy of any single experiment. Fluctuations of this general type tend, of course, to be noticeable in any experiment where data have to be obtained in a very short time interval.

The primary kinetic data consisted of plots of peak height of N_2O^+, O_2^+, N_2^+, and NO^+ versus time from shock arrival. These mass spectral peak heights were assumed to be proportional to gas concentrations. We found it impracticable to obtain absolute (and constant) sensitivity factors for converting peak heights to concentrations. The measurement of absolute concentrations was, however, possible using relative sensitivity factors and the known initial concentration of N_2O. These relative sensitivity factors were determined under conditions as close as possible to those used in the kinetic investigations. Mass spectra of various gas mixtures of known composition were recorded under shock wave conditions. This procedure was used because an apparent temperature dependence of the mass spectra of some larger molecules has been found under similar conditions in other work (95). Also, diffusive separation of the gases may take place during their expansion into the ion source (36, 37), and this effect may be temperature dependent. Our experimentally-obtained sensitivity factors may reasonably be assumed to take these effects into account. The sensitivity to N_2 was rather low, mainly because of the high ionization potential of that molecule (15.6 eV). Hence the results for N_2 concentration are less accurate and more subject to statistical fluctuation than for the other gases.

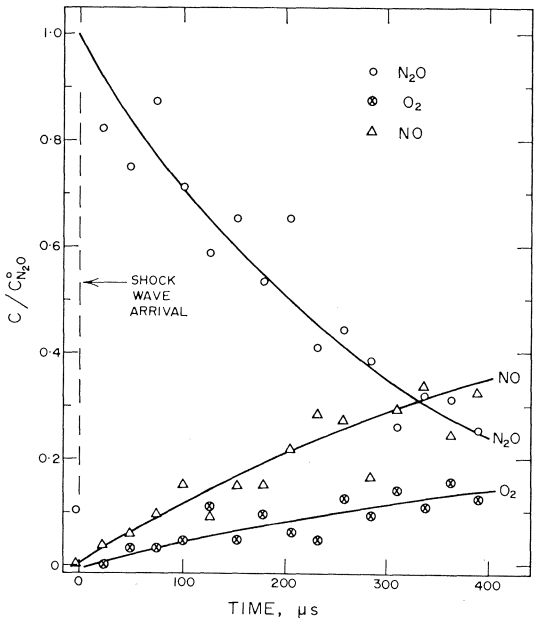

FIG. 5. Experimental concentration profiles of N_2O, NO, and O_2. The concentrations have been normalized by dividing by the initial concentration of N_2O. T_5 = 2370 °K.

The concentration profiles obtained in a typical successful experiment are shown in Fig. 5.

Overall Rate of Decomposition of N_2O

The results of previous workers indicate that the unimolecular reaction will be of the second order under our conditions. Then, neglecting for the moment the occurrence of possible secondary reactions, the rate of disappearance of N_2O will be given by

$$-\frac{d[N_2O]}{dt} = k_0[M][N_2O],$$

and hence

$$\log_{10}[N_2O] = \log_{10}[N_2O]_0 - k_0[M]t/2.303$$

[M] is the total concentration and is assumed to remain constant during a given experiment.

A typical plot of the logarithm of the N_2O peak height against time is shown in Fig. 6. These plots could be fitted fairly well to a straight line whose slope was used to obtain a value of k_0.

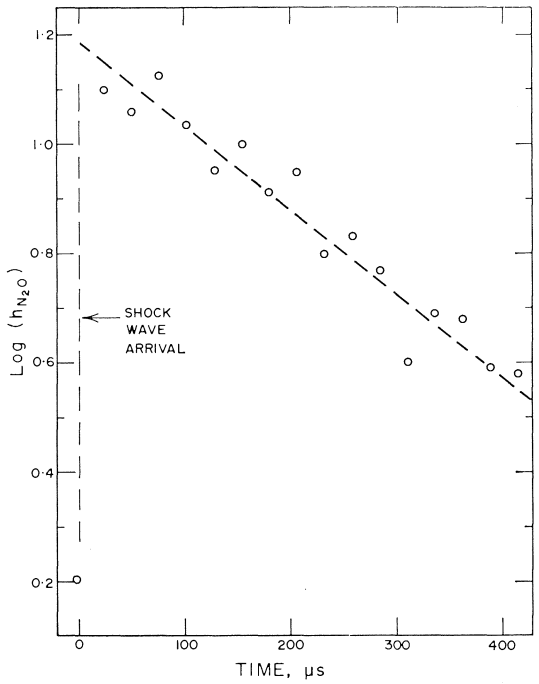

FIG. 6. Logarithm of the experimentally observed mass spectrometric peak height of N_2O (in arbitrary units), plotted as a function of time from shock arrival.

The values of k_0 at various temperatures were then fitted to an Arrhenius form by a least mean squares procedure, resulting in

$$k_0 = 5.8 \times 10^{12} \exp(-37\,000/RT)$$

in cm^3 mole s units (which are used throughout this paper), and with the energy of activation in cal $mole^{-1}$. The relation of this overall rate constant to the rate constant for the unimolecular reaction will be discussed later.

Discussion

The Reaction Mechanism

This and other investigations suggest that the reactions which may be important in the mechanism at high temperatures include:

[1] $N_2O + M \rightarrow N_2 + O + M$

[2] $O + N_2O \rightarrow N_2 + O_2$
$\Delta H_0^0 = -79.3$ kcal

[3] $O + N_2O \rightarrow 2NO$
$\Delta H_0^0 = -36.3$ kcal

[4] $NO + N_2O \rightarrow NO_2 + N_2$
$\Delta H_0^0 = -33.1$ kcal

[5] $O + NO + M \rightarrow NO_2 + M$
$\Delta H_0^0 = -71.8$ kcal

[−5] $NO_2 + M \rightarrow NO + O + M$

[6] $O + O + M \rightarrow O_2 + M$
$\Delta H_0^0 = -118.0$ kcal

[7] $O + NO_2 \rightarrow O_2 + NO$
$\Delta H_0^0 = -46.2$ kcal

[8] $NO_2 + N_2O \rightarrow NO + O_2 + N_2$
$\Delta H_0^0 = -7.5$ kcal

We have made calculations using the literature values of the rates of the two termolecular processes, reaction [5] (38–43) and reaction [6] (44) which show that both of these will be negligibly slow under the relatively low density conditions of our experiments. Calculations on reaction [4] using literature data (16, 18, 45, 46) show that its rate will be at most of the order of 1% of that of reaction [1] and hence it also can be neglected. These calculations are supported by the fact that we did not observe NO_2 in any of our experiments. Consequently we have omitted reactions [4], [5], and [6], and all processes involving NO_2, from the analysis of our own data.

Relative Values of k_2 and k_3

It is convenient next to evaluate k_3/k_2 from our data. It may readily be shown that in any experiment, $[NO]/[O_2] = 2k_3/k_2$. The average value of this quantity in all our experiments was 2.0 ± 0.7. Therefore we find $k_3/k_2 = 1.0 \pm 0.35$, in very good agreement with Belford *et al.* (20) who obtained 1.2 ± 0.2. The standard deviation which we quote represents deviations attributable to small fluctuations in the ion source conditions with consequent variations in the relative sensitivity to NO and O_2. There may be a small trend of k_3/k_2 with temperature, since we find 0.85 ± 0.3 in the range 1960–2100 °K, 1.0 ± 0.4 from 2100 to 2500°, and 1.15 ± 0.3 from 2500 to 2800°. However the trend, if any, lies within the standard deviations of the various values. We note that Belford found no trend with temperature, but that Kaufman *et al.* (46) found a difference of 1 kcal $mole^{-1}$ in the activation energies of the two reactions, which would predict a very small trend in the same direction as ours.

The results of experiments below 1960° were not used in the evaluation of k_3/k_2, since the amount of product formed during the observation time was too small to permit accurate measurement of $[NO]/[O_2]$.

Can. J. Chem. Downloaded from www.nrcresearchpress.com by 210.87.254.5 on 09/05/12
For personal use only.

Can. J. Chem. Downloaded from www.nrcresearchpress.com by 210.87.254.5 on 09/05/12
For personal use only.

Relative Values of k_1 and $(k_2 + k_3)$

The mechanism to be considered thus consists of reactions [1], [2], and [3]. The differential equations to which these give rise,

$$[9] \quad -\frac{d[N_2O]}{dt} = k_1[M][N_2O] + (k_2 + k_3)[O][N_2O]$$

$$[10] \quad \frac{d[O]}{dt} = k_1[M][N_2O] - (k_2 + k_3)[O][N_2O]$$

do not seem to have any straightforward analytic solution which would give the concentrations as an explicit function of time (47). However, it can readily be seen that if the secondary reactions [2] and [3] are very slow, the overall rate of disappearance of N_2O will be the rate of the unimolecular reaction. If reactions [2] and [3] are very rapid, a steady state in oxygen atoms will quickly be set up, and the overall rate will be twice the unimolecular rate. Therefore, in order to obtain the rate of reaction [1], we expect that we shall have to apply a correction factor, whose value lies between $\frac{1}{2}$ and 1, to the observed rate.

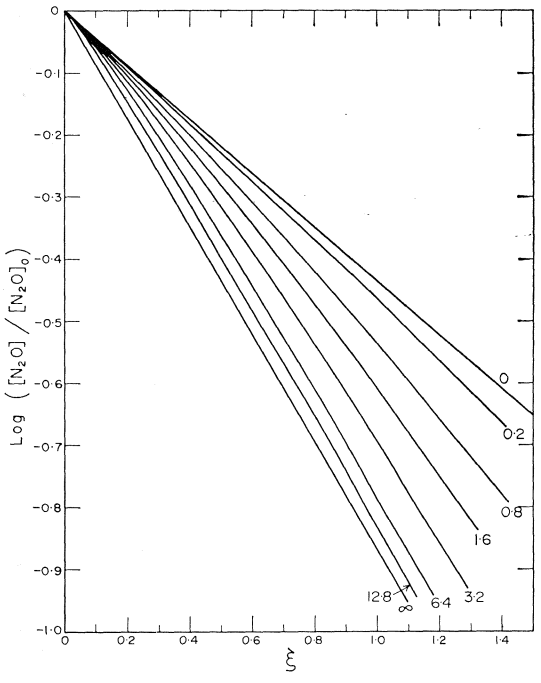

FIG. 7. Concentration profile obtained by computer solution of eqs. [9] and [10]. Logarithm of dimensionless N_2O concentration is plotted against dimensionless reaction time $\xi = k_1[M]t$, for various indicated values of $Y = (k_2 + k_3)[N_2O]_0/k_1[M]$.

Careful inspection of the experimental records, and preliminary calculations based on the literature data on reactions [2] and [3] (46, 48–51) indicated that we could not safely assume that a steady state in O atoms was rapidly established in all of our experiments. Therefore, in order to evaluate k_1, and also, if possible to obtain information about the rates of the secondary reaction, the reaction scheme needs to be considered in detail. In order to reach conclusions of general validity, it is convenient to transform the rate equations into dimensionless form. We define the following two quantities

$$\xi = k_1[M]t$$

and

$$Y = \frac{(k_2 + k_3)[N_2O]_0}{k_1[M]}$$

where $[N_2O]_0$ is the initial concentration. ξ is a dimensionless reaction time; it expresses the elapsed time in terms of $1/k_1[M]$, the time constant for reaction [1]. The equations then become

$$-\frac{d}{d\xi}\frac{[N_2O]}{[N_2O]_0} = \frac{[N_2O]}{[N_2O]_0} + Y \cdot \frac{[N_2O]}{[N_2O]_0} \cdot \frac{[O]}{[N_2O]_0}$$

and

$$\frac{d}{d\xi}\frac{[O]}{[N_2O]_0} = \frac{[N_2O]}{[N_2O]_0} - Y \cdot \frac{[N_2O]}{[N_2O]_0} \cdot \frac{[O]}{[N_2O]_0}$$

The solutions of these equations express the dimensionless concentrations $[O]/[N_2O]_0$ and $[N_2O]/[N_2O]_0$ in terms of the dimensionless time ξ, and depend only on the initial conditions and on the value of Y. We have solved these equations by numerical integration on a computer, using the initial conditions $[O]/[N_2O]_0 = 0$ and $[N_2O]/[N_2O]_0 = 1$, for Y values in the range 0.2 to 25.6. Some results of these computations are shown in Figs. 7 to 10. These graphs can be converted into plots in real time by a straight-forward linear scaling of the ξ-axis, if a value of $k_1[M]$ is known or assumed.

We now seek to establish values of Y, and hence of $(k_2 + k_3)/k_1$, by comparing the computed solutions with our experimental data. This may be done in several ways such as (*i*) comparing the shape of log $[N_2O]$ vs. time plots

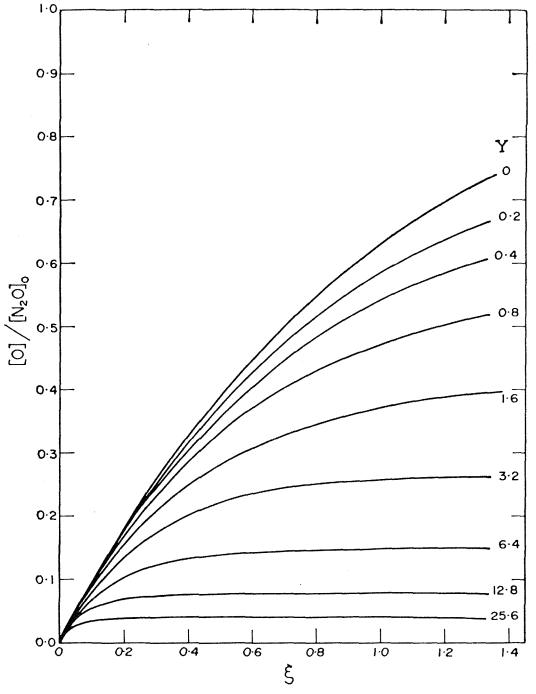

FIG. 8. Computed dimensionless O atom concentration plotted against dimensionless reaction time, ξ, for various values of *Y*.

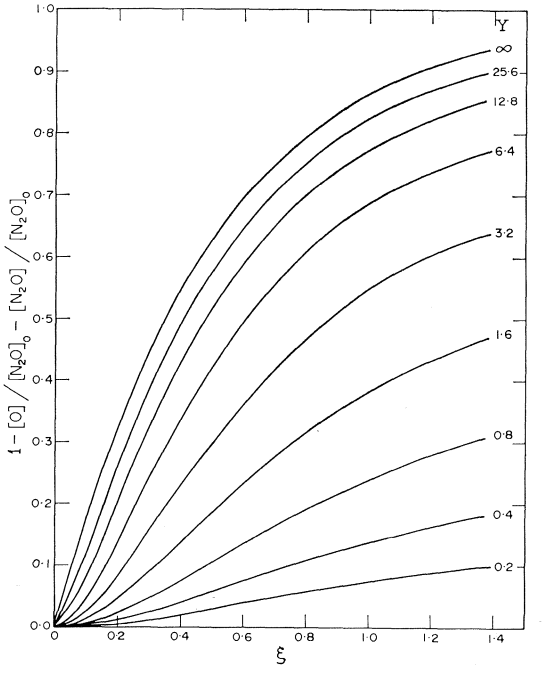

FIG. 9. Computed values of $s = 1 - [O]/[N_2O]_0 - [N_2O]/[N_2O]_0$ plotted as a function of ξ for various values of *Y*. *s* represents the fractional amount of total oxygen, originally present as N_2O, which has been converted to secondary products (NO and O_2) at any given time.

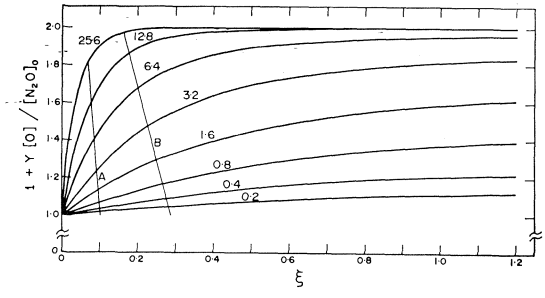

FIG. 10. Computed values of $1 + Y[O]/[N_2O]_0$ plotted against ξ for various values of *Y*. This graph can also be regarded as a plot of $d(\ln [N_2O])/dt$ against ξ, or as a plot of the ratio of the total rate of disappearance of N_2O to the unimolecular rate. The lines A and B represent times at which 10 and 25% of the initial N_2O have reacted.

(cf. Fig. 7), (*ii*) by observing the O-atom concentration (cf. Fig. 8), or (*iii*) by studying the formation of secondary products (cf. Fig. 9). Evidently none of these methods will be successful if *Y* is very small or very large, since the experimental results then become very insensitive to the actual value of *Y*.

A number of our log $[N_2O]$ plots appeared to be appreciably curved in such a manner as to suggest an acceleration in rate due to a build-up of O atoms. However, it is not easy to determine values of *Y* from such curves, partly because of statistical scatter in the experimental concentration plots; even a moderate scatter will tend to mask the curvature of any of the lines of Fig. 7. A more fundamental difficulty is that such curvature can arise in 2 quite distinct ways. If *Y* happens to be moderately small, the O atom concentration builds up gradually and this causes curvature of the log $[N_2O]$ plot, as explained above. The overall reaction is then approximately thermoneutral, as we show later, so that there is no appreciable temperature effect on the rate of N_2O disappearance. On the other hand, if *Y* is large, the O atom concentration quickly approaches a steady state but the overall reaction is exothermic. The temperature will rise as the reaction proceeds, so that in this case also there will be an increase in the relative rate of reactant consumption, and curved plots

Can. J. Chem. Downloaded from www.nrcresearchpress.com by 210.87.254.5 on 09/05/12
For personal use only.

of log $[N_2O]$ will again occur. Considerable care is therefore needed in the analysis of the results, in order to separate the effects of exothermicity from those of the secondary reactions. Because of the danger of employing a circular argument in the interpretation, we did not rely on the N_2O plots alone for our determinations of Y. However, we did note that if the apparent curvature was assumed to be mainly due to build-up of O atoms, then a value of Y of about 6 at 2300 °K was indicated in our experiments. This is in quite good agreement with values obtained in a different manner, as described below.

In principle, a more satisfactory method of finding Y is to study the O atom concentration directly. Provided that Y is sufficiently large (cf. Fig. 8), the value of $[O]/[N_2O]_0$ tends to the stationary value $1/Y$. Unfortunately it is not easy to obtain a reliable mass spectrometric calibration factor for O atoms, in order to make concentration measurements. In any case, the mass spectrometric peaks for $m/e = 16$ were small and hence very subject to statistical fluctuation and unsuitable for quantitative evaluation. The sensitivity of the mass spectrometer to O atoms under our conditions is expected to be relatively low, because of the small cross section and relatively high ionization potential of this species, because of mass spectrometer discrimination against light atoms, and because of the possibility of loss of O from the sampled beam by diffusive separation (36). Using an estimated sensitivity for O atoms of 0.2 relative to O_2, we found a Y value of about 10 in the temperature range 2550 to 2750 °K. This rather rough estimate is also in satisfactory agreement with the results described below.

The third method of evaluating Y is to study the disappearance of N_2O and to compare it with the formation of NO and O_2. The mass spectrometer has good sensitivity to these 3 species, and relative sensitivity factors are of course known from our experiments. The method includes, essentially, an evaluation of the O atom concentration from the difference between the amount of N_2O decomposed and the NO and O_2 formed, though the actual calculation is not cast in exactly that form. Evidently such a calculation will only be successful if the quantity to be found is sufficiently large, compared with the probable errors in the quantities whose difference is to be taken. Fortunately this condition appears to be reasonably well fulfilled in our experiments, so that an approximate value of Y can be obtained. The calculation was actually made by matching our experimental data with the appropriate concentration profiles from the computed solutions of the rate equations (cf. Fig. 7 and 9). From each experiment we obtained plots of log $[N_2O]/[N_2O]_0$ and $s = ([NO] + 2[O_2])/[N_2O]_0$ against time. The quantity s represents the fraction of total oxygen which is present as secondary products, and is, therefore, to be directly compared with the computed profile of $1 - [O]/[N_2O]_0 - [N_2O]/[N_2O]_0$. Since the forms of the curves of log $[N_2O]/[N_2O]_0$ and s against time have different dependences on Y, only for one particular value of Y is it possible to match both of the experimental curves to their computed counterparts. A value of Y was found in this manner for each experiment. The results are plotted as log (Y) against $1/T$ in Fig. 11. One experiment that gave an extremely large value of Y has been omitted from the graph; presumably this high value was caused by an uncontrolled fluctuation in the ion source conditions, which would change the effective relative sensitivity factors.

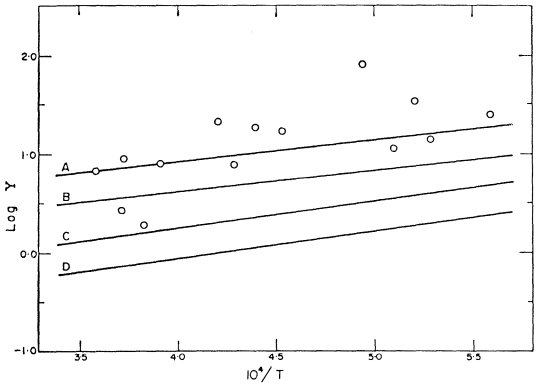

FIG. 11. Experimental values of log Y, obtained in the present work. The lines A and B are logarithmic plots of $(k_2 + k_3)[N_2O]_0/0.5k_0[M]$ and $(k_2 + k_3)[N_2O]_0/k_0[M]$, using data of Fenimore and Jones (49) for k. The lines C and D are similar plots using the data of Fishburne and Edse (51) for $(k_2 + k_3)$.

There are 2 previous determinations of the rates of the secondary reactions in a temperature range close to that of the present work. Fenimore and Jones (49) have measured k_3 over the range

Can. J. Chem. Downloaded from www.nrcresearchpress.com by 210.87.254.5 on 09/05/12
For personal use only.

Can. J. Chem. Downloaded from www.nrcresearchpress.com by 210.87.254.5 on 09/05/12
For personal use only.

1400 to 2200 °K and find a value of 1×10^{14} exp $[(-28\,000 \pm 3\,000)/RT]$ cm^3 mole^{-1} s^{-1}. Fishburne and Edse (51) find that $(k_2 + k_3) = (2.3 \pm 0.4) \times 10^{13}$ exp $[(-25\,000 \pm 800)/RT]$ from 1700 to 2300 °K. If it is assumed that $k_2 \simeq k_3$, then the rates found by Fenimore and Jones are about 4 times as great as those of Fishburne and Edse.

Our values of Y can be compared with the earlier work in the following way. We believe that k_1 lies between $0.5k_0$ and k_0. Therefore Y should lie between $(k_2 + k_3)[N_2O]_0/0.5k_0[M]$ and $(k_2 + k_3)[N_2O]_0/k_0[M]$. The 2 lower lines in Fig. 11 are these two quantities plotted using $(k_2 + k_3)$ from Fishburne and Edse's data, and using $[N_2O]_0$, [M], and k_0 from our own experiments. The 2 upper lines are the corresponding quantities using Fenimore and Jones' data for $(k_2 + k_3)$, assuming that $k_2 = k_3$. To agree with Fishburne and Edse, our data points should lie between the 2 lower lines, whereas to agree with Fenimore and Jones, they should lie between the 2 upper ones. In fact, in the latter case the correction factor to k_0 is found to be fairly near to 0.5, so that the points should lie close to the upper line if Fenimore and Jones' value is correct. Our data are rather scattered, since the measurement is a difficult one, depending upon differences between measured quantities. Nevertheless, it will be seen that the value of Fenimore and Jones is strongly favored by our results.

It should be pointed out that the method just described for finding Y will not be very seriously affected by minor changes in temperature due to slight endothermicity or exothermicity of the reaction. It would be expected that the value of Y obtained would simply be an average over a small temperature range. Since Y depends on a ratio of rate constants, its temperature dependence is not particularly large. Of course, large temperature changes would considerably distort the shapes of the curves and would affect the results, probably making it difficult to obtain a match for any value of Y.

There has been no agreement among previous workers on the N_2O pyrolysis, about the rates of reactions [2] and [3]. Two groups (7, 17, 20) have previously considered that their rate data fitted the results of Fenimore and Jones, though they did not report any actual determination of the secondary rates. Several other workers have favored lower values for the rates of the secondary reactions (16, 18, 19). However the results of Kaufman, Gerri, and Bowman (46) for reactions [2] and [3], which were at one time held to favor the lower values, have now been reconciled with the data of Fenimore and Jones (49, 50, 52).

Determination of k_1

When the mechanism and the values of k_2 and k_3 are known, k_1 can be found by correcting the observed rate for the effects of exothermicity or endothermicity and secondary reactions. We will assume for the present that the thermal effects are small, and will justify this assumption later.

To correct for the secondary reactions, we use the experimental results in conjunction with the computed solutions of the rate equations. Essentially we fit a curve of the appropriate shape to the N_2O concentration points for a given experiment, by making a suitable linear scaling of the ξ-axis. A value of $k_1[M]$ is then derived from the scale factor which has to be applied to ξ. The shape of curve to be used is found from the computer solution for the relevant value of Y. This value of Y could have been our own value, determined as described in the previous section. However, we decided instead to use the value of Fenimore and Jones for k_3, and to assume that $k_2 = k_3$, as found in our own experiments.

In order to obtain Y from $(k_2 + k_3)$, we needed also an estimate of k_1. Therefore we employed a method of successive approximations, using $(k_2 + k_3)[N_2O]_0/0.6k_0[M]$ as our first estimate of Y. This was used to obtain a more accurate value of k_1, and a new value of Y was then found. Two complete iterations were found to be quite sufficient for k_1 to converge to a closely constant value. Additional calculations showed that, for given values of k_2 and k_3, the final value of k_1 by this successive approximation procedure was not appreciably dependent on the value of Y that was initially assumed; this is reasonable, because of the relative insensitivity of the correction to the value of Y.

Corrected values of log k_1 are plotted against $1/T$ in Fig. 12. The line is a least mean squares fit of the data to an Arrhenius form, and can be expressed as

$$k_1 = 10^{12.86 \pm 0.09} \exp [(-40\,700 \pm 900)/RT]$$

Using the above correction procedure, we

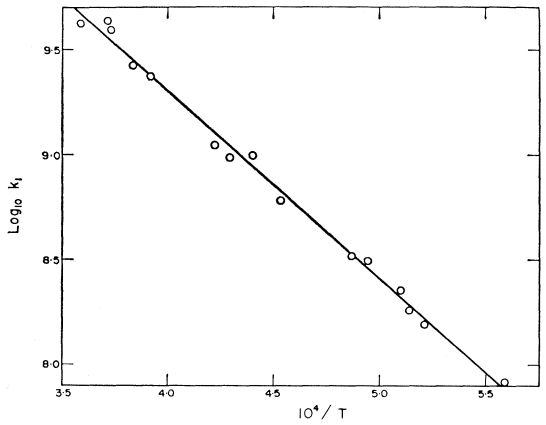

FIG. 12. Arrhenius plot of experimental values of k_1 obtained in the present work.

found that the value of k_1/k_0 was not the same in all experiments, though it was generally about 0.55 to 0.6. The final value of k_1 is somewhat affected by the values assumed for the rates of the secondary reactions. Therefore we also tried the effect of using Fishburne and Edse's values (51), which are about $\frac{1}{4}$ of those of Fenimore and Jones, for the secondary rates. The experimental curves then did not fit the computed ones quite as well, but it was still possible to obtain a corrected value of k_1 which ranged from about $0.6k_0$ at the lower end of the temperature range of our work to about $0.8k_0$ at the higher temperatures.

Throughout these calculations, we had set [M] equal to the total initial concentration of the shock-compressed gas. The results of Volmer and Bogdan (53) below 1000 °K show that the efficiencies of various monatomic and diatomic gases in energizing N_2O are not extremely different from that of N_2O itself; the differences may well be smaller still at higher temperatures (54). Therefore, we believe that our rate constant can, without serious error, be considered that for Kr as M. We believe also that our rates should be comparable, without large correction, to those in otherwise similar experiments which use argon as diluent.

Thermal Effects

Reaction [1] is endothermic by at least 38 kcal, so that the overall reaction will always be endothermic in the initial stages. The secondary reactions [2] and [3] are, however, exothermic. The overall endo- or exothermicity will therefore be decided by the relative effects of these 3 reactions. In considering this point, it is useful to note that at the low densities and short reaction times of the present work, d[O]/dt cannot become negative. This can be seen by consideration of eqs. [9] and [10], or from Fig. 8. Thus O atoms are always present, even when the decomposition of N_2O is essentially complete; for small values of Y, the predicted proportion of O atoms is quite large (Fig. 8).

Calculations show that in the range studied by us, the overall reaction is in fact very nearly thermoneutral, and that thermal effects are therefore probably quite negligible. As an example, at 1900 °K, where $Y = 12$, about 10% of the N_2O has decomposed when $\xi = 0.0777$. The reaction can then be written as

$$N_2O \rightarrow 0.900\ N_2O + 0.048\ O + 0.087\ N_2 + 0.026\ NO + 0.013\ O_2$$

$$\Delta H^0 = 1.37 \text{ kcal}$$

corresponding to a temperature change of $-6°$ due to endothermicity in a 2% mixture. When 40% of the N_2O has decomposed, the temperature change is calculated to be $+1.5°$. At 2600°, the temperature changes at 10 and 40% reaction are calculated to be -9 and $-8°$ respectively. Incidentally, in calculating these temperature changes we actually used values of Y obtained from Fenimore and Jones' data and our own final k_1. However, essentially the same conclusion would have been reached if we had used our own values of Y, derived by methods (*ii*) and (*iii*) above without the assumption of negligible thermal effects, so that our conclusion that temperature changes are small is not reached by circular argument.

In experiments at much higher densities, where the recombination reactions are fast, the figures given here will not apply and the overall reaction will tend to be much more exothermic.

Discussion of k_1 Values

Our values of k_1 are compared with those of several other workers (7, 18, 20) in Fig. 13. Fishburne and Edse (F.E.) (18) quoted first order rate constants for the total rate of N_2O disappearance. Their constants have accordingly been divided by total gas concentration and multiplied by 0.5 (approximately the expected value of k_1/k_0) to bring them to a convenient form for comparison. Of their data, only the results for their lowest total concentration, 13×10^{-6} mole cm^{-3}, are shown on this

Can. J. Chem. Downloaded from www.nrcresearchpress.com by 210.87.254.5 on 09/05/12
For personal use only.

Can. J. Chem. Downloaded from www.nrcresearchpress.com by 210.87.254.5 on 09/05/12
For personal use only.

graph. It will be seen that as regards the magnitude of the observed rates at about 2000° there is fair agreement among the various workers. However, there is not very good agreement about the temperature coefficient of the rate, and in particular the results of Olschewski, Troe, and Wagner (O.T.W.) (7) (see also Jost, Michel, Troe, and Wagner (17)), show a substantially larger temperature dependence than any of the other results in Fig. 13.

Making a more detailed comparison, we note that F.E. found, as is usual in unimolecular reactions, that the Arrhenius activation energy is appreciably dependent on total gas concentration. As shown in Fig. 14, our own result for the activation energy appears consistent with the trend found by F.E. It should be pointed out, however, that the usual theories of unimolecular reaction predict that the energy of activation should level out again at low concentrations, and it is not clear from Fig. 14 whether this is happening. The difference between high and low pressure activation energies also appears rather large, as discussed below. On the other hand,

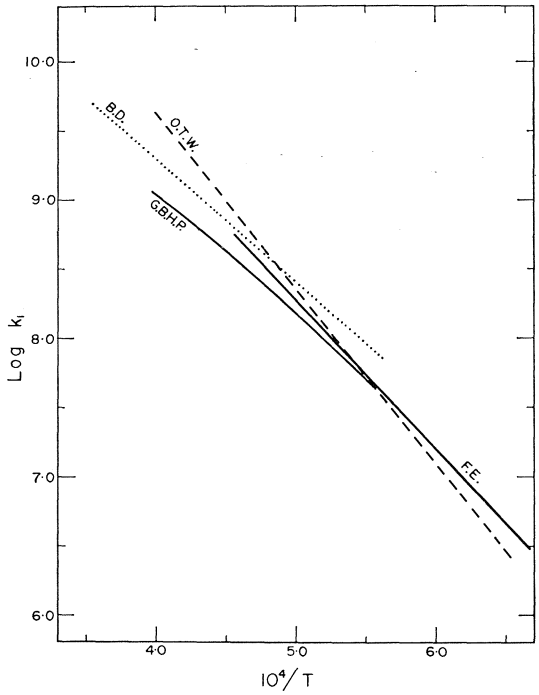

FIG. 13. Comparison of various experimental values of k_1 in the temperature range 1600 to 2800 °K. B.D., this work. F.E., Fishburne and Edse (18). G.B.H.P., Gutman, Belford, Hay, and Pancirov (20). O.T.W., Olschewski, Troe, and Wagner (7).

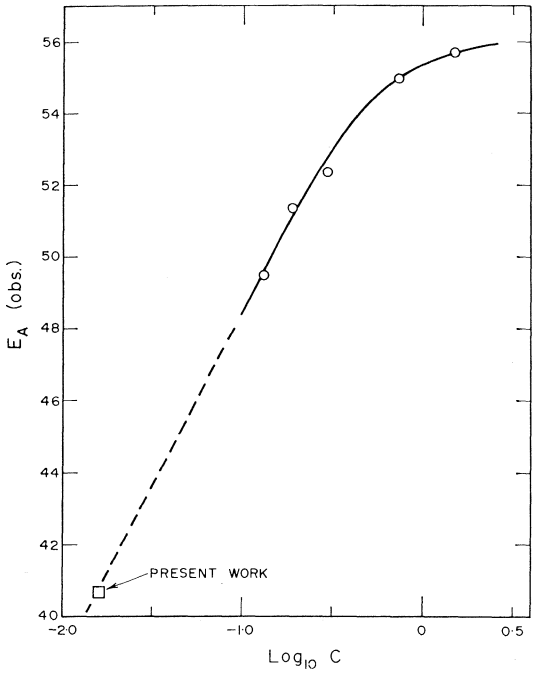

FIG. 14. Experimentally observed Arrhenius activation energies, plotted as a function of concentration. The circles are data of Fishburne and Edse (18).

it must also be admitted that there is relatively little experimental evidence to show whether the expected levelling out of the activation energy at low concentrations does in general occur under high temperature conditions such as those used in our work. When F.E.'s k_1 is plotted against total concentration, for a fixed temperature, a curve which is always concave upwards is obtained, as is expected on theoretical grounds (55). Again our result lies on a plausible extrapolation of their curve, as is shown for one representative temperature in Fig. 15. Accordingly we conclude that our values of k_1 are in general reasonably consistent with those of F.E., though some points remain to be clarified. Also, Kistiakowsky and co-workers (56) have briefly reported some work on N_2O decomposition, and find agreement with F.E.

Gutman, Belford, Hay, and Pancirov (G.B.H.P.) (20) expressed their k_1 in a different functional form

$$k_1 = 1.2 \times 10^7 (T)^{\frac{1}{2}} (60\,000/RT)^{5.09} \times \exp(-60\,000/RT) \text{ cm}^3 \text{ mole}^{-1}\text{s}^{-1}$$

However, their Arrhenius activation energy can be written as $E_A = 60\,000 - 4.59RT$, and this

gives a temperature coefficient very close to ours. For example, at 2200 °K, in the middle of our temperature range, the value obtained from their results is 39.9 kcal mole^{-1}, compared with our figure of 40.7. Our rate constants are, however, consistently about 1.8 times as large as theirs. In looking for a possible explanation of this discrepancy, we note that G.B.H.P. expected that the reaction would be appreciably exothermic. Therefore, to eliminate interference from exothermicity and from possible thermal boundary layer effects, they extrapolated their rate constants to zero time. The extrapolated constant was interpreted as $2k_1$, and was accordingly divided by 2 before plotting. Figure 10 shows a graph of k'/k_1 against dimensionless reaction time. k' is the effective overall rate constant for N_2O destruction. Clearly any procedure which efficiently extrapolates the rate constant towards zero time will tend to give k_1 rather than $2k_1$. However, the Y values of G.B.H.P. would be rather large; we estimate for their conditions 60 at 1500° and 13 at 2500°, so that the extrapolation would have to be carried rather close to the shock front in order to give a result substantially smaller than $2k_1$.

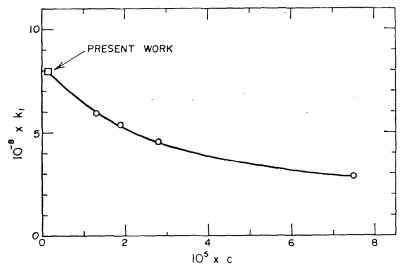

FIG. 15. Experimentally observed rate constants at 2200 °K, plotted as a function of concentration. The circles are taken from the data of Fishburne and Edse (18) and represent $0.5k/c$, where k is their measured first order rate constant for overall consumption of N_2O, and c is the total gas concentration.

The remarks of the previous paragraph will need some modification if the results of Fishburne and Edse (51) are used for the secondary reactions. Then the Y values will be considerably smaller, and almost any extrapolation towards zero time will give an apparent rate coefficient less than $2k_1$. In such a case, as mentioned above, our own results for k_1 would also have to be revised upwards by a small amount.

Comparing our results with O.T.W. (7), we find good agreement in the actual rates at about 2000 °K. At higher temperatures, O.T.W. find much higher rates than the other groups. This difference, which leads also to a difference in the energy of activation, is a major discrepancy which we have not been able to understand. It might be suggested that some of the gases used were impure. It is difficult to see how in our work an impurity could have passed unnoticed in the mass spectrometric records and yet have been present in sufficient amount to *reduce* our high temperature rates enough to account for the difference. O.T.W. used rather low concentrations of reactant, and this would tend to make their results susceptible to the presence of small amounts of catalytic impurity. It is clear, however, that they took considerable pains with cleanliness and purity. Moreover, their rate constants do not show the degree of scatter that might be expected if impurities were being accidentally introduced.

One other aspect of the comparison with O.T.W. is hard to understand. They report seeing effects due to non-stationary O atom concentrations only if the initial N_2O percentage was lowered to 0.02%. Accepting the values of F.J. for the secondary rates or, *a fortiori*, those of Fishburne and Edse (51), we would have expected non-stationary effects at much higher percentages of N_2O. For example, with 1% N_2O at 2500 °K, F.J.'s and O.T.W.'s rates imply a Y value of about 1.6. Figures 7 to 10 show that the non-stationary effects should be quite noticeable. With lower percentages of N_2O, the effects would be very marked, even at considerably lower temperatures. O.T.W.'s results may imply that all currently available values of k_2 and k_3, including our own, are too small. Alternatively, some re-interpretation of their results may be necessary. However, we do not believe that the differences between our results and those of O.T.W. can be due mainly to such non-stationary effects.

Drummond and Hiscock (21) have recently reported a unimolecular rate and activation energy for N_2O that closely agree with O.T.W. Unfortunately this does not help to resolve the difference between our results and those of O.T.W., because Drummond and Hiscock also report that if they were to correct their own results for the effects of temperature changes in

Can. J. Chem. Downloaded from www.nrcresearchpress.com by 210.87.254.5 on 09/05/12
For personal use only.

the reacting mixture, they believe that the activation energy would be reduced to a value close to 40 kcal mole^{-1}. This latter value would, of course, agree with ours.

Low pressure unimolecular rate constants are often expressed in the simplified classical Kassel form. If we do this with our results, we obtain, assuming a minimum critical energy of 60 kcal mole^{-1},

$$k_1 = 10^{7.475}(T)^{\frac{1}{2}}(60\,000/RT)^{4.96} \times \exp(-60\,000/RT)$$

However, we are somewhat dubious of the theoretical significance or value of using this form of the rate constant, since it implies six contributing classical oscillators for a light molecule with only 4 vibrations. Moreover, this expression is already an approximation which is only valid when $6RT \ll 60\,000$ cal mole^{-1}. Since the inequality is not very well obeyed in the present case, we must use (57) the more complete form

$$k = PZ \sum_{r=0}^{s-1} \frac{1}{r!}\left(\frac{E_0}{RT}\right)^r \exp(-E_0/RT)$$

where s is the number of contributing oscillators. Because the addition of the extra terms reduces the overall temperature dependence of the expression, one needs to use $s = 7$ to represent the results. This number of oscillators can scarcely have any direct physical significance.

Several other recent experimental studies of the high temperature dissociation of triatomic molecules have found energies of activation that could not be accounted for in terms of reasonable numbers of Kassel oscillators. A summary of data is given in Table I. For CO_2 and CS_2, as well as N_2O, direct dissociation into ground state products is spin-forbidden. For none of these cases is the minimum critical energy known *a priori*. However, the minimum critical energy E^* must be at least as great as the bond dissociation energy D for a truly unimolecular process, and may be much greater than D. In the case of CO_2, quite unreasonable numbers of Kassel oscillators are required to account for the results, even if $E^* = D$. For CS_2, the number of oscillators can be just within reason, but only if E^* is assumed to be very close to D. Of the spin-allowed processes, NOCl also requires too many oscillators; for SO_2, the number of oscillators may be normal, assuming that $E^* = D$.

TABLE I

Experimental data on high temperature energies of activation for dissociation of some triatomic molecules

Molecule	E_A* (kcal mole^{-1})	T (°K)	Reference	D† (kcal mole^{-1})
N_2O	62*	888	14	38.7
	59.5*	1400–2500	7	
	58	1400–2500	7	
	40.7	1800–2800	§	
	40.9	1800–2500	20	
	49.5–55.7	1500–2200	18	
CO_2	110‡	2800–3700	58	125.8
	87	3000–5500	59	
	99	2800–4400	60,64	
	83	2550–2860	61	
	79	3500–6000	62	
	76	6000–11000	63	
	83–88	3000–5000	65	
CS_2	87‡	1950–2800	58	92
	81.8	2250–3350	66	
	80.3	1800–3700	67	
NOCl	26.8	880–1350	68	37
SO_2	110	5000–7000	69	129

*E_A = Arrhenius energy of activation. Where the rate constant was not quoted in Arrhenius form, E_A has been evaluated at the temperature corresponding to the mean value of $1/T$.
†D = dissociation energy, into ground state products, of the bond which is broken. Data are taken from refs. 9–11, 70, and 71.
‡Quoted in the original paper as a "high pressure" value for energy of activation.
§This work.

Several of these results suggest an analogy with the thermal dissociation of diatomic molecules, where Arrhenius activation energies much lower than the energy of dissociation are frequently observed. These low values of the activation energy are very likely to be due to the occurrence of deviations from a Boltzmann distribution of vibrational energy amongst molecules which have insufficient energy to dissociate (72, 73). Similar deviations (20) might occur also for small polyatomic molecules at high temperatures.

The existence of deviations from Boltzmann equilibrium amongst molecules having *more than* the minimum critical energy is, of course, well known in unimolecular reactions, and is one of the principal topics of the theory of such reactions. The possibility of similar deviations amongst molecules of energy less than E^* seems to have been generally ignored or discounted because of the use of the "strong collision" assumption. According to this assumption, relatively large amounts of energy are exchanged during the collisions which energize molecules to levels above E^*. This in turn implies that

Can. J. Chem. Downloaded from www.nrcresearchpress.com by 210.87.254.5 on 09/05/12
For personal use only.

Can. J. Chem. Downloaded from www.nrcresearchpress.com by 210.87.254.5 on 09/05/12
For personal use only.

energization can occur with appreciable probability from each of many different levels below E^*. Then, in order to explain with this model any large non-equilibrium effect on the reaction rate, we would have to propose that a substantial proportion of these levels can simultaneously be considerably out of Boltzmann equilibrium. Because of the very large number of vibrational levels in a polyatomic molecule, such widespread disequilibrium is highly unlikely.

If we examine the evidence for the strong collision assumption, it appears that direct experimental evidence of collisional transfer of large amounts of energy from highly energized molecules has been obtained only for much more complex molecules than N_2O (74–80). There is indeed already some indication that for small molecules, the strong collision mechanism does not operate (81). Certainly, in the case of diatomic molecules, it is generally assumed that most of the energy transfer occurs by transitions among neighboring levels (82). Moreover, in the shock tube experiments which are considered here, the triatomic species is in high dilution. Therefore most of the energizing collisions are expected to be between a molecule and an atom, rather than between two molecules. An atom as collision partner would in general be less likely to exchange large amounts of energy than a molecule of the same mass, simply because the atom has fewer degrees of freedom available for such an exchange.

If we assume that a "weak collision" mechanism operates in N_2O, direct energization to states above E^* will occur only from a relatively few states which have energy just less than E^*. At very low pressures and high temperatures, these levels will become heavily depleted by the unbalanced demand from above. Energy transfer among levels below E^* will then tend to become a rate-determining factor, and the low pressure rate will be less than that predicted for a strong collision mechanism. Incidentally, though O.T.W. do suggest a weak collision mechanism for N_2O, they use an equilibrium energy distribution function to calculate energization rates, and therefore their treatment does not appear to be applicable to the study of possible disequilibrium below E^*.

Unfortunately, if the strong collision assumption is not used, the theoretical treatment of energization rates becomes much more difficult. In order to calculate unimolecular reaction rates in the fall-off and low pressure regions, detailed information about intermolecular energy transfer will be needed. At present, the data for a calculation of the actual energy distributions during unimolecular reaction in such a system are not available. Even when such data are obtained, it is likely that each reaction will have to be treated as a separate different case. The observations quoted in Table I already hint at such a situation.

Experimental Errors

There are several possible sources of error which might give rise to systematic deviations in our experimental results. These possible sources of error include non-ideal behavior of the shock waves, thermal boundary layer effects, and accumulation of sampled gas in the ion source region.

Non-ideal behavior of reflected shocks has been reported by a number of workers (see, e.g., refs. 83–92). However, the deviations from ideality are relatively small in the case of gas mixtures whose specific heat ratio, γ, is close to 1.67, as in the present work. It appears that for such mixtures, the actual shock temperatures may be about 30° lower than calculated (89). However, there is not complete agreement in the literature about the extent or even the direction of the deviation. Consequently we have not attempted to correct our reported temperatures for this effect. A systematic deviation of 30° would change our reported rate constant at 2000 °K by about 10%, and would have only a negligible effect on the observed energy of activation.

The possibility that a substantial proportion of the sampled gas might come from the thermal boundary layer near the end wall of the shock tube has been considered by a number of workers (16, 19, 20, 23, 56, 93). The general conclusion has been that in the range of temperatures and reaction times used in our work, interference by the thermal boundary layer is not very serious. In particular, Belford and coworkers (20) have reported an observed cooling rate of less than 5° per 100 μs at 2000°, and 50° per 100 μs at 2500 °K. These cooling rates would not be sufficient to affect our reaction rates very seriously. Moreover, these estimates of cooling rates were based on an observed

Can. J. Chem. Downloaded from www.nrcresearchpress.com by 210.87.254.5 on 09/05/12
For personal use only.

deceleration of the rate of reaction, and included an allowance for the expected exothermicity. If, as we believe, the reaction is less exothermic than they estimated, the true cooling rate would be less than mentioned above. Also, our sampling orifice was larger than that used by Belford, so that the influence of the thermal boundary layer on our results would in any case be expected to be less. Thus we conclude that, on evidence currently available, our results are probably not seriously affected by the thermal boundary layer. Nevertheless our opinion is that the general question of the effects of the thermal boundary layer on sampling in systems of this type is not by any means entirely closed, and that it would be desirable to find additional methods of studying these effects, particularly at temperatures above 2500 °K.

If substantial amounts of sampled gas build up in the ionization region of the mass spectrometer, the observed concentration profiles could be distorted. Calculations[4] of the gas flow in this region, based on the known geometry of the ion source, indicate that this effect is negligible. In these calculations, the gas flow from the orifice was treated as a freely expanding jet (36). Part of this flow was backscattered by the ion grids. The backscattered gas was then assumed to leave the ionization region by molecular flow. We have not made detailed calculations of the possibility of effects due to ion–molecule reactions, or elastic scattering of ions during flight to the detector; however, the calculations of Diesen and co-workers (94) show that such effects would almost certainly not cause appreciable errors under our conditions. This conclusion is supported by the fact that we did not observe any systematic deviations which could be attributed to elastic scattering or to ion–molecule reactions or to reactions of metastable krypton atoms, during our calibration experiments.

Acknowledgments

This work was supported by the National Research Council of Canada, Imperial Oil Limited, and the Ontario Research Foundation. S.C.B. thanks the National Research Council of Canada for the award of a Studentship. J.E.D. wishes to acknowledge his great indebtedness to Dr. George B. Kistiakowsky, in whose laboratory he began work on this area of research. We thank the Institute of Computer Science, University of Toronto, for the use of their facilities, and Drs. R. L. Belford, J. Troe, D. McL. Moulton, and J. V. Michael for helpful correspondence and discussion.

[4]We thank Mr. M. A. Di Valentin for making these calculations.

1. E. K. Gill and K. J. Laidler. Can. J. Chem. **36**, 1570 (1958).
2. E. K. Gill and K. J. Laidler. Proc. Roy. Soc. London, Ser. A, **250**, 121 (1959).
3. E. E. Nikitin. Dokl. Akad. Nauk SSSR, **129**, 157 (1959).
4. A. I. Osipov. Dokl. Akad. Nauk SSSR, **137**, 883 (1961).
5. G. M. Wieder and R. A. Marcus. J. Chem. Phys. **37**, 1835 (1962).
6. D. L. Bunker. J. Chem. Phys. **40**, 1946 (1964).
7. H. A. Olschewski, J. Troe, and H. Gg. Wagner. Ber. Bunsenges. Physik. Chem. **70**, 450 (1966).
8. E. E. Nikitin. Theory of thermally induced gas phase reaction. Indiana University Press, Bloomington. 1966. Chap. 2.
9. JANAF Thermochemical Tables. U.S. Department of Commerce, Natl. Bur. Stds. Washington, D.C. Revised to 1966.
10. F. Kaufman. J. Chem. Phys. **46**, 2449 (1967).
11. V. H. Dibeler. J. Chem. Phys. **47**, 2191 (1967).
12. F. J. Lindars and Sir Cyril Hinshelwood. Proc. Roy. Soc. London, Ser. A, **231**, 162, 178 (1955).
13. B. G. Reuben and J. W. Linnett. Trans. Faraday Soc. **55**, 1543 (1959).
14. H. S. Johnston. J. Chem. Phys. **19**, 663 (1951).
15. H. S. Johnston and J. R. White. J. Chem. Phys. **22**, 1969 (1954).
16. J. N. Bradley and G. B. Kistiakowsky. J. Chem. Phys. **35**, 256 (1961).
17. W. Jost, K. W. Michel, J. Troe, and H. Gg. Wagner. Z. Naturforsch. **19a**, 59 (1964).
18. E. S. Fishburne and R. Edse. J. Chem. Phys. **41**, 1297 (1964).
19. A. P. Modica. J. Phys. Chem. **69**, 2111 (1965).
20. D. Gutman, R. L. Belford, A. J. Hay, and R. Pancirov. J. Phys. Chem. **70**, 1793 (1966).
21. L. J. Drummond and S. W. Hiscock. Australian J. Chem. **20**, 815 (1967).
22. G. B. Kistiakowsky and P. H. Kydd. J. Am. Chem. Soc. **79**, 4825 (1957).
23. J. E. Dove and D. McL. Moulton. Proc. Roy. Soc. London, Ser. A, **283**, 216 (1965).
24. R. W. Diesen and W. J. Felmlee. J. Chem. Phys. **39**, 2115 (1963).
25. R. T. Meyer. J. Chem. Phys. **46**, 967 (1967).
26. R. T. Meyer. The time-of-flight mass spectrometer. *Edited by* D. Price and J. E. Williams. The Pergamon Press, Ltd., Oxford. (In the press).
27. I. I. Glass. UTIAS Review No. 26, Part 2. Institute for Aerospace Studies. University of Toronto, Toronto. 1965.
28. H. Mirels and S. W. King. AIAA J. **4**, 782 (1966). (Earlier references there.)
29. W. C. Wiley and I. H. McLaren. Rev. Sci. Instr. **26**, 1150 (1955).
30. D. B. Harrington. Advances in mass spectrometry. *Edited by* J. D. Waldron. The Pergamon Press, Ltd., London. 1959. p. 249.

Can. J. Chem. Downloaded from www.nrcresearchpress.com by 210.87.254.5 on 09/05/12
For personal use only.

31. G. T. SKINNER. Report No. RM-1396-A-1. Cornell Aeronautical Laboratory, Buffalo, New York. 1961.
32. S. C. BARTON, M. A. DI VALENTIN, and J. E. DOVE. Paper presented at the 5th Intern. Shock Tube Symp. Div. Fluid Dyn. Am. Phys. Soc. U.S. Naval Ordnance Laboratory, Silver Spring, Maryland. 1965.
33. M. PHISTER. Logical design of digital computers. John Wiley and Sons, Inc., New York. 1958.
34. NAVWEPS 16-1-519-5. Handbook, preferred circuits, Navy aeronautical electronic equipment. Vol. II. Semiconductor device circuits. Natl. Bur. Stds. Washington, D.C. 1962.
35. C. D. JOHNSON and D. BRITTON. J. Chem. Phys. **38**, 1455 (1963).
36. F. S. SHERMAN. Phys. Fluids, **8**, 773 (1965).
37. D. E. ROTHE. Phys. Fluids, **9**, 1643 (1966).
38. F. KAUFMAN. Proc. Roy. Soc. London, Ser. A, **247**, 123 (1958).
39. P. HARTECK, R. R. REEVES, and G. MANNELLA. J. Chem. Phys. **29**, 1333 (1958).
40. E. A. OGRYZLO and H. I. SCHIFF. Can. J. Chem. **37**, 1690 (1959).
41. H. P. BROIDA, H. I. SCHIFF, and T. M. SUGDEN. Trans. Faraday Soc. **57**, 259 (1961).
42. M. A. A. CLYNE and B. A. THRUSH. Proc. Roy. Soc. London, Ser. A, **269**, 404 (1962).
43. F. S. KLEIN and J. T. HERRON. J. Chem. Phys. **41**, 1285 (1964).
44. K. L. WRAY. 10th Intern. Symp. Comb. 1964. The Combustion Institute, Pittsburgh, Pennsylvania. 1965. p. 523. (Earlier references there.)
45. F. KAUFMAN and J. R. KELSO. J. Chem. Phys. **23**, 602 (1955).
46. F. KAUFMAN, N. J. GERRI, and R. E. BOWMAN. J. Chem. Phys. **25**, 106 (1956).
47. H. T. DAVIS. Introduction to nonlinear differential and integral equations. Dover Publications, New York. 1962. Chap. 5.
48. C. P. FENIMORE and G. W. JONES. J. Phys. Chem. **62**, 178 (1958).
49. C. P. FENIMORE and G. W. JONES. 8th Intern. Symp. Comb. 1960. The Williams and Wilkins Co., Baltimore, Md. 1962. p. 127.
50. F. KAUFMAN. Progr. Reaction Kinetics, **1**, 1 (1961).
51. E. S. FISHBURNE and R. EDSE. J. Chem. Phys. **44**, 515 (1966).
52. C. P. FENIMORE. J. Chem. Phys. **35**, 2243 (1961).
53. M. VOLMER and M. BOGDAN. Z. Phys. Chem. B, **21**, 257 (1933).
54. V. N. KONDRAT'EV. *Translated by* J. M. Crabtree and S. N. Carruthers. Chemical kinetics of gas reactions. Addison-Wesley Publishing Co., Inc., Reading, Mass. 1964. Chap. 6.
55. H. S. JOHNSTON. Gas phase reaction rate theory. The Ronald Press Co., New York. 1966. Chap. 15.
56. I. D. GAY, G. B. KISTIAKOWSKY, J. V. MICHAEL, and H. NIKI. J. Chem. Phys. **43**, 1720 (1965).
57. N. B. SLATER. Theory of unimolecular reactions. Cornell Univ. Press, Ithaca, New York. 1959. Chap. 2.
58. H. A. OLSCHEWSKI, J. TROE, and H. GG. WAGNER. Ber. Bunsenges. Physik. Chem. **70**, 1060 (1966).
59. S. A. LOSEV, N. A. GENERALOV, and V. A. MAKSIMENKO. Dokl. Akad. Nauk SSSR, **150**, 839 (1963).
60. K. W. MICHEL, H. A. OLSCHEWSKI, H. RICHTERING, and H. GG. WAGNER. Z. Phys. Chem. Frankfurt, **39**, 129 (1963).
61. T. A. BRABBS, F. E. BELLES, and S. A. ZLATARICH. J. Chem. Phys. **38**, 1939 (1963).
62. W. O. DAVIES. J. Chem. Phys. **41**, 1846 (1964).
63. W. O. DAVIES. J. Chem. Phys. **43**, 2809 (1965).
64. K. W. MICHEL, H. A. OLSCHEWSKI, H. RICHTERING, and H. GG. WAGNER. Z. Phys. Chem. Frankfurt, **44**, 160 (1965).
65. E. S. FISHBURNE, K. R. BILWAKESH, and R. EDSE. J. Chem. Phys. **45**, 160 (1966).
66. A. G. GAYDON, G. H. KIMBELL, and H. B. PALMER. Proc. Roy. Soc. London, Ser. A, **279**, 313 (1964).
67. H. A. OLSCHEWSKI, J. TROE, and H. GG. WAGNER. Z. Phys. Chem. Frankfurt, **45**, 329 (1965).
68. P. DEKLAU and H. B. PALMER. 8th Intern. Symp. Comb. 1960. The Williams and Wilkins Co., Baltimore, Md. 1962. p. 139.
69. H. A. OLSCHEWSKI, J. TROE, and H. GG. WAGNER. Z. Phys. Chem. Frankfurt, **44**, 173 (1965).
70. B. J. MCBRIDE, S. HEIMEL, J. G. EHLERS, and S. GORDON. Thermodynamic properties to 6000 °K for 210 substances involving the first 18 elements. NASA SP-3001. Natl. Aeronautics Space Admin. Washington, D.C. 1963.
71. V. I. VEDENEEV, L. V. GURVICH, V. N. KONDRAT'YEV, V. A. MEDVEDEV, and YE. L. FRANKEVICH. Bond energies, ionization potentials and electron affinities. Edward Arnold and Co., London. 1966.
72. C. A. BRAU, J. C. KECK, and G. F. CARRIER. Phys. Fluids, **9**, 1885 (1966).
73. H. J. KOLKER. J. Chem. Phys. **44**, 582 (1966). (Earlier references there.)
74. R. E. HARRINGTON, B. S. RABINOVITCH, and M. R. HOARE. J. Chem. Phys. **33**, 744 (1960).
75. G. H. KOHLMAIER and B. S. RABINOVITCH. J. Chem. Phys. **38**, 1692 (1963).
76. G. H. KOHLMAIER and B. S. RABINOVITCH. J. Chem. Phys. **38**, 1709 (1963).
77. G. H. KOHLMAIER and B. S. RABINOVITCH. J. Chem. Phys. **39**, 490 (1963).
78. D. W. SETSER, B. S. RABINOVITCH, and J. W. SIMONS. J. Chem. Phys. **40**, 1751 (1964).
79. J. H. CURRENT and B. S. RABINOVITCH. J. Chem. Phys. **40**, 2742 (1964).
80. J. W. SIMONS, B. S. RABINOVITCH, and D. W. SETSER. J. Chem. Phys. **41**, 800 (1964).
81. F. J. FLETCHER, B. S. RABINOVITCH, K. W. WATKINS, and D. J. LOCKER. J. Chem. Phys. **70**, 2823 (1966).
82. J. F. CLARKE and M. MCCHESNEY. The dynamics of real gases. Butterworths, London. 1964. Chap. 7.
83. J. P. TOENNIES and E. F. GREENE. J. Chem. Phys. **26**, 655 (1957).
84. H. MARK. J. Aeron. Sci. **24**, 304 (1957).
85. G. SKINNER. J. Chem. Phys. **31**, 268 (1959).
86. R. A. STREHLOW and A. COHEN. J. Chem. Phys. **30**, 257 (1959).
87. G. RUDINGER. J. Chem. Phys. **30**, 1507 (1959).
88. R. A. STREHLOW and C. T. CASE. J. Chem. Phys. **35**, 1506 (1961).
89. C. D. JOHNSON and D. BRITTON. J. Chem. Phys. **38**, 1455 (1963).
90. E. S. FISHBURNE, D. M. BERGBAUER, and R. EDSE. Phys. Fluids, **7**, 1391 (1964).
91. S. TSUCHIYA and K. KURATANI. J. Chem. Phys. **44**, 2986 (1966).
92. E. H. CARNEVALE, S. WOLNIK, G. LARSON, C. CAREY, and G. W. WARES. Phys. Fluids, **10**, 1459 (1967).
93. R. W. DIESEN. J. Chem. Phys. **44**, 3662 (1966).
94. W. J. FELMLEE, R. V. PETRELLA, and R. W. DIESEN. Technical Report SL 175311a. The Dow Chemical Company, Midland, Michigan. 1966.
95. M. A. DI VALENTIN and J. E. DOVE. To be published.

Can. J. Chem. Downloaded from www.nrcresearchpress.com by 210.87.254.105 on 09/05/12
For personal use only.

Molar excess Gibbs free energies of benzene – *m*-xylene mixtures[1]

T. BOUBLÍK[2] AND G. C. BENSON
Division of Pure Chemistry, National Research Council of Canada, Ottawa, Canada

Received September 25, 1968

Vapor–liquid equilibria for the system benzene – *m*-xylene were measured in a circulation still at 25, 37, and 50 °C. Excess free energy data were analyzed in terms of Flory's theory of non-polar mixtures.

Canadian Journal of Chemistry, **47**, 539 (1969)

Introduction

Values of the excess enthalpies and excess volumes of the three systems formed by mixing benzene with *o*-, *m*-,and *p*-xylene (at 25 °C) were presented in a previous publication (1). It was found that the Flory theory (2) of non-polar mixtures provided a reasonable framework for interpretation of these results. However, a similar treatment (3) of data for aromatic–alicyclic systems showed that, although the theory appears to correlate enthalpy and volume changes fairly well, excess free energies are generally overestimated. Analogous behavior has been observed for mixtures of *n*-alkanes by Orwoll and Flory (4) who suggested that the equation for the excess free energy in the original formulation of the theory should be amended to include an empirical interaction entropy contribution.

The present paper continues our investigation of the thermodynamic properties of benzene–xylene systems by reporting results for the vapor–liquid equilibrium of benzene – *m*-xylene mixtures at 25, 37, and 50 °C. Excess free energies derived from these data are considered in the light of the Flory theory and its recent modification.

Experimental

Materials

Spectroquality benzene from Matheson, Coleman and Bell was used without further purification since gas chromatographic analysis failed to show any significant impurities. Values of the density, refractive index (μ_D), and vapor pressure, determined for this material at 25 °C, were 0.87340 g cm^{-3}, 1.49777, and 95.20 Torr respectively.

The *m*-xylene (primary material also Matheson, Coleman and Bell spectroquality reagent) was purified chromatographically using a 4 in. column packed with 20% PEG 20M on Chromosorb W. At 25 °C the density of the final product was equal to 0.85988 g cm^{-3} and μ_D was equal to 1.49464.

Description of Apparatus

The vapor–liquid equilibrium was studied by the dynamical method. The equilibrium still (capacity 120 cc), shown schematically in Fig. 1, is similar to that described by Dvořák and Boublík (5). The design of the temperature chamber and separator ensures good thermal equilibrium, and stirrers in both the vapor condensate and liquid sampling vessels prevent the occurrence of density gradients.

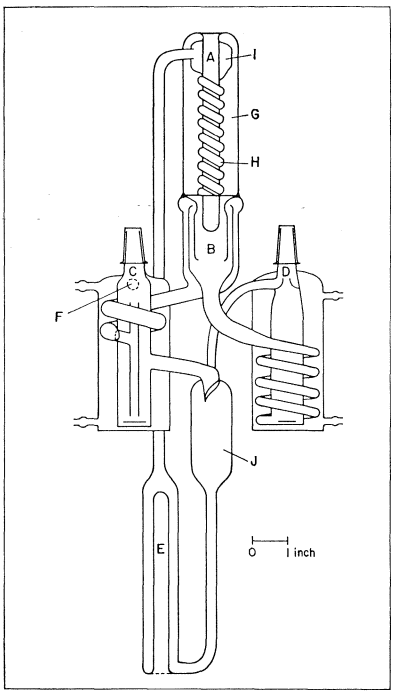

FIG. 1. Vapor–liquid equilibrium still. A, thermometer well; B, separator; C, D, vapor and liquid samplers; E, heater; F, connection to the pressure vessel; G, evacuated mantle; H, spiral tube carrying vapor and liquid from expansion chamber I to separator and ensuring good thermal contact with thermometer well; J, collector for condensate and liquid.

[1]Issued as NRCC No. 10 460.

[2]NRCC Postdoctorate Fellow 1967–1968. Present address: Institute of Chemical Process Fundamentals, Czechoslovak Academy of Science, Prague, Czechoslovakia.

Can. J. Chem. Downloaded from www.nrcresearchpress.com by 210.87.254.105 on 09/05/12
For personal use only.

The still and a water ebullioscope were attached to a large pressure vessel which could be maintained at any required pressure. The equilibrium value of the pressure was calculated from the boiling point of the water in the ebullioscope. The latter could be determined with an accuracy of 0.005 °C using a standardized Leeds and Northrup platinum resistance thermometer in a Mueller bridge circuit. The temperature in the still was measured to 0.02 °C with a mercury thermometer which had been calibrated against the resistance thermometer.

Analysis

The usual methods of analysis based on density or refractive index are unsatisfactory for the present system since they would necessitate measuring relatively small differences in the values of these properties. Gas chromatography has proved to be useful in determining the compositions of benzene – alkylbenzene systems where similar conditions prevail (6) and this technique was adopted in the present investigation.

Preliminary tests indicated that an equilibrium state was reached within the still after it had been operating for about 1½ h under steady conditions. Samples of the liquid phase and vapor condensate were removed with syringes and analyses carried out using a Perkin–Elmer gas chromatograph with hot wire detector and a column containing 4% squalane on Chromosorb (G-AW-DMCS). With the output from the thermal conductivity bridge connected to an integrating recorder, the mean of 10 analyses was reproducible to 0.1 mole %. A calibration curve was established over the whole concentration range; the compositions of the equilibrium phases were then determined as the mean of 10 analyses. The overall accuracy of the compositions is estimated to be 0.3 mole %.

Results

Pressures and compositions (expressed as mole fractions x_1 and y_1 of benzene in the liquid and vapor respectively) measured for the equilibrium phases at 25, 37, and 50 °C are listed in Table I. Activity coefficients γ_i were calculated from the equilibrium data using the relation

$$[1]\quad RT \ln \gamma_i = RT \ln (y_i p / x_i p_i^0) + (B_{ii} - v_i^0)(p - p_i^0) + (1 - y_i)^2 p\delta$$

where R is the gas constant, T the absolute temperature, p the pressure of the system, and x_i and y_i are the mole fractions of component i in the liquid and vapor phases. The vapor pressure and molar volume of pure component i are denoted by p_i^0 and v_i^0 respectively. The quantity δ is related to the virial coefficients (B_{11} and B_{22}) of the pure species and to the cross term (B_{12}) between the species by the equation

$$[2]\quad \delta = 2B_{12} - B_{11} - B_{22}$$

Vapor pressures of the component liquids were calculated from the Antoine equation with values of the coefficients taken from the API tables (7). Values of the molar volumes were based on the experimental densities at 25 °C and on data at other temperatures from refs. (7) and (8). Haggenmacher's formula (9) was used to estimate values of the virial coefficients from critical data (7); the simple mixing rules outlined by O'Connell and Prausnitz (10) were adopted in the case of the cross coefficient. Table II summarizes the results of these calculations.

TABLE I

Comparison of experimental and calculated values for the vapor–liquid equilibria of the system benzene (1) – *m*-xylene (2)

x_1	y_1	p	$y_{1\ \mathrm{calcd}}$	p_{calcd}
		25.00 °C		
0.244	0.786	29.54	0.789	29.97
0.252	0.790	30.35	0.796	30.68
0.380	0.874	41.69	0.876	41.83
0.470	0.909	49.58	0.910	49.57
0.556	0.931	57.32	0.934	56.97
0.645	0.955	64.97	0.953	64.63
0.719	0.967	71.27	0.966	70.94
0.820	0.981	79.72	0.980	79.63
0.927	0.993	88.75	0.993	88.87
		37.00 °C		
0.037	0.296	22.08	0.285	21.80
0.042	0.314	22.80	0.308	22.45
0.072	0.446	27.07	0.441	26.93
0.085	0.501	29.44	0.488	28.97
0.137	0.619	36.58	0.616	36.56
0.268	0.782	55.06	0.786	55.78
0.394	0.866	73.66	0.865	74.03
0.474	0.900	85.68	0.899	85.64
0.535	0.916	94.76	0.918	94.32
0.651	0.948	111.40	0.947	110.97
0.745	0.967	125.10	0.966	124.50
0.819	0.977	135.50	0.977	135.18
0.928	0.991	150.70	0.992	150.96
		50.00 °C		
0.044	0.308	42.63	0.291	42.03
0.088	0.464	52.61	0.461	52.88
0.095	0.488	54.42	0.481	54.52
0.146	0.603	66.47	0.601	67.05
0.274	0.769	97.07	0.766	97.79
0.388	0.848	125.20	0.845	125.21
0.480	0.890	147.20	0.887	147.19
0.538	0.911	161.50	0.908	160.87
0.654	0.943	189.40	0.941	188.47
0.749	0.962	211.80	0.961	210.95
0.804	0.975	224.80	0.971	224.17
0.826	0.976	230.40	0.975	229.40
0.929	0.993	254.30	0.991	254.09

Values of the excess Gibbs free energy of the liquid phase as given by

$$[3]\quad G^E = RT(x_1 \ln \gamma_1 + x_2 \ln \gamma_2)$$

were fitted with an expression of the form

$$[4]\quad G^E = x_1 x_2 [c_1 + c_2(x_2 - x_1) + c_3(x_2 - x_1)^2 + \ldots]$$

Can. J. Chem. Downloaded from www.nrcresearchpress.com by 210.87.254.105 on 09/05/12
For personal use only.

TABLE II

Virial coefficients calculated for the system benzene (1) – *m*-xylene (2)

Temperature (°C)	Coefficients*		
	B_{11}	B_{22}	δ
25.0	−1691	−3130	189
37.0	−1563	−2892	174
50.0	−1440	−2664	161

*Units: $cm^3\ mole^{-1}$.

where the constants c_j were calculated for each temperature by a least squares method with weights assigned according to estimated errors of the primary experimental data. In point of fact the values of ln γ_i were fairly small and differences between the experimental results (i.e. from eq. [1]) and those calculated from the fit of G^E (i.e. from differentiation of eq. [4]) were relatively large. The experimental accuracy did not warrant using more than one coefficient in eq. [4] and a single value of this ($c_1 = 113 \pm 19$) described the free energy behavior of the system within the limit of the experimental error over the temperature range studied. This is illustrated by the comparison of calculated and experimental values of y_1 and p given in Table I. Use of a single temperature independent coefficient in eq. [4] should not be interpreted as indicating that the excess entropy is zero but only that the temperature variation of G^E is less than the error of its determination from the present measurements.

Application of Flory's Theory

As originally presented (2) Flory's theory permits the evaluation of the excess properties of a binary system from the properties of the pure components, provided the value of one parameter, X_{12}, characterizing the interaction of unlike species in the mixture, is known. In practice this parameter is generally estimated from data for the mixture.

In our earlier work on benzene – isomeric xylene systems (1), the values of X_{12} which minimized the integral

$$[5]\quad \sigma_H^2(X_{12}) = \int_0^1 (H^E_{exptl} - H^E_{Flory}(X_{12}))^2 dx_1$$

were determined. The integrand in this equation represents the square of the difference between the experimental excess enthalpy and the value obtained from the Flory theory (see eq. 34′ of ref. (2)) for any particular value of X_{12}. Using the values of X_{12} obtained in this way for the three benzene–xylene systems, excess volumes of the right order of magnitude were calculated and the observed order meta > ortho > para was reproduced, although differences between the systems were underestimated.

The expression for the excess free energy derived by Flory (2) on the basis of an ideal combinatory entropy, is

$$[6]\quad G^E_{Flory}(0) = \sum_1^2 x_i\left[v_i^* p_i^*(\tilde{v}_i^{-1} - \tilde{v}) + 3v_i^* p_i^* \tilde{T}_i \ln\left(\frac{\tilde{v}_i^{1/3} - 1}{\tilde{v}^{1/3} - 1}\right)\right] + x_1 v_1^* \theta_2 X_{12} \tilde{v}^{-1}$$

where p_i^*, T_i^*, and v_i^* are characteristic values of the pressure, temperature, and hard-core volume per mole which can be calculated from the molar volume, coefficient of expansion, and isothermal compressibility of pure component i at a given temperature. From these the reduced volume per mole of segments $\tilde{v}_i$, and the reduced temperature $\tilde{T}_i$ are readily obtainable. At zero pressure the reduced volume per mole of segments in the solution $\tilde{v}$, and the reduced temperature defined by

$$[7]\quad \tilde{T} = (\phi_1 p_1^* \tilde{T}_1 + \phi_2 p_2^* \tilde{T}_2)/(\phi_1 p_1^* + \phi_2 p_2^* - \phi_1 \theta_2 X_{12})$$

satisfy the simple equation of state

$$[8]\quad \tilde{T} = (\tilde{v}^{1/3} - 1)/\tilde{v}^{4/3}$$

In eqs. [6] and [7] ϕ_i and θ_i are the segment fractions and site fractions which can be calculated from the relations

$$[9]\quad \phi_2 = 1 - \phi_1 = x_2/(x_2 + x_1 r_1/r_2)$$

and

$$[10]\quad \theta_2 = 1 - \theta_1 = \phi_2/(\phi_2 + \phi_1 s_1/s_2)$$

where r_i is the effective number of segments in a molecule of component i, and s_i is the mean number of contact points per segment.

As in our previous calculation it is assumed that

$$[11]\quad r_1/r_2 = v_1^*/v_2^*$$

and

$$[12]\quad s_1/s_2 = (v_2^*/v_1^*)^{1/3}$$

Using the above relations and the properties of

benzene and *m*-xylene at 25° as summarized in ref. (1) along with the value of $X_{12} = 11.51$ J cm^{-3} derived therein, the values of G^E plotted as a broken curve in Fig. 2 were calculated. These values are considerably higher than the experimental results represented by the solid curve in Fig. 2; for an equimolar solution the difference amounts to nearly a factor of 8. This may be compared with our earlier calculations (3) for benzene–cyclopentane, benzene–cyclohexane, and toluene–cyclohexane where discrepancies in the excess free energies amounting to factors of the order of 2 were found.

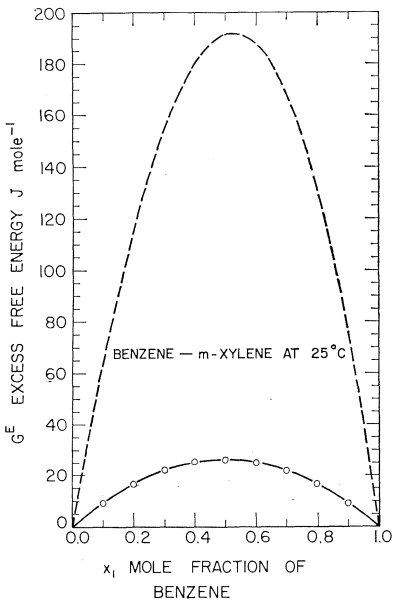

FIG. 2. Excess Gibbs free energy of the system benzene–*m*-xylene at 25 °C. Solid curve represents experimental results obtained from data for vapor–liquid equilibria. Broken curve calculated from Flory theory with $Q_{12} = 0$; the points ⊙ at 0.1 intervals in x_1 are theoretical values calculated with $Q_{12} = 0.02824$ J cm^{-3} deg^{-1}.

Recently Orwoll and Flory (4) pointed out that interaction between neighboring species can be expected to contribute to the entropy of the mixture as well as to the enthalpy. To allow for this contribution they added an empirical term containing a second adjustable parameter Q_{12} to the original free energy equation. The resulting expression

$$[13] \quad G^E_{\text{Flory}}(Q_{12}) = G^E_{\text{Flory}}(0) - x_1 v_1^* \theta_2 T Q_{12}$$

was fitted to our experimental data for G^E by minimizing the integral

$$[14] \quad \sigma_G^2(Q_{12}) = \int_0^1 [G^E_{\text{exptl}} - G^E_{\text{Flory}}(Q_{12})]^2 dx_1$$

It was found that the experimental data could be represented within the experimental error by eq. [13] using a value of $Q_{12} = 0.02824$ J cm^{-3} deg^{-1}. Values calculated in this way at 0.1 intervals in x_1 are indistinguishable from the experimental curve in Fig. 2.

In the same way the excess free energies of aromatic–alicyclic systems considered previously (3) can be fitted quite well using values of $Q_{12} =$ 0.03362, 0.04807, and 0.02675 J cm^{-3} deg^{-1} for benzene–cyclopentane, benzene–cyclohexane, and toluene–cyclohexane respectively. Thus it appears that the use of Q_{12} as a second adjustable parameter in the Flory theory leads to a useful representation of excess free energy data.

Acknowledgment

We are grateful to Mr. C. J. Halpin for purifying the *m*-xylene and for technical assistance throughout the course of this investigation.

1. J. SINGH, H. D. PFLUG, and G. C. BENSON. J. Phys. Chem. **72**, 1939 (1968).
2. P. J. FLORY. J. Am. Chem. Soc. **87**, 1833 (1965).
3. G. C. BENSON and J. SINGH. J. Phys. Chem. **72**, 1345 (1968).
4. R. A. ORWOLL and P. J. FLORY. J. Am. Chem. Soc. **89**, 6822 (1967).
5. K. DVOŘÁK and T. BOUBLÍK. Coll. Czech. Chem. Commun. **28**, 1249 (1963).
6. W. D. KESSELMAN, G. E. HOLLENBACH, A. L. MYERS, and A. E. HUMPHREY. J. Chem. Eng. Data, **13**, 35 (1968).
7. American Petroleum Institute. Research Project 44. Selected values of properties of hydrocarbons and related compounds. Carnegie Press, Carnegie Institute of Technology, Pittsburgh. 1953, and later revisions.
8. J. TIMMERMANS. Physico-chemical constants of pure organic compounds. Vol. I and II. Elsevier Press, Inc., New York. 1950 and 1965.
9. J. E. HAGGENMACHER. J. Am. Chem. Soc. **68**, 1123 (1946).
10. J. P. O'CONNELL and J. M. PRAUSNITZ. Ind. Eng. Chem., Process Des. Develop. **6**, 245 (1967).

Can. J. Chem. Downloaded from www.nrcresearchpress.com by 210.87.254.105 on 09/05/12
For personal use only.

Can. J. Chem. Downloaded from www.nrcresearchpress.com by 210.87.254.40 on 09/05/12
For personal use only.

Excess thermodynamic properties of isopropanol–*n*-decanol mixtures[1]

JASWANT SINGH[2], H. D. PFLUG[3], AND G. C. BENSON
Division of Pure Chemistry, National Research Council of Canada, Ottawa, Canada

Received October 2, 1968

Molar excess Gibbs free energies, obtained from static vapor pressure measurements on isopropanol–*n*-decanol mixtures over the temperature range 20–50 °C, are reported. Results of direct determinations of heats and volumes of mixing at 25 °C are also presented.

Canadian Journal of Chemistry, **47**, 543 (1969)

Introduction

Previous studies of the thermodynamic properties of binary alcohol mixtures (1–5) have been continued by investigating the system isopropanol–*n*-decanol. The new measurements comprise determinations of total vapor pressures over the range 20–50 °C and of heats and volumes of mixing at 25 °C.

Experimental

(i) Vapor Pressures

Static vapor pressures for systems of known total composition and known total volume were measured with a precision quartz gauge (Texas Instruments). Details of the experimental procedure and of the method of calculating the compositions of the individual liquid and vapor phases have been described in earlier communications (3–4).

Assumptions similar to those made in ref. (3) were also adopted in the present investigation. Thus, the equation of state employed for the vapor phase was

$$[1] \qquad V^g = n^g\left(\frac{RT}{p} + B + Dp^2\right)$$

where V^g is the volume of n^g moles of material and B and D are the second and fourth virial coefficients respectively. For isopropanol vapor, Kretschmer and Wiebe (6) have found that this form is more appropriate than one involving second and third virial coefficients. In all of the vapor phases studied, the mole fraction of decanol, y_2, was small (< 0.015) and the second and fourth virial coefficients were approximated by the values for pure isopropanol. Also, since the vapor pressure of decanol was relatively small at all of the temperatures considered, the partial pressure, p_2, of decanol in the vapor phase was estimated from that of pure decanol, p_2^0, by means of the Raoult expression

$$[2] \qquad p_2 = x_2 p_2^{\,0}$$

where x_2 is the mole fraction of decanol in the liquid phase in equilibrium with the vapor.

(ii) Excess Enthalpies and Excess Volumes

The enthalpy and volume changes for mixing isopropanol with *n*-decanol were measured at 25 °C by continuous dilution techniques. The same calorimeter and dilatometer were used as in our previous studies (1, 2).

(iii) Materials

Purification of the *n*-decanol used in this investigation has been described in ref. (3). The isopropanol (Eastman Organic Chemicals) was purified chromatographically with a column containing PEG 4000 supported on Chromosorb W. Density measurements on the alcohols at 25 °C yielded values of 0.7808_6 and 0.8268_7 g cm^{-3} for isopropanol and decanol respectively.

Results and Discussion

Vapor pressures of pure isopropanol were fitted with an Antoine form of equation

$$[3] \qquad \log_{10} p\,(\text{Torr}) = 8.1838 - 1591.08/[218.028 + t\,(^\circ\text{C})]$$

The standard error of the estimate is 0.047 Torr. Values of the vapor pressure of isopropanol calculated at rounded temperatures are given in Table I along with the observed vapor pressures of decanol. The values of other properties of the pure alcohols needed for analysis of the vapor pressure measurements on mixtures are also collected in Table I. The molar volumes at 25 °C are based on the densities quoted above; the variation of the molar volumes with temperature was derived from the work of Costello and Bowden (7). Equations given by Kretschmer and Wiebe (6) were used to calculate the virial coefficients of isopropanol; this usage involved an extrapolation to temperatures 40 °C lower than investigated experimentally.

Results for the liquid–vapor equilibrium of isopropanol–decanol mixtures at 20, 25, 30, 35, 40, and 50 °C are summarized in Table II (x_1

[1]Issued as NRCC No. 10 513.

[2]NRCC Postdoctorate Fellow 1965–67. Present address: 112 College Complex Circle, Rochester, New York 14615.

[3]NRCC Postdoctorate Fellow 1965–67. Present address: Metallgesellschaft-AG, Frankfurt/M, Germany.

TABLE I

Properties of pure component liquids

Temperature (°C)	Isopropanol p_1^0 (Torr)	Isopropanol V_1^0 (cm^3 mole^{-1})	Isopropanol B_{11} (cm^3 mole^{-1})	Isopropanol D_{1111} (cm^3 mole^{-1} Torr^{-2})	*n*-Decanol p_2^0 (Torr)	*n*-Decanol V_2^0 (cm^3 mole^{-1})
20	31.58	76.544	−3900	−0.1417	0.016	190.644
25	43.35	76.962	−3417	−0.0837	0.026	191.428
30	58.74	77.392	−3023	−0.0503	0.042	192.207
35	78.65	77.834	−2679	−0.0307	0.060	192.980
40	104.12	78.290	−2396	−0.0191	0.089	193.748
50	176.85	79.237	−1940	−0.0077	0.210	195.278

TABLE II

Liquid vapor equilibrium for isopropanol–decanol mixtures*

T	x_1	p	y_1	ln γ_1	T	x_1	p	y_1	ln γ_1
20	0.0691	2.57	0.9942	0.1658	25	0.0690	3.50	0.9931	0.1587
	0.1241	4.56	0.9969	0.1565		0.1239	6.22	0.9963	0.1508
	0.1958	7.11	0.9982	0.1432		0.1956	9.69	0.9978	0.1381
	0.2773	9.93	0.9988	0.1293		0.2771	13.54	0.9986	0.1240
	0.3999	13.98	0.9993	0.1051		0.3996	19.10	0.9992	0.1010
	0.4988	17.14	0.9995	0.0868		0.4986	23.42	0.9994	0.0835
	0.5870	19.83	0.9997	0.0695		0.5868	27.11	0.9996	0.0665
	0.6088	20.41	0.9997	0.0618		0.6087	27.91	0.9996	0.0589
	0.6974	23.01	0.9998	0.0455		0.6974	31.49	0.9998	0.0430
	0.8120	26.25	0.9999	0.0246		0.8119	35.94	0.9999	0.0226
	0.8652	27.72	0.9999	0.0152		0.8652	37.98	0.9999	0.0137
30	0.0689	4.70	0.9917	0.1511	35	0.0687	6.24	0.9910	0.1445
	0.1237	8.37	0.9956	0.1448		0.1234	11.10	0.9953	0.1393
	0.1953	13.03	0.9974	0.1327		0.1950	17.31	0.9972	0.1276
	0.2768	18.21	0.9983	0.1188		0.2764	24.20	0.9982	0.1138
	0.3993	25.73	0.9990	0.0969		0.3990	34.24	0.9989	0.0929
	0.4984	31.59	0.9993	0.0801		0.4980	42.09	0.9993	0.0767
	0.5866	36.60	0.9995	0.0636		0.5864	48.81	0.9995	0.0609
	0.6085	37.70	0.9996	0.0563		0.6083	50.30	0.9995	0.0539
	0.6972	42.56	0.9997	0.0409		0.6971	56.84	0.9997	0.0391
	0.8119	48.63	0.9998	0.0210		0.8118	65.00	0.9998	0.0198
	0.8651	51.40	0.9999	0.0126		0.8651	68.75	0.9999	0.0118
40	0.0685	8.17	0.9899	0.1376	50	0.0680	13.58	0.9856	0.1236
	0.1231	14.56	0.9946	0.1337		0.1222	24.24	0.9924	0.1232
	0.1946	22.72	0.9968	0.1224		0.1934	37.89	0.9955	0.1127
	0.2759	31.79	0.9980	0.1089		0.2745	53.12	0.9971	0.1002
	0.3985	45.05	0.9988	0.0889		0.3972	75.54	0.9983	0.0818
	0.4976	55.44	0.9992	0.0734		0.4965	93.20	0.9989	0.0674
	0.5861	64.39	0.9994	0.0584		0.5852	108.55	0.9992	0.0543
	0.6080	66.37	0.9995	0.0518		0.6072	112.02	0.9993	0.0485
	0.6969	75.08	0.9996	0.0376		0.6964	126.99	0.9995	0.0356
	0.8117	85.95	0.9998	0.0190		0.8115	145.73	0.9997	0.0184
	0.8651	90.94	0.9999	0.0113		0.8650	154.34	0.9998	0.0112

*x_1, y_1 are the mole fractions of isopropanol in liquid and vapor phase respectively; p in Torr, T in °C.

TABLE III

Coefficients* for eqs. [5] and [6]

Temperature (°C)	C_1	C_2	C_3	C_4	$\sigma_{\ln\gamma}$	σ_G
20	595.5	−240.9	128.2	−62.5	0.0016	0.85
25	582.4	−232.8	114.6	−55.1	0.0013	0.70
30	567.4	−225.3	105.0	−52.4	0.0011	0.64
35	552.8	−217.9	100.1	−52.8	0.0011	0.62
40	537.5	−211.5	98.5	−58.0	0.0011	0.63
50	506.8	−201.9	104.0	−82.5	0.0012	0.69

*C_i and σ_G in J mole^{-1}.

Can. J. Chem. Downloaded from www.nrcresearchpress.com by 210.87.254.40 on 09/05/12
For personal use only.

Can. J. Chem. Downloaded from www.nrcresearchpress.com by 210.87.254.40 on 09/05/12
For personal use only.

and y_1 are the mole fractions of isopropanol in the liquid and vapor phases respectively). The activity coefficients of isopropanol in the liquid phase were calculated from the equation

$$[4] \quad \ln \gamma_1 = \ln\left(\frac{y_1 p}{x_1 p_1^0}\right) + \frac{(p - p_1^0)(B_{11} - V_1^0)}{RT} + D_{1111}\frac{(4y_1^3 - 3y_1^4)[p^3 - (p_1^0)^3]}{3RT}$$

A least squares procedure was used to fit these values with the form

$$[5] \quad \ln \gamma_1 = \frac{x_2^2}{RT}\sum_{r=1}^{n} C_r(1 - 2rx_1)(x_2 - x_1)^{r-2}$$

which corresponds to representation of the excess free energy by the relation

$$[6] \quad G^E = x_1 x_2 \sum_{r=1}^{n} C_r(x_2 - x_1)^{r-1}$$

At each temperature an adequate fit of the data by eq. [5] was obtained with four coefficients. The values of these are given in Table III along with $\sigma_{\ln \gamma}$ and σ_G, the standard errors of estimates of $\ln \gamma_1$ and G^E by eqs. [5] and [6].

Results of the calorimetric and dilatometric measurements are given in Table IV. These data are represented by the equations

$$[7] \quad H^E\,(\text{J mole}^{-1}) = x_1x_2[1183.23 - 305.38(x_2 - x_1) + 231.43(x_2 - x_1)^2 - 192.6(x_2 - x_1)^3]$$

and

$$[8] \quad V^E\,(\text{cm}^3\ \text{mole}^{-1}) = x_1x_2[0.10552 + 0.08710(x_2 - x_1) + 0.01035(x_2 - x_1)^2 - 0.01656(x_2 - x_1)^3]$$

TABLE IV

Excess enthalpies and volumes* of isopropanol–*n*-decanol mixtures at 25 °C

x_1	H^E	x_1	V^E
0.0926	83.4	0.0460	0.0084
0.1750	149.1	0.1128	0.0171
0.2734	212.5	0.1859	0.0243
0.3845	265.1	0.2796	0.0287
0.4836	293.4	0.3704	0.0301
0.5755	302.5	0.4273	0.0290
0.6177	300.2	0.4551	0.0278
0.6428	297.3	0.5039	0.0264
0.6704	293.3	0.5277	0.0253
0.6998	284.2	0.5709	0.0232
0.7196	278.6	0.5900	0.0219
0.7510	264.3	0.6261	0.0198
0.7728	254.6	0.6423	0.0189
0.7910	242.8	0.6727	0.0169
0.8197	224.5	0.6857	0.0163
0.8684	183.4	0.7103	0.0146
0.9103	138.8	0.7199	0.0141
0.9465	91.1	0.7486	0.0124
0.9710	54.2	0.8530	0.0067
0.9885	23.9	0.8860	0.0052
		0.9176	0.0040
		0.9452	0.0028
		0.9674	0.0017
		0.9828	0.0008
		0.9946	0.0003

*x_1, mole fraction of isopropanol, H^E in J mole^{-1}, V^E in cm^3 mole^{-1}.

with standard errors of 1.17 J mole^{-1} and 0.0003 cm^3 mole^{-1} respectively.

The curve for G^E shown in Fig. 1 was calculated from eq. [6] with coefficients for 25 °C taken from Table III; eq. [7] was used to construct the curve for H^E. In principle, excess entropies (and enthalpies) can be obtained from the variation of the excess free energy with tem-

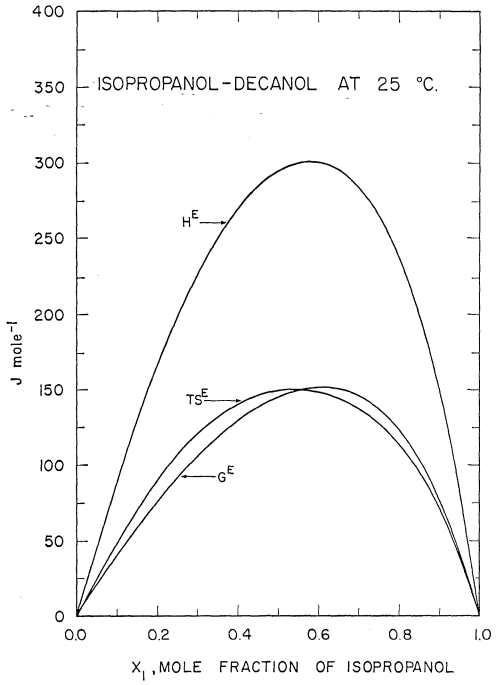

FIG. 1. Excess thermodynamic properties of isopropanol–decanol mixtures at 25 °C, G^E is derived from vapor pressures; H^E represents calorimetric results; TS^E is calculated from eq. [9].

perature. However values obtained in this way are subject to relatively large errors. For the present system, values of H^E at 25 °C calculated from the free energy data are all larger than the calorimetric results; the difference amounts to 58 J mole^{-1} for an equimolar solution. Similar discrepancies were noted for the ethanol–decanol and *n*-propanol–decanol systems (3, 4). Accordingly the TS^E curve shown in Fig. 1 was calculated from the relation

$$[9] \qquad TS^E = H^E - G^E$$

using the values of H^E measured calorimetrically.

The excess free energies of isopropanol–decanol mixtures at 25 °C are slightly lower than those of the *n*-propanol–decanol mixtures studied previously (4). However, the present heats of mixing, and as a consequence the TS^E values, are noticeably larger than those for the *n*-propanol system[4]. This suggests that the formation of the isopropanol mixtures results in the breaking of more hydrogen bonds and is accompanied by greater structural changes than in the case of *n*-propanol. On the other hand the excess volumes for isopropanol–decanol mixtures are considerably smaller than those for *n*-propanol–decanol (8) (0.026 cm^3 mole^{-1} compared to 0.089 cm^3 mole^{-1} for equimolar mixtures).

[4]In an equimolar mixture of isopropanol–decanol (at 25 °C) G^E = 145.6 J mole^{-1}, H^E = 295.8 J mole^{-1}, and TS^E = 150.2 J mole^{-1}. The corresponding values for the *n*-propanol–decanol system are 158.0, 252.0, and 94.0 J mole^{-1} respectively.

Acknowledgments

We are indebted to Mr. P. J. D'Arcy and to Mr. C. J. Halpin for invaluable technical assistance throughout the course of this investigation.

1. A. E. Pope, H. D. Pflug, B. Dacre, and G. C. Benson. Can. J. Chem. **45**, 2665 (1967).
2. H. D. Pflug and G. C. Benson. Can. J. Chem. **46**, 287 (1968).
3. J. Singh and G. C. Benson. Can. J. Chem. **46**, 1249 (1968).
4. J. Singh and G. C. Benson. Can. J. Chem. **46**, 2065 (1968).
5. H. D. Pflug, A. E. Pope, and G. C. Benson. J. Chem. Eng. Data, **13**, 408 (1968).
6. C. B. Kretschmer and R. Wiebe. J. Am. Chem. Soc. **76**, 2579 (1954).
7. J. M. Costello and S. T. Bowden. Rec. Trav. Chim. **77**, 36 (1958).
8. G. C. Benson and H. D. Pflug. Unpublished data.

Can. J. Chem. Downloaded from www.nrcresearchpress.com by 210.87.254.40 on 09/05/12
For personal use only.

Can. J. Chem. Downloaded from www.nrcresearchpress.com by 210.87.254.105 on 09/05/12
For personal use only.

Conductance and viscosity of *n*-alkylamine hydrobromides in water at 25 °C: influence of hydrophobic hydration

JACQUES E. DESNOYERS, MARCEL AREL, AND PAUL-ANDRÉ LEDUC
Department of Chemistry, University of Sherbrooke, Sherbrooke, Quebec

Received April 30, 1968

The equivalent conductivities and viscosities of the homologous salts RNH_3Br, where R varies from H to *n*-octyl, have been measured in water at 25 °C. The data in the submicellar region can be represented adequately by the semi-empirical relations

$$\Lambda = \Lambda_0 - A_\Lambda c^{1/2} + B_\Lambda c \text{ and } \eta/\eta_0 - 1 = A_\eta c^{1/2} + B_\eta c + D_\eta c^2$$

The parameters $B_\eta{}^+$ and $\lambda_0{}^+$ are both functions of the effective size of the organic ions in solutions, while the parameters D_η and B_Λ can be interpreted through structural salting-in of the hydrophobic cations. Viscosities and conductivities can be used equally well to study the micelle formation of *n*-octylamine hydrobromide.

Canadian Journal of Chemistry, **47**, 547 (1969)

Introduction

Recent reviews (1–5) on the properties of aqueous solutions have stressed the importance of structural changes induced by the solute. Small ions attract water molecules (hydrophilic hydration), most large organic ions and molecules strengthen the hydrogen bonds of the neighboring water molecules (hydrophobic hydration), and intermediate ions break the structure of water. Much of the information on hydrophobic hydration was provided by the quaternary ammonium salts with the general formula R_4NX, since these salts are reasonably soluble in water and their hydrophobic character can be varied by changing the size and nature of the R group. The homologous salts RNH_3Br have also proven to be very informative (6, 7) since the true distance of closest approach is approximately the same with all the larger homologs, and this series goes from a relatively simple (NH_4Br) to a micellar salt (*n*-octylamine hydrobromide). These salts are therefore very useful in examining the influence of certain factors, such as association and hydration, on the concentration dependence of physico-chemical properties of electrolyte solutions.

The principal conclusion we have reached in previous studies (1, 6, 7) of the concentration dependence of hydrophobic ions is that activity coefficients, excess entropies, and volumes are ruled to a large extent by structural salting-in and salting-out effects: attractive forces (salting-in) between two hydrophobic ions and repulsive forces (salting-out) between a hydrophobic and a hydrophilic ion are induced by structural changes in water (8). The purpose of the present work is to extend these studies to viscosities and conductivities; a systematic investigation of aqueous RNH_3Br solutions, when R is lengthened, should disclose the influence of structural interactions on the concentration dependence of these properties.

Experimental

The preparation and purification of the amine salts have been described elsewhere (7). In all measurements, water was redistilled from an alkaline permanganate solution using an all-glass still and was equilibrated with atmospheric CO_2. All solutions were made by weight (molalities) and converted to molarities c from the known densities (7). These densities were also used for calculating viscosities. For the viscosity measurements the solutions were in addition filtered through a fine sintered glass disk. All measurements were made at 25.000 ± 0.003 °C.

Conductivities

The resistances were obtained with an Industrial Instrument Conductivity Bridge (model RC-18) using a Scientific Glass Apparatus cell (model E-4100-4). The platinum electrodes were platinized following the method of Jones and Bollinger (9). The cell constant was determined in the usual manner (10) from KCl solutions. Corrections were made for the conductivity of water and for the slight dependence of the resistance on frequency. As a check of the technique, the equivalent conductivity of NaCl was determined as a function of concentration. Extrapolation to infinite dilution by the method described later in the text gives a value $\Lambda_0 = 126.43$ conductance units which compares well with the value quoted by Robinson and Stokes (10) as 126.45. In general a reproducibility of 0.05 conductance units has been realized.

Viscosities

A viscometer of the Ubbelohde type, similar to the one described by Tuan and Fuoss (11), was fitted with a plexiglass jacket in which thermostated water was circulated. The instrument was supported perpendicularly

Can. J. Chem. Downloaded from www.nrcresearchpress.com by 210.87.254.105 on 09/05/12
For personal use only.

by a steel rod mounted on a bearing system, the viscometer could thus be easily inverted to initiate a run.

The viscometer was kept wet when not in use to insure cleanliness. Whenever adsorption of impurities in capillary became noticeable, the viscometer was cleaned with alkaline ethanol solution and then with a 1:1 mixture of hot sulfuric and nitric acid. The flow time of water was 811.05 ± 0.08 s at 25 °C which indicates a reproducibility of 0.01%. To avoid errors from the formation of drops at the end of the capillary the viscometer was slanted at a fixed angle of about 7° during all measurements. The flow time correction mentioned by Kay *et al.* (12) for solutions of large organic ions was not found necessary.

The viscometer was calibrated with the equation $\eta/d = at + b/t$, where a and b are constants determined from the known densities and viscosities of water at 20, 25, and 30 °C (13). As a check, the viscosities of NaCl, KCl, NaBr, and KBr solutions were measured at 25 °C in the region 0.05 to 0.7 molar, and the relative viscosities were given by

$$\eta/\eta_0(\text{NaCl}) = 1 + 0.0060c^{\frac{1}{2}} + 0.0810c + 0.0033c^2$$

$$\eta/\eta_0(\text{KCl}) = 1 + 0.0050c^{\frac{1}{2}} - 0.0117c + 0.0015c^2$$

$$\eta/\eta_0(\text{NaBr}) = 1 + 0.0061c^{\frac{1}{2}} + 0.0458c + 0.0106c^2$$

$$\eta/\eta_0(\text{KBr}) = 1 + 0.0050c^{\frac{1}{2}} - 0.0461c + 0.0108c^2$$

The B_η coefficients are all slightly more positive than the literature values (13); this is presumably a consequence of the different methods of plotting. Still the differences are: $B_\eta(\text{NaCl}) - B_\eta(\text{KCl}) = 0.0927$ and $B_\eta(\text{NaBr}) - B_\eta(\text{KBr}) = 0.0919$ l mole^{-1}. This additivity test indicates that the B_η coefficients are probably reliable to ±0.001.

Results and Discussion

It was shown (7) that the apparent molal volumes ϕ_v of the salts RNH_3Br can be represented below the critical micelle concentration (c.m.c.) by a relation of the type

$$[1] \qquad \phi_v = \phi_v^0 + A_v c^{\frac{1}{2}} + B_v c$$

where A_v can be calculated from the limiting Debye–Huckel theory. The apparent molal volume at infinite dilution ϕ_v^0 and the parameter B_v can be obtained from a plot of $\phi_v - A_v c^{\frac{1}{2}}$ versus c. By analogy with eq. [1] we may possibly expect similar relations for Λ and η

$$[2] \qquad \Lambda = \Lambda_0 - A_\Lambda c^{\frac{1}{2}} + B_\Lambda c + \cdots$$

and

$$[3] \qquad \eta/\eta_0 - 1 = A_\eta c^{\frac{1}{2}} + B_\eta c + D_\eta c^2 + \cdots$$

Since the left-hand side of eq. [3] is not a reduced function of c, an extra term in c^2 is required to retain the analogy between eqs. [1], [2], and [3].

The conductance data is now commonly interpreted from the Fuoss–Onsager equation which bears the form

$$[4] \qquad \Lambda = \Lambda_0 - A_\Lambda c^{\frac{1}{2}} + Ec \log c + Jc$$

The term in $c \log c$ is essential for the treatment of the data in very dilute solutions, but the approximations leading to this term are not valid (10) at intermediate concentrations where most of our measurements were made. It is probably for this reason that the present data could not be fitted adequately with eq. [4] while the semi-empirical eq. [2] was applicable over most of the concentration range as it will be shown. Kay (15) has shown that the effect of the log term is to raise Λ_0 by about 0.06 conductance units; since our experimental error is about 0.05 conductance units, eq. [2] is acceptable as a basis for extrapolation.

If eqs. [2] and [3] are applicable to our system, then the parameters A_Λ and A_η must be the theoretical values predicted from the interionic theory since the Debye–Huckel theory is valid at infinite dilution. There is, therefore, no need to determine A_Λ and A_η experimentally. A plot of $\Lambda + A_\Lambda c^{\frac{1}{2}}$ versus c and $(\eta/\eta_0 - 1 - A_\eta c^{\frac{1}{2}})/c$ versus c should be essentially linear at low concentration with the slopes B_Λ and D_η and the intercepts Λ_0 and B_η respectively. It was established (7) that B_v is related to the mutual salting-in of the organic cations; the analogous parameters B_Λ and D_η can also be expected to depend on these structural salting-in effects.

Equivalent Conductivities

The equivalent conductivities have been measured[1] at 25 °C for the salts RNH_3Br where R varies from H to *n*-octyl. Since the parameter A_Λ of eq. [2] is a function of Λ_0 (10), a first approximation for Λ_0 is obtained from a plot of Λ against $c^{\frac{1}{2}}$. The parameter A_Λ is then calculated, and a better value for Λ_0 is obtained from the method of plotting described above. This procedure may be repeated as often as desired but one or two cycles were usually found sufficient to obtain reliable Λ_0. The final plots are shown in Fig. 1 and the derived parameters Λ_0 and B_Λ obtained by a least-square fit are given in Table I. The

[1]Photocopies of the actual experimental conductivity and viscosity data may be obtained free of charge, upon request, from: Depository of Unpublished Data, National Science Library, National Research Council of Canada, Ottawa, Canada.

Can. J. Chem. Downloaded from www.nrcresearchpress.com by 210.87.254.105 on 09/05/12
For personal use only.

TABLE I

Conductance parameters of the equation $\Lambda = \Lambda_0 - A_\Lambda c^{\frac{1}{2}} + B_\Lambda c$ and derived apparent distances of closest approach

Salt	Λ_0	A_Λ	B_Λ	$\mathring{a}$
NH_4Br	152.10	95.53	95.51	1.64
$MeNH_3Br$	135.85	91.85	76.38	1.47
$EtNH_3Br$	124.24	89.14	67.32	1.40
n-$PrNH_3Br$	118.22	87.88	65.68	1.38
n-$BuNH_3Br$	114.55	86.98	60.68	1.32
n-$PenNH_3Br$	111.83	86.38	52.42	1.19
n-$HexNH_3Br$	109.85	85.87	48.86	1.14
n-$HepNH_3Br$	108.25	85.51	45.40	1.08
n-$OctNH_3Br$	106.52	85.12	42.95	1.04

complete curve for *n*-octylamine hydrobromide is shown in Fig. 2.

The parameters Λ_0 and ϕ_v^0 should both be functions of the effective size of the hydrated ions in solution. Near hydrophobic solutes there is little free space (7), and ϕ_v^0 (RNH_3^+) should be proportional to r^3, where r is a mean effective radius of the ion. Similarly, if Stokes law is applicable to hydrophobic ions, λ_0^+ should be inversely proportional to r. After subtraction of the Br^- contribution to ϕ_v^0 and Λ_0, ϕ_v^0 (Br^-) = 30.9 ml $mole^{-1}$ (16) and λ_0^- (Br^-) = 78.14 (10), $1/\lambda_0^+$ was plotted against the cube-root of ϕ_v^0 (RNH_3^+) in Fig. 3. Except for NH_4^+, all points fall on a straight line given by the relation

$$[5] \qquad 1/\lambda_0^+ = 0.0083\,(\phi_v^0)^{1/3} - 0.0082$$

This behavior illustrates the self-consistency of the conductivity and density measurements and indicates that both λ_0^0 and ϕ_v^0 are related to the effective size of the ions in solution. The significance of these functions in terms of hydration models has been discussed elsewhere (7, 16, 17).

The slopes B_Λ in Fig. 1 are all positive but decrease with chain length. These slopes are more difficult to interpret than Λ_0 since none of the existing theories of conductance can be considered reliable in the concentration range we are concerned with, and little correlation has been made between hydrophobic hydration and the concentration dependence of Λ. The parameter B_Λ

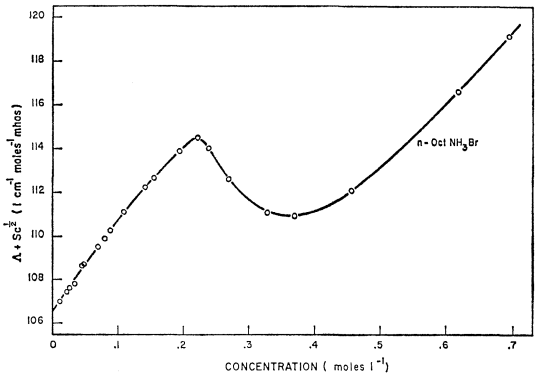

FIG. 2. Equivalent conductivity of *n*-octylamine hydrobromide in water at 25 °C.

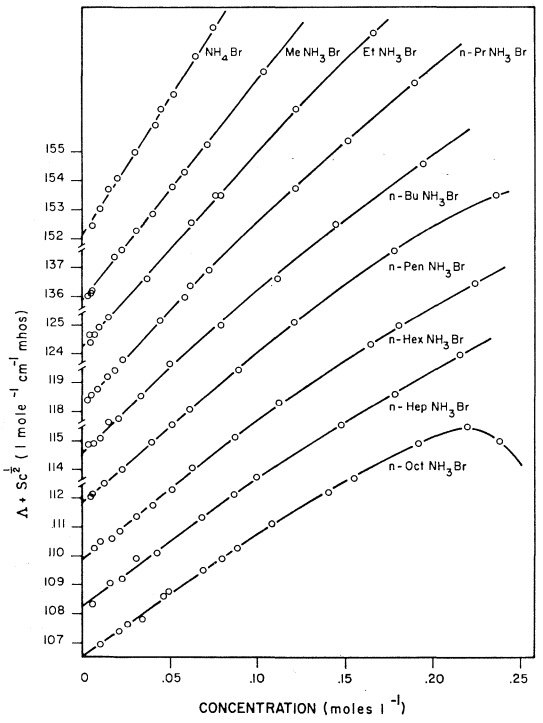

FIG. 1. Equivalent conductivities of *n*-alkylamine hydrobromides in water at 25 °C.

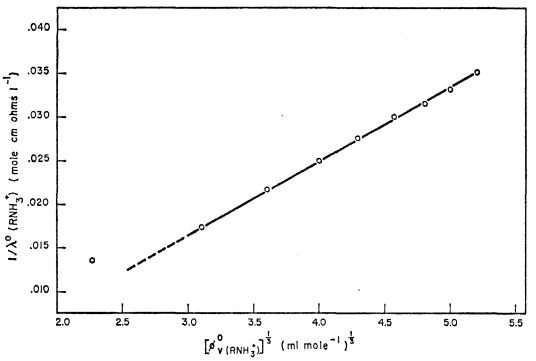

FIG. 3. Relation between the ionic conductivities and the apparent ionic volumes of *n*-alkylammonium ions.

should be a function of Λ_0, the distance of closest approach and all other sources of deviations between the limiting Onsager theory and the experimental data. In an attempt to eliminate the dependence of B_Λ on Λ_0, *apparent* distances of closest approach $\mathring{a}$ were calculated (see Table I) assuming that the B_Λ coefficient was equivalent to the J parameter of the Fuoss–Onsager theory (14). At 25 °C

$$[6] \quad J = 0.4583\Lambda_0\left(\frac{\mathring{a}}{3.575} + \frac{\mathring{a}^2}{25.57} - \frac{\mathring{a}^3}{365.6} - \ln \mathring{a} - 0.2052\right) + 13.79 + 18.15\,\mathring{a} - 17.66\,(\ln \mathring{a} - 0.0956)$$

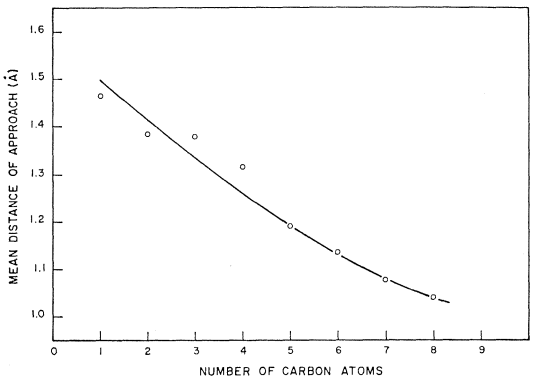

FIG. 4. Apparent distances of closest approach of *n*-alkylamine hydrobromides as a function of chain length.

The derived ion-size parameters were plotted as a function of the chain length in Fig. 4. Similar $\mathring{a}$ and trends are also obtained if other extensions of the Onsager theory, such as those mentioned by Robinson and Stokes (10), are used[2].

As a first approximation, the true distance of closest approach of this homologous series should be constant, since, except for the lower members, the hydrophilic hydration of the $-NH_3^+$ group is similar. As seen from Fig. 4, the apparent distances of closest approach, on the other hand, decrease markedly with chain length and reach unrealistically low values. The same observations have been made by Evans and Kay (17) in their study of symmetrical quaternary ammonium salts; all values of $\mathring{a}$ are of the order of 1 Å, but while the ion-size parameters increase with the size of the cations R_4N^+ with the chlorides, they remain approximately constant with the bromides and decrease with the iodides.

Evans and Kay (17) attribute the anomalous $\mathring{a}$ to some type of ion association. Levien (18) and Evans and Broadwater (19) reach similar conclusions. We prefer to interpret the small size of $\mathring{a}$ and its variations with the size of the cations to structural attractive and repulsive forces. In a recent review (1), it was shown that structural salting-out predominates between strong hydrophobic cations (large R_4N^+) and strong hydrophilic anions (F^- and Cl^-), while structural salting-in of hydrophobic cations is observed when the anions are only weakly hydrophilic (I^-). The data of Evans and Kay is in complete agreement with this model; with R_4NCl structural salting-out causes $\mathring{a}$ to increase with the size of the cations (with the fluorides the effect should be even more pronounced), while with R_4NI the influence of I^- is small and structural salting-in between R_4N^+ ions is observed. The structural salting-in is larger with the larger cations and for the same reason $\mathring{a}$ is smallest with (*n*-butyl)$_4$NI. Therefore structural salting-in causes a decrease in $\mathring{a}$ and structural salting-out causes an increase. The results with the RNH_3Br salts are also consistent with this model. The Br^- has little effect, and, as the chain increases in length, the hydrophobic character increases and so does the mutual structural salting-in between the cations. This is

[2]It has been pointed out by one of the referees that it is incorrect to compare the $\mathring{a}$ parameters obtained from the Fuoss–Onsager theory with those from any other theory which neglects the c log c term. We have verified this by fitting Λ of $MeNH_3Br$, $EtNH_3Br$, and *n*-$BuNH_3Br$, where sufficient data below 0.01 molar are available, with the Fuoss–Onsager equation. The derived $\mathring{a}$ parameters are respectively 2.8, 2.5, and 2.4 Å compared with the values 1.47, 1.38, and 1.32 Å of Table I. These new values are closer to but still lower than the expected distance of closest approach. In addition, they still decrease as the length of the hydrophobic chain increases. Therefore the conclusions reached in this paper are to a large extent independent of the equation used to obtain $\mathring{a}$.

It should be noted also that the Λ_0 parameters obtained from the Fuoss–Onsager equation, using the data below 0.01 molar for the above salts, are all as expected, larger than the Λ_0 of Table I by a factor which varies between 0.05 to 0.2 conductance units. Because of the larger uncertainty in the data below 0.01 molar we prefer to use the Λ_0 derived from eq. [2] for the study of trends in this homologous series.

Can. J. Chem. Downloaded from www.nrcresearchpress.com by 210.87.254.105 on 09/05/12
For personal use only.

Can. J. Chem. Downloaded from www.nrcresearchpress.com by 210.87.254.105 on 09/05/12
For personal use only.

reflected in a decreasing $\mathring{a}$. The conductance data of trialkyl sulfonium iodides in water (19) can also be interpreted in a similar way.

Structural salting-in is an attractive force between hydrophobic solutes and may lead to association as a limiting case, e.g. micelle formation, hydrophobic bonding (20). However, as evidenced from the concentration dependence of ϕ_v for RNH_3Br salts (7), structural salting-in may occur without association. Therefore, an abnormal decrease in the ion-size parameter of hydrophobic solutes may be taken as an indication of predominance of attractive forces over the long-range coulombic forces but does not necessarily mean association. With the ϕ_v of hydrophobic solutes, structural salting-in and association act in opposite direction. Unfortunately, in the case of conductance, both have similar effects. For example, association is clearly indicated in the case of *n*-octylamine hydrobromide above the c.m.c. (Fig. 2). Therefore much caution should be taken before interpreting as association negative deviations from the Onsager or Fuoss–Onsager theories when hydrophobic solutes are involved.

Structural effects such as structural salting-out and salting-in are very pronounced with large quaternary ammonium salts. They are also present to a lesser extent in all aqueous electrolyte solutions (1, 21). It therefore seems of little value to attempt interpreting quantitatively the concentration dependence of Λ in water unless structural effects are taken into account.

The present method of plotting equivalent conductivities is very useful for the study of micelle formation. Usually Λ is plotted as a function of $c^{\frac{1}{2}}$ and a slight change in slope is seen at the c.m.c. In Fig. 2, the range over which a micelle is formed is very well defined and corresponds closely to that obtained from density measurements (7).

Viscosities

The viscosities of the homologous series have been measured at 25 °C and are plotted as a function of concentration in Figs. 5 and 6. The parameter A_η was calculated from Falkenhagen's theory (13) using the above λ_0^+ and λ_0^-. The derived parameters B_η and D_η are given in Table IV.

Most works on electrolyte theories have neglected the D_η term of eq. [3]. The reason is that the method of plotting the data, $(\eta/\eta_0 - 1)/c^{\frac{1}{2}}$ versus $c^{\frac{1}{2}}$, does not reveal this term at low concentration. With a correction for the A_η term the ordinate in Figs. 5 and 6 becomes analogous to the reduced viscosity used with polymer solutions and more confidence can be given to the B_η coefficient; the D_η coefficient is obtained at the same time from

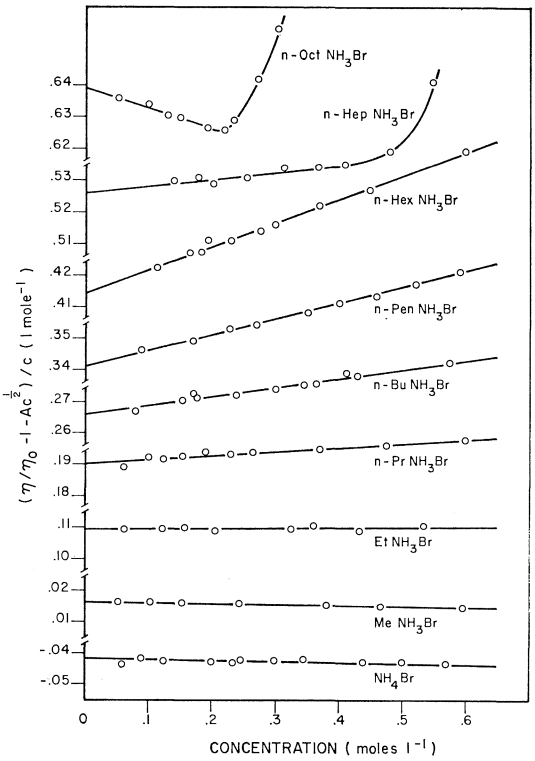

FIG. 5. Viscosities of *n*-alkylamine hydrobromides in water at 25 °C.

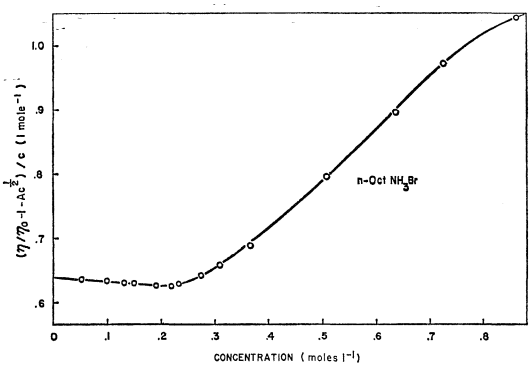

FIG. 6. Viscosity of *n*-octylamine hydrobromide in water at 25 °C.

the slope. The B_η coefficient should be proportional to the effective size of the ions (13). A straight line (or smooth curve) is therefore expected if B_η is plotted against ϕ_v^0. As seen from Fig. 7 a linear relation given by

$$[7] \qquad B_\eta = 4.9\ \phi_v^0 - 0.03$$

is observed except for the two highest homologs; these two salts fall above the line. This break is unexpected since it was not observed in Fig. 3. The anomaly with *n*-heptylamine and *n*-octylamine hydrobromides is even more obvious when the D_η parameters are examined in Fig. 5 and Table II; the slopes increase in a regular fashion except for the two higher homologs. To elucidate this irregularity, the viscosities of the symmetrical salts R_4NBr were examined (22) and D_η was found to increase in a regular way with the size of the cation. Therefore hydrophobic hydration seems to give a positive contribution to D_η. This would indicate that the behavior of B_η up to *n*-hexylamine hydrobromide is normal and reveals the presence of structural salting-in.

Ion association cannot be responsible for the behavior of *n*-heptylamine and *n*-octylamine hydrobromides since association causes an increase in viscosity as witnessed by the micelle formation in Fig. 6. A more plausible explanation is that the flow becomes non-Newtonian when the chain reaches a certain length. An attempt was made to verify this hypothesis by repeating the viscosities of these salts with a viscometer with a shorter flow time. Unfortunately the experimental error was larger with this viscometer and the results were not conclusive. Measurements with a very sensitive Couette type viscometer would possibly solve this dilemma. Until such measurements are made available, the data for these two salts must be considered doubtful. They are still included since the anomaly before the c.m.c. does not seem to affect the determination of micelle formation and good agreement is found between Figs. 2 and 6.

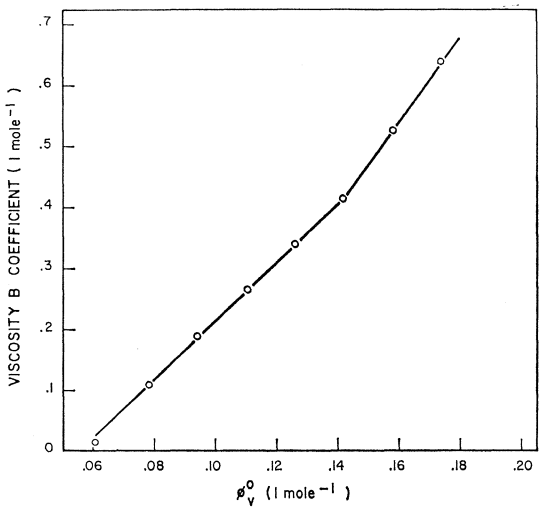

FIG. 7. Relation between the B_η viscosity coefficients and the apparent molal volumes of *n*-alkylamine hydrobromides.

TABLE II

Viscosity parameters of the equation $\eta/\eta_0 = 1 + A_\eta c^{\frac{1}{2}} + B_\eta c + D_\eta c^2$

Salt	A_η	B_η	D_η
NH_4Br	0.0050	−0.042	−0.004
$MeNH_3Br$	0.0056	0.016	−0.003
$EtNH_3Br$	0.0061	0.109	0.013
n-$PrNH_3Br$	0.0065	0.190	0.013
n-$BuNH_3Br$	0.0067	0.266	0.028
n-$PenNH_3Br$	0.0069	0.341	0.051
n-$HexNH_3Br$	0.0070	0.414	0.074
n-$HepNH_3Br$	0.0071	0.527	0.019
n-$OctNH_3Br$	0.0073	0.639	−0.063

Since the D_η coefficients have been ignored by most authors, little is known about its significance. It is reasonable to expect that structural salting-in would produce an increase in viscosity since all attractive forces will make the slipping of one molecule past another more difficult. An increase in D_η with increasing hydrophobic character is therefore normal. The negative sign of D_η with CH_3NH_3Br could be an indication that this pair of ions breaks the water structure. Work is presently under way (22) to study the significance of this coefficient with other systems.

Acknowledgment

Grateful acknowledgment is made to the National Research Council of Canada for financial assistance.

1. J. E. DESNOYERS and C. JOLICOEUR. Modern aspects of electrochemistry. Vol. 5. *Edited by* J. O'M. Bockris and B. E. Conway. Butterworths, London. 1968. (In press.)
2. B. E. CONWAY. Ann. Rev. Phys. Chem. **17**, 481 (1966).
3. F. FRANKS and D. J. G. IVES. Quart. Rev. London, **20**, 1 (1966).
4. W. DROST-HANSEN. Advan. Chem. Ser. **67**, 70 (1967).

Can. J. Chem. Downloaded from www.nrcresearchpress.com by 210.87.254.105 on 09/05/12
For personal use only.

5. J. L. KAVANAU. Water and solute-water interactions. Holden-Day, Inc., San Francisco. 1964.
6. J. E. DESNOYERS, G. E. PELLETIER, and C. JOLICOEUR. Can. J. Chem. **43**, 3232 (1965).
7. J. E. DESNOYERS and M. AREL. Can. J. Chem. **45**, 359 (1967).
8. H. S. FRANK. J. Phys. Chem. **67**, 1554 (1963).
9. G. JONES and D. BOLLINGER. J. Am. Chem. Soc. **57**, 280 (1935).
10. ROBINSON and STOKES. Electrolyte solutions. Butterworths, London. 1959. Chap. 5 and 7.
11. D. F.-T. TUAN and R. M. FUOSS. J. Phys. Chem. **67**, 1343 (1963).
12. R. L. KAY, T. VITUCCIO, C. ZAWOYSKI, and D. F. EVANS. J. Phys. Chem. **70**, 2336 (1966).
13. R. H. STOKES and R. MILLS. Viscosity of electrolytes and related properties. The Pergamon Press, Ltd., New York. 1965.
14. R. M. FUOSS and F. ACCASCINA. Electrolytic conductance. Interscience Publishers, Inc., New York. 1959.
15. R. L. KAY. J. Am. Chem. Soc. **82**, 2099 (1960).
16. B. E. CONWAY, R. E. VERRALL, and J. E. DESNOYERS. Trans. Faraday Soc. **62**, 2738 (1966).
17. D. F. EVANS and R. L. KAY. J. Phys. Chem. **70**, 366 (1966). See also R. L. KAY. Advan. Chem. Ser. **73**, 1 (1968).
18. B. J. LEVIEN. Australian J. Chem. **18**, 1161 (1965).
19. D. F. EVANS and T. L. BROADWATER. J. Phys. Chem. **72**, 1037 (1968).
20. G. NEMETHY and H. A. SCHERAGA. J. Chem. Phys. **36**, 3401 (1962).
21. H. S. FRANK. Z. Phys. Chem. Leipzig, **228**, 364 (1965).
22. J. E. DESNOYERS and M. AREL. In preparation.

Can. J. Chem. Downloaded from www.nrcresearchpress.com by 210.87.254.105 on 09/05/12
For personal use only.

Electron paramagnetic resonance studies on copper(II) benzoate

F. G. HERRING AND R. C. THOMPSON
Department of Chemistry, The University of British Columbia, Vancouver 8, British Columbia

AND

C. F. SCHWERDTFEGER
Department of Physics, The University of British Columbia, Vancouver 8, British Columbia

Received August 16, 1968

An electron paramagnetic resonance (e.p.r.) study at 9.1 and 12.0 GHz on polycrystalline copper(II) benzoate has given the following Spin Hamiltonian parameters for the binuclear molecule: $D = 0.3311 \pm 0.0006$ cm^{-1}, $E = 0.0147 \pm 0.0003$ cm^{-1}, $g_x = 2.048 \pm 0.004$, $g_y = 2.074 \pm 0.004$, $g_z = 2.345 \pm 0.004$. Using the average g value of 2.160 ± 0.004 obtained from e.p.r. and previously published magnetic susceptibility studies, $2J$ is estimated to be 333 cm^{-1}.

Canadian Journal of Chemistry, **47**, 555 (1969)

Can. J. Chem. Downloaded from www.nrcresearchpress.com by 210.87.254.105 on 09/05/12
For personal use only.

Introduction

The magnetic properties of binuclear copper(II) alkyl- and aryl-carboxylates, molecules in which two copper ions are connected by four bridging carboxylate groups, have been studied extensively (1–7). The first e.p.r. studies, on single crystals of copper(II) acetate monohydrate were carried out by Bleaney and Bowers (1), Kumagi, Abe, and Shimada (2), and by Abe and Shimada (3). These workers found that the e.p.r. spectra could be accounted for by employing the appropriate Spin Hamiltonian for a $S = 1$ system. The lack of extensive e.p.r. studies on analogous systems is no doubt due to the fact that many of the complexes in question here do not readily form single crystals.

The work of Wasserman, Snyder, and Yager (8) has shown that it is possible to obtain the Spin Hamiltonian parameters of a triplet state from the e.p.r. spectra observed in polycrystalline samples. The object of the present work was to apply these techniques to the Cu(II) benzoate system, which can be obtained only in a polycrystalline form, and to determine the appropriate Spin Hamiltonian parameters for this molecule in its triplet state. In order to do this, it proved necessary to carry out experiments at two microwave frequencies.

During the course of this work two similar studies appeared on copper(II) cyanoacetate (9) and copper(II) propionate monohydrate (10). These studies also demonstrated the feasibility of obtaining the Spin Hamiltonian parameters of an inorganic $S = 1$ system from the e.p.r. spectra of a polycrystalline sample.

Experimental

Whereas copper(II) acetate apparently exists only in a binuclear form with magnetic properties of a system with a singlet ground state and a triplet excited state, such is not the case for copper(II) benzoate where the magnetic properties depend on the method of preparation (6, 7). The samples studied in the present work were obtained from acetone solution as described previously (6). This method yields material which is largely binuclear but which contains a small (ca. 5%) and slightly variable percentage of copper ions in a form in which the magnetic concentration is weaker than in the binuclear form. The e.p.r. work described below has shown that the Spin Hamiltonian parameters of the binuclear species are unaffected (to within experimental error) by this fact (Table II).

Electron paramagnetic resonance spectra were obtained at 9.1 GHz and 12.0 GHz.

Results and Discussion

The spectrum of polycrystalline copper(II) benzoate observed at 77 °K with a microwave frequency of 9.1 GHz is shown in Fig. 1. This spectrum is typical of a triplet state in which $D > h\nu$, i.e. we observe resonances (designated using the notation of Wasserman *et al.* (8)) H_{z1}, H_{z2}, H_{x2}, H_{y2}; these are shown in Fig. 1. The resonance observed at about 3000 G is due to copper ions in a different form to the binuclear species. This was confirmed by variable temperature studies which showed, as is to be expected, that the signals due to the triplet decrease as the temperature is lowered whereas the other resonance increases in intensity. We have made no attempt to analyze this part of the spectrum but note the similarity between it and the spectrum of polycrystalline Zn doped copper(II) acetate (11). We note that the four resonances are insufficient

to determine unambiguously the Spin Hamiltonian parameters. Consequently, we carried out measurements at the second frequency. In this case $D < h\nu$ and therefore we should observe all six $\Delta m = \pm 1$ transitions. Unfortunately it was not possible to observe the H_{z2} and H_{y1} transition due to the lack of sensitivity of the instrument at 12.0 GHz. However, those lines observed and their assignments are given in Table II.

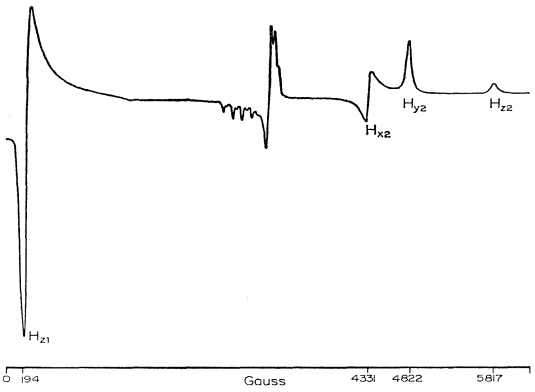

FIG. 1. Electron paramagnetic resonance spectrum of copper(II) benzoate (sample 1) at 77 °K. $H_0 = 3266.8$ G.

The Spin Hamiltonian parameters were obtained from the experimental data at both frequencies by employing an extended Newton–Raphson (12) technique to eq. [13] of Wasserman *et al.* (8). These calculations have been put in the form of a FORTRAN program for an IBM 7044. This program uses any five resonances at the corresponding microwave frequencies and solves for D, E, g_x, g_y, and g_z. A word of caution is necessary here; if one chooses five resonances that are far away from zero field (e.g. H_{x2}, and H_{y2} at 12.0 GHz and H_{x2}, H_{y2}, and H_{z2} at 9.1 GHz), then the technique employed converges on a local minimum which gives D, E, g_x, g_y, and g_z which are in error to $\pm 20\%$. However, if any one of the lower lines (i.e. H_{x1}, H_{y1}, H_{z1}) is employed with the high field lines, then reliable parameters are obtained. Presumably this condition arises because of the long extrapolation required to zero field when using exclusively high field lines.

The values of the Spin Hamiltonian parameters obtained are given in Table I, together with the values for Cu(II) acetate for comparison. Table II gives the observed and calculated resonances.

The foregoing experimental work has tacitly assumed that the D tensor and g tensor are

TABLE I

Spin Hamiltonian parameters for $Cu_2(C_6H_5CO_2)_4$ and $Cu_2(CH_3CO_2)_4(H_2O)_2$ (3)

	Value	
Parameter	$Cu_2(C_6H_5CO_2)_4$	$Cu_2(CH_3CO_2)_4(H_2O)_2$
D	0.3311 ± 0.0006 cm^{-1}	0.345 ± 0.005 cm^{-1}
E	0.0147 ± 0.0003 cm^{-1}	0.007 ± 0.003 cm^{-1}
g_x	2.048 ± 0.004	2.053 ± 0.005
g_y	2.074 ± 0.004	2.093 ± 0.005
g_z	2.345 ± 0.004	2.344 ± 0.01

diagonal in the same axis system. We note that Kokoszka, Allen, and Gordon (4) observed that the D and g tensors of dichlorobispyridine-*N*-oxide copper(II) are not diagonal in the same axis system. However, as was pointed out in ref. 4, the pseudodipolar interaction has the same set of principal axes as the dipolar interaction in the copper acetate monohydrate complex and since we expect copper(II) benzoate to be similar to the acetate homologue, as is evidenced by the similarity in magnetic data, we conclude that most probably the g and D tensors have the same principal axis system. The fact that E for the benzoate is twice as large as that for the acetate suggests that there is a greater deviation from tetragonal symmetry in the former molecule.

Magnetic susceptibility data on a number of preparations of copper(II) benzoate have been reported in the literature. Using curve-fitting techniques, Lewis and Mabbs (7) were able to fit their magnetic susceptibility data for copper(II) benzoate (preparation 5, ref. 7) to the theoretical expression for binuclear copper(II) molecules. Using our average g value of 2.160 and the data of Lewis and Mabbs, a good fit is obtained with $2J$ (singlet–triplet separation) $= 333$ cm^{-1} and $N\alpha$ [temperature-independent paramagnetic contribution for copper(II)] $= 80 \times 10^{-6}$ c.g.s.e.m.u. (Fig. 2). For two other preparations of copper(II) benzoate previously reported, it is possible to account for the magnetic data in terms of a mixture of the binuclear form with a small percentage of magnetically dilute copper(II) for which $X_{Cu} = 0.43/T + 80 \times 10^{-6}$ (Fig. 2). For those preparations which yielded samples of even higher magnetic susceptibilities, attempts to account for their magnetic properties in the manner described above were unsuccessful. It appears that as the percentage of binuclear species decreases the assumption that the remaining

Can. J. Chem. Downloaded from www.nrcresearchpress.com by 210.87.254.105 on 09/05/12
For personal use only.

TABLE II

Computed and observed resonances for $Cu_2(C_6H_5CO_2)_4$

	Resonance					
	Sample 1* (H_0 = 3.2668 kG)		Sample 2* (H_0 = 3.2701 kG)		Sample 2 (H_0 = 4.2850 kG)	
Line	Observed	Calcd.	Observed	Calcd.	Observed	Calcd.
H_{x1}	†	†	†	†	1.982	1.986
H_{x2}	4.331	4.333	4.344	4.337	5.404	5.396
H_{y1}	†	†	†	†	†	1.469
H_{y2}	4.822	4.822	4.822	4.825	5.852	5.850
H_{z1}	0.194	0.196	0.197	0.193	‡	0.618
H_{z2}	5.817	5.820	5.824	5.823	†	6.691

*By visual comparison of relative peak heights sample 1 contained a higher percentage of the binuclear form.
†Not observed.
‡Not measured precisely (estimated at ca. 0.6 kG).

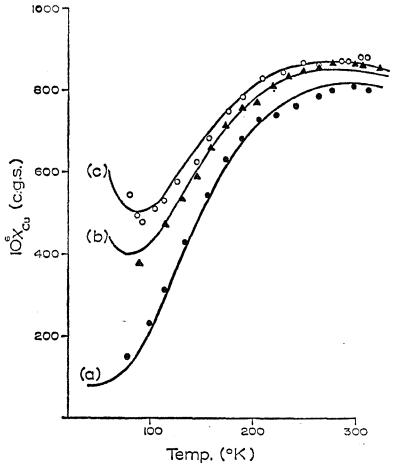

FIG. 2. Observed and calculated X_{Cu} vs. T curves.
Experimental data: ●, preparation 5, ref. 7; ▲, ref. 6; ○, preparation 4, ref. 7.
The solid lines are calculated on the basis of (*a*) 100%, (*b*) 95%, and (*c*) 93% of the copper ions in the binuclear form and the remaining copper ions in the magnetically dilute form.

copper ions are magnetically dilute is incorrect. For these samples it is possible that those copper ions which are not coupled in pairs are bonded together in a highly polymeric form of copper(II) benzoate in which "super-exchange" takes place via bridging carboxylate groups. It has been suggested that interactions of this type occur in some forms of copper(II) formate (13).

Similar e.p.r. studies on pyridine and aniline adducts of copper(II) arylcarboxylates are now in progress.

Acknowledgments

The authors thank the National Research Council of Canada for financial assistance and C. R. Byfleet for helpful discussions.

1. B. BLEANEY and K. D. BOWERS. Phil. Mag. **43**, 372 (1952).
2. H. KUMAGI, H. ABE, and J. SHIMADA. Phys. Rev. **86**, 385 (1952).
3. H. ABE and J. SHIMADA. Phys. Rev. **90**, 316 (1953).
4. G. F. KOKOSZKA, H. C. ALLEN, JR., and G. GORDON. J. Chem. Phys. **46**, 3013 (1967), and references cited therein.
5. M. KATO, H. B. JONASSEN, and J. C. FANNING. Chem. Rev. **64**, 99 (1964).
6. J. LEWIS, Y. C. LIN, L. K. ROYSTON, and R. C. THOMPSON. J. Chem. Soc. 6464 (1965).
7. J. LEWIS and F. MABBS. J. Chem. Soc. 3894 (1965).
8. E. WASSERMAN, L. C. SNYDER, and W. A. YAGER. J. Chem. Phys. **41**, 1763 (1964).
9. J. R. WASSON, C. SHYR, and C. TRAPP. Inorg. Chem. **7**, 469 (1968).
10. G. F. KOKOSZKA, M. LINZER, and G. GORDON. Inorg. Chem. **7**, 1730 (1968).
11. G. KOKOSZKA, H. C. ALLEN, JR., and G. GORDON. J. Chem. Phys. **42**, 3693 (1965).
12. A. RALSTON. A first course in numerical analysis. McGraw-Hill Book Co., Inc., London. 1965. p. 348.
13. R. L. MARTIN and H. WATERMAN. J. Chem. Soc. 1359 (1959).

Can. J. Chem. Downloaded from www.nrcresearchpress.com by 210.87.254.105 on 09/05/12
For personal use only.

Can. J. Chem. Downloaded from www.nrcresearchpress.com by 210.87.254.40 on 09/05/12
For personal use only.

Mass spectra of organometallic compounds. VI. Some indenylmetal derivatives and related compounds[1]

R. B. KING[2]
Mellon Institute, Pittsburgh, Pennsylvania
and
Department of Chemistry, University of Georgia, Athens, Georgia

Received June 12, 1968

The mass spectra of the following complexes have been investigated: (*a*) the indenylmolybdenum carbonyl derivatives $CH_3Mo(CO)_3C_9H_7$, π-$C_3H_5Mo(CO)_2C_9H_7$, π-$CH_3SCH_2Mo(CO)_2C_5H_5$, and $C_9H_7Mo(CO)_2I$; (*b*) the bisindenyl derivative $(C_9H_7)_2Fe$; (*c*) the series of compounds $C_5H_5FeC_9H_7$, $C_5H_5FeC_9H_9$, and $C_5H_5FeC_9H_{11}$ with different degrees of hydrogenation of the π-indenyl ligand. The following features of particular interest were noted: (*a*) evidence for the existence of small amounts of the new compound π-$C_3H_5Mo(CO)_2C_9H_6C_3H_5$ in the sample of π-$C_3H_5Mo(CO)_2C_9H_7$; (*b*) evidence for the pyrolysis of $C_9H_7Mo(CO)_2I$ to give $[C_9H_7MoI_2]_2$ and $(C_9H_7)_2MoCOI$; (*c*) evidence for the fragmentation of $C_9H_7Fe^+$ to give the ion $C_9H_7^+$ and a neutral iron atom; (*d*) evidence for parallel pathways for fragmentation of the parent ion from $C_5H_5FeC_9H_{11}$ involving elimination of CH_3, C_2H_4, C_3H_5, C_5H_6, and H_2. Diagnostic features from the mass spectrum for the presence of a π-indenyl ligand in a complex appear to be the ions $C_9H_8^+$, $C_9H_7^+$, $C_7H_5^+$, $C_5H_3^+$, and $C_9H_7^{2+}$.

Canadian Journal of Chemistry, **47**, 559 (1969)

Introduction

Previous papers have discussed the mass spectra of a great variety of π-cyclopentadienyl derivatives including metallocenes (2–8) and cyclopentadienylmetal carbonyl derivatives (9–11). Fusion of a benzene ring to a π-cyclopentadienyl ligand gives the π-indenyl ligand (**1**), which like the π-cyclopentadienyl ligand forms a variety of metal complexes. This paper reports the mass spectra of several π-indenyl derivatives.

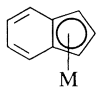

1

Experimental

The mass spectra were run on a standard Associated Electrical Industries, Ltd., MS-9 mass spectrometer located at the Mellon Institute. Tables containing these mass spectral data may be obtained upon request[3]. In addition Fig. 1 depicts the mass spectra of four representative compounds. The operating conditions were 70 eV electron energy, 200–230° inlet temperature, resolution of 1000, and 8 kV accelerating voltage. Samples were introduced directly into the ion source using a metal probe. The standard galvanometer recorder was used to measure the output signal from the electron multiplier. The relative ion intensities were estimated by measurement of the heights of the peaks on the galvanometer recorder chart with a millimeter scale. Values relative to an arbitrary value of 100.0 assigned to a selected intense metal-containing ion are reported in the Tables.

This work dealt entirely with compounds of iron or molybdenum. Natural iron contains 91.6% of the isotope ^{56}Fe. The *m/e* values reported for ions containing iron are for ions containing ^{56}Fe. Natural molybdenum contains a mixture of isotopes forming a characteristic pattern that is diagnostic of the presence of molybdenum in a given ion. The *m/e* values for ions containing molybdenum are given just for the ions containing ^{96}Mo, although in all cases the characteristic multiline pattern containing ions with different molybdenum isotopes was observed.

For transitions not involving ions of the multiisotopic metal molybdenum, metastable ions were sometimes observed as much weaker and broader peaks often at non-integral *m/e* values. These metastable ions provide excellent corroboratory evidence regarding suggested modes of fragmentation of certain of the observed ions (12). Because of the weakness and breadth of the metastable ions, they were only unequivocally observed for transitions involving the strongest ions of the spectrum and for those involving only essentially monoisotopic elements.

Except for $C_5H_5FeC_9H_9$, the compounds used in this study were prepared by methods adequately described in the literature[4].

Preparation of $C_5H_5FeC_9H_9$

A suspension of 50 mmoles of ferrous chloride was prepared by boiling for 16 h under reflux 33 mmoles of

[1]For Part V of this series, see ref. 1.
[2]Fellow of the Alfred P. Sloan Foundation, 1967–1969.
[3]Photocopies may be obtained free of charge, upon request, from: Depository of Unpublished Data, National Science Library, National Research Council of Canada, Ottawa, Canada.

[4]For $CH_3Mo(CO)_3C_9H_7$, π-$C_3H_5Mo(CO)_2C_9H_7$, π-$CH_3SCH_2Mo(CO)_2C_9H_7$, and $C_9H_7Mo(CO)_2I$, see ref. 13.
For $(C_9H_7)_2Fe$, $C_5H_5FeC_9H_7$, and $C_5H_5FeC_9H_{11}$, see ref. 14.

Can. J. Chem. Downloaded from www.nrcresearchpress.com by 210.87.254.40 on 09/05/12
For personal use only.

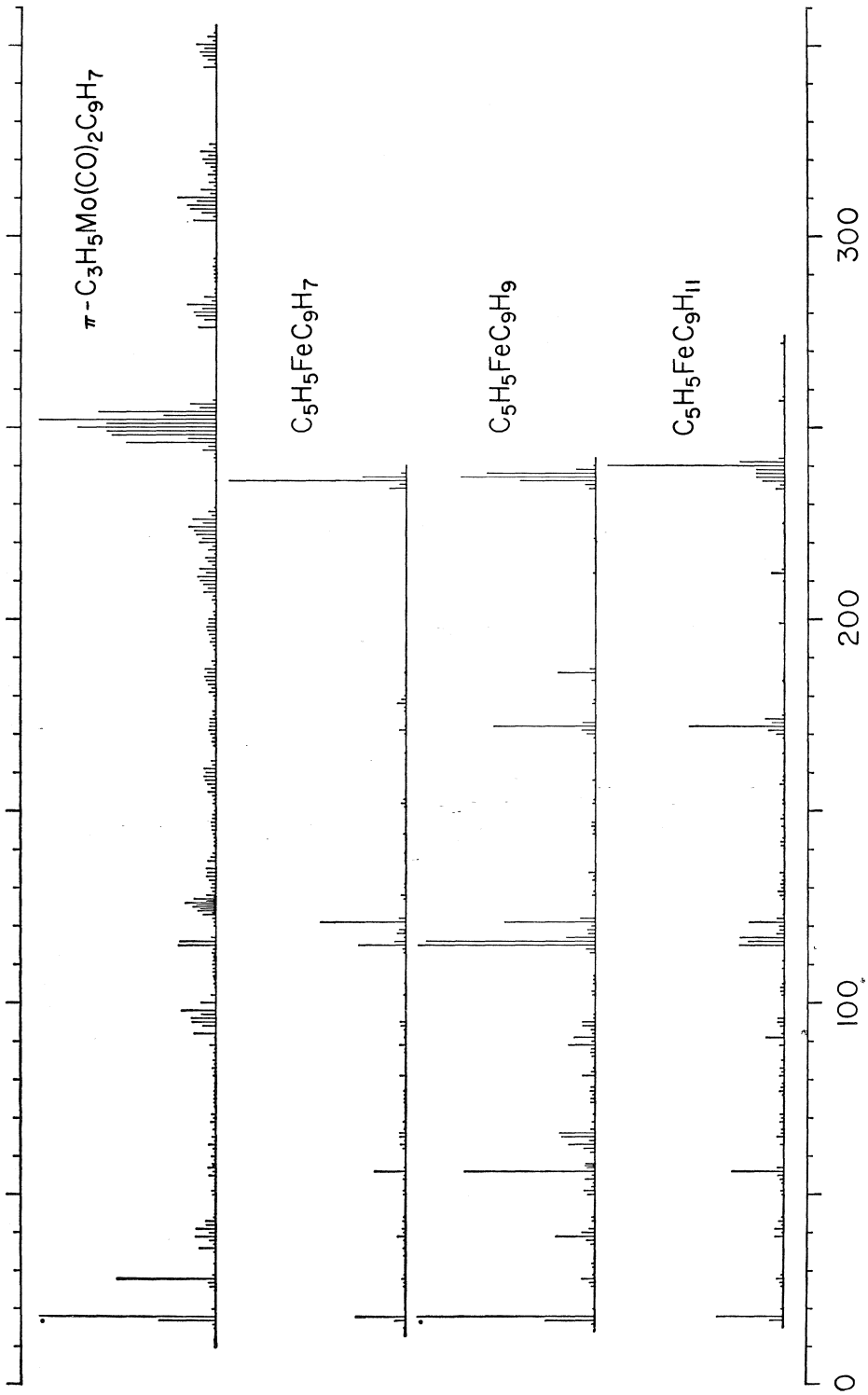

FIG. 1. Mass spectra of π-$C_3H_5Mo(CO)_2C_9H_7$, $C_5H_5FeC_9H_7$, $C_5H_5FeC_9H_9$, and $C_5H_5FeC_9H_{11}$.

Can. J. Chem. Downloaded from www.nrcresearchpress.com by 210.87.254.40 on 09/05/12
For personal use only.

anhydrous ferric chloride, 17 mmoles of iron powder, and 250 ml of redistilled tetrahydrofuran. A purple-brown suspension apparently (15) containing lithium cyclononatetraenide was obtained by stirring for 20 h at room temperature a mixture of 100 mmoles of lithium wire, 50 mmoles of chlorobicyclo[6,1,0]-nonatriene (15), and 150 ml of redistilled tetrahydrofuran. A solution of sodium cyclopentadienide was prepared by treatment of a suspension of 50 mmoles of sodium dispersion in 100 ml redistilled tetrahydrofuran with excess cyclopentadiene.

The ferrous chloride suspension was cooled in a $-78°$ bath and treated first with the lithium cyclononatetraenide and then with the sodium cyclopentadienide. The reaction mixture was allowed to warm to room temperature and finally boiled 16 h under reflux.

After cooling to room temperature solvent was removed at $\sim 25°/25$ mm. The residue was extracted with 400 ml of dichloromethane in four portions. The extracts were filtered through alumina. Solvent was removed from the filtrate at $\sim 25°/25$ mm. The resulting orange-brown residue was extracted with ~ 200 ml of pentane. After reducing the volume of these extracts to ~ 100 ml, the solution was chromatographed on a 2×50 cm alumina column. The chromatogram was developed with pentane. A yellow-orange band of ferrocene followed by a smaller orange band of $C_5H_5FeC_9H_9$ was observed. Both bands were eluted with pentane. From the first band 1.3 g (14% yield) of ferrocene was obtained. The product from the second band was dissolved in pentane and the filtered solution cooled overnight at $-78°$. The orange crystals which formed were separated and sublimed at 70°/0.25 mm to give 0.038 g ($\sim 0.3\%$ yield) of red-orange $C_5H_5FeC_9H_9$, m.p. 107–109°. This meager yield was very erratic; this preparation often failed completely.

Anal. Calcd. for $C_{14}H_{14}Fe$: C, 70.6; H, 5.9; Fe, 23.5. Found: C, 69.9; H, 5.9; Fe, 23.6.

Infrared spectrum: (Perkin–Elmer Model 21 spectrometer, sodium chloride optics): ν(CH) at 3060 (vw) and 2950 (m) cm^{-1}; ν(C=C) at 1632 (m) cm^{-1}; other bands at 1420 (w), 1389 (w), 1356 (vw), 1334 (m), 1188 (vw), 1180 (w), 1161 (w), 1015 (w), 1000 (w), 988 (vw), 978 (vvw), 965 (vvw), 956 (vw), 940 (w), 928 (w), 913 (vw), 893 (m), 886 (m,sh), 856 (w), 853 (vw,sh), 830 (sh), 820 (m), 795 (s), 763 (s), and 718 (m) cm^{-1}.

Discussion

A. General Comments

The mass spectra of π-cyclopentadienylmetal derivatives (2–11) generally exhibit the metal-free ions $C_5H_6^+$, $C_5H_5^+$, and $C_3H_3^+$ arising from the π-cyclopentadienyl ligand. Apparently the π-C_5H_5 ligand can either come off as such or abstract a proton from elsewhere and be removed as $C_5H_6^+$. Furthermore, the $C_5H_5^+$ ion can eliminate a neutral acetylene (C_2H_2) fragment forming $C_3H_3^+$. Related acetylene-elimination processes are well-established to occur in normal benzenoid aromatic compounds (16).

The data obtained in this work indicate that typical metal-free ions in the mass spectra of π-indenyl derivatives arising from the π-indenyl ligand include $C_9H_8^+$, $C_9H_7^+$, $C_7H_5^+$, and $C_5H_3^+$. A π-C_9H_7 ligand can thus either come off as such or abstract a proton from elsewhere and be removed as $C_9H_8^+$. The $C_9H_7^+$ ion can undergo two successive acetylene (C_2H_2) eliminations giving first $C_7H_5^+$ and then $C_5H_3^+$. In some cases the acetylene eliminations were supported by the presence of appropriate metastable ions. The fragmentation of the C_9H_7 ligand in π-indenyl derivatives thus appears to follow a pattern similar to the fragmentation of the C_5H_5 ligand in π-cyclopentadienyl derivatives.

A further feature of the mass spectra of certain π-indenyl derivatives is the presence of metal-free ions of the type $C_{18}H_n^+$ (n = mostly 14 but sometimes 13 or 12). These apparently arise from coupling of two indenyl groups possibly after pyrolytic cleavage of the metal–indenyl bond. Analogous ions of the type $C_{10}H_n^+$ (n = 10, 9, and/or 8) have occasionally been observed in the mass spectra of π-cyclopentadienyl derivatives.

In many compounds doubly charged ions of the type $C_9H_n^{2+}$ (n = most often 7 but occasionally also 8 or 6) are also observed. Similar doubly charged ions of the type $C_5H_n^{2+}$ have not been reported to occur in the mass spectra of π-C_5H_5 derivatives.

B. Indenylmolybdenum Carbonyl Derivatives

1. $CH_3Mo(CO)_3C_9H_7$: The parent ion in the mass spectrum of $CH_3Mo(CO)_3C_9H_7$ (**2**) exhibits stepwise loss of its carbonyl groups. However, after one carbonyl group is lost, fragmentation of the methyl group competes with further loss of carbonyl groups. Also loss of the last carbonyl group from the monocarbonyl ion $CH_3MoCOC_9H_7^+$ (*m/e* 254) is accompanied by dehydrogenation giving the carbonyl-free ion $C_{10}H_8Mo^+$ (*m/e* 224). The involvement of the methyl hydrogens in this dehydrogenation is suggested by the fact that the loss of the last carbonyl group from the methyl-free monocarbonyl ion $C_9H_7MoCO^+$ (*m/e* 239) gives the carbonyl-free ion $C_9H_7Mo^+$ (*m/e* 211) without accompanying dehydrogenation.

The carbonyl-free ions $C_{10}H_8Mo^+$ (*m/e* 224) and $C_8H_7Mo^+$ (*m/e* 211) both undergo acetylene (C_2H_2) eliminations giving $C_8H_6Mo^+$ (*m/e* 198) and $C_7H_5Mo^+$ (*m/e* 185), respectively. The remaining molybdenum ions in the mass spectrum

of $CH_3Mo(CO)_3C_9H_7$ appear to arise from some $Mo(CO)_6$ present as an impurity or decomposition product.

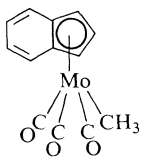

2

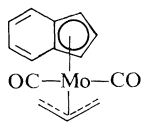

3

The usual metal-free ions found in the mass spectra of π-indenyl derivatives (see above) are also observed in the mass spectrum of $CH_3Mo(CO)_3C_9H_7$. These include $C_9H_8^+$, $C_9H_7^+$, $C_7H_5^+$, $C_5H_3^+$, $C_9H_8^{2+}$, and $C_9H_7^{2+}$. In addition there appears to be a strong tendency for the formation of an acetyl ion CH_3CO^+ (*m/e* 43). Also the ion $CH_3COC_9H_7^+$ (*m/e* 158) appears to come from acetylation of the π-indenyl ligand. The ion $C_{10}H_{10}^+$ (*m/e* 130) can arise by methylation of a π-indenyl ligand. It appears to undergo dehydrogenation to give $C_{10}H_9^+$ (*m/e* 129) and $C_{10}H_8^+$ (*m/e* 128).

2. π-$C_3H_5Mo(CO)_2C_9H_7$ (3): The parent ion $C_3H_5Mo(CO)_2C_9H_7^+$ (*m/e* 308) first loses one carbonyl group giving the monocarbonyl ion $C_3H_5MoCOC_9H_7^+$ (*m/e* 280). Loss of the second carbonyl group is accompanied by dehydrogenation giving the carbonyl-free ion $C_3H_3MoC_9H_7^+$ (*m/e* 250). This fragmentation scheme is completely analogous to that observed (11) for the corresponding π-cyclopentadienyl derivative $C_3H_5Mo(CO)_2C_5H_5$.

One further fragmentation pathway in this mass spectrum involves loss of the π-allyl ligand giving the ion $C_9H_7Mo^+$ (*m/e* 211). Successive eliminations of acetylene (C_2H_2) from $C_9H_7Mo^+$ (*m/e* 211) give the ions $C_7H_5Mo^+$ (*m/e* 185) and $C_5H_3Mo^+$ (*m/e* 159). Similar successive eliminations of acetylene (C_2H_2) from $C_3H_3MoC_7H_5^+$ ($=C_{10}H_8Mo^+$, *m/e* 224) give the ions $C_8H_6Mo^+$ (*m/e* 198) and $C_6H_4Mo^+$ (*m/e* 172). The doubly charged ions $C_3H_3MoC_9H_7^{2+}$ (*m/e* 125), $C_3H_3MoC_7H_5^{2+}$ (*m/e* 112), and $C_8H_7Mo^{2+}$ (*m/e* 105.5) are also observed.

The usual metal-free ions found in the mass spectra of π-indenyl derivatives (see above) are also observed in the mass spectrum of $C_3H_5Mo(CO)_2C_9H_7$ (**3**). The additional metal-free ions $C_6H_n^+$ ($n = 9$ or 11), $C_3H_nCO^+$ ($n = 5$ or 7), $C_3H_5^+$, and $C_3H_3^+$ arise from coupling, carbonylation, cleavage, and dehydrogenation of the π-allyl ligand, respectively.

The mass spectrum of $C_3H_5Mo(CO)_2C_9H_7$ (**3**) also exhibited the ions $C_3H_5Mo(CO)_2C_9H_6C_3H_5^+$ (*m/e* 348), $C_3H_5MoCOC_9H_6C_3H_5^+$ (*m/e* 320), and $C_3H_3MoC_9H_6C_3H_5^+$ (*m/e* 290) in relatively low abundances. These ions appear to arise from π-allyl-π-(allylindenyl)-molybdenum dicarbonyl, $C_3H_5Mo(CO)_2C_9H_6C_3H_5$, present as an impurity. This impurity could either have been present in the original sample or could have been produced by a pyrolysis reaction in the mass spectrometer. In the latter case the allyl group of one molecule of $C_3H_5Mo(CO)_2C_9H_7$ would allylate the π-indenyl group of another molecule producing the compound $C_3H_5Mo(CO)_2C_9H_6C_3H_5$. The mass spectral data give no indication of the position of allyl substitution in the indenyl system.

The former possibility that the $C_3H_5Mo(CO)_2C_9H_7$ used for this work contains a small amount of $C_3H_5Mo(CO)_2C_9H_6C_3H_5$ raises an interesting point. The compound $C_3H_5Mo(CO)_2C_9H_7$ was prepared by the published procedure (13). This consists of reducing the binuclear compound $[C_9H_7Mo(CO)_3]_2$ with sodium amalgam in tetrahydrofuran followed by addition of allyl chloride. The reduction of $[C_9H_7Mo(CO)_3]_2$ with sodium amalgam in tetrahydrofuran has been assumed to give the sodium salt $Na[Mo(CO)_3C_9H_7]$. However, it is conceivable that some of the disodium derivative $Na[Mo(CO)_3C_9H_6Na]$ might be formed. This disodium derivative would be expected to react with allyl chloride to give $C_3H_5Mo(CO)_2C_9H_6C_3H_5$. If the assumption of equal ionization efficiencies for $C_3H_5Mo(CO)_2C_9H_7$ and $C_3H_5Mo(CO)_2C_9H_6C_3H_5$ is made, then the amount of $C_3H_5Mo(CO)_2C_9H_6C_3H_5$ present in the sample of $C_3H_5Mo(CO)_2C_8H_7$ would be about 2%. In the previous work on $C_3H_5Mo(CO)_2C_9H_7$ an impurity of ~ 2% of $C_3H_5Mo(CO)_2C_9H_6C_3H_5$ would have escaped detection.

3. π-$CH_3SCH_2Mo(CO)_2C_9H_7$: Much of the mass spectrum of π-$CH_3SCH_2Mo(CO)_2C_9H_7$ (**4**) is very similar to that of its π-cyclopentadienyl analogue π-$CH_3SCH_2Mo(CO)_2C_5H_5$ (17). The parent ion (*m/e* 328) first undergoes stepwise loss of carbonyl groups giving the carbonyl-free ion $CH_3SCH_2MoC_9H_7^+$ (*m/e* 272). This ion then appears to lose methane (CH_4) giving the ion $C_{10}H_8SMo^+$ (*m/e* 256), which is the most

Can. J. Chem. Downloaded from www.nrcresearchpress.com by 210.87.254.40 on 09/05/12
For personal use only.

Can. J. Chem. Downloaded from www.nrcresearchpress.com by 210.87.254.40 on 09/05/12
For personal use only.

abundant metal-containing ion in the mass spectrum. This behavior exactly parallels that of π-$CH_3SCH_2Mo(CO)_2C_5H_5$ where $C_6H_6SMo^+$ is the most abundant metal-containing ion in the mass spectrum (17).

The other significant metal-containing ion in the mass spectrum of π-$CH_3SCH_2Mo(CO)_2C_9H_7$ is $C_9H_7MoSH^+$ (*m/e* 244) apparently formed by elimination of ethylene from $CH_3SCH_2MoC_9H_7^+$ (*m/e* 272). The formation of $C_9H_7MoSH^+$ (*m/e* 244) in the mass spectrum of π-$CH_3SCH_2Mo(CO)_2C_9H_7$ closely parallels the formation (17) of $C_5H_5MoSH^+$ in the mass spectrum of the π-cyclopentadienyl analogue π-$CH_3SCH_2Mo(CO)_2C_5H_5$.

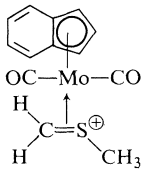

4

The usual metal-free ions found in the mass spectra of π-indenyl derivatives are observed in the mass spectrum of π-$CH_3SCH_2Mo(CO)_2C_9H_7$. Also observed are the ions $C_9H_7CO^+$ (*m/e* 143) and CH_3CO^+ (*m/e* 43), arising from carbonylation of the indenyl ligand and methyl substituent, respectively. The ions $C_{10}H_9^+$ (*m/e* 129) and $C_{10}H_8^+$ (*m/e* 128) may arise from insertion of a carbon atom of the π-CH_3SCH_2 ligand into the C_9H_7 ligand. The assignments of several of the metal-free ions were unclear.

4. $C_9H_7Mo(CO)_2I$: Reaction of the binuclear compound $[C_9H_7Mo(CO)_3]_2$ with iodine gives a brown solid formulated as the dicarbonyl $C_9H_7Mo(CO)_2I$ on the basis of analytical data. The mass spectrum (Table IV) of this brown solid indicated that the $C_9H_7Mo(CO)_2I$ had completely decomposed by pyrolysis in the mass spectrometer.

The highest *m/e* ion in the mass spectrum of this brown solid could be assigned to $(C_9H_7)_2Mo_2I_4^+$ (*m/e* 930). This corresponds to the parent ion of an unknown compound $[C_9H_7MoI_2]_2$ of structure **5**. This structure **5** would correspond to structure **6** for the organosulfur derivative $[C_5H_5Mo(SCH_3)_2]_2$, (18). Structure **5** is related to structure **6** by substituting π-indenyl rings for π-cyclopentadienyl rings and by substituting bridging iodine atoms for bridging CH_3S groups.

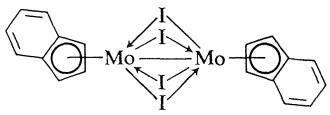

5

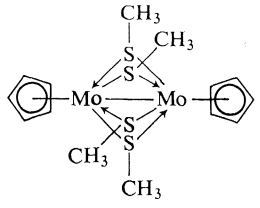

6

The parent ion of **5**, $(C_9H_7)_2Mo_2I_4^+$ (*m/e* 930), appears to undergo stepwise loss of iodine atoms resulting finally in $(C_9H_7)_2Mo_2^+$ (*m/e* 422). The iodine bridges can thus be removed in $[C_9H_7MoI_2]_2$ (**5**) without disturbing the molybdenum–molybdenum bond believed to be in **5** by analogy with $[C_5H_5Mo(SCH_3)_2]_2$ (**6**), where a molybdenum–molybdenum bond is required to explain the diamagnetism. The intermediate ions $(C_9H_7)_2Mo_2I_n^+$ (n = 3, 2, and 1) can also undergo π-C_9H_7 cleavage giving the corresponding ions $C_9H_7Mo_2I_n^+$ (n = 3, 2, and 1). The doubly-charged ions $(C_9H_7)_2Mo_2I_n^{2+}$ (n = 4 or 3) were also observed.

An additional series of ions containing one carbonyl group is observed in the mass spectrum which cannot arise from $[C_9H_7MoI_2]_2$. The highest *m/e* ion in this second series corresponds to $(C_9H_7)_2MoCOI^+$ (*m/e* 481) suggesting that bisindenylmolybdenum carbonyl iodide is a second pyrolysis product of $C_9H_7Mo(CO)_2I$. The presence of ions from $[C_9H_7MoI_2]_2$ and from $(C_9H_7)_2MoCOI$ in the mass spectrum of $C_9H_7Mo(CO)_2I$ suggests that its pyrolysis proceeds according to the following equation:

$$6C_9H_7Mo(CO)_2I \xrightarrow{\Delta} [C_9H_7MoI_2]_2 + 2(C_9H_7)_2MoCOI + 2Mo + 10CO$$

The ion $(C_9H_7)_2MoCOI^+$ (*m/e* 481) appears to fragment either by loss of its carbonyl group giving $(C_9H_7)_2MoI^+$ (*m/e* 453) or by loss of its iodine atom giving $(C_9H_7)_2MoCO^+$ (*m/e* 354).

The mass spectrum of this brown solid also exhibits some metal-containing ions which can arise either from $[C_9H_7MoI_2]_2$ or from

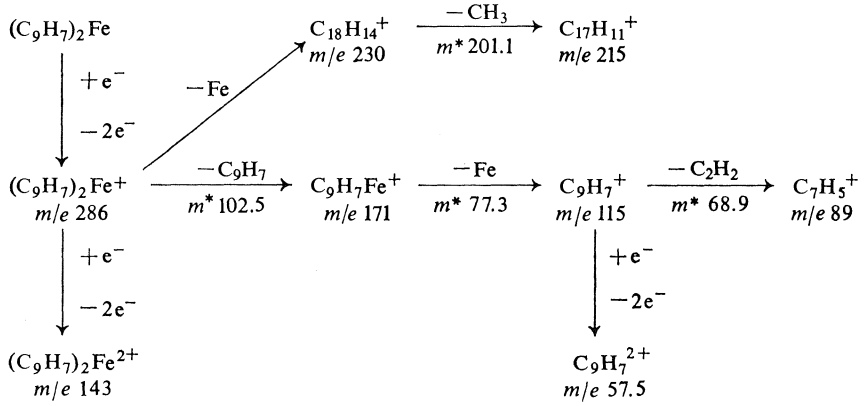

FIG. 2. Fragmentation scheme of $(C_9H_7)_2Fe$.

$(C_9H_7)_2MoCOI$, since they correspond to fragments of either species. The highest *m/e* ion among these "ambiguous" ions is $C_9H_7MoI^+$ (*m/e* 338). This ion $C_9H_7MoI^+$ (*m/e* 338) can eliminate acetylene (C_2H_2) giving the ion $C_7H_5MoI^+$ (*m/e* 312). The ion $(C_9H_7)_2Mo^+$ (*m/e* 326) can arise by processes such as molybdenum elimination from $(C_9H_7)_2Mo_2^+$ (*m/e* 422) (a fragment of $[C_9H_7MoI_2]_2$) or by carbon monoxide elimination from $(C_9H_7)_2MoCO^+$ (*m/e* 354) (a fragment of $(C_9H_7)_2MoCOI$). The great ease of carbon monoxide elimination from metal carbonyl ions suggests the latter process to be much more likely. The ion $(C_9H_7)_2Mo^+$ (*m/e* 326) can undergo a second ionization giving the dipositive ion $(C_9H_7)_2Mo^{2+}$ (*m/e* 163). The two remaining metal-containing ions are $C_9H_7Mo^+$ (*m/e* 211) and its acetylene-elimination product $C_7H_5Mo^+$ (*m/e* 185) expected to be present in the mass spectra of all π-indenylmolybdenum derivatives.

The usual metal-free ions found in the mass spectra of π-indenyl derivatives are also observed in the mass spectrum of this brown solid. These include $C_9H_8^+$, $C_9H_7^+$, $C_7H_5^+$, $C_5H_3^+$, and $C_9H_7^{2+}$. In addition the ion $C_{18}H_{14}^+$ (*m/e* 230) arising from the coupling of two indenyl ligands is observed in relatively high abundance. Such coupling of indenyl ligands would be expected to occur readily in $(C_9H_7)_2MoCOI$ owing to the presence of two indenyl ligands on one metal atom. Most of the remaining hydrocarbon ions are possible fragmentation products of $C_{18}H_{14}^+$ (*m/e* 230). The iodide ligand in both $[C_9H_7MoI_2]_2$ and $(C_9H_7)_2MoCOI$ can account for the ions HI^+ (*m/e* 128) and I^+ (*m/e* 127).

C. Indenyliron Derivatives and Hydrogenation Products

1. $(C_9H_7)_2Fe$: Figure 2 depicts the main features of the fragmentation scheme of $(C_9H_7)_2Fe$ (7). The parent ion in this mass spectrum first loses one of its indenyl ligands giving the ion $C_9H_7Fe^+$ (*m/e* 171). This ion then loses its iron atom giving the indenyl ion $C_9H_7^+$ (*m/e* 115). Both of these processes are supported by the presence of appropriate metastable ions. The only other iron ion present in significant abundance is the doubly charged parent ion $(C_9H_7)_2Fe^{2+}$ (*m/e* 143). The "bare" iron ion Fe^+ (*m/e* 56) is only observed in low abundance. Apparently the indenyliron ion ($C_9H_7Fe^+$, *m/e* 171) fragments almost exclusively by elimination of a neutral iron atom according to the following equation

$$\underset{m/e\ 171}{C_9H_7Fe^+} \xrightarrow{m^*\ 77.4} \underset{m/e\ 115}{C_9H_7^+} + Fe$$

This contrasts with the behavior of the corresponding cyclopentadienyliron ion ($C_5H_5Fe^+$, *m/e* 121) which fragments mainly by elimination of a neutral C_5H_5 fragment according to the following equation

$$\underset{m/e\ 121}{C_5H_5Fe^+} \xrightarrow{m^*\ 25.8} \underset{m/e\ 56}{Fe^+} + C_5H_5$$

Metal-free ions in the mass spectrum of $(C_9H_7)_2Fe$ (7) include the usual ions present in π-indenyl complexes (see above). In addition the ion $C_{18}H_{14}^+$ (*m/e* 230) arising from the coupling of two C_9H_7 groups is observed. This $C_{18}H_{14}^+$ (*m/e* 230) ion appears to fragment by loss of a

Can. J. Chem. Downloaded from www.nrcresearchpress.com by 210.87.254.40 on 09/05/12
For personal use only.

Can. J. Chem. Downloaded from www.nrcresearchpress.com by 210.87.254.40 on 09/05/12
For personal use only.

neutral methyl (CH_3) fragment giving the $C_{17}H_{11}^+$ (*m/e* 215) ion.

2. $C_5H_5FeC_9H_7$: Figure 3 depicts the main features of the fragmentation scheme of $C_5H_5FeC_9H_7$ (**8**). The parent ion in this mass spectrum can lose either its indenyl ligand giving the ion $C_5H_5Fe^+$ (*m/e* 121) or its cyclopentadienyl ligand giving the ion $C_9H_7Fe^+$ (*m/e* 171). The ratio of the relative abundance of $C_9H_7Fe^+$ to that of $C_5H_5Fe^+$ is only 0.071, indicating that the tendency for the parent ion to lose its π-indenyl ligand is much greater than the tendency for the parent ion to lose its π-cyclopentadienyl ligand, in accord with the chemical indications (14) of the lower stability of metal-π-indenyl bonds compared with the analogous metal-π-cyclopentadienyl bonds. Further fragmentation of $C_5H_5Fe^+$ (*m/e* 121) results in elimination of a C_5H_5 fragment giving Fe^+ (*m/e* 56) whereas further fragmentation of $C_9H_7Fe^+$ (*m/e* 171) results in elimination of a neutral iron atom giving $C_9H_7^+$ (*m/e* 115) as discussed above.

The metal-free ions $C_9H_7^+$ (*m/e* 115), $C_7H_5^+$ (*m/e* 89), and $C_5H_3^+$ (*m/e* 63) result from the π-indenyl ligand as discussed above. The metal-free ions $C_5H_6^+$ (*m/e* 66), $C_5H_5^+$ (*m/e* 65), and $C_3H_3^+$ (*m/e* 39) result from the π-cyclopentadienyl ligand. The ions $C_{14}H_{11}^+$ (*m/e* 179) and

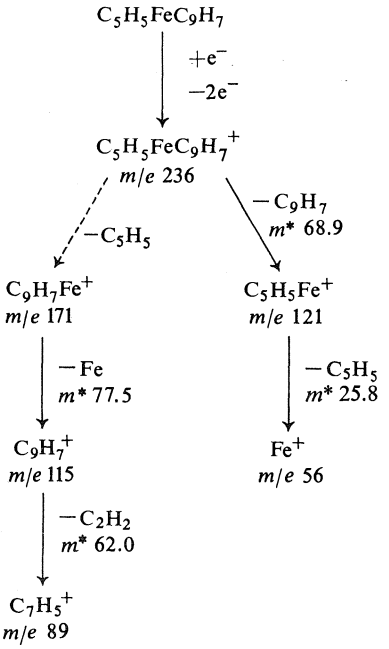

FIG. 3. Fragmentation scheme of $C_5H_5FeC_9H_7$.

$C_{14}H_{10}^+$ (*m/e* 178) result from coupling of the indenyl and cyclopentadienyl ligands followed by dehydrogenation.

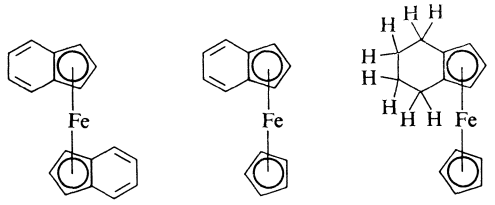

7 8 9

3. $C_5H_5FeC_9H_{11}$: Hydrogenation of $C_5H_5FeC_9H_7$ (**8**) at atmospheric pressure in the presence of a palladium catalyst has been shown to give $C_5H_5FeC_9H_{11}$ (**9**). The mass spectrum of the hydrogenated product $C_5H_5FeC_9H_{11}$ (**9**) was compared with that of $C_5H_5FeC_9H_7$ (**8**) and found to be somewhat more complex owing to possibilities of dehydrogenation processes. Figure 4 depicts the principal features of the fragmentation scheme of $C_5H_5FeC_9H_{11}$ (**9**).

Four decomposition processes for the parent ion in the mass spectrum of $C_5H_5FeC_9H_{11}$ were identified from metastable ions:

1. Elimination of CH_3 (methyl)

$$\underset{m/e\ 240}{C_5H_5FeC_9H_{11}^+} \xrightarrow{m^*210.6} \underset{m/e\ 225}{C_5H_5FeC_8H_8^+} + CH_3$$

This process must necessarily involve a hydrogen shift.

2. Elimination of C_2H_4 (ethylene)

$$\underset{m/e\ 240}{C_5H_5FeC_9H_{11}^+} \xrightarrow{m^*\ 187.4} \underset{m/e\ 212}{C_5H_5FeC_7H_7^+} + C_2H_4$$

Two adjacent sp^3 carbon atoms in the six-membered ring of the C_9H_{11} ligand can be eliminated as ethylene.

3. Elimination of C_3H_5 (allyl)

$$\underset{m/e\ 240}{C_5H_5FeC_9H_{11}^+} \xrightarrow{m^*\ 164.9} \underset{m/e\ 199}{C_5H_5FeC_6H_6^+} + C_3H_5$$

The $C_5H_5FeC_6H_6^+$ ion formed in this reaction has also been isolated in the form of stable salts (19, 20).

4. Elimination of $C_5H_6 + H_2$ in one step

$$\underset{m/e\ 240}{C_5H_5FeC_9H_{11}^+} \xrightarrow{m^*\ 123.2} \underset{m/e\ 172}{C_9H_8Fe^+} + C_5H_6 + H_2$$

The presence of an appreciable abundance of $C_9H_{10}Fe^+$ (*m/e* 174) also suggests elimination of

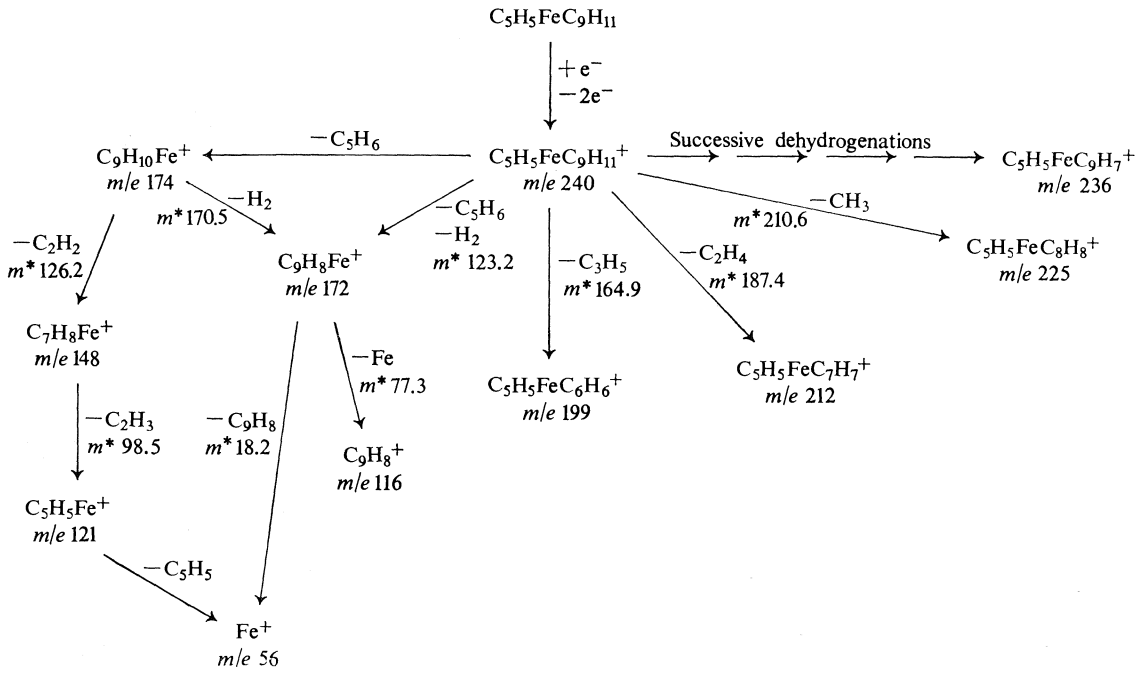

FIG. 4. Fragmentation scheme of $C_5H_5FeC_9H_{11}$.

C_5H_6 from the parent ion $C_5H_5FeC_9H_{11}^+$ (*m/e* 240).

The presence of the ions $C_5H_5FeC_9H_n^+$ (n = 10, 9, 8, and 7) in the mass spectrum of $C_5H_5FeC_9H_{11}$ (**9**) suggests that the parent ion can undergo dehydrogenation of its sp^3 carbon atoms giving sp^2 carbon atoms. Similar dehydrogenation processes involving carbonyl-free ions have been noted in the mass spectra of olefin-metal carbonyl derivatives (21).

The ion $C_7H_8Fe^+$ (*m/e* 148) can result by acetylene (C_2H_2) elimination from the ion $C_9H_{10}Fe^+$ (*m/e* 174). Other fragmentation processes of several types can result in the iron-containing ions $C_6H_6Fe^+$ (*m/e* 134) and $C_5H_5Fe^+$ (*m/e* 121). The "bare" iron ion Fe^+ (*m/e* 56) is also observed as the third most abundant metal-containing ion.

The metal-free ions arising from a π-C_9H_{11} ligand differ from those arising from a π-C_9H_7 ligand discussed above. A negligible abundance of $C_9H_{11}^+$ (*m/e* 119) is observed suggesting that the π-C_9H_{11} ligand undergoes dehydrogenation before the C_9H_{11} can be eliminated as an ion. The ions arising from the π-C_9H_{11} ligand in the mass spectrum of $C_5H_5FeC_9H_{11}$ include at least $C_9H_9^+$, $C_9H_8^+$, $C_9H_7^+$, $C_7H_7^+$, and $C_3H_5^+$. The ions $C_5H_5^+$ and $C_3H_3^+$ appear to arise from the π-C_5H_5 ligand. The fragment ions with 10, 11, and 12 carbon atoms probably arise from coupling both the C_5H_5 and C_9H_{11} ligands followed by various elimination processes.

4. $C_5H_5FeC_9H_9$: The mass spectral studies on $C_5H_5FeC_9H_7$ (**8**, Fig. 3) and $C_5H_5FeC_9H_{11}$ (**9**, Fig. 4) made interesting the study of a partially hydrogenated derivative $C_5H_5FeC_9H_9$. Such a compound has not yet been reported in the literature. However, a study of the reaction of ferrous chloride with a mixture of lithium cyclononatetraenide (15) and sodium cyclopentadienide had yielded a few mg of a material of apparent composition $C_5H_5FeC_9H_9$. The mass spectrum of this very rare compound of unknown structure was investigated. The composition $C_5H_5FeC_9H_9$ was confirmed. Main features of the fragmentation scheme of this complex are depicted in Fig. 5.

The parent ion in the mass spectrum of $C_5H_5FeC_9H_9$ undergoes both dehydrogenation giving $C_5H_5FeC_9H_8^+$ (*m/e* 237) and $C_5H_5FeC_9H_7^+$ (*m/e* 236) and acetylene elimination giving $C_5H_5FeC_7H_7^+$ (*m/e* 212). A second acetylene

Can. J. Chem. Downloaded from www.nrcresearchpress.com by 210.87.254.40 on 09/05/12
For personal use only.

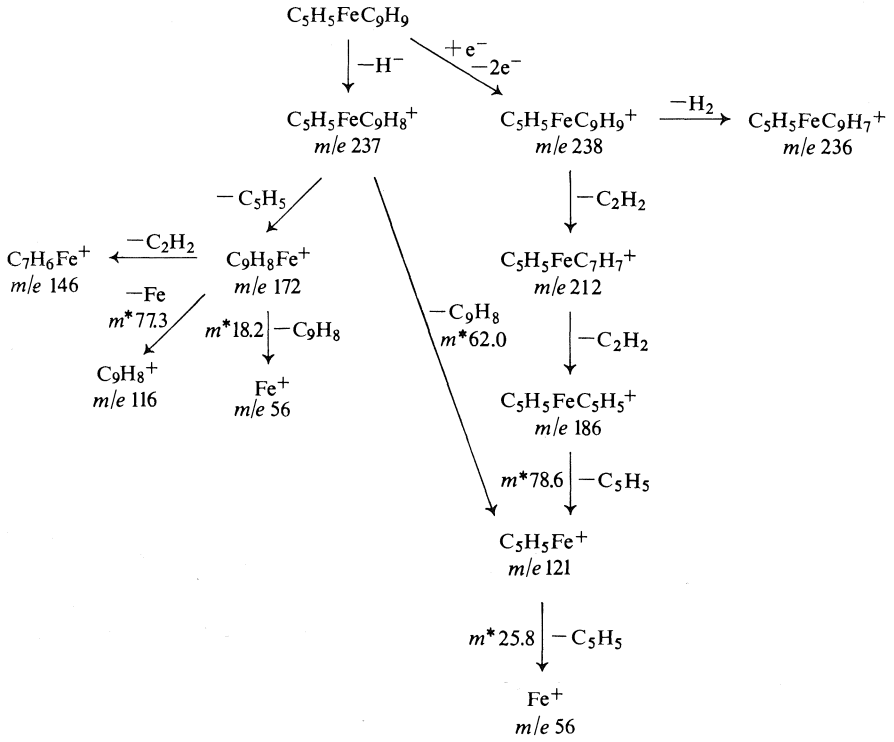

FIG. 5. Fragmentation scheme of $C_5H_5FeC_9H_9$.

elimination gives $C_5H_5FeC_5H_5^+$ (*m/e* 186). This ion (possibly the ferrocene ion) loses successively its two C_5H_5 rings giving first $C_5H_5Fe^+$ (*m/e* 121) and then the "bare" iron ion Fe^+ (*m/e* 56).

The most abundant iron-containing ion in the mass spectrum of $C_5H_5FeC_9H_9$ is $C_5H_5FeC_9H_8^+$ (*m/e* 237). Its formation may occur by hydride elimination from the parent neutral compound, e.g.

$$\underset{m/e\ 238}{C_5H_5FeC_9H_9} \longrightarrow \underset{m/e\ 237}{C_5H_5FeC_9H_8^+} + H^-$$

The $C_5H_5FeC_9H_8^+$ (*m/e* 237) ion can either lose its C_9H_8 ligand giving $C_5H_5Fe^+$ (*m/e* 121) or its C_5H_5 ligand giving $C_9H_8Fe^+$ (*m/e* 172). Further fragmentation of the $C_9H_8Fe^+$ (*m/e* 172) ion involves rupture of the bond between the C_9H_8 ligand and the iron atom giving a C_9H_8 fragment and an Fe fragment. The positive charge can remain with either fragment; both possibilities are supported by the appropriate metastable ions.

The most abundant hydrocarbon ions in the mass spectrum of $C_5H_5FeC_9H_9$ are $C_9H_8^+$ (*m/e* 116) and $C_9H_7^+$ (*m/e* 115). The $C_9H_7^+$ (*m/e* 115) ion appears to undergo stepwise loss of two acetylene (C_2H_2) fragments giving first $C_7H_5^+$ (*m/e* 89) and then $C_5H_3^+$ (*m/e* 63). Both of these acetylene eliminations are supported by the presence of appropriate metastable ions. The $C_5H_6^+$ (*m/e* 66), $C_5H_5^+$ (*m/e* 65), and $C_3H_3^+$ (*m/e* 39) ions are generally observed in the mass spectra of π-cyclopentadienyl derivatives and thus probably arise (at least partially) from the π-C_5H_5 ligand in $C_5H_5FeC_9H_9$. The $C_{14}H_{10}^+$ (*m/e* 178) ion appears to arise by coupling of the C_5H_5 and C_9H_9 ligands followed by dehydrogenation.

The mass spectral data on this new but very rare complex $C_5H_5FeC_9H_9$ do not provide unequivocal structural evidence. Prior observations on various π-allyl (11) and olefin (21) complexes suggest that in carbonyl-free ions carbon atoms bearing two hydrogen atoms tend to lose easily one of these hydrogen atoms. The parent ion $C_5H_5FeC_9H_9^+$ tends to lose two hydrogen atoms easily. This suggests that it contains two CH_2 groups and has a bicyclic structure. The relative abundances of the $C_9H_8Fe^+$ and $C_5H_5Fe^+$ ions are nearly equal suggesting that

Can. J. Chem. Downloaded from www.nrcresearchpress.com by 210.87.254.40 on 09/05/12
For personal use only.

the C_9H_9 ligand is as strongly bonded to the iron atom as the π-C_5H_5 ligand. The π-C_9H_9 ligand is probably a substituted π-cyclopentadienyl ligand. The most probable structure for $C_5H_5FeC_9H_9$ appears to be **10**. The more symmetrical placement of the uncomplexed double bond in the six-membered ring of the C_9H_9 ligand is chosen because the melting point (107°) of $C_5H_5FeC_9H_9$ is higher than that of either $C_5H_5FeC_9H_7$ (72°) or $C_5H_5FeC_9H_{11}$ (40°) and because of the greater abundance of $C_5H_5FeC_9H_8^+$ than that of either $C_5H_5FeC_9H_9^+$ or $C_5H_5FeC_9H_7^+$. In this structure (**10**) for $C_5H_5FeC_9H_9$ with non-adjacent CH_2 groups in the C_9H_9 ligand, elimination of two hydrogen atoms to give $C_5H_5FeC_9H_7^+$ is likely to occur individually rather than simultaneously as H_2. Individual rather than simultaneous elimination of hydrogen atoms from $C_5H_5FeC_9H_9$ is more consistent with the observed greater abundance of $C_5H_5FeC_9H_8^+$ than either $C_5H_5FeC_9H_9^+$ or $C_5H_5FeC_9H_7^+$.

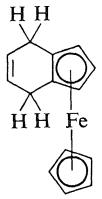

10

Acknowledgments

I am indebted to the National Science Foundation for partial support under Grant No. GP-3954 of the portion of this work performed at the Mellon Institute. I am also indebted to Mr. R. E. Rhodes and Mr. J. R. Boal for running these spectra on the Mellon Institute MS-9 mass spectrometer.

1. R. B. KING. Appl. Spectry. In press.
2. L. FRIEDMAN, A. P. IRSA, and G. WILKINSON. J. Am. Chem. Soc. **77**, 3689 (1955).
3. H. EGGER. Monatsh. Chem. **97**, 602 (1966).
4. R. I. REED and F. M. TABRIZI. Appl. Spectry. **17**, 124 (1963).
5. A. MANDELBAUM and M. CAIS. Tetrahedron Letters, 3847 (1964).
6. D. J. CLANCY and I. J. SPILNERS. Anal. Chem. **34**, 1839 (1962).
7. D. W. SLOCUM, R. LEWIS, and G. J. MAINS. Chem. Ind. London, 2095 (1966).
8. J. MÜLLER and L. D'OR. J. Organometal. Chem. **10**, 313 (1967).
9. R. E. WINTERS and R. W. KISER. J. Organometal. Chem. **4**, 190 (1965).
10. E. SCHUMACHER and R. TAUBENEST. Helv. Chim. Acta, **49**, 1447 (1966).
11. R. B. KING. J. Am. Chem. Soc. **90**, 1417 (1968).
12. H. BUDZIKIEWICZ, C. DJERASSI, and D. H. WILLIAMS. Interpretation of mass spectra of organic compounds. Holden-Day, Inc., San Francisco. 1964. p. xiii. J. H. BEYNON. Mass spectrometry and its applications to organic chemistry. Elsevier Publishing Co., Amsterdam. 1960. pp. 251–262; and references cited therein.
13. R. B. KING and M. B. BISNETTE. Inorg. Chem. **4**, 475 (1965).
14. R. B. KING and M. B. BISNETTE. Inorg. Chem. **3**, 796 (1964).
15. T. J. KATZ and P. J. GARRATT. J. Am. Chem. Soc. **86**, 5194 (1964).
16. R. I. REED. Applications of mass spectrometry to organic chemistry. Academic Press, Inc., New York. 1966. p. 67.
17. R. B. KING. J. Am. Chem. Soc. **90**, 1429 (1968).
18. R. B. KING. J. Am. Chem. Soc. **85**, 1587 (1963).
19. M. L. H. GREEN, L. PRATT, and G. WILKINSON. J. Chem. Soc. 989 (1960).
20. A. N. NESMEYANOV, N. A. VOL'KENAU, and I. N. BOLESOVA. Tetrahedron Letters, 1725 (1963).
21. R. B. KING. In preparation.

Can. J. Chem. Downloaded from www.nrcresearchpress.com by 210.87.254.40 on 09/05/12
For personal use only.

Can. J. Chem. Downloaded from www.nrcresearchpress.com by 210.87.254.6 on 09/05/12
For personal use only.

Dimethylboric anhydride: a convenient preparation and full characterization

G. F. LANTHIER AND W. A. G. GRAHAM
Department of Chemistry, University of Alberta, Edmonton, Alberta

Received June 25, 1968

Dimethylboric anhydride, $(CH_3)_2BOB(CH_3)_2$, has been prepared by limited hydrolysis of dimethylboron chloride and complete characterization has been carried out. The Lewis acid character of boron and the donor strength of oxygen have been studied using tensimetric and nuclear magnetic resonance techniques.

Evidence for boron–oxygen π-bonding obtained from complex formation studies, using trimethylboron as a reference acid, is presented and discussed. The reduced acidity of the boron atoms, in comparison with trimethylboron, is discussed in terms of boron–oxygen π-bonding.

Canadian Journal of Chemistry, 47, 569 (1969)

Introduction

Dimethylboric anhydride, $(CH_3)_2BOB(CH_3)_2$, contains two electron-accepting atoms bridged by one electron-donating atom, and could conceivably behave as either a Lewis acid or a Lewis base. In the former case, both mono- and di-adducts might be possible. Although this interesting compound was first prepared by McKennon in 1936 (1), very few references to it are found in the literature (2–4).

In view of the interesting Lewis amphoteric character of the compound, some studies of complex formation have also been carried out using tensimetric (5) and nuclear magnetic resonance (n.m.r.) techniques.

Experimental

A. Apparatus

Preparation and purification of the compounds were carried out in a standard high vacuum apparatus to which a gas–liquid chromatography system was attached. The gas–liquid chromatography system comprised a Gow–Mac stainless steel gas-density thermistor detector Model #140, used in conjunction with a Gow–Mac power supply #9999. The sample introduction system, connected to the high vacuum apparatus by a Teflon valve, was operated by a pair of 3-way valves (Hoke, C-415K). Nitrogen carrier gas was rerouted through the introduction system by simultaneously closing a bypass 2-way valve (Hoke, C-413K) and opening both 3-way valves. Good separation characteristics were found for a 10-ft, 7-mm inner diameter column, packed with 30–60 mesh celite and containing 20% by weight of Fisher paraffin oil. Purified sample was collected in two U-traps lightly packed with glass wool, through which the effluent gases could be directed and frozen out at liquid nitrogen temperatures.

The mass spectrum was obtained using an Associated Electrical Industries (A.E.I.) MS-9 spectrometer. The infrared spectrum was obtained using a Perkin–Elmer Model 421 spectrometer in conjunction with a 5 cm gas cell with potassium bromide windows. Nuclear magnetic resonance spectra were run on a Varian A-60 spectrometer; sample tubes were flamed lightly under vacuum, and were sealed off after the components of the solution had been distilled in from the vacuum system.

B. Materials

Dimethylboron chloride was prepared by reacting equimolar quantities of boron trichloride (Matheson of Canada, Ltd., C.P. grade) with tetramethyltin (M & T Chemicals, Inc.) in a stainless steel Hoke cylinder at 140 °C for 12 h. The use of alkyltin compounds for the preparation of alkylboron halides has been described in the literature (6, 7). The reaction conditions employed in this study gave an improved yield (approximately 95% based on boron trichloride). The other major product was dimethyltin dichloride. The crude dimethylboron chloride was purified chromatographically to remove small amounts of hydrogen chloride, trimethylboron, methylboron dichloride, and boron trichloride. Dimethylboric anhydride was prepared by reacting appropriate quantities of dimethylboron chloride and water in a Pyrex vessel. Although the reaction is rapid at room temperature, repeated condensation and re-warming facilitates complete mixing of the two phases. Essentially quantitative yields of HCl and crude dimethylboric anhydride are obtained. Purification is best carried out by initial trap-to-trap distillation through a −78.5 °C trap to remove hydrogen chloride, followed by sublimation of the material from a cold trap (allowed to warm from −196 °C to room temperature by simply removing the liquid nitrogen) into a −78.5 °C trap, through which traces of more volatile materials readily pass. After purification, the yields of pure dimethylboric anhydride were approximately 85%.

Trimethylboron was prepared by the reaction of 2 moles of boron trichloride with 3 moles of tetramethyltin. Chromatography indicated yields greater than 95% in all experiments. Trimethylphosphine was prepared by the Grignard route using dibutylether solvent, and purified through its silver iodide complex (8). Both of these compounds, as well as commercially available trimethylamine, dimethylether, and dimethylsulfide, were purified chromatographically. As an indication of purity of the aforementioned compounds, the vapor pressures at specific temperatures are listed, along with the literature

values: dimethylboron chloride, 635 mm at 0 °C (lit. (9), 634 mm at 0 °C); trimethylboron, 85.5 mm at −63.5 °C (lit. (10), 85.6 mm at −63.5 °C); trimethylphosphine, 158 mm at 0 °C (lit. (8), 158.5 mm at 0 °C); trimethylamine, 681 mm at 0 °C (lit. (11), 681.7 mm at 0 °C); dimethylether, 33.8 mm at −78. 5 °C (lit. (12), 34.4 mm at −78.5 °C); and dimethylsulfide, 166.8 mm at 0 °C (lit. (13), 167 mm at 0 °C).

Results

A. Characterization

Dimethylboric anhydride as prepared and purified above was found to have a molecular weight of 97.5 using the gas density method (calculated 97.72). The vapor pressure of the liquid was measured at several temperatures between −20.2 and +10.0 °C, with results as given in Table I. Values calculated using the least square equation $\log P_{liq} = 8.459 - 1718/T$ are also given. From the equation, the heat of vaporization is calculated as 7.86 kcal, the boiling point +34.8 °C, and the Trouton constant 25.5. The melting point is −21.2 °C using the magnetic plunger of Stock (14). The vapor pressure of the solid material was determined at three temperatures as shown in Table I. These values determine the equation $\log P_{solid} = 13.63 - 3028/T$, from which the heat of sublimation is calculated to be 13.86 kcal.

Mass spectral data are reported in Table II. While the molecular ion is too weak for a mass determination at high resolution, the fragment at 83 *m/e* was shown in this way to be $C_3H_9B_2{}^{11}O$. The observed and calculated masses differ by less than 1 p.p.m.

Infrared data are reported in Table III, where tentative assignments have been made as discussed later.

The ambient temperature proton n.m.r. spectrum of dimethylboric anhydride in CS_2, $CHCl_3$, $CFCl_3$, and C_7D_{14} consisted of a single broad resonance (half-width: 3.5 c.p.s.) 0.43 p.p.m. downfield from tetramethylsilane (TMS). Varying the concentration between 2 and 20 mole % did not affect the chemical shift.

TABLE I

Vapor pressure data for dimethylboric anhydride

Temperature (°C)	Observed pressure (mm)	Calculated pressure (mm)
Liquid		
+10.0	244.0	247.2
+ 8.0	224.6	223.9
+ 5.5	195.9	197.2
0.0	150.0	148.3
− 7.0	102.4	101.2
−15.0	63.2	63.8
−20.2	46.3	46.6
Solid		
−22.9	33.6	34.2
−35.0	8.0	8.3
−45.3	2.3	2.2

TABLE II

Mass spectrum of dimethylboric anhydride[a]

m/e	Ion	*I*(%)[b]	*m/e*	Ion	*I*(%)[b]
10	B^{10}	0.3	40	$C_2H_6B^{10}$	27.0
11	B^{11}	1.1	41	$C_2H_6B^{11}$	85.0
13	CH	1.3	42	$CH_4B^{10}O$	31.3
15	CH_3	5.8	43[c]	$CH_4B^{11}O$	100
25	CH_2B^{11}	1.1	44	$C^{13}H_4B^{11}O$	1.6
26	C_2H_2, $B^{10}O$	1.8	51	$CH_3B^{10}B^{10}O$	0.3
26.5[e]	$CH_3B^{11}B^{11}O$	0.1	52	$CH_3B^{10}B^{11}O$	0.5
27	$B^{10}OH$, $B^{11}O$	2.8	53	$CH_3B^{11}B^{11}O$	1.1
28	$B^{11}OH$	3.3	57	$C_2H_7B^{10}O$	0.4
29	C_2H_5	4.0	58	$C_2H_7B^{11}O$	1.6
33[e]	$C_2H_6B^{10}B^{10}O$	1.3	81	$C_3H_9B^{10}B^{10}O$	3.0
33.5[e]	$C_2H_6B^{10}B^{11}O$	4.0	82	$C_3H_9B^{10}B^{11}O$	21.3
34[e]	$C_2H_6B^{11}B^{11}O$	4.2	83[d]	$C_3H_9B^{11}B^{11}O$	42.3
34.5[e]	$C^{13}CH_6B^{11}B^{11}O$	0.1	84	$C^{13}C_2H_9B^{11}B^{11}O$	1.5
36	$C_2H_2B^{10}$	1.2	96	$C_4H_{12}B^{10}B^{10}O$	≃0
37	$C_2H_2B^{11}$	3.8	97	$C_4H_{12}B^{10}B^{11}O$	≃0
38	$CB^{10}O$	2.5	98	$C_4H_{12}B^{10}B^{11}O$	0.1
39	$CB^{11}O$	8.3			

[a]Peaks of less than 1% of the base peak are not listed unless considered pertinent.
[b]% intensity relative to the base peak.
[c]Exact mass calculated, 43.0355; found, 43.0351.
[d]Exact mass calculated, 83.0839; found, 83.0840.
[e]Doubly charged ion.

Can. J. Chem. Downloaded from www.nrcresearchpress.com by 210.87.254.6 on 09/05/12
For personal use only.

Can. J. Chem. Downloaded from www.nrcresearchpress.com by 210.87.254.6 on 09/05/12
For personal use only.

TABLE III

Vibrational frequencies and suggested assignments for dimethylboric anhydride[a]

Frequencies (cm^{-1})	Suggested assignments
2990 m, *ca* 2920 sh	C—H sym. and asym.
	CH_3 def. asym.
1405 vsb[b]	B—O asym.
	B—O sym.
1320 vs	CH_3 def. sym.
1165 sh	CH_3 rock
1135 s	B—C asym.
940 m	CH_3 rock
730 w	B—C sym.

[a]Abbreviations: w = weak, m = medium, s = strong, v = very, b = broad, sh = shoulder; sym. = symmetric, asym. = asymmetric.
Spectra taken in the gas phase at 4 mm and 16 mm pressure in a 5 cm cell.
[b]Approximate half-width at 16 mm is 200 cm^{-1}.

B. Complex Formation

Trimethylamine – Dimethylboric Anhydride

The saturation pressures obtained from a 4.5 cc[1] sample of dimethylboric anhydride treated with a carefully matched volume of trimethylamine are recorded in Table IV. Values are substantially less than calculated for an ideal solution, presumably the result of complex formation by the equilibrium

$$(CH_3)_2BOB(CH_3)_2 \cdot N(CH_3)_3 \rightleftarrows (CH_3)_2BOB(CH_3)_2 + N(CH_3)_3$$

The saturation pressures in Table IV correspond to the equation $\log P_{mm} = 10.43 - 2816/T$, implying a "boiling point" of 99.5 °C and a Trouton constant of 34.6.

TABLE IV

Saturation pressures of trimethylamine – dimethylboric anhydride

Temperature (°C)	Observed pressure (mm)	Calculated pressure[a] (mm)
24.6	9.6	9.5
28.3	12.4	12.5
34.6	19.2	19.4
36.3	21.4	21.7
42.5	32.0	32.8
44.8	37.7	38.0
54.3	69.3	68.9
58.3	87.4	87.4

[a]Calculated from $\log P_{mm} = 10.43 - 28.6/T$.

[1]The abbreviation cc in this paper refers to gas volumes at standard temperature and pressure. Pressures were measured using a cathetometer reading to 0.01 mm and errors in the calculated volumes are considered to be about 1%.

The 1:1 adduct (4.5 cc) was treated with an additional 4.5 cc of trimethylamine. After standing for 15 h at −78.5 °C, 4.5 cc of trimethylamine were recovered by pumping through a −196 °C trap, while the sample remained at −78.5 °C, indicating that a 2:1 complex, if it does exist at this temperature, is very weak.

The above equilibrium was studied in the gas phase using a sample prepared by treating 2.7 cc of dimethylboric anhydride with a matched volume of trimethylamine. In the temperature range 47.0 to 72.0 °C, dissociation ranged from 72 to 85%. The variation of pressure with temperature and other data are recorded in Table V. A check of the dissociation pressures as the sample was cooled showed that no decomposition had taken place. Variation of the equilibrium constant with temperature is represented by the equation $\log K_p(\text{atm}) = 5.007 - 2073/T$. Therefore, for the above reaction, the enthalpy and entropy of dissociation are: $\Delta H^0 = 9.5$ kcal and $\Delta S^0 = +22.9$ e.u.

Trimethylphosphine – Dimethylboric Anhydride

The addition compound was formed in the tensimeter by bringing together 18.8 cc of dimethylboric anhydride and a matched volume of trimethylphosphine. In the gas phase at room temperature, the complex was found to be 98% dissociated. The saturation pressures of the liquid reported in Table VI determine the equation $\log P_{mm} = 9.077 - 2019/T$, from which one calculates a "boiling point" of 52.6 °C and the Trouton constant as 28.4.

Dimethylether – Dimethylboric Anhydride

Dimethylether was treated with a matched volume of dimethylboric anhydride. The volumes in the gas phase at room temperature were found to be additive. Furthermore when the mixture was cooled to −78.5 °C the pressure above the liquid was slightly greater (6%) than that calculated using Raoult's law. It may be concluded that an adduct does not form down to −78.5 °C.

Dimethylsulfide – Dimethylboric Anhydride

Dimethylsulfide was treated with a matched volume of dimethylboric anhydride. The volumes in the gas phase at room temperature were found to be additive. At temperatures below −45.2 °C, the pressures observed were only 10% below those expected for pure dimethylsulfide. This presumably indicates some degree of insolubility of dimethylboric anhydride in dimethylsulfide at

TABLE V

Gas phase dissociation trimethylamine – dimethylboric anhydride

Temperature (°C)	Observed P_{mm}	Calculated P_{mm}[a]	α	K_p[b] (atm)	Calculated K_p[c] (atm)
47.0	25.10	14.62	0.717	0.0330	0.0341
50.0	25.57	14.75	0.733	0.0390	0.0392
53.0	26.08	14.89	0.751	0.0444	0.0449
55.0	26.38	14.98	0.761	0.0478	0.0491
57.0	26.84	15.07	0.781	0.0551	0.0536
60.0	27.22	15.21	0.789	0.0592	0.0611
63.0	27.67	15.35	0.803	0.0659	0.0693
65.0	28.08	15.44	0.819	0.0750	0.0755
67.0	28.47	15.53	0.833	0.0849	0.0820
70.0	28.88	15.67	0.843	0.0934	0.0927
72.0	29.17	15.76	0.851	0.101	0.100

[a]Calculated pressure for no dissociation.
[b]Calculated from observed data.
[c]Calculated from $\log K_p = 5.007 - 2073/T$.

TABLE VI

Saturation pressures of trimethylphosphine–dimethylboric anhydride

Temperature (°C)	Observed P_{mm}	Calculated P_{mm}[a]
−15.0	18.1	18.1
−10.0	25.7	25.5
− 6.0	33.2	33.2
− 4.0	36.4	37.8
0.0	48.6	48.6
4.0	61.1	62.2
5.0	65.8	66.0
7.4	75.4	76.1
10.0	89.6	88.7
15.0	119.9	118.9
20.0	156.5	155.2

[a]Calculated from $\log P_{mm} = 9.077 - 2019/T$.

these temperatures and it may be concluded that a complex is not formed.

Trimethylboron – Dimethylboric Anhydride

A 49.6 cc sample of trimethylboron was treated with an equivalent amount of dimethylboric anhydride in the tensimeter. Below −78.5 °C, the observed pressures were within 5% of those expected for pure trimethylboron. These data would suggest that dimethylboric anhydride is quite insoluble in trimethylboron at these temperatures and it may be concluded that a complex is not formed.

Dimethylboron Chloride – Dimethylboric Anhydride

A 24.1 cc sample of dimethylboron chloride was treated with a matching volume of dimethylboric anhydride in the tensimeter. After standing 6 h at −78.5 °C, the observed pressure was 7.7 mm, essentially the same as that of pure dimethylboron chloride at −78.5 °C. We conclude that no complex is formed and that dimethylboric anhydride is insoluble in dimethylboron chloride in this temperature region.

Nuclear Magnetic Resonance Studies of Complexes

Room temperature n.m.r. data are listed in Table VII. Chemical shifts of the protons on dimethylboric anhydride show shifts to high field when complexed to a Lewis base, while the Lewis base protons are shifted to lower field. Comparing this data to the tensimetric data shows the magnitude of the chemical shift increases as the strength of the complex increases,

TABLE VII

60 Mc n.m.r. chemical shifts of some acid–base systems

System	Proton chemical shifts[a]	
	Me_4B_2O	Other
Me_4B_2O	0.43	
Me_3N		2.23
Me_4B_2O:NMe_3	0.03	2.45
Me_3P		1.02[b]
Me_4B_2O:Me_3P	0.38	1.13[c]
Me_2O		3.30
Me_4B_2O:Me_2O	0.43	3.30
Me_2S		2.12
Me_4B_2O:Me_2S	0.43	2.12
Me_3B		0.77
Me_4B_2O:Me_3B	0.43	0.77
Me_2BCl		0.97
Me_4B_2O:Me_2BCl	0.62[d]	0.62[d]

[a]In p.p.m. relative to TMS. All samples 10% in chloroform.
[b]Doublet $J_{P-C-H} = 8.0$ c.p.s.
[c]Doublet $J_{P-C-H} = 6.7$ c.p.s.
[d]Single peak indicating rapid exchange.

Can. J. Chem. Downloaded from www.nrcresearchpress.com by 210.87.254.6 on 09/05/12
For personal use only.

Can. J. Chem. Downloaded from www.nrcresearchpress.com by 210.87.254.6 on 09/05/12
For personal use only.

in agreement with work done by other workers (15–17). The single resonance observed for the dimethylboron chloride – dimethylboric anhydride system will be discussed in the next section.

Discussion

The original synthesis of dimethylboric anhydride involved dehydration of dimethylboric acid using phosphorus pentoxide (1):

$$2(CH_3)_2BOH + P_2O_5 \rightarrow 2HPO_3 + (CH_3)_2BOB(CH_3)_2$$

In our hands, this method proved unsatisfactory. The products obtained were highly variable, and a pure compound exhibiting the reported vapor pressure of 118 mm at 0 °C (1) could not be isolated. We were thus led to seek an alternative route, and report here a convenient, reproducible method involving partial hydrolysis of dimethylboron chloride, which gives rise to easily separable products:

$$2(CH_3)_2BCl + H_2O \rightarrow (CH_3)_2BOB(CH_3)_2 + 2HCl$$

A similar reaction has been used to prepare diphenylboric anhydride (18) and di-*n*-butylboron anhydride (19).

Although an elemental analysis of dimethylboric anhydride was not carried out, the preparative method, the gas density molecular weight, and the accumulated spectroscopic data establish the identity of the compound beyond all doubt.

Mass Spectrum

It is evident from the spectrum that rearrangements are taking place. For example, the base peak at 43 *m/e* was shown by its exact mass to be $CH_4B^{11}O$. Only one metastable peak at 20.3 *m/e* was observed, corresponding to

$$(CH_3)_2B^{11}OB^{11}(CH_3)^+ \rightarrow (CH_3)_2B^{11+} + (CH_3)B^{11}O$$

Suggested assignments of other peaks are listed in Table II. The presence of only one observable metastable peak, coupled with occurrence of rearrangement, allows little interpretation of the fragmentation pattern. The isotopes of boron simplify identification of boron-containing ions.

The region of 33, 33.5, and 34 *m/e* is of some interest. The peak at 33.5 must be due to a doubly charged ion, and $(CH_3)B^{10}OB^{11}(CH_3)^{2+}$ is our assignment. The peak at 34 has a C^{13} isotope peak at 34.5, indicating it is also a doubly charged ion, assigned to be $(CH_3)B^{11}OB^{11}(CH_3)^{2+}$. Any C^{13} isotope peak of the peak at 33 is masked by the 33.5 peak mentioned. The removal of two electrons from a molecule is facilitated by the presence of π-electron density (20). The presence of these peaks, and also a small peak at 26.5 attributed to $CH_3B^{11}B^{11}O^{2+}$, support the evidence for B–O π interaction recently reported for this compound (21).

Infrared Spectrum

The C—H stretching frequencies require no comment. In accord with Lehmann *et al.* (22), who place all B—C asymmetric stretching frequencies in the range from 1116 to 1138 cm^{-1}, we assign the 1135 cm^{-1} absorption to the B—C asymmetric stretch. The B—C symmetric stretch is assigned to the weak absorption at 730 cm^{-1}, following Ulmschneider and Goubeau (23), who have similarly assigned absorptions at 718 and 738 cm^{-1} in dimethylboric acid. From the work of Lehmann *et al.* on trimethylboron (22) and tetramethyldiborane (24), it is clear that the absorptions at 1165 and 940 cm^{-1} may be assigned to CH_3 rocking modes.

There is general agreement that in methylboron compounds the asymmetric methyl deformation occurs in the region of 1450 cm^{-1}, while the symmetric mode occurs in the region 1350–1300 cm^{-1} (25). On this basis, we assign the absorption at 1320 cm^{-1} to the symmetrical methyl deformation, while the band due to asymmetric methyl deformation presumably lies within the very broad absorption centered at 1405 cm^{-1}.

The B—O stretching frequencies are somewhat difficult to assign. Ulmschneider and Goubeau (23) assign a weak shoulder at 1276 cm^{-1} in the spectrum of dimethylboric acid to the B—O stretch. No equivalent exists in the spectrum of the anhydride. Abel *et al.* (26) report two B—O stretching frequencies[2] for diphenylboric anhydride at 1262 and 1378 cm^{-1}. It is conceivable that both symmetric and asymmetric modes of the B—O—B group, as well as the symmetric CH_3 deformation mentioned previously, are contained in the broad band at 1405 cm^{-1}.

Complex Formation

The results of the tensimetric studies provide interesting information about the donor strength

[2]Diphenylboric anhydride, as synthesized in this laboratory, exhibited a strong absorption at 1262 cm^{-1}, although there was no appreciable absorption at 1378 cm^{-1}.

of the oxygen atom towards acceptor molecules, and the acceptor strength of the boron atoms toward strong Lewis bases, such as trimethylamine. This information, when examined with reference to other acceptor–donor systems, provides some insight into the B—O bond, and the effects of π-bonding in this bond (21).

Examining first the data on oxygen base strength, it is evident that dimethylboric anhydride does not behave as a Lewis base towards trimethylboron. This is not unexpected, since no complex is formed between dimethylether and trimethylboron under equivalent conditions (27). Unfortunately, the boron trihalides, which are stronger Lewis acids, cannot be used since the following cleavage reaction occurs (2):

$$3(CH_3)_2BOB(CH_3)_2 + 2BX_3 \rightarrow 6(CH_3)_2BX + B_2O_3$$

However, if a dimethylboron halide were used, the products would be identical with the reactants:

$$(CH_3)_2BOB(CH_3)_2 + (CH_3)_2B^*Cl \rightleftarrows (CH_3)_2B^*OB(CH_3)_2 + (CH_3)_2BCl$$

In fact, the single resonance observed in the room temperature spectrum of this system (Table VII) is consistent with a rapidly exchanging system of this nature. Dimethylboron chloride, a stronger acceptor than trimethylboron, shows no indication of complex formation, and it may be concluded that the basicity of oxygen in dimethylboric anhydride is rather low.

The results of the study of the Lewis acid characteristics of dimethylboric anhydride show that it is considerably weaker than trimethylboron. The enthalpies of dissociation of $(CH_3)_2BOB(CH_3)_2 \cdot N(CH_3)_3$ and $(CH_3)_3B \cdot N(CH_3)_3$ are 9.5 and 17.62 kcal (28), respectively. The trimethylphosphine adduct of dimethylboric anhydride is completely dissociated in the gas phase, while $(CH_3)_3B \cdot P(CH_3)_3$ is not (29). Finally dimethylsulfide forms a recognizable adduct at −78.5 °C with trimethylboron (27) but not with dimethylboric anhydride.

Nuclear Magnetic Resonance Data

The n.m.r. data support the tensimetric results fully. Tensimetric studies show that only trimethylamine, of the bases studied, was strong enough to form a measurable complex in the gas phase. The large upfield shift of the B–methyl resonance in the 1:1 $Me_4B_2O \cdot NMe_3$ sample, as compared to the B–methyl resonance in the free Me_4B_2O, is consistent with the formation of a strong complex (15). The large downfield shift of the N–methyl resonance in the 1:1 $Me_4B_2O \cdot NMe_3$, as compared to the N–methyl resonance of free NMe_3 is also to be expected (16, 17). The lack of any change of chemical shift for all resonances in the samples involving dimethylether, dimethylsulfide, and trimethylboron indicate little or no complex formation, in accord with the results of the tensimetric studies. In the case of trimethylphosphine the small shifts of the P-methyl and B-methyl resonance are in accord with the weak complexing found in tensimetric work.

It is feasible to discuss these results in terms of the boron–oxygen bond, presuming that two competitive effects are involved. Purely inductive effects would be expected to increase the acceptor strength of the boron atoms relative to trimethylboron, oxygen being more electronegative than CH_3; this effect would also increase the donor strength of the oxygen atom relative to dimethylether, since $B(CH_3)_2$ is more electropositive than CH_3. On the other hand the effect of π-bonding involving oxygen lone pairs and the vacant boron 2p orbitals would be to weaken both the Lewis acidity of boron and the Lewis basicity of oxygen.

Nuclear magnetic resonance studies of hindered rotation in dimethylmethoxyboron and dimethylboric anhydride indicate a significant amount of π-bonding in these compounds (21). It is, therefore, reasonable to attribute the lower Lewis acidity of dimethylboric anhydride to this effect. The lack of evidence for a 2:1 complex between trimethylamine and dimethylboric anhydride is not inconsistent with this interpretation. When one of the two boron atoms is "electronically saturated" due to complexing with trimethylamine, the vacant p orbital is no longer available to an oxygen lone pair. Therefore, the decreased delocalization of oxygen lone-pair electrons should increase the double bond character between oxygen and the remaining uncomplexed boron atom, thereby lowering the Lewis acidity towards excess trimethylamine.

Further studies involving variable temperature n.m.r. techniques which support the above interpretations are in progress and will shortly be completed.

Acknowledgments

This research was supported in part by the Defence Research Board of Canada, Grant num-

Can. J. Chem. Downloaded from www.nrcresearchpress.com by 210.87.254.6 on 09/05/12
For personal use only.

ber 9530-49. The authors wish to thank Dr. M. G. Hogben for information concerning the gas–liquid chromatography system, and Mr. Roger S. Gay for helpful discussion about the infrared data.

1. F. L. McKennon. Ph.D. Dissertation. University of Chicago, Chicago, Illinois. 1936.
2. A. B. Burg. J. Am. Chem. Soc. **52**, 2228 (1940).
3. J. Goubeau and R. Epple. Chem. Ber. **90**, 171 (1957).
4. J. Goubeau and H. Lehmann. Z. Anorg. Allgem. Chem. **322**, 224 (1963).
5. A. B. Burg and H. I. Schlesinger. J. Am. Chem. Soc. **59**, 780 (1937).
6. F. E. Brinckmann and F. G. A. Stone. J. Am. Chem. Soc. **82**, 6218 (1960).
7. W. Gerrard, E. F. Mooney, and R. G. Rees. J. Chem. Soc. 740 (1964).
8. R. Thomas and K. Eriks. Inorganic synthesis. Vol. IX. McGraw-Hill Book Co., Inc., New York. 1967. p. 59.
9. L. Gmelin. Handbook. Supplementary volume on boron. Verlag Chemie, GMBH Weinheim/Bergstrasse, Germany. 1954. p. 247.
10. A. Stock and F. Zeidler. Ber. **54**, 531 (1921).
11. J. G. Aston, M. L. Sagenkahn, G. J. Szasz, G. W. Moessen, and H. F. Zahr. J. Am. Chem. Soc. **66**, 1171 (1944).
12. R. Kennedy, M. Sagenkahn, and J. Aston. J. Am. Chem. Soc. **63**, 2267 (1941).
13. N. Davidson and H. C. Brown. J. Am. Chem. Soc. **64**, 316 (1942).
14. A. Stock. Chem. Ber. **50**, 156 (1917).
15. T. D. Coyle and F. G. A. Stone. J. Am. Chem. Soc. **83**, 4138 (1961).
16. C. W. Heitsch. Inorg. Chem. **4**, 1019 (1965).
17. J. M. Miller and M. Onyszchuk. Can. J. Chem. **42**, 1518 (1964).
18. E. W. Abel, W. Gerrard, and M. F. Lappert. J. Chem. Soc. 5051 (1957).
19. W. Gerrard, M. F. Lappert, and R. Shafferman. J. Chem. Soc. 3828 (1957).
20. K. Biemann. Mass spectrometry, organic chemical applications. McGraw-Hill Book Co., Inc., New York. 1962. p. 158.
21. G. F. Lanthier and W. A. G. Graham. Chem. Commun. 715 (1968).
22. W. J. Lehmann, C. O. Wilson, Jr., and I. Shapiro. J. Chem. Phys. **28**, 777 (1958).
23. D. Ulmschneider and J. Goubeau. Z. Physik. Chem. Frankfurt, **14**, 56 (1958).
24. W. J. Lehmann, C. O. Wilson, Jr., and I. Shapiro. J. Chem. Phys. **34**, 783 (1961).
25. W. Gerrard. The organic chemistry of boron. Academic Press, Inc., New York. 1967. p. 226.
26. E. W. Abel, W. Gerrard, and M. F. Lappert. J. Chem. Soc. 3833 (1957).
27. W. A. G. Graham and F. G. A. Stone. J. Inorg. Nucl. Chem. **3**, 164 (1956).
28. H. C. Brown, H. Bartholomay, Jr., and M. D. Taylor. J. Am. Chem. Soc. **66**, 435 (1944).
29. S. Sujishi. Ph.D. Thesis. Purdue University, Lafayette, Indiana. 1949.

Can. J. Chem. Downloaded from www.nrcresearchpress.com by 210.87.254.6 on 09/05/12
For personal use only.

A theory of circular dichroism

V. LAWETZ AND D. A. HUTCHINSON
Department of Chemistry, Queen's University, Kingston, Ontario

Received May 7, 1968

An expression for circular dichroism is derived by a method in which the radiation field, in addition to the molecules, is quantized. From the total scattering cross sections for right and for left circularly polarized photons, the respective absorption coefficients are determined. A formula for the circular dichroism is obtained from the difference between the absorption coefficients. The present result is in agreement with the semi-classical result of Condon, Altar, and Eyring.

Canadian Journal of Chemistry, 47, 577 (1969)

Can. J. Chem. Downloaded from www.nrcresearchpress.com by 210.87.254.105 on 09/05/12
For personal use only.

Introduction

The phenomenon of circular dichroism is a manifestation of the difference in absorption coefficients for left and right circularly polarized light. This difference is measured near an absorption peak in the spectrum of an optically active molecule (1). Usually electronic transitions are involved so that measurements are made in the visible or ultraviolet region.

The parameter used to express the extent of circular dichroism, analogous to the angle of rotation per unit length in optical rotation, is the ellipticity Ψ per unit path length. The ellipticity is defined by an angle whose tangent is the ratio of the minor to the major amplitude of the emergent light beam. From this definition, it can be shown that (2)

$$[1] \qquad \tan \Psi = \tanh \frac{\varepsilon_l - \varepsilon_r}{4} l$$

where ε_l and ε_r are the absorption coefficients for left and right circularly polarized light, respectively, and l is the path length. If, as is usually the case, the arguments in eq. [1] are small the circular dichroism is

$$[2] \qquad \Psi/l = (\varepsilon_l - \varepsilon_r)/4$$

Several authors (3–5) have discussed circular dichroism using classical theories; others (2, 6) have used the semiclassical approach in which the molecules are treated by quantum mechanics but the radiation is treated classically. Condon, Altar, and Eyring (6), used the latter approach and obtained the following expression for the ratio of the difference $\varepsilon_l - \varepsilon_r$ to the mean $\varepsilon = (\varepsilon_l + \varepsilon_r)/2$

$$[3] \qquad \frac{\varepsilon_l - \varepsilon_r}{\varepsilon} = \frac{2k}{mck_{ng}} \frac{\text{Im } \langle n|\hat{\boldsymbol{L}}|g\rangle \cdot \langle g|\hat{\boldsymbol{R}}|n\rangle)}{|\langle n|\hat{\boldsymbol{R}}|g\rangle|^2}$$

In this expression, m is the mass of an electron, c is the velocity of light, $\hbar\boldsymbol{k}$ is the momentum of a photon in the incident light beam and the term $\hbar ck_{ng}$ is the energy difference between an excited state $|n\rangle$ and the ground state $|g\rangle$ of the molecule. $\hat{\boldsymbol{L}}$ and $\hat{\boldsymbol{R}}$ are the angular momentum operator and the coordinate operator respectively.

Condon *et al.* (6) give expressions for both the optical rotation and circular dichroism; the expressions are valid for all frequencies of the incident light. Condon's results are obtained by an intuitive extension of the classical theory of light dispersion.

More recently a number of papers have appeared in which the problem of optical birefrigence is treated from a general point of view. Stephen (7) introduced the idea of treating double refraction as a scattering problem in quantum field theory; Stephen's approach used the Stokes operator and did not require the idea of refractive index. Hameka (8) used the Heitler–Ma (9) perturbation method to attack the problem. Atkins and Barron (10) gave a general discussion based on the *S*-matrix approach, the use of Stokes operators, and diagrammatic perturbation theory. Go (11, 12) extended the work of Stephen (7) and Hameka (8) to a situation where the orientational distribution of the solute molecules is arbitrary.

The point of view taken in this paper is more restricted. The method used is essentially that of an earlier paper (13) on optical rotation. For the problem of circular dichroism it yields the result in a fairly direct manner.

The model consists of a system sufficiently dilute so that multiple photon scattering processes are unimportant. In addition, the attenuation of a light beam, on passing through the system, is

Can. J. Chem. Downloaded from www.nrcresearchpress.com by 210.87.254.105 on 09/05/12
For personal use only.

taken to be a consequence only of scattering. From this idealized model it can be shown that the attenuation of intensity $I(\boldsymbol{k})$ of a light beam is given by

$$\frac{dI(\boldsymbol{k})}{dz} = -N\bar{\sigma}_T(\boldsymbol{k})I(\boldsymbol{k})$$

where N is the number of molecules per unit volume and $\bar{\sigma}_T(\boldsymbol{k})$ is the Euler angle average of the total photon scattering cross section $\sigma_T(\boldsymbol{k})$ of a molecule. Since the absorption coefficient $\varepsilon(\boldsymbol{k})$ is defined by

$$\frac{dI(\boldsymbol{k})}{dz} = -\varepsilon(\boldsymbol{k})I(\boldsymbol{k})$$

the result

$$[4] \qquad \varepsilon(\boldsymbol{k}) = N\bar{\sigma}_T(\boldsymbol{k})$$

follows immediately. Thus if the total scattering cross sections for right and left circularly polarized light are known, the respective absorption coefficients and the circular dichroism are readily obtained. A description of the method of calculation is given in the next section.

Calculations and Results

The circular dichroism is large when the frequency of the incident light is near an absorption frequency of the molecule. Thus if the theory of circular dichroism is to be developed by scattering theory, a resonance scattering description is required. As given by Dirac (14), the total scattering cross section for photons is

$$[5] \quad \sigma_T(\boldsymbol{k}) = 4\pi\left(\frac{2\pi}{\hbar c}\right)^2 \frac{b}{2}\frac{|\langle 0n|\,\hat{V}|\boldsymbol{k}g\rangle|^2}{(k - k_{ng} - a)^2 + (b/2)^2}$$

where $$a = (\hbar c)^{-2}\sum_r \int d\boldsymbol{k}'' \frac{|\langle 0n|\,\hat{V}|\boldsymbol{k}''r\rangle|^2}{k - k_{ng} - k''}$$

and $$\frac{b}{2} = \pi\sum_r\left(\frac{k'}{\hbar c}\right)^2 \int\int d\Omega|\langle 0n|\,\hat{V}|\boldsymbol{k}'r\rangle|^2$$

$$k' = k - k_{ng}$$

The kinetic energy of an incident photon is $\hbar ck$, $|0n\rangle$ represents an excited state of the molecule with no photons present, $|\boldsymbol{k}g\rangle$ describes the ground state of the molecule and a photon of momentum $\hbar\boldsymbol{k}$ and $|\boldsymbol{k}''r\rangle$ describes the r-th state of the molecule and a photon of momentum $\hbar\boldsymbol{k}''$. $\hat{V}$ is the interaction of the radiation field with an electron. The quantities a and $b/2$ are identified, respectively, with the level shift and the half-width of a transition.

The interaction potential, in terms of the photon creation operators $\hat{s}_\sigma(\boldsymbol{k})$ and annihilation operators $\hat{s}_\sigma\dagger(\boldsymbol{k})$, is (13)

$$[6] \quad \hat{V} = (\alpha^{\frac{1}{2}}\hbar/2\pi m)\sum_\sigma\sum_{\boldsymbol{k}} k^{-\frac{1}{2}}[\hat{s}_\sigma(\boldsymbol{k})e^{-i\boldsymbol{k}\cdot\hat{\boldsymbol{r}}}\hat{p}_\sigma\dagger + \hat{s}_\sigma\dagger(\boldsymbol{k})e^{i\boldsymbol{k}\cdot\hat{\boldsymbol{r}}}\hat{p}_\sigma]\rho_\sigma{}^{-\frac{1}{2}}(\boldsymbol{k})$$
$$+ (\alpha\hbar^2/8\pi^2 m)\sum_\sigma\sum_{\boldsymbol{k}}\sum_{\sigma'}\sum_{\boldsymbol{k}'} k^{-\frac{1}{2}}k'^{-\frac{1}{2}}[\hat{s}_\sigma(\boldsymbol{k})e^{-i\boldsymbol{k}\cdot\hat{\boldsymbol{r}}}\hat{s}_{\sigma'}(\boldsymbol{k}')e^{-i\boldsymbol{k}'\cdot\hat{\boldsymbol{r}}}\boldsymbol{e}_\sigma\cdot\boldsymbol{e}_{\sigma'}$$
$$+ \hat{s}_\sigma(\boldsymbol{k})e^{-i\boldsymbol{k}\cdot\hat{\boldsymbol{r}}}\hat{s}_{\sigma'}\dagger(\boldsymbol{k}')e^{i\boldsymbol{k}'\cdot\hat{\boldsymbol{r}}}\boldsymbol{e}_\sigma\cdot\boldsymbol{e}_{\sigma'}{}^* + \hat{s}_\sigma\dagger(\boldsymbol{k})e^{i\boldsymbol{k}\cdot\hat{\boldsymbol{r}}}\hat{s}_{\sigma'}(\boldsymbol{k}')e^{-i\boldsymbol{k}'\cdot\hat{\boldsymbol{r}}}\boldsymbol{e}_\sigma{}^*\cdot\boldsymbol{e}_{\sigma'}$$
$$+ \hat{s}_\sigma\dagger(\boldsymbol{k})e^{i\boldsymbol{k}\cdot\hat{\boldsymbol{r}}}\hat{s}_{\sigma'}\dagger(\boldsymbol{k}')e^{i\boldsymbol{k}'\cdot\hat{\boldsymbol{r}}}\boldsymbol{e}_\sigma{}^*\cdot\boldsymbol{e}_{\sigma'}{}^*]\rho_\sigma{}^{-\frac{1}{2}}(\boldsymbol{k})\rho_{\sigma'}{}^{-\frac{1}{2}}(\boldsymbol{k}')$$

In the above, $\alpha = e^2/\hbar c$ is the fine structure constant and $\rho(\boldsymbol{k})$ is the density of states function used in replacing an integration by a summation in the description of the radiation field. The $\boldsymbol{e}_\sigma$ are unit vectors describing the states of polarization: $\boldsymbol{e}_+ = 2^{-\frac{1}{2}}(\boldsymbol{e}_1 - i\boldsymbol{e}_2)$ for left circularly polarized light and $\boldsymbol{e}_- = 2^{-\frac{1}{2}}(\boldsymbol{e}_1 + i\boldsymbol{e}_2)$ for right circularly polarized light. The unit vectors $\boldsymbol{e}_1$, $\boldsymbol{e}_2$, and the propagation vector $\boldsymbol{k}$ form a right-handed cartesian system. The quantities a and $b/2$ can be treated as constants as they both involve integration over all photon states. Therefore only the term $|\langle 0n|\,\hat{V}|\boldsymbol{k}g\rangle|^2$ is needed in order to show the difference between the absorption coefficients.

Due to the previous limitation to one photon processes, only the first two terms of $\hat{V}$ are retained. Firstly consider

$$\langle 0n|\,\hat{V}|\boldsymbol{k}g\rangle = (\alpha^{\frac{1}{2}}\hbar/2\pi mk)^{\frac{1}{2}}\langle n|e^{i\boldsymbol{k}\cdot\hat{\boldsymbol{r}}}\hat{p}_\sigma|g\rangle$$

Now $e^{i\boldsymbol{k}\cdot\hat{\boldsymbol{r}}}$ is approximated to $\hat{\mathbf{1}} + i\boldsymbol{k}\cdot\hat{\boldsymbol{r}}$, then

$$[7] \qquad \langle 0n|\,\hat{V}|\boldsymbol{k}g\rangle = (\alpha/k)^{\frac{1}{2}}(\hbar/2\pi m)(\langle n|\hat{p}_\sigma|g\rangle + i\langle n|\boldsymbol{k}\cdot\hat{\boldsymbol{r}}\hat{p}_\sigma|g\rangle)$$

Hence

$$[8] \qquad |\langle 0n|\,\hat{V}|\boldsymbol{k}g\rangle|^2 = (\alpha/k)(\hbar/2\pi m)^2[|\langle n|\hat{p}_\sigma|g\rangle|^2 - 2\,\mathrm{Im}\,(\langle n|\boldsymbol{k}\cdot\hat{\boldsymbol{r}}\hat{p}_\sigma|g\rangle\langle g|\hat{p}_\sigma\dagger|n\rangle)]$$

The square of the last term in eq. [7] is neglected in eq. [8] because it is an order of magnitude smaller than those which have been retained.

The method described by Hameka (15) is used to evaluate the quantities in eq. [8]. The result is

$$[9]\quad |\langle 0n|\hat{V}|kg\rangle|^2 = (\hbar c k_{ng}/2\pi)^2[k^{-1}|\langle n|\hat{x}_o|g\rangle|^2 - \mathrm{Im}\,(\langle n|\hat{x}_o\hat{x}_\sigma|g\rangle\langle g|\hat{x}_\sigma\dagger|n\rangle) \pm (mck_{ng})^{-1}\,\mathrm{Im}\,(\langle n|\hat{l}_\sigma|g\rangle\langle g|\hat{x}_\sigma\dagger|n\rangle)]$$

where in the last quantity the plus sign refers to a left circularly polarized incident light beam and the minus sign to a right circularly polarized incident light beam. $\hat{l}_\sigma$ is the σ-component of the orbital angular momentum operator $\hat{\mathbf{l}}$ and $\hat{x}_\sigma$ is the σ-component of the coordinate operator $\hat{r}$. The o-component of a vector operator is parallel to the propagation vector $\boldsymbol{k}$ of the incident light.

An Euler angle average is calculated for all of the terms in eq. [9] in order to account for the different orientations of the molecule. The required formulae for determining the Euler angle averages are

$$(a_\pm b_\mp)_{\mathrm{avg}} = (\boldsymbol{a}\cdot\boldsymbol{b})/3$$

$$(a_+ b_- c_o)_{\mathrm{avg}} = -i(\boldsymbol{a}\times\boldsymbol{b})\cdot\boldsymbol{c}/6$$

where $\boldsymbol{a}$, $\boldsymbol{b}$, $\boldsymbol{c}$ are any three vectors. If two or more of the vectors $\boldsymbol{a}$, $\boldsymbol{b}$, $\boldsymbol{c}$ are identical, the scalar triple product vanishes. Thus the Euler angle average of the electric dipole – electric quadrupole term of eq. [9] vanishes. Thus the following results are obtained for the Euler angle average of the total scattering cross sections from eq. [9]

$$[10]\quad \bar{\sigma}_T(\boldsymbol{k},\pm) = \frac{(4\pi\alpha k_{ng}/3)(b/2)}{(k-k_{ng}-a)^2+b/2)^2}\,[(k_{ng}/k)|\langle n|\hat{\mathbf{R}}|g\rangle|^2 \pm (mc)^{-1}\,\mathrm{Im}\,(\langle n|\hat{\mathbf{L}}|g\rangle\cdot\langle g|\hat{\mathbf{R}}|n\rangle)]$$

In eq. [10], capital letters are used for the operators to indicate that the matrix elements of their components are evaluated with respect to a coordinate system fixed in the molecule.

From eqs. [4] and [10], the circular dichroism is

$$[11]\quad \frac{\Psi}{l} = \frac{2\pi N\alpha k_{ng}}{3mc}\,\frac{b}{2}\,\frac{\mathrm{Im}\,(\langle n|\hat{\mathbf{L}}|g\rangle\cdot\langle g|\hat{\mathbf{R}}|n\rangle)}{(k-k_{ng}-a)^2+(b/2)^2}$$

The results of Condon, Altar, and Eyring (6), eq. [3], follow in a similar way. If Condon's (2) expression for the circular dichroism, which is applicable for all frequencies, is restricted to frequencies near resonance it reduces to eq. [11]. This, along with the rederivation of Condon, Altar, and Eyring's result, suggests that the method of this paper is valid in so far as it goes.

Acknowledgments

One of the authors (V.L.) gratefully acknowledges the financial support provided him by a Province of Ontario Graduate Fellowship award; the other (D.A.H.) acknowledges the National Research Council of Canada for an operating grant.

1. A. Abu-Shumays and J. J. Duffield. Anal. Chem. **38**, 29A (1966).
2. E. U. Condon. Rev. Mod. Phys. **9**, 432 (1937).
3. A. M. Cotton. Ann. Chim. et Phys. **8**, 347 (1896).
4. P. Drude. Ann. Physik, **48**, 536 (1896).
5. J. Natanson. J. Phys. **8**, 321 (1909).
6. E. U. Condon, W. Altar, and H. Eyring. J. Chem. Phys. **5**, 753 (1937).
7. M. J. Stephen. Proc. Cambridge Phil. Soc. **54**, 81 (1958).
8. H. F. Hameka. Ann. Phys. **26**, 122 (1964).
9. W. Heitler and S. T. Ma. Proc. Roy. Irish Acad. Sect. B. **52**, 109 (1949).
10. P. W. Atkins and L. D. Barron. Proc. Roy. Soc. London, Ser. A, **304**, 303 (1968).
11. N. Go. J. Chem. Phys. **43**, 1275 (1965).
12. N. Go. J. Phys. Soc. Japan, **23**, 88 (1967).
13. D. A. Hutchinson. Can. J. Chem. **46**, 599 (1968).
14. P. A. M. Dirac. The principles of quantum mechanics. 4th ed. Oxford University Press, London. 1958. pp. 201–206; pp. 239–244.
15. H. F. Hameka. Advanced quantum chemistry. Addison-Wesley Publishing Co., Inc., Reading, Mass. 1965. pp. 123–124.

Can. J. Chem. Downloaded from www.nrcresearchpress.com by 210.87.254.105 on 09/05/12
For personal use only.

Heats of formation of RuO_4, RuO_4^{2-}, and related compounds[1]

E. E. Mercer and D. T. Farrar[2]
Department of Chemistry, University of South Carolina, Columbia, South Carolina 29208
Received June 25, 1968

The heat of reaction of ruthenium metal with bromine in basic solution, according to the equation

$$Ru(c) + 3Br_2(l) + 8OH^-(aq) = RuO_4^{2-}(aq) + 6Br^-(aq) + 4H_2O$$

has been measured calorimetrically. In addition, the heat of oxidation of barium ruthenate hydrate by sodium periodate to form RuO_4(aq) has been determined. From these heats of reaction, and several other heats measured here, the heats of formation of several ruthenium species have been calculated. The more important of these are: Na_2RuO_4(aq), $\Delta H_f = -224.1 \pm 0.8$; RuO_4^{2-}(aq), $\Delta H_f = -109.4 \pm 1.0$; RuO_4(aq), $\Delta H_f = -57.5 \pm 1.1$; RuO_4(l), $\Delta H_f = -57.0 \pm 1.1$ kcal/mole.

Canadian Journal of Chemistry, 47, 581 (1969)

Can. J. Chem. Downloaded from www.nrcresearchpress.com by 210.87.254.105 on 09/05/12
For personal use only.

There is a paucity of thermodynamic data on compounds of ruthenium. The heats of formation of only a few compounds have been reported. The heats of formation of RuO_2 and $RuCl_3$ have been determined. Several investigations have led to the heat of formation of RuO_4. In two of these (1–3), lengthy temperature extrapolations were required to obtain the heat of formation of the compound at 25°. This resulted in rather large limits of uncertainty. In the third investigation (4) the heat of formation was determined by measuring the heat of the reduction of RuO_4 by ammonia. A later paper (5) questioned the validity of the reported reaction products. In addition to the above enthalpy data, the potentials of three couples, Ru^{2+}–Ru^{3+} (6), $Ru(NH_3)_6^{2+}$–$Ru(NH_3)_6^{3+}$ (7), and RuO_4^{2-}–RuO_4^- (8) have been reported. The polarographic potential of the RuO_4^-–RuO_4 couple is also known (9).

The enthalpies of formation of aqueous species of ruthenium are extremely desirable, since so much of the chemistry of this element is performed in that medium. It is necessary to have a reliable enthalpy of formation of at least one well-characterized compound or ion, which can be related through chemical reactions to other aqueous species. Both RuO_2 and $RuCl_3$ are unsatisfactory compounds on this basis. For this reason we have made an independent determination of the heat of formation of RuO_4 and also that of RuO_4^{2-}.

Experimental

The Calorimeter

This has been described previously (10). To facilitate the complete removal of the ampul contents into the solution, 40 mesh silicon carbide was added on top of the solid sample in some cases. No heat effect was observed when ampuls containing only the silicon carbide were broken under normal reaction conditions. In all calorimetric runs a volume of 45.1 ml of solution was used. Electrical determinations of the energy equivalent were made in every run. In all cases, except the reaction of ruthenium with bromine, the electrical calibration was performed after the chemical reaction. Experimentally it was shown that the energy equivalent determined before and after the chemical reaction was the same within experimental accuracy.

Reagents

Bromine was obtained from Michigan Chemical Corporation with a stated purity of 100.0%. Sodium periodate, $NaIO_4$, was Baker and Adamson reagent grade. This was washed with dilute nitric acid and dried for 2 h at 105°. Titration with sodium thiosulfate of the iodine liberated in the reduction of the sodium periodate in acid solution gave an assay of 100.04%.

G. F. Smith reagent grade perchloric acid was used. All solutions were standardized with standard sodium hydroxide solution.

Sodium hydroxide solutions were made carbonate-free by dilution of a concentrated solution. In cases where barium ion would not interfere, a small amount of barium chloride was added to the solution of base. These solutions were filtered prior to use.

Ruthenium metal powder was obtained from K and K Laboratories with a purity of 99.9%. Some samples of this metal were reduced with hydrogen at 500° for 1–2 h prior to use. There was no observable difference in the heats measured in these runs.

Sodium ruthenate solutions were prepared from ruthenium chloride (Engelhard Industries). The ruthenium chloride was suspended in 1.0 *M* NaOH and bromine was added dropwise until the solid dissolved completely. The resulting ruthenate–perruthenate solution was filtered and 30% hydrogen peroxide was added

[1]This work was taken from the Ph.D. thesis of D. T. Farrar, University of South Carolina, and was supported by the U.S. Atomic Energy Commission, under Contract No. AT-(40-1)-3542.
[2]National Defense Fellow, 1964–1967.

Can. J. Chem. Downloaded from www.nrcresearchpress.com by 210.87.254.105 on 09/05/12
For personal use only.

dropwise. After reduction of the perruthenate to ruthenate was complete, the solution was heated to destroy excess hydrogen peroxide. The concentration and purity of the ruthenate solutions were determined spectrophotometrically. For a pure ruthenate solution the ratio of absorbance at 465 mμ to that at 385 mμ is 2.06 (11). In all solutions used this ratio was within 1% of the desired value. The absorbance at the isosbestic point, 415 mμ, was used to determine the total concentration.

$BaRuO_4 \cdot H_2O$ (12) was prepared by adding barium chloride solution slowly with stirring to the basic ruthenate solution described above. The red solid which separated from solution was separated by filtration and washed with 0.01 *M* NaOH. The solid was dried and stored in a vacuum desiccator with P_2O_5.

Anal. Calcd. for $BaRuO_4 \cdot H_2O$: 42.86% Ba, 31.54% Ru. Found: 43.2% Ba, 30.8% Ru.

Calorimetric Reactions

The key reaction in determining the heats of formation reported herein is that between bromine and ruthenium metal in an alkaline solution. An excess of ruthenium metal powder was suspended with rapid stirring in 0.97 *M* sodium hydroxide. A weighed sample of liquid bromine was sealed in the sample ampul. The chemical reaction was initiated by breaking the ampul to introduce the bromine into solution. The calorimeter was opened and an aliquot of the solution was removed for analysis, as soon as a sufficient drift line for extrapolation purposes had been recorded. The solution was analyzed spectrophotometrically for ruthenate, after centrifuging to remove excess ruthenium metal. The yield was calculated from the ruthenium analysis and the weight of bromine used.

Results

Several chemical reactions of ruthenium metal, to produce RuO_4(aq) under conditions attainable within the calorimeter, were investigated. Several attempts were also made to find reactions in which well characterized aqueous species could be reduced to the free metal. None of these resulted in reactions which met all of the criteria necessary to yield a useful heat of formation.

It was found, however, that the addition of Br_2(l) to a 1.0 *M* NaOH solution, in which finely divided ruthenium metal was suspended, produced a solution in which all of the metal oxidized was in the form of ruthenate ion. Unfortunately, the reaction was not quantitative. The yield, based on moles of bromine added, depended upon stirring speed, particle size, and the excess of ruthenium present. In the calorimetric runs the yield of ruthenate ranged from 21.5 to 43.8%. In trial runs performed in normal glassware the course of the reaction was followed visually. The solution first became green, the color of RuO_4^-. This changed within a few minutes to the red color of ruthenate ion. The spectrum of the solution, after removal of the excess metal, proved to be that of pure ruthenate within 10 min after initiating the reaction. The spectrum also revealed the absence of BrO^- ion, *only* when an excess of metal was present. On this basis, it was assumed that all bromine which did not oxidize ruthenium to ruthenate underwent disproportionation to BrO_3^- and Br^-. It would appear that the mechanism leading to the final reaction products is quite complicated. In Table I the heats of reaction observed, when Br_2(l) is added to the basic suspension of ruthenium metal, have been summarized. The yield was determined by spectrophotometric analysis of the solution, after centrifuging to remove the ruthenium metal, and is also given in Table I.

The following interpretation of this heat data has been made. Consider the reactions

$$[1] \quad Ru(c) + 3Br_2(l) + [a\text{NaOH}, b\text{H}_2\text{O}] = [\text{Na}_2\text{RuO}_4, 6\text{NaBr}, (a-8)\text{NaOH}, (b+4)\text{H}_2\text{O}]$$

$$[2] \quad 3Br_2(l) + [a\text{NaOH}, b\text{H}_2\text{O}] = [5\text{NaBr}, \text{NaBrO}_3, (a-6)\text{NaOH}, (b+3)\text{H}_2\text{O}]$$

in which the square brackets are used to indicate the composition of the solution. Both of these reactions are competing during the calorimetric run. The observed heat is therefore given by the expression

$$[3] \quad \Delta H_{\text{obs}}(\text{kcal/mole Br}_2) = \frac{\Delta H_1}{3} + \frac{f_D}{3}(\Delta H_2 - \Delta H_1)$$

where f_D is the fraction of Br_2 undergoing disproportionation and the number subscripts on ΔH refer to the number of the reaction equation.

The data in Table I was fit by the best least squares straight line. This is shown in Fig. 1. By equating the intercept of this line to $\Delta H_1/3$ and the slope to $(\Delta H_2 - \Delta H_1)/3$, we calculate $\Delta H_1 = -121.8 \pm 0.8$ kcal and $\Delta H_2 = -41.1 \pm 1.4$ kcal, which is in good agreement with the value of -41.0 kcal calculated from the National Bureau of Standards Tables (13). In the calculation the tabulated heats of formation at infinite dilution were used. This excellent agreement tends to substantiate the validity of reaction [2] as the competing side reaction.

The heats for the following reactions are necessary to complete the thermochemical cycle for

[4] $Na(c) + 1/2Br_2(l) + 1/6[Na_2RuO_4, (a - 8)NaOH, (b + 4)H_2O] = 1/6[Na_2RuO_4, 6NaBr, (a - 8)NaOH, (b + 4)H_2O]$

[5] $Na(c) + 1/8[(a - 8)NaOH, (b + 4)H_2O, Na_2RuO_4] = 1/2H_2(g) + 1/8[aNaOH, (b - 4)H_2O, Na_2RuO_4]$

[6] $H_2(g) + 1/2O_2(g) + 1/4[aNaOH, (b - 4)H_2O, Na_2RuO_4] = 1/4[aNaOH, bH_2O, Na_2RuO_4]$

TABLE I

Heat of reaction of Ru(c) with $Br_2(l)$ in 0.97 *M* NaOH at 25.00 °C

Weight $Br_2(l)$ (mg)	RuO_4^{2-} yield (%)	Heat evolved (cal)	$-\Delta H_{obs}$ (kcal/mole Br_2)
121.47	21.5	14.753	19.41
109.51	22.3	13.430	19.60
123.59	22.7	15.211	19.67
125.56	23.5	15.729	20.02
123.52	24.3	15.491	20.04
119.25	23.0	15.002	20.11
124.54	25.2	16.108	20.67
127.77	26.6	16.693	20.88
123.60	28.8	16.615	21.48
123.12	29.2	16.642	21.60
128.33	29.2	17.486	21.78
124.93	30.6	17.096	21.87
117.80	36.4	17.176	23.30
116.92	38.0	17.479	23.89
118.35	41.9	18.291	24.70
117.40	43.8	18.844	25.65

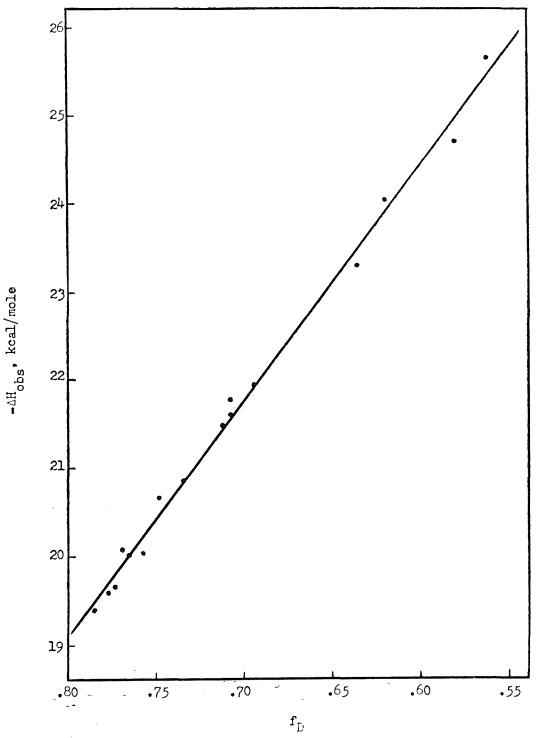

FIG. 1. The observed heat of reaction of bromine with ruthenium metal as a function of the reaction yield: f_D is the fraction of the bromine undergoing reaction [2], the line shown was calculated by least squares.

evaluation of the desired enthalpy of formation. The enthalpy changes for reactions [4] and [5] are the apparent heats of formation in the medium used. It was assumed that the heat of formation of NaBr(aq) in 0.97 *M* NaOH was not significantly different from that in 0.97 *M* NaBr. The heat of formation of water in the solution is not significantly different from that of pure water, −68.315 kcal/mole. The appropriate summation of reactions [1] and [4] through [6] leads to the equation

[7] $$Ru(c) + 2Na(c) + 2O_2(g) + [aNaOH, bH_2O] = [Na_2RuO_4, aNaOH, bH_2O]$$

$$\Delta H_7 = \Delta H_1 - \Delta 6H_4 + 8\Delta H_5 + 4\Delta H_6 = (-121.8) - 6(-86.67) + 8(43.63) + 4(-68.315)$$

$$= -224.1 \pm 0.8 \text{ kcal/mole}$$

ΔH_7 is the enthalpy of formation of sodium ruthenate in the basic solution. We estimate this formal enthalpy to be within a few tenths of a kcal of that at infinite dilution. Using the heat of formation of $Na^+(aq)$ at infinite dilution we calculate the heat of formation of $RuO_4^{2-}(aq)$ as −109.4 kcal/mole. Once again this is expected to be very close to the standard enthalpy of formation for ruthenate ion.

To obtain the heat of formation of $RuO_4(aq)$ a means of transferring ruthenate ion from basic solution to an acidic solution containing sodium periodate was necessary. For this purpose we chose to use $BaRuO_4 \cdot H_2O$. The addition of excess barium chloride dihydrate to a ruthenate solution causes the precipitation of this compound. Precipitation is incomplete under the conditions used in our calorimetric runs. Experimentally a solution of ruthenate was analyzed spectrophotometrically and an accurately measured volume (45.1 ml) was placed in the calorimeter. After adjusting the temperature to 25.00°

Can. J. Chem. Downloaded from www.nrcresearchpress.com by 210.87.254.105 on 09/05/12
For personal use only.

Can. J. Chem. Downloaded from www.nrcresearchpress.com by 210.87.254.105 on 09/05/12
For personal use only.

the ampul containing a weighed sample of $BaCl_2 \cdot 2H_2O$ was broken. Following the calorimetric run, an aliquot of the solution was filtered and its spectrum recorded. The number of moles of solid formed was calculated from the change in ruthenium concentration. The measured heats are summarized in Table II. In Table III is the heat of solution of $BaCl_2 \cdot 2H_2O$ in 0.97 *M* NaOH in the absence of ruthenate ion. The heat of precipitation of $BaRuO_4 \cdot H_2O$ was calculated by attributing the appropriate portion of the heat observed to the heat of solution of $BaCl_2 \cdot 2H_2O$ and the remainder of the heat to the reaction:

[8] $[Na_2RuO_4, a\text{NaOH}, (b + 2)H_2O, BaCl_2] = BaRuO_4 \cdot H_2O(c) + [2\text{NaCl}, a\text{NaOH}, (b + 1)H_2O]$

This is the enthalpy change shown in the last column of Table II.

TABLE II

Heat of precipitation of $BaRuO_4 \cdot H_2O(c)$ from sodium ruthenate in 0.97 *M* NaOH solution at 25.00 °C

Weight of $BaCl_2 \cdot 2H_2O$ (mg)	Heat absorbed (cal)	Moles $BaRuO_4 \cdot H_2O$ precipitated $\times 10^4$	$-\Delta H_8$ (kcal/mole)
107.93	0.862	2.51	3.72
110.30	0.952	2.38	3.72
108.60	0.930	2.32	3.78
113.20	1.052	2.30	3.62
110.91	0.826	2.77	3.68
110.48	0.850	2.69	3.67
		Average	3.70±0.04*

*Uncertainties cited in this and subsequent tables represent the average deviation, except where noted otherwise.

TABLE III

Heat of solution of $BaCl_2 \cdot 2H_2O$ in 0.97 *M* NaOH at 25.00 °C

Sample weight (mg)	Heat absorbed (cal)	ΔH_{10} (kcal/mole)
162.10	2.689	4.052
110.10	1.821	4.040
112.80	1.890	4.093
111.78	1.865	4.076
	Average	4.065±0.019

The conversion of the barium ruthenate into ruthenium tetroxide in aqueous solution was accomplished by dissolution of the compound in a solution which was 1.019 *M* $HClO_4$ and 0.100 *M* $NaIO_4$. These conditions were found to be the best for achieving a rapid reaction and avoiding formation of a barium iodate precipitate. The concentration of ruthenium tetroxide was measured spectrophotometrically, following each run. Under the conditions used the ruthenium tetroxide found was within 0.5% of the quantity of barium ruthenate which was dissolved. The reaction which takes place is

[9] $BaRuO_4 \cdot H_2O(c) + [c\text{HClO}_4, d\text{NaIO}_4, eH_2O] = [RuO_4, Ba(ClO_4)_2, (c - 2)\text{HClO}_4, \text{NaIO}_3, (d - 1)\text{NaIO}_4, (e + 1)H_2O]$

Because there is a possibility that the barium ruthenate is slightly contaminated by barium carbonate, the limits of error have been estimated to include any uncertainty arising from this impurity. The heats for the following additional reactions are needed to calculate the heat of formation of RuO_4 in this acidic solution

[10] $BaCl_2 \cdot 2H_2O(c) + [a\text{NaOH}, bH_2O, Na_2RuO_4] = [BaCl_2, a\text{NaOH}, (b + 2)H_2O, Na_2RuO_4]$

[11] $\text{Na(c)} + 1/2Cl_2(g) + 1/2[a\text{NaOH}, (b + 1)H_2O] = 1/2[2\text{NaCl}, a\text{NaOH}, (b + 1)H_2O]$

[12] $H_2(g) + 1/2O_2(g) + [a\text{NaOH}, bH_2O] = [a\text{NaOH}, (b + 1)H_2O]$

[13] $1/2H_2(g) + 1/2Cl_2(g) + 1/2[RuO_4, Ba(ClO_4)_2, (c - 2)\text{HClO}_4, (d - 1)\text{NaIO}_4, \text{NaIO}_3, (e + 1)H_2O] = 1/2[RuO_4, BaCl_2, c\text{HClO}_4, (d - 1)\text{NaIO}_4, \text{NaIO}_3, (e + 1)H_2O]$

[14] $BaCl_2 \cdot 2H_2O(c) + [RuO_4, c\text{HClO}_4, (d - 1)\text{NaIO}_4, \text{NaIO}_3, (e - 1)H_2O] = [RuO_4, BaCl_2, c\text{HClO}_4, (d - 1)\text{NaIO}_4, \text{NaIO}_3, (e + 1)H_2O]$

[15] $\text{NaIO}_4(c) + [RuO_4, c\text{HClO}_4, (d - 1)\text{NaIO}_4, \text{NaIO}_3, (e - 1)H_2O] = [RuO_4, c\text{HClO}_4, d\text{NaIO}_4, \text{NaIO}_3, (e - 1)H_2O]$

[16] $\text{NaIO}_3(c) + [RuO_4, d\text{NaIO}_4, c\text{HClO}_4, (e - 1)H_2O] = [RuO_4, c\text{HClO}_4, d\text{NaIO}_4, \text{NaIO}_3, (e - 1)H_2O]$

[17] $H_2(g) + 1/2O_2(g) + [RuO_4, c\text{HClO}_4, d\text{NaIO}_4, (e - 1)H_2O] = [RuO_4, c\text{HClO}_4, d\text{NaIO}_4, eH_2O]$

[18] $\text{Na(c)} + 1/2I_2(c) + 2O_2(g) = \text{NaIO}_4(c)$

[19] $\text{Na(c)} + 1/2I_2(c) + 3/2O_2(g) = \text{NaIO}_3(c)$

The appropriate sum of these equations gives the reaction

[20] $\mathrm{Ru(c)} + 2\mathrm{O_2(g)} + [c\mathrm{HClO_4}, d\mathrm{NaIO_4}, e\mathrm{H_2O}] = [\mathrm{RuO_4}, c\mathrm{HClO_4}, d\mathrm{NaIO_4}, e\mathrm{H_2O}]$

$$\Delta H_{20} = \Delta H_7 + \Delta H_8 + \Delta H_9 + \Delta H_{10} - 2\Delta H_{11} - \Delta H_{12} + 2\Delta H_{13} - \Delta H_{14} + \Delta H_{15} - \Delta H_{16} + \Delta H_{17} + \Delta H_{18} - \Delta H_{19}$$

TABLE IV

Heat of reaction of $BaRuO_4 \cdot H_2O$ with 0.100 *M* $NaIO_4$ in 1.019 *M* $HClO_4$ at 25.00 °C

Sample weight (mg)	Heat evolved (cal)	$-\Delta H_9$ (kcal/mole)
42.52	2.069	15.59
43.13	2.089	15.52
42.16	2.051	15.59
42.22	2.048	15.54
	Average	15.56±0.11*

*The uncertainty cited includes error due to the possible presence of barium carbonate impurity.

TABLE V

Heat of solution of $BaCl_2 \cdot 2H_2O$(c) in 0.100 *M* $NaIO_4$, 1.019 *M* $HClO_4$ solution at 25.00 °C

Sample weight (mg)	Heat absorbed (cal)	ΔH_{14} (kcal/mole)
110.30	2.011	4.454
110.42	2.036	4.504
110.37	2.017	4.464
110.30	2.020	4.474
	Average	4.474±0.016

TABLE VI

Heat of solution of $NaIO_4$(c) in solutions of $NaIO_4$ in 1.019 *M* $HClO_4$ at 25.00 °C

Sample weight (mg)	Initial $NaIO_4$ (*M*)	Heat evolved (cal)	ΔH_{16} (kcal/mole)
68.66	0.095	1.152	3.589
68.69	0.095	1.154	3.593
27.66	0.097	0.466	3.602
27.59	0.097	0.465	3.602
		Average	3.597±0.005

The enthalpy changes in reactions [12] and [17] were assumed to be equal to the heat of formation of pure water, −68.315 kcal/mole. The heats of reactions [9], [10], [14], [15], and [16] are closely approximated by the experimentally measured heats reported in Tables III to VII. The apparent heats of formation of sodium chloride and hydrochloric acid in the reaction media were calculated to be −97.52 and −39.34 kcal/mole, respectively. These calculations were made using the data from the National Bureau of Standards (13) using the same assumptions made above with sodium bromide. The heat of formation of $NaIO_4$(c) used was set equal to −105.15 kcal/mole, in accord with previous calorimetric studies in our laboratory (10). The enthalpy change of reaction [19] was calculated from tabulated data (13), using the heat of solution of $NaIO_3$(c) in water that was measured by Spencer and Hepler (14). Using these data the heat of formation of RuO_4 in 1 *M* $HClO_4$ is found to be −57.5 ± 1.1 kcal/mole.

TABLE VII

Heat of solution of $NaIO_3$(c) in 1.019 *M* $HClO_4$ at 25.00 °C

Sample weight (mg)	Heat absorbed (cal)	ΔH_{15} (kcal/mole)
89.63	2.171	4.793
89.89	2.179	4.797
89.34	2.162	4.789
	Average	4.793±0.003

The heat of solution of RuO_4(l) in 1 *M* $HClO_4$ was measured to obtain a heat of formation of the pure compound. Because the melting point of RuO_4 is 25.5° these calorimetric runs were made at 26° to be sure of the physical state of the compound. The results of these runs are given in Table VIII. The heat of formation of RuO_4(l) is thus found to be −57.0 ± 1.1 kcal/mole. The heat of formation of RuO_4(c) and RuO_4(g) were calculated from heats of vaporization and sublimation reported by Nikol'skii (15, 16). The heats of formation as determined in this work are summarized in Table IX.

TABLE VIII

Heat of solution of RuO_4(l) in 1.019 *M* $HClO_4$ at 26.00 °C

Sample (moles × 10^4)*	Heat evolved (cal)	$-\Delta H_{obs}$ (kcal/mole)
2.87	0.155	0.54
3.02	0.123	0.41
4.49	0.226	0.50
4.11	0.163	0.40
	Average	0.46±0.06

*Because RuO_4 is somewhat unstable, the size of the sample was calculated from the concentration of the solution, after completion of the calorimetric run. The weight of the sample was not determined.

Can. J. Chem. Downloaded from www.nrcresearchpress.com by 210.87.254.105 on 09/05/12
For personal use only.

TABLE IX

Heats of formation of some ruthenium compounds at 25 °C

Substance	ΔH_f (kcal/mole)
Na_2RuO_4(aq)	-224.1 ± 0.85
RuO_4^{2-}(aq)	-109.4 ± 1.0
$BaRuO_4\cdot H_2O$(c)	-309.8 ± 0.9
RuO_4(aq)	-57.5 ± 1.1
RuO_4(l)	-57.0 ± 1.1
RuO_4(c)	-59.6 ± 1.3
RuO_4(g)	-46.4 ± 1.4

Discussion

The heat of formation for ruthenium tetroxide reported here does not have as high a precision as we had initially hoped to obtain. The inability to find a "clean" reaction for the oxidation of the metal accounts for most of the uncertainty in the final number. The value we have determined is more negative by 2.0 kcal/mole than that obtained in the previous calorimetric work by Nikol'skii and Ryabov (4). The agreement with the value given by Bell and Tagami, however, is excellent (3).

The heat of formation of ruthenate ion is the first value of that quantity which has been reported. A comparison of the heat of formation of RuO_4^{2-}(aq) to that of other tetrahedral dinegative ions such as CrO_4^{2-}(aq), MoO_4^{2-}(aq), and WO_4^{2-}(aq), is initially somewhat surprising. For the Group VI transition elements the heats of formation of these ions are all more negative than -213 kcal/mole and become more negative with increasing atomic number. Heat of formation data for other MO_4^{2-} ions, where M is a transition metal, is presently unavailable. The free energy of formation of MnO_4^{2-}(aq) is given by Latimer (17) as -120.42 kcal/mole. By combining this with an estimated entropy of 4 cal deg^{-1} mole^{-1} for the ion, a value of -160 kcal/mole may be calculated for the heat of formation of manganate ion. Based on the chemical behavior of ferrate(VI) ion and the potential data of Grube and Gmelin (18) obtained in 40% sodium hydroxide, a lower limit of the heat of formation of this ion may be estimated to be -100 kcal/mole. Admittedly these numbers are very crude estimates, but they are sufficient to establish a definite trend, and make the measured value for ruthenate ion seem quite reasonable.

1. H. Schafer, G. Schneidereit, and W. Gerhardt. Z. Anorg. Allgem. Chem. **319**, 327 (1963).
2. H. Schafer, A. Tebben, and W. Gerhardt. Z. Anorg. Allgem. Chem. **321**, 41 (1963).
3. W. E. Bell and M. Tagami. J. Phys. Chem. **67**, 2432 (1963).
4. A. B. Nikol'skii and A. N. Ryabov. Zh. Neorgan. Khim. **9**, 3 (1964).
5. G. W. Watt and W. G. McMordie. J. Inorg. Nucl. Chem. **27**, 262 (1955).
6. R. R. Buckley and E. E. Mercer. J. Phys. Chem. **70**, 3102 (1966).
7. J. F. Endicott and H. Taube. Inorg. Chem. **4**, 437 (1965).
8. R. E. Connick and C. R. Hurley. J. Am. Chem. Soc. **74**, 5012 (1952).
9. M. D. Silverman and H. A. Levy. J. Am. Chem. Soc. **76**, 3319 (1954).
10. E. E. Mercer and D. T. Farrar. Can. J. Chem. **46**, 2679 (1968).
11. J. L. Woodhead and J. M. Fletcher. J. Chem. Soc. 5039 (1961).
12. H. Debray and A. Joly. Compt. Rend. **106**, 1499 (1888).
13. *a*. U.S. Natl. Bur. Stds. Tech. Note 270–3 (1968). *b*. U.S. Natl. Bur. Stds. Circ. 500. 1952.
14. J. G. Spencer, Jr. and L. G. Hepler. J. Phys. Chem. **64**, 499 (1960).
15. A B. Nikol'skii. Zh. Neorgan. Khim. **8**, 1045 (1963).
16. A. B. Nikol'skii and A. N. Ryabov. Zh. Neorgan. Khim. **10**, 290 (1965).
17. W. M. Latimer. Oxidation potentials. 2nd ed. Prentice-Hall, Inc., New York. 1952.
18. G. Grube and H. Gmelin. Z. Electrochem. **26**, 416 (1920).

Can. J. Chem. Downloaded from www.nrcresearchpress.com by 210.87.254.105 on 09/05/12
For personal use only.

Can. J. Chem. Downloaded from www.nrcresearchpress.com by 210.87.254.42 on 09/05/12
For personal use only.

Effect of metal–oxygen bond on the sensitivity of atomic-absorption spectroscopic technique[1]

VEDULA S. SASTRI, CHUNI L. CHAKRABARTI[2], AND DOUGLAS E. WILLIS
Chemistry Department, Carleton University, Ottawa 1, Canada

Received July 4, 1968

Studies on sensitivity in atomic absorption spectroscopy of nickel, tin, titanium, zirconium, hafnium, niobium, and tantalum, as metallocenes and as simple salts or oxy-salts, have shown that the metal–oxygen bonded species in solution (as in the case of simple salts or oxy-salts or complexes with ligands having oxygen atom as the donor) contributes to the total amount of metal oxide in flames, and hence, depopulates the ground electronic state of the atom in flames. In the case of the metals which form oxides of high dissociation energy, sensitivity is enhanced if the metals in solution are not bonded to oxygen as in metallocenes or fluoro complexes. The importance of the dissociation equilibrium and the reduction equilibrium in populating the ground electronic state of the atom has been assessed, and an irregular correlation has been established of enhancement in sensitivity with the metal–oxygen dissociation energy.

Canadian Journal of Chemistry, **47**, 587 (1969)

Introduction

A flame is most commonly used for atomization of samples in atomic absorption spectroscopy. The number of free atoms that exist in the flame per unit time (1) is governed by three factors: (*a*) the solution flow rate into the flame; (*b*) the aspiration efficiency (2) of the aspirator–burner–flame combination; and (*c*) the fraction of the sample salt existing as atoms in flame gases. The latter fraction, called the atomization efficiency (3), is influenced by ionization, incomplete dissociation of the salts introduced, and compound formation of the atom of interest with flame gas products. The atomization efficiency for 22 elements in an acetylene–air flame has been measured by de Galan and Winefordner (4), and atomization problems have been studied by Willis (5). Also, the degree of dissociation of many elements in flames has been investigated (6–8). The depressing effect of phosphate and aluminium on calcium when present in the same solution and the absence of the depressing effect when calcium and phosphate or aluminium are introduced simultaneously but through separate atomizers in the flame shows the importance of the state of combination of the metal at the time of evaporation of the solvent (9). Amos and Willis (10), and also, Bond and O'Donnell (11) reported enhancement of the absorption signal of titanium, tantalum, hafnium, and zirconium, in the presence of fluoride ion as compared to the absorption signal of these elements in the absence of fluoride ion. The objective of the present work is to elucidate the role played by the metal–oxygen bonded species in the sensitivity of the atomic-absorption spectroscopic technique so that such knowledge can be used to enhance the sensitivity of this technique.

[1]Presented at the 51st Annual Conference and Exhibition of the Chemical Institute of Canada, Vancouver, British Columbia, June 2–6, 1968.

[2]All correspondence should be addressed to this author.

Theory

The chemistry of titanium, zirconium, hafnium, niobium, and tantalum shows that these elements exist in solution as oxy or hydroxy species (11–13). These elements also readily form complexes with ligands containing oxygen atom as the donor, and also form fluoro or oxo-fluoro complexes in highly acidic solution (13). Since the metal–oxygen bond energies for the oxides of these elements are high (ranging from 157 to 194 kcal $mole^{-1}$), poor sensitivities are obtained when simple hydrolyzed salts are used in atomic absorption spectroscopy. Free atoms are formed (9) in flames by thermal dissociation of the metal oxide and reduction of the oxide by carbonaceous flame gases. The dissociation energy of the oxide, and the temperature and the reducing nature of the flame, would determine the relative importance of the dissociation equilibrium and the reduction equilibrium. The various equilibria involved—starting from the dissolution of a sample in a solvent to the formation of atoms by thermal dissociation of the oxide and reduction of the oxide by carbonaceous flame gases are as follows. Hydrated metal ion in aqueous solution undergoing the hydrolysis reaction:

$$[1] \qquad M(H_2O)_x^{n+} \rightleftharpoons [M(OH)(H_2O)_{x-1}]^{(n-1)+}$$

Can. J. Chem. Downloaded from www.nrcresearchpress.com by 210.87.254.42 on 09/05/12
For personal use only.

[2] Vaporization of the solvent

Vaporization of the solute MX to form gaseous particles:

[3] $$MX(s) \rightleftharpoons MX(g)$$

The formation of the gaseous metal atoms from the gaseous solute:

[4] $$MX(g) \rightleftharpoons M(g) + X(g)$$

The reaction of the gaseous metal with oxygen in the flame to form the metal oxide:

[5] $$M(g) + O(g) \rightleftharpoons MO$$

The metal oxide undergoes reduction by carbonaceous material in the flame to form gaseous metal atoms:

[6] $$MO + C \rightleftharpoons M(g) + CO(g)$$

In the above equilibria, M stands for the metallic part; X stands for the non-metallic part including oxygen; O stands for oxygen; g stands for the gaseous state; and s stands for the solid state.

The reactions [2–6] are kinetically controlled in the sense that the efficiency of reaction [2] and the combined efficiency of reactions [3–6] to form free metal atoms will depend on the time taken for the particles to pass through the part of the flame traversed by the light beam. Hence, for the determination of elements which form refractory compounds, it was important to choose a flame which had both low burning velocity and high temperature. Such a flame was nitrous oxide – acetylene flame, which was used for titanium, zirconium, hafnium, niobium, and tantalum, whereas air–acetylene flame was used for tin and nickel.

Dissociation Equilibrium

It is well-known from the flame emission spectra (14–16) of tin, nickel, titanium, zirconium, hafnium, niobium, and tantalum, that when these elements are introduced into flames which are normally used, they form more or less refractory oxides, e.g., SnO, NiO, TiO, ZrO, HfO, NbO, and TaO. Pungor (17) and Pungor and Konkoly-Thege (18) confirmed that the same oxide (and in the case of some alkali metals, to some extent, the same hydroxide) is produced irrespective of the anion present. Molecular compounds and oxides other than monoxides can also be formed but only monoxides will be considered here for the sake of simplicity. The concentration of atoms, under normal circumstances, is determined by the degree of dissociation of the molecular compounds, introduced or formed in the flame (19). The degree of dissociation of several oxides (BaO, AlO, TiO) in flames normally used is extremely small (7, 15–17, 19). The dissociation constants are computed as follows:

For the dissociation equilibrium

[7] $$XY \rightleftharpoons X + Y$$

of a diatomic molecule XY the dissociation constant K_n is defined as

[8] $$K_n = \frac{[X][Y]}{[XY]}$$

where all concentrations are expressed as number per cm^3. K_n is computed (20) from the equation:

[9] $$\log K_n = 20.432 + \frac{3}{2}\log\frac{M_x M_y}{M_{xy}} + \log Z_x Z_y + \log B - \log g + \frac{1}{2}\log T + \log\left(1-10^{-0.625\omega/T}\right) - \frac{5040}{T}V_d$$

where M is the molecular weight; Z is the partition function; B is the rotational constant; g is the statistical weight of XY; T is the absolute temperature; ω is the vibrational constant; and V_d is the dissociation energy. It is assumed that only the lowest electronic level contributes substantially to the partition function of the molecule XY and that the excited electronic states of XY do not contribute to its electronic partition function.

Equation [9] shows that K_n is dependent exponentially on both the dissociation energy and the temperature.

Experimental

Reagents

Reagents used were analytical-reagent grade: nickel(ous) chloride, stannic chloride, titanium oxy-oxalate, zirconium oxy-chloride, hafnium oxy-chloride, niobium oxalate, tantalum oxalate, cyclopentadienyl compounds of nickel, titanium, zirconium, hafnium, and in the case of tin, niobium, and tantalum, the compounds

TABLE I

Experimental conditions

Element and the line (Å)	Height above burner-top traversed by light-beam (cm)	Oxidant	Pressure of oxidant (p.s.i.)	Acetylene flow rate with aqueous solution (l/min)	Acetylene flow rate with organic solvents (l/min)	Flame temperature (°C)	Flame velocity (10) (cm s^{-1})	Burner type	Lamp current (mA)	Spectral width (Å)
Ni (2320)	0.2	Air	15	1.5	0.7	2100	160	*	8.0	1.7
Sn (2863)	0.2	Air	15	2.0	—	2100	160	*	10	3.3
Ti (3643)	0.2	Nitrous oxide	10	3.75	3.5	2955	180	†	20	3.3
Zr (3601)	0.2	”	10	3.75	3.5	2955	180	†	15	3.3
Hf (3073)	0.2	”	10	3.75	3.5	2955	180	†	15	3.3
Nb (4058)	0.2	”	10	3.5	—	2955	180	†	15	3.3
Ta (2714)	0.2	”	10	3.75	—	2955	180	†	15	3.3

*Techtron AB41 10 cm laminar flow burner (air–acetylene).
†Techtron AB40 5 cm laminar flow burner (nitrous oxide – acetylene).

TABLE II

Flow rates of solvents

Solvent	Flow rate of solvent with nitrous oxide – acetylene burner (ml/min)	Flow rate of solvent with air–acetylene burner (ml/min)
Distilled water	0.5	0.4
Distilled water containing 20% ethanol	0.5	Not used in this study
Methyl isobutyl ketone	1.2	”
Methanol	1.4	”
Ethanol	1.1	1.0
Acetylacetone	1.2	Not used in this study
Acetone	2.8	”

$Sn(CH_3)_2Cl_2$, $KNbF_6$, and $KTaF_6$, respectively. Other reagents included chemically pure acids, freshly distilled organic solvents, and doubly distilled water.

Apparatus

A Techtron AA-3 spectrophotometer was used with a meter readout and a Sargent recorder Model SRL. A Techtron 5 cm nitrous oxide – acetylene burner was used in the case of titanium, zirconium, hafnium, niobium, and tantalum. A Techtron 10 cm air–acetylene burner was used in the case of nickel and tin. Standard hollow cathode lamps were used for all the elements except nickel, for which a high-intensity hollow cathode lamp was used.

Experimental Conditions

Experimental details pertaining to the lines of the elements, the height above the burner-top traversed by the light beam, lamp current, spectral width, fuel flow rates, type of flame, and flame velocity are summarized in Table I. Table II shows the flow rates of the solvents at the constant flow rate of the aspirating gas (as shown in Table I). The nitrous oxide – acetylene flame had a feather 2 cm high without the samples (including the solvents).

Procedure for Solvent Extraction

(*a*) Titanium, which was present in aqueous solution containing an excess of cupferron, was extracted with an equal volume of methyl isobutyl ketone according to the procedure given by Furman *et al.* (21).

(*b*) Zirconium and hafnium, which were present singly in aqueous solution, were extracted with an equal volume of acetylacetone according to the procedure given by Stary (22).

Can. J. Chem. Downloaded from www.nrcresearchpress.com by 210.87.254.42 on 09/05/12
For personal use only.

TABLE III

Dissociation constants

Element and absorption line (Å)	Metal–oxygen bond energy (24–29) (kcal mole^{-1})	Atomizer-burner temperature (°C)	Dissociation constant K_n of metal oxides
Ni (2320)	<99	Premix 10 cm (Techtron) air–acetylene; 2100	3.7×10^{15}
Sn (2863)	125	"	1.7×10^{13}
Ti (3643)	157	Premix 5 cm (Techtron) nitrous oxide – acetylene; 2955	3.5×10^{14}
Zr (3601)	180	"	1.1×10^{13}
Hf (3073)	182	"	7.9×10^{12}
Nb (4058)	173	"	3.1×10^{13}
Ta (2714)	194	"	1.4×10^{12}

Results and Discussion

The optimum experimental conditions shown in Table I were established separately for each element. The absorbance produced under the optimum experimental conditions was the gross absorbance, from which the blank absorbance value for each solution nebulized was subtracted in order to arrive at the net absorbance, which was recorded.

Sensitivity (defined as the concentration in p.p.m./1 % absorption, obtained under optimized experimental conditions) has been shown in the Tables instead of absorbance values because sensitivity data offer direct comparison of the elements, whereas absorbance data have to be converted to the sensitivity data before comparison. The sensitivity data were calculated by extrapolation of the absorbance values obtained with the lowest concentrations of the elements. It was experimentally established for each element that the absorbance varied linearly with the concentration in the region of low absorbances.

In order to assess the contributions of the various equilibria to the total amount of the metal oxide introduced and formed in flames, and hence, to the sensitivity of the metals, absorption signals given by nickel, tin, titanium, zirconium, hafnium, niobium, and tantalum, present as different compounds (listed below) were studied. The compounds were: (*1*) cyclopentadienyl compounds in which the metal was not bonded to oxygen (23); (*2*) complexes containing ligands with oxygen atom as the donor; and (*3*) simple or oxy-salts. In the case of both (*2*) and (*3*) the metal was bonded to oxygen (12–13). Also, the effect of variation of other experimental parameters, e.g., solvents, and flow rates of fuels and oxidants were studied. In arriving at the net contribution of the metal–oxygen bonding (reaction [1]) to the sensitivity, the experimental conditions were so adjusted as to eliminate marked change in the flame caused by switching solvents. This was done in every case and the net effect of the metal–oxygen bonding on the sensitivity was assessed.

Table III shows the values of the dissociation constants calculated by means of eq. [9] and the dissociation energy of the metal oxide and the temperatures of the two flames. If one inserts into the dissociation constant expression (eq. [8]) the concentration of atomic oxygen 1×10^{17} (expressed as number per cm^3) found in slightly reducing air–acetylene flames (30–33) (similar to the air–acetylene flame used in this study), one obtains, as a rough estimate, the ratio, metal oxide/free metal atom, equal to 10^2/1 for the least refractory oxide, NiO. The concentration of atomic oxygen in the nitrous oxide – acetylene flame was not known, and so the ratio, metal oxide/free metal atom, in nitrous oxide – acetylene flame could not be estimated.

Reduction Equilibrium

The reaction $2C + O_2 \rightleftarrows 2CO$ releases 256 kcal mole^{-1} at 25 °C. One can make approximate

Can. J. Chem. Downloaded from www.nrcresearchpress.com by 210.87.254.42 on 09/05/12
For personal use only.

TABLE IV
Effect of variation of fuel flow rate

Flow rate of fuel (C_2H_2) (l/min)	Pressure of oxidant (N_2O) (p.s.i.)	Sensitivity (p.p.m./1% absorption)			
		$K_2TiO(C_2O_4)_2$ in aqueous solution	$(C_5H_5)_2TiCl_2$ in ethanol	$ZrOCl_2$ in aqueous solution	$(C_5H_5)_2ZrCl_2$ in aqueous solution
3.2	10	16.3	1.44	90	65
3.5	10	16.3	1.40	77	44
4.0	10	27.2	1.59	102	65
4.5	10	40.8	2.05	172	97

comparison of the free energies of formation of the oxides under standard conditions by using enthalpy change instead of free energy change in the thermodynamic relationship:

[10] $$\Delta G^0 = \Delta H^0 - T\Delta S^0$$

where ΔG^0 stands for free energy change; ΔH^0 stands for enthalpy change; ΔS^0 stands for entropy change; and T stands for absolute temperature.

The dissociation energy of almost all metal oxides is less than 200 kcal $mole^{-1}$. When both the metal and carbon compete for the oxygen in a flame, carbon should undergo the reaction $2C + O_2 \rightarrow 2CO$ in preference to the metal undergoing the reaction $2M + O_2 \rightarrow 2MO$. However, if one were to use rigorously eq. [10] by taking into account also the entropy change, carbon becomes an even better competitor than metal for the oxygen, as can be seen from reactions [11–13] below. Because of the favorable entropy change in the reaction:

[11] $$2MO(c) + C \rightarrow 2M\ (s\ or\ g) + CO_2$$

and particularly in the reaction:

[12] $$2MO(c) + 2C \rightarrow 2M\ (s\ or\ g) + 2CO$$

where (c) stands for crystalline solid, reduction with carbon becomes more and more favorable as the temperature of the flame is increased (34). If the temperature of the flame is less than the boiling point of the metal oxide, then the increase of entropy in the following reaction, [13], favors still more the reduction of the metal oxide by carbon, especially when the temperature of the flame is greater than the boiling point of the metal. Thus, at the boiling point of tin (2270 °C) the entropy for the reaction:

[13] $$2Sn + O_2 \rightarrow 2SnO\ (s)$$

decreases further, as the reaction now involves the ordering of three gaseous molecules into the solid oxide. Thus, at temperatures around 2000 °C carbon is thermodynamically capable of reducing almost all metal oxides (34). This is why a reducing flame not only greatly increases the sensitivity but is also essential even for detection of some of the elements that form refractory oxides. However, theoretical considerations given earlier have shown that high temperature and low burning velocity are also important; even the reduction process becomes more favorable at high temperature.

The effect of the reducing nature of the nitrous oxide – acetylene flame is shown in Table IV. Since the flame becomes stoichiometric (and hazardous) around the acetylene flow rate of 3.0 l/min (with the pressure of nitrous oxide held constant at 10 p.s.i.) the flow rate of acetylene was not decreased below 3.2 l/min. The Table shows moderate enhancement of sensitivity with increase of the acetylene flow rate from 3.2 l/min to 3.5 l/min; at the latter flow rate the flame had a feather 2 cm high. The sensitivity fell off with further increase in the flow rate of acetylene.

The contribution of the metal–oxygen bonding in the solution (reaction [1]) to the total amount of the metal oxide introduced and formed in the flame was assessed from Tables V–IX. It can be seen from these tables that the sensitivity was enhanced when the metals were present as metallocenes or fluoride complexes. This enhancement of sensitivity could not be accounted for by the increased flow rate of the solvents (see Table IX). Since the flow-rate of acetylene was adjusted (holding the flow rate of the oxidant constant) to eliminate any change in the flame caused by switching the solvents (see Table I), this enhancement could not be attributed to the temperature or the reducing nature of the flames. Such enhancements can be explained satisfactorily in the following way. In the case of the elements with

Can. J. Chem. Downloaded from www.nrcresearchpress.com by 210.87.254.42 on 09/05/12
For personal use only.

TABLE V
Sensitivity

Element and absorption line (Å)	Metal–oxygen bond energy (24–29) (kcal mole^{-1})	Sensitivity in p.p.m./1% absorption				Enhancement in sensitivity expressed as a ratio		
		Simple salt in aqueous solution	Metal complex with oxygen atom as the donor	Metal cyclopentadienyl compound		Metal complex/ simple salt	Metal cyclopentadienyl compound/ simple salt	Metal cyclopentadienyl compound/ metal complex
Ni (2320)	<99	0.13	—	0.11‖		—	1.18	—
Sn (2863)	125	11.2	—	8.7¶		—	1.29	—
Ti (3643)	157	16.0	16.9*	1.3‖	2.2‡	0.95	12.3; 7.3	13.0; 7.7
Zr (3601)	180	118	30†	51¶	17§	3.9	2.3; 7.0	1.8
Hf (3073)	182	146	49†	28‖	22§	3.0	5.2; 6.6	1.8; 2.2
Nb (4058)	173	225	—	126**		—	1.8	—
Ta (2714)	194	244.5	—	54**		—	4.5	—

*Titanium cupferrate in methyl isobutyl ketone.
†Zirconium and hafnium as acetylacetonates in acetylacetone.
‡$(C_5H_5)_2TiCl_2$ in methyl isobutyl ketone.
§$(C_5H_5)_2ZrCl_2$ and $(C_5H_5)_2HfCl_2$ in acetylacetone.
‖Metal–cyclopentadienyl compounds in ethanol.
¶Metal–cyclopentadienyl compounds in aqueous solutions.
**Metal–fluoro complexes in aqueous solutions.

high M—O bond energies and a great tendency to exist as oxo or hydroxo complexes in solution, or which form complexes with ligands having oxygen atom as the donor, the usual process of obtaining the elements or their compounds in aqueous solution or in organic solvents results in the M—O species being present in the solution (11–13). When such a solution is aspirated into a flame, the M—O species in the solution contributes greatly to the total amount of the metal oxide in the flame, and hence, reduces greatly the population of the free metal atoms in the flame. However, if the metal atoms can be present in the solution without being bonded to oxygen, as in metallocenes (23), then the total amount of the metal oxide is formed entirely in the flame as a result of the equilibrium (reaction [5]), and is thus much less than that present in the former case. That this hypothesis is, at least, qualitatively correct is borne out by the data of Tables V and IX, in which comparison has been made of the enhancement obtained with the metal present, as oxo or hydroxo complexes or as complexes having oxygen atom as the donor, and as metallocenes or fluoride complexes. The greatest enhancements were obtained when the metals were present as metallocenes or fluoride complexes. This hypothesis is further supported by the authors' work (35) on the nature of "chemical" interferences with the elements which form oxo or hydroxo species in solution; in the case of the element which forms with another element refractory compounds ("chemical" interference) when both are present in the same solution, the former bonded to oxygen as in oxo or hydroxo complexes, no interference was observed when the former was present as a metallocene in solution (absence of metal–oxygen bond).

Enhancement of sensitivity with metallocenes or fluoro-complexes would occur only with those metals for which the degree of atomization is very small at the flame temperature and the flame velocity, if simple salts or oxy-salts or complexes of the metals containing metal–oxygen bonds, are used. If the temperature of the flame is below the boiling point and the latent heat of vaporization of the solvent and the solute, and if the flame furnishes energy less than the dissociation energy of the metal oxide formed, then the degree of atomization will be very small. Thus, the dissociation of metal oxides having dissociation energy roughly over 130 kcal mole^{-1} will not be

Can. J. Chem. Downloaded from www.nrcresearchpress.com by 210.87.254.42 on 09/05/12
For personal use only.

TABLE VI

Effect of organic solvents on the sensitivity of titanium

Solvent	Sensitivity of $(C_5H_5)_2TiCl_2$ (p.p.m./1% absorption)	Sensitivity of $K_2TiO(C_2O_4)_2$ (p.p.m./1% absorption)	Flow rate of solvent (ml/min)	Flow rate of fuel C_2H_2 (l/min)	Pressure of oxidant N_2O (p.s.i.)
Distilled water		16	0.5	3.5	10
Distilled water containing 20% ethanol*	3.5	—	0.5	3.5	10
Methanol	1.7	—	1.4	3.2	10
Ethanol	1.3	—	1.1	3.2	10
Methyl isobutyl ketone	2.2	—	1.2	3.2	10
Acetone	2.8	—	2.8	3.2	10

*$(C_5H_5)_2TiCl_2$ was not soluble in water but soluble in ethanol, and was therefore dissolved in ethanol, and the solution diluted with distilled water to the maximum possible extent.

TABLE VII

Effect of organic solvents on the sensitivity of zirconium

Solvent	Sensitivity of $(C_5H_5)_2ZrCl_2$, (p.p.m./1% absorption)	Sensitivity of $ZrOCl_2$ (p.p.m./1% absorption)	Flow rate of solvent (ml/min)	Flow rate of fuel C_2H_2 (l/min)	Pressure of oxidant N_2O (p.s.i.)
Distilled water	51	118	0.5	3.75	10
Acetylacetone	30	—	1.2	3.50	10
Acetone	99	—	2.8	3.50	10
Methyl isobutyl ketone	85	—	1.2	3.50	10

complete in a flame which has a temperature of ~ 3000 °C. It is in the case of the metals which form oxides of high dissociation energy that the sensitivity can be enhanced if the metals are present as metallocenes or fluoro-complexes. The smaller the degree of atomization is, the greater would be the enhancement of sensitivity given by the metallocenes or fluoro-complexes as compared to simple salts or oxy-salts or complexes of the metals containing metal–oxygen bond. The dissociation process described earlier is an important part of the complex atomization process. In the case where the other factors of the atomization process have minor influence on the degree of atomization, there should exist a correlation between the dissociation energy of the oxide and the degree of atomization. However, the above assumption, and the picture of bonding in solution, and the molecular compounds formed in flames, although conceptually correct, is a vast over-simplification. In actual solutions, other species also may be formed. In actual flames, compounds other than oxides would also be formed, ionization at high temperature would not be negligible, etc., and all these equilibria would influence the degree of atomization. However, the experimental evidence shown in Table V points to a correlation (although an irregular one) between the dissociation energy of the oxide and the enhancement ratio; nickel and tin showing the smallest enhancement ratio, titanium, and tantalum showing the largest enhancement ratio.

Tables VI, VII, and VIII show the effect of organic solvents on titanium, zirconium, and hafnium. In many of these cases the enhancement in sensitivity given by an element used as a particular compound e.g., $(C_2H_5)_2TiCl_2$ in different solvents roughly parallels the flow rate of the solvents, the exceptions being acetone in Table VI, and methyl isobutyl ketone in Tables VI and VII, where a decrease in the sensitivity was noted. Besides, the flow rates of solvents there are other parameters, e.g., solution viscosity, surface tension, density, and volatility of the solution, which directly influence the aspiration efficiency and

Can. J. Chem. Downloaded from www.nrcresearchpress.com by 210.87.254.42 on 09/05/12
For personal use only.

TABLE VIII

Effect of organic solvents on the sensitivity of hafnium

Solvent	Sensitivity of $(C_5H_5)_2HfCl_2$ (p.p.m./1% absorption)	Sensitivity of $HfOCl_2$ (p.p.m./1% absorption)	Flow rate of solvent (ml/min)	Flow rate of fuel C_2H_2 (l/min)	Pressure of oxidant N_2O (p.s.i.)
Distilled water	—	146	0.5	3.75	10
Acetylacetone	22	—	1.2	3.50	10
Ethanol	28	—	1.1	3.50	10

TABLE IX

The enhancement ratios with the same solvents for both compounds

Element	Solvent	Observed enhancement ratio	Compounds compared
Sn	Aqueous solution	1.29	Sn : simple salt and $(CH_3)_2SnCl_2$
Ti	Methyl isobutyl ketone	7.7	Ti-cupferrate and $(C_5H_5)_2TiCl_2$
Zr	Acetylacetone	1.8	Zr-acetylacetonate and $(C_5H_5)_2ZrCl_2$
Zr	Aqueous solution	2.3	Zr-oxy salt and $(C_5H_5)_2ZrCl_2$
Hf	Acetylacetone	2.2	Hf-acetylacetonate and $(C_5H_5)_2HfCl_2$
Nb	Aqueous solution	1.8	Nb-oxalato complex and Nb-fluoro complex
Ta	Aqueous solution	4.5	Ta-oxalato complex and Ta-fluoro complex

thereby, also the atomization efficiency. This complex interrelationship of the parameters involved makes it difficult to isolate quantitatively the effect of one variable such as the flow rate of the solvent on the sensitivity.

Table IX shows the enhancement ratios (given in Table V) for the same element in two different compounds present in the same solvent. Because the same solvent was used the effect of the solvent was assumed to cancel out. The enhancement may be attributed to the fact that the metals in the form of cupferrate, acetylacetonate, simple or oxy-salts, are bonded to oxygen atom (i.e., the metal–oxygen bond is present in solution), whereas the metal–oxygen bond is absent in the solutions of metallocenes and fluoro-complexes. Such enhancements should be observable in the case of all metals which in aqueous solution exist as oxo and hydroxo complexes or which form complexes with ligands having oxygen atom as the donor, and which have high metal–oxygen bond energies, and also provided that the corresponding metallocenes are soluble in the solvents of interest.

Besides the physical properties of the solvents mentioned above, chemical reactions with the solvents, such as formation of solvates, alteration of the chemical equilibria in flames by products of combustion, etc. must also be taken into account. Organic solvents may also change slightly the temperature of the flame in spite of the measures taken in this study to keep the flame conditions constant (which was to decrease the acetylene flow rate to match the amount of organic solvents introduced into the flame). However, the enhancement ratios (see Table IX) obtained with the same solvent (either aqueous or organic) provide conclusive evidence that any change in the flame conditions caused by switching solvents under the experimental conditions maintained could have only a minor effect on the sensitivity. Thus, the major cause for the enhancement effect must be the well-established fact (12, 13, 23) that when the metals were present as metallocenes or fluoro-complexes in aqueous or organic solvents there was no metal–oxygen bond present in the solutions, whereas when the metals were present as oxo or hydroxo complexes or as complexes with ligands with oxygen atom as the donor there was metal–oxygen bond in solution.

An alternative interpretation has been suggested by a referee. The alternative interpretation is given in this paragraph and is followed by the authors' comments given in the next paragraph. In this interpretation, the reactions involved in the mechanism of atomization can be divided into the rate-controlled processes and the equilibrium-

Can. J. Chem. Downloaded from www.nrcresearchpress.com by 210.87.254.42 on 09/05/12
For personal use only.

Can. J. Chem. Downloaded from www.nrcresearchpress.com by 210.87.254.42 on 09/05/12
For personal use only.

controlled processes. The rate-controlled processes are the processes of solvent dispersion, solvent evaporation, and solute volatilization—the last is also the most important process. The process of solute volatilization is dependent on the form of the metal compound introduced into the flame. Therefore, the differences between M—O bonded species and M—X bonded species, could be the effect on solute volatilization rather than the effect on dissociation equilibrium, i.e. nonvolatile solutes could be formed.

The alternative interpretation given in the above paragraph is applicable to cases when nonvolatile molecular compounds are formed, but is less satisfactory in the cases of metallocenes and metal complexes dealt with in this paper. For example, the metal acetylacetonates and cupferrates are as readily volatilized as the metallocenes at the flame temperature used, but the cleavage of the bond in the vapor state occurs thus:

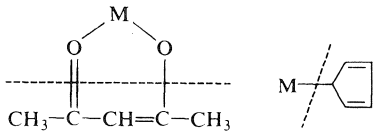

Metal acetylacetonate Metallocene

This is the reason why the metallocenes give a higher sensitivity compared to metal acetylacetonates and cupferrates. However, there is no conflict between these two interpretations—the difference is on the emphasis placed on different processes in the mechanism of atomization. The interpretation given in the body of the paper emphasizes the dissociation and reduction equilibria in the cases of the molecular compounds with high dissociation energy, where these equilibria are important; whereas the interpretation given in this paragraph emphasizes the rate of solute volatilization in the cases of nonvolatile molecular compounds, where the rate of volatilization is important. However, both the interpretations are extreme cases, and neither of them is applicable to all systems. In most cases, perhaps, the actual mechanism involves both in varying degrees, as has been separately reported by Chakrabarti *et al.* (36).

Conclusions

1. For the metals which form refractory oxides in flames, low sensitivities are obtained if the metals are used as simple or oxy-salts, or as complexes with ligands having oxygen atom as the donor, dissolved in aqueous or organic solvents; this is due to the presence of metal–oxygen bond in solution which adds to the metal oxides formed in flames.

2. In the case of the above metals, the sensitivities can be enhanced if the metal–oxygen bond in solution can be avoided or reduced by using metallocenes or fluoro-complexes in aqueous or organic solvents.

Acknowledgments

The authors are indebted to the National Research Council of Canada, and the Ontario Department of University Affairs, for research grants, and to the referee for the alternative interpretation.

1. M. L. Parsons and J. D. Winefordner. Appl. Spectry. **21**, 368 (1967).
2. J. D. Winefordner, C. T. Mansfield, and T. J. Vickers. Anal. Chem. **35**, 1607 (1963).
3. J. D. Winefordner and T. J. Vickers. Anal. Chem. **36**, 1939 (1964).
4. L. De Galan and J. D. Winefordner. J. Quant. Spectry. Radiative Transfer, **7**, 251 (1967).
5. J. B. Willis. Spectrochim. Acta, **23A**, 811 (1967).
6. F. W. Hoffmann and H. Kohn. J. Opt. Soc. Am. **51**, 512 (1961).
7. E. Hinnov and H. Kohn. J. Opt. Soc. Am. **47**, 156 (1957).
8. C. G. James and T. M. Sugden. Proc. Roy. Soc. London, Ser. A, **227**, 312 (1955).
9. R. Herrmann and C. T. J. Alkemade. Chemical analysis by flame photometry. *Translated by* P. T. Gilbert, Jr. Interscience Publishers, Inc., New York. 1963.
10. M. D. Amos and J. B. Willis. Spectrochim. Acta, **22**, 1325 (1966).
11. A. M. Bond and T. A. O'Donnell. Anal. Chem. **40**, 560 (1968).
12. A. Clearfield. Rev. Pure Appl. Chem. **14**, 91 (1964).
13. F. A. Cotton and G. Wilkinson. Advanced inorganic chemistry. 2nd ed. Interscience Publishers, Inc., New York. 1966. pp. 796–808, 913–930.
14. R. W. B. Pearse and A. G. Gaydon. The identification of molecular spectra. 3rd ed. Chapman and Hall, Ltd., London. 1963.
15. V. G. Alexseeva and S. L. Mandelshtam. Zh. Tekhn. Fiz. **17**, 765 (1947).
16. E. V. Vietz and L. V. Gurvitch. Opt. i Spektroskopiya, **1**, 22 (1956); Dokl. Akad. Nauk SSSR, **108**, 659 (1956).
17. E. Pungor. Flame photometry theory. *Translated and edited by* R. A. Chalmers. D. Van Nostrand Co., Ltd., New York. 1967. p. 140.
18. E. Pungor and I. Konkoly-Thege. Acta Chim. Acad. Sci. Hung. **11**, 23 (1957); Magy. Kem. Folyoirat, **62**, 17 (1956).
19. B. V. L'Vov. Spectrochim. Acta, **17**, 761 (1961).
20. P. W. J. M. Boumans. Theory of spectrochemical excitation. Hilger and Watts Ltd., London. 1966. p. 328.

21. N. H. FURMAN, W. B. MASON, and J. S. PEKOLA. Anal. Chem. **21**, 1325 (1949).
22. J. STARY. The solvent extraction of metal chelates. The Pergamon Press, Ltd., London. 1964. pp. 57, 60.
23. F. A. COTTON and G. WILKINSON. Advanced inorganic chemistry. 2nd ed. Interscience Publishers, Inc., New York. 1966. pp. 761–775.
24. T. L. COTTRELL. The strengths of chemical bonds. 2nd ed. Butterworths Scientific Publications, London. 1958. p. 280.
25. L. BREWER. Univ. Calif. Radiation Lab. Rept. 8356 (1958).
26. R. MAVRODINEAU and H. BOITEUX. Flame spectroscopy. John Wiley and Sons, Inc., New York. 1965.
27. L. L. AMES. Ph.D. Thesis, Ohio State University, Columbus, Ohio, 1965.
28. V. A. FASSEL and D. W. GOLIGHTLY. Anal. Chem. **39**, 466 (1967).
29. P. W. J. M. BOUMANS. Theory of spectrochemical excitation. Hilger and Watts Ltd., London. 1966. p. 326.
30. R. MAVRODINEAU and H. BOITEUX. Flame spectroscopy. John Wiley and Sons, Inc., New York. 1965. pp. 536–537.
31. C. G. JAMES and T. M. SUGDEN. Nature, **175**, 252 (1955).
32. R. M. FRISTROM. 9th Symp. Comb. Cornell University, Ithaca. Academic Press, Inc., New York. 1963. p. 560.
33. M. A. A. CLYNE. 9th Symp. Comb. Cornell University, Ithaca. Academic Press, Inc., New York. 1963. p. 211.
34. C. S. G. PHILLIPS and R. J. P. WILLIAMS. Inorganic chemistry. Part I. Oxford University Press, New York and Oxford. 1965. pp. 242–245.
35. V. S. SASTRI, C. L. CHAKRABARTI, and D. E. WILLIS. Talanta. In press.
36. C. L. CHAKRABARTI and S. P. SINGHAL. Can. J. Chem. In press.

Can. J. Chem. Downloaded from www.nrcresearchpress.com by 210.87.254.42 on 09/05/12
For personal use only.

Spectrofluorometric studies. V. 1,2,4- and 1,3,5-Trifluorobenzene

G. P. SEMELUK, R. D. S. STEVENS, AND I. UNGER
Department of Chemistry, University of New Brunswick, Fredericton, New Brunswick

Received July 24, 1968

The variation of fluorescence yield as a function of exciting wavelength for the title compounds has been examined. 1,3,5-Trifluorobenzene shows a maximum in fluorescence yield at an exciting wavelength λ_{ex} = 2680 Å; for 1,2,3-trifluorobenzene, this maximum occurs near 2740 Å. Triplet yields for both molecules, based on the biacetyl sensitized emission technique, have been determined at various exciting wavelengths. The maximum triplet yield of 1,3,5-trifluorobenzene = 0.40 and occurs at λ_{ex} = 2640 Å, while that of 1,2,4-trifluorobenzene = 0.64 at λ_{ex} = 2780 Å. The triplet of the 1,2,4 isomer appears to lie below the triplet of *cis*-butene-2 and thus the olefin *cis–trans* isomerization technique cannot be used as a diagnostic for the triplet state of this molecule. The effect of two inert gases, cyclohexane and *cis*-butene-2, on both fluorescence and triplet yield has been studied.

Canadian Journal of Chemistry, 47, 597 (1969)

Can. J. Chem. Downloaded from www.nrcresearchpress.com by 210.87.254.6 on 09/05/12
For personal use only.

Introduction

Recently, Wilzbach, Harkness, and Kaplan (1) reported that benzene-1,3,5-d_3 irradiated at 2480 and 2537 Å in both liquid and gas phases undergoes intramolecular rearrangement. That benzene and benzene derivatives excited in the 2500 Å region undergo this type of reaction has been known for some time (2–5). There has been some speculation about a possible connection between quantum deficit $[1 - (\Phi_s + \Phi_T)]$ and quantum yield of intramolecular rearrangement (6). It has also been suggested that vibrational excitation in upper electronic states may play a role in this type of reaction (1). We have been quite interested in the above mentioned effect and have chosen the fluorinated benzenes as model compounds, for reasons given elsewhere (7). If any correlation is to be established between quantum deficit and/or extent of vibrational excitation, and phototransposition of ring carbon atoms, then obviously it will first be necessary to determine singlet and triplet yields of the molecules involved, and the dependence of these yields on exciting wavelength and pressure. 1,3,5-Trifluorobenzene (1,3,5-TFB) and 1,2,4-trifluorobenzene (1,2,4-TFB) are particularly interesting to study, since the former has D_{3h} symmetry while the latter possesses C_s symmetry. This paper presents a summary of a study of the type outlined above, carried out in the gas phase, for 1,3,5- and 1,2,4-TFB.

Experimental

The 1,2,4-TFB used was obtained from two sources, K and K Laboratories, Inc., and Peninsular Chemresearch Inc. The 1,2,4-TFB obtained from K and K Laboratories was purified by preparative vapor phase chromatography while the material obtained from Peninsular Chemresearch was found to be sufficiently pure to be used without further treatment. The 1,3,5-TFB was also obtained from Peninsular Chemresearch and found to be chromatographically pure. Biacetyl was obtained from the Aldrich Chemical Company and was purified by bulb-to-bulb distillation, and stored in a blackened bulb. Fluorometric grade benzene and cyclohexane obtained from the Hartman–Ledden Company were used without further purification. Similarly, Philips research grade *cis*-butene-2 having less than 0.1% impurity was used without further purification.

A grease and mercury free high vacuum line, equipped with Hoke packless metal diaphragm valves exclusively, was employed in this study. The pumping section of the high vacuum system was of conventional design.

Pressure measurements were carried out by means of a spiral gauge obtained from National Research Council (NRC) in Ottawa. Pressures below 5 Torr were obtained by expansion into an accurately calibrated volume. The cell used was a flow-through cuvette type, 1 cm × 1 cm × 4.5 cm, polished on all four sides, and was obtained from Aminco.

Mixing was accomplished by an all glass circulating pump obtained from NRC Ottawa. All emission measurements were performed on a modified Aminco–Bowman spectrofluorometer. Experimental details concerning the modification, light source, procedures of emission and absorption measurements have been given previously (7).

Singlet yields for directly excited fluorinated benzenes can be arrived at directly from fluorescence measurements. These molecules, however, do not exhibit any phosphorescence in the gas phase and thus indirect techniques must be used to estimate triplet yields. In the present instance, the biacetyl sensitized emission technique (8) was used to determine triplet yields. The quantum yields of fluorescence of TFB and of sensitized emission of Biacetyl (BiA) were obtained by a relative method, which has been described in detail elsewhere (9).

Results

A. 1,2,4-Trifluorobenzene

The absorption spectrum of 1,2,4-TFB taken

TABLE I

Fluorescent yield dependence on wavelength and pressure of 1,2,4-trifluorobenzene and biacetyl

Excitation wavelength (Å)	Pressure (Torr) BiA	Pressure (Torr) 1,2,4-TFB	Equation
2540	0	4.8–47.6	$1/\phi_f = 48.1+4.20\times10^3$[TFB]*$\pm 6.2\%$, max.$=12.2\%$
2540	0.1–20.7	31.3	$1/\phi_f = 46.2+2.17\times10^3$[BiA]*$\pm 1.8\%$, max.$=5.4\%$
2580	0	5.0–47.3	$1/\phi_f = 7.18+6.43\times10^3$[TFB]$\pm 14.0\%$, max.$=22.3\%$
2620	0	5.3–47.3	$1/\phi_f = 3.28+4.57\times10^3$[TFB]$\pm 14.0\%$, max.$=\pm 26.5\%$
2660	0	5.3–47.5	$1/\phi_f = 3.37+2.36\times10^3$[TFB]$\pm 7.9\%$, max.$=16\%$
2700	0	5.1–47.5	$1/\phi_f = 2.69+1.13\times10^3$[TFB]$\pm 1.4\%$, max.$=3.0\%$
2700	0.10–16.0	30.9	$1/\phi_f = 4.65+2.17\times10^3$[BiA]$\pm 2.2\%$, max.$=5.8\%$
2740	0	5.3–47.5	$1/\phi_f = 2.94+5.68\times10^2$[TFB]$\pm 0.7\%$, max.$=1.2\%$
2780	0	5.3–47.5	$1/\phi_f = 3.48+2.87\times10^2$[TFB]$\pm 1.9\%$, max.$=5\%$
2780	0.22–20.5	31.6	$1/\phi_f = 4.20+3.23\times10^3$[BiA]$\pm 1.5\%$, max.$=2.8\%$

*[TFB] and [BiA] represent the concentration, in moles per l, of 1,2,4-trifluorobenzene and biacetyl, respectively.

TABLE II

Effect of *cis*-butene-2 and cyclohexane on the fluorescent yield of 1,2,4-trifluorobenzene

Excitation wavelength (Å)	Pressure (Torr) 1,2,4-TFB	Pressure (Torr) *cis*-B-2	Pressure (Torr) CH	Fluorescent yield
2540	39.9	0	0–39.4	0.026 ± 0.0006
2540	40.1	0–48.5	0	0.026 ± 0.0008
2700	19.6	0	0–48.5	$0.23\ \pm0.004$
2700	20.1	0–48.4	0	$0.23\ \pm0.006$
2780	19.9	0	0–48.1	$0.22\ \pm0.004$
2780	19.9	0–48.3	0	$0.22\ \pm0.009$

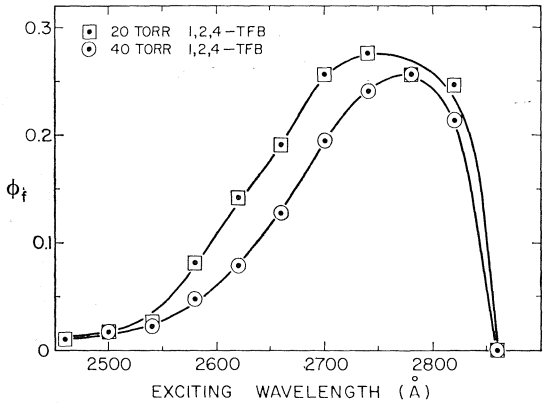

FIG. 1. Fluorescent yield ϕ_f of 1,2,4-trifluorobenzene as a function of exciting wavelength.

on a Coleman, Model EPS-3T Hitachi spectrophotometer shows that the molecule absorbs between 2800 and 2250 Å apparently into a closely spaced vibrational band system. The maximum fluorescence yield, ϕ_f, is produced by $\lambda_{ex} \simeq$ 2780 Å. Figure 1 shows how the fluorescence yield varies with the exciting wavelength. Fluorescence of 1,2,4-TFB is selfquenched at $\lambda_{ex} >$ 2540 Å and plots of I/ϕ_f versus [1,2,4-TFB] are linear. Plots of $1/\phi_f$ versus [BiA] at constant [1,2,4-TFB] are also linear. These quenching data are summarized in Table I. Addition of *cis*-butene-2 (*cis*-B-2) or cyclohexane (CH) to 1,2,4-TFB has no effect on the fluorescence yield, as is indicated in Table II.

The triplet yield of 1,2,4-TFB was examined at three exciting wavelengths 2540, 2700, and 2780 Å. Excitation at any of these wavelengths in the presence of BiA produces a sensitized emission of BiA. Additions of *cis*-B-2 to mixtures of BiA and 1,2,4-TFB have no significant effect on sensitized emission yield (Table III). On the other hand, addition of CH to mixtures of BiA and 1,2,4-TFB increases the sensitized emission yield. A satisfactory linear representation of this functional dependence is obtained when total pressure divided by sensitized emission yield is plotted against cyclohexane pressure, as illustrated in Fig. 2. At constant pressure of 1,2,4-TFB the

Can. J. Chem. Downloaded from www.nrcresearchpress.com by 210.87.254.6 on 09/05/12
For personal use only.

TABLE III

Effect of *cis*-butene-2 on the sensitized emission yield from mixtures of 1,2,4-trifluorobenzene and biacetyl

Excitation wavelength (Å)	Pressure (Torr) 1,2,4-TFB	BiA	*cis*-B-2	Sensitized emission yield
2540	30.2	10.1	0–49.6	0.053±0.003
2700	31.8	10.1	0–49.6	0.22 ±0.007
2780	31.0	11.0	0–49.9	0.22 ±0.02

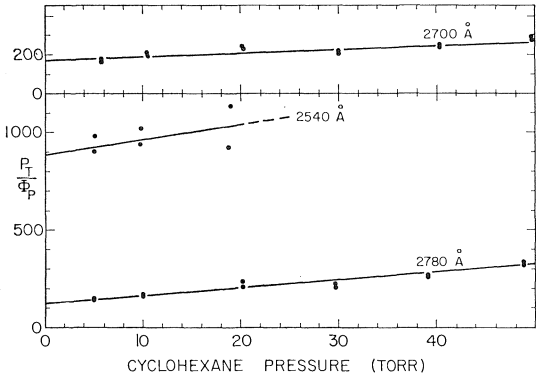

FIG. 2. Dependence of sensitized emission yield ϕ_P in mixtures of biacetyl and 1,2,4-trifluorobenzene on total pressure P_T, and cyclohexane pressure P_{CH} for some exciting wavelengths.

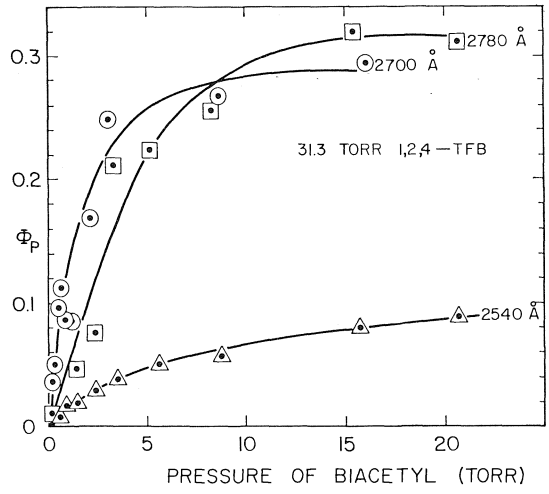

FIG. 3. Variation of sensitized emission yield ϕ_P as a function of biacetyl pressure at constant pressure of 1,2,4-trifluorobenzene.

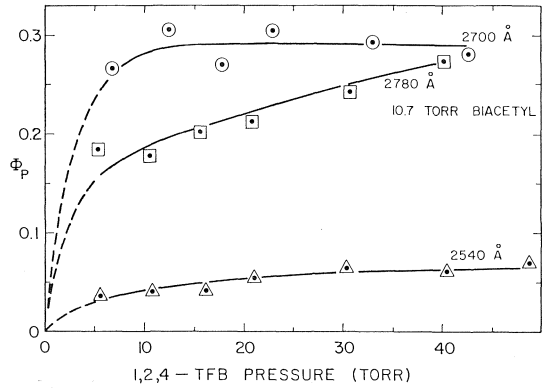

FIG. 4. Variation of sensitized emission yield ϕ_P as a function of 1,2,4-trifluorobenzene pressure at a constant biacetyl pressure of 10.7 Torr.

sensitized emission yield increases rapidly with increasing biacetyl pressure. It then levels off, but does not appear to go through a maximum for the exciting wavelengths examined. The same phenomenon is observed when the biacetyl pressure is held constant while the 1,2,4-TFB pressure is increased. These results are given in Figs. 3 and 4. The triplet yields at the highest biacetyl pressure used are 0.1 for λ_{ex} = 2540 Å, 0.44 at λ_{ex} = 2700 Å, and 0.64 at λ_{ex} = 2780 Å.

B. 1,3,5-Trifluorobenzene

The absorption spectrum of 1,3,5-TFB shows weak absorption ($\varepsilon \simeq 120$) in the 2700 to 2200 Å region, with a closely spaced (30 to 40 Å) vibration band system. Fluorescence resulting from excitation in the 2700–2200 Å region is very weak. In contrast to the behavior of the less highly fluorine-substituted benzenes, the fluorescent yield versus λ_{ex} curve shows only one structural feature, a maximum at 2680 Å (Fig. 5). The fluorescence excited at 2640 and 2680 Å is self-quenched, giving linear plots for $1/\phi_f$ vs. 1,3,5-TFB pressure (Fig. 6).

Because of the combination of very weak absorption with very weak fluorescence our experimental conditions did not allow a systematic

Can. J. Chem. Downloaded from www.nrcresearchpress.com by 210.87.254.6 on 09/05/12
For personal use only.

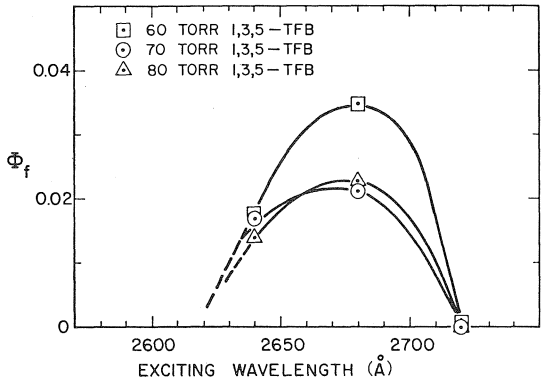

FIG. 5. Variation of fluorescent yield of 1,3,5-trifluorobenzene as a function of exciting wavelength for three different pressures.

investigation of the effect of biacetyl on the fluorescent yield. Thus, relatively large pressures of 1,3,5-TFB (50/100 Torr) must be used in order to obtain appreciable emission. This limited the maximum biacetyl pressure to about 8 Torr, since pressures in excess of this produced condensation on the cell windows.

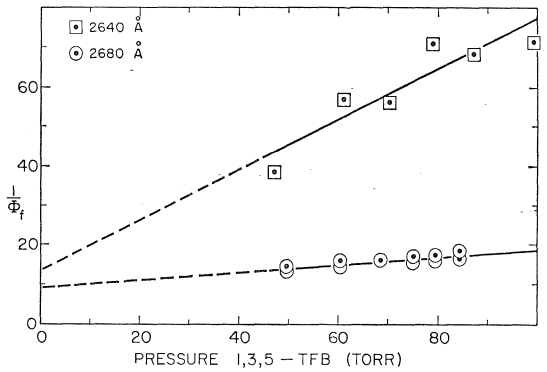

FIG. 6. Stern–Volmer type plots for 1,3,5-trifluorobenzene fluorescent yield at two wavelengths.

A series of experiments, however, did show that cyclohexane and *cis*-butene-2 were ineffective as quenchers of the fluorescence. The addition of up to 50 Torr cyclohexane to 81 Torr of 1,3,5-trifluorobenzene did not affect the fluorescent yield by more than 1%, while up to 60 Torr of *cis*-butene-2 added to 81 Torr of 1,3,5-TFB, did not alter the yield by more than 5%. Similarly, the addition of up to 28 Torr of cyclohexane to a mixture of 81 Torr 1,3,5-TFB and 8 Torr biacetyl did not change the yield by more than 1%.

TABLE IV

Effect of *cis*-butene-2 and cyclohexane on the triplet yield* of 1,3,5-trifluorobenzene

Pressure (Torr)				Sensitized emission yield
1,3,5-TFB	BiA	CH	*cis*-B-2	
88.8	10.1	0	9.95	0.14
88.8	10.1	0	20.0	0.12
88.8	10.1	0	29.9	0.11
88.8	10.1	0	39.9	0.07
88.8	10.1	0	49.9	0.08
81.0	8.17	0	0	0.33
81.0	8.17	4.50	0	0.32
81.0	8.17	9.60	0	0.32
81.0	8.17	14.5	0	0.36
81.0	8.17	19.4	0	0.35
81.0	8.17	23.8	0	0.35
81.0	8.17	28.8	0	0.35

*Exciting wavelength 2680 Å.

A sensitized emission of BiA is observed in mixtures of 1,3,5-TFB and BiA excited by 2640 and 2680 Å radiation. This sensitized emission rises rapidly with increasing BiA pressure, then appears to level off, but does not go through a maximum, presumably because the biacetyl pressure is limited experimentally to about 8 Torr. These data are summarized graphically in Fig. 7. The maximum triplet yield (uncorrected for biacetyl quenching of the singlet) under these experimental limitations is about 0.4, at λ_{ex} = 2640 Å.

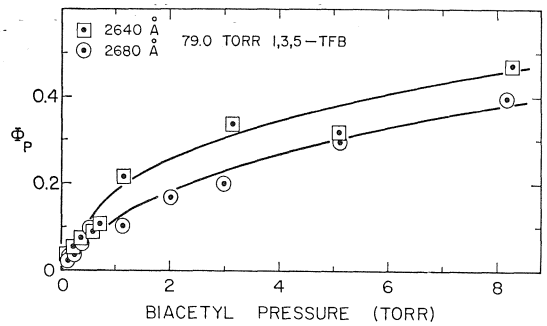

FIG. 7. Variation of sensitized emission yield ϕ_p for mixtures of 1,3,5-trifluorobenzene with biacetyl as a function of biacetyl pressure at two exciting wavelengths.

When excitation is at 2680 Å, increasing pressures of 1,3,5-TFB at constant biacetyl pressure produce a decrease in the triplet yield. The relationship is adequately summarized by the equation

$$\frac{1}{\phi_p} = 2.29 + 1.49 \times 10^2 P_{TFB}(\text{Torr})$$

Can. J. Chem. Downloaded from www.nrcresearchpress.com by 210.87.254.6 on 09/05/12
For personal use only.

TABLE V

Values of rate constants and quenching cross sections for 1,3,5- and 1,2,4-trifluorobenzene at various exciting wavelengths

Exciting wavelength (Å)	k_2 (s^{-1})	k_3 (s^{-1})	k_4 (l $mole^{-1}$ s^{-1})	TFB cross section (Å²)	k_7 (l $mole^{-1}$ s^{-1})	Biacetyl cross section (Å²)
			1,2,4-Trifluorobenzene			
2580	1.7×10^{8}	1.1×10^{9}	1.1×10^{12}	190		
2620	1.0×10^{8}	2.3×10^{8}	4.6×10^{11}	78		
2660	7.5×10^{7}	1.8×10^{8}	1.8×10^{11}	31		
2700	5.6×10^{7}	9.5×10^{7}	6.4×10^{10}	11	1.2×10^{11}	19
2740	5.2×10^{7}	1.0×10^{8}	3.0×10^{10}	5.1		
2780	5.7×10^{7}	1.4×10^{8}	1.6×10^{10}	2.8	1.8×10^{11}	28
2820	5.8×10^{7}	1.6×10^{8}	1.0×10^{10}	1.8		
			1,3,5-Trifluorobenzene			
2640	9.1×10^{7}	1.2×10^{9}	1.1×10^{12}	18		
2680	7.5×10^{7}	6.2×10^{8}	1.4×10^{11}	24		

where P_{TFB} refers to the pressure of 1,3,5-TFB. Addition of *cis*-butene-2 to mixtures of 1,3,5-TFB and BiA sharply reduces the triplet yield, while addition of cyclohexane to these mixtures slightly increases the yield (Table IV).

Discussion

In a previous communication from this laboratory (10) a mechanism for the photochemical reactions of monofluorobenzene was presented. The same mechanism, which appears to hold equally well for 1,2,4- and 1,3,5-trifluorobenzene, is presented below to make it easier for the reader to follow the discussion.

[1] $F + h\nu \rightarrow {}^1F^I$

[2] ${}^1F^I \rightarrow F + h\nu$

[3] ${}^1F^I (+ M) \rightarrow {}^3F^I (+ M)$

[4] ${}^1F^I + F \rightarrow 2F$

[5] ${}^1F^I \rightarrow$ isomerization

[6] ${}^3F^I (+ M) \rightarrow F (+ M)$

[7] ${}^1F^I + BiA \rightarrow {}^1BiA^{II} + F$

[8] ${}^3F^I + BiA \rightarrow {}^3BiA^{I*} + F$

[9] ${}^3BiA^{I*} \rightarrow$ dissociation

[10] ${}^3BiA^{I*} + M \rightarrow {}^3BiA^I + M$

[11] ${}^1BiA^{II} \rightarrow$ dissociation

[12] ${}^1BiA^{II} + M \rightarrow {}^1BiA^I + M$

[13] ${}^1BiA^I \rightarrow {}^3BiA^I$

[14] ${}^1BiA^I \rightarrow BiA + h\nu_f$

[15] ${}^3BiA^I \rightarrow BiA + h\nu_p$

[16] ${}^3BiA^I \rightarrow BiA$

[17] ${}^3F^I \rightarrow$ isomerization

In the scheme shown above, F represents either a 1,3,5- or 1,2,4-TFB molecule in its ground state. BiA denotes ground state biacetyl. The Arabic numerals indicate spin multiplicity while the Roman numerals denote first and second excited states. M represents any quenching molecule, and the asterisk denotes a vibrationally excited molecule. Quenching of ${}^3BiA^I$ by BiA has been omitted from this scheme, even though recently it has been shown to occur (11), since the rate constant for this step is very small.

Application of steady state treatment to the mechanism gives for the fluorescent yield ϕ_f

$$[18] \quad \frac{1}{\phi_f} = \frac{k_2 + k_3 + k_5}{k_2} + \frac{k_4[F]}{k_2} + \frac{k_7[BiA]}{k_2}$$

Equation [18] predicts that plots of $1/\phi_f$ versus [F] at zero [BiA] should be linear and that plots of $1/\phi_f$ versus [BiA] at constant [F] should also be linear. This is observed experimentally, as indicated in Fig. 2 and Table I.

The integrated molar absorptivities of both 1,2,4- and 1,3,5-TFB have been given (12). These values were used to determine τ_0, the mean radiative lifetime of the two species. From the fluorescence yields, τ, the actual radiative lifetime, may now be determined (13); and from these, k_2, the reciprocal of τ. All the reported studies on phototransposition of ring carbon atoms show that k_5 is very small (14). Assuming that it is likewise negligible in the present case, k_3, k_4, k_7, and quenching cross sections can be calculated at various exciting wavelengths. These are summarized in Table V, and are, of course, somewhat dependent on mechanistic details. For example, if it is not assumed that fluorescence and intersystem crossover and isomerization

Can. J. Chem. Downloaded from www.nrcresearchpress.com by 210.87.254.6 on 09/05/12
For personal use only.

occur from the same vibrational level, as is implied by reactions [2], [3], and [5], and if rate constants for vibrational deactivation to these *different* levels from some higher level are included, then the quenching cross sections given in Table V will be somewhat high. The precision of our measurements does not justify the inclusion of such mechanistic refinements.

In applying the steady state approximation to the case of sensitized emission, [12] and [13] may be neglected (15). The sensitized yield ϕ_p is then given by

$$[19] \qquad \frac{1}{\phi_p} = \frac{(k_{15}+k_{16})(k_9+k_{10}[M])(k_6+k_{17}+k_8[BiA])(k_2+k_3+k_4[F]+k_5+k_7[BiA])}{k_{15}k_{10}k_8k_3[M][BiA]}$$

No further approximation need be made to explain the effect of cyclohexane on the sensitized emission yield of mixtures of the TFB and BiA as is summarized, for example, in Fig. 2, since eq. [19] predicts that at constant [F] and [BiA], plots of P_T/ϕ_p vs. P_{CH}, where P_T is the total pressure and P_{CH} the pressure of cyclohexane, should be linear with positive intercept at $P_{CH} = 0$ and relatively small positive slopes.

In the absence of cyclohexane but at moderate pressures of either BiA or F or both, it is expected that $k_{10}[M] > k_9$, so that eq. [19] may be approximated by

$$[20] \qquad \frac{1}{\phi_p} = \frac{(k_{15}+k_{16})(k_6+k_{17}+k_8[BiA])(k_2+k_3+k_4[F]+k_5+k_7[BiA])}{k_3k_{15}k_8[BiA]}$$

Equation [20] predicts that at low biacetyl pressures, ϕ_p should increase linearly with [BiA], and that as the pressure of BiA becomes larger, it should eventually reach a maximum and decrease. Although our experimental observations on 1,2,4-TFB confirm the low pressure predictions, the higher pressure behavior could not be studied because it was not possible to introduce high enough pressures into the system. This suggests that for this molecule reaction [6] remains competitive with reaction [8] throughout the range under study and is in contrast to the behavior of benzene (8) and fluorobenzene (10). There is as yet no evidence for the relative importance of reaction [17], although it is expected that k_{17} will be small (14).

Equation [20] also describes to a satisfactory extent the behavior of the sensitized emission from mixtures of 1,3,5-TFB and BiA. At constant biacetyl pressure, $1/\phi_p$ was a linear function of [TFB]. However, as is evident from Fig. 7, it is not possible to say with certainty that there is a well defined initial linear portion to the ϕ_p vs. biacetyl pressure curve at constant TFB pressure. The biacetyl pressures experimentally possible were not high enough to observe a maximum in this plot.

It is worth noting the several features of the photochemistry of these two trifluorobenzenes which are distinctly different from those of other fluorinated benzenes.

1. The fluorescent yield as a function of exciting wavelength shows only the one maximum, rather than the combination of minima and maxima observed in the other fluorinated benzenes which we have investigated. This is presumably due to the closer spacing of the vibrational band systems in these two molecules. The relatively large band pass used in the present study ensures that excitation will occur simultaneously into at least two vibrational bands, thus obscuring any differences in behavior due to different vibrational excitation.

2. Our data indicate that the triplet of 1,2,4-TFB must be relatively short-lived and thus considerably larger pressures of BiA are required to pick up all the 1,2,4-TFB. They also suggest that reaction [6] of the proposed mechanism must be unimolecular, otherwise the triplet yield would behave differently with increasing pressures of 1,2,4-TFB, CH, and BiA. It should be noted, however, that a mechanism more detailed in its handling of the vibrational deactivation steps, such as has been mentioned, does not necessarily require the latter conclusion.

3. *cis*-Butene-2 readily quenches the triplet of benzene (16), monofluorobenzene (17), metadifluorobenzene (7), ortho- and para-difluoroben-

Can. J. Chem. Downloaded from www.nrcresearchpress.com by 210.87.254.6 on 09/05/12
For personal use only.

zene (9), and that of 1,3,5-trifluorobenzene. It does not, however, quench the triplet of 1,2,4-TFB. Therefore, it seems likely that the triplet energy of *cis*-B-2 is either very close to, or slightly below that of 1,2,4-TFB. Cundall (18) estimates the triplet energy of *cis*-B-2 to be about 72 kcal mole^{-1}. A simple Hückel molecular orbital calculation (7) indicates that the singlet of 1,2,4-TFB may lie about 10% lower in energy than the singlet of benzene, and lower than the singlet of any of the above mentioned fluorinated benzenes. The shifts in the 0,0 band position in the ultraviolet spectra of these compounds (19) confirm this calculation qualitatively, although not to the extent of 10%. If the triplet energy of 1,2,4-TFB happens to be 10% lower than that of benzene, it would lie at approximately 73.5 kcal mole^{-1}, making energy transfer from it to triplet *cis*-B-2 very unlikely.

The somewhat unsatisfactory nature of the data on 1,3,5-TFB indicates the exercise of caution in reaching any firm conclusions regarding this molecule. A reinvestigation using a much higher intensity source and a much narrower exciting band width is obviously necessary. This will be carried out as soon as it becomes experimentally feasible.

Acknowledgments

The authors gratefully acknowledge a grant from the Associated Alumni of the University of New Brunswick towards the purchase of the instrumentation used in this study, and financial and other assistance from the National Research Council of Canada.

1. K. E. Wilzbach, A. L. Harkness, and L. Kaplan. J. Am. Chem. Soc. **90**, 1116 (1968).
2. L. Kaplan, K. E. Wilzbach, W. G. Brown, and S. S. Yang. J. Am. Chem. Soc. **87**, 675 (1965).
3. I. Haller. J. Am. Chem. Soc. **88**, 2070 (1966); J. Chem. Phys. **47**, 1117 (1967).
4. J. M. Blair and D. Bryce-Smith. Proc. Chem. Soc. 287 (1957).
5. H. R. Ward and J. S. Wishnok. J. Am. Chem. Soc. **90**, 1085 (1968).
6. W. A. Noyes, Jr. and C. S. Burton. Ber. Bunsenges. Physik. Chem. **72**, 146 (1968).
7. F. W. Ayer, F. Grein, G. P. Semeluk, and I. Unger. Ber. Bunsenges. Physik. Chem. **72**, 282 (1968).
8. H. Ishikawa and W. A. Noyes, Jr. J. Chem. Phys. **39**, 583 (1962).
9. J. L. Durham, G. P. Semeluk, and I. Unger. Can. J. Chem. Submitted for publication.
10. M. E. MacBeath, G. P. Semeluk, and I. Unger. J. Phys. Chem. Submitted for publication.
11. M. E. Garabedian and D. A. Dows. J. Am. Chem. Soc. **90**, 2468 (1968).
12. M. Ballester, J. Palan, and J. Riera. J. Quant. Spectry. Radiative Transfer, **4**, 819 (1964).
13. J. G. Calvert and J. N. Pitts, Jr. Photochemistry. John Wiley and Sons, Inc., New York. 1966. p. 174.
14. W. A. Noyes, Jr. 8th Informal Conf. Photochem. Ottawa, June 17–19, 1968.
15. J. Lemaire. J. Phys. Chem. **71**, 2653 (1967).
16. R. B. Cundall, F. G. Fletcher, and D. G. Milne. Trans. Faraday Soc. **60**, 1146 (1964).
17. I. Unger. J. Phys. Chem. **69**, 4284 (1965).
18. R. B. Cundall. 8th Informal Conf. Photochem. Ottawa, June 17–19, 1968.
19. H. Sponer. J. Chem. Phys. **22**, 234 (1954).

Can. J. Chem. Downloaded from www.nrcresearchpress.com by 210.87.254.6 on 09/05/12
For personal use only.

Can. J. Chem. Downloaded from www.nrcresearchpress.com by 210.87.254.6 on 09/05/12
For personal use only.

Complexing, exchange, and redistribution reactions of some Group III and Group V fluorides and their anions[1]

S. BROWNSTEIN
Division of Applied Chemistry, National Research Council of Canada, Ottawa, Canada

Received July 18, 1968

Complexing, fluorine exchange, and redistribution reactions were studied for systems containing BF_3, PF_5, AsF_5, SbF_5, and their anions BF_4^-, PF_6^-, AsF_6^-, and SbF_6^-. Fluorine resonance spectra were obtained for $PSbF_{11}^-$ and $AsSbF_{11}^-$. Silver and tetrabutylammonium were used as cations in methylene chloride as solvent.

Canadian Journal of Chemistry, 47, 605 (1969)

Introduction

Complexing and fluorine exchange reactions have been reported for the fluorides of boron and phosphorus in methylene chloride solution (1–3). Although $B_2F_7^-$ was the only fluorine bridged species which could be identified, in those cases where the mechanism of fluorine exchange could be investigated, fluorine bridged intermediates were suggested. Fluorine bridging of SbF_5 with itself and with SbF_6^- has been reported in more polar solvents (4, 5). This study concerns the other Group V fluorides and mixtures of them, since it was thought that fluorine bridging should be a common phenomenon amongst these compounds.

Experimental

Tetra-*n*-butylammonium hexafluoroarsenate ($TBAAsF_6$) and hexafluoroantimonate were prepared in the same way that the hexafluorophosphate had been made previously (6). Vapor pressure measurements and fluorine resonance spectra, as well as reagent purification and storage, were accomplished as described in earlier papers already cited. However, in two instances it was necessary to obtain fluorine resonance spectra at 25.1 MHz as well as 94.1 MHz to confirm details of spectral interpretation. Antimony pentafluoride was twice fractionally distilled under vacuum in an interconnected distillation assembly (5). Samples were transferred by distillation on a vacuum system and at no time was the reagent allowed to come in contact with the atmosphere.

Results and Discussion

A summary of the results of this and previous studies is presented in Table I. In each case where reactions of the type $MF_{x+1}^- + NF_y \rightarrow MF_x + NF_{y+1}^-$ are reported, this conclusion was reached by pressure measurements of the gas evolved during the reaction. This was accomplished in the same apparatus used for determining complex formation with BF_3 (1). The solubility difference between the different gases was quite sufficient to make this distinction. In addition the non-volatile products were isolated and their identities confirmed by X-ray powder diffraction patterns. As an example of the information used to determine complex formation, the uptakes of BF_3, PF_5, and AsF_5 by $TBASbF_6$ at -20 °C are shown in Fig. 1.

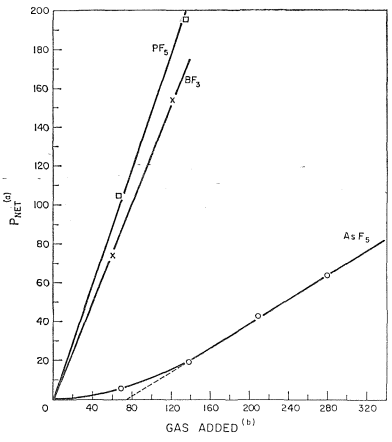

FIG. 1. Pressure above a $TBASbF_6$ solution at -20 °C. (*a*) *P* in mm Hg, (*b*) arbitrary units.

The presence or absence of fluorine exchange was established by fluorine resonance spectroscopy, where either a single averaged line was observed with rapid exchange or separate lines from the various species were observed in the absence of exchange. Figure 2 is the fluorine resonance spectrum of a CH_2Cl_2 solution of BF_3 and $TBAAsF_6$. The characteristic resonance lines of BF_3 and AsF_6^- indicate that fluorine exchange between them is slow on the nuclear

[1]Issued as NRCC No. 10 447.

TABLE I

Reactions of boron, phosphorus, arsenic, and antimony fluorides

System	Product	Comment	Reference
$BF_3+TBABF_4$[a]	$TBAB_2F_7$	Rapid fluorine exchange	(1)
$BF_3+TBAPF_6$	None	Rapid fluorine exchange	(3)
$TBABF_4+PF_5$	$BF_3+TBAPF_6$		(3)
$BF_3+TBAAsF_6$	None	No fluorine exchange	[b]
$TBABF_4+AsF_5$	$BF_3+TBAAsF_6$		[b]
$BF_3+TBASbF_6$	None	No fluorine exchange	[b]
$AgBF_4+SbF_5$	$BF_3+AgSbF_6$		[b]
PF_5+PF_5	None	Probably fluorine exchange	(2)
$PF_5+TBAPF_6^-$	None	Rapid fluorine exchange	(3)
$PF_5+TBAAsF_6$	None	Rapid fluorine exchange	[b]
$TBAPF_6+AsF_5$	$PF_5+TBAAsF_6$		[b]
$PF_5+TBASbF_6$	None at 30 °C	Rapid fluorine exchange	[b]
	$TBAPSbF_{11}$ at −96 °C	Slow fluorine exchange	[b]
$AsF_5+TBAAsF_6$	$TBAAs_2F_{11}$	Rapid fluorine exchange	[b]
$AsF_5+TBASbF_6$	$TBAAsSbF_{11}$	Rapid fluorine exchange 30 °C	[b]
		Slow fluorine exchange −96 °C	[b]
$AsF_5+AgSbF_6$	$AgAsSbF_{11}$		[b]
SbF_5+HSbF_6	HSb_2F_{11}		(5)

[a]TBA is used as an abbreviation for tetra-*n*-butylammonium.
[b]This work.

magnetic resonance (n.m.r.) time scale. Only a single broad line was observed for $TBAAsF_6^-$ at −60 °C because of averaging of arsenic–fluorine spin coupling due to quadrupole relaxation (7). At room temperature the rate of quadrupole relaxation had slowed sufficiently to allow the observation of four very broad lines. This is in accord with the theory of quadrupole relaxation (8).

At room temperature the fluorine resonance spectrum of an equimolar solution of PF_5 and $TBASbF_6$ in methylene chloride is a single broad line. On lowering the sample temperature to −60 °C, two broad lines are observed. At −96 °C a pair of relatively sharp lines and a pair of broad lines are observed. The sharp doublet (half width of 14 Hz) has $J = 940$ Hz and $\delta = 70.2$. The broad doublet (half width of 120 Hz) has five times the total area of the sharp one and $J = 913$ Hz, $\delta = 65.2$. The chemical shifts and spin coupling constants were confirmed by measurements at both 94.1 and 25.1 MHz. In all the spectra a sharp doublet is present from POF_3. This is an impurity in the PF_5 employed and is produced after long storage of PF_5 in glass vessels. It appears to be inert in the present samples. Both sets of lines, not arising from POF_3, are attributed to fluorine directly bonded to phosphorus.

The chemical shifts and phosphorus–fluorine spin coupling constants for PF_6^- are $\delta = 71.0$ and $J = 711$ Hz (3). For PF_5 the corresponding values are $\delta = 65.4$ and $J = 947$ Hz (2). The values of 916 (9) and 930 Hz (10) previously reported for PF_5 were the peak separations of broadened and somewhat coalesced lines, and are therefore smaller than the actual spin coupling constant.

It is rationalized that a signal is not observed from fluorine bonded to antimony because the quadrupole broadening of the antimony–fluorine spin coupling produces an unobservably broadened line. With $TBASbF_6$ alone in methylene chloride and with solutions of BF_3 and $TBASbF_6$, the signal expected for fluorine bonded to antimony is also not observed. The bonding of PF_5 to SbF_6^- is much weaker than that of AsF_5 and SbF_5 since vapor pressure measurements give no evidence of complex formation at −20 °C. Perhaps this weak bond does not cause a sufficient distortion of the octahedral symmetry of SbF_6^- to allow a narrowed signal because of rapid quadrupole averaging.

If the structure of $PSbF_{11}^-$ is that of two octahedra joined at one corner by a bridging fluorine, there will be three types of fluorine bonded to phosphorus. The assignment of the bridging fluorine, four equatorial fluorines, and one apical fluorine among the two sets of peaks is not straightforward. One possible assignment is that the apical and equatorial fluorines give rise to the broad peak. A large spin coupling and small chemical shift between these fluorine nuclei would

Can. J. Chem. Downloaded from www.nrcresearchpress.com by 210.87.254.6 on 09/05/12
For personal use only.

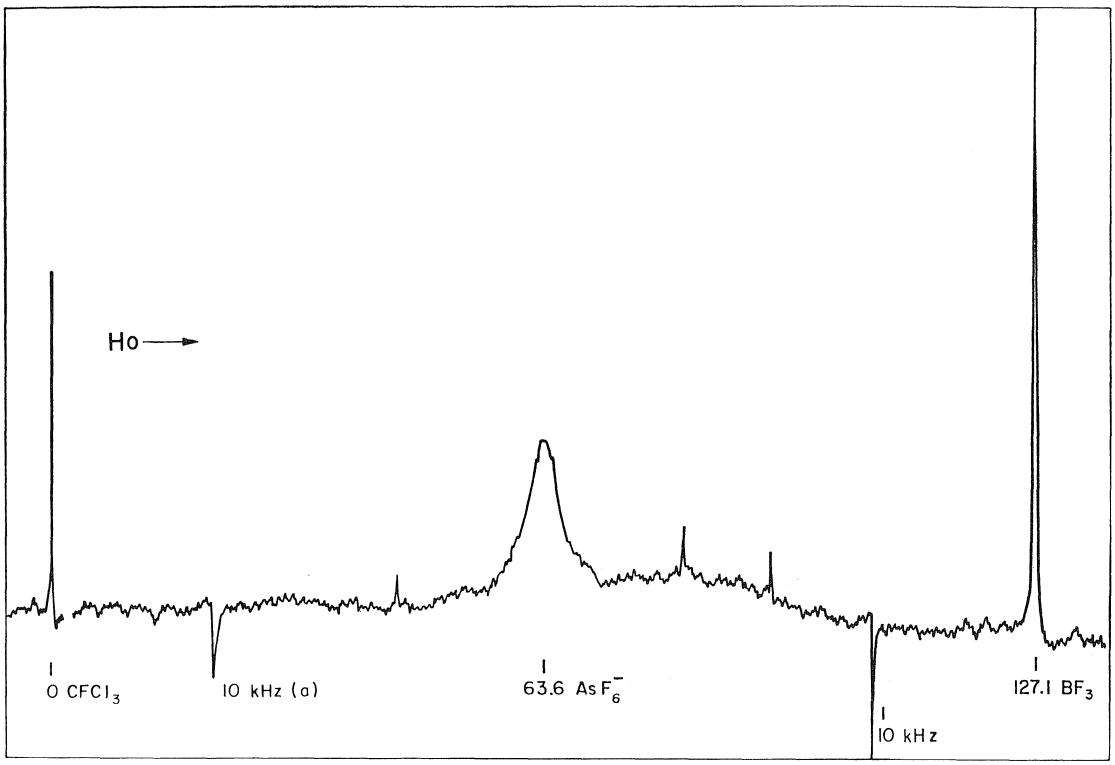

FIG. 2. The fluorine resonance spectrum of a CH_2Cl_2 solution of BF_3 and $TBAAsF_6$ at -60 °C. (*a*) The 10 kHz peaks of reversed phase are sidebands which occur because of operation in a "time division" mode.

give rise to many lines. Further spin coupling to the fluorines on antimony would produce a still greater multiplicity and yield a single broad envelope. The absence of further observable spin coupling in the two sharp peaks attributed to the bridging fluorine is not readily explicable. It is to be expected that the bridging fluorine will occur at higher magnetic field, between the position for fluorine on phosphorus and that for fluorine on antimony. The fluorine resonance spectrum of $PSbF_{11}^-$ is shown in Fig. 3.

At room temperature the fluorine resonance spectrum of an equimolar solution of AsF_5 and $TBASbF_6$ is a broad structureless line. As the temperature is lowered, two prominent lines appear and gradually sharpen. By -96 °C, four sets of well-resolved lines are observed. Chemical shift and spin coupling constants were confirmed from spectra at both 25.1 and 94.1 MHz. The 94.1 MHz spectrum of $AsSbF_{11}^-$ at -95 °C is shown in Fig. 4. Since it was found that $CFCl_3$ was not inert as an internal reference in this system, CF_4 was used as internal reference and a correction made for the chemical shift between it and $CFCl_3$. The assignment of chemical shifts and spin coupling constants is presented in Table II. Evidently there is sufficient asymmetry of the electric field about the arsenic and antimony nuclei for quadrupole relaxation to average all traces of arsenic or antimony–fluorine spin coupling. The two most intense absorption regions at 50.5 and 118 p.p.m. are assigned to fluorine on arsenic and antimony, respectively. This agrees with the values of 63.6 p.p.m. for AsF_6^- and 107 p.p.m. for the equatorial fluorines in the complex $SbF_5 \cdot SO_2$ (11). The quintet centered at 138.9 p.p.m. is assigned to the terminal fluorine on antimony, in agreement with a chemical shift of 141 p.p.m. for the apical fluorine in $SbF_5 \cdot SO_2$ (11). The remaining quintet at 92.9 p.p.m. is then assigned to the terminal fluorine on arsenic. By comparison, the apical fluorine in $AsF_5 \cdot (CH_3)_2O$ has a chemical shift of 83 p.p.m. (12). Spin coupling between the terminal and equatorial

Can. J. Chem. Downloaded from www.nrcresearchpress.com by 210.87.254.6 on 09/05/12
For personal use only.

Can. J. Chem. Downloaded from www.nrcresearchpress.com by 210.87.254.6 on 09/05/12
For personal use only.

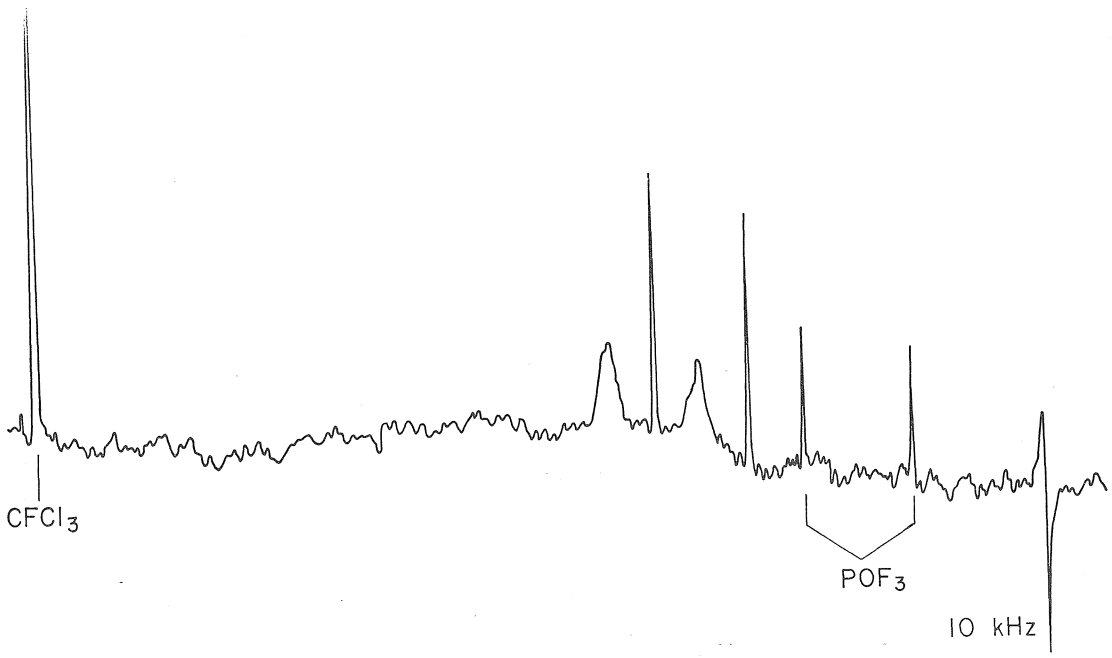

FIG. 3. The fluorine resonance spectrum of a CH_2Cl_2 solution of PF_5 and $TBASbF_6$ at −96 °C.

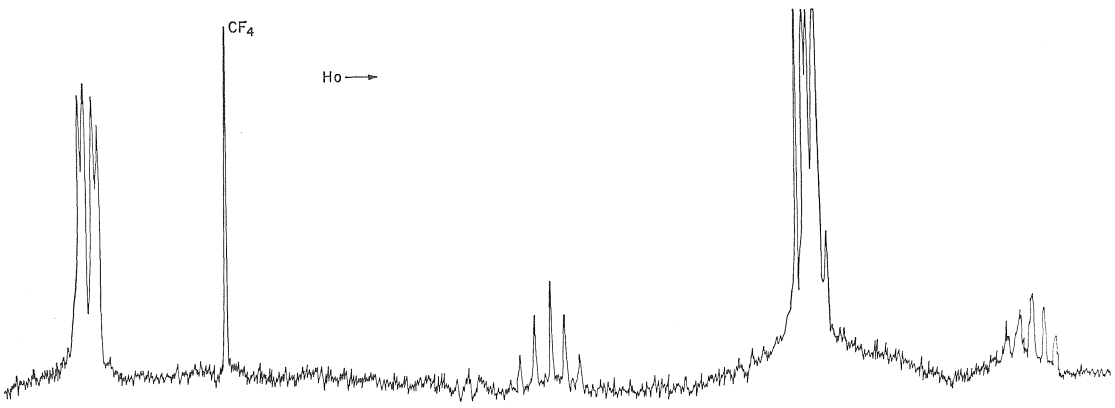

FIG. 4. The fluorine resonance spectrum of a CH_2Cl_2 solution of AsF_5 and $TBASbF_6$ at −96 °C.

TABLE II

Chemical shifts and spin coupling constants for $AsSbF_{11}^-$

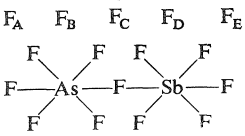

	δ^a	$J_{AB}{}^b$	J_{BC}	J_{DE}
F_A	92.9	126		
F_B	50.5	126	47	
F_C	118		47	
F_D	118			112
F_E	138.9			112

[a]Chemical shifts are in p.p.m. to high field of $CFCl_3$.
[b]Spin coupling constants are in Hz.

fluorines on arsenic is observed in the multiplets of both species. However, spin coupling between the equatorial and bridging fluorines is only observed in the peaks of the equatorial fluorines on arsenic, since the bridging fluorine and the equatorial fluorines on antimony overlap in a complex multiplet. Similarly, spin coupling between the equatorial fluorines and the terminal fluorine on antimony can only be observed for the peaks attributed to the terminal fluorine. The absence of spin coupling between terminal and bridging fluorines is consistent with results for complexes of boron, phosphorus, and arsenic fluorides with proton containing Lewis bases where long range coupling to an apical fluorine is not observed (12, 13).

Additional evidence for the formation of $AsSbF_{11}^-$ comes from the infrared spectrum of a KBr pellet containing the solid product obtained after evaporation of all readily volatile material from a methylene chloride solution of equimolar quantities of AsF_5 and $TBASbF_6$. The infrared spectra for $TBAAsF_6$, $TBASbF_6$, and $TBAAsSbF_{11}$ are shown in Fig. 5. It was not possible to isolate pure solid $TBAAsSbF_{11}$ by evaporation of solvent from a solution, since varying amounts of AsF_5 were lost by this procedure. Therefore, the infrared spectrum is not that of a compound with stoichiometric composition.

Conclusion

In addition to B—F—B and Sb—F—Sb fluorine bridge bonding, which has previously been reported, evidence is presented for P—F—Sb, As—F—As, and As—F—Sb bridge bonding. At room temperature the fluorines exchange rapidly between the different chemical environments.

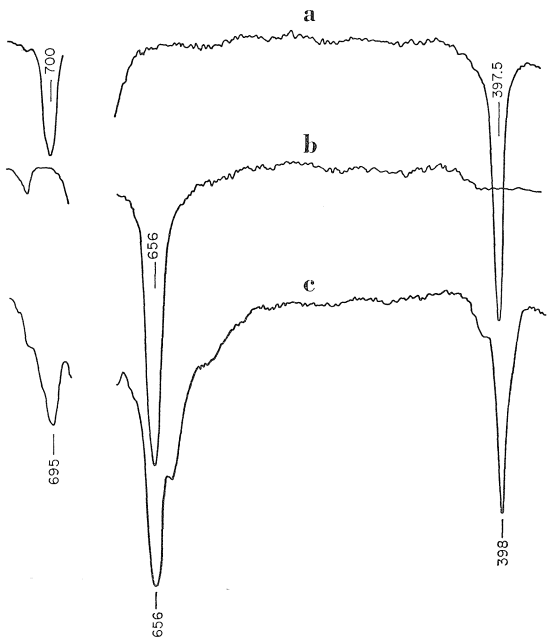

FIG. 5. The infrared spectra of complex tetrabutylammonium fluorides. Frequencies are in cm^{-1}. (*a*) $TBAAsF_6$, (*b*) $TBASbF_6$, (*c*) $TBAAsSbF_{11}$.

1. (*a*) S. BROWNSTEIN and J. PAASIVIRTA. Can. J. Chem. **43**, 1645 (1965). (*b*) J. PAASIVIRTA and S. BROWNSTEIN. J. Am. Chem. Soc. **87**, 3593 (1965).
2. S. BROWNSTEIN. Can. J. Chem. **45**, 1711 (1967).
3. S. BROWNSTEIN and J. BORNAIS. Can. J. Chem. **46**, 225 (1968).
4. C. J. HOFFMAN, B. E. HOLDER, and W. L. JOLLY. J. Phys. Chem. **62**, 364 (1958).
5. R. J. GILLESPIE and K. C. MOSS. J. Chem. Soc. A, 1170 (1966).
6. S. BROWNSTEIN. Can. J. Chem. **45**, 2403 (1967).
7. K. J. PARKER and E. L. MUETTERTIES. Proc. Chem. Soc. 147 (1964).
8. J. BACON, R. J. GILLESPIE, and J. W. QUAIL. Can. J. Chem. **41**, 3063 (1963).
9. E. L. MUETTERTIES and W. D. PHILLIPS. J. Am. Chem. Soc. **81**, 1084 (1959).
10. H. S. GUTOWSKY, D. W. MCCALL, and C. P. SLICHTER. J. Chem. Phys. **21**, 279 (1953).
11. S. BROWNSTEIN. Unpublished results.
12. L. LUNAZZI and S. BROWNSTEIN. J. Magnetic Resonance. In press.
13. A. G. MASSEY and A. J. PARK. J. Organometal. Chem. Amsterdam, **5**, 218 (1966).

Can. J. Chem. Downloaded from www.nrcresearchpress.com by 210.87.254.6 on 09/05/12
For personal use only.

The silver–calcium phase diagram[1]

W. A. ALEXANDER[2], L. D. CALVERT, A. DESAULNIERS, H. S. DUNSMORE[3], AND D. F. SARGENT[4]
Division of Applied Chemistry, National Research Council of Canada, Ottawa, Canada

Received September 23, 1968

The silver–calcium system has been reinvestigated over the whole composition range by thermal analysis, X-ray diffraction, and metallography. A novel technique has been used to prepare and examine these reactive alloys. In the course of this project four intermetallic compounds have been observed for the first time; while two others, viz., Ag_2Ca and AgCa, which were reported before by others, have been confirmed. Three of the new compounds are: Ag_8Ca_3, Ag_3Ca_5, and $AgCa_3$, while the fourth was not isolated or examined in detail. Two other compounds which were described in earlier work as Ag_4Ca and Ag_3Ca, have been found to be Ag_9Ca_2 and Ag_7Ca_2, respectively. Major modifications have been made in the liquidus curve and possible reactions in the solid state are indicated.

Canadian Journal of Chemistry, 47, 611 (1969)

Can. J. Chem. Downloaded from www.nrcresearchpress.com by 210.87.254.5 on 09/05/12
For personal use only.

Introduction

The application of silver–calcium alloys to the preparation of skeletal silver catalysts for the oxidation of ethylene to ethylene oxide provided the initial incentive for this work. The calcium is removed from the silver–calcium alloys by oxidation at 350 °C in steam, followed by leaching in 20% acetic acid. Occasional variability in catalyst activities suggested that the crystal structure of the calcium–silver alloy might be a factor worth investigation. Since the available phase diagram was obviously incomplete and possibly in error in the part of major interest to us, the reinvestigation of the whole system was undertaken.

The only thermal analysis of this system is that of Baar (1) whose results are uncertain for part of the system and his procedure casts some doubt on all the results. According to Hansen and Anderko (2) a number of other partial investigations have been made, principally the X-ray examination of Degard (3). Several others (4–8) have made limited examinations of the system by various methods including X-ray diffraction. Elliott (9) mentions the review of Kripyakevich (10), who discusses the results of Calvert *et al.* (11) on the CaAg structure and relates them to similar structures. Other than the structure determinations of Calvert and Rand (12) and Rand and Calvert (13), no other work on this system has been found.

[1]NRCC No. 10 479.
[2]To whom correspondence should be addressed.
[3]NRCC Postdoctorate Fellow 1953–1956; present affiliation: Chemistry Department, University of Glasgow, Glasgow, Scotland.
[4]Present address: c/o Department of Biophysics, University of Western Ontario, London, Ontario.

Experimental

All alloys were prepared from high purity metals. The silver was "Mint Grade" granules with the following spectrographic analysis, in parts per million (p.p.m.) (13): Pb, 10; Fe, 4; Si, 5; Cd, 20; Ca, 1; Mg, 1; Cu, Sn, and Na, not visible. The calcium was made by Dominion Magnesium Limited by thermal reduction and was distilled six times before use. Spectrographic analysis showed (13): Mg, 2; Fe, 2.5; Mn, 1; Si, 2; Ba, 2.5; Sr, 2.5 p.p.m.; while Cu, Pb, Zn, Cd, Ni, Sb, Li, Cr, Al, and Ag were not visible. The nitrogen content of the calcium varied from 100 to 260 p.p.m., but was only about 100 to 110 p.p.m. in the alloy, even after observing six cooling curves. Although Bevan and Richardson (14) state that oxygen will have only a slight effect on the melting point, others, particularly Smith *et al.* (15), Wolfson (16), and Messing *et al.* (17), have indicated the importance of extreme care in melting calcium and its alloys.

The apparatus is similar to that used by Freeth and Raynor (18) for a similarly reactive system and is shown in Fig. 1. After completing the cooling curves, the stirrer was withdrawn, the alloy superheated 100 – 150 °C, mixed by tilting the furnace, and cast into the cold mold in the side-arm. An argon atmosphere purified by slow passage over calcium shavings at 650 – 700 °C was maintained over the alloy at a positive pressure of about 2 cm Hg. The melt was stirred at about 40 r.p.m.

In some early work at low calcium contents the charges weighed in argon were dropped into the melt vessel with a stream of argon issuing from it. It was soon evident that greater precautions were needed and a simple distillation tube was adopted. This comprised a tube 2.3 cm internal diameter (i.d.) with a 1 mm wall, made into a right angled assembly, each leg being about 25 cm long. The first leg was cut at 45° at one end and made up as shown in Fig. 1 later to form the lower 18 cm of this vessel. The second half of the vessel was a simple tube welded at the bottom and also cut at 45° to match the first half. A small iron baffle with two thin plates was fixed in this tube above the calcium. A screen with 6.4 mesh per cm was welded into the 45° joint between the two tubes. A stainless steel tube 7.9 mm i.d., with about 0.5 mm wall and about 8 cm long, was welded over a hole near the 45° joint for evacuation and sealing off. The charge of silver granules, too large to pass through the

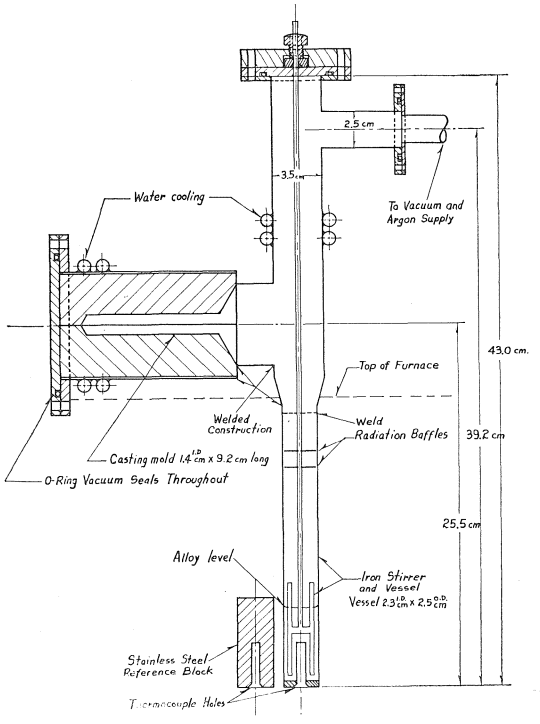

FIG. 1. Melting and casting vessel. The heated portion and mold were of mild steel, while the upper portion of the case was partly of stainless steel. The O-rings were lightly lubricated, while the stirrer shaft ring was well lubricated with "Myvane" from Distillation Products Co., Rochester, New York.

screen, was placed in the end with the thermocouple well. The required weight of calcium crystals, pressed into pellets if necessary, was put in the opposite end with the baffle to prevent the possible entrainment of oxide or nitride in the vapor stream. The whole vessel was degassed at suitable elevated temperatures and the side-arm sealed off at less than one micron pressure (19). Three of these tubes could be placed in a vacuum furnace at one time in a temperature gradient. With the calcium at about 940 °C and the silver or the alloy at about 830 °C distillation of the calcium was complete in about two weeks. Any leaks were indicated by a "mushroom" growth of calcium oxide on the outside and such alloys were discarded.

The tubes were opened in an argon-filled "dry box" by sawing off the thermocouple or alloy end, which was then stoppered. This stoppered end was removed from the dry box and welded to the cooling curve vessel with a vigorous stream of argon flowing over the alloy surface. Thus only the top surface of the ingot could be exposed to a somewhat impure argon atmosphere and the results were reasonably reproducible.

The cooling curves using platinum–rhodium thermocouples were recorded automatically at 6 s intervals with a six point recorder, both directly and in a differential manner, with the stainless steel block as the reference temperature. The thermocouple was calibrated in pure metal baths after each alloy. There was no systematic drift and the variations from alloy to alloy were almost always less than ± 0.3 °C. The cooling rate was automatically controlled at about $\frac{1}{2} - \frac{3}{4}°$ per min by a chromel–alumel differential thermocouple arrangement between the alloy and the furnace winding. The setup was sufficiently sensitive to show reproducibly the Curie point of the mild steel container, or the energy imput due to the stirring.

Top and bottom analyses were made for each casting. These differed up to a few tenths wt. % in most cases with the maximum being about 1 wt. %. The analyses accounted for 99.6 – 99.9 wt. % as calcium and silver, the remainder being undoubtedly oxide and nitride formed during sampling and weighing for analysis, which were done in air. No other metals were found by the wet chemical analysis. No correction has been applied to the calcium contents from chemical analysis.

The errors in our measurements are evidently additive and may be estimated as follows. The thermocouple calibration error due to temperature gradients in the bath, loss along the wires and the like, are estimated to be $\pm 0.3°$. The recorder errors were minimized by comparison with a sensitive (± 0.01 °C) potentiometer at regular 9 min intervals and are estimated at about ± 0.2 °C. Thus the error in a temperature read from the chart is believed to be about ± 0.5 °C. The errors in estimating an arrest point are larger for a liquidus — up to ± 1 °C, and smaller for a eutectic arrest — usually about ± 0.1 °C, since these lasted for several minutes and the temperature was essentially constant. Thus the error in estimating a liquidus is believed to be not greater than ± 1.5 °C and a eutectic about ± 0.6 °C. The reproducibility is of course somewhat better due to some of these errors being constant or systematic.

Results and Discussion

It is probable that small amounts of impurities such as calcium oxide, nitride, or hydride have only a minor effect on the arrests of alloys with low calcium content. Some early experiments without the final careful techniques confirmed the data of Baar (1) in this region. Up to 18% Ca[5] the system in Fig. 2 is drawn from these and two later experiments. In Fig. 2 the actual points are all from later experiments with the higher accuracy. The liquidus points are evidently reasonably consistent but the eutectic or solid state arrests are not very reproducible from alloy to alloy. These arrests sometimes changed in duration for successive observations with the same alloy, especially in the case of the more reactive alloys with about 60–75% calcium. The probable cause is gradual contamination by impurities from the upper part of the vessel. This must be small since

[5]Unless otherwise specified all percentages are atomic percent.

Can. J. Chem. Downloaded from www.nrcresearchpress.com by 210.87.254.5 on 09/05/12
For personal use only.

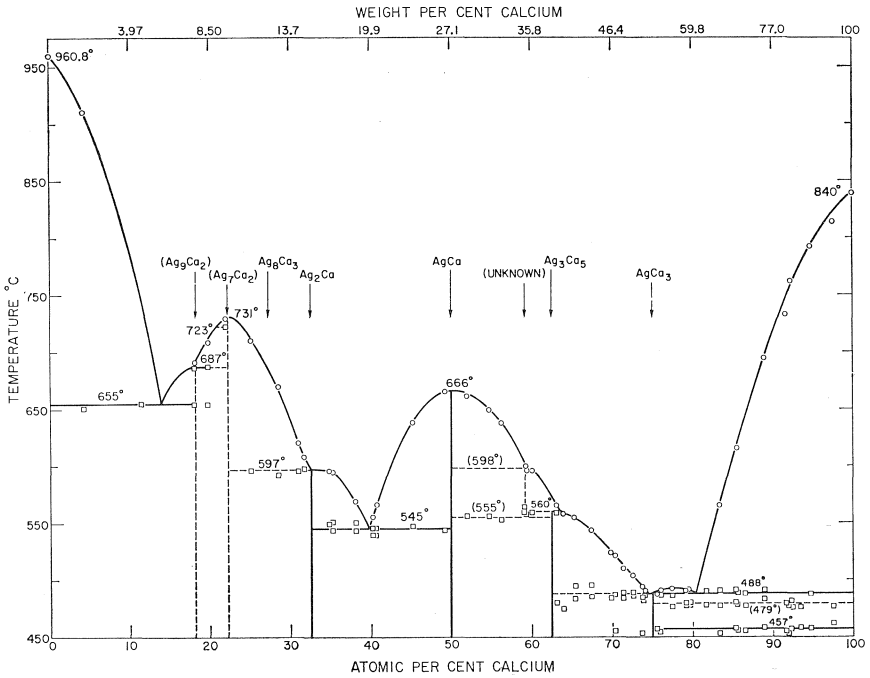

FIG. 2. The calcium–silver system. ○, liquidus or first arrests; □, solid state or secondary arrests.

the transformation temperature of calcium is very sensitive to impurities (15) and these arrests remained reasonably constant. Also high temperature X-ray examination of various alloys with more than 75% calcium showed a constant transformation temperature for the calcium phase of about 450 °C.

Figure 2 has been drawn to fit the experimental data of the later experiments and the data and confirmations from X-ray diffraction. In some instances and especially in the solid state reactions much further work is desirable, which would amplify and probably modify our results. It would also appear that a higher order of purity of the alloys, avoiding the pickup of impurity during melting, would be necessary for this purpose. The same is true of metallography. We examined alloys only up to 53% calcium, both chill-cast and after various annealing treatments, and the results were in agreement with the diagram proposed here. Beyond this composition the brittleness and high reactivity of the alloys make metallography very difficult. At 53% calcium, the alloys were suitably etched by a few minutes' exposure to moist laboratory air.

The low calcium eutectic was found at 655 °C in essential agreement with Baar (1) and the composition was not redetermined. The peritectic reaction at 687 °C and about 18% Ca also is not in great disagreement with Baar's values of 683 °C and 15%. The cooling curves indicate a maximum of about 731 °C at 22% Ca and a pronounced second arrest at 723 °C on the lower calcium side. Some early X-ray diffraction examination of single crystals from a chill cast ingot showed the compounds Ag_9Ca_2 and Ag_7Ca_2 in place of Ag_4Ca and Ag_3Ca. The compound Ag_8Ca_3 has been described in detail from X-ray single crystal analysis by Calvert and Rand (12), although thermal analysis has shown no indication of its presence. The crystal was obtained from an ingot containing 22.2% Ca which was annealed at 695 °C for 4 days and quenched. It is thus probable that solid state reactions occur in this composition and temperature range which we have not observed.

The peritectic at 597 °C, the low slope of the liquidus at the Ag_2Ca composition, and the eutectic at 545 °C are all essentially the same as those of Baar (1). A eutectic near 33% Ca and the

Can. J. Chem. Downloaded from www.nrcresearchpress.com by 210.87.254.5 on 09/05/12
For personal use only.

Can. J. Chem. Downloaded from www.nrcresearchpress.com by 210.87.254.5 on 09/05/12
For personal use only.

formation of Ag_2Ca by congruent melting are also possibilities. The eutectic composition indicated at 39.8% is also in agreement with Baar (1). The compound AgCa melting at 666 °C is also in close agreement with the results of Baar (1). X-ray photographs agree (11) with these results for Ag_2Ca and AgCa and in addition high temperature X-ray observations indicate the existence of two crystal forms of AgCa.

In the region from 50–80% Ca our results differ very considerably from the previous work. On the basis of X-ray powder diffraction photographs of as-cast alloys with no annealing, a new compound of unknown composition has been observed between AgCa and Ag_3Ca_5 and in the same sample with either or both of these compounds. Moreover, the unknown compound is sometimes absent from a sample containing AgCa and Ag_3Ca_5. There is a possibly fortuitous indication of a peritectic at about 59% Ca and 598 °C and the diagram is drawn concordantly.

The compound Ag_3Ca_5 has been analyzed by single crystal X-ray diffraction (13) and hence the indication of its formation at 560 °C by peritectic reaction is probably accurate. The relationships of the unknown compound with the neighboring AgCa and Ag_3Ca_5 are tentatively drawn to fit our experimental data. It is also quite possible that further examination would show a different relation such as the existence of the unknown down to room temperature. On the other hand the compound X was not always present when expected, which might indicate some complexity in the reactions by which it is formed or disappears.

Between the compound Ag_3Ca_5 and pure calcium the data suggest the presence of two eutectics with the congruently melting compound $AgCa_3$. The latter's structure has been clearly elucidated by X-ray diffraction[6]. $AgCa_3$ was always found in association with the pure calcium phase in alloys with higher calcium content and with Ag_3Ca_5 on the opposite side. Although the X-ray crystal structure analysis indicates a nominal composition of 75% for $AgCa_3$, congruent melting of a compound at about 77.5% is still possible since the stoichiometry of the compound was not specifically studied in the X-ray work, but no variation in lattice parameter was observed. Regarding the solid state arrests in this region, viz., two at about 455 °C between 70 and 75% and the scattered ones at about 479 °C from about 77 to 98%, which were not always observed, these are most probably indications of solid state transformations which we did not investigate further.

The liquidus arrests from pure calcium to the first eutectic at about 80.5% are very weak and sometimes were not observed at all, even with the sensitivity we achieved. However, there seems to be little doubt of the general course of this liquidus line. The melting point of calcium at 840 °C is in agreement with what we believe to be the most reliable literature values (17, 20).

The X-ray photographs of these alloys indicated little or no range of solid solution in all cases, including that of the terminal metals with the adjacent compounds.

[6]Unpublished investigation.

Acknowledgments

The assistance of Mr. R. H. Gamble and Mr. F. Liuzzo in the experimental work is gratefully acknowledged. Mr. Michel Bouchard assisted with the metallography.

1. N. Baar. Z. Anorg. Allgem. Chem. **70**, 352 (1911).
2. M. Hansen and K. Anderko. Constitution of binary alloys. McGraw-Hill Book Co., Inc., New York. 1958.
3. C. Degard. Z. Krist. **90**, 399 (1935).
4. E. Zintl and G. Brauer. Z. Physik. Chem. B, **20**, 245 (1933).
5. H. Nowotny. Z. Metallk. **37**, 34 (1946).
6. A. Iandelli. Rend. seminar. fac. sci. univ. Cagliari, **19**, 133 (1949).
7. R. H. Kremann, H. Wostall, and H. Schöpfer. Forschungsarb. Metallk. No. 5. 1922; J. Inst. Metals, **32**, 529 (1924).
8. C. A. Kraus and H. F. Kurtz. J. Am. Chem. Soc. **47**, 43 (1925).
9. R. P. Elliott. Constitution of binary alloys. 1st Suppl. McGraw-Hill Book Co., Inc., New York. 1965.
10. P. I. Kripyakevich. Kristallografiya, **6**, 626 (1961).
11. L. D. Calvert, H. S. Dunsmore, L. V. Kuhi, and R. S. Tse. Acta Cryst. **10**, 775 (1957).
12. L. D. Calvert and C. Rand. Acta Cryst. **17**, 1175 (1964).
13. R. P. Rand and L. D. Calvert. Can. J. Chem. **40**, 705 (1962).
14. D. J. M. Bevan and F. D. Richardson. Australian At. Energy Symp. Proc. Sydney. 1958. p. 586.
15. J. F. Smith, O. N. Carlson, and R. W. Vest. J. Electrochem. Soc. **103**, 409 (1956); **106**, 448 (1959).
16. M. R. Wolfson. Trans. Am. Soc. Metals, **49**, 794 (1957).
17. A. F. Messing, M. D. Adams, and R. K. Steunenberg. Trans. Am. Soc. Metals **56**, 345 (1963).
18. W. E. Freeth and G. V. Raynor. J. Inst. Metals, **82**, 569 (1953).
19. W. A. Alexander and F. Liuzzo. J. Sci. Instr. **40**, 338 (1963).
20. J. C. Schotmiller, A. J. King, and F. A. Kanda. J. Phys. Chem. **62**, 1446 (1958).

Kinetics of the thermal decomposition of cyclobutanone[1]

ARTHUR T. BLADES
Research Council of Alberta, Edmonton, Alberta

Received May 17, 1968

The thermal decomposition of cyclobutanone into cyclopropane and carbon monoxide has been shown to occur simultaneously with the major decomposition to ethylene and ketene. The relative rate constant expression is given by $k_{C_3H_6}/k_{C_2H_4} = 0.65 \exp(-6000/RT)$. Both reactions are pressure sensitive below 10 Torr and this quasi-unimolecular behavior is most pronounced in the cyclopropane forming reaction, consistent with the higher activation energy. The data are also discussed in relation to the photochemical decomposition and it is shown that cyclopropane formation from the ground singlet is an important feature of the photolysis at 3130 Å.

Canadian Journal of Chemistry, 47, 615 (1969)

Can. J. Chem. Downloaded from www.nrcresearchpress.com by 210.87.254.40 on 09/05/12
For personal use only.

Introduction

The photochemical decomposition of cyclobutanone yields ethylene, ketene, cyclopropane, propylene, and carbon monoxide (1, 2). Recent studies (3, 4) suggest that these products arise from the two primary reactions

[1] $\text{cyclo-}C_4H_6O \xrightarrow{h\nu} C_2H_4 + CH_2CO$

and

[2] $\text{cyclo-}C_4H_6O \xrightarrow{h\nu} \text{cyclo-}C_3H_6 + CO$

In reaction [2], the partitioning of the residual energy of the photon between the products is such that some of the cyclopropane may isomerize to propylene. The formation of this product is therefore favored by low pressure and short wavelength.

On the basis of benzene photosensitization studies, Denschlag and Lee (5) have proposed that the cyclopropane arises from the excited triplet cyclobutanone. The formation of ethylene on the other hand, has been attributed (6) to the decomposition of the vibrationally excited ground singlet following internal conversion from the first excited singlet. The relative rates of the two processes [1] and [2] may, therefore, be determined not by the rates of chemical processes but by the rates of change of the electronic configuration, processes which might be expected to be less sensitive to absorbed energy. The invariance of the product ratio with wavelength under certain conditions (3, 4) is in keeping with this evaluation.

From the variation of the quantum yields of ethylene, cyclopropane, and propylene, Magee (7) has proposed that only propylene arises from the triplet while the other products arise from the excited singlet. While these data are somewhat compelling, the suggestion that the cyclopropane, formed with energies in excess of the activation energy for its conversion to propylene (3, 4), does not isomerize at low pressures, is untenable.

In the pyrolysis of cyclobutanone, the major process is reaction [1], only 0.5% of the hydrocarbon product being cyclopropane (8). The major reaction has been shown to be homogeneous and first order over the pressure range 10–88 Torr, the rate constant being given by

$$k = 3.6 \times 10^{14} \exp(-52\,000/RT)\ \text{s}^{-1}$$

There is no evidence that the cyclopropane arises by reaction [2] but this would seem to be a reasonable assumption by analogy with the photolysis. Since the pyrolysis involves only the ground singlet, however, and the source of the cyclopropane is believed to be the triplet, some inconsistency exists between the pyrolytic and photolytic systems. This paper is concerned with the kinetics of the pyrolytic formation of cyclopropane.

Experimental

The pyrolyses were carried out in a Pyrex reactor (84 cc) employing standard high vacuum techniques. The commercial cyclobutanone was purified by gas chromatography and was degassed prior to use. In the gas chromatographic analysis of the products (35 ft diisooctyl phthalate on firebrick, 0 °C, 30 cc/min, H_2 carrier), the flame ionization detector response was monitored by a digital integrator.

Results

The products of the pyrolysis were confirmed to be ethylene and ketene, with about 0.5% cyclopropane (and CO). Propylene was always detected but was less than 1% of the cyclopropane.

[1]Contribution No. 429 from the Research Council of Alberta, Edmonton, Alberta.

Can. J. Chem. Downloaded from www.nrcresearchpress.com by 210.87.254.40 on 09/05/12
For personal use only.

At constant temperature (350°) and pressure (10 Torr) the ratio of products was independent of reaction time up to 75% reaction. Rate constants for ethylene formation agreed within experimental error with those previously reported (8).

The effect of pressure on the rate of ethylene formation was determined in the range 0.7 to 16 Torr and on the relative rates of cyclopropane and ethylene formation in the range 1.3–19.5 Torr. These data are shown in Fig. 1. The temperature coefficient of the relative rates of the two processes was determined from 316–393° at 15 Torr, and an Arrhenius plot of this data is shown in Fig. 2. The relative rate expression derived from this data is

$$k_{C_3H_6}/k_{C_2H_4} = 0.65 \exp(-6000 \pm 500/RT)$$

When combined with the rate expression for the major reaction (8), the rate constant for cyclopropane formation is

$$k = 2.34 \times 10^{14} \exp(-58\,000/RT)\,s^{-1}$$

Similar behavior was observed in various reaction vessels of different surface to volume ratio and the rates were independent of the presence of a 100-fold excess of toluene.

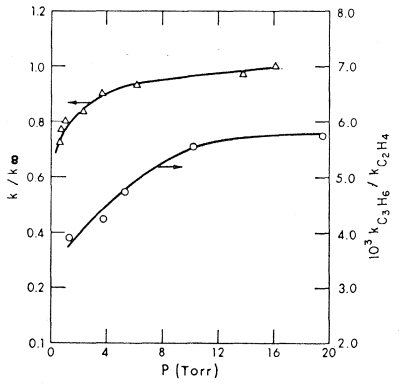

FIG. 1. Pressure effects in the decomposition of cyclobutanone. Δ, left hand scale, k/k_∞ for ethylene formation; ○, right hand scale, $10^3 k_{C_3H_6}/k_{C_2H_4}$.

Discussion

Cyclopropane might arise in the pyrolysis of cyclobutanone either by a direct decomposition or by a series of consecutive reactions of the major products, ketene and ethylene. This latter possibility is ruled out since reaction time did not affect the product ratio and the formation of cyclopropane, like ethylene, must be first order. Since the chain-inhibitor, toluene, and surface to volume ratio also failed to influence the rates of either process, both reactions must be homogeneous unimolecular decompositions.

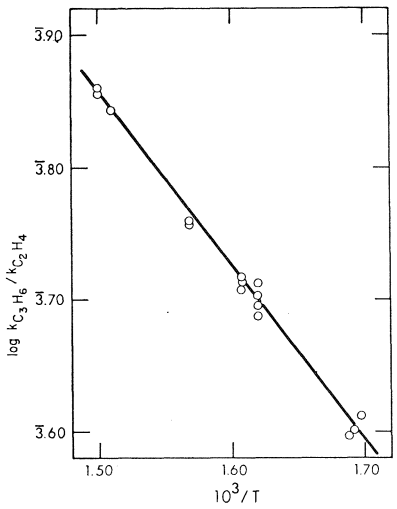

FIG. 2. Arrhenius plot of the relative rates of cyclopropane and ethylene formation.

The pressure effects in these competitive homogeneous reactions illustrate an effect previously observed in intramolecular hydrogen isotope effects (9). The decline in the rate constant for ethylene formation below 10 Torr implies pseudo-unimolecular behavior for this reaction, while the decline in the relative rate constants implies that the cyclopropane-forming reaction is more susceptible to pressure decrease. Since the latter process has the higher activation energy, and these products arise preferentially from the more highly excited cyclobutanone, such behavior is to be expected independent of subtle differences between the two mechanisms. Calculations of Rice–Ramsperger–Kassel (R.R.K.) theory "S" value, the number of degrees of freedom contributing to activation, are therefore not meaningful for the minor process.

The Arrhenius parameters for the decomposition of cyclobutanone to ethylene and ketene have been estimated by O'Neal and Benson (10) on the basis of a mechanism involving the intermediate diradical $\cdot CH_2CH_2COCH_2\cdot$. Resonance in this diradical contributes significantly in reducing the

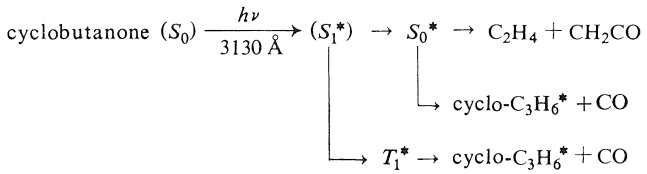

entropy of activation and the activation energy. If the decomposition to cyclopropane occurs via the diradical $\cdot CH_2CH_2CH_2CO\cdot$, such resonance does not exist, and the activation energy for this process would be expected to be greater by the carbonyl resonance energy which has been estimated at about 8 kcal/mole (10). This difference is in reasonable agreement with the 6 kcal/mole observed. The accompanying higher entropy change would be partially offset by a smaller entropy increase due to internal rotation in the radical formation, and hence the frequency factors for the two processes are similar. The activated complex must lead directly to cyclopropane and CO since the intermediate formation of trimethylene is energetically forbidden.

This pyrolysis study has shown that cyclopropane is an alternate decomposition product of ground singlet cyclobutanone. Since the photolysis mechanism of Lee *et al.* (6) involves the decomposition of this species, but allows only for ethylene as a product, it is desirable to estimate how significant an error this implies. Using the R.R.K. theory expression for the specific rate constants, assuming 15 Kassel oscillators (6), it can be estimated that for photolysis at 3130 Å, about 7% of the ground singlet will decompose to cyclopropane. The ratio of ethylene to cyclopropane at 3130 Å is 2.45 (6) and therefore, of the cyclopropane formed, about 18% would be predicted to arise from the ground singlet decomposition. Evidence for this significant contribution to the cyclopropane in photolysis is provided by the quenching studies of Lee *et al.* (6). They observed a 10% decrease in C_3H_6 formation in the same pressure range where ethylene had decreased about 66%. While they attribute this to a minor quenching of the cyclobutanone triplet, an alternate explanation would be that this results from quenching of that part of the ground singlet which would otherwise have produced the cyclopropane. On this basis, it would appear that about 15% of the cyclopropane arises from the ground singlet at 3130 Å, in excellent agreement with that predicted from the pyrolysis data, and modification of the photolysis mechanism seems justified.

At shorter wavelengths, the proportion of the ground singlet decomposing to cyclopropane would be greater and this prediction is in keeping with a slight decrease in the C_2H_4 to C_3H_6 ratio with decreasing wavelength. This decrease is, however, twice that predicted on the basis of the classical theory and may result wholly or in part from a variation in the relative rates of intersystem cross-over and internal conversion with absorbed energy.

1. S. W. Benson and G. B. Kistiakowsky. J. Am. Chem. Soc. **64**, 80 (1942).
2. F. E. Blacet and A. Miller. J. Am. Chem. Soc. **79**, 4327 (1957).
3. R. F. Klemm, D. N. Morrison, P. Gilderson, and A. T. Blades. Can. J. Chem. **43**, 1934 (1965).
4. R. J. Campbell, E. W. Schlag, and B. W. Ristow. J. Am. Chem. Soc. **89**, 5098 (1967).
5. H. O. Denschlag and E. K. C. Lee. J. Am. Chem. Soc. **89**, 4795 (1967).
6. N. E. Lee, H. O. Denschlag, and E. K. C. Lee. J. Chem. Phys. **48**, 3334 (1968).
7. T. H. Magee. J. Phys. Chem. **72**, 1621 (1968).
8. M. N. Das, F. Kern, T. D. Coyle, and W. D. Walters. J. Am. Chem. Soc. **76**, 6271 (1954).
9. A. T. Blades, P. W. Gilderson, and M. G. H. Wallbridge. Can. J. Chem. **40**, 1526 (1962).
10. H. E. O'Neal and S. W. Benson. J. Phys. Chem. **72**, 1866 (1968).

Can. J. Chem. Downloaded from www.nrcresearchpress.com by 210.87.254.40 on 09/05/12
For personal use only.

Can. J. Chem. Downloaded from www.nrcresearchpress.com by 210.87.254.105 on 09/05/12
For personal use only.

Heats of mixing and dielectric constants of some partially miscible liquid pairs

A. N. CAMPBELL AND E. M. KARTZMARK
Department of Chemistry, University of Manitoba, Winnipeg, Manitoba

Received May 2, 1968

The physical properties mentioned in the title have been determined for the six systems: (*a*) aniline–hexane, (*b*) methanol–cyclohexane, (*c*) methanol – carbon disulfide, (*d*) acetic anhydride – carbon disulfide, (*e*) acetic anhydride – cyclohexane, and (*f*) triethylamine–water, over the complete range of composition. All six systems are partially miscible, above or below a critical solution temperature (c.s.t.).

From the experimental data, the partial molal heats of mixing have been calculated, using the Redlich and Kister equations. The enthalpy of hydrogen bonding in the triethylamine–water compound appears to be about −1.33 kcal per hydrogen bond.

The orientation polarization, according to the Syrkin formula, appears always to exhibit negative deviation from ideality, at least over part of the concentration range.

Canadian Journal of Chemistry, 47, 619 (1969)

Previous work from this laboratory has dealt with congruent concentrations (1) of the six systems, (*a*) aniline–hexane, (*b*) methanol–cyclohexane, (*c*) methanol – carbon disulfide, (*d*) acetic anhydride – carbon disulfide, (*e*) acetic anhydride – cyclohexane, and (*f*) triethylamine–water. Another paper (2) is confined to the system aniline–hexane, and deals with excess volume, vapor pressure, surface tension, and viscosity. The present work deals with the same systems and studies the properties mentioned in the title.

For those liquid systems which form two layers, the change of volume on mixing is usually positive but this is not always the case. That it should not be true of the system triethylamine–water, where both ΔV and ΔH are strongly negative, is not surprising since we have shown that here a compound is formed (3), which probably continues to exist, to some extent undissociated, even at room temperature.

The density measurements, however, show that ΔV is negative over the whole concentration range for the system aniline–hexane, and over a part of the range for methanol – carbon disulfide, and there is no possibility of compound formation between aniline and hexane. According to Bellemans (4), upper critical solution phenomena occur in endothermal mixtures but a lower critical point can only occur in exothermal mixtures.

Experimental

The method of determining heat of mixing has been described previously (5, 6). The purity of materials was the same as previously described (1).

The dielectric constants were determined with a Sargent oscillometer, the sample being thermostated at a temperature high enough or low enough to ensure homogeneity over the complete concentration range (7). Determinations with this instrument cannot be made on substances having higher electrical conductances than the alcohols, although we found it possible to use conductance water as a calibration point. No measurements could, however, be made on mixtures of triethylamine and water, containing considerable quantities of water, because of the high electric conductance. Dilute solutions of triethylamine in water gave apparent dielectric constants as high as 120, obviously due to the electric conductance.

Results

TABLE I

Heats of mixing

Acetic anhydride – carbon disulfide*

Composition	ΔH	Composition	ΔH
4.26	207.5	53.03	434.5
8.89	274.5	59.70	393.7
12.93	291.8	69.41	358.9
18.98	327.2	70.84	380.0
25.16	398.0	74.30	347.7
31.55	442.8	85.83	212.3
39.78	449.4		

*Composition in mole % acetic anhydride, ΔH in cal/mole mixture, $T = 34.2$ °C.

Methanol – carbon disulfide*

Composition	ΔH	Composition	ΔH
15.20	147.4	51.23	192.0
28.47	195.6	69.93	162.8
39.15	192.7	79.52	151.3
44.34	194.8	82.74	127.0
47.55	189.0	95.48	40.56

*Composition in mole % methanol, ΔH in cal/mole mixture, $T = 36.5$ °C.

Drucker and Weissbach (8) have determined the heats of mixing of solutions of methanol and carbon disulfide outside of the gap, at 20 °C. Insofar as the results are comparable, they are in good agreement.

TABLE I (*Concluded*)

Methanol–cyclohexane*

Composition	ΔH	Composition	ΔH
6.99	205.0	63.14	270
13.01	240.3	72.33	247.1
24.26	284.0	80.52	198.1
31.26	296.4	86.80	155.5
41.90	293.5	90.80	133.4
52.05	296.7	95.83	69.6

*Composition in mole % methanol, ΔH in cal/mole mixture, $T = 50.5$ °C.

According to Mondain–Monval (9) the heat of mixing of methanol–cyclohexane has a value of 4 cal/g, at the maximum. This amounts to 253 cal/mole and is to be compared with our value of 300 cal at the maximum (40 mole % methanol). Wood (10) calculates a value of 800 cal/mole mixture, a value which is obviously absurd.

Acetic anhydride – cyclohexane*

Composition	ΔH	Composition	ΔH
3.60	236.9	50.86	705.2
10.45	378.0	63.22	646.7
19.49	543.7	71.21	549.6
37.28	711.3	82.36	380.0
39.24	715.8	90.52	296.6
44.05	733.4		

*Composition in mole % acetic anhydride, ΔH in cal/mole mixture, $T = 59.0$ °C.

Hexane–aniline*

Composition	ΔH	Composition	ΔH
5.02	166.4	39.51	676.7
12.57	382.3	40.04	654.2
23.58	580.3	51.04	733.0
26.20	633.4	60.13	667.3
26.58	599.5	66.25	717.6
27.71	586.1	68.70	603.6
33.00	629.9	80.00	590.0
38.42	662.3		

*Composition in mole % hexane, ΔH in cal/mole mixture, $T =$ 66.5 °C.

Triethylamine–water*

Composition	ΔH	Composition	ΔH
0.59	−47.0	28.85	−537.8
3.62	−220.7	41.41	−575.1
6.18	−250.7	55.87	−357.4
7.52	−248.7	57.08	−408.0
22.98	−515.9	67.20	−331.3

*Composition in mole % triethylamine, ΔH in cal/mole mixture $T = 10$ °C.

The results of Copp and Everett (11) are in fair agreement with ours, as regards the shape of the curve and the value H^E at the maximum, but whereas they obtain a maximum value of −595 cal/mole at a composition of 25 mole % triethylamine, our maximum value is −580 cal at 41 mole % triethylamine. Copp and Everett's curve is, however, buite flat at the top and a small error on their part or ours would qring the compositions into agreement.

TABLE II

Dielectric constant (ε), molar polarization (P in cc), ΔP ($P_{obsd} - P_{calcd}$), and Syrkin's orientation polarization (P_i) for various mixtures

Acetic anhydride – carbon disulfide*

Composition	ε	P (cc)	ΔP	P_i
0.00 (pure CS_2)	2.612	21.28	—	0
100.00	20.55	82.92	—	243.7
7.83	4.15	32.91	+6.81	15.6
16.06	5.70	41.12	9.94	31.4
23.00	6.85	46.19	10.73	43.7
33.11	8.40	53.08	11.4	63.4
39.62	10.5	57.68	11.98	77.9
50.96	13.0	63.91	11.21	116.7
61.54	14.6	68.01	8.80	139.4
75.10	16.8	73.24	5.67	174.0
85.67	18.3	77.49	3.40	201.7

*Composition in mole % acetic anhydride, $T = 32$ °C.

Methanol – carbon disulfide*

Composition	ε	P (cc)	ΔP	P_i
0.00 (pure CS_2)	2.45	20.11	—	0
100.00	30.3	37.65	—	165.9
14.14	3.73	27.98	+5.39	11.5
28.61	5.53	33.59	8.43	22.1
38.12	7.85	37.81	11.02	41.3
50.85	12.5	41.47	12.44	73.5
60.28	15.5	41.85	11.17	90.0
68.38	17.9	41.32	9.21	105.4
78.00	20.5	40.49	6.68	118.0
85.24	24.0	39.77	4.71	135.9
92.92	26.6	38.67	2.27	135.0

*Composition in mole % methanol, $T = 40$ °C.

Methanol–cyclohexane*

Composition	ε	P (cc)	ΔP	P_i
0.00 (pure cyclohexane)	1.82	24.23	—	0
13.35	2.17	29.09	0.06	4.2
22.80	2.75	35.77	5.84	15.5
40.32	4.57	46.13	14.40	37.1
52.20	6.48	49.46	16.62	54.6
63.72	9.3	49.73	15.75	74.5
73.31	13.2	49.40	14.46	100.8
80.02	15.6	47.01	11.41	111.6
86.44	18.2	44.12	7.88	120.7
91.72	20.5	41.86	5.11	128.4
96.11	24.2	39.77	2.59	142.3
100.00	26.6	37.59	—	147.3

*Composition in mole % methanol, $T = 50.0$ °C.

Can. J. Chem. Downloaded from www.nrcresearchpress.com by 210.87.254.105 on 09/05/12
For personal use only.

TABLE II (*Concluded*)

Acetic anhydride – cyclohexane*

Composition	ε	P (cc)	ΔP	P_i
0.00 (cyclohexane)	1.97	27.83	—	0
11.68	3.00	45.3	10.89	20.0
22.09	4.07	56.2	16.46	38.0
34.37	5.90	67.3	20.1	65.2
43.61	7.32	73.2	20.8	86.2
51.68	8.90	77.3	20.3	107.7
62.94	11.65	81.4	18.1	142.8
70.85	13.15	83.3	15.6	162.4
81.67	15.50	84.6	10.8	191.4
90.89	17.20	84.7	5.7	214.3
100.00	18.75	84.19	—	226.8

*Composition in mole % acetic anhydride, T = 58.5 °C.

Hexane–aniline*

Composition	ε	P (cc)	ΔP	P_i
0 (aniline)	5.85	58.56	—	43.3
7.65	5.34	57.77	1.79	40.0
14.29	4.96	56.62	2.87	36.9
23.70	4.50	55.20	4.63	33.3
32.40	4.06	53.27	5.63	29.2
42.07	3.63	51.44	7.07	26.7
52.53	3.16	48.14	7.30	20.4
60.84	2.74	43.42	5.38	14.1
74.76	2.30	37.49	4.15	7.1
86.99	1.98	32.11	2.89	1.25
100.00	1.68	24.83	—	0

*Composition in % hexane, T = 67.5 °C.

Discussion

The heats of mixing can be represented by the Redlich and Kister equation (12), viz.

$$H^E = X_1X_2[A + B(X_1 - X_2) + C(X_1 - X_2)^2]$$

where X_1 = mole fraction of the component first named.

The constants for the above equation were determined from our data, using a least squares fit, on the computer. The program was essentially that of Myers and Scott (13). The constants, together with the σ values, or deviations of the constants, are given in Table III.

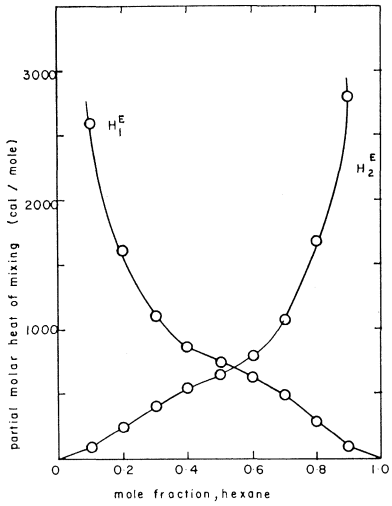

FIG. 1. Partial molar excess enthalpies: aniline–hexane.

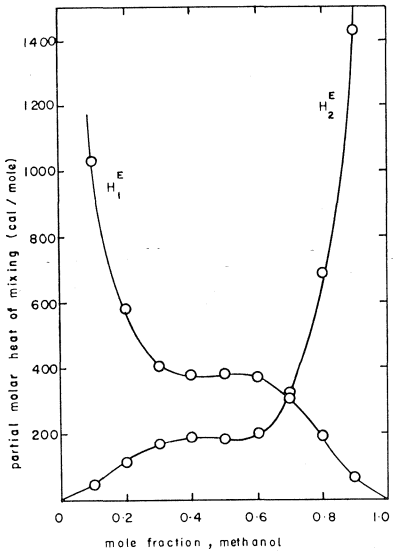

FIG. 2. Partial molar excess enthalpies: methanol–cyclohexane.

TABLE III

Constants of the Redlich and Kister equation and their deviations

System	A	σ	B	σ	C	σ
Acetic anhydride – carbon disulfide	1708	79	442.2	138	1195	352
Methanol – carbon disulfide	761.0	11	158.6	27	588.6	59
Methanol–cyclohexane	1134	49	411.2	88	1203	196
Acetic anhydride – cyclohexane	2822	76	703.7	167	1167	362
Hexane–aniline	2779	58	−206.6	123	1713	345
Triethylamine–water	−1683	178	−1315	677	−2304	1520

Can. J. Chem. Downloaded from www.nrcresearchpress.com by 210.87.254.105 on 09/05/12
For personal use only.

Using the above constants, the partial molar heats of mixing can be calculated from the equations

$$H_1^E = (1 - X_1)^2[(A + B(4X_1 - 1) + C(2X_1 - 1)(6X_1 - 1)]$$

$$H_2^E = X_1^2[A + B(4X_1 - 3) + C(2X_1 - 1)(6X_1 - 5)]$$

The results are expressed graphically in Figs. 1 to 6.

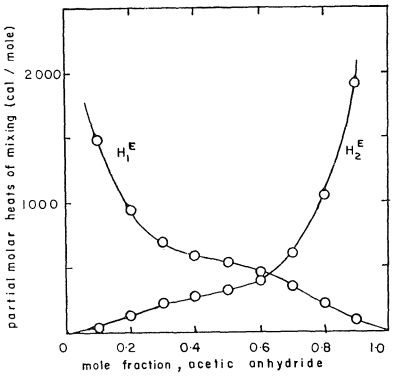

FIG. 3. Partial molar excess enthalpies: acetic anhydride – carbon disulfide.

All heats of mixing are positive except those of triethylamine–water, which are strongly negative[1]. The partial molar heats of mixing require no comment, except those of triethylamine–water. In view of the equilibrium existing in solution, viz.

$$(C_2H_5)_3N + 2H_2O \rightleftarrows (C_2H_5)N_3 \cdot 2H_2O$$

the limiting value of the partial molar heat of mixing of triethylamine in infinite excess of water may represent the enthalpy of formation of the compound. The calculation was therefore carried out for low mole fractions of triethylamine (0.01 and 0.05). The limiting value is -2650 cal. This gives a value of -1.325 kcal for the hydrogen bond.

When dielectric constant is plotted against mole fraction, negative deviation from straight line behavior is usually observed. The exception to this is the system acetic anhydride – carbon disulfide,

[1]This is in agreement with the predictions of Haase and Rehage (14) who state that an upper critical solution temperature is associated with a positive enthalpy of mixing and a lower critical solution temperature with a negative.

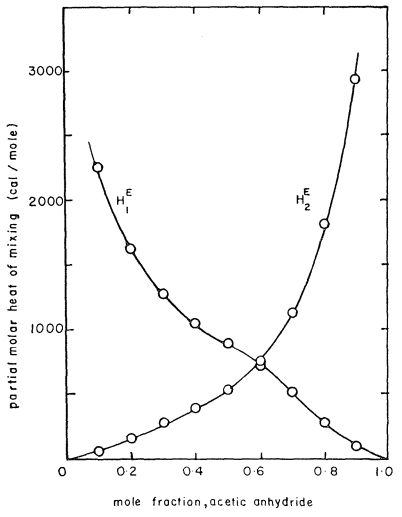

FIG. 4. Partial molar excess enthalpies: acetic anhydride – cyclohexane.

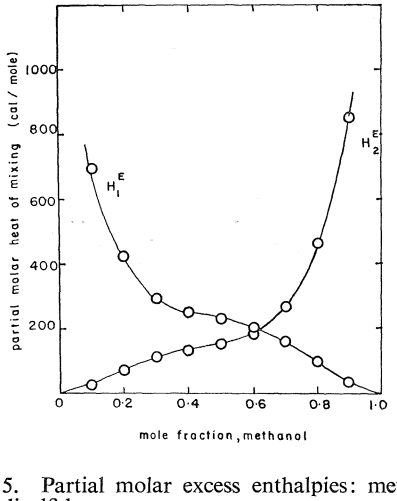

FIG. 5. Partial molar excess enthalpies: methanol – carbon disulfide.

which shows slightly positive deviation. We have not used our results for triethylamine–water, because we do not think these results are reliable in the presence of appreciable amounts of water.

The molar polarization,

$$P = \left(\frac{\varepsilon - 1}{\varepsilon + 2}\right) \cdot \left(\frac{X_1M_1 + X_2M_2}{d}\right)$$

as a function of mole fraction, shows strong positive deviation from linearity. Finally, we

Can. J. Chem. Downloaded from www.nrcresearchpress.com by 210.87.254.105 on 09/05/12
For personal use only.

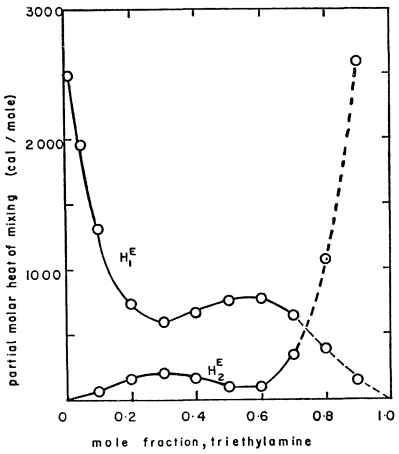

FIG. 6. Partial molar excess enthalpies: triethylamine–water.

owe to Syrkin (16) a formula for orientation polarization, viz.

$$P_i = \frac{P - X_1R_1 - X_2R_2}{1 - \left(\frac{\varepsilon - 1}{\varepsilon + 2}\right)^2}$$

where P is the molar polarization and R_1, R_2 are the molar refractions of the pure components. When these results are plotted against mole fraction, negative deviation is always observed, at least over part of the concentration range, a behavior which, according to Syrkin, is attributable to dipole – induced dipole interaction, dipole association, or a decrease in hydrogen bonding with dilution. It does not necessarily follow, however, that a mixture of polar and non-polar liquids shows negative deviation from additivity of Syrkin polarization. Thus, the behavior of a benzene–nitrobenzene mixture is ideal and this mixture does not show partial miscibility. On the other hand, mixtures of acetic acid with carbon tetrachloride, which are completely miscible, show marked negative deviation from additivity.

We determined the refractive indices of all solutions at the temperatures of investigation of the other properties (above the c.s.t.). In every case, the molar refraction was so close to that calculated from the mixture rule that the slight differences might be attributed to experimental error. This is to be expected if, as the Clausius–Mosotti theory teaches, the molar refraction represents the true volume of matter in a mole.

1. A. N. CAMPBELL and E. M. KARTZMARK. Can. J. Chem. **45**, 2433 (1967).
2. A. N. CAMPBELL, E. M. KARTZMARK, S. C. ANAND, Y. CHENG, H. P. DZIKOWSKI, and S. M. SKRYNYK. Can. J. Chem. **46**, 2399, 1968.
3. E. M. KARTZMARK. Can. J. Chem. **45**, 1089 (1967).
4. A. BELLEMANS. J. Chem. Phys. **21**, 369 (1953).
5. A. N. CAMPBELL, E. M. KARTZMARK, and H. FRIESEN. Can. J. Chem. **39**, 735 (1961).
6. A. N. CAMPBELL and J. M. T. M. GIESKES. Can. J. Chem. **43**, 1004 (1964).
7. A. N. CAMPBELL and J. M. T. M. GIESKES. **42**, 1379 (1964).
8. C. DRUCKER and H. WEISSBACH. Z. Physik. Chem. **117**, 209 (1925).
9. P. MONDAIN-MONVAL. Compt. Rend. **183**, 1104 (1926).
10. S. E. WOOD. J. Am. Chem. Soc. **68**, 1963 (1946).
11. J. L. COPP and D. H. EVERETT. Discussions Faraday Soc. **15**, 174 (1953).
12. O. REDLICH and A. T. KISTER. Ind. Eng. Chem. **40**, 345 (1948).
13. D. B. MYERS and R. L. SCOTT. Ind. Eng. Chem. **55**, 431 (1963).
14. R. HAASE and G. REHAGE. Z. Elektrochem. **59**, 994 (1955).
15. J. LAURANSON, P. PINEAU, and M. L. JOSIEN. Ann. Chim. **9**, 213, (1964). J. H. LADY and K. B. WHETSEL. J. Phys. Chem. **64**, 1001 (1964).
16. Y. K. SYRKIN. Compt. Rend. U.R.S.S. **35**, 43 (1942).

Can. J. Chem. Downloaded from www.nrcresearchpress.com by 210.87.254.105 on 09/05/12
For personal use only.

Medium effects in nuclear magnetic resonance. VII. Vapor phase studies of hydrogen bonding in methanol and methanol–trimethylamine mixtures[1]

A. D. H. Clague[2], G. Govil[3], and H. J. Bernstein
Division of Pure Chemistry, National Research Council of Canada, Ottawa 2, Canada

Received September 20, 1968

The self association of methanol, and the intermolecular association of methanol and trimethylamine have been examined in the vapor phase using nuclear magnetic resonance spectroscopy. Values of ΔH and ΔS for the two systems have been found to be -4.1 ± 0.5 kcal/mole and -17.5 ± 3 e.u., and -5.8 ± 0.7 kcal/mole and -22.6 ± 3 e.u., respectively.

Canadian Journal of Chemistry, 47, 625 (1969)

Can. J. Chem. Downloaded from www.nrcresearchpress.com by 210.87.254.105 on 09/05/12
For personal use only.

Introduction

While extensive nuclear magnetic resonance (n.m.r.) studies (1, 2) have been made on hydrogen bonding in the condensed phase, little work has been done in the gas phase. Thermodynamic studies in the gas phase are especially valuable since the hydrogen bond will be least modified by a medium effect. Further, in such systems it is possible (3–5) to estimate the contributions of interactions other than hydrogen bonding, to the observed chemical shifts in n.m.r. Recently (6), we have shown that n.m.r. can be used with success for the study of hydrogen bonding in the gas phase. In this paper, we report the n.m.r. results on the self association in methanol and its association with trimethylamine (TMA).

Experimental

Spectroquality methanol and Matheson Co. trimethylamine (99.0% minimum purity) were used without further purification. All sample handling was carried out on a vacuum line.

All spectra were recorded on a Varian A-60A spectrometer fitted with a variable temperature probe calibrated with ethylene glycol. Owing to the construction of the probe assembly of the Varian A-60A the portion of a normal n.m.r. tube surrounded by the plastic spinner cone remains at a different temperature than the portion below it. There was a tendency for methanol to condense on this cooler portion, resulting in loss of signal. Thus, to maintain the reactants in the vapor phase as well as to prevent a temperature gradient along the tube it is necessary to encapsulate them entirely within the temperature controlled portion of the probe. A normal 5 mm outer diameter 4 mm inner diameter n.m.r. tube was modified in the following way. The closed end of the tube was removed and the tube was extended by about 5 cm with a piece of Pyrex tubing having the same diameter. Using standard glass blowing techniques a glass plug was formed in the original portion of the tube about 9.5 cm from the position of the joint. A benzene capillary was inserted via the Pyrex extension and a constriction was pulled at the position of the joint. The tube was attached to the line by means of the Pyrex extension.

A known pressure of each gas was allowed into a bulb of known volume then condensed into the tube using a liquid nitrogen bath. The tube was sealed at the point of the constriction. Every effort was made to ensure as symmetric a seal as possible since this point represents the bottom of the tube and any asymmetry would interfere with the spinning qualities of the tube. A separate tube was used for each experiment, and the tube volumes were determined volumetrically after the n.m.r. data had been recorded.

In order to relate accurately the pressure of methanol to its concentration, the bulb of measured volume was filled with a series of different pressures of methanol; in each case the gas was condensed in a weighing bottle and weighed on a Mettler Microgramatic balance. By plotting the weight of methanol against pressure a calibration curve was obtained from which the true weight of methanol in any sample could be read. Trimethylamine has practically no tendency for self-association and therefore its concentration was determined from the ideal gas laws.

Spectra were recorded at intervals up to 200 °C. In samples containing a high concentration of methanol, the starting temperature was about 100 °C to ensure complete vaporization of the sample. For samples containing methanol alone, the shift of the hydroxyl proton was measured relative to the signal from benzene using 4 observations and the standard deviation was found to be between 0.5 to 1.0 Hz, depending on the temperature and pressure. In most of the mixtures with TMA it was found necessary to enhance the signals using a Varian time average computer (CAT-1024). About 9 to 25 traces were added by triggering the CAT on a side band of the benzene signal, generated by an audio oscillator close to the expected position of the OH signal. The audio oscillator was calibrated by a frequency counter. The instabilities in the spectrometer caused a further broadening of the accumulated signal and therefore the accuracy of the shift measurements was no better than $\sim \pm 1.5$ Hz. In each case, the measured shifts were converted relative to the shift of ethane gas at 10 atm pressure using the relation between temperature and chemical shift of benzene relative to above standard described previously in ref. (6).

[1]Issued as NRCC No. 10 461.
[2,3]Post Doctoral Fellow 1966–68.

TABLE I

Observed and calculated chemical shifts of the hydroxyl proton in methanol

Sample number	Concentration (g-moles/l)	Temperature (°K)	Observed* shift, δ_0 (Hz)	Calculated* † shift, δ_c (Hz)	$\delta_c - \delta_0$ (Hz)	Corrected* ‡ shift for the monomer, δ_M
1	0.0277	333.2	50.8±1.0	52.0	1.2	57.7
		353.2	53.5±1.0	53.3	−0.2	57.7
		373.2	54.5±1.0	54.2	−0.3	57.7
2	0.0546	353.2	49.6±0.7	49.7	0.1	57.5
		368.2	50.8±0.7	50.8	0.0	57.5
		388.2	51.2±1.0	52.0	0.8	57.4
		413.2	52.7±0.7	53.2	0.5	57.5
		443.2	54.0±1.0	54.1	0.1	57.5
3	0.1210	383.2	47.4±0.5	46.5	−0.9	56.8
		413.2	49.0±0.5	48.7	−0.3	56.9
		443.2	50.3±0.5	50.4	0.1	57.0
		468.2	51.0±1.0	51.4	0.4	57.1

*Relative to the resonance line in ethane gas at 10 atm.
†Using eqs. [1], [2], and [3] with $\Delta H_1 = -4152$ cal/mole, $\Delta S_1 = -17.47$ e.u., $\delta_{MM} = 0.0$ Hz.
‡From eq. [4] using the value of σ^{MM} from Appendix.

Results and Discussion

(A) Self Association of Methanol

The reaction for the dimerization of methanol (M) can be written as

$$\underset{a-x}{M} \rightleftharpoons \underset{x/2}{\tfrac{1}{2}(MM)}$$

where a is the total concentration of methanol in g-moles/l (dimer + monomer) and $x/2$ is the amount present as dimer. The equilibrium constant (K_{C_1}) for dimerization is given by

$$[1] \qquad K_{C_1} = \frac{x}{2(a-x)^2}$$

and is related to the enthalpy (ΔH_1) and entropy (ΔS_1) for the reaction by

$$[2] \qquad R \ln (K_{C_1}/RT) = \Delta S_1 - \Delta H_1/T$$

where R is the gas constant and T is the absolute temperature.

Since the rate (on the n.m.r. scale) at which the hydrogen bonds are formed and broken is fast, one observes only one signal from the proton involved in hydrogen bond formation. The observed chemical shift (δ_0) of this proton is related to that in the free form (δ_M) and the bonded form (δ_{MM}) by the relation

$$[3] \qquad \delta_0 = [(a-x)\delta_M + x\delta_{MM}]/a$$

Thus, if δ_M and δ_{MM} are known, a knowledge of δ_0 enables one to calculate x and vice versa.

The chemical shift for the OH signal at zero pressure ($\delta_M{}^0$) in free methanol can be obtained by extrapolation of the high temperature shifts for samples 1–3 in Table I. This gives $\delta_M{}^0 = 58 \pm 2$ Hz relative to C_2H_6, which corresponds to 208 Hz relative to the CH_3 peak in methanol. The corresponding value (7) in CCl_4 solution is 172 Hz indicating the presence of some additional interactions which affect the chemical shift in CCl_4 solutions.

At higher pressures δ_M in the vapor can be estimated from eq. [4]

$$[4] \qquad \delta_M = \delta_M{}^0 + (p_M/RT)\sigma^{MM}$$

where σ^{MM} is a correction for the diamagnetic anisotropy, electric field, and van der Waal interactions and p_M is the pressure of methanol. σ^{MM} can be calculated provided certain molecular parameters are known. Details of such calculations are given in Appendix and the calculated shifts δ_M for the three samples at different temperatures are given in Table I.

From eqs. [1–3] one sees that these involve three unknowns, namely ΔH_1, ΔS_1, and δ_{MM}. It is possible to solve for them from the experimental data on δ_0 using a minimization procedure given in a previous paper [6]. One obtains

$$\delta_{MM} = 0 \pm 40 \text{ Hz relative to } C_2H_6$$

$$\Delta H_1 = -4152 \pm 500 \text{ cal/mole}$$

$$\Delta S_1 = -17.47 \pm 3.0 \text{ e.u.}$$

The calculated shifts using the mean values of the above parameters have been included in Table I for comparison.

Can. J. Chem. Downloaded from www.nrcresearchpress.com by 210.87.254.105 on 09/05/12
For personal use only.

Can. J. Chem. Downloaded from www.nrcresearchpress.com by 210.87.254.105 on 09/05/12
For personal use only.

Self association in methanol has been studied earlier by other physical methods. Weltner and Pitzer (8) using P–V–T curves and heat capacity measurement showed that methanol exists in dimeric and tetrameric forms with ΔH and ΔS values of -3220 cal/mole and -16.5 e.u. for dimer and $-24\,200$ cal/mole and -81.3 e.u. for tetramer. More accurate measurements of Kretschmer and Wiebe (9) gave ΔH as -4000 and $-22\,100$ cal/mole, respectively, for dimer and tetramer. Using these values it is seen that the amount of tetramer present under the conditions used in this experiment is negligible, hence the good fit between observed and calculated chemical shifts using only 3 variables. If an appreciable amount of tetramer is present one has to use three additional parameters in the minimization but the accuracy in the estimate of six unknowns from the observed chemical shift is unlikely to be good (10).

The enthalpies of dimerization and tetramerization for methanol have also been measured by an infrared method (11) (-3500 and $-18\,400$ cal/mole, respectively). Again the measured values are in good agreement with the n.m.r. result.

Using the infrared values for equilibrium constant Becker, Liddel, and Shoolery (12) estimated $\delta_{MM} - \delta_M$ for alcohols as -2.3 p.p.m. for cyclic dimer and -1.2 p.p.m. for open dimer in CCl_4 solutions. The latter value is in good agreement with the observed result of -1 ± 0.7 p.p.m. for the difference in gas phase where open dimers are known to exist (7).

(B) Methanol–Trimethylamine System

For such a system, there are two competing reactions

$$\underset{a-x-y}{\mathrm{M}} \rightleftharpoons \underset{x/2}{\tfrac{1}{2}(\mathrm{MM})}$$

and

$$\underset{a-x-y}{\mathrm{M}} + \underset{b-y}{\mathrm{N}} \rightleftharpoons \underset{y}{\mathrm{MN}}$$

where b is the starting concentration of TMA (referred to as subscript N) in g-moles/l. We have

$$[5] \qquad K_{C_1} = \frac{x}{2(a-x-y)^2}$$

for the first reaction, and corresponding to eqs. [1–4] we have for the second reaction

$$[6] \qquad K_{C_2} = \frac{y}{(a-x-y)(b-y)}$$

$$[7] \qquad R \ln (K_{C_2}/RT) = \Delta S_2 - \Delta H_2/T$$

$$[8] \qquad \delta_0 = [(a-x-y)\delta_M + x\delta_{MM} + y\delta_{MN}]/a$$

with

$$[9] \qquad \delta_M = \delta_M{}^0 + [p_M\sigma^{MM} + p_N\sigma^{MN}]/RT$$

where K_{C_2}, ΔH_2, and ΔS_2 are the equilibrium constant, enthalpy, and entropy for the second reaction, p_M and p_N are the partial pressures of methanol and TMA respectively, δ_{MN} is the shift of the hydroxyl proton in the complex MN, and σ^{MN} is a correction similar to σ^{MM} whose value has been calculated in the Appendix.

One can eliminate y from eqs. [5] and [8] to obtain eq. [10]

$$[10] \qquad x^2 + 2(f-g)x + f^2 = 0$$

where

$$f \equiv a \cdot \frac{\delta_0 - \delta_{MN}}{\delta_{MN} - \delta_{MM}}$$

and

$$g \equiv \frac{(\delta_M - \delta_{MN})^2}{4K_{C_1}(\delta_{MN} - \delta_{MM})^2}$$

Selecting the physically acceptable solution of x gives

$$[11] \qquad x = g - f - [g^2 - 2gf]^{1/2}$$

while rearrangement of [8] gives y in terms of x

$$[12] \qquad y = a\left(\frac{\delta_M - \delta_0}{\delta_M - \delta_{MN}}\right) - x\left(\frac{\delta_M - \delta_{MM}}{\delta_M - \delta_{MN}}\right)$$

Since K_{C_1}, δ_{MM}, and δ_M are known, eqs. [6], [7], [11], and [12] again involve three unknowns only, namely, δ_{MN}, ΔS_2, and ΔH_2.

A graphical method for estimating δ_{MN} has been suggested (13) using data for mixtures where $b > a$. In such cases the self association is suppressed e.g. $y > x$ and $b \gg y$. Using these approximations in eqs. [6], [8], and [12] one obtains

$$[13] \qquad \frac{a}{y(\delta_M - \delta_{MN})} \simeq \frac{1}{\delta_M - \delta_0} \simeq \frac{1}{\delta_M - \delta_{MN}} + \frac{1}{bK_{C_2}(\delta_M - \delta_{MN})}$$

Thus, the double reciprocal plot of $(\delta_M - \delta_0)$ and b at a constant temperature, gives $\delta_M - \delta_{MN}$. Using such a technique one obtains

$$\delta_{MN} = -250 \pm 100 \text{ Hz}$$

Can. J. Chem. Downloaded from www.nrcresearchpress.com by 210.87.254.105 on 09/05/12
For personal use only.

The values of ΔH_2 and ΔS_2 can now be obtained by a least squares method using the data on the observed chemical shifts (δ_0). For all the mixtures, x and y are estimated using eqs. [11] and [12] for each sample and temperature at which δ_0 has been measured and substituted in eq. [6] to obtain values of K_{C_2} at different temperatures. ΔH_2 and ΔS_2 are solved by the linear least squares fitting to the values of R ln K_{C_2} as estimated above.

The values thus obtained are

$$\Delta H_2 = -5847 \pm 700 \text{ cal/mole}$$

$$\Delta S_2 = -22.64 \pm 3.0 \text{ e.u.}$$

The calculated chemical shifts δ_c with the above values of δ_{MN}, ΔH_2, and ΔS_2 are given in Table II along with the observed chemical shifts. These fit within the standard error ($\Delta\delta_0$) in the measurement of δ_0. The possible errors in ΔH_2 and ΔS_2 have been estimated using the criterion that the overall fit between the observed and calculated chemical shifts, $\phi = \sum_i(\delta_c - \delta_0)_i^2$, where i runs over all the experimental measurements, is less than $\sum_i(\Delta\delta_0)_i^2$. The accuracy of ΔH_2 and ΔS_2 measurements compares favorably with that expected by other physical methods.

The accuracy in the estimation of δ_{MN} can be improved if the OH chemical shift in methanol in samples containing higher proportions of TMA could be studied. Under the present experimental conditions this was not feasible.

Appendix

For gases having low quadrupole moments σ^{MM} and σ^{MN} in eqs. [4] and [9] can be estimated from the equation (3)

$$[A\text{-}1]\quad \sigma^{ij} = \tfrac{2}{3}\pi\chi_{vj} - (N\pi/1080)(\chi_{\parallel} - \chi_{\perp})_j \{\tau^2 H_9(y) + (y^4\tau^4/70)H_{15}(y) + \ldots.\}$$
$$- (\pi NA/6y^2)[\mu_j\{(\tau/3)H_6(y) + (y^4\tau^3/200)H_{12}(y) + \ldots.\} + (4a_j\mu_i/r_0{}^3y^2)\{H_6(y) + (\tau^2y^4/40)H_{12}(y) + \ldots.\}]$$
$$- (\pi NB/3y^4)[(2\mu_j{}^2/r_0{}^3)\{H_6(y) + (\tau^2y^4/40)H_{12}(y) + \ldots.\} + (a_j\mu_i\mu_j/r_0{}^6)\{y^2\tau H_{12}(y) + \tau^3y^6/60)\,H_{18}(y) + \ldots.\}]$$
$$- (\pi NB/y^4r_0{}^3)a_jI_j[H_6(y) + (y^4\tau^2/48)H_{12}(y) + \ldots.]$$

where μ_i, μ_j are the dipole moments, a_j the polarizability, I_j the ionization potential, χ_{vj} the volume susceptibility, and $(\chi_{\parallel} - \chi_{\perp})_j$ is the magnetic anisotropy, N is the Avogadro's number, and A and B are the bond parameters. τ and y are related by [A-2] and [A-3] to the parameters ε and r_0 of the "Stockmayer potential" tabulated by Hirschfelder *et al.* (14) for a number of gases while the functions $H_n(y)$ have been tabulated by Buckingham and Pople (15).

$$[A\text{-}2]\qquad \tau = \mu_i\mu_j/(\varepsilon r_0{}^3)$$

$$[A\text{-}3]\qquad y = (4\varepsilon/kT)^{1/2}$$

Following values were used for the calculation of σ^{MM} and σ^{MN}

Variable	Values for M (CH_3OH)	Values for N (TMA)
χ_m	-21.4×10^{-6}	-63.0×10^{-6} e.m.u.
$(\chi_{\parallel} - \chi_{\perp})$	0	0
ε/k	452	425
μ_0	1.70×10^{-18}	0.67×10^{-18} e.s.u.
r_0	3.67	4.34 A
a	3.23×10^{-24}	7.93×10^{-24} cm^3
I	17.4×10^{-12}	15.05×10^{-12} ergs

One also needs the bond parameters A and B for such calculations. Terms involving B make only little contribution and its values show comparatively small variations from one compound to another from its mean value of 0.5×10^{-18} e.s.u. The value of A changes significantly from one bond type to another (3–5). We have estimated an approximate value of A for the O—H bond by assuming that in intramolecular hydrogen bonds (orthophenols) the chemical shift change (from ortho to meta) is caused by electric field and magnetic anisotropy effect. Using the known molecular geometry for such molecules and $B = 0.5 \times 10^{-18}$ e.s.u. we find $A \simeq 25 \times 10^{-12}$ e.s.u. Substituting these values we obtain

$$\sigma^{MM} = -178.5 \text{ p.p.m. at } 343\ ^\circ\text{K}$$
$$-138.5 \text{ p.p.m. at } 443\ ^\circ\text{K}$$
$$\sigma^{MN} = -226.9 \text{ p.p.m. at } 343\ ^\circ\text{K}$$
$$-204.1 \text{ p.p.m. at } 443\ ^\circ\text{K}$$

Since these terms account for less than 10% of the observed shift an error in A of 100% is tolerable.

TABLE II

Observed and calculated chemical shifts of the hydroxyl proton in methanol in presence of trimethylamine

Sample number	Concentration (mole/l)		Temperature (°K)	Observed* † shift, δ_0 (Hz)	Calculated† ‡ shift, δ_c (Hz)	$\delta_c - \delta_0$ (Hz)	Corrected† § shift for the monomer, δ_M
	a	*b*					
1	0.0432	0.0263	343.2	38.6	39.7	1.1	57.2
			373.2	46.0	45.9	−0.1	57.2
			383.2	48.6	47.3	−1.3	57.2
			423.2	52.0	51.0	−1.0	57.2
2	0.0504	0.0417	363.2	39.0	39.3	0.3	56.9
			383.2	44.4	43.5	−0.9	56.9
			403.2	46.5	46.6	0.1	57.0
			433.2	48.0	49.6	1.6	57.1
3	0.0447	0.0545	363.2	37.4	36.5	−0.9	57.1
			393.2	43.7	43.5	−0.2	57.1
			423.2	47.2	47.8	0.6	57.2
			463.2	50.7	50.9	0.2	57.2
4	0.0343	0.1017	353.2	14.4	18.8	4.4	56.2
			373.2	28.1	28.9	0.8	56.3
			393.2	36.2	35.7	−0.5	56.3
			418.2	41.2	41.5	0.3	56.4
			453.2	46.0	46.4	0.4	56.4
5	0.0399	0.2059	363.2	−3.9	−0.3	3.6	54.8
			373.2	4.2	7.2	3.0	55.0
			383.2	14.8	13.5	−1.3	55.0
			393.2	21.2	18.7	−2.5	55.0
			413.2	26.0	27.0	1.0	55.1

*Correct to about ±1.5 Hz.
†Relative to resonance line in ethane gas at 10 atm.
‡From eqs. [7], [8], and [5] using $\Delta H_1 = -4152$ cal/mole, $\Delta S_1 = -17.47$ e.u., $\delta_{MM} = 0.0$ Hz, $\Delta H_2 = -5847$ cal/mole, $\Delta S_2 = -22.64$, $\delta_{MN} = -250$ Hz.
§Using eq. [9] with σ^{MM} and σ^{MN} from Appendix.

1. J. A. POPLE, W. G. SCHNEIDER, and H. J. BERNSTEIN. High resolution nuclear magnetic resonance. McGraw-Hill Book Co., Inc., New York. 1959.
2. J. W. EMSLEY, J. FEENEY, and L. H. SUTCLIFFE. High resolution nuclear magnetic resonance spectroscopy. The Pergamon Press, Ltd., New York. 1965.
3. W. T. RAYNES, A. D. BUCKINGHAM, and H. J. BERNSTEIN. J. Chem. Phys. **36**, 3481 (1962).
4. L. PETRAKIS and H. J. BERNSTEIN. J. Chem. Phys. **37**, 2731 (1962); **38**, 1562 (1963).
5. F. H. A. RUMMENS and H. J. BERNSTEIN. J. Chem. Phys. **43**, 2971 (1965).
6. G. GOVIL, A. D. H. CLAGUE, and H. J. BERNSTEIN. J. Chem. Phys. **49**, 2821 (1968).
7. J. C. DAVIS, K. S. PITZER, and C. N. R. RAO. J. Phys. Chem. **64**, 1744 (1960).
8. W. WELTNER, JR. and K. S. PITZER. J. Am. Chem. Soc. **73**, 2606 (1951).
9. C. B. KRETSCHMER and R. WIEBE. J. Am. Chem. Soc. **76**, 2579 (1954).
10. G. GOVIL and H. J. BERNSTEIN. J. Chem. Phys. **47**, 2818 (1967).
11. R. G. INSKEEP, F. E. DICKSON, and H. M. OLSON. J. Mol. Spectry. **5**, 284 (1960).
12. E. D. BECKER, U. LIDDEL, and J. N. SHOOLERY. J. Mol. Spectry. **2**, 1 (1958).
13. R. MATHUR, E. D. BECKER, R. B. BRADLEY, and N. C. LI. J. Phys. Chem. **67**, 2190 (1963).
14. J. O. HIRSCHFELDER, C. F. CURTISS, and R. B. BIRD. Molecular theory of gases and liquids. John Wiley and Sons, Inc., New York. 1965.
15. A. D. BUCKINGHAM and J. A. POPLE. Trans. Faraday Soc. **51**, 1173 (1955).

Can. J. Chem. Downloaded from www.nrcresearchpress.com by 210.87.254.105 on 09/05/12
For personal use only.

Can. J. Chem. Downloaded from www.nrcresearchpress.com by 210.87.254.105 on 09/05/12
For personal use only.

Normal coordinate analysis of dialkyldithiocarbamate and its selenium analogue

G. DURGAPRASAD, D. N. SATHYANARAYANA, AND C. C. PATEL
Department of Inorganic and Physical Chemistry, Indian Institute of Science, Bangalore, India

Received August 20, 1968

The infrared spectrum of N,N-dimethyldithiocarbamate complex of nickel(II) has been recorded in the range 2000–250 cm^{-1}. Normal coordinate analyses have been made for nickel dimethyldithiocarbamate and nickel dimethyldiselenocarbamate complexes and their infrared spectra indexed. The frequency shifts observed on alkyl substitution have been discussed. The M—Se stretching frequency occurs about 100 cm^{-1} lower in the diselenocarbamate complex as compared to M—S frequency of the dithiocarbamate.

Canadian Journal of Chemistry, 47, 631 (1969)

A few papers (1–9) have appeared since the publication of the infrared spectral studies of dithiocarbamate complexes of metals by Chatt *et al.* (10), where dithiocarbamate acts as a uninegative bidentate ligand. The chief interest has been the C=N stretching frequency which occurs around 1480–1550 cm^{-1}, which helps in estimating the contribution of each of the three canonical forms to the total structure. Very few investigators (5–9) mention one or two bands other than C=N. Nakamoto *et al.* (5), however, studied the infrared spectra of metal complexes of $S_2CNH_2^-$ and S_2CNHR^- (R being an alkyl group) and assigned their spectra on the basis of a normal coordinate treatment made for $Pt(S_2CNH_2)_2$, 1:1 complex. In spite of this, it has been found difficult to assign metal–sulfur and other frequencies in dialkyldithiocarbamate complexes (7, 8). A normal coordinate calculation has, therefore, been made for nickel dimethyldithiocarbamate to guide our assignments. The change observed on alkyl substitution has been pointed out from a comparison with the spectra of $S_2CNH_2^-$ complexes.

Since the spectra of selenium compounds are very similar to their corresponding sulfur compounds (vide infra), the calculations have also been made for nickel dimethyldiselenocarbamate with the same set of force constants as those of nickel dimethyldithiocarbamate.

Experimental

N,N-Dimethyldithiocarbamate complex of nickel(II) was prepared by adding aqueous solution of sodium dimethyldithiocarbamate to an aqueous solution of $NiCl_2.6H_2O$. The precipitate obtained was purified by washing with water followed by ether, and dried. The infrared spectra of the complex were recorded by Perkin–Elmer spectrophotometers models 137 and 21. The spectrum in the region 1800–250 cm^{-1} is given in Fig. 1

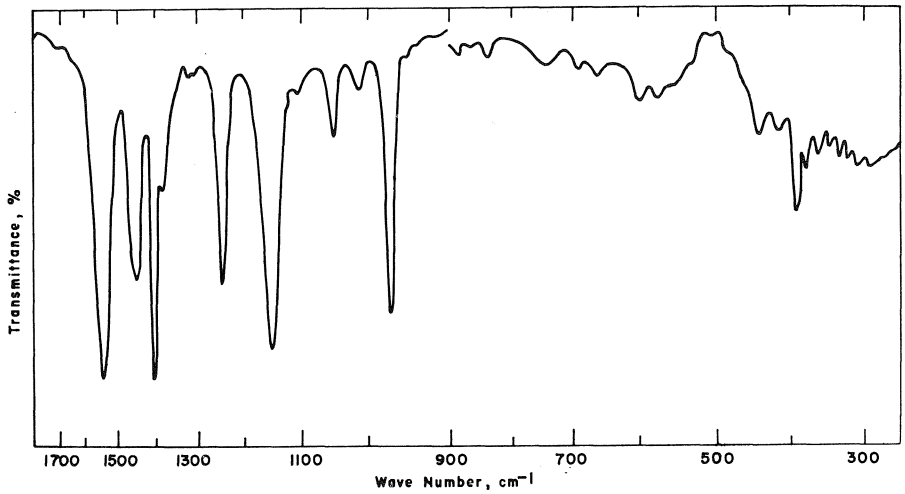

FIG. 1. Infrared spectrum of bis(N,N-dimethyldithiocarbamato)nickel(II).

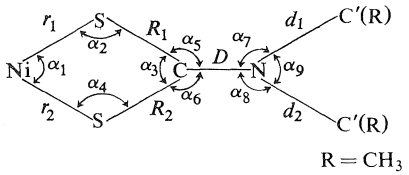

FIG. 2. Internal coordinates of nickel dimethyldithiocarbamate (1:1).

Normal Coordinate Treatment

The calculation has been made for 1:1 complex as shown in Fig. 2. In the present calculations, the methyl groups are treated as "point masses". The molecule is planar and belongs to the point group C_{2v}. The 15 vibrations are grouped into 11 in-plane vibrations ($6A_1 + 5B_2$) and 4 out-of-plane vibrations ($2A_2 + 2B_1$). Only the in-plane vibrations are considered here. The structural parameters for dithiocarbamate (11) and diselenocarbamate (12) are taken from the literature and are given in Table I.

TABLE I

Structural parameters

Nickel dithiocarbamate parameters	Nickel diselenocarbamate parameters
$r_1=r_2=2.212$ Å	$r_1=r_2=2.404$ Å
$R_1=R_2=1.707$ Å	$R_1=R_2=1.91$ Å
$D=1.33$ Å	$D=1.36$ Å
$d_1=d_2=1.485$ Å	$d_1=d_2=1.52$ Å
$\alpha_1=79°$	$\alpha_1=80°$
$\alpha_2=\alpha_4=85°$	$\alpha_2=\alpha_4=86°$
$\alpha_3=111°$	$\alpha_3=108°$
$\alpha_5=\alpha_6=124.5°$	$\alpha_5=\alpha_6=126°$
$\alpha_7=\alpha_8=121°$	$\alpha_7=\alpha_8=\alpha_9=120°$
$\alpha_9=118°$	

The symmetry coordinates with their approximate description are given in Table II. The method used is Wilson's **GF** matrix method (13). The secular equations for both A_1 and B_2 involve one redundant coordinate, each of which gives zero frequency in the solution.

The potential field used is of Urey–Bradley type (14). The best set of force constants obtained after several trials of computation is given in Table III. The force constants are of the same order as that used by Nakamoto *et al.* (5). The observed and calculated frequencies of nickel dimethyldithiocarbamate are given in Table IV. Potential energy distribution for this complex is given in Table V.

The calculations were carried out on a National Elliott 803 computer.

TABLE III

Force constants in mdyn/Å

Force constant	Value	Force constant	Value	Force constant	Value
K_r	2.02	H_{α_1}	0.30	F_{SS}	0.62
K_R	2.78	H_{α_2}	0.10	F_{SN}	0.28
K_D	6.68	H_{α_3}	0.52	F_{CM}	0.10
K_d	4.36	H_α	0.26	F_{RC}	0.48
		H_{α_7}	0.20	F_{RR}	0.32
		H_{α_9}	0.36		

Discussion

(a) Dithiocarbamate

The observed and calculated frequencies listed in Table IV agree fairly well, the maximum deviation being about 2%. The effect of alkyl substitution may be realized by comparing the present

TABLE II

Symmetry coordinates and their approximate description

Mode	Symmetry coordinate	Approximate description
A_1		
	$S_1 = (1/\sqrt{2})\ (\Delta r_1+\Delta r_2)$	M—S stretching
	$S_2 = (1/\sqrt{2})\ (\Delta R_1+\Delta R_2)$	C—S stretching
	$S_3 = \Delta D$	C—N stretching
	$S_4 = (1/\sqrt{2})\ (\Delta d_1+\Delta d_2)$	N—C′ stretching
	$S_5 = (1/\sqrt{12})\ (3\Delta\alpha_1-\Delta\alpha_2-\Delta\alpha_3-\Delta\alpha_4)$	Ring deformation
	$S_6 = (1/\sqrt{6})\ (\Delta\alpha_2+\Delta\alpha_4-2\Delta\alpha_3)$	Ring deformation
	$S_7 = (1/\sqrt{6})\ (2\Delta\alpha_9-\Delta\alpha_7-\Delta\alpha_8)$	C′—N—C′ bending
B_2		
	$S_1 = (1/\sqrt{2})\ (\Delta r_1-\Delta r_2)$	M—S stretching
	$S_2 = (1/\sqrt{2})\ (\Delta R_1-\Delta R_2)$	C—S stretching
	$S_3 = (1/\sqrt{2})\ (\Delta d_1-\Delta d_2)$	N—C′ stretching
	$S_4 = (1/\sqrt{2})\ (\Delta\alpha_2-\Delta\alpha_4)$	Ring deformation
	$S_5 = (\Delta\alpha_5-\Delta\alpha_6)$(unnormalized)	S_2C rocking
	$S_6 = (1/\sqrt{2})\ (\Delta\alpha_7-\Delta\alpha_8)$	C′—N—C bending

Can. J. Chem. Downloaded from www.nrcresearchpress.com by 210.87.254.105 on 09/05/12
For personal use only.

TABLE IV

Frequencies (cm^{-1}) of nickel dimethyldithiocarbamate and their assignment

Mode	Frequencies: Representation	Frequencies: Obsd.	Frequencies: Calcd.	Assignment
A_1	λ_1	1550	1551	C═N str.
	λ_2	1010	990	C′—N str.
	λ_3	600	605	C—S str. + 0.45 C′—N str. + 0.53 C′NC′ bend.
	λ_4	570	567	M—S str. + 0.86 ring def.
	λ_5	438	435	M—S str. + 0.82 ring def. + 0.86 C′NC′ bend.
	λ_6	285	284	Ring def. + 0.62 C′NC′ bend. + 0.51 ring def. + 0.45 M—S str.
B_2	λ_7	1245	1269	C′—N str.
	λ_8	975	980	C═S str.
	λ_9	410	408	M—S str.
	λ_{10}	385	386	CNC′ bend. + 0.65 M—S str. + 0.43 C═S str.
	λ_{11}	—	155	S_2C rock. + 0.7 CNC′ bend.

TABLE V

Potential energy distribution, $F_{ii}l_i^2\lambda$, for nickel dimethyldithiocarbamate

Mode	Symmetry coordinate	$F_{ii}l_i^2\lambda$: λ_1	λ_2	λ_3	λ_4	λ_5	λ_6
A_1	S_1	0	0.002	0.001	1.000	1.000	0.445
	S_2	0.108	0.217	1.000	0.180	0.202	0.118
	S_3	1.000	0.010	0.154	0.022	0.043	0.229
	S_4	0.121	1.000	0.448	0.066	0.011	0.011
	S_5	0	0.003	0.207	0.044	0.817	0.505
	S_6	0.110	0.179	0.031	0.859	0.039	1.000
	S_7	0.052	0.106	0.530	0.167	0.858	0.624

Mode	Symmetry coordinate	$F_{ii}l_i^2\lambda$: λ_7	λ_8	λ_9	λ_{10}	λ_{11}
B_2	S_1	0	0.002	1.000	0.650	0.070
	S_2	0.035	1.000	0.187	0.431	0.016
	S_3	1.000	0.182	0.023	0.088	0.009
	S_4	0.001	0.037	0.049	0.128	0.010
	S_5	0.119	0.273	0.149	0.194	1.000
	S_6	0.156	0.100	0.068	1.000	0.703

data with those of the complexes of $S_2CNH_2^-$ (5). The C═N stretching frequency which is a pure band is raised by more than 100 cm^{-1} (from ~1430 cm^{-1}) on alkylation. Since the alkyl groups are electron donating, the increase in frequency can be taken to indicate an increase in the C═N bond order.

The C═S stretch in $Pt(S_2CNH_2)_2$ occurs at 820 cm^{-1} as coupled vibration, coupling being with NH_2 rock (5). In the deuterated complex, the band is lowered to 710 cm^{-1} and is coupled with ND_2 rock (5). In nickel dimethyldithiocarbamate, the C═S band is practically pure and occurs at 975 cm^{-1}. The shift of C═S frequency is in the opposite direction to that observed for C—S vibration, which is a fairly coupled vibration. The increase of C═S frequency may indicate increased $p\pi$–$p\pi$ bonding of carbon and sulfur. It has been noted by Chatt *et al.* that in dithiocarbamate ligand, the —NR_2 group acts as a very strong electron releasing moiety, forcing the sulfur atoms to accept electrons from it (10). This electron drift into sulfur atoms will increase their electron donor capacity, which makes the formation of strong complexes with metals possible. It may, therefore, be expected that dialkyldithiocarbamates should be stronger donors than $S_2CNH_2^-$. This is also borne out by the M—S

Can. J. Chem. Downloaded from www.nrcresearchpress.com by 210.87.254.105 on 09/05/12
For personal use only.

Can. J. Chem. Downloaded from www.nrcresearchpress.com by 210.87.254.105 on 09/05/12
For personal use only.

frequencies of the respective nickel(II) complexes of these ligands. The M—S frequency of the nickel complex of the former ligand occurs at 410 cm^{-1}, while that of the latter (5) near 380 cm^{-1}. The assignment of 975 cm^{-1} band for C═S is justified from infrared spectra of the selenium analogue in which the band has been found to shift to lower frequency (15) as expected. The C—S frequency in the nickel dimethyldithiocarbamate has been found at 600 cm^{-1}, while it occurs at 622 cm^{-1} in platinum dithiocarbamate (5), $Pt(S_2CNH_2)_2$.

The M—S stretching frequencies occurring in the A_1 vibrations are strongly coupled with ring deformation and other bending modes of vibrations, while the M—S stretching frequency occurring at 410 cm^{-1} in the B_2 vibrations is a pure band. It may be noted that Moore and Larson (7) place the probable M—S stretching frequencies around 500 cm^{-1} in molybdenum dialkyldithiocarbamates, and Bagnall *et al.* (8) around 300 cm^{-1} in actinide complexes of dialkyldithiocarbamates, but definite assignment was not made by the latter investigators because of the occurrence of too many bands in the region. The M—S stretch occurs in the region 405–410 cm^{-1} in copper and zinc complexes, which have different structures. Thus the band is quite insensitive. The band at 385 cm^{-1} for C—N—C′ bending is justified since a strong band at 360 cm^{-1} has been assigned to similar C—N—C′ bending in N,N′-dimethylformamide (16).

A comparison of dithiocarbamates and N-alkyldithiocarbamates with N,N-dialkyldithiocarbamates is interesting. The bands at 1438, 820, 622, and 375 cm^{-1} in $Pt(S_2CNH_2)_2$ for C⋯N stretching, C═S stretching, C—S stretching, and M—S stretching, respectively, are observed at 1560, 665, 612, and 357 cm^{-1} in N-methyldithiocarbamate complex (5). It is argued that since the electron donating tendency of the alkyl group is expected to increase the C═N bond order and "decrease the C—S and Pt—S bond orders", the direction of the band shifts in N-alkyldithiocarbamate is in accordance with the predictions (5). In dialkyldithiocarbamates, the bands are observed at 1550, 975, 600, and 410 cm^{-1} region for the respective vibrations mentioned above. It is clear that the above argument for the C═S and M—S bond orders being decreased on electron donation from alkyl groups does not seem to hold. In fact, an increase in C═N, C═S, and M—S stretching frequencies is expected. Coucouvanis and Fackler found that dithiocarbamate square planar complex of nickel(II) forms adducts with nitrogen bases more easily than do the dialkyldithiocarbamates (4). This indicates that dialkyldithiocarbamates are better donors than dithiocarbamates. This is in accordance with the prediction that dialkyldithiocarbamate should be a better donor because of electron flow from $—NR_2$ group, as discussed before. The trend in the shift of M—S and C—S frequencies in N-alkyldithiocarbamate is unexpected. Since the molecule lacks symmetry, coupling of the vibrations not possible in dithiocarbamate and its dialkyl derivatives may be held responsible for this shift.

Apart from the bands discussed above, the well-known methyl deformation modes, asymmetric and symmetric, occur at 1445 (s) and 1400 (vs) cm^{-1}, and the methyl rocking vibrations at 1148 (s) and 1050 (m) cm^{-1} in nickel dimethyldithiocarbamate. The other bands observed for the same complex in the region 700–300 cm^{-1} are 676, 650, 590, 550, 375, 355, 341, 327, 315, and 302 cm^{-1}. All these bands are weak or very weak in intensity.

(b) Nickel Dimethyldiselenocarbamate

The substitution of selenium for sulfur, called "selenation" similar to deuteration, can be useful for assignment of the infrared bands. Jensen and Nielsen (17) have observed that the spectra of sulfur and their corresponding selenium compounds are almost identical except that the bands connected with sulfur are shifted by about 30–100 cm^{-1} lower in the selenium compounds. The force field for selenium compound is not expected to differ widely from that of the sulfur compounds. We have, therefore, carried out normal coordinate analysis for nickel dimethyldiselenocarbamate, using the force constants of nickel dimethyldithiocarbamate. The chief interest in these calculations is the assignment of the metal–ligand vibrations, in particular, and the shift in other frequencies, in general. The calculated frequencies along with their assignments are given in Table VI. Unfortunately, we could not get the spectrum of nickel dimethyldiselenocarbamate to "evaluate" the data. However, we

TABLE VI

Frequencies (cm^{-1}) of nickel dimethyldiselenocarbamate and their assignment

Mode	Calcd. frequency	Assignment
A_1	1547	C═N str.
	977	C′—N str.
	574	C′NC′ bend. + 0.42 C—Se str. + 0.44 C′—N str.
	390	M—Se str.
	348	Ring def. (S_5) + 0.97 C—Se str. + 0.52 C′NC′ bend.
	276	Ring def. (S_6) + 0.47 ring def. (S_5) + 0.39 C′NC′ bend.
B_2	1278	C′—N str.
	946	C═Se str.
	344	CNC′ bend. + 0.7 C═Se str.
	308	M—Se str.
	136	Se_2C rock. + 0.55 CNC′ bend.

were able to get the infrared spectra of nickel diethyldiselenocarbamate in the NaCl and KBr regions (18). The spectrum has bands at 1520, 987, 570, and 415 cm^{-1} which could be assigned to ν(C═N), ν(C′—N) coupled with δ(C′NC′), ν(C—Se), and ν(C′—N) coupled with ν(M—Se), respectively, in the A_1 vibrations, the calculated frequencies being 1547, 977, 574, and 390 cm^{-1}. The bands are also observed at 1278 and 950 cm^{-1}, the calculated frequencies being 1278 and 946 cm^{-1}, for ν(C′—N) and ν(C═Se), respectively, for the B_1 type of vibrations. In the spectra of ethyl and methyl compounds, no major changes in the bands listed above are expected unless coupling with CH_2 or C—C vibrations affects these bands. The above comparison is therefore taken to be valid. The agreement between the calculated and available observed frequencies lends confidence to the assignment of the bands of diselenocarbamate. The assignment of the infrared frequencies in the selenium compound is similar to that of the sulfur compound, the C═S stretching frequency being lowered on selenation by about 35 cm^{-1}. The lowering is in conformation with the observation of Jensen *et al.* (15). Some of the bands are not affected as expected and only the metal–ligand frequency seems to have been affected largely. The metal–selenium stretching frequency occurring at 308 cm^{-1} (B_2) is lower by about 100 cm^{-1} as compared to the metal–sulfur frequency at 410 cm^{-1}. The calculation is thus of particular interest in assigning the metal–ligand stretching frequency and other frequencies in the far infrared region.

Acknowledgments

The authors wish to thank Professor M. R. A. Rao for his keen interest in the work. The help of Dr. K. J. Rao, Indian Institute of Technology, Kanpur, in recording a spectrum, is warmly acknowledged. Thanks are also due to Messrs. A. M. Pathan and B. S. N. Murthy of Hindustan Aeronautics Ltd., Bangalore, for their assistance in computation.

1. M. Delépine. Bull. Soc. Chim. France, 5 (1958).
2. R. Colton, R. Levitus, and G. Wilkinson. J. Chem. Soc. 5275 (1960).
3. F. A. Cotton and J. A. McCleverty. Inorg. Chem. **3**, 1398 (1964).
4. D. Coucouvanis and J. P. Fackler, Jr. Inorg. Chem. **6**, 2047 (1967).
5. K. Nakamoto, J. Fujita, R. A. Condrate, and Y. Morimoto. J. Chem. Phys. **39**, 423 (1963).
6. M. L. Shankaranarayana and C. C. Patel. Spectrochim. Acta, **21**, 95 (1965).
7. F. W. Moore and M. L. Larson. Inorg. Chem. **6**, 998 (1967).
8. K. W. Bagnall, D. Brown, and D. G. Holah. J. Chem. Soc. A, 1149 (1968).
9. J. P. Bibler and D. G. Karraker. Inorg. Chem. **7**, 982 (1968).
10. J. Chatt, L. A. Duncanson, and L. M. Venanzi. Suomen Kemistilehti, **29B**, 75 (1956).
11. M. Bonamico, G. Dessy, C. Mariani, A. Vaciago, and L. Zambonelli. Acta Cryst. **19**, 619 (1965).
12. M. Bonamico and G. Dessy. Chem. Commun. 1114 (1967).
13. E. B. Wilson, J. C. Decius, and P. C. Cross. Molecular vibrations. McGraw-Hill Book Co., Inc., New York. 1955.
14. T. Shimanouchi. J. Chem. Phys. **17**, 245 (1949).
15. K. A. Jensen, J. B. Carlsen, A. Holm, and P. H. Nielsen. Acta Chem. Scand. **17**, 550 (1963).
16. G. Kaufmann and M. J. F. Leroy. Bull. Soc. Chim. France, 402 (1967).
17. K. A. Jensen and P. H. Nielsen. Acta Chem. Scand. **20**, 597 (1966).
18. V. Krishnan and M. L. Shankaranarayana. Private communications.

Can. J. Chem. Downloaded from www.nrcresearchpress.com by 210.87.254.105 on 09/05/12
For personal use only.

Can. J. Chem. Downloaded from www.nrcresearchpress.com by 210.87.254.42 on 09/05/12
For personal use only.

Phenoxo complexes of copper(II)

J. F. HARROD[1]
General Electric Research & Development Center, Schenectady, New York 12301

Received August 14, 1968

A series of phenoxo complexes of copper(II) containing a variety of halophenoxo ligands and a variety of amine ligands has been prepared. The thermal stability of the complexes with regard to the decomposition reaction:

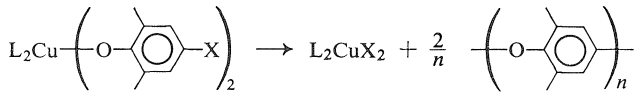

was found to be lower with those ligands, L, which increase the oxidizing power of the copper(II) and vice versa.

The intense absorption bands in the visible region exhibited by these complexes have been assigned to a metal-to-ligand charge transfer process.

Canadian Journal of Chemistry, 47, 637 (1969)

Introduction

The preparation and properties of transition metal alkoxo derivatives have been studied in great detail (1). The aryloxo derivatives, on the other hand, have been virtually ignored, except for chelating ligands which utilize an aryloxy function. Although innumerable compounds are known containing such chelating ligands as salicylaldehydate, 8-hydroxyquinolinate, and 2-azophenolate, the specific properties of the aryloxy–metal bond have not been investigated.

A series of simple phenoxotitanium complexes was prepared by Funk *et al.* (2), from a variety of substituted phenols. More recently, a structural study by Watenpaugh and Caughlin (3) has shown the dimeric dichlorodiphenoxotitanium-(IV) to contain both linear and bridging phenoxo groups, as well as titanium in an unusual five-coordinate state. The latter authors commented on the unusual color of phenoxotitanium complexes, but did not advance a satisfactory explanation.

The classical use of iron(III) for the colorimetric determination of phenols has prompted several investigations (4, 5) to seek the origin of the characteristic intense colors obtained. There is general agreement that phenoxoiron(III) complexes are responsible for the colors, but the evidence is largely circumstantial and no stoichiometric complex has ever been isolated, or characterized.

A series of bis(phenoxo)bis(pyridine)copper-(II) complexes was prepared and characterized by Blanchard *et al.* (6) using a variety of substituted phenols. Such complexes are of considerable chemical interest because of the important industrial (7) and biological (8) role of copper(II) in the selective catalytic oxidation of phenols. A remarkable property of certain 4-halophenoxocopper(II) complexes is their tendency to undergo thermal decomposition (6), according to the generalized reaction [1], where L represents a neutral ligand and X is a halogen atom. It has been suggested (6) that the initiating step, both in reaction [1] and in the catalytic oxidative coupling of phenols (7), is ligand-to-

[1] 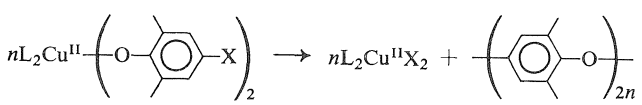

metal charge transfer to produce a phenoxy radical and a copper(I) species.

The present study was undertaken to answer two questions. Firstly, what is the dependence of the thermal stability of phenoxocopper(II) complexes on the nature of the neutral ligand. Secondly, what is the cause of the intense colors

[1]Present address: Chemistry Department, McGill University, Montreal, Quebec.

TABLE I

Analytical data for some phenoxocopper(II) complexes

Phenol	Amine	C		H		N		Chloride	
		Calcd.	Found	Calcd.	Found	Calcd.	Found	Calcd.	Found
2,4,6-Trichloro	Pyridine*	43.0	43.2	2.28	2.30	4.6	4.5	34.7	34.8
,,	NH_3†	29.3	28.8	2.04	2.2	5.7	5.8	43.4	43.8
,,	$C_2H_5NH_2$†	35.1	35.2	3.29	3.25	5.1	5.1	38.9	39.4
,,	Tetramethylen*	37.7	37.6	3.50	3.43	4.9	5.0	37.2	38.2
,,	Tetraethylen*	42.0	41.8	4.45	4.45	4.5	4.4	33.9	34.5
,,	2,2′-Dipyridyl†	43.1	42.1	1.96	2.00	4.6	4.7	34.8	35.0
,,	*o*-Phenanthroline†	45.2	45.2	1.88	2.03	4.4	4.4	33.4	33.6
Pentachloro	Tetramethylen*	30.4	30.5	2.25	2.28	4.0	3.8	49.9	50.4
2,4-Dichloro	,, *	42.9	42.6	4.37	4.42	5.6	5.5	28.2	28.6

*Prepared by aqueous solution method.
†Prepared by exchange with pyridine complex.

of phenoxocopper(II) complexes. (They are brown to purple in solution, dark brown to black crystals.)

Experimental

(1) Preparation of Phenoxo Complexes from Aqueous Solutions

Complexes derived from acidic phenols (in the present work this means those with at least two halide substituents) were prepared easily and in high yield from aqueous solutions of reagents. The standard procedure was to add the required amount of neutral ligand to a solution of $CuSO_4.5H_2O$ (0.02 mole) in distilled water (50 ml). A second solution containing the phenol (0.04 mole) and sodium hydroxide (0.04 mole) in water (50 ml) was then slowly added to the copper solution with vigorous stirring. The resulting dark brown slurry was filtered, washed with water, and dried. Recrystallization of pyridine complexes was effected by dissolution in a minimum of hot benzene, filtration, and addition of excess methanol to the hot benzene filtrate. The tetramethyl- and tetraethylethylenediamine complexes were recrystallized from hot toluene–hexane solutions. The yields of these complexes were essentially quantitative. Analyses of some representative complexes are given in Table I.

(2) Preparation of Complexes from Bis(2,4,6-trichlorophenoxo)bis(pyridine)copper(II)

The high solubility of the pyridine complex in benzene permitted the simple preparation of other complexes by displacement of the pyridine in benzene solution.

Treatment of a hot saturated solution of the pyridine complex in benzene (about 5.0 g of complex in 50 ml of benzene) with a boiling solution of 2,2′-dipyridyl (1.6 g in 10 ml benzene), followed by dilution of the mixture with an equal volume of boiling hexane, yielded black crystals of the dipyridyl complex on cooling to room temperature. The yield (5.0 g) was essentially quantitative. The *o*-phenanthroline complex was prepared by the same method.

The ammonia, ethylamine, and ethylenediamine complexes were quite insoluble in benzene and could be precipitated by careful addition of the appropriate ligand to a benzene solution of the pyridine complex at room temperature. The ammonia complex was best prepared by bubbling gaseous ammonia into the benzene solution. The other amine ligands were added as solutions in benzene. Addition of excess of these saturated amine ligands resulted in the formation of ionic complexes by expulsion of the phenoxo ligand from the coordination sphere. The ionic complexes were blue, whereas the neutral complexes were light brown in the case of ammonia and ethylamine, and bright orange in the case of ethylenediamine.

Analyses of some derivatives prepared from the pyridine complex are given in Table I.

The orange bis(ethylenediamine) complexes with trihalophenols were also easily prepared by the aqueous solution method described above.

(3) Spectra of Complexes

Visible and ultraviolet spectra were measured with a Perkin–Elmer 202 recording spectrophotometer.

Infrared spectra were measured with a Perkin–Elmer Model 521 grating spectrometer. Samples were studied in carbon tetrachloride solution and dispersed in potassium bromide pellets.

Results

Types of Phenoxocopper(II) Compounds

Most amine ligands were found to yield tetracoordinate complexes of the type $L_2Cu(OPh)_2$ (L = monofunctional amine ligand; OPh = halosubstituted phenoxo ligand) using the methods described above. A notable exception was ethylenediamine which yielded complexes containing two ethylenediamine ligands per copper(II) ion by both synthetic methods.

Saturated aliphatic amines (including ethylenediamine) in excess yielded blue ionic complexes, soluble in water, in which the phenoxo ligand had presumably been expelled from the coordination sphere. This phenomenon was not

Can. J. Chem. Downloaded from www.nrcresearchpress.com by 210.87.254.42 on 09/05/12
For personal use only.

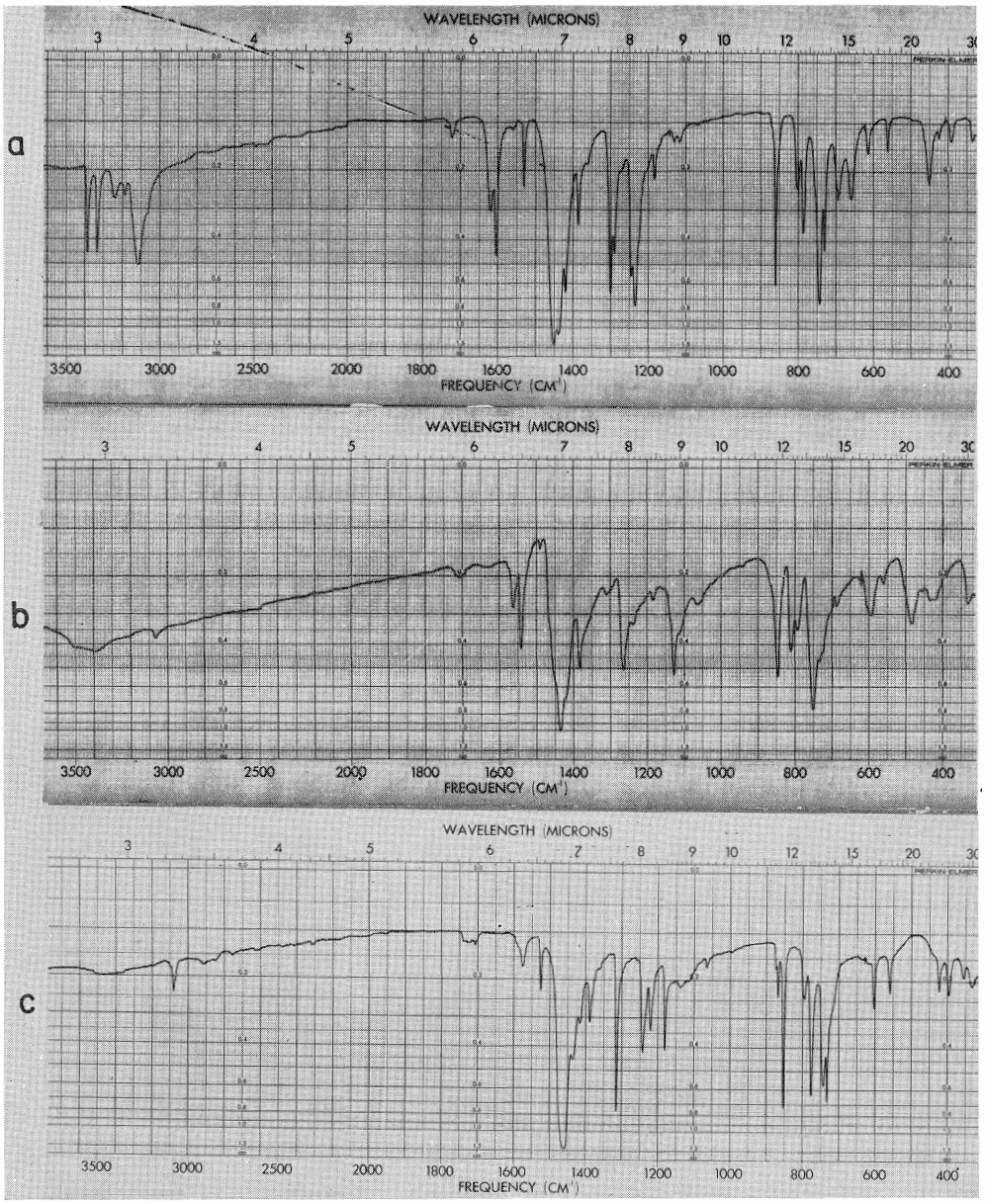

FIG. 1. Infrared spectra of (*a*) bis(trichlorophenoxo)diamminecopper(II), (*b*) copper(II)trichlorophenolate, and (*c*) sodium trichlorophenolate.

observed with unsaturated aromatic bases. In fact pyridine was found to be an excellent solvent for the $Py_2Cu(OPh)_2$ complexes and their spectra were qualitatively the same in pyridine as in benzene. It may thus be concluded that pyridine has virtually no tendency to increase the coordination number of these tetracoordinate complexes, nor to displace the phenoxo ligand.

A fourth type of complex was obtained by the aqueous solution method if the reaction was carried out in the absence of any added neutral ligand. The dark brown amorphous compounds

Can. J. Chem. Downloaded from www.nrcresearchpress.com by 210.87.254.42 on 09/05/12
For personal use only.

Can. J. Chem. Downloaded from www.nrcresearchpress.com by 210.87.254.42 on 09/05/12
For personal use only.

TABLE II

Infrared data for trichlorophenoxocopper(II) complexes*

Neutral ligand	Absorption frequency (cm^{-1})													
$C_2H_5.NH_2$		1530		1450		1295	1240	1220			845	800, 785	740
NH_3		1530		1450		1298	1240	1230			858	800, 785	740
None		1540		1435		1265			1130		848	810, 790	750
2,2′-Dipyridyl		1530		1460–1440		1312	1250				855	800, 790	750
$(CH_3)_2N.CH_2.CH_2.N(CH_3)_2$		1525		1460		1310, 1280	1245	1230			858	800, 780	750
$H_2N.CH_2CH_2.NH_2$		1515		1465		1300	1240				840	790, 770	730
Pyridine	1605	1527	1489	1455	1445	1305	1245	1210		1068	1040	855, 845	800, 785	760, 750
$(Py)_2CuBr_2$	1605, 1600		1490		1445			1220		1078	1040			753
Sodium trichlorophenolate		1525		1450		1310	1240	1220	1180			855	780	740

*Data cited for spectra in KBr pellets. Spectra in chloroform showed only minor shifts and intensity changes.

TABLE III

Thermal stability of trichlorophenoxocopper(II) complexes

Neutral ligand	Thermal behavior
Biquinolyl, triphenylphosphine	Complexes too unstable to be isolated
2,6-Dimethylpyridine	Stable enough to be isolated as solid. Lifetime in benzene ~ hours at room temperature*
Ammonia ethylamine	Rapid decomp. at ~ 90 °C in solid state. Lifetime in benzene ~ days at room temperature*
Pyridine	Sharp decomp. at 125–127 °C in solid. Lifetime in benzene ~ months at room temperature,* ~ 12 h at 80 °C
None	Sharp decomp. at 143–145 °C in solid
2,2′-Dipyridyl	m.p., 175–177 °C; decomp. ~ 195 °C
Tetraethylethylenediamine	m.p., 167–168 °C
Tetramethylethylenediamine	m.p., 182–184 °C. Lifetime in benzene ~ years†
o-Phenanthroline	m.p., 220 °C; decomp. ~ 220 °C

*These observations were made on numerous solutions prepared for spectroscopic and other measurements.
†One solution of this complex which had been stored for two years, was found to be completely decomposed. The isolated polymer was found to have $M_n \sim 80\,000$, by far the highest molecular weight ever obtained by thermal decomposition of phenoxy complexes.

obtained had the stoichiometry $Cu(OPh)_2$, and were characterized by their almost complete insolubility. The only solvent found for these compounds was dimethylformamide and reprecipitation by addition of water to dimethylformamide solutions gave dark brown crystalline compounds containing coordinated dimethylformamide.

Infrared Spectra of the Tetracoordinate Complexes

Table II lists some of the principal infrared absorptions exhibited by a series of trichlorophenoxocopper(II) complexes. A comparison between the spectrum of the pyridine complex and the spectra of sodium trichlorophenolate and dibromobis(pyridine)copper(II), indicates that all of the bands of the former may be accounted for in terms of complexed pyridine and a trichlorophenolate anion, except for minor frequency shifts. The same is true of the other complexes, including the bis(ethylenediamine) complex. The only obvious deviation occurs with the simple copper trichlorophenolate which contains no neutral ligands.

The spectra of sodium trichlorophenolate, copper trichlorophenolate, and bis(trichlorophenoxo)diamminecopper(II) are shown in Fig. 1. The most significant variations in these spectra occur in the 1200–1300 cm^{-1} region, the region in which the C—O vibrations of the phenoxy group are expected to occur. Although the ammine complex spectrum is somewhat different from that of sodium trichlorophenolate in this region, the difference is small compared to that of the copper trichlorophenolate.

Thermal Stability of (Trichlorophenoxo)-copper(II) Complexes

All of the trichlorophenoxo complexes thus far prepared were found to decompose according to eq. [1]. The ease of decomposition was found qualitatively to vary to a considerable degree, depending on the nature of the neutral ligand. Addition of biquinolyl, or triphenyl phosphine to benzene solutions of the pyridine complex resulted in rapid production of poly(dichlorophenyleneoxide) at room temperature, whilst the dipyridyl complex was stable for several years in benzene solution. Some qualitative data on the thermal decomposition of solutions, or pure compounds are shown in Table III.

In all cases of decomposition, the poly(dichlorophenyleneoxide) was isolated and characterized according to previously described procedures (6). The copper chloride complexes resulting from decomposition were only characterized in the case of the pyridine complex (Py_2CuCl_2), the uncomplexed copper trichlorophenolate ($CuCl_2$), and the tetramethylethylenediamine complex referred to in footnote (marked †) to Table III (dichlorotetramethylethylenediaminecopper(II)).

Electronic Spectra of Phenoxocopper(II) Complexes

The spectrum of bis(trichlorophenoxo)bis-(pyridine)copper(II) is shown in Fig. 2. This spectrum was typical of all the phenoxo complexes examined and may be discussed in terms of four regions.

A ligand band system in the 40 to 50 kK (1 kK = 1000 cm^{-1}) region was observed in

Can. J. Chem. Downloaded from www.nrcresearchpress.com by 210.87.254.42 on 09/05/12
For personal use only.

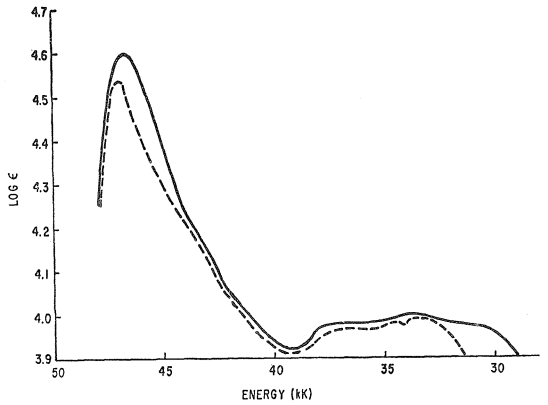

FIG. 2. Ultraviolet spectra of: ------, trichlorophenol; and ——, bis(trichlorophenoxo)bis(pyridine)copper(II) (in methanol solution).

methanol solution. Within the sensitivity and resolution of the instrument, these high energy ligand bands were not significantly altered by complexing and were not studied in any detail.

In benzene all of the complexes examined obeyed the Beer–Lambert law. Three band systems were observed at $\lambda_{max} \sim 35$, ~ 27, and ~ 20 kK. The spectrum of the tetramethylethylenediamine complex is shown in Fig. 3. The 35 kK band system, arising, at least partly, from a phenolate ligand transition, was strongly perturbed by varying the neutral ligands of the complex. The changes occurring in this band, with trichlorophenoxocopper(II) complexes, are illustrated for several neutral ligands in Fig. 4. The 27 kK band appeared as a shoulder on the low energy tail of the 35 kK band, and was present in all of the complexes examined. This band did not appear to change intensity, or position, on varying the neutral ligands.

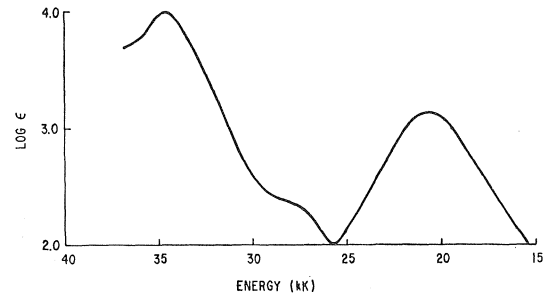

FIG. 3. Spectrum of bis(trichlorophenoxo)-*N*,*N*,*N*′,-*N*′-tetramethylethylenediaminecopper(II) in the ultraviolet–visible region (in benzene solution).

The band in the 19 to 23 kK region is mainly responsible for the intense colors of the phenoxocopper(II) complexes. The absorption maximum for this band was found to undergo shifts on substituting different neutral ligands into a given phenoxo complex. Data for a number of complexes in benzene and other solvents are given in Table IV.

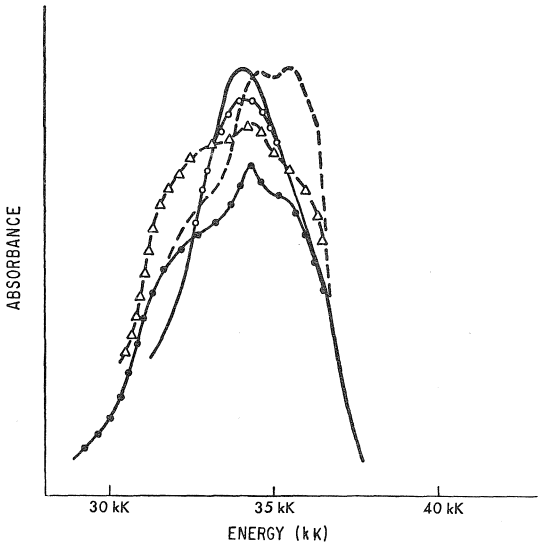

FIG. 4. Effect of amine ligands on the 35 kK band system of trichlorophenoxocopper(II) complexes. ------, pyridine; —●—●—, NH_3; —△—, $C_2H_5NH_2$; —○—, tetramethylethylenediamine; ——, tetraethylethylenediamine.

The Structure of Phenoxocopper(II) Complexes

Chemical analysis, molecular weight data, and infrared spectra obtained in the present study and those reported in ref. 6, all indicate that the majority of phenoxocopper(II) complexes are four-coordinated and monomeric.

A determination of the crystal structure of bis(trichlorophenoxo)*N*,*N*,*N*′,*N*′tetramethylethylenediaminecopper(II) has recently been completed (9). In this complex the copper(II) ion is coordinated by two nitrogens and two oxygens in an approximately square planar arrangement. There is a small tetrahedral distortion giving an angle of ca. 20° between the N—Cu—N and the O—Cu—O planes. A schematic representation of the molecule is shown in Fig. 5.

Perhaps the most important property of this molecule, as far as the present study is concerned,

Can. J. Chem. Downloaded from www.nrcresearchpress.com by 210.87.254.42 on 09/05/12
For personal use only.

TABLE IV

Spectroscopic data for phenoxocopper(II) complexes

Neutral ligand	Solvent	Phenol	ν_{max} (kK) (±0.02)	$\varepsilon_{max} \times 10^{-3}$
$(C_2H_5)_2N.CH_2.CH_2.N(C_2H_5)_2$	Benzene	2,4,6-Trichloro	19.76	3.3
o-Phenanthroline	,,	,,	20.14	3.1
2,2′-Dipyridyl	,,	,,	20.35	2.0
$(CH_3)_2N.CH_2.CH_2.N(CH_3)_2$	,,	,,	20.54	2.5
Pyridine	,,	,,	22.51	1.1
NH_3	,,	,,	22.55	1.3
$C_2H_5.NH_2$	,,	,,	22.65	1.3
2,6-Lutidine*	,,	,,	24.18	—
$(CH_3)_2.N.CH_2.CH_2.N(CH_3)_2$	,,	Pentachloro	20.40	—
,,	,,	2,4-Dichloro	20.85	—
,,*	,,	4-Chloro	22.00	—
Pyridine	Pyridine	2,4,6-Trichloro	21.9	1.0
,,	Hexane	,,	22.7	1.0
,,	Tetrahydrofuran	,,	22.9	1.0
,,	Chloroform	,,	22.7	1.2
,,	Ethanol	,,	~25.0	0.7
,,	Methanol	,,	~25.0	0.5

*Due to their instability, these solutions were of doubtful purity.

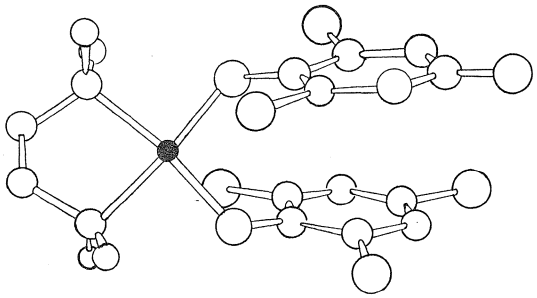

FIG. 5. Structure of bis(trichlorophenoxo)tetramethylethylenediaminecopper(II). (After Vogt, La Placa, and Bednowitz, see ref. 9.)

is the Cu—O—C bond angle of ca. 120° and the resulting very close approach of the two rings of the phenoxo ligands. That this close approach was not primarily responsible for the charge transfer bands observed in the present study may be concluded from the fact that these bands were also observed in the complexes with monodentate ligands. The pyridine complex had no detectable dipole moment and must be *trans*, a configuration which would make close approach of the ligand rings impossible.

Discussion

Thermal Stability of Trichlorophenoxo Complexes

If, as has been previously suggested (6), the initiation step in the thermal decomposition reaction [1] is a ligand-to-metal electron transfer, the nature of the neutral ligand should strongly influence the thermal stability of the starting complex. After a thorough study of the effect of amine ligands on the redox potential of the Cu(II)/Cu(I) system, James and Williams (10) concluded that the order for stabilization of Cu(II) was ethylenediamine ≫ 2,2′-bipyridyl > 1,10-phenanthroline > pyridine ~ ammonia ≫ 2,2′-biquinolyl. The most important factors governing this sequence were the chelate effect (Cu(II) forms chelates readily, Cu(I) is reluctant to form chelates) and the π-acceptor property of the ligand. The latter was invoked by James and Williams (10) to explain the order of potentials of the dipyridyl and phenanthroline complexes. The anomalous position of the biquinolyl ligand in the series was attributed to its poor ability to chelate, due to steric interference by the 8,8′ hydrogens.

In the present study a striking correlation was found to exist between the thermal stability of phenoxocopper(II) complexes and the position of the amine ligand in the James and Williams sequence of oxidation potentials. Those complexes containing amine ligands which preferentially stabilize copper(I) were found to be markedly less stable than those containing ligands expected to enhance the stability of copper(II). Although no oxidation potential data are available for tetraalkylethylenediamine complexes, they would certainly be expected to stabilize copper(II) and the phenoxo complexes

Can. J. Chem. Downloaded from www.nrcresearchpress.com by 210.87.254.42 on 09/05/12
For personal use only.

containing such ligands were found to be exceptionally resistant to thermal decomposition.

The Electronic Spectra of Phenoxocopper(II) Complexes

The outstanding feature of the visible–ultraviolet spectra of phenoxocopper(II) complexes is the general occurrence of an intense band in the 20 kK region. The intensity of this band is too high for a simple d → d transition and at first sight it was tempting to assign the band to a ligand-to-metal charge transfer process. Examination of the experimental observations argued against such an assignment. The evidence may be summarized as follows:

(*i*) Complexes with a low energy ligand-to-metal charge transfer would be expected to decompose more readily than those with a higher energy charge transfer. In fact, complexes which have absorption at lower energy have been found to be much more thermally stable than complexes with absorption at high energy.

(*ii*) The thermal stability of complexes follows the sequence of oxidation potentials for Cu(I)/Cu(II) couples in the presence of various amine ligands. For example, the thermal stability of 2,4,6-trichlorophenoxo complexes was found to be in the sequence: *o*-phenanthroline ~ bipyridyl > pyridine ~ NH_3 > biquinolyl. The energy of the 20 kK band followed the inverse of this sequence.

(*iii*) In the series of complexes of 4-chloro-, 2,4-dichloro-, 2,4,6-trichloro-, and pentachlorophenol, with the same neutral ligand, the absorption moves progressively to lower energy. This shift is in a direction contrary to that expected for a ligand-to-metal charge transfer, on the basis of the expected ease of oxidation of the corresponding phenoxide ion.

This evidence strongly suggests the origin of the 20 kK band to be a metal-to-ligand charge transfer, rather than the reverse. On the basis of chemical intuition, the latter proposition seems unlikely. In effect, it requires the donation of an electron by Cu(II), a good oxidizing agent, to a phenoxide ion, already carrying negative charge and normally considered to be a reducing species. However, a qualitative study of the ligand and metal energy levels indicates that such a transition is not unlikely.

The existence of metal-to-ligand charge transfer has been postulated and discussed at some length by Jørgensen (11). He suggested that charge transfer bands in certain pyridine and *o*-phenanthroline complexes may originate from the excitation of an electron in an atomic-like orbital on the metal ion to an antibonding π* orbital on the ligand. Such a transition could certainly be postulated to occur in phenoxo complexes.

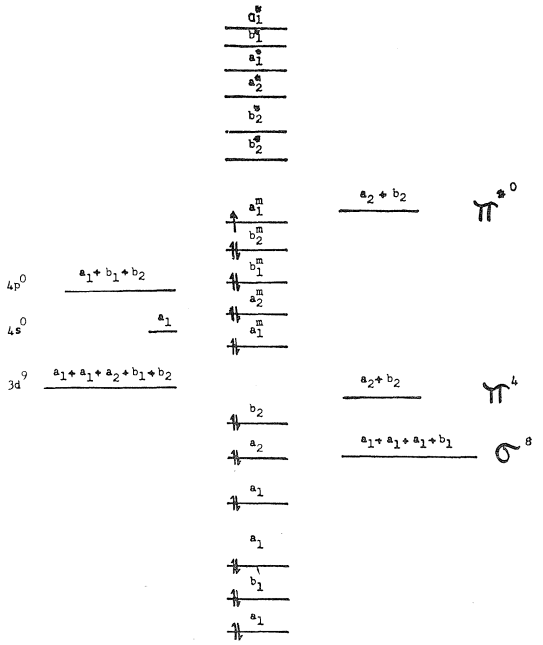

FIG. 6. Schematic molecular orbital diagram for a *cis*-bis(phenoxo)copper(II) complex.

A qualitative molecular orbital energy level diagram for *cis*-bis(trichlorophenoxo) complexes is shown in Fig. 6. It is assumed that the molecule exhibits ideal C_{2v} symmetry and that the neutral ligands only contribute orbitals of σ symmetry. The phenoxo ligands were assumed to contribute σ-orbitals, a set of low energy and a set of high energy π-orbitals. The molecular orbital diagram for a *trans*-complex (D_{2h}) would not differ qualitatively from Fig. 5, nor would the inclusion of π-orbitals from the neutral ligands cause serious change.

The existence of metal-to-ligand charge transfer may be understood in terms of excitation from $b_2{}^m$, or $a_1{}^m$ orbitals (largely associated with the metal) to $b_2{}^*$, or $a_2{}^*$ orbitals (ligand antibonding π-orbitals associated largely with oxygen). Similarly, a ligand-to-metal charge

Can. J. Chem. Downloaded from www.nrcresearchpress.com by 210.87.254.42 on 09/05/12
For personal use only.

transfer band would be expected as a result of excitations from the highest energy a_1 σ-bonding orbital, and/or the a_2 and b_2 π-bonding orbitals to a_1^m. Such transitions are almost certainly responsible for the manifold of bands in the 35 kK region (c.f. Fig. 3). It is interesting to note that the latter bands do in fact extend to lower energy in those complexes exhibiting poor thermal stability. The shifts of the 20 and 35 kK band systems in opposing directions suggest that the primary effect of the amine ligands is to raise, or lower, the metal orbitals relative to the phenoxo ligand orbitals.

The effect of solvent on the metal-to-ligand charge transfer is not easily interpreted. Solvation at the vacant coordination positions above and below the plane of the complex should raise the average energy of the metal orbitals. The low value for the transition energy in pyridine compared to hexane, benzene, and chloroform is in accord with such an interpretation. The slightly higher value in tetrahydrofuran and the much higher values in methanol or ethanol, must, however, be considered anomalous. In the latter solvents a specific effect, such as hydrogen bonding to the phenoxy oxygen, may be operative.

Conclusions

The properties of phenoxocopper(II) complexes indicates that phenolate ligands can participate in both metal-to-ligand and ligand-to-metal charge transfer. In the case of copper(II) complexes, both types of transition are at relatively low energy and the energies of the transitions are quite sensitive to the character of both the phenolate and the other ligands present in the complex.

At present the most probable initiation step for decomposition of phenoxocopper(II) complexes involves homolysis of the Cu—O bond via ligand-to-metal charge transfer. There is no evidence to date to suggest that the low energy metal-to-ligand charge transfer has any relationship to the chemistry of decomposition. A detail study of the kinetics and mechanism of this reaction is in progress.

Acknowledgment

The author would like to thank L. H. Vogt, S. La Placa, and A. Bednowitz for a private communication of their results prior to publication.

1. D. C. Bradley. *In* Progress in inorganic chemistry. Vol. II. *Edited by* F. A. Cotton. Interscience Publishers, Inc., New York. 1960. p. 303.
2. H. Funk, A. Schlegel, and K. Zimmermann. J. Prakt. Chem. **3**, 320 (1956).
3. K. Watenpaugh and C. N. Caughlin. Inorg. Chem. **5**, 1782 (1966).
4. M. Nageswara Rao and Bh. S. V. Raghava Rao Z. Physik. Chem. Leipzig, **212**, 267 (1959); Z. Physik. Chem. Frankfurt, **21**, 388 (1959).
5. W. R. Brode and W. J. Wesp. J. Am. Chem. Soc. **56**, 1037 (1934).
6. H. S. Blanchard, H. L. Finkbeiner, and G. A. Russel. J. Polymer Sci. **58**, 469 (1962).
7. A. S. Hay, J. S. Blanchard, G. F. Endres, and J. W. Eustance. J. Am. Chem. Soc. **81**, 6335 (1959).
8. W. Brackman and E. Havinga. Rec. Trav. Chim. **74**, 1107 (1955).
9. L. H. Vogt, S. La Placa, and A. Bednowitz. Am. Chem. Soc. Meeting; Inorg. Div. San Francisco. March, 1968.
10. B. R. James and R. J. P. Williams. J. Chem. Soc. 2007 (1961).
11. C. K. Jørgensen. Acta Chem. Scand. **11**, 166 (1957).

Can. J. Chem. Downloaded from www.nrcresearchpress.com by 210.87.254.42 on 09/05/12
For personal use only.

Can. J. Chem. Downloaded from www.nrcresearchpress.com by 210.87.254.6 on 09/05/12
For personal use only.

Ion–molecule reactions in vinyl chloride and vinyl bromide

J. A. HERMAN[1], J. J. MYHER[2], AND A. G. HARRISON
Department of Chemistry, University of Toronto, Toronto 5, Ontario

Received June 24, 1968

The following ion–molecule reactions involving fragment ions in vinyl chloride have been studied and rate constants measured for ions of 2.4 eV exit energy.

$$C_2H_2^+ + C_2H_3Cl \rightarrow C_2H_3Cl^+ + C_2H_2 \qquad k = 1.9 \times 10^{-9}\ cm^2\ molecule^{-1}\ s^{-1}$$

$$C_2H_3^+ + C_2H_3Cl \rightarrow C_2H_4Cl^+ + C_2H_2 \qquad k = 1.5 \times 10^{-10}\ cm^3\ molecule^{-1}\ s^{-1}$$

$$C_2H_3^+ + C_2H_3Cl \rightarrow C_4H_5^+ + HCl \qquad k = 5.6 \times 10^{-10}\ cm^3\ molecule^{-1}\ s^{-1}$$

The reaction of the $C_2H_3Cl^+$ molecule–ion produces $C_3H_4Cl^+$, $C_4H_5Cl^+$, and $C_4H_6Cl^+$ both in a second order and a third order reaction. The apparent rate coefficient for the second order reaction is approximately $1 \times 10^{-11}\ cm^3\ molecule^{-1}\ s^{-1}$ while that for the third order reaction is approximately $1 \times 10^{-25}\ cm^6\ molecule^{-2}\ s^{-1}$. The product distributions from both the second and third order reactions have been determined.

In vinyl bromide the $C_2H_3^+$ ion produces $C_4H_5^+$, $C_4H_6^+$, and $C_2H_4Br^+$ while the $C_2H_3Br^+$ ion reacts to form $C_4H_6Br^+$ both in a second order and a third order reaction.

Canadian Journal of Chemistry, 47, 647 (1969)

Introduction

Recently Baldeschwieler *et al.* (1), using ion cyclotron resonance (i.c.r.) spectroscopy, have studied the ion–molecule reactions occurring in gaseous vinyl chloride subject to electron bombardment. They have shown that reaction of $C_2H_3Cl^+$ with neutral vinyl chloride yields three products: $C_3H_4Cl^+$, $C_4H_5Cl^+$, and $C_4H_6Cl^+$, while reaction of $C_2H_3^+$ yields $C_4H_5^+$ and $C_2H_4Cl^+$. In addition to identifying the primary reactions they have followed the consecutive reactions to a high order at relatively low pressure by using appropriate ion trapping conditions to increase the reaction time. However, they have not reported rate constants for the primary reactions. As part of our study (2–4) of the ionic reactions in unsaturated systems we have investigated the ionic reactions in vinyl chloride using a conventional medium pressure mass spectrometer. Our reaction identification is essentially in agreement with that made previously; however, we find that the $C_2H_3Cl^+$ ion disappears both by second and third order reactions. The rate constants (and product distributions) for both reactions have been determined as well as the rate constants for the other primary reactions.

The ion–molecule reactions of vinyl bromide have been investigated briefly.

[1]Visiting scientist 1967–1968, permanent address: Department of Chemistry, Laval University, Quebec.
[2]Holder of NRCC Studentships 1963–1966.

Experimental

The experiments were carried out on the medium pressure mass spectrometer previously described (5). The pertinent operating conditions were a source temperature of approximately 100 °C and a primary ion travel distance of 0.54 cm. Pressure studies were carried out at repeller fields corresponding to either 2.4 or 3.4 eV ion exit energy. The ionizing electron beam was pulsed and primary ion residence times were measured directly by the deflection technique previously described (5). Source pressures were measured directly using an MKS Baratron capacitance micromanometer.

The vinyl chloride and vinyl bromide were obtained from Matheson Company and were purified by bulb-to-bulb distillation prior to use. No impurities were detected in the mass spectra.

Results and Discussion

Vinyl Chloride

Figures 1 and 2 show a typical pressure plot obtained at 2.4 eV ion exit energy and 20 eV nominal electron energy. The normalized intensities of the $C_2H_2^+$, $C_2H_3^+$, and $C_2H_2Cl^+$ ions show the exponential decrease with increasing pressure characteristic of reactive primary ions, while the intensity of the $C_2H_3Cl^+$ ion shows an initial increase followed by a decrease, indicating that it is the product of an ion–molecule reaction as well as a reactant ion. The product ions observed are $C_2H_4Cl^+$, $C_4H_5^+$, $C_3H_4Cl^+$, $C_4H_5Cl^+$, and $C_4H_6Cl^+$. The intensities of the first two increase in the manner expected for secondary ions; however, the shape of the curves for the latter three suggest that they are formed by a

Can. J. Chem. Downloaded from www.nrcresearchpress.com by 210.87.254.6 on 09/05/12
For personal use only.

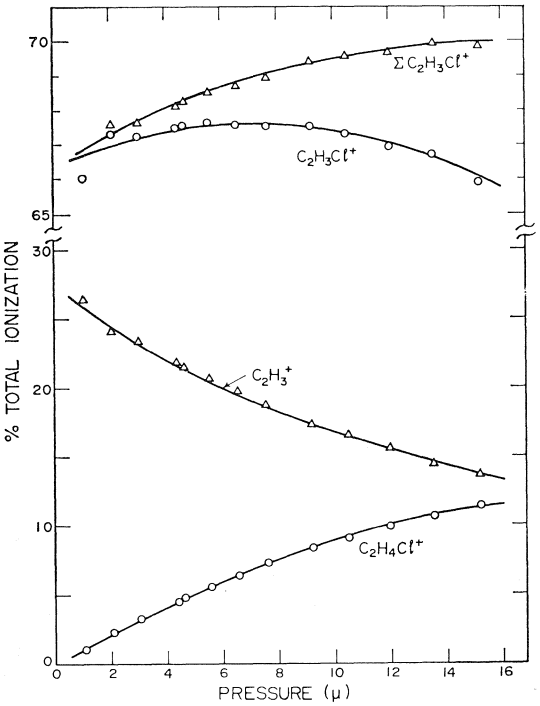

FIG. 1. Pressure plot vinyl chloride, 2.4 eV ion exit energy, 20 eV electron energy.

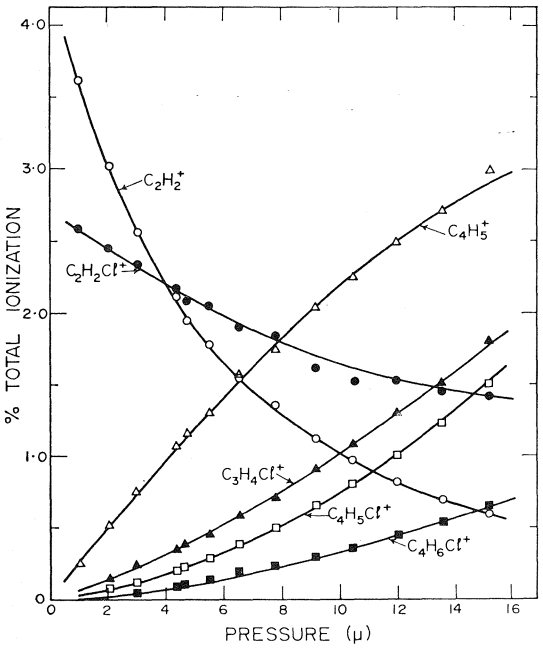

FIG. 2. Pressure plot vinyl chloride; conditions as for Fig. 1.

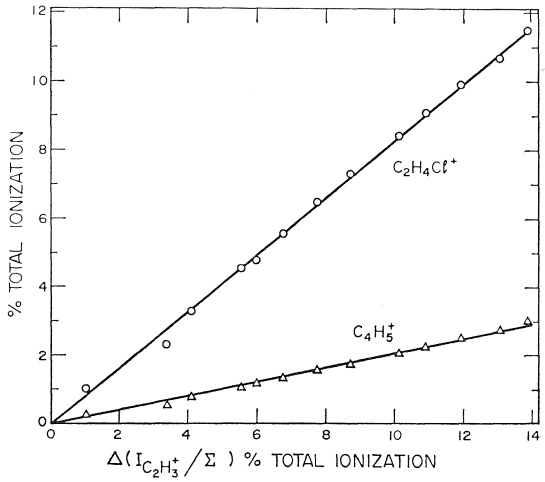

FIG. 3. $C_2H_4Cl^+$ and $C_4H_5^+$ intensities as function of $C_2H_3Cl^+$ reacted.

reaction which is second order in neutral vinyl chloride concentration.

Plots of the normalized $C_2H_4Cl^+$ and $C_4H_5^+$ intensities versus $\Delta(I_{C_2H_3^+/\Sigma})$ (i.e. the $C_2H_3^+$ reacted) are linear (Fig. 3) and give slopes which sum to approximately unity, indicating that $C_2H_3^+$ reacts to give only these products (reactions [1] and [2]).

[1] $C_2H_3^+ + C_2H_3Cl \rightarrow C_2H_4Cl^+ + C_2H_2$

[2] $C_2H_3^+ + C_2H_3Cl \rightarrow C_4H_5^+ + HCl$

Four runs at 2.4 eV ion exit energy gave a total rate constant for the disappearance of $C_2H_3^+$ of $7.1 \pm 0.3 \times 10^{-10}$ cm^3 molecule^{-1} s^{-1} with approximately 21% of the total reaction yielding $C_4H_5^+$. Three runs at 3.4 eV ion exit energy gave a total disappearance rate constant of $5.7 \pm 0.2 \times 10^{-10}$ cm^3 molecule^{-1} s^{-1} with approximately 18% of the reaction yielding $C_4H_5^+$.

The rate constant for disappearance of the small $C_2H_2Cl^+$ ion current was found to be approximately 5×10^{-10} cm^3 molecule^{-1} s^{-1}; however, the products of the reaction could not be identified and the ion may react either by proton transfer or by charge transfer.

Since the reaction of $C_2H_3^+$ accounts for the formation of both $C_4H_5^+$ and $C_2H_4Cl^+$ and no other significant products were observed, we conclude that $C_2H_2^+$ reacts by charge transfer. Indeed, if we assume, in agreement with earlier work (1) and the results presented below, that $C_3H_4Cl^+$, $C_4H_5Cl^+$, and $C_4H_6Cl^+$ originate

Can. J. Chem. Downloaded from www.nrcresearchpress.com by 210.87.254.6 on 09/05/12
For personal use only.

from the reaction of $C_2H_3Cl^+$, we observe that the sum of the reactant and product ion currents, labelled $\sum C_2H_3Cl^+$ in Fig. 1, increases significantly with pressure, the increase being of the same magnitude as the decrease in the $C_2H_2^+$ ion current. Two determinations at 2.4 eV ion exit energy gave a rate constant of 1.9×10^{-9} cm^3 $molecule^{-1}$ s^{-1} and two determinations at 3.4 eV ion exit energy gave a rate constant of 1.8×10^{-9} cm^3 $molecule^{-1}$ s^{-1} for the charge transfer reaction [3].

[3] $C_2H_2^+ + C_2H_3Cl \rightarrow C_2H_3Cl^+ + C_2H_2$

As mentioned above, the shapes of the curves (Fig. 2) for the $C_3H_4Cl^+$, $C_4H_5Cl^+$, and $C_4H_6Cl^+$ product ions suggest that these products are formed in reactions which are predominantly second order in neutral molecule concentration. However, the interpretation of the results in Figs. 1 and 2 is complicated by the fact that the precursor $C_2H_3Cl^+$ ion is itself formed by reaction [3]. Therefore, we have carried out a number of runs at low electron energy where $C_2H_3Cl^+$ was the only significant primary ion. A typical pressure plot is shown in Fig. 4 for ions of 2.4 eV exit energy produced by electrons of 10.5 eV nominal electron energy, where

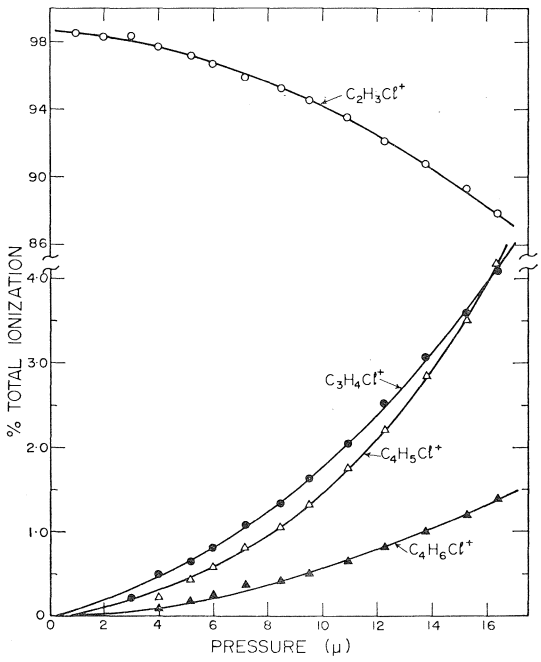

FIG. 4. Pressure plot vinyl chloride, 2.4 eV ion exit energy, 10.5 eV electron energy.

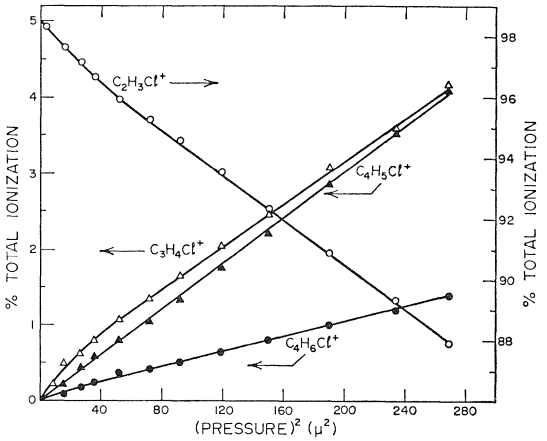

FIG. 5. Ion intensities vs. P^2.

$C_2H_3Cl^+$ comprises > 98% of the total ionization at low pressures. Neither the decrease of the $C_2H_3Cl^+$ intensity with pressure nor the increase of the product ion intensities with pressure are characteristic of reactions which are first order in neutral reactant concentration. Figure 5 shows a plot of the normalized product ion intensities as a function of the square of the ion source pressure. All plots are linear at higher pressures with a slight drop-off at lower pressures indicating that these ions are produced predominantly by reactions second order in neutral concentration with a possible small first order contribution at low pressures. Similarly the disappearance of $C_2H_3Cl^+$ is linear with P^2 at higher pressures, the initial non-linear portion indicating a small contribution from a reaction which is first order in neutral C_2H_3Cl. We, therefore, conclude that the formation of the $C_3H_4Cl^+$, $C_4H_5Cl^+$, and $C_4H_6Cl^+$ products is the sum of two reactions, one first order in C_2H_3Cl (reaction [4]) and one second order in C_2H_3Cl (reaction [5]).

[4] $C_2H_3Cl^+ + C_2H_3Cl \rightarrow C_3H_4Cl^+ + CH_2Cl$
$\rightarrow C_4H_5Cl^+ + HCl$
$\rightarrow C_4H_6Cl^+ + Cl$

[5] $C_2H_3Cl^+ + 2C_2H_3Cl \rightarrow C_3H_4Cl^+ + \text{neutrals}$
$\rightarrow C_4H_5Cl^+ + \text{neutrals}$
$\rightarrow C_4H_6Cl^+ + \text{neutrals}$

For the two concurrent reactions [4] and [5] at low total conversion of reactant we may write

$$[6] \qquad \frac{I_{S_x^+}}{\Sigma I_{p^+} \cdot P} = k_{4X}tK + k_{5X}tK^2P$$

TABLE I

Rate constants and product distribution from reaction of $C_2H_3Cl^+$

Run	Nominal electron energy (eV)	% of second order reaction			k_4 (total) ($\times 10^{11}$)	% of third order reaction			k_5 (total) ($\times 10^{25}$)
		$C_3H_4Cl^+$	$C_4H_5Cl^+$	$C_4H_6Cl^+$		$C_3H_4Cl^+$	$C_4H_5Cl^+$	$C_4H_6Cl^+$	
A	20	59	23	18	1.87	37	49	14	0.68
B	20	63	19	18	1.75	35	50	15	0.80
C	15	68	16	16	1.35	37	48	15	1.1_1
D	10.5	85	0	15	1.03	36	49	15	1.4_4

where $I_{S_{x^+}}$ is the ion current for product ion X^+ formed by second order and third order reactions with rate constants k_{4X} and k_{5X} respectively, ΣI_{p^+} is the sum of reactant and product ion intensities, P is the ion source pressure, t is the reaction time, and K is the proportionality constant relating the source concentration to the measured source pressure. A plot of the left hand side of eq. [6] vs. the source pressure for each product ion should lead to straight lines, the slope of each being proportional to the third order rate constant and the intercept proportional to the second order rate constant. The data from Figs. 4 and 5 are plotted in this manner in Fig. 6 where it can be seen that satisfactory straight lines result. The results for this plot and others carried out at higher electron energies are summarized in Table I.

The total second order rate constant k_4 is of the order of 10^{-11} cm^3 molecule^{-1} s^{-1}, a factor of 10^2 less than is normally observed for exothermic bimolecular ion–molecule reactions. The rate constant as well as the product distribution appear to be dependent on the ionizing electron energy. The reasons for the low bimolecular rate

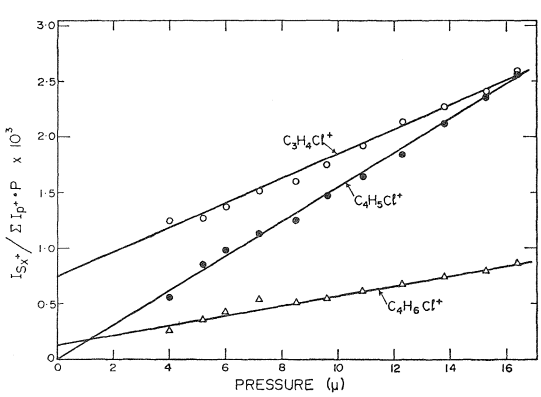

FIG. 6. $I_{S_X^+}/\Sigma I_{p^+}\cdot P$ vs. pressure, vinyl chloride.

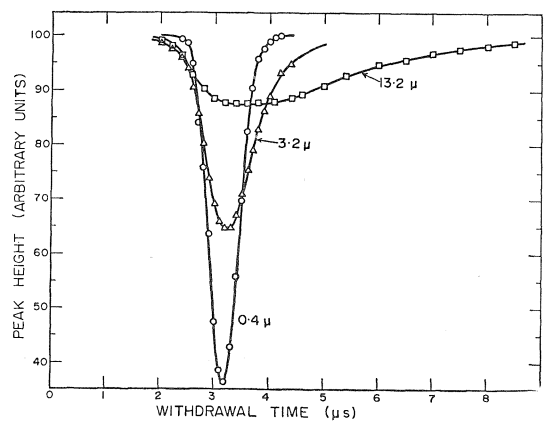

FIG. 7. Withdrawal curves for $C_2H_3Cl^+$ as function of pressure.

are not readily apparent. A possible explanation will be discussed below. In any event it is apparent that the majority of collisions do not lead to reaction but to reversion to reactants with or without charge exchange. In this regard it is significant that the withdrawal curves for $C_2H_3Cl^+$ (Fig. 7) show significant broadening and extend to very long withdrawal times as the source pressure is increased. This indicates that at the higher pressures a significant fraction of the $C_2H_3Cl^+$ ions have been retarded in their passage out of the ionization chamber through formation of a collision complex of finite lifetime which reverts to reactants with or without charge transfer. The charge transfer reaction has been detected in the i.c.r. work (1). The rate constant for the third order reaction shows a small but significant increase with decreasing electron energy, the opposite effect to that shown for the second order reaction. On the other hand, the product distribution from the third order reaction is independent of electron energy and is distinctly different from the distribution observed for the

Can. J. Chem. Downloaded from www.nrcresearchpress.com by 210.87.254.6 on 09/05/12
For personal use only.

Can. J. Chem. Downloaded from www.nrcresearchpress.com by 210.87.254.6 on 09/05/12
For personal use only.

second order reaction. The mechanism of the third order reaction cannot be elucidated from the present work.

Following the completion of our work Dr. T. O. Tiernan communicated to us the results (6) of a study of the ion–molecule reactions in vinyl chloride, using a tandem mass spectrometer (7), which provide considerable insight on the reactions of the vinyl chloride molecule ion. It is appropriate to compare our results obtained by conventional mass spectrometric techniques with those obtained by the tandem instrument.

Using the tandem instrument, Tiernan *et al.* (6) have bombarded C_2H_3Cl with $C_2D_3Cl^+$ ions of 0.3 eV energy. At low pressures of C_2H_3Cl (5 μ), where higher order ionic reactions should not occur, they observed the isotopically mixed products $C_3H_xD_{4-x}Cl^+$, $C_4H_xD_{5-x}Cl^+$, and $C_4H_3D_3Cl^+$ in the ratio 0.73:0.11:0.15. At high pressures of C_2H_3Cl (25 μ) in addition to the above products, they observed $C_3H_4Cl^+$, $C_4H_5Cl^+$, and $C_4H_6Cl^+$ in the ratio 0.42:0.36:0.23. Obviously the complex decomposing to form these latter products cannot contain deuterium and must be formed from two molecules of C_2H_3Cl. They propose the following mechanism, written in the present case for non-deuterated reactants

$$[7] \quad C_2H_3Cl + e \rightarrow C_2H_3Cl^{+*} + 2e$$

$$[8] \quad C_2H_3Cl^{+*} + C_2H_3Cl \rightarrow (C_4H_6Cl_2)^{+*} \rightarrow \text{products}$$

$$[9] \quad C_2H_3Cl^{+*} + C_2H_3Cl \rightarrow C_2H_3Cl + C_2H_3Cl^{+}‡$$

$$[10] \quad C_2H_3Cl^{+}‡ + C_2H_3Cl \rightarrow (C_4H_6Cl_2)^{+} \rightarrow \text{products}$$

The initial electron impact process is considered to lead to internally excited vinyl chloride ions $C_2H_3Cl^{+*}$ which react to form complexes (reaction [8]), which, because of their high excitation, revert to reactants so rapidly that only a small fraction survives for a sufficient length of time to undergo the structural rearrangements necessary to produce the condensation products. The vinyl chloride ion produced in the charge transfer reaction [9] is considered to be of lower energy content, with the result that the collision complex of reaction [10] is much longer lived and forms the observed products with high efficiency.

In general our results are consistent with this reaction scheme although they do suggest some modification of the details. Our product distribution from the second order reaction (Table I) is in quite good agreement with the distribution observed at low pressures of C_2H_3Cl in the tandem experiments. Further, our distribution for the third order reaction is also in reasonable agreement with that observed for the non-deuterated products formed at high C_2H_3Cl pressures in the tandem instrument.

As discussed above, the withdrawal curves (Fig. 7) indicate that a significant fraction of the $C_2H_3Cl^+$ ions have been retarded in their passage out of the ionization chamber. However, this broadening of the withdrawal curves is not consistent with a charge transfer reaction proceeding without momentum transfer as is implied by reaction [9] of the Tiernan mechanism. For such a charge transfer reaction simple kinematic considerations indicate that the product ions should have withdrawal times peaked relatively sharply at times a factor of 1.4 greater than the unreacted primary ions. The curves in Fig. 7 show no such contribution peaked[3] at 4.5 μs and we conclude that charge transfer without momentum transfer does not occur. On the other hand charge transfer through complex formation would lead to product ions with average withdrawal times approximately 1.1 times greater than the reactant ions and the broadening in Fig. 7 is consistent with this mechanism. Thus we would suggest that the charge transfer reaction, written as reaction [9], is better written as an alternative mode of fragmentation of the complex formed in reaction [8]. It is, of course, possible that a significant fraction of the complexes revert to reactants without charge transfer. In any event, since the collision rate constant k_8 is probably of the order of 10^{-9} cm^3 molecule^{-1} s^{-1} while the rate of formation of condensation products, $k_4 = 1 \times 10^{-11}$ cm^3 molecule^{-1} s^{-1}, only $\sim 1\%$ of the complexes form the observed C-3 and C-4 products. Thus we would suggest that the mechanism is more properly written as follows.

$$[7] \quad C_2H_3Cl + e \rightarrow C_2H_3Cl^{+*} + 2e$$

$$[8] \quad C_2H_3Cl^{+*} + C_2H_3Cl \rightarrow (C_2H_3Cl)_2^{+*}$$

$$[9a] \quad [C_2H_3Cl]_2^{+*} \rightarrow \text{products}$$

$$[9b] \quad \rightarrow C_2H_3Cl + C_2H_3Cl^{+}†$$

[3]In argon and krypton, where charge transfer without momentum transfer does occur, large peaks are observed in the withdrawal curves peaked at withdrawal times a factor of 1.4 greater than primary ions for gas pressures of ~ 4 μ (Jones and Harrison, unpublished results).

[10] $C_2H_3Cl^+\dagger + C_2H_3Cl \rightarrow [C_2H_3Cl]_2{}^+\dagger$

[11*a*] $[C_2H_3Cl]_2{}^+\dagger \rightarrow$ products

[11*b*] $\rightarrow C_2H_3Cl^+\dagger + C_2H_3Cl$

In the initial stages reaction [9*b*] will be much faster than reaction [10] leading to an overall third order rate constant for formation of $[C_2H_3Cl]_2{}^+\dagger$ $k = k_{9b}k_{10}t$ where t is the reaction time. The assumptions that $k_{9b} \approx 10^{-9}$ cm^3 molecule^{-1} s^{-1} (i.e., that 99% of the initial collision complexes lead to $C_2H_3Cl^+\dagger$) and that all the complexes of reaction [10] lead to observed products, leads to a predicted third order rate constant approximately a factor of 10 greater than the experimental rate constant. This suggests that a significant fraction (up to 90%) of the complexes, $[C_2H_3Cl]_2{}^+\dagger$, do not lead to observed products and leads us to include reaction [11*b*] in the reaction scheme.

Tiernan *et al.* (6) have suggested that the complex formed in reaction [8] is very short lived because of its high internal excitation energy while that formed in reaction [10] has a longer lifetime because of its lower energy content and that the differing product distributions in the second and third order reactions are determined by this internal excitation. Our results on the effect of electron energy on the second order reaction are not entirely consistent with this suggestion. One would expect on this basis that as the electron energy is lowered the internal excitation of the complex formed in reaction [8] should decrease with a corresponding increase in the lifetime and the rate of formation of observable products. In fact the observed rate constant (Table I) decreases. Further if the product distribution of the third order reaction represents that for "cool" complexes one would expect, as the electron energy is decreased, that the product distribution from the second order reaction should approach that observed for the third order reaction. Such is obviously not the case. In these two aspects our results do not support the suggestions of Tiernan *et al.* (6). One possible explanation is that the ions formed in the initial electron impact process are in various electronic states which react to form the observed products with different efficiencies and with different product distributions and the ion formed by charge transfer is in an electronic state (or states) distinctly different from those formed by electron impact.

Vinyl Bromide

The ion–molecule reactions in vinyl bromide were investigated briefly at low electron energies where $C_2H_3{}^+$ and $C_2H_3Br^+$ were the only significant primary ions. The products observed were $C_4H_5{}^+$, $C_4H_6{}^+$ (in minor yield), $C_2H_4Br^+$, and $C_4H_6Br^+$. The $C_4H_5{}^+$, $C_4H_6{}^+$, and $C_2H_4Br^+$ appeared to originate predominantly from reaction of the $C_2H_3{}^+$ fragment ion although in all cases the plot of the product ions intensity versus the $C_2H_3{}^+$ disappearance showed on upward curvature at higher pressures. Further the log plots for the disappearance of $C_2H_3{}^+$ were not linear and the explanation of both phenomena may be that $C_2H_3{}^+$ is formed by a third order reaction of $C_2H_3Br^+$. The $C_4H_6Br^+$ ion originated from the reaction of $C_2H_3Br^+$ and, as in the vinyl chloride system, the overall reaction is the sum of a second order and a third order contribution. Figure 8 shows a typical plot of the data in the form of eq. [6]. Three such determinations gave the following rate constants for ions of 2.4 eV exit energy.

[12] $C_2H_3Br^+ + C_2H_3Br \rightarrow C_4H_6Br^+ + Br$

$k = 6.5 \pm 0.2 \times 10^{-12}$ cm^3 molecule^{-1} s^{-1}

[13] $C_2H_3Br^+ + 2C_2H_3Br \rightarrow C_4H_6Br^+ + ?$

$k = 5.5 \pm 0.2 \times 10^{-26}$ cm^6 molecule^{-2} s^{-1}

It is probable that the mechanism of reaction [13] is similar to that of the third order reaction in vinyl chloride. The $C_3H_4Br^+$ and $C_4H_5Br^+$, analogous to the $C_3H_4Cl^+$ and $C_4H_5Cl^+$ ions formed in vinyl chloride, were not observed. A more detailed comparison of the reactions in the vinyl halides and in ethylene will be made in the following paper (8).

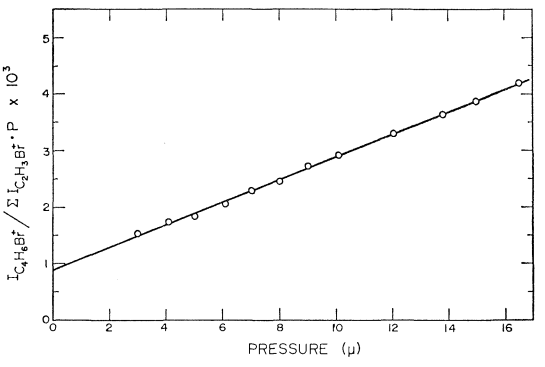

FIG. 8. $I_{C_4H_6Br^+}/\Sigma I_{C_2H_3Br^+}\cdot P$ vs. pressure, vinyl bromide.

Can. J. Chem. Downloaded from www.nrcresearchpress.com by 210.87.254.6 on 09/05/12
For personal use only.

Acknowledgments

The authors are indebted to the National Research Council of Canada for financial support of this work. They are also indebted to Dr. T. O. Tiernan for communication of results prior to publication and to a referee for many helpful suggestions.

1. J. L. Beauchamp, L. R. Anders, and J. D. Baldeschwieler. J. Am. Chem. Soc. **89**, 4569 (1967).
2. J. J. Myher and A. G. Harrison. Can. J. Chem. **46**, 101 (1968).
3. J. J. Myher and A. G. Harrison. Can. J. Chem. **46**, 1795 (1968).
4. J. J. Myher and A. G. Harrison. J. Phys. Chem. **72**, 1905 (1968).
5. S. K. Gupta, E. G. Jones, A. G. Harrison, and J. J. Myher. Can. J. Chem. **45**, 3107 (1967).
6. B. M. Hughes, T. O. Tiernan, and J. H. Futrell. J. Phys. Chem. In press.
7. J. H. Futrell and C. D. Miller. Rev. Sci. Instr. **37**, 1521 (1966).
8. J. A. Herman and A. G. Harrison. Can. J. Chem. This issue.

Can. J. Chem. Downloaded from www.nrcresearchpress.com by 210.87.254.6 on 09/05/12
For personal use only.

Recoil studies of some light-mass products from the proton-induced fission of ^{238}U at intermediate energies[1]

G. B. SAHA AND L. YAFFE
Radiochemistry Laboratory, Department of Chemistry, McGill University, Montreal, Quebec
Received August 15, 1968

The recoil properties of ^{66}Ni, ^{67}Cu, and ^{72}Zn produced in the fission of ^{238}U by protons of 40–85 MeV energy have been studied radiochemically by the thick target – thick catcher technique. The average kinetic energy of each product has been calculated from the ranges by use of known range–energy relationships. The calculated impact velocity $v_{\parallel}$ shows that these fission products are formed predominantly via a compound nucleus mechanism in this energy region. The average total kinetic release in fission is found to be insensitive to the bombarding energy.

Canadian Journal of Chemistry, **47**, 655 (1969)

Can. J. Chem. Downloaded from www.nrcresearchpress.com by 210.87.254.40 on 09/05/12
For personal use only.

Introduction

The study of recoil ranges of fission products has proved to be of considerable interest in providing useful information about the fission process. A number of investigations involving measurements of recoil ranges (1–8) have been made by the use of a thick target – thick catcher technique. All these experiments involve the measurement of the average ranges of fission products and the subsequent conversion of the ranges into kinetic energies of these products by the use of a suitable range–energy relationship. Attempts have been made to correlate these results with the fission mechanism. In some of these studies (1, 5, 7, 8), additional information about the cascade deposition energy and the angular distribution of fission fragments has also been gathered. All these experiments have, however, been performed for either thermal fission or high-energy proton fission (> 150 MeV) of heavy elements. We have investigated the recoil properties of fission products in the energy range of 40–85 MeV. This study is of particular interest since a transition from compound nucleus formation to a direct interaction is generally believed to take place in this energy range.

We have measured the recoil ranges of the low-mass fission products, ^{66}Ni, ^{67}Cu, and ^{72}Zn, in 40–85 MeV proton fission of ^{238}U by the thick target – thick catcher technique. The kinetic energies of the fission products have been calculated and attempts have been made to explain these energies in terms of coulombic repulsion between two charged centers at the moment of scission. Information about the momentum transfer in the initial impact between the incident proton and ^{238}U nucleus has been obtained. In addition a correlation between our results and higher energy data has been attempted.

Experimental Procedure

The targets used in the present work consisted of uranium foils of normal isotopic composition having a superficial density of about 140 mg/cm^2. High purity aluminium foils (0.0008 in. thick) were used as catchers. The target foil was cleaned with nitric acid prior to bombardment, and then sandwiched between two aluminium catcher foils. The dimensions of the catcher foils were larger than that of the target so that any recoils originating in the edge of the target were all caught. An additional aluminium foil was introduced in the stack in order to determine the activation correction due to impurities in the catcher. The entire assembly was wrapped with a 0.0008 in. thick aluminium foil and then fixed on a target holder which in turn was attached to the cyclotron probe for irradiation.

Irradiations were performed in the internal circulating beam of protons in the McGill synchrocyclotron. The duration of bombardment was about 1 h and the beam current was of the order of 1 μA. The activation correction amounted to about 2% for all the nuclides studied. In the forward–backward recoil experiments the target assembly was irradiated perpendicular to the beam and in the "perpendicular" experiments irradiations were performed with the target stack at about 10° to the beam. The beam energy was selected by placing the stack at a radius corresponding to a desired energy and irradiations were made at 40, 55, 70, and 85 MeV. In view of the energy spread in the beam ($\sim \pm 2$ MeV) the energy degradation in the stack was calculated to be small and therefore neglected.

After irradiation, the appropriate foils were separated and dissolved in suitable acids. The chemical procedures for the separation of Ni, Cu, and Zn are given elsewhere (9).

The characteristic radiations and half-lives (10) of all nuclides that have been studied are given in Table I. Also

[1]This research received financial support from the National Research Council of Canada.

TABLE I

Pertinent decay properties of the nuclides of interest

Nuclide	Half-life	β^- radiation (MeV)	Abundance (%)	Remarks
^{66}Ni	55 h	0.20	100	maintains secular equilibrium with 5.1 min ^{66}Cu
^{67}Cu	61.5 h	0.40	45	
		0.48	35	
		0.58	20	
^{72}Zn	46.5 h	0.30	95	maintains transient equilibrium with ^{72}Ga
		1.60	5	
^{72}Ga	14.1 h	0.96	35	
		0.66	17	
		0.68	24	
		1.51	7	
		2.53	5	
		3.17	5	
^{66}Cu	5.1 min	1.59	9	
		2.63	91	

given in the table are the relevant decay properties of the daughters of some of these nuclides since they were measured along with their precursors.

The beta activities of ^{66}Ni, ^{67}Cu, and ^{72}Zn were measured by a low-background beta proportional counter. The counter had a background of less than 1 count/min and a dead time of about 300 μs. The characteristic behavior of the counter was monitored regularly with a ^{36}Cl standard source.

In general, in a recoil experiment, three samples of each nuclide, corresponding to the activities of the target and two catchers, are measured. Thus three samples each of ^{66}Ni, ^{67}Cu, and ^{72}Zn were measured over several half-lives and the activity ratios obtained after correcting for the chemical yield. The activity ratios obtained at different intervals agreed within 1–2% with each other and an average of these ratios was taken. Since ^{72}Zn maintains a transient equilibrium with ^{72}Ga, the shapes of the growth–decay curves for all three samples must be identical with respect to the time axis for proper comparison. This was ensured by precipitating $ZnHg(SCN)_4$ from the target and the catchers at the same time.

The ^{66}Ni and ^{72}Zn nuclides decay by emitting low-energy beta rays and thus self-absorption in the solid samples makes the activity measurements difficult. However, these nuclides are in equilibrium with their daughters which emit high-energy beta radiation. These two nuclides were, therefore, measured with a 200 mg/cm^2 thick aluminium absorber in order to stop all low energy beta rays, thus obviating any self-absorption correction. A self-absorption correction was, however, applied to the activities of ^{67}Cu.

Results

(a) Treatment of Recoil Data

In a typical forward–backward recoil experiment, the fractions F and B of the total activity of a given nuclide that were found in the forward and backward Al catcher foils, respectively, were measured. Similarly in the perpendicular experiments, where the foils lie at about 10° to the beam, the fractions P of the total activity of a given nuclide observed in the top or bottom catchers were also measured. In the latter experiment the activities in the top and bottom catchers were almost the same and were averaged. The fractions F, B, and P were corrected for the scattering of the recoils at the uranium–aluminium interface and for the edge-effect of the target. These effects have been investigated by Panontin and Sugarman (11). Following Niday's (3) suggestion, Sugarman *et al.* (8) gave the following expression for the scattering correction factor

$$[1] \quad W_{(Pb)}(F, B, \text{or } P)_{(Pb)} = [0.922 + 3.4 \times 10^{-4}A]\, W_{(Al)}(F, B, \text{or } P)_{(Al)}$$

Here A is the mass member of the fission product of interest, W is the thickness of the catcher, and the subscripts Pb and Al refer to the quantities as measured with lead or aluminium catchers, respectively. This expression assumes that the scattering effect is the same in both uranium and lead foils. The correction factor for the edge effect for the uranium foil used was taken to be 0.97 as suggested by Sugarman and co-workers (8, 11). Thus the quantities F, B, and P were corrected by multiplying by 0.97 and the factor given by eq. [1]. Corrections for fission products produced by secondary neutrons and protons arising from nuclear interactions in the target and other foils were calculated to be small and were neglected.

Can. J. Chem. Downloaded from www.nrcresearchpress.com by 210.87.254.40 on 09/05/12
For personal use only.

TABLE II

Measured recoil parameters

Energy (MeV)	$2W(F+B)$ (mg/cm² U)	$4WP$ (mg/cm² U)	$W(F-B)$ (mg/cm² U)	R (mg/cm² U)	$\eta_{\parallel}$	b/a
			^{66}Ni			
40	16.0±3.5	14.1±3.1	0.321±0.071	14.7±3.2	0.0187	+0.621
55	15.3±3.3	13.2±2.9	0.321±0.071	13.9±3.0	0.0197	+0.754
70	14.1±3.1	12.7±2.8	0.355±0.078	13.2±2.9	0.0232	+0.492
85	12.1±2.7	12.3±2.7	0.420±0.092	12.5±2.7	0.0293	+0.165
			^{67}Cu			
40	16.7±3.7	13.8±3.0	0.330±0.073	14.8±3.3	0.0190	+0.612
55	14.4±3.2	12.8±2.8	0.362±0.080	13.3±2.9	0.0233	+0.567
70	13.4±2.9	14.4±3.2	0.419±0.092	14.1±3.1	0.0263	−0.263
85	14.3±3.1	14.3±3.1	0.456±0.101	14.3±3.1	0.0281	−0.004
			^{72}Zn			
40	12.5±2.7	12.3±2.7	0.312±0.069	12.4±2.7	0.0222	+0.063
55	13.7±3.0	14.5±3.2	0.330±0.073	14.2±3.1	0.0206	−0.211
70	13.4±2.9	13.1±2.9	0.401±0.088	13.2±2.9	0.0267	+0.090
85	12.6±2.8	13.8±3.0	0.430±0.095	13.4±2.9	0.0287	−0.324

Sugarman and co-workers (8) and Winsberg (12) have independently derived equations relating F, B, and P with three other important quantities, the range R, the velocity parameter η, and the anisotropy parameter b/a. Sugarman *et al.* (8) have analyzed their results on the basis of a vector model. The vector model assumes that the incident particle imparts an average velocity v to the struck nucleus in the cascade process. Then the struck nucleus undergoes fission either before or after the evaporation of neutrons. The fission fragments acquire an average velocity V in the moving frame of reference and the angular distribution of V is given by the form $a + b\cos^2\theta$. The velocity parameter η is given by v/V. The components of η along the parallel and perpendicular directions to the beam are denoted by $\eta_{\parallel}$ and $\eta_{\perp}$ respectively. One assumes a range–energy relationship given by $R = kV^N$ where k and N are empirical constants.

With $\eta_{\perp} = 0$, the Sugarman (8) equations were solved by successive approximations of various values for R, $\eta_{\parallel}$, and b/a until these values did not change. The derived values of the range R, the velocity parameter $\eta_{\parallel}$, and the anisotropy parameter b/a are given in Table II. Sugarman *et al.* (8) have deduced $\eta_{\perp}$ from a knowledge of the dependence of $\eta_{\perp}$ on $\eta_{\parallel}$ at 450 MeV. In the absence of such information we have not attempted to obtain a value for $\eta_{\perp}$ in the present energy range.

In column 1 of Table II are given the proton bombarding energies in MeV. Columns 2, 3, and 4 present the experimentally determined data for $2W(F+B)$, $4WP$, and $W(F-B)$ in units of mg/cm² of uranium. The values of R, $\eta_{\parallel}$, and b/a are shown in columns 5, 6, and 7, respectively.

Errors have been estimated, on the basis of random uncertainty involved in the determination of activities, chemical yields, and target thickness, for W, F, and B. An estimated total error of ±22% has been uniformly quoted for the values of $2W(F+B)$, $4WP$, and $W(F-B)$ for all nuclides at all energies even though it may be somewhat larger at the lowest energies because of the low activity produced. Since R is proportional to the above measured quantities, the error in R will be of the same order. Based on the same considerations as above, the error estimated for $\eta_{\parallel}$ is ±30%.

(b) Range–Energy Relationship

The average range R, given in mg/cm², can be used to calculate the kinetic energy of the fission fragments. In order to do this a suitable range–energy relationship is necessary. An empirical range–energy relationship often used by Sugarman *et al.* (8) and others is of the form

$$[2] \qquad R = CT_p^{N/2}$$

where C and N are constants dependent on mass numbers of both recoiling ions and stopping atoms. The values of C and N have been deduced by fitting to the experimental results. T_p is the average kinetic energy of the recoiling ion.

Recently Lindhard, Scharff, and Schiøtt (13)

Can. J. Chem. Downloaded from www.nrcresearchpress.com by 210.87.254.40 on 09/05/12
For personal use only.

Can. J. Chem. Downloaded from www.nrcresearchpress.com by 210.87.254.40 on 09/05/12
For personal use only.

(hereafter denoted by L.S.S.) have deduced a universal range–energy relationship

$$[3] \qquad \rho(\varepsilon) = (2/k)\,\varepsilon^{1/2} - \Delta(k,\varepsilon)$$

where $\rho(\varepsilon)$ and ε are the dimensionless variables of the range and kinetic energy respectively; k is a parameter dependent on the masses and charges of the recoiling ions and stopping atoms; $\Delta(k,\varepsilon)$ is a term which corresponds to the nuclear stopping and is given by L.S.S. in their paper. The values of $\rho(\varepsilon)$, ε, and k are given by

$$[4] \qquad \rho(\varepsilon) = 4\pi a^2 NRM_1M_2(M_1 + M_2)^{-2}$$

$$[5] \qquad \varepsilon = aT_pM_2[Z_1Z_2e^2(M_1 + M_2)]^{-1}$$

$$[6] \qquad k = \frac{0.0793\xi Z_1^{1/2}Z_2^{1/2}(M_1 + M_2)^{3/2}}{M_1^{3/2}M_2^{1/2}(Z_1^{2/3} + Z_2^{2/3})^{3/4}}$$

Here a is $0.8853\,a_0(Z_1^{2/3} + Z_2^{2/3})^{-1/2}$, where a_0 is the Bohr radius in the hydrogen atom; R is the range in cm; ξ is approximately given by $Z_1^{1/6}$; N is the number of stopping atoms per cc; Z_1 and Z_2 are the charge numbers; and M_1 and M_2 are the mass numbers of the recoiling ions and stopping atoms, respectively.

Equation [3] can be used to calculate T_p provided $\Delta(k,\varepsilon)$ is known. On the other hand, ε, that is, T_p, must be known before $\Delta(k,\varepsilon)$ can be calculated. In a recoil experiment, only R is known and T_p is to be calculated. Therefore, eq. [3] is relatively complicated to apply in our case. Noshkin and Sugihara (7) analyzed the recoil data of thermal-neutron fission of ^{235}U for different catchers such as Al, Zr, Au, and U. They used the kinetic energy data of Milton and Fraser (14) for several mass numbers and checked the applicability of the L.S.S. range–energy relationship. They showed by this analysis that all the thermal fission data could be fitted by the following relationship

$$[7] \qquad \rho(\varepsilon) = \frac{1.3}{k}\,\varepsilon^{1/2}$$

We have used eqs. [2] and [7] for the determination of the kinetic energy of the individual fission products studied.

(c) Kinetic Energy Calculation

It is to be noted that eq. [7] has a charge dependence of the range–energy relationship through eqs. [4], [5], and [6]. The average charge, $\bar{Z}$, for an isobaric chain is the most probable charge, Z_p, at a given bombarding energy. For a cumulatively-formed species, which is the case for all nuclides in the present study, the average charge $\bar{Z}$, i.e. the charge of each member of the chain weighted by its independent fractional yield is

$$[8] \qquad \bar{Z} = \frac{\sum f_i Z_i}{\sum f_i}$$

where f_i is the fractional yield of the ith member of the chain and summations are taken over isobaric nuclides of charges less than and equal to that of the observed nuclide.

The fractional yield, f_i, can be obtained from the charge dispersion curves of fission products. The charge dispersion curves have often (15, 16) been assumed to have the following Gaussian form

$$[9] \qquad P(Z) = \frac{1}{\sqrt{(c\pi)}}\exp\left[\frac{-(Z - Z_p)^2}{c}\right]$$

The standard deviation, c, is related to the full-width at half-maximum, d_i, by the relation $c = 0.361\,d_i^2$ (17). If this is substituted into eq. [9], the following results

$$[10] \qquad f_i(Z_i) = \left(\frac{0.940}{d_i}\right)\exp\{-2.77[(Z_i - Z_p)/d_i]^2\}$$

where Z_i is the nuclear charge of the nuclide of interest, and Z_p is the most probable charge for the chain. Davies and Yaffe (18) and Parikh *et al.* (19) gave the full-width at half-maximum of the charge dispersion for masses 130–144 in ^{238}U fission by protons of energies 20–85 MeV. Unfortunately, there is yet no such information available regarding the width of the charge dispersion for the low-mass region at these energies. However, it can easily be shown that although $f_i(Z_i)$ changes with variation in d_i, the average charge $\bar{Z}$ remains almost unchanged. Under these circumstances we chose arbitrarily the data of Davies and Yaffe and the values are given in Fig. 1.

The most probable charges, Z_p, to be used in eq. [10], for different isobaric chains were calculated using both the equal charge displacement (e.c.d.) and unchanged charge division (u.c.d.) postulates (20). These give

$$[11] \qquad \text{for e.c.d., } Z_p = \tfrac{1}{2}(Z_c + Z_A - Z_{(A_c - A - \bar{\nu}_T)})$$

$$[12] \qquad \text{for u.c.d., } Z_p = \frac{Z_c A}{A_c - \bar{\nu}_T}$$

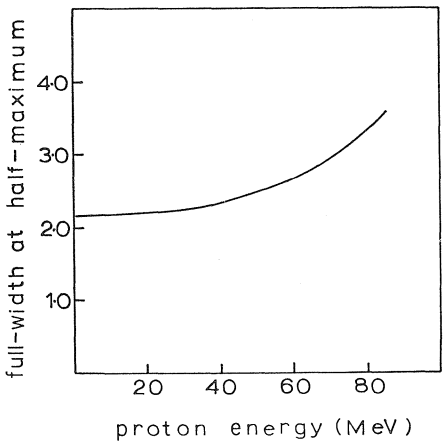

FIG. 1. Variation of full-width at half-maximum of charge dispersion curves (A = 130–144) with proton bombarding energy (ref. 18).

Here Z_c and A_c are the charge and mass numbers of the fissioning nucleus; Z_A is the most stable charge associated with the chain mass A; $\bar{\nu}_T$ is the average total number of neutrons emitted in fission. $\bar{\nu}_T$ was obtained from an energy-dependent relationship given by Unik and Huizenga (21, 22)

$$[13] \qquad \bar{\nu}_T = 1.9 + 0.12E^* \qquad \text{where } E^* \text{ is the excitation energy of the fissioning nucleus calculated on the basis of compound nucleus formation.}$$

Using the above information we have calculated $\bar{Z}$ for a measured fission product with the Z_p values obtained by both e.c.d. and u.c.d. methods. The appropriate value for $\bar{Z}$ was substituted in eqs. [5] and [6], and the kinetic energy, T_p, of each of the observed fission products was calculated from eq. [7] and the range R given in Table II. The kinetic energies of different products are listed in Table IV along with average charges $\bar{Z}$. The error in T_p is $\pm$ 22%.

We have also calculated the kinetic energies of the observed fission products by the use of eq. [2]. The values of C and N have been taken from Sugarman *et al.* (8). These authors have listed these values as a function of mass number through the analysis of range–energy data for heavy ions and fission fragments in thermal fission. The values chosen for C and N are given in Table III. The kinetic energies calculated by eq. [2] are also included in Table IV. It should be pointed out that for the mass region of our interest, no charge dependence of the range–energy relationship has been postulated in using eq. [2].

TABLE III

Values of C and N (8)*

A	C	N
66	0.453	1.44
67	0.455	1.44
72	0.475	1.40

*C and N are empirical constants shown in eq. [2].

TABLE IV

Kinetic energies of fission products

Energy (MeV)	$\bar{Z}$ (e.c.d.)	$\bar{Z}$ (u.c.d.)	Kinetic energy of fission product T_p (MeV) (e.c.d.)	(u.c.d.)	eq. [2]	Impact velocity $v_{\|\|}$ (MeV/a.m.u.)$^{1/2}$ (e.c.d.)	(u.c.d.)	eq. [2]	v_{CN} (MeV/a.m.u.)$^{1/2}$
					^{66}Ni				
40	27.2	26.5	134	127	126	0.0376	0.0367	0.0365	0.0374
55	27.3	26.6	120	115	116	0.0376	0.0368	0.0370	0.0438
70	27.3	26.7	108	103	108	0.0418	0.0411	0.0419	0.0495
85	27.3	26.7	96	93	100	0.0501	0.0491	0.0510	0.0545
					^{67}Cu				
40	27.7	26.9	137	130	126	0.0383	0.0374	0.0368	0.0374
55	27.9	27.1	113	107	109	0.0427	0.0417	0.0420	0.0438
70	28.0	27.2	126	120	117	0.0509	0.0497	0.0491	0.0495
85	28.0	27.3	130	125	120	0.0555	0.0543	0.0533	0.0545
					^{72}Zn				
40	29.4	28.8	99	95	105	0.0368	0.0362	0.0380	0.0374
55	29.4	28.9	131	127	129	0.0393	0.0387	0.0390	0.0438
70	29.5	29.0	113	110	116	0.0474	0.0467	0.0479	0.0495
85	29.4	28.9	116	112	118	0.0515	0.0508	0.0520	0.0545

Can. J. Chem. Downloaded from www.nrcresearchpress.com by 210.87.254.40 on 09/05/12
For personal use only.

Can. J. Chem. Downloaded from www.nrcresearchpress.com by 210.87.254.40 on 09/05/12
For personal use only.

Once the kinetic energy, T_p, of a fission product is known, its average velocity, V, can be calculated from the expression $T_p = \frac{1}{2}AV^2$. The impact velocity $v_{\parallel}$ imparted to the struck nucleus is then obtained by multiplying the measured $\eta_{\parallel}$ values by V. The error in $v_{\parallel}$ (from $\eta_{\parallel}$) is $\pm 30\%$. The values of $v_{\parallel}$ as deduced from the e.c.d. and u.c.d. methods, and eq. [2] are tabulated in Table IV. The last column of Table IV gives the impact velocity, v_{CN}, of the compound nucleus.

Discussion

From our recoil experiment we have derived three important quantities, viz. the kinetic energy T_p of the fission product, the initial velocity component $v_{\parallel}$ imparted to the fissioning nucleus along the beam direction, and the anisotropy parameter b/a for the angular distribution of the fission velocity V. An attempt will be made in the following section to obtain from these quantities relevant information about the fission mechanism and other related properties.

The kinetic energies of the fission products, ^{66}Ni, ^{67}Cu, and ^{72}Zn have been calculated by three methods as described earlier. Considering the uncertainties involved ($\pm 22\%$) as seen from Table IV, one cannot discriminate between the values obtained by the use of the three methods. This is also true for the values of the impact velocity, $v_{\parallel}$.

As can be seen from Table II, there is no systematic trend in the variation of the values of b/a with bombarding energy, which can be applied equally well to all nuclides. The anisotropy factor b/a is very sensitive to the $(F + B)$ and P values and a small variation in either of these introduces a large error in b/a. It is known (7, 8), however, that the anisotropy factor does change with bombarding energy and the mass number of the fission product. It would be expected that the b/a values should be large for products arising from highly asymmetric fission, and they are in general seen to be large in magnitude, except in the case of ^{72}Zn.

The impact velocity $v_{\parallel}$ of the struck nucleus along the beam direction has been used at higher energies to deduce the average deposition energy of the fissioning nucleus (5, 7, 8). This has usually been done from analysis of the Monte Carlo cascade calculation of Metropolis *et al.* (23) made by Porile (24) at 460 MeV and higher energies. Although we could make such an analysis for our energy region from the results of Metropolis *et al.* (23), a comparison between the values of v_{CN} and $v_{\parallel}$ indicates that this analysis is not worthwhile. It is apparent from Table IV that, in general, the compound nucleus velocity v_{CN} is the same as $v_{\parallel}$ at all bombarding energies. Any discrepancy that is observed between v_{CN} and $v_{\parallel}$ is attributable to the errors in the determination of $v_{\parallel}$. We can conclude that ^{66}Ni, ^{67}Cu, and ^{72}Zn or the corresponding primary fission fragments arise from the compound nuclei formed in the interaction of the protons with ^{238}U nuclei. This conclusion was also drawn from the excitation function studies of these nuclides (9). As $\eta_{\perp}$ is zero in compound nucleus information, no inconsistency is thus introduced by our neglect of $\eta_{\perp}$. Correlation with the compound nucleus mechanism does not, however, mean that no direct interaction takes place at these energies. It has been pointed out by several authors (5, 7, 8, 25) that the light-mass products such as ^{66}Ni, ^{67}Cu, and ^{72}Zn probably arise from a fissioning nucleus having high deposition energy. Thus it appears that that fraction of the total reaction which forms compound nuclei yields these products, whereas those leading to partial energy transfer would give rise to relatively more symmetric fission products.

The kinetic energies of ^{66}Ni, ^{67}Cu, and ^{72}Zn obtained on the basis of the u.c.d. hypothesis have been plotted in Fig. 2. Also included in the figure are the data of Noshkin and Sugihara (7) at 150 MeV and those of Alexander *et al.* (5) at 720 MeV. Regardless of the slight mass difference, the kinetic energies of these products in the bombarding regions of 40–85 MeV are nearly the same within experimental error. At higher energies, however, there may be a small decrease in kinetic

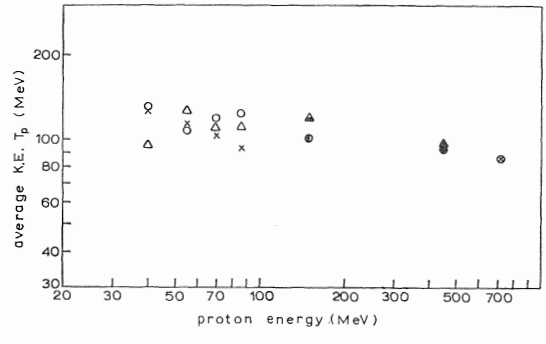

FIG. 2. Variation of average kinetic energy, T_p, as a function of proton bombarding energy. ^{67}Cu: ○, this work; ◐, ref. 7; ●, ref. 8; ^{72}Zn: △, this work; ▲, ref. 7; ▲, ref. 8; ^{66}Ni: ×, this work; ⊗, ref. 5.

TABLE V

Total kinetic energy release at different energies

Bombarding energy (MeV)	Measured kinetic energy of the products T_p (MeV)			Total kinetic energy T_0 (MeV)			Average total kinetic energy $\overline{T}_0$ (MeV)
	^{66}Ni	^{67}Cu	^{72}Zn	^{66}Ni	^{67}Cu	^{72}Zn	
40	127	130	95	172	183	139	150±33
55	115	107	127	156	151	185	180±40
70	103	120	110	144	169	160	160±35
85	93	125	112	129	176	164	160±35

energies. A smaller share of the kinetic energy for these products at higher bombarding energy would probably indicate the emission of relatively massive charged particles carrying various amounts of kinetic energies.

The kinetic energy T_p of the fission products measured can be used to calculate the total kinetic energy release in fission. Because of conservation of momentum, the total kinetic energy is shared by the fragments in the ratio of their masses. Thus the total kinetic energy T_0 is related to that of the primary fragments of masses A_1 and A_2 by the following expression

$$[14] \qquad T_0 = T_{\text{prim}}\left(1 + \frac{A_2}{A_1}\right)$$

If the u.c.d. hypothesis is again invoked, then A_2/A_1 is equal to $(93 - Z_1)/Z_1$ with Z_1 and $(93 - Z_1)$ as the charges of the primary fragments. Since only neutrons rather than any charged particles are expected to be evaporated from the primary fragments, the average charge of the primary fragments should be equal to that of the products observed. Moreover, as neutron evaporation will not cause a very appreciable change in the kinetic energy of the fragments, the average kinetic energy T_p of the products can be approximated to be that of the primary fragments. Thus, from the measured T_p values of each observed product and the average charges, $\overline{Z}$, of the chain, as calculated on the basis of the u.c.d. hypothesis, the total kinetic energies corresponding to each observed fission product have been calculated from eq. [14]. They are given in Table V along with the T_p values of the individual products. Finally the average total kinetic energy $\overline{T}_0$ at a given bombarding energy can be calculated from

$$[15] \qquad \overline{T}_0 = \frac{\sum \sigma_i (T_0)_i}{\sum \sigma_i}$$

by weighting the T_0 values with the yield σ_i of each product. The values of σ_i have been given elsewhere (9). With these values, the $\overline{T}_0$ values have been calculated and are given in Table V and in Fig. 3. These values have an uncertainty of ±22%. Also included in Fig. 3 are published data at higher energies. However, the average $\overline{T}_0$ value given by us is not a very representative average value of the total kinetic energy release in fission in the sense that it has been weighted only with respect to the yields of a very narrow region of light-mass fission products.

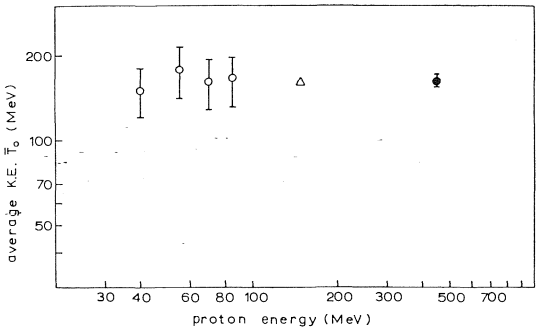

FIG. 3. Variation of average total kinetic energy, $\overline{T}_0$, as a function of proton bombarding energy: ○, this work; △, ref. 7; ●, ref. 8.

It is apparent from Fig. 3 that the total kinetic energy of the fragments is insensitive to the bombarding energy. It has been maintained that the kinetic energy of the fragments results from the Coulombic repulsion between two complementary fragments at scission. The insensitivity of $\overline{T}_0$ to the bombarding energy indicates that this Coulomb energy does not depend on excitation energy. In other words, the average distance between the two charge centers of the fragments at the point of scission would seem to be the same at all these excitation energies (22, 26).

Can. J. Chem. Downloaded from www.nrcresearchpress.com by 210.87.254.40 on 09/05/12
For personal use only.

A value of 163 MeV has been obtained for the average kinetic energy release in fission of ^{238}U by protons of energy 40–85 MeV. This value is comparable with other data (7, 8).

Acknowledgments

We are grateful to Dr. R. E. Bell, Director of the Foster Radiation Laboratory, for ready access to the cyclotron and associated facilities. Mr. R. H. Mills, as always, cheerfully performed the irradiations.

1. N. T. Porile and N. Sugarman. Phys. Rev. **107**, 1410 (1957); **111**, 1746 (1958).
2. J. M. Alexander and M. F. Gazdik. Phys. Rev. **120**, 874 (1960).
3. J. B. Niday. Phys. Rev. **121**, 1471 (1961).
4. F. Brown and B. H. Oliver. Can. J. Chem. **39**, 616 (1961).
5. J. M. Alexander, C. Baltzinger, and M. F. Gazdik. Phys. Rev. **129**, 1826 (1963).
6. J. M. Alexander, M. F. Gazdik, A. R. Trips, and S. Wasif. Phys. Rev. **129**, 2659 (1963).
7. V. E. Noshkin, Jr. and T. T. Sugihara. J. Inorg. Nucl. Chem. **27**, 943 (1965); **27**, 959 (1965).
8. N. Sugarman, H. Münzel, J. A. Panontin, K. Wielgoz, M. V. Ramaniah, G. Lange, and E. Lopez-Menchero. Phys. Rev. **143**, 952 (1966).
9. A. H. Khan, G. B. Saha, and L. Yaffe. Can. J. Chem. **46**, 3565 (1968).
10. C. M. Lederer, J. M. Hollander, and I. Perlman. Table of isotopes. 6th ed. John Wiley and Sons, Inc., New York. 1967.
11. J. A. Panontin and N. Sugarman. J. Inorg. Nucl. Chem. **25**, 1321 (1963).
12. L. Winsberg. UCRL-8618 (1959). Unpublished.
13. J. Lindhard, M. Scharff, and H. E. Schiøtt. Kgl. Danske Videnskab Selskab Mat. Fys. Medd. **33**, No. 14 (1963).
14. J. C. D. Milton and J. S. Fraser. Can. J. Phys. **40**, 1626 (1962).
15. A. C. Wahl. J. Inorg. Nucl. Chem. **6**, 263 (1958).
16. A. C. Wahl, R. L. Ferguson, D. R. Nethaway, D. E. Troutner, and K. Wolfsberg. Phys. Rev. **126**, 1112 (1962).
17. R. D. Evans. The atomic nucleus. McGraw-Hill Book Co., Inc., New York. 1955. p. 749.
18. J. H. Davies and L. Yaffe. Can. J. Phys. **41**, 762 (1963).
19. S. Parikh, D. A. Marsden, N. T. Porile, and L. Yaffe. Can. J. Chem. **45**, 1863 (1967).
20. C. D. Coryell, M. Kaplan, and R. D. Fink. Can. J. Chem. **39**, 646 (1961).
21. J. P. Unik and J. R. Huizenga. Phys. Rev. **134**, B90 (1964).
22. J. R. Huizenga, and R. Vandenbosch. Nuclear reactions. Vol. II. *Edited by* P. M. Endt and P. B. Smith. North-Holland Publishing Company, Amsterdam. 1962.
23. N. Metropolis, R. Bivins, M. Storm, A. Turkevich, J. M. Miller, and G. Friedlander. Phys. Rev. **110**, 185 (1958). N. Metropolis, R. Bivins, M. Storm, J. M. Miller, G. Friedlander, and A. Turkevich. Phys. Rev. **110**, 204 (1958).
24. N. T. Porile. Phys. Rev. **120**, 572 (1960).
25. E. Hagebø, A. C. Pappas, and P. Aagaard. J. Inorg. Nucl. Chem. **26**, 1639 (1964). A. C. Pappas and E. Hagebø. J. Inorg. Nucl. Chem. **28**, 1769 (1966).
26. I. Halpern. Ann. Rev. Nucl. Sci. **9**, 245 (1959).

Can. J. Chem. Downloaded from www.nrcresearchpress.com by 210.87.254.40 on 09/05/12
For personal use only.

Neutralization of dilute aqueous aluminium sulfate solutions with a base[1]

S. Shah Singh
Soil Research Institute, Canada Department of Agriculture, Ottawa, Canada
Received July 30, 1968

A theoretical treatment of the neutralization of dilute $Al_2(SO_4)_3$ solutions with a base is presented and is supported by the experimental data. The formation of soluble complex $AlSO_4^+$; the first-stage hydrolysis product, $AlOH^{2+}$, and the precipitation of amorphous aluminium hydroxy sulfate are the reactions controlling the conditions in solution up to 80% of neutralization with respect to aluminium. Beyond 80% of neutralization there is slow replacement of SO_4^{2-} by OH^- in the amorphous precipitate of aluminium hydroxy sulfate.

Canadian Journal of Chemistry, **47**, 663 (1969)

Can. J. Chem. Downloaded from www.nrcresearchpress.com by 210.87.254.105 on 09/05/12
For personal use only.

Introduction

The hydrolysis of aluminium salts has been the subject of extensive investigations. The products of hydrolysis reported range from monomers to a variety of complex aluminium species, ionic and neutral, mononuclear and polynuclear. Chernov (1) found that the monomeric hydrolysis mechanism adequately described the chemistry of dilute aqueous aluminium chloride in the concentration range of 10^{-4} to 10^{-2} *M*. Frink and Sawhney (2) reported that potentiometric titration curves of dilute aluminium salt solutions can be predicted by a simple reaction scheme which combines the first-stage hydrolysis reaction, the formation of $AlOH^{2+}$, with the concomitant precipitation of $Al(OH)_3$. From a general treatment of the titration of aluminium chloride with a base, Turner (3) concluded that the relative rates of hydrolysis, formation of polynuclear hydroxy-aluminium cations, precipitation and crystallization had an important effect on the shape of the experimental titration curves. However, with fast titrations, hydrolysis to monomers and precipitation of amorphous $Al(OH)_3$ played the major roles in controlling conditions in solution. Turner (3) did not give any treatment for the neutralization of dilute aqueous solutions of aluminium sulfate. Frink and Sawhney (2), although they did not show any neutralization curves for aluminium sulfate, claimed in their text that their simple treatment of hydrolysis to monomers and concomitant precipitation of $Al(OH)_3$ could be applied to neutralization curves of dilute aqueous aluminium sulfate solutions. It has been reported in the literature (4) that an amorphous precipitate of aluminium hydroxy sulfate is formed when a solution of aluminium sulfate is neutralized with a base, and that this precipitate has a fairly constant solubility (5). It is apparent, therefore, that Frink and Sawhney's (2) conclusions obviously are not consistent with this result.

Evidence reported in this paper indicates that curves for the fast titration of dilute aluminium sulfate solutions can be predicted by the first-stage hydrolysis reaction (6, 7), the formation of soluble complex $AlSO_4^+$ (8), and the precipitation of aluminium hydroxy sulfate, which has a constant ionic product $[Al][OH]^{3-x}[SO_4]^{x/2}$. They cannot be predicted from the first-stage hydrolysis reaction and the precipitation of $Al(OH)_3$ as concluded by Frink and Sawhney (2).

Theoretical

The assumptions used to calculate the curves for the neutralization of aqueous solutions of aluminium sulfate with a base are that the soluble complex $AlSO_4$, the first-stage hydrolysis product, AlOH, and an amorphous precipitate of aluminium hydroxy sulfate, $[Al(OH)_{3-x}(SO_4)_{x/2}]$, are formed and that the precipitate has a definite solubility product. The charges on the ions are omitted for the sake of convenience. The equilibrium constants relationship used are

$$[1] \qquad [Al][OH]^{3-x}[SO_4]^{x/2} = K_s$$

$$[2] \qquad \frac{[AlSO_4]}{[Al][SO_4]} = K_{SO_4}$$

$$[3] \qquad \frac{[AlOH][H]}{[Al]} = K_1$$

$$[4] \qquad [H][OH] = K_w$$

where square brackets denote concentrations in

[1]Contribution No. 283.

moles/l, the K's are constant for any given ionic strength. Equation [1] expresses the concentration solubility product of amorphous aluminium hydroxy sulfate, K_w is the ionic product of water at any given ionic strength, K_1 is the constant of first stage of hydrolysis of aluminium, and K_{SO_4} is the equilibrium constant of reaction

$$Al + SO_4 \rightleftharpoons AlSO_4$$

According to the assumptions mentioned above, since all of the aluminium and sulfate are present in some form of ions or as the precipitate aluminium hydroxy sulfate, it follows that

$$[5] \quad [Al]_t = [Al] + [AlOH] + [AlSO_4] + [Al(OH)_{3-x}(SO_4)_{x/2}]$$

$$[6] \quad [SO_4]_t = [SO_4] + [AlSO_4] + x/2[Al(OH)_{3-x}(SO_4)_{x/2}]$$

where $[Al]_t$ and $[SO_4]_t$ denote the total Al and SO_4 in the system. From the formula of each species in eq. [5] it also follows that

$$[7] \quad B = [AlOH] + (3 - x)[Al(OH)_{3-x}(SO_4)_{x/2}] - [H]$$

where B is the amount of base added in equivalents/l of the system. Subtracting $1/(3 - x)$ of eq. [7] from eq. [5] it gives

$$[8] \quad [Al]_t - \frac{1}{3-x}B = [Al] + \frac{2-x}{3-x}[AlOH] + [AlSO_4] + \frac{1}{3-x}[H]$$

It can be seen from eqs. [1] and [4], that

$$[9] \quad [Al] = \frac{K_s[H]^{3-x}}{K_w{}^{3-x}[SO_4]^{x/2}}$$

from eq. [3]

$$[10] \quad [AlOH] = \frac{K_1[Al]}{[H]}$$

and from eqs. [2] and [6]

$$[11] \quad [AlSO_4] = \frac{K_{SO_4}\{[Al]\}\{[SO_4]_t - x/2[Al(OH)_{3-x}(SO_4)_{x/2}]\}}{1 + K_{SO_4}[Al]}$$

$\{[SO_4]_t - x/2[Al(OH)_{3-x}(SO_4)_{x/2}]\}$ in eq. [11] will be referred to as $[SO_4]_t'$ in the following equations for simplicity.

Equations [8], [9], [10], and [11] can be combined to give

$$[12] \quad [Al]_t - \frac{1}{3-x}B = \frac{K_s[H]^{3-x}}{K_w{}^{3-x}[SO_4]^{x/2}} + \frac{2-x}{3-x}\frac{K_sK_1[H]^{2-x}}{K_w{}^{3-x}[SO_4]^{x/2}} + \frac{K_sK_{SO_4}[SO_4]_t'[H]^{3-x}}{K_w{}^{3-x}[SO_4]^{x/2} + K_sK_{SO_4}[H]^{3-x}} + \frac{1}{3-x}[H]$$

Equation [12] is a general equation, which can be solved for a given value of x and the neutralization curve of a particular concentration of Al in aluminium sulfate can be constructed provided K_s in eq. [1] is known for that value of x. Equation [12] will be simplified for two values of x and calculated curves will be compared with experimental curves for different concentrations of Al.

If x is zero, eq. [1] becomes

$$[13] \quad [Al][OH]^3 = K_s'$$

and accordingly eq. [12] can be simplified to

$$[14] \quad [Al]_t - \frac{1}{3}B = \frac{K_s'[H]^3}{K_w{}^3} + \frac{2}{3}\frac{K_s'K_1[H]^2}{K_w{}^3} + \frac{K_s'K_{SO_4}[SO_4]_t'[H]^3}{K_w{}^3 + K_s'K_{SO_4}[H]^3} + \frac{1}{3}[H]$$

Can. J. Chem. Downloaded from www.nrcresearchpress.com by 210.87.254.105 on 09/05/12
For personal use only.

Can. J. Chem. Downloaded from www.nrcresearchpress.com by 210.87.254.105 on 09/05/12
For personal use only.

Equation [14] is similar to that of Frink and Sawhney (2) except that [14] contains an extra term to take account of soluble complex $AlSO_4$.

The other form to which eq. [12] is simplified, is for the precipitation of amorphous aluminium hydroxy sulfate of an approximate composition $[Al(OH)_{2.5}(SO_4)_{0.25}]$. The value of x in this case is 0.5. With this assumption eq. [1] becomes

$$[15] \qquad [Al][OH]^{2.5}[SO_4]^{0.25} = K_s''$$

and by using [15], eq. [12] can be simplified to

$$[16] \qquad [Al]_t - 0.4B = \frac{K_s''[H]^{2.5}}{K_w{}^{2.5}[SO_4]^{0.25}} + 0.6\,\frac{K_s''K_1[H]^{1.5}}{K_w{}^{2.5}[SO_4]^{0.25}} + \frac{K_s''K_{SO_4}[SO_4]_t'[H]^{2.5}}{K_w{}^{2.5}[SO_4]^{0.25} + K_s''K_{SO_4}[H]^{2.5}} + 0.4\,[H]$$

Equation [15] can be simplified, where $[Al][OH]^{2.5}$ becomes a constant for a particular concentration of aluminium sulfate solution. The maximum variation in sulfate concentration due to its precipitation from zero neutralization to 100% neutralization of Al is 17% and, as is apparent from eq. [15], SO_4 is raised to the power of 0.25; any change in SO_4 is thus insignificant in eq. [15]. For a particular concentration of aluminium sulfate solution, therefore,

$$[17] \qquad [Al][OH]^{2.5} = \frac{K_s''}{[SO_4]^{0.25}} = K_s'''$$

Combining eqs. [16] and [17] gives

$$[18] \qquad [Al]_t - 0.4B = \frac{K_s'''[H]^{2.5}}{K_w{}^{2.5}} + 0.6\,\frac{K_s'''K_1[H]^{1.5}}{K_w{}^{2.5}} + \frac{K_s'''K_{SO_4}[SO_4]_t'[H]^{2.5}}{K_w{}^{2.5} + K_s'''K_{SO_4}[H]^{2.5}} + 0.4\,[H]$$

Equations [14] and [18] can be used for calculations up to 100% neutralization. For calculations beyond 100%, an extra term for $Al(OH)_4$ can be introduced, and the following relationship given by Kittrick (9) can be used in solving the equations.

$$\frac{(Al(OH)_4)(H)^4}{(Al)} = 10^{-23.30}$$

The numerical values used for various equilibrium constants at zero ionic strength to solve eqs. [14] and [18] are $K_{SO_4} = 10^{3.20}$ (8); $K_1 = 10^{-5.02}$ (6); $K_w = 10^{-14.00}$; $K_s' = 10^{-31.80}$ (2); and $K_s'' = 10^{-28.60}$. These values were corrected for the different ionic strength by using ionic activity coefficients calculated from the Debye–Hückel equation with values for the parameter a_i "the distance of closest approach" taken from Klotz (10).

Experimental

A stock solution of concentration 0.1 N was prepared from analytical grade $Al_2(SO_4)_3.18H_2O$ in CO_2-free distilled water. This stock solution was used to prepare a second stock solution of 10^{-2} M Al. The concentration of aluminium in the second stock solution was determined by an 8-quinolinolate extraction method (11). Appropriate aliquots of the second stock solution were diluted to concentrations of 1.00×10^{-3} and 1.00×10^{-4} M Al. Twenty ml portions were titrated with CO_2-free NaOH. The 10^{-2}, 10^{-3}, and 10^{-4} M solutions were titrated with 1 N, 0.1 N, and 0.01 N NaOH, respectively. A combination of a Beckman expanded-scale pH meter and a motor driven Metrohm buret was used to follow the titration curves. Absolute accuracy of the buret was ± 0.002 ml. The drop rate of NaOH from the buret was adjusted so that a titration to 100% of neutralization was completed in about 25 min.

At different degrees of neutralization of aluminium the suspensions were filtered through 10 mμ pore size millipore filters. The liquid phase was collected in a test tube and the solid precipitate remained on the filter membrane. The liquid phase was analyzed for aluminium and sulfate. Aluminium was determined by 8-quinolinolate extraction method (11) and sulfate was determined by direct titration with barium perchlorate, using thorin as an indicator (12).

Results and Discussion

The experimental neutralization curves and the calculated curves according to eqs. [14] and [18] for solution concentrations 1.00×10^{-2}, 10^{-3}, and 10^{-4} M Al as $Al_2(SO_4)_3$ are shown in Fig. 1.

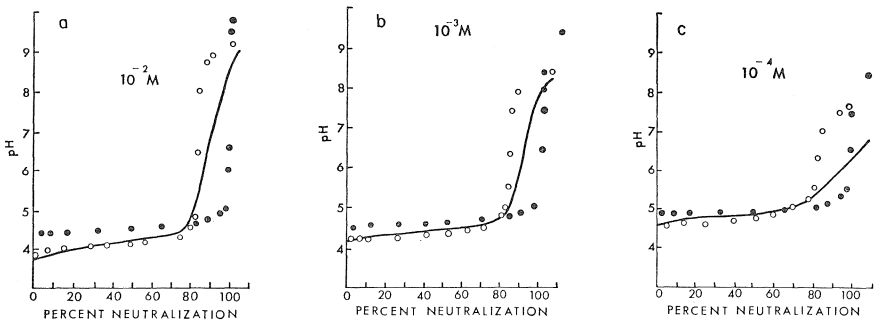

FIG. 1. Neutralization of dilute aqueous solutions of $Al_2(SO_4)_3$ with NaOH: (*a*) 10^{-2} *M* Al; (*b*) 10^{-3} *M* Al; (*c*) 10^{-4} *M* Al. Smooth curve, experimental; closed circles, calculated according to eq. [14], and open circles, calculated according to eq. [18].

A precipitate was visible to the naked eye during the neutralization of dilute solutions of aluminium sulfate with NaOH. Smooth solid curves in the figure are experimental ones; closed and open circles represent eqs. [14] and [18].

It is apparent that eq. [18], which is based on the assumption that $Al(OH)_{2.5}(SO_4)_{0.25}$ is the precipitate formed, fits the experimental data well to about 80% of neutralization[2] but beyond this degree of neutralization the experimental pH values do not increase as rapidly as shown by the calculated curve. The calculated curves according to eq. [14], in which it was assumed that $Al(OH)_3$ is the precipitate formed, do not agree at all with the experimental values for the 10^{-2} and 10^{-3} *M* Al solutions. For the 10^{-4} *M* solution the agreement is fairly good with both calculated curves to 80% of neutralization but a close examination shows that the agreement with eq. [18] is the better of the two.

It can be concluded, therefore, that first-stage hydrolysis to AlOH, formation of the soluble complex $AlSO_4$ and precipitation of an aluminium hydroxy sulfate controls conditions in solution during the first 80% of neutralization of dilute solutions of $Al_2(SO_4)_3$ with NaOH.

The fact that the curve calculated from eq. [14] also agrees with the experimental results for the first 80% of neutralization does not mean that the reactions at the low concentration are different from those at the two higher concentrations. The curves represented by eqs. [14] and [18] agree rather well at the 10^{-4} concentration, because under these conditions $[Al][OH]^{2.5}[SO_4]^{0.25}$ is $10^{-28.6}$, and $[Al][OH]^3$ is $10^{-32.1}$, a value not greatly different from the ion product $10^{-31.8}$, which was used in the calculations for eq. [14] for the solubility product of the $Al(OH)_3$ precipitated (2). With the 10^{-2} and 10^{-3} *M* solutions $[Al][OH]^3$ values calculated from $10^{-28.6}$ for $[Al][OH]^{2.5}[SO_4]^{0.25}$ are $10^{-33.0}$ and $10^{-32.7}$, respectively, which are considerably lower than $10^{-31.8}$. This is the main cause of the differences at these concentrations between the experimental curves and those calculated from eq. [14].

Beyond about 80% of neutralization, the deviation of the experimental curves from those calculated according to eq. [18] indicates a significant change in the reactions. The pH of the experimental curves is lower than the calculated pH. This is due to slow replacement of SO_4 by OH in the amorphous precipitate of aluminium hydroxy sulfate, because of the heterogeneous nature of the system. If it were a homogeneous system, one would expect a rapid replacement.

In order to test the validity of this explanation the liquid phase was analyzed for SO_4 and Al concentration during the neutralization. It was found (Table I) that the Al concentration was decreased to a greater extent than that expected if $Al(OH)_3$ were formed, until at about a degree of neutralization of 80% or higher, the Al concentration was essentially zero. The SO_4 concentration in the liquid phase decreased as titration progressed to about 80% of neutralization and then increased. These results from the chemical analysis thus agree with the explanation that up to 80% of neutralization a precipitate of aluminium hydroxy sulfate of an approximate composition of $Al(OH)_{2.5}(SO_4)_{0.25}$ is formed and

[2]% of neutralization means always with respect to aluminium.

Can. J. Chem. Downloaded from www.nrcresearchpress.com by 210.87.254.105 on 09/05/12
For personal use only.

TABLE I

Concentration of aluminium and sulfate in liquid phase at different degrees of neutralization

% neutralization	Al (mmoles/l) $Al(OH)_3$*	$Al(OH)_{2.5}(SO_4)_{0.25}$*	Experimental	SO_4 (mmoles/l)
0	10.37	10.37	10.37	16.24
15	8.82	8.50	8.25	15.40
30	7.26	6.64	6.20	14.90
40	6.22	5.39	5.22	14.53
50	5.19	4.15	3.89	13.72
65	3.63	2.28	2.10	12.63
75	2.59	1.04	0.65	11.98
80	2.07	0.41	0.13	11.76
85	1.56	—	0.002	12.30
90	1.04	—	—	12.95
95	0.52	—	—	13.60
100	0	—	0.24	14.00

*Calculated assuming all the base added formed $Al(OH)_3$ or $Al(OH)_{2.5}(SO_4)_{0.25}$.

beyond this degree of neutralization the reaction is the replacement of SO_4 from the amorphous precipitate with OH. The results reported by Hsu and Bates (4) also agree with this interpretation. They found that over the range of NaOH/Al = 0.3 to 2.1 the amount of precipitate increased with increasing ratio but the composition of the precipitate was approximately constant.

The presence of polynuclear aluminium in the liquid phase was checked by extracting with 8-quinolinol for different length of time (11). Okura *et al.* (11) found that with 10 s extraction time, only aluminium ions with the degree of polymerization at or very close to unity were determined in the chloroform extraction and any delay caused considerable depolymerization of the higher aluminium complex. In the present investigation, there was a very small change in the aluminium concentration determined in the chloroform separation, when extraction time with 8-quinolinol was 24 h as compared with zero time. This change was, however, not enough to cause any significant influence on the shape of the neutralization curve, or the calculated composition of the precipitate.

In summary, it is concluded that the first-stage hydrolysis of aluminium, the formation of $AlSO_4$, and the precipitation of aluminium hydroxy sulfate of the approximate composition $Al(OH)_{2.5}(SO_4)_{0.25}$ were the reactions responsible for controlling the conditions in solution up to 80% of neutralization when aqueous solutions in the concentration range of 10^{-2} to 10^{-4} *M* Al as aluminium sulfate were neutralized with a base. Beyond 80% of neutralization, there was replacement of SO_4 by OH in the precipitate.

Acknowledgment

The author is grateful to Dr. R. C. Turner for valuable discussions during the preparation of the manuscript.

1. V. A. Chernov. The nature of soil acidity. Press of the Academy of Sciences, U.S.S.R. 1947, Moscow. Translated by Soil Sci. Soc. Am., Madison, Wis.
2. C. R. Frink and B. L. Sawhney. Soil Sci. **103**, 144 (1967).
3. R. C. Turner. Soil Sci. **106**, 291 (1968).
4. P. H. Hsu and R. F. Bates. Mineral. Mag. **33**, 749 (1964).
5. S. S. Singh. Soil Sci. **104**, 433 (1967).
6. C. R. Frink and M. Peech. Inorg. Chem. **2**, 473 (1963).
7. R. K. Schofield and A. W. Taylor. J. Chem. Soc. 4445 (1954).
8. B. Behr and H. Wendt. Z. Elektrochem. **66**, 223 (1962).
9. J. A. Kittrick. Soil Sci. Soc. Am. Proc. **30**, 595 (1966).
10. I. M. Klotz. Chemical thermodynamics. Prentice-Hall, Inc., New York. 1950.
11. T. Okura, K. Goto, and T. Yotuyanagi. Anal. Chem. **34**, 581 (1962).
12. J. S. Fritz and S. S. Yamura. Anal. Chem. **27**, 1461 (1955).

Can. J. Chem. Downloaded from www.nrcresearchpress.com by 210.87.254.105 on 09/05/12
For personal use only.

Isomerization of methyl isocyanide sensitized by vibrationally excited ethane

D. H. SHAW, B. K. DUNNING, AND H. O. PRITCHARD
Centre for Research in Experimental Space Science, York University, Toronto, Ontario

Received September 5, 1968

The isomerization of methyl isocyanide in the presence of methyl radicals takes place by two mechanisms. One is the simple free-radical displacement reaction which has been described previously. The other is through a direct transfer of energy from vibrationally excited ethane molecules. The vibrationally sensitized component can be quenched by increasing the total pressure.

Canadian Journal of Chemistry, **47**, 669 (1969)

Can. J. Chem. Downloaded from www.nrcresearchpress.com by 210.87.254.6 on 09/05/12
For personal use only.

In the past five years, numerous examples have been found in which a vibrationally excited haloethane eliminates a hydrogen halide molecule (1, 2). Typically, the excited ethane is formed when two methyl-type radicals combine, e.g.

$$CH_3 + CCl_3 \rightarrow CH_3CCl_3^*$$

although other methods of formation have also been tried (3, 4); then, if the pressure is not too high, an elimination, e.g.

$$CH_3CCl_3^* \rightarrow CH_2{:}CCl_2 + HCl$$

takes place before the ethane can be stabilized by collisions with the surrounding gas. However, no reaction of vibrationally excited ethane formed by the combination of methyl radicals has yet been reported. Two reactions seem possible, viz.

$$C_2H_6^* \rightarrow C_2H_4 + H_2$$

and

$$C_2H_6^* \rightarrow CH_2 + CH_4$$

but neither of them has been observed despite the fact that efforts have been made on several occasions to find them (5). In the experiments described below, we set out to determine whether a vibrationally excited ethane molecule could transfer sufficient energy to another molecule to sensitize a chemical reaction, and we chose the isomerization of methyl isocyanide to test this idea. To avoid complications due to electronic excitation of molecules in the system, the thermal decomposition of di-*tert*-butyl peroxide was used as the source of methyl radicals.

Materials and Experimental Technique

Methyl isocyanide, ethyl isocyanide, di-*tert*-butyl peroxide, and carbon dioxide were prepared and/or purified as described previously (6, 7); 1,1-difluoroethane was obtained from Matheson of Canada Ltd.

Experiments were performed in the temperature range 85–130 °C by heating mixtures of methyl isocyanide, di-*tert*-butyl peroxide (DTBP), and CO_2 in a 10 cc Hoke stainless steel pressure vessel. Initial quantities of about 2×10^{-4} and 3×10^{-5} moles, respectively, of isocyanide and peroxide were chosen to give some 10–20% isomerization (6), and pressures of CO_2 up to 60 atm were added to the reaction mixture. At the end of the reaction, the contents of the pressure vessel were pumped into the vacuum system; the methane, ethane, and CO_2 were removed by careful distillation with two Leroy stills (7); and the residue was analyzed by gas chromatography (6) for the final concentrations of methyl isocyanide, acetone, methyl cyanide, and di-*tert*-butyl peroxide. No methyl acetate was detected, even at the highest pressures, indicating that methyl radicals do not react significantly with CO_2 at these temperatures.

Results and Discussion

The sequence of reactions previously proposed (6) for the methyl-radical catalyzed isomerization of methyl isocyanide is

[1] $$DTBP \rightarrow 2CH_3 + 2CH_3COCH_3$$

[2] $$CH_3 + CH_3 \rightarrow C_2H_6$$

[3] $$CH_3 + CH_3NC \rightarrow CH_3CN + CH_3$$

whence, by using the integrated form of the rate expression, the apparent rate constant

$$k_3^* = \frac{1}{t}\left(\frac{k_2 v}{k_1[\mathrm{DTBP}]_{av}}\right)^{\frac{1}{2}} \ln \frac{[CH_3NC]_i}{[CH_3NC]_f}$$

where t is the length of the run, v is the volume of the reaction vessel, and the value for k_1 is that taken from ref. 7.

Without the addition of CO_2, the apparent rate constants k_3^* which we obtained are very similar to those found previously (6). However, as the CO_2 pressure is increased, k_3^* falls and eventually becomes constant above about 10 atm total pressure, as shown in Fig. 1. We postulate that this behavior can be accounted

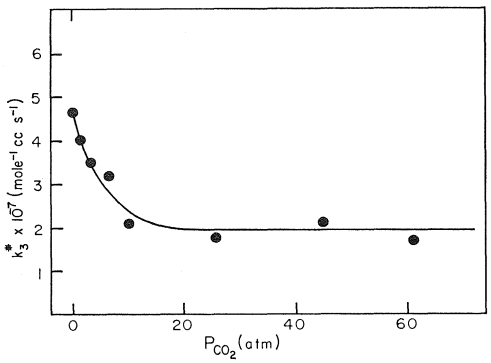

FIG. 1. Pressure dependence of the rate of isomerization of methyl isocyanide by methyl radicals at 110 °C.

for by the following modification to the above sequence of reactions

[2*a*] $CH_3 + CH_3 \rightarrow C_2H_6^*$

[2*b*] $C_2H_6^* + M \rightarrow C_2H_6$

[4] $C_2H_6^* + CH_3NC \rightarrow C_2H_6 + CH_3CN$

We envisage that process [2*b*] involves a series of stepwise deactivations, and in this reaction C_2H_6 represents an ethane molecule which has had sufficient of its vibrational energy removed so as to make it ineffective in reaction [4]. Reaction [4] as written also represents an overall process, which in detail probably takes place by a sharing of the vibrational excitation between the two partners, producing $CH_3NC\dagger$, which may then isomerize, or may be deactivated. Whilst some information is available (8) on the lifetime of vibrationally excited $CH_3NC\dagger$, we are not yet in a position to be able to make a theoretical analysis of the pressure dependence of k_3^*. All we can say at the moment is that at sufficiently high pressure, reaction [4] will be suppressed, as observed in Fig. 1.

The pressure dependence of k_3^* is not altered by using a 75 cc reaction vessel, indicating that no major surface effect is involved. Behavior similar to that shown in Fig. 1 was observed at all temperatures in the range 85–130 °C, except that the pressure dependence was slightly less marked at the higher temperatures. The result of this is that the high-pressure limit of the rate constant is represented by

$$k_3^{(\infty)} \approx 10^{17} \exp\,[-(16\,400 \pm 1000)/RT] \text{ mole}^{-1} \text{ cc s}^{-1}$$

We believe that this rate-constant expression requires further substantiation before it is accepted with confidence, since previous examples of "high" frequency factors in free-radical reactions have eventually proved to be incorrect (9, 10). In fact, it appears likely that it may be due to a certain amount of self-heating at the highest temperatures, since at 130 °C, the rate of production of heat is of the order of 5×10^{-5} cal cc^{-1} s^{-1}.

These experiments were then repeated using ethyl isocyanide, which is similarly isomerized by methyl radicals according to the reaction scheme (6)

[3*a*] $CH_3 + C_2H_5NC \rightarrow CH_3CN + C_2H_5$

[3*b*] $C_2H_5 + C_2H_5NC \rightarrow C_2H_5CN + C_2H_5$

It was found that both the rates of formation of methyl cyanide and isomerization of ethyl isocyanide were independent of pressure. This is consistent with our proposal since, being a more complicated molecule, the vibrationally excited $C_2H_5NC\dagger$ would have perhaps 100 times the lifetime of $CH_3NC\dagger$ with respect to isomerization. Hence the isomerization of C_2H_5NC would be at its high-pressure limit at rather less than 1 atm, and as the total pressure in most of the unpressurized experiments was about 0.1 atm, no conspicuous effect would be expected on increasing the pressure. Since methyl and ethyl isocyanide are so similar, both as regards their rates and heats of isomerization, their different behavior in this respect effectively rules out self-heating as the direct cause of the pressure effect described above.

The most unusual aspect of our proposed reaction scheme is the apparent existence of energy chains. If we compare the final compositions after a pair of comparable 2 h runs at 110 °C, we find

	Composition $\times 10^6$ moles			
Condition	DTBP	C_2H_6	CH_3NC	CH_3CN
No CO_2	31	(0.4)	181	32
45 atm CO_2	29	(0.4)	150	10

whence k_3^* works out to be 4.5×10^7 and 2.1×10^7 mole^{-1} cc s^{-1}, respectively; the ethane concentrations were not measured in these particular experiments, but were calculated from

Can. J. Chem. Downloaded from www.nrcresearchpress.com by 210.87.254.6 on 09/05/12
For personal use only.

the previously known behavior of the system (6, 7). Assuming that at the high pressure, all the isomerization takes place by reaction [3], we conclude that at low pressure, some kind of chain occurs, since the pressure effect far exceeds the number of moles of C_2H_6* which can partake directly in reaction [4]. Since reaction [3] is only 15 kcal/mole exothermic, and the activation energy for the thermal isomerization is 38 kcal/mole (11), no amount of internal excitation of the products could lead to a sensitization reaction; nor is it likely, since the activation energy of [3] is probably around 8–10 kcal/mole, that the CH_3 radical produced in [3] could carry sufficient excitation to react spontaneously with another isocyanide molecule. Thus, we are forced to conclude that it is only those vibrationally hot $CH_3CN‡$ formed in reaction [4] that can propagate a chain; reaction [4] must, therefore, be rewritten as

[4*a*] $C_2H_6^* + CH_3NC \rightarrow C_2H_6 + CH_3NC†$

[4*b*] $CH_3NC† \rightarrow CH_3CN‡$

[4*c*] $CH_3CN‡ + CH_3NC \rightarrow 2CH_3CN‡$

whence the chain length in essentially undiluted CH_3NC appears to be of the order of 30–50. (In this respect, it should be remembered that we found it necessary to postulate reaction [4*c*] in the ultraviolet photolysis of CH_3NC (12) to account for a quantum yield in excess of unity.)

We also decomposed di-*tert*-butyl peroxide in the presence of 1,1-difluoroethane to see if vibrationally excited ethane would sensitize the elimination of hydrogen fluoride. No vinyl fluoride was found. Hence either the lifetime of $CH_3CHF_2†$ is too long at 0.1 atm, or else the hot ethane molecule does not impart sufficient vibrational energy to the difluoroethane to cause it to decompose; since the critical energy for this process is greater than 50 and probably nearer 60 kcal (13) as opposed to the 38 kcal required to isomerize the isocyanide (11), the latter is probably the more meaningful explanation.

1. D. M. Tomkinson and H. O. Pritchard. J. Phys. Chem. **70**, 1579 (1966).
2. G. O. Pritchard and R. L. Thommarson. J. Phys. Chem. **71**, 1674 (1967).
3. G. O. Pritchard, J. T. Bryant, and R. L. Thommarson. J. Phys. Chem. **69**, 2804 (1966).
4. J. A. Kerr, A. W. Kirk, B. V. O'Grady, D. C. Phillips, and A. F. Trotman-Dickenson. Discussions Faraday Soc. **44**, 263 (1967).
5. G. O. Pritchard. Private communication.
6. D. H. Shaw and H. O. Pritchard. Can. J. Chem. **45**, 2749 (1967).
7. D. H. Shaw and H. O. Pritchard. Can. J. Chem. **46**, 2721 (1968).
8. D. C. Tardy and B. S. Rabinovitch. J. Chem. Phys. **48**, 1282 (1968).
9. H. O. Pritchard. Rec. Trav. Chim. **74**, 779 (1955).
10. G. C. Fettis, J. H. Knox, and A. F. Trotman-Dickenson. J. Chem. Soc. 4177 (1960).
11. F. W. Schneider and B. S. Rabinovitch. J. Am. Chem. Soc. **84**, 4215 (1962).
12. D. H. Shaw and H. O. Pritchard. J. Phys. Chem. **70**, 1230 (1966).
13. J. T. Bryant and G. O. Pritchard. J. Phys. Chem. **71**, 3439 (1967).

Can. J. Chem. Downloaded from www.nrcresearchpress.com by 210.87.254.6 on 09/05/12
For personal use only.

Can. J. Chem. Downloaded from www.nrcresearchpress.com by 210.87.254.105 on 09/05/12
For personal use only.

Coordination compounds of methyl gallium hydrides[1]

A. STORR AND V. G. WIEBE
Chemistry Department, University of British Columbia, Vancouver 8, British Columbia

Received August 15, 1968

Although the organo hydride derivatives of boron and aluminium are well characterized, little work has been reported on the corresponding gallium systems. The present study was initiated to determine the relative stabilities of organo gallium hydride derivatives as compared to the stabilities of the corresponding compounds of boron and aluminium. Various preparative routes in this new class of gallium compounds have been investigated. These include the use of organo mercury and organo lithium reagents in reactions with gallium hydride compounds and their halogen substituted derivatives, and also equlibration reactions between gallium hydride and organo gallium compounds. Both infrared and proton magnetic resonance spectroscopy techniques have been used extensively in following the progress of these reactions and in the characterization of the products.

Canadian Journal of Chemistry, **47**, 673 (1969)

Introduction

Coordination compounds of gallane, GaH_3, and halogenogallanes, $GaH_{3-n}X_n$ (where X = halogen and $n = 1$ or 2), with amines and phosphines have been investigated extensively over the past few years (1–5). Similarly the coordination chemistry of the simpler gallium alkyls has been thoroughly studied (6, 7). In contrast, however, very little work has been carried out on the chemistry of organogallanes and none has been reported on coordination compounds of the type $D{\cdot}GaH_{3-n}R_n$, (where D represents a Lewis base, e.g. Me_3N; R represents a simple alkyl group, Me and Et; and $n = 1$ or 2).

The low thermal stability of known uncoordinated alkyl gallanes, of the type R_2GaH (8), suggested that the most profitable line of approach to the desired compounds would be via substitution reactions involving introduction of organo groups into coordinated gallium compounds. Several methods of synthesis were attempted, the first of which involved the reaction of trimethylamine-gallane with dimethylmercury in benzene or ether as solvent.

[1] $$Me_3NGaH_2Me + \tfrac{1}{2}H_2 + \tfrac{1}{2}Hg \xrightarrow[(ii)C_6H_6]{(i)Et_2O} Me_3NGaH_3 + \tfrac{1}{2}Me_2Hg$$

A second method involved the lithium hydride reductions of trimethylamine adducts of methylgallium halides.

[2] $$Me_3NGaMe_2Cl + LiH \xrightarrow{Et_2O} Me_2NGaMe_2H + LiCl$$

$$Me_3NGaMeCl_2 + 2LiH \xrightarrow{Et_2O} Me_3NGaMeH_2 + 2LiCl$$

A third and more advantageous route employed the reaction of lithium methyl with halogenogallanes.

[3] $$Me_3NGaH_2Cl + LiMe \xrightarrow{Et_2O} Me_3NGaH_2Me + LiCl$$

$$Me_3NGaHCl_2 + 2LiMe \xrightarrow{Et_2O} Me_3NGaHMe_2 + 2LiCl$$

Finally, equilibration reactions between trimethylamine-gallane and trimethylamine trimethyl gallium, in either ether or benzene as solvent, gave quantitative yields of the methylgallanes.

[4] $$Me_3NGaH_3 + 2Me_3NGaMe_3 \longrightarrow 3Me_3NGaHMe_2$$

$$2Me_3NGaH_3 + Me_3NGaMe_3 \longrightarrow 3Me_3NGaH_2Me$$

Experimental

Materials were handled in a conventional high vacuum line or in a glove box under an atmosphere of oxygen-free dry nitrogen. All solvents were thoroughly dried and redistilled before use.

Starting Materials

Trimethylamine-gallane and trimethylamine-trideuteriogallane were prepared as previously described (2). Trimethylamine-chlorogallanes were also obtained by

[1]Presented in part at the Third International Symposium on Organometallic Chemistry, Munich, 1967. Abstracts, p. 270.

Can. J. Chem. Downloaded from www.nrcresearchpress.com by 210.87.254.105 on 09/05/12
For personal use only.

standard procedures (4). Trimethyl gallium was prepared by reacting a slight excess of gallium metal with dimethyl mercury in a sealed Carius tube (9). Methylgallium chlorides were prepared by standard procedures (10–12). Trimethylamine trimethyl gallium and trimethylamine methyl gallium chlorides were prepared by condensing excess trimethylamine onto the appropriate gallium acceptor moiety, followed by removal of excess amine at −10 °C under vacuum. Trimethylamine-alane was prepared by the method of Ruff and Hawthorne (13). Trimethylamine trimethyl aluminium was prepared from trimethyl aluminium and trimethylamine. Trimethyl boron was prepared by a Grignard reaction (14) and its trimethylamine adduct by the above method. Trimethylamine-borane was obtained by reacting lithium borohydride with trimethylamine hydrochloride in ether solution (15). Dimethyl mercury and lithium methyl were obtained from Alfa Inorganics. The latter reagent was obtained as an ether solution, the concentration of which was determined prior to each experiment.

Preparations of Methyl Gallane Derivatives

Method A

In a typical reaction trimethylamine-gallane (0.373 g, 2.83 mmoles) and dimethyl mercury (0.328 g, 1.42 mmoles) were dissolved in 50 ml of benzene and the solution refluxed under a nitrogen atmosphere. Graying occurred after a short time and the reaction was terminated after about 1 h and the reaction mixture filtered. The filtrate was concentrated by removal of benzene at low temperature (−20 °C) and the resulting solution examined by infrared (i.r.) and nuclear magnetic resonance (n.m.r.) techniques to establish the presence of the desired product, Me_3NGaH_2Me.

Method B

Trimethylamine-dichloromonomethylgallane, $Me_3NGaMeCl_2$, (0.178 g, 0.828 mmole) in 50 ml of ether was reacted with excess lithium hydride (0.032 g, 4.0 mmoles), initially at −20 °C, and then at room temperature for 2 h. The reaction mixture was then filtered and the ether solvent removed from the filtrate held at −40 °C. The paste-like product, "Me_3NGaH_2-Me", was dissolved in benzene and examined spectroscopically (i.r. and n.m.r.).

To prepare the dimethyl derivative, "$Me_3NGaHMe_2$", by this method trimethylamine-monochlorodimethylgallane, Me_3NGaMe_2Cl (0.271 g, 1.395 mmoles) in 50 ml of ether was reacted with lithium hydride (0.0274 g, 3.42 mmoles) and the product again examined spectroscopically.

Method C

In a typical experiment trimethylamine-monochlorogallane Me_3NGaH_2Cl (0.369 g, 2.22 mmoles) dissolved in 30 ml of ether was reacted with an ether solution of lithium methyl (3.51 ml of 0.63 *M*, 2.21 mmoles). The reaction mixture was stirred for several hours at room temperature and then the lithium chloride was filtered off. The ether solvent was removed from the filtrate at low temperature (−40 °C) to leave a liquid product. This product could be sublimed, and analyzed for Me_3NGaH_2-Me.

Anal. Calcd. for $C_4H_{14}GaN$, (mol. wt. 145.7): Ga, 47.8; H (hydrol.), 1.37. Found, (mol. wt. 175): Ga, 46.9; H (hydrol.), 1.38.

In an analogous manner, $Me_3NGaHCl_2$, (0.247 g, 1.23 mmoles) in 50 ml of ether, and an ether solution of LiMe (1.3 ml of 1.89 *M*, 2.46 mmoles) were reacted for several hours to yield an oily product after removal of the lithium chloride precipitate and the ether solvent. Again the product could be sublimed, and analyzed correctly for $Me_3NGaHMe_2$.

Anal. Calcd. for $C_5H_{16}GaN$, (mol. wt. 159.7): Ga, 43.6; H (hydrol.), 0.62. Found, (mol. wt. 172): Ga, 42.9; H (hydrol.), 0.62.

Method D

Trimethylamine-monomethylgallane, Me_3NGaH_2Me, was prepared by simply mixing together trimethylamine-gallane (0.608 g, 4.62 mmoles) and trimethylamine trimethyl gallium (0.398 g, 2.30 mmoles) in benzene solution. Similarly for the preparation of the dimethyl derivative, $Me_3NGaHMe_2$, trimethylamine-gallane (0.232 g, 1.76 mmoles) and trimethylamine trimethyl gallium (0.612 g, 3.51 mmoles) were mixed together in benzene. The resultant clear solutions were then examined spectroscopically (i.r. and n.m.r.).

To obtain a solvent-free species by this method ether was found to be a superior solvent since it could be removed at much lower temperatures from the product solution. The products obtained on removal of ether solvent had identical physical characteristics to those of the compounds obtained via route C.

The deuterated analogues, trimethylamine-monomethylbideuteriogallane, Me_3NGaD_2Me, and trimethylamine-dimethylmonodeuteriogallane, $Me_3NGaDMe_2$, were prepared by method D using trimethylamine-trideuteriogallane, Me_3NGaD_3, and trimethylamine trimethyl gallium, Me_3NGaMe_3, as starting materials.

The corresponding alane compounds, Me_3NAlH_2Me and $Me_3NAlHMe_2$, were also obtained by route D as previously described by Peters *et al.* (16). Investigation of the borane systems gave no indication of equilibration between Me_3NBH_3 and Me_3NBMe_3 as evidenced by p.m.r. data.

Analytical Methods

The samples were analyzed for hydrolyzable hydrogen, (i.e. Ga—H), by treatment with water using a method similar to the one previously described (2). Gallium was determined by the 8-hydroxyquinolate method (2) after first removing the methyl groups from the metal by boiling the sample for several hours with concentrated hydrochloric acid (17).

Cryoscopic molecular weight determinations were carried out in benzene solution under strictly anhydrous conditions in a nitrogen-flushed system.

Spectra

Definitive i.r. spectra were recorded on a Perkin–Elmer model 457 spectrometer (4000–250 cm^{-1}) and routine spectra on Perkin–Elmer infrared models 137E and K24.

Proton magnetic resonance spectra were obtained on Varian HA-100 and A-60 instruments. The benzene (or cyclohexane) solutions were prepared in the glove box and the sample tubes sealed off to avoid atmospheric hydrolysis. All τ values are referred to benzene as $\tau_{C_6H_6}$ = 2.84 p.p.m. or to cyclohexane as $\tau_{C_6H_{12}}$ = 8.54 p.p.m.; (τ_{TMS} = 10.00 p.p.m.). Cyclohexane has the advantage

Can. J. Chem. Downloaded from www.nrcresearchpress.com by 210.87.254.105 on 09/05/12
For personal use only.

that all the proton peaks in this solvent are concentration independent, but it has the disadvantage that the solvent peak often obscures the N—Me peak which appears at $\tau \simeq 8.0$ p.p.m. At higher concentrations, the proton signals in benzene solutions show a concentration dependence but in this work this effect was minimized by working at lower concentrations. In addition, with benzene as solvent, the N—Me region is no longer obscured in the spectra.

Signals due to Ga—H and Al—H protons were not observed, principally because of the low concentrations but also perhaps because of nuclear quadrupole broadening (3, 5).

Results and Discussion

Synthetic Methods

No reaction was observed between Me_2Hg and Me_3NGaH_3 (Method A) in benzene or ether solvent at room temperature, and at higher temperatures the yield of product was low due to thermal instability of both the gallane starting material (2) and the methylgallane product. The presence of finely divided gallium metal from the initial thermal decomposition of starting material probably catalyzes the decomposition of the product. This type of autocatalytic process has been noted in other gallium systems (18, 19). That a definite reaction did take place, rather than merely decomposition of starting material, is evidenced by both the p.m.r. and i.r. spectra of the product solution and the appearance of mercury in the product mixture. The low yields in this reaction are in contrast to the corresponding system in alane chemistry where quite high yields are reported from the reaction at elevated temperatures (16).

The reduction of methylchlorogallanes (Method B) with lithium hydride proved to be a very unsatisfactory route to the methylgallane derivatives, and, although some reduction was evident from the p.m.r. and i.r. spectra of the products, compounds free from chlorine could not be isolated. Even with higher reaction temperatures and longer reaction times similar incomplete reductions were noticed in the alane systems (16). Higher reaction temperatures in the gallane systems are prohibited because of the thermal instability of the products.

The reactions involving lithium methyl (Method C) proceed smoothly at room temperature and yield pure products free from chlorine. The equilibration reactions (Method D) gave quantitative yields of the methyl-gallanes. In both methods C and D, the products could be purified by sublimation under high vacuum.

Physical Properties

The trimethylamine-methylgallanes are liquids at room temperature and exhibit extended melting point ranges (approx. 0–20 °C). These long melting point ranges may indicate that there is a change in the degree of polymerization in going from the solid to the liquid, a behavior observed for compounds of the type Me_2NGaMe_2, (20), or perhaps that some dissociation or disproportionation of the complexes occurs.

The molecular weights of the compounds Me_3NGaH_2Me and $Me_3NGaHMe_2$ were determined cryoscopically in benzene solution. The results indicate a slight degree of association (1.20 and 1.08, respectively) which probably occurs via dipole–dipole interaction rather than through bridged dimers, which would involve unstable 5-coordinate gallium species. These results may, however, represent only a *mean* molecular weight in each case, since, as is described later, a number of different gallium species probably co-exist in the benzene solutions.

Proton Magnetic Resonance Data

The p.m.r. spectra of Me_3NGaH_2Me and $Me_3NGaHMe_2$, in benzene or cyclohexane, both show, at the same positions, three distinct Ga—Me signals which have different integrated intensities in the two samples (Fig. 1). The approximate Ga—Me peak separations were ~ 5 c.p.s. at 60 Mc/s and ~ 8 c.p.s. at 100 Mc/s, thus demonstrating that signals arise from three

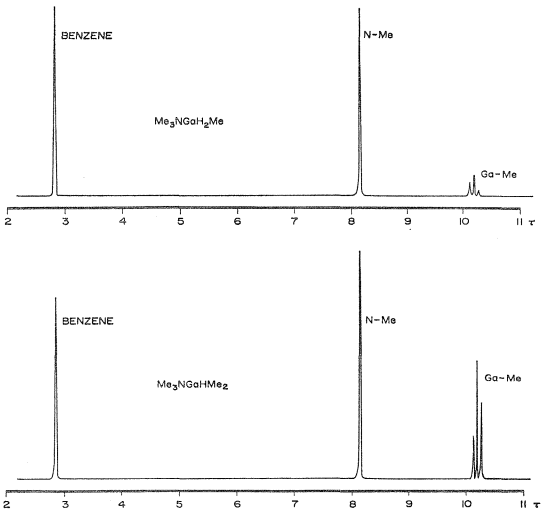

FIG. 1. Nuclear magnetic resonance spectra of Me_3NGaH_2Me and $Me_3NGaHMe_2$ in benzene at 60 Mc/s.

Can. J. Chem. Downloaded from www.nrcresearchpress.com by 210.87.254.105 on 09/05/12
For personal use only.

different species and not from spin–spin coupling. It seems probable, therefore, that an equilibrium is established in solution in which all four possible species are present: Me_3NGaMe_3, Me_3NGaH_2Me, $Me_3NGaHMe_2$, and Me_3NGaH_3.

Thus for Me_3NGaH_2Me in benzene the three Ga—*Me* signals appear at τ = 10.24, 10.17, and 10.09 p.p.m. with the single N—Me resonance occurring at τ = 8.10 p.p.m. The signals are assigned in Table I which also includes the percentage of each compound in solution. The signal at 10.24 occurs at the same position as the Ga—Me signal in an authentic sample of Me_3NGaMe_3 and its assignment follows directly. The monomethyl- and dimethyl-gallane derivatives are assigned on the basis of peak area ratios and on chemical shifts expected on substituting hydrogen for methyl on gallium. Thus with the introduction of the more electronegative hydrogen atom the remaining methyl groups become less shielded and give signals at lower field positions. The percentages given in Table I are calculated from the area ratios of the Ga—Me signals and the area ratio of the single N—Me signal. For the compound $Me_3NGaHMe_2$ in benzene solution the data listed in Table II were obtained. Similarly, three Ga—Me signals were observed for each of the deuterated compounds Me_3NGaD_2Me and $Me_3NGaDMe_2$ in benzene solution and almost identical proportions of the various species were present as compared to the hydrido compounds. In cyclohexane a similar pattern resulted with the three Ga—*Me* signals appearing at τ = 10.57, 10.51, and 10.42 p.p.m. for the hydrido compounds.

TABLE I

Proton magnetic resonance data for Me_3NGaH_2Me in benzene solution

Species	τ (Ga—Me)	Peak area ratio	% of species
Me_3NGaMe_3	10.24	1.00	3.1
$Me_3NGaHMe_2$	10.17	4.85	22.9
Me_3NGaH_2Me	10.09	5.00	47.0
Me_3NGaH_3	—	—	27.0

TABLE II

Proton magnetic resonance data for $Me_3NGaHMe_2$ in benzene solution

Species	τ (Ga—Me)	Peak area ratio	% of species
Me_3NGaMe_3	10.24	1.60	16.0
$Me_3NGaHMe_2$	10.16	3.10	46.4
Me_3NGaH_2Me	10.08	1.00	30.0
Me_3NGaH_3	—	—	7.6

This same set of three Ga—Me signals was observed in the product solutions from all four experimental routes (A–D). Solutions obtained via route B, however, gave additional Ga—Me signals which are probably due to partially reduced species of the type $Me_3NGaHClMe$, or to compounds of the form $LiGaH_3Me$. The equilibria between the four species does not appear to be time dependent since two spectra taken on the same sample one month apart showed no change. Variation of the solvent from benzene to cyclohexane seems to have little effect on the percentage of each species present but merely displays the Ga—Me signals at higher field.

It is interesting to note that in all the spectra taken only a single sharp peak was observed for the N—Me resonance. In solutions of Me_3NGaH_2Me and $Me_3NGaHMe_2$, the Me_3N groups must be exchanging rapidly, and indeed the N—Me peak positions appear to be in the average position between the extremes of Me_3NGaMe_3 and Me_3NGaH_3.

The p.m.r. of the chloro compounds, Me_3NGaMe_2Cl and $Me_3NGaMeCl_2$, in benzene solution showed only a single resonance in the Ga—Me region of the spectrum at room temperature. Presumably the greater efficiency of the chlorine as a bridging group over methyl or hydrogen (21) leads to a specific single compound or to a very rapid exchange process.

The behavior of the methylgallanes in benzene and cyclohexane solutions at room temperature prompted us to re-examine the corresponding alane compounds, Me_3NAlH_2Me and $Me_3NAlHMe_2$, under similar conditions. Peters *et al.* (16) explained the "doublet" appearing above 10τ in the p.m.r. spectra of these compounds in cyclohexane solution in terms of dimerization involving hydrogen and/or methyl bridging groups. A close re-examination of this p.m.r. study showed not two, but three distinct signals in the Al—Me region of the spectrum in both benzene and cyclohexane solutions. Figure 2 depicts the Al—Me region of the spectra observed in benzene solution at 100 Mc/s and Table III collects the data obtained from both solvents. Examination of the spectra showed a

TABLE III

Proton magnetic resonance data for $Me_3NAlH_{3-n}Me_n$ species

Species	τ values in C_6H_6 solvent		τ values in C_6H_{12} solvent	
	N—Me	Al—Me	N—Me	Al—Me
Me_3NAlMe_3	8.31	10.58	7.61	10.92
$Me_3NAlHMe_2$	8.26	10.47, 10.53, 10.58	7.62	10.81, 10.87, 10 92
Me_3NAlH_2Me	8.06	10.47, 10.53, 10.58	7.61	10.80, 10.87, 10.92
Me_3NAlH_3	7.94	—	7.71	—

TABLE IV

Proton magnetic resonance data for Me_3NAlH_2Me and $Me_3NAlHMe_2$ in benzene solution

	Species	τ, Al—Me	Peak area ratio	% of species
Me_3NAlH_2Me	Me_3NAlMe_3	10.58	1.00	4.3
	$Me_3NAlHMe_2$	10.53	3.43	21.8
	Me_3NAlH_2Me	10.47	3.00	38.5
	Me_3NAlH_3	—	—	35.4
$Me_3NAlHMe_2$	Me_3NAlMe_3	10.58	4.14	29.3
	$Me_3NAlHMe_2$	10.53	3.57	38.3
	Me_3NAlH_2Me	10.47	1.00	21.2
	Me_3NAlH_3	—	—	11.2

peak separation of ~ 5.5 c.p.s. at 100 Mc/s and ~ 3.5 c.p.s. at 60 Mc/s showing the Al—Me peaks to be field dependent as were the Ga—Me peaks. These trimethylamine–methylalane spectra show a close resemblance to the corresponding gallane spectra and lead us to propose a similar set of aluminium compounds co-existing in solution. Table IV lists the various proportions of each species present worked out on the above assumption.

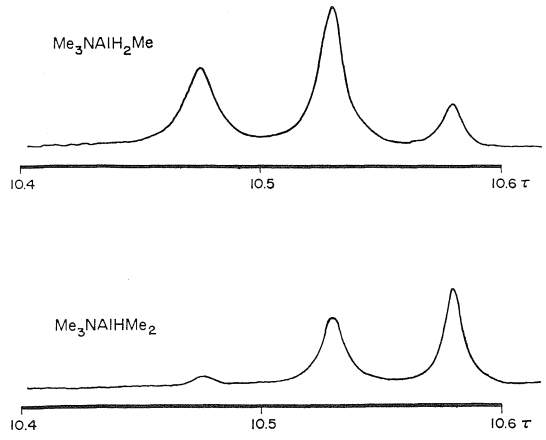

FIG. 2. Nuclear magnetic resonance spectra (Al—Me region) of Me_3NAlH_2Me and $Me_3NAlHMe_2$ in benzene at 100 Mc/s.

On the basis that the trimethylamine adducts of methylgallanes and methylalanes yield a series of equilibrium products in solution an examination of the analogous boron systems was carried out. The compounds Me_3NBMe_3 and Me_3NBH_3 were mixed in 1:2 and 2:1 mole ratios in benzene but no exchange of either Me_3N groups or Me/H groups was evident from the n.m.r. spectra (Fig. 3). The data are summarized in Table V. The slight shift in Me—N and B—Me peaks in the mixtures is due probably to dipole–dipole interactions rather than to alkyl or amine exchange.

Infrared Data

The i.r. spectra of the compounds Me_3NGaH_2-Me, $Me_3NGaHMe_2$, and their deuterated analogues Me_3NGaD_2Me and $Me_3NGaDMe_2$ were recorded in benzene solution. As observed in previously reported spectra of gallane derivatives (2, 4), the strongest absorptions were attributable to Ga—H(D) stretching and deformation frequencies. These are listed and assigned in Table VI. The expected decrease by a factor of about $\sqrt{2}$ in going from Ga—H to Ga—D frequencies was observed. Two distinct Ga—H stretching frequencies were evident for the compounds Me_3NGaH_2Me and $Me_3NGaHMe_2$. The band

Can. J. Chem. Downloaded from www.nrcresearchpress.com by 210.87.254.105 on 09/05/12
For personal use only.

TABLE V

Proton magnetic resonance data for mixtures of Me_3NBMe_3 and Me_3NBH_3 in benzene solution

Species	τ values				$J_{^{11}B-H}$(c.p.s.)
	N—Me		B—Me	B—H	
Me_3NBMe_3		8.24	9.99	—	—
$2Me_3NBMe_3 + Me_3NBH_3$	7.96	8.19	10.00	7.76	99
$Me_3NBMe_3 + 2Me_3NBH_3$	7.91	8.16	10.05	7.82	98
Me_3NBH_3	7.81		—	7.89	99

TABLE VI

Infrared data for methylgallane derivatives in benzene solution*

Infrared data				
Me_3NGaH_2Me	Me_3NGaD_2Me	$Me_3NGaHMe_2$	$Me_3NGaDMe_2$	Assignment
1845 vs	1313 vs, br	1840 vs	1295 vs, br	Ga—H(D) stretch
1775 vs		1770 vs		
745 vs	538 vs	745 vs	538 vs	Ga—H(D)deformation
495 s	490 s	490 s	488 s	Ga—N stretch

*Bands are recorded in cm^{-1} and vs = very strong, s = strong, br = broad.

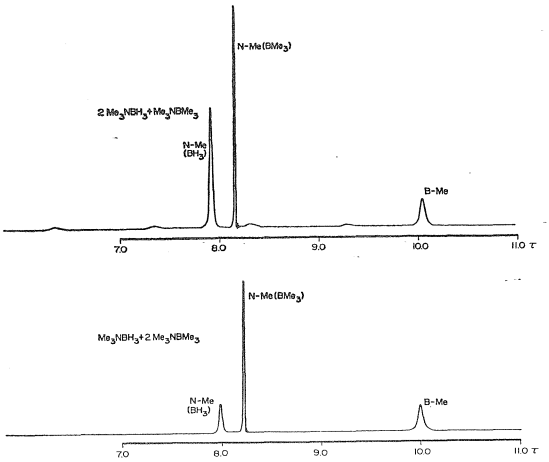

FIG. 3. Nuclear magnetic resonance spectra of mixtures of Me_3NBH_3 and Me_3NBMe_3 in benzene at 60 Mc/s.

at 1840 cm^{-1} is very close to the one occurring in the spectrum of Me_3NGaH_3 in benzene solution (4) and could be due to this species in the equilibrium mixture. The strong absorption at 1770 cm^{-1} could then be assigned to methylgallanes in the solutions.

Mechanism of Exchange

From the p.m.r. and i.r. data there is strong evidence that the four compounds $Me_3NGaH_{3-n}Me_n$, where n = 0, 1, 2, or 3, co-exist in solution. The intermediate that gives rise to these species must presumably be reached via a bridged gallium species

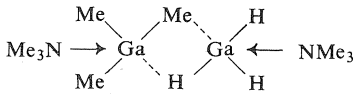

This bridged intermediate could then dissociate to give the original compounds or to give new species. The latter can then lead to a mixture containing all the four different species postulated.

An alternative mechanism could involve a bridged dimer containing both five-coordinate and four-coordinate gallium atoms

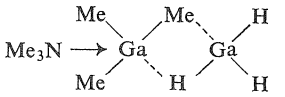

In this case the four-coordinate gallium is derived from a three-coordinate gallium atom, e.g. GaH_3, $GaHMe_2$, etc. from which the Me_3N has dissociated. Both these mechanisms have been proposed for exchange reactions involving adducts of the type Me_3NAlMe_3 and Me_3NAlMe_2X where X = halogen (22).

Can. J. Chem. Downloaded from www.nrcresearchpress.com by 210.87.254.105 on 09/05/12
For personal use only.

A further possibility would be for both compounds to dissociate in solution to yield free amine and three-coordinate gallium species. The gallium entities could then form a dimer species which, on dissociation, could produce mixed methylgallanes or the original species. Finally recombination with amine would yield the series of trimethylamine methylgallanes

$$Me_3NGaMe_3 \rightarrow Me_3N + GaMe_3$$

$$Me_3NGaH_3 \rightarrow Me_3N + GaH_3$$

$$GaMe_3 + GaH_3 \rightleftarrows \begin{matrix} Me & Me & H \\ & Ga \cdots Ga & \\ Me & H & H \end{matrix}$$

$$\rightleftarrows Me_2GaH + MeGaH_2$$

$$Me_3N + Me_2GaH \rightarrow Me_3NGaMe_2H$$

$$Me_3N + MeGaH_2 \rightarrow Me_3NGaMeH_2$$

A dissociation mechanism of this type has been proposed by DeRoos and Oliver to account for the exchange reaction occurring between Me_3NGaMe_3 and excess Me_3Ga (23).

In the present case the latter mechanisms, involving three-coordinate gallium species, seem unlikely, since benzene solutions of Me_3NGaH_2Me were found not to hydrogallate ethylene, a process to be expected if three-coordinate species of the type, GaH_2Me, are present in the solution (24).

Similar mechanisms can be proposed for the observed behavior of the methylalane adducts. The absence of exchange in the boron systems is presumably due on the one hand to the inability of boron to form five-coordinate intermediates of this type, and on the other to the absence of three-coordinate BH_3 and BMe_3 units (from dissociation of the adducts). If these three-coordinate species were *both* formed they would readily rearrange to give a series of methylboranes (25, 26) and hence, on recombination with amine, the mixed adducts.

In summary, it appears that the compounds Me_3NGaH_2Me and $Me_3NGaHMe_2$ are comparable to Me_3NGaH_3 in thermal stability and much more stable thermally than the uncoordinated alkylgallanes (8, 27). However, the gallane derivatives are much less stable than the corresponding borane (15) and alane (16) compounds.

Acknowledgment

Thanks are due to the National Research Council of Canada for financial support.

1. N. N. GREENWOOD, A. STORR, and M. G. H. WALLBRIDGE. Proc. Chem. Soc. 249 (1962).
2. N. N. GREENWOOD, A. STORR, and M. G. H. WALLBRIDGE. Inorg. Chem. **2**, 1036 (1963).
3. N. N. GREENWOOD, E. J. F. ROSS, and A. STORR. J. Chem. Soc. 246 (1965).
4. N. N. GREENWOOD and A. STORR. J. Chem. Soc. 620 (1965).
5. N. N. GREENWOOD, E. J. F. ROSS, and A. STORR. J. Chem. Soc. A, 706 (1966).
6. G. E. COATES. J. Chem. Soc. 2003 (1951).
7. A. LEIB, M. T. EMERSON, and J. P. OLIVER. Inorg. Chem. **4**, 1825 (1965).
8. J. J. EISCH. J. Am. Chem. Soc. **84**, 3830 (1962).
9. K. C. WILLIAMS and T. L. BROWN. J. Am. Chem. Soc. **88**, 5460 (1966).
10. G. E. COATES and J. GRAHAM. J. Chem. Soc. 233 (1963).
11. H. SCHMIDBAUR and W. FINDEISS. Chem. Ber. **99**, 2187 (1966).
12. B. ARMER and H. SCHMIDBAUR. Chem. Ber. **100**, 1521 (1967).
13. J. K. RUFF and M. F. HAWTHORNE. J. Am. Chem. Soc. **82**, 2141 (1960).
14. G. BRAUER (*Editor*). Handbook of preparative inorganic chemistry. Vol. 1. Academic Press, Inc. New York. 1963. p. 798.
15. K. NIEDENZU and J. W. DAWSON. Boron–nitrogen compounds. Academic Press, Inc., New York. 1965. p. 18.
16. F. M. PETERS, B. BARTOCHA, and A. J. BILBO. Can. J. Chem. **41**, 1051 (1963).
17. J. R. JENNINGS, I. PATTERSON, K. WADE, and B. K. WYATT. J. Chem. Soc. 1608 (1967).
18. J. J. EISCH. J. Am. Chem. Soc. **84**, 3605 (1962).
19. H. I. SCHLESINGER, H. C. BROWN, and G. W. SCHAEFER. J. Am. Chem. Soc. **65**, 1786 (1943).
20. O. T. BEACHLEY, G. E. COATES, and G. KOHNSTAM. J. Chem. Soc. 3248 (1965).
21. E. A. JEFFREY, T. MOLE, and J. K. SAUNDERS. Australian J. Chem. **21**, 649 (1968).
22. N. S. HAM, E. A. JEFFREY, T. MOLE, and J. K. SAUNDERS. Australian J. Chem. **21**, 659 (1968).
23. J. B. DEROOS and J. P. OLIVER. J. Am. Chem. Soc. **89**, 3970 (1967).
24. Annual surveys of organometallic chemistry. Vol. 3. Elsevier Publ. Co., Inc., Amsterdam. 1966. p. 139.
25. H. I. SCHLESINGER and A. O. WALKER. J. Am. Chem. Soc. **57**, 621 (1935).
26. H. I. SCHLESINGER, N. W. FLODIN, and A. B. BURG. J. Am. Chem. Soc. **61**, 1078 (1939).
27. H. SCHMIDBAUR, W. FINDEISS, and E. GAST. Angew. Chem. **77**, 170 (1965).

Can. J. Chem. Downloaded from www.nrcresearchpress.com by 210.87.254.105 on 09/05/12
For personal use only.

Can. J. Chem. Downloaded from www.nrcresearchpress.com by 210.87.254.5 on 09/05/12
For personal use only.

Dielectric studies. Part XXIII. Relaxation data and apparent dipole moments of aniline and some disubstituted aromatic amines

S. W. TUCKER (MISS)
Chemistry Department, University of Aston in Birmingham, England

AND

S. WALKER
Chemistry Department, Lakehead University, Port Arthur, Ontario

Received August 13, 1968

Dielectric studies have been carried out at microwave frequencies on dilute solutions of aniline, *p*-chloro-, *p*-bromo-, and *m*-chloro-anilines, and *o*-, *m*-, and *p*-toluidines at 25 °C in cyclohexane and *p*-xylene. The static dielectric constant has also been measured at 2 MHz. In addition *o*- and *m*-toluidines have been measured at 50 °C and *p*-toluidine at 15, 35, and 50 °C.

The dielectric results, particularly those at 70.01 GHz, establish that there is more than one relaxation process present and the data have been analyzed on a two relaxation time model, the longer of which τ_1, is identified as molecular relaxation. The cause of the lower electric dipole moments found from this method as opposed to the non-dielectric absorption methods is discussed. It follows that there is either an additional higher frequency dispersion or (and) a high atomic polarization for aniline and *o*-, *m*-, and *p*-toluidines. Work at still higher frequencies is required to study this further and to establish more precise values of τ_2.

Canadian Journal of Chemistry, **47**, 681 (1969)

When two polar solutes of similar size and shape are independently examined in a particular non-polar solvent and the solute is present at low concentration, then, providing there is no appreciable molecular interaction and the solute molecules undergo no intramolecular motion (such as group re-orientation), similar observed relaxation times are to be expected. The observed relaxation time would then be the molecular relaxation time. Such considerations were embodied in the work of Fischer (1) and used to identify the lack of rigidity in certain molecules. In general, when the observed relaxation time is shorter than that anticipated, it suggests a contribution from an additional relaxation process(es). This appears the case for aniline in benzene (2) at 20 °C since the observed relaxation time is 4.3×10^{-12} s which is to be compared with a molecular relaxation time of 7.5×10^{-12} s for chlorobenzene in cyclohexane (3) at 25 °C.

This present work aimed to examine whether such a shortening of the relaxation time of primary aromatic amines in non-polar solvents was a general phenomenon. Further, it seemed likely that measurements at 70.01 GHz would help to establish any contribution from a short relaxation time more precisely. It was considered worthwhile to carry out measurements in the two solvents in order to assess whether the dipole moments and relaxation times were highly dependent on specific solvent effects.

Experimental

The apparatus and procedure for determining the dielectric constant and loss have been described previously (4).

Materials

The liquid amines were all distilled from a spinning band column of 35 theoretical plates and then dried. The observed boiling points were compared with literature values, and the compounds were shown to have no detectable amounts of impurities by infrared and gas chromatographic techniques.

The solids were recrystallized from appropriate solvents and dried until their melting points agreed with those in the literature.

Experimental Results

ε_∞ was estimated from the high frequency intercept of the Cole–Cole plot and the accuracy of this procedure has been considered previously (5). The dielectric data at different frequencies were then analyzed into contributory relaxation times by assuming that each relaxation process undergoes Debye behavior. The theory has been given by Budó (6).

Consideration of the real and imaginary parts of the complex dielectric constant yields

$$[1] \qquad \frac{\varepsilon''}{\varepsilon_0 - \varepsilon_\infty} = \frac{C_1\omega\tau_1}{1 + \omega^2\tau_1^2} + \frac{C_2\omega\tau_2}{1 + \omega^2\tau_2^2}$$

TABLE I

Dielectric constant and loss data

Frequency (GHz)	ε'_{obsd}	ε''_{obsd}	ε'_{calcd}	ε''_{calcd}
Aniline in cyclohexane at 25 °C, $w_2 = 0.0846$				
9.313	2.21_4	0.035_9	2.21_2	0.036_2
16.20	2.20_1	0.050_8	2.19_3	0.049_5
23.98	2.17_9	0.055_7	2.17_5	0.054_3
34.86	2.16_3	0.053_6	2.15_7	0.054
70.01	2.13_7	0.044_9	2.12_9	0.045_2
Aniline in cyclohexane at 25 °C, $w_2 = 0.1190$				
9.313	2.31_2	0.062_5	2.30_5	0.058_4
16.20	2.28_2	0.073_2	2.27_4	0.077_4
23.98	2.24_2	0.083_7	2.24_5	0.083_1
34.86	2.21_1	0.081_9	2.21_6	0.080_2
70.01	2.20_6	0.070_7	2.20_8	0.065
Aniline in *p*-xylene at 25 °C, $w_2 = 0.0683$				
9.313	2.44_4	0.048	2.44_4	0.047
16.20	2.41_7	0.061_9	2.41_8	0.060_5
23.98	2.39	0.060_2	2.39_4	0.061_6
34.86	2.36_9	0.051	2.38_5	0.059_8
70.01	2.36_2	0.043_8	2.35_6	0.041_6
p-Chloroaniline in cyclohexane at 25 °C, $w_2 = 0.0194$				
9.313	2.09_6	0.046_4	2.09_5	0.046_3
16.20	2.06_9	0.043_1	2.07_1	0.043_3
23.98	2.06	0.036_6	2.05_9	0.036
34.86	2.04_9	0.028_5	2.05_1	0.028_8
70.01	2.04_5	0.018_8	2.04_3	0.015_6
p-Chloroaniline in *p*-xylene at 25 °C, $w_2 = 0.0193$				
9.313	2.34_8	0.063_7	2.36_6	0.064_8
16.20	2.32_3	0.059_9	2.33_1	0.062_2
23.98	2.30_5	0.043	2.31_2	0.052
34.86	2.29_5	0.033_8	2.30_1	0.040_8
70.01	2.28_5	0.022_1	2.28_7	0.017_4
p-Bromoaniline in cyclohexane at 25 °C (saturated solution)				
9.313	2.09_8	0.054_7	2.09_4	0.053_1
16.20	2.07_1	0.047_4	2.06_8	0.046_6
23.98	2.06	0.038	2.05_6	0.038_2
34.86	2.05_1	0.030_4	2.04_8	0.030_6
70.01	2.04_5	0.019_2	2.03_9	0.019_1
p-Bromoaniline in *p*-xylene at 25 °C, $w_2 = 0.0422$				
9.313	2.38_8	0.104_1	2.39	0.106_2
16.20	2.34_7	0.087_1	2.34_3	0.084_2
23.98	2.32	0.063	2.32_4	0.064_8
34.86	2.30_1	0.048_3	2.31_3	0.049_2
70.01	2.30	0.031_1	2.30_2	0.029_4
m-Chloroaniline in *p*-xylene at 25 °C, $w_2 = 0.0295$				
9.313	2.36_6	0.077	2.37_1	0.077_2
16.20	2.33_7	0.066_5	2.33_4	0.065
23.98	2.31_6	0.049_5	2.31_7	0.051_1
34.86	2.29_9	0.038_9	2.30_8	0.039_1
70.01	2.29_5	0.025_5	2.29_9	0.023_4
m-Chloroaniline in cyclohexane at 25 °C, $w_2 = 0.0352$				
9.313	2.14	0.062_2	2.14_3	0.062_7
16.20	2.11_3	0.064_9	2.10_9	0.063_5
23.98	2.08_5	0.054	2.08_8	0.055
34.86	2.07_2	0.044_4	2.07_5	0.044_6
70.01	2.06_3	0.028_2	2.06_1	0.027_8
o-Toluidine in cyclohexane at 25 °C, $w_2 = 0.0595$				
9.313	2.13_4	0.029_8	2.13_9	0.030_3
16.20	2.12_4	0.035_9	2.12_2	0.036_1
23.98	2.10_1	0.036_2	2.11	0.035_7
34.86	2.09_1	0.032_5	2.09_9	0.032_8
70.01	2.08_9	0.026_1	2.08_4	0.024_7

Frequency (GHz)	ε'_{obsd}	ε''_{obsd}	ε'_{calcd}	ε''_{calcd}
o-Toluidine in *p*-xylene at 25 °C, $w_2 = 0.0530$				
9.313	2.38_4	0.041_8	2.38_7	0.041
16.20	2.36_2	0.047_8	2.36_4	0.046_2
23.98	2.33_8	0.042_1	2.34_8	0.043_1
34.86	2.33_5	0.037_1	2.33_6	0.036_9
70.01	2.32_2	0.027_4	2.32_2	0.024
o-Toluidine in *p*-xylene at 50 °C, $w_2 = 0.0729$				
9.313	2.38_5	0.042_6	—	—
16.20	2.36_2	0.057_1	—	—
23.98	2.32_8	0.055_4	—	—
34.86	2.32_5	0.052	—	—
70.01	2.28_9	0.031_4	—	—
m-Toluidine in cyclohexane at 25 °C, $w_2 = 0.0678$				
9.313	2.13_6	0.026_7	2.13_9	0.024_6
16.20	2.12	0.028_8	2.12_6	0.028_8
23.98	2.11_2	0.027_7	2.11_6	0.028_4
34.86	2.10_4	0.025_8	2.10_7	0.026_1
70.01	2.09	0.021_2	2.09_8	0.021_2
m-Toluidine in *p*-xylene at 25 °C, $w_2 = 0.0540$				
9.313	2.36_6	0.032_9	2.36_7	0.033_5
16.20	2.35	0.036_4	2.35	0.034_7
23.98	2.33_1	0.029_8	2.33_9	0.031_4
34.86	2.33_2	0.027_5	2.33_1	0.027_3
70.01	2.31_7	0.021	2.32	0.019_7
m-Toluidine in *p*-xylene at 50 °C, $w_2 = 0.0695$				
9.313	2.34_6	0.031_9	2.34_6	0.032_4
16.20	2.33_3	0.040_5	2.32_8	0.038_8
23.98	2.31_2	0.038_8	2.31_4	0.037_9
34.86	2.30	0.032_2	2.30_3	0.034_2
70.01	2.29	0.027_2	2.28_9	0.026_4
p-Toluidine in cyclohexane at 25 °C, $w_2 = 0.0583$				
9.313	2.10_6	0.014_1	—	—
16.20	2.10	0.016	—	—
23.98	2.09_5	0.016	—	—
34.86	2.08_9	0.016_1	—	—
70.01	2.08	0.110	—	—
p-Toluidine in *p*-xylene at 15 °C, $w_2 = 0.0763$				
9.313	2.41_8	0.037_1	—	—
16.20	2.39_2	0.042_8	—	—
23.98	2.37_1	0.033	—	—
34.86	2.36_1	0.033_1	—	—
70.01	2.35	0.029_1	—	—
p-Toluidine in *p*-xylene at 25 °C, $w_2 = 0.0740$				
9.313	2.39_3	0.032	—	—
16.20	2.37_1	0.038_7	—	—
23.98	2.35_4	0.031_4	—	—
34.86	2.34_4	0.031_1	—	—
70.01	2.32_1	0.030	—	—
p-Toluidine in *p*-xylene at 35 °C, $w_2 = 0.0759$				
9.313	2.37_6	0.028_8	—	—
16.20	2.35_5	0.037	—	—
23.98	2.34	0.032_2	—	—
34.86	2.33_3	0.032	—	—
70.01	2.32	0.030	—	—
p-Toluidine in *p*-xylene at 50 °C, $w_2 = 0.0763$				
9.313	2.33	0.023_1	—	—
16.20	2.31	0.026_9	—	—
23.98	2.30_7	0.026_8	—	—
34.86	2.28_8	0.026	—	—
70.01	2.27_5	0.024	—	—

Can. J. Chem. Downloaded from www.nrcresearchpress.com by 210.87.254.5 on 09/05/12
For personal use only.

TABLE II

Static dielectric constant, dielectric constant at very high frequency, relaxation time, distribution coefficient, and apparent dipole moment (in Debye units) data for solutions of weight fraction w_2 for aniline and some substituted anilines

Solvent	w_2	t (°C)	$\tau_0 \times 10^{12}$	$\tau_1 \times 10^{12}$	$\tau_2 \times 10^{12}$	C_1	ε_0	ε_∞	α	μ_m
				Aniline						
Cyclohexane	0.0846	25	5.1	7.5	2.1	0.66	2.2259	2.09_8	0.07	1.28
Cyclohexane	0.1190	25	6.6	8.5	2.5	0.70	2.3301	2.15	0.03	1.28
p-Xylene	0.0693	25	7.5	8.1	3.3	0.90	2.4659	2.33_9	0.02	1.27
				p-Chloroaniline						
Cyclohexane	0.0194	25	13.5	15.3	2	0.89	2.1358	2.03_4	0.06	2.80
p-Xylene	0.0193	25	16.9	18.0	3	0.94	2.4199	2.28_3	0.04	2.92
				p-Bromoaniline						
Cyclohexane	sat.soln.	25	15.4	18.0	2	0.90	2.1477	2.03_8	0.02	—
p-Xylene	0.0422	25	20.7	21.5	2	0.94	2.5210	2.29_3	0.05	2.95
				m-Chloroaniline						
Cyclohexane	0.0352	25	12.4	13.2	2	0.90	2.1901	2.05_1	0.10	2.43
p-Xylene	0.0295	25	18.1	18.7	2	0.94	2.4537	2.29	0.04	2.57
				o-Toluidine						
Cyclohexane	0.0595	25	7.6	10.5	2.7	0.70	2.1557	2.07	0.09	1.33
p-Xylene	0.0530	25	11.0	11.0	3.2	0.85	2.4124	2.31_3	0.03	1.38
p-Xylene	0.0729	50	7.6	—	—	—	2.3998	2.28_4	0	1.35
				m-Toluidine						
Cyclohexane	0.0678	25	9.3	11.5	3.0	0.65	2.1533	2.08_7	0.08	1.19
p-Xylene	0.0540	25	10.6	13.4	2.6	0.77	2.3920	2.30_8	0.12	1.25
p-Xylene	0.0695	50	8.0	9.8	1.6	0.75	2.3634	2.27	0.07	1.24
				p-Toluidine*						
p-Xylene	0.0763	15		13	2		2.4428			
p-Xylene	0.0740	25		12	3.5		2.4135			
p-Xylene	0.0759	35		10	2		2.3897			
p-Xylene	0.0763	50		8	3		2.3375			

*The τ_1 and τ_2 estimates for *p*-toluidine in *p*-xylene were obtained from the limiting slopes of the plot of ε' vs. $\varepsilon''\omega$.

$$[2] \quad \frac{\varepsilon' - \varepsilon_\infty}{\varepsilon_0 - \varepsilon_\infty} = \frac{C_1}{1 + \omega\tau_1^2} + \frac{C_2}{1 + \omega^2\tau_2^2}$$

and eq. [1] was solved using an Elliott 803 computer for the weight factor C_1 and the two relaxation times τ_1 and τ_2.

Dipole moments were obtained from the Debye equation for dilute solutions

$$[3] \quad \mu_m = 0.012812\,\{[(\varepsilon_0 - \varepsilon_\infty)/w_2] \times [3TM_2/(\varepsilon_1 + 2)^2 d_1]\}^{1/2}$$

where ε_1 is the static dielectric constant of the solvent, d_1 is its density, T is the absolute temperature, M_2 the molecular weight of the solute, and w_2 the weight fraction of the solute.

The mean relaxation times τ_0 were deduced from the equation

$$\frac{v}{u} = (\omega\tau_0)^{1-\alpha}$$

in which v is the distance on the Cole–Cole plot between the static dielectric constant (ε_0) and the experimental point, u is that between the point and the very high frequency value ε_∞; α is the distribution coefficient.

The dielectric constant and loss data are presented in Table I. The experimental values ε'_{obsd} and ε''_{obsd} are compared with those calculated from eqs. [1] and [2]. The terms ε'_{calcd} and ε''_{calcd} calculated using the τ_1, τ_2, and C_1 values given by computer analysis are listed in Table II, together with the mean relaxation time and electric dipole moment.

The absorption of *p*-xylene has been subtracted at 23.98, 34.86, and 70.01 GHz from the measured results and these corrected values are quoted as ε'_{obsd} and ε''_{obsd}.

Plots of ε' vs. $\varepsilon''\omega$ can be useful for indicating the presence of more than one relaxation process (7). For Debye behavior, the plot is a straight line of slope τ but for two relaxation times, sufficiently distinct in magnitude, a curve is obtained. The extremes of slope then indicate τ_1 and τ_2 but the steeper slope gives a value less than the true τ_1 and the lesser slope longer than τ_2.

The results for *p*-toluidine gave extended Cole–Cole plots, and because of insufficient accuracy

Can. J. Chem. Downloaded from www.nrcresearchpress.com by 210.87.254.5 on 09/05/12
For personal use only.

TABLE III

τ_0 and τ_1 values of each amine in cyclohexane at 25 °C compared with τ_1 values of rigid molecules of the same size and shape

Amine	$\tau_0 \times 10^{12}$	$\tau_1 \times 10^{12}$	Analogous rigid molecule (3)	Molecular relaxation time $\times 10^{12}$
Aniline	5.1	7.5	Chlorobenzene	7.5
p-Chloroaniline	13.5	15.3	*p*-Chlorotoluene	16.8
p-Bromoaniline	15.4	18.0	*p*-Bromotoluene	21.0
m-Chloroaniline	12.4	13.2	*m*-Chlorotoluene	14.0
o-Toluidine	7.6	10.5	*o*-Xylene	11.4
			o-Dichlorobenzene	9.4
m-Toluidine	9.3	11.5	*m*-Xylene	11.8
			m-Dichlorobenzene	10.0
p-Toluidine	6.7	—	*p*-Chlorotoluene	16.8

TABLE IV

A comparison* of literature dipole moments with μ_m

Solute	Solvent	w_2	μ_{lit}	$\varepsilon_{\infty\ calcd}$	μ_m	$\varepsilon_{\infty\ obsd}$
Aniline	Cyclohexane	0.0846			1.28	2.09_8
	Benzene		1.50			
p-Chloroaniline	Cyclohexane	0.0194	2.95	2.02_3	2.92	2.03_4
p-Chloroaniline	*p*-Xylene	0.0193	3.00	2.27_6	2.80	2.28_3
p-Bromoaniline	*p*-Xylene	0.0422	3.00	2.28_7	2.95	2.29_3
m-Chloroaniline	Cyclohexane	0.0352	2.65	2.02_5	2.43	2.05_1
m-Chloroaniline	*p*-Xylene	0.0295	2.70	2.27_5	2.57	2.29_0
o-Toluidine	Cyclohexane	0.0595	1.55	2.04_2	1.33	2.07_0
	p-Xylene	0.0530	1.60	2.27_8	1.38	2.31_3
m-Toluidine	Cyclohexane	0.0678	1.42	2.04_4	1.19	2.08_7
	p-Xylene	0.0540	1.47	2.27_6	1.25	2.30_8

*$\varepsilon_{\infty calcd}$ values estimated from literature dipole moments are compared with the microwave $\varepsilon_{\infty obsd}$ values at 25 °C. The static dielectric constants of cyclohexane and *p*-xylene at 25 °C are 2.016 and 2.263 respectively.

of the 70.01 GHz results it was not possible to determine ε_∞ with sufficient accuracy to deduce τ_1 and τ_2 from eq. [2]. Estimates of the two relaxation times were obtained from ε' vs. $\varepsilon''\omega$ plots. The τ_1 and τ_2 values derived from the limiting slopes of these plots for *p*-toluidine are given in Table II.

Discussion

The results at 25 °C for substituted anilines yield estimates for two relaxation times. Courtauld models indicate that the methyl and chloro groups are of similar sizes to that of the amino group and thus, the τ_1 value of the amine, for example, may be compared with that of the corresponding chloro-substituent where the latter can be regarded as a rigid molecule characterized by a molecular relaxation time in the microwave region. Justification for the analyses may be gained by comparison of the τ_1 values for the amines with those of the corresponding methyl or chloro substituents (see Table III).

Since Williams (8) has recently given a comprehensive account of the internal re-orientation motion feasible for the τ_2 process of aniline and alkylamines the actual mechanism will not be considered further here except to note that his treatment expresses τ_2 in terms of τ_1 and an internal re-orientation time. It should be noted though that the error in τ_2 could be appreciable and work at higher frequencies (e.g. in the far infrared region) is desirable to establish more precise values.

From Table II it may be observed that the α values for a given solute in cyclohexane and *p*-xylene tend to be less in the latter solvent. However, within our experience, relaxation time values are up to $\sim 10\%$ longer in *p*-xylene than cyclohexane for molecular relaxation of rigid molecules. For a constant C_1,α would increase with the

Can. J. Chem. Downloaded from www.nrcresearchpress.com by 210.87.254.5 on 09/05/12
For personal use only.

Can. J. Chem. Downloaded from www.nrcresearchpress.com by 210.87.254.5 on 09/05/12
For personal use only.

τ_1/τ_2 ratio (9) and, thus, it follows that the variable α in the solvents cyclohexane and *p*-xylene is more likely to be due to an intermolecular effect. This also fits in better with the variable C_2 values in the two solvents.

For the halo-substituted anilines where the moment is high (> 2.5 D), the C_2 values are ~0.1 or less, whereas for aniline, *o*-, *m*-, and *p*-toluidine whose moments are less than ~ 1.5 D, the C_2 values are ~ 0.2 or greater. Thus, the τ_2 process becomes more detectable when the moment is low and for *p*-toluidine, which has the lowest moment of ~ 1.1 D an ε' vs. $\varepsilon''\omega$ plot clearly indicates the presence of more than one relaxation process.

The dipole moments obtained by the microwave method are lower than those from the non-dielectric absorption procedure (see Tables IV and V). This is particularly so when the moment of the compound is ~ 1.5 D or less for *o*-, *m*-, and *p*-toluidine but this discrepancy is much smaller for those compounds the dipole moment of which is ~ 3D.

TABLE V

Apparent dipole moments calculated from the data of Smyth and co-workers in benzene at 20 °C compared with literature values

Solute	Maximum mole fraction	μ_m	μ_{lit}
Aniline	0.05	1.43	1.50
1-Naphthylamine	0.026	1.46	1.55
2-Naphthylamine	0.027	1.53	—
p-Toluidine	0.057	1.07	1.33

For small solutes at low concentrations, the alteration in the ε_∞ value for slight increases in concentration is very small and in the absence of any additional dispersion ε_∞ would tend to ε_1. Inspection of the experimental ε_∞ values in Table II, bearing in mind that at 25 °C, ε_1 (cyclohexane) = 2.016, ε_1 (*p*-xylene) = 2.263, indicates significant differences between ε_∞ and ε_1. In conjunction with eq. [3] this could account for the evaluation of apparently low dipole moments. Table IV gives ε_∞ values which have been calculated for the solutions from (*a*) literature dipole moments obtained by non-dielectric absorption methods and (*b*) our measured values. The non-dielectric absorption methods and non-microwave methods such as the Guggenheim (10) for determining dipole moments involves n_D^2 in place of ε_∞. However, this approximation cannot be justified when there is an unusually high atomic polarization and would result in the value for the dipole moment being too high. The microwave method for evaluating dipole moments does not involve such an approximation although, if an additional higher frequency dipole relaxation existed, then our ε_∞ values would not be the ones required for eq. [3] but would be too large and would account for the μ_m being too small. Thus, two possible explanations may be advanced to account for the divergent dipole moment values.

Schneider (11) has measured the dielectric absorption of aniline in dilute benzene solution at 20 °C and found its dipole moment to be 1.30 D and the molecular relaxation time to be 5.4×10^{-12} s in the molar fraction range, 0.001 to 0.01. The dielectric loss curve showed a Debye type relaxation process characterized by a single relaxation time and the equation

$$\varepsilon'' = m(a_0 - a_\infty)\frac{\omega\tau}{1 + \omega^2\tau^2}$$

where m is the molar fraction of aniline and a_∞ is the slope of the straight line when the dielectric constant measured in the far infrared region is plotted against molar fraction. He suggests that the low dipole moment value, as opposed to that obtained by the non-dielectric absorption method, could be explained by the presence of an unusually large atomic polarization arising from a low frequency vibration of the amino group. The good agreement between our apparent moments for aniline in *p*-xylene and cyclohexane and Schneider's in benzene, where the concentration was appreciably lower, suggests that the major cause of the lower moment is not association.

Smyth and his co-workers have not quoted their dipole moments. From their microwave data we have calculated the moments (see Table V) from the equation

$$\mu_m = 0.012812\,\{(a_0 - a_\infty)\,TM_1/(\varepsilon_1 + 2)^2 d_1\}^{1/2}$$

where M_1 is the molecular weight of the solvent, and a_0 and a_∞ are the slope of ε_0 and ε_∞ vs. mole fraction of solute respectively. It should be noted that for 1- and 2-naphthylamine the difference between a_D (the slope of n_D^2 vs. mole fraction) and a_∞ has been taken "to indicate a second dispersion region at higher frequencies" (2).

Hadni (12) observed a band at 269.5 cm^{-1} in the far infrared spectrum of methylamine. Stewart (13) has calculated a torsional frequency of 225 cm^{-1} for methylamine, assuming a large moment of inertia of the alkyl group along the C—N axis, and a sinusoidal two minima rotational potential function having a barrier height of 3.3 kcal/mole. This torsional oscillation band is not found in the gas phase and is not observed for secondary aliphatic amines.

Evans (14) has observed a band at 420 cm^{-1} for dilute solutions of aniline in benzene which in the vapor phase appears at 440 cm^{-1}. He has assigned this band to the first overtone of a torsional mode of the C—NH_2 group, and by a similar method to Stewart, has calculated the fundamental frequency of the torsional mode to be 216 cm^{-1} and the barrier height to internal rotation to be 3.54 kcal/mole, which is similar to that of methylamine.

Torsional movement in aniline and substituted anilines could account for our dipole moments being lower than those calculated by the Guggenheim and Halverstadt–Kumler methods.

When all the available evidence is taken into account, it is not clear whether the dipole moment difference by the two approaches is to be attributed to a high atomic polarization contribution as favored by Schneider (11) for aniline or to a second dispersion at higher frequencies as proposed by Grubb and Smyth (2) for 1- and 2-naphthylamine.

In conclusion, the present work on aromatic amines in the inert solvent cyclohexane and the weakly donor solvent *p*-xylene establishes the presence of (at least) one shorter relaxation (τ_2) process other than that for molecular relaxation. This is readily apparent from an ε' vs. $\varepsilon''\omega$ plot for *p*-toluidine by virtue of the 70.01 GHz point. In addition, the dipole moment by the non-dielectric absorption approach differs from that obtained here. Either an additional higher frequency dispersion or a high atomic polarization exists for aniline, *o*-, *m*-, and *p*-toluidine.

1. E. Fischer. Physik. Z. **40**, 645 (1939).
2. E. L. Grubb and C. P. Smyth. J. Am. Chem. Soc. **83**, 4879 (1961).
3. W. F. Hassell. Ph.D. Thesis, University of Aston in Birmingham, Birmingham, England. 1966.
4. W. F. Hassell, M. D. Magee, S. W. Tucker, and S. Walker. Tetrahedron, **20**, 2137 (1964).
5. M. D. Magee and S. Walker. Trans. Faraday Soc. **62**, 3093 (1966).
6. A. Budó. Physik. Z. **39**, 706 (1938).
7. W. P. Purcell, K. Fish, and C. P. Smyth. J. Am. Chem. Soc. **82**, 6299 (1960).
8. G. Williams. Trans. Faraday Soc. **64**, 1219 (1968).
9. J. Crossley, W. F. Hassell, and S. Walker. J. Chem. Phys. **48**, 1261 (1968).
10. E. A. Guggenheim. Trans. Faraday Soc. **45**, 714 (1949).
11. J. Schneider. J. Chem. Phys. **32**, 665 (1960).
12. A. Hadni. J. Phys. Radium, **15**, 375 (1954).
13. J. E. Stewart. J. Chem. Phys. **30**, 1259 (1959).
14. J. C. Evans. Spectrochim. Acta, **16**, 428 (1960).

Can. J. Chem. Downloaded from www.nrcresearchpress.com by 210.87.254.5 on 09/05/12
For personal use only.

Can. J. Chem. Downloaded from www.nrcresearchpress.com by 210.87.254.105 on 09/05/12
For personal use only.

A novel aromatic ketone photoproduct: para-coupling of a phenyl-ketyl radical

B. D. CHALLAND[1]
Chemistry Department, University of Western Ontario, London, Ontario

Received September 18, 1968

Three minor products from the irradiation of acetophenone in ether are described, and the mechanism of their formation is discussed.

Canadian Journal of Chemistry, **47**, 687 (1969)

Irradiations of aromatic ketones in hydrogen-donating solvents have long been known to give mixtures of reduction products, predominantly pinacols (1), and recent publications concerning the mechanism of the photoreduction of benzophenone to benzopinacol (2–5) have prompted this report. During the course of other investigations it was found that irradiation of acetophenone in ether/cyclohexane solvent gave, as expected, the acetophenone pinacols in good yield (6). The product mixture also contained three minor constituents which were separated chromatographically and identified.

Two butan-2-ol derivatives were isolated in 6% yield each and the gross structure **1**, for both of them, was assigned from their spectra. The infrared (i.r.) spectra of each showed a monosubstituted phenyl, a hydroxyl group (probably tertiary) and no carbonyl, and differed only in details of the "fingerprint region". The proton magnetic resonance (p.m.r.) spectra, however, differed appreciably. Both showed the presence of one singlet, one doublet, and one triplet methyl group, but in one case (compound **1*a***) the doublet and triplet were well-separated, and in the other (compound **1*b***) almost superimposed. Three protons on carbon adjacent to oxygen appeared as complex multiplets in each, the patterns differing in detail. These were consistent with the A, B, and A′ portion of an ABX_3 pattern superimposed on an $A'X'_3$ (7, 8). Five aromatic protons and one hydroxyl were present in each compound. The compounds **1*a*** and **1*b*** were evidently diastereoisomeric and on the basis of the relative chemical shifts of the methyl groups, and the anticipated preferred conformations (9), the structures were tentatively proposed as shown.

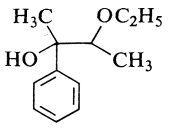

1

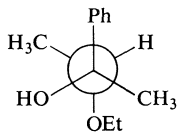

1*a*

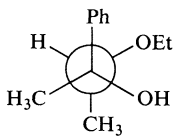

1*b*

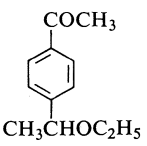

2

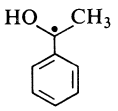

3

4

The third minor product, **2** (3% yield after purification), was also identified by its spectra. Ultraviolet (u.v.) and i.r. spectra showed that the compound was a substituted aromatic ketone, and all the non-equivalent protons were clearly resolved in the p.m.r. spectrum. The *p*-substitution of the acetophenone was apparent from

[1]Present address: Chemistry Department, University of Southampton, Southampton, SO9 5NH, England.

the pattern of the aromatic protons, two symmetrical doublets of two protons each. The possibility of a dimeric structure was considered to be incompatible with the observed p.m.r. spectrum, which was very well-defined.

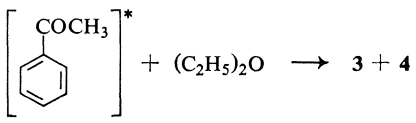

The generally accepted mechanism for photoreduction of aromatic ketones involves abstraction of a hydrogen atom from the solvent by the ketone in the excited triplet state to give two radicals, in this case **3** and **4**. Subsequent combination of these radicals would give the two butan-2-ol derivatives, **1**, which were observed. Such compounds are well-known as minor products from photoreduction reactions; for example, irradiation of benzophenone in toluene, which acts as a hydrogen donor, gives **5** as well as benzopinacol (10).

The substituted acetophenone, **2**, however, is apparently a photoproduct of a new type. Its formation can be rationalized by postulating that the delocalized ketyl radical, **3**, is attacked at the *p*-position by the ethoxyethyl radical, **4**, to give the enolic intermediate **6**, which would be expected to be oxidized by air to the observed product, **2**, during workup of the reaction mixture. Alternatively the dehydrogenation might have been effected by acetophenone in the excited triplet state. The intermediate is analogous to **7** and **8**, both of which have been reported to be the oxygen-sensitive intermediate in the photoreduction of benzophenone by alcohols (3–5). The isolation of **2**, therefore, tends to confirm the mechanism of benzophenone photoreduction as recently proposed (3–5), and suggests that this mechanism is common to aromatic ketone photoreduction by hydrogen donors other than alcohols.

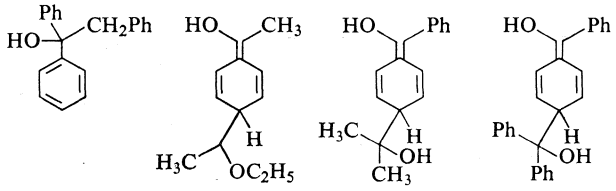

5 **6** **7** **8**

Experimental

Nitrogen was bubbled through a solution of acetophenone (4.73 g) in 50% ether/cyclohexane (250 ml) for 1 h, and the solution was then irradiated under nitrogen with light of λ_{max} 350 nm ("black light" phosphor lamps through Pyrex; Rayonet reactor) for 2¼ h. Evaporation of the solution and chromatography on a silicic acid column (5% ether/benzene eluent) afforded recovered acetophenone (2.54 g), ***1a*** (162 mg, 7% yield), ***1b*** (150 mg, 6% yield), **2** (70 mg, 3% yield), and a mixture of the acetophenone pinacols (1.30 g).

*Compound **1a*** had p.m.r. peaks at τ 9.16 (3H, d, J = 6.5 Hz), 8.84 (3H, t, J = 7 Hz), 8.49 (3H, s), 7.30 (1H, exchanges with D_2O, s), 6.1–6.9 (3H, m), 2.5–3.0 (5H, m); u.v. λ_{max}^{hexane} at 206 nm (ε 8600), 258 nm (ε 190).

Anal. Calcd. for $C_{12}H_{18}O_2$: C, 74.19; H, 9.34. Found: C, 74.17; H, 9.42.

*Compound **1b*** had p.m.r. peaks at τ 9.00 (3H, d, J = 6.5 Hz), 8.93 (3H, t, J = 7 Hz), 8.61 (3H, s), 7.21 (1H, exchanges with D_2O, s), 6.2–7.1 (3H, m), 2.5–3.0 (5H, m); u.v. λ_{max}^{hexane} at 206 nm (ε 8400), 258 nm (ε 200).

Anal. Found: C, 74.35; H, 9.32.

p-(1-Ethoxyethyl)acetophenone, **2**, had i.r. ν_{max} 1685 cm^{-1}; p.m.r. peaks at τ 8.83 (3H, t, J = 7 Hz), 8.62 (3H, d, J = 6.5 Hz), 7.51 (3H, s), 6.69 (2H, q, J = 7 Hz), 5.62 (1H, q, J = 6.5 Hz), 2.68 (2H, d, J = 8 Hz), 2.18 (2H, d, J = 8 Hz); u.v. λ_{max}^{hexane} at 248 nm (ε 15 000), 320 nm (ε 670).

Anal. Calcd. for $C_{12}H_{16}O_2$: C, 74.97; H, 8.39. Found: C, 75.07; H, 8.45.

1. A. SCHONBERG and A. MUSTAFA. Chem. Rev. **40**, 181 (1947).
2. J. N. PITTS, R. L. LETSINGER, R. P. TAYLOR, J. M. PATTERSON, G. RECKTENWALD, and R. B. MARTIN. J. Am. Chem. Soc. **81**, 1068 (1959).
3. G. O. SCHENCK, M. CZIESLA, K. EPPINGER, G. MATTHIAS, and M. PAPE. Tetrahedron Letters, 193 (1967). G. O. SCHENCK and G. MATTHIAS. Tetrahedron Letters, 699 (1967).
4. H. MAUSER, B. NICKEL, U. SPROESSER, and V. BIHL. Z. Naturforsch. **22b**, 903 (1967).
5. N. FILIPESCU and F. L. MINN. J. Am. Chem. Soc. **90**, 1544 (1968).
6. C. WEIZMANN, E. BERGMANN, and Y. HIRSHBERG. J. Am. Chem. Soc. **60**, 1530 (1938).
7. F. A. L. ANET. Can. J. Chem. **39**, 2262 (1961).
8. R. W. FESSENDEN and J. S. WAUGH. J. Chem. Phys. **30**, 944 (1959).
9. J. H. STOCKER, D. H. KERN, and R. M. JENEVEIN. J. Org. Chem. **33**, 412 (1968).
10. G. S. HAMMOND, W. P. BAKER, and W. M. MOORE. J. Am. Chem. Soc. **83**, 2795 (1961).

Can. J. Chem. Downloaded from www.nrcresearchpress.com by 210.87.254.105 on 09/05/12
For personal use only.

Abstraction of hydrogen from hydrogen sulfide by methyl radicals

PETER GRAY, A. A. HEROD[1], AND L. J. LEYSHON[2]
School of Chemistry, Leeds University, Leeds 2, England

Received August 27, 1968

The methyl radical attack on H_2S has been investigated briefly using azomethane as the radical source. The results indicate that the previous rate-constants for the abstraction reaction are too high and that CF_3 radicals may react with H_2S faster than CH_3 radicals.

Canadian Journal of Chemistry, 47, 689 (1969)

Can. J. Chem. Downloaded from www.nrcresearchpress.com by 210.87.254.40 on 09/05/12
For personal use only.

The reaction of methyl radicals with hydrogen sulfide has been investigated using the photolysis of azomethane as the source of methyl radicals. Previous workers generated methyl radicals from acetone (1) and acetaldehyde (2, 3) and obtained conflicting results. These earlier data are open to objection on several grounds: in the acetone work (1) the temperature range (50 to 200 °C) included a region (50 to 120 °C) where the Arrhenius relationship for methyl radical attack on acetone is non-linear; no account was taken of this. Furthermore, it was necessary to decompose large amounts of H_2S; the assumption that SH radicals reformed H_2S is unlikely since hydrogen sulfide was consumed during the reaction, other secondary reactions producing methane could be important. Secondary reactions may also have interfered in the work using acetaldehyde (2, 3) because the aldehyde decomposition is complex in the presence of thiols (4). Although the present work is not conclusive, it indicates that the previous rate-constants are too high.

The experimental method was basically as has been described previously (5) although some modification was necessary because ethane and hydrogen sulfide cannot be separated by low-temperature fractionation. In the bulk of the experiments the ethane content of the C_2H_6/H_2S mixtures was estimated by gas chromatography using an alumina column which retained H_2S. Two samples of azomethane were employed; one had been used in previous experiments (5) and the second yielded Arrhenius parameters for the attack of methyl radicals on azomethane of $\log_{10} A = 10.98 \pm 0.04$ (A in $cm^3\ mole^{-1}\ s^{-1}$) and $E = 7.65 \pm 0.08$ kcal $mole^{-1}$ over the temperature range 93 to 174 °C. H_2S (Matheson C.P. grade) was distilled through a trap at −80 °C. The purity of the reactants was checked by gas chromatography and mass spectrometry. From 10 experiments between 99 and 171 °C Arrhenius parameters for the reaction

$$CH_3 + H_2S \rightarrow CH_4 + SH$$

were found to be $\log_{10} A = 10.7 \pm 0.4$ and $E = 2.9 \pm 0.7$ kcal $mole^{-1}$, with $\log_{10} k = 9.20$ at 150 °C. Support for these results is afforded by experiments where ethane was estimated differently; before measurement of the ethane, the C_2H_6/H_2S mixture was treated with KOH pellets after which mass spectrometry indicated the complete removal of H_2S. Using this technique, $\log_{10} k$ (k in $cm^3\ mole^{-1}\ s^{-1}$) was 8.87 at 147 °C, which can be compared with the corresponding figure of 9.19 by the first method. The agreement is satisfactory considering the rapid rates of reaction and the small amounts of ethane produced. H_2S decomposition was limited to between 6 and 10% throughout the work.

The present results are compared with previous work and related systems in Table I (all rate-constants are relative to Shepp's rate-constant for methyl radical combination (6)). It is clear that the present rate-constants are lower than previous values by about an order of magnitude at 150 °C. We have already drawn attention to possible sources of error in the earlier work. The apparently normal isotope effect (3) between H_2S and D_2S ($A_H/A_D = 0.75$, $E_D - E_H = 1.15$ kcal $mole^{-1}$) is of little consequence since a "normal" isotope effect has been found for the hydroxyl group of isopropanol (9) although secondary reactions interfere there also. The same feature has been demonstrated for the amino group of formamide (10). The lower reactivity of H_2S can be supported by reference to the literature. The overall reactivity of the alkyl thiols (4, 11) CH_3SH, C_2H_5SH, and i-C_3H_7SH increases with

[1]Present address: Lash-Miller Chemical Laboratories, University of Toronto, Toronto 5, Ontario.
[2]Present address: Kodak Research Laboratories, Harrow, Middlesex, England.

TABLE I

CH_3 and CF_3 radical attack on SH bonds

Reaction	$\log_{10} A$ (A in cm^3 $mole^{-1}$ s^{-1})	E (kcal $mole^{-1}$)	$\log_{10} k$ (at 150 °C)	Reference
$CH_3 + H_2S$	10.7	2.9	9.2	This work
$CH_3 + H_2S$	11.4	2.6	10.1	1
$CH_3 + H_2S$	12.1	3.5	10.3	2, 3*
$CH_3 + D_2S$	12.2	4.5	9.9	3*
$CH_3 + CH_3SH$†	11.0	4.1	8.9	7
$CF_3 + H_2S$	11.6	3.9	9.6	8

*Parameters modified according to ref. 7.
†Abstraction from the SH group.

increasing molecular weight, and by analogy with alcohols, amines, and hydrocarbons, the first member of the series (H_2S) is expected to be the least reactive. The earlier results for H_2S indicate that this compound is the most reactive of the series but we find that the SH bond reactivity of H_2S is the same as for methane thiol (7). The S—H bond strengths in H_2S and CH_3SH are about the same (and probably near 90 kcal $mole^{-1}$ (12)) so that similar reactivities would be expected.

Further support for the low rate-constants reported here comes from the CF_3 radical attack on H_2S (8). It is to be expected that the A-factor ratio (A_{CF_3}/A_{CH_3}) for attack on a substrate should be unity. The normally higher activation energy for H abstraction from hydrocarbons by CH_3 radicals as against CF_3 radicals leads to a difference in reactivity which may be reduced or even reversed with polar substrates such as H_2S (8, 13). The present results show that the CF_3 radical is slightly more reactive than the CH_3 radical to H_2S; the literature indicates that CF_3 and CH_3 radicals show similar reactivities to HI (14, 15) where A_{CF_3}/A_{CH_3} is 0.17, $E_{CH_3} - E_{CF_3}$ is 1.8 kcal $mole^{-1}$ and k_{CF_3}/k_{CH_3} is 1.4 at 150 °C, but that CF_3 radicals are less reactive than CH_3 to HBr (13, 14, 16) where A_{CH_3}/A_{CF_3} is 8.3, $E_{CF_3} - E_{CH_3}$ is 1.5 kcal $mole^{-1}$, and k_{CH_3}/k_{CF_3} at 150 °C is 50, and to $SiHCl_3$ (17, 18) where A_{CH_3}/A_{CF_3} is 20, $E_{CH_3} - E_{CF_3}$ is 1.6 kcal $mole^{-1}$, and k_{CH_3}/k_{CF_3} is 2.7 at 150 °C. The Arrhenius parameters obtained here contain large standard errors since the temperature range investigated was small, however, if A_{CF_3}/A_{CH_3} is set equal to unity (8) then our rate-constants yield an activation energy of about 5 kcal $mole^{-1}$, a more reasonable value than the low measured ones and one that compares well with the alkyl thiols.

Acknowledgments

We thank the Ministry of Aviation and the National Rubber Producers' Research Association of England for financial support.

1. N. Imai and O. Toyama. Bull. Chem. Soc. Japan, **33**, 652 (1960).
2. N. Imai and O. Toyama. Bull. Chem. Soc. Japan, **33**, 1120 (1960).
3. N. Imai, T. Dohmaru, and O. Toyama. Bull. Chem. Soc. Japan, **38**, 639 (1965).
4. R. N. Birrell, R. F. Smith, and A. F. Trotman-Dickenson. J. Chem. Soc. 2807 (1957).
5. P. Gray and A. A. Herod. Trans. Faraday Soc. **63**, 2489 (1967).
6. A. Shepp. J. Chem. Phys. **24**, 939 (1956).
7. G. Greig and J. C. J. Thynne. Trans. Faraday Soc. **62**, 379 (1966).
8. N. L. Arthur and T. N. Bell. Can. J. Chem. **44**, 1445 (1966).
9. P. Gray and A. A. Herod. Trans. Faraday Soc. **64**, 2723 (1968).
10. P. Gray and L. J. Leyshon. Trans. Faraday Soc. To be published.
11. J. A. Kerr and A. F. Trotman-Dickenson. J. Chem. Soc. 3322 (1957).
12. J. A. Kerr. Chem. Rev. **66**, 465 (1966).
13. B. G. Tucker and E. Whittle. Trans. Faraday Soc. **61**, 866 (1965).
14. J. C. Amphlett and E. Whittle. Trans. Faraday Soc. **63**, 2695 (1967).
15. M. C. Flowers and S. W. Benson. J. Chem. Phys. **38**, 882 (1963).
16. G. C. Fettis and A. F. Trotman-Dickenson. J. Chem. Soc. 3037 (1961).
17. T. N. Bell and B. B. Johnson. Australian J. Chem. **20**, 1545 (1967).
18. J. A. Kerr, D. H. Slater, and J. C. Young. J. Chem. Soc. A, 104 (1966).

Can. J. Chem. Downloaded from www.nrcresearchpress.com by 210.87.254.40 on 09/05/12
For personal use only.

Concerning the so-called "isohydric point"

W. A. E. McBryde
Department of Chemistry, University of Waterloo, Waterloo, Ontario

Received July 25, 1968

Evaluation of the formation function $\bar{n}$ for a system of monomeric and polymeric (condensed) acids in mutual equilibrium can account for the appearance of a network of formation curves with a crossover point at a fixed value of the coordinates $\bar{n}$, pH. The value of $\bar{n}$ at this isohydric point is equal to $1 - z/n$, where n is the degree of condensation and z the basicity of the condensed acid. A third formation curve is unlikely to pass through the same isohydric coordinates, so that the system is very probably restricted to two predominant species in equilibrium. These conclusions confirm the work of Carpéni and collaborators, but appear to have been derived in a different way.

Canadian Journal of Chemistry, 47, 691 (1969)

Can. J. Chem. Downloaded from www.nrcresearchpress.com by 210.87.254.6 on 09/05/12
For personal use only.

In a recent article in this journal Carpéni (1) has given an account summarizing the experimental and theoretical aspects of almost 20 years of work by himself and his associates concerning the interpretation of titration curves for solutions of acids in which condensation or association has taken place[1]. The distinctive feature of Carpéni's work has been the observation and interpretation of a point of convergence among titration curves in various suitably concentrated solutions of the acids believed to undergo condensation. The presence of such a convergence point, called by Carpéni an isohydric point, is regarded as symptomatic of the presence in the titrated solution of a single isopoly condensed species in equilibrium with the starting acid (or, in principle, two different isopoly species in equilibrium with one another), and to rule out significant concentrations of other species. Moreover, the degree of neutralization, X, as defined by the author, found where the isohydric point occurs is said to be capable of defining the degree of condensation (n) and the charge (z) of the condensed species in accordance with the relationship $X_i = (z/n)_m$, in which m is a multiplicity index that can be found from the data.

While the occurrence of isohydric networks in the systems investigated cannot be seriously questioned as an experimental fact, the inferences to be drawn from the appearance and coordinates of an isohydric point may not be immediately obvious to the reader encountering them for the first time. A somewhat different explanation of the origin of the isohydric point than that outlined by Carpéni has occurred to the writer, and is offered here in corroboration of that already published (1, and references therein).

[1]Copies of an English translation of (1) may be obtained, upon request, from the author.

To begin with, it may be desirable to point out that the quantity x defined by Carpéni is indeed the fraction of the (monomer) acid titrated, and thus the relationship between pH and x is a true titration curve. The quantity X is equivalent to the degree of deprotonation of the acid, and for a monobasic simple acid HA is in fact equal to $1 - \bar{n}$, where $\bar{n}$ is the formation function, or average number of protons bound per atom of A (2, 3). While it is quite true that values of x and X often coincide, it may nevertheless not be desirable, in the interest of precise definition, to describe the relationship between pH and X as a "titration curve". In what follows it is intended to develop the relationship between pH and $\bar{n}$, but it will be evident that this does bear directly on the function studied by Carpéni. Perhaps also it should be mentioned that the expression pH in this paper, as in Carpéni's, is used with the significance as identically equal to $-\log [H^+]$.

Suppose we consider a primitive acid HA which undergoes reversible polymerization to form an acid $(HA)_n$ or H_nA_n which is z-basic. Suppose the polyacid undergoes ionization to form $H_{n-1}A_n$, $H_{n-2}A_n, \cdots, H_{n-z}A_n$ by the transfer of $1, 2, \cdots, z$ protons to the solvent. It is recognized that other hydrogen atoms may be eliminated in the course of condensation reactions

$$(\text{e.g. } 5H_3BO_3 \rightleftarrows 2H^+ + HB_5O_9^{2-} + 6H_2O)$$

but what is proposed here in general can readily be adapted to such specific instances.

The equilibria and associated equilibrium constants which must be considered are then defined by eqs. [1] to [3].

$$[1] \quad nHA \rightleftarrows H_nA_n \qquad k_{cn} = [H_nA_n]/[HA]^n$$

$$[2] \quad HA \rightleftarrows H + A \qquad k_{11} = [H][A]/[HA]$$

[3] $H_nA_n \rightleftarrows H + H_{n-1}A_n$

$$k_{n1} = [H][H_{n-1}A_n]/[H_nA_n] = \beta_{n1}$$

. . . . .

. . . . . .

$$H_nA_n \rightleftarrows zH + H_{n-z}A_n$$

$$\beta_{nz} = [H]^z[H_{n-z}A_n]/[H_nA_n]$$

These equilibrium constants are written as concentration quotients, incorporating the assumption that the experimental data to which they relate have been secured under conditions predisposing to the maintenance of constant activity coefficients. Charges have been omitted from the formulae for simplicity and for generality.

We may put for C_A, the total analytical concentration of acid in all forms

$$[4] \qquad C_A = [HA] + [A] + n\{[H_nA_n] + [H_{n-1}A_n] + \cdots + [H_{n-z}A_n]\}$$

$$[5] \qquad C_A = [HA]\left\{1 + \frac{k_{11}}{[H]}\right\} + nk_{cn}[HA]^n\left\{1 + \frac{\beta_{n1}}{[H]} + \frac{\beta_{n2}}{[H]^2} + \cdots + \frac{\beta_{nz}}{[H]^z}\right\}$$

For the formation function, $\bar{n}$ (degree of protonation)

$$[6] \qquad \bar{n} = \frac{[HA] + n[H_nA_n] + (n-1)[H_{n-1}A_n] + \cdots + (n-z)[H_{n-z}A_n]}{C_A}$$

$$[7] \qquad \bar{n} = \frac{1 + k_{cn}[HA]^{n-1}\left\{n + (n-1)\frac{\beta_{n1}}{[H]} + \cdots + (n-z)\frac{\beta_{nz}}{[H]^z}\right\}}{1 + \frac{k_{11}}{[H]} + nk_{cn}[HA]^{n-1}\left\{1 + \frac{\beta_{n1}}{[H]} + \cdots + \frac{\beta_{nz}}{[H]^z}\right\}}$$

Equation [7] shows that in a system of acids such as we are considering, the formation function $\bar{n} = f([H])$ is not independent of [HA], and accordingly will not be independent of C_A. This is analogous to the case of metal complexes: for mononuclear complexes $\bar{n}$ is independent of C_M, but this no longer applies when polynuclear complexes form.

We should now consider three particular cases:

Case 1. Suppose k_{cn} is extremely small, so that practically no polymerization occurs. In this case we may neglect all the terms of higher order in [HA] in eq. [7], and put

$$[8] \qquad \bar{n} \approx \frac{1}{1 + k_{11}/[H]} \approx \frac{[H]}{[H] + k_{11}}$$

The variation in $\bar{n}$ with pH in this case is well known, and is shown in Fig. 1(*a*), and that for $1 - \bar{n}$, in Fig. 1(*b*).

Case 2. Suppose k_{cn} is extremely large, so that practically all the original acid is converted to and remains as polymer. If this were to happen we

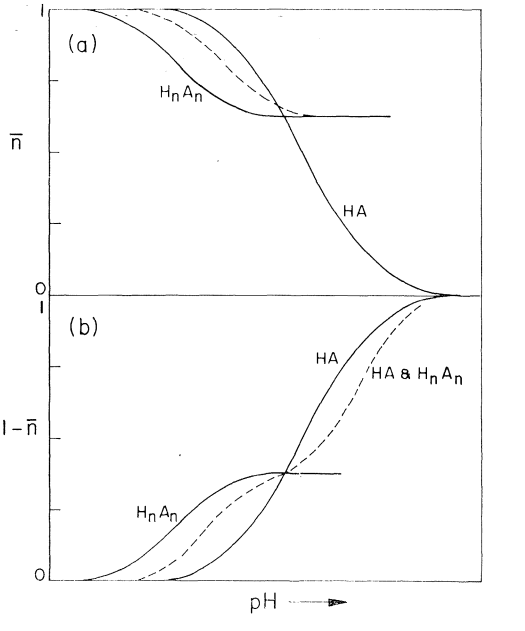

FIG. 1. Plot of $\bar{n}$ and $1 - \bar{n}$ versus pH of HA and H_nA_n.

Can. J. Chem. Downloaded from www.nrcresearchpress.com by 210.87.254.6 on 09/05/12
For personal use only.

could neglect the first terms in numerator and denominator of eq. [7] and put

$$[9] \quad \bar{n} \approx \frac{n + (n-1)\frac{\beta_{n1}}{[H]} + \cdots + (n-z)\frac{\beta_{nz}}{[H]^z}}{n\left\{1 + \frac{\beta_{n1}}{[H]} + \cdots + \frac{\beta_{nz}}{[H]^z}\right\}}$$

This function will have unity as its maximum value when [H] is large compared to the several β's, and will have its minimum value when [H] becomes small compared to the values of β. The minimum value will be $\bar{n}_{min} = (n - z)/n = 1 - z/n$. We show a representative plot for $\bar{n}$ in Fig. 1(*a*) and for $1 - \bar{n}$ in Fig. 1(*b*).

As Carpéni has pointed out, the polymerized acids will generally be stronger than the corresponding primitive acids, so accordingly we show the formation function in a region of lower pH in Fig. 1(*a*) and 1(*b*). The relative position of these curves, in consequence of these differences in strength, imposes the requirement that there must be a crossover point in the $\bar{n}$ or $1 - \bar{n}$ curves as shown in Fig. 1 by the solid lines.

The crossover point suggested by Fig. 1 will occur at $1 - \bar{n} = z/n$. Should the strength of the polymerized acid not be markedly greater than that of the monomer, the formation curve will be like that shown by the broken line in Fig. 1(*a*) and in this event the crossover could occur at a slightly different value of $\bar{n}$ or $1 - \bar{n}$.

Case 3. The situation described in Case 2 is really rather improbable, in the sense that in the course of a titration of this mixture of acids the concentration of HA will decrease, and that of H_nA_n will decrease even faster (an x-fold decrease in [HA] will be matched by an x^n-fold decrease in $[H_nA_n]$). This is the alkaline degradation of which Carpéni speaks. So it is clear that we must consider mixtures of monomer and polymer together. In this event we must use the entire expression for $\bar{n}$ [7]. This may be more simply represented as

$$[10] \quad \bar{n} = \frac{ac + pkc^n}{bc + qkc^n}$$

in which $c = [HA]$, $k = k_{cn}$, and a, b, p, and q are functions of [H]. In the case being discussed a has the value of unity, but this is only the case for a monobasic primitive acid.

Now as Fig. 1 shows, there is a single value of pH or [H] at which the $\bar{n}$ or $1 - \bar{n}$ curves intersect. For this particular value, [H]′, there will be corresponding fixed values a', b', p', and q', and from the limiting cases just considered it follows that

$$[11] \quad \bar{n}' = a'/b' = p'/q'$$

In general, eqs. [8], [9], and [10] will lead to different values of $\bar{n}$ for the same pH. But at the single value pH′ it is obvious from combining [10] and [11] that $\bar{n} = \bar{n}'$.

For mixtures of monomer and polymer in any proportions resulting from a titration or from various initial values of C_A, it follows that the functions $\bar{n}$ or $1 - \bar{n}$ will lie intermediate between those suggested by eqs. [8] and [9], but that at one particular value, pH′, the corresponding value, $\bar{n}'$, will be independent of the concentration of the acid taken. The course of such an intermediate function $1 - \bar{n}$ is shown in Fig. 1(*b*) as a broken line. Several such curves could be drawn, each for a different value of C_A, to produce a network with a common crossover point.

This derivation seems to account for the appearance of an isohydric point in such a system of acids; and the coordinates X_i and pH_i for this point in Carpéni's notation are identical with $1 - \bar{n}'$ and pH′. Moreover in most cases the crossover point in the network of $1 - \bar{n}$ curves will occur, as explained previously, at $1 - \bar{n} = z/n$, which is the same conclusion as that reached by Carpéni.

As we have noted, the situation described under Case 2 is not apt to be encountered just as described; in other words, a solution of pure polymeric acid is not apt to arise and remain polymerized to generate a formation curve throughout a range of pH in the manner suggested by Fig. 1(*b*). Consequently the network of formation curves observed will probably not include this particular limiting case.

Finally we turn to another aspect of the isohydric phenomenon reported by Carpéni, namely the inference from the appearance of an isohydric point that the condensation equilibria involve only *two* predominating species, any others being in negligible proportions. What we have done is to show that if two species, a monomeric and a polymeric acid, are present, an isohydric network must result; and Carpéni said as much. Now we must ask what would happen if another polymeric species, say H_vA_v, were included in significant

Can. J. Chem. Downloaded from www.nrcresearchpress.com by 210.87.254.6 on 09/05/12
For personal use only.

concentrations with the constituents already assumed? For an isohydric point to arise in this case it would be necessary for the formation curve of the third species to pass through the coordinates $\bar{n}'$, pH′. For this to happen it would be necessary in the formation function

$$\bar{n} = \frac{ac + pk_nc^n + rk_vc^v}{bc + qk_nc^n + sk_vc^v}$$

for the ratio r/s, the analogue of [9] for H_vA_v, to achieve the same value as p/q when [H] = [H]′. We cannot say categorically that this is impossible, but can assert that it is highly improbable, except for the case where H_vA_v generates the same $\bar{n}_{min}$ as H_nA_n and both polymeric acids are stronger than HA. Moreover the coincidence of three formation curves at pH′ would be altogether impossible if H_vA_v led at high pH to a minimum value of $\bar{n}$ that was larger than $\bar{n}_{min}$ for H_nA_n, for in that event $1 - \bar{n}$ for H_vA_v would always be smaller than $1 - \bar{n}'$.

From the foregoing considerations it seems highly probable that an isohydric point in a network of formation curves does signify in most cases the presence of two principal species in solution. One could modify the treatment given above to include the possibility of an isohydric network arising from equilibria between two condensed species, but in that case the monomer would have to be in negligible concentration. There does seem, however, to be a possible risk in applying this inference to a system of condensible acids where an isohydric point is not clearly defined. (In the accounts given by Carpéni of experiments on such systems it is admitted that the coordinates of the isohydric point are not always sharply defined by the data.) It seems quite possible that two different polymeric species might arise whose formation curves would lead to minimum values of $\bar{n}$ that are not very different. These would intersect the formation curve of the primitive acid at nearly the same pH. For instance, suppose we had the following cases:

$$H_5A_5 \rightleftarrows 2H^+ + H_3A_5^{2-} \quad z/n = 0.40$$
$$H_7A_7 \rightleftarrows 3H^+ + H_4A_7^{3-} \quad z/n = 0.43$$

Would we be prepared to conclude from an indistinct isohydric "point" at, say, $1 - \bar{n} = 0.41$ that we had one or other of the above species in our solution, and not perhaps both according to the value of C_A, etc.? It has been shown that in hydrolysis of metal cations it is often difficult from the data to make a choice from among two or more possible polynuclear species (4).

1. G. Carpéni. Can. J. Chem. **46**, 1787 (1968).
2. L. G. Sillén. *In* Treatise on analytical chemistry. *Edited by* I. M. Kolthoff and P. J. Elving. Interscience Publishers, Inc., New York. 1959. pp. 290–1.
3. J. N. Butler. Ionic equilibrium. Addison–Wesley, Reading, Mass. 1964. pp. 213–223.
4. Åke Olin. Svensk Kemisk Tidskrift, **73**, 9 (1961).

Mechanism of oxidation of alcohols with N-bromo succinimide

N. Venkatasubramanian and V. Thiagarajan
Department of Chemistry, Vivekananda College, Madras, India

Received August 20, 1968

The kinetics of the oxidation of a number of aliphatic and aromatic secondary alcohols with N-bromo succinimide has been investigated. Electron-withdrawing substituents retard the reaction considerably and electron-releasing substituents increase the rate of oxidation. The Taft ρ* value is −2.56. *Cis*- and *trans*-4-*t*-butyl cyclohexanols are oxidized at nearly the same rates. There is also a good correlation between the rates of the NBS oxidations and Br_2 oxidations of these alcohols. The results are interpreted in terms of a cyclic mechanism involving a rate-determining abstraction of the alpha hydrogen as a hydride anion.

Canadian Journal of Chemistry, **47**, 694 (1969)

The mechanism of the N-bromo succinimide (NBS) oxidation of alcohols has not yet been established, though the use of NBS as a versatile oxidizing agent is well known (1). It is generally accepted that in polar solvent media a "positive" bromine is the attacking species (2, 3). The following tentative mechanisms have been proposed on the basis of preparative work (see ref. (2) for reaction [1], and ref. (3) for reaction [2]). Langbein and Steinert (4) concluded in a kinetic investigation on the oxidation of 3,17-α-dihydroxy-21-bromo-11,20-pregnane-dione by NBS,

Can. J. Chem. Downloaded from www.nrcresearchpress.com by 210.87.254.6 on 09/05/12
For personal use only.

concentrations with the constituents already assumed? For an isohydric point to arise in this case it would be necessary for the formation curve of the third species to pass through the coordinates $\bar{n}'$, pH′. For this to happen it would be necessary in the formation function

$$\bar{n} = \frac{ac + pk_nc^n + rk_vc^v}{bc + qk_nc^n + sk_vc^v}$$

for the ratio r/s, the analogue of [9] for H_vA_v, to achieve the same value as p/q when [H] = [H]′. We cannot say categorically that this is impossible, but can assert that it is highly improbable, except for the case where H_vA_v generates the same $\bar{n}_{min}$ as H_nA_n and both polymeric acids are stronger than HA. Moreover the coincidence of three formation curves at pH′ would be altogether impossible if H_vA_v led at high pH to a minimum value of $\bar{n}$ that was larger than $\bar{n}_{min}$ for H_nA_n, for in that event $1 - \bar{n}$ for H_vA_v would always be smaller than $1 - \bar{n}'$.

From the foregoing considerations it seems highly probable that an isohydric point in a network of formation curves does signify in most cases the presence of two principal species in solution. One could modify the treatment given above to include the possibility of an isohydric network arising from equilibria between two condensed species, but in that case the monomer would have to be in negligible concentration. There does seem, however, to be a possible risk in applying this inference to a system of condensible acids where an isohydric point is not clearly defined. (In the accounts given by Carpéni of experiments on such systems it is admitted that the coordinates of the isohydric point are not always sharply defined by the data.) It seems quite possible that two different polymeric species might arise whose formation curves would lead to minimum values of $\bar{n}$ that are not very different. These would intersect the formation curve of the primitive acid at nearly the same pH. For instance, suppose we had the following cases:

$$H_5A_5 \rightleftarrows 2H^+ + H_3A_5^{2-} \quad z/n = 0.40$$
$$H_7A_7 \rightleftarrows 3H^+ + H_4A_7^{3-} \quad z/n = 0.43$$

Would we be prepared to conclude from an indistinct isohydric "point" at, say, $1 - \bar{n} = 0.41$ that we had one or other of the above species in our solution, and not perhaps both according to the value of C_A, etc.? It has been shown that in hydrolysis of metal cations it is often difficult from the data to make a choice from among two or more possible polynuclear species (4).

1. G. Carpéni. Can. J. Chem. **46**, 1787 (1968).
2. L. G. Sillén. *In* Treatise on analytical chemistry. *Edited by* I. M. Kolthoff and P. J. Elving. Interscience Publishers, Inc., New York. 1959. pp. 290–1.
3. J. N. Butler. Ionic equilibrium. Addison–Wesley, Reading, Mass. 1964. pp. 213–223.
4. Åke Olin. Svensk Kemisk Tidskrift, **73**, 9 (1961).

Mechanism of oxidation of alcohols with N-bromo succinimide

N. Venkatasubramanian and V. Thiagarajan
Department of Chemistry, Vivekananda College, Madras, India

Received August 20, 1968

The kinetics of the oxidation of a number of aliphatic and aromatic secondary alcohols with N-bromo succinimide has been investigated. Electron-withdrawing substituents retard the reaction considerably and electron-releasing substituents increase the rate of oxidation. The Taft ρ* value is −2.56. *Cis*- and *trans*-4-*t*-butyl cyclohexanols are oxidized at nearly the same rates. There is also a good correlation between the rates of the NBS oxidations and Br_2 oxidations of these alcohols. The results are interpreted in terms of a cyclic mechanism involving a rate-determining abstraction of the alpha hydrogen as a hydride anion.

Canadian Journal of Chemistry, **47**, 694 (1969)

The mechanism of the N-bromo succinimide (NBS) oxidation of alcohols has not yet been established, though the use of NBS as a versatile oxidizing agent is well known (1). It is generally accepted that in polar solvent media a "positive" bromine is the attacking species (2, 3). The following tentative mechanisms have been proposed on the basis of preparative work (see ref. (2) for reaction [1], and ref. (3) for reaction [2]). Langbein and Steinert (4) concluded in a kinetic investigation on the oxidation of 3,17-α-dihydroxy-21-bromo-11,20-pregnane-dione by NBS,

Can. J. Chem. Downloaded from www.nrcresearchpress.com by 210.87.254.42 on 09/05/12
For personal use only.

[1] 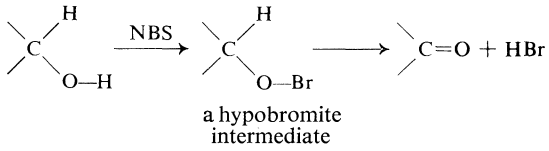

a hypobromite intermediate

[2] 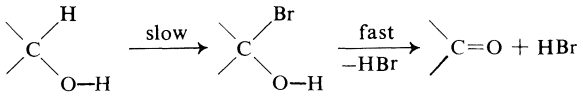

a substituted intermediate

that the oxidation was brought about by molecular bromine:

[3] $\rangle CHOH + 2\rangle N{-}Br \rightarrow \rangle C{=}O + 2\rangle NH + Br_2$

[4] $\rangle CHOH + Br_2 \rightarrow \rangle C{=}O + 2HBr$

[5] $2HBr + 2\rangle N{-}Br \rightarrow 2\rangle NH + 2Br_2$

It is believed that [5] is 10^4 times faster than [4]. These authors proposed a cyclic mechanism involving the attack of the steroidal molecule by a Br_2 molecule embodying a rate-determining breakage of the secondary hydrogen as a hydride ion.

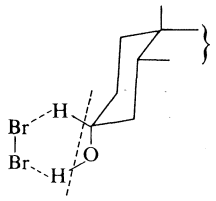

In a previous communication (5) we reported that the NBS oxidation of alcohols is composed of two stages, an initial slow reaction superceded by a faster one involving the attack of Br_2 molecules on the alcohol moiety. We have further shown that the second stage is completely suppressed by added mercuric acetate[1].

TABLE I

Second order rate constants for NBS oxidation of some aliphatic and aromatic secondary alcohols*

Alcohol	$k_2 \times 10^4$ l mole^{-1} s^{-1}
Aliphatic	
Propanol-2	1.51
Butanol-2	2.70
Pentanol-2	2.73
Hexanol-2	3.63
Octanol-2	3.95
1,3-Dichloro-propanol-2	0.45
1-Methoxy-propanol-2	0.88
1-*n*-Butoxy-propanol-2	1.12
Aromatic	
α-Phenyl ethanol	8.54
Benzhydrol	15.17
4-Chloro-benzhydrol	6.04

*[ROH] = 0.1 *M*, [NBS] = 0.01 *M*, and [Hg(OAc)$_2$] = 0.01 *M*.

In this communication, we wish to report the results of the rate measurements on the NBS oxidation of a number of alcohols with suitable electronegative and electropositive substituents. All these reactions were carried out in the presence of Hg^{2+}. This would mean that what has been followed by us is the pure NBS oxidation, uncontaminated with any Br_2 oxidation. It must be pointed out that the kinetic work of Langbein and Steinert (4) differs from our work in that no attempt was made in the former to prevent the product HBr from reacting with NBS. Table I consists of the second order rate constants for the oxidation of the alcohols in 70% HOAc – 30% H_2O at 45 °C and at pH = 4. The alcohols chosen here are smoothly and quantitatively oxidized to the corresponding

[1]One of the referees has suggested that added mercuric acetate would buffer the Br_2 concentration at a low level as follows, and that bromine is actually the reactant:

(*i*) NBS + Br^- → Br_2 + S

(*ii*) $2Br^- + Hg(OAc)_2 \leftrightarrows HgBr_2 + 2OAc^-$

We feel that this is unlikely for the following reasons. (*a*) Equilibrium (*ii*) is most unlikely in the solvent system of 70% HOAc – H_2O with a sodium acetate concentration of 0.2 *M*. (*b*) The Br^- formed is most likely to exist as $HgBr_4^{2-}$ or $Hg(OAc)_2Br_2^{2-}$. (*c*) The reaction exhibits identical kinetics in the presence of added $HgCl_2$ also. (*d*) If the oxidation were to proceed by buffered bromine, the reaction order would not be as simple as observed. Further, the rate constants for NBS and Br_2 oxidation must be identical, whereas they actually differ markedly.

Can. J. Chem. Downloaded from www.nrcresearchpress.com by 210.87.254.42 on 09/05/12
For personal use only.

TABLE II

Second order rate constants for the NBS and Br_2 oxidations of *cis*- and *trans*-4-*t*-butyl cyclohexanols*

Alcohol	$k_2 \times 10^2$ (l mole^{-1} s^{-1}) NBS oxidation	Br_2 oxidation
cis-4-*t*-Butyl cyclohexanol	0.198	6.70
trans-4-*t*-Butyl cyclohexanol	0.180	6.48

*[ROH] = 0.1 *M*, [NBS] = 0.01 *M*, and [Hg(OAc)$_2$] = 0.01 *M*.

ketones by NBS. Preliminary runs on the bromination of the products, ketones, were found to be very slow compared to the rate of oxidation. Further, as the order of the oxidations with respect to the organic substrate was shown to be one in preliminary runs, the oxidations were generally carried out with a large excess of alcohol, whereby product bromination was reduced to the minimum. The kinetics were followed by estimation of unreacted NBS by iodometry.

We find in the aliphatic series that electronegative substituents(—Cl,—OCH_3,—*n*-OC_4H_9, etc.) decrease the oxidation rate, while electropositive substituents (alkyl groups) increase the rate of oxidation. A Taft plot for the NBS oxidation shows points for the aliphatic alcohols lying on the same line and $\rho^* = -2.56$, pointing to an electron deficient carbon center in the transition state of the oxidation. It is interesting to observe that the value for Br_2 oxidation of the same series of alcohols reported earlier (6) was more or less the same ($\rho^*_{Br_2\ oxidation} = -2.6$).

A point-to-point correspondence between the Br_2 oxidation of these secondary alcohols and the NBS oxidation of the same alcohols is well brought out by Fig. 1, wherein log $k_{Br_2\ oxidation}$ is plotted against log $k_{NBS\ oxidation}$. This linear free-energy correlation would, therefore, point to a close similarity between the mechanisms for Br_2 and NBS oxidations.

Table II gives the second order rate constants

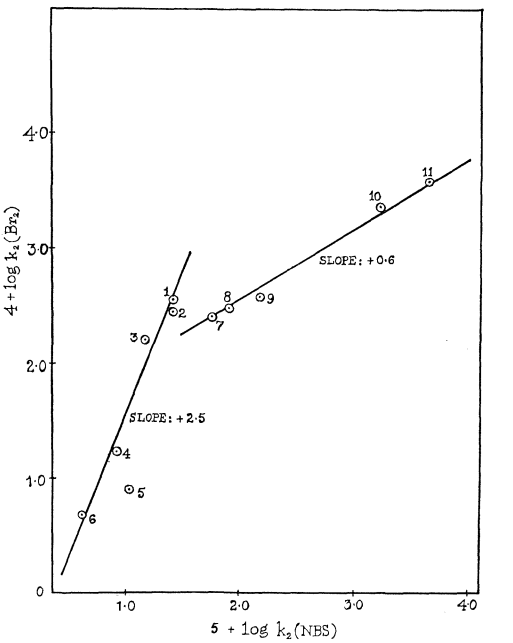

FIG. 1. Linear free-energy correlation in the oxidation of aliphatic and aromatic secondary alcohols with Br_2 and NBS. 1, Pentanol-2; 2, butanol-2; 3, propanol-2; 4, 1-methoxy propanol-2; 5, 1-*n*-butoxy propanol-2; 6, 1,3-dichloro-propanol-2; 7, 4-chloro-benzhydrol; 8, α-phenyl ethanol; 9, benzhydrol; 10, α-tetralol; 11, naphthyl-1-methyl carbinol.

for the NBS and Br_2 oxidations of a pair of stereoisomeric alcohols, *cis*- and *trans*-4-*t*-butyl cyclohexanols. As in the case of Br_2 oxidation, we observe an insensitivity of the NBS oxidation to the configuration of the alcohol. In the Br_2 oxidation, this insensitivity is traced to the cyclic nature of the transition state (7). We may thus conclude that the NBS and Br_2 oxidations proceed by similar mechanistic pathways.

We propose from the evidence detailed above, the following *cyclic* mechanism for the NBS oxidation of alcohols involving a rate-determining loss of the secondary hydrogen as a hydride ion

[6]

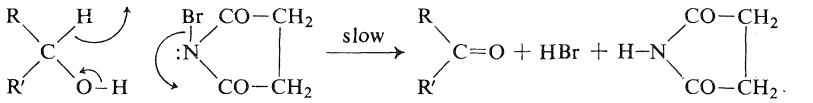

This is further substantiated by the fact that ω, the slope of a Bunnett plot (8) (log $k + H_0$ vs. log a_{H_2O}), has a large negative value pointing to considerable carbonium ion character in the transition state.

It is also interesting to observe from Fig. 1 that while the points for the aliphatic alcohols fall on the same line (slope = +2.5), the points for those alcohols which have a phenyl or naphthyl ring directly attached to the reaction center fall on yet

Can. J. Chem. Downloaded from www.nrcresearchpress.com by 210.87.254.42 on 09/05/12
For personal use only.

another straight line with a smaller slope (slope = +0.6). In the mechanism proposed above, the transition state possesses a carbonium ion character. In the case of alcohols having an aryl ring attached to the reaction center, this positive charge will be stabilized by a resonance participation and the reduced positive slope can be attributed to this effect.

Acknowledgment

We thank the Department of Atomic Energy, Government of India, for a grant-in-aid for this work.

1. R. FILLER. Chem. Rev. **63**, 21 (1963).
2. P. F. KRUSE, JR., K. L. GRIST, and T. A. MCCOY. Anal. Chem. **26**, 139 (1954).
3. J. LECOMTE and H. GAULT. Compt. Rend. **238**, 2538 (1954).
4. G. LANGBEIN and B. STEINERT. Ber. **95**, 1873 (1962).
5. N. VENKATASUBRAMANIAN and V. THIAGARAJAN. Tetrahedron Letters, **35**, 3349 (1967).
6. N. VENKATASUBRAMANIAN and V. THIAGARAJAN. Tetrahedron Letters, **14**, 1711 (1968).
7. I. R. L. BARKER, W. G. OVEREND, and G. W. REES. J. Chem. Soc. 3263 (1964).
8. J. F. BUNNETT. J. Am. Chem. Soc. **83**, 4956 (1961).

Calculation of the bond lengths in sulfur-containing heterocyclic systems

T. ŽIVKOVIĆ AND N. TRINAJSTIĆ[1]

Institute "Rudjer Bošković", Zagreb, Croatia, Yugoslavia

Received August 20, 1968

The equations $l_{CC} = 1.532 - \frac{0.242p_{CC}}{1 + 0.240p_{CC}}$ and $l_{CS} = 1.829 - 0.262p_{CS}$ are proposed for use in the calculation of bond lengths in sulfur heterocycles.

Canadian Journal of Chemistry, **47**, 697 (1969)

We propose the following equations for use in the calculation of the carbon–carbon and carbon–sulfur bond lengths in sulfur-containing heterocyclic compounds

$$[1] \qquad l_{CC} = 1.532 - \frac{0.242p_{CC}}{1 + 0.240p_{CC}}$$

$$[2] \qquad l_{CS} = 1.829 - 0.262p_{CS}$$

where l_{ij} is the bond length of the bond i–j, and p_{ij} is the corresponding bond order.

Equation [1] is a different form of the first theoretical expression for this phenomenon developed by Coulson in 1938 and published (1) in 1939. We have derived eq. [1] in the following manner: if one considers that the bond length in the first approximation is proportional to the π-electron density between the atoms i and j, one should take into account not only the bond orders p_{ij}, but also the product $p_{ij}S_{ij}$, where S_{ij} is the overlap integral for pπ orbitals centered on atoms i and j. Therefore, we propose to use the following relationship

$$[3] \qquad l_{ij} = l_0 - k\,p_{ij}\,S_{ij}$$

In the first approximation S_{ij} can be expressed as:

$$[4] \qquad S_{ij} = S_0 + S_1\,\Delta l_{ij}$$

By substituting [4] into [3] and using

$$[5] \qquad c_0 = k\,S_0$$

and

$$[6] \qquad c_1 = -k\,S_1$$

we obtain

$$[7] \qquad l_{ij} = l_0 - c_0\,p_{ij} - c_1\,\Delta l_{ij}\,p_{ij}$$

If one now considers the carbon–carbon bonds, constants l_0, c_0, and c_1 are obtained by using experimental data for C—C bond lengths in ethane 1.5324 Å (2), ethylene 1.337 Å (3), and acetylene 1.205 Å (4), respectively. Bond orders for C—C bonds in these compounds are 0, 1, and 2, respectively. Equation [1], thus obtained, has been checked on a number of hydrocarbons and has reproduced experimental bond lengths quite well. It gives the best agreement with experimental values for the bond lengths between sp^2 hybridized carbon atoms. Therefore, we suggest that

[1]Present address: University of Texas, Department of Chemistry, Austin, Texas 78712, U.S.A.

Can. J. Chem. Downloaded from www.nrcresearchpress.com by 210.87.254.42 on 09/05/12
For personal use only.

another straight line with a smaller slope (slope = +0.6). In the mechanism proposed above, the transition state possesses a carbonium ion character. In the case of alcohols having an aryl ring attached to the reaction center, this positive charge will be stabilized by a resonance participation and the reduced positive slope can be attributed to this effect.

Acknowledgment

We thank the Department of Atomic Energy, Government of India, for a grant-in-aid for this work.

1. R. FILLER. Chem. Rev. **63**, 21 (1963).
2. P. F. KRUSE, JR., K. L. GRIST, and T. A. MCCOY. Anal. Chem. **26**, 139 (1954).
3. J. LECOMTE and H. GAULT. Compt. Rend. **238**, 2538 (1954).
4. G. LANGBEIN and B. STEINERT. Ber. **95**, 1873 (1962).
5. N. VENKATASUBRAMANIAN and V. THIAGARAJAN. Tetrahedron Letters, **35**, 3349 (1967).
6. N. VENKATASUBRAMANIAN and V. THIAGARAJAN. Tetrahedron Letters, **14**, 1711 (1968).
7. I. R. L. BARKER, W. G. OVEREND, and G. W. REES. J. Chem. Soc. 3263 (1964).
8. J. F. BUNNETT. J. Am. Chem. Soc. **83**, 4956 (1961).

Calculation of the bond lengths in sulfur-containing heterocyclic systems

T. ŽIVKOVIĆ AND N. TRINAJSTIĆ[1]

Institute "Rudjer Bošković", Zagreb, Croatia, Yugoslavia

Received August 20, 1968

The equations $l_{CC} = 1.532 - \frac{0.242p_{CC}}{1 + 0.240p_{CC}}$ and $l_{CS} = 1.829 - 0.262p_{CS}$ are proposed for use in the calculation of bond lengths in sulfur heterocycles.

Canadian Journal of Chemistry, **47**, 697 (1969)

We propose the following equations for use in the calculation of the carbon–carbon and carbon–sulfur bond lengths in sulfur-containing heterocyclic compounds

$$[1] \qquad l_{CC} = 1.532 - \frac{0.242p_{CC}}{1 + 0.240p_{CC}}$$

$$[2] \qquad l_{CS} = 1.829 - 0.262p_{CS}$$

where l_{ij} is the bond length of the bond i–j, and p_{ij} is the corresponding bond order.

Equation [1] is a different form of the first theoretical expression for this phenomenon developed by Coulson in 1938 and published (1) in 1939. We have derived eq. [1] in the following manner: if one considers that the bond length in the first approximation is proportional to the π-electron density between the atoms i and j, one should take into account not only the bond orders p_{ij}, but also the product $p_{ij}S_{ij}$, where S_{ij} is the overlap integral for pπ orbitals centered on atoms i and j. Therefore, we propose to use the following relationship

$$[3] \qquad l_{ij} = l_0 - k\,p_{ij}\,S_{ij}$$

In the first approximation S_{ij} can be expressed as:

$$[4] \qquad S_{ij} = S_0 + S_1\,\Delta l_{ij}$$

By substituting [4] into [3] and using

$$[5] \qquad c_0 = k\,S_0$$

and

$$[6] \qquad c_1 = -k\,S_1$$

we obtain

$$[7] \qquad l_{ij} = l_0 - c_0\,p_{ij} - c_1\,\Delta l_{ij}\,p_{ij}$$

If one now considers the carbon–carbon bonds, constants l_0, c_0, and c_1 are obtained by using experimental data for C—C bond lengths in ethane 1.5324 Å (2), ethylene 1.337 Å (3), and acetylene 1.205 Å (4), respectively. Bond orders for C—C bonds in these compounds are 0, 1, and 2, respectively. Equation [1], thus obtained, has been checked on a number of hydrocarbons and has reproduced experimental bond lengths quite well. It gives the best agreement with experimental values for the bond lengths between sp^2 hybridized carbon atoms. Therefore, we suggest that

[1]Present address: University of Texas, Department of Chemistry, Austin, Texas 78712, U.S.A.

Can. J. Chem. Downloaded from www.nrcresearchpress.com by 210.87.254.5 on 09/05/12
For personal use only.

TABLE I

Comparison of calculated and observed bond lengths (all results in Å)

Molecule	Bond	Bond order	Bond length		Δl
			Calculated	Observed	
1,4-Thiophthene	1—2	0.4066	1.722	1.72	0.002
	1—7	0.3612	1.734	1.74	0.006
	2—3	0.8210	1.366	1.36	0.006
	3—8	0.4921	1.426	1.41	0.016
	7—8	0.6871	1.389	1.36	0.029
2,2′-Bithiophene	1—2	0.4738	1.705	1.717	0.012
	1—5	0.4933	1.700		
	2—3	0.7286	1.382	1.357	0.025
	2—2′	0.3075	1.463	1.480	0.017
	3—4	0.5757	1.410	1.433	0.023
	4—5	0.7635	1.376		

this formula be used for predicting the carbon–carbon bond lengths only in planar conjugated systems.

On the other hand, eq. [2] is obtained by a least-squares linear fit to the bond order – bond length curve presented in our earlier work (5). This formula is useful for calculating the bond lengths between the σ-bivalent sulfur and the sp^2 hybridized carbon atom.

Results

We have considered 1,4-thiophthene (**1**) and 2,2′-bithiophene (**2**) (a topology of these two molecules is given in Fig. 1) as examples. The l.c.a.o.-s.c.f.-m.o. π-bond orders, calculated, and experimental (6, 7) values for carbon–carbon and carbon–sulfur bond lengths are given in Table I. Generally speaking, the agreement between the calculated and observed values is quite good. The difference between the calculated and experimental values is in the range of 0.002–0.025 Å. This is within the limits of the experimental error. Only the result for the bond 7–8 in 1,4-thiophthene is out of this range. This particular bond has been rather extensively studied (8–11), but the theoretical results obtained for the bond length were always too large. The best agreement was obtained when Schomaker (10) corrected the calculated result for distortion; he obtained 1.38 Å. Results from different m.o. calculations are greater by 0.030 Å or more than the experimentally observed value 1.36 Å (6). On the other hand, our calculations for 2,2′-bithiophene predict different values for lengths of all bonds in the thiophene ring. But, experimental measurements (electron diffraction studies in gas phase (7)) indicate that the bonds 1–2 and 1–5 are of equal lengths and that 2–3 and 4–5 are also of equal lengths[2].

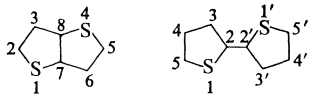

1 **2**

FIG. 1. Atomic skeletal structure and numbering of atoms for 1,4-thiophthene (**1**) and 2,2′-bithiophene (**2**).

Finally, we would like to comment on the results for 1,4-thiophthene reported by Clark[3] (12). It seems to us that his equation ($l_{CS} = 1.802 - 0.229p_{CS}$) slightly underestimates the experimental values for C—S bonds. At the same time his results for C—C bonds are in agreement with ours.

Acknowledgments

We would like to thank Professor C. A. Coulson (Oxford) for helpful comments concerning eq. [1]. We would also like to thank Dr. B. Matković (Zagreb) and Professor M. Randić (Zagreb) for helpful discussions.

[2]Recent X-ray measurements by Visser, Heeres, Wolters, and Vos (13) have given different values for lengths of all bonds in the thiophene ring, but unfortunately their results are not very accurate (the estimated standard deviations are approximately 0.02 Å for C—S and 0.03 Å for C—C bonds).

[3]We thank Dr. Clark for sending us preprint of his results from m.o. calculations on three isomeric thiophthenes.

Can. J. Chem. Downloaded from www.nrcresearchpress.com by 210.87.254.5 on 09/05/12
For personal use only.

1. C. A. COULSON. Proc. Roy. Soc. London, Ser. A, **169**, 413 (1939).
2. L. S. BARTELL and H. K. HIGGINBOTTOM. J. Chem. Phys. **42**, 851 (1965).
3. H. C. ALLEN and E. K. PLYLER. J. Am. Chem. Soc. **80**, 2673 (1958).
4. M. T. CHRISTENSEN, D. R. EATON, B. A. GREEN, and H. W. THOMPSON. Proc. Roy. Soc. London, Ser. A, **238**, 15 (1956).
5. N. TRINAJSTIĆ. Tetrahedron Letters, 1529 (1968).
6. E. G. COX, R. J. H. GILLOT, and G. A. JEFFREY. Acta Cryst. **2**, 350 (1949).
7. A. ALMENINGEN, O. BASTIANSEN, and P. SVENDSÅS. Acta Chem. Scand. **12**, 1671 (1958).
8. M. G. EVANS and J. DE HEER. Acta Cryst. **2**, 363 (1949).
9. H. C. LONGUET-HIGGINS. Acta Cryst. **3**, 79 (1950).
10. V. SCHOMAKER. Acta Cryst. **4**, 158 (1951).
11. D. T. CLARK. Tetrahedron Letters, 2889 (1967).
12. D. T. CLARK. J. Mol. Spectry. **26**, 181 (1968).
13. G. J. VISSER, G. J. HEERES, J. WOLTERS, and A. VOS. Acta Cryst. **B24**, 467 (1968).

Thermochemistry of the aqueous manganous ion[1]

L. M. GEDANSKY[2] AND L. G. HEPLER
Department of Chemistry, University of Lethbridge, Lethbridge, Alberta

Received September 23, 1968

Heats of solution of $MnSO_4$(c) have been measured and combined with heats of dilution to yield $\Delta H^0 = -15.3$ kcal/mole for the standard heat of solution. This value leads to $\Delta H_f^0 = -52.9$ kcal/mole for Mn^{2+}(aq). Calculations with data from the literature give $\Delta G_f^0 = -55.1$ kcal/mole for Mn^{2+}(aq). Combination of this value with our ΔH_f^0 gives $\bar{S}_2^0 = -16.2$ gibbs/mole for Mn^{2+}(aq). Our ΔH_f^0 value for Mn^{2+}(aq) is compared with other values derived from calculations based on data taken from the literature.

Canadian Journal of Chemistry, **47**, 699 (1969)

Introduction

Thermodynamic data already available now provide a means of calculating ΔG_f^0 for Mn^{2+}(aq) and thence E^0 for the Mn/Mn^{2+} oxidation potential. But the situation with respect to the ΔH_f^0 and $\bar{S}_2^0$ for Mn^{2+}(aq) is not nearly so satisfactory and should be resolved experimentally for several reasons. For example, once the ΔH_f^0 of Mn^{2+}(aq) is reliably known, heat of solution data permit calculation of ΔH_f^0 values for a number of compounds of manganese. It will also be useful to have complete and reliable thermodynamic data for Mn^{2+}(aq) because of its d^5 electronic configuration and its consequent use as a "reference" divalent ion with Ca^{2+}(aq) and Zn^{2+}(aq) in connection with consideration of ligand field stabilization effects.

Largely as a result of considerations outlined above, measurements of the heat of solution of $MnSO_4$(c) in water and the calculations reported here have been carried out.

Experimental

Three samples of $MnSO_4$(c) were prepared for calorimetric measurements. The first was prepared by recrystallization of Baker analyzed reagent, followed by drying at 400 °C for several days. The second was prepared in exactly the same manner from Fisher certified reagent. The third sample was prepared by further heating of a portion of the second sample at 450 °C overnight. All three samples appeared to be identical and led to consistent heats of solution.

The calorimetric apparatus used for these measurements was patterned after one previously described (1). The calorimeter consisted of a Dewar vessel suspended in a brass can submerged in a water bath which was maintained at constant temperature. Temperature in the calorimeter was determined with two 100 Ω thermistors wired in parallel and connected to a Leeds and Northrup G-2 Mueller bridge with a Liston–Becker model 14 breaker amplifier and zero-center meter. The thermistors and a manganin heater (300 Ω) were contained in a glass spiral filled with mineral oil. All of the calorimetric data (in terms of the defined calorie, 4.184 J) reported here were obtained with 950 ml of water in the Dewar at 25.00 ± 0.15 °C. Operation of the calorimeter was checked by heats of solution of THAM and KCl, with results indicating that uncertainties range from about 0.05 to 0.10 cal. The heat associated with breaking sample bulbs was 0.03 ± 0.02 cal, which was taken into account in calculating reported ΔH values.

Results and Calculations

The results of our determinations of the heat of solution of $MnSO_4$(c) in water are summarized in Table I.

Since the most dilute solution formed in our measurements was about 1×10^{-3} *M*, there is

[1]The experimental work reported here was carried out at the Carnegie Institute of Technology and the University of Louisville.
[2]Present address: Scott Paper Company, Philadelphia, Pennsylvania.

Can. J. Chem. Downloaded from www.nrcresearchpress.com by 210.87.254.5 on 09/05/12
For personal use only.

1. C. A. COULSON. Proc. Roy. Soc. London, Ser. A, **169**, 413 (1939).
2. L. S. BARTELL and H. K. HIGGINBOTTOM. J. Chem. Phys. **42**, 851 (1965).
3. H. C. ALLEN and E. K. PLYLER. J. Am. Chem. Soc. **80**, 2673 (1958).
4. M. T. CHRISTENSEN, D. R. EATON, B. A. GREEN, and H. W. THOMPSON. Proc. Roy. Soc. London, Ser. A, **238**, 15 (1956).
5. N. TRINAJSTIĆ. Tetrahedron Letters, 1529 (1968).
6. E. G. COX, R. J. H. GILLOT, and G. A. JEFFREY. Acta Cryst. **2**, 350 (1949).
7. A. ALMENINGEN, O. BASTIANSEN, and P. SVENDSÅS. Acta Chem. Scand. **12**, 1671 (1958).
8. M. G. EVANS and J. DE HEER. Acta Cryst. **2**, 363 (1949).
9. H. C. LONGUET-HIGGINS. Acta Cryst. **3**, 79 (1950).
10. V. SCHOMAKER. Acta Cryst. **4**, 158 (1951).
11. D. T. CLARK. Tetrahedron Letters, 2889 (1967).
12. D. T. CLARK. J. Mol. Spectry. **26**, 181 (1968).
13. G. J. VISSER, G. J. HEERES, J. WOLTERS, and A. VOS. Acta Cryst. **B24**, 467 (1968).

Thermochemistry of the aqueous manganous ion[1]

L. M. GEDANSKY[2] AND L. G. HEPLER
Department of Chemistry, University of Lethbridge, Lethbridge, Alberta

Received September 23, 1968

Heats of solution of $MnSO_4$(c) have been measured and combined with heats of dilution to yield $\Delta H^0 = -15.3$ kcal/mole for the standard heat of solution. This value leads to $\Delta H_f^0 = -52.9$ kcal/mole for Mn^{2+}(aq). Calculations with data from the literature give $\Delta G_f^0 = -55.1$ kcal/mole for Mn^{2+}(aq). Combination of this value with our ΔH_f^0 gives $\bar{S}_2^0 = -16.2$ gibbs/mole for Mn^{2+}(aq). Our ΔH_f^0 value for Mn^{2+}(aq) is compared with other values derived from calculations based on data taken from the literature.

Canadian Journal of Chemistry, **47**, 699 (1969)

Introduction

Thermodynamic data already available now provide a means of calculating ΔG_f^0 for Mn^{2+}(aq) and thence E^0 for the Mn/Mn^{2+} oxidation potential. But the situation with respect to the ΔH_f^0 and $\bar{S}_2^0$ for Mn^{2+}(aq) is not nearly so satisfactory and should be resolved experimentally for several reasons. For example, once the ΔH_f^0 of Mn^{2+}(aq) is reliably known, heat of solution data permit calculation of ΔH_f^0 values for a number of compounds of manganese. It will also be useful to have complete and reliable thermodynamic data for Mn^{2+}(aq) because of its d^5 electronic configuration and its consequent use as a "reference" divalent ion with Ca^{2+}(aq) and Zn^{2+}(aq) in connection with consideration of ligand field stabilization effects.

Largely as a result of considerations outlined above, measurements of the heat of solution of $MnSO_4$(c) in water and the calculations reported here have been carried out.

Experimental

Three samples of $MnSO_4$(c) were prepared for calorimetric measurements. The first was prepared by recrystallization of Baker analyzed reagent, followed by drying at 400 °C for several days. The second was prepared in exactly the same manner from Fisher certified reagent. The third sample was prepared by further heating of a portion of the second sample at 450 °C overnight. All three samples appeared to be identical and led to consistent heats of solution.

The calorimetric apparatus used for these measurements was patterned after one previously described (1). The calorimeter consisted of a Dewar vessel suspended in a brass can submerged in a water bath which was maintained at constant temperature. Temperature in the calorimeter was determined with two 100 Ω thermistors wired in parallel and connected to a Leeds and Northrup G-2 Mueller bridge with a Liston–Becker model 14 breaker amplifier and zero-center meter. The thermistors and a manganin heater (300 Ω) were contained in a glass spiral filled with mineral oil. All of the calorimetric data (in terms of the defined calorie, 4.184 J) reported here were obtained with 950 ml of water in the Dewar at 25.00 ± 0.15 °C. Operation of the calorimeter was checked by heats of solution of THAM and KCl, with results indicating that uncertainties range from about 0.05 to 0.10 cal. The heat associated with breaking sample bulbs was 0.03 ± 0.02 cal, which was taken into account in calculating reported ΔH values.

Results and Calculations

The results of our determinations of the heat of solution of $MnSO_4$(c) in water are summarized in Table I.

Since the most dilute solution formed in our measurements was about 1×10^{-3} *M*, there is

[1]The experimental work reported here was carried out at the Carnegie Institute of Technology and the University of Louisville.
[2]Present address: Scott Paper Company, Philadelphia, Pennsylvania.

Can. J. Chem. Downloaded from www.nrcresearchpress.com by 210.87.254.5 on 09/05/12
For personal use only.

TABLE I

Heats of solution of $MnSO_4$(c)

g $MnSO_4$/950 ml H_2O	ΔH (kcal/mole)
0.22383	−15.04
0.23575	−14.94
0.48412	−14.72
0.50792	−14.76
0.55871	−14.77
0.58379	−14.72
1.04654	−14.65
1.27342	−14.62

an appreciable heat of dilution to zero concentration that must be considered in obtaining the desired ΔH^0 of solution. No relevant data for $MnSO_4$(aq) are available, but we do have data (2, 3) for aqueous sulfates of Cd^{2+}, Cu^{2+}, Ni^{2+}, and Zn^{2+}. We use these as a guide in graphical estimation of the heats of dilution, which are then combined with the data in Table I to give $\Delta H^0 = -15.3$ kcal/mole for the standard heat of solution of $MnSO_4$(c) to yield Mn^{2+}(aq) and SO_4^{2-}(aq). The total uncertainty (due to uncertainties in calorimetric measurements and in estimated heats of dilution) is not more than ± 0.2 kcal/mole.

Calorimetric determinations by Southard and Shomate (4) of the heats of solution of Mn(c) and $MnSO_4$(c) in aqueous sulfuric acid permitted them to calculate a ΔH_f^0 value for $MnSO_4$(c). We have used more recent data (5) for aqueous sulfuric acid in combination with their data to obtain $\Delta H_f^0 = -254.9$ kcal/mole for $MnSO_4$(c). Combination of this ΔH_f^0 with the most recent (5) ΔH_f^0 for SO_4^{2-}(aq) and our ΔH^0 of solution of $MnSO_4$(c) leads to $\Delta H_f^0 = -52.9$ kcal/mole for Mn^{2+}(aq). Total uncertainty in this value is about ± 0.3 kcal/mole. It should be noted that uncertainties in the data for sulfuric acid and sulfate ion largely cancel out in evaluation of the desired ΔH_f^0 for Mn^{2+}(aq).

We now turn to calculation of the ΔG_f^0 for Mn^{2+}(aq). Mah (6) has reviewed data on MnO_2(c) and recommended adoption of $\Delta H_f^0 = -124.4$ kcal/mole for this compound. Combination of this ΔH_f^0 with entropies from Kelley and King (7) gives $\Delta G_f^0 = -111.3$ kcal/mole for MnO_2(c). On the basis of earlier investigations and the careful experimental work of Covington, Cressey, Lever, and Thirsk (8), we adopt $E^0 = -1.239$ V for the standard oxidation potential to be associated with the Mn^{2+}/MnO_2(c) half reaction in acidic solution. Combination of this potential with $\Delta G^0 = -nFE^0$ and the ΔG_f^0 value for MnO_2(c) cited above gives us $\Delta G_f^0 = -55.1$ kcal/mole for Mn^{2+}(aq). This ΔG_f^0 leads to $E^0 = 1.20$ V for the standard oxidation potential for

[1] $$Mn(c) = Mn^{2+}(aq) + 2e^-$$

We combine the ΔG_f^0 and ΔH_f^0 values for Mn^{2+}(aq) with entropies of manganese and hydrogen to obtain its $\bar{S}_2^0 = -16.2$ gibbs/mole[3].

Now we turn to brief consideration of earlier investigations that have yielded data relevant to our measurements and calculations.

Two investigations (9, 10) are in good agreement for the heat of solution of $MnCl_2$(c). Combinations of these values with small estimated heats of dilution give $\Delta H^0 = -17.5$ kcal/mole for the standard heat of solution of $MnCl_2$(c). Other heat of solution measurements (11) have led to $\Delta H_f^0 = -115.2$ kcal/mole for $MnCl_2$(c), and high temperature data (12, 13) lead to $\Delta H_f^0 = -116.9$ kcal/mole. Combination of these values with the ΔH^0 of solution leads to $\Delta H_f^0 = -52.8$ and -54.4 kcal/mole for Mn^{2+}(aq). Walkley (14) has reported $\Delta H_f^0 = -53.2$ and -52.8 (recalculated by Zordan and Hepler (15)) kcal/mole for Mn^{2+}(aq). Our $\Delta H_f^0 = -52.9$ kcal/mole for Mn^{2+}(aq) is in excellent agreement with all but one of the values cited in this paragraph, and it is probable that the disagreement between our value and that derived from high temperature data (12, 13) is almost entirely due to uncertainties in the high temperature data.

There is one other path by which the ΔH^0 of Mn^{2+}(aq) can be calculated. Zordan and Hepler (15) have used E^0 for the MnO_2/MnO_4^-(aq) potential with the ΔG_f^0 of MnO_2(c) to obtain $\Delta G_f^0 = -107.6$ kcal/mole for MnO_4^-(aq). Then the ΔG^0 of solution of $KMnO_4$(c) calculated from its solubility and activity coefficient in saturated solution was combined with its ΔH^0 of solution to yield ΔS^0 of solution and thence $\bar{S}_2^0 = 46.5$ gibbs/mole for MnO_4^-(aq). Combination of this $\bar{S}_2^0$ with the ΔG_f^0 gave $\Delta H_f^0 = -129.9$ kcal/mole for MnO_4^-(aq). Still further combination of this

[3]Although we know of no action yet taken by the I.U.P.A.C. or other international organization, we follow W. F. Giauque (and others, more recently) in using *gibbs* to represent the combination cal/deg.

Can. J. Chem. Downloaded from www.nrcresearchpress.com by 210.87.254.5 on 09/05/12
For personal use only.

ΔH_f^0 with a calorimetrically determined heat of reduction of MnO_4^-(aq) to Mn^{2+}(aq) led to $\Delta H_f^0 = -53.4$ kcal/mole for Mn^{2+}(aq). Considering the many different data and steps in this calculation, this latter value agrees well with the value derived directly from our data.

Acknowledgments

We are grateful to Mr. T. A. Zordan for helpful discussions and to the United States National Science Foundation for support of much of this research.

1. W. F. O'Hara, C. H. Wu, and L. G. Hepler. J. Chem. Educ. **38**, 512 (1961).
2. E. Lange. *In* The structure of electrolyte solutions. *Edited by* W. J. Hamer. John Wiley and Sons, Inc., New York. 1959.
3. E. Lange and W. Miederer. Z. Electrochem. **60**, 34 (1956).
4. J. C. Southard and C. H. Shomate. J. Am. Chem. Soc. **64**, 1770 (1942).
5. D. D. Wagman, W. H. Evans, V. B. Parker, I. Halow, S. M. Bailey, and R. H. Schumm. Natl. Bur. Std. Tech. Note 270-3, U.S. Government Printing Office, Washington, D.C. 1968.
6. A. D. Mah. Bureau of Mines Report of Investigations No. 5600, U.S. Government Printing Office, Washington, D.C. 1960.
7. K. K. Kelley and E. G. King. Bureau of Mines Bulletin No. 592, U.S. Government Printing Office, Washington, D.C. 1961.
8. A. K. Covington, T. Cressey, B. G. Lever, and H. R. Thirsk. Trans. Faraday Soc. **58**, 1975 (1962).
9. P. Ehrlich, F. W. Koknat, and H. J. Seifert. Z. Anorg. Allgem. Chem. **341**, 281 (1965).
10. P. Paoletti and A. Vacca. Trans. Faraday Soc. **60**, 50 (1964).
11. M. F. Kohler and J. P. Coughlin. J. Phys. Chem. **63**, 605 (1959).
12. L. Rossemyr and T. Rosenqvist. Trans. AIME, **224**, 140 (1962).
13. H. Schafer. Z. Anorg. Allgem. Chem. **278**, 300 (1955).
14. A. Walkley. J. Electrochem. Soc. **93**, 316 (1948); **94**, 41 (1948).
15. T. A. Zordan and L. G. Hepler. Chem. Rev. **68**, 737 (1968).

Can. J. Chem. Downloaded from www.nrcresearchpress.com by 210.87.254.5 on 09/05/12
For personal use only.

Can. J. Chem. Downloaded from www.nrcresearchpress.com by 210.87.254.105 on 09/05/12
For personal use only.

COMMUNICATIONS

Hydrodynamically induced crystallization of isotactic polystyrene

A. G. WIKJORD AND R. ST.JOHN MANLEY
Physical Chemistry Division, Pulp and Paper Research Institute of Canada
and
Department of Chemistry, McGill University, Montreal, Quebec

Received November 8, 1968

This report provides a brief preliminary account of the solution crystallization of isotactic polystyrene under the influence of velocity gradients. During crystallizations from 1,3,5-trimethylbenzene and cyclohexanol solutions, the polymer appears in a number of morphological forms which are composed of microfibrillar units. In isotactic polystyrene produced by heterogeneous Ziegler–Natta catalysis, similar microfibrillar units are observed. It is suggested, therefore, that these two apparently different processes have a common underlying mechanism in the formation of the microfibrils. The possible mechanisms of fibril formation are discussed.

Canadian Journal of Chemistry, **47**, 703 (1969)

There have been relatively few reports of the crystallization of isotactic polystyrene from solution (1–3). It crystallizes from solution only with difficulty, perhaps because of substantial steric hindrance of the bulky phenyl groups (4).

The purpose of the present communication is to report preliminary observations on the crystallization of isotactic polystyrene from solutions subjected to shear forces. It is now recognized that fibrillar structures are generally produced when linear and stereoregular polymers are crystallized under conditions in which the chain molecules are oriented (5–7). Similar structures are often generated in heterogeneous Ziegler–Natta catalysis (8). In regard to both of these processes, polyethylene has received the most attention to date. The results presented here for polystyrene may help to clarify the mechanism of fibril formation in these systems.

The polystyrene used was a high molecular weight sample (Dow Chemical Company) which was extracted with methyl ethyl ketone prior to use to remove atactic and stereoblock components. The resulting polymer had a viscosity-average molecular weight of 2×10^6. In the crystallization experiments, two solvents, 1,3,5-trimethylbenzene, a good solvent, and cyclohexanol, a poor solvent, were employed. In a typical experiment, a 0.5% solution was prepared by refluxing the polymer in the appropriate solvent; the polymer was then crystallized in the turbulent flow created by a stirring rod rotating at a constant speed of 2000 r.p.m. Crystallizations were conducted isothermally: in 1,3,5-trimethylbenzene, appreciable yields were obtained at temperatures ranging from −25 to 125 °C; in cyclohexanol, it was only feasible to operate between the theta point (83.5 °C) and 140 °C. Above the latter temperature, recovery was negligible.

When the crystallized polystyrene was viewed in the swollen state under the light microscope, it appeared as distinct structural entities or "macrostructures". The morphology of the macrostructure varied with the conditions of growth. For example, in crystallizations from trimethylbenzene over a 150 °C temperature range (at 25 °C intervals), the following macrostructures were observed: spherical particles 15–40 μ in diameter (−25 °C), irregularly shaped globules 100–500 μ in size (0 °C), fibres with diameters up to 1 mm (25–125 °C), and ring-shaped structures (100–125 °C). The detailed morphology of these macrostructures will be discussed in a separate paper. However, it may be noted here that they are not the primary products of crystallization but apparently result from the hydrodynamically induced aggregation of finer fibrillar elements of structure. These microfibrillar units will be discussed in the following.

Regardless of the temperature of growth of the macrostructures, upon mechanical disruption, they broke up exclusively into microfibrillar

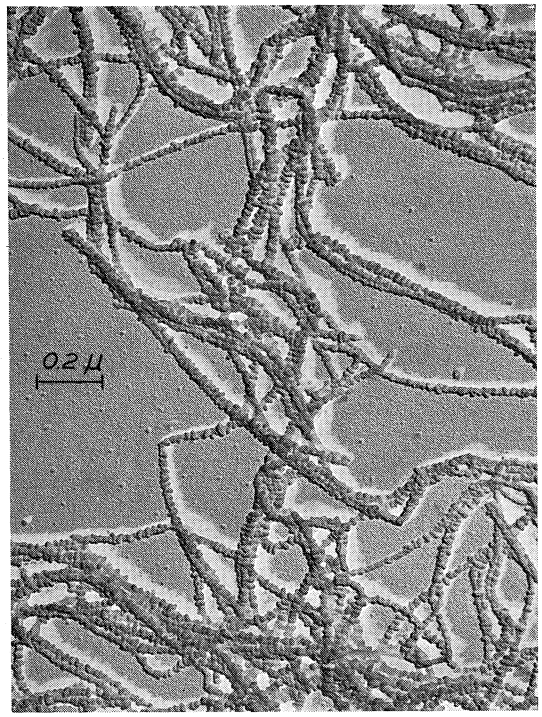

FIG. 1. Microfibrils crystallized under shear from a 0.5% solution of isotactic polystyrene in 1,3,5-trimethylbenzene at 100 °C. Electron micrograph, Pt shadowed.

units as depicted in Fig. 1. These constituent microfibrils were also found in the early stages of the crystallization when the macrostructures were not yet developed. The microfibrils showed little variation in diameter within a given preparation or from one preparation to another; they are characterized by overgrowths periodically spaced along their lengths, a feature common to many fibrillar polymer crystals (5–8).

It is noteworthy that there is a close parallel between the stirrer-crystallization of polystyrene and the heterogeneous Ziegler–Natta polymerization of this polymer (8). The polystyrene produced in both of these processes have similar morphological features as seen in the polarizing microscope and consist of elementary microfibrils which are essentially indistinguishable in the electron microscope. Both processes, apparently, are characterized by a remarkable facility of the crystallization process in comparison to crystallizations from solution under quiescent conditions. One is therefore led to believe that similar growth mechanisms operate in the two processes.

The crystallization of the polystyrene chains into microfibrils occurs virtually simultaneously to the application of the shear field in the stirred systems or to the initiation of the polymerization reaction in the Ziegler–Natta systems. This step is the most fundamental one in terms of the crystallization process and allows for a number of interesting interpretations. In the shear-induced crystallizations, hydrodynamic forces may play the role of decreasing the conformational entropy of the system by uncoiling molecules into more extended and ordered conformations, the 3_1 helix being the most favored energetically. Alignment of these helical chains in the streamlines of flow would promote nucleation. In the case of Ziegler–Natta catalysis, local convection currents created by the heat of reaction at the active sites may play a similar role. Alternatively, it is possible that the catalyst promotes nucleation by the helical placement of monomer units, one at a time, to the growing chain. In this way, the polystyrene chains would grow directly into the conformation which they assume in the solid state and not the random coil which requires a subsequent conformational change for crystallization. The possibility that the catalyst may play a role in preserving the symmetry of the helix was originally proposed about a decade ago by Szwarc (9). However, a recent report (10) suggests that polystyrene may exist under certain conditions in the helical conformation in solution in the absence of any perturbing forces (i.e. shear or catalyst). Under conditions where a large part of the molecule already exists in a helical conformation, the shear stresses or catalyst surface would have the more limited function of bringing the helical chains into close proximity so that they may crystallize.

This work appears to support the proposition derived earlier on the basis of studies on polyethylene (7) that hydrodynamically-induced crystallizations and fluid-bed Ziegler–Natta polymerizations have similar underlying crystallization mechanisms.

1. V. A. KARGIN, N. F. BAKEEV, LI LI-SHEN, and T. S. OCHAPOVSKAYA. Vysokomolekul. Soedin. **2**, 1280 (1960).
2. P. BLAIS and R. ST.JOHN MANLEY. J. Polymer Sci. **A4**, 1022 (1966).
3. H. D. KEITH, F. J. PADDEN, and R. G. VADIMSKY. Bull. Am. Phys. Soc. Ser. 11, Vol. 12, No. 3, March 1967.

Can. J. Chem. Downloaded from www.nrcresearchpress.com by 210.87.254.105 on 09/05/12
For personal use only.

4. PAUL J. FLORY. Principles of polymer chemistry. Cornell Univ. Press, Ithaca, N.Y. 1953. p. 246–249.
5. A. J. PENNINGS and A. M. KIEL. Kolloid-Z. **205**, 160 (1965).
6. A. KELLER and M. J. MACHIN. J. Macromol. Sci. **B1**, 41 (1967).
7. A. G. WIKJORD and R. ST.JOHN MANLEY. J. Macromol. Sci. **B2**, 501 (1968).
8. P. BLAIS and R. ST.JOHN MANLEY. J. Polymer Sci. **A6**, 291 (1968).
9. M. SZWARC. Chem. Ind. London, 1589 (1958).
10. CLAUDE REISS. J. Chim. Phys. 1319 (1966).

The crystal structure of tetraphenylcyclobutadiene molybdenum dicarbonyl bromide

M. MATHEW AND GUS J. PALENIK
Department of Chemistry, University of Waterloo, Waterloo, Ontario

Received November 25, 1968

The crystal structure of tetraphenylcyclobutadiene molybdenum dicarbonyl bromide has been determined by X-ray diffraction. Previously, the compound has been formulated incorrectly as tetraphenylcyclobutadiene molybdenum tricarbonyl bromide.

Canadian Journal of Chemistry, **47**, 705 (1969)

Can. J. Chem. Downloaded from www.nrcresearchpress.com by 210.87.254.105 on 09/05/12
For personal use only.

Tetraphenylcyclobutadiene molybdenum dicarbonyl bromide, the first proven example of a cyclobutadiene ring bonded to a second or third row transition element, is a novel compound containing bromine bridges, the cyclobutadiene moiety, and a strong metal–metal interaction. Not only was the compound incorrectly formulated by Maitlis and Games (1) as a tricarbonyl, **1**, but also the presence of the cyclobutadiene rings was questioned by Cotton and Wilkinson (2) in a popular textbook. Recently, Baird (3) has cited the incorrectly formulated compound as an example of a molybdenum–molybdenum bond. To prevent further errors regarding this compound, we wish to report that our crystal structure study has shown that the compound is correctly formulated as the dimer, **2**, which contains only two carbonyl groups per molybdenum atom.

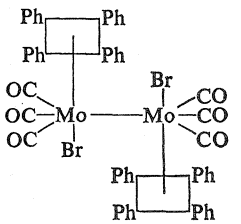

1

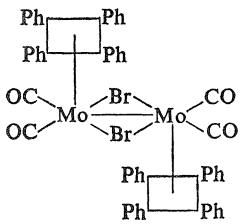

2

Crystal data: triclinic with $a = 11.306 \pm 0.004$, $b = 13.681 \pm 0.004$, $c = 17.561 \pm 0.010$ Å, $\alpha = 105.58 \pm 0.01°$, $\beta = 91.14 \pm 0.02°$, $\gamma = 108.50 \pm 0.05°$, $d_m = 1.59$ g/cm^3, $d_c = 1.585$ g/cm^3, $Z = 2$ dimers. The space group $P\bar{1}$ was indicated by the intensity statistics and the subsequent analysis confirms this choice.

A small, equidimensional crystal (0.10 mm) was used for intensity measurements. Intensity data were collected on a General Electric XRD-6 automated by Datex Corporation, using the stationary crystal – stationary counter method. Of the 8851 reflections within the range of $2\theta \leq 135.0°$ (Cu K_α), 8089 were observed above the threshold count. No absorption corrections were applied.

A three dimensional Patterson synthesis was computed and the positions of 2 molybdenum and 2 bromine atoms were located. A Fourier synthesis, phased with the 2 molybdenum and 2 bromine atoms, revealed the positions of all the light atoms. A difference Fourier synthesis using all 68 atoms for phasing did not indicate the presence of any additional carbonyl groups. The refinement was completed by the method of least squares using the full matrix. After four cycles of least squares refinement with individual isotropic thermal parameters, the *R*-index was 0.091.

The compound crystallizes as a dimer, **2**. The 2 molybdenum atoms are linked through bromine bridges (average Mo—Br distance 2.638 ± 0.001 Å). The Mo—Mo distance of 2.954 ± 0.001 Å is shorter than the distance of 3.222 Å found in $[C_6H_5Mo(CO)_3]_2$ (4). The short Mo—Mo distance together with the reported diamagnetism suggests the presence of a metal–metal bond. Each molybdenum is also

4. PAUL J. FLORY. Principles of polymer chemistry. Cornell Univ. Press, Ithaca, N.Y. 1953. p. 246–249.
5. A. J. PENNINGS and A. M. KIEL. Kolloid-Z. **205**, 160 (1965).
6. A. KELLER and M. J. MACHIN. J. Macromol. Sci. **B1**, 41 (1967).
7. A. G. WIKJORD and R. ST.JOHN MANLEY. J. Macromol. Sci. **B2**, 501 (1968).
8. P. BLAIS and R. ST.JOHN MANLEY. J. Polymer Sci. **A6**, 291 (1968).
9. M. SZWARC. Chem. Ind. London, 1589 (1958).
10. CLAUDE REISS. J. Chim. Phys. 1319 (1966).

The crystal structure of tetraphenylcyclobutadiene molybdenum dicarbonyl bromide

M. MATHEW AND GUS J. PALENIK
Department of Chemistry, University of Waterloo, Waterloo, Ontario

Received November 25, 1968

The crystal structure of tetraphenylcyclobutadiene molybdenum dicarbonyl bromide has been determined by X-ray diffraction. Previously, the compound has been formulated incorrectly as tetraphenylcyclobutadiene molybdenum tricarbonyl bromide.

Canadian Journal of Chemistry, **47**, 705 (1969)

Can. J. Chem. Downloaded from www.nrcresearchpress.com by 210.87.254.42 on 09/05/12
For personal use only.

Tetraphenylcyclobutadiene molybdenum dicarbonyl bromide, the first proven example of a cyclobutadiene ring bonded to a second or third row transition element, is a novel compound containing bromine bridges, the cyclobutadiene moiety, and a strong metal–metal interaction. Not only was the compound incorrectly formulated by Maitlis and Games (1) as a tricarbonyl, **1**, but also the presence of the cyclobutadiene rings was questioned by Cotton and Wilkinson (2) in a popular textbook. Recently, Baird (3) has cited the incorrectly formulated compound as an example of a molybdenum–molybdenum bond. To prevent further errors regarding this compound, we wish to report that our crystal structure study has shown that the compound is correctly formulated as the dimer, **2**, which contains only two carbonyl groups per molybdenum atom.

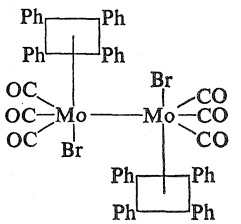

1

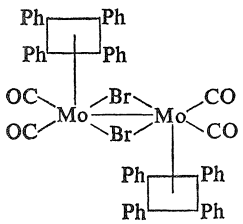

2

Crystal data: triclinic with $a = 11.306 \pm 0.004$, $b = 13.681 \pm 0.004$, $c = 17.561 \pm 0.010$ Å, $\alpha = 105.58 \pm 0.01°$, $\beta = 91.14 \pm 0.02°$, $\gamma = 108.50 \pm 0.05°$, $d_m = 1.59$ g/cm^3, $d_c = 1.585$ g/cm^3, $Z = 2$ dimers. The space group $P\bar{1}$ was indicated by the intensity statistics and the subsequent analysis confirms this choice.

A small, equidimensional crystal (0.10 mm) was used for intensity measurements. Intensity data were collected on a General Electric XRD-6 automated by Datex Corporation, using the stationary crystal – stationary counter method. Of the 8851 reflections within the range of $2\theta \leq 135.0°$ (Cu K_α), 8089 were observed above the threshold count. No absorption corrections were applied.

A three dimensional Patterson synthesis was computed and the positions of 2 molybdenum and 2 bromine atoms were located. A Fourier synthesis, phased with the 2 molybdenum and 2 bromine atoms, revealed the positions of all the light atoms. A difference Fourier synthesis using all 68 atoms for phasing did not indicate the presence of any additional carbonyl groups. The refinement was completed by the method of least squares using the full matrix. After four cycles of least squares refinement with individual isotropic thermal parameters, the *R*-index was 0.091.

The compound crystallizes as a dimer, **2**. The 2 molybdenum atoms are linked through bromine bridges (average Mo—Br distance 2.638 ± 0.001 Å). The Mo—Mo distance of 2.954 ± 0.001 Å is shorter than the distance of 3.222 Å found in $[C_6H_5Mo(CO)_3]_2$ (4). The short Mo—Mo distance together with the reported diamagnetism suggests the presence of a metal–metal bond. Each molybdenum is also

bonded to 2 carbonyl groups and the tetraphenylcyclobutadiene ring, thus attaining the inert gas configuration.

The average C—C distance in the cyclobutadiene is 1.461 ± 0.013 Å with an average C—C—C angle of 90.0°, comparing favorably with the two other cyclobutadiene structures reported to date (5, 6). The molybdenum atoms are equidistant from the carbon atoms of the cyclobutadiene rings, the average Mo—C (ring) distance being 2.252 ± 0.009 Å. The distances between the center of the cyclobutadiene rings and the molybdenum atoms are 1.995 and 2.008 Å. The cyclobutadiene rings are planar within the present experimental error. The 4 phenyl groups on each cyclobutadiene ring are tilted out of the plane of the ring away from the molybdenum atom.

Acknowledgments

We wish to thank the National Research Council of Canada for the support of this research. We are also grateful to Dr. A. Efraty for the compound and to the University Computing Centre for the exclusive use of the IBM-360 Model 75 for the refinement of the structure.

1. P. M. Maitlis and M. L. Games. Chem. Ind. London, 1624 (1963).
2. F. A. Cotton and G. Wilkinson. Advanced inorganic chemistry. 2nd ed. Interscience Publishers, Inc., New York. 1966. p. 769.
3. M. C. Baird. *In* Progress in inorganic chemistry. Vol. 9. *Edited by* F. A. Cotton. Interscience Publishers, Inc., New York. 1968. p. 1.
4. F. C. Wilson and D. P. Shoemaker. J. Chem. Phys. **27**, 809 (1957).
5. J. D. Dunitz, H. C. Mez, O. S. Mills, and H. M. M. Shearer. Helv. Chim. Acta, **45**, 647 (1962).
6. R. P. Dodge and V. Schomaker. Acta Cryst. **18**, 614 (1965).

Can. J. Chem. Downloaded from www.nrcresearchpress.com by 210.87.254.42 on 09/05/12
For personal use only.

Pyrrolidone hydrotribromide: a brominating agent with selectivity for ketones

D. V. C. Awang and Saul Wolfe
Department of Chemistry, Queen's University, Kingston, Ontario

Received January 13, 1969

The relative reactivities of a ketone, an olefin, and an enol acetate towards bromination in tetrahydrofuran by "pyrrolidone–bromine complex", (pyrrolidone)$_3$·HBr$_3$ (PHT), are ketone ≫ olefin ≫ enol acetate. The conversion of benzalacetone to $C_6H_5CH{=}CHCOCH_2Br$ is given as an example. The selectivity of PHT is enhanced by dilution and is diminished upon addition of pyrrolidone to the reaction mixtures. The selectivity of phenyltrimethylammonium tribromide (PTAT) is not as great as that of PHT and is subject to acid catalysis.

At a sufficiently low concentration in a nonpolar solvent, the enol of cyclohexanone reacts at least 1 000 000 times faster with molecular bromine than does cyclohexene. This observation suggests that the selectivity of perbromides may be due to their ability to furnish a low equilibrium concentration of bromine when dissolved in solvents of low polarity.

Canadian Journal of Chemistry, **47**, 706 (1969)

Selective bromination of a ketone in the presence of a double bond has been achieved by the action of phenyltrimethylammonium tribromide (PTAT) (1, 2) upon dihydrocarvone (3) and by the action of cupric bromide upon several unsaturated steroidal ketones (4). The purpose of this communication is to demonstrate that pyrrolidone hydrotribromide (PHT), a new reagent (5), possesses selectivity for ketones superior to that of PTAT, and that molecular bromine, in low concentration and in a solvent of low dielectric constant, also displays selectivity for ketones.

PHT is a stable red crystalline solid, m.p. 89–91°, whose analysis corresponds to a molecular formula $(C_4H_7NO)_3{\cdot}HBr_3$. The compound is soluble in tetrahydrofuran and its reaction with cyclohexene in this solvent proceeds as follows

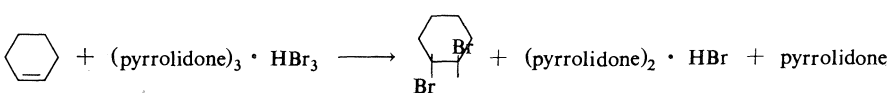

1

bonded to 2 carbonyl groups and the tetraphenylcyclobutadiene ring, thus attaining the inert gas configuration.

The average C—C distance in the cyclobutadiene is 1.461 ± 0.013 Å with an average C—C—C angle of 90.0°, comparing favorably with the two other cyclobutadiene structures reported to date (5, 6). The molybdenum atoms are equidistant from the carbon atoms of the cyclobutadiene rings, the average Mo—C (ring) distance being 2.252 ± 0.009 Å. The distances between the center of the cyclobutadiene rings and the molybdenum atoms are 1.995 and 2.008 Å. The cyclobutadiene rings are planar within the present experimental error. The 4 phenyl groups on each cyclobutadiene ring are tilted out of the plane of the ring away from the molybdenum atom.

Acknowledgments

We wish to thank the National Research Council of Canada for the support of this research. We are also grateful to Dr. A. Efraty for the compound and to the University Computing Centre for the exclusive use of the IBM-360 Model 75 for the refinement of the structure.

1. P. M. Maitlis and M. L. Games. Chem. Ind. London, 1624 (1963).
2. F. A. Cotton and G. Wilkinson. Advanced inorganic chemistry. 2nd ed. Interscience Publishers, Inc., New York. 1966. p. 769.
3. M. C. Baird. *In* Progress in inorganic chemistry. Vol. 9. *Edited by* F. A. Cotton. Interscience Publishers, Inc., New York. 1968. p. 1.
4. F. C. Wilson and D. P. Shoemaker. J. Chem. Phys. **27**, 809 (1957).
5. J. D. Dunitz, H. C. Mez, O. S. Mills, and H. M. M. Shearer. Helv. Chim. Acta, **45**, 647 (1962).
6. R. P. Dodge and V. Schomaker. Acta Cryst. **18**, 614 (1965).

Can. J. Chem. Downloaded from www.nrcresearchpress.com by 210.87.254.5 on 09/05/12
For personal use only.

Pyrrolidone hydrotribromide: a brominating agent with selectivity for ketones

D. V. C. Awang and Saul Wolfe
Department of Chemistry, Queen's University, Kingston, Ontario

Received January 13, 1969

The relative reactivities of a ketone, an olefin, and an enol acetate towards bromination in tetrahydrofuran by "pyrrolidone–bromine complex", (pyrrolidone)$_3$·HBr$_3$ (PHT), are ketone ≫ olefin ≫ enol acetate. The conversion of benzalacetone to $C_6H_5CH{=}CHCOCH_2Br$ is given as an example. The selectivity of PHT is enhanced by dilution and is diminished upon addition of pyrrolidone to the reaction mixtures. The selectivity of phenyltrimethylammonium tribromide (PTAT) is not as great as that of PHT and is subject to acid catalysis.

At a sufficiently low concentration in a nonpolar solvent, the enol of cyclohexanone reacts at least 1 000 000 times faster with molecular bromine than does cyclohexene. This observation suggests that the selectivity of perbromides may be due to their ability to furnish a low equilibrium concentration of bromine when dissolved in solvents of low polarity.

Canadian Journal of Chemistry, **47**, 706 (1969)

Selective bromination of a ketone in the presence of a double bond has been achieved by the action of phenyltrimethylammonium tribromide (PTAT) (1, 2) upon dihydrocarvone (3) and by the action of cupric bromide upon several unsaturated steroidal ketones (4). The purpose of this communication is to demonstrate that pyrrolidone hydrotribromide (PHT), a new reagent (5), possesses selectivity for ketones superior to that of PTAT, and that molecular bromine, in low concentration and in a solvent of low dielectric constant, also displays selectivity for ketones.

PHT is a stable red crystalline solid, m.p. 89–91°, whose analysis corresponds to a molecular formula $(C_4H_7NO)_3{\cdot}HBr_3$. The compound is soluble in tetrahydrofuran and its reaction with cyclohexene in this solvent proceeds as follows

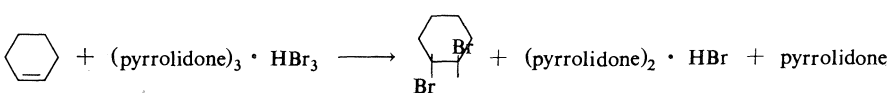

1

TABLE I

Selectivities of PHT and PTAT in competitive bromination experiments in tetrahydrofuran at 25°[a]

Entry	Substrate mixture[b]	Brominating agent (molarity)	Product ratio[c]
1	A+B	PTAT (0.5)	1.38[f]
2	A+B	PTAT (0.1)	6.14[f]
3	A+B	PTAT (0.05)	>100.[f]
4	A+B	PTAT (0.1)[d]	2.57[f]
5	A+B	PHT (0.5)	5.67[f]
6	A+B	PHT (0.1)[d]	>199.[f]
7	A+C	PTAT (0.1)[d]	0.053[f]
8	A+C	PTAT (0.1)	0.22[f]
9	A+C	PTAT (0.1)[e]	>100.[f]
10	A+C	PHT (0.1)[d]	3.0[f]
11	A+C	PHT (0.1)	>100.[f]
12	A+C	PHT (0.05)[d]	>100.[f]
13	A+D	PHT (0.1)[d]	>100.[g]
14	B+E	PHT (0.1)[d]	>100.[h]
15	D+F	PHT (0.1)[d]	>100.[i]

[a]A solution of the brominating agent of the stated molarity (20 ml) was added dropwise in the dark to a solution containing equimolar quantities of the two substrates in tetrahydrofuran (20 ml).
[b]A, cyclohexene; B, cyclohexanone; C, 3-pentanone; D, cyclohexenyl acetate; E, 4-methylcyclohexenyl acetate; F, 4-methylcyclohexanone.
[c]Determined by quantitative gas chromatography.
[d]One mole-equivalent of pyrrolidone was added to the substrate mixture.
[e]One drop of concentrated H_2SO_4 was added to the substrate mixture.
[f]Bromoketone/dibromoolefin.
[g]The product is dibromoolefin.
[h]The product is 2-bromocyclohexanone.
[i]The product is 2-bromo-4-methylcyclohexanone.

the hemihydrobromide **1** being precipitated from the solution as colourless needles as the reaction proceeds. The precipitation of **1** provides a convenient visual assay of the extent of reaction and also facilitates isolation of the product.

Entries 1–12 of Table I summarize the results of competition experiments in which PTAT or PHT were allowed to react, in tetrahydrofuran, with a mixture of an olefin and a ketone. Entries 13–15 show the results of competition experiments with PHT in which an enol acetate was included. Several conclusions follow immediately: (*i*) PHT exercises greater "ketoselectivity" than does PTAT (cf. entries 1 and 5; 4 and 6 for cyclohexanone–cyclohexene competitions, and entries 8 and 11; 7 and 10 for 3-pentanone–cyclohexene competitions); (*ii*) the selectivity of both reagents is enhanced upon dilution of the perbromide solutions (cf. entries 1, 2, and 3; 10 and 12); (*iii*) a catalytic amount of acid dramatically enhances the selectivity of PTAT (entries 8 and 9); (*iv*) under the conditions of these experiments the relative susceptibilities towards bromination are ketone ≫ olefin ≫ enol acetate. The synthetic implications of such a reactivity sequence are clear. Thus, benzalacetone was smoothly converted with PHT in tetrahydrofuran to bromomethylstyryl ketone, **2**, m.p. 46–47° (Found: C, 52.92; H, 4.25.). Previous attempts to achieve selective bromination of benzalacetone have led to the dibromide (6).

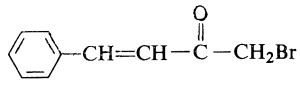

2

In both PTAT and PHT brominations the hydrogen bromide or acetyl bromide liberated as a result of bromoketone formation can be trapped effectively as the insoluble compound **1** or as the insoluble acetylium salt of pyrrolidone by prior addition to the reaction mixture of an equimolar amount of pyrrolidone. Although this causes some loss of selectivity (entries 2 and 4; 7 and 8; 10 and 11), the selectivity can be restored by dilution of the brominating agent (entries 10 and 12). It is then possible to brominate a ketone in the presence of both a double bond and an acid

Can. J. Chem. Downloaded from www.nrcresearchpress.com by 210.87.254.5 on 09/05/12
For personal use only.

TABLE II

Effects of solvent and concentration upon the relative reactivities towards bromine of cyclohexene and cyclohexanone at 25°[a]

Run	Solvent	Substrate solution Moles	Substrate solution Volume (ml)	Bromine solution Moles	Bromine solution Volume (ml)	Maximum effective bromine concentration (M)[b]	Ratio of bromoketone to dibromoolefin[c]
1	CCl_4	0.01	20	0.01	20	1×10^{-3}	0.43
2	CCl_4	0.01	100	0.01	100	5×10^{-5}	0.54
3	CCl_4	0.01	1000	0.01	1000	5×10^{-7}	3.17
4	CCl_4	0.005	500	0.0025[d]	500	5×10^{-7}	13.3
5	CCl_4	0.0025	500	0.00125	500	2.5×10^{-7}	>199
6	C_2H_5OH	0.01	20	0.01	20	1×10^{-3}	0.14
7	CH_3COOH	0.01	20	0.01	20	1×10^{-3}	0.16
8	tetrahydrofuran[e]	0.01	20	0.01	20	1×10^{-3}	1.0

[a]The bromine solution was added dropwise in the dark to a rapidly stirred solution of olefin and ketone.
[b]Calculated on the basis that each drop was efficiently dispersed and reacted before the addition of the next drop.
[c]Determined by quantitative gas chromatography.
[d]An induction period of 30 min was observed after the addition of the first few drops of the bromine solution. The color was suddenly discharged and the reaction then proceeded as in [a].
[e]About 60% of the HBr liberated in the substitution reaction reacted with the solvent to form 4-bromo-1-butanol. For this reason tetrahydrofuran was not used for the detailed concentration studies although this would have permitted a closer approximation of the conditions usually employed for perbromide brominations.

sensitive group. Thus, the production of 4-bromo-1-butanol or 1-acetoxy-4-bromobutane, usually formed by cleavage of the solvent by the liberated HBr or AcBr, is completely suppressed under these conditions as is the hydrolysis of an enol acetate if bromination of a ketone function is occurring elsewhere in the molecule. However, enol ethers react readily with a saturated tetrahydrofuran solution of **1** to regenerate the parent ketones.

The difference in selectivity between PHT and PTAT can be understood in terms of acid catalysis of enolization since the hemipyrrolidonium ion is an acid and the tetrasubstituted ammonium ion is not. In the latter case, catalysis of enolization has to be achieved by the HBr produced when the small amount of enol originally present undergoes bromination. If this is trapped by base, enolization is effectively stalled; conversely, as with free bromine reactions (7), a small amount of acid catalyzes the reaction.

We suggest that the phenomenon which we have termed ketoselectivity may result from the ability of these various reagents to furnish a low equilibrium concentration of molecular bromine when dissolved in solvents of low dielectric constant. For example, with PTAT equilibria [1]–[4] can be written (8). The forward reactions of [1] and [3], and, therefore, [4], can be expected to be discouraged in media of low polarity with the result that [2], which produces molecular bromine, becomes the most significant relationship.

$$[R_4N^+Br_3^-] \rightleftarrows R_4N^+ + Br_3^- \quad [1]$$

$$[R_4N^+Br_3^-] \rightleftarrows [R_4N^+Br^-] + Br_2 \quad [2]$$

$$[R_4N^+Br^-] \rightleftarrows R_4N^+ + Br^- \quad [3]$$

$$Br_2 + Br^- \rightleftarrows Br_3^- \quad [4]$$

If this reasoning is correct it should be possible to observe ketoselectivity even with molecular bromine by employing a sufficiently dilute solution in a solvent of low polarity. The cyclohexene vs. cyclohexanone competition experiments which are summarized in Table II demonstrate that in carbon tetrachloride addition to the double bond can be completely suppressed by lowering the effective concentration of molecular bromine. Taking into account the fact that the ketone contains only 10^{-2}–10^{-6}% of enol (9) it appears that under these conditions the enol is at least 1 000 000 times as reactive as the olefin.

It is hoped that further studies will provide an acceptable explanation of this rate difference. An intriguing speculation is that under the conditions where ketoselectivity is observed the enol reacts via a cyclic six-membered transition state (10, 11).

Acknowledgment

Support of this work by the National Research Council of Canada is gratefully acknowledged.

Can. J. Chem. Downloaded from www.nrcresearchpress.com by 210.87.254.5 on 09/05/12
For personal use only.

1. A. MARQUET and J. JACQUES. Tetrahedron Letters, 24 (1959).
2. A. MARQUET, M. DVOLAITSKY, H. B. KAGAN, L. MAMLOK, C. OUANNES, and J. JACQUES. Bull. Soc. Chim. France, 1822 (1961).
3. A. MARQUET and J. JACQUES. Bull. Soc. Chim. France, 90 (1962).
4. E. R. GLAZIER. J. Org. Chem. **27**, 4397 (1962).
5. W. E. DANIELS, M. E. CHIDDIX, and S. A. GLICKMAN. J. Org. Chem. **28**, 573 (1963).
6. P. L. SOUTHWICK, L. A. PURSGLOVE, and P. NUMEROF. J. Am. Chem. Soc. **72**, 1600 (1950).
7. P. B. D. DE LA MARE and R. BOLTON. Electrophilic addition to unsaturated systems. Elsevier Publ. Co., Inc., Amsterdam. 1966. Chaps. 6 and 7.
8. A. MARQUET, J. JACQUES, and B. TCHOUBAR. Bull. Soc. Chim. France, 511 (1965).
9. N. L. ALLINGER, L. W. CHOW, and R. A. FORD. J. Org. Chem. **32**, 1994 (1967).
10. M. S. NEWMAN. J. Am. Chem. Soc. **73**, 4993 (1951).
11. W. A. WATERS. Mechanisms of oxidation of organic compounds. Methuen and Co. Ltd., London. 1964. p. 92.

Can. J. Chem. Downloaded from www.nrcresearchpress.com by 210.87.254.5 on 09/05/12
For personal use only.

Luminescence in the thermal decomposition of 3,3,4-trimethyl-1,2-dioxetane

KARL R. KOPECKY AND CEDRIC MUMFORD
Department of Chemistry, University of Alberta, Edmonton, Alberta

Received November 25, 1968

Luminescence is observed during the thermal decomposition of 3,3,4-trimethyl-1,2-dioxetane to acetone and acetaldehyde. The wavelength maximum of the luminescence is at 430–440 mμ when the decomposition is carried out at 60° in benzene solution. This shows that the decomposition of the dioxetane is a concerted electrocyclic reaction which forms a carbonyl compound in the excited singlet state, and confirms the suggestion that bioluminescence is due to the decomposition of 1,2-dioxetanes.

Canadian Journal of Chemistry, **47**, 709 (1969)

Acetone and acetaldehyde are produced in quantitative yield (1) from the thermal decomposition of 3,3,4-trimethyl-1,2-dioxetane, **1**, according to eq. [1]. In carbon tetrachloride the reaction has an activation energy of 25 kcal/mole.

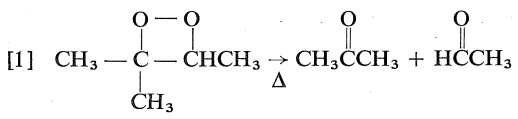

[1] $CH_3-\underset{\displaystyle CH_3}{\overset{\displaystyle O-O}{\underset{|}{C}}}-CHCH_3 \xrightarrow[\Delta]{} CH_3\overset{\displaystyle O}{\overset{\|}{C}}CH_3 + H\overset{\displaystyle O}{\overset{\|}{C}}CH_3$

1

This is a surprisingly large value in view of the weak oxygen–oxygen bond, the probable strain in the molecule, and the stability of the products. It has been suggested (2) on the basis of orbital symmetry rules (3) that the concerted decomposition of a 1,2-dioxetane must produce one of the carbonyl products in an excited electronic state. This would also account for the relative stability of **1**. We wish to report the direct confirmation of this prediction.

A faint bluish luminescence is observed when a benzene solution of **1** is heated above 70° in the dark. The luminescence wavelength maximum is at 430–440 mμ when **1** is decomposed in benzene at 60°, see Fig. 1. The position of the maximum appears to be dependent upon the concentration

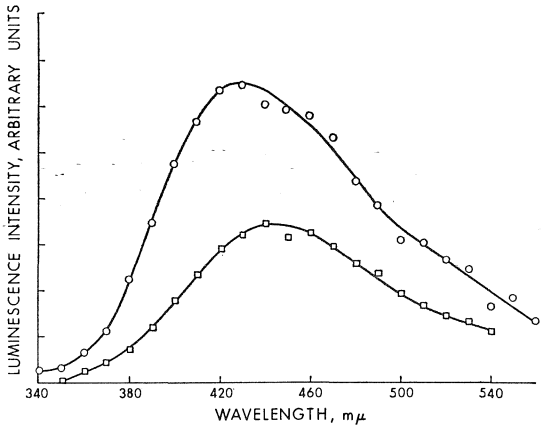

FIG. 1. Spectrum of luminescence from solutions of **1** in benzene at 60°. Initial concentrations: □, 0.21 *M*; ○, 0.021 *M*. The two curves are not on the same scale. The spectra were scanned manually using a Bausch and Lomb 500 mm monochrometer in conjunction with an RCA 1P28 photomultiplier tube. The emission intensity is corrected for photomultiplier response.

of the products, shifting to somewhat longer wavelength with increasing initial concentration of **1** and with time during a run. Comparison of the position of this maximum with the positions of the fluorescence wavelength maxima of acetone (4, 5) and acetaldehyde (6) makes it apparent that

1. A. MARQUET and J. JACQUES. Tetrahedron Letters, 24 (1959).
2. A. MARQUET, M. DVOLAITSKY, H. B. KAGAN, L. MAMLOK, C. OUANNES, and J. JACQUES. Bull. Soc. Chim. France, 1822 (1961).
3. A. MARQUET and J. JACQUES. Bull. Soc. Chim. France, 90 (1962).
4. E. R. GLAZIER. J. Org. Chem. **27**, 4397 (1962).
5. W. E. DANIELS, M. E. CHIDDIX, and S. A. GLICKMAN. J. Org. Chem. **28**, 573 (1963).
6. P. L. SOUTHWICK, L. A. PURSGLOVE, and P. NUMEROF. J. Am. Chem. Soc. **72**, 1600 (1950).
7. P. B. D. DE LA MARE and R. BOLTON. Electrophilic addition to unsaturated systems. Elsevier Publ. Co., Inc., Amsterdam. 1966. Chaps. 6 and 7.
8. A. MARQUET, J. JACQUES, and B. TCHOUBAR. Bull. Soc. Chim. France, 511 (1965).
9. N. L. ALLINGER, L. W. CHOW, and R. A. FORD. J. Org. Chem. **32**, 1994 (1967).
10. M. S. NEWMAN. J. Am. Chem. Soc. **73**, 4993 (1951).
11. W. A. WATERS. Mechanisms of oxidation of organic compounds. Methuen and Co. Ltd., London. 1964. p. 92.

Luminescence in the thermal decomposition of 3,3,4-trimethyl-1,2-dioxetane

KARL R. KOPECKY AND CEDRIC MUMFORD
Department of Chemistry, University of Alberta, Edmonton, Alberta

Received November 25, 1968

Luminescence is observed during the thermal decomposition of 3,3,4-trimethyl-1,2-dioxetane to acetone and acetaldehyde. The wavelength maximum of the luminescence is at 430–440 mμ when the decomposition is carried out at 60° in benzene solution. This shows that the decomposition of the dioxetane is a concerted electrocyclic reaction which forms a carbonyl compound in the excited singlet state, and confirms the suggestion that bioluminescence is due to the decomposition of 1,2-dioxetanes.

Canadian Journal of Chemistry, **47**, 709 (1969)

Acetone and acetaldehyde are produced in quantitative yield (1) from the thermal decomposition of 3,3,4-trimethyl-1,2-dioxetane, **1**, according to eq. [1]. In carbon tetrachloride the reaction has an activation energy of 25 kcal/mole.

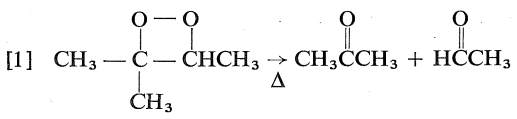

[1] $CH_3-\underset{\displaystyle CH_3}{\overset{\displaystyle O-O}{\underset{|}{\overset{|}{C}}}}-CHCH_3 \xrightarrow[\Delta]{} CH_3\overset{\displaystyle O}{\overset{\|}{C}}CH_3 + H\overset{\displaystyle O}{\overset{\|}{C}}CH_3$

1

This is a surprisingly large value in view of the weak oxygen–oxygen bond, the probable strain in the molecule, and the stability of the products. It has been suggested (2) on the basis of orbital symmetry rules (3) that the concerted decomposition of a 1,2-dioxetane must produce one of the carbonyl products in an excited electronic state. This would also account for the relative stability of **1**. We wish to report the direct confirmation of this prediction.

A faint bluish luminescence is observed when a benzene solution of **1** is heated above 70° in the dark. The luminescence wavelength maximum is at 430–440 mμ when **1** is decomposed in benzene at 60°, see Fig. 1. The position of the maximum appears to be dependent upon the concentration

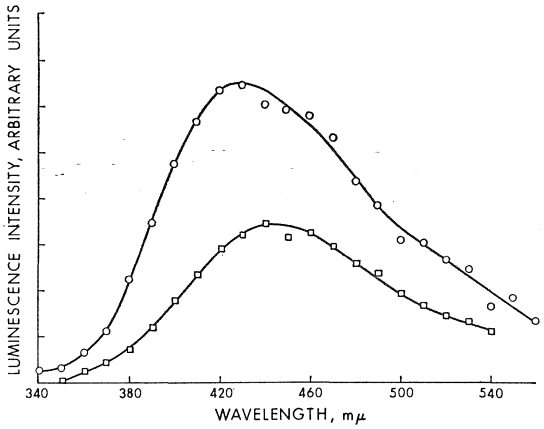

FIG. 1. Spectrum of luminescence from solutions of **1** in benzene at 60°. Initial concentrations: □, 0.21 *M*; ○, 0.021 *M*. The two curves are not on the same scale. The spectra were scanned manually using a Bausch and Lomb 500 mm monochrometer in conjunction with an RCA 1P28 photomultiplier tube. The emission intensity is corrected for photomultiplier response.

of the products, shifting to somewhat longer wavelength with increasing initial concentration of **1** and with time during a run. Comparison of the position of this maximum with the positions of the fluorescence wavelength maxima of acetone (4, 5) and acetaldehyde (6) makes it apparent that

Can. J. Chem. Downloaded from www.nrcresearchpress.com by 210.87.254.105 on 09/05/12
For personal use only.

one of these compounds is produced in the excited singlet state upon decomposition of **1**. Two types of fluorescence (4) are observed from acetone: monomer emission with wavelength maximum at 345 mμ (4) at low concentrations and eximer emission with wavelength maximum reported at 405 (4) and 415 mμ (5) at higher concentrations (0.02 and 0.2 *M*, respectively) in hexane at 25°. The fluorescence wavelength maximum of acetaldehyde is at about 420 mμ (6), and it is likely that the position of the maximum in solution is also concentration dependent (4). Short wavelength luminescence corresponding to emission from a "monomeric" excited carbonyl compound (4) is not expected from the decomposition of **1** at any initial concentration, because the excited carbonyl compound is necessarily formed together with another carbonyl compound in the same solvent cage.

The position of the O→O band of neither acetaldehyde (6) nor acetone (5) is known so that it is not yet possible to decide which of these compounds is produced in the excited state from **1**.

Further evidence that the luminescence observed in the decomposition of **1** is the result of emission from a decomposition product and not as a result of an emission from **1** during the act of decomposition is obtained from energy transfer experiments. The faint blue luminescence from a 0.07 *M* degassed benzene solution of **1** at 80° becomes invisible to the eye beside the very much brighter greenish-white luminescence from a degassed benzene solution 0.07 *M* in **1** and 0.0036 *M* in biacetyl. The intensity of emission from the latter solution is clearly many times greater than that from the former. This greatly increased intensity of luminescence is not the result of an induced decomposition of **1** by biacetyl. The first order rate constant, k_d, for decomposition of **1**, 0.1 *M* in benzene, is 5.5×10^{-4} s^{-1} at 60°. In the presence of 0.2 *M* biacetyl the rate is still first order and k_d is 11×10^{-4} s^{-1}. These results indicate that there is energy transfer to biacetyl from the fairly long-lived triplet state (formed by intersystem crossing from the excited singlet state) of one of the carbonyl products of the decomposition of **1**. Energy transfer to biacetyl from the excited singlet state of acetone becomes very inefficient when the concentration of biacetyl is below 0.01 *M*, while energy transfer from the triplet state of acetone remains efficient even at much lower concentrations of biacetyl (7).

Significantly greater intensities and changes in the color of luminescence are also observed from decomposition of solution of **1** containing 0.1 *M* anthracene (deep blue luminescence) and pyrene (light blue luminescence), indicating energy transfer from the excited singlet state of one of the carbonyl compounds from **1**. Intensities are greater because these materials fluoresce much more efficiently, ϕ ca. 0.5 (8), than does acetone, $\phi = 0.01$ (5).

The results indicate that the decomposition of **1** is a concerted process and confirm the prediction (2) that an electronically excited carbonyl compound must be formed in the decomposition of 1,2-dioxetanes. They also lend strong support to the proposal (2, 9) that luminescence observed in many biological systems (see refs. 9*c* and 10 for reviews), model compounds (11) and many other systems (2, 12) may result from the decomposition of transient 1,2-dioxetanes.

The 1,2-dioxetanes from many of these latter systems seem to have a very transitory existence at ambient temperatures. The excited singlet state of acetone appears to lie between 83 and 87 kcal/mole above the ground state (5) and that of acetaldehyde must have a similar energy. The carbonyl compounds formed during luminescence of the biological and model systems are highly conjugated (9–11) and their excited singlet states should lie at energies much lower than those of the excited singlet states of acetone and acetaldehyde. Also, the 1,2-dioxetanes in these systems would be substituted by groups more bulky than the methyl groups of **1** and should thus be more strained. The extremely high rates of decomposition of these 1,2-dioxetanes (which must be several orders of magnitude greater than that of **1**) then become understandable.

Acknowledgments

This research was supported in part by a grant from the National Research Council of Canada. We wish to express our thanks to Professor O. P. Strausz and Dr. G. Greig for the use of and help with the spectrometer and to Mr. A. Clement for technical assistance.

1. K. R. KOPECKY and C. MUMFORD. 51st Annual Conf. Chemical Institute of Canada, Vancouver, British Columbia. June, 1968. Abstr. p. 41.
2. F. MCCAPRA. Chem. Commun. 155 (1968).
3. R. HOFFMANN and R. B. WOODWARD. J. Am. Chem. Soc. **87**, 2047 (1965).

Can. J. Chem. Downloaded from www.nrcresearchpress.com by 210.87.254.105 on 09/05/12
For personal use only.

4. M. O'SULLIVAN and A. C. TESTA. J. Am. Chem. Soc. **90**, 6245 (1968).
5. R. F. BORKMAN and D. R. KEARNS. J. Chem. Phys. **44**, 945 (1966).
6. G. W. ROBINSON. J. Chem. Phys. **22**, 1147 (1954).
7. F. WILKINSON and J. T. DUBOIS. J. Chem. Phys. **39**, 377 (1963).
8. E. J. BOWEN and A. H. WILLIAMS. Trans. Faraday Soc. **35**, 765 (1939).
9. (*a*) F. MCCAPRA and D. G. RICHARDSON. Tetrahedron Letters, 3167 (1964). (*b*) E. H. WHITE and M. J. C. HARDING. J. Am. Chem. Soc. **86**, 5686 (1964). (*c*) F. MCCAPRA. Quart. Rev. London, **20**, 485 (1966).
10. T. GOTO and Y. KISHI. Angew. Chem. Intern. Ed. **7**, 407 (1968).
11. (*a*) F. MCCAPRA and R. WRIGGLESWORTH. Chem. Commun. 1256 (1968). (*b*) F. MCCAPRA, Y. C. CHANG, and V. P. FRANCOIS. Chem. Commun. 22 (1968). (*c*) F. MCCAPRA and Y. C. CHANG. Chem. Commun. 1011 (1967). (*d*) T. A. THOMPKINS, H. H. SELIGER, E. H. WHITE, and M. W. CASS. J. Am. Chem. Soc. **89**, 7148 (1967). (*e*) F. MCCAPRA and Y. C. CHANG. Chem. Commun. 522 (1966).
12. L. J. BOLLYKY, R. H. WHITMAN, B. G. ROBERTS, and M. M. RAUHUT. J. Am. Chem. Soc. **89**, 6523 (1967), and previous papers.

Evidence for reversible intermediate formation in cyclopentenone cycloaddition[1]

P. DE MAYO, A. A. NICHOLSON, and M. F. TCHIR
Department of Chemistry, University of Western Ontario, London, Ontario

Received November 18, 1968

The usual kinetics for product formation lead to variable values of k_d, the rate constant for decay of the responsible triplet. On the assumption that at least one intermediate is formed which gives either products, or reverts to starting materials, a value near 10^8 s^{-1} is obtained for k_d both from cyclopentene and hex-3-ene cycloadditions.

Canadian Journal of Chemistry, **47**, 711 (1969)

Recent work (1–4) has shown that cyclopentenone cycloaddition proceeds through a triplet[2]. On the assumption that the triplet reacts irreversibly with the substrate to give the product, and with the usual steady state assumptions the expression

$$[1] \qquad \frac{1}{\Phi} = \frac{1}{\Phi_{ic}} + \frac{1}{\Phi_{ic}} \cdot \frac{k_d}{k_r} \frac{1}{[\text{olefin}]}$$

may be derived (3) for the quantum yield of cycloaddition. A plot of the reciprocal quantum yield versus the reciprocal of the olefin concentration should give the efficiency of triplet formation (intercept) and the ratio of k_d/k_r. Previous results (3) and those recorded in Table I clearly indicate that the triplet yield is variable for different olefins, and does not approach the value of near unity determined by the triplet counting technique. Further, the determined values of k_d (3) varied with the olefin concentration.

If the assumption is made that k_r refers to the formation of an intermediate which may either, directly or by a number of intramolecular steps, go on to give product, or may itself (or a subsequent intermediate) decay to regenerate starting materials, then it may be shown that

$$[2] \qquad \frac{1}{\Phi} = \frac{1}{k} + \frac{1}{k}\left(\frac{k_d}{k_r}\right)\frac{1}{[\text{olefin}]}$$

where $$k = \Phi_{ic}\left(\frac{k_1}{k_1 + k_2}\right)$$

Here k_1 is the (composite) rate constant for

TABLE I
Dilution of olefin

Olefin	Intercept	Slope	Φ_{ic}[d]	k_d/k_r[e]
Cyclohexene[a]	2.1	< .1	.48	—
Cyclopentene[b]	3.8	.43	.27	.11
trans-3-Hexene[c]	4.7	.89	.21	.19

[a]See ref. 3.
[b]Done point by point on an optical bench using light of 313 mμ. Hexane was used as diluant.
[c]Irradiations were done at 20 °C on a 'merry-go-round' apparatus. The light from a 450 W mercury lamp was filtered through Pyrex and $NiSO_4$ (a band from 350–300 mμ). A sample of ketone in neat olefin acted as the actinometer. The samples were degassed by nitrogen purge. The diluant was *n*-hexane.
[d]Calculated on the basis of eq. [1].
[e]Calculated on the basis of eq. [2].

[1]Photochemical Synthesis, 26. For Part 25, see ref. 15.
[2]The exact nature of this triplet (2, 3) is not relevant to the present discussion.

Can. J. Chem. Downloaded from www.nrcresearchpress.com by 210.87.254.105 on 09/05/12
For personal use only.

4. M. O'SULLIVAN and A. C. TESTA. J. Am. Chem. Soc. **90**, 6245 (1968).
5. R. F. BORKMAN and D. R. KEARNS. J. Chem. Phys. **44**, 945 (1966).
6. G. W. ROBINSON. J. Chem. Phys. **22**, 1147 (1954).
7. F. WILKINSON and J. T. DUBOIS. J. Chem. Phys. **39**, 377 (1963).
8. E. J. BOWEN and A. H. WILLIAMS. Trans. Faraday Soc. **35**, 765 (1939).
9. (*a*) F. MCCAPRA and D. G. RICHARDSON. Tetrahedron Letters, 3167 (1964). (*b*) E. H. WHITE and M. J. C. HARDING. J. Am. Chem. Soc. **86**, 5686 (1964). (*c*) F. MCCAPRA. Quart. Rev. London, **20**, 485 (1966).
10. T. GOTO and Y. KISHI. Angew. Chem. Intern. Ed. **7**, 407 (1968).
11. (*a*) F. MCCAPRA and R. WRIGGLESWORTH. Chem. Commun. 1256 (1968). (*b*) F. MCCAPRA, Y. C. CHANG, and V. P. FRANCOIS. Chem. Commun. 22 (1968). (*c*) F. MCCAPRA and Y. C. CHANG. Chem. Commun. 1011 (1967). (*d*) T. A. THOMPKINS, H. H. SELIGER, E. H. WHITE, and M. W. CASS. J. Am. Chem. Soc. **89**, 7148 (1967). (*e*) F. MCCAPRA and Y. C. CHANG. Chem. Commun. 522 (1966).
12. L. J. BOLLYKY, R. H. WHITMAN, B. G. ROBERTS, and M. M. RAUHUT. J. Am. Chem. Soc. **89**, 6523 (1967), and previous papers.

Evidence for reversible intermediate formation in cyclopentenone cycloaddition[1]

P. DE MAYO, A. A. NICHOLSON, and M. F. TCHIR
Department of Chemistry, University of Western Ontario, London, Ontario

Received November 18, 1968

The usual kinetics for product formation lead to variable values of k_d, the rate constant for decay of the responsible triplet. On the assumption that at least one intermediate is formed which gives either products, or reverts to starting materials, a value near 10^8 s^{-1} is obtained for k_d both from cyclopentene and hex-3-ene cycloadditions.

Canadian Journal of Chemistry, **47**, 711 (1969)

Recent work (1–4) has shown that cyclopentenone cycloaddition proceeds through a triplet[2]. On the assumption that the triplet reacts irreversibly with the substrate to give the product, and with the usual steady state assumptions the expression

$$[1] \qquad \frac{1}{\Phi} = \frac{1}{\Phi_{ic}} + \frac{1}{\Phi_{ic}} \cdot \frac{k_d}{k_r} \frac{1}{[\text{olefin}]}$$

may be derived (3) for the quantum yield of cycloaddition. A plot of the reciprocal quantum yield versus the reciprocal of the olefin concentration should give the efficiency of triplet formation (intercept) and the ratio of k_d/k_r. Previous results (3) and those recorded in Table I clearly indicate that the triplet yield is variable for different olefins, and does not approach the value of near unity determined by the triplet counting technique. Further, the determined values of k_d (3) varied with the olefin concentration.

If the assumption is made that k_r refers to the formation of an intermediate which may either, directly or by a number of intramolecular steps, go on to give product, or may itself (or a subsequent intermediate) decay to regenerate starting materials, then it may be shown that

$$[2] \qquad \frac{1}{\Phi} = \frac{1}{k} + \frac{1}{k}\left(\frac{k_d}{k_r}\right)\frac{1}{[\text{olefin}]}$$

where $$k = \Phi_{ic}\left(\frac{k_1}{k_1 + k_2}\right)$$

Here k_1 is the (composite) rate constant for

TABLE I
Dilution of olefin

Olefin	Intercept	Slope	Φ_{ic}[d]	k_d/k_r[e]
Cyclohexene[a]	2.1	< .1	.48	—
Cyclopentene[b]	3.8	.43	.27	.11
trans-3-Hexene[c]	4.7	.89	.21	.19

[a]See ref. 3.
[b]Done point by point on an optical bench using light of 313 mμ. Hexane was used as diluant.
[c]Irradiations were done at 20 °C on a 'merry-go-round' apparatus. The light from a 450 W mercury lamp was filtered through Pyrex and $NiSO_4$ (a band from 350–300 mμ). A sample of ketone in neat olefin acted as the actinometer. The samples were degassed by nitrogen purge. The diluant was *n*-hexane.
[d]Calculated on the basis of eq. [1].
[e]Calculated on the basis of eq. [2].

[1]Photochemical Synthesis, 26. For Part 25, see ref. 15.
[2]The exact nature of this triplet (2, 3) is not relevant to the present discussion.

Can. J. Chem. Downloaded from www.nrcresearchpress.com by 210.87.254.40 on 09/05/12
For personal use only.

TABLE II

Stern–Volmer data[a]

[Olefin]	$k_q\tau$[b,c]	Intercept[b,c]	$k_q \times 10^{-10}$[d] (M^{-1} s^{-1})	$k_d \times 10^{-7}$ (s^{-1})	$k_r \times 10^{-8}$ (M^{-1} s^{-1})
Trans-3-hexene[e]					
3.98	14.6	0.85	2.3	8.0	2.8
1.99	33.1	0.78	2.6	5.7	3.7
0.75	64.6	0.72	2.6	8.5	4.9
0.31	116.5	0.45	2.7	8.8	4.5
Cyclopentene[f]					
0.998	11.6	0.91	1.9	16	14
8.8	1.22	0.96	1.8	18	15
1.52	8.22	0.84	1.9	16	14

[a]Determined as for footnote *c* in Table I.
[b]Determined by a least squares calculation.
[c]The number represents the average of two runs.
[d]Calculated from the Debye equation using viscosities of the solutions determined at 20 °C.
[e]Pentane used as diluant.
[f]Hexane used as diluant.

product formation from the intermediate, and k_2 that of its decay. If Φ_{ic} is taken as unity (3) then the intercept of a plot of $1/\Phi$ vs. reciprocal olefin concentration represents that portion of the intermediate that closes to give adducts.

From Stern–Volmer plots[3] and those of $1/\Phi$ vs. reciprocal olefin concentration (3) k_d and k_r may be evaluated (Table II).

The values of K_d obtained may be compared with that of 5.7×10^6 s^{-1} obtained by Chapman *et al.* (5) for isophorone and 3.9×10^7 s^{-1} by Zimmerman *et al.* (6) for a hydrophenanthrone[4,5].

The value is now independent of olefin concentration and (approximately[4]) of olefin[6].

The values of k_r are much higher than those recorded (5), for instance, for isophorone dimerization (10^6 M^{-1} s^{-1}) and, indeed, are faster than the rate constant for the addition of thiyl radicals to pent-2-ene (8)[7]. They approach radical recombination rates (9). Whether the intermediate is of the π-complex type supposed by Corey *et al.* (10) or is the 1,4-diradical, or whether both are involved, remains to be ascertained. It is noteworthy that the existence of a reversible step in cycloaddition in the literature has hitherto received little serious attention[8]. Experiments are in progress to define more accurately the nature of the intermediate.

[3]Using 2,5-dimethyl-2,4-hexadiene as quencher.

[4]Professor P. Wagner (Michigan State) has informed us that he has obtained a value of k_d for cyclopentenone near 10^8 s^{-1} from a study of its dimerization. We thank Professor Wagner most cordially for this information. It should be noted that the absolute value of k_d depends on a number of factors such as the method used for computing diffusion rates and the efficiency of exothermic quenching (7) and so is subject to some uncertainty.

[5]The value of k_d seems high for decay of a spectroscopic triplet to the ground state (by two orders of magnitude) but slow for an internal conversion (12).

[6]Although cyclopentene was used immediately after purification it was found extremely difficult to maintain this condition.

[7]Schuster *et al.* (13) give 3×10^8 M^{-1} s^{-1} for cyclopentenone dimerization.

[8]For the relevance of such processes in oxetane formation see the discussion by Yang *et al.* (11). See also ref. 14.

1. P. E. Eaton and W. S. Hurt. J. Am. Chem. Soc. **88**, 5038 (1966).
2. P. de Mayo, J.-P. Pete, and M. Tchir. J. Am. Chem. Soc. **89**, 5712 (1967).
3. P. de Mayo, J.-P. Pete, and M. Tchir. Can. J. Chem. **46**, 2535 (1968).
4. J. L. Ruhlen and P. A. Leermakers. J. Am. Chem. Soc. **89**, 4944 (1967).
5. O. L. Chapman, P. J. Nelson, R. W. King, D. J. Trecker, and A. A. Griswold. Record. Chem. Progr. Kresge-Hooker Sci. Lib. **28**, 167 (1967).
6. H. E. Zimmerman, R. G. Lewis, J. J. McCullough, A. Padwa, S. W. Staleg, and M. Semmelhack. J. Am. Chem. Soc. **88**, 1965 (1966).
7. P. J. Wagner and I. Kochevar. J. Am. Chem. Soc. **90**, 2232 (1968).
8. C. Sivertz. J. Phys. Chem. **63**, 84 (1959).
9. D. J. Carlsson and K. V. Ingold. J. Am. Chem. Soc. **90**, 1055 (1968).
10. E. J. Corey, J. D. Bass, R. LeMahieu, and R. B. Mitra. J. Am. Chem. Soc. **86**, 5570 (1964).
11. N. C. Yang, J. I. Cohen, and A. Shani. J. Am. Chem. Soc. **90**, 3264 (1968).
12. R. S. H. Liu and J. R. Edman. J. Am. Chem. Soc. **90**, 213 (1968).
13. D. I. Schuster, A. C. Fabian, N. P. Kong, W. C. Barringer, W. V. Curran, and D. H. Sussman. J. Am. Chem. Soc. **90**, 5027 (1968), (footnote 13).
14. S. Toki and H. Sakurai. Bull. Chem. Soc. Japan, **40**, 2885 (1967).
15. B. D. Challand, H. Hikino, G. Kornis, G. Lange, and P. de Mayo. J. Org. Chem. In press.

Can. J. Chem. Downloaded from www.nrcresearchpress.com by 210.87.254.40 on 09/05/12
For personal use only.

Inefficiency and reversibility in the photodimerization of 2-cyclopentenone

PETER J. WAGNER[1] AND DAVID J. BUCHECK[2]
Chemistry Department, Michigan State University, East Lansing, Michigan 48823

Received November 26, 1968

The maximum efficiency for photodimerization of cyclopentenone in acetonitrile is 36%. The intermediacy of metastable dimeric species, 64% of which revert to two ground state molecules, is indicated.

Canadian Journal of Chemistry, 47, 713 (1969)

Can. J. Chem. Downloaded from www.nrcresearchpress.com by 210.87.254.40 on 09/05/12
For personal use only.

The photodimerization of cyclopentenone has been shown to proceed from an excited triplet state (1). The dependence of the HH/HT product ratio on concentration apparently reflects a polar solvent effect (1, 2).

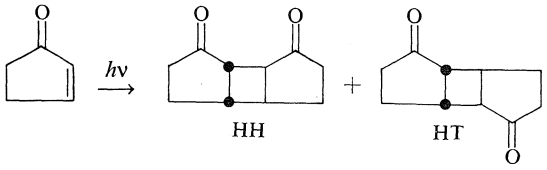

We have performed kinetic studies on the photodimerization in acetonitrile, with the following results. First, the HT/HH dimer ratio is 55/45 from 0.1 to 3.0 *M* ketone. Apparently the acetonitrile is sufficiently polar that varying concentrations of ketone do not change the effective solvent polarity.

TABLE I

Kinetic results for photodimerization of cyclopentenone in acetonitrile

[Cyclopentenone], M^{-1}	Φ_{DIM}*	$k_q\tau$, M^{-1}	$1/\tau$, 10^8 s^{-1}
1.52	—	9.1	10.5
1.00	0.34	12.5	7.7
0.75	—	16.5	5.9
0.50	0.32	26.5	3.7
0.375	0.31	—	—
0.25	0.29	—	—

*Absolute values ±0.02; relative values ±0.002.

Table I contains values for quantum yields of dimer formation and cyclopentenone triplet state lifetimes as a function of cyclopentenone concentration. These values were determined as follows. Degassed samples containing 0.003 *M* isophthalonitrile as internal standard and varying amounts of 1,3-pentadiene as quencher were irradiated in parallel at 3130 Å. Yields of dimer formation at <4% conversion were determined by vapor-phase chromatographic analysis. The acetophenone sensitized *cis*-to-*trans* isomerization of 1,3-pentadiene (3) was used to measure light intensity. Stern–Volmer analysis of relative quantum yields as a function of quencher concentration yielded values of $k_q\tau$, where k_q is taken to be 1.0×10^{10} M^{-1} s^{-1} (4, 5).

To the common mechanism for photodimerization, which assumes irreversible addition,

$$[1] \qquad CP_0 \xrightarrow{h\nu} CP^{1*} \longrightarrow CP^{3*}$$

$$[2] \qquad CP^{3*} \xrightarrow{k_i} CP_0$$

$$[3] \qquad CP^{3*} + CP_0 \xrightarrow{k_a} \text{dimers}$$

the following familiar kinetic expressions apply, where Φ_{isc} is the quantum yield

$$[4] \qquad \tau^{-1} = k_i + k_a[CP]$$

$$[5] \qquad \Phi_{DIM}^{-1} = \Phi_{isc}^{-1}(1 + k_i k_a^{-1}[CP]^{-1})$$

of intersystem crossing.

Analysis of the lifetime data according to eq. [4] yields values of $7.6 \pm 2 \times 10^7$ s^{-1} for k_i and 6.7×10^8 M^{-1} s^{-1} for k_a. Analysis of the quantum yield data according to eq. [5] yields an intercept of 0.36^{-1} and a k_i/k_a value of 0.06, the latter in good agreement with the individual values.

The important point we wish to make is that the moderately low quantum yields are not due to rapid physical decay of the triplet nor to a low intersystem crossing efficiency. Extrapolation of the efficiency with which 0.5 *M* cyclopentenone sensitized the *cis*-to-*trans* isomerization of 1,3-pentadiene to infinite diene concentration indicates that Φ_{isc} is unity, in agreement with de Mayo's recent report (6) and Leermakers' earlier data (2).

[1]Fellow of the Alfred P. Sloan Foundation, 1968–1970.
[2]N.I.H. Predoctoral Fellow, 1966–1969.

These results reveal that a major source of inefficiency is missing from the above mechanistic scheme. Furthermore, the majority of return to ground state ketone must occur after the triplet state has reacted. Consequently, a two-step photodimerization mechanism is indicated. Only 36% of the initial dimeric photoproduct, quite possibly a 1,4-biradical (7, 8), proceeds to stable dimer, the rest dissociating to two ground state cyclopentenone molecules.

$$[6] \qquad CP^{3}* + CP_0 \xrightarrow{k_a} *CP\text{–}CP*$$

$$[7] \qquad *CP\text{—}CP* \xrightarrow{k_{-a}} 2\ CP_0$$

$$[8] \qquad *CP\text{—}CP* \xrightarrow{k_c} \text{dimers}$$

$$[9] \qquad \Phi_{DIM}^{-1} = \Phi_{isc}^{-1}\phi_c^{-1}(1 + k_i k_a^{-1}[CP]^{-1})$$

$$[10] \qquad \phi_c = k_c(k_c + k_{-a})$$

Equation [4] is not a good general expression for the quantum yield of photocycloaddition; eq. [9] replaces it (9, 10). de Mayo has reached the identical conclusion in his studies of the photocycloaddition of cyclopentenone to various olefins (6, 11). As is the case in Type II photoelimination (7), the relationship between quantum efficiencies and triplet state reactivities is not direct. This phenomenon apparently is widespread among nonconcerted triplet state reactions.

It should be pointed out that there are probably two ϕ_c values, one for head-to-tail dimerization and one for head-to-head dimerization. Therefore solvent effects on product ratios are a composite of effects on two competing k_a values and two ϕ_c's. Further work will be devoted to separating these effects.

Acknowledgments

This work was supported by the National Science Foundation. We are indebted to Professor Paul de Mayo for sharing with us his related thoughts and results.

1. P. E. Eaton and W. S. Hurt. J. Am. Chem. Soc. **88**, 5038 (1966).
2. J. L. Ruhlen and P. A. Leermakers. J. Am. Chem. Soc. **89**, 4944 (1967).
3. A. A. Lamola and G. S. Hammond. J. Chem. Phys. **43**, 2129 (1965).
4. P. J. Wagner. J. Am. Chem. Soc. **89**, 5898 (1967).
5. P. J. Wagner and I. Kochevar. J. Am. Chem. Soc. **90**, 2232 (1968).
6. P. de Mayo, J-P. Pete, and M. Tchir. Can. J. Chem. **46**, 2535 (1968).
7. P. J. Wagner and A. E. Kemppainen. J. Am. Chem. Soc. **90**, 5896 (1968).
8. N. C. Yang, J. I. Cohen, and A. Shani. J. Am. Chem. Soc. **90**, 3266 (1968).
9. S. Toki and H. Sakurai. Bull. Chem. Soc. Japan, **40**, 2885 (1967).
10. P. J. Wagner and D. J. Bucheck. J. Am. Chem. Soc. **90**, 6530 (1968).
11. P. de Mayo, A. A. Nicholson, and M. F. Tchir. Can. J. Chem. This issue.

Can. J. Chem. Downloaded from www.nrcresearchpress.com by 210.87.254.40 on 09/05/12
For personal use only.

Can. J. Chem. Downloaded from www.nrcresearchpress.com by 210.87.254.105 on 09/05/12
For personal use only.

Canadian Journal of Chemistry

Published by THE NATIONAL RESEARCH COUNCIL OF CANADA

VOLUME 47 MARCH 1, 1969 NUMBER 5

Metal ion initiated halogenation reactions of *N*-haloamines[1]

DENNIS D. TANNER AND MELVYN W. MOSHER[2]

Department of Chemistry, University of Alberta, Edmonton, Alberta

Received July 5, 1968

The metal ion catalyzed chlorination of hydrocarbon substrates by *N*-chloroamines and imides in acid media proceeds by a free radical chain mechanism. Reactions of four different *N*-chloro halogenating reagents with cuprous chloride, ferrous sulfate, and ferrous chloride initiators have been investigated. Contrary to the previously reported observations no experimental differences were observed in the halogenation reactions of individual *N*-halo compounds or with the different initiators. The chain carrying species in all cases was shown to be the chlorine atom and the radical chain process showed identical reactivity to that of photo-chlorination by molecular chlorine.

Canadian Journal of Chemistry, 47, 715 (1969)

Introduction

In recent years considerable attention has been given to the radical chain reactions of *N*-haloamines, amides, and imides. Divalent nitrogen species have been proposed as reactive intermediates in the free radical addition reactions of these positive halogen compounds with olefins (1–14) as well as in their halogenation reactions involving hydrogen abstraction.

The reactions leading to abstraction by nitrogen radicals fall into two classifications, those involving intramolecular abstraction and those involving intermolecular abstraction. In the case of the intramolecular reactions (i.e. to give δ halogenation) a further division can be noted; whether they proceed by a chain sequence with or without acid catalysis. The acid-catalyzed reactions comprise the reactions of *N*-haloamines and are usually referred to under the general heading of the Hofmann–Löffler–Freytag Reaction (15, 16). The intramolecular reactions (i.e. to give δ halogenation) proceeding under neutral conditions are the reactions of *N*-haloimides (17) and *N*-haloamides (18, 19) and can be generally referred to as "Barton type" reactions for these classes of compounds.

Since it has been established that the intermolecular free radical halogenation reactions of *N*-haloamides and *N*-haloimides proceed under neutral conditions by a process involving halogen atom abstraction in the chain propagating step (20–22), only examples of acid-catalyzed intermolecular chain halogenation reactions can claim to involve nitrogen radical abstraction. The photo-initiated reaction of *N*-iodosuccinimide in trifluoroacetic acid to abstract hydrogen from trifluoroacetic acid (23), and the metal ion initiated, acid-catalyzed chain halogenation reactions of *N*-haloamines (24–28), which have been extensively studied by Minisci and co-workers, remain to our knowledge the only examples of chain reactions involving intermolecular hydrogen transfer by divalent nitrogen.

The metal ion initiated halogenation reactions of *N*-haloamines, as reported, seemed a unique, synthetically useful, and theoretically interesting reaction. Minisci has proposed the mechanism of the reaction to involve hydrogen abstraction by a protonated aminium radical (see Scheme 1) (24–28).

The relationship between the reactivity (i.e., the ability of the aminium radical to differentiate between different hydrogens in the same molecule) of the nitrogen radical and the structure of the starting *N*-chloro- and *N*-bromoamine has been studied (24, 25, 28). The authors reported varying distributions of products in the chlorina-

[1]Presented in part at the 51st national meeting of the Chemical Institute of Canada, Organic Chemistry Section, June 1968.

[2]University of Alberta Postdoctoral Fellow (1967–1969).

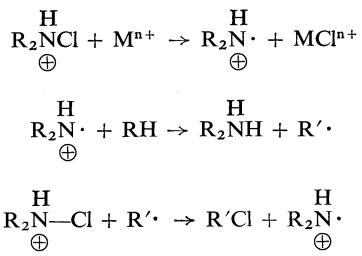

Scheme 1

tion of chlorocyclohexane with several *N*-chloroamines (25). Furthermore they claim that by varying the metal ion used to initiate the reaction (27), variations in the product compositions were obtained for a number of organic halogenations.

A proper selection of *N*-haloamine, initiator, and substrate would allow one to selectively substitute chlorine or bromine at a desired position in the substrate molecule. In order to realize the full synthetic usefulness of this reaction a more detailed investigation of these halogenations has been undertaken.

It was immediately apparent that an inconsistency in the proposed mechanism for these reactions existed. The variability of the product distribution with the initiator used argues for a more complicated sequence of reactions than had been proposed, since no account had been taken of the role of the metal ion in the product determining abstraction reaction.

Results and Discussion

The ferrous sulfate initiated chlorination of methyl butyrate with *N*-chlorodiethylamine in sulfuric acid – acetic acid solvent has been reported to give the distribution of products seen in Table I, reaction 1 (27). Comparison of this product distribution with that found for the photo-initiated chlorination of the ester in carbon tetrachloride with molecular chlorine is seen in Table I, reaction 3. When reaction 1 was repeated the product distribution shown in reaction 2 was obtained.

It was found, however, that when the mixture of chlorinated esters obtained in reaction 3 was placed in the sulfuric acid – acetic acid solvent, allowed to stand for the same length of time, and temperature as was reported for the *N*-chloroamine halogenation, after re-isolation of the resultant mixture and re-analysis by gas–liquid partition chromatography, the product distribution was seen to change, reaction 4, Table I. An analogous test of the stability of the brominated esters showed similar results.

TABLE I

Comparison of the isomer distribution for the halogenation of methyl butyrate* at 25°

		$CH_3OC(=O)-CH_2-CH_2-CH_3$			
1†	$R_2\overset{\oplus}{N}HCl/Fe^{++}$	—	—	86.4	13.6
2	$R_2\overset{\oplus}{N}HCl/Fe^{++}$	—	—	77.6	23.4
3	Cl_2/CCl_4	1.6	12.7	60.9	24.3
4	$2,H_2SO_4$	—	2.1	64.3	33.6

*Values are averages of the results of three or more independent experiments. Duplicate analyses were obtained for each experiment; the individual experimental values agreed to within ±5%.
†Taken from ref. 27.

The mechanism proposed for halogenation by *N*-haloamines was based on the comparison of the differences in product distributions reported for halogenation reactions between molecular halogen and the *N*-chloroamine, and that *N*-bromodimethylamine and *N*-chlorodimethylamine gave the same isomer distributions (26). The obvious instability of the brominated and chlorinated esters in sulfuric acid – acetic acid mixtures casts some doubt on the reliability of these mechanistic conclusions.

The halogenation products from the chlorination in acid media of 1-chlorobutane or 1-chloropropane were found to be stable for the length of time required for the completion of the reaction. These substrates were used to determine the relative reactivity of the different hydrogens in the reactants towards the abstracting radical in the halogenation process.

It was found for *N*-chlorodiethylamine that catalytic amounts of cuprous chloride (2%) were sufficient to cause a 96% conversion of the active halogen to halogenated 1-chloropropane in 7 h, while under identical conditions in the absence of cuprous ions no halogenation could be detected. The catalytic effect of trace amounts of cuprous ion was convincing evidence for a radical chain process.

The photo-chlorination of 1-chloropropane (0.1 *M*) with molecular chlorine (1.4×10^{-4} *M*) in the sulfuric acid – acetic acid mixture gave a quantitative yield of the three chlorinated 1-chloropropanes; in the presence of cuprous chloride (5×10^{-5} *M*) identical results were obtained. The cuprous chloride (8.4×10^{-4} *M*)

Can. J. Chem. Downloaded from www.nrcresearchpress.com by 210.87.254.105 on 09/05/12
For personal use only.

Can. J. Chem. Downloaded from www.nrcresearchpress.com by 210.87.254.105 on 09/05/12
For personal use only.

initiated chlorination of 1-chloropropane (0.1 *M*) with *N*-chlorodiethylamine (3.5×10^{-3} *M*) in the acid media gave a 96% yield of the chlorinated substrate. The high yield of chlorides in the copper-catalyzed chlorinations by both molecular chlorine and the chloroamine was good evidence for the lack of copper-catalyzed oxidation of the intermediate radicals (Scheme 2) (29–32).

$$R_2\overset{\oplus}{N}HCl + M^{n+} \rightarrow R_2\overset{\oplus}{N}H + MCl^{n+}$$

$$R_2\overset{\oplus}{N}H + R'H \rightarrow R_2\overset{\oplus}{N}H_2 + R'\cdot$$

$$R'\cdot + M^{(n+1)+} \rightarrow R'^{\oplus} + M^{n+}$$

$$R'^{\oplus} + Y^{\ominus} \rightarrow R'Y$$

Scheme 2

The production of carbonium ion intermediates in concentrated sulfuric acid – acetic acid was inconsistent with the formation of high yields of chlorination products in this media. The possibility of the inclusion of an oxidation–reduction process in the mechanistic scheme for halogenation, therefore, seems unlikely.

The product distributions for chlorination of the methyl esters reported by Minisci *et al.* (27) were compared to the distributions found by Singh and Tedder (33) for the chlorination of these same esters by molecular chlorine in carbon tetrachloride solvent. Since dramatic solvent effects have been noted for chlorinations of hydrocarbons with molecular chlorine (34–36), the photo-initiated chlorination of 1-chlorobutane and 1-chloropropane was carried out in carbon tetrachloride and in the sulfuric acid – acetic acid solvent. The halogenation patterns for the two substrates in these solvents are compared in Table II.

TABLE II

Comparison of the isomer distribution for 1-chloropropane and 1-chlorobutane with solvent*

	Cl—CH_2—CH_2—CH_3			
Cl_2/CCl_4	11.8	57.6	30.7	
Cl_2,H_2SO_4/HOAc	16.0	54.1	29.9	
	Cl—CH_2—CH_2—CH_2—CH_3			
Cl_2/CCl_4	10.5	27.6	45.3	13.7
Cl_2,H_2SO_4/HOAc	5.4	20.9	52.0	21.6

*Values are averages of the results of 3 or more independent experiments and duplicate analyses were obtained for each experiment. The individual experimental values agreed to within ±5%.

The variation in the product distribution for the two substrates in the two different solvents was small. As a check on the analytical procedure (i.e. isolation and analysis), and to rule out the possibility of any larger effects with other substrates, the comparisons of the isomer distributions and relative reactivities for the halogenations studied were made with the results obtained from photo-initiated halogenations run in the acid solvent.

Attempts to obtain hydrogen selectivities for the abstracting radical in the *N*-chloroamine halogenations proved unsuccessful. When halogenations of isobutane (1°/3° abstraction ratios) were attempted in the acid media isobutyl chloride was obtained and only traces of *t*-butyl chloride could be detected by g.l.p.c. analysis. Similar results were obtained in the chlorination of 2,3-dimethylbutane. These results illustrated the instability of the tertiary chlorides to the acid media.

Hydrogen abstraction from negatively substituted hydrocarbons has been shown to be substantially influenced by polar interactions between the abstracting radical and the electron withdrawing substituent (37–39). Aminium radicals generated from chloroamines derived from amines having a wide range of basicities would be expected to show a varying range of polar interactions with substituted hydrocarbons. The cuprous ion initiated halogenation patterns for the chlorination of 1-chloropropane with *N*-chlorodiethylamine, *N*,*N*-dichloropropylamine, *N*-chloropiperidine, and *N*-chlorosuccinimide are shown in Table III.

TABLE III

Comparison of the isomer distribution for 1-chloropropane with various halogenation agents*

	Cl—CH_2—CH_2—CH_3		
N,*N*-Dichloropropylamine	16.9	51.6	31.5
N-Chloropiperidine	16.8	51.7	31.4
N-Chlorodiethylamine	16.6	51.4	32.0
N-Chlorosuccinimide	16.9	51.6	31.3
Cl_2/hν	17.2	50.7	32.2
N-Bromodiethylamine	39.2	60.8	Trace
Br_2/hν	40.4	59.6	Trace

*Values are averages of the results of 3 or more independent experiments and duplicate analyses were obtained for each experiment. The individual experimental values agreed to within ±1%.

It can be seen that within experimental error the *N*-chloroamines, *N*-chlorosuccinimide, and the photo-initiated chlorination reactions with molecular chlorine gave identical results.

Can. J. Chem. Downloaded from www.nrcresearchpress.com by 210.87.254.105 on 09/05/12
For personal use only.

The photo-initiated bromination of 1-chloropropane with molecular bromine and its cuprous ion initiated bromination with *N*-bromodiethylamine gave the same distribution of brominated products. The isomer distributions for the bromination and chlorination reactions are clearly different and in the case of the two *N*-halodiethylamines must proceed through two intermediates which differ in their selectivities (see Table III).

Furthermore, it was found that cuprous chloride, ferrous sulfate, and ferrous chloride initiation of the four *N*-chloro compounds studied gave isomer distributions for the halogenation of 1-chloropropane which were indistinguishable experimentally from the results obtained for the photo-initiated chlorination of that substrate with molecular chlorine in solvent sulfuric acid (see Table IV).

TABLE IV

Comparison of the isomer distribution of 1-chloropropane with various initiators*

	Cl—CH_2—	—CH_2—	—CH_3
$FeSO_4$	15.6	53.9	30.5
$FeCl_2$	15.9	55.2	29.7
CuCl	16.9	51.4	32.0
hν (without acid)	17.6	51.0	31.2
$Cl_2h\nu$	17.2	50.7	32.2

*Values are averages of the results of 3 or more independent experiments and duplicate analyses were obtained for each experiment. The individual experimental values agreed to within ±4%.

The results clearly show, at least with the substrate investigated, that neither the *N*-chloro reagent involved nor the initiator used shows any effect on the isomer distribution for halogenation. The evidence indicates that the mechanisms for the reactions studied were all radical chain reactions involving atomic chlorine as the abstracting species. The radical chain proposed for the chlorination reactions is identical with the reaction sequence established in neutral media for halogenation by *N*-bromo- and *N*-chlorosuccinimide (20–22, 40), (see Scheme 3).

$$RH + Cl\cdot \rightarrow R\cdot + HCl$$

$$HCl + R'_2\overset{\oplus}{N}HCl \rightarrow Cl_2 + R'_2\overset{\oplus}{N}H_2$$

$$Cl_2 + R\cdot \rightarrow RCl + Cl\cdot$$

Scheme 3

The chlorine atom chain mechanism was considered by the earlier workers in their studies, but was rejected on the basis of their previously discussed results. They furthermore rejected the possibility of the operation of the halogen atom chain, since they reported that in sulfuric acid – acetic acid media anhydrous hydrogen chloride did not react with the *N*-chloroamines they studied (27). Contrary to their findings we found that when excess anhydrous hydrogen chloride was stirred with an acid solution of the *N*-chloroamines, an immediate reaction took place with the liberation of a nearly quantitative yield of molecular chlorine. The observed reaction between hydrogen chloride and *N*-chloroamines in acid media is in agreement with the observation of Komori *et al.* (41) in the same systems.

Further evidence for the chlorine atom chain was obtained by the competitive halogenation of a series of substituted and unsubstituted hydrocarbons. The relative rates of the cuprous chloride initiated reactions of cyclohexane to the various substrates with the four *N*-halo compounds are compared with the photo-initiated reaction with molecular chlorine. The results are listed in Table V.

TABLE V

Relative reactivities of hydrocarbons toward *N*-chlorodiethylamine and molecular chlorine*

	Relative reactivity/molecule†	
	N-Chlorodiethylamine	Cl_2
Cyclohexane	1.00	1.00
Cyclopentane	0.84±0.07‡	0.83±0.04
2,3-Dimethylbutane	0.83±0.10‡	0.89±0.06
Norbornane	0.68±0.03	0.74±0.08
2,2,3,3-Tetramethylbutane	0.59±0.03	0.65±0.01
1-Chlorobutane	0.36±0.03‡	0.36±0.08

*Values are averages of the results of 3 or more independent experiments and duplicate analyses were obtained for each.
†The experimental errors were those reported for *N*-chlorodiethylamine.
‡Identical results were obtained with *N*-chlorosuccinimide and *N*,*N*-dichloropropylamine.

The use of relative reactivities as a probe for the investigation of the intermolecular selectivities of a specific radical has the advantage that the ratio of rate constants is obtained from the determination of the relative consumption of the two substrates, and that this value is not affected by the subsequent fate of the intermediates involved. Within experimental error the

Can. J. Chem. Downloaded from www.nrcresearchpress.com by 210.87.254.105 on 09/05/12
For personal use only.

relative rates for the cuprous chloride initiated halogenation reactions of *N*-chlorodiethylamine, *N*-chlorosuccinimide, and *N,N*-dichloropropylamine were found to be identical with the relative rates determined for the photo-initiated chlorination reactions of molecular chlorine.

The initiation reaction for the production of chlorine atoms by the interaction of the appropriate metal ion and an *N*-halo compound can arise by one of two paths; either (1) the reduction of the *N*-chloroammonium salt to the neutral amine and a chlorine atom, or (2) the production of an aminium radical and a chloride ion. The chloride ion can subsequently react with the *N*-halo compound to produce molecular chlorine (see Scheme 4). No direct evidence is available for a choice between either of these initiation reactions.

$$(1)\quad \overset{\oplus}{R_2NHCl} + M^{n+} \rightarrow R_2NH + Cl + M^{(n+1)+}$$

or

$$(2)\quad \overset{\oplus}{R_2NHCl} + M^{n+} \rightarrow R_2NH + M^{(n+1)+} + Cl^-$$

$$R_2\overset{\oplus}{N}HCl + Cl^- \rightarrow Cl_2 + R_2NH$$

Scheme 4

Conclusion

The metal ion catalyzed chlorination of hydrocarbon substrates by *N*-chloroamines and imides proceeds by a free radical chain mechanism. The chain carrying species in these halogenations is the chlorine atom, and the selectivity and reactivity of the reagents are unaffected by the structure of the *N*-halogenating agent or the metal ion catalyst used to initiate the reaction. No evidence is found for metal ion promoted oxidation–reduction reactions of the intermediates involved.

Experimental

Materials

The method of Coleman (42) was used to prepare the *N*-haloamines. These were used without further purification. Iodometric titration showed a purity of 90–102%. Phillips research grade cyclohexane, 2,3-dimethylbutane, cyclopentane, *n*-butane, and *i*-butane were used without further purification. All other substrates were commercially available; their purity was checked by gas–liquid partition chromotography and they were distilled when necessary.

Chlorination of Methyl Butyrate

Methyl butyrate (0.1 *M*) in carbon tetrachloride was added to a solution of chlorine (0.04 *M*) in carbon tetrachloride. The solution was degassed by the freeze–thaw method and then irradiated in sealed Pyrex ampoules until the chlorine color had disappeared. The reaction mixture was analyzed upon a 10 ft × $\frac{1}{8}$ in. DEGS g.l.p.c. column. Three of the four chlorination product peaks were identified by their identical retention times on 2 different g.l.p.c. columns with commercially available compounds. The chloromethyl butyrate was assigned by elimination and by comparison of this substitution pattern with that obtained from the reaction of molecular chlorine.

Methyl butyrate was chlorinated by the method of Minisci *et al.* (27, 28) using *N*-chlorodiethylamine and iron sulfate. The reaction products were isolated and analyzed on a 10 ft × $\frac{1}{8}$ in. DEGS g.l.p.c. column.

Effect of Sulfuric Acid – Acetic Acid upon Chlorinated Methyl Butyrate, 1-Chloropropane, and 1-Chlorobutane

The mixture obtained in the chlorination of methyl butyrate with molecular chlorine in carbon tetrachloride was subjected to the reaction reported for the *N*-chloroamine chlorination and the resultant mixture was reisolated using this isolation procedure (24) and reanalyzed.

When this procedure was repeated for the monochlorinated 1-chloropropanes and 1-chlorobutanes the reanalyzed isomer distributions were found to remain unchanged. The monochlorinated 1-chloropropanes and 1-chlorobutanes were identified and quantitated by the method previously reported by this laboratory (39).

Bromination of 1-Chloropropane

Bromination products of 1-chloropropane were analyzed on a 25 ft × $\frac{1}{8}$ in. 5% Polar g.l.p.c. column. The products were identified by comparison with the previously reported bromination of 1-chloro-propane with molecular bromine (33).

Catalytic Effect of Cuprous Chloride

The formation of the three dichlorinated 1-chloropropanes was observed from the reaction of *N*-chlorodiethylamine (2.9×10^{-3} *M*), 1-chloropropane (0.1 *M*), and cuprous chloride (5.2×10^{-5} *M*). The mixture was degassed and shaken for 7 h, 1,4-dichlorobutane was added as an external standard and the organic layer analyzed as above. Molar amounts of the chlorination products were calculated from calibration plots of area ratios vs. mole ratios for 1,4-dichlorobutane vs. the authentic samples. The yield of the three dichlorinated 1-chloropropanes was found to be 96%.

Photo-initiated Chlorination of 1-Chloropropane and 1-Chlorobutane with Molecular Chlorine in Sulfuric Acid/Acetic Acid

Heterogeneous mixtures of a solution of 1-chloropropane (0.1 *M*) and chlorine (1.4×10^{-4} *M*) and 10 ml of 85/15 sulfuric acid/acetic acid solution were placed in Pyrex ampoules, degassed and sealed. The mixtures were continuously shaken and irradiated at room temperature for 15 min. The yield of the three dichlorinated 1-chloropropanes was determined to be 98% based upon 1,4-dichlorobutane as an external standard.

Heterogeneous mixtures of a solution of 1-chloropropane (0.1 *M*) and chlorine (1.4×10^{-4} *M*) and 10 ml of 85/15 sulfuric acid/acetic acid solution containing

Can. J. Chem. Downloaded from www.nrcresearchpress.com by 210.87.254.105 on 09/05/12
For personal use only.

cuprous chloride (5×10^{-5} *M*) were placed in Pyrex ampoules, degassed and sealed. The mixtures were continuously shaken and irradiated at room temperature for 15 min. The yield of the three dichlorinated 1-chloropropanes was determined to be 96% based upon 1,4-dichlorobutane as an external standard.

An identical procedure was carried for the photoinitiated chlorination and isolation of the halogenation products of 1-chlorobutane. The four dichlorinated butanes were analyzed by the method previously reported (39).

Chlorination of 1-Chloropropane by N-Chlorodiethylamine

To 1-chloropropane (0.1 *M*) – and *N*-chlorodiethylamine (3.5×10^{-3} *M*) in a Pyrex ampoule were added 10 ml of sulfuric – acetic acid (85/15) containing cuprous chloride (8.4×10^{-4} *M*). The ampoules were degassed and shaken for 3 h. The yield of the three dichlorinated 1-chloropropanes was determined to be 96% using 1,4-dichlorobutane as an external standard.

Chlorination of 1-Chloropropane and 1-Chlorobutane with Molecular Chlorine in Carbon Tetrachloride

The 1-chlorohydrocarbons were chlorinated and quantitated by the method previously reported (39).

Chlorination with N-Haloamines and Imides

To a mixture of the accurately weighed *N*-haloamine or imide (0.126 *M*) in 50 ml of sulfuric acid/acetic acid (85/15) were added the hydrocarbon (1.9 *M*) and the finely powdered metal ion initiator (0.126 *M*). The reaction mixture was stirred rapidly at room temperature for 2 h and then poured on ice, and the organic layer was separated, washed with 5% sodium bicarbonate solution, and dried over magnesium sulfate. The dried reaction mixture was then examined by gas–liquid partition chromatography. The isolation method was shown to be suitable for this analysis by subjecting known synthetic mixtures to this procedure.

In an alternative method an accurately weighed portion of the *N*-haloamine or imide (0.126 *M*) was added to the hydrocarbon (1.9 *M*) in Pyrex ampoules. The solution was frozen and a solution of the metal initiator in sulfuric acid/acetic acid (85/15) was added to give a metal ion concentration between 0.0126 and 0.063 *M*. The tubes were degassed by the freeze–thaw method and the sealed ampoules were continuously shaken for 1–4 h. The ampoules were opened and the organic layer was examined by gas–liquid partition chromatography.

The values obtained by both of the above methods gave results within experimental error. The latter method was used exclusively in the competition reactions.

Detection of Chlorine from N-Chloroamines

In a Pyrex ampoule was placed a standard solution containing 2×10^{-3} *M* of the *N*-chloroamine in sulfuric acid/acetic acid (85/15). The contents were frozen and dry hydrogen chloride was condensed on the frozen solution. The ampoule was connected to a vacuum line and the system evacuated and allowed to warm. An instant reaction commenced with the evolution of a gas. The gas was fractionated through a series of traps and found to freeze at between −98 and −105° as a yellow solid. The literature value reported for chlorine was −101.5° (43). The material was identified as chlorine by comparison of its retention on a Polypak 1 (6 ft × $\frac{1}{8}$ in.) g.l.p.c. column and by its mass spectrum. The yield of chlorine was approximated to be 100% by comparing peak areas obtained from known concentrations of chlorine with the areas of the gas obtained from the reaction.

Competitive Chlorination of Hydrocarbons

The competitive chlorinations using molecular chlorine, *N*-chloroamines, or imides were carried out by the method previously reported (39). The relative reactivities were calculated by the method previously reported in this laboratory (44). The values obtained are reported in Table V.

Acknowledgments

The authors wish to thank the National Research Council of Canada and the University of Alberta for their generous support of this work.

1. Y. Ogata, Y. Izawa, and H. Tomioka. Tetrahedron, **23**, 1509 (1967).
2. F. Minisci, R. Galli, and M. Cecere. Tetrahedron Letters, 3163 (1966), and references cited therein.
3. F. Minisci, R. Galli, and M. Cecere. Tetrahedron Letters, 4663 (1965).
4. F. Minisci and R. Galli. Tetrahedron Letters, 167 (1964).
5. R. S. Neale and N. L. Marcus. J. Org. Chem. **32**, 3273 (1967).
6. R. S. Neale. J. Org. Chem. **32**, 3263 (1967).
7. G. H. Coleman, R. L. Paterson, and G. E. Goheen. J. Am. Chem. Soc. **58**, 1874 (1936).
8. R. S. Neale. Tetrahedron Letters, 483 (1966).
9. F. Minisci and R. Galli. Tetrahedron Letters, 3197 (1964).
10. F. Minisci and R. Galli. Chim. Ind. Milan, **46**, 546 (1964).
11. F. Minisci, R. Galli, and G. Pollena. Chim. Ind. Milan, **47**, 736 (1965).
12. R. S. Neale and R. L. Hinman. J. Am. Chem. Soc. **85**, 2666 (1963).
13. R. S. Neale. J. Am. Chem. Soc. **86**, 5340 (1964).
14. F. Minisci and R. Galli. Tetrahedron Letters, 1679 (1965).
15. M. E. Wolff. Chem. Rev. **63**, 55 (1963), and references cited therein.
16. E. J. Corey and W. R. Hertler. J. Am. Chem. Soc. **82**, 1657 (1960).
17. R. C. Patterson and A. Wambsgans. J. Am. Chem. Soc. **86**, 1648 (1964).
18. D. H. R. Barton and L. R. Margan, Jr. J. Chem. Soc. 622 (1962).
19. D. H. R. Barton and A. J. L. Beckwith. Proc. Chem. Soc. 335 (1963).
20. C. Walling, A. L. Rieger, and D. D. Tanner. J. Am. Chem. Soc. **85**, 3129 (1963).
21. R. E. Pearson and J. C. Martin. J. Am. Chem. Soc. **85**, 3142 (1963).
22. G. A. Russell and K. M. Damond. J. Am. Chem. Soc. **85**, 3139 (1963).
23. D. D. Tanner. J. Am. Chem. Soc. **86**, 4674 (1964).
24. R. Bernardi, R. Galli, and F. Minisci. J. Chem. Soc. B, 324 (1968).
25. F. Minisci, R. Galli, and R. Bernardi. Chim. Ind. Milan, **49**, 594 (1967).

26. F. MINISCI, R. GALLI, and R. BERNARDI. Chem. Commun. 903 (1967).
27. F. MINISCI, R. GALLI, A. GALLI, and R. BERNARDI. Tetrahedron Letters, 2207 (1967).
28. F. MINISCI, R. GALLI, M. PERCHINUNNO, and R. BERNARDI. Chim. Ind. Milan, **50,** 453 (1968).
29. J. K. KOCHI. Tetrahedron, **18**, 483 (1962), and references cited therein.
30. J. K. KOCHI. Record Chem. Progr. Kresge–Hooker Sci. Lib. **27**, 207 (1966).
31. C. WALLING and A. A. ZAVITSAS. J. Am. Chem. Soc. **85**, 2084 (1963).
32. A. G. BERNIS and J. K. KOCHI. Abstr. Papers Am. Chem. Soc. Meeting, Chicago. 1967. Abstract: S 077.
33. H. SINGH and J. M. TEDDER. J. Chem. Soc. 4737 (1964).
34. G. A. RUSSELL. J. Am. Chem. Soc. **79**, 2977 (1957).
35. C. WALLING and M. F. MAYAHI. J. Am. Chem. Soc. **81**, 1485 (1959).
36. M. L. POUTSMA and R. L. HINMAN. J. Am. Chem. Soc. **86**, 3807 (1964).
37. P. S. FREDRICKS and J. M. TEDDER. Chem. Ind. London, 490 (1959).
38. P. S. FREDRICKS and J. M. TEDDER. J. Chem. Soc. 144 (1960).
39. D. D. TANNER and P. VAN BOSTELEN. J. Org. Chem. **32**, 1517 (1967).
40. J. ADAMS, P. A. GOSSOLAIN, and P. GOLDFINGER. Bull. Soc. Chim. Belges, **65**, 523 (1956).
41. S. KOMORI, M. OKAHARA, and Y. HORADA. Kogyo Kagaku Zasshi, **66**, 1850 (1963).
42. G. H. COLEMAN. J. Am. Chem. Soc. **55**, 3001 (1933).
43. N. A. LANGE. Handbook of chemistry. Handbook Pubs. Inc., Sandusky, Ohio. 1956.
44. D. D. TANNER and E. PROTZ. Can. J. Chem. **44**, 1555 (1966).

Can. J. Chem. Downloaded from www.nrcresearchpress.com by 210.87.254.105 on 09/05/12
For personal use only.

Can. J. Chem. Downloaded from www.nrcresearchpress.com by 210.87.254.40 on 09/05/12
For personal use only.

Lignin and related compounds.[1] I. A comparative study of catalysts for lignin hydrogenolysis[2]

J. M. Pepper and Y. W. Lee

Department of Chemistry and Chemical Engineering, University of Saskatchewan, Saskatoon, Saskatchewan

Received August 16, 1968

A detailed comparative study has been made of the effectiveness of various catalysts for the hydrogenolysis of spruce wood lignin. The catalysts studied were Raney nickel, 10% palladium–charcoal, 5% rhodium–charcoal, 5% rhodium–alumina, 5% ruthenium–charcoal, and 5% ruthenium–alumina. Lignin degradation products were obtained initially as a chloroform-soluble fraction which was then divided and studied as diethyl ether-soluble and -insoluble fractions. Gas–liquid chromatographic separation of the ether-soluble fraction made possible the characterization and quantitative estimation of many of the lower molecular weight lignin degradation products.

The data indicate that rhodium, palladium, and a limited amount of Raney nickel produce similar results as do ruthenium and an excess of Raney nickel; however, with the latter catalysts the degradation is more severe. In particular, rhodium–charcoal and palladium–charcoal appear to offer interesting advantages as catalysts for lignin hydrogenolysis.

Canadian Journal of Chemistry, 47, 723 (1969)

Previous work in these and other laboratories (1–3), has contributed to the acceptance of catalytic hydrogenolysis as a valuable approach to the study of lignin structure through the production of significant lignin degradation products. The production of 3-guaiacyl-1-propanol (dihydroconiferyl alcohol) and/or 2-guaiacyl-1-ethanol from softwoods and of the corresponding 4-hydroxy-3,5-dimethoxyphenyl (syringyl) analogues from hardwoods have added strong support to the belief that oxygen ether linkages exist in positions both β and γ to the guaiacyl and/or syringyl nuclei. This realization coupled with the appreciable yields (up to 25% of the lignin) of such products retaining, as essentially they do, the 3-carbon propyl side chain, have led to a continuation of this procedure as a method of study of lignin structure in these laboratories.

In this earlier work (2) it was shown that, under similar conditions of hydrogenolysis, there was little difference in the yields and in the nature of the products obtained whether Raney nickel catalyst (10 g/50 g wood meal) or 10% Pd—C (1 g/10 g wood meal) were used. It was noted, however, that under conditions wherein the relative amount of Raney nickel catalyst was increased (10 g/10 g wood meal) significant differences appeared in the nature of the products and, in particular, the amount of dihydroconiferyl alcohol markedly decreased while at the same time the amounts of two unidentified compounds increased.

It was therefore of interest to examine more closely the effect of the relative amount of Raney nickel catalyst and also of other catalysts which might be expected to have similar or related catalytic properties. To this end a study was made of the hydrogenolysis of preextracted spruce sapwood (10 g) under conditions that were reported previously (4) but with the following catalyst systems: Raney nickel (RaNi, 1 g), Raney nickel (RaNi, 10 g), 10% palladium–charcoal (Pd—C, 1 g), 5% rhodium–charcoal (Rh—C, 1 g), 5% rhodium–alumina (Rh–alumina, 1 g), 5% ruthenium–charcoal (Ru—C, 1 g), and 5% ruthenium–alumina (Ru–alumina, 1 g). After removing the residual pulp and catalysts by filtration, the dioxane water solution was extracted thoroughly with chloroform, the excess solvents removed, and the residue, labelled the chloroform-soluble fraction was weighed. Results recorded in Table I, and indicate to a first approximation the efficiency of lignin extraction. In certain cases, small samples were removed for determination of the methoxyl content.

Preliminary experiments involving gas–liquid chromatography had shown that a diethyl ether extraction of the chloroform-soluble fraction, permitted an essentially complete separation of

[1]Several previous publications dealing with the chemistry of lignin and related compounds have resulted from work done in these laboratories. A list of such references is available from J. M. Pepper.

[2]Presented at the 51st annual conference of the Chemical Institute of Canada, Vancouver, British Columbia, June 3–5, 1968.

TABLE I

Catalytic hydrogenolysis of spruce wood*

Catalyst (g)	Chloroform soluble fraction		Amount of residue used for ether extraction (g)	Ether extraction yields				Loss (%)
				Ether-soluble		Ether-insoluble		
	Yield (g)	Percent OMe		g	%OMe	g	%OMe	
Raney Ni (1)	1.97	18.4	1.72	0.72	17.5	0.93	19.6	4.1
(1)	1.87†		1.87	0.63	15.7	1.08	16.8	8.6
(10)	1.60	15.8	1.48	0.55	9.5	0.93‡	21.9	
(10)	1.61	14.7	1.38	0.65	8.6	0.68	13.3	3.6
10% Pd–C (1)	1.62		1.62	0.91	14.8	0.70	16.0	0.6
5% Rh–C (1)	2.58		2.58	1.85		0.60		5.0
(1)	2.53	17.1	2.33	1.48	15.5	0.85‡	17.8	
(1)	2.47		2.47	1.68		0.50		11.8
(1)	2.52							
(1)	2.33§							
5% Rh–alumina (1)	1.14	15.9	1.07	0.53	15.5	0.54‡	15.0	
(1)	1.76		1.76	0.85		0.73		10.3†
5% Ru—C (1)	1.78		1.68	0.91	12.1	0.77‡	14.7	
5% Ru–alumina (1)	1.53		1.41	0.59	10.5	0.82‡	15.6	
(1)	1.91		1.85	0.68		1.13‡		

*Preextracted spruce wood meal (10 g); dioxane–water (1:1 v/v, 150 ml); initial hydrogen pressure, 500 p.s.i.g.; temperature, 195°; time, 5 h.
†After storing 10 days in desiccator over Drierite.
‡By difference.
§After storing 8 days in desiccator over Drierite.

the lower from the higher molecular weight lignin degradation products. Accordingly, to facilitate subsequent study, each chloroform-soluble fraction was divided into a diethyl ether-soluble and a diethyl ether-insoluble portion. The weights of such fractions and some representative methoxy contents are also presented in Table I.

The poor reproducibility in some cases is believed to be due primarily to the difficulty in controlling the loss of lower boiling products during the procedure of removing the excess solvent systems. Although this would affect the relative abundance of the lower molecular weight to the higher molecular weight derivatives so obtained, it is the relative amounts of the compounds in the latter group which are perhaps of more significance (*vide infra*).

Of the seven catalytic systems, that of 5% Rh on charcoal appears to be significantly different from the others and appears to possess an activity which encourages further study. The readily reproducible high yields of the chloroform-soluble fraction, which, because of its high methoxyl content may be considered to be lignin in origin, represent essentially complete lignin recovery from the original wood meal. For this product, too, the amount that is ether-soluble (ca. 70%) is much greater than the percent ether-solubility of the $CHCl_3$-soluble fractions obtained using the other catalysts. Assuming that such greater ether-solubility reflects the greater abundance of lower molecular weight substances, this fraction would enable one, through a more detailed chemical examination, to identify a larger portion of the lignin degradation products.

To complete this comparable study of these different catalysts, representative samples of the ether-soluble fractions obtained by the use of each catalyst system, were chromatographed using a 6 ft × $\frac{1}{8}$ in. column packed with 10% UCW98 on Chromosorb W (DMCS treated, acid washed, 60–80 mesh). Details of these chromatograms are given in Figs. 1 and 2. The indicated identity of the compounds represented by the major peaks has been determined by a comparison of the retention times with those of authentic samples.

Using coumarin as the internal standard, the relative abundance of each of these compounds was determined and is given in Table II in terms of the percentage, by weight, of the original Klason lignin that it represents.

From the data recorded in Figs. 1 and 2 and in Table II, the following conclusions may be drawn. There is a significant difference between the hydrogenolysis products obtained using any of Raney Ni (1 g), Pd—C, Rh—C, and Rh–alumina on the one hand and those obtained

Can. J. Chem. Downloaded from www.nrcresearchpress.com by 210.87.254.40 on 09/05/12
For personal use only.

Can. J. Chem. Downloaded from www.nrcresearchpress.com by 210.87.254.40 on 09/05/12
For personal use only.

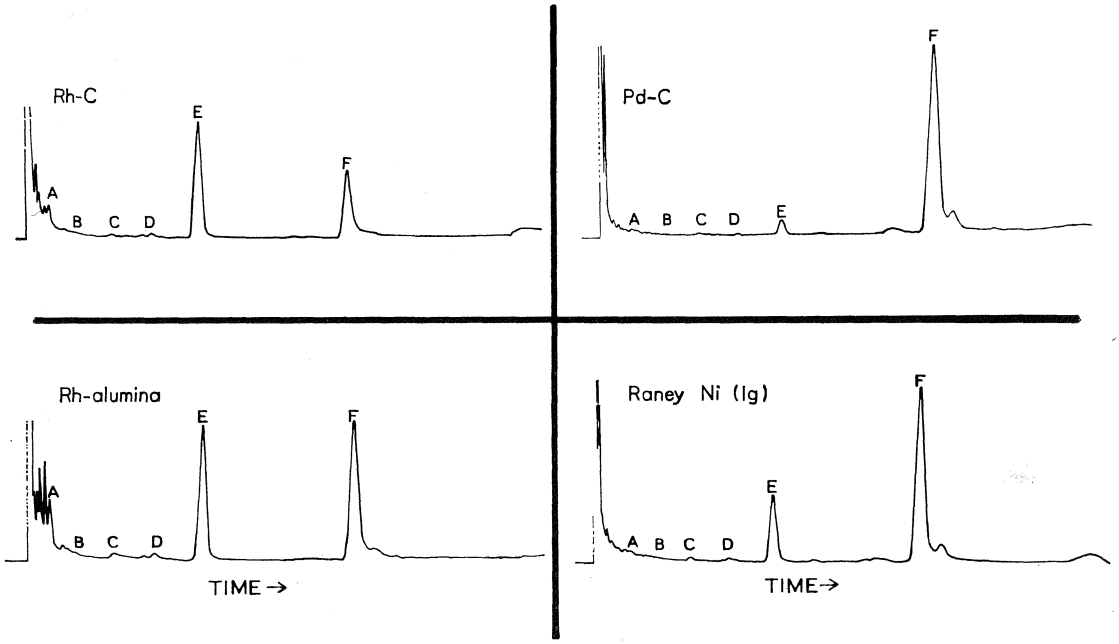

FIG. 1. Gas–liquid chromatograms of spruce lignin hydrogenolysis products: A, phenol; B, guaiacol; C, 4-methylguaiacol; D, 4-ethylguaiacol; E, 4-*n*-propylguaiacol; F, dihydroconiferyl alcohol.

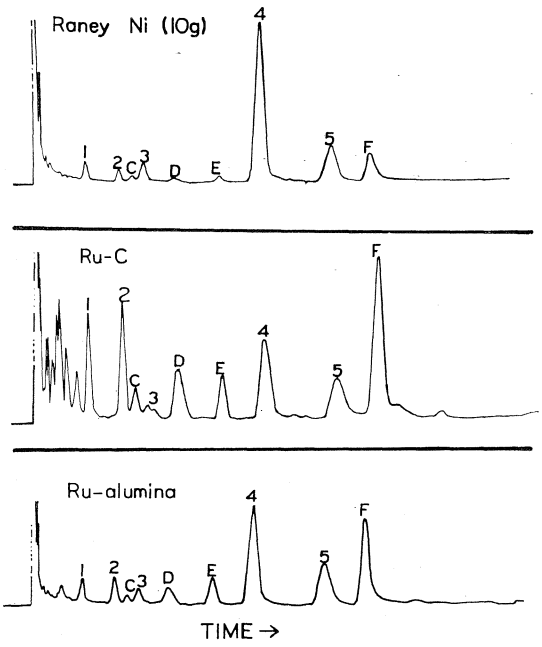

FIG. 2. Gas–liquid chromatograms of spruce lignin hydrogenolysis products: C, 4-methylguaiacol; D, 4-ethylguaiacol; E, 4-*n*-propylguaiacol; F, dihydroconiferyl alcohol; compounds **1**, **2**, **3**, **4**, **5** unidentified cyclohexyl derivatives.

using any of Raney Ni (10 g), Ru—C, and Ru–alumina on the other. For each of the former type, 4-*n*-propylguaiacol and dihydroconiferyl alcohol are the two major products, the relative amount in each case being different, whereas for members of the latter type several products are obtained in addition to these two. A preliminary examination of the unidentified compounds represented by the peaks 1–5 reveals that they are cyclohexyl derivatives, probably resulting from the further reduction and hydrogenolysis of dihydroconiferyl alcohol. Details of the chemical nature of these compounds and their relationship to dihydroconiferyl alcohol will be reported in a forthcoming publication. It is clear that the three catalyst systems making up this group may be regarded as more severe and although of possible interest for synthetic studies would appear of less value for studies in lignin chemistry. The possibility exists though that other new and significant results may be obtained using catalysts as yet untested, or in amounts different to those previously studied.

It is particularly interesting to note that, using the Pd—C catalyst, about 68% of the total ether-soluble fraction, representing some 24% of the

TABLE II

Gas–liquid chromatographic analysis of ether-soluble spruce lignin hydrogenolysis products

Catalyst	Abundance of chromatographable products*†						Total	Yield of recovered lignin‡
	A	B	C	D	E	F		
Raney–Ni (1 g)	1.85	0.23	0.31	0.36	6.92	56.7	66.3	16.4
Rh—C	3.36	0.18	0.29	0.57	16.5	31.3	52.2	33.8
Rh–alumina	3.08	0.49	0.38	0.27	9.53	34.0	47.8	12.5
Pd—C	1.81	0.22	0.19	0.17	1.33	67.9	71.6	23.9

*Percent of total ether-soluble fraction.
†Product identity: A, phenol; B, guaiacol; C, 4-methylguaiacol; D, 4-ethylguaiacol; E, 4-*n*-propylguaiacol; F, dihydroconiferyl alcohol.
‡Percent of original Klason lignin.

lignin, is accounted for as the one compound, dihydroconiferyl alcohol. In the case of the Rh—C catalyst it may be noted that over 90% of the ether-soluble fraction is accounted for by two compounds, 4-*n*-propylguaiacol and dihydroconiferyl alcohol, which together represent some 34% of the original lignin. The increased recovery of lignin degradation products in the case of Rh—C over Pd—C is accounted for almost exactly by the second product, 4-*n*-propylguaiacol, with the yields of dihydroconiferyl alcohol essentially the same in each case (20–23%). If it is assumed that these monomeric fractions are released as a result of an ether cleavage reaction, the above observations could be interpreted as follows. Two types of ether linkages may exist in the lignin: $-CH_2-O-X$ and $-CH_2-O-Y$, where X and Y represent chemically different species. Hydrogenolysis, using Pd—C, may result in the selective cleavage of the $-O-\vdots X$ bond of only the $-CH_2-O-X$ type of linkage, thereby releasing dihydroconiferyl alcohol. With Rh—C, on the other hand, cleavage of this linkage occurs in a similar way to produce the dihydroconiferyl alcohol, but, as well, cleavage of the $-CH_2-O-Y$ type occurs at the $-CH_2-\vdots O-Y$ bond, releasing the 4-*n*-propylguaiacol.

Experimental

White spruce sapwood (*Picea glauca* Moench (Voss)) was ground to ca. 20 mesh in a Wiley mill, extracted 48 h with ethanol–benzene (1:1), and air dried. Found: Klason lignin, 27.3; moisture, 2.18.

Raney nickel catalyst was prepared according to Pavlic and Adkins (5) with the exception that the washing under a hydrogen atmosphere was omitted. The catalyst was stored under cold dioxane. The dioxane was purified according to Fieser (6). The rhodium and ruthenium catalysts were obtained from K & K Laboratories, Inc., and the palladium catalyst was obtained from Matheson, Coleman and Bell.

General Reaction Procedure

Preextracted, air-dried spruce wood meal (10 g), catalyst (1 g or 10 g), and dioxane:oxygen-free water (1:1 v/v, 150 ml) were mixed in a 1410-ml capacity bomb of an Aminco hydrogenator. The reactor was flushed twice with hydrogen and then filled to an initial pressure of 500 p.s.i.g. The temperature was raised (about 120°/h) and controlled automatically at 195 ± 5° for 5 h. During this heating period and later until the room temperature had been reached, the reactor was rocked continuously.

The reactor contents were suction-filtered. The residual wood meal and catalyst were washed with dioxane–water (1:1) until the washings were colorless. The washings and original filtrate were combined, transferred to a separatory funnel, and extracted with 4 × 200 ml portions of chloroform. This extract was dried over anhydrous sodium sulfate, filtered, and concentrated under reduced pressure keeping the temperature below 50°. This chloroform-soluble fraction was dried to essentially constant weight in a desiccator over Drierite.

Either this total chloroform-soluble portion, or the residue remaining after the removal of a small sample for methoxyl analysis, was then extracted under reflux with anhydrous ether (2 × 200 ml). Both the ether-soluble fraction obtained by removal of the excess ether under reduced pressure and the residual ether-insoluble fraction were dried to essentially constant weight in a vacuum desiccator over Drierite.

Gas–liquid Chromatographic Analysis of the Ether-soluble Products

All analyses were conducted using an F & M Chromatograph, model 5750 with hydrogen flame detector and temperature programming. The column (⅛ in. × 6 ft) was packed with 10% UCW98 (silicone rubber) on Chromosorb W (60/80 mesh, DMCS treated, acid washed). The chromatograms were obtained under identical conditions of a helium flow rate of 40 ml/min; temperature programmed from 100 to 200 °C at 4°/min; injection temperature 260°; detector temperature 270°; and recorder chartspeed, 0.5 in./min. Identification of peaks was made by comparison of retention times with those obtained from authentic samples under identical conditions.

Can. J. Chem. Downloaded from www.nrcresearchpress.com by 210.87.254.40 on 09/05/12
For personal use only.

The quantitative analytical data reported in Table II were obtained as follows using coumarin as the internal standard. The thermal response factor, f, for each compound was first determined from a mixture of known amounts of the authentic sample and internal standard using the formula $f = A_i/A_s \cdot W_s/W_i$ where A_i and A_s are peak areas of the coumarin and pure sample and W_i and W_s are the corresponding weights of coumarin and sample comprising the mixture. Subsequently using a known weight of the ether-soluble fraction to which has been added a known weight of coumarin, from the peak areas and calculated response factors for each compound, the relative abundance of the products was obtained.

Reference Compounds

Guaiacol, 4-methylguaiacol, 4-ethylguaiacol, 4-*n*-propylguaiacol, and dihydroconiferyl alcohol were available, their source or preparation having been reported previously (4). Dihydroconiferyl alcohol, which, until recently, had been prepared in these laboratories as a viscous oil, was now obtained as a white solid, recrystallized from ethanol, m.p. 62–64.5°.

Acknowledgments

The authors wish to record their appreciation of the support provided by a grant from the Department of Forestry of Canada, and of financial assistance provided by the National Research Council of Canada.

1. I. A. PEARL. The chemistry of lignin. Marcel Dekker, Inc., New York. 1967. pp. 210–220.
2. J. M. PEPPER, W. F. STECK, R. SWOBODA, and J. C. KARAPALLY. Lignin structure and reactions. Advan. Chem. Ser. **59**, 205 (1966).
3. L. S. NAHUM. Ind. Eng. Chem. Prod. Res. Develop. **4**, 71 (1965).
4. J. M. PEPPER and W. F. STECK. Can. J. Chem. **41**, 2867 (1963).
5. A. A. PAVLIC and H. ADKINS. J. Am. Chem. Soc. **68**, 1471 (1946).
6. L. F. FIESER. Experiments in organic chemistry. 3rd ed. D. C. Heath and Co., Boston. 1955.

Can. J. Chem. Downloaded from www.nrcresearchpress.com by 210.87.254.40 on 09/05/12
For personal use only.

Can. J. Chem. Downloaded from www.nrcresearchpress.com by 210.87.254.5 on 09/05/12
For personal use only.

Meisenheimer complexes of some 1-substituted-3,5-dinitrobenzenes

M. I. Foreman and R. Foster
Chemistry Department, University of Dundee, Dundee, Scotland

Received July 10, 1968

It has been shown by nuclear magnetic resonance spectroscopy that both 3,5-dinitrobenzonitrile and 3,5-dinitrobenzotrifluoride form Meisenheimer-type σ-complexes with various nucleophiles in solution. In some cases attack appears to occur at both the 2- and 4-positions.

Canadian Journal of Chemistry, **47**, 729 (1969)

σ-Complexes formed by the action of nucleophiles on aromatic systems containing electron-accepting groups have received considerable attention recently (1). Products of this type were first described by Meisenheimer (2) who prepared them by the action of alkali metal alkoxides on picryl ethers. Such products are now often referred to as Meisenheimer complexes (or salts, or compounds). The stable products which were prepared by Meisenheimer are now generally represented by the structure **1** (1). Recently Servis (3) has shown that in certain cases the ion **2** is formed initially, which is then rapidly converted to **1**. The structures of these complexes are most readily determined by high resolution nuclear magnetic resonance (n.m.r.) spectroscopy of solutions of the ions (1). By such means it has also been conclusively demonstrated that the ion **3** is formed by the action of the alkoxide ion OR′ on 1,3,5-trinitrobenzene (4).

Although Meisenheimer complexes have been obtained from various 1-X-substituted-2,4,6-trinitrobenzenes (1), very few complexes derived from 1-X-3,5-dinitrobenzenes have been studied (5). If the substituent X is an electron-attracting group then the compound would be expected to behave in a similar fashion to 1,3,5-trinitrobenzene. However, due to the non-equivalence of the 2- and 4-positions in the former group of compounds, two products are possible by attack of a nucleophile Nu^- at an unsubstituted position, namely **4** and **5**. The visible absorption spectra of a number of 1-X-3,5-dinitrobenzenes in the presence of nucleophiles show two maxima not present in the spectra of the original substituted nitrobenzenes in the absence of nucleophile, see ref. 5, where it has been suggested that these extra absorptions may be due one each to two products corresponding to structures **4** and **5**. However, argument as to the structure of the product based on such observations cannot be conclusive.

In the present work evidence for the structures of σ-complexes formed in solution by the action of nucleophiles on 1-X-3,5-dinitrobenzenes (where X = —CN and —CF_3) has been obtained by n.m.r. spectroscopy. In corresponding systems where X = —I, —COOEt, and —NMe_2, no evidence of σ-complex formation was obtained. In no case was it found possible to isolate the solid salt.

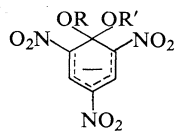

1

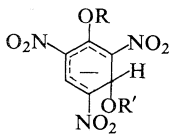

2

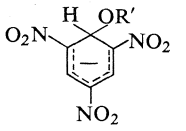

3

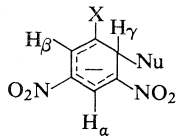

4

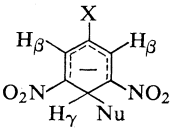

5

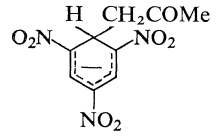

6

Results and Discussion

Reaction of 3,5-Dinitrobenzonitrile with Methoxide in DMSO

Addition of solid sodium methoxide to solutions of 3,5-dinitrobenzonitrile in dimethyl sulfoxide (DMSO) produces a deep red color. The

TABLE I

Chemical shifts and coupling constants (J) for protons in various ions with the general formula **4** or **5** in dimethyl sulfoxide solution

Structure			Chemical shift (δ)† and coupling constants (J)‡		
Formula*	X	Nu	H_α	H_β	$H\gamma$
4	—CN	—OMe	8.08 (d,J=2Hz)	7.35 (d,J=2Hz)	5.4 (broad s)
4	—CN	—OH	8.21 (d,J=2Hz)	7.52 (d,J=2Hz)	5.5 (broad s)
4	—CN	—CH_2COMe	8.05 (d,J=2Hz)	7.17 (d,J=2Hz)	4.24 (t,J=5Hz)
4	—CN	—CH(Me)COEt	8.18 (d,J=2Hz)	7.35 (d,J=2Hz)	4.33 (d,J=4Hz)
4	—CF_3	—OMe	8.02 (d,J=2Hz)	7.13 (d,J=2Hz)	5.44 (broad s)
4	—CF_3	—OH	8.15 (d,J=2Hz)	7.31 (d,J=2Hz)	§
4	—CF_3	—CH_2COMe	7.95 (d,J=2Hz)	7.00 (d,J=2Hz)	4.29 (t,J=4Hz)
5	—CN	—CH_2COMe		7.40 (s)	4.91 (t,J=5Hz)
5	—CN	—CH(Me)COEt		7.55 (s)	4.5 (d,J=4Hz)
5	—CF_3	—CH_2COMe		7.32 (s)	§

*See text for structures **4** and **5**.
†δ measured in p.p.m. downfield from internal tetramethylsilane.
‡s,d,t in parentheses denote singlet, doublet, and triplet splittings respectively.
§In these cases the peak intensities were too low to permit a definite assignment to be made.

n.m.r. spectrum shows the effectively instantaneous disappearance, at 33.5°, of the absorptions of the parent aromatic compound, an AB_2 spectrum of five lines centered at $\delta \simeq 9.10$, and the rapid formation of new absorptions. The relative intensities of the lines indicate that two species are present, the product in major abundance having doublets at $\delta = 8.08$ and $\delta = 7.35$ and a broader absorption at $\delta = 5.40$, whilst the product in lesser amount shows a very similar spectrum but with doublets at $\delta = 8.21$ and $\delta = 7.52$, and a broader absorption at $\delta \simeq 5.5$ (see Table I). All these observations are consistent with the formation of two products, **4** (X = —CN, Nu = —OMe) and **4** (X = —CN and Nu = —OH), the latter being formed by the attack of hydroxide ion derived from a small water impurity remaining in the DMSO.[1]

Reaction of 3,5-Dinitrobenzonitrile with Acetone and Triethylamine in DMSO

When 3,5-dinitrobenzonitrile is added to a solution of triethylamine and acetone in DMSO, an immediate red coloration is obtained which changes to blue after a few hours. Initially, the proton magnetic resonance (p.m.r.) spectrum shows only broad peaks which suggest that some exchange reaction with a free-radical species is occurring. However, after about 45 min at the probe temperature (33.5°) peaks become discernible and eventually become well resolved (Table I and Fig. 1). These absorptions are consistent with the formation of the ions **4** (X = —CN, Nu = —CH_2COMe) and **5** (X = —CN, Nu = —CH_2COMe). The relative intensities of the absorptions suggest that these ions are formed in the approximate ratio 2:1. Evidence for attack by the nucleophilic species $CH_3COCH_2^-$ in similar circumstances has been reported earlier. The assignment of the singlet at $\delta = 7.40$ to the protons H_β in **5** (X = —CN, Nu = —CH_2COMe), and the two doublets at $\delta = 8.05$ and $\delta = 7.17$ to the protons H_α, H_β respectively in **4** (X = —CN, Nu = —CH_2COMe), is consistent with the spin–spin splitting observed in the latter case, where these two protons are non-equivalent. The proton H_α between the two nitro groups in **4** (X = —CN, Nu = —CH_2COMe) would be expected to absorb at lower fields than H_β which lies between a nitro and a cyano group. In both ions the triplet splitting of H_γ is the result of spin–spin coupling with the methylene protons of the acetonyl group. Under very high resolution, the n.m.r. spectrum indicates that H_α is also weakly coupled with H_α in **4** (X = —CN, Nu = —CH_2COMe) and with H_β in **5** (X = —CN, Nu = —CH_2COMe) (in both cases $J \approx 0.8$ Hz). No coupling is observed between H_γ and H_β in **4** (X = —CN, Nu = —CH_2COMe).

Reaction of 3,5-Dinitrobenzonitrile with Acetone and Diethylamine in DMSO

Previously it had been shown that the ion **6** formed in acetone solutions containing 1,3,5-

[1]The authors are grateful to one of the referees for suggesting this possibility.

Can. J. Chem. Downloaded from www.nrcresearchpress.com by 210.87.254.5 on 09/05/12
For personal use only.

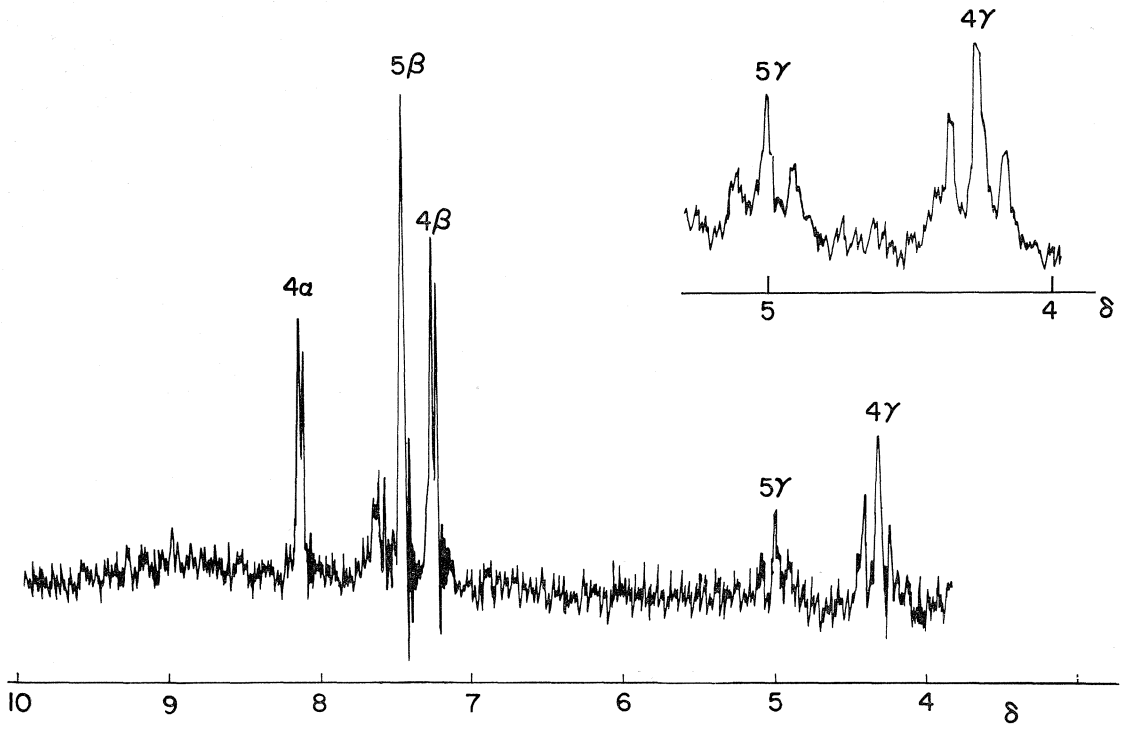

FIG. 1. Nuclear magnetic resonance spectrum below δ = 4.0 p.p.m. of the adducts **4** (X = —CN, Nu = —CH_2COMe) and **5** (X = —CN, Nu = —CH_2COMe) in DMSO solution at 33.5° (measured at 60.004 MHz).

trinitrobenzene and diethylamine reacts further with diethylamine in acetone to form *N*,*N*-diethyl-4-nitroaniline (6). It was thought that the ions **4** (X = —CN, Nu = —CH_2COMe) and **5** (X = —CN, Nu = —CH_2COMe) might undergo comparable reactions and thereby possibly yield information which would help to elucidate the mechanism of the reaction. However, addition of diethylamine to solutions containing these ions in acetone caused the collapse of the n.m.r. absorptions, presumably owing to free-radical formation.

Reaction of 3,5-Dinitrobenzonitrile with Diethyl Ketone and Triethylamine in DMSO

The behavior of this system is very similar to the reaction involving acetone. The deep red solution has a n.m.r. spectrum which is accounted for by the presence of the ions **4** (X = —CN, Nu = —CH(Me)COEt) and **5** (X = —CN, Nu = —CH(Me)COEt) (Table I). The intensities of the absorptions slowly change with time in favor of the former species.

Reaction of 3,5-Dinitrobenzotrifluoride with Sodium Methoxide in DMSO

The proton n.m.r. spectrum of the red solution formed by the addition of solid sodium methoxide to a solution of 3,5-dinitrobenzotrifluoride in DMSO shows a stronger set and a weaker set of absorptions which may be accounted for in terms of the ions **4** (X = —CF_3, Nu = —OMe) and **4** (X = —CF_3, Nu = —OH), the latter being the minor component (Table I). The parent compound in DMSO shows an AB_2 spectrum of seven lines centered at δ ≃ 9.00. The spectrum of the solution obtained by adding methoxide to 3,5-dinitrobenzotrifluoride shows free-radical broadening and collapses after a few minutes. The ^{19}F n.m.r. spectrum shows a similar broadening, which after a further lapse of time develops new maxima in the region of the original 3,5-dinitrobenzotrifluoride peak. It would therefore appear that although Meisenheimer-type complexes are formed at first, further reaction is more complicated. These changes are paralleled by the rapid decay of the initial visible spectrum

Can. J. Chem. Downloaded from www.nrcresearchpress.com by 210.87.254.5 on 09/05/12
For personal use only.

which is characteristic of a Meisenheimer complex.

Reaction of 3,5-Dinitrobenzotrifluoride with Acetone and Triethylamine in DMSO

This reaction is analogous to the corresponding system involving 3,5-dinitrobenzonitrile. The absorptions correspond to the ions **4** (X = $-CF_3$, Nu = $-CH_3COMe$) and **5** (X = $-CF_3$, Nu = $-CH_2COMe$). Although there is some evidence for absorption at higher fields due to H_γ in **5** (X = $-CF_3$, Nu = $-CH_2COMe$) no positive identification has been made. With time these weaker absorptions disappear. These observations indicate that the ion **4** is more stable than the ion **5** in this case.

As in the case of the methoxide reaction the ^{19}F n.m.r. spectrum of the reaction mixture is complicated. However, an intense peak is observed 70 Hz upfield from the parent $-CF_3$ peak. This may be due to the species **4** (X = $-CF_3$, Nu = $-CH_2COMe$). From the relative intensities, a very much weaker absorption 55 Hz upfield from the parent $-CF_3$ peak may be accounted for by **5** (X = $-CF_3$, Nu = $-CH_2COMe$).

Experimental

Solutions of 3,5-dinitrobenzonitrile and 3,5-dinitrobenzotrifluoride (25% v/v in DMSO), were treated with equimolar amounts of the appropriate reagents. The nuclear magnetic resonance (n.m.r.) spectrum was then repeatedly scanned at intervals of a few minutes. Because of the high concentrations used, side-reactions occasionally gave rise to small absorptions in the n.m.r. spectra which could not be assigned in the above scheme.

In attempts to isolate solid products, the solutions in DMSO were treated with excess anhydrous ether. In every case an intractable, deep red, ether-insoluble oil was obtained. Addition of dilute aqueous acid to the oils regenerated the parent nitro compound in each case.

Where X = —I and X = —COOEt, both the addition of methoxide, and of acetone plus triethylamine produced deep red solutions. In the case of X = $-NMe_2$, a dark green solution was obtained with methoxide. In all these cases the n.m.r. absorptions collapsed. On long standing the absorptions due to the starting materials slowly reappeared. However, no peaks assignable to Meisenheimer complexes were observed. In the case of X = $-NMe_2$, addition of acetone plus triethylamine produced no color and the n.m.r. spectrum gave no evidence of reaction.

Materials

3,5-Dinitrobenzonitrile was prepared by the method of Bennett and Wain (7) recrystallized twice from ethanol, m.p. 127–128°. 3,5-Dinitrobenzotrifluoride was prepared by the method of Finger and Reed (8) recrystallized twice from ethanol, m.p. 49–50°. Dimethyl sulfoxide was dried by refluxing over calcium hydride and stored over 5A molecular sieve.

Nuclear Magnetic Resonance Spectra

^1H spectra were measured at 60.004 MHz and ^{19}F spectra at 56.462 MHz using a Perkin–Elmer R.10 spectrometer at 33.5°. All proton spectra are given as shifts in p.p.m. downfield from an internal tetramethylsilane reference ($\delta = 0$).

Acknowledgment

This work was carried out during the tenure (by M.I.F.) of a Science Research Council Grant.

1. R. Foster and C. A. Fyfe. Rev. Pure Appl. Chem. **16**, 61 (1966). E. Buncel, A. R. Norris, and K. E. Russell. Quart. Rev. Chem. Soc. London, **22**, 123 (1968) and references therein.
2. J. Meisenheimer. Ann. **323**, 205 (1902).
3. K. L. Servis. J. Am. Chem. Soc. **87**, 5495 (1965); J. Am. Chem. Soc. **89**, 1508 (1967).
4. M. R. Crampton and V. Gold. J. Chem. Soc. 4293 (1964); J. Chem. Soc. B, 893 (1966).
5. R. J. Pollitt and B. C. Saunders. J. Chem. Soc. 4615 (1965).
6. R. Foster and C. A. Fyfe. Tetrahedron, **22**, 1831 (1966).
7. G. M. Bennett and R. L. Wain. J. Chem. Soc. 1108 (1936).
8. G. C. Finger and F. H. Reed. J. Am. Chem. Soc. **66**, 1972 (1944).

Can. J. Chem. Downloaded from www.nrcresearchpress.com by 210.87.254.5 on 09/05/12
For personal use only.

Le dimère de la *cis* dihydroxy-5,6 cyclohexène-2 dione-1,4

J. Y. Savoie et P. Brassard
Département de Chimie, Université Laval, Québec, Québec

Reçu le 15 août 1968

On reconnaît depuis longtemps que le produit d'oxydation de la *p*-benzoquinone par le chlorate de sodium en présence d'acide osmique est un dimère. Par le choix de conditions de plus en plus rigoureuses, il est possible d'en tirer trois acétates qui correspondent au dimère lui même et à ses produits de déshydratation et d'aromatisation. Ces substances ont été reconnues comme les tétra-acétates de la tétrahydroxy-1,2,6,7 dibenzo *p*-dioxinne (**2***a*), de l'oxo-2 tétrahydroxy-1,4*a* (*trans*), 6,7 tétrahydro-1,2,4*a*,10*a* dibenzo *cis* *p*-dioxinne (**3**) et du dimère monohémiacétal de la *cis* dihydroxy-5,6 cyclohexène-2 dione-1,4 (**4***b*). La structure du dimère à l'état solide et en solution y est discutée.

The osmic acid catalyzed oxidation of *p*-benzoquinone by sodium chlorate has long been recognized to yield a dimeric substance. By using progressively more vigorous conditions of acetylation, it has been possible to prepare from it three acetates corresponding to the dimer and to products of increasing degrees of dehydration and aromatization. The compounds have now been identified as the tetraacetates of 1,2,6,7-tetrahydroxydibenzo-*p*-dioxine (**2***a*), of 2-oxo-1,4*a* (*trans*),6,7-tetrahydroxy-1,2,4*a*,10*a*-tetrahydrodibenzo-*cis*-*p*-dioxinne (**3**) and of the monohemiacetal dimer of *cis*-5,6-dihydroxycyclohex-2-ene-1,4-dione (**4***b*). The structure of the dimer in the solid state and in solution is discussed.

Canadian Journal of Chemistry, **47**, 733 (1969)

L'oxydation de la *p*-benzoquinone par le chlorate de sodium en présence d'acide chlorhydrique et d'une quantité catalytique d'acide osmique donne une substance microcristalline insoluble dans les solvants organiques (1). On a alors cru que celle-ci était le produit dihydroxylé correspondant, mais on a suggéré depuis qu'il s'agissait bien du dimère de cette substance (2). Nous avons préparé la *cis* dihydroxy-5,6 cyclohexène-2 dione-1,4 (3) et vérifié qu'effectivement elle se transforme en un produit identique à celui déjà obtenu. L'étude des divers dérivés acétylés de ce dimère[1] nous a permis d'en préciser la structure.

Il est clair que l'acétate de p.f. 227–228° [litt. 217–218° (1)] obtenu dans des conditions rigoureuses ne peut être qu'une dibenzo *p*-dioxinne (**2***a*). Le spectre de masse indique un poids moléculaire de 416 et montre quatre groupes acétates. Le spectre de résonance magnétique nucléaire (r.m.n.) par ailleurs ne révèle que deux signaux pour ces acétates et un troisième singulet à 6.86 p.p.m. Après l'hydrolyse acide de cette substance en tétrahydroxy-1,2,6,7 dibenzo *p*-dioxinne (**2***b*), le signal correspondant aux protons aromatiques se présente comme un doublet dédoublé (J = 9.1 Hz). Ces données ne conviennent qu'à une structure très symétrique ayant deux paires identiques de protons vicinaux aromatiques.

Un deuxième acétate (**3**) de formule moléculaire $C_{20}H_{18}O_{11}$ obtenu par acétylation en présence d'une trace d'acide sulfurique se présente sous deux formes allotropiques (identiques aux points de vue analytiques et spectrales) de p.f. 140° et 182°. Il s'agit ici sans doute de l'"acétate d'apionol" et du composé $C_{24}H_{22}O_{13}$ décrits par Terry et Milas (1). L'authentique acétate d'apionol ne se forme qu'en présence de catalyseurs basiques.

Le spectre de masse de cette substance indique quatre fonctions acétates et un poids moléculaire de 434. Son spectre de r.m.n. révèle d'intéressantes analogies avec celui de la cétone de Pummerer (**1**) (6) et confirme sa formation à partir du dimère par perte d'une molécule d'eau et aromatisation d'un des cycles carbonés. En plus des quatre signaux dus aux acétates et du pic unique attribué aux deux protons aromatiques, ce spectre se compose de deux doublets et de deux doublets dédoublés correspondant à quatre protons. Les protons éthyléniques en 3 et 4 se reconnaissent aisément par leur déplacement chimique et leur constante de couplage. La valeur élevée (J = 2.6 Hz) de la constante de couplage à longue distance entre les protons en 4 et 10*a* ne laisse aucun doute sur la position

[1]Lors de la préparation de ce mémoire, Thompson et Anderson (4) ont également proposé pour ce dimère une structure tricyclique qui diffère au point de vue stéréochimique de celle que nous avons déjà communiquée (5).

Can. J. Chem. Downloaded from www.nrcresearchpress.com by 210.87.254.5 on 09/05/12
For personal use only.

Can. J. Chem. Downloaded from www.nrcresearchpress.com by 210.87.254.5 on 09/05/12
For personal use only.

équatoriale de ce dernier (7), tandis que l'absence d'un tel couplage entre ceux en 1 et 3 et la configuration du monomère original font assigner au proton en 1 une position axiale. Il en résulte donc que la jonction des cycles en 4*a* et 10*a* ne peut être que *cis*, relation qui doit se retrouver dans le dimère.

Un troisième acétate de p.f. 196.0–196.5° fut obtenu à partir du même dimère par action de l'anhydride acétique à 90°, seul, ou mieux en présence d'une trace d'acide *p*-toluènesulfonique. Cette substance semble inédite et son analogie avec les α-hydroxy cétones (8) laisserait supposer qu'il s'agit du dioxanne tricyclique. En effet, son spectre de masse indique un poids moléculaire de 452 et la présence de quatre groupes acétates. Le spectre de r.m.n. par ailleurs permet de déceler les douze pics caractéristiques de l'arrangement des quatre protons en 1, 3, 4, et 10*a* du composé **3** superposés à un autre système de quatre protons couplés essentiellement de la même façon. Mais toute tentative d'interpréter ce spectre en fonction d'une structure tricyclique se heurte à des difficultés du fait de la faible différence de déplacements chimiques observée pour la seconde paire de protons éthyléniques et de l'absence d'un deuxième proton qui résonnerait vers 5 p.p.m.

Ces données concordent bien si l'on considère avoir affaire à un monohémiacétal (**4***b*). Une preuve supplémentaire à l'appui de cette proposition est tirée de la présence dans le spectre de masse de pics importants à *m/e* 322 (M — AcOH, CH_2CO, CO) et 321 (M — AcOH, CH_2CO, CHO) qui indiquent un mode de décomposition caractéristique des quinones (9). Le couplage à longue distance qui se manifeste entre deux protons de la partie cyclohexènedione de la molécule permet également de déterminer la conformation de ce cycle. En effet, le proton tertiaire le plus déblindé, celui en 6′ montre un dédoublement secondaire et doit en conséquence être équatorial; le proton en 5′ ne montre par contre aucune interaction de spin avec celui en 3′ et serait donc axial. La partie cyclohexènone doit avoir essentiellement la même conformation que dans l'acétate **3** puisqu'on n'observe que de faibles divergeances entre les déplacements chimiques et les constantes de couplage attribuées aux protons de chaque système.

Nous avons de plus cherché à étayer ces preuves de structure par l'étude d'un dimère portant un plus petit nombre de protons. L'oxydation de la chlorohydroquinone n'a pas donné un produit homogène. Il est tout de même possible, suivant les conditions, d'obtenir deux acétates de ce mélange. La méthode employée pour la préparation du composé **4***b* produit un acétate (**4***c*) qui présente des caractéristiques (spectre infrarouge) comparables à celles de **4***b*. Son spectre de r.m.n. ne révèle aucun dédoublement secondaire et montre que les atomes de chlore sont en 3 et 2′. Il semble logique que, dans le monomère original, le groupe hydroxyle en 5 soit le plus nucléophile et réagisse de préférence avec le carbonyle voisin de l'halogène.

Dans des conditions plus rigoureuses, le dimère chloré fournit un autre acétate qui ne montre pas de ressemblance dans son spectre de r.m.n. avec le composé **3** quoique la substance s'avère partiellement aromatique. L'absence d'un proton qui résonne aux environs de 5 p.p.m. alors que les caractéristiques spectrales de la partie cyclohexènedione persistent, indique que l'aromatisation a suivi un autre cours pour aboutir à la structure **5**.

Les structures proposées pour ces différents acétates rendent également bien compte des propriétés et des réactions de ces composés. En effet, les conditions requises pour produire l'acétate **2***a* à partir du dimère **6***a* conduisent également à l'aromatisation du produit **3**. Par contre, il a été impossible de transformer la substance **4***b* en l'un ou l'autre des produits **3** et **2***a*.

Conformément aux données de Terry et Milas (1), plus tard niées par Baker et Munk (2), nous avons trouvé que le dimère original se dissoût lentement dans l'eau bouillante et y cristallise inchangé. Le spectre de r.m.n. de la substance (dans D_2O ou DMSO) indique clairement qu'elle existe en solution sous forme de monohémiacétal. Sous cette forme, le dimère est passablement soluble et la lenteur de la dissolution ne s'explique que si celle-ci est accompagnée d'une isomérisation. Il est d'ailleurs bien établi que les dimères des α-hydroxy cétones se dépolymérisent dans l'eau (10).

L'obtention facile de substances tricycliques à partir du dimère solide ne laisse pas de doute qu'il s'agit bien d'un di-hémiacétal. Un des produits de dégradation (**3**) indique qu'une des jonctions de cycles doit être *cis*, tandis que la

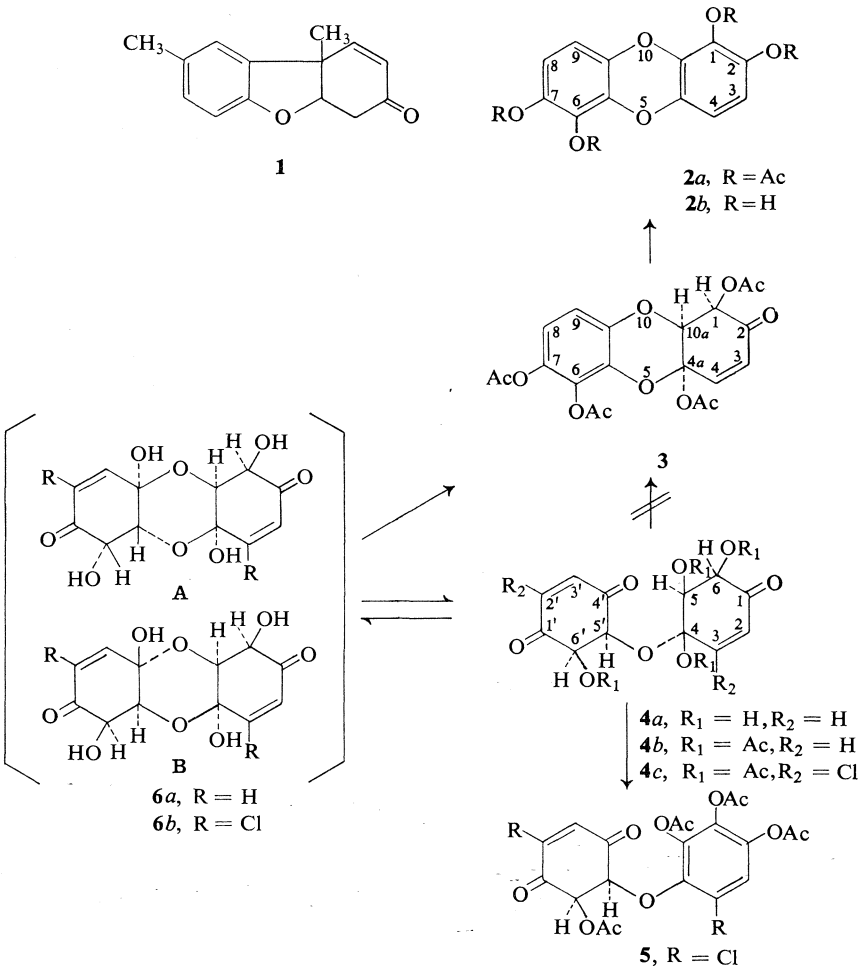

facilité de l'aromatisation partielle par perte d'une molécule d'eau laisse présumer que l'autre est *trans*. L'examen de modèles révèle que deux isomères *cis*, *trans* sont possibles (**6***a*; **A** ou **B**) sans qu'il soit possible dans l'état de nos connaissances actuelles de préciser davantage la structure tricyclique du dimère.

Partie expérimentale

Les points de fusion ont été déterminés en tube capillaire à l'aide d'un thermomètre calibré (appareil Thomas–Hoover). Les spectres infrarouges ont été réalisés sur un appareil Beckman, modèle IR-4. Les spectres ultraviolets ont été déterminés sur un appareil Beckman, modèle DK-1A. Les spectres de résonance magnétique nucléaire (r.m.n.) ont été enregistrés sur un appareil Varian A 60; les déplacements chimiques sont mesurés en δ par rapport au tétraméthyl silane (δ = 0) et ne sont pas corrigés. Les spectres de masse ont été déterminés sur un spectrographe Varian M 66.

Le dimère de la cis dihydroxy-5,6 cyclohexène-2 dione-1,4 (6a)

A une solution de chlorate de sodium (10.0 g) dans l'eau (50 ml) contenant de l'acide osmique (1.3 ml d'une solution aqueuse à 1%), on ajoute de l'acide chlorhydrique concentré (1 ml) puis de la *p*-benzoquinone (10.8 g; 0.1 mole) et on maintient le milieu réactionnel sous forte agitation pendant 48 h. Le dimère (3.0 g; 21%) obtenu par filtration est presque pur et peut être recristallisé en petites quantités dans l'eau ou encore mieux dans le diméthylsulfoxyde. Si l'on prolonge la durée de réaction à 8 jours ou si l'on ajoute de l'acétone (50 ml) au mélange 12 heures avant la fin de la préparation, les rendements s'élèvent à 43% (6.1 g) et à 50% (7.1 g) respectivement, p.f. 210–212° (décomp.) (chauffage rapide) (litt. p.f. 177–178°) (1).

Spectre infrarouge (KBr): bandes à 2.89, 3.07, 5.89 et 6.15 μ.

Can. J. Chem. Downloaded from www.nrcresearchpress.com by 210.87.254.5 on 09/05/12
For personal use only.

Can. J. Chem. Downloaded from www.nrcresearchpress.com by 210.87.254.5 on 09/05/12
For personal use only.

Spectre de résonance magnétique nucléaire (DMSO) (**4***a*): un triplet (doublet dédoublé) à 3.96 p.p.m., $J = 2.5$, 2.5 Hz (CH 5); un pic large à 4.44 p.p.m. qui rétrécit par deutériation (CH 6,5′,6′; OH); un doublet à 6.15 p.p.m., $J = 10.0$ Hz (CH 2); un quadruplet à 6.58 p.p.m., $J = 10.0$, 2.5 Hz (CH 3); un singulet correspondant à deux protons à 6.86 p.p.m. (CH 2′, 3′). Le spectre comprend en outre trois pics larges à 5.3, 6.0 et 7.4 p.p.m. qui disparaissent par deutériation et un signal à 6.90 p.p.m. dû à un produit de décomposition (son intensité est fonction de la durée de chauffage).

Anal. Calc. pour $C_{12}H_{12}O_8$: C, 50.71; H, 4.26. Trouvé: C, 50.37; H, 4.44.

Tétrahydroxy-1,2,3,4 benzène (apionol)

On chauffe au bain-marie pendant 20 min un mélange du dimère **6***a* (5.0 g) et de pyridine (40 ml). Après refroidissement on le verse dans 100 ml d'une solution d'acide chlorhydrique à 20%. Par extraction continue de la solution avec de l'éther on obtient de l'apionol (2.0 g; 40%) p.f. 158–160° (litt. 161° (11)). Cette substance est identique (spectre infrarouge) à celle obtenue par déméthylation ($AlCl_3$) du diméthoxy-1,2 dihydroxy-3,4 benzène (11).

*Tétra-acétoxy-1,2,6,7 dibenzo p-dioxinne (**2***a)*

A une suspension du dimère (**6***a*) de la *cis* dihydroxy-5,6 cyclohexène-2 dione-1,4 (5.0 g) dans de l'anhydride acétique (25 ml), on ajoute de l'acide sulfurique concentré (1 ml) et on chauffe le mélange au bain-marie pendant 15 min. Après l'hydrolyse de l'excès de l'anhydride, on obtient le tétra-acétate **2***a* (6.2 g; 85%) qui cristallise en aiguilles dans le benzène p.f. 227–228° (litt. p.f. 217–218° (1)). Ce composé s'obtient également à partir du tétra-acétate **3** dans les mêmes conditions, p.f. mixte 226–227°.

Spectre infrarouge (KBr): bandes à 5.60 μ et 6.71 μ.

Spectre ultraviolet (EtOH): bandes à 288 mμ, log ε = 3.41 et à 229 mμ, log ε = 4.53.

Spectre de résonance magnétique nucléaire (acétone-d_6): un singulet à 6.86 p.p.m. (CH aromatique).

Spectre de masse: pic moléculaire à *m/e* 416; pics à *m/e* 374, 332, 290 et 248.

Anal. Calc. pour $C_{20}H_{16}O_{10}$: C, 57.69; H, 3.87. Trouvé: C, 57.29; H, 4.01.

*Tétrahydroxy-1,2,6,7 dibenzo-p-dioxinne (**2***b)*

On porte à ébullition pendant 24 h un mélange du composé précédent (**2***a*) (6.0 g), de méthanol (50 ml) et d'acide chlorhydrique concentré (0.3 ml). Après dilution à froid avec du chloroforme (20 ml), le tétrahydroxy-1,2,6,7 dibenzo *p*-dioxine cristallise en aiguilles incolores (3.0 g; 84%), p.f. 335–337°.

Spectre d'infrarouge (KBr): bandes à 2.80, 3.07, 6.04, 6.20, 6.50 et 6.68 μ.

Spectre résonance magnétique nucléaire (acétone-d_6): centré à 6.46 p.p.m., un système AB, $J = 9.1$ Hz et $\Delta\nu = 0.05$ p.p.m.; un singulet disparaissant par deutériation.

Spectre de masse: pic moléculaire à *m/e* 248.

*Oxo-2 tétraacétoxy-1,4a(trans), 6,7, tétrahydro-1,2,4a, 10a dibenzo cis p-dioxinne (**3**)*

On chauffe au bain-marie pendant 30 min un mélange du dimère **6***a* (1.0 g), d'anhydride acétique (15 ml) et d'acide sulfurique concentré (1 goutte). Après l'hydrolyse de l'excès de l'anhydride et recristallisation dans l'acétate d'éthyle, on obtient 1.1 g du tétra-acétate **3** de p.f. 140–142°. Cette forme est métastable et se transforme en une autre de p.f. 182°. Les spectres infrarouges et de r.m.n. sont identiques.

Spectre infrarouge (KBr): 5.63, 5.70, 5.81 μ.

Spectre ultraviolet (EtOH): 275 mμ, log ε = 3.30; 217 mμ, log ε = 4.25.

Spectre de résonance magnétique nucléaire (acétone-d_6): quatre singulets à 2.20, 2.22, 2.25 et 2.27 p.p.m. ($OCOCH_3$); un quadruplet centré à 4.88 p.p.m., $J = 2.2$, 2.6 Hz (CH 10*a*); un doublet centré à 6.04 p.p.m., $J = 2.2$ Hz (CH 1); un doublet centré à 6.27 p.p.m., $J = 10.5$ Hz (CH 3); un singulet à 6.86 p.p.m. (CH 8, 9); un quadruplet centré à 7.33 p.p.m., $J = 10.5$, 2.6 (CH 4).

Spectre de masse: pic moléculaire à *m/e* 434; pics à *m/e* 392, 350, 308, 290, 266 et 248.

Anal. Calc. pour $C_{20}H_{18}O_{11}$: C, 55.30; H, 4.18. Trouvé: C, 55.45; H, 4.16.

*Tétra-acétate du dimère (hémiacétal) de la cis dihydroxy-5,6 cyclohexène-2 dione-1,4 (**4***b)*

On chauffe au bain-marie pendant 48 h un mélange du dimère (**6***a*) (1.0 g), d'acide *p*-toluènesulfonique (2 mg) et d'anhydride acétique (15 ml). Après hydrolyse de l'excès de l'anhydride et recristallisation du produit dans de l'éther anhydre, on obtient 0.9 g du tétra-acétate **4***b* de p.f. 196.0–196.5°.

Spectre infrarouge (KBr): 5.65, 5.77 et 6.08 μ.

Spectre ultraviolet (EtOH): 218 mμ, log ε = 4.24.

Spectre de résonance magnétique nucléaire (acétone-d_6): trois singulets à 2.06, 2.14 et 2.20 p.p.m. correspondant respectivement à 3,6 et 3 protons ($OCOCH_3$) un doublet dédoublé à 5.16 p.p.m., $J = 2.3$, 4.2 Hz (CH 5); un doublet à 5.76 p.p.m., $J = 2.8$ Hz (CH 5′); un doublet dédoublé à 5.91 p.p.m., $J = 2.1$, 2.8 Hz (CH 6′); un doublet à 6.11 p.p.m., $J = 4.1$ Hz (CH 6); un doublet à 6.23 p.p.m., $J = 10.4$ Hz (CH 2); un doublet à 6.31 p.p.m., $J = 10.2$ Hz (CH 3′); un doublet dédoublé à 6.56 p.p.m., $J = 2.1$, 10.2 Hz (CH 2′); un doublet dédoublé à 7.04 p.p.m., $J = 2.3$, 10.4 Hz (CH 3). La double irradiation de ce proton provoque la disparition du dédoublement secondaire du signal de CH 5.

Spectre de masse: pic moléculaire à *m/e* 452, pics à *m/e* 350, 322, 321, 308, 279, 266, 248.

Anal. Calc. pour $C_{20}H_{20}O_{12}$: C, 53.10; H, 4.46. Trouvé: C, 53.30; H, 4.32.

*Le dimère de la cis dihydroxy-5,6 chloro-2 cyclohexène-2 dione-1,4 (**6***b)*

On ajoute très lentement à 0° et sous forte agitation de la chlorohydroquinone (26 g) à un mélange de chlorate de sodium (37.5 g), d'acide chlorhydrique concentré (1 ml), d'acide osmique (3 ml d'une solution aqueuse à 1%), d'acétone (25 ml) et d'eau (75 ml). Après 5 jours, on recueille le dimère chloré (**6***b*) par filtration et on le lave successivement avec de l'eau, du méthanol et de l'acétone. La substance (1.3 g) se décompose à 172° et ne semble pas homogène.

*Le tétra-acétate du dimère (monohémiacétal) du cis dihydroxy-5,6 chloro-2 cyclohexène-2 dione-1,4 (**4***c)*

La substance se prépare de la même façon que le

tétra-acétate **4***b* si ce n'est que l'on élimine le dimère inchangé avant l'hydrolyse de l'excès du réactif. Elle cristallise dans l'acétate d'éthyle, p.f. 222.0–222.5°.

Spectre infrarouge (KBr): bandes à 5.63, 5.81 et 6.17 μ.

Spectre de résonance magnétique nucléaire (dioxanne): trois singulets à 2.07, 2.13 et 2.25 p.p.m. correspondant respectivement à 3,6 et 3 protons ($OCOCH_3$); un doublet à 5.17 p.p.m., $J = 4.0$ Hz (CH 5); un singulet à 5.84 p.p.m. (CH 5′,6′); un doublet à 6.18 p.p.m., $J = 4.0$ Hz (CH 6); deux singulets à 6.63 et 6.72 p.p.m. (CH 2′,3′). Dans le diméthylsulfoxyde les protons en 5 et 6 ne sont plus fortuitement équivalents: deux doublets à 6.12 et 6.29 p.p.m., $J = 2.8$ Hz.

Spectre de masse: pic moléculaire à *m/e* 520; pics à *m/e* 485, 418, 376, 341, 331, 316.

[Triacétoxy-2,3,4 chloro-6 phénoxy]-5 acétoxy-6 chloro-2 cyclohexène-2 dione-1,4 (5)

La préparation de ce composé à partir du dimère chloré (**6***b*) est analogue à celle du tétra-acétate **3**. Recristallisé dans l'acétate d'éthyle, ce tétra-acétate (**5**) fond à 186–187°.

Spectre infrarouge (KBr): 5.57, 5.64, 5.79, et 6.18 μ.

Spectre de résonance magnétique nucléaire (acétone-d_6): quatre singulets à 2.06, 2.25, 2.28 et 2.32 p.p.m. ($OCOCH_3$); un doublet à 5.77 p.p.m., $J = 2.9$ Hz (CH 5); un doublet à 6.07 p.p.m., $J = 2.9$ Hz, deux singulets à 6.73 et 7.15 p.p.m. (CH 3 et CH aromatique).

Spectre de masse: pic moléculaire à *m/e* 502, pics à *m/e* 460, 418, 376, 358, 334, 316, 282, 176, 160.

Remerciements

Nous remercions le Conseil National de Recherches du Canada pour l'octroi d'une bourse de recherche à l'un de nous (J.Y.S.) et de subventions.

1. E. M. Terry et N. A. Milas. J. Am. Chem. Soc. **48**, 2647 (1926).
2. W. Baker et I. Munk. J. Chem. Soc. 1092 (1940).
3. J. Y. Savoie et P. Brassard. Résultats inédits.
4. H. A. Thompson et R. H. Anderson. J. Chem. Soc. C, 2152 (1967).
5. J. Y. Savoie et P. Brassard. Annales de l'A.C.F.A.S. **34**, 38 (1967.)
6. J. Shoji. Chem. Pharm. Bull. Tokyo, **10**, 483 (1962).
7. S. Sternhell. Rev. Pure Appl. Chem. **14**, 15 (1964).
8. A. Wohl et C. Neuberg. Chem. Ber. **33**, 3099 (1900).
9. J. H. Bowie, D. W. Cameron, R. G. F. Giles et D. H. Williams. J. Chem. Soc. B, 335 (1966).
10. R. P. Bell et E. C. Baughan. J. Chem. Soc. 1947 (1937).
11. A. Einhorn, J. Cobliner et H. Pfeiffer. Chem. Ber. **37**, 106 (1904).
12. W. Baker, E. H. T. Jukes et C. A. Subrahmanyam. J. Chem. Soc. 1681 (1934).

Can. J. Chem. Downloaded from www.nrcresearchpress.com by 210.87.254.5 on 09/05/12
For personal use only.

Can. J. Chem. Downloaded from www.nrcresearchpress.com by 210.87.254.42 on 09/05/12
For personal use only.

Reductions with sulfurated borohydrides. II. Reduction of typical aldehydes

J. M. LALANCETTE AND A. FRÊCHE
Department of Chemistry, Faculty of Sciences, University of Sherbrooke, Sherbrooke, Quebec

Received October 2, 1968

Aromatic and aliphatic aldehydes can be reduced by sulfurated sodium borohydride to the corresponding alcohols. The reduction gives a quantitative yield of alcohol, without secondary products, if the reaction is performed at 0–10 °C. At higher temperatures (60°), the reduction is accompanied by the formation of disulfide. A good selection of the two possible reactions is obtained by adjusting the operating temperature. A mechanism explaining the reduction and the formation of sulfurated product is presented.

Canadian Journal of Chemistry, 47, 739 (1969)

We have indicated in a previous article that the product obtained from the reaction of sodium borohydride with sulfur, $NaBH_2S_3$, behaves as a reducer towards many organic functions (1). We wish to report the reduction of typical aldehydes with this new reagent.

Like $NaBH_4$, where all hydrogen atoms are available for reduction, the two hydrogens carried by the boron atom in $NaBH_2S_3$ are capable of acting as reducer. This conclusion is confirmed by the yield of alcohol observed in the course of reduction of benzaldehyde at low temperature; with a 2:1 molar ratio of aldehyde and sulfurated hydride, an almost quantitative yield of benzyl alcohol is obtained. If a 100% excess of aldehyde is used, a 50% yield of alcohol is observed. The very high yield of intermediate borate, as it will be reported later, is also an indication that both hydrogens are available for reduction.

The reduction must take place through a hydride shift from the boron atom to the positive carbon of the carbonyl group, as it is the case with other borohydrides. This hypothesis has been confirmed by reduction of benzaldehyde with deuterated, sulfurated borohydride. This reaction gave the expected deuterated alcohol, eq. [1].

In this sequence of reaction, when both deuteride or hydride ions have been used up,

[1]

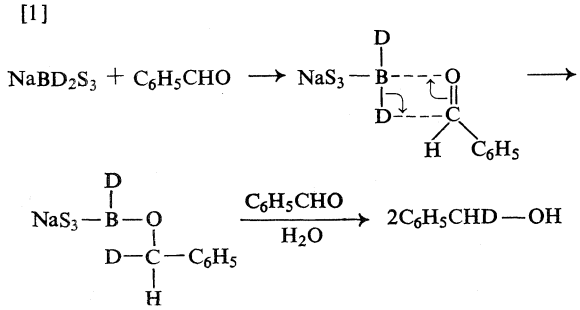

the intermediate ester must be a mixed orthothioborate : $NaS_3B—(O—CHD—C_6H_5)_2$ or $NaS_3B—(O—CH_2—C_6H_5)_2$. We have not been able to isolate this asymmetric boric ester but we have indirect evidence of the existence of a precursor to the symmetrical borate. The nuclear magnetic resonance (n.m.r.) measurement on a fresh reaction mixture, after the reduction of benzaldehyde by $NaBH_2S_3$, gave peaks that could not be related to any starting material or reaction products. Upon heating or simply keeping at room temperature, these peaks faded, as the expected peaks of the benzyl orthoborate appeared. This behavior is in accordance with the chemistry of the asymmetric orthoborates which are known to disproportionate spontaneously and very rapidly to symmetrical species rending their preparation impossible, except in the case of extreme steric hindrance (2). The disproportionation of an asymmetric borate is represented by eq. [2].

[2] $3\,RO—B—(OR')_2 \rightarrow (RO)_3—B + 2(R'O)_3—B$

The disproportionation should be eased greatly if B—S and B—O bonds are present on the same boron atom as it is the case with $NaS_3B(OCH_2C_6H_5)_2$. Following this spontaneous rearrangement, the orthoborate can be obtained in quantitative yield, by extraction of the crude reduction mixture with petroleum ether. This technique offers a very simple method of eliminating sulfur and inorganic residue from the organic substrate, since the sodium salt of the thioboric acid is completely insoluble in petroleum ether. Subsequent hydrolysis of the borate by water gives the expected alcohol, eq. [3].

[3] $3\,NaS_3—B—(OR)_2 \rightarrow Na_3S_9B\downarrow + 2B—(OR)_3$

$2\,B—(OR)_3 + 6\,H_2O \rightarrow 2\,H_3BO_3 + 6\,R—OH$

[4] 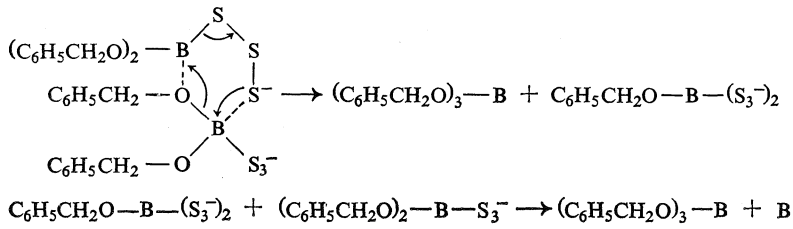

$$C_6H_5CH_2O{-}B{-}(S_3^-)_2 + (C_6H_5CH_2O)_2{-}B{-}S_3^- \longrightarrow (C_6H_5CH_2O)_3{-}B + B{-}(S_3^-)_3$$

[5] 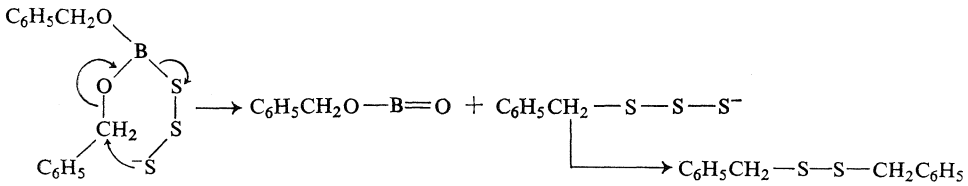

The most appropriate experimental method of reduction with $NaBH_2S_3$ calls for short contact time and low temperature. Under these conditions, the percentage of reduction is always above 95%, the yield very high, and secondary product almost nonexistent. Cinnamaldehyde was reduced to cinnamyl alcohol, with a 95% yield; *p*-nitro- and *m*-nitrobenzaldehyde were reduced quantitatively to the corresponding alcohol without interference by, or attack on the nitro group. When an equimolar mixture of *meta* and *para* nitrobenzaldehyde was treated with half the required amount of $NaBH_2S_3$, for complete reduction, the resulting mixture of alcohols was 60% *para*- and 40% *meta*-nitrobenzyl alcohol. This competitive reaction, where relative steric factors were identical, indicates the preferred attack of the hydride ion on the more positive C-1 carbon of *para*-nitrobenzaldehyde. With simple aliphatic aldehydes the reaction led exclusively to the corresponding alcohols, even in the case of pivaldehyde, a somewhat hindered aldehyde.

Under more drastic experimental conditions such as reflux in tetrahydrofuran or a long period of contact, secondary reactions appear, leading to the production of sulfurated products and degradation of these products. With benzaldehyde, for example, a variable ratio of benzyl alcohol and benzyl disulfide can be obtained by adjusting the time of contact and the temperature of reaction. Yields as high as 50% of disulfide have been observed. When the crude mixture of reduction is distilled, after reflux at high temperature (80°) the disulfide is decomposed into olefin; for example, with benzyl disulfide, *trans*-stilbene is obtained. This production of sulfurated products was observed to be general with all aldehydes when high temperature was used. The critical stage of the reaction, as far as secondary products are concerned, must be at the level of the asymmetric orthoborate. The hydride shift must be the first step of the reaction, since in the case of benzaldehyde for instance, the benzyl group is found in either alcohol or sulfurated by-product as the sole constituent. On the other hand, the symmetric orthoborate cannot be the entity responsible for the production of sulfurated products. This has been verified by treating benzyl orthoborate with large excess of $NaBH_2S_3$ or B_2S_3 at reflux temperature in tetrahydrofuran. In all cases, the boric orthoester has been recovered unaffected by the treatment.

Different mechanisms for the disproportionation represented by eq. [3] must then prevail, depending on the temperature, to explain the presence, or absence, of product incorporating sulfur. We believe that at low temperature, the disproportionation must take place through intermolecular reaction. With such a mechanism, the asymmetric borate is transformed into a symmetric orthoester, all the sulfur being concentrated on the same boron atom, eq. [4].

But if the temperature is high enough, a pattern of reaction calling for an intramolecular rearrangement of the asymmetric borate explains the incorporation of sulfur in the reaction products, eq. [5].

The metaborate upon hydrolysis, yields the corresponding alcohol and the polysulfide can

Can. J. Chem. Downloaded from www.nrcresearchpress.com by 210.87.254.42 on 09/05/12
For personal use only.

Can. J. Chem. Downloaded from www.nrcresearchpress.com by 210.87.254.42 on 09/05/12
For personal use only.

rearrange to give the disulfide and the olefin. If this explanation is true, when the reaction is completely intramolecular, the yield of alcohol should be equal to the yield of sulfurated product. We have observed that as the temperature of reflux increases, the ratio of alcohol to secondary product decreases to reach a 50:50 value and then remains constant as expected from the proposed mechanism.

Conclusion

It can be seen, from these results that sulfurated sodium borohydride, at low temperature, behaves as a good reducer towards aldehydes, without any undesirable side reaction.

It is certainly surprising that such a sharp distinction can be made between pure reduction (intermolecular mechanism) and sulfuration (intramolecular mechanism) by a mere 50° increase in temperature. The rationale for such different reactions must be found in the thermodynamics of the system. An increase in reaction temperature, increasing the entropy of the system, should hamper an intermolecular reaction and at the same time favor intramolecular rearrangement of the transitory asymmetric thioborate.

Experimental

Nuclear magnetic resonance (n.m.r.) measurements were made with a Varian, A-60 apparatus. Infrared (i.r.) measurements were made with a Perkin–Elmer, model 137 spectrophotometer. Vapor-phase chromatography (v.p.c.) measurements were made with a Microteck, model GC2000R apparatus using an Se30, 4 ft column.

Optimal Conditions for Reduction

(1) Reduction of Benzaldehyde

To a suspension of 0.20 mole (26.4 g) of $NaBH_2S_3$ in tetrahydrofuran (125 ml), 0.40 mole (42.4 g) of benzaldehyde was added dropwise. The reaction mixture was stirred and kept at 5–10° for 1 h. This contact was followed by acid hydrolysis with 50 ml of 10% hydrochloric acid. The precipitated sulfur was filtered off and the filtrate extracted with chloroform. After drying over magnesium sulfate, the evaporation of chloroform gave a yield of 95% of benzyl alcohol. The i.r. and v.p.c. of this product, from comparison with authentic benzyl alcohol, indicated that the reduction was complete and that the alcohol was the sole product (99%) of the reaction.

Following the same procedure, a 50% yield of benzyl alcohol was obtained with a $\frac{1}{4}$ molar ratio of reducer and benzaldehyde.

(2) Reduction of Typical Aldehydes

Following the procedure cited in *(1)*, butyraldehyde, pivaldehyde, cinnamaldehyde, *p*-nitrobenzaldehyde, and *m*-nitrobenzaldehyde were reduced to the corresponding alcohols. The alcohols were identified by comparison with i.r. spectra of authentic samples. The absence (traces, less than 0.5%) of sulfurated product was shown by v.p.c. The yields were of the order of 95%. When a mixture of *p*-nitrobenzaldehyde (0.10 mole, 15.1 g) and *m*-nitrobenzaldehyde (0.10 mole, 15.1 g) was treated with 0.05 mole (6.60 g) of $NaBH_2S_3$, following the above procedure, a mixture of alcohols and unreduced aldehyde was obtained. From the relative intensity of the aldehydic hydrogens at 10.28 δ (*meta*) and 10.33 δ (*para*) observed with the reaction mixture, 1.5 mole of *p*-nitrobenzaldehyde was reduced for each mole of *m*-nitrobenzaldehyde.

(3) Identification of the Intermediate Orthoborate

In an experiment similar to *(1)*, 0.40 mole (42.4 g) of benzaldehyde was reduced by 0.20 mole (26.4 g) of $NaBH_2S_3$. The crude mixture given by the reduction, before hydrolysis, was evaporated to dryness under reduced pressure. The yellow lumps were then extracted by 200 ml of petroleum ether and the extract, after filtration, was evaporated, giving an oily liquid, benzyl orthoborate. The weight of the crude borate was 44 g (0.14 mole), a quantitative yield according to eq. [3]. The i.r., n.m.r., and v.p.c. of the borate were identical with the same measurements made on a pure sample of benzyl orthoborate prepared from benzyl alcohol and boric acid, by the azeotropic method.

(4) Indication of the Presence of an Asymmetric Borate in the Reaction Mixture

The crude reaction mixture (as in *(1)*) was examined by n.m.r. immediately after the reaction subsided. Three peaks were observed at 6.38, 6.68, and 6.92 δ. There was a weak singlet at 4.96 δ. Upon standing at room temperature, the peak at 4.96 δ increased and the other peaks decreased; after 18 h, all peaks, between 4.0 and 7.0 δ had disappeared except the singlet at 4.96 δ. The n.m.r. of the reaction mixture was then identical with the same measurement made on authentic benzyl orthoborate, in tetrahydrofuran.

(5) Reduction with Deuterated Hydride

The preparation of $NaBD_2S_3$ and the reduction procedure of benzaldehyde was identical with the procedure cited above, the reaction being carried on a 200 mg scale. The n.m.r. of the orthoborate $(C_6H_5CHDO)_3$—B was showing a rather wide singlet (or an ill defined multiplet) at 4.80 δ. The ratio of aromatic protons to aliphatic protons at 4.80 δ was 5.5:1, instead of the 5:2 ratio for $(C_6H_5CH_2O)_3$—B.

Production of Sulfurated Products

(a) Production of Benzyl Disulfide

The reaction was repeated as in *(1)* except that the initial mixture was kept at 60° for several hours, under a nitrogen atmosphere. After cooling, the reaction mixture was hydrolyzed with 3% HCl, at 5–10 °C. The crude mixture was extracted with chloroform and benzyl disulfide crystallized out upon evaporation of the solvent. Most of benzyl alcohol was eliminated by filtration and the disulfide was recrystallized from ethanol to give light rosy crystals, m.p. 70°; n.m.r. singlet at 3.53 δ, singlet at 7.20 δ.

Anal. Calcd. for $C_{14}H_{14}S_2$: C, 68.25; H, 5.75; S, 26.00. Found: C, 68.47; H, 6.00; S, 26.19.

The aqueous phase contained the expected benzyl

alcohol, extracted with chloroform and identified as in *(1)*. The reduction of carbonyl was complete (no trace of aldehyde left in the crude mixture, before hydrolysis, as shown by the infrared). The relative yield of alcohol to benzyl disulfide decreased, as time of contact was increased. After 20 h of contact, there was no significant increase in the yield of benzyl disulfide which remained in the 50% range. A higher temperature of reaction or a faster addition of aldehyde, as a rule, increased the percentage of sulfurated product which, in all cases levelled when a 1:1 ratio of benzyl disulfide to benzyl alcohol was reached.

The formation of disulfide was observed with all aldehydes under experimental conditions as in *(a)*.

(b) Production of Stilbene

If the crude mixture obtained after hydrolysis in *(a)* was extracted with chloroform, and distilled under vacuum, two fractions were obtained. The first one, b.p. 88°/0.8 mm, was benzyl alcohol. The second one, b.p. 180–190°/0.8 mm was stilbene (100% *trans* by n.m.r.).

(c) Stability of Various Intermediates

Benzyl orthoborate—Pure, redistilled benzyl orthoborate (5 g) was treated with 1.0 g of $NaBH_2S_3$ at 60 °C for 5 h. After removal of solid material by filtration, the residual material gave an i.r. identical with the same measurement made on the starting boric ester, indicating the absence of reaction.

A similar experiment, using boron sulfide, left the benzyl orthoborate unaffected.

Benzyl disulfide—Pure, recrystallized benzyl disulfide (0.500 g) was decomposed to stilbene, and another product by heating in a test tube for 15 min at 200°, under nitrogen atmosphere. The presence of stilbene (*trans*) was confirmed by the presence of the typical pattern for the *trans* isomer, in n.m.r. and by v.p.c.

Acknowledgments

We thank the National Research Council of Canada and the Defence Research Board of Canada (grant no. 9530–30) for financial assistance.

1. J. M. LALANCETTE, A. FRÊCHE, and R. MONTEUX. Can. J. Chem. 46, 2754 (1968).
2. H. STEINBERG. Organoboron chemistry. Vol. I. Interscience Publishers, Inc., New York. 1964. p. 852.

Can. J. Chem. Downloaded from www.nrcresearchpress.com by 210.87.254.42 on 09/05/12
For personal use only.

Anisotropic effects on proton magnetic resonance frequencies of substituted barbituric acids[1]

GEORGE A. NEVILLE AND DENYS COOK
Research Laboratories, Food and Drug Directorate, Department of National Health and Welfare, Ottawa, Canada
Received June 14, 1968

Several pharmacologically important barbituric acids were examined by proton magnetic resonance spectroscopy in trifluoroacetic acid, *p*-dioxane, and dimethyl sulfoxide-d_6. The data obtained greatly facilitate identifying and distinguishing barbiturates. Variations in chemical shift with alkyl substitution have been discussed, and the suggestion has been put forward that—the CH_3(Et) protons may be a sensitive probe for detecting changes in anisotropy (both ring and C=O) in a series of barbiturates. Evidence for the preferred configuration of C-5 phenyl, ethyl, and isopropyl substituents was obtained. Concentration studies by both proton magnetic resonance and infrared spectroscopy indicate that the barbiturates examined exist predominantly as solvated monomers rather than as dimers or oligomers.

Canadian Journal of Chemistry, 47, 743 (1969)

Can. J. Chem. Downloaded from www.nrcresearchpress.com by 210.87.254.40 on 09/05/12
For personal use only.

Introduction

This proton magnetic resonance study of substituted barbituric acids was undertaken to obtain chemical shift and coupling data (*i*) to aid the identification of barbiturates that have very similar infrared spectra or melting points, (*ii*) to gain some insight into the possible existence of a partial ring current or localized anisotropic effects from a study of magnetic shielding and deshielding of ring substituents, and (*iii*) to determine if any tautomerism could be detected by proton magnetic resonance (p.m.r.) under normal conditions. When this work was begun, no comprehensive p.m.r. study of well-known barbiturates had been reported although some use of p.m.r. had been made in conjunction with the synthesis of new barbiturates (1). In the meantime, Rücker (2) published a qualitative analysis of barbituric acid derivatives by p.m.r. and noted the superiority of p.m.r. over other spectroscopic methods for distinguishing between barbiturates.

Results

Frequency data from p.m.r. studies are given in Tables I–III for several barbiturates in trifluoroacetic acid, *p*-dioxane, and dimethyl sulfoxide-d_6. Trifluoroacetic acid and *p*-dioxane solutions of 5-ethyl-5-phenylbarbituric acid (phenobarbital) and of 1-methyl-5-ethyl-5-phenylbarbituric acid (mephobarbital) have been examined by p.m.r. for a concentration effect while the same solutes have been examined by infrared (i.r.) spectroscopy in chloroform solution for a concentration effect.

[1]Presented in part at the Canadian Symposium on Applied Spectroscopy, Montreal, October 26, 1966.

Discussion

It is assumed that the barbiturate ring in the 5-substituted compounds discussed here is planar, as has been shown for 5,5-diethylbarbituric acid (**1**) (3) and its potassium salt (4). In **1** and **2** there is a barely perceptible fine structure in the CH_2(Et) and CH_3(Et) resonances which has been attributed to long range coupling ($J \sim 0.01$ p.p.m.). If, in fact, the fine structure is due to non-planarity of the ring, and therefore to non-equivalence of the two Et groups, then this small difference in chemical shift is barely significant when compared with chemical shift differences arising from substituent and solvent effects.

(a) Inductive and Anisotropy Effects

Effect of N-Substitution on CH_3(Et) and CH_2(Et) Chemical Shifts

Although the changes in chemical shift for the methyl protons, of the ethyl substituents, i.e. CH_3(Et), in the C-5 position of the barbiturate ring (Table I) amount to only a few (3–5) Hz with *N*-substitution, these changes appear to be real. The chemical shift (0.83 p.p.m., $CDCl_3$) for the CH_3(Et) of **2** shows weak shielding of these protons relative to the value (~0.90 p.p.m., $CDCl_3$) (5) for methyl protons in saturated hydrocarbons. When the latter value is corrected for the deshielding effect from β-substituents like CO_2H and CO_2Alkyl, which result in a shift of 0.25 p.p.m. (5) to lower frequencies, then the model chemical shift becomes 1.15 p.p.m., in close agreement with the observed chemical shifts for

Can. J. Chem. Downloaded from www.nrcresearchpress.com by 210.87.254.40 on 09/05/12
For personal use only.

TABLE I

Proton magnetic resonance frequencies of some substituted barbituric acids in chloroform-*d* (CHL), trifluoroacetic acid (TFA), *p*-dioxane (DOX) and dimethyl sulfoxide-d_6 (DMS) (chemical shifts (δ) in p.p.m. downfield from tetramethylsilane (TMS))

	Substitution				N—H				N—CH_3				—CH_2—(Et)				—CH_3(Et)				—C_6H_5			
No.	1	3	5	5	CHL	TFA	DOX	DMS	CHL	TFA	DOX	DMS	CHL	TFA	DOX	DMS	CHL	TFA	DOX	DMS	CHL	TFA	DOX	DMS
1	H	H	Et	Et	—	10.1	10.1	11.4	—	—	—	—	—	2.23	1.93	1.87	—	1.02	0.83	0.80	—	—	—	—
2	Me	H	Et	Et	9.40	10.2	10.1	11.6	3.32	3.45	3.22	3.18	2.07	2.22	1.90	1.87	0.83	0.95	0.78	0.75	—	—	—	—
3	H	H	Et	Ph	8.70	10.1	10.2	11.7	—	—	—	—	2.50	2.70	2.42	2.35	1.00	1.12	0.92	0.90	7.37	7.43	7.35	7.37
4	Me	H	Et	Ph	8.81	10.2	10.2	11.9	3.33	3.50	3.23	3.23	2.50	2.70	2.40	2.38	0.97	1.07	0.90	0.88	7.31	7.40	7.32	7.37
5	H	H	Et	*i*-Pr	—	10.1	10.0	11.3	—	—	—	—	—	2.42	2.00	1.90	—	0.97	0.80	0.73	—	—	—	—
5	H	H	Et	*i*-Pr		—C(H)—										>C(CH_3)$_2$								
						TFA	DOX	DMS						TFA	DOX	DMS								
						2.47	2.23	2.05						1.17	1.00	0.93								

TABLE II

Proton magnetic resonance frequencies of some substituted barbituric acids in trifluoroacetic acid (TFA), *p*-dioxane (DOX), and dimethyl sulfoxide-d_6 (DMS)

	Substitution				N—H			—C_6H_5			—CH_2—(5)			N—CH_3			—CH_3(5)		
No.	1	3	5	5	TFA	DOX	DMS	TFA	DOX	DMS	TFA	DOX	DMS	TFA	DOX	DMS	TFA	DOX	DMS
6*	H	H	H	H	9.97	9.92	11.0	—	—	—	4.00	†	3.50	—	—	—	—	—	—
7	H	H	Me	Ph	10.0	10.0	11.4	7.43	7.35	7.38	—	—	—	—	—	—	2.08	1.77	1.82
8	Me	Me	H	H	—	—	—	—	—	—	4.08	†	3.70	3.47	3.20	3.12	—	—	—
9	Ph	H	H	H	10.0	10.2	11.5	7.25‡	8.05‡	7.35‡	4.10	†	3.78	—	—	—	—	—	—

*Anhydrous.
†Peaks obscured by solvent.
‡Complex multiplet centered at indicated frequency.

Can. J. Chem. Downloaded from www.nrcresearchpress.com by 210.87.254.40 on 09/05/12
For personal use only.

TABLE III

Proton magnetic resonance frequencies of some substituted barbituric acids in trifluoroacetic acid (TFA), *p*-dioxane (DOX), and dimethyl sulfoxide-d_6 (DMS)

	Substitution				N—H			>C=CH			—CH_2 (Ring)			—CH_2(Et)			—CH_3(Et)		
No.	1	3	5	5	TFA	DOX	DMS	TFA	DOX	DMS	TFA	DOX	DMS	TFA	DOX	DMS	TFA	DOX	DMS
10	H	H	Et		10.0	10.0	—	6.05	5.75	—	2.9–1.9 1.8–1.5 1.4–1.0	2.2–1.8 1.8–1.4 1.1–0.6	— — —	2.40	1.98	—	1.02	0.81	—
11	Me	H	Me		10.1	9.93	11.4	6.05	5.67	5.63	2.4–1.5	2.2–1.7 1.7–1.4	2.3–1.7 1.7–1.3	—	—	—	—	—	—

					N—CH_3			—CH_3(5)		
					TFA	DOX	DMS	TFA	DOX	DMS
11	Me	H	Me		3.45	3.17	3.12	1.80	1.48	1.47

Can. J. Chem. Downloaded from www.nrcresearchpress.com by 210.87.254.40 on 09/05/12
For personal use only.

the CH_3(Et) protons of *n*-propionamide (1.13 p.p.m., $CDCl_3$) (6) and *sym*-diethylurea (1.10 p.p.m., $CDCl_3$)[2]. Since any inductive electron withdrawal from the CH_3(Et) protons in the barbiturate ring is exerted as a γ-substituent effect, a much better model for comparison purposes is *N*,*N*′-dimethyl-α,α-diethyl malonamide. In this compound the CH_3(Et) protons absorb at 1.00 p.p.m. ($CDCl_3$); thus, the CH_3(Et) protons in **2** are shielded by 11 Hz relative to the same protons in the malonamide model. This is, perhaps, the best obtainable model for substituents at the C-5 position of the barbiturate ring since it represents both the inductive effects of γ-substitution and the anisotropy effects of the amide grouping also present in the barbiturate ring. In the barbiturate ring, however, delocalization of the π-electron system in the amide linkages is expected to generate a partial ring current (incomplete because of the C-5 methylene unit) which could induce diamagnetic shielding above and below the planar (3, 4) barbiturate ring. The CH_3(Et) protons in the C-5 position, therefore, might provide a sensitive probe for detecting changes in anisotropy (both ring and/or C=O) in a series of barbiturates. Comparison of the chemical shifts for the CH_3(Et) protons in Table I shows these protons to be shielded by 0.05–0.07 p.p.m. in 1-methyl-5,5-diethylbarbituric acid (**2**) relative to 5,5-diethylbarbituric acid (**1**), by 0.02–0.05 p.p.m. in 1-methyl-5-ethyl-5-phenylbarbituric acid (**4**) relative to 5-ethyl-5-phenylbarbituric acid (**3**), and by 0.03–0.07 p.p.m. in 5-ethyl-5-isopropylbarbituric acid (**5**) relative to 5,5-diethylbarbituric acid (**1**). This weak shielding in **2** and **4** is attributed to electron release by the 1-methyl substituents, assuming no conformational changes in the planar barbiturate. The crystal structures of the potassium salt of 5,5-diethylbarbituric acid (4) and of 5,5-diethylbarbituric acid (3) are known, and show that the methyl protons (Et), in their preferred configuration (**12**), are fully exposed to the shielding effects of the (nearly planar) ring π-electrons. The weak shielding effects observed above suggests that the same configuration, (**12**) for C-5 ethyl substituents exists in solution as in the solid state.

The chemical shift data in Table I for the methylene protons of the ethyl substituents, i.e. CH_2(Et), in the C-5 position show that no change occurs for the CH_2(Et) proton frequencies with methyl substitution at N-1 of the barbiturate ring. In the suggested preferred configuration (**12**) the CH_2(Et) protons are remotely exposed to the deshielding regions of the C-4 and C-6 carbonyl groups and little better oriented towards the deshielding region that might arise from a partial ring current in the planar ring. Any anisotropic effects arising from these carbonyl groups due to *N*-methylation might be expected to have little effect on the poorly oriented CH_2(Et) protons, particularly when the shielding effects observed for the more favorably oriented CH_3(Et) protons are so small.

Effects of an Isopropyl Substituent at C-5

When an isopropyl substituent is introduced at C-5 of the barbiturate ring as in **5**, the methyl protons of the isopropyl group, i.e. CH_3(*i*-Pr), are deshielded by 0.20 p.p.m. relative to the CH_3(Et) protons in the same molecule. While the barbiturate molecule appears to tolerate one methyl group hovering over its ring (~2.1 Å^3 between a CH_3 proton and the plane), the possibility of two methyl groups, as in the isopropyl substituent, over the ring appears to involve too much steric repulsion (~1.1 Å,[3] minimum distance between a CH_3 proton and the C-4 or C-6 carbonyl oxygen atom). Since the CH_3(*i*-Pr) protons are deshielded relative to the CH_3(Et) protons, it appears that the isopropyl methyl groups must be oriented away from the ring (i.e. *exo* conformation) such that the CH_3(*i*-Pr) protons are exposed to the deshielding regions of the C-4 and C-6 carbonyl groups and of the ring itself. In the *exo* conformation the minimum distance between the methyl (*i*-Pr) protons and the carbonyl oxygen atoms, and also between both types of protons, CH_3(Et) and CH_3(*i*-Pr), is approximately 1.7 Å^3.

It is also noteworthy that the 5-isopropyl substituent in **5** results in shielding of the CH_3(Et) protons of **5** equal to that produced by the 1-methyl substituent of **2**. This shielding in **5** relative to **1** is attributed to the greater electron release of an isopropyl group ($\sigma^* = -0.19$) to the C-5 carbon atom compared to that from an ethyl group ($\sigma^* = -0.10$) (7) which could then produce an increased anisotropy effect from the C-4 and C-6 carbonyl groups. The deshielding

[2]George A. Neville. Unpublished data.

[3]Distances estimated from Dreiding models.

of the methylene protons (Et) in **5** relative to **1** may be due in part to the above difference in inductive effects and in part to steric hindrance by the isopropyl group in the *exo*-conformation, proposed above, resulting in longer conformational lifetimes for the CH_2(Et) protons in the deshielding regions of the C-4 and C-6 carbonyl groups.

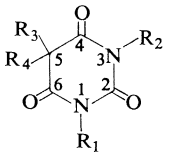

No.	R_1	R_2	R_3	R_4
		Substitution		
1	H	H	C_2H_5	C_2H_5
2	CH_3	H	C_2H_5	C_2H_5
3	H	H	C_2H_5	C_6H_5
4	CH_3	H	C_2H_5	C_6H_5
		Substitution		
No.	R_1	R_2	R_3	R_4
5	H	H	C_2H_5	$(CH_3)_2CH$
6	H	H	H	H
7	H	H	CH_3	C_6H_5
8	CH_3	CH_3	H	H
9	C_6H_5	H	H	H
10	H	H	C_2H_5	
11	CH_3	H	CH_3	

Effect of a Phenyl Substituent at C-5

Comparison of the chemical shift values for the CH_3(Et) and CH_2(Et) protons of **3** are deshielded by 0.47–0.49 p.p.m. and by 0.09–0.10 p.p.m. respectively relative to **1**. These shifts would appear to be due largely to the effect of the C-5 phenyl group being in the same plane as the C_{2v} mirror plane of the barbiturate ring. In this configuration the methylene and methyl protons are exposed to the deshielding region of the phenyl ring but this deshielding would be increased somewhat by inductive electron withdrawal by the phenyl ring ($\sigma^* = +0.60$) (7) from the C-4 and C-6 carbonyl groups. Also, in this configuration, the 1-methyl protons of **4** are exposed to the deshielding region of the phenyl ring; thus, the small downfield shift (0.01–0.05 p.p.m.) for these protons in **4** compared to **2** is supporting evidence for this configuration as the preferred one.

The introduction of a 1-methyl substituent in **4** results in shielding (relative to **3**) of 0.02–0.05 p.p.m. in the CH_3(Et) protons and this effect is due to the anisotropy of the C-4 and C-6 carbonyl groups as described above. It is interesting that the phenyl proton frequencies of **3** and of **7** (Table II) are identical whereas those of **4** show a slight shielding effect attributable to weak anisotropic shielding by the C-4 and C-6 carbonyl groups from introduction of the 1-methyl group.

The C-5 methyl protons of 5-methyl-5-phenylbarbituric acid (**7**) (Table II) are deshielded by 0.28–0.35 p.p.m. compared to those of 5-(1-cyclohexenyl)-1,5-dimethylbarbituric acid (**11**) (Table III). This shift is due mainly to the larger paramagnetic anisotropy from a benzene ring than from an isolated double bond having its plane in the C_{2v} mirror plane of the barbiturate ring.

(b) Concentration Effects

The effects of varying the concentration of an acid in solution were investigated by both proton magnetic resonance and infrared spectroscopy. In dilute alcohol-free chloroform solution (0.003 *M*) **3** and **4** gave infrared spectra in which the NH stretching frequency was at 3380 cm^{-1}, clearly not involved in hydrogen bonding, and therefore indicative of each acid being in its monomeric state. In the more concentrated solutions (up to 0.024 *M*, i.e., near saturation) a low intensity band developed near 3210 cm^{-1} showing the presence of a small amount of some more complicated species, possibly a dimer. The same infrared frequencies and behavior on dilution of mephobarbital, i.e. **4**, in chloroform (alcohol-free?) were recently reported by Kyogoku *et al.* (8). It is assumed, therefore, that the p.m.r. spectra of nearly saturated $CDCl_3$ solutions are those of predominantly monomeric molecules.

The effect of varying concentration on p.m.r. frequencies was examined with two representative barbiturates. 5-Ethyl-5-phenyl-barbituric acid and 1-methyl-5-ethyl-5-phenylbarbituric acid were chosen because the former can exist as long hydrogen bonded chains whereas the latter can only form dimers. The fact that no significant change occurs in the chemical shift values for either of these barbiturates with variation of concentration (from 160–10 mg/ml) in trifluoroacetic acid and in *p*-dioxane is taken as an indication that the solute is monomeric in the solvents over the concentration ranges examined. In the more dilute TFA samples (40 mg/ml and less) the NH peak was too broad to be seen. However, because of the sensitivity of the resonances of the

Can. J. Chem. Downloaded from www.nrcresearchpress.com by 210.87.254.40 on 09/05/12
For personal use only.

Can. J. Chem. Downloaded from www.nrcresearchpress.com by 210.87.254.40 on 09/05/12
For personal use only.

methyl protons to changes in shielding caused by substituent and solvent effects, the frequencies of these protons provide a more reliable index to concentration effects. Since the chemical shifts for the barbiturates in dimethyl sulfoxide closely parallel those in *p*-dioxane, one may safely assume that the solutes are completely solvated as monomers in both these solvents. Trifluoroacetic acid *p*-dioxane and dimethyl sulfoxide, having relatively large dielectric constants, would be expected to break up any dimers or oligomers in solvating these barbiturates over the concentration range used.

(c) Solvent Effects

The CH_2(Et) protons of the C-5 ethyl substituents are more sensitive to solvent effects than the CH_3(Et) protons. Table I shows these shifts to be in the order, δ for TFA > $CDCl_3$ > DOX > DMS. These values would be in keeping with the solute–solvent interactions depicted in **13**, **14**, and **15**. In such hydrogen-bonded interactions the CH_2(Et) protons are expected to be less effected by anisotropy changes than the CH_3(Et) protons and more dependent on inductive effects than the CH_3(Et) protons.

Chloroform would form only a weak hydrogen bond to a carbonyl oxygen atom of the barbiturate ring (**13**) which would result in electron displacement away from the ring thus slightly deshielding the CH_2(Et) protons relative to the isolated molecule. DMS and dioxane would have the opposite effect (**14**) since they would enhance the tendency of the NH group to ionize. This would result in shielding of the CH_2(Et) protons. Since DMS is probably a little better donor than dioxane this accounts for the slightly smaller chemical shift values in DMS. In TFA the complex **15** is probably formed,[4] and the overall deshielding effect (relative to $CDCl_3$ solution) would be due to a balance between the good COOH proton donor and the rather weakly basic CO group in TFA.

Inductive effects due to solvent interactions would give rise to shifts in the CH_3(Et) resonances in the same direction as those induced by ring currents. The changes due to inductive effects are expected to be small because of the large number of bonds involved.

The *N*-methyl proton resonances can be analyzed in a similar manner. Inductive effects on these protons due to solvent interactions will be the same as just discussed for the CH_2(Et) and CH_3(Et) protons. Thus Table I shows the *N*—CH_3 resonances for **2** and **4** at about the same δ-value in DOX and DMS with both slightly upfield from $CDCl_3$, and downfield from $CDCl_3$ in TFA. These values are again quite consistent with the solvent interactions shown in **13**, **14**, and **15**. It is difficult to separate the inductive and ring current effects since they both operate in the same direction.

(d) Tautomerism

No indications of the presence of two tautomeric forms (lactam ⇌ lactim) could be seen in the p.m.r. spectra of the free barbituric acids listed in Tables I–III. A single, sometimes broad,[5] peak near 10 δ has been attributed to the NH proton. This, however, does not preclude the possibility of tautomerism because the concentration of tautomers in equilibrium in the solvents employed could be too small to be detected. However, peaks which we have attributed to NH protons have been found in the monosodium salts of 5,5-diethyl- and 5-ethyl-5-phenylbarbituric acids at 3.53 and 5.82 δ respectively in dimethyl sulfoxide-d_6. Although these anomalously high field absorptions occur in the same range (4.00–6.01 δ) as hydroxyl proton resonances in dimethyl sulfoxide (11) they do not necessarily indicate the existence of tautomerism since the negative charge in the salts would shift the resonance to higher field.

As a corollary to the concentration study, these results would reinforce the conclusion that no

[4]In glacial acetic acid (AcOH), **2** shows the same chemical shift value for the CH_3(Et) and N—CH_3 protons as in chloroform-*d* solution. Ma and Warnhoff (9) observed that the N—CH_3 signal of *N*-methyl amides was shifted downfield by nearly 0.2 p.p.m. in TFA relative to $CDCl_3$ with little or no change in AcOH relative to $CDCl_3$ solution whereas the *N*—CH_3 signal of aliphatic tertiary and secondary amines is shifted downfield by 0.6–0.8 and by 0.45–0.6 p.p.m. respectively in TFA. It would appear from this data that little protonation of amides occurs in TFA and that less protonation of barbiturates occurs than with amides. Hydrogen bonding between TFA and carboxylic acid esters has been reported (10). In the hydrogen bonded complex (**15**) a certain amount of proton transfer may occur but the extent of this cannot be deduced from the present measurements.

[5]The NH band is moderately sharp in both dimethyl sulfoxide and dioxane solution spectra relative to the broad band commonly seen for amides in chloroform solution. The band is broadened in trifluoroacetic acid solution spectra.

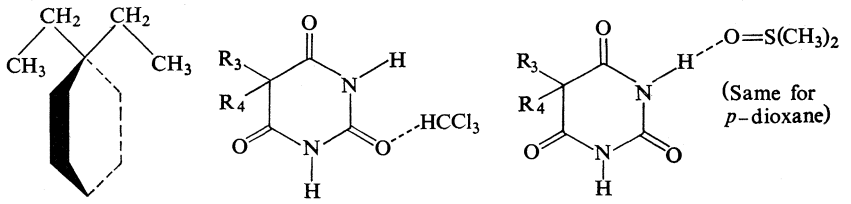

12 13 14

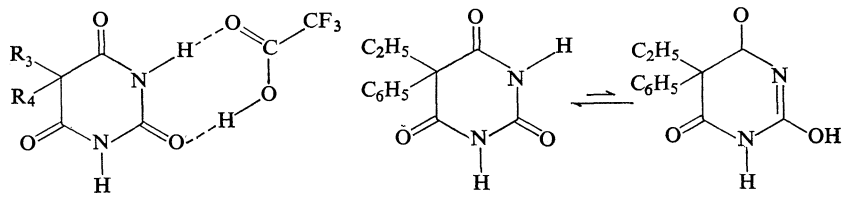

15 16

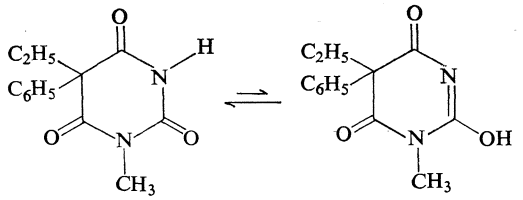

17

tautomerism, detectable by p.m.r., occurs in the barbiturates examined. If two tautomeric forms occurred (**16** and **17**) it might be expected that they would have different ring anisotropies which would be detected in the tautomeric proton resonances, and more particularly, in the CH_3(Et) proton frequencies. Tautomerism, however, could be masked in p.m.r. by rapid exchange of protons between the tautomers.

Experimental

Proton magnetic resonance spectra were obtained from a Varian A-60A spectrometer with ambient probe temperature at $40\pm2°$. Chemical shifts (δ) were measured downfield from tetramethylsilane (TMS), used as an internal reference, and are considered to be accurate to ±0.02 p.p.m. The NH chemical shift was taken as the center of the broad band, and is estimated to be accurate to ±0.05 p.p.m. Sweep width calibration was periodically checked against the 7.27 δ chloroform signal downfield from TMS. Concentrations of solutions were approximately 100 mg solute per ml solvent unless stated otherwise.

Infrared spectra were recorded on a Perkin–Elmer 621 grating spectrometer using 1.0 mm cells. The frequency counter was checked against established indene calibration frequencies. Alcohol-free chloroform was prepared from Mallinckrodt AR chloroform (containing ~0.75% ethanol) by (*i*) extraction with concentrated sulfuric acid, (*ii*) washing with distilled water until neutral, (*iii*) drying overnight over anhydrous magnesium sulfate, and (*iv*) distilling the dried solvent. The main fraction, b.r. 60.8–61.0°, was stored in the dark and used within two days after distillation.

All barbiturates except two were pharmaceutical grade having been obtained from various pharmaceutical manufacturers. All gave melting ranges in accordance with reported values, and were used without further purification. 1-Phenylbarbituric acid was obtained from the Aldrich Chemical Co., and was used without further purification. 1,3-Dimethylbarbituric acid (m.p. 122°) was prepared by the method of Biltz and Wittek (12).

N,N'-Dimethyl-α,α-diethylmalonamide was prepared by the method of Cohn (13) with modification. After 5,5-diethylbarbituric acid (0.0263 moles) had been heated under reflux for $3\frac{1}{2}$ h in aqueous sodium hydroxide solution (0.064 moles NaOH/40 ml water) with dimethyl sulfate (0.0640 moles), the crude product was ground up with concentrated hydrochloric acid. The acid insoluble solid was recrystallized from chloroform – petroleum ether mixed solvent to give the product m.p. 151–153°. Cohn reported a m.p. of 149°. The p.m.r. spectrum of the product showed a triplet (6H), a quartet (4H), a doublet (6H), and a broad band (2H) centered at 0.82, 1.92, 2.83, and 7.0 p.p.m. respectively downfield from TMS in

Can. J. Chem. Downloaded from www.nrcresearchpress.com by 210.87.254.40 on 09/05/12
For personal use only.

$CDCl_3$. The infrared spectrum ($CHCl_3$, 0.1 mm cell) showed a free (sharp) and an associated (broad) amide NH stretching band at 3470 and 3300 cm^{-1} respectively and a strong carbonyl band at 1665 cm^{-1} with a shoulder at 1630 cm^{-1}.

Acknowledgments

We are grateful to Mr. H. W. Avdovich for assistance with the preparative work; to Mr. Z. R. Regnier for recording the infrared spectra; and to Mr. P. Hanbury for some of the nuclear magnetic resonance spectra. We would like to acknowledge the kindness of many manufacturers in generously making samples available to us.

1. A. K. Bose and G. Mina. J. Org. Chem. **30**, 812 (1965).
2. G. Rücker. Archiv. der Pharm. **299**, 688 (1966).
3. F. Bertinotti, M. Bonamico, A. Braibauti, F. Coppola, and G. Giacomello. Ann. Chim. (Rome) **49**, 825 (1959).
4. J. Berthou, B. Rérat, and C. Rérat. Acta Cryst. **18**, 768 (1965).
5. L. M. Jackman. Nuclear magnetic resonance spectroscopy. 4th impression. The Pergamon Press, Ltd., New York. 1964. pp. 52–53.
6. N. S. Bhacca, L. F. Johnson, and J. N. Shoolery. Varian NMR Spectra Catalog, 1962. Spectrum #40.
7. R. W. Taft, Jr. *In* Steric effects in organic chemistry. *Edited by* M. S. Newman. John Wiley & Sons, Inc., New York. 1956. p. 591.
8. Y. Kyogoku, R. C. Lord, and A. Rich. Nature, **218**, 69 (1968).
9. J. C. N. Ma and E. W. Warnhoff. Can. J. Chem. **43**, 1849 (1965).
10. I. M. Ginzburg. Spektroskopiya Metody i Primenenie, Akad. Nauk SSSR, Sibirsk. Otd. 167 (1964).
11. O. L. Chapman and R. W. King. J. Am. Chem. Soc. **86**, 1256 (1964).
12. H. Biltz and H. Wittek. Ber. **54**, 1035 (1921).
13. G. Cohn. Pharm. Zentral. **53**, 27 (1912).

Can. J. Chem. Downloaded from www.nrcresearchpress.com by 210.87.254.40 on 09/05/12
For personal use only.

Can. J. Chem. Downloaded from www.nrcresearchpress.com by 210.87.254.5 on 09/05/12
For personal use only.

Etude de résonance magnétique nucléaire dans la série des pregnane et D-homopregnane

KRZYSZTOF JANKOWSKI ET CASIMIR BERSE
Département de Chimie, Université de Montréal, Montréal, Québec

Reçu le 13 septembre 1968

L'influence d'environnement sur le déplacement chimique du méthyle-20 dans les spectres de résonance magnétique nucléaire (r.m.n.) a été étudiée pour la série des dérivés du prégnane. Les différences dans le déplacement chimique du méthyle-20 des produits examinés par rapport aux produits modèles ont été calculés. Le méthyle-20 a été transposé en le méthyle-17 ou -17*a* par la D-homoannulation et les spectres de r.m.n. de tous les isomères ont été interprétés.

Canadian Journal of Chemistry, **47**, 751 (1969)

Au cours de nos études précédentes (1),[1] nous avons fait quelques observations concernant l'influence des envrionnements chimiques sur le déplacement chimique du méthyle-20 des stéroides dans le spectre de résonance magnétique nucléaire (r.m.n.). Le déplacement chimique du méthyle-20 des stéroides différemment substitué réflète les changements dans leur structure parfois mieux que celles des méthyles-10 et -13.

Nous avons complété nos études et le Tableau I résume nos observations en donnant la position du méthyle-20, la correction $\Delta\delta$ due à la présence des substituants, la différence entre le méthyle-20 des acétyles-17 α ou β, la différence entre les déplacements chimiques des méthyles des acétyles et des cétales correspondantes. L'hydroxy-3β pregnène-5 one-20 (**1**) et son cétal (**2**) ont été utilisés comme produits de référence.

La différence entre le méthyle d'acétyl-17 α ou β varie entre 0.19–0.20 p.p.m. Le cétal correspondant donne la différence analogue entre 0.10–0.15 p.p.m.

La différence pour le méthyle-20 entre les paires des composés (cétal–acétyl, par exemple, **1–2**, **3–8** etc....) varie entre 0.67–0.89 p.p.m.

Nous voulons signaler que le déplacement chimique du méthyle-20 dans la série du prègnane même, donc un stéroide portant l'éthyle dans la position-17, réflète aussi le changement dans l'environnement.

Ensuite le méthyle-20 des certains stéroides (**3**, **6**) a été transformé en méthyle-17 ou -17*a* par la réaction de la D-homoannulation.

Les spectres de r.m.n. des D-homostéroides n'ont pas été étudiés.

Les seuls récents travaux qu'on peut citer sont des articles de Pivnitsky et Torgov (2), Trenner *et al.* (3) et Neudert et Röpke (4). Nos essais consistent à lier le déplacement chimique des méthyles-17 ou -17*a* avec leur position dans l'espace. Les données de r.m.n. des produits sont résumées dans le Tableau III.

Les stéroides hydroxy-17 acétyl-17 sont très sensibles en milieu basique ou en présence des acides de Lewis donnent les D-homo-17 ou -17*a* cétones. Ce réarrangement a été étudié par plusieurs auteurs (5^2–7) pour les différents stéroides. Nous avons effectué (voir le Tableau II) l'isomérisation des produits acétyl-17β hydroxy-17α (**3**) et acétyl-17α hydroxy-17β (**6**) en utilisant les bases classiques (KOH dans l'alcool) ou les acides de Lewis (BF_3, Al_2O_3 etc...).

Les quatre produits D-homo possibles dans les réactions ont été nommés **A**, **B**, **C** et **D**:

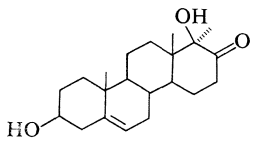

A

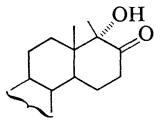

B

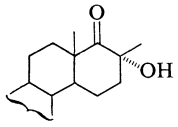

C

[1]Voir aussi la bibliographie de cet article.

[2]Voir aussi la bibliographie de ce chapitre.

Can. J. Chem. Downloaded from www.nrcresearchpress.com by 210.87.254.5 on 09/05/12
For personal use only.

TABLEAU I

Résonance magnétique nucléaire du méthyle-20 des dérivés* dans la série des hydroxy-3β pregnènes-5 substitués (δ (p.p.m.) dans $CDCl_3$)

Composé	R	R′	R″	R‴	Autres	C-20	Δδ C-20	Δδ C-20 α/β acétyl	Δδ C-20 acétyl–cétal	Ref.
1	CH_3CO	H	H	H		2.15	0	—	+0.87	1
2	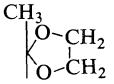	H	H	H		1.28	0	—	—	1
3	CH_3CO	OH	H	H		2.27	+0.12	—	+0.89	1
4	CH_3CO	OH	OH	H		2.10	−0.17	—	+0.80	1
5	CH_3CO	OH	$NHCH_2COOC_2H_5$	H		2.03	−0.24	—	+0.71	1
6	OH	CH_3CO	H	H		2.08	—	−0.19	+0.80	1
7	H	CH_3CO	H	H		1.95	—	−0.20	+0.67	1
8	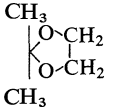	OH	H	H		1.38	+0.10	—	—	1
9	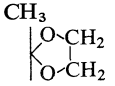	OH	OH	H		1.30	−0.08	—	—	1
10	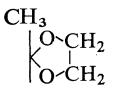	OH	$NHCH_2COOC_2H_5$	H		1.38	−0.06	—	—	1
11	OH	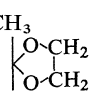	H	H		1.28	—	−0.10	—	1
12	H	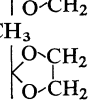	H	H		1.13	—	−0.15	—	1
13	CH_3CO	OH	H	CH_3		2.24	+0.09	—	—	4
14	CH_3CO	H	H	CH_3		2.11	+0.03	—	—	4
15	CH_3CO	H	H	—	Δ^{15}	2.23	+0.08	—	0.74	4
16	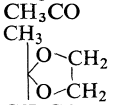	H	H	—	Δ^{15}	1.49	+0.21	—	—	4
17	CH_3CO	—	H	—	Δ^{14}, Δ^{16}	2.35	+0.20	—	—	16
18	CH_3CO	H	CH_3	H		2.19	+0.04	—	—	17

*Composés du forme 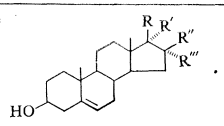

.

TABLEAU II

Résultats de la D-homoannulation

	Catalyseur	Rendement % A	B	C	D*
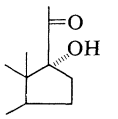 3	BF_3	—	—	17	—
	$(t\text{-}C_4H_9O)_3Al$	—	23	14	—
	5% KOH/MeOH	10	—	—	2
	$HgCl_2$	—	15	16	—
	5% KOH/EtOH	14	4	—	2
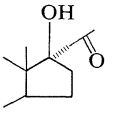 6	BF_3	18	—	—	—
	$HgCl_2$	14	—	—	—
	5% KOH/MeOH	—	16	—	—
	Al_2O_3 (basic)	15	—	—	2
	$(t\text{-}C_4H_9O)_3Al$	7	—	—	—
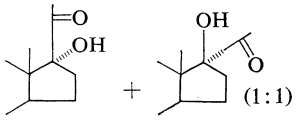 3 + 6 (1:1)	5% KOH/MeOH	5	4	—	—

*La quantité de produit **D** a été évaluée d'après le spectre de résonance magnétique nucléaire.

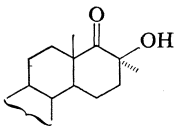

D

A—le méthyl-17*aα* dihydroxy-3β, 17*aβ* D-homo-pregnène-5 one-17

B—le méthyl-17*aβ* dihydroxy-3β, 17*aα* D-homo-pregnène-5 one-17

C—le méthyl-17β dihydroxy-3β, 17α D-homo-pregnène-5 one-17*a*

D—le méthyl-17*a* dihydroxy-3β, 17β D-homo-pregnène-5 one-17*a*

Les produits **A** et **B** correspondant à la migration du lien C_{13}–C_{17}; produits **C** et **D** du lien C_{16}–C_{17}.

Le produit **D** n'a jamais été obtenu à l'état pur. Il faut souligner que le produit **D** est *a priori* le moins stable de tous les quatre isomères.

Nous avons isolé, par isomérisation du produit **3** avec les acides de Lewis, le composé **C** comme le principal et le composé **B**. Avec le KOH, le même produit **3** a donné les composés **A** et **D**. Par contre, l'isomérisation par les acides de Lewis ou la solution de KOH du produit **6** donne comme les principaux produits **A** ou **B** respectivement. Nos résultats sont soutenus par la littérature (5–8). Il n'y a aucune analogie entre la D-homoannulation faite par les acides de Lewis ou les bases avec ce réarrangement effectué à la façon thermique (les quantités équivalentes des produits, par exemple **A** et **C** sont les produits (9)).

Les quatre produits D-homo isolés dans les différentes réactions des deux séries montrent que le déplacement chimique (Tableau III) des protons du méthyle-10 se diffère très peu l'un à l'autre. On a observé pour les quatre produits que, si le groupement OH et cétonique sont du même côté du cycle, le déplacement chimique du méthyle-13 est légèrement déplacé vers le champ plus bas (1.016 par exemple) par rapport aux produits où la cétone et OH sont des côtés opposés.

Dans ce cas, une possibilité d'avoir la résolution des problèmes structuraux est une examination du déplacement chimique des méthyles-17 ou -17*a* provenant de la transformation du méthyle-20.

Le méthyle en question absorbe vers 1.46 p.p.m. pour le composé **A** et vers 1.43 p.p.m. pour le composé **C**. Pour la structure **B** son signal tombe

Can. J. Chem. Downloaded from www.nrcresearchpress.com by 210.87.254.5 on 09/05/12
For personal use only.

Can. J. Chem. Downloaded from www.nrcresearchpress.com by 210.87.254.5 on 09/05/12
For personal use only.

TABLEAU III

Résonance magnétiques nucléaires des produits **A**, **B**, **C** et **D***

Composé	p.f.	R	R′	R″	R‴	Méthyles C-10	Méthyles C-13	Méthyles C-17	Δδ C-17 α/β	Analyse: Pour le produit	Analyse: Calculé	Analyse: Trouvé
A (6)	179–182°	OH	CH_3	C=O		0.74	1.016	1.46	0.14	$C_{21}H_{32}O_3$ (332.5)	C, 75.85 H, 9.71	C, 75.75 H, 9.77
B (7)	275–277°	CH_3	OH	C=O		0.73	0.98	1.32	—	$C_{21}H_{32}O_3$ (332.5)	C, 75.85 H, 9.71	C, 75.81 H, 9.88
C (8)	187–189°	C=O		CH_3	OH	0.99	1.13	1.43	0.15	$C_{21}H_{32}O_3$ (332.5)	C, 75.85 H, 9.71	C, 75.63 H, 9.64
D	—	C=O		OH	CH_3	1.02	1.19	1.28	—	—	—	—

*Composés du forme

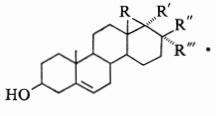

Can. J. Chem. Downloaded from www.nrcresearchpress.com by 210.87.254.5 on 09/05/12
For personal use only.

à 1.32 p.p.m. Par l'isomérisation avec le KOH, le produit **D** a été fait. Son déplacement chimique du méthyle-17 tombe vers 1.28 p.p.m. Ce produit a été obtenu en mélange avec le composé **A**.

Nous avons essayé d'interpréter l'isomérisation des produits **3** et **6** par les acides de Lewis ou par les bases. On observe généralement que le groupement cétonique formé reste de même côté que l'hydroxyle du produit de départ (rétention de la configuration de la fonction oxygénique) par rapport au cycle si on fait l'isomérisation à l'aide des acides de Lewis. Si on effectue l'isomérisation avec le KOH, il y a l'inversion de la fonction oxygénique par rapport au produit de départ.

Le produit **C** formé principalement par l'isomérisation du produit **3** possède le groupement OH α éloigné au maximum du carbonyle et du cycle **C** du stéroide donc dans la position du minimum d'énergie. Ce problème a été discuté par Elphimoff–Felkin (10)[3] et Wendler *et al.* (11).[4] Le réactif comme KOH produit le composé **A** qui est aussi stable (OH équatorial).

L'isomérisation du produit **6** par les acides de Lewis, fournit principalement le composé **A** qui est relativement stable. La formation du produit **B** à partir du même composé s'explique par l'attaque *trans*-coûplanaire de la part de base. Dans le cas du produit **3**, la présence des isomères **B** et **C** ensemble (isomérisation avec les acides de Lewis) et la présence des produits **A** et **D** ensemble (isomérisation avec des bases) ainsi que l'absence des mêmes paires d'isomères pour le composé **6** prouve notre suggestion. En plus on a observé que les différences dans le déplacement chimique du méthyle-17 et -17*a* pour les paires des isomères **A**–**B** et **C**–**D** restent constantes

pour les isomères **A**–**B** 0.14 p.p.m.
pour les isomères **C**–**D** 0.15 p.p.m.

Cette valeur est une mesure d'une différence énergétique entre la position α et β-axiale et équatoriale-du méthyle. L'approche de ces deux valeurs est une confirmation additionnelle d'exactitude de la structure **D** supposée. Les produits suivants: le méthyl-17*a*β dihydroxy-3β, 17*a*α D-homopregnène-5 (**19**) et le méthyl-17*a*α dihydroxy-3β, 17*a*β D-homopregnène-5 (**20**)—donc les composés ne contenant pas de carbonyle dans le noyau D—ont été examinés en vue de démontrer l'importance secondaire de l'effet électronique sur le déplacement chimique du méthyle-17*a*. Leur déplacement chimique tombe à 1.31 et 1.44 p.p.m. respectivement et la différence est de 0.13 p.p.m.

Les résultats obtenus pour les stéroides **19** et **20** ainsi que les stéroides nommés dans les références (4) démontrent que la présence du méthyle dans le plan du carbonyle (structure **B** et **D**) n'est pas une cause de la différence entre le déplacement chimique des paires des isomères **A**–**B** et **C**–**D**. L'avantage de notre méthode a aussi été démontrée pour la série de la décaline ou des autres stéroides; le déplacement chimique du diméthyl-9β,10 hydroxy-9α décalinène-4 one-3 (21) ou le méthyle 9β est équatoriale tombe à 1.33 p.p.m. (12).

Les mêmes corrélations entre les déplacements chimiques des méthyles ont été observées aussi pour quelques stéroides normales ayant le méthyle et l'hydroxyle dans les positions-3 ou -17 sur le même atome de carbone (4).

Cependant, la série des *tert*-butyl-méthylcyclohexanols—même que la rigidité du squelette est comparable à celle des stéroides—ne se subordonne pas à nos prévisions (13).

Partie expérimentale

Les points de fusion ne sont pas corrigés. Les spectres de résonance magnétique nucléaire (r.m.n.) ont été enregistrés à l'aide de spectrophotomètre Varian A-60 dans $CDCl_3$ (concentration environ 10%). L'éthynyl-17α dihydroxy-3β, 17β androstène-5 (**22**), l'hydroxy-3β pregnène-5 one-20 (**1**), le dihydroxy-3β, 17α pregnène-5 one-20 (**3**) ainsi que le *tert*-butylate d'aluminium ont été des produits commerciaux.

Les *N*-(oxo-20 dihydroxy-3β, 17α pregnène-5 yl)-16β glycinate d'éthyle (**5**) et son cétal (**10**), le trihydroxy-3β,-16β,17α pregnène-5 one-20 (**4**) et son cétal (**9**) ont été synthétisé par nous récemment (1).

Les cétales de l'hydroxy-3β pregnène-5 one-20 (**2**) (14) et dihydroxy-3β, 17α pregnène-5 one-20 (**8**) (15) ont été faites par la méthode habituelle à partir des cètones correspondants par l'action du glycol éthylénique dans le benzène en présence d'acide *p*-toluènesulfonique. L'estimation sur la quantité des produits isomériques **A**, **B**, **C** et **D** dans chaque préparation a été faite par l'examen des spectres des r.m.n. des mélanges réactionnels cristallisés en les comparant avec les spectres des produits purs. Les produits purs ont été obtenus par la chromatographie sur les couches minces préparatives.

D-Homoannulation du produit 6 à l'aide de l'alumine

Le produit **6** (100 mg, ~0.3 mmole) a été chromatographié sur une colonne d'alumine basique (act. II, 150 g). L'élution avec l'éthanol–benzène 1:99 (3000 ml) a

[3]Voir aussi la bibliographie de cet article.
[4]Voir aussi la bibliographie de ect article.

donné après avoir évaporé les solvants, les cristaux blancs des produits **A** et **D**.

*D-Homoannulation des produits **3** ou **6** par trifluorure de bore*

La suspension du produit (500 mg, 1.3 mmole) dans l'acide acétique (80 ml) a été mélangée avec l'anhydride acétique (3 ml) et le trifluorure de bore dans l'éther (4 ml). Le mélange a été agité pendant 24 h dans la température de la pièce. (Après 1 h environ, on observe la dissolution complète du produit cristallin). Ensuite l'eau (100 ml) a été ajouté. Environ la moitié des solvants a été évaporée *in vacuo* et le restant a été extrait trois fois à l'éther (500 ml). La solution éthérée a été lavée avec le bicarbonate de sodium à 5% (50 ml) et séchée avec le sulfate de magnésium. L'éther a été évaporé et le résidu a été chromatographié sur l'alumine acide. Après le contrôle sur les couches minces, les fractions de benzène–éther 9:1 (400 ml) et benzène–acétone 4:1 (500 ml) ont été combinés ensemble. Les solvants ont été évaporés *in vacuo* et le résidu a été traité avec l'hydroxyde de sodium à 10% dans l'éthanol (25 ml). La solution a été agitée dans la température de la pièce pendant 12 h, saturée avec le chlorure de sodium et extraite à l'éther. La phase éthérée a été séchée avec le sulfate de sodium anhydre, évaporée *in vacuo* et le résidu a été recristallisé de l'acétone.

*D-Homoannulation des produits **3** et **6** à l'aide de KOH*

La solution des produits **3** ou **6** (100 mg, ~0.3 mmole) a été portée à reflux avec l'hydroxyde de potassium à 5% dans le méthanol (ou éthanol) (25 ml) pendant 24 h. La solution a été traitée avec le carbonate de potassium à 5% (20 ml) et l'acide chlorhydrique à 5% (30 ml) et avec l'eau (50 ml); puis refroidi à 4° pendant 2 h. Les petites quantités des produits de la D-homoannulation ont été filtrées. La solution a été extraite deux fois à l'éther (50 ml), séchée avec le sulfate de magnésium, évaporée *in vacuo* et le résidu cristallin a été combiné ensemble avec les cristaux filtrés et recristallisés de l'acétone.

*D-Homoannulation des produits **3** et **6** à l'aide du butyle tertiaire d'aluminium*

La solution des produits **3** ou **6** (500 mg, 1.3 mmole) dans le toluène anhydre (40 ml) a été portée à reflux avec le butylate tertiaire d'aluminium (500 mg, 2 mmoles) pendant 6 h. Ensuite, la solution a été refroidie à 0° et neutralisée avec l'acide chlorhydrique à 5% (20 ml). Le matériel organique a été extrait à l'éther (200 ml), séché avec le sulfate de sodium anhydre et la solution a été évaporée *in vacuo*. Le résidu cristallise après refroidissement.

*D-Homoannulation des produits **3** et **6** à l'aide de $HgCl_2$*

La suspension des produits **3** ou **6** (1 g, 3 mmoles) et de chlorure de mercure (2 g) dans l'aniline (1 ml), l'eau (20 ml) et le benzène (70 ml) a été chauffée dans une bouteille à pression pendant 10 h à 100°. L'aniline et le benzène ont été séparés par l'entraînement à vapeur d'eau et le résidu aqueux a été traité avec le sulfure d'hydrogène gazeux. Le précipité noir a été filtré et séché à l'air, puis extrait à l'éther (250 ml) dans un appareil de Soxhlet. L'éther a été évaporé et le résidu a été filtré par une colonne de charbon activé. Après évaporation du solvant, le résidu cristallise.

Remerciements

Les auteurs remercient le Conseil National de Recherches du Canada et l'Université de Montréal de l'aide financière de ce travail.

1. K. JANKOWSKI et C. BERSE. Can. J. Chem. **46**, 1835 (1968).
2. K. K. PIVNITSKY et I. V. TORGOV. Tetrahedron, **22**, 1407 (1966).
3. N. R. TRENNER, B. H. ARISON, D. TAUB et N. J. WENDLER. Proceedings Roy. Chem. Soc. 214 (1961).
4. W. NEUDERT et H. RÖPKE. Atlas of steroids spectra. Springer-Verlag, Berlin–Hamburg, New York, 1965. N. S. BHACCA et D. H. WILLIAMS. Application of n.m.r. spectroscopy in organic chemistry. Holden–Day, San Francisco. 1964.
5. L. F. FIESER et M. FIESER. Steroids. Reinhold Publishing Corp., Chapman and Hall, Ltd., New York. pp. 577–583, 1959.
6. H. E. STAVELY. J. Am. Chem. Soc. **63**, 3127 (1941).
7. H. E. STAVELY. J. Am. Chem. Soc. **62**, 489 (1940).
8. H. E. STAVELY. J. Am. Chem. Soc. **61**, 79 (1939).
9. J. VON EUW and T. REICHSTEIN. Helv. Chim. Acta, **24**, 280 (1941).
10. I. ELPHIMOFF-FELKIN. Bull. Soc. Chim. France, 1845 (1956). I. ELPHIMOFF-FELKIN et A. SKROBEK Bull. Soc. Chim. France, 742 (1959). R. B. TURNER. J. Am. Chem. Soc. **75**, 3483 (1953).
11. N. L. WENDLER, D. TAUB et R. FIRESTONE. Experientia **15**, 237 (1959).
12. J. GAUTHIER. Université de Montréal, communiqué personnel.
13. C. LAMARRE. Université de Montréal, communiqué personnel.
14. K. B. BHARUCHA, G. C. BUCKLEY, C. K. CROSS, L. J. RUBIN et P. ZIEGLER. Can. J. Chem. **34**, 982 (1958).
15. P. JULIEN, E. W. MEYER et I. RYDEN. J. Am. Chem. Soc. **71**, 756 (1949).
16. A. J. SOLO et B. SINGH. J. Med. Chem. **9**, 179 (1966).
17. J. ROMO, J. LEPE et M. ROMERO. Bol. Inst. Quim. Univ. Nal. Auton. Mex. **4**, 125 (1952).

Can. J. Chem. Downloaded from www.nrcresearchpress.com by 210.87.254.5 on 09/05/12
For personal use only.

Can. J. Chem. Downloaded from www.nrcresearchpress.com by 210.87.254.40 on 09/05/12
For personal use only.

Photo-additions of aromatic hydrocarbons—indene and naphthalene with acrylonitrile

JOHN J. MCCULLOUGH AND C. W. HUANG
Department of Chemistry, McMaster University, Hamilton, Ontario

Received September 23, 1968

The photolyses of indene and naphthalene with acrylonitrile have been studied, and the products characterized. Indene reacts with acrylonitrile when the hydrocarbon absorbs light, or when a triplet sensitizer (acetophenone) is absorbing. Photolysis under the former conditions in ethanol yields 2-(1-indenylpropionitrile) (70%), 2-(3-indenylpropionitrile) (10%), and 6-cyano-2,3-benzobicyclo[3,2,0]hept-2-ene (20%). Base-catalyzed isomerizations of the substituted indenes are reported. On sensitization, *cis*- and *trans*-isomers of 7-cyano-2,3-benzobicyclo[3,2,0]hept-2-ene are formed, with a minor amount of indene dimer. The former isomers can be equilibrated with strong base. Adducts of 1,1-dimethyl- and 1,1-diphenylindene with acrylonitrile are also described, and nuclear magnetic resonance data reported. Naphthalene adds acrylonitrile on photolysis in *t*-butyl alcohol (pyrex filter) to afford *trans*-8-cyano-2,3-benzobicyclo-[4,2,0]-octa-2,4-diene (90%) and 1- and 2-naphthyl-2-propionitrile (10%). Sensitization with acetophenone gave no detectable products. Irradiation of the major product at 253.7 mμ through Vycor gave naphthalene. The preparative value of these reactions is considered and possible mechanisms are proposed.

Canadian Journal of Chemistry, **47**, 757 (1969)

Introduction

Photocycloaddition reactions of aromatic hydrocarbons (1) constitute an important branch of organic chemistry. The dimerizations of anthracene (2), acenaphthylene (3), and indene (4) may be cited as examples. A number of interesting cross-additions leading to cyclic structures are also known. These include the additions of maleic anhydride and derivatives to benzene (5*a–c*), indene (5*d*), phenanthrene (6), and anthracene (7), and the reactions of benzene with alkenes (8), acrylonitrile (9), dienes (10), and acetylenes (11).

Cross additions of the bicyclic hydrocarbon naphthalene which have been reported are few in number. Naphthalene reportedly does not react with maleic anhydride on irradiation (12) but does form a photo-adduct with diphenylacetylene (13). Also, reactions have been observed on photolysis of naphthalene and dienes (14).

In our work in this area, initial experiments showed that indene and acrylonitrile react on irradiation, and subsequent work with naphthalene and acrylonitrile revealed similar reactions. We are reporting here the structures of the products of these reactions, and the evidence for our assignments.

Acrylonitrile is a suitable ethylene derivative to use in trapping other excited molecules in a bimolecular reaction. First, it is transparent over much of the ultraviolet spectrum, having λ_{max} (EtOH) 215.5 mμ, log ε 1.69 (15), and therefore may be present in high concentration without restricting the choice of light-absorbing partner. Also, no charge–transfer absorption is observed in solutions containing acrylonitrile and benzene ((9) and references cited), naphthalene, or indene. No ambiguities regarding the excitation process should arise in future mechanistic work with the latter hydrocarbons, cf. maleic anhydride reactions (7, 16).

Results

Schemes I, II, and IV show that both indene and naphthalene form two kinds of adducts on

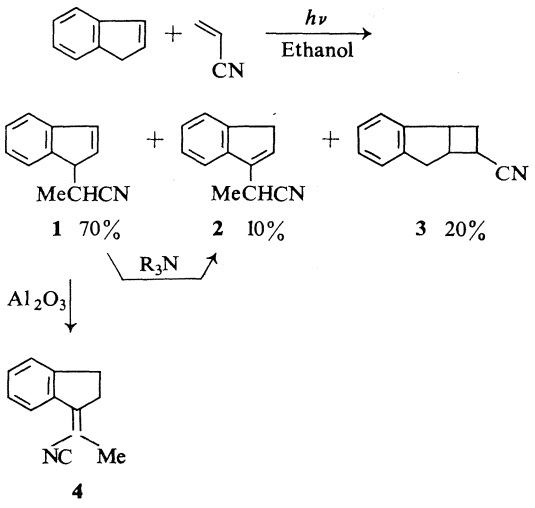

Scheme I

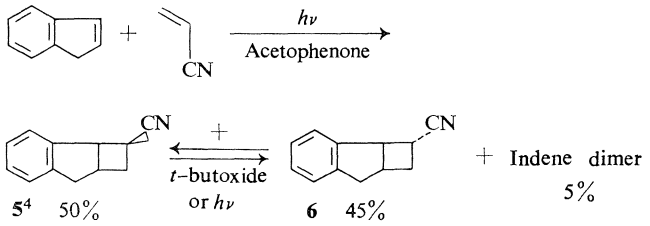

Scheme II

photoreaction with acrylonitrile. These are (*i*) cyanocyclobutane derivatives and (*ii*) cyanoethyl derivatives of the hydrocarbons, indene and naphthalene. The behavior of these two hydrocarbons will be described separately.

Indene and Acrylonitrile

Photolysis[1] of indene and acrylonitrile in ethanol, using a mercury lamp and a Vycor filter so that indene was the sole absorbing species, led to the formation of adducts which were detected and the ratio determined by gas–liquid chromatography. Analysis of aliquots (Column A, 175°)[1] revealed three major peaks of retention times 2.5, 3.3, and 3.8 min. If the mixture was allowed to stand, the 3.8 min peak increased at the expense of the major 2.5 min component, which eventually disappeared; the change was accelerated by heating or on adding triethylamine. Accordingly, vacuum distillation of the mixture allowed purification of the 3.8 min component, b.p. 100–115°/1 mm; these fractions crystallized, m.p. 80–82° from ethanol.

This product had infrared absorption at 2240 cm^{-1} (nitrile), and in the nuclear magnetic resonance (n.m.r.)[2] spectrum, resonances appeared at 1.56, doublet (J = 7.0) area 3, (methyl); at 3.26, broad peak, area 2, (methylene); quartet at 3.52 (J = 7.0) area 1, (methine); triplet at 6.44, area 1, (vinylic); the aromatic protons gave rise to a multiplet at 7.20, area 4. This n.m.r. spectrum is consistent with structure (**2**), but some doubt remained as to the location of the cyanoethyl substituent in the indene nucleus. Since it is known that protons at C-1 and C-3 of indene can be exchanged by treatment with deuterium oxide and triethylamine (17), while the C-2 proton is unaffected, this product was treated with triethylamine and deuterium oxide in dioxan at 20°. The doublet at 3.26 had disappeared in 27 h, but there was no change in the vinylic peak, hence the cyanoethyl group is at C-3 and structure (**2**) for the 3.8 min product was confirmed.

On alumina, (**2**) isomerized to a conjugated unsaturated nitrile, m.p. 114–115°, which had infrared absorption at 2201 cm^{-1}, and the ultraviolet spectrum[3] (18) had λ_{max} (EtOH) 274 mμ, log ε 4.20. The n.m.r. of this product is consistent with structure (**4**); the allylic protons of the methyl group gave a peak at 1.99, area 3, while the four methylene protons were included in a broad multiplet centered at 2.89, area 4. The downfield region is interesting because it showed one proton of the aromatic system as a doublet of doublets (J = 6.5 and 3.0) at 8.28, well downfield from the remaining three, which gave a multiplet centered at 7.27. The downfield shift of one proton has been reported (19) in compounds related to (**4**), and its observation here assures us of the *cis* relationship of the nitrile and phenyl groups.

Isolation of the 3.3 min and the major, labile 2.5 min components was achieved by careful chromatography on silica gel. These adducts were both liquids, which had the infrared nitrile band at 2240 cm^{-1}. The major 2.5 min product isomerized cleanly to (**2**) on treatment with water and triethylamine in dioxan (17), suggesting that it was the less stable tautomer, 2-(1-indenyl)-propionitrile (**1**). The n.m.r. of this major component was in agreement with structure (**1**), and showed a resonance at 1.10, doublet (J = 7.0), area 3 (methyl); one-proton multiplets at 3.0 and

[1]For details see Experimental.

[2]Chemical shifts are in p.p.m. downfield from tetramethylsilane; coupling constants are in c.p.s. Spectra of the substituted indenes were obtained on a Varian A-60 spectrometer in $CDCl_3$ solution.

[3]Compare *cis*-cinnamonitrile which has λ_{max} 273 mμ, log ε 4.22.

[4]In Table (I), **5** is labelled (B) and **6** is (A).

Can. J. Chem. Downloaded from www.nrcresearchpress.com by 210.87.254.40 on 09/05/12
For personal use only.

TABLE I

Nuclear magnetic resonance spectral data* for cyclobutane adducts of acrylonitrile and indene derivatives

Cyclobutane Derivative	Chemical shifts†				
	H-1	H-5	H-6	H-7	Other
R = —H; m.p. 50°, (A) (**6**)	3.98 b‡	2.76 m	2.16, 2.51 m	3.36 m	2.86, 3.08 benzylic CH_2
R = —H; m.p. 70°, (B) (**5**)	3.84 b	—§	1.95, 2.50 m	3.35 q	—§
R = —CH_3, m.p. 72°, (A′)	3.92 d	2.64 q	2.20 m	3.14 q	1.04, 1.26 (methyls)
R = —CH_3, m.p. 59°, (B′)	3.82 quin	2.69 q	1.99, 2.19 m	3.24 q	1.00, 1.24 (methyls)
R = —C_6H_5, m.p. 224° (B″)	4.18 quin	3.24 q	1.3–2.0 m	3.74 q	

*All spectra recorded in $CDCl_3$ at 100 M c.p.s. on a Varian HA-100 instrument.
†Chemical shifts given in p.p.m. downfield from tetramethylsilane.
‡m = multiplet; q = quartet; d = doublet; quin = quintet; s = singlet; b = broad peak.
§benzylic methylene and H-5 signals overlap.

3.6 (methines); one-proton multiplets at 6.35 and 6.88 (vinylic), and the aromatic protons gave multiplets at 7.25 and 7.59, total area 4.

The component of retention time 3.3 min was difficult to obtain pure, and the n.m.r. alone was not of great value in assigning the structure. It was possible to exclude the benzonorbornene system, as no resonances at high field (<2.0 p.p.m.) were observed (20). The n.m.r. did resemble[1] the spectra of the two adducts of the sensitized addition, although it was not identical with either of them; since the latter were subsequently shown to be cyclobutane derivatives we assign structure (**3**) to the 3.3 min adduct, but do not specify the stereochemistry of the cyano group.

Turning now to the products of the sensitized addition of indene and acrylonitrile, gas–liquid chromatography showed that three products, none of which was formed in the direct irradiation were produced, and these had retention times of 1.7, 2.0, and 8.0 min (Column A, 200°). Separation of the three components was readily achieved on a column of alumina; the 8.0 min product which was eluted first was identified as the product of sensitized dimerization of indene, m.p. 109–110°, lit. 109.5–111° (*4b*).

The two nitrilic adducts had m.p. 70° and m.p. 50°, and both showed a band in the infrared at 2240 cm^{-1}. They were interconverted by treatment with potassium *t*-butoxide in *t*-butyl alcohol, showing that they were epimers. The n.m.r. spectra (see Table I) were difficult to interpret, but were consistent with cyclobutane structures rather than benzonorbornenes (20). Their photochemical behavior also supports the cyclobutane structure for these adducts, and in addition, allows an assignment of the location of the nitrile group. Irradiation of either of the nitriles through Vycor resulted in formation of a mixture of the two. This reaction is interpreted by the mechanism shown in Scheme III. Excitation followed by uncoupling of the C_1—C_7 bond (numbering as shown), rotation about the C_6—C_7 bond, and closure to regenerate the four-membered ring seems to be a reasonable sequence. The photolytic isomerization would not occur by this

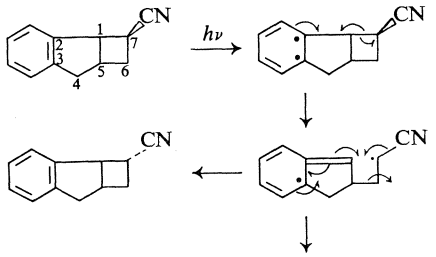

Scheme III

Can. J. Chem. Downloaded from www.nrcresearchpress.com by 210.87.254.40 on 09/05/12
For personal use only.

Can. J. Chem. Downloaded from www.nrcresearchpress.com by 210.87.254.40 on 09/05/12
For personal use only.

mechanism if the nitrile group were at C-6, and the reaction therefore allows us to place the substituent at C-7. Hence these products are the *cis*- and *trans*-isomers of 7-cyano-2,3-benzobicyclo[3,2,0]hept - 2 - ene. Prolonged irradiation caused other products to form, probably via decomposition of the cyclobutane derivative to indene and acrylonitrile (21, 22).

Related adducts were prepared by addition of 1,1-dimethylindene and 1,1-diphenylindene with acrylonitrile. The former were obtained either on sensitization or direct irradiation, the latter by direct irradiation. Some of their properties are summarized in Table I, in which data for the indene–acrylonitrile adducts is also given. Consideration of the n.m.r. data allows a tentative assignment of nitrile group stereochemistry in these derivatives.

First, the methine proton resonance at lowest field (close to 4.0 p.p.m.) was shown to be that of H-1, the benzylic methine. 3-Deuterio-1,1-diphenyl-indene was prepared[1] and in the n.m.r. of the adduct with acrylonitrile (B″) no signal was observed at 4.18 p.p.m. This shows that the 4.18 peak is due to H-1 in this adduct. In Table I it can be seen that adducts A and A′ have the H-1 resonance at somewhat lower field than the corresponding epimers, B and B′. This probably means that H-1 is *cis* to the cyano group in A and A′, since the deshielding effect of this group should be stronger for a vicinal proton on the same side of the four-membered ring.[5] Consistent with this argument is the fact that the H-1 signal in A′ is essentially a doublet (J = 6.5 c.p.s.), while B′ has this signal as a broad quintet. In the case where H-1 is *cis* to the cyano group, it will strongly couple to one other proton H-5, and J will be a vicinal *cis*- coupling constant.[6] Examination of models[7] shows that in this isomer the dihedral angle between the bonds to H-1 and H-7 is close to 90°, and should cause negligible coupling of these protons (25*a*).

On the other hand, the structure in which H-1 and the cyano group are *trans* will have H-1 *cis*-coupled to two vicinal protons H-5 and H-7, and the signal from H-1 should be more complex than a doublet. Hence on the basis of these features in the n.m.r. spectra, adducts B, B′, and B″ are assigned the *cis*-configuration of the five-membered ring and the cyano group.

It was considered that equilibration studies might help in assigning the stereochemistry, and adducts (A) and (B) were equilibrated with *t*-butoxide. The ratio of A:B was 30:70 at 25°, corresponding to a small free energy difference of 0.5 kcal/mole, and was of no help in settling the stereochemical problem.

Naphthalene and Acrylonitrile

The photo-additions of naphthalene and indene to acrylonitrile in which the hydrocarbon absorbs radiation are interesting in that analogous products are formed in the two reactions. Photolysis (Pyrex filter) of naphthalene and acrylonitrile in ethanol or *tert*-butyl alcohol gave two peaks when subjected to gas–liquid chromatography (Column A, 175°) of retention times 2.4 and 2.8 min. The ratio of the peak areas varied with conditions, but was approximately 1:9 for short photolysis times. The two components were separated by chromatography on silica gel. The component giving the 2.4 min peak appeared to be a mixture of 1-naphthyl- and 2-naphthyl-2-propionitrile, as the n.m.r. had two methyl signals (doublets), two methine resonances (quartets), and complicated signals in the aromatic region. 2-(1-Naphthyl)-propionitrile prepared by methylation of 2-(1-naphthyl)-acetonitrile with sodium amide (26) and methyl iodide had methyl, methine, and aromatic proton resonances corresponding to one set of peaks in the n.m.r. of the 2.4 min component. From the latter a crystalline compound, m.p. 64–66° from ethanol, was isolated which gave rise to the second set of n.m.r. peaks, and clearly is 2-(2-naphthyl)-propionitrile.

The component of retention time 2.8 min was obtained as a single compound m.p. 98–99°. This product had infrared absorption at 2235 cm^{-1}, and the mass spectrum showed a molecular ion of *m/e* 181. The ultraviolet spectrum had λ_{max} (EtOH) 269 mμ, log ε 3.91 with some absorption to longer wavelength than 300 mμ, suggesting that the aromatic ring was conjugated with a double bond.[8]

---

[5]In the nuclear magnetic resonance (23) of 2-methylacrylonitrile, the signals of the two vinyl protons are reported at 5.73 and 5.82 p.p.m., the latter is assigned to the proton *cis*- to the nitrile group.

[6]Steinmetz, Hartmann, and Schenck (24) give *cis* vicinal coupling constants ranging from 6.7–11.5 c.p.s. for a series of cyclobutane derivatives.

[7]Courtauld Atomic Models, available from Griffin and George Ltd., Wembley, Middlesex, England.

[8]The spectrum of 1,2-dihydronaphthalene has λ_{max} (EtOH) 259 mμ, log ε 3.98 (27).

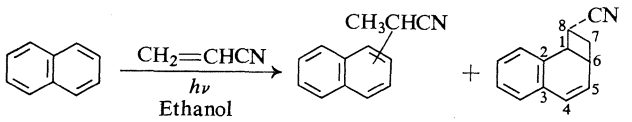

8 and **9** **7**

Scheme IV

The n.m.r. spectrum ($CDCl_3$) at 100 Mc.p.s. showed a multiplet at 7.14, area 4, (aromatics), a multiplet at 3.54, area 3, (methines), and a multiplet at 2.65, area 2 (methylenes).

In the vinyl region, two doublets (J = 5 c.p.s.) appeared at 6.63 (area 1) and at 5.93 (area 1). The doublet at higher field showed some further splitting, and spin decoupling demonstrated that this was due to coupling with the protons of the methylene group. Thus, irradiation of the 2-proton multiplet at 2.65 caused the higher-field doublet to become much sharper. Structure (**7**) is consistent with the spectral data. The vinyl protons would be coupled with J_{cis} for ethylene, which is in the 6–14 c.p.s. range (25*b*). The higher-field doublet, assigned to the vinyl proton at C-5 might reasonably be expected to be coupled to a proton[9] at C-7, but not to protons at C-8. The spin-decoupling experiment therefore demonstrates that the methylene group is at C-7. This adduct is 8-cyano-2,3-benzobicyclo[4,2,0]-octa-2,4-diene (**7**) and one stereoisomer is formed, which has the *trans*-configuration, deduced from steric considerations of the unit cell packing (1*b*). Consistent with this conclusion is the observation that (**7**) could not be equilibrated with *t*-butoxide, in contrast to the cyanocyclobutanes from indene. This suggests the more stable, *trans*-structure for (**7**). Comparison of space-filling models[3] of *cis*-(**7**) and the *cis*-adduct of indene (**5**), shows that *cis*- (**7**) is the more strained due to steric interaction of the aromatic ring with the cyano group, and this could account for the difference in equilibrium position in the two systems.

Finally, it should be mentioned why the n.m.r. data point to the cyclobutane structure for (**7**) rather than an isomeric benzobicyclo[2,2,2]octadiene derivative. First, as stated above, the ultraviolet spectrum of (**7**) is very similar to 1,2-dihydronaphthalene (27). Second, it is difficult to see why a cyano-compound derived from benzobicyclo[2,2,2]octane would not isomerize on equilibration with strong base. Third, the n.m.r. spectrum is not consistent with the latter structure.[10]

The adduct (**7**) when irradiated at 253.7 mμ or with a Corex filter transmitting above 250 mμ, decomposed to naphthalene (and presumably, acrylonitrile).

No reaction was observed on attempted (acetophenone) sensitization of the naphthalene–acrylonitrile addition.

Discussion

We will consider first the preparative value of some of the reactions reported in the Results section. Scheme I shows two indene derivatives which are readily obtained by this photochemical route; they are (**2**) and (**4**). If the 3-substituted indene (**2**) is the desired product, the photolysis mixture is evaporated, then heated or treated with an amine to convert (**1**) to (**2**), and distilled. If the unsaturated nitrile (**4**) is required, the mixture after being heated is chromatographed slowly on alumina. The less stable indene derivative (**1**) and the cyclobutane (**3**) can also be obtained, but their isolation requires careful work or recovery is poor. It is to be noted that neither of the cyclobutane derivatives formed by sensitized addition were found in the direct photolysis.

The products of triplet sensitization (**5**) and (**6**) are efficiently produced by the reaction in Scheme II, and their separation is not troublesome. These comments also apply to the products of the addition of 1,1-dimethylindene and acrylonitrile, which are the same in the direct and sensitized reactions.

From the naphthalene–acrylonitrile reaction, the cyclobutane derivative (**7**) may be obtained by using a Pyrex filter in the photolysis. If excitation is by shorter wavelength light e.g. using a Corex

[9]Snyder and Franzus (28) report 4-bond coupling in 7-substituted norbornenes between the olefinic and *anti*-7 protons ($J \sim 0.8$ c.p.s.).

[10]For example, the bridgehead protons of benzobicyclo[2,2,2]octadiene are further downfield (3.91) than any methine resonance in this adduct. Also the splitting of the vinyl resonances is inconsistent with the bicyclo-[2,2,2]octane system (29).

Can. J. Chem. Downloaded from www.nrcresearchpress.com by 210.87.254.40 on 09/05/12
For personal use only.

filter, the mixture of substituted naphthalenes (**8**) and (**9**) can be prepared.

No mechanistic studies of these photoreactions have been made so far, but such work will be reported in a future paper. However, we wish to make the following observations on the mechanistic aspects of the photo-additions described above.

The products of the triplet sensitized reaction of indene and acrylonitrile are in accord with other triplet state addition reactions such as the dimerization of indene (4) and additions of dienes and halogenated ethylenes (3). A reasonable biradical mechanism depicted in Scheme V

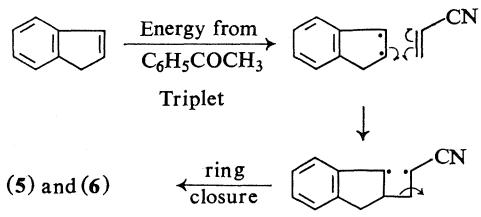

Scheme V

consists of energy transfer from the triplet state of the sensitizer (acetophenone) to the indene, followed by attack of indene triplet on acrylonitrile to produce the more stable biradical (30), which can close to a four-membered ring forming both epimers, as observed.

It seems likely that the sequence in the direct irradiation of indene (Scheme I) is initiated by a singlet excited state of the hydrocarbon.[11] In support of this is the observation that indene (and naphthalene) fluorescence is quenched efficiently by acrylonitrile (31) and the rate constant for the bimolecular quenching process (k_q) is similar to that reported by Hammond *et al.* (14) using dienes as quenchers, k_q being 10^8–10^9 l mole^{-1}s^{-1}. We may use this rate constant to estimate the rate of intersystem crossing for the indene singlet. Two of the processes competing for the latter in a steady state are (*i*) intersystem crossing and (*ii*) bimolecular capture by acrylonitrile. Since we do not observe the products of triplet addition in the direct irradiation, we will assume that they are formed in 1% yield, (this being an upper limit). Ignoring other processes such as fluorescence and radiationless decay of the triplet, the following equation holds to an approximation:

$$\frac{\text{Amount triplet products}}{\text{Amount singlet products}} \leqslant \frac{1}{100} = \frac{k_{ic}\ s^{-1}}{k_q[\text{Acrylonitrile}]s^{-1}}$$

where k_{ic} is the intersystem crossing rate constant for indene, k_q is the bimolecular quenching constant for indene singlet, and the acrylonitrile concentration is in square brackets. Setting $k_q = 10^8$ l mole^{-1} s^{-1}, and [Acrylonitrile] = 1 mole/l, this gives k_{ic} of 10^6 s^{-1}. This figure is of the same order as the estimated value for naphthalene, 1.5–4.4 × 10^6 s^{-1} (32). It appears then that the sluggish intersystem crossing and the high rate of singlet capture excludes the formation of products of triplet reaction.

The nature of later processes in the transformations leading to substituted indenes (and naphthalenes) is unknown. At first it was thought that the labile hydrogens of the indene methylene group might be involved, but since naphthalene undergoes a similar reaction, considerable doubt is thrown on this explanation. Mechanistic routes being considered as possibilities are concerted 1,3- and 1,5-hydrogen shifts, or such shifts in biradical intermediates, and intervention of the solvent acting as a proton donor.

Finally, it should be mentioned that the substituted indene derivatives may arise by photo-initiated, free radical chain reactions. This type of pathway seems unlikely, since none of the latter products are formed on heating indene and acrylonitrile with benzoyl peroxide, but a free radical mechanism cannot be rigorously excluded at present.

Experimental

The nuclear magnetic resonance spectra were obtained with a Varian HA-100 or A-60 spectrometer. The chemical shifts are δ values (p.p.m.) measured downfield from tetramethylsilane (δ = 0) as internal standard. Infrared spectra were run on a Beckman IR-5 or on a Perkin–Elmer 521 instrument and ultraviolet spectra were determined on a Cary model 14 spectrophotometer. Mass spectra were measured on a Hitachi Perkin–Elmer MRU 6 instrument. Gas–liquid chromatography was performed with a Varian 204B dual column instrument with 35 ml/min helium, using column A (5 ft × $\frac{1}{8}$ in. 5% SE-30 on Chromosorb W). Melting points were taken on a Kofler hot stage and are uncorrected.

[11]The ultraviolet absorption spectra of indene and naphthalene were unchanged by the addition of 0.47 *M* acrylonitrile. Although ground-state complexes are probably formed, cf. benzene and acrylonitrile, references cited in (9), the hydrocarbon is the absorbing species. We thank a referee for bringing the benzene–acrylonitrile case to our attention.

Can. J. Chem. Downloaded from www.nrcresearchpress.com by 210.87.254.40 on 09/05/12
For personal use only.

Can. J. Chem. Downloaded from www.nrcresearchpress.com by 210.87.254.40 on 09/05/12
For personal use only.

Nitrogen was Canadian Liquid Air certified grade and was further purified by successive passage through vanadous sulfate solution (33), concentrated sulfuric acid, and potassium hydroxide pellets.

Alumina used was Absorption, Fisher Alumina and the silica gel was Grace, 923 (100–200 mesh).

Unless specifically stated, all column chromatography was performed with a 2.5 × 90 cm column, slurry-packed in 10% benzene–hexane. Elution was begun with this mixture, and the benzene concentration was increased 5% for every additional liter of eluant; 250 ml fractions were collected.

Yields in photolysis reactions are not absolute yields, but are based on unrecovered hydrocarbon starting material.

Indene was J. T. Baker, Practical Grade, twice distilled, b.p. 65°/15 mm. Naphthalene (Fisher Reagent) was crystallized twice from benzene and had m.p. 79–80°. Acrylonitrile was Eastman Practical Grade, distilled four times, b.p. 75–76°. Acetophenone (Eastman Reagent) was distilled and had b.p. 87–90°/15 mm. Solvents were distilled before use.

Deuterium oxide was obtained from Columbia Organic Chemicals, Inc., and was specified at 99.7% D_2O. 1,1-Diphenylindene was prepared as described previously (34) and 3-deuterio-1,1-diphenylindene was obtained using sodium borodeuteride (Merck, Sharp and Dohme of Canada Ltd.) in the reduction of 3,3-diphenyl-1-indanone.

Microanalyses were by the Sprang Microanalytical Laboratory, Ann Arbor, Michigan.

Photo-condensation of Indene and Acrylonitrile

Indene (2.0 g; 0.0172 mole) and acrylonitrile (20.0 g; 0.377 mole) in 95% ethanol (400 ml) were stirred and purged with nitrogen for 30 min prior to and during the 2 h photolysis. The latter was carried out using a Hanovia type L 450W lamp in a conventional quartz immersion apparatus, which had an outlet for withdrawing aliquots. A Vycor sleeve was used. Gas–liquid chromatography of aliquots showed that three products were formed, having retention times (Column A, 175°) 2.5, 3.3 and 3.8 min, labelled **1**, **2**, and **3** respectively in the ratio 70:10:20 as measured from peak areas. After the 2 h photolysis, the mixture was filtered through silica gel to remove a small amount of polymer, and the solvent and residual indene were removed under vacuum at room temperature. The mixtures from nine such runs were combined and the three components were separated by chromatography on a 2.5 × 90 cm column of silica gel, slurry-packed in 10% benzene–hexane, using the gradient elution procedure described above. The fractions were monitored by gas–liquid chromatography. Fractions 1–6 contained indene (0.5 g); fractions 10–18 contained (**1**) 2.03 g; fractions 20–24 contained (**1**) and (**3**), 0.197 g; 25–29 were mixtures of (**2**) and (**3**), 1.297 g, and 30–37 contained (**2**) 0.807 g, m.p. 80.5–81.5° from ethanol.

Fractions 25–29 were combined and chromatographed on a 4.0 × 90 cm column of silica gel, slurry-packed in 50% benzene–hexane, and eluted with this solvent, 250 ml fractions being collected. Fractions 9–22 contained (**3**), 0.883 g, and 27–41 contained (**2**), 0.313 g. By this procedure (**1**) was obtained as an oil, 2.03 g; 21.6%, identified as 2-(1-indenyl)-propionitrile. Component (**2**) had m.p. 80.5–81.5°, 1.22 g; 13.0%, and was shown to be 2-(3-indenyl)-propionitrile as described in the Results section.

Anal. Calcd. for $C_{12}H_{11}N$: C, 85.17; H, 6.55; N, 8.28. Found: C, 85.35; H, 6.38; N, 8.35.

Compound (**3**) was also an oil, 1.08 g; 11.5%, which had a nitrile band at 2240 cm^{-1}, and the nuclear magnetic resonance (n.m.r.) spectrum (100 M c.p.s.) which had at 7.23, mult. area 4 (aromatics); 3.83, broad peak area 1 (benzylic methine) and at 2.00, mult. area 1 (alicyclic methylene). The remaining proton signals were superimposed in a complex multiplet from 2.50–3.50 p.p.m. This resembled the spectra of the sensitized reaction products. Also, the mass spectrum of (**3**) was almost identical with the spectra of the latter products, having a weak molecular ion, *m/e* 169, a base peak, *m/e* 116 (100) and a second strong peak, *m/e* 115 (35). From these comparisons, (**3**) is identified as 6-cyano-2,3-benzobicyclo[3,2,0]hept-2-ene.

*Isomerization of 2-(1-Indenyl)-propionitrile (**1**)*

Treatment of (**1**) (0.1 g; 0.0006 mole) with triethylamine (1.0 g) (17) in water (1.0 ml) and dioxane (5.0 ml) for 12 h was followed by the addition of water and ether, and separation of the ether layer, which was washed with saturated salt (NaCl) solution, and dried ($MgSO_4$). Evaporation of the solvent afforded 2-(3-indenyl)-propionitrile (**2**), 0.9 g (90%), m.p. 80.5–81.5° (from ethanol).

*Deuteration of (**2**)*

The procedure of Bergson (17) was followed. To a solution of (**2**) (50 mg) in dioxane (5.0 ml) was added 2 ml of a 1:1 mixture of deuterium oxide and triethylamine. The mixture was stirred at 25° for 27 h, when the reaction was poured into water, and immediately extracted with ether. The ether layer was washed with salt (NaCl) solution, and dried ($MgSO_4$). The n.m.r. of the residue on evaporating the ether showed a vinylic proton peak at 6.44 but the benzylic methylene peak 3.26 p.p.m. had disappeared, confirming the structure 2-(3-indenyl)-propionitrile for (**2**).

*Isolation of 2-(3-Indenyl)-propionitrile (**2**) by Distillation*

If (**2**) is the desired product in the above photolysis, the ethanol is distilled at atmospheric pressure, and the residue is then distilled at 2.0 mm. From 11.0 g of photolysis mixture, distillation gave 5.27 g of 2-(3-indenyl)-propionitrile, b.p. 100–115°/1 mm, m.p. 80–81°, from ethanol.

Isomerization of 2-(3-Indenyl)-propionitrile on Alumina

A solution of 2-(3-indenyl)-propionitrile (0.5 g) in benzene was left on a 2.5 × 30 cm column of alumina for one week. The column was eluted with 3 l of benzene to obtain 0.42 g (84%) of needles, m.p. 114.5–115° (from benzene–hexane). This was identified[12] as 2-(1-indanylidene)-propionitrile (**4**).

---

[12]C. K. Ingold and J. F. Thorpe (35) ioslated a compound by elimination of the carbethoxyl group from ethyl 2-(3-indenyl)-2-cyanopropionate, for which they reported m.p. 118°, and assigned it the structure 2-(3-indenyl)-propionitrile (**2**). We have repeated their experiments, and have found that their product is identical with the nitrile m.p. 114.5–115°, to which we assign structure (**4**).

Can. J. Chem. Downloaded from www.nrcresearchpress.com by 210.87.254.40 on 09/05/12
For personal use only.

Anal. Calcd. for $C_{12}H_{11}N$: C, 85.17; H, 6.55; N, 8.28. Found: C, 84.97; H, 6.58; N, 8.22.

Acetophenone Sensitized Photolysis of Indene and Acrylonitrile

Acetophenone (5.0 g; 0.0417 mole), indene (5.0 g; 0.0431 mole), and acrylonitrile (15 g; 0.283 mole) in ethanol (400 ml) were photolyzed as above, with a Corex filter. After the 3 h photolysis, the solvent and most of the residual starting materials were distilled. The residue was chromatographed on alumina by the above general procedure. Fractions 1–5 contained indene dimer (0.11 g), m.p. 109–110°, lit. (46) m.p. 109.5–111°. Fractions 7–14 contained (**6**), 0.90 g, m.p. 48.5–50° from benzene–hexane, identified as *trans*-7-cyano-2,3-benzobicyclo[3,2,0]hept-2-ene (A in Table I).

Anal. Calcd. for $C_{12}H_{11}N$: C, 85.17; H, 6.55; N, 8.28. Found: 85.08; H, 6.54; N, 8.22.

Fractions 19–26 contained (**5**), 0.44 g, m.p. 70.5–72° from benzene–hexane, identified as *cis*-7-cyano-2,3-benzobicyclo[3,2,0]hept-2-ene (**5**) (B in Table I).

Anal. Calcd. for $C_{12}H_{11}N$: C, 85.17; H, 6.55; N, 8.28. Found: C, 85.29; H, 6.60; N, 8.28.

Fractions 15–18 were mixtures of (**5**) and (**6**) total 0.475 g, which were separated by further chromatography on a 2.5 × 30 cm column of alumina, eluted with the usual benzene–hexane mixtures. Fractions 4–11 contained 0.115 g of (**6**), while 0.360 g of (**5**) was found in fractions 14–21.

The ratios reported in Scheme II were measured by gas–liquid chromatography (Column A, 200°) on the photolysis solution before work-up. Retention times were (**6**), 1.7 min; (**5**), 2.0 min and indene dimer 8.0 min.

*Base-catalyzed Epimerization of the 7-Cyano-2,3-benzobicyclo[3,2,0]hept-2-enes (**5** and **6**)*

Under a blanket of nitrogen, (**5**) (the *cis*-isomer) (0.8 g; 0.00473 mole) in tetrahydrofuran (10 ml) was added to potassium *t*-butoxide, from *tert*-butyl alcohol (30 ml) and potassium (1.0 g). The mixture was stirred at room temperature, and aliquots were withdrawn at 15 min intervals. These were added to dilute hydrochloric acid, and ether extracted. The ether solution was washed with salt (NaCl) solution, and dried ($MgSO_4$). This solution was monitored by gas–liquid chromatography (Column A, 200°). The same peaks as are obtained in the photolysis of retention times 1.7 and 2.0 min were observed, and an equilibrium was reached in 1 h. No change in ratio occurred in 48 h, and after this time the reaction was quenched with dilute HCl, and ether extracted. The mixture obtained on ether evaporation was chromatographed on alumina (2.5 × 30 cm column). The usual benzene–hexane mixtures were used as eluant; fractions 3–8 contained the *trans*-isomer (**6**), 0.23 g, m.p. 48–50°. The *cis*-isomer (**5**) was eluted in fractions 11–20, 0.56 g, m.p. 71–72°. The gas–liquid chromatographic *cis*:*trans* ratio at equilibrium was 70:30. An identical experiment was performed using pure (**6**), the *trans*-isomer, as starting material, and the same equilibrium mixture was obtained.

Photo-epimerization of the 7-Cyano-2,3-benzobicyclo-[3,2,0]hept-2-enes

A solution of the *cis*-compound, **5** (0.5 g, 0.003 mole) in ethanol (400 ml) was irradiated with the 450W Hanovia lamp, fitted with a Vycor sleeve. The progress of the reaction was followed by gas–liquid chromatography (g.l.c.) (Column A, 200°). In 9 h a photostationary state of *cis*/*trans* ratio 45/55 appeared to be reached. This ratio did not change on 12 h photolysis, but the g.l.c. showed slow decomposition of (**5**) and (**6**) resulting in the appearance of several other peaks.

An identical run, starting with 0.5 g, 0.003 mole of the *trans*-isomer (**6**) gave the same stationary state composition, measured by g.l.c., which was apparently reached more quickly (3 h) than with the *cis*-compound.

Photo-addition of 1,1-Dimethylindene and Acrylonitrile

1,1-Dimethylindene (2.0 g; 0.014 mole) (36) and acrylonitrile (3.7 g, 0.07 mole) in ethanol (400 ml) were irradiated (Vycor sleeve) in the usual apparatus for 6 h. The solvent was distilled and the products from five of these runs were combined and chromatographed on alumina. Fractions 7–18 contained A′ (Table I), 1.176 g, needles m.p. 70.5–72°, from benzene–hexane. This was assigned the structure *trans*-7-cyano-4,4-dimethyl-2,3-benzobicyclo[3,2,0]hept-2-ene.

Anal. Calcd. for $C_{14}H_{15}N$: C, 85.24; H, 7.66; N, 7.10. Found: C, 85.37; H, 7.79; N, 6.99.

Fractions 24–37 contained 1.16 g of B′, m.p. 58–59°, needles from benzene–hexane, identified as the *cis*-isomer, as described in the Results section.

Anal. Calcd. for $C_{14}H_{15}N$: C, 85.24; H, 7.66; N, 7.10. Found: C, 85.35; H, 7.76; N, 6.93.

Fractions 19–23 were mixtures of the two isomers, total 0.98 g which were further chromatographed on a 2.5 × 30 cm column of alumina to obtain 0.49 g of *cis*- and 0.49 g of *trans*-isomer.

The *cis*:*trans* ratio in the photolysis was measured by g.l.c. (Column A, 200°) and was approximately 40:60.

Acetophenone Sensitized Photo-addition of 1,1-Dimethylindene and Acrylonitrile

Acrylonitrile (3.7 g; 0.07 mole), 1,1-dimethylindene (2.0 g; 0.014 mole), and acetophenone (2.0 g; 0.0167 mole) in ethanol were photolyzed with the Hanovia lamp and a Corex filter for 5.5 h.

The solutions from five such reactions were combined, the solvent and residual starting materials distilled, and the mixture chromatographed on alumina as in the previous experiment to obtain 4.60 g of *cis*-adduct and 2.94 g of *trans*-compound, identical with the products of the direct photolysis by m.p. and n.m.r. and infrared spectra.

Photoaddition of 1,1-Diphenylindene and Acrylonitrile

Acrylonitrile (20.0 g; 0.377 mole) and 1,1-diphenylindene (1.349 g; 0.00503 mole) (34) in ethanol (400 ml) were photolyzed in the usual way (Vycor filter) for 2 h. After solvent evaporation, the mixture was chromatographed on a 4.0 × 90 cm column of alumina, slurry-packed in 10% benzene–hexane. The column was eluted with 2 l of 10%, 2 l of 20%, 2 l of 30% benzene–hexane and finally with 4 l of benzene, and 250 ml fractions were collected. Fractions 5–13 contained 1,1-diphenyl-indene 360 mg, m.p. 90–92° (from light petroleum, b.p. 80–110°).

Fractions 31–34 contained a nitrile adduct infrared band at 2420 cm^{-1}, 300 mg, m.p. 219–222° (from ethyl

acetate). This had a molecular ion of *m/e* 321, and is assigned the structure *cis*-7-cyano-4,4-diphenyl-2,3-benzobicyclo[3,2,0]hept-2-ene (B″) from the n.m.r. spectrum (Table I).

Anal. Calcd. for $C_{24}H_{19}N$: C, 89.68; H, 5.96. Found: C, 89.33; H, 6.11.

Preparation of 1-deuterio-B″

3-Deuterio-1,1-diphenylindene (1.45 g; 0.00542 mole) and acrylonitrile (20.0 g; 0.377 mole) in ethanol (400 ml) were photolyzed and chromatographed as above to afford 1-deuterio-B″ 137 mg, m.p. 220–222°. The quintet at 4.18 in the n.m.r. spectrum of B″ (Table I) was absent from the spectrum of 1-deuterio-B″, identifying the quintet as the resonance of H-1 in this adduct.

Photo-condensation of Naphthalene and Acrylonitrile

Acrylonitrile (2.0 g; 0.0377 mole) and naphthalene (0.1 g; 0.00078 mole) in *tert*-butyl alcohol (80 ml) (under nitrogen at 30°) were irradiated through Pyrex with the Hanovia 450W lamp for 40 min. Gas–liquid chromatography (Column A, 175°) showed two peaks at 2.4 and 2.8 min, in the ratio of 8:92 respectively. The mixtures from five such reactions were evaporated and combined, and the mixture was chromatographed on a 2.5 × 30 cm column of silica gel, slurry-packed in benzene. The column was eluted with benzene, and 250 ml fractions were collected. Fractions 1–3 contained naphthalene (0.286 g); fractions 4–20 contained 0.461 g of naphthalene and 3 mg of the 2.4 min product separated by sublimation. The latter was identical with the product from photolysis using a Corex filter or longer photolysis times and is described in the next experiment. Fractions 23–36 contained the 2.8 min product, 50 mg, m.p. 98–99° from ether. This is assigned the structure *trans*-8-cyano-2,3-benzobicyclo[4,2,0]octa-2,4-diene (**7**), from the data described in the Results.

Anal. Calcd. for $C_{13}H_{11}N$: C, 86.15; H, 6.12; N, 7.73. Found: C, 86.19; H, 6.14; N, 7.82.

Attempted Sensitization of the Naphthalene–Acrylonitrile Reaction with Acetophenone

Naphthalene (0.5 g; 0.00391 mole), acrylonitrile (10.0 g; 0.189 mole), and acetophenone (5.0 g; 0.0417 mole) were photolyzed through Pyrex for 4 h. Much polymer was formed, but no products were observed by g.l.c. (Column A, 175°).

Identification of the 2.4 Min Component

Photolysis of naphthalene (0.5 g; 0.00391 mole) and acrylonitrile (10 g; 0.189 mole) in ethanol (400 ml) with a Pyrex sleeve for 2.5 h (use of a Corex sleeve for 2 h gave similar results) gave a solution containing much polymer. This appeared after 40 min and was not observed in the previous small scale reactions. The polymer was removed by filtration (7.6 g), and the mixtures from ten reactions were combined and chromatographed on a 2.5 × 90 cm column of silica gel, slurry-packed in and eluted with benzene, 250 ml fractions being collected. Fractions 1–4 contained naphthalene 0.599 g, m.p. 79°. Fractions 6–19 were the 2.4 min component 0.239 g; 20–28 were a mixture of the 2.4 min component and (**7**), 0.616 g, while fractions 26–42 were pure (**7**), 1.743 g, m.p. 98°. Fractions 6–19 were combined, dissolved in the minimum volume of ethanol and kept in the refrigerator for several days. Crystals were deposited which were filtered and recrystallized from ethanol and had m.p. 64–66°. This compound had peaks at 7.58 p.p.m. mult., area 7 (aromatics); 3.92, quartet, area 1 (methine); 1.67, doublet, area 3 (methyl). This compound is assigned the structure 2-(2-naphthyl)-propionitrile from the n.m.r. spectrum and by its non-identity with authentic 2-(1-naphthyl)-propionitrile (26).

Anal. Calcd. for $C_{13}H_{11}N$: C, 86.15; H, 6.12; N, 7.73. Found: C, 86.00; H, 6.18; N, 7.59.

The mother liquors from the above crystallization were mainly 2-(1-naphthyl)-propionitrile, having peaks at 7.55, mult., area 7 (aromatic); 4.49, quartet, area 1 (methine), and at 1.72, doublet, area 3 (methyl). This n.m.r. was identical with that of an authentic sample, prepared by methylation of (1-naphthyl)-acetonitrile (26), which had b.p. 136–138/0.5 mm, lit. b.p. 125–127°/0.5 mm (26). The ratio of the 1- and 2-substituted naphthalenes formed in the photolysis was 2:1, estimated from the n.m.r. spectrum of the mixture.

Photolysis of trans-8-Cyano-2,3-benzobicyclo[4,2,0]-octa-2,4-diene (7)

A solution of the cyano compound (**7**) (80 mg, 4.42×10^{-4} mole) in ethanol (80 ml) was photolyzed for 10 min using a low-pressure Hanovia 87A-45 mercury lamp (Vycor envelope) giving 95% of the radiation at 253.7 mμ. On distillation of the solvent, and sublimation of the residue, 54 mg (95%) of naphthalene were obtained, m.p. and mixed melting point 78.5–79.5°.

Attempted Base-catalyzed Epimerization of trans-8-Cyano-2,3-benzobicyclo[4,2,0]octa-2,4-diene (7)

The adduct (**7**) (100 mg) in *tert*-butyl alcohol (10 ml) was added under nitrogen to potassium *t*-butoxide from potassium (1.0 g) and *tert*-butyl alcohol (20.0 ml). The mixture was stirred at 60° for 5 h, poured into cold acid (HCl), ether extracted, and the extracts dried ($MgSO_4$). Gas–liquid chromatography (Column A, 175°) did not show any peaks other than starting material. The solution was filtered through silica gel, and a quantitative recovery of starting material (**7**), m.p. 98–99° was obtained. A similar experiment was conducted as above, with a reflux time of 20 h. Gas–liquid chromatography showed no new peaks, but it was observed that the starting material gradually disappeared, and no identifiable material was isolated from the experiment.

Effects of Added Acrylonitrile on the Ultraviolet Absorptions of Indene and Naphthalene

The ultraviolet spectra of the following solutions were examined (1 mm path length) using the Cary 14 spectrometer.

(a) Naphthalene (0.125 g; 9.765×10^{-4} mole) in in ethanol, (to make 100 ml).

(b) Naphthalene (0.125 g; 9.765×10^{-4} mole), and acrylonitrile (2.5 g; 4.7×10^{-2} mole) in ethanol (to make 100 ml).

(c) Indene (0.05 g; 4.3×10^{-4} mole) in ethanol (to make 100 ml of solution).

(d) Indene (0.05 g; 4.3×10^{-4} mole) and acrylonitrile (0.5 g; 9.43×10^{-3} mole) in 100 ml ethanol solution.

The spectra of *(a)* and *(b)* were identical, as were

Can. J. Chem. Downloaded from www.nrcresearchpress.com by 210.87.29.10 on 08/31/12
For personal use only.

those of *(c)* and *(d)*, the absorption being measured from 200–800 mμ. No long wavelength band appeared on adding acrylonitrile to the hydrocarbon. Dilution of these solutions to allow measurement of the molar absorbance at the hydrocarbon λ_{max} showed that acrylonitrile had no effect on either of these properties.

Acknowledgments

We thank the Uniroyal Co. Ltd. for a grant with which the gas chromatograph was purchased, and the Imperial Oil Co. Ltd., and the National Research Council of Canada for financial support.

1. *(a)* J. J. McCULLOUGH and C. W. HUANG. Chem. Commun. 815 (1967), and *(b)* J. J. McCULLOUGH, C. CALVO, and C. W. HUANG. Chem. Commun. 1176 (1968).
2. A. SCHÖNBERG. Preparative organic photochemistry. Springer–Verlag, New York, Inc., 1968, p. 97–99.
3. *(a)* K. DZIEWONSKI and G. RAPALSKI. Ber. **45**, 2491 (1912); *(b)* K. DZIEWONSKI and C. PASCHALSKI. Ber. **46**, 1986 (1913); *(c)* G. O. SCHENCK and R. WOLGAST. Naturwissenschaften **48**, 737 (1961); *(d)* G. O. SCHENCK and R. WOLGAST. Naturwissenschaften **49**, 36 (1962); *(e)* I.-M. HARTMANN, W. HARTMANN, and G. O. SCHENCK. Ber. **100**, 3146 (1967).
4. *(a)* G. O. SCHENCK, W. HARTMANN, S.-P. MANNSFELD, W. METZNER, and C. H. KRAUCH. Ber. **95**, 1642 (1962); *(b)* J. BOWYER and Q. N. PORTER. Australian J. Chem. **19**, 1455 (1966).
5. *(a)* H. J. F. ANGUS and D. BRYCE-SMITH. J. Chem. Soc. 4791 (1960); *(b)* E. GROVENSTEIN, JR., D. V. RAO, and J. W. TAYLOR. J. Am. Chem. Soc. **83**, 1705 (1961); *(c)* G. B. VERMONT, P. X. RICCOBONO, and J. BLAKE. J. Am. Chem. Soc. **87**, 4024 (1965); *(d)* W. METZNER, H. PARTALE, and C. H. KRAUCH. Ber. **100**, 3156 (1967).
6. D. BRYCE-SMITH and B. VICKERY. Chem. and Ind. (London), 429 (1961).
7. J. P. SIMONS. Trans. Faraday Soc. **56**, 391 (1960).
8. *(a)* K. E. WILZBACH and L. KAPLAN. J. Am. Chem. Soc. **88**, 2066 (1966); *(b)* D. BRYCE-SMITH, A. GILBERT, and B. H. ORGER. Chem. Commun. 512 (1966).
9. B. E. JOB and J. D. LITTLEHAILES. J. Chem. Soc. (C), 886 (1968).
10. G. KOLTZENBURG and K. KRAFT. Tetrahedron Letters, 389 (1966).
11. *(a)* D. BRYCE-SMITH and J. E. LODGE. J. Chem. Soc. 695 (1963); *(b)* E. GROVENSTEIN, JR. and D. V. RAO. Tetrahedron Letters, 148 (1961); *(c)* J. G. ATKINSON, D. E. AYER, G. BUCHI, and E. W. ROBB. J. Am. Chem. Soc. **85**, 2257 (1963).
12. G. O. SCHENCK, J. KUHLS, S.-P. MANNSFELD, and C. H. KRAUCH. Ber. **96**, 813 (1963).
13. W. H. F. SASSE, P. J. COLLIN, and G. SUGOWDZ. Tetrahedron Letters, 3373 (1965).
14. L. M. STEPHENSON, D. G. WHITTEN, G. F. VESLEY, and G. S. HAMMOND. J. Am. Chem. Soc. **88**, 3665 (1966); *(b)* K. KRAFT and G. KOLZENBURG. Tetrahedron Letters, 4723 (1967).
15. M. T. ROGERS. J. Am. Chem. Soc. **69**, 2544 (1947).
16. D. BRYCE-SMITH and J. E. LODGE. J. Chem. Soc. 2675 (1962).
17. G. BERGSON. Acta Chem. Scand. **17**, 2691 (1963).
18. W. E. PARKAM, W. N. MOULTON, and A. ZUCKERBRAUN. J. Org. Chem. **21**, 72 (1956).
19. *(a)* G. JONES and W. J. ROE. Tetrahedron Letters, **22**, 3021 (1966); *(b)* F. BELL and J. SPANSWICK. J. Chem. Soc. (C), 1887 (1966).
20. K. TORI, K. AONA, Y. HATA, R. MUVEYUKI, T. TSUJI, and H. TANIDA. Tetrahedron Letters, 9 (1966).
21. P. YATES, S. N EĞE, G. BUCHI, and D. KNUTSEN. Can. J. Chem. **45**, 2927 (1967).
22. W. G. BROWN and R. L. MARKEZICH. 153rd Meeting, American Chemical Society, Miami Beach, Florida, April 1967. Abstr. 0–139.
23. NMR Spectra Catalog, Varian Associates, Palo Alto, California, 1962. Spectrum 97.
24. R. STEINMETZ, W. HARTMANN, and G. O. SCHENCK. Ber. **98**, 3854 (1965).
25. *(a)* L. M. JACKMAN. Applications of nuclear magnetic resonance spectroscopy in organic chemistry, Pergamon Press, Oxford (1959), p. 87. *(b)* L. M. JACKMAN. Applications of nuclear magnetic resonance spectroscopy in organic chemistry. Pergamon Press, Oxford. (1959). p. 85.
26. S. CASADIO and G. PALA. Instituto de Angeli Societa per Azioni, Brit. Pat. 969, 068. Chem. Abstr. **61**, 16026*h* (1964).
27. W. HÜCKEL, E. VEVERA, and U. WÖRFEL. Ber. **90**, 901 (1957).
28. E. I. SNYDER and B. FRANZUS. J. Am. Chem. Soc. **86**, 1166 (1964).
29. K. TORI, Y. TAKANO, and K. KITAHONAKI. Ber. **97**, 2798 (1964).
30. N. J. TURRO and P. D. BARTLETT. J. Org. Chem. **30**, 1849 (1965).
31. J. McCULLOUGH and C. W. HUANG. Unpublished results.
32. T. D. S. HAMILTON and J. P. RAY. Photochem. Photobiol. **4**, 269 (1965).
33. L. MEITES and T. MEITES. Anal. Chem. **20**, 984 (1948).
34. R. F. BROWN and L. M. JACKMAN. J. Chem. Soc. 3147 (1960); also J. J. McCULLOUGH. Can. J. Chem. **46**, 43 (1968).
35. C. K. INGOLD and J. F. THORPE. J. Chem. Soc. **115**, 143 (1919).
36. A. BOSCH and R. K. BROWN. Can. J. Chem. **42**, 1718 (1964).

Can. J. Chem. Downloaded from www.nrcresearchpress.com by 210.87.254.40 on 09/05/12
For personal use only.

Some metabolites of *Alternaria solani* [1,2]

A. STOESSL
Research Institute, Canada Department of Agriculture, London, Ontario
Received August 19, 1968

Pigments isolated from culture filtrates and mycelia of *Alternaria solani* were shown to be 5-hydroxy-7-methoxy-2-methylanthraquinone (**1**, 2-methylxanthopurpurin-7-methylether), 7-methoxy-2-methyl-3,4,5-trihydroxyanthraquinone (**2**), 3,5-dihydroxy-7-methoxy-2-methylanthraquinone (**3**, macrosporin), 7-methoxy-2-methyl-1,2,3,4,5-pentahydroxy-1,2,3,4-tetrahydroanthraquinone (**5**, altersolanol A) and 7-methoxy-2-methyl-1,2,3,4-tetrahydro-2,3,5-trihydroxyanthraquinone (**8**, altersolanol B). **3** has been described previously and may have chemotaxonomic significance. Compounds **5** and **8** represent a new type of naturally occurring, reduced anthraquinone.

Canadian Journal of Chemistry, **47**, 767 (1969)

Can. J. Chem. Downloaded from www.nrcresearchpress.com by 210.87.254.105 on 09/05/12
For personal use only.

Alternaria solani, a pathogen of solanaceous plants (2) which produces alternaric acid (3, 4), has been reported (3, 5) to yield also an antibiotically active substance, of unelucidated structure, together with some ill-defined pigments (5). Ergosterol and a dihydro-coenzyme Q have also been isolated (6), but little further knowledge of the mold's chemistry appears to be available. An interest in this Institute in phytotoxins led to the re-isolation of alternaric acid as a reference compound and thus gave an opportunity for a fresh examination of the culture filtrates and mycelia.

The antibiotic substance described earlier (5) could not be detected, possibly because a different strain of mold or different cultural conditions were employed, but five pigments were isolated and characterized (Table I). Two of them, altersolanol A and altersolanol B, represent a new type of naturally occurring, reduced anthraquinone while the three others are classical anthraquinones into which the altersolanols can be transformed. These interrelations in turn facilitated the structural studies on each. Thus all five compounds exhibit bands in their nuclear magnetic resonance (n.m.r.) spectra which can be assigned to an aromatic methoxyl group and a pair of *meta*-coupled aromatic protons, while the infrared spectra show absorption due to chelated phenol and both chelated and free quinone carbonyl groups. Since these bands account completely for the aromatic moiety of the altersolanols (see below), it is evident that all five compounds contain the same ring system (AB).

The simplest compound of the series is anthraquinone A, $C_{16}H_{12}O_4$. Its n.m.r. spectrum (Table II) shows signals, in addition to those already discussed, which can be assigned to one chelated phenol ($\tau -2.87$, subject to deuterium exchange) in (AB); and to three aromatic protons (in a 1,3,4 relation) and an aromatic *C*-methyl group arranged as in part structure (C). Evidence on hand from studies on anthraquinone B, indicates that fragment (C) is to be attached to (AB) in the sense implied by the numbering. Structure **1** for anthraquinone A follows and was confirmed by synthesis. Selective methylation at the 7-position of the readily accessible 2-methylxanthopurpurin (**1***a*) (7) gave **1** which was shown to be identical with anthraquinone A in every respect.

Anthraquinone B, $C_{16}H_{12}O_6$, has only one proton directly attached to the moiety (C) (Table II). This absorbs as a slightly broadened singlet (long-range coupling to the methyl group) at comparatively low field (deshielding by carbonyl). Three phenolic protons are manifested as a broad band at $\tau -2.5$ to -0.8 and can be attributed to system (D). As required by the catechol moiety present in this system, the pigment, alone of the five studied, gives an olive-brown color with ferric chloride. Anthraquinone B must therefore have structure **2**. This conclusion was verified when exhaustive methylation of the pigment gave a compound with the melting point and ultraviolet spectrum reported for 3,4,5,7-tetramethoxy-2-methylanthraquinone (**2***a*) (8).

Incomplete methylation of anthraquinone B led to the isolation of a small amount of the dimethyl ether (**2***b*), which shows three methoxyl groups in the n.m.r. spectrum (Table II) and a deuterium-exchangeable proton absorbing at

---

[1]Contribution No. 387 from the Research Institute.
[2]Part of this work has been reported in a preliminary communication (1).

TABLE I

Pigments of *Alternaria solani**

Structure	Trivial name	R_f†	Filtrate	Mycelium
1	Methylxanthopurpurin-7-methylether	0.74	0.01 g	0.12 g
2	—	0.62	0.03 g	0.91 g
3	Macrosporin	0.51	0.10 g	5.79 g
5	Altersolanol A	0.03	3.46 g	—
8	Altersolanol B	0.14	0.15 g	—

*Grown in 70 Roux bottles each containing 150 ml culture medium.
†Determined simultaneously on thin layer of silica gel (Camag DF-5) with methanol – chloroform – 90% formic acid (5:95:2) as irrigant (mean of 4 runs).

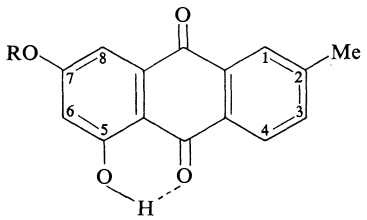

(**1**, R = Me)
(**1***a*, R = H)

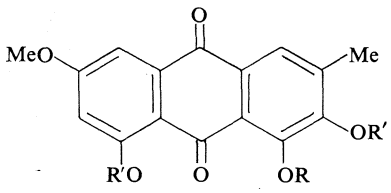

(**2**, R = R′ = H)
(**2***a*, R = R′ = Me)
(**2***b*, R = H, R′ = Me)

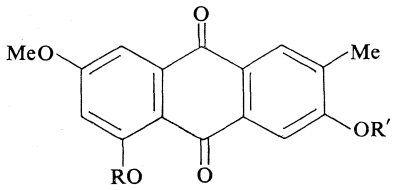

(**3**, R = R′ = H)
(**3***a*, R = R′ = COMe)
(**3***b*, R = H, R′ = Me)
(**3***c*, R = R′ = Me)

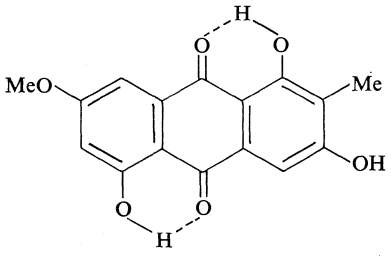

(**4**)

τ −3.4. Isolation of the same substance from a different precursor (see following communication (9)) allows placement of the phenolic hydroxyl at the 4-position rather than the 5-position. The melting point of **2***b* suggests that it is identical with the by-product, m.p. 220°, isolated by Briggs and regarded as a dihydroxydimethoxy compound (8).

Anthraquinone C, $C_{16}H_{12}O_5$, was too insoluble even in dimethyl sulfoxide to allow obtention of its n.m.r. spectrum. However, it furnished a soluble diacetate (**3***a*) which exhibits two broadened singlets which must be assigned to two weakly (i.e., *para*-) coupled protons on ring C. Since this ring must also accommodate one of the acetate groups and a *C*-methyl group, the pigment has structure **3**, already known as that of macrosporin (10*a–d*). Its identity with this compound was confirmed by the ultraviolet spectrum (10*a*) and by the preparation of the mono- and dimethylethers (**3***b* and *c* respectively) (10*b*). The pigment and its three derivatives were found to have melting points a few degrees higher than those reported, but all four compounds gave infrared spectra which match those published in the literature (10*a,b*).

Altersolanol A, which is optically active, has an ultraviolet spectrum resembling those of some naphthoquinones without oxygen substituents on the quinone double bond (e.g., 2-carbomethoxymethyl-3-methyl-5,7,8-trimethoxynaphthoquinone (11) and the quinone A methyl ether[3] obtained from protaphin (12)). Elemental analysis and integration of the n.m.r. spectrum gave its constitution as $(C_{16}H_{16}O_8)_n$. On acetylation in the presence of perchloric acid, it afforded a highly crystalline and chloroform-soluble pentaacetate which was shown to have the constitu-

[3]Structure **4** in the following paper (9).

Can. J. Chem. Downloaded from www.nrcresearchpress.com by 210.87.254.105 on 09/05/12
For personal use only.

TABLE II

Nuclear magnetic resonance data of anthraquinone derivatives

Anthraquinone	A (1)	(1*a*)	B§(2)	(2*a*)	(2*b*)	(3*a*)	(4)
τ values*							
H-1	1.95 d	2.36 d	2.77	2.13	2.38	1.93†	—
H-3	2.42 dxd	2.52 dxd	—	—	—	—	—
H-4	1.82 d	2.19 d	—	—	—	2.18†	2.23
H-6	3.31 d	3.55 d	3.47 d	3.23 d	3.22 d	3.16 d	3.22 d
H-8	2.66 d	3.06 d	3.15 d	2.64 d	2.52 d	2.32 d	2.54 d
C_2—CH_3	7.47	7.62	7.85	7.63	7.62	7.56	7.57
$ArOCH_3$	6.05	—	6.17	6.04	6.00	6.07	6.00
				6.02	5.97		
				5.98	5.97		
				5.98			
$ArOCOCH_3$	—	—	—	—	—	7.67	—
						7.69	
Couplings‡ (Hz)							
$J_{1,3}$	2.0	2.0	—	—	—	—	—
$J_{3,4}$	7.5	7.5	—	—	—	—	—
$J_{6,8}$	2.5	2.5	2.5	2.5	2.5	2.5	2.5

*In deuteriochloroform except where marked § for hexadeuteriodimethyl sulfoxide, with TMS as internal reference; all bands singlets‖ except where marked d for doublets;‖ resonance positions measured at geometrical centers.
†H-4 in this compound assigned at higher field than H-1 because of its *ortho* relation to OH.
‡J = apparent coupling constant = observed splitting.
‖Long-range splittings neglected.

tion $C_{26}H_{26}O_{13}$ by elemental analysis and a molecular weight determination. Mild alkaline hydrolysis of this derivative regenerated appreciable amounts of altersolanol A of unchanged optical rotation; therefore, neither skeletal rearrangements nor disruption into two identical fragments had intervened and the parent compound must also be monomeric ($n = 1$).

The n.m.r. spectrum of altersolanol A (in hexadeuteriodimethyl sulfoxide) shows broadened signals from four alcoholic hydroxyl groups at τ 5.8 to 4.9 and a sharp singlet (1H, chelated phenol) at τ −2.17, which vanish on deuteration or acetylation. An aromatic methoxyl group (3H, singlet, τ 6.13) and a pair of *meta*-coupled aromatic protons (doublets, 1H each, J[4] 2.5 Hz, centered at 3.07 and 3.28) are accommodated by part structure (AB). A broadened singlet (1H, τ 5.62) and a pair of doublets (1H each, $J \sim 7$ Hz, centered at τ 5.46 and 6.32) are shifted downfield by acetylation; together with the only remaining signal, a singlet (3H, τ 8.69) corresponding to an aliphatic methyl group deshielded by a geminal oxygen atom, they require assignment as in part structure (E). All the atoms of the pigment are now accounted for. On heating *in vacuo* at moderate temperatures, altersolanol A was dehydrated to two anthraquinones. The major product, which was also obtained as a by-product of the deacetylation of the pentaacetate, is identical with anthraquinone B (**2**). The minor product could be characterized only by its spectroscopic properties (Table II and Experimental) but these left no doubt that it is 7-methoxy-2-methyl-1,3,5-trihydroxyanthraquinone (**4**). These facts establish that altersolanol A has structure **5**, which also accounts for the following observations.

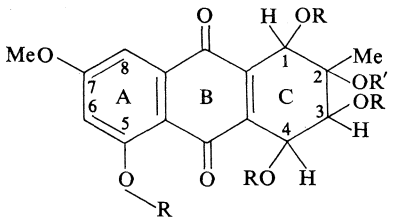

(**5**, R = R′ = H)
(**5***a*, R = COMe, R′ = H)
(**5***b*, R = R′ = COMe)

Acetylation of altersolanol A in pyridine gave a tetraacetate (**5***a*),[5] further acetylable to the pentaacetate (**5***b*),[5] whose properties (exchangeable alcoholic proton at τ 7.12 not coupled to vicinal hydrogen) require the presence of a tertiary hydroxyl group. Oxidation of altersolanol A with

[4]J = apparent coupling constant = observed splitting throughout this paper.

[5]The nuclear magnetic resonance spectra of these compounds will be considered in detail in the following communication (9).

Can. J. Chem. Downloaded from www.nrcresearchpress.com by 210.87.254.105 on 09/05/12
For personal use only.

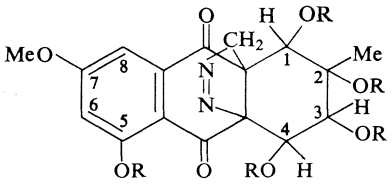

(7, R = COMe)

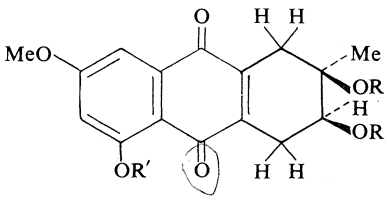

(8, R = R′ = H)
(8*a*, R = R′ = COMe)
(8*b*, R = COMe, R′ = H)

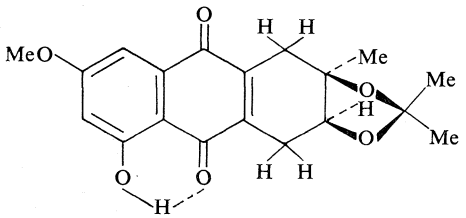

(9)

sodium periodate furnished almost one mole-equivalent each of formic and acetic acids. Attempted methylation with diazomethane led to several benzindazoles of which only one, **6** or an isomer, was obtained in substantial amounts. One of the minor products is the corresponding 4-desmethyl compound; the two others appear to be isomers of **6**.

The addition of diazomethane to naphthoquinones is well known (13) and, in the present instance, presumably is followed by an elimination of the type illustrated in Scheme I. This view is supported by the following observations. First, apart from the brightly colored indazoles, the reaction also yielded a colorless, intractable product which was very soluble in water and which furnished an equally unworkable mixture of precipitates on addition of 2,4-dinitrophenylhydrazine. Secondly, altersolanol A pentaacetate also reacted with diazomethane but gave only a single, colorless product. This compound is the adduct (**7** or equivalent structure) by elemental analysis and spectroscopic data (see Experimental). Acetylation has evidently blocked the dealdolization possible in altersolanol A itself. As required by this postulate, compound **7** reacted rapidly with dilute sodium hydroxide at

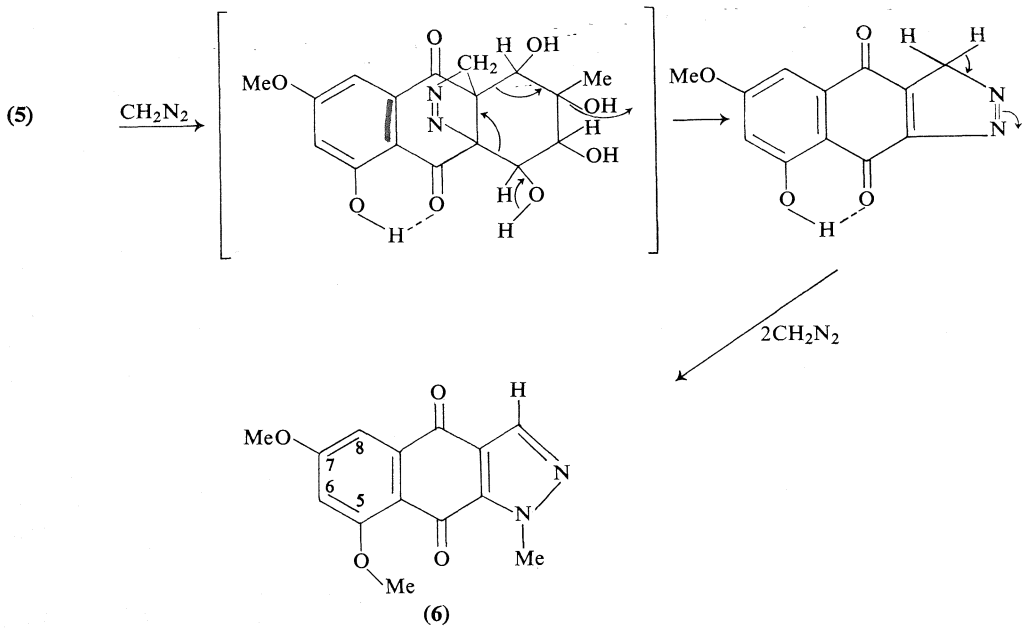

SCHEME I

Can. J. Chem. Downloaded from www.nrcresearchpress.com by 210.87.254.105 on 09/05/12
For personal use only.

Can. J. Chem. Downloaded from www.nrcresearchpress.com by 210.87.254.105 on 09/05/12
For personal use only.

room temperature, to afford a mixture of yellow benzindazoles. These lacked *C*-methyl and acetoxyl groups and on methylation with diazomethane, gave the 4-desmethyl compound mentioned above, as major product.

The stereochemistry of altersolanol A, and further coincidental correlations with its cometabolites, will be discussed in the following communication (9).

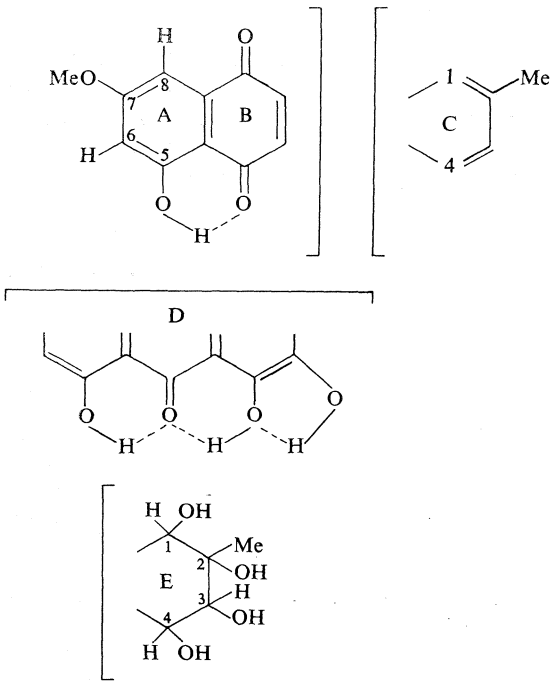

Altersolanol B was found to have the constitution $C_{16}H_{16}O_6$, with two oxygen atoms fewer than altersolanol A, but resembles the latter in the ultraviolet spectrum. On aromatization with thionyl chloride in pyridine, it furnished anthraquinone A (**1**). Assignment of structure **8** to altersolanol B follows from the following further evidence: The n.m.r. spectrum (in hexadeuteriodimethyl sulfoxide), with bands at τ −2.12 (1H, s, exchangeable), 3.08 and 3.29 (1H each, d, *J* 2.75 Hz) and 6.12 (3H, s), and the infrared spectrum (KBr; 1679 (free CO), 1635 (chelated CO) and 1619 (aromatic) cm^{-1}) confirm the presence of part structure (AB). Other bands in the n.m.r. spectrum correspond to two alcoholic hydroxyl groups (τ 5.33 and 5.65, 1H each, broad, exchangeable), a deshielded *C*-methyl (τ 8.80, 3H, s) and —C*H*(OH)— (τ 6.75, 1H, m). The only remaining signal is a multiplet (4H?, partly submerged under solvent peak) at τ 7.27 to 7.62 which evidently represents two methylene groups in similar environments. Acetylation gave altersolanol B triacetate (**8***a*) which lacks protons readily exchangeable for deuterium. The n.m.r. spectrum of this compound, in deuteriochloroform, can be assigned as follows: τ 2.52 (1H, d, *J* 2.75 Hz; H-8), 3.22 (1H, d, *J* 2.75 Hz; H-6), 6.06 (3H, s; ArOMe), 7.59 (3H, s; ArOAc), 7.93 (3H, s; ROAc), 8.02 (3H, s; ROAc), and 8.42 (3H, s; C_2—Me). The essentially equivalent methylene groups at C-1 and C-4 again absorb as a complex multiplet in the relatively narrow range τ 6.67 to 7.33, while only the resonance of the proton assigned to C-3 has been moved downfield to τ 4.67 (1H, multiplet approximating a triplet).

As a by-product of the acetylation, there was isolated altersolanol B-2,3-diacetate (**8***b*) which was probably formed from **8***a* by facile hydrolysis of the reactive 5-acetoxyl during work-up. The free phenol at C-5, chelated to the carbonyl group, was easily detected in the ultraviolet and infrared spectra. Further hydrolysis, *via* a monoacetate which was not isolated, regenerated **8**.

Location of the secondary hydroxyl group in altersolanol B at C-4 rather than C-3 would have been more attractive on biogenetic considerations. Unfortunately, insufficient purified pigment was available to allow investigation of this point by degradative studies. However, the assignment to C-3 is strongly supported by a comparison of the relevant resonance positions in altersolanol A and B derivatives, as in Table III. Further confirmation of the vicinal diol system at C_2—C_3 in altersolanol B was obtained by the ready formation of an isopropylidene derivative (**9**) which, in analogy with altersolanol A acetonide (see following communication (9)) presumably has a dioxolane rather than dioxane structure. This also requires that the hydroxyl groups should be *cis* to one another. A complete analysis of the rather complex n.m.r. spectrum of this substance will be undertaken in the near future;[6] it is hoped that this will confirm the assigned structure and throw light on the possible conformations of altersolanol B and its derivatives.

[6]Dr. J. B. Stothers of the University of Western Ontario has kindly consented to undertake this analysis.

Can. J. Chem. Downloaded from www.nrcresearchpress.com by 210.87.254.105 on 09/05/12
For personal use only.

TABLE III

Comparison of resonance positions[a] in altersolanols A and B

Proton	H-3	H-4	H-1
C_3—OH free or in ether linkage			
B[c]	6.75	7.22–7.62	
A[c]	6.32	5.46	5.62
B acetonide	5.69	6.33–7.92	
A-2,3-acetonide[b]	5.53	4.81	5.18
A-2,3-acetonide-4,5-dimethylether[b]	5.50	5.04	5.22
A-2,3-acetonide-4,5-dimethylether-1-acetate[b]	5.61	5.07	3.83
A-2,3-acetonide triacetate[b]	5.63	3.81	3.79
A-1,4,5-triacetate[b]	6.13	3.95	3.82
C_3—OH acetylated			
B triacetate	4.67	6.67–7.33	
A-1,3,4,5-tetraacetate	4.65	3.71	3.81
A-pentaacetate	4.47	3.70	2.83
A-pentaacetate diazomethane adduct	4.72	4.26	3.03

[a]As in Table II.
[b]Described in the following communication (9).
[c]Hexadeuteriodimethyl sulfoxide was used as solvent.

Macrosporin (**3**), earlier isolated from *A. porri* (10*a*), has recently also been obtained from cultures of *A. cucumerina* by Dr. A. N. Starratt of this Institute.[7] It may have chemotaxonomic significance since it does not appear to have been found in other fungal genera or plants. Pigments **2** and **1** do not appear to have been found in nature before, although the corresponding phenols, (**2***a*) and 2-methylxanthopurpurin (**1***a*) respectively, have been isolated but only from higher plants (7, 8). The altersolanols are clearly closely related to their co-metabolites since they have the same ring A and a *C*-methyl group in the biogenetic 2-position. It is indeed possible that **2** is formed from altersolanol A, and **1** from altersolanol B, by dehydration brought about enzymatically or by acid catalysis within the mold tissue.[8]

The question arises whether the altersolanols in turn could have been formed from anthraquinone precursors. While this may be the case, it is at least equally probable that **5** and **8** are on branches of the metabolic pathway leading to macrosporin. It is generally accepted (15) that fungal anthraquinones are biosynthesized from acetate and malonate but the detailed sequence of condensation, dehydration, and hydroxylation steps is not well known. For this reason, a thorough investigation of altersolanol biogenesis might be of general significance.

[7]Dr. A. N. Starratt. Private communication.
[8]The compounds are unlikely to be artifacts generated during work-up; extraction conditions, with temperatures not exceeding 80°, were too mild to dehydrate **5** and **8** which could be dried for several days at 100° without apparent damage.

TABLE IV

Nuclear magnetic resonance data for benzindazoles*

		A	B	C	D
H-8 (1H, d, *J* 2.5 Hz)		2.49	2.53	2.66	2.47
H-6 (1H, d, *J* 2.5 Hz)		3.33	3.22	3.26	3.22
$ArOCH_3$	(3H, s)	6.08	6.00	6 05	6.01
	(3H, s)	—	5.97	6.02	6.01
OH	(1H, s)	−2.73	—	—	—
—C*H*=N—	(1H, s)	1.99	2.00	2.07	2.04
NCH_3	(3H, s)	5.69	5.48	5.72	5.91

*As in Table II.

Experimental

Analyses were by Dr. C. Daesslé, Montreal. Melting points were taken on the Köfler stage and infrared spectra with a Perkin–Elmer 21 spectrophotometer. Ultraviolet spectra, in 96% ethanol, were determined with a Beckman DK instrument. Nuclear magnetic resonance (n.m.r.) spectra (tetramethylsilane (TMS) as internal reference) were obtained on Varian A60 and A60A spectrometers with, where necessary, the use of a Varian C1024 computer. Compounds were deuterated, either by shaking their solution in deuteriochloroform with deuterium oxide, or by precipitation from hexadeuteriodimethyl sulfoxide with deuterium oxide. The latter method was convenient for compounds insoluble in chloroform but soluble in anhydrous dimethyl sulfoxide. Rotations were measured optically with a 1-dm path length. Petroleum ether was of b.p. 40–70°. Evaporations were done at the pressure of the water pump. Analytical and preparative thin-layer chromatography (t.l.c.) was on silica gel (Camag DMF) with methanol – chloroform – 90% formic acid (2:98:2) as the most useful irrigant; others are noted as required.

Growth and Harvesting of Alternaria solani

An alternaric acid producing strain of *A. solani* (P. W. Brian's strain No. 408 (3)) obtained from the American Type Culture Collection, Rockeville, Maryland, as ATCC No. 11078, has been maintained by Mr. C. H. Unwin in this Institute since 1962. It was used in the usual manner to inoculate 70 Roux bottles, each containing 150 ml of Brian's medium T (10% glucose, casein hydrolyzate and mineral salts (16)), which were then kept at 25° in the dark for 18 days. The mycelial mats were filtered off, squeezed dry, and washed twice by suspending in water and filtering. The compressed filtered cake was broken up and dried in air at 80° to give 206 g of product sufficiently dry to be ground to a coarse powder in a mortar.

Isolation of Pigments from Culture Filtrates

The culture filtrates and washings (pH ca. 5.6) obtained above were extracted continuously during 3 days with ethyl acetate distilling under reduced pressure from a

Can. J. Chem. Downloaded from www.nrcresearchpress.com by 210.87.254.105 on 09/05/12
For personal use only.

suitably connected reservoir (2 l, bath temperature ca. 55°) in which the extracts were also collected. After concentration to approximately 1 l, the extracts were washed with sodium hydrogen carbonate solution (5%; 100 and 50 ml) and water (3 × 50 ml). The aqueous phases were reextracted in turn with several portions of ethyl acetate, the ethyl acetate layers were bulked and concentrated to about 300 ml. Essentially homogeneous altersolanol A (2.44 g) crystallized out. The mother liquors were evaporated to dryness and the residue (2.85 g) distributed between water (3 × 500 ml) and chloroform (3 × 500 ml). A little methanol was added to the first funnel to aid solution. The chloroform layers were combined, evaporated to dryness and the residue redistributed in a similar manner. The combined aqueous layers were concentrated to half-volume and extracted 5 times with equal volumes of ethyl acetate which gave another 1.02 g of essentially homogeneous altersolanol A on evaporation. The chloroform layers were concentrated and chromatographed on thin layers of silica gel (200 plates 20 × 20 cm) in the usual solvent. Well-separated bands corresponding, in order of decreasing R_f, to pigments **1** (about 10 mg), **2** (30 mg), and **3** (96 mg) were collected, moistened with dilute hydrochloric acid, and eluted with chloroform. The coalesced bands extending from the origin were similarly eluted and the product rechromatographed in methanol – chloroform – 90% formic acid (4:96:2) to give crude altersolanol B (148 mg) and at least 8 other incompletely resolved pigments (183 mg) which were not further examined.

When the culture filtrates were extracted by shaking with ethyl acetate at room temperature, essentially similar results were obtained but the yield of altersolanol A was reduced. When chloroform was used (3) instead of ethyl acetate, pigments **1**, **2**, **3**, and **8** were isolated but not altersolanol A. In contrast to the main experiment, these two runs yielded crystalline alternaric acid from the sodium hydrogen carbonate fraction.[9]

Isolation of Pigments from the Mycelium

The ground mycelium was extracted in a Soxhlet apparatus with petroleum ether during 5 days, to give an oil (18.4 g, ν_{max} (liquid) 1748 cm^{-1}), contaminated with only traces of pigments, which was not further examined. Extraction was continued for 10 days with ethyl acetate containing methanol (5–15%). The extracts (ca. 1 l) were filtered from precipitated solids which were refluxed with five successive portions (250 ml each) of methanol – ethyl acetate (1:4), to leave an olive-brown powder (4.8 g, not investigated). The combined ethyl acetate extracts were evaporated, the residue was suspended in petroleum ether, filtered off, and washed with more of the solvent. Filtrate and washings yielded an oil (35.7 g) essentially identical (infrared spectrum) with that obtained earlier. The solids (17.5 g) were Soxhlet-extracted for 5 days with benzene, the material which separated on cooling the extract was returned to the thimble, and extraction was continued for 3 days with chloroform (1.5 l, replaced by fresh solvent after 1 day with return of precipitated solids to the thimble). The residue in the thimble was combined with the solid which separated on cooling the second chloroform extract and was crystallized twice from pyridine to give pigment **3** (3.55 g) and mother liquor A.

The benzene extracts were evaporated to dryness, the residue was dissolved in chloroform (1.5 l) and stirred with basic magnesium carbonate (200 g). After filtration, chromatography of the material from the filtrates on silica gel (BDH; 100 g) gave pigment **1** (107 mg, eluted by benzene and chloroform–benzene (5:95) and further purified by preparative t.l.c.). The column was then stripped with acetone containing a little acetic acid, to give eluate A.

The chloroform Soxhlet extracts were treated with magnesium carbonate (several portions) as above. Evaporation of the filtrates gave **3** (1.10 g).

The filter cakes of magnesium carbonate from the preceding paragraphs were dissolved in a slight excess of 6 *N* hydrochloric acid. The precipitated pigments were combined with mother liquor A and eluate A, evaporated, and chromatographed on silica gel (BDH; 800 g). 0.5 l fractions were collected. Fractions 11–20 (benzene) contained pigment **1** (11 mg); benzene–chloroform (1:1) eluted **2** (0.685 g, fractions 32–46), a mixture A of **2** and **3** (fractions 47–55), and **3** (0.79 g, fractions 56–61). The column was then stripped with acetone containing a little acetic acid and methanol. On concentration, the eluate deposited **2** and **3** (mixture B). The mother liquors, on preparative t.l.c., gave more **2** (46 mg) and mixtures containing very small to trace amounts of **3** and at least eight other pigments. Analysis of mixtures A and B, by t.l.c. and spectrophotometry, showed that they contained 177 mg of **2** and 351 mg **3**.

Anthraquinone A (1)

Recrystallized from acetic acid, **1** had m.p. 184–185°; $\lambda\lambda_{max}$ 409, 279, 261, 252 and 226 mμ (log ε 3.71, 4.23, 4.23, 4.25 and 4.12); ν_{max} ($CHCl_3$) 3400–2400 (broad, chelated OH), 1676 (s, free CO), 1635 (vs, chelated CO) and 1610 (vs, aromatic) cm^{-1}.

Anal. Calcd. for $C_{16}H_{12}O_4$: C, 71.63; H, 4.51. Found: C, 71.58; H, 4.35.

Synthesis

2-Methylxanthopurpurin was prepared as in the literature (7) and further characterized by its n.m.r. spectrum (Table II). On methylation with diazomethane in ether–methanol (repeated addition of reagent until all starting material had been consumed), it gave **1**, identified by m.p., mixture m.p., t.l.c., infrared, and ultraviolet spectra.

Anthraquinone B (2)

Recrystallized from pyridine, the pigment had m.p. 267–268°; $\lambda\lambda_{max}$ 425, 312, 280, and 229 mμ (log ε 4.03, 4.00, 4.43, and 4.36); ν_{max} (KBr) 3480 (s), 1665 (m), and 1622 (vs) cm^{-1}.

Anal. Calcd. for $C_{16}H_{12}O_6$: C, 64.00; H, 4.03. Found: C, 63.67; H, 3.79.

The substance (100 mg) was methylated as described by Briggs (8) but reaction time was extended to 2.5 h, additional dimethyl sulfate (0.2 ml in 1 ml acetone) being added twice. The product (**2***a*) was extracted from water with ethyl acetate and crystallized on concentration. Recrystallized from chloroform–ethanol or acetic acid, it had m.p. 180–181.5°; $\lambda\lambda_{max}$ 367, 276, and 223 mμ (log ε 3.71, 4.36, and 4.34); ν_{max}(KBr) 1673 (s) and 1602 (vs)

[9]I thank Dr. G. A. White for informing me of this result.

Can. J. Chem. Downloaded from www.nrcresearchpress.com by 210.87.254.105 on 09/05/12
For personal use only.

cm^{-1} (ref. (8) gives m.p. 181–182°; $\lambda\lambda_{max}$ 367, 278, and 225.5 mμ (log ε 3.80, 4.45, and 4.39)).

Anal. Calcd. for $C_{19}H_{18}O_6$: C, 66.85; H, 5.01. Found: C, 66.84; H, 5.04.

In methylation experiments in which literature conditions were followed precisely, a more complex product was obtained which was separated by preparative t.l.c. into **2***a* and a second major product (**2***b*). **2***b*, recrystallized from acetic acid, had m.p. 222–223°; $\lambda\lambda_{max}$ 418, 300 (sh), 274, and 226 mμ (log ε 4.04, 4.07, 4.49, and 4.54); ν_{max}(KBr) 1668 (m), 1632 (s), and 1600 (vs) cm^{-1}.

Anal. Calcd. for $C_{18}H_{16}O_6$: C, 65.84; H, 4.91. Found: C, 65.92; H, 4.81.

*Anthraquinone C (**3**)*

Recrystallized from pyridine, the substance had m.p. 308–316° (sealed capillary, decomp. with prior charring; lit. (10*a*) m.p. 300–302°); $\lambda\lambda_{max}$ 379, 305, 284, 251 (inf), and 225 mμ (log ε 3.74, 4.03, 4.45, 4.03, 4.00, and 4.23).

Anal. Calcd. for $C_{16}H_{12}O_5$: C, 67.60: H, 4.25; O, 28.14. Found: C, 67.30; H, 4.07; O, 28.37.

The pigment (30 mg) was acetylated overnight at 5° with acetic anhydride (2 ml) containing 70% perchloric acid (3 drops). The product (**3***a*) crystallized from chloroform–ethanol with m.p. 213–216° (lit. (10*a*), m.p. 209–210°) and $\lambda\lambda_{max}$ 331 and 270 mμ (log ε 3.71 and 4.67).

Anal. Calcd. for $C_{20}H_{16}O_7$ (mol. wt., 368.4): C, 65.21; H, 3.99. Found (mol. wt., (osmometer) 338): C, 64.90; H, 4.15.

Methylation with diazomethane in methanol–ether until reaction was complete, gave macrosporin monomethylether (**3***b*), crystallized from chloroform–ethanol; m.p. 211–214° (lit. (10*b*, *c*), m.p. 209–210°); $\lambda\lambda_{max}$ 410 (inf), 377, 308, 281, and 225 mμ (log ε 3.83, 4.12, 4.56, and 4.35).

Anal. Calcd. for $C_{17}H_{14}O_5$: C, 68.45; H, 4.73. Found: C, 68.53; H, 4.63.

Methylation with dimethyl sulfate in acetone as described in the literature (9*a*) gave the dimethyl ether (**3***c*), m.p. 270–271° (lit., m.p. 260–261°).

Altersolanol A

The substance was obtained free of an impurity by recrystallization from dioxane. It had m.p. 218–218.5° (capillary; charring from 205°); $\lambda\lambda_{max}$ 422, 268, 240, and 219 mμ (log ε 3.65, 4.15, 3.96, and 4.57) and λ_{inf} 285 mμ (log ε 3.84); ν_{max}(KBr) 3650–3000, 1671 (m), 1635 (s), 1603 (vs) and 1595 (vs) cm^{-1}; $[\alpha]_D^{23°}$ −292° (*c*, 0.25 in pyridine).

Anal. Calcd. for $C_{16}H_{16}O_8$: C, 57.14; H, 4.80; O, 38.06; OCH_3, 9.23. Found: C, 56.70, 56.79; H, 4.85, 4.90; O, 38.41; OCH_3, 11.95.

Altersolanol A Pentaacetate

Altersolanol A (76 mg) was added to ice-cold acetic anhydride (5 ml) containing a few drops of 70% perchloric acid. After 2 h in the refrigerator, the solution was poured on ice, the product extracted into ethyl acetate and crystallized from ethanol. Recrystallized it had m.p. 169–173°; $\lambda\lambda_{max}$ 383, 268, and 210 mμ (log ε 3.41, 4.34, and 4.51); ν_{max}(CCl_4) 1750 (vs), 1669 (s) and 1603 (vs) cm^{-1}; $[\alpha]_D^{23°}$ −108° (*c*, 0.25 in chloroform).

Anal. Calcd. for $C_{26}H_{26}O_{13}$ (mol. wt., 546.5): C, 57.14; H, 4.80; O, 38.06. Found (mol. wt., 534 (Mechrolab osmometer; in chloroform, with benzil as reference)): C, 56.89; H, 4.57; O, 38.41.

A suspension of the pentaacetate (85 mg) in 0.05 *N* aqueous sodium hydroxide was stirred under nitrogen at room temperature until solution was complete (ca. 4 h) and then for a further 3 h. After addition of a slight excess of 0.05 *N* hydrochloric acid, the product was extracted, first with 2 portions of chloroform, then with ethyl acetate until the aqueous layer was almost colorless. The chloroform extracts (17 mg) were found by t.l.c. to contain some starting material and several colored products. A major component, corresponding to pigment **2** (2.6 mg), was isolated by preparative t.l.c. and identified by m.p. and mixture m.p. The combined ethyl acetate extracts contained altersolanol A (8.5 mg) which was isolated similarly and identified by m.p., mixture m.p., infrared, and ultraviolet spectra. Its specific rotation was identical with that of altersolanol A within the experimental error.

Altersolanol A Tetraacetate

Altersolanol A (67 mg) in ice-cold pyridine (3 ml) was treated with acetic anhydride (2 ml) and allowed to warm to room temperature. After 2 days, the solution was poured on ice and extracted with ethyl acetate. The major product, isolated by preparative t.l.c., was obtained microcrystalline by careful addition of petroleum ether to its solution in ether. It had m.p. 188–192° (capillary, prior charring); $\lambda\lambda_{max}$ 380, 266, and 210 mμ (log ε 3.44, 4.34, and 4.46); ν_{max}(CCl_4) 3600 (sharp), 3500 (broad), 1755, 1752 (vs), 1666 (s), and 1604 (vs) cm^{-1}; $[\alpha]_D^{23°}$ −84° (*c*, 0.25 in chloroform).

Anal. Calcd. for $C_{24}H_{24}O_{12}$: C, 57.14; H, 4.80. Found: C, 57.38; H, 4.82.

Periodate Degradation of Altersolanol A

The pigment (35.5 mg; 0.106 millimole) was shaken with 0.02 *M* aqueous sodium periodate (25 ml; 0.50 millimole) at room temperature for 48 h, when the solution was distilled to dryness *in vacuo* at room temperature. The distillate, collected at −70°, was rendered slightly alkaline with 0.10 *N* sodium hydroxide, concentrated to 4 ml, acidified (0.5 ml 1.0 *N* sulfuric acid) and distilled at atmospheric pressure and constant volume until no more acid passed over. The distillate was carefully neutralized (1.95 ml 0.100 *N* sodium hydroxide; 0.195 millimole) and evaporated to dryness. The n.m.r. spectrum of the product in deuterium oxide, with TMS as external reference, had bands only at τ 7.27 (singlet) and 3.48 (singlet) of relative area 3:1.07. The salts obtained by evaporating a mixture of 0.98 ml 0.100 *N* sodium formate and 0.98 ml 0.100 *N* sodium acetate gave singlets at 7.28 and 3.48 of relative area 3:1.04. The authentic mixture was indistinguishable from the degradation product by t.l.c. (cellulose; *n*-propanol – concentrated ammonium hydroxide 3:2; silver nitrate spray).

Sublimation of Altersolanol A

The pure pigment (42.6 mg) was sublimed in a high vacuum at 120–130° during 17 days, an almost black residue (17 mg) remaining. The orange sublimate was crystallized from pyridine to give **2** (12 mg), identified by m.p., mixture m.p., t.l.c., and infrared and ultraviolet spectra. The mother liquors, on preparative t.l.c., gave more of the substance (4 mg), material which remained at the origin, and a pigment ((**4**), ca. 2 mg crude yield) which,

Can. J. Chem. Downloaded from www.nrcresearchpress.com by 210.87.254.105 on 09/05/12
For personal use only.

after recrystallization from petroleum ether, had m.p. 179–181°; $\lambda\lambda_{max}$ 428, 300 (sh), 275, 256, and 227 mμ (log ε 3.91, 3.91, 4.17, 4.19, and 4.39). The infrared spectrum ($CHCl_3$) exhibited a single band in the carbonyl region at 1612 cm^{-1} (shoulders at 1629 and 1597 cm^{-1}). In addition to the resonances listed (Table II), the time-averaged n.m.r. spectrum had sharp singlets (1 H each) at τ −3.00 and −2.93. The expected signal from a further phenolic hydroxyl group (at C-3) could not be observed, probably because of broadness.

Reaction of Altersolanol A with Diazomethane

Successive portions (10 ml at a time) of ethereal diazomethane were added to altersolanol A (200 mg) in methanol (10 ml) at room temperature until the starting material had been consumed (t.l.c.). After evaporation to dryness, the product was distributed between chloroform (10 ml, 5 ml) and water (3 × 5 ml). Evaporation of the aqueous layers furnished a brown lac (99 mg) which was treated with 2,4-dinitrophenylhydrazine in dilute hydrochloric acid. The precipitated solid was separated by t.l.c. into numerous components but none accrued in amounts sufficient for investigation.

The combined chloroform layers (140 mg) on preparative t.l.c. gave four yellow bands which furnished crystalline residues on elution and evaporation: A, 6.4 mg; B, 3.3 mg; C, 50.3 mg; D, 6.9 mg (in order of increasing polarity).

Indazole A, recrystallized from chloroform–ethanol, had m.p. 212–215°; $\lambda\lambda_{max}$ 416, 290 (sh), 266, 262, and 223 mμ (log ε 3.72, 4.01, 4.31, 4.30, and 4.45); ν_{max}(KBr) 1678 (s, free CO), 1634 (vs, chelated CO) and 1615 (sh, aromatic) cm^{-1}; n.m.r. data, Table IV. Methylation (dimethyl sulfate/potassium carbonate in refluxing acetone) gave indazole C, identified by t.l.c., m.p., and mixture melting point.

Indazole B, recrystallized from benzene, melted indistinctly above 190°; $\lambda\lambda_{max}$ 401, 270, and 215 mμ (E_{1cm}(1%) 157, 605, and 785); ν_{max}(KBr) 1665 (vs, 2 free CO) and 1600 (vs, aromatic) cm^{-1}; n.m.r. data, Table IV.

Indazole C was recrystallized from chloroform as orange needles, m.p. 214–215.5°; $\lambda\lambda_{max}$ 406 and 263 mμ (log ε 3.58 and 4.33); ν_{max}(KBr) 1671 (s, free CO), 1651 (s, free CO) and 1589 (vs, aromatic) cm^{-1}; n.m.r. data, Table IV.

Anal. Calcd. for $C_{14}H_{12}N_2O_4$: C, 61.76; H, 4.44; N, 10.29; two OCH_3, 22.81. Found: C, 61.99; H, 4.57; N, 10.07; OCH_3, 20.86.

The substance was recovered unchanged from acetic anhydride – perchloric acid.

Indazole D, recrystallized from aqueous acetic acid, sublimed without melting at 275–285°. It had $\lambda\lambda_{max}$ 391, 270, 255, and 220 mμ (log ε 3.63, 4.37, 4.26, and 4.29); ν_{max}(KBr)1683 (m, free CO), 1672 (s, free CO) and 1599 (vs, aromatic) cm^{-1}; n.m.r. data, Table IV.

Anal. Calcd. for $C_{14}H_{12}N_2O_4$: N, 10.29. Found: N, 10.07.

Reaction of Altersolanol A Pentaacetate with Diazomethane

To the pentaacetate (50 mg) in methanol (10 ml) was added an ethereal solution of diazomethane (10 ml) at room temperature. Reaction was complete after 15 min (t.l.c.). The homogeneous product crystallized on evaporation and trituration under ether and was recrystallized from methanol – ether – light petroleum ether, to give colorless needles, m.p. 145–156°; $[\alpha]_D^{23°}$ +200° (*c*, 0.25 in $CHCl_3$); $\lambda\lambda_{max}$ 322, 275 (sh), and 250 mμ (log ε 3.59, 4.02, and 4.38); ν_{max}($CHCl_3$) 1760 (vs, acetate), 1692 (s, free CO) and 1608 (vs, aromatic) cm^{-1}; τ 2.34 and 2.97 (lH each, d, *J* 2.5 Hz; H-8 and H-6 respectively), 3.03 (lH, s; H-1), 4.10 and 5.42 (lH each, d, *J* 18 Hz; —CH_2—N=N—), 4.26 and 5.28 (1H each, d, *J* 9.5 Hz; H-4 and H-3 respectively), 6.02 (3H, s; $ArOCH_3$), 7.68 (3H, s; $ArOCOCH_3$), 7.93, 7.95, and 7.96 (3H each, s; 3 $ROCOCH_3$), 8.26 (3H, s; shielded $ROCOCH_3$) and 8.48 (3H, s; C—CH_3).

Anal. Calcd. for $C_{27}H_{28}N_2O_{13}$: C, 55.10; H, 4.80; N, 4.76. Found: C, 55.22; H, 4.97; N, 4.97.

To a solution of the compound (10 mg) in ethanol (2 ml) was added sodium hydroxide (1 *N*; 2 ml) with the immediate appearance of a deep orange color. After 16 h (no noticeable change) the solution was acidified and extracted with ethyl acetate. The extracts were washed with water and evaporated. The n.m.r. spectrum of the yellow product showed absorption from aromatic protons and methoxyl but none attributable to acetate or *C*-methyl. The substance was dissolved in methanol – ethyl acetate (1:1, 4 ml) and treated with ethereal diazomethane (4 ml) for 10 min. Evaporation and isolation of the main product by preparative t.l.c. gave indazole A (2 mg), identified by m.p., mixture m.p., t.l.c., and infrared spectrum. One of the two minor products was indistinguishable from indazole C by chromatographic behavior.

Altersolanol B

The pigment crystallized from ethanol as lustrous red-brown plates, m.p. 228–230°; $\lambda\lambda_{max}$ 421, 285, 265, and 217 mμ (log ε 3.58, 3.97, 4.14, and 4.52); ν_{max} (KBr)3490, 3420, 1679 (m), 1635 (s), 1619 (s), and 1599 (m) cm^{-1}.

Anal. Calcd. for $C_{16}H_{16}O_6$: C, 63.15; H, 5.30; O, 31.55. Found: C, 63.12; H, 5.14; O, 32.01.

Acetylation of Altersolanol B

Altersolanol B (35 mg), suspended in acetic anhydride (2 ml) at ice temperature, was treated with 3 drops of 70% perchloric acid and kept overnight at 5°. The product was poured on ice, extracted with chloroform and separated by preparative t.l.c. into yellow and orange components (23 and 9 mg respectively).

The yellow substance was recrystallized from chloroform–ethanol to give altersolanol B triacetate; m.p. 182–185°; $\lambda\lambda_{max}$ 379, 348, and 265 mμ (log ε 3.39, 3.36, and 4.38); ν_{max}($CHCl_3$) 1768 (m), 1735 (vs), 1660 (vs) and 1605 (vs) cm^{-1}; $[\alpha]_D^{23°}$ −44° (*c*, 0.25 in $CHCl_3$).

Anal. Calcd. for $C_{22}H_{22}O_9$: C, 61.39; H, 5.15; O, 33.46. Found: C, 61.30; H, 5.05; O, 33.32.

The orange substance, on recrystallization from aqueous acetic acid, gave altersolanol B diacetate, m.p. 141–145°; $\lambda\lambda_{max}$ 423, 282, 267, and 217 mμ (log ε 3.62, 3.96, 4.15, and 4.54); ν_{max}($CHCl_3$) 3300–2600 (broad, chelated OH), 1734 (vs), 1660 (m), 1644 (s), and 1615 cm^{-1}.

Anal. Calcd. for $C_{20}H_{20}O_8$: C, 61.85; H, 5.19. Found: C, 61.92; H, 5.25.

Hydrolysis of Altersolanol B Triacetate

The triacetate (8 mg) was refluxed in a mixture of methanol (0.45 ml), chloroform (0.45 ml), and 6 *N* hydrochloric

acid (0.1 ml) for 20 h. Evaporation of the solution and recrystallization of the residue from ethanol gave altersolanol B, identified by m.p., mixture m.p. and infrared spectrum. Monitoring of the hydrolysis by t.l.c. indicated that it proceeded in the stages: triacetate → orange diacetate → a more polar compound, presumably the 3-monoacetate → altersolanol B.

Dehydration of Altersolanol B

The compound (10 mg) in ice-cold pyridine (1 ml) was treated with 3 drops of thionyl chloride, allowed to warm to room temperature and poured into water after a further hour. The product was extracted with chloroform and isolated from minor components by preparative t.l.c. After recrystallization, it was indistinguishable from pigment **1** by t.l.c., m.p., mixture m.p., ultraviolet, and infrared spectra.

Attempted dehydration by heating *in vacuo* at 145° gave only a trace of **1** (t.l.c.), most of the sublimate corresponding to starting material.

Altersolanol B Acetonide

A suspension of altersolanol B (30 mg) in dry acetone (3 ml) containing sulfuric acid (0.11 ml) was shaken until dissolved and for a further hour. The product was poured into dilute sodium hydrogen carbonate solution, extracted with ethyl acetate and separated from a little starting material by preparative t.l.c. Recrystallization from acetone–ethanol gave the acetonide, m.p. 133–134°; $\lambda\lambda_{max}$ 425, 287, 266, and 217 mμ (log ε 3.62, 3.90, 4.11, and 4.53); $\nu_{max}(CHCl_3)$ 2800–2300 (w, chelated OH), 1660 (sh, free CO), 1640 (s, chelated CO) and 1611 (vs, aromatic) cm^{-1}; τ −2.20 (1H, s; chelated phenol), 2.83 (1H, d, *J* 2.75 Hz; H-8), 3.48 (1H, d, *J* 2.75; H-6), 5.61 (1 H, m; H-3), 6.12 (3H, s; $ArOCH_3$), 6.33–7.92 (4H, several multiplets; H-1 and H-4), 8.57 (3 H, s (sharp); R—CH_3), 8.65 and 8.78 (2 × 3 H, s (broadened); *gem*-dimethyl); $[\alpha]_D^{23°}$ −16° (*c*, 0.25 in $CHCl_3$).

Anal. Calcd. for $C_{19}H_{20}O_6$: C, 66.27; H, 5.85. Found: C, 66.20; H, 6.04.

Acknowledgments

I thank the Director, Dr. E. Y. Spencer, for support of this work, Dr. G. A. White for providing culture filtrates for preliminary investigations, C. H. Unwin for growing the mold for large scale extraction, Mrs. M. H. H. Thomson for her patient assistance with tedious separations, and G. Rock for excellent experimental support throughout.

1. A. Stoessl. Chem. Commun. 307 (1967).
2. C. Chupp and A. F. Sherp. Vegetable diseases and their control. Roland Press, New York. 1960. p. 541.
3. P. W. Brian, P. J. Curtis, H. G. Hemming, E. G. Jefferys, C. H. Unwin, and Joyce M. Wright. J. Gen. Microbiol. **5**, 619 (1951).
4. J. F. Grove. J. Chem. Soc. 4056 (1952); J. R. Bartels-Keith. J. Chem. Soc. 860, 1662 (1960).
5. H. Darpoux, A. Faivre-Amiot, and L. Roux. Compt. Rend. **230**, 993 (1950).
6. W. V. Lavate and R. Bentley. Arch. Biochem. Biophys. **108**, 287 (1964).
7. F. K. Beilstein. Handbuch der Organischen Chemie. 3rd ed. Voss, Hamburg, 1906. **H 8** p. 473.
8. L. H. Briggs, F. E. Jacombs, and G. A. Nicholls. J. Chem. Soc. 3069 (1953).
9. A. Stoessl. Can. J. Chem. This issue.
10. *a*) R. Suemitsu, Y. Matsui, and M. Hiura. Bull. Agr. Chem. Soc. Japan, **21**, 1 (1957); *b*) R. Suemitsu and M. Hiura. Bull. Agr. Chem. Soc. Japan, **21**, 337 (1957); *c*) R. Suemitsu, M. Nakajima, and M. Hiura. Bull. Agr. Chem. Soc. Japan, **23**, 547 (1959); *d*) R. Suemitsu, M. Nakajima, and M. Hiura. Agr. Biol. Chem. (Tokyo) **25**, 100 (1961).
11. E. Hardegger, K. Steiner, E. Widmer, and T. Schmidt. Helv. Chim. Acta **47**, 2017 (1964).
12. D. W. Cameron, R. I. T. Cromartie, D. J. Kingston, and Lord Todd. J. Chem. Soc. 51 (1964).
13. F. M. Dean, Peter G. Jones, and P. Sidisunthorn. J. Chem. Soc. 5186 (1963) and subsequent papers; H. Brockmann, Kirsten Van Der Merwe, and A. Zeeck. Chem. Ber. **97**, 2555 (1964).
14. A. C. Neish. Biochemistry of phenolic compounds. *Edited by* J. B. Harborne. Academic Press. London. 1964. p. 302.
15. P. W. Brian, P. J. Curtis, and H. G. Hemming. Proc. Roy. Soc. (London) Ser. B. **135**, 106 (1947).

Can. J. Chem. Downloaded from www.nrcresearchpress.com by 210.87.254.105 on 09/05/12
For personal use only.

Relative stereochemistry of altersolanol A[1]

A. STOESSL
Research Institute, Canada Department of Agriculture, London, Ontario

Received August 19, 1968

Altersolanol A (**1**) forms a monoisopropylidene derivative which in turn yields a triacetate and a dimethylether monoacetate. Both of the latter compounds can be aromatized but the products indicate that either an acyl or a methyl migration has taken place. The former possibility is considered to be much more likely. This and other considerations lead to structure **2** for altersolanol A acetonide. Analysis of the nuclear magnetic resonance spectra of **1** and **2** and their derivatives allows assignments of their relative configurations and conformations as **7** and **8** respectively.

Canadian Journal of Chemistry, 47, 777 (1969)

Can. J. Chem. Downloaded from www.nrcresearchpress.com by 210.87.254.40 on 09/05/12
For personal use only.

Altersolanol A was shown in the preceding communication (1) to be represented by **1** but its stereochemistry remained unassigned. An approach to this problem was found in the preparation of an isopropylidene derivative whose structure must be considered in some detail.

The substance, altersolanol A acetonide (**2**), has the elemental composition corresponding to the addition of C_3H_4 to altersolanol A, and an ultraviolet spectrum essentially identical with that of the parent compound. It forms a triacetate (**2***a*) on acetylation in pyridine. The nuclear magnetic resonance (n.m.r.) spectrum (Fig. 1) shows signals from a chelated phenol (τ −2.00,s), two alcohols (τ 5.75–6.05,m) and those listed in Table I. Appropriate bands can be assigned unambiguously to the naphthoquinone moiety and the C_2—methyl group familiar from **1**, and to the *gem*-dimethyl group of an isopropylidene residue. The latter group must therefore be attached in ketal form to two of the oxygen atoms on ring C. The spectrum also indicates that carbon atom C-1 is the site of a free hydroxyl group because the signal from H-1 at τ 5.14 (doublet collapsing to a characteristic broadened singlet on deuteration) undergoes a pronounced downfield shift on acetylation. A similar situation prevails with respect to the signals at τ 4.80 (approximate quartet collapsing to approximate doublet on deuteration; downfield shift on acetylation), while those at τ 5.50 are unaffected. One of these two bands must represent H-3 and the other, H-4. Because it is adjacent to the quinone ring, it is reasonable to expect H-4 to be the more deshielded proton and therefore responsible for the absorption at τ 4.80. Similar assignments of resonance position have been made in the eleutherin series (e.g., (**3**)) and for derivatives (e.g., (**4**)) of the protoaphins (2). It then follows from the properties of the bands on deuteration and acetylation that H-4 is geminal to free hydroxyl, which must therefore be placed at C-4, while the other proton is attached to one terminus of the isopropylidene bridge at C-3. The second terminus is necessarily at C-2, since all other positions are accounted for. However, it remained conceivable that one of the oxygen functions in the vicinity[2] could deshield H-3 to a resonance position lower than that of H-4 so that the assignments would require reversal. Also, an inspection of Dreiding models suggested that neither steric repulsion nor steric strain would be present in an altersolanol-2,4-acetonide to a significantly greater extent than in a 2,3-acetonide.[3] Such effects therefore could not be invoked to clarify the position and it was necessary to confirm structure **2** by more extended studies.

Partial hydrolysis of the acetonide triacetate gave altersolanol A triacetate which has acetoxyl groups at C-1 and C-5 (ultraviolet and n.m.r. spectra) and at either C-3 or C-4. A ready reaction with periodate would have implied free hydroxyls at positions-2 and -3 but, when put to the test, the compound was not attacked by periodate in aqueous acetonitrile during 24 h at room temperature. More severe conditions

[1]Contribution No. 388 from the Research Institute.

[2]I am greatly indebted to Dr. J. B. Stothers for an informative discussion on this aspect.

[3]From numerous examples (3) from carbohydrate chemistry, it appears that six-membered ketal rings fused to a pyranose are obtained only when C-6 of the sugar, which is exocyclic to the pyranose ring, is a terminus. Six-membered cyclic ketals have also been considered (4) to be unobtainable from cyclitols for steric reasons which are not necessarily applicable in the present instance. On the other hand, at least one such compound has recently been reported (5) as a derivative of a 7,9-dihydroxyanthracyclinone.

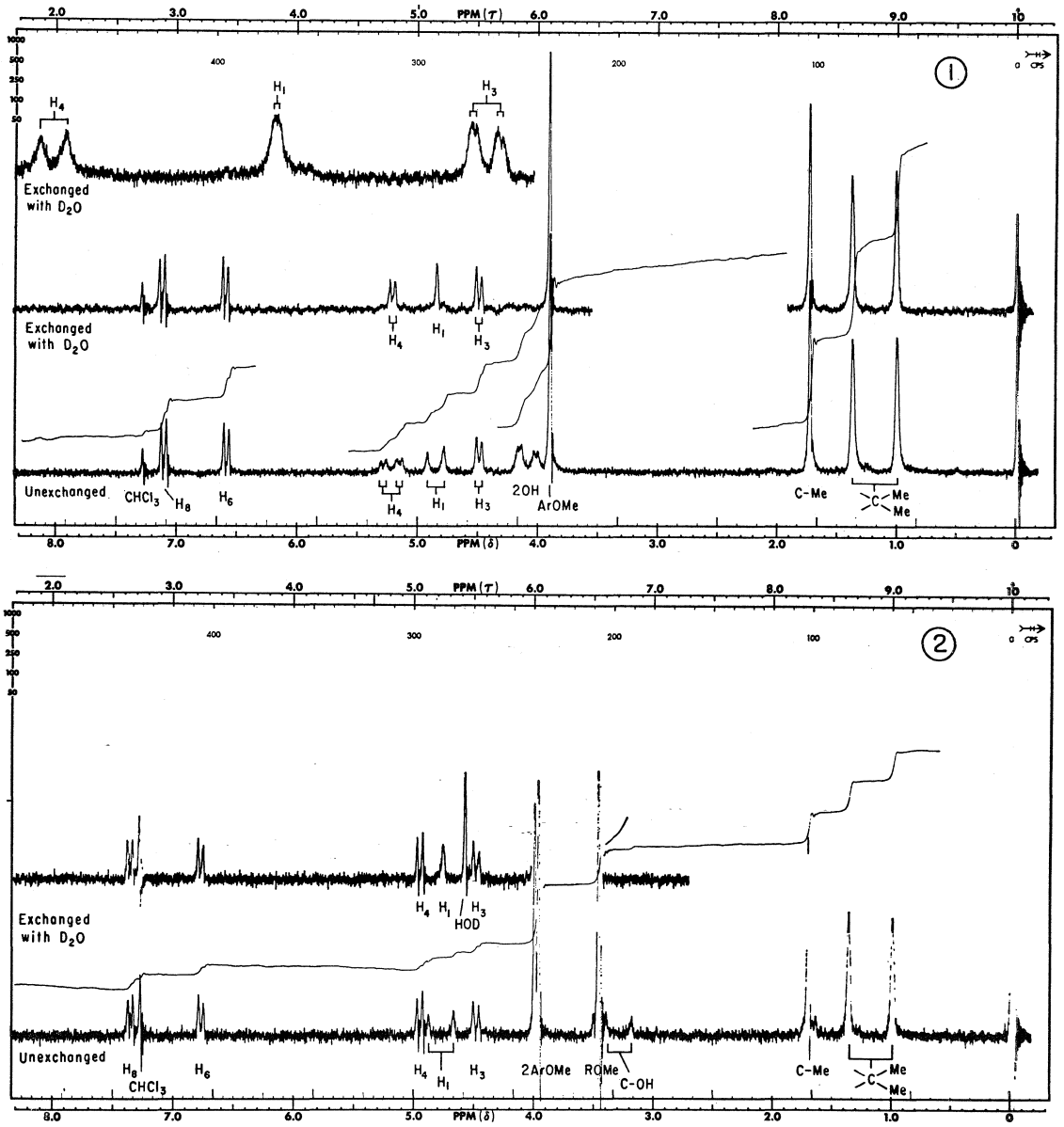

FIG. 1. The nuclear magnetic resonance spectrum of altersolanol A acetonide, obtained in deuteriochloroform with tetramethylsilane as internal reference. Expanded portions were determined with 100 Hz sweep-width and are off-set.
FIG. 2. The nuclear magnetic resonance spectrum of altersolanol A acetonide dimethylether.

seemed inadvisable and experimentation with the substance, which could not be obtained in satisfactory yields, was not continued. Similarly, in another experiment, the acetonide triacetate (**2***a*), on heating in pyridine at steam-bath temperature, deposited a substance which was readily characterized as 3-acetoxy-4,5-dihydroxy-7-methoxy-2-methylanthraquinone (**5***a*). At first sight, both these results appeared to require that the tentative assignment of band positions for H-3 and H-4 in the acetonide should indeed be reversed. However, the formation of **5***a* might have involved an acyl migration from the *peri*-position to C_3—O, while the failure of altersolanol A triacetate to be cleaved by periodate could possibly be ascribed to steric hindrance at C-2

Can. J. Chem. Downloaded from www.nrcresearchpress.com by 210.87.254.40 on 09/05/12
For personal use only.

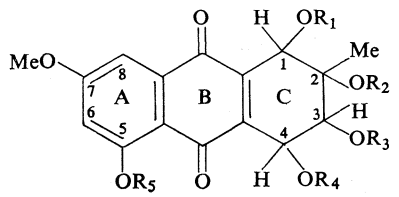

(**1**, $R_1 = R_2 = R_3 = R_4 = R_5 = H$)
(**1***a*, $R_1 = R_2 = R_3 = R_4 = R_5 = COMe$)
(**1***b*, $R_1 = R_3 = R_4 = R_5 = COMe$, $R_2 = H$)
(**1***c*, $R_1 = R_4 = R_5 = COMe$, $R_2 = R_3 = H$)

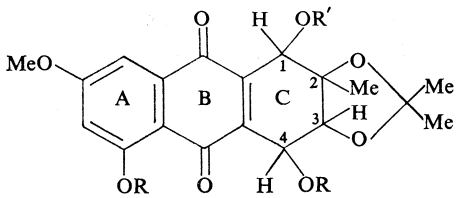

(**2**, $R = R' = H$)
(**2***a*, $R = R' = COMe$)
(**2***b*, $R = Me$, $R' = H$)
(**2***c*, $R = Me$, $R' = COMe$)

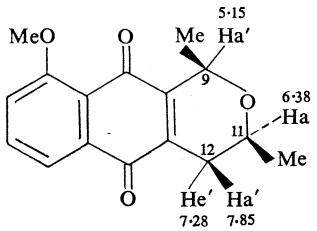

(**3**, τ values as indicated.
$J^{11,12}_{a'e'}$ 2.9 Hz; $J^{11,12}_{a'a}$ 9.2 Hz)

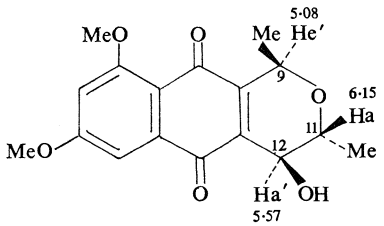

(**4**, τ values as indicated.
$J^{11,12}_{a'a}$ 8.0 Hz)

and not to the lack of a vicinal glycol system. Thus, both results had to be regarded with suspicion.

A potentially more informative approach was sought in the preparation of a dihydro compound by reduction of the quinone double bond. Such hydrogenations have been realized in the case of juglone (6, 7) but, unfortunately, could not be accomplished in this instance. Altersolanol A pentaacetate (**1***a*), as a model substance, proved inert to hydrogenation in benzene in the presence of Wilkinson's catalyst (6). It reacted rapidly with zinc dust in ether – acetic acid or in ether – dilute sulfuric acid (7), but the only compound isolated under either set of conditions was the 5-acetate (**6***a*) of 7-*O*-methyl-2-methylxanthopurpurin (**6***b*), recognized by its n.m.r. spectrum and identical with a synthetic specimen. Obviously, the reaction which had occurred involved a succession of reduction–elimination steps and could not be usefully applied to the acetonide.

Attention was therefore turned to a derivative unlikely to rearrange under aromatization conditions. A dimethylether of altersolanol A acetonide was obtained by methylation over silver oxide in acetone; comparison of its n.m.r. spectrum (Fig. 2; Table I) with others shows that it is a di-*O*-methyl derivative with a free hydroxyl group at C-1 (τ 6.70, d, J[4] 13 Hz, exchangeable; H-1 before deuteration appearing as a doublet, J 13 Hz). Acetylation of the dimethylether gave the syrupy monoacetate (n.m.r. spectrum (Fig. 3)) which, on aromatization[5] by heating in pyridine at 105°, afforded two compounds. The major product was shown to be 3-hydroxy-2-methyl-4,5,7-trimethoxyanthraquinone (**5***b*) by analytical and spectroscopic data and by facile methylation with diazomethane to **5***c*. The minor product, on the basis of spectroscopic data, is a monodemethylation product of **5***b* (see Experimental; in order to conserve the small amount available, the compound was not submitted to elemental analysis). It gave the color reactions associated with the catechol system of **5** (1) and therefore can only be **5***d*. Methylation with diazomethane readily gave the 3-*O*-methyl derivative (**5***e*), the chelated phenol at C-4 remaining unattacked, which is identical with the dimethylation product obtained earlier (1) from **5**.

The two compounds which are directly relevant

[4]J = apparent coupling constant = observed splitting throughout this paper.

[5]The dimethylether (**2***b*) itself was not aromatized under these conditions but instead was transformed into a compound which retained both the acetonide grouping and optical activity. This product appeared to be pure, as judged from its chromatographic behavior and nuclear magnetic resonance spectrum, which suggested that it was a monoanhydro derivative. Nevertheless, despite repeated runs, the substance did not yield satisfactory elemental analyses and elucidation of its structure must be deferred until fresh supplies of starting material become available.

Can. J. Chem. Downloaded from www.nrcresearchpress.com by 210.87.254.40 on 09/05/12
For personal use only.

TABLE I

Nuclear magnetic resonance data of altersolanol A derivatives*

	m	**1***a*	**1***b*	**1***c*	**2**	**2***a*	**2***b*	**2***c*
τ Values								
H-1	s	2.83	3.82	3.82	5.14	3.80	5.22	3.83
H-3	d	4.47	4.66	6.13	5.50	5.62	5.50	5.61
H-4	d	3.70	3.73	3.95	4.80	3.76	5.04	5.07
H-6	d	3.12	3.18	3.18	3.40	3.10	3.21	3.23
H-8	d	2.46	2.57	2.55	2.87	2.39	2.63	2.67
C_2-Me	s	8.40	8.72	8.62	8.23	8.48	8.28	8.47
ArOMe	s	6.05	6.10	6.12	6.09	6.04	5.99	6.00
	s						6.02	6.05
ROMe	s	—	—	—	—	—	6.52	6.53
CMe_2	s	—	—	—	8.59	8.62	8.62	8.62
	s				8.97	8.88	9.00	8.92
ArOCOMe	s	7.62	7.64	7.64	—	7.55	—	—
ROCOMe	s	7.85	7.86	7.85	—	7.93	—	7.97
	s	7.87	7.90	7.92		7.95		
	s	7.94	7.96					
	s	8.02						
splittings (Hz)								
$J_{6,8}$		2.7	2.6	2.7	2.7	2.7	2.7	2.7
$J_{3,4}$		7.7	7.6	6.8	2.6	2.5	2.8	2.5

*Values determined after exchange with D_2O, relative to TMS as internal reference, in $CDCl_3$; m = apparent multiplicity (neglect of long-range couplings) determined from a 500 Hz sweep (s = singlet, d = doublet); J = apparent coupling constant = observed splitting.

to this discussion are **5***a* and **5***b*. The formation of one of them must have involved a migration; either of acetyl from C_4—O to C_3—O or of methyl from C_3—O to C_4—O. To confirm the unlikelihood of a methyl migration, the trimethoxy compound (**5***e*) was treated with pyridine under the same conditions as the dimethylether acetate. It remained largely unattacked, yielding only negligible amounts of the monodemethylation product (**5***d*) and an unidentified, polar material. Only a minute trace, barely visible on thin-layer chromatograms, of a compound corresponding to **5***b* in R_f value and color, could be detected. Methyl migration, at any rate after aromatization, therefore cannot account for the substantial formation of **5***b* from the dimethylether acetate. On the other hand, the facility of acyl migration to suitably disposed hydroxyl groups is well attested (8). It is therefore almost certain that altersolanol A triacetate is **1***c*, while the acetonide dimethylether and its acetate must be **2***b* and **2***c* respectively. Thus, the original assignment of structures **2** and **2***a*, to altersolanol A acetonide and its triacetate respectively, can no longer be in serious doubt.

Examination of Dreiding models revealed the requirement for a *pseudo*-boat conformation for the acetonides (**2**, **2***a–c*) and, as expected (4), for a *cis*-configuration of the oxygen atoms at C-2 and C-3. The n.m.r. spectra indicate that one of the *gem*-dimethyl groups of the isopropylidene residue experiences considerable shielding which is clearly attributable to its position above the quinone double bond. This necessitates a diaxial disposition for the oxygen atoms at positions-2 and -3 in the acetonides. The apparent coupling constants associated with the interaction of the protons attached to C-3 and C-4, are about 2.6 Hz and are compatible with an equatorial – *pseudo*equatorial arrangement.

On the other hand, the apparent coupling constants for H-3, H-4 in altersolanol A and its acetates are 6.8 to 7.7 Hz. By analogy with eleutherin and related compounds (2), these values strongly suggest a *trans*-axial – *pseudo*-axial relation of these protons in **1**,**1***a–c*. Mild hydrolysis of **2** regenerated **1** which had the specific rotation of the natural substance. The change in coupling constants in the transformation (**1**) → (**2**) thus reflects a conformational rather than a more deep-seated rearrangement and all configurations must have remained unchanged. A further important fact is that the resonance position of H-1 in altersolanol A tetraacetate (**1***b*) (Fig. 4) at τ 3.82 was moved downfield by acetylation of the vicinal tertiary hydroxyl and appears at τ 2.83 in the pentaacetate (**1***a*) (Fig. 5). Analogous effects, previously observed in other compounds (9, 10), were studied quite recently in steroid derivatives (11) and correlated with those

Can. J. Chem. Downloaded from www.nrcresearchpress.com by 210.87.254.40 on 09/05/12
For personal use only.

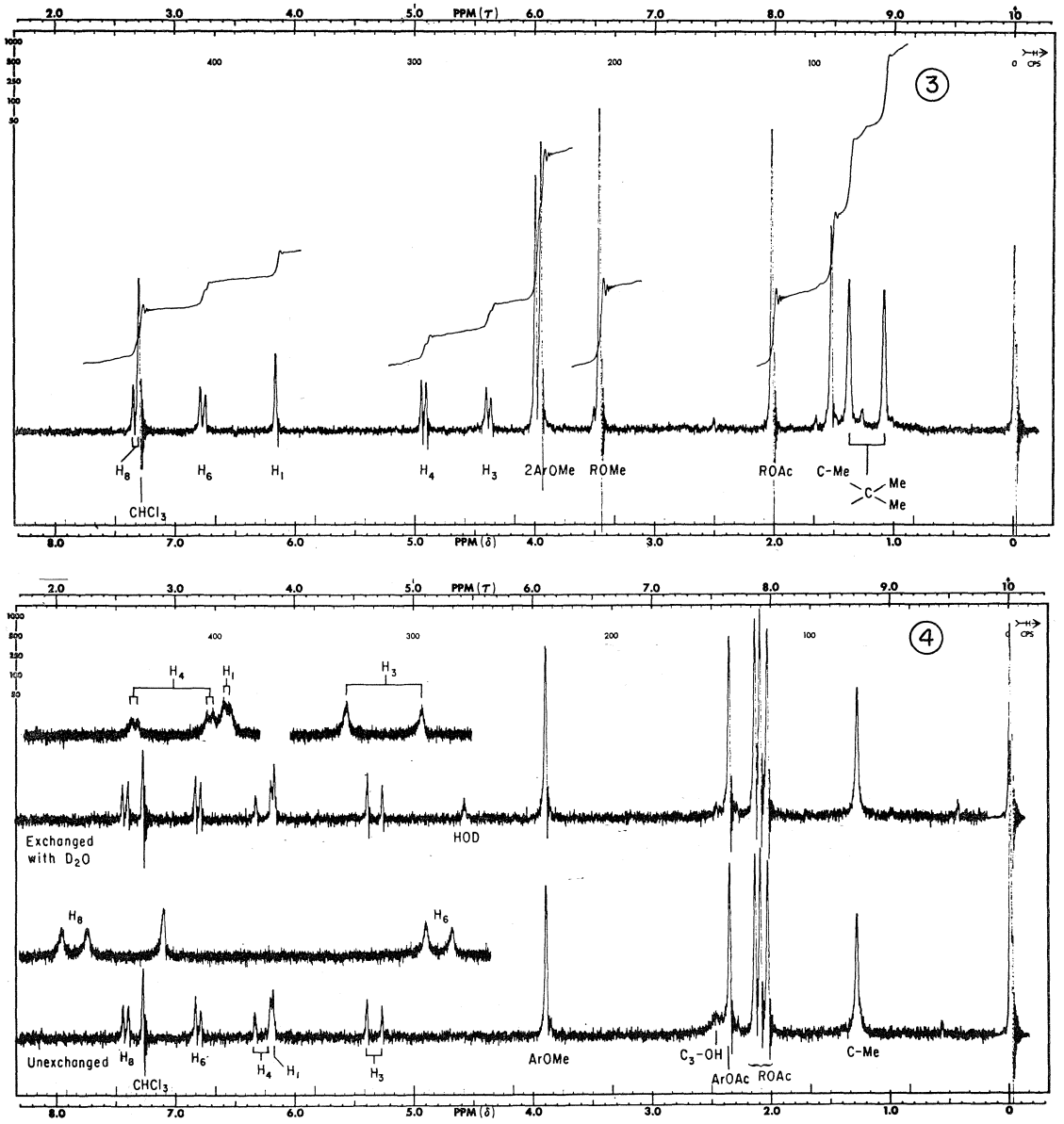

FIG. 3. The nuclear magnetic resonance spectrum of altersolanol A acetonide dimethylether acetate.
FIG. 4. The nuclear magnetic resonance spectrum of altersolanol A tetraacetate.

situations, in which the deshielded protons were equatorial, and vicinal to axial tertiary acetoxyl groups.

Thus, in altersolanol A and its acetates, H-1 is *pseudo*equatorial, C_2—O axial and *cis* to C_3—O, and H_3,H_4 are *trans*-axial – *pseudo*axial. These conditions lead to only one stereochemical expression (**7** or mirror-image) for altersolanol A and its acetates. Similarly, only one representation (**8** or mirror-image) satisfies the properties of the acetonides.

Corroboration for these conclusions was obtained from some other observations. The acetoxyl groups attached to saturated carbon atoms in the acetonide triacetate are magnetically almost equivalent ($\Delta\tau = 0.02$) as expected of their di*pseudo*axial dispositions in **8**, (R = Ac). In altersolanol A pentaacetate (**7**, R = Ac), the

Can. J. Chem. Downloaded from www.nrcresearchpress.com by 210.87.254.40 on 09/05/12
For personal use only.

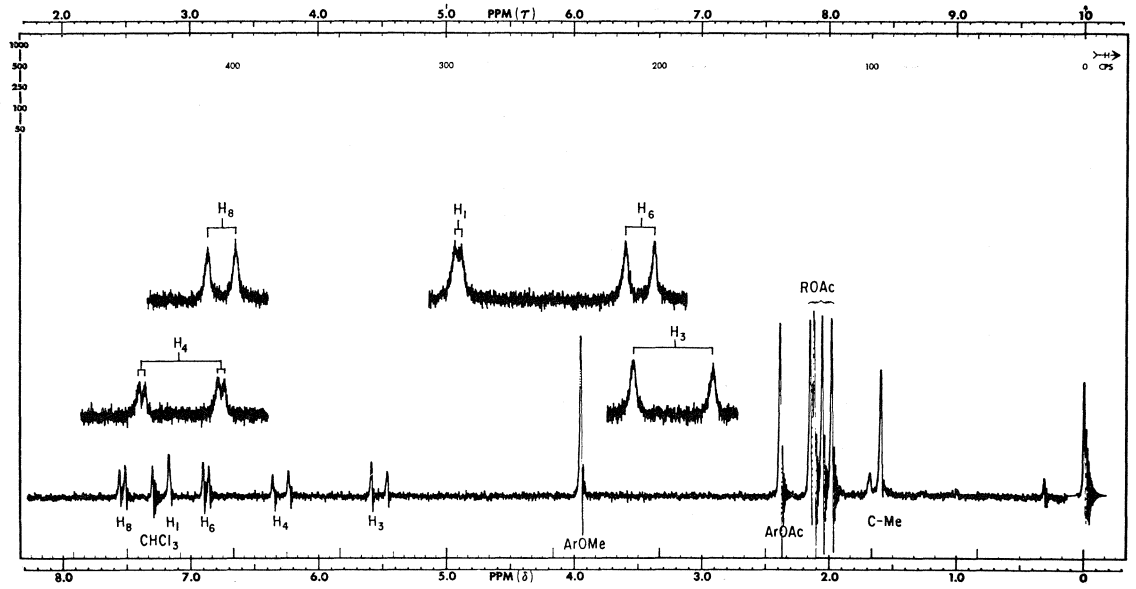

FIG. 5. The nuclear magnetic resonance spectrum of altersolanol A pentaacetate.

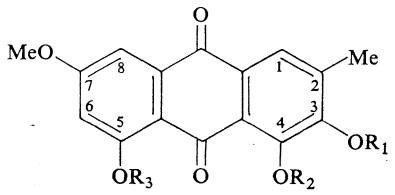

(**5**, $R_1 = R_2 = R_3 = H$)
(**5***a*, $R_1 = COMe$, $R_2 = R_3 = H$)
(**5***b*, $R_1 = H$, $R_2 = R_3 = Me$)
(**5***c*, $R_1 = R_2 = R_3 = Me$)
(**5***d*, $R_1 = R_2 = H$, $R_3 = Me$)
(**5***e*, $R_1 = R_3 = Me$, $R_2 = H$)

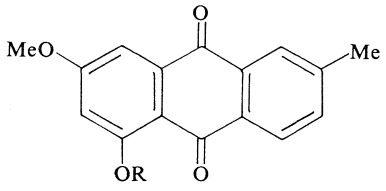

(**6***a*, R = COMe)
(**6***b*, R = H)

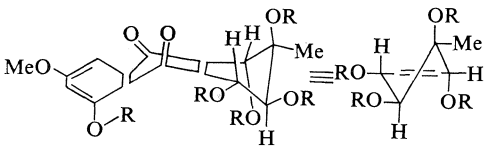

7

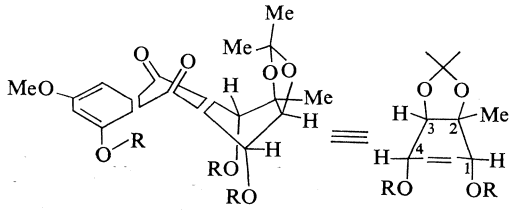

8

corresponding resonances range through $\Delta\tau = 0.17$, consistent with the presence of both equatorial and axial acetyl functions (12). However, this effect is less clearly evident in the tetraacetate ($\Delta\tau = 0.10$) and triacetate ($\Delta\tau = 0.07$). A comparison of the resonance positions of H-1 and H-4 is complicated by the need to consider neighboring group effects and was not attempted in detail; however, the values observed are compatible with the structural proposals (**7** and **8**). Finally, some moment can be attached to the smooth formation of the acetonide from altersolanol A. The sole by-product of this reaction accrued in less than 1% yield; it is thus improbable that more than one *cis*-glycol is available for acetonation.

One difficulty, however, remained. Cameron *et al.* (2) found that eleutherin and its analogues exhibit long-range coupling effects whose magni-

Can. J. Chem. Downloaded from www.nrcresearchpress.com by 210.87.254.40 on 09/05/12
For personal use only.

Can. J. Chem. Downloaded from www.nrcresearchpress.com by 210.87.254.40 on 09/05/12
For personal use only.

tudes vary with the character of the bonds. Thus, they could readily distinguish between *pseudo*-axial–*pseudo*equatorial ($J > 1.5$ Hz) and di*pseudo*-equatorial ($J < 1$ Hz) interactions through five bonds (H—C—C═C—C—H) in the non-aromatic ring. In altersolanol A derivatives, long-range interactions through both four and five bonds are discernible in the nuclear magnetic resonance spectra (see Figures) but all the effects are small (half-band widths of signals from H-4 < 1.2 Hz). If H-1, H-4 were always di*pseudo*-equatorial, then, irrespective of the configurations assigned to any center, acetonation would have to proceed without conformational rearrangement. This is clearly against all the evidence. Any differential long-range coupling effects in altersolanol A derivatives are therefore smaller than in eleutherin and thus eluded observation.

Experimental

General conditions were as described in the preceding paper (1).

Altersolanol A Acetonide

To a suspension of altersolanol A (40 mg) in dry acetone (4 ml) was added a cold solution of sulfuric acid (0.144 ml) in the same solvent (4 ml). After shaking at room temperature for 1.5 h, the solution was poured into dilute sodium hydrogen carbonate and extracted with ethyl acetate. The product crystallized on removal of the solvent and was recrystallized from methanol. It had m.p. 163–164°, with resetting and was recrystallized from methanol. It had m.p. 163–164°, with resetting and a second m.p. 180–183°; $\lambda\lambda_{max}$429, 285 (sh), 268 and 218 mμ (log ε 3.68, 3.75, 4.11, and 4.58; $\nu_{max}(CHCl_3)$ 3590 (sharp), 3310 (broad), 1662 (m), 1641 (s) and 1612 (vs) cm^{-1}; $[\alpha]_D^{23°}$ +32° (*c*, 0.25 in $CHCl_3$).

Anal. Calcd. for $C_{19}H_{20}O_8$: C, 60.63; H, 5.36. Found: C, 60.49; H, 5.28.

In a like experiment, the crude product from 2 mg altersolanol A was separated into its components by preparative thin-layer chromatography. The three colored bands obtained were eluted and the amounts estimated spectrophotometrically at 420 mμ. The ratio (altersolanol A acetonide: recovered altersolanol A: unidentified product) was (110:2:1).

The acetonide (10 mg) was refluxed for 18 h in ethanol (0.8 ml) containing hydrochloric acid (1 *N*; 0.2 ml). The solution was shaken with a slight excess of silver carbonate and filtered. Evaporation and recrystallization from ethyl acetate gave altersolanol A (t.l.c., m.p., and mixture m.p.) of unchanged specific rotation.

Altersolanol A Acetonide Triacetate

The acetonide (50 mg) was kept overnight in pyridine (1.2 ml) and acetic anhydride (0.9 ml). The product crystallized on removing the solvent and reevaporation from ethanol. Recrystallized from acetone–ethanol, it had m.p. 214–217°; $\lambda\lambda_{max}$ 384, 265, and 210 mμ (log ε 3.48, 4.31, and 4.49); $\nu_{max}(CHCl_3)$ 1743 (vs), 1666 (s) and 1605 (vs) cm^{-1}; $[\alpha]_D^{23°}$ +44° (*c*, 0.25 in $CHCl_3$).

Anal. Calcd. for $C_{25}H_{26}O_{11}$: C, 59.76; H, 5.22. Found: C, 59.10; H, 5.24.

Reaction of Altersolanol A Pentaacetate with Zinc Dust

The pentaacetate (35 mg) in ether (10 ml) was stirred with dilute sulfuric acid (5 ml) and zinc dust (Fisher Scientific, 300 mg) for 40 min. After dilution with ether, the organic phase was washed with water and evaporated. The product, recrystallized from ethyl acetate, had m.p. 171–173°; $\lambda\lambda_{max}$360, 328, and 267 mμ (log ε 3.55, 3.61, and 4.58); $\nu_{max}(CHCl_3)$ 1772 (s, ArOCOCH_3), 1673 (s, free CO), 1665 (sh), and 1606 (vs, aromatic) cm^{-1}; τ $CDCl_3$ 1.85 (1 H, d, *J* 8 Hz, H-4), 1.92 (1 H, s, H-1), 2.24 (1 H, d, *J* 2.5 Hz, H-8), 2.42 (1 H, broadened d, *J* 8 Hz, H-3), 3.08 (1 H, *J* 2.5 Hz, H-6), 6.00 (3 H, s, ArOCH_3), 7.47 (3 H, s, ArCH_3) and 7.51 (3H, s, ArOCOCH_3).

Anal. Calcd. for $C_{18}H_{14}O_5$: C, 69.67; H, 4.55. Found: C, 69.46; H, 4.51.

The same compound (m.p., mixture m.p., and t.l.c.) was also obtained when altersolanol A pentaacetate (25 mg) in ether (10 ml) containing acetic acid (0.5 ml) was stirred with zinc dust for 2 h. The substance was also identical by t.l.c., m.p., mixture m.p., ultraviolet, and infrared spectra with the product obtained by acetylation (acetic anhydride/perchloric acid) of the 7-methylether of 2-methylxanthopurpurin (1).

Altersolanol A Triacetate

Altersolanol A acetonide triacetate (120 mg) in acetonitrile (9 ml) and aqueous hydrochloric acid (3 *N*; 3 ml) was heated at 70° for 30 min. The solution was poured on ice and the product extracted with chloroform and washed with dilute sodium hydrogen carbonate solution and water. Preparative t.l.c. (methanol–chloroform – 90% formic acid; 10:90:2) gave starting material (ca. 60%) and crude triacetate (**1***c*) (R_f 0.49) which crystallized from isopropanol (14.5 mg, 16%). After repeated recrystallizations from the same solvent, it had m.p. 188–192°; $\lambda\lambda_{max}$384 and 267 mμ (log ε 3.43 and 4.31); $\nu_{max}(CHCl_3)$ 3520 (broad), 1755 (vs), 1671 (vs), and 1608 (vs) cm^{-1}.

Anal. Calcd. for $C_{22}H_{22}O_{11}$: C, 57.14; H, 4.80. Found: C, 57.28; H, 4.83.

The compound (2.2 mg) did not undergo a noticeable reaction (t.l.c.) when kept for 24 h at room temperature in acetonitrile (0.9 ml) containing sodium periodate solution (0.1 *M*; 0.1 ml).

Dehydration of Altersolanol A Acetonide Triacetate

A solution of the acetonide triacetate (34 mg) in pyridine (0.34 ml; stored over sodium hydroxide and distilled before use) was heated on the steam bath for 4 h. The crystalline product was filtered off, washed with hot pyridine, and recrystallized from the same solvent. It had m.p. 283–286°; $\lambda\lambda_{max}$ 428, 272 (broad), and 222 mμ (log ε 3.94, 4.15, and 4.33); ν_{max} (Nujol) 2800–2500 (w, chelated OH), 1754 (vs, acetate), 1675 (s, free CO), 1631 (vs, chelated CO), and 1608 (vs, aromatic) cm^{-1}; τ (saturated solution in $CDCl_3$, 81 accumulations) −2.33 (1 H, s, chelated phenol), −2.22 (1 H, s, chelated phenol), 2.32 (1 H, s, H-1), 2.64 (1 H, d, *J* 2.5 Hz, H-8),

Can. J. Chem. Downloaded from www.nrcresearchpress.com by 210.87.254.40 on 09/05/12
For personal use only.

3.32 (1 H, d, J 2.5 Hz, H-6), 6.07 (3 H, s, ArOCH_3), 7.60 (3 H, s, ArCH_3), and 7.68 (3 H, s, ArOCOCH_3).

Anal. Calcd. for $C_{18}H_{14}O_7$: C, 63.16; H, 4.12. Found: C, 63.24; H, 4.21.

A solution of this product (0.7 mg) in sodium hydroxide (0.10 N; 1 ml) was acidified after 1 h. The resulting compound, extracted with ethyl acetate, was indistinguishable from 7-methoxy-2-methyl-3,4,5-trihydroxyanthraquinone (anthraquinone B) (1) by R_f and characteristic lake formation on t.l.c.

Altersolanol A Acetonide Dimethylether

Altersolanol A acetonide (120 mg) in dry acetone (12 ml) containing methyl iodide (0.18 ml) was shaken for 48 h at room temperature over silver oxide (420 mg). The suspension was filtered, the filter cake washed with acetone, the combined filtrates and washings concentrated, diluted with water, and extracted with ethyl acetate. The major band obtained on preparative t.l.c. of the product was crystallized from ether – light petroleum ether to give altersolanol A acetonide dimethylether (69 mg). After recrystallization from methanol, it had m.p. 173–175°; $\lambda\lambda_{max}$413, 267, and 217 mμ (log ε 3.61, 4.17, and 4.58); ν_{max}($CHCl_3$) 3470 (OH), 1659 (s, 2 free CO), and 1600 (s, aromatic) cm^{-1}; $[\alpha]_D^{23°}$ +40° (c, 0.25 in $CHCl_3$).

Anal. Calcd. for $C_{21}H_{24}O_8$: C, 62.37; H, 5.98. Found: C, 62.28; H, 6.34.

Aromatization of Altersolanol A Acetonide Dimethylether Acetate

The dimethylether (52 mg) was kept overnight at room temperature in pyridine (2.5 ml) containing acetic anhydride (1.5 ml). Evaporation in the usual manner and preparative t.l.c. gave altersolanol A acetonide dimethylether acetate as a syrup which was characterized by its nuclear magnetic resonance spectrum.

The substance was heated in pyridine (1 ml, dried over sodium hydroxide and distilled before use) at 105° until all the starting material had been consumed (48 h, no transient product revealed by t.l.c.). After removal of the solvent, the product, on preparative t.l.c., gave two major bands, yellow and orange respectively.

The yellow substance was recrystallized from chloroform–ether to give needles (16.5 mg), m.p. 226–235° (unchanged by recrystallization); $\lambda\lambda_{max}$374, 295 (inf), 280 and 226 mμ (log ε 3.96, 4.21, 4.52, and 4.46); ν_{max} ($CHCl_3$) 3470 and 3420 (OH), 1663 (s, 2 free CO) and 1590 (vs, aromatic) cm^{-1}; τ $CDCl_3$ 2.60 (1 H, d, J 2.5 Hz, H-8), 3.21 (1 H, s, exchangeable, non-chelated phenol), 3.24 (1 H, d, J 2.5 Hz, H-6), 5.96, 6.01 and 6.03 (3 × 3H, s, 3 ArOCH_3), and 7.62 (3 H, s, ArCH_3).

Anal. Calcd. for $C_{18}H_{16}O_6$: C, 65.84; H, 4.91. Found: C, 65.62; H, 4.79.

Ethereal diazomethane (2 ml) was added to ca. 2 mg of the substance in methanol (1 ml). Reaction was complete after 5 min. Recrystallization of the product from chloroform–ethanol gave 2-methyl-3,4,5,7-tetramethoxyanthraquinone, identical with an authentic specimen (1) by m.p., mixture m.p., and infrared spectrum.

The orange substance (11 mg), in chloroform–ethanol, was washed with dilute hydrochloric acid to remove inorganic material. Recrystallization from acetic acid (R_f and color unchanged throughout) gave the pure product, m.p. 266–267°; $\lambda\lambda_{max}$419, 302 (sh), 277, and 226 mμ (log ε 3.96, 4.05, 4.47, and 4.36); ν_{max} (Nujol) 3370 (bonded OH), 2700–2300 (w, chelated OH), 1655 (sh, free CO), 1636 (s, chelated CO) and 1593 (vs, aromatic) cm^{-1}; τ (saturated solution in $CDCl_3$, 16 accumulations) −3.40 (1 H, s, exchangeable, chelated phenol), 2.36 (1 H, s, H-1), 2.40 (1 H, d, J 2.5 Hz, H-8), 3.26 (1 H, d, J 2.5 Hz, H-6), 3.62 (1 H, broad, exchangeable, non-chelated phenol), 5.96 (3 H, s, ArOCH_3), 6.00 (3 H, s, ArOCH_3) and 7.62 (3 H, s, ArCH_3). The compound resembled 7-methoxy-2-methyl-3,4,5-trihydroxyanthraquinone (1) in giving an olive-brown color with alcoholic ferric chloride and in the reversible formation of purple lakes on thin layers of silica gel on evaporation of the acidic solvent.

The foregoing orange compound, in methanol – ethyl acetate (1:1), was methylated with ethereal diazomethane (2 ml) during 10 min. The product, recrystallized from chloroform–methanol, was identical with the dimethylether, m.p. 222–223°, obtained by partial methylation of anthraquinone B (1), by m.p., mixture m.p., nuclear magnetic resonance and infrared spectra.

The above methylation product (2 mg) in pyridine (0.15 ml) was heated at 105° for 48 h. Chromatograms of the product showed a very intense spot corresponding to starting material and three faint to very faint spots assigned as in the text.

Acknowledgments

I am grateful to Dr. J. B. Stothers for a stimulating discussion and for helpful comments on the manuscript; to Dr. E. Y. Spencer for encouraging this research; and to Mr. G. Rock for valuable experimental help.

1. A. Stoessl. Can. J. Chem. This issue.
2. D. W. Cameron, D. G. I. Kingston, N. Sheppard, and Lord Todd. J. Chem. Soc. 98 (1964).
3. A. N. de Belder. Advances in Carbohydrate Chem. **20**, 219 (1965).
4. E. L. Eliel, N. L. Allinger, S. J. Angyal, and G. A. Morrison. Conformational analysis, Interscience, New York. 1966. p. 360.
5. F. Arcamone, G. Cassinelli, G. Franceschi, P. Orezzi, and R. Mondelli. Tetrahedron Letters, 3353 (1968).
6. A. J. Birch and K. A. M. Walker. Tetrahedron Letters, 3457 (1967).
7. Y. P. Volkov, M. N. Kolosov, V. G. Korobko, and M. M. Shemyakin. Chem. Abstr. **60**, 15799*a* (1964).
8. R. U. Lemieux. Molecular rearrangements, Vol. 2. *Edited by* P. de Mayo. Interscience, New York. 1967. p. 763.
9. K. Yamada, S. Takada, S. Nakamura, and Y. Hirata. Tetrahedron, **24**, 1267 (1968).
10. S. M. Kupchan, J. H. Block, and A. C. Isenberg. J. Am. Chem. Soc. **89**, 1189 (1967).
11. C. R. Narayanan and M. R. Sarma. Tetrahedron Letters, 1553 (1968).
12. E. L. Eliel, N. L. Allinger, S. J. Angyal, and G. A. Morrison. Conformational analysis. Interscience, New York. 1966. p. 399.

Reaction of propionaldehyde with *N'*-methyl-2,6-dimethylphenylhydrazine hydrochloride. The dienone–imine intermediate in the Fischer indole synthesis and its conversion to the indole structure[1]

G. S. Bajwa and R. K. Brown
Department of Chemistry, University of Alberta, Edmonton, Alberta

Received August 9, 1968

When *N'*-methyl-2,6-dimethylphenylhydrazine hydrochloride was condensed with propionaldehyde by azeotropic removal of water in refluxing benzene for 10–12 min, a solid mixture was obtained which contained no aromatic ring system but instead possessed features indicative of a dienone–imine structure. When this mixture, or the original combination of *N'*-methyl-2,6-dimethylphenylhydrazine hydrochloride and propionaldehyde, was heated in refluxing benzene for 20 h there was obtained 1,3,7-trimethylindole in 36 and 31% yield respectively. Evidence indicated that a substantial amount of 3,7-dimethylindole was also produced.

The results support the view that an intermediate dienone–imine is formed as one step in the Robinson mechanism of the Fischer indole synthesis.

Canadian Journal of Chemistry, **47**, 785 (1969)

Can. J. Chem. Downloaded from www.nrcresearchpress.com by 210.87.254.5 on 09/05/12
For personal use only.

In a recent communication from this laboratory (1) it was shown that the condensation of isobutyraldehyde with *N'*-methyl-2,6-dimethylphenylhydrazine hydrochloride, **1**, by azeotropic removal of water in refluxing dry benzene, led to the formation of an isolable dienone–imine, **4** (Scheme 1). The expected enamine, **2**, the product of the first step of the condensation, could not be obtained.

Elemental analysis, ultraviolet (u.v.), and infrared (i.r.) spectra supported either of the two dienone–imines, **3** and **4**, but the nuclear magnetic resonances (n.m.r.) spectrum clearly showed that **4** was the compound obtained. It was the presence of the methyl groups at the C-2 and C-6 positions of the aromatic ring of the hydrazine, and the two methyl groups on C-2 of the aldehyde which prevented final formation of the indole ring system and thus permitted isolation of this dienone–imine.

We have now condensed *propionaldehyde* with *N'*-methyl-2,6-dimethylphenylhydrazine hydrochloride by azeotropic removal of water in refluxing dry benzene. When this mixture was refluxed for 10–12 min, water collected in the trap and a solid appeared in the reaction flask. This was isolated and crystallized from alcohol–ether (m.p. 147–148°, 31% yield). The n.m.r. spectrum (Fig. 1) in D_2O showed the *absence* of aromatic proton signals expected in the region τ 2.0–3.3. Several features of this spectrum were similar to those found in the n.m.r. spectrum (Fig. 2) of the dienone–imine, **4**, previously described (1). These were, notably, (*a*) the signals for the olefinic protons of the former aromatic ring, between τ 3.3–4.2, (*b*) the high field signals for the aliphatic methyl protons between τ 8.5–9.4, (*c*) the signal for the protons of the methyl group attached to a C=C (~τ 8.0), (*d*) the signal for the protons of a methyl group attached to nitrogen (τ 7.0–7.3), and (*e*) the anomeric proton signal(s) in the region τ 4.8–5.2. The presence of *two* signals for N—CH_3 protons at τ 7.0–7.3 (Fig. 1) and the multiplicity of signals at τ 8.5–9.3 clearly showed that the solid contained more than one compound.[2] Attempts to purify the material by further crystallization or by chromatography were unsuccessful because of its susceptibility to decomposition. Because the material was impure, spin decoupling experiments were not carried out.

The u.v. spectrum in 95% ethanol showed a narrow band at λ_{max}, 204 mμ (ε = 3600) and a broad band at λ_{max}, 315 mμ (ε = 1200). This u.v.

[1]Taken from the Thesis of G. S. Bajwa presented to the Faculty of Graduate Studies, University of Alberta, Edmonton, Alberta, as part of the requirements for the Degree of Doctor of Philosophy.

[2]Possible isomeric compounds, one or more of which might be present as impurities, are shown in Scheme 2. These are structures **6**, **7**, and **8**. The presence of a small amount of the dienone–imine hydrochloride, **6**, is indicated by the N—H absorption shown in the region 3100–3300 cm^{-1} of the i.r. spectrum. That compound **8** (shown in Fig. 1) might be a significant impurity is indicated by the fact that the chief product obtained upon prolonged heating of this material is 1,3,7-trimethylindole, which can arise only from a structure such as **8**.

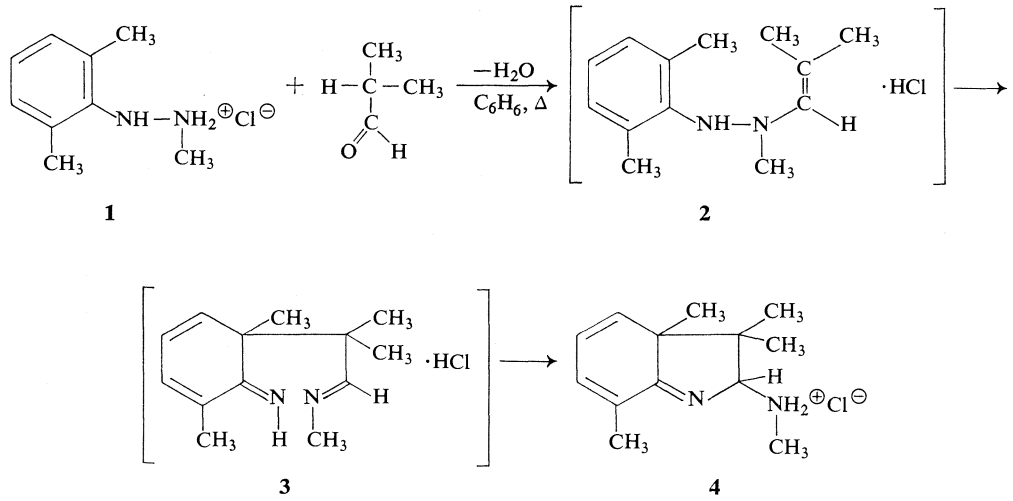

SCHEME 1

spectrum is closely similar to that found for the dienone–imine, **4**, previously reported (1). The i.r. spectrum (in Nujol) showed weak absorption in the region 3100–3300 cm^{-1} (NH) and strong bands at 1580 and 2700 cm^{-1} ($NH_2^{\oplus}$) (2).

In addition to the above evidence, the elemental analysis also agreed with the dienone–imine structure indicated below (**5**), and thus the impurity present must have a closely similar if not identical elemental composition.[2]

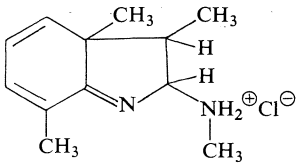

5

When this impure dienone–imine hydrochloride was suspended in dry benzene and the mixture refluxed for 20 h, a precipitate was obtained. This was removed by filtration and dried. It melted at 299–320°. The n.m.r. spectrum of this crude material in D_2O showed only two signals—a singlet at τ 7.31 (NCH_3) and a singlet at τ 5.13 (DOH). These signals and their integrated areas, along with the melting point observed above, indicated that the precipitate was a mixture of ammonium chloride and methylammonium chloride in the molar ratio of 3:1.

Removal of the benzene from the filtrate above gave a dark yellowish oil whose i.r. spectrum showed a weak, though sharp band at 3490 cm^{-1} (NH for the indole molecule, ref. 2, p. 251). The n.m.r. spectrum in $CDCl_3$ (Fig. 3) showed that this oil was a mixture containing some of the dienone–imine (signals at τ 8.5–9.3, τ 8.0, τ 3.5–4.2) along with one or more compounds possessing aromatic protons as part of their structure (multiplet at τ 2.5–3.3). From this oil, after removal of the dienone–imine by aqueous acid wash, there was obtained by fractional crystallization, a solid melting at 46°. The yield, based on the dienone–imine hydrochloride, was 36%. This was assigned the structure 1,3,7-trimethylindole for the following reasons.

The elemental analysis agreed well with the proposed structure. The i.r. spectrum in CCl_4 showed no absorption in the N—H region. The u.v. spectrum in hexane showed two bands—a sharp band at λ_{max}, 226 mμ (ε = 39 200), and a broad band at λ_{max}, 281 mμ (ε = 6900). This u.v. spectrum was closely similar to that obtained for indole (3). The n.m.r. spectrum (Fig. 4) in $CDCl_3$ provided clear evidence that this was indeed 1,3,7-trimethylindole. The three signals at τ 6.08 (singlet, 3H), τ 7.29 (singlet, 3H) and τ 7.73 (narrow doublet, 3H) are readily assigned to the *N*-methyl, C-7 methyl, and C-3 methyl protons respectively. The three aromatic protons provide the multiplet at τ 2.5–3.2. The broad singlet at τ 3.32 is due to the C-2 proton. That C-2 rather than C-3 of the indole structure was unsubstituted, was corroborated by the large

Can. J. Chem. Downloaded from www.nrcresearchpress.com by 210.87.254.5 on 09/05/12
For personal use only.

Can. J. Chem. Downloaded from www.nrcresearchpress.com by 210.87.254.5 on 09/05/12
For personal use only.

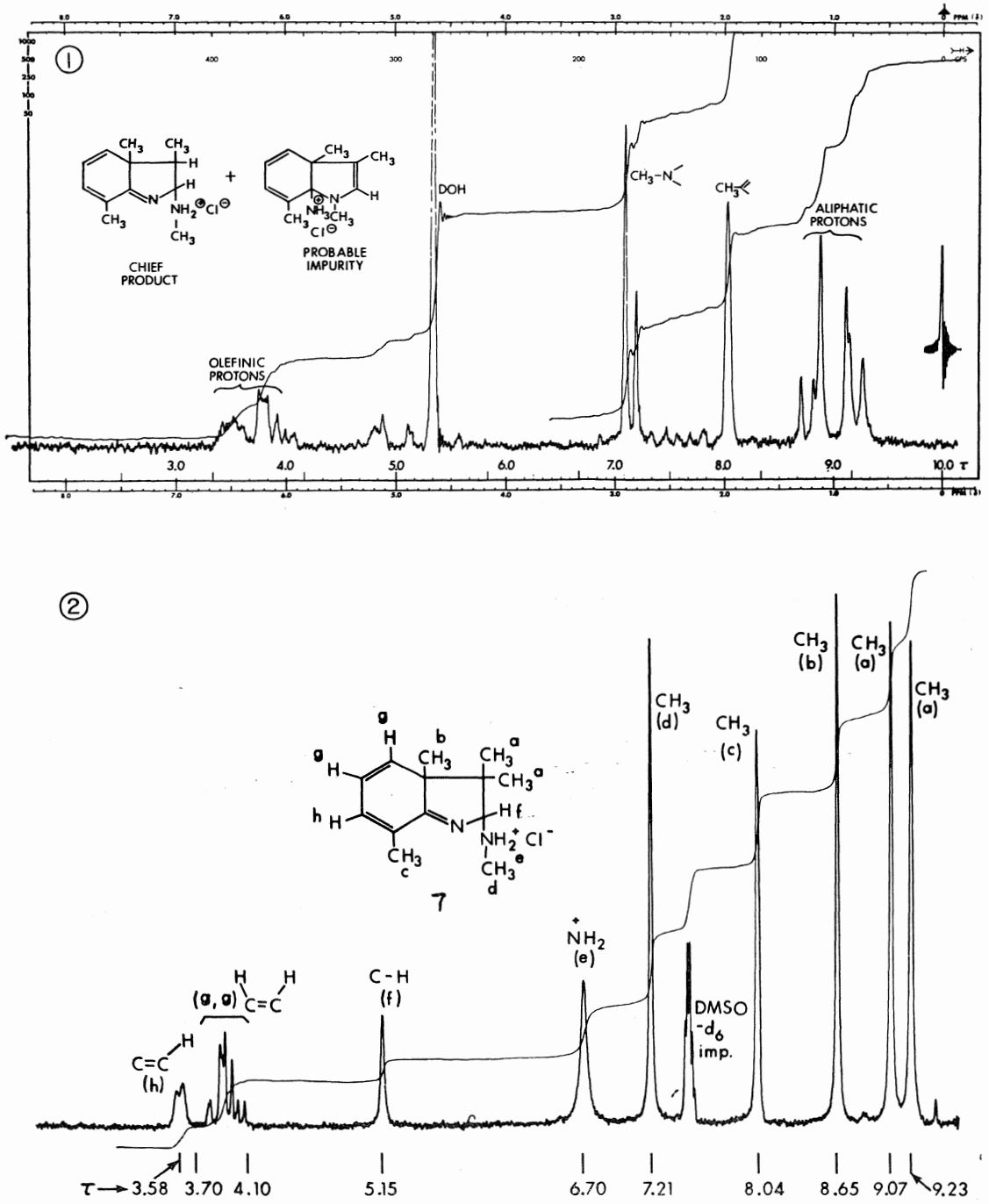

FIG. 1. The nuclear magnetic resonance spectrum (60 MHz in D_2O; reference, tetramethylsilane) of the solid (m.p. 147–148°) obtained from the 10–12 min reaction between *N'*-methyl-2,6-dimethylphenylhydrazine hydrochloride and propionaldehyde in refluxing dry benzene.

FIG. 2. The nuclear magnetic resonance spectrum (100 MHz in dimethyl sulfoxide-d_6; reference, tetramethylsilane) of the dienone–imine hydrochloride obtained from the reaction of *N'*-methyl-2,6-dimethylphenylhydrazine hydrochloride and isobutyraldehyde. Taken from ref. 1.

Can. J. Chem. Downloaded from www.nrcresearchpress.com by 210.87.254.5 on 09/05/12
For personal use only.

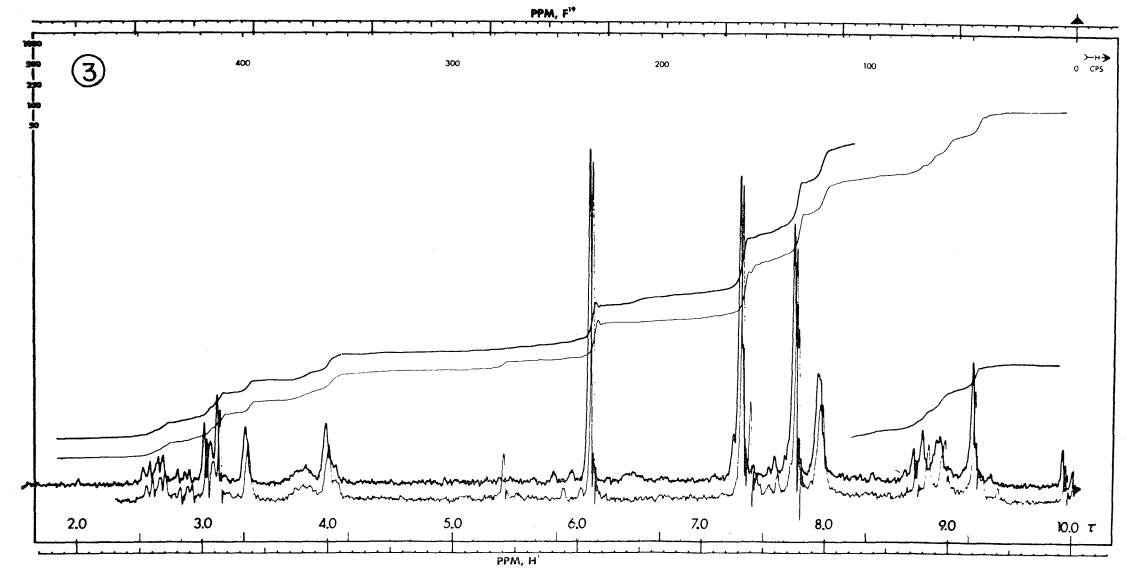

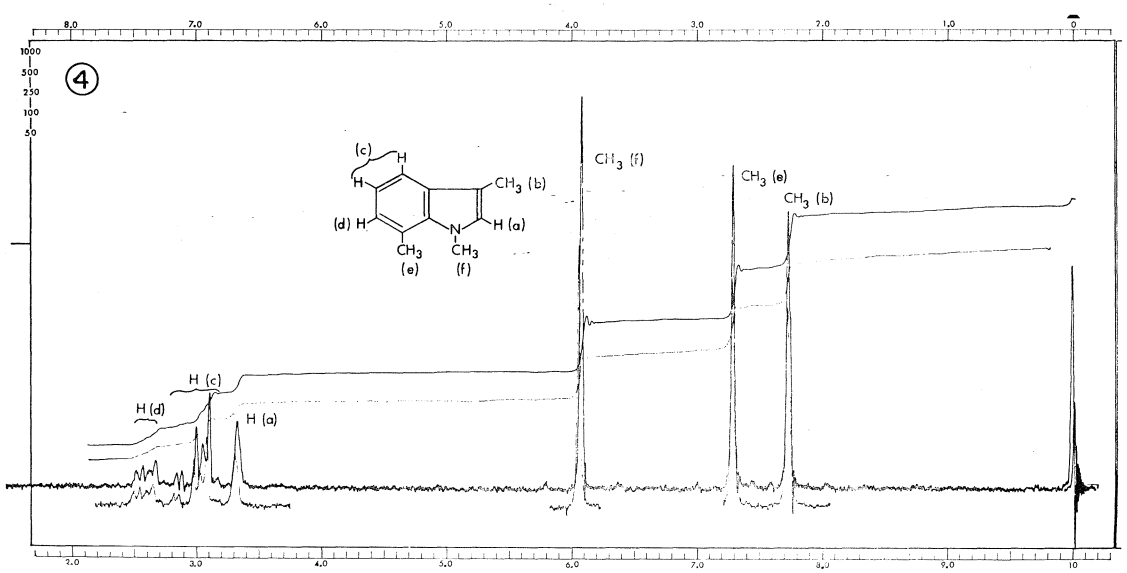

FIG. 3. The nuclear magnetic resonance spectrum (60 MHz in $CDCl_3$; reference, tetramethylsilane) of the oil obtained when the solid, melting at 147–148°, was heated in refluxing dry benzene for 20 h, and the precipitated mixture of ammonium chloride and methylammonium chloride was removed. Lower tracing obtained after the addition (shaken) of a small amount of D_2O.

FIG. 4. The nuclear magnetic resonance spectrum (60 MHz in $CDCl_3$; reference, tetramethylsilane) of 1,3,7-trimethylindole obtained from the 20 h heating in refluxing benzene of the 147–148° melting solid *or* of the mixture of *N'*-methyl-2,6-dimethylphenylhydrazine hydrochloride and propionaldehyde. Lower tracing obtained after the addition (shaken) of a small amount of D_2O.

Can. J. Chem. Downloaded from www.nrcresearchpress.com by 210.87.254.5 on 09/05/12
For personal use only.

shift of the signal for this proton downfield to τ 3.05 ($\Delta\tau = 0.27$) when the more polar solvent dimethyl sulfoxide-d_6 was used. Such large signal shifts in the n.m.r. spectrum due to change in solvent are characteristic of the C-2 proton but not of the C-3 proton of the indole structure (4). Spin decoupling experiments supported the structure. Irradiation of the nucleus of H_a (τ 3.32) showed no effect on the signals of H_d (τ 2.5–2.7) but did cause a sharpening of the signal for the

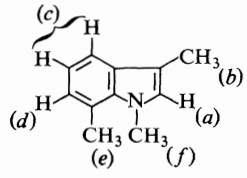

methyl group *b* at τ 7.73. Irradiation of the methyl protons, *b*, at τ 7.73 changed the broad singlet ($w/2 \approx 3$ Hz) at τ 3.32 (H_a) to sharp singlet. This, along with the solvent shift of the signal for H_a when dimethyl sulfoxide-d_6 was used rather than $CDCl_3$ provides evidence that H_a and CH_3(*b*) give rise to the signals at τ 3.32 and 7.73 respectively. Irradiation at τ 7.29 (CH_3, *e*) changed the multiplet at τ 2.5–2.7 to two doublets centered at τ 2.98 and τ 2.91 ($J \approx 2$ Hz) which are believed to be due to H_d (1). As well, simplification occurred in the multiplet at τ 2.8–3.2 (protons *c*).

Authentic 1,3,7-trimethylindole was made by *N*-methylation of 3,7-dimethylindole. The synthesis of this latter compound has been reported previously (5–7). Our efforts to prepare 3,7-dimethylindole via cyclization of propionaldehyde *o*-tolylhydrazine by following the published directions (6, 7) have not been successful. The directions given by Marion and Oldfield (6) led to an oil boiling in the range reported (6).[3] However, the n.m.r. spectrum clearly showed that it was a mixture of substances. Of the several catalysts normally used to effect the cyclization of phenylhydrazones to indoles (9) we have found that boron trifluoride etherate in acetic acid was somewhat better, but this still gave a mixture. Both the procedures of Marion and Oldfield and that using the boron trifluoride etherate gave oils which showed absorption in the i.r. spectrum at 3490 cm^{-1} characteristic of the NH absorption of indoles (ref. 2, p. 251) thus showing that the 3,7-dimethylindole had been formed as one compound in the mixture of products, but our attempts to purify it by fractional distillation or chromatography have as yet been unsuccessful. However, a more fruitful route to 3,7-dimethylindole via Fischer cyclization was devised. This involved heating a mixture of *N'*-methyl-*o*-tolylhydrazine hydrochloride and propionaldehyde in refluxing, dry benzene, following the method described for the analogous reaction using *N'*-methyl-2,6-dimethylphenylhydrazine hydrochloride (1, 10). From this reaction there was obtained in 24% yield, an oil whose n.m.r. spectrum (Fig. 5) was consistent with that expected for 3,7-dimethylindole. But here also it was clear from this spectrum that small amounts of impurities were present. All attempts to eliminate these by fractional distillation or chromatography were unsuccessful. The elemental analysis clearly reflected the impure state.

Pure 3,7-dimethylindole was prepared by the method of Cornforth and Robinson (5) wherein 7-methylindole was heated in an autoclave at 215° with sodium methoxide in methanol. The material obtained was a solid, melting at 56–57°. That reported (5), melted at 56°. Its n.m.r. spectrum was practically identical with that shown in Fig. 5 but devoid of the slight impurities indicated by the very weak signals in the region τ 8.7 to τ 9.2.

N-Methylation of 3,7-dimethylindole by the published procedure (10) gave in very low yield authentic 1,3,7-trimethylindole identical in all respects (m.p., i.r., and n.m.r. spectra) with the compound obtained from the dienone–imine hydrochloride as described above.

We were particularly interested in preparing authentic 3,7-dimethylindole since the i.r. spectrum of the oil obtained from the benzene filtrate above (after removal of the ammonium chloride and methylammonium chloride from the mixture resulting from the 20-h heating of the dienone–imine hydrochloride in refluxing benzene) showed a band at 3490 cm^{-1}. This, along with the formation of a substantial proportion of methylammonium chloride, strongly indicated that the

[3]Marion and Oldfield report a melting point of 64° in Table I, page 2 of ref. 6. Their experimental details (page 5, ref. 6) of the preparation of 3,7-dimethylindole via the Fischer cyclization state that a boiling point of 80–95° at 0.5 mm was obtained for this compound. No melting point was reported in the Experimental and no indication was provided that a solid was obtained. Hence it is not clear where their figure of 64° was obtained.

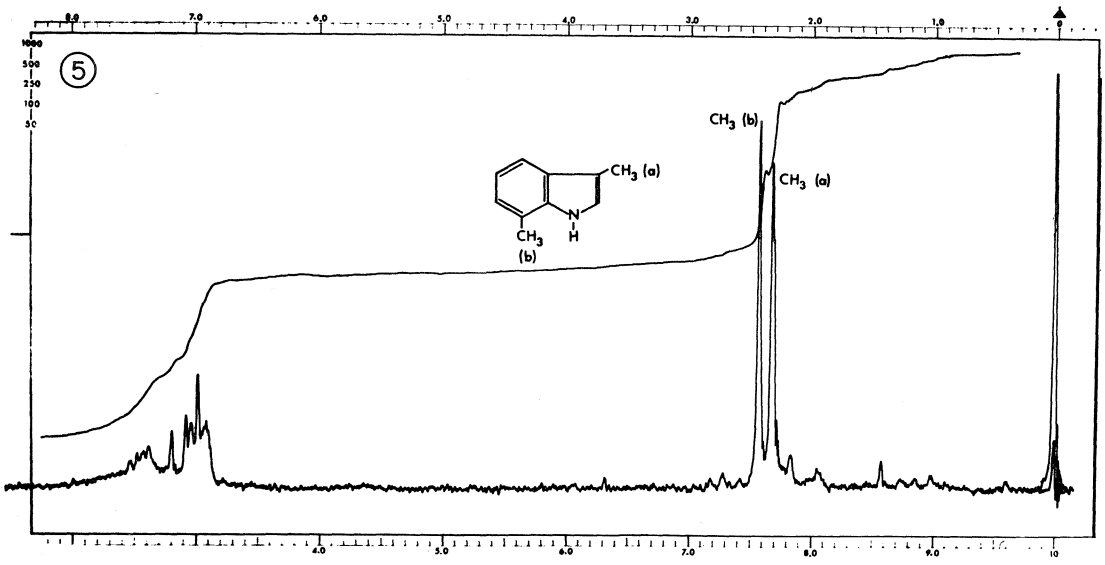

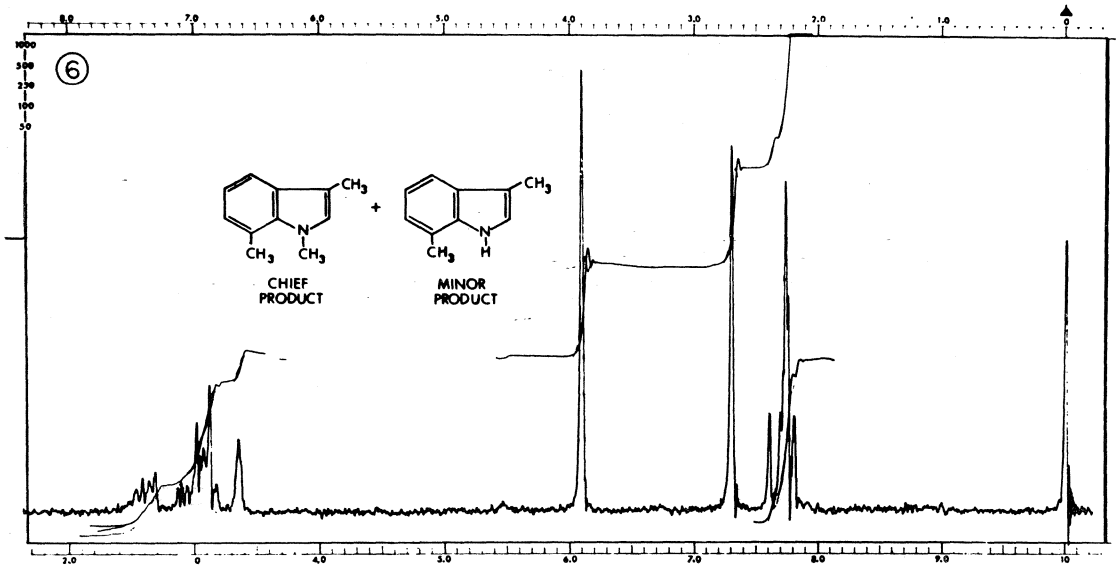

FIG. 5. The nuclear magnetic resonance spectrum (60 MHz in $CDCl_3$; reference, tetramethylsilane) of 3,7-dimethylindole prepared by the reaction of *N'*-methyl-*o*-tolylhydrazine hydrochloride with propionaldehyde in refluxing dry benzene.

FIG. 6. The nuclear magnetic resonance spectrum (60 MHz in $CDCl_3$; reference, tetramethylsilane) of the oil obtained from the 19 h reaction in refluxing benzene of the mixture of *N'*-methyl-2,6-dimethylphenylhydrazine hydrochloride and propionaldehyde.

other significant product formed by prolonged heating of this dienone–imine hydrochloride was 3,7-dimethylindole. The 3,7-dimethylindole synthesized above possessed characteristic signals in the n.m.r. spectrum which were clearly apparent (Fig. 5). In $CDCl_3$ these signals were at τ 7.57 (singlet, 3H) and τ 7.68 (narrow doublet, 3H) for the C-7 and C-3 methyl protons respectively. These were not obvious in the n.m.r. spectrum in $CDCl_3$ (Fig. 3) of the crude oil obtained when

Can. J. Chem. Downloaded from www.nrcresearchpress.com by 210.87.254.5 on 09/05/12
For personal use only.

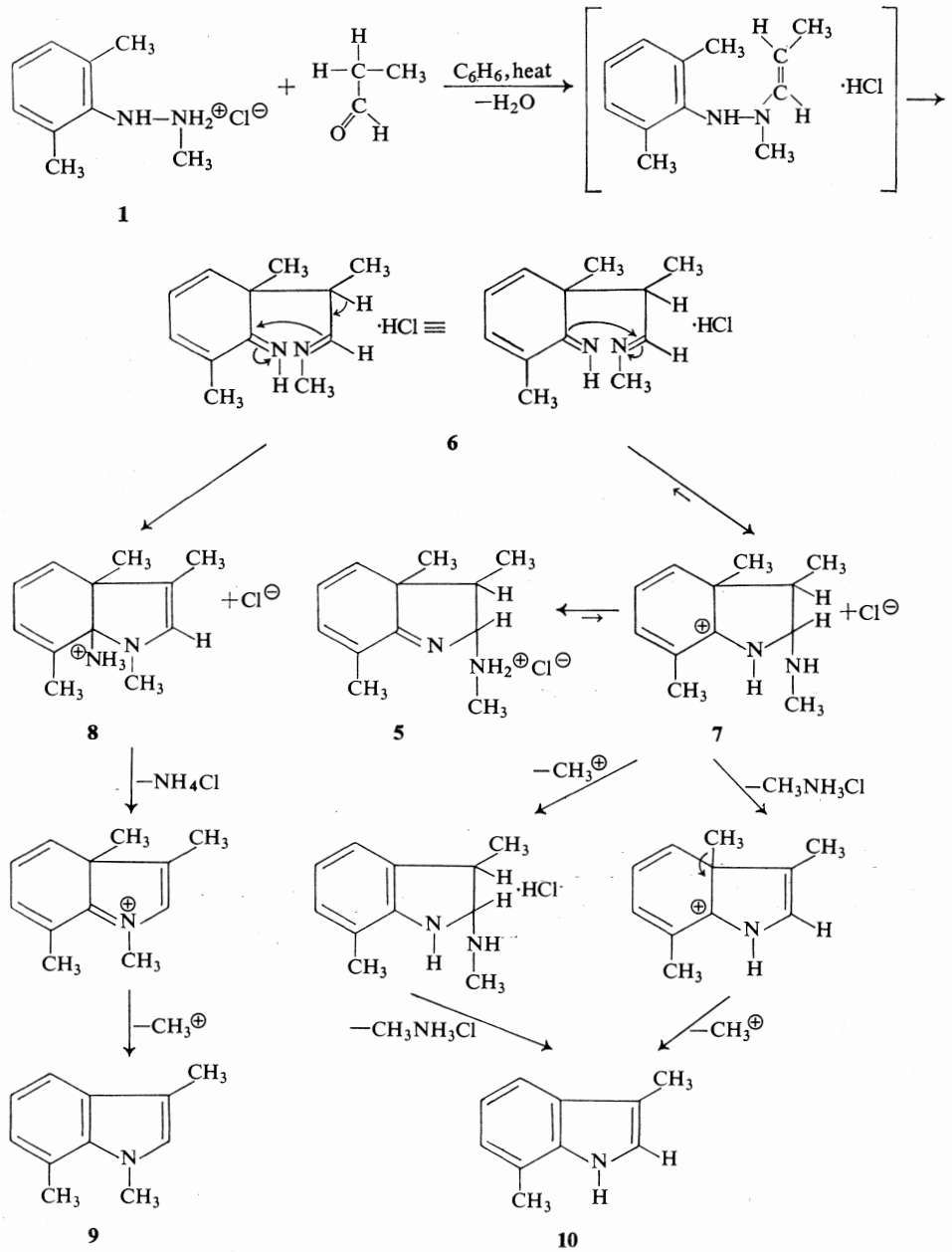

SCHEME 2

the dienone–imine hydrochloride had been heated for 20 h. The small signals at τ 7.58 and 7.68 could be due to 3,7-dimethylindole. This is more clearly shown in the following work.

A mixture of *N'*-methyl-2,6-dimethylphenylhydrazine hydrochloride and excess propionaldehyde was heated for 19 h in refluxing dry benzene. Water was observed to collect in the trap. The mixture was then filtered and gave a gelatinous solid. This, when crystallized from ethanol–ether, gave a colorless solid which by its melting point characteristics and n.m.r. spectrum proved to be largely ammonium chloride contaminated with a small amount of methylammonium chloride.

Can. J. Chem. Downloaded from www.nrcresearchpress.com by 210.87.254.5 on 09/05/12
For personal use only.

Can. J. Chem. Downloaded from www.nrcresearchpress.com by 210.87.254.5 on 09/05/12
For personal use only.

Apparently some of the latter compound had been lost during this crystallization due to its greater solubility. The benzene filtrate gave an oil which was distilled. The n.m.r. spectrum in $CDCl_3$ (Fig. 6) of the first fraction clearly showed that this was chiefly 1,3,7-trimethylindole (signals at τ 6.10, 7.30, and 7.74) containing a substantial quantity of 3,7-dimethylindole (signals at τ 7.60 and 7.69). The bulk of the trimethylindole was found in the second fraction. From both fractions, by crystallization, there was obtained a 31% yield of 1,3,7-trimethylindole (after accounting for some recovered unchanged *N'*-methyl-2,6-dimethylphenylhydrazine hydrochloride) identical with that obtained above. We were unable to isolate pure 3,7-dimethylindole from either of these fractions.

It is clear from the above work that *N'*-methyl-2,6-dimethylphenylhydrazine hydrochloride and propionaldehyde have reacted to produce first a non-aromatic intermediate (or intermediates) which in turn, upon further reaction, is converted into the indole structure. The reaction can be rationalized according to the Robinson mechanism (8, 9) as shown in Scheme 2, by routes similar to those utilized to explain the products reported in our previous communications (1, 10).

This scheme requires the loss of a methyl group from the aromatic ring under relatively mild conditions. However, such an elimination of a methyl group under similar conditions has been demonstrated previously for the reaction of *N'*-methyl-2,6-dimethylphenylhydrazine (or its hydrochloride) with cyclohexanone to produce 8,9-dimethyl-1,2,3,4-tetrahydrocarbazole (10). The fate of this lost methyl group is as yet unknown.

A significant point which must be considered with respect to Scheme 2, is the correlation between the structure of the dienone–imine, **5**, and the products actually obtained from its conversion to the indoles **9** and **10**. It was concluded that the mixture obtained from the 10–12 min condensation of propionaldehyde with *N'*-methyl-2,6-dimethylphenylhydrazine hydrochloride contains a predominance of the dienone–imine, **5**. Possible contaminating products are the compounds **6**, **7**, and/or **8**. Structure **5** should then give 3,7-dimethylindole as the main product. But as actually found, the product was a mixture containing 3,7-dimethylindole and 1,3,7-trimethylindole in the approximate proportion of 1:4 respectively. This suggests that in Scheme 2, there exists an equilibrium between compounds **5**–**8**. It is quite apparent that in structure **8**, there is much more strain than exists in any of the other structures (**5**–**7**). Models show that in **8** the C-7*a* substituent, $-NH_3^+Cl^\ominus$, is quite crowded. Hence, when heat is applied, structure **8** should lose ammonium chloride and subsequently $CH_3^\oplus$ to become 1,3,7-trimethylindole much more readily than structure **7** (or **5**) would lose methylammonium chloride to become 3,7-trimethylindole. This would explain the results obtained, and why the nitrogen atom adjacent to the aromatic ring of the hydrazine is lost in preference to that more remote from the ring (cf. ref. 9).

Experimental

Melting points and boiling points are uncorrected. Elemental analyses were made by Mrs. Darlene Mahlow of this Department.

Ultraviolet spectra of 1,3,7-trimethylindole were obtained with a JASCO model ORD/UV-5 spectrometer and of the dienone–imine hydrochloride with a Perkin–Elmer 202 ultraviolet–visible spectrometer. Infrared spectra were obtained with a Perkin–Elmer 421 grating spectrometer.

The 60 MHz n.m.r. spectra were made by Mr. R. Swindlehurst; the 100 MHz spectra and spin decoupling experiments were made by Mr. Glen Bigham of this Department. The instruments employed were the 60 MHz and 100 MHz Varian spectrometers.

Solvents were removed by rotary evaporator under vacuum unless otherwise stated.

Condensation of N'-Methyl-2,6-dimethylphenylhydrazine Hydrochloride with Propionaldehyde

(a) Limited Reaction—The Hydrochloride of the Dienone–imine Intermediate

A mixture of 1.5 g (0.008 mole) of *N'*-methyl-2,6-dimethylphenylhydrazine hydrochloride (1) and 0.9 g (0.016 mole) of propionaldehyde in 20 ml of dry benzene was refluxed for 10 min using a Dean–Stark water collection apparatus (11). To the solution was added a further quantity (1 g) of propionaldehyde and then refluxing was continued for 2 min longer. Water was observed in the Dean–Stark trap. The white insoluble precipitate was removed by filtration under vacuum and washed with ether. When air-dried, the crude material weighed 625 mg (36%) and melted at 143–145°. It was crystallized by solution in 95% ethyl alcohol followed by the addition of ether till a faint turbidity appeared. The white precipitate obtained weighed 520 mg (29%) and melted at 147–148°. A second crystallization was difficult because of the tendency for decomposition. But by using a minimum quantity of solvents and thorough cooling of the solution in a refrigerator for 2 days, crystals were obtained which melted at 147–148°.

Anal. Calcd. for $C_{12}H_{19}N_2Cl$: C, 63.58; H, 8.38; N, 12.36; Cl, 15.67. Found: C, 63.08; H, 8.37; N, 12.28; Cl, 16.17.

The n.m.r. spectrum in D_2O is shown in Fig. 1 and has been described in the discussion. The significant

Can. J. Chem. Downloaded from www.nrcresearchpress.com by 210.87.254.5 on 09/05/12
For personal use only.

absorptions of the spectrum in 95% ethanol and the i.r. spectrum in Nujol have also been described in the discussion.

(b) Longer Reaction Time—1,3,7-Trimethylindole

A mixture of 10 g (0.054 mole) of *N'*-methyl-2,6-dimethylphenylhydrazine hydrochloride (1) and 3.1 g (0.054 mole) of propionaldehyde in 150 ml of dry benzene was refluxed for 19 h in the Dean–Stark apparatus (11). Water collected in the trap. The color of the reaction mixture became dark after 1 h of reflux. After the 19 h of reflux, the mixture was cooled and filtered free of a dark gelatinous material (~1 g). This was dissolved in 95% ethyl alcohol and diluted with ether to faint turbidity. A white water soluble solid (700 mg) was obtained melting at 290–320 °C. Its n.m.r. spectrum in D_2O showed only two signals, a small singlet at τ 7.4 (N—CH_3) and a large singlet at τ 5.4 (DOH). From the integrated areas and the above evidence it was certain that the solid was ammonium chloride contaminated with ~3% of methylammonium chloride.

The benzene filtrate was freed from solvent and the residual dark oil was treated with 150 ml of water. The aqueous material was extracted with ether (3 × 100 ml). The ether extracts were washed with 300 ml of 12% HCl in water and then with water (3 × 100 ml). The dried ether solution ($MgSO_4$, 2 h) was then freed from solvent. The resulting yellow oil was distilled to give two fractions. The first fraction boiled at 80–125 ° at 8 mm (1.6 g of yellow oil). Its n.m.r. spectrum (Fig. 6) indicated that it was chiefly 1,3,7-trimethylindole contaminated with 3,7-dimethylindole along with other very minor amounts of impurities. The second fraction boiled at 136–138° at 8 mm (2.5 g of viscous yellow oil). The latter fraction was twice crystallized from petroleum ether (b.p., 60–70°) and gave 1.8 g of *1,3,7-trimethylindole* melting at 46°. The first fraction (1.6 g) showed a sharp, weak band in the i.r. spectrum at 3490 cm^{-1} characteristic of the N—H stretching band found in indole (ref. 2, p. 251). Crystallization of this fraction from petroleum ether gave 300 mg of 1,3,7-trimethylindole. The total yield was 2.1 g, 31% based on the 8 g of *N'*-methyl-2,6-dimethylphenylhydrazine hydrochloride consumed (see below).

Anal. Calcd. for $C_{11}H_{13}N$: C, 83.02; H, 8.19; N, 8.80. Found: C, 83.10; H, 8.00; N, 8.66.

The i.r. spectrum in CCl_4 showed no absorption in the NH region (3100–3600 cm^{-1}). The u.v. spectrum in hexane, λ_{max}, 226 mμ (ε = 39 200), 281 mμ (ε = 6900) was nearly identical with that of indole (3). The 60 MHz n.m.r. spectrum in $CDCl_3$ (Fig. 4) and spin decoupling experiments are described in the discussion and support the structure as 1,3,7-trimethylindole.

The aqueous acidic solutions obtained from the ether extraction and water washes above were basified with aqueous sodium hydroxide and the mixture then extracted with ether (2 × 100 ml). The ether extract was washed with water (3 × 30 ml) and dried ($MgSO_4$) overnight while it was kept cold in a refrigerator. The drying agent was separated and the ether filtrate treated with dry hydrogen chloride. The resulting precipitate was crystallized from 95% ethyl alcohol, diluted with ether to faint turbidity, and gave 2.0 g of *N'-methyl-2,6-dimethylphenylhydrazine hydrochloride.*

Conversion of the Dienone–imine to 1,3,7-Trimethylindole

One gram of the above dienone–imine hydrochloride was heated in refluxing benzene for 20 h. The precipitate (113 mg) was removed (m.p. 299–320°) and found to be ammonium chloride contaminated with some methylammonium chloride (~3:1). The benzene filtrate was freed from solvent. The dark residue gave an n.m.r. spectrum in $CDCl_3$ (Fig. 3) which indicated that it was a mixture of 1,3,7-trimethylindole and some starting dienone–imine hydrochloride (see Discussion). The i.r. spectrum in CCl_4 showed a sharp, weak band at 3490 cm^{-1} indicative of the presence of an indole with a free NH group.

The dark oil was suspended in 50 ml of water and the mixture extracted with ether (2 × 50 ml). The ether solution was in turn washed with 20 ml of 10% aqueous HCl and then with water (3 × 20 ml). The ether solution was dried ($MgSO_4$, 2 h) and freed from the drying agent and then from the solvent. The residue deposited crystals (310 mg) melting at 38–42° which showed weak absorption at 3490 cm^{-1} in the i.r. spectrum. This solid was crystallized twice from petroleum ether (60–70°) and gave 250 mg of pure 1,3,7-trimethylindole, melting at 46°. The n.m.r. spectrum in $CDCl_3$ is shown in Fig. 4 and is described in the discussion. The i.r. spectrum in CCl_4 showed no absorption for N—H. The u.v. spectrum in hexane is very closely similar to that for indole itself (see Discussion).

Preparation of 3,7-Dimethylindole

To a solution of *o*-tolylhydrazine (58 g, 0.475 mole) in 150 ml of glacial acetic acid was added, over a period of 0.5 h, 21.4 g (0.476 mole) of formamide. The solution was stirred for 3 h at room temperature, and then diluted with 150 ml of water and allowed to stand for about 15 min. The solid which accumulated was removed and when air-dried weighed 40 g and melted at 115–118°. Two crystallizations from 95% ethanol gave 35 g of *N'-formyl-o-tolylhydrazine*, m.p. 120°; lit. m.p. 120° (12). The n.m.r. spectrum in $CDCl_3$ supported the structural assignment.

To a solution of *N'*-formyl-*o*-tolylhydrazine (35 g, 0.233 mole) in 150 ml of dimethyl sulfoxide was added, simultaneously in a dropwise fashion over a period of 0.5 h, equimolar quantities of dimethyl sulfate (29.5 g) and sodium hydroxide (9.3 g in 10 ml of water). The reaction mixture was stirred for 2.5 h and then diluted with 200 ml of water. The ether extract (3 × 100 ml) was washed with water and dried ($MgSO_4$, 1 h). The drying agent was separated and the solvent removed from the filtrate. The yellow oil so obtained darkened rapidly hence was not subjected to further purification or to elemental analysis. The i.r. spectrum (CCl_4) showed a band of medium strength at 3320 cm^{-1} (N—H) and a strong band at 1685 cm^{-1} (C=O). The n.m.r. spectrum in $CDCl_3$ clearly showed that *N*-methylation had occurred (singlet at τ 6.93 for N—CH_3). But the relative areas of the signal of the aromatic methyl group at τ 7.82 (singlet) and that for the N—CH_3 group at τ 6.93 were in the ratio 3:2, thus showing that methylation was incomplete. Hence this oil was approximately a 1:2 mixture of *N'-formyl-o-tolylhydrazine* and *N'-formyl-N'-methyl-o-tolylhydrazine.*

The mixture (14 g) was hydrolyzed by heating in 56 ml of a 1:1 solution (v/v) of concentrated hydrochloric acid and 95% ethanol under reflux for 6 h. The solution, when cooled and then allowed to stand in a refrigerator overnight, deposited a dark yellow solid (3 g) melting at

Can. J. Chem. Downloaded from www.nrcresearchpress.com by 210.87.254.5 on 09/05/12
For personal use only.

130–140°. This was thrice crystallized by solution in 95% ethanol and addition of ether till a faint turbidity appeared. To avoid decomposition the crystallization had to be carried out quickly by effecting solution at room temperature and cooling in a refrigerator. In this manner 1.5 g of a solid hydrazine hydrochloride was obtained, melting at 144–146°. No elemental analysis was made because of the strong tendency of this material to decompose. The i.r. spectrum in Fluorolube showed two sharp bands at 3200 and 3300 cm^{-1} (N—H) and a broad band at 2700 (NH_2^+). The n.m.r. spectrum in D_2O showed a singlet at τ 7.02 (N—CH_3) and two closely spaced singlets at τ 7.80 and τ 7.82 (CH_3—C=C), as well as the DOH peak at τ 5.30 and the aromatic proton multiplet at τ 2.5–3.2. The relative area of the methyl proton signals at τ 7.02 and τ 7.80–7.82 was in the ratio 3:8 indicating that in the hydrolysis and crystallization there had been some loss of *N'*-methylated material, and that the material melting at 144–146° was a mixture primarily of two substances—*N'-methyl-o-tolylhydrazine hydrochloride* and *o-tolylhydrazine hydrochloride*. We were unable to separate these readily, hence proceeded to the cyclization.

A mixture of the above impure *N'*-methyl-*o*-tolylhydrazine hydrochloride (1 g, 0.0058 mole) and propionaldehyde (0.34 g, 0.0058 mole) was heated in refluxing dry benzene (50 ml) for 17 h in an apparatus equipped to collect the azeotropically distilled water. The dark solid which was formed was separated and thrice crystallized by solution in 95% ethanol followed by addition of ether to faint turbidity. There was obtained 52 mg of pure methylamine hydrochloride melting (with sublimation) at 225–230°. The n.m.r. spectrum in D_2O showed only two signals—a relatively large singlet at τ 7.34 (N—CH_3) and a small singlet at τ 5.18 (DOH).

The filtrate obtained after removal of the methylammonium chloride was freed from benzene and the residue was dissolved in 200 ml of ether. The ether solution was washed with 2% hydrochloric acid (15 × 100 ml), then with water (3 × 100 ml) and then dried ($MgSO_4$, 1 h). The $MgSO_4$ was separated and the ether removed from the filtrate to give 500 mg of a dark oil which, according to its n.m.r. spectrum, consisted of essentially 3,7-dimethylindole. The oil was distilled and gave 200 mg of *3,7-dimethylindole* boiling at 90–92°, 0.5 mm; lit. b.p., 85–95° (6) of what is now known to be a mixture containing some 3,7-dimethylindole. The i.r. spectrum in CCl_4 showed a sharp band at 3490 cm^{-1} (N—H). The n.m.r. spectrum in $CDCl_3$ (Fig. 5) showed signals at τ 7.68 (narrow doublet, $J \approx 1$ Hz, 3 H for CH_3 at C-3); τ 7.58 (singlet, 3 H for CH_3 at C-7); a narrow multiplet at τ 3.08 (1 H for H at C-2), and a multiplet for the aromatic protons and NH proton between τ 2.4–3.1. The spectrum showed evidence of the presence of impurities.

Anal. Calcd. for $C_{10}H_{11}N$: C, 82.75; H, 7.58; N, 9.66. Found: C, 79.84; 80.13; H, 10.25, 10.13; N, 9.52, 10.16.

Preparation of 1,3,7-Trimethylindole

The published procedure for *N*-methylation of 8-methyl-1,2,3,4-tetrahydrocarbazole (10) was followed for the *N*-methylation of 3,7-dimethylindole. However, the work-up procedure, following the addition of the concentrated ammonium hydroxide, was modified since the filtered solution failed to deposit any solid even when cooled in a refrigerator overnight. This ammoniacal filtrate was diluted with water and twice extracted with ether. The dried ether solution ($MgSO_4$) was freed from solid and ether.

From 0.5 g of 3,7-dimethylindole there was obtained 0.4 g of an oil whose n.m.r. spectrum in $CDCl_3$ showed it to be a mixture of 3,7-dimethylindole and 1,3,7-trimethylindole in the approximate proportion of 55:45. A petroleum ether (60–70°) solution of this mixture when cooled in a ice–salt bath for 6 h, deposited 44 mg of crystals melting at 43–46°. The n.m.r. spectrum showed that this was essentially 1,3,7-trimethylindole but contaminated with a small amount of 3,7-dimethylindole. The i.r. spectrum verified this contamination by the weak absorption band at 3490 cm^{-1}. A second crystallization from 1 ml of petroleum ether (cooled in a refrigerator overnight) gave 12 mg of pure 1,3,7-trimethylindole melting at 45–46°; mixture m.p. with that previously obtained was undepressed. The n.m.r. spectrum in $CDCl_3$ was identical to that in Fig. 4. No absorption for NH was evident in the i.r. spectrum (CCl_4).

Acknowledgment

The authors are grateful to the National Research Council of Canada for financial support throughout the course of this work.

1. G. S. Bajwa and R. K. Brown. Can. J. Chem. **46**, 3105 (1968)
2. L. J. Bellamy. The infra-red spectra of complex molecules. 2nd ed. John Wiley and Sons, Inc., New York. 1958. p. 260.
3. G. M. Badger. *In* The chemistry of heterocyclic compounds. Academic Press, Inc., New York. 1961. p. 17.
4. R. V. Jardine and R. K. Brown. Can. J. Chem. **41**, 2067 (1963).
5. R. H. Cornforth and R. Robinson. J. Chem. Soc. 680 (1942).
6. L. Marion and C. W. Oldfield. Can. J. Res. **25B**, 1 (1947).
7. F. Mendlik and J. P. Wibaut. Rev. Trav. Chim. **50**, 109 (1931).
8. G. M. Robinson and R. Robinson. J. Chem. Soc. **113**, 639 (1918).
9. B. Robinson. Chem. Rev. **63**, 373 (1963).
10. G. S. Bajwa and R. K. Brown. Can. J. Chem. **46**, 1927 (1968).
11. E. W. Dean and D. D. Stark. Ind. Eng. Chem. **12**, 486 (1920).
12. I. Heilbron and H. M. Bunbury. Dictionary of organic compounds. Vol. IV. Eyre and Spottiswoode Ltd. London. 1953. p. 532.

Syntheses of 8-acetoxy-4-twistanone, twistane, 1-twistanol, 1-twistylamine, and 1-twistane carboxylic acid

A. BÉLANGER, Y. LAMBERT, AND P. DESLONGCHAMPS
Département de Chimie, Université de Sherbrooke, Sherbrooke, Québec

Received October 1, 1968

8-Acetoxy-4-twistanone (**8**) has been obtained in one-step from decalin dione **4** and a rigorous chemical proof has been obtained by chemical conversion of **8** into 4-twistanone (**6**). Twistane (**1**), 1-twistanol (**15**), 1-twistane carboxylic acid (**17**), and 1-twistylamine (**20**) have also been synthesized from compound **8** and chemical proofs are included.

Canadian Journal of Chemistry, 47, 795 (1969)

Can. J. Chem. Downloaded from www.nrcresearchpress.com by 210.87.254.42 on 09/05/12
For personal use only.

The chemistry of tricyclo[$4\cdot4\cdot0\cdot0^{3,8}$]decane **1** (twistane), the twist boat isomer of adamantane, was started by Whitlock (1) who achieved an elegant and unambiguous synthesis of this hydrocarbon *via* the internal cyclization of the bicyclo[2·2·2]system **2** yielding 2-twistanone (**3**).

In order to study the chemistry of this new polycyclic system more thoroughly, it was necessary to develop complementary synthetic schemes which would afford twistane derivatives monofunctionalized at the other alternative positions of the twistane skeleton which are C-4 and the bridgehead.[1] Also shorter syntheses of twistane (**1**) itself were desirable and since its chemical structure was well established, more simple but *a priori* less trivial scheme could be theoretically conceived and tested in the laboratory.

Recently, we have reported (2) a seven-step synthesis of twistane (**1**) utilizing the readily available decalin dione **4**. The key step in this scheme was the internal cyclization of keto mesylate **5** yielding the previously unknown 4-twistanone (**6**).

The high yield obtained in the internal irreversible cyclization step (**5** → **6**) led us to suspect that in strong acidic medium, the decalin dione **4** might well be in equilibrium with the isomeric hydroxy tricyclic ketone **7**. We further anticipated that even if such isomer **7** could be present in small amount at equilibrium, one could take advantage of the presence of a hydroxyl group in **7** by trapping it in order to shift irreversibly the equilibrating system (**4** ⇌ **7**) toward the twistane compound **8**.

If such process can be realized, a twistane derivative would be obtained in one-step directly from the readily available decalin dione **4**. With its two functional groupings, such derivative **8** would permit the synthesis of a large variety of previously unknown twistane compounds.

In this paper, we wish to describe our successful investigation in this area.[2]

By treating decalin dione **4** with boron trifluoride ethereate in acetic acid containing acetic anhydride at room temperature and utilizing chromatography, the crystalline 8-acetoxy-4-twistanone (**8**) was obtained. Spectral as well as analytical data supported entirely structure **8**. In order to provide an unambiguous chemical proof, 8-acetoxy-4-twistanone (**8**) was converted into the known 4-twistanone (**6**).

Ketalization of 8-acetoxy-4-twistanone (**8**) in the usual manner with ethylene glycol, benzene, and *p*-toluenesulfonic acid gave the oily ketal acetate **9** which by reductive hydrolysis with lithium aluminium hydride in ether gave the expected ketal alcohol **10** in an almost quantitative yield.

Bromination of ketal alcohol **10** with thionyl bromide in pyridine (4) and chromatography gave bromoketal **11**. Hydrogenolysis of compound **11** with Raney nickel in methanol containing sodium hydroxide (4) yielded the corresponding ketal **12** which after acid hydrolysis gave a high yield of 4-twistanone (**6**) as shown by comparison with an authentic sample. This new six-step synthesis of 4-twistanone (**6**) is, however, inferior to our first synthesis (2) because of experimental difficulties encountered at the bromination step (**10** → **11**).

[1]In twistane, the bridgehead C-1, C-3, C-6, and C-8; C-2 and C-7; and C-4, C-5, C-9, and C-10 are all respectively equivalent.

[2]For a preliminary account on part of this work, see ref. 3.

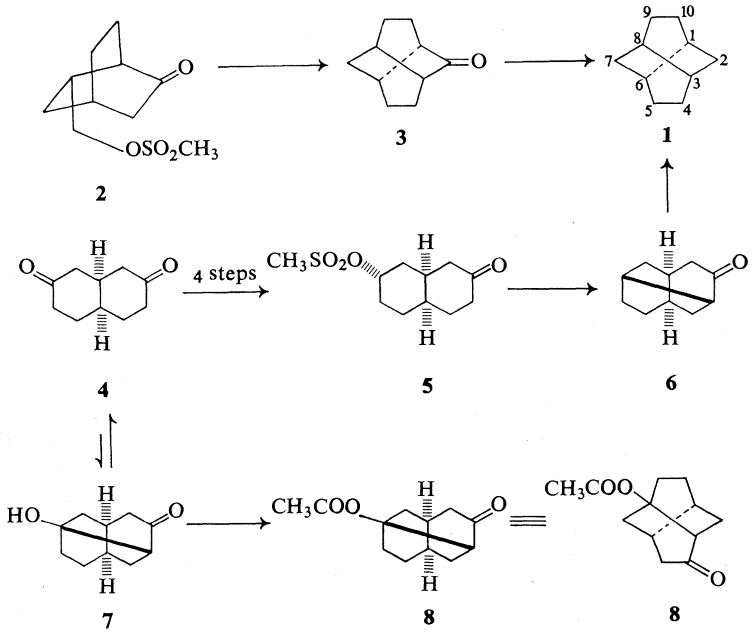

It was of interest to find out if the intermediate hydroxy tricyclic ketone **7** (8-hydroxy-4-twistanone) could be isolated. We had in hand an ideal precursor, the ketal alcohol **10** which could possibly generate the intermediate **7** by a very mild acid hydrolysis.

Consequently, ketal alcohol was submitted to mild hydrolysis condition and was found to give two compounds as judged by thin-layer chromatography. One compound had an identical R_f value with the one of decalin dione **4**, the other compound had a lower R_f value which was a good indication for the presence of the intermediate **7**. This result was further supported by the infrared spectrum of the mixture which showed a strong absorption at 3450 cm^{-1}.

Therefore, an attempt was made to isolate these two compounds by preparative thin-layer chromatography with silica gel. A very neat separation of the two compounds was obtained on the preparative chromatogram and both compounds were isolated by the usual extraction procedure. As expected, the first compound (~25% yield) was found identical to authentic decalin dione **4** by comparison of R_f values (t.l.c.) and infrared spectra. Very surprisingly, the second compound (~75% yield) was also found to have an R_f value identical with the one of decalin dione **4** and its infrared spectra was also identical to an authentic spectra of decalin dione **4**.

Consequently, a logical explanation for such result is that mild hydrolysis of ketal alcohol **10** gives decalin dione **4** and the isomeric hydroxy tricyclic ketone **7**. The tricyclic isomer **7** appears to survive during the elution on silica gel, but it is so sensitive that it is readily transformed into decaline dione **4** either by a prolonged contact with silica gel or during the extraction procedure.

With a rigorous structural proof in hand for 8-acetoxy-4-twistanone (**8**), the synthesis of twistane derivatives with functions at the bridgehead position was next investigated.

Reaction of 8-acetoxy-4-twistanone (**8**) with ethane dithiol and boron trifluoride in acetic acid at room temperature gave crude thioketal acetate **13** which could be obtained crystalline with petroleum ether. Desulfurization of crude thioketal **13** with a large excess of Raney nickel in boiling ethanol for two days gave the liquid 1-twistyl acetate (**14**). Reductive hydrolysis of compound **14** with lithium aluminium hydride in ether yielded the highly crystalline 1-twistanol (**15**).

Attempts to obtain directly 1-twistanol from 8-acetoxy-4-twistanone (**8**) by the tosylhydrazone – sodium borohydride method (5) followed by lithium aluminium hydride were not as success-

Can. J. Chem. Downloaded from www.nrcresearchpress.com by 210.87.254.42 on 09/05/12
For personal use only.

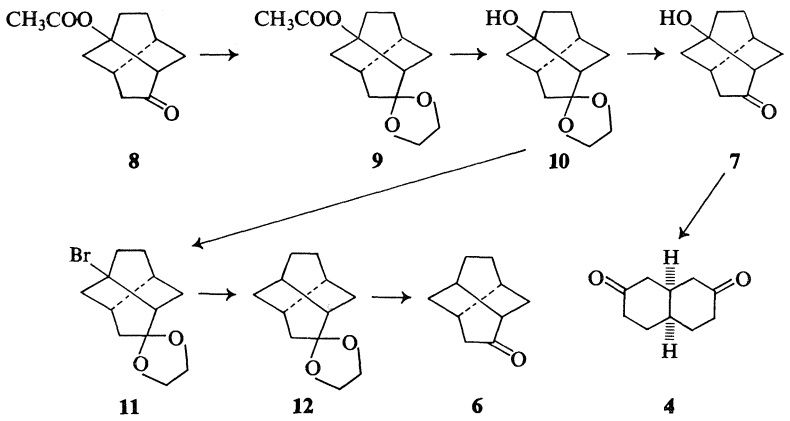

ful. Yields of approximately 50% were obtained by this method while the thioketal route provided an overall yield of 80%. The Wolff–Kischener reduction procedure, although more esthetical, cannot be applied on 8-acetoxy-4-twistanone (**8**) since the removal of the acetoxy group either by hydroxide ion or hydrazine would destroy the twistane skeleton. Other alternative procedures were also not successful. Reductive hydrolysis of thioketal acetate **13** with lithium aluminium hydride gave the crystalline thioketal alcohol **13** ($CH_3CO{=}H$) which did not yield 1-twistanol (**15**) by desulfurization with Raney nickel or with sodium in liquid ammonia. Similarly, a Birch reduction on thioketal acetate **13** in order to obtain 1-twistanol (**15**) directly was also unsuccessful.

Treatment of 1-twistanol (**15**) with thionyl chloride at reflux temperature gave the crystalline 1-twistyl chloride (**16**) in 95% yield. Reduction of 1-twistyl chloride (**16**) by sodium in liquid ammonia and ether (6) gave a crystalline hydrocarbon which after one sublimation had its physical and spectral properties in complete agreement with those of authentic twistane (**1**). We consider this new six-step synthesis of twistane (**1**), the best practical route to produce the hydrocarbon (1, 2).

Reaction of 1-twistanol with formic acid in sulfuric acid, the Koch–Haaf carboxylation (7), proceeded with remarkable ease giving an excellent yield of a tricyclic tertiary carboxylic acid to which structure **17** was assigned. Because of a theoretically possible rearrangement of 1-twistanol into the adamantane skeleton during this reaction (8), compound **17** was compared and shown to be a different compound than 1-adamantane carboxylic acid. In order to eliminate any other possible structural isomers, a rigorous chemical proof for 1-twistane carboxylic acid (**17**) was necessary and it was achieved in the following manner. By reacting compound **17** with methyl lithium in ether, a quantitative yield of the corresponding methyl ketone **18** was obtained. Baeyer–Villiger oxidation of **18** with *m*-chloroperbenzoic acid in boiling chloroform gave in high yield a liquid identified as 1-twistyl acetate (**14**) which afforded after reductive hydrolysis the crystalline 1-twistanol (**15**) as shown by comparison with an authentic sample.

Similarly, the Ritter reaction proceeded with great facility. Treatment of 1-twistanol (**15**) with acetonitrile and sulfuric acid (9) at room temperature gave the highly crystalline 1-acetamidotwistane (**19**) with a 93% yield. Hydrolysis of compound **19** with diethylene glycol and sodium hydroxide (9) gave 1-twistylamine (**20**) which was obtained crystalline by sublimation. The crystalline hydrochloride salt **21** was obtained by treating an ethereal solution of 1-twistylamine (**20**) with dry hydrogen chloride.

Compounds **19**, **20**, and **21** were respectively compared with 1-acetamido-adamantane, 1-adamantylamine, and its hydrochloride salt.[3] They were shown to be different compounds on

[3]1-adamantylamine hydrochloride was obtained from Aldrich Chemical. 1-Acetamido-adamantane was produced by treating 1-adamantylamine with pyridine and acetic anhydride (m.p. 149–150 °C, reported m.p. 149 °C (9)).

Can. J. Chem. Downloaded from www.nrcresearchpress.com by 210.87.254.42 on 09/05/12
For personal use only.

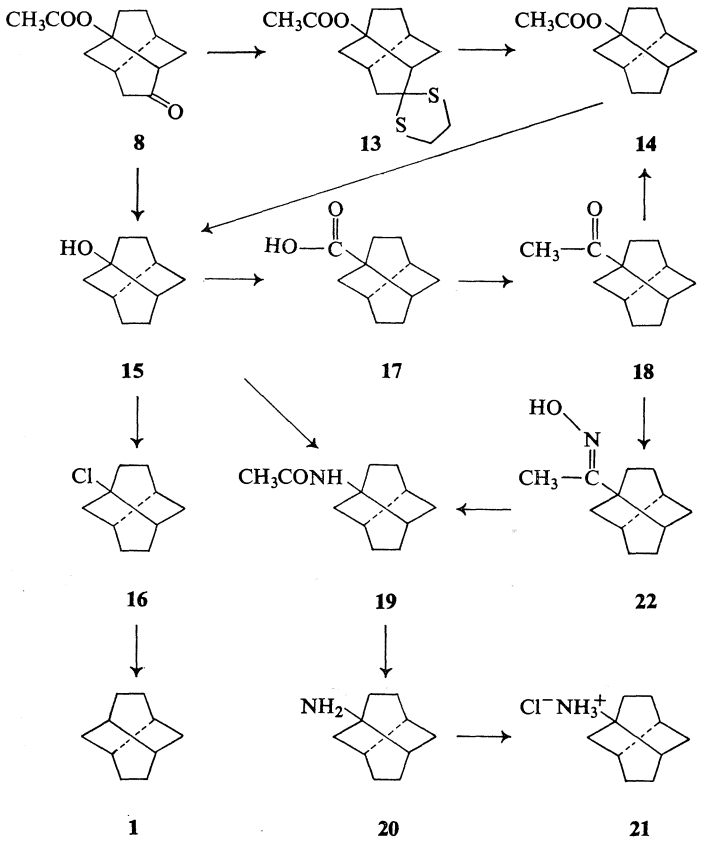

the basis of their melting point and the finger print region of their respective infrared and nuclear magnetic resonance spectra. Furthermore, the spectral absorption (infrared and n.m.r.) of the functional groups of the adamantane derivatives (10) were found useful to confirm the presence of a primary acetamido group, a primary amino group and a primary ammonium group in compounds **19**, **20**, and **21** respectively.

Again, there remained a possibility that compound **19**, could belong to another tricyclic decane system isomeric with the twistane skeleton, consequently, a rigorous chemical proof was necessary.

Treatment of methyl twistyl ketone (**18**) with hydroxylamine gave the crystalline oxime **22** which was then transformed into the corresponding oxime mesylate (**22**, H=CH_3SO_2). The crude mesylate was heated at reflux in aqueous dioxane (11) and gave a high yield of an amide which was found completely identical to 1-acetamidotwistane (**19**), thus affording a rigorous chemical proof for 1-twistylamine (**20**) and its derivatives.

1-Twistylamine hydrochloride (**21**) is the only other possible skeletal isomer of the important antiviral agent, 1-adamantylamine hydrochloride (12) which possesses three six-membered rings. Biological results on 1-twistylamine and its derivatives will be reported elsewhere.

Experimental

Melting points are not corrected. Infrared spectra (ν_{max}) were recorded on Perkin–Elmer Infracord, model 137 spectrophotometer. Nuclear magnetic resonance spectra (n.m.r., τ values) were taken on a Varian A60 spectrometer with tetramethylsilane as an internal standard. Aluminium oxide G was used for thin-layer chromatography (t.l.c.) and the chromatograms were developed with iodine. Woelm alumina (neutral, grade II) was utilized for column chromatography unless otherwise stated. Anhydrous magnesium sulfate was used as the drying agent in working up reactions. Petroleum ether boiling point 30–60 °C was used.

Can. J. Chem. Downloaded from www.nrcresearchpress.com by 210.87.254.42 on 09/05/12
For personal use only.

Can. J. Chem. Downloaded from www.nrcresearchpress.com by 210.87.254.42 on 09/05/12
For personal use only.

8-Acetoxy-4-twistanone (8)

Decalin dione **4** (10 g, 63 mmoles) was added to a mixture of freshly distilled boron trifluoride ethereate (86 ml), acetic acid (150 ml), and acetic anhydride (80 ml). After 24 h at room temperature, water was added (700 ml) and the mixture was extracted with chloroform. The organic phase was washed twice with water, aqueous sodium carbonate solution (5%), and water. Evaporation of the dried organic phase yielded a reddish oil (12.79 g) which was purified by column chromatography. Elution with benzene – petroleum ether (15%) gave crystalline 8-acetoxy-4-twistanone **8** (7.54 g). Recrystallization with petroleum ether gave the analytical sample; m.p. 66–68 °C; t.l.c.: R_f value, 0.6, benzene–ether (1:3); mol. wt. (mass spectroscopy) 208; infrared: ν_{max} (CCl_4) 1725 and 1245 cm^{-1}; n.m.r.: τ ($CDCl_3$) 7.32 (1H, broad doublet, CHCO), and 8.05 (3H, singlet, CH_3COO).

Anal. Calcd. for $C_{12}H_{16}O$: C, 69.20; H, 7.74. Found: C, 69.44; H, 7.77.

The 2,4-dinitrophenylhydrazone had m.p. 184–185 °C.

Anal. Calcd. for $C_{18}H_{20}O_6N_4$: C, 55.66; H, 5.19; N, 14.42. Found: C, 55.53; H, 5.14; N, 14.44.

Ketal Acetate (9)

A mixture containing 8-acetoxy-4-twistanone **8** (5.93 g, 28.4 mmoles), ethylene glycol (9.31 g), and *p*-toluenesulfonic acid (210 mg) in benzene (225 ml) was heated at reflux for 24 h with continuous azeotropic removal of water and excess ethylene glycol by means of a Dean–Stark trap. The cooled mixture was washed with saturated aqueous sodium carbonate and water. The dried organic phase was evaporated *in vacuo* to give crude liquid ketal acetate (7.30 g). The analytical sample was obtained by distillation *in vacuo*; t.l.c.: R_f value, 0.9, benzene–ether (1:3); mol. wt. (mass spectroscopy) 252; infrared: ν_{max} (CCl_4) 1725 and 1245 cm^{-1}; n.m.r.: τ ($CDCl_3$) 6.14 (4H, multiplet, OCH_2CH_2O), and 8.03 (3H, singlet, CH_3COO).

Anal. Calcd. for $C_{14}H_{20}O_4$: C, 66.64; H, 8.00. Found: C, 66.53; H, 8.13.

Ketal Alcohol (10)

Crude ketal acetate **9** (6.62 g) was dissolved in ether (250 ml) and lithium aluminium hydride (4.95 g) was added. After a reflux of 3 h, the excess hydride was destroyed by careful addition of water. Magnesium sulfate was added and the inorganic insoluble material was removed by filtration. The organic phase was evaporated to dryness yielding the crude liquid ketal alcohol (4.65 g). The analytical sample was obtained by column chromatography (benzene as eluent) followed by microdistillation *in vacuo*; t.l.c.: R_f value, 0.8, benzene–ether (1:3); mol. wt. (mass spectroscopy) 210; infrared: ν_{max} (CCl_4) 3590 cm^{-1}; n.m.r.: τ($CDCl_3$) 5.96 (4H, multiplet, OCH_2CH_2O) and 7.90 (1H, singlet, OH).

Anal. Calcd. for $C_{12}H_{18}O_3$: C, 68.55; H, 8.63. Found: C, 68.72; H, 8.69.

Bromoketal (11)

A cooled solution (0 °C) of ketal alcohol **10** (750 mg, 3.5 mmoles) in pyridine (7 ml) was added dropwise to a cooled (0 °C) mixture of thionyl bromide (1.45 ml) in pyridine (7 ml) with magnetic stirring. The mixture was then heated (oil bath temperature 90–93 °C) for 90 min. The cooled mixture was mixed with dichloromethane (200 ml) and washed with saturated aqueous sodium carbonate solution and brine. The dried organic phase was evaporated to dryness yielding crude bromoketal (730 mg). Pure liquid bromoketal **11** (640 mg, 66% yield) was obtained by column chromatography with Fisher florisil (100–200 mesh) by elution with benzene. Distillation *in vacuo* gave the analytically pure sample; t.l.c.: R_f value, 0.9, benzene–ether (1:3); mol. wt. (mass spectroscopy) 272 and 274; infrared (CCl_4) no hydroxyl absorption; n.m.r.: τ (CCl_4) 6.08 (4H, multiplet, OCH_2CH_2O).

Anal. Calcd. for $C_{12}H_{17}O_2Br$: C, 52.76; H, 6.28. Found: C, 52.72; H, 6.37.

4-Twistanone (4)

Bromoketal **11** (771 mg, 2.82 mmoles) was hydrogenolyzed in methanol (20 ml) containing sodium hydroxide (124 mg) and Raney nickel (250 mg) under an atmosphere of hydrogen at 50 °C during 12 h. During this period, new portion of Raney nickel (~200 mg) was added twice. The catalyst was removed by filtration and the solvent evaporated *in vacuo*. Ether was added and the solution was washed with brine. The dried ethereal solution was evaporated to dryness to give crude ketal **12** (430 mg).

A solution of crude ketal (340 mg) in tetrahydrofuran (7 ml) was mixed with a hydrochloric acid solution (*N*, 35 ml) and left for 3 h at room temperature. Sodium chloride was added and the mixture was extracted with ether. The dried extract was evaporated to dryness yielding crude 4-twistanone (**6**). This crude product was purified by column chromatography. Elution with benzene gave pure 4-twistanone **6** (160 mg) which after one sublimation was found identical (mixed melting point, t.l.c., infrared, and n.m.r. spectra) with an authentic sample (2).

Acid Hydrolysis of Ketal Alcohol (10)

p-Toluenesulfonic acid (9 mg) and water (5 drops) were added to an ethereal solution (10 ml) of ketal alcohol **10** (80 mg, 0.38 mmole). The mixture was magnetically stirred at room temperature. The reaction was followed by thin-layer chromatography analyses and after 12 h, ketal alcohol **10** was completely hydrolyzed. The reaction mixture was washed with an aqueous solution of sodium bicarbonate (0.5 *N*). The dried organic phase was evaporated to dryness at room temperature to give a mixture of two compounds (70 mg). This mixture was separated by preparative thin-layer chromatography with Silica Gel G as adsorbent and benzene–ether (1:3).

The compound having an R_f value of 0.6 was extracted with ether. Evaporation of the solvent gave a compound (12 mg) which was found completely identical with authentic diketone **4** by comparison of their R_f value (t.l.c.), infrared, and n.m.r. spectra.

The product having an R_f value of 0.5 was extracted with ether. Evaporation of the solvent gave a product (33 mg) which had an identical R_f value with the one of diketone **4**. The infrared spectrum was almost completely identical to the infrared spectrum of diketone **4**. This material was submitted again to preparative thin-layer chromatography and yielded a product having an

Can. J. Chem. Downloaded from www.nrcresearchpress.com by 210.87.254.42 on 09/05/12
For personal use only.

infrared spectrum which was completely identical to the one of authentic diketone **4**.

*Thioketal Acetate (**13**)*

Boron trifluoride ethearate (12 ml) and ethane dithiol (10 ml) was added to a solution of 8-acetoxy-4-twistanone **8** (10 g, 48 mmoles) in acetic acid (600 ml). After 17 h at room temperature, water (5 l) was added and the mixture was extracted with ether. The ethereal extract was washed with a saturated solution of sodium carbonate and the dried organic phase was evaporated to dryness. This material (17.7 g) was heated (oil bath temperature, 100 °C) *in vacuo* (0.5 mm) during 3 h to remove excess of ethane dithiol. The crude oily material (14.4 g) was suitable for the next reaction. Pure crystalline thioketal acetate **13** was obtained by crystallization with petroleum ether; m.p. 71–72 °C; t.l.c.: R_f value, 0.4, petroleum ether – benzene (1:1); mol. wt. (mass spectroscopy) 284; infrared: ν_{max} (CCl_4) 1735 cm^{-1}; n.m.r.: τ (CCl_4) 6.60 (4H, multiplet, SCH_2CH_2S) and 8.02 (3H, singlet, CH_3COO).

Anal. Calcd. for $C_{14}H_{20}O_2S_2$: C, 59.15; H, 7.04; S. 22.54. Found: C, 59.15; H, 7.17; S, 22.83.

*Thioketal Alcohol (**13**, $CH_3CO{=}H$)*

Lithium aluminium hydride (1.1 g) was added to a solution of crude thioketal acetate (900 mg) in ether (150 ml) and the mixture was refluxed during 4 h. The excess hydride was destroyed by careful addition of water, magnesium sulfate was added, and the insoluble material was removed by filtration. The ethereal solution was evaporated to dryness yielding a crude product (860 mg) which was purified by column chromatography. Elution with benzene – petroleum ether (10%) gave unidentified material. Elution with mixtures of benzene – petroleum ether (25% and 50%) gave crystalline thioketal alcohol **13** (450 mg). Recrystallization with petroleum ether gave the analytical sample; m.p. 111–112 °C; t.l.c.: R_f value, 0.5, benzene; infrared: ν_{max} (CCl_4) 3480 cm^{-1}; n.m.r.: τ ($CDCl_3$) 6.65 (4H, complex multiplet, SCH_2CH_2S).

Anal. Calcd. for $C_{12}H_{18}OS_2$: C, 59.49; H, 7.48; S, 26.41. Found: C, 59.37; H, 7.67; S, 26.19.

*1-Twistyl Acetate (**14**)*

*(a) from Thioketal Acetate (**13**)*

Crude thioketal acetate **13** (14.4 g) was dissolved in absolute ethanol (1.5 l), Raney nickel (225 g) was added and the mixture was mechanically stirred and refluxed for 24 h. The catalyst was removed by filtration and a new portion of catalyst (150 g) was added and the mixture was refluxed for 24 h. After removal of the Raney nickel by filtration, the ethanol was evaporated *in vacuo* yielding pure 1-twistyl acetate **14** (7.3 g, 80% overall yield from 8-acetoxy-4-twistanone). The analytical sample was obtained by distillation *in vacuo* (80 °C, 0.5 mm). t.l.c.: R_f value, 0.6, petroleum ether – benzene (1:1); infrared: ν_{max} (film) 1735 cm^{-1}; n.m.r.: τ (CCl_4) 8.11 (3H, singlet, CH_3COO).

Anal. Calcd. for $C_{12}H_{18}O_2$: C, 74.23; H, 9.28. Found: C, 74.48; H, 9.62.

*(b) from Methyl Twistyl Ketone (**22**)*

Methyl twistyl ketone **22** (192 mg, 1.08 mmoles) was dissolved in dichloromethane (20 ml) containing *m*-chloroperbenzoic acid (400 mg) and the mixture was refluxed for seven days. An aqueous sodium hydroxide solution (0.5 *N*) was added and the organic phase was separated, washed with water, and dried. The solvent was evaporated *in vacuo* to give a crude liquid (200 mg) which showed one spot on thin-layer chromatography having a R_f value corresponding to 1-twistyl acetate. A small quantity (40 mg) was purified by column chromatography using a mixture of petroleum ether – dichloromethane (1:1) and was shown to be identical to authentic 1-twistyl acetate (**14**) by comparison of infrared and n.m.r. spectra. Crude 1-twistyl acetate **14** (200 mg) was hydrolyzed with lithium aluminium hydride in ether and after the usual work-up gave crude crystalline 1-twistanol (120 mg). This product was recrystallized in petroleum ether (m.p. 216–217 °C) and was shown to be identical with authentic 1-twistanol by mixed melting point determination and by comparison of infrared and nuclear magnetic resonance spectra.

*1-Twistanol (**15**)*

*(a) from 1-Twistyl Acetate (**14**)*

Lithium aluminium hydride (15 g) was added to an ethereal solution (2 l) of 1-twistyl acetate (14.5 g, 75 mmoles) and the mixture was refluxed for 12 h. The excess hydride was carefully destroyed by addition of moist ether and a hydrochloric acid solution (*N*) was added. The organic phase was separated, dried, and evaporated to dryness to give quantitatively 1-twistanol **15** (11.4 g). Recrystallization with petroleum ether gave the analytical sample; m.p. 215–216 °C; t.l.c.: R_f value, 0.7, ether; infrared: ν_{max} (CCl_4) 3600 and 3400 cm^{-1}.

Anal. Calcd. for $C_{10}H_{16}O$: C, 78.95; H, 10.53. Found: C, 78.75; H, 10.81.

*(b) from 8-Acetoxy-twistanone (**8**)*

p-Toluenesulfonylhydrazine (559 mg, 3 mmoles) was added to methanol (50 ml) containing 8-acetoxy-4-twistanone (500 mg, 2.4 mmoles) and the mixture was refluxed for 20 h. Most of the solvent was removed and the residue was recrystallized with methanol (750 mg, 83% yield). The *p*-toluenesulfonylhydrazone derivative was recrystallized with methanol to give the analytical sample; m.p. 165.5–167.5 °C.

Anal. Calcd. for $C_{19}H_{24}N_2O_4S$: C, 60.64; H, 6.38; N, 7.45. Found: C, 60.32; H, 6.88; N, 7.88.

The crude *p*-toluenesulfonylhydrazone derivative (1.26 g) obtained from 8-acetoxy-4-twistanone (1.15 g, 2.76 mmoles) was dissolved in dry dioxane (50 ml), sodium borohydride (786 mg, 20.7 mmoles) was added, and the mixture was refluxed for 10 h. Excess lithium aluminium hydride was added and the mixture was heated at reflux during 12 h. The excess hydride was destroyed by addition of acetone and water. The insoluble material was filtered, dissolved in hydrochloric acid solution (*N*, 10 ml), and extracted with ether. The dried dioxane filtrate was evaporated to dryness and combined with the ethereal extract which was evaporated to dryness (638 mg). This crude material was distilled *in vacuo* to yield an oil (480 mg) which was purified by column chromatography. Elution with petroleum ether and benzene gave no desired product. Elution with ether–benzene (2%) gave pure crystalline 1-twistanol **15** (207 mg, 52% yield from **8**) which was found to be identical with an authentic sample by comparison of their infrared spectra.

Can. J. Chem. Downloaded from www.nrcresearchpress.com by 210.87.254.42 on 09/05/12
For personal use only.

*1-Twistyl Chloride (**16**)*

1-Twistanol **15** (1.6 g, 10.5 mmoles) was slowly added to freshly distilled thionyl chloride (35 ml) with an efficient stirring. When the solution was homogeneous, it was refluxed for 2 h. The solution was evaporated to dryness giving a yellow oil which was dissolved in pentane (500 ml), washed with water, and saturated sodium carbonate solution. The dried pentane solution was evaporated to dryness yielding a slightly yellow crystalline residue (1.75 g). This material was purified by column chromatography using pentane – petroleum ether (1:1). The analytical sample was obtained by sublimation, m.p. 147–148 °C.

Anal. Calcd. for $C_{10}H_{15}Cl$: C, 70.38; H, 8.80. Found: C, 69.31; H, 8.90.

*Twistane (**1**)*

An ethereal solution (350 ml) of 1-twistyl chloride **16** (5.16 g, 30.3 mmoles) was mixed with liquid ammonia (750 ml) and sodium (2.7 g) was added in small pieces over a period of 4 h. Ethanol was added to destroy the excess of sodium and the ammonia was allowed to evaporate at room temperature. A solution of hydrochloric acid (*N*) was added to the residue and extracted with pentane. The pentane solution was washed with water, dried, and distilled at atmospheric pressure giving semi-crystalline residue. One sublimation (120–124 °C, 12 mm) gave pure twistane (3.46 g, 85% yield) which was found to be identical (t.l.c., infrared, and n.m.r.) with an authentic sample (1, 2).

*1-Twistane Carboxylic Acid (**17**)*

A mixture of 1-twistanol **15** (2.18 g, 182 mmoles) and formic acid (97%+, 4.7 ml) in hexane (47 ml) cooled at 0 °C was slowly added during a period of 1 h in cold sulfuric acid (0 °C). Vigourous stirring was maintained during the addition and for a period of 3 h at room temperature. The mixture was poured on ice, sodium chloride was added, and the mixture was extracted with ether. The organic phase was extracted with an aqueous sodium hydroxide solution (*N*). The basic aqueous phase was acidified with hydrochloric acid solution (3 *N*) and extracted with ether. The dried organic phase was evaporated to dryness yielding a semi-crystalline product (2.2 g, 80% yield) which was shown homogeneous by thin-layer chromatography. This product was obtained crystalline with methanol–water. Recrystallization and sublimation *in vacuo* gave the analytical sample, m.p. 85–87 °C; t.l.c. (silicagel G): R_f value, 0.5, methanol–ether (10%); infrared: ν_{max} (CCl_4) 1710 cm^{-1}; n.m.r.: τ ($CDCl_3$) −1.34 (1H, broad singlet, COOH).

Anal. Calcd. for $C_{11}H_{16}O_2$: C, 73.26; H, 8.94. Found: C, 73.02; H, 9.12.

*Methyl Twistyl Ketone (**18**)*

An ethereal solution of methyl lithium (60 ml, 0.6 *N*) was added to 1-twistane carboxylic acid **17** (2.0 g, 11.1 mmoles) dissolved in dry ether (80 ml). This mixture was refluxed for 3 h, the excess methyl lithium was destroyed by addition of moist ether and brine was added. The dried ethereal phase was evaporated *in vacuo* to give a liquid (1.96 g, 100% yield) which was shown homogeneous by thin-layer chromatography. A pure sample was obtained by microdistillation *in vacuo*; t.l.c.: R_f value, 0.6, benzene; infrared: ν_{max} (CCl_4) 1700 cm^{-1}; n.m.r.: τ (CCl_4) 8.01 (3H, singlet, CH_3CO) 2,4-dinitrophenylhydrazone, m.p. 175–177 °C.

Anal. Calcd. for $C_{18}H_{22}N_4O_4$: C, 60.30; H, 6.20; N, 15.65. Found: C, 60.01; H, 6.52; N, 15.89.

*Methyl Twistyl Ketone Oxime (**23**)*

Hydroxylamine hydrochloride (10.24 g), sodium acetate (15.35 g), and methyl twistyl ketone **18** (1.454 g, 8.2 mmoles) was dissolved in methanol (150 ml) and the mixture was refluxed for 5 h. A part of the methanol was evaporated *in vacuo*, water was added, and the mixture was extracted with ether. The dried organic phase was evaporated to dryness yielding a crystalline product (1.734 g). Recrystallization with petroleum ether gave the analytical sample; m.p. 150–151 °C; t.l.c.: R_f value, 0.6, benzene; infrared: ν_{max} (CCl_4) 3250 and 1660 (weak) cm^{-1}; n.m.r. τ (CCl_4) 8.23 (3H, singlet, CH_3).

Anal. Calcd. for $C_{12}H_{19}OH$: C, 74.57; H, 9.90; N, 7.24. Found: C, 74.37; H, 10.13; N, 7.43.

*1-Acetamidotwistane (**19**)*

*(a) from 1-Twistanol (**15**)*

Concentrated sulfuric acid (3.8 ml) was slowly added to cold acetonitrile (10 ml, ice-bath) and this solution was added drop-by-drop (30 min) to a solution of 1-twistanol **15** (579 mg, 3.8 mmoles) in acetonitrile (10 ml) while magnetically stirred and cooled with an ice-bath. The reaction mixture was left at room temperature for 12 h. The mixture was then cooled with an ice–bath and a solution of sodium hydroxide (6 g) in water (20 ml) was slowly added. The mixture was extracted with ether and the organic extract was washed once with brine. The dried organic phase was evaporated *in vacuo* to give a crystalline product **19** (741 mg; 100% yield). 1-Acetamidotwistane **19** was recrystallized with ether – petroleum ether to give the analytical sample (686 mg, 93% yield); m.p. 129–131 °C, t.l.c.: R_f value, 0.5, ether; mol. wt. (mass spectroscopy) 193; infrared: ν_{max} (CCl_4) 3230 and 1670 cm^{-1}; n.m.r.: τ (CCl_4) 3.55 (1H, broad singlet, CONH) and 8.18 (3H, singlet, CH_3CO).

Anal. Calcd. for $C_{12}H_{19}NO$: C, 74.57; H, 9.91; N, 7.25. Found: C, 74.22; H, 9.76; N, 7.16.

*(b) from Methyl Twistyl Ketone Oxime (**22**)*

A cold solution of methyl twistyl ketone oxime **22** (68 mg, 0.35 mmole) in dichloromethane (0.6 ml) was added to a cold mixture of methanesulfonyl chloride (68 mg), pyridine (0.2 ml), and dichloromethane (2 ml). After 36 h in the cold, dichloromethane was added, the mixture was washed twice with saturated aqueous sodium carbonate, and with water. The dried organic phase was evaporated to dryness yielding the crude methyl twistyl ketone oxime mesylate (75 mg). This crude product (70 mg) was dissolved in a mixture of dioxane (4 ml) and water (3 ml) and heated at reflux for 4 h. Brine was added and the mixture was extracted with ether. The dried organic phase was evaporated to dryness to give crude crystalline 1-acetamido twistane (52 mg). This product was further purified by column chromatography and recrystallized with ether–petroleum ether to give a compound which was found identical (m.p., t.l.c., infrared, and n.m.r. spectra) to 1-acetamido twistane **19** obtained from procedure *a*.

*1-Twistylamine (**20**) and its Hydrochloride Salt (**21**)*

1-Acetamidotwistane **19** (522 mg, 2.7 mmoles) was dissolved by heating in diethylene glycol (10 ml) and then cooled at room temperature. Sodium hydroxide (1 g) was added and the mixture was heated (oil bath temperature 240–250 °C) under a nitrogen atmosphere during 4 h. The reaction mixture was cooled at room temperature, brine (40 ml) was added and the mixture was extracted with ether. The dried extract was evaporated to dryness to give crude 1-twistyl amine (560 mg) which slowly solidified on standing. Pure 1-twistylamine **20** was obtained by sublimation; m.p. 184–185 °C; t.l.c.: R_f value 0.25, methanol–ether (7%); infrared: ν_{max} (NaCl) 3300 (broad) and 1600 (broad) cm^{-1}; n.m.r. τ (CCl_4) 9.02 (2H, singlet, NH_2).

Crude 1-twistylamine (560 mg) was dissolved in dry ether and dry hydrogen chloride gas was passed through the solution until the precipitation of 1-twistylamine hydrochloride **21** was completed (392 mg, 80% yield). Recrystallization with methanol–ether gave the analytical sample; m.p. above 360 °C; mol. wt. (mass spectroscopy) 151 (M^+-HCl); n.m.r.: τ ($CDCl_3$), 1.65 (3H, broad singlet, NH_3^+).

Anal. Calcd. for $C_{10}H_{18}NCl$: C, 64.34; H, 9.65; N, 7.50. Found: C, 64.03; H, 9.62; N, 7.48.

Acknowledgments

The assistance of Miss J. Poupart in the early part of this investigation is gratefully acknowledged. This research was supported by the National Research Council of Canada, Ayerst Laboratories, Montreal and the Ministère de l'Education, Québec.

1. H. W. Whitlock, Jr. J. Am. Chem. Soc. **84**, 3412 (1962); H. W. Whitlock, Jr. and M. W. Siefken. J. Am. Chem. Soc. **90**, 4929 (1968).
2. J. Gauthier and P. Deslongchamps. Can. J. Chem. **45**, 297 (1967).
3. A. Bélanger, J. Poupart, and P. Deslongchamps. Tetrahedron Letters, 2127 (1968).
4. H. Stetter, P. Tacke, and J. Gartner. Chem. Ber. **97**, 3480 (1964).
5. L. Gaglioti. Tetrahedron, **22**, 487 (1966).
6. H. Dugas, M. E. Hazenberg, Z. Valenta, and K. Wiesner. Tetrahedron Letters, 4931 (1967).
7. H. Koch and W. Haaf. Angew. Chem. **72**, 628 (1960).
8. R. C. Fort and P. von R. Schleyer. Chem. Rev. **64**, 277 (1964).
9. H. Stetter, J. Mayer, M. Schwarz, and K. Wulff. Chem. Ber. **93**, 226 (1960).
10. R. C. Fort and P. von R. Schleyer. J. Org. Chem. **30**, 789 (1965).
11. R. E. Ireland and L. N. Mander. Tetrahedron Letters, 2627 (1965).
12. W. L. Davies, R. R. Grunert, R. F. Haff, J. W. McGahen, E. M. Neumayer, M. Paulshock, J. C. Watts, T. R. Wood, E. C. Hermann, and C. E. Hoffman. Science, **144**, 862 (1964).

Can. J. Chem. Downloaded from www.nrcresearchpress.com by 210.87.254.42 on 09/05/12
For personal use only.

Can. J. Chem. Downloaded from www.nrcresearchpress.com by 210.87.254.42 on 09/05/12
For personal use only.

Nuclear magnetic resonance study of intramolecular electronic effects in diphenyl sulfides, sulfoxides, and sulfones[1]

J. B. Hyne and J. W. Greidanus

Fundamental Sulphur Research Group, Alberta Sulphur Research Ltd., and Department of Chemistry, University of Calgary, Calgary, Alberta

Received August 13, 1968

A nuclear magnetic resonance (n.m.r.) method has been applied to the study of variations in electron density in the aromatic rings of *para*-disubstituted diphenyl sulfides, sulfoxides and sulfones. The n.m.r. response of the aromatic ring protons has been determined as a function of the nature of the *para* substituents and particularly as a function of the nature of the bridging group between the rings. Certain diphenyl ethers and diphenyl methanes have been investigated for comparison purposes. The results establish that a transmission mechanism is operative through sulfur in diphenyl sulfides that is not effective when the bridging function is sulfoxide or sulfone. The extent to which transmission is operative even in the sulfides is dependent on the precise nature of the *para* substituents, in particular whether they are donors or acceptors and the manner in which they interact with the remainder of the molecule.

Canadian Journal of Chemistry, **47** 803 (1969)

Introduction

Many experimental techniques have been applied to the study of transmission of electronic effects through a sulfur bridge. In any bridged system we may expect σ-conduction which rapidly diminishes with distance. The potentially much stronger transmission of effects through a system of delocalized π-bonds in particular has attracted much attention; for instance the question of whether a bridging sulfur atom linking two π-bonded systems, one a potential electron donor, the other a potential acceptor, permits "leakage" of electron density from one ring to the other:

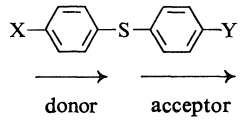

In general the state of hybridization of the bridging atom is fundamental to the question of transmission across a bridging atom or group located between potential donor and acceptor functions in a molecule. When the energy differences between the various possible states of hybridization of the bridging function become small, as is the case in sulfur compared with oxygen, it also becomes increasingly difficult to establish whether there exists sufficient "incentive" for the molecule to promote electrons from lower lying orbital energy levels to slightly higher ones, i.e. undergo rehybridization. The possibility of expansion of the sulfur valence shell has been discussed by many workers and reviews covering this topic up to a recent date have been published (2, 3).

Mangini and co-workers, studying the ultraviolet spectra of a large variety of aromatic sulfides found no evidence for transmission of electronic effects (4–6). Szmant and McIntosh (7) have, on the basis of similar studies, come to the conclusion that there was indeed evidence for this type of transmission when there was sufficient driving force in the form of both a powerful electron donating and an electron accepting potential within the molecule. The conclusion that interaction through the sulfur atom in various diphenyl sulfides was very limited was reached by other workers as a result of infrared and polarographic studies (8, 9). The effect of various ring substituents on the acid strengths of β-phenylthio, β-phenylsulfinyl, and β-phenylsulfonyl acrylic acids led Hogeveen (10) to the conclusion that the effects were more efficiently transmitted through the sulfide *S*-bridge than through the sulfinyl or sulfonyl bridges. Litvinenko and co-workers (11–14) studied the reactivity of the primary amino group in di-*para*-substituted compounds of the type $Y—C_6H_4—X—C_6H_4—NH_2$, where X = S, Se or NH. These authors suggested that the ability to transmit electronic effects decreases in the order —NH—>—S—>—Se—>—O—.

In any experimental investigation of the possible transmission of electronic effects through a bridging sulfur atom the question as to whether

[1]Preliminary results were presented at the Princeton University Conference on "The Chemistry of Sulfides", June 1966 (1).

TABLE I

Average chemical shift* of the aromatic protons† of some diphenyl compounds ("whole molecules") and of the corresponding *para*-substituted "half molecules"‡

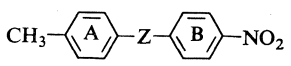

		A ring		B ring
Z = S	Half molecule	429.3	Half molecule	461.8
	Whole molecule	440.9	Whole molecule	455.1
	Change§	−11.6	Change	+6.7
Z = SO	Half molecule	444.3	Half molecule	486.5
	Whole molecule	445.2	Whole molecule	484.0
	Change§	−0.9	Change	+2.5
Z = SO_2	Half molecule	455.3	Half molecule	497.5
	Whole molecule	456.1	Whole molecule	493.8
	Change§	−0.8	Change	+3.7

*All figures in c.p.s. from tetramethylsilane internal standard in $CDCl_3$, calibrated on singlet peak of residual $CHCl_3$ at 435 c.p.s.
†The shift of the center of the aromatic multiplet was taken.
‡For explanation see text.
§A negative change indicates a downfield shift, the protons being less shielded in the diphenyl compound.

excited states are involved in the study must be clearly established. Transmission mechanisms operative in excited states may not be important in the ground state. Any evidence obtained from the study of ultraviolet spectra and reactivity differences must be considered to be in a different class from that obtained in studies where ground states are involved, such as dipole moment, infrared, and nuclear magnetic resonance studies. In a recent paper Wehry (15) discussed the results of his measurement of acid dissociation constants of various phenols with sulfur-containing substituents in the ground state, the lowest triplet and the first excited singlet state. He obtained good evidence for both $3p_\pi$ donor and $3d_\pi$ acceptor conjugation of sulfide sulfur in the ground state.

Because the nature of the transmission process is subtle and may be energetically of minor magnitude, the proper choice of the experimental tool to be applied would seem to be important. It is therefore not surprising that in recent times nuclear magnetic resonance techniques have been increasingly used in studies of sulfur bonding (6, 16–18). We also chose to use this tool to study the transmission of electronic effects in di-*para*-substituted diphenyl compounds of the sulfide, sulfoxide, sulfone, ether and methylene types.

Methods and Results

The specific aim of our study was to investigate changes in the electron density of the aromatic rings of disubstituted diphenyl systems by measuring the chemical shifts associated with the protons of each aromatic ring. Almost all compounds contained unsymmetrically *para*-disubstituted rings only and the splitting pattern associated with the n.m.r. response of each set of four ring protons, although strictly of the A_2B_2 type, may be considered as two superimposed identical AB patterns, yielding a typical AB quartet. The average n.m.r. shift associated with the four ring protons was obtained by measuring the position of the center of the multiplet. The value of this shift was then taken as a measure of the relative electron density in each aromatic ring in the various compounds studied. The further approach chosen to find an answer to the basic question of whether a bridging function Z acts as an insulator or a transmitter of electronic effects will be illustrated by reference to a specific set of compounds.

The average n.m.r. shifts observed for the aromatic protons in the "whole molecule" were compared with those of the corresponding "half molecules", where Z = S, SO, or SO_2:

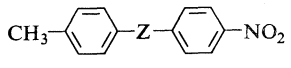

"whole molecule"

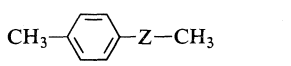

"half molecules"

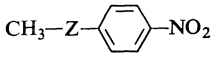

Can. J. Chem. Downloaded from www.nrcresearchpress.com by 210.87.254.42 on 09/05/12
For personal use only.

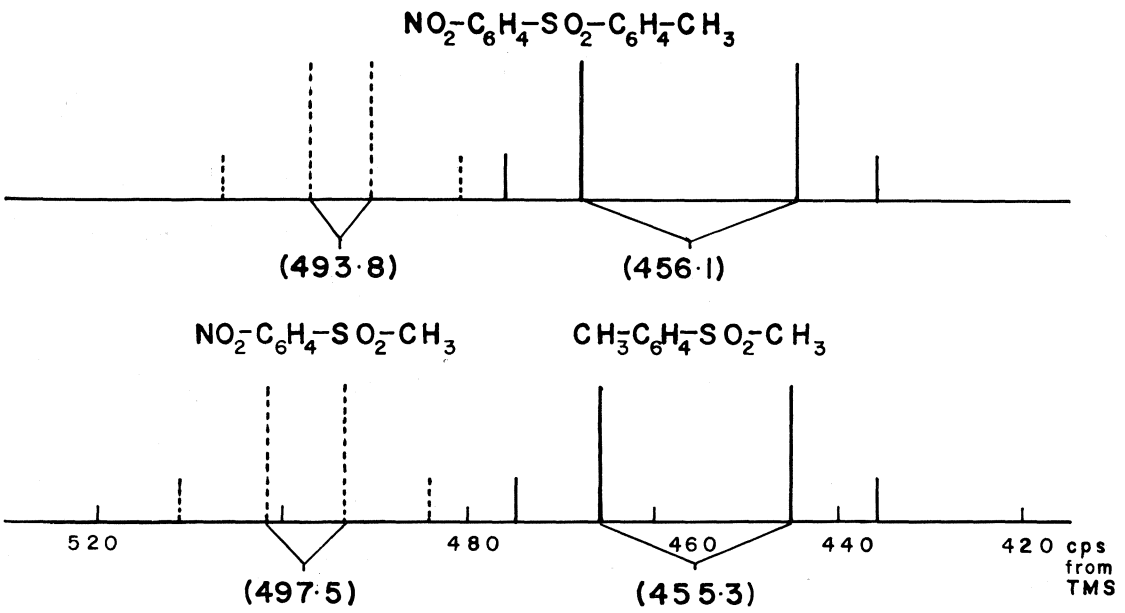

FIG. 1. Diagrammatic representation of the nuclear magnetic resonance spectra for 4-(*p*-nitrophenylsulfonyl)-toluene.

If the sum of the n.m.r. ring spectra of the "half molecules" shows no significant difference from that of the "whole molecule", it must be concluded that the Z-function bridge acts as an insulator between the two phenyl rings. Even if there is no transmission across the Z-function, it is to be expected that strict additivity will not be observed, since replacing the terminal methyl group in the "half molecules" by a substituted phenyl ring, as in the "whole molecule", must lead to minor changes in electron density due to inductive effects (σ-conduction). The shifts observed for the three sets of compounds under consideration are presented in Table I. The sign convention used for the differences is indicated in this Table.

In these three systems it was found that in the sulfone and sulfoxide cases (Z = SO_2 or SO) there was little difference between the ring proton shifts in the "half molecules" compared with the "whole molecule" as manifest in the small value of the "change". Such was not the case where Z = S (Figs. 1, 2, and 3). In the diphenyl sulfide (Z = S) the electron density of the methyl-carrying ring was significantly decreased, while that of the nitro-substituted ring was increased when compared with the n.m.r. data obtained for the "half molecules".

Based on the initial analysis described above the study was extended to cover a wider range of *para*-substituents and the corresponding oxygen- and methylene-bridged compounds. The complete n.m.r. data are presented in Tables II and III. In Table IV the differences in chemical shifts for the aromatic protons, calculated in exactly the same way as the "change" entry in Table I, are tabulated.

Discussion

The n.m.r. results for 4-(*p*-nitrophenylthio)-toluene (Table I, Z = S) are in agreement with transmission through the sulfur bridge, the electron density in the methyl-substituted ring having decreased, that in the nitro-substituted ring having increased in the "whole molecule" compared with two "half molecules". This can only arise if the molecule is polarized along its entire length, permitting electron density to leak from the donor ring to the acceptor ring. In the case of the corresponding sulfoxide and sulfone (Table I, Z = SO or SO_2) the changes in shift are comparatively minor and may be due to inductive effects. These results clearly established the fact that a transmission effect is operative in the sulfide that is not operative in the sulfoxide or sulfone. This trend is also evident from the data

Can. J. Chem. Downloaded from www.nrcresearchpress.com by 210.87.254.42 on 09/05/12
For personal use only.

Can. J. Chem. Downloaded from www.nrcresearchpress.com by 210.87.254.42 on 09/05/12
For personal use only.

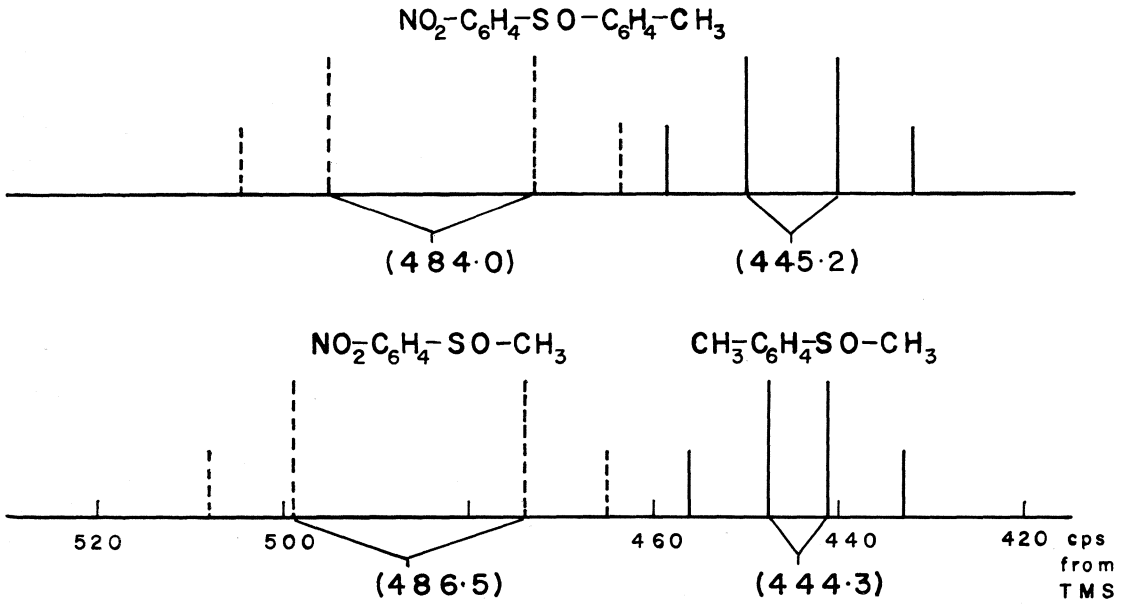

FIG. 2. Diagrammatic representation of the nuclear magnetic resonance spectra for 4-(*p*-nitrophenylsulfinyl)-toluene.

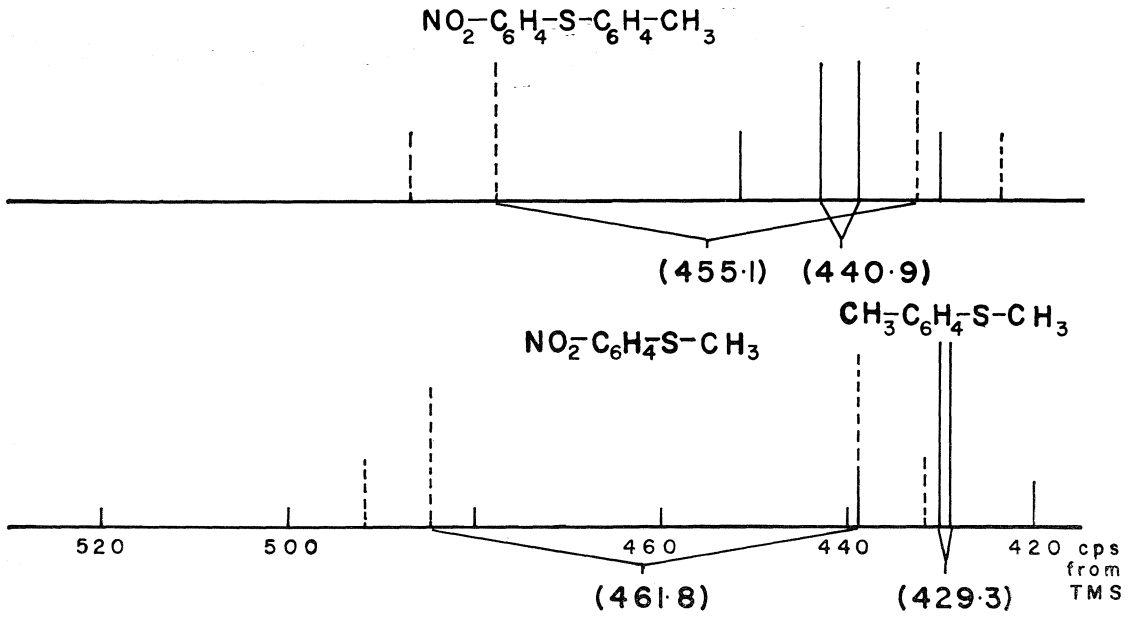

FIG. 3. Diagrammatic representation of the nuclear magnetic resonance spectra for 4-(*p*-nitrophenylthio)toluene.

Can. J. Chem. Downloaded from www.nrcresearchpress.com by 210.87.254.42 on 09/05/12
For personal use only.

TABLE II

Chemical shift of the aromatic multiplet of diphenyl compounds ("whole molecules")

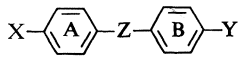

Compound	Z	Substituents X	Substituents Y	Chemical shift in c.p.s.* of center of AB quartet Ring A	Ring B
1	S	CH_3O	NO_2	433.4	454.0
2	S	NH_2	NO_2	421.2	454.2
3	S	CH_3O	CH_3	427.0	427.0
4	S	CH_3	NO_2	440.9	455.1
5	S	CH_3	H	433.9	436.0
6	S	H	NO_2	449.0	457.0
7	S	$(CH_3)_2N$	NO_2	423.4	453.2
8	S	NH_2	CH_3	417.8	424.2
9	S	Cl	NO_2	445.9	458.1
10	S	CH_3	Br	433.4	433.8
11	S	CH_3	Cl	433.5	432.2
12	SO	CH_3O	NO_2	435.4	482.2
13	SO	NH_2	NO_2	421.2	481.0
14	SO	CH_3O	CH_3	434.2	441.6
15	SO	CH_3	NO_2	445.2	484.0
16	SO_2	CH_3O	NO_2	446.1	492.4
17	SO_2	NH_2	NO_2	431.2	490.0
18	SO_2	CH_3O	CH_3	443.5	451.7
19	SO_2	CH_3	NO_2	456.1	493.8
20	O	CH_3O	NO_2	418.2	454.5
21	O	NH_2	NO_2	407.1	452.5
22	O	CH_3O	CH_3	414.2	417.7
23	O	CH_3	NO_2	425.5	455.7
24	CH_2	CH_3O	NO_2	417.5	463.5
25	CH_2	NH_2	NO_2	407.2	462.8
26	CH_2	CH_3O	CH_3	417.8	425.1

*All figures in c.p.s. from tetramethylsilane internal standard in $CDCl_3$ solution (2.5% W/W), calibrated on singlet peak of residual $CHCl_3$ at 435 c.p.s.

collected for the three other diphenyl sulfides whose sulfoxides and sulfones were used in this study together with their corresponding ethers and methylenes (see Table IV, first four lines). There are some notable exceptions, however.

In general the changes in the shifts are largest for the sulfide-bridged molecules with the exception of the 4-methoxy-4′-methyl-disubstituted sulfide; here the behavior is more comparable with the shift changes observed for the sulfoxides and sulfones. This may be a reflection of the fact that both substituents are electron donors, working against each other. The necessary "incentive" for the bridging sulfur to transmit may therefore be missing in this case, as was suggested by Szmant and McIntosh (7) in their study of the ultraviolet spectra of some other diphenyl sulfides.

The methylene-bridged compounds were included in this study because it was not expected that they would transmit by other than an inductive mechanism, and therefore would serve as a useful reference. Indeed, all changes in the shifts for both rings in the substituted diphenylmethane compounds are positive. This strongly suggests that these changes arise from a diamagnetic anisotropy effect resulting from the replacement of the terminal methyl group in the "half molecule" by the aromatic ring in the "whole molecule". Since this shift effect is extraneous to the transmission effect, these data serve to establish the fact that changes in shift of the order of 2 c.p.s. can not be considered as meaningful as far as the study of transmission is concerned. This would conveniently account for many of the minor shift variations listed in Table IV but it does not account for the very sizeable negative variations (decreased electron density) in the shifts observed in the X-substituted ring of the oxygen-bridged compounds (see Table IV). There is no corresponding positive variation

TABLE III

Chemical shift of the aromatic multiplet of *para*-disubstituted benzenes ("half molecules")

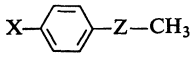

Compound	Z	X	Chemical shift in c.p.s.* of center of AB quartet
27	S	CH_3	429.3
28	S	CH_3O	423.5
29	S	NH_2	413.2
30	S	NO_2	461.8
31	S	H	435.4
32	S	$(CH_3)_2N$	418.8
33	S	Br	434.8
34	S	Cl	432.6
35	SO	CH_3	444.3
36	SO	CH_3O	436.2
37	SO	NH_2	423.6
38	SO	NO_2	486.5
39	SO_2	CH_3	455.3
40	SO_2	CH_3O	445.0
41	SO_2	NH_2	430.6
42	SO_2	NO_2	497.5
43	O	CH_3	416.4
44	O	CH_3O	408.9
45	O	NH_2	399.8
46	O	NO_2	454.7
47	CH_2	CH_3	426.9
48	CH_2	CH_3O	418.3
49	CH_2	NH_2	408.4
50	CH_2	NO_2	464.9

*All figures in c.p.s. from tetramethylsilane internal standard in $CDCl_3$ solution (2.5% W/W), calibrated on singlet peak of residual $CHCl_3$ at 435 c.p.s.

Can. J. Chem. Downloaded from www.nrcresearchpress.com by 210.87.254.42 on 09/05/12
For personal use only.

TABLE IV

Changes in chemical shifts (in c.p.s.)* associated with the center of aromatic multiplets, calculated as in Table I ("whole molecule" compared with "half molecule")†

		Z									
		S		SO		SO_2		O		CH_2	
X	Y	X-C_6H_4-	Y-C_6H_4-	X-C_6H_4-	Y-C_6H_4-	X-C_6H_4-	Y-C_6H_4-	X-C_6H_4-	Y-C_6H_4-	X-C_6H_4-	Y-C_6H_4-
CH_3	NO_2	−11.6	+6.7	−0.9	+2.5	−0.8	+3.7	−9.1	−1.0		
CH_3O	NO_2	− 9.9	+7.8	+0.8	+4.3	−1.1	+5.1	−9.3	+0.2	+0.8	+1.4
NH_2	NO_2	− 8.0	+7.6	+2.4	+5.5	−0.6	+7.5	−7.3	+2.2	+1.2	+2.1
CH_3O	CH_3	− 3.5	+2.3	+2.0	+2.7	+1.5	+3.6	−5.3	−1.3	+0.5	+1.8
CH_3	H	− 4.6	−0.6								
H	NO_2	−13.6	+4.8								
$(CH_3)_2N$	NO_2	− 4.6	+8.6								
NH_2	CH_3	− 4.6	+5.1								
Cl	NO_2	−13.3	+3.7								
CH_3	Br	− 4.1	+1.0								
CH_3	Cl	− 4.2	+0.4								

*A negative change indicates a downfield shift, i.e., the protons in the diphenyl compound are less shielded than in the corresponding ring in the "half molecule".

†Compounds of structure 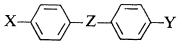

.

Can. J. Chem. Downloaded from www.nrcresearchpress.com by 210.87.254.42 on 09/05/12
For personal use only.

(increase in electron density) observed in the Y-substituted ring as is the case in the sulfides.

At first sight it is hardly conceivable that the flow of electron density from the donor ring of the oxygen-bridged compounds would find its way on to the oxygen without being subsequently transmitted to the acceptor ring by some mechanism. The findings of Marcus *et al.* (18) are of interest in this regard. These authors concluded on the basis of results of their own n.m.r. study as well as of the work of others that in conjugative roles sulfur is a better transmitter than oxygen when acting as an acceptor or acceptor–donor of negative charge, but that the situation is reversed when only conjugative donation by the bridging atom is called for. When this conclusion is accepted it is clear that the relative order of the sulfur and oxygen bridge-effects may depend to a great extent on the role these atoms are called upon to play by the specific relative nature of the two *para*-substituents on the aromatic rings. Indeed, it is possible using these conclusions by Marcus *et al.* to account qualitatively for the marked differences in the shift changes (Table IV) obtained for sulfur and oxygen-bridged compounds where strong donor and acceptor groups are present as substituents, i.e. in the case of the combinations of CH_3O— with NO_2—, and of NH_2— with NO_2—. In the other two cases where comparison is possible between O and S as a bridging atom, i.e. in the case of the combinations of CH_3— with NO_2—, and of CH_3O— with CH_3— as *para*-substituents, the predictions on the basis of the same conclusions of Marcus *et al.* (18) do not always agree with the changes in the shift.

There are probably many interesting facts relevant to the problem hidden within the many minor changes in shift as tabulated in Table IV. However, there are also a number of minor perturbing factors at work which are not directly related to the transmission problem. We are obliged therefore to restrict our attention to *the more salient features of the data* and accordingly limit our conclusion to the fact that there is evidence for the existence of a transmission mechanism across the sulfide bridge that is absent in the cases of the sulfoxide, sulfone and methylene bridges. There does not appear to be a similar transmission mechanism operative in the oxygen bridge but some type of deshielding of the donor ring protons takes place when oxygen is flanked by two π-electron systems.

In the case of the sulfides, where transmission appears to be operative, the study was extended to cover a wider range of substituents (see Table IV). In all but one of these compounds the donor ring is deshielded and the acceptor ring shows increased shielding. The exception is the case where CH_3— and H— are the substituents; conjugative interaction would be expected to be weaker.

The deshielding of the donor ring in the *p*-nitro-substituted diphenyl sulfide coupled with the increase in shielding in the nitro-substituted acceptor ring provides evidence for a transmission process and is in contrast with the conclusion reached by Szmant and McIntosh (7). On the basis of their ultraviolet studies, there is no evidence for involvement of the resonance structure:

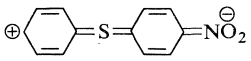

Wehry (15) found that when donor–acceptor type conjugation is present in the ground state of sulfides it must be expected to increase upon excitation, unless electron releasing p_π conjugation is sterically inhibited.

The data obtained for the 4-chloro-4′-nitro-substituted diphenyl sulfide (see Table IV) indicate that in the presence of the powerful electron withdrawing nitro group the chloro substituent is also forced to act as a donor.

Conclusion

The n.m.r. evidence presented supports the conclusion that intramolecular transmission of electronic effects between a donor and acceptor moiety occurs more readily across a sulfide bridge than across sulfoxide, sulfone, ether or methylene bridges. The extent to which such transmission occurs, however, is strongly dependent upon the nature of the donor and acceptor functions and the availability of a mechanism for establishing a sufficient degree of polarization across the bridging function to provide sufficient "incentive" for the bridging function to act as a conductor as opposed to an insulator.

Experimental

Nuclear magnetic resonance spectra were recorded on a Varian A-60 spectrometer. The concentration of the solutions was 2.5% (W/W) in $CDCl_3$, with tetramethylsilane as an internal reference. All spectra were run at a

Can. J. Chem. Downloaded from www.nrcresearchpress.com by 210.87.254.42 on 09/05/12
For personal use only.

sweep width of 500 c.p.s., but the aromatic multiplets were always re-run at sweep widths of 100 or 50 c.p.s. In this region the residual $CHCl_3$ in the solvent served as a convenient standard for calibration (at 435 c.p.s. from tetramethylsilane).

Microanalyses were carried out by Mrs. S. Bagley, and the nuclear magnetic resonance spectra were recorded by Mrs. V. Boon, both of the Department of Chemistry, The University of Calgary.

Most of the compounds used in this study had been reported previously and several were commercially available. The data for those prepared follow. Melting points are not corrected. Numbers given to compounds refer to the listing in Tables II and III.

Preparation of Sulfides

(a) Methyl Phenyl Sulfides

Most of the methyl phenyl sulfides were prepared by methylation of the corresponding thiols, using the procedure of Gilman and Beaber (19): 1-bromo-4-(methylthio)benzene (**33**), m.p. 38–39° from aqueous methanol (lit. m.p. 38° (20)); 1-chloro-4-(methylthio)-benzene (**34**), b.p. 87° at 5 mm (lit. b.p. 170° (21)); 4-(methylthio)toluene (**27**), b.p. 82° at 6 mm (lit. 104–105° at 20 mm (19)); 1-(methylthio)-4-nitrobenzene (**30**), m.p. 71–72° from methanol (lit. m.p. 72° (22)); 4-(methylthio)-anisole (**28**), b.p. 100° at 5 mm (lit. b.p. 99° at 4 mm (23)); *N,N*-dimethyl-4-(methylthio)aniline (**32**), b.p. 74–77° at 0.13–0.20 mm (lit. b.p. 140° at 3 mm (5)).

4-(Methylthio)aniline (**29**) was prepared as reported (24), b.p. 74° at 0.15 mm (lit. b.p. 155° at 23 mm (24)).

(b) Diphenyl Sulfides

The procedure given by Gilman and Broadbent (25) was used for the preparation of the following sufides: 4-(*p*-nitrophenylthio)anisole (**1**), m.p. 67–68° from ethanol (lit. m.p. 67–68° (26)); 4-(*p*-nitrophenylthio)-toluene (**4**), m.p. 80–82° from ethanol (lit. m.p. 80–81° (25)); (*p*-nitrophenylthio)benzene (**6**), m.p. 55–56° from ethanol (lit. m.p. 55° (25)); *N,N*-dimethyl-4-(*p*-nitrophenylthio)aniline (**7**), m.p. 181.5–183° from ethanol–chloroform (lit. m.p. 181° (4)); 1-chloro-4-(*p*-nitrophenylthio)benzene (**9**), m.p. 85–87° from ethanol (lit. m.p. 83–84° (25), 88° (27)).

Diazotization of *p*-anisidine, *p*-bromoaniline, and *p*-chloraniline, followed by reaction with a solution of the appropriate sodium thiolate (28, 29) gave the following sulfides respectively: 4-(*p*-tolylthio)anisole (**3**), b.p. 145–149° at 0.8 mm, m.p. 43–45° from 95% ethanol (lit. b.p. 181–182° at 4 mm, m.p. 45–46° (28)); 4-(*p*-bromophenylthio)toluene (**10**), m.p. 82.5–83.5° from methanol (lit. m.p. 82.5° (30)); 4-(*p*-chlorophenylthio)toluene (**11**), m.p. 72–74° from methanol (lit. m.p. 72–73° (31)).

The method described by Campbell (32) was used for the preparation of *p*-(phenylthio)toluene (**5**), b.p. 137–140° at 3.2 mm (lit. 169° at 13 mm (29)).

4-(*p*-Nitrophenylthio)aniline (**2**) was prepared from *p*-chloronitrobenzene (33), m.p. 144–145.5° from ethanol (lit. m.p. 145° (33)). Acetylation of this amine gave 4′-(*p*-nitrophenylthio)acetanilide, m.p. 196.5–198° from methanol (lit. m.p. 198° (33)).

4-(*p*-Tolylthio)aniline (**8**) was prepared by reduction of the corresponding nitro compound with stannous chloride (34), m.p. 72.5–73.5° from 50% ethanol, as reported (35).

Preparation of Sulfoxides

A variety of oxidation methods was used for the preparation from the corresponding sulfides.

(a) Methyl Phenyl Sulfoxides

4-(Methylsulfinyl)toluene (**35**) was prepared by oxidation with sodium periodate (36), m.p. 42–44° (lit. m.p. 42–43° (37)). 1-(Methylsulfinyl)-4-nitrobenzene (**38**) was prepared by oxidation with H_2O_2 in glacial acetic acid (38), m.p. 147–149° after repeated crystallizations from benzene (lit. m.p. 151–152° from benzene (38)).

4-(Methylsulfinyl)anisole (**36**) was prepared by oxidation with H_2O_2 in acetone as described by Ghersetti and Palotti (39), b.p. 110–115° at 0.1 mm, m.p. 44–45° from low-boiling petroleum ether (lit. m.p. 43°, b.p. 153–154° at 5 mm (37)). This oxidation method was also used for the preparation of 4-(methylsulfinyl)aniline (**37**). In this case it was found to be advantageous to keep the reaction mixture in the dark for 2–4 days. It was necessary to purify the crude sulfoxide by chromatography on an alumina column as described by Ghersetti and Palotti (39) for some other sulfoxides. Using the eluents benzene, benzene–chloroform (1:1), chloroform and finally ethanol, the sulfoxide was isolated from the ethanol fraction, m.p. 96–96.5° from chloroform – petroleum ether (1:1); lit. m.p. 95–96° (39).

(b) Diphenyl Sulfoxides

Most required diphenyl sulfoxides were prepared using the same procedure: the sulfide and the theoretically required quantity of hydrogen peroxide (30% aqueous solution) were mixed, and glacial acetic acid was added until the mixture had become homogeneous after thorough mixing. The mixture was left standing for 4–7 days at about 20°. Water was added and the mixture was extracted with chloroform, from which the sulfoxide was isolated. The following sulfoxides were prepared by this method.

4-(*p*-Nitrophenylsulfinyl)toluene (**15**), m.p. 125.5–126.5° after crystallization from methanol (2 times) and petroleum ether.

Anal. Calcd. for $C_{13}H_{11}NO_3S$: C, 59.76; H, 4.24; N, 5.36. Found: C, 59.92; H, 3.93; N, 5.05.

4-(*p*-Tolylsulfinyl)anisole (**14**), m.p. 69–70° after crystallization from aqueous methanol and petroleum ether.

Anal. Calcd. for $C_{14}H_{14}O_2S$: C, 68.26; H, 5.73. Found: C, 67.98; H, 5.69.

4-(*p*-Nitrophenylsulfinyl)anisole (**12**), m.p. 122° from petroleum ether.

Anal. Calcd. for $C_{13}H_{11}NO_4S$: C, 56.31; H, 4.00; N, 5.05. Found: C, 56.01; H, 3.90; N, 4.93.

Deacetylation of crude 4′-(*p*-nitrophenylsulfinyl)-acetanilide with m.p. 194–196°, prepared according to Gabel and Grinberg (40), gave 4-(*p*-nitrophenylsulfinyl)-aniline (**13**), m.p. 130–131° from water, as reported (7).

Preparation of Sulfones

All sulfones, except where indicated, were prepared by oxidation of the corresponding sulfides with hydrogen peroxide in refluxing glacial acetic acid.

(a) Methyl Phenyl Sulfones

4-(Methylsulfonyl)toluene (**39**), m.p. 88–89° from ethanol, as reported (41); 4-(methylsulfonyl)anisole

Can. J. Chem. Downloaded from www.nrcresearchpress.com by 210.87.254.42 on 09/05/12
For personal use only.

(**40**), m.p. 120–121° from water (lit. m.p. 121° (42)); 1-(methylsulfonyl)-4-nitrobenzene (**42**), m.p. 142–143° from methanol (lit. m.p. 142.5° (43)). Low pressure hydrogenation of the latter compound using Raney nickel catalyst as described by Gilman and Broadbent (25) gave an 80% yield of 4-(methylsulfonyl)aniline (**41**), m.p. 136.5–137.5° from water (lit. m.p. 134–135° (44)).

(b) Diphenyl Sulfones

4-(*p*-Nitrophenylsulfonyl)toluene (**19**), m.p. 171–172.5° from ethanol, as reported (25); 4-(*p*-tolylsulfonyl)-anisole (**18**), m.p. 102.5–104° from petroleum ether containing 5% *p*-dioxane (lit. m.p. 103–104.5° (45)); 4′-(*p*-nitrophenylsulfonyl)acetanilide, m.p. 227–229° from tetrahydrofuran (lit. m.p. 229–230° (33)). Deacetylation of this compound (46) gave 4-(*p*-nitrophenylsulfonyl)-aniline (**17**), m.p. 170–171° from methanol (lit. m.p. 168–169° (46)).

4-(*p*-Nitrophenylsulfonyl)anisole (**16**), a compound not yet reported to our knowledge, was also prepared by oxidation of the corresponding sulfide. After crystallization from ethanol m.p. 162–163.5°.

Anal. Calcd. for $C_{13}H_{11}NO_5S$: C, 54.16; H, 3.85; N, 4.86. Found: C, 53.93; H, 4.01; N, 4.84.

Preparation of Diphenyl Ethers

4-(*p*-Nitrophenoxy)aniline (**21**) was prepared from 4′-hydroxyacetanilide and 1-bromo-4-nitrobenzene according to Ikawa (47), m.p. 134° from ethanol (lit. m.p. 133° (47)). The same method was used for the preparation of 1-methoxy-4-(*p*-nitrophenoxy)benzene (**20**), m.p. 111° from methanol, as reported (48), and for the preparation of 1-methoxy-4-(*p*-tolyloxy)benzene (**22**). Even after many recrystallizations the m.p. 52–53° reported by Tomita and Ikawa (49) for the last compound could not be duplicated, but remained at 46–47° (from petroleum ether), in agreement with the m.p. 47–48° reported by Harrington (50). 4-(*p*-Nitrophenoxy)toluene (**23**) was prepared as reported (51), m.p. 67° (sharp) from petroleum ether. Tomita and Ikawa (52) report a m.p. 82°. This could not be duplicated, but our m.p. is in better agreement with another reported value, m.p. 69° (53).

Preparation of Diphenyl Methanes

α-(*p*-Nitrophenyl)*p*-toluidine (**25**) was prepared by nitration of *p*-benzylaniline (54, 55), m.p. 98–99° from ethanol (lit. 97.5–98.5° (54)). The required *p*-benzylaniline was prepared by reduction of the corresponding nitro compound with iron powder in aqueous acetic acid (56) and isolated as its *N*-acetyl derivative, m.p. 120° for the crude product (lit. m.p. 125–126° (57)). 4-(*p*-Methylbenzyl)anisole (**26**), prepared as reported by Pratt *et al.* (58) was found to be impure and contaminated with what seemed to be 2-(*p*-methylbenzyl)anisole, on the basis of the n.m.r. spectrum of the distilled product. An attempt to separate the two isomers on an alumina column failed. The compound was finally prepared by a method described by Houston (59). In this preparation a mixture of the two isomers was obtained again, but the pure *para* isomer could be obtained after careful distillation:

To a well stirred mixture of 30.5 g (0.25 mole) of *p*-methylbenzyl alcohol, and 39 g (0.36 mole) of anisole in 100 ml of low-boiling petroleum ether were added 18.8 g (0.14 mole) of aluminium trichloride in small portions over a period of 30 min. The temperature was kept at 15–25°. After standing overnight, ice, water and hydrochloric acid were added, as well as ether. After work-up and distillation of the products (a fore-run of anisole was collected) two main fractions were collected. The first fraction, weighing 19.75 g, collected at 99–101° (0.13–0.15 mm), n_D^{25} 1.5696 contained again a mixture of the *ortho* and *para* isomers. The second fraction, weighing 5.80 g, distilling at 103–109° (0.08–0.15 mm), n_D^{25} 1.5691, was the desired 4-(*p*-methylbenzyl)anisole (lit. b.p. 140–145° at 2.7 mm, n_D^{25} 1.5671 (58)).

4-(*p*-Nitrobenzyl)anisole (**24**) was prepared according to Blackwell and Hickinbottom (60). The crude product, a yellow oil, was purified by chromatography on aluminium oxide, and the compound was isolated from the first eluent fraction (petroleum ether – benzene 5:1). After recrystallization from methanol m.p. 70–71° (lit. m.p. 61° (60)).

Acknowledgment

The authors wish to acknowledge the capable technical assistance of Mrs. D. J. Bird who did most of the preparative work.

1. J. B. Hyne and J. W. Greidanus. *In* Chemistry of sulfides. *Edited by* A. V. Tobolsky. Interscience Publishers, Inc., New York. 1968. p. 83.
2. G. Cilento. Chem. Rev. **60**, 147 (1960).
3. C. C. Price and S. Oae. Sulfur bonding. The Ronald Press Co., New York. 1962.
4. A. Mangini and R. Passerini. J. Chem. Soc. 1168 (1952).
5. A. Mangini and R. Passerini. J. Chem. Soc. 4954 (1956).
6. A. Mangini. Pure Appl. Chem. 103 (1963).
7. H. H. Szmant and J. J. McIntosh. J. Am. Chem. Soc. **73**, 4356 (1951).
8. R. Zahradnik and K. Bocek. Collection Czech. Chem. Commun. **26**, 1733 (1961).
9. K. Bocek, A. Mangini, and R. Zahradnik. J. Chem. Soc. 225 (1963).
10. H. Hogeveen. Rec. Trav. Chim. **83**, 813 (1964).
11. L. M. Litvinenko, R. S. Cheshko, and S. V. Tsukerman. Dokl. Akad. Nauk SSSR **118**, 946 (1958); Chem. Abstr. **52**, 12810*h* (1958).
12. L. M. Litvinenko, S. V. Tsukerman, R. S. Cheshko, and B. M. Kolesnikova. Zh. Obshch. Khim. **27**, 1663 (1957); Chem. Abstr. **52**, 4546*c* (1958).
13. L. M. Litvinenko and R. S. Cheshko. Zh. Obshch. Khim. **30**, 3682 (1960); Chem. Abstr. **55**, 19846*g* (1961).
14. L. M. Litvinenko. Izv. Akad. Nauk SSSR, Otd. Khim. Nauk, 1737 (1962); Chem. Abstr. **58**, 12397*c* (1963).
15. E. L. Wehry. J. Am. Chem. Soc. **89**, 41 (1967).
16. L. Goodman and R. W. Taft. J. Am. Chem. Soc. **87**, 4385 (1965).
17. M. C. Caserio, R. E. Pratt, and R. J. Holland. J. Am. Chem. Soc. **88**, 5747 (1966).
18. S. H. Marcus, W. F. Reynolds, and S. I. Miller. J. Org. Chem. **31**, 1872 (1966).
19. H. Gilman and N. J. Beaber. J. Am. Chem. Soc. **47**, 1449 (1925).
20. F. G. Bordwell and H. M. Andersen. J. Am. Chem. Soc. **75**, 6019 (1953).
21. K. Brand and W. Groebe. J. Prakt. Chem. **108**, 1 (1924); Chem. Abstr. **18**, 3180 (1924).

22. H. J. BACKER and J. GROOT. Rec. Trav. Chim. **69**, 1323 (1950).
23. C. M. SUTER and H. L. HANSEN. J. Am. Chem. Soc. **54**, 4100 (1932).
24. R. L. LANTZ, G. MINGASSON, and H. DELARUE. Bull. Soc. Chim. France, 1201 (1957).
25. H. GILMAN and H. S. BROADBENT. J. Am. Chem. Soc. **69**, 2053 (1947).
26. A. MANGINI, R. PASSERINI, and S. SERRA. Gazz. Chim. Ital. **84**, 47 (1954).
27. H. BURTON and E. HOGGARTH. J. Chem. Soc. 468 (1945).
28. G. E. HILBERT and T. B. JOHNSON. J. Am. Chem. Soc. **51**, 1526 (1929).
29. M. ROLLA, M. SANESI, and G. LEANDRI. Ann. Chim. Rome, **42**, 664 (1952).
30. E. BOURGEOIS and A. FOUASSIN. Rec. Trav. Chim. **30**, 426 (1911).
31. F. KROLLPFEIFFER and A. WISSNER. Ann. Chem. **572**, 195 (1951).
32. J. R. CAMPBELL. J. Org. Chem. **29**, 1830 (1964).
33. G. W. RAIZISS, L. W. CLEMENCE, M. SEVERAC, and J. C. MOETSCH. J. Am. Chem. Soc. **61**, 2763 (1939).
34. C. C. PRICE, N. J. LEONARD, and G. W. STACY. J. Am. Chem. Soc. **69**, 855 (1947).
35. G. H. LAW and T. B. JOHNSON. J. Am. Chem. Soc. **52**, 3623 (1930).
36. N. J. LEONARD and C. R. JOHNSON. J. Org. Chem. **27**, 282 (1962).
37. A. CERNIANI and G. MODENA. Gazz. Chim. Ital. **89**, 843 (1959).
38. G. LEANDRI, A. MANGINI, and R. PASSERINI. J. Chem. Soc. 1386 (1957).
39. S. GHERSETTI and M. PALOTTI. Gazz. Chim. Ital. **93**, 1000 (1963).
40. Y. O. GABEL and F. L. GRINBERG. J. Appl. Chem. USSR English Transl. **12**, 1481 (1939); Chem. Abstr. **34**, 6244 (1940).
41. L. KATZ, L. S. KARGER, W. SCHROEDER, and M. S. COHEN. J. Org. Chem. **18**, 1380 (1953).
42. A. MANGINI, L. RUZZIER, and A. TUNDO. Boll. Sci. Fac. Chim. Ind. Bologna, **14**, 81 (1956).
43. W. R. WALDRON and E. E. REID. J. Am. Chem. Soc. **45**, 2399 (1923).
44. L. M. YAGUPOLSKII and M. S. MARENETS. Zh. Obshch. Khim. **27**, 1395 (1957); Chem. Abstr. **52**, 2781 *i* (1958).
45. H. H. SZMANT and G. SULD. J. Am. Chem. Soc. **78**, 3400 (1956).
46. M. S. ZHEDEK. Zh. Prikl. Khim. **25**, 109 (1952); Chem. Abstr. **47**, 867*a* (1953).
47. K. IKAWA. Yakugaku Zasshi, **79**, 764 (1959); Chem. Abstr. **53**, 21761*h* (1959).
48. K. IKAWA. Yakugaku Zasshi, **79**, 1493 (1959); Chem. Abstr. **54**, 10922*h* (1960).
49. M. TOMITA and K. IKAWA. J. Pharm. Soc. Japan, **74**, 1061 (1954); Chem. Abstr. **49**, 11591*a* (1955).
50. C. R. HARRINGTON. Biochem. J. **20**, 300 (1926).
51. R. Q. BREWSTER and T. GROENING. *In* Organic syntheses. Coll. Vol. II. *Edited by* A. H. Blatt. John Wiley and Sons, Inc., New York. 1943. p. 445.
52. M. TOMITA and K. IKAWA. J. Pharm. Soc. Japan, **74**, 1065 (1954); Chem. Abstr. **49**, 11592*a* (1955).
53. C. HAEUSSERMANN and O. SCHMIDT. Chem. Ber. **34**, 3769 (1901).
54. R. S. TSEKHANSKII. Izv. Vysshikh Uchebn. Zavedenii, Khim. i Khim. Tekhnol. **4**, 691 (1961); Chem. Abstr. **56**, 3383*h* (1962).
55. R. S. TSEKHANSKII and L. I. VINOGRADOV. Zh. Obshch. Khim. **32**, 3802 (1962); Chem. Abstr. **58**, 12444*b* (1963).
56. R. N. CASTLE and D. B. COX. J. Org. Chem. **19**, 1117 (1954). J. C. E. SIMPSON, C. M. ATKINSON, K. SCHOFIELD, and O. STEPHENSON. J. Chem. Soc. 646 (1945). J. C. E. SIMPSON. J. Chem. Soc. 94 (1946).
57. F. G. MANN and F. H. C. STEWART. J. Chem. Soc. 4127 (1954).
58. E. F. PRATT, R. K. PRESTON, and J. D. DRAPER. J. Am. Chem. Soc. **72**, 1367 (1950).
59. R. C. HOUSTON. J. Am. Chem. Soc. **46**, 2775 (1924).
60. J. BLACKWELL and W. J. HICKINBOTTOM. J. Chem. Soc. 366 (1963).

Can. J. Chem. Downloaded from www.nrcresearchpress.com by 210.87.254.42 on 09/05/12
For personal use only.

Can. J. Chem. Downloaded from www.nrcresearchpress.com by 210.87.254.42 on 09/05/12
For personal use only.

Tetrazolylacetic acids

R. RAAP AND J. HOWARD[1]
R. and L. Molecular Research Limited, 8045 Argyll Road, Edmonton 82, Alberta
Received June 3, 1968

The syntheses of several 1-,2- and 5-tetrazolylacetic acids are described. Isomeric tetrazolylacetic esters can be separated by fractional distillation or crystallization. 5-Hydroxytetrazole reacts with ethyl bromoacetate in the presence of triethylamine to give 1,4-dicarbethoxymethyl-5-tetrazolone. The use of nuclear magnetic resonance spectroscopy for the assignment of structural isomers is discussed.

Canadian Journal of Chemistry, **47**, 813 (1969)

In our search for precursors for arylmethylpenicillins (1) we recently prepared several 1-, 2-, and 5-tetrazolylacetic acids. This report describes the syntheses and some of the properties of these acids.

Alkylation of the triethylammonium salt of the tetrazole **1** with either ethyl bromoacetate or methyl chloroacetate generally provided a mixture of the 1- and 2-tetrazolylacetic esters **2** and **3**. Separation of the isomers was effected by fractional crystallization (the 2-isomers were more soluble in organic solvents than the corresponding 1-isomers) or by fractional distillation. The boiling points of the 2-isomers were considerably below those of the corresponding 1-isomers, a behavior which had been noted before in similar instances (2, 3). The predominance of the 1- or 2-isomer depended strongly on the 5-substituent R. Whereas from 5-methyltetrazole and ethyl bromoacetate more than twice as much ethyl 5-methyl-1-tetrazolylacetate than ethyl 5-methyl-2-tetrazolylacetate was obtained, 5-chlorotetrazole gave under the same conditions at least seven times as much 2-isomer than 1-isomer. This effect has been observed before (3–5) and is probably a result of electrostatic interactions giving rise to localization of the negative charge of the tetrazole anion in the 1- or 2-position, depending on the electropositive or electronegative character of the 5-substituent.

Alkylation of the triethylammonium salt of methyl 5-tetrazolylacetate with an alkyl halide provided a mixture of the isomeric 5-tetrazolylacetic esters **4** and **5**, which again could be separated by fractional distillation. Whereas the reaction with methyl iodide gave a 1:1 mixture of the 1- and 2-isomer, with isopropyl bromide this ratio was 3:1 in favor of the 2-isomer, indicating that not only electronic factors control the isomer distribution, but that steric factors can also play an important role.

The reaction of 5-hydroxytetrazole and ethyl bromoacetate in the presence of triethylamine

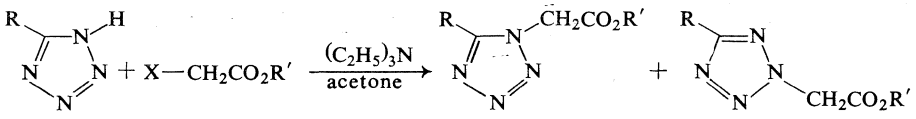

1 **2** **3**

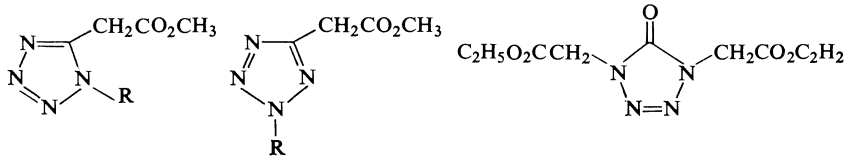

4 **5** **6**

[1]Present address: Research Department, Rayonier Inc., Shelton, Washington.

TABLE I

1-Tetrazolylacetic acids, 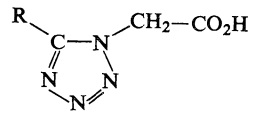

R	Empirical formula	Method of isolation	Melting point, °C	% C Calcd. (Found)	% H Calcd. (Found)	% N Calcd. (Found)
H*	$C_3H_4N_4O_2$	*a*	127–129	28.13 (28.31)	3.15 (3.31)	43.74 (44.01)
CH_3*	$C_4H_6N_4O_2$	*a*	184–186 (decomp.)	33.81 (33.78)	4.26 (4.33)	39.43 (39.41)
C_2H_5†	$C_5H_8N_4O_2$	*b*	135–136	38.52 (38.65)	5.17 (5.40)	35.88 (36.22)
n-C_3H_7†	$C_6H_{10}N_4O_2$	*b*	106–108	42.34 (42.35)	5.92 (6.12)	32.92 (33.12)
C_6H_5	$C_9H_8N_4O_2$	*c*	148–150 (decomp.)	52.94 (52.58)	3.95 (3.85)	27.44 (27.50)
$(CH_3)_2N$-CH_2	$C_6H_{11}N_5O_2$		187–189 (decomp.)	38.91 (38.98)	5.99 (6.00)	37.83 (38.40)
CF_3‡	$C_4H_3F_3N_4O_2$	*a*	Oil	24.62 (25.08)	2.07 (2.27)	35.90 (36.40)
CH_3S*	$C_4H_6N_4O_2S$	*b, c*	173–174 (decomp.)	27.58 (27.60)	3.47 (3.66)	32.16 (32.00)
NH_2	$C_3H_5N_5O_2$	*a*	202–203 (decomp.)	25.18 (25.22)	3.52 (3.65)	48.96 (49.22)
Cl§	$C_3H_3ClN_4O_2$	*a*	—	22.30 (22.94)	2.50 (2.95)	43.36 (42.80)
Br‖	$C_3H_3BrN_4O_2$	*a*	—	17.49 (17.57)	1.96 (1.85)	34.00 (34.30)

*Recrystallization solvent: ethyl acetate.
†Recrystallization solvent: ethyl acetate – hexane.
‡The analysis was obtained on the amide, $C_4H_4F_3N_5O$, m.p. 146–147° (recrystallized from ethyl acetate).
§The analysis was obtained on the amide, $C_3H_4ClN_5O$, m.p. 125–127° (recrystallized from ethyl acetate).
‖The analysis was obtained on the amide, $C_3H_4BrN_5O$, m.p. 145–146° (decomp.) (recrystallized from ethyl acetate).

TABLE II

2-Tetrazolylacetic acids, 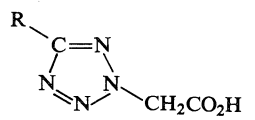

R	Empirical formula	Method of isolation	Melting point, °C	% C Calcd. (Found)	% H Calcd. (Found)	% N Calcd. (Found)
H*	$C_3H_4N_4O_2$	*a*	175–176	28.13 (28.46)	3.15 (3.34)	43.74 (44.08)
CH_3†	$C_4H_6N_4O_2$	*a*	155–156	33.81 (33.90)	4.26 (4.45)	39.43 (39.62)
C_2H_5†	$C_5H_8N_4O_2$	*b*	95–97	38.52 (38.69)	5.17 (5.29)	35.88 (36.21)
n-C_3H_7‡	$C_6H_{10}N_4O_2$	*b*	91–93	42.34 (42.59)	5.92 (5.92)	32.92 (33.20)
C_6H_5†	$C_9H_8N_4O_2$	*c*	182–184 (decomp.)	52.94 (52.48)	3.95 (3.96)	27.44 (27.41)
CF_3‖	$C_4H_3F_3N_4O_2$	*a*	Oil	24.62 (24.78)	2.07 (2.40)	35.90 (36.30)
CH_3S§	$C_4H_6N_4O_2S$	*c*	127–129	27.58 (27.37)	3.47 (3.40)	32.16 (32.40)
CH_3SO_2†	$C_4H_6N_4O_4S$	*b*	102–105	23.31 (23.06)	2.93 (3.26)	27.18 (27.40)
NH_2¶	$C_3H_5N_5O_2$	*a*	185–186 (decomp.)	35.08 (35.20)	5.30 (5.14)	40.92 (41.18)
Cl§	$C_3H_3ClN_4O_2$	*a, b*	100–101	22.16 (22.36)	1.86 (2.11)	34.47 (34.70)
Br§	$C_3H_3BrN_4O_2$	*a, b*	111–113	17.41 (17.63)	1.46 (1.63)	27.06 (26.95)

*Recrystallization solvent: ethyl acetate.
†Recrystallization solvent: ethyl acetate – hexane.
‡Recrystallization solvent: benzene–hexane.
§Recrystallization solvent: chloroform.
‖The analysis was obtained on the amide, $C_4H_4F_3N_5O$, m.p. 115–116° (recrystallized from ethyl acetate – hexane).
¶The analysis was obtained on the ethyl ester, $C_5H_9N_5O_2$, m.p. 106–107°.

provided only 1,4-dicarbethoxymethyl-5-tetrazolone **6** both with one and two equivalents of the bromoacetate. This result was not too surprising in view of previously reported results on the alkylation of 1-alkyl-5-aminotetrazole (6) and the reaction of diazomethane with 5-acetamidotetrazole (7) and 5-hydroxytetrazole (8).

Tables I–III list the various 1-, 2-, and 5-tetrazolylacetic acids prepared from the corresponding esters by hydrolysis with methanolic sodium hydroxide.

Apart from the isomer assignment on basis of physical behavior, the position of the substituents in a few cases was determined by an

Can. J. Chem. Downloaded from www.nrcresearchpress.com by 210.87.254.42 on 09/05/12
For personal use only.

TABLE III

5-Tetrazolylacetic acids, 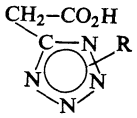

R*	Empirical formula	Method of isolation	Melting point, °C	% C Calcd. (Found)	% H Calcd. (Found)	% N Calcd. (Found)
H	$C_3H_4N_4O_2$	*a*	176–177 (decomp.)	28.13 (28.27)	3.15 (3.18)	43.74 (44.00)
1-CH_3	$C_4H_6N_4O_2$	*a*	83–84	33.81 (34.02)	4.26 (4.13)	39.43 (39.65)
2-CH_3	$C_4H_6N_4O_2$	*a*	119–121	33.81 (34.29)	4.26 (4.25)	39.43 (39.28)
1-C_2H_5	$C_5H_8N_4O_2$	*a*	96–98	38.52 (38.70)	5.17 (4.99)	35.88 (35.49)
2-C_2H_5	$C_5H_8N_4O_2$	*a*	99–101	38.52 (38.53)	5.17 (5.02)	35.88 (35.78)
1-*iso*-C_3H_7	$C_6H_{10}N_4O_2$	*b*	100–101	42.34 (42.33)	5.92 (5.78)	32.92 (32.61)
2-*iso*-C_3H_7	$C_6H_{10}N_4O_2$	*b*	109–112	42.34 (42.39)	5.92 (6.00)	32.92 (32.50)

*5-Tetrazolylacetic acid was recrystallized from aqueous acetic acid; all other acids were recrystallized from benzene – *n*-hexane mixtures.

unequivocal synthesis. *t*-Butyl 1-tetrazolylacetate was prepared from *t*-butyl isocyanoacetate and hydrazoic acid. The acid obtained from this ester was identical with the one prepared from the highest boiling ethyl tetrazolylacetate. This latter ester in turn was also obtained by reductive deamination of the ethyl 5-aminotetrazolylacetate isomer which was least soluble in organic solvents. Methyl 5-trifluoromethyl-1-tetrazolylacetate was prepared from trifluoroacetonitrile and methyl azidoacetate under the conditions given by Carpenter (9). The reaction between sodium 5-trifluoromethyltetrazole and ethyl bromoacetate gives rise to only one of the isomers of ethyl 5-trifluoromethyltetrazolylacetate. The acids and amides prepared from these esters were different, indicating that in the latter reaction the 2-isomer was produced. The reaction of methyl (methoxy-*N*-ethylcarbimino)-acetate (**7**) (10) with sodium azide in glacial acetic acid, conditions described by Hagedorn and Winkelmann (11), provided methyl 1-ethyl-5-tetrazolylacetate (**8**), identical with the higher boiling isomer obtained from methyl 5-tetrazolylacetate and ethyl bromide.

Nuclear magnetic resonance spectroscopy represents an excellent tool for assigning structural isomers in the tetrazole series. It has already been shown that 1- and 2-methyltetrazoles can readily be distinguished from one another as the signal of the 1-methyl group appears at a higher field than the 2-methyl group in the corresponding isomer (except in the 1- and 2-methyl-5-tetrazolylhydrazones where the signals coincide) (12–16). The 5-methyl group experiences approximately the same chemical shift in dimethyltetrazoles (12), the 5-proton in 1- and 2-alkyltetrazoles is however distinctively more shielded in the 2-isomer than in the corresponding 1-isomer (13, 17). The chemical shifts of some representative tetrazolylacetic acids and esters are listed in Table IV and similar trends as the above-mentioned ones are clearly noticeable. The carboxymethylene signals for the 1- and 2-tetrazolylacetic acids and esters appear at τ 4.60–4.95 and τ 4.29–4.67 respectively (for isomer pairs: $\Delta\tau$ = 0.23–0.33). Also interesting to note is the comparatively large difference in the degree of shielding of the 5-hydrogen, 5-carboxymethylene and 5-amino between corresponding 1- and 2-substituted isomers ($\Delta\tau$ = 0.30, 0.13–0.23, and 0.73 respectively) whereas this difference is small for the 5-methyl and the 5-methylthio group ($\Delta\tau$ = 0.05 and 0.10 respectively).

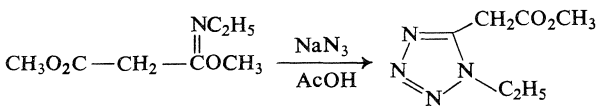

7 **8**

Can. J. Chem. Downloaded from www.nrcresearchpress.com by 210.87.254.42 on 09/05/12
For personal use only.

Can. J. Chem. Downloaded from www.nrcresearchpress.com by 210.87.254.42 on 09/05/12
For personal use only.

TABLE IV

Nuclear magnetic resonance parameters of certain tetrazolylacetic acids and esters, 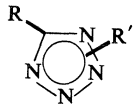

R	R′	CH_2—CO_2— 1-isomer	CH_2—CO_2— 2-isomer	Chemical shift (τ) others 1-isomer	Chemical shift (τ) others 2-isomer	Solvent
H	CH_2CO_2H	4.60	4.29	0.80(C^5—H)	1.10(C^5—H)	D_2O
CH_3	CH_2CO_2H	4.70	4.47	7.48(C^5—CH_3)	7.53(C^5—CH_3)	D_2O
Cl	CH_2CO_2H	4.64	4.40			D_2O
NH_2	CH_2CO_2H	4.89	4.63			D_2O
NH_2	$CH_2CO_2C_2H_5$	4.90	4.57	3.23(NH_2)	3.96(NH_2)	DMSO-d_6
CH_3S	$CH_2CO_2C_2H_5$	4.95	4.67	7.23(S—CH_3)	7.33(SCH_3)	CCl_4
CH_3SO_2	$CH_2CO_2C_2H_5$		4.30		6.54(SO_2CH_3)	$CDCl_3$
CF_3	$CH_2CO_2CH_3$	4.63		6.14(OCH_3)		$CDCl_3$
CF_3	$CH_2CO_2C_2H_5$		4.38		5.64(qu, CH_2); 8.67(t, CH_3)	CCl_4
CH_2CO_2H	H	5.86				D_2O
CH_2CO_2H	CH_3	5.84	6.07	5.97(N^1—CH_3)	5.65(N^2—CH_3)	DMSO-d_6*
CH_2CO_2H	C_2H_5	5.84	6.07	5.62(N^1—CH_2); 8.56(C—CH_3)	5.32(N^2—CH_2); 8.48(C—CH_3)	DMSO-d_6*
CH_2CO_2H	*iso*-C_3H_7	6.04	6.17	5.23(N^1—CH); 8.45($C(CH_3)_2$)	4.89(N^2—CH); 8.40($C(CH_3)_2$)	D_2O + K_2CO_3

*In D_2O solutions the carboxymethylene signal of the 1-isomer rapidly disappeared, indicating exchange of hydrogen for deuterium.

TABLE V

Tetrazolylacetic esters*

R	R′	X	Boiling point (mmHg), °C 1-isomer†	Boiling point (mmHg), °C 2-isomer	Yield, % 1-isomer†	Yield, % 2-isomer	Reaction conditions‡
H	$CH_2CO_2C_2H_5$	Br		85–87 (0.5)§	55	22	30 min at 0°, 1–3 h at 25°
CH_3	$CH_2CO_2C_2H_5$	Br	m.p. 75–77‖	81–83 (1.0)	49	22	30 min at 0°, 1–3 h at 25°
C_2H_5	$CH_2CO_2C_2H_5$	Br	158–163 (1.0)	100–107 (1.0)	37	28	30 min at 0°, 1–3 h at 25°
n-C_3H_7	$CH_2CO_2C_2H_5$	Br	139–141 (0.5)	79–85 (0.5)	46	26	30 min at 0°, 1–3 h at 25°
Cl	$CH_2CO_2CH_3$	Cl	m.p. 42–46	88–92 (1.0)	18	63	18 h reflux in acetonitrile
Cl	$CH_2CO_2C_2H_5$	Br	m.p. 54–58	91–93 (1.0)	9	66	18 h at 25°
Br	$CH_2CO_2CH_3$	Cl		95–100 (0.5)	21	64	18 h reflux in acetonitrile
CH_3S	$CH_2CO_2C_2H_5$	Br	124–125 (0.3)¶	96–97 (0.3)¶		91¶	30 min at 0°, 1–3 h at 25°
CH_3SO_2—	$CH_2CO_2C_2H_5$	Br		m.p. 72–74**	<10	62	48 h at 25°
CF_3	$CH_2CO_2C_2H_5$	Br		72–77 (1.0)	0	76	3 h reflux (Na–salt)
$CH_2CO_2CH_3$	CH_3	I	130–146 (0.5)††	89–92 (0.1)	40	41	18 h reflux
$CH_2CO_2CH_3$	C_2H_5	Br	174–175 (4)	119–121 (4)	30	58	18 h reflux
$CH_2CO_2CH_3$	*iso*-C_3H_7	Br		85–87 (0.3)	20	62	18 h reflux

* 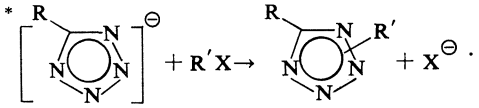

†The 1-isomer could not always be distilled; the yield in these instances refers to the amount of crude isomer.
‡Acetone was used as solvent except when indicated.
§m.p. 49–52°; reported b.p. 83.5–84°; m.p. 51–52° (26).
‖Reported m.p. 73–74° (27); the 1-isomer crystallized from the isomer mixture by the addition of ether.
¶The product mixture (b.p. 120–130° (0.4 mm)), the n.m.r. spectrum indicated a 3:5 ratio of 1- and 2-isomer, could be only separated by careful fractional distillation using a spinning band column but much material was lost due to decomposition. A mixture of the acids however could be separated on basis of the different solubilities of the acids in ethyl acetate. Whereas 5-methylthio-2-tetrazolylacetic acid is very soluble in this solvent at room temperature, the 1-isomer is almost completely insoluble. The n.m.r. spectra of the esters are given in Table IV.
**The crude product mixture (the n.m.r. spectrum showed the predominance of the 2-isomer by at least a factor of six) was recrystallized from a benzene – *n*-hexane (5:2) mixture to give the 2-isomer as long white needles. This same product was also obtained by hydrogen peroxide oxidation of ethyl 5-methylthio-2-tetrazolylacetate. The n.m.r. spectrum is given in Table IV.
††The compound decomposed extensively upon distillation.

Experimental

The nuclear magnetic resonance (n.m.r.) spectra were recorded on a Varian Associates model A-60 Spectrometer, with tetramethylsilane as a reference. Melting and boiling points are uncorrected. The elemental analyses were performed by Dr. G. Weiler and Dr. F. B. Strauss, Micro-analytical Laboratory, Oxford, England. Elemental analyses were only obtained on the acetic acids (Tables I–III) or, in those instances where the acid was either not crystalline or difficult to purify, on a derivative.

Starting Materials

Most of the tetrazoles were prepared by standard procedures. The reaction of a nitrile with ammonium azide according to the procedure of Finnegan, Henry, and Lofquist (18) provided: 5-ethyltetrazole (m.p. 90–91°), 5-*n*-propyltetrazole, 5-phenyltetrazole, 5-methylthiotetrazole and 5-carbomethoxymethyltetrazole (m.p. 152–155°). 5-Methyltetrazole (12) and sodium 5-trifluoromethyltetrazole (3) were prepared by reaction of acetonitrile and trifluoroacetonitrile with sodium azide. From 5-aminotetrazole (19) were prepared: tetrazole by reductive deamination (2, 20) and 5-chloro- and 5-bromotetrazole by a Sandmeyer reaction (21).

5-Methylsulfonyltetrazole

A mixture of 5-methylthiotetrazole (10.0 g, 0.086 mole), 30% aqueous hydrogen peroxide (22.7 ml, 0.20 mole) and glacial acetic acid (150 ml) was allowed to react at room temperature for three days. The solvent was removed under reduced pressure and the residue recrystallized from an ethyl acetate – *n*-hexane (1:1) mixture to give 11.4 g (90%) of white crystals, m.p. 127–128° (decomp.). Reported m.p. 110–120° (22).

Tetrazolylacetic Esters (General Procedure)

A solution of alkyl halide (0.1 mole) in 50 ml of acetone was added to a mixture of the tetrazole (0.1 mole) and triethylamine (0.1 mole) in 50 ml of acetone. When the reaction was completed the triethylammonium hydrochloride was filtered off and the acetone removed from the filtrate. The residue was dissolved in 100 ml of methylene chloride and this solution washed with an aqueous sodium carbonate solution. The residue obtained after drying and removal of the methylene chloride was generally fractionally distilled *in vacuo*. Table V lists some of the esters prepared by this procedure, together with the reaction conditions employed. The products for which the work-up differed or that were prepared by a different method are described separately.

t-Butyl 1-Tetrazolylacetate

To *t*-butyl isocyanoacetate (2.7 g, 0.019 mole) (23) were added 46 ml of a 1.16 *M* solution of hydrazoic acid (0.053 mole) in benzene. The mixture was heated under reflux for 24 h. The residue obtained after removal of the solvent, solidified and was recrystallized from *n*-hexane – ethyl acetate to give 2.4 g (68%) of product, m.p. 82–84°.

Can. J. Chem. Downloaded from www.nrcresearchpress.com by 210.87.254.42 on 09/05/12
For personal use only.

Can. J. Chem. Downloaded from www.nrcresearchpress.com by 210.87.254.42 on 09/05/12
For personal use only.

1-Tetrazolylacetic Acid

t-Butyl 1-tetrazolylacetate (10.0 g, 0.054 mole) was dissolved in 100 ml of acetic acid and heated under reflux for 4 h. The residue obtained after removal of the acetic acid was recrystallized from ethyl acetate to give 4.4 g (64%) of acid, m.p. 127–129°, identical with the acid prepared from ethyl 1-tetrazolylacetate (mixture m.p. 127–129°, the infrared spectra were superimposable). The elemental analyses are reported in Table I.

t-Butyl 5-N,N-Dimethylaminomethyl-1-tetrazolylacetate

To a suspension of dimethylamine hydrochloride (3.25 g, 0.040 mole) in 40 ml of acetone, cooled in an ice–salt bath, was added successively 3.0 ml of 40% aqueous formaldehyde (0.040 mole), a solution of sodium azide (2.6 g, 0.040 mole) in 10 ml of water, and *t*-butyl isocyanoacetate (5.5 g, 0.040 mole) (23). The reaction mixture was stirred for 45 min at −10°, then for 3 h at room temperature. After the addition of 150 ml of water the mixture was cooled. The product precipitated as fine white needles which were filtered off; yield: 6.2 g (65%); m.p. 50–52°. Two recrystallizations from ether – *n*-hexane raised the melting point to 53–54°.

5-N,N-Dimethylaminomethyl-1-tetrazolylacetic Acid

The *t*-butyl ester (6.1 g, 0.025 mole) was dissolved in 60 ml of acetic acid and this mixture was heated under reflux for 45 min. The solvent was removed and the residue recrystallized from ethanol–ether to give 4.3 g (93%) of the acid, m.p. 187–189° (decomp.). The elemental analyses are reported in Table I.

5-Phenyl-1-tetrazolylacetic Acid and 5-Phenyl-2-tetrazolylacetic Acid

To a mixture of the two isomeric esters, prepared from 5-phenyltetrazole (14.6 g, 0.1 mole), triethylamine (10.8 g, 0.105 mole) and ethyl bromoacetate (16.7 g, 0.1 mole), were added 50 ml of 3 *N* methanolic sodium hydroxide. After the reaction mixture was left at room temperature for 2 h, the methanol was removed and the salt mixture dissolved in 300 ml of water. Upon acidification, 5-phenyl-2-tetrazolylacetic acid (14 g, 69%), m.p. 176–181° (decomp.) crystallized. An analytical sample, m.p. 182–184° (decomp.), was obtained after one recrystallization from ethyl acetate – *n*-hexane. The aqueous filtrate was extracted with two 100-ml portions of ether. After drying, the ethereal solution was treated with cyclohexylamine (7 ml). The precipitated cyclohexylamine salt was recrystallized from methanol–ether to give 1.7 g of cyclohexylammonium 5-phenyl-1-tetrazolylacetate, m.p. 157–159° (decomp.). A solution of the salt in hot water was acidified. Upon cooling pure 5-phenyl-1-tetrazolylacetic acid (1.0 g, m.p. 148–150° (decomp.)) precipitated. Both acids had the correct neutralization equivalent. The analytical results are recorded in Tables I and II.

Ethyl 5-Amino-1-tetrazolylacetate and Ethyl 5-Amino-2-tetrazolylacetate

A solution of ethyl bromoacetate (20.0 g, 0.12 mole) in 50 ml of acetone was added to a mixture of 5-aminotetrazole monohydrate (12.4 g, 0.12 mole), triethylamine 12.1 g, 0.12 mole) and 50 ml of acetone. Upon shaking, the mixture rapidly became homogeneous and the exothermic reaction necessitated cooling with water. When the reaction subdued the reaction mixture was left at room temperature for an additional 3 h. The isomer mixture, obtained after filtering off the triethylamine hydrobromide and removal of the acetone from the filtrate, was dissolved in 250 ml of warm ethyl acetate. The warm ethyl acetate solution, after washing with small amounts of water and aqueous bicarbonate, was dried, then concentrated to a volume of approximately 100 ml. Chloroform (75 ml) was added and the mixture was kept under refrigeration overnight. The solid (10.0 g) was filtered off and recrystallized from ethyl acetate to give 7.4 g (36%) of ethyl 5-amino-1-tetrazolylacetate, m.p. 145–148°. The filtrate was concentrated to dryness and the solid residue (4.0 g) was heated with 50 ml of chloroform. Some insoluble material (1-isomer) was filtered off and 75 ml of carbon tetrachloride was added to the filtrate. Upon cooling, 2.8 g (14%) of white crystalline ethyl 5-amino-2-tetrazolylacetate, m.p. 96–103° (could be raised to 105–107° by an additional recrystallization from carbon tetrachloride) was obtained. Ethyl 5-amino-1-tetrazolylacetate upon treatment with methanolic ammonia could readily be converted to 5-amino-1-tetrazolylacetamide, m.p. 211–212° (decomp.). Treatment of a solution of ethyl 5-amino-1-tetrazolylacetate in dilute hypophosphorous acid with a sodium nitrite solution at room temperature gave rise to the formation of ethyl 1-tetrazolylacetate (characterized as the amide, m.p. 150–152° (decomp.)).

Methyl 5-Amino-1-tetrazolylacetate

Methyl chloroacetate (27.1 g, 0.25 mole) was added to a mixture of 5-aminotetrazole monohydrate (25.7 g, 0.25 mole), triethylamine (25.3 g, 0.25 mole), and 150 ml of acetone. The resulting mixture was refluxed for 1 h, then left at room temperature overnight. After cooling the solid precipitate was collected, followed by concentration of the solution to a volume of approximately 75 ml. Upon cooling some more solid precipitated. The combined solids were twice recrystallized from 200 ml of water to give 13.9 (36%) of white plates, m.p. 179–181°.

Methyl 5-Trifluoromethyl-1-tetrazolylacetate

A mixture of methyl azidoacetate (4.9 g, 0.043 mole; prepared by the procedure of Forster and Fierz (24) for the ethyl ester) and trifluoroacetonitrile (approximately 5 ml at −70°) (25) in a 250 ml autoclave was heated at 140–150° for 20 h. The product was distilled *in vacuo* to give 7.0 g (78%) of colorless liquid, b.p. 72–73° (0.5 mm); n.m.r. ($CDCl_3$): τ 4.63 (s, 2H), 6.14 (s, 3H.)

Methyl 1-Ethyl-5-tetrazolylacetate

A mixture of methyl (methoxy-*N*-ethylcarbimino)-acetate (8.0 g, 0.050 mole) (10), sodium azide (16.2 g, 0.25 mole) and glacial acetic acid (100 ml) was heated at 45° for 18 h. The reaction mixture was poured into 200 ml of ice-water and the product extracted with ether (2 × 100 ml). The ether extracts were dried, the solvent removed, and the residue distilled *in vacuo* to give 2.5 g (29%) of the desired product, b.p. 152–153° (1.0 mm). The infrared spectrum was superimposable with that of the high boiling fraction obtained from the reaction of methyl 5-tetrazolylacetate with ethyl bromide in the presence of triethylamine (Table V).

General Procedure for the Preparation of Tetrazolylacetic Acids from Tetrazolylacetic Esters

Tetrazolylacetic ester (0.010 mole) was dissolved in approximately 5 ml of methanol, followed by the addition of 4 ml of a 3 *N* methanolic sodium hydroxide solution. In most instances the sodium salt precipitated. The mixture was left at room temperature for 1 h, whereafter the methanol was removed. The sodium salt was converted to the acid by method *a*, *b*, or *c* (see Tables I–III): *a*.) An aqueous solution of the salt was passed through a column of DOWEX 50W-X8 H^+ form ion exchange resin, followed by removal of the water of the eluate under reduced pressure. *b*.) The sodium salt was dissolved in a small amount of water and this solution was acidified. The acid was extracted with ethyl acetate. *c*.) A solution of the sodium salt in a small amount of water was acidified. The precipitated acid was collected by filtration.

The acids prepared in this manner are listed in Tables I–III. The experimental neutralization equivalents were all within 5% of the theoretical value.

5-Tetrazolone-1,4-diacetic Acid

To a mixture of 5-hydroxytetrazole (3.0 g, 0.035 mole) (8), triethylamine (7.05 g, 0.070 mole) and 20 ml of acetone, cooled in ice, was added a solution of ethyl bromoacetate (11.7 g, 0.070 mole) in 20 ml of acetone. The reaction mixture was left at room temperature overnight, followed by the usual work-up. There were obtained 6.8 g (76%) of crystalline material, m.p. 87–89° (after recrystallization from carbon tetrachloride). The same product was obtained when equimolar amounts of reactants were employed. The infrared spectrum did not show any absorption in the 3600–3000 cm^{-1} range, indicating the absence of OH, but showed strong absorption in the 1720–1750 cm^{-1} region. The n.m.r. spectrum ($CDCl_3$) showed a singlet at τ 5.17, a quartet at τ 5.65, and a triplet at τ 8.68, with an integrated area ratio of 2:2:3. The ester, 1,4-dicarbethoxymethyl-5-tetrazolone, was converted in 90% yield to the diacid by following the general procedure outlined above (method *a*). The diacid, m.p. 213–215°, could be recrystallized from ethyl acetate and was found to have a neutralization equivalent of 102 (calcd. 101).

Anal. Calcd. for $C_5H_6N_4O_5$: C, 29.71; H, 2.99; N, 27.72. Found: C, 29.78; H, 3.09; N, 27.85.

Acknowledgments

The authors are indebted to Professor R. U. Lemieux for guidance and advice in the conduct of this research and to Messrs. V. R. Baker, M. Donelly, H. Müller, and P. K. Wolfert for technical assistance.

1. R. Raap and R. G. Micetich. J. Med. Chem. **11**, 70 (1968).
2. W. G. Finnegan and R. A. Henry. J. Org. Chem. **24**, 1565 (1959).
3. W. P. Norris. J. Org. Chem. **27**, 3248 (1962).
4. R. A. Henry and W. G. Finnegan. J. Am. Chem. Soc. **76**, 923 (1954).
5. R. N. Butler and F. L. Scott. J. Org. Chem. **31**, 3182 (1966).
6. R. A. Henry, W. G. Finnegan, and E. Lieber. J. Am. Chem. Soc. **76**, 2894 (1954).
7. V. P. Shchipanov. Zh. Organ. Khim. **2**, 356 (1966); Chem. Abstr. **65**, 2248 (1966).
8. K. Hattori, E. Lieber, and J. P. Horwitz. J. Am. Chem. Soc. **78**, 411 (1956).
9. W. R. Carpenter. J. Org. Chem. **27**, 2085 (1962).
10. R. Raap. Can. J. Chem. **46**, 2255 (1968).
11. I. Hagedorn and H. D. Winkelmann. Chem. Ber. **99**, 850 (1966).
12. J. H. Markgraf, W. T. Bachmann, and D. P. Hollis. J. Org. Chem. **30**, 3472 (1965).
13. G. B. Barlin and T. J. Batterham. J. Chem. Soc. (B), 516 (1967).
14. R. N. Butler and F. L. Scott. J. Org. Chem. **31**, 3182 (1966).
15. R. N. Butler and F. L. Scott. J. Org. Chem. **32**, 1224 (1967).
16. F. L. Scott and R. N. Butler. J. Chem. Soc. (B), 919 (1967).
17. D. W. Moore and A. G. Whittaker. J. Am. Chem. Soc. **82**, 5007 (1960).
18. W. G. Finnegan, R. A. Henry, and R. Lofquist. J. Am. Chem. Soc. **80**, 3908 (1958).
19. J. S. Mihina and R. M. Herbst. J. Org. Chem. **15**, 1082 (1950).
20. R. A. Henry and W. G. Finnegan. J. Am. Chem. Soc. **76**, 290 (1954).
21. R. Stollé. Ber. **62**, 1118 (1929).
22. M. Freund and T. Paradies. Ber. **34**, 3110 (1901).
23. I. Ugi, W. Betz, U. Fetzer, and K. Offermann. Ber. **94**, 2814 (1961).
24. M. O. Forster and H. E. Fierz. J. Chem. Soc. **93**, 72 (1908).
25. H. Gilman and R. G. Jones. J. Am. Chem. Soc. **65**, 1458 (1943).
26. J. Cohen, W. G. Finnegan, and R. A. Henry. U.S. Patent 3,073,731 (Jan. 15, 1963).
27. C. R. Jacobson and E. D. Amstutz. J. Org. Chem. **21**, 311 (1956).

Can. J. Chem. Downloaded from www.nrcresearchpress.com by 210.87.254.42 on 09/05/12
For personal use only.

Can. J. Chem. Downloaded from www.nrcresearchpress.com by 210.87.254.40 on 09/05/12
For personal use only.

Structure of crotonic acid dimers and higher polymers with partial stereochemistry of the dimers[1]

MARTIN B. HOCKING
Exploratory Research Laboratory, Dow Chemical of Canada, Limited, Sarnia, Ontario

Received June 5, 1968

Heating *trans*-crotonic acid (CH_3—CH=CH—CO_2H) yields labile high boiling compounds which have received some attention in the past. These have now been conclusively characterized as the two geometric isomers of a dimer of crotonic acid. In addition trimers and tetramers discovered in the thermally polymerized crotonic acid were isolated as their methyl esters and positively identified.

Canadian Journal of Chemistry, 47, 821 (1969)

Introduction

Partial dimerization by heat of crotonic acid has been given the attention of a number of early workers (1–3) who have attributed at least two possible structures, **1** and **2**, to the compound obtained.

In the most recent publication on the subject, Skau and Saxton (4) conduct a critical reappraisal of earlier results with consideration of new data of their own and reservedly suggest that structure **2** fits the compound best. We confirm with new evidence the latter authors' structural assignment and have also determined the orientations of two geometrical isomers of this dimer. In addition we have obtained conclusive evidence of some higher polymers of crotonic acid.

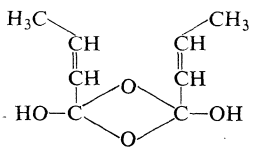

1

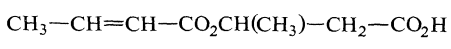

2

Results and Discussion

The primary difficulty encountered with the dimer of crotonic acid has been its isolation. To bring about its formation, a quantity of *trans*-crotonic acid is heated at around 150° for a few days. Most of the unchanged *trans* isomer is separated from the dimer by allowing the mixture to cool to ambient and then draining the dimer, as an oil, from the crystallized *trans* compound. It is the remainder of the dissolved *trans* acid, together with some *cis*-crotonic acid also present, that is very difficult to remove from this oil. At distillation pressures low enough to avoid cracking of the dimer (around 0.01 mm), the *trans*-crotonic acid still present in the crude mixture undergoes ready sublimation, fouling and blocking distillation passages. Clean distillation of *trans*-crotonic acid from the dimer can be accomplished at 40 mm, but this makes pot temperatures severe enough to cause simultaneous cracking of the dimer.

This difficulty was initially circumvented by esterifying all of the mixture. Vacuum distillation of this mixture of methyl esters then cleanly separated them. Characterization of the methyl-(*trans*-crotonate)-3-hydroxybutyrate (**2***a*, methyl ester) by infrared (i.r.), nuclear magnetic resonance (n.m.r.), elemental analysis, and molecular weight confirmed its structure. The geometry of the still unsaturated portion of the molecule was

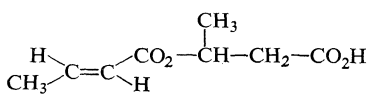

2*a*

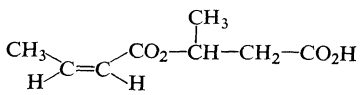

2*b*

[1]Contribution No. 163.

TABLE I

Nuclear magnetic resonance spectra of crotonic acid dimers and ester of *trans*-dimer*

Assignment	Multiplicity—relative areas in parentheses	Dimer **2***a*, methyl ester Shift p.p.m.	Dimer **2***a*, methyl ester Coupling c.p.s.	Dimer **2***a*, (*trans*-crotonate) Shift p.p.m.	Dimer **2***a*, (*trans*-crotonate) Coupling c.p.s.	Dimer **2***b*, (*cis*-crotonate) Shift p.p.m.	Dimer **2***b*, (*cis*-crotonate) Coupling c.p.s.
δ_a	Doublet pair (3, *cis* + *trans*)	1.84	J_{ab} = 6.7 J_{ac} = 1.5	1.86	J_{ab} = 6.8 J_{ac} = 1.7	2.12	J_{ab} = 7.0 J_{ac} = 1.6
δ_b	Overlapping quartet pair (1)	6.97	J_{ba} = 6.7 J_{bc} = 15.0	7.00	J_{ba} = 6.8 J_{bc} = 15.4	6.35	J_{ba} = 7.0 J_{bc} = 11.4
δ_c	Well differentiated quartet pair (1)	5.80	J_{ca} = 1.5 J_{cb} = 15.0	5.82	J_{ca} = 1.7 J_{cb} = 15.4	5.7†	J_{ca} = 1.6 See note †
δ_d	Sextet‡ (ratio of 1:5:10:10:5:1) (1)	5.30	J_{de} = 6.2	5.32	J_{de} = 6.2	5.32	J_{de} = 6.2
δ_e	Doublet (3)	1.29	J_{ed} = 6.2	1.32	J_{ed} = 6.2	1.32	J_{ed} = 6.2
δ_f	Two double doublets,§ center two doublets overlapping, (ratio 1:1:21:20:22:19:1:1) (2)	2.59	J_{f_1d} = 6.2 $J_{f_1f_2}$ = 15.3 J_{f_2d} = 6.6	2.66	J_{f_1d} = 6.0 $J_{f_1f_2}$ = 15.6 J_{f_2d} = 6.6	2.66	J_{f_1d} = 6.0 $J_{f_1f_2}$ = 15.6 J_{f_2d} = 6.6
δ_{CH_3}(ester)	Singlet (3)	3.65	—	—	—		
δ_{OH}	Singlet (1)	—	—	12.16		Not determined	

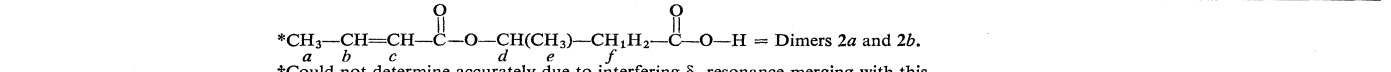

†Could not determine accurately due to interfering δ_c resonance merging with this.

‡Due to two quartets the proximate two peaks of each which have merged. A more complex spin–spin coupling due to the adjacent non-equivalent methylene protons has not been resolved because their respective coupling constants are too similar, and too close to that of the saturate methyl.

§Shift difference between the diastereomeric non-equivalent hydrogens ($\delta_{H1} - \delta_{H2}$), taken from the calculated centers of gravity of each of the two pairs of doublets (5), was found to be 7.8 c.p.s. Calculation of the relative intensities of the inner and outer peaks of this multiplet, using this shift difference, gave ratios of 1:18.9 (5*a*) and 1:18.4 (5*b*) which confirmed the interpretation. Geminal diastereomeric hydrogen calculated shift differences of the magnitude observed here are common (6).

TABLE II

Nuclear magnetic resonance shifts of *cis*- and *trans*-crotonic acids and their methyl esters*

Assignment	Multiplicity	*cis*-Crotonic acid (7) Shift	*cis*-Crotonic acid (7) Coupling	Methyl *cis*-crotonate† (8) Shift	Methyl *cis*-crotonate† (8) Coupling	*trans*-Crotonic acid (7) Shift	*trans*-Crotonic acid (7) Coupling	Methyl *trans*-crotonate† (8) Shift	Methyl *trans*-crotonate† (8) Coupling
δ_a	Doublet pair	2.15	J_{ab} = 7.1 J_{ac} = 1.1	2.10	J_{ab} = 7.0 J_{ac} = 1.5	1.89	J_{ab} = 6.7 J_{ac} = 1.5	1.86	J_{ab} = 7.0 J_{ac} = 1.5
δ_b	Overlapping quartet pair	6.50	J_{ba} = 7.1 J_{bc} = 11.6	6.25	J_{ba} = 7.0 J_{bc} = 11.0	7.12	J_{ba} = 6.7 J_{bc} = 15.0	6.87	J_{ba} = 7.0 J_{bc} = 15.5
δ_c	Quartet pair	5.82	J_{ca} = 1.1 J_{cb} = 11.7	5.73	J_{ca} = 1.5 J_{cb} = 11.0	5.83	J_{ca} = 1.5 J_{cb} = 15.1	5.76	J_{ca} = 1.5 J_{cb} = 15.5
δ_d	Singlet			3.61				3.61	

†Spectra in carbon tetrachloride.

expected to be *trans*, due to the preponderant presence of this monomer, and indeed the chemical shifts in the n.m.r. of appropriate protons were virtually the same as those found for the analogous protons in methyl *trans*-crotonate (Tables I and II).

After isolation of the ester, attention turned again to isolation of the dimer free acid since a differential hydrolysis of the methyl over the 3-hydroxybutyric acid ester group was not an attractive proposition. At least isolation and identification of the ester first made it much easier to determine whether or not procedures used to isolate the free acid were being applied successfully. Several careful aqueous acetone titrations of the crude mixtures were tried. Unfortunately, only one plateau at pH 4.9 was evident (p*K*a of *trans*-crotonic acid is 4.60; (9))

Can. J. Chem. Downloaded from www.nrcresearchpress.com by 210.87.254.40 on 09/05/12
For personal use only.

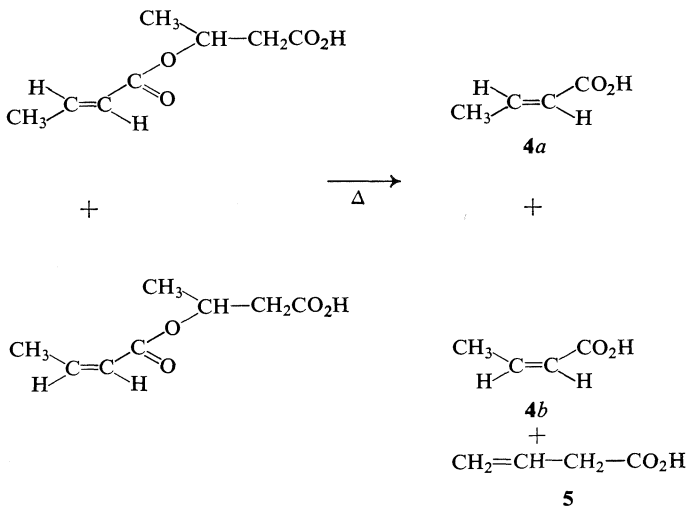

indicating that **2** and monomeric *trans* acid were being neutralized together.

Pure dimer **2** was eventually obtained on a relatively large scale by taking advantage of the ready sublimation of the *trans* acid. First, *trans*-crotonic acid (plus a small amount of the *cis* isomer) was sublimed and distilled from the crude oil under moderate conditions in a rotary evaporator until no further sublimation occurred. The vacuum was then improved and the temperature was raised just sufficiently to allow the dimer to distil. Titration of the material obtained by this method gave an acid equivalence of 0.515, an improvement on the best material obtained by Skau and Saxton (4), which gave an acid equivalence of 0.535. Bromination and catalytic hydrogenation established chemically the presence of one double bond per molecule. Physical data on the compound confirmed its identity as compound **2** (not its structural isomer **3**: CH_3—CH=CH—CO_2—$CH(CH_2$—$CH_3)CO_2H$) and verified its purity. The molecular weight of **2** determined in acetone was 190 (near the theoretical 172). In benzene a value of 377 was obtained, twice that observed in the polar solvent. This doubling of molecular weight of carboxylic acids in solutions of nonpolar solvents is a demonstration of the strong intermolecular hydrogen bonding (10).

Earlier papers by others (11) deal with the formation of *cis*-crotonic acid on heating the *trans*, so it was not surprising when it was found that the unsaturated portion of dimer **2** was in fact a mixture of *trans*- (**2***a*) and *cis*- (**2***b*) crotonate moieties. The percent of *cis*-crotonate in the mixture ranged between 15 and 19, which was about the same as the ratio of *cis* to *trans* monomeric acids present in the thermally equilibrated mixtures (7). As in the case of the methyl ester of **2** the identities and reasonably accurate proportions of the two isomeric free acids were readily confirmed and determined by n.m.r. by comparison of the appropriate shifts with those of the respective monomeric free acids (see Tables I and II). That the n.m.r. evidence for the presence of **2***b* was not due to this amount of dissolved *cis*-crotonic acid coming through the isolation procedure was confirmed by several vigorous water (in which both monomers are very soluble (12)) washes which caused negligible change in the n.m.r. but did improve the acid equivalence to a figure of 0.504. The absence of *cis* ester in the methyl ester of **2** was probably due to the shorter heating time for the starting *trans* acid (giving less time for *cis* equilibration).

Degradative experiments helped to confirm the identity of **2**. Cracking the mixture of dimers **2***a* and **2***b* by heat was expected to yield *trans*-crotonic acid **4***a* plus a little *cis* **4***b* resulting from the crotonate moiety of **2***b*. From the butyric portion of **2***a* and **2***b*, appreciable further proportions of *cis*-crotonic acid and at least detectable amounts of vinylacetic acid **5** were also anticipated, based on the statistical distribution of protons available for a leaving crotonate

Can. J. Chem. Downloaded from www.nrcresearchpress.com by 210.87.254.40 on 09/05/12
For personal use only.

TABLE III

Product distribution on cracking mixtures of dimers **2***a* and **2***b*

% Dimer **2***b* in mixture, and conditions	Monomeric acid yielded		
	trans-Crotonic	*cis*-Crotonic	Vinylacetic
16%; calcd.* yield	92.0	8.0	0.0
16%; cracked at 250 mm	86.7	11.8 (7.6)†	1.5
16%; cracked at 760 mm	86.0	12.8 (9.6)	1.2
6%; calcd. yield*	97.0	3.0	0.0
6%; cracked at 760 mm	92.1	7.9 (9.8)	0.0
	92.9	7.1 (8.2)	0.0

*Calculations are assuming butyrate portion of dimer goes entirely to *trans*-crotonic acid.
†The percent of the dimer butyrate converted to *cis*-crotonic acid, taking into account the *cis* unsaturated half present in **2***b*, is given in parentheses.

moiety. Early tautomeric studies gave analogy for the anticipated formation of vinylacetic acid in at least strongly basic systems (13).

Initially the mixture of dimers **2***a* and **2***b* was cracked under reduced pressure to decrease the tendency of *cis* to isomerize to *trans* or vice versa, and to approximate the cracking temperatures existing during the formation of the dimer. The distillate contained 11.8% *cis*-crotonic, and 1.5% vinylacetic acid (by n.m.r.) in addition to the expected *trans*. This represents conversion of 7.6% of the saturated half of dimer **2** to *cis*-crotonic and about 3% to vinylacetic acids (Table III).

However, one other consequence of the lower temperature cracking under reduced pressure should be the favoring of initial formation of the thermodynamically more stable product, *trans*-crotonic acid, over a statistical product distribution. This would act in opposition to the slower *cis* to *trans* isomerization expected at lower temperatures and may in fact give less *cis* compound than would higher temperature cracking. To test this theory a further sample of a mixture of dimers **2***a* and **2***b* was cracked at atmospheric pressure. A small amount of unchanged dimer came over, but correcting for this, 12.8% *cis*-crotonic and 1.2% vinylacetic acid were obtained. The changes detected in product ratios were insufficient to permit any conclusions to be drawn.

For clarification of the degradative experiments an effort was made to obtain pure dimer **2***a* so that none of the *cis*-crotonate moiety would be present in the dimer to contribute to the *cis*-crotonic acid arising from the saturated portion of the dimer on cracking it. Preliminary thin-layer chromatographic experiments to establish whether or not column chromatography was likely to be successful in physically separating **2***a* from **2***b* were not promising. Using dimerization conditions such that dimer **2***a* should form exclusively, an increase in the concentration of **2***a* from 84 to 94% was obtained. Cracking this mixture yielded about the same proportion of *cis*-crotonic acid via the butyrate as did the 84% pure **2***a* (Table III), but surprisingly no vinylacetic acid. This may be an indication, as suggested earlier, that the vinylacetic acid is largely arising via tautomerization of *cis*-crotonic acid (7) and not directly from the saturated portion of the dimers.

An attempt to crack the methyl esters of a mixture of dimers **2***a* and **2***b* by distillation up a column at atmospheric pressure was unsuccessful.

Saponification of the dimer **2**, which has been carried out previously (1) but details of which are inaccessible, in our hands yielded a good material balance of nearly equivalent amounts of the component monomeric acids present, *cis*- and *trans*-crotonic acids and β-hydroxybutyric acid. The identity of the latter was confirmed by comparison of its physical properties with those of an authentic sample. Many of the interesting features of the n.m.r. of β-hydroxybutyric acid are relevant to, and help confirm the n.m.r. interpretations of dimers **2***a* and **2***b*.

Trimers and Tetramers of Crotonic Acid

The n.m.r. spectra of the crude oils obtained from some of the longer duration or higher temperature dimer preparations showed 4–6 additional bands at the approximate chemical shift of the doublet due to the saturated methyl (*e*) of the dimer, four additional bands at the

Can. J. Chem. Downloaded from www.nrcresearchpress.com by 210.87.254.40 on 09/05/12
For personal use only.

TABLE IV

Elemental analyses and ebullioscopic molecular weights for methyl crotonate and polymers

	Methyl crotonate		Dimer **2**		Trimer		Tetramer	
	Calcd.	Found	Calcd.	Found	Calcd.	Found	Calcd.	Found
C	59.98	59.94 60.28	58.05	57.91 57.87	57.34	57.24 57.20	56.97	56.83 56.78
H	8.05	8.09 8.16	7.58	7.51 7.55	7.40	7.51 7.39	7.31	7.44 7.30
Mol. wt.	100.1	—	186	180 180	272	251 260	358	320 312

$CH_3—CH=CH—CO_2—\underset{d}{CH}(CH_3)—\underset{e}{CH_2}—\underset{f}{CO_2H}$

2

$CH_3—CH=CH—CO_2\text{-}[\text{-}CH(CH_3)—CH_2—CO_2\text{-}]_n\text{-}CH(CH_3)—CH_2—CO_2H$

6 trimer, $n = 1$
tetramer, $n = 2$

shift of the methylene protons (f) of the dimer, and broadening with fine structure of the bands which appeared in the region of the methine (d) of the dimer. On the basis of this n.m.r. evidence, i.e. no additional n.m.r. resonances other than those easily attributable to repetition of the unit —$CH(CH_3)—CH_2—CO_2$— above, and the i.r. band at 1745 cm^{-1} (saturated ester carbonyl) which was relatively stronger in partially enriched material than the band at 1720 cm^{-1} (saturated acid and unsaturated ester carbonyls), it was suspected that simple higher polymers were being obtained.

After early attempts to isolate the free acids of these materials were unsuccessful, the ester route was satisfactorily employed for isolation of the suspected higher polymers. Distillation of the mixture of polymer esters thus obtained, initially gave fractions of dimer methyl ester, followed by trimer and tetramer esters with about 50° increments in the boiling points with each crotonyl unit. Characterization of these materials was by elemental analyses and molecular weights (Table IV), mass spectral analyses, i.r., n.m.r., and chemically by catalytic hydrogenation.

Mass spectral analyses gave small signals for the mass numbers corresponding to the molecular weights of the parent ions of the dimer, trimer, and tetramer methyl esters (Tables V and VI). Fragmentation was quite severe for the telomers however, as is evident by the much larger relative abundance of the parent ion of methyl crotonate than those of the polymer parent ions.

Nuclear magnetic resonance confirmed in two ways the structures of the trimer and tetramer. The first was by the absence in these spectra of any bands with a large shift difference from any already present in spectra of the dimers' methyl esters. Any structural isomer of the trimer or tetramer different from that shown, for example such as the orientation of dimer **3**, would be expected to lead to spectra with at least two multiplet groups at shifts quite different from those of the dimers' methyl esters. The change most clearly evident was an increase in the apparent multiplicity of the resonance due to the butyric type methyl, details of which are given in the Experimental. Integration reaffirmed the other n.m.r. interpretations. Table VII shows how well the proton integral ratios of ester methyl and crotonate moieties to butyrate moieties in the polymers agree with the structures suggested for the crotonic acid polymers.

Catalytic hydrogenation of the polymer esters established, by the equimolar consumption of hydrogen (Table VIII), the presence of one olefinic double bond per molecule. The answers obtained for the dimer ester are slightly lower than could be explained on the basis of experimental error, but this could perhaps have been caused by the presence of traces of trimer ester.

Experimental

trans-Crotonic acid used was practical grade material purchased from Matheson, Coleman, and Bell. Melting points and boiling points are not corrected. Microanalyses and molecular weights are by A. B. Gygli, Toronto, Ontario, and L. E. Swim, The Dow Chemical Company, Midland, Michigan.

Infrared spectra were recorded on Beckman IR-9 and Perkin–Elmer 337 spectrophotometers and are quoted in reciprocal centimeters. Ultraviolet (u.v.) data were obtained on a Beckman DK-2 Ratio Recording Spectrophotometer. A Varian A60 nuclear magnetic resonance

Can. J. Chem. Downloaded from www.nrcresearchpress.com by 210.87.254.40 on 09/05/12
For personal use only.

TABLE V

Mass spectral cracking patterns of the methyl esters of *trans*-crotonic acid,* crotonic acid dimer, trimer, and tetramer

Mol. wt.	Probable molecular ion	Relative abundances: Methyl *trans*-crotonate* (mol. wt. 100)	Dimer **2** methyl ester (mol. wt. 186)	Trimer methyl ester (mol. wt. 272)	Tetramer methyl ester (mol. wt.358)
358	Tetramer P⊕				0.02
343	Tetramer P⊕–CH_3				0.04
289	Tetramer P⊕–$CH_3CH{=}CH{-}CO$			—	0.12
273	Tetramer P⊕–$CH_3CH{=}CH{-}CO_2$			—	0.31
272	Trimer P⊕			0.06	—
257	Trimer P⊕–CH_3			0.13	0.15
241	Trimer P⊕–CH_3O			0.16	0.81
203	Trimer P⊕–$CH_3{-}CH{=}CH{-}CO$			3.87	1.73
200	Trimer P⊕–$CH_3{-}O_2C{-}CH$			0.32	—
188	Trimer P⊕–$CH_3CH{=}CH{-}CO_2H$		—	—	3.08
187	Trimer P⊕–$CH_3{-}CH{=}CH{-}CO_2$		—	5.16	—
186	Dimer P⊕		0.05	3.55	—
171	Dimer P⊕–CH_3		0.14	1.94	1.92
155	$CH_3{-}CH{=}CH{-}CO_2{-}CH(CH_3){-}CH_2CO$⊕		—	22.58	23.08
154	$CH_3CH{=}CH{-}CO_2CH(CH_3){-}CHCO$⊕		0.42	24.19	—
145	$CH_3O_2C{-}CH_2{-}CH(CH_3){-}CO_2$⊕		—	0.61	0.77
127	$CH_3CH{=}CH{-}CO_2CH(CH_3){-}CH_2$⊕		0.10	—	—
126	$CH_3CH{=}CH{-}CO_2CH(CH_3)CH_2$⊕		—	1.26	0.73
117	$CH_3O_2CCH_2{-}CH(CH_3)O$⊕		17.34	9.03	4.23
113	$CH_3CH{=}CH{-}CO_2CH(CH_3)$⊕		0.68	—	—
101	$CH_3{-}CH{-}CH_2{-}CO_2CH_3$⊕	0.84	—	43.55	26.92
100	$CH_3{-}CH{=}CHCO_2CH_3$⊕	16.63	20.73	—	—
87	$CH_3CH{-}CH_2{-}CO_2H$⊕	—	—	11.94	8.46
85	$CH_3CH{=}CH{-}CO_2$⊕	19.17	10.22	8.06	4.61
69	$CH_3CH{=}CH{-}CO$⊕	100.00	100.00	100.00	100.00
59	CH_3O_2C⊕	5.30	14.55	45.16	23.07
41	$CH_3{-}CH{=}CH$⊕	50.00	18.70	32.26	18.08

*See Table VI for ions of methyl crotonate observed but not included here.

TABLE VI

Additional mass spectral ions of methyl crotonate

Molecular weight	Relative abundance	Molecular weight	Relative abundance
15	13.47	40	5.18
16	0.14	42	3.59
24.5	0.40	43	0.67
25	0.29	44	0.41
26	1.94	45	0.64
27	2.84	50	0.15
28	5.67	53	1.03
29	5.38	54	0.18
30	0.57	55	0.92
31	1.11	56	0.14
32	0.31	57	0.30
33	0.13	66	0.13
36	0.23	67	0.25
37	2.89	68	3.15
38	5.76	70	4.72
39	31.88	71	0.46
		72	0.53
		86	0.78
		99	0.23

(n.m.r.) spectrometer fitted with a phase detector integrator, and with a Hewlett–Packard oscillator and electronic counter (models 200CD and 5212A respectively) for sweep width calibration was used to measure the n.m.r. data. The latter were recorded at room temperature in deuteriochloroform. Shifts are those of the centers of multiplets given in p.p.m. downfield from internal tetramethylsilane and coupling constants, which were measured on spectra expanded to 50 or 100 cycle sweep width, are quoted in c.p.s. Mass spectra of the methyl esters of *trans*-crotonic acid, and its dimer and trimer were run on a Westinghouse 90° sector machine, and that of the tetramer on a Consolidated Electrodynamics 21-110B high resolution instrument all at 70 eV.

Separation of Ester Mixture

trans-Crotonic acid (250 g) was heated in a thermostatted bath at 180° for 28 h; crystallization from hexane (250 ml) recovered 112 g of unchanged *trans* acid. Evaporation of the solvent from the filtrate left 116 g of brown oil, a mixture of dimer **2***a*, polymers **6**, and *cis*- and *trans*-crotonic acids (by n.m.r. approximate weight percentages: 47, 10, 10, and 33 respectively). This oil was dissolved in ammonium hydroxide (640 ml of 2 *N*) with cooling in an ice bath. In subdued light aqueous

Can. J. Chem. Downloaded from www.nrcresearchpress.com by 210.87.254.40 on 09/05/12
For personal use only.

TABLE VII

Integral ratios of proton nuclear magnetic resonance spectra of esters of polymers of crotonic acid

Compound		Integral proton equivalence						
		Proton						
		CH_3—CH=CH—C(=O)—O—CH(CH_3)—CH_2—C(=O)—O—CH_3						
		a	*b*	*c*	*d*	*e*	*f*	*g*
Dimer	Calcd.	3	1	1	1	3	2	3
	Found	3	1	1	1	3.2	2	3
Trimer	Calcd.	3	1	1	2	6	4	3
	Found	3	1	1	2	6.4	4	3.2
Tetramer	Calcd.	3	1	1	3	9	6	3
	Found*	3	1	1	3	8.5	5.5	3
		3	1	1	3.1	9.6	5.8	3

*Integrals of spectra of two consecutive fractions in the distillation.

TABLE VIII

Catalytic hydrogenations of methyl esters of crotonate polymers

Compound	Amount (mmoles)	$NaBH_4$ molarity	Solution (ml)	F.S.E.*	H_2 uptake (mmoles)
Dimer methyl ester	26.5	1.08	5.4	0.40	23.7
	5.80	0.0960	11.0	0.48	4.70 av.
			11.1		
Trimer methyl ester	2.02	0.108	4.35	0.194	2.07
Tetramer methyl ester	3.08	0.0960	7.3	0.332	3.13

*Free space equivalent, or the mmole equivalent for the volume of hydrogen displaced by olefin and borohydride addition. Determination: (ml olefin + ml borohydride) × 0.04.

silver nitrate (1.29 l of 1.1 *N*) was then added with stirring to the solution of ammonium salts, and the precipitated silver salts then filtered off and washed with water. These salts were dried in the dark azeotropically with benzene (1500 ml) using a Dean and Stark apparatus and occasional agitation. When dry, methyl iodide (60 ml plus 40 ml after 1 h) was added and boiling under reflux continued for 1½ h. The reaction mixture was filtered and the benzene removed up a 40 cm Vigreux column under slightly reduced pressure leaving 110 g of brown oil. This was distilled up a Todd column (90 × 2.5 cm, 10:1 reflux ratio) packed with ⅛ in. glass helices. After a forerun (about 30 ml), taken off at about 100 mm pressure consisting of a mixture of benzene and the *cis*- and *trans*-crotonates, methyl-(*trans*-crotonate)-3-hydroxybutyrate (**2***a*, methyl ester; 45 g, b.p. 70°/0.03 mm) was obtained. On a stainless steel gas chromatographic column (6 ft × ⅛ in.) packed with 5% FFAP (mono-ester of 2-nitroterephthallic acid with 20 000 mol. wt. polyethylene glycol) on 90–100 mesh Anachrome ABS support, at 250° with 1 cm^3/min nitrogen flow, a single peak of retention time 1½ min was observed for this compound.

Anal. Calcd. for $C_9H_{14}O_4$ (mol. wt., 186.2): C, 58.05; H, 7.58. Found (mol. wt., ebulliometric in $CHCl_3$, 214): C, 58.1, 57.9; H, 7.38, 7.41.

Spectroscopic examination of a thin film in the i.r. showed for aliphatic C—H a broad weak multiplet 2850 to 3050, saturated and unsaturated ester C=O strong bands at 1750 and 1725 and olefinic C=C stretch at 1665 cm^{-1}. The u.v. spectrum in ethanol showed no maximum above 212 mμ and the complete unambiguous structural correlation of the n.m.r. spectrum is given in Table I.

Separation of Mixtures of trans-Crotonic Acid and Dimers

(a) By Titration

Solutions of mixtures of dimers **2***a* and **2***b* with about 17% of *trans*-crotonic acid present, in acetone–water (30:70, v/v), were titrated with 0.100 *N* sodium hydroxide. Using a pH meter to observe the progress only one plateau with mid-point at pH 5.25 was observed. There was a reproducible marginal point of inflection in this plateau about ⅕ from the low pH end (pH 4.8) which may have been caused by complete formation of monomer sodium salt and the beginning of the neutralization of the dimer acid. This was too slight a difference to be useful in separating mixtures of the two. However, after successful separation of the dimer from monomer by the method immediately following pH determinations confirmed this interpretation of the titrations. Solutions of the dimer **2***a* (0.0098 *M*) and *trans*-crotonic acid (0.01008 *M*) in water at 26.2° gave pH readings of 3.18 and 3.40 respectively (Radiometer type PHM 28 instrument). In acetone–water (30:70, v/v) pH readings of 2.40 and 2.65 respectively were obtained for 1.000 *M* solutions at 26.6°.

Can. J. Chem. Downloaded from www.nrcresearchpress.com by 210.87.254.40 on 09/05/12
For personal use only.

Can. J. Chem. Downloaded from www.nrcresearchpress.com by 210.87.254.40 on 09/05/12
For personal use only.

(b) By Rotary Evaporation

About 500 g of a crude mixture of dimers **2***a* and **2***b* (together about $\frac{1}{3}$ of total, by n.m.r.) and *cis*- and *trans*-crotonic acids, obtained from 2 kg of *trans*-crotonic acid heated at 180 °C for 7 days, was distilled under reduced pressure. Using a 1 m × 2 cm vacuum jacketed column packed with $\frac{1}{8}$ in. glass helices, and a 4:1 reflux ratio, a total of 300 g of a mixture of monomeric acids (b.p. 80°/10 mm to 93°/0.5 mm at pot temperatures of 118–168°) were obtained in the distillate. The residue (140 g) contained less than 10% of the monomeric acids (by n.m.r.) and was predominantly dimer **2** with a higher polymer content than the starting mixture. Distillation of this residue without a column (100–115°/0.1–0.2 mm; pot 120–165°) under conditions such that the vapor temperature was kept as close as possible to that of the distilland yielded only a distillate (114 g in six fractions) comprised largely of the cracking products of dimer **2** and there was no sign of higher polymers in either the distillate or residue. The last four fractions (70 g), containing the largest proportion of dimer, were then combined and worked up using a Büchi vacuum rotary evaporator. The monomeric acids (52 g oily crystals) were first sublimed and distilled out by heating with a boiling water bath (5–0.1 mm Hg). When no further sublimate could be obtained under these conditions, the vacuum was improved to 0.01 mm and the temperature of an oil bath heat source was very gradually raised. At 135° dimer began to come over and 15 g were collected as a colorless oil at 135–140°. No impurities were detectable by n.m.r. Later preparations using rotary evaporation immediately after the initial rough removal of the monomeric acid by distillation gave recoveries of 100–120 g of the dimers **2** from 500 g of the crude oil.

Anal. Calcd. for $C_8H_{12}O_4$ (mol. wt., 172.2): C, 55.8; H, 7.0. Found (mol. wt., ebullioscopic; in acetone 189, 191; in benzene, 377): C, 55.3, 55.7; H, 6.9, 7.0.

The i.r. spectrum of a thin film showed OH stretch at 3500, 3150, and 2650, CH stretch at 2925 and 2975, C=O stretch at 1720 and 1745, and C=C stretch at 1655. The portion of the n.m.r. spectrum of the mixture of *cis* and *trans* dimers attributed to the *trans* (**2***a*), correlated with that of the *trans* monomer methyl ester, and no higher polymer was present (see Table I).

Bromination of the dimer acid at room temperature in CCl_4 failed to reach completion in 8 days. However, in glacial acetic acid (5 ml) at room temperature over 6 days bromine (0.10 g; 0.625 mmoles) was decolorized by 0.125 g (0.728 mmoles) of dimer, and was not decolorized by 0.090 g (0.525 mmoles) of dimer.

A methylene chloride solution of the dimers **2** (17.2 g) as obtained above was washed with water (2 × 10 ml). On drying ($MgSO_4$) and evaporation of the solvent the dimers **2** (15.7 g) were obtained free of monomeric acids. Confirmation of the purity improvement was obtained by titration for acid equivalence. Values of 0.519 and 0.504 (theory = 0.500; crotonic acid = 1) were obtained before and after washing. The only apparent indication by n.m.r. was slight net loss, from 15.9 to 14.7, in the percentage of dimer **2***b* present.

Thermal Cracking of Mixtures of Dimers 2a and 2b

(a) At 250 mm

Dimer mixture (containing 16% **2***b*; 3.8 g) was placed in a short-path micro distillation apparatus, the pressure in the system reduced to 250 mm and heat applied with a mantle at such a rate that distillation was complete in 15 min. The distillate (3.3 g; vapor temperature 157–162°, pot temperature 180–204°) consisted of these acids: *trans*-crotonic, 86.7%; *cis*-crotonic, 11.8%; vinylacetic, 1.5% (by n.m.r). The pot residue (0.4 g) was dimer mixture plus a small amount of *trans*-crotonic acid.

(b) At Atmospheric Pressure

Dimer mixture (as in (*a*); 4 g) was cracked in the same apparatus and at the same rate as in (*a*). The distillate (3.5 g; vapor temperature 182–218°, pot temperature 220–258°) consisted of the following monomeric acids; *trans*-crotonic 81.5%, *cis*-crotonic 12.1%, vinylacetic 1.2%, and in addition 5.2% (by weight) of unchanged dimer. Recalculation of these results correcting for the dimer still present gave the figures quoted in Table III.

(c) Control Experiment

Recrystallized *trans*-crotonic acid (4.6 g) was distilled over the same time in the same apparatus as in (*a*) and (*b*) above, except that the condenser was only air cooled and the receiving flask was cooled in an ice–water bath. The distillate (4.1 g; vapor temperature 179–190°, pot temperature 182–200°) contained no vinylacetic acid and only a trace (0.5% or less) of *cis*-crotonic acid.

Attempted Thermal Cracking of 2a, Methyl Ester

Methyl-(3-*trans*-crotonate)-butyrate (**2***a*, methyl ester; 2.1 g) in the same apparatus as the preceding cracking experiments was distilled over in 10 min (vapor temperature 224–230°, pot temperature 228–240°). The distillate (2 g) consisted entirely of unchanged starting material.

Saponification of Mixture of 2a and 2b

The mixture of dimers (containing 16% **2***b*; 22 g) was boiled in 10% aqueous caustic (120 ml) for $1\frac{1}{2}$ h, and acidified to pH 4 with concentrated hydrochloric acid while cooling in an ice bath, then saturated with sodium chloride. Crystals of *trans*-crotonic acid (6.2 g, m.p. 66–70°) came out of the brine solution, which when recrystallized from hexane melted at 70–72°. The brine solution was then extracted with ether (1 × 50 + 3 × 30 ml) which when dried (Na_2SO_4) and concentrated under reduced pressure, yielded 10.9 g of pale-yellow oil. Distillation of this oil yielded crotonic acid (some *cis*, 2 g, b.p. 99°/16 mm) and, after a middle fraction consisting of a mixture of the crotonic and butyric acids (0.2 g, b.p. 94–149/10 mm), 1.2 g of 3-hydroxybutyric acid (b.p. 149–149.5°/10 mm; lit. b.p. 130°/12–14 mm (9)) was obtained.

Anal. Calcd. for $C_4H_8O_3$: C, 46.15; H, 7.75. Found: C, 46.0, 45.9; H, 8.21, 7.90.

Its identity was confirmed by comparison of its n.m.r. (*vide infra*) and i.r. spectra with those of a redistilled sample of authentic material.[2] The water was then carefully removed from the brine solution on a steam bath under reduced pressure; no crotonic or butyric acid came off with the water (determined by i.r.). The residual oily crystals were washed with ether (3 × 20 ml) and filtered. Drying and evaporation of the ether from the filtrate gave a further 6.7 g of 3-hydroxybutyric acid (as determined by n.m.r.). Total crude yields obtained were 8.3 g (76%) and 8.0 g (61%) of the crotonic acids and 3-hydroxybutyric acid respectively.

[2]Purchased from Aldrich Chemicals Limited.

Can. J. Chem. Downloaded from www.nrcresearchpress.com by 210.87.254.40 on 09/05/12
For personal use only.

The n.m.r. spectrum of 3-hydroxybutyric acid showed: for the methyl protons, a doublet at 1.25 p.p.m., $J = 6.0$ c.p.s.; for the methine proton, a sextet (footnote‡, Table I) at 4.27 p.p.m., $J = 6.0$ c.p.s.; for the methylene protons, a doublet at 2.51 p.p.m., $J = 6.0$ c.p.s.; and for the hydroxyl and carboxyl, a singlet at 7.57 p.p.m. The less complex spin–spin splitting pattern observed here, over that of protons *f* in dimer (Table I), has two possible explanations. Either the diastereomeric methylene hydrogens are equivalent in this special case, or more complex positive and negative coupling constants operate (14). This net effect has invariably been observed where a diastereomeric methylene is adjacent to an optically active R—CHOH-group (6).

Separation of Dimers **2***a and* **2***b*

(a) Thin-Layer Chromatography

A mixture of the dimers **2***a* and **2***b* containing about 15% **2***b* was duplicate spotted on Kodak prepared silica gel plates. They were developed using various appropriate solvent systems (15) with aqueous $KMnO_4$ as the visualizing agent. The R_f values for **2***a* and **2***b* were the same for the solvent systems chloroform with 4 volume % acetic acid, benzene – methanol – acetic acid 45:8:4 by volume, and ethyl acetate – hexane – acetic acid 50:50:1 by volume and were found to be 0.47, 0.78, and 0.65 respectively. Only the system ethanol – water – concentrated ammonium hydroxide (100:12:16 by volume) showed any promise by yielding R_f values of 0.77 for **2***a* and 0.63 for **2***b* (values for ammonium salts). The difficulties expected in scaling this up for elution chromatography to obtain sufficient for one or two cracking experiments made us discontinue this approach.

(b) Preparation of Dimer **2***a Alone*

trans-Crotonic acid was dimerized under conditions such that an insignificant amount of *cis*-crotonic acid would be present (7) and hence avoid even the formation of **2***b* as the dimer was made. *trans*-Crotonic acid (3.5 kg) was heated at 116–119° for 21 days. Generally during this interval the *cis* monomer concentration in the pot was kept below 2% though on two occasions it rose to 5% for a few hours. After cooling, the dimer oil (1300 ml) was decanted from the crystallized *trans*-crotonic acid. This brown oil was diluted with methylene chloride (800 ml) and vigorously washed with cold water (6 × 600 ml), dried, and the solvent removed on a boiling water bath under reduced pressure leaving 1220 g of brown oil. Rotary evaporation of this oil (100–110° oil bath; 0.1 mm) removed 335 g of *trans*-crotonic acid. Continuation of rotary evaporation (130–150° oil bath, 0.05 mm) yielded 526 g of the dimers **2***a* and **2***b* (5.75% of the latter) as a very pale-yellow viscous oil, and a residue of 338 g of viscous brown oil which consisted almost entirely of higher polymers of crotonic acid.

*Preparation of Methyl Esters of Trimer and Tetramer (***6***)*

After a successful dummy run using methanol/sulfuric acid to esterify the dimer, this procedure was used with a portion of the 338 g of higher polymer obtained in the preparation of *trans*-dimer (**2***a*).

Polymer mixture (25.5 g), methanol (64 g), and concentrated sulfuric acid (1 ml) were boiled together under reflux for 6 h. At the end of this time it was allowed to cool and diluted with methylene chloride (30 ml). This solution was washed with dilute brine (2 × 400 ml), saturated aqueous sodium bicarbonate (2 × 100 ml), and water (1 × 100 ml), and then dried ($MgSO_4$), and solvent removed. About 13 g of pale-brown oil remained which was distilled at 0.01 mm pressure using a short path apparatus. Six fractions of the esters were taken: fractions 1 and 2, b.p. 82–95°, 2.8 ml of colorless oil consisting largely of dimer; fraction 3, b.p. 95–128°, 0.7 ml of colorless oil, mixture of dimer and trimer; fraction 4, b.p. 128–136°, 3.9 ml of colorless oil which was trimer (93%, 7% dimer); fraction 5, b.p. 136–175°, 1.5 ml of pale-yellow oil consisting of trimer (38%) and tetramer (62%); fraction 6, b.p. 175–202°, 2.0 ml tetramer pale-yellow oil. The compositions reported above were obtained by gas–liquid chromatography using the same conditions reported under the analysis of the pure dimer ester, except that carrier gas flow rate was 17 cm^3/min here. Trimer methyl ester retention time was 2 min, tetramer 8 min. The elemental analyses, molecular weights, mass spectra, and n.m.r. data on these methyl esters are given in Tables IV, V, and VI. The distinguishing feature noticed in n.m.r. spectra of the methyl esters of the trimer and tetramer over those of the dimer was an increase in the multiplicity of the resonance ascribed to a butyric type methyl. Whereas the dimer yielded a doublet attributable to this moiety, the trimer apparently gave rise to three doublets, each with the same splitting as the dimer doublet, but with the first pair shifted about one cycle downfield and the second, a further cycle downfield. The tetramer additionally gave a further doublet one cycle downfield of the lowest field pair of the trimer.

Unsaturation in Crotonate Polymers by Quantitative Catalytic Hydrogenation

Using a published (16) method the methyl esters of the crotonate dimer, trimer, and tetramer were quantitatively hydrogenated. An unsupported platinum catalyst was prepared *in situ* by treating 10% aqueous chloroplatinic acid (2 ml) in ethanol (40 ml), which in a special borohydride hydrogenation flask had been previously purged with nitrogen, with a 1 *M* stabilized solution of sodium borohydride (10 ml). Excess 6 *N* hydrochloric acid (8 ml) was then added to the flask, followed shortly after by the injection of the olefin, neat. The hydrogenation then proceeded rapidly by the action of the acid present on the standardized sodium borohydride solution as it was added. The rate of borohydride addition was automatically regulated by the hydrogen uptake. Standardization of the borohydride solutions used was by duplicate runs against octene-1 and ethyl crotonate. The average of the four results, which agreed to within 2%, was taken as the molarity.

Acknowledgments

The author thanks Mr. H. D. Mak for obtaining the n.m.r. spectra required for this work and Dr. L. A. Shadoff for the mass spectra. He is also indebted to Dr. J. G. Smith for carrying out the thin-layer chromatography experiments.

1. THACKRAH. Dissertation, Leipzig (1891).
2. J. A. WISLICENUS. Dissertation, Leipzig (1892); Chem. Zentr. I, 413 (1893).
3. J. A. WISLICENUS. Chem. Zentr. II, 259 (1897).

4. E. L. SKAU and B. SAXTON. J. Am. Chem. Soc. **52**, 335 (1930).
5. (*a*) L. M. JACKMAN. Applications of nuclear magnetic resonance in organic chemistry. The Pergamon Press, Ltd., New York. 1959. p. 89. (*b*) K. B. WIBERG and B. J. NIST. The interpretation of n.m.r. spectra. W. A. Benjamin, Inc., New York. 1962. p. 3.
6. C. G. CARLSON and S. J. KUHN. Unpublished results. 1967.
7. M. B. HOCKING. To be published.
8. H. O. HOUSE, V. K. JONES, and G. A. FRANK. J. Org. Chem. **29**, 3327 (1964).
9. Handbook of Chemistry and Physics. 45th ed. *Edited by* R. C. Weast. The Chemical Rubber Co., Cleveland. 1964. p. D77.
10. L. J. BELLAMY. Infra-red spectra of complex molecules. John Wiley and Sons, Inc., New York. 1956. p. 162.
11. R. S. MORRELL and E. K. HANSON. J. Chem. Soc. **85**, 1520 (1904).
12. C. BULK. Ann. **139**, 64 (1866). J. A. WISLICENUS. Chem. Zentr. II, 260 (1897).
13. R. P. LINSTEAD and E. P. NOBLE. J. Chem. Soc. 614 (1934). D. J. G. IVES. J. Chem. Soc. 81 (1938), and references cited therein.
14. M. RABAN. Tetrahedron Letters, 3105 (1966), and references cited therein.
15. K. RANDERATH. Thin-layer chromatography. *Translated by* D. D. Libman. Academic Press, Inc., New York. 1966.
16. H. C. BROWN, K. SIVASANKARAN, and C. A. BROWN. J. Org. Chem. **28**, 214 (1963), and references cited therein.

Can. J. Chem. Downloaded from www.nrcresearchpress.com by 210.87.254.40 on 09/05/12
For personal use only.

Total synthesis of (±)-aristolone[1]

EDWARD PIERS, RONALD W. BRITTON, AND WILLIAM DE WAAL
Department of Chemistry, University of British Columbia, Vancouver 8, British Columbia

Received August 28, 1968

A novel and efficient total synthesis of the racemic form of the sesquiterpene (−)-aristolone (**1**) is presented. The key step involves the cupric sulfate catalyzed intramolecular cyclization of the diazoketone **27**, which produces a mixture of products, the major component of which is (±)-aristolone.

Canadian Journal of Chemistry, **47**, 831 (1969)

Can. J. Chem. Downloaded from www.nrcresearchpress.com by 210.87.254.5 on 09/05/12
For personal use only.

The sesquiterpene (−)-aristolone was initially isolated from *Aristolochia debilis* Sieb. *et* Zucc. in 1955 (1). The structure determination of this interesting natural product was reported (2) some six years later and, in 1962, Büchi and co-workers (3), on the basis of an indirect correlation with maaliol (4), of known absolute configuration, established the absolute configuration of (−)-aristolone as depicted in **1**. We previously carried out, and reported in preliminary form (5), a model study involving the synthesis of (±)-4-demethylaristolone. In this paper we describe the total synthesis of (±)-aristolone.

In any consideration of possible approaches to the total synthesis of (±)-aristolone, it is obvious that the most difficult and complex part of the synthesis would involve the construction of ring B, containing the olefinic double bond and the *gem* dimethylcyclopropyl moiety conjugated to the carbonyl. Of the number of possible routes which might be employed in the construction of these functionalities, we chose the scheme which can be illustrated, in general terms, by the hypothetical conversion of **2** into **3**. This conversion, involving an intramolecular cyclization of an olefinic diazoketone, appeared at first sight to be a potentially efficient method for the synthesis of the required substituted bicyclo[4·1·0]heptanone system. The use of olefinic diazoketones in intramolecular cyclizations was already well documented (6), and success of the above proposed conversion (**2** into **3**) appeared, in our opinion, quite likely.

The starting material which was chosen for the synthesis of the required crucial intermediate of type **2** was the readily available 2,3-dimethylcyclohexanone (7). Conversion of the latter into its 6-*n*-butylthiomethylene derivative **5**, *via* the corresponding hydroxymethylene compound **4**, was readily accomplished by standard procedures (8). Alkylation of **5** with methallyl chloride in *t*-butyl alcohol in the presence of potassium *t*-butoxide (8) gave, in 87% yield, a mixture of the corresponding alkylated products (**6**). Removal of the *n*-butylthiomethylene blocking group by treatment of **6** with potassium hydroxide in refluxing aqueous diethylene glycol (8) provided, in 90% yield, a mixture of *cis*-(**7**) and *trans*-2,3-dimethyl-2-methallylcyclohexanone (**8**). Analysis of this mixture by gas–liquid chromatography (g.l.c.) indicated that these two compounds were present in a ratio of approximately 4:1, respectively. An analytical sample of each epimer was obtained by preparative g.l.c. and each exhibited spectral data which were fully in accord with the assigned structure.

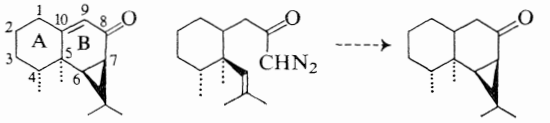

1 **2** **3**

Since the factors which affect the stereochemical outcome of the alkylation of cyclohexanone derivatives are not well understood in detail and were, in fact, the subject of very recent discussion (9), it was rather difficult to predict with certainty the stereochemistry of the alkylation products **7** and **8**. We therefore felt it necessary to obtain unambiguous proof concerning this point and showed that the major alkylation product was, in fact, the desired *cis* compound **7**.

Reaction of the well known and readily available (10) *trans*-10-methyl-2-decalone (**9**) with excess methyllithium in refluxing ether provided a high yield of a semicrystalline material,

[1]Presented at the 51st Annual Conference and Exhibition of the Chemical Institute of Canada, Vancouver, British Columbia, June 3–6, 1968.

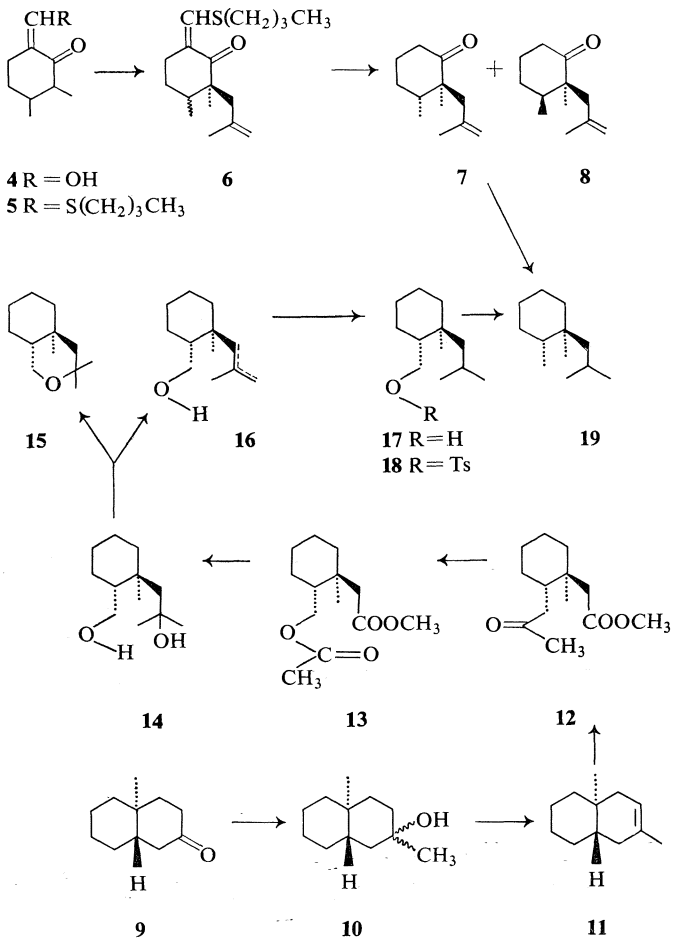

consisting of a mixture of the epimeric tertiary alcohols **10**. Dehydration of this material with a catalytic amount of *p*-toluenesulfonic acid in refluxing benzene produced 2,10-dimethyl-*trans*-2-octalin (**11**) (see ref. 11). The latter was obtained as a clear, colorless oil and was shown by g.l.c. analysis to be greater than 95% pure. Furthermore, the nuclear magnetic resonance (n.m.r.) spectrum exhibited only one olefinic proton signal, an unresolved multiplet at τ 4.72, with a half-height width of 8 Hz. This was clearly in accord with the octalin structure having the olefinic double bond at the 2-position.

The octalin **11** was subjected to a modified ozonolysis reaction (12) and the resulting crude keto-aldehyde was immediately oxidized with Jones reagent (13). The keto-acid thus obtained was esterified with ethereal diazomethane, affording an overall 68% yield (from the octalin **11**) of the keto ester **12**.

In order to obtain, from the keto-ester **12**, a compound suitable for appropriate comparison with the alkylation products (**7** and/or **8**), it can readily be seen that the acetic ester side chain of **12** required conversion to an *iso*butyl-type group, while the keto containing side chain required degradation to a methyl group. This was accomplished as follows.

Baeyer–Villiger oxidation of the keto-ester **12** with trifluoroperacetic acid in dichloromethane in the presence of disodium hydrogen phosphate (see ref. 14) gave, in 83% yield, the diester **13**. Interestingly, the n.m.r. spectrum of this compound exhibited, in addition to the expected signals, a pair of quartets (AB of ABX system) between τ 5.65 and τ 6.32, readily attributable to

Can. J. Chem. Downloaded from www.nrcresearchpress.com by 210.87.254.5 on 09/05/12
For personal use only.

Can. J. Chem. Downloaded from www.nrcresearchpress.com by 210.87.254.5 on 09/05/12
For personal use only.

the methylene protons on the carbon bearing the acetate group. However, the magnetic non-equivalence of methylene protons found in an asymmetric environment is a well-established phenomenon (15), and this therefore deserves no further comment.

Reaction of the diester **13** with excess refluxing ethereal methyllithium afforded the diol **14** in 97% yield. Treatment of the latter with a catalytic amount of *p*-toluenesulfonic acid in refluxing benzene, followed by careful distillation of the crude product, gave, in addition to the cyclic ether **15** (44%, b.p. 64–66° at 0.1 mm), a mixture of the olefinic alcohols **16** (46%, b.p. 104–108° at 0.1 mm). Hydrogenation of the latter over Adam's catalyst in ethanol at room temperature and atmospheric pressure provided the primary alcohol **17**. This material was converted, by treatment with *p*-toluenesulfonyl chloride in pyridine at 0°, into the corresponding tosylate (**18**) and the crude material thus obtained was subjected to lithium aluminium hydride reduction in refluxing tetrahydrofuran. The product, *cis*-1,2-dimethyl-1-*iso*butylcyclohexane (**19**) was obtained in 66% overall yield from the alcohol **17**.

When the major alkylation product (**7**) was subjected to successive catalytic hydrogenation (ethanol, Adam's catalyst) and Huang–Minlon reduction (16), the corresponding hydrocarbon was obtained in high yield. The latter was shown to be identical (refractive index, infrared and n.m.r. spectra, g.l.c. retention time) with *cis*-1,2-dimethyl-1-*iso*butylcyclohexane (**19**) obtained from alcohol **17** as described above. This comparison unambiguously proved that the major alkylation product was, in fact, the desired *cis*-2,3-dimethyl-2-methallylcyclohexanone (**7**).

Having obtained a suitable synthetic intermediate with appropriate stereochemistry, it became necessary at this point, bearing in mind the initially proposed synthetic approach, to convert the methallyl group of **7** into the methylpropenyl moiety. In this connection, we had found in a model study (5) that 2-methyl-2-methallylcyclohexanone was smoothly converted, by treatment with *p*-toluenesulfonic acid in refluxing benzene, into a mixture consisting mainly of the starting material and 2-methyl-2-methylpropenylcyclohexanone in a ratio of approximately 1:3, respectively. This procedure was therefore adopted in the present work.

A solution of compound **7** in benzene containing *p*-toluenesulfonic acid was refluxed for three days and the reaction mixture was then subjected to aqueous work-up. Gas–liquid chromatographic analysis of the crude product showed that it consisted of a mixture, containing the starting material **7** (approximately 12%), the desired cyclohexanone derivative **20** (46%), the cyclic hemiketal **21** (37%) and an unidentified compound (5%). Distillation of this material (b.p. 66–68° at 2.8 mm) allowed the isolation (see Experimental) of a small amount of the crystalline hemiketal **21**, m.p. 74–74.5°. The spectral data of this compound was in full accord with the assigned structure. It should be noted that the hemiketal **21**, when heated at temperatures greater than 120° readily dihydrated to afford the corresponding cyclic enol-ether **22** (see below).

When the bulk of the material obtained from the above distillation was redistilled, at 53 mm pressure, through a spinning band column, the initial fractions consisted of a mixture of water and the enol ether **22** (the dehydration product of hemiketal **21**). The structure assigned to compound **22**, b.p. 128° at 53 mm, was fully substantiated by spectral data. It should be noted that this compound was extremely sensitive to moisture and, even upon exposure to the atmosphere, readily hydrated to re-form the crystalline hemiketal **21**.

A later fraction from the above spinning-band distillation consisted of nearly pure desired *cis*-2,-3-dimethyl-2-methylpropenylcyclohexanone **20**, b.p. 143–144° at 53 mm. The isolated yield of this compound was approximately 22% and thus, in contrast to the equivalent reaction in the model study (5), the direct acid-catalyzed conversion of compound **7** into compound **20** was not particularly efficient.[2] The n.m.r. spectrum of compound **20**, particularly when compared with that of the starting material **7**, clearly showed that the carbon–carbon double bond had undergone the desired migration. Thus, while **7**

[2]We were subsequently able to show (E. Piers and W. de Waal, unpublished results) that the conversion of **7** into **20** could be carried out more efficiently by use of a modified sequence in which the keto group of **7** was first protected by formation of the corresponding ethylene ketal. Subsequent acid-catalyzed isomerization of the carbon–carbon double bond, followed by removal of the ketal protecting group (*p*-toluenesulfonic acid in refluxing dry acetone) and separation of isomers allowed the isolation of cyclohexanone **20** in 50% overall yield (from **7**).

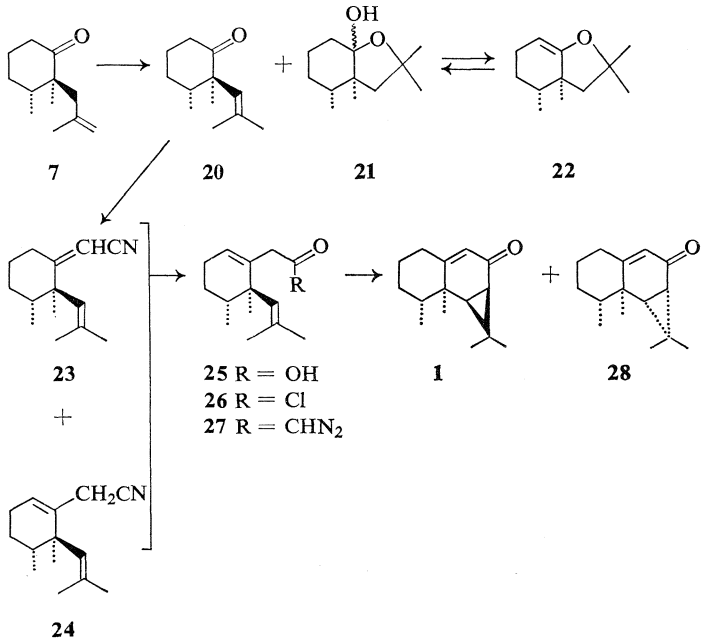

exhibited signals for two olefinic protons (τ 5.17 and τ 5.27) and one vinyl methyl group (τ 8.38), the isomerized material **20** showed signals for only one olefinic proton (τ 4.59) and two vinyl methyl groups (τ 8.27 and τ 8.57).

Having obtained in sufficient quantity a cyclohexanone derivative with the desired functionality and stereochemistry, we planned to use the keto group of **20** as a "handle" for the introduction of the required diazoketone-containing side chain. We initially considered for this purpose the reaction of **20** with the modified Wittig reagent, triethyl phosphonoacetate (17). However, this reaction proved very sluggish and even when carried out at elevated temperatures, produced no useful result. Since we felt that the failure of this reaction was due, at least in part, to the sterically hindered nature of the carbonyl group in **20**, we decided to attempt the use of a reagent which was sterically less demanding, namely, diethyl cyanomethylphosphonate (17). This approach proved successful. Thus, reaction of cyclohexanone **20** with diethyl cyanomethylphosphonate in the presence of methylsulfinyl carbanion in dimethyl sulfoxide (18) at 100° for 1 h, produced, in 87% yield, a mixture of the α,β-unsaturated nitrile **23** and the β,γ-unsaturated nitrile **24**, in a ratio of approximately 2:1, respectively.[3] The fact that these compounds were isomeric was clearly shown by the spectral data. The α,β-unsaturated isomer **23** exhibited a strong ultraviolet absorption at 220.5 mμ (ε = 12 300) and, in the n.m.r. spectrum, showed a one-proton singlet at τ 4.75 (=CHCN). The β,γ-unsaturated isomer **24**, on the other hand, gave no strong ultraviolet absorption and, in the n.m.r. spectrum, exhibited a broad one-proton signal at τ 4.07 (γ-vinyl H) and a two-proton multiplet at τ 7.01 (—CH_2CN).

Hydrolysis of the mixture of nitriles (**23** and **24**) with potassium hydroxide in refluxing aqueous ethanol afforded, in 82% yield, the β,γ-unsaturated carboxylic acid **25**. That the double bond had now completely isomerized into the β,γ-position was again clearly shown by the lack of an appropriate absorption in the ultraviolet and by the n.m.r. spectrum which showed, in addition to a two-proton multiplet at τ 7.07 (—CH_2COOH), the γ-vinyl proton as a poorly resolved triplet at τ 4.35. Although the

[3]The relative amounts of these two isomers in the product depended somewhat on the reaction conditions and reaction time.

Can. J. Chem. Downloaded from www.nrcresearchpress.com by 210.87.254.5 on 09/05/12
For personal use only.

Can. J. Chem. Downloaded from www.nrcresearchpress.com by 210.87.254.5 on 09/05/12
For personal use only.

base-promoted equilibration of α,β- and β,γ-unsaturated carboxylic acids is a well-known process (19), it is interesting that in the present case the equilibrium lies completely on the side of the β,γ-unsaturated isomer. One of the major factors contributing to this phenomenon may well be the $A^{(1,3)}$ strain (20) which would be associated with the exocyclic double bond in the α,β-unsaturated isomer.

The carboxylic acid **25** was converted into its sodium salt and the latter was reacted with oxalyl chloride in benzene at 0°. The crude acid chloride **26** (λ_{max} 5.62 μ) thus obtained was, due to its instability, immediately converted, by reaction with dry ethereal diazomethane, into the corresponding diazoketone **27** (λ_{max} 4.79, 6.15 μ). The n.m.r. spectrum of the crude diazoketone indicated that during the sequence **25** → **26** → **27**, the olefinic double bond had remained in the β,γ-position with respect to the carbonyl group. This was of some importance since any migration of the double bond into conjugation with the carbonyl would undoubtedly have resulted in a large predominance of the geometric isomer having the diazoketone moiety *trans* to the ring carbon bearing the methylpropenyl substituent, thus making the subsequent intramolecular cyclization (see below) of the diazoketone impossible.

When the crude diazoketone **27** was refluxed in cyclohexane in the presence of cupric sulfate (6) and the crude product distilled under reduced pressure, a clear oil (70%, based on the carboxylic acid **25**) was obtained. This material was shown by g.l.c. analysis to consist of approximately 42% (±)-aristolone (**1**), 20% (±)-6,7-epi-aristolone (**28**) and a number of minor unidentified components. Purification of this mixture by a combination of preparative thin-layer chromatography and preparative g.l.c. allowed the isolation of both of the major products. Thus, (±)-aristolone (**1**) was obtained as a crystalline solid which, upon recrystallization from petroleum ether, exhibited m.p. 62–63°. This material was shown to be identical (m.p., mixed m.p., infrared, and n.m.r.[4] spectra) with a recrystallized (petroleum ether) 1:1 mixture of (−)-aristolone and α-ferulone [(+)-aristolone] (22).

(±)-6,7-Epi-aristolone (**28**) was obtained as an oil. It was shown to be isomeric with (±)-aristolone by high resolution mass spectrometry, and gave spectral data in complete accord with the assigned structure.

It should be noted that very recently another synthesis of (±)-aristolone by a sequence completely different from that described above, was reported (23).

Experimental

Melting points, which were determined on a Kofler block, and boiling points are uncorrected. Ultraviolet spectra were, unless otherwise noted, measured in methanol solution on either a Cary, model 14, or a Unicam, model SP. 800, spectrophotometer. Routine infrared spectra were recorded on a Perkin–Elmer Infracord model 137 spectrophotometer, while all comparison spectra were recorded on a Perkin–Elmer model 421 spectrophotometer. Nuclear magnetic resonance spectra were taken in dueteriochloroform solution on Varian Associates spectrometers, model A-60 and/or model HA-100. Line positions are given in the Tiers τ scale, with tetramethylsilane as an internal standard; the multiplicity, integrated peak areas, and proton assignments are indicated in parentheses. Gas–liquid chromatography (g.l.c.) was carried out on an Aerograph Autoprep, model 700. The following columns (10 ft × 1/4 in., unless otherwise noted) were employed, with the inert, supporting material being 60/80 mesh Chromosorb W in each case: column A, 20% FFAP; column B (10 ft × 3/8 in.), 30% FFAP; column C, 15% QF-1; column D, 3% SE-30; column E, 20% SE-30; column F (10 ft × 3/8 in.), 30% Apiezon J; column G, 10% Apiezon J; column H, 10% FFAP; column I (20 ft × 3/8 in.), 30% SE-30. The specific column used, along with column temperature and carrier gas (helium) flow-rate (in ml/min), are indicated in parentheses. Microanalyses were performed by Mr. P. Borda, Microanalytical Laboratory, University of British Columbia, Vancouver.

*6-Hydroxymethylene-2,3-dimethylcyclohexanone (**4**)*

To an ice-cooled, stirred suspension of powdered sodium methoxide 78 g, 1.44 moles) in 800 ml of dry benzene, kept under an atmosphere of dry nitrogen, was added 71 g (0.564 mole) of 2,3-dimethylcyclohexanone. The resulting mixture was stirred for 10 min, and then 70 g (0.945 mole) of ethyl formate was added. The mixture was warmed to room temperature and allowed to stand overnight. Water was added, the mixture was thoroughly shaken, and the layers separated. The organic layer was extracted with two portions of 10% aqueous sodium hydroxide. The combined aqueous layer and alkaline extracts were cooled, acidified with 6 *N* hydrochloric acid, and thoroughly extracted with ether. The combined extracts were washed with water and dried over anhydrous magnesium sulfate. Removal of the solvent, followed by distillation of the residual oil under reduced pressure, gave 77.5 g (90%) of the hydroxymethylene derivative **4** as a pale-yellow oil, b.p. 60–63° at 2 mm,

[4]For an analysis of the n.m.r. spectrum of (−)-aristolone, see ref. 21.

n_D^{20} 1.5135. Ultraviolet, λ_{max} 281 mμ, λ_{max} (NaOH added) 316 mμ; infrared (film), λ_{max} 6.05, 6.25 μ. The instability of this compound precluded the acquisition of satisfactory analytical data.

6-n-Butylthiomethylene-2,3-dimethylcyclohexanone (5)

A solution of the hydroxymethylene derivative (**4**) (77.5 g, 0.504 mole), *n*-butyl mercaptan (55.5 g, 0.615 mole), and *p*-toluenesulfonic acid (50 mg) in 500 ml of dry benzene was refluxed in a nitrogen atmosphere under a Dean–Stark water separator for 6 h, at which time 6 ml of water had been collected. The cooled solution was washed with saturated aqueous sodium bicarbonate, then with water and finally dried over anhydrous magnesium sulfate. Removal of the solvent gave an oil which, upon distillation under reduced pressure, afforded 99.4 g (87%) of the *n*-butylthiomethylene derivative (**5**), b.p. 116–118° at 0.3 mm, n_D^{20} 1.5368; ultraviolet, λ_{max} 309 mμ (ε = 15 400); infrared (film), λ_{max} 6.01, 6.48 μ.

Anal. Calcd. for $C_{13}H_{22}OS$: C, 68.97; H, 9.79. Found: C, 68.59; H, 9.71.

2,3-Dimethyl-2-methallyl-6-n-butylthiomethylenecyclohexanone (6)

The *n*-butylthiomethylene derivative **5** (99.4 g, 0.440 mole) was added to 1800 ml of dry *t*-butanol containing 144 g (1.40 moles) potassium *t*-butoxide and the resulting solution was stirred at room temperature for 10 min and then cooled to 0°. Freshly distilled methallyl chloride (255 g, 2.82 moles) was added slowly and the reaction mixture was refluxed under an atmosphere of dry nitrogen for 2 h. Most of the solvent was removed under reduced pressure and the residue was diluted with water. The resulting mixture was extracted thrice with ether. The combined ether extracts were washed with water and dried over anhydrous magnesium sulfate. Removal of the solvent gave an oil which, upon distillation under reduced pressure, afforded 107 g (87%) of 2,3-dimethyl-2-methallyl-6-*n*-butylthiomethylenecyclohexanone (**6**) (mixture of epimers), b.p. 106–109° at 0.25 mm, n_D^{20} 1.5043; ultraviolet, λ_{max} 281 mμ (ε = 14 700); infrared (film), λ_{max} 6.00, 6.32, 11.10 μ.

Anal. Calcd. for $C_{17}H_{28}OS$: C, 72.80; H, 10.06. Found: C, 73.09; H, 10.11.

cis- and trans-2,3-Dimethyl-2-methallylcyclohexanone (7 and 8)

To a solution of the above alkylated material (**6**) (107 g) in 700 ml of diethylene glycol was added 650 ml of 25% aqueous potassium hydroxide and the resulting solution was refluxed under nitrogen for 18 h. The reaction mixture was steam distilled until the distillate was clear. The distillate was saturated with salt and extracted thrice with ether. The combined ether extracts were washed with water, dried (anhydrous magnesium sulfate), and evaporated. The residual oil, upon distillation under reduced pressure, gave 66 g (96%) of a mixture of *cis*- and *trans*-2,3-dimethyl-2-methallyl cyclohexanone, (**7** and **8**), b.p. 76–80° at 3.6 mm. Analysis of this mixture by g.l.c. (column A, 140°, 85) indicated that the ratio of the *cis* compound (**7**) to the *trans* compound (**8**) was approximately 4:1. An analytical sample of each epimer was obtained by preparative g.l.c. (column B, 250°, 120). The desired *cis* epimer **7** exhibited n_D^{20} 1.4809. Infrared (film), λ_{max} 5.89, 6.13, 11.25 mμ; n.m.r., τ 5.17, 5.27 (unresolved multiplets, 2H, $=CH_2$), 7.33, 7.84 (broadened AB-type pair of doublets, 2H, vinyl $—CH_2$, J = 14 Hz), 8.38 (broad singlet, 3H, vinyl methyl), 9.13 (singlet, 3H, tertiary methyl), 9.28 (doublet, 3H, secondary methyl, J = 6.5 Hz).

Anal. Calcd. for $C_{12}H_{20}O$: C, 80.01; H, 11.11. Found: C, 79.78; H, 11.31.

The *trans* epimer (**8**) exhibited n_D^{20} 1.4812; infrared (film), λ_{max} 5.88, 6.11, 11.28 μ; n.m.r., τ 5.22, 5.32 (unresolved multiplets, 2H $=CH_2$), 7.62, 8.04 (broadened AB-type pair of doublets, 2H, vinyl $—CH_2$, J = 14 Hz), 8.42 (broad singlet, 3H, vinyl methyl), 8.84 (singlet, 3H, tertiary methyl), 9.27 (doublet, 3H, secondary methyl, J = 5.8 Hz).

Anal. Calcd. for $C_{12}H_{20}O$: C, 80.01; H, 11.11. Found: C, 79.78; H, 11.27.

2,10-Dimethyl-trans-2-octalin (11)

To a solution of *trans*-10-methyl-2-decalone (10) (**9**, 44.5 g, 0.236 mole) in 1 l of dry ether was added 9 g (0.41 mole) of methyllithium in 200 ml of ether. The solution was refluxed for 8 h, cooled, and the excess methyllithium was destroyed by careful addition of dilute hydrochloric acid. The ether layer was washed with water, dried (anhydrous magnesium sulfate), and evaporated. Distillation of the residual material under reduced pressure gave 42.7 g (88%) of a mixture of epimeric alcohols (**10**) as a semi-crystalline mass, b.p. 62–67° at 0.2 mm. This material was not further purified, but was used directly for the next step.

A solution of the above mixture of alcohols (**10**) (2.0 g) and *p*-toluenesulfonic acid (25 mg) in 25 ml of dry benzene was refluxed under a Dean–Stark water separator until the required amount of water had been collected. The solution was cooled, washed with dilute aqueous sodium hydroxide, and evaporated. Distillation of the residual oil afforded 1.15 g (70%) of 2,10-dimethyl-*trans*-2-octalin (**11**) as a clear colorless oil, b.p. 91–93° at 11 mm. Gas–liquid chromatographic analysis (column C, 170°, 85) indicated that this material was greater than 95% pure. An analytical sample, collected by preparative g.l.c. (column C, 150°, 85) exhibited n_D^{20} 1.4873. Infrared (film), λ_{max} 6.94, 7.33, 12.73 μ; n.m.r., τ 4.72 (unresolved multiplet, 1H, olefinic proton, width at half-height = 8 Hz), 8.37 (broad singlet, 3H, vinyl methyl), 9.23 (singlet, 3H, tertiary methyl).

Anal. Calcd. for $C_{12}H_{20}$: C, 87.73; H, 12.27. Found: C, 87.58; H, 12.40.

Preparation of Keto-ester 12

A solution of the octalin **11** (19.6 g, 0.12 mole) in 1 l of dry methanol was cooled by means of a dry ice – acetone bath. Ozone was bubbled through the solution until a permanent blue color persisted, and then continued for an additional 15 min. Dimethyl sulfide (11.9 ml, 0.162 mole) was added and the solution was allowed to warm to room temperature. The methanol and excess dimethyl sulfide were removed under reduced pressure and the residue was taken up in ether. The ether solution was washed with water, dried (anhydrous magnesium sulfate), and evaporated. The residual crude keto-aldehyde was immediately oxidized with Jones reagent (13) (30 ml) and, after

Can. J. Chem. Downloaded from www.nrcresearchpress.com by 210.87.254.5 on 09/05/12
For personal use only.

Can. J. Chem. Downloaded from www.nrcresearchpress.com by 210.87.254.5 on 09/05/12
For personal use only.

the normal work-up, afforded 22.7 g of the corresponding keto-acid. Treatment of the latter crude material with excess ethereal diazomethane, followed by removal of the ether and distillation of the residual oil, gave 18.2 g (68%) of the desired keto-ester (**12**), b.p. 85–85.5° at 0.1 mm. An analytical sample isolated by preparative g.l.c. (column D, 160°, 80), showed n_D^{20} 1.4712. Infrared (film), λ_{max} 5.83, 6.97, 9.83 μ; n.m.r., τ 6.34 (singlet, 3H, —$COOCH_3$), 7.73 (singlet, 2H, —CH_2COOCH_3), 7.85 (singlet, 3H, —$COCH_3$), 9.07 (singlet, 3H, tertiary methyl).

Anal. Calcd. for $C_{13}H_{22}O_3$: C, 68.99; H, 9.79. Found: C, 69.30; H, 10.01.

The 2,4-dinitrophenylhydrazone derivative of the keto-ester **12** exhibited m.p. 111–112°.

Anal. Calcd. for $C_{19}H_{26}N_4O_6$: C, 56.15; H, 6.44; N, 13.78. Found: C, 55.85; H, 6.65; N, 13.61.

*Preparation of Diester **13***

To a solution of the keto-ester **12** (18.2 g, 85 mmoles) in 1.7 l of dichloromethane was added 220 g of anhydrous disodium hydrogen phosphate. The resulting mixture was stirred vigorously and a solution of trifluoroperacetic acid (prepared by adding 13.5 ml of 90% hydrogen peroxide to 86.5 ml of trifluoroacetic anhydride in 42 ml of dichloromethane) was added. The mixture was stirred at room temperature for 1.5 h and then at reflux for 3.5 h. Ethyl acetate (500 ml) was added and the mixture was washed with saturated aqueous sodium bicarbonate, water, saturated brine, and then dried over anhydrous magnesium sulfate. Removal of the solvents, followed by distillation of the residual oil afforded 16.2 g (83%) of the diester **13**, b.p. 96–102° at 0.1 mm. An analytical sample, collected by preparative g.l.c. (column D, 190°, 90), exhibited n_D^{20} 1.4658; infrared (film), λ_{max} 5.77, 6.97, 9.71 μ; n.m.r., τ 5.65–6.32 (pair of quartets, 2H, —CH_2—OAc, AB of ABX system), 6.35 (singlet, 3H, —$COOCH_3$), 7.64 (singlet, 2H, CH_2COOCH_3), 7.96 (singlet, 3H, —$OCOCH_3$), 9.03 (singlet, 3H, tertiary methyl).

Anal. Calcd. for $C_{13}H_{22}O_4$: C, 64.43; H, 9.14. Found: C, 64.28; H, 9.23.

*Preparation of Diol **14***

To a solution of the diester **13** (15.8 g, 65.5 mmoles) in 250 ml of dry ether was added 300 ml of 1.7 *M* methyllithium in ether. The solution was refluxed overnight, cooled, and quenched by careful addition of water. The ether solution was dried over anhydrous magnesium sulfate. Removal of the ether and distillation of the residual oil provided 12.6 g (97%) of the diol **14**, b.p. 109–110° at 0.15 mm; infrared (film), λ_{max} 3.08, 6.89, 9.80 μ; n.m.r., τ 6.17–6.83 (pair of quartets, 2H, —CH_2OH, AB of ABX system), 6.65 (singlet, 2H, OH | 2—O—H), 8.15, 8.54 (doublets, 2H, —CH_2—$C(CH_3)_2$, AB system, J = 15 Hz), 8.64, 8.76 (singlets, 6H, OH | —$C(CH_3)_2$), 9.12 (singlet, 3H, tertiary methyl). Due to the ease with which this compound dehydrated, it was virtually impossible to obtain pure diol which was not contaminated with small amounts of its dehydration products. Satisfactory analytical data was therefore not obtained.

*Dehydration of Diol **14***

A solution of the diol **14** (5.0 g) in 250 ml of dry benzene containing 50 mg of *p*-toluenesulfonic acid was refluxed under a Dean–Stark water separator for 4 h, at which time the required amount of water had been collected. The solution was cooled, washed with dilute aqueous sodium bicarbonate, and dried over anhydrous magnesium sulfate. Removal of the benzene gave an oil, which, upon distillation gave two distinct fractions. The first fraction (2.0 g, 44%, b.p. 64–66° at 0.1 mm) was shown by g.l.c. analysis (column E, 135°, 100) to consist of nearly pure cyclic ether **15**. An analytical sample was collected by preparative g.l.c. (column F, 230°, 150), and exhibited n_D^{20} 1.4747; infrared (film), λ_{max} 6.97, 7.30, 9.40, 9.57 μ; n.m.r., τ 6.25–6.80 (diffuse, 2H, —CH_2—O—, overlapped AB of ABX system), 8.71, 8.81, 8.97 (singlets, 9H, tertiary methyls).

Anal. Calcd. for $C_{12}H_{22}O$: C, 79.07; H, 12.15. Found: C, 79.19; H, 12.17.

The second fraction (2.1 g, 46%) was a mixture of the two olefinic alcohols **16**, b.p. 104–108° at 0.1 mm, n_D^{20} 1.4919; infrared (film), λ_{max} 3.05, 6.12, 6.98, 9.80, 10.19, 11.28 μ.

Anal. Calcd. for $C_{12}H_{22}O$: C, 79.07; H, 12.15. Found: C, 79.17; H, 12.35.

*Preparation of Alcohol **17***

The hydrogenation of the mixture of the olefinic alcohols **16** was carried out in ethanol at room temperature and atmospheric pressure using platinum as the catalyst. From 1.85 g of **16** there was obtained 1.23 g (71%) of pure saturated alcohol **17**, b.p. 110–115° (bath temperature) at 0.15 mm, n_D^{20} 1.4749. Infrared (film), λ_{max} 6.04, 6.90, 9.83 μ; n.m.r., τ 6.12–6.88 (pair of quartets, 2H, —CH_2OH, AB of ABX system), 9.07 (doublet, 6H, —$CH(CH_3)_2$, J = 6.2 Hz), 9.22 (singlet, 3H, tertiary methyl).

Anal. Calcd. for $C_{12}H_{24}O$: C, 78.19; H, 13.12. Found: C, 78.33; H, 13.20.

*cis-1,2-Dimethyl-1-isobutylcyclohexane (**19**)*

*(a) From Alcohol **17***

A solution of alcohol **17** (1 g, 5.4 mmoles) in 5 ml of dry pyridine was cooled to 0° and 1.09 g (5.75 mmoles) of *p*-toluenesulfonyl chloride was added. The solution was stirred at 0° for 1.5 h and then diluted with ice-cold water. The mixture was extracted with ether and the ether solution was washed with saturated aqueous sodium bicarbonate, water, saturated brine, and then dried over anhydrous magnesium sulfate. Removal of the ether gave 1.77 g of the crude tosylate **18** as a pale-yellow oil. The latter was dissolved in 32 ml of dry tetrahydrofuran and 380 mg (10 mmoles) of lithium aluminium hydride was added. The mixture was refluxed, with stirring, for 22 h, cooled, and the excess hydride was destroyed by careful addition of ice-cold water. Ether was added and the organic layer was separated and dried over anhydrous magnesium sulfate. Removal of the solvents, followed by distillation of the residual oil, afforded 500 mg (66%) of *cis*-1,2-dimethyl-1-*iso*butylcyclohexane (**19**), b.p. 110° at 10 mm. An analytical sample was collected by preparative g.l.c. (column G, 165°, 85) and exhibited n_D^{20} 1.4544. The n.m.r. spectrum of this compound showed signals only in the expected region, between τ 8.0 and τ 9.3.

Can. J. Chem. Downloaded from www.nrcresearchpress.com by 210.87.254.5 on 09/05/12
For personal use only.

Anal. Calcd. for $C_{12}H_{24}$: C, 85.63; H, 14.37. Found: C, 85.73; H, 14.41.

(b) From cis-2,3-Dimethyl-2-methallylcyclohexanone (7)

Hydrogenation of 202 mg of *cis*-2,3-dimethyl-2-methallylcyclohexanone (**7**) in ethanol at room temperature and atmospheric pressure, using platinum as the catalyst, gave 195 mg of undistilled *cis*-2,3-dimethyl-2-*iso*butylcyclohexanone, which exhibited one component by g.l.c. (column G, 200°, 80). The latter was not further purified, but was directly subjected to Huang–Minlon reduction (16). Thus, a solution of the cyclohexanone (190 mg) in diethylene glycol (1.5 ml) containing 0.5 g of potassium hydroxide and 0.2 ml of hydrazine hydrate was refluxed for 2 h. The reflux condensor was removed and replaced by a distillation head, and the temperature of the reaction mixture was slowly raised to 195° and kept at this temperature for 1 h. The distillate and the cooled reaction mixture were combined, diluted with water, and thoroughly extracted with ether. The combined ether extracts were washed with dilute hydrochloric acid, water, saturated brine, and dried over anhydrous magnesium sulfate. Careful removal of the ether afforded 176 mg (94%) of a pale-yellow oil which exhibited one component by g.l.c. (column G, 155°, 80). An analytical sample, collected by preparative g.l.c. (column G, 155°, 80), exhibited refractive index, infrared and n.m.r. spectra, and g.l.c. retention time identical with those of *cis*-1,2-dimethyl-1-*iso*butylcyclohexanone (**19**) obtained from the alcohol **17**, as described above.

Acid-catalyzed Isomerization of cis-2,3-Dimethyl-2-methallylcyclohexanone (7)

A solution of compound **7** (62 g, containing approximately 5% of its epimer **8**) in 1 l of dry benzene containing 1 g of *p*-toluenesulfonic acid was refluxed under an atmosphere of nitrogen for 3 days. The cooled solution was extracted twice with saturated aqueous sodium bicarbonate, then with water, and finally with saturated brine. After drying (anhydrous magnesium sulfate) the benzene was removed, yielding a yellow oil, which was shown by g.l.c. analysis (column H, 140°, 85) to consist of approximately 46% of the desired cyclohexanone **20**, 12% of the starting material, 37% of the cyclic hemiketal **21**,[5] and 5% of an unidentified compound. Distillation of the oil under reduced pressure (2.8 mm) gave the following fractions: fraction 1, b.p. 66–66.5°, 7 g; fraction 2, b.p. 66.5°, 7 g; fraction 3, b.p. 66.5–67.5°, 37.5 g; fraction 4, b.p. 67.5–68°, 3.5 g. Fraction 3 contained a small amount of crystalline material, while fraction 4 was nearly entirely crystalline. Isolation of this material, followed by recrystallization from petroleum ether (b.p. 60–80°) gave pure hemiketal **21** (3.2 g), m.p. 74–74.5°. Infrared (Nujol), λ_{max} 2.92, 6.92, 7.28, 9.16, 9.85, 10.08 μ; n.m.r., τ 7.69 (broad singlet, 1H, —O—H, D_2O exchange), 8.14 (singlet, 2H, —C—CH_2—C—), 8.58, 8.65, 9.06 (singlets, 9H, 3 tertiary methyls), 9.13 (doublet, 3H, secondary methyl J = 6.2 Hz).

Anal. Calcd. for $C_{12}H_{22}O_2$: C, 72.68; H, 11.18. Found: C, 73.00; H, 11.00.

Fraction 2 and the oil of fraction 3 from the above distillation were combined and subjected to careful fractional distillation through a spinning band column (stainless steel, 8 mm × 24 in.). The distillation was carried out at a pressure of 53 mm, and the various fractions were subjected to g.l.c. analysis (column H, 140°, 85). The initial three fractions (5.5 g) consisted mainly of a mixture of the cyclic enol-ether **22** and water (due to dehydration of the hemiketal **21**). Fraction 4 (11.1 g, b.p. 128°) was nearly pure enol-ether **22**, fraction 7 (13.7 g, b.p. 143–144°) was shown to be greater than 90% pure ketone **20**, while fractions 5 and 6 (6.4 g, b.p. 128–143°) consisted of a mixture of compounds **20** and **22**. Fractions 8 and 9 (5 g, b.p. 144–147°) contained ketone **20** and starting material **7** in a ratio of approximately 5:2, respectively.

An analytical sample of the cyclic enol ether **22** was obtained from fraction 4 by preparative g.l.c. (column B, 200°, 110). This compound was extremely sensitive to moisture and, even upon exposure to the atmosphere, readily hydrated to afford the crystalline hemiketal **21**. The pure enol-ether exhibited n_D^{20} 1.4760. Ultraviolet (cyclohexane) λ_{max} 200 mμ (ε = 8 760); infrared (film), λ_{max} 5.92 μ; n.m.r., τ 5.36 (triplet, 1H, olefinic H, J = 3.5 Hz), 8.57, 8.74, 8.90 (singlets, 9H, tertiary methyls), 9.10 (doublet, 3H, secondary methyl, J = 6 Hz).

Anal. Calcd. for $C_{12}H_{20}O$: C, 80.01; H, 11.11. Found: C, 80.19; H, 11.10.

An analytical sample of *cis*-2,3-dimethyl-2-methylpropenylcyclohexanone (**20**) was obtained from fraction 7 by preparative g.l.c. (column B, 200°, 110) and exhibited n_D^{20} 1.4822. Infrared (film), λ_{max} 5.85 μ; n.m.r., τ 4.59 (multiplet, 1H, vinyl H), 8.27, 8.57 (doublets, 6H, vinyl methyls, J = 1.5, 1.3 Hz, respectively), 8.91 (singlet, 3H, tertiary methyl), 9.17 (doublet, 3H, secondary methyl, J = 7 Hz).

Anal. Calcd. for $C_{12}H_{20}O$: C, 80.01; H, 11.11. Found: C, 80.08; H, 11.02.

Reaction of Ketone 20 with Diethyl Cyanomethylphosphonate

A stirred suspension of sodium hydride (9.3 g, 0.387 mole) in dry dimethyl sulfoxide (200 ml) was slowly heated under an atmosphere of nitrogen, to 75° and kept at this temperature until frothing had ceased (approximately 45 min). The solution was cooled to room temperature and a solution of diethyl cyanomethylphosphonate (72.6 g, 0.387 mole) in 125 ml of dimethyl sulfoxide was added. The solution was stirred for 10 min and then a solution of compound **20** (13 g, 64.2 mmoles) in 125 ml of dimethyl sulfoxide was added. The reaction mixture was heated at 100° for 1 h, cooled, diluted with water, and then thoroughly extracted with petroleum ether (b.p. 30–60°). The combined extracts were washed twice with water, once with saturated brine, and then dried over anhydrous magnesium sulfate. Removal of the solvent, followed by distillation of the residual oil under reduced

[5]It should be noted that the hemiketal **21** was not stable to the high temperatures used in the g.l.c. analysis, but, in fact, dehydrated to the enol-ether **22**. Thus, both authentic hemiketal and enol-ether exhibited identical g.l.c. retention times. However, distillation of the crude reaction product under reduced pressure at a relatively low temperature clearly showed that none of the relatively low boiling enol-ether was present in the initially obtained mixture.

Can. J. Chem. Downloaded from www.nrcresearchpress.com by 210.87.254.5 on 09/05/12
For personal use only.

pressure yielded 12.7 g (89%) of a pale-yellow oil, b.p. 86–91° at 0.25 mm. This material was shown, by g.l.c. analysis (column C, 190°, 100), to consist of a mixture of the α,β-unsaturated nitrile **23** and the β,γ-unsaturated nitrile **24**, in a ratio of approximately 2:1, respectively. An analytical sample of each of these compounds was isolated by preparative g.l.c. (column F, 230°, 120). The α,β-unsaturated nitrile **23** exhibited n_D^{20} 1.5109. Ultraviolet, λ_{max} 220.5 mμ (ε = 12 300); infrared (film), λ_{max} 4.53, 6.20 μ; n.m.r., τ 4.75 (singlet, 1H, =CHCN), 4.82 (unresolved multiplet, 1H, vinyl H), 8.25, 8.44 (doublets, 6H, vinyl methyls, J = 1.4, 1.6 Hz, respectively), 8.84 (singlet, 3H, tertiary methyl), 9.13 (doublet, 3H, secondary methyl, J = 6.5 Hz).

Anal. Calcd. for $C_{14}H_{21}N$: C, 82.70; H, 10.41. Found: C, 82.85; H, 10.25.

The β,γ-unsaturated nitrile **24** exhibited n_D^{20} 1.4981. Infrared (film), λ_{max} 4.48, 6.06 μ; n.m.r., τ 4.07 (unresolved multiplet, 1H, γ-vinyl H), 4.94 (unresolved multiplet, 1H, vinyl H), 7.01 (unresolved multiplet, 2H, —CH_2CN) 8.31, 8.40 (doublets, 6H, vinyl methyls, J = 1.5, 1.7 Hz respectively), 9.00 (singlet, 3H, tertiary methyl), 9.11 (doublet, 3H, secondary methyl).

Anal. Calcd. for $C_{14}H_{21}N$: C, 82.70; H, 10.41. Found: C, 82.71; H, 10.45.

Preparation of Carboxylic Acid ***25***

Potassium hydroxide (77 g) was dissolved in a mixture of ethanol (380 ml) and water (20 ml), and a mixture of the two nitriles (**23** and **24**) (13.2 g) was added. The solution was refluxed under an atmosphere of nitrogen for 3 days and then most of the solvent was removed under reduced pressure. The residual material was diluted with water and the resulting solution was washed with ether. The aqueous layer was acidified with 6 *N* hydrochloric acid and extracted thoroughly with ether. The combined extracts were washed with water, saturated brine, and then dried over anhydrous sodium sulfate. Removal of the solvent gave a viscous yellow oil which, upon distillation under reduced pressure, yielded 12 g (82%) of the β,γ-unsaturated carboxylic acid **25** as a clear viscous oil, b.p. 130–134° at 0.25 mm, n_D^{20} 1.5040; infrared ($CHCl_3$), λ_{max} 2.9–4.2 (broad), 5.88 μ; n.m.r., τ 4.35 (poorly resolved triplet, 1H, γ-vinyl H), 4.93 (unresolved multiplet, 1H, vinyl H), 7.07 (unresolved multiplet, 2H,—CH_2C-OOH), 8.32, 8.38 (doublets, 6H, vinyl methyls, J = 1.5, 1.3 Hz, respectively), 8.99 (singlet, 3H, tertiary methyl), 9.11 (doublet, 3H, secondary methyl, J = 6.5 Hz).

Anal. Calcd. for $C_{14}H_{22}O_2$: C, 75.63; H, 9.97. Found: C, 75.61; H, 10.00.

*(±)-Aristolone (**1**) and (±)-6,7-Epi-aristolone (**28**)*

The β,γ-unsaturated carboxylic acid **25** (5.0 g, 22.4 mmoles) was dissolved in aqueous sodium hydroxide (25.0 mmoles), the water was evaporated under reduced pressure, and the residue was dried in a vacuum oven at 70°. A stirred suspension of the resulting dry sodium salt in 140 ml of dry benzene containing 0.5 ml of pyridine was cooled to 0° and 56 g (0.44 mole) of oxalyl chloride was added. The reaction mixture was stirred at 0° for 15 min, filtered, and evaporated under reduced pressure (vacuum pump). The solution was kept at 0° during this process. The crude acid chloride **26** [infrared (film), λ_{max} 5.62 μ; n.m.r., very similar to that of the carboxylic acid] thus obtained was taken up in 250 ml of dry ether and the resulting solution was added to excess alcohol free ethereal diazomethane which had been dried over potassium hydroxide. The solution was stirred for 15 min and evaporated under reduced pressure affording the crude diazoketone **27**. Infrared (film), λ_{max} 4.79, 6.15 μ. The crude diazoketone **27** was dissolved in 600 ml of cyclohexane and cupric sulfate (15 g) was added. The resulting suspension was refluxed, with stirring, until the infrared absorption at 4.79 μ had disappeared (approximately 4 h). The cooled mixture was filtered and the filtrate was washed with saturated aqueous sodium bicarbonate, water, saturated brine, and then dried over anhydrous sodium sulfate. Removal of the solvent, followed by distillation of the residual material under reduced pressure, yielded 3.5 g (approximately 70%, based on the acid **25**) of a clear oil, b.p. 100–110° (bath temperature) at 0.1 mm. This material was shown by g.l.c. analysis (column G, 220°, 110) to consist of approximately 42% of (±)-aristolone (**1**), 20% of (±)-6,7-epi-aristolone (**28**) and a number of minor unidentified components. This mixture was partially purified by preparative thin-layer chromatography. Neutral alumina plates (20 × 60 cm, 0.5 mm thick) were used, with 3:2 *n*-hexane – ether being employed as developing solvent. Approximately 150 mg of the distilled material was applied per plate and the appropriate band of each plate, containing (±)-aristolone (**1**) and its isomer **28**, was eluted with ether. From 3.5 g of distilled material there was thus obtained 2.1 g of a clear oil which consisted mainly of (±)-aristolone (**1**) and its isomer **28**, in a ratio of approximately 2.4:1, respectively. Final purification was effected by preparative g.l.c. (column I, 240°, 110). Crystalline (±)-aristolone (**1**), thus obtained was recrystallized from petroleum ether (b.p. 60–80°), and exhibited m.p. 62–63°. Ultraviolet, λ_{max} 236 mμ (ε = 10 300); infrared ($CHCl_3$), λ_{max} 6.09 μ; n.m.r., τ 4.28 (unresolved multiplet, 1H, —C^9H, width at half-height = 3.5 Hz), 8.28 (pair of doublets, 1H, —C^7H, J = 8 and 1.2 Hz), 8.61 (doublet, 1H, —C^6H, J = 8 Hz), 8.74, 8.80, 8.81 (singlets, 9H, tertiary methyls), 8.93 (doublet, 3H, secondary methyl, J = 6.5 Hz). This material was found to be identical (m.p., mixed m.p., infrared, n.m.r., g.l.c. retention time) with authentic (±)-aristolone, prepared by recrystallizing, from petroleum ether (b.p. 60–80°), a 1:1 mixture of (−)-aristolone and α-ferulone [(+)-aristolone] (23).

Mol. Wt. Calcd. for $C_{15}H_{22}O$: 218.167. Found (high resolution mass spectrometry): 218.166.

Pure (±)-6,7-epi-aristolone (**28**) was obtained as a colorless oil. Ultraviolet, λ_{max} 233 (ε = 10 000); infrared ($CHCl_3$), λ_{max} 6.08 μ; n.m.r., τ 4.24 (unresolved multiplet, 1H, —C^9H, width at half-height = 2.5 Hz), 8.38 (pair of doublets, 1H, —C^7H, J = 8 and 1.1 Hz), 8.45 (doublet, 1H, —C^6H, J = 8 Hz), 8.80, 8.81, 8.84 (singlets, 9H, tertiary methyls), 9.02 (doublet, 3H, secondary methyl, J = 6.0 Hz).

Mol. Wt. Calcd. for $C_{15}H_{22}O$: 218.167. Found (high resolution mass spectrometry): 218.167.

Acknowledgments

We are very grateful to Professor A. Marsili for generous samples of (−)-aristolone and

α-ferulone, and to Professor F. Sorm for a generous quantity of (−)-aristolone. Financial support from the National Research Council of Canada, and a National Research Council of Canada Studentship (to W. de W.) are gratefully acknowledged.

1. T. KARIYONE and S. NAITO. J. Pharm. Soc. Japan, **75**, 1511 (1955).
2. S. FURUKAWA and N. SOMA. J. Pharm. Soc. Japan, **81**, 559 (1961); S. FURUKAWA, K. OYAMADA, and N. SOMA. J. Pharm. Soc. Japan, **81**, 565 (1961); S. FURUKAWA. J. Pharm. Soc. Japan, **81**, 570 (1961).
3. G. BÜCHI, F. GREUTER, and T. TOKOROYAMA. Tetrahedron Letters, 827 (1962).
4. G. BÜCHI, M. SCHACH v. WITTENAU, and D. M. WHITE. J. Am. Chem. Soc. **81**, 1968 (1959); R. B. BATES, G. BÜCHI, T. MATSUURA, and R. R. SHAFFER. J. Am. Chem. Soc. **82**, 2327 (1960).
5. E. PIERS, W. DE WAAL, and R. W. BRITTON. Chem. Comm. 188 (1968).
6. M. M. FAWZI and C. D. GUTSCHE. J. Org. Chem. **31**, 1390 (1966), and references therein.
7. H. E. ULERY and J. H. RICHARDS. J. Am. Chem. Soc. **86**, 3113 (1964).
8. R. E. IRELAND and J. A. MARSHALL. J. Org. Chem. **27**, 1615 (1962), and references therein.
9. H. O. HOUSE, B. A. TEFERTILLER, and H. D. OLMSTEAD. J. Org. Chem. **33**, 935 (1968), and references therein.
10. J. A. MARSHALL, N. COHEN, and K. R. ARENSON. J. Org. Chem. **30**, 762 (1965), and references therein.
11. J. A. MARSHALL and M. J. WURTH. J. Am. Chem. Soc. **89**, 6788 (1967).
12. J. J. PAPPAS, W. P. KEAVENEY, E. GANCHER, and M. BERGER. Tetrahedron Letters, 4273 (1966).
13. K. BOWDEN, I. M. HEILBRON, E. R. H. JONES, and B. C. L. WEEDON. J. Chem. Soc. 39 (1946).
14. W. S. JOHNSON, J. C. COLLINS, JR., R. PAPPO, M. B. RUBIN, P. J. KROPP, W. F. JOHNS, J. E. PIKE, and W. BARTMANN. J. Am. Chem. Soc. **85**, 1409 (1963).
15. L. M. JACKMAN. Applications of nuclear magnetic resonance spectroscopy in organic chemistry. The Pergamon Press, Ltd. Oxford, 1959. pp. 99–103.
16. HUANG-MINLON. J. Am. Chem. Soc. **68**, 2487 (1946).
17. W. S. WADSWORTH and W. D. EMMONS. J. Am. Chem. Soc. **83**, 1733 (1961).
18. E. J. COREY and M. CHAYKOVSKY. J. Am. Chem. Soc. **87**, 1345 (1965), and references therein.
19. R. R. RANDO and W. VON E. DOERING. J. Org. Chem. **33**, 1671 (1968).
20. S. K. MALHOTRA and F. JOHNSON. Chem. Comm. 1149 (1968), and references therein.
21. L. BAUER, C. L. BELL, J. E. GEARIEN and H. TAKEDA. J. Pharm. Sci. **56**, 336 (1967).
22. S. CARBONI, A. DA SETTIMO, V. MALAGUZZI, A. MARSILI, and P. L. PACINI. Tetrahedron Letters, 3017 (1965).
23. C. BERGER, M. FRANCK-NEUMANN, and G. OURISSON. Tetrahedron Letters, 3451 (1968).

Can. J. Chem. Downloaded from www.nrcresearchpress.com by 210.87.254.5 on 09/05/12
For personal use only.

Enzymic deacylation of esterified mono- and disaccharides.[1] 2. The chemical synthesis of 2,3-di-*O*-acetyl-D-glucopyranose

A. L. FINK[2] AND G. W. HAY[3]
Department of Chemistry, Queen's University, Kingston, Ontario
Received July 9, 1968

2,3-Di-*O*-acetyl-D-glucopyranose was synthesized by catalytic (paladium on carbon) hydrogenation of benzyl 2,3-di-*O*-acetyl-4,6-*O*-benzylidene-β-D-glucoside.

Canadian Journal of Chemistry, **47**, 841 (1969)

Can. J. Chem. Downloaded from www.nrcresearchpress.com by 210.87.254.42 on 09/05/12
For personal use only.

The synthesis of 2,3-di-*O*-acetyl-D-glucopyranose (**1**) was prompted by the need for a partially acetylated glucose derivative for use in assessing the suitability of methods for identifying partially acetylated sugars (1). Benzyl 2,3-di-*O*-acetyl-4,6-*O*-benzylidene-β-D-glucoside (**2**) was prepared from glucose by the route shown in Scheme 1, using standard procedures. Hydrogenation of **2**, performed using a suspension in ethyl ether (methanol, chloroform, or methanol–acetic acid, proved to be unsatisfactory) at room temperature under a small positive pressure, removed the benzylidene and/or benzyl groups to give **1** and 2,3-di-*O*-acetyl-4,6-*O*-benzylidene-β-D-glucose (**3**). Careful preparation of the catalyst, palladium on carbon, by hydrogenation of the chloride salt, was essential and uniformity of reactivity with different batches of catalyst was difficult to attain. The hydrogenation was conducted under strictly anhydrous, neutral conditions to minimize the possibility of any acetyl migration. The progress of the reaction was followed conveniently by thin-layer chromatography of the reaction mixture, and by gas–liquid partition chromatography of trimethylsilyl ether derivatives of aliquots (Table I).

A rapid initial consumption of hydrogen occurred until approximately 40% of the theoretical amount of hydrogen had been incorporated, whereupon the rate diminished to a lower value for a brief period of time. This lull was most pronounced with less active batches of catalyst. Evaporation of the filtrate of the reaction mixture at that point afforded a crystalline product which, upon recrystallization from ethyl ether, had a nuclear magnetic resonance (n.m.r.) spectrum and an elemental analysis consistent with structure **3**.

TABLE I

Retention times for acetyl trimethylsilyl and methyl derivatives of glucose

Derivative of D-glucoside	Relative retention time
Trimethylsilyl 2,3,4,6-tetrakis-*O*-trimethylsilyl-β-	1.5
Trimethylsilyl 2-*O*-acetyl-3,4,6-tris-*O*-trimethylsilyl-β-	2.7
Trimethylsilyl 2,3-di-*O*-acetyl-4,6-bis-*O*-trimethylsilyl-β-	3.8
Methyl 2,3,4,6-tetra-*O*-methyl-α-	0.14
Methyl 2,3,4,6-tetra-*O*-methyl-β-	0.10
Methyl 3,4,6-tri-*O*-acetyl-2-*O*-methyl-α-	1.71
Methyl 3,4,6-tri-*O*-acetyl-2-*O*-methyl-β-	2.60
Methyl 4,6-di-*O*-acetyl-2,3-di-*O*-methyl-α-	1.00
Methyl 4,6-di-*O*-acetyl-2,3-di-*O*-methyl-β-	0.77

NOTE: Column *a*; 180 °C; 100 ml per min. Retention times relative to trimethylsilyl tetrakis-*O*-trimethylsilyl-α-D-glucopyranoside for the trimethylsilyl derivatives, and methyl 4,6-di-*O*-acetyl-2,3-di-*O*-methyl-α-D-glucopyranoside for the methyl derivatives.

The continuation of hydrogenation after the initial lull in the rate of hydrogen uptake resulted in a gradual decrease until the uptake was almost negligible. Further hydrogenation caused an increase in the rate of hydrogen uptake which thereafter slowly diminished to zero. The total consumption at that point was greater than the theoretical amount. Evaporation of the filtrate obtained when the hydrogenation rate first became negligible (ca. 100% of theoretical) gave a white, amorphous powder. Attempts to crystallize the compound failed. On the basis of the n.m.r. spectrum, elemental analysis, thin-layer chromatographic behavior, and the gas–liquid chromatographic analysis of the trimethylsilyl derivative, the compound was assigned structure **1**.

[1]This project was supported by the National Research Council of Canada, Operating Grant A1921. Abstracted from the Ph.D. Thesis of A. L. Fink, Queen's University, Kingston, Ontario, December, 1967.
[2]Present address: Department of Chemistry, Northwestern University, Evanston, Illinois 60201.
[3]To whom enquiries should be addressed.

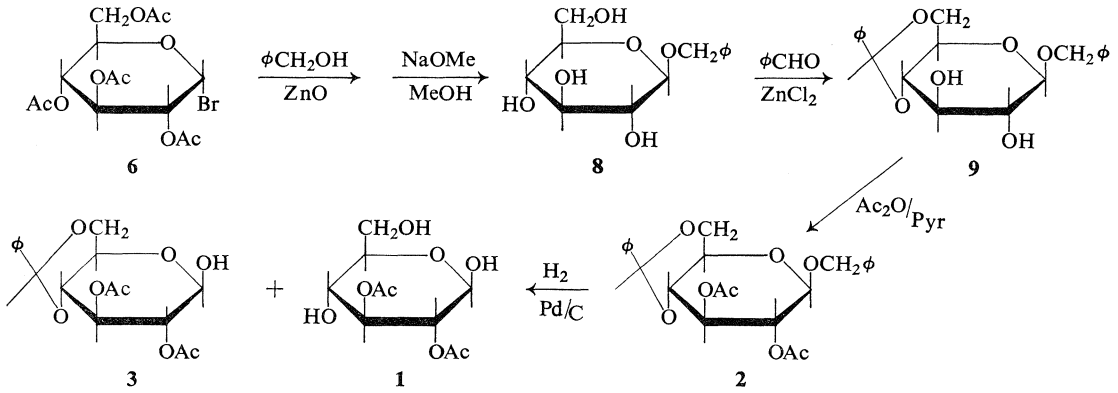

SCHEME 1. The reaction sequence for the synthesis of 2,3-di-*O*-acetyl-D-glucopyranose.

In the amorphous state, **1** underwent spontaneous decomposition into 2-*O*-acetyl-D-glucopyranose (**4**) and D-glucose (**5**), even at −1 °C. This chemical lability greatly hindered the unequivocal establishment of the identity of **1**. Compound **1** was very sensitive to alcoholysis. Thus, if the catalyst was washed with methanol or ethanol during the work-up following hydrogenation the amount of decomposition of **1** into **4** and **5** greatly increased. Furthermore, elution with methanol during preparative thin-layer chromatography resulted in complete deacetylation of **1**. Methanol also has been found to cause deacetylation during the hydrogenation of benzyl 2-*O*-acetyl-4-*O*-methyl-β-D-xyloside (2).

Preparative thin-layer or paper partition chromatography could be used to purify **1** and **3**. Freshly prepared **1** was homogeneous by thin-layer chromatography. An aged sample afforded three closely adjacent compounds in the region of the chromatogram where diacetates were expected. This observation, and the finding that a random mixture of glucose acetates was resolved by thin-layer chromatography into groups of components in the vicinity of each product from the enzymic deacetylation of glucose pentaacetate, inferred that the technique was capable of distinguishing some, if not all, of the isomeric acetate derivatives.

Gas–liquid partition chromatographic analysis of the trimethylsilyl derivative from **1** revealed one major and two minor products. Only the major product had a retention time consistent with a di-*O*-acetyl derivative. The retention times of the minor products corresponded to those of the trimethylsilyl derivatives of **4** and **5**. Thus, whereas trimethylsilylation may have caused some deacetylation no evidence of acetyl group migration was obtained.

Paper partition chromatographic analysis of the hydrogenation product from **2** disclosed only three products with migration rates corresponding to those of **1**, **2**, and **3**.

The detection of **1** and **3** but not glucose pentaacetate by *p*-anisidine spray reagent was taken as presumptive evidence for the absence of substitution at C-1 in **1** and **3**.

These chromatographic data argue for the ability of the methods to discriminate between similar or isomeric acetyl derivatives, and aver either that no acetyl group migration occurred or that a quantitative, selective migration of acetyl groups occurred to yield only one of the potentially numerous isomers.

The n.m.r. spectrum of **1** in dimethyl sulfoxide (DMSO)-d_6 revealed the ratio of acetoxy protons (8.05 τ) to ring protons to be 6:10. The resonance at 3.3 τ was assigned to O_1H (3.5 τ in β-D-glucopyranose), that at 5.6 τ to C_1H (5.7 τ in β-D-glucopyranose), and that at 5.54 τ to O_6H (5.58 τ in β-D-glucopyranose). The same ratio of acetoxy to ring protons was obtained in acetone-d_6(acetoxy protons 8.22 τ). In D_2O the acetoxy resonance occurred at 7.94 τ. The chemical shifts for acetoxy resonance are in accord with equatorial acetoxy groups (3) and bear the correct ratio with ring protons for a hexose diacetate. The chemical shifts for O_1H and O_6H in DMSO-d_6 are consistent with the β configuration, but are too low for the α anomer (3).

Elemental analysis of **1** was consistent with a di-*O*-acetylhexose.

Can. J. Chem. Downloaded from www.nrcresearchpress.com by 210.87.254.42 on 09/05/12
For personal use only.

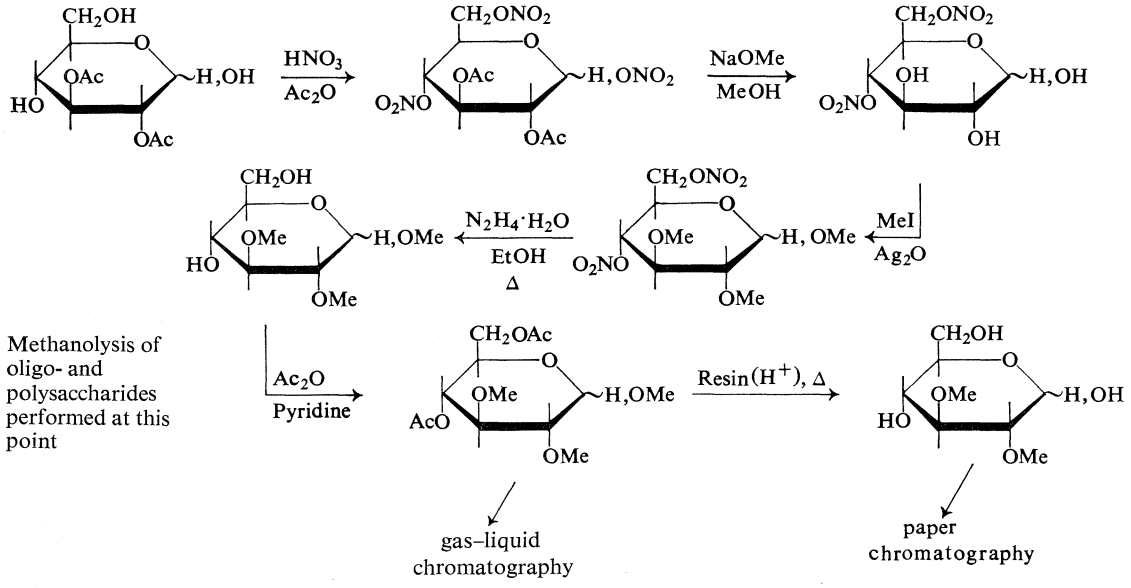

SCHEME 2. Reaction sequence for the location of acetyl groups in partially acetylated sugars.

Compound **1** was subjected to a sequence of reactions designed to locate the positions of acetate esters in carbohydrates (1). The major product was identified as methyl 4,6-di-*O*-acetyl-2,3-di-*O*-methyl-D-glucoside which is in agreement with the structure proposed for **1** (Scheme 2). The literature (4, 5) indicates that nitrate esters and methyl ethers do not migrate under the conditions utilized in Scheme 2. Consequently only acetyl migration prior to nitration is to be expected. However, to obtain the 2,3-di-*O*-methyl derivative, either a migration of nitrate esters in the direction opposite to that observed with acetate groups must have occurred, or deacetylation must have caused a concurrent loss of certain nitrate esters and methylation must have been almost quantitatively ineffective at C-4 and/or C-6 while being quantitatively effective at C-2 and C-3.

Experimental

Unless stated otherwise the chemicals used were reagent grade products. Melting points were determined on a Fisher–Johns apparatus and are uncorrected. Optical rotations were measured with a Bendix automatic polarimeter (sodium lamp) at 25 ± 1 °C. Nuclear magnetic resonance (n.m.r.) spectra were obtained with a Varian A-60 spectrometer using tetramethylsilane as external standard. Paper partition chromatography was performed by the descending technique using butanone-water azeotrope on Whatman No. 1 paper. Thin-layer chromatography was performed on Silica Gel G or Silica Gel HF254 (preparative) irrigated with methanol:benzene 1:9 (v/v). Gas–liquid partition chromatography was carried out with an F and M model 402 chromatograph with hydrogen flame detector. Compounds were identified by co-chromatography with authentic specimens or by comparison of retention times. The columns (6 ft × 1/8 in. I.D., U-shaped) used were 5% (Column *a*) and 10% (w/w) LAC-4R-886 on Chromosorb W, 100–120 mesh.

Tetra-O-acetyl-1-bromo-1-deoxy-α-D-glucopyranose (6)

Compound **6** was prepared by the method of Scheurer and Smith (6); m.p. 88–89 °C (lit. 88–89 °C); yield, 67%.

Benzyl Tetra-O-acetyl-β-D-glucopyranoside (7)

Compound **7** was prepared from **6** by the method of Helferich and Wedemeyer (7); m.p. 95–97 °C (lit. 95–101 °C); yield, 54%.

Benzyl β-D-glucopyranoside (8)

Compound **8** was prepared from **7** by deacetylation with sodium methoxide – methanol; m.p. 121–122 °C (lit. (8) 123–125 °C); yield, 88%.

Benzyl 4,6-O-Benzylidene-β-D-glucoside (9)

Compound **9** was prepared from **8** by the method of Klemer (9); m.p. 158–159 °C (lit. 159–160 °C); yield, 75%.

Benzyl 2,3-Di-O-acetyl-4,6-O-benzylidene-β-D-glucoside (2)

Compound **9** (7.0 g) was dissolved in 45 ml dry pyridine, 35 ml acetic anhydride added, and the solution allowed to stand at room temperature for 24 h. A white precipitate formed after a few hours. The reaction mixture was filtered, the residue washed with ice-water, and

Can. J. Chem. Downloaded from www.nrcresearchpress.com by 210.87.254.42 on 09/05/12
For personal use only.

recrystallized from ethyl acetate to give **2**, m.p. 211–212 °C (lit. (10) 208–209 °C); yield, 66%.

Anal. Calcd. for $C_{24}H_{26}O_8$: C, 65.0; H, 5.9. Found: C, 64.7; H, 6.0.

The n.m.r. spectrum of **2** showed acetoxy resonance at 8.15 τ in acetone-d_6, and at 7.98 τ and 8.02 τ in deuteriochloroform.

2,3-Di-O-acetyl-4,6-O-benzylidene-β-D-glucose (3)

Palladium on carbon catalyst was prepared from palladium chloride on carbon (11) (0.5 g), by slurrying in methanol, and hydrogenating until the uptake of hydrogen ceased. The catalyst was washed 10 times with methanol, 5 times with glacial acetic acid, and 10 times with ethyl ether on a sintered glass funnel. The catalyst was added to 125 mg **2** as a slurry in ethyl ether and hydrogenation carried out until a lull in the rate of hydrogen uptake occurred (ca. 40% of theoretical). The mixture was filtered through a sintered glass funnel and the filtrate evaporated to dryness under reduced pressure at room temperature. The resulting syrup was crystallized from ethyl ether as fine white needles, m.p. 162–163 °C, $[\alpha]_D^{25}$ −7.0° (*c*, 1.0 in acetone). The compound was insoluble in water, sparingly soluble in ethyl ether, and soluble in acetone or DMSO. Thin-layer chromatography detected only one component, which was identified as a reducing sugar by its reaction with *p*-anisidine (12). Analysis by n.m.r., in acetone-d_6 detected the presence of resonance at 2.20 τ (aromatic ring protons), at 8.14 τ (acetoxy protons), as well as that due to protons on the sugar ring. Integration indicated a ratio of 5:6:9, respectively, which is in accord with the proposed structure, **3**. The elemental analysis was consistent with this conclusion.

Anal. Calcd. for $C_{17}H_{20}O_8$: C, 58.1; H, 5.7. Found: C, 58.3; H, 5.9.

2,3-Di-O-acetyl-β-D-glucopyranose (1)

If hydrogenation of **2** was continued until the rate of hydrogen uptake became negligible (ca. 100% of theoretical), or if **3** was subjected to similar hydrogenation conditions and work-up, an amorphous, white compound, (yield: 82%, $[\alpha]_D$ +10.9° (*c*, 2.2 in H_2O)), was isolated which could not be crystallized. The compound was soluble in water and in acetone. Thin-layer chromatographic analysis of the compound detected only one compound, R_3 0.16. This compound (**1**) was visualizable with *p*-anisidine spray reagent. Gas–liquid chromatography of the trimethylsilyl ether of **1** revealed only one major component with a retention time relative to that of pentakis-*O*-trimethylsilyl-α-D-glucopyranose (R_T) of 3.2, and two minor components with R_T 2.7 and 1.5, respectively. The elemental analysis was as follows:

Anal. Calcd. for $C_{10}H_{16}O_8$: C, 45.5; H, 6.1. Found: C, 45.75; H, 6.5.

Products Obtained from Compound 1 via Scheme 2

Compound **1** was subjected to the sequence of reactions outlined in Scheme 2 (1). Gas–liquid partition chromatographic analysis (Column *a*; 180 °C; 100 ml/min) of the products (1) revealed that the major product was a mixture of methyl 4,6-di-*O*-acetyl-2,3-di-*O*-methyl-α- and β-D-glucosides with retention times of 1.00 and 0.77 respectively, relative to an authentic sample of the α-anomer. Either peak could be exclusively augmented by co-chromatography with an authentic sample.

Acknowledgments

The authors are grateful for the generous gifts of reference standards from Professor J. K. N. Jones.

1. A. L. Fink and G. W. Hay. Can. J. Chem. This issue.
2. P. J. Garegg. Acta Chem. Scand. **16**, 1849 (1962).
3. B. Casu, M. Reggiani, G. G. Gallo, and A. Vigevani. Tetrahedron Letters, 2253 (1965).
4. J. Honeyman and J. W. Morgan. Chem. Ind. (London), 1035 (1953).
5. J. Honeyman and J. W. Morgan. Advan. Carbohydrate Chem. **12**, 117 (1957).
6. P. Scheurer and F. Smith. J. Am. Chem. Soc. **76**, 3224 (1954).
7. B. Helferich and K. F. Wedemeyer. Ann. **563**, 139 (1949).
8. W. J. Hickenbottom. J. Chem. Soc. 3140 (1928).
9. A. Klemer. Chem. Ber. **92**, 218 (1959).
10. A. L. Raymond, R. S. Tipson, and R. A. Levine. J. Biol. Chem. **130**, 47 (1939).
11. A. L. Vogel. Textbook of practical organic chemistry. 3rd ed. Longmans, Green and Co., London. 1964. p. 950.
12. L. Hough, J. K. N. Jones, and W. H. Wadman. J. Chem. Soc. 1702 (1950).

Can. J. Chem. Downloaded from www.nrcresearchpress.com by 210.87.254.42 on 09/05/12
For personal use only.

Enzymic deacylation of esterified mono- and disaccharides.[1] 3. The location of acetylated positions in partially acetylated sugars[2]

A. L. FINK[3] AND G. W. HAY[4]
Department of Chemistry, Queen's University, Kingston, Ontario

Received July 9, 1968

The nitrate ester, formed by reaction with fuming nitric acid in acetic anhydride at 0 °C, was suitable to block free hydroxyl groups in partially acetylated sugars without acetyl migration. This allowed the acetylated positions in partially acetylated mono- and disaccharides to be located by the reaction sequence: nitration, deacetylation, methylation, de-nitration, disaccharide hydrolysis and methyl glycosylation (initial product identification by paper partition chromatography), acetylation, and analysis of the products by gas–liquid partition chromatography. D-Glucose, penta-*O*-acetyl-D-glucopyranose, and 2,3-di-*O*-acetyl-β-D-glucopyranose were used as test compounds in the evaluation of this scheme.

Canadian Journal of Chemistry, 47, 845 (1969

Can. J. Chem. Downloaded from www.nrcresearchpress.com by 210.87.254.42 on 09/05/12
For personal use only.

Introduction

In connection with studies on the enzymic deacylation of some esterified sugars (1), it became necessary to identify partially acylated sugar derivatives, particularly the partially acetylated derivatives of glucose and disaccharides of glucose. Techniques to locate the acetylated positions in such compounds are complicated by the mobility and lability of the acetyl group. The results of various investigations of means of locating the acetylated positions are reported herein.

Results and Discussion

The facile migrations of acyl groups in partially acylated polyhydroxylic compounds first noted by Fischer (2), have been observed under neutral, basic, and acidic conditions, and have been reported to originate at all positions except C-6 in the hexose series (3, 4). As a consequence, the number of reactions that may be carried out in the partially acetylated sugars without affecting the acetylated positions is severely limited.

With the exception of the methylation of acidic hydroxyls by diazomethane, all the procedures currently used in carbohydrate chemistry for methylation involve basic conditions (5) which could lead to hydrolysis or migration of the acetyl groups (4, 6). Indeed, the migration of acetyl groups during methylation has been used advantageously in some syntheses (7). Attempts to permethylate sugars using the diazomethane – boron trifluoride reagent resulted in incomplete methylation (8) and although methyl glycosides have been prepared by such a method the yields were low. Recently the methylation of some tetra-*O*-acetylhexopyranosides and a hepta-*O*-acetylmaltose with diazomethane and boron trifluoride etherate has been reported (9, 10). No migration or hydrolysis of acetate was observed.

As an initial test, the diazomethane – boron trifluoride etherate methylation method was applied to D-glucose (**1**) and to penta-*O*-acetyl-β-D-glucopyranose (**2**). Some replacement of acetyl by methyl occurred as a result of the boron trifluoride – catalyzed hydrolysis of some acetate groups of **2**, and no conditions were found under which **1** was fully methylated.

The sodium *t*-butoxide-catalyzed deacetylation of **2** was very slow. Methylation by the use of methyl iodide and sodium *t*-butoxide in dimethyl sulfoxide permethylated **1** rapidly, but afforded methyl tetra-*O*-methyl-α- and β-D-glycopyranosides as the major products from **2**. Presumably the sodium *t*-butoxide reacted with dimethyl sulfoxide to form methylsulfinylcarbanion (11) which can cause deacetylation (12).

The general reaction sequence whereby acetate groups can be located in carbohydrates is shown in Scheme 1*a*. Model compounds were used to determine the suitability of potential protective groups. A partial list of the various protective

[1]This project was supported by the National Research Council of Canada, Operating Grant A1921. Abstracted from the Ph.D. Thesis of A. L. Fink, Queen's University, Kingston, Ontario, December, 1967.
[2]Presented at the 155th National Meeting, American Chemical Society, Division of Carbohydrate Chemistry, San Francisco, April, 1968.
[3]Present address: Department of Chemistry, Northwestern University, Evanston, Illinois 60201.
[4]To whom enquiries should be addressed.

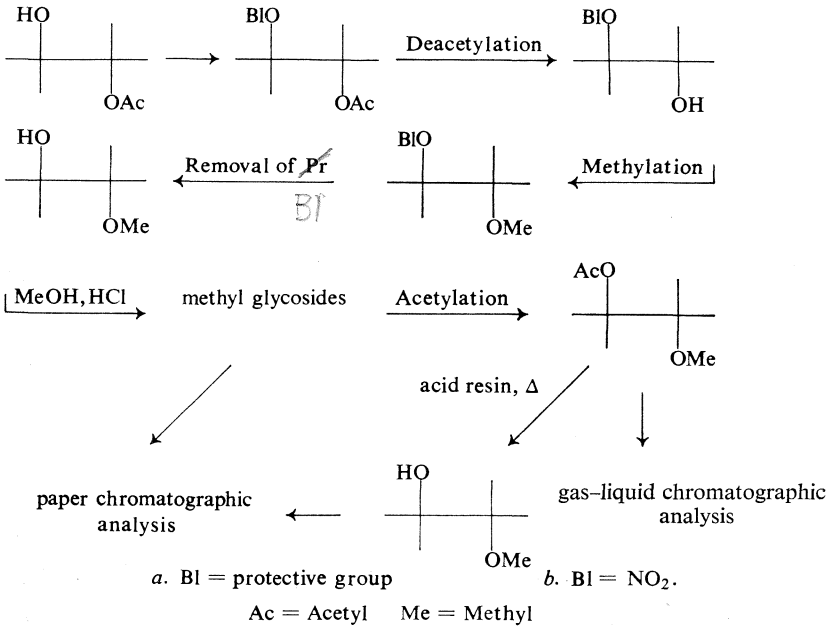

SCHEME 1. The reaction sequence used to locate the acetylated positions in partially acetylated glucoses or disaccharides of glucose.

groups considered follows; the stage in the reaction series at which the protective group was considered unsuitable is given in parentheses: alkyl, aryl, allyl (13), vinyl (14), and alkoxy–alkyl ethers (15) (formation); carbonate, thiocarbonate (16), formyl, trifluoroacetyl, and benzoyl esters (17) (formation, deacetylation); 2,4-dinitrobenzenesulfinyl esters (18) (deacetylation, methylation); sulfonates and sulfates (19) (deacetylation, removal); and alkylhalogenomethyl ethers (20) and phenylcarbanilates (21) (methylation).

Trimethylsilyl ethers of sugars may be formed rapidly and quantitatively (22) and have found much use in gas–liquid partition chromatographic analysis. The trimethylsilyl ethers are susceptible to alcoholysis except in neutral solvents, and are sensitive to acid- and base-catalyzed hydrolysis. Methanolysis has been found to occur much more rapidly at C-6 than at the secondary hydroxyl positions in **4** (23). Consequently, whereas sodium methoxide – catalyzed deacetylation would affect the trimethylsilyl groups at C-6, other methods of deacetylation such as reduction, acid hydrolysis, and reaction with Grignard reagents were precluded since they would cause general cleavage of the oxygen–silicon bond (24).

1 could be completely trimethylsilylated in a few minutes at 0 °C (22), and **2** could be recovered unaltered after the reaction. However, with 2,3-di-*O*-acetyl-β-D-glucopyranose (**3**) trimethylsilylation in this fashion caused some replacement of acetyl by trimethylsilyl groups as revealed by the formation of some trimethylsilyl 2-*O*-acetyl-3,4,6-tris-*O*-trimethylsilyl- and 2,3,4,6-tetrakis-*O*-trimethylsilyl-β-D-glucopyranosides. Trimethylsilylation of the products from the enzymic deacetylation of penta-*O*-acetyl-α and β-D-glucopyranoses with a purified esterase from wheat germ lipase (1) gave 12 well-resolved peaks on gas–liquid partition chromatographic analysis. These *O*-acetyl-*O*-trimethylsilyl derivatives tentatively were assigned identities from their relative retention times (Table I).

The conditions used for the synthesis of **5** were very similar to those of deacetylation (25). The effects of sodium methoxide/methanol on **2** and **6** at various temperatures and catalyst concentrations were followed conveniently by thin-layer chromatography. At temperatures above 15 °C hydrolysis of trimethylsilyl ethers proceeded faster than deacetylation, whereas below 15 °C the order was reversed. The effect of catalyst concentration was similar in both reactions.

Can. J. Chem. Downloaded from www.nrcresearchpress.com by 210.87.254.42 on 09/05/12
For personal use only.

Can. J. Chem. Downloaded from www.nrcresearchpress.com by 210.87.254.42 on 09/05/12
For personal use only.

Erratum: Enzymic deacylation of esterified mono- and disaccharides. 3. The location of acetylated positions in partially acetylated sugars

A. L. FINK AND G. W. HAY
Department of Chemistry, Queen's University, Kingston, Ontario

Received March 17, 1969
(Ref. Can. J. Chem. 47, 845 (1969))

Canadian Journal of Chemistry, 47, 2490 (1969)

In Scheme 1 p. 846, the second line is:

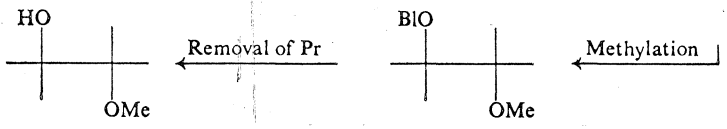

This should be changed to:

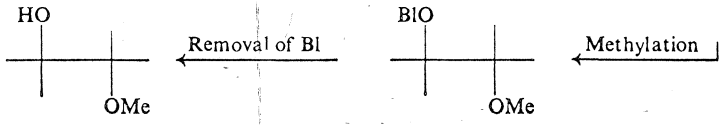

In Table I p. 847, "pentakis" should replace "pentabis" in the names of the top two compounds as well as in the compound of footnote†, Table I: in the same table, "tetrakis" should replace "tetrabis" in the names of the third ar fourth compounds.

On p. 850, lines 40 and 41 should include tl prefix "penta-kis" and not "penta-bis".

Can. J. Chem. Downloaded from www.nrcresearchpress.com by 210.87.254.42 on 09/05/12
For personal use only.

TABLE I

The retention times of some trimethylsilylated acetylated glucopyranoses on gas–liquid partition chromatography

Assigned identity*	Relative† retention time
1,2,3,4,6-Pentakis-*O*-trimethylsilyl-α-D-glucose	1.0
1,2,3,4,6-Pentakis-*O*-trimethylsilyl-β-D-glucose	1.5
2-*O*-Acetyl-1,3,4,6-tetrakis-*O*-trimethylsilyl-α-D-glucose	2.2
2-*O*-Acetyl-1,3,4,6-tetrakis-*O*-trimethylsilyl-β-D-glucose	2.7
2,3-Di-*O*-acetyl-1,4,6-tris-*O*-trimethylsilyl-α-D-glucose	3.3
2,3-Di-*O*-acetyl-1,4,6-tris-*O*-trimethylsilyl-β-D-glucose	3.8
2,3,4-Tri-*O*-acetyl-1,6-bis-*O*-trimethylsilyl-α-D-glucose	4.5
2,3,4-Tri-*O*-acetyl-1,6-bis-*O*-trimethylsilyl-β-D-glucose	5.6
2,3,4,6-Tetra-*O*-acetyl-1-*O*-trimethylsilyl-α-D-glucose	5.2
2,3,4,6-Tetra-*O*-acetyl-1-*O*-trimethylsilyl-β-D-glucose	7.2

*See text.
†Relative to pentakis-*O*-trimethylsilyl-α-D-glucopyranose.
NOTE: Column 5% LAC-4R-886, 180° C, 100 ml/min.

Dissolving the substrate in acetone prior to the addition of methanol – sodium methoxide decreased the rate of deacetylation. Replacement of sodium methoxide by sodium *t*-butoxide or sodium isopropoxide resulted in much slower reactions and, at temperatures resulting in complete deacetylation within a reasonable time, detrimethylsilylation proceeded faster than deacetylation.

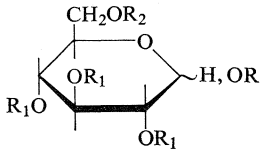

4 R = Me $R_1 = R_2$ = TMS
5 R = Me R_1 = TMS R_2 = H
6 R = R_1 R_2 = TMS
7 R = R_1 = TMS R_2 = H
8 R = Me $R_1 = R_2$ = H
TMS = Trimethylsilyl
Me = Methyl

The use of methanolic piperidine solutions (26) caused deacetylation of **2** and detrimethylsilylation of **6**. The optimum conditions for complete deacetylation of **2** and minimum loss of trimethylsilyl groups from **6** required 10–20% methanol in piperidine at 70 °C. However, even these conditions gave starting material and **7** as the major products from **6**. The deacetylation of **2** by reduction with diborane or by sodium methoxide/chloroform (conditions which had no effect on **6**) failed.

Although the phenylcarbamoyl group has been used as a protective agent for locating the position of acetyl groups in partially acetylated (1 → 4)-linked polysaccharides (21, 27, 28), the method is unsuitable if the C-4 hydroxyl is not blocked because migration of the phenylcarbamoyl group may occur during methylation (21). The benzylthiocarbonyl group (29) was not investigated but might be suitable if not liable to migration.

Dihydropyran forms ethers of tetrahydropyran by acid-catalyzed condensation with alcohols. The products are sensitive to acid but stable to base (30). The reaction has been used to block free positions in some partially acetylated carbohydrates (31–33) although the yields were not quantitative. None of the reports specifically mentioned any replacement of acetyl by tetrahydropyranyl groups. The effect of the reaction on **1** and **2** was followed conveniently by infrared spectroscopy. Experiments with various catalysts, and various catalyst concentrations showed that the rate of tetrahydropyranyl ether formation increased with increasing catalyst concentration, that sufficient catalyst for complete substitution of **1** resulted in some replacement of acetyl by tetrahydropyranyl groups in **2**, and that *p*-toluenesulfonic acid catalysis appeared to cause the least replacement of acetyl groups. No conditions were found in which both complete etherification of the free hydroxyl groups of **1**, and complete retention of acetyl groups of **2** were achieved. Evidence of deacetylation upon the addition of trifluoroacetic acid alone was observed by infrared spectroscopy.

Both dimethyl sulfoxide and dimethylformamide reacted with **6**, but Purdie methylation conditions (5) had no effect. However, the Purdie methylation of the products obtained by subjecting **6** to the optimum deacetylation conditions (sodium methoxide/methanol, −15 °C) gave methyl tetra-*O*-methyl-α- and β-D-glucopyranosides as major products.

Of the several procedures used to prepare nitrate esters of carbohydrates (34) the mildest, fuming nitric acid in acetic anhydride at or below 0 °C, has been shown to have no effect on acetyl groups (35). Neither fuming nitric acid/acetic

FOR ERRATA SEE
V.47 1969 P. 2499

Can. J. Chem. Downloaded from www.nrcresearchpress.com by 210.87.254.42 on 09/05/12
For personal use only.

anhydride nor dinitrogen pentoxide/chloroform (36) had any effect on **2**. Reaction of **1** and **8** with fuming nitric acid/acetic anhydride yielded penta-*O*-nitro-D-glucopyranose (**9**) and methyl penta-*O*-nitro-D-glucopyranoside (**10**), respectively. The infrared spectra of **9** and **10** exhibited the characteristic strong absorptions of the nitrate bands I, II, and III (37), and detected no free hydroxyl groups. Thus, nitration under these conditions did not affect acetylated positions and reacted quantitatively with free hydroxyl groups. Mildly basic conditions cause hydrolysis of the nitrate group on C-1. Accordingly, treatment of **9** with sodium methoxide/methanol, followed by methylation gave a product with an infrared spectrum indistinguishable from that of **10**. However, nitrate groups can be removed quantitatively and conveniently by refluxing with ethanolic hydrazine hydrate, a reagent which has no effect on methyl groups (38). Other substituents on the sugar ring may exert a strong influence on the ease of formation and removal of nitrate esters, and *vice-versa* (39–41).

When **1** was subjected to the reaction sequence: nitration, deacetylation, methylation, de-nitration, and acetylation, product analysis by gas–liquid partition and thin-layer chromatography revealed only methyl tetra-*O*-acetyl-α- and β-D-glucopyranosides. This suggested that nitration of **1** proceeded quantitatively, the deacetylation conditions caused removal of the nitrate group only on C-1, and that the methylation of free hydroxyl groups and the hydrazine denitration proceeded quantitatively. When **2** was put through the reaction sequence the only products were the anticipated methyl tetra-*O*-methyl-α- and β-D-glucopyranosides.

Compound **3** (42), which affords opportunities for both acetyl migration and hydrolysis, was put through the reaction sequence as a further test. **3** was rather unstable and underwent spontaneous deacetylation to give a mono-acetyl derivative, and **1** (42). Consequently, in spite of purification by preparative thin-layer chromatography, the starting sample probably was contaminated with some decomposition products. The products of the above reaction sequence and subsequent acetylation were identified as methyl 4,6-di-*O*-acetyl-2,3-di-*O*-methyl-α- and β-D-glucopyranosides, with traces of the tri-*O*-acetyl-2-*O*-methyl and tetra-*O*-acetyl derivatives. These results suggested that the starting compound was **3**, which contained traces of 2-*O*-acetyl-β-D-glucopyranose and **1**, resulting from deacetylation prior to nitration.

On the basis of these results, the reliability of the reaction sequence outlined in Scheme 1*b* was judged satisfactory for locating the acetylated position in partially acetylated glucoses and disaccharides of glucose. The reaction sequence is not capable of locating acetyl groups on C-1 at the reducing end of the sugar. However, the presence of a reducing sugar may be determined independently by other methods. Thus, the use of maltose-1-^{14}C permits the reducing and non-reducing glucose moieties to be distinguished readily. The method has been used to identify the partially acetylated products from the enzymic and solvolytic deacetylation of some per-acetylated disaccharides and per-acetylated glucose (1).

Experimental

Several Methods

Unless otherwise stated, materials were commercially available reagent grade products. Melting points were measured with a Fisher–Johns apparatus and are uncorrected. Optical rotations were measured with a Bendix automatic polarimeter at 25 ± 1 °C. All solutions were concentrated under reduced pressure at or below 40 °C. Infrared spectra were recorded using a Perkin–Elmer model 21 or Beckman model IR-5A instrument. Samples were analyzed in 5–10% (w/v) solutions. Paper partition chromatograms were developed by the descending technique using Whatman #1 paper and butanone–water azeotrope, or 1-butanol:acetic acid:water 4:1:5 (v/v). The spray reagent used was *p*-anisidine (43). Thin-layer chromatography was done on Silica Gel G using methanol–benzene (1:9 v/v). A 5% solution of sulfuric acid in ethanol and/or *p*-anisidine was used to detect compounds. Gas–liquid partition chromatography was performed with an F and M model 402 chromatograph equipped with a hydrogen flame detector. Compounds were identified with the aid of authentic specimens either by simultaneous injection, or by comparison of retention times (44). Six-foot, 4 mm I.D. glass columns of LAC-4R-886 (Column *a*, 5%; Column *b*, 10%) on Chromosorb W, 100–120 mesh, were used at various isothermal temperatures between 150 °C and 200 °C, and programmed between 150 °C and 200 °C. Standard procedures were employed for nitration (35), hydrolysis of nitrate esters (38), methylation (9, 45, 46), trimethylsilylation (22) and acetylation (47, 48), unless otherwise stated. 2,3-Di-*O*-acetyl-D-glucopyranose was prepared by the method of Fink and Hay (42).

Formation of Tetrahydropyranyl (THP) Ethers

A sample (100 mg) was dissolved in dichloromethane (2 ml) or in dimethyl sulfoxide or 1,4-dioxane, and dihydropyran (distilled from sodium hydroxide pellets) (10 ml) was added. Alternatively, dihydropyran was used as solvent in some reactions. Catalyst (0.02 to 0.2 ml) was

TABLE II

Conditions under which substitution of acetyl by tetrahydropyranyl groups in penta-*O*-acetyl-β-D-glucopyranose occurred

Solvent	Temperature °C	Catalyst	Catalyst concentration *M*	Replacement %	Replacement Observed time (h)
DCM*	30	conc. HCl	5×10^{-2}	90	1
DCM	30	$POCl_3$	5×10^{-2}	95	1
DCM	25, 30	*p*TsOH§	2×10^{-3}	80	1
DMSO†	25	*p*TsOH	2×10^{-3}	50	1
1,4-Dioxane	30	conc. HCl	5×10^{-2}	40	18
DHP‡	40	TFA‖	6×10^{-3}	90	20
DHP	40	$POCl_3$	5×10^{-2}	95	20
DCM	40	Anhydrous HCl 5 *N* in 1,4-dioxane	1.5×10^{-1}	93	15
DCM	25	Anhydrous HCl 5 *N* in 1,4-dioxane	5×10^{-2}	96	4
DCM	25	Anhydrous HCl 5 *N* in 1,4-dioxane	1.3×10^{-2}	87	4
DCM	25	TFA	7×10^{-5}	47	24
DCM	25	$POCl_3$	2×10^{-4}	55	24
DMSO	25	*p*TsOH	3×10^{-2}	18	1.75

*DCM, dichloromethane.
†DMSO, dimethyl sulfoxide.
‡DHP, dihydropyran.
§*p*TsOH, *p*-toluenesulfonic acid.
‖TFA, trifluoroacetic acid.

added, and the solution was stirred at 25 °C in a water bath. When etherification was complete, anhydrous potassium carbonate (1 g) was added. After 15 min the mixture was filtered and evaporated to dryness under reduced pressure. The residue was extracted with chloroform and dried over anhydrous potassium carbonate.

Catalysts used were concentrated hydrochloric acid, trifluoroacetic acid, *p*-toluenesulfonic acid, phosphorus oxychloride, and anhydrous HCl/dioxane (5 *N*). The reaction was followed by changes observed in the infrared spectrum at wavelengths at which absorption was absent or negligible except in the compounds of interest:

2.8–3.0 μ (OH)	Decreasing presence of **1**
3.5 μ (C—H)	THP ether formation
8.9, 9.8, 10.3 μ	THP ether formation
5.7 μ	Presence of **2**
6.1, 12.0 μ	Presence of dihydropyran

The decrement in the ratio of absorbance at 2.8 μ relative to that at 3.5 μ was used as an estimation of the proportion of THP ether formed from **1**, whereas the ratio of intensities at 3.5 and 5.7 μ was used as a measure of the replacement of acetyl by THP groups in **2**. Figure 1 shows the results of a typical experiment plotted in such a manner.

The use of this assay revealed that a 4-fold increase in *p*-toluenesulfonic acid concentration caused a small but significant increase in the rate of both THP ether formation and of substitution of acetyl by THP groups. This replacement was confirmed by thin-layer chromatographic analysis of the product after deacetylation. A series of components having mobilities relative to **2** (R_2) of 0.0 (**1**) – 1.4 were detected.

The effect of catalyst was studied by treating 100 mg **2** with 5.0 ml 0.025 *M* trifluoroacetic acid in dichloromethane. The infrared spectrum showed no change after 4.5 h, but revealed variations in the relative intensities of absorption at 2.8, 3.5, and 5.7 μ after 24 h which indicated that some deacetylation had occurred.

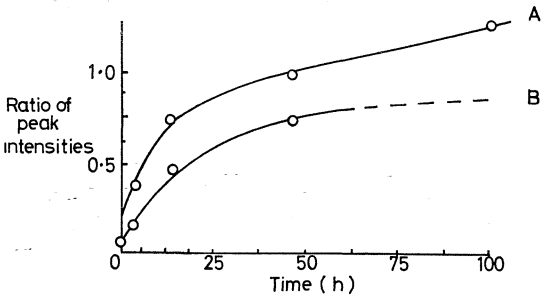

FIG. 1. The ratios of the intensities of infrared absorption at 3.5 μ relative to 3.0 μ (A), and at 3.5 μ relative to 5.7 μ (B), during the reaction of dihydropyran with **1** (A) and **2** (B), respectively. The catalyst used was 0.03 *M* *p*-toluenesulfonic acid.

The conditions under which substitution of acetyl by THP groups in **2** occurred prior to complete etherification of **1** are summarized in Table II. In each case 100 mg substrate was dissolved in 4:1 (v/w) solvent:dihydropyran. The volume was such that the weight ratio of dihydropyran:substrate was 5:1.

Deacetylation

Sodium methoxide-catalyzed deacetylation (Zemplen procedure) was used (49). Similar procedures were utilized with sodium isopropoxide and *t*-butoxide except for substitution of the appropriate alkoxide/alcohol mixture.

Can. J. Chem. Downloaded from www.nrcresearchpress.com by 210.87.254.42 on 09/05/12
For personal use only.

Can. J. Chem. Downloaded from www.nrcresearchpress.com by 210.87.254.42 on 09/05/12
For personal use only.

The reactions were monitored by thin-layer chromatography.

With piperidine as catalyst, the sugar acetate (25 mg) was dissolved in dry methanol (1.0 ml). Dry, redistilled piperidine (10.0 ml) and a few grains of crushed Drierite were added, and the mixture heated at 65 °C for 5 h. The reaction mixture was filtered through a layer of activated carbon, and evaporated to dryness.

Deacetylation of D-*Glucose Pentaacetate with Sodium Methoxide/Chloroform*

To 10 g **2** was added 1.0 ml $CHCl_3$ solution containing 0.2 mg NaOMe and 0.02 MeOH per ml. The solution was allowed to stand at room temperature and was analyzed at intervals by thin-layer chromatography. After 6 h the chromatogram revealed compounds having R_2 1.0, 0.5, 0.36, 0.18, 0.05, and 0.0. Reference standards of **1** and **2** had R_2 0.0 and 1.0 respectively. A control experiment using MeOH in place of $CHCl_3$ gave only **1** (R_2 0.0) after 0.5 h.

*The Attempted Reduction of Penta-O-acetyl-*β-D-*glucose by Diborane*

Compound **2** (25 mg) was dissolved in 2.0 ml tetrahydrofuran (THF) in a magnetically stirred flask thermostatted at 25 °C. The system was purged with dry nitrogen, 1.2 ml 0.5 *M* B_2H_6 in THF was added, and the solution stirred for 2 h. Excess diborane was removed by reaction with ethylene glycol, water was added, and the solution evaporated to dryness. Thin-layer chromatographic analysis revealed a series of compounds with R_2: 0.24, 0.10, and 0.0.

Methylation

Sodium *t*-butoxide – dimethyl sulfoxide – methyl iodide: The sample (50 mg) was dissolved in dry dimethyl sulfoxide (1.0 ml). Methyl iodide (5.0 ml) and a few grains of crushed Drierite were added, and the mixture was stirred at 25 °C. Dry sodium *t*-butoxide was added at a rate sufficient to maintain an excess of sodium *t*-butoxide. The reaction was followed by thin-layer chromatography, and worked up by the usual procedures (50).

*The Effect of Various Methylating Reagents on Penta-bis-O-trimethylsilyl-*α-D-*glucopyranose*

Compound **6** was prepared from **1** by the method of Sweeley *et al.* (22). A chloroform solution of **6** was placed in several nitrogen-filled vials. Methylation reagents were added and the solutions allowed to stand at room temperature. Contents were analyzed by gas–liquid partition chromatography (Column *a*, 180 °C, 100 ml/min). The results have been summarized in Table III.

Disaccharide Hydrolysis and Methyl Glycosylation

A solution of 1.5% HCl in methanol (15 ml) was added to the sample (100 mg) and refluxed overnight. The solution was neutralized by the addition of Duolite 101D resin (OH form), filtered, the resin washed with methanol, and combined filtrate and washings evaporated to dryness under reduced pressure.

Hydrolysis of Methyl O-Acetyl-O-methylglucosides

The sample was heated in a sealed glass vial with Duolite C20 resin. The combined solutions were evaporated to dryness under reduced pressure.

FOR ERRATA SEE
V. 47 ... 19 69 ... p. 2490

TABLE III

Effect of various methylating reagents on pentabis-*O*-trimethylsilyl-α-D-glucopyranose

Reagent	Products R_6^* after 2 h	Products R_6^* after 1 week
Dimethyl sulfoxide	1.0, 1.9	—
Dimethyl sulfate	Precipitated **6**	Precipitated **6**
Dimethylformamide	1.0	1.0, 2.3
Methyl iodide	1.0	1.0
Silver oxide	1.0	1.0
Methanol	1.0	1.0

*Retention time relative to compound **6**.

Reaction Sequence to Locate Acetylated Positions

The dry sample was subjected to the following series of reactions: (1) nitration; (2) deacetylation (sodium methoxide – methanol); (3) methylation (method *a*); (4) denitration; (5) disaccharide hydrolysis and methyl glycosylation (in the case of disaccharide derivatives); (6) acetylation, analysis by gas–liquid partition chromatography; (7) hydrolysis of the acetyl groups and analysis by paper partition chromatography (alternatively the analysis could have been done at step (5) (Scheme 1*b*).)

*Identification of the Products from Esterase-catalyzed Deacetylation of Penta-O-acetyl-*β-D-*glucopyranose*

A solution containing approximately 100 mg of a mixture of glucose acetates was lyophilized and cooled in an ice-brine bath at $\leqslant 5$ °C. Colorless, fuming nitric acid, and acetic anhydride were cooled to < -5 °C and 2.0 ml of the acid were added to 5.0 ml of acetic anhydride to form the nitrating reagent, which was held at -5 °C. Cold acetic anhydride (2.0 ml) and 0.5 ml nitrating reagent were added in sequence to the glucose acetate mixture and the solution stirred 1 h at $\leqslant 5$ °C. The reaction solution was added to a large excess of ice-water and extracted with chloroform. The chloroform extract was washed free of acid and dried over anhydrous magnesium sulfate in the usual manner. The chloroform was evaporated and the residue dissolved in 5.0 ml anhydrous methanol. A 0.2 *M* solution (0.2 ml) of sodium methoxide in methanol was added and stirred at room temperature for 1 h. Sodium ions were removed by treatment with Rexyn 101 (H-form) cation exchange resin. The solvent was evaporated and the residue methylated three times by the modified Purdie technique (45, 46) using small amounts of powdered Drierite to maintain anhydrous conditions in the reaction solution. The product was dissolved in 10 ml ethanol, 1.5 ml 64% aqueous hydrazine was added, and the solution refluxed for 2 h. Excess hydrazine was decomposed by boiling the solution with Raney nickel for 15 min. The catalyst was filtered, washed with ethanol, and the combined filtrate and wash solutions evaporated to dryness. Cold (0 °C) pyridine (2.5 ml) and 0.5 ml acetic anhydride were added to the residue and allowed to react at room temperature for 18 h prior to warming to 60–70 °C for 1 h. The solution was poured into ice-water and the products isolated by chloroform extraction in the usual manner. The product was con-

TABLE IV

Retention times of *O*-acetyl and/or *O*-methyl derivatives of methyl D-glucoside

Derivative of methyl D-glucoside	Column *a*	Column *b*	Relative peak area
2,3,4,6-Tetra-*O*-methyl-β-	0.11	0.10	96
-α-	0.14	0.16	10
6-*O*-Acetyl-2,3,4-tri-*O*-methyl-β-	0.37	0.35	14
-α-	0.29	0.25	20
4-*O*-Acetyl-2,3,6-tri-*O*-methyl-β-	0.31	0.28	74
-α-	0.44	0.38	5
4,6-Di-*O*-acetyl-2,3-di-*O*-methyl-β-	0.77	0.72	3.5
-α-	1.00	1.00	2
3,4,6-Tri-*O*-acetyl-2-*O*-methyl-β-	2.60	2.34	2
-α-	1.70	1.65	1
2,3,4,6-Tetra-*O*-acetyl-β-	4.10	3.5	8
-α-	3.2	2.85	9
Artifact	0.56	0.52	12

centrated to a syrup and examined by gas–liquid partition chromatography. The mixture was resolved into components which were identified by co-chromatography with authentic samples or by comparison of retention times. Column *a* was used at 180 °C and Column *b* at 195 °C, both with a flow rate of 100 ml/min. The retention times relative to that of methyl 4,6-di-*O*-acetyl-2,3-di-*O*-methyl-α-D-glucoside, and the identities of the methyl D-glucosides are given in Table IV.

Products Obtained from Scheme 1b Sequence with 2,3-Di-O-acetyl-β-D-glucopyranose

A sample of **3** (42) was subjected to the reaction sequence of Scheme 1*b*. Analysis of the product by gas–liquid partition chromatography gave peaks with the following retention times relative to methyl 4,6-di-*O*-acetyl-2,3-di-*O*-methyl-α-D-glucoside:

Column *a*: 0.77, 1.00, 1.61, 1.70, 3.20, 4.05;

Column *b*: 0.72, 1.00, 1.67, 2.30, 2.85, 3.60,

corresponding to the anomers of methyl 4,6-di-*O*-acetyl-2,3-di-*O*-methyl-D-glucoside, methyl 3,4,6-tri-*O*-acetyl-2-*O*-methyl-D-glucoside, and methyl 2,3,4,6-tetra-*O*-acetyl-D-glucoside, respectively.

1. A. L. FINK and G. W. HAY. Can. J. Biochem. **47**, 135 (1969).
2. E. FISCHER. Ber. **53**, 1621 (1920).
3. P. J. GAREGG. Arkiv Kemi, **23**, 255 (1965).
4. W. A. BONNER. J. Org. Chem. **24**, 1388 (1959).
5. E. L. HIRST and E. PERCIVAL. *In* Methods in carbohydrate chemistry. Vol. V. *Edited by* R. L. Whistler. Academic Press, Inc., New York. 1965. pp. 287–296.
6. J. K. HAMILTON and H. W. KIRCHER. J. Am. Chem. Soc. **80**, 4703 (1958).
7. P. A. FINAN and C. D. WARREN. J. Chem. Soc. 4214 (1962).
8. L. HOUGH and R. S. THEOBALD. *In* Methods in carbohydrate chemistry. Vol. II. *Edited by* R. L. Whistler and M. L. Wolfrom. Academic Press, Inc., New York. 1963. pp. 162–166.
9. J. O. DEFERRARI, E. G. GROS, and I. O. MASTRONARDI. Carbohydrate Res. **4**, 432 (1967).
10. W. E. DICK, B. G. BAKER, and J. E. HODGE. Carbohydrate Res. **6**, 52 (1968).
11. E. J. COREY and M. CHAYKOVSKY. J. Am. Chem. Soc. **84**, 866 (1962).
12. G. A. RUSSELL and H. D. BECKER. 142nd Meeting, American Chemical Society, Atlantic City, New Jersey. 1962. Abstr. Papers. p. 3Q.
13. J. CUNNINGHAM, R. GIGG, and C. D. WARREN. Tetrahedron Letters, 1191 (1964).
14. S. CHLADEK and J. SMRT. Chem. Ind. London, 1719 (1964).
15. A. HAMPTON. J. Am. Chem. Soc. **87**, 4654 (1965).
16. L. HOUGH, J. E. PRIDDLE, and R. S. THEOBALD. Advan. Carbohydrate Chem. **15**, 91 (1960).
17. J. STANEK, M. CERNY, J. KOCOUREK, and J. PACAK. The monosaccharides. Academic Press, Inc., New York. 1963.
18. R. L. LETSINGER, J. FONTAINE, V. MAHADEVAN, D. A. SCHEXNAYDER, and R. E. LEONE. J. Org. Chem. **29**, 2615 (1964).
19. R. S. TIPSON. Advan. Carbohydrate Chem. **8**, 108 (1953).
20. G. R. AMES, H. M. BLACKMORE, and T. A. KING. J. Appl. Chem. **14**, 503 (1964).
21. H. O. BOUVENG. Acta Chem. Scand. **15**, 96 (1961).
22. C. C. SWEELEY, R. BENTLEY, M. MAKITA, and W. W. WELLS. J. Am. Chem. Soc. **85**, 2479 (1963).
23. A. G. MCINNES. Can. J. Chem. **43**, 1998 (1965).
24. V. BAZANT, V. CHVALOVSKY, and J. RATHOUSKY. Organosilicon compounds. Academic Press, Inc., New York. 1965.
25. D. T. HURST and A. G. MCINNES. Can. J. Chem. **43**, 2004 (1965).
26. J. SOKOLOWSKI and Z. PILARSKI. Zeszyty Nauk Mat., Fiz. Chem., Wyzsza Szkola. Pedagog. Gdansku, **1**, 107 (1961); Chem. Absts. **60**, 1827 (1964).
27. W. LEIGH and Z. KRZEMINSKI. J. Chem. Soc. 1700 (1966).
28. G. KATZ. Tappi, **48**, 134 (1965).
29. J. J. WILLARD, J. S. BRIMACOMBE, and R. P. BRUETON. Can. J. Chem. **42**, 2650 (1964).
30. D. N. ROBERTSON. J. Org. Chem. **25**, 431 (1960).
31. S. J. ANGYAL and S. D. GERO. J. Chem. Soc. 5255 (1965).
32. J. W. MENCH and M. S. LOUNSBERY. U.S. Patent 2,639,280.
33. A. N. DEBELDER, P. J. GAREGG, B. LINDBERG, G. PETROPAVLOVSKII, and O. THEANDER. Acta Chem. Scand. **16**, 623 (1962).

Can. J. Chem. Downloaded from www.nrcresearchpress.com by 210.87.254.42 on 09/05/12
For personal use only.

34. J. HONEYMAN and J. W. MORGAN. Advan. Carbohydrate Chem. **12**, 117 (1957).
35. J. HONEYMAN and J. W. MORGAN. Chem. Ind. London, 1035 (1953).
36. G. V. CAESAR and M. GOLDFRANK. J. Am. Chem. Soc. **68**, 372 (1946).
37. R. D. GUTHRIE and H. SPEDDING. J. Chem. Soc. 953 (1960).
38. K. S. ENNOR and J. HONEYMAN. J. Chem. Soc. 2586 (1958).
39. D. J. BELL and R. L. M. SYNGE. J. Chem. Soc. 1711 (1937).
40. J. DEWAR and G. FORT. J. Chem. Soc. 469 (1944).
41. D. O'MEARA and D. M. SHEPHERD. J. Chem. Soc. 3377 (1957).
42. A. L. FINK and G. W. HAY. Can. J. Chem. This issue.
43. L. HOUGH, J. K. N. JONES, and W. H. WADMAN. J. Chem. Soc. 1702 (1950).
44. H. G. JONES. Ph.D. Thesis. Queen's University, Kingston, Ontario. 1964.
45. W. E. TREVELYAN, D. D. PROCTOR, and J. S. HARRISON. Nature, **166**, 444 (1950).
46. H. G. WALKER, M. GEE, and R. M. MCCREADY. J. Org. Chem. **27**, 2100 (1962).
47. M. L. WOLFROM and A. THOMPSON. *In* Methods in carbohydrate chemistry. Vol. II. *Edited by* R. L. Whistler and M. L. Wolfrom. Academic Press, Inc., New York, 1963. pp. 211–215.
48. M. L. WOLFROM and A. THOMPSON. *In* Methods in carbohydrate chemistry. Vol. 1. *Edited by* R. L. Whistler and M. L. Wolfrom. Academic Press, Inc., New York, 1962. pp. 334–335.
49. A. THOMPSON and M. L. WOLFROM. *In* Methods in carbohydrate chemistry. Vol. II. *Edited by* R. L. Whistler and M. L. Wolfrom. Academic Press, Inc., New York, 1963. pp. 215–220.
50. D. M. W. ANDERSON and G. M. CREE. Carbohydrate Res. **2**, 162 (1966).

Can. J. Chem. Downloaded from www.nrcresearchpress.com by 210.87.254.42 on 09/05/12
For personal use only.

Can. J. Chem. Downloaded from www.nrcresearchpress.com by 210.87.254.6 on 09/05/12
For personal use only.

Monomolecular films of compounds with potential dermophilic and prophylactic properties. Esters of dihydroxyacetone

RONALD P. QUINTANA, LORRIN R. GARSON, AND ANDREW LASSLO
Department of Medicinal Chemistry, College of Pharmacy, University of Tennessee Medical Units, Memphis, Tennessee 38103

Received August 30, 1968

The synthesis of 1,3-diundecanoyloxyacetone (**1**) and 1-undecanoyloxy-3-hydroxyacetone (**2**) is reported. The properties of **1**, spread as a pure monomolecular film and in mixed films with stearic acid, were determined and evaluated. Compound **2** did not form films. The compounds were designed to exert, potentially, long-lasting insect-repellent activity subsequent to anchoring to the skin.

Canadian Journal of Chemistry, **47**, 853 (1969)

During the past few years, we have been concerned with the development of agents exerting *perdurable* insect-repellent and other types of prophylactic activity subsequent to topical or systemic administration (1–6). Currently, our efforts are focused on compounds designed to provide long-lasting prophylactic efficacy by means of the *gradual* release of an active component from a precursor-type molecule anchored to the epidermal surface (3). Figure 1 illustrates this concept schematically.

In this communication, we report the synthesis of two novel precursor-type molecules (**1** and **2**), and their effects upon monolayers of stearic acid, a known dermal constituent (7). Their molecular structures incorporate undecanoic acid and

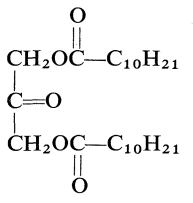

1

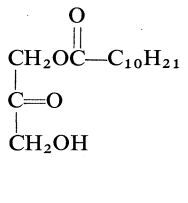

2

dihydroxyacetone; undecanoic acid is a proven insect-repellent (8), and the ability of dihydroxyacetone, and of some structurally related entities, to interact with skin is well established (9–12).

Experimental

Melting points are corrected; they were determined with a Büchi melting point apparatus. Infrared (i.r.) spectra were obtained with a Perkin–Elmer model 137B spectrophotometer. Mass-spectral analyses were carried out by the Morgan–Schaffer Corporation of Montreal, Canada, employing a Hitachi Perkin–Elmer RMU-GD mass spectrometer. Combustion analyses were performed by Drs. G. Weiler and F. B. Strauss, Oxford, England.

Synthetic Work

*1,3-Diundecanoyloxyacetone (**1**)*

To a stirred solution of 25.0 g (0.277 mole) of dry 1,3-dihydroxyacetone in 250 ml of dry freshly distilled pyridine, 56.7 g (0.277 mole) of undecanoyl chloride was added dropwise over a period of 1.5 h. After standing at room temperature for 22 h, the reaction mixture was poured into 600 ml of cold 6 *N* sulfuric acid, precipitating a white solid which was collected by filtration and washed with water. The product was recrystallized three times from hexane and once from 95% ethanol, affording 35.3 g (59.7%) of pure **1**, m.p. 67.4–68.0°, $\nu_{max}(CHCl_3)$ 1750 cm^{-1} (ester carbonyl).

Anal. Calcd. for $C_{25}H_{46}O_5$: C, 70.38; H, 10.87. Found: C, 70.62; H, 10.81.

The method described by Schlenk, Lamp, and DeHaas (13) for the preparation of a similar compound, was employed in the synthesis of compound **2**.

*Undecanoyloxyacetic Acid (**3**)*

This was prepared employing the procedure described for the preparation of **1**. A solution of 25.0 g (0.329 mole) of glycolic acid in 250 ml of pyridine was allowed to react with 67.2 g (0.328 mole) of undecanoyl chloride, affording 83.5 g of product. Four recrystallizations of a 10 g sample from hexane yielded 8.4 g of pure **3**, m.p. 71.2–71.9°, $\nu_{max}(CHCl_3)$ 1748 cm^{-1} (ester and carboxylic acid carbonyl).

Anal. Calcd. for $C_{13}H_{24}O_4$: C, 63.91; H, 9.90. Found: C, 63.78; H, 9.81.

*1-Undecanoyloxy-3-diazoacetone (**4**)*

A mixture of 24.4 g (0.100 mole) of **3** (recrystallized once from hexane; m.p. 71.4–71.9°), 50.8 g (0.400 mole) of oxalyl chloride, and 100 ml of dry benzene was refluxed for 2 h. The solvent and excess oxalyl chloride were removed by distillation *in vacuo* affording brown, liquid undecanoyloxyacetyl chloride. After drying *in vacuo* for 2 h, the acid chloride was dissolved in 150 ml of anhydrous ether, the solution was cooled to −3°, and 0.256 mole of dry, alcohol-free diazomethane in 950 ml of ether was added over a period of 1.2 h. After standing at −2° for an additional 1.5 h, the ether solution was concentrated *in vacuo* to 300 ml, dried over anhydrous magnesium sulfate, and filtered. The filtrate was evaporated *in vacuo* yielding a mobile, oily liquid which solidified upon storage in a refrigerator (24 h). The solid was recrystallized once from hexane affording 19.2 g

Can. J. Chem. Downloaded from www.nrcresearchpress.com by 210.87.254.6 on 09/05/12
For personal use only.

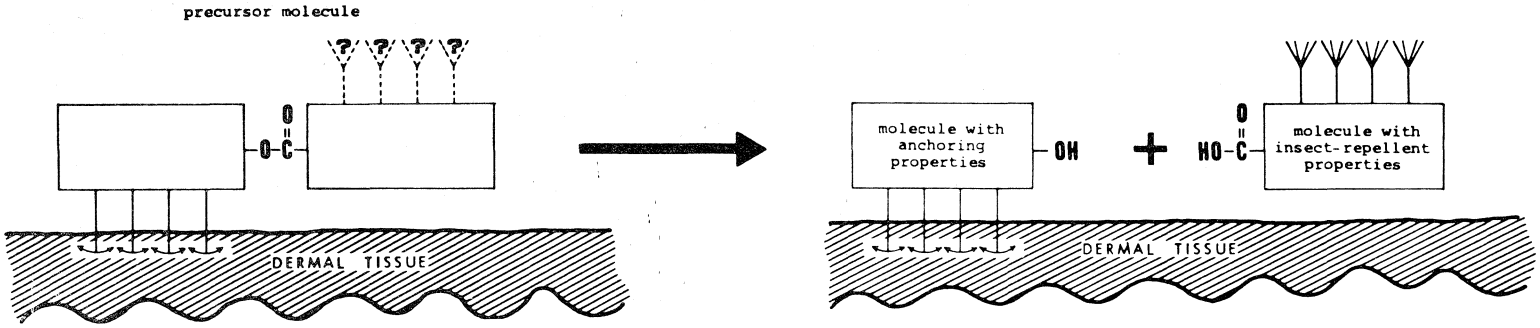

FIG. 1. In the schematic illustration, the precursor molecule itself, anchored to dermal tissue, may or may not have repellent activity; this is indicated by the broken-line symbol for repellency and by the question marks. The release is effected by moisture, pH, esterases or other enzymes, and bacterial flora on and in the epidermal structure.

Can. J. Chem. Downloaded from www.nrcresearchpress.com by 210.87.254.6 on 09/05/12
For personal use only.

(71%) of **4**, m.p. 29.2–31.7°, $\nu_{max}(CHCl_3)$ 2128 (diazo group), 1754 (ester carbonyl), 1653 cm^{-1} (ketone carbonyl). The product was employed, without further purification, in the preparation of **2**.

1-Undecanoyloxy-3-hydroxyacetone (2)

To a hot (80°) solution of 15.0 g (0.056 mole) of **4** in 100 ml of *p*-dioxane, a solution containing 75 ml of water and 15.0 g of 75% aqueous perchloric acid, also heated to 80°, was added. The resulting solution was heated at 80–85° for 2 min, during which time evolution of nitrogen occurred and then ceased. The reaction mixture was rapidly chilled to 5°, poured into cold (0°) water, and was extracted with benzene. The benzene extracts were evaporated *in vacuo* to yield a yellow, viscous liquid. After standing for 10 weeks, the desired product was purified by three recrystallizations from hexane, affording 715 mg (4.9%) of pure **2**, m.p. 81.4–82.3° (sealed capillary), $\nu_{max}(CHCl_3)$ 3546 (O—H stretching), 1736 cm^{-1} (ester and ketone carbonyl).

Anal. Calcd. for $C_{14}H_{26}O_4$: C, 65.09; H, 10.14. Found: C, 65.07; H, 10.09.

Monolayer Studies

Specific details of the film balance, ancillary equipment, and general methods employed in our monolayer studies have already been described (2, 4–6).

In the currently reported work, spectrograde chloroform was utilized as the spreading solvent; solutions of the individual compounds (0.070 μmole/0.02 ml) and of the mixtures (0.070 μmole of each component/0.02 ml) were prepared immediately before they were deposited on the aqueous subphase surface. The compression procedure previously reported (5, 6) was employed. At low pressures the compression barrier was moved in 2 mm decrements, while at higher pressures 1 mm decrements were used; one-minute intervals were employed between each decrement. The subphase temperature was 25.5 ± 1.4°. At least three independent determinations were used to determine average pressure–area curves. The experimental curves deviated from the average curves normally by no more than 0.5 $Å^2$ per molecule, at a given surface pressure.

Results and Discussion

The structure assignments made for compounds **1** and **2** were based upon their combustion analyses and their infrared (i.r.) and mass spectra. The molecular weight of 426 for 1,3-diundecanoyloxyacetone (**1**) was confirmed by the appearance of the molecular ion at *m/e* 426. The fragmentation pattern obtained for this compound was also consistent with the proposed structure. The findings of Schlenk, Lamp, and DeHaas (13), in their work with 1-palmitoxy-3-hydroxyacetone, imply the possibility that we could have obtained 1-undecanoyloxy-3-hydroxyacetone (**2**) in a dimeric form. Further work on the nature of monomer and dimer formation is currently in progress and will be reported later.

Experimentally derived pressure–area isotherms for compound **1**, stearic acid, and an equimolar mixture[1] of **1** and stearic acid are illustrated in Fig. 2 along with the calculated average obtained by assuming additivity of the curves for **1** and for stearic acid.

The isotherm for **1** indicates that the film is expanded; this, along with the relatively low collapse pressure (14.5 dynes/cm), is consistent with curves obtained for some triglycerides with alkyl chains of intermediate length (14, pp. 245–249). Considering that **1** has only two such chains, the observed limiting area per molecule (62.5 $Å^3$) appears also to be compatible with published data (14, pp. 245–249). Examination of accurate, space-filling molecular models[2] supports the view that molecules of **1**, at pressures close to collapse, are anchored to the aqueous subphase surface by their polar ketonic and ester oxygen atoms; the ester alkyl groups project upwards but in a somewhat tilted manner.

In the mixed film containing compound **1** and stearic acid, **1** controls the properties of the film at low pressures (up to 15 dynes/cm), while stearic acid exerts prominent influence at higher pressures.[3] At low pressures, the experimentally derived isotherm for the mixture is shifted toward slightly higher area-per-molecule values, compared with the calculated-average curve; although the displacement is quite limited, it reflects non-additive behavior. Molecules of **1** are ejected from area-determining positions in the film during the plateau portion of the curve. In the latter region, the congruence of the calculated and experimental curves may be indicative of phase separation (14, p. 285). The difference (i.e., 10.6 dynes/cm) between the collapse pressure of pure stearic acid and the high-pressure region of the mixed film suggests that **1** has a pronounced influence upon the collapse process.[4]

---

[1]Area-per-molecule values for the mixture were obtained by dividing the area occupied by the film by the total number of molecules in the film.

[2]Godfrey molecular models; cf. ref. 5.

[3]The compressibility (15) of **1** (0.0168) was virtually identical with that of the mixed-film curve (0.0173), at pressures up to 15 dynes/cm; similarly, the compressibility of stearic acid (0.0023) was essentially the same as that for the high-pressure portion of the mixed-film isotherm (0.0026).

[4]In addition to the quintuplicate determination for the pressure–area curve of pure stearic acid (Fig. 2), the behavior of the latter was determined under kinetic conditions paralleling those of stearic acid in the mixed film. Two sets of duplicate control experiments with *pure* stearic acid, with the same rate of compression as in the *mixed* film, indicated unequivocally that the collapse pressure of stearic acid *per se* was not affected by the rates of compression employed in the experiments reported here.

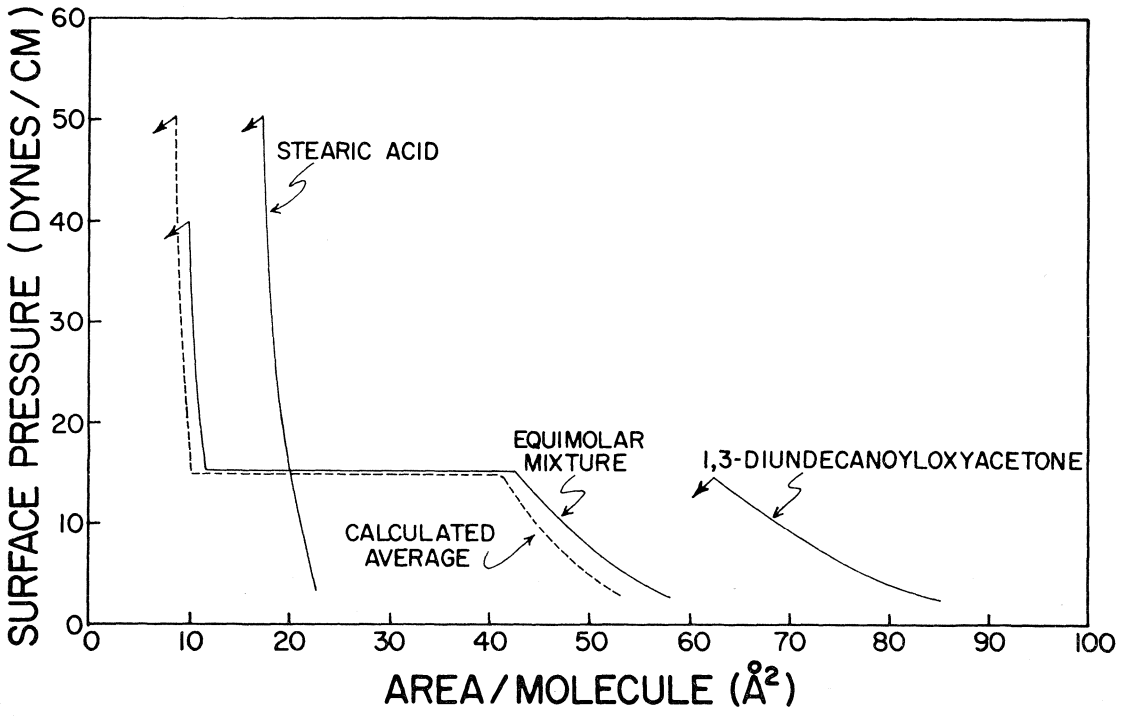

FIG. 2. Pressure–area isotherms for 1,3-diundecanoyloxyacetone (**1**), stearic acid, an equimolar mixture, and the calculated average for the mixture.

While the physicochemical properties of **2** are consistent with all desired characteristics for a precursor molecule, the compound's polarity did not lend itself to evaluation within the system suited for the study of the first compound (**1**) of this series. Attempts to evaluate pure and mixed films of **2** revealed, in two sets of independent determinations, that this compound did not form a monolayer. It was not retained in area-determining positions when mixed films (1:1) with stearic acid were spread; the pressure–area curve was identical, in all respects, with that of stearic acid. The comparative potentialities for anchoring affinity of the two compounds, with particular reference to the effect of one free hydroxyl function, will be investigated in the near future.

Acknowledgments

This investigation was supported by the United States Army Medical Research and Development Command, Washington, D.C., through Research Contract No. DA-49-193-MD-2636.

The authors gratefully acknowledge the assistance of Mrs. P. L. Sanders in determining the pressure–area isotherms reported in this communication.

1. V. DEV, R. P. QUINTANA, and A. LASSLO. J. Med. Chem. **9**, 242 (1966).
2. R. P. QUINTANA, A. LASSLO, P. P. BOGGS, and E. D. YEAGLIN. J. Pharm. Sci. **57**, 230 (1968).
3. R. P. QUINTANA, L. R. GARSON, and A. LASSLO. Can. J. Chem. **46**, 2835 (1968).
4. R. P. QUINTANA, A. LASSLO, and S. L. OUSLEY. J. Pharm. Sci. **56**, 1193 (1967).
5. R. P. QUINTANA, A. LASSLO, and P. P. BOGGS. J. Colloid Interface Sci. **26**, 166 (1968).
6. R. P. QUINTANA and R. M. OWENS. J. Colloid Interface Sci. To be published.
7. S. ROTHMAN. Physiology and biochemistry of the skin. Univ. Chicago Press, Chicago. 1954. pp. 313–318.
8. W. V. KING (*Compiler*). Chemicals evaluated as insecticides and repellents at Orlando, Fla. Agriculture Handbook No. 69. Entomology Research Branch, Agricultural Research Service, United States Department of Agriculture, Washington, D.C. 1954. p. 185.
9. E. WITTGENSTEIN and H. K. BERRY. J. Invest. Dermatol. **36**, 283 (1961).
10. E. WITTGENSTEIN and H. K. BERRY. Science, **132**, 894 (1960).
11. L. GOLDMAN, J. BARKOFF, D. BLANEY, T. NAKAI, and R. SUSKIND. J. Invest. Dermatol. **35**, 161 (1960).
12. H. I. MAIBACH and A. M. KLIGMAN. Arch. Dermatol. **82**, 505 (1960).
13. H. SCHLENK, B. G. LAMP, and B. W. DEHAAS. J. Am. Chem. Soc. **74**, 2550 (1952).
14. G. L. GAINES, JR. Insoluble monolayers at liquid–gas interfaces. Interscience Publishers, Inc., New York. 1966.
15. H. E. RIES, JR. and H. D. COOK. J. Colloid Sci. **9**, 535 (1954).

Can. J. Chem. Downloaded from www.nrcresearchpress.com by 210.87.254.6 on 09/05/12
For personal use only.

Can. J. Chem. Downloaded from www.nrcresearchpress.com by 210.87.254.105 on 09/05/12
For personal use only.

One-step conversion of isatins to oxindoles and phthalonimides to homophthalimides

J. M. MUCHOWSKI
Bristol Laboratories of Canada Ltd., Candiac, Quebec

Received October 7, 1968

The palladium-catalyzed hydrogenation of isatins and phthalonimides in acetic acid containing perchloric acid produced oxindoles and homophthalimides directly.
A general, one-step synthesis of phthalonimides from isocarbostyrils is described.

Canadian Journal of Chemistry, **47**, 857 (1969)

The conversion of isatin to oxindole was first effected by von Baeyer and Knop (1) in 1866 in connection with studies which culminated in the first rational synthesis (2) of the important dyestuff indigo. The transformation was achieved by the reduction of isatin (**1**) with sodium amalgam in water to dioxindole (**2**), which, without isolation, could be further reduced to oxindole (**3**) with the same reagent in aqueous acidic medium. Since von Baeyer's original work, numerous methods have been developed[1] for the preparation of **3** from **1**, but to date, only one of these has not involved a two-step process,[2] i.e. in 1942 Sakurai (4) showed that electrolysis of isatin in aqueous sodium sulfate at a mercury cathode gave a mixture which was comprised of oxindole, dioxindole, and isatide (3,3′-dihydroxy-3,3′-*bi*-oxindole).

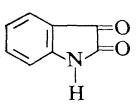

1

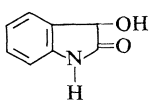

2

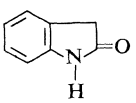

3

We have found that oxindole can be prepared in one step by the palladium-catalyzed hydrogenation (at 60°) of isatin in glacial acetic acid containing approximately two equivalents of perchloric acid. The reduction evidently proceeds in two stages, since the first equivalent of hydrogen is absorbed rapidly and the second slowly. The reduction is also applicable to the synthesis of *N*-methyloxindole (see Table I) and presumably could be used for the preparation of other oxindoles bearing substituents stable to the reaction conditions.

Under somewhat milder conditions (see Table I) the reaction can be utilized for the synthesis of homophthalimides (**6**) from the corresponding readily available (see below) phthalonimides (**5**),

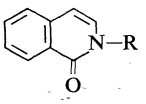

4

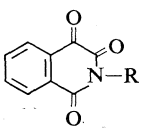

5

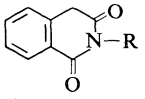

6

but this method will probably not be extensively applied to simple homophthalimides inasmuch as these are easily prepared from homophthalic acid and ammonia or primary amines (for example see refs. 5 and 6). On the other hand, it should find use in the synthesis of homophthalimides substituted in the benzene ring since the requisite homophthalic acids are relatively difficult to obtain.

Phthalonimides, a long known but comparatively rare class of compounds, have heretofore been synthesized by the chromic acid oxidation of tetrahydroisoquinolines (7), the nitric acid oxidation of 4-hydroxyisocarbostyrils (8, 9), and recently, by the selenium dioxide oxidation of homophthalimides (5). We have found that phthalonimides are generally available by the oxidation of isocarbostyrils (**4**) with chromic acid in acetic acid at room temperature. A number of examples of this oxidation are shown in Table II.

Several synthetic consequences of the results

[1]For a summary of these methods through 1952, see ref. 3.

[2]*Note added in proof:*—After this manuscript was accepted for publication, Beckett, Daisley, and Walker (12) described the palladium-catalyzed hydrogenation, at atmospheric pressure, of isatin to oxindole, and Foglia and Swern (13) showed that zinc–copper couple in refluxing acetic acid converted isatins to oxindoles.

TABLE I

Catalytic reduction of isatins and phthalonimides

Reactant	Temperature (°C)	Time (h)	Product	% Yield*	Melting point (°C) Observed	Literature
Isatin	60	16	Oxindole	63	124–126†	127‡
N-Methylisatin	60	14	*N*-Methyloxindole	73	85.5–87§	88‡
Phthalonimide	25	8.5	Homophthalimide	40	234–236‖	230–233¶
N-Methylphthalonimide	25	5	*N*-Methylhomophthalimide	81	120–121	121–122**
N-Ethylphthalonimide	25	10.5	*N*-Ethylhomophthalimide	76	102–103	106††
N-Benzylphthalonimide	25	12	*N*-Benzylhomophthalimide	91	124–126#	—

*Unless specified otherwise, the yields and melting points refer to crude, unrecrystallized products.
†See Experimental.
‡See ref. 10.
§After one crystallization from cyclohexane.
‖After one crystallization from acetic acid.
¶See ref. 6.
**See ref. 11.
††See ref. 5.
‡‡After one crystallization from cyclohexane followed by sublimation at 110°/0.001 mm, the m.p. was raised to 128–130°.
Anal. Calcd. for $C_{16}H_{13}NO_2$: C, 76.42; H, 5.22. Found: C, 76.52; H, 5.38.

TABLE II

Chromic acid oxidation of isocarbostyrils to phthalonimides

Reactant*	Product	% Yield†	Melting point (°C) Observed	Literature
Isocarbostyril	Phthalonimide	45	221–223	224‡
N-Methylisocarbostyril	*N*-Methylphthalonimide	81	185–186	186–187§
N-Ethylisocarbostyril	*N*-Ethylphthalonimide	67	102.5–103.5	101‖
N-Benzylisocarbostyril	*N*-Benzylphthalonimide	75¶	181.5–183.5¶	—

*The isocarbostyrils described herein are known and were synthesized according to published procedures.
†Unless specified otherwise, the yields and melting points refer to crude, unrecrystallized products.
‡See ref. 8.
§See ref. 7.
‖See ref. 5.
¶After crystallization from benzene–cyclohexane 3:1.
Anal. Calcd. for $C_{16}H_{11}NO_3$: C, 72.44; H, 4.18. Found: C, 72.44; H, 4.50.

described herein will be submitted for publication in due course.

Experimental

The melting points were determined in a Gallenkamp melting point apparatus and are not corrected.

Oxindole

The following method was typical for the reduction of isatins.

A mixture consisting of isatin (5.98 g, 40 mmoles), glacial acetic acid (192 ml), 60–62% perchloric acid (8 ml), and 600 mg of 10% palladium on charcoal was hydrogenated in a Parr apparatus at 60° and an initial hydrogen pressure of 60 p.s.i.g. The theoretical amount of hydrogen was absorbed in 16 h. The cooled mixture was filtered through Celite, and the filtrate was concentrated to a small volume *in vacuo* at 40°. The residue was diluted with 300 ml of water and then extracted with ethyl acetate. The extract was washed with water, dried over sodium sulfate, and evaporated *in vacuo*. The solid thus obtained was boiled with 200 ml of cyclohexane to give an insoluble residue which was collected by filtration and dried. It weighed 1.669 g and had m.p. 124–126°; mixture m.p. with oxindole was undepressed. The cyclohexane solution on cooling deposited 1.681 g of a cream-colored solid, m.p. 122.5–124°; mixture m.p. with oxindole, 123–126°. The total yield of oxindole was 3.35 g or 63%.

N-Methylhomophthalimide

The following procedure was typical for the reduction of phthalonimides.

A mixture of *N*-methylphthalonimide (7.57 g, 40 mmoles), glacial acetic acid (192 ml), 60–62% perchloric acid (8 ml), and 760 mg of 10% palladium on charcoal was hydrogenated at room temperature and an initial hydrogen pressure of 60 p.s.i.g. After 5 h, the catalyst was removed by filtration through Celite, and the filtrate was evaporated to a volume of ca. 10 ml *in vacuo* at 40°. The solution was carefully diluted with 300 ml of water with swirling, whereupon a white, crystalline solid separated from solution. After being cooled in ice, the product was collected by filtration, washed well with ice-cold water, and dried *in vacuo*. The product weighed

Can. J. Chem. Downloaded from www.nrcresearchpress.com by 210.87.254.105 on 09/05/12
For personal use only.

5.68 g (81%) and had m.p. 120–121°. A mixture melting point with an authentic specimen of *N*-methylhomophthalimide was undepressed.

N-Methylphthalonimide

The following procedure was typical for the oxidation of isocarbostyrils.

A magnetically stirred solution of *N*-methylisocarbostyril (20.0 g, 125.8 mmoles) in 200 ml of glacial acetic acid was titrated with 0.649 *M* sodium dichromate in 2.5 *M* sulfuric acid (194 ml, 377.7 m eq.) at a rate such that the reaction temperature did not exceed 30°. When the addition was completed the mixture was stirred for an additional ½ h at room temperature, and then it was poured with stirring into ca. 1.5 l of ice-cold water. The precipitated yellow solid was collected by filtration, washed well with ice-cold water, and dried *in vacuo*. The yellow solid obtained in this way had m.p. 185–186° (lit. (7), m.p. 186–187°), and weighed 19.2 g (81%).

1. A. VON BAEYER and C. KNOP. Ann. Chem. **140**, 1 (1866).
2. A. VON BAEYER. Chem. Ber. **11**, 582 (1878).
3. P. L. JULIAN, E. W. MEYER, and H. C. PRINTY. Heterocyclic compounds. Vol. III. *Edited by* R. C. Elderfield. John Wiley and Sons, Inc., New York. 1952. pp. 126–130.
4. B. SAKURAI. J. Chem. Soc. Japan, **17**, 269 (1942); Chem. Abstr. **41**, 4486 (1947).
5. N. P. BUU-HOI, G. SAINT-RUF, and J. C. BOURGEADE. J. Heterocyclic Chem. **5**, 545 (1968).
6. B. R. HARRIMAN, R. S. SHELTON, M. G. VAN CAMPEN, and M. R. WARREN. J. Am. Chem. Soc. **67**, 1481 (1945).
7. M. FREUND and H. BECK. Chem. Ber. **37**, 1942 (1904).
8. S. GABRIEL and J. COLEMAN. Chem. Ber. **35**, 2421 (1902).
9. W. FINDEKLEE. Chem. Ber. **38**, 3542 (1905).
10. R. STOLLE, R. BERGDOLL, M. LUTHER, A. AUERHAHN, and W. WACKER. J. Prakt. Chem. **128**, 1 (1930).
11. J. M. MUCHOWSKI. Tetrahedron Letters, 1773 (1966).
12. A. H. Beckett, R. W. Daisley, and J. Walker. Tetrahedron, **24**, 6093 (1968).
13. T. A. Foglia and D. Swern. J. Org. Chem. **33**, 4440 (1968).

Facile preparation of thioacetals in neutral medium starting from sodium borohydride

J. M. LALANCETTE AND A. LACHANCE
Department of Chemistry, Faculty of Sciences, University of Sherbrooke, Sherbrooke, Quebec

Received October 23, 1968

Sodium borohydride can be sulfurated to give $NaBH_2S_3$. The sulfurated hydride, when treated with a mercaptan, gives an orthothioborate: $(RS)_3B$. The orthoborates react with aldehydes and ketones to give the corresponding thioacetals with quantitative yields, in neutral medium.

Canadian Journal of Chemistry, **47**, 859 (1969)

We have reported (1) the preparation of thioacetals in neutral media (benzene or petroleum ether) using alkyl orthothioborates (eq. [1]).

[1] $2(RS)_3B + 3R'COR'' \rightarrow$ 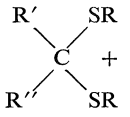 $+ \quad B_2O_3$

The orthothioesters can be prepared from boron sulfide (2) or boron halides (3) but in both cases, these preparations are somewhat tedious. Recently, we have reported the partial sulfuration of sodium borohydride to give a sulfurated borohydride formulated as $NaBH_2S_3$ (4).

This sulfurated borohydride reacts very easily with mercaptans to give the corresponding orthothioborates, according to eq. [2]:

[2] $NaBH_2S_3 + RSH \rightarrow (RS)_3B + H_2 + RSSR + NaS_3H$

The sulfuration of the borohydride is an extremely simple reaction; a mixture of $NaBH_4$ (1 mole) and sulfur (3 moles) is treated by anhydrous tetrahydrofuran and the solvent is evaporated under vacuum after a short contact. This sulfurated hydride is then treated with an excess of the selected mercaptan in petroleum ether. The use of a stoichiometric amount of mercaptan gives rather low yields of orthothioborate (10–20%) but a 100% excess of mercaptan brings the yield in the 50–60% range. In petroleum ether the sodium polysulfide is insoluble and the organic fraction can be filtered off. Due care must be exercized in the course of this filtration since orthothioborates are very hygroscopic. The orthothioborate is then separated from the disulfide by distillation and can be used for the preparation of the thioacetal.

This sequence of reactions besides giving a new

Can. J. Chem. Downloaded from www.nrcresearchpress.com by 210.87.254.105 on 09/05/12
For personal use only.

5.68 g (81%) and had m.p. 120–121°. A mixture melting point with an authentic specimen of *N*-methylhomophthalimide was undepressed.

N-Methylphthalonimide

The following procedure was typical for the oxidation of isocarbostyrils.

A magnetically stirred solution of *N*-methylisocarbostyril (20.0 g, 125.8 mmoles) in 200 ml of glacial acetic acid was titrated with 0.649 *M* sodium dichromate in 2.5 *M* sulfuric acid (194 ml, 377.7 m eq.) at a rate such that the reaction temperature did not exceed 30°. When the addition was completed the mixture was stirred for an additional ½ h at room temperature, and then it was poured with stirring into ca. 1.5 l of ice-cold water. The precipitated yellow solid was collected by filtration, washed well with ice-cold water, and dried *in vacuo*. The yellow solid obtained in this way had m.p. 185–186° (lit. (7), m.p. 186–187°), and weighed 19.2 g (81%).

1. A. VON BAEYER and C. KNOP. Ann. Chem. **140**, 1 (1866).
2. A. VON BAEYER. Chem. Ber. **11**, 582 (1878).
3. P. L. JULIAN, E. W. MEYER, and H. C. PRINTY. Heterocyclic compounds. Vol. III. *Edited by* R. C. Elderfield. John Wiley and Sons, Inc., New York. 1952. pp. 126–130.
4. B. SAKURAI. J. Chem. Soc. Japan, **17**, 269 (1942); Chem. Abstr. **41**, 4486 (1947).
5. N. P. BUU-HOI, G. SAINT-RUF, and J. C. BOURGEADE. J. Heterocyclic Chem. **5**, 545 (1968).
6. B. R. HARRIMAN, R. S. SHELTON, M. G. VAN CAMPEN, and M. R. WARREN. J. Am. Chem. Soc. **67**, 1481 (1945).
7. M. FREUND and H. BECK. Chem. Ber. **37**, 1942 (1904).
8. S. GABRIEL and J. COLEMAN. Chem. Ber. **35**, 2421 (1902).
9. W. FINDEKLEE. Chem. Ber. **38**, 3542 (1905).
10. R. STOLLE, R. BERGDOLL, M. LUTHER, A. AUERHAHN, and W. WACKER. J. Prakt. Chem. **128**, 1 (1930).
11. J. M. MUCHOWSKI. Tetrahedron Letters, 1773 (1966).
12. A. H. Beckett, R. W. Daisley, and J. Walker. Tetrahedron, **24**, 6093 (1968).
13. T. A. Foglia and D. Swern. J. Org. Chem. **33**, 4440 (1968).

Facile preparation of thioacetals in neutral medium starting from sodium borohydride

J. M. LALANCETTE AND A. LACHANCE

Department of Chemistry, Faculty of Sciences, University of Sherbrooke, Sherbrooke, Quebec

Received October 23, 1968

Sodium borohydride can be sulfurated to give $NaBH_2S_3$. The sulfurated hydride, when treated with a mercaptan, gives an orthothioborate: $(RS)_3B$. The orthoborates react with aldehydes and ketones to give the corresponding thioacetals with quantitative yields, in neutral medium.

Canadian Journal of Chemistry, **47**, 859 (1969)

We have reported (1) the preparation of thioacetals in neutral media (benzene or petroleum ether) using alkyl orthothioborates (eq. [1]).

[1] $2(RS)_3B + 3R'COR'' \rightarrow \begin{matrix} R' & SR \\ & C \\ R'' & SR \end{matrix} + B_2O_3$

The orthothioesters can be prepared from boron sulfide (2) or boron halides (3) but in both cases, these preparations are somewhat tedious. Recently, we have reported the partial sulfuration of sodium borohydride to give a sulfurated borohydride formulated as $NaBH_2S_3$ (4).

This sulfurated borohydride reacts very easily with mercaptans to give the corresponding orthothioborates, according to eq. [2]:

[2] $NaBH_2S_3 + RSH \rightarrow (RS)_3B + H_2 + RSSR + NaS_3H$

The sulfuration of the borohydride is an extremely simple reaction; a mixture of $NaBH_4$ (1 mole) and sulfur (3 moles) is treated by anhydrous tetrahydrofuran and the solvent is evaporated under vacuum after a short contact. This sulfurated hydride is then treated with an excess of the selected mercaptan in petroleum ether. The use of a stoichiometric amount of mercaptan gives rather low yields of orthothioborate (10–20%) but a 100% excess of mercaptan brings the yield in the 50–60% range. In petroleum ether the sodium polysulfide is insoluble and the organic fraction can be filtered off. Due care must be exercized in the course of this filtration since orthothioborates are very hygroscopic. The orthothioborate is then separated from the disulfide by distillation and can be used for the preparation of the thioacetal.

This sequence of reactions besides giving a new

Can. J. Chem. Downloaded from www.nrcresearchpress.com by 210.87.254.40 on 09/05/12
For personal use only.

preparative method of orthothioborates, offers a new, simple and rapid technique of preparation of thioacetals, under neutral conditions. The side reactions resulting from acid catalysis, as required by the standard methods of preparation of thioacetals, can be avoided with this new procedure.

Experimental

In a dry 500 ml flask, a mixture of 7.6 g (0.2 mole) of sodium borohydride and 19.2 g (0.6 mole) of sulfur was stirred with 50 ml of anhydrous tetrahydrofuran (slow addition). After the initial reflux had subsided, heat was applied, for a total reflux time of 1½ h. The tetrahydrofuran was then evaporated under vacuum at room temperature and 200 ml of dry petroleum ether, b.p. 30–60° was added to the hydride, with 137 g (1.8 mole) of 1-propanethiol. The reaction mixture was then refluxed overnight.

The crude mixture was then filtered on a carefully dried sintered glass filter (medium porosity). It is advantageous to keep the system dry during the filtration, using a stream of dry nitrogen flowing through an inverted funnel over the filter. After evaporation of the solvent at atmospheric pressure under dry nitrogen, the residue (56.0 g) was then fractionated under vacuum. The first fraction was di-*n*-propyl disulfide, 20.3 g, b.p. 44°/0.5 mm, n_D^{29} 1.4980. Reported for di-*n*-propyl disulfide, b.p. 193.5°/750 mm, n_D^{20} 1.4981. The second fraction, 25.8 g (55% yield based on $NaBH_4$) was *n*-propyl orthothioborate, b.p. 110–118° /0.6 mm, n_D^{29} 1.5341. Reported (5) for *n*-propyl orthothioborate, b.p. 110°/0.6 mm, n_D^{25} 1.5346. This second fraction had an infrared spectrum showing the typical B—S bands at 910 cm^{-1}.

In a dry 250 ml flask, 6.7 g (0.93 mole) of butanone were mixed with 16.1 g (0.82 mole) of ethyl orthoborate. Upon warming, the mixture assumed a gel-like appearance. After a 1h- contact, the mass was extracted with petroleum ether. The boric anhydride was filtered off, the solvent evaporated, and the crude thioacetal distilled. The main fraction was the ethyl thioacetal of butanone, b.p. 73°/0.15 mm, n_D^{28} 1.4959. Reported (2), b.p. 205–208°/750 mm, n_D^{25} 1.4955. The yield of thioacetal was 86%. The reaction could be reproduced with other simple orthothioborates, such as propyl, butyl, and pentyl, with similar yields.

1. F. Bessette, J. Brault, and J. M. Lalancette. Can. J. Chem. **43**, 307 (1965).
2. J. Brault and J. M. Lalancette. Can. J. Chem. **42**, 2903 (1964).
3. B. M. Mikhailov, T. A. Schegoleva, E. M. Shashkova, and V. D. Sheludyakov. Bull. Acad. Sci. USSR, Div. Chem. Sci. English Transl. **7**, 1143 (1962).
4. J. M. Lalancette, A. Frêche, and R. Monteux. Can. J. Chem. **46**, 2754 (1968).
5. A. Cabana, J. Brault, and J. M. Lalancette. Spectrochim. Acta, **22**, 377 (1966).

Can. J. Chem. Downloaded from www.nrcresearchpress.com by 210.87.254.40 on 09/05/12
For personal use only.

α-Metallation and subsequent alkylation of alkyl alkanesulfonates

W. E. Truce and D. J. Vrencur
Purdue University, Lafayette, Indiana 47907

Received October 3, 1968

Strong bases affect α-metallation of alkyl alkanesulfonates; subsequent alkylation offers a useful approach to esters of the higher sulfonic acids.

Canadian Journal of Chemistry, **47**, 860 (1969)

In further pursuing the synthesis utility of sulfur group-stabilized carbanions as in alkylations (1), acylations (2), halogenations (3), nitrations (4), and sulfonylations,[1] it has been found that alkyl alkanesulfonates can be metallated and subsequently alkylated in fair to excellent yields.[2,3]

Interest in this area was cultivated by the discovery in this laboratory (6) that the azasultone **1** could be alkylated to yield two different products depending on the conditions employed. Also, the related 1,3-diphenyl-1,4-butanesultone was methylated under the first set of conditions (6).

Following this, attention was turned to a series of neopentyl alkanesulfonates (**2**–**4** in Table I), the neopentyl group being used initially to preclude the possibility of such undesirable side reactions on the alkyl unit as elimination and displacement. With neopentyl α-toluenesulfonate (**2**), where a benzylic carbanion is formed, *n*-

[1]W. E. Truce and L. W. Christensen. Unpublished results.
[2]E. J. Corey and T. Durst (5) have studied the formation of $LiCH_2SO_3CH_3$ and its reaction with carbonyl compounds.
[3]We were recently made aware of related work by T. Durst and J. du Manoir on reactions of α-metallated sultones with alkyl halides and with carbonyl compounds.

preparative method of orthothioborates, offers a new, simple and rapid technique of preparation of thioacetals, under neutral conditions. The side reactions resulting from acid catalysis, as required by the standard methods of preparation of thioacetals, can be avoided with this new procedure.

Experimental

In a dry 500 ml flask, a mixture of 7.6 g (0.2 mole) of sodium borohydride and 19.2 g (0.6 mole) of sulfur was stirred with 50 ml of anhydrous tetrahydrofuran (slow addition). After the initial reflux had subsided, heat was applied, for a total reflux time of 1½ h. The tetrahydrofuran was then evaporated under vacuum at room temperature and 200 ml of dry petroleum ether, b.p. 30–60° was added to the hydride, with 137 g (1.8 mole) of 1-propanethiol. The reaction mixture was then refluxed overnight.

The crude mixture was then filtered on a carefully dried sintered glass filter (medium porosity). It is advantageous to keep the system dry during the filtration, using a stream of dry nitrogen flowing through an inverted funnel over the filter. After evaporation of the solvent at atmospheric pressure under dry nitrogen, the residue (56.0 g) was then fractionated under vacuum. The first fraction was di-*n*-propyl disulfide, 20.3 g, b.p. 44°/0.5 mm, n_D^{29} 1.4980. Reported for di-*n*-propyl disulfide, b.p. 193.5°/750 mm, n_D^{20} 1.4981. The second fraction, 25.8 g (55% yield based on $NaBH_4$) was *n*-propyl orthothioborate, b.p. 110–118° /0.6 mm, n_D^{29} 1.5341. Reported (5) for *n*-propyl orthothioborate, b.p. 110°/0.6 mm, n_D^{25} 1.5346. This second fraction had an infrared spectrum showing the typical B—S bands at 910 cm^{-1}.

In a dry 250 ml flask, 6.7 g (0.93 mole) of butanone were mixed with 16.1 g (0.82 mole) of ethyl orthoborate. Upon warming, the mixture assumed a gel-like appearance. After a 1h- contact, the mass was extracted with petroleum ether. The boric anhydride was filtered off, the solvent evaporated, and the crude thioacetal distilled. The main fraction was the ethyl thioacetal of butanone, b.p. 73°/0.15 mm, n_D^{28} 1.4959. Reported (2), b.p. 205–208°/750 mm, n_D^{25} 1.4955. The yield of thioacetal was 86%. The reaction could be reproduced with other simple orthothioborates, such as propyl, butyl, and pentyl, with similar yields.

1. F. Bessette, J. Brault, and J. M. Lalancette. Can. J. Chem. **43**, 307 (1965).
2. J. Brault and J. M. Lalancette. Can. J. Chem. **42**, 2903 (1964).
3. B. M. Mikhailov, T. A. Schegoleva, E. M. Shashkova, and V. D. Sheludyakov. Bull. Acad. Sci. USSR, Div. Chem. Sci. English Transl. **7**, 1143 (1962).
4. J. M. Lalancette, A. Frêche, and R. Monteux. Can. J. Chem. **46**, 2754 (1968).
5. A. Cabana, J. Brault, and J. M. Lalancette. Spectrochim. Acta, **22**, 377 (1966).

Can. J. Chem. Downloaded from www.nrcresearchpress.com by 210.87.254.40 on 09/05/12
For personal use only.

α-Metallation and subsequent alkylation of alkyl alkanesulfonates

W. E. Truce and D. J. Vrencur
Purdue University, Lafayette, Indiana 47907

Received October 3, 1968

Strong bases affect α-metallation of alkyl alkanesulfonates; subsequent alkylation offers a useful approach to esters of the higher sulfonic acids.

Canadian Journal of Chemistry, **47**, 860 (1969)

In further pursuing the synthesis utility of sulfur group-stabilized carbanions as in alkylations (1), acylations (2), halogenations (3), nitrations (4), and sulfonylations,[1] it has been found that alkyl alkanesulfonates can be metallated and subsequently alkylated in fair to excellent yields.[2,3]

Interest in this area was cultivated by the discovery in this laboratory (6) that the azasultone **1** could be alkylated to yield two different products depending on the conditions employed. Also, the related 1,3-diphenyl-1,4-butanesultone was methylated under the first set of conditions (6).

Following this, attention was turned to a series of neopentyl alkanesulfonates (**2**–**4** in Table I), the neopentyl group being used initially to preclude the possibility of such undesirable side reactions on the alkyl unit as elimination and displacement. With neopentyl α-toluenesulfonate (**2**), where a benzylic carbanion is formed, *n*-

[1]W. E. Truce and L. W. Christensen. Unpublished results.
[2]E. J. Corey and T. Durst (5) have studied the formation of $LiCH_2SO_3CH_3$ and its reaction with carbonyl compounds.
[3]We were recently made aware of related work by T. Durst and J. du Manoir on reactions of α-metallated sultones with alkyl halides and with carbonyl compounds.

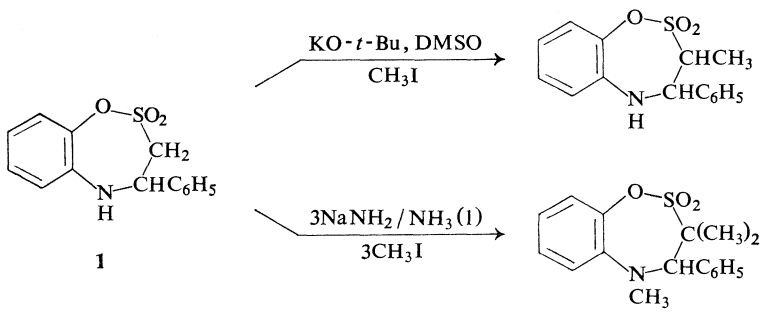

TABLE I

$RCH_2SO_3CH_2R'' + R'X \rightarrow RR'CHSO_3CH_2R''$

$RCH_2SO_3CH_2C(CH_3)_3$	R′X	Base	$RR'CHSO_3CH_2C(CH_3)_3$	
R = C_6H_5 (**2**)	CH_3I	*n*-BuLi	73%	b.p. 110–113°/0.25 mm
R = C_6H_5	$(CH_3)_2CHI$	*n*-BuLi	86%	b.p. 112–115°/0.25 mm
R = H (**3**)	*p*-$CH_3C_6H_4CH_2Br$	*n*-BuLi/TMEDA	40% by n.m.r. 15% isolated	m.p. 51–52°
R = H	$C_6H_5CH_2Cl$	KH	38%	b.p. 131–137°/0.45 mm
R = CH_3 (**4**)	CH_3I	KH	46%	b.p. 51–52°/0.20 mm
$C_6H_5CH_2SO_3CH_2CH_3$ (**5**)	CH_3I	*n*-BuLi	$C_6H_5CHSO_3CH_2CH_3$ CH_3 79%	b.p. 99–101°/0.20 mm

butyllithium in hexane was found to be a satisfactory metallating agent. Subsequent reaction of the α-metallated species with methyl or isopropyl iodide led to alkylation product in excellent yield.

With neopentyl methanesulfonate (**3**) or neopentyl ethanesulfonate (**4**), where the α-position being metallated is not benzylic, best yields were obtained with potassium hydride in tetrahydrofuran or *n*-butyllithium complexed with *N,N,N′,N′*-tetramethylethylenediamine (TMEDA) (7–9) as metallating agent.

Most recently,[4] ethyl-α-toluenesulfonate (**5**) has been prepared, and shows, by its conversion to its α-methyl derivative in high yield, that the presence of the neopentyl "protective group" is not necessary to obtain high yields when a benzylic position is being alkylated. That is, α-metallation is preferred over elimination or displacement in these systems.

[4]Recently, we extended the use of α-metallated sulfonate esters to the preparation of cyclopropanesulfonates from γ-chloropropanesulfonates by internal alkylation, e.g., neopentyl cyclopropanesulfonate from γ-chloropropanesulfonate, see ref. 10.

Experimental

All reactions described herein were carried out in thoroughly dried apparatus under an atmosphere of nitrogen. *n*-Butyllithium in hexane was purchased from the Foote Mineral Co., and potassium hydride, as a 50% suspension in mineral oil, from Alfa Inorganics. Starting sulfonates were prepared by the reaction of the appropriate sulfonyl chloride and alcohol in the presence of triethylamine in benzene or diethyl ether solvent. These consisted of: neopentyl α-toluenesulfonate, m.p. 71–73°; neopentyl methanesulfonate, b.p. 94–96°/10 mm; neopentyl ethanesulfonate, b.p. 58–60°/0.15 mm; and ethyl α-toluenesulfonate, b.p. 129–130°/0.04 mm. Infrared (i.r.) spectra were recorded on an Infracord spectrophotometer and nuclear magnetic resonance (n.m.r.) spectra on a Varian Associates A-60A spectrophotometer. Microanalyses were carried out by Dr. C. S. Yeh and staff.

Neopentyl 1-Phenylethanesulfonate

A solution of 7.27 g (0.030 mole) of neopentyl α-toluenesulfonate dissolved in 40 ml of tetrahydrofuran was added dropwise to 20.7 ml of a 1.6 *M* solution (0.033 mole) of *n*-butyllithium in hexane at −65 °C over a 35 min period. As soon as the addition was complete, 4.69 g (0.033 mole) of methyl iodide were added portionwise resulting in the precipitation of finely divided lithium iodide. After 15 min stirring at −65°, the reaction mixture was allowed to warm to room temperature, was quenched with 100 ml of H_2O, and the resulting suspension was extracted with chloroform. The chloroform

Can. J. Chem. Downloaded from www.nrcresearchpress.com by 210.87.254.40 on 09/05/12
For personal use only.

Can. J. Chem. Downloaded from www.nrcresearchpress.com by 210.87.254.40 on 09/05/12
For personal use only.

extracts were combined, dried, and evaporated *in vacuo* yielding a yellow oil which was chromatographed on a 3 × 25 cm column of alumina with chloroform as eluent. The neopentyl 1-phenylethanesulfonate thus obtained was distilled yielding 5.62 g (73.1%) of pure material, b.p. 110–113°/0.25 mm; i.r. (neat): 2950 (s), 1470 (s), 1360 (s), 1175 (s), 980 (b), 840 (b), and 700 cm^{-1} (s); n.m.r. ($CDCl_3$): δ 0.84 (s, 9H, $C(CH_3)_3$), 1.77 (d, 3H, $CH—CH_3$) J = 7 c.p.s., 3.62 (sym m, 2H, $O—CH_2C(CH_3)_3$), 4.37 (quartet, 1H, $CHCH_3$) J = 7 c.p.s., and 7.35 (m, 5H, ArH).

Anal. Calcd. for $C_{10}H_{14}O_3S$: C, 60.90; H, 7.86; S, 12.51. Found: C, 61.10; H, 8.14; S, 12.52.

Neopentyl 2-Methyl-1-phenylpropanesulfonate

In a manner completely analogous to that above, the title compound was prepared from neopentyl α-toluenesulfonate and isopropyl iodide in 86% yield, b.p. 112–115°/0.25 mm; i.r. (neat): 3000 (s), 1460 (s), 1180 (s), 975 (b), and 704 cm^{-1} (s); n.m.r. ($CDCl_3$): δ 0.75 (s, 9H, $C(CH_3)_3$), 0.98 (d, 3H), and 1.22 (d, 3H), the two non-equivalent methyl groups of the isopropyl group, δ 2.62 (m, 1H, $CH(CH_3)_2$), 3.51 (sym m, 2H, $OCH_2C(CH_3)_3$), 3.98 (d, 1H, C_6H_5CH), and 7.35 (s, 5H, C_6H_5).

Anal. Calcd. for $C_{15}H_{24}O_3S$: C, 63.34; H, 8.51; S, 11.28. Found: C, 63.55; H, 8.81; S, 11.64.

Neopentyl 2-p-Tolylethanesulfonate

To 0.050 mole of the *n*-butyllithium – TMEDA complex prepared as described by Peterson (9), were added 8.31 g (0.050 mole) of neopentyl methanesulfonate. After 2.25 h stirring, a solution of 9.25 g (0.050 mole) of *p*-methylbenzylbromide in 30 ml of tetrahydrofuran was added. After 1.5 h additional stirring, the reaction was quenched with 100 ml of H_2O and extracted with chloroform. The chloroform extracts were combined, dried, and evaporated *in vacuo* yielding a yellow oil. The oil was dissolved in a small amount of 95% ethanol, and the solution cooled to −78°. The white solid that separated was recrystallized from isopropanol–water yielding 2.05 g (15.1%) of the title compound, m.p. 51–52°; i.r. (solid film): 3000 (s), 1530 (s), 1370 (s), 1170 (s), and 970 cm^{-1} (b); n.m.r. ($CDCl_3$): δ 0.98 (s, 9H, $C(CH_3)_3$), 2.28 (s, 3H, $ArCH_3$), 3.20 (sym m, 4H, CH_2CH_2), 3.82 (s, 2H, OCH_2), and 7.08 (s, 4H, ArH).

Neopentyl 2-Phenylethanesulfonate

A solution of 7.07 g (0.0425 mole) of neopentyl methanesulfonate dissolved in 20 ml of tetrahydrofuran was added to a suspension of 0.0425 mole of potassium hydride in 30 ml of tetrahydrofuran. The reaction mixture was stirred at room temperature for 5.5 h, and then heated to 60° until hydrogen evolution ceased. The reaction mixture was then cooled to 0°, and 5.37 g (0.0425 mole) of benzyl chloride were added dropwise. After 12 h stirring, 200 ml of water were added, and the resulting suspension was extracted with chloroform. The chloroform extracts were combined, dried, and evaporated *in vacuo* yielding a light oil. Upon distillation, 4.0 g (38%) of the title compound, contaminated with a small amount of mineral oil was obtained, b.p. 131–137°/0.45 mm; i.r. (neat): 2950 (s), 1360 (s), 1175 (s), 970 (b), and 700 cm^{-1} (s); n.m.r. ($CDCl_3$): δ 0.94 (s, 9H, $C(CH_3)_3$), 3.19 (sym m, 4H, CH_2CH_2), 3.78 (s, 2H, OCH_2), and 7.21 (s, 5H, ArH).

Neopentyl 2-Propanesulfonate

To 0.105 mole of potassium hydride suspended in tetrahydrofuran were added 9.5 g (0.052 mole) of neopentyl ethanesulfonate, and the reaction mixture was stirred for 48 h. After this time, 15 g of methyl iodide (0.105 mole) were added and stirring continued for 24 h before the reaction mixture was quenched with 100 ml of water and extracted with chloroform. The chloroform extracts were combined, dried, and evaporated *in vacuo* leaving a light oil that was chromatographed on acid-washed alumina with chloroform as eluent. The product obtained was distilled under vacuum yielding 4.72 g (46.2%) of neopentyl 2-propanesulfonate, b.p. 51–52°/0.20 mm; i.r. (neat): 3020 (s), 1370 (s), 1190 (s), 1170 (s), 975 (b), and 835 cm^{-1} (b); n.m.r. ($CDCl_3$): δ 0.98 (s, 9H, $C(CH_3)_3$), 1.43 (d, 6H, $(CH_3)_2CH$), 3.37 (septet, 1H, $(CH_3)_2CH$), and 3.89 (s, 2H, OCH_2).

Ethyl 1-Phenylethanesulfonate

In a manner completely analogous to that used for the preparation of neopentyl 1-phenylethanesulfonate, the title compound was prepared in 79% yield from ethyl α-toluenesulfonate and methyl iodide with *n*-butyllithium as metallating agent, b.p. 99–101°/0.20 mm; i.r. (neat): 3000 (w), 1350 (s), 1175 (s), 1005 (s), 920 (b), and 700 cm^{-1} (s); n.m.r. ($CDCl_3$): δ 1.17 (t, 3H, CH_2CH_3), 1.76 (d, 3H, $CHCH_3$), 3.98 (m, 2H, CH_2CH_3), 4.33 (m, 1H, $CHCH_3$), and 7.37 (m, 5H, ArH).

Anal. Calcd. for $C_{10}H_{14}O_3S$: C, 56.05; H, 6.58; S, 14.97. Found: C, 55.77; H, 6.54; S, 15.12.

1. W. E. Truce and L. B. Lindy. J. Org. Chem. **26**, 1463 (1961).
2. W. E. Truce and F. E. Roberts. J. Org. Chem. **28**, 961 (1963).
3. W. E. Truce and R. W. Lagally. Abstr. 153rd Meeting Amer. Chem. Soc. Miami Beach, Florida. April 1967. No. O 102.
4. W. E. Truce and L. W. Christensen. Tetrahedron, To be published.
5. E. J. Corey and T. Durst. J. Am. Chem. Soc. **90**, 5548 (1968).
6. J. W. Fieldhouse. Ph.D. Thesis, Purdue University. Lafayette, Indiana. June 1968.
7. G. G. Eberhardt and W. A. Butte. J. Org. Chem. **29**, 2928 (1964).
8. A. W. Langer, Jr. Trans. New York Acad. Sci. [II], **27**, 741 (1965).
9. B. J. Peterson. J. Org. Chem. **32**, 1717 (1967).
10. C. T. Goralski. Ph.D. Thesis, Purdue University. Lafayette, Indiana. January 1969.

Ultraviolet absorption maxima, both calculated and observed, for some α-benzoyl-*trans*-benzalacetones, ethyl α-benzoyl-*trans*-cinnamates, and some α-cyano-*trans*-benzalacetophenones

D. J. Currie and H. L. Holmes
The Chemistry Section, Defence Research Establishment Suffield, Ralston, Alberta

Received September 9, 1968

The equation for the calculation of absorption maxima for conjugated heteroenoid compounds has been extended to include a number of α-benzoyl-*trans*-benzalacetones and ethyl α-benzoyl-*trans*-cinnamates and has been used to assign configuration to the α-cyano-*trans*-benzalacetophenones. The method for calculating the substituent constant, *D*, has been refined to give more accurate values.

Canadian Journal of Chemistry, 47, 863 (1969)

Can. J. Chem. Downloaded from www.nrcresearchpress.com by 210.87.254.42 on 09/05/12
For personal use only.

A method for calculating the long wavelength absorption maxima for conjugated heteroenoid compounds with the generalized formula **1** has already been presented (1) and eq. [1] has now

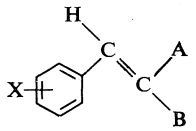

1

been extended and refined to calculate the long wavelength maxima, λ(mμ), of the title compounds.

$$[1]\quad \lambda\left(\mathrm{X{-}C_6H_4{-}CH{=}C(A)(B)}\right) = \lambda(\mathrm{C_6H_5{-}CH{=}CH_2}) + \Delta\lambda_A + \Delta\lambda_B{}^1 + \Sigma\Delta\lambda^{11} + D$$

where $\Delta\lambda_A$ is the conjugative effect (mμ) of the A group, $\Delta\lambda_B{}^1$ is the inductive effect (mμ) of the B group, $\Delta\lambda^{11}$ is the sum of the steric effects (mμ) of the A, B, and phenyl groups, and *D* is the increment (mμ) for the X substituent.

The values for the inductive and steric effects of the benzoyl group presented earlier (1) are based upon an estimated value for the inductive effect of this group in 2-benzal-1,3-diphenyl-1,3-propanedione. The long wavelength ultraviolet absorption maxima for a series of α-benzoyl-*trans*-benzalacetones, **2***a* (Table I),[1] ethyl α-benzoyl-*trans*-cinnamates, **2***b* (Table I), and α-cyano-*trans*-benzalacetophenones, **3** (Table I), have provided new values for these two effects.

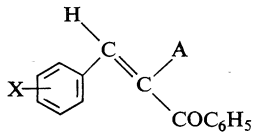

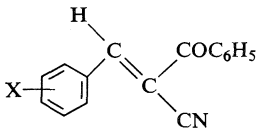

2*a*, A = $COCH_3$
2*b*, A = $CO_2C_2H_5$
2*c*, A = CN

3

Absence of an upfield shift for the CH_3 protons in A of C_2-substituted **2***a* compounds and for the CH_2 and CH_3 protons in A of the C_2-substituted **2***b* compounds assigns the configurations of **2***a* and **2***b* to these compounds (2). Inductive and steric effects of +52 mμ and −30 mμ respectively for the *cis*-benzoyl group provide satisfactory long wavelength absorption maxima for the **2***a* and **2***b* compounds and for 2-benzal-1,3-diphenyl-1,3-propanedione (λ_{obs} = 295 mμ).

The calculated absorption maximum for **3**, X = H (317 mμ) while not good, agrees much better with the observed value (310 mμ) than does that for the alternate **2***c* configuration. In fact this difference is quite constant for substituted derivatives of **3** and may be accounted for by the additional steric effect resulting from interaction of the *trans*-benzoyl group with the ethylenic hydrogen atom. Models indicate that steric factors in 2-benzal-1,3-diphenyl-1,3-propanedione preclude the conformation where such interference can become operative and so the agreement between λ_{obs} and λ_{calcd} is good. This could account for the similar deviation in benzalcyanoacetanilide and its absence in benzalacetoacetanilide (2).

The contribution of an electron donating X

[1]A photocopy of Table I may be obtained, upon request, from The Depository of Unpublished Data, National Science Library, National Research Council of Canada, Ottawa, Canada.

group at C-4 to the resonance system of this general class of compounds will depend upon the polarization of the rest of the conjugated system which in turn is reflected in the long wavelength absorption maximum of the parent compound. Hence a more accurate estimation of the *D* values for electron donating groups at C-4 is given by the equation

$$D^1 = \frac{\lambda^1 \text{ parent}}{\lambda \text{ parent}} \times D$$

where λ^1 parent is the absorption maximum of the unsubstituted compound in the given series and λ parent is that from which the *D* value was derived. The *D* value for the 4-acetamido group is a case in point (Table I). Using the 4-acetamidobenzalmalononitrile as reference, the D^1 values so obtained for the C_4-acetamido group provides an absorption maximum in agreement with the observed value for 4-acetamido-3-benzal-2,4-pentanedione while that calculated for 4-acetamido-α-cyano-*trans*-benzalacetophenone is 8.5 mμ too high.

The spectra of the ethanolic solutions of these compounds were recorded on a model 15 Cary spectrophotometer. Calculated and observed maxima, and extinction coefficients are listed in Table I.

All of these compounds were prepared by the method of Horning *et al.* (4) with the exception of 4-acetamidobenzalmalononitrile which was prepared by the method of Corson and Stoughton (5) and the α-cyano-*trans*-benzalacetophenones which were prepared by the method of Kauffmann (3). Melting and boiling points and analytical figures for these compounds are listed in Table I.

Acknowledgments

The assistance of Mr. R. F. Silver in the synthesis of these compounds and of Mr. C. E. Lough in recording their ultraviolet absorption spectra is gratefully acknowledged. Microanalyses were done by Mr. R. P. Hicken.

1. D. J. Currie, C. E. Lough, R. F. Silver, and H. L. Holmes. Can. J. Chem. **45**, 1567 (1967).
2. W. M. Phillips, F. K. McClusky, and D. J. Currie. Unpublished data.
3. H. Kauffmann. Ber. **50**, 515 (1917).
4. E. C. Horning, J. Koo, M. S. Fish, and G. N. Walker. Org. Syn. **31**, 56 (1951).
5. B. Corson and R. W. Stoughton. J. Am. Chem. Soc. **50**, 2825 (1928).
6. E. Knoevenagel and A. Erler. Ber. **36**, 2134 (1900).
7. S. Ruhemann. J. Chem. Soc. **83**, 720 (1903).

Reaction of 6,7-dimethoxy-3-isochromanone with hydrazine

Gerald Rosen and Frank D. Popp
Department of Chemistry, Clarkson College of Technology, Potsdam, New York 13676

Received September 19, 1968

The reaction of the title compound with hydrazine resulted in the formation of the hydroxy hydrazide **5**. Alkylation of **5** took place on both oxygen and nitrogen. Compound **5** can be reconverted to the title compound or to the corresponding isoquinolone.

Canadian Journal of Chemistry, **47**, 864 (1969)

Recently Finkelstein and Brossi (1) reported the synthesis of 6,7-dimethoxy-3-isochromanone (**1**). In view of the reported[1] conversion of compounds of the types **2** and **3** to diazepines on reaction with hydrazine, it was felt that **1** might be an attractive intermediate for the synthesis of 2,3-benzodiazepines of the type **4**.

Reaction of **1** with hydrazine in ethanol gave a compound, $C_{11}H_{16}N_2O_4$, whose analysis would suggest the formation of a hydrate of the desired

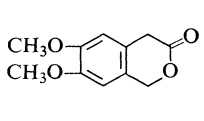

1

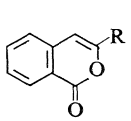

2

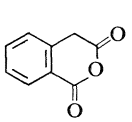

3

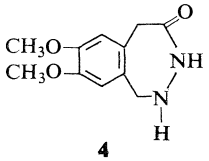

4

[1]See ref. 2 for references to this type of conversion.

Can. J. Chem. Downloaded from www.nrcresearchpress.com by 210.87.254.42 on 09/05/12
For personal use only.

group at C-4 to the resonance system of this general class of compounds will depend upon the polarization of the rest of the conjugated system which in turn is reflected in the long wavelength absorption maximum of the parent compound. Hence a more accurate estimation of the *D* values for electron donating groups at C-4 is given by the equation

$$D^1 = \frac{\lambda^1 \text{ parent}}{\lambda \text{ parent}} \times D$$

where λ^1 parent is the absorption maximum of the unsubstituted compound in the given series and λ parent is that from which the *D* value was derived. The *D* value for the 4-acetamido group is a case in point (Table I). Using the 4-acetamidobenzalmalononitrile as reference, the D^1 values so obtained for the C_4-acetamido group provides an absorption maximum in agreement with the observed value for 4-acetamido-3-benzal-2,4-pentanedione while that calculated for 4-acetamido-α-cyano-*trans*-benzalacetophenone is 8.5 mμ too high.

The spectra of the ethanolic solutions of these compounds were recorded on a model 15 Cary spectrophotometer. Calculated and observed maxima, and extinction coefficients are listed in Table I.

All of these compounds were prepared by the method of Horning *et al.* (4) with the exception of 4-acetamidobenzalmalononitrile which was prepared by the method of Corson and Stoughton (5) and the α-cyano-*trans*-benzalacetophenones which were prepared by the method of Kauffmann (3). Melting and boiling points and analytical figures for these compounds are listed in Table I.

Acknowledgments

The assistance of Mr. R. F. Silver in the synthesis of these compounds and of Mr. C. E. Lough in recording their ultraviolet absorption spectra is gratefully acknowledged. Microanalyses were done by Mr. R. P. Hicken.

1. D. J. Currie, C. E. Lough, R. F. Silver, and H. L. Holmes. Can. J. Chem. **45**, 1567 (1967).
2. W. M. Phillips, F. K. McClusky, and D. J. Currie. Unpublished data.
3. H. Kauffmann. Ber. **50**, 515 (1917).
4. E. C. Horning, J. Koo, M. S. Fish, and G. N. Walker. Org. Syn. **31**, 56 (1951).
5. B. Corson and R. W. Stoughton. J. Am. Chem. Soc. **50**, 2825 (1928).
6. E. Knoevenagel and A. Erler. Ber. **36**, 2134 (1900).
7. S. Ruhemann. J. Chem. Soc. **83**, 720 (1903).

Reaction of 6,7-dimethoxy-3-isochromanone with hydrazine

Gerald Rosen and Frank D. Popp
Department of Chemistry, Clarkson College of Technology, Potsdam, New York 13676

Received September 19, 1968

The reaction of the title compound with hydrazine resulted in the formation of the hydroxy hydrazide **5**. Alkylation of **5** took place on both oxygen and nitrogen. Compound **5** can be reconverted to the title compound or to the corresponding isoquinolone.

Canadian Journal of Chemistry, **47**, 864 (1969)

Recently Finkelstein and Brossi (1) reported the synthesis of 6,7-dimethoxy-3-isochromanone (**1**). In view of the reported[1] conversion of compounds of the types **2** and **3** to diazepines on reaction with hydrazine, it was felt that **1** might be an attractive intermediate for the synthesis of 2,3-benzodiazepines of the type **4**.

Reaction of **1** with hydrazine in ethanol gave a compound, $C_{11}H_{16}N_2O_4$, whose analysis would suggest the formation of a hydrate of the desired

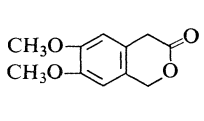

1

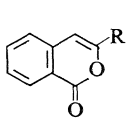

2

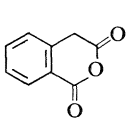

3

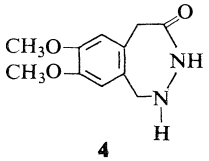

4

[1]See ref. 2 for references to this type of conversion.

Can. J. Chem. Downloaded from www.nrcresearchpress.com by 210.87.254.42 on 09/05/12
For personal use only.

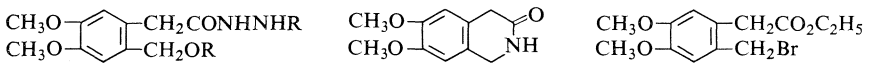

5, R = H
6, R = alkyl

7

8

diazepine **4**. Examination of the infrared (i.r.) and nuclear magnetic resonance (n.m.r.) spectra and reactions of this product, however, indicates that rather it is the hydroxy hydrazide **5**. This type of product is similar to those observed (1) from the reaction of **1** with amines. When the reaction with hydrazine was carried out in ethanol containing a trace of acetic acid, **5** was still the major product; however, the reaction of **1** with hydrazine in acetic acid (hot or cold) gave only **1**. It was noted that **5** can be converted to **1** on heating in glacial acetic acid.

Alkylation of **5**, with alkyl halides and sodium hydride in dimethyl formamide, occurred both at nitrogen and oxygen to give compounds of the type **6** as indicated in Table I. Treatment of **5** with 10% hydrochloric acid gave a 76% yield of 6,7-dimethoxy-1,4-dihydro-3(2*H*)isoquinolone (**7**) together with 5% of **1**; with formic acid, **1** was the major product, and as noted above with acetic acid, **1** was the exclusive product.

In a further attempt to convert **1** to **4**, compound **1** was converted to **8** (1) and without isolation the crude **8** was reacted with hydrazine. This reaction gave **7** as the only pure product isolated.

Experimental

Reaction of 6,7-Dimethoxy-3-isochromanone with Hydrazine

To 1 g (0.0048 mole) of **1** dissolved in 20 ml of ethanol was added, slowly, 0.154 g (0.0048 mole) of hydrazine. After 6 h of reflux, the mixture was evaporated to one-half volume and cooled to give 0.945 g (82%) of a white solid (**5**), m.p. 163–165° from ethanol. Infrared (KBr): 3300, 3100, 3000, 1680, 1610 cm^{-1}.

Anal. Calcd. for $C_{11}H_{16}N_2O_4$: C, 54.99; H, 6.71; N, 11.66. Found: C, 54.71; H, 6.64; N, 11.66.

Addition of a trace of acetic acid to the ethanol in the above sequence gave a 68% yield of **5**. Replacement of the ethanol by glacial acetic acid in the above sequence gave a 74% recovery of **1** when the reaction was run in the cold and a 78% recovery of **1** when the reaction was run on the steam bath (in these cases the reaction mixture was poured on ice and the product extracted with methylene chloride).

*Preparation of **6** by Alkylation of **5***

To 0.75 g (0.00312 mole) of **5** dissolved in 15 ml of dimethyl formamide was added at room temperature with stirring 0.25 g (0.00312 mole) of 30% sodium hydride. To the resulting yellow solution was added an excess of the alkyl iodide (or benzyl chloride). After stirring for 1 h, the solution was poured on ice and extracted with chloroform. Evaporation of the dried ($MgSO_4$) extract gave an oil, infrared: 1650 cm^{-1}, which was converted to the picrate as recorded in Table I. (The benzyl product was obtained as a solid.)

*Reaction of **5** with Acid*

To 1 g (0.00415 mole) of **5** were added 20 ml of 10% hydrochloric acid and the solution was refluxed for 2 h. Upon cooling and the addition of water, 0.65 g (76%) of **7**, m.p. 227–228° (from ethanol), was obtained. Infrared (KBr): 3400 and 1660 cm^{-1}; n.m.r. (DMSO-d_6): 2.7 (Ar), 4.9 (NH), 5.9 (CH_3O), 6.45 (CH_2), and 7.8 τ (CH_2).

Anal. Calcd. for $C_{11}H_{13}NO_3$: C, 63.75; H, 6.32; N, 6.76. Found: C, 63.53; H, 5.96; N, 6.62.

Extraction of the remaining solution with methylene chloride gave a 5% yield of **1**.

TABLE I
Alkylation of **5***

R	Yield (%)	Melting point† (°C)	Analyses† Calculated C	H	N	Found C	H	N
CH_3	25	149–150	45.88	4.66	14.08	45.41	4.86	13.89
C_2H_5	80	134–135	48.00	5.18	13.33	48.04	4.99	13.39
n-C_3H_7	45	155–158	49.90	5.65	12.65	49.91	5.58	12.56
n-C_4H_9	53	134–135	51.63	6.07	12.04	51.59	5.99	12.06
$C_6H_5CH_2$	42	144–145‡	71.40‡	6.71	6.66	71.34‡	6.71	6.60

* 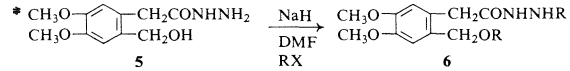

5 **6**

†Melting points and analyses of picrates unless otherwise noted.
‡Melting point and analysis of free base.

Can. J. Chem. Downloaded from www.nrcresearchpress.com by 210.87.254.42 on 09/05/12
For personal use only.

Replacement of the hydrochloric acid by acetic acid gave a 74.5% yield of **1** and no **7**, while replacement of the hydrochloric acid by formic acid gave a 67% yield of **1** and a 5% yield of **7**.

Acknowledgment

We should like to thank Finkelstein and Brossi (1) for making the details of the procedure for the synthesis of **1** available to us before publication.

1. J. FINKELSTEIN and A. BROSSI. J. Heterocyclic Chem. **4**, 315 (1967).
2. F. D. POPP and A. C. NOBLE. Advan. Heterocyclic Chem. **8**, 32 (1968).

Can. J. Chem. Downloaded from www.nrcresearchpress.com by 210.87.254.42 on 09/05/12
For personal use only.

cis-Crotonaldehyde and related compounds

D. E. MCGREER AND B. D. PAGE
Department of Chemistry, The University of British Columbia, Vancouver, British Columbia

Received September 23, 1968

cis-Crotonaldehyde (**1**) has been prepared as a mixture with *trans*-crotonaldehyde (**2**) by irradiation of **2** with 3000 Å light. The thermodynamic equilibrium value for **1** to **2** was determined to be 1:50. Conditions for attaining this equilibrium and the structural factors contributing to its position are discussed.

Canadian Journal of Chemistry, **47**, 866 (1969)

In one reported attempt to prepare *cis*-crotonaldehyde (**1**) by irradiation of an acid solution of *trans*-crotonaldehyde (**2**) no evidence could be found for the formation of **1** (1). The photodecomposition (2–6) and photooxidation (7) of **2** has been studied without reports of the formation of **1**. On the other hand irradiation of *trans*-α,β-unsaturated ketones readily leads to the *cis*-isomers (5, 8, 9). As part of a general study on the chemistry of α,β-unsaturated carbonyl compounds we have investigated the conversion of **2** to **1**.

Irradiation at room temperature of **2** sealed in a 4 mm tube in a Rayonet Srinivasan-Griffin reactor using 16 RPR-3000 Å lamps gave after 4 days a mixture of **1** and **2** in the ratio of 29:71. Further irradiation did not increase the proportion of **1**. Detection of **1** in **2** was possible by nuclear magnetic resonance (n.m.r.) and the spectra of **1** and **2** are given in Table I.[1]

cis-Crotonaldehyde (**1**) was found to be particularly sensitive to acids being converted rapidly with a trace of acid to **2**. The separation of **1** from **2** has as yet been unsuccessful by distillation or vapor-phase chromatography with a variety of columns including DIDP, DNP, Ucon P, silver nitrate-glycerol, DEGS and Poropak Q. Samples collected from the chromatograph (Varian Aerograph A-90P) remained unchanged. Heating samples of **1** and **2** indicated **1** to be also thermally labile with half-life of 2 h at 160°. This value however is a minimum due to the sensitivity of **1** to acid.

The thermodynamic equilibrium of **1** and **2**, attained at room temperature with a trace of dry hydrochloric acid or by heating mixtures to 200 °C for 5 h, contains 2.0% of **1**. No evidence was found for the presence of 3-butenal which would be expected to be less than 0.5% based on the results of Sifniades (11) who found 0.35% of 3-butenal in equilibrium with crotonaldehyde when **1** was heated in the gas phase at 150° and 1% at 210°. For comparison we have determined the acid-catalyzed equilibrium of angelaldehyde with tiglaldehyde to be 1:100 and of *cis*-3-methyl-3-penten-2-one with *trans*-3-methyl-3-pentene-2-one to be 1.5:100.

The marked stability of the *trans*-conjugated forms of these compounds implies a high resonance stabilization in this form. This stabilization apparently is reduced in the *cis* form by distortion from planarity of the carbonyl group of the conjugated system. The importance of this destabilizing interaction is emphasized in angelaldehyde and *cis*-3-methyl-3-pentenoate where the stable isomer involves a *cis* arrangement of two methyl groups rather than a *cis* arrangement of a methyl and the smaller formyl or acetyl groups (the conformational free energy difference $-\Delta G$ for the formyl group on a cyclohexane ring is 1.35 (12) compared to 1.7 for methyl (13)).

The conjugative stabilization in esters is expected to be less than that for ketones and aldehydes and this is supported by the fact that the

[1]The spectrum of **2** is reported in ref. 10.

Replacement of the hydrochloric acid by acetic acid gave a 74.5% yield of **1** and no **7**, while replacement of the hydrochloric acid by formic acid gave a 67% yield of **1** and a 5% yield of **7**.

Acknowledgment

We should like to thank Finkelstein and Brossi (1) for making the details of the procedure for the synthesis of **1** available to us before publication.

1. J. FINKELSTEIN and A. BROSSI. J. Heterocyclic Chem. **4**, 315 (1967).
2. F. D. POPP and A. C. NOBLE. Advan. Heterocyclic Chem. **8**, 32 (1968).

Can. J. Chem. Downloaded from www.nrcresearchpress.com by 210.87.254.5 on 09/05/12
For personal use only.

cis-Crotonaldehyde and related compounds

D. E. MCGREER AND B. D. PAGE
Department of Chemistry, The University of British Columbia, Vancouver, British Columbia

Received September 23, 1968

cis-Crotonaldehyde (**1**) has been prepared as a mixture with *trans*-crotonaldehyde (**2**) by irradiation of **2** with 3000 Å light. The thermodynamic equilibrium value for **1** to **2** was determined to be 1:50. Conditions for attaining this equilibrium and the structural factors contributing to its position are discussed.

Canadian Journal of Chemistry, **47**, 866 (1969)

In one reported attempt to prepare *cis*-crotonaldehyde (**1**) by irradiation of an acid solution of *trans*-crotonaldehyde (**2**) no evidence could be found for the formation of **1** (1). The photodecomposition (2–6) and photooxidation (7) of **2** has been studied without reports of the formation of **1**. On the other hand irradiation of *trans*-α,β-unsaturated ketones readily leads to the *cis*-isomers (5, 8, 9). As part of a general study on the chemistry of α,β-unsaturated carbonyl compounds we have investigated the conversion of **2** to **1**.

Irradiation at room temperature of **2** sealed in a 4 mm tube in a Rayonet Srinivasan-Griffin reactor using 16 RPR-3000 Å lamps gave after 4 days a mixture of **1** and **2** in the ratio of 29:71. Further irradiation did not increase the proportion of **1**. Detection of **1** in **2** was possible by nuclear magnetic resonance (n.m.r.) and the spectra of **1** and **2** are given in Table I.[1]

cis-Crotonaldehyde (**1**) was found to be particularly sensitive to acids being converted rapidly with a trace of acid to **2**. The separation of **1** from **2** has as yet been unsuccessful by distillation or vapor-phase chromatography with a variety of columns including DIDP, DNP, Ucon P, silver nitrate-glycerol, DEGS and Poropak Q. Samples collected from the chromatograph (Varian Aerograph A-90P) remained unchanged. Heating samples of **1** and **2** indicated **1** to be also thermally labile with half-life of 2 h at 160°. This value however is a minimum due to the sensitivity of **1** to acid.

The thermodynamic equilibrium of **1** and **2**, attained at room temperature with a trace of dry hydrochloric acid or by heating mixtures to 200 °C for 5 h, contains 2.0% of **1**. No evidence was found for the presence of 3-butenal which would be expected to be less than 0.5% based on the results of Sifniades (11) who found 0.35% of 3-butenal in equilibrium with crotonaldehyde when **1** was heated in the gas phase at 150° and 1% at 210°. For comparison we have determined the acid-catalyzed equilibrium of angelaldehyde with tiglaldehyde to be 1:100 and of *cis*-3-methyl-3-penten-2-one with *trans*-3-methyl-3-pentene-2-one to be 1.5:100.

The marked stability of the *trans*-conjugated forms of these compounds implies a high resonance stabilization in this form. This stabilization apparently is reduced in the *cis* form by distortion from planarity of the carbonyl group of the conjugated system. The importance of this destabilizing interaction is emphasized in angelaldehyde and *cis*-3-methyl-3-pentenoate where the stable isomer involves a *cis* arrangement of two methyl groups rather than a *cis* arrangement of a methyl and the smaller formyl or acetyl groups (the conformational free energy difference $-\Delta G$ for the formyl group on a cyclohexane ring is 1.35 (12) compared to 1.7 for methyl (13)).

The conjugative stabilization in esters is expected to be less than that for ketones and aldehydes and this is supported by the fact that the

[1]The spectrum of **2** is reported in ref. 10.

TABLE I

The nuclear magnetic resonance spectra of **1** and **2** neat with internal tetramethylsilane reference

	β-CH_3	β-H	α-H	—CHO
1	7.90 τ *J* 7.6, 1.8 Hz	3.36 τ 11.4, 7.6 Hz	4.19 τ 11.4, 8.0, 1.8 Hz	−0.04 τ 8.0 Hz
2	8.07 τ *J* 6.7, 1.5 Hz	3.15 τ 15.4, 6.7 Hz	4.01 τ 15.4, 7.6, 1.5 Hz	0.60 τ 7.6 Hz

equilibrium achieved from the crotonates is 83:12:5 for *trans*:*cis*:β, γ at 300° (14).

The formation of *cis*-crotonaldehyde from the *trans*-isomer may be a key step in the photoisomerization of crotonaldehyde to 3-butenal, which is an important step in the photochemical breakdown of this 4 carbon unit (6). The deconjugated isomer is expected to be formed photochemically from the *cis*-isomer rather than from the *trans*-isomer for precedent is available for this preference in the ketone series (8). The ready isomerization of **1** in acid accounts for its absence in normal methods for preparation of crotonaldehyde (15) and for the lack of detection by Blacet *et al.* (1). By extrapolation citral and other naturally occurring α,β-unsaturated aldehydes can be expected to isomerize thermally and with acid. An equilibrium of citral *a* to citral *b* of 61:39 is in fact achieved at 140°.

Acknowledgment

A grant from the National Research Council of Canada is gratefully acknowledged.

1. F. E. Blacet, W. G. Young, and J. G. Roof. J. Am. Chem. Soc. **59**, 608 (1937).
2. F. E. Blacet and J. G. Roof. J. Am. Chem. Soc. **58**, 73 (1936).
3. F. E. Blacet and J. E. Luvalle. J. Am. Chem. Soc. **61**, 273 (1939).
4. D. H. Volman, P. A. Leighton, F. E. Blacet, and R. K. Brenton. J. Chem. Phys. **18**, 203 (1950).
5. R. Tolberg and J. Pitts. J. Am. Chem. Soc. **80**, 1304 (1958).
6. C. A. McDowell and S. Sifniades. J. Am. Chem. Soc. **84**, 4606 (1962).
7. F. E. Blacet and D. H. Volman. J. Am. Chem. Soc. **61**, 582 (1939).
8. N. C. Yang and M. J. Jorgenson. Tetrahedron Letters, **19**, 1203 (1964).
9. R. A. Schneider and J. Meinwald. J. Am. Chem. Soc. **88**, 2023 (1967).
10. A. W. Douglas and J. H. Goldstein. J. Mol. Spectry **16**, 1 (1965).
11. S. Sifniades. Ph.D. Thesis. The University of British Columbia. Vancouver, British Columbia. May, 1965.
12. G. W. Buchanan and J. B. Stothers. Chem. Commun. 179 (1967).
13. E. L. Eliel, N. L. Allinger, S. J. Angyal, and G. A. Morrison. Conformation analysis. Interscience, New York. 1965. p. 44.
14. D. E. McGreer, W. Wai, and G. Carmichael. Can. J. Chem. **38**, 2410 (1960).
15. J. E. Fernandez and T. W. Solomons. Chem. Rev. **62**, 485 (1962).

Reaction of diphenylphosphine and 1,2-dichlorotetrafluorocyclobutene

Richard F. Stockel

Research and Development, Organic Chemicals Division, American Cyanamid Company, Bound Brook, New Jersey 08805

Received September 27, 1968

Diphenylphosphine and 1,2-dichlorohexafluorocyclobutene react in a solvent medium of dimethyl formamide to give both the mono (**3**) and 1,2-disubstituted (**2**) derivatives as products. In contrast, these same reactants give entirely different products when the reaction is conducted in the absence of a solvent.

Analytical and spectroscopic data are presented for the proposed structures.

Canadian Journal of Chemistry, **47**, 867 (1969)

The reactions of secondary phosphines and perhalocyclobutene have been investigated recently (1). While diethylphosphine reacts with either perfluorocyclobutene or 1,2-dichlorotetrafluorocyclobutene to give the monosubstituted tertiary phosphine **1**, diphenylphosphine reacts with perfluorocyclobutene to give only the disubstituted tertiary phosphine **2**. Interestingly, diphenylphosphine did not give an analogous product with 1,2-dichlorotetrafluorocyclobutene,

Can. J. Chem. Downloaded from www.nrcresearchpress.com by 210.87.254.5 on 09/05/12
For personal use only.

TABLE I

The nuclear magnetic resonance spectra of **1** and **2** neat with internal tetramethylsilane reference

	β-CH_3	β-H	α-H	—CHO
1	7.90 τ *J* 7.6, 1.8 Hz	3.36 τ 11.4, 7.6 Hz	4.19 τ 11.4, 8.0, 1.8 Hz	−0.04 τ 8.0 Hz
2	8.07 τ *J* 6.7, 1.5 Hz	3.15 τ 15.4, 6.7 Hz	4.01 τ 15.4, 7.6, 1.5 Hz	0.60 τ 7.6 Hz

equilibrium achieved from the crotonates is 83:12:5 for *trans*:*cis*:β, γ at 300° (14).

The formation of *cis*-crotonaldehyde from the *trans*-isomer may be a key step in the photoisomerization of crotonaldehyde to 3-butenal, which is an important step in the photochemical breakdown of this 4 carbon unit (6). The deconjugated isomer is expected to be formed photochemically from the *cis*-isomer rather than from the *trans*-isomer for precedent is available for this preference in the ketone series (8). The ready isomerization of **1** in acid accounts for its absence in normal methods for preparation of crotonaldehyde (15) and for the lack of detection by Blacet *et al.* (1). By extrapolation citral and other naturally occurring α,β-unsaturated aldehydes can be expected to isomerize thermally and with acid. An equilibrium of citral *a* to citral *b* of 61:39 is in fact achieved at 140°.

Acknowledgment

A grant from the National Research Council of Canada is gratefully acknowledged.

1. F. E. Blacet, W. G. Young, and J. G. Roof. J. Am. Chem. Soc. **59**, 608 (1937).
2. F. E. Blacet and J. G. Roof. J. Am. Chem. Soc. **58**, 73 (1936).
3. F. E. Blacet and J. E. Luvalle. J. Am. Chem. Soc. **61**, 273 (1939).
4. D. H. Volman, P. A. Leighton, F. E. Blacet, and R. K. Brenton. J. Chem. Phys. **18**, 203 (1950).
5. R. Tolberg and J. Pitts. J. Am. Chem. Soc. **80**, 1304 (1958).
6. C. A. McDowell and S. Sifniades. J. Am. Chem. Soc. **84**, 4606 (1962).
7. F. E. Blacet and D. H. Volman. J. Am. Chem. Soc. **61**, 582 (1939).
8. N. C. Yang and M. J. Jorgenson. Tetrahedron Letters, **19**, 1203 (1964).
9. R. A. Schneider and J. Meinwald. J. Am. Chem. Soc. **88**, 2023 (1967).
10. A. W. Douglas and J. H. Goldstein. J. Mol. Spectry **16**, 1 (1965).
11. S. Sifniades. Ph.D. Thesis. The University of British Columbia. Vancouver, British Columbia. May, 1965.
12. G. W. Buchanan and J. B. Stothers. Chem. Commun. 179 (1967).
13. E. L. Eliel, N. L. Allinger, S. J. Angyal, and G. A. Morrison. Conformation analysis. Interscience, New York. 1965. p. 44.
14. D. E. McGreer, W. Wai, and G. Carmichael. Can. J. Chem. **38**, 2410 (1960).
15. J. E. Fernandez and T. W. Solomons. Chem. Rev. **62**, 485 (1962).

Reaction of diphenylphosphine and 1,2-dichlorotetrafluorocyclobutene

Richard F. Stockel

Research and Development, Organic Chemicals Division, American Cyanamid Company, Bound Brook, New Jersey 08805

Received September 27, 1968

Diphenylphosphine and 1,2-dichlorohexafluorocyclobutene react in a solvent medium of dimethyl formamide to give both the mono (**3**) and 1,2-disubstituted (**2**) derivatives as products. In contrast, these same reactants give entirely different products when the reaction is conducted in the absence of a solvent.

Analytical and spectroscopic data are presented for the proposed structures.

Canadian Journal of Chemistry, **47**, 867 (1969)

The reactions of secondary phosphines and perhalocyclobutene have been investigated recently (1). While diethylphosphine reacts with either perfluorocyclobutene or 1,2-dichlorotetrafluorocyclobutene to give the monosubstituted tertiary phosphine **1**, diphenylphosphine reacts with perfluorocyclobutene to give only the disubstituted tertiary phosphine **2**. Interestingly, diphenylphosphine did not give an analogous product with 1,2-dichlorotetrafluorocyclobutene,

Can. J. Chem. Downloaded from www.nrcresearchpress.com by 210.87.254.42 on 09/05/12
For personal use only.

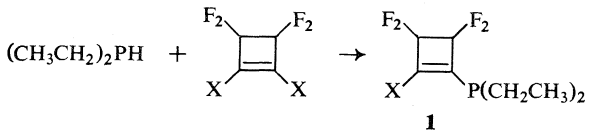

1

where X = Cl or F

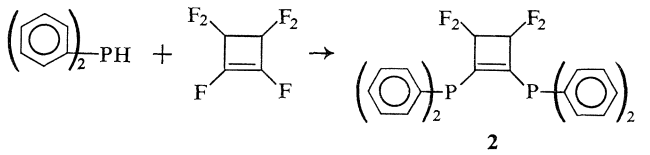

2

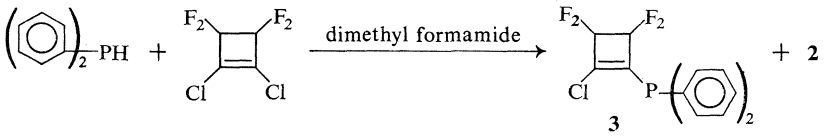

3

but instead hydrogen chloride, trifluorodiphenylphosphorane, and diphenylphosphinic fluoride were found. All of these experiments were carried out in the absence of solvent (neat). The reaction of 1,2-dichlorotetrafluorocyclobutene and diphenylphosphine was of particular interest in view of some recent work which this laboratory has just published (2).

The effect of the reaction medium, in which similar type nucleophilic reactions have been carried out (3), indicates that the judicious choice of a solvent can play a dominant role in product(s) formation. The reason for this is that the chemical potential of the various species involved in the reaction can be altered by the dipolar aprotic solvent (4).

With dimethyl formamide as the solvent, diphenylphosphine and 1,2-dichlorotetrafluorocyclobutene gave both **3** (46.3%) and **2** (20.0%). This result is in contrast to the work of Cullen *et al.* (1), where the reaction was run in the absence of a solvent.

Based on the reactions of phosphites and 1,2-dichlorohexafluorocyclopentene (5), the formation of **2** might not have been predicted. With phosphites as the nucleophile, the 1,2-disubstituted products are exclusively found due to a conjugative effect by the phosphonate group which renders C-2 susceptible to further nucleophilic attack (**4**). Although this electronic effect is not possible with **3**, a 1,2-disubstituted product is still found.

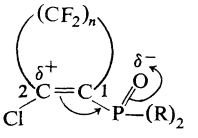

$n = 3$

4

Recent studies involving cyclic perhaloolefins and alkoxides (6, 7) suggest that the products can be predicted on the basis of the stability of the intermediate carbanions formed. Undoubtedly, as illustrated in this and other studies (1, 2, 6–8) the actual product distribution must definitely depend on other factors like ring size, nucleophilicity of the reactant, steric hindrance, polarity of the reaction medium, as well as electronic effects. Much more work is needed before the role of each variable can be deduced, and its role in the mechanistic pathway be understood.

Experimental

The infrared (i.r.) spectra were determined as mineral oil mulls on a Perkin–Elmer model 317 spectrophotometer. Phosphorus nuclear magnetic resonance (n.m.r.) spectra were measured as 10% solutions using triethylphosphate as the reference on a Varian HR-60 instrument.

Preparation of **3** *(2-Chloro-3,3,4,4-tetrafluoro-1-cyclobuten-1-yl)diphenylphosphine and* **2** *(3,3,4,4-Tetrafluorocyclobuten-1,2-ylene)bisdiphenylphosphine*

A solution of 19.5 g (0.1 mole) of 1,2-dichlorotetrafluorocyclobutene and 18.6 g (0.1 mole) of diphenylphosphine (9) in 100 ml of dimethyl formamide was stirred at 65 °C for 10 h, then poured into 300 ml water. The organic materials were extracted twice with 100 ml

Can. J. Chem. Downloaded from www.nrcresearchpress.com by 210.87.254.42 on 09/05/12
For personal use only.

ether and the combined ethereal extracts were washed three times with 50 ml portions of water. The ether solution was dried over anhydrous $MgSO_4$ and concentrated to dryness. The crude consisted of solid and an oil. Approximately 10 g of solid (**2**) were filtered off and 16 g of oil (**3**) remained. The oil was distilled at 114–116 °C/0.1 mm and the solid was recrystallized from ethanol and had m.p. 127–127.5 °C (lit. (1), m.p. 129.5–130.5°). A vapor-phase chromatography analysis employing an F and M model 810 equipped with a 3 ft silicon gum rubber column indicated that the crude mixture had at least two other minor components representing less than 5% of the total besides **2** and **3**.

Anal. Calcd. for **3**, $C_{16}H_{10}ClF_4P$: C, 55.76; H, 2.90; Cl, 10.28; P, 8.99. Found: C, 55.36; H, 3.14; Cl, 10.41; P, 8.78.

Infrared spectrum (neat): some of the more significant peaks are 3060w, 1575m, 1480m, 1320s, 1120vs, 1070w, 1030w, 1000m, 860s, 835s, 745s, 693s. Nuclear magnetic resonance: the phosphorus spectrum shows only one peak at +25.1 p.p.m., which is in agreement for a tertiary phosphine (10).

Anal. Calcd. for **2**, $C_{28}H_{20}P_2F_4$: C, 68.03; H, 4.04; P, 12.54. Found: C, 68.29; H, 4.38; P, 12.71.

Infrared spectrum (mull): some of the more significant peaks are 1595w, 1435m, 1375w, 1295s, 1220s, 1155s, 1085s, 1065w, 1025w, 1000w, 830m, 822m, 758m, 740s, 730w, 725m, 694s. Nuclear magnetic resonance: the phosphorus spectrum shows only one peak at 22.7 p.p.m. which is in agreement for a tertiary phosphine (10). A sample of **2** was obtained from Professor W. R. Cullen (1) and it was shown by i.r., ^{31}P n.m.r., and a mixture melting point, to be identical to that obtained in this work.

Acknowledgments

The author wishes to acknowledge the assistance of Dr. J. E. Lancaster and Mrs. M. Neglia of the American Cyanamid Company's Central Research Laboratories for the phosphorus nuclear magnetic resonance spectra.

I would also like to thank Professor W. R. Cullen of the University of British Columbia for a generous sample of (3,3,4,4-tetrafluorocyclobuten-1,2-ylene)bisdiphenylphosphine.

1. W. R. Cullen, D. S. Dawson, and P. S. Dhahival. Can. J. Chem. **45**, 683 (1967).
2. R. F. Stockel. Can. J. Chem. **46**, 2625 (1968).
3. R. F. Stockel, M. T. Beachem, and F. H. Megson. J. Org. Chem. **30**, 1629 (1965).
4. A. J. Parker. *In* Advances in physical organic chemistry. Vol. 5. *Edited by* V. Gold. Academic Press, Inc., New York. 1967. p. 173.
5. A. W. Frank. J. Org. Chem. **30**, 3663 (1965).
6. J. D. Park, R. J. McMurtry, and R. Sullivan. J. Org. Chem. **33**, 33 (1968).
7. W. J. Feast, D. R. A. Perry, and R. Stephens. Tetrahedron, **22**, 433 (1966).
8. D. J. Burton and R. L. Johnson. Tetrahedron Letters, 2681 (1966).
9. L. Horner and H. Hoffmann. Newer methods of preparative organic chemistry. Vol. II. *Edited by* W. Foerst. Academic Press, Inc., New York. 1963.
10. K. Moedritzer, L. Maier, and L. C. D. Groenvegh. J. Chem. Eng. Data, **7**, 310 (1962).

Can. J. Chem. Downloaded from www.nrcresearchpress.com by 210.87.254.42 on 09/05/12
For personal use only.

7-*O*-β-D-Glucosyl-3′,4′,5-trihydroxy-6-methyl flavanone—a new *C*-methyl flavanone glycoside from Douglas-fir [*Pseudotsuga menziesii* (Mirb.) Franco] roots

G. M. Barton

Forest Products Laboratory, Forestry Branch, Department of Fisheries and Forestry, Vancouver, British Columbia

Received September 13, 1968

A new *C*-methyl flavanone, 7-*O*-β-D-glucosyl-3′,4′,5-trihydroxy-6-methyl flavanone, has been obtained from healthy Douglas-fir [*Pseudotsuga menziesii* (Mirb.) Franco] root bark in a high yield of 2.6%. Its structure was elucidated by high resolution and mass spectrometry together with a variety of chemical and physical tests and confirmed by synthesis of its methylated aglycone. Pathological testing of this new glucoside against *Poria weirii* Murr. is being undertaken.

Canadian Journal of Chemistry, **47**, 869 (1969)

The first new *C*-methyl flavanone, poriol, to be discovered in Douglas-fir [*Pseudotsuga menziesii* (Mirb.) Franco] roots has been described in a previous paper (1). In contrast to poriol, which was obtained in low yield (0.2%) from diseased (*Poria weirii* Murr.) Douglas-fir root bark, the new *C*-methyl flavanone glucoside (**1**) was obtained in high yield (2.6%) from healthy Douglas-fir root bark. The structure of this new *C*-methyl flavanone glucoside (**1**) is proposed as 7-*O*-β-D-glucosyl-3′,4′,5-trihydroxy-6-methyl flavanone.

Flavanone glucoside (**1**) crystallized from an ethyl acetate extract of healthy Douglas-fir root bark. This bark had been previously extracted

ether and the combined ethereal extracts were washed three times with 50 ml portions of water. The ether solution was dried over anhydrous $MgSO_4$ and concentrated to dryness. The crude consisted of solid and an oil. Approximately 10 g of solid (**2**) were filtered off and 16 g of oil (**3**) remained. The oil was distilled at 114–116 °C/0.1 mm and the solid was recrystallized from ethanol and had m.p. 127–127.5 °C (lit. (1), m.p. 129.5–130.5°). A vapor-phase chromatography analysis employing an F and M model 810 equipped with a 3 ft silicon gum rubber column indicated that the crude mixture had at least two other minor components representing less than 5% of the total besides **2** and **3**.

Anal. Calcd. for **3**, $C_{16}H_{10}ClF_4P$: C, 55.76; H, 2.90; Cl, 10.28; P, 8.99. Found: C, 55.36; H, 3.14; Cl, 10.41; P, 8.78.

Infrared spectrum (neat): some of the more significant peaks are 3060w, 1575m, 1480m, 1320s, 1120vs, 1070w, 1030w, 1000m, 860s, 835s, 745s, 693s. Nuclear magnetic resonance: the phosphorus spectrum shows only one peak at +25.1 p.p.m., which is in agreement for a tertiary phosphine (10).

Anal. Calcd. for **2**, $C_{28}H_{20}P_2F_4$: C, 68.03; H, 4.04; P, 12.54. Found: C, 68.29; H, 4.38; P, 12.71.

Infrared spectrum (mull): some of the more significant peaks are 1595w, 1435m, 1375w, 1295s, 1220s, 1155s, 1085s, 1065w, 1025w, 1000w, 830m, 822m, 758m, 740s, 730w, 725m, 694s. Nuclear magnetic resonance: the phosphorus spectrum shows only one peak at 22.7 p.p.m. which is in agreement for a tertiary phosphine (10). A sample of **2** was obtained from Professor W. R. Cullen (1) and it was shown by i.r., ^{31}P n.m.r., and a mixture melting point, to be identical to that obtained in this work.

Acknowledgments

The author wishes to acknowledge the assistance of Dr. J. E. Lancaster and Mrs. M. Neglia of the American Cyanamid Company's Central Research Laboratories for the phosphorus nuclear magnetic resonance spectra.

I would also like to thank Professor W. R. Cullen of the University of British Columbia for a generous sample of (3,3,4,4-tetrafluorocyclobuten-1,2-ylene)bisdiphenylphosphine.

1. W. R. Cullen, D. S. Dawson, and P. S. Dhahival. Can. J. Chem. **45**, 683 (1967).
2. R. F. Stockel. Can. J. Chem. **46**, 2625 (1968).
3. R. F. Stockel, M. T. Beachem, and F. H. Megson. J. Org. Chem. **30**, 1629 (1965).
4. A. J. Parker. *In* Advances in physical organic chemistry. Vol. 5. *Edited by* V. Gold. Academic Press, Inc., New York. 1967. p. 173.
5. A. W. Frank. J. Org. Chem. **30**, 3663 (1965).
6. J. D. Park, R. J. McMurtry, and R. Sullivan. J. Org. Chem. **33**, 33 (1968).
7. W. J. Feast, D. R. A. Perry, and R. Stephens. Tetrahedron, **22**, 433 (1966).
8. D. J. Burton and R. L. Johnson. Tetrahedron Letters, 2681 (1966).
9. L. Horner and H. Hoffmann. Newer methods of preparative organic chemistry. Vol. II. *Edited by* W. Foerst. Academic Press, Inc., New York. 1963.
10. K. Moedritzer, L. Maier, and L. C. D. Groenvegh. J. Chem. Eng. Data, **7**, 310 (1962).

Can. J. Chem. Downloaded from www.nrcresearchpress.com by 210.87.254.40 on 09/05/12
For personal use only.

7-*O*-β-D-Glucosyl-3′,4′,5-trihydroxy-6-methyl flavanone—a new *C*-methyl flavanone glycoside from Douglas-fir [*Pseudotsuga menziesii* (Mirb.) Franco] roots

G. M. Barton

Forest Products Laboratory, Forestry Branch, Department of Fisheries and Forestry, Vancouver, British Columbia

Received September 13, 1968

A new *C*-methyl flavanone, 7-*O*-β-D-glucosyl-3′,4′,5-trihydroxy-6-methyl flavanone, has been obtained from healthy Douglas-fir [*Pseudotsuga menziesii* (Mirb.) Franco] root bark in a high yield of 2.6%. Its structure was elucidated by high resolution and mass spectrometry together with a variety of chemical and physical tests and confirmed by synthesis of its methylated aglycone. Pathological testing of this new glucoside against *Poria weirii* Murr. is being undertaken.

Canadian Journal of Chemistry, **47**, 869 (1969)

The first new *C*-methyl flavanone, poriol, to be discovered in Douglas-fir [*Pseudotsuga menziesii* (Mirb.) Franco] roots has been described in a previous paper (1). In contrast to poriol, which was obtained in low yield (0.2%) from diseased (*Poria weirii* Murr.) Douglas-fir root bark, the new *C*-methyl flavanone glucoside (**1**) was obtained in high yield (2.6%) from healthy Douglas-fir root bark. The structure of this new *C*-methyl flavanone glucoside (**1**) is proposed as 7-*O*-β-D-glucosyl-3′,4′,5-trihydroxy-6-methyl flavanone.

Flavanone glucoside (**1**) crystallized from an ethyl acetate extract of healthy Douglas-fir root bark. This bark had been previously extracted

Can. J. Chem. Downloaded from www.nrcresearchpress.com by 210.87.254.40 on 09/05/12
For personal use only.

(soxhlet) with chloroform to remove interfering substances. White crystals were obtained, melting at 228.5 °C (Mettler FP 1). After recrystallization from aqueous methanol, the melting point was raised to 255.1 °C.

Flavanone glucoside (**1**) gave positive phenolic tests with Barton's reagent (2) (blue) and diazotized sulfanilic acid (3) (yellow). The 3-hydroxy flavanone test (4) developed for thin-layer chromatography (t.l.c.) proved negative, but the Shinoda test (5) was positive (violet). Its infrared (i.r.) spectrum was similar to flavanone glucosides such as hesperedin. Principal absorption peaks were ν(KBr) 530 (w), 545 (w), 565 (w), 615 (w), 625 (w), 690 (m), 720 (m), 740 (m), 760 (m), 785 (w), 815 (s), 865 (m), 880 (m), 890 (m), 915 (s), 960 (s), 1030 (m), 1070 (m), 1080 (m), 1130 (m), 1170 (s), 1190 (m), 1240 (m), 1290 (s), 1320–1350 (br, m), 1435 (m), 1450 (m), 1490 (m), 1540 (m), 1580 (m), 1605 (w), 1635 (s), 2920 (m), 2940 (m), 2960 (w), 3000–3560 (br, s).

Its ultraviolet (u.v.) spectrum was typical of a substituted flavanone λ_{max} 288 (log ε 4.31) λ_{min} 251 mμ (isopropanol).

The 100 Mc.p.s. nuclear magnetic resonance (n.m.r.) spectrum of its acetate (**2**) in deuteriochloroform showed clearly that it was a monoglucoside with 4 free aromatic protons. The AB part of the expected ABX absorption pattern of ring C protons was easily discernable, centered at 7.2 τ. Mold hydrolysis of **1** (300 mg) with a mixture of hydrochloric – acetic acid (0.2 ml concentrated hydrochloric acid, 5 ml of glacial acetic acid) for 30 min at 100 °C gave two main fragments, glucose and aglycone (**3**) which were identified by t.l.c. The first preparations of the glycosides (**1**) after hydrolysis gave, in addition to glucose, a small quantity of rhamnose. Recrystallization of the glucoside (**1**) from ethanol (trace of water) resulted in only glucose and aglycone (**4**) being formed. It has not been determined whether the rhamnose was present as a free sugar impurity or whether a small quantity of rhamnoside co-crystallized with the glucoside. Lack of an extra methyl group (required for the C-6 position of rhamnose) in the n.m.r. spectrum of the glycoside acetate (**2**) precluded the possibility of a rutinoside. High-resolution nuclear magnetic resonance of the methylated aglycone (**4**) enabled probable assignments to be made as follows: τ (deuteriochloroform): 2.06 (1H, singlet, hindered hydroxyl group C-5), 3.10 (3H, multiplet, aromatic protons ring B), 3.95 (1H, singlet, aromatic proton C-8), 4.60, 4.73 (1H, doublets, X part of ABX, J_{BX} = 3.5 c.p.s. proton C-2), 6.10 (3H, singlet, methoxyl C-3′ or C-4′), 6.13 (3H, singlet, methoxyl C-3′ or C-4′), 6.20 (3H, singlet, methoxyl C-7), 7.07 (2H, mulitplet, AB part of ABX, J_{AB} = 17.5 c.p.s., J_{AX} = 12.5 c.p.s., C-3), 8.01 (3H, singlet, methyl, C-6).

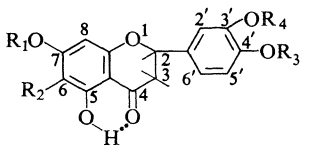

1 R_1 = glucose, R_2 = CH_3, R_3 = R_4 = H
2 R_1 = glucose acetate, R_2 = CH_3, R_3 = R_4 = acetate
3 R_1 = R_3 = R_4 = H, R_2 = CH_3
4 R_1 = R_2 = R_3 = R_4 = CH_3
6 R_1 = R_2 = R_3 = H, R_4 = CH_3

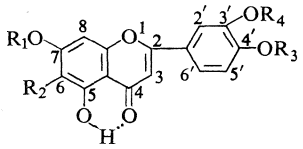

5 R_1 = R_2 = R_3 = R_4 = CH_3

The high value (12.5 c.p.s.) for the coupling constant J_{AX} is indicative of an axial–axial coupling only. Therefore, the C-2 hydrogen is axial and ring B is equatorial (6).

The mass spectrum of **4** showed a strong parent ion peak at *m/e* 330 (100) and 3 main fragments at *m/e* 164 (99), 151 (86), and 133 (43). The abundance of the 164 fragment indicates great stability of 3,4-dimethoxystyrene arising from the expected cleavage between C-1 and the heterocyclic oxygen and between C-3 and C-4. The fragments are consistent with structure **4**.

Since the n.m.r. spectrum of **4** had shown the presence of three methoxyl groups and color tests (7) indicated that compound **1** had vicinal phenolic hydroxyl groups, it must be concluded that the glucoside was formed at the non-vicinal hydroxyl group. Subsequent experiments showed that this hydroxyl group was on C-7 and hence the sugar moiety was associated with ring A at C-7. The successful hydrolysis of compound **1** by emulsin showed that it was a β-glucoside.

Final proof of structure was obtained in two ways. It was shown that dehydrogenation of the methylated aglycone (**4**) with iodine and glacial

acetic acid (30 mg of **4** was refluxed for 2 h with 30 mg of iodine in 5 ml of glacial acetic acid) followed by purification on t.l.c. (silica gel, carbon tetrachloride – methanol (7:1) R_f 0.61) resulted in the known compound 6-methyl-luteolin, 7,3′,4′-trimethylether (**5**) melting at 197.6 °C. It was also shown that nuclear methylation of hesperetin (**6**) at C-6 with methyl iodide and sodium methoxide (8) resulted in the methylated aglycone (**4**). This result was confirmed by quantitative i.r. comparison and mixture melting point 176.8 °C. Thus the structure of the new *C*-methyl flavanone glucoside is 7-*O*-β-D-glucosyl-3′,4′,5-trihydroxy-6-methyl flavanone. Pathological testing of this glucoside (**1**) against *Poria weirii* is currently being undertaken by Dr. G. W. Wallis at the Forest Research Laboratory, Victoria, British Columbia.

Acknowledgments

The author thanks Dr. Wallis and his staff for the collection of the Douglas-fir roots. Technical assistance by Mr. C. R. Daniels of the Wood Chemistry Section, Forest Products Laboratory, is gratefully acknowledged.

1. G. M. BARTON. Can. J. Chem. **45**, 1020 (1967).
2. G. M. BARTON, R. S. EVANS, and J. A. F. GARDNER. Nature, **170**, 249 (1952)
3. I. SMITH. Chromatographic techniques, clinical and biochemical applications. W. Heinemann Medical Books, Ltd., London. 1958. p. 145.
4. G. M. BARTON. J. Chromatog. **34**, 562 (1968).
5. J. SHINODA. J. Pharm. Soc. Japan, **48**, 214 (1928).
6. J. MASSICOT and J. P. MARTHE. Bull. Soc. Chim. France, **10**, 1962 (1962).
7. H. A. SCHROEDER. J. Chromatog. **30**, 537 (1967).
8. R. N. GOEL, A. C. JAIN, and T. R. SESHADRI. Proc. Indian Acad. Sci. Sect. A, **48**, 180 (1958).

Can. J. Chem. Downloaded from www.nrcresearchpress.com by 210.87.254.40 on 09/05/12
For personal use only.

Can. J. Chem. Downloaded from www.nrcresearchpress.com by 210.87.254.40 on 09/05/12
For personal use only.

Canadian Journal of Chemistry

Published by THE NATIONAL RESEARCH COUNCIL OF CANADA

VOLUME 47 MARCH 15, 1969 NUMBER 6

Nucleophilic decomposition of α-disulfones

PAUL ALLEN, JR. AND PATRICK J. CONWAY

The Department of Chemistry and Chemical Engineering, Stevens Institute of Technology, Hoboken, New Jersey 07030

Received June 18, 1968

The sulfur–sulfur bond of α-disulfones is attacked by hydroxide ion in alcohol to yield sulfinate and sulfonate ion by a second-order reaction, first order in each of the reactants. With aromatic disulfones the ρ value of the Hammett equation is 0.2. The Arrhenius activation energy of the reaction of *p*-tolyl disulfone is 7.95 kcal/mole.

Canadian Journal of Chemistry, **47**, 873 (1969)

Although α-disulfones are very stable towards acids, they readily undergo nucleophilic attack. *p*-Tolyl α-disulfone reacts with potassium hydroxide (2) according to eq. [1].

[1] $$C_7H_7SO_2\cdot SO_2C_7H_7 + 2KOH \rightarrow C_7H_7SO_2K + C_7H_7SO_3K + H_2O$$

and with piperidine (3) to give *p*-tolylsulfopiperidide and piperidinium *p*-toluene-sulfinate.

The kinetics and mechanism of this reaction have not been investigated.

Kharasch and Parker (4), Kice (5), and others have studied the nucleophilic fission of the sulfur–sulfur bond in disulfides, sulfinyl sulfones, and other sulfur compounds and found that it takes place by a second-order reaction.

The reaction of one aliphatic and several aromatic disulfones with sodium hydroxide in alcohol has now been studied and shown to be second order, first order in disulfone and first order in hydroxide ion. The initial reaction is, therefore

[2] $$(RSO_2)_2 + OH^- \rightarrow RSO_2^- + RSO_3H$$

followed immediately by neutralization of the sulfonic acid.

Ultraviolet absorption afforded a suitable method of analysis since aromatic α-disulfones, in most cases, have strong and characteristic absorptions, different from those of the corresponding sulfinates and sulfonates, see Table I. All the substances obey the Beer–Lambert law.

TABLE I

Ultraviolet absorption* of $(ArSO_2)_2$, $ArSO_2^-$, and $ArSO_3^-$

		$(ArSO_2)_2$		$ArSO_2^-$		$ArSO_3^-$
Compound	Ar	λ_{max}	log ε	λ_{max}	log ε	λ_{max}
1	C_6H_5	237†	4.30†	272	3.04	262
2	*p*-$CH_3C_6H_4$	250†	4.36†	270	3.10	260
3	*p*-$CH_3OC_6H_4$	277†	4.45†	267	3.40	272
4	*p*-BrC_6H_4	262†	4.29†	285	3.05	
5	*m*-BrC_6H_4	235†‡	4.18†	248	3.37	
6	*p*-$HO_2CC_6H_4$	270‡	3.73†	‡	2.28§	
7	*m*-$HO_2CC_6H_4$	None		None		
8	*p*-$O_2NC_6H_4$	260		264		264
9	*m*-$O_2NC_6H_4$	250		253		256

*Given in mμ.
†From ref. 6.
‡Broad shoulder.
§Absorption measured at 280 mμ.

TABLE II

Rate constants of eq. [2] at 23 °C

Compound	By ultraviolet absorption: Initial concentration × 10^4 of (moles l^{-1}) Disulfone	Hydroxide	k_2 (av.) (l $mole^{-1}$ s^{-1})	By permanganimetry: Initial concentration × 10^4 of (moles l^{-1}) Disulfone	Hydroxide	k_2 (av.) (l $mole^{-1}$ s^{-1})
1	0.425	2.000	7.14	0.500	1.260	7.14
2	0.450	2.826	6.52			
3	0.300	1.844	6.08	0.500	1.260	6.11
4	0.506	1.844	7.47	0.500	1.260	7.58
5	0.750	1.844	8.38	0.500	1.260	8.55
6	1.358*	5.000	7.79	0.500*	1.260	7.78
7				0.500*	1.260	8.15
8				0.500	1.260	9.93
9				0.500	1.260	9.54
$(C_{12}H_{25}SO_2)_2$				0 500	5.250	4.32

*As sodium salt.

The disulfones were made by cobalt(III) oxidation of sulfinic acid (6).

The reaction was followed by measuring the absorbance of the solution at suitable time intervals at the λ_{max} of the disulfone and at the λ_{max} of the sulfinate ion, with an allowance for the very small absorption of the sulfonate ion at these wavelengths. Three disulfones and the corresponding sulfinate ions had absorption maxima so close to each other that they could not be analyzed by this method. With these, using others as a check, and with *n*-dodecyl disulfone, the concentration of sulfinate was determined at intervals by permanganimetry. The permanganate and absorption methods gave essentially the same second-order rate constants, see Tables II and III.

To determine the activation energy, the rate of reaction of hydroxide ion and *p*-tolyl α-disulfone was measured at several temperatures, see Table IV. A plot of $\log k_2$ vs. $1/T$ gives an excellent straight line. Calculation by least-squares gives an Arrhenius activation energy of 7.95 kcal/mole. According to the formula $\Delta S^{\ddagger}/4.576 = \log k - 10.753 - \log T + E_a/4.576T$ (see ref. 7), the entropy of activation is about −30 e.u.

Hammett Function

The logarithms of the rate constants of the substituted disulfones, $(XC_6H_4SO_2)_2$, were plotted against the Hammett substituent constants σ of the groups X, using the rate constants determined by permanganimetry, except for the tolyl disulfone. If the meta and para $—CO_2^-$ groups are omitted, the points are fairly close to a straight line of which the slope, ρ, is 0.2. (If the two $—CO_2^-$ groups are included, the slope by the least-squares method becomes 1.23, but it seems advisable to omit these groups.)

It is of interest to compare these results with those for the ionization of sulfinic acids. Unfortunately, there is considerable disagreement between the published values. Burkhard *et al.* (8) determined the pK_a of a few aromatic sulfinic acids taking great care to avoid oxidation to the stronger sulfonic acids. They gave two figures for the pK_a of benzene sulfinic acid, 1.84 and 2.16; for the pK_a of *p*-toluene sulfinic acid they gave 1.99. Other workers have found that the benzene is stronger than the toluene acid. Ritchie, Saltiel, and Lewis (9) found pK_a's considerably lower than those published by Burkhard; their data agreed with fair precision with the equation $\log K_a = 0.976\sigma - 1.23$. A plot of Burkhard's results vs. σ, excluding the pK_a of benzene sulfinic acid, gives a moderately good line with a slope of about 0.15; according to this line the pK_a of benzenesulfinic acid should be 1.94. In the plot of our rate constants, if solvent or other effects make the σ values of the $—CO_2^-$ groups sufficiently uncertain for them to be left out, the slope of the line σ vs. $\log k_2$, about 0.2, is quite like that of σ vs. $\log K_a$ of Burkhard's data. These figures indicate that substituents on the aromatic ring do not greatly affect the sulfur atom in these reactions. However, one would expect more

Can. J. Chem. Downloaded from www.nrcresearchpress.com by 210.87.254.40 on 09/05/12
For personal use only.

Can. J. Chem. Downloaded from www.nrcresearchpress.com by 210.87.254.40 on 09/05/12
For personal use only.

TABLE III

Rate of reaction of *p*-methoxyphenyl α-disulfone at 23 °C

Ultraviolet absorption				Permanganate method				
Time (s)	Disulfone moles $l^{-1} \times 10^4$	Hydroxide ion moles $l^{-1} \times 10^4$	k_2 1 mole^{-1} s^{-1}	Time (s)	Disulfone moles $l^{-1} \times 10^4$	Sulfinate ion moles $l^{-1} \times 10^4$	Hydroxide ion moles $l^{-1} \times 10^4$	k_2 1 mole^{-1} s^{-1}
0	0.300	1.844		0	0.500	0	1.260	
90	0.275	1.794	6.00	120	0.457	0.043	1.174	6.13
210	0.239	1.722	6.06	240	0.421	0.079	1.102	6.09
300	0.220	1.684	5.89	360	0.389	0.111	1.038	6.10
510	0.177	1.598	6.06	480	0.360	0.140	0.980	6.16
720	0.143	1.530	6.18	600	0.337	0.163	0.934	6.10
900	0.124	1.492	6.02	900	0.287	0.213	0.834	6.09
				1200	0.248	0.252	0.756	6.10
1980	0.048	1.340	6.15					
		av. of 12	6.08					av. 6.11

TABLE IV

Rate of reaction of *p*-tolyl disulfone with OH^- ion vs. temperature

Temp. (°K)	k_2	Temp. (°K)	k_2
288.1	4.661	300.3	7.750
289.1	4.875	306.1	10.050
292.9	5.769	307.6	10.543
293.7	5.969	308.7	11.152
295.9	6.500	309.6	11.573
296.1	6.518	313.7	13.288
299.7	7.644	333.1	27.248

effect when the sulfur is directly attacked, as in the reaction between OH^- and disulfones, than when the reaction is removed from the sulfur, as in ionization of sulfinic acids. On the other hand, Kice (ref. 5, p. 62) found that substituents on the ring had a large effect in both the spontaneous and acid-catalyzed hydrolysis of sulfinyl sulfones.

Mechanism

The data indicate that the hydroxide ion attacks one of the sulfur atoms, displacing a sulfinate ion by scission of the sulfur–sulfur bond,

$$[3]\quad HO^- + \underset{\underset{R}{|}}{SO_2}\text{—}SO_2R \rightarrow [HO\cdots \underset{\underset{R}{|}}{SO_2} \cdots SO_2R]^- \rightarrow RSO_3H + RSO_2^-$$

As expected, the rate of reaction increases as the sulfur of the disulfone is made more positive by introduction of electron attracting groups into the aromatic ring.

Experimental Section

Sulfinic Acids

Benzene- and *p*-toluene-sulfinic and sulfonic acid sodium salts were Eastman products. *m*-Bromobenzenesulfinic acid was made by diazotizing *m*-bromoaniline and adding sulfur dioxide in the presence of copper. The other sulfinic acids were prepared by reducing the sulfonyl chlorides with sodium sulfite.

Sulfonic Acids

When not available from other sources, these were made by peroxide oxidation of sulfinic acids in dilute hydrochloric acid.

α-Disulfones

Sulfinic acids or their sodium salts were oxidized by cobaltic(III) sulfate directly to disulfones (6).

The disulfones were very slightly soluble in ethanol, sparingly soluble in cold, but soluble in hot carbon tetrachloride, benzene, and benzene–xylene, soluble in dioxane and in acetonitrile. Constancy of melting point, analyses, and spectral data confirmed the purity and structure of the compounds.

Ultraviolet Absorption

A recording DK 2A Beckman spectrophotometer was used. The absorbances of α-disulfones, sodium sulfinates, and sodium sulfonates were determined in absolute alcohol at various concentrations. From the absorbance curves the values of the extinction coefficients were calculated by the method of least squares. In all cases the Beer–Lambert law was obeyed.

Temperature

For the calculation of the activation energy of the reaction of *p*-tolyl disulfone the temperatures were controlled within 0.03°. In all other runs the temperature was kept at 23.00 ± 0.05 °C.

Determination by u.v. Absorbance

Solutions of known strength of sodium hydroxide and of disulfone in absolute ethanol at 23 °C were mixed in a silica absorption cell. At intervals, timed by a stopwatch, absorption curves were recorded from 200–360 mμ. The intervals varied from 1–5 min. Calculations of disulfone concentration were made from the absorbances at two wavelengths, the λ_{max} of the disulfone and that of the sodium sulfinate, and the extinction coefficients of the disulfone, sulfinate, and sulfonate at these wavelengths. The sodium sulfonates showed little absorption; nevertheless their small absorbances were included. At the initial concentrations given in Table II, the reactions were 75% complete in about 25 min. For each run, 10–12 absorption curves were taken; second-order rate constants were calculated according to eq. [2] and gave excellent straight lines.

Determination by Permanganimetry in Alkaline Solution (10)

Solutions of known strength of base and of disulfone in absolute alcohol at 23° were mixed in a flask at 23° and kept at this temperature. At known intervals, 2–5 min, 100 cc samples were pipetted into water containing a few drops of sodium hydroxide. Standard 0.01 *N* permanganate was added from a microburette to a potentiometric end point shown on a pH meter with an expanded scale, using a platinum and a calomel electrode. The method of titration was checked against purified Eastman sodium benzenesulfinate. Tests showed that the reaction of disulfone and base stopped completely when the alcoholic solution was added to water. Seven or eight samples were withdrawn for titration in each run and second-order rate constants calculated. Second-order plots gave excellent straight lines. At the initial concentrations listed in Table II, the reactions of aromatic disulfones were 50% complete in 15–20 min. The reaction of dodecyl disulfone was 50% complete in 5 min and 90% in 20 min, but the concentration of base was relatively larger than in the reaction of the aromatic disulfones.

1. Presented before the Division of Physical Chemistry, 152nd Meeting Am. Chem. Soc. New York. Sept. 11–16, 1966.
2. E. P. KOHLER and M. B. MACDONALD. Am. Chem. J. **22**, 219 (1899).
3. H. J. BACKER. Rec. Trav. Chim. **70**, 254 (1951).
4. N. KHARASCH and A. J. PARKER. J. Org. Chem. **24**, 1029 (1959); A. J. PARKER and N. KHARASCH.

Can. J. Chem. Downloaded from www.nrcresearchpress.com by 210.87.254.40 on 09/05/12
For personal use only.

Chem. Rev. **59**, 583 (1959); J. Am. Chem. Soc. **82**, 3071 (1960).
5. J. L. KICE. Accounts Chem. Res. **1**, 58 (1968). This article has numerous relevant references.
6. G. C. DENZER, JR., P. ALLEN, JR., P. CONWAY, and J. M. VAN DER VEEN. J. Org. Chem. **31**, 3418 (1966).
7. A. WEISSBERGER (*Editor*). Technique of organic chemistry. Vol. VIII. Interscience Publishers, Inc., New York. 1961. p. 201.
8. R. K. BURKHARD, D. E. SELLERS, F. DECOU, and J. L. LAMBERT. J. Org. Chem. **24**, 767 (1959).
9. C. D. RITCHIE, J. D. SALTIEL, and E. S. LEWIS. J. Am. Chem. Soc. **83**, 4601 (1961).
10. P. ALLEN, JR. J. Org. Chem. **7**, 28 (1942).

Can. J. Chem. Downloaded from www.nrcresearchpress.com by 210.87.254.40 on 09/05/12
For personal use only.

Low temperature Raman spectrum of rhombic sulfur

A. Anderson and Y. T. Loh
Department of Physics, University of Waterloo, Waterloo, Ontario

Received October 2, 1968

Raman spectra of polycrystalline samples of rhombic sulfur have been recorded at 100 and 300 °K, with excitation by the 5145 Å line of an argon ion laser. Spectra of sulfur solutions in carbon disulfide and bromoform were also obtained to aid in assignments. Experimental confirmation is presented of the frequencies of two intramolecular fundamental vibrations, suggested from normal coordinate analysis (one at very low frequency, the other inactive in both Raman and infrared for the free molecule). The spectra are analyzed in terms of the static and correlation crystal field perturbations, and for all except the weakest bands, substantial agreement is obtained. It is concluded that the effects of the two types of interaction are comparable in magnitude, and that a correct analysis must take account of the full symmetry of the unit cell.

Canadian Journal of Chemistry, 47, 879 (1969)

Can. J. Chem. Downloaded from www.nrcresearchpress.com by 210.87.254.6 on 09/05/12
For personal use only.

Introduction

Infrared and Raman spectra of rhombic sulfur have been reported previously. The results are conveniently summarized in a recent monograph (1). Only recently, however, have experimental techniques become adequate to obtain high resolution results, such as might reveal the crystal field splittings. All the 11 fundamental vibrations of the S_8 molecule have frequencies below 500 cm^{-1}. In the infrared, this is a region where low energy and insensitive detectors make high resolution studies difficult by conventional techniques. The difficulties are compounded in this case as crystalline sulfur absorbs very strongly. Some evidence of splitting in two of the fundamentals was, however, reported recently with the use of interferometric methods (2), but no specific conclusions were possible.

For Raman spectra, measurements near the exciting line have also presented problems because of excessive Rayleigh scattering. The advent of the laser as exciting source, and the use of double monochromators (3) have largely overcome these difficulties. In a recent paper, Ward (4) presented high resolution Raman results on rhombic sulfur using a helium–neon laser, and observed certain splittings. The research described here covers the same ground, but differs in three important respects. (*a*) The more powerful argon ion laser was used, giving greater scattering intensity, and allowing additional weak features to be recorded. (*b*) The sulfur was cooled to liquid nitrogen temperature, resulting in considerable sharpening of the observed bands, and permitting additional splittings to be detected. (*c*) Discussion of these splittings is in terms of both the static field effect, responsible for the removal of degeneracy of certain vibrations because of the lower site symmetry, and the correlation field effect, which results from coupling of vibrating molecules within the same unit cell.

Experimental

Raman spectra were excited by the Spectra-Physics Argon Ion Laser, model 140, using the 5145 Å line which has a power level of about 900 mW. A Spex Double Monochromator, model 1400, fitted with Bausch and Lomb 1200 lines/mm gratings, and a photomultiplier (model FW 130, manufactured by IT and T Co.) cooled by a flow of cold nitrogen gas, were used to measure the scattered radiation. The signal was recorded by the photon counting technique, and processed in a 400 Channel Analyzer (Nuclear Chicago Co.) with output through a rate-meter and chart recorder.

Because of difficulties in growing good quality single crystals of rhombic sulfur and their fragility, particularly with respect to thermal shock, pressed discs of powdered sulfur (Fisher, U.S.P. grade) were used. These were 1 cm in diameter and about 0.5 mm thick. In the absence of a perfect crystal suitable for a complete polarization analysis, a powdered sample has the advantage of a completely random orientation of crystallites, so that spurious intensity dependence from a partially oriented sample is avoided.

The sulfur pellet was positioned at an angle of 30° to the vertical in a brass sample holder which was connected through a Kovar–Pyrex seal to the reservoir of liquid nitrogen in a simple cylindrical glass cryostat with plate glass end disc. A thin layer of vacuum grease between the back surface of the sample and the holder improved thermal contact. The temperature, as measured by a copper–constantan thermocouple soldered on the holding ring, was 85 °K, rising to 90 °K in the laser beam. Local heating of the sample by the laser undoubtedly occurred, but was not appreciable, since the sulfur loses its characteristic yellow color at low temperatures and absorption is correspondingly small. The appreciable sharpening of the bands in the liquid nitrogen experiments confirmed that the sample was, in fact, cold, and its temperature is estimated at approximately 100 °K.

The unfocused laser beams entered the cryostat vertically upwards, and the main reflected beam emerged at

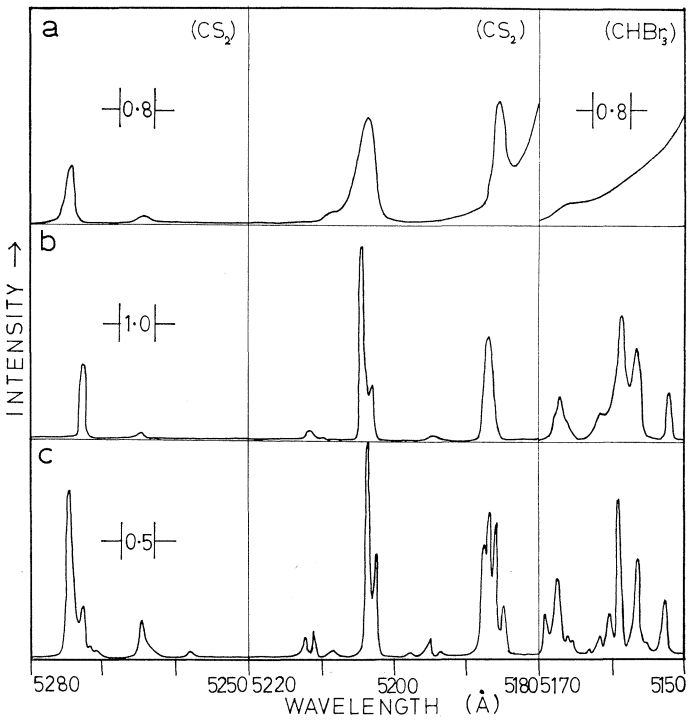

FIG. 1. Raman spectra of sulfur excited by 5145 Å argon line. (*a*) Solution in CS_2 and $CHBr_3$, (*b*) crystal at 300 °K, (*c*) crystal at 100 °K.

60° to the vertical. Scattered radiation was observed horizontally through a standard optical system mounted in front of the entrance slit of the monochromator.

Several solution spectra were also recorded. Saturated solutions of sulfur in CS_2 and $CHBr_3$ were placed in flat-ended Pyrex tubes. As sample warming was no problem here, the laser beam was focused in the solution at the focal point of the entrance optics, and horizontal scattering again observed.

Calibration was effected by noting the positions of non-lasing argon lines of known wavelength, when a small fraction of the beam was scattered directly into the monochromator. This also revealed the presence of two grating ghosts near the exciting line ($\Delta\nu$ = 13 and 23 cm^{-1}), similar to those reported by Ward (4). The resolution of the instrument as a function of slit widths was also checked using these sharp argon lines.

Results

In Fig. 1 are shown the spectra recorded from (*a*) room temperature saturated solutions of sulfur in CS_2 and $CHBr_3$, (*b*) the solid at room temperature, and (*c*) the solid at liquid nitrogen temperature. The bromoform spectrum is included only for the low temperature region, where the Rayleigh wing of carbon disulfide is very intense. In other regions, there is overlap between most of the sulfur peaks and those from $CHBr_3$.

The numbers inside slit symbols indicate the instrumental resolution in wavenumbers used for the different spectra. The frequencies of scattering intensity maxima are collected in Table I, and are estimated to be accurate to within ± 2 cm^{-1}. Results from other workers (refs. 4 and 5) are also included. The assignments and symmetry classifications of the normal vibrations of the isolated molecule are those of Scott, McCullough, and Kruse (5).

Additional spectra, not reproduced here, showed that (*a*) raising the temperature of the bromoform to just below its boiling point ($\sim$ 150 °C) and adding more sulfur to obtain a near saturated solution, increased the intensity of the band present as a shoulder in the room temperature experiment, thus confirming this as a fundamental of the isolated sulfur molecule; (*b*) room temperature experiments of the sulfur in solution and as a pressed disc, run under identical slit conditions, confirmed that none of the splittings

Can. J. Chem. Downloaded from www.nrcresearchpress.com by 210.87.254.6 on 09/05/12
For personal use only.

TABLE I

Raman spectra of sulfur

Mode and species	Raman frequencies at maximum intensity (cm^{-1})						
	Previous work			This work			
	Solution (5)	Crystal 300 °K (5)	Crystal 300 °K (4)	Solution	Crystal (300 °K)	Crystal (100 °K)	Suggested assignments
Lattice			26		28	29	R_z $b_{2g}b_{3g}$
			42.5		44	39 44	T_xT_y $b_{1g}b_{2g}b_{3g}$ a_g
		49	49.5 61		51 63	53 59 63 68	R_xR_y a_g b_{1g} b_{2g} b_{3g}
ν_9 (e_2)	86	85	82 86	80	84	77 79 85 91	ν_9 b_{2g} b_{3g} a_g b_{1g}
ν_8 (e_2)	152	152	147 151	152	157	149 152 156 159	ν_8 b_{2g} b_{3g} a_g b_{1g}
ν_6 (e_1)	184	184	189 194	—	186	182 187 197	ν_6 b_{1g} a_g $b_{2g}b_{3g}$
ν_2 (a_1)	218	216	215 219	218	217 221	214 218	ν_2 b_{1g} a_g
ν_4 (b_2)					241	236	ν_4 $b_{2g}b_{3g}$
ν_{11} (e_3)	248	243	247 251.5	245	249	246 250	ν_{11} a_gb_{1g} $b_{2g}b_{3g}$
ν_3 (b_1)						417	ν_3 a_gb_{1g}
ν_{10} (e_3)	437	434	434 441	440	442	441	ν_{10} a_gb_{1g} $b_{2g}b_{3g}$
ν_5 (e_1) ν_7 (e_2)						464 466	ν_7 (or ν_5) ?
ν_1 (a_1)	475	470	470 474	475	471	470 477	ν_1 b_{1g} a_g

NOTE: Combination and overtone bands above 500 cm^{-1} omitted.

observed in the crystal spectra were present in solution, thus eliminating isotopic species as a possible cause.

Discussion

(a) General

The molecular and crystal structures of sulfur in the orthorhombic modification are well known (6, 7). There are 16 S_8 puckered octagon molecules in the face-centered orthorhombic unit cell with space group D_{2h}^{24} (*Fddd*). However, in the primitive unit cell (the smallest volume from which the entire lattice can be generated by translations alone), this is reduced to 4 molecules. The only sites available with this occupancy number are C_2 and C_i, and the latter is excluded because it is not a sub-group of the molecular symmetry, D_{4d}. The two-fold axis is along the crystalline z axis, which lies in the nodal planes of the molecules, and thus does not correspond to the principal four-fold molecular axis. Hence, in the discussion which follows, the site symmetry is taken as C_2'. The distinction is important when the correlation table is constructed, as different predictions of infrared and Raman activity can result (8). Ward's assumption that there are only two types of molecule in the unit cell is incorrect (4). In any case, his analysis in terms of site symmetry only should be independent of the number of non-equivalent molecules present. The activities of the normal modes of the unit cell may be found by standard methods (9, 10). The correlation table relating the representations of the molecular, site, and unit cell symmetries is obtained by a comparison of their character tables, or more directly by using the standard compilations of

Can. J. Chem. Downloaded from www.nrcresearchpress.com by 210.87.254.6 on 09/05/12
For personal use only.

TABLE II

Number of optically active components predicted from group theory

Mode and species		Isolated molecule		Static field approximation, infrared and Raman	Static and correlation fields		Raman peaks observed
		Infrared	Raman		Infrared	Raman	
ν_1, ν_2	(a_1)	0	1	1	1	2	2, 2
ν_3	(b_1)	0	0	1	1	2	1
ν_4	(b_2)	1	0	1	2	2	1
ν_5, ν_6	(e_1)	1	0	2	3	4	0*, 3
ν_7, ν_8, ν_9	(e_2)	0	1	2	3	4	2, 4, 4
ν_{10}, ν_{11}	(e_3)	0	1	2	3	4	1, 2
R_z	(a_2)	0	0	1	2	2	1
(R_xR_y)	(e_3)	0	1	2	3	4	4
T_z	(b_2)	0†	0	1	1†	2	0‡
(T_xT_y)	(e_1)	0†	0	2	1†	4	2
Total		3	8	24	33	48	29

*Overlaps with ν_1.
†Translational modes corresponding to zero frequency have been subtracted.
‡Possible overlap with R_xR_y.

Wilson, Decius, and Cross (11). The result is shown in Fig. 2, which also includes the classification of the 11 internal and 4 external modes of S_8, and their optical activities. For convenience, the numbers of infrared and Raman components predicted for all the fundamental molecular and lattice vibrations are summarized in Table II, with the final column listing the Raman components actually observed in this study.

As indicated, group theory predicts 48 Raman and 33 infrared bands for vibrations within the unit cell. Together with 12 inactive components, these total 93, all non-degenerate. This agrees with the formula $3nN - 3$ where $n = 8$, the number of atoms per molecule, and $N = 4$, the number of molecules per unit cell. The 3 zero frequency modes, corresponding to translations of the entire lattice, are subtracted. Usually, many of these 48 components will be either too weak to be observed, or too close to other bands to be resolved. However, one would at least hope to observe the splitting of those bands which are strongly Raman active in the isolated molecule, and the appearance of weak bands corresponding to those modes which are active only under the crystal symmetry selection rules. As indicated by Ward (4), the degree of perturbation on the spectrum of the isolated molecule is governed by the relative strength of the intermolecular van der Waals forces compared to the covalent intramolecular sulfur bonds.

In fact a total of 29 peaks were observed. These will now be classified, using as basis the assignments of the isolated molecule by Scott *et al.* (5).

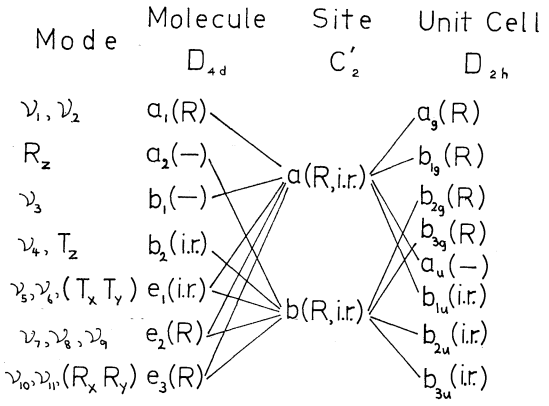

FIG. 2. Correlation between the molecular, site, and unit cell symmetries of orthorhombic sulfur. R, Raman active; i.r., infrared active; —, inactive.

The convention suggested by Herzberg (12) will be adopted: the modes are numbered with suffices from 1 to 11 in order of decreasing symmetry, and, for those having the same representation (e.g. e_2), in order of decreasing frequency. There is an initial problem of separating lattice from intramolecular modes. It is known from normal coordinate analysis (5), that there is a very low frequency molecular mode of e_2 species, ν_9, its most likely position, for consistency with vapor pressure data, being 56 cm^{-1}. The only experimental evidence for this vibration appears to be from the work of Gerding and Westrik (13), who observed a band at 86 cm^{-1} from a solution of sulfur in naphthalene at 110 °C and at 92 cm^{-1} from liquid sulfur at 120 °C. Because of the strong

Can. J. Chem. Downloaded from www.nrcresearchpress.com by 210.87.254.6 on 09/05/12
For personal use only.

Can. J. Chem. Downloaded from www.nrcresearchpress.com by 210.87.254.6 on 09/05/12
For personal use only.

scattering from the wing of the Rayleigh peak of CS_2, the band could not be detected in this solvent. However, the peak observed at 80 cm^{-1} from sulfur in bromoform at room temperature in this work puts the assignment of ν_9 on a more substantial basis as there is some evidence of breakage of the puckered rings of S_8 at elevated temperatures (6). The frequency is expected to increase with the extent of perturbation (5), and so the multiplet centered at 85 cm^{-1} in the low temperature crystal spectrum is assigned to ν_9 and all peaks below 75 cm^{-1} are assigned to lattice vibrations.

(b) Non-degenerate Vibrations

There are two totally symmetric vibrations, ν_1 (stretch) and ν_2 (bend). Both of these are split into well-resolved doublets as predicted. The splittings at 100 °K are 7 and 4 cm^{-1}, respectively. The strong component of each doublet is presumably the a_g mode and occurs at the higher frequency in each case. The b_1 mode, ν_3, which is completely inactive in the isolated molecule, should have two Raman components in the crystal. Normal coordinate analysis (5) predicts this frequency to be near 412 cm^{-1}, but experimental confirmation is indirect, relying on a combination band in the infrared (14). A weak band is observed in this work at 417 cm^{-1}, which may be the first direct sighting of ν_3. The b_2 mode, ν_4, is also Raman inactive in the molecule but has been observed in the infrared at 239 cm^{-1} (2). The weak band observed here at 236 cm^{-1} is probably the unresolved doublet predicted from the correlation table.

(c) Degenerate Vibrations

The two e_1 modes, ν_5 and ν_6, are also Raman active only through violation of the selection rules for the free molecule. A weak doublet is observed on the low frequency side of ν_1 which is close to the value observed for ν_5 in the infrared spectrum of the crystal at low temperature (15). However, the situation is complicated by an accidental degeneracy between ν_1 and ν_7 (e_2). Since ν_7 is nominally active for the free molecule, it is perhaps more likely that the weak doublet is really the unresolved quartet predicted for this mode. Three peaks are observed in the 180–200 cm^{-1} region, which is where ν_6 is observed in the far infrared (2). The strongest of these appears asymmetric on the high frequency side, and probably conceals a weak fourth component, so that again the agreement with theory is close.

There are three e_2 vibrations, one of which, ν_7, has been discussed above. At 100 °K, ν_8 is beautifully resolved into the four predicted components, the separations being of the order of 3 cm^{-1}. The low lying vibration, ν_9, is also well resolved into four components at low temperature, but here the assignment is not quite so clear-cut because of possible overlap with lattice modes. The splittings here range from 3 to 6 cm^{-1}.

The two e_3 modes appear only weakly in the solution spectra, and are not resolved into the predicted quartets in the crystal: ν_{10} is the rather broad band at 441 cm^{-1} with a low frequency tail; ν_{11} is observed as a doublet near 250 cm^{-1}, the splitting being 4 cm^{-1}. For this mode, it appears that either the static or correlation field is dominant, but as has been seen from the above analysis, in general the two effects give comparable splittings.

(d) Lattice Vibrations

Analysis of the lattice region is complicated by four factors. (*a*) The predicted Raman spectrum is rich, with 12 peaks lying in a narrow frequency region (between 10 and 75 cm^{-1}). (*b*) Strong grating ghosts may obscure certain very low frequency peaks. (*c*) There is a strong possibility of mixing between translational and torsional modes of like symmetry and similar frequency. (*d*) No normal coordinate analysis is available to aid in assignments.

Certain theoretical factors which should help in the analysis will first be considered. Of the six torsional modes, the two originating from motions about the principal molecular axis (R_z) are expected to be at low frequencies. Not only is the moment of inertia larger ($I_z:I_{xy} = 1.8:1$), but the restoring force about this axis should be weak (4). The other four torsional modes may be expected to be relatively strong, since the degenerate rotation from which they originate (R_xR_y) is formally Raman active for the free molecule. In particular, the in-phase totally symmetric component (a_g) should be more intense than the others.

A recent paper by Walmsley (16) suggests an approximate method for calculating the optically active translational frequencies of molecular crystals in terms of the intermolecular distance, static lattice energy at 0 °K, and molecular weight. Although strictly applicable only to face-centered cubic lattices, extension to crystals where neighboring molecules are almost equidistant is

Can. J. Chem. Downloaded from www.nrcresearchpress.com by 210.87.254.6 on 09/05/12
For personal use only.

possible. From the crystallographic data, the mean nearest neighbor intermolecular distance of rhombic sulfur is calculated to be 6.8 Å. The static lattice energy at 0 °K is the sum of the heat of sublimation at 0 °K and the zero-point energy. These quantities can be calculated using standard thermodynamic formulae (17) and the experimental data of Nernst (18), Norris (19), and Bradley (20). In this way, values of the two translational modes are estimated to be 35 and 52 cm^{-1}. For sulfur, there are in total eight optically active translational modes, and so the above frequencies serve merely as a guide to the general position of these bands and precise agreement is not expected. It is known that orthorhombic crystals of S_8 cleave readily across the 001 face (6). This suggests that translations in the crystallographic z direction (which corresponds to components of the molecular translation, T_xT_y) experience weak restoring forces and hence have low frequencies of vibration. Since no translational modes of the free molecule are Raman active, only weak bands in the crystal are probable. Similar to the torsions, however, the a_g component, originating from T_xT_y, might be more intense than the others.

With these factors in mind, the most plausible assignment of the seven observed lattice peaks appears to be as follows: R_z, 29 cm^{-1}; R_xR_y, 53, 59, 63, 68 cm^{-1}; T_z, $\sim$ 52 cm^{-1} (obscured by R_xR_y); T_xT_y, 39, 44 cm^{-1}. It is recognized that this is at best tentative. Further experiments such as polarization studies on a single crystal (Raman and infrared) would resolve some of the ambiguities, but probably not the basic problem of separating translational and torsional modes, since, as mentioned earlier, these have like symmetries.

Conclusions

The Raman spectrum of rhombic sulfur at 100 °K has been observed, and analyzed in terms of the normal modes of the unit cell. All except one of the intramolecular fundamentals are observed directly[1]. General confirmation of the assignments of Scott *et al.* (5) is obtained. In particular, there is new experimental verification of the frequencies of two modes (ν_3 and ν_9) deduced from their normal coordinate analysis. The splittings observed for the strongly Raman active fundamentals are entirely consistent with the group theoretical analysis in terms of the static and correlation crystal fields. The observed bands are never more than predicted, and the indications are that under ideal conditions of intensity, instrumental resolution, and sharp non-overlapping bands, the agreement would be complete. In general, the effects from the two types of field appear comparable, and a correct analysis must take account of both.

[1]At the suggestion of a referee, who pointed out that several weak spectral features may be caused by long chain molecules of sulfur stabilized by small amounts of impurity, the experiments were repeated with Gallard–Schlesinger sulfur stated to be 99.9999% pure. Identical spectra were obtained. The co-existence of S_8 rings and S_n chains is discussed in a recent paper (21). We are grateful to the referee for his advice, and to Mr. T. S. Sun for help with these later experiments.

Acknowledgments

The authors thank Dr. B. H. Torrie and Mr. L. Y. Wong for useful discussions, and Mr. J. Beke and Mr. D. Chandler for technical assistance. This research was supported in part by grants from the National Research Council of Canada and the Ontario Department of University Affairs.

1. H. L. Strauss and J. A. Greenhouse. Elemental sulphur. *Edited by* B. Meyer. Interscience Publishers, Inc., New York. 1965. p. 241.
2. G. W. Chantry, A. Anderson, and H. A. Gebbie. Spectrochim. Acta, **20**, 1223 (1964).
3. D. O. Landon and S. P. S. Porto. Appl. Opt. **4**, 762 (1965).
4. A. T. Ward. J. Phys. Chem. **72**, 744 (1968).
5. D. W. Scott, J. P. McCullough, and F. H. Kruse. J. Mol. Spectry. **13**, 313 (1964).
6. B. E. Warren and J. T. Burwell. J. Chem. Phys. **3**, 6 (1935).
7. C. Lu and J. Donohue. J. Am. Chem. Soc. **66**, 818 (1944).
8. A. Anderson and W. H. Smith. J. Chem. Phys. **44**, 4216 (1966).
9. D. F. Hornig. J. Chem. Phys. **16**, 1063 (1948).
10. H. Winston and R. S. Halford. J. Chem. Phys. **17**, 607 (1949).
11. E. B. Wilson, J. C. Decius, and P. C. Cross. Molecular vibrations. McGraw-Hill Book Co., Inc., New York. 1955. p. 333.
12. G. Herzberg. Infrared and Raman spectra. D. Van Nostrand Co., Inc., New York. 1945. pp. 163, 271.
13. H. Gerding and R. Westrik. Rec. Trav. Chim. **62**, 68 (1943).
14. V. D. Neff and T. H. Walnut. J. Chem. Phys. **35**, 1723 (1961).
15. A. A. Anderson and L. Y. Wong. Unpublished work, this laboratory.
16. S. H. Walmsley. Mol. Phys. **14**, 165 (1968).
17. R. H. Beaumont, H. Chihaha, and J. A. Morrison. Proc. Phys. Soc. **78**, 1462 (1961).
18. W. Nernst. Ann. Phys. **36**, 395 (1911).
19. R. Norris. Proc. Indian Acad. Sci. Sect. A, **13**, 291 (1941).
20. R. S. Bradley. Proc. Roy. Soc. London, Ser. A, **205**, 553 (1951).
21. A. T. Ward. J. Phys. Chem. **72**, 4133 (1968).

Can. J. Chem. Downloaded from www.nrcresearchpress.com by 210.87.254.6 on 09/05/12
For personal use only.

The effect of pressure on the radiation-induced conductance of liquid hydrocarbons

D. W. Brazier and G. R. Freeman
Chemistry Department, University of Alberta, Edmonton, Alberta

Received September 26, 1968

An attempt was made to test the cavity model of electron localization in liquid hydrocarbons by measuring the effect of pressures up to 4000 bars on the radiation induced conductance of *n*-pentane, *n*-hexane, *n*-octane, cyclopentane, methylcyclohexane, and 2,2-dimethylbutane at 30°. Measurements at 3 and 56° were also made on *n*-hexane and *n*-octane. The relative induced conductance, i.e. the ratio of the induced conductance at pressure *p* to that at 1 bar, decreased with increasing pressure. The amount of decrease was slightly greater at low than at high temperatures. The behavior of 2,2-dimethylbutane was complex and is not understood. For the other liquids, it was concluded that the free ion yields remained constant or decreased somewhat with increasing pressure. An appreciable increase in the free ion yields, which is a possible implication of the cavity model of electron localization, did not occur. Therefore, either (*a*) the cavity model of electron localization in hydrocarbons is wrong, or (*b*) application of pressures up to 4000 bars did not appreciably alter the cavity concentrations in the liquids. Perhaps the cavity concentration is greatly reduced only by pressures great enough to cause a solid phase (glass or crystal) to form.

Canadian Journal of Chemistry, **47**, 885 (1969)

Introduction

The cavity model for the structure of solvated electrons in liquid hydrocarbons (1) is useful in the interpretation of various effects that indicate that extra electrons are localized in these liquids (2). One of the implications of the model is that the range of a low energy secondary electron might be significantly dependent on the concentration of cavities in the liquid, i.e. the range might increase as the concentration of cavities decreases. An increasing range would result in an increasing free ion yield (2*b*).

It was thought that the application of several thousands of atmospheres pressure to a liquid might reduce the cavity concentration. For this reason, the effect of pressure on the radiation-induced conductance of several hydrocarbons was measured. Increasing the pressure on a hydrocarbon also increases the density, dielectric constant, and viscosity of the liquid. The first two of these factors affect the induced conductance through the free ion yield, and the third affects it through the ion mobilities. The influence of pressure on the cavity concentration must be sorted out from the other factors.

The hydrocarbons used in the present work were *n*-pentane, *n*-hexane, *n*-octane, cyclopentane, methylcyclohexane, and 2,2-dimethylbutane. The pressure dependences of the density, dielectric constant, and viscosity of these liquids were also measured and the results are reported in the following paper (3).

Experimental

High Pressure System

Full details of the high pressure system are given elsewhere (4). The pressure in the system was measured with a 14 in. dial Heise gauge that was calibrated in 100 p.s.i. divisions; 1 bar = 14.504 p.s.i. The temperature of the thermostated pressure vessel was controllable to within ±0.5 °C.

Three electrical connections to the pressure vessel interior were passed through the closure plunger. The connectors, obtained from American Instrument Co., were of the self-sealing cone design.

High Pressure Conductance Cells

Glass-to-metal seals made from all combinations of tungsten, platinum, and Kovar, with Pyrex, soda, and uranium glasses usually failed when the pressure was released, so glass cells were unsatisfactory.

The bellows cell employed is illustrated in Figs. 1 and 2. The cell electrodes (Fig. 1) were 16 mm in diameter and were made from stainless steel. The electrodes were separated (2–10 mm) by an interchangeable spacer made of Supramica 500 Ceramoplastic (Mycalex Corp.). The

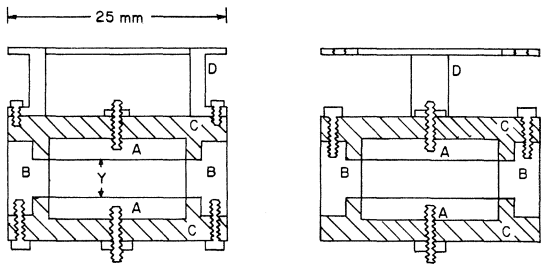

Fig. 1. Conductance cell (two sections at 90°). A, electrodes (2 mm thick); B, Supramica Ceramoplastic spacer; C, Supramica electrode holder; D, support post; Y, the interelectrode separation, varied from 2 to 10 mm.

Can. J. Chem. Downloaded from www.nrcresearchpress.com by 210.87.254.6 on 09/05/12
For personal use only.

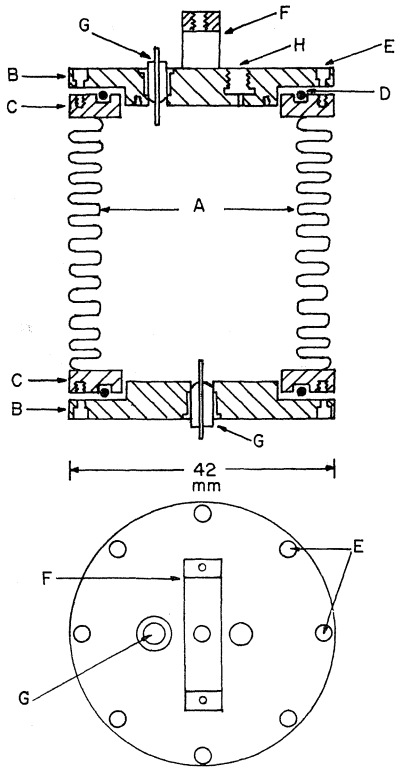

FIG. 2. Bellows assembly. A, stainless steel bellows; B, stainless steel closure cap; C, "O" ring seat; D, "O" ring; E, compression bolts; F, bracket to attach bellows to pressure vessel piston; G, terminal seal; H, filling aperture.

cell was enclosed in a bellows (Robertshaw Controls Ltd.) that was closed at each end as shown in Fig. 2. The "O" ring seats were silver soldered to the bellows.

Electrical connections into the bellows were made through Latronics Corp. metal-to-ceramic terminal seals. The conductance cell was rigidly attached to the lower surface of the top cap of the bellows. The filling aperture was closed by a needle valve type of screw.

Prior to assembly of the cell, all components were washed in a large Soxhlet apparatus for several days. Either hexane or the hydrocarbon under investigation was used for washing.

Materials

The hydrocarbons used for conductance measurements were Phillips Research Grade. Olefinic impurities were removed by concentrated sulfuric acid. The hydrocarbon was then washed with 5% sodium hydroxide and with doubly distilled water. After preliminary drying over anhydrous magnesium sulfate, the liquid was distilled from lithium aluminium hydride.

Radiation Sources and Dosimetry

A 5500 Ci ^{60}Co γ source could be reproducibly positioned near the pressure vessel. The dose rate within the vessel was 10^{14}–10^{15} eV/cm^3 s, determined using the Fricke dosimeter. The dose rate was very dependent on the position of the sample within the vessel, because of the variable path length of the radiation through the steel vessel wall.

Conductance Measurements

Currents were measured with an E. H. Laboratories Model 240 micromicroammeter. The meter was calibrated by applying known voltages across Victoreen precision resistors.

An extra (dummy) cable was used on the current measuring side of the circuit to check whether currents that did not originate in the conductance cell were negligible. The extra cable paralleled the actual measuring cable and passed into the interior of the pressure vessel, but terminated just prior to the conductance cell electrode.

The method of shielding the connections at the pressure vessel head, to reduce the amount of ion collection from the surrounding ionized air, is shown in Fig. 3. In this way the current that passed through the ionized air was reduced to a negligible level.

Electrical connections were spot welded, when possible.

Cell Filling and Experimental Procedure

The cleaned and assembled bellows cell was connected to a vacuum manifold, using a Kovar seal and a special hollow screw which fitted into the needle valve closure of the bellows cap.

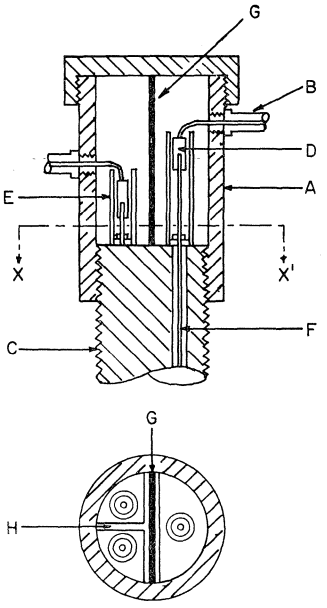

FIG. 3. Shielding of cables at pressure vessel head. A, brass cap; B, BNC coaxial cable connector; C, pressure vessel closure piston; D, brass sleeve; E, polyethylene tubing; F, electrical connection through closure piston; G, grounded copper plate; H, rubber sheet.

Can. J. Chem. Downloaded from www.nrcresearchpress.com by 210.87.254.6 on 09/05/12
For personal use only.

The chemically purified and degassed hydrocarbon was electrolyzed for several hours between platinum electrodes, with fields up to 5 kV/cm. The liquid was then transferred to the radiolysis cell; if its conductance was greater than 10^{-14} mho at 200 V/cm, it was transferred back to the electrolysis cell for further purification. The liquid was transferred back and forth between the electrolysis and radiolysis cells by a special device (4), to prevent contamination. When the sample in the radiolysis cell had a sufficiently low intrinsic conductance, an atmosphere of dry argon was allowed into the vacuum manifold. The cell was removed and the needle valve screw closure inserted whilst maintaining an argon atmosphere around the cell.

The cell current, in the presence and absence of radiation, was measured as a function of voltage up to a maximum of 500 V. The pressure was then changed to a new value and the system was allowed to sit for at least 20 min before taking the new conductance measurements.

Measurements were made during both the pressure increasing and the pressure decreasing parts of the cycle. If the conductance values obtained at atmospheric pressure were different before and after the pressure cycle, the cycle was repeated. The "before" and "after" readings were different if there had been a shift in the position of the closure piston before it became tightly seated.

Results

At all pressures and temperatures employed in the present work, a linear relationship was found between the cell current and the applied voltage. Typical results are shown in Fig. 4. The plots exhibited voltage intercepts that varied in a non-reproducible manner between 0.5 and 10 V. The non-zero intercepts were probably due to induced currents in the cables and to contact potentials, and had been noted earlier (5, 6). The conductance of the sample was taken from the slope of the current–voltage plot. The radiation induced conductance was assumed to be equal to the difference between the conductances measured in the presence and absence of radiation.

In general, the induced conductance decreased with increasing pressure. A typical plot is shown in Fig. 5.

In order to correlate the results obtained under different conditions, the relative conductance is used: the relative conductance is the ratio of the conductance at pressure p to that at 1 bar, at the same temperature.

Within the $\pm 3\%$ experimental error, the relative conductance was independent of electrode separation (2–10 mm) and of dose rate (1–6 $\times$ 10^{14} eV/cm^3 s) for all the hydrocarbons studied.

The induced conductances of all the hydrocarbons except 2,2-dimethylbutane were independent of the absorbed dose. The induced conductance of 2,2-dimethylbutane varied in a peculiar fashion with absorbed dose (Fig. 6).

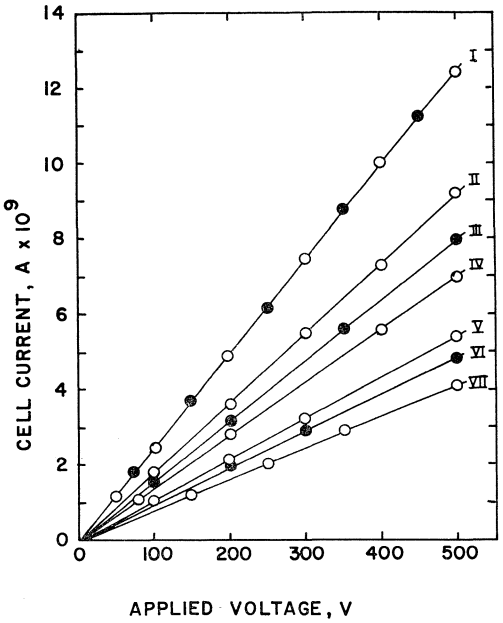

FIG. 4. Cell current vs. applied voltage in hexane at 30 °C. Electrode spacing 3.2 mm; dose rate 4.3 $\times$ 10^{14} eV/cm^3 s. I–VII results at pressures of 1, 747, 1140, 1600, 2690, 3450, and 4068 bars, respectively. Open points, pressure increasing cycle; closed points, pressure decreasing cycle.

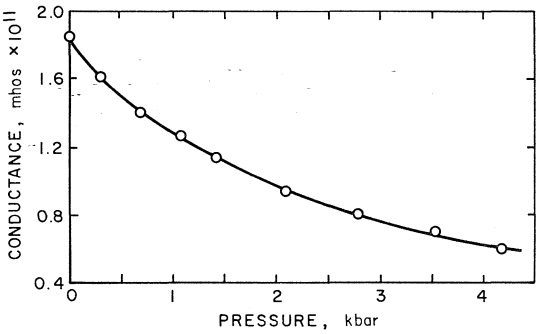

FIG. 5. Conductance vs. pressure in hexane at 30 °C. Electrode spacing 2 mm; dose rate 1.5 $\times$ 10^{14} eV/cm^3 s.

The relative induced conductances of n-hexane and n-octane were measured up to 4000 bars at each of the temperatures 3, 30, and 56°, and the results are recorded in Table I. Each number in the Table is the average of several results obtained with different electrode spacings and at different

TABLE I

Relative induced conductances of *n*-hexane and *n*-octane at 3, 30, and 56 °C

Pressure (bar)	Relative induced conductance					
	n-Hexane			*n*-Octane		
	3°	30°	56°	3°	30°	56°
1	1.00	1.00	1.00	1.00	1.00	1.00
500	0.82	0.82	0.81	0.77	0.79	0.81
1000	0.70	0.69	0.69	0.64	0.66	0.67
1500	0.61	0.60	0.60	0.54	0.57	0.58
2000	0.53	0.53	0.53	0.45	0.48	0.51
2500	0.47	0.48	0.48	0.39*	0.43	0.45
3000	0.42	0.42	0.43	—	0.37	0.39
3500	0.38	0.38	0.40	—	0.32	0.33
4000	0.34	0.35	0.37	—	0.29	0.31

*Freezes above 2500 bars.

dose rates. The relative conductances are essentially independent of temperature. The value for *n*-octane decreases slightly more rapidly with pressure than does that for *n*-hexane.

The relative induced conductances of *n*-pentane, cyclopentane, methylcyclohexane, and 2,2-dimethylbutane up to 4000 bars at 30° are given in Table II. The tabulated values are the averages obtained from several experiments. Methylcyclohexane shows a greater pressure effect than does either *n*-pentane or cyclopentane. The conductance of 2,2-dimethylbutane was dose dependent at doses below 2×10^{19} eV/cm^3 (Fig. 6), so two sets of values are included for this compound in Table II. The first set corresponds to the average of the values obtained during the pressure increasing and pressure decreasing parts of a cycle, starting with a fresh sample. During this experiment the sample received a dose of about 1.4×10^{18} eV/cm^3. The second set was obtained from a sample that had previously been irradiated to 3.8×10^{19} eV/cm^3, and the conductance had become independent of the dose (see Fig. 6). The pressure effect was somewhat greater for the high than for the low dose sample (Table II).

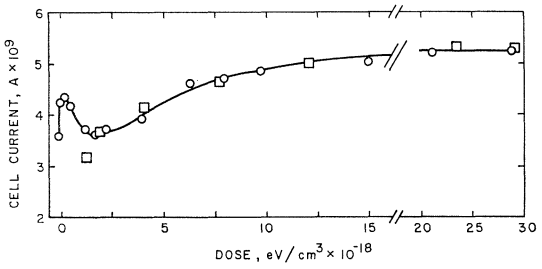

FIG. 6. Dose dependence of current in 2,2-dimethylbutane at 30 °C: dose rate, 4.2×10^{14} eV/cm^3 s; field strength, 260 V/cm; ○, fresh sample; □, after 1.4×10^{18} eV/cm^3 irradiation during a pressure cycle up to 4000 bars.

Discussion

The free ion yield G_{fi} in a liquid under irradiation is related to the induced conductance κ by the following equation (5, 7).

$$[1] \qquad G_{fi} = \frac{100k\kappa^2}{Ru^2}$$

where k is the ion neutralization rate constant (cm^3/ion s), R is the absorbed radiation dose rate (eV/cm^3 s), and u is the sum of the positive and negative ion mobilities (cm^2/V s). The appropriate units for κ in eq. [1] are ion/cm V s.

One can show from equations presented earlier (5, 7) that, theoretically,

$$[2] \qquad k/u = 1.81 \times 10^{-6}/\varepsilon \quad \text{V/cm}$$

where ε is the dielectric constant of the liquid. Hence,

$$[3] \qquad G_{fi} = \frac{1.81 \times 10^{-4}\kappa^2}{Ru\varepsilon}$$

The yield of free ions at pressure p, $G_{fi}{}^p$, is related to the yield at 1 bar, $G_{fi}{}^1$, by eq. [4].

$$[4] \qquad \frac{G_{fi}{}^p}{G_{fi}{}^1} = \frac{R_1u_1\varepsilon_1}{R_pu_p\varepsilon_p}\left(\frac{\kappa_p}{\kappa_1}\right)^2$$

Can. J. Chem. Downloaded from www.nrcresearchpress.com by 210.87.254.6 on 09/05/12
For personal use only.

TABLE II

Relative induced conductance of *n*-pentane, cyclopentane, methylcyclohexane, and 2,2-dimethylbutane at 30°

Pressure (bar)	Relative induced conductance				
	n-Pentane	Cyclopentane	Methylcyclohexane	2,2-Dimethylbutane	
1	1.00	1.00	1.00	1.00*	1.00†
500	0.79	0.82	0.76	0.80*	0.68†
1000	0.68	0.72	0.63	0.67*	0.51†
1500	0.59	0.63	0.53	0.57*	0.38†
2000	0.53	0.56	0.45	0.48*	0.31†
2500	0.48	0.51	0.38	0.41*	0.25†
3000	0.44	0.45	0.33	0.35*	0.23†
3500	0.41	0.41	0.29	0.30*	0.21†
4000	0.38	0.38	0.23	0.26*	0.19†

*Fresh sample.
†High dose sample (see text).

However, the dose rate is directly proportional to the density ρ of the liquid, so one may write

$$[5] \qquad \frac{G_{fi}{}^{p}}{G_{fi}{}^{1}} = \frac{\rho_1 u_1 \varepsilon_1}{\rho_p u_p \varepsilon_p}\left(\frac{\kappa_p}{\kappa_1}\right)^2$$

The pressure dependences of the densities and dielectric constants of the liquids used in the present work are reported elsewhere (3).

The pressure dependences of the radiolytic ion mobilities are not known, and there is conflicting evidence about the relationship between the ion mobilities and the liquid viscosity η at atmospheric pressure (8, 9). Therefore, two sets of calculations were done to answer the following questions: (*a*) if the ion mobilities obey the Stokes–Walden relationship,

$$[6] \qquad u_1/u_p = \eta_p/\eta_1$$

how does the value of G_{fi} change with pressure; (*b*) if G_{fi} is independent of pressure, how do the ion mobilities vary with pressure?

(a) Assume that the Stokes–Walden Relationship is Obeyed

Then,

$$[7] \qquad \frac{G_{fi}{}^{p}}{G_{fi}{}^{1}} = \frac{\rho_1 \eta_p \varepsilon_1}{\rho_p \eta_1 \varepsilon_p}\left(\frac{\kappa_p}{\kappa_1}\right)^2$$

The pressure dependence of η is reported elsewhere (3), along with those of ρ and ε.

The dependence of G_{fi} on pressure, as calculated from eq. [7], is illustrated in Fig. 7 for all the hydrocarbons studied except 2,2-dimethylbutane. In every instance, G_{fi} decreases with increasing pressure. The decrease at 4000 bars amounts to 33% for *n*-pentane and *n*-hexane, 30% for *n*-octane, and about 20% for the two cyclic hydrocarbons, all at 30°. The curves of $G_{fi}{}^{p}/G_{fi}{}^{1}$ for *n*-hexane at 3 and 56° are also shown in Fig. 7. The variation with temperature is small.

The induced conductance of 2,2-dimethylbutane was dose dependent at low doses, but became independent of dose above about 2×10^{19} eV/cm^3 (Fig. 6). In a low dose sample, the apparent value of $G_{fi}{}^{p}/G_{fi}{}^{1}$ increased at first with increasing pressure, then went through a maximum (Fig. 8). This behavior is probably associated with the dose dependence of the conductance. In a high dose sample (3.8×10^{19} eV/cm^3), the apparent value of $G_{fi}{}^{p}/G_{fi}{}^{1}$ decreased at first with increasing pressure and passed through a minimum at 2500 bars. The viscosity of this liquid increased abnormally rapidly with pressure (3), so the complex behavior displayed by the high dose curve in Fig. 8 may represent changes in the liquid structure.

(b) Assume that G_{fi} is Independent of Pressure

The mobilities of positive and negative radiolytic ions have been measured at atmospheric pressure in many hydrocarbon liquids with widely different viscosities (8, 9). The viscosity dependences of the mobilities were expressed in the form

$$[8] \qquad u_+ = a_+ \eta^{-b_+}$$

$$[9] \qquad u_- = a_- \eta^{-b_-}$$

where a_+, a_-, b_+, and b_- are constants. The Stokes–Walden relationship corresponds to $b_+ = b_- = 1.0$. The reported values of b_+ lie between 1.5 (8) and 0.94 (10), whereas those of b_- are between 1.00 (8) and 0.83 (9). Thus, in the

Can. J. Chem. Downloaded from www.nrcresearchpress.com by 210.87.254.6 on 09/05/12
For personal use only.

Can. J. Chem. Downloaded from www.nrcresearchpress.com by 210.87.254.6 on 09/05/12
For personal use only.

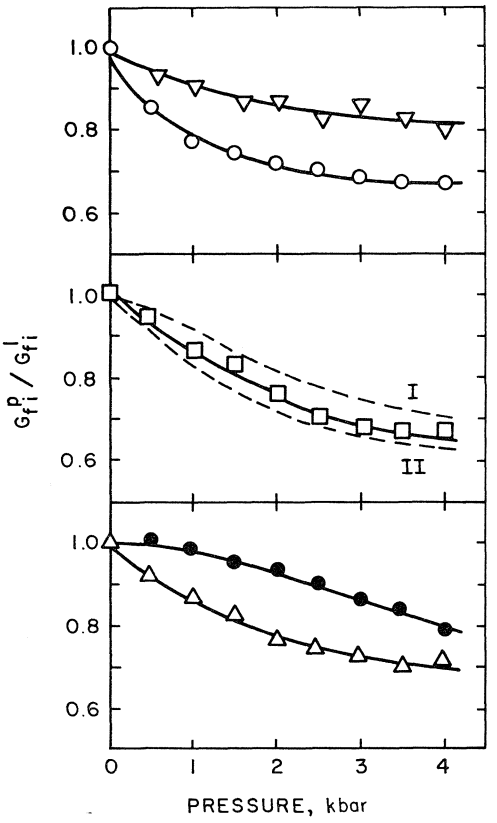

FIG. 7. $G_{fi}{}^{p}/G_{fi}{}^{1}$ vs. pressure. Temperature 30° unless otherwise specified: ○, *n*-pentane; ▽, methylcyclohexane; □, *n*-hexane (line I, 3°; line II, 56°); ●, cyclopentane; △, *n*-octane. Dose rate range 1–6 × 10^{14} eV/cm^3 s.

majority of cases the Stokes–Walden rule does not accurately correlate the mobilities of radiolytic ions in different liquids at atmospheric pressure.

We now assume that

$$[10] \qquad u = u_+ + u_- = a\eta^{-b}$$

then assume that G_{fi} is independent of pressure and calculate the value of b that is required to fit the results at different pressures. The relationship used is

$$[11] \qquad \left(\frac{\eta_p}{\eta_1}\right)^b = \frac{\rho_p\varepsilon_p}{\rho_1\varepsilon_1}\left(\frac{\kappa_1}{\kappa_p}\right)^2$$

and the values of η, ρ, and ε are taken from ref. 3. The pressure dependences of the power b for all the hydrocarbons used except 2,2-dimethylbutane are shown in Fig. 9. The value of b is 1.2 at all pressures above 1 kbar in *n*-hexane and *n*-octane. In *n*-pentane b decreases from 1.4 at 0.5 kbar to 1.2 at 4 kbar; in cyclopentane b increases from 1.0 to 1.1, while in methylcyclohexane it decreases from 1.2 to 1.1 over this pressure range.

The variation of b with pressure in 2,2-dimethylbutane, assuming G_{fi} to be independent of pressure, is shown in Fig. 10. For the low dose sample, b appeared to vary between 0.8 and 1.0, whereas for the high dose sample b varied between 1.2 and 1.5 with a maximum at about 2 kbar.

In all the compounds studied, the values of b are within the range of values previously obtained from measurements at atmospheric pressure. Although it is not necessary that the value of b obtained by varying the pressure on a given liquid would be the same as that obtained from a series of compounds with different viscosities at atmospheric pressure, it appears that G_{fi} in liquid hydrocarbons is not greatly dependent on the pressure, up to 4000 bars.

(c) Nonhomogeneous Kinetics Model Calculations

By assuming that the electron ranges in a liquid at different pressures are simply inversely proportional to the liquid density, one can calculate the variation of G_{fi} with pressure that is predicted by our nonhomogeneous kinetics model (2*b*, 11). The required values of the densities and dielectric constants are given in ref. 3.

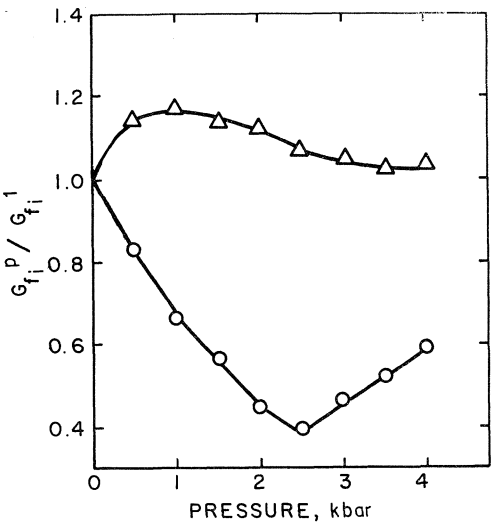

FIG. 8. $G_{fi}{}^{p}/G_{fi}{}^{1}$ vs. pressure in 2,2-dimethylbutane at 30 °C: electrode spacing, 3.9 mm; dose rate, 4.2 × 10^{14} eV/cm^3 s; △, low dose sample; ○, high dose sample (see text).

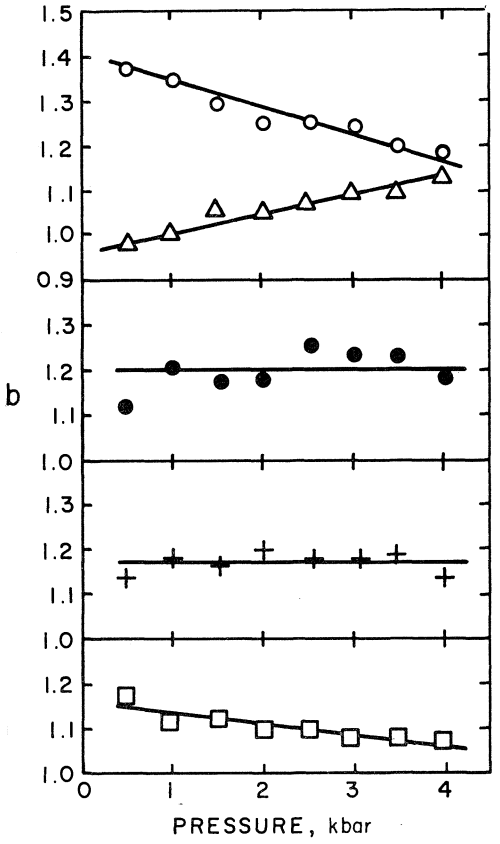

FIG. 9. Power b vs. pressure at 30 °C: ○, n-pentane; △, cyclopentane; ●, n-hexane; +, n-octane; □, methylcyclohexane.

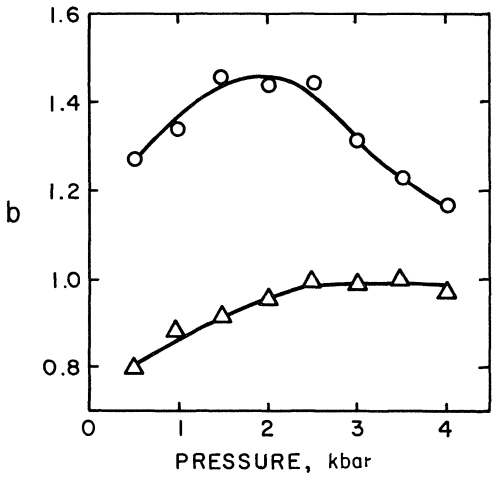

FIG. 10. Pressure dependence of b in 2,2-dimethylbutane at 30 °C. △, low dose sample; ○, high dose sample.

The model calculations for n-hexane give the result that G_{fi} at 4000 bars is 6% smaller than at 1 bar. The estimated variation of G_{fi} is small because the effect of the increasing density, and hence the decreasing electron range, is nearly cancelled by the effect of the increasing dielectric constant. The same is true of the other hydrocarbons.

Comments and Conclusions

1. The free ion yield in liquid hydrocarbons may remain constant or it may decrease somewhat as the pressure is increased from 1 to 4000 bars. An appreciable *increase* in the yield, which is a possible implication of the cavity model of electron localization, does not occur.

2. Either (*a*) the cavity model of electron localization is wrong, or (*b*) compression of the liquids by a pressure of 4000 bars did not appreciably alter the cavity concentrations. The molar volumes of the hydrocarbons at 4000 bars are about 20% smaller than those at 1 bar (3), and most of this contraction should correspond to a decrease in the "free volume" of the liquids. Thus the sizes of the cavities should be smaller at 4000 bars than those at 1 bar, but the decrease in size may not have been great enough to affect the electron capture cross sections of the cavities beyond the present limits of detection. Furthermore, if the compressibility of the cavities is about the same as that of the average free volume, the cavity concentration would not be greatly reduced by pressure until the pressure was great enough to cause a change of phase, i.e. to cause glass formation or crystallization. Unfortunately, the present conductance technique is not applicable to solid phase samples, because the ion mobilities are too low in solids.

3. The complex behavior of 2,2-dimethylbutane is not understood.

Acknowledgments

This work received financial assistance from the National Research Council of Canada. The assistance of E. B. Cairns of the Radiation Research Center with the electronic equipment and of R. G. Cox of the Chemistry Department with the construction of the pressure systems is gratefully acknowledged.

Can. J. Chem. Downloaded from www.nrcresearchpress.com by 210.87.254.6 on 09/05/12
For personal use only.

1. G. R. FREEMAN. *In* Radiation research. *Edited by* G. Silini. Interscience Publishers, Inc., New York. 1967. p. 113.
2. (*a*) F. WILLIAMS. J. Am. Chem. Soc. **86**, 3954 (1964). (*b*) G. R. FREEMAN and J. M. FAYADH. J. Chem. Phys. **43**, 86 (1965).
3. D. W. BRAZIER and G. R. FREEMAN. Can. J. Chem. This issue.
4. D. BRAZIER. Ph.D. Thesis, University of Alberta, Edmonton, Alberta. 1968.
5. A. O. ALLEN and A. HUMMEL. Discussions Faraday Soc. **36**, 95 (1963).
6. G. R. FREEMAN. Discussions Faraday Soc. **36**, 250 (1963).
7. G. R. FREEMAN. J. Chem. Phys. **39**, 988 (1963).
8. I. ADAMCZEWSKI. Brit. J. Appl. Phys. **16**, 759 (1965).
9. I. ADAMCZEWSKI and B. JACHYM. Acta Phys. Polon. **30**, 767 (1967).
10. P. H. TEWARI and G. R. FREEMAN. J. Chem. Phys. **49**, 4934 (1968).
11. G. R. FREEMAN. J. Chem. Phys. **46**, 2822 (1967).

Downloaded from www.nrcresearchpress.com by 210.87.254.6 on 09/05/12
For personal use only.

The effects of pressure on the density, dielectric constant, and viscosity of several hydrocarbons and other organic liquids

D. W. Brazier and G. R. Freeman
Chemistry Department, University of Alberta, Edmonton, Alberta
Received September 26, 1968

The effects of pressures up to 4 kbar on the density, dielectric constant, and viscosity of *n*-pentane, *n*-hexane, *n*-octane, cyclopentane, methylcyclohexane, and 2,2-dimethylbutane (DMB) were measured at 30 °C. The pressure effects on the viscosities of *n*-hexane and *n*-octane were also determined at 0 and 60°. The densities of diethyl ether and cyclopentanone and the dielectric constant of carbon tetrachloride at high pressures are also recorded. The densities of the hydrocarbons increased by 20–30% and the dielectric constants increased by 11–16% as the pressure was increased from 1 to 4000 bars at 30°, but the viscosities increased by 695–2352% over the same pressure range. Carbon tetrachloride froze at 1500 bars at 30°, and cyclopentanone froze at 3500 bars at about 20°. In agreement with earlier work on other liquids, the value of the Clausius–Mosotti function $(\varepsilon - 1)V/(\varepsilon + 2)$ for the present compounds decreased slightly with increasing pressure. The viscosity at a given pressure decreased slightly with increasing temperature, and temperature effect increased with increasing pressure. In general, the smaller the compressibility of the liquid, the greater was the effect of pressure on the viscosity; DMB was an exception because its viscosity increased abnormally rapidly with pressure. Molecular structure and liquid structure have greater influences on the pressure dependence of viscosity than on that of density or dielectric constant.

Canadian Journal of Chemistry, **47**, 893 (1969)

Can. J. Chem. Downloaded from www.nrcresearchpress.com by 210.87.254.42 on 09/05/12
For personal use only.

Introduction

As part of an investigation of the effect of pressure on the radiation induced conductance of liquid hydrocarbons (1), it was necessary to measure the variation of the density, dielectric constant, and viscosity of the liquids. The hydrocarbons used in the conductance study were *n*-pentane, *n*-hexane, *n*-octane, cyclopentane, methylcyclohexane, and 2,2-dimethylbutane. These and several other compounds were used in the present work. Values of pressure coefficients of physical properties of many liquids have been reported earlier (2–9).

Experimental

High Pressure System

The high pressure system is described briefly in ref. 1 and in detail in ref. 10. The pressure vessel temperature was controlled to within ±0.5° over the range 0–60 °C.

Materials

The *n*-pentane, *n*-hexane, *n*-heptane, *n*-octane, *n*-decane, cyclopentane, methylcyclohexane, and 2,2-dimethylbutane were Phillips Research Grade and were purified as described earlier (1). Phillips Research Grade benzene was purified by repeated partial recrystallization. Eastman Spectroscopic Grade carbon tetrachloride and diethyl ether were used as supplied. Dodecane, tetradecane (both from Eastman Organic Chemicals), and octadecane (Matheson, Coleman and Bell) were also used as supplied. Eastman White Label cyclopentanone was distilled twice through a 45 cm column packed with glass helices, retaining the middle 50% each time.

A series of viscometric standard oils, which were mixtures of high boiling straight chain hydrocarbons, were obtained from the Cannon Instrument Co. This company also supplied the precalibrated Ubbelohde viscometers. Silicone oils from Dow Corning Co. were also used during the calibration of the rolling ball viscometer. The viscosities of the silicone oils were measured with the Ubbelohde viscometers.

Density Measurements

The change of liquid volume with pressure was measured using a bellows dilatometer (3, 11). A detailed description of the apparatus is given elsewhere (10). The internal volume of the dilatometer was 20 ml. The change of volume of the bellows was measured with a slide wire, using the potential ratio technique (11). The dilatometer operation was calibrated at atmospheric pressure, using a special apparatus (10).

Dielectric Constant Measurements

The dielectric constants of the hydrocarbons were measured at pressures up to 4 kbar in the cell shown in Fig. 1. Pressure was transmitted to the cell interior by a teflon piston and cylinder of the type described by Jamieson (12). The leads from the cylindrical platinum electrodes through the Supramica plug (Fig. 1) were cemented with Armstrong Epoxy Resin cement. Samples of the latter cement, cured for 4 days at 80°, were placed in contact with the hydrocarbon liquids for 4 months and no change in the dielectric constants of the liquids was observed.

Capacitance measurements were made with a General Radio Impedence Bridge, Model 1608-A. The bridge was calibrated with an accuracy of ±0.02 pF. The capacitance measurements were conducted at 1 kc. The total system capacitance at 30° and atmospheric pressure was determined with a series of standard dielectrics between the cell plates. The standards used were air ($\varepsilon = 1.0005$),

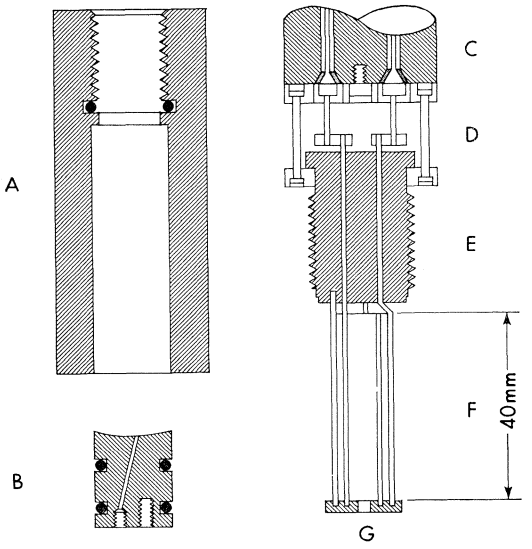

FIG. 1. Dielectric constant cell (not to scale): A, teflon cylindrical cell walls; B, teflon piston with "O" ring seals; C, pressure vessel closure piston; D, stainless steel and teflon cell holder; E, Supramica Ceramoplastic plug; F, cylindrical platinum electrodes (0.25 mm thick); G, teflon cap.

cyclohexane ($\varepsilon = 2.023$), carbon tetrachloride ($\varepsilon = 2.239$), benzene ($\varepsilon = 2.274$), and diethyl ether ($\varepsilon = 4.335$). The total capacitances at atmospheric pressure ranged from 40 to 70 pF. A calibration graph was plotted of total capacitance vs. dielectric constant of the liquid in the cell.

Viscosity Measurement

A rolling ball viscometer (13, 14) was used to measure the viscosities of the liquids at pressures up to 4 kbar. The principle of operation was to measure the amount of time required for a ball to roll a given distance down a tilted tube full of liquid. A steel ball, 6.35 mm diameter, and a precision bore quartz tube, 7.99 ± 0.01 mm internal diameter, were used. The roll tube with ball-detector coils is illustrated in Fig. 2. The roll tube was inserted in a tiltable pressure vessel.

Full details of the viscometer construction and operation are given elsewhere (10). Briefly, the roll tube and detector device were placed within a cylindrical stainless steel holder that contained a bellows section for the transmission of pressure. Electrical connections to the interior of the holder, through end plate H (Fig. 2), were made with Latronics Corp. metal to ceramic terminal seals. The detector coils, in slots E, were each 100 turns of 30 gauge magnet wire (Belden Wire Co.). The coils were wound in series.

The electrical circuit and timing device used in conjunction with the detector coils are described in ref. 10. The time required for the ball to roll between the two detector coils was measurable with a precision of ±0.3%.

All the components of the viscometer and holder were cleaned in a Soxhlet extractor before being assembled. The solvent used was either hexane or the hydrocarbon to be investigated. Soldered components underwent a preliminary extraction with water.

The assembled viscometer and holder were tested for leaks on a vacuum line, then filled by a technique similar to that used for the filling of the conductance cells (10).

The viscometer was calibrated with a series of liquids of known viscosity. The calibration plot for 30 °C is shown in Fig. 3. The variables of the system were correlated with the expression (14)

$$[1] \qquad \eta = \kappa(\rho_S - \rho_L)t$$

where η is the viscosity, κ is the viscometer coefficient, ρ_S and ρ_L are the densities of the ball and the liquid, respectively, and t is the roll time. The variation of ρ_S with

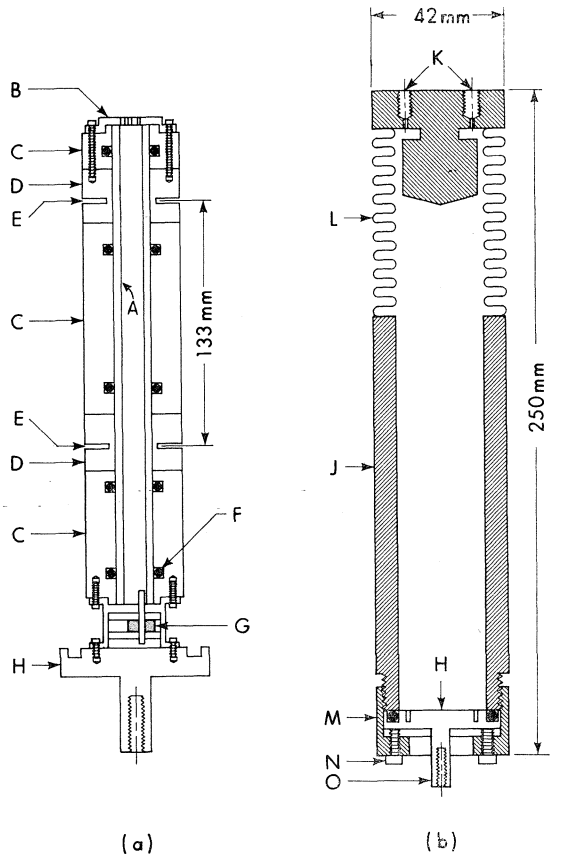

FIG. 2. (*a*) Viscometer roll tube assembly (not to scale): A, quartz roll tube; B, perforated cap; C, aluminium cylinder section, slotted on the outside to allow liquid to flow to the bottom of the cell holder; D, Lucite detector coil bobbin; E, detector coil slot; F, "O" ring; G, electromagnet; H, stainless steel base plate.

(*b*) Viscometer roll tube holder (not to scale): Constructed of stainless steel; H, base plate; J, cylinder; K, filling apertures in cap, to be closed by needle valve type screws; L, bellows; M, compression screw cap; N, compression screw (8 in all); O, tapped stem, to fix viscometer to pressure vessel closure piston.

Can. J. Chem. Downloaded from www.nrcresearchpress.com by 210.87.254.42 on 09/05/12
For personal use only.

TABLE I

Pressure dependences of relative volumes of several hydrocarbons at 30 °C

Pressure (bars)	Relative volume						
	n-Pentane	*n*-Hexane	*n*-Heptane	*n*-Octane	Cyclo-pentane	Methyl-cyclohexane	2,2-Dimethyl-butane*
1	1.000	1.000	1.000	1.000	1.000	1.000	1.000
500	0.930	0.941	0.945	0.953	0.947	0.956	0.935
1000	0.889	0.905	0.909	0.921	0.914	0.928	0.900
1500	0.859	0.877	0.882	0.898	0.888	0.906	0.872
2000	0.836	0.858	0.863	0.879	0.867	0.888	0.853
2500	0.821	0.841	0.848	0.863	0.850	0.872	0.837
3000	0.804	0.826	0.834	0.848	0.837	0.858	0.823
3500	0.791	0.814	0.823	0.837	0.825	0.846	0.812
4000	0.778	0.803	0.813	0.827	0.815	0.836	0.802
4500	0.767	0.796	—	—	0.807	0.828	—
Molar volume (cm^3) at 1 bar	117.03	132.46	148.38	164.53	95.32	129.08	134.9
Density (g/cm^3) at 1 bar	0.6165	0.6505	0.6753	0.6942	0.7357	0.7606	0.639

*Estimated from data in ref. 3.

pressure and temperature was negligible; $\rho_S = 7.78 \pm 0.02$ g/cm³ under all conditions used. Values of ρ_L were taken from Table I.

The variation of $(\rho_S - \rho_L)t$ with η was determined at several temperatures in the range 0–60 °C for each of the two angles of inclination. The values of $(\rho_S - \rho_L)t$ plotted in Fig. 3 were obtained for 30 °C by graphical interpolation. Similar plots were made for 0 and 60 °C. The values of η were taken from ref. 15 or were measured with an Ubbelohde viscometer. All of the standards used, except the two cyclic hydrocarbons, fell on a smooth curve at each temperature (Fig. 3). The cause of the deviation of the cyclic compounds is unknown, but it may have to do with an effect of liquid structure on eddy currents. The flow of liquid past the ball in the tube was probably turbulent, indicated by the fact that the value of κ was viscosity dependent under the present conditions (see ref. 14).

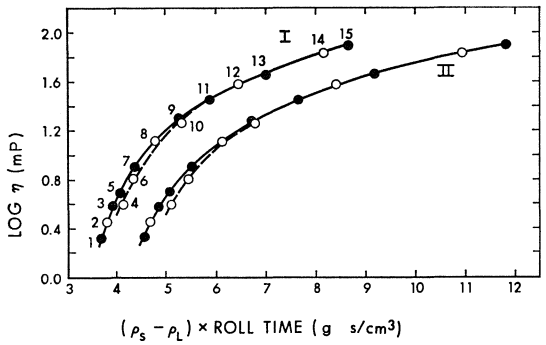

FIG. 3. Viscometer calibration plot, 30 °C: I, 30° angle of inclination; II, 20° angle. The liquids used were: *1*, *n*-pentane; *2*, *n*-hexane; *3*, 2,2-dimethylbutane; *4*, cyclopentane; *5*, *n*-octane; *6*, methylcyclohexane; *7*, *n*-decane; *8*, *n*-dodecane; *9*, *n*-tetradecane; *10*, Dow silicone oil (2 cts); *11*, Cannon standard oil S3; *12*, *n*-octadecane; *13*, Dow silicone oil (5 cts); *14*, Cannon standard oil S6; *15*, Dow silicone oil (10 cts).

The viscosities of the hydrocarbons under pressure at 30 °C were obtained by evaluating $(\rho_S - \rho_L)t$ and reading the corresponding values of log η from Fig. 3. It was assumed that the calibration plot obtained at atmospheric pressure was valid at higher pressures, the change in the roll time arising only from the increased viscosity. This assumption is reasonable because the dimensions of the ball and of the roll tube were reduced by only 0.1 and 0.3%, respectively, at 4.5 kbar.

Results and Discussion

Pressure Dependence of Density

The pressure–volume relationships were determined for *n*-pentane, *n*-hexane, *n*-heptane, *n*-octane, cyclopentane, and methylcyclohexane at 30° and pressures up to 4.5 kbar. The results are reported as relative volumes, i.e. the ratio of the volume at pressure p to that at 1 bar, and are listed in Table I. The absolute densities and molar volumes at 1 bar are also given.

There was no hysteresis in the measurements. The value of the potential ratio obtained from the dilatometer at atmospheric pressure after a pressure cycle agreed with the value obtained before the pressure was applied, to within 0.1%. At least two runs were done for each compound, and the results were averaged. The reproducibility of the relative volumes measured from one experiment to the next was ±0.25% at 4000 bars, and was better at lower pressures.

Can. J. Chem. Downloaded from www.nrcresearchpress.com by 210.87.254.42 on 09/05/12
For personal use only.

Can. J. Chem. Downloaded from www.nrcresearchpress.com by 210.87.254.42 on 09/05/12
For personal use only.

TABLE II

Pressure dependences of relative volumes of diethyl ether and cyclopentanone

Pressure (bars)	Relative volume: Diethyl ether (30°)	Relative volume: Cyclopentanone (25°)
1	1.000	1.000
500	0.939	0.964
1000	0.893	0.938
1500	0.866	0.899
2000	0.842	0.884
2500	0.824	0.872
3000	0.811	0.860
3500	0.799	0.850
4000	0.786	0.841
Molar volume (cm^3) at 1 bar	105.61	89.2
Density (g/cm^3) at 1 bar	0.7018	0.943

Pressure–volume measurements on 2,2-dimethylbutane were not done. The relative volumes of this compound at 30° at different pressures were estimated graphically from Bridgman's data (3), and are listed in Table I.

Table II lists the relative volumes measured for diethyl ether at 30° and cyclopentanone at 25°. These measurements are related to other studies in this laboratory. It was also noted that if the temperature of cyclopentanone at 3500 bars was lowered to 20°, the sample froze. This tends to support the interpretation (16) that the rapid decrease in the radiation yield of isomerization of cyclopentanone to 4-pentenal, as the pressure was increased from 3000 to 5000 bars at about 25°, was due to the solidification of the sample.

Where comparison with other literature values is possible (3, 5, 6), the present results agree with them to within 0.2%. The only exception was *n*-pentane, for which the present result at 4 kbar was 1% higher than that estimated graphically from Bridgman's data at 0, 50, and 95° (3).

Pressure Dependence of Dielectric Constant

The total capacitance of the system was determined as a function of pressure with a given liquid in the cell, and the dielectric constant was read directly from the calibration graph. The sensitivity of the system was approximately 10 pF per unit change in dielectric constant. The agreement between the total capacitance values before and after a pressure cycle was usually within 0.5%, unless a phase change had occurred. The cell became distorted if the sample froze in it. The change in cell capacitance caused by the decrease in the electrode dimensions with increasing pressure amounted to an error of 0.06% in the measured capacitance at 4 kbar. This was calculated using the volume compressibility of platinum, which is (2)

$$[2] \qquad \beta = 3.6 \times 10^{-7} - 3.6 \times 10^{-12} p$$

where p is the pressure in kg/cm^2 (1 bar = 1.02 kg/cm^2).

Values of the relative dielectric constant, i.e. the

TABLE III

Pressure dependences of relative dielectric constants at 30°

Pressure (bars)	Relative dielectric constants: *n*-Pentane	*n*-Hexane	*n*-Octane	Cyclopentane	Methylcyclohexane	2,2-Dimethylbutane	Carbon tetrachloride
1	1.000	1.000	1.000	1.000	1.000	1.000	1.000
500	1.045	1.036	1.026	1.037	1.028	1.039	1.034
1000	1.074	1.060	1.047	1.060	1.047	1.068	1.055
1500	1.096	1.078	1.064	1.079	1.063	1.087	1.069§
2000	1.114	1.094	1.077	1.094	1.074	1.102	—
2500	1.129	1.107	1.087	1.108	1.089	1.116	—
3000	1.142	1.118	1.096	1.121	1.099	1.128	—
3500	1.153	1.129	1.106	1.133	1.108	1.139	—
4000	1.163	1.138	1.113	1.144	1.116	1.149	—
Dielectric constant* at 1 bar	1.83†	1.875†	1.935‡	1.96†	2.01†	1.86†	2.217†

*Estimated from reported values or from the square of the refractive index. The latter values are reported to only three significant figures. The source references are cited.
†See ref. 21.
‡See ref. 22.
§Freezes at 1500 bars at 30°; see ref. 23.

TABLE IV

Pressure dependence of relative viscosity of *n*-hexane and *n*-octane

Pressure (bars)	Relative viscosity					
	n-Hexane			*n*-Octane		
	0°	30°	60°	0°	30°	60°
1	1.00	1.00	1.00	1.00	1.00	1.00
500	1.63	1.58	1.61	1.70	1.62	1.56
1000	2.20	2.18	2.24	2.43	2.26	2.23
1500	2.91	2.81	2.82	3.30	3.12	2.95
2000	3.67	3.44	3.45	4.38	4.09	3.73
2500	4.54	4.35	4.17	6.25*	5.28	4.62
3000	5.70	5.30	4.98	—	6.83	5.79
3500	7.01	6.47	5.69	—	8.85	7.58
4000	8.63	7.75	6.82	—	11.64	9.95
η(cP) at 1 bar	0.381	0.285	0.223	0.712	0.487	0.359

*Freezes above 2500 bars.

ratio of the dielectric constant at pressure p to that at 1 bar, are listed for *n*-pentane, *n*-hexane, *n*-octane, cyclopentane, methylcyclohexane, 2,2-dimethylbutane, and carbon tetrachloride at 30° in Table III. The absolute values of the dielectric constant at atmospheric pressure are also given.

The present results for *n*-pentane and *n*-hexane agree with those of earlier workers (8, 9). Our values of the relative dielectric constant at 30° and 2 kbar for *n*-pentane and *n*-hexane are 1.114 and 1.094, respectively, whereas those estimated from the literature are 1.113 (8) and 1.096 (9), respectively.

The Clausius–Mosotti (C.M.) function is

$$[3] \qquad \frac{\varepsilon - 1}{\varepsilon + 2} V = \frac{4}{3}\pi N\alpha$$

where ε is the dielectric constant, V is the molar volume of the liquid, N is Avogadro's number, and α is the molecular polarizability. This function is frequently used to describe the relationship between the molar volume, or density, and the dielectric constant of a medium. It is usually assumed that the C.M. function is independent of the density of the medium, but plots of the left-hand side of eq. [3] against the densities of liquids at high pressures have slightly negative slopes (see Fig. 4 and refs. 2, 7–9). Two possible explanations of the negative slope are (*a*) that the form of the C.M. function is incorrect at high densities (17), and (*b*) that the molecular polarizabilities decrease with increasing pressure (18, 19). Both (*a*) and (*b*) may contribute to the observed effect.

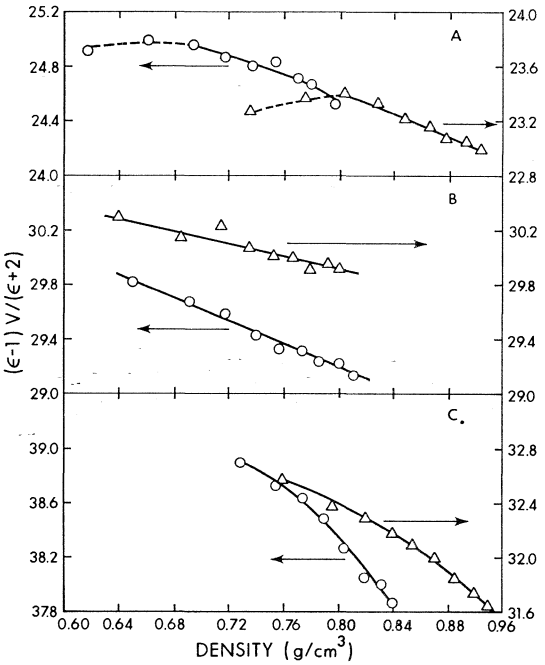

FIG. 4. Clausius–Mosotti function plotted against density at 30 °C. A: ○, *n*-pentane; △, 2,2-dimethylbutane. B: ○, *n*-hexane; △, cyclopentane. C: ○, *n*-octane; △, methylcyclohexane; ○, left hand scale; △, right hand scale.

Pressure Dependence of Viscosity

The relative viscosities, i.e. values of the ratio of the viscosity at pressure p to that at 1 bar at the same temperature, of *n*-hexane and *n*-octane at 0, 30, and 60 °C are listed in Table IV. The relative viscosity increased greatly as the pressure was

Can. J. Chem. Downloaded from www.nrcresearchpress.com by 210.87.254.42 on 09/05/12
For personal use only.

TABLE V

Pressure dependence of relative viscosity of *n*-pentane, cyclopentane, methylcyclohexane, and 2,2-dimethylbutane at 30°

Pressure (bars)	Relative viscosity			
	n-Pentane	Cyclopentane	Methylcyclohexane	2,2-Dimethylbutane
1	1.00	1.00	1.00	1.00
500	1.53	1.64	1.67	2.00
1000	2.08	2.36	2.50	3.03
1500	2.73	3.00	3.59	4.44
2000	3.47	3.87	5.18	6.05
2500	4.17	4.64	7.10	8.33
3000	5.00	5.62	10.30	12.06
3500	5.93	6.90	14.23	16.57
4000	6.95	8.10	18.41	23.52
η(cP) at 1 bar	0.216	0.390	0.641	0.330

increased from 1–4000 bars; it decreased slightly as the temperature was increased from 0–60°. The temperature effect increased with increasing pressure.

The absolute values of the viscosities at 1 bar are given at the bottom of Table IV.

The relative viscosities of *n*-pentane, cyclopentane, methylcyclohexane, and 2,2-dimethylbutane at 30° and pressures up to 4000 bars are listed in Table V. The absolute viscosities at 1 bar are also given.

The present 30° data for *n*-pentane, *n*-hexane, *n*-octane, and methylcyclohexane may be compared with results of Bridgman (2). The present results for hexane and octane are 6% lower than Bridgman's at 4000 bars, but the discrepancy decreases with decreasing pressure. The cause of the difference is not known. The present result for pentane is 1% lower and that for methylcyclohexane is 2% lower than Bridgman's at 4000 bars.

Although the relative volumes of similar organic compounds are similar at a given pressure, the relative viscosities of the compounds at a pressure of several thousand bars vary over a wide range (2). In the current work the relative volumes of the hydrocarbons at 4000 bars were all in the range from 0.836 to 0.778, whereas the relative viscosities at this pressure varied from 6.95 to 23.5. With the exception of 2,2-dimethylbutane, which has been exceptional throughout this work (1), the relative viscosity at 4000 bars increases with the relative volume at that pressure (Fig. 5). A "large" value of the relative volume at a high pressure implies a small compressibility of the liquid. Thus, when comparing several similar liquids, a large relative viscosity is linked to a small compressibility; both of these properties are probably linked to a close molecular packing in the liquid.

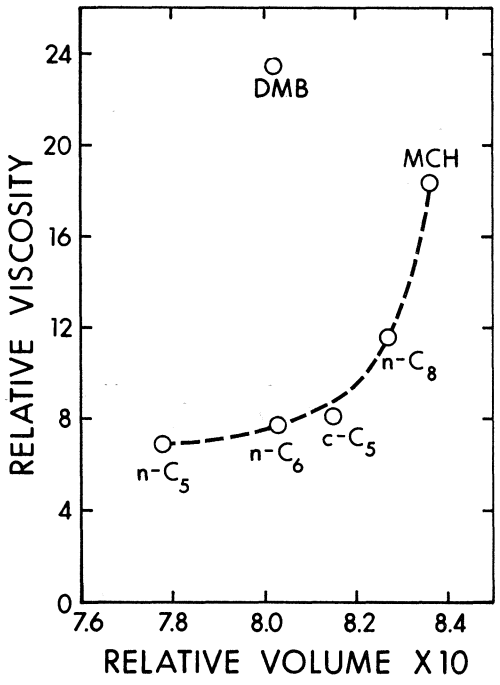

FIG. 5. Relative viscosity vs. relative volume for several hydrocarbons at 4000 bars and 30 °C. DMB is 2,2-dimethylbutane and MCH is methylcyclohexane.

The abnormally high value of the relative viscosity of 2,2-dimethylbutane (Fig. 5) supports the observation of Bridgman (2) that the vis-

Can. J. Chem. Downloaded from www.nrcresearchpress.com by 210.87.254.42 on 09/05/12
For personal use only.

cosity–pressure effects are largest for those liquids with the most complicated molecules. For example, isocompounds showed larger viscosity increases than did the isomeric normal compounds (2). It is clear that molecular structure and liquid structure have great influences on the magnitude of the effect of pressure on viscosity.

The free volume theory of liquids adequately describes the pressure and temperature dependences of the viscosities of the liquids *n*-pentane, *n*-hexane, and *n*-octane, provided one assumes that the "limiting specific volume" increases with increasing temperature and decreases with increasing pressure in ways similar to the changes in the specific volume of a solid (20). The theory was applied only to liquids whose viscosities were not described by the Arrhenius equation (20). The theory utilizes empirical constants which cannot be evaluated for the other hydrocarbons used in the current work, due to lack of appropriate data. It would be especially interesting to attempt to apply the theory to 2,2-dimethylbutane.

Acknowledgments

The financial assistance from the National Research Council of Canada is gratefully acknowledged. We also thank E. B. Cairns of the Radiation Research Center for planning and constructing much of the electronic equipment and R. G. Cox of the Chemistry Department for assistance in the planning and construction of the pressure systems.

1. D. W. Brazier and G. R. Freeman. Can. J. Chem. This issue.
2. P. W. Bridgman. The physics of high pressure. 2nd ed. Bell and Sons, Ltd., London. 1958.
3. P. W. Bridgman. Proc. Am. Acad. Arts Sci. **66**, 185 (1931).
4. P. W. Bridgman. Proc. Am. Acad. Arts Sci. **61**, 57 (1926).
5. H. E. Eduljee, D. M. Newitt, and K. E. Weale. J. Chem. Soc. 3086 (1951).
6. J. W. M. Boelhouwer. Physica, **26**, 1021 (1960).
7. F. Waibel. Ann. Physik, **72**, 161 (1923).
8. W. E. Danforth. Phys. Rev. **38**, 1224 (1931).
9. F. I. Mopsik. J. Res. Natl. Bur Std. A, **71**, 287 (1967).
10. D. W. Brazier. Ph.D. Thesis, University of Alberta, Edmonton, Alberta. 1968.
11. N. L. Brown. Ann. Rept. Conf. Electrical Insulation, Natl. Acad. Sci. National Research Council Publication #1238 (1954).
12. J. C. Jamieson. J. Chem. Phys. **21**, 1385 (1953).
13. A. E. Flowers. Proc. Am. Soc. Testing Materials, **14**, 565 (1914).
14. R. M. Hubbard and G. G. Brown. Ind. Eng. Chem. Anal. Ed. **15**, 212 (1943).
15. F. D. Rossini, K. S. Pitzer, R. L. Arnett, R. M. Braun, and G. C. Pimentel. Selected values of physical and thermodynamic properties of hydrocarbons and related compounds. American Petroleum Institute Research Project #44, Carnegie Press, Pittsburgh. 1953.
16. D. L. Dugle and G. R. Freeman. J. Phys. Chem. **70**, 1256 (1966).
17. H. G. David, S. D. Hamann, and J. F. Pease. J. Chem. Phys. **19**, 1491 (1951).
18. A. Michels, J. de Boer, and A. Bijl. Physica, **4**, 981 (1937).
19. C. A. Ten Seldam and S. R. de Groot. Physica, **18**, 905 (1952); **18**, 910 (1952).
20. A. J. Matheson. J. Chem. Phys. **44**, 695 (1966).
21. J. Timmermans. Physico-chemical constants of pure organic compounds. Elsevier Publishing Co., New York. 1950. See also Vol. 2. 1965.
22. R. W. Dornte and C. P. Smythe. J. Am. Chem. Soc. **52**, 3546 (1930).
23. P. W. Bridgman. Phys. Rev. **3**, 153 (1914).

Can. J. Chem. Downloaded from www.nrcresearchpress.com by 210.87.254.42 on 09/05/12
For personal use only.

Infrared studies on rotational isomerism. III. 2-Chloro- and 2-bromo-ethanol

PAUL BUCKLEY, PAUL A. GIGUÈRE, AND MICHEL SCHNEIDER
Département de Chimie, Université Laval, Québec, Québec

Received August 19, 1968

The relative intensities of the C—X stretching bands of the *gauche* and *trans* isomers in the vapor were measured as a function of temperature up to 165 °C for 2-chloroethanol, and up to 130 °C for 2-bromoethanol. From these the enthalpy differences between the two isomers were found to be 1.20 and 1.45 ± 0.1 kcal mole^{-1} respectively for the two halogenated ethanols. Similar measurements on the O—H stretching bands gave values higher than the above by 0.45 kcal mole^{-1} for both compounds. This apparent discrepancy is interpreted as due to a second *gauche* isomer, the OH group of which is not engaged in intramolecular hydrogen bonding, and which is less stable than the *trans* isomer.

A study of the isotopic molecule $ClCH_2$—CH_2OD has led to unambiguous assignment of the OH bending and torsional frequencies. The spectra of the solid show that 2-chloroethanol can exist in two different crystalline phases: a stable one consisting of *gauche* molecules only, and a metastable one containing both isomers.

L'intensité relative des bandes de valence C—X dans le spectre infrarouge de la vapeur a été mesurée en fonction de la température jusqu'à 165 °C pour le 2-chloroéthanol et jusqu'à 130 °C pour le 2-bromoéthanol. De ces mesures on tire les valeurs 1.20 et 1.45 ± 0.1 kcal mole^{-1} respectivement pour les différences d'enthalpie entre les isomères *gauche* et *trans*. Par contre des mesures semblables faites sur les bandes de valence O—H conduisent à des valeurs de ΔH plus élevées d'environ 0.45 kcal mole^{-1} pour les deux composés. Ce désaccord est probablement dû à la présence d'un troisième isomère, de configuration *gauche*, mais sans liaison hydrogène intramoléculaire.

Une étude de la molécule isotopique $ClCH_2$—CH_2OD a permis d'identifier sans ambiguité les bandes de déformation OH. Les spectres du 2-chloroéthanol à l'état solide ont révélé deux phases cristallines distinctes: l'une stable, ne contenant que l'isomère *gauche*, l'autre métastable, faite d'un mélange des deux isomères.

Canadian Journal of Chemistry, 47, 901 (1969)

Can. J. Chem. Downloaded from www.nrcresearchpress.com by 210.87.254.5 on 09/05/12
For personal use only.

Introduction

The question of rotational isomerism in 2-chloro- and 2-bromo-ethanol (also called ethylene chloro- and bromo-hydrin) was settled much sooner, at least qualitatively, than in the case of ethylene glycol discussed in Part I of this series (1). Indeed, the very first spectroscopic studies revealed the presence of more than one conformer in the liquid (2, 3) and the vapor as well (4, 5). Further studies have led to the correct structure for the *gauche* and the *trans* isomers, the former being the most abundant owing to its stabilization by internal hydrogen bonding. Quantitatively, however, there remains some uncertainty as to the energy difference ΔH between the two conformers. Zumwalt and Badger (5) found this to be 2 kcal mole^{-1} for 2-chloroethanol based on the temperature dependence of the relative intensities of the second overtone O—H bands, whereas similar measurements by Mizushima *et al.* (6), but on the fundamental C—Cl stretching bands, led to a value only half as large. Still a third value, 1.20 ± 0.09 kcal mole^{-1}, has been reported by Krueger and Mettee (7) from high resolution studies of the fundamental O—H bands in dilute solutions in carbon tetrachloride.

2-Bromoethanol has not received nearly as much attention as 2-chloroethanol. The last named authors found its enthalpy of isomerization to be about the same as that for 2-chloroethanol within the accuracy of their measurements. In contrast Kuhn *et al.* (8) estimated it to be practically zero. At the time the present work was carried out no infrared spectra of the pure compound had been published. A recent paper on the four 2-haloethanols (9) has just come to our attention.

In view of the above, and considering that the low-frequency vibrations of these molecules are strongly affected by rotational isomerism, it seemed to us that a systematic study extending into the far infrared, and covering the three physical states was desirable. This is reported here except for crystalline 2-bromoethanol which could not be obtained despite numerous attempts.

Experimental

The experimental conditions were essentially the same as before (1). For the intensity measurements special care

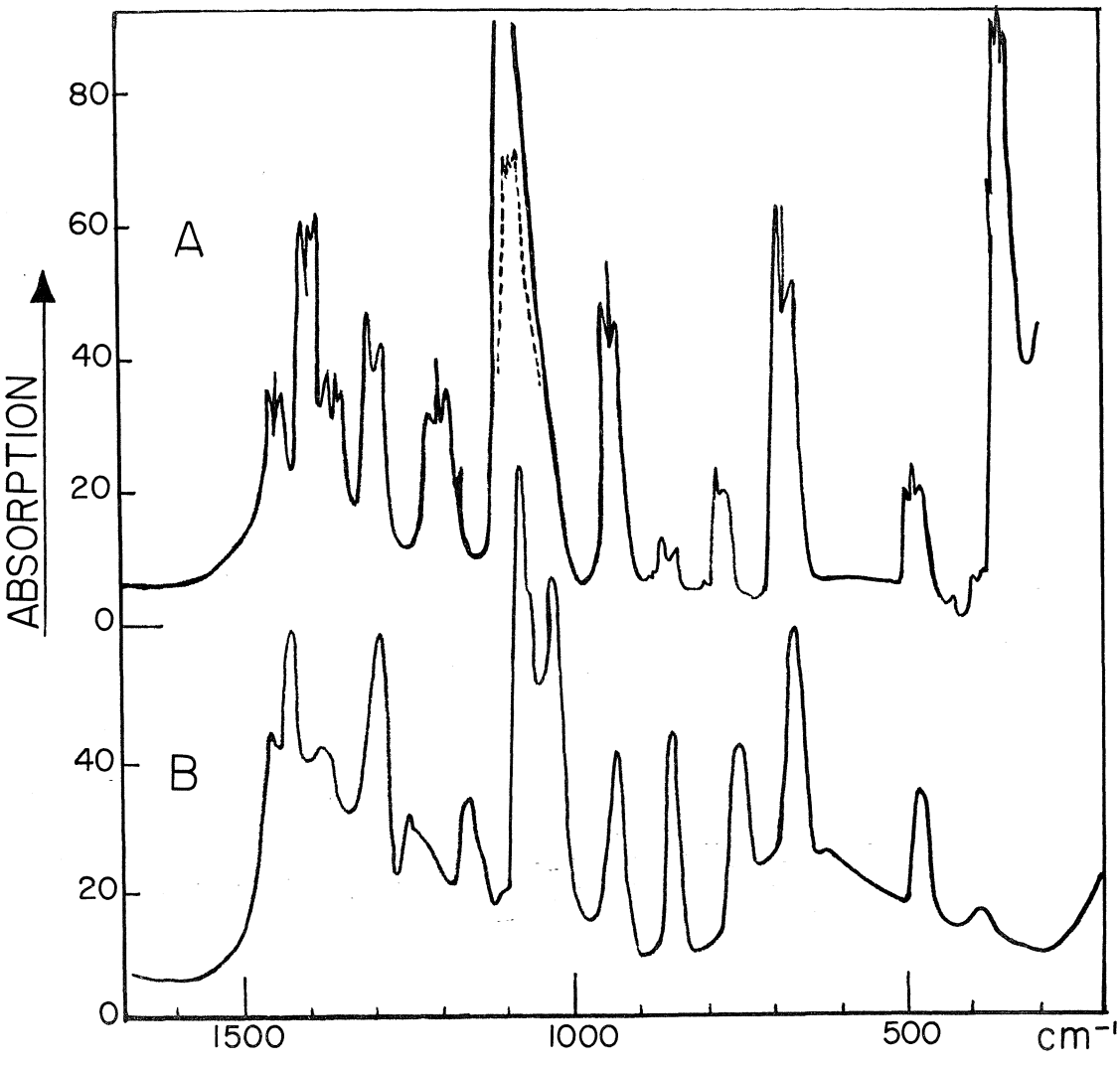

FIG. 1. Infrared spectra of 2-chloroethanol in the vapor (A) and liquid (B) at room temperature.

was exercised to insure that the temperature of the absorption cells was uniform throughout. Calibrated copper–constantan thermocouples and a precision potentiometer gave readings of more than sufficient accuracy. A short absorption cell 10 cm long made of brass was used for 2-chloroethanol. The cell and the liquid sample in a side tube were placed in an oven at 65 °C for about 1 h to reach equilibrium. Thereafter only the temperature of the cell was raised. A multiple reflection cell of 2.5 m total path was also used. With 2-chloroethanol the evacuated cell was briefly put in contact with the liquid at room temperature (vapor pressure of about 6 mm Hg). This operation had to be repeated periodically for over 1 h as appreciable absorption took place on the walls of the cell. For 2-bromoethanol, which is less volatile, a flow system with nitrogen as carrier gas was needed to reach equilibrium within reasonable time. Decomposition was noticeable at the higher temperatures after a while, as shown by weak absorption bands at 1760, 1135, and 860 cm^{-1} (aldehydes and ketones). However, these did not interfere with intensity measurements. The commercial samples of 2-chloroethanol (Eastman Organic Chemicals) and 2-bromoethanol (Matheson, Coleman and Bell) were vacuum distilled, the latter three times to remove all traces of impurities from the spectra. The sample of OD substituted 2-chloroethanol was prepared through synthesis of the borate ester (10) followed by hydrolysis with 99.6% pure D_2O. The operations were

Can. J. Chem. Downloaded from www.nrcresearchpress.com by 210.87.254.5 on 09/05/12
For personal use only.

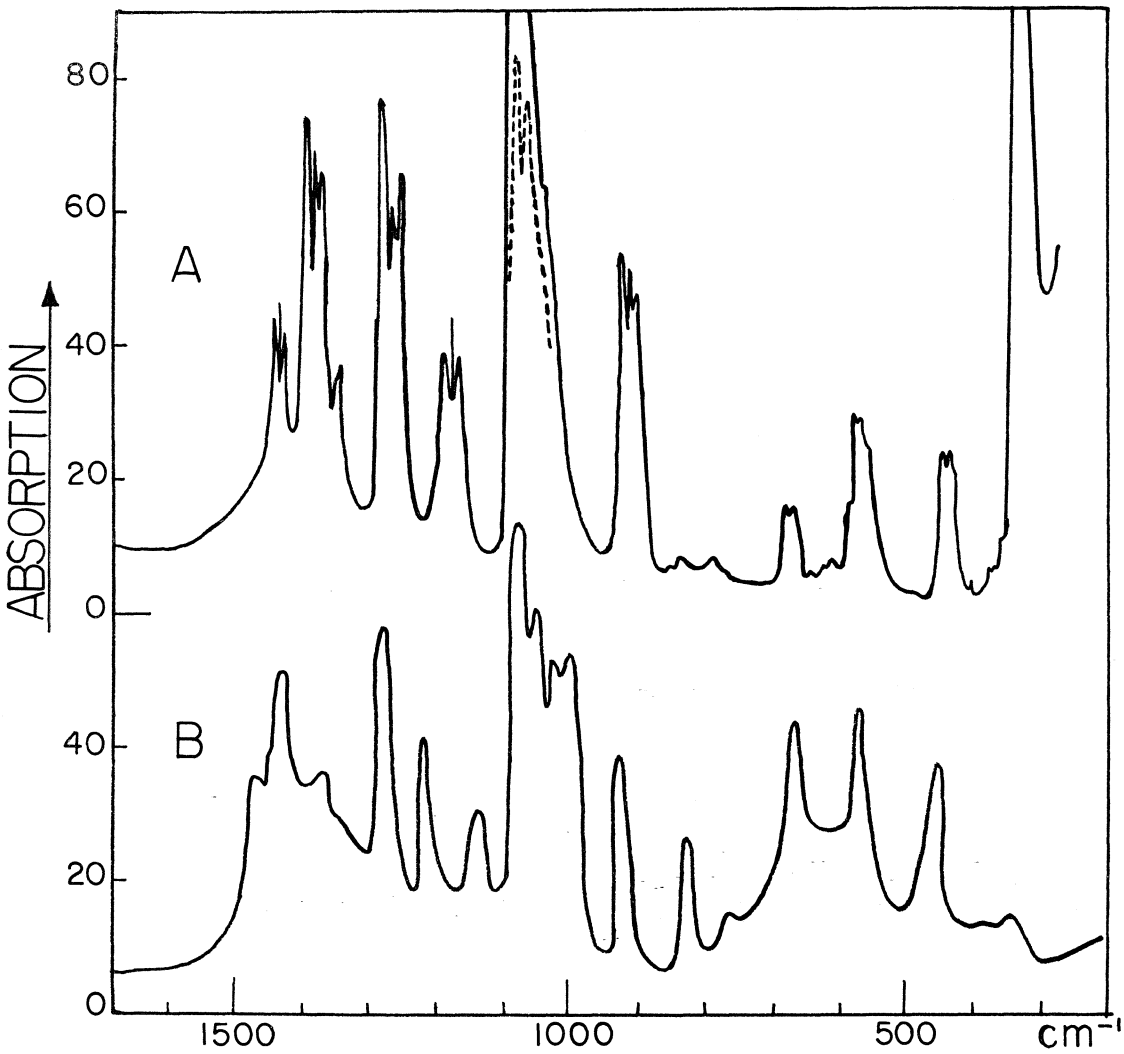

FIG. 2. Infrared absorption of 2-bromoethanol vapor (A) and liquid (B) at ordinary temperature.

carried out under controlled atmosphere to exclude moisture. From the intensity of the residual OH bands the extent of deuteration was of the order of 90%.

Results

The absorption spectra at room temperature of the two compounds between 1500 and 200 cm^{-1} are shown in Figs. 1 and 2 for both vapor and liquid. The 3 μ region is shown separately in Fig. 3.

Vibrational Spectra

Detailed assignment of the bands to normal modes of these two molecules is not feasible in all cases because of strong coupling or near coincidence of certain bands. At any rate the assignments given in Table I seem straightforward and need not be discussed further except in connection with rotational isomerism. For that purpose the O—H and the C—X stretching modes are the most useful. Both give rise to two distinct bands with temperature dependent relative intensities. Approximate calculations of the P–R branch maximum separation (Table II) based on moments of inertia from microwave spectra (11)

Can. J. Chem. Downloaded from www.nrcresearchpress.com by 210.87.254.5 on 09/05/12
For personal use only.

TABLE I

Infrared spectra of 2-chloro- and 2-bromo-ethanol

Frequencies				
CH_2ClCH_2OH		CH_2BrCH_2OH		
Liquid	Vapor	Liquid	Vapor	Assignments
	13 723, 13 635, 13 461 *			
	10 546, 10 485, 10 367 †		10 527, 10 470, 10 318 †	
	7 101, 7 072, 7 029 ‡			
	3 675, 3 661 w		3 674, 3 666 m	
3500 sh		3500 sh		O—H stretching (t)
3365 s	3 636, 3 621 vs	3350 vs	3 625, 3 615 vs	O—H stretching (g)
3000	3 007 §	3010	3 027 §	
2957	2 956 §	2955	2 954 §	
2932 s	2 927 s	2930	2 926 s	C—H stretching
2876	2 882	2865	2 880	
	1 446	1457	1 436	
1454 w	1 436, 1 429 m	1451 m	1 430, 1 423 m	CH_2 scissoring
	1 400		1 391	
1430 m	1 394, 1 386 s	1420 s	1 385, 1 379 s	CH_2 wagging
	1 362		1 362	
1384 w	1 352, 1 344 m	1378 m	1 356, 1 351, 1 345 w	OH bending (g)
1297 m	1 299, 1 286 m	1275 s	1 269, 1 263, 1 257 s	CH_2 twisting (g)
	1 208		1 189	
1237 w	1 200, 1 193 m	1212 m	1 182, 1 176 m	CH_2 twisting (t) OH bending (t)
1252 w	1 176	1140 w	1 160 vw	
1162 w	1 160 vw			
	1 082		1 083	
1073 s	1 065 vs	1068 vs	1 076 vs	C—O stretching
1055 s	1 070	1048	1 071	
	1 060	1022 s	1 049	
1029 s	1 045 m	1002 s	1 035 m	C—C stretching
	937		923	
938 m	930, 924 s	925 m	917, 911 s	CH_2 rocking (g)
	859			
869 vw	851 vw	827 w	~840 vw	CH_2 rocking (t)
846 m	844			
	773		690	
748 m	762 w	665 m	681 w	C—X stretching (t)
	679		595, 592	
661 m	672, 664 s	566 m	581, 577, 570 m	C—X stretching (g)
	480		456	
474 w	472, 465 w		451, 445 m	CCO bending (g)

Can. J. Chem. Downloaded from www.nrcresearchpress.com by 210.87.254.5 on 09/05/12
For personal use only.

TABLE I (*Concluded*)

Frequencies				
CH_2ClCH_2OH		CH_2BrCH_2OH		
Liquid	Vapor	Liquid	Vapor	Assignments
~650 mb		~625 mb		O—H torsion
395 vw	390 vw	~340 vw		CCO bending (t)
	340 vs		338 vs	O—H torsion
	~280 w			CCCl bending (g)
	~250 w			CCCl bending (t)
162 m	153 m			C—C torsion

*Mizushima *et al.* (4).
†Zumwalt and Badger (5).
‡In solution in CCl_4. Piccolini and Winstein (19).
§Kuhn *et al.* (8).

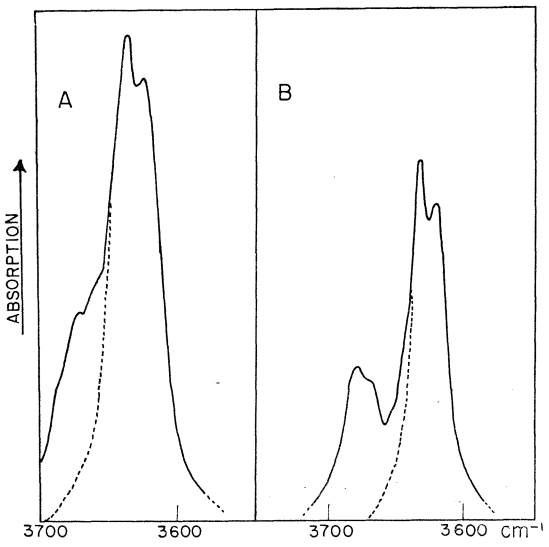

FIG. 3. Fundamental O—H stretching bands of 2-chloroethanol (A) and 2-bromoethanol (B) at 70 °C.

confirm that the high- and the low-frequency components of the C—X pairs of bands must be assigned to the *trans* and the *gauche* conformers respectively, in agreement with previous inferences.

In the spectra of the deuterated chloroalcohol the band at 1352 cm^{-1} has disappeared and is replaced by a weak pair at 985–1005 cm^{-1}, which confirms our assignment to the OH bending mode of the *gauche* isomer. The corresponding bands of the *trans* conformer are not so readily identified owing to their relative weakness. However, an appreciable decrease in intensity of the band at 1200 cm^{-1} upon deuteration indicates some contribution from an OH vibration. Normally this should be shifted to about 900 cm^{-1} in the OD compound, which coincides with a strong, slightly displaced CH_2 rocking band. As for the OH torsion, the strong peak at 340 cm^{-1} has now vanished almost completely, whereas absorption in the 220 to 250 cm^{-1} region has increased markedly.

Intensity Measurements

The band intensities were compared by the two methods of optical density at the maximum and integrated absorption intensities (Figs. 4, 5). Besides the well-known limitations of these methods, the method of optical density of the C—Br stretching bands in the *gauche* isomer presented further difficulty because of the irregular contour near the maximum. This may be due to an isotope effect, although it is not clear why

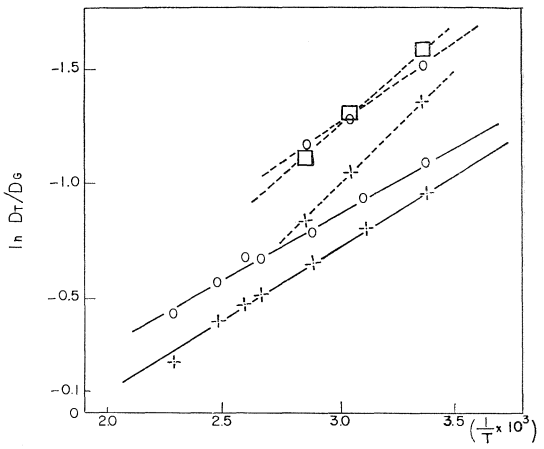

FIG. 4. Relative intensity measurements for 2-chloroethanol. Solid lines, C—Cl bands; broken lines, O—H bands. ○, Integrated intensities; +, optical densities; □, optical densities corrected for overlapping bands.

Can. J. Chem. Downloaded from www.nrcresearchpress.com by 210.87.254.5 on 09/05/12
For personal use only.

TABLE II

Structural and thermodynamic data for the *gauche* and *trans* conformers

Molecule	P–R branch separation of C—X bands (cm^{-1})			Relative populations		
					Temperature (°C)	
	Gauche	*Trans*	Reference	Conformers	25	75
$ClCH_2CH_2OH$	20	13	Calcd.	*Gauche*	100	100
	15	12	Found	*Trans*	34	46
				Non-hydrogen bonded *gauche*	~3	8–9
$BrCH_2CH_2OH$	13.5	8	Calcd.	*Gauche*	100	100
	11	8	Found	*Trans*	45	65
				Non-hydrogen bonded *gauche*	~3	15–20

Molecule	State	ΔH (kcal $mole^{-1}$)				ΔS (e.u.)			
		O—H	Reference	C—X	Reference	O—H	Reference	C—X	Reference
$ClCH_2CH_2OH$	Vapor	2.0 ±0.5	5	0.95±0.02	6			3.7±0.4	6
		1.65±0.20	This work	1.20±0.1	This work			3.3±0.3	This work
	Solution	1.20±0.09	7			3.9	7		
$BrCH_2CH_2OH$	Vapor	1.90±0.20	This work	1.45±0.10	This work			4.7±0.5	This work
	Solution	3.9	7			4.7	7		

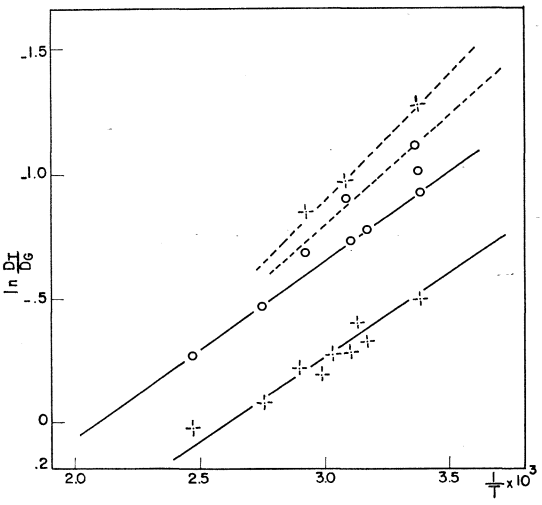

FIG. 5. Relative intensity measurements for 2-bromoethanol vapor. Solid lines, C—Br bands; broken lines, O—H bands. ○, Integrated intensities; ⊹, optical densities.

the *trans* band is not similarly affected. At any rate the optical density measured at 570 cm^{-1}, corresponding roughly to the R branch maximum of one of the presumed isotope bands, gives roughly the same slope of the ln D_t/D_g curve (Fig. 5) as that from integrated intensity measurements. Treatment of the data by the least squares method led to the values of ΔH shown in Table II along with those of previous workers. The entropy differences were evaluated by the method of Mizushima (12) using the optical density measurements, and as standard, or reference band, one of the C—H stretching at 2890 cm^{-1}. The possible effect of some slight decomposition of the vapor at the higher temperatures is exaggerated in the plotting of Fig. 6.

Spectra of the Solid

The first few spectra of 2-chloroethanol in the solid state were obtained by the usual technique of deposition from the vapor on a salt plate cooled to about −170°. This invariably yielded a glassy transparent solid with roughly the same absorption spectrum as the liquid. Annealing by controlled warming induced crystallization, as did also a fast deposition rate. The spectra of these crystals (I, in Fig. 7) show quite conspicuously the disappearance of the characteristic bands of the *trans* isomer in the liquid as observed previously in Raman effect (3). Then, on one occasion, while warming very slowly a sample deposited on a polyethylene disc for the far infrared spectra, a new crystalline form (crystal II) was obtained accidentally which exhibited four absorption bands, instead of only two, below 300 cm^{-1}. Duplication of this phenomenon on a salt disc

Can. J. Chem. Downloaded from www.nrcresearchpress.com by 210.87.254.5 on 09/05/12
For personal use only.

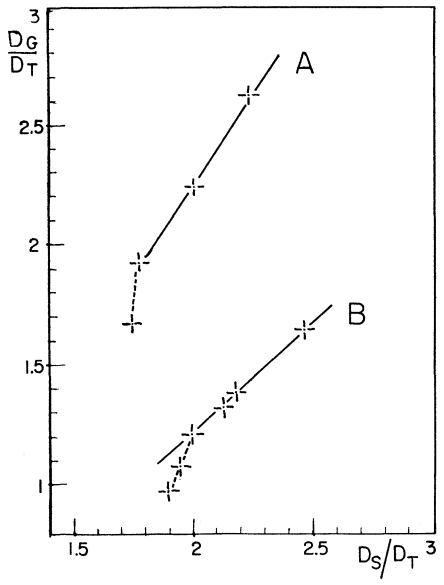

FIG. 6. Entropy relationships for 2-chloroethanol (A) and 2-bromoethanol isomers (B).

(CsBr) turned out to be extremely difficult. This may be due partly to the strongly polar nature of the ionic crystal, as opposed to a molecular solid, and also partly to the greater thermal conductivity of the salt plate. With a poor heat conductor like polyethylene a temperature gradient could develop between the center and the rim of the support, which seemed to favor formation of the metastable phase. Eventually another method was found for preparing crystal II by very slow cooling of crystal I below −90°. As far as could be judged from visual observation (crystal II has a powdery aspect), the transition occurred through melting, somewhere around −120°. On warming up, crystal II changed into an amorphous translucent solid in the neighborhood of −100° well before melting for the second time. The complex nature of the new crystalline phase is confirmed by the reappearance of the strong bands of the *trans* isomer (Table III).

As for 2-bromoethanol, as previously experienced (13), it could not be crystallized in spite of numerous attempts, for instance by quick quenching in liquid nitrogen, rubbing and shearing of a film of the supercooled liquid (around −100°), application of ultrasonics, etc. This is all the more surprising as the three other 2-haloethanols can be crystallized without difficulty.

TABLE III

Principal infrared bands in the two crystalline forms of 2-chloroethanol

Infrared frequencies		
Crystal I	Crystal II	Assignments
3320 s	3360 s, 3300 s	O—H stretching
2963 m, 2934 m, 2872 w	2932 s, 2875 s	C—H stretching
1460 sh, 1431 s	1449 s, 1425 s	CH_2 scissoring
1398 vw	1391 sh	
1379 m	1370 s	OH bending
1302 s	1295 vs	CH_2 wagging
1245 s	1245 sh, 1226 vs	CH_2 twisting (g)
	1185 w, 1169 sh	CH_2 twisting (t)
	1117 s, 1100 m	C—O stretching (t)
1079 vs	1070 s, 1061 s	C—O stretching (g)
1038 s, 1030 s	1033 sh, 1029 s, 981 w	C—C stretching
942 s	939 vs	CH_2 rocking (g)
849 s	847 s	CH_2 rocking (t)
	720 s	C—Cl stretching (t)
657 m	661 vs	C—Cl stretching (g)
610 w	611 s	OH torsion
473 m	470 vs	CCO bending (g)
	392 w	CCO bending (t)
315 m	307 s, 295 sh	CCCl bending (g)
	276 s	CCl bending (t)
162 s	162 s	C—C torsion (g)
	115 s	C—C torsion (t)

Discussion

Our knowledge of the problem of rotational isomerism in the 2-haloethanols rests mainly on spectroscopic evidence (14) as the other methods have not provided complete or unambiguous evidence. For instance, an electron diffraction study (15) has established the structure of the *gauche* isomer with an intramolecular hydrogen bond, but the results were interpreted in terms of that isomer only. An independent reinvestigation (16) has led to essentially the same conclusions. It would seem that the method is not sensitive enough to detect the less abundant conformer. One fundamental difficulty here is the uncertainty as to temperature of the vapor at the moment of diffraction (17).

It is interesting to compare the frequency

Can. J. Chem. Downloaded from www.nrcresearchpress.com by 210.87.254.5 on 09/05/12
For personal use only.

Can. J. Chem. Downloaded from www.nrcresearchpress.com by 210.87.254.5 on 09/05/12
For personal use only.

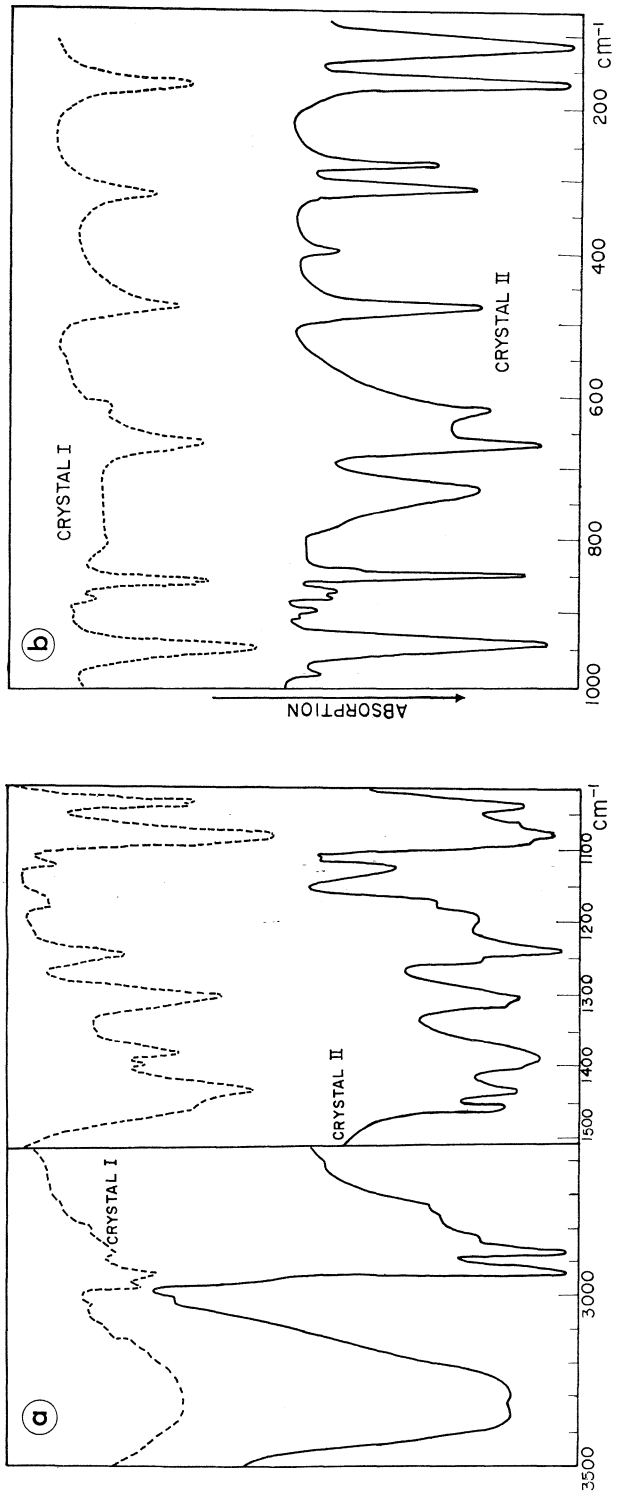

FIG. 7. Infrared spectra of the two crystalline forms of 2-chloroethanol.

Can. J. Chem. Downloaded from www.nrcresearchpress.com by 210.87.254.5 on 09/05/12
For personal use only.

difference between the "free" and the "bonded" O—H stretching fundamentals for the chloro (40 cm^{-1}) and the bromo compound (50 cm^{-1}) with that for ethylene glycol (33 cm^{-1}). As explained before, these relatively small shifts are due to the non-linearity of the intramolecular hydrogen bond. By contrast the OH bending frequencies are strongly shifted. As for the OH torsional frequency in the *gauche* conformer, it shows surprisingly little correlation with the strength of the hydrogen bond, by comparison with the values in ethylene glycol, 375 cm^{-1}, and in 2-fluoroethanol, 343 cm^{-1} (18). On that basis the barrier to free rotation of the hydroxyl in the *gauche* conformer would have roughly the same height, 3–4 kcal $mole^{-1}$ in these four molecules.

Regarding our intensity measurements the following points are noteworthy. (*a*) Both the data from O—H and C—X stretching bands give a higher ΔH for the bromo than for the chloro alcohol. The difference seems real as it lies outside the uncertainty of our measurements. This is in agreement with the magnitude of the *gauche*-to-*trans* shifts of the O—H stretching frequencies (40 cm^{-1} in the chloro vs. 50 cm^{-1} in the bromo alcohol). Presumably, this could be due to the larger size of the Br atom, which brings it closer to the proton in a strained intramolecular hydrogen bond, and (or) to the greater mass of Br (more than double that of Cl) which changes the force constants throughout the whole molecule. In that connection it is interesting that both 2-haloethanols have been found recently by microwave spectroscopy (11) to have the same azimuthal angle in the *gauche* configuration, 64 $\pm$ 2°. This is appreciably smaller than first believed, 74°, from electron diffraction data (15, 16). Intuitively one would expect that angle to be a bit smaller than in 1,2-dichloroethane, 71°.

(*b*) Our results show definitely that the ΔH based on the O—H stretching bands are greater than those from the C—X bands for both haloethanols. (The discrepancy between our value for 2-chloroethanol and that of Zumwalt and Badger (5) is understandable considering the vagaries of the photometric method.) The explanation suggested before (6) of a third isomer, that is *gauche* but without intramolecular hydrogen bond, in the vapor seems the most plausible. In fact other experimental evidence points to the possibility of more than two orientations for the OH group in these molecules. For instance three distinct O—H stretching bands have been reported in the second and third overtones for the vapor (4, 5) as well as in the first overtone for dilute solutions (19). This multiplet structure seems to be a common occurrence, as found long ago (20), in saturated primary alcohols. Pending more complete data on this non-hydrogen-bonded *gauche* conformer, its relative energy may be taken as about 1 kcal $mole^{-1}$ above that of the *trans* by analogy with 1,2-dichloroethane. Based on our optical density data the relative populations of the three species are estimated to be as shown in Table II.

Lastly the existence of two distinct crystalline phases in 2-chloroethanol, and the transition into an amorphous, or plastic state prior to melting are rather surprising. Such behavior has been observed so far only in the so-called globular molecules, i.e. molecules which describe a symmetrical figure of revolution in space, such as a spheroid, e.g. CH_4, or an ellipsoid, e.g. $(CH_2CN)_2$. Now, 2-chloroethanol is not a globular molecule in either conformation. It may be that in condensed phases the *gauche* and the *trans* conformers have nearly equal energy due to stabilization by intermolecular hydrogen bonding. This would make orientation into the most stable crystalline arrangement rather sluggish, and a metastable phase could ensue under certain conditions. The same explanation may account for the observation that the relative intensity of the *gauche* and *trans* C—Cl stretching bands changes very little with temperature (21). In conclusion, this phenomenon certainly deserves further investigation by other physical methods such as calorimetry and X-ray diffraction.

Acknowledgments

The authors are grateful to the National Research Council of Canada for a research grant; also to Dr. Azrak for permission to quote unpublished data, to Professor P. Brassard for preparation of the deutero compound, and to Professor D. Yamamoto for assistance with the spectra of the solid.

1. P. Buckley and P. A. Giguère. Can. J. Chem. **45**, 397 (1967).
2. K. W. F. Kohlrausch and G. P. Ypsilanti. Z. Physik. Chem. B, **29**, 274 (1935).
3. S. Mizushima, Y. Morino, and S. Nakamura. Sci. Papers Inst. Phys. Chem. Res. **37**, 205 (1940).

4. S. MIZUSHIMA, T. KUBOTA, and Y. MORINO. Bull. Chem. Soc. Japan, **14**, 15 (1939).
5. L. R. ZUMWALT and R. M. BADGER. J. Am. Chem. Soc. **62**, 305 (1940).
6. S. MIZUSHIMA, T. SHIMANOUCHI, T. MIYAZAWA, K. ABE, and M. YASUMI. J. Chem. Phys. **19**, 1477 (1951).
7. P. J. KRUEGER and H. D. METTEE. Can. J. Chem. **42**, 326 (1964).
8. M. KUHN, W. LÜTTKE, and R. MECKE. Z. Anal. Chem. **170**, 106 (1959).
9. E. WYN-JONES and W. ORVILLE-THOMAS. J. Mol. Structure, **1**, 79 (1967–68).
10. C. G. SWAIN, A. D. KETLEY, and R. F. W. BADER. J. Am. Chem. Soc. **81**, 2357 (1959).
11. R. G. AZRAK. Symp. Mol. Structure Spectry., Columbus, Ohio, 1966.
12. S. MIZUSHIMA, T. SHIMANOUCHI, K. KURATANI, and T. MIYAZAWA. J. Am. Chem. Soc. **74**, 1378 (1952).
13. S. NAKAMURA. J. Chem. Soc. Japan, **60**, 1010 (1939).
14. S. MIZUSHIMA. Structure of molecules and internal rotation. Academic Press, Inc., New York. 1954.
15. O. BASTIANSEN. Acta Chem. Scand. **3**, 415 (1949).
16. M. YAMAHA. Bull. Soc. Chem. Japan, **29**, 865 (1956).
17. O. BASTIANSEN. Intramolecular motion and conformation problems in free molecules as studied by electron diffraction. *In* Structural chemistry and molecular biology. W. H. Freeman and Co., San Francisco. 1948. p. 649.
18. P. BUCKLEY, P. A. GIGUÈRE, and D. YAMAMOTO. Can. J. Chem. **46**, 2917 (1968).
19. R. PICCOLINI and S. WINSTEIN. Tetrahedron Letters, No. 13, 4 (1959).
20. R. M. BADGER and S. H. BAUER. J. Chem. Phys. **4**, 711 (1936).
21. M. MAZUMDER. Indian J. Phys. **29**, 361 (1955).

Can. J. Chem. Downloaded from www.nrcresearchpress.com by 210.87.254.5 on 09/05/12
For personal use only.

The Wallach rearrangement. Part V.[1] Acid catalyzed hydrolysis of azobenzene-4-hydrogen sulfate[2]

E. BUNCEL AND W. M. J. STRACHAN
Department of Chemistry, Queen's University, Kingston, Ontario

Received September 18, 1968

In relation to the intermediacy of azobenzene-4-hydrogen sulfate in the Wallach rearrangement of azoxybenzene, the potassium salt has been characterized and subjected to examination under acidic conditions. A pK_a value of -2.14 has been obtained, for N-protonation. The sulfate salt hydrolyzes to *p*-hydroxyazobenzene in acid media and the rate of the reaction has been measured over the region 22–42% H_2SO_4 at 25° spectrophotometrically. A correlation between rate and acidity function indicates that a two-proton process is involved; a reactive species is proposed having a nitrogen and the phenolic oxygen protonated. The relevance of these findings to Wallach rearrangement studies is discussed.

Canadian Journal of Chemistry, **47**, 911 (1969)

Can. J. Chem. Downloaded from www.nrcresearchpress.com by 210.87.254.6 on 09/05/12
For personal use only.

The mechanism of the acid-catalyzed Wallach rearrangement, the conversion of azoxybenzene and its derivatives into *p*-hydroxyazobenzenes in strong sulfuric acid solutions, has received considerable attention recently (1–10). Discussion has centered mainly on the intermediacy of an N,N-oxide intermediate **1**, or its protonated forms (5), as opposed to a dicationic intermediate **2** (4, 9). Some authors have proposed mechanisms which involve both **1** and **2** in the reaction schemes (3, 6). Of direct consequence to the reaction mechanism was the observation of a two-proton process in a kinetic study of the rearrangement of azoxybenzene (10), which was subsequently confirmed and extended to substituted azoxybenzenes (2, 3).

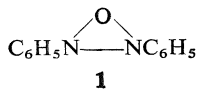

1

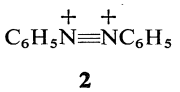

2

There appears to be general agreement that in the product-forming step the reaction intermediate(s) reacts with a nucleophile derived from the solvent. However, opinions on the nature of the nucleophile are divided: some authors consider solvent water to act as the nucleophilic species (4, 6), others consider bisulfate ion to be the effective nucleophile (2, 3, 9), while still others do not differentiate between these (5). In one recent study (3) bisulfate ion was ascribed a specific role in hydrogen-bond formation when attached to an ortho position of the protonated N,N-oxide intermediate, in the "abnormal" cases when the Wallach rearrangement leads to *o*-hydroxyazo product. Since an arylazo hydrogen sulfate has never been isolated in a Wallach rearrangement reaction, it has generally been assumed (2, 3, 8, 9) that the postulated hydrogen sulfate becomes hydrolyzed to the hydroxyazo product in the reaction medium or during isolation. There has only been one report of an indirect observation of an azoaryl hydrogen sulfate: cryoscopic, conductivity, and spectral evidence was given that in the rearrangement of azoxybenzene in $\geqslant$ 100% H_2SO_4 the first product formed was the hydrogen sulfate (2).

Previously we suggested (4) the possibility that the dication **2** might become stabilized in anhydrous acids where water as nucleophile is not available. In order to obtain further information on the intermediacy of azobenzene-4-hydrogen sulfate for azoxybenzene rearragement in sulfuric acid we have now prepared this material, as the stable potassium salt, and subjected it to examination under acidic conditions. We report here the spectral characterization of this compound, its protonation behavior, and the kinetics of its hydrolysis to *p*-hydroxyazobenzene in aqueous sulfuric acid solutions.

Results and Discussion

Spectral Characterization

Azobenzene-4-hydrogen sulfate was prepared by sulfonation of *p*-hydroxyazobenzene and was isolated as the potassium salt, as described in the Experimental section. The ultraviolet–visible spectrum of this compound in 95% ethanol is similar to that of *p*-hydroxyazobenzene, but in basic medium the spectra are widely different.

[1]Part IV: Tetrahedron, **24**, 6671 (1968).
[2]A more systematic name for the title compound would be 4-phenylazophenyl hydrogen sulfate.

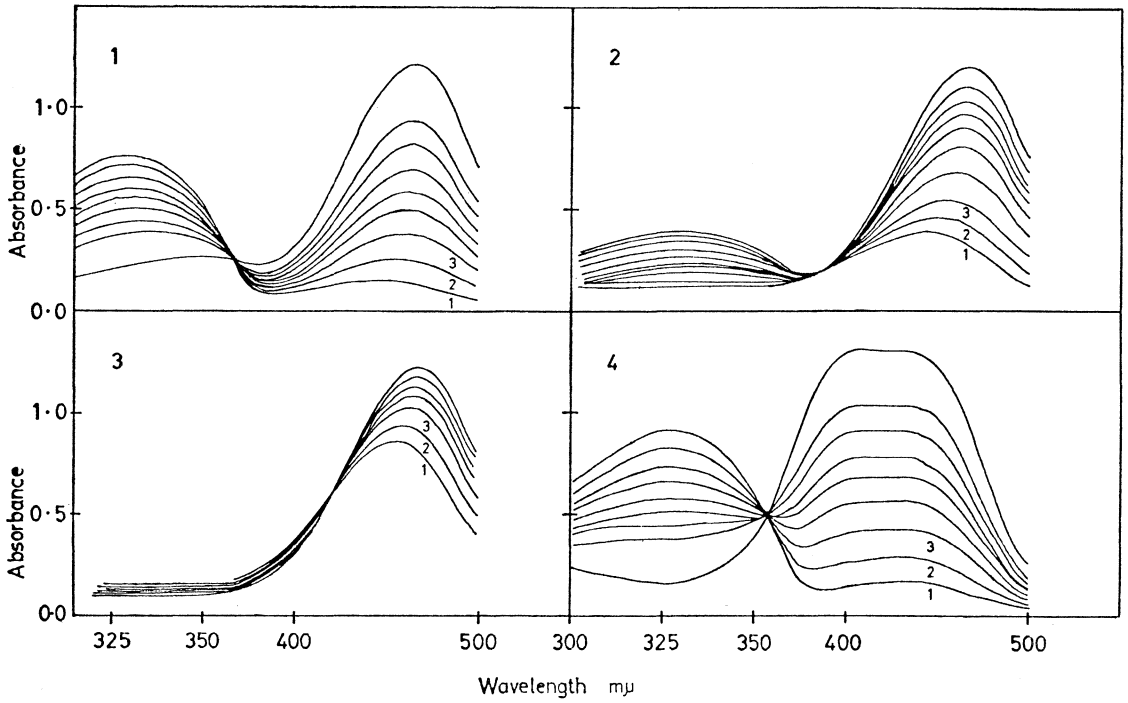

FIGS. 1–4. Sample kinetic runs for the acid hydrolysis of azobenzene-4-sulfate at 25 °C.

Figure 1, reaction medium, 24.0% H_2SO_4; substrate concentration, 38.8×10^{-5} *M*; followed in situ in 0.100 cm cell. Scan times noted are: 1–5 min, 2–26 min, 3–55 min, final scan 22 h. Figure 2, reaction medium, 34.3% H_2SO_4; substrate concentration, 3.22×10^{-5} *M*; followed in situ in 1.00 cm cell. Scan times noted are: 1–1 min, 2–2.5 min, 3–4.5 min, final scan 4.5 h. Figure 3, reaction medium, 41.1% H_2SO_4; substrate concentration, 3.22×10^{-5} *M*; followed in situ in 1.00 cm cell. Scan times noted are: 1–1.2 min, 2–2 min, 3–3 min, final scan 23 min. Figure 4, reaction medium, 24.0% H_2SO_4; substrate concentration, 38.8×10^{-5} *M*; base-quenched and followed in 4.00 cm cell (1.55×10^{-5} *M*). Scan times noted are: 1–6 min, 2–27 min, 3–56 min, final scan 22 h.

The respective absorption maxima and molar extinctions are given in Table I. The shift in absorption maximum for *p*-hydroxyazobenzene which accompanies basification is due to formation of the azophenolate anion, which is structurally not possible with the hydrogen sulfate derivative.

TABLE I

Spectral characteristics of azobenzene-4-sulfate and of *p*-hydroxyazobenzene in neutral and basic solution

	Spectral characteristics in			
	95% Ethanol		1 *N* aq. KOH	
Compound	λ_{max} (mμ)	$\varepsilon \times 10^4$	λ_{max} (mμ)	$\varepsilon \times 10^4$
Azobenzene-4-sulfate	329	2.08	325	1.46
p-Hydroxyazobenzene	348	2.50	400	2.19[a]
			440	2.17[a]

[a]In 1 *N* aqueous KOH, *p*-hydroxyazobenzene exhibits a broad absorption covering the range 400–440 mμ over which the extinction is practically invariant (see also Fig. 4).

Kinetic Measurements

The acid hydrolysis of azobenzene-4-hydrogen sulfate is characterized by certain spectral changes, dependent on the acid concentration. This is illustrated in the following kinetic runs at 25° which were followed by periodic scanning of the visible spectrum. (*i*) 24.0% H_2SO_4 (Fig. 1). In this medium protonation of reactant (on azo function, *vide infra*) is only slight and the initial absorption is mainly in the 325 mμ region. Reaction leads to a gradual decrease in the 325 mμ absorption and an increase in absorption in the 460 mμ region, due to *p*-hydroxyazobenzene formation (extensively protonated in this medium). (*ii*) 34.3% H_2SO_4 (Fig. 2). Protonation of substrate in this medium is appreciable and the initial spectrum now shows roughly equal absorption in the 325 and 440 mμ regions, of which the latter is characteristic of protonated substrate. The reaction is accompanied by an increase in the 460 mμ absorption, as previously

Can. J. Chem. Downloaded from www.nrcresearchpress.com by 210.87.254.6 on 09/05/12
For personal use only.

TABLE II

Kinetic data for hydrolysis of azobenzene-4-sulfate in aq. H_2SO_4 at 25°

Weight % H_2SO_4	$-H_0$	c_{SH^+}[a] / ($c_S + c_{SH^+}$)	c_S[a] / ($c_S + c_{SH^+}$)	$10^5 k$ (s^{-1})
21.8[b]	−1.15	0.091	0.909	7.17
24.0	−1.31	0.129	0.871	7.91[c]
				8.42[d]
				8.25[e]
				8.28[d,e]
26.2	−1.46	0.173	0.827	14.3
				14.7
27.2	−1.54	0.200	0.800	21.9[f]
29.8	−1.72	0.277	0.723	38.6[f]
32.0	−1.86	0.344	0.656	71.3[f]
32.9[b]	−1.93	0.382	0.618	65.4[c]
				65.0[d]
				62.1[e]
				61.9[d,e]
34.3	−2.02	0.431	0.569	126[f]
34.6	−2.04	0.443	0.557	124
				127
				129
35.4	−2.10	0.477	0.523	175[f]
36.3	−2.16	0.512	0.488	178
37.2	−2.22	0.545	0.455	247
				247
				278[f]
41.1	−2.53	0.711	0.289	656[f]
42.0	−2.60	0.795	0.205	684[f]

[a]Calculated from the relationship $\log c_{SH^+}/c_S = pK_s - H_0$.
[b]Rate constants at these acidities err considerably from the linear rate $-H_0$ relationship and are not included in slope values.
[c]Reactions performed in 0.100 cm cells.
[d]Rate data obtained from $\log (A_\infty - A_t)$ plots (the remaining rate constants were evaluated by the Guggenheim method).
[e]Rate data obtained by base analysis.
[f]Rate data obtained using aliquots of a single stock solution (the remaining rate constants were obtained on individually prepared reaction solutions).

mentioned. (*iii*) 41.1% H_2SO_4 (Fig. 3). The substrate now exists largely as the protonated form, so that the initial absorption is largely shifted to the 440 mμ region. A sharp isosbestic point defines the rate process for the conversion between the two absorbing species and was observed in every kinetic run with this compound. The spectral data obtained in the above runs readily lend themselves to analysis by the Guggenheim method. The first order rate constants for formation of the spectral absorptions at 460 mμ due to *p*-hydroxyazobenzene are 7.91×10^{-5}, 126×10^{-5}, and 656×10^{-5} s^{-1}, in 24.0, 34.3, and 41.1% H_2SO_4 respectively.

As an alternative to the above kinetic method the reaction may be followed by quenching of aliquots of the reaction solution in base, thus taking advantage of the considerably different spectral absorptions of reactant and product in basic medium. An illustrative run is shown in Fig. 4, for 24.0% H_2SO_4. The rate constant for the appearance of the azophenolate ion absorption at 440 mμ is found to be 8.25×10^{-5} s^{-1} by the Guggenheim method. The more usual $\log (A_\infty - A_t)$ vs. time plot, where A_∞ is the theoretical expected absorbance based on *p*-hydroxyazobenzene, gave 8.28×10^{-5} s^{-1} for the rate constant. Hence the rate constants obtained by the alkaline quenching procedure are in satisfactory agreement with those obtained when the reaction is followed directly in the acid medium, and confirm the validity of that method. The total kinetic data obtained by the various methods are listed in Table II.

pK Determination

In order to evaluate quantitatively the extent of protonation of azobenzene-4-hydrogen sulfate in the various acid media, "zero time" spectra were obtained by extrapolation of the spectral sweeps for the various kinetic runs. The family of curves so obtained passes through a fairly sharp

Can. J. Chem. Downloaded from www.nrcresearchpress.com by 210.87.254.6 on 09/05/12
For personal use only.

Can. J. Chem. Downloaded from www.nrcresearchpress.com by 210.87.254.6 on 09/05/12
For personal use only.

isosbestic point and shows absorption maxima at 326 and 440 mμ, due to the neutral and protonated forms of substrate. The zero time extrapolated absorbances at these wavelengths are given in Table III. Plots of A^{326} vs. H_0 and A^{440} vs. H_0 (11) are sigmoid, with some scatter of the points. An approximate value of -2.1 is obtained for the pK_a, corresponding to the H_0 value at the inflexion point of each curve. Treatment of the data at 440 mμ, which fell more closely on the absorbance vs. H_0 curve, by the convergence method of Arnett and Wu (12) yields a value of -2.14 for the pK_a of azobenzene-4-sulfate. The pK_a of *p*-hydroxyazobenzene itself is -0.93 (13).

There seems little doubt that the basic center in the equilibrium protonation measured here is the azo function, rather than the negatively charged oxygen of the sulfate moiety. It is likely that the sulfate salt remains completely dissociated throughout the acid region covered in Table III. The dissociation constant of an aryl hydrogen sulfate should not be vastly different from the first dissociation constant of sulfuric acid itself, which is known to be very large, though estimates of its actual magnitude vary (14, 15). Further evidence for nitrogen protonation in the present system is derived from the shift in λ_{max} on protonation, which is very similar to corresponding shifts observed with other azobenzene derivatives (13, 16–18). The azobenzene sulfate ion is a weaker base than *p*-hydroxyazobenzene due to the electron withdrawing character of the SO_3^- group (14, 19). Azobenzene-4-sulfonate has a pK of -3.13 (18). The probable site of protonation is the nitrogen furthest removed from the OSO_3^- substituent, by analogy with considerations applied previously to related azo derivatives (13, 20).

TABLE III

Protonation behavior of azobenzene-4-sulfate

Weight %H_2SO_4	H_0	$\varepsilon^{326} \times 10^4$	$\varepsilon^{440} \times 10^4$
2.0[a]	0.49	2.06	0.17
4.8[a]	0.11	2.07	0.14
13.0[a]	−0.52	2.08	0.23
21.8[a]	−1.15	2.03	0.32
27.2	−1.54	1.63	0.63
29.8	−1.72	1.52	0.69
32.0	−1.86	1.47	0.85
34.3	−2.02	1.37	0.98
35.4	−2.10	1.31	1.18
36.3[a]	−2.16	1.38	1.30
37.2	−2.22	1.20	1.44
41.1	−2.53	(0.56)[b]	(2.06)[b]
42.1	−2.60	(0.47)[b]	(1.90)[b]

[a]Except for these determinations which were obtained by spectral measurement on individually prepared solutions, all of the above data were obtained by using a stock solution as described in the Experimental section.

[b]These values are dubious due to the very fast hydrolysis of the substrate and the accompanying uncertainty in extrapolation, and hence were not employed in the pK_a determination.

Mechanism of Hydrolysis

Several possible modes of hydrolysis of azobenzene sulfate ion need to be considered. First there is the mechanism described by eqs. [1] and [2], which is essentially similar to the mechanism proposed by Kice and Anderson (19) for the hydrolysis of sodium phenyl sulfate. Among the evidence presented by these authors for the formation of a reactive species by aryl-oxygen protonation was the solvent isotope effect ($k_{D_2O}/k_{H_2O} = 2.43$), an increase in rate with decreased dielectric constant, and the unit slope in the log $k - H_0$ plot. In the present case, an equilibrium protonation on the phenolic oxygen yields the reactive zwitterion SH'^+, which decomposes to products by a unimolecular (A-1) mechanism. The concentration of SH'^+ would be very small over the range of acid concentration studied, so that the N-protonated substrate (eq. [3]) would represent a storage of material in an unreactive form.

[1] $$PhN{=}N.C_6H_4.OSO_3^- + H^+ \underset{K_{SH'^+}}{\overset{\text{fast}}{\rightleftharpoons}} PhN{=}N.C_6H_4.\overset{\overset{H}{|}}{\underset{+}{O}}{-}SO_3^- \ (SH'^+)$$

[2] $$PhN{=}N.C_6H_4.\overset{\overset{H}{|}}{\underset{+}{O}}{-}SO_3^- \xrightarrow[k]{\text{slow}} PhN{=}N.C_6H_4.OH + SO_3$$

The second mechanism involves an initial protonation on nitrogen, to give the species SH^+, followed by a second equilibrium protonation on phenolic oxygen to give the reactive species SH_2^{2+} which decomposes unimolecularly; this is shown in eqs. [3] – [5].

[3] $$PhN{=}N.C_6H_4.OSO_3^- + H^+ \underset{K_{SH^+}}{\overset{\text{fast}}{\rightleftharpoons}} \underset{+}{\overset{H}{\overset{|}{PhN}}}{=}N.C_6H_4.OSO_3^- \ (SH^+)$$

[4] $$\underset{+}{\overset{H}{\overset{|}{PhN}}}{=}N.C_6H_4.OSO_3^- + H^+ \underset{K_{SH_2{}^{2+}}}{\overset{\text{fast}}{\rightleftharpoons}} \underset{+}{\overset{H}{\overset{|}{PhN}}}{=}N.C_6H_4.\underset{+}{\overset{H}{\overset{|}{O}}}{-}SO_3^- \ (SH_2^{2+})$$

[5] $$\underset{+}{\overset{H}{\overset{|}{PhN}}}{=}N.C_6H_4.\underset{+}{\overset{H}{\overset{|}{O}}}{-}SO_3^- \xrightarrow[k']{\text{slow}} Ph{-}\underset{+}{\overset{H}{\overset{|}{N}}}{=}N.C_6H_4.OH + SO_3$$

Thirdly, there is the possibility that the reaction involves C—O bond fission, rather than S—O bond fission as depicted in the above two mechanisms. The last proposal, which would presumably involve nucleophilic attack by H_2O on aromatic carbon, would normally be considered unlikely but cannot be ruled out since the acid catalyzed hydrolysis of certain azoaryl ethers was in fact shown to involve aryl–oxygen bond cleavage (17, 21). In the absence of further evidence, such as from isotopic tracer studies, the last possibility will not be considered further at this time.

The mechanisms of eqs. [1], [2], and [3] – [5] can be tested by means of acidity function correlations (22–25). The rate expression given by eq. [6] can readily be derived (23) for the mechanism of eqs. [1] and [2]. In eq. [6], k_{obs} is the measured pseudo first order rate constant, $c_S/(c_S + c_{SH^+})$ represents the fraction of substrate present in the unprotonated form in a given reaction medium, f_S and $f_{\neq}$ refer to the activity coefficients of neutral substrate and of the activated complex, while f_B and f_{BH^+} refer to the activity coefficients of the standard amine base used to define H_0. The activity coefficient term in eq. [6] is assumed to be zero (22, 23) so that one would expect a plot of the two left hand terms against $-H_0$ to be linear of unit slope.

[6] $$\log k_{obs} - \log \frac{c_S}{c_S + c_{SH^+}} = -H_0 + \log \frac{k}{K_{SH'^+}} + \log \frac{f_S f_{BH^+}}{f_{\neq} f_B}$$

The mechanism of eqs. [3] – [5] is reminiscent of the two-proton process previously considered for the rearrangement of azoxybenzene (4), and analogous rate expressions (eqs. [7] and [8]) can be derived. In eqs. [7] and [8], H_+ is the acidity function applicable to the protonation of a positively charged base, C^+. The available evidence indicates that H_0 and H_+ are parallel functions (26, 27) so that one would expect a plot of the two left hand terms of eq. [7] against H_0 to be linear of unit slope, while the two left hand terms of eq. [8] plotted against $-H_0$ should give a slope of +2, assuming that the activity coefficient terms cancel as is probable at least in eq. [7].

[7] $$\log k_{obs} - \log \frac{c_{SH^+}}{c_S + c_{SH^+}} = -H_+ + \log \frac{k'}{K_{SH_2{}^{2+}}} + \log \frac{f_{SH^+} f_{CH^{2+}}}{f_{\neq}' f_{C^+}}$$

[8] $$\log k_{obs} - \log \frac{c_S}{c_S + c_{SH^+}} = -H_0 - H_+ + \log \frac{k'}{K_{SH^+} K_{SH_2{}^{2+}}} + \log \frac{f_S f_{BH^+} f_{CH^{2+}}}{f_{\neq}' f_B f_{C^+}}$$

The relevant plots are presented in Fig. 5. It is seen that $\log k_{obs} - \log c_S/(c_S + c_{SH^+})$ vs. $-H_0$ gives a linear plot with a slope of 1.97, while $\log k_{obs} - \log c_{SH^+}/(c_S + c_{SH^+})$ vs. $-H_0$ is linear with a slope of 0.97. These results are not consistent with the mechanism of eqs. [1] and [2] but are in good accordance with the predicted values on the basis of eqs. [3] – [5]. Furthermore, examination of eqs. [7] and [8] shows that one should be able to calculate K_{SH^+} by combining the intercepts of the two plots, provided the activity coefficient terms are zero. The value obtained for

Can. J. Chem. Downloaded from www.nrcresearchpress.com by 210.87.254.6 on 09/05/12
For personal use only.

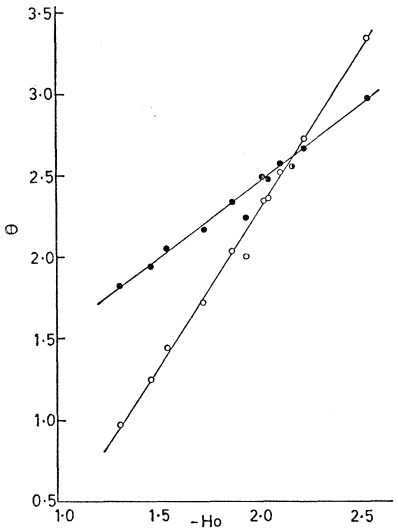

FIG. 5. Correlation between acidity function and rate for the acid hydrolysis of azobenzene-4-sulfate. ○, $\theta = 5 + \log k_{obs} - \log c_S/(c_S + c_{SH^+})$; ●, $\theta = 5 + \log k_{obs} - \log c_{SH^+}/(c_S + c_{SH^+})$.

K_{SH^+} in this manner is 133 which agrees satisfactorily with the experimentally determined value of 138 ($pK_a = -2.14$).

Azobenzene-4-hydrogen Sulfate as an Intermediate in the Wallach Rearrangement

The question of the intermediacy of azobenzene-4-hydrogen sulfate in the Wallach rearrangement of azoxybenzene has to be considered in the light of the present study. This has shown that hydrolysis of the sulfate salt proceeds readily over the region 22–42% H_2SO_4, with the half-life in the upper acid region being about 2 min. If the dependence of rate on acidity continued to obey the same function of H_0 then the estimated half-life for reaction in 90% H_2SO_4 would be of the order of 10^{-4} s. It is of course conceivable that a discontinuity between rate and acidity can arise over such a large extrapolation. A few exploratory experiments were performed to test this possibility. Spectra were taken of solutions of the sulfate salt in 56.1, 75.3, and 89.3% H_2SO_4 within minutes of their preparation: the spectra were virtually identical with the *p*-hydroxyazobenzene spectrum in these media.

Despite the above considerations one may not conclude that azobenzene hydrogen sulfate is not initially formed in the Wallach rearrangement. In strong sulfuric acid solutions the nucleophilic species present predominantly is the bisulfate ion. According to the calculations of Robertson and Dunford (28), when hydration of the hydrogen ion is taken into account, the bisulfate ion concentration exceeds that of the available water above 40% H_2SO_4. The water activity diminishes by about 10^4 on going from 40 to 95% H_2SO_4 but the bisulfate ion concentration remains within a factor of 10 over the same acid range (28). It would seem probable that unless there was a dramatic reversal in the relative reactivities of the two nucleophiles, then bisulfate ion would be the actual nucleophilic species in Wallach rearrangement studies, generally carried out in 65–95% H_2SO_4. However, the azobenzene hydrogen sulfate initially formed would, under these conditions, become rapidly hydrolyzed to *p*-hydroxyazobenzene which would then be the observed product.

Experimental

Materials

The potassium salt of azobenzene-4-hydrogen sulfate was prepared by a modification of the method described by Burkhardt and Lapworth (29). Pyridine – sulfur trioxide adduct was prepared from pyridine (3.33 g) and stabilized SO_3 (2.78 g) under nitrogen at 0°. The white solid was suspended in 20 ml benzene and after heating till reflux, *p*-hydroxyazobenzene (4.95 g) was added as a suspension in 15 ml benzene. After 4 h refluxing, the suspension of yellow-orange precipitate which had formed was poured into an excess (40 ml) of 1 *N* KOH. After stirring for 2 h the solid was filtered, washed extensively with absolute ethanol, followed by ether, and then dried over P_2O_5 at 0.1 mm/25°. The bright-yellow powder decomposed over the temperature range 200–235°.

Anal. Calcd. for $C_{12}H_9N_2O_4SK$: C, 45.56; H, 2.85; N, 8.85; S, 10.13. Found: C, 45.22; H, 2.63; N, 8.73; S, 9.80.

p-Hydroxyazobenzene (Eastman) was recrystallized from 40% ethanol, m.p. 154.5–155.5° (lit. (30) 155–156°). Sulfuric acid solutions were made up by dilution of Reagent grade acid and standardized by titration with sodium hydroxide.

Kinetic Procedures

Rate data were generally obtained by spectral examination of the reaction solutions contained in a thermostatted cell (25.00 ± 0.03°) mounted in a Unicam SP800B ultraviolet–visible spectrophotometer. These kinetics were conducted by two main methods. In the first method a 1.00 ml sample of a 1.61×10^{-3} *M* aqueous solution of azobenzene-4-sulfate was placed in a 50 ml volumetric flask in a thermostatted bath and made up with pre-thermostatted sulfuric acid, the resulting acid concentration being determined by titration at the end of the kinetic run. This reaction solution was placed in the thermostatted cell and spectra were recorded periodically

Can. J. Chem. Downloaded from www.nrcresearchpress.com by 210.87.254.6 on 09/05/12
For personal use only.

over the region 300–500 mμ. In the second method the reaction solution was prepared by direct addition of a weighed quantity of the potassium salt to a given sulfuric acid medium and then transferred to the cell. Most of the kinetic runs were carried out in 1.00 cm cells but in a few runs 0.100 cm cells were used, in order to compare directly (at the given concentration of acid and substrate) the rate constant obtained by the above method with the value obtained by the base-dilution method described below.

The base-dilution procedure was similar to that employed previously (4). In a typical run, 1.227 mg of azobenzene-4-sulfate was dissolved in 10.0 ml of 24.0% H_2SO_4 at 25°, to give a 3.88×10^{-4} *M* solution of substrate. This reaction solution, contained in a flask in the thermostatted bath, was sampled periodically and the aliquots (1.00 ml) quenched by adding to precooled 1 *N* KOH solution which was subsequently made up to 25 ml with the aqueous base. The spectra of these quenched solutions were recorded in 4.00 cm cells over the range 300–500 mμ.

Rate constants were calculated either by the Guggenheim method or from $(A_\infty - A_t)$ vs. time plots. In the case of runs monitored *in situ* the absorbance changes at 460 mμ were used, while in the case of the base-quenched runs the absorbance changes at 440 mμ were so treated; these wavelengths correspond to λ_{max} for *p*-hydroxyazobenzene in acidic and basic medium (see footnote in Table I), respectively.

Examination of Azobenzene-4-sulfate in Intermediate Acid Concentrations

The stability of the above potassium salt was examined spectrally in the media 56.1, 75.3, and 89.3% H_2SO_4, at 25°, within minutes of preparation of the reaction solutions. For the last acid concentration, in addition to recording the spectrum in the acid medium, the reaction solution was diluted with base (1.00 ml of 4.18×10^{-4} *M* reaction solution made up to 50 ml with 1 *N* KOH and run in a 4.00 cm cell) and the basic spectrum taken. The above spectra were compared with corresponding spectra of *p*-hydroxyazobenzene over this acid region and were found to be identical within experimental error. The spectral absorptions in the acid media all fell in the range λ_{max} 460 ± 1 mμ, ε 3.87 ± 0.09 × 10^4. The base-quenched solution of azobenzene-4-sulfate after exposure to 89.3% H_2SO_4 showed λ_{max} 400 mμ, ε 2.22 × 10^4; and λ_{max} 440 mμ, ε 2.19 × 10^4 (cf. Table I).

Acknowledgments

This research was supported by a grant from the National Research Council of Canada. The award of an Ontario Graduate Fellowship to W.M.J.S. is also acknowledged.

1. E. BUNCEL. *In* Mechanisms of molecular migrations. *Edited by* B. S. Thyagarajan. John Wiley and Sons, Inc., New York. In press.
2. D. DUFFEY and E. C. HENDLEY. J. Org. Chem. **33**, 1918 (1968).
3. C. S. HAHN, K. W. LEE, and H. H. JAFFÉ. J. Am. Chem. Soc. **89**, 4975 (1967).
4. E. BUNCEL and B. T. LAWTON. Can. J. Chem. **43**, 862 (1965).
5. M. M. SHEMYAKIN, T. E. AGADZHANYAN, V. I. MAIMIND, and R. V. KUDRYAVTSEV. Bull. Acad. Sci. USSR, 1216 (1963).
6. S. OAE, T. FUKUMOTO, and M. YAMAGAMI. Bull. Chem. Soc. Japan, **36**, 601 (1963).
7. (*a*) B. T. NEWBOLD. J. Chem. Soc. 6972 (1965). (*b*) B. T. NEWBOLD and M. H. AKHTAR. Private communication.
8. J. SINGH, P. SINGH, J. L. BOIVIN, and P. E. GAGNON. Can. J. Chem. **41**, 499 (1963).
9. P. H. GORE. Chem. Ind. London, 191 (1959).
10. E. BUNCEL and B. T. LAWTON. Chem. Ind. London, 1835 (1963).
11. M. A. PAUL and F. A. LONG. Chem. Rev. **57**, 1 (1957).
12. E. M. ARNETT and C. Y. WU. J. Am. Chem. Soc. **82**, 5660 (1960).
13. (*a*) I. M. KLOTZ, H. A. FIESS, J. Y. C. HO, and M. MELLODY. J. Am. Chem. Soc. **76**, 5136 (1954). (*b*) E. SAWICKI. J. Org. Chem. **22**, 365 (1957).
14. R. P. BELL. The proton in chemistry. Cornell University Press, Ithaca, New York. 1959. Chap. 7.
15. R. A. ROBINSON and R. H. STOKES. Electrolyte solutions. 2nd ed. Butterworths, London. 1959. p. 383.
16. H. H. JAFFÉ and R. W. GARDNER. J. Am. Chem. Soc. **80**, 319 (1958).
17. J. F. BUNNETT and E. BUNCEL. J. Am. Chem. Soc. **83**, 1117 (1961).
18. R. L. REEVES. J. Am. Chem. Soc. **88**, 2240 (1966).
19. J. L. KICE and J. M. ANDERSON. J. Am. Chem. Soc. **88**, 5242 (1966).
20. F. GERSON and E. HEILBRONNER. Helv. Chim. Acta, **45**, 51 (1962).
21. J. F. BUNNETT, E. BUNCEL, and K. V. NAHABEDIAN. J. Am. Chem. Soc. **84**, 4136 (1962).
22. L. P. HAMMETT. Physical organic chemistry. McGraw-Hill Book Co., Inc., New York. 1940. pp. 262–277.
23. F. A. LONG and M. A. PAUL. Chem. Rev. **57**, 935 (1957).
24. J. F. BUNNETT. J. Am. Chem. Soc. **83**, 4956 (1961); **83**, 4968 (1961); **83**, 4973 (1961); **83**, 4978 (1961).
25. J. F. BUNNETT and F. OLSEN. Can. J. Chem. **44**, 1917 (1966).
26. T. G. BONNER and J. C. LOCKHART. J. Chem. Soc. 364 (1957).
27. M. W. FULLER and W. M. SCHUBERT. J. Am. Chem. Soc. **85**, 108 (1963).
28. E. B. ROBERTSON and H. B. DUNFORD. J. Am. Chem. Soc. **86**, 5080 (1964).
29. G. N. BURKHARDT and A. LAPWORTH. J. Chem. Soc. 684 (1926).
30. H. H. JAFFÉ and S. Y. YEH. J. Am. Chem. Soc. **81**, 3274 (1959).

Can. J. Chem. Downloaded from www.nrcresearchpress.com by 210.87.254.6 on 09/05/12
For personal use only.

Mass spectrometry of ozonides

J. CASTONGUAY, M. BERTRAND[1], J. CARLES, S. FLISZÁR, AND Y. ROUSSEAU[2]
Département de Chimie, Université de Montréal, Montréal, Québec

Received August 9, 1968

The mass spectra of some ozonides are reported, and the modes of formation of the major fragment ions tentatively described. The use of ^{18}O-labelled compounds has proven to be useful in establishing fragmentation patterns. It is concluded that these follow a characteristic path, which is common to all the ozonides studied and permits mass spectrometric identification.

Les spectres de masse d'une série d'ozonides sont rapportés ainsi qu'une rationalisation des modes de fragmentation conduisant aux principaux ions. Dans certains cas, des ozonides marqués avec ^{18}O ont servi à établir plus fermement les divers modes de fragmentation. Il s'avère que tous les produits étudiés se décomposent par impact électronique, selon un mode qui leur est caractéristique et qui permet leur identification par spectrométrie de masse.

Canadian Journal of Chemistry, **47**, 919 (1969)

Can. J. Chem. Downloaded from www.nrcresearchpress.com by 210.87.254.40 on 09/05/12
For personal use only.

We have recently reported on the general behavior of cyclic organic peroxides (**B**), when submitted to electron impact (1), and the present communication reports an analogous study on some selected ozonides (**A**).

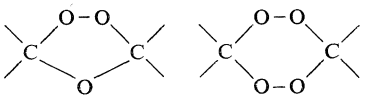

(A) (B)

The behavior of a number of ozonides towards electron impact and the characteristics of the fragmentation patterns are of considerable interest both for comparative purposes, for example, with peroxides containing ring (**B**), and for mass spectral identification. The identification of the fragment ions in the mass spectra of the ozonides, in particular of those suitably labelled with ^{18}O, provides additional evidence as to the position of incorporation of the aldehydic oxygen in the ozonide molecule [1]. This evidence may be used as suitable support for the mechanism of ozonolysis now under consideration (2). The compounds listed in Table I and referred to as compounds **1** to **8**, were selected for study, as suitable substituents are attached to the ozonide ring. The effect of these substituents on the fragmentation patterns will indicate the possibility of aromatic stabilization and the path of any bond cleavage.

The fact that the compounds chosen are unstable is a serious disadvantage for mass spectrometric study. In fact, there is a possibility that the recorded spectra may arise from the decomposition products of the ozonides and not from the ozonides. Two observations, however, verified that the recorded spectra were those of the ozonides. First, the spectra of the compounds did not differ when the same sample was subjected to a number of consecutive analyses. If decomposition did occur, the spectra would be expected to change due to the formation of ions of the more stable products. Second, stilbene ozonide was intentionally pyrolyzed in the mass spectrometer by using the standard metal inlet system. In these experiments, the temperature of the sample was raised slowly and consecutive spectra were taken. They showed a completely different pattern when compared to the spectrum of the stilbene ozonide. The ions at *m/e* 196 and 122 disappeared, and peaks at *m/e* 18, 28, 44, 78, and 106, showing the presence of H_2O^+, CO^+, CO_2^+, $C_6H_6^+$, and $PhCHO^+$, were very intense. The pattern from one spectrum to the other was found to vary in favor of these ions. Furthermore, since the spectrum of styrene ozonide was reproducible and had ions at *m/e* 122 (8.2% Σ) and at the right molecular weight (this compound having the lowest thermal stability of all) it supports the conclusion that decomposition by means other than electron impact could not play a significant role in the present conditions.

[1]Holder of a postgraduate "Hydro-Québec" scholarship.

[2]Author to whom the correspondence should be addressed.

TABLE I

List of compounds studied

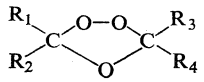

Compound number	Nature of substituents	Name
1	$R_1=R_3=R_4=H$, $R_2=Ph$	Styrene ozonide
2	$R_1=R_3=H$, $R_4=CH_3$, $R_2=Ph$	β-Methylstyrene ozonide (*cis–trans*-mixture)
3	$R_1=R_3=H$, $R_2=R_4=Ph$	Stilbene ozonide (*cis–trans*-mixture)
4	$R_2=R_3=R_4=Ph$, $R_1=H$	Triphenylethylene ozonide
5	$R_1=R_3=H$, $R_2=R_4=n\text{-}C_3H_7$-	4-Octene ozonide (*cis–trans*-mixture)
6	$R_1=R_3=H$, $R_2=R_4=Ph\text{-}CH_2$-	1,4-Diphenyl-2-butene ozonide (*cis–trans*-mixture)
7	$R_1=R_3=H$, $R_2=R_4=Cl\text{-}CH_2$	1,4-Dichloro-2-butene ozonide (*cis–trans*-mixture)
8	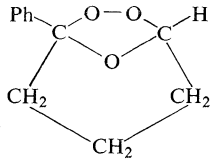	1-Phenyl-cyclopentene ozonide

Experimental

All spectra were obtained by using a single focussing Hitachi RMU-6D mass spectrometer with the MG-150 direct introducing system. The compounds have sufficiently high vapor pressures to eliminate the need for external heat on the sample holder. The ionization chamber was maintained between 150 and 170 °C and the ionizing electrons were accelerated by a 70 V potential.

Compounds **1**, **3**, **5**, **6**, and **7** were prepared and purified according to literature (3–5).

Styrene Ozonide

Five mmoles of styrene dissolved in 25 ml of CCl_4 were ozonized at room temperature with 80% of the theoretical amount of ozone. Isolation of the styrene and the stilbene ozonides was performed by column chromatography, using Baker silica gel. The unreacted olefin was collected in the CCl_4 fraction. With a benzene–hexane (9:10) mixture, the stilbene ozonide (m.p. 74 °C) was collected initially and then the styrene ozonide, m.p. −12 °C (lit. (5) −15 °C), n_D^{25} 1.4482 (lit. (5) n_D^{20} 1.4511).

Stilbene Ozonide

Five mmoles of *cis*- or *trans*-stilbene dissolved in 25 ml of CCl_4 were ozonized at room temperature with 80% of the theoretical amount of ozone. After evaporation of the solvent, the product was crystallized several times in hot methanol. Fine needles of the ozonide (m.p. 74 °C, lit. (5) 74 °C) were obtained and the nuclear magnetic resonance (n.m.r.) spectrum of this product showed a multiplet at 2.7 and two signals at 3.79 and 3.83 (methine protons), which are attributed (2) to the *cis*-ozonide and *trans*-ozonide, respectively. On the 100 c.p.s. scale, the signals for the *cis*- and the *trans*-ozonides can be integrated separately. Measurements made with *cis–trans* mixtures in known proportions prepared from the pure isomers (2) confirm that the ozonide (m.p. 74 °C) is a 1:1 *cis–trans*-ozonide mixture. The stilbene ozonide, obtained as cross ozonide during the ozonization of styrene, has been shown to be identical with the product, m.p. 74 °C.

β-Methylstyrene Ozonide

Five mmoles of *trans*-β-methylstyrene in 25 ml of CCl_4 or pentane were ozonized at room temperature with 80% of the theoretical amount of ozone. For experiments at −78 °C, pentane was used as solvent. The initial separation of the unreacted olefin in the CCl_4 fraction was effected by column chromatography, using Baker silical gel. From a *n*-hexane–benzene mixture (1:1), the stilbene ozonide which can be purified by recrystallization in methanol (m.p. 74 °C) was first obtained. The subsequent fraction contained the β-methylstyrene ozonide, which can be purified further by repeating the chromatography.

Anal. Calcd. for $C_9H_{10}O_3$ (m.p. 19 °C): C, 65.05; H, 6.07. Found: C, 65.4; H, 6.25, 6.00.

The n.m.r. spectrum showed the following signals: 9.48 (d), 4.52 (q), and 2.6 (m). The two signals at 4.04 and 4.00 (methine protons) indicated that this ozonide was a *cis–trans* mixture. By comparison with similar systems (2, 7), it is reasonable to assign the 4.04 signal to the *trans*-ozonide and the 4.00 signal to the *cis*-ozonide.

Triphenylethylene Ozonide

Five mmoles of triphenylethylene in 25 ml of CCl_4 or pentane were ozonized at room temperature with 80% of the theoretical amount of ozone. The unreacted olefin was recovered in column chromatography, using Baker silica gel, in the CCl_4 fraction. The ozonide was recovered in the benzene–hexane (1:1) fraction. After evaporation of the solvent, the triphenylethylene ozonide was recrystallized in methanol. The colorless crystals obtained had a m.p. of 95 °C.

Can. J. Chem. Downloaded from www.nrcresearchpress.com by 210.87.254.40 on 09/05/12
For personal use only.

Can. J. Chem. Downloaded from www.nrcresearchpress.com by 210.87.254.40 on 09/05/12
For personal use only.

Anal. Calcd. for $C_{20}H_{16}O_3$: C, 78.95; H, 5.33. Found: C, 79.11; H, 5.45.

The n.m.r. spectrum shows a multiplet at 2.7 and a singlet (methine proton) at 3.72.

1-Phenyl-cyclopentene Ozonide

A solution of 1.0 mmole of 1-phenyl-cyclopentene in 10 ml of CCl_4 was ozonized with the theoretical amount of ozone at room temperature. After evaporation of the solvent, the ozonide was recovered in almost quantitative yield. For purification, the cyclic compound was dissolved in a 1:1 mixture of benzene–hexane and passed through a Baker silica gel column. The waxy crystalline compound obtained after removal of the solvent under vacuum, had a m.p. of 34 °C.

Anal. Calcd. for $C_{11}H_{12}O_3$: C, 68.73; H, 6.29. Found: C, 68.74; H, 6.42.

Benzaldehyde ^{18}O

This aldehyde, which was used to label the ozonides **1** to **4**, was prepared by an exchange reaction (6).

In a nitrogen atmosphere, 2.0 g of $H_2{}^{18}O$ (67.17% ^{18}O), 5.3 g of freshly distilled benzaldehyde, and a trace of *p*-toluenesulfonic acid were stirred together at room temperature. After 12 h, the organic layer, together with the ether extract of the water, was distilled at 15 Torr. The aldehyde obtained (5 g) contained 44.6% ^{18}O.

Ozonides Labelled with ^{18}O

If the formation of ozonides proceeds via the Criegee mechanism (8), the ^{18}O atom of the benzaldehyde will be located only in the ether position of the ozonide:

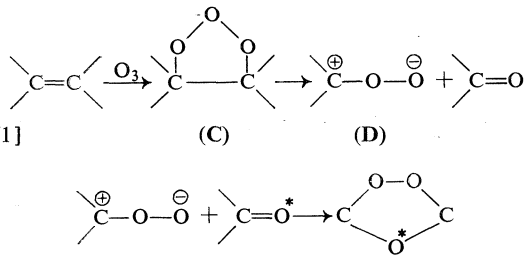

[1] (C) (D)

The key zwitterion intermediate (**D**) formed during the cleavage of the molozonide (**C**) can react equally well with the ^{18}O-labelled PhCHO or with the carbonyl compound formed during the cleavage of (**C**).

The present results indicate that all of the ^{18}O incorporation is located in the ether position of the ozonides. It must be stressed, however, that this does not prove that the Criegee mechanism is necessarily the correct one, since other pathways (2) would also yield the same labelled molecule[3]. Owing to the instability of the molozonides, even at very low temperatures, it is reasonable to assume that no molozonide–aldehyde mechanism will compete with the Criegee mechanism at room temperature.

The labelled ozonides were obtained by ozonizing 25 ml of 0.2 *M* olefin in the presence of 0.2 *M* $PhCH^{18}O$ (44.6% ^{18}O) at room temperature. The solvents used were CCl_4 and pentane, and no difference in incorporation was detected between the solvents. The amounts of ozone used were limited to 80% of the theoretical amount to prevent the formation of peracids due to the autoxidation of the aldehydes, the probability of this being enhanced by the presence of ozone. The isolation of the ozonides by the column chromatography work-up procedure was described previously for the nonlabelled compounds.

Results and Discussion

The spectra[4] of compounds **1** to **8** are shown in Figs. 1–8. In many cases the sample introduced into the mass spectrometer contained a mixture of *cis*- and *trans*-ozonide. However, examination of the spectra of pure *cis*- and pure *trans*-stilbene enriched in ^{18}O (5%), from Fig. 9, shows that the cracking patterns are very similar for the two isomers. This is not unreasonable since both of these compounds give the same ion on primary fragmentation.

A general fragmentation scheme (Scheme 1) is proposed to explain the spectra obtained with ozonides **1** to **7**. Compound **8**, which has a different structure, will be discussed separately and will permit comparisons to be made. Although in specific cases the substituent groups affect the intensity of certain fragments, it can be seen that fragmentation of the molecular ion occurs by two distinct paths, both of which involve a rupture of the heterocycle. The first involves the cleavages of an O—O and a C—O bond, whereas the second, which occurs less frequently, proceeds by the rupture of two C—O bonds. These differences are also clearly illustrated by the spectra of the labelled compounds, which will be discussed later. These two major modes of fragmentation are depicted in Scheme 1. The ions reported in that figure account for most of the ionic current recorded. In some cases the elimination of a radical (R_1, R_2, R_3, or R_4) from the molecular ion was detected but this process gave rise to peaks of very low intensity.

With the exception of the $[M - 32]^+$ peak, processes 1 and 2 of Scheme 1 give rise to ions having the same *m/e* ratio. Nevertheless, the spectra of ^{18}O-labelled ozonides show clearly

[3]A detailed study of the mechanism of ozonolysis, including the formation of *cis*- or *trans*-ozonides and the stereospecifical dependence of the ozonides *cis*/*trans* ratio on the olefin geometry, is now being conducted in one of our laboratories (S. Fliszár).

[4]In many cases low intensity peaks (<0.5% Σ) have been omitted in the figures.

Can. J. Chem. Downloaded from www.nrcresearchpress.com by 210.87.254.40 on 09/05/12
For personal use only.

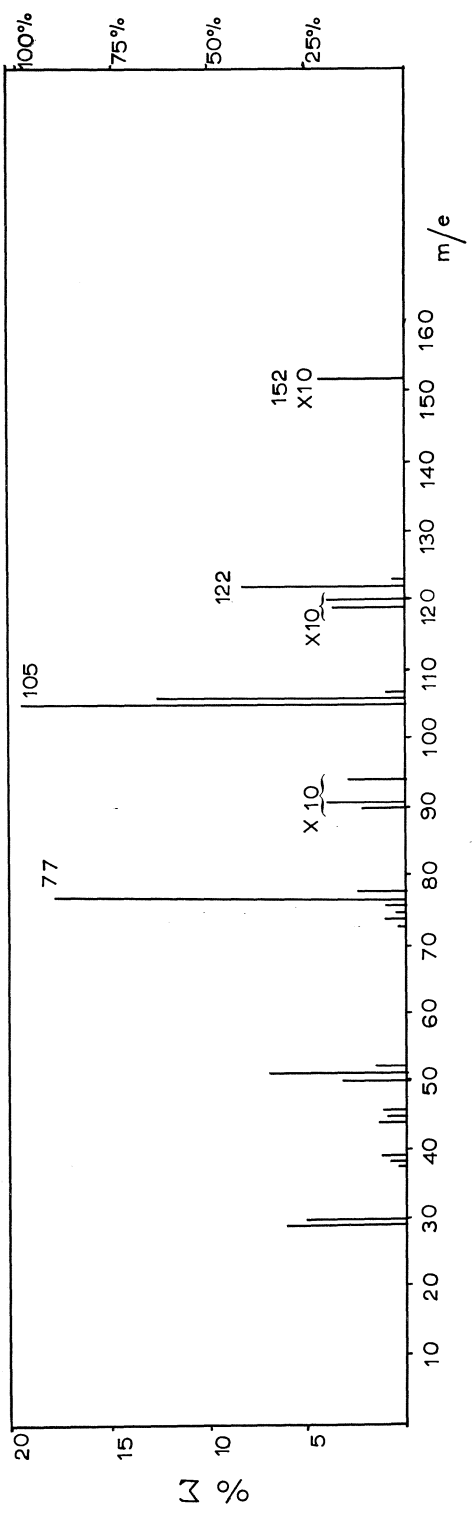

FIG. 1. Mass spectrum of styrene ozonide.

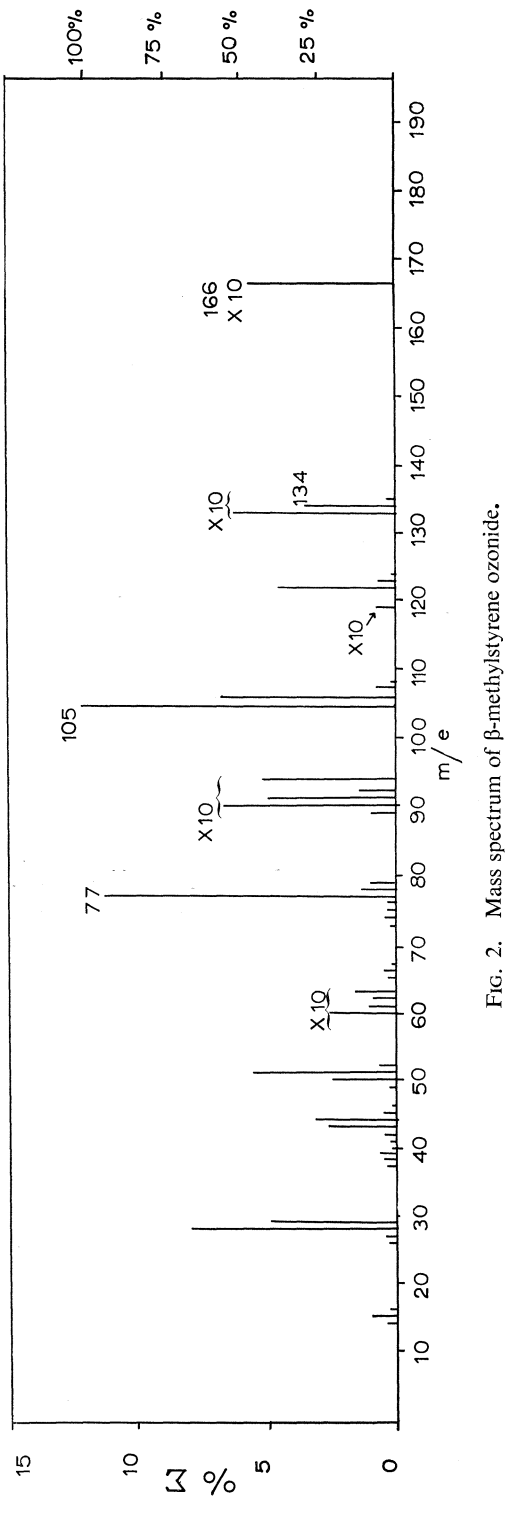

FIG. 2. Mass spectrum of β-methylstyrene ozonide.

Can. J. Chem. Downloaded from www.nrcresearchpress.com by 210.87.254.40 on 09/05/12
For personal use only.

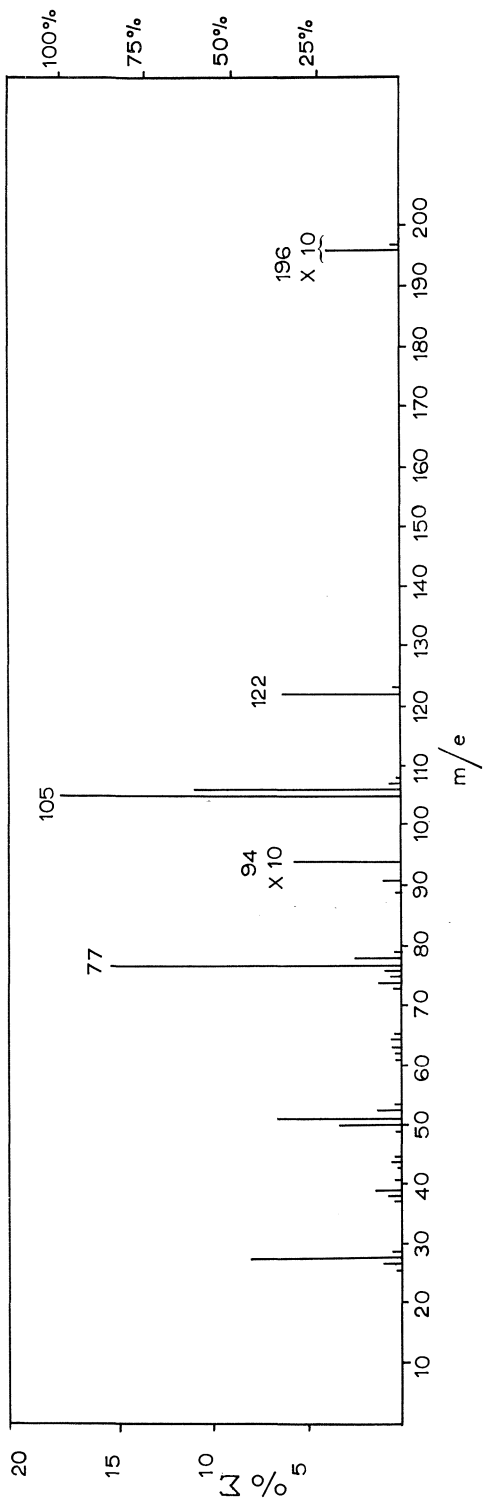

FIG. 3. Mass spectrum of stilbene ozonide.

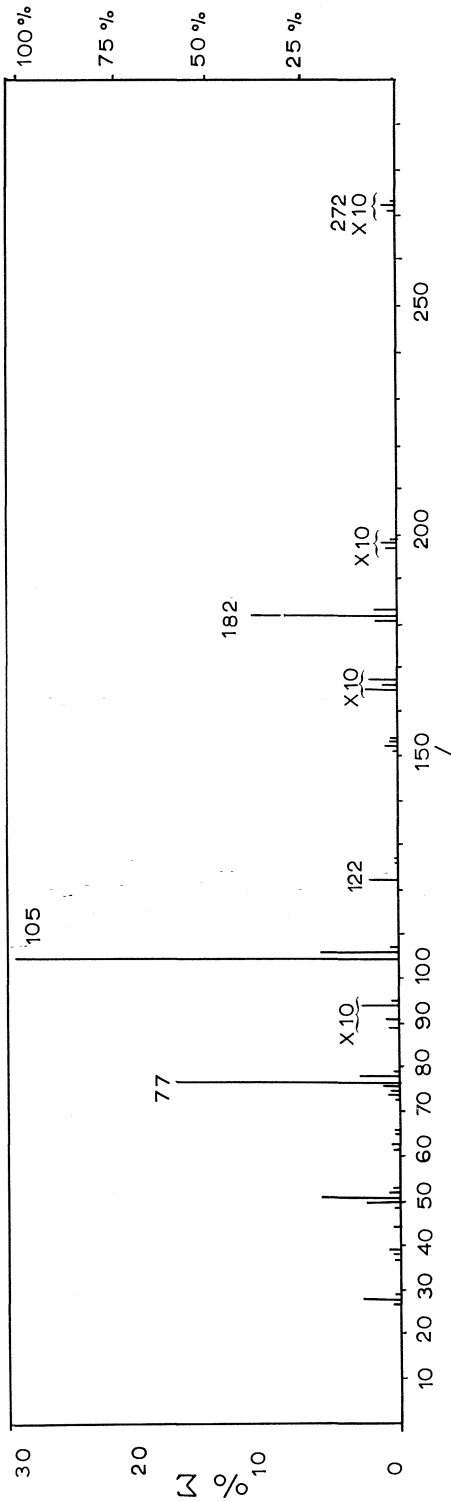

FIG. 4. Mass spectrum of triphenylethylene ozonide.

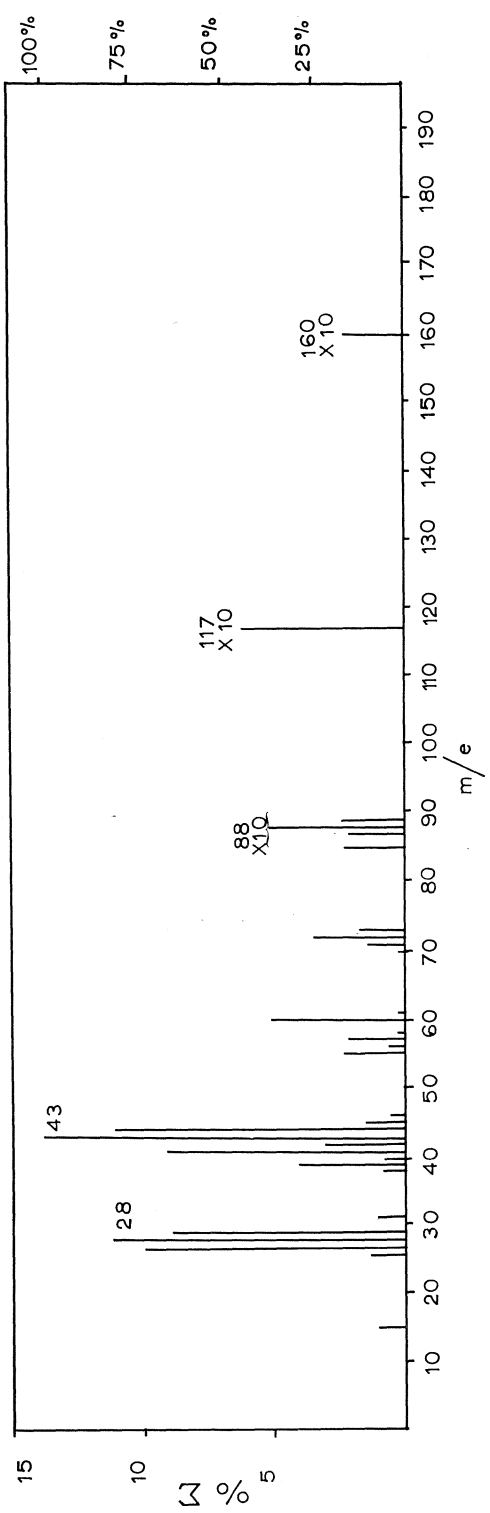

FIG. 5. Mass spectrum of 4-octene ozonide.

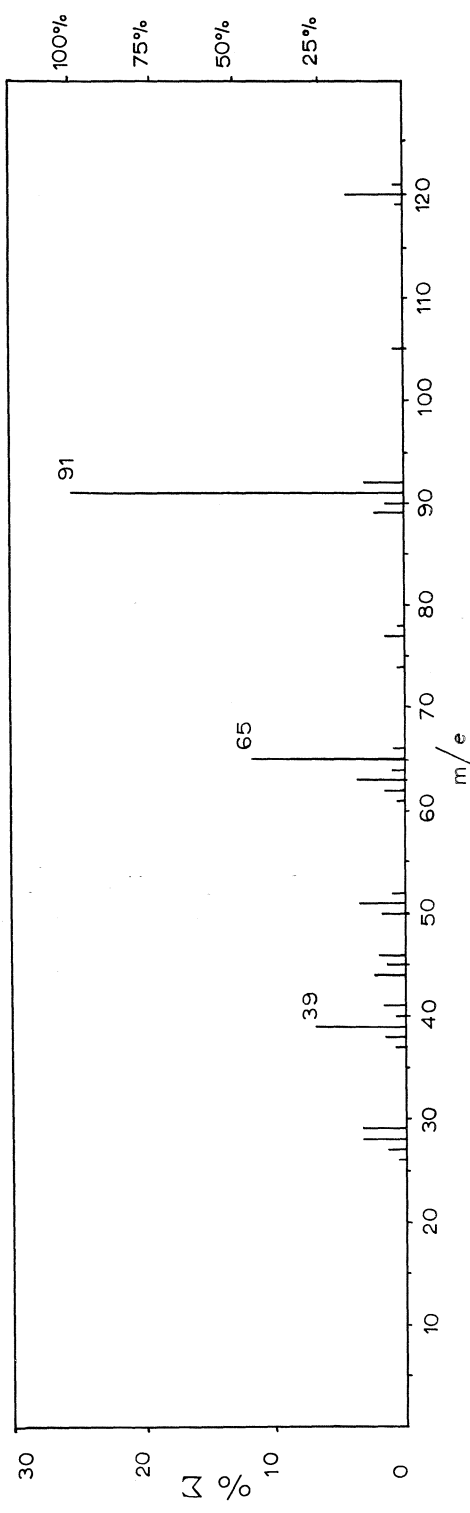

FIG. 6. Mass spectrum of 1,4-diphenyl 2-butene ozonide.

Can. J. Chem. Downloaded from www.nrcresearchpress.com by 210.87.254.40 on 09/05/12
For personal use only.

Can. J. Chem. Downloaded from www.nrcresearchpress.com by 210.87.254.40 on 09/05/12
For personal use only.

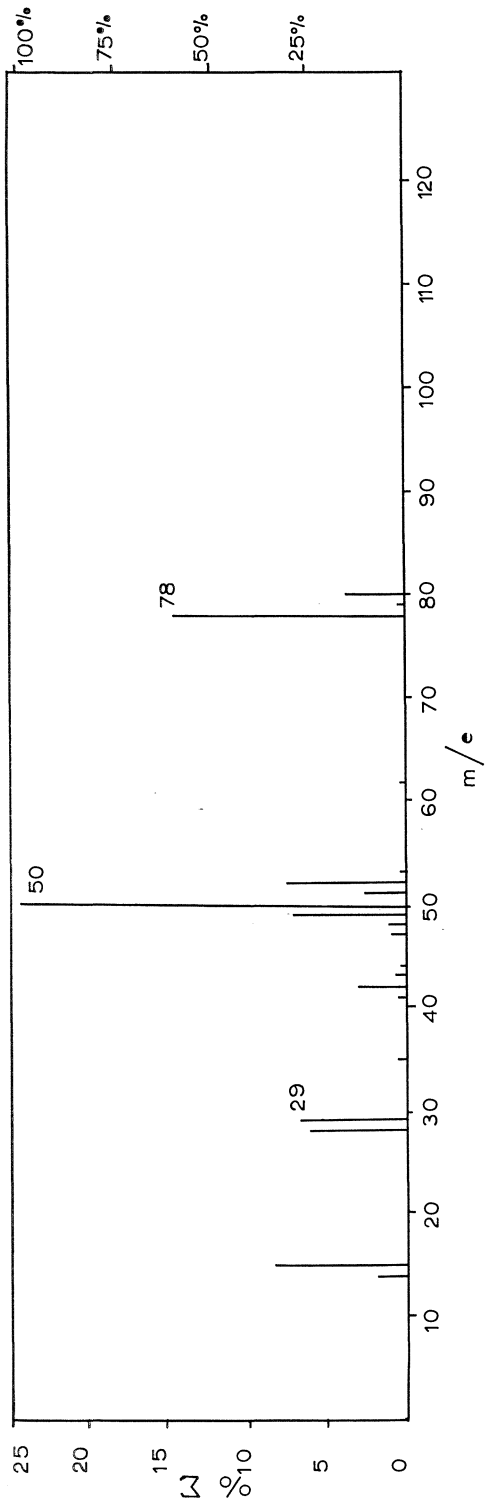

FIG. 7. Mass spectrum of 1,4-dichloro 2-butene ozonide.

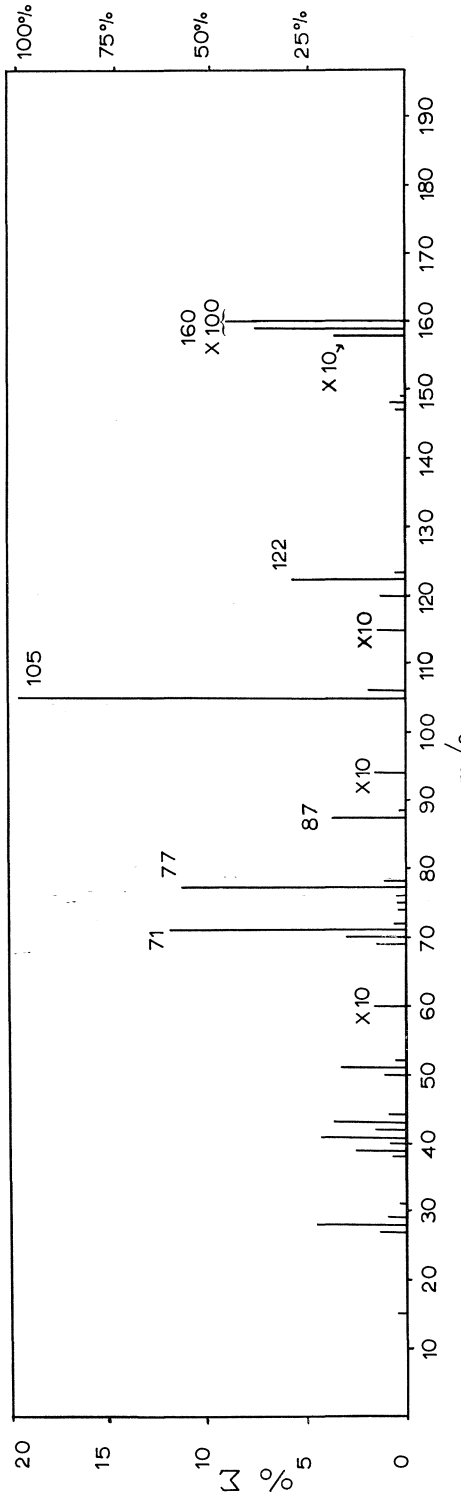

FIG. 8. Mass spectrum of 1-phenyl cyclopentene ozonide.

Can. J. Chem. Downloaded from www.nrcresearchpress.com by 210.87.254.40 on 09/05/12
For personal use only.

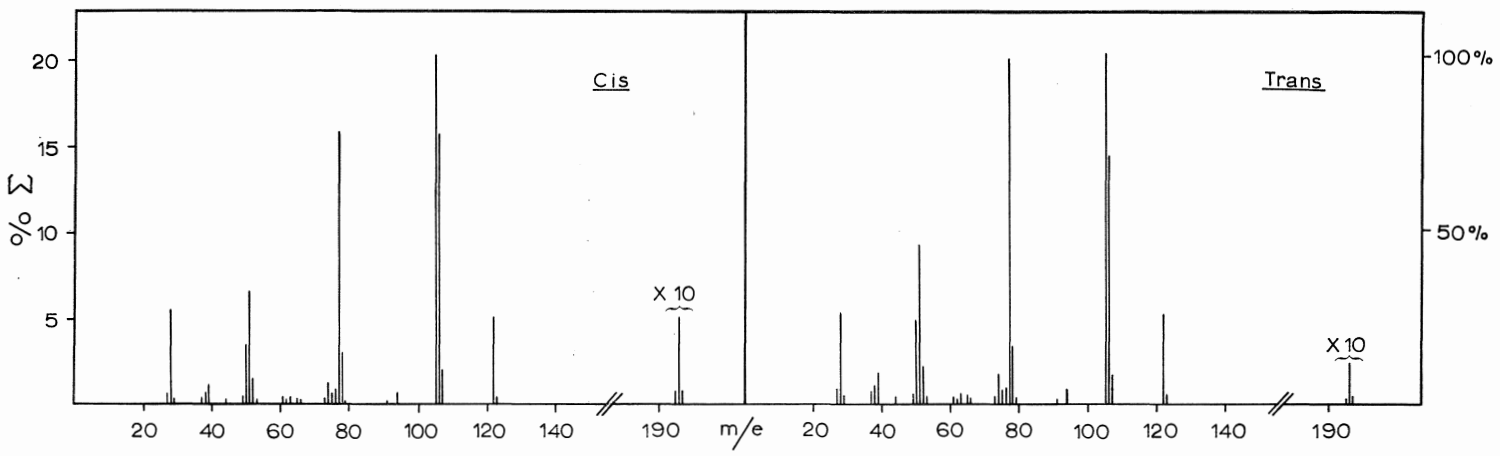

FIG. 9. Mass spectra of *cis*- and *trans*-stilbene ozonides enriched 5% in ^{18}O.

TABLE II
Intensity of major ions

Compound number	$R_1R_2C{=}O^{+\cdot}$ *m/e*	%Σ	$[R_1R_2C{\cdot}{-}O{-}O^{\cdot}]^+$ *m/e*	%Σ	$R_1R_2C(O^{\cdot})O^{\cdot}$ *m/e*	%Σ	$R_3R_4C{=}O^{+\cdot}$ *m/e*	%Σ	$[R_3R_4C{\cdot}{-}O{-}O^{\cdot}]^+$ *m/e*	%Σ	$[R_3R_4C(O^{\cdot})O^{\cdot}]^+$ *m/e*	%Σ	$R_1R_2C{-}O{-}CR_3R_4$ *m/e*	%Σ	M^+ *m/e*	%Σ
1	106	12.07	122	8.23	30	4.77	46	1.11	120	0.39	152	0.43				
2	106	8.77	122	5.00	44	3.54*	60	0.58	134	0.47	160	0.66				
3	106	11.1	122	6.55	106	11.10	122	6.55	196	0.42	228	—				
4	106	6.38	122	2.21	182	11.63	198	0.11	272	0.11	304	—				
5	72	3.81	88	0.522	72	3.81	88	0.522	128	—	160	0.26				
6	120	4.8	136	—	120	4.8	136	—	224	—	256	—				
7	78	11.43	94	—	78	11.43	94	—	140	—	172	—				

*Not only due to above ion.

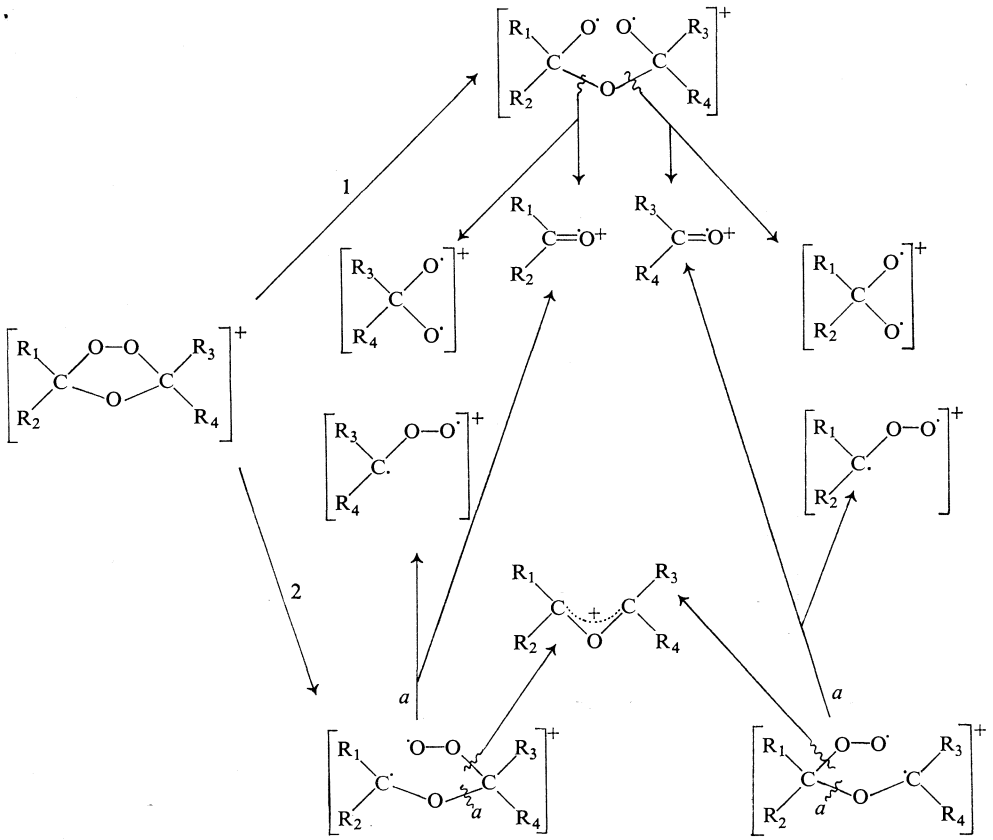

SCHEME 1. General fragmentation pattern for the ozonides **1–7**

that there are two different ions, i.e. (**E**) and (**G**) of the same *m/e* ratio:

[2]

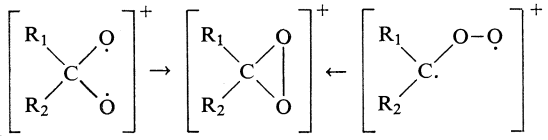

(**E**) (**F**) (**G**)

Structures (**E**) and (**G**) are shown to indicate the original ions produced by ruptures 1 or 2 of Scheme 1. It is possible that one or both of these ions can exist in the (**F**) form, although no definite indication of this has been obtained.

Further fragmentation of the carbonyl fragments usually occurs by the well-established mechanism (9)

[3] 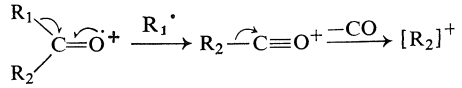

The decomposition of the $[M - 32]^+$ and the $[RR'CO_2]^+$ ions[5] depends on the R substituents and this decomposition will be specified in particular cases. For compounds **1** to **7**, the major ions produced by the general fragmentation scheme are given in Table II.

The spectra of compounds **1–4** (Figs. 1–4) exhibit breakdown patterns found to be in agreement with the general mechanism of Scheme 1. Whenever a phenyl radical is substituted directly onto the ozonide ring, the most intense peak is at *m/e* 105. The ionic intensity distribution reflects the relative stability of the secondary ions. On the basis of a unimolecular fragmentation pattern, the relative abundance of the major ions can be qualitatively estimated by considering the charge stabilization effect of the substituents. From Table II, the intensity ratio $R_3R_4CO^+/PhCHO^+$

[5] $RR'CO_2^+$ through the text stands for $R_1R_2CO_2^+$ and $R_3R_4CO_2^+$.

Can. J. Chem. Downloaded from www.nrcresearchpress.com by 210.87.254.40 on 09/05/12
For personal use only.

for compounds **1**, **2**, and **4** is, respectively, 0.3, 0.5, and 2. Therefore, it is possible to classify the following ions by order of their increasing ease of formation from the molecular ion

[4] $H_2CO^+ < CH_3CHO^+ < PhCHO^+ < Ph_2CO^+$

In all four spectra, the presence of a fragment ion at $[M - 32]^+$ which results from the elimination of O_2 from the molecular ion, can be seen. This elimination is believed to occur in a way similar to that observed for the peroxides (1) in that this elimination of O_2 is from the peroxidic bridge of the ozonide ring. However, in the present study, molecular elimination of O_2 is not indicated by the presence of ions of *m/e* 32, unlike in the case of the peroxides (1). Further decomposition of the $[M - 32]^+$ occurs most probably as in ethers (10) by α or β cleavages

[5]

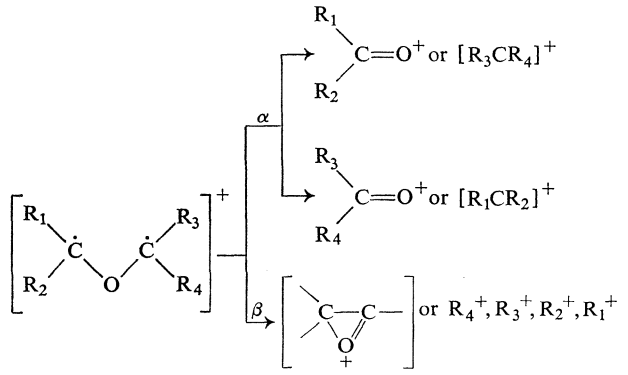

Process α gives rise to ions of low intensity at *m/e* 90, $[Ph—CH]^+$, for compounds **1**–**4** and to an ion at *m/e* 166, $[Ph—C—Ph]^+$, for compound **4**. Process β is responsible for ions at *m/e* 119 for compound **2**

[6]

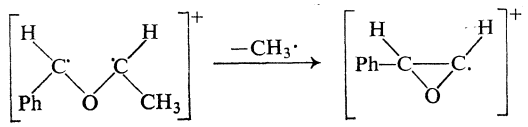

m/e 134 *m/e* 119

This β cleavage is also responsible for the presence of an $[M - 33]^+$ ion in the spectrum of compounds **1**–**4**. The transition

[7] $$[M - 32]^+ \xrightarrow{-H\cdot} [M - 33]^+$$

is characterized by metastable peaks at *m/e* 270 ($272^+ \rightarrow 271^+$) and at *m/e* 194 ($196^+ \rightarrow 195^+$) for compounds **4** and **3**, respectively. The $[M - 33]^+/[M - 32]^+$ intensity ratio depends on the compounds and is found to be 0.97, 1.6, 0.15, and 0.43 for compounds **1**–**4**, respectively.

In competition with the above processes it is possible to detect a β cleavage coupled with a hydrogen atom transfer, as shown below:

[8]

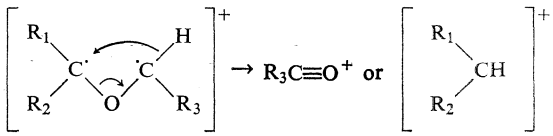

This rearrangement is indicated by the presence of ions at *m/e* 91 in compounds **1** to **4** and *m/e* 167 $[R_3R_4CH]^+$ in compound **4**.

It has been established that the base peak[6] in the spectrum of benzoic acid is at *m/e* 105 (11). This ion was found to result from an OH· elimination from the molecular ion at *m/e* 122 (12). Fragments ions at *m/e* 122 from the ozonides also undergo hydroxyl elimination, as indicated by a metastable peak (*m**) at 90.4

[9]

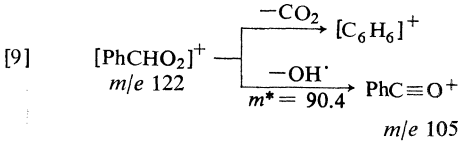

[6]Throughout the text the term "base peak" is used to designate the most intense peak.

Can. J. Chem. Downloaded from www.nrcresearchpress.com by 210.87.254.40 on 09/05/12
For personal use only.

TABLE III

Relative intensity of important fragments from the spectra of ^{18}O-labelled ozonides*, corrected for naturally-occurring heavy-isotopic abundance (%)

Compound **1**			Compound **2**			Compound **3**			Compound **4**		
	Relative intensity			Relative intensity			Relative intensity			Relative intensity	
m/e	A	B	*m/e*	A	B	*m/e*	A	B	*m/e*	A	B
105	100.00	100.00	105	100.00	100.00	105	100.00	100.00	105	100.00	100.00
106	65.77	72.92	106	76.84	83.10	106	83.69	75.65	106	14.14	12.62
107	3.82	4.43	107	9.33	6.94	107	7.17	9.72	107	8.37	7.66
108	1.21	1.64	108	4.30	3.82	108	5.44	4.57	108	1.71	1.82
122	25.99	18.51	122	13.33	17.02	122	9.34	14.94	122	7.64	5.88
124	3.91	3.16	124	3.54	3.74	124	3.70	6.22	124	3.06	2.36
119	3.33	1.55	44	20.00	31.56	196	1.19	1.54	182	33.35	63.53
			46	2.38	3.55	198	0.623	0.821	184	1.21	2.51
121	0.620	0.297	60	2.21	4.04	228	—	—	198	0.303	0.598
			62†	0.675	0.930	230	—	—	200	0.073	0.129
152	4.07	2.00	133	0.476	2.91				271	0.364	0.549
154	0.735	0.395	134	0.310	1.41				272	0.940	1.29
			135	0.177	0.840				273	0.171	0.266
			136	0.111	0.393				274	0.463	0.602
			166	0.500	1.62				304	—	—
			168	0.186	0.461				306	—	—

*A and B represent two labelled ozonides, differently synthesized.
†Corrected to represent the intensity of the $[R_3R_4CO_2]^+$ ion exclusively.

Furthermore, these *m/e* 122 ions also undergo rearrangement to give the phenol ion at *m/e* 94. This transition has been characterized previously (1, 11).

Isotopic Labelling

A minimum of two differently synthesized labelled ozonides were studied for each of the compounds **1**–**4**. The labelled ozonides studied were found to contain only one labelled oxygen atom, as the $(M + 4)^+$ ion was accounted for entirely with the natural isotopic abundance. Table IV reports the percentages of incorporation calculated as follows from Table III

$$[10] \qquad \% = \frac{H_{(M+2)}}{H_{(M)} + H_{(M+2)}} \times 100$$

where $H_{(M)}$ and $H_{(M+2)}$ represent the peak heights of the ^{16}O and ^{18}O containing ions, respectively. The ^{18}O isotope was found to appear exclusively in the ether position of the ozonide ring. For compounds **1** and **2** this conclusion is readily verified, since the percentages of ^{18}O incorporation for the $[M]^+$, $[M - 32]^+$, and/or $[M - 33]^+$ ions are the same within experimental error. For compounds **3** and **4**, it can be seen that the sum of incorporation for the $RR'CO^+$ and $R''R'''CO_2^+$ fragment ions, i.e. % enrichment in $R_1R_2CO^+$ + % enrichment in $R_3R_4CO_2^+$, or % enrichment in $R_3R_4CO^+$ + % enrichment in $R_1R_2CO_2^+$, is equal to the % enrichment in ^{18}O for the $[M - 32]^+$ ion. It is evident that the sum of the ^{18}O incorporation of the two sets of fragments given above must represent the total percentage of ^{18}O incorporation. It can, therefore, be concluded that the ^{18}O incorporation took place exclusively at the ether position of the ozonide ring. A study which will be published shortly, of the reaction of these labelled ozonides with triphenylphosphine, indicates that the carbonyl compounds formed on reduction retain all the ^{18}O and that the triphenylphosphine oxide formed does not retain ^{18}O. These results thus indicate that only the peroxidic oxygens of the ozonides are attacked by the triphenylphosphine and further confirm that only the ether oxygen of the ozonide is labelled by ^{18}O.

The incorporation in the $[M - 32]^+$ ion can be verified by using the $[M - 33]^+$ peak, which, as shown earlier in reaction [7], contains the ether oxygen. This proved to be useful also for compound **1** where the labelled counterpart of the $[M - 32]^+$ ion is at *m/e* 122, the same *m/e* value as $PhHCO_2^+$. In that particular case, the incorporation was calculated by using the $[M - 33]^+$ ion.

The observation that the enrichment in ^{18}O

Can. J. Chem. Downloaded from www.nrcresearchpress.com by 210.87.254.40 on 09/05/12
For personal use only.

TABLE IV

Percentages of ^{18}O incorporation in various fragments

Compound	% of ^{18}O						
	$[M]^+$	$[M-32]^+$	$[M-33]^+$	$[R_1R_2CO]^+$	$[R_3R_4CO_2]^+$	$[R_1R_2CO_2]^+$	$[R_3R_4CO]^+$
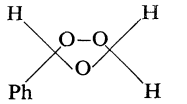	15.3±0.4	—*	15.7±0.4	1.8±0.4	*	13.1±0.4	*
	16.5±0.4	—*	16.1±0.5	2.2±0.4	*	14.6±0.4	*
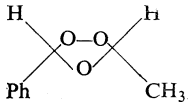	27.1±0.4	26.3±0.4	27.1±0.4	5.3±0.4	23.4±0.5	21.0±0.5	6.1±0.6
	22.2±0.4	21.8±0.4	22.4±0.4	4.4±0.4	18.7±0.5	18.0±0.5	4.0±0.6
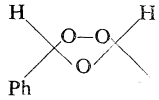	—	34.4±0.5	—	6.1±0.4	28.4±0.4	28.4±0.4	6.1±0.4
	—	34.8±0.5	—	5.7±0.4	29.4±0.5	29.4±0.5	5.7±0.4
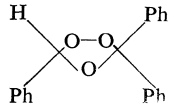	—	33.0±0.5	32.0±0.5	10.8±0.5	19.3±0.5	28.6±0.5	3.5±0.4
	—	31.8±0.5	32.6±0.5	12.6±0.5	17.7±0.5	28.6±0.5	3.8±0.4

*Not computable because of interference from other ions.

occurs exclusively at the ether position of the ozonide ring supports what has been previously stated regarding the structure and decomposition of the $[RR'CO_2]^+$ fragments. It is apparent that if these ions were all of type (**E**), then the incorporation at the *m/e* 122 peak should be the same as that of the molecular ion, because it would be formed exclusively with the ether oxygen. From Table V, which is computed from data of Table IV, it can be readily observed that the incorporation of the $[RR'CO_2]^+$ ion is always less than that of $[M]^+$. This supports the presence of *m/e* 122 ions of the form (**G**), i.e., $[RR'C^{\cdot}—OO^{\cdot}]^+$, which has no ^{18}O incorporation. The ^{18}O spectra confirm that for the $[PhHCO_2]^+$ fragments at *m/e* 122, the (**E**) form eliminates an $OH^{\cdot}$ radical; metastable peaks are recorded for the following transitions

[11] 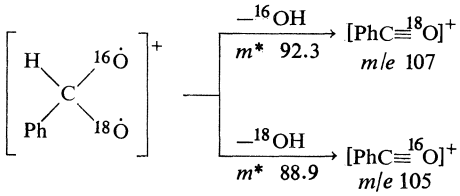

Furthermore, the ^{18}O incorporation, calculated for the phenol ion, is about 20% of that calculated at *m/e* 122. This indicates that, although the (**E**) form rearranges to give the phenol ion, the (**G**) form undergoes the same rearrangement to a much greater extent. Since the $PhCHO^+$ and $PhCO_2^+$ ions are common to spectra of compounds **1** to **4**, the amount of incorporation of ^{18}O given in Table IV can be used to calculate the relative intensities of ions given in Table V. It can be seen that the aldehydic ion $PhCHO^+$ usually includes an oxygen from the peroxidic bridge. This implies rupture of a C—O and an O—O bond as in process (1) of Scheme 1. This process is most probable for compounds **1**–**4** inclusively. The $PhCHO^+$ ion formed with the ether oxygen implies rupture of two C—O bonds and this process seems to be less frequent for all ozonides **1**–**4**. Nevertheless this process appears to be more probable for compound **4** than for the other three. Now, for the $[PhCHO_2]^+$ ion, it can be seen, also from Table V, that the (**E**) form is predominant, thus confirming the possibility of process (1) rather than (2) (Scheme 1).

From these data, it thus appears that even

Can. J. Chem. Downloaded from www.nrcresearchpress.com by 210.87.254.40 on 09/05/12
For personal use only.

TABLE V

Relative intensities of ions from compound

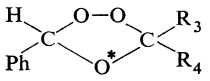

Compounds	Relative intensity of the fragmentation			
			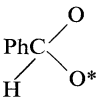	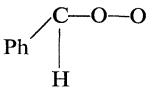
$R_3=R_4=H$	14	86	85	15
$R_4=CH_3$, $R_3=H$	20	80	79	21
$R_4=Ph$, $R_3=H$	17	83	83	17
$R_3=Ph$, $R_4=Ph$	36	64	88	12

NOTE: O* to differentiate the ether oxygen from the other two.

though the substituents influence the relative intensities of the major ions, they have little influence on the primary fragmentation processes of the ozonide ring for compounds **1** to **4**. Every time, the rupture implying the more vulnerable O—O bond occurs predominantly.

Although compounds **5** to **7** fall under the common structural formula given in Table I, they can also be visualized in terms of substituents as

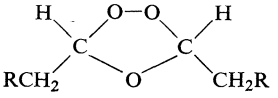

where R is C_2H_5, Ph, and Cl for compounds **5**, **6**, and **7**, respectively. In other words, it is considered that the heterocycle is directly substituted by two methylene groups and the effects of the R group can be studied as a function of intensity distribution. An interesting feature of these compounds is that, even though their spectra can be interpreted according to the general scheme proposed in Scheme 1, most of the ionic current recorded is due to ions of lower *m/e* ratio. In this series, the only molecular ion recorded is that of compound **5** (0.26% Σ at *m/e* 160). The $[M-32]^+$ ion is not seen in any of these spectra, but further fragmentation indicates that it is present as an intermediate. The $[RR'CO_2]^+$ fragment is only recorded in the spectrum of compound **5** (0.5% Σ at *m/e* 88). The only ion that appears in all three spectra is the aldehydic fragment, which is unique when the symmetry of the substituents is considered. It therefore appears that these structures exhibit a lack of charge stabilization on the major ions issued from Scheme 1, when these are compared to the ions from compounds **1** to **4**, where aromatic stabilization was strongly indicated. Even in these cases where the intensities of the ions of higher masses are very low, the general fragmentation scheme can be used to explain the obtained spectra. These explanations are based on the presence of the aldehydic fragments in the spectra and on the prescence of the $[RR'CO_2]^+$ type ion in the spectra of compound **5**. In fact, the absence of the $[RR'CO_2]^+$ ion in compounds **6** and **7** can be interpreted in terms of substituents effects. For compound **6**, where the *m/e* 91 ion is 25.8% Σ, it is expected that transition [12] would be preferred.

[12] 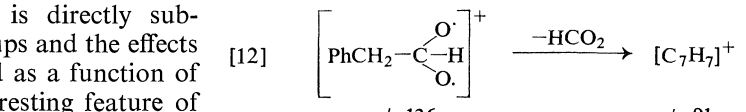

m/e 136 *m/e* 91

With compound **7**, the intensity of $[CH_3 — Cl]^+$ is 24.7% Σ at *m/e* 50 and it is proposed that a similar mechanism for the fast decomposition of the $RR'CO_2{}^+$ occurs

[13] 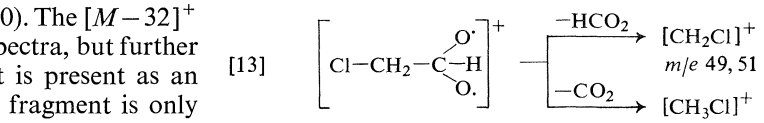

m/e 94, 96 *m/e* 50, 52

In fact, comparison of this ion (*m/e* 94, 96) with the monochloroacetic acid molecular ion (13) indicates that both have the *m/e* 50 ion as the most intense peak. As for the $[C_4H_8O_2]^+$ ion, it is

Can. J. Chem. Downloaded from www.nrcresearchpress.com by 210.87.254.40 on 09/05/12
For personal use only.

proposed that it decomposes in a way similar to the corresponding acid

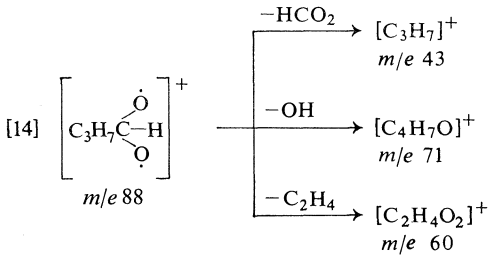

The high intensities of the ion at *m/e* 44 (11.2% Σ) is explained by decomposition of aldehydic fragments:

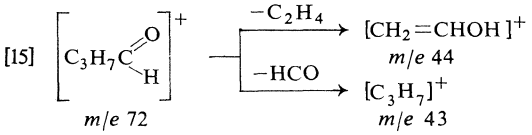

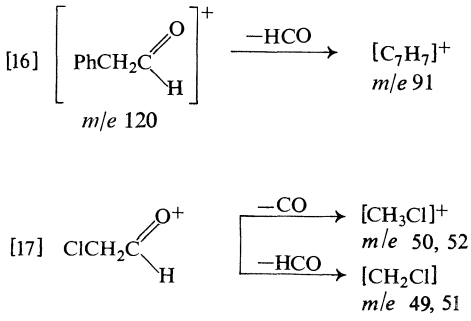

The $[M-32]^+$ ion, not recorded in these spectra, can be identified by its decomposition fragments: the spectrum of compound **5**, for example, exhibits peaks at *m/e* 73 and 31 which most probably evolve by the following sequence

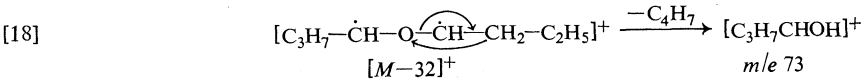

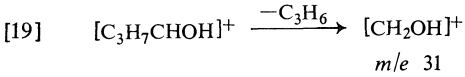

These processes are similar to those reported for ethers (10). Process [18] also gives rise to ions at *m/e* 121 and 79 for compounds **6** and **7**, respectively. However, for these ozonides (**6** and **7**), reaction [19] is not detected, as these lack a β hydrogen necessary for this process to occur. The $[R_1R_2CH]^+$ ions are recorded at *m/e* 57 and 105 for compounds **5** and **6**, and the $[R_1R_2C]^+$ ions at *m/e* 56, 104, and 62 for compounds **5**, **6**, and **7**. All these ions occur from decomposition of the $[M-32]^+$ ions as shown previously for compounds **1–4**. Therefore, the general scheme appears to be valid for ozonides **1** to **7** as the effect of substituents is reflected mainly in the ionic distribution.

Compound **8**, which can be represented as indicated in Table I, cannot be included in the general formula since the aliphatic bridging between the two carbon atoms on the ring is not comparable with the structures of compounds **1–7**. It is of interest, however, to determine if fragmentation of compound **8** will occur in a similar manner to the one observed for compounds **1** to **7**, or if its particular structure will favor a competitive process. Spectrum 8 (Fig. 8) shows ions at *m/e* 160, 148, 122, 120, 105, 87, 77, and 71. The ions at lower *m/e* ratio are decomposition fragments of the above ions. The $[M-32]^+$ ion is seen at *m/e* 160, but with a very low intensity (0.1% Σ). As shown in Scheme 2, the opening of the ozonide ring proceeds in a similar fashion to that found for compounds **1** to **7** (Scheme 2, ruptures *a* and *c*), but there is a competitive process (*b*) which involves a C—C cleavage to give the ion at *m/e* 122 (5.7% Σ). This cleavage initiates a process involving a six-membered ring intermediate, characterized by a metastable peak at *m/e* 77.5. Ions at *m/e* 87, 71, and 70 are believed to be cyclic because of their high intensity (11.8% Σ at *m/e* 71). In fact, the cyclic structure has been found to be more stable (14) than the biradical equivalent. Charge stabilization in the cyclic structure is enhanced by resonance with the oxygen, whereas the biradical form would readily eliminate a neutral fragment. Thus, it is apparent that the different structure of compound **8** favors a fragmentation pattern which differs from that of Scheme 1. Process (*b*), Scheme 2, must be of some importance if the relative height of the *m/e* 122 peak is considered.

Can. J. Chem. Downloaded from www.nrcresearchpress.com by 210.87.254.40 on 09/05/12
For personal use only.

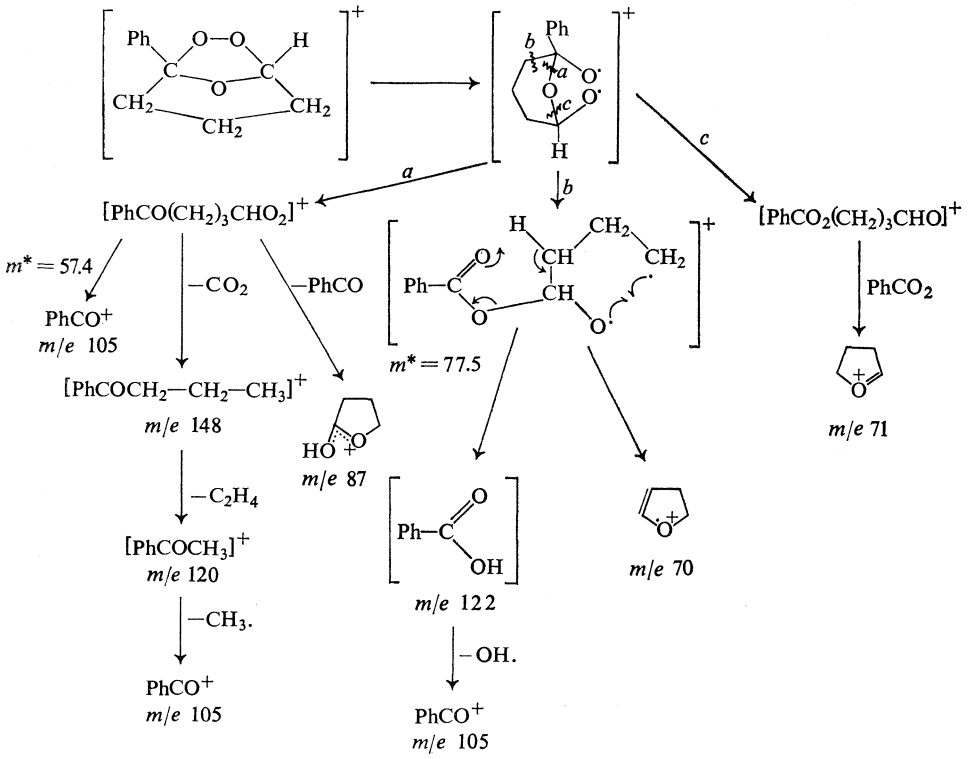

SCHEME 2. Fragmentation pattern of compound **8**

However, the spectrum still indicates that the primary cleavage predominantly involves rupture of the O—O bond, although further decomposition differs as a result of aliphatic bridging which does not permit fragmentation via simple carbonyl or $RR'CO_2$ type fragments, as in the case of compounds **1** to **7**.

Conclusions

The mass spectra recorded for compounds **1** to **7** were found to include ions such as $[M - 32]^+$, $[RR'CO_2]^+$, and the carbonyl ions, that are characteristic of these ozonides. A comparison of the spectra of compounds **1** to **4** with those of compounds **5** to **7** shows that there is a net effect on the charge stabilization, due to the substituents, which is reflected in the ionic current distribution. For compounds **1** to **4**, which have aromatic stabilization, most of the ionic current is due to the carbonyl fragments, whereas for compounds **5** to **7**, the carbonyl fragment ions are less intense and more ions due to secondary decomposition are observed. The fact that the $[M - 32]^+$ ion is present in the spectra of compounds **1** to **4** and not in those of compounds **5** to **7** indicates that aromatic substituents have a large influence on the intensity of this ion. The molecular ion is present only in the spectra of compounds **1** and **2**, which have only one phenyl group as substituent on either side of the ring. This observation indicates that carbonyl fragments containing phenyl groups are of sufficient stability so that decomposition through them is favored.

In compounds **5**, **6**, and **7**, where substituents are in the β position, the substituent effects are inferred by the non-appearance of the $[M - 32]^+$ ion in their spectra, and also by the non-appearance of the $[M]^+$ and $[RR'CO_2]^+$ ions in the spectra of compounds **6** and **7**. It is also seen for compounds **6** and **7** that the phenyl group favors the formation of the tropylium ion whereas the presence of chlorine atoms in the molecule favors the formation of $[CH_3Cl]^+$ ion.

In all of these compounds (**1**–**7**), the mode of fragmentation is similar, as indicated by ^{18}O

Can. J. Chem. Downloaded from www.nrcresearchpress.com by 210.87.254.40 on 09/05/12
For personal use only.

isotopic labelling. Rupture of the ozonide ring proceeds predominantly by an O—O and a C—O bond split. The influence of molecular structure on the fragmentation pattern of the ozonides is clearly indicated by comparison of the spectrum of compound **8** with the spectra of compounds **1**–**7**. However, even for compound **8**, the O—O bond appears to be the most easily opened by electron impact. It is also concluded that the ^{18}O incorporation in the ozonide molecules studied occurs exclusively at the ether position of the ring.

Acknowledgments

The authors wish to thank the National Research Council of Canada and the Department of Defence Production of Canada, for their financial assistance.

1. M. BERTRAND, S. FLISZÁR, and Y. ROUSSEAU. J. Org. Chem. **33**, 1931 (1968).
2. S. FLISZÁR, J. CARLES, and J. RENARD. J. Am. Chem. Soc. **90**, 364 (1968).
3. S. FLISZÁR and J. B. CHYLIŃSKA. Can. J. Chem. **45**, 29 (1967).
4. S. FLISZÁR and J. B. CHYLIŃSKA. Can. J. Chem. **46**, 783 (1968).
5. R. CRIEGEE, A. KERCKOV, and H. ZINKE. Chem. Ber. **88**, 1878 (1955).
6. K. BIEMANN. Mass spectrometry, organic chemical application. McGraw-Hill Book Co., Inc., New York. 1962. p. 237.
7. L. M. JACKMANN. Application of nuclear magnetic resonance spectroscopy in organic chemistry. The Pergamon Press, Ltd., New York. 1959. p. 126.
8. R. CRIEGEE and G. WERNER. Ann. **564**, 9 (1949). R. CRIEGEE. Ann. **583**, 1 (1953). R. CRIEGEE. Record Chem. Progr. Kresge–Hooker Sci, Lib. **18**, 111 (1957).
9. K. BIEMANN. Mass spectrometry, organic chemical application. McGraw-Hill Book Co., Inc., New York. 1962. p. 101.
10. F. W. MCLAFFERTY. Anal. Chem. **29**, 1782 (1957).
11. A. CORNU and R. MASSOT. Application of mass spectrometry to organic chemistry. Heyden and Son Ltd., and P.U.F., London. 1966. p. 33-B.
12. (*a*) S. MEYERSON and J. L. CORBIN. J. Am. Chem. Soc. **87**, 3045 (1965). (*b*) J. H. BEYNON, B. E. JOB, and A. E. WILLIAMS. Z. Naturforsch. **20***a*, 883 (1965).
13. A. CORNU and R. MASSOT. Application of mass spectrometry to organic chemistry. Heyden and Son Ltd., and P.U.F., London. 1966. p. 16-B.
14. R. I. REED. Application of mass spectrometry to organic chemistry. Academic Press, Inc., New York. 1966. p. 119.

Can. J. Chem. Downloaded from www.nrcresearchpress.com by 210.87.254.40 on 09/05/12
For personal use only.

On the in-plane vibration frequencies of the vinylidene, d_1-, and d_2-vinylidene halides. I. Force fields and normal modes. II. Characteristic group vibrations

J. M. FREEMAN AND T. HENSHALL
Department of Chemistry and Applied Chemistry, University of Salford, Salford 5, Lancashire, England
Received October 15, 1968

An investigation has been undertaken of the characteristic in-plane group vibrations of the vinylidene and d_2-vinylidene groups from the viewpoints both of approximation methods of the vibrational analysis of, and aids to assignments in, molecules containing such groups.

The need in these studies for reliable force fields for the vinylidene halides has caused us to undertake a normal coordinate analysis of the in-plane vibrations of these molecules using a modified valence force field, and including all the available information from the hydrogen and deuterium isotopically substituted species.

Canadian Journal of Chemistry, **47**, 935 (1969)

Can. J. Chem. Downloaded from www.nrcresearchpress.com by 210.87.254.5 on 09/05/12
For personal use only.

I. Force Fields and Normal Modes

In continuation of our investigations of characteristic group frequencies from the viewpoint both of approximation methods of vibrational analysis and as aids to frequency assignments (1), we have undertaken a study of the vinylidene group.

However, for the approximation methods we required reliable force fields for the vinylidene halides, but surprisingly little work has been published on them. These include an early determination of a symmetry force field by Manneback and Rahman (2), calculations of a Urey–Bradley potential by Scherer and Overend (3), and by Enomoto and Ichinohe (4), but no valence force constants have so far been reported. Accordingly we have also undertaken a normal coordinate analysis of the in-plane vibrations of the vinylidene halides using a modified valence force field, and including all the available information from the hydrogen and deuterium isotopically substituted species.

The internal coordinates used are shown in Fig. 1. The symmetry coordinates for in-plane vibrations of CH_2CX_2 and CD_2CX_2 under the covering operations of the C_{2v} point group are listed in Table I, which also includes the coordinates for the isotopic species $CHDCX_2$ under C_s.

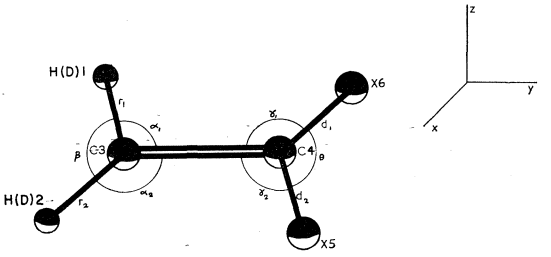

FIG. 1. Internal coordinates of vinylidene halide.

TABLE I
Symmetry coordinates for the in-plane vibrations

	Symmetry coordinates		
Species	CH_2CX_2, CD_2CX_2 (C_{2v})	$CHDCX_2$(C_s)	Form
A_1	S_1	S_2	$(\Delta r_1 + \Delta r_2)/\sqrt{2}$
	S_2	S_4	$(2\Delta\beta - \Delta\alpha_1 - \Delta\alpha_2)/\sqrt{6}$
	S_3	S_3	ΔR
	S_4	S_7	$(\Delta d_1 + \Delta d_2)/\sqrt{2}$
	S_5	S_9 (A')	$(2\Delta\theta - \Delta\gamma_1 - \Delta\gamma_2)/\sqrt{6}$
B_2	S_6	S_1	$(\Delta r_1 - \Delta r_2)/\sqrt{2}$
	S_7	S_5	$(\Delta\alpha_1 - \Delta\alpha_2)/\sqrt{2}$
	S_8	S_6	$(\Delta d_1 - \Delta d_2)/\sqrt{2}$
	S_9	S_8	$(\Delta\gamma_1 - \Delta\gamma_2)/\sqrt{2}$

TABLE II

Molecular geometries of vinylidene halides

Molecule	Bond distance, Å			Bond angles	
	C—H	C—X	C=C	HĈH	XĈX
CH_2CF_2	1.10	1.32	1.31	110°	109° 18′
CH_2CCl_2	1.07	1.71	1.32	117°	114° 30′
CH_2CBr_2	1.07	1.90	1.31	117°	114° 0′

TABLE III

The valence force field

$2V$	r_1	r_2	R	d_1	d_2	β	α_1	α_2	θ	γ_1	γ_2
r_1	F_r	f_{rr}	0	0	0	0	$(f_{r\alpha})$	0	0	0	0
r_2		F_r	0	0	0	0	0	$(f_{r\alpha})$	0	0	0
R			F_R	0	0	0	$f_{R\alpha}$	$f_{R\alpha}$	0	$f_{R\gamma}$	$f_{R\gamma}$
d_1				F_d	f_{dd}	0	$(f_{d\alpha})$	0	$f_{d\theta}$	$f_{d\gamma}$	0
d_2					F_d	0	0	$(f_{d\alpha})$	$f_{d\theta}$	0	$f_{d\gamma}$
β						H_β	0	0	0	0	0
α_1							H_α	0	0	0	0
α_2			(symmetrical)					H_α	0	0	0
θ									H_θ	0	0
γ_1										H_γ	0
γ_2											H_γ

The molecular geometries were taken mainly from ref. 5 but with some minor modifications, and are presented in Table II. The **G** matrices for the complete solutions for CH_2CX_2, $CHDCX_2$, and CD_2CX_2 (X = F, Cl, Br) were calculated on an English-Electric KDF-9 computer using the program described in ref. 6. The valence force field of Table III was chosen on the basis of calculations on the "standard vinylidene molecule" of Part II. Those force constants in parentheses, viz. $f_{r\alpha}$ and $f_{d\alpha}$, were included in an attempt to fit the observed frequencies for the fluoro compounds; they were not used for the bromides and chlorides. The corresponding symmetry force field for CH_2CX_2, CD_2CX_2 is given in Table IV, from which that for $CHDCX_2$ is easily constructed by combining the elements in the A_1 and B_2 species, with due regard for the renumbering of the coordinates in Table I.

The observed frequencies of the fluorides and bromides were taken from refs. 7, 8, and 9 respectively, but with some slight amendments suggested by Scherer and Overend (3); the assignments quoted in Tables V–VII were made on the basis of their approximate potential energy distributions (p.e.d.) derived from a Urey–Bradley potential. In our calculations, the force constants of Table IX were determined by an iterative procedure (10), so that a force field could be obtained corresponding to a chosen assignment.

In the case of the vinylidene chlorides, no observed frequencies are available for the monodeuterated species $CHDCCl_2$. The results are, therefore, confined to the symmetrically substituted molecules. But even for CD_2CCl_2 the assignment is incomplete; the unknown frequencies were therefore accorded zero weight in the iteration process. The first estimate of the valence force constants was made by interpolation of the values for vinylidene fluoride and bromide, and the results of this zero-order calculation came surprisingly close to the observed frequencies apart from the bands at 980 cm^{-1} in the A_1 species and 815 cm^{-1} in the B_2 species of CD_2CCl_2, for which the calculated values were 1035 and 960 cm^{-1} respectively.

These bands correspond respectively to δ(DCD) and δ(DCC). Their values in the fluoride are 1076 and 807 cm^{-1}, and are 1019 and 932 cm^{-1} in the bromide. It is perhaps indicative of an error in assignment in the chloride, that while the observed frequency of 980 cm^{-1} for the deuterated molecule does not lie between those of

Can. J. Chem. Downloaded from www.nrcresearchpress.com by 210.87.254.5 on 09/05/12
For personal use only.

TABLE IV

Symmetry force field for vinylidene halides

Species		Force field				
A_1	$2V$	S_1	S_2	S_3	S_4	S_5
	S_1	$[F_r + f_{rr}]$	$-(f_{r\alpha})/\sqrt{3}$	0	0	0
	S_2		$[2H_\beta + H_\alpha]/3$	$-2f_{R\alpha}/\sqrt{6}$	$-(f_{d\alpha})/\sqrt{3}$	0
	S_3			F_R	0	$-2f_{R\gamma}/\sqrt{6}$
	S_4		(symmetrical)		$[F_d + f_{dd}]$	$[2f_{d\theta} - f_{d\gamma}]/\sqrt{3}$
	S_5					$[2H_\theta + H_\gamma]/3$
B_2	$2V$	S_6	S_7	S_8	S_9	
	S_6	$[F_r - f_{rr}]$	$(f_{r\alpha})$	0	0	
	S_7		H_α	$(f_{d\alpha})$	0	
	S_8	(symmetrical)		$[F_d - f_{dd}]$	$f_{d\gamma}$	
	S_9				H_γ	

the fluoride and bromide, the calculated frequency of 1035 cm^{-1} does! Some doubt on the accuracy of this observed frequency is also expressed in ref. 3, where it is estimated that such a low frequency for the bending mode excludes any contributions from the force constants of the CX_2 group. The components of δ(DCD) in d_2-vinylidene chloride are shown by the zero-order calculation to be almost identical to those in d_2-vinylidene bromide, and it is, therefore, unlikely that any change in the force constants can remove the contributions (of S_2 and S_5) from the CX_2 group, since the transition from the force field of the bromide to that of the chloride has had but little effect on them. However, no such correlation is possible for the band at 815 cm^{-1} in the B_2 species because of the complex nature of this frequency. The high value of 932 cm^{-1} in the d_2-vinylidene bromide arises from a measure of coupling with the frequency at 625 cm^{-1}, whereas little vibrational coupling of this kind occurs in the fluoride. Thus a large degree of coupling in the chloride would be expected to raise the DĈC deformation frequency in the B_2 species; indeed the calculation revealed a very strong degree of coupling between those frequencies at 680 and 960 cm^{-1}. It seemed reasonable, therefore, to question the validity of the observed frequency of 815 cm^{-1} in CD_2CCl_2, which is at 117 cm^{-1} less than the corresponding frequency in CD_2CBr_2. Accordingly, two iterative calculations were made, one in which the observed frequency of 815 cm^{-1} in CD_2CCl_2 was included in the data, and given normal weighting (I), and another in which it was assigned a zero weight (II). Examination of the results in Table VI reveals a considerable improvement in the agreement of the remaining calculated and observed frequencies in the latter case. This provides a further indication of a possible error in the assignment of the frequency at 815 cm^{-1}. Since there is still a discrepancy of 63 cm^{-1} in the frequency at 980 cm^{-1} in the A_1 species of CD_2CCl_2, the doubt expressed above on the reliability of this frequency is re-emphasized. Finally, in view of the lack of a complete vibrational assignment for the deuterated compounds it was considered to be unprofitable to attempt any further refinement of the force field.

Discussion

The vinylidene halides are so vibrationally dissimilar that it is more convenient to discuss them separately.

(i) Vinylidene Fluoride

The observed and calculated frequencies for CH_2CF_2, $CHDCF_2$, and CD_2CF_2 are presented in Table V. The assignments of the bands at 1359 and 1076 cm^{-1} to δ(HCH) and δ(DCD) respectively have been taken from ref. 3, and were made on the basis of a close agreement with calculated values when the frequencies were accorded a zero weight. Our calculations, however, give values of 1374 and 1050 cm^{-1} for these modes, which are closer to the original assignments of 1380 and 1060 cm^{-1} by Edgell and

Can. J. Chem. Downloaded from www.nrcresearchpress.com by 210.87.254.5 on 09/05/12
For personal use only.

Can. J. Chem. Downloaded from www.nrcresearchpress.com by 210.87.254.5 on 09/05/12
For personal use only.

TABLE V

In-plane frequencies and potential energy distribution for CH_2CF_2, $CHDCF_2$, and CD_2CF_2

Molecule	Species	Approximate description of mode	Observed frequencies (cm^{-1})(3)	Calculated frequencies (cm^{-1})				Approximate p.e.d.
				Complete	Framework	First-order simple	First-order degenerate	
CH_2CF_2	A_1	ν(C—H)(s)	3060	3078	—	3074	—	$0.98S_1 + 0.01S_3$
		ν(C=C)	1734	1736	1734	1675	1699	$0.62S_3 + 0.30S_4 + 0.07S_5$
		δ(HCH)	1359	1374	—	1401	1371	$0.98S_2 + 0.02S_4$
		ν(C—F)(s)	926	917	937	—	—	$0.02S_2 + 0.35S_3 + 0.61S_4 + 0.01S_5$
		δ(FCF)	550	550	552	—	—	$0.02S_3 + 0.07S_4 + 0.91S_5$
	B_2	ν(C—H)(a)	3103	3135	—	3137	—	$1.00S_6$
		ν(C—F)(a)	1302	1301	1302	—	—	$0.18S_7 + 0.79S_8 + 0.03S_9$
		δ(HCC)	955	969	970	—	—	$0.76S_7 + 0.22S_8 + 0.02S_9$
		δ(FCC)	438	427	426	—	—	$0.06S_7 + 0.94S_9$
$CHDCF_2$	A'	ν(C—H)	3133	3108				$0.54S_1 + 0.45S_2$
		ν(C—D)	2325	2305				$0.44S_1 + 0.51S_2 + 0.04S_3 + 0.01S_5$
		ν(C=C)	1715	1722				$0.01S_1 + 0.03S_2 + 0.58S_3 + 0.31S_7 + 0.08S_9$
		ν(C—F)(a)	1298	1306				$0.19S_4 + 0.17S_5 + 0.61S_6 + 0.02S_8$
		δ(HCD)	1224	1224				$0.01S_3 + 0.68S_4 + 0.01S_5 + 0.27S_6 + 0.02S_7$
		ν(C—F)(s)	929	924				$0.28S_3 + 0.17S_5 + 0.04S_6 + 0.48S_7 + 0.01S_8 + 0.01S_9$
		δ(CCD)	829	818				$0.01S_1 + 0.07S_3 + 0.1S_4 + 0.53S_5 + 0.09S_6 + 0.12S_7 + 0.06S_8$
		δ(FCF)	542	547				$0.02S_3 + 0.01S_4 + 0.06S_7 + 0.90S_9$
		δ(CCF)	392	400				$0.01S_4 + 0.11S_5 - 0.01S_6 + 0.89S_8$
CD_2CF_2	A_1	ν(C—D)(s)	2274	2274	—	2264	—	$0.91S_1 + 0.08S_3$
		ν(C=C)	1705	1705	1691	1659	1667	$0.07S_1 + 0.54S_3 + 0.32S_4 + 0.08S_5$
		δ(DCD)	1076	1050	—	1035	1022	$0.01S_1 + 0.70S_2 + 0.10S_3 + 0.17S_4 + 0.02S_5$
		ν(C—F)(s)	858	851	907	—	—	$0.28S_2 + 0.26S_3 + 0.45S_4$
		δ(FCF)	543	543	547	—	—	$0.01S_2 + 0.03S_3 + 0.06S_4 + 0.90S_5$
	B_2	ν(C—D)(a)	2354	2339	—	2345	—	$0.98S_6 + 0.01S_7 + 0.01S_9$
		ν(C—F)(a)	1284	1281	1285	—	—	$0.08S_7 + 0.89S_8 + 0.03S_9$
		δ(DCC)	807	792	795	—	—	$0.01S_6 + 0.75S_7 + 0.12S_8 + 0.11S_9$
		δFCC	374	380	380	—	—	$0.15S_7 - 0.01S_8 + 0.86S_9$

Can. J. Chem. Downloaded from www.nrcresearchpress.com by 210.87.254.5 on 09/05/12
For personal use only.

TABLE VI

In-plane frequencies and potential energy distribution for CH_2CCl_2 and CD_2CCl_2

Molecule	Species	Approximate description of mode	Observed frequencies (cm^{-1})(4)	Calculated frequencies (cm^{-1}) Complete I	Complete II	Framework	First-order simple	First-order degenerate	Approximate p.e.d.
CH_2CCl_2	A_1	ν(C—H)(s)	3035	3035	3035	—	3032	—	I $0.99S_1 + 0.01S_2$ II
		ν(C=C)	1616	1620	1624	1597	1626	1626	I $0.09S_2 + 0.78S_3 + 0.08S_4 + 0.04S_5$ II $0.13S_2 + 0.75S_3 + 0.07S_4 + 0.04S_5$
		δ(HCH)	1391	1384	1402	—	1403	1403	I $0.91S_2 + 0.06S_3 + 0.02S_4$ II $0.86S_2 + 0.09S_3 + 0.03S_4 + 0.02S_5$
		ν(C—Cl)(s)	601	594	586	600	—	—	I $0.01S_2 + 0.15S_3 + 0.68S_4 + 0.16S_5$ II $0.01S_2 + 0.14S_3 + 0.70S_4 + 0.15S_5$
		δ(ClCCl)	299	298	308	308	—	—	I $0.22S_4 + 0.78S_5$ II $0.20S_4 + 0.79S_5$
	B_2	ν(C—H)(a)	3130	3127	3127	—	3129	—	I $1.00S_6$ II
		δ(HCC)	1088	1025	1098	1101	—	—	I $0.83S_7 + 0.11S_8 + 0.05S_9$ II $0.72S_7 + 0.19S_8 + 0.09S_9$
		ν(C—Cl)(a)	788	735	798	798	—	—	I $0.12S_7 + 0.96S_8 - 0.08S_9$ II $0.24S_7 + 0.77S_8 - 0.01S_9$
		δ(CCCl)	375	352	375	374	—	—	I $0.05S_7 - 0.07S_8 + 1.02S_9$ II $0.04S_7 + 0.04S_8 + 0.92S_9$
CD_2CCl_2	A_1	ν(C—D)(s)	2230	2231	2231	—	2229	—	I II $0.92S_1 + 0.01S_2 + 0.07S_3$
		ν(C=C)	1576	1575	1573	1534	1576	1576	I II $0.07S_1 + 0.02S_2 + 0.77S_3 + 0.09S_4 + 0.05S_5$
		δ(CDC)	980*	1026	1042	—	1045	1044	I II $0.93S_2 + 0.04S_4 + 0.02S_5$
		ν(C—Cl)(s)	—†	570	563	587	—	—	I $0.04S_2 + 0.16S_3 + 0.66S_4 + 0.14S_5$ II $0.04S_2 + 0.15S_3 + 0.68S_4 + 0.13S_5$
		δ(ClCCl)	—†	297	306	306	—	—	I $0.01S_3 + 0.20S_4 + 0.79S_5$ II $0.01S_3 + 0.19S_4 + 0.80S_5$
	B_2	ν(C—D)(a)	2330	2339	2340	—	2346	—	I $0.99S_6 + 0.01S_7$ II $0.98S_6 + 0.01S_7 + 0.01S_9$
		Mixture of δ(DCC) and ν(C—Cl)(a)	815*‡	889	988§	997§	—	—	I $0.01S_6 + 0.49S_7 + 0.44S_8 + 0.06S_9$ II $0.01S_6 + 0.37S_7 + 0.50S_8 + 0.12S_9$
			698	671	697	698			I $0.01S_6 + 0.38S_7 + 0.63S_8 - 0.02S_9$ II $0.01S_6 + 0.51S_7 + 0.49S_8 - 0.01S_9$
		δ(CCCl)	—†	309	331	331	—	—	I $0.11S_7 - 0.07S_8 + 0.96S_9$ II $0.11S_7 + 0.01S_8 + 0.88S_9$

*Assignment considered to be incorrect.
†Accorded zero weight in iteration process.
‡Accorded zero weight in calculation II only.
§Note difference in assignment according to p.e.d. for calculations I and II.

Can. J. Chem. Downloaded from www.nrcresearchpress.com by 210.87.254.5 on 09/05/12
For personal use only.

TABLE VII

In-plane vibrations for CH_2CBr_2, $CHDCBr_2$, and CD_2CBr_2

Molecule	Species	Approximate description of mode	Observed frequencies (cm^{-1})(3)	Calculated frequencies (cm^{-1})				Approximate p.e.d.
				Complete	Framework	First-order simple	First-order degenerate	
CH_2CBr_2	A_1	ν(C—H)(s)	3023	3027	—	3025	—	$0.99S_1 + 0.01S_3$
		ν(C=C)	1593	1601	1531	1589	1603	$0.29S_2 + 0.63S_3 + 0.04S_4 + 0.03S_5$
		δ(HCH)	1379	1364	—	1381	1365	$0.70S_2 + 0.23S_3 + 0.04S_4 + 0.03S_5$
		ν(C—Br)(s)	467	474	486	—	—	$0.01S_2 + 0.14S_3 + 0.61S_4 + 0.25S_5$
		δ(BrCBr)	184	182	182	—	—	$0.31S_4 + 0.69S_5$
	B_2	ν(C—H)(a)	3108	3112	—	3114	—	$1.0S_6$
		δ(HCC)	1065	1070	1074	—	—	$0.83S_7 + 0.09S_8 + 0.07S_9$
		ν(C—Br)(a)	696	698	698	—	—	$0.13S_7 + 0.86S_8 + 0.01S_9$
		δ(CCBr)	322	324	323	—	—	$0.03S_7 + 0.05S_8 + 0.92S_9$
$CHDCBr_2$	A'	ν(C—H)	3061	3072				$0.56S_1 + 0.43S_2$
		ν(C—D)	2282	2274				$0.42S_1 + 0.53S_2 + 0.03S_3$
		ν(C=C)	1563	1558				$0.03S_2 + 0.73S_3 + 0.12S_4 + 0.06S_7 + 0.02S_9$
		δ(HCD) or δ(HCC)	1258	1260				$0.09S_3 + 0.73S_4 + 0.13S_5 + 0.03S_7 + 0.02S_9$
		δ(DCC)	949	947				$0.11S_4 + 0.55S_5 + 0.21S_6 + 0.11S_8$
		ν(C—Br)(a)	655	662				$0.25S_5 + 0.75S_6$
		ν(C—Br)(s)	458	463				$0.14S_3 + 0.60S_7 + 0.23S_9$
		δ(CCBr)	300	302				$0.06S_5 + 0.03S_6 + 0.91S_8$
		δ(BrCBr)	184	182				$0.30S_7 + 0.70S_9$
CD_2CBr_2	A_1	ν(C—D)(s)	2230	2223	—	2221	—	$0.93S_1 + 0.06S_3$
		ν(C=C)	1545	1528	1453	1525	1531	$0.07S_1 + 0.06S_2 + 0.76S_3 + 0.07S_4 + 0.05S_5$
		δ(DCD)	1019	1028	—	1036	1028	$0.91S_2 + 0.03S_3 + 0.04S_4 + 0.02S_5$
		ν(C—Br)(s)	453	453	477	—	—	$0.03S_2 + 0.15S_3 + 0.60S_4 + 0.23S_5$
		δ(BrCBr)	183	182	182	—	—	$0.30S_4 + 0.70S_5$
	B_2	ν(C—D)(a)	2339	2329	—	2335	—	$0.98S_6 + 0.01S_7 + 0.01S_9$
		δ(DCC)	932	922	933	—	—	$0.01S_6 + 0.56S_7 + 0.30S_8 + 0.13S_9$
		ν(C—Br)(a)	625	631	630	—	—	$0.34S_7 + 0.68S_8 - 0.03S_9$
		δ(CCBr)	283	284	283	—	—	$0.08S_7 + 0.01S_8 + 0.90S_9$

Can. J. Chem. Downloaded from www.nrcresearchpress.com by 210.87.254.5 on 09/05/12
For personal use only.

Ultee (7), but although this agreement may be considered as supporting evidence for this latter assignment, the results are not really sufficiently conclusive.

The most interesting feature of the approximate p.e.d. of Table V is the purity of δ(HCH) in CH_2CF_2. This is due to the much wider separation of δ(HCH) and ν(C═C) in this molecule than in the other vinylidene halides; the contribution from ν(C═C) is considerable in the bromide, though less marked in the chloride. Hence δ(HCH) can be considered as a true group frequency only in vinylidene fluoride. No such purity is apparent in the C═C stretching frequencies to which the symmetric C—X stretching vibration contributes 30% in CH_2CF_2, 8% in CH_2CCl_2, and only 4% in CH_2CBr_2. As the mass of atom X increases through F to Br, the contributions to ν(C═C) from the coordinate S_4 are gradually replaced by those from S_2.

In CD_2CF_2, the DĈD bending mode is highly complex in contrast to CD_2CCl_2 and CD_2CBr_2 where the mode is relatively pure. The composition of ν(C═C) in CD_2CF_2 is similar to that in CH_2CF_2, whilst in the vibrations of species B_2 considerable mixing occurs between ν(C—F) (a) and δ(HCC) or δ(DCC), but replacement of H by D does lead to slightly purer δ(DCC) and ν(C—F) (a) vibrational modes.

TABLE VIII

Valence force constants for the vinylidene halides*

Force constants	Values in F	Cl I	Cl II	Br
F_r	5.252	5.170	5.168	5.131
F_R	8.509	8.397	8.396	7.622
H_α	0.524	0.470	0.509	0.507
F_d	7.175	3.613	3.716	3.098
H_γ	0.707	0.726	0.812	0.745
H_β	0.367	0.381	0.384	0.382
H_θ	1.552	1.257	1.252	1.192
f_{rr}	0.032	0.016	0.017	0.029
f_{dd}	0.992	0.232	0.133	−0.039
$f_{d\gamma}$	0.646	0.829	0.633	0.651
$f_{R\alpha}$	0.362	0.254	0.236	0.121
$f_{d\theta}$	0.435	0.346	0.340	0.244
$f_{R\gamma}$	0.371	0.106	0.110	−0.104
$(f_{r\alpha})$	−0.008	—	—	—
$(f_{d\alpha})$	−0.012	—	—	—

*Stretching force constants, e.g. F_r, are in mdyn Å^{-1}; bending force constants, e.g. H_γ, are in mdyn Å rad^{-2}; stretch–stretch interaction constants, e.g. f_{rr}, are in mdyn Å^{-1}; stretch–bend interaction constants, e.g. $f_{d\gamma}$, are in mdyn rad^{-1}.

An estimate provided by the iterative program of the relative importance of the constants in the valence force field indicates that $f_{r\alpha}$ and $f_{d\alpha}$ make very little contribution to the determination of the frequencies. The reason lies in the very small values for these constants (Table VIII), and there is no indication that these values are only weakly determined by the data. These constants were only included in an attempt to obtain agreement between observed and calculated values of ν(C—H) and ν(C—D), and the failure of this attempt may serve to indicate that the discrepancies are more probably due to the effects of anharmonicity in the vibrations, which will clearly be more important for ν(C—H) than for ν(C—D).

The interaction constant $f_{R\gamma}$ has a relatively large effect on the calculated frequencies, but the value of the expression (10),

$$Q = (\Sigma_{q=1}(JZ)^*P(JZ))_{ii}$$

for this constant indicates that it is only weakly determined.

The values of F_r and F_R, the force constants for the C—H and C═C stretching vibrations compare favorably with those reported in ref. 3, but our value for F_d, the constant for the CF stretching vibration of 7.175 mdyn Å^{-1}, does not compare favorably with their value of 4.660 mdyn Å^{-1}. The reasons for this discrepancy may lie in the different types of force field used, with the resultant arbitrary allocations of neglected force constants amongst those remaining, and in the large uncertainty of 0.63 mdyn Å^{-1} reported (3) for the F—F interaction constant.

However, our values of F_d and f_{dd} appear to be well determined, the former having the largest relative importance of all the constants in the valence force field, although such considerations should strictly be applied only to interaction constants. The reliabilities of F_d and f_{dd} are also indicated by the fact that, during the iteration process, F_d remained sensibly constant, whilst f_{dd} oscillated only very slightly.

(ii) Vinylidene Chloride

Due to the paucity of experimental data for the chlorides, the results of the calculations on these compounds are not as reliable as those for the fluorides and bromides. This is emphasized by the smaller values of Q for the interaction constants f_{dd}, $f_{d\theta}$, and $f_{R\gamma}$ compared with the

values obtained for the fluorides and bromides, which indicates that these force constants are only weakly determined in this case by the experimental data.

Scherer and Overend (3) point to the close correspondence of the frequencies for ν(C═C) and δ(HCH) in both vinylidene chloride and bromide, and suggest that in consequence these modes will be considerably mixed in both cases. However, our calculations only partly confirm this suggestion; the p.e.d. in Tables VI and VII indicate that the amounts of vibrational coupling are less for the chlorides than the bromides.

For the B_2 species of CD_2CCl_2, the force constants under I and II (Table VIII) correspond to different assignments of δ(DCC) and ν(C—Cl) (a), and calculation II is really contrary to the chosen assignment. However, the extent of vibrational mixing is so great that it is questionable whether any such assignment should be made.

Little evidence is available to enable a choice to be made between the results of the calculations in I and II, but the force constants from II do lead to closer agreement between calculated and observed frequencies, and the values of H_α and $f_{d\gamma}$ from II are more consistent with those for the fluorides and bromides than are those from I. For these reasons we chose to use the force constants under II in our considerations of group frequencies in Part II.

(iii) Vinylidene Bromide

The observed and calculated frequencies of vinylidene and d_2-vinylidene bromides are compared in Table VII; the agreement is satisfactory in all cases, with a maximum error of 1.46% for the band at 476 cm^{-1} in the A_1 species of CH_2CBr_2. The calculations show that the interaction constant $f_{R\gamma}$ is of little importance in determining the calculated frequencies, even though its value is -0.103 mdyn $Å^{-1}$; the conclusion, therefore, is that this value is unreliable.

The **L** matrices indicate a considerable degree of mixing between the coordinates S_2 and S_3 in both CH_2CBr_2 and CD_2CBr_2, but the marked vibrational coupling between S_7 and S_8 in the latter molecule is not so pronounced in the former. Similar conclusions may be drawn from the p.e.d. of Table VII. This vibrational coupling of S_7 and S_8 as noted above is the reason for the high values of the δ(HCC) and δ(DCC) modes in the B_2 species.

The use by Scherer and Overend (3) of a Urey–Bradley potential makes a comparison of the force constants difficult. However, similar values are obtained for the C—H and C═C stretching force constants, but their value is 2.225 mdyn $Å^{-1}$ for F_d against 3.098 mdyn $Å^{-1}$ in this study. Again the discrepancy may lie in the very different character of the force fields, and in the extremely large uncertainty of 2.4 mdyn $Å^{-1}$ reported (3) for the Br—Br interaction constant.

Both F_d and F_{dd} appear to be well determined in our calculations. Their values were decreasing only very slowly in the last stages of the iteration process, which indicates that the convergence was almost complete. The final value of 3.098 mdyn $Å^{-1}$ for F_d is, however, considerably lower than the value 3.54 mdyn $Å^{-1}$ reported by Manneback and Rahman (2), and the small value, -0.039 mdyn $Å^{-1}$, for f_{dd} implies that its inclusion in the force field will have little effect on the calculated frequencies.

II. Characteristic Group Vibrations

The vinylidene halides are reported (11) to exhibit four in-plane group vibrations: two ν(C—H), a δ(HCH), and a ν(C═C). The shifts in δ(HCH) and ν(C═C) with changes in molecular structure have been discussed by many authors (11) in terms of inductive and mesomeric effects within the molecule. However, on the basis of a normal coordinate analysis using a Urey–Bradley potential, Scherer and Overend (3) have shown that the use of ν(C═C) in such attempted correlations can lead to erroneous conclusions regarding the relative strengths of C═C bonds. The reason lies in a strong and variable degree of vibrational coupling between the nearly degenerate C═C stretching and HĈH bending modes in some molecules containing vinylidene groups. This coupling is most pronounced in vinylidene bromide, but almost absent from the corresponding fluoride. Its occurrence precludes the applications both of a first-order perturbation treatment of these "group frequencies" (12), and the method of Wilson *et al.* (13) for the reduction in the order of the vibrational secular determinants for the vinylidene halides by factorization of these frequencies from them.

However, Needham and Overend (14) have discussed the application to the vinylidene halides of a first-order perturbation theory for

Can. J. Chem. Downloaded from www.nrcresearchpress.com by 210.87.254.5 on 09/05/12
For personal use only.

the nearly degenerate case, and their method has been combined with that of King and Crawford (12) in an investigation of group frequencies in vinylidene and d_2-vinylidene halides.

The starting point for the calculations was the "standard molecule" defined in Fig. 1, in which angles of 120° were assumed, and with the following bond lengths (5): r(C—H) = r(C—D) = 1.07 Å; r(C=C) = 1.31 Å; r(C—X) = 1.50 Å, as for a C—C bond in a similar environment. The symmetry coordinates under the operations of C_{2v} point group symmetry are listed in Table I; they are orthogonal to the redundant coordinate, and conform to the convention proposed by Cyvin *et al.* (15).

The force field for the standard molecule (Table IX) was constructed from that for vinylidene bromide (3), but in which the force constants in the $=CX_2$ group were replaced by values representative of the group $=C—C_2$, in view of the possible application of the group frequency factorization procedure to organic molecules to which the vinylidene group is so attached.

The secular equations for the standard molecules derived both from the vinylidene and d_2-vinylidene groups were solved on an English-Electric KDF-9 computer. The resulting **L** matrices and calculated frequencies are given in Table X, and the corresponding inverse **L** matrices in Table XI. Both the **L** and $\mathbf{L}^{-1}$ matrices indicate that ν(C—H), 3100 and 3020 cm^{-1} and ν(C—D), 2328 and 2209 cm^{-1} are characteristic of the vinylidene and d_2-vinylidene groups, respectively, but that ν(C=C), 1602 and 1564 cm^{-1}; δ(HCH), 1398 cm^{-1}; and δ(DCD), 1041 cm^{-1} are expressions of considerably mixed

TABLE IX

Symmetry force field for the "standard molecule"*

$2V(A_1)$	S_1	S_2	S_3	S_4	S_5
S_1	5.16	0	0	0	0
S_2		0.416	−0.200	0	0
S_3			7.550	0	0
S_4	(symmetrical)			5.27	−0.375
S_5					1.080

$2V(B_2)$	S_6	S_7	S_8	S_9
S_6	5.040	0	0	0
S_7		0.522	0	0
S_8			4.730	0
S_9	(symmetrical)			1.330

*See footnote to Table VIII for units.

TABLE X

The L matrices for the "standard molecules", CH_2CX_2 and CD_2CX_2

Molecule	Species	Symmetry coordinates	Matrix elements for frequency $\bar{\nu}$ (cm^{-1})			
			3020	1602	1398	537
CH_2CX_2	A_1	S_1	−1.0155	−0.0494	−0.0064	−0.0054
		S_2	0.1582	−0.6923	−1.5559	0.0424
		S_3	0.0768	−0.3879	0.0724	−0.0701
		S_4	−0.0066	0.1564	−0.0732	−0.1084
		S_5	0.0131	−0.3128	0.1464	0.2169
			3100	1224	848	359
	B_2	S_6	−1.0564	0.0271	−0.0093	−0.0045
		S_7	0.1956	0.8705	−0.6436	0.0741
		S_8	0.0051	0.2780	0.2123	0.0498
		S_9	−0.1153	−0.4634	−0.1802	0.1917
			2209	1564	1041	504
CD_2CX_2	A_1	S_1	−0.7219	−0.1273	−0.0221	−0.0091
		S_2	0.2562	−0.3358	−1.1987	0.1124
		S_3	0.1486	−0.3741	−0.0074	−0.0663
		S_4	−0 0261	0.1657	−0.0612	−0 0987
		S_5	0.0522	−0.3313	0.1225	0.1975
			2328	1158	688	311
	B_2	S_6	−0.7866	0.0440	−0.0212	−0.0056
		S_7	0.2737	0.5859	−0.5946	0.1050
		S_8	0.0138	0.3206	0.1435	0.0361
		S_9	−0.1677	−0.4901	−0.0330	0.1671

Can. J. Chem. Downloaded from www.nrcresearchpress.com by 210.87.254.5 on 09/05/12
For personal use only.

TABLE XI

The $\mathbf{L}^{-1}$ matrices for the "standard molecule"

Molecule	Species	$\nu(cm^{-1})$	Matrix elements			
			S_1	S_2	S_3	S_4
CH_2CX_2	A_1	3020	−0.9755	0.0094	0.1020	−0.0074
		1602	−0.1686	−0.1392	−1.8455	0.6228
		1398	−0.0287	−0.5747	0.7451	−0.3829
		537	−0.1648	0.1868	−3.1710	−3.8485
			S_6	S_7	S_8	S_9
	B_2	3100	−0.9404	0.0180	−0.0090	−0.0265
		1224	0.1546	0.5146	1.1482	−0.4933
		848	−0.1108	−0.7937	2.0956	−0.2401
		359	−0.2959	0.5088	4.7390	3.7816
			S_1	S_2	S_3	S_4
CD_2CX_2	A_1	2209	−1.2954	0.0267	0.3723	−0.0547
		1564	−0.4558	−0.0450	−1.9129	0.6918
		1041	−0.1784	−0.7784	0.2884	−0.5773
		504	−0.3116	0.4003	−3.4870	−3.9645
			S_6	S_7	S_8	S_9
	B_2	2328	−1.2416	0.0447	−0.0137	−0.0670
		1158	0.2808	0.3870	1.5158	−0.5610
		689	−0.3826	−1.1104	2.3515	0.1765
		311	−0.4979	0.9601	4.8958	4.3061

TABLE XII

The **A** Matrices (**D** = **A***S)

Molecule		Matrix				
CH_2CX_2	A_1	D_1	D_2	D_3	D_4	D_5
	S_1	−0.9945	0.0729	−0.0717	0.0209	−0.0088
	S_2	0.0096	−0.5624	−0.7857	−0.2374	0.1000
	S_3	0.1040	0.7172	−0.6144	0.2875	−0.1210
	S_4	−0.0075	−0.3732	−0.0092	0.9272	0.0307
	S_5	0.0032	0.1572	0.0039	0.0307	0.9871
	B_2	D_6	D_7	D_8	D_9	
	S_6	−0.9994	0.0192	−0.0096	−0.0282	
	S_7	0.0192	−0.4136	−0.2932	−0.8617	
	S_8	−0.0086	−0.2932	−0.8534	0.4309	
	S_9	−0.0282	−0.8617	0.4309	0.2664	
CD_2CX_2	A_1	D_1	D_2	D_3	D_4	D_5
	S_1	−0.9600	0.0725	−0.2612	0.0651	−0.0274
	S_2	0.0198	−0.7669	−0.4174	−0.4490	0.1891
	S_3	0.2759	0.2113	−0.8463	0.3721	−0.1567
	S_4	−0.0405	−0.5545	0.1874	0.8056	0.0818
	S_5	0.0171	0.2335	−0.0789	0.0818	0.9655
	B_2	D_6	D_7	D_8	D_9	
	S_6	−0.9978	0.0360	−0.0110	−0.0539	
	S_7	0.0360	−0.4015	−0.1828	−0.8967	
	S_8	−0.0110	−0.1828	−0.9442	0.2740	
	S_9	−0.0540	−0.8967	0.2740	0.3435	

Can. J. Chem. Downloaded from www.nrcresearchpress.com by 210.87.254.5 on 09/05/12
For personal use only.

TABLE XIII

Effective inverse mass matrices, $(\mathbf{M}^{-1})_{cc}{}^{+}$ for C_3 and C_4

Molecule	Matrix (a.m.u.$^{-1}$)							
CH_2CX_2	C_3	x	y	z	C_4	x	y	z
	x	0.0731	0	0	x	0.0832	0	0
	y	0	0.0777	0	y	0	0.0724	0
	z	0	0	0.0833	z	0	0	0.0833
CD_2CX_2	C_3	x	y	z	C_4	x	y	z
	x	0.0639	0	0	x	0.0831	0	0
	y	0	0.0620	0	y	0	0.0744	0
	z	0	0	0.0833	z	0	0	0.0833

vibrations, the first being the more highly contaminated with contributions from the skeletal modes, and the latter two contaminated to a lesser degree with the XĈX bending mode.

However, despite the unfavorable degree of vibrational coupling, an attempt was made to factorize the ν(CH) or ν(CD), ν(C═C) and δ(HCH) or δ(DCD) frequencies from the secular determinant for the A_1 vibrational species by the method of King and Crawford (12). As expected, large corrections were required to the inverse masses and force constants for the skeletal modes, and this is usually considered to be a possible source of difficulty, even of failure, in an application of the method. However, satisfactory results were obtained for vinylidene and d_2-vinylidene bromides, but not so for the corresponding fluorides in which the degree of vibrational coupling was relatively small, and which did not therefore so closely resemble the conditions in the "standard molecule".

A second approach was suggested by the more pronounced vinylidene and d_2-vinylidene group character of δ(HCH) and δ(DCD) than of ν(C═C). This involved the inclusion of ν(C═C) in the skeletal modes and of ν(CH), δ(HCH), and their deuterium counterparts in the group vibrations in the factorization procedure.

The **A** matrices of the orthogonal transformation (12) are presented in Table XII for both the A_1 and B_2 vibrational species, and were calculated from $\mathbf{L}^{-1}$ matrices of Table XI. It is noteworthy that in the construction of $\mathbf{A}(A_1)$ an unusual situation arises in that ν(CH) and δ(HCH) are not the two highest frequencies, so that in this case it is the first and third rows of $\mathbf{L}^{-1}(A_1)$ that are used. Examination of the $\mathbf{A}(A_1)$ matrices reveals that the only potential source of difficulty in the application of the group frequency factorization method lies in the relatively large matrix elements which couple the coordinate S_2 with ν(C═C) in D_3, and with ν(C—X) in D_4. No such difficulty was anticipated for the B_2 vibrations, since there are no abnormally large elements coupling group and framework coordinates in this species.

The effective inverse mass matrices for atoms C_3 and C_4 (Fig. 1) are presented in Table XIII and the corrections, $\mathbf{\Phi}_{ff}$, to the force constants for the framework vibrations in Table XIV. Although some of the elements in $\mathbf{\Phi}_{ff}(A_1)$ are larger than is desirable in the method, they are nonetheless far smaller than those arising in the first calculations in which ν(C═C) was included in the group vibrations, and the corrections, $\mathbf{\Phi}_{ff}(B_2)$, are so small as to be negligible.

Since the skeletal vibrations involve only the system C═CX$_2$, it is unnecessary to define effective inverse hydrogen or deuterium masses for the A_1 species. The derivation of the reduced **G** matrices ($\mathbf{G}_{ff}{}^{+}$) is therefore particularly simple here, and the results for bond angles of 120° are quoted in Table XV. However, care should be taken in calculations not to confuse the two effective inverse carbon masses; viz. $\mu^{+}{}_{C_3(y)}$, $\mu^{+}{}_{C_4(y)}$ refer respectively to the motions of C_3 and C_4 in the y direction. On the other hand, the derivations of the reduced secular equations for the B_2 species do strictly require the definition of inverse hydrogen and deuterium masses, but the corrections are so small as to be negligible.

The construction of the approximate group frequency equations for ν(C—H) and ν(C—D) is straightforward, but the inclusion of several

Can. J. Chem. Downloaded from www.nrcresearchpress.com by 210.87.254.5 on 09/05/12
For personal use only.

TABLE XIV

The corrections, Φ_{ff}, to the force constants

Molecule	Species	Matrix			
CH_2CX_2	A_1	Φ_{ff}	S_3	S_4	S_5
		S_3	0.2472	−0.2326	0.0979
		S_4		0.1852	−0.0780
		S_5	(symmetrical)		0.0328
	B_2	Φ_{ff}	S_7	S_8	S_9
		S_7	0.0019	−0.0009	−0.0027
		S_8		0.0005	0.0014
		S_9	(symmetrical)		0.0040
CD_2CX_2	A_1	Φ_{ff}	S_3	S_4	S_5
		S_3	0.3620	−0.0329	0.0139
		S_4		0.2377	−0.1001
		S_5	(symmetrical)		0.0421
	B_2	Φ_{ff}	S_7	S_8	S_9
		S_7	0.0065	−0.0020	−0.0098
		S_8		0.0006	0.0030
		S_9	(symmetrical)		0.0147

elements of ΔG_{ij} is necessary to achieve a satisfactory degree of accuracy when the equations are applied to molecules with bond angles differing from 120°. The following equations contain all the significant terms in the first-order perturbation treatment (12):

vinylidene group

$$\lambda_1 = 5.3713 + 1.0312\Delta F_{11} + 0.0250\Delta F_{22} + 5.1113\Delta G_{11} - 0.0988\Delta G_{12}$$

$$\lambda_6 = 5.6621 + 1.1160\Delta F_{66} + 5.0073\Delta G_{66}$$

d_2-vinylidene group

$$\lambda_1 = 5.3713 + 1.0312\,\Delta F_{11} + 0.0250\,\Delta F_{22} + 5.1113\,\Delta G_{11} - 0.0988\,\Delta G_{12}$$

$$\lambda_6 = 5.6621 + 1.1160\,\Delta F_{66} + 5.0073\,\Delta G_{66}$$

$$\lambda_1 = 2.8757 + 0.5211\Delta F_{11} + 0.0656\Delta F_{22} + 0.0221\Delta F_{33} + 0.0761\Delta F_{23} + 4.8257\Delta G_{11} - 0.1990\Delta G_{12}$$

$$\lambda_6 = 3.1931 + 0.6187\Delta F_{66} + 4.9224\Delta G_{66}$$

$$(\Delta F_{ij} = F_{ij} - F_{ij}^{\circ} \qquad \Delta G_{ij} = G_{ij} - G_{ij}^{\circ})$$

where superscript 0 refers to the standard molecule.

The C=C stretching and HĈH (DĈD) bending frequencies were then treated by the method of ref. 14. This method is applicable to two or more frequencies which, although they may involve some mixing among themselves, are relatively independent of the other vibrations of the same symmetry species. Thus, if the subscript 0 refers to the standard molecule, then for a perturbed system

$$\mathbf{G} = \mathbf{G}_0 + \Delta\mathbf{G} \qquad \mathbf{F} = \mathbf{F}_0 + \Delta\mathbf{F}$$

and to first-order,

$$\mathbf{H} = \mathbf{GF} = \mathbf{G}_0\mathbf{F}_0 + \mathbf{G}_0\Delta\mathbf{F} + \Delta\mathbf{G}\mathbf{F}_0$$

$$= \mathbf{H}_0 + \Delta\mathbf{H}$$

Can. J. Chem. Downloaded from www.nrcresearchpress.com by 210.87.254.5 on 09/05/12
For personal use only.

TABLE XV
Reduced G matrices $\mathbf{G}_{ff}{}^{+}$

A_1	S_3	S_4	S_5
S_3	$[\mu^+{}_{C_3(y)} + \mu^+{}_{C_4(y)}]$	$-\mu^+{}_{C_4(y)}/\sqrt{2}$	$3\mu^+{}_{C_4(y)}/\sqrt{2}d$
S_4		$[\frac{1}{2}\mu^+{}_{C_4(y)} + \mu_X]$	$-3\mu^+{}_{C_4(y)}/2d$
S_5	(symmetrical)		$3[\mu_X + 3\mu^+{}_{C_4(y)}/2]/d^2$
B_2	S_7	S_8	S_9
S_7	$\{\frac{1}{2}[2/R + 1/r]^2\mu^+{}_{C_3(x)} + 2\mu^+{}_{C_4(x)}/R^2 + \mu_{H(D)}/r^2\}$	$[3\mu^+{}_{C_4(x)}/r]$	$\{-[(2/R + 1/r)\mu^+{}_{C_3(x)} + (2/R + 1/d)\mu^+{}_{C_4(x)}]/R\}$
S_8		$[3\mu^+{}_{C_4(x)}/2 + \mu_X]$	$[-\sqrt{3}(2/R + 1/d)\mu^+{}_{C_4(x)}/2]$
S_9	(symmetrical)		$[2\mu^+{}_{C_3(x)}/R^2 + (2/R + 1/d)^2\mu^+{}_{C_4(x)}/2 + \mu_X/d^2]$

Then on transforming **H** into the representation in which $\mathbf{H}_0$ is diagonal there results:

$$\mathscr{H} = \mathbf{L}_0{}^{-1}\mathbf{H}\mathbf{L}_0 = \mathbf{\Lambda}_0 + \mathbf{L}_0{}^*\Delta\mathbf{F}\mathbf{L}_0 + \mathbf{L}_0{}^{-1}\Delta\mathbf{G}(\mathbf{L}^{-1})^*\mathbf{\Lambda}_0$$
$$= \mathbf{\Lambda}_0 + \Delta\mathscr{H}$$

wherein the asterisk denotes the transpose.

The matrix elements of $\Delta\mathscr{H}$ for the required frequencies are thus determined from the eigenvectors of the zero-order problem, in this case the standard molecule, and from the perturbed **G** and **F** matrices. The diagonal elements of $\mathscr{H}$ are the frequency parameters obtained from first-order perturbation theory, and the off-diagonal elements usually contribute to the next higher order of approximation. In those cases for which $|\Delta\mathscr{H}_{ij}| \sim |\mathscr{H}_{ii} - \mathscr{H}_{jj}|$, the off-diagonal elements are important, and the submatrix $\mathscr{H}$ must be diagonalized to obtain the frequency parameters of the perturbed system. The application of the method to ν(C═C) and δ(HCH) or δ(DCD) leads to a second-order secular determinant involving the corresponding eigenvectors from the standard molecule. Since ν(C═C) is obtained from the treatment of both the skeletal and group vibrations, a convenient internal check for self-consistency is available, and a close agreement between the results from the two methods of calculation is an indication that the values so obtained are satisfactory. The results of the calculations by this, and by the other methods described above are collected in Tables V–VII. It is apparent that a simple first-order perturbation treatment gives excellent results for all those frequencies for which it is strictly applicable, i.e. in the absence of near degeneracy, and the values obtained for ν(C═C) and δ(HCH) or δ(DCD) in $CH_2{=}CF_2$, $CD_2{=}CF_2$, and $CH_2{=}CBr_2$ are expectedly in poor agreement with the observed frequencies due to the very complex nature of the vibrational modes in these compounds.

However, the first-order perturbation method for the degenerate case gives excellent agreement for ν(C═C) and δ(HCH) or δ(DCD) in all the molecules studied, with the exceptions of CH_2CF_2 where there is a difference of 37 cm^{-1} in ν(C═C), and of CD_2CF_2 where the calculated values of ν(C═C) and δ(DCD) are in error by 38 and 28 cm^{-1}, respectively. These discrepancies arise from a very high degree of participation of the symmetric C—F stretching vibration in these modes, which is not expected to occur to such a marked extent in compounds containing the groups $CH_2{=}CC_2$ and $CD_2{=}CC_2$. Even so, the results obtained by this method are an improvement on those from the simple first-order theory except for δ(DCD) in $CD_2{=}CF_2$, but it should be noted that the solutions of the reduced secular equations for the fluorides give reliable values for the C═C stretching frequencies.

Although the approximation methods described above have not proved completely successful in the vibrational analysis of the vinylidene halides, nevertheless the results do suggest criteria for the choice of method suitable for the treatment of individual cases. Thus the results obtained for the bromide and chloride indicate that for those molecules in which δ(HCH) or δ(DCD) and symmetric ν(C—X) are widely separated, the solution of the reduced equation in the method of King and Crawford (12) will give reliable results for all frequencies except ν(C═C), and that the first-order perturbation method for the case of near degeneracy will then give accurate values for this frequency and for δ(HCH) or δ(DCD).

Can. J. Chem. Downloaded from www.nrcresearchpress.com by 210.87.254.5 on 09/05/12
For personal use only.

Can. J. Chem. Downloaded from www.nrcresearchpress.com by 210.87.254.5 on 09/05/12
For personal use only.

On the other hand, the results for the fluoride suggest that for those molecules having a high value for the C—X stretching force constant so that δ(HCH) or δ(DCD) and symmetric ν(C—X) are very close, then it is the solution of the reduced secular equation which gives the more reliable value for ν(C=C). In such cases first-order perturbation theory for the degenerate case also provides accurate values for δ(HCH) in $CH_2{=}CF_2$, but gives only moderate agreement for δ(DCD) in $CD_2{=}CF_2$.

However, simple first-order perturbation theory provides satisfactory results for ν(C—H) and ν(C—D) in all cases, provided only that account is taken of changes in molecular geometry.

Finally, we consider the calculation of the skeletal frequencies for CH_2CX_2 and CD_2CX_2 by solution of the reduced secular determinant $|\mathbf{G}_{ff}{}^{+}\mathbf{F}_{ff}{}^{+} - \lambda\mathbf{E}_{ff}| = 0$ (12) wherein $\mathbf{F}_{ff}{}^{+} = \mathbf{F}_{ff} + \mathbf{\Phi}_{ff}$, with $\mathbf{F}_{ff}$ the force constants in Table VIII, and $\mathbf{\Phi}_{ff}$, the "corrections" of Table XIV. For convenience, the $\mathbf{G}_{ff}{}^{+}$ matrices were calculated on the computer using the program in ref. 6, since the analytical expressions of Table XV apply only to the simplified geometry with bond angles of 120°.

The determinants for the reduced problem were solved on the computer. The results of the calculations are presented in Tables V–VII, and inspection of Table VII for CH_2CBr_2 and CD_2CBr_2 reveals that the only significant error in the frequencies of the framework vibrations obtained by the approximation method lies in ν(C=C). This applies to both "light" and "heavy" isotopic molecules, but the results are slightly better in the former. The approximate value of ν(C=C) is about 70 cm^{-1} too low in both molecules, and as indicated by the **L** matrix, is most probably due to an unusually large contribution from δ(HCH) and δ(DCD). But reliable values for ν(C=C) are available from the other approximation methods described above.

A similar situation occurs in the chlorides, but the contributions to ν(C=C) from δ(HCH) and δ(DCD) are much smaller, with consequent reduction in the errors of ν(C=C) to 35 cm^{-1}. Both of the first-order perturbation calculations again give reliable results for ν(C=C).

However, the results of the approximation methods for the fluorides are quite different. Here, only skeletal modes contribute to ν(C=C), and the values obtained for this frequency in both "light" and "heavy" isotopic molecules are satisfactory. The remaining framework frequencies for the "light" molecule are generally satisfactory, the only significant error being one of 20 cm^{-1} in ν(C—F) (s). The discrepancy in this frequency in the "heavy" molecule is 56 cm^{-1}, and arises from a 28% contribution for δ(DCD). However, it is not expected that an application of the approximation method to molecules containing the groups $Y_2C{=}C(C_2)$ (Y = H, D) would encounter this difficulty, since ν(C=C) and δ(YCY) (Y = H, D) are more widely separated in these cases; for the effect is due mainly to the high value, 7.175 mdyn $Å^{-1}$, for F_d, and not to the mass of the fluorine atom.

Acknowledgments

The authors thank the Council of Salford University for the award of a Demonstratorship to J.M.F., and the staff of the Computation Laboratory for their assistance.

1. J. H. Carter, J. M. Freeman, and T. Henshall. J. Mol. Spectry. **20**, 402 (1966); **22**, 18 (1967). J. M. Freeman and T. Henshall. J. Mol. Struct. **1**, 31 (1967); Can. J. Chem. **46**, 2129, 2134, 2175 (1968).
2. C. Manneback and A. Rahman. Ann. Soc. Sci. Bruxelles, Ser. I, **67**, 140 (1953).
3. J. R. Scherer and J. Overend. J. Chem. Phys. **32**, 1720 (1960).
4. S. Enomoto and S. Echinohe. Nippon Kagaku Zasshi, 1343 (1958).
5. Tables of interatomic distances. Chem. Soc. Spec. Publ. No. 11, 1958, and Suppl. Chem. Soc. Spec. Publ. No. 18, 1959.
6. J. H. Carter, J. M. Freeman, and T. Henshall. Spectrochim. Acta, **23A**, 1463 (1966).
7. F. Edgell and C. J. Ultee. J. Chem. Phys. **22**, 1983 (1954).
8. D. C. Smith, J. Rud Nielsen, and H. H. Claason. J. Chem. Phys. **18**, 326 (1950).
9. M. de Hemptine, C. Velghe, and R. van Riet. Bull. Classe Sci. Acad. Roy. Belg. **30**, 40 (1944).
10. J. M. Freeman and T. Henshall. J. Mol. Spectry. **25**, 101 (1968).
11. L. J. Bellamy. The infrared spectra of complex molecules. Methuen and Co., London. 1956.
12. W. T. King and B. L. Crawford, Jr. J. Mol. Spectry. **5**, 421 (1960); **8**, 58 (1962).
13. E. B. Wilson, Jr., J. C. Decius, and P. C. Cross. Molecular vibrations. McGraw-Hill Book Co., Inc., New York. 1955.
14. C. D. Needham and J. Overend. Spectrochim. Acta, **21**, 417 (1965).
15. S. J. Cyvin, J. Brunvoll, B. N. Cyvin, I. Elvebredd, and G. Hagen. Mol. Phys. **14**, 43 (1968).

Can. J. Chem. Downloaded from www.nrcresearchpress.com by 210.87.254.105 on 09/05/12
For personal use only.

Circular dichroism of some bis(halogenoacetato)bis(ethylenediamine)cobalt(III) complexes

ROLAND A. HAINES AND EDWARD B. KIPP
Department of Chemistry, University of Western Ontario, London, Ontario

Received August 22, 1968

Compounds of the general type *cis*-bis(halogenoacetato)bis(ethylenediamine)cobalt(III) are discussed for the cases where the halogenoacetate ion is monochloroacetate, dichloroacetate, trichloroacetate, or dibromoacetate. For the first time these complexes have been resolved into their optical isomers and a study has been made of the circular dichroism data obtained.

The positions of circular dichroism and absorption bands have been interpreted by calculating relative values of the σ and π interactions for the halogenoacetate ligands.

Canadian Journal of Chemistry, **47**, 949 (1969)

Introduction

Both *cis*- and *trans*-isomers of the type $[Co(en)_2(halac)_2]^+$ (where en is ethylenediamine and halac is the anion of a halogenoacetic acid) have been reported in the literature (1–5).Their absorption spectra have been given and from the shifts in absorption maxima, the various acids have been arranged into a spectrochemical series.

Although these compounds are of the general type $[Co(en)_2X_2]^{n+}$, for which many examples are known, very significant differences are present which justify a detailed study. For most compounds of this type the X groups can vary over a wide range of size, charge, coordinating atom, π-bonding properties, etc.; in fact, generally the X groups have little in common for any given series. However, when halogenoacetate ions are the X groups, greater similarities are present since all involve the carboxylate grouping as the common coordinating species. The sole changes are due to the degree of halogen substitution on the acetic acid, resulting in changes of basicity of the carboxylate anion. Scale molecular models indicate that the halogen substituted groups do not interfere with each other and thus effects due to interaction of these groups will not be significant. Hence it should be possible to study the effect of *small* changes in the donor properties of the ligand on the various spectral properties of the complex.

For the *cis*-compounds two d–d absorption bands have been reported (2) and small differences are observed in the absorption maxima. However, it is well known that in complexes such as these, with C_2 symmetry, splitting of the various energy levels should occur. Such splitting is usually not apparent from absorption spectra but circular dichroism (c.d.) spectra have frequently been able to show the features. Thus it should be possible to obtain more information regarding these ligands if the c.d. spectra could be obtained.

In this paper we report the resolution of several of the *cis*-complexes into their optical isomers and discuss the results derived from the c.d. curves.

Experimental

Racemic complexes with the general formula *cis*-$[Co(en)_2(halac)_2]^+$ (where halac is monochloroacetate, dichloroacetate, trichloroacetate, and dibromoacetate) were prepared by previous methods (1, 3). Optically active sodium arsenyl tartrate was prepared by the method of Henderson and Ewing (6). Starting chemicals were obtained from Fisher Scientific Co., with the exception of dibromoacetic acid which was purchased from K and K Laboratories.

Ultraviolet and visible absorption spectra were obtained from a Beckman DK-1 recording spectrophotometer, while optical rotatory dispersion (o.r.d.) and circular dichroism data were measured on a Durrum-Jasco ORD/UV/5 spectropolarimeter. Microanalyses were performed by Alfred Bernhardt, West Germany, or A. Gygli, Toronto.

Resolution of the cis-$[Co(en)_2(CH_2ClCO_2)_2]^+$ Ion

cis-$[Co(en)_2(CH_2ClCO_2)_2]I$ (8.0 g) in 40 ml of water at 60 °C was converted to the acetate by stirring for 10 min with 2.68 g of silver acetate. The silver salts were filtered and washed with 20 ml of warm water. Three drops of glacial acetic acid were added to the filtrate, followed by 4.84 g of $(+)_{589}$-$NaAsOC_4H_4O_6.2H_2O$, then 30 ml of ethanol. The solution was allowed to stand 1 h in an ice bath, then was placed in a freezer for 20 min, and finally was allowed to stand at 0 °C overnight, after the beaker was scratched vigorously with a glass rod. The pink crystals of the diastereoisomer $(-)_{589}$-$[Co(en)_2(CH_2ClCO_2)_2][(+)_{589}$-$AsOC_4H_4O_6].2\frac{1}{2}H_2O$ were filtered, washed with small amounts of ethanol and ether, and air dried. Yield: 2.72 g. $[\alpha]_{546} = -331°$.

Anal. Calcd. for $[Co(en)_2(CH_2ClCO_2)_2][AsOC_4H_4O_6]$: C, 23.82; H, 4.00; N, 9.26; Cl, 11.72; As, 12.52.

Can. J. Chem. Downloaded from www.nrcresearchpress.com by 210.87.254.105 on 09/05/12
For personal use only.

Found: C, 23.65; H, 4.08; N, 9.14; Cl, 11.75; As, 12.52.

To a solution of 2.35 g of $(-)_{589}$-$[Co(en)_2(CH_2ClCO_2)_2][(+)_{589}$-$AsOC_4H_4O_6].2\frac{1}{2}H_2O$ in 140 ml of water was added a solution of 1.35 g of $NaB(C_6H_5)_4$ in 40 ml of water. Acetone (2 ml) was added slowly and the solution was stirred for a few minutes. The pink precipitate of $(-)_{589}$-$[Co(en)_2(CH_2ClCO_2)_2]B(C_6H_5)_4.H_2O$ was filtered, washed with water, sucked dry, and dried in a vacuum desiccator. Yield: 1.76 g. $[\alpha]_{546} = -278°$.

Recrystallization was accomplished by *partially* dissolving 1.20 g of crude material in a minimum amount of methanol. The clear red solution was separated from the undissolved solid. To the solution, water was added dropwise with stirring until a permanent cloudiness remained on mixing. The solution was poured into another beaker, and the major part of the complex precipitated by adding water quickly. The pink crystals of the $(-)_{589}$-isomer were filtered, washed with water, sucked dry, and dried in a vacuum desiccator. Yield: 0.73 g. $[\alpha]_{546} = -278°$.

Anal. Calcd. for $[Co(en)_2(CH_2ClCO_2)_2]B(C_6H_5)_4$: C, 56.08; H, 5.88; N, 8.18; Cl, 10.35. Found: C, 56.27; H, 6.12; N, 8.23; Cl, 10.18.

Resolution of the cis-$[Co(en)_2(CHCl_2CO_2)_2]^+$ Ion

cis-$[Co(en)_2(CHCl_2CO_2)_2]I$ (4.0 g) in 65 ml of water at 60 °C was converted to the acetate by stirring for 10 min with 1.19 g of silver acetate. The silver salts were filtered and washed with 12 ml of warm water. Three drops of glacial acetic acid were added to the filtrate, followed by 2.12 g of $(+)_{589}$-$NaAsOC_4H_4O_6.2H_2O$, then 30 ml of ethanol. The solution was allowed to stand in an ice–salt–water bath at −7 °C for $1\frac{1}{4}$ h. The pink crystals of the diastereoisomer $(+)_{589}$-$[Co(en)_2(CHCl_2CO_2)_2][(+)_{589}$-$AsOC_4H_4O_6].H_2O$ were filtered, sucked dry, washed with ethanol, then ether[1], and dried in a desiccator. Yield: 0.80 g. $[\alpha]_{546} = +53.4°$.

Anal. Calcd. for $[Co(en)_2(CHCl_2CO_2)_2][AsOC_4H_4O_6]$: C, 21.39; H, 3.29; N, 8.31; Cl, 21.04; As, 11.12. Found: C, 21.54; H, 3.10; N, 8.25; Cl, 21.02; As, 11.36.

To a filtered solution of 0.76 g of the diastereoisomer $(+)_{589}$-$[Co(en)_2(CHCl_2CO_2)_2][(+)_{589}$-$AsOC_4H_4O_6].H_2O$ in 40 ml of water was added a solution of 0.38 g of $NaB(C_6H_5)_4$ in 10 ml of water. Acetone ($\frac{1}{2}$ ml) was added slowly with stirring and the solution was allowed to stand $\frac{1}{2}$ h. The pink crystals of $(+)_{589}$-$[Co(en)_2(CHCl_2CO_2)_2]B(C_6H_5)_4.H_2O$ were filtered, washed with water, sucked dry, and dried in a vacuum desiccator. Yield: 0.69 g.

The crude material (0.35 g) was dissolved in the minimum amount of methanol. The solution was filtered, and the complex crystallized by adding water slowly to the filtrate with stirring. The pink crystals of the $(+)_{589}$-isomer were filtered, washed with water, sucked dry, and dried in a vacuum desiccator. Yield: 0.20 g. $[\alpha]_{546} = +46.4°$.

Anal. Calcd. for $[Co(en)_2(CHCl_2CO_2)_2]B(C_6H_5)_4$: C, 50.96; H, 5.08; N, 7.43; Cl, 18.80. Found: C, 51.30; H, 5.12; N, 7.29; Cl, 18.77.

[1]During washing with ethanol and ether, some of the diastereoisomer may change into a sticky residue and the crystalline material remaining must be manually separated.

Resolution of the cis-$[Co(en)_2(CCl_3CO_2)_2]^+$ Ion

cis-$[Co(en)_2(CCl_3CO_2)_2]Cl$ (4.0 g) in 200 ml of water at 60 °C was converted to the acetate by stirring for 10 min with 1.38 g of silver acetate. The silver salts were filtered and washed with 10 ml of warm water. Four drops of glacial acetic acid were added to the filtrate, followed by 2.21 g of $(+)_{589}$-$NaAsOC_4H_4O_6.2H_2O$ and 80 ml of ethanol. The solution was allowed to stand in an ice–salt–water bath at −5 °C for $1\frac{1}{4}$ h. The pink crystals of the diastereoisomer $(-)_{589}$-$[Co(en)_2(CCl_3CO_2)_2][(+)_{589}$-$AsOC_4H_4O_6]$ were filtered, washed with ethanol and ether, and dried in a desiccator. Yield: 0.80 g. $[\alpha]_{546} = -228°$.

A second fraction of the $(-)_{589}$-diastereoisomer was obtained by taking the filtrate from the first fraction and cooling it for 1–$1\frac{1}{2}$ h in a freezer. When a precipitate began to form, the solution was allowed to stand at 0 °C overnight. The diastereoisomer was filtered, washed with ethanol and ether, and dried in a desiccator. Yield: 0.50 g. $[\alpha]_{546} = -236°$.

Anal. Calcd. for $[Co(en)_2(CCl_3CO_2)_2][AsOC_4H_4O_6]$: C, 19.40; H, 2.71; N, 7.54; Cl, 28.63; As, 10.08. Found: C, 19.60; H, 2.85; N, 7.43; Cl, 28.46; As, 10.16.

To a filtered solution of 0.92 g of the diastereoisomer $(-)_{589}$-$[Co(en)_2(CCl_3CO_2)_2][(+)_{589}$-$AsOC_4H_4O_6]$ in 550 ml of water was added a solution of 0.50 g of $NaB(C_6H_5)_4$ in 20 ml of water. Acetone (2 ml) was added slowly with stirring and the solution was allowed to stand $\frac{1}{2}$ h. The pink crystals of $(-)_{589}$-$[Co(en)_2(CCl_3CO_2)_2]B(C_6H_5)_4$ were filtered, washed with water, sucked dry, and dried in a vacuum desiccator. Yield: 0.82 g.

The crude material (0.65 g) was dissolved in the minimum amount of methanol. The solution was filtered, and the complex caused to crystallize by adding water slowly to the solution with stirring. The pink crystals of the $(-)_{589}$-isomer were filtered, washed with water, sucked dry, and dried in a vacuum desiccator. Yield: 0.20 g. $[\alpha]_{546} = -240°$.

Anal. Calcd. for $[Co(en)_2(CCl_3CO_2)_2]B(C_6H_5)_4$: C, 46.70; H, 4.41; N, 6.81; Cl, 25.81. Found: C, 47.04; H, 4.56; N, 6.79; Cl, 25.72.

Resolution of the cis-$[Co(en)_2(CHBr_2CO_2)_2]^+$ Ion

cis-$[Co(en)_2(CHBr_2CO_2)_2]I$ (4.0 g) in 120 ml of water at 60 °C was converted to the acetate by stirring for 10 min with 0.92 g of silver acetate. The silver salts were filtered off and washed with 10 ml of warm water. Three drops of glacial acetic acid were added to the filtrate, followed by 1.62 g of $(+)_{589}$-$NaAsOC_4H_4O_6.2H_2O$, then 30 ml of ethanol. The solution was allowed to stand in an ice–salt–water bath at −7 °C for $1\frac{1}{4}$ h. The pink crystals of the diastereoisomer $(+)_{589}$-$[Co(en)_2(CHBr_2CO_2)_2][(+)_{589}$-$AsOC_4H_4O_6]$ were filtered, washed with ethanol and ether, and dried in a desiccator. Yield: 1.10 g. $[\alpha]_{546} = +39.7°$.

Anal. Calcd. for $[Co(en)_2(CHBr_2CO_2)_2][AsOC_4H_4O_6]$: C, 16.92; H, 2.60; N, 6.58; Br, 37.52; As, 8.79. Found: C, 16.85; H, 2.56; N, 6.45; Br, 37.52; As, 9.01.

To a filtered solution of 0.94 g of the diastereoisomer $(+)_{589}$-$[Co(en)_2(CHBr_2CO_2)_2][(+)_{589}$-$AsOC_4H_4O_6]$ in 100 ml of water was added a solution of 0.39 g of $NaB(C_6H_5)_4$ in 20 ml of water. Acetone ($\frac{1}{2}$ ml) was added slowly with stirring and the solution was allowed to

TABLE I

Comparison of circular dichroism and absorption data

Compound	Absorption		Circular dichroism*	
	ν_{max} (cm^{-1})	ε_{max}	ν_{max} (cm^{-1})	$(\varepsilon_l - \varepsilon_d)$
$[Co(en)_2(CH_2ClCO_2)_2]^+$	19 840	144	17 480	−0.092
			20 360	+1.210
	27 320	118	27 340	−0.259
$[Co(en)_2(CHCl_2CO_2)_2]^+$	19 920	147	17 580	−0.032
			20 350	+0.190
	27 400	130	27 230	−0.050
$[Co(en)_2(CCl_3CO_2)_2]^+$	20 000	133	17 430	−0.030
			20 270	+0.961
	27 470	123	27 030	−0.120
$[Co(en)_2(CHBr_2CO_2)_2]^+$	19 880	148	17 650	−0.022
			20 470	+0.180
	27 400	122	27 430	−0.030

*All c.d. data are for the $(+)_{589}$-isomer.

stand ½ h. The pink crystals of $(+)_{589}$-$[Co(en)_2(CHBr_2CO_2)_2]B(C_6H_5)_4$ were filtered, washed with water, sucked dry, and dried in a vacuum desiccator. Yield: 0.75 g.

The crude material (0.70 g) was dissolved in the minimum amount of methanol. The solution was filtered, and the complex caused to crystallize by adding water slowly with stirring. The pink crystals of the $(+)_{589}$-isomer were filtered, washed with water, sucked dry, and dried in a vacuum desiccator. Yield: 0.56 g. $[\alpha]_{546} = +28.0°$.

Anal. Calcd. for $[Co(en)_2(CHBr_2CO_2)_2]B(C_6H_5)_4$: C, 41.24; H, 4.11; N, 6.01; Br, 34.29. Found: C, 40.96; H, 4.19; N, 5.95; Br, 34.37.

For all complexes the optical isomer of opposite configuration was obtained by using $(-)_{589}$-$NaAsOC_4H_4O_6$ as the resolving agent.

All measurements were made on methanol solutions of the resolved complex.

Results and Discussion

The absorption spectra, o.r.d., and c.d. curves for each of the compounds studied are shown in Figs. 1–4 and a comparison of the absorption and circular dichroism data is given in Table I. Previous workers (2) have examined the absorption spectra of these complexes and have arranged the various acids into a spectrochemical series on the basis of shifts in absorption maxima. The relative ordering of the ligands was $CH_2ClCO_2^- < CHCl_2CO_2^- \sim CHBr_2CO_2^- < CCl_3CO_2^-$ and was the reverse of that expected on purely electrostatic grounds, thus suggesting that other effects were more predominant. An examination of the c.d. results presented below provides additional information on the matter.

To begin our discussion it is necessary to recall both the interrelationship of c.d. and absorption spectra and the splitting of absorption bands in complexes of low symmetry. For each electronic transition which is magnetic dipole allowed, strong circular dichroism will be observed and since c.d. is only a difference in absorbance of left and right

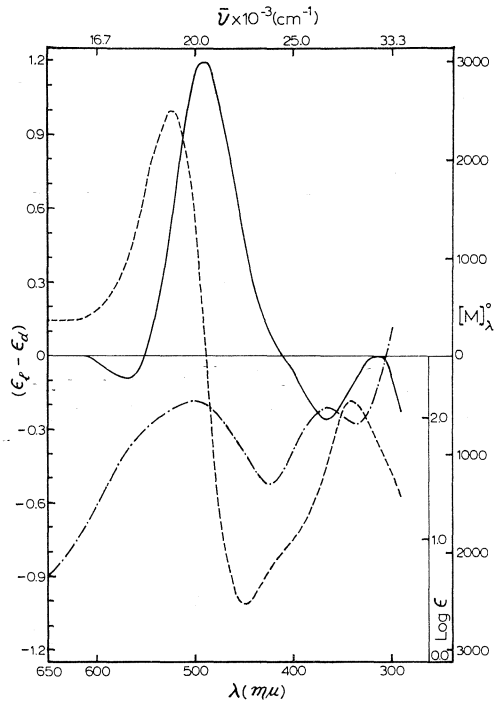

FIG. 1. Absorption spectrum (-·-·-), o.r.d. (---), and c.d. curve (—) for $(+)_{589}$-$[Co(en)_2(CH_2ClCO_2)_2]B(C_6H_5)_4.H_2O$.

Can. J. Chem. Downloaded from www.nrcresearchpress.com by 210.87.254.105 on 09/05/12
For personal use only.

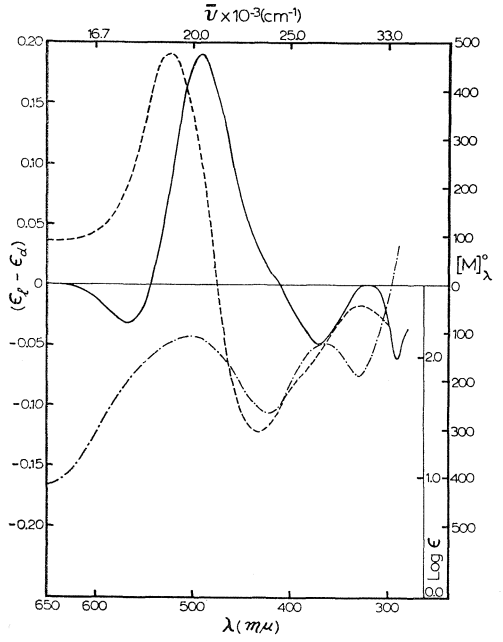

FIG. 2. Absorption spectrum (-·-·-), o.r.d. (---), and c.d. curve (—) for $(+)_{589}$-$[Co(en)_2(CHCl_2CO_2)_2]B(C_6H_5)_4.H_2O$.

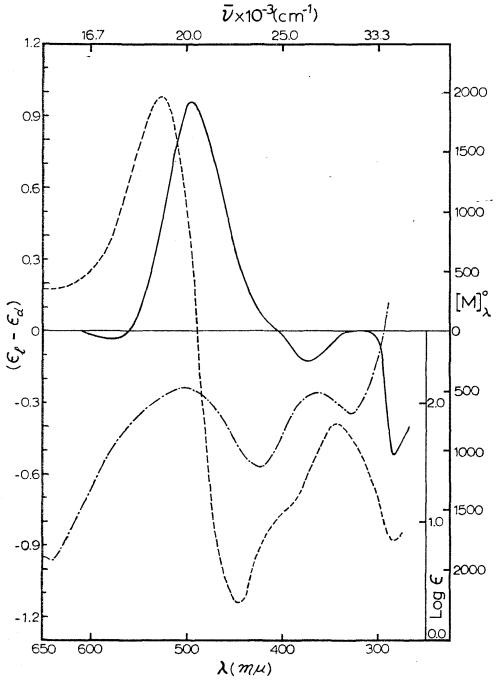

FIG. 3. Absorption spectrum (-·-·-), o.r.d. (---), and c.d. curve (—) for $(+)_{589}$-$[Co(en)_2(CCl_3CO_2)_2]B(C_6H_5)_4$.

circularly polarized light at any particular wavelength, the position of the c.d. and absorption maxima should be identical. Octahedral cobalt(III) complexes have two d–d absorption bands, corresponding to the $^1A_{1g} \rightarrow {}^1T_{1g}$ and $^1A_{1g} \rightarrow {}^1T_{2g}$ transitions, and theory predicts that in complexes of lower symmetry these bands become split. Thus two components are predicted for each band in complexes of D_3 symmetry, while three are expected for complexes of C_2 and C_{2v} symmetry. However, in many cases these component bands are not seen since the energy differences are rather small. Hence only the envelope of the combined absorption bands is observed and these results have suggested that the symmetry could be regarded as O_h to a first approximation.

The use of c.d. spectra has permitted some of the component bands to be located in certain compounds, this being largely due to the fact that c.d. bands are narrower than absorption bands and also may be of different sign. Thus in $[Co(en)_3]^{3+}$, which has D_3 symmetry, two c.d. bands of opposite sign are observed in the region of the low energy absorption band. For com-

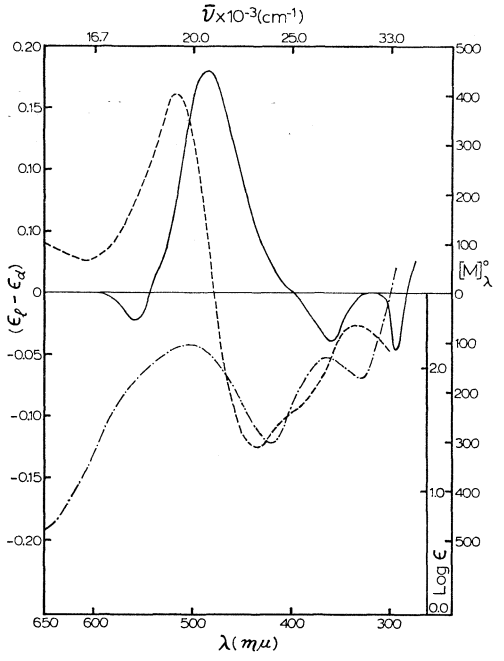

FIG. 4. Absorption spectrum (-·-·-), o.r.d. (---), and c.d. curve (—) for $(+)_{589}$-$[Co(en)_2(CHBr_2CO_2)_2]B(C_6H_5)_4$.

Can. J. Chem. Downloaded from www.nrcresearchpress.com by 210.87.254.105 on 09/05/12
For personal use only.

TABLE II

Values of δ_σ and δ_π derived from c.d. data*

Compound	δ_σ (cm^{-1})	δ_π (cm^{-1})	$\delta_\sigma+\delta_\pi$ (cm^{-1})
$[Co(en)_2(CH_2ClCO_2)_2]^+$	−6660	+2810	−3850
$[Co(en)_2(CHCl_2CO_2)_2]^+$	−7260	+3370	−3890
$[Co(en)_2(CCl_3CO_2)_2]^+$	−7980	+3770	−4200
$[Co(en)_2(CHBr_2CO_2)_2]^+$	−6780	+3380	−3400

*Expressed as displacements from the absorption maxima in $[Co(en)_3]^{3+}$.

plexes of C_2 or C_{2v} symmetry three c.d. bands are predicted in this region but only for $[Co(en)(mal)_2]^-$ (mal = malonate ion) are all three clearly defined (8), and the number observed in other compounds is strongly dependent on the ligands.

The two low energy c.d. bands observed for the $[Co(en)_3]^{3+}$ complex correspond to transitions to a doubly degenerate E level and to one with A_2 symmetry. In the C_2 complexes one transition has A symmetry while the remaining two have B symmetry. One of the B components derives from the A_2 transition in the corresponding $[Co(en)_3]^{3+}$ compound, while the other B component and the one with A symmetry result from the breakdown of the E level in that complex (7).

The octahedral T_{2g} level is also broken down for $[Co(en)_3]^{3+}$ and a symmetry forbidden A_1 state which shows no c.d. and a double degenerate E level are produced. The degeneracy of the latter becomes further broken down into two components with A and B symmetry in C_2 complexes.

The compounds reported here are all of the type $[Co(en)_2XX]^{n+}$ and possess C_2 symmetry. Two c.d. bands of opposite sign are found in the region of the low energy absorption band and this is similar to that often observed when X is a monodentate ligand. The band of lower energy corresponds to the B component derived from A_2 in $[Co(en)_3]^{3+}$, while the other is a combination of the A and B transitions which are obtained from the E band in that complex and are very similar in energy (7, 9). For most complexes of this general type the shifts of these bands upon changing the X group parallel the shifts in absorption maxima, but for the series of halogenoacetic acids such was not found to be the case. This may be due to the fact that most ligands in the spectrochemical series differ quite markedly from one another and hence any changes observed on substitution of ligands are quite distinct. This is not the situation for the halogenoacetate ligands which all bear a strong similarity to one another and hence present much smaller changes at the coordination site. All are uninegative, unidentate, and possess the same carboxylate grouping, thus eliminating some of the problems encountered in comparing ligands. Hence the differences observed should be related directly to properties of the particular halogenoacetate ion.

Yamatera (9) has predicted the relative magnitudes of splitting in absorption bands as the symmetry is lowered from O_h. Accordingly each shift can be attributed to some combination of σ and π interactions in complexes of the type *cis*-$[Coa_4b_2]$ of C_{2v} symmetry, and the arguments are readily extended to similar complexes with C_2 symmetry. From his arguments it can be seen that in the low energy region the net shift of the B component should be twice that of the combined A and B transition. Other equations apply to the shifts observed in the region of the higher energy absorption band. The positions of our c.d. maxima were considered as shifts relative to the absorption maxima of $[Co(en)_3]^{3+}$, which has O_h point symmetry and D_3 overall symmetry. The equations presented in Table II of Yamatera's paper were then employed and two quantities, δ_σ and δ_π, were calculated for each of the complexes. These two terms are measures of the effect of changes in σ and π interactions respectively on the spectral band shifts. Since the c.d. data is derived from overlapping Gaussian curves, probably not too much significance should be attached to the actual numerical values. However, the trends should give indications of the relative importance of each term to the observed shifts. It can be seen from Table II presented below that δ_σ and δ_π individually have different trends but their sum produces the observed variations in c.d. maxima.

The δ_σ term becomes more negative as chlorine substitution on the acid is increased, while the dibromoacetate compound has a δ_σ value which

Can. J. Chem. Downloaded from www.nrcresearchpress.com by 210.87.254.105 on 09/05/12
For personal use only.

Can. J. Chem. Downloaded from www.nrcresearchpress.com by 210.87.254.105 on 09/05/12
For personal use only.

is less than that of the dichloroacetate species. This term is an indication of the shift produced if only σ interactions are involved and a possible explanation can be put forward using an electrostatic argument. The relative acid strengths of the free acids follow the order $CH_2ClCO_2H < CHCl_2COOH \sim CHBr_2CO_2H < CCl_3CO_2H$. Thus the trichloroacetate ion is the poorest Lewis base and will present the weakest field to the metal ion. Hence a shift to the lowest energies (or most negative δ_σ values) should occur for this ligand. The remaining acid anions should cause a smaller shift toward lower energies in proportion to their basicity and such is found to be the case.

The δ_π term, which indicates the contributions from π bonding effects, follows a trend toward more positive values as the chlorine substitution on the ligand is increased, while the dibromoacetate compound has a value which is similar to that for the dichloroacetate complex. According to Yamatera (9) the δ_π term should become more positive as π bonding is increased, and hence the metal–ligand π bonding would be greatest in the trichloroacetate compound and least in the monochloroacetate. The dichloroacetate and dibromoacetate compounds have values which are similar to each other and indicate π bonding which is intermediate between the two extremes. Thus the trend is the reverse of that for δ_σ and it is possible that the σ effects produced by increasing halogen substitution render the carboxylate group a better π acceptor of electron density from the metal. This seems logical if simple ligand field theory is applied. As the field presented by the ligand becomes weaker, the donor atom may approach the metal more closely and hence better overlap is possible in the π system.

The positions of either absorption or c.d. spectra depend on the relative importance of each term. As predicted (9), the δ_σ term is always predominant but as δ_π changes the combination can produce different trends which are reflected in positions of the c.d. maxima. The absorption spectra show an average effect due to band overlap (of the same sign) and the location of the band maximum depends on the actual energy separation of the components. For this series these vary only by small amounts and produce small changes in absorption maxima. A more meaningful picture can be obtained by considering the interrelationship of all the component bands as located by c.d. spectra.

The intensities of the c.d. spectra vary considerably and detailed calculations are needed before a satisfactory argument can be put forward. Two major problems contribute to the observed c.d. intensity in these complexes, (*a*) band overlap and (*b*) mixing of transitions with the same symmetry. It has been shown previously (10) that in $[Co(en)_3]^{3+}$ the bands cancel each other to within 5%. Such cancellation would obtain for these complexes also, since the energy separation is almost the same or in some cases even less than that in $[Co(en)_3]^{3+}$. Thus the intensity could vary considerably, depending on the energy separation.

An even more important contribution could be due to configuration interaction which occurs between transitions of the same symmetry. Thus in the region of the low energy absorption band the two *B* components should have rotational strengths which are a combination of the two "pure" *B* rotational strengths. Although limits have been set on the extent of such mixing (7), for any given compound it has remained an unknown quantity. Examination of the equations describing the interaction shows that the resultants vary widely in both sign and magnitude for small changes in mixing coefficients, and thus casual examination of the relative c.d. intensities may not be too useful.

All of these complexes may be assigned an absolute configuration on the basis of their c.d. curves. It has been shown (7) that for complexes of this type the predominant c.d. band is the *A* component, and hence may be related to the *E* band of the compound $[Co(en)_3]^{3+}$ for which an absolute configuration is known (11). On this basis, all complexes of $[Co(en)_2(halac)_2]^+$ which have a positive *A* component of c.d. may be assigned the *D* or Λ configuration which is related directly to the *D* or Λ isomer of $[Co(en)_3]^{3+}$, as shown in Fig. 5.

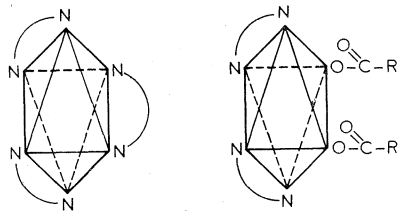

FIG. 5. Configuration of the *D* or Λ isomers of $[Co(en)_3]^{3+}$ and $[Co(en)_2(halac)_2]^+$.

This study emphasizes the fact that absorption spectra frequently do not give detailed information concerning metal complexes but rather present an average effect. Although in many cases this is sufficient, for this particular series with very similar ligands it is not. We have shown how c.d. spectra can be used to gain information concerning the metal–ligand interactions.

Acknowledgment

We are grateful to the Department of University Affairs (Province of Ontario) for financial support of this work.

1. M. LINHARD and G. STERN. Z. Anorg. Allgem. Chem. **268**, 105 (1952).
2. K. KURODA and P. S. GENTILE. J. Inorg. Nucl. Chem. **27**, 155 (1965).
3. K. KURODA and P. S. GENTILE. Bull. Chem. Soc. Japan, **38**, 1362 (1965).
4. K. KURODA and P. S. GENTILE. Bull. Chem. Soc. Japan, **38**, 1368 (1965).
5. V. CARUNCHIO, G. ILLUMINATI, and F. MASPERO. J. Inorg. Nucl. Chem. **28**, 2693 (1966).
6. G. G. HENDERSON and A. R. EWING. J. Chem. Soc. 102 (1895).
7. A. J. MCCAFFERY, S. F. MASON, and B. J. NORMAN. J. Chem. Soc. 5094 (1965).
8. B. E. DOUGLAS, R. A. HAINES, and J. G. BRUSHMILLER. Inorg. Chem. **2**, 1194 (1963).
9. H. YAMATERA. Bull. Chem. Soc. Japan, **31**, 95 (1958).
10. A. J. MCCAFFERY and S. F. MASON. Mol. Phys. **6**, 359 (1963).
11. Y. SAITO, K. NAKATSU, M. SHIRO, and H. KUROYA. Acta Cryst. **8**, 729 (1955).

Can. J. Chem. Downloaded from www.nrcresearchpress.com by 210.87.254.105 on 09/05/12
For personal use only.

Can. J. Chem. Downloaded from www.nrcresearchpress.com by 210.87.254.105 on 09/05/12
For personal use only.

Ion–molecule reactions in vinyl fluoride

J. A. HERMAN[1] AND A. G. HARRISON
Department of Chemistry, University of Toronto, Toronto 5, Ontario

Received June 24, 1968

The ion–molecule reactions in vinyl fluoride have been studied as a function of pressure and electron energy. The $C_2H_2^+$ and C_2HF^+ fragment ions react predominantly by charge transfer while $C_2H_3^+$ produces $C_2H_4F^+$ and $C_4H_5^+$. The $C_2H_2F^+$ fragment forms $C_2H_4F^+$, CHF_2^+, $C_2H_3F_2^+$, $C_4H_4F^+$, and probably $C_2H_3^+$. The rate constants for the individual reactions have been measured. The $C_2H_3F^+$ ion reacts to form $C_3H_5^+$, $C_3H_4F^+$, $C_3H_3F_2^+$, and $C_4H_5F^+$ (in minor yield), both by a second order and by a third order reaction. The rate constants and product distributions from the individual reactions have been evaluated. A number of consecutive reactions have been identified and shown to be third order processes.

Canadian Journal of Chemistry, 47, 957 (1969)

Introduction

The ion–molecule reactions in vinyl chloride have been studied recently both by ion cyclotron resonance spectrometry (1) and by conventional mass spectrometric techniques (2). The reaction of $C_2H_3Cl^+$ leads to $C_3H_4Cl^+$, $C_4H_5Cl^+$, and $C_4H_6Cl^+$. The $C_3H_4Cl^+$ and $C_4H_6Cl^+$ products are analogous to the $C_3H_5^+$ and $C_4H_7^+$ products observed from reaction of $C_2H_4^+$ in ethylene (3), while the $C_4H_5Cl^+$ product is distinctive. The vinyl chloride system is also distinctive in that the bimolecular reaction of $C_2H_3Cl^+$ is very slow, the majority of those $C_2H_3Cl^+$ ions which react disappearing by a reaction which is second order in neutral vinyl chloride. A similar third order reaction has been observed in vinyl bromide (2). In view of the large effect which substitution of chlorine or bromine has on the reaction course and rates, it appeared of interest to study the ionic reactions in vinyl fluoride. The present work reports the results we have obtained in such a study.

Experimental

The experimental work was carried out on the medium pressure instrument recently described (4). The pertinent operating conditions were a source temperature of approximately 100 °C, a primary ion travel distance of 0.54 cm, and a repeller field corresponding to 2.4 eV ion exit energy. The ionizing electron beam was pulsed and primary ion residence times were measured by the deflection technique previously described (4). The source pressures were measured directly using an MKS Baratron capacitance micromanometer.

The vinyl fluoride was obtained from Matheson and Co. and was purified by bulb-to-bulb distillation in vacuo before use. No impurities were detected in the mass spectrum.

Results and Discussion

Figure 1 shows the dependence of the primary ion intensities (% total ionization) on the ion source pressure for impact of 50 eV electrons at 2.4 eV ion exit energy. The $C_2H_2F^+$, C_2HF^+, and $C_2H_2^+$ primary ion intensities decrease with

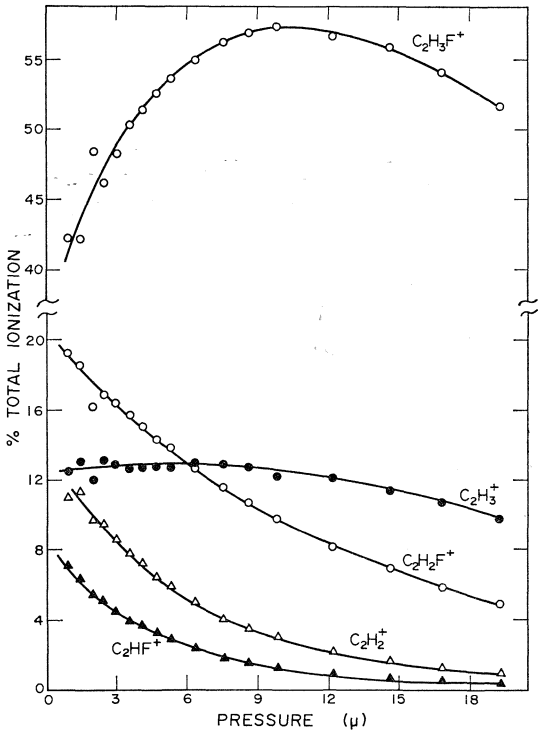

FIG. 1. Pressure plot for primary ions 50 eV electron energy, 2.4 eV ion exit energy.

[1]Visiting scientist, 1967–1968. Permanent address: Department of Chemistry, Laval University, Quebec, Quebec.

Can. J. Chem. Downloaded from www.nrcresearchpress.com by 210.87.254.105 on 09/05/12
For personal use only.

increasing pressure in the exponential manner expected of reactive primary ions. On the other hand, the $C_2H_3^+$ and $C_2H_3F^+$ intensities show an initial increase followed by a decrease at higher pressures, indicating that these ions are products of ion–molecule reactions as well as being reactive ions.

Figure 2 shows the product ion intensities as a function of pressure. The products $C_2H_4F^+$, CHF_2^+, $C_2H_3F_2^+$, $C_4H_5^+$, and $C_4H_4F^+$ show an increase in intensity with pressure which is characteristic of the products of bimolecular reactions. On the other hand, the curves for $C_3H_5^+$, $C_3H_4F^+$, and $C_3H_3F_2^+$ suggest that they are formed predominantly, if not exclusively, by third order reactions. The curve for $C_4H_6F^+$ also shows a pronounced upward curvature, indicating a high kinetic order for the reaction producing this ion. In addition to the products shown in Fig. 2 very small intensities were observed for $C_3H_3^+$ and $C_4H_5F^+$. From observations of the ion intensities as a function of electron energy and from ratio plot (5) studies, the reaction identifications summarized in Table I were obtained. The reactions of the individual primary ions are considered in detail in the following.

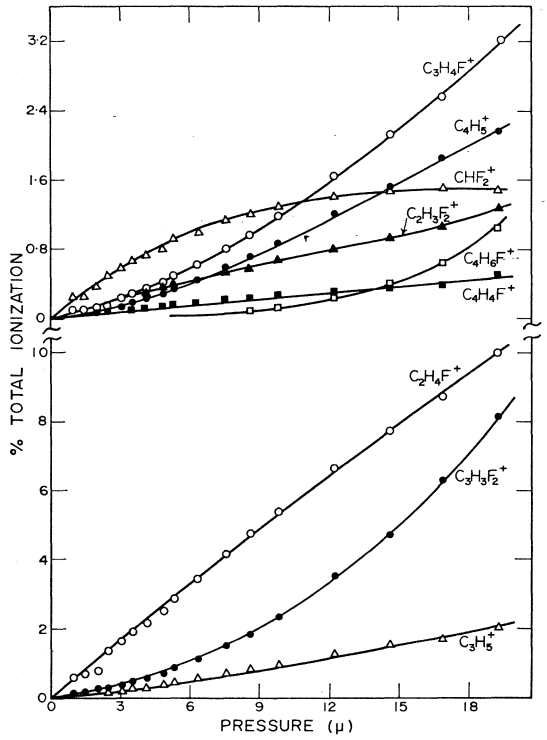

FIG. 2. Pressure plot for product ion, conditions as for Fig. 1.

TABLE I

Reaction identification in vinyl fluoride

Reactant	Products
$C_2H_2^+$	$C_3H_3^+$, $C_2H_3F^+$
$C_2H_3^+$	$C_2H_4F^+$, $C_4H_5^+$
C_2HF^+	$C_2H_3F^+$
$C_2H_2F^+$	$C_2H_4F^+$, CHF_2^+, $C_2H_3F_2^+$, $C_4H_4F^+$
$C_2H_3F^+$	$C_3H_5^+$, $C_3H_4F^+$, $C_4H_5F^+$, $C_3H_3F_2^+$

$C_2H_2^+$

A typical log plot of the normalized $C_2H_2^+$ intensity versus pressure is shown in Fig. 3. Several such plots gave an average total rate constant for the disappearance of $C_2H_2^+$ of $(19.5 \pm 0.3) \times 10^{-10}$ cm^3 molecule^{-1} s^{-1}. The $C_3H_3^+$ ion was found to originate from reaction of $C_2H_2^+$ (reaction [1]), the rate constant being 0.5×10^{-10} cm^3 molecule^{-1} s^{-1}. No other products were observed and we conclude that the majority of the $C_2H_2^+$ ions charge transfer to vinyl fluoride (reaction [2]). Since $I(C_2H_2) = 11.42$ eV (6) and $I(C_2H_3F) = 10.37$ eV (7), the reaction is exothermic. A similar rapid charge transfer reaction of $C_2H_2^+$ has been observed in the vinyl chloride system (2)

$$[1] \quad C_2H_2^+ + C_2H_3F \rightarrow C_3H_3^+ + CH_2F \qquad k = 0.5 \times 10^{-10} \text{ cm}^3 \text{ molecule}^{-1} \text{ s}^{-1}$$

$$[2] \quad C_2H_2^+ + C_2H_3F \rightarrow C_2H_3F^+ + C_2H_2 \qquad k = 19.0 \times 10^{-10} \text{ cm}^3 \text{ molecule}^{-1} \text{ s}^{-1}$$

$C_2H_3^+$

No total rate constants for the disappearance of $C_2H_3^+$ could be obtained since this ion appears to be produced in an ion–molecule reaction. Ratio plots showed that both $C_2H_3^+$ and $C_2H_2F^+$ reacted to form $C_2H_4F^+$. A typical ratio plot obtained over the electron energy range 13 to 18.8 eV nominal is shown in Fig. 3. The non-zero slope and intercept clearly indicate the occurrence of both reactions [3] and [4] with the average rate constants indicated.

$$[3] \quad C_2H_3^+ + C_2H_3F \rightarrow C_2H_4F^+ + C_2H_2 \qquad k = (3.0 \pm 0.5) \times 10^{-10} \text{ cm}^3 \text{ molecule}^{-1} \text{ s}^{-1}$$

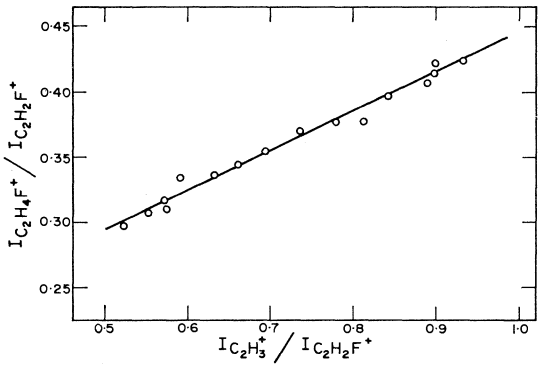

FIG. 3. Ratio plot for formation of $C_2H_4F^+$ [M] = 2.66×10^{14} molecules cm^{-3}.

[4] $C_2H_2F^+ + C_2H_3F \rightarrow C_2H_4F^+ + C_2HF$

$k = (1.7 \pm 0.2) \times 10^{-10}$ cm^3 $molecule^{-1}$ s^{-1}

The $C_2H_3^+$ ion also reacts to form $C_4H_5^+$. However, the ratio $I_{C_4H_5^+}/\sum I_{C_2H_3^+}$ was not linear with pressure as expected but showed an upward curvature. It is not known whether another reaction of higher order also produces $C_4H_5^+$ or whether the $C_2H_3^+$ ions produced by ion–molecule reaction react at a faster rate than those produced by dissociative ionization. No rate constant could be evaluated for reaction [5].

[5] $C_2H_3^+ + C_2H_3F \rightarrow C_4H_5^+ + HF$

C_2HF^+

No products of the reaction of this ion were observed and we conclude that it reacts exclusively by charge transfer to vinyl fluoride (reaction [6]). A typical log plot is shown in Fig. 4 and leads to $k_6 = 19.5 \times 10^{-10}$ cm^3 $molecule^{-1}$ s^{-1}.

[6] $C_2HF^+ + C_2H_3F \rightarrow C_2H_3F^+ + C_2HF$

$C_2H_2F^+$

The following reactions of $C_2H_2F^+$ were observed (all rate constants in cm^3 $molecule^{-1}$ s^{-1}).

[4] $C_2H_2F^+ + C_2H_3F \rightarrow C_2H_4F^+ + C_2HF$

$k = (1.7 \pm 0.2) \times 10^{-10}$

[7] $C_2H_2F^+ + C_2H_3F \rightarrow CHF_2^+ + C_3H_4$

$k = (1.1 \pm 0.1) \times 10^{-10}$

[8] $C_2H_2F^+ + C_2H_3F \rightarrow C_2H_3F_2^+ + C_2H_2$

$k = (0.50 \pm 0.1) \times 10^{-10}$

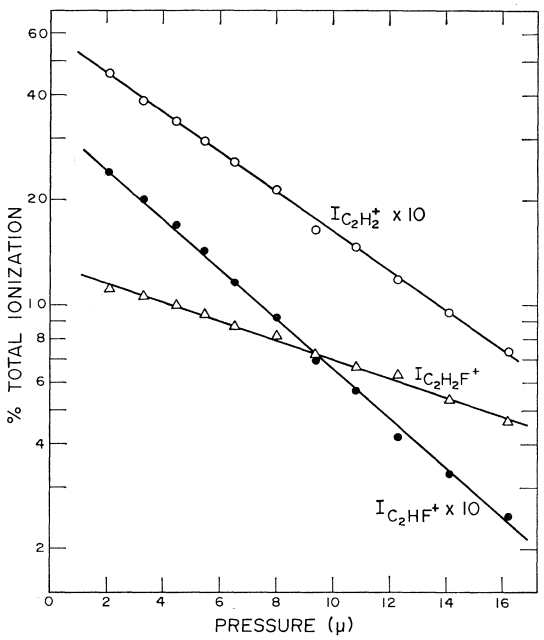

FIG. 4. log (I_{X^+}/Σ) versus pressure.

[9] $C_2H_2F^+ + C_2H_3F \rightarrow C_4H_4F^+ + HF$

$k = (0.20 \pm 0.1) \times 10^{-10}$

The total rate constant for the disappearance of $C_2H_2F^+$ (see typical log plot in Fig. 4) was found to be $(7.5 \pm 0.3) \times 10^{-10}$ cm^3 $molecule^{-1}$ s^{-1} while the sum of the rate constants for the above four reactions is only $\sim 3.5 \times 10^{-10}$ cm^3 $molecule^{-1}$ s^{-1}, indicating a further undetected reaction. It is probable that this is reaction [10], leading to formation of $C_2H_3^+$, with a rate constant of approximately 4×10^{-10} cm^3 $molecule^{-1}$ s^{-1}.

[10] $C_2H_2F^+ + C_2H_3F \rightarrow C_2H_3^+ + C_2H_2F_2$

$C_2H_3F^+$

In addition to being formed in reactions [1] and [6] $C_2H_3F^+$ reacts to produce $C_3H_3F_2^+$, $C_3H_4F^+$, $C_3H_5^+$, and $C_4H_5F^+$ in order of decreasing yield. The data in Fig. 2 suggest that the first three are formed predominantly by third-order reactions, although the partial secondary character of the $C_2H_3F^+$ makes this interpretation uncertain. Figure 5 shows a pressure plot obtained at 10.4 eV nominal electron energy where $C_2H_3F^+$ is the only significant primary ion. In addition to the expected products, $C_5H_7^+$,

Can. J. Chem. Downloaded from www.nrcresearchpress.com by 210.87.254.105 on 09/05/12
For personal use only.

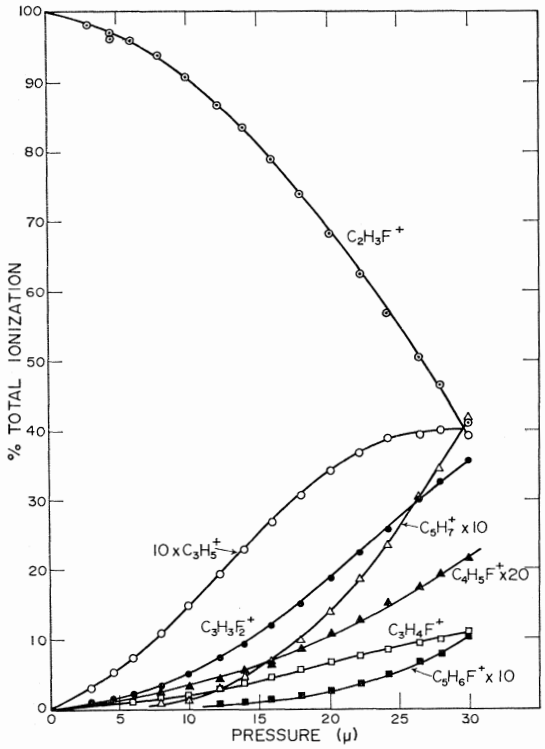

FIG. 5. Pressure plot 10.4 eV electron energy, 2.4 eV ion exit energy.

$C_5H_6F^+$, and, in minor yield, $C_4H_3F_3^+$ (not shown on graph) are found at high pressures, presumably as a result of the following consecutive reactions.

$$C_2H_3F^+ \rightarrow C_3H_5^+ \rightarrow C_5H_7^+$$
$$C_2H_3F^+ \rightarrow C_3H_4F^+ \rightarrow C_5H_6F^+$$
$$C_2H_3F^+ \rightarrow C_3H_3F_2^+ \rightarrow C_4H_3F_3^+$$

Both the shape of the curve for the reactant $C_2H_3F^+$ and the shapes of the curves for the product ions indicate that the major part of the reaction of $C_2H_3F^+$ is second order in concentration of the neutral reactant. The order of the reaction is shown more clearly by the data in Fig. 6, which cover a smaller range of pressure with the result that the consecutive reactions are unimportant. At higher pressures both the reactant ion intensity and the product ion intensities are linear functions of the square of the source pressure, indicating a predominant third-order reaction. The curvature in the initial region for the product ions indicates a small contribution from a second-order reaction.

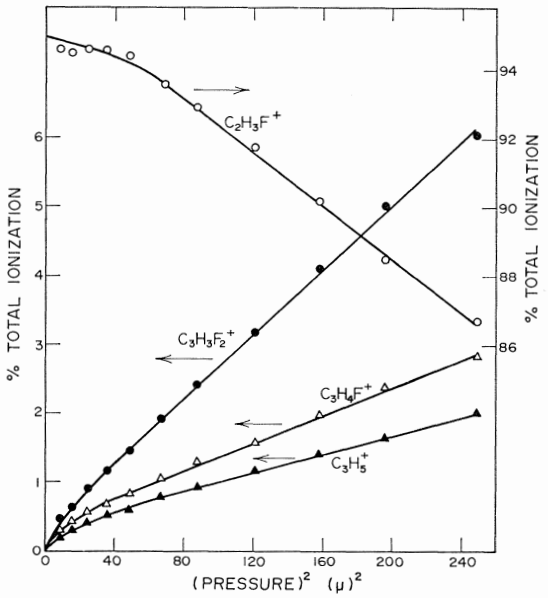

FIG. 6. Ion intensities versus P^2.

For the concurrent second-order and third-order reactions, [11] and [12] respectively,

[11] $C_2H_3F^+ + C_2H_3F \rightarrow C_3H_5^+ + CHF_2$
$\rightarrow C_3H_4F^+ + CH_2F$
$\rightarrow C_3H_3F_2^+ + CH_3$

[12] $C_2H_3F^+ + 2C_2H_3F \rightarrow C_3H_5^+ + ?$
$\rightarrow C_3H_4F^+ + ?$
$\rightarrow C_3H_3F_2^+ + ?$

we may write for each product ion at low total conversions

$$[13] \qquad \frac{I_{X^+}}{\sum I_{p^+} \cdot P} = k_{11_x} tK + k_{12_x} tK^2 P$$

where I_{X^+} is the ion current for product X^+, $\sum I_{p^+}$ is the sum of reactant and product ion currents, t is the reaction time, P is the ion source pressure, and K is the proportionality constant relating the source pressure to the source concentration in molecules cm^{-3}. Figure 7 shows the data of Fig. 6 plotted in the manner indicated by eq. [13]; satisfactory straight lines are obtained[2]. From the slopes and intercepts of such plots we have obtained the rate constants for formation of

[2]The $C_4H_5F^+$ product has been omitted from this analysis because of its low intensity (<1% of total product).

Can. J. Chem. Downloaded from www.nrcresearchpress.com by 210.87.254.105 on 09/05/12
For personal use only.

TABLE II

Rate constants and product distributions from reaction of $C_2H_3F^+$

Run	Nominal electron energy (eV)	% of second order reaction $C_3H_5^+$	$C_3H_4F^+$	$C_3H_3F_2^+$	k_{11} (total) $\times 10^{11}$	% of third order reaction $C_3H_5^+$	$C_3H_4F^+$	$C_3H_3F_2^+$	k_{12} (total) $\times 10^{25}$
A	19	28.0	30.8	41.2	3.0	13.0	23.5	63.5	0.8
B	15	30.6	33.1	36.3	2.7	12.4	22.5	65.1	1.1
C	12	27.0	35.0	38.0	2.5	13.7	21.4	64.8	1.2
D	11	24.8	34.5	40.7	2.4	15.5	22.4	62.1	1.2
E	11	26.4	33.8	39.8	2.2	13.3	23.6	63.1	1.4

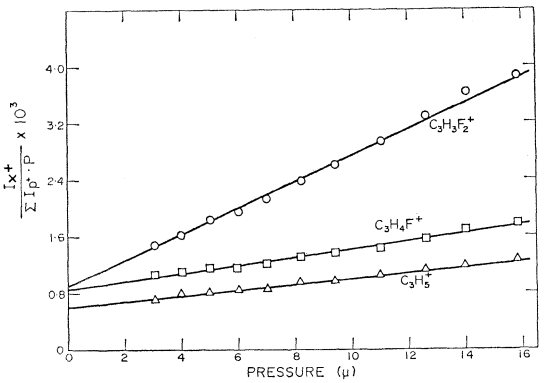

FIG. 7. $I_{X^+}/\Sigma I_{p^+} \cdot P$ versus P.

each product by both reaction [11] and reaction [12]. The results are summarized in Table II as total reaction rate constants and product distributions[3].

The bimolecular rate constant $k_{11} = 2.6 \times 10^{-11}$ cm^3 molecule^{-1} s^{-1} is approximately a factor of 20 lower than that measured (3) for the analogous reaction [14] in ethylene

[14] $\quad C_2H_4^+ + C_2H_4 \rightarrow C_3H_5^+ + CH_3$

The bimolecular rate constant for vinyl fluoride is only slightly larger than that observed (2) for vinyl chloride ($\sim 1 \times 10^{-11}$ cm^3 molecule^{-1} s^{-1}), although the product distribution is different. For vinyl chloride the only C_3 ion observed was $C_3H_4Cl^+$ ($\sim$85% of total), the remaining product being $C_4H_6Cl^+$. In addition, in vinyl chloride both the product distribution and the bimolecular rate constant appeared to be dependent on the ionizing electron energy. No such trend is evident in the vinyl fluoride system.

The apparent third order rate constant $k_{12} = 1.2 \times 10^{-25}$ cm^6 molecule^{-2} s^{-1} is approximately the same as the third order rate constant in vinyl chloride. The product distribution is distinctly different, the third-order reaction in vinyl chloride leading to $C_3H_4Cl^+$ ($\sim$36%), $C_4H_5Cl^+$ (49%), and $C_4H_6Cl^+$ (15%) with no $C_3H_5^+$ or $C_3H_3Cl_2^+$ being observed.

The reasons for the slow bimolecular reaction and the mechanism of the third-order reaction are not known with certainty; however, a reaction scheme similar to that proposed (8) for the vinyl chloride system can explain the results. Reactions [15] to [19] outline this scheme as modified in the light of our results (2) for the vinyl chloride system.

[15] $\quad C_2H_3F + e \rightarrow C_2H_3F^{+*} + 2e$

[16] $\quad C_2H_3F^{+*} + C_2H_3F \rightarrow (C_2H_3F)_2^{+*}$

[17a] $\quad (C_2H_3F)_2^{+*} \rightarrow$ Products

[17b] $\quad \rightarrow C_2H_3F^+\dagger + C_2H_3F$

[18] $\quad C_2H_3F^+\dagger + C_2H_3F \rightarrow (C_2H_3F)_2^+\dagger$

[19a] $\quad (C_2H_3F)_2^+\dagger \rightarrow$ Products

[19b] $\quad \rightarrow C_2H_3F^+\dagger + C_2H_3F$

The collision complex formed in reaction [16] produces the observed products with low efficiency ($\sim$1%), the majority of the complexes taking part in the charge transfer reaction [17b]. The analogous charge transfer reaction is known (8) to occur rapidly in vinyl chloride, and it has been shown (2) that it must occur through complex formation. The broadening of the withdrawal curves for the $C_2H_3F^+$ ion indicates a similar charge transfer in vinyl fluoride. The product of the charge transfer reaction, $C_2H_3F^+\dagger$, undergoes reactions [18] and [19] to form the observed products with an efficiency of $\sim$10%, somewhat

[3]It might be noted that the product distributions do not correspond to random loss of H and F from the $C_4H_6F_2^+$ intermediate. Such a statistical loss would predict 10.7% $C_3H_5^+$, 53.6% $C_3H_4F^+$, and 35.7% $C_3H_3F_2^+$.

Can. J. Chem. Downloaded from www.nrcresearchpress.com by 210.87.254.105 on 09/05/12
For personal use only.

higher than for the ions produced directly by electron impact.

For the vinyl chloride system it has been suggested (8) that the overall efficiency of the condensation reaction and the distribution of products therefrom depend on the internal excitation of the collision complex, and that the complex formed in reaction [16] has a greater internal energy than that formed in reaction [18], presumably because $C_2H_3X^+$* is more highly excited than $C_2H_3X^+$†. As pointed out in the previous paper (2) the effect of ionizing electron energy on the second order rate constant and product distribution does not entirely support the suggestion. The present results do not either. If the internal energy of the complex is important in determining the rate and product distribution, one would expect both to vary as the ionizing electron energy is changed, whereas, in fact, both are independent of electron energy in the vinyl fluoride system. This is in contrast to the vinyl chloride system where a variation with electron energy was observed, but in a direction opposite to that predicted if vibrational excitation of the reactant ion plays an important role. The reasons for the low efficiencies of the second-order reactions in the vinyl halides and for the differences in the two vinyl halide systems are not readily apparent. Our results would certainly indicate that excess vibrational energy of the reactant ion is not an important factor in determining the fate of the collision complex; however, they do not preclude the possibility that excited electronic states may play an important role.

Consecutive Reactions in Vinyl Fluoride

In addition to the primary reactions discussed above, the following reactions of product ions have been observed in the vinyl fluoride system

[20] $C_2H_4F^+ + 2C_2H_3F \rightarrow C_4H_6F^+ + ?$

[21] $C_3H_5^+ + 2C_2H_3F \rightarrow C_5H_7^+ + ?$

[22] $C_3H_4F^+ + 2C_2H_3F \rightarrow C_5H_6F^+ + ?$

In each case the reaction corresponds formally to the type $A^+ + C_2H_3F \rightarrow AC_2H_2^+ + HF$, a reaction type whose importance was first pointed out by Baldeschwieler *et al.* (1); however, for all three reactions we find that the rate is second order in neutral vinyl fluoride pressure. The relevant plots are shown in Figs. 8 to 10 where in each case a good linear plot versus P^2 is obtained. For reactions [20] and [22] the extent of reaction

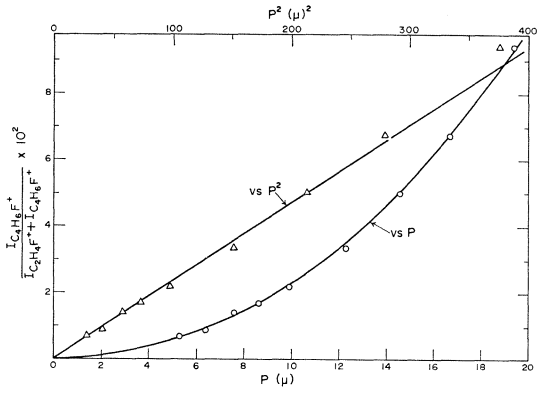

FIG. 8. $I_{C_4H_6F^+}/(I_{C_2H_4F^+} + I_{C_4H_6F^+})$ as a function of pressure.

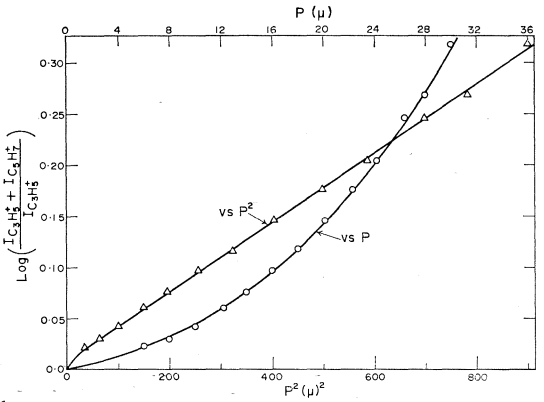

FIG. 9. log $(I_{C_3H_5^+} + I_{C_5H_7^+})/I_{C_3H_5^+}$ as a function of pressure.

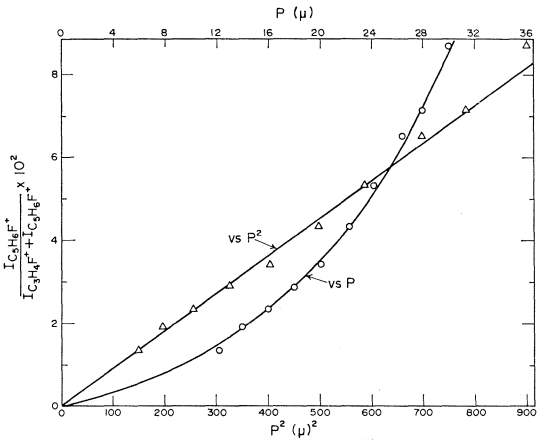

FIG. 10. $I_{C_5H_6F^+}/(I_{C_2H_4F^+} + I_{C_5H_6F^+})$ as a function of pressure.

Can. J. Chem. Downloaded from www.nrcresearchpress.com by 210.87.254.105 on 09/05/12
For personal use only.

TABLE III

Products of reaction $C_2X_2^+ + C_2X_4$

Reactants		Product %		
Ion	Neutral	$C_2X_4^+$	$C_3X_3^+$	Reference
$C_2H_2^+$	C_2H_4	70	8.2	9
$C_2H_2^+$	C_2H_3Cl	100 ($C_2H_3Cl^+$)	—	2
$C_2H_2^+$	C_2H_3F	97.5 ($C_2H_3F^+$)	2.5 ($C_3H_3^+$)	This work
C_2HF^+	C_2H_3F	100 ($C_2H_3F^+$)	—	This work
$C_2F_2^+$	C_2F_4	Observed (?)	Observed	10

TABLE IV

Products of reaction $C_2X_3^+ + C_2X_4$

Reactants		Product %		
Ion	Neutral	$C_2X_5^+$	$C_4X_5^+$	Reference
$C_2H_3^+$	C_2H_4	85	8	9
$C_2H_3^+$	C_2H_3Cl	82 ($C_2H_4Cl^+$)	18 ($C_4H_5^+$)	2
$C_2H_3^+$	C_2H_3F	Obs. ($C_2H_4F^+$)	Obs. ($C_4H_5^+$)	This work
$C_2H_2F^+$	C_2H_3F	29 ($C_2H_4F^+$, $C_2H_3F_2^+$)	3 ($C_4H_4F^+$)	This work
$C_2H_3^+$	C_2H_3Br	Obs. ($C_2H_4Br^+$)	Obs. ($C_4H_5^+$)	2
$C_2F_3^+$	C_2F_4	Obs. ($C_2F_5^+$)	—	10

is low and we have plotted I(product)/(I(reactant) + I(product)) as a function of pressure. For reaction [21] the extent of reaction is large and a logarithmic plot is necessary. Since the reactant ions are themselves produced by ion–molecule reactions, their residence times in the ion source cannot be determined accurately and therefore accurate third order rate constants cannot be evaluated. If we estimate the reaction times to be a few microseconds (compare 3 μs for the withdrawal time of $C_2H_3F^+$), we calculate third order rate constants in the region 10^{-25} to 10^{-24} cm^6 molecule^{-2} s^{-1}. While the third-order reaction of $C_2H_3F^+$ can readily be accommodated by the mechanism outlined above, no simple rationale can be advanced for the third-order reactions [20] to [22]. It appears that the collision complex in each case must be collisionally stabilized before decomposition to the observed products occurs.

Comparison of Ionic Reactions of Vinylic Compounds

The ion–molecule reactions in C_2H_4, C_2H_3Cl, C_2H_3F, C_2H_3Br, and C_2F_4 have now been studied and it is of interest to compare the reactions which occur in these various vinylic systems. The comparisons for the reactions of the $C_2X_2^+$, $C_2X_3^+$, and $C_2X_4^+$ ions (X = H or halogen) are summarized in Tables III to V. The $C_2X_2^+$ ion reacts chiefly by reactions [23] and [24],

$$[23] \quad C_2X_2^+ + C_2X_4 \rightarrow C_2X_4^+ + C_2X_2$$

$$[24] \quad \rightarrow C_3X_3^+ + CX_3$$

although in ethylene a third reaction yielding $C_4H_5^+$ has been reported (9). The summary in Table III shows that the charge transfer reaction [23] is the most important in all systems and, indeed, is the only reaction observed for $C_2H_2^+$ in vinyl chloride and C_2HF^+ in vinyl fluoride. For both vinyl fluoride and chloride the reaction of $C_2X_2^+$ has a rate constant comparable to the Langevin prediction, although for ethylene the reaction is slower. The $C_2F_2^+$ ion intensity in C_2F_4 is low and only the $C_3F_3^+$ product has been definitely identified (10); however, the charge transfer reaction is exothermic and probably occurs.

The reaction of $C_2X_3^+$ with C_2X_4 forms two products by reactions [25] and [26].

$$[25] \quad C_2X_3 + C_2X_4 \rightarrow C_2X_5^+ + C_2X_2$$

$$[26] \quad \rightarrow C_4X_5^+ + X_2$$

In all cases (see Table IV) reaction [25] is the most important with reaction [26] being of minor

Can. J. Chem. Downloaded from www.nrcresearchpress.com by 210.87.254.105 on 09/05/12
For personal use only.

TABLE V
Products of reaction $C_2X_4^+ + C_2X_4$

Reactant		Product %			
Ion	Neutral	$C_3X_5^+$	$C_4X_7^+$	$C_4X_6^+$	Reference
$C_2H_4^+$	C_2H_4	84	10	0.04	9
$C_2H_3Cl^+$	C_2H_3Cl	36–85 ($C_3H_4Cl^+$)	15–18 ($C_4H_6Cl^+$)	0–49 ($C_4H_5Cl^+$)	2
$C_2H_3F^+$	C_2H_3F	~99 ($C_3H_5^+$, $C_3H_4F^+$, $C_3H_3F_2^+$)		~1 ($C_4H_5F^+$)	This work
$C_2H_3Br^+$	C_2H_3Br		100 ($C_4H_6Br^+$)		2
$C_2F_4^+$	C_2F_4	~99	~1		10

importance. Reaction [25] involves H^+ transfer except for $C_2H_2F^+$ as a reactant in the vinyl fluoride system where both $C_2H_4F^+$ and $C_2H_3F_2^+$ are observed as products. Reaction [26] proceeds in all the vinyl halides with formation of the corresponding hydrogen halide as the X_2 neutral fragment. A number of other minor products are observed in the ethylene, tetrafluoroethylene, and vinyl fluoride systems. In the latter system the most important extra reaction is

[10] $C_2H_2F^+ + C_2H_3F \rightarrow C_2H_3^+ + C_2H_2F_2^+$

and it is interesting to note that the analogous reaction in ethylene, reaction [27], has been reported recently (9).

[27] $C_2H_3^+ + C_2D_4 \rightarrow C_2H_3D + C_2D_3^+$

Three different reactions, [28] to [30], have been observed for the $C_2X_4^+$ molecule-ion

[28] $C_2X_4^+ + C_2X_4 \rightarrow C_3X_5^+ + CX_3$

[29] $C_2X_4^+ + C_2X_4 \rightarrow C_4X_7^+ + X$

[30] $\rightarrow C_4X_6^+ + X_2$

As shown in Table V, reaction [28] is the major reaction in all cases except vinyl bromide where only $C_4H_6Br^+$ (reaction [29]) is observed. Reaction [30] is significant in vinyl chloride and of minor importance in vinyl fluoride. The reaction $C_2H_3F^+ + C_2H_3F$ produces the full range of possible $C_3X_5^+$ ions consistent with extensive, but not complete, scrambling of the hydrogens and fluorines. In all other reactions of the vinyl halide molecule-ions, one halogen atom is found in the ionic product and one in the neutral product.

From the above comparisons it is evident that the major features of the ionic reactions in ethylene and in the halogen-substituted ethylenes are very similar. The most noticeable difference lies in the low efficiency of the second-order reaction of the molecule-ion in the vinyl halides. It might be noted that in C_2F_4 it has been suggested (10) that the $C_3F_5^+$ and $C_4F_7^+$ products are also produced by higher order reactions involving the molecule-ion.

Acknowledgments

The authors are indebted to the National Research Council of Canada for financial support of this work. The authors are deeply indebted to Dr. T. O. Tiernan for communication of results prior to publication and for illuminating discussions concerning ion–molecule reaction mechanisms, and to a referee for helpful suggestions.

1. J. L. Beauchamp, L. R. Anders, and J. D. Baldeschwieler. J. Am. Chem. Soc. **89**, 4569 (1967).
2. J. A. Herman, J. J. Myher, and A. G. Harrison. Can. J. Chem. In press.
3. J. J. Myher and A. G. Harrison. Can. J. Chem. **46**, 101 (1968).
4. S. K. Gupta, E. G. Jones, A. G. Harrison, and J. J. Myher. Can. J. Chem. **45**, 3107 (1967).
5. T. W. Shannon and A. G. Harrison. J. Chem. Phys. **43**, 4201 (1965).
6. F. H. Field and J. L. Franklin. Electronic impact phenomena and the properties of gaseous ions. Academic Press, Inc., New York. 1957.
7. J. Momigny. Etude de quelques aspects de l'ionization dans les gaz rarefies. Extrait des Mem. Soc. Roy. Sci. Liege, Ser. 5, Vol. XIII (1966).
8. B. M. Hughes, T. O. Tiernan, and J. H. Futrell. J. Phys. Chem. In press.
9. T. O. Tiernan and J. H. Futrell. J. Phys. Chem. **12**, 3080 (1968).
10. G. A. W. Derwish, A. Galli, A. Giardini-Guidoni, and G. G. Volpi. J. Am. Chem. Soc. **86**, 4563 (1964).

Can. J. Chem. Downloaded from www.nrcresearchpress.com by 210.87.254.105 on 09/05/12
For personal use only.

Electromotive force studies of liquid uranium–zinc alloys

Y. HOSHINO[1] AND J. A. PLAMBECK
Department of Chemistry, University of Alberta, Edmonton, Alberta

Received September 3, 1968

The electromotive force of cells of the type U(s)/LiCl–KCl (eutectic) + UCl_3/(U + Zn) (liquid alloy) have been measured over the temperature range 450–550 °C, in the zinc-rich region of alloy composition. Thermodynamic functions for the limiting uranium–zinc intermetallic compound existing in this region are: ΔG_f^0, −23.0 kcal/mole; ΔS_f^0, −37.1 cal/deg mole; ΔH_f^0, −52.9 kcal/mole at 535 °C. These values are compared with those previously reported by other workers.

Canadian Journal of Chemistry, **47**, 965 (1969)

Can. J. Chem. Downloaded from www.nrcresearchpress.com by 210.87.254.5 on 09/05/12
For personal use only.

Introduction

The processing of spent nuclear reactor fuel is one of the most important problems in nuclear technology. Although aqueous processes are currently used, there has been considerable recent interest in pyrometallurgical processes and reviews of this work are available (1–6). In some of these processes, spent fuel is first dissolved in liquid bismuth or zinc metal at high temperatures. This liquid metal is then contacted with a fused salt; the fission products distribute themselves between the salt and metal phases. Although this process has generally been considered (5, 6, 11, 12, 14) from the point of view of distribution equilibria, the material in the salt phase (metal ions) is related to that in the metal phase (metal alloys) through electrochemical as well as distributive equilibria. The use of electrochemical cells could well lead to improvements in the effectiveness and/or selectivity of these separations. The electrochemical properties of metal ions in fused salts have been extensively studied (7, and references cited therein). The electrochemical and thermodynamic properties of the alloys have been studied less extensively, but it is clear that they cannot, in general, be treated as merely ideal solutions of one metal in another. In view of the obvious central importance of the U–Zn system and the existence of prior studies of it, the zinc-rich portion of this system was chosen for initial investigation.

The phase diagram of the zinc-rich region of the U–Zn binary system (8) has a liquidus line rising sharply near the melting point of zinc. The stoichiometry of the solid phase existing in equilibrium with dilute liquid U–Zn alloy has been the subject of considerable recent controversy; this has been reviewed by Pascal (9). For the purpose of this paper, we will consider the stoichiometry of the limiting U–Zn compound to be $UZn_{8.5}$; our data are given in a form which permits recalculation in terms of other stoichiometric compositions.

The thermodynamic behavior of U–Zn alloys in the zinc-rich portion of the phase diagram has previously been studied by United States Atomic Energy Commission workers. Chiotti and co-workers (10–14) have used vapor pressure and electromotive force (e.m.f.) measurements, and Johnson and co-workers (15, 16) have used e.m.f. measurements to obtain thermodynamic data on the $UZn_{8.5}$ phase in general agreement with our own. The study of solutions in the more dilute range is less extensive (16). Carbide and oxycarbide formation have also been studied in this system by e.m.f. methods (17, 18).

Experimental

Materials

The fused LiCl–KCl eutectic was prepared by the method of Laitinen *et al.* (19) and ampuled under argon for future use. Reagent grade zinc shot (Allied Chemical, New York) was cast into a small ingot under fused zinc chloride for future use. Uranium wire (0.1 in. diameter, 99.9%, A. D. MacKay Inc., New York) was cut into small pieces which were weighed and stored in small zinc wire capsules for ease in handling. Argon gas was purified by passage over hot copper wires followed by a magnesium perchlorate drying tube.

Instruments

All potential measurements were made with a K-3 potentiometer (Leeds and Northrup Co., Philadelphia, Pennsylvania). The entire cell envelope was contained in a 3 in. internal diameter vertical tube furnace equipped with an indicating temperature controller (Models 54231A, 59344; Lindberg-Hevi-Duty Heating Equipment Co., Watertown, Wisconsin). The temperature within the

[1]Present address: Department of Chemistry, Tokyo Institute of Technology, O-okayama, Meguro-ku, Tokyo, Japan.

Can. J. Chem. Downloaded from www.nrcresearchpress.com by 210.87.254.5 on 09/05/12
For personal use only.

cell was monitored by a calibrated chromel–alumel thermocouple in a Pyrex sheath immersed in the melt; its output was read on a Model 3440A digital voltmeter (Hewlett–Packard, Palo Alto, California) or the K-3 potentiometer. Coulometric oxidations were carried out with a Model IV current source (E. H. Sargent and Co., Chicago, Illinois).

Cell and Electrodes

All parts of the cell and associated apparatus were of Pyrex glass unless otherwise specified. The cell proper consisted of a high-wall crucible with a central bottom depression to hold the U–Zn pool; this contained the LiCl–KCl melt. Contact with the pool was made by a tungsten lead sealed in a Pyrex tube to insulate it from other leads. Other electrodes were suspended in the melt from the outer glass envelope cap.

The outer glass envelope consisted of a closed-end tube with a 60/50 male standard taper joint at the top, which extended above the furnace. The cell crucible rested on Pyrex wool at the bottom of the outer envelope. The envelope was capped with a female standard taper joint, closed off, into which were blown one 10/30 and four 14/20 standard taper female joints to permit insertion of electrodes, gas inlets, or other apparatus. The outer glass envelope was airtight and was maintained at a slight positive pressure of argon during experiments, to prevent entry of air.

In addition to the zinc pool electrode, the cell always contained a uranium rod electrode. This rod (0.1 in. diameter) was attached to a flexible copper lead well above the melt level. It could be raised and lowered into the melt by rotating a horizontal Pyrex rod around which the wire was wound. The Pyrex rod entered through a standard taper joint, and electrical contact was made through a Kovar seal to ensure airtight operation. A counter electrode and auxiliary reference electrode were sometimes required as well as the uranium rod. These consisted of tungsten or silver wires, respectively, held in isolation compartments made from 10 mm sealing tubes (D porosity, Ace Glass Co., Vineland, New Jersey) and allowed to fill with melt before addition of uranium or zinc. The silver reference wire was anodized to produce a solution of about 0.1 *M* Ag^+ within the compartment; this reference electrode has been discussed (20).

The small zinc capsules containing uranium were lined up in a horizontal sealed side tube with a small piece of iron behind them. To add a capsule to the U–Zn pool, an external magnet was used to move the iron so that the leading capsule was pushed out of the side tube. It then fell through a vertical Pyrex guide tube ending just above the melt, and through the melt into the pool. This method permitted successive additions of uranium without exposure of the melt to air.

Procedure

An ampul of the previously prepared eutectic was taken, melted, subjected to HCl for 1 h, purged with argon, and evacuated. Argon was then introduced and a positive pressure maintained throughout each experiment. If changes in the electrodes necessitated opening the cell for a few moments, the cell was evacuated and argon re-introduced before continuing with the experiment.

Uranium trichloride solutions were prepared by anodization of the uranium rod at 20 mA to the extent of 200 mC against an isolated counter electrode. The e.m.f. of the cell was, as expected, independent of the concentration of U(III) so produced, provided that a reasonable concentration was generated; all experimental runs used approximately 0.012 *M* U(III) solutions. The activity of U(III) was also checked against the auxiliary Ag/Ag(I) reference to ensure that approximately 100% current efficiency had been attained. The melt was stirred with argon bubbling to destroy the electrolytic concentration gradient before any potential measurements were made.

The U–Zn pool was made by adding individual weighed zinc capsules containing weighed uranium metal, through the addition apparatus described above, to a pool made from a weighed small zinc ingot. Previous attempts to prepare the alloys by coulometric deposition of uranium were successful but potentials were not reproducible, the current efficiency being less than 100% for the deposition, and hence this method was discarded. Several hours were generally required to reach equilibrium (e.m.f. change less than 0.1 mV in 30 min). Several composition values were obtained in each run by addition of successive zinc capsules.

In the measurements of e.m.f. as a function of temperature, values were taken both with increasing and with decreasing temperature. The time required to return to equilibrium after a temperature change was several times longer when cooling than when heating, although the equilibrium e.m.f. was the same; this indicates that the dissolution of the solid U–Zn phase is more rapid than its formation.

Results and Discussion

Typical results of the e.m.f. measurements of the cell U(s)/LiCl–KCl (eutectic) + UCl_3/U in Zn(I) at 808 °K are shown in Fig. 1. The break point in this curve is considered to be the point at which the solid compound $UZn_{8.5}$ begins to precipitate from the liquid U–Zn alloy, and occurs at 2.2×10^{-2} mole % uranium. This does not agree with corresponding value of 8.1×10^{-2}

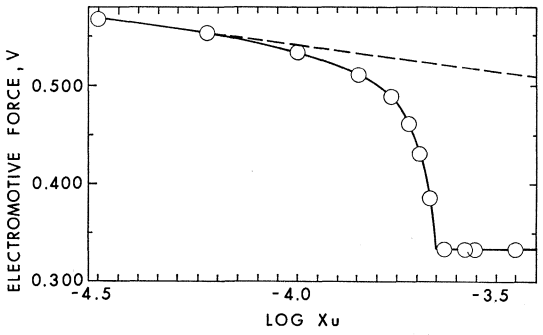

FIG. 1. Cell e.m.f. as a function of the mole fraction uranium in the alloy. Dashed line indicates Henrian behavior, horizontal region formation of solid compound.

Can. J. Chem. Downloaded from www.nrcresearchpress.com by 210.87.254.5 on 09/05/12
For personal use only.

mole % we calculate from early solubility data of Chiotti *et al.* (21), but is in considerably better agreement with the value of 1.2×10^{-2} mole % we calculate from the more recent direct solubility measurements analyzed by Johnson and Dillon (22).

The thermodynamics of the region preceding the break point (unsaturated region) and following it (saturated region) must be treated separately. In the unsaturated region, the excess partial molal free energy of uranium (excess chemical potential) is related to the e.m.f. of the cell studied through the well-known thermodynamic equation

$$\Delta\bar{G}_U^{XS} = -nFE - RT\mathrm{d}\ln X_U$$

Values of $\Delta\bar{G}_U^{XS}$ are calculated in Table I, and their relation to Henry's law is shown in Fig. 1. It is clear that positive deviations from Henry's law exist for all solutions of uranium in zinc more concentrated than 1×10^{-2} mole %. Large negative deviations from Raoult's law are always observed, as expected. The data reported here do not agree with the report of Johnson and Feder (15) that the excess partial molal free energy of uranium was independent of uranium concentration in the unsaturated region at 450 °C; it is probable that these workers did not take experimental data in the comparatively small region where Henry's law is not obeyed.

TABLE I

Excess chemical potential of uranium in liquid zinc unsaturated region, 808 °K

X_U ($\times 10^4$)	Observed e.m.f.* (V)	Calculated $\Delta\bar{G}_U^{XS}$ (kcal/mole)
0.315	0.5676	−22.62
0.423†	0.5663	−23.01
0.595	0.5537	−22.68
0.950†	0.5427	−22.68
1.001	0.5339	−22.15
1.43	0.5106	−21.11
1.72	0.4885	−19.88
1.91	0.4615	−18.17
2.01†	0.4074	−16.52
2.03	0.4307	−16.14
2.15	0.3847	−13.05
2.36	0.3319	—
2.62†	0.3338	—
2.65	0.3321	—
2.81	0.3321	—
3.25†	0.3340	—
3.54	0.3321	—

*Mean of several observations differing only by tenths of mV. Values where $X_U(\times 10^4)$ is greater than 2.2 are in the saturated region (see text).
†Data from run 1; all other data from run 2.

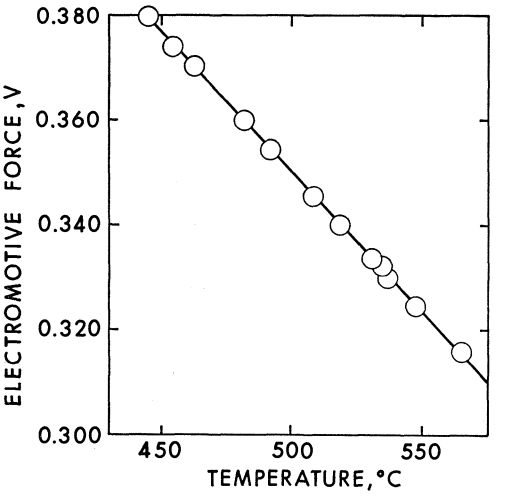

FIG. 2. Behavior of cell e.m.f. in saturated region as a function of temperature. Points taken randomly with increasing and decreasing temperature.

The excess chemical potential of zinc can be calculated from that of uranium by use of the Gibbs–Duhem equation, and is found from our data to be 2.5 cal/mole at $X_U = 2.2 \times 10^{-4}$, which is negligible. We can therefore assume ideal (Raoultian) behavior for zinc.

The thermodynamics of the saturated region are quite different since we are now concerned with the solid alloy $UZn_{8.5}$. A typical e.m.f. – temperature plot for this region is shown in Fig. 2. A least squares analysis of the results of several such runs gives the equation:

$$E = 0.7646 - 5.36 \times 10^{-4}\,T$$

where E is the e.m.f. (V) and T the temperature (°K); the standard deviation is 0.0011 V.

Since the cell reaction corresponding to this potential is $U(s) + 8.5\,Zn(l, alloy) \rightarrow UZn_{8.5}(s)$, the standard free energy of formation of the compound $UZn_{8.5}(s)$ will be given by

$$\Delta G_f^0 = \Delta G + 8.5RT \ln a_{Zn}$$

where ΔG is the free energy change of the cell and a_{Zn} is the activity of zinc metal in the alloy. Standard states are taken as pure (solid) uranium, pure (liquid) zinc, pure (solid) $UZn_{8.5}$. Using the Gibbs–Duhem equation discussed above for a_{Zn}, the term $8.5\,RT \ln a_{Zn}$ is found to be only −6.3 cal/mole so that we may neglect it and

TABLE II

Standard free energy of formation of $UZn_{8.5}$ solid

Temperature (°C)	ΔG_f^0, kcal/mole				
	Present work	Johnson (15)	Chiotti (18)	Chiotti (10, 18)	Chiotti (10)
450	26.09	26.51	27.70	28.53*	28.85*
500	24.23	24.60	25.82	26.54*	27.03*
550	22.38	22.69	23.94	24.54*	25.12*
600	20.52*	20.78	22.06	22.55*	23.14*
650	18.67*	18.87	20.19	20.55	21.07
700	16.81*	16.96	18.31	18.56	18.95
750	14.96*	15.05*	16.43	16.56	16.74
800	13.11*	13.13*	14.55*	14.56	14.48
850	11.25*	11.22*	12.67*	12.57	12.14
900	9.40*	9.31*	10.80*	10.57	9.75

*Beyond temperature range of experimental measurements; extrapolated using equation given by authors.

use $\Delta G_f^0 = \Delta G$. The least-squares equation then becomes

$$\Delta G_f^0{}_{UZn_{8.5}} = -52.90 + 37.08 \times 10^{-3} T\ (°K) \text{ kcal/mole}$$

over the temperature range 450–550 °C, standard deviation 0.076 kcal/mole. The values given by this equation are compared to those given by previous authors (10, 15, 18) in Table II. Values calculated beyond the actual temperature range of the author's experiments are indicated by asterisks. Our work confirms that of Johnson (15, 16) but differs more from that of Chiotti and Kilp (10) even using the recalculated values of Chiotti *et al.* (18). Chiotti *et al.* (18), in discussing Johnson's work, suggested that the contamination of the uranium electrode surface by impurities might explain the discrepancy. We cannot accept this criticism, however, since the potential of the U–Zn pool against a uranium electrode which had been in the melt for several days was the same as its potential against a freshly prepared uranium electrode.

The standard entropy and enthalpy of the formation of $UZn_{8.5}$ were calculated from the temperature dependence of the potential given above; their values are $\Delta S_f^0 = -37.1$ cal/deg mole, $\Delta H_f^0 = -52.9$ kcal/mole. These are in good agreement with the values we calculate from the work of Johnson (15, 16), −38.2 cal/deg mole and −54.2 kcal/mole respectively. The vapor pressure data of Chiotti and Kilp (10) gives, for ΔH_f^0, −54.6 kcal/mole at 450 °C and −55.9 kcal/mole at 500°, and −35.6 cal/deg mole and −37.3 cal/deg mole for ΔS_f^0 at the same temperatures.

Since completion of this study, Volkovich *et al.* (23) have published a study at 700–950 °C in fused NaCl–KCl from which we calculate

$$\Delta G_f^0{}_{UZn_{8.5}} = -53.43 + 37.4 \times 10^{-3} T\ (°K) \pm 0.035 \text{ kcal/mole}$$

This, extrapolated to our lower temperature range, is in agreement with the results of the present study.

Conclusion

Uranium in liquid zinc is a solute which retains ideal Henrian behavior only up to 1×10^{-2} mole % U at 808 °K. Positive deviations then occur up to 2.2×10^{-2} mole % U at which point a solid U–Zn phase precipitates. The thermodynamic properties of the liquid and solid phases have been measured and these measurements compared with those of other workers.

Acknowledgments

The authors are grateful to the National Research Council of Canada for support of this research. We are indebted to Dr. I. Johnson of Argonne National Laboratory, United States Atomic Energy Commission, for access to his unpublished data.

1. L. Burris, Jr., K. M. Harmon, G. E. Brand, E. W. Murbach, and R. K. Steunenberg. Proc. Intern. Conf. Peaceful Uses At. Energy. 3rd. Geneva, 1964. Vol. 10. p. 501. (pub. 1965).
2. R. D. Pierce and L. Burris, Jr. U.S. At. Energy Comm. TID-8540, (1964).

Can. J. Chem. Downloaded from www.nrcresearchpress.com by 210.87.254.5 on 09/05/12
For personal use only.

3. S. LAWROSKI and L. BURRIS, JR. At. Energy Rev. **2**, 3 (1964).
4. L. BURRIS, JR., I. G. DILLON, and R. K. STEUNENBERG. U.S. At. Energy Comm. ANL-6818, (1964).
5. F. J. SALZANO and F. B. HILL. U.S. At. Energy Comm. BNL-639, (1962).
6. S. YAMAGISHI and Y. KAMEMOTO. J. At. Energy Soc. Japan, **6**, 158 (1964).
7. J. A. PLAMBECK. J. Chem. Eng. Data, **12**, 77 (1967).
8. M. HANSEN and K. ANDERKO. Constitution of binary alloys. 2nd ed. McGraw-Hill Book Co., Inc., New York. 1958. p. 1249.
9. P. PASCAL (*Editor*). Nouveau traité de chimie minèrale. Vol. 15. Part 4. Uranium. Masson et Cie, Paris. 1967. pp. 228–229; also Vol. 20. Metal alloys.
10. P. CHIOTTI and G. R. KILP. Trans. AIME, **218**, 41 (1960).
11. P. CHIOTTI and S. J. S. PARRY. J. Less-Common Metals, **4**, 315 (1962).
12. P. CHIOTTI. U.S. At. Energy Comm. IS-660. (1963).
13. P. CHIOTTI and J. S. KLEPFER. Ind. Eng. Chem. Process Design Develop. **4**, 232 (1965).
14. P. CHIOTTI. Ind. Eng. Chem. Process Design Develop. **4**, 299 (1965).
15. I. JOHNSON and H. M. FEDER. Thermodynamics of nuclear materials. International Atomic Energy Agency, Vienna. 1962. p. 319.
16. I. JOHNSON. Private communication.
17. W. C. ROBINSON and P. CHIOTTI. J. Less-Common Metals, **10**, 190 (1966).
18. P. CHIOTTI, W. C. ROBINSON, and M. KANNO. J. Less-Common Metals, **10**, 273 (1966).
19. H. A. LAITINEN, W. S. FERGUSON, and R. A. OSTERYOUNG. J. Electrochem. Soc. **104**, 516 (1957).
20. R. A. BAILEY and G. J. JANZ. The chemistry of nonaqueous solvents. Vol. I. *Edited by* J. J. Lagowski. Academic Press, Inc., New York. 1966. p. 292.
21. P. CHIOTTI, H. H. KLEPFER, and K. J. GILL. Trans. AIME, **209**, 51 (1957).
22. I. JOHNSON and I. G. DILLON. U.S. At. Energy Comm. ANL-7083, p. 99 (1965).
23. A. V. VOLKOVICH, I. F. NICHKOV, S. P. RASPOPIN, V. I. TITARENKO, and V. A. LEBEDEV. Zh. Fiz. Khim. **42**, 682 (1968).

Can. J. Chem. Downloaded from www.nrcresearchpress.com by 210.87.254.5 on 09/05/12
For personal use only.

Pyrochlores. V. Thermoanalytic, X-ray, neutron, infrared, and dielectric studies of $A_2Ti_2O_7$ titanates[1]

OSVALD KNOP AND FRANÇOIS BRISSE[2]
Department of Chemistry, Dalhousie University, Halifax, Nova Scotia

AND

LOTTE CASTELLIZ
Department of Chemical Engineering, Nova Scotia Technical College, Halifax, Nova Scotia

Received August 14, 1968

A number of compositions $A_2^{3+}Ti_2^{4+}O_7$ and of related mixed phases were prepared and investigated. For the trivalent lanthanons from Sm to Lu, and for Y, the homogeneous $A_2Ti_2O_7$ phases were of the cubic pyrochlore type. Their lattice parameters gave a very good linear relationship when plotted against the Templeton–Dauben radii of A^{3+}. The room-temperature stability region of the pyrochlore titanates at ordinary pressures extends from an Ahrens radius ratio, $r(A^{3+}):r(Ti^{4+})$, of about 1.22 to about 1.50, taking into account homogeneous mixed phases. The compositions $Bi_2Ti_2O_7$, $In_2Ti_2O_7$, and $Cr_2Ti_2O_7$ were not cubic pyrochlores; the results of an X-ray and neutron examination of $Sc_2Ti_2O_7$ indicate that further work is needed to clarify its structural properties.

The structures of Lu, Y, Gd, and Sm titanates were refined from X-ray powder data and that of $Y_2(Ti_{0.64}Zr_{0.36})_2O_7$, from neutron powder data. The structure of $Er_2Ti_2O_7$ was re-refined from previously published data without significant improvement. The positional parameter of the majority oxygen atom, $x(O_2)$, in $A_2B_2O_7$ pyrochlores has been found to increase, and the distortion of the BO_6 octahedra to decrease, with the increasing $r(A^{3+}):r(B^{4+})$ ratio. This is in agreement with a similar result obtained earlier from Mössbauer spectra for A_2FeSbO_7 pyrochlores.

The variation of the frequencies of the principal absorption bands in the infrared spectra of the titanates has been correlated with $r(A^{3+})$. No evidence of ferroelectricity was found in Sm and Er titanates between room temperature and 4.2 °K.

The Templeton–Dauben set of empirical crystal radii for trivalent lanthanons has been supplemented by values for Sc, In, Tl, and Bi derived from the *C*-type sesquioxides and the pyrochlores. The self-consistency and applicability of the expanded set have been tested on several series of isostructural compounds.

Canadian Journal of Chemistry, 47, 971 (1969)

Can. J. Chem. Downloaded from www.nrcresearchpress.com by 210.87.254.40 on 09/05/12
For personal use only.

In a previous paper (1) it was established that $Er_2Ti_2O_7$, which is a typical representative of the cubic $A_2^{3+}B_2^{4+}O_7$ phases, is isostructural with pyrochlore, (NaCa)(NbTa)O_6F. The crystal structures of another 4 members of the $A_2Ti_2O_7$ series (A = Y, Lu, Gd, and Sm) have now been refined from X-ray powder diffractometer data, and the systematic study (2) of the cubic pyrochlore stannates, $A_2Sn_2O_7$, has been extended to the titanate series. For reasons similar to those stated in ref. 2, a mixed phase, $Y_2(Ti_{0.64}Zr_{0.36})_2O_7$, was also prepared and investigated by neutron powder diffraction.

The main points of interest, as with the stannates, have been the variation of the positional parameter $x(O_2)$ of the majority oxygen atom (and thus the distortion of the TiO_6 octahedra) with the size of A^{3+}, and the limits of existence of the cubic pyrochlore structure. Results of preliminary work on the latter problem were reported earlier (3).

Experimental

The origin and purity of the starting materials have been described in ref. 2. In addition, MnO_2 (Fisher Certified Reagent), Ga_2O_3 (4 *N*) and ZrO_2 (3 *N*) (Koch–Light Laboratories Limited), GeO_2 (K & K Laboratories, Inc.), and $ZrO(NO_3)_2$ (Tizon Chemical Corporation; stated to contain less than 100 p.p.m. Si) were used. Solutions of titanyl oxalate were prepared from $TiCl_4$ that had been purified by the method described in ref. 4.

Titanates of series D (dry-mixed) were prepared as in ref. 1. The individual firing schedules are listed in Table I. The progress of the solid-state reaction was followed by powder photography. In series C (coprecipitated, or totally precipitated) the hydroxides were precipitated with NH_4OH from mixed solutions of the A nitrate and titanyl oxalate of correct stoichiometries. The resulting slurry was dried at 120°, calcined at 900° for 1 h, ground to pass 400 mesh, and calcined at 1100° for 10 h. The calcine was pressed to pellets and fired at 1300° for 2 h, ground, pressed again, and fired at 1400° for 2 h. When the heat treatment differed from the standard procedure details are given in Table I (La, Y, Sc).

---

[1]For Part IV, see ref. 37.

[2]Present address: Division of Pure Chemistry, National Research Council of Canada, Ottawa, Canada.

TABLE I

Lattice parameters of cubic $A_2Ti_2O_7$ titanates and related phases

A (or intended composition)	$a_0(P)$, Å	Preparation*	Reference†
La		1000/24, 1400/16; not *P*	C
Sm	10.44±3	Fusion in electric arc	13
	10.228	1550/1, air-quenched	15
	10.2303±6‡		3
	10.211±1		17
	10.2329±3		C
	10.2331±8	1200/8, 1350/6, 1400/18	D
Eu	10.195		18
	10.192±1		17
	10.1988±4		C
	10.1962±11	950/6, 1000/36, 1100/12, 1400/48	D
Gd	10.181	1550/2, air-quenched	15
	10.1857±5‡		3
	10.180	1700?	19
	10.171±1		17
	10.1825±4		C
	10.1852±9	1000/2, 1350/8, 1400/8, 1450/4	D
Tb	10.148±1		17
	10.1560±9		C
	10.1515±9	1400/2, 1400/24	D
Dy	10.106	1425/1, air-quenched	15
	10.1245±4‡		3
	10.110	1700?	19
	10.119±1		17
	10.1226±3		C
	10.1237±9	950/6, 1000/36, 1100/12, 1400/48	D
Ho	10.0979±2‡		3
	10.098		18
	10.095±1		17
	10.0998±5	1000/2, 1350/8, 1400/8, 1450/4	D
Er	10.0759±5‡	1400/2, slow cooling in furnace	3
	10.075		18
	10.069±1		17
	10.0766±6‡	1400/2, slow cooling in furnace	1
	10.0869±1		C
Tm	10.055		18
	10.050±1		17
	10.0533±3		C
	10.0538±8	950/6, 1000/36, 1100/12, 1400/48	D
Yb	10.030	1550/2, air-quenched	15
	10.0309±3‡		3
	10.028±1		17
	10.0298±3	950/6, 1000/36, 1100/12, 1400/48	D
Lu	10.023		18
	10.011±1		17
	10.0258±3		C
	10.0180±9	1000/2, 1350/8, 1400/8, 1450/4	D
Y	10.08±3	Fusion in electric arc	13
	10.095	1200	14
	10.093	1525/½, air-quenched	15
	10.24	600/11, 1200/12§	33
	10.0950±5‡		3
	10.080±1		17
	10.100±1	1500	20
	10.0949±5	950/24, 1100/24, 1400/48	C
	10.0949±5	1400/4, 1450/4	D
Sc	9.801±1		17
	4.9042±5	950/6, 1000/36, 1100/12, 1400/48	D

Can. J. Chem. Downloaded from www.nrcresearchpress.com by 210.87.254.40 on 09/05/12
For personal use only.

TABLE I (*concluded*)

A (or intended composition)	$a_0(P)$, Å	Preparation*	Reference†
	Mixed compositions (this work)		
$Sm_{1-x}La_x$ (x = 0.1, 0.2)		1350/12, 1350/12, 1400/12; "$La_2Ti_2O_7$"	
$Lu_{1-x}Sc_x$ x = 0.2	9.9762±12	1400/24, 1500/18	
0.4	9.9351±18	1400/24, 1500/18	
0.6	9.8833±5	1400/24, 1500/18; P+ ?	
0.8		1400/24, 1500/18; P+ ?	
HoY	10.0961±3	1400/3, 1400/8	
YbNd	10.1695±7	1350/3, 1400/2, 1600/1	
$Y_{0.9}Ga_{0.1}$	10.0888±11	1350/36, 1400/24; P+ ?	D
$Y_{1-x}In_x$ (x = 0.2 to 0.8)		950/1 week, 1000/24, 1100/24, 1250/12; not P	
$Y_{1-x}Cr_x$ x = 0.2	10.0897±12	950/6, 1000/12, 1350/9; P+$Cr_2Ti_2O_7$	
0.4		950/6, 1000/12, 1350/9; P+$Cr_2Ti_2O_7$	
$Y_{1-x}Bi_x$ x = 0.2	10.1485±14	950/6, 1000/12, 1000/12	
0.4	10.2027±14	950/6, 1000/12, 1000/12	
0.5	10.2240±20	950/6, 1000/12, 1000/12	
0.6	10.2522±23	950/6, 1000/12, 1000/12	
0.8	10.2957±15	950/6, 1000/12, 1000/12; P+ ? (or distorted P)	
$Sm_2(Ti_{1-x}Ge_x)_2O_7$ x = 0.2	10.2316±9	1000/24, 1100/24, 1350/24, 1400/12; P+ ?	
0.3	10.2316±14	1000/24, 1100/24, 1350/24, 1400/12; P+ ?	
$Y_2(Ti_{1-x}Ge_x)O_7$ x = 0.1	10.0817±16	950/24, 1200/24, 1450/24	
0.2	10.0719±15	950/24, 1200/24, 1450/24	
0.3	10.0490±9	950/24, 1200/24, 1450/24	
0.6	10.0396±16	950/24, 1200/24, 1450/24; P+ ?	
$Er_2(Ti_{1-x}Ge_x)_2O_7$ x = 0.2	10.0414±25	1000/24, 1100/24, 1350/24, 1400/12	
0.4	10.0036±9	1000/24, 1100/24, 1350/24, 1400/12	
0.6	10.0040±15	1000/24, 1100/24, 1350/24, 1400/12; P+ ?	
$Y_2(Ti_{1-x}Zr_x)_2O_7$ x = 0.36	10.2178±19	950/24, 1200/24, 1450/24	C
0.5	10.2461±9	950/24, 1200/24, 1450/24	C
0.64	10.3169±28	950/24, 1200/24, 1450/24	C
$Er_2Ge_2O_7$		1000/12, 1200/4, 1300/4, 1400/8; not P	
$Y_2Ge_2O_7$		1000/12, 1100/24, 1350/24, 1350/24; not P	
$Sc_2Ge_2O_7$		950/12, 1200/8, 1400/12; not P	

*1000/24 stands for 1000°/24 h. Reference 3: 1000/16, 1000–1400/5, 1400/2, cooled in the furnace; the temperature dropped from 1400 to 1060° during the first hour. Reference 17: 1200–1350/10–14.
†C, this work, coprecipitated; D, this work, dry-mixed.
‡Converted to present λ (Cu Kα) (cf. ref. 2).
§$Y_2Ti_2O_7$ fired at 1420/20 is reported to be weberite + ? (34).

Not listed in Table I are the following firing schedules: Ln_2O_3 + 2TiO_2 (Ln = Pr, Nd); Bi_2O_3 + 2TiO_2 (950/6, 1000/12, 1000/12)[3]; Cr_2O_3 + 2TiO_2 (950/12, 1200/3, 1300/8, 1400/2); Y_2O_3 + 2GeO_2 (1000/24, 1100/24, 1350/24, 1350/24); and Er_2O_3 + 2GeO_2 (1000/12, 1200/4, 1300/4, 1400/8). Preparative firing was not carried out for MnO_2 + TiO_2 (only thermogravimetric analysis (t.g.a.) up to 1310° at 6°/min)[4] and In_2O_3 + 2TiO_2 (only differential thermal analysis (d.t.a.) up to 1600° at 20°/min).

Terbium presented a complication in that the commercial brown oxide is not Tb_2O_3 but a phase of uncertain composition usually referred to as Tb_4O_7. To determine the actual Tb content a sample of the oxide was heated in a thermobalance in stagnant air (for details see ref. 1). The t.g.a. curve showed an intermediate plateau between 600 and 940°. When the final plateau (above 1130°) is taken to correspond to Tb_2O_3, the composition of the intermediate oxide would be $TbO_{1.692}$, i.e. almost Tb_7O_{12}, and the initial composition would be $TbO_{1.790}$, i.e. almost Tb_5O_9. The endothermic peaks in the d.t.a. curve corresponded with the plateaus of the t.g.a. curve. The final product, Tb_2O_3, could be reoxidized almost reversibly. When the heating was carried out in a stream of oxygen, the positions of the t.g.a. plateaus shifted toward higher temperatures (Fig. 1, Table II).

A similar investigation was carried out on the commercial black Pr_6O_{11}. The t.g.a. and d.t.a. curves were more complicated than for TbO_x (Fig. 1, Table II). Pr_2O_3 appears to be stable in atmospheric air above 1360°.

[3]950/6 stands for 950° for 6 h, etc.
[4]MnO_2 goes over to Mn_2O_3 between 880 and 960°. The sesquioxide, which exists above 1085°, is stable on further heating in stagnant air (6°/min) to at least 1320°.

Can. J. Chem. Downloaded from www.nrcresearchpress.com by 210.87.254.40 on 09/05/12
For personal use only.

TABLE II

Thermogravimetric analysis of TbO_x and PrO_x (2°/min)

Plateau (heating)	x	Plateau (cooling)	x
	TbO_x (stagnant air)		
Room temp.–520°	1.790	1280–1190°	1.500
600–940°	1.692	700–530°	1.695
1130–1280°	1.500	390°–room temp.	1.798
	TbO_x (flowing oxygen)		
Room temp.–575°	1.790	1400–1280°	1.500
660–1015°	1.687	760–585°	1.689
1340–1400°	1.500	480°–room temp.	1.791
	PrO_x (stagnant air)		
Room temp.–460°	1.833	1400–1180°	1.500
480–720°	1.805–1.768	*ca.* 990°	1.674
770–1035°	1.702–1.698	920–730°	1.712–1.715
1070–1260°	1.654–1.604	500°–room temp.	1.833
1360–1400°	1.500		

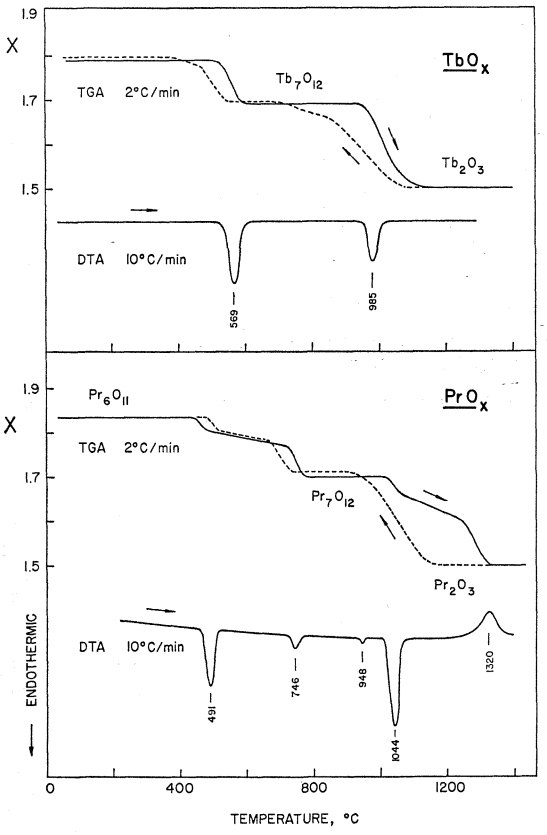

FIG. 1. Differential thermal analysis and thermogravimetric analysis curves of TbO_x and PrO_x in stagnant air. The formulae Tb_7O_{12} and Pr_7O_{12} are only approximations (see text).

The information from t.g.a. and d.t.a. was used merely to ensure that correct amounts of Tb and Pr were introduced to yield products of the intended compositions. However, the analyses were done with care, and the results concerning the intermediate stability levels can be used to verify the findings on the systems Tb–O and Pr–O reported by other authors (5–7).

The process of formation of some of the titanates was followed by thermogravimetry as well as by d.t.a. There was no loss of weight on heating intimate mixtures of $Ln_2O_3 + 2TiO_2$ (Ln = La, Nd, Sm, Er) to 1400° in air. For $TbO_x + TiO_2$ and $PrO_{1.833} + TiO_2$ the total weight decreased with increasing temperature till the sesquioxides formed, but there was no further loss on continued heating and no gain on cooling. This was confirmed for $TbO_x + TiO_2$ by d.t.a.

Differential Thermal Analysis

A Deltatherm Model 2000-16 differential thermal analyzer (Technical Equipment Corporation, Denver, Colorado) was capable of reaching 1600° in non-reducing atmospheres. The heating rate could be varied in steps from 2 to 20°/min. The Pt–Rh sample block was designed to accommodate 4 samples plus 4 alumina references. Some of the d.t.a. experiments were carried out with a home-made differential thermal analyzer of the Mineral Sciences Division, Department of Energy, Mines and Resources, in Ottawa, Canada.

Infrared Spectra

Infrared spectra were recorded from 4000 to 250 cm^{-1} on a Perkin–Elmer model 521 spectrophotometer using KBr pellets (1 mg sample/200 mg KBr) with a KBr reference.

Permittivity Measurements

These were performed by Y. S. Lim of the Physics Department, Dalhousie University, Halifax, Nova Scotia. For details see ref. 2.

X-ray and Neutron Diffraction

Details will be found in refs. 1, 2, and 8. No foreign

Can. J. Chem. Downloaded from www.nrcresearchpress.com by 210.87.254.40 on 09/05/12
For personal use only.

Can. J. Chem. Downloaded from www.nrcresearchpress.com by 210.87.254.40 on 09/05/12
For personal use only.

lines were visible in well-exposed powder photographs of the pyrochlore titanates. Films of Gd, Sm, Nd, and Eu titanates taken with Ni-filtered CuK radiation had exceptionally dark backgrounds. A Rigaku–Denki high-temperature X-ray camera was used in the examination of $La_2Ti_2O_7$.

For details of the least-squares refinement, ref. 2 may be consulted. Neutral and ionic scattering factors and dispersion corrections were taken from the following sources:

Y, Sm, Gd, Er, Lu (neutral and 3+), and Ti^{4+}: *f*, ref. 9; dispersion corrections, ref. 10.

O, Ti, and Ti^{3+}: *f* and dispersion corrections, ref. 11.

O^{2-}: *f*, ref. 12.

Results and Discussion

In agreement with previous reports (3, 13–20) the lanthanons from Lu to Sm as well as Y were found to form cubic $A_2Ti_2O_7$ pyrochlores (Table I), whereas Nd, Pr, and La gave X-ray powder patterns of a different type. A notable exception is the finding of Padurow and Schusterius (21), who stated that $La_2Ti_2O_7$ had a cubic pyrochlore structure with $a = 10.60$ Å. We have been unable to confirm this result. All attempts to prepare a cubic $La_2Ti_2O_7$ pyrochlore failed, be it by solid-state reaction or by firing the coprecipitated hydroxides. The possibility of a phase transformation was examined with a high-temperature X-ray camera. There was no significant change in the powder pattern of $La_2Ti_2O_7$ (coprecipitated and fired at 1400°) as the temperature was continuously raised from room temperature to 1490°. $(Sm_{1-x}La_x)_2Ti_2O_7$ compositions gave patterns of the same type as $La_2Ti_2O_7$. Moreover, compared with the a_0 values obtained for $La_2Ti_2O_7$ by extrapolating the lattice parameters of the cubic pyrochlores (Fig. 2), the value of 10.60 Å is about 0.19 Å too high and thus improbable, quite apart from the impurities in Padurow and Schusterius's La_2O_3 which would tend to lower the a_0 of the cubic phase.

All the reflections observed in the powder pattern of $Sc_2Ti_2O_7$ could be indexed on a fluorite unit cell. Because of the similarity of the atomic scattering factors of Sc^{3+} and Ti^{4+}, it was not possible to decide whether the product had the pyrochlore or the disordered fluorite-type structure[5]. With $b(Sc) = 1.18$, $b(Ti) = -0.34$,

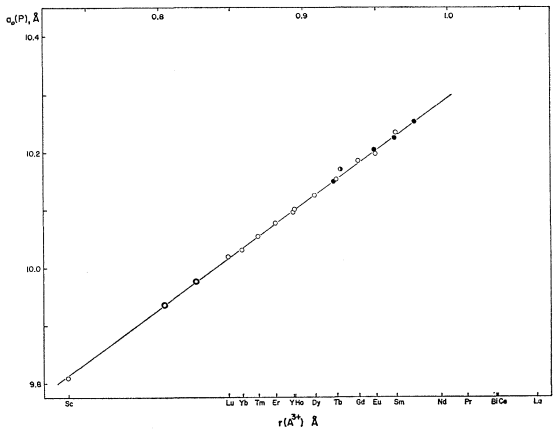

FIG. 2. Dependence of $a_0(A_2Ti_2O_7)$ on the radius of A^{3+}. Full circles, $(Y_{1-x}Bi_x)_2Ti_2O_7$; double circles, $(Lu_{1-x}Sc_x)_2Ti_2O_7$; half-full circle, $YbNdTi_2O_7$. The value for Sc is $2a_0$ of the fluorite pattern.

and $b(O) = 0.577$ (all in 10^{-12} cm (22)), neutron diffraction ought to make the distinction possible.

To this end a large batch of $Sc_2Ti_2O_7$ was prepared by coprecipitation (1000/24, 1200/24, 1400/24, 1400/24, 950/2 days, cooled with the furnace). The neutron diffraction pattern of the product was neither that of pyrochlore nor that of fluorite, but X-ray powder photographs taken before and after the neutron diffraction experiment contained only lines of a fluorite-type pattern. The films were of very good quality, with sharp diffraction lines.

These results are at variance with what would be expected from the investigation of the system Sc_2O_3–TiO_2 by Komissarova *et al.* (23). These authors concluded that there is no phase of the composition $Sc_2O_3 \cdot 2TiO_2$. The phase closest to TiO_2 is the δ phase $2Sc_2O_3 \cdot 3TiO_2$, which is rhombohedral ($a_{rh} = 7.742 \pm 5$ Å, $\alpha_{rh} = 71.94 \pm 0.10°$) below $1150 \pm 50°$, and of the defect fluorite type above this temperature. The composition $Sc_2O_3 \cdot 2TiO_2$ should thus correspond to a mixture of $\delta(Sc_2O_3$–$TiO_2)$ and rutile if cooled slowly or annealed below 1150°, or to a single phase of the fluorite type if quenched from temperatures above 1150°.

The conflicting evidence from the X-ray and neutron diffraction patterns of our sample fitted neither case. A possible explanation might be that the high-temperature disordered fluorite phase did not transform, under the above annealing conditions, into a mixture of δ and TiO_2 but had

[5]Brixner (17), who had prepared $Sc_2Ti_2O_7$ earlier, listed it with the cubic pyrochlore titanates and quoted an a_0 that corresponds to a double fluorite cell (Table I).

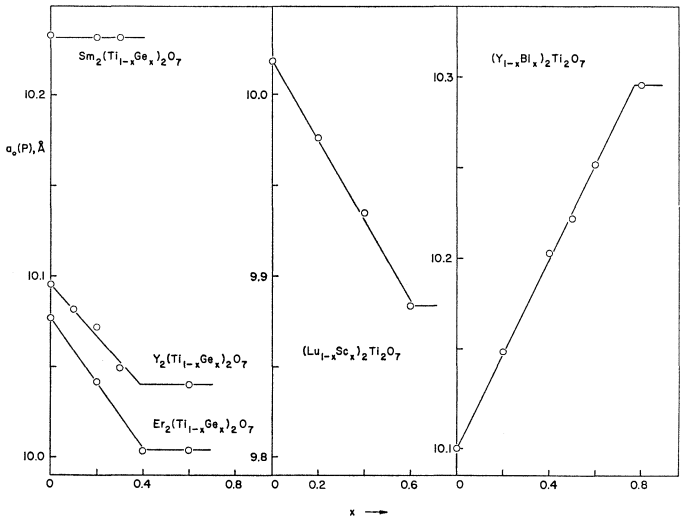

FIG. 3. Lattice parameter $a_0(P)$ vs. composition. *Left*, $A_2(Ti_{1-x}Ge_x)_2O_7$ (A = Sm, Y, Er); *center*, $(Lu_{1-x}Sc_x)_2Ti_2O_7$; *right*, $(Y_{1-x}Bi_x)_2Ti_2O_7$.

nevertheless attained a considerable degree of short-range order. This, as well as vacancy ordering in the anion sublattice, might give rise to extra neutron diffraction maxima but not necessarily to additional X-ray reflections. A situation of this kind has recently been described for the phase $Y_2O_3 \cdot 2CeO_2$ by Barker and Wilson (25). Further work to clarify the discrepancy is underway, but even on the evidence available at present it is clear that the $Sc_2Ti_2O_7$ sample was not a cubic pyrochlore.

Chromium and indium titanates apparently had formed (cf. Fig. 5) but they did not have the pyrochlore structure[6]. The In compound was greyish, the Cr compound was dark brown. No compound appeared to form on firing $InAlO_3$ (*C*-type, $a_0 = 10.1070 \pm 9$ Å) + $2TiO_2$ at 1400° for 12 h. $MnTiO_3$ with the ilmenite structure rather than $Mn_2Ti_2O_7$ was obtained by firing $MnO_2 + TiO_2$ or $Mn_2O_3 + 2TiO_2$ in air; this result was confirmed by t.g.a.

The structure of Bi titanate appeared to be related to that of pyrochlore (cf. $Bi_2Sn_2O_7$, refs. 15 and 2). The extra lines present in the X-ray powder pattern could not be accounted for on a cubic pyrochlore cell. However, mixed phases $(Y_{1-x}Bi_x)_2Ti_2O_7$ that contained up to $x = 0.75$ bismuth were prepared as cubic pyrochlores (Table I, Fig. 3).

The $(Lu_{1-x}Sc_x)_2Ti_2O_7$ system was investigated to determine the lower limit of existence of the pyrochlore phase. The limit is approximately at $x = 0.55$ (Table I, Fig. 3), which corresponds to an average Ahrens ionic radius of about 0.83 Å.

Although Cr^{3+} is too small to form a pyrochlore phase in its own right, the slight lowering of $a_0(P)$ of $Y_2Ti_2O_7$ on introducing chromium (Table I) would seem to indicate that a small amount of Cr had entered the pyrochlore structure. A similar observation was made with gallium. In spite of the similarity of the Ahrens ionic radii of In and Sc, a mixed Y–In pyrochlore titanate did not appear to form.

The two mixed titanates $HoYTi_2O_7$ and $YbNdTi_2O_7$ were pyrochlores, as expected.

Mixed Phases $A_2(Ti_{1-x}M_x)_2O_7$ (M = Ge, Zr)

No pyrochlore pattern was obtained for pure $Y_2Ge_2O_7$, $Er_2Ge_2O_7$, or $Sc_2Ge_2O_7$,[7] but it was possible to estimate the extent to which Ge could

[6]Roth (15) did not obtain a compound on firing $In_2O_3 + 2TiO_2$ at 1550° for 3 h. Hamelin (24) stated $Cr_2Ti_2O_7$ to form by firing the dry-mixed oxides at 1440° in air for 10 min as well as under other firing conditions. She reported the *d* spacings of the phase but made no attempt at indexing.

[7]Recently Shannon and Sleight (26) prepared high-pressure cubic $A_2Ge_2O_7$ pyrochlores (A = Gd, Dy, Ho, Tl, Er, Tm, Yb, Lu, Y, In, and Sc); a corresponding Sm phase did not form. The lattice parameters of $Y_2Ge_2O_7$ (9.897 ± 2 Å) and $Er_2Ge_2O_7$ (9.864 ± 2 Å) would fall 0.03–0.05 Å below the points obtained for the corresponding $A_2(Ti_{1-x}Ge_x)_2O_7$ phases by extrapolating the $a_0(P)$ vs. x straight lines of Fig. 3 to $x = 1$.

Can. J. Chem. Downloaded from www.nrcresearchpress.com by 210.87.254.40 on 09/05/12
For personal use only.

Can. J. Chem. Downloaded from www.nrcresearchpress.com by 210.87.254.40 on 09/05/12
For personal use only.

be accommodated in Er, Y, and Sm titanates as host structures (Table I, Fig. 3):

Very little Ge was present in the homogeneous Sm phase at the saturation limit. Assuming that the stability of the pyrochlore structure in $A_2Ti_2O_7$ is determined primarily by the radius ratio $r(A^{3+}):r(B^{4+})$, the upper limit of the ratio can be estimated from $Sm_2(Ti_{0.92}Ge_{0.08})_2O_7$ as 1.50 (Ahrens). The largest value of $r(A^{3+})$ in combination with $r(Ge^{4+}) = 0.53$ Å would then be $1.50 \times r(Ge^{4+}) = 0.80$ Å, which is smaller than $r(Lu^{3+})$. The lanthanons and scandium would thus not be expected to form pyrochlores with Ge. In a similar manner one can estimate the average maximum values of $r(B^{4+})_{calcd} = r(A^{3+})/1.50$ appropriate to Y and Er in the mixed germanates. As Table III shows, the estimates,

TABLE III

A	x (limit)	$\bar{r}(B^{4+})$, Å: limit	$\bar{r}(B^{4+})$, Å: calcd.	$r(A^{3+}):r(B^{4+})$ (limit)
		Ahrens radii		
Sm	0.08	0.668	0.668	1.50
Y	0.36	0.626	0.613	1.45
Er	0.40	0.620	0.593	1.44
		"Improved" radii		
Sm	0.08	0.616	0.616	1.56
Y	0.36	0.602	0.571	1.48
Er	0.40	0.600	0.565	1.47

though lower, are reasonably close to the average radii $\bar{r}(B^{4+})_{limit}$ calculated from the experimental saturation limits.

When "improved" radii are used, the upper limit of the radius ratio becomes 1.56 and the largest value of $r(A^{3+})$, 0.89 Å[8]. This value falls between $r(Er^{3+})$ and $r(Y^{3+})$ (cf. ref. 2), which would suggest that a cubic $Er_2Ge_2O_7$ ought to exist. Since neither Y nor Er form pure germanate pyrochlores at ordinary pressures, the implication is that the effective size of the oxygen ion exerts a controlling influence on the upper stability limit of the pyrochlore structure even when the radius ratio is favorable, similar to the way in which it controls the lower limit (8), and prevents the germanates from existing as pyrochlores. In other words, the value of the upper limit of the radius ratio decreases with decreasing $r(A^{3+})$ and $r(B^{4+})$, which is the reason for $\bar{r}(B^{4+})_{calcd}$ being increasingly lower than $\bar{r}(B^{4+})_{limit}$ (cf. Table III). The same is of course true of the Ahrens radii, even disregarding the fact that the Ahrens radius of Sc^{3+}, 0.81 Å, is much too large (cf. next section). The upper limit can, however, be extended to include the pure germanates by application of high pressure (cf. footnote 7).

The three $Y_2(Ti_{1-x}Zr_x)_2O_7$ phases ($x = 0.36$, 0.5, and 0.64) were pyrochlores (Table I).

Other Compositions

An attempt was made to prepare, by firing the dry-mixed oxides, mixed titanate pyrochlores of the type $M^{2+}N^{4+}Ti_2O_7$. The combinations tried were CaGe (1200°), SrGe (1200°), CaSn (1500°), CaZr (1400°), SrZr (1400°), CaCe (1400°), and SrCe (1400°). The average ionic size of the combination CaSn is about the same as $r(Lu^{3+})$, and CaZr would correspond to Er^{3+}. SrZr, CaCe, and SrCe are still within the size range of the trivalent lanthanons (Ahrens radii), and compounds are known in which $Ca^{2+}Sn^{4+}$ or $Ca^{2+}Zr^{4+}$ substitute for a trivalent ion of similar size. Examples are $CaSn(BO_3)_2$ (nordenskiöldite) and $La(Ca_{0.5}Zr_{0.5})O_3$, though $CaZrTi_2O_7$ has previously been reported to have a symmetry lower than cubic (28), in fact tetragonal (calzirtite, ref. 29).

None of the products gave a pyrochlore pattern.

Lattice Parameters

The agreement with the literature values was on the whole good (Table I). The differences between corresponding $a_0(P)$ values in series C and D were within 3σ, with the exception of $Er_2Ti_2O_7$ and $Lu_2Ti_2O_7$. The final a_0 is probably affected by the method of preparation and the firing cycle.

The overall agreement of the lattice parameters reported in refs. 15, 2, and 17 with those of series D was compared by regressing the a_0 sets on each other. Very high correlation coefficients were obtained, the highest one being that for series D and the a_0 values of ref. 3 (Table IV). Regression of series D on $a_0(A_2Sn_2O_7)$ (2) also gave a very high correlation coefficient, the slopes of the regression and reverse regression lines being very nearly unity. As with the stannates (2), the relationship between the lattice parameters of the titanates and $r(A^{3+})$ was linear (Table IV, Fig. 2). For the D series least squares gave the equations

[8]A set of empirical $r(B^{4+})$ for six-coordination has been derived from the lattice parameters and stability limits of cubic $A_2^{3+}B_2^{4+}O_7$ pyrochlores and BO_2 rutiles that leads to a more satisfactory description of the crystal chemistry of such compounds (27). Provisional values for Ge and Ti are 0.57 and 0.62 Å respectively. These values together with the $r(A^{3+})$ of Templeton and Dauben (cf. ref. 2) constitute the above "improved" radii.

TABLE IV

Standard deviations and correlation coefficients of a_0 and $r(A^{3+})$ regressions*

Regression of $a_0(P)$ of	$10^4\sigma$, Å	Correlation coefficient	$10^4\sigma$, Å (reverse regression)
Series D on $a_0(P)$ (15)	53	0.9970	51
Series D on $a_0(P)$ (17)	54	0.9988	53
Series D on $a_0(P)$ (series C)	38	0.9985	37
Series D on $a_0(P)$ (3)†	11	0.9998	11
Series D on $a_0(A_2Sn_2O_7)$ (2)	14	0.9997	14
Ref. 17 on $r(A^{3+})$	42	0.9978	23
Ref. 15 on $r(A^{3+})$	64	0.9954	36
Series D on $r(A^{3+})$	41	0.9981	22

*Templeton–Dauben radii (cf. ref. 2).
†Converted to present λ(Cu Kα) (cf. ref. 2).

$$a_0(P) = 8.45913 + 1.8344r(A^{3+})$$

$$r(A^{3+}) = -4.5910 + 0.54312a_0(P)$$

with standard deviations of the same order as were obtained for the stannates (2).

When the lattice parameters of the homogeneous $(Lu_{1-x}Sc_x)_2Ti_2O_7$ phases ($x = 0.2, 0.4$) are substituted in the last equation, effective crystal radii of the "$(Lu_{1-x}Sc_x)^{3+}$" ion are obtained, from which an average value of $r(Sc^{3+})$, 0.742 ± 2 Å, can be calculated. Extrapolating the correlation of $a_0(C)$ and the Templeton–Dauben radii (2) to Sc_2O_3 ($a_0 = 9.8455$ Å (30)) gave $r(Sc^{3+}) = 0.733$ Å.

The accuracy of these linear extrapolations may be questioned and the radius obtained from the mixed Lu–Sc titanates may be too high. Lu, as the larger ion of the two, may tend to dominate the lattice parameters in a situation which is marginal with respect to the stability of the pyrochlore phase. But there can be little doubt that the effective radius of Sc^{3+} in six or near-six coordination is much smaller than the value of 0.81 Å ascribed to it by Ahrens. We have adopted the average of the above two values, 0.737 ± 7 Å, as a provisional working value to be used in the pyrochlore chemistry.

In a similar manner a value can be obtained for the radius of Bi(III) from homogeneous $(Y_{1-x}Bi_x)_2Ti_2O_7$ phases ($x = 0.2, 0.4, 0.5, 0.6$; Table I). The average for the four compositions, 1.033 ± 3 Å, is again quite different from the "ionic" radius listed for trivalent bismuth by Ahrens, 0.93 Å, but the straight-line fit of Fig. 3 justifies accepting this figure as a provisional working value for $r(Bi(III))$ in pyrochlores. The extrapolated lattice parameter of $Bi_2Ti_2O_7$ would be 10.354 Å. Similarly, extrapolating for $Bi_2Sn_2O_7$ (cf. ref. 2) would yield 10.642 Å, which is not too far from the dimension of the cubic pseudocell quoted for the stannate by Roth (15), 10.68 Å.

It should be noted that these radii are for six-coordination, since they have been arrived at from the linear relationship of $a_0(P)$ and the $r(A^{3+})$ of Templeton and Dauben, but the actual coordination of A in the pyrochlore structure is 2 + 6.

Mechanism of Formation of the Pyrochlore Phase

Differential thermal analysis experiments with dry-mixed $A_2O_3 + 2TiO_2$ at heating rates of 10 and 20°/min in stagnant air revealed two exothermic peaks of roughly equal intensity (Fig. 4, curve 1). While the position of the first peak varied little with A, the temperature corresponding to the second peak maximum depended markedly on A and passed through a minimum at Gd or Sm (Fig. 5).

The presence of two exothermic peaks indicates that the formation of the final product, $A_2Ti_2O_7$, proceeds in two or more steps. A likely possibility is the formation of A_2TiO_5 as the precursory phase. To test this hypothesis d.t.a. curves of dry-mixed $Gd_2O_3 + TiO_2$ (Fig. 4, curve 2) and $Gd_2TiO_5 + TiO_2$ (Fig. 4, curve 3) were recorded under similar conditions[9]. The curve for $Gd_2O_3 + TiO_2$ contained a single broad exothermic peak with a maximum at *ca.* 1152°. Similarly, only one broad exothermic peak was observed in the curve for $Gd_2TiO_5 + TiO_2$, with a maximum at *ca.*

[9]Gd_2TiO_5 was prepared by firing $Gd_2O_3 + TiO_2$ at 1350° for 24 h. The powder pattern of the product was different from those of rutile, Gd_2O_3 and $Gd_2Ti_2O_7$ (cf. refs. 19, 31, and 32).

Can. J. Chem. Downloaded from www.nrcresearchpress.com by 210.87.254.40 on 09/05/12
For personal use only.

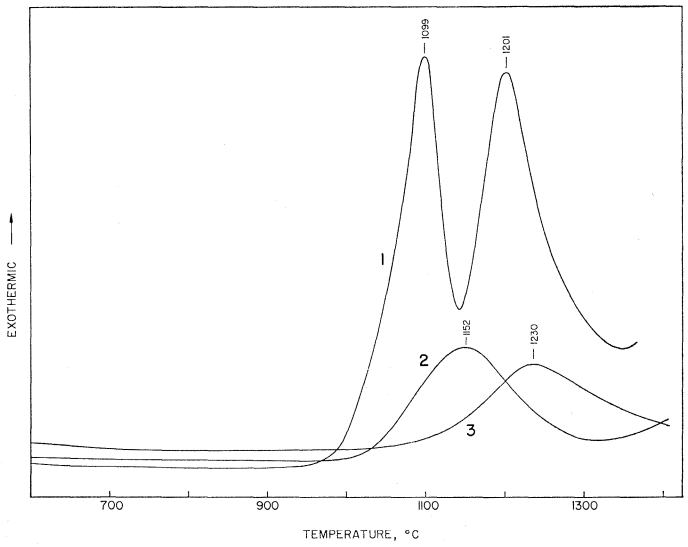

FIG. 4. Differential thermal analysis curves of dry-mixed $Gd_2O_3 + 2TiO_2$ (*1*), $Gd_2O_3 + TiO_2$ (*2*), and $Gd_2TiO_5 + TiO_2$ (*3*) in stagnant air. Rate of heating, 20°/min.

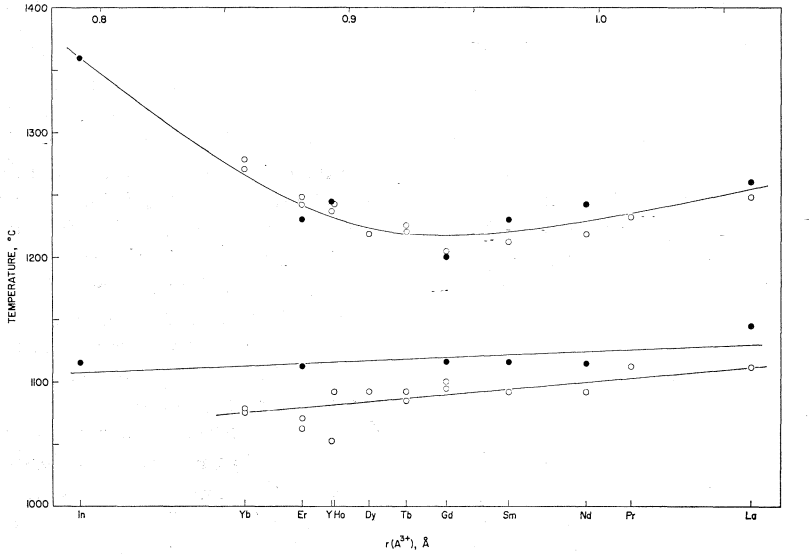

FIG. 5. Temperatures of the d.t.a. maxima of curve *1* (Fig. 4) plotted against the radius of A^{3+}. Heating rates in stagnant air: open circles, 10°/min; full circles, 20°/min.

1230°. When allowance is made for the difficulties in attempting to reproduce d.t.a. conditions with sufficient accuracy from one sample to another, and for the different solid state reactivities of the three mixtures (different reacting species, particle size, extent of surface contact, thermal conductivity), it may be concluded that the 1152° peak corresponds to the 1099° peak of curve 1 and thus to the formation of the 1:1 compound, Gd_2TiO_5, while the 1230° peak corresponds to the 1201° peak of curve 1 and to the formation of the 1:2 compound, $Gd_2Ti_2O_7$. The latter in turn is of course the 1:1 product of the reaction $Gd_2TiO_5 + TiO_2$.

Can. J. Chem. Downloaded from www.nrcresearchpress.com by 210.87.254.40 on 09/05/12
For personal use only.

TABLE V

Results of least squares structure refinements of $A_2^{3+}Ti_2^{4+}O_7^{2-}$ (Cu Kα; full matrix)

	Lu	Er	Y	Gd	Sm
			Overall temperature factor		
After cycle	10	9	10	10	9
K	1.015±6	1.021±5	0.990±4	1.009±11	1.007±10
$x(O_2)$	0.4221±16	0.4207±11	0.4218±7	0.4271±19	0.4259±20
B, Å^2	0.77±4	0.61±3	0.56±3	0.67±7	0.40±7
R(initial), %	6.02	3.73	1.83	4.28	2.27
R(final), %	1.74	1.30	1.37	1.98	1.50
e.s.d.(w)	2.60	1.67	1.39	3.21	3.08
			Individual isotropic temperature factors		
After cycle	10	9	10	4	9
K	1.016±7	1.020±4	0.990±5	1.005±11	1.004±6
$x(O_2)$	0.4201±24	0.4194±14	0.4201±10	0.4263±34	0.4230±28
B(A), Å^2	0.75±9	0.62±5	0.54±7	0.74±23	0.57±12
B(Ti), Å^2	0.76±25	0.64±13	0.54±15	0.58±52	−0.08±29
$B(O_1)$, Å^2	1.78±217	−0.60±64	2.06±120	−1.57±115	0.57±183
$B(O_2)$, Å^2	1.51±85	1.95±45	0.83±41	2.84±126	1.75±74
R(initial), %	10.04	7.76	3.64	2.32	2.94
R(final), %	1.60	1.02	1.15	1.82	1.39
e.s.d.(w)	2.81	1.43	1.14	3.16	2.40

The appreciable overlap of the two maxima of curve 1 indicates that the two stages were not clearly separated and that some $Gd_2Ti_2O_7$ had formed already at temperatures within the first peak. That the two-stage process of formation of $Ln_2Ti_2O_7$ in d.t.a. experiments is essentially dynamic in character was demonstrated from an X-ray photograph of the product obtained by firing a mixture of $Er_2O_3 + 2TiO_2$ at 1100° for 10 h. This temperature corresponds to the minimum between the two peaks in the d.t.a. curve of $Er_2O_3 + 2TiO_2$; the firing was an isothermal subsolidus process. There was no evidence of Er_2TiO_5. All the lines of the composite pattern could be accounted for by $Er_2Ti_2O_7$, Er_2O_3, and TiO_2.

The appearance of the two exothermic peaks in the d.t.a. curve of $In_2O_3 + 2TiO_2$ is additional evidence of compound formation in this system. The dry-mixed oxides in Roth's experiment (15) may have been brought to too high a temperature too quickly for a reaction to begin before the In_2O_3 volatilized.

The d.t.a. curve of $TbO_{1.79} + TiO_2$ showed that $Tb_2Ti_2O_7$ formed after the higher oxide had decomposed to Tb_2O_3.

Least-Squares Refinement

The structures of Lu, Gd, Sm, and Y titanates were refined from X-ray powder diffractometer data (Cu Kα) using (I) individual isotropic temperature factors and a block-diagonal approximation F-program written for IBM 1620/40K (cf. ref. 1); (II) individual isotropic temperature factors and an *ad hoc* full-matrix F-program written for IBM 360/50; and (III) an overall temperature factor and program II. The weighting scheme was W3 of ref. 35. One set of initial parameter values was employed in all the refinements: $K = 1.000$, $x(O_2) = 0.4200$, B(A) = 0.15 Å^2, B(Ti) = 0.60 Å^2, $B(O_1) = B(O_2) = 1.50$ Å^2, and B(overall) = 0.50 Å^2. In addition the structure of $Er_2Ti_2O_7$ (1) was re-refined to see the effect of a different weighting scheme and a different set of scattering factors.

The refinement was relatively insensitive to the choice of weighting scheme and, for each of the three programs, to the assumed degree of ionicity of the constituent atoms. On Hamilton's $\mathcal{R}$ criterion (36) there was no significant difference between the results obtained with f's for neutral atoms, for (A^{3+}, Ti^{3+}, O^{2-}), and for (A^{3+}, Ti^{4+}, O^{2-}). However, program I gave consistently lower $x(O_2)$ values than II or III (Fig. 6), with large e.s.d.'s of $B(O_1)$ and $B(O_2)$, while some of the $B(O_1)$ obtained with II were (positive or negative) indefinite (Table V). The overall temperature factors obtained with III were always physically reasonable and the $x(O_2)$ values were closely similar to those obtained with II, in fact always within 1σ (Table V and Fig. 6). On the whole, the ionic model with Ti^{4+} yielded the lowest-correlated parameters.

As for $Er_2Ti_2O_7$, there were small differences

Can. J. Chem. Downloaded from www.nrcresearchpress.com by 210.87.254.40 on 09/05/12
For personal use only.

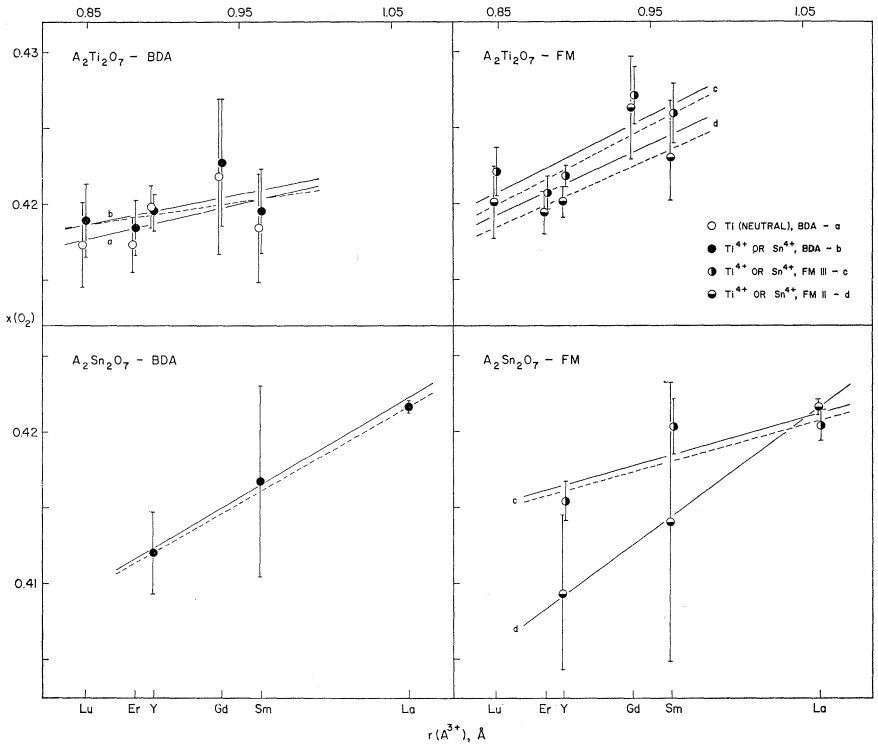

FIG. 6. Variation of the positional parameter $x(O_2)$ with $r(A^{3+})$. BDA, block-diagonal approximation (refinement I); FM II and FM III, full-matrix refinements II and III. The points are slightly displaced to facilitate plotting.

in the final values of the temperature factors, but the $x(O_2)$ values obtained with $f(Er^{3+}, Ti^{4+}, O^{2-})$ from all three programs were the same within 1σ of the individual values. The refinement results quoted in ref. 1 were not different within 2σ, and mostly within 1σ, from those obtained with refinement I in the present work.

The similarity of the $x(O_2)$ values obtained from II and III indicated that the success of refining with program II, which is physically more reasonable than III, was not prejudiced by the relatively small number of $|F_o|$ used in the refinement. The final R(II) values were slightly lower than R(III), and the slopes of the best $x(O_2)$ vs. $r(A^{3+})$ lines were practically the same for II and III, and similar to the corresponding lines for the stannates (2) (Fig. 6)[10]. The final $x(O_2)$ values from II (Table V) have therefore been adopted as the best set. The observed and calculated structure factors based on II are compared in Table VI.

When the $x(O_2)$ values are plotted against $r(A^{3+})$ there is an appreciable scatter, but the increase of $x(O_2)$ with the size of A^{3+} is reasonably evident. While it is true that the trend disappears when the uncertainty intervals are increased to $3\sigma(x)$, corresponding plots for the stannates (Fig. 6) and for two hafnates (27) show similar behavior. One may conclude that $x(O_2)$ increases with $r(A^{3+})$ in both the titanate and the stannate series, even though the accuracy of the refinements is perhaps not quite high enough to demonstrate this unambiguously. Thus the larger A^{3+} the smaller the distortion of the BO_6 octahedron for a particular B^{4+}, and the larger the B^{4+} ion, for a particular A^{3+}, the greater the distortion. In other words, the greater the $r(A^{3+}):r(B^{4+})$ ratio, the less distorted is the BO_6

[10]For comparison, the refinements of the three stannates (2) were repeated with II and III. For II the final $x(O_2)$, B(A), B(Ti), $B(O_1)$, $B(O_2)$, R, and e.s.d.(w) values respectively were: Y, 0.4093 ± 52, 0.85 ± 31, 0.12 ± 18, −0.68 ± 129, 2.75 ± 123, 0.85%, 2.215; Sm, 0.4140 ± 92, 0.63 ± 73, 0.80 ± 91, 0.63 ± 213, 3.25 ± 227, 0.81%, 3.536; La, 0.4216 ± 5, 1.32 ± 32, −0.22 ± 31, 4.17 ± 71, −0.21 ± 21, 0.71%, 0.170. For III the final $x(O_2)$, B(overall), R and e.s.d.(w) values respectively were: Y, 0.4154 ± 13, 0.40 ± 3, 1.03%, 2.467; Sm, 0.4203 ± 18, 0.71 ± 3, 1.17%, 3.661; La, 0.4204 ± 10, 0.77 ± 22, 1.92%, 0.391.

Can. J. Chem. Downloaded from www.nrcresearchpress.com by 210.87.254.40 on 09/05/12
For personal use only.

TABLE VI

Observed and calculated structure factors (Cu Kα, Ti^{4+}, refinement II)

	$Lu_2Ti_2O_7$		$Er_2Ti_2O_7$		$Y_2Ti_2O_7$		$Gd_2Ti_2O_7$		$Sm_2Ti_2O_7$	
hkl	$\|F_o\|$	F_c	$\|F_o\|$	F_c	$\|F_o\|$	F_c	$\|F_o\|$	F_c	$\|F_o\|$	F_c
111	285	−299	253	−252	90	−97	221	−223	230	−237
220	—	25	—	23	—	23	—	15	—	22
311	251	257	217	209	54	67	188	185	191	197
222	1123	1125	1044	1039	754	753	1064*	995	1021	1024
400	819	810	732	726	450	445	697	696	714	716
331	393	391	354	353	217	218	323	334	347	342
422	†	−59	†	−54	†	−60	†	−52	†	−55
440	1088	1084	1012	1021	784	785	953	954	1014	1010
531	266	251	215	219	92	95	186	200	215	203
620	—	36	—	41	—	41	—	50	—	40
533	228	202	167	159	63	55	224*	156	167	147
622	858	853	780	782	577	576	737	748	799	797
444	734	746	662	667	467	472	671	656	705	699
642	—	−4	—	−10	—	−6	—	−15	—	−9
800	806	811	751	750	575	581	731	717	780	777
733	275	−279	251	−244	167	−164	249	−225	231	−239
662	685	685	622	626	478	471	609	600	670	662
840	621	629	560	565	414	418	542	546	597	611
664	—	27	—	33	—	33	—	35	—	29
931	165	172	132	136	66	70	†	146	†	157
844	631	626	591	587	442	443	571	556	615	619
953	139	152	117	134	†	75	†	147	†	148
10.4.2	—	17	—	24	—	22	—	21	—	18
880	512	521	499	493	374	375	419*	474	527	540
10.6.2	509	489	457	452	363	357	425	435	528	515
12.4.0	455	460	438	439	345	348	426	433		

*Not used in the refinement.
†Not measured.

octahedron. An independent and striking confirmation of the decrease of the distortion of BO_6 with increasing $r(A^{3+})$ in the A_2FeSbO_7 pyrochlore series has been obtained from the Mössbauer spectra of these phases at room temperature (37). The quadrupole splitting at the Fe^{57} nucleus decreases with increasing $r(A^{3+})$, thus indicating a progressively smaller distortion of the FeO_6 octahedron.

Compared with the other titanates, the values of $x(O_2)$ for $Gd_2Ti_2O_7$ and $Sm_2Ti_2O_7$ are less reliable because of the exceptionally high backgrounds and low peak-to-background ratios of most reflections in the diffractometer patterns of these two phases, and also because of the large and probably uncertain dispersion corrections for f(Gd) for Cu Kα radiation.

The powder intensity data for the five titanates have been submitted to the American Society for Testing and Materials (ASTM) powder diffraction file.

Refinement of $Y_2(Ti_{0.64}Zr_{0.36})_2O_7$ from Neutron Data

Twelve $|F_o|$ were extracted from the neutron powder pattern (Fig. 7) by Gaussian analysis (cf. ref. 2) and utilized in refinements I, II, and III. The initial parameter values were the same as for the refinements from X-ray data except for B(overall), which was 0.70 Å^2. The neutron scattering amplitudes were taken as b(Ti) = −0.34, b(Zr) = 0.62, b(O) = 0.577, and b(Y) = 0.80 (all in 10^{-12} cm) (22).

None of the refinements was completely satisfactory. Some of the temperature factors were (positive or negative) indefinite or even negative. No significant difference resulted on using $b(Y) = 0.788 \times 10^{-12}$ cm (38).

The best $x(O_2)$ value was that from III, 0.4177 ± 21. It was identical with that from II, while the value obtained in refinement I was considerably lower. The final R values were in the range 6–9%.

Interatomic Distances and Bond Angles

The apparent interatomic distances and bond angles (not corrected for thermal motion) are listed in Table VII. They have been calculated from the final $x(O_2)$ (II). The uncertainty limits are based on $3\sigma(x)$, and on $4\sigma(a_0)$ for distances independent of $x(O_2)$.

The shortest Ti–O distances in the five titanates

Can. J. Chem. Downloaded from www.nrcresearchpress.com by 210.87.254.40 on 09/05/12
For personal use only.

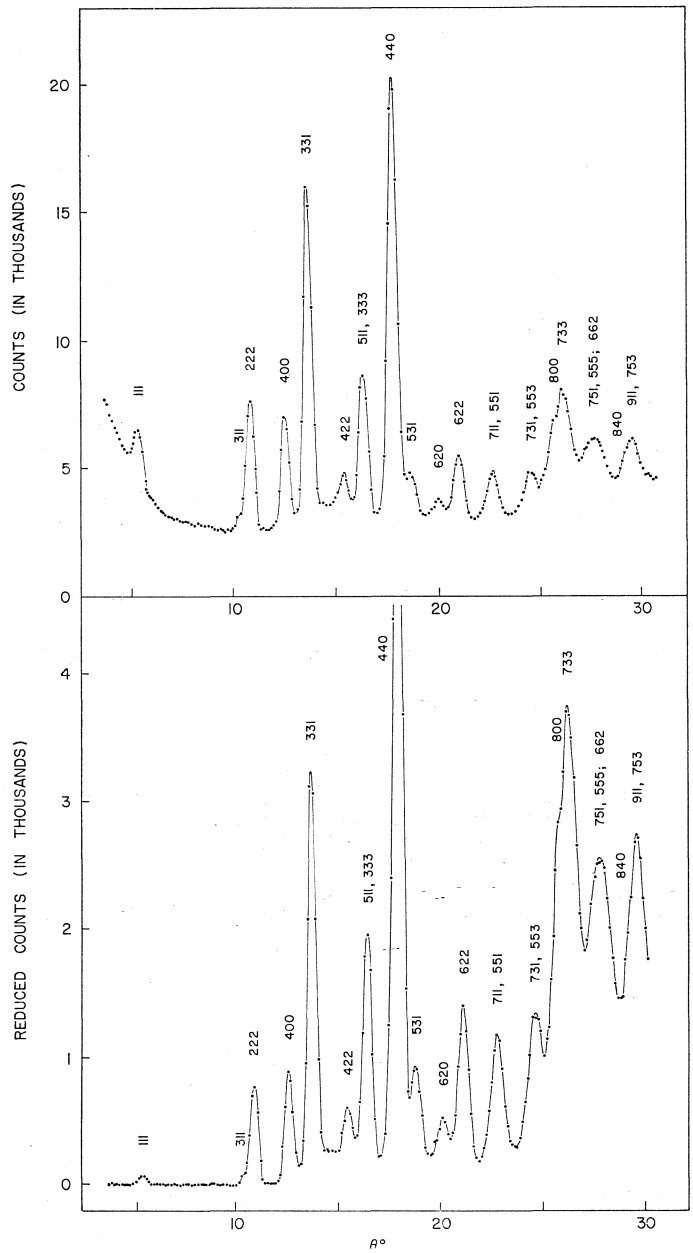

FIG. 7. Raw (*top*) and reduced (*bottom*) neutron diffraction patterns of $Y_2(Ti_{0.64}Zr_{0.36})_2O_7$ (monochromator, Al(111); $\lambda = 1.10$ Å; counting time per point, 10 min).

all fall between the two Ti–O distances reported by Baur for rutile, 1.944 ± 4 and 1.988 ± 6 Å (cf. ref. 1), and they are all within the range known from TiO_6 octahedra in other compounds (Table VIII and ref. 1).

Comparison of the A–O distances is more difficult to make. The $A–O_1$ distance depends only on a_0. It is thus shorter in the titanate than in the stannate pyrochlores. For example, the $Y–O_1$ distance in the stannate is 2.2457 ± 10 Å (2), while in the titanate it is 2.1856 ± 6 Å, which is one of the shortest Y–O distances reported (Table VIII, and Table V of ref. 2). The $A–O_1$ distances are on the whole rather short, as might

Can. J. Chem. Downloaded from www.nrcresearchpress.com by 210.87.254.40 on 09/05/12
For personal use only.

TABLE VII

Apparent interatomic distances and bond angles in $A_2Ti_2O_7$ pyrochlores*

Distance or angle	Lu	Er	Y	Gd	Sm
			Distances, Å		
$Ti–O_2$	1.943±30	1.958±18	1.958±12	1.951±39	1.973±33
$Ti–O_2$	3.749±63	3.778±36	3.778±27	3.756±90	3.804±75
$A–O_1 = a_0\sqrt{3}/8$	2.1690±8	2.1816±8	2.1856±6	2.2052±8	2.2155±8
$A–O_2$	2.458±51	2.467±30	2.476±21	2.543±72	2.531±60
$O_2(5)–O_2(6)$	2.585±24	2.597±15	2.604±12	2.651±42	2.651±33
$O_2(4)–O_2(5)$	2.903±102	2.930±60	2.925±42	2.862±147	2.923±123
$O_1(1)–O_2(3)$	2.956±72	2.966±42	2.979±30	3.069±105	3.049±87
$O_1(1)–O_2(2)$	3.571±9	3.591±6	3.598±4	3.639±15	3.651±12
$O_1–O_1 = a_0\sqrt{3}/4$	4.3379±16	4.3634±12	4.3712±8	4.4103±12	4.4311±12
			Bond angles, (degrees)†		
$O_2(4)–Ti(1)–O_2(5)$	96.64±17	96.89±10	96.64±7	94.38±24	95.60±20
$O_2(2)–A(1)–O_2(3)$	63.45±14	63.52±8	63.45±6	62.84±19	63.16±16
$O_1(1)–A(1)–O_2(3)$	79.16±10	79.04±6	79.16±4	80.19±13	79.65±11
$O_2(2)–O_1(1)–O_2(3)$	45.46±19	45.44±11	45.46±8	45.59±26	45.52±22

*For atomic positions see Table IV of ref. 1; $O_5(2)$ is now $O_2(5)$ etc. (the same applies to Table IV of ref. 2).
†$[O_2(4)–Ti(1)–O_2(5)] + [O_2(5)–Ti(1)–O_2(6)] = 2R$; $[O_1(1)–A(1)–O_2(3)] + [O_1(1)–A(1)–O_2(2)] = 2R$; $A(1)–O_1(1)–A(2) = 109.47°$ (tetrahedral angle); Ti–Ti, A–A, Ti–A $= a_0\sqrt{2}/4$.

TABLE VIII

M–O distances in some compounds of Gd, Er, Lu, Y, and Ti(IV)*

Compound	Coordination	Distance, Å	Reference
		Gd–O distances	
$Gd(HCOO)_3$	3O+6O	2.30; 2.50	39
$GdFeO_3$	1O+1O+2O+2O+2O (12-coordinated; shortest distances only)	2.26±5; 2.36±4; 2.38±2; 2.39±2; 2.82±2	40
$Gd_3Fe_5O_{12}$ (garnet)	4O+4O+4O+4O (shortest distances only)	2.38; 2.47; 2.67; 2.87 (all ±8)	41
		Er–O distances	
$Er(EtSO_4)_3\cdot 9H_2O$	$6H_2O+3H_2O$	2.37; 2.52	42
		Lu–O distances	
$LuMnO_3$	3O+3O+1O	2.18; 2.35; 2.42	43
ULu_6O_{12}	1O+1O+1O+2O+1O	2.20; 2.22; 2.23; 2.25; 2.27 (all ±2)	44
		Y–O distances	
Y_2BeO_4	1O+2O+1O+2O 2O+1O+1O+2O	2.212±3; 2.274±2; 2.280±3; 2.337±2 2.245±2; 2.271±3; 2.276±3; 2.342±2	45
		Ti(IV)–O distances	
$ThTi_2O_6$	1O+1O+2O+1O+1O	1.83±5; 1.84±4; 1.94±7; 2.06±4; 2.20±7	46
$NaTi_2Al_5O_{12}$	1O+2O+2O+1O	1.843±16; 1.952±18; 1.973±17; 2.167±19	47

*For Sm–O distances see ref. 2. For additional values of Er–O, Y–O, and Ti(IV)–O distances see refs. 1 and 2.

be expected from the tetrahedral coordination of the O_1 atom, and hence not typical. Subtracting $r(A^{3+})$ for six-coordination from the $A–O_1$ distances gives values from 1.321 Å (Lu) to 1.252 Å (Sm) for the radius of the oxygen atom; in view of the quite small uncertainties in the $A–O_1$ distances these differences must be considered as meaningful. By contrast, subtracting $r(A^{3+})$ from the $A–O_2$ distances leaves residues that do not significantly differ within the 3σ, and in fact within the 2σ limits, the average value of the "oxygen radius" being about 1.59 Å.

The $A–O_2$ distances increase progressively from Lu to Sm. As in the stannates, they are longer than the corresponding distances reported for six-coordinated A, but within the range for higher coordination. In the two cases where they are known for both series, they are not signif-

Can. J. Chem. Downloaded from www.nrcresearchpress.com by 210.87.254.40 on 09/05/12
For personal use only.

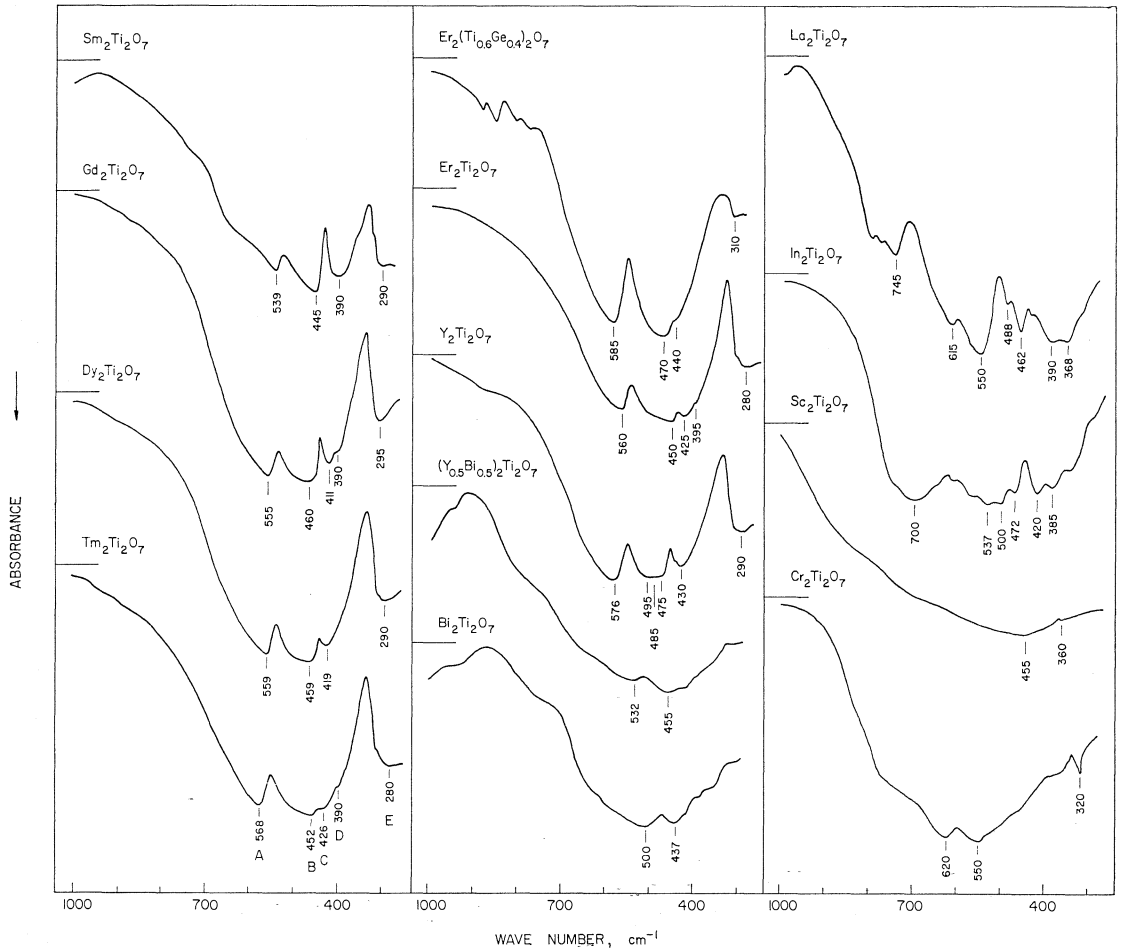

FIG. 8. Infrared transmission spectra of representative pyrochlore titanates and related compounds.

icantly different within 3σ (Sm) or even within 2σ (Y). This seems to indicate that the O_1 atom, for which the A–O distance varies with B^{4+}, is under constraint in a "forced" coordination, and the $A–O_1$ distance is not free to adjust in the same way as the $A–O_2$ distance does through change in $x(O_2)$. As a consequence the O_1 atom will be polarized by the same nearest neighbor A to an extent that will depend on the size of B^{4+}.

The difference between $A–O_1$ and $A–O_2$ introduces an ambiguity into attempts to assign an "effective radius" to A^{3+} in the 2 + 6 coordination. The standard radii for six-coordination leave O_1 undersized and O_2 too large, thus leading to the conclusion that the effective "shape" of the A atom in this coordination is an oblate spheroid.

Infrared Spectra

Compared with the spectra of the pyrochlore stannates in the 1600–250 cm^{-1} region (2), the features of the corresponding titanate spectra were not nearly as well defined. This applies also to the spectrum of $BaTiO_3$ (1) compared with $BaSnO_3$ (2), and to rutile compared with SnO_2. The main feature of the titanate spectra in this region is a very strong band with a wide, flat maximum exhibiting shallow fine structure peaks at 540–575 (*A*), 440–460 (*B*), 390–440 (*C*), and about 390 cm^{-1} (*D*) (Fig. 8). Another band was sometimes observed at 280–295 cm^{-1}, but its position could not be determined accurately because it was too close to the limit of the instrument range.

When the trivalent cation in the titanate

Can. J. Chem. Downloaded from www.nrcresearchpress.com by 210.87.254.40 on 09/05/12
For personal use only.

changes, the frequency of the *B* band does not appear to change, but the frequencies of *A* and *C* are shifted (Fig. 9). The *A* and *B* frequencies of $Y_2Ti_2O_7$ are noticeably above the corresponding frequencies of the lanthanon titanates. This is in contrast with the stannate series (2), where the peak frequencies of the yttrium member were indistinguishable from those of Ho and Er stannates. The assumption that was made for the stannates does not seem to hold for the titanates. That is, the Ti atom is not sufficiently heavy to provide, together with Y, a quasi-stationary framework for the oxygen atoms. Consequently the effect of approximately halving the mass of the lanthanon atoms makes itself felt in the increased frequencies of $Y_2Ti_2O_7$, even though the increase may not be as much as would appear from Fig. 9 because of the spread of the points about the least-squares straight lines.

Changes of frequency of the absorption bands in the expected direction were observed on replacing Ti in $Er_2Ti_2O_7$ partially with Ge, and Y in $Y_2Ti_2O_7$ with Bi. The mass average of

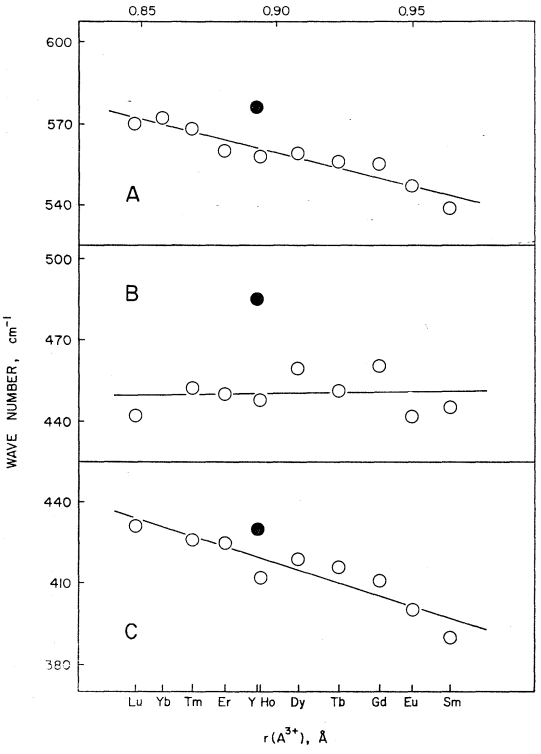

FIG. 9. Variation of the frequencies of the *A*, *B*, and *C* absorption maxima with $r(A^{3+})$. Full circles, $Y_2Ti_2O_7$.

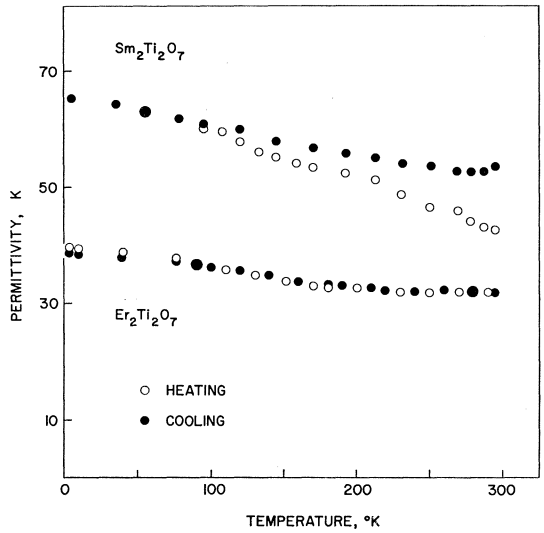

FIG. 10. Permittivity vs. temperature relationships for $Sm_2Ti_2O_7$ and $Er_2Ti_2O_7$.

$Y_{0.5}Bi_{0.5}$ is very close to the mass of Sm, but the general features of the spectrum of the mixed phase resemble more those of $Bi_2Ti_2O_7$ (which is not a cubic pyrochlore) than those of $Sm_2Ti_2O_7$. The spectrum of $La_2Ti_2O_7$ may be viewed as derived from the spectrum of $Sm_2Ti_2O_7$ by splitting of the main absorption bands and an appreciable increase in the intensity of the shoulder between 700 and 800 cm^{-1}; a detailed correlation cannot be offered at present.

The spectra of the In and Cr phases, which are believed to be homogeneous phases, are also shown in Fig. 8. The $Sc_2Ti_2O_7$ phase which gave a fluorite-type pattern had a spectrum with no distinct features but resembling, in a general way, the spectrum of $Sc_4Sn_3O_{12}$ (2).

Dielectric Properties

Permittivity measurements on two pyrochlore titanates, $Sm_2Ti_2O_7$ and $Er_2Ti_2O_7$, from room temperature to 4.2 °K gave no indication of ferroelectric transitions (Fig. 10).

Conclusions

(1) The linear relationship, which exists between a_0 of the pyrochlore titanates and the Templeton–Dauben radii of A^{3+}, makes it possible to derive provisional values of the crystal radii of Sc^{3+} and Bi(III) for six-coordination. Similarly, linear extrapolation for *C*-type sesquioxides (2) provides a check on the compatibility,

Can. J. Chem. Downloaded from www.nrcresearchpress.com by 210.87.254.40 on 09/05/12
For personal use only.

TABLE IX

Ionic (crystal) radii of A^{3+} in six-coordination, in Å*

A^{3+}	Goldschmidt	Pauling	Ahrens	Zachariasen	T and D†	Others	This work‡ (provisional)
Fe	0.67		0.64				*0.640(±3)*
Sc	0.83	0.81	0.81	0.68			*0.737±7*
In	0.92	0.81	0.81			0.779 (48)	*0.791*
Lu	0.99		0.85		*0.848*		
Yb	1.00		0.86		*0.858*		
Tm	1.04		0.87		*0.869*		
Er	1.04		0.89		*0.881*		
Tl	1.05	0.95	0.95				*0.881*
Y	1.06	0.93	0.92	0.88		*0.893* (48)	
Ho			0.91		*0.894*		
Dy			0.92		*0.908*		
Tb			0.93		*0.923*		
Gd	1.11		0.97		*0.938*		
Cf						0.949 (49); 0.976 (57)	*0.947*
Eu			0.98		*0.950*		
Bk						0.954 (49)	*0.954*
Sm			1.00	0.97	*0.964*		
Pm					0.979		*0.978(±3)*
Cm						0.979 (49)	*0.979±5*
Am						0.985 (49)	*0.984±3*
Pu						0.987 (49)	*0.986±5*
Nd			1.04		*0.995*		
Pr	1.16		1.06		*1.013*		
Bi(III)			0.93				*1.033±3*
Ce	1.18		1.07		*1.034*		
La	1.22	1.15	1.14	1.04	*1.061*		

*Values in italics constitute the best set (adopted in the present work).
†Templeton and Dauben (cf. ref. 2).
‡The lattice parameters of the *C*-type oxides used in the calculation were: Tl, 10.543 (50); In, 10.117±1 (51); β-Fe_2O_3, 9.40 (52); Am, 11.03±1 (53); Pu, 11.04±2 (54); Cm, 11.01±2 (55); Pm, 10.99 (56); and Bk, 10.8865 (49) (all in Å). For Cf the *B*-type sesquioxide was used (57); its exact stoichiometry was, however, not known.

with the Templeton–Dauben set, of the values quoted for the crystal radii of some other six-coordinated trivalent ions. Comparing the radii derived in this way for Tl^{3+}, In^{3+}, and Fe^{3+} (Table IX) with the corresponding Ahrens values reveals a major discrepancy for $r(Tl^{3+})$, but only a small difference for In^{3+}; the values for Fe^{3+} are identical[11].

Linear extrapolation using the same relationship leads to crystal radii for six-coordinated trivalent Pu, Am, Cm, and Bk which differ only insignificantly, or not at all, from the values listed recently by Peterson and Cunningham (49). It also shows that Espinosa's a_0 of Pr_2O_3 (*C*-type), 11.152 ± 3 Å (66), though higher than the 11.140 ± 2 Å quoted by Eyring and Baenziger (69), is still below the calculated value, 11.165 ± 5 Å. The lattice parameter reported by Sastry *et al.* (70), 11.160 ± 6 Å, is however in close agreement.

Whatever the precise significance and applicability of empirical crystal radii, if a consistent set for a particular coordination is available, it can serve for correlation, verification, and prediction of various metric properties of crystal structures. The usefulness and self-consistency of the Templeton–Dauben set, augmented by Geller's value for Y^{3+}, has been demonstrated earlier (2). The enlarged set of Table IX has been tested on several isostructural series of compounds (Fig. 11)[12]. The straight-line fits are seen to be very satisfactory for coordination numbers from 6 to 8 and for structure types as different as CrB and the

[11]Shannon (71) has suggested that the effective radius of Tl^{3+} in the 3–3 perovskites is considerably smaller than the Ahrens value, and probably less than 0.85 Å; for Sc^{3+} he uses a value of 0.73 Å and for In^{3+}, 0.77 Å (estimated from his Fig. 2). Shannon's values thus corroborate the validity of the effective crystal radii in six-coordination deduced for the three ions in the present work.

[12]The unit-cell dimensions of the compounds shown in Fig. 11 were taken mostly from ref. 58. In addition the following references were used: A_2O_3 (*B*-type), 56, 57, 61, 62; A_2O_3 (high-pressure corundum), 63; AUO_4, 64; $A_2Ge_2O_7$ (high-pressure pyrochlore), 26; Fe and Ga garnets, 65, 66; $Ca_3Al_2Si_3O_{12}$, 59, 60; Sr hydrogarnets, 59; AGa, 67, 68.

Can. J. Chem. Downloaded from www.nrcresearchpress.com by 210.87.254.40 on 09/05/12
For personal use only.

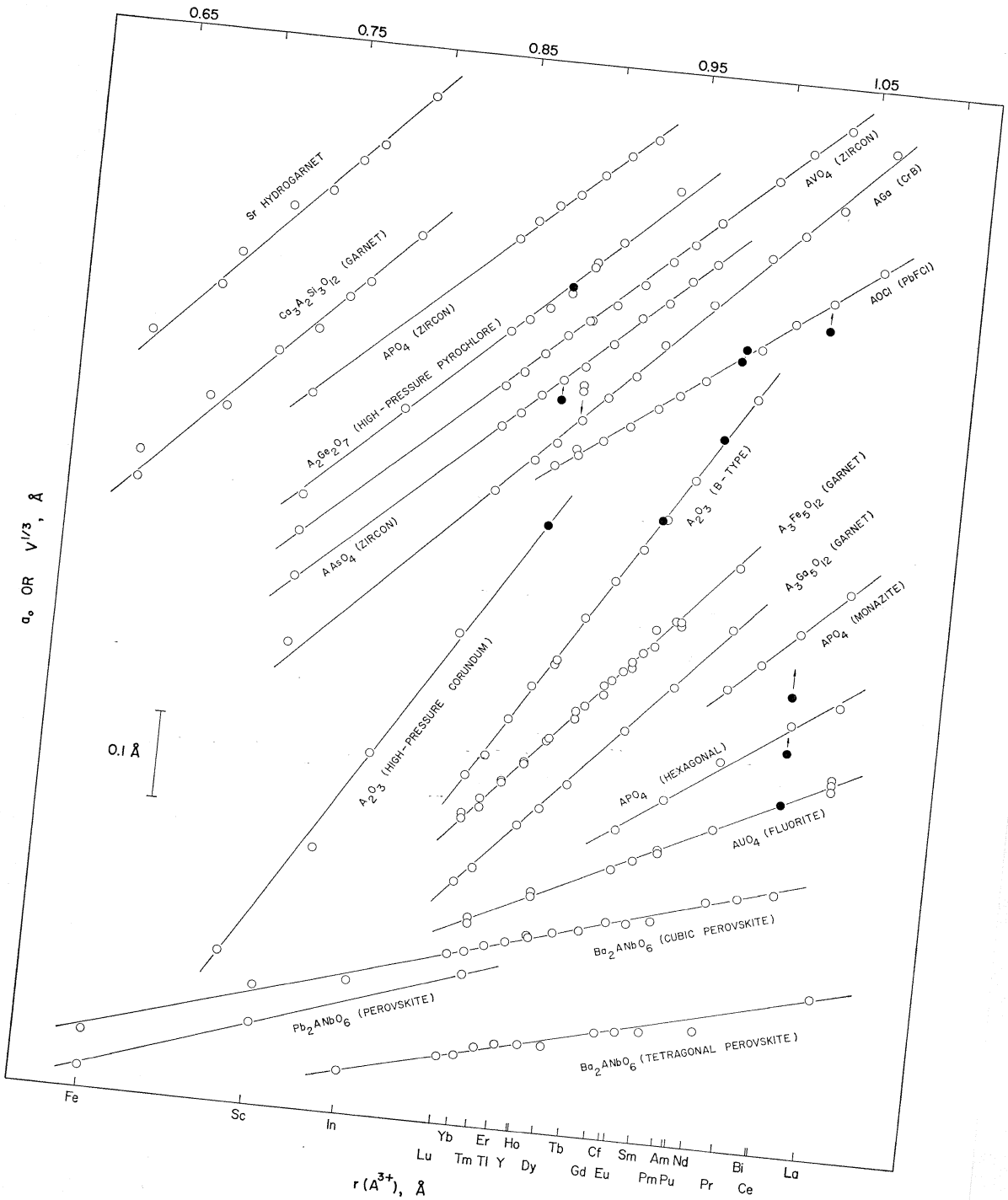

FIG. 11. Lattice parameters or $V^{1/3}$ values of various A^{3+} compounds plotted against $r(A^{3+})$. The a_0 and $V^{1/3}$ values are on the correct scale but the ordinates have been arbitrarily shifted to facilitate plotting. Full circles: Tl, Bi, and the transuranium elements.

Can. J. Chem. Downloaded from www.nrcresearchpress.com by 210.87.254.40 on 09/05/12
For personal use only.

Can. J. Chem. Downloaded from www.nrcresearchpress.com by 210.87.254.40 on 09/05/12
For personal use only.

garnets. It is probably true, however, that these radii will in general give best linear correlations for oxygen compounds with structures of high symmetries, in which variations of the positional parameters from one member of an isostructural series to next are relatively insignificant compared with the variations of the unit-cell volume. Where appreciable covalency and pronounced asymmetric orbital occupancies are involved, the radii lose their universality. An example is Bi. When occupying sites of highly regular coordination at random, such as in mixed phases of the pyrochlore or fluorite type (Fig. 11), Bi(III) falls in the $r(A^{3+})$ sequence just below Ce^{3+}. In other structures, where the coordination is less regular and the degree of covalency higher, the apparent size of the Bi atom decreases, approaching perhaps that of Pr^{3+} or even Nd^{3+}. This is evident in Fig. 11. Although there may be some doubt about the exact composition of at least one of the two forms of $BiPO_4$ referred to in the drawing, BiOCl illustrates this point adequately. A similar tendency may exist for Tl.

Successful correlation of the Templeton–Dauben radii with the empirical crystal radii of the smaller trivalent ions (Al, Ga, Ti, V, Cr, Mn, Co, Rh) is handicapped by the paucity of suitable isostructural series that would include compounds of Sc and In and at least a few of the smaller lanthanons; the spin configurations of the *d* electrons may also have to be taken into consideration in some cases.

(2) The stability region of the pyrochlore titanates extends from an Ahrens radius ratio, $r(A^{3+}):r(B^{4+})$, of about 1.22 (in mixed Lu–Sc phases) to about 1.47 ($Sm_2Ti_2O_7$); or, using the "improved" radii, from about 1.27 to about 1.55. The upper limit is slightly extended in Sm titanate–germanate phases to 1.50 (Ahrens) or 1.56 ("improved").

Although $Bi_2Ti_2O_7$ is not a cubic pyrochlore, in mixed Y–Bi titanates the pyrochlore phase extends to about $Y_{0.5}Bi_{1.5}Ti_2O_7$, i.e. to a radius ratio of *ca.* 1.36 (Ahrens) or 1.61 ("improved"). The corresponding values for a pure Bi pyrochlore would be 1.37 and 1.67.

If the present value proposed for r(Bi(III)), 1.033 Å, is accepted, the upper limit in the Y–Bi titanates is higher than in the Ln compounds, though pure Bi titanate should be, on the radius-ratio criterion, outside the pyrochlore field, as is in fact the case. However, $Bi_2Sn_2O_7$, which is not a pyrochlore either, has a radius ratio of 1.31 (Ahrens) or 1.44 ("improved"), and is thus inside the upper ratio limit for the pyrochlore stannates, 1.61 (Ahrens) or 1.48 ("improved") (in $La_2Sn_2O_7$).

These observations again demonstrate the exceptional behavior of bismuth as a potential pyrochlore former.

(3) The positional parameter $x(O_2)$ in the titanates increases with $r(A^{3+})$ and has larger values than in the corresponding stannates. Consequently the distortion of the BO_6 octahedra decreases with the increasing $r(A^{3+}):r(B^{4+})$ ratio.

(4) No evidence of ferroelectric transitions in Sm and Er titanates was found by permittivity measurements between room temperature and 4.2 °K.

(5) Unlike in $Y_2Sn_2O_7$, in $Y_2Ti_2O_7$ the atoms of the two metals are not sufficiently heavy for their sublattices to behave like a stationary framework with respect to the oxygen atoms. Some of the absorption maxima of $Y_2Ti_2O_7$ in the 600–300 cm^{-1} region have therefore frequencies significantly higher than those of the corresponding maxima of Er and Ho titanates.

Acknowledgments

We should like to express our gratitude to the following individuals and agencies:

The staff of the Neutron Physics Branch, Atomic Energy of Canada Limited, for permission to use their neutron diffraction facilities; Dr. F. R. Ahmed, for making available to us the least-squares program of ref. 1; Dr. M. Falk, for placing at our disposal the infrared spectrometer; Mr. Y. S. Lim, for carrying out the dielectric measurements; Dr. M. H. Jericho, for making possible the dielectric study at low temperatures; Dr. N. F. H. Bright and Mr. R. H. Lake, for the differential thermal analysis of the $Gd_2O_3 + TiO_2$ mixtures; Drs. R. D. Shannon and W. W. Barker, for seeing the manuscripts of their papers (refs. 26 and 25) before publication; Dr. V. Seidl and Mr. C. Ayasse, for assistance with some of the computations; and Drs. B. I. Pokrovskiĭ and F. M. Spiridonov of the Moscow State University, for encouraging us to investigate $Sc_2Ti_2O_7$ in detail and for a generous gift of high-purity scandium oxide.

Financial support of this investigation by the Defence Research Board and the National Research Council of Canada through grants to the first-named author is hereby acknowledged. Some of the preparative work and a part of the

X-ray study were carried out under Defence Research Board contract No. 800107/200024 and are reported in the present form with the permission of the Board.

Last but not least we should like to thank the staff of the Dalhousie Computing Centre for their unfailing assistance with machine computation.

1. O. KNOP, F. BRISSE, L. CASTELLIZ, and SUTARNO. Can. J. Chem. **43**, 2812 (1965).
2. F. BRISSE and O. KNOP. Can. J. Chem. **46**, 859 (1968).
3. L. CASTELLIZ and O. KNOP. 13th Progress Report, December 31st, 1963; and 14th Progress Report, June 30th, 1964. Defense Research Board Contract No. 200024. Nova Scotia Technical College, Halifax, Nova Scotia.
4. W. S. CLABAUGH, R. T. LESLIE, and R. GILCHRIST. J. Res. Natl. Bur. Std. **55**, 261 (1955).
5. N. C. BAENZIGER, H. A. EICK, H. S. SCHULDT, and L. EYRING. J. Am. Chem. Soc. **83**, 2219 (1961).
6. R. E. FERGUSON, E. D. GUTH, and L. EYRING. J. Am. Chem. Soc. **76**, 3890 (1954).
7. E. D. GUTH, J. R. HOLDEN, N. C. BAENZIGER, and L. EYRING. J. Am. Chem. Soc. **76**, 5239 (1954).
8. F. BRISSE and O. KNOP. Can. J. Chem. **45**, 609 (1967).
9. D. T. CROMER and J. T. WABER. Acta Cryst. **18**, 104 (1965).
10. D. T. CROMER. Acta Cryst. **18**, 17 (1965).
11. International tables for X-ray crystallography. Vol. III. Kynoch Press, Birmingham. 1962.
12. M. TOKONAMI. Acta Cryst. **19**, 486 (1965).
13. D. GIUŞCĂ and I. POPESCU. Bull. soc. roumaine phys. **40**, 13 (1939).
14. F. JONA, G. SHIRANE, and R. PEPINSKY. Phys. Rev. **98**, 903 (1955).
15. R. S. ROTH. J. Res. Natl. Bur. Std. **56**, 17 (1956).
16. J. B. MACCHESNEY and H. A. SAUER. J. Am. Ceram. Soc. **45**, 416 (1962).
17. L. H. BRIXNER. Inorg. Chem. **3**, 1065 (1964).
18. J. L. WARING and S. J. SCHNEIDER. Am. Ceram. Soc. Bull. **43**, 4, 263 (1964).
19. F. QUEYROUX. Compt. Rend. **259**, 1527 (1964).
20. J. D. AULT and A. J. E. WELCH. Acta Cryst. **20**, 410 (1966).
21. N. N. PADUROW and C. SCHUSTERIUS. Ber. Deut. Keram. Ges. **31**, 391 (1954).
22. G. E. BACON. Neutron diffraction. 2nd ed. Oxford University Press, Oxford. 1962.
23. L. N. KOMISSAROVA, B. I. POKROVSKĬĬ, and V. V. NECHAEVA. Dokl. Akad. Nauk SSSR, **168**, 1076 (1966).
24. M. HAMELIN. Bull. Soc. Chim. France, [5] **24**, 1421 (1957).
25. W. W. BARKER and A. F. WILSON. J. Inorg. Nucl. Chem. **30**, 1415 (1968).
26. R. D. SHANNON and A. W. SLEIGHT. Inorg. Chem. **7**, 1649 (1968).
27. O. KNOP and F. BRISSE. To be published.
28. L. W. COUGHANOUR, R. S. ROTH, S. MARZULLO, and F. E. SENNETT. J. Res. Natl. Bur. Std. **54**, 191 (1955).
29. YU. A. PYATENKO and Z. V. PUDOVKINA. Kristallografiya, **9**, 98 (1964); Soviet Phys.-Cryst. English Transl. **9**, 76 (1964).
30. O. KNOP and J. M. HARTLEY. Can. J. Chem. **46**, 1446 (1968).
31. J. L. WARING and S. J. SCHNEIDER. J. Res. Natl. Bur. Std. A, **69**, 255 (1965).
32. F. QUEYROUX, A. HARARI, and R. COLLONGUES. Bull. Soc. Franc. Ceram. [72], 37 (1966).
33. E. ALESHIN and R. ROY. J. Am. Ceram. Soc. **45**, 18 (1962).
34. E. ALESHIN. M.Sc. Thesis. The Pennsylvania State University, State College, Pennsylvania. 1959.
35. SUTARNO, O. KNOP, and K. I. G. REID. Can. J. Chem. **45**, 1391 (1967).
36. W. C. HAMILTON. Acta Cryst. **18**, 502 (1965).
37. O. KNOP, F. BRISSE, R. E. MEADS, and J. BAINBRIDGE. Can. J. Chem. **46**, 3829 (1968).
38. M. G. PATON and E. N. MASLEN. Acta Cryst. **19**, 679 (1965).
39. A. PABST. J. Chem. Phys. **11**, 145 (1943).
40. P. COPPENS and M. EIBSCHÜTZ. Acta Cryst. **19**, 524 (1965).
41. J. WEIDENBORNER. Acta Cryst. **14**, 1051 (1961).
42. D. R. FITZWATER and R. E. RUNDLE. Z. Krist. **112**, 362 (1959).
43. H. L. YAKEL, W. C. KOHLER, E. F. BERTAUT, and E. F. FORRAT. Acta Cryst. **16**, 957 (1963).
44. S. F. BARTRAM. Inorg. Chem. **5**, 749 (1966).
45. L. A. HARRIS and H. L. YAKEL. Acta Cryst. **22**, 354 (1967).
46. R. RUTH and A. D. WADSLEY. Acta Cryst. **21**, 974 (1966).
47. W. G. MUMME and A. D. WADSLEY. Acta Cryst. **23**, 754 (1967).
48. S. GELLER. Acta Cryst. **10**, 248 (1957).
49. J. R. PETERSON and B. B. CUNNINGHAM. Inorg. Nucl. Chem. Letters, **3**, 327 (1967).
50. H. E. SWANSON and R. K. FUYAT. Natl. Bur. Std Circ. No. 539. **2**, 28 (1953).
51. M. MAREZIO. Acta Cryst. **20**, 723 (1966).
52. M. BONNEVIE SVENDSEN. Naturwiss. **45**, 542 (1958).
53. D. H. TEMPLETON and C. H. DAUBEN. J. Am. Chem. Soc. **75**, 4560 (1953).
54. L. B. ASPREY, F. H. ELLINGER, S. FRIED, and W. H. ZACHARIASEN. J. Am. Chem. Soc. **77**, 1707 (1955).
55. J. C. WALLMAN. J. Inorg. Nucl. Chem. **26**, 2053 (1964).
56. F. WEIGEL and V. SCHERER. Radiochim. Acta, **4**, 197 (1965).
57. J. L. GREEN and B. B. CUNNINGHAM. Inorg. Nucl. Chem. Letters, **3**, 343 (1967).
58. R. W. G. WYCKOFF. Crystal structures. 2nd ed. Vols. I–III. Interscience Publishers, Inc., New York. 1963–1965.
59. JUN ITO. Private communication. 1967.
60. B. J. SKINNER. Am. Mineralogist, **41**, 428 (1956).
61. R. S. ROTH and S. J. SCHNEIDER. J. Res. Natl. Bur. Std. A, **64**, 309 (1960).
62. H. R. HOEKSTRA. Inorg. Chem. **5**, 754 (1966).
63. R. D. SHANNON. Solid State Commun. **4**, 629 (1966).
64. W. RÜDORFF, H. ERFURTH, and S. KEMMLER-SACK. Z. Anorg. Allgem. Chem. **354**, 273 (1967).
65. F. BERTAUT and F. FORRAT. Compt. Rend. **244**, 96 (1957).
66. G. D. ESPINOSA. J. Chem. Phys. **37**, 2344 (1962).
67. A. E. DWIGHT, J. W. DOWNEY, and R. A. CONNER, JR. Acta Cryst. **23**, 860 (1967).
68. O. SCHOB and E. PARTHÉ. Acta Cryst. **19**, 214 (1965).
69. L. EYRING and N. C. BAENZIGER. J. Appl. Phys. **33**, 428 (1962).
70. R. L. N. SASTRY, P. N. MEHROTRA, and C. N. R. RAO. Trans. Faraday Soc. **62**, 1632 (1966).
71. R. D. SHANNON. Inorg. Chem. **6**, 1474 (1967).

Can. J. Chem. Downloaded from www.nrcresearchpress.com by 210.87.254.40 on 09/05/12
For personal use only.

Determination of the bond dissociation energy, $D(CH_3Hg—CH_3)$, by the toluene carrier method

R. J. KOMINAR[1] AND S. J. PRICE
Department of Chemistry, University of Windsor, Windsor, Ontario
Received October 11, 1968

The thermal decomposition of $Hg(CH_3)_2$ has been studied in a toluene carrier flow system over the pressure range 4.5 to 323 mm at temperatures of 422 to 527 °C. The Arrhenius equation for the pressure independent region,

$$k = 5.5 \times 10^{15} \exp(-57\,500/RT)\ s^{-1}$$

is in excellent agreement with earlier work on the fully inhibited decomposition at lower temperatures. The region of fall off of the unimolecular rate constant is in agreement with a classical Kassel calculation using $s = 16$–18, but the rate of fall off requires the use of a curve with $s = 3$, displaced five log units to the left. This is consistent with the previous results for the dissociation of ethane into two methyl radicals and is further evidence of the inability of the classical Kassel equation to represent the behavior of systems with high pre-exponential factors.

Canadian Journal of Chemistry, 47, 991 (1969

Can. J. Chem. Downloaded from www.nrcresearchpress.com by 210.87.254.42 on 09/05/12
For personal use only.

Introduction

The available high pressure Arrhenius parameters for the pyrolysis of dimethylmercury in the presence of suitable inhibitors are in reasonable agreement (1–4). The results of Russell and Bernstein (1), $k = 5.0 \times 10^{15} \exp(-57\,900/RT)\ s^{-1}$, and of Kallend and Purnell (2), $k = 5.0 \times 10^{15} \exp(-57\,600/RT)\ s^{-1}$ are in excellent agreement. However, Weston and Seltzer (3) report $k = 7.0 \times 10^{16} \exp(-61\,200/RT)\ s^{-1}$ and a previous benzene carrier study from this laboratory (4) gave $k = 6.3 \times 10^{14} \exp(-53\,700/RT)\ s^{-1}$. The results of Weston and Seltzer cover approximately the same temperature range as those of Russell and Bernstein and the actual rate constants, particularly at higher decompositions, are in good agreement. The benzene carrier work represented an attempt to extend the data on the fully inhibited high pressure decomposition to considerably higher temperatures. An extrapolation of the Arrhenius plot obtained by combining the results of Russell and Bernstein and of Kallend and Purnell indicated that the benzene carrier results are in excellent agreement with those studies at high decomposition, but become progressively poorer with decreasing conversion. This may indicate that benzene was not a sufficiently effective scavenger. A reinvestigation using toluene as carrier has therefore been carried out.

[1]Present address: Division of Pure Chemistry, National Research Council, Ottawa, Canada.

Experimental

Materials

(*a*) Dimethylmercury was prepared by adding methyl magnesium iodide to an ether slurry of mercuric chloride (4).

(*b*) Toluene from sulfonic acid (Eastman Organic X325) was prepared for use by refluxing over sodium under vacuum for 24 h and then degassing twice by bulb-to-bulb distillation.

Apparatus and Procedure

The experiments were carried out using the same system previously used in studying the decomposition of dimethylmercury in a benzene carrier (4). The gaseous products were analyzed using a Perkin–Elmer 154 gas chromatograph equipped with a $\frac{1}{4}$ in. × 6 in. silica gel column. The column was maintained at 80 °C and a helium flow rate of 20 cc/min was used.

The liquid products condensed along with the toluene in an acetone–dry ice trap were analyzed using a P.E. model 800 gas chromatograph equipped with a 150 ft × 0.02 in. inside diameter Golay Column coated with poly(propylene glycol) (isothermal operation at 50 °C, inlet pressure of N_2 carrier is 7 lb).

Results and Discussion

The thermal decomposition of $Hg(CH_3)_2$ has been studied over the temperature range 422–554 °C at pressures of 111–318 mm, and 507–580 °C at 4.5 mm.

The major processes occurring in the thermal decomposition of dimethylmercury in a toluene carrier system may be represented by the following mechanism

[1] $$Hg(CH_3)_2 \rightarrow CH_3^{\cdot} + HgCH_3^{\cdot}$$

[2] $$HgCH_3^{\cdot} \rightarrow Hg + CH_3^{\cdot}$$

TABLE I

P (mm)	T (°K)	Time* (min)	Toluene (g)	Toluene/alkyl (molar ratio)	Concentration of products (moles × 10^5) Alkyl	CH_4	C_2H_6†	Ethyl benzene	Xylenes‡	t_c (s)	log k (s^{-1})
111	777.0	5,20,5	7.84	205	27.8	46.38	0.82	4.2	0.8	8.29	−0.370
111	750.1	5,15,5	4.67	30	100.3	108.05	3.48	15.3	1.4	12.07	−1.036
112	744.0	3,15,3	5.56	146	29.6	26.38	0.45	1.7	0.3	8.58	−1.088
110	733.0	3,15,3	5.01	73	53.2	31.92	0.67	2.9	0.3	7.29	−1.353
108	734.2	5,15,5	5.16	40	83.3	47.48	1.11	6.5	0.8	10.83	−1.400
109	714.7	5,15,5	5.67	44	84.1	18.69	0.39	1.8	0.9	10.19	−1.849
112	714.5	5,15,5	5.79	47	79.4	19.18	0.41	1.7	0.4	10.21	−1.868
111	695.1	5,20,5	7.01	53	94.9	7.9	0.12	0.5	0.3	10.38	−2.324
201	776.8	5,20,5	17.40	125	100.7	166.01	2.95	15.6	2.6	6.74	−0.364
205	776.8	5,15,5	14.98	146	66.6	110.90	1.80	7.7	1.7	6.65	−0.396
209	754.1	7,15,3	14.02	37	244.3	245.60	4.94	30.7	3.4	7.46	−0.907
206	753.6	7,15,4	14.25	37	240.9	240.92	7.67	31.9	3.0	7.53	−0.896
211	751.4	5,15,5	12.85	37	227.7	232.80	5.28	26.6	2.9	8.25	−0.942
207	743.9	3,10,3	9.32	125	50.8	42.99	0.59	1.3	0.4	7.21	−1.084
201	733.0	3,10,3	9.11	105	58.7	32.91	0.43	1.8	0.3	7.29	−1.297
208	732.9	7,15,3	13.68	36	245.7	118.90	2.55	13.5	1.4	7.84	−1.396
209	732.8	7,15,3	13.72	38	232.3	115.06	2.50	11.8	1.3	7.86	−1.368
205	714.0	7,15,3	13.52	37	239.8	50.08	0.81	4.0	0.5	8.03	−1.802
209	713.8	7,15,3	13.97	41	219.2	43.43	0.61	3.3	0.7	7.94	−1.826
203	712.0	5,10,5	11.61	126	49.9	10.73	0.12	0.5	—	7.44	−1.784
192	697.2	3,15,3	11.38	128	68.8	6.41	0.11	0.2	0.3	7.67	−2.143
330	755.2	7,10,3	18.15	58	170.0	183.10	5.00	15.8	3.4	7.29	−0.863
317	754.7	7,10,3	17.48	49	191.4	217.77	7.59	22.8	3.8	7.27	−0.796
319	742.3	5,09,3	15.60	191	46.9	39.27	0.61	1.8	0.5	7.09	−1.084
316	735.0	7,15,3	22.03	69	211.1	97.00	2.66	9.4	1.8	7.38	−1.256
315	734.9	7,10,3	17.60	53	178.5	101.18	2.86	8.9	1.8	7.37	−1.260
308	733.2	3,09,3	13.20	103	83.3	46.58	0.57	2.2	0.4	7.21	−1.308
313	714.8	7,15,3	21.75	91	154.9	36.09	0.77	1.8	0.6	7.61	−1.739
315	714.1	7,15,3	21.93	95	150.7	34.66	0.86	1.6	0.8	7.60	−1.739
306	712.0	3,09,3	13.15	159	54.0	11.42	0.11	0.2	—	7.41	−1.791
321	698.7	7,20,3	27.31	123	159.5	13.18	0.31	0.4	0.5	7.64	−2.218
323	698.7	7,20,3	26.91	122	159.4	15.56	0.35	0.3	—	7.78	−2.147

*Prerun, duration of alkyl flow, post run.
†C_2H_4 and C_3H_8 negligible in all runs.
‡Ethyl toluenes, propyl benzenes, and styrene negligible in all runs.

[3] $CH_3^{\cdot} + C_6H_5CH_3 \rightarrow CH_4 + C_6H_5CH_2^{\cdot}$

[4] $2CH_3^{\cdot} \rightarrow C_2H_6$

[5] $2C_6H_5CH_2^{\cdot} \rightarrow$ dibenzyl

[6] $CH_3^{\cdot} + C_6H_5CH_2^{\cdot} \rightarrow C_6H_5C_2H_5$

plus other minor reactions including

[7] $CH_3^{\cdot} + C_2H_6 \rightarrow CH_4 + C_2H_5^{\cdot}$

[8] $C_2H_5^{\cdot} \rightarrow C_2H_4 + H^{\cdot}$

[9] $CH_3^{\cdot} + C_2H_5^{\cdot} \rightarrow C_3H_8$

[10] $C_6H_5CH_2^{\cdot} + C_2H_5^{\cdot} \rightarrow C_6H_5CH_2CH_2CH_3$

and reactions analogous to reactions [3], [5], [6], and [10] resulting from ring abstraction.

The results obtained above 100 mm are shown in Table I. Rate coefficients were calculated from the usual first order equation, $k = 2.3/t_c \log (a/a - x)$. Under the experimental conditions used, the only minor reactions of any importance are those leading to the formation of xylenes. The extent of decomposition was therefore calculated from

$$\text{fraction decomposed} = \frac{\frac{1}{2}\,\text{moles}\,(CH_4 + C_6H_5C_2H_5 + \text{xylenes}) + \text{moles}\ C_2H_6}{\text{moles}\ Hg(CH_3)_2}$$

The first-order rate coefficients are approximately independent of pressure above 100 mm. At any given temperature the values at 318, 206, and 111 mm agree within ±8%. The least mean squares equation obtained using the rate data at these three pressures is $k = 5.5 \times 10^{15}$ exp

Can. J. Chem. Downloaded from www.nrcresearchpress.com by 210.87.254.42 on 09/05/12
For personal use only.

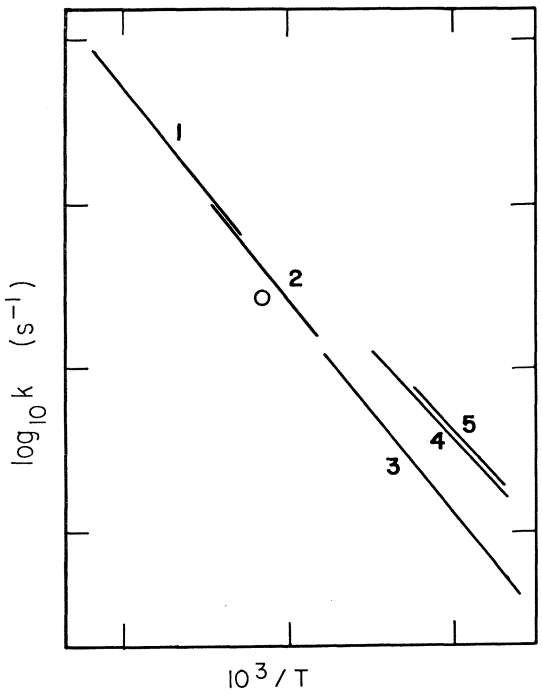

FIG. 1. Arrhenius plots for the decomposition of dimethylmercury. All rate constants are at or near the high pressure limit. If a radical scavenger has been used it is shown in brackets: 1, this work (toluene); 2, Kallend and Purnell (propylene); 3, Russell and Bernstein (cyclopentane); 4, Russell and Bernstein; 5, Laurie and Long; O, point calculated from steady state equation of Kallend and Purnell.

$(-57\,500/RT)\,s^{-1}$ (422–527 °C). This result should represent the fully inhibited decomposition and should be a good approximation to k_∞, the rate constant at infinite pressure.

It is compared with previous work in Fig. 1. The agreement with the work of Russell and Bernstein and of Kallend and Purnell is excellent.

Curves 4 (1) and 5 (5) in Fig. 1 represent studies on the decomposition of $Hg(CH_3)_2$ in uninhibited systems. The uninhibited decomposition is faster than the fully inhibited decomposition by a factor of 5 to 15. Russell and Bernstein (1) propose short chain processes, while work by Laurie and Long (5, 6) and Cattanach and Long (7) seems to contradict this. At the present time, no mechanism has been proposed for the uninhibited decomposition that can explain all the observed facts. It is possible that surface reactions either chain, nonchain, or a mixture of both, play a significant role.

Taking $\Delta H_f^\circ{}_{298}(CH_3,g) = 33.2$ kcal mole^{-1} (8), $\Delta H_f^\circ{}_{298}(Hg,g) = 14.7$ kcal mole^{-1} (9), and $\Delta H_f^\circ{}_{298}(Hg(CH_3)_2,g) = 22.4$ kcal mole^{-1} (10) gives for the reaction

$$Hg(CH_3)_2,g \rightarrow Hg,g + 2CH_3,g$$

a value of $\Delta H^\circ{}_{298} = 58.6$ kcal mole^{-1}. If this is a sufficient approximation to ΔH_0° then

$$D(CH_3Hg - CH_3) + D(Hg - CH_3) = 58.6 \text{ kcal mole}^{-1}$$

The observed Arrhenius activation energy for reaction [1] in the fully inhibited system at the high pressure limit, $E_1 = 57.5$ kcal mole^{-1}, should be within the limits $D_1 \leqslant E_1 \leqslant D_1 + 1.5$ kcal mole^{-1} (assuming E_1 contains no experimental error). This would yield $D_2 = 1.1$ to 2.6 kcal mole^{-1}. However, a conservative estimate of the accumulated experimental error in D_2 would be ± 2 kcal mole^{-1} so that although D_2 may have a small finite value, the value $D_2 = 0$ is a possibility.

The work at 4.5 mm is not primarily concerned with the pyrolysis of $Hg(CH_3)_2$ and is therefore not reported in detail here. It will appear shortly in conjunction with another study. However, some pertinent features should be noted. At the toluene/alkyl ratios used, approximately 10/1, all the minor reactions previously proposed play a significant role as well as limited pyrolysis of the ethylbenzene formed in reaction [6]. In the temperature range 507–589 °C the Arrhenius equation for the decomposition is

$$\log k = 13.6 - 51\,800/2.3RT$$

If the equation is extrapolated to 360 °C, $k = 5 \times 10^{-5}\,s^{-1}$. This is in close agreement with the results of Russell and Bernstein (1) under fully inhibited conditions, $4.5 \times 10^{-5}\,s^{-1}$, indicating that the present equation is a good approximation to that representing the fully inhibited decomposition at this pressure.

The present results for the region of fall-off of the first-order rate constant agree reasonably well with Kassel theory predictions if 17 ± 1 effective oscillators are assumed. However, the fall-off is much faster than predicted by Kassel theory with $s = 17$, due to the inadequacy of the classical theory for reactions with high frequency factors. For ethane the Rice, Ramsperger, Kassel, Marcus theory shows that the experimental data should in fact fit a classical Kassel curve with $s = 3$ when this curve is shifted 5.6 logarithmic units to the left (11). The pre-exponential factor for the

Can. J. Chem. Downloaded from www.nrcresearchpress.com by 210.87.254.42 on 09/05/12
For personal use only.

$Hg(CH_3)_2$ decomposition is of the same order of magnitude as that for the dissociation of ethane into two methyl radicals, $5.5 \times 10^{15}\ s^{-1}$ vs. $2 \times 10^{16}\ s^{-1}$ (11), and the best fit for the present data would also be obtained using classical Kassel theory if the curve for $s = 3$ shifted approximately 5 logarithmic units to the left was used.

Acknowledgment

This work has been supported by a grant from the National Research Council of Canada.

1. M. R. Russell and R. B. Bernstein. J. Chem. Phys. **30**, 607 (1959).
2. A. S. Kallend and J. H. Purnell. Trans. Faraday Soc. **60**, 103 (1964).
3. R. E. Weston and S. Seltzer. J. Chem. Phys. **66**, 2192 (1962).
4. M. Krech and S. J. Price. Can. J. Chem. **41**, 224 (1963).
5. C. M. Laurie and L. H. Long. Trans. Faraday Soc. **51**, 665 (1955).
6. L. H. Long. Trans. Faraday Soc. **51**, 673 (1955).
7. J. Cattanach and L. H. Long. Trans. Faraday Soc. **56**, 1286 (1960).
8. Selected values of chemical thermodynamic properties. Natl. Bur. Std. U.S. Tech. Note, No. 270–3. 1968.
9. Handbook of chemistry and physics. 47th ed. The Chemical Rubber Co., Cleveland, Ohio. 1966–67.
10. A. S. Carson, E. S. Carson, and B. Willmhurst. Nature, **170**, 320 (1952).
11. A. B. Trenwith. Trans. Faraday Soc. **62**, 1538 (1966).

Can. J. Chem. Downloaded from www.nrcresearchpress.com by 210.87.254.42 on 09/05/12
For personal use only.

Dimethyl and diphenyl formamide complexes of lanthanide perchlorates

S. S. KRISHNAMURTHY AND S. SOUNDARARAJAN
Department of Inorganic and Physical Chemistry, Indian Institute of Science, Bangalore 12, India

Received September 9, 1968

N,N-Dimethyl formamide (DMF) and N,N-diphenyl formamide (DPF) complexes of six lanthanide perchlorates of the composition $M(DMF)_8(ClO_4)_3$ and $M(DPF)_6(ClO_4)_3$ where M = La, Ce, Pr, Nd, Sm, or Y have been prepared and characterized. The infrared spectra show that the amide is bonded to the metal through oxygen. Conductivity, molecular weight, and spectral studies indicate coordination numbers of eight and six for DMF and DPF complexes respectively, with the perchlorate groups remaining ionic.

Canadian Journal of Chemistry, **47**, 995 (1969)

Can. J. Chem. Downloaded from www.nrcresearchpress.com by 210.87.254.42 on 09/05/12
For personal use only.

Introduction

The ligating properties of N,N-disubstituted tertiary amides have been well investigated in recent years (1–6). We had previously described the preparation and the properties of lanthanide nitrate complexes with N,N-dimethyl formamide (DMF) and inferred that the nitrato groups are covalently bound to the metal (6). It is to be expected that if the nitrate is replaced by an ion having low coordinating tendencies such as the perchlorate, the metal atom would tend to add on to itself the maximum number of organic ligands. Consequently a study of the lanthanide perchlorate complexes with DMF was undertaken. The study was extended to cover diphenyl formamide (DPF) in order to investigate the electronic and steric effects (if any) of the phenyl groups on the coordination behavior of the lanthanides.

Experimental

Materials

Dimethylformamide (E. Merck L. R. Grade), nitromethane, and nitrobenzene (both B.D.H. L. R. grade) were purified by standard methods (7).

Diphenyl formamide was prepared by formylating diphenylamine with 99% formic acid (8) (E. Merck) and recrystallizing the product from hot petroleum ether (boiling range 50–60°), m.p. 73 °C (lit. 73–74 °C (8)).

The starting materials for the rare earth complexes were the oxides (99.9% pure) obtained from Lindsay Chem. Co., U.S.A. Cerous chloride (A. R.), used for preparing Ce(III) perchlorate, was obtained from Atomic Energy Commission, India.

Preparation of the Complexes

Except for that of cerium, the rare earth perchlorates were prepared by dissolving the oxides in 60% perchloric acid (E. Merck "proanalyze" grade) and crystallizing them from water. Cerium(III) perchlorate was prepared by dissolving freshly precipitated Ce(III) hydroxide in perchloric acid in the presence of small quantities of hydrogen peroxide to reduce any Ce(IV) formed by atmospheric oxidation.

DMF Complexes

About 2–3 g of rare earth perchlorate were dissolved in 5 ml of DMF, and the excess DMF was pumped off, avoiding contamination with moisture. The complexes were left behind as glistening hygroscopic crystals. The complexes were soluble in polar solvents such as nitromethane, nitrobenzene, and acetone.

DPF Complexes

A solution of rare earth perchlorate (1 g) in A. R. acetone (3 ml) was added dropwise to a solution of 3.2 g of DPF in 5 ml acetone. The mixture was warmed to 50 °C and then cooled at 0 °C for 12 h. Since no precipitate was obtained, the solvent was pumped off and the residue dried over P_2O_5 under vacuum. The solid residue was washed 3 or 4 times with 10 ml portions of petroleum ether and then thrice with 10 ml portions of CCl_4, in order to remove the excess ligand. The complex was finally dried over P_2O_5 and analyzed.

Unlike the parent perchlorates the complexes were not hygroscopic. It was, however, found that the ligand and the complexes, when exposed to direct sunlight, were photoactive and turned green. When light exposure was minimized the complexes could be preserved without any apparent change.

Analyses

The metal content of the complexes was estimated by precipitation as oxalate and subsequent ignition to the oxide. The perchlorate determination was carried out by Kurtz's method (9). The DMF content was determined as described in an earlier publication (6). In the case of DPF complexes the carbon content in a few representative cases was determined by using a conventional semimicro combustion apparatus. The analytical data are summarized in Table I.

Conductivity Measurements

The molar conductance of the complexes in DMF, nitromethane, and nitrobenzene solutions was determined in a Siemen's conductivity bridge at 30 °C, using an immersion cell (Type LTA) previously calibrated with standard KCl solutions. The data are presented in Table II.

Molecular Weight Measurements

The molecular weights of the DMF complexes in water and nitrobenzene and those of DPF complexes in nitrobenzene were determined by the freezing point method.

TABLE I

Analytical data for Ln perchlorate complexes with DMF and DPF

Compound	Found (%)			Calculated (%)		
	Metal	Perchlorate	DMF	Metal	Perchlorate	DMF
$La(DMF)_8(ClO_4)_3$	13.85	29.70	57.71	13.60	29.2	57.23
$Ce(DMF)_8(ClO_4)_3$	14.05	29.60	57.00	13.70	29.18	57.10
$Pr(DMF)_8(ClO_4)_3$	13.71	28.91	56.30	13.76	29.14	57.10
$Nd(DMF)_8(ClO_4)_3$	14.09	29.38	55.90	14.05	29.05	56.90
$Sm(DMF)_8(ClO_4)_3$	14.50	28.77	55.80	14.54	28.85	56.70
$Y(DMF)_8(ClO_4)_3$	9.23	30.30	59.60	9.15	30.70	60.15
$La(DPF)_6(ClO_4)_3$	8.73	19.00	57.3*	8.57	18.41	57.80*
$Ce(DPF)_6(ClO_4)_3$	8.50	18.38	—	8.65	18.40	—
$Pr(DPF)_6(ClO_4)_3$	8.58	18.60	—	8.71	18.38	—
$Nd(DPF)_6(ClO_4)_3$	9.00	18.71	—	8.88	18.35	—
$Sm(DPF)_6(ClO_4)_3$	9.03	18.01	—	9.22	18.28	—
$Y(DPF)_6(ClO_4)_3$	5.60	18.72	59.10*	5.66	19.00	59.63*

*The values refer to the percentage of carbon.

While using nitrobenzene as the solvent, a mercury seal stirrer was employed to exclude moisture. The data are tabulated in Table II.

Infrared Spectra

The infrared (i.r.) spectra of the complexes were recorded in Nujol mulls and KCl pellets employing a Carl–Zeiss UR-10 automatic infrared spectrophotometer. Some of the spectra were also recorded on a Perkin–Elmer Infracord. The principal absorption peaks and their assignments are shown in Table III.

Results and Discussion

The analytical data show that the DMF complexes have the formula $M(DMF)_8(ClO_4)_3$ where M = La, Ce, Pr, Nd, Sm, or Y. The corresponding DPF complexes analyze for the composition $M(DPF)_6(ClO_4)_3$ (Table I).

The conductivities of all the complexes in DMF, nitromethene, and nitrobenzene lie in the range expected for 1:3 electrolytes (Table II). This suggests that the perchlorate groups are not covalently bound to the metal. In nitrobenzene the complexes are dissociated into 4 species as shown by molecular weight data (Table II), confirming the ionic nature of the perchlorate. The molecular weight data for DMF complexes in water reveal the presence of 12 species (Table II) implying that the complex breaks down into its components in water.

The i.r. spectra of the complexes with the same ligand are very similar, exhibiting no significant dependence on the nature of the metal. The highest frequencies at 1650 and 1645 cm^{-1} in the spectra of DMF and DPF complexes respectively are attributed to carbonyl stretching vibrations. These are about 30 and 35 cm^{-1} lower than the carbonyl frequencies in the free amides (Table III). The decrease in carbonyl frequency suggests coordination through oxygen (2, 6).

There is considerable confusion in the literature regarding the assignment of ν(C—N) frequency in DMF and its complexes (14). While Randall *et al.* (14) opine that either 1389 or 1255 cm^{-1} band is to be attributed to ν(C—N), a recent normal coordinate treatment (15) shows that the 1499 band must be ν(C—N). Randall *et al.* (14) have also pointed out that in DMF complexes, shifts of ν(C=O) to lower frequencies are accompanied by shifts to lower frequencies of the two bands 1389 and 1255 cm^{-1}, one of which must be ν(C—N). Perhaps the group frequency approximation is inadmissible here due to some coupling of ν(C—N) and ν′(C—N) with ν(C=O) (14). However, the 1680 cm^{-1} band has been shown to be essentially due to C=O stretching vibration with very little contribution from C—N stretch (15). Table III shows the best possible assignment in the light of available literature data on the spectra of tertiary amides and their complexes.

The shifts in the case of DPF complexes compared with the free ligand are slightly greater than the corresponding shifts in the spectra of DMF complexes. This suggests that the phenyl groups on the nitrogen increase the basicity of the carbonyl. It is likely that the larger shifts observed in DPF complexes are due to the greater extent of delocalization of the positive charge on nitrogen arising from the flow of the electrons from the carbonyl to the metal. This is

Can. J. Chem. Downloaded from www.nrcresearchpress.com by 210.87.254.42 on 09/05/12
For personal use only.

Can. J. Chem. Downloaded from www.nrcresearchpress.com by 210.87.254.42 on 09/05/12
For personal use only.

TABLE II

Conductivity and molecular weight data for Ln perchlorate complexes with DMF and DPF*

	DMF complexes				DPF complexes		
Metal	λ_m in $MeNO_2$† (Ω^{-1} cm^2 mole^{-1})	λ_m in DMF‡ (Ω^{-1} cm^{-2} mole^{-1})	Mol. wt. in $PhNO_2$	Mol. wt. in water	λ_m in $MeNO_2$ (Ω^{-1} cm^2 mole^{-1})	λ_m in $PhNO_2$§ (Ω^{-1} cm^2 mole^{-1})	Mol. wt. in $PhNO_2$
La	208.5	210.6	269	84.0	210.2	74.8	420
Ce	207.6	208.7	—	—	208.6	73.1	—
Pr	205.2	215.3	—	—	209.0	74.2	—
Nd	210.4	210.4	265	83.5	205.2	75.6	424
Sm	202.6	206.3	—	—	207.8	79.1	—
Y	200.8	204.7	261	80.1	204.6	73.0	402

*All conductivity measurements were carried out using solutions of concentration 0.001 *M*.

†In nitromethane, 1:1 electrolytes have a molar conductance in the range 80–100 Ω^{-1} cm^2 mole^{-1} (10, 11); 2:1 electrolytes have λ_m in the range 140–160 (11). It can be expected that 3:1 electrolytes will show a molar conductance around 210 in $MeNO_2$.

‡In DMF, the molar conductance of 1:1, 2:1, and 3:1 electrolytes are 85–100, 140–170, and 200–260 Ω^{-1} cm^2 mole^{-1}, respectively (12).

§In nitrobenzene, 1:1 electrolytes exhibit λ_m values in the range 25–35 and 2:1 electrolytes around 45–60. From these values it is reasonable to anticipate a value around 80 for 3:1 electrolytes (13).

TABLE III

The principal absorption maxima in the infrared spectra* of DMF and DPF complexes of Ln perchlorates

DMF	DMF complex	DPF	DPF complex	Assignment	Reference
1680 (vs)	1650 (vs)	1681 (vs)	1645 (vs)	ν(C═O)	1, 6, 15
1498 (m)	1502 (w)	—	—	ν(C—N) ?	15
1382 (s)	1388 (s)	1375 (w)	1372 (s)	ν(C—N)	1, 14
1255 (s)	1250 (m)	1333 (m)	1350 (m)		
		1323 (m)			
—	1152 (s, sh)		1100 (s)	$\nu_3(ClO_4^-)$	18, 19
	1122 (s)	—			
	1092 (s)				
—	932 (w)	—	—	$\nu_1(ClO_4^-)$	18, 19
660 (s)	675 (s)	—	—	NCO bending	3
—	625 (s)		625 (m)	$\nu_4(ClO_4^-)$	18, 19
	635 (sh, m)				

*vs, very strong; s, strong; m, medium; w, weak; sh, shoulder; wavenumber in cm^{-1}.

borne out by the perturbations of the aromatic ring vibrations. The phenyl band at 1602 cm^{-1} in the free amide, shifts to 1590 cm^{-1} in the complexes with enhanced intensity. An increased resonance involving electrons of the carbonyl and phenyl groups can account for this behavior (16). Further as in the case of the N,N-diphenylacetamide (DPA) complex with BCl_3 (17), the C—H out of plane deformations appear as doublets at 766 and 758 cm^{-1} (free DPF) and at 764 and 749 cm^{-1} (complex). This has been interpreted as implying double bond character in the C—N bond of (—CO.N<) in both the amide and the complex, and would thus be consistent with oxygen coordination.

The i.r. spectra also throw light on the nature of the perchlorate groups in the complexes. In the DPF complexes the ν_3 and the ν_4 bands of the perchlorate ion (18) at 1100 and 625 cm^{-1} respectively, are sharp and unsplit indicating retention of the T_d symmetry for the ion.

In the case of DMF complexes, however, the ν_3 band at 1096 cm^{-1} undergoes splitting. There seems to be a strong interaction between this perchlorate mode and the ligand vibration appearing around 1120 cm^{-1}. Actually a triplet is observed in this region (Table III). The ν_4 band is also split except in the case of Ce complex. The splitting of both ν_3 and ν_4 bands definitely indicates the loss of T_d symmetry of the perchlorate ion. The possible causes (19) for such a lowering of symmetry are (*a*) a covalent bonding of the perchlorate ion to the metal through one or two of its oxygen atoms, (*b*) a non-uniform field due to the ligand molecules round the cation, and (*c*) distortion of the perchlorate tetrahedron in the crystal lattice. If the observed splittings were the result of covalent bonding of the perchlorate, then both ν_1 and ν_2 must become i.r. active. These frequencies are not observed in the spectra except for a weak kink at 930 cm^{-1} attributable to ν_1 mode. Hathaway and Underhill (18) have shown that ν_1 at 930 cm^{-1} can appear for complexes with ionic perchlorate due to distortion of the ion by the crystal lattice. Also, Moeller and Vicentini (25) reported a splitting of the ν_3 band for the N,N-DMA complexes of lanthanide perchlorates in KBr pellets. Further, the known instability of the covalent perchlorate complexes (20), the very few instances of their occurrence (21, 22), and the completely altered spectrum of the covalent perchlorates (22) rule out the possibility of covalent bonding of the perchlorate in DMF complexes of the present study. While the effect of coordination of the perchlorate must be to bring about major differences in the i.r. spectra, minor shifts or splittings such as those observed may result from the other two causes listed above. The i.r. spectra thus confirm the non-coordinating nature of the perchlorate groups in the complexes.

With the perchlorate groups remaining ionic, it emerges that the coordination number of the rare earth ion is eight and six in DMF and DPF complexes respectively. The difference in behavior is attributable to steric considerations. The bulkier phenyl groups in DPF preclude the close approach of more than six ligand molecules

Can. J. Chem. Downloaded from www.nrcresearchpress.com by 210.87.254.42 on 09/05/12
For personal use only.

to the metal. The effect of ligand size in lowering the coordination number of rare earths is also reflected in the decrease of coordination number from eight in DMSO complexes (23) to six in analogous diphenyl sulfoxide complexes (24).

Acknowledgment

The authors thank Professor M. R. A. Rao for his kind interest and encouragement. One of the authors (S.S.K.) thanks University Grants Commission (India) for a fellowship during the course of this investigation.

1. J. ARCHAMBAULT and R. RIVEST. Can. J. Chem. **38**, 1331 (1960).
2. W. E. BULL, S. K. MADAN, and J. E. WILLIS. Inorg. Chem. **2**, 303 (1963).
3. M. A. JUNGBAUER and C. CURRAN. Nature, **202**, 290 (1964).
4. G. VICENTINI and E. DE CARVALHO FILHO. J. Inorg. Nucl. Chem. **28**, 2987 (1966).
5. K. W. BAGNALL, D. BROWN, and P. J. JONES. J. Chem. Soc. A, 1763 (1966).
6. S. S. KRISHNAMURTHY and S. SOUNDARARAJAN. J. Inorg. Nucl. Chem. **28**, 1689 (1966); and references therein.
7. A. WEISSBERGER and E. S. PROSKAUER. Organic solvents, techniques of organic chemistry. Vol. VII. Interscience Publishers, Inc., New York. 1961.
8. H. BEILSTEIN. Handbuch der Organischen Chemie. Series IV. Vol. 12. Springer Verlag, Berlin. 1929. p. 235.
9. E. KURZ, G. KOBER, and M. BERL. Anal. Chem. **30**, 1983 (1958).
10. A. K. R. UNNI, L. ELIAS, and H. I. SCHIFF. J. Phys. Chem. **67**, 1216 (1963).
11. D. B. FOX, J. R. HALL, and R. A. PLOWMAN. Australian J. Chem. **18**, 691 (1965).
12. J. V. QUAGLIANO, J. FUJITA, G. FRANZ, D. J. PHILLIPS, J. WALMSLEY, and S. Y. TYREE. J. Am. Chem. Soc. **83**, 3770 (1961).
13. J. A. WALMSLEY and S. Y. TYREE. Inorg. Chem. **2**, 312 (1963).
14. E. W. RANDALL, C. N. SILCOX YODER, and J. J. ZUCKERMAN. Inorg. Chem. **5** (12), 2240 (1966).
15. V. VENKATACHALAPATHI and K. VENKATARAMIAH. Proc. Indian Acad. Sci. Sect. A, **58**, 109 (1968).
16. (*a*) L. J. BELLAMY. The infrared spectra of complex molecules. John Wiley and Sons, Inc., New York. 1958. pp. 60–63.
(*b*) B. P. SUZS and P. CHALANDON. Hel. Chim. Acta, **41**, 1332 (1958).
17. W. GERRARD, M. F. LAPPERT, H. PYSZOVA, and J. W. WALLIS. J. Chem. Soc. 2144 (1960).
18. B. J. HATHAWAY and A. E. UNDERHILL. J. Chem. Soc. 309 (1961).
19. S. D. ROSS. Spectrochim. Acta, **18**, 225 (1962).
20. J. MAYER and W. SPORMANN. Z. Anorg. Allgem. Chem. **228**, 34 (1936).
21. A. S. WICKENDEN and R. A. KRAUSE. Inorg. Chem. **4**, 404 (1965).
22. F. A. COTTON and D. L. WEAVER. J. Am. Chem. Soc. **87**, 4189 (1965).
23. V. N. KRISHNAMURTHY and S. SOUNDARARAJAN. J. Inorg. Nucl. Chem. **29**, 517 (1967).
24. S. K. RAMALINGAM and S. SOUNDARARAJAN. Bull. Chem. Soc. Japan, **41**, 106 (1968).
25. T. MOELLER and G. VICENTINI. J. Inorg. Nucl. Chem. **27**, 1477 (1965).

Can. J. Chem. Downloaded from www.nrcresearchpress.com by 210.87.254.42 on 09/05/12
For personal use only.

Theoretical considerations bearing on the evaluation and interpretation of the dielectric behavior of physically adsorbed polar gases[1]

T. McMullen[2] and R. McIntosh
Department of Chemistry, Queen's University, Kingston, Ontario
Received May 22, 1968

This paper consists of Part I and Part II. Part I contains a discussion of the evaluation of the dielectric constant of an adsorbed phase for a system which contains a small volume fraction of adsorbing solid. The method is similar to one employed earlier, but treats the case of spherical particles rather than spherical voids and employs the volume average macroscopic field of a phase rather than the volume average internal field. Part II contains the application of the correlation function method of Kubo to the assignment of the macroscopic dielectric properties of the adsorbed phase. The correlation function is developed for a system of rigid harmonic oscillators and used to establish the formulae for the static polarization and the resonance behavior of such a system. The results agree with earlier derivations by Kurbatov, by Benson, Channen, and McIntosh, and by Fröhlich.

Canadian Journal of Chemistry, **47**, 1001 (1969)

Can. J. Chem. Downloaded from www.nrcresearchpress.com by 210.87.254.5 on 09/05/12
For personal use only.

Introduction

Many authors have reported the results of measurements of dielectric constant and loss of adsorbent–adsorbate systems (1). These measurements should provide a good deal of information about the structure of the adsorbed layer, since the dielectric behavior depends upon the interactions of an adsorbed molecule with its neighbors, and with the surface on which it lies. Unfortunately, the heterogeneous dielectric composed of the solid, adsorbed phase, and gas phase, is not easily treated theoretically, so that although the dielectric behavior of liquids and solids is in principle well understood, the same cannot be said for adsorbent–adsorbate systems. Consequently, many investigators have restricted themselves to qualitative interpretations of dielectric isotherms, and have emphasized features such as changes in the rate of increase of the dielectric constant of the overall system with amount adsorbed between points on a single isotherm, and the temperature coefficients of these slopes. Other investigators have used other methods of comparing dielectric isotherms of different adsorbates. A recent and interesting approach is discussed by Gröbner (2).

Any attempt at comparison of different adsorbates must encounter the obstacle which prevents proper interpretation of the dielectric behavior of any particular adsorbent–adsorbate system. The polarization of an adsorbed molecule depends on two factors: its net polarizability at the appropriate frequency, and the electric field at its location in the sample. This field is not generally the same as the external applied field. The experimentally measured quantity is essentially the total polarization of the sample, or more precisely the ratio of this quantity to the magnitude of the applied field. One wishes to obtain from this measurement the polarizability of an adsorbate molecule, which contains the useful information about the structure of the adsorbed layer. In the case of a homogeneous sample of solid or liquid, a model is assumed, and the macroscopic response of the system to the applied field is calculated in terms of molecular properties. However, a similar approach to heterogeneous dielectrics of the type at present employed in adsorption studies is considerably more difficult, and has not yet been attempted.

Several methods to establish approximate solutions have been tried, and these are reviewed by McIntosh (1). One which has been reasonably successful, and has some theoretical basis, is the extension of the Böttcher powder treatment (3, 4) by McIntosh and his associates (5, 6). These authors assume that a dielectric constant can be assigned to the adsorbed phase, and in the case of porous adsorbents, they obtain values for the adsorbates which appear reasonable when compared with liquid state values. However, there is reason to believe that their model is not applicable to powdered adsorbents of low packing fraction, since their method has been found to assign negative dielectric constants to the adsorbed phase

[1]Based on a thesis by T. McMullen which was presented in partial fulfilment of the requirements of the Ph.D. degree.

[2]Present address: H. H. Wills Laboratory, Department of Physics, Bristol University, Bristol, England.

Can. J. Chem. Downloaded from www.nrcresearchpress.com by 210.87.254.5 on 09/05/12
For personal use only.

when applied to the results of some recent measurements employing hydrogen and ethyl chlorides adsorbed on nonporous sodium chloride (7).

Because of the complexity of the problem, the retention of the assumption that a dielectric constant can be assigned to the adsorbed phase is attractive. This permits separation into two independent problems: the evaluation of this dielectric constant from experimental data, and, also, the interpretation of its behavior in terms of molecular properties. Consequently, in the first part of the present paper, we describe a modification of the extended Böttcher powder treatment which does appear to be applicable to powder samples with a low volume fraction of solid. In the second part, we show how the approach of Cole (8) can be modified in order to interpret the dielectric constant of the adsorbed phase which, by the above assumption, may now be considered to be a "two-dimensional" liquid (or gas) in an external potential which is chosen to represent the effect of the solid surface. No other property of the actual sample, such as its geometry, need be included. The "rotational oscillator model" of Kurbatov (9) and of Benson, Channen, and McIntosh (10) is considered explicitly, and the results of these authors are rederived by the correlation function method, which permits somewhat easier physical interpretation. In addition, the relaxation behavior of the model is discussed.

Part I
The Extended Böttcher Powder Treatment

Consider a sample of dielectric containing several distinct phases, each denoted by an index k. The polarization of this sample is

$$[1] \qquad \boldsymbol{P} = \boldsymbol{M}/V$$

with $\boldsymbol{M}$ the total moment, and V the volume. Because of the inhomogeneity of the sample, the polarization at any point is not a constant throughout, but may nevertheless be defined as

$$[2] \qquad \boldsymbol{P}(\boldsymbol{x}) = \Delta\boldsymbol{M}(\boldsymbol{x})/\Delta V(\boldsymbol{x})$$

where $\Delta\boldsymbol{M}(\boldsymbol{x})$ is the moment of a microscopically large, macroscopically small volume ΔV not including a phase boundary situated around a position defined by the position vector $\boldsymbol{x}$. With this definition, $\boldsymbol{P}(\boldsymbol{x})$ is continuous within a phase. Furthermore, we have

$$[3] \qquad \boldsymbol{P} = \frac{1}{V}\int_V \mathrm{d}^3x\, \boldsymbol{P}(\boldsymbol{x}) = \sum_k \frac{V_k}{V}\cdot\frac{1}{V_k}\cdot\int_{V_k} \mathrm{d}^3x\, \boldsymbol{P}(\boldsymbol{x})$$

which may be rewritten as

$$[4] \qquad \langle\boldsymbol{P}\rangle = \sum_k \delta_k\langle\boldsymbol{P}\rangle_k$$

where δ_k is the volume fraction of the kth phase, $\langle\rangle_k$ represents a volume average over the kth phase, and $\langle\rangle$, a volume average over the entire sample.

The macroscopic electric field may also be written as a volume average

$$[5] \qquad \boldsymbol{E}(\boldsymbol{x}) = 1/\Delta V\int_{\Delta V} \mathrm{d}^3x'\, \boldsymbol{F}(\boldsymbol{x}')$$

where $\boldsymbol{F}(\boldsymbol{x}')$ is the internal, or microscopic, field at the point $\boldsymbol{x}'$. In the same way, then

$$[6] \qquad \langle\boldsymbol{E}\rangle = \sum_k \delta_k\langle\boldsymbol{E}\rangle_k$$

which, from [5], is identical to

$$[7] \qquad \langle\boldsymbol{F}\rangle = \sum_k \delta_k\langle\boldsymbol{F}\rangle_k$$

McIntosh and co-workers (5, 6) consider a medium, the adsorbent, which contain spherical inclusions, and adsorption occurs on the walls of these interstices. For powder samples of low packing fraction, however, a model in which the solid is considered to be composed of spherical particles, seems preferable. (This may, for convenience, be called the "spherical particle model", and the former the "spherical void model".) The reason for this is that in the development, it is necessary to assume that the volume average field in the non-spherical region (whether it is the gas or the solid phase) remains constant on adsorption, and this is probably more nearly true for the phase occupying the largest volume.

Let the solid, adsorbed phase, and gas phase be denoted by the subscripts 1, 2, and 3 respectively. The average polarization is then written in terms of an average or overall dielectric constant ε found from the experimental data, so that [4] becomes

$$[8] \qquad \frac{\varepsilon - 1}{4\pi}\langle\boldsymbol{E}\rangle = \sum_k \delta_k\langle\boldsymbol{P}\rangle_k$$

Previous authors have used [7] as a second relation, and expressed the internal fields in terms of the macroscopic fields by the Lorentz relation. The same result is obtained for the

Can. J. Chem. Downloaded from www.nrcresearchpress.com by 210.87.254.5 on 09/05/12
For personal use only.

spherical particle model if [6] is employed instead of [7]; this makes it unnecessary to assume the Lorentz field.

If the polarization of the kth phase is written

$$[9] \qquad \langle \boldsymbol{P} \rangle_k = \chi_k \langle \boldsymbol{E} \rangle_k = \frac{\varepsilon_k - 1}{4\pi} \langle \boldsymbol{E} \rangle_k$$

we have, in the case of no adsorption:

$$[10] \qquad \frac{\varepsilon_0 - 1}{4\pi} \langle \boldsymbol{E} \rangle = \delta_1 \chi_1 \langle \boldsymbol{E} \rangle_1{}^0$$

$$[11] \qquad \langle \boldsymbol{E} \rangle = \delta_1 \langle \boldsymbol{E} \rangle_1{}^0 + (1 - \delta_1) \langle \boldsymbol{E} \rangle_3{}^0$$

where ε_0 is the overall dielectric constant of the powder sample without adsorbate, and the superscript zero indicates that $\delta_2 = 0$. Now $\langle \boldsymbol{E} \rangle_3$ is assumed to be unchanged on adsorption, so that

$$[12] \qquad \langle \boldsymbol{E} \rangle_3 = \frac{\langle \boldsymbol{E} \rangle}{1 - \delta_1} \left[1 - \frac{\varepsilon_0 - 1}{4\pi\chi_1} \right]$$

Considering the particles to be spherical and embedded in a medium of dielectric constant ε,

$$[13] \qquad \langle \boldsymbol{E} \rangle_1 = \frac{3\varepsilon}{2\varepsilon + \varepsilon_1} \langle \boldsymbol{E} \rangle$$

so that, from [4] and [9], one has

$$[14] \qquad \delta_2 \chi_2 \langle \boldsymbol{E} \rangle_2 = \frac{\varepsilon - 1}{4\pi} \langle \boldsymbol{E} \rangle - \delta_1 \chi_1 \frac{3\varepsilon}{2\varepsilon + \varepsilon_1} \langle \boldsymbol{E} \rangle$$

if ε_3 is assumed to be unity. Also [6] then becomes

$$[15] \qquad \delta_2 \langle \boldsymbol{E} \rangle_2 = \langle \boldsymbol{E} \rangle - \delta_1 \frac{3\varepsilon}{2\varepsilon + \varepsilon_1} \langle \boldsymbol{E} \rangle - \frac{\delta_3 \langle \boldsymbol{E} \rangle}{1 - \delta_1} \left[1 - \frac{\varepsilon_0 - 1}{4\pi\chi_1} \right]$$

Division yields an expression for χ_2, which is related to the complex dielectric constant ε_2 by [9]. A solution employing [7] instead of [6] yields an identical result for this model; this is not the case, however, if the "spherical void" model is used.

The spherical particle model has been used to determine the dielectric constant of butane adsorbed on sodium chloride (7), where $\delta_1 \simeq 0.1$ and δ_2 was calculated from the liquid state density. Good agreement with the liquid state dielectric constant indicates that the method is applicable, at least for adsorbates of low dielectric constant. Also, reasonable values for the dielectric constants of hydrogen and ethyl chlorides on sodium chloride were found, in contrast to the negative dielectric constants found from the spherical void model of McIntosh and his associates.

Part II
The Rotational Oscillator

If a dielectric constant is assigned to an adsorbed phase by a method similar to that described in the preceding section, the behavior should then be interpreted in terms of molecular properties. The adsorbed phase was considered in the development given in Part I to have the liquid state density. However, the intermolecular interactions are not as in the liquid, but, at least in the case of a gas-like film, are weakened by the increased distances between adsorbed molecules. In the treatment of the adsorbed film which follows, the most general and powerful approach to dielectric theory now available is applied. It is the adaptation of the correlation function method of Kubo (11, 12) by Glarum (13), and Cole (8).

Consider as a model of an adsorbate molecule the description given by Cole, in which each of the N molecules is assumed to have a permanent moment $\boldsymbol{\mu}$ and an induced moment represented by harmonic oscillator displacements $\boldsymbol{r}_i$ of charge e. We employ the change of origin introduced by Cole (14) in which these displacements are expressed in terms of the displacements $\boldsymbol{r}_i'$ from the equilibrium values $\boldsymbol{r}_{iE}$ in the presence of the field $\boldsymbol{E}_0$ due to external charges, so that

$$[16] \qquad e\boldsymbol{r}_i = e\boldsymbol{r}_i' + e\boldsymbol{r}_{iE}$$

and

$$[17] \qquad k\boldsymbol{r}_{iE} = e \left[\boldsymbol{E}_0(t) - \nabla_i \sum_{j \neq i} \frac{e\boldsymbol{r}_{jE} \cdot \boldsymbol{R}_{ij}}{|R_{ij}|^3} \right]$$

where k is the oscillator force constant and $\boldsymbol{R}_{ij}$ the vector separation of molecules i and j. Cole assumes cubic symmetry of the spherical sample, or an isotropic medium, so that the sum in [17] may be considered to vanish. This is not permissible in the case of a thin adsorbed film, however, and the optical polarizability of the medium must now be identified with the average value of a tensor $\tilde{\boldsymbol{\alpha}}$ defined by

$$[18] \qquad e\boldsymbol{r}_{iE} = \tilde{\boldsymbol{\alpha}}_i(p, q) \boldsymbol{E}_0$$

Also, the result given by Cole (8) for the mean moment in the field direction is generalized to

$$[19]\quad \langle \boldsymbol{M}(t)\cdot\boldsymbol{e}\rangle = N\langle\tilde{\boldsymbol{\alpha}}\boldsymbol{e}\rangle\cdot\boldsymbol{e}E_0 - \frac{1}{kT}\int_0^\infty d\tau \left\langle \dot{\boldsymbol{M}}(\tau)\cdot\boldsymbol{e}\sum_i\left[\boldsymbol{\mu}_i(0)\cdot\boldsymbol{e} - \mu_i(0)\cdot\nabla_i\sum_{j\neq i}\frac{\tilde{\boldsymbol{\alpha}}_i\boldsymbol{e}\cdot\boldsymbol{R}_{ij}}{|R_{ij}|^3}\right]\right\rangle_0 E_0(t-\tau)$$

where the applied field is written as $\boldsymbol{E}_0 = E_0\boldsymbol{e}$, and the subscript zero indicates an average over the unperturbed distribution, which is assumed to be canonical.

We now consider explicitly the rotational oscillator model employed by Kurbatov (9) and Benson, Channen, and McIntosh (10). The adsorbate molecules are assumed to be well separated so that there are no adsorbate–adsorbate interactions, and [19] reduces to

$$[20]\quad \langle \boldsymbol{M}(t)\cdot\boldsymbol{e}\rangle = N\alpha E_0 - N\left\langle\frac{\boldsymbol{M}(0)\cdot\boldsymbol{\mu}(0)}{3kT}\right\rangle_0 \times\int_0^\infty d\tau\, E_0(t-\tau)\dot{\Phi}(\tau)$$

where $\dot{\Phi}(\tau)$ indicates differentiation with respect to time of $\Phi(\tau)$ defined as

$$\Phi(t) = \langle\boldsymbol{\mu}(0)\cdot\boldsymbol{M}(t)\rangle_0/\langle\boldsymbol{\mu}(0)\cdot\boldsymbol{M}(0)\rangle_0$$

Some of the assumptions and transformations leading to [20] are worthwhile to indicate. We start with

$$\langle \boldsymbol{M}(t)\cdot\boldsymbol{e}\rangle = \int dpdq\sum_i(\boldsymbol{\mu}_i + e\boldsymbol{r}_{iE} + e\boldsymbol{r}_i')\times ef(p,q,t)$$
$$= N\alpha E_0 + \langle\sum_i(\boldsymbol{\mu}_i + e\boldsymbol{r}_i')\times ef(p,q,t)\rangle$$

The Hamiltonian of the system may be written as

$$H(p,q,t) = H^0(p,q) - \sum_i(\boldsymbol{\mu}_i + e\boldsymbol{r}_i)\cdot\boldsymbol{E}_0$$

and, if the change of origin employed by Cole (14) is utilized,

$$H(p,q,t) = H^0(p,q') - \sum_i\boldsymbol{\mu}_i\cdot\boldsymbol{E}_0 - \tfrac{1}{2}N\alpha E_0^2$$

We next take advantage of the fact that the time variation of the distribution function, given by $\partial f/\partial t = iLf$, is satisfied by the equation

$$f(t) = f_0 + \int_{-\infty}^t dt'\, e^{i(t-t')L_0}\{H_1(t'),f(t')\}$$

where f_0 is the equilibrium distribution function in the absence of the applied field. There is then obtained the integral equation for the distribution function

$$f(p,q,t) = f_0(p,q) - \int_{-\infty}^t dt'\, e^{iL_0(t-t')}\{\sum_i\mu_i(t'),f(t')\}E_0(t') - \frac{N}{2}\int_{-\infty}^t dt'\, e^{iL_0(t-t')}\{\alpha(t'),f(t')\}E_0^2(t')$$

where $\{\}$ are Poisson brackets, L_0 is the Liouville operator of the unperturbed system, and the field is applied subsequent to $t = -\infty$. To first order in the field E_0, the distribution function then becomes

$$f(t) = f_0(t) - \int_{-\infty}^t dt'\, e^{iL_0(t-t')}\{\sum_i\mu_i(t'),f_0(t')\}E_0(t')$$
$$= f_0(t) + \int_\infty^0 d\tau\, e^{iL_0\tau}\{\sum_i\mu_i(0),f_0\}E_0(t-\tau) \qquad \text{where}\quad \tau = t - t'$$

Since the distribution function is initially canonical,

$$f_0 = \frac{1}{Z}e^{-H^0/kT}\ , \qquad \{\sum_i\mu_i, f_0\} = -\frac{1}{kT}f_0\sum\dot{\mu}_i$$

Can. J. Chem. Downloaded from www.nrcresearchpress.com by 210.87.254.5 on 09/05/12
For personal use only.

Can. J. Chem. Downloaded from www.nrcresearchpress.com by 210.87.254.5 on 09/05/12
For personal use only.

and $$f(t) = f_0(t) + \frac{1}{kT}\int_0^\infty d\tau\, e^{iL_0\tau} \sum_i \dot{\mu}_i(0) E_0(t-\tau)$$

whence $$\langle \boldsymbol{M}(t)\cdot \boldsymbol{e}\rangle = N\alpha E_0 + \frac{1}{kT}\int_0^\infty d\tau \,\langle \boldsymbol{M}(0)\cdot \boldsymbol{e}\, e^{iL_0\tau}\sum_i \dot{\mu}_i(0)\cdot E_0(t-\tau) f_0\rangle$$

$$= N\alpha E_0 + \frac{1}{kT}\int_0^\infty d\tau\, \langle e^{-iL_0\tau} M(0) \times (-iL_0 \textstyle\sum_i \mu_i(0) f_0)\rangle E_0(t-\tau)$$

$$= N\alpha E_0 - \frac{N}{kT}\int_0^\infty d\tau \langle \dot{\boldsymbol{M}}(\tau)\cdot \boldsymbol{e}\mu_i(0)\cdot \boldsymbol{e}\rangle_0 E_0(t-\tau)$$

For systems in which the moment $\boldsymbol{M}$ and the dipoles $\boldsymbol{\mu}_i$ may be considered to lie in random directions with respect to the field, in the present case because of randomly oriented adsorption sites, we finally obtain

[21] $$\langle \boldsymbol{M}(t)\cdot \boldsymbol{e}\rangle = N\alpha E_0 - \frac{N}{3kT}\int_0^\infty d\tau \langle \dot{\boldsymbol{M}}(\tau)\cdot \boldsymbol{\mu}(0)\rangle_0 E_0(t-\tau)$$

We postpone for the present a discussion of the evaluation of the average $\langle \boldsymbol{\mu}(0)\cdot \boldsymbol{M}(0)\rangle_0$ and use [20] to obtain the relation among dielectric constant and distortion and orientational polarization. We note that $\boldsymbol{E}_0(t)$ is the external applied field, and introduce a definitition of dielectric constant in the usual way by consideration of a spherical sample. In this case the macroscopic field inside the sample is related to $E_0(t)$, which may be taken to be sinusoidal,

$$E_0(t) = E_0\, e^{-i\omega t}$$

so that $$E\, e^{-i\omega t} = \frac{3}{\varepsilon + 2} E_0\, e^{-i\omega t}$$

Thus we have

$$\frac{\varepsilon - 1}{4\pi} E e^{-i\omega t} = \frac{\langle \boldsymbol{m}(t)\cdot \boldsymbol{e}\rangle}{V}$$

and

[22] $$\frac{\varepsilon - 1}{\varepsilon + 2} = \frac{4\pi}{3}\frac{N\alpha}{V} - \frac{4\pi N}{9kTV}\langle \boldsymbol{M}(0)\cdot \boldsymbol{\mu}(0)\rangle_0 \int_0^\infty d\tau\, e^{i\omega\tau}\dot{\Phi}(\tau)$$

$$= \frac{4\pi N\alpha}{3V} - \frac{4\pi N}{9kTV}\sqrt{(2\pi)}\langle \boldsymbol{M}(0)\cdot \boldsymbol{\mu}(0)\rangle_0 \hat{\dot{\Phi}}(\omega)$$

where $\hat{\dot{\Phi}}(\omega)$ is the Fourier transform of $\dot{\Phi}(\tau)$, namely

$$\hat{\dot{\Phi}}(\omega) = \frac{1}{\sqrt{(2\pi)}}\int_0^\infty e^{i\omega\tau}\dot{\Phi}(\tau)\, d\tau$$

Using the conditions for very high frequency and for a static field, there results

$$\frac{\varepsilon_0 - 1}{\varepsilon_0 + 2} - \frac{\varepsilon_\infty - 1}{\varepsilon_\infty + 2} = \frac{4\pi N}{9kTV}\langle \boldsymbol{M}(0)\cdot \boldsymbol{\mu}(0)\rangle_0$$

which, after extensive re-arrangement, may be written

[23] $$\frac{\varepsilon(\omega) - \varepsilon_\infty}{\varepsilon_0 - \varepsilon_\infty} = \left[1 + \frac{\varepsilon_0 + 2}{\varepsilon_\infty + 2}\left(-\frac{1}{\sqrt{(2\pi)}}\frac{1}{(\hat{\dot{\Phi}}(\omega))} - 1\right)\right]^{-1}$$

Given the causal correlation function $\dot{\Phi}(\tau)$, the macroscopic response of the dielectric as a function of frequency may be ascertained.

It is now necessary to evaluate expressions of the form $\langle \boldsymbol{M}(t)\cdot \boldsymbol{\mu}(0)\rangle_0$. This is done by separating the expression into two terms,

[24] $$\langle M(t)\cdot\mu(0)\rangle_0 = \langle[\mu_i(t)+er_i'(t)]\cdot\mu_i(0)\rangle_0 + \sum_{j\neq i}\langle[\mu_j(t)+er_j'(t)\cdot\mu_i(0)]\rangle_0$$

In this connection it is convenient to identify the dipoles by the orientation of the sites on which they are located, that is to say, by the solid angle Ω_i which defines the orientation of the ith dipole. When this is done it may be seen that

$$\langle M(t)\cdot\mu(0)\rangle_0 = \langle[\mu_{\Omega_i}(t)+er'_{\Omega_i}(t)]\cdot\mu_{\Omega_i}(0)\rangle_0 + \langle[\mu_{-\Omega_i}(t)+er'_{-\Omega_i}(t)]\cdot\mu_{\Omega_i}(0)\rangle_0 + \sum_{\Omega_j\neq\Omega_i,-\Omega_i}\langle[\mu_{\Omega_j}(t)+er'_{\Omega_j}(t)]\cdot\mu_{\Omega_i}(0)\rangle_0$$

Consideration of the last term results in the conclusion that contributions from the Ω_j and $-\Omega_j$ positions cancel out and as it is assumed that terms of the form $er_i'\cdot\mu_i$ also make no contributions to the average, one obtains

[25] $$\langle M(t)\cdot\mu(0)\rangle = \langle\mu_\Omega(t)\cdot\mu_\Omega(0)\rangle_0 + \langle\mu_{-\Omega}(t)\cdot\mu_\Omega(0)\rangle_0$$

We now apply [25] in the case of rigid dipoles which perform rotational harmonic oscillations about the equilibrium positions so that

$$H^0 = \tfrac{1}{2}\sum_i(I\dot\gamma_i^2 + k_\gamma\gamma_i^2) = \tfrac{1}{2}\sum_i(P_{\gamma_i}^2/I + k_\gamma\gamma_i^2)$$

where I is the moment of inertia. We calculate first the moment

$$\langle M\cdot e\rangle = N\alpha E_0 - \frac{N}{3kT}\langle M(0)\cdot\mu(0)\rangle_0 \times\int_0^\infty d\tau\,\dot\Phi(\tau)E_0(t-\tau) = NE_0\left(\alpha+\frac{1}{3kT}\langle M(0)\cdot\mu(0)\rangle_0\right)$$

for the static case. The first term in [25] yields μ^2 and the second term

$$\langle\mu_{-\Omega}\cdot\mu_\Omega\rangle_0 = \int dpdq\, e^{-H0/kT}\,\mu_{-\Omega}\cdot\mu_\Omega \Big/ \int dpdq\, e^{-H0/kT}$$

The integrations over momenta, and over the position coordinates of all other dipoles, may be carried out immediately and cancel in numerator and denominator. There results

$$\langle\mu_{-\Omega}\cdot\mu_\Omega\rangle_0 = \frac{\int d\gamma_1\,d\gamma_2\, e^{-(k_\gamma\gamma_1^2+k_\gamma\gamma_2^2)/2kT}\,\mu(\gamma_1)\cdot\mu(\gamma_2)}{\int d\gamma_1\,d\gamma_2\, e^{-(k_\gamma\gamma_1^2+k_\gamma\gamma_2^2)/2kT}} = -\mu^2\frac{\int d\gamma_1\,d\gamma_2\,(\cos\gamma_1\cos\gamma_2-\sin\gamma_1\sin\gamma_2)\,e^{-k_\gamma(\gamma_1^2+\gamma_2^2)/2kT}}{\int d\gamma_1\,d\gamma_2\, e^{-k_\gamma(\gamma_1^2+\gamma_2^2)/2kT}}$$

The situation is illustrated in Fig. 1.

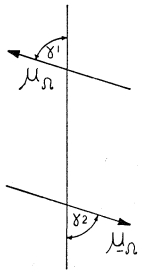

FIG. 1. Rotational oscillators.

For large k_γ, the limits of integration may be made $\pm\infty$. The integrals over odd functions vanish and there results

[26] $$\langle\mu_{-\Omega}\cdot\mu_\Omega\rangle_0 = -\mu^2\, e^{-kT/k_\gamma}$$

so that the static polarizability becomes

[27] $$\frac{\langle M\cdot e\rangle}{E_0} = N\alpha + \frac{N\mu^2}{3kT}(1-e^{-kT/k_\gamma})$$

which is the result given by Kurbatov (9). Expansion of the exponential term gives

[28] $$\frac{\langle M\cdot e\rangle}{E_0} = N\alpha + \frac{N\mu^2}{3k_\gamma}\left[1-\frac{1}{2}\frac{kT}{k_\gamma}+\frac{1}{3!}\left(\frac{kT}{k_\gamma}\right)^2+\ldots\right]$$

Can. J. Chem. Downloaded from www.nrcresearchpress.com by 210.87.254.5 on 09/05/12
For personal use only.

Can. J. Chem. Downloaded from www.nrcresearchpress.com by 210.87.254.5 on 09/05/12
For personal use only.

which, to first order in kT/k_γ is the result of Benson, Channen, and McIntosh (10).

We now consider the frequency dependence of the polarizability. This is determined by the correlation function involving two times t and t', so that we seek to evaluate $\langle \boldsymbol{M}(t) \cdot \boldsymbol{\mu}(t') \rangle_0$. As before, we recognize that the value will be given by the two terms

$$[29] \quad \langle \boldsymbol{M}(t) \cdot \boldsymbol{\mu}(t') \rangle_0 = \langle (\boldsymbol{\mu}_\Omega(t) + e\boldsymbol{r}'_\Omega(t)) \cdot \boldsymbol{\mu}_\Omega(t') \rangle_0 + \langle (\boldsymbol{\mu}_{-\Omega}(t) + e\boldsymbol{r}'_{-\Omega}(t)) \cdot \boldsymbol{\mu}_\Omega(t') \rangle_0$$
$$= \langle \boldsymbol{\mu}_\Omega(t) \cdot \boldsymbol{\mu}_\Omega(t') \rangle_0 + \langle \boldsymbol{\mu}_{-\Omega}(t) \cdot \boldsymbol{\mu}_\Omega(t') \rangle_0$$

if the electron and nuclear motions are uncorrelated with the rotational motion.

To evaluate the first term, which is the correlation of the dipole with itself, we should average over all phase angles in order to obtain the stationary value of the correlation function. The rigorous way to do this is to average over positions and momenta, since these determine the phase angle uniquely. A less rigorous method which seems equivalent is to find the correlation function for a given phase angle and then to average over phase angles assuming each to be equally probable.

The equation of motion of the oscillator is taken to be

$$[30] \quad \gamma(t) = \frac{\gamma_0}{2} \left(e^{i(\omega t + \alpha)} + e^{-i(\omega t + \alpha)} \right)$$

where γ_0 and α are respectively the amplitude and the phase angle. These are given by the initial conditions expressed in the relation

$$[31] \quad \frac{1}{2} k_\gamma \gamma_0^2 = \frac{1}{2} I \dot{\gamma}^2(0) + \frac{1}{2} k_\gamma \gamma(0)^2$$

and

$$\tan \alpha = -\omega \frac{\dot{\gamma}(0)}{\gamma(0)}$$

We next consider an oscillator of given phase angle, arbitrarily chosen to be zero.

$$[32] \quad \langle \boldsymbol{\mu}(t) \cdot \boldsymbol{\mu}(t') \rangle_0 \Big|_{\alpha = 0} = \frac{\int dp dq \, \mu^2 \cos [\gamma(t) - \gamma(t')] \, e^{-H_0/kT}}{\int dp dq \, e^{-H_0/kT}}$$

and

$$\gamma(t) - \gamma(t') = \gamma(t') \left[\frac{e^{i\omega t} + e^{-i\omega t}}{e^{i\omega t'} + e^{-i\omega t'}} - 1 \right]$$
$$= \gamma(t') b$$

We perform the integration for time t', extending the limits of integration for γ to $\pm \infty$.

$$\langle \boldsymbol{\mu}(t') \cdot \boldsymbol{\mu}(t) \rangle_0 = \frac{\int_{-\infty}^{\infty} d\gamma \, \mu^2 \cos b\gamma \, e^{-k_\gamma \gamma^2 / 2kT}}{\int_{-\infty}^{\infty} d\gamma \, e^{-k_\gamma \gamma^2 / 2kT}}$$

since b is assumed to be independent of γ and $\dot{\gamma}$ and the integrals over $\dot{\gamma}$ cancel in numerator and denominator. The result is

$$[33] \quad \langle \boldsymbol{\mu}(t) \cdot \boldsymbol{\mu}(t') \rangle_0 \Big|_{\alpha = 0} = \mu^2 \, e^{-kTb^2/2k\gamma}$$

In dealing with the second term of the correlation function we again consider one oscillator with a zero value of its phase angle, but because the phase angles are independent, we must consider the second to have a value of phase angle between $\pm \pi$ and which may be randomly chosen.

$$[34] \quad \langle \boldsymbol{\mu}_{-\Omega}(t) \cdot \boldsymbol{\mu}_\Omega(t') \rangle_0 = \langle \boldsymbol{\mu}_{\gamma_2}(t) \cdot \boldsymbol{\mu}_{\gamma_1}(t') \rangle_0 = \frac{\int d\dot{\gamma}_1 \, d\dot{\gamma}_2 \, d\gamma_1 \, d\gamma_2 \, e^{-H_0/kT} \, \mu^2 \cos [\gamma_1(t') + \pi - \gamma_2(t)]}{\int d\dot{\gamma}_1 \, d\dot{\gamma}_2 \, d\gamma_1 \, d\gamma_2 \, e^{-H_0/kT}}$$

We now use

$$\gamma_1(t) = \gamma_1^0 \cos \omega t, \qquad \gamma_2(t) = \gamma_2^0 \cos (\omega t + \alpha),$$

so that

$$\gamma_1(t') - \gamma_2(t) = \gamma_1(t') - \gamma_2(t') \left[\frac{e^{i(\omega t + \alpha)} + e^{-i(\omega t + \alpha)}}{e^{i(\omega t' + \alpha)} + e^{-i(\omega t' + \alpha)}} \right]$$
$$= \gamma_1(t') - C\gamma_2(t')$$

The averaging may now be carried out over the equilibrium distribution at t'. Since $\cos(\gamma_1 - C\gamma_2) = \cos\gamma_1 \cos C\gamma_2 + \sin\gamma_1 \sin C\gamma_2$, and the integral over $\sin\gamma_1$ will vanish since H^0 is an even function of γ_1, and assuming C to be independent of γ_1, γ_2, $\dot{\gamma}_1$, $\dot{\gamma}_2$, we arrive at

$$[35] \qquad \langle \boldsymbol{\mu}_{\gamma_1}(t) \cdot \boldsymbol{\mu}_{\gamma_2}(t') \rangle_0 \Big|_{\alpha_1 = 0, \alpha_2 = \alpha} = - \frac{\int d\gamma_1\, d\gamma_2\, e^{-k_\gamma(\gamma_1^2 + \gamma_2^2)/2kT}\, \mu^2 \cos\gamma_1 \cos C\gamma_2}{\int d\gamma_1\, d\gamma_2\, e^{-k_\gamma(\gamma_1^2 + \gamma_2^2)/2kT}}$$

$$= - \mu^2 e^{[-kT(1+C^2)]/2k_\gamma}$$

We now have $$\langle \boldsymbol{M}(t) \cdot \boldsymbol{\mu}(t') \rangle_0 = + \mu^2 e^{-kTb^2/2k\gamma} - \mu^2 e^{-kT(1+C^2)/2k\gamma}$$

Expanding the exponentials and keeping only those terms of first order in kT/k_γ gives

$$[36] \qquad \langle \boldsymbol{M}(t) \cdot \boldsymbol{\mu}(t') \rangle_0 \Big|_{\alpha_1 = 0, \alpha_2 = \alpha} \simeq \frac{\mu^2 kT}{2k_\gamma} [1 - b^2 + c^2]$$

To average over all values of α_2 is the same as averaging over all values of initial times t' assuming that these are equally probable within the period

$$-\frac{\pi}{\omega} < t' < \frac{\pi}{\omega}$$

We set $t = t' + \tau$ and obtain

$$1 - b^2 + c^2 = 2\cos\omega\tau - 2\tan\omega t' \sin\omega\tau + 2\cos\omega\tau \sin\omega\tau[\tan\omega t' - \tan(\omega t' + \alpha)] + \sin^2\omega\tau[\tan^2(\omega t' + \alpha) - \tan^2\omega t']$$

The averages over $t' = -\pi/\omega$ to $t' = \pi/\omega$ vanish for the terms $\int dt' \tan\omega t'$, $\int dt' [\tan\omega t' - \tan(\omega t' + \alpha)]$, and $\int dt' [\tan^2(\omega t' + \alpha) - \tan^2\omega t']$ for any value of α. Thus we obtain

$$[37] \qquad \langle \boldsymbol{M}(t) \cdot \boldsymbol{\mu}(t') \rangle_0 \simeq \frac{\mu^2 kT}{k_\gamma} \cos\omega\tau$$

which is now stationary.

However, dielectric loss must be accounted for, and in the present case of an isolated dipole, arises purely from interaction with the crystal surface. An appropriate model for this interaction would appear to be a small fluctuating random force on the dipole, caused by the thermal vibrations of the atoms composing the crystal, and the resulting deviations from linearity of the force binding the dipole. This additional perturbation to the Hamiltonian should properly be included at an early stage in the calculation.

Nevertheless, it is not obvious that the present calculation, with its other rather drastic simplifying assumptions, merits a detailed treatment of a loss mechanism. Also, one of our purposes was to rederive eq. [37] as obtained by other authors. Thus, in order to give an explicit expression for the susceptibility, we introduce loss by assuming an exponential decay of correlation, which is mathematically the simplest way of allowing for the effect. We write

$$[38] \qquad \langle \boldsymbol{M}(t) \cdot \boldsymbol{\mu}(t') \rangle_0 \simeq \frac{\mu^2 kT}{k_\gamma} e^{-\tau/\tau_0} \cos\omega\tau$$

This behavior results from the assumption that correlation is destroyed by a Poisson process, and exists for a mean free time τ_0. A process of this type would occur if the lattice vibrations were sharp impulses, randomly distributed in time with mean free time τ_0, and each sufficiently large to randomize completely the oscillator phases. Such a mechanism is similar to that of strong collisions in gases employed by Van Vleck and Weisskopf (16), but may not be a particularly good model for the physical situation considered here.

Equation [38] for the correlation function leads to the expression for the complex susceptibility of a rotational oscillator. We may write

$$\langle \Delta\boldsymbol{M} \cdot \boldsymbol{e} \rangle = \langle \boldsymbol{M} \cdot \boldsymbol{e} \rangle - N\alpha E_0$$

$$= - \frac{N}{3kT} \langle \boldsymbol{\mu}(0) \cdot \boldsymbol{M}(0) \rangle_0 \times \int_0^\infty d\tau\, \dot{\Phi}(\tau) E_0(t - \tau)$$

Can. J. Chem. Downloaded from www.nrcresearchpress.com by 210.87.254.5 on 09/05/12
For personal use only.

Can. J. Chem. Downloaded from www.nrcresearchpress.com by 210.87.254.5 on 09/05/12
For personal use only.

If a sinusoidal field is assumed we have $E_0\, e^{-i\omega t}$, and the susceptibility may be defined by

$$\chi(\omega) = \frac{\langle \Delta \boldsymbol{M} \cdot \boldsymbol{e} \rangle}{E_0\, e^{-i\omega t}}$$

$$= -\frac{N}{3kT} \langle \boldsymbol{M}(0) \cdot \boldsymbol{\mu}(0) \rangle_0 \int_0^\infty d\tau\, e^{i\omega\tau}\, \dot{\Phi}(\tau)$$

$$= -\frac{\sqrt{(2\pi)N}}{3kT} \langle \boldsymbol{M}(0) \cdot \boldsymbol{\mu}(0) \rangle_0 \hat{\dot{\Phi}}(\omega) \quad (39)$$

For the rotational oscillator this becomes

$$\chi(\omega) = -\frac{\sqrt{(2\pi)N}}{3k_\gamma} \mu^2 \hat{\dot{\Phi}}(\omega)$$

with $\Phi(\tau) = e^{-\tau/\tau_0} \cos \omega_0 \tau$

or

$$\Phi(t) = e^{-t/\tau_0} \cos \omega_0 t$$

with $\omega_0^2 = k_\gamma / I$

$$\hat{\dot{\Phi}}(\omega) = \frac{1}{\sqrt{(2\pi)}} \int_0^\infty dt \left[\left(\frac{i\omega_0 - 1/\tau_0}{2} \right) e^{i(\omega + \omega_0 + i/\tau_0)t} - \left(\frac{i\omega_0 + 1/\tau_0}{2} \right) e^{-i(\omega_0 - \omega - i/\tau_0)t} \right]$$

$$= -\frac{1}{2i\sqrt{(2\pi)}} \left[\frac{i\omega_0 - 1/\tau_0}{(\omega + \omega_0) + i/\tau_0} + \frac{i\omega_0 + 1/\tau_0}{(\omega_0 - \omega) - i/\tau_0} \right]$$

After some rearrangement this yields for $\chi(\omega)$

$$\chi(\omega) = \frac{N\mu^2}{6k_\gamma} \left[\frac{\omega_0(\omega + \omega_0) + (1/\tau_0)^2 + i\omega/\tau_0}{(\omega + \omega_0)^2 + (1/\tau_0)^2} + \frac{\omega_0(\omega_0 - \omega) + (1/\tau_0)^2 + i\omega/\tau_0}{(\omega - \omega_0)^2 + (1/\tau_0)^2} \right]$$

If we set

$$\Delta\chi = \frac{N\mu^2}{3k_\gamma}$$

we have

$$\mathrm{Re}\, \chi(\omega) = \frac{\Delta\chi}{2} \left[\frac{1 + \omega_0(\omega + \omega_0)\tau_0^2}{(\omega + \omega_0)^2 \tau_0^2 + 1} + \frac{1 - \omega_0(\omega - \omega_0)\tau_0^2}{(\omega - \omega_0)^2 \tau_0^2 + 1} \right]$$

$$\mathrm{Im}\, \chi(\omega) = \frac{\Delta\chi}{2} \left[\frac{\omega\tau_0}{(\omega + \omega_0)^2 \tau_0^2 + 1} + \frac{\omega\tau_0}{(\omega - \omega_0)^2 \tau_0^2 + 1} \right]$$

These results are in agreement with the expressions given by Fröhlich (15).

Appendix

If the sum in [17] is retained, the additional terms arising in the expression for the mean moment may be obtained as follows. Cole (14) gives the perturbed Hamiltonian to first order in the field, expressed in the primed coordinates as

$$[A1] \quad H(p, q, t) = H^0(p, q) - \textstyle\sum_i (\boldsymbol{\mu}_i + \boldsymbol{e}\boldsymbol{r}_i) \cdot \boldsymbol{E}_0$$

$$= H^0(p, q') - \textstyle\sum_i \boldsymbol{\mu}_i \cdot \boldsymbol{E}_0 + \sum_i \boldsymbol{\mu}_i \cdot \nabla_i \sum_{j \neq i} \dfrac{\boldsymbol{e}\boldsymbol{r}_{jE} \cdot \boldsymbol{R}_{ij}}{|R_{ij}|^3} + \sum_i \boldsymbol{e}\boldsymbol{r}_{iE} \cdot \nabla_i \sum_{j>i} \phi_{ij}$$

since r_{iE} is dependent on the field strength. A short range interaction term is included, and in the last term the potential ϕ_{ij} is considered to include all terms of higher order than dipole. The expression simplifies somewhat if this is disregarded, so that only dipole interactions are considered. Use of the definition [18] permits [A1] to be rewritten as

$$[A2] \qquad H(p, q, t) = H^0(p, q') - \sum_i \boldsymbol{\mu}_i \cdot \boldsymbol{E}_0 + \sum_i \boldsymbol{\mu}_i \cdot \nabla_i \sum_{j \neq i} \frac{\tilde{\alpha}_j \boldsymbol{E}_0 \cdot \boldsymbol{R}_{ij}}{|R_{ij}|^3}$$

$$= H^0(p, q') - \sum_i \left[\boldsymbol{\mu}_i \cdot \boldsymbol{e} - \boldsymbol{\mu}_i \cdot \nabla_i \sum_{j \neq i} \frac{\tilde{\alpha}_j \boldsymbol{e} \cdot \boldsymbol{R}_{ij}}{|R_{ij}|^3} \right] E_0$$

$$= H^0 + H^1(t)$$

where $\boldsymbol{E}_0 = \boldsymbol{e}E_0$. Thus H^1 is of the form

$$[A3] \qquad H^1(t) = -AE_0(t)$$

where A is a dynamical variable not explicitly dependent on time. We now evaluate the mean moment in the field direction, if $\boldsymbol{M}(t)$ is the total moment of the system

$$[A4] \qquad \langle \boldsymbol{M}(t) \cdot \boldsymbol{e} \rangle = \int \mathrm{d}p\mathrm{d}q \sum_i (\boldsymbol{\mu}_i + e\boldsymbol{r}_i) \cdot e f(p, q, t)$$

$$= N\langle \tilde{\alpha} \boldsymbol{e} \rangle E_0 \cdot \boldsymbol{e} + \int \mathrm{d}p\mathrm{d}q \times (\boldsymbol{\mu}_i + e\boldsymbol{r}_i') \cdot e f(p, q, t)$$

Solution of Liouville's equation by the method of Kubo (11, 12) yields [19], when only terms to first order in the field are assumed to be equally probable, and gives for the first term $N\alpha E_0$, where α may be defined as the optical polarizability of the medium. The second term in the correlation function is the electrostatic interaction of a permanent dipole with all other induced dipoles. If this is written explicitly in terms of the gradient of a dipole field, it is easily shown to vanish if the medium is isotropic; that is, if the pair distribution function is spherically symmetric.

Acknowledgments

Grateful acknowledgment is made to the National Research Council of Canada for the support of this work and for graduate fellowships to T. McMullen. Important help was rendered by C. Carter in the checking of the mathematical developments.

1. R. L. McIntosh. Dielectric behaviour of physically adsorbed gases. Marcel Dekker, Inc., New York. 1966.
2. Oswald Gröbner. J. Chem. Phys. **46**, 4381 (1967).
3. C. J. F. Böttcher. Rec. Trav. Chim. **64**, 47 (1945).
4. C. J. F. Böttcher. Theory of electric polarization. Elsevier Publ. Co., Inc., Amsterdam. 1952.
5. E. W. Channen and R. McIntosh. Can. J. Chem. **33**, 172 (1955).
6. R. McIntosh, E. K. Rideal, and J. A. Snelgrove. Proc. Roy. Soc. London, Ser. A, **208**, 292 (1951).
7. T. McMullen, R. D. Crozier, and R. McIntosh. Can. J. Chem. **46**, 2945 (1968).
8. R. H. Cole. J. Chem. Phys. **42**, 637 (1965).
9. L. N. Kurbatov. J. Phys. Chem. Acad. Science USSR, **24**, 899 (1950).
10. G. C. Benson, E. W. Channen, and R. McIntosh. J. Colloid Sci. **11**, 593 (1956).
11. R. Kubo. J. Phys. Soc. Japan, **12**, 570 (1957).
12. R. Kubo. *In* Lectures in theoretical physics. Boulder, 1958. Interscience Publishers, Inc., New York. 1959.
13. S. H. Glarum. J. Chem. Phys. **33**, 1371 (1960).
14. R. H. Cole. J. Chem. Phys. **27**, 33 (1957).
15. H. Fröhlich. Theory of dielectrics. The Clarendon Press, Oxford. 1949. p. 101.
16. J. H. Van Vleck and V. F. Weisskopf. Rev. Mod. Phys. **17**, 227 (1945).

Can. J. Chem. Downloaded from www.nrcresearchpress.com by 210.87.254.5 on 09/05/12
For personal use only.

Vibrational spectra of thiocarbonyl chlorofluoride and a normal coordinate analysis of thiocarbonyl chlorofluoride and thiocarbonyl difluoride

D. C. MOULE AND C. R. SUBRAMANIAM
Department of Chemistry, Brock University, St. Catharines, Ontario

Received September 26, 1968

The previously unreported infrared and Raman spectra of thiocarbonyl chlorofluoride have been obtained and analyzed. An assignment has been made for the in-plane fundamental frequencies. The frequency of the out-of-plane fundamental has been obtained from a partial analysis of the near ultraviolet (π^*n) system. Normal coordinate analyses for thiocarbonyl fluoride and thiocarbonyl chlorofluoride have been carried out using the Urey–Bradley potential field. The value of the CS stretching force constant is found to show a marked change with the halogen substitution in contrast to the CO stretching constant in the carbonyl halides. This is attributed to the presence of ionic valence bond structures in the thiocarbonyl halides which are not significant in the carbonyl halides.

Canadian Journal of Chemistry, 47, 1011 (1969)

Can. J. Chem. Downloaded from www.nrcresearchpress.com by 210.87.254.6 on 09/05/12
For personal use only.

Introduction

The study of the vibrational spectrum of thiophosgene, $CSCl_2$, and the normal coordinate analysis have been carried out by many authors (1–6), with the most recent one giving a revised assignment for ν_3 and ν_4 (6). The electronic spectrum in absorption of thiophosgene has been analyzed in considerable detail (6) and from the combination differences of the vibrational levels in the lower electronic state, precise values of certain fundamental frequencies have been obtained. The infrared spectrum of thiocarbonyl fluoride has been reported by Downs (7) who has been able to assign the fundamental vibrational modes satisfactorily. From this analysis, Pillai and Ramaswamy (8) have carried out a normal coordinate analysis using an empirical valence force field.

The infrared and the Raman spectra of thiocarbonyl chlorofluoride have been obtained and the vibrational analysis carried out. The analysis of the ground state vibrations was undertaken as a necessary prelude to a detailed study of the electronic spectrum. In order to carry out a normal coordinate analysis of CSFCl required in a Franck–Condon analysis of the (π^*n) electronic transition, it was felt necessary to carry out first a normal coordinate analysis of CSF_2 and $CSCl_2$ in the Urey–Bradley force field, from which a transfer of force constants could then be made.

Experimental

Thiocarbonyl chlorofluoride was prepared by fluorinating thiophosgene, $CSCl_2$, using antimony trifluoride in the solvent tetrahydrothiophene-1,1-dioxide. A mixture of 5 ml of thiophosgene, 25–30 g of SbF_3, and 50 g of the solvent was refluxed at atmospheric pressure for more than 48 h at 78–80 °C.

After the reaction, the products were condensed and purified by trap-to-trap distillation followed by a low temperature distillation. The purified sample still contained small quantities of COS, CCl_3F, and CS_2. The sample and the impurities were identified by their mass spectral pattern.

The infrared spectrum was recorded in the gaseous phase using a Perkin–Elmer model 225 grating spectrophotometer which was provided with a dry air purging unit.

The Raman spectrum of liquid CSClF was excited by a 50 mW He–Ne laser and recorded with a Spexs double monochromator. The spectrum was recorded both with the polarized light parallel and perpendicular to the incident electric vector direction.

Results and Assignment

No structural data for CSClF have been reported, although electron diffraction data (9) modified by infrared data (6) are available for $CSCl_2$. The molecules CSF_2 and CSClF are presumably planar and belong to the point groups C_{2v} and C_s, respectively. The geometrical parameters assumed for CSClF were transferred from $CSCl_2$ (6) and COF_2 (10). They are: r(CS), 1.63 Å; r(CF), 1.32 Å; r(CCl), 1.746 Å; α(ClCF), 111° 54′; and α(SCCl), 124° 18′, where r and α are the interatomic distances and the bond angles, respectively.

TABLE I

Principal moments of inertia of thiocarbonyl chlorofluoride

	Moments of inertia (10^{-40}g cm^2)		
Molecule	I_A	I_B	I_C
CSClF	149.81	268.1	417.8

TABLE II

Observed fundamental frequencies of CSClF

Infrared frequency, gas (cm^{-1})	Intensity*	Raman frequency, liquid (cm^{-1})	Intensity†	Assignment
1257	100	1242	32 (P)	ν_1
1014	75	992	8 (P)	ν_2
612	28	608	100 (P)	ν_3
427	4	426	10 (P)	ν_4
323	2	326	50 (P)	ν_5

*The intensity of the band at 1257 cm^{-1} was arbitrarily taken as 100 and the other band intensities are normalized with respect to this band.
†The Raman line at 608 cm^{-1} is the most intense and is taken as of intensity 100; P stands for polarized.

There are five vibrations of a' species and one vibration of a'' species expected for CSClF. Both species are infrared and Raman active. Table I gives the principal moments of inertia of CSClF. Figure 1 shows the orientation of the inertial axis with respect to the molecule. The five in-plane vibrations of a' species will be polarized with their electric dipole vector in the ab plane, and their resulting rotational contours will consist of a superposition of type A and type B bands. The remaining vibration of a' species will give rise to a type C band.

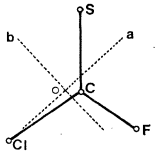

FIG. 1. Orientation of inertial axes of CSClF.

The infrared spectrum of CSClF obtained in the gas phase is shown in Fig. 2. Table II lists the observed infrared and Raman fundamental frequencies for CSClF. The strongest bands in the infrared spectrum of CSClF vapor are located at 1257 and 1014 cm^{-1}, and are found at 1242 and 992 cm^{-1}, respectively, in the Raman spectrum of the liquid. Both of the infrared bands have an AB type rotational envelope and their corresponding Raman lines are polarized. The 1257 cm^{-1} mode can be assigned to the CS stretch, $\nu_1(a_1)$; the corresponding modes in Cl_2CS and F_2CS appearing at 1139 and 1368 cm^{-1}, respectively. The assignment of the second band at 1014 cm^{-1} to $\nu_2(a_1)$, the CF stetching mode, was also straightforward.

The weaker infrared band at 612 cm^{-1} displays a complicated rotational band envelope containing five principal maxima which can not be rationalized in terms of type AB hybridization or an isotope effect, although it could be interpreted as a fundamental with several sequence bands superimposed on it. The corresponding intense Raman line at 608 cm^{-1} is polarized and must be assigned to $\nu_3(a_1)$, the CCl stretch.

The infrared band at 427 cm^{-1} has a rotational envelope similar to ν_1 and ν_3 and was assigned to $\nu_4(a_1)$, an in-plane bending mode. The remaining $\nu_5(a_1)$ mode was assigned to the weak infrared band at 323 cm^{-1} which had a contour different from that of the 427 cm^{-1} band. The corresponding Raman lines were at 426 and 326 cm^{-1}, respectively, and were found to be polarized.

The out-of-plane modes for $CSCl_2$ and CSF_2 have been found to be 471 and 622 cm^{-1}, respectively. Hence, the out-of-plane vibration is expected to be about 540–550 cm^{-1}. It has not been possible to identify this mode either in the infrared or in the Raman spectra because of the presence of certain strong impurity bands in this region. The sample contained small quantities of CS_2, COS, and CCl_3F. Information about ν_6 was obtained from a partial analysis of certain progressions observed in the ultraviolet spectra of CSClF. Attached to most of the prominent bands in the electronic spectra were hot band progressions extending to lower wavenumbers in the interval of 540 cm^{-1}. This progression can be assigned to the ν_6 mode on Franck–Condon ground since, as in the case of $CSCl_2$, CSClF is expected to assume a non-planar configuration in the excited electronic state (6).

Normal Coordinate Analysis

The normal coordinate analysis was carried out by the Wilson's [**F**] and [**G**] matrix method.

Can. J. Chem. Downloaded from www.nrcresearchpress.com by 210.87.254.6 on 09/05/12
For personal use only.

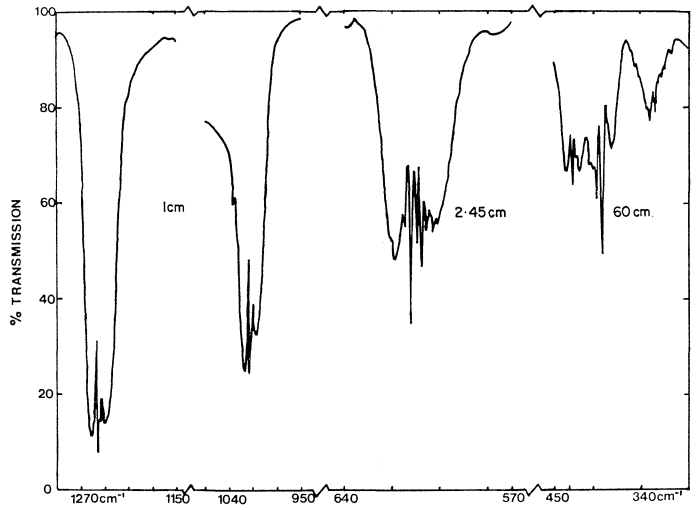

FIG. 2. Infrared bands of thiocarbonyl chlorofluoride vapor.

In order to reduce the number of force constants to a manageable size, the Urey–Bradley force field was employed and is given by

$$[1]\quad V = \sum_i [\tfrac{1}{2}K_i(\Delta r_i)^2 + K'_i r_i(\Delta r_i) + \sum_{i<j} [\tfrac{1}{2}H_{ij}r^2{}_{ij}(\Delta\alpha_{ij})^2 + H'_{ij}r^2{}_{ij}(\Delta\alpha_{ij})] + \sum_{i<j} [\tfrac{1}{2}F_{ij}(\Delta q_{ij})^2 + F'_{ij}q_{ij}(\Delta q_{ij})]$$

Here Δr_i, $\Delta\alpha_i$, and Δq_i are the changes in bond lengths, bond angles, and distances between non-bonded atoms, respectively. The symbols K_i, K'_i, H_{ij}, H'_{ij}, F_{ij}, and F'_{ij} represent the stretching, bending, and non-bonded interaction force-constants.

The [**G**] matrix elements were constructed by the method given by Wilson, Decius, and Cross (10). The [**F**] matrix elements were obtained from the transformation

$$[2]\qquad [\mathbf{F}] = [\mathbf{Z}][\mathbf{\Phi}]$$

where [**Z**] is a matrix representing a transformation between a vector of Urey–Bradley force constants [$\mathbf{\Phi}$] and a vector of valence force field constants.

In the case of CSF_2 both the [**F**] and [**G**] matrices were symmetrized and the secular equation

$$[3]\qquad [\mathbf{G}][\mathbf{F}][\mathbf{L}] = [\mathbf{L}][\lambda]$$

solved for the eigenvectors [**L**] and eigenvalues [λ]. The [**L**] matrix relates the normal coordinates [**Q**] to the internal coordinates [**R**] by the relation

$$[4]\qquad [\mathbf{R}] = [\mathbf{L}][\mathbf{Q}]$$

The initial set of force constants were transferred from similar molecules with the assumption that $F'_{ij} = 0.1F_{ij}$ (10), and then were refined using a Jacobian least squares procedure to obtain good agreement between the experimental and calculated values.

Table III shows the in-plane force constants for the three thiocarbonyl halides while Table IV shows the calculated frequencies for CSF_2 and

TABLE III

Urey–Bradley force constants for the thiocarbonyl halides

Force constant	Value (mdyn/Å)		
	CSF_2	CSClF	$CSCl_2$*
K_{CS}	6.27	5.739	5.327
K_{CF}	4.483	3.936	
K_{CCl}		2.632	2.352
H_{FF}	0.425		
H_{ClCl}			0.08
H_{SF}	0.158	0.158	
H_{SCl}		0.101	0.101
H_{FCl}		0.321	
F_{FF}	1.143		
F_{ClCl}			0.74
F_{SF}	0.97	0.97	
F_{SCl}		0.681	0.681
F_{FCl}		0.761	

*This set of force constants was recalculated and is in good agreement with the values in ref. 6.

Can. J. Chem. Downloaded from www.nrcresearchpress.com by 210.87.254.6 on 09/05/12
For personal use only.

TABLE IV

Calculated and observed in-plane fundamental frequencies of CSF_2 and $CS^{35}ClF$

CSF_2					$CS^{35}ClF$				
Frequency		Obsd.	Calcd.	Obsd. − Calcd.	Frequency		Obsd.	Calcd.	Obsd. − Calcd.
a_1	ν_1	1368	1367.9	0.1	a'	ν_1	1257.7	1257.6	0.1
	ν_2	787	786.5	0.5		ν_2	1014.7	1014.7	0.0
	ν_3	526	526.9	−0.9		ν_3	611.9	611.8	0.1
b_2	ν_5	1189	1189.3	−0.3		ν_4	427.1	426.9	0.2
	ν_6	417	416.8	0.2		ν_5	322.6	323.5	0.9

TABLE V

Elements of the [**L**] matrix for CSF_2

	Matrix elements for modes				
	ν_1	ν_2	ν_3	ν_5	ν_6
δrCS	+0.318578	+0.105741	−0.043700	0	0
δrCF(2)	−0.187675	+0.129584	+0.004818	+0.289177	+0.017435
δrCF(1)	−0.187675	+0.129584	+0.004818	−0.289177	−0.017435
δθFCF	+0.349801	+0.046810	+0.260994	0	0
δθSCF(1)	−0.174900	−0.023405	−0.130497	+0.261040	−0.218827
δθSCF(2)	−0.174900	−0.023405	−0.130497	−0.261040	+0.218827

TABLE VI

Elements of the [**L**] matrix for $CS^{35}ClF$

	Matrix elements for modes				
	ν_1	ν_2	ν_3	ν_4	ν_5
δrCS	−0.320219	−0.078796	+0.073504	−0.016635	+0.012399
δrCF	+0.229433	−0.278747	+0.073818	+0.009306	−0.009401
δrCCl	+0.119397	+0.255010	+0.165564	+0.067413	+0.025730
δθClCF	−0.293056	−0.091432	−0.068246	+0.192538	−0.075773
δθFCS	+0.128366	+0.295144	+0.145330	−0.160613	−0.117230
δθClCS	+0.164691	−0.203710	−0.077091	−0.031925	+0.193007

CSClF. Tables V and VI give the elements of the [**L**] matrix for CSF_2 and CSClF, respectively. The potential energy distribution in the Urey–Bradley coordinate space was calculated by the equation

$$[5] \qquad [\mathbf{V}] = [\mathbf{J}][\lambda]^{-1}[\Phi^*]$$

where $[\Phi^*]$ is a diagonal matrix with elements Φ_i. Tables VII and VIII list the distribution of potential energy in Urey–Bradley space for CSF_2 and CSClF, respectively. The mass-weighted cartesian displacement vector diagrams, which give a pictorial representation of the normal coordinates, are given in Figs. 3 and 4 for CSF_2 and CSClF respectively.

The number of Urey–Bradley force constants to be determined for CSF_2 and CSClF was 6 and 9, respectively, for the in-plane vibrations. The observed number of in-plane vibrations was 5 for each molecule. Hence, it was necessary to constrain certain force constants in order to see the variation of the Urey–Bradley force constant of CSF_2 and $CSCl_2$ as a function of the constrained force constants. The latter were varied

Can. J. Chem. Downloaded from www.nrcresearchpress.com by 210.87.254.6 on 09/05/12
For personal use only.

TABLE VII

Potential energy distribution of thiocarbonyl fluoride in Urey–Bradley space

Frequency (cm^{-1})	Potential energy distribution (%)					
	K_{CS}	K_{CF}	H_{FCF}	H_{SCF}	F_{SF}	F_{FF}
787	19.23	41.31	0.44	0.10	19.69	19.19
526	7.32	0.12	30.84	7.03	21.33	33.30
1368	57.72	28.64	8.21	1.87	0	3.50
417	0	2.66	0	31.61	65.61	0.04
1189	0	89.97	0	5.52	5.88	1.41
[Φ] (md/Å)	6.27	4.483	0.425	0.157	0.969	1.143

TABLE VIII

Potential energy distribution of thiocarbonyl chlorofluoride in Urey–Bradley space

Frequency (cm^{-1})	Potential energy distribution (%)								
	K_{CS}	K_{CF}	K_{CCl}	H_{FCl}	H_{SF}	H_{ClS}	F_{FCl}	F_{SF}	F_{SCl}
1257.7	63.16	22.23	4 02	6.81	0.59	0.83	2.10	−0.44	0.66
1014.7	5.87	50.42	28.22	1.01	4.85	1.96	0.04	6.34	1.25
611.9	14.06	9.72	32.72	1.56	3.23	0.77	6.15	23.54	8.21
427.1	1.47	0.31	11.13	25.53	8.11	0.27	36.40	16.29	0.44
322.6	1.43	0.56	2.82	6.88	7.52	17.36	4.26	12.92	46.20
[Φ] (md/Å)	5.739	3.936	2.632	0.321	0.157	0.101	0.761	0.969	0.680

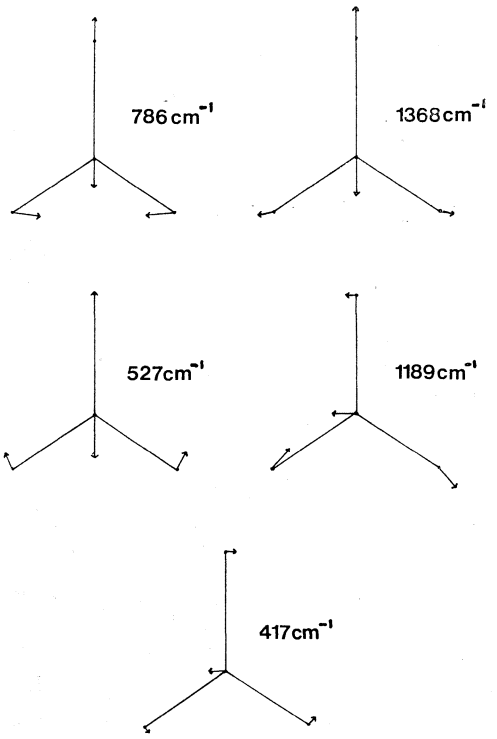

FIG. 3. Mass-weighted cartesian displacement vector diagram for CSF_2.

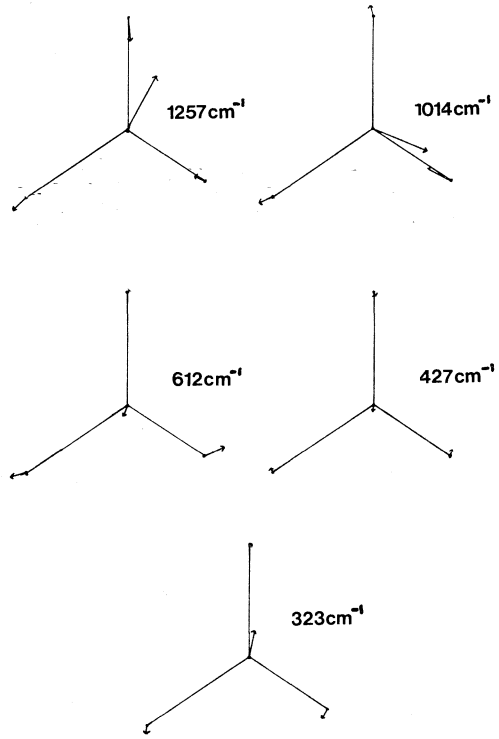

FIG. 4. Mass-weighted cartesian displacement vector diagram for CSClF.

Can. J. Chem. Downloaded from www.nrcresearchpress.com by 210.87.254.6 on 09/05/12
For personal use only.

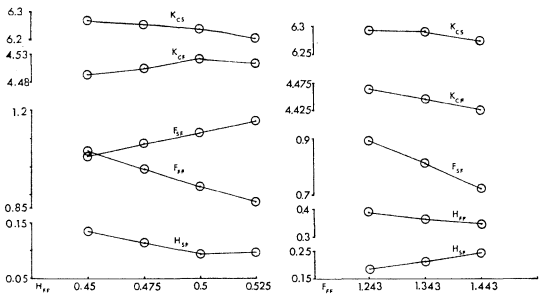

Fig. 5. Urey–Bradley force constants for CSF_2 as functions of H_{FF} and F_{FF}.

over a reasonable range and the other five constants calculated. Figure 5 shows the variation graphically for CSF_2.

Discussion

Although small variations in the bending and nonbonded interaction force constants are not very significant because of their dependence on the value of the constrained force constant, it is interesting to compare the stretching force constants in Cl_2CS, F_2CS, and ClFCS which are relatively independent of the value of the constrained force constant. In contrast to a variation of 2% in the value of K_{CO} in the carbonyl halides (11), the value of K_{CS} varies by 18% between CSF_2 and $CSCl_2$. This can be explained in terms of the valence bond structures for the thiocarbonyl halides. For $CSCl_2$ the possible resonance structures are

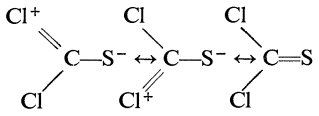

1a **1b** **1c**

Similarly for CSClF the plausible structures are

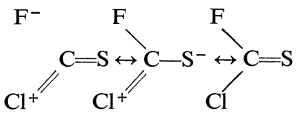

2a **2b** **2c**

For CSF_2, the structures similar to **1***a* and **1***b* would make very little contribution to the overall structure since they would require the presence of a positive charge on a fluorine atom. The prominent valence bond structure will be

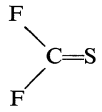

3*a*

From a study of the infrared spectra of amides and thioamides, Jensen (12) has shown that structures of the form

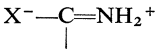

have greater weight than structures

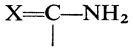

when X = S, whereas the reverse is true when X = O. A linear combination of atomic orbitals/molecular orbitals calculation on the CS molecule has likewise demonstrated that electron back donation should be easier to sulfur than it would be to the oxygen atom (13). Thus, the ionic structures like **1***a* and **1***b* play a greater role in determining the overall structure of the thiocarbonyl compounds than they do in the carbonyl compounds. Hence the C=S bond order and the K_{CS} force constant will be lower in $CSCl_2$ than in CSClF or CSF_2 because of the contribution of structures **1***a* and **1***b*. Likewise K_{CS} in CSClF will be lower than in CSF_2 because of the contribution of structure **2***b*.

The variation of K_{CCl} and K_{CF} with halogen substitution is more difficult to understand. One explanation for the increase in the value of K_{CCl} from $CSCl_2$ to CSClF is the presence of structure **2***a* in CSClF which is absent in $CSCl_2$. Likewise the decrease in K_{CF} in CSClF over CSF_2 can be attributed to structure **2***a* in CSClF which would not contribute to CSF_2.

Acknowledgments

The authors wish to thank Dr. G. W. King for use of the 20 foot Ebert spectrograph and for the Laser Raman spectrophotometer.

1. H. W. Thompson. J. Chem. Phys. **6**, 748 (1938); Trans. Faraday Soc. **37**, 251 (1941).
2. J. Duschesne. Acad. Roy. Belg., Classe Sci. Mem. **28**, no. 8 (1955).
3. M. G. K. Pillai and F. F. Cleveland. J. Mol. Spectry. **6**, 465 (1961).
4. D. A. Long and D. T. L. Jones. Trans. Faraday Soc. **59**, 577 (1963).
5. D. Papousek and J. Pliva. Collection Czech. Chem. Commun. **28**, 755 (1963).

Can. J. Chem. Downloaded from www.nrcresearchpress.com by 210.87.254.6 on 09/05/12
For personal use only.

6. J. C. D. BRAND, J. H. CALLOMON, D. C. MOULE, J. TYRRELL, and T. H. GOODWIN. Trans. Faraday Soc. **61**, 2365 (1965).
7. A. J. DOWNS. Spectrochim. Acta, **19**, 1165 (1963).
8. M. G. KRISHNA PILLAI and A. RAMASWAMY. J. Annanalai Univ. Pt. B. **25**, 115 (1964).
9. L. O. BROCKWAY, J. Y. BEACH, and L. PAULING. J. Am. Chem. Soc. **57**, 2693 (1935).
10. E. B. WILSON, J. C. DECIUS, and P. C. CROSS. Molecular vibrations. McGraw-Hill Book Co., Inc., New York. 1955.
11. J. OVEREND and J. R. SCHERER. J. Chem. Phys. **32**, 1289 (1960).
12. A. K. JENSEN. Acta. Chem. Scand. **17**, 551 (1963).
13. W. G. RICHARDS. Trans. Faraday, Soc. **63**, 257 (1967).

Can. J. Chem. Downloaded from www.nrcresearchpress.com by 210.87.254.6 on 09/05/12
For personal use only.

Nuclear recoil reactions in polynuclear metal carbonyls

S. R. NARAYAN AND D. R. WILES
Chemistry Department, Carleton University, Ottawa, Canada

Received August 30, 1968

Nuclear recoil reactions have been studied in the compounds $Ru_3(CO)_{12}$, $Fe_3(CO)_{12}$, $Fe(CO)_5$, and $W(CO)_6$, with the objective of testing the hypothesis that the retention would be closely related to the molecular complexity. Retention values were found to be 41, 26, 41, and 52%, respectively, after exhaustive purification, and the hypothesis is concluded to be invalid for these compounds. A recoil yield of 26% is found for $Fe_3(CO)_{12}$ in $Fe(CO)_5$, and 17% for $Fe(CO)_5$ in $Fe_3(CO)_{12}$. Some reactions are suggested which can account qualitatively for the observed results. The critical stage of the reaction is assumed to be the hot-zone formation of a mononuclear radioactive species $M(CO)_3$ or $M(CO)_4$, which reacts further by various stepwise reactions.

A retention of 52 or 64% was found for $W(CO)_6$, depending on whether column chromatography or vacuum sublimation was used as the first step in the separation. The lower value is preferred.

Canadian Journal of Chemistry, **47**, 1019 (1969)

Can. J. Chem. Downloaded from www.nrcresearchpress.com by 210.87.254.42 on 09/05/12
For personal use only.

Neutron irradiation of metal carbonyls gives rise to the production of the parent carbonyl, re-formed with a radioisotope of the metal atom. However, the mechanism whereby this re-formation occurs is unknown, and although some aspects of the reaction have been discussed in the literature, no general mechanism has been proposed. It has been calculated (1) that the strict billiard-ball re-formation could be as high as a few %, but this is far too low to account for the experimental data, and we are driven to try to find out more about the fundamental nature of the reaction. One of the intriguing aspects of those carbonyls which have been studied is that the mononuclear $Cr(CO)_6$, $Mo(CO)_6$, and $W(CO)_6$ have retentions which are much higher than is common among organometal compounds, and in some cases are quite high, while the retention in $Mn_2(CO)_{10}$, the only binuclear metal carbonyl which has been studied to date, is considerably lower. The retention values for such compounds have been found to vary widely according to the conditions of the irradiation, and are thus difficult to intercompare when the work has been done at different laboratories, but the above-mentioned grouping seems to be quite valid and outside of all reasonable uncertainties. The approximate ranges of the retention values found in the literature for metal carbonyls are given in Table I. Also shown in this Table are the values found for the yields of two metal carbonyls from neutron-irradiated arenemetal carbonyls.

Assuming that these data reflect the kinetic processes by which the molecules are reformed, we were led to the following postulate: *The extent of formation, or of re-formation, of metal carbonyls following nuclear transformation is closely related to the structural simplicity of the molecule.*

TABLE I

Reported retention and yield values for metal carbonyls and related compounds*

Compound	Retention (%)	Reference
$Cr(CO)_6$	35–70	2,3,4,5
$Mo(CO)_6$	23–74	3,4
$W(CO)_6$	26–52	6,7
$Mn_2(CO)_{10}$	9.8, 12	6,7

Target	Compound	Yield (%)	Reference
$C_6H_6Cr(CO)_3$	$Cr(CO)_6$	13.5	8
$C_5H_5Mn(CO)_3$	$Mn_2(CO)_{10}$	0.2	6
$CH_3C_5H_4Mn(CO)_3$	$Mn_2(CO)_{10}$	0.1	6
$Mn_2(CO)_{10}$	$\cdot Mn(CO)_5$	4.1	7
$C_5H_5Mn(CO)_3$	$\cdot Mn(CO)_5$	4.2	7

*Retention and yield, in this and the other Tables, is the fraction of the radioactivity appearing in the form of the target compound and any other compound, respectively.

This amounts to the imposition of an activation entropy for the re-formation reaction. The activation energy is clearly no barrier in a hot-zone. If this postulate were found to have any validity, one would predict the mononuclear carbonyls to have high retentions and the binuclear carbonyls to have markedly lower retentions. Similarly, one would expect the yield of a mononuclear carbonyl to be considerably higher than that of a binuclear carbonyl from the respective arenemetal carbonyls. Table I indicates that both of these anticipated results of our postulate are supported by the experimental data. Moreover,

TABLE II

Irradiation conditions used in the present work

Facility	Flux ($cm^{-2}s^{-1}$)	Cd ratio	Dose rate (rads h^{-1})	Temperature (°C)
AECL Pool	3×10^8		10^6	20
AECL Mobile	2.8×10^8		10^6	20
NRX Self-serve	5×10^{12}	1:50	13×10^6	65

as would be expected from the postulate, the yield of the mononuclear $\cdot Mn(CO)_5$ is higher than that of $Mn_2(CO)_{10}$. The fact that this radical is formed in rather lower yield than is $Cr(CO)_6$ in neutron-irradiated benzenechromium tricarbonyl, is perhaps not a serious challenge to the postulate since the systems are different. Moreover, the radical would be susceptible to destruction by various extraneous reactions which might not affect the more stable molecule.

It is this postulate which gave impetus to the present work, which was designed to test some further extrapolations:

The retention in the trinuclear $Ru_3(CO)_{12}$ and $Fe_3(CO)_{12}$ should be extremely low, perhaps 1% or less.

The retention in $Fe(CO)_5$ should be high, and very much greater than that in $Fe_3(CO)_{12}$.

The yield of $Fe(CO)_5$ in neutron-irradiated $Fe_3(CO)_{12}$ should be moderately high, while the yield of $Fe_3(CO)_{12}$ in neutron irradiated $Fe(CO)_5$ should be quite small.

Similarly, the yields of $Ru(CO)_5$ in irradiated $Ru_3(CO)_{12}$, and $Ru_3(CO)_{12}$ in irradiated $Ru(CO)_5$ should be high and very low, respectively. Unfortunately, we were unable to procure a sample of $Ru(CO)_5$, so that this last prediction could not be tested.

Experimental

Reagents

The target materials and carriers were commercially obtained and were repurified as follows:

$W(CO)_6$ was obtained from Metallomer Laboratories. It was resublimed in vacuo (10^{-3} Torr) at 50 °C, through a column of glass wool, and collected on a cold finger at 0 °C.

$Ru_3(CO)_{12}$ was obtained from K and K Laboratories, and was purified by column chromatography using neutral alumina (Woelm, grade 1) and cyclohexane.

$Fe(CO)_5$, from Alfa Inorganics, Inc., was repeatedly distilled in vacuo under subdued light, and the middle fraction was further purified by vapor–phase chromatography.

$Fe_3(CO)_{12}$, obtained from Strem Chemicals, Inc., was recrystallized from benzene and subsequently from petroleum ether. It was further purified by column chromatography on Florisil, using pentane as eluant. All these operations were done in subdued light.

All other reagents were the best available. Solvents were distilled under an atmosphere of dry air.

Separation Methods

In experiments of this sort, the exact value of the result is often less important than the purity of the separated products. Moreover, in systems such as these, it is not uncommon to produce radioactive compounds which are quite unexpected and often extremely difficult to identify. Thus, we have taken the precaution in several cases to apply a number of different separation methods to each sample, often varying the order of the methods in successive experiments. Generally the separation and purification methods were the following:

1. column chromatography on alumina
2. column chromatography on Florisil
3. vacuum sublimation at 50 °C for $W(CO)_6$ and at 80 °C for $Ru_3(CO)_{12}$
4. vapor–phase chromatography
5. pumping on the solid at room temperature
6. scavenging the solution with iodine during dissolution (6, 7)
7. fractional distillation

While no work was done below room temperature, we avoided any unnecessary rise in temperature, especially during the early stages of the separation.

Irradiations

The tungsten and ruthenium carbonyls were irradiated in the antimony–beryllium neutron facility of Atomic Energy of Canada, Ltd., Commercial Products Division, in Ottawa (9) while the iron carbonyls were irradiated for 10 h in a self-serve position in the NRX reactor at Chalk River. The conditions of irradiation are given in Table II, insofar as the information is available.

All samples were sealed in vacuo in quartz ampoules before irradiation. Samples were normally held at room temperature for the hour or so between the end of the irradiation and the time of chemical treatment. The iron samples, some of which were processed only after several weeks, were kept in dry ice in the dark after being received from Chalk River.

Results

The results are shown for tungsten carbonyl in Table III. These data are in general agreement with previous results, but are important in that they show a significant difference from one type

Can. J. Chem. Downloaded from www.nrcresearchpress.com by 210.87.254.42 on 09/05/12
For personal use only.

Can. J. Chem. Downloaded from www.nrcresearchpress.com by 210.87.254.42 on 09/05/12
For personal use only.

of separation to the other. In all cases, the use of sublimation as a first step results in a distinctly higher retention value. It is our feeling that the lower values, obtained by the use of chromatography as a first step, are closer to the real value. It may be that sublimation at even moderate temperatures causes the production of $W(CO)_6$ by pyrolysis of more complex species, perhaps unstable polymers. If this is so, then all results obtained from sublimation separations are to be viewed with caution, even though they may be reproducible, since the data could represent the sum of the original retention and the production by pyrolysis.

The results for ruthenium carbonyl are given in Table IV, and for the iron carbonyls in Table V. From Table IV it is evident that although the exact value of the retention is not to be deduced with great precision, the retention value for $Ru_3(CO)_{12}$ is surely between 35 and 45%. It is our opinion that the variation in results is to a

TABLE III

Retention values found in $W(CO)_6$ with various combinations of purification methods

Purification method*	Retention (%)	Purification method*	Retention (%)
1	52	3	68
1,4	51	3,3	67
1	52	3,3,3	63
1,4	50	3	54
6,1	51	3,4	62
6,1,4	55	3	62
	Av. 51.8	3,4	62
		3,4	65
		3,4	64
			Av. 63.8

*Each number represents a separate step using the methods as listed by number previously. Thus, 3,3,3 signifies three separate, successive sublimations.

TABLE IV

Retention values found in $Ru_3(CO)_{12}$ with various combinations of purification methods*

Separation method	Retention (%)	Separation method	Retention (%)
2, 5†	63.7	1,5	36.5
1,1,5	47.8	1,1,5	43.4
1,1,1,5	47.7	1,1,3 collected at 20 °C	36.1, 37.5, 33.4
1,5	45.4	1,1,3 " " −196 °C	46.7, 31.8
1,1	32.5	1,1,3 " " 0 °C	43.1
1,1	37.2	3† " " 0 °C	60.4, 55.7
1,1,1	42.5	3† " " 0 °C	First fraction: 51.4, 48.6, 47.5
1,1,1,1	42.8	3,3† " " 0 °C	Second fraction: 41.9, 42.9
1	51.1		
1,1	43.7	6,1,1	41.4
1,1	40.8	6,1,1,3	43.0
1,1,5	41.4	6,1,1,3,3	40.1

*The average of all values except those in experiments marked (†) is 41%.

TABLE V

Retention and yield values found in the iron carbonyls*

Target	Separation method	Retention (%)	Compound	Purification method	Yield (%)
$Fe_3(CO)_{12}$	2	22.5	$Fe(CO)_5$	2,7,4	(8.1)
	2,2	(16.4)		2,7,4	(21.6)
	2,2,2	27.2		1,4	16.8
	2,2	27.6		1,4	14.7
	2,2,2	27.7		1,4	11.5
	6,2	23.8		1,4	8.3
		Av. 25.8		6,1,4	22.6
					Av. 16.8
			$Fe_2(CO)_9$	Not determined	
$Fe(CO)_5$	1,1,4	39.0	$Fe_3(CO)_{12}$	2	26
	1,1,4	39.6		2	24
	1,1,4	42.9		2	26
		Av. 40.5	$Fe_2(CO)_9$	*	(2.8, 3.5)

*This is a very crude experiment in which the chemical recovery could not be measured, although the product appeared to be pure. It is likely that these values represent the lower limit of the recoil yield. Values in parentheses are from experiments of doubtful reliability, and were not used in computing the averages.

Can. J. Chem. Downloaded from www.nrcresearchpress.com by 210.87.254.42 on 09/05/12
For personal use only.

large extent caused by fluctuations in the conditions of irradiation, although we have not been able to test this speculation. Recoil studies on ruthenocene (10, 11) show retention values of 5–8%, suggesting at least 95% bond breakage. From this evidence, it seems clear that in the present case some type of re-formation process is required. We draw attention to the results from experiments starting with sublimation and those starting with chromatography. We note also that the difference between the first and second fractions in the sublimation experiments suggests the presence of a radioactive compound more volatile than the parent compound—perhaps $Ru(CO)_5$.

Retention values in the iron carbonyls can be evaluated in the same approximate fashion. Retention values in $Fe(CO)_5$ and $Fe_3(CO)_{12}$ are approximately 41 and 26%, respectively. The yield of $Fe(CO)_5$ in irradiated $Fe_3(CO)_{12}$ was found to be 17%. The yield of $Fe_3(CO)_{12}$ in irradiated $Fe(CO)_5$ was rather difficult to determine unambiguously, since the target compound was decomposed somewhat, presumably by the gamma radiation, to give $Fe_3(CO)_{12}$. This radiolysis is well known, and its mechanism has been fairly well elucidated (12, 13). The extent of the decomposition was determined to be approximately 2%. After correcting for this direct chemical production, we estimate the activity of ^{59}Fe found as $Fe_3(CO)_{12}$ to be 24% of the total. The results shown for the yield of $Fe_3(CO)_{12}$ must be regarded as only approximate values.

Discussion[1]

The retention found in $Fe(CO)_5$ is seen in Table IV to be high, in satisfactory agreement with expectations. Moreover, the yield of radioactive $Fe(CO)_5$ found in $Fe_3(CO)_{12}$ is seen to be qualitatively in agreement with prediction. It seems very likely that a rapid condensation of CO molecules on the metal atom occurs, much as was suggested in connection with the formation of the $Mn(CO)_5$ radical (6):

[1] $$M + nCO \rightarrow \rightarrow \rightarrow M(CO)_x$$

or, more specifically,

[1a] $$Fe + nCO \rightarrow \rightarrow \rightarrow Fe(CO)_5$$

[1]When it is useful in the following discussion to distinguish the radioactive atom from the others, an asterisk will be used. The asterisk thus does not imply a chemically excited species.

The earlier stages of this chain are purely speculative, including the starting point (14), but the later stages are supported by the results of recent annealing studies (5) on $Cr(CO)_6$, and by studies of the photo- and radiation chemistry of $Fe(CO)_5$ (12, 13). That the chain must quite rapidly go all the way to $Fe(CO)_5$ in the hot-zone is suggested by contrast with the known reaction of $Fe(CO)_4$ radicals with $Fe(CO)_5$ to give $Fe_2(CO)_9$ (13). It is possible, of course, that an S_N2-like exchange process occurs, at a temperature still too high for $Fe_2(CO)_9$ to be stable. Thus

[2] $$*Fe(CO)_4 + Fe(CO)_5 \rightarrow [*FeFe(CO)_9] \rightarrow *Fe(CO)_5 + Fe(CO)_4$$

although there seems to be no experimental evidence on this point.

From this point on, however, everything seems to be contradictory to our expectations, and we now examine the data and our postulates to seek reasons for the discrepancies. The test assumption as set forth is surely valid for cases in which the molecule is totally re-created from separated fragments in a single grand step, and there seems to be some suggestion that the distribution of products in the arenemetal carbonyls can be interpreted in this way (15). Since this appears not to be the case in these systems, however, we look for the alternative, perhaps stepwise, reactions. The stepwise nature of these more complex reactions is perhaps to be expected, since even the simpler mononuclear species are to some extent re-formed stepwise (3).

We suggest reaction [1] as the fundamental reaction leading to reconstitution. The test postulate can thus accommodate a high yield of $M(CO)_x$ fragments, where x could be 4 or 5. Following this one can write down plausible, although perhaps not unique, mechanisms to account for the observed results. Reactions involving this type of fragment have been suggested on occasion as short-lived reaction intermediates. Cohen and Basolo (16) have inferred the existence of the fragment $Fe(CO)_4$ to be formed during substitution reactions of $Fe(CO)_4X_2$.

For the formation of radioactive $Fe_3(CO)_{12}$ in neutron-irradiated $Fe(CO)_5$ we must find a mechanism different from that devised for the description of the same reaction induced by radiolysis or photolysis, since the yield of the radioactive product is some ten times higher than

Can. J. Chem. Downloaded from www.nrcresearchpress.com by 210.87.254.42 on 09/05/12
For personal use only.

that of the non-radioactive form. Thus, the diffusive recombination of three $Fe(CO)_4$ groups (12, 13) can be eliminated. The reaction of one $*Fe(CO)_4$ with the bulk $Fe(CO)_5$ is known to give $Fe_2(CO)_9$, which does not react further. The instantaneous reaction of three $Fe(CO)_4$ radicals in the hot-zone is presumably ruled out by the failure of our initial hypothesis to predict the yields and retentions. We are left, then, with the following scheme for formation of $Fe_3(CO)_{12}$:

[3] $$*Fe(CO)_4 + Fe(CO)_4 \rightarrow *FeFe(CO)_8$$

[4] $$*FeFe(CO)_8 + Fe(CO)_5 \rightarrow *FeFe_2(CO)_{12} + CO$$

The second stage (reaction [3]) could well occur with fragments formed in the hot-zone; fragments which are only partially re-formed by the chain of reaction [1]. The final step (reaction [4]) would plausibly occur after some diffusion. No positive evidence can be adduced at present to test the validity of this suggested mechanism. It is apparent that a combination of $Fe(CO)_3$ and $Fe(CO)_4$ to give $Fe_2(CO)_7$ in reaction [3] would be equally defensible.

Less can be said, unfortunately, about the reactions in the trinuclear target compounds. Once again, our hypothesis would suggest that the retention should be very low, so we are led to search for stepwise reactions of greater specificity. Of the possibilities, most can be eliminated in the same way as was discussed above. One, however, remains plausible

[1] $$*M + nCO \rightarrow \rightarrow \rightarrow *M(CO)_x \qquad x = 3, 4$$

[5] $$*M(CO)_x + M_3(CO)_{12} \rightleftarrows *MM_2(CO)_{12} + M(CO)_x$$

The first of these, the reconstruction of the metal polycarbonyl radical or molecule is, as before, assumed to occur in the hot-zone. It seems likely that this reaction leads to the observed $*Fe(CO)_5$. The exchange step could well occur during the cooling stages or, less likely, later at ambient temperature. The little which can be drawn from the literature on these solid state exchanges suggests that it must occur in the hot- (or warm-) zone, if at all.

It has been shown (7) that the exchange reaction

[6] $$*Mn(CO)_5 + Mn_2(CO)_{10} \rightleftarrows *MnMn(CO)_{10} + Mn(CO)_5$$

does not occur subsequent to the irradiation time. The results found by Zahn, Collins, and Collins (5) for $Cr(CO)_6$, in which the retention was found to increase as a result of thermal annealing, could be explained as being an exchange, but in this case only a single carbonyl group need be transferred

[7] $$*Cr(CO)_5 + Cr(CO)_6 \rightleftarrows *Cr(CO)_6 + Cr(CO)_5$$

Thus, this reaction does not compare with the post-irradiation exchange of the type shown in reactions [5] and [6].

It is possible that the exchange shown in reaction [5] could be induced by the γ-radiation, especially in the case of $Fe_3(CO)_{12}$, in which photolytic excitation of the bridging carbonyls would weaken the ring structure. We have regrettably been unable to determine the effect of γ dose on the retention, and invite others to extend our experiments in this direction.

In summary, we have shown that the yields and retentions of the trinuclear carbonyls are far higher than can be accommodated by a simple single-stage hot-zone reconstitution mechanism. We have thus examined other possibilities and have concluded that the reaction must start with the hot-zone formation of a reactive radical, such as $M(CO)_4$, which reacts further in a stepwise, more selective reaction.

It is interesting to speculate that through these recoil studies a possible new area for investigation of inorganic exchange reactions has been revealed. Virtually all the exchange reactions of metal carbonyls studied to date (17) are those of a CO molecule with a metal carbonyl molecule (or a substituted metal carbonyl). We have here suggested two further reactions: the transfer of a carbonyl group from a molecule to a radical, as exemplified by reaction [2], and the transfer of larger groups, as exemplified by reactions [5] and [6]. It is suggested that recoil studies in scavenged liquid systems may provide a good approach to studying these new reactions.

Acknowledgments

We are grateful to Imperial Oil Ltd. and to the National Research Council of Canada for financial assistance. Atomic Energy of Canada, Ltd., has been most generous in extending to us the use of their Sb–Be neutron facilities, in which connection Mr. Pat Kennedy and Mr. Roger Murphy have been extremely helpful. We thank Professor K. E. Collins for a prepublication copy of ref. 5.

1. W. H. WONG and D. R. WILES. Can. J. Chem. **45**, 1813 (1967).
2. F. BAUMGÄRTNER and U. ZAHN. Z. Elektrochem. **64**, 1046 (1960).
3. P. REICHOLD and H. P. ANDERS. Radiochim. Acta, **5**, 44 (1966).
4. G. HARBOTTLE and U. ZAHN. Radiochim Acta, **8**, 114 (1967).
5. U. ZAHN, K. E. COLLINS, and C. H. COLLINS. Radiochim Acta, in press.
6. I. G. DE JONG and D. R. WILES. Chem. Commun. 519 (1968).
7. I. G. DE JONG, S. C. SRINIVASAN, and D. R. WILES. Can. J. Chem. In press.
8. F. BAUMGÄRTNER and U. ZAHN. Radiochim. Acta, **1**, 51 (1963).
9. R. COURTEMANCHE and S. A. KUSHNERIAK. Can. Nucl. Technol. **5**(2), 32 (1966).
10. G. HARBOTTLE and U. ZAHN. *In* Chemical effects of nuclear transformations. Vol. II. I.A.E.A. Symp. Vienna. 1964. p. 133.
11. S. R. NARAYAN. Unpublished work.
12. E. K. VON GUSTORF, M.-J. JUN, and G. O. SCHENK. Z. Naturforsch. **18b**, 767 (1963).
13. H. BARZYNSKI and D. HUMMEL. Z. Phys. Chem. **38**, 103 (1963).
14. I. C. YANG and D. R. WILES. Can. J. Chem. **45**, 1357 (1967).
15. S. C. SRINIVASAN and D. R. WILES. To be published.
16. I. A. COHEN and F. BASOLO. J. Inorg. Nucl. Chem. **28**, 511 (1966).
17. C. H. LANGFORD and M. PARRIS. Substitution reactions of labile complexes. To be published in Comprehensive chemical kinetics. *Edited by* C. H. Bamford. Elsevier Publ. Co., Inc., Amsterdam. 1969.

Can. J. Chem. Downloaded from www.nrcresearchpress.com by 210.87.254.42 on 09/05/12
For personal use only.

Can. J. Chem. Downloaded from www.nrcresearchpress.com by 188.143.235.115 on 09/06/12
For personal use only.

Phosphinohydrazines. Part II. Reactions of N,N-dimethylhydrazine and trimethylhydrazine with substituted phosphines[1]

L. K. Peterson, G. L. Wilson, and K. I. Thé
Department of Chemistry, Simon Fraser University, Burnaby 2, British Columbia

Received September 3, 1968

Reactions between trimethylhydrazine and $(CF_3)_2PI$, and between N,N-dimethylhydrazine and CF_3PI_2 have been utilized as synthetic routes to phosphinohydrazine compounds. Two new compounds, trimethylhydrazino-bis(trifluoromethyl) phosphine (m.p. −47.00°, b.p. 130.5° extrapolated) and bis-(N,N-dimethylhydrazino)-trifluoromethylphosphine (m.p. 49.20°, b.p. 184° extrapolated), are described.

Canadian Journal of Chemistry, 47, 1025 (1969)

Discussion

The fundamental features of interest in the chemistry of metalloid-substituted hydrazines were described in Part I (1). We now report an extension of this work, describing reactions between hydrazines and phosphines of varied functionality. The hydrazinolysis of the P—Cl bond was first demonstrated by Nielson and Sisler (2) in the synthesis of $(C_6H_5)_2PNHNMe_2$ and related compounds. Our work shows the feasibility of this process in the reactions of fluoroalkylhalophosphines, $(CF_3)_2PX$ and CF_3PX_2, with alkyl-substituted hydrazines Me_2NNH_2 and Me_2NNHMe, in a suitable solvent such as ether. With hydrazine itself, the products were too unstable to be characterized (1).

Trimethylhydrazino-bis(trifluoromethyl) phosphine, $Me_2NN(Me)P(CF_3)_2$, **1**, obtained according to the equation

[1] $$2Me_2NNHMe + (CF_3)_2PI \rightarrow Me_2NN(Me)P(CF_3)_2 + Me_2NNHMeHI$$

was a colorless liquid (m.p. $-47.00 \pm 0.20°$) which was identified by its mass spectrum (parent peak: obsd., 242; calcd., 242), its nuclear magnetic resonance (n.m.r.) spectrum, and its quantitative cleavage by anhydrous hydrogen chloride into $(CF_3)_2PCl$ and $Me_2NNHMe2HCl$. The ^1H n.m.r. spectrum revealed the six protons of the Me_2N group (at τ 7.50, reference internal $SiMe_4$) and the three protons of the Me—N—P group. The latter absorption (τ, mid-point, 7.13) was split into a doublet by long range *P*—N—C—*H* coupling (J_{P-H}, 3 c.p.s.). This value is considerably smaller than the coupling constants reported by Pople *et al.*(3) for other P—N—C—H systems (viz. ca. 10 c.p.s.), reflecting electron withdrawal from the intervening bonds by the electronegative CF_3 groups attached to phosphorus. The peaks of the doublet showed further fine structure due to long range proton—fluorine coupling (J_{H-F}, ~0.7 c.p.s.), and were recognizable as two overlapping septets. The overall intensity ratio of 2:1 was consistent with our formulation of compound **1**. The familiar ^{19}F doublet was also observed (δ, mid-point, 63.4 p.p.m. above internal $CFCl_3$; J_{P-CF_3}, 82 c.p.s.). The main features of the infrared spectrum, given in Table I, are indicative of bands due to methyl, CF_3, and N—N.

In theory, reaction between two difunctional species such as CF_3PI_2 and Me_2NNH_2 should provide potential synthetic routes to at least three distinct systems

(*a*) the molecular species,

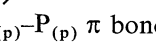

involving the $N_{(p)}$–$P_{(p)}$ π bond

(*b*) the linear polymer

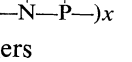

and (*c*) cyclic oligomers

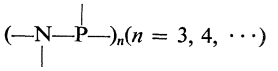

via the possible intermediates

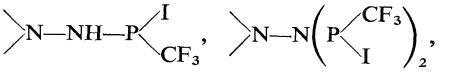

and

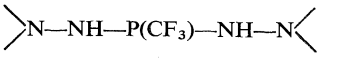

The nature of the preferred product should provide clues about the mechanistic, stereochemical,

[1]Presented at the Annual Conference, Chemical Institute of Canada, Vancouver, British Columbia, June 1968.

TABLE I

Infrared spectrum* of $Me_2NN(Me)P(CF_3)_2$

Wavelength (cm^{-1})	Intensity	Wavelength (cm^{-1})	Intensity	Wavelength (cm^{-1})	Intensity	Wavelength (cm^{-1})	Intensity
422	8	658	7	1153	100	2788	14
449	13	738	2	1198	70	2825	15
473	23	848	20	1222	(Shoulder)	2853	13
475	23	868	8	1280	(Shoulder)	2875	(Shoulder)
540	4	1000	7	1456	12	2912	11
560	8	1020	7	2244	4	2690	25
563	8	1109	68	2300	2	2995	16

*Intensities are quoted relative to the strongest band, at 1153 cm^{-1}, with a value of 100 arbitrary units.

and electronic factors controlling the reaction. In our work we found that solvent effects were of prime importance. Thus, in ether, cyclohexane, or tetrachloroethylene, reactions between CF_3PI_2 and Me_2NNH_2 afforded intractable, apparently polymeric, involatile materials, ranging in character from yellow oils to sticky brown solids. These products are probably analogous to the phosphonitrilic polymers derived from the thermal decomposition of $C_6H_5P(NHNMe_2)_2$ (4). With chlorobenzene as solvent, however, the new compound bis(N,N - dimethylhydrazino) - trifluoromethylphosphine, $CF_3P(NHNMe_2)_2$, **2**, was created in good yield according to the equation:

[2] $$CF_3PI_2 + 4H_2NNMe_2 \rightarrow CF_3P(NHNMe_2)_2 + 2Me_2NNH_2HI$$

The absence of CF_3H and nitrogen indicates stability against molecular rupture and fragmentation, in contrast to the analogous reactions involving N_2H_4 (1). Because of its low volatility, compound **2** is difficult to handle in the vacuum system. However, mass spectral data, as well as structural evidence from n.m.r., are consistent with our formulation. The ^1H spectrum consisted of distinct resonance adsorptions in 6:1 ratio, corresponding to 12 methyl protons [at τ 7.59, single sharp peak], and a doublet corresponding to the NH protons split by coupling with spin 1/2 ^{31}P (τ, mid-point, 5.92; J_{P-H}, 20 c.p.s.). The ^{19}F resonance was a doublet (δ, mid-point, +65.4 p.p.m.; J_{P-CF_3}, 83 c.p.s.). Our efforts to locate $Me_2N—N{=}PCF_3$, a system containing the unstable —P=N— bonding situation (5–7), were unsuccessful. Thus, the stability of compound **2**, $CF_3P(NHNMe_2)_2$, must stem from an enhancement of $N(p_\pi) \rightarrow P(d_\pi)$ π-bonding, a bonding situation favored by the electronegative CF_3 group on phosphorus (8, 9).

Experimental

Volatile materials were handled in a vacuum system, while dry-box techniques were used where nonvolatile substances were encountered. Reactions were carried out in specially constructed sealed Pyrex vessels, fitted with in situ filtration facilities. Nuclear magnetic resonance spectra were determined with a Varian A56/60 instrument, infrared spectra with a Beckmann I.R. 12 spectrophotometer, and mass spectra with a double focusing RMU-6E Hitachi Perkin–Elmer instrument.

The iodophosphines and dimethylhydrazines were obtained as previously described (1), and all solvents were rigorously dried and distilled. Trimethylhydrazine was prepared by the method of Class *et al.* (10). We found that the final stage, viz. the reduction of $Me_2NN{=}CH_2$ with lithium aluminium hydride, yielded dimethylhydrazine as well as trimethylhydrazine. Purification was effected by vacuum distillation, using a 36 in. low temperature distillation column.

Reaction of $(CF_3)_2PI$ with Me_2NNHMe

In a typical synthesis, a mixture of trimethylhydrazine (0.9179 g) in ether (1.4100 g) was treated with $(CF_3)_2PI$ (1.2068 g) in a filtration reaction vessel. After 12 h at room temperature, the products were separated by filtration and vacuum fractionation. The components isolated were $Me_2NNHMeHI$ (0.7977 g); excess Me_2NNHMe (0.2230 g); "ether fraction" (1.5671 g); and $Me_2NN(Me)P(CF_3)_2$, **1** (0.8143 g, 83% yield). The latter product was identified by its mass spectrum (parent peak: obsd., 242; calcd., 242); major fragments were Me_2NNMe (*m*, 73), CF_3 (*m*, 69), and Me_2N (*m*, 44). Infrared (Table I) and n.m.r. spectra were consistent with our formulation of compound **1**. In addition, compound **1** (0.0678 g) reacted quantitatively with anhydrous hydrogen chloride (0.0373 g) in chlorobenzene solution, yielding $(CF_3)_2PCl$ (0.0548 g; m_{obsd}, 202; m_{calcd}, 204.5) and $Me_2NNHMe2HCl$ (0.0402 g), determining the stoichiometry

[3] $$Me_2NNMeP(CF_3)_2 + 3HCl \rightarrow (CF_3)_2PCl + Me_2NNHMe2HCl$$

Physical Properties of $Me_2NN(Me)P(CF_3)_2$

The melting point of compound **1**, determined on samples sealed into capillary tubes, was $-47.00 \pm 0.20°$.

Saturated vapor pressures were measured with a mercury tensimeter. Compound **1** was stable at least to 110°, as shown by reproducible vapor pressures. Data for

Can. J. Chem. Downloaded from www.nrcresearchpress.com by 188.143.235.115 on 09/06/12
For personal use only.

TABLE II

Saturated vapor pressure data* for liquid $Me_2NN(Me)P(CF_3)_2$

T, °C	P_{mm}(obsd.)	P_{mm}(calcd.)	T, °C	P_{mm}(obsd.)	P_{mm}(calcd.)
26.6	15.4	14.8	63.0	83.7	83.8
29.7	17.8	17.4	69.2	108	108
38.8	27.9	27.9	76.5	144	143
47.0	41.6	41.4	81.2	170	170
54.5	58.3	58.3	91.4	247	242

*$\text{Log } P_{mm} = 6.7566 - 0.005896T + 1.75 \log T - 2445/T$.

TABLE III

Saturated vapor pressure data* for $CF_3P(NHNMe_2)_2$

T, °C	P_{mm}(obsd.)	P_{mm}(calcd.)	T, °C	P_{mm}(obsd.)	P_{mm}(calcd.)
49.4	1.70	1.75	93.2	21.4	21.4
63.1	4.10	4.13	115.0	56.4	59.2
72.5	7.00	7.11	134.0	128	130
86.6	15.3	15.3	151.0	248	249

*$\text{Log } P_{mm} = 5.9707 - 0.002678T + 1.75 \log T - 2985/T$.

the liquid–vapor equilibria are given in Table II. The extrapolated boiling point is 130.5°; the latent heat of vaporization at the boiling point is 8200 cal mole^{-1}; and the Trouton constant is 20.3 cal deg^{-1}.

The infrared spectrum over the range 400 to 4000 cm^{-1}, measured in the gas phase (10 cm cell, KBr windows), is given in Table I.

Reaction of CF_3PI_2 with Me_2NNH_2

In the solvents ether, cyclohexane, and tetrachloroethylene, CF_3PI_2 and Me_2NNH_2 reacted to form intractable, nonvolatile materials, ranging from yellow oils to dark brown, sticky solids. But when CF_3PI_2 (0.5635 g) was mixed with a solution of Me_2NNH_2 (0.9681 g) in chlorobenzene (2.8921 g), no discoloration was observed, even after 12 h at room temperature. The products were Me_2NNH_2HI (0.7486 g); "chlorobenzene fraction" (C_6H_5Cl plus excess Me_2NNH_2, 3.4730 g); and colorless, crystalline needles of $CF_3P(NHNMe_2)_2$, **2**, in good yield. The mass spectral pattern of compound **2** indicated a parent molecular weight corresponding to $CF_3P(NHNMe_2)_2$ (m_{obsd}, 218; m_{calcd}, 218), and intense peaks indicative of the fragments $CF_3PNHNMe_2$ (m, 159) and $NHNMe_2$ (m, 59). The n.m.r. spectrum, measured in chlorobenzene solution, was consistent with the above formulation for compound **2**.

Physical Properties of $CF_3P(NHNMe_2)_2$

The melting point of compound **2**, determined on samples sealed into capillary tubes, was 49.20 ± 0.20°.

Saturated vapor pressures were measured with a mercury tensimeter. At elevated temperatures (>100°), compound **2** was unstable; hence measurements were made on fresh samples in the minimal time required to establish equilibrium. The data are given in Table III. The extrapolated boiling point is 184°, and the latent heat of vaporization is 12 700 cal mole^{-1}.

Acknowledgments

The authors gratefully acknowledge the financial support from the National Research Council of Canada, and from the President's Research Fund of Simon Fraser University.

1. L. K. Peterson and G. L. Wilson. Can. J. Chem. **46**, 685 (1968).
2. R. P. Nielson and H. H. Sisler. Inorg. Chem. **2**, 753 (1963).
3. J. A. Pople, W. G. Schneider, and H. J. Bernstein. High resolution nuclear magnetic resonance. McGraw-Hill Book Co., Inc., New York. 1959. p. 351.
4. M. Winyall and H. H. Sisler. Inorg. Chem. **4**, 655 (1965).
5. A. J. Kirby and S. G. Warren. The organic chemistry of phosphorus. Elsevier Publ. Co., Inc., Amsterdam. 1967.
6. E. Fluck. *In* Topics in phosphorus chemistry. *Edited by* M. Grayson and E. J. Griffith. Interscience Publishers, Inc., New York. 1967.
7. J. R. van Wazer. Phosphorus and its compounds. Vol. 1. Interscience Publishers, Inc., New York. 1958. pp. 328–344.
8. E. Fluck. *In* Topics in phosphorus chemistry. *Edited by* M. Grayson and E. J. Griffith. Interscience Publishers, Inc., New York. 1967. p. 312.
9. A. B. Burg and J. Heners. J. Am. Chem. Soc. **87**, 3092 (1965).
10. J. B. Class, J. G. Aston, and T. S. Oakwood. J. Am. Chem. Soc. **75**, 2937 (1953).

Can. J. Chem. Downloaded from www.nrcresearchpress.com by 188.143.235.115 on 09/06/12
For personal use only.

Can. J. Chem. Downloaded from www.nrcresearchpress.com by 210.87.254.42 on 09/05/12
For personal use only.

γ-Radiolysis of disulfides in aqueous solution. II. D-Penicillamine disulfide[1]

J. W. PURDIE[2]
Defence Research Establishment Ottawa, Defence Research Board, Ottawa, Canada

Received July 10, 1968

The γ-radiolysis of D-penicillamine disulfide (PenSSPen) in 3×10^{-4} *M* aqueous solution has been studied under aerated and deaerated conditions. G values were determined for the following products: penicillamine sulfinic acid ($PenSO_2H$), penicillaminic acid ($PenSO_3H$), β-hydroxyvaline (PenOH), 2-amino-3-methylbut-3-enoic acid ($HOOC \cdot CH(NH_2) \cdot C(CH_3)=CH_2$), penicillamine (PenSH), penicillamine disulfide-*S*-monoxide (PenS(O)SPen), valine (PenH), penicillamine trisulfide (PenSSSPen), and ammonia. The low yield of $PenSO_3H$ in aerated solution indicated that PenSOH did not react with oxygen or O_2^-. The trisulfide, which was obtained in high yield, was found to come mainly from the reactions:

$$PenSSPen + \cdot OH \rightarrow PenSSOH + Pen\cdot$$

$$PenSSOH + PenSH \rightarrow PenSSSPen + H_2O$$

Experiments with ·OH radicals produced chemically ($TiCl_3/H_2O_2$) and irradiations with cysteine or penicillamine present were used to confirm these reactions. These and the other reactions were tested with radical scavengers; formate and monochloroacetate ions and nitrous oxide.

Canadian Journal of Chemistry, 47, 1029 (1969)

Introduction

In a previous communication (1) the γ-radiolysis of cystine in aqueous solution was reported and a mechanism proposed. Studies of cystine and related disulfides in aqueous solutions have been reported by several other workers recently (2–8) and the earlier literature has been reviewed (9).

The present paper reports a study of the radiolysis of D-penicillamine disulfide (2,2,5,5-tetramethylcystine) in dilute aqueous solutions. This compound was of particular interest for comparison with cystine since cysteine is a radioprotective compound whereas penicillamine is not radioprotective. Radiolysis of penicillamine disulfide has not been reported previously although the thiol, penicillamine, has been examined by several workers. Henriksen (10, 11) studied irradiated penicillamine in frozen aqueous solutions and in polycrystalline samples by electron spin resonance (e.s.r.) spectroscopy. Braams (12) obtained rate constants for reaction of the solvated electron with penicillamine using pulse radiolysis. It has also been investigated in solution by Armstrong and Humphreys (4) using e.s.r. spectroscopy. In this paper, the symbol "Pen" is used to represent $HOOCCH(NH_2)C(CH_3)_2S$— in structural formulae and hence PenSH is penicillamine and PenSSPen is the disulfide. The usual abbreviations, CySH and CySSCy, are used for cysteine and cystine respectively.

Experimental

A Technicon amino acid analyzer model NC-1 was employed with the modifications described previously (13). Columns of the following resins were used for analytical purposes: "Chromobeads" type A, 150 × 0.6 cm; "Chromobeads" type C2, 75 × 0.6 cm; Dowex 1-x8 (200–400 mesh) 150 × 0.6 cm. The nuclear magnetic resonance (n.m.r.) spectra were run on a Varian HA60I and infrared spectra on a Perkin–Elmer 221 G. Mass spectra and interpretations were performed by Morgan Schaffer Corp., Montreal.

D-Penicillamine (A grade) was purchased from Calbiochem and used for the preparation of the disulfide. Penicillaminic acid and β-hydroxyvaline were obtained from Calbiochem. Valine and other reference amino acids were purchased from Mann Research Labs. Nitrous oxide gas was supplied by Matheson, Coleman and Bell Ltd. and was purified by trap-to-trap distillation just before use. Monochloroacetic acid and sodium formate were Fisher certified reagents.

D-*Penicillamine Disulfide (PenSSPen)*

This compound was prepared by bubbling oxygen through an alkaline aqueous solution of penicillamine until a negative test was obtained with Ellman's reagent for thiols (14). The solution was neutralized, evaporated to dryness, and the product (crystallized from aqueous ethanol) had m.p. 198–199°.

Anal. Calcd. for $C_{10}H_{20}N_2O_4S_2$: C, 40.5; H, 6.7; N, 9.45; S, 21.6. Found: C, 40.3; H, 6.9; N, 9.5; S, 21.8.

This sample was chromatographically pure except for traces of the trisulfide (PenSSSPen) and was used for

[1]Presented in part at the 15th Annual Meeting of the Radiation Research Society, San Juan, May, 1967. Issued as DREO Report No 572.

[2]Present address: Division of Biology, National Research Council of Canada, Ottawa, Canada.

TABLE I

Elution times and color yields of products

Compound	Column	Elution time (min)	Color yield hw, 0.25 μE*	Notes
Glutamic	Dowex 1	200	15.3	Reference standard
$PenSO_2H$	Dowex 1	245	9.2	hw assumed equal to $PenSO_3H$
$PenSO_3H$	Dowex 1	300	9.2	
PenOH	Chromobeads A	180	9.3	
COOH CH_3 | | $CH(NH_2)C{=}CH_2$	Chromobeads A	250	12.1	Yield same as valine
PenSH	Chromobeads A	315	1.25	
PenS(O)SPen	Chromobeads A	370	7.5	Assumed equal to PenSSPen
PenH	Chromobeads A	460	12.1	
PenSSPen	Chromobeads A	590	7.5	
Norleucine	Chromobeads A	660	13.8	Reference standard
PenSSSPen	Chromobeads A	725	6.7	
NH_3	Chromobeads A	830	7.5	

*E = equivalent weight with respect to ninhydrin positive groups.

most of the radiation experiments. The nuclear magnetic resonance spectrum, run in trifluoroacetic acid, showed a broad peak at $\tau = 2.38$ due to the NH_3^+ and peaks at $\tau = 5.65$ (CH), $\tau = 8.21$ (CH_3), and $\tau = 8.38$ (CH_3).

Penicillamine Trisulfide (β,β′-divalyltrisulfide; PenSSSPen)

Preparation of this compound was attempted by the methods described by Fletcher and Robson for preparation of cystine trisulfide (CySSSCy) (15). The following preparation was the most successful. Sulfur (216 mg) was dissolved in chloroform (50 ml) and ethanol (200 ml) added. The solution was made alkaline by addition of concentrated ammonium hydroxide solution (5 ml) and penicillamine (1 g in 25 ml water) was added. The solution was stirred for 4 h and evaporated to dryness.

The product was purified by chromatography on a column of Dowex 50W-x8 cation-exchange resin using volatile buffers (16) and had m.p. 185° (corrected) after crystallization from aqueous ethanol; yield, 280 mg from half the starting material (40%).

Anal. Calcd. for $C_{10}H_{20}N_2O_4S_3$: C, 36.53; H, 6.09; N, 8.53; S, 29.26. Found: C, 36.34; H, 5.82; N, 8.44; S, 29.15.

The n.m.r. spectrum of the pure trisulfide was run in trifluoroacetic acid. It had peaks at $\tau = 2.40$ (NH_3^+) $\tau = 5.44$ (—C(H)—) and methyl peaks at $\tau = 8.17$ and 8.41 with integrals in the ratio 3:1:3:3 as required by the assignment given. This spectrum is very similar to that of the disulfide except for slight shifts and a greater separation of the methyl peaks. The occurrence of two sharp methyl peaks in the spectrum shows that it is a linear trisulfide.

Irradiation and Analysis

Irradiations were performed using 25 ml samples in 25 ml round-bottom flasks as described previously. Thrice-distilled water was used for all solutions and the irradiation flasks were cleaned with hot chromic acid, rinsed thoroughly and steamed before use. A total dose of 10 000 rads at a dose rate of 800 rads/min was used except where otherwise stated. The irradiated solutions were analyzed as described previously (1). In order to measure ammonia yields, samples were pumped directly into a "Chromobeads" C2 column without freeze drying and then eluted in the usual way.

Order of Elution of Products and Color Yields

The elution times and color yields for the products and reference compounds are listed in Table I. These are for a flow rate of 30 ml of eluent per h. The Dowex 1 column was operated at room temperature and the "Chromobead" type A column was maintained at 60° throughout the run.

Isolation of Products

The products were separated by chromatography on a column of Dowex 50W-x8 cation-exchange resin using volatile buffer systems (16). A solution of penicillamine disulfide (2.4 g) in 4 l of water was irradiated with a total dose of 100 000 rads, concentrated, and chromatographed with acetic acid – pyridine buffers. A small portion of the effluent was drawn into the amino acid analyzer by the proportioning pump so as to provide a continuous record of the separation. Nine major peaks were observed, including unchanged disulfide and ammonia. Each product was purified by re-running it on the same column, operated at 45 °C, until chromatographically pure samples were obtained.

Seven products were obtained in quantities sufficient to allow examination.

Results

Identification of Products

Products 1 and 2 (penicillaminic and penicillamine sulfinic acids) both occurred in the first group. They were resolved by chromatography on a column of Dowex 1 anion-exchange resin using aqueous formic acid as eluent (17). The first product eluted was a strong acid which decolorized iodoplatinic acid. This result, together

Can. J. Chem. Downloaded from www.nrcresearchpress.com by 210.87.254.42 on 09/05/12
For personal use only.

Can. J. Chem. Downloaded from www.nrcresearchpress.com by 210.87.254.42 on 09/05/12
For personal use only.

with its chromatographic behavior, showed that it was penicillamine sulfinic acid, (valine-β-sulfinic acid), ($PenSO_2H$). The second product, also a strong acid, was found to co-chromatograph with commercial penicillaminic acid ($PenSO_3H$).

Product No. ***4*** contained sulfur but was not identified.

Anal. Found: S, 17.2.

Mass spectrometric analysis of the acid and of the ethyl ester indicated a molecular weight of 161 for the acid.

Product No. ***5*** *(β-Hydroxyvaline)*

The infrared spectrum of this product had a sharp peak at 3410 cm^{-1} indicating a hydroxy group. β-Hydroxyvaline appeared to be a likely product so it was synthesized as described by Mix (18) and compared with the isolated product. The infrared spectra (KBr) differed considerably. However, the two compounds co-chromatographed on paper and with the amino acid analyzer. Both gave identical n.m.r. spectra when run in trifluoroacetic acid. The infrared spectrum of the synthetic compound differed from the radiolysis product because the former was a racemic mixture whereas the latter was a pure optical isomer (19). The n.m.r. spectrum had a broad band at $\tau = 2.48$ (NH_3), a broad band at

$$\begin{array}{c} | \\ \text{5.65 (—CH)} \\ | \end{array}$$

which could be decoupled from the NH_3 to give a sharp peak, and two sharp peaks at $\tau = 8.28$ and $\tau = 8.50$ (2 CH_3 groups).

Product No. ***6*** *(2-Amino-3-methylbut-3-enoic Acid)*

This compound will be referred to as the "vinyl" derivative for convenience.

The infrared spectrum of this product indicated it was a neutral amino acid without other functional groups and analysis showed sulfur was absent. The mass spectrum of the ethyl ester showed that the compound was a vinyl derivative of valine: $CH_2{=}C(CH_3)CH(NH_2)COOH$. A weak n.m.r. spectrum was obtained (capillary sample tube) which was consistent with this structure: peaks; $\tau = 8.05$ (CH_3); $\tau = 5.1$

$$\begin{array}{c} \diagdown \\ \text{(broad, —CH)} \\ \diagup \end{array}$$

$\tau = 4.62$ ($CH_2{=}$). Further evidence for the structure was obtained by catalytic hydrogenation. A mixture of the unknown and alanine in water was hydrogenated (H_2/Pt) and a portion of the solution examined using the amino acid analyzer before and after hydrogenation. The radiolysis product was reduced completely to valine whereas the alanine was unchanged.

Product No. ***8*** *(Penicillamine Trisulfide)*

The infrared spectrum of the product was very similar to that of penicillamine disulfide. The most noticeable difference was a sharp peak at 1695 cm^{-1} and another at 1270 cm^{-1} in the spectrum of the product. The n.m.r. spectrum was also very similar to penicillamine disulfide. The unknown had peaks at $\tau = 2.40$, 5.44, 8.17, 8.41, and 7.77. The peak at 7.77 was sharp and appeared to be due to acetic acid which had not evaporated during the freeze drying.

Anal. Calcd. for $C_{10}H_{20}N_2O_4S_3 \cdot CH_3CO_2H$: N, 7.22; S, 24.8. Found: N, 7.56; S, 23.54.

Penicillamine trisulfide (PenSSSPen) was synthesized and found to be identical with the radiolysis product as shown by infrared and n.m.r. spectra, and by chromatography. The synthetic sample also retained acetic acid when isolated by the same procedure.

Product No. ***9*** *(Valine)*

This product was shown to be identical to valine (PenH) by infrared analysis and chromatography.

Products not Isolated

The main product which was not isolated by the procedures described above was penicillamine. A peak was present in aerated and deaerated solutions which co-chromatographed with penicillamine but it was presumably oxidized to the disulfide during the preparative-scale chromatography and evaporations. The presence of penicillamine was confirmed using Ellman's reagent (5,5′-dithio-bis-(2-nitrobenzoic acid)) and the yields were checked by this method (14, 20). The other significant peak which remained unaccounted for appeared on chromatograms between penicillamine and valine. PenS(O)SPen seemed a likely possibility for this compound and it was found to decompose if the solution was made alkaline. Disulfide-*S*-monoxides are unstable in solutions above pH 6 and decompose to yield sulfinic acid and disulfide.

A double peak frequently appeared in the chromatograms corresponding to β-hydroxyvaline (PenOH). This may have been due to the presence of PenOOH which is probably the precursor of the PenOH.

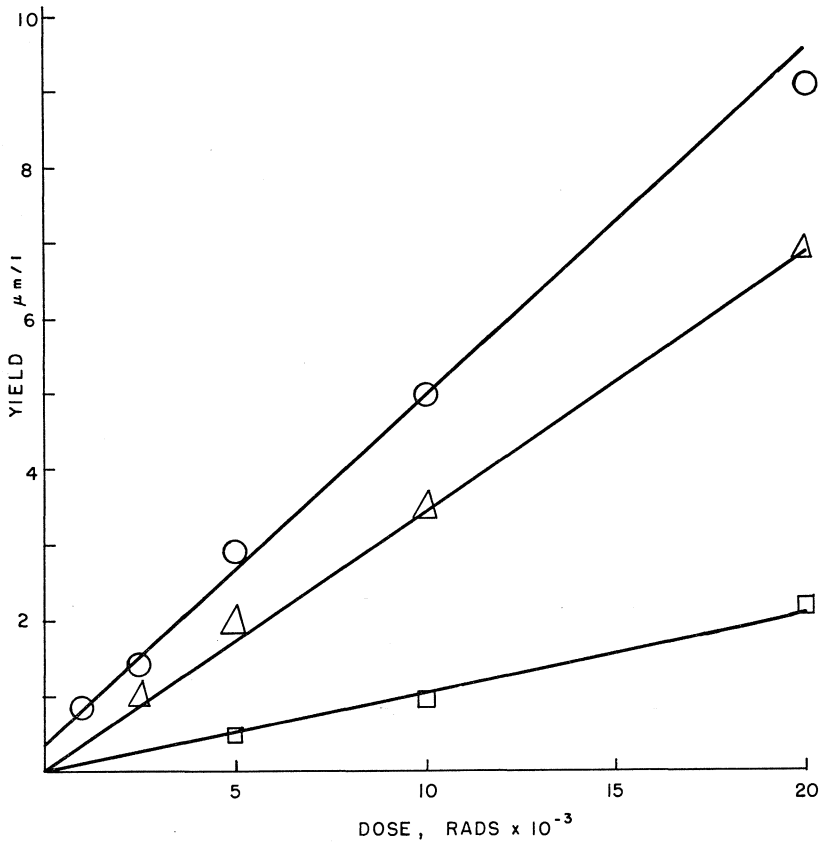

FIG. 1. Yield–dose plots for the major products of radiolysis of penicillamine disulfide in aerated solution: PenSSSPen (○); $PenSO_2H$ (△); $PenSO_3H$ (□).

TABLE II

Radiolysis of PenSSPen: G values and nitrogen balance for products after irradiation with 10 000 rads at ambient temperature

	Aerated			Deaerated		
Product	G value	Average deviation (±)	G(N)	G value	Average deviation (±)	G(N)
$PenSO_2H$	0.5	0.1	0.5	0.3	0.1	0.3
$PenSO_3H$	0.10	0.01	0.1	Trace	—	0.0
$PenSSO_3H$	0.05	—	0.05	0.05	—	0.05
PenOH	0.20	0.02	0.2	Trace	—	0.0
COOH CH₃ | | CH(NH₂)C=CH₂	0.11	0.01	0.11	0.33	0.08	0.33
PenSH	0.45	0.05	0.45	2.3	0.4	2.3
PenS(O)SPen	0.27	0.1	0.54	0.22	0.04	0.44
PenH	0.0	—	0.0	0.13	0.01	0.13
PenSSSPen	0.6	0.1	1.2	1.0	0.1	2.0
NH_3	1.5	—	1.5	0.75	—	0.75
TOTAL N			4.65			6.30
PenSSPen	−3.3	0.3	−6.6	−4.0	0.3	−8.0
RECOVERY			70%			80%

Can. J. Chem. Downloaded from www.nrcresearchpress.com by 210.87.254.42 on 09/05/12
For personal use only.

TABLE III

G values in the presence of radical scavengers

Scavenger	Concentration of scavenger	$PenSO_2H$	PenOH	Vinyl	PenSH	PenS(O)SPen	PenH	PenSSSPen
				Aerated				
No scavenger	0	0.49	0.19	0.11	0.46	0.22	0	0.6
Formate	10^{-4} *M*	0.31	0.20	0.14	0.4	0.36	0	0.4
	10^{-3} *M*	0.24	Trace	Trace	Trace	0.07	0	0.26
Chloroacetate	10^{-4} *M*	0.38	0.11	0.12	0.62	0.24	0	0.59
	10^{-3} *M*	0.24	0.07	0.10	0.3	—	0	0.23
Scavenger	Concentration of scavenger	$PenSO_2H$	PenOH	Vinyl	PenSH	PenS(O)SPen	PenH	PenSSSPen
				Deaerated				
No scavenger	0	0.3	Trace	0.33	2.3	0.22	0.13	1.0
Chloroacetate	10^{-4} *M*	0.50	Trace	0.23	2.3	0.17	0.09	0.77
	10^{-3} *M*	0.34	Trace	0.2	Trace	0.11	0.04	0.3
N_2O	2×10^{-3} *M*	0.30	Trace	0.28	1.7	0.24	0.08	1.35
	2×10^{-2} *M*	0.41	Trace	0.29	Trace	0.2	0.09	1.5

Yields of Radiolysis Products

The yields of the main products in aerated solutions were measured at various doses between 1 000 rads and 20 000 rads. The results are shown in Fig. 1. The yields measured were linear with dose up to 20 000 rads.

The yields of all products identified were measured or estimated after irradiation of PenSSPen with 10 000 rads. The results for both aerated and deaerated solutions are listed in Table II. The figures are average values from a number of experiments and the average deviation is given. Table II also gives the G values in terms of nitrogen atoms in order to estimate the product balance. The nitrogen was used rather than the sulfur since products were measured with ninhydrin which reacts with amino groups and ammonia.

Dose-Rate Effects

The effect of dose rate was examined in aerated solution in view of the fact that it had a remarkable effect on the yields of sulfinic and sulfonic acids from cystine (1). With penicillamine disulfide however, there was no measurable change in the yields of $PenSO_2H$ and $PenSO_3H$ when the dose rate was reduced from 800 rads/min to 10 rads/min. Disulfide concentration and total dose were kept constant at $3 \times 10^{-4}M$ and 10 000 rads respectively, while dose rates of 800, 600, 300, 100, and 10 rads/min were employed.

Effect of Radical Scavengers on Yields

The effect of radical scavengers on the yields was investigated using formate ions and monochloroacetate ions in aerated solution, and monochloroacetate ions and nitrous oxide in deaerated solutions (21). Formate ions react readily with ·H and ·OH radicals but relatively slowly with e^-_{aq}. Monochloroacetate ions react rapidly with e^-_{aq}. Nitrous oxide reacts with e^-_{aq} but gives rise to an ·OH radical. The results of these experiments are given in Table III.

Effect of CySH and PenSH

Experiments were carried out with CySH or PenSH present during the irradiation in order to evaluate the mechanism proposed for trisulfide formation. The mercaptans were present in low concentrations (10^{-6} and 10^{-5} *M*) so as to avoid significant competition with the disulfide ($3 \times 10^{-4}M$) for the primary ·OH and e^-_{aq} radicals. The results are presented in Table IV. The irradiations without mercaptans present were performed at about the same time and using the same solution of disulfide. (Small variations were frequently encountered between irradiations performed at different times.)

Discussion

Radiolysis of penicillamine disulfide differs from radiolysis of cystine mainly in the relative

Can. J. Chem. Downloaded from www.nrcresearchpress.com by 210.87.254.42 on 09/05/12
For personal use only.

TABLE IV

Effect of PenSH and CySH on G values of trisulfides

	Aerated					Deaerated	
		PenSH		CySH			
	No RSH	$10^{-6}M$	$10^{-5}M$	$10^{-6}M$	$10^{-5}M$	No RSH	CySH $10^{-5}M$
PenSH	0.53	0.64	0.67	0.62	0.86	3.3	3.5
CySSCy	—	—	—	0.02	0.24	—	0.06
CySSPen	—	—	—	0.02	0.21	—	0.31
CySSSCy	—	—	—	0	0	—	0
CySSSPen	—	—	—	0.06	0.22	—	0.08
PenSSSPen	0.60	0.58	0.68	0.52	0.41	1.00	0.80

amounts of the various products. The yields of sulfonic acid and trisulfide were significantly changed; the sulfonic acid yield was much lower and the trisulfide yield much higher (Table II). The yields reported previously (1) for cystine trisulfide were high by a factor of four due to an error in calculation. As before it was difficult to measure the loss of disulfide accurately at low dose and this may account for some of the discrepancy in the nitrogen balance in Table II. Also, some assumptions had to be made with respect to the color yields of certain products as indicated in Table I. Some minor products remained unidentified and these could have contributed significantly to the nitrogen balance if their color yields with ninhydrin were very low. The peak which was thought to be PenOOH was not included in the Table. It was usually similar to PenOH in color yield.

The disulfide is attacked mainly at the sulfur atoms by e^-_{aq} and ·OH radicals with splitting of the sulfur–sulfur bond or a carbon–sulfur bond. Scission of the sulfur–sulfur bond probably occurs as follows:

[1] $\text{PenSSPen} + \cdot\text{OH} \rightarrow \text{PenSOH} + \text{PenS}\cdot$

[2] $\text{PenSSPen} + e^-_{aq} \rightarrow \text{PenS}^- + \text{PenS}\cdot$

Reaction [2] should occur mainly in deaerated solutions as the oxygen will scavenge the e^-_{aq} in aerated solutions. However, the solvated electron reacts rapidly with penicillamine ($k = 5.1 \times 10$ $M^{-1}\,s^{-1}$) (12), so it probably reacts rapidly with the disulfide also, allowing the latter to compete effectively with oxygen. (Solvated electrons react with cystine faster than with cysteine (12).) The PenS· radical has been detected in aqueous solutions by Armstrong and Humphreys using electron spin resonance spectroscopy (4). It was produced when ·OH radicals, from the $TiCl_3 - H_2O_2$ reaction, reacted with penicillamine in a flow system. Adams *et al.* (5) have suggested that the radical $RS\dot{S}R$ is an important intermediate in the radiolysis of cysteamine and cystamine. They observed a species with an absorption maximum at 4100 Å, obtained by ·OH oxidation and e^-_{aq} reduction of cysteamine and cystamine respectively. Since the $RS\dot{S}R$ decays to give the same products as reaction [2] it represents an intermediate in that reaction. With disulfides the radical anion is not produced by ·OH radicals so reaction [1] is satisfactory to explain the attack by ·OH at this position. A radical cation ($RS\dot{S}R^+$) has been suggested as an intermediate in the radiolysis of disulfides (7), but in the absence of any supporting evidence reaction [1] seems preferable since RS· is the only radical which has been identified in acidic solutions.

Sulfenic acids are unstable and usually decompose to sulfinic acid and disulfide. The following reactions are suggested for the decomposition of PenSOH in the irradiated solution:

[3] $2\,\text{PenSOH} \rightarrow \text{PenSO}_2\text{H} + \text{PenSH}$

[4] $\text{PenSOH} + \text{PenSSPen} \rightarrow \text{PenS(O)SPen} + \text{PenSH}$

[5] $\text{PenSOH} + \text{PenSH} \rightarrow \text{PenSSPen} + \text{H}_2\text{O}$

The sulfenic acid does not react with O_2 or O_2^- to form sulfonic acid as appeared to be the case with cysteine sulfenic acid. The PenS· radicals produced in reactions [1] and [2] may combine to give disulfide, or react with oxygen (in aerated solution) to produce sulfinic and sulfonic acids (1).

Rupture of the carbon–sulfur bond in the disulfide during radiolysis leads to products such

Can. J. Chem. Downloaded from www.nrcresearchpress.com by 210.87.254.42 on 09/05/12
For personal use only.

Can. J. Chem. Downloaded from www.nrcresearchpress.com by 210.87.254.42 on 09/05/12
For personal use only.

as trisulfide, valine, etc. In discussing the radiolysis of cystine (1) it was suggested that RS· radicals attacked the disulfide:

[6] $RS\cdot + RSSR \rightarrow RSSSR + R\cdot$

This seems unlikely in the light of results obtained with penicillamine disulfide. It appears that the carbon–sulfur bond is attacked by the ·OH radical giving an intermediate which reacts to yield trisulfide:

[7] $RSSR + \cdot OH \rightarrow RSSOH + R\cdot$

[8] $RSSOH + RSH \rightarrow RSSSR + H_2O$

In deaerated solution the disulfide may also be attacked at the same site by e^-_{aq} or ·H radicals with formation of a hydrodisulfide (22) and hence, trisulfide:

[9] $RSSR + e^-_{aq} \rightarrow RSS^- + R\cdot$

[10] $RSS^- + RSOH \rightarrow RSSSR + OH^-$

The tertiary radical Pen· formed from penicillamine disulfide should be more stable than the primary radical Cy· formed in the case of cystine and this may be the reason for the larger yield of trisulfide from penicillamine disulfide. Reaction [7] appears to be more important than [9] since the yield of trisulfide was increased in deaerated solution by addition of nitrous oxide. The Pen· radical produced in reactions [7] and [9] (in the case of penicillamine disulfide) could react with oxygen in aerated solution to form, eventually, hydroxyvaline (PenOH). In deaerated solutions it may react with e^-_{aq} or ·H to give valine (PenH). In both aerated and deaerated solutions it may lose a hydrogen to yield the vinyl compound: e.g.

[11] $HOOCCH(NH_2)\text{—}\dot{C}(CH_3)\text{—}CH_3 + PenS\cdot \rightarrow HOOCCH(NH_2)\text{—}C(CH_3)=CH_2 + PenSH$

An alternative mechanism which was considered for formation of trisulfides was production of RSS· radicals by the primary species followed by combination with RS· radicals: e.g.

[12] $RSSR + \cdot OH \rightarrow RSS\cdot + ROH$

However, this reaction is unsatisfactory since the yield of ROH (hydroxyvaline) is always much lower than the yield of trisulfide. Also, since hydroxyvaline is produced only in aerated solution, it must be formed by a different mechanism. Similar arguments apply in the case of e^-_{aq} or ·H atoms reacting with the disulfide to form RSS· and valine.

The formation of trisulfides was also investigated by reacting ·OH radicals (produced chemically from $TiCl_3$ and H_2O_2) with disulfides in solution, using a flow system similar to that described by Armstrong and Humphreys (4). Good yields of trisulfides were produced when a disulfide (CySSCy or PenSSPen) was present in solution when the ·OH radicals were produced. If the disulfide was added after a short time (3 s) no trisulfide was obtained. When ·OH radicals were reacted with a disulfide and a mercaptan added after 3 s, the yield of trisulfide was not significantly changed. However, if the mercaptan of a different disulfide was used, a mixed trisulfide was also produced. Thus when PenSSPen was reacted with ·OH radicals followed by addition of CySH, both PenSSSPen and PenSSSCy were produced. But when PenSSPen was reacted with ·OH and CySSCy was added, PenSSSPen was obtained with only trace amounts of CySSSPen. Reactions [7] and [8] provide a reasonable explanation of these results.

The experiments with PenSH and CySH present during the radiolysis offer further support for reaction [8]. As shown in Table IV, the presence of PenSH had almost no effect on the yield of trisulfide in aerated solution. Thus, reaction [8] is either very fast or else it is the only important reaction of the PenSSOH intermediate. This explains why the dose–yield plot of the trisulfide is linear within the limits of experimental error. When CySH was present, there was a decrease in the yield of PenSSSPen together with a yield of CySSSPen of similar magnitude in aerated solutions, but little change in deaerated solutions. The high yield of PenSH from reaction [2] probably swamped the CySH added in deaerated solutions. Only a small amount of the CySH and PenSH reacted directly with the primary radical as shown by the low yield of CySSCy in deaerated solution. The mixed disulfide produced in deaerated solution probably came from CySH and PenSOH (analogous to reaction [5]).

The effect of radical scavengers on the yields provided some information on the reactions

suggested (Table III). In aerated solutions, formate (·OH scavenger) reduced the yields of $PenSO_2H$ and PenSSSPen significantly. In deaerated solutions, the yield of $PenSO_2H$ increased slightly in the presence of chloroacetate and N_2O (both e^-_{aq} scavengers). However, the most significant change was the increase in PenSSSPen with N_2O present in deaerated solutions. At the same time the yield of PenSH was reduced to a trace while other products were virtually unchanged. This is consistent with reactions [7] and [8] being the main source of trisulfide. PenSH is produced in reactions [2] [3], and [4] and it may also be an intermediate in others.

The mechanism outlined above is sufficient to explain the main features of the radiolysis of penicillamine disulfide. The significance of these results to the theories of radiation protection will be discussed in the following paper on radiolysis of cysteine–penicillamine mixed disulfide.

Acknowledgments

The author is indebted to Dr. M. A. Weinberger for assistance in nuclear magnetic resonance spectroscopy and to Mr. W. A. Armstrong for advice on the use of $TiCl_3$ and H_2O_2. Thanks are extended to Mr. R. A. Gravelle and Mrs. D. E. Hanafi for technical assistance. The work of Mr. S. C. Wallace (Summer assistant 1967) is also gratefully acknowledged.

1. J. W. PURDIE. J. Am. Chem. Soc. **89**, 226 (1967).
2. S. ROKUSHIKA, S. GANNO, K. SUMIZU, and H. HATANO. J. Radiation Res. Tokyo, **7**, 47 (1966).
3. C. J. DIXON and D. W. GRANT. Biochem. J. **105**, 8c (1967).
4. W. A. ARMSTRONG and W. G. HUMPHREYS. Can. J. Chem. **45**, 2589 (1967).
5. G. E. ADAMS, G. S. MCNAUGHTON, and B. D. MICHAEL. *In* The chemistry of ionization and excitation. *Edited by* G. R. A. Johnson and G. Scholes. Taylor and Francis, London. 1967. p. 281.
6. P. M. DORELLO, M. BOCCACCI, and M. QUINTILIANI. Estrat. Rend. Instituto Superiore di Sanita, Rome, **27**, 126 (1964).
7. G. G. JAYSON, T. C. OWEN, and A. C. WILBRAHAM. J. Chem. Soc. B, 944 (1967).
8. T. C. OWEN, M. RODRIGUEZ, B. G. JOHNSON, and J. A. G. ROACH. J. Am. Chem. Soc. **90**, 196 (1968).
9. W. E. SAVIGE and J. A. MACLAREN. *In* The chemistry of organic sulfur compounds. Vol. 2. *Edited by* N. Kharasch and C. Y. Meyers. The Pergamon Press, Ltd., London. 1966. p. 367.
10. T. HENRIKSEN. J. Chem. Phys. **38**, 1926 (1963); **37**, 2189 (1962).
11. T. HENRIKSEN and T. SANNER. Radiation Res. **32**, 164 (1967).
12. R. BRAAMS. Radiation Res. **27**, 319 (1966).
13. J. W. PURDIE, J. P. FARANT, and R. A. GRAVELLE. J. Chromatog. **23**, 242 (1966).
14. G. L. ELLMAN. Arch. Biochim. Biophys. **82**, 70 (1959).
15. J. C. FLETCHER and A. ROBSON. Biochem. J. **87**, 553 (1963).
16. W. A. SCHROEDER, R. T. JONES, J. CORMICK, and K. MCKALLA. Anal. Chem. **34**, 1570 (1962).
17. C. DAVIES, R. D. HARTLEY, and G. J. LAWSON. J. Chromatog. **18**, 47 (1965).
18. H. MIX. Z. Physiol. Chem. **327**, 41 (1961).
19. D. K. DOUGALL, G. G. F. NEWTON, and E. P. ABRAHAM. Biochem J. **66**, 30P (1957).
20. E. BEUTLER, A. DURON, and B. M. KELLY. J. Lab. Clin. Med. **61**, 882 (1963).
21. M. ANBAR and P. NETA. Intern. J. Appl. Radiation Isotopes, **18**, 493 (1967).
22. B. MILLIGAN, B. SAVILLE, and J. M. SWAN. J. Chem. Soc. 4850 (1961).

Can. J. Chem. Downloaded from www.nrcresearchpress.com by 210.87.254.42 on 09/05/12
For personal use only.

γ-Radiolysis of disulfides in aqueous solution. III. L-Cysteine-D-penicillamine mixed disulfide[1]

J. W. PURDIE[2]

Defence Research Establishment Ottawa, Defence Research Board, Ottawa, Canada

Received July 10, 1968

L-Cysteine-D-penicillamine mixed disulfide (CySSPen) was irradiated in aerated and deaerated aqueous solutions with ^{60}Co γ-rays. G values were determined for all products identified after exposure to 10 000 rads. The major products were the sulfinic and sulfonic acids ($CySO_2H$, $CySO_3H$, and $PenSO_2H$), the sulfhydryl derivatives (CySH and PenSH), symmetrical disulfides (CySSCy and PenSSPen), three trisulfides (CySSSCy, CySSSPen, and PenSSSPen), and ammonia. Each half of the disulfide behaved in exactly the same way as the corresponding symmetrical disulfide. Products from the CyS— part of the disulfide were dose rate dependent while products from the PenS— part were independent of dose rate. The reactions proposed for the symmetrical disulfides were adequate to explain radiolysis of the unsymmetrical disulfide.

Radiolysis of a mixture of cystine and penicillamine disulfide was examined for comparison with the unsymmetrical disulfide and was found to give very similar results. It was concluded that the free radicals produced from the water attack each half at approximately equal rates.

Canadian Journal of Chemistry, 47, 1037 (1969)

Can. J. Chem. Downloaded from www.nrcresearchpress.com by 210.87.254.6 on 09/05/12
For personal use only.

Introduction

Detailed studies of the γ-radiolysis of cystine (1) and penicillamine disulfide (2) have already been reported. In an extension of the investigation, the mixed disulfide of cysteine and penicillamine has been examined under similar conditions. This provided a direct comparison of the CyS and PenS sub-units which was of particular interest since cysteine is a radio-protective compound whereas penicillamine is non-protective. One object of this work was to determine the difference in reactivity, if any, between the cysteine and penicillamine sulfur atoms. Also, further information on the mechanism of radiolysis could be obtained since formation of disulfides from RS· radicals etc. would result in production of some symmetrical disulfides. Information on this aspect was not available from studies of the symmetrical disulfides. Studies of disulfides of cysteine in aqueous solution also contribute to an understanding of the effects of radiation on proteins containing sulfur.

Radiolysis of unsymmetrical disulfides related to cystine has not been reported previously. The recent literature on radiolysis of cystine, penicillamine, and related compounds is covered in the preceding paper in this series (2). The abbreviation CySSPen is used for the cysteine–penicillamine mixed disulfide (1,6-diamino-2,2-dimethyl-3,4-dithiahexane-1,6-dicarboxylic acid) i.e.:

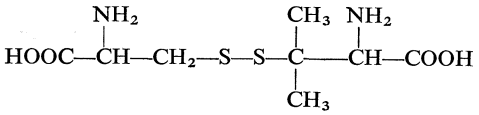

CySSCy and PenSSPen are used to represent cystine and penicillamine disulfide respectively.

Experimental

Materials

Reference amino acids were obtained from Mann Research or Calbiochem as before. Sodium formate and chloroacetic acid were Fisher certified reagents and nitrous oxide was purchased from Matheson, Coleman and Bell.

Cysteine–Penicillamine Mixed Disulfide (CySSPen)

This compound was synthesized from cystine-*S*-monoxide by reaction with penicillamine.

$$CyS(O)SCy + 2\ PenSH \rightarrow 2\ CySSPen + H_2O$$

The monoxide of cystine was prepared as described by Savige *et al.* (3). Cystine (4.8 g) was dissolved in 2 *N* sulfuric acid (50 ml) and cooled to 0 °C. Performic acid, prepared by mixing 5 ml H_2O_2 (30%) with 50 ml formic acid (98%) and allowing the solution to stand 30 min, was added to the solution of cystine and the mixture kept at 5 °C for 3 h. The solution was filtered and adjusted to pH 4 with cold pyridine (28 ml). Addition of cold ethanol (100 ml) precipitated the monoxide. After 30 min at 0 °C the product was filtered off, washed with 50% ethanol (100 ml) and absolute ethanol (100 ml), and dried *in vacuo*. The crude product crystallized from 0.5 *N* acetic acid (500 ml) at 0 °C after addition of an equal

[1]Presented in part at the 15th Annual Meeting of the Radiation Research Society, San Juan, May 1967. Issued as DREO Report No. 573.

[2]Present address: Division of Biology, National Research Council of Canada, Ottawa, Canada.

volume of ethanol; yield 2.9 g (57%). The infrared spectrum had a strong absorption peak at 1060 cm^{-1} characteristic of an *S*-monoxide. The monoxide was stored at −18 °C.

Cystine-*S*-monoxide (1.3 g) in water (10 ml) was mixed with penicillamine (1.58 g) in water (10 ml). The mixture was stirred for 30 min then the precipitate was filtered off and washed with water. The product was recrystallized from 1 *N* HCl by raising the pH to 7 with pyridine; yield 1.0 g (37%), m.p. 198–199°.

Anal. Calcd. for $C_8H_{16}N_2O_4S_2$: C, 35.82; H, 5.97; N, 10.44; S, 23.88. Found: C, 35.64; H, 6.22; N, 10.3; S, 23.99.

This sample was chromatographically pure except for minor traces of impurities and was used for all the radiation experiments.

The nuclear magnetic resonance (n.m.r.) spectrum was run in trifluoroacetic acid. It had peaks at $\tau = 2.30$ ($NH_3^+ \times 2$), 5.23 (CH of CyS half), 5.47 (CH of PenS half), 6.32 (doublet, CH_2), 8.20 (CH_3), and 8.32 (CH_3).

All other amino acids were purchased or prepared as described in the preceding paper (2).

Methods for the preparation of solutions and irradiations were as described previously (2). Solutions of the mixed disulfide were prepared in 200 ml batches and kept at 5 °C. Fresh solutions were prepared each week although blank runs (unirradiated samples) indicated that disproportionation of the mixed disulfide did not occur in unbuffered aqueous solutions (pH 5.5). After storage for two weeks, solutions of CySSPen did not contain any symmetrical disulfide (CySSCy or PenSSPen). Solutions of disulfide 3×10^{-4} *M* were used in all experiments except those where the effect of disulfide concentration was being studied.

The analytical methods employed, ion-exchange chromatography with an amino acid analyzer, have been described in the preceding paper and in previous publications (4). Typical color yields were reported for the various amino acids used or resulting from the radiolysis.

Specimen analyses on "Chromobead" type A cation-exchange resin are illustrated in Fig. 1 for irradiations with 10 000 rads. The unirradiated sample (upper curve) showed only the mixed disulfide peak, ammonia, and slight irregularities in the baseline near the beginning. The middle chart was irradiated–aerated solution and the bottom chart was irradiated–deaerated solution. The irradiated solutions were also examined using Dowex 1 anion-exchange resin (4) in order to separate the sulfinic and sulfonic acids which co-chromatograph as peak 1 in the runs illustrated. Cysteine was usually measured using the absorption at 440 mμ (broken line on lower chart) rather than the usual 570 mμ absorption.

Results

Yields of the principal products were measured in aerated solutions at different total doses in the range 2 500 to 20 000 rads. Figure 2 illustrates the results for cystine, penicillamine disulfide, and the unsymmetrical trisulfide CySSSPen. The yields of the other products measured, CySSSCy, PenSSSPen, and the combined sulfinic and

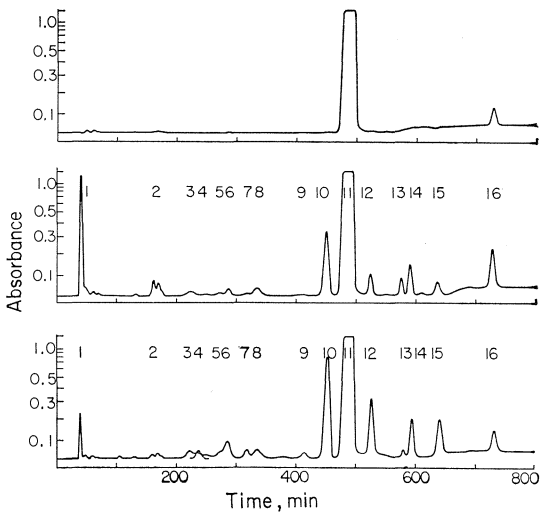

FIG. 1. Amino acid analyzer charts of CySSPen. Top, unirradiated solution; middle, aerated solution irradiated with 10 000 rads; bottom, deaerated solution after 10 000 rads. Peaks are: 1, sulfinic and sulfonic acids; 2, β-hydroxyvaline; 3, $CH_2{=}C(CH_3)CH(NH_2)$-COOH; 4, CySH (broken line); 5, alanine; 6, PenSH; 7, unknown; 8, PenS(O)SPen; 9, valine; 10, CySSCy; 11, CySSPen; 12, PenSSPen; 13, CySSSCy; 14, CySSS-Pen; 15, PenSSSPen; 16, NH_3.

sulfonic acids peak, were also linear with dose up to at least 20 000 rads. Thus 10 000 rads was a suitable dose to use for a general study of the radiolysis of cysteine–penicillamine mixed disulfide.

The yields of all products identified were measured in aerated and deaerated solutions after a dose of 10 000 rads at approximately 700 rads/min. The results are given in Table I in G values. The G values in terms of nitrogen atoms were used to calculate the product balance since the color reaction used in the amino acid analyzer, ninhydrin, detects amines and ammonia. The products of deamination have not been investigated. Values for G (—CySSPen) were 3.6 and 4.7 in aerated and deaerated solutions respectively. Minor products, e.g. lanthionine, (CySCy), cysteine thiosulfonic, and cysteine thiosulfuric acids ($CySO_2SH$ and $CySSO_3H$), which have been detected in irradiated cystine solutions, were probably present in small amounts. Similarly, $PenSSO_3H$ was probably produced in trace amounts. As with radiolysis of PenSSPen, β-hydroxyvaline was produced in aerated solutions together with an adjacent peak believed to be the peroxyvaline derivative (PenOOH). Trace

Can. J. Chem. Downloaded from www.nrcresearchpress.com by 210.87.254.6 on 09/05/12
For personal use only.

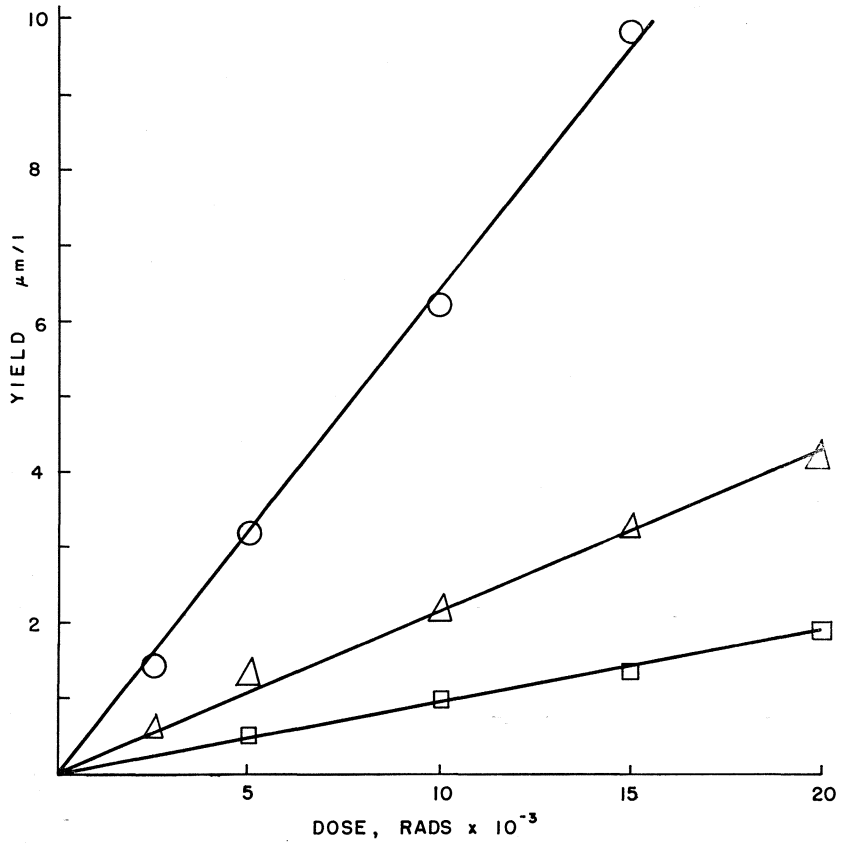

FIG. 2. Dose-yield plots for γ-radiolysis of CySSPen in aerated solution; CySSCy (○); CySSSPen (△); PenSSPen (□).

amounts of serine (CyOH) were also detected in aerated solutions. Estimates for the G value of these minor products and the PenOOH in aerated solutions gave a total of 0.2. When this was included, the nitrogen balance was approximately 80% in aerated solution and 90% in deaerated solution. In view of the number of products and the combined experimental errors this seems reasonably satisfactory. Some minor products remained unidentified and are not included in Table I. The average deviation for a number of experiments was ±0.05 for CySSCy, ±0.02 for PenSSPen, ±0.02 for the trisulfides, ±0.03 for $CySO_3H$ (aerated) and the sulfinic acids, and ±0.35 for PenSH (deaerated). The other products were estimated to be reproducible to within ±5%.

The yields followed the same general pattern obtained previously with the symmetrical disulfides, PenSSPen (preceding paper), and CySSCy (1). For example, sulfinic acids but not sulfonic acids were obtained in deaerated solution while in aerated solution the yields were in the following order:

$$CySO_3H > CySO_2H > PenSO_2H > PenSO_3H$$

High yields of the mercaptans, CySH and PenSH, were obtained in deaerated solutions. Cystine was obtained in much higher yield than penicillamine disulfide and the yield of each was higher in deaerated than in aerated solution. Variations in the yields of the trisulfides were unusual. In changing from aerated to deaerated solution, CySSSCy decreased, CySSSPen remained almost constant, and PenSSSPen increased. These effects were consistent and can be observed on the charts reproduced in Fig. 1 (peaks 13, 14, and 15 respectively).

In view of the fact that the yields from the mixed disulfide resembled those from the two

Can. J. Chem. Downloaded from www.nrcresearchpress.com by 210.87.254.6 on 09/05/12
For personal use only.

TABLE I

Radiolysis of disulfides. G values for CySSPen and comparison with CySSCy and PenSSPen

Compound	Aerated solutions			Deaerated solutions		
	CySSPen	Mixture*	CySSCy or PenSSPen	CySSPen	Mixture*	CySSCy or PenSSPen
$CySO_2H$	0.30	0.39	0.9	0.26	0.60	1.2
$CySO_3H$	0.34	0.36	1.2	Trace	Trace	Trace
$PenSO_2H$	0.19	0.16	0.5	0.11	0.14	0.3
$PenSO_3H$	0.10	0.10	0.10	Trace	Trace	Trace
PenOH	0.11	0.06	0.2	Trace	Trace	Trace
$CH_2{=}C(CH_3)CH(NH_2)COOH$	0.03	0.04	0.11	0.06	0.06	0.33
CySH	Trace	Trace	0.7	0.72	0.84	2.5
PenSH	0.76	0.80	0.45	2.50	2.0	2.3
Alanine	0	0	0	0.10	0.10	0.1
Valine	0	0	0	0.07	0.05	0.13
PenS(O)SPen	0.19	0.2	0.27	0.07	0.1	0.22
CySSCy	0.58	—	—	1.18	—	—
CySSPen	—	0.24	—	—	1.16	—
PenSSPen	0.10	—	—	0.19	—	—
CySSSCy	0.10	0.09	0.15	0.06	0.13	0.25
CySSSPen	0.21	0.26	—	0.26	0.23	—
PenSSSPen	0.07	0.22	0.6	0.27	0.24	1.0
NH_3	0.93	—	—	0.57	—	—

*Mixture = CySSCy + PenSSPen (each 1.5×10^{-4} *M*).

symmetrical disulfides, a solution containing a mixture of CySSCy and PenSSPen was irradiated for comparison. The concentration of each disulfide was 1.5×10^{-4} *M* giving a total disulfide concentration of 3×10^{-4} *M*, which was the concentration used for experiments described above. The mixture was irradiated with 10 000 rads and analyzed as before. The yields measured are reported in Table I. The Table also contains G values from the cystine and penicillamine disulfide studies. However, the concentration of each CyS and PenS unit would be twice that of the mixture, and comparison of the symmetrical disulfides with the mixture or the unsymmetrical disulfide does not allow for reactions between intermediates from the different halves which could occur in the latter cases. As can be seen from Table I, the yields from the mixture were very close to those from the unsymmetrical disulfide and similar to half the values from CySSCy or PenSSPen.

Dose-Rate Effects

The effect of irradiating at different dose rates was investigated by irradiating solutions with 10 000 rads at dose rates of 800, 650, 330, 110, 40, and 10 rads/min. The yields of the disulfides, CySSCy, and PenSSPen, and the three trisulfides, were independent of dose rate in both aerated and deaerated solutions. Yields of the acidic products, however, followed the pattern observed with the symmetrical disulfides. The yields of $PenSO_2H$ and $PenSO_3H$ in aerated solution and the yield of $PenSO_2H$ in deaerated solution, were independent of dose rate. In aerated solution, the yield of $CySO_3H$ decreased from 0.35 at 800 rads/min to 0.15 at 10 rads/min while the yield of $CySO_2H$ increased from 0.30 at 800 rads/min to 0.5 at 10 rads/min. In deaerated solution, the yield of $CySO_2H$ decreased from 0.30 to 0.10 at 800 and 10 rads/min respectively. The observation that the two halves of the disulfide behave independently with respect to dose rate is in agreement with reactions proposed earlier to explain the dose-rate effect in the radiolysis of cystine. The dose-rate effect must be due to competition between intermediates and not to the initial reactions of free radicals with the disulfide.

Disulfide Concentration

A disulfide concentration of 3×10^{-4} *M* was used in this and previous studies as this was the maximum concentration which could be obtained with cystine in neutral solution. The same concentration was used in all studies so that results could be compared without complications from concentration effects. The low concentra-

Can. J. Chem. Downloaded from www.nrcresearchpress.com by 210.87.254.6 on 09/05/12
For personal use only.

TABLE II
Yields of main products at various concentrations of CySSPen in aerated solutions

Product	Disulfide concentration			
	1×10^{-4}	3×10^{-4}	6×10^{-4}	9×10^{-4}
Sulfinic and sulfonic acids	1.1	1.25	1.31	1.3
PenS(O)SPen	0.13	0.19	0.17	0.25
CySSCy	0.36	0.56	0.84	1.00
PenSSPen	0.04	0.06	0.14	0.16
CySSSCy	0.07	0.09	0.12	0.16
CySSSPen	0.14	0.18	0.24	0.26
PenSSSPen	0.03	0.04	0.07	0.08

tion used was also suitable as it minimized the chance of direct radiation effects. However, since the mixed disulfide was much more soluble than cystine, a study was made of the effect of different concentrations on the results. The results are presented in Table II and these show a general increase with concentration. The total dose was 10 000 rads at all concentrations. Thus it appears that a higher concentration than 3×10^{-4} *M* would be necessary in order to trap all the primary species formed in the water.

Radical Scavengers

Radical scavengers were employed to test the reactions postulated to explain the mechanism of the radiolysis. Experiments were carried out using deaerated solutions with formate ions present to react with ·OH radicals, chloroacetate ions to scavenge e^-_{aq}, or nitrous oxide which scavenges e^-_{aq} and produces an ·OH radical. From the results, listed in Table III, it can be seen that the combined yield of sulfinic and sulfonic acids is effectively reduced by formate ions, unaffected by chloroacetate ions, and increased with nitrous oxide present. This is also true for CySSSCy and CySSSPen and indicates that the ·OH radical is necessary for formation of these compounds. PenSSSPen appears to be an exception as it is not affected by chloroacetate or nitrous oxide but is slightly increased by formate ions. The yields of PenSH and CySH were reduced but not eliminated by nitrous oxide. The disulfides, CySSCy and PenSSPen, increased considerably with formate present but were little affected by chloroacetate or nitrous oxide.

Discussion

The reactions giving rise to the products obtained have been discussed in detail in the previous papers dealing with the symmetrical disulfides (1, 2). The same reactions are probably involved in the case of CySSPen with some changes due to interaction between cysteine and penicillamine intermediates. The following appear to be the more important of those discussed:

[1] $RSSR + \cdot OH \rightarrow RSOH + RS\cdot$

[2] $RSSR + e^-_{aq} + H^+ \rightarrow RSH + RS\cdot$

[3] $RSOH + RSOH \rightarrow RSO_2H + RSH$

[4] $RSOH + RSSR \rightarrow RS(O)SR + RSH$

[5] $RSOH + RSH \rightarrow RSSR + H_2O$

[6] $RSOH + O^-_2 \rightarrow RSO^-_3 + H\cdot$

[7] $RS\cdot + RS\cdot \rightarrow RSSR$

[8] $RSSR + \cdot OH \rightarrow RSSOH + R\cdot$

[9] $RSSOH + RSH \rightarrow RSSSR + H_2O$

Reactions [1] and [2] seem to occur with both cystine and penicillamine disulfide although reaction [8] may be more important than [1] in the case of penicillamine disulfide. Reactions [3], [4], and [5] probably occur with both CySOH and PenSOH and reaction [5] could be one of the reactions leading to the symmetrical disulfides. Reaction [6] is more specific as it does not occur with PenSOH. The details of this reaction are not clear but it was established that $CySO_3H$ was only produced when oxygen was present in solution and the yield was reduced by e^-_{aq} scavengers (1). It is possible that e^-_{aq} or O^-_2 has a catalytic effect on oxidation of CySOH by oxygen or perhaps the O^-_2 reacts with the initial disulfide – radical complex, i.e.:

[10] $RSSR \overset{\cdot OH}{+} O^-_2 \rightarrow RSO^-_3 + RSH$

Such a reaction would be favored by high dose rates leading to higher sulfonic acid yields, as was

Can. J. Chem. Downloaded from www.nrcresearchpress.com by 210.87.254.6 on 09/05/12
For personal use only.

TABLE III

Effect of radical scavengers on yields: deaerated CySSPen solution

Product	No scavenger	Formate		Chloroacetate		Nitrous oxide	
		10^{-4} *M*	10^{-3} *M*	10^{-4} *M*	10^{-3} *M*	2×10^{-3} *M*	2×10^{-2} *M*
Sulfinic and sulfonic acids	0.53	0.24	0.05	0.55	0.58	0.98	1.10
CySH	1.3	0.5	0.8	1.0	—	0.40	(0.01)
PenSH	2.4	1.6	2.9	2.9	2.6	1.6	1.4
Alanine	0.09	0.10	0.17	0.10	0.08	0.07	0.07
PenS(O)SPen	0.07	0.33	0.52	0.13	0.16	0.10	0.15
Valine	0.08	0.07	0.16	0.09	0.06	0.05	0.04
CySSCy	1.2	1.5	1.9	1.3	1.3	1.23	1.1
PenSSPen	0.21	0 44	0.90	0.20	0.17	0.19	0.16
CySSSCy	0.06	0.03	(0.01)	0.07	0.02	0.11	0.18
CySSSPen	0.28	0.18	0.11	0.25	0.18	0 41	0.47
PenSSSPen	0.27	0.41	0.37	0.28	0.27	0.26	0.27

observed with $CySO_3H$ from both CySSPen and CySSCy.

Reaction [7] is probably the main source of symmetrical disulfides (CySSCy and PenSSPen) from the unsymmetrical disulfide. The yields of PenSSPen were lower than those of CySSCy which may be due to steric hindrance by the two methyl groups adjacent to the sulfur atom in the penicillamine radical:

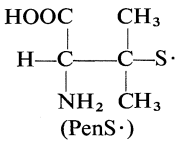

(PenS·)

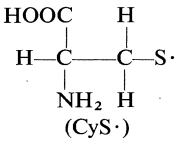

(CyS·)

When a mixture of CySSCy and PenSSPen was irradiated, a moderate yield of CySSPen was obtained (Table II).

It is difficult to establish a mechanism for formation of trisulfides. Reactions [8] and [9] appear to satisfy the experimental results better than the alternatives, as discussed in the previous paper. The results with nitrous oxide strongly indicate that the ·OH radical is involved in the initial step leading to the trisulfides. The work with the ·OH and e^-_{aq} scavengers, formate and chloroacetate, also supports this view although the effects are less dramatic. The variations in the yields of the three trisulfides are also noteworthy. In changing from aerated to deaerated solutions, CySSSCy decreases, CySSSPen remains approximately constant, and PenSSSPen increases. In the previous work on cystine and penicillamine disulfide, the trisulfide yield increased in deaerated solution. The explanation of this phenomenon may be that the high yield of PenSH in deaerated solutions (approximately 2.5×10^{-5} *M* after 10 000 rads) swamps the CySH in the competing reactions:

[9*a*] $\quad CySSOH + CySH \rightarrow CySSSCy + H_2O$

[9*b*] $\quad CySSOH + PenSH \rightarrow CySSSPen + H_2O$

[9*c*] $\quad PenSSOH + CySH \rightarrow CySSSPen + H_2O$

[9*d*] $\quad PenSSOH + PenSH \rightarrow PenSSSPen + H_2O$

A high concentration of PenSH would favor reactions [9*b*] and [9*d*], leading to the effect observed.

Comparison of the mixed disulfide, CySSPen, with the mixture, CySSCy + PenSSPen, (Table II) leads to some important conclusions. In studying the radiolysis of an unsymmetrical disulfide such as CySSPen it was thought that the two sulfur atoms would react at different rates with the primary free radicals, ·OH and e^-_{aq}. If such a difference did exist there should be a measurable difference in yield between the products from the mixed disulfide and those from the mixture. However, since the yields from the mixed disulfide were approximately equal to those from the mixture and half the yields from the pure disulfides, it follows that the two sulfur atoms react at almost equal rates with the primary species from water. Hence differences between cystine and penicillamine disulfide are due to different reactions following the initial attack. This conclusion will apply irrespective of the exact mechanism involved.

As mentioned above, cysteine is a radioprotective compound whereas penicillamine is not. Thus, studies of the radiolysis of these two compounds and of the corresponding disulfides

Can. J. Chem. Downloaded from www.nrcresearchpress.com by 210.87.254.6 on 09/05/12
For personal use only.

contribute to an understanding of the mechanism of radiation protection and of the effect of radiation on sulfur-containing proteins. The most outstanding difference observed between cystine and penicillamine disulfide was the almost complete absence of sulfonic acid from among the radiolysis products of the latter. Since the sulfonic acid is formed by reaction with ·OH radicals and oxygen (as O^-_2) this may be one of the important properties which determines whether or not a compound is radio-protective. In this connection it is interesting to note that Vos *et al.* (5) found that penicillamine protected cells almost as well as cysteine under anoxic conditions (i.e. in the absence of O^-_2). One possibility is that the amino group attracts and binds the O^-_2 to the protective molecule where it eventually reacts with the sulfur. This would explain the necessity for an amino group and the fact that the chain length between the nitrogen and the sulfur is very critical for protection (two or three carbon atoms).

The other notable differences observed were the low yields of penicillamine disulfide compared with cystine and the high yields of penicillamine (PenSH) and the trisulfide (PenSSSPen). There is no obvious connection between these observations and radio-protective properties other than the possibility that steric hindrance, which may be responsible for the low yield of PenSSPen, may also render the sulfur inaccessible at a critical stage in the radiation protection process.

It has been suggested that RS· radicals react with many disulfides in proteins causing a "scrambling" of disulfide bonds (6). This hypothesis was based on the high G values, up to 25 (7), reported for polymerization of lipoic acid which has a cyclopentane ring containing a disulfide unit. However, for the amino acid, cysteine-penicillamine mixed disulfide, the G value for reformed disulfides in aerated solutions was only about 1. Even in deaerated solutions the G value for regenerated disulfides was about 2.5. Since these disulfides could all result from reactions of the primary radicals followed by recombinations, it is clear that RS· radicals do not cause extensive rearrangement of disulfide bonds in proteins.

Acknowledgments

Thanks are extended to Mr. R. A. Gravelle and Mrs. D. E. Hanafi for technical assistance and to Dr. M. A. Weinberger for assistance in magnetic resonance spectroscopy.

1. J. W. PURDIE. J. Am. Chem. Soc. **89**, 226 (1967).
2. J. W. PURDIE. Can. J. Chem. This issue.
3. W. E. SAVIGE, J. EAGER, J. A. MACLAREN, and C. M. ROXBURGH. Tetrahedron Letters, 3289 (1964).
4. J. W. PURDIE, J. P. FARANT, and R. A. GRAVELLE. J. Chromatog. **23**, 242 (1966).
5. A. J. VERGROESEN, L. BUDKE, and O. Vos. Intern. J. Radiation Biol. **13**, 77 (1967).
6. T. C. OWEN, M. RODRIGUEZ, B. G. JOHNSON, and J. A. G. ROACH. J. Am. Chem. Soc. **90**, 196 (1968).
7. T. C. OWEN and A. C. WILBRAHAM. Chem. Commun. 624 (1967).

Can. J. Chem. Downloaded from www.nrcresearchpress.com by 210.87.254.6 on 09/05/12
For personal use only.

The $CdO–CdCl_2$ reaction studied by thermal analysis and X-ray diffraction: X-ray diffractogram and infrared spectrum of $CdCl_2 \cdot 2CdO$

P. Ramamurthy and E. A. Secco

Chemistry Department, St. Francis Xavier University, Antigonish, Nova Scotia

Received September 6, 1968

CdO and molten $CdCl_2$ react to form $CdCl_2 \cdot 2CdO$ according to the equation:

$$2CdO_{(s)} + CdCl_{2(l)} \xrightarrow{560\ °C} CdCl_2 \cdot 2CdO_{(s)} \qquad \Delta H = -5.3 \text{ kcal/mole}$$

The compound $CdCl_2 \cdot 2CdO$ dissociates to the oxide and chloride at 680 °C. CdO and $CdCl_2$ form a solid solution of partial miscibility of 15% by weight of CdO.

The X-ray diffractogram of $CdCl_2 \cdot 2CdO$ was indexed to the orthorhombic system. The unit cell dimensions are calculated to be $a = 4.38$ Å, $b = 11.47$ Å, $c = 9.93$ Å with 4 molecules in the unit cell. The infrared spectrum shows a band structure of two doublets and a well-defined band in the region 370–550 cm^{-1}.

Canadian Journal of Chemistry, 47, 1045 (1969)

Can. J. Chem. Downloaded from www.nrcresearchpress.com by 210.87.254.105 on 09/05/12
For personal use only.

Introduction

Our knowledge of the reaction between cadmium oxide and cadmium chloride is incomplete. This limitation became evident to us when a recent study (1) on the decomposition of CdOHCl by differential thermal analysis (d.t.a.) revealed three unknown endotherms which were tentatively assigned to oxide–chloride interactions. The sole literature item on this interaction appears in Mellor (2) as an unconfirmed reference to the existence of cadmium oxychloride, $CdCl_2 \cdot 2CdO$. The purpose of this communication is to fill the existing gap and report on a study of the $CdO–CdCl_2$ reaction over the entire composition range.

Experimental

CdO and $CdCl_2 \cdot 2\frac{1}{2}H_2O$ used in this work were Fisher Certified and Baker Analyzed reagent grade, respectively. The $CdCl_2 \cdot 2\frac{1}{2}H_2O$ was dehydrated at 125 °C for 12 h before mixing with CdO to obtain the requisite composition. The physical mixtures of various compositions were prepared by thorough manual grinding and storing in a dessicator to preclude the uptake of moisture and subsequent formation of CdOHCl on long standing.

Most thermograms were recorded on a duPont thermal analyzer, DTA-900 using a low temperature cell (850 °C) as previously reported (1). Some experiments were carried out with the duPont 1200 °C cell. In all thermograms, the heating rate used was 20 °C/min with an ambient atmosphere of dry air. Cooling curves were obtained by self-cooling with dry air flowing through the d.t.a. cell. The peak temperatures reported here are reproducible within ±5 °C.

The X-ray diffractograms of the specimens were recorded on a Norelco X-ray diffractometer unit using CuK_α radiation and Ni filter as previously described (3). To obtain accurate values of θ for the compound $CdCl_2 \cdot 2CdO$ a slow scanning rate of $\frac{1}{4}° - 2\theta$/min was used.

The infrared (i.r.) spectra were recorded on the Perkin–Elmer 521 grating instrument using the standard KCl pellet technique. The compound $CdCl_2 \cdot 2CdO$ was prepared by heating a physical mixture of CdO:$CdCl_2$ in 2:1 mole ratio at 560 °C for 1 h as described above.

Results and Discussion

Heating thermograms at selected compositions to illustrate the salient features of thermal behavior with composition are shown in Fig. 1. Physical mixtures of composition greater than 85% by weight of $CdCl_2$ showed only the melting endotherm of $CdCl_2$ at the peak temperature of 560 °C; the peak temperature shifted slightly to 570 °C as the oxide content of the mixture reached 15% by weight. At the 85:15 $CdCl_2–CdO$ composition, a weak unidentified endotherm appeared at 680 °C accompanying the 560 °C endotherm. Increasing the CdO content in the mixture causes a decrease in the intensity (or area) of the 560 °C endotherm with a concomitant increase in the 680 °C endotherm until the $CdCl_2–CdO$ composition 35:65 is attained. Where the 680 °C endotherm attains a maximum area while the 560 °C endotherm is barely discernible and always accompanied by a weak exotherm at 565 °C. Further enrichment in oxide content effects a decrease in the 680 °C endotherm intensity and the appearance of a sharp weak endotherm at 640 °C above 75% by weight of CdO.

Can. J. Chem. Downloaded from www.nrcresearchpress.com by 210.87.254.105 on 09/05/12
For personal use only.

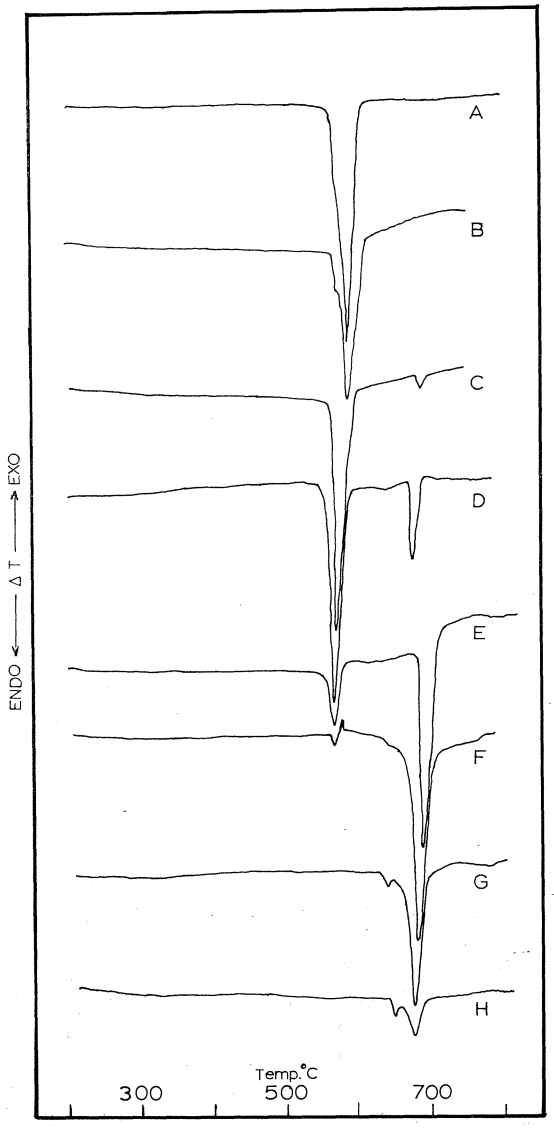

FIG. 1. Thermograms of CdO–$CdCl_2$ mixtures at different composition to display pertinent features as a function of composition (% by weight).
A, 100% $CdCl_2$; B, 90% $CdCl_2$, 10% CdO; C, 80% $CdCl_2$, 20% CdO; D, 60% $CdCl_2$, 40% CdO; E, 50% $CdCl_2$, 50% CdO; F, 35% $CdCl_2$, 65% CdO; G, 20% $CdCl_2$, 80% CdO; H, 10% $CdCl_2$, 90% CdO.

The disappearance of the $CdCl_2$ melting endotherm above 65% by weight of CdO was tentatively interpreted in terms of immediate interaction between the oxide and molten $CdCl_2$, where the fusion endotherm of $CdCl_2$ is exactly compensated by the oxide–chloride reaction exotherm. The possibility that the reduced heat requirement due to the decreasing $CdCl_2$ content might escape the instrumental sensitivity was ruled out when a physical mixture of 35% by weight of $CdCl_2$ in an inert matrix of 65% by weight of Al_2O_3 exhibited an intense endotherm at 560 °C.

The 65:35 CdO–$CdCl_2$ composition lies very near to 2:1 molar ratio in agreement with the compound $CdCl_2 \cdot 2CdO$ cited by Mellor (2). The thermogram of 2:1 molar CdO–$CdCl_2$ mixture heated to 600 °C showed a weak endotherm at 560 °C and a weak exotherm at 565 °C. The cooling curve from 600 °C to room temperature, Fig. 2, exhibited no thermal effect, therefore confirming an irreversible oxide–chloride interaction up to 600 °C. A second heating of the same sample to 700 °C produced the 680 °C endotherm. On cooling from 700 °C to room temperature, two exotherms appeared at 620 and 530 °C. These facts were interpreted in terms of decomposition of the compound $CdCl_2 \cdot 2CdO$ to its components at 680 °C on heating and the subsequent partial recombination of CdO and $CdCl_2$ to form $CdCl_2 \cdot 2CdO$ occurs at 620 °C on cooling. The unreacted $CdCl_2$ displays its exothermic effect due to crystallization with slight undercooling at 530 °C.

The areas of the weak endotherm at 560 °C and weak exotherm at 565 °C observed in the combination of 1 mole of $CdCl_2$ with 2 moles of CdO cancel out to show a net zero thermal effect. That is, the endothermic heat of fusion for 1 mole of

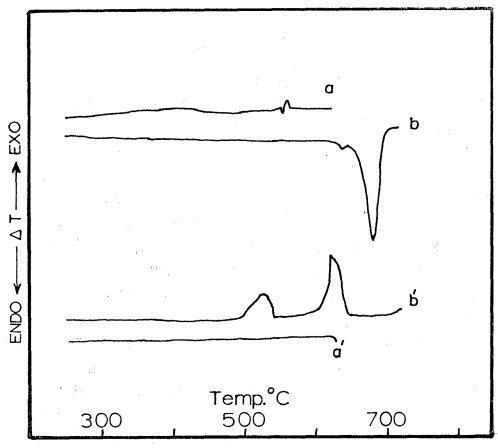

FIG. 2. Heating and cooling thermograms of 2:1 CdO–$CdCl_2$ molar composition. *a*, *a′*, first heating and cooling thermograms, respectively; *b*, *b′*, second heating and cooling thermograms, respectively.

Can. J. Chem. Downloaded from www.nrcresearchpress.com by 210.87.254.105 on 09/05/12
For personal use only.

$CdCl_2$, 5.3 kcal/mole, exactly equals the exothermic heat of reaction between molten $CdCl_2$ and solid CdO. The reaction given in equation form reads as follows:

$$2CdO_{(s)} + CdCl_{2(l)} \xrightarrow{560\ ^\circ C} CdCl_2 \cdot 2CdO_{(s)}$$
$$\Delta H = -5.3 \text{ kcal/mole}$$

Evidence from X-ray diffractograms presented in Fig. 3 confirm the above interpretation of $CdCl_2 \cdot 2CdO$ dissociation at 680 °C with partial recombination on cooling. $CdCl_2$–CdO physical mixture of 1:2 molar ratio heated to 500 °C gave a diffractogram which is a sum of the characteristic peaks due to CdO and $CdCl_2$. Heating the mixture of 565 °C yields a diffractogram distinctly different from the combined CdO and $CdCl_2$ pattern. The resultant diffractogram at 565 °C cannot be found in the literature and is assigned to the compound $CdCl_2 \cdot 2CdO$; the pattern remains unchanged to 660 °C. Heating the compound to 700 °C and recooling yields a diffractogram with peaks common to CdO, $CdCl_2$, and the compound.

The absence of the 680 °C dissociation endotherm in d.t.a. up to 15% by weight CdO was a point of interest and merited clarification by X-ray diffraction. Untreated $CdCl_2$–CdO mixtures up to 15% CdO showed characteristic CdO and $CdCl_2$ diffraction peaks, whereas the fused mixture revealed only $CdCl_2$ diffraction peaks. Furthermore, a fused mixture of 5% by weight of $CdCl_2 \cdot 2CdO$ in $CdCl_2$ gave diffraction peaks characteristic of both species, i.e. compound and chloride. We conclude, therefore, that a solid solution of limited miscibility of 15% CdO and $CdCl_2$ occurs prior to compound formation.

The additional endotherms at 745 and 796 °C for 1:1 mole ratio assigned earlier (1) to volatilization processes have been confirmed using a Mettler simultaneous d.t.a.–t.g.a. instrument, Fig. 4. Instead of distinct endotherms, we observe a broad endotherm, 720–820 °C, which arises from the volatilization of $CdCl_2$ from a system of variable composition, i.e. a two phase system of a saturated solution of CdO–$CdCl_2$ and excess liquid $CdCl_2$.

Cooling thermograms of mixtures were studied in more detail to account for the partial recombination. Alternate heating and cooling curves for a 55:45 $CdCl_2$–CdO mixture are presented in Fig. 5*a*; the decreasing intensity trend of the

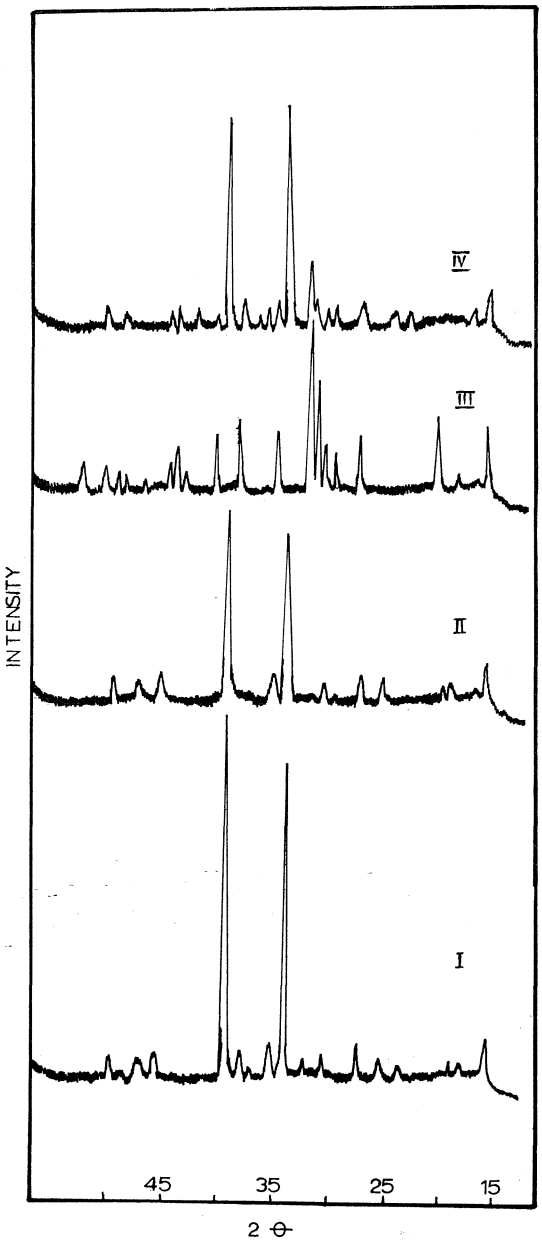

FIG. 3. X-ray powder diffractograms of 2:1 CdO–$CdCl_2$ molar mixture, recorded at room temperature following heat treatment. I, untreated; II, after heating to 500 °C; III, after heating to 565 °C; IV, after heating to 700 °C.

680 °C endotherm and the 620 °C exotherm accompanied by an increasing intensity trend of the 560 °C endotherm and the 530 °C exotherm with each heat–cool cycle are evident. In addition

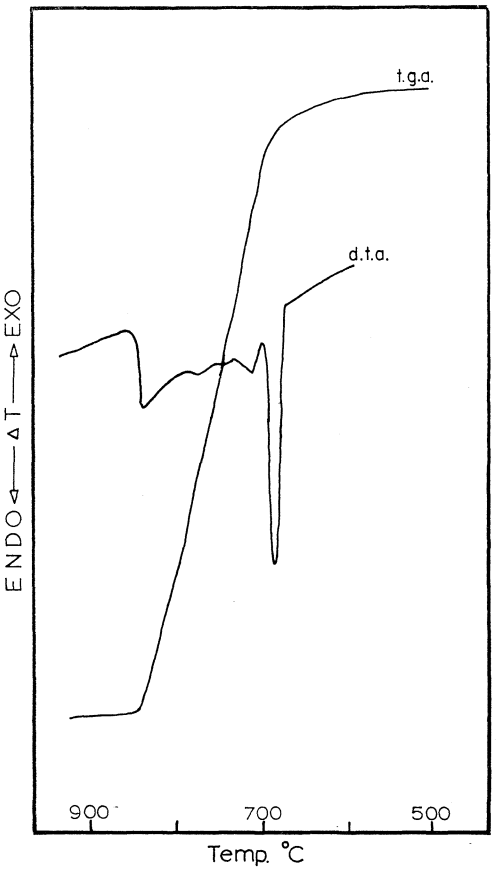

FIG. 4. Thermogram of 1:1 CdO–$CdCl_2$ molar mixture recorded by Mettler simultaneous d.t.a.–t.g.a. instrument.

to a kinetic factor responsible for only partial return of the compound after dissociation, the heat–cool cycle inactivates the oxide by particle growth, most likely through a solubility–precipitation sequence, thereby liberating previously bound $CdCl_2$ to intensify the $CdCl_2$ endo- and exo-therms at the expense of compound endo- and exo-therms. Cooling thermograms of mixtures containing excess CdO relative to the $CdCl_2 \cdot 2CdO$ composition reveal only the exotherm due to compound formation as shown in Fig. 5*b*.

Attempts to identify conclusively the sharp weak endotherm at 640 °C in oxide excess mixtures, i.e. above 65% CdO, have failed. We can only speculate on the possible origins of such an endotherm: (*i*) melting point of $CdCl_2 \cdot 2CdO$ prior to dissociation; (*ii*) phase transition of the $CdCl_2 \cdot 2CdO$; (*iii*) presence of higher oxychloride, i.e. $CdCl_2 \cdot nCdO$ where $n > 2$.

In summary, CdO and molten $CdCl_2$ react to form $CdCl_2 \cdot 2CdO$ according to the equation:

$$2CdO_{(s)} + CdCl_{2(l)} \xrightarrow{560\ ^\circ C} CdCl_2 \cdot 2CdO_{(s)}$$
$$\Delta H = -5.3 \text{ kcal/mole}$$

which is followed by the reverse reaction at 680 °C

$$CdCl_2 \cdot 2CdO_{(s)} \xrightarrow{680\ ^\circ C} 2CdO_{(s)} + CdCl_{2(l)}$$

CdO and $CdCl_2$ form a solid solution of partial miscibility of 15% by weight of CdO.

The X-ray powder lines were indexed to orthorhombic system using the Hesse–Lipson method (4, 5). The observed and calculated $\sin^2\theta$ values according to orthorhombic system along with their relative intensities and *hkl* values are given in

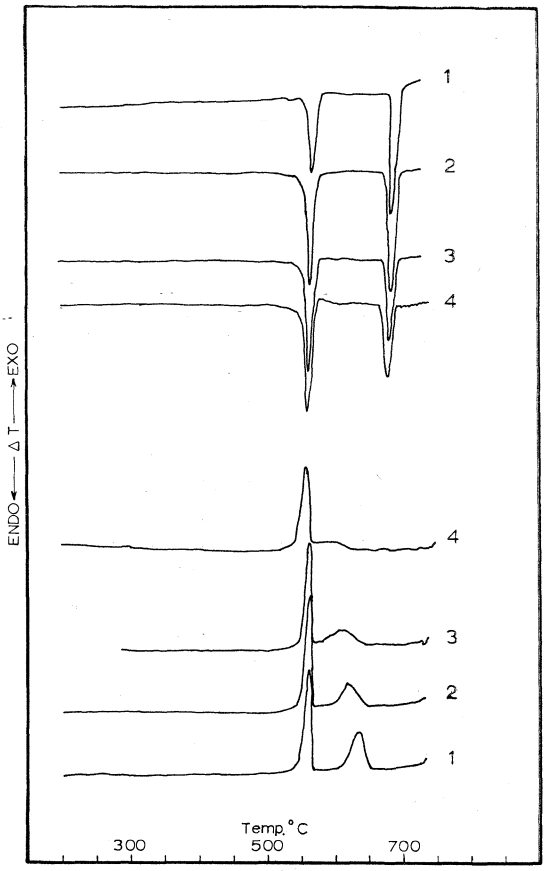

FIG. 5*a*. Heating and cooling thermograms of 55:45 $CdCl_2$–CdO composition by weight percent.

Can. J. Chem. Downloaded from www.nrcresearchpress.com by 210.87.254.105 on 09/05/12
For personal use only.

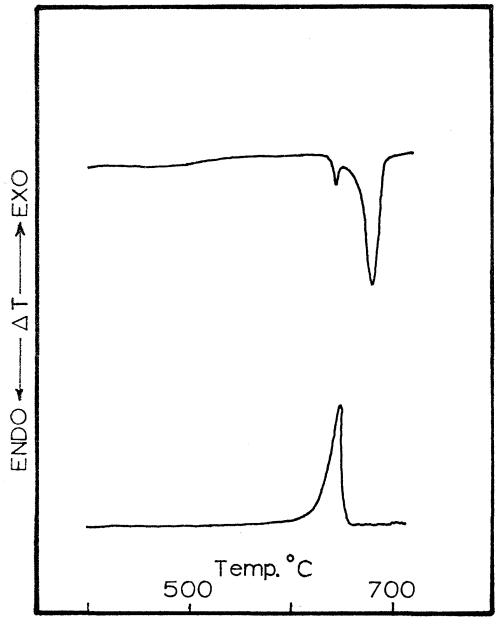

FIG. 5*b*. Heating and cooling thermograms of $CdCl_2$–CdO mixture with CdO in excess of 2:1 CdO–$CdCl_2$ molar ratio.

Table I. The unit cell dimensions are calculated to be $a = 4.38$, $b = 11.47$, and $c = 9.93$ Å.

The density of the compound was determined by the displacement method at 25 °C using benzene and dibutyl phthalate as displacing liquids. The average density value from six measurements in both liquids with its mean deviation was found to be 5.85 ± 0.03 g/cc. Water could not be used as a displacing solvent, because the compound decomposes in water with the evolution of heat.

With the density value of 5.85 g/cc, the number of molecules in the unit cell was calculated to be $3.994 \approx 4$. As there is no systematic absence of *hkl* values, the space group of the compound could not be assigned.

The i.r. spectrum of the compound, Fig. 6, showed a band structure consisting of two doublets and a well-defined band in the range between 370–550 cm^{-1}. Both $CdCl_2$ and CdO show no absorption in this region (6), and we conclude, therefore, that the observed bands are characteristic of the compound $2CdO \cdot CdCl_2$. In the absence of a point group, the factor group analysis could not be carried out, and under these circumstances it is very difficult to assign a structure and to give proper and complete assignments to these bands.

TABLE I
X-ray data

Line number	$\sin^2 \theta_{obsd}$	$\sin^2 \theta_{calcd}$	*hkl*	I/I_0
1	0.01810	0.01810	020	16
2	0.02862	0.02862	012	48
3	0.03100	0.03100	100	15
4	0.05423	0.05422	003	40
5	0.06480	0.06482	032	25
6	0.07163	0.07172	130	70
7	0.07247	0.07240	040	100
8	0.08551	0.08522	103	35
9	0.08970	0.08974	113	25
10	0.1029	0.1034	140	40
		0.1033	123	
11	0.1080	0.1094	141	35
12	0.1142	0.1131	050	8
13	0.1198	0.1190	051	10
14	0.1308	0.1300	201	40
15	0.1340	0.1320	114	20
16	0.1380	0.1372	034	8
17	0.1773	0.1782	203	12
18	0.1862	0.1855	115	10
19	0.1914	0.1913	035	7
20	0.2007	0.1998	144	8
		0.2001	161	
21	0.2159	0.2169	006	6
22	0.2284	0.2277	072	4
23	0.2338	0.2350	026	12
24	0.2369	0.2371	250	10
25	0.2492	0.2483	163	15
26	0.2590	0.2593	064	8
27	0.2797	0.2790	300	10

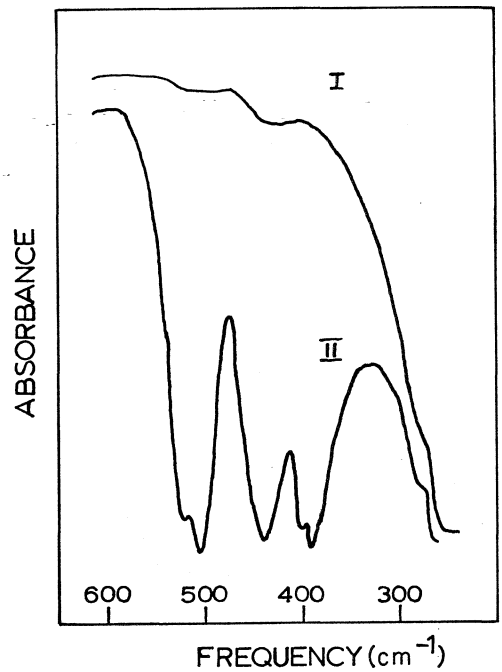

FIG. 6. Infrared spectra: I, 2:1 molar ratio of CdO–$CdCl_2$ mixture; II, compound $2CdO \cdot CdCl_2$.

Can. J. Chem. Downloaded from www.nrcresearchpress.com by 210.87.254.105 on 09/05/12
For personal use only.

Acknowledgments

The authors are indebted to the National Research Council of Canada for financial support of this research program and to Dr. M. Falk, Atlantic Regional Laboratory, Halifax, for providing the infrared facilities. They also acknowledge the contribution of Mr. Nicholas Edbrooke on the early d.t.a. measurements, and the assistance of Mr. Paul Gagnon on the density measurements. The authors are most grateful to the Mettler Analytical and Precision Balance of Zürich, Switzerland for the simultaneous d.t.a.–t.g.a. trace in Fig. 4.

1. O. K. Srivastava and E. A. Secco. Can. J. Chem. **45**, 579 (1967).
2. J. N. Mellor. Comprehensive treatise on inorganic and theoretical chemistry. Vol. IV. Longmans, Green and Co., Ltd., London. 1923. p. 456.
3. E. A. Secco. Can. J. Chem. **42**, 2143 (1964).
4. R. Hesse. Acta Cryst. **1**, 200 (1948).
5. H. Lipson. Acta Cryst. **2**, 43 (1949).
6. T. McDevitt and L. Baun. Spectrochim. Acta, **20**, 799 (1964).

Downloaded from www.nrcresearchpress.com by 210.87.254.105 on 09/05/12
For personal use only.

Can. J. Chem. Downloaded from www.nrcresearchpress.com by 210.87.254.5 on 09/05/12
For personal use only.

Kinetics and mechanism of the oxidation of formaldehyde by hexacyanoferrate(III) ion

V. N. SINGH, M. C. GANGWAR, B. B. L. SAXENA, AND M. P. SINGH
Chemical Laboratories, University of Allahabad, Allahabad, India

Received April 8, 1968

The kinetics of the reaction between formaldehyde and hexacyanoferrate(III) ion in alkaline medium has been investigated at four temperatures. The data show that the reaction is rapid initially, then follows a simple first order rate with respect to each of the hexacyanoferrate(III) ion, formaldehyde, and hydroxide ion. Calculations reveal that only 0.27% of the formaldehyde corresponds to the initial rapid reaction; the remaining 99.73% follows the kinetics described. The net rate of the oxidation of formaldehyde as measured by the consumption of hexacyanoferrate(III) ion, is given by

$$-\frac{d[Fe(CN)_6^{3-}]}{dt} = \frac{2k_1k_2[HC(OH)_2][OH^-][Fe(CN)_6^{3-}]}{k_{-1}[H_2O] + k_2[Fe(CN)_6^{3-}]}$$

Canadian Journal of Chemistry, 47, 1051 (1969)

Introduction

Potassium permanganate and the ferricyanide are the most common reagents used as oxidants in alkaline medium for a number of organic compounds. However, the kinetic features of the oxidation of formaldehyde are not well known. Conant and co-workers (1) were first to observe that there is no appreciable oxidation of formaldehyde with ferricyanide below pH 11. Holluta and co-workers (2) have studied the kinetics of oxidation of this organic substrate with neutral permanganate and found that it was base catalyzed. The present study aims at getting more definite information regarding the mechanism of the oxidation of formaldehyde with alkaline ferricyanide ion.

Results and Discussion

The oxidation of formaldehyde in basic aqueous solution has been investigated kinetically at constant ionic strength. Our measurements, covering a much wider concentration and temperature range, confirm that this reaction is strictly first order with respect to each reactant under the conditions used. The kinetic data for the oxidation of formaldehyde have been collected into Tables I to IX. The course of the reaction was followed by estimating the amount of ferrocyanide ion produced at different intervals of time, with the help of a standard solution of ceric sulfate and

TABLE I

Pseudo first order rate constants* in ferricyanide at 40°

$10^3 \times [K_3Fe(CN)_6]$†	$10^3 \times k''$
1.00	3.60
1.30	3.20
2.00	2.24
2.50	2.90
4.00	2.64
5.00	2.60
10.00	1.84

*Rate constants in min^{-1}; [NaOH] = 1.00 *M*; [HCHO] = 0.02 *M*; μ = 2.0 *M*.
†Initial concentrations in mole l^{-1}.

TABLE II

Pseudo first order rate constants* in hexacyanoferrate(III) ion at 40°

$10^3 \times$ [HCHO]†	$10^3 \times k''$	$10 \times \frac{k''}{[HCHO]}$
20.00	3.60	1.80
14.00	2.54	1.81
10.00	1.82	1.82
7.00	1.26	1.80
5.00	0.91	1.82

*Rate constants in min^{-1}; [NaOH] = 1.00 *M*; $[K_3Fe(CN)_6] = 1.00 \times 10^{-3}$ *M*; μ = 2.0 *M*.
†Concentration in mole l^{-1}.

TABLE III

Pseudo first order rate constants* in hexacyanoferrate(III) ion at 40°

[NaOH]†	$10^3 \times k''$	$10^3 \times k''/[OH^-]$
2.00	7.28	3.60
1.50	5.42	3.61
1.00	3.60	3.60
0.75	2.72	3.62
0.50	1.82	3.64

*Rate constants in min^{-1}; [HCHO] = 2.00×10^{-2} *M*, $[K_3Fe(CN)_6] = 1.00 \times 10^{-3}$ *M*; μ = 2.0 *M*.
†Concentrations in mole l^{-1}.

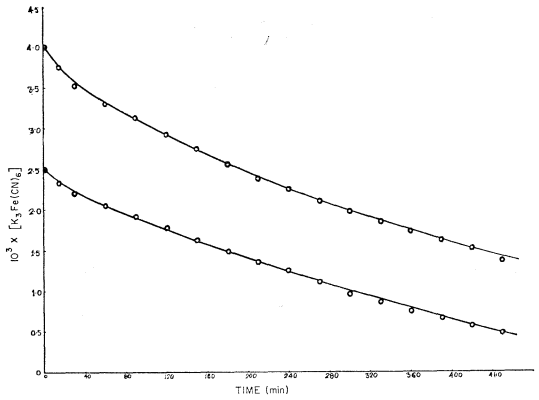

FIG. 1. Nature of the reaction in terms of the decreasing concentration of hexacyanoferrate(III) ion; temperature = 40°, [HCHO] = 0.02 *M*, [NaOH] = 1.0 *M*.

the use of ferroin as a redox indicator. The first order rate constants (k'') given in Tables I to III are the averages obtained from the slope of the first order plot made for ferricyanide. The actual nature of the reaction is also shown graphically in Fig. 1. Figure 2 shows the first order plot for different runs of ferricyanide. It indicates that there is a possibility of two parallel reactions producing a common product, and shows similarity to the explanation of Brown and Fletcher

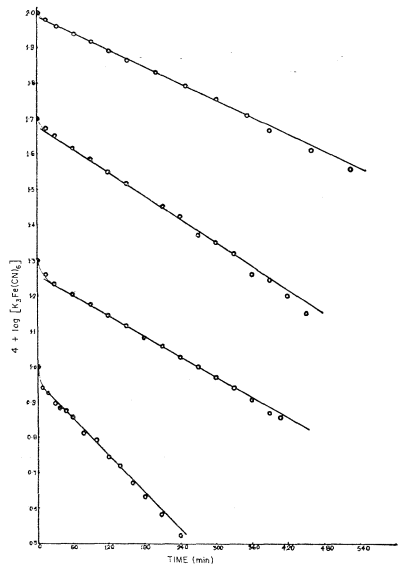

FIG. 2. First order plot for the rate of oxidation of formaldehyde by hexacyanoferrate(III) ion; temperature = 40°, [HCHO] = 0.02 *M*, [NaOH] = 1.0 *M*.

(3) for the hydrolysis of mixed tertiary aliphatic chlorides. The curves become linear and follow simple first order kinetics after some time, because the more reactive component has disappeared. From their intercepts, the concentration of the more reactive component (which is half the concentration of ferricyanide consumed) is estimated to be 0.27%. Thus the relative proportions of the components likely to be the hydrate and nonhydrate forms of formaldehyde are 99.73% and 0.27% of the original mixture.

Table I collects the values of k'' (first order rate constant values obtained from the slope) for different initial concentrations of ferricyanide. These values appear to be constant at moderate concentrations but there is some retarding effect at higher concentrations. They continue to decrease as the concentration of ferricyanide ion is increased. At least part of this decrease must be due to the fact that psuedo first order kinetics do not apply at high concentrations of hexacyanoferrate(III) ion. But the retarding effect of the hexacyanoferrate(III) ion cannot be omitted on this ground only, as the effect is apparent even in the initial part of the reaction where there is negligible change in the reductant concentration.

Table II contains the first order rate constants for different concentrations of formaldehyde. The last column shows that the second order rate constants obtained by dividing k'' by the initial formaldehyde concentrations are indeed constant. This confirms that the reaction is first order with respect to formaldehyde.

Similarly Table III demonstrates the effect of variation of hydroxide ion on the rate of the reaction. The last column shows that $k''/[OH^-]$ is almost constant for these base concentrations and thus confirms the first order dependence of the reaction rate on base concentration.

Further confirmation of the order has also been made by studying the reaction with respect to formaldehyde. The reaction velocity was again measured by estimating the amount of ferrocyanide produced after different intervals of time. It was observed that 2 equivalents of ferrocyanide ions are produced for 1 mole of formaldehyde. The first order rate constants (k'), in this case, were calculated from the standard integrated first order equation. Summarized data are given in Tables IV to VIII. The average deviation of k' given in these tables is $\pm 0.04 \times 10^{-2}$ units. Under these conditions the possibility of Can-

Can. J. Chem. Downloaded from www.nrcresearchpress.com by 210.87.254.5 on 09/05/12
For personal use only.

Can. J. Chem. Downloaded from www.nrcresearchpress.com by 210.87.254.5 on 09/05/12
For personal use only.

TABLE IV

Pseudo first order constants* in formaldehyde at 40°

Initial concentrations $10^3 \times$ [HCHO]†	$10^3 \times k'$
10.00	12.56
5.00	10.08
4.00	11.93
2.50	13.48
2.00	13.45
1.33	13.12
1.00	13.18

*Rate constants in min^{-1}; [NaOH] = 1.00 M; $[K_3Fe(CN)_6] = 0.20\ M$; $\mu = 2.2\ M$.
†Concentrations in mole l^{-1}.

TABLE V

Pseudo first order rate constants* in formaldehyde at 40°

Initial concentrations $10^3 \times$ [HCHO]†	$10^3 \times k'$
5.00	30.10
4.00	28.01
2.50	30.81
2.00	31.62
1.00	29.32

*Rate constants in min^{-1}; [NaOH] = 2.00 M; $[K_3Fe(CN)_6] = 0.10\ M$; $\mu = 2.6\ M$.
†Concentrations in mole l^{-1}.

TABLE VI

Pseudo first order rate constants* in formaldehyde for different ferricyanide concentrations at constant ionic strength at 40°

$10^2 \times [K_3Fe(CN)_6]$†	$10^3 \times k'$	$10 \times \frac{k'}{[K_3Fe(CN)_6]}$
20.00	65.19	3.25
15.00	53.58	3.57
10.00	48.84	4.88
7.50	31.86	4.14
5.00	26.40	5.28
4.00	20.00	5.00
2.00	13.02	6.50

*Rate constants in min^{-1}; [NaOH] = 2.0 M; [HCHO] = 1.00 × 10^{-3} M; $\mu = 3.2\ M$.
†Concentrations in mole l^{-1}.

nizzaro reaction (4) is negligible. Tables IV and V show that the first order rate constant values are practically the same over a ten-fold range of formaldehyde concentration.

A standard first order plot between $\log (a - x)$ and time is also shown in Fig. 3 [$(a - x)$ = concentration of formaldehyde]. The reaction is first order to more than 90% completion. Though in this case the complete course of the reaction is

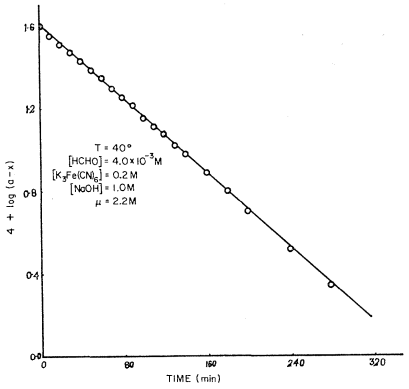

FIG. 3. First order plot for the rate of oxidation of formaldehyde by hexacyanoferrate(III) ion.

followed by a 4% change in the ferricyanide concentration, no apparent change in the first order rate constant is observed. In addition, the effect of the formation of the acid on the concentration of the base must be considered. The decrease in ferricyanide concentration increases the first order rate constants (Table I) while the decrease in base concentration will lower them. Probably these two effects counteract one another and no apparent change in the velocity constant is observed. These observations, therefore, confirm the first order dependence of the reaction rate on formaldehyde concentration.

Tables VI and VII show the k' values for different concentrations of ferricyanide, both at constant and varying values of μ. When μ is not constant the reaction shows a first order dependence on ferricyanide concentration, but at constant μ the $k'/[Fe(CN)_6^{3-}]$ values decrease with increasing concentration of ferricyanide. In this case some association of ferricyanide ion

TABLE VII

Pseudo first order rate constants* in formaldehyde for different ferricyanide concentrations at non-constant ionic strength at 40°

$10^2 \times [K_3Fe(CN)_6]$†	$10^3 \times k'$	$10 \times \frac{k'}{[K_3Fe(CN)_6]}$
20.00	65.19	3.25
15.00	45.96	3.06
12.50	39.94	3.33
10.00	31.62	3.16
5.00	15.20	3.04

*Rate constant in min^{-1}; [NaOH] = 2.0 M; [HCHO] = 2.00 × 10^{-3} M.
†Concentrations in mole l^{-1}.

TABLE VIII

Pseudo first order rate constants* in formaldehyde for different hydroxide concentrations at 40°

[OH⁻]	$10^3 \times k'$	$10^3 \times \frac{k'}{[OH^-]}$
2.00	29.32	14.66
1.50	20.50	13.67
1.00	13.50	13.50
0.75	10.00	13.33
0.50	6.60	13.20

*Rate constants in min^{-1}; $[K_3Fe(CN)_6] = 10.00 \times 10^{-2}$ *M*; $[HCHO] = 1.00 \times 10^{-3}$ *M*; $\mu = 2.6$ *M*.
†Concentrations in mole l^{-1}.

with Na^+ or K^+ ion may also occur but the error involved is difficult to estimate at higher $[Fe(CN)_6^{3-}]$. Nevertheless, it is quite evident from Tables VI and VII that, if μ of the medium is kept constant, $k'/[Fe(CN)_6^{3-}]$ will not remain constant but will show the same dependence as is observed in Table I. All these observations clearly indicate that the reaction is first order at low ferricyanide concentrations, but it proceeds with a retarded velocity at higher concentrations.

Table VIII contains the k' values obtained for different concentrations of hydroxide ion. The almost constant $k'/[OH^-]$ values again show that the reaction is first order with respect to hydroxide ion.

Scheme of Oxidation of Formaldehyde by Alkaline Ferricyanide

From the experimental results it is clear that after a rapid initial reaction, the velocity follows a good first order dependence on ferricyanide concentration. It has been observed that 99% of the formaldehyde in aqueous medium is in the hydrated form (5). In many ways its oxidation resembles that of aliphatic alcohols (6). In the present case, one might assume that the hydrate has a lower rate than the non-hydrate as the oxidation of the alcohols is slower than that of the aldehydes. However, consider the equilibrium

$$H_2CO + H_2O \rightleftharpoons H_2C(OH)_2$$

The rapid initial reaction seen in Fig. 2 could not be the result of oxidation of the non-hydrate of formaldehyde unless the rate of oxidation of the hydrate was faster than that of its dehydration. Since the rate of oxidation is relatively slow, this does not seem to be a likely situation and this part of the problem still remains questionable.

Further, the probable scheme of the ferricyanide oxidation of the hydrated formaldehyde in alkaline medium might be considered as follows

[1] 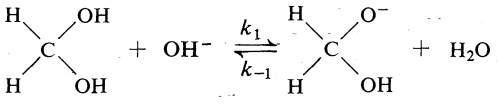

[2] 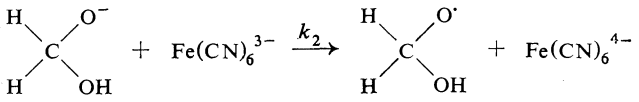

[3] 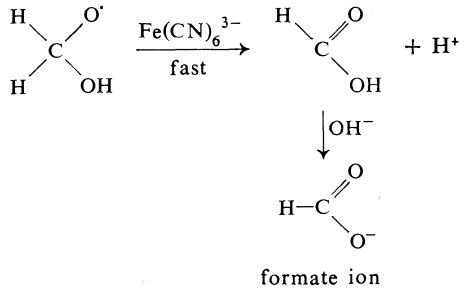

formate ion

Can. J. Chem. Downloaded from www.nrcresearchpress.com by 210.87.254.5 on 09/05/12
For personal use only.

Can. J. Chem. Downloaded from www.nrcresearchpress.com by 210.87.254.5 on 09/05/12
For personal use only.

If the concentration of the anion formed in step [1] reaches a steady state, the net rate of disappearance of ferricyanide is

$$[4] \quad -\frac{d[Fe(CN)_6^{3-}]}{dt} = \frac{2k_1k_2[HC(OH)_2][OH^-][Fe(CN)_6^{3-}]}{k_{-1}[H_2O] + k_2[Fe(CN)_6^{3-}]}$$

This rate law [4] predicts the observed retardation at higher concentrations of ferricyanide. Since k_1/k_{-1} equals K, the equilibrium constant for the step [1], the rate law reduces to

$$[5] \quad -\frac{d[Fe(CN)_6^{3-}]}{dt} = \frac{2Kk_2[HC(OH)_2][OH^-][Fe(CN)_6^{3-}]}{[H_2O] + \frac{k_2}{k_{-1}}[Fe(CN)_6^{3-}]}$$

If the concentration of ferricyanide is sufficiently small,

$$[H_2O] \gg \frac{k_2}{k_{-1}}[Fe(CN)_6^{3-}]$$

and eq. [5] becomes

$$[6] \quad -\frac{d[Fe(CN)_6^{3-}]}{dt} = \frac{2Kk_2}{[H_2O]}[HC(OH)_2][OH^-][Fe(CN)_6^{3-}]$$

The observed third order rate constant would then be $2Kk_2/[H_2O]$. This has been calculated taking two different sets of conditions having approximately the same ionic strength. From Table I, the value of the third order rate constant is 0.092 mole^{-2} l^2 min^{-1} when $[Fe(CN)_6] = 0.01$ M, and from the Table IV it is 0.065 mole $^{-2}$ l^2 min^{-1} when $[Fe(CN)_6] = 0.20$ M. This degree of agreement is taken to substantiate the above mechanism.

The free radical

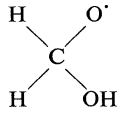

is rapidly oxidized to formic acid by reaction with more ferricyanide. Oxygen has a greater electron affinity than hydrogen; it shares immediately the hydrogen bonded electron of the carbon and the proton separates with simultaneous abstraction of the electron by hexacyanoferrate(III) ion. Although it is difficult to discuss the details of the oxidation of this free radical, it is apparent from the kinetic data that it is rapidly attacked by hexacyanoferrate(III) ion to yield formic acid as the final product. The formate ion is much more stable towards oxidation due to its mesomeric structure. A stoichiometric equation can be written as follows

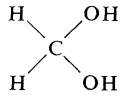

$$[7] \quad + 3OH^- + 2Fe(CN)_6^{3-} \rightarrow HCO_2^- + 2Fe(CN)_6^{4-} + 3H_2O$$

The work has been extended to three temperatures and the summarized data are given in Table IX. The energy of activation is 12.0 kcal/mole.

TABLE IX

Effect of variation of temperature* on the psuedo first order rate constants† in formaldehyde

Temperature	$10^5 \times k'$
30	11.74
35	15.81
40	19.88
45	31.36

*Temperature in °C; [HCHO] = 0.25 × 10^{-2} M; [$K_3Fe(CN)_6$] = 0.20 M; [NaOH] = 1.00 M; μ = 2.2 M.
†Rate constants in s^{-1}.

Experimental

The kinetic study of the reaction was done with Analar (B.D.H.) grade samples. The reaction was initiated by mixing the requisite amount of formaldehyde solution with a solution of potassium ferricyanide and sodium hydroxide kept in a bottle coated with black Japan. The temperature of the reaction mixture was kept constant (±0.1°) using an electrically operated thermostat. The course of the reaction was followed at different intervals of time by estimating the amount of ferrocyanide ion produced. This was done by titration with a standard solution of ceric sulfate using ferroin as a redox indicator. The ionic strength of the medium was kept constant with a standard solution of sodium perchlorate.

Product Study

After complete reduction of the hexacyanoferrate(III) ion the organic acid was separated by extracting into ether followed by aqueous ammonia. The ammoniacal solution was employed to detect the anion of the organic acid by

paper chromatography. The stoichiometry of the reaction supports the conclusion that formic acid is the final product.

Acknowledgment

One of the authors (V. N. Singh) is thankful to the Ministry of Education, Government of India, for a research training scholarship.

1. J. B. CONANT, J. C. ASTON, and C. O. TONBERG. J. Am. Chem. Soc. **52**, 407 (1930).
2. J. HALLUTA and A. MUTSCHIN. Z. Phys. Chem. **150**, 381 (1930).
3. H. C. BROWN and R. S. FLETCHER. J. Am. Chem. Soc. **71**, 1845 (1949).
4. H. V. EULER and T. LOVGREN. Z. Anorg. Allgem. Chem. **147**, 127 (1925).
5. R. BIEBER and G. TRÜMPLER. Helv. Chim. Acta, **30**, 1860 (1947).
6. T. J. KEMP and W. A. WATERS. Proc. Roy. Soc. London, Ser. A, **274**, 480 (1963).

Can. J. Chem. Downloaded from www.nrcresearchpress.com by 210.87.254.5 on 09/05/12
For personal use only.

Nuclear magnetic resonance spectra of ortho-, meta-, and para-difluorobenzenes in a nematic liquid crystal solvent

C. T. YIM AND D. F. R. GILSON
Department of Chemistry, McGill University, Montreal, Quebec
Received October 4, 1968

The proton and fluorine magnetic resonance spectra of ortho-, meta-, and para-difluorobenzene dissolved in a nematic liquid crystal solvent have been analyzed. Expressions for the anisotropy of the fluorine chemical shift were obtained but an attempt to fit these to the Karplus and Das theory failed. Hydrogen atoms *ortho* to fluorine show small displacements from their expected positions.

Canadian Journal of Chemistry, 47, 1057 (1969)

Can. J. Chem. Downloaded from www.nrcresearchpress.com by 210.87.254.40 on 09/05/12
For personal use only.

Introduction

The use of nematic liquid crystal solvents for studying the nuclear magnetic resonance spectra of partially oriented solute molecules permits the determination of the anisotropies of chemical shifts, the absolute signs of indirect coupling constants, and, in certain cases, the geometry of the solute molecule (1–3). Saupe (4) has developed expressions for the average orientation of a solute molecule in terms of an order matrix $\boldsymbol{S}$, which Snyder (5) has re-defined in terms of the probability function of the orientation expanded in real spherical harmonics. In Snyder's notation the chemical shift in the nematic phase is given by

$$[1]\quad \bar{\sigma}_{zzi} = \tfrac{1}{3}(\sigma_{zzi} + \sigma_{xxi} + \sigma_{yyi}) + C_{3z^2-r^2}\frac{2}{3\sqrt{5}}[\sigma_{zzi} - \tfrac{1}{2}(\sigma_{xxi} + \sigma_{yyi})] + C_{x^2-y^2}\frac{1}{\sqrt{(15)}}(\sigma_{xxi} - \sigma_{yyi}) + C_{xz}\frac{1}{\sqrt{(15)}}(\sigma_{xzi} + \sigma_{zxi}) + C_{yz}\frac{1}{\sqrt{(15)}}(\sigma_{yzi} + \sigma_{zyi}) + C_{xy}\frac{1}{\sqrt{(15)}}(\sigma_{xyi} + \sigma_{yxi})$$

where $\sigma_{\alpha\beta}$ are the components of the nuclear shielding tensor, and the C terms are the motional constants.

The direct dipole coupling constants are given by

$$[2]\quad D_{ij} = \frac{\gamma_i\gamma_j}{\pi\sqrt{5}}\left\{C_{3z^2-r^2}\left[\left\langle\frac{(\Delta z_{ij})^2}{r_{ij}^5}\right\rangle - \frac{1}{2}\left\langle\frac{(\Delta x_{ij})^2}{r_{ij}^5}\right\rangle - \frac{1}{2}\left\langle\frac{(\Delta y_{ij})^2}{r_{ij}^5}\right\rangle\right] + C_{x^2-y^2}\frac{\sqrt{3}}{2}\left[\left\langle\frac{(\Delta x_{ij})^2}{r_{ij}^5}\right\rangle - \left\langle\frac{(\Delta y_{ij})^2}{r_{ij}^5}\right\rangle\right] + C_{xz}\sqrt{3}\left[\left\langle\frac{(\Delta x_{ij})(\Delta z_{ij})}{r_{ij}^5}\right\rangle\right] + C_{yz}\sqrt{3}\left[\left\langle\frac{(\Delta y_{ij})(\Delta z_{ij})}{r_{ij}^5}\right\rangle\right] + C_{xy}\sqrt{3}\left[\left\langle\frac{(\Delta x_{ij})(\Delta y_{ij})}{r_{ij}^5}\right\rangle\right]$$

where Δx_{ij}, Δy_{ij}, and Δz_{ij} are the components of the vector $\boldsymbol{r}_{ij}$ joining nuclei i and j, and the angular brackets indicate averages over the internal motions of the molecule.

For molecules with a threefold or higher axis of symmetry only one of the five possible motional constants is non-zero. Thus, for benzene (6), hexafluorobenzene (7), and 1,3,5-trifluorobenzene (2, 8) the anisotropy of the chemical shift can be determined directly. If a molecule has two perpendicular planes of symmetry but less than threefold symmetry, a suitable choice of axes leads to two non-zero motional constants and the anisotropy of the chemical shift is not

Can. J. Chem. Downloaded from www.nrcresearchpress.com by 210.87.254.40 on 09/05/12
For personal use only.

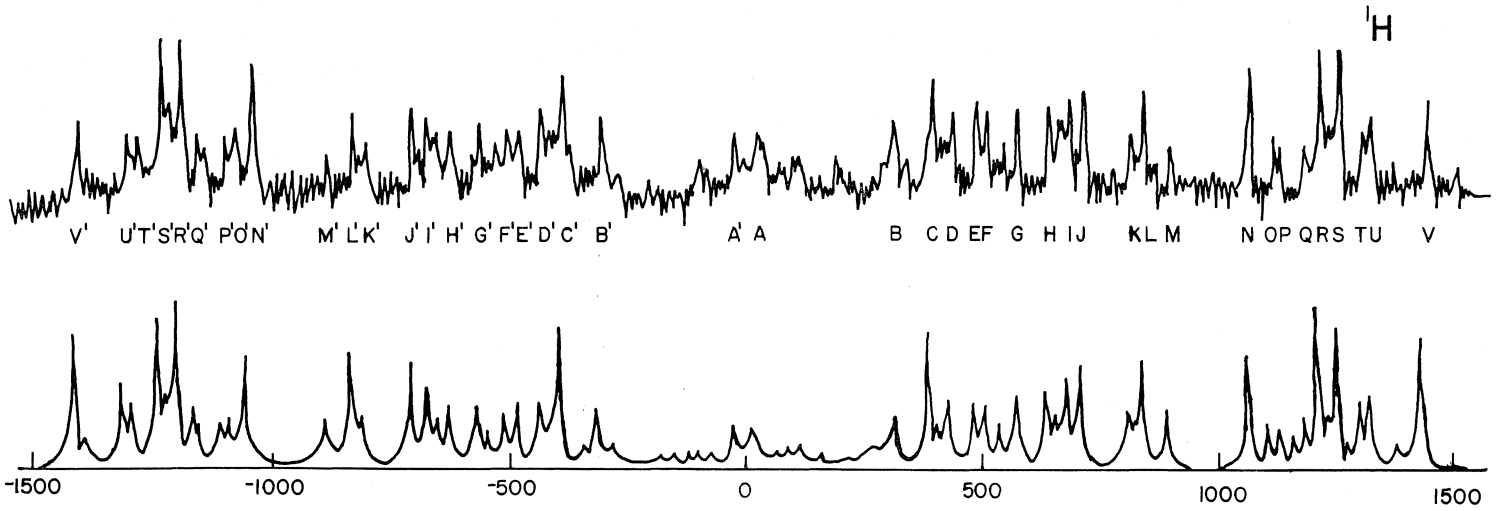

FIG. 1*a*. The proton magnetic resonance spectra of *ortho*-difluorobenzene. Computer simulated spectra are shown below the experimental spectra.

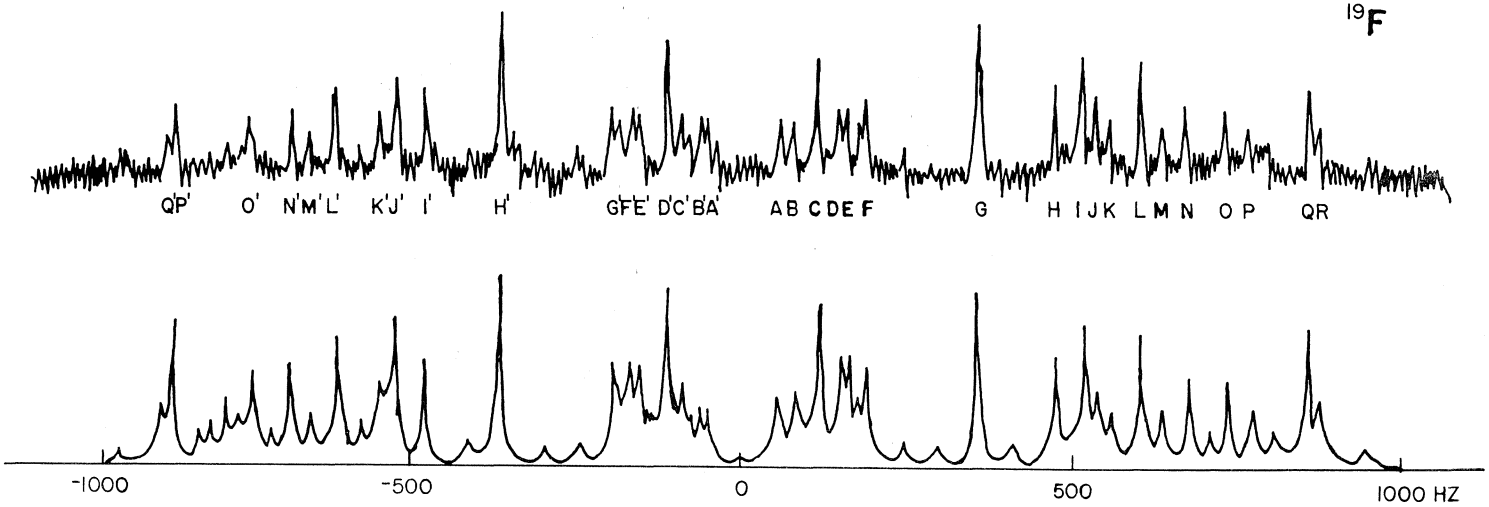

FIG. 1*b*. The fluorine magnetic resonance spectra of *ortho*-difluorobenzene. Computer simulated spectra are shown below the experimental spectra.

Can. J. Chem. Downloaded from www.nrcresearchpress.com by 210.87.254.40 on 09/05/12
For personal use only.

immediately defined. Snyder (5) has calculated the anisotropy of the fluorine chemical shift in monofluorobenzene by assuming that the C—F bonds in fluorobenzene and hexafluorobenzene are similar. The magnitude of the anisotropy obtained in this way was in reasonable agreement with the value obtained by Chan and Dubin (9) from molecular beam magnetic resonance measurements, but the values of $(\sigma_{yy} - \sigma_{xx})$ from the two methods were in considerable disagreement. Applications of the Karplus and Das theory (10) predicted the direction of the anisotropy found by Snyder but the relative magnitudes of σ_{xx} and σ_{yy} as found by Chan and Dubin.

In the present study we report the analyses of the proton and fluorine magnetic resonance spectra of ortho-, meta-, and para-difluorobenzene dissolved in a mixed nematic liquid crystal.

Experimental

Samples of difluorobenzenes were obtained from commercial sources and used without further purification. Spectra were recorded with a modified Varian DP60 spectrometer as previously reported (8). Solute concentrations and the temperatures of measurement were as follows

Compound	Amount (mole %)	Temperature (°C)
o-Difluorobenzene	36	64
m-Difluorobenzene	37	64
p-Difluorobenzene	33	67

Trifluoroacetic acid was used as an external reference for fluorine resonances. A solution of carbon tetrafluoride (4%) in the liquid crystal solvent showed a 13 Hz high field shift (at 56.4 MHz) on going from the nematic phase (65 °C) to the isotropic phase (104 °C) and a corresponding correction was made to all observed anisotropic shifts (11, 12).

Results

ortho-Difluorobenzene

The proton and fluorine magnetic resonance spectra of ortho-difluorobenzene are given in Fig. 1. The spectra are not symmetrical with respect to their centers due to the difference between the proton chemical shifts. Theoretical spectra were computed, using the program described previously (8), with initial values of the direct coupling constants calculated for a regular molecular structure with bond distances of C—C = 1.39 Å, C—H = 1.08 Å, and C—F = 1.31 Å, all bond angles were assumed to be 120°. The appearance of the spectra depend essentially on the ratio of the two motional constants. Trial calculations were commenced with an arbitrarily chosen value of −0.25 for $C_{3z^2-r^2}$ and neglecting the indirect spin coupling constants and proton chemical shift difference. After approximate values of $C_{3z^2-r^2}$ and $C_{x^2-y^2}$ were obtained, the indirect coupling constants and proton shifts were included, and the theoretical spectrum was recalculated. Examination of the spectrum showed that certain lines bore simple fixed relationships to the coupling constants, viz.

$$\nu_Q(F) \text{ and } \nu_{P'}(F) = 1/2(D_{12} + D_{13} + D_{25} + D_{26} + J_{12} + J_{13} + J_{25} + J_{26}) + 3/4D_{23}$$

$$\nu_I(F) \text{ and } \nu_{J'}(F) = 1/2(D_{12} + D_{13} + D_{25} + D_{26} + J_{12} + J_{13} + J_{25} + J_{26}) - 3/4D_{23}$$

The spectral parameters were optimized while maintaining a reasonable fit to the positions of the lines. The best fit to the fluorine spectrum was obtained with all J_{ij}, except J_{35} and J_{56}, positive with respect to D_{ij}, but for the proton spectrum the agreement between theoretical and experimental spectra was not as satisfactory under the combined variation of the two motional constants and the chemical shift with both possible

TABLE I

Spectral parameters for ortho-difluorobenzene

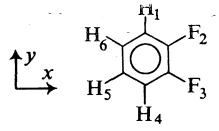

i	j	D_{ij}	J_{ij} This work	J_{ij} Ref. 15
1	2	−970.8	11.0	10.44
1	3	−98.0	9.0	7.87
1	4	−41.6	0	0.29
1	5	−115.0	1.5	1.62
1	6	−1108.4	8.3	8.30
2	3	−225.5	−20.0	−20.43
2	5	−115.6	−1.5	−1.39
2	6	−219.4	3.5	4.33
5	6	−332.8	7.6	7.62

$C_{3z^2-r^2} = -0.2418$

$C_{x^2-y^2} = 0.0857$

^{19}F: $\bar{\sigma}$ nematic (64 °C) = 67.87 ± 0.05 p.p.m. (internal standard, CF_4)
$\bar{\sigma}$ isotropic (90 °C) = 78.81 ± 0.04 p.p.m.

^1H: $\nu_{1,4} = 0$ Hz $\nu_{5,6} = -4.0$ Hz at 56.4 MHz

Can. J. Chem. Downloaded from www.nrcresearchpress.com by 210.87.254.40 on 09/05/12
For personal use only.

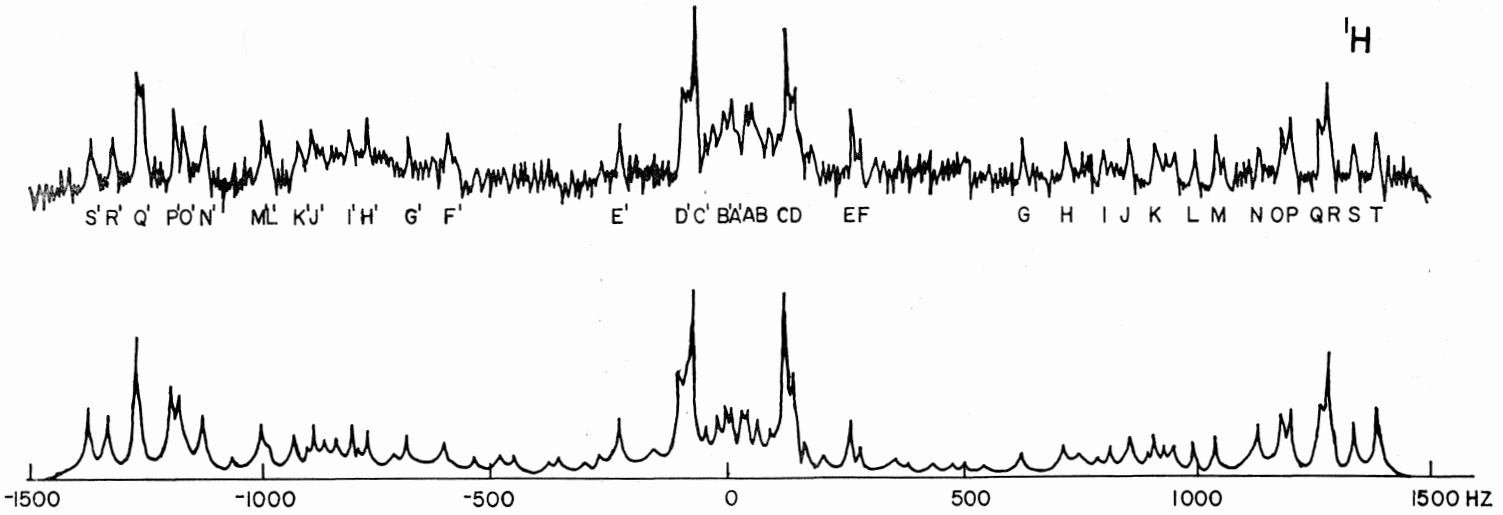

FIG. 2*a*. The proton magnetic resonance spectra of meta-difluorobenzene. Computer simulated spectra are shown below the experimental spectra.

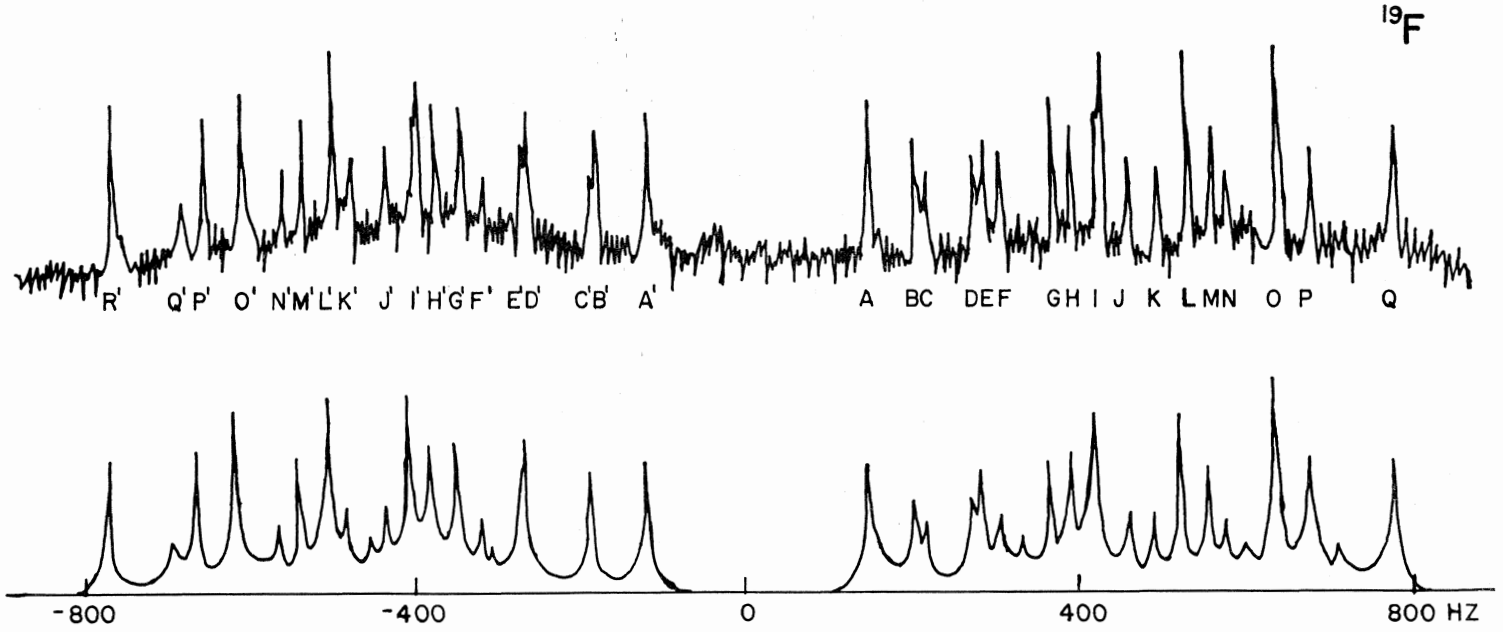

FIG. 2*b*. The fluorine magnetic resonance spectra of meta-difluorobenzene. Computer simulated spectra are shown below the experimental spectra.

Can. J. Chem. Downloaded from www.nrcresearchpress.com by 210.87.254.40 on 09/05/12
For personal use only.

signs of J_{ij}. The final stage of computation included the pseudo-dipole coupling constants and further optimization of the spectral parameters to give the best overall fit to both fluorine and proton spectra. The parameters are given in Table I and the computer simulated spectra in Fig. 1. The r.m.s. deviation of all observed lines from their calculated frequencies was 2.8 Hz.

meta-Difluorobenzene

The proton and fluorine spectra are given in Fig. 2. The same procedure for analysis was employed with the following lines used for optimization

$$\nu_Q(F) \text{ and } \nu_{R'}(F) = 1/2(D_{12} + D_{23} + D_{24} + D_{25} + J_{12} + J_{23} + J_{24} + J_{25}) + 3/4D_{26}$$

$$\nu_L(F) \text{ and } \nu_{L'}(F) = 1/2(D_{12} + D_{23} + D_{24} + D_{25} + J_{12} + J_{23} + J_{24} + J_{25}) - 3/4D_{26}$$

The final parameters are listed in Table II and the computer simulated spectra are given in Fig. 2. The r.m.s. deviation of all observed lines was 2.3 Hz.

TABLE II

Spectral parameters for meta-difluorobenzene

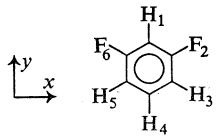

i	j	D_{ij}	J_{ij} This work	J_{ij} Ref. 14
1	2	−917.0	9.2	9.23
1	3	−100.2	2.5	2.45
1	4	−31.4	0.3	0.33
2	3	−209.8	8.2	8.16
2	4	−86.0	6.5	6.46
2	5	−108.7	−0.9	−0.86
2	6	−173.2	6.6	6.57
3	4	−1028.0	8.4	8.4
3	5	−216.1	0.9	0.86

$C_{3z^2-r^2} = -0.2216$

$C_{x^2-y^2} = 0.0872$

^{19}F: $\bar{\sigma}$ nematic (64 °C) = 43.10 ± 0.06 p.p.m. (internal standard, CF_4)
$\bar{\sigma}$ isotropic (85 °C) = 48.00 ± 0.02 p.p.m.

^1H: $\nu_1 = 25.0$ Hz, $\nu_{3,5} = 15.0$ Hz, $\nu_4 = 0$ Hz at 56.4 MHz

para-Difluorobenzene

The higher molecular symmetry of para-difluorobenzene led to a simpler method of spectral analysis. Instead of computing a theoretical spectrum and comparing it with the experimental spectrum, a perturbation method was used which gave simple expressions for the transition energies. This was possible because the spectrum was dominated by the dipole coupling between the ortho protons. Recently Bulthuis, Gerritsen, Hilbers, and McLean (13) have given a detailed discussion of this method and its application to the analysis of the spectra of symmetrically para-disubstituted benzenes, including para-difluorobenzene, dissolved in nematic 4,4′-di-*n*-hexyloxyazoxybenzene[1].

In the first order approximation the proton half-spectrum should consist of five triplets with a splitting equal to $1/2(D_{12} + D_{13} + J_{12} + J_{13})$. In the actual spectrum, Fig. 3*a*, only four triplets were observed, due to coincidence of lines C and D, H and I, M and N.

The fluorine spectrum, Fig. 3*b*, consisted essentially of ten lines based on a quintet, with a splitting $1/2(D_{12} + D_{13} + J_{12} + J_{13})$, each line of which was further split into a doublet with separation $3/2D_{14}$. A further small splitting due to second order effects was also observed. Analysis of the spectra only gave values of D_{14}, D_{23}, D_{25}, D_{26}, and $1/2(D_{12} + D_{13} + J_{12} + J_{13})$ and the magnitudes and signs of the remaining indirect coupling constants could not be obtained.

This perturbation method has been applied to the analysis of the spectra of some partially oriented para-substituted fluorobenzene derivatives and will be discussed further in a subsequent publication.

Final parameters for para-difluorobenzene are given in Table III and the computer simulated spectra are shown in Fig. 3.

Discussion

Indirect Coupling Constants

The magnitudes and absolute signs of the indirect coupling constants are listed in Tables I, II, and III and are in agreement with those reported from isotropic spectra in the literature (14–16). The signs of the indirect proton–fluorine

[1]We are indebted to the referees for bringing this paper to our attention.

Can. J. Chem. Downloaded from www.nrcresearchpress.com by 210.87.254.40 on 09/05/12
For personal use only.

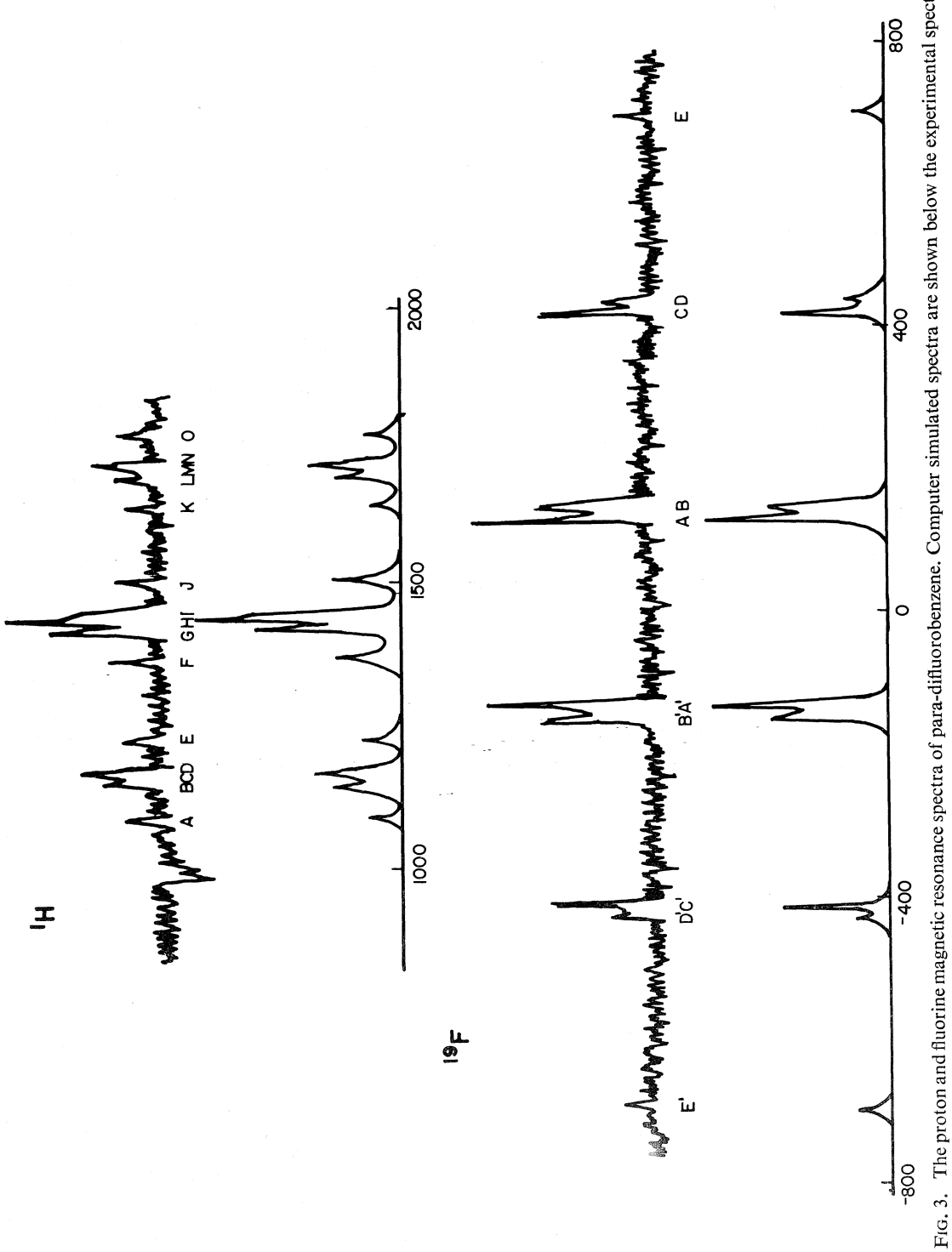

FIG. 3. The proton and fluorine magnetic resonance spectra of para-difluorobenzene. Computer simulated spectra are shown below the experimental spectra.

TABLE III

Spectral parameters for para-difluorobenzene

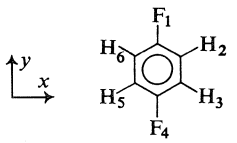

i	j	D_{ij}	J_{ij} This work	J_{ij} Ref. 13
1	2	−344.5	8.1	7.6
1	3	−233.2	4.6	4.6
1	4	−170.8		
2	3	−1907.9		
2	5	−35.8		
2	6	59.9		

$C_{3z^2-r^2} = -0.2413$

$C_{x^2-y^2} = -0.1899$

^{19}F: $\bar{\sigma}$ nematic (67 °C) = 55.32 ± 0.05 p.p.m. (internal standard, CF_4)
$\bar{\sigma}$ isotropic (90 °C) = 57.62 ± 0.02 p.p.m.

^{1}H: $\bar{\sigma}$ nematic (67 °C) = −6.31 ± 0.03 p.p.m. (internal standard, TMS)
$\bar{\sigma}$ isotropic (93 °C) = −6.46 ± 0.03 p.p.m.

coupling constants are all positive except J_{HF}^{para} which is negative. J_{FF} in ortho-difluorobenzene is negative.

Anisotropy of the Fluorine Chemical Shifts

As discussed earlier, when two motional constants are required, the anisotropy of the chemical shift cannot be obtained directly. In Table IV the anisotropies are expressed as equations of the form

$$[4] \qquad A\sigma_{aa} + B\sigma_{bb} + C\sigma_{cc} = D$$

where the molecule fixed axes x, y, and z have been transformed to axes; a (perpendicular to the molecular plane), b (along the C—F bond), and c (in the molecular plane and perpendicular to the C—F bond). It is assumed that a, b, and c are the principal axes of the paramagnetic shielding tensor, which is an approximation for the ortho and meta derivatives. Also included in Table IV are the results for monofluorobenzene (5), 1,3,5-trifluorobenzene (8), and hexafluorobenzene (7). If, as Snyder has assumed, these results are consistent, then the expressions for any two molecules can be used to determine the anisotropy. Snyder obtained $(\sigma_{bb} - \sigma_{cc}) = 259$ p.p.m. for monofluoro- and hexafluorobenzene. With the most favorable cases, i.e. those without orthosubstituents, the values of $(\sigma_{bb} - \sigma_{cc})$ are; 96 p.p.m. (monofluorobenzene and meta-difluorobenzene), 70 p.p.m. (monofluorobenzene and para-difluorobenzene), 83 p.p.m. (meta-difluorobenzene and para-difluorobenzene), 123 p.p.m. (monofluorobenzene and 1,3,5-trifluorobenzene), and 162 p.p.m. (meta-difluorobenzene and 1,3,5-trifluorobenzene). The assumption that the carbon–fluorine bonds are sufficiently similar is not justified and this may account for the apparent disagreement between the results of Snyder (5) and those of Chan and Dubin (9). The latter results, however, disagreed in sign with the predictions of the Karplus and Das theory (10). This theory, originally intended for the calculation of isotropic chemical shifts, can be used to express the shielding tensor components, and hence the anisotropy, in terms of the bond parameters; hybridization s, ionic character I, and double bond character ρ.

$$[5] \qquad \sigma_{aa} = \frac{3}{2}\sigma_0\{1 - s - I + Is\}$$

$$[6] \qquad \sigma_{bb} = \frac{3}{2}\sigma_0\{\rho\}$$

$$[7] \qquad \sigma_{cc} = \frac{3}{2}\sigma_0\{1 - s - I + Is + \rho(s + I)\}$$

TABLE IV

Anisotropy expressions for fluorine chemical shifts

	A	B	C	D	σ_{0calcd} (p.p.m.)
ortho-Difluorobenzene	1	−0.653	−0.347	123.9	—
meta-Difluorobenzene	1	−0.670	−0.330	74.4	3560
para-Difluorobenzene	1	−1.184	0.184	31.7	234
Fluorobenzene	1	−0.076	−0.924	50.0	524
1,3,5-Trifluorobenzene	1	−0.500	−0.500	102.0	—
Hexafluorobenzene	1	−0.500	−0.500	154.0	—

Can. J. Chem. Downloaded from www.nrcresearchpress.com by 210.87.254.40 on 09/05/12
For personal use only.

where

$$\sigma_0 = -\left(\frac{2e^2h^2}{3m^2c^2\Delta E}\right)\left\langle\frac{1}{r^3}\right\rangle_{2p}$$

ΔE = average excitation energy

$\left\langle\frac{1}{r^3}\right\rangle_{2p}$ = the expectation value of $\frac{1}{r^3}$ for the 2p orbital.

For monofluorobenzene, Karplus and Das assumed values of $s = 0.05$, $I = 0.75$ (from electronegativity considerations), and $\rho = 0.126$ (from Hückel molecular orbital calculations). For the difluorobenzenes double bond character was calculated but the changes in ionic character were obtained empirically. The value for ortho-difluorobenzene was unacceptable and will not be considered in the present study. If the values for s, I, and ρ given by Karplus and Das are substituted in eqs. [5]–[7] and the resulting σ_{aa}, σ_{bb}, and σ_{cc} substituted in eq. [4], acceptable values of σ_0 are not obtained. The calculated anisotropy in 1,3,5-trifluorobenzene is zero. There remain more unknown than known terms in the Karplus and Das treatment and it is possible that the adjustment of a sufficient number of empirical parameters could lead to agreement with the experimental results. It is also possible that the theory is strained too far in applying it to the calculation of chemical shift anisotropies. It should be noted that we have assumed that the anisotropies measured in nematic solvents represent the true values and do not involve large contributions due to the highly anisotropic environment (11, 12). The average excitation energy and the average inverse cube function for a p orbital are also assumed to be constant, and, for the difluorobenzenes these should be valid approximations.

Various other methods have been used to calculate isotropic chemical shifts in substituted fluorobenzenes (17–20). The trends in chemical shifts have been correlated with π electron densities with moderate success, although Emsley (20) remains sceptical that reliable predictions can be made by these methods. In all cases assumptions are made: an invariant sigma framework, empirical values for ionic character, empirical (sometimes negative) average excitation energies, which render these methods unsuitable for calculation of anisotropies.

Molecular Geometry

The optimized direct dipole coupling constants can be used to recalculate the molecular geometry but, since the nuclear coordinates in eq. [2] are multiplied by the motional constants, the derived distances are all relative and a linear change in the molecular geometry will be compensated by changes in the motional constants, and it is necessary to assume fixed values for certain nuclear coordinates. The direct dipole coupling constants, calculated for "ideal" geometry based on a regular hexagonal carbon skeleton, with C—C = 1.390 Å, C—H = 1.080 Å, and C—F = 1.310 Å, all bond angles 120°, disagreed with experimental values in some cases. For para-difluorobenzene a positive pseudo-dipole coupling constant of about 100 Hz occurred for the ortho hydrogen atoms; the geometry, therefore, is not ideal. The hydrogen atom positions were determined with respect to fixed fluorine atoms placed 2.700 Å from the origin at the center of the molecule. Trial values of the x and y coordinates were used to determine the motional constants from experimental values of D_{23} and D_{26} and then the motional constants and trial coordinates were used to calculate D_{25} and $(D_{12} + D_{13})$, which were compared with experiment. The process was repeated until agreement was within the experimental error. The final coordinates are given in Table V. The departure from ideal geometry is such that the hydrogen atoms are displaced toward neighboring fluorine atoms. In para-difluorobenzene this positional change cannot be accounted for by altering the C—C—H bond angle only, but also requires changes in the carbon–carbon bond lengths. Since, in this analysis, the fluorine coordinates were fixed, the changes appear as increases in the C_1—C_2, C_1—C_6, and C_3—C_4, C_4—C_5 bond distances but a decrease in C_2—C_3 and C_5—C_6 bonds could also be involved. These are the changes expected from a contribution from the quinoid type structure arising from conjugation of the fluorine substituent with the ring. To determine the actual bond shortening and lengthening and angular distortion would require further assumptions regarding nuclear coordinates and is not justified.

McLean *et al.* (13) have computed the geometry of para-difluorobenzene from their experimental dipolar coupling constants but by a different procedure. They compared the ratios

Can. J. Chem. Downloaded from www.nrcresearchpress.com by 210.87.254.40 on 09/05/12
For personal use only.

TABLE V

Nuclear coordinates* in difluorobenzenes

	ortho		meta		para	
	x	y	x	y	x	y
1	0.008	2.480	0	2.470	0	(2.700)
2	2.338	1.350	(2.338)	1.350	2.141	1.261
3	2.338	−1.350	2.166	−1.228	2.141	−1.261
4	0.008	−2.480	0	−2.470	0	(−2.700)
5	−2.139	(−1.235)	−2.166	−1.228	−2.141	−1.261
6	−2.139	(1.235)	(−2.338)	1.350	−2.141	1.261

*Assumed coordinates are in parentheses.

of the distances r_{26} to r_{23}, and r_{14} to r_{13}. These ratios are 1.6988 and 2.1335, respectively. The corresponding values from our analysis are 1.6979 and 2.1412.

The nuclear coordinates of ortho- and meta-difluorobenzene were calculated by a similar procedure and are given in Table V. A similar effect was observed. The hydrogen atoms ortho to fluorine were displaced toward the fluorine atom. If distortion of the carbon skeleton is assumed for ortho-difluorobenzene, it is in the direction opposite to that expected as a result of fluorine conjugation. The displacements are small but consistent and a similar effect has been reported for para-dichlorobenzene (21). In the discussion of internuclear distances derived from nuclear magnetic resonance spectra in nematic solvents it should be noted that a value appropriate to $(r^3)^{1/3}$, not r_0, is obtained, and then an average is taken over all internal motions of the molecule. Snyder and Meiboom (22) have explained discrepancies in bond lengths in cyclopropane as due to large amplitudes of vibration but the harmonic and anharmonic corrections to $(r^{-3})^{1/3}$ are of opposite sign (23) and cannot be applied without knowledge of their magnitudes from a complete vibrational analysis.

Acknowledgments

We are grateful to the National Research Council of Canada, for financial support. C.T.Y. thanks McGill University for the award of a University Graduate Fellowship.

1. A. D. Buckingham and K. A. McLauchlan. Progr. Nucl. Magn. Res. Spectry. **2**, 63 (1967).
2. A. Saupe. Angew Chem. Intern. Ed. **7**, 97 (1968).
3. G. R. Luckhurst. Quart. Rev. London, **22**, 179 (1968).
4. A. Saupe. Z. Naturforsch. **19**a, 161 (1964).
5. L. C. Snyder. J. Chem. Phys. **43**, 4041 (1965).
6. A. Saupe. Z. Naturforsch. **20**a, 572 (1965).
7. L. C. Snyder and E. W. Anderson. J. Chem. Phys. **42**, 3336 (1965).
8. C. T. Yim and D. F. R. Gilson. Can. J. Chem. **46**, 2783 (1968).
9. S. I. Chan and A. S. Dubin. J. Chem. Phys. **46**, 1745 (1967).
10. M. Karplus and T. P. Das. J. Chem. Phys. **34**, 1683 (1961).
11. A. D. Buckingham and E. E. Burnell. J. Am. Chem. Soc. **89**, 3341 (1967).
12. R. A. Bernheim and T. R. Krugh. J. Am. Chem. Soc. **89**, 6784 (1967).
13. J. Bulthuis, J. Gerritsen, C. W. Hilbers, and C. MacLean. Rec. Trav. Chim. **87**, 417 (1965).
14. W. G. Patterson and E. J. Wells. J. Mol. Spectry. **14**, 101 (1964).
15. D. B. Macdonald. Chem. Commun. 686 (1967).
16. J. E. Loemker, J. H. Goldstein, and J. M. Read. Junr. Chem. Commun. 744 (1968).
17. F. Prosser and L. Goodman. J. Chem. Phys. **38**, 374 (1963).
18. D. W. Davies. Mol. Phys. **13**, 465 (1967).
19. B. P. Dailey and T. K. Wu. J. Chem. Phys. **41**, 2796 (1964).
20. J. W. Emsley. J. Chem. Soc. A, 2018 (1968).
21. A. Saupe. Mol. Cryst. **1**, 527 (1966).
22. L. C. Snyder and S. Meiboom. J. Chem. Phys. **47**, 1480 (1967).
23. J. A. Ibers and D. P. Stevenson. J. Chem. Phys. **28**, 929 (1958).

Can. J. Chem. Downloaded from www.nrcresearchpress.com by 210.87.254.40 on 09/05/12
For personal use only.

Can. J. Chem. Downloaded from www.nrcresearchpress.com by 210.87.254.6 on 09/05/12
For personal use only.

NOTES

Gas phase photochlorination of perfluorocyclohexene

J. J. Cosa, C. A. Vallana, and E. H. Staricco

Departamento de Fisicoquímica, Instituto de Ciencias Químicas, Universidad Nacional de Córdoba, Ciudad Universitaria, Córdoba, Argentina

Received September 9, 1968

The kinetics of the gas phase photochemical reaction between perfluorocyclohexene and chlorine was studied between 10 and 50 °C. The system was irradiated with light of 4360 Å. The rate of the photochlorination was independent of the perfluorocyclohexene pressure and of the total pressure. It was found to be proportional to the first power of the pressure of Cl_2 and to the square root of the intensity of absorbed light. At 30 °C, the quantum yield was found to be 200 when the initial Cl_2 pressure was 100 Torr, and intensity of light absorbed 9.89×10^{-9} einstein l^{-1} s^{-1}.

An activation energy of 5.1 kcal/mole could be assigned to the reaction $C_6F_{10}Cl + Cl_2$.

Canadian Journal of Chemistry, **47**, 1067 (1969)

Introduction

Much attention has been devoted to the gas phase photochlorination of olefins (1, 2) and recently some new contributions have been made (3, 4). It cannot, however, be regarded as yet completely understood in all respects. It was thought that studies on the photochlorination of cyclic olefins may contribute to the knowledge of the radical reactions involved subsequently to the addition of a chlorine atom to an olefin.

We found that cyclohexene and cyclopentene readily reacted in the gas phase when mixed with Cl_2 in the dark at room temperature, and that neither reaction was inhibited by NO or O_2. The replacement of the hydrogen atoms by fluorine decreased the thermal reaction and in fact, between Cl_2 and perfluorocyclohexene no thermal reaction took place up to 70 °C.

When the gaseous mixture was irradiated with light of 4360 Å a reaction occurred with a lowering of the total pressure. The present paper is concerned with the kinetics of the photochlorination of perfluorocyclohexene.

Experimental

Experiments were performed in a conventional high vacuum system. The reactor was a Pyrex cylinder 10 cm long, 174 ml in volume, and fitted with number 7740 Corning glass windows.

The course of the reaction was followed manometrically with a quartz spiral manometer connected to the reactor by a quartz glass graded seal. This manometer was used as a null instrument in connection with a mercury manometer.

The light source was an Osram HBO 200 mercury lamp. A practically parallel and homogeneous beam of wavelength 4360 Å was obtained by employing quartz lens, diaphragms, and Schott filters. The intensity of the incident light was measured with a compensated Kipp thermopile and a Microva galvanometer.

The use of any type of grease in the reaction system was avoided, and instead of stopcocks, aluminium valves with Teflon gaskets and nickel needles were employed.

The perfluorocyclohexene was purchased from Imperial Smelting Corp. It was purified by refluxing over KOH, distilled under nitrogen atmosphere, and then injected into a gas chromatograph equipped with a Porapak Q column at 180 °C. It was finally trap to trap distilled in vacuum at low temperature and stored in a trap cooled with liquid air. Chlorine and carbon dioxide were obtained from cylinders and conventionally purified.

Runs were performed in a darkened room and the reactor was protected against stray radiation. The experiments were carried out in the range of temperatures from 10–50 °C. Temperature was controlled by means of a circulating thermostat and the reactor was housed in such a way that the water did not intersect light beam.

Results

The variation of pressure of the system indicated that the stoichiometry of the reaction was

$$C_6F_{10} + Cl_2 = C_6F_{10}Cl_2$$

as could be proved in runs with excess Cl_2 and carried out to full conversion. Infrared and gas chromatographic determinations showed that the only product was $C_6F_{10}Cl_2$.

In order to determine the rate law, experiments were performed at 30 °C with variation of the initial pressure of Cl_2 between 25–200 Torr, and that of C_6F_{10} between 25–100 Torr. Most

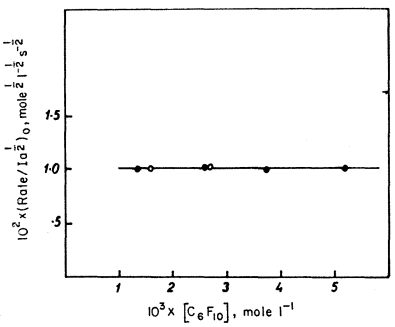

FIG. 1. Initial rate/$I_{abs}^{\frac{1}{2}}$ vs. initial pressure of C_6F_{10}. ○, runs with addition of 400 Torr CO_2. In all experiments pressure of Cl_2 = 50 Torr and temperature = 30 °C.

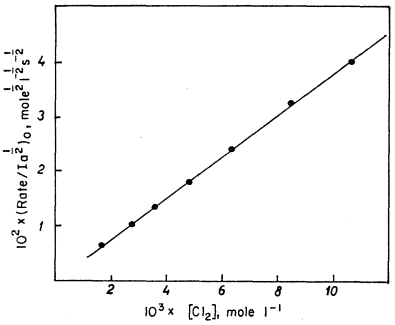

FIG. 2. Initial rate/$I_{abs}^{\frac{1}{2}}$ vs. initial pressure of Cl_2. Pressure of C_6F_{10} = 100 Torr in all experiments and temperature = 30 °C.

of the runs were performed up to 50% conversion or more. They showed excellent reproducibility and had no induction period.

In Fig. 1 it is shown that the rate of photochlorination for a given pressure of Cl_2 is independent of the pressure of C_6F_{10}. The plot of Fig. 2 shows that the rate was proportional to the first power of the pressure of Cl_2. In both figures the initial rate was obtained by the method of Letort (5).

The variation of total pressure by means of the addition of inert gases such as CO_2 does not affect the rate, as is also shown in Fig. 1.

The dependence of rate on the intensity of light was determined by inserting a calibrated neutral filter in the light beam. The filter transmitted 51% of the incident light and it was found that the rate of photochlorination diminished to 71% of the rate of runs carried out without the filter and with the same initial pressure of reactants, showing that the rate varied with the square root of the intensity of absorbed light. Therefore the rate of photochlorination can be represented by the following expression

$$[A] \qquad \frac{d(C_6F_{10}Cl_2)}{dt} = k(Cl_2)(I_{abs})^{\frac{1}{2}}$$

This rate law proved to be valid up to 25% conversion in runs with 100 Torr Cl_2 and 25 Torr C_6F_{10}, and to 80% conversion in runs with 200 Torr Cl_2 and 100 Torr C_6F_{10}.

Experiments carried out at 10, 20, 30, 40, and 50 °C enable one to obtain an apparent activation energy of 5.1 kcal/mole from the Arrhenius plot (Fig. 3). The value of k was calculated from the above equation with Cl_2 in units of mole l^{-1} and I_{abs} in einstein l^{-1} s^{-1}.

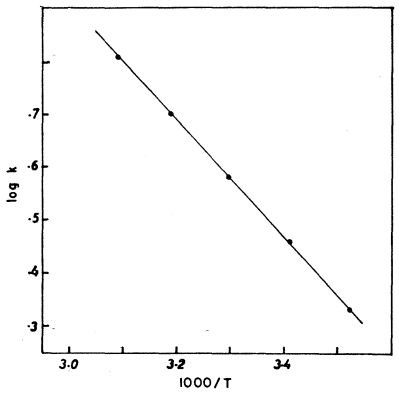

FIG. 3. Arrhenius plot of the reaction, k in mole^{-1} $l^{\frac{1}{2}}$ $s^{-\frac{1}{2}}$.

The light measurements gave a value for the intensity of the incident light to be 5.465×10^{-8} einstein l^{-1} s^{-1}. For a run at 30 °C, 100 Torr initial pressure of Cl_2, and 9.89×10^{-9} einstein l^{-1} s^{-1} of absorbed light, it was evident that a chain reaction took place with a quantum yield of 200.

Discussion

The results obtained support the following mechanism:

$$[1] \qquad Cl_2 + h\nu \rightarrow 2Cl$$

$$[2] \qquad Cl + C_6F_{10} \rightarrow C_6F_{10}Cl$$

$$[3] \qquad Cl_2 + C_6F_{10}Cl \rightarrow C_6F_{10}Cl_2 + Cl$$

$$[4] \qquad 2C_6F_{10}Cl \rightarrow C_6F_{10} + C_6F_{10}Cl_2$$

Can. J. Chem. Downloaded from www.nrcresearchpress.com by 210.87.254.6 on 09/05/12
For personal use only.

Stationary state treatment gives

$$\frac{d\,C_6F_{10}Cl_2}{dt} = (k_3/k_4^{\frac{1}{2}})(Cl_2)(I_{abs})^{\frac{1}{2}}$$

which is in agreement with [A] if one puts $k = k_3/k_4^{\frac{1}{2}}$.

The length of the chain does not permit an insight, from a kinetic point of view, of the nature of reaction [4], although experimental evidence of the product of the reaction rather supports a disproportionation. To a first approximation the value of the activation energy of reaction [4] may be considered negligible, and therefore the experimental value of 5.1 kcal can be assigned to the reaction $C_6F_{10}Cl + Cl_2$. This value is comparable with the corresponding activation energies for the reaction between the chloroalkyl radical and Cl_2 in the photochlorination of perfluoro-2-butene (6), tetrachloro- (7, 8) and trichloro-ethylene (8–10), and 1,1-dichloro-2,2-difluoroethylene (4).

From the values of $k_3/k_4^{\frac{1}{2}}$ and of the activation energy one obtains log $A_3/A_4^{\frac{1}{2}} = 4.3$ mole$^{-\frac{1}{2}}$ l$^{\frac{1}{2}}$ s$^{-\frac{1}{2}}$.

In a comparative study of the photochlorination of chloroethylenes, Dainton *et al.* (3) assume that a repulsive effect between the chlorine atoms on the carbon bearing the unpaired electron, and the chlorine molecule accounts for an increment in activation energy of the propagation reaction as the number of chlorine atoms in the chloroalkyl radical increases. If this view is also taken as valid in the interpretation of the data on the photochlorination of chlorofluoroethylenes (4, 11, 12) it may be concluded that the repulsive effect of fluorine atoms is lower than that of chlorine atoms. The rather high values of 5.1 kcal found in the present case can be justified assuming a repulsive effect between the ring and the chlorine molecule. An activation energy of approximately 5 kcal in the photochlorination of perfluorocyclopentene (13) supports, to some extent, this view.

Acknowledgment

We thank the Consejo Nacional de Investigaciones Científicas y Técnicas (República Argentina) for financial support.

1. E. W. R. Steacie. Atomic and free radical reactions. Reinhold Publishing Corp., New York. 1954.
2. R. J. Cvetanovic. *In* Advances in photochemistry. Vol. 1. Interscience Publishers, Inc., New York. 1961.
3. P. B. Ayscough, F. S. Dainton, and B. E. Fleischfresser. Trans. Faraday Soc. **62**, 1838 (1966).
4. C. A. Vallana, E. Castellano, and H. J. Schumacher. Z. Physik. Chem. Frankfurt, **46**, 294 (1965).
5. M. Letort. J. Chim. Phys. **34**, 206 (1937).
6. M. E. Roselli and H. J. Schumacher. Z. Physik. Chem. Frankfurt, **38**, 326 (1963).
7. C. Schott and H. J. Schumacher. Z. Physik. Chem. B, **49**, 107 (1941).
8. P. Goldfinger, G. Huybrecht, and G. Martens. Trans. Faraday Soc. **57**, 2210 (1961).
9. F. S. Dainton, D. A. Lomax, and M. Weston. Trans. Faraday Soc. **53**, 460 (1957).
10. K. L. Muller and H. J. Schumacher. Z. Physik. Chem. B, **35**, 455 (1937).
11. E. Castellano, N. R. Bergamin, and H. J. Schumacher. Z. Physik. Chem. Frankfurt, **27**, 112 (1961).
12. N. R. Bergamin, E. Castellano, and H. J. Schumacher. Z. Physik. Chem. Frankfurt, **40**, 246 (1964).
13. Z. Alberto, J. J. Cosa, C. A. Vallana, and E. H. Staricco. To be published.

Preparation of β-rhenium tetrachloride

P. W. Frais, A. Guest, and C. J. L. Lock[1]

Department of Chemistry and Institute for Materials Research, McMaster University, Hamilton, Ontario

Received October 21, 1968

β-Rhenium tetrachloride has been prepared by three different methods. Infrared, magnetic, and X-ray powder diffraction data are reported.

Canadian Journal of Chemistry, **47**, 1069 (1969)

Introduction

There are a number of reports of rhenium tetrachloride in the literature. However, early reports of the preparation of this compound (1–3) have been discounted (4, 5). More recently, Brown and Colton claimed to have prepared rhenium tetrachloride (6), but no detailed report on the properties of this material has been given. Cotton *et al.*

[1]Author to whom correspondence should be addressed.

Can. J. Chem. Downloaded from www.nrcresearchpress.com by 210.87.254.6 on 09/05/12
For personal use only.

Stationary state treatment gives

$$\frac{d\,C_6F_{10}Cl_2}{dt} = (k_3/k_4^{\frac{1}{2}})(Cl_2)(I_{abs})^{\frac{1}{2}}$$

which is in agreement with [A] if one puts $k = k_3/k_4^{\frac{1}{2}}$.

The length of the chain does not permit an insight, from a kinetic point of view, of the nature of reaction [4], although experimental evidence of the product of the reaction rather supports a disproportionation. To a first approximation the value of the activation energy of reaction [4] may be considered negligible, and therefore the experimental value of 5.1 kcal can be assigned to the reaction $C_6F_{10}Cl + Cl_2$. This value is comparable with the corresponding activation energies for the reaction between the chloroalkyl radical and Cl_2 in the photochlorination of perfluoro-2-butene (6), tetrachloro- (7, 8) and trichloro-ethylene (8–10), and 1,1-dichloro-2,2-difluoroethylene (4).

From the values of $k_3/k_4^{\frac{1}{2}}$ and of the activation energy one obtains log $A_3/A_4^{\frac{1}{2}} = 4.3$ mole$^{-\frac{1}{2}}$ l$^{\frac{1}{2}}$ s$^{-\frac{1}{2}}$.

In a comparative study of the photochlorination of chloroethylenes, Dainton *et al.* (3) assume that a repulsive effect between the chlorine atoms on the carbon bearing the unpaired electron, and the chlorine molecule accounts for an increment in activation energy of the propagation reaction as the number of chlorine atoms in the chloroalkyl radical increases. If this view is also taken as valid in the interpretation of the data on the photochlorination of chlorofluoroethylenes (4, 11, 12) it may be concluded that the repulsive effect of fluorine atoms is lower than that of chlorine atoms. The rather high values of 5.1 kcal found in the present case can be justified assuming a repulsive effect between the ring and the chlorine molecule. An activation energy of approximately 5 kcal in the photochlorination of perfluorocyclopentene (13) supports, to some extent, this view.

Acknowledgment

We thank the Consejo Nacional de Investigaciones Científicas y Técnicas (República Argentina) for financial support.

1. E. W. R. Steacie. Atomic and free radical reactions. Reinhold Publishing Corp., New York. 1954.
2. R. J. Cvetanovic. *In* Advances in photochemistry. Vol. 1. Interscience Publishers, Inc., New York. 1961.
3. P. B. Ayscough, F. S. Dainton, and B. E. Fleischfresser. Trans. Faraday Soc. **62**, 1838 (1966).
4. C. A. Vallana, E. Castellano, and H. J. Schumacher. Z. Physik. Chem. Frankfurt, **46**, 294 (1965).
5. M. Letort. J. Chim. Phys. **34**, 206 (1937).
6. M. E. Roselli and H. J. Schumacher. Z. Physik. Chem. Frankfurt, **38**, 326 (1963).
7. C. Schott and H. J. Schumacher. Z. Physik. Chem. B, **49**, 107 (1941).
8. P. Goldfinger, G. Huybrecht, and G. Martens. Trans. Faraday Soc. **57**, 2210 (1961).
9. F. S. Dainton, D. A. Lomax, and M. Weston. Trans. Faraday Soc. **53**, 460 (1957).
10. K. L. Muller and H. J. Schumacher. Z. Physik. Chem. B, **35**, 455 (1937).
11. E. Castellano, N. R. Bergamin, and H. J. Schumacher. Z. Physik. Chem. Frankfurt, **27**, 112 (1961).
12. N. R. Bergamin, E. Castellano, and H. J. Schumacher. Z. Physik. Chem. Frankfurt, **40**, 246 (1964).
13. Z. Alberto, J. J. Cosa, C. A. Vallana, and E. H. Staricco. To be published.

Preparation of β-rhenium tetrachloride

P. W. Frais, A. Guest, and C. J. L. Lock[1]

Department of Chemistry and Institute for Materials Research, McMaster University, Hamilton, Ontario

Received October 21, 1968

β-Rhenium tetrachloride has been prepared by three different methods. Infrared, magnetic, and X-ray powder diffraction data are reported.

Canadian Journal of Chemistry, **47**, 1069 (1969)

Introduction

There are a number of reports of rhenium tetrachloride in the literature. However, early reports of the preparation of this compound (1–3) have been discounted (4, 5). More recently, Brown and Colton claimed to have prepared rhenium tetrachloride (6), but no detailed report on the properties of this material has been given. Cotton *et al.*

[1]Author to whom correspondence should be addressed.

Can. J. Chem. Downloaded from www.nrcresearchpress.com by 210.87.254.40 on 09/05/12
For personal use only.

Can. J. Chem. Downloaded from www.nrcresearchpress.com by 210.87.254.40 on 09/05/12
For personal use only.

(7) subsequently reported a series of reactions on a material they called β-rhenium tetrachloride to distinguish it from Colton's material. Cotton *et al.* obtained β-rhenium tetrachloride under the name of rhenium(III) chloride from the Shattuck Chemical Company. The preparation conditions had not been recorded and the company was not able to make any more of the material. Thus, there exists the anomaly of an extensive chemistry of a material for which no preparative method is available. We now report three ways of making β-rhenium tetrachloride.

Experiments

Analyses for rhenium and chlorine were performed by neutron activation analysis in the McMaster University Reactor using a method described by us previously (8). Carbon and hydrogen analyses were performed by A. B. Gygli, Toronto.

Infrared (i.r.) spectra were recorded for solid samples ground into a mull with Nujol. The Nujol had been dried by reflux with phosphorous pentoxide followed by vacuum distillation. The mull samples were mounted between potassium bromide or polyethylene plates and spectra were recorded on Perkin–Elmer 337 and 301 spectrometers. X-ray diffraction photographs of powdered samples were recorded on a Debye–Scherrer camera. Samples were sealed inside quartz tubes. Copper radiation was used for recording the photographs. Line intensities were measured from the powder photographs using a Joyce–Loebl microdensitometer.

Measurements of magnetic susceptibility were made by the Gouy method. The apparatus used was based on the Gouy System sold by Alpha Scientific Laboratories, Inc., Berkeley, California. The cooling and temperature control were changed to a system similar to that described by Earnshaw (9)[2]. The electronic bridge was designed and built by Schonfeld of this University. Sample temperatures could be maintained to ± 0.01 °C at -180 °C and to ± 0.1 °C at 0 °C. Sample weight changes were recorded on a Sartorius Electrono I microbalance. Sample tubes were 3 mm outer diameter quartz tubes. The tubes were filled with finely ground sample in a dry-box and sealed. Packing errors in these small tubes were limited to $\sim 5\%$ by vibrating the tubes in the vibrator of a Hoover (Philadelphia) Unimelt melting point apparatus. The tubes and field were calibrated with powdered mercuric tetrathiocyanotocobaltate(II) (10). The magnetic apparatus is described in detail elsewhere (11).

Preparation (a)

Powdered rhenium metal (0.5 g) (99.9% pure by weight) and antimony pentachloride (mole ratio $Re:SbCl_5 \simeq 1:2.5$) were sealed in a "Vycor" tube. The tube was constricted in the middle so that it was composed of two sections, A and B, joined by a narrow neck. The sealed tube was heated in a tube-furnace at 600° C until all the metal had reacted (about 48 h). The tube was moved along the furnace, so that the end B was out of the furnace and at room temperature. Material condensed in B. When this material no longer increased in amount, the furnace temperature was reduced to 250 °C and the tube was reversed, so that B was at the furnace temperature and A was at room temperature. Excess antimony pentachloride and some antimony trichloride distilled into A, leaving a black solid in B. The tube was opened in a dry-box and the black solid transferred to a test-tube fitted with a ground-glass joint. The tube was stoppered, removed from the dry-box, and transferred rapidly to a vacuum line. The black solid was kept under vacuum at room temperature for 12 h. The temperature was raised slowly to 160 °C (4 h) and held at 160 °C for 48 h to remove all traces of volatile impurity. A small amount of impurity volatized at 160 °C and condensed at a cold spot in the vacuum line. Neutron activation analysis of the volatile material showed that the Re:Cl atom ratio was $1:5.2 \pm 0.1$, suggesting that it was mainly rhenium pentachloride. A black crystalline residue was left in the tube. The tube was sealed and the product stored in a dry-box. Yields up to 75% have been recorded.

Preparation (b)

Approximately equimolar quantities of rhenium pentachloride and antimony trichloride were sealed in a Pyrex glass tube similar to the tube used in preparation (*a*). The tube was heated for 48 h at 300 °C, and the resulting black product was purified in a manner similar to that described above. The yield was nearly quantitative.

Preparation (c)

Rhenium trichloride (0.25 g) and rhenium pentachloride (0.5 g) were sealed in a Vycor tube in a dry-box. The tube was heated to 600 °C for 24 h, then allowed to cool to room temperature. A black powder was obtained. The material was shown to be β-rhenium tetrachloride by comparison of an X-ray powder photograph of the product with that of a pure sample. The contaminants were rhenium pentachloride and rhenium trichloride. The yield was about 20%. No attempt was made to vary the conditions as the only purpose of the preparation was to confirm a possible way in which β-rhenium tetrachloride could have been made accidentally by the Shattuck Chemical Company. It may be possible to obtain better yields of a more pure product by this method but preparation (*b*) is a more satisfactory way of preparing β-rhenium tetrachloride[3].

The materials obtained from preparations (*a*) and (*b*) were shown to give identical powder photographs. Analysis of a number of samples showed the Re:Cl atom ratio was $1:4.01 \pm 0.08$. Exposure to air gave a sticky black mess. The material was insoluble in acetonitrile, tetrahydrofuran, benzene, and carbon tetrachloride. The material dissolved slowly in methanol, ethanol, acetone, and dimethyl sulfoxide, and, from the color changes, subsequently decomposed. The material reacted with hydrochloric acid to give a blue solution which later decomposed. Heating the material at 300 °C in nitrogen

[2]Variable-temperature Gouy balance system. Newport Instruments Ltd., Newport Pagnell, Buckinghamshire, England, 1966.

[3]Canterford and Colton have recently prepared β-$ReCl_4$ by a similar method (18).

TABLE I

X-ray diffraction data for a powdered sample of β-$ReCl_4$

d_{hkl}*	d_{hkl}†	Intensity‡	hkl†	d_{hk}*	d_{hkl}†	Intensity‡	hkl†
6.288	6.282	7	010	1.894	1.892	~9	$\bar{2}15$
6.012	6.073	43	002	1.831	1.834	6	$\bar{2}24$
5.528	5.580	100	001	1.791	1.797	20	$\bar{1}33$
4.478	4.468	18	110	1.768	1.767	12	224
4.225	4.274	31	$\bar{1}11$	1.751	1.756	14	320
3.386	3.403	<3	013		1.752		$\bar{2}06$
3.151	3.141	~10	020	1.719	1.717	7	$\bar{3}14$
3.036	3.037	~10	004	1.703	1.702	10	026
2.939	2.944	~10	113	1.671	1.673	~5	017
2.774	2.800	16	022	1.625	1.625	~5	126
2.721	2.728	32	121	1.585	1.585	~5	323
2.674	2.683	~9	104	1.550	1.552	~4	$\bar{3}24$
2.606	2.620	~11	$\bar{2}12$	1.510	1.510	~9	141
2.559	2.558	~11	$\bar{1}14$	1.487	1.489	~5	330
2.367	2.379	<3	$\bar{2}13$		1.485		$\bar{3}31$
2.270	2.271	~9	213	1.463	1.464	~5	043, $\bar{3}16$
2.227	2.234	~7	220	1.439	1.440	~5	$\bar{2}35$
2.161	2.170	<3	$\bar{1}15$	1.414	1.415	~5	413
2.094	2.094	16	030	1.393	1.393	~5	325
2.067	2.064	17	031	1.376	1.377	~5	404
2.034	2.036	11	$\bar{3}02$	1.365	1.366	~11	422
1.991	1.989	20	$\bar{2}23$, $\bar{1}30$		1.364		242
1.957	1.957	11	131	1.331	1.334	<3	$\bar{4}15$

*Values calculated from our photographs.
†Values calculated from unit cell parameters of Cotton *et al.* (13).
‡Values measured from our photographs.

caused slow decomposition to Re_3Cl_9 and Re_2Cl_{10}. These were separated in a thermal gradient and identified by neutron activation analysis. Rapid reaction of the material dissolved in concentrated hydrochloric acid with tetra(*n*-butyl)ammonium bromide gave blue tetra(*n*-butyl)ammonium octachlorodirhenate(III). The product was identical with that of an authentic sample prepared by a standard method (7).

Anal. Calcd. for $C_{32}H_{72}Cl_8N_2Re_2$: C, 33.6; H, 6.4; Cl, 24.8. Found: C, 33.1; H, 6.4; Cl, 23.1.

This reaction is considered by Cotton to be characteristic of β-$ReCl_4$. The i.r. spectrum of β-rhenium tetrachloride showed no bands between 4000 and 400 cm^{-1}. Observed bands were 369 cm^{-1}, strong; 294 cm^{-1}, weak; 244 cm^{-1}, weak; 166 cm^{-1}, shoulder; 158 cm^{-1}, medium.

Results and Discussion

Many properties of β-rhenium tetrachloride have been described (7) but no preparative method has been published. The black material produced by us appears to be identical to β-rhenium tetrachloride described by Cotton *et al.* (7). Analysis shows that the Re:Cl atom ratio was 1:4 and the absence of bands in the i.r. spectrum from 4000 to 400 cm^{-1} suggests that groups such as Re—O, Re—O—Re, Re=O, and O=Re=O which might be expected to cause absorption in this region (12), are absent. The far-infra-red spectrum was recorded for a Nujol mull of β-rhenium tetrachloride mounted between polyethylene plates and four bands were observed between 400 and 150 cm^{-1}. However, the polyethylene plates were attacked so that it cannot be stated whether the bands observed are caused by β-rhenium tetrachloride or decomposition products. The strong band at 369 cm^{-1} is in the range associated with metal–chlorine vibrations but is higher than the 318 cm^{-1} of ν_{Re-Cl} in the hexachlororhenates (14) and ν_{Re-Cl} observed in this laboratory for several rhenium complexes (15). However, 369 cm^{-1} is the frequency found for ν_{Re-Cl} in rhenium oxotetrachloride which might be present as a decomposition product (11).

The chemical reactions of the material are identical to those described by Cotton *et al.* (7) and it has proved possible to index the powder pattern of the material using the unit cell parameters given by Cotton for β-rhenium tetrachloride (13). These were a = 6.366 (5) Å, b = 6.282 (6) Å, c = 12.165 (6) Å, β = 93.17 (10)° space group Pc or $P2/c$. The calculation was done on an IBM 7040 computer using the program DESLID written by Robertson. The results are presented in Table I.

The magnetic susceptibility of β-rhenium tetrachloride was measured over the range 100–300 °K

Can. J. Chem. Downloaded from www.nrcresearchpress.com by 210.87.254.40 on 09/05/12
For personal use only.

at 20 °K temperature intervals. The susceptibility is independent of temperature and was 1010 × 10^{-6} c.g.s.u. in all measurements. The magnetic results can be interpreted as an indication that β-$ReCl_4$ contains no unpaired electrons in the ground state. Cotton *et al.* (13) cite a minimum Re–Re interatomic distance of 2.73 Å and consider this to be short enough to indicate some metal–metal interaction. Our observations also require such an interaction to force pairing of the unpaired electrons of pairs of d^3 Re(IV) atoms.

The mechanism of formation appears to be a simple reduction

$$2ReCl_5 + SbCl_3 \rightarrow 2ReCl_4 + SbCl_5$$

and the metal might also react through a similar path

$$SbCl_5 \rightarrow SbCl_3 + Cl_2$$

$$2Re + 5Cl_2 \rightarrow Re_2Cl_{10}$$

Further evidence in favor of this mechanism is that Re_2Cl_{10} and $SbCl_5$ do not give $ReCl_4$ even after heating to 600 °C for a week. In addition, the yield of $ReCl_4$ is reduced very greatly if chlorine is added to the Re + $SbCl_5$ reaction mixture. It has been stated (16) that rhenium metal is not attacked by chlorine when sealed in a static system, but this is not true as we have prepared $ReCl_5$ from the metal in this manner.

The original sample of rhenium tetrachloride was isolated from a reaction designed to give rhenium trichloride (7). It was noted that the temperature of reaction was somewhat lower than normal and we suspect that the flow rate of nitrogen was very low. Probably conditions were just right for the occurrence of reactions of the type

$$3Re_2Cl_{10} \rightarrow 2Re_3Cl_9 + 6Cl_2$$

$$3Re_2Cl_{10} + 2Re_3Cl_9 \rightarrow 6Re_2Cl_8$$

The reasons for failure to prepare $ReCl_4$ in subsequent preparations can be seen when it is realized that the last reaction proceeds from right to left at 300 °C if the products are allowed to separate. The normal conditions for the preparation of rhenium trichloride require a temperature of 450 °C (17) and a flow of nitrogen gas over the reactants which gives a facile separation of rhenium trichloride and rhenium pentachloride in the thermal gradient. It is hardly surprising that no rhenium tetrachloride is formed. Reaction of rhenium trichloride and rhenium pentachloride in a closed system produced some rhenium tetrachloride suggesting that this postulate is probably correct.

We conclude that we have successfully synthesized the elusive β-rhenium tetrachloride.

Acknowledgment

We acknowledge the financial support of the National Research Council of Canada in this work and the grant of a scholarship to one of us (A.G.).

1. I. Noddack and W. Noddack. Das Rhenium. Leipzig, 1933. p. 65.
2. D. M. Yost and G. O. Schull. J. Am. Chem. Soc. **54**, 4657 (1932).
3. (*a*) H. V. A. Briscor, P. L. Robinson, and E. M. Stoddart. J. Chem. Soc. 2263 (1931). (*b*) H. V. A. Briscor, P. L. Robinson, and A. J. Rudge. J. Chem. Soc. 1104 (1932).
4. D. Hogenschmidt and R. Sachtlehen. Z. Anorg. Allgem. Chem. **191**, 309 (1930).
5. W. Geilmann, F. W. Wrigge, and W. W. Blitz. Z. Anorg. Allgem. Chem. **214**, 244, 248 (1933).
6. D. Brown and R. Colton. Nature, **198**, 300 (1963); J. Chem. Soc. 714 (1964).
7. F. A. Cotton, W. R. Robinson, and R. A. Walton. Inorg. Chem. **6**, 223 (1967).
8. W. D. Courrier, A. Guest, C. J. L. Lock, and R. H. Tomlinson. Can. J. Chem. **46**, 2965 (1968).
9. A. Earnshaw. Personal communication.
10. J. Lewis. *In* Modern co-ordination chemistry. *Edited by* J. Lewis and R. G. Wilkins. Interscience Publishers, Inc., New York. 1960. p. 415.
11. A. Guest. Ph.D. Thesis, McMaster University, Hamilton, Ontario. 1968.
12. C. A. Barraclough, J. Lewis, and R. S. Nyholm. J. Chem. Soc. 3552 (1959). (*b*) N. P. Johnson, C. J. L. Lock, and G. Wilkinson. J. Chem. Soc. 1054 (1964).
13. M. J. Bennett, F. A. Cotton, B. M. Foxman, and P. F. Stokely. J. Am. Chem. Soc. **89**, 2759 (1967).
14. L. A. Woodward and M. J. Ware. Spectrochim. Acta, **20**, 71 (1964).
15. W. Courrier and C. J. L. Lock. Unpublished work.
16. R. Colton. The chemistry of rhenium and technetium. Interscience Publishers, Inc., London. 1965. p. 74.
17. L. C. Hurd and E. Brimar. Inorganic syntheses. Vol. I. McGraw Hill Book Co., Inc., New York. 1939. p. 182.
18. Canterford and R. Colton. Inorg. Nucl. Chem. Letters, **4** (11), 607 (1968).

Can. J. Chem. Downloaded from www.nrcresearchpress.com by 210.87.254.40 on 09/05/12
For personal use only.

Infrared studies of *cis*- and *trans*-bis(halogenoacetato)bis(ethylenediamine)-cobalt(III) complexes

EDWARD B. KIPP AND ROLAND A. HAINES
Department of Chemistry, University of Western Ontario, London, Ontario

Received September 3, 1968

The infrared spectra have been studied for *cis*- and *trans*-isomers of complexes of the type $[Co(en)_2(halac)_2]ClO_4$, where en = ethylenediamine and halac = $CH_3CO_2^-$, $CH_2ClCO_2^-$, $CHCl_2CO_2^-$, $CCl_3CO_2^-$, $CHBr_2CO_2^-$, and $CF_3CO_2^-$. Characteristic differences between the spectra of *cis*- and *trans*-isomers have been examined and correlated with data for similar complexes. The most consistent variations are in the 500–610 cm^{-1} region where Co—N stretching modes occur.

Canadian Journal of Chemistry, **47**, 1073 (1969)

Can. J. Chem. Downloaded from www.nrcresearchpress.com by 210.87.254.6 on 09/05/12
For personal use only.

Several methods (1) have been applied with varying degrees of success to the problem of differentiating between *cis*- and *trans*-isomers of bis(ethylenediamine)cobalt(III) complexes. Visible, ultraviolet, infrared, and proton magnetic resonance spectra all may be employed and have given reliable data when used in conjunction with one another. However, each method has shown some irregularities and it is desirable to examine more complexes of this type in order to evaluate the utility of any particular technique. A series of complexes of the type $[Co(en)_2(halac)_2]^+$ have been prepared[1] (2) and the geometric configurations have been assigned on the basis of visible and ultraviolet spectra (3). In the course of our studies on the resolution of the *cis*-isomers of these complexes, we have found interesting features in the infrared spectra of the *cis*- and *trans*-isomers which can be of help in assessing infrared assignments of isomerism and we wish to report them here.

Recently attempts have been made to correlate the configurations of bis(ethylenediamine)-cobalt(III) complexes with the positions and multiplicity of infrared absorption bands. Most of the interest has been centered on the vibrational modes of the NH_2 and CH_2 groups of the ethylenediamine cobalt ring system.

Merritt and Wiberley (4) have suggested that differentiation between *cis*- and *trans*-isomers of bis(ethylenediamine)cobalt(III) complexes may be made on the basis of a shift of the NH_2 asymmetric deformation in the 1550 – 1600 cm^{-1} region to larger frequencies, on changing from *cis*- to *trans*-isomers. The differences in the spectra of the complexes $[Co(en)_2(halac)_2]^+$ are in general agreement with this as indicated by the data in Table I. The one exception was the *trans*-dichloroacetato complex, where the band for the *trans*-isomer was at a lower frequency than that for the corresponding *cis*-isomer. However, with the series of complexes reported here, there is a possibility of the NH_2 asymmetric deformation mode overlapping with the CO asymmetric stretching mode of the halogenoacetato group and this could possibly cause some differences in this region.

Attempts have also been made to correlate configuration with the multiplicity (5) of bands in the 1600 cm^{-1} region. The *cis*-isomer has a lower symmetry than the *trans*-isomer and thus should have a more complex band structure. No such correlation could be made with the complexes studied, perhaps as a result of overlapping of the vibrational modes mentioned previously.

Baldwin (6) has suggested that the most consistent variations between the spectra of *cis*- and *trans*-isomers are found in the CH_2 rocking region (870–900 cm^{-1}). The *cis*-isomers always show two peaks, whereas the *trans*-isomers usually have only one. These bands are insensitive to changes in the ligands or anions. The data in Table I indicate that generally the complexes studied followed the previous trends. The drawback with this region is due to the fact that the CH_2 rocking bands are usually weak and are thus difficult to observe. This is shown with the trichloroacetato complex where both *cis*- and *trans*-isomers show only one band in this region. This is due to the weak CH_2 rocking mode being partially obscured by a strong band at 843 cm^{-1}

[1]Where en is ethylenediamine and halac is the anion of a halogenoacetic acid.

TABLE I

Infrared data for complexes of the type $[Co(en)_2(halac)_2]ClO_4$

	Infrared data					
	1550 – 1600 cm^{-1}		870 – 900 cm^{-1}		500 – 610 cm^{-1}	
halac	*cis*	*trans*	*cis*	*trans*	*cis*	*trans*
$CH_3CO_2^-$	1570 s	1577 s	897 w 878 w	900 m 876 w	584 w 567 w 534 sh 524 sh 506 w	578 sh 568 s 522 s
$CH_2ClCO_2^-$	1563 s	1583 s	895 w 881 w	896 sh 887 m	584 s 569 sh 516 sh 504 m	595 s 572 m 521 m
$CHCl_2CO_2^-$	1573 s	1569 s	896 w 881 w	889 w	587 sh 577 m 523 sh 509 w–m	592 s 560 sh 520 m
$CCl_3CO_2^-$	1569 s	1589 s	895 w	893 w	587 m 572 sh 553 w 510 w	597 m 581 m 553 m 514 m
$CHBr_2CO_2^-$	1559 s	1570 s	897 w 882 w	891 w	592 s 569 sh 525 sh 510 w	591 m 565 w 537 w
$CF_3CO_2^-$	1577 s	1584 s	897 w 882 w	895 w	586 m 570 sh 521 m 508 sh	592 m 561 m 526 s

which can be assigned to the CCl_3 symmetric stretching mode (7).

The significant exception for this region is the *trans*-acetato complex which shows two bands, one of medium intensity. The presence of two distinct bands for this isomer may be due to coupling of the NH_2 and CH_2 rocking vibrations (8).

A satisfactory correlation between infrared spectra differences and geometric configuration can best be obtained from the 500–610 cm^{-1} region. Hughes and McWhinnie (9) found that in this region no *trans*-complex had more than three strong bands, while all *cis*-complexes had at least four bands, sometimes occurring as shoulders. These observations were also found in the complexes in this study, as indicated in Table I, the exception here being the *trans*-trichloroacetato complex which has one extra band. The band patterns also differ from *cis*- to *trans*-isomers, as shown in Fig. 1. The bands for the *trans*-complexes are generally evenly distributed in the range 500–610 cm^{-1}, whereas for the *cis*-complexes the bands in this region tend to occur in two groups with wide separation between them.

Tentative assignments were made by Hughes and McWhinnie for bands in the 500–610 cm^{-1} region to Co—N stretching modes (9). This was based on the work of Powell and Sheppard (10) on some ethylenediamine complexes of transition metals. A study of the single crystal spectrum of *trans*-$[Co(en)_2Cl_2]Cl$ (8) has supported these assignments. Of the six *cis*-isomers and six *trans*-isomers examined, all could be identified as such either by the number of bands or by the spacing of the bands in the 500–610 cm^{-1} region of the infrared spectrum.

Thus, although all three of the infrared regions which have been considered are useful for identifying *cis*- and *trans*-isomers, only spectra from 500–610 cm^{-1} region gave complete differentiation. This region is applicable to most complexes of the type $[Co(en)_2X_2]^+$ regardless of the ligands or anions involved. The data for the series of complexes studied in this note support the conclusions made by Hughes and McWhinnie (9) and give the same assignments

Can. J. Chem. Downloaded from www.nrcresearchpress.com by 210.87.254.6 on 09/05/12
For personal use only.

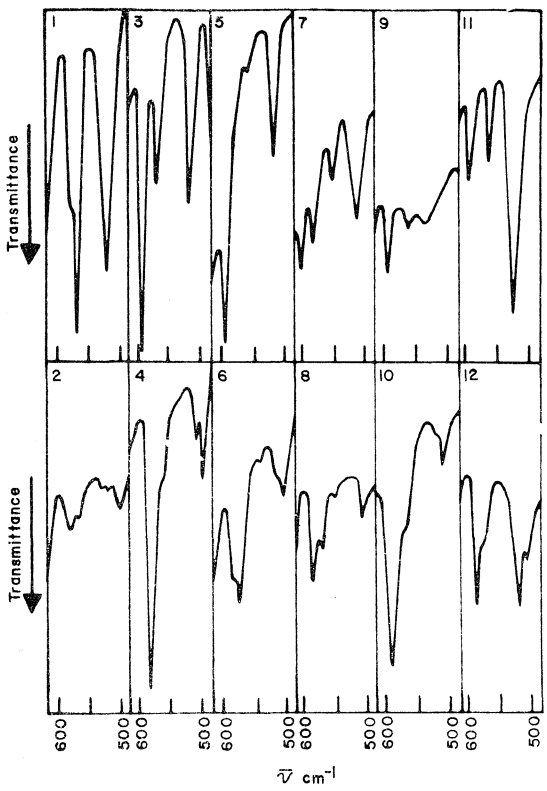

FIG. 1. The infrared spectra (500–610 cm^{-1}) of some *cis*- and *trans*-bis(ethylenediamine)cobalt(III) complexes: 1, *trans*-$[Co(en)_2(CH_3CO_2)_2]ClO_4$; 2, *cis*-$[Co(en)_2(CH_3CO_2)_2]ClO_4$; 3, *trans*-$[Co(en)_2(CH_2ClCO_2)_2]ClO_4$; 4, *cis*-$[Co(en)_2(CH_2ClCO_2)_2]ClO_4$; 5, *trans*-$[Co(en)_2(CHCl_2CO_2)_2]ClO_4$; 6, *cis*-$[Co(en)_2(CHCl_2CO_2)_2]ClO_4$; 7, *trans*-$[Co(en)_2(CCl_3CO_2)_2]ClO_4$; 8, *cis*-$[Co(en)_2(CCl_3CO_2)_2]ClO_4$; 9, *trans*-$[Co(en)_2(CHBr_2CO_2)_2]ClO_4$; 10, *cis*-$[Co(en)_2(CHBr_2CO_2)_2]ClO_4$; 11, *trans*-$[Co(en)_2(CF_3CO_2)_2]ClO_4$; 12, *cis*-$[Co(en)_2(CF_3CO_2)_2]ClO_4$.

as obtained from visible and ultraviolet absorption data (3).

Experimental

The complexes were prepared by previously reported methods (2). Samples were prepared as potassium bromide discs or Nujol mulls (between KBr plates) and the infrared spectra were recorded on a Beckman IR 10 spectrophotometer.

Acknowledgments

We are grateful to the Department of University Affairs (Province of Ontario) for financial support of this work.

1. (*a*) R. G. WILKINS and M. J. G. WILKINS. *In* Modern coordination chemistry. Chap. 3. *Edited by* J. Lewis and R. G. Wilkins. Interscience Publishers, Inc. New York. 1960. (*b*) D. A. BUCKINGHAM, L. DURHAM, and A. M. SARGESON. Australian J. Chem. **20**, 257 (1967). (*c*) I. R. LANTZKE and D. W. WATTS. Australian J. Chem. **20**, 35 (1967).
2. (*a*) K. KURODA and P. S. GENTILE. Bull. Chem. Soc. Japan, **38**, 1362 (1965); **38**, 1368 (1965); **38**, 2159 (1965). (*b*) M. LINHARD and G. STIRN. Z. Anorg. Allgem. Chem. **268**, 105 (1952).
3. K. KURODA and P. S. GENTILE. J. Inorg. Nucl. Chem. **27**, 155 (1965); **27**, 1289 (1965).
4. P. E. MERRITT and S. E. WIBERLEY. J. Phys. Chem. **59**, 55 (1955).
5. M. L. MORRIS and D. H. BUSCH. J. Am. Chem. Soc. **82**, 1521 (1960).
6. M. E. BALDWIN. J. Chem. Soc. 4369 (1960).
7. E. SPINNER. J. Chem. Soc. 4217 (1964).
8. N. TANAKA, N. SATO, and J. FUJITA. Spectrochim. Acta, **22**, 577 (1966).
9. M. N. HUGHES and W. R. MCWHINNIE. J. Inorg. Nucl. Chem. **28**, 1659 (1966).
10. D. B. POWELL and N. SHEPPARD. Spectrochim. Acta, **17**, 68 (1961).

Diffusion of gases in liquids: the constant size bubble method

WING Y. NG AND JOHN WALKLEY

Simon Fraser University, Department of Chemistry, Burnaby 2, British Columbia

Received August 28, 1968

A method is described by which the diffusion of a gas in a liquid is measured by maintaining a bubble of the gas at constant size in the liquid. A steady state solution to the diffusion equation is seen to fit the observed experimental data. The measured diffusion coefficients for nitrogen, oxygen, and carbon dioxide in water at 25 °C are found in good agreement with previously determined values.

Canadian Journal of Chemistry, **47**, 1075 (1969)

Introduction

The diffusion of gases in liquids has recently become the study of several research groups. Together with accurate saturation solubility and entropy of solutions studies, such data are necessary for a fuller, theoretical understanding of the

Can. J. Chem. Downloaded from www.nrcresearchpress.com by 210.87.254.6 on 09/05/12
For personal use only.

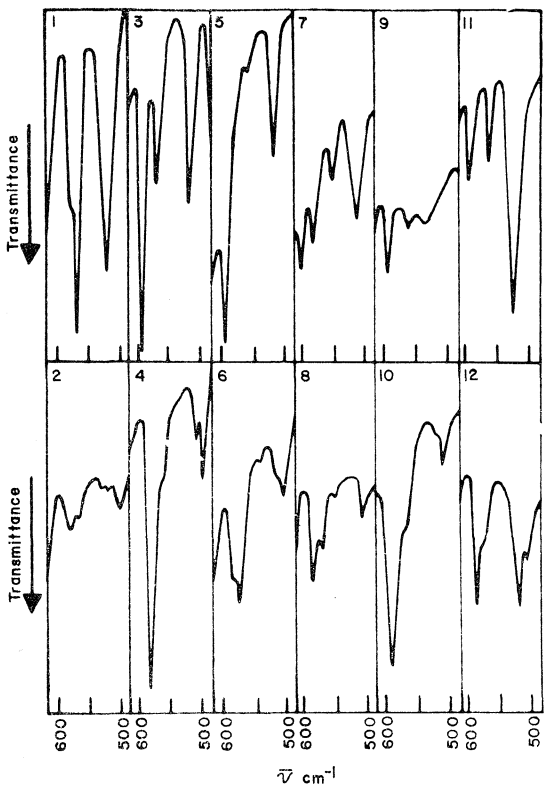

FIG. 1. The infrared spectra (500–610 cm^{-1}) of some *cis*- and *trans*-bis(ethylenediamine)cobalt(III) complexes: 1, *trans*-$[Co(en)_2(CH_3CO_2)_2]ClO_4$; 2, *cis*-$[Co(en)_2(CH_3CO_2)_2]ClO_4$; 3, *trans*-$[Co(en)_2(CH_2ClCO_2)_2]ClO_4$; 4, *cis*-$[Co(en)_2(CH_2ClCO_2)_2]ClO_4$; 5, *trans*-$[Co(en)_2(CHCl_2CO_2)_2]ClO_4$; 6, *cis*-$[Co(en)_2(CHCl_2CO_2)_2]ClO_4$; 7, *trans*-$[Co(en)_2(CCl_3CO_2)_2]ClO_4$; 8, *cis*-$[Co(en)_2(CCl_3CO_2)_2]ClO_4$; 9, *trans*-$[Co(en)_2(CHBr_2CO_2)_2]ClO_4$; 10, *cis*-$[Co(en)_2(CHBr_2CO_2)_2]ClO_4$; 11, *trans*-$[Co(en)_2(CF_3CO_2)_2]ClO_4$; 12, *cis*-$[Co(en)_2(CF_3CO_2)_2]ClO_4$.

as obtained from visible and ultraviolet absorption data (3).

Experimental

The complexes were prepared by previously reported methods (2). Samples were prepared as potassium bromide discs or Nujol mulls (between KBr plates) and the infrared spectra were recorded on a Beckman IR 10 spectrophotometer.

Acknowledgments

We are grateful to the Department of University Affairs (Province of Ontario) for financial support of this work.

1. (*a*) R. G. WILKINS and M. J. G. WILKINS. *In* Modern coordination chemistry. Chap. 3. *Edited by* J. Lewis and R. G. Wilkins. Interscience Publishers, Inc. New York. 1960. (*b*) D. A. BUCKINGHAM, L. DURHAM, and A. M. SARGESON. Australian J. Chem. **20**, 257 (1967). (*c*) I. R. LANTZKE and D. W. WATTS. Australian J. Chem. **20**, 35 (1967).
2. (*a*) K. KURODA and P. S. GENTILE. Bull. Chem. Soc. Japan, **38**, 1362 (1965); **38**, 1368 (1965); **38**, 2159 (1965). (*b*) M. LINHARD and G. STIRN. Z. Anorg. Allgem. Chem. **268**, 105 (1952).
3. K. KURODA and P. S. GENTILE. J. Inorg. Nucl. Chem. **27**, 155 (1965); **27**, 1289 (1965).
4. P. E. MERRITT and S. E. WIBERLEY. J. Phys. Chem. **59**, 55 (1955).
5. M. L. MORRIS and D. H. BUSCH. J. Am. Chem. Soc. **82**, 1521 (1960).
6. M. E. BALDWIN. J. Chem. Soc. 4369 (1960).
7. E. SPINNER. J. Chem. Soc. 4217 (1964).
8. N. TANAKA, N. SATO, and J. FUJITA. Spectrochim. Acta, **22**, 577 (1966).
9. M. N. HUGHES and W. R. MCWHINNIE. J. Inorg. Nucl. Chem. **28**, 1659 (1966).
10. D. B. POWELL and N. SHEPPARD. Spectrochim. Acta, **17**, 68 (1961).

Diffusion of gases in liquids: the constant size bubble method

WING Y. NG AND JOHN WALKLEY

Simon Fraser University, Department of Chemistry, Burnaby 2, British Columbia

Received August 28, 1968

A method is described by which the diffusion of a gas in a liquid is measured by maintaining a bubble of the gas at constant size in the liquid. A steady state solution to the diffusion equation is seen to fit the observed experimental data. The measured diffusion coefficients for nitrogen, oxygen, and carbon dioxide in water at 25 °C are found in good agreement with previously determined values.

Canadian Journal of Chemistry, **47**, 1075 (1969)

Introduction

The diffusion of gases in liquids has recently become the study of several research groups. Together with accurate saturation solubility and entropy of solutions studies, such data are necessary for a fuller, theoretical understanding of the

Can. J. Chem. Downloaded from www.nrcresearchpress.com by 210.87.254.6 on 09/05/12
For personal use only.

Can. J. Chem. Downloaded from www.nrcresearchpress.com by 210.87.254.6 on 09/05/12
For personal use only.

liquid state. We have recently developed a method which appears to allow a rapid and accurate determination of the diffusion coefficient. A bubble of the gas is maintained at a constant size in the solvent under investigation. The rate of solution of the gas from the bubble into the solution is compensated by introducing a known amount of gas into the bubble. The amount of gas required to do this is measured, as a function of time, using a micro-pipette. In previous work the diffusion of the gas into the liquid has been measured by observing the change in radius of the bubble as a function of time (1). This latter method has associated with it complicated hydrodynamic conditions existing at the interface and makes the results of this method difficult to interpret quantitatively (2, 3).

The steady state solution for the Fick's law of spherical diffusion (4) viz.

$$\frac{\partial c}{\partial t} = D\left(\frac{\partial^2 c}{\partial r^2} + \frac{2}{r}\cdot\frac{\partial c}{\partial r}\right) = 0$$

is given by

$$C = C_0(a/r)$$

where $C = C_0$ when $r = a$, with C_0 the equilibrium saturation concentration of the gas studied. This equation holds for $0 \leqslant t < \infty$. If a (the bubble radius) is kept constant then the rate of solution of the gas from the bubble is given as

$$V = \frac{4\pi a C_0 D}{\rho}\cdot t$$

where ρ is the density of the gas in the bubble. The above expression, implying a steady-state diffusion process, allows the diffusion coefficient of the gas in the liquid, D, to be found, upon knowing the experimental relationship between V, the volume of gas required to keep the bubble at constant radius, and the time t.

Experimental

The gas bubble is generated in the liquid under investigation at the tip of a micro-pipette (Manostat Corp: Digitpette). The pipette was pre-calibrated with mercury, and the capillary of the pipette was coated with "siliclad" (Clay–Adams Inc.) to prevent it from wetting. For the present experiments the solvent used is distilled water, thoroughly degassed at a low pressure. The apparatus is so designed that the pipette can be repeatedly flushed with the gas under investigation before being immersed into the solvent. The whole apparatus is thermostated to ± 0.01 °C, and mounted on a heavy concrete block to eliminate mechanical vibration.

The diameter of the bubble is measured with a microscope fitted with a calibrated filar eyepiece, (Gaertner Scientific Corporation). It has been observed that bubbles under 2.5 mm in diameter remain perfectly spherical at the tip of the pipette with less than 0.5% of contact area to the capillary. No correction is made for the bubble area in contact with the capillary since the uncertainty is much less than the uncertainty in the gas solubility data. The rate of solution of the gas into the solvent is compensated by operating the plunger of the pipette, so keeping the bubble at a constant size. The change in the position of the calibrated plunger is measured as a function of time.

Results

Measurements have so far been made on the rate of diffusion of N_2, O_2, and CO_2 in water at 25 °C. In each of these systems a steady state diffusion equation is seen to be obeyed. Typical results are plotted in Fig. 1 and the calculated diffusion coefficients for the three gases in this single solvent are given in Table I. Values taken from the literature for these systems are also given in Table I and agreement with these is seen to be good (5).

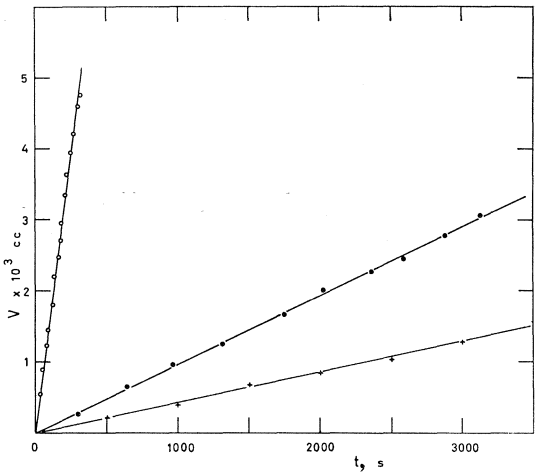

FIG. 1. Rates of absorption of constant size gas bubbles into water at 25 °C: ○, CO_2, $a = 0.767$ mm; ●, O_2, $a = 0.924$ mm; +, N_2, $a = 0.978$ mm.

Conclusion

The method described above has been found to be quick and accurate. It has the distinct advantage over the "open-tube" and more so over the "diaphragm" methods (6, 7) in that it allows diffusion coefficients to be measured for systems in which the solute gas has an exceedingly low saturation solubility. The apparatus can be easily

TABLE I

Diffusion coefficients of O_2, N_2, and CO_2 in water at 25 °C

Gas	Diffusion coefficients ($\times 10^5$ cm^2/s)		
	This work	Vivian and King (8)	Selected literature values
O_2	2.65	2.41	2.25 (ref. 9)
N_2	2.19	—	2.25 (ref. 10)
CO_2	1.99	2.00	1.90 (ref. 11)

adapted so that D can be measured over a wide temperature range. It could easily be designed to fit into a pressure bomb so that systems at a high pressure could be investigated. The advantages of this method over the dissolving bubble method, apart from the simplicity of the mathematics of the diffusion process, are that the "streaming" problem is reduced and that by retaining the constant bubble size we are not concerned with the convection problem associated with a changing size bubble.

1. I. M. KRIEGER, G. W. MULHOLLAND, and C. S. DICKEY. J. Phys. Chem. **71**, 1123, (1967).
2. V. G. LEVICH. Physicochemical hydrodynamics. Prentice-Hall, Inc., Englewood Cliffs. 1962.
3. L. E. JOHNS. J. Phys. Chem. **71**, 4566 (1967).
4. H. S. CARSLAW and J. C. JAEGAR. Conduction of heat in solids. The Clarendon Press, Oxford. 1959.
5. D. M. HIMMELBLAU. Chem. Rev. **64**, 527 (1964).
6. L. BENNETT, W. NG., and J. WALKLEY. J. Phys. Chem. **72**, 4699 (1968).
7. M. ROSS and J. H. HILDEBRAND. J. Chem. Phys. **40**, 2397 (1964). K. NAKANISHI, E. M. VOIGT, and J. H. HILDEBRAND. J. Chem. Phys. **42**, 1860 (1965).
8. J. E. VIVIAN and C. J. KING. J.A.I.Ch.E. **10**, 220 (1964).
9. J. JORDAN, E. ACKERMAN, and C. L. BERGER. J. Am. Chem. Soc. **78**, 2979 (1956).
10. R. E. SMITH, E. T. FRIESS, and M. F. MORALES. J. Phys. Chem. **59**, 382 (1955).
11. Y. P. TANG and D. M. HIMMELBLAU. J.A.I.Ch.E. **9**, 630 (1963).

Interactions of formic acid, formaldehyde, and methanol with germania surfaces

J. C. MCMANUS, KUN-ICHI MATSUSHITA, AND M. J. D. LOW
Department of Chemistry, New York University, New York, New York 10453

Received August 15, 1968

Infrared studies of the interaction of, respectively, formic acid, formaldehyde, and methanol with hydroxylated germania gel surfaces were made. Formic acid was dissociatively adsorbed to give covalently bonded formate species and new surface hydroxyl groups. Monomeric formic acid could not be observed. Degassing the treated sample at 246° removed most of the surface formate and the perturbing effects on the surface hydroxyls were also decreased. Two adsorbed species were observed when germania was exposed to high pressures (~10 Torr) of formaldehyde at room temperature. One species was very weakly bonded; it was removed by degassing at room temperature and its structure is tentatively taken as formaldehyde hydrogen-bonded to the surface hydroxyl groups. The other species had a spectrum very similar to polyoxymethylene, and it is proposed that it was in fact a surface polymer formed through the catalytic effect of the surface hydroxyl groups. Methanol was dissociatively adsorbed on germania surfaces. A species attributed to surface methoxide was formed and the concentration of the surface hydroxyl groups increased. Also, small concentrations of two other species were observed which gave absorptions at 2195 and 1727 cm^{-1}, respectively. The band at 2195 cm^{-1} is assigned to a Ge—H species formed, possibly, at non-stoichiometric portions of the surface, while the latter species is tentatively ascribed to a surface formate species.

Canadian Journal of Chemistry, **47**, 1077 (1969)

Somewhat surprisingly, in view of the great interest in germanium junction devices, there is relatively little direct information about the nature and structure of materials adsorbed on "real" germanium surfaces, perhaps because experimental emphasis has so far been placed on the measurement of electronic properties. Germania is, however, transparent to infrared radiation over a wide range, so that infrared spectroscopic techniques can be used to study

Can. J. Chem. Downloaded from www.nrcresearchpress.com by 210.87.254.6 on 09/05/12
For personal use only.

TABLE I

Diffusion coefficients of O_2, N_2, and CO_2 in water at 25 °C

Gas	Diffusion coefficients ($\times 10^5$ cm^2/s)		
	This work	Vivian and King (8)	Selected literature values
O_2	2.65	2.41	2.25 (ref. 9)
N_2	2.19	—	2.25 (ref. 10)
CO_2	1.99	2.00	1.90 (ref. 11)

adapted so that D can be measured over a wide temperature range. It could easily be designed to fit into a pressure bomb so that systems at a high pressure could be investigated. The advantages of this method over the dissolving bubble method, apart from the simplicity of the mathematics of the diffusion process, are that the "streaming" problem is reduced and that by retaining the constant bubble size we are not concerned with the convection problem associated with a changing size bubble.

1. I. M. KRIEGER, G. W. MULHOLLAND, and C. S. DICKEY. J. Phys. Chem. **71**, 1123, (1967).
2. V. G. LEVICH. Physicochemical hydrodynamics. Prentice-Hall, Inc., Englewood Cliffs. 1962.
3. L. E. JOHNS. J. Phys. Chem. **71**, 4566 (1967).
4. H. S. CARSLAW and J. C. JAEGAR. Conduction of heat in solids. The Clarendon Press, Oxford. 1959.
5. D. M. HIMMELBLAU. Chem. Rev. **64**, 527 (1964).
6. L. BENNETT, W. NG., and J. WALKLEY. J. Phys. Chem. **72**, 4699 (1968).
7. M. ROSS and J. H. HILDEBRAND. J. Chem. Phys. **40**, 2397 (1964). K. NAKANISHI, E. M. VOIGT, and J. H. HILDEBRAND. J. Chem. Phys. **42**, 1860 (1965).
8. J. E. VIVIAN and C. J. KING. J.A.I.Ch.E. **10**, 220 (1964).
9. J. JORDAN, E. ACKERMAN, and C. L. BERGER. J. Am. Chem. Soc. **78**, 2979 (1956).
10. R. E. SMITH, E. T. FRIESS, and M. F. MORALES. J. Phys. Chem. **59**, 382 (1955).
11. Y. P. TANG and D. M. HIMMELBLAU. J.A.I.Ch.E. **9**, 630 (1963).

Interactions of formic acid, formaldehyde, and methanol with germania surfaces

J. C. MCMANUS, KUN-ICHI MATSUSHITA, AND M. J. D. LOW
Department of Chemistry, New York University, New York, New York 10453

Received August 15, 1968

Infrared studies of the interaction of, respectively, formic acid, formaldehyde, and methanol with hydroxylated germania gel surfaces were made. Formic acid was dissociatively adsorbed to give covalently bonded formate species and new surface hydroxyl groups. Monomeric formic acid could not be observed. Degassing the treated sample at 246° removed most of the surface formate and the perturbing effects on the surface hydroxyls were also decreased. Two adsorbed species were observed when germania was exposed to high pressures (~10 Torr) of formaldehyde at room temperature. One species was very weakly bonded; it was removed by degassing at room temperature and its structure is tentatively taken as formaldehyde hydrogen-bonded to the surface hydroxyl groups. The other species had a spectrum very similar to polyoxymethylene, and it is proposed that it was in fact a surface polymer formed through the catalytic effect of the surface hydroxyl groups. Methanol was dissociatively adsorbed on germania surfaces. A species attributed to surface methoxide was formed and the concentration of the surface hydroxyl groups increased. Also, small concentrations of two other species were observed which gave absorptions at 2195 and 1727 cm^{-1}, respectively. The band at 2195 cm^{-1} is assigned to a Ge—H species formed, possibly, at non-stoichiometric portions of the surface, while the latter species is tentatively ascribed to a surface formate species.

Canadian Journal of Chemistry, **47**, 1077 (1969)

Somewhat surprisingly, in view of the great interest in germanium junction devices, there is relatively little direct information about the nature and structure of materials adsorbed on "real" germanium surfaces, perhaps because experimental emphasis has so far been placed on the measurement of electronic properties. Germania is, however, transparent to infrared radiation over a wide range, so that infrared spectroscopic techniques can be used to study

Can. J. Chem. Downloaded from www.nrcresearchpress.com by 210.87.254.105 on 09/05/12
For personal use only.

Can. J. Chem. Downloaded from www.nrcresearchpress.com by 210.87.254.105 on 09/05/12
For personal use only.

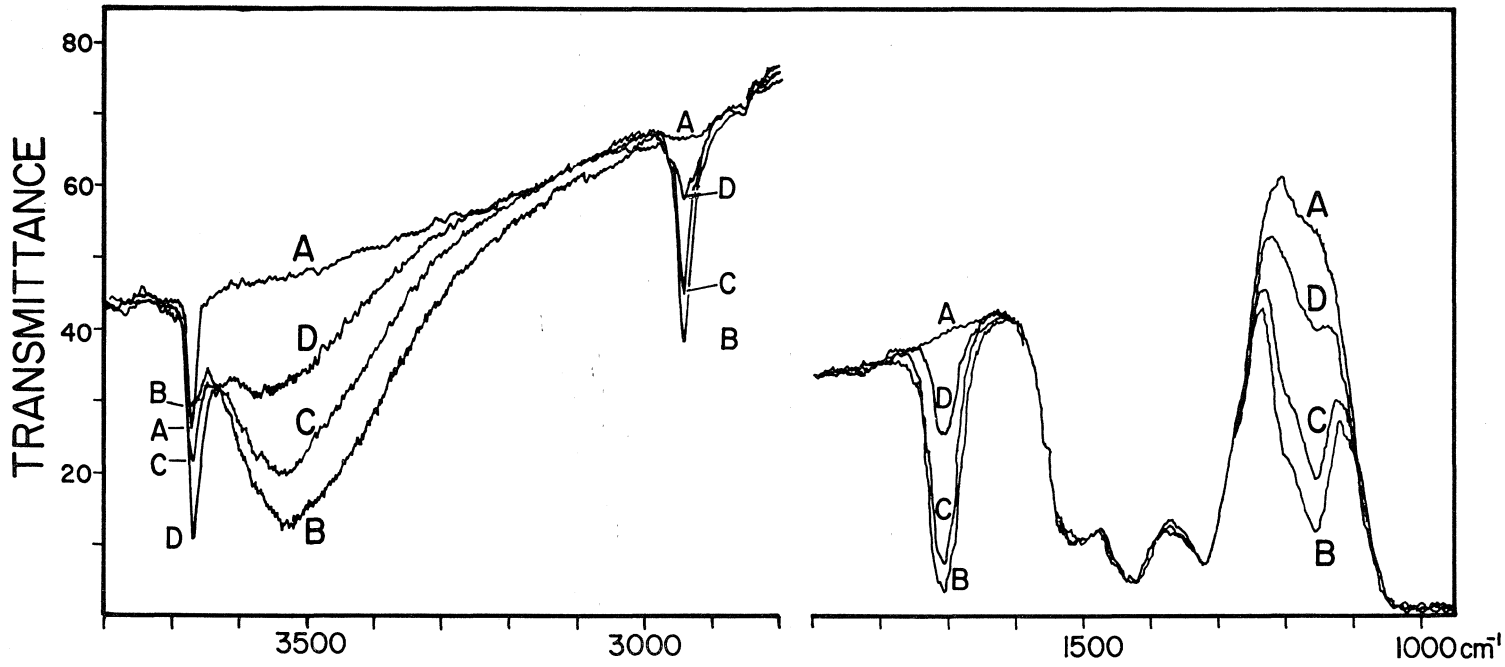

FIG. 1. Interaction of formic acid and germania. A germania sample was heated in 30 Torr O_2 at 520° for 6 h and degassed at 580° overnight (spectrum A). The sample was then exposed to 7 Torr formic acid at room temperature for 30 min and degassed for 1 h at room temperature (spectrum B). The sample was then degassed for 1 h at 146° (spectrum C) and at 230° (spectrum D).

reactions occurring on oxidized germanium. Using germania gel as analogue for real germanium, some information has recently been obtained about the surface species formed when water (1, 2), hydrogen (2), and propionic and acetic acids (3) were sorbed on germania. Those studies were extended in order to examine the interactions of formic acid, formaldehyde, and methanol with germania.

Experimental

The procedures for preparing germania gel and compacted pellets suitable for infrared studies have already been described (2, 3). Methanol and formic acid were dried under vacuum with anhydrous copper sulfate and were degassed by freeze–pump–thaw cycles. Formaldehyde was prepared from paraformaldehyde according to the method of Spence and Wild (4). Spectra were recorded with a Perkin–Elmer Model 621 spectrophotometer using cells similar to those of Peri and Hannan (5). Contributions from the gas phase were nulled, in most instances, by the use of a reference cell.

Results and Discussion

Formic Acid–GeO_2

Spectrum A of Fig. 1 is that of pure germania after treatment with oxygen and degassing (2) at 550°. The sharp band at 3672 cm^{-1}, hereafter termed the free Ge—OH band, has been previously assigned to ν(OH) of "free" or isolated hydroxyls attached to surface germanium atoms. The intense absorptions in the 1600–1200 cm^{-1} region are caused by the oxide. Exposing the germania to 7 Torr formic acid at room temperature (spectrum B) decreased the free Ge—OH band intensity and caused the formation of a broad band centering near 3530 cm^{-1}, attributed to perturbed hydroxyls (2); also, taking into account the sloping background in the 1500–1000 cm^{-1} region, bands were observed at 2944, 1707, 1201 (shoulder), and 1157 cm^{-1}. Degassing at increasingly higher temperatures resulted in a marked decrease of the latter bands at temperatures greater than 100° and showed that they could all be related to the same surface species. The bands were completely removed by degassing at 270°. On degassing, the intensity of the free Ge—OH band increased and became greater than its initial value, while the broad band shifted from 3530 cm^{-1} to higher wavenumbers and decreased in intensity.

The bands at 2944, 1707, 1201, and 1157 cm^{-1} can best be interpreted in terms of a covalent formate species formed by dissociative chemisorption,

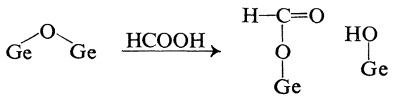

Although there are no published spectra of germyl esters, such compounds exist (6). Moreover, comparison of the present spectra with those of silyl formates (7) and organic formates (8) shows very good agreement, so that it is reasonable to make band assignments in an analogous fashion. On this basis, the band at 2944 cm^{-1} is attributed to ν_a(C—H), that at 1707 cm^{-1} to ν(C═O), while those at 1201 and 1157 cm^{-1} are the results of coupled modes with the main contribution coming from ν(C—O). The possibility that the surface species was solely monomeric formic acid held to the surface by hydrogen bonding is not given much credence. For gaseous monomeric formic acid it has been shown (9, 10) that, although there is much coupling of the modes, bands at 1229 and 1105 cm^{-1} are due mainly to δ(OH) and ν(C—O), respectively. Hydrogen bonding would be expected to shift these modes to higher frequencies and may cause a decrease in the intensity of δ(OH), but this model does not give a convincing explanation of the results. Also, hydrogen-bonding forces of the strength expected from the Δν(OH) shift would not be considered large enough to hold monomeric acid molecules to the surface at temperatures of 150–200°. Parenthetically, the model of a covalently bonded carboxylate species best explained the results obtained when acetic and propionic acids reacted with germania (3).

It seems clear that the adsorption of formic acid was dissociative and that the final products were formate and hydroxyl species. Comparison with previous work (2) seems to indicate that while Ge—OH groups were formed in the adsorption process, the band at 3530 cm^{-1} decreased to a greater extent with increasing temperature than would be expected if it were caused solely by OH—OH interactions. There may thus have been some hydrogen-bonding interaction between the carbonyl group of the surface formate and a neighboring Ge—OH group.

When the germania was exposed to 7 Torr formic acid at 270° (the temperature at which surface formate would be removed completely)

Can. J. Chem. Downloaded from www.nrcresearchpress.com by 210.87.254.105 on 09/05/12
For personal use only.

Can. J. Chem. Downloaded from www.nrcresearchpress.com by 210.87.254.105 on 09/05/12
For personal use only.

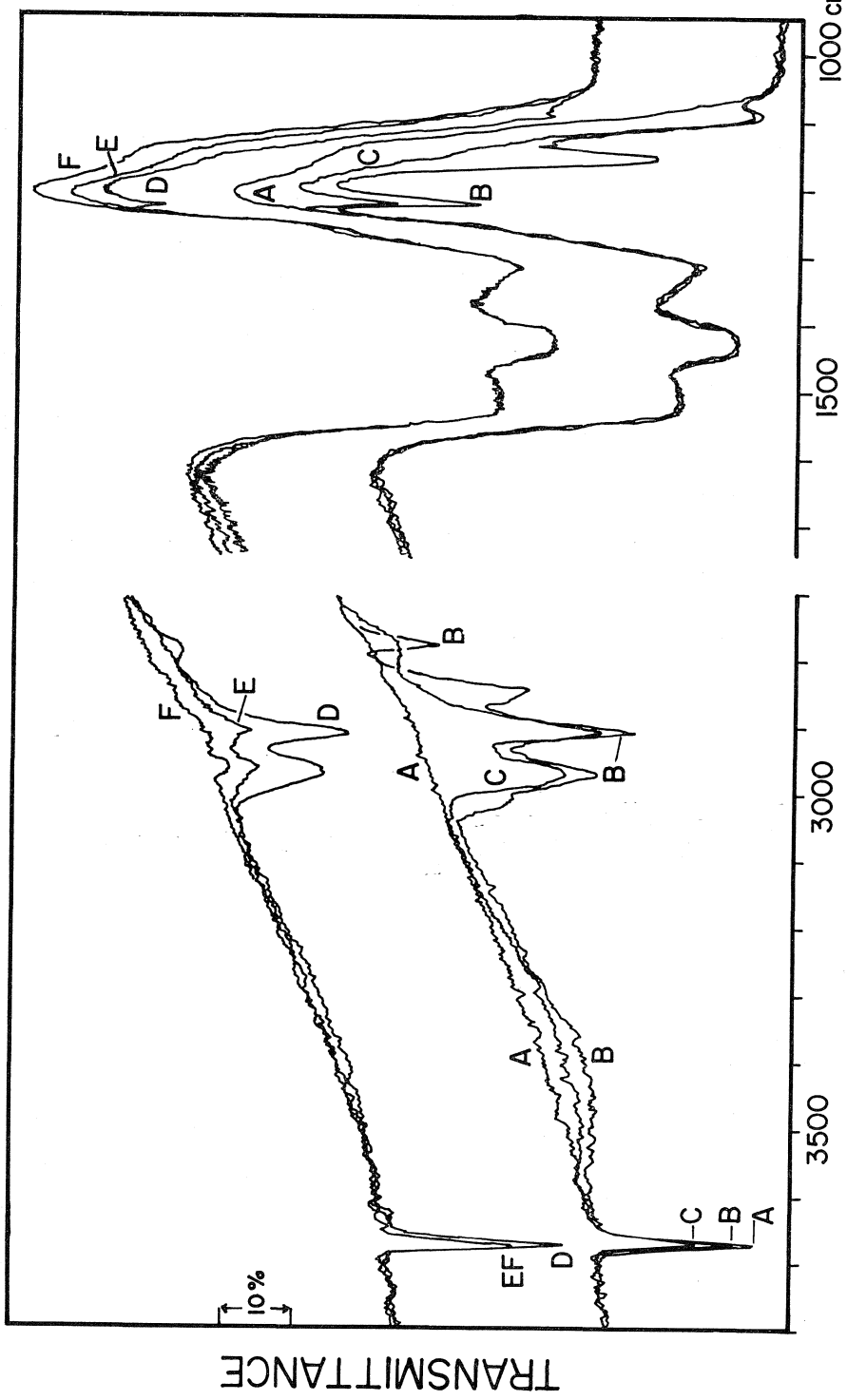

FIG. 2. Interaction of formaldehyde and germania. A well-degassed germania sample (spectrum A) was exposed to 9 Torr formaldehyde at room temperature for 1 h (spectrum B). The pressure was then reduced to 4 μ by pumping at room temperature (spectrum C). The sample was then degassed at the following temperatures and times in hours to obtain spectrum D, room temperature, 15; E, 125°, 1; F, 200°, 0.5. The ordinate of the group of spectra D, E, F is displaced to avoid overlapping of traces.

Can. J. Chem. Downloaded from www.nrcresearchpress.com by 210.87.254.105 on 09/05/12
For personal use only.

and degassed for 30 min at 100°, the intensity of the band due to perturbed hydroxyls at 3530 cm^{-1} compared to those due to surface formate, was much greater than that observed when germania was exposed to 7 Torr formic acid at room temperature and degassed at 140°. Thus, while there is no evidence against the adsorption process being reversible to some extent, it is clear that there was a decomposition involving a dehydration process.

Formaldehyde–GeO_2

From the spectra it is clear that two surface species were formed when germania was exposed to formaldehyde at room temperature (Fig. 2). One was weakly bound and could easily be desorbed by degassing at room temperature. Bands due to this species were observed at 3015, 2849, 2785, and 1167 cm^{-1}; in addition, it was noted that the free Ge—OH band increased and the band due to perturbed hydroxyls, which was formed in the region 3350–3400 cm^{-1}, decreased when the weakly bound species was removed. There was no evidence for a band in the 1750–1700 cm^{-1} region, but this could have been obscured by imperfect compensation of the reference beam. However, in spite of the fact that there was no band attributable to ν(C=O), we think that the bands can be best interpreted in terms of formaldehyde molecules, hydrogen-bonded to surface hydroxyl groups by means of the carbonyl groups, because there is good agreement with the spectra of formaldehyde (11, 12) recorded at 77 and 273 °K. However, the failure to observe ν(C=O) is disturbing and no satisfactory reason can be given for this.

The second species was much more strongly bound and was removed only by degassing at 200°. It gave rise to bands at 2972–2979, 2913, 2785, 1233, and 1100 cm^{-1}. These positions compare very favorably with those found in the spectrum of polyoxymethylene (13). Consequently, it seems probable that a polymerization had occurred on the surface. As the intensity of the free Ge—OH band was dependent on the surface concentration of the polymer, it is likely that the latter was bonded, at least in part, to surface hydroxyls by hydrogen bonds; with such a big molecule, van der Waals – London forces may also play an important role. The main details of the mechanism are obscure, but it was found that when the sample (upon which only the polymer was adsorbed) was heated in a closed cell, formaldehyde was present in the gas phase on cooling and the concentration of polymer was reduced quite markedly. Thus, the polymerization rate was sensitive to the formaldehyde pressure, so that a weakly bound form of formaldehyde, whose surface concentration is pressure-dependent, may play an important intermediate role in polymerization. It is well known that formaldehyde polymerization is catalyzed by acids (14), and so it may be that surface OH groups act as sites for a process such as

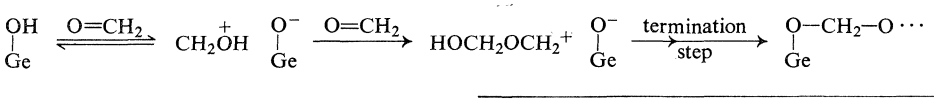

Methanol–GeO_2

Exposure of a highly dehydroxylated surface to 1 Torr methanol followed by evacuation at room temperature for 1 h (Fig. 3) resulted in the formation of new bands at 2999, 2952, 2848, 1475, 1360, 1180, 677, 1727, and 2195 cm^{-1}. Also, the intensity of the free Ge—OH band remained essentially unchanged, but a broad band centering near 3500–3450 cm^{-1} was formed and is attributed to perturbed OH. Intensity measurements made under different degassing conditions showed that each of the bands at 1727 and 2195 cm^{-1} belonged to a separate species and that the rest of the bands belonged to a third species. The band at 2195 cm^{-1} disappeared after evacuation at 230° and was formed only when the methanol was contacted at room temperature with a surface containing very few hydroxyl groups. Thus, in accordance with previous work (2), the 2195 cm^{-1} band was probably caused by a Ge—H structure which was formed only when methanol reacted with a non-stoichiometric portion of the germania surface.

An early study (15) of the spectrum of $Ge(OMe)_4$ showed strong bands at 2955, 1460, 1181, 1040, 897, and 670 cm^{-1}. Thus the main surface species observed in our work showed marked similarities with this, apart from the failure to correlate the band at 1370 cm^{-1}. Also, the present spectra are very similar to those of

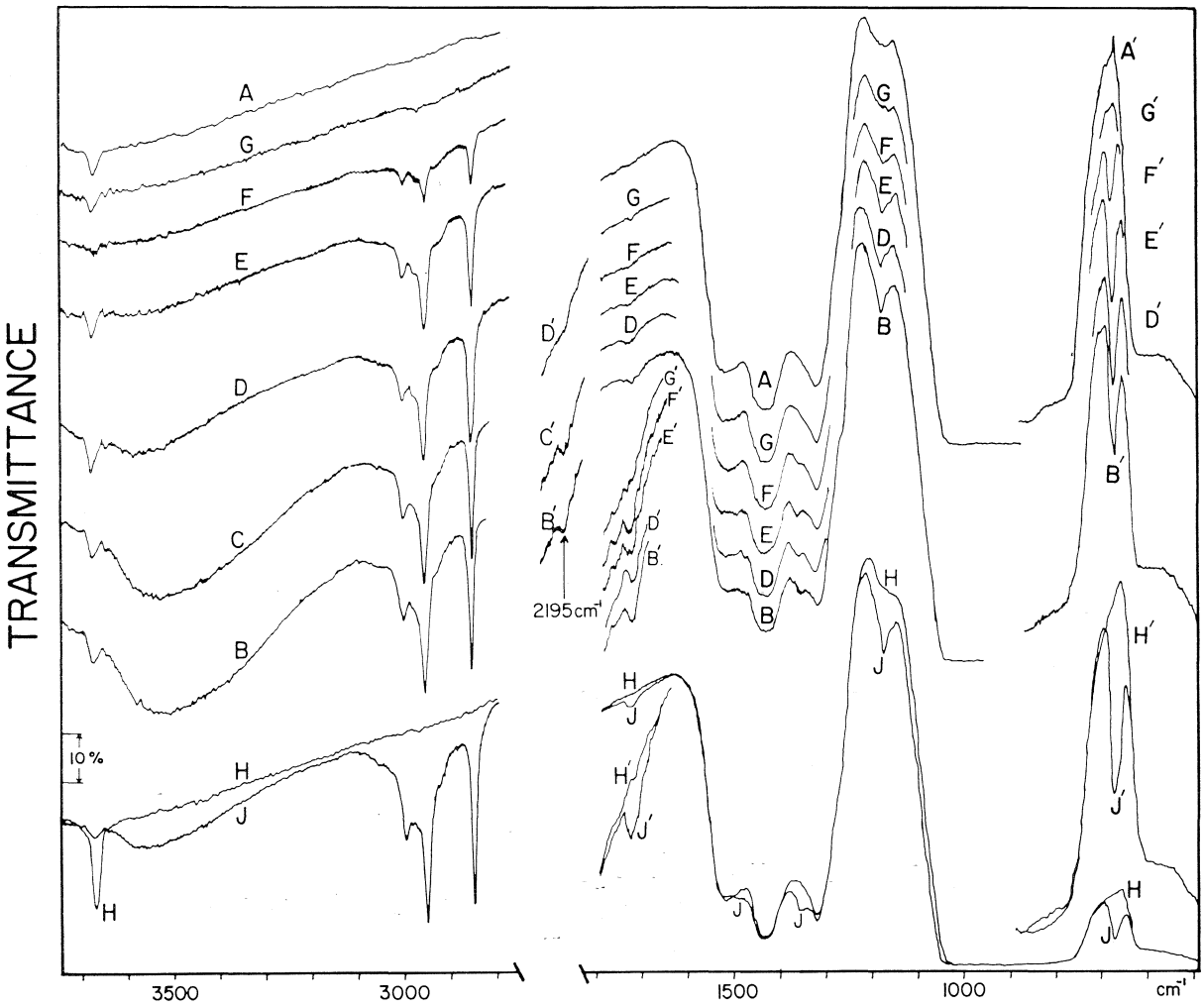

FIG. 3. Interaction of methanol and germania. A well-degassed germania sample (spectrum A) was exposed to 1 Torr methanol at room temperature for 1 h and degassed at room temperature for 1 h (spectrum B). The sample was then degassed at the following temperatures and times in hours to give spectrum C, room temperature, 9; D, 210°, 1; E, 300°, 0.5; F, 400°, 0.5; G, 450°, 0.5. A second well-degassed sample (spectrum H) was exposed to 5 Torr methanol at 210° for 1 h and was then degassed for 30 min at 210°(spectrum J). The ordinates of spectra A to G were displaced to prevent overlapping of traces. Letters marked with a prime indicate that the portion of the spectrum was re-recorded with 5 times ordinate scale expansion.

methoxide formed on siliceous surfaces (16). We therefore think that the spectrum of the surface species can be interpreted best in terms of a surface methoxide.

Intensity measurements show that there was no relation between the surface methoxide bands and that at 3500 cm^{-1}, indicating that hydrogen-bonding forces were involved with the methoxide only to a slight extent, if at all. The band at 3500 cm^{-1} disappeared on degassing at a much quicker rate than found when a hydrated fresh gel surface was degassed for the first time (2). Even so, the band was probably due almost in its entirety to perturbed hydroxyl groups which were formed together with methoxide radicals when the methanol was adsorbed. These hydroxyl groups were removed from the surface at a quite rapid rate. This was probably due to the fact that the sample was initially almost completely dehydroxylated. Previous work (2) showed that hydroxyl groups formed on a dehydroxylated surface were not as stable as those formed on a

Can. J. Chem. Downloaded from www.nrcresearchpress.com by 210.87.254.105 on 09/05/12
For personal use only.

partially dehydroxylated surface, although the cause of this is not known.

At room temperature the predominant reaction appeared to involve a disruption of the germania surface:

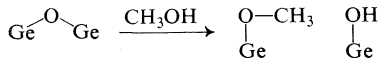

The direct surface esterification,

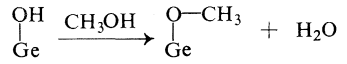

appeared to be minimal. Only at higher reaction temperatures was there any significant removal of free Ge—OH groups (spectra H, J, Fig. 3).

The nature of the species giving the band at 1727 cm^{-1} is uncertain. Possibly the band indicates the presence of some type of carbonyl group. The stability of the surface species immediately rules out the presence of ketones, aldehydes, or esters. It has been shown by Greenler (17) that surface formate was formed when an alumina surface was heated at 170° in methanol. Our system is similar in that surface methoxide was formed when germania was exposed to methanol, although surface hydroxyl groups, rather than hydrogen, were also produced. We feel that it is possible that the reactions on alumina and germania are similar, although there are two factors against this. The formate species on germania surfaces were not stable at temperatures greater than 240°, whereas the 1727 cm^{-1} band was not removed until degassing temperatures of 300° were used; and the band positions do not agree in that formate species absorb at 1707–1717 cm^{-1}. However, these are not overwhelming objections and we think that the interpretation of surface formate is the best available.

Acknowledgment

Support from the National Center for Air Pollution Control is gratefully acknowledged.

1. M. J. D. Low and P. Ramamurthy. Chem. Commun. 733 (1966).
2. M. J. D. Low, N. Madison, and P. Ramamurthy. Surface Sci. In press.
3. J. C. McManus and M. J. D. Low. J. Phys. Chem. **72**, 2378 (1968).
4. R. Spence and W. Wild. J. Chem. Soc. 338 (1935).
5. J. B. Peri and R. B. Hannan. J. Phys. Chem. **64**, 1526 (1960).
6. H. H. Anderson. J. Am. Chem. Soc. **72**, 2089 (1950).
7. A. G. E. Robiette and J. C. Thompson. Spectrochim. Acta, **21**, 2023 (1965).
8. A. R. Katritzky, J. M. Lagowski, and J. A. T. Beard. Spectrochim. Acta, **16**, 964 (1960).
9. R. C. Millikan and K. S. Pitzer. J. Chem. Phys. **27**, 1305 (1957).
10. D. Hadzi and M. Pintar. Spectrochim. Acta, **12**, 162 (1958).
11. H. H. Blan and H. H. Nielsen. J. Mol. Spectry. **1**, 124 (1957).
12. K. B. Harvey and J. F. Ogilvie. Can. J. Chem. **40**, 85 (1962).
13. H. Tadokoro, M. Kobayashi, Y. Kawaguchi, and A. Kobayashi. J. Chem. Phys. **38**, 703 (1963).
14. J. C. Bevington and R. G. W. Norrish. Proc. Roy. Soc. London, Ser. A, **250**, 516 (1951).
15. O. H. Johnson and H. E. Fritz. J. Am. Chem. Soc. **75**, 718 (1953).
16. M. J. D. Low and Y. Harano. J. Res. Inst. Catalysis, Hokkaido Univ. In press.
17. R. Greenler. J. Chem. Phys. **37**, 2094 (1962).

Hydroboration of acyclic allenes with disiamylborane

D. S. Sethi, G. C. Joshi, and D. Devaprabhakara

Department of Chemistry, Indian Institute of Technology, Kanpur, India

Received June 10, 1968

The present investigation demonstrates the hydroboration of 1,2-nonadiene, phenylpropadiene, 3-phenyl-1,2-butadiene, 4,5-nonadiene, and tetramethylallene with disiamylborane. All the allenes except tetramethylallene underwent 100% conversion. Examination of the products indicated preferential electrophilic attack of boron on the least substituted terminal carbon atom in the case of 1,2-nonadiene, phenylpropadiene, 3-phenyl-1,2-butadiene, and on the central carbon atom in 4,5-nonadiene. In tetramethylallene boron, attack was exclusively on the central carbon atom. These results have been explained in terms of steric effects on a four-centered transition state.

Canadian Journal of Chemistry, 47, 1083 (1969)

In our preceding publication (1), the effect of ring size on hydroboration of cyclic allenes with disiamylborane has been demonstrated. In continuation of this study we undertook the hydroboration of representative acyclic allenes with disiamylborane, to achieve monohydroboration,

Can. J. Chem. Downloaded from www.nrcresearchpress.com by 210.87.254.105 on 09/05/12
For personal use only.

partially dehydroxylated surface, although the cause of this is not known.

At room temperature the predominant reaction appeared to involve a disruption of the germania surface:

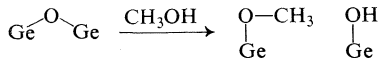

The direct surface esterification,

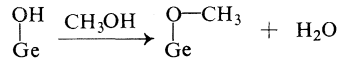

appeared to be minimal. Only at higher reaction temperatures was there any significant removal of free Ge—OH groups (spectra H, J, Fig. 3).

The nature of the species giving the band at 1727 cm^{-1} is uncertain. Possibly the band indicates the presence of some type of carbonyl group. The stability of the surface species immediately rules out the presence of ketones, aldehydes, or esters. It has been shown by Greenler (17) that surface formate was formed when an alumina surface was heated at 170° in methanol. Our system is similar in that surface methoxide was formed when germania was exposed to methanol, although surface hydroxyl groups, rather than hydrogen, were also produced. We feel that it is possible that the reactions on alumina and germania are similar, although there are two factors against this. The formate species on germania surfaces were not stable at temperatures greater than 240°, whereas the 1727 cm^{-1} band was not removed until degassing temperatures of 300° were used; and the band positions do not agree in that formate species absorb at 1707–1717 cm^{-1}. However, these are not overwhelming objections and we think that the interpretation of surface formate is the best available.

Acknowledgment

Support from the National Center for Air Pollution Control is gratefully acknowledged.

1. M. J. D. Low and P. Ramamurthy. Chem. Commun. 733 (1966).
2. M. J. D. Low, N. Madison, and P. Ramamurthy. Surface Sci. In press.
3. J. C. McManus and M. J. D. Low. J. Phys. Chem. **72**, 2378 (1968).
4. R. Spence and W. Wild. J. Chem. Soc. 338 (1935).
5. J. B. Peri and R. B. Hannan. J. Phys. Chem. **64**, 1526 (1960).
6. H. H. Anderson. J. Am. Chem. Soc. **72**, 2089 (1950).
7. A. G. E. Robiette and J. C. Thompson. Spectrochim. Acta, **21**, 2023 (1965).
8. A. R. Katritzky, J. M. Lagowski, and J. A. T. Beard. Spectrochim. Acta, **16**, 964 (1960).
9. R. C. Millikan and K. S. Pitzer. J. Chem. Phys. **27**, 1305 (1957).
10. D. Hadzi and M. Pintar. Spectrochim. Acta, **12**, 162 (1958).
11. H. H. Blan and H. H. Nielsen. J. Mol. Spectry. **1**, 124 (1957).
12. K. B. Harvey and J. F. Ogilvie. Can. J. Chem. **40**, 85 (1962).
13. H. Tadokoro, M. Kobayashi, Y. Kawaguchi, and A. Kobayashi. J. Chem. Phys. **38**, 703 (1963).
14. J. C. Bevington and R. G. W. Norrish. Proc. Roy. Soc. London, Ser. A, **250**, 516 (1951).
15. O. H. Johnson and H. E. Fritz. J. Am. Chem. Soc. **75**, 718 (1953).
16. M. J. D. Low and Y. Harano. J. Res. Inst. Catalysis, Hokkaido Univ. In press.
17. R. Greenler. J. Chem. Phys. **37**, 2094 (1962).

Hydroboration of acyclic allenes with disiamylborane

D. S. Sethi, G. C. Joshi, and D. Devaprabhakara
Department of Chemistry, Indian Institute of Technology, Kanpur, India

Received June 10, 1968

The present investigation demonstrates the hydroboration of 1,2-nonadiene, phenylpropadiene, 3-phenyl-1,2-butadiene, 4,5-nonadiene, and tetramethylallene with disiamylborane. All the allenes except tetramethylallene underwent 100% conversion. Examination of the products indicated preferential electrophilic attack of boron on the least substituted terminal carbon atom in the case of 1,2-nonadiene, phenylpropadiene, 3-phenyl-1,2-butadiene, and on the central carbon atom in 4,5-nonadiene. In tetramethylallene boron, attack was exclusively on the central carbon atom. These results have been explained in terms of steric effects on a four-centered transition state.

Canadian Journal of Chemistry, 47, 1083 (1969)

In our preceding publication (1), the effect of ring size on hydroboration of cyclic allenes with disiamylborane has been demonstrated. In continuation of this study we undertook the hydroboration of representative acyclic allenes with disiamylborane, to achieve monohydroboration,

Can. J. Chem. Downloaded from www.nrcresearchpress.com by 210.87.254.40 on 09/05/12
For personal use only.

TABLE I

Results of the hydroboration–oxidation of the representative acyclic allenes

	% yield					
	Ketone		Unsaturated alcohol		Olefins	
Allene	Compound	%	Compound	%	Compound	%
1,2-Nonadiene	2-Nonanone	16.9	2-Nonen-1-ol	38.6	1-Nonene	5.5
					2-Nonene, *cis* and *trans*	15.8
Phenylpropadiene	1-Phenyl-2-propanone	16.8	—		Allylbenzene	22.9
					1-Phenyl-1-propene, *cis* and *trans*	44.1
3-Phenyl-1,2-butadiene	3-Phenyl-2-butanone	10.6	—		3-Phenyl-1-butene	19.1
					2-Phenyl-2-butene, *cis* and *trans*	60.3
4,5-Nonadiene	5-Nonanone	60.5	5-Nonen-4-ol	20.4	4-Nonene, *cis* and *trans*	8.7
Tetramethylallene	Diisopropyl ketone	73.1				

to examine the relative rates of reaction, and to study the selectivity in the direction of addition.

It has been shown by Brown and Zweifel (2) that the hydroboration of 1-hexene and styrene with disiamylborane followed by alkaline hydrogen peroxide oxidation provides 98–99% primary alcohols. From this observation, the authors have concluded not only the steric equivalence of phenyl and *n*-alkyl groups but also the absence of electrical effect by the phenyl substituent. In view of this, 1,2-nonadiene, phenylpropadiene, 3-phenyl-1,2-butadiene, 4,5-nonadiene, and tetramethylallene were subjected to hydroboration–oxidation under identical conditions, and the nature of the product(s) was explored.

Results and Discussion

Disiamylborane was prepared by the hydroboration of 2-methyl-2-butene under a static pressure of nitrogen (3). A solution of appropriate allene in diglyme was added to the above solution within 3–4 min. The mixture was allowed to attain room temperature (approx. 3 h). After stirring for a further 2 h at room temperature, the mixture was hydrolyzed by careful addition of water till hydrogen was no longer evolved. The resulting organoboranes were oxidized with alkaline hydrogen peroxide in the usual manner. The conversion of the allene to product(s) as determined by gas chromatography (4) was found to be 100% except in the case of tetramethylallene. The latter underwent conversion only to the extent of 30%.

A general scheme for the hydroboration of acyclic allenes may be represented as follows and the results are summarized in Table I.

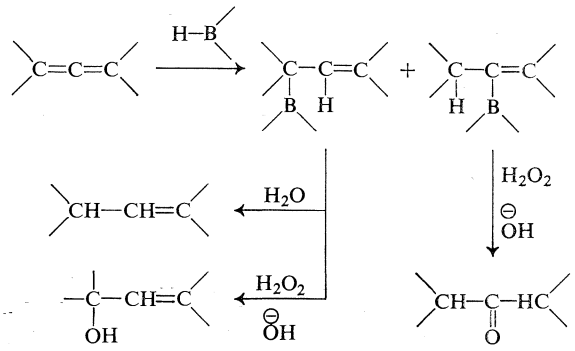

The identity of each product was established by comparison of gas liquid chromatographic (g.l.c.) retention times (using several columns) and infrared spectra (i.r.) with those of an authentic sample. Wherever necessary, elemental analysis and preparation of known derivatives were also used in the characterization of products.

The ratio of electrophilic attack of boron on the terminal and central carbon atoms of the allenic linkage as calculated from the molar ratio of the products for each allene is shown in Table II.

The electrophilic attack of boron on the central vs. terminal carbon atom of the allenic linkage in the case of 1,2-nonadiene and phenylpropadiene suggests that the steric requirement of the phenyl group is almost the same as that of *n*-alkyl group, even in acyclic allenes when disiamylborane is used as the hydroborating reagent. The observed difference in the reactivity and selectivity in the

Can. J. Chem. Downloaded from www.nrcresearchpress.com by 210.87.254.40 on 09/05/12
For personal use only.

TABLE II

Molar ratio of products resulting from the electrophilic attack of boron on terminal and central carbon atoms of the allenic linkage

Allene	Molar ratio (terminal C/central C)
1,2-Nonadiene	3.54
Phenylpropadiene	3.99
3-Phenyl-1,2-butadiene	7.47
4,5-Nonadiene	0.48
Tetramethylallene	0.00

direction of addition of disiamylborane to these acyclic allenes could solely be dictated by the difference in steric requirements of the allenes in the Brown's well-known postulated transition state for hydroboration (5). The electronic effect seems to be of minor importance here. Our result with tetramethylallene suggests that complete selectivity in the hydroboration of a tetrasubstituted allene is possible using disiamylborane.

The formation of olefins is in complete agreement with our previous observation (6), where we have shown that allylic organoboranes undergo slow hydrolytic cleavage at the boron–carbon bond. The ready hydrolysis of allylic organoboranes from phenylpropadiene and 3-phenyl-1,2-butadiene may be interpreted through the formation of an extensive stabilized carbanion, which in turn picks up a proton to give a mixture of possible olefins. The most thermodynamically stable isomer was found to be the major product in each olefinic mixture. In particular it is interesting to know that the predominant formation of *cis*-2-phenyl-2-butene over its *trans* isomer is in complete agreement with Cram's observation (7).

Experimental

Boiling points are uncorrected. Melting points were performed in open capillaries and are uncorrected. All infrared spectra were recorded on a Perkin–Elmer model 521 spectrophotometer from compounds as films between salt plates or in cells. Gas chromatographic analyses were made with Aerograph model 90P instrument using 6 ft by $\frac{1}{4}$ in. columns. The following liquid phases were employed (percentage by weight on 60/80 mesh chromosorb W): 15% silicone rubber, 15% carbowax 20M, 15% ucon, and 15% carbowax 20M – silver nitrate. Samples were collected by g.l.c. for i.r. spectra. Microanalyses were carried out by Mr. A. H. Siddiqui of the Department of Chemistry, Indian Institute of Technology, Kanpur, India.

Materials

Diglyme (Ansul Co.) was kept over calcium hydride for 24 h, decanted, and distilled from slightly excess of lithium aluminium hydride under reduced pressure. Boron trifluoride ethyl etherate (Eastman) was treated with a small quantity of dry ethyl ether (to ensure an excess of this component) and distilled under reduced pressure from calcium hydride. Sodium borohydride from Metal Hydrides Inc. (98%) was used without purification. 2-Methyl-2-butene (Aldrich Co.) was used for the preparation of disiamylborane.

Tetramethylallene (K & K Co.) was used for hydroboration. It showed no detectable impurities by g.l.c. 1,2-Nonadiene, phenylpropadiene, 3-phenyl-1,2-butadiene, and 4,5-nonadiene were prepared by two-step sequence starting from a suitable olefin in each case according to the procedure of Moore and Ward (8). Their properties corresponded well with those reported (9–11).

Monohydroboration of 1,2-Nonadiene

Pulverized sodium borohydride (3.2 g, 0.083 mole) in dry diglyme (50 ml), and 2-methyl-2-butene (15.4 g, 0.22 mole) were placed in 250 ml three-necked flask equipped with a condenser, an equilibrating dropping funnel, a low temperature thermometer, and an inlet and outlet for dry nitrogen gas. Hydroboration was achieved by adding boron trifluoride etherate (15.8 g, 0.111 mole) in diglyme (20 ml) to the well stirred mixture kept at 0 to $-5°$ over a period of 0.5 h. Throughout the reaction a static pressure of nitrogen gas was maintained. After leaving the reaction mixture for 1 h at 0°, 1,2-nonadiene (12.4 g, 0.10 mole) was added in 3 min. The reaction mixture was allowed to attain the room temperature (approx. 3 h). The excess of the hydride was destroyed by careful addition of water until hydrogen was no longer evolved. The oxidation of the intermediate organoboranes was accomplished in the usual manner by adding 3 *N* sodium hydroxide (pH 9–10) followed by 30% hydrogen peroxide. The products were extracted with ether, dried over anhydrous magnesium sulfate and ether distilled over. At this stage the percentage conversion of allene to products was determined by g.l.c.

Fractionation of the reaction mixture afforded 2.68 g (21.3% yield) of olefinic product with a b.p. 40–42° at 15 mm, 2.4 g (16.9% yield) of 2-nonanone with a b.p. 87–90° at 15 mm, n_D^{30} 1.4182 (lit. (12), b.p. 195° at 760 mm, n_D^{20} 1.4211) and 5.48 g (38.6% yield) of 2-nonen-1-ol with a b.p. 107–109° at 15 mm, n_D^{30} 1.4461 (lit. (13), b.p. 98–99° at 10 mm, n_D^{19} 1.4480). Gas chromatographic analysis of the olefinic product on a carbowax – silver nitrate column indicated the presence of 1-nonene (26%), *cis*-2-nonene (4%), and *trans*-2-nonene (70%). The identity of the individual product(s) was established by comparison of g.l.c. retention times and i.r. spectra with those of the authentic samples. The 2,4-dinitrophenylhydrazone derivative with a m.p. 58–59°, did not depress the m.p. of authentic 2-nonanone 2,4-dinitrophenylhydrazone (lit. (12), m.p. 58–59°).

Anal. Calcd. for C_9H_{18}: C, 85.71; H, 14.29. Found: C, 85.64; H, 14.21.

Anal. Calcd. for $C_{15}H_{22}N_4O_4$: C, 55.90; H, 6.83; N, 17.39. Found: C, 55.76; H, 6.58; N, 17.21.

Monohydroboration of Phenylpropadiene

The procedure described for monohydroboration of 1,2-nonadiene was followed without any change. From phenylpropadiene (11.6 g, 0.1 mole), 2-methyl-2-butene

Can. J. Chem. Downloaded from www.nrcresearchpress.com by 210.87.254.40 on 09/05/12
For personal use only.

Can. J. Chem. Downloaded from www.nrcresearchpress.com by 210.87.254.40 on 09/05/12
For personal use only.

(15.4 g, 0.22 mole), sodium borohydride (3.2 g, 0.083 mole), and boron trifluoride etherate (15.88 g, 0.111 mole), we obtained 2.7 g (22.9% yield) of allylbenzene with a b.p. 65–66° at 40 mm, n_D^{32} 1.5038 (lit. (14), b.p. 72.5–73.5° at 45 mm, n_D^{25} 1.5071), 5.2 g, (44.1% yield) of 1-phenyl-1-propenes (*cis* and *trans*) with a b.p. 58–60° at 10 mm (lit. (15), b.p. 53° at 8 mm), and 2.25 g (16.8% yield) of 1-phenyl-2-propanone with a b.p. 96–97° at 10 mm, n_D^{32} 1.5126 (lit. (16), b.p. 122–125° at 50 mm, n_D^{28} 1.5136). Gas chromatographic analysis of the olefinic mixture showed 6% of *cis* isomer and 94% of *trans* isomer. The identity of each product was established on the basis of the comparison of g.l.c. retention times and i.r. spectra with those of authentic samples. The 2,4-dinitrophenylhydrazone of the ketone had m.p. and mixture m.p. 152–153° (lit. (16), 152–153°).

Anal. Calcd. for C_9H_{10}: C, 91.53; H, 8.47. Found: C, 91.34; H, 8.38.

Anal. Calcd. for $C_{15}H_{14}N_4O_4$: C, 57.32; H, 4.46; N, 17.84. Found: C, 57.21; H, 4.42; N, 17.68.

Monohydroboration of 3-Phenyl-1,2-butadiene

Following the procedure described for 1,2-nonadiene, from 3-phenyl 1,2-butadiene (9.75 g, 0.075 mole), 2-methyl-2-butene (11.5 g, 0.165 mole), sodium borohydride (2.4 g, 0.062 mole), and boron trifluoride etherate (11.8 g, 0.083 mole), there was obtained 7.86 g (79.4% yield) of olefinic mixture containing 3-phenyl-1-butene (24%), *cis*-2-phenyl-2-butene (62%), and *trans*-2-phenyl-2-butene (14%) with a b.p. 65–75° at 20 mm and 1.18 g (10.6% yield) of 3-phenyl-2-butanone with a b.p. 103° at 20 mm, n_D^{29} 1.5060 (lit. (17), b.p. 107–108° at 22 mm, n_D^{25} 1.5074). The products were identified by comparison of their g.l.c. retention times and i.r. spectra with those of authentic samples. The semicarbazone derivative of the ketone had m.p. and mixture m.p. 169–170° (lit. (17), m.p. 173°).

Anal. Calcd. for $C_{10}H_{12}$: C, 90.91; H, 9.09. Found: C, 90.82; H, 9.21.

Anal. Calcd. for $C_{11}H_{15}N_3O$: C, 64.39; H, 7.32; N, 20.49. Found: C, 64.34; H, 7.21; N, 20.23.

Monohydroboration of 4,5-Nonadiene

Following the procedure described previously for hydroboration–oxidation, 4,5-nonadiene (6.2 g, 0.05 mole), 2-methyl-2-butene (7.7 g, 0.11 mole), sodium borohydride (1.6 g, 0.041 mole), and boron trifluoride etherate (7.9 g, 0.055 mole) afforded 0.55 g (8.7% yield) of 4-nonene with a b.p. 50–51° at 15 mm, 4.3 g (60.5% yield) of 5-nonanone with a b.p. 76–78° at 15 mm, n_D^{30} 1.4186 (lit. (18), b.p. 186–187° at 760 mm, n_D^{15} 1.4210), and 1.45 g (20.4% yield) of 5-nonen-4-ol with a b.p. 85–86° at 15 mm, n_D^{30} 1.4398 (lit. (19), b.p. 96–100° at 35 mm, n_D^{20} 1.4405). The g.l.c. analysis of 4-nonene showed 97% *trans* isomer and only 3% *cis* isomer. Only *trans* isomer was separated by g.l.c. and identified by comparison of i.r. spectra with that of an authentic sample. The *cis* isomer was identified only by comparison of g.l.c. retention times with those of an authentic sample. On the basis of i.r. and g.l.c. analysis data of the authentic samples, the ketone and the alcohol were shown to be 5-nonanone and 5-nonen-4-ol respectively. The semicarbazone derivative of the ketone had m.p. and mixture m.p. 89–90° (lit. (18), m.p. 89–90°).

Anal. Calcd. for C_9H_{18}: C, 85.71; H, 14.29. Found: C, 85.61; H, 14.36.

Anal. Calcd. for $C_{10}H_{21}N_3O$: C, 60.3; H, 10.55; N, 21.10. Found: C, 60.21; H, 10.41; N, 20.93.

Monohydroboration of Tetramethylallene

Following the procedure described previously for 1,2-nonadiene, from tetramethylallene (9.6 g, 0.1 mole), 2-methyl-2-butene (15.4 g, 0.22 mole), sodium borohydride (3.2 g, 0.083 mole), and boron trifluoride etherate (15.8 g, 0.111 mole), there was obtained only 2.5 g (73.1% yield based on consumed starting material) of diisopropyl ketone with a b.p. 122–124° at 742 mm, n_D^{31} 1.3950 (lit. (20), b.p. 121–126° at 760 mm, n_D^{20} 1.4001). The percentage conversion of tetramethylallene to the products as established by g.l.c. was 30%. The identity of the ketone was established by comparison of g.l.c. retention times and i.r. spectra with those of an authentic sample. The m.p. and mixture m.p. of the 2,4-dinitrophenylhydrazone of the ketone was observed to be 88–89° (lit. (20), m.p. 87–88°).

Anal. Calcd. for $C_{13}H_{18}N_4O_4$: C, 53.06; H, 6.12; N, 19.04. Found: C, 52.84; H, 6.10; N, 18.87.

Acknowledgment

We thank the Council of Scientific and Industrial Research, New Delhi, India, for the financial support of this work.

1. D. S. Sethi, G. C. Joshi, and D. Devaprabhakara. Can. J. Chem. **46**, 2632 (1968).
2. H. C. Brown and G. Zweifel. J. Am. Chem. Soc. **83**, 1241 (1961).
3. H. C. Brown and G. Zweifel. J. Am. Chem. Soc. **82**, 3222 (1960).
4. S. D. Nogare and R. S. Juvet, Jr. Gas-liquid chromatography—theory and practice. Interscience Publishers Inc., New York. 1962. p. 259.
5. H. C. Brown and G. Zweifel. J. Am. Chem. Soc. **83**, 2544 (1961).
6. D. S. Sethi and D. Devaprabhakara. Can. J. Chem. **46**, 1165 (1968).
7. D. J. Cram. J. Am. Chem. Soc. **71**, 3883 (1949).
8. W. R. Moore and H. R. Ward. J. Org. Chem. **27**, 4179 (1962).
9. L. Skattebol. Acta Chem. Scand. **17**, 1683 (1961).
10. K. Alder, R. Braden, and F. H. Flock. Chem. Ber. **94**, 456 (1961).
11. T. V. Stadnichuk, V. A. Korner, and A. A. Petrov. Zh. Obshch. Khim. **34**, 3279 (1964); Chem. Abstr. **62**, 3913 (1965).
12. T. Shenton and J. C. Smith. Chem. Ind. London, 1510 (1958).
13. F. Zobrist and H. Schinz. Helv. Chim. Acta, **35**, 2380 (1952); Chem. Abstr. **48**, 1974b (1954).
14. A. C. Cope and L. Bumgardner. J. Am. Chem. Soc. **79**, 960 (1957).
15. W. R. R. Park and G. F. Wright. J. Org. Chem. **19**, 1435 (1954).
16. F. C. Whitmore and T. K. Sloat. J. Am. Chem. Soc. **64**, 2968 (1942).
17. K. Mislow and J. Brenner. J. Am. Chem. Soc. **75**, 2318 (1953).
18. G. Vavon and D. Ivanoff. Compt. Rend. **127**, 453 (1923).
19. R. Delaby and S. G. Allegre. Bull. Soc. Chim. France, **53**, 301 (1933).
20. M. Hamell and R. Levine. J. Org. Chem. **15**, 162 (1950).

The infrared absorption spectra of thiosemicarbazide and related compounds: NH_2 and NH vibrations[1]

D. M. WILES AND T. SUPRUNCHUK
Division of Applied Chemistry, National Research Council of Canada, Ottawa, Canada

Received August 8, 1968

In the infrared absorption spectra of thiosemicarbazide (I), aldehyde thiosemicarbazones (II), and N-methyl derivatives of these compounds, the following assignments are proposed: $\nu_a(N^dH_2)$ absorbs in the vicinity of 3400 cm^{-1}; N^aH_2 vibrations are observed in the region of 1630 cm^{-1}; there is a significant contribution from $\nu(N^bH)$ at or near 3170 cm^{-1}. These conclusions probably apply to other thioamides and amides having related structures.

Canadian Journal of Chemistry, **47**, 1087 (1969)

Can. J. Chem. Downloaded from www.nrcresearchpress.com by 210.87.254.6 on 09/05/12
For personal use only.

Much information is available in the literature concerning the infrared spectra of amines and amides. Although less is known about infrared absorption by thioamides and thiosemicarbazones, studies have been published of the hydrogen bonding in these compounds (1), and of the C=S absorption in thiourea (2, 3) and in thioformamide (4). Mashima (5) has discussed in detail the infrared spectra of hydrazine-N,N′-bis-thiocarbonic acid amide, thiosemicarbazide, formyl thiosemicarbazide, and acetyl thiosemicarbazide and the spectra of the deuterated analogues. In this latter work, some success was achieved in attributing particular absorption bands to particular bonds, e.g., C=S, NH, and NH_2. Some of the assignments, however, are ambiguous, owing in part to the complexity of the molecules and the coupling between bond vibrations.

In earlier work from these laboratories (6, 7), the major contribution by C=S stretching vibrations to the infrared spectra of thiosemicarbazones was established as being in the 830 to 805 cm^{-1} region. In the present work we have used a similar approach to locate the absorption by

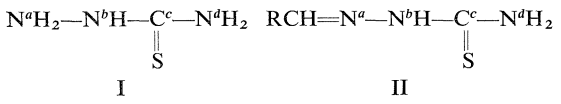

I II

N^aH_2, N^bH, and N^dH_2 both in thiosemicarbazide (I) and in thiosemicarbazones (II) of aliphatic and aromatic aldehydes (R = C_6H_{13}, C_7H_{15}, $C_{10}H_{21}$, and C_6H_5). Infrared spectra of these compounds were compared with those of the N^b-methyl, N^d-methyl, and N^d-dimethyl analogues in order to identify with some confidence the desired absorptions. The advantage of using the thiocarbonyl compounds rather than the corresponding carbonyl compounds is that the C=S stretching vibrations do not give rise to absorptions in the conventional "double-bond region", thus simplifying the spectra in this region.

Experimental

Thiosemicarbazide was obtained from commercial sources and was recrystallized from water, m.p. 183 °C.

All the methyl-substituted thiosemicarbazides were prepared by standard methods (8–12) and had melting points identical with those reported previously.

The aliphatic and aromatic aldehydes for synthesizing the thiosemicarbazones (II) were obtained from commercial sources and were used without further purification. The preparation of all but one of the aldehyde thiosemicarbazones listed in Table I has been reported previously (13).

Undecanal 4,4-dimethylthiosemicarbazone was synthesized as follows. To a solution of 4,4-dimethylthiosemicarbazide (0.036 mole) in warm water (100 ml) was added a solution of undecanal (0.036 mole) in ethanol (100 ml) containing 1 ml of glacial acetic acid. This reaction mixture was heated gently on the steam bath for 15 min, then cooled, and neutralized with 1 *N* NaOH solution. The white solid which was recovered, following evaporation of the solvents, was recrystallized repeatedly from *n*-hexane; m.p. 49 °C, yield 40%.

Anal. Calcd. for $C_{14}H_{28}N_3S$: C, 62.80; H, 10.02; N, 15.33; S, 11.67. Found: C, 62.57; H, 10.50; N, 15.37; S, 12.00.

The infrared spectra of the compounds described in this work were obtained from KBr pellets with a model 21 Perkin–Elmer double-beam spectrophotometer (NaCl prism) and with a Beckman IR-8 grating instrument. The frequency range 3500 to 700 cm^{-1} was covered. The frequencies reported in Table I are expected to be accurate within the following limits: for the region 3400 to 3000 cm^{-1}, ± 7 cm^{-1} (model 21), ± 2 cm^{-1} (IR-8); for the region 1700 to 1600 cm^{-1}, ± 5 cm^{-1} (model 21), ± 2 cm^{-1} (IR-8). The reproducibility in all cases was within the limits ± 2 cm^{-1}.

Results and Discussion

Table I lists the important bands in two regions

[1]Issued as NRCC No. 10 485.

TABLE I

Main infrared absorption bands in the 3500 to 3000 and 1650 to 1550 cm^{-1} regions

	Compound	Wavenumber					
1	$N^aH_2N^bHC^cSN^dH_2$	3370 s	3260 s	3170 s	1645 s	1620 s	
2	$NH_2NCH_3CSNH_2$	3410 s	3290 s	3170 m	1620 s (doublet)		
3	$NH_2NHCSNHCH_3$	—	3280 m	3180 m	1640 s	—	
4	$NH_2NHCSN(CH_3)_2$	—	3280 s	3210 m	1630 s	—	
5	$NH_2NCH_3CSNHCH_3$	—	3280 s	3170 w	1630 s	—	
6	$CH_3(CH_2)_5CH{=}N^aN^bHC^cSN^dH_2$	3400 s	3280 s	3160 s	—	—	1595 s
7	$CH_3(CH_2)_6CH{=}NNCH_3CSNH_2$	3420 s	3240 s	3130 m	—	—	1590 s
8	$CH_3(CH_2)_6CH{=}NNHCSNHCH_3$	—	3260 s	3160 m	—	—	1560 br
9	$CH_3(CH_2)_5CH{=}NNCH_3CSNHCH_3$	—	3280 s	—	—	—	1565 br
10	$CH_3(CH_2)_9CH{=}NNHCSN(CH_3)_2$	—	3200 s	3080 w	—	—	1610 m
11	$C_6H_5CH{=}N^aN^bHC^cSN^dH_2$	3400 s	3240 s	3160 s	—	—	1600 s
12	$C_6H_5CH{=}NNCH_3CSNH_2$	3440 s	3260 s	3120 w	—	—	1580 s
13	$C_6H_5CH{=}NNCH_3CSNHCH_3$	—	3340 s	—	—	—	1560 s
14	$C_6H_5CH{=}NNHCSNHCH_3$	—	3325 s	3170 m	—	—	1550 br
15	$C_6H_5CH{=}NNHCSN(CH_3)_2$	—	3260 m	3180 m	—	—	1610 m

of the spectra of N-methyl substituted thiosemicarbazides and N-methyl substituted aldehyde thiosemicarbazones: 3500 to 3000 cm^{-1}, and 1650 to 1550 cm^{-1}. The concept here is that it should be possible to identify a contribution to these spectral regions by the vibration of a particular N—H or NH_2 group by comparison of the absorption bands for the compound with those observed when the relevant hydrogen atom has been replaced by a methyl group.

For thiosemicarbazide (compound **1**), strong bands at 3370, 3260, 3170, 1645, and 1620 cm^{-1} are observed. Replacement of either or both of the hydrogens on N^d by a methyl group (compounds **3** to **5**) results in loss of the 3370 band completely. Replacement of N^b—H by N^b—CH_3 results in a significant intensity loss of the band at 3170 cm^{-1}. It is reasonable to assume that the 3370 band should be attributed to $\nu(N^dH_2)$, presumably the asymmetric mode (14), and that there is a considerable contribution to the 3170 cm^{-1} band by $\nu(N^bH)$; the remainder probably includes N^dH_2 symmetric stretch. In the spectra of the aldehyde thiosemicarbazones (compounds **6** to **15**, Table I), the same phenomena are observed, i.e., methyl substitution at N^d eliminates the band at 3400 cm^{-1} and methyl substitution at the N^b position reduces the absorption in the 3140 to 3170 cm^{-1} region.

The bands near 1645 and at 1620 cm^{-1} are ascribed to $\delta(N^aH_2)$ and $\delta(N^dH_2)$ respectively, since the band near 1645 cm^{-1} occurs only when N^aH_2 is present and the 1620 cm^{-1} band appears only for compound **1** when N^dH_2 remains unsubstituted. The question remains as to why no absorption is observed in the 1620 cm^{-1} region for N^dH_2 deformations in compounds **6**, **7**, **11**, and **12**. The suggestion may be made that such absorption is at a lower frequency here, owing to the electron-withdrawing nature of the groups on the "left" of the thiocarbonyl group, and is obscured by C=N and other absorption bands. These conclusions appear to agree with the data of Campbell and Grzeskowiak (15), although not, apparently, with their interpretation of them.

In the spectra of all of the compounds, except **1** and **11**, appropriate strong absorptions for symmetric methyl group stretching vibrations are observed in the 2960 to 2930 cm^{-1} region. Finally, a medium to strong band for C=N stretch appears in the 1610 to 1560 cm^{-1} region of the spectra of all the thiosemicarbazones. There is likely to be overlap with aromatic ring absorptions in this latter region for compounds **11** to **15**.

Sadler (1) has reported bonded N—H frequencies at 3400 and 3200 cm^{-1} for the 3-thiosemicarbazone, the 3-4′-phenylthiosemicarbazone, and the 3-4′,4′-dimethylthiosemicarbazone of 1-methylisatin. According to the present work, there should be no absorption at 3400 cm^{-1} for the latter compound. It may be, however, that the degree of hydrogen bonding, the complexity, and the asymmetry of the molecule result in ν(NH) absorption at frequencies as high as 3400 cm^{-1}. These reasons could not account for the 3400 cm^{-1} band reported by Sadler (1) for benzaldehyde 4,4′-dimethylthiosemicarbazone; this absorption was not observed in the present work.

Can. J. Chem. Downloaded from www.nrcresearchpress.com by 210.87.254.6 on 09/05/12
For personal use only.

Most of the absorption bands and the assignments of them by Mashima (5) for thiosemicarbazide and related compounds are in agreement with the results shown in Table I and the conclusions based on them. In Mashima's work, however, the band at 3270 cm^{-1} in the spectrum of thiosemicarbazide is said to be "associated with the $\nu(N^aH_2)$ vibration of the $-NHNH_2$ group", i.e., with $\nu(N^aH_2)$. In the present work, there appears to be no contribution, or at most a very small one, to this band from $\nu(N^aH_2)$.

Further evidence for the validity of the assignments made here can be obtained from the absorptions characteristic of other compounds related to thiosemicarbazide. For example, in the infrared spectrum of ethylene dithiosemicarbazide, there are bands at 3340, 3200, and 1645 cm^{-1}; there is no thioamide N^dH_2 group in such dithiosemicarbazides. This is additional support, therefore, for the claim that $\nu_a(N^dH_2)$ absorbs in the 3400 cm^{-1} region and that the amine N^aH_2 group absorbs in the 1645 cm^{-1} region. It is probable that similar considerations apply in the case of related carbonyl compounds (e.g. 5, 16).

Acknowledgments

The authors are indebted to Dr. E. Whalley and Dr. Yoshinori Kato for helpful discussions and to Mr. R. Ironside for measuring some of the infrared spectra.

1. P. W. Sadler. J. Chem. Soc. 957 (1961).
2. A. Yamaguchi, R. B. Penland, S. Mizushima, T. J. Lane, C. Curran, and J. V. Quagliano. J. Am. Chem. Soc. **80**, 527 (1958).
3. K. Swaminathan and H. M. N. H. Irving. J. Inorg. Nucl. Chem. **26**, 1291 (1964).
4. I. Suzuki. Bull. Chem. Soc. Japan, **35**, 1286 (1962).
5. M. Mashima. Bull. Chem. Soc. Japan, **37**, 974 (1964).
6. D. M. Wiles, B. A. Gingras, and T. Suprunchuk. Can. J. Chem. **45**, 469 (1967).
7. D. M. Wiles and T. Suprunchuk. Can. J. Chem. **45**, 2258 (1967).
8. A. H. Greer and G. B. L. Smith. J. Am. Chem. Soc. **72**, 874 (1950).
9. J. Bernstein, W. A. Lott, and F. Y. Wiselogle. U.S. patent 2 635 115 (1953).
10. E. Lieber and P. Ramchandran. Can. J. Chem. **37**, 101 (1959).
11. K. A. Jensen. J. Prakt. Chem. **159**, 189 (1941).
12. G. Traverso. Gazz. Chim. Ital. **83**, 1027 (1953).
13. B. A. Gingras, R. W. Hornal, and C. H. Bayley. Can. J. Chem. **38**, 712 (1960).
14. N. B. Colthup, L. H. Daly, and S. E. Wiberley. Introduction to infrared and Raman spectroscopy. Academic Press, Inc., New York. 1964.
15. M. J. Campbell and R. Grzeskowiak. J. Chem. Soc. A, 396 (1967).
16. D. M. Wiles and T. Suprunchuk. Can. J. Chem. **46**, 701 (1968).

Can. J. Chem. Downloaded from www.nrcresearchpress.com by 210.87.254.6 on 09/05/12
For personal use only.

Can. J. Chem. Downloaded from www.nrcresearchpress.com by 210.87.254.40 on 09/05/12
For personal use only.

Conversion of tetracyclic triterpenes to steroids[1]

GEORGE R. PETTIT AND JERRY R. DIAS[2]
Department of Chemistry, Arizona State University, Tempe, Arizona 85281

Received January 24, 1969

An alternative procedure for converting the typical 3-hydroxy-4,4-dimethyl-substituted triterpene A-ring to a steroidal 3-oxo-4-ene system has been outlined. Application of the new method to 3β-hydroxy-5α-lanostane (**1**) was used for illustration. Key reaction steps involved Baeyer–Villiger oxidation of ketone **3** to lactone **4** and the latter to carboxylic acid **5** employing Jones' reagent. Proceeding *via* enol–lactone (**6**) and diketone (**7**) led to 3-oxo-14α-methyl-cholest-4-ene (**8**). The first example of an oxa-14α-methyl-steroid was also reported.

Canadian Journal of Chemistry, 47, 1091 (1969)

Lanosterol, a typical tetracyclic triterpene (1) contains the 3β-hydroxy-4,4-dimethyl substituted A-ring characteristic of many triterpenes. Synthetic transformation (2–4) of lanosterol to 14α-methyl-steroids requires extensive reconstruction of the A-ring. Indeed, removing the 4,4-dimethyl substituent is a major obstacle in triterpene → steroid conversions. Except for improvements (e.g. see 4) in experimental conditions, the important and useful procedure of Voser and colleagues (5) has remained sole chemical method for obtaining 3-oxo-4-ene-type steroids from triterpenes. Prior attempts[3] (e.g. 3, 6) to make available another method led instead to results more useful in other areas. Now we wish to report a comparable (yield) but potentially more versatile alternative.

Preparation of 3-oxo-14α-methyl-cholest-4-ene illustrates the new route. Isocholesterol (crude lanosterol) was used to synthesize 3β-hydroxy-5α-lanostane (**1**) as previously described (7). Wagner–Meerwein type rearrangement of alcohol **1** to olefin **2** (62% yield, m.p. 110–113°, reported in ref. 3, m.p. 110–112°) was conducted (at 0°) in benzene-toluene containing phosphorous pentachloride. Oxidative (ozone) cleavage of olefin **2** was performed essentially as reported (3) earlier. The product, 5β-ketone **3** (50%, m.p. 126.5–127.5°, positive Cotton effect optical rotatory dispersion curve) was treated (overnight at approximately 10°) with trifluoroperacetic acid (8) and lactone **4** (78%, plates from methanol, m.p. 170.5–172.5°, M^+ 402)[4] was isolated by chromatographing the product on silica gel. A new technique was devised for oxidizing lactone **4** to carboxylic acid **5**. Allowing lactone **4** (2.9 g) to react in acetone (300 ml) with Jones' reagent (4 ml, 8 *N* chromium trioxide, ref. 9) during 3 h afforded (80%) 2.4 g of acid **5** (m.p. 121–123°, needles from diethyl ether – ligroin). Brief contact between acid **5** in ethyl acetate with acetic anhydride-perchloric acid (10) gave enol–lactone **6** (55%, needles from methanol, m.p. 124–125°, M^+ 400). Adding precisely 4 equivalents, of methyl magnesium iodide (11) (in ether) to lactone **6** (0.25 g) in benzene–ether (at ice–salt temperature) over a 3 h period led to diketone **7** which, without further purification, was added to methanol (20 ml) containing 2 ml of 10% sodium hydroxide. The mixture was heated at reflux 1.5 h and ketone **8** (0.15 g, 58%, m.p. 113.5–115°, M^+ 399, reported: ref. 3, m.p. 113–114°) was isolated by preparative thin layer chromatography on silica gel HF_{254} with 5:1 benzene – ethyl acetate as mobile phase.

---

[1]Steroids and Related Natural Products. Part XLVII. For part XLVI, see J. C. Knight and G. R. Pettit, Phytochemistry, **8**, 477 (1969). This investigation was supported by PHS research grants CA-04074-06 and CA-10612-01 from the National Cancer Institute.

[2]National Institutes of Health Predoctoral Fellow 1968–1969.

[3]Recently Professor C. W. Shoppee kindly informed us of his studies toward the same objective.

[4]Acceptable elemental analyses, proton magnetic resonance and infrared spectra were obtained for each new compound. The yields reported correspond to material displaying one spot on a thin-layer chromatogram. Mass spectra were obtained using an Atlas CH-4B mass spectrometer equipped with a molecular beam type inlet system.

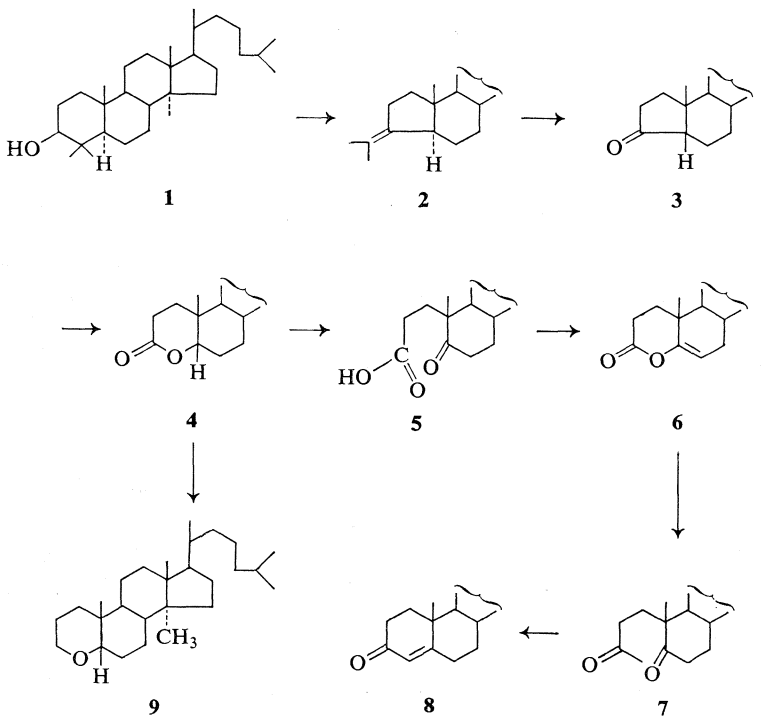

FIG. 1. Conversion of tetracyclic triperpenes to steroids.

The preceding method for transforming certain tetracyclic triterpenes to steroids also allows ready access to 4-oxa-5β-steroids. For example, boron trifluoride – sodium borohydride reduction (12) of lactone **4** easily led to 14α-methyl-4-oxa-5β-cholestane (**9**, 75%, m.p. 55–57°, M^+ 388).

1. G. OURISSON, P. CRABBÉ, and O. RODIG. Tetracyclic triterpenes. *Edited by* E. LEDERER, Holden-Day, Inc., Publ. 1964.
2. W. VOSER, H. HEUSSER, O. JEGER, and L. RUZICKA. Helv. Chim. Acta, **36**, 299 (1953).
3. D. H. R. Barton, D. A. J. IVES, and B. R. THOMAS. J. Chem. Soc. 903 (1954).
4. G. R. PETTIT and P. HOFER. Helv. Chim. Acta, **46**, 2142 (1963); G. R. Pettit and P. HOFER. J. Chem. Soc. 4439 (1963).
5. W. VOSER, D. E. WHITE, H. HEUSSER, O. JEGER, and L. RUZICKA. Helv. Chim. Acta, **35**, 830 (1952).
6. G. R. PETTIT, R. E. KADUNCE, P. SUNDER-PLASSMANN, and J. OCCOLOWITZ. Can. J. Chem. **43**, 2872 (1965).
7. G. R. PETTIT, D. S. ALKALAY, P. HOFER, and P. A. WHITEHOUSE. Tetrahedron, **20**, 1755 (1964).
8. W. D. EMMONS and G. B. LUCAS. J. Am. Chem. Soc. **77**, 2287 (1955).
9. K. BOWDEN, I. M. HEILBRON, E. R. H. JONES, and B. C. L. WEEDON. J. Chem. Soc. 39 (1946).
10. B. E. EDWARDS and P. NARASIMHA RAO. J. Org. Chem. **31**, 324 (1966).
11. R. B. WOODWARD, F. SONDHEIMER, D. TAUB, K. HEUSLER, and W. M. MCLAMORE. J. Am. Chem. Soc. **74**, 4223 (1952).
12. G. R. PETTIT and W. J. EVERS. Can. J. Chem. **44**, 1293 (1966).

Can. J. Chem. Downloaded from www.nrcresearchpress.com by 210.87.254.40 on 09/05/12
For personal use only.

A distorted tetrahedral copper(II) complex: 1,2-bis(diphenylphosphineoxido)ethane copper(II) chloride

M. MATHEW AND GUS J. PALENIK
Department of Chemistry, University of Waterloo, Waterloo, Ontario

Received January 21, 1969

The crystal structure of 1,2-bis(diphenylphosphineoxido)ethane copper(II) chloride has been determined by X-ray diffraction techniques. The compound is the first structual determination of a $CuCl_2$–phosphineoxide adduct and exhibits some very large distortions from the ideal tetrahedral symmetry. The Cl—Cu—O angle is 140.2° and the Cu—Cl distance of 2.195 Å is shorter than in other $CuCl_2$ complexes.

Canadian Journal of Chemistry, 47, 1093 (1969)

Can. J. Chem. Downloaded from www.nrcresearchpress.com by 210.87.254.5 on 09/05/12
For personal use only.

The bis-phosphine oxide adducts of copper(II) halides are assumed to be tetrahedral although no structural studies are available. Since a copper(II) ion in a tetrahedral field is subject to Jahn–Teller distortions, the structural details of tetrahedral copper(II) species are therefore of importance in understanding the Jahn–Teller theorem. We wish to report the first crystal structure determination of a bis-phosphine oxide adduct of copper(II) chloride, 1,2-bis(diphenylphosphineoxido)ethane copper(II) chloride, $CuCl_2$·DPPO. This compound, $CuCl_2$·DPPO, exhibits some of the largest distortions found in a nominally tetrahedral molecule as well as one of the shortest Cu—Cl bonds found in a copper(II) complex.

The reaction of 1,2-bis(diphenylphosphino)-ethane, DPP, with copper(II) chloride yields a product which is rapidly oxidized in air to the compound 1,2-bis(diphenylphosphineoxido)ethane copper(II) chloride (1). The preparation of $CuCl_2$·DPPO provided an opportunity to test the hypothesis of Goodgame and Cotton (2) that the bis(triphenylphosphine oxide) copper(II) chloride complex was tetrahedral. In addition, the presence of a seven-membered chelate ring involving the DPPO moiety was an interesting possibility.

Recrystallization of $CuCl_2$·DPPO from *n*-butanol yielded greenish-blue crystals. Preliminary measurements indicated the crystals to be monoclinic with $a = 12.206 \pm 0.002$, $b = 20.172 \pm 0.004$, $c = 10.559 \pm 0.002$ Å, and $\beta = 97.26 \pm 0.02°$. The density calculated for 4 molecules per unit cell is 1.454 g/cm^3, in good agreement with the measured value of 1.46 g/cm^3. The space group is either *Cc* or *C*2/*c* with the latter indicated by intensity statistics. Intensity data were measured from a small equidimensional crystal (0.15 mm an edge) using a General Electric XRD-6 automatic diffractometer. The stationary crystal – stationary counter method was used to measure all the reflections with $2\theta \leq 135°$ with copper radiation. A total of 2161 reflections was considered observed and used in the analysis.

A three-dimensional Patterson function was computed from which the positions of the copper, chlorine, and phosphorus were determined. A subsequent Fourier synthesis was used to locate the lighter atoms and a second Fourier synthesis used to refine the atomic positions. The refinement was completed by 3 cycles of least-squares with individual isotropic thermal parameters followed by 4 cycles with anisotropic thermal parameters for all atoms, bringing the usual residual (R) to 0.058. Atomic scattering factors for all atoms were taken from the International tables for X-ray crystallography (3).

The copper atom is situated on a twofold axis with the DPPO molecules being located on a center of symmetry. The resulting structure is an infinite polymer with the DPPO molecules linking $CuCl_2$ units. The copper atom is coordinated to two O atoms from two different DPPO molecules and two Cl atoms. The distances and angles illustrated in Fig. 1 demonstrate that the copper atom is definitely distorted from a tetrahedral configuration. In fact the Cl—Cu—O angle of 140.2° is the largest reported angle for a tetrahedral copper molecule. The large angle is not due to a steric effect since DPPO has only two phenyl rings per phosphorus compared to triphenylphosphine. Furthermore, the O—Cu—O angle is 91.3° while a repulsion between the phosphine–oxide groups might be expected to open the angle. The opening of the Cl—Cu—O angle, therefore, appears to be an electronic

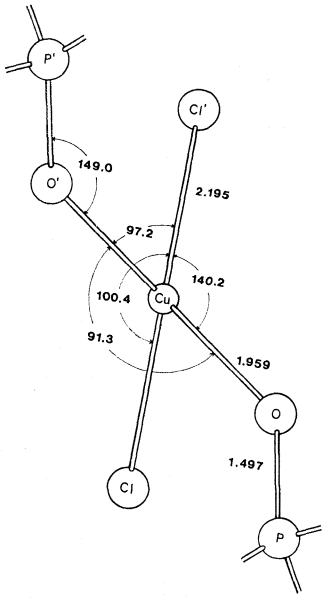

FIG. 1. The coordination around the copper(II) atom is illustrated, together with the pertinent bond distances (in Å) and angles (in degrees). The primed atoms are related by a two-fold axis to the unprimed atoms.

effect. The triphenylphosphine oxide adducts will probably be very distorted also and should only be considered as tetrahedral molecules in the widest sense.

The criteria, suggested by Cruickshank and Robertson (4), indicate that the Cu—Cl distance of 2.195 ± 0.001 Å is significantly shorter than that found in dimeric-μ-(pyridine oxide)-bis(dichlorocopper(II)), 2.211 ± 0.005 Å (5). The Cu—O distance of 1.959 ± 0.003 Å is also significantly shorter than the average Cu—O distance of 2.007 ± 0.011 Å found in the pyridine oxide complex (5). These observations are of importance since the magnetic moment of the pyridine oxide adduct is abnormally low. Therefore, any mechanism used to explain the low moment in the pyridine oxide compound must not involve a shortening of the Cu—O bonds since the bond distances are representative or longer than those found in other four-coordinated copper(II) complexes.

1. A. J. CARTY. Private communication.
2. D. M. L. GOODGAME and F. A. COTTON. J. Chem. Soc. 2298 (1961).
3. International tables for X-ray crystallography. Vol. III. The Kynoch Press, Birmingham, England. 1962. p 203.
4. D. W. J. CRUICKSHANK and A. P. ROBERTSON. Acta Cryst. **6**, 698 (1953).
5. R. S. SAGER, R. J. WILLIAMS, and W. H. WATSON. Inorg. Chem. **6**, 951 (1967).

Can. J. Chem. Downloaded from www.nrcresearchpress.com by 210.87.254.5 on 09/05/12
For personal use only.

Can. J. Chem. Downloaded from www.nrcresearchpress.com by 210.87.254.105 on 09/05/12
For personal use only.

Canadian Journal of Chemistry

Published by THE NATIONAL RESEARCH COUNCIL OF CANADA

VOLUME 47 APRIL 1, 1969 NUMBER 7

Synthesis of 9-β-D-arabinofuranosyl-9*H*-purine-6(1*H*)-thione-5′-phosphate[1]

JOHN PERKINS BELL

Life Sciences Research, Stanford Research Institute, Menlo Park, California 94025

Received June 10, 1968

The 5′-phosphate of 9-β-D-arabinofuranosyl-9*H*-purine-6(1*H*)-thione was obtained by selective protection of the 2′- and 3′-positions followed by phosphorylation with β-cyanoethyl phosphate.

Canadian Journal of Chemistry, **47**, 1095 (1969)

Nucleosides possessing D-arabinofuranose in place of D-ribofuranose moieties have received increasing attention (1) as antimetabolites. Of central importance in pharmacological studies of these nucleoside analogues, is the question of nucleotide formation as an activation step *in vivo*. 9-β-D-arabinofuranosyl-9*H*-purine-6(1*H*)-thione(ara-6MP, **1**) has been shown to have metabolic effects (2) which cannot be easily rationalized by its negligible conversion to a "nucleotide-like" metabolite *in vivo* (3). To resolve this problem the synthesis of the 5′-phosphate of **1** was undertaken.

The first approach utilized the direct phosphorylation of the unprotected nucleoside as successfully applied (4) to the 6-amino analogue of **1** using Tener's β-cyanoethyl phosphate(β-CEP) procedure (5). A high yield of a triphosphate of **1** was isolated; however, analyses indicated the absence of labile phosphate which suggested that the phosphorylation had occurred at the 2′-, 3′-, and 5′-positions (6).

A second, more rational approach involved the selective protection of the 2′- and 3′-hydroxyls prior to phosphorylation (7). Thus, reaction of ara-6MP (**1**) with triphenylchloromethane (trityl chloride) at room temperature gave 5′-trityl-ara-6MP (**2**) as the only product as indicated by t.l.c. (thin-layer chromatography) analysis. No evidence for tritylation of the 6-thio group was found; tritylation of 9-β-D-ribofuranosyl-9*H*-purine-6(1*H*)-thione (the ribosyl analogue of ara-6MP) occurs at both the 5′-OH and the 6-thio groups under more forcing conditions (8). One trityl group was revealed in the n.m.r. (nuclear magnetic resonance) spectrum of compound **3**, the acetylated trityl-ara-6MP. Furthermore, as an indication that tritylation occurred only at the 5′-position, the 5′-proton multiplet in the n.m.r. spectrum of **3** shifted 0.3 p.p.m. downfield in the de-tritylated intermediate **4** obtained by mild aqueous acetic acid treatment. In contrast, only minor shifts were observed for the acetate and nucleoside protons. These findings are similar to experiences in the arabinosyl cytosine series (7).

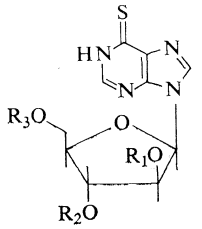

1 $R_1 = R_2 = R_3 = H$
2 $R_1 = R_2 = H$; $R_3 = \phi_3C$
3 $R_1 = R_2 = Ac$; $R_3 = \phi_3C$
4 $R_1 = R_2 = Ac$; $R_3 = H$

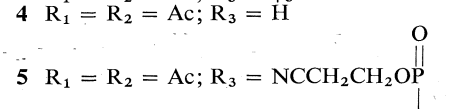

5 $R_1 = R_2 = Ac$; $R_3 = NCCH_2CH_2OP(O)(OH)$

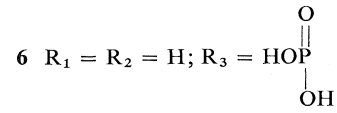

6 $R_1 = R_2 = H$; $R_3 = HOP(O)(OH)$

[1]This work was supported by Contract No. PH 43-65-575 with the Cancer Chemotherapy National Service Center, National Cancer Institute, United States National Institutes of Health.

Can. J. Chem. Downloaded from www.nrcresearchpress.com by 210.87.254.105 on 09/05/12
For personal use only.

2′,3′-diacetyl-ara-6MP (**4**) underwent phosphorylation by the Tener procedure only with a large excess of reagents. This may be partly explained by the water of hydration found in **4**. The β-cyanoethyl phosphorylated intermediate **5** was not isolated but was directly treated with ammonium hydroxide which removed both the β-cyanoethyl and acetyl protecting groups. The resulting 5′-phosphate **6** was purified by standard procedures, and was found to possess the expected mobilities on paper chromatograms. Analyses revealed one "bound" phosphate group, and compound **6** was found to be a substrate for crude snake venom phosphomonoesterase, yielding only ara-6MP (**1**) under conditions favoring 5′-nucleotidase activity. Radiosulfur labeled ara-6MP phosphate was easily prepared by exchange of the thione group with rhombic sulfur-35.

Studies of the metabolic fate and effects of the labeled ara-6MP phosphate in extracts of mouse ascites tumor cells are now in progress.

Experimental

General

Paper chromatography by the descending technique was performed on Whatman 3 MM paper with the following solvent systems: solvent *a*, isopropyl alcohol – concentrated NH_4OH–H_2O (7:1:2 v/v); solvent *b*, isobutyric acid – concentrated NH_4OH–H_2O (15:1:10 v/v); solvent *c*, 95% ethanol – saturated NaB_4O_7 – 5*M* NH_4OAc – 0.25*M* EDTA (660:240:60:3); solvent *d*, 5% KH_2PO_4.

Thin-layer chromatography (t.l.c.) was performed on microscope slides coated with Silica Gel HF. Spots of tritylated derivatives were located by ultraviolet (u.v.) absorption and coloration with HCl fumes. Spots of phosphate derivatives were located on paper chromatograms with the Hanes–Isherwood spray, followed by u.v. irradiation (9). Paper chromatograms of radioactive compounds were cut into 1 × 3.5 cm strips and counted in a toluene fluor on a Nuclear-Chicago scintillation instrument.

Reagent grade pyridine was stored over KOH pellets before use. Melting points were taken on a Fisher–Johns hot stage and are uncorrected. Elemental analyses were carried out by Stanford Research Institute Analytical Services. Infrared (i.r.) spectra were recorded on a Perkin–Elmer 137 spectrometer, and ultraviolet spectra were recorded on a Gary model 11 spectrophotometer. Nuclear magnetic resonance (n.m.r.) spectra were taken on a Varian instrument at 60 Mc.p.s. with chemical shifts given in p.p.m. relative to external tetramethylsilane. Pertinent n.m.r. data are listed as chemical shift, number of protons, multiplicity (s, d, t, q, and m, indicating singlet, doublet, triplet, quartet, and multiplet, respectively), and coupling constant (*J*) in that order. Compounds were dried by storing *in vacuo* at room temperature over NaOH flakes and concentrated H_2SO_4; pyridine was removed in the same way.

9-(5′-O-Trityl-β-D-arabinofuranosyl)-9H-purine-6(1H)-thione (2)

A solution of 284 mg (1 mmole) of ara-6MP (**1**) and recrystallized (10) triphenylchloromethane (306 mg, 1.1 mmole) in 5 ml of dry pyridine was held at room temperature until t.l.c. analysis of evaporated samples (20% ethanol in chloroform) showed that ara-6MP was replaced by a single faster moving, trityl-positive component in 24 h. The pyridine was removed and the glassy residue triturated in water to remove traces of pyridine and starting material. After thorough drying, the solid was freed of triphenylcarbinol by trituration in ether to afford 413 mg of a white powder (79% yield). For analysis, a sample was recrystallized from methanol–chloroform; m.p. 192–196; i.r. λ_{max} (mull) 3.0–3.2, 6.28, 6.55, and 10.35 μ; u.v. λ_{max} (95% EtOH) 323 mμ (ε 19 500).

Anal. Calcd. for $C_{29}H_{26}N_4O_4S \cdot CH_3OH$: C, 64.50; H, 5.42; N, 10.02; S, 5.74. Found: C, 64.84; H, 5.14; N, 9.97; S, 5.29.

9-(2′,3′-Diacetyl-5′-O-trityl-β-D-arabinofuranosyl)-9H-purine-6(1H)-thione (3)

A solution of 583 mg (1.04 mmole) of crude trityl-ara-6MP (**2**) plus 1.5 ml of acetic anhydride in 8.5 ml of dry pyridine was stirred over night. Evaporation and trituration of the residue in methanol gave 262 mg (38%) of colorless **3** containing traces of triphenyl carbinol and a non-trityl containing component (possibly 2′,3′,5′-triacetytated ara-6MP) as indicated by t.l.c. in 10% ethanol in chloroform. Recrystallization was accomplished by adding $CHCl_3$ to a suspension of **3** in hot methanol until solubilization occurred; partial evaporation initiated crystallization: m.p. 258–263 (dried overnight); i.r. λ_{max} (mull) 5.70, 6.28, 6.37, 8.20, 8.33, and 10.24 μ; u.v. λ_{max} (95% EtOH) 323 mμ (ε 17 850); n.m.r. (DMSO-d_6), 1.7 (3H, s), 2.07 (3H, s), 3.44 (2H, broad s), 4.28 (1H, m), 5.53 (2H, broad m, 5 c.p.s. wide), 6.53 (1H, d, J = 4.5 c.p.s.), 7.32 (15H, broad s), 8.12 (1H, s), 8.22 (1H, s), and 13.8 (0.75 H, broad s).

Anal. Calcd. for $C_{33}H_{30}N_4O_6S \cdot 0.5\ CHCl_3$: C, 60.17; H, 4.59; N, 8.38; S, 4.78. Found: C, 59.68; H, 4.57; N, 8.47; S, 4.51.

9-(2′,3′-Diacetyl-β-D-arabinofuranosyl)-9H-purine 6(1H)-thione (4)

Pure diacetyl-trityl-ara-6MP (**3**) (450 mg, 0.673 mmole) was stirred in 200 ml of 80% aqueous acetic acid at room temperature until t.l.c. analysis (10% EtOH in $CHCl_3$) showed the disappearance of starting material and the appearance of a new, non-tritylated derivative, plus triphenyl carbinol. After 18 h, the clear solution was rotary evaporated *in vacuo* (45° bath) and further dried *in vacuo* at room temperature over night. Trituration of the crystalline residue in boiling ether gave 227 mg of colorless (**4**) (89% yield). A sample was recrystallized from methanol for analysis: m.p. 234–244 (decomp.); i.r. λ_{max} (mull) 2.92, 3.03, 5.70, 6.22, 6.35, 6.51, 8.05, 8.12, and 8.27 μ; u.v. λ_{max} (95% EtOH) 323 mμ (ε 23 100) and λ shoulder 225 mμ (ε 7650); n.m.r. (DMSO-d_6), 1.74 (3H, s), 2.06 (3H, s), 3.70 (2H, m), 4.12 (1H, m), 5.50 (2H, broad m, 7 c.p.s. wide), 6.50 (1H, d, J = 3.5 c.p.s.), 8.22 (1H, s), 8.48 (1H, s).

Anal. Calcd. for $C_{14}H_{16}N_4O_6S \cdot 0.5\ H_2O$: C, 44.56; H, 4.54; N, 14.85; S, 8.50. Found: C, 44.75; H, 4.41; N, 14.99; S, 8.09.

9-β-D-Arabinofuranosyl-9H-purine-6(1H)-thione-5′-phosphate (6)

A mixture of 286 mg (0.76 mmole) of crude 2′,3′-diacetyl-ara-6MP (**4**) and 9.1 ml of β-CEP (4.55 mmole) in pyridine (5) was dried overnight. The residue was stirred with 2.85 g (13.7 mmole) of dicyclohexylcarbodiimide in 38 ml of dry pyridine until t.l.c. analysis (10% ethanol in chloroform) showed that the starting material had disappeared (24 h). Water was added (9 ml) and stirring was continued for another hour. Water was added (20 ml) to precipitate most of the dicyclohexylurea, and after 2 h of stirring, the filtrate was rotary-evaporated under high vacuum to a yellow residue, assumed to be the intermediate **5**. To remove the acetyl and β-cyanoethyl protecting groups, the above residue was stirred in 30 ml of 9 *N* NH_4OH at 55–60° for 1 h. Dicyclohexylurea was filtered off and rotary evaporation of the filtrate carried out under high vacuum (45° bath temp) to a volume suitable for application to a 2 × 7.5 cm Dowex-50-H^+ column. Elution with deionized water until neutral (90 ml) and addition of saturated $Ba(OH)_2$ to attain pH 8 gave a precipitate of barium phosphate which was filtered off after refrigeration overnight. The volume of the filtrate was reduced to 20 ml; adding 2 volumes of ethanol at 0 °C precipitated the crude barium salt of ara-6MP-5′-phosphate (**6**) which was separated by centrifugation and washed with ethanol, acetone, and then ether: 474 mg (> 100% yield) of a white powder. Analysis for inorganic phosphate indicated 0.03% contamination on a molar basis; i.r. λ_{max} (mull) 3.1 (broad), 4.4 (weak, β-CEP), 6.26, 6.5, 8.35 (broad), 9.2 (very broad), and 10.15 (broad) μ; u.v. λ_{max} (pH 1), 324 mμ (ε 7370 assuming a molecular weight of 571.7 (11)). Chromatography in solvents *a* and *b* indicated the presence of β-CEP.

The free phosphate **6** was regenerated from its crude barium salt by absorbing 230 mg on a 1 × 10 cm Dowex-50-H^+ column and eluting at 1 ml/min with deionized water. One-millilitre fractions were collected, and those containing the β-CEP (by analysis of a replicate chromatography of β-CEP) and initial amounts of the desired phosphate **6** (by u.v. analysis) were discarded. Fractions 11 to 30 were pooled and rotary evaporated under high vacuum at 30–40 °C to afford 53 mg of yellow **6**. The analytical sample was recrystallized from water. Analysis for esterified phosphate (12) revealed 1.005 equivalents per mole of ara-6MP-phosphate·$2H_2O$; i.r. λ_{max} (mull) 3.0 (shoulder), 3.2, 6.15, 6.40, 7.95, 8.30, 8.75, 9.30, 9.70, and 10.5 μ; u.v. λ_{max} (pH 7.0) 319 mμ (ε 24 100) and 226 mμ (ε 9 800).

Anal. Calcd. for $C_{10}H_{13}N_4O_7PS \cdot 2H_2O$: C, 30.00; H, 4.28; N, 14.00; S, 8.01. Found: C, 30.23; H, 4.26; N, 13.66; S, 7.69.

Radiosulfur-labeled ara-6MP-5′-phosphate (**6**) was prepared by exchange of its thione group with rhombic sulfur-^{35}S in refluxing pyridine (13) as follows: A suspension of 52.5 mg (0.131 mmole) of **6** and 16 mg (0.5 mmole) of rhombic-^{35}S (The Radiochemical Centre, Amersham, England) in 10 ml of dry pyridine was gently refluxed for 2 h. The pyridine was removed; the residue was taken up in water, filtered to remove the insoluble ^{35}S, and the filtrate was evaporated *in vacuo* at 35°. This process was repeated two more times; 25 mg of the ^{35}S labeled ara-6MP-5′-phosphate **6** crystallized from 3 ml of water as yellow leaflets. The spectral and chromatographic characteristics were the same as those of unlabeled **6**. The specific activity was 1.5 × 10^6 cpm/μmole, and the radiochemical purity was >92%. One-fourth of the impurities was identified as ara-6MP by paper chromatographic analyses in the following solvents.

Solvent	R_f of ara-6MP	R_f of ara-6MP-5′-phosphate
a	0.37	0.05
b	0.47	0.26
c	0.51	0.09
d	0.62	0.73

Following a standard procedure (14), the labeled phosphate **6** (0.3 μmoles) was 20% dephosphorylated with 0.1 mg of crude snake venom phosphomonoesterase and 43% dephosphorylated with 0.2 mg of the enzyme after 1 h incubation at 37 °C in a pH 8.2 buffer containing magnesium chloride (15). Chromatography in solvent *c* revealed ara-6MP (**1**) as the only product.

Acknowledgments

The author wishes to thank Dr. G. A. LePage, in whose laboratory this work was carried out, for helpful discussions, and Dr. Leon Goodman for generous supplies of ara-6MP and for his critique of the manuscript.

1. S. S. Cohen. Introduction to the biochemistry of D-arabinosyl nucleosides. *Edited by* J. N. Davidson and W. E. Cohn. *In* Progress in nucleic acid research and molecular biology. Vol. 5. Academic Press, Inc., New York. 1966. pp. 1–88.
2. A. P. Kimball, B. Bowman, P. S. Bush, J. Herriot, and G. A. LePage. Cancer Research **26**, 1337 (1966).
3. A. P. Kimball, G. A. LePage, and B. Bowman. Can. J. Biochem., **42**, 1753 (1964).
4. J. J. Furth and Seymour S. Cohen. Cancer Research **27**, 1528 (1967).
5. G. M. Tener. J. Am. Chem. Soc. **83**, 159 (1961).
6. A. P. Kimball. Unpublished results.
7. William J. Wechter. J. Med. Chem. **10**, 762 (1967).
8. H. Jeanette Thomas, Kathleen Hewson, and John A. Montgomery. J. Org. Chem. **27**, 192 (1962).
9. R. M. C. Dawson, Daphne C. Elliott, W. H. Elliott, and R. M. Jones (*Editors*). Data for biochemical research. Oxford University Press, Fair Lawn, New Jersey. 1959. p. 250.
10. W. E. Bachmann. Org. Syn. Coll. Vol. 3, 841 (1955).
11. J. A. Montgomery and H. J. Thomas. J. Org. Chem. **26**, 1926 (1961).
12. G. A. LePage. Methods for the analysis of phosphorylated intermediates. W. W. Umbreit, R. H. Burris, and J. F. Stauffer. *In* Manometric techniques, Burgess Publishing Co., Minneapolis, Minnesota. 1957. pp. 272–273.
13. J. Moravek and Z. Nejedly. Chem. and Ind. 530 (1960).
14. A. P. Kimball, G. A. LePage, and P. S. Allinson. Cancer Research **27**, 106 (1967).
15. L. A. Heppel and R. J. Hilmore. 5′-Nucleotidases *Edited by* S. P. Colowick and N. O. Kaplan. *In* Methods of enzymology. Vol. II, Academic Press Inc., New York. 1955. p. 549.

Can. J. Chem. Downloaded from www.nrcresearchpress.com by 210.87.254.105 on 09/05/12
For personal use only.

Acetoacetyl pyrroles and their boron complexes

M. W. ROOMI[1]

Organisch-Chemisches Institut, der Technische Hochschule, München, West Germany

Received September 19, 1968

Various boron complexes of acetoacetyl pyrrole have been synthesized and their nuclear magnetic resonance and infrared spectra showed that the complexes formed are six member chelate.

Canadian Journal of Chemistry, **47**, 1099 (1969)

Complexes of boron with acetylacetone are well known (1–3). In contrast no studies on boron complexes with acetoacetyl pyrroles have been recorded. This paper describes the preparation of the boron complexes of various 2- and 3-acetoacetyl pyrroles and an investigation of their structures utilizing nuclear magnetic resonance (n.m.r.) and infrared spectroscopy in addition to the chemical degradation. The 2-acetoacetyl pyrroles can form two types of complexes. In one case the complex is formed entirely with the acetoacetyl moiety resulting in the formation of a six member chelate (4–6), while in the other the pyrrole nitrogen participates with the complex formation resulting in a five member chelate (7).

The various acetoacetyl pyrroles used in this investigation were prepared by the reaction of the parent pyrroles with ketene dimer as described by Treibs and Michl (4). The particular pyrroles were chosen to provide three structurally distinct types having functional groups as follows (*i*) a 2-acetoacetyl group and an N—H, (*ii*) a 3-acetoacetyl group and an N—H but with methyl groups at 2 and 5, (*iii*) a 2-acetoacetyl group and an N—CH_3 group.

The infrared spectra of **1–4** showed a sharp band in the 3300 cm^{-1} region and a broad strong band in the 1600–1640 cm^{-1} region characteristic of the N—H and β-diketone function respectively. The spectrum of **5** lacked the N—H absorption but showed an absorption at 1600 cm^{-1} attributed to the free carbonyl.

The n.m.r. spectrum of **1** in $CDCl_3$ showed it to be a mixture of enol **1***ii* or **1***iii* (62%) and keto-1 (38%) tautomers. Similarly **2–5** were observed to be mixtures of enol and keto in the following ratios; 68:22, 62:38, 53:47 and 60:40.

On treatment with boron trifluoride etherate in benzene or ether the acetoacetyl pyrroles **1–5** all gave boron complexes in 80–90% yield. The infrared spectrum of **1***a* has bands at 3378 cm^{-1} (N—H) and 1565 cm^{-1} (chelated carbonyl (8, 9)). It is of special importance to point out that the N—H band showed an increase in frequency and the β-diketone band showed a decrease in frequency relative to those of **1**. This increase in frequency is attributed to the absence of hydrogen bonding to the N—H group in the complex. The N—H is hydrogen bonded in the original compound. The decrease in frequency of the β-diketone is attributed to the coordination of the acetoacetyl group to boron. The decrease in frequency is a measure of the degree of coordination (9) and quite strong coordination is indicated in this case. The infrared evidence points towards a complex involving only the acetoacetyl moiety.

The infrared spectra of **2***a*–**5***a* all resemble that of **1***a* and show the same shift relative to the starting material. That of **5***a* is similar except that it of course lacks the absorption of the N—H at 3200 cm^{-1}. This indicates that they too have structures analogous to **1***a*.

The n.m.r. spectra of **1** (Fig. 1) in $CDCl_3$ exhibit signals at (δ values) 2.05, 2.3, 3.85, 5.9, 6.3, 7.0, and 9.83 p.p.m. with relative intensities of 3:3:2:1:2:1. A comparison of the spectrum with that of the pyrrole leads to the assignment of the signals at 7.0 and 6.3 to the α- and β-hydrogen of the pyrrole ring respectively. The signals at 2.05 and 2.3 are assigned to the protons of the enolic and keto methyl groups, while those at 3.85 and 5.9 are attributed to the —CH= and —CH_2 groups in the keto and enol form.

The n.m.r. spectra of **1***a* (Fig. 2) in $CDCl_3$ exhibit signals at 2.25, 6.2, 6.7, 7.25, and 9.76 p.p.m. with relative intensities of 3:1:1:2:1. A comparison of this with the spectrum of **1** leads to the assignment of the signals at 7.25 and 6.7 to the α- and β-hydrogen of the pyrrole and the signals at 6.2 and 2.25 to the —CH= and methyl protons of the acetoacetyl moiety respectively. The disappearance of the peaks

[1]Present address: Division of Pure Chemistry, National Research Council of Canada, Ottawa, Canada.

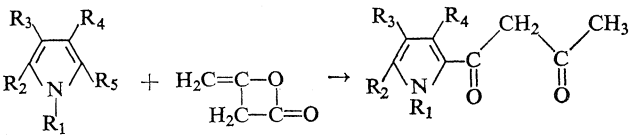

1-5

	R_1	R_2	R_3	R_4	R_5
1	H	H	H	H	Acac*
2	H	CH_3	H	CH_3	Acac
3	H	CH_3	C_2H_5	CH_3	Acac
4	H	CH_3	H	Acac	CH_3
5	CH_3	CH_3	H	CH_3	Acac

*Acac—C(=O)—CH_2—C(=O)—CH_3.

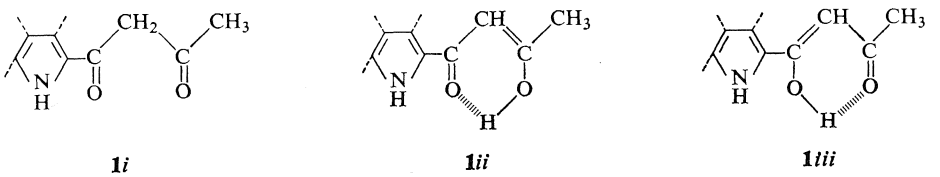

1*i* **1*ii*** **1*iii***

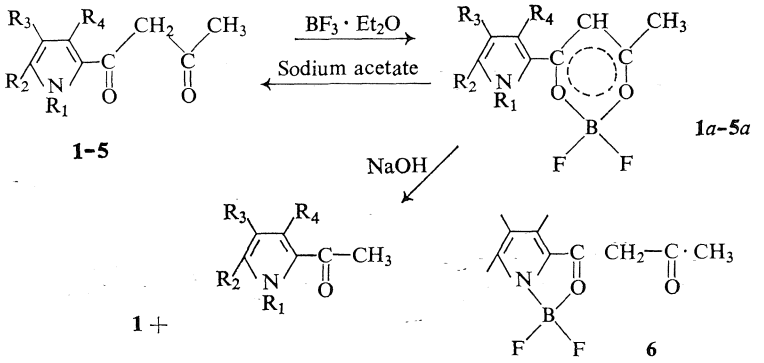

1-5 **1*a*-5*a***

1 + **6**

at 2.3 and 3.85 and a broadening of the signal for N—H at 9.76 p.p.m. in conjunction with the frequency shift observed in the infrared spectra clearly show that the complex has formed on the acetoacetyl moiety in the formation of a six member chelate and does not involve reaction with the nitrogen.

The n.m.r. spectra of the complexes derived from **2**–**5** similarly show only the signals attributed to the enol form of the acetoacetyl groups. This shows they all have the same type of structure as postulated for **1***a*.

Refluxing the boron complexes with aqueous sodium acetate regenerated the starting acetoacetyl pyrroles (10, 11). Similar treatment with aqueous sodium hydroxide gave both the starting acetoacetyl pyrrole and the corresponding acetyl compound, presumably due to ketonic cleavage of the regenerated starting material.

Experimental

All melting points are uncorrected. Nuclear magnetic resonance (n.m.r.) measurements were carried out in $CDCl_3$ containing tetramethylsilane as internal standard using Varian A-60 machine. Infrared spectra were obtained in Nujol on Perkin–Elmer Infracord model 137E.

*1,3-Butanedione-1(2-pyrryl) (**1**)*

This compound was prepared according to the method of Treibs and Michl (4) m.p. 85–87°. Infrared spectrum (Nujol): N—H 3268 cm^{-1}, C=O 1639 cm^{-1}.

Anal. Calcd. for $C_8H_9NO_2$: C, 63.50; H, 6.00; N, 9.27. Found: C, 63.58; H, 5.98; N, 9.23.

*Difluoro[1(2-pyrryl)-1,3-butanediono]borane (**1a**)*

A solution of **1** (75 mg) in benzene (5 ml) was treated with $BF_3{\cdot}Et_2O$ (90 mg) and stirred, the complex separated

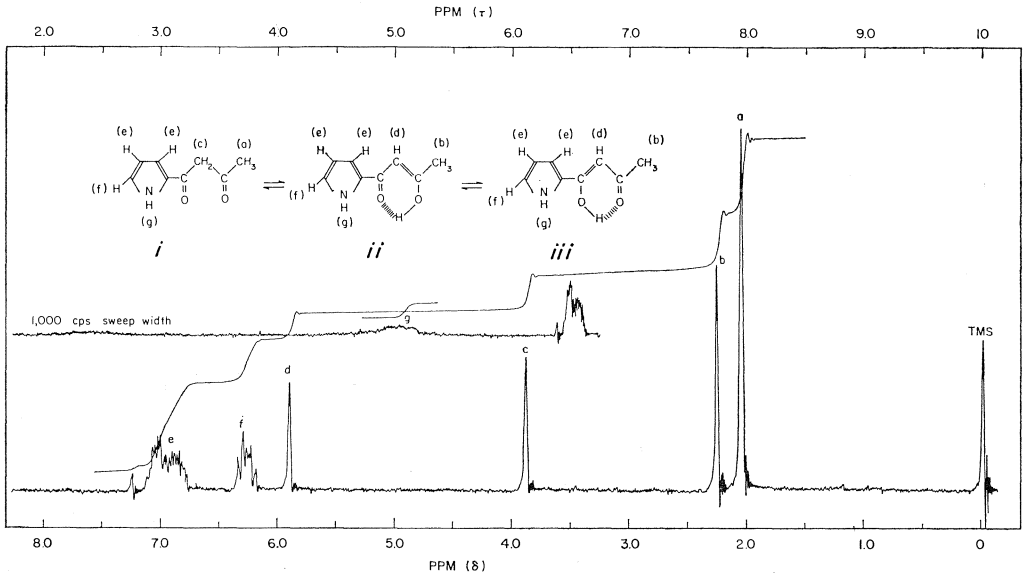

FIG. 1. The nuclear magnetic resonance spectrum of **1** (**1***i*, **1***ii*, and **1***iii*) in $CDCl_3$.

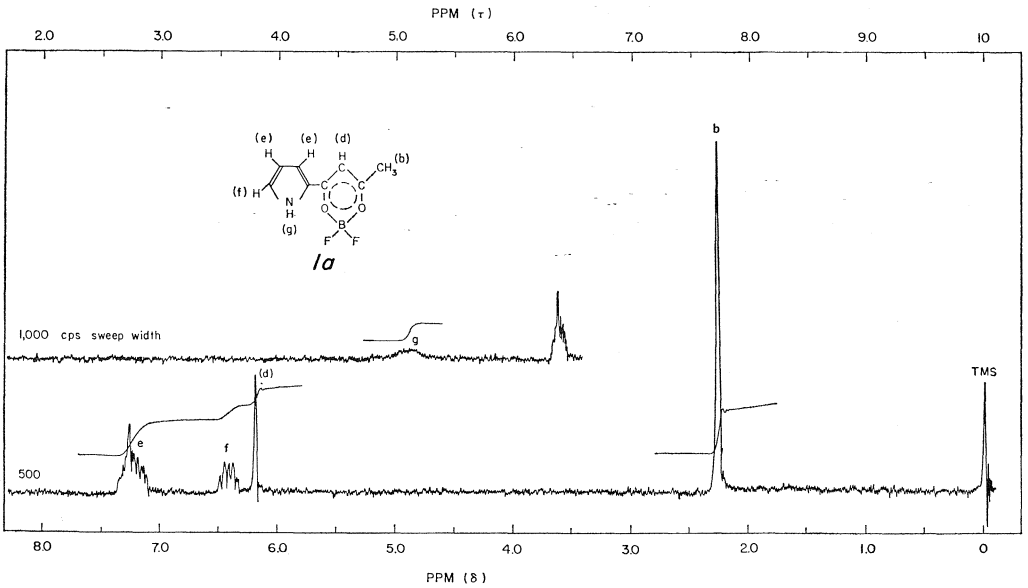

FIG. 2. The nuclear magnetic resonance spectrum of **1***a* in $CDCl_3$.

out, was filtered, washed, dried, and crystallized from benzene gave (75 mg) of the boron complex m.p. 144–146°; infrared spectrum (Nujol): N—H 3378 cm^{-1}, C=O 1565 cm^{-1}.

Anal. Calcd. for $C_8H_8NO_2BF_2$: C, 48.31; H, 4.05; N, 7.03; B, 5.44; F, 19.10. Found: C, 48.24; H, 4.12; N, 7.21; B, 5.24; F, 18.65.

1,3-Butanedione-1(2,4-dimethyl 5-pyrryl) (2)

2 was prepared by reacting 2,4-dimethyl pyrrole with diketene dimer (4) m.p. 106–108°. Infrared spectrum (Nujol): N—H 3279 cm^{-1}, C=O 1639 cm^{-1}. Nuclear magnetic resonance spectrum in $CDCl_3$ showed signals at 2.1, 2.26, 2.3, and 2.35 (singlets, 3H each, enol CH_3, keto CH_3 α- and β-CH_3) 3.9 (singlet, 2H, keto CH_2)

5.86 (broad triplet, enol H and β-H) and 9.83 p.p.m. (singlet, 1H, NH).

Anal. Calcd. for $C_{10}H_{13}NO_2$: C, 67.00; H, 7.31; N, 7.82. Found: C, 66.91; H, 7.23; N, 8.12.

*Difluoro[1(2,4-dimethyl 5-pyrryl)-1,3-butanediono]-borane (**2a**)*

A solution of **2** (1.5 g) in benzene (10 ml) was treated with $BF_3{\cdot}Et_2O$ (1.8 g) the yellow complex separated, was filtered, washed, and crystallized from alcohol (1.9 g) as yellow needles m.p. 216–218°. Infrared spectrum (Nujol): N—H 3367 cm^{-1}, C=O 1575 cm^{-1}. Nuclear magnetic resonance spectrum in pyridine ($CDCl_3$ insoluble) 2.16, 2.26, and 2.33 (singlets, 3H each, enol CH_3, α- and β-CH_3) 5.96 (doublets, β-H), and 6.16 p.p.m. (singlet, enol H).

Anal. Calcd. for $C_{10}H_{12}NO_2BF_2$: C, 52.90; H, 5.29; N, 6.17; B, 4.76; F, 16.76. Found: C, 52.81; H, 5.54; N, 6.23; B, 4.36; F, 15.75.

*1,3-Butanedione-1(2,4-dimethyl 3-ethyl 5-pyrryl) (**3**)*

2,4-Dimethyl 3-ethyl pyrrole was treated with diketene (4) to give **3** m.p. 86–88°. Infrared spectrum (Nujol): N—H 3279 cm^{-1}, C=O 1629 cm^{-1}. Nuclear magnetic resonance spectrum in $CDCl_3$ 6.2 (triplet, 3H, CH_3—CH_2) 2.8, 2.16, 2.26 (singlets, 3H each) 2.5 (quartet, 2H, CH_3—CH_2) 3.86 (singlet, 2H, keto CH_2) 5.83 (singlet, 1H, enol H) and 9.65 p.p.m. (singlet, NH).

Anal. Calcd. for $C_{12}H_{17}NO_2$: C, 69.55; H, 8.26; N, 6.79. Found: C, 69 43; H, 8.18; N, 6.59.

*Difluoro[1(2,4-dimethyl 3-ethyl 5-pyrryl)-1,3-butanediono] borane (**3a**)*

This was prepared from **3** (56 mg) in benzene (5 ml) and $BF_3{\cdot}Et_2O$ (45 mg), the complex separated, was filtered, washed, and crystallized from benzene (54 mg) as yellow needles m.p. 150–152°. Infrared spectrum (Nujol): N—H 3356 cm^{-1}, C=O 1577 cm^{-1}. Nuclear magnetic resonance spectrum in $CDCl_3$ 6.2 (triplet, 3H, CH_3CH_2) 2.21, 2.33 (singlet, 3H, 6H) 2.5 (quartet, 2H, CH_3CH_2) 6.05 (singlet, 1H, enol H) and 9.43 p.p.m. (singlet, N—H).

Anal. Calcd. for $C_{12}H_{16}NO_2BF_2$: C, 56.52; H, 6.31; N, 5.49. Found: C, 56.65; H, 6.14; N, 5.56.

*1,3-Butanedione-1(2,5-dimethyl 3-pyrryl) (**4**)*

2,5-Dimethyl pyrrole was reacted with diketene (4) to give **4**, m.p. 87–88°. Infrared spectrum (Nujol): N—H 3270 cm^{-1}, C=O 1630 cm^{-1}.

Anal. Calcd. for $C_{10}H_{13}NO_2$: C, 67.00; H, 7.31; N, 7.82. Found: C, 67.18; H, 7.21; N, 7.76.

*Difluoro[1(2,5-dimethyl 3-pyrryl)-1,3-butanediono]-borane (**4a**)*

A solution of **4** (90 mg) in benzene (10 ml) was treated with $BF_3{\cdot}Et_2O$ (90 mg) and allowed to stand at room temperature. The complex separated, was filtered, washed, and crystallized from benzene (95 mg) as yellow needles m.p. 155–157°. Infrared spectrum (Nujol): N—H 3370 cm^{-1}, C=O 1570 cm^{-1}. Nuclear magnetic resonance spectrum in $CDCl_3$ 2.25 and 2.57 (singlets, 6H, 2 times CH_3, α- and α′-CH_3 and 3H, enol CH_3) 6.08 (singlet, 1H, enol H) 6.3 (multiplet, 1H, β-H) and 9.16 p.p.m. (singlet N—H).

Anal. Calcd. for $C_{10}H_{12}NO_2BF_2$: C, 52.90; H, 5.29; N, 6.17; B, 4.76; F, 16.76. Found: C, 52.78; H, 5.35; N, 6.25; B, 4.36; F, 15.98.

*1,3-Butanedione-1(1,2,4-trimethyl 5-pyrryl) (**5**)*

1,2,4-Trimethylpyrrole (12) was treated with diketene to give **5**, m.p. 58–60°. Infrared spectrum (Nujol): C=O 1600 cm^{-1}. Nuclear magnetic resonance spectrum in $CDCl_3$ 2.08, 2.2, 2.3 (singlets, 3H, 3H and 2 times 3H) 3.76 (singlet, 3H N—CH_3) 3.85 (singlet, 2H, keto CH_2) 5.72 (singlet, 1H, enol H) 5.8 p.p.m. (multiplet, 1H, β-H).

Anal. Calcd. for $C_{11}H_{15}NO_2$: C, 68.38; H, 7.82. Found: C, 68.20; H, 7.52.

*Difluoro[1-(1,2,4-trimethyl 5-pyrryl)-1,3-butanediono]-borane (**5a**)*

A solution of **5** (96 mg) in benzene (5 ml) was treated with $BF_3{\cdot}Et_2O$ (90 mg) and stirred, the complex separated, was filtered, washed, and crystallized from benzene (1.02) as yellow needles m.p. 135–137°. Infrared spectrum (Nujol): C=O 1580 cm^{-1}. Nuclear magnetic resonance spectrum in $CDCl_3$ 2.25, 2.28, 2.36 (singlets 3H each, enol CH_3, α- and β-CH_3) 3.83 (singlet, 3H, N—CH_3) 6.01 p.p.m. (multiplet, 2H, enol and β-H).

Anal. Calcd. for $C_{11}H_{14}NO_2BF_2$: C, 54.80; H, 5.85; N, 5.81. Found: C, 54.72; H, 5.96; N, 5.78.

*Hydrolysis of **2a***

(i) By Sodium Acetate

2*a* (20 mg) was refluxed with 10% sodium acetate (10 ml) for 10 min, allowed to cool, the solid separated, was filtered, washed, dried, and identified as **2** m.p. and mixture m.p. 108°.

(ii) By Sodium Hydroxide

2*a* (20 mg) was heated with dilute sodium hydroxide (5 ml) for 10 min. It was cooled, the colorless crystalline precipitate separated, was filtered, washed, dried and identified as 2,4-dimethyl 5-acetyl pyrrole m.p. and mixture m.p. 120°. The mother liquor was acidified with dilute acetic acid, the precipitate separated, was filtered, washed, dried, and identified as **2** m.p. and mixture m.p. 108°.

Acknowledgments

The author wishes to thank Professor Dr. A. Treibs for his keen interest during the progress of the work and Alexander von Humboldt–Stiftung for the award of the Fellowship.

1. W. Dilthey, F. Eduardoff, and F. J. Schumacher. Ann. Chem. **344**, 300 (1906).
2. G. T. Morgan and R. B. Tunstall. J. Chem. Soc. 1963 (1924).
3. A. N. Sagredos. Ann. Chem. **700**, 29 (1966).
4. A. Treibs and K. H. Michl. Ann. Chem. **577**, 129 (1952).
5. E. M. Larsen and G. A. Terry. J. Am. Chem. Soc. **73**, 500 (1951).
6. Howard Steinberg. Organoboron chemistry. Vol. 1. Boron–oxygen and boron–sulfur compounds. Interscience Publishers, John Wiley & Sons, New York. 1964.
7. K. Niedenzu and J. W. Bawson. Boron–nitrogen compounds. Academic Press, Inc., New York. 1965.
8. H. F. Holtzclaw, Jr. and J. P. Collman. J. Am. Chem. Soc. **79**, 3318 (1957).
9. K. Nakamoto, P. J. McCarthy, and A. E. Martell. J. Am. Chem. Soc. **83**, 1272 (1961).
10. C. E. Denoon, Jr. Organic Synthesis Coll. Vol. **3**, 16 (1955).
11. C. R. Hauser, F. W. Swamer, and J. T. Adams. Organic reactions, **8**, 59 (1954).
12. A. Treibs and A. Dietl. Ann. Chem. **619**, 80 (1958).

Can. J. Chem. Downloaded from www.nrcresearchpress.com by 210.87.254.40 on 09/05/12
For personal use only.

Alkaloids of fumariaceous plants. LVII. Miscellaneous observations

R. H. F. MANSKE
Research Laboratories, Uniroyal Limited, Guelph, Ontario

Received November 8, 1968

The isolation of a number of new alkaloids from plants previously investigated is reported. Several known alkaloids have been encountered for the first time in plants also previously examined.

Canadian Journal of Chemistry, **47**, 1103 (1969)

A further investigation of plants already reported upon has disclosed a number of new alkaloids and a number of new sources of known alkaloids. These were recovered from new lots of plant material and from a further study of some mother liquors. Several alkaloids which had been given F-numbers have been shown to be mixtures or have been identified with known bases.

Fumaria officinalis L.

This much investigated plant has been subjected to further study in that a new lot of plant material had become available. The alkaloids already reported (1) were again obtained but the combined mother liquors gave the known scoulerine and two new alkaloids, fumariline, $C_{20}H_{17}O_5N$ and F63, $C_{20}H_{21}O_5N$ which may be identical with fumaritine isolated from *F. schleicheri* Soyer-Willem (2). A request to the senior author (P. S. Massagetov) for a specimen for direct comparison remains unanswered. The structures and properties of F37 (fumaricine), fumaritine, and fumariline have been reported (4).

Corydalis ochroleuca Koch (3)

Five alkaloids, none new but, not previously isolated, isocorydine, l-sinactine, *d*-glaucine, l-scoulerine, and adlumidine were obtained.

Corydalis tuberosa DC. (5)

In addition to the alkaloids which had been shown to be elaborated by this plant there were obtained, capnoidine, domestine, and narcotine. There were also obtained a number of fractions of alkaloids of doubtful homogeneity which are currently under study.

Corydalis pallida (Thunb.) Pers. (6)

Corydaline, cryptopine, and *dl*-stylopine were obtained.

Corydalis sibirica (L.) Pers. (7)

The alkaloid F16 proved to be not quite pure adlumidine. After another recrystallization from chloroform it melted sharply at 237° either alone or in admixture with authentic adlumidine.

Experimental

The mother liquors from previous examinations, together with fresh alkaloids from additional plant material, were reworked by the procedure (8) which has been generally satisfactory. The fractions BS and BSE refer respectively to non-phenolic and phenolic bases whose hydrochlorides are *not* extractable from aqueous solution by chloroform. The fractions BC and BCE are respectively non-phenolic and phenolic bases whose hydrochlorides are extractable from aqueous solution by chloroform. All melting points are corrected.

Fumana officinalis

The bases in the filtrate from which alkaloid F37 (fumaricine) had been crystallized were redissolved in dry chloroform and passed through a long column of ca. 250 g neutral alumina. Four eluates of approximately 200 ml each were obtained, pale-yellow, colorless, pale-orange, and colorless. The two last fractions yielded some more F37. The first two fractions were converted to hydrochlorides and yielded a salt from which the free base was regenerated. When recrystallized from methanol, fumariline (F64), obtained in stout prisms, melted at 138°.

Anal. Calcd. for $C_{20}H_{17}O_5N$: C, 68.37; H, 4.84; N, 3.99; NMe, 4.27. Found: C, 68.29; H, 4.93; N, 3.88; NMe, 4.74.

When this alkaloid was treated with carbon disulfide in concentrated ether solution, there was rapid separation of pale-yellow stout prisms which melted at 92° with gas evolution. A test for carbon disulfide was strongly positive (9) and when this compound was admixed with that melting at 138°, the mixture m.p. was 138°, when slowly heated. The infrared (i.r.) and nuclear magnetic resonance (n.m.r.) spectra of the two compounds were superimposable. The yield of this alkaloid was about 0.3 g from 110 kg of dried plant material, and the yields of scoulerine and fumaritine were about 0.1 and 0.5 g respectively.

The total phenolic base fraction from the above amount of plant material weighed only several grams. It was converted to hydrochloride in methanol and then precipitated with excess dry ether with which the pasty residue was repeatedly triturated. When in contact with acetone containing a trace of methanol it became crystalline and was recrystallized from methanol–acetone and then consisted of a mixture of two hydrochlorides.

Can. J. Chem. Downloaded from www.nrcresearchpress.com by 210.87.254.40 on 09/05/12
For personal use only.

The portion very sparingly soluble in water proved to be the hydrochloride of 1-scoulerine (free base, m.p. and mixture m.p. 205°). The very soluble hydrochloride (m.p. 248°) was converted to free base and this crystallized readily from dry ether in fine colorless needles melting at 157°. Fumaritine, so obtained, gave a nondescript dirty green color with concentrated sulfuric acid.

Anal. Calcd. for $C_{20}H_{21}O_5N$: C, 67.60; H, 5.92; N, 3.94; 1 OMe, 8.73. Found: C, 67.87, 68.00; H, 5.32, 5.56; N, 3.83, 4.13; OMe, 9.00, 9.60.

When a solution of fumaritine in methanol was treated with diazomethane there was rapid evolution of nitrogen and the non-phenolic base isolated from the reaction mixture was identical with fumaricine.

Corydalis ochroleuca

The more soluble fraction from which 1-isocorypalmine had been separated was converted to hydrobromide and the base was then regenerated from the sparingly soluble salt. The free base was recrystallized from methanol–ether and then consisted of colorless plates, m.p. 184°, either alone or mixed with *d*-isocorydine.

The fraction from which the 1-tetrahydropalmatine had been separated was dissolved in dry chloroform and passed through a long column of (ca. 250 g) neutral alumina. The base from the front zone of ca. 100 ml solvent was converted to hydrobromide (m.p. 248° decomp.) and the base regenerated again. When recrystallized from methanol it melted at 175–176°. The m.p. was unchanged when admixed with a specimen of 1-sinactine.

The subsequent eluates gave a fraction which yielded a mixture of perchlorates, pale-yellow needles and stout dark polyhedra. The former, more soluble in acetone, proved to be 1-tetrahydropalmatine perchlorate. The less soluble salt was recrystallized from methanol–acetone (m.p. 233°) and the m.p. was not lowered when the salt was admixed with *d*-glaucine perchlorate. The free base, prepared from the perchlorate, was recrystallized from dry ether and then melted at 120° either alone or mixed with *d*-glaucine.

The combined mother liquors from which the protopine and ochroberine had been separated were dissolved in dilute hydrochloric acid and the bases regenerated and dissolved in dry ether. The solution was filtered through a short column of alumina and then deposited a sparingly soluble base which, when recrystallized from chloroform–methanol, melted at 237° either alone or mixed with adlumidine.

The phenolic fraction BSE in contact with methanol yielded some isocorydine. The bases in the soluble fraction were dissolved in dry chloroform and passed through a column of ca. 250 g neutral alumina. When continued percolation with chloroform removed nothing further, the column was eluted with 4% methanol in chloroform. The residue from the eluate crystallized readily when dissolved in hot methanol. It melted at 208° (*in vacuo*) and the m.p. was unchanged when mixed with 1-scoulerine.

Corydalis tuberosa

The somewhat less basic fraction (BC) from which thalictricavine had been separated was converted to perchlorate in methanol. The sparingly soluble salt which separated proved to be the perchlorate of corycavine. The base in the soluble portion was converted to l-tartrate and the sparingly soluble salt thus obtained was recrystallized first from hot methanol (sparingly soluble) and then from water–methanol. The *l*-tartrate then melted at 223° and the base regenerated from it melted at 140° when recrystallized from dry ether in which it was sparingly soluble.

Anal. Calcd. for $C_{20}H_{21}O_4N$: C, 70.80; H, 6.20; 2 OMe, 18.30. Found: C, 71.32, 71.03; H, 6.05, 5.99; OMe, 18.64, 18.39.

The tartrate analyzed satisfactorily for $C_{20}H_{21}O_4N \cdot C_4H_6O_4 \cdot 1/2$ MeOH. The methine, prepared in the usual way from the methiodide, melted at 130° (lit. (10), m.p. 133°) when recrystallized from ether. A specimen of domestine received from Professor Tatsuo Ohta (Tokyo College of Pharmacy, Shinjuku-ku, Japan) melted at 139° and a mixture of it with the above base melted at the same temperature.

The mother liquors from the crystallization of the corydaline were also divided into a number of fractions of progressively weaker bases by successive elution with hydrochloric acid from ether solution. The middle fractions were converted to nitrates in methanol and the salt, which separated and proved to consist largely of corydaline nitrate, was removed. The bases in the soluble portion were regenerated and the portion which then crystallized from ether was recrystallized from chloroform–methanol.

Anal. Calcd. for $C_{22}H_{23}O_7N$: C, 63.91; H, 5.61. Found: C, 64.20, 64.40; H, 5.82, 5.82.

Infrared and n.m.r. spectra showed the presence of a lactone carbonyl, three methoxyls, one *N*-methyl, and one methylenedioxy group. Its m.p. (176°) and the above properties suggest that this alkaloid is narcotine and a mixture m.p. confirmed its identity.

The mother liquors from the separation of the corycavine were converted to oxalates a second time in methanol. The mixture of salts thus obtained consisted largely of the sparingly soluble corycavine oxalate and a second minor component which was removed by warming with water. The base, regenerated from the soluble portion, was recrystallized from chloroform–methanol and then melted at 238°, either alone or mixed with capnoidine. When some of this and an equal weight of adlumidine were recrystallized from chloroform–methanol there was formed *dl*-capnoidine which melted at 206°, either alone or mixed with an authentic specimen.

Corydalis pallida

The mother liquors from which *d*-tetrahydropalmatine had crystallized were converted to hydrochloride and another crop separated. The soluble portion was converted to free base and its solution in ether was dried over potassium hydroxide. Removal of the ether and contact of the residue with methanol yielded a crop of *d*-corydaline which, alone or mixed with an authentic specimen, melted at 135°.

The filtrate from the corydaline was converted to acid oxalate in methanol–acetone. The sparingly soluble salt which slowly separated was washed with acetone and the base regenerated from it crystallized in contact with methanol and proved to be cryptopine (m.p. and mixture m.p., 223°).

The oxalates which remained in solution from the above

experiment were reconverted to the free base mixture. A methanol solution of these yielded a mixture of crystalline bases. The portion sparingly soluble in warm methanol was recrystallized from chloroform–methanol and the resultant *dl*-stylopine (m.p. 220°) was identified by a mixture m.p. determination.

1. R. H. F. MANSKE. Can. J. Res. **B16**, 438 (1938).
2. T. F. PLATONOVA, P. S. MASSAGETOV, A. D. KUZOVKOV, and L. M. UTKIN. Zh. Obshch. Khim. **26**, 173 (1956).
3. R. H. F. MANSKE. Can. J. Res. **B17**, 95 (1939); Can. J. Chem. **46**, 2873 (1968).
4. J. K. SAUNDERS, R. A. BELL, C.-Y. CHEN, D. B. MACLEAN, and R. H. F. MANSKE. Can. J. Chem. **46**, 2873, 2876 (1968).
5. R. H. F. MANSKE. J. Am. Chem. Soc. **75**, 4928 (1953).
6. R. H. F. MANSKE. Can. J. Res. **B18**, 80 (1940).
7. R. H. F. MANSKE. Can. J. Res. **B14**, 354 (1936).
8. R. H. F. MANSKE. Can. J. Res. **8**, 210 (1933).
9. F. FEIGL and K. WEISSELBERG. Z. anal. Chem. **83**, 101 (1931).
10. H. SHISHIDO. Bull. Chem. Soc. Japan, **13**, 247 (1938).

Can. J. Chem. Downloaded from www.nrcresearchpress.com by 210.87.254.40 on 09/05/12
For personal use only.

Synthesis of exaltone and *dl*-muscone based on 1,5,9-cyclododecatriene

H. NOZAKI, H. YAMAMOTO, AND T. MORI
Department of Industrial Chemistry, Kyôto University, Kyôto, Japan

Received August 13, 1968

Bicyclo[9·4·1]hexadecan-16-one is prepared from cyclododecanone *via* four steps: ethoxycarbonylation, condensation with 1,4-dibromobutane, saponification, and decarboxylation. Photolysis of the bicyclic ketone yields a ketene which is trapped with methanol to afford methyl cyclopentadecanecarboxylate or alternatively oxidized to exaltone directly. The ester is also converted into exaltone *via* five steps. *dl*-Muscone is prepared by applying the same scheme to cyclotridecanone with 14-methylbicyclo-[10·3·1]hexadecan-16-one as the key intermediate.

Canadian Journal of Chemistry, 47, 1107 (1969)

Can. J. Chem. Downloaded from www.nrcresearchpress.com by 210.87.254.5 on 09/05/12
For personal use only.

Owing to Wilke's discovery of butadiene-cyclotrimerization, 1,5,9-cyclododecatriene and cyclododecanone (**1**) have become readily accessible. Ohloff, Eschenmoser and others (1, 2) have recently published elegant syntheses of exaltone (cyclopentadecanone) (**12**) and *dl*-muscone (3-methylcyclopentadecanone) (**25**) starting from these 12-membered cyclic compounds. We wish to describe a different route which involves the key intermediates, **4** and **18**, both containing a 15-membered ring bridged by a carbonyl group. Photolysis of **4** and **18** has been shown to afford cyclopentadecanecarboxylates **7** and **20**, which are converted to **12** and **25** in 44 and 19% overall yields based on **4** and **18**, respectively.[1] A similar photolysis of bicyclo[5·2·1]decan-10-one was previously recorded by Gutsche *et al.* (4).

Ethoxycarbonylation of **1** (5) gave **2** which was treated with sodium hydride and 1,4-dibromobutane in toluene to afford the cyclized ketoester **3**. Heating of **3** with sulfuric acid in glacial acetic acid furnished the desired bicycloketone **4** as a sharp melting solid in 72% overall yield based on **2**. Attempted condensation of **1** with 1,4-dibromobutane yielded an approximately 1:1 mixture of **4** and a spiro isomer **5**.[2]

The ketone **4** proved homogeneous upon attempted thin-layer chromatographic (t.l.c.) and gas–liquid chromatographic (g.l.c.) separation and, therefore, is assumed to be the thermodynamically more stable isomer of the possible *cis* and *trans* isomers. The stereochemistry has not been determined yet. Any carbonyl derivatives of **4** could not be obtained and this was ascribed to the steric hindrance around the carbonyl group, as inspection of Dreiding models indicated that the preferred conformation should be the one with the carbonyl group almost buried in the nonamethylene group for either the *cis* or *trans* isomer. The observed inertness of **4** towards ring cleavage by oxidizing agents can be explained in the same way.

The n,π^*-excitation of the hindered ketone **4** was found to cause the ring-cleavage in the desired way. Irradiation of a 3% methanolic solution of **4** was carried out by means of a 200 W high pressure mercury arc with a Pyrex filter for 20–30 h. The volatile product (80% recovery by weight) consisted of a C_{15}-hydrocarbon fraction (32%) and methyl cyclopentadecanecarboxylate (**7**) (68%) by g.l.c. analysis. The hydrocarbon fraction was not investigated in detail.

Irradiation of **4** was examined in several solvents, and the use of halogenated ones such as methylene bromide or carbon tetrachloride was found to decrease the amount of hydrocarbon byproducts remarkably. Thus, irradiation of a 2% solution of **4** in a mixture of methanol and carbon tetrachloride (1:6 by volume) gave **7** as the only distillable product in 73% yield.

In support of Gutsche's mechanism (4) on this kind of photolytic ring cleavage, irradiation of **4** in cyclohexane gave a solution, whose infrared spectrum (i.r.) showed absorption at 2140 cm^{-1} characteristic of the ketene **6**.[3]

Oxidation of this ketene with oxygen should

[1]The exaltone synthesis has appeared in a preliminary form (3).

[2]Opitz and Mildenberger obtained bicyclic ketones homologous to **4** from the reactions of dihalides with enamines of 5, 6, and 7 membered cyclic ketones (6). We thank one of the referees for this suggestion.

[3]Chapman and Lassila (7) claim the first identification of a ketene intermediate in the type I cleavage of ketone photolysis. See, however, refs. 3 and 4.

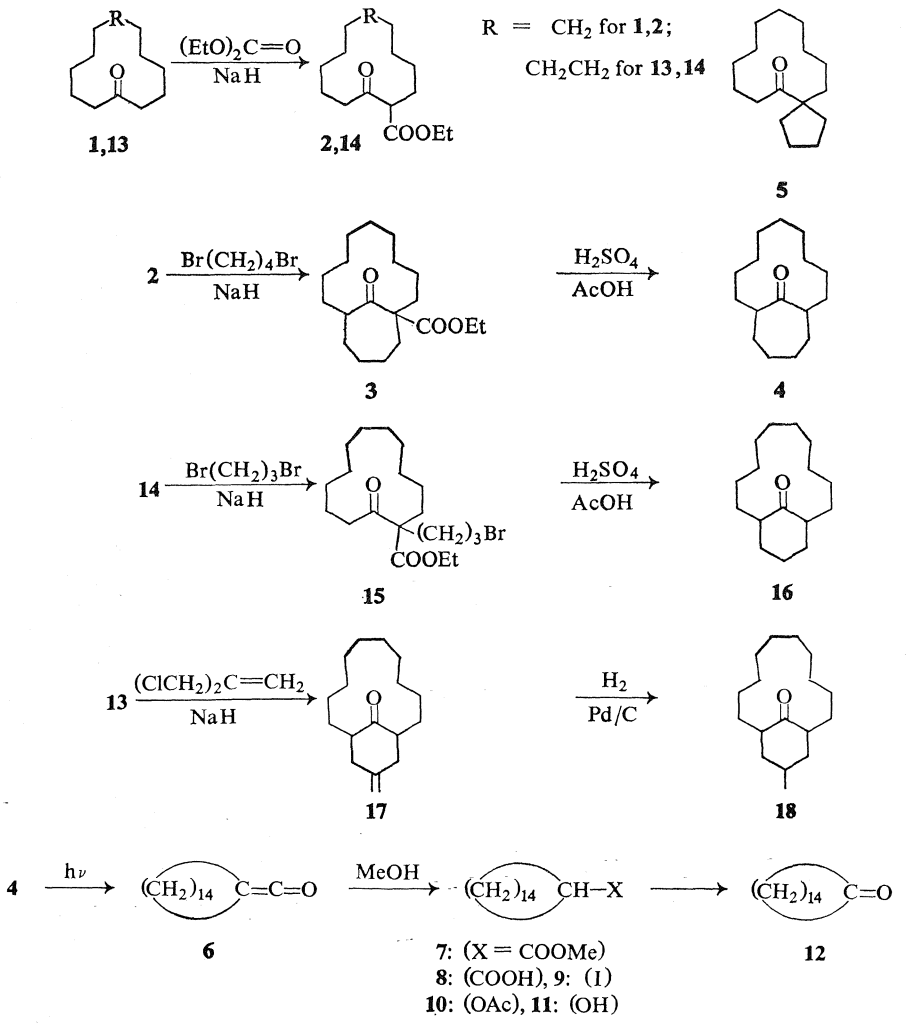

furnish exaltone (**12**) directly. Irradiation of a 3% solution of **4** in cyclohexane while bubbling oxygen through the solution afforded **12** in 20–30% yields, but hydrocarbon by-products and polymeric substances were produced together with **12** and separation gave rise to some difficulties. In contrast, the isolated ester **7** gave better yields of **12** by successive treatments mentioned below.

Hydrolysis of **7** followed by decarboxylation according to Barton's procedure (8) gave a mixture of iodocyclopentadecane (**9**) and its acetolysis product **10**. The acetolysis was completed by the action of mercuric acetate in acetic acid, and the resulting acetate **10** was hydrolyzed to cyclopentadecanol (**11**). Oxidation of **11** by Brown's method (9) gave exaltone (**12**) in 61% overall yield based on **7**.

Theoretically *dl*-muscone (**25**) should be obtained by using methyl-substituted **4** as an intermediate. In order to minimize the possibility of obtaining methylcyclopentadecanone having the methyl group at unsuitable positions, it seemed more appropriate to go through **18**. First we prepared the bicycloketone **16** to examine its photochemistry as a model experiment.

Cyclotridecanone (**13**) has been prepared from 1,5,9-cyclododecatriene by several methods (10). Attempted condensation of the ethoxycarbonylated ketone **14** with 1,3-dibromopropane in the presence of 2 mole equivalents of sodium

Can. J. Chem. Downloaded from www.nrcresearchpress.com by 210.87.254.5 on 09/05/12
For personal use only.

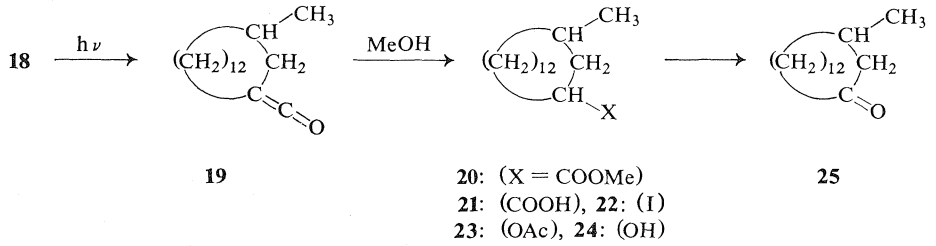

19 **20**: (X = COOMe) **25**
21: (COOH), **22**: (I)
23: (OAc), **24**: (OH)

hydride failed to afford the desired cyclization product due to side reactions. Condensation in the presence of one mole equivalent of sodium hydride gave the 3-bromopropyl-substituted ketoester **15**, which was not isolated. Treatment of the crude **15** with sulfuric acid was found to effect the cyclization as well as the elimination of the ethoxycarbonyl group simultaneously. The bicycloketone **16** was isolated as a sharp melting solid in a 31% overall yield based on **14** and proved to be homogeneous upon t.l.c. and g.l.c. analyses. This bicycloketone is also assumed to be the thermodynamically more stable isomer. In contrast to **4**, the isomer **16** gave an oxime. Irradiation of **16** in methanolic solution furnished methyl cyclopentadecanecarboxylate (**7**) in a 55% yield.

Attempted synthesis of **18** by means of the reaction of **14** with 1,3-dibromo-2-methylpropane failed, as this halide proved to be inert under the usual conditions for the condensation, possibly due to the steric hindrance of the methyl group (11). Direct condensation of cyclotridecanone (**13**) with 3-chloro-2-chloromethylpropene proceeded smoothly to afford the cyclized product **17** in a 57% yield. Catalytic hydrogenation of **17** gave quantitatively the desired ketone **18**. Both ketones **17** and **18** gave one peak upon g.l.c., but two spots (ca. 1:1) on t.l.c. analysis. The stereochemistry is open to research in the future.

Photolysis of **18** in methanol gave methyl 3-methylcyclopentadecanecarboxylate (**20**) in a 33% yield. This was transformed into *dl*-muscone in a 58% overall yield based on **20** by means of a similar sequence of reactions as used in the exaltone synthesis. The stereochemistry of compounds **20**–**24** has not been determined.

Experimental

All temperatures are uncorrected. Nuclear magnetic resonance (n.m.r.) spectra were obtained on JOEL C-60-H spectrometer in CCl_4 solutions with tetramethylsilane as reference. Chemical shifts are given in p.p.m. from this reference together with the multiplicity of signals indicated in an abbreviated form: s for singlet, d for doublet, t for triplet, and m for multiplet, respectively. Gas–liquid chromatography analyses were performed on a 2 m column of SE 30 on Chromsorb W (10%) with helium as a carrier gas at 160–180°. Thin-layer chromatography analyses were conducted on Silica-gel G with *n*-hexane and ethyl acetate (10:1) as a developing solvent.

Bicyclo[9·4·1]hexadecan-16-one (4)

To a suspension of sodium hydride (7.2 g, 0.3 mole) in anhydrous xylene mixture (30 ml) was slowly added a solution of 2-carbethoxycyclododecanone (**2**) (5) (38.1 g, 0.15 mole) in xylenes (80 ml) with stirring at room temperature under nitrogen atmosphere. After evolution of hydrogen was complete, 1,4-dibromobutane (32.4 g, 0.15 mole) was added in one portion. On heating the mixture at 80–90° another mole equivalent of hydrogen evolved. Heating and stirring were continued until hydrogen evolution had subsided (15 h). After cooling, the mixture was treated with water and extracted with ether. The organic layer was washed with water, dried (Na_2SO_4), and concentrated *in vacuo* to give crude **3** (48.3 g) as a yellow viscous oil. Alkaline hydrolysis of this oily ketoester and subsequent recrystallization from benzene–hexane gave bicyclo[9·4·1]hexadecan-16-one-1-carboxylic acid as colorless crystals, m.p. 141–142° (decomp.). Infrared (Nujol): 3600–2400, 1720–1690 cm^{-1} (C=O, COOH).

Anal. Calcd. for $C_{17}H_{28}O_3$: C, 72.8; H, 10.1. Found: C, 72.3; H, 10.2.

The crude **3** (48.3 g) was dissolved in a mixture of acetic acid (300 ml), water (120 ml), and concentrated sulfuric acid (80 ml), and the solution was heated at reflux for 10 h. After cooling and treatment with water, the mixture was extracted with *n*-hexane. The extracts were combined, washed with water, dried (Na_2SO_4), and concentrated *in vacuo*. Vacuum distillation of the resulting semisolid gave **4** (25.4 g: 72% based on **2**) as a colorless solid, b.p. 110–115°/0.1 mm, m.p. 80–84°. Recrystallization from methanol afforded an analytical sample melting at 86–87°. Infrared (Nujol): 1700 cm^{-1} (C=O). Nuclear magnetic resonance: δ 3.2–2.6 m (2H), 2.3–0.9 m (a peak at 1.25) (26H).

Anal. Calcd. for $C_{16}H_{28}O$: C, 81.3; H, 11.9. Found: C, 81.4; H, 12.2.

In another procedure, a mixture of sodium hydride (4.8 g: 0.2 mole), cyclododecanone (**1**) (18.2 g: 0.1 mole), 1,4-dibromobutane (21.6 g: 0.1 mole), and anhydrous xylenes (50 ml) was stirred at 80–90° under nitrogen

Can. J. Chem. Downloaded from www.nrcresearchpress.com by 210.87.254.5 on 09/05/12
For personal use only.

Can. J. Chem. Downloaded from www.nrcresearchpress.com by 210.87.254.5 on 09/05/12
For personal use only.

atmosphere for 40 h, when hydrogen evolution was complete. After cooling and treatment with water, the mixture was extracted with *n*-hexane. The extracts were combined, washed with water, dried (Na_2SO_4), and concentrated. Distillation of the resulting oil gave a colorless oil (10.3 g), b.p. 110–120°/0.15 mm, which solidified on standing, m.p. 40–70°. Fractional recrystallization from methanol gave two crystalline materials, **4** (3.1 g: 13%) melting at 86–87° and a spiroketone **5** (4.5 g: 19%) melting at 50–52°. The structure of **5** was based on the following data. Infrared (Nujol): 1710 cm^{-1} (C=O). Nuclear magnetic resonance: δ 2.5 diffused *t* (2H), 2.3–1.0 m (a peak at 1.25) (26 H).

Anal. Calcd. for $C_{16}H_{28}O$: C, 81.3; H, 11.9. Found: C, 81.1; H, 12.1.

Photolysis of Bicyclo[9·4·1]hexadecan-16-one (4)

A solution of **4** (8.3 g: 0.035 mole) in methanol (280 ml) was well degassed and subjected to irradiation with an immersion type 200 W high pressure mercury arc sealed in a cooling water mantle made of Pyrex glass. The photo-reaction was monitored by means of i.r., and the irradiation was interrupted when the 1700 cm^{-1} band characteristics to the starting bicyclic ketone had disappeared (20–30 h). Evaporation of the solvent followed by vacuum distillation gave a colorless oil (6.6 g), b.p. 70–130°/0.1 mm. Gas–liquid chromatography analysis indicated that this oil consisted of a 32:68 mixture of C_{15}-hydrocarbons and methyl cyclopentadecanecarboxylate (**7**). The mixture was subjected to alkaline hydrolysis, and free carboxylic acid **8** was separated (4.2 g: 47% yield based on **4**), m.p. 65–66° (from ethanol) (reported (12) m.p. 52–54°). Infrared (Nujol): 3300–2400, 1710–1690 cm^{-1} (COOH). The *p*-phenylphenacyl ester of **8** was obtained by the usual method, m.p. 101.5–102° (from ethanol).

Anal. Calcd. for $C_{30}H_{40}O_3$: C, 80.3; H, 9.0. Found: C, 80.3; H, 9.1.

The hydrocarbon mixture, b.p. 70–80°/0.3 mm, consisted of at least three components (g.l.c.) and absorbed about 0.3 mole equivalent of hydrogen on catalytic hydrogenation.

Anal. Calcd. for $C_{15}H_{28}$: C, 86.5; H, 13.5. Found: C, 86.9; H, 13.4.

In another procedure, a solution of the bicyclic ketone **4** (4.7 g: 0.02 mole) in methanol (30 ml) and carbon tetrachloride (180 ml) was similarly photolyzed. Evaporation of the solvent followed by vacuum distillation gave methyl cyclopentadecanecarboxylate (**7**) as a colorless oil (3.9 g: 73%), b.p. 117–120°/0.1 mm, which proved to be homogeneous on g.l.c. and t.l.c. Infrared (neat): 1750, 1195, 1160 cm^{-1} ($COOCH_3$). Nuclear magnetic resonance: δ 3.60 s (3H), 2.5–2.1 m (1H), 1.35 s (28H).

Anal. Calcd. for $C_{17}H_{32}O_2$: C, 76.1; H, 12.0. Found: C, 76.5; H, 11.9.

Direct conversion of **4** to **12** was attained as follows: into a solution of **4** (2 g) in cyclohexane (70 ml) placed in a Pyrex tube, oxygen gas was bubbled through a narrow inlet tube at a rate of 60–70 ml/min at room temperature under external irradiation with a 200 W high pressure mercury arc for 30 h. Distillation of the mixture gave a colorless oil (1.0–1.3 g), b.p. 100–130°/0.3 mm, which was a mixture of several components (g.l.c.). Purification by preparative g.l.c. yielded cyclopentadecanone (**12**) as a colorless solid, m.p. and mixed m.p. 61–62° (reported (13) m.p. 63°), semicarbazone, m.p. and mixed m.p. 187–188° (from ethanol) (reported (13) m.p. 188°). Infrared of **12** was completely superimposable with that of authentic exaltone. The yields ranged from 20 to 30% (determined from the peak area of g.l.c.).

The intermediacy of a ketene in this photolysis was shown as follows. A solution of **4** (1 g) in cyclohexane (70 ml) was irradiated for 20 h with a high pressure mercury arc through a Pyrex filter. The i.r. of the cyclohexane solution showed an absorption band at 2140 cm^{-1}. Attempted isolation of the ketene failed.

Cyclopentadecyl Acetate (10)

A mixture of cyclopentadecanecarboxylic acid (**8**) (5.1 g: 0.02 mole) and mercuric acetate (25.4 g: 0.08 mole) in benzene (200 ml) was heated at reflux with stirring in a nitrogen atmosphere while being irradiated by a 500 W tungsten lamp for 30 min. To this mixture under the same condition was added dropwise a saturated solution of iodine in benzene until the color-discharge was no longer observed (1.5 h). After cooling, the inorganic substances were removed by filtration. The filtrate was washed with aqueous sodium thiosulfate solution and then with water, dried (Na_2SO_4), and concentrated *in vacuo*. The residual oil (5.5 g) gave two spots on t.l.c. and strong i.r. bands at 1750 and 1250 cm^{-1}. This crude oil was dissolved in acetic acid (100 ml), and the solution was heated on a steam bath with mercuric acetate (10 g) for 3 h. After treatment with water, the mixture was extracted with benzene. The extracts were combined, washed with water, dried (Na_2SO_4), and concentrated to about 10 ml. The concentrated solution was passed through a short alumina column and distilled *in vacuo* to give **10** (4.0 g: 74%) as a colorless oil, b.p. 105–108°/0.06 mm. Infrared (neat): 1750, 1250 cm^{-1} (OAc). Nuclear magnetic resonance: δ 5.0–4.5 m (1H), 1.89 s (3H), 1.35 s (28H).

Anal. Calcd. for $C_{17}H_{32}O_2$: C, 76.1; H, 12.0. Found: C, 76.1; H, 12.1.

Cyclopentadecanol (11)

Alkaline hydrolysis of the acetate **10** (2.5 g) in the usual manner afforded cyclopentadecanol (**11**) (2.0 g: 95%) as a colorless solid, m.p. 74–76° (from *n*-hexane) (reported (14) m.p. 81°). The i.r. of **11** was superimposable on that of an authentic sample prepared from exaltone by lithium aluminium hydride reduction. The phenylurethane of **11** was prepared in the usual way and recrystallized from methanol, m.p. and mixed m.p. 102–103° (reported (14) m.p. 104°).

Cyclopentadecanone (12)

To a solution of **11** (1.1 g: 5 mmoles) in ether (20 ml) was added a mixture of sodium dichromate dihydrate (1.0 g: 3.4 mmoles), water (10 ml), and concentrated sulfuric acid (0.8 ml) in the course of 0.5 h under stirring at room temperature. Stirring was continued for an additional 3 h. The ethereal layer was washed with water, dried (Na_2SO_4), and concentrated *in vacuo*. Distillation gave **12** as a colorless solid (1.0 g: 91%), b.p. 101–103°/0.2 mm, m.p. 57–60°. Recrystallization from methanol gave an analytically pure sample, m.p. and mixed m.p. 61–62°, semicarbazone, m.p. and mixed m.p. 187–188°.

Can. J. Chem. Downloaded from www.nrcresearchpress.com by 210.87.254.5 on 09/05/12
For personal use only.

Comparison of i.r. of **12** with that of the authentic exaltone also confirmed the identity.

*2-Carbethoxycyclotridecanone (**14**)*

To a mixture of sodium hydride (4.8 g: 0.2 mole) and diethyl carbonate (150 ml) was added a solution of cyclotridecanone (**13**) (19.6 g: 0.1 mole) in diethyl carbonate (30 ml) in the course of 2 h with stirring under nitrogen atmosphere. Stirring was continued at room temperature until hydrogen evolution had ceased (15 h). After treatment with water and acidification with dilute hydrochloric acid, the mixture was extracted with ether. The organic layer was washed with water, dried (Na_2SO_4), and concentrated. Distillation of the residue gave **14** (25.1 g: 94%) as a colorless solid, b.p. 130–135°/0.15 mm, m.p. 63–66°. Recrystallization from methanol afforded colorless needles melting at 66–67°. Infrared (Nujol): 1750, 1195 (COOR), 1708 cm^{-1} (C=O).

Anal. Calcd. for $C_{16}H_{28}O_3$: C, 71.6; H, 10.5. Found: C, 71.5; H, 10.6.

*Bicyclo[10·3·1]hexadecan-16-one (**16**)*

Condensation of **14** with 1,3-dibromopropane attempted similarly as mentioned for the preparation of **4** gave an intractable oily mixture instead of the desired cyclization product. The following procedure was found to give the best results. A mixture of **14** (20.8 g: 0.0776 mole), sodium hydride (1.87 g: 0.078 mole), and xylenes (35 ml) was stirred until hydrogen evolution was complete, and then 1,3-dibromopropane (47 g: 0.23 mole) was added in one portion. The whole mixture was stirred at 80–90° for 30 h. Treatment with water and extraction with ether followed by concentration of the extracts gave a yellow oil, which was dissolved in a mixture of acetic acid (160 ml), water (80 ml), and concentrated sulfuric acid (80 ml). This solution was heated to reflux for 5 h. After cooling, the mixture was diluted with water and extracted with *n*-hexane. The organic layer was washed, dried (Na_2SO_4), and distilled to give **16** (5.7 g: 31%) as a colorless solid, b.p. 122–126°/0.2 mm, m.p. 49–53°. Thin-layer chromatography and g.l.c. indicated the homogeneity of **16**. Recrystallization from methanol gave an analytically pure sample melting at 54–55°. Infrared (Nujol): 1710 cm^{-1} (C=O). Nuclear magnetic resonance: all protons appeared at δ 3.0–1.0 with poor resolution (a peak at 1.28).

Anal. Calcd. for $C_{16}H_{28}O$: C, 81.3; H, 11.9. Found: C, 81.1; H, 12.2.

The oxime of **16** was obtained in the usual manner, m.p. 143–144° (from ethanol). Infrared (Nujol): 3300 cm^{-1} (OH).

Anal. Calcd. for $C_{16}H_{29}NO$: C, 76.4; H, 11.6; N, 5.6. Found: C, 75.7; H, 11.5; N, 5.5.

The unsatisfactory analysis of carbon might possibly be ascribed to the presence of some impurity, but further purification was impossible due to the lack of material.

*Photolysis of Bicyclo[10·3·1]hexadecan-16-one (**16**)*

A solution of **16** (2.4 g) in methanol (200 ml) was photolyzed as described for the photolysis of **4** while monitoring by g.l.c. The crude reaction mixture was immediately hydrolyzed with ethanolic potassium hydroxide, and the acidic fraction was secured in the usual manner. Reesterification of the latter with diazomethane followed by vacuum distillation gave methyl cyclopentadecanecarboxylate (**7**) (1.5 g: 55%), which was identical with the specimen obtained from **4** upon comparison of i.r., retention time on g.l.c., and m.p. of *p*-phenylphenacyl ester of the free acid (**8**).

*14-Methylenebicyclo[10·3·1]hexadecan-16-one (**17**)*

A mixture of cyclotridecanone (**13**) (19.6 g: 0.1 mole), sodium hydride (4.8 g: 0.2 mole), 3-chloro-2-chloromethylpropene (15) (12.5 g: 0.1 mole), and toluene (30 ml) was stirred at 90–100° after nitrogen flushing, until hydrogen evolution was complete (60 h). The reaction mixture was treated with water and extracted with *n*-hexane. The extracts were combined, washed with water, dried (Na_2SO_4), and concentrated. On vacuum distillation of the residue, cyclotridecanone (**13**) (3.9 g) boiling at 80–100°/0.3 mm was recovered, and **17** (11.3 g: 57% based on consumed **13**) was obtained as a colorless solid, b.p. 115–120°/0.3 mm, m.p. 57–62° which showed a single peak on g.l.c. Recrystallization from ethanol gave a sample melting at 63–66.5°, but further recrystallizations failed to give a sharper melting point. Thin-layer chromatography of recrystallized **17** gave two equal spots. Infrared (Nujol): 3090, 1650, 895 (=CH_2), 1710 cm^{-1} (C=O). Nuclear magnetic resonance: δ 4.79 s (2H), 2.8–1.9 m (6H), 1.6–0.8 m (a peak at 1.25) (20 H).

Anal. Calcd. for $C_{17}H_{28}O$: C, 82.2; H, 11.4. Found: C, 81.9; H, 11.7.

*14-Methylbicyclo[10·3·1]hexadecan-16-one (**18**)*

A solution of the unsaturated ketone **17** (11 g) in ethanol (100 ml) was stirred under an atmospheric pressure of hydrogen in the presence of palladium-on-carbon (10%) (0.5 g). It took 23 h for completion of hydrogen absorption. The catalyst was removed by filtration, and the filtrate was distilled *in vacuo* to give **18** (10.8 g: 98%) as a colorless solid, b.p. 135–137°/0.4 mm, m.p. 49–53°. Recrystallization was not attempted. Infrared (Nujol): 1710 cm^{-1} (C=O). Nuclear magnetic resonance: all protons appeared at δ 3.0–0.8 with poor resolution (peaks at 1.30, 0.98, 0.88).

Anal. Calcd. for $C_{17}H_{30}O$: C, 81.5; H, 12.1. Found: C, 81.5; H, 12.3.

*Methyl 3-Methylcyclopentadecanecarboxylate (**20**)*

A solution of **18** (9.5 g) in methanol (500 ml) was photolyzed as mentioned above. The crude product was hydrolyzed with ethanolic potassium hydroxide and the acidic substance was separated and reesterified with diazomethane to methyl ester, which was distilled *in vacuo* to give **20** (3.5 g: 33%), b.p. 104°/0.04 mm. Gas–liquid chromatography and thin-layer chromatography gave a single peak and spot, respectively. Infrared (neat): 1740, 1195, 1160 cm^{-1} ($COOCH_3$). Nuclear magnetic resonance: δ 3.60 s (3 H), 2.6–2.1 m (1 H), 1.7–1.1 m (a peak at 1.35) (27 H), 0.88 diffused d (3 H).

Anal. Calcd. for $C_{18}H_{34}O_2$: C, 76.5; H, 12.1. Found: C, 76.8; H, 11.8.

The use of halogenated solvents in this photolysis did not improve the yield of **20**.

The methyl ester **20** was hydrolyzed again with ethanolic potassium hydroxide to give free acid **21** (96% yield) as a colorless viscous liquid.

*3-Methylcyclopentadecyl Acetate (**23**)*

The acid **21** (2.68 g: 0.01 mole) was converted into a

mixture of iodide **22** and acetate **23** with mercuric acetate (12.7 g: 0.04 mole) in benzene (100 ml) and a saturated benzene solution of iodine by the method mentioned above for **8**. The mixture was acetolyzed to pure **23** with mercuric acetate (10 g) in acetic acid (100 ml) as before. Vacuum distillation gave **23** (2.3 g: 82%) as a colorless oil, b.p. 107–110°/0.08 mm. Infrared (neat): 1740, 1240 cm^{-1} (OAc). Nuclear magnetic resonance: δ 5.0–4.5 m (1 H), 1.90 s (3 H), 1.8–1.1 m (a peak at 1.34) (27 H), 0.88 diffused d (3 H).

Anal. Calcd. for $C_{18}H_{34}O_2$: C, 76.5; H, 12.1. Found: C, 76.8; H, 12.0.

3-Methylcyclopentadecanol (24)

Alkaline hydrolysis of the acetate **23** (2.0 g) in the usual manner gave crude alcohol **24** (1.6 g: 94%) as an oil, which was subjected immediately to the next oxidation reaction without further purification. Infrared (neat): 3350 cm^{-1} (OH).

3-Methylcyclopentadecanone (25)

To the crude alcohol **24** (0.6 g: 2.5 mmoles) dissolved in ether (10 ml) was added under stirring a mixture of sodium dichromate dihydrate (0.5 g: 1.7 mmoles), concentrated sulfuric acid (0.4 ml), and water (5 ml) in one portion. After stirring the whole mixture for 2 h, working-up followed by distillation gave **25** (0.47 g: 78%), b.p. 106–107°/0.2 mm. Infrared (neat): 1710 cm^{-1} (C=O). Nuclear magnetic resonance: δ 2.6–2.2 m (4 H), 2.1–1.1 m (a peak at 1.30) (23 H), 0.90 diffused d (3 H).

Anal. Calcd. for $C_{16}H_{30}O$: C, 80.6; H, 12.7. Found: C, 80.4; H, 12.8.

The semicarbazone of **25** melted at 130–131° (from methanol) (reported (16) m.p. 131–132°).

Anal. Calcd. for $C_{17}H_{33}N_3O$: C, 69.1; H, 11.3; N, 14.2. Found: C, 68.9; H, 11.3; N, 13.7.

Acknowledgments

The authors are thankful to Prof. K. Sisido for generous help and to Dr. R. Noyori for valuable suggestions. They acknowledge with pleasure financial support by the Scientific Grant-in-Aid of the Ministry of Education, Japanese Government.

1. G. Ohloff, J. Becker, and K. H. Schulte-Elte. Helv. Chim. Acta, **50**, 705 (1967).
2. A. Eschenmoser, D. Felix, and G. Ohloff. Helv. Chim. Acta, **50**, 708 (1967).
3. H. Nozaki, T. Mori, and R. Noyori. Tetrahedron Letters, 779 (1967).
4. (*a*) C. D. Gutsche and C. W. Armbruster. Tetrahedron Letters, 1297 (1962). (*b*) C. D. Gutsche and J. W. Baum. Tetrahedron Letters, 2301 (1965). C. D. Gutsche and J. W. Baum. J. Am. Chem. Soc. **90**, 5862 (1968).
5. S. J. Rhoads, J. C. Gilbert, A. W. Decora, T. R. Garland, R. J. Spangler, and M. J. Urbigkeit. Tetrahedron, **19**, 1625 (1963).
6. G. Opitz and H. Mildenberger. Ann. Chem. **650**, 115 (1961).
7. O. L. Chapman and J. D. Lassila. J. Am. Chem. Soc. **90**, 2449 (1968).
8. D. H. R. Barton, H. P. Faro, E. P. Serebryakov, and N. F. Woolsey. J. Chem. Soc. 2438 (1965).
9. H. C. Brown and C. P. Garg. J. Am. Chem. Soc. **83**, 2952 (1961).
10. (*a*) H. Nozaki, S. Kato, and R. Noyori. Can. J. Chem. **44**, 1021 (1966). (*b*) W. Kirchhof, W. Stumpf, and W. Franke. Ann. Chem. **681**, 32 (1965). (*c*) M. Mühlstädt and J. Graefe. Chem. Ber. **100**, 223 (1967). (*d*) W. E. Parham and R. J. Sperley. J. Org. Chem. **32**, 926 (1967).
11. E. S. Gould. Mechanism and structure in organic chemistry. Henry Holt and Co., New York. 1959. p. 276.
12. S. A. Rhone-Poulenc. Brit. Patent 989,476. Chem. Abstr. **63**, 9837 (1965).
13. L. Ruzicka, M. Stoll, and H. Schinz. Helv. Chim. Acta, **9**, 249 (1926).
14. M. Kobelt, P. Barman, V. Prelog, and L. Ruzicka. Helv. Chim. Acta, **32**, 256 (1949).
15. L. F. Hatch, J. J. Russ, and L. B. Gordon. J. Am. Chem. Soc. **69**, 2614 (1947).
16. M. S. R. Nair, H. H. Mathur, and S. C. Bhattacharyya. J. Chem. Soc. 4154 (1964).

Can. J. Chem. Downloaded from www.nrcresearchpress.com by 210.87.254.5 on 09/05/12
For personal use only.

On the reduction of the ozonides of selected phenylethylenes by triphenylphosphine

JACQUES CARLES AND SÁNDOR FLISZÁR[1]
Department of Chemistry, University of Montreal, Montreal, Quebec

Received November 6, 1968

Triphenylphosphine has been found to reduce ^{18}O labelled ozonides of styrene, stilbene, β-methylstyrene, and triphenylethylene by a very selective attack on the peroxidic oxygen atoms of the ozonides. The presence of an electron withdrawing phenyl group attached to a C atom of the ozonide ring enhances the attack on the peroxidic oxygen adjacent to this C atom, whereas the presence of an electron releasing methyl group enhances the attack on the other peroxidic oxygen atom.

La réduction, par la triphénylphosphine, des ozonides du styrène, stilbène, β-méthylstyrène et du triphényléthylène, marqués par ^{18}O dans la position éther, montre que l'attaque a lieu très sélectivement sur les oxygènes peroxydiques. Le groupe phényle, relié à un atome de carbone du noyau ozonique, favorise l'attaque sur l'atome d'oxygène péroxydique voisin à cet atome de carbone. Le groupe méthyle exerce une influence contraire.

Canadian Journal of Chemistry, 47, 1113 (1969)

The reduction of ozonides by triphenylphosphine has been investigated by Lorenz and Parks (1, 2). This reaction was found to proceed quantitatively and was thus applicable to the determination of unknown quantities of ozonide (2).

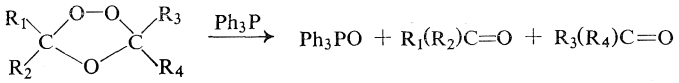

In addition, the nature of the ozonide submitted to this reduction may be determined from the analysis of the carbonyl compounds which are formed during this reduction (1).

In some cases, the reaction proceeds at different rates when *cis*- and *trans*-ozonide isomers are reduced (1). The *cis*-isomer of 2,5-dimethyl-3-hexene ozonide is reduced more rapidly than the *trans*-isomer, whereas, in the case of the 2-butene ozonides, the *trans*-isomer appears to be reduced more rapidly than the *cis*-isomer.

By analogy with the reaction of triphenylphosphine with sulfur (3), the attack of Ph_3P on the ozonide ring is believed to occur via a nucleophilic attack on a peroxidic oxygen of the ozonide ring (1). As no unambiguous experimental proof was available for this hypothesis, this study has attempted to determine the position of attack of the Ph_3P on the ozonide ring. The use of ^{18}O labelled ozonides, in which the isotopic oxygen is situated exclusively in the ether position, has permitted the reaction to be followed and the selectivity of the attack to be determined.

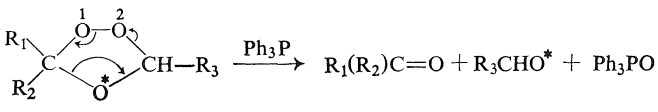

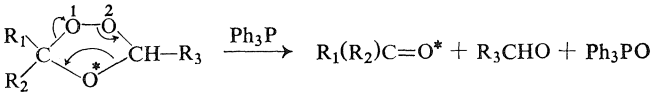

[1]To whom enquiries should be addressed.

Can. J. Chem. Downloaded from www.nrcresearchpress.com by 210.87.254.6 on 09/05/12
For personal use only.

TABLE I

Measured ^{18}O incorporations

R_1	R_2	R_3	% incorporation of ^{18}O in ozonide	Ph_3PO	$R_1(R_2)CO$	R_3CHO	% reaction on position-1
Ph	H	H	15.5	0.0	8.5	—*	55
Ph	H	Ph	34.6	0.0	16.4	16.4	50
Ph	H	CH_3	30.4	0.0	18.3	12.3	60
Ph	Ph	Ph	32.0	0.0	0.1	32.2	0

*Not determined.

The preparation of the ^{18}O labelled ozonides of styrene, stilbene, β-methylstyrene, and triphenylethylene has been described previously (4–6), and the exclusive location of the oxygen isotope in the ether position has been established (5, 6)[2] by mass spectrometry.

The reduction of these ozonides by Ph_3P was carried out under conditions similar to those indicated by Lorenz and Parks (1). The carbonyl compounds and the triphenylphosphine oxide formed were isolated and purified. The percentage ^{18}O content of these compounds, as determined by mass spectrometry, is indicated in Table I. The percentage labelling of the ozonides submitted to this reduction was determined by mass spectrometry, using the methods described elsewhere (5, 6).

The results indicate that in no case is the triphenylphosphine oxide labelled. This indicates that the attack of triphenylphosphine takes place very selectively on the peroxidic oxygens of the ozonides of those phenylethylenes which have been examined.

The results given in Table I also show that, within experimental error, a satisfactory mass balance for the oxygen isotope is obtained. For example, in the reduction of stilbene ozonide, the expected percentage ^{18}O labelling of the benzaldehyde is half that of the original ozonide, since two molecules of benzaldehyde are formed upon reduction of one molecule of ozonide, one of these molecules retaining a peroxidic oxygen, and the other retaining the labelled ether oxygen of the original ozonide. Similar mass balances for the oxygen isotope are also obtained for the products formed upon reduction of the β-methylstyrene and triphenylethylene ozonides. Within experimental error, the sum of the percentage labelling of the two carbonyl compounds is found, in each case, to be equal to the percentage labelling of the ozonide used.

The reduction of ozonides obtained from unsymmetrical olefins, after examination of the ^{18}O content of the carbonyl compounds formed, also enables the peroxidic oxygen, which is preferentially attacked by the triphenylphosphine, to be determined.

The results obtained with the ozonide of triphenylethylene indicate that most of the ether oxygen is retained in the benzaldehyde formed upon reduction. This indicates that the peroxidic oxygen in position-2 is selectively attacked by the triphenylphosphine. Both electronic and steric factors may be responsible for this selective attack. The steric hindrance contributed by the two phenyl groups (R_1 and R_2) obscures, in this case, the contribution of the electronic effects in distributing the sites of attack of the Ph_3P among the two peroxidic oxygens.

In the reduction of the styrene ozonide, approximately 55% of the attack takes place on the peroxidic oxygen identified by **1**. This is an indication of the participation of the electron withdrawing phenyl group in directing the position of attack of the peroxidic oxygens by triphenylphosphine. In β-methylstyrene ozonide, the electron releasing methyl group tends to increase the electron density at the oxygen identified by **2**. Under the combined influence of the phenyl and the methyl groups, the proportion of attack on the peroxidic oxygen in position-1 is thus favored. This is confirmed by the results given in Table I, which indicate that in the reduction of β-methylstyrene ozonide the positions of attack are distributed as follows: 60% on the oxygen in position-1, and, consequently, 40% on the other peroxidic oxygen.

The present results thus indicate that electron withdrawing groups attached to a carbon atom

[2]The mechanistic implications concerning the formation of ozonides are discussed in refs. 4 and 6.

Can. J. Chem. Downloaded from www.nrcresearchpress.com by 210.87.254.6 on 09/05/12
For personal use only.

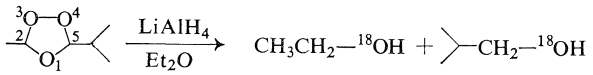

of the ozonide ring favor the attack by Ph_3P on the peroxidic oxygen adjacent to this carbon atom, whereas electron releasing groups exert the opposite influence.

Similar leaving characteristics of the peroxide-bridge oxygens have been observed by Bishop and Story (7) for the reduction of 1,2-dimethylcyclopentane ozonide by lithium aluminium hydride. This ozonide was labelled exclusively in the ether oxygen by ^{18}O and gave, upon reduction, the 2,6-heptanediol which retained essentially all the isotopic label of the ozonide. Hence the selectivity of attack of the peroxide oxygens by $LiAlH_4$ is clearly established in this case, and it is assumed (7), by extension, that the hydride reduction of other saturated alkyl-substituted ozonides occurs with loss of oxygen only from the peroxide bridge. Their detailed mechanism explains clearly why, with $LiAlH_4$, the peroxide oxygens are favored to leave the ozonide. This selectivity is now found to occur in the ozonide reduction by Ph_3P.

However, little is known about the preferential position of $LiAlH_4$ attack on the peroxidic oxygens of ozonides of unsymmetrical olefins. The most detailed study, by Story *et al.* (8), concerned the hydride reduction of the ^{18}O labelled ozonide of 4-methylpentene-2 (*cis–trans* mixture).

Owing to the mode of preparation of this ozonide from the ozonolysis of *trans* diisopropylethylene in the presence of acetaldehyde-^{18}O, only the oxygen atoms in positions-1 and -3 are labelled. The preferential position of attack (0–3 or 0–4) can be calculated from the published data (8). Let x be the proportion of labelling in 0–3 and, hence, $1 - x$ the proportion of labelling in 0–1. Let y be the proportion of 0–3 abstraction by the reducing agent, and $1 - y$ the proportion of abstraction of 0–4. Thus the labelling of ethanol and isobutyl alcohol, referred to the total ozonide labelling, is expressed by eqs. [1] and [2].

[1] (ethanol) $y(1 - x) + (1 - y)x = 25.4/47.8$

[2] (isobutanol) $(1 - y)(1 - x) = 7.6/47.8$

Owing to the fact that these equations lead to quadratic expressions for x (or y), two solutions are obtained:[3]

(*i*) $x_1 = 0.43$; $y_1 = 0.72$

(*ii*) $x_2 = 0.72$; $y_2 = 0.43$

A consideration of electronic and steric factors favors solution (*i*), which indicates that 43% of the labelling is found in 0–3 and that 0–3 is abstracted in preference (~72%) to 0–4 (~28%).

Electronic factors due to the combined effects of the methyl and the isopropyl groups probably play only a minor role in distributing the sites of attack among 0–3 and 0–4. The results obtained in the reduction of β-methylstyrene ozonide by Ph_3P (Table I) support this view. However, if any small effect occurs, the mechanism of hydride reduction proposed by Story (7) indicates that the attack of H^- on the less negative oxygen atom, i.e. 0–3, and hence its elimination, would be favored.

The steric effects, however, appear to play a more important role in the reduction of ozonides. Story's mechanism predicts that a steric effect should function so as to cause excessive loss of 0–3 rather than 0–4. The results obtained in the reduction of triphenylethylene ozonide by triphenylphosphine also illustrates the significance of the steric effect, since, in this reduction, the peroxidic oxygen adjacent to the carbon atom bearing the two phenyl groups is not attacked by the reducing agent.

Although these limited experimental data do not permit definite conclusions to be drawn, it appears that ozonide rings undergo similar modes of reduction when reacted with lithium aluminium hydride or triphenylphosphine. First, the same selectivity of attack on the peroxide bridge is observed for both reducing agents. Secondly, the electronic effects due to the substituents seem to play a minor role in the distribution of the sites of attack. Story's mechanism

[3]The ^{18}O content of 0–3 calculated here differs from the value (68%) calculated by Story *et al.* (8) because these authors had assumed, to a first approximation, equal proportions of abstraction of 0–3 and 0–4.

Can. J. Chem. Downloaded from www.nrcresearchpress.com by 210.87.254.6 on 09/05/12
For personal use only.

for hydride reduction indicates the same trends as those which have been observed for Ph_3P, namely a preferential loss of the least negative peroxidic oxygen atom. Finally, the importance of any steric effect is of equal significance for both $LiAlH_4$ and Ph_3P reduction of the least hindered peroxidic oxygen atom.

Experimental

The preparation of the ^{18}O labelled ozonides, and the determination of the ^{18}O content of the ozonides by mass spectrometry, have been described elsewhere (4–6).

The mass spectra of the compounds obtained upon reduction of the ozonides by triphenylphosphine were recorded using a single focussing Hitachi RMU-6D mass spectrometer, with a direct introduction system MG 158. The vapor pressures of the compounds examined were sufficiently high, so that no external heat on the sample holder was required. The ionization chamber was maintained between 150 and 170 °C, and the ionizing electrons were accelerated by a 70 V potential.

Reduction of the Stilbene Ozonide

Ninety mg of the stilbene ozonide (1:1 *cis–trans* mixture, m.p. 74°) were dissolved, under an N2 atmosphere, in 5 ml of hexane and 150 mg of triphenylphosphine were added. The solution was boiled, under N_2, for 1 h. Cooling to 0° caused the triphenylphosphine oxide (m.p. 160°) to crystallize, and it was isolated by filtration and further purified by recrystallization. The filtrate was distilled under reduced pressure, in N_2 atmosphere, and the benzaldehyde collected. The benzaldehyde was further purified by column chromatography, using Baker Silica-Gel and a benzene–hexane mixture (1:3).

Reduction of Triphenylethylene Ozonide

The procedure is similar to the one described for the stilbene ozonide. One hundred and six mg ^{18}O-triphenylethylene ozonide and 150 mg triphenylphosphine were used. After isolation of the triphenylphosphine oxide and of the benzaldehyde, the benzophenone was isolated from the distillation residue by fractional crystallization in methanol.

Reduction of the β-Methylstyrene Ozonide

One-hundred and twenty-three mg ozonide, 300 mg triphenylphosphine and 5 ml heptane were placed in a "V"-shaped Carius tube and ca. 1 ml of liquid N_2 was added. The Carius tube was sealed, and the mixture was heated at 70° for 1 h. On cooling to room temperature, the mixture was retained in one branch of the "V"-shaped tube. This branch was cooled by a dry ice – acetone bath to collect all the volatile products. After warming to room temperature, the other branch of the tube was cooled rapidly in liquid nitrogen. The acetaldehyde condensed in the cold branch of the Carius tube, which was then cut off. The acetaldehyde was transferred to the mass spectrometer for analysis. The triphenylphosphine oxide was isolated from the heptane solution as described previously by cooling the solution to 0°. By distillation under reduced pressure, the benzaldehyde was isolated, and further purified by column chromatography.

Reduction of the Styrene Ozonide

The work-up procedure for this ozonide was similar to that described for β-methylstyrene ozonide. Seventy mg of ozonide and 200 mg of triphenylphosphine were used. The formaldehyde could not be isolated.

Acknowledgment

The financial support given by the National Research Council of Canada is gratefully acknowledged.

1. O. Lorenz and C. R. Parks. J. Org. Chem. **30**, 1976 (1965).
2. O. Lorenz. Anal. Chem. **37**, 101 (1965).
3. P. D. Bartlett and G. Meguerian. J. Am. Chem. Soc. **78**, 3710 (1956).
4. S. Fliszár, J. Carles, and J. Renard. J. Am. Chem. Soc. **90**, 1364 (1968).
5. J. Castonguay, M. Bertrand, J. Carles, S. Fliszár, and Y. Rousseau. Can. J. Chem. To be published.
6. S. Fliszár and J. Carles. J. Am. Chem. Soc. To be published.
7. C. E. Bishop and P. R. Story. J. Am. Chem. Soc. **90**, 1905 (1968).
8. P. R. Story, C. E. Bishop, J. R. Burgess, R. W. Murray, and R. D. Youssefyeh. J. Am. Chem. Soc. **90**, 1907 (1968).

Can. J. Chem. Downloaded from www.nrcresearchpress.com by 210.87.254.6 on 09/05/12
For personal use only.

Can. J. Chem. Downloaded from www.nrcresearchpress.com by 210.87.254.42 on 09/05/12
For personal use only.

Thiohydantoins. VII. Ionization and ultraviolet spectra of 4-thiohydantoins and 2,4-dithiohydantoins

J. T. Edward and J. K. Liu
Department of Chemistry, McGill University, Montreal, Quebec

Received August 27, 1968

The acid and base dissociation constants of 5,5-pentamethylene-4-thiohydantoin, 5,5-pentamethylene-2,4-dithiohydantoin, and their 1-methyl derivatives, have been determined by ultraviolet studies in basic and acid media. In aqueous sulfuric acid the 4-thiohydantoins are protonated on oxygen at the 2-position, so that the extent of protonation varies with the H_A function of the acid solution, while the 2,4-dithiohydantoins are protonated on sulfur at the 2-position, so that the extent of their protonation varies with H_0'''. The importance of using acidity functions appropriate to the different types of compounds when comparing their basicities is emphasized.

Les constantes d'ionization acides et basiques des pentamethylene-5,5 thio-4 hydantoïne, pentamethylene-5,5 dithio-2,4 hydantoïne, et leur méthyle-1 derivés, ont été déterminés par études d'absorbance ultraviolète dans les milieux basiques et acides. Dans l'acide sulfurique aqueux les thio-4 hydantoïnes sont protonnés sur l'atome d'oxygène à la position-2, parce que le degré d'ionization suit la fonction d'acidité H_A. Les dithio-2,4 hydantoïnes sont protonnés sur l'atome de soufre à la position-2, et le degré d'ionization suit la fonction H_0'''. Ce travail démontre la necessité d'utiliser les fonctions d'acidité appropriées pour des classes différentes de composés, si on veut comparer leurs basicités.

Canadian Journal of Chemistry, **47**, 1117 (1969)

A knowledge of the ionization constants of 2-thiohydantoins and of the changes in their ultraviolet (u.v.) absorption spectra brought about by ionization (1) has proved useful in elucidating the structures of their oxidation products (2). In the present paper we are concerned with extending this knowledge to representative 4-thiohydantoins and 2,4-dithiohydantoins; some use of the results is made in the following paper (3).

The compounds chosen for study were 5,5-pentamethylene-4-thiohydantoin (**2**; R = H), 5,5-pentamethylene-2,4-dithiohydantoin (**5**; R = H), and their 1-methyl derivatives (**2**; R = Me; and **5**; R = Me). The preparation of these compounds has been described by Carrington and Waring (4), who showed that they do not exist, to any appreciable extent, in other tautomeric forms. Their u.v. characteristics in various solvents are listed in Table I; an attempt has been made to classify the absorption bands as Type I, II, or IV, according to a scheme of Janssen (5, 6).

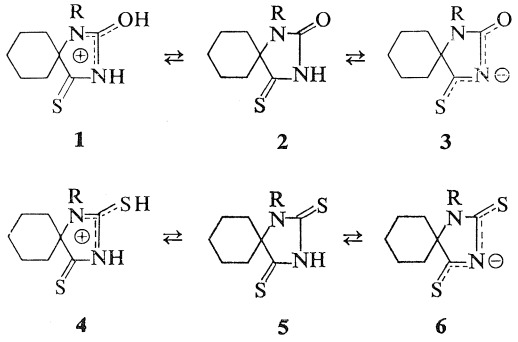

1 **2** **3**

4 **5** **6**

Reaction Scheme 1

For solutions of the neutral compounds in methanol, Carrington and Waring (4) reported the peaks which we classify as Types II and IV. They further reported that the compounds are yellow, but did not observe the Type I peaks responsible for the yellow color. These weak peaks were not observed in water because the compounds are too sparingly soluble, nor in sulfuric acid when they are lost in the trailing edge of the more intense Type II peaks. However, the absorption curve of **5** (R = Me) in 96% sulfuric acid shows an inflexion at about 450 mμ which is probably due to a submerged Type I peak. These peaks are almost certainly the result of $n \rightarrow \pi^*$ transitions of the 4-thiocarbonyl group; $n \rightarrow \pi^*$ transitions of the 2-thiocarbonyl group should take place at shorter wavelengths (6, 7). As expected (6), the Type I peaks of the 2,4-dithiohydantoins are at longer wavelengths than the similar peaks of the 4-thiohydantoins, because the 2-thiocarbonyl group pulls electrons more strongly than the 2-carbonyl group (6). The bathochromic effects of the methyl groups at the 1-position are unexpected and without any obvious explanation.

The Type II bands are undoubtedly due to $\pi \rightarrow \pi^*$ transitions of the thioamide function

TABLE I

Effect of solvent and ionization on ultraviolet absorption bands

Compound	Band type	Ethanol λ_{max} (mμ)	Ethanol ε_{max}	Water λ_{max} (mμ)	Water ε_{max}	H_2SO_4 λ_{max} (mμ)	H_2SO_4 ε_{max}	Alkaline solution λ_{max} (mμ)	Alkaline solution ε_{max}
2; R = H	I	375	25.8						
	II	277	14 800	273	10 800	269	7 900*	287	11 800§
	IV	228	4 800	229	3 700	240	10 400		
2; R = Me	I	389	30						
	II	285.5	10 700	286	12 500	283	4 650†	292	11 500‖
	IV	235	5 700	237	6 650	240	9 300		
5; R = H	I	393	45.4						
	II	297	31 000	295	28 200	290	16 900‡	317.5	32 000¶
	IV	227	5 540	209	9 340	245	12 200		
5; R = Me	I	404	36						
	II	300	28 800	296.5	24 300	299	16 000‡	316	24 000¶
	IV	226	8 000	206	12 000	245	14 400		

*Solvent used: 96.0% H_2SO_4.
†Solvent used: 95.5% H_2SO_4.
‡Solvent used: 71.4% H_2SO_4.
§Solvent used: 0.1 *N* NaOH.
‖In buffer, pH 10.80.
¶In buffer, pH 9.11.

(7–9) in the molecules, and the Type IV bands possibly to $n \rightarrow \sigma$ transitions (7).

In sufficiently acid or alkaline solution the compounds **2** (R = H and Me) and **5** (R = H and Me) form the ions shown in Reaction Scheme 1. The ionization can be followed from changes in the spectra of the compounds (see Table I), most conveniently at suitable wavelengths in the neighborhood of the intense Type II peaks.

Ionization of **2** (R = H) in alkaline solution is expected to take place at N_3—H and not at N_1—H (6). In the present instance this view is supported by the similarity of the spectra of the anions **1** (R = H and Me). Similar considerations apply to the ionization of **5** (R = H). The acid strength of **5** (R = H) (Table II), found by the usual spectrophotometric method, proved to be about the same as that of 5,5-dimethyl-2,4-dithiohydantoin (10); the acid-weakening effect of a 1-methyl group (about 0.5 p*K* unit) is about the same as its effect on the acidity of 2-thiohydantoins (1), and has about the magnitude anticipated (11). The ionization constant pK_{HA} of **2** (R = H) (Table II) showed it to be a stronger acid than the corresponding 2-thiohydantoin (1) but (as expected (6)) a weaker acid than the corresponding 2,4-dithiohydantoin (**5**; R = H).

Protonation of **5** (R = H or Me) (B) would be expected to take place on the 2-thiocarbonyl sulfur to give the cation **4** (R = H or Me) (BH^+), because this permits the maximum delocalization of the positive charge (12). The structure **4** (R = H) is supported by the similarity of the spectrum of 5,5-pentamethylene-2,4-dithiohydantoin in 96% sulfuric acid (see Table I) to that of 2-methylthio-5,5-pentamethylene-2-imidazol-4-thione (**7**)[1] in 5% acid (λ_{max} at 263 and 296 mμ; ε_{max} 11 600 and 16 600). Protonation of the latter should give **8**, which differs from **4** (R = H) only in having a S—Me in place of a S—H group; the bathochromic effect of this methyl group on

TABLE II

Ionization constants of 4-thiohydantoins and 2,4-dithiohydantoins as acids (pK_{HA}) and bases (pK_{BH^+})

Compound	pK_{HA}	pK_{BH^+}
2; R = H	8.12	−4.76*
2; R = Me	—	−4.57*
5; R = H	7.64	−6.02†
5; R = Me	8.15	−5.83†

*Referred to H_A scale.
†Referred to H_0''' scale.

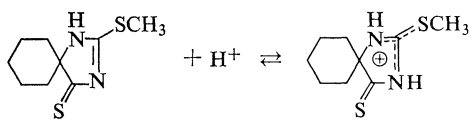

7 **8**

[1]Only one of two possible tautomeric forms is shown. The tautomerism of this compound will be discussed in a later paper.

Can. J. Chem. Downloaded from www.nrcresearchpress.com by 210.87.254.42 on 09/05/12
For personal use only.

Can. J. Chem. Downloaded from www.nrcresearchpress.com by 210.87.254.42 on 09/05/12
For personal use only.

the Type IV band is large but has many precedents.[2]

The change in spectra of the two compounds **5** (R = H and Me) in different concentrations of acid allowed their ionization to be followed in the usual way (13). The plots of log $[B]/[BH^+]$ against H_0 had slopes greater than unity (Fig. 1*A*), showing that protonation of 2,4-dithiohydantoins does not follow this acidity function. However, plots against H_0''' (15) had slopes close to unity (Fig. 1*B*). It had been shown previously that the ionization of thioamides and thiolactams, which are protonated on sulfur (12), follows H_0''',[2] and it would seem that the same is true for 2,4-dithiohydantoins.

The ionization constants pK_{BH^+} of the 2,4-dithiohydantoins **5** (R = H and CH_3), determined in the usual way from the plots in Fig. 1*B*. are recorded in Table II, and show them to be about ten times weaker bases than the corresponding 2-thiohydantoins,[2] just as they are about ten times stronger acids (1). The difference in both cases depends on the thiocarbonyl group being more polarized, and hence more strongly electron-attracting, than the carbonyl group (6). The base-strengthening effect of the 1-methyl group (about 0.2 pK unit) is the same as that found by Janssen (11) for the methyl groups of *N*,*N*′-dimethylethylenethiourea. Janssen has shown that this effect is probably composite, being made up of an electronic effect (base-strengthening) and a steric effect on solvation (base-weakening). This would explain the greater effect of the 1-methyl group (about 0.5 pK unit) on the basicity of the anion **6** (R = Me), if the methyl group hinders the solvation of this anion less than it does the solvation of the cation **4** (R = Me). This might be expected because of the different distribution of charge in anion and cation.

Lactams are more basic than thiolactams (16), and hence 4-thiohydantoins would be expected to be protonated in strong acid on the 2-carbonyl oxygen to give the cations **1** (R = H or Me). In such a case their ionization would be expected to follow better H_A than H_0; as a parallel case, we have found this to be true for the ionization of *N*-phenylurea (compare Fig. 1*A* and Fig. 1*B*).[3]

[2]J. T. Edward and I. Lantos, unpublished research.

[3]The slope (0.85) of the plot for *N*-phenylurea in Fig. 1*B* shows that the ionization does not follow H_A exactly; however, the deviation of the slope from unity is no worse than in many other cases cited in the literature (18). From Fig. 1*B*, *N*-phenylurea has $pK_{BH^+} = -1.45$.

The ionization of the 4-thiohydantoins (**2**; R = H and Me) takes place only in very strongly acidic solution, beyond the range in which the H_A scale was established by Katritzky *et al.* (17) using amide indicators. However, it can be seen from Fig. 2 that plots of log $[BH^+]/[B]$ against % sulfuric acid for the two 4-thiohydantoins (**2**; R = H and Me) show reasonably good parallelism to the plot for 2,4,6-trinitrobenzamide, the most weakly basic amide indicator acid used by Katritzky *et al.* (17); the parallelism is at least as satisfactory as that of the immediately more strongly basic amide indicators used by these authors, and shown in Fig. 2. Such behavior indicates that the ionization of the 4-thiohydantoins (**2**; R = H and Me) follows H_A, and hence that the compounds are *O*-protonated to give the cations **1** (R = H and Me).[4] Furthermore, the parallelism of the plots of log $[BH^+]/[B]$ with that of phenazine 5,10-dioxide (Fig. 2) is also reasonably good. Johnson *et al.* (18) have recently used this compound as an indicator to extend the H_A scale into higher concentrations of sulfuric acid, justifying its use by the argument that the ionization of more strongly basic *N*-oxides had been found previously to follow the H_A scale reasonably well. The present results with the 4-thiohydantoins (**2**; R = H and Me) support this argument.

The ionization constants pK_{BH^+} of the 4-thiohydantoins, obtained from the plots in Fig. 1*B*, are recorded in Table II, and show them to be considerably stronger bases than the corresponding 2,4-dithiohydantoins. This is to be expected from the greater basicity of lactams as compared with thiolactams (16). A comparison of Fig. 1*B* with Fig. 1*A* shows the dangers of obtaining relative basicities from H_0 values of half-protonation.[5,6] Although the theoretical inadequacy of such a method is well known (19), it continues to be used (e.g. ref. 20). At a more naive level, it is evident from Fig. 1*A* that the 4-thiohydantoins (*a* and *b*) require more concentrated sulfuric acid

[4]This would appear to be the first instance in which the site of protonation in a molecule (frequently a disputed point: see Katritzky and Jones (12)) has been decided on the basis of acidity function behavior.

[5]pK_{BH^+} Values based on H_0 are: *a*, −7.55; *b*, −7.22; *c*, −4.55; *d*, −4.43.

[6]It should be pointed out that a slope s = 1 (as in Fig. 1*b*) is a necessary but not a sufficient condition for the numerical validity of a measured pK_{BH^+} in this region of acidity: see Arnett (19) for a good discussion of this point.

Can. J. Chem. Downloaded from www.nrcresearchpress.com by 210.87.254.42 on 09/05/12
For personal use only.

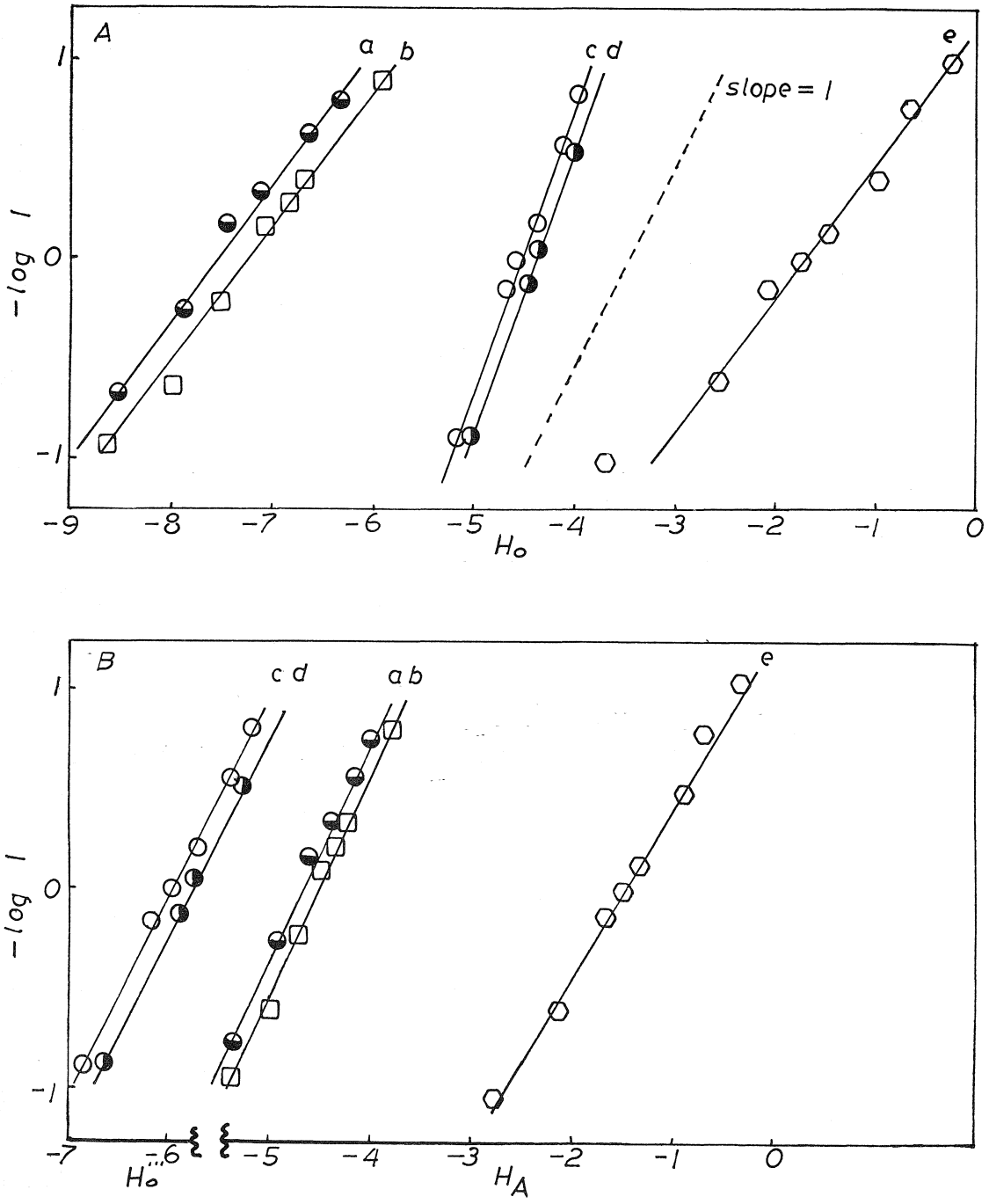

FIG. 1. Plots of $-\log I$ (= log [B]/[BH$^+$]) against H_0 (A) or H_0''' or H_A (B) of the following compounds; slopes S_A or S_B of lines given: *a*: 2 (R = H); S_A, 0.73; S_B, 0.99. *b*: 2 (R = Me); S_A, 0.75; S_B, 0.98. *c*: 5 (R = H); S_A, 1.46; S_B, 1.04. *d*: 5 (R = Me); S_A, 1.43; S_B, 1.04. *e*: *N*-phenylurea; S_A, 0.66; S_B, 0.85.

Can. J. Chem. Downloaded from www.nrcresearchpress.com by 210.87.254.42 on 09/05/12
For personal use only.

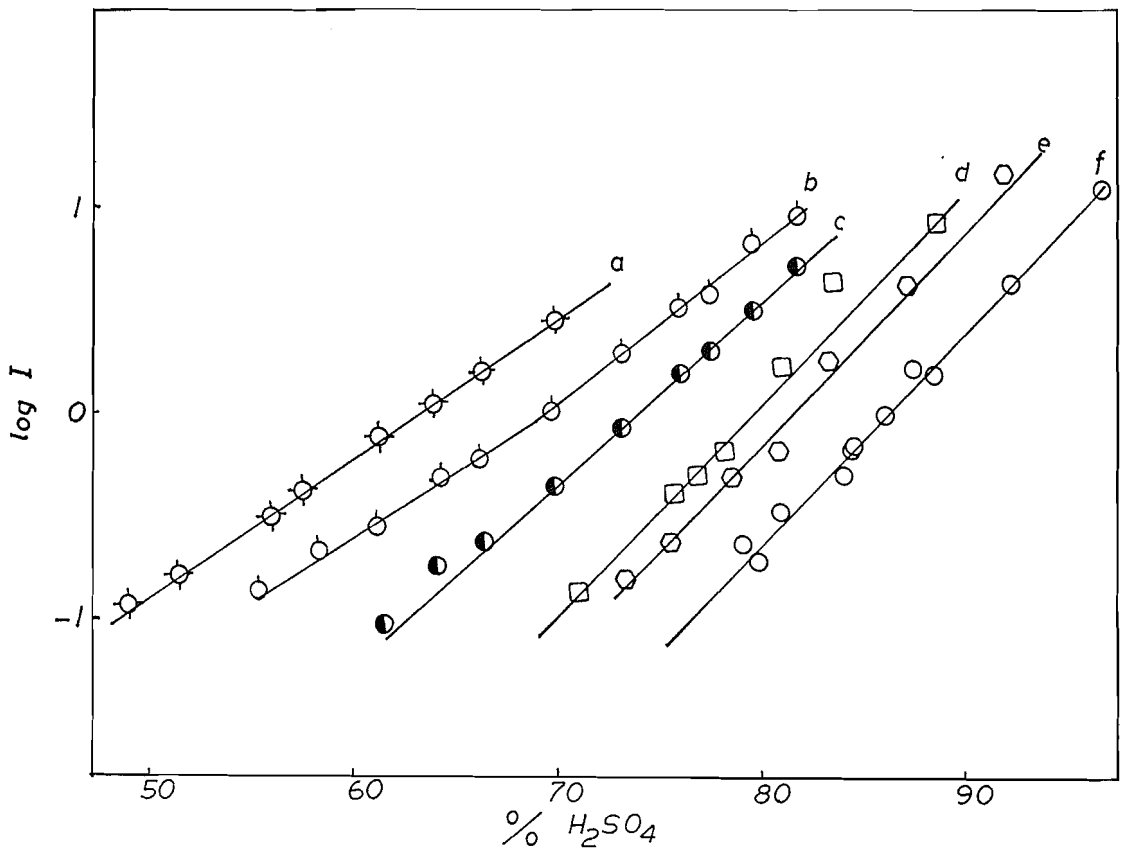

FIG. 2. Plots of log I against % sulfuric acid of the following compounds: *a*: 2,3,6-trichlorobenzamide (ref. 17); *b*: 2,4-dichloro-3,5-dinitrobenzamide (ref. 17); *c*: 2,4,6-trinitrobenzamide (ref. 17); *d*: 1-methyl-5,5-pentamethylene-4-thiohydantoin; *e*: 5,5-pentamethylene-4-thiohydantoin; *f*: phenazine 5,10-dioxide (ref. 18).

to bring about their half-protonation than the 2,4-dithiohydantoins (*c* and *d*), and it might be inferred (erroneously) that for this reason the 4 thiohydantoins are weaker bases. The importance of determining the correct acidity functions for different classes of compounds is apparent.

Experimental

The 4-thiohydantoins and 2,4-dithiohydantoins were prepared according to procedures in the literature (4), and had melting points close to those reported. Spectral measurements for all compounds were made with a Unicam SP 800 spectrophotometer having the cell compartment thermostated at 25.0±0.1°. Ionization constants were obtained by methods described previously (1, 16) and are reproducible to within ±0.05 pK units. The ionic strengths of buffers used in obtaining measurements for pK_{HA} values were about 0.01.

Acknowledgments

We are grateful to Mr. Wayne Congdon for experimental assistance, and to the National Research Council of Canada and the Petroleum Research Fund, administered by the American Chemical Society, for financial assistance.

1. J. T. EDWARD and S. NIELSEN. J. Chem. Soc. 5075 (1957).
2. J. T. EDWARD and S. NIELSEN. J. Chem. Soc. 2327 (1959).
3. J. T. EDWARD and J. K. LIU. Can. J. Chem. This issue.
4. H. C. CARRINGTON and W. S. WARING. J. Chem. Soc. 354 (1950).
5. M. J. JANSSEN. Rec. Trav. Chim. 79, 454, 464 (1960).
6. J. T. EDWARD. *In* The chemistry of organic sulfur compounds. Vol. II. *Edited by* C. Y. Meyers and N.

Kharasch. The Pergamon Press, Ltd., Oxford. 1966. pp. 287–309.
7. R. MAYER and J. FABIAN. Angew. Chem. Intern. Ed. **3**, 277 (1964).
8. M. J. JANSSEN. Rec. Trav. Chim **79**, 1066 (1960).
9. J. SANDSTROM. Acta Chem. Scand. **16**, 1616 (1962).
10. J. T. EDWARD and O. J. CHIN. Can. J. Chem. **41**, 1650 (1963).
11. M. J. JANSSEN. Rec. Trav. Chim. **81**, 650 (1962).
12. A. R. KATRITZKY and R. A. Y. JONES. Chem. Ind. London, 722 (1961).
13. L. A. FLEXSER, L. P. HAMMETT, and A. DINGWALL. J. Am. Chem. Soc. 57, 2103 (1935).
14. L. P. HAMMETT and A. J. DEYRUP. J. Am. Chem. Soc. **54**, 2721 (1932). M. A. PAUL and F. A. LONG. Chem. Rev. **57**, 1 (1957).
15. E. M. ARNETT and G. W. MACH. J. Am. Chem. Soc. **82**, 2677 (1964).
16. J. T. EDWARD and H. STOLLAR. Can. J. Chem. **41**, 721 (1963).
17. A. R. KATRITZKY, J. B. STEVENS, and K. YATES. Can. J. Chem. **42**, 1957 (1964).
18. C. D. JOHNSON, A. R. KATRITZKY, and N. SHAKIR. J. Chem. Soc. **B**, 1235 (1967).
19. E. M. ARNETT. *In* Progress in physical organic chemistry. Vol. I. *Edited by* S. G. Cohen, A. Streitwieser, and R. W. Taft. Interscience Publishers, Inc., New York. 1963. pp. 223–403.
20. P. HAAKE, R. D. COOK, and G. H. HURST. J. Am. Chem. Soc. **89**, 2650 (1967).

Can. J. Chem. Downloaded from www.nrcresearchpress.com by 210.87.254.42 on 09/05/12
For personal use only.

Can. J. Chem. Downloaded from www.nrcresearchpress.com by 210.87.254.42 on 09/05/12
For personal use only.

Thiohydantoins. VIII. Structure of the reported 5-phenyl-2,4-dithiohydantoin and its benzylation products

J. T. EDWARD AND J. K. LIU
Department of Chemistry, McGill University, Montreal, Quebec

Received February 23, 1968

The supposed 5-phenyl-2,4-dithiohydantoin (**3**) actually exists as its tautomer 5-mercapto-4-phenyl-4-imidazolin-2-thione (**12**). The reactions of the compound have been clarified by spectral studies of the products; in particular, mono- and dibenzylation have been shown to take place on sulfur and not (as reported) on nitrogen.

Le composé décrit comme phényle-5 dithio-2,4 hydantoïne (**3**) est actuellement son tautomère mercapto-5 phényle-4 imidazoline-4 thione-2 (**12**). Les produits de quelques reactions de ce composé ont été étudiés par spectroscopie. L'action du chlorure de benzyle attache un ou deux groupements benzyliques aux soufres, et non à l'azote.

Canadian Journal of Chemistry, **47**, 1123 (1969)

The products formed by the alkylation of ambident ions are generally (but not always (1)) predicted by the theory of Kornblum *et al.* (2). In particular, the theory is in accord with the general tendency of thiohydantoins to be *S*-methylated by methyl iodide in alkaline solution and *N*-methylated by diazomethane in ether solution (3, 4). An apparent exception is provided by the report of Cook *et al.* (5) that 5-phenyl-2,4-dithiohydantoin (**3**) is *N*-benzylated by benzyl chloride in alkaline solution to give a monobenzyl derivative (**6** or **7**) (λ_{max} = 277 mμ) and a dibenzyl derivative (**8**) (λ_{max} = 277 mμ). However, it has already been pointed out (4) that these *N*-benzyl structures are excluded by the ultraviolet (u.v.) absorption spectra which Cook *et al.* reported for their compounds,[1] and by the fact that the dibenzyl compound forms a hydrochloride; the compound **8** would be much too weakly basic to do this (7). Consequently, it became of interest to establish the correct structures of the benzylated compounds.

The procedure followed by Cook *et al.* in preparing 5-phenyl-2,4-dithiohydantoin (**3**) is shown in Reaction Scheme 1. A similar procedure is known to be successful in giving 5,5-disubstituted 2,4-dithiohydantoins (8), and evidence for the structure **3** was obtained by converting the compound by treatment with Raney nickel into 4-phenylimidazole (**4**). On oxidation with air or various oxidizing agents in alkaline solution it gave a compound $C_{18}H_{14}N_4S_4$, assigned the structure **5** by analogy with the structure of the product obtained by oxidizing 5-phenylhydantoin in alkaline solution (9). However, a spectral examination of these various compounds shows the structures assigned to all of them to require modification, except for **1** and **4**.

The structure **2** for the compound formed by the reaction of the aminonitrile **1** with carbon disulfide seems much less likely than **9**, in the light of our present knowledge of relative stabilities of thioamides and their iminothiol tautomers (3, 4, 10), and indeed no S—H stretching band (11) could be detected in the infrared (i.r.) spectrum of the compound. Furthermore, in ethanol solution its u.v. absorption spectrum (λ_{max} = 336 mμ, ε_{max} = 10 600) is distinctly different from that of its *S*-methyl derivative **10** (λ_{max} = 296 mμ, 224 mμ; ε_{max} = 12 200, 14 300); the spectra of **2** and **10** would be expected to be fairly similar (10). The compound must consequently exist as the tautomer **9** and not **2**. In sulfuric acid **9** and **10** have similar spectra, protonation of the first compound giving **11** (R = H) (λ_{max} 290 mμ and 245 mμ; ε_{max} 8280 and 11 500) and protonation of the second compound giving **11** (R = Me) (λ_{max} 303 mμ and 248 mμ; ε_{max} = 1.22 × 10^4 and 1.13 × 10^4). The bathochromic shift of 13 mμ on going from **11**

[1]These structures would require strong absorption peaks at about 305 mμ. 2,4-Dithiohydantoins show a strong peak at about 300 mμ (3, 4), and 5-phenyl-2,4-dithiohydantoin would be expected to show a peak at about 305 mμ (6) (cf. 5,5-diphenyl-2,4-dithiohydantoin in ethanol: $\lambda\lambda_{max}$ 410, 310, 235 mμ; $\varepsilon\varepsilon_{max}$ 81, 19 200, 10 900). *N*-Benzylation should have little effect on the ultraviolet absorption of 5-phenyl-2,4-dithiohydantoin (4, 6).

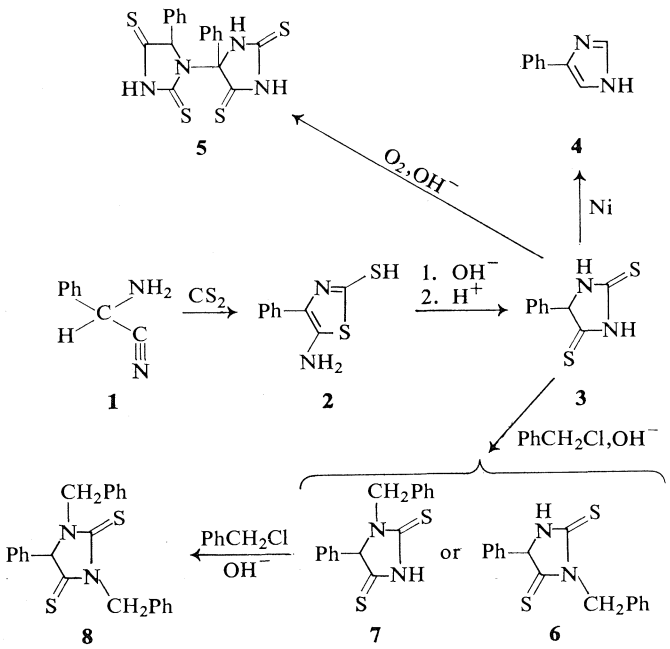

REACTION SCHEME 1

(R = H) to **11** (R = Me) is of the magnitude found for other examples of *S*-methylation,[2] while the strong hypsochromic shift on protonating the thiocarbonyl sulfur of **9** is similar to the shifts noticed on protonating other thiocarbonyl compounds (12).

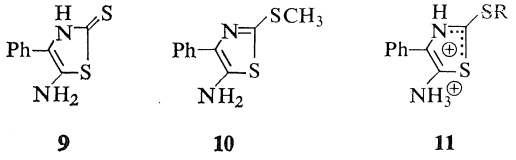

Cook's second compound (the supposed 5-phenyl-2,4-dithiohydantoin) has the structure **12** (Reaction Scheme 2) and not **3**. Its u.v. spectrum (Table I) does not exhibit a strong peak at about 305 mμ, as would be required by **3**.[1] Its i.r. spectrum showed S—H stretching bands at 2400 cm^{-1} and 2355 cm^{-1} (Nujol). This is lower than the usual frequency for the S—H band (11), but recently we have observed even lower values.[3] The assignment of the band to S—H was

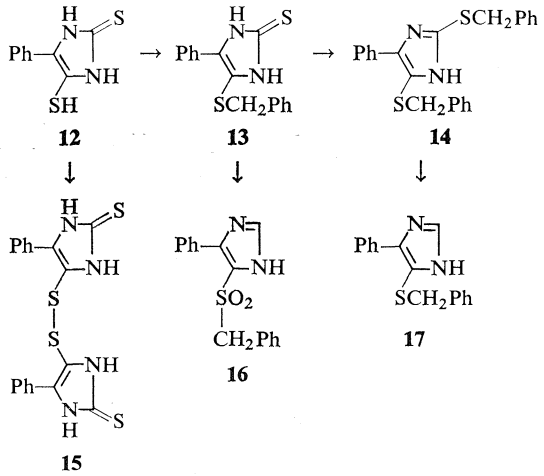

REACTION SCHEME 2

confirmed by treating the compound with deuterium oxide. The peaks at 2400 cm^{-1} and 2355 cm^{-1} disappeared and S—D peaks at 1660 cm^{-1} and 1640 cm^{-1} appeared. The structure **12** also accords with the nuclear magnetic resonance (n.m.r.) spectrum of the compound (Table II), which shows only SH, NH, and aromatic CH peaks. The structure **3** would require a C_5—H singlet at about δ = 5.5 p.p.m.; such singlets are

[2]J. T. Edward and I. Lantos. Unpublished observations.

[3]J. T. Edward and R. Sheffler. Unpublished observations.

Can. J. Chem. Downloaded from www.nrcresearchpress.com by 210.87.254.42 on 09/05/12
For personal use only.

TABLE I

Ultraviolet absorption spectra

Compound	Un-ionized* λ_{max} (mμ)	Un-ionized* ε_{max}	Cation BH^+† λ_{max} (mμ)	Cation BH^+† ε_{max}	Anion A^-† λ_{max} (mμ)	Anion A^-† ε_{max}
12	277	16 200	262	9 350	280	14 000
	(345)‡				(315)‡	11 500
13	277	17 000	260	17 200	260	12 100
	(313)‡				(302)‡	8 800
4	258	12 800	248	17 750	277	11 200
17	277	9 500	245	11 100	290	8 900
	250	9 220				
16	252	9 800	243	9 300	260	7 800
14	277	14 400	277	15 000	282	13 400

*In ethanol.
†In water.
‡Shoulder.

TABLE II

Proton magnetic resonance spectra

Compound	Solvent*	Chemical shift δ (p.p.m.) (relative areas) NH‡	SH‡	CH_2	Aromatic H
12	D	12.92 (1)‖	3.42 (1)‖	—	7.42 (5)‖
		13.00 (1)‖			
13	D	12.17 (2)†	—	3.88 (2)‖	7.0 (10)§
14	D	8.03 (1)†	—	4.01 (2)‖	7.5 (15)§
				4.37 (2)‖	
16	D	7.80 (1)‖	—	4.42 (2)‖	7.1 (11)§
17	C	10.23 (1)†	—	3.88 (2)‖	7.2 (11)§

*D = $(CD_3)_2SO$; C = $CDCl_3$.
†Broad peak.
‡Eliminated by treatment of solution with D_2O.
§Multiplet.
‖Singlet.

shown in the spectra of the hydrochloride of **1** (δ = 5.81 p.p.m.) and of 1-acetyl-5-phenyl-2-thiohydantoin (δ = 5.51 p.p.m.), and are unaffected by treating the compounds with deuterium oxide.

The structure **12** is further supported by measurements of the acid and base dissociation constants of the compound (Table III). The acidity (pK_{HA} 8.1) is about that expected for an unsaturated thiol (cf. pK_{HA} of 6.52 for thiophenol, 10–11 for alkane thiols (13)), and the basicity (pK_{BH^+} −3.15, referred to the H_O''' scale (14)), is about that expected for a thiourea.[4] A compound of structure **3** would be a much weaker base, having a pK_{BH^+} of about −6 (7).

TABLE III

Ionization constants

Compound	pK_{HA}	pK_{BH^+}
12	8.15±0.04	−3.16±0.01
13	9.55±0.09	−3.31±0.09
14	10.93±0.15	2.70±0.10
17	11.97±0.03	5.43±0.09
4	12.96±0.04	6.12±0.01*

*Kirby and Neuberger (26) obtained a pK_{BH^+} of 6.00±0.04 (zero ionic strength) from potentiometric measurements.

The occurrence of Cook's supposed 5-phenyl-2,4-dithiohydantoin as its tautomer **12** is interesting in view of the fact that 5-phenylhydantoin and 5-phenyl-2-thiohydantoin, which also have a hydrogen atom at C-5, do not tautomerize in the same way. (The n.m.r. signal in the spectrum of 1-acetyl-5-phenyl-2-thiohydantoin due to this hydrogen has been mentioned above.) It has been

[4]Janssen (15) reported a pK_{BH^+} of −1.9 for ethylenethiourea, the ionization of which he assumed to follow H_O; referred to the H_O''' scale, this would represent a pK_{BH^+} of −2.7.

Can. J. Chem. Downloaded from www.nrcresearchpress.com by 210.87.254.42 on 09/05/12
For personal use only.

Can. J. Chem. Downloaded from www.nrcresearchpress.com by 210.87.254.42 on 09/05/12
For personal use only.

claimed that thiones are more extensively enolized than ketones (16), although quantitative data to support this claim seem to be lacking, and this would seem to be a further example.

The thiol formulation **12** for Cook's second compound makes the disulfide structure **15** more plausible than **5** for its oxidation product $C_{18}H_{14}N_4S_4$. This disulfide structure is supported by the i.r. spectrum, which is similar to that of **12** except for the absence of the S—H band, and the u.v. spectrum, which lacks a peak at about 305 mμ. (The u.v. spectra of this and related compounds will be discussed in detail later.)

The disulfide structure **15** better accommodates some of the properties of the compound (e.g. the formation of 4-phenylimidazole by treatment with Raney nickel) already reported by Cook *et al.* (5). In particular, their report that the compound when treated with alkali gave about 80% yield of 5-phenyl-2,4-dithiohydantoin (**3**) would be most remarkable on the basis of the structure **5**, from which one would expect a maximum yield of 50% (17). It becomes understandable on the basis of **15**, since alkaline hydrolysis of disulfides can give thiols (theoretical yield 75%) and sulfinic acids (18):

$$2RSSR + 2H_2O \rightarrow 3RSH + RSO_2H$$

Benzylation of **12** gives the *S*-benzyl derivative **13**, and not the *N*-benzyl derivative **6** or **7**. The structure **13** is required by the u.v. spectrum (Table I), which, as mentioned above, excludes structures **6** and **7**, by the infrared and n.m.r. (Table II) spectra, which show the thiol group of the starting material **12** to have disappeared, and by the basicity of the compound (Table III), which is about 10^3 times stronger than would be expected for **6** or **7** (7). The absence of the thiol grouping is shown also by the weakened acidity (pK_{HA} 9.5) of the compound, as compared with **12**. The experimental pK_{HA} is probably a composite value, ionization of **13** yielding both **18** and **19**. Because ionization of **12** in basic solution takes place at the SH group, and of **13** at NH groups, their spectra in alkaline solution are different. However, in strongly acidic solution both are protonated on the thiourea sulfur, and have similar u.v. spectra (Table I) and ionization constants (Table III).

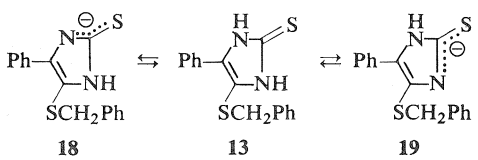

18 **13** **19**

Treatment of the monobenzyl derivative with Raney nickel gave 4-phenylimidazole, the product anticipated from **13** but not from **6** or **7**. Treatment with hydrogen peroxide in acetic acid gave the ω-toluenesulfonyl derivative **16**, whose structure follows from its n.m.r. spectrum (Table II) and u.v. spectrum (Table I). The latter shows a fairly strong similarity to that of 4-phenylimidazole. The oxidative removal of sulfur from a thiourea function (as in **13** → **16**) finds ample analogy in the literature (19).

The dibenzyl derivative (pK_{BH^+} +2.70) is about one million times more strongly basic than the monobenzyl derivative, and hence can form a crystalline hydrochloride, as noted by Cook *et al.* (5). Similar changes in basicity have been observed following the *S*-alkylation of thiourea (4), and in the present instance indicate the structure **14** for the dibenzyl derivative. This structure is compatible with the n.m.r. (Table II) and u.v. (Table I) spectra of the compound. The latter shows some similarity to the spectrum of **4**, although the perturbing effect of the two benzylthio groups is perhaps greater than expected.

Treatment of the dibenzyl compound with a deactivated Raney nickel gave 4-phenylimidazole and 5-benzylthio-4-phenylimidazole (**17**). No 2-benzylthio-4-phenylimidazole, a known compound (20), was detected. The preferential removal of the 2-benzylthio group may perhaps be explained by the hindered character of the 5-benzylthio group. The spectral (Tables I and II) and ionization characteristics (Table III) of **17** accord with the structure assigned it. The acidity (pK_{HA}) of the compounds **4**, **17**, and **14** changes in the direction and by about the magnitudes to be expected from the inductive effects of the benzylthio groups. The basicity (pK_{BH^+}) also changes in the direction expected, but the change on going from **17** to **14** (Table III) is unexpectedly large; steric hindrance to solvation of the cation from **14** may be involved (15).

Experimental

General Preparation of Compounds

5-Amino-4-phenyl-2-thiazolin-2-thione (**9**), 4-mercapto-5-phenyl-2-imidazolin-2-thione (**12**), di-(4-phenyl-2-thioxo-4-imidazolinyl) disulfide (**15**), 4-benzylthio-5-

Can. J. Chem. Downloaded from www.nrcresearchpress.com by 210.87.254.42 on 09/05/12
For personal use only.

phenyl-2-imidazolin-2-thione (**13**), 2,4-dibenzylthio-5-phenylimidazole (**14**), and 5-amino-2-methylthio-4-phenylthiazole (**10**) were prepared according to Cook *et al.* (5). 1-Acetyl-5-phenyl-2-thiohydantoin was prepared according to Swan (21). Melting points were in satisfactory agreement with those reported.

5-Phenylmethanesulfonyl-4-phenylimidazole (16)

Hydrogen peroxide (50%; 1 ml) was added dropwise to a solution of 4-benzylthio-5-phenyl-2-imidazolin-2-thione (**13**), (0.5 g) in acetic acid (10 ml) at room temperature. After 1 h the solution was diluted with water (20 ml) and evaporated to dryness at reduced pressure. The residue was crystallized from methanol, giving colorless needles of 5-phenylmethanesulfonyl-4-phenylimidazole (0.13 g), m.p. 212–213°, ν_{max}(KBr) 1330 and 1130 cm^{-1} (sulfonyl: ref. 22).

Anal. Calcd. for $C_{16}H_{14}N_3O_2S$ (mol. wt., 298): C, 64.4; H, 4.7; N, 9.4. Found (mol. wt., 298; mass spectry.): C, 64.1; H, 4.9; N, 10.2.

Desulfurization of 4-Benzylthio-5-phenyl-2-imidazolin-2-thione (13)

The thione (0.32 g) in ethanol (25 ml) was treated with Raney nickel (1.5 g) of W-4 activity (23) for 30 min at 60°. The mixture was filtered, and the filtrate taken to dryness. The residue was extracted with ether, the ether evaporated, and the residue crystallized from benzene, giving colorless plates of 4-phenylimidazole (59 mg; 41% yield), m.p. 133–134°, λ_{max}(EtOH) 258 mμ, ε_{max} = 12 800 (lit. m.p. 133–134° (5), λ_{max}(EtOH) 257 mμ, ε_{max} = 16 000 (24)).

5-Benzylthio-4-phenylimidazole (17)

A solution of 2,4-dibenzylthio-5-phenylimidazole (**14**) (6.3 g) in methanol (100 ml) containing a suspension of deactivated W-2 Raney nickel (23) was refluxed for 4 h. The mixture was filtered, the filtrate evaporated, and the residue chromatographed on neutral alumina. Elution with chloroform–methanol 95:5 (v/v) gave 5-benzylthio-4-phenylimidazole (0.14 g), m.p. 162–163°.

Anal. Calcd. for $C_{16}H_{14}N_2S$: C, 72.2; H, 5.3; N, 10.5. Found: C, 71.7; H, 5.4; N, 10.3.

Conditions for obtaining this compound were extremely critical. Treatment of 2,4-dibenzylthio-5-phenyi-imidazole with W-2 Raney nickel in ethanol, with W-4 nickel in methanol or ethanol, or with deactivated W-4 nickel in methanol gave only low yields of 4-phenylimidazole.

Spectral Measurements

Infrared spectra were obtained with a Perkin–Elmer Infracord 317 instrument, using KBr discs. Nuclear magnetic resonance spectra were obtained with a Varian HA-60 instrument, using tetramethylsilane as an internal standard. Ultraviolet spectra were obtained with a Unicam SP 800 spectrophotometer having the cell compartment maintained at 25.0 ± 0.1°. For u.v. measurements the compounds were dissolved in ethanol, in aqueous sulfuric acid of varying concentration, or in buffer solutions of 0.05–0.1 ionic strength; pH values of the buffer solutions were measured with a Radiometer pH meter No. 23. The spectral characteristics of the un-ionized compound (B or HA), the protonated compound (BH^+), and the deprotonated compound (A^-) were obtained by measurements at appropriate pH or H_O''' values, and the ionization constants pK_{BH+} (= pH or H_O''' + log [BH^+]/[B]) and pK_{HA} (= pH + log [HA]/[A^-]) obtained by absorbance measurements at intermediate pH or H_O''' values according to well-established procedures (25). No correction was made for the effects of ionic strength for compounds ionizing in the pH range 1–14; the pK_{BH+} value of 4-phenylimidazole is in reasonable agreement with the value reported by Kirby and Neuberger (26) when ionic strength is taken into account.

Acknowledgment

Grateful acknowledgment is made to the National Research Council of Canada for financial support.

1. W. J. Le Noble and J. E. Puertor. Tetrahedron Letters, 1087 (1966).
2. N. Kornblum, R. A. Smiley, R. A. Blackwood, and D. C. Iffland. J. Am. Chem. Soc. **77**, 6269 (1955).
3. H. C. Carrington and W. S. Waring. J. Chem. Soc. 354 (1950).
4. J. T. Edward. *In* The chemistry of organic sulfur compounds. Vol. 2. *Edited by* N. Kharasch and C. Y. Meyers. The Pergamon Press, Ltd., Oxford. 1966. p. 287.
5. A. H. Cook, Sir I. Heilbron, and A. L. Levy. J. Chem. Soc. 1598 (1947).
6. J. T. Edward and S. Nielsen. J. Chem. Soc. 5075 (1957).
7. J. T. Edward and J. K. Liu. Can. J. Chem. This issue.
8. R. A. Jacobson. J. Am. Chem. Soc. **67**, 1996 (1945); H. C. Carrington. J. Chem. Soc. 1619 (1948).
9. S. Gabriel. Ann. **350**, 118 (1906); A. Pinner. Ann. **350**, 135 (1906).
10. A. R. Katritzky and J. M. Lagowski. *In* Advances in heterocyclic chemistry. Vol. 1. *Edited by* A. R. Katritzky. Academic Press, Inc., New York. 1963. pp. 341 *ff.*
11. L. J. Bellamy. *In* The chemistry of organic sulfur compounds. Vol. I. *Edited by* N. Kharasch. The Pergamon Press, Ltd., Oxford. 1961. p. 51. R. B. Nannan, J. H. Lieblich, and A. G. Renfrew. J. Am. Chem. Soc. **71**, 3733 (1959).
12. M. J. Janssen. Rec. Trav. Chim. **79**, 454, 464 (1960).
13. M. M. Kreevoy, E. T. Harper, R. E. Duval, H. S. Wilgus, and L. T. Ditsch. J. Am. Chem. Soc. **82**, 4899 (1960).
14. E. M. Arnett and G. W. Mach. J. Am. Chem. Soc. **86**, 2671 (1964).
15. M. J. Janssen. Rec. Trav. Chim. **81**, 650 (1962).
16. R. Mayer and J. Fabian. Angew. Chem. Intern. Ed. Engl. **3**, 277 (1964).
17. J. T. Edward and S. Nielsen. J. Chem. Soc. 2327 (1959).
18. D. S. Tarbell. *In* The chemistry of organic sulfur compounds. Vol. I. *Edited by* N. Kharasch. The Pergamon Press, Ltd., New York. 1961. p. 97. O. Foss; p. 84. N. Kharasch; p. 375.
19. R. M. Evans, P. G. Jones, P. S. Polmer, and F. F. Stevens. J. Chem. Soc. 4106 (1956).

20. R. M. DODSON. J. Am. Chem. Soc. **70**, 2754 (1945).
21. J. SWAN. Australian J. Sci. Res. **A5**, 711 (1952).
22. A. D. CROSS. Introduction to practical infrared spectroscopy. Butterworths, London. 1960. p. 72.
23. R. MOZINGO. Org. Syn. **21**, 15 (1941).
24. H. E. UNGNADE. (*Editor*). Organic electronic spectral data. Vol. 2. Interscience Publishers, Inc., New York. 1960. p. 165.
25. L. A. FLEXSER, L. P. HAMMETT, and A. DINGWALL. J. Am. Chem. Soc. **57**, 2103 (1935).
26. A. H. M. KIRBY and A. NEUBERGER. Biochem. J. **32**, 1146 (1938).

Can. J. Chem. Downloaded from www.nrcresearchpress.com by 210.87.254.42 on 09/05/12
For personal use only.

Can. J. Chem. Downloaded from www.nrcresearchpress.com by 210.87.254.5 on 09/05/12
For personal use only.

Purine analogues. I. The status of Hückel molecular orbital calculations as predictors of proton shifts, basic strengths, and reactivity[1]

BRIAN M. LYNCH,[2] ALLAN J. ROBERTSON,[3] AND JOHN G. K. WEBB[4]
Organic Chemistry Laboratory, Saint Francis Xavier University, Antigonish, Nova Scotia

Received June 17, 1968

A detailed series of molecular orbital calculations based on the HMO method has been made for the various possible ionic species of purine, pyrazolo(3,4-*d*)pyrimidine, v-triazolo(4,5-*d*)pyrimidine, and pyrazolo(3,4-*b*)pyridine. π-Electron densities and localization and delocalization energies for nucleophilic substitution have been derived.

The results are compared with the observed proton chemical shifts in the conjugate acids of these molecules, with the relative rates of nucleophilic piperidinodehalogenations in the neutral molecules, and with the ionization constants.

It is concluded that it is possible to reconcile the calculations with experimental results for the various positions within a six-membered ring, but that positions in six- and five-membered rings cannot be directly compared. The electron densities seem to be of little value in correlating the observed ionization patterns of purines and their analogues.

Canadian Journal of Chemistry, **47**, 1129 (1969)

Introduction

As a consequence of their involvement as determinants of biological processes, the purine components of nucleic acids and their analogues have received much attention from synthetic organic chemists (1, 2) and from quantum chemists (3). However, there is little constructive interaction between the two groups: uncritical applications of molecular orbital (MO) calculations by synthetic chemists (4) often suggest that the calculations have little value, while defences of the value of simple MO treatments (5, 6) often quote irrelevant or incorrect supporting data. In this paper, we seek to show where simple MO calculations on appropriate ionic species of purines and their analogues are of correlative or predictive value, and also to indicate areas where the simple approach gives predictions at variance with experimental facts.

We have chosen three areas where detailed comparisons between theory and experiment are possible: calculated π-electron densities and observed proton chemical shifts (cf. 7, 8); π-electron densities and ionization constants (cf. 9); and localization energies (10) and delocalization energies (11) for nucleophilic substitution as compared with observed activation parameters for piperidinodehalogenations (cf. 12).

Results and Discussion

Molecular Orbital Calculations

The simple Hückel method (HMO) (13) was used, employing a standard matrix diagonalization program with an IBM 1620 40K computer (14, 15). The following electronegativity parameters h (16) were used: carbon and anionic nitrogen, 0; pyridine-type nitrogen, +0.5; pyridinium- and pyrazole-type NH, +1. All resonance integrals were assumed equal to β_{CC}. The output of the calculations consisted of the orbital energies, π-electron densities, and π-bond orders. ω-Technique calculations (17), using $\omega = 1.4$, were performed using the electron densities from the HMO calculations as input.

Localization energies for nucleophilic substitution at the various positions were evaluated by subtraction of the energies of electrons in the occupied orbitals in the residual systems from those in the parent species, and delocalization energies for nucleophilic piperidinodechlorinations were evaluated following Beltrame *et al.* (11).

The results for purine **1** and the purine analogues 1*H*-pyrazolo(3,4-*d*)pyrimidine **2**, 3*H*-v-triazolo(4,5-*d*)pyrimidine **3**, and 1*H*-pyrazolo-

---

[1]Presented in part at the International Congress of Heterocyclic Chemistry, Albuquerque, New Mexico, June 14, 1967.

[2]Enquiries should be addressed to this author. Address until September 1969: Department of Medical Chemistry, John Curtin School of Medical Research, Australian National University, Box 334, Canberra City, A.C.T. 2601, Australia.

[3]Graduate Research Assistant, 1965–1967. Present address: Cyanamid of Canada Ltd., St. Catharines, Ontario.

[4]Graduate Research Assistant, 1966–1968. Present address: Queen's University, Kingston, Ontario.

(3,4-*b*)pyridine **4** are summarized in Tables I through III.

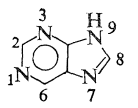

1

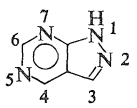

2

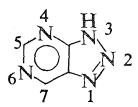

3

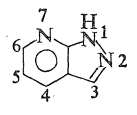

4

π-Electron Densities and Proton Chemical Shifts

Previous work has established qualitative and quantitative correlations between proton chemical shifts and HMO π-electron densities for pyridinium and diazolium ions (7), and for the amino protons in carbocyclic and heterocyclic aromatic amines (8), and Black, Brown, and Heffernan (18) have analyzed the proton chemical shifts of a series of heteroaromatic nitrogen compounds, establishing "empirical" electron density distributions after allowing for the effects of ring currents, lone-pair anisotropy, and non-adjacent charges.

Although the proton and carbon-13 magnetic resonance spectra of purine have received considerable attention (19–22), little success has been achieved in correlating electron densities directly with the proton shifts. In view of the fairly wide range of proton shifts available in the series purine, pyrazolo(3,4-*d*)pyrimidine, and v-triazolo(4,5-*d*-)pyrimidine, and also pyrazolo-(3,4-*b*)pyridine (23), we have attempted such a correlation for the protons in the six-membered rings employing the proton chemical shifts observed in trifluoroacetic acid-*d* (in this solvent, many paramagnetic effects of n–π^* transitions will disappear (cf. 7)), and using ring-current corrections of 0.20 p.p.m. for the influence of the five-membered rings at positions α to them, and a further correction of 0.30 p.p.m. for the influence of a pyridine-type nitrogen in a position *peri* to protons α to a five-membered ring. We have used π-electron densities appropriate to models assuming that protonation has occurred at positions analogous to position-1 of purine (which we expect to be the predominant basic site (cf. 9, 21)).

We find that the chemical shifts of the protons in this series of compounds are linearly related to the calculated electron densities, and the correlation coefficient meets the acceptable standard of $r = 0.96$, set by Jaffe (24): the least-squares regression line is defined by

$$\delta = 14.86 - 6.64q\pi \; (r = 0.972)$$

and the average deviation is ca. 0.1 p.p.m. (see Table IV, and Fig. 1).

Thus, the calculated HMO π-electron densities for assumed models of the conjugate acids of purine and purine analogues are excellent predictors for the proton chemical shifts within the six-membered rings. Since very few points are available for correlations within the five-membered rings, no analysis was made in these instances. We point out, however, that the proton shifts are well downfield from the values predicted from the calculated electron densities using the regression line given above, suggesting that the deshielding effect of the ring current in the six-membered ring on protons in five-membered rings is significantly greater than 0.20 p.p.m. (cf. 18).

MO Quantities and Ionization Behavior

As Clark and Perrin (25) have noted, many difficulties beset quantitative correlations of the base strengths of nitrogen heterocycles with MO quantities, although there are correlations between pK_a and electron density at nitrogen with aza-derivatives of alternant hydrocarbons and with polycyclic aromatic amines (26, 27). Thus, although the total HMO π-electron densities at the nitrogen atoms in the pyrimidine rings of the neutral molecules of pyrazolo(3,4-*d*)pyrimidine, purine, and 3*H*-v-triazolo(4,5-*d*)-pyrimidine decrease in the same order as the basic strengths of these compounds (electron densities: 2.491, 2.480, 2.473 (cf. Table I) pK_a of cations: 2.8, 2.4, ca. −0.1), the absolute changes are very small and may have little significance.

Nakajima and the Pullmans (28, 29) have suggested that correlations between relative SCF-MO ionization potentials for the lone-pair electrons on ring nitrogen atoms and pK_a values, which are observed for other nitrogen heterocyclic compounds, allow predictions of the basic strengths of purines and their analogues. We find that these predictions are of very limited

Can. J. Chem. Downloaded from www.nrcresearchpress.com by 210.87.254.5 on 09/09/12
For personal use only.

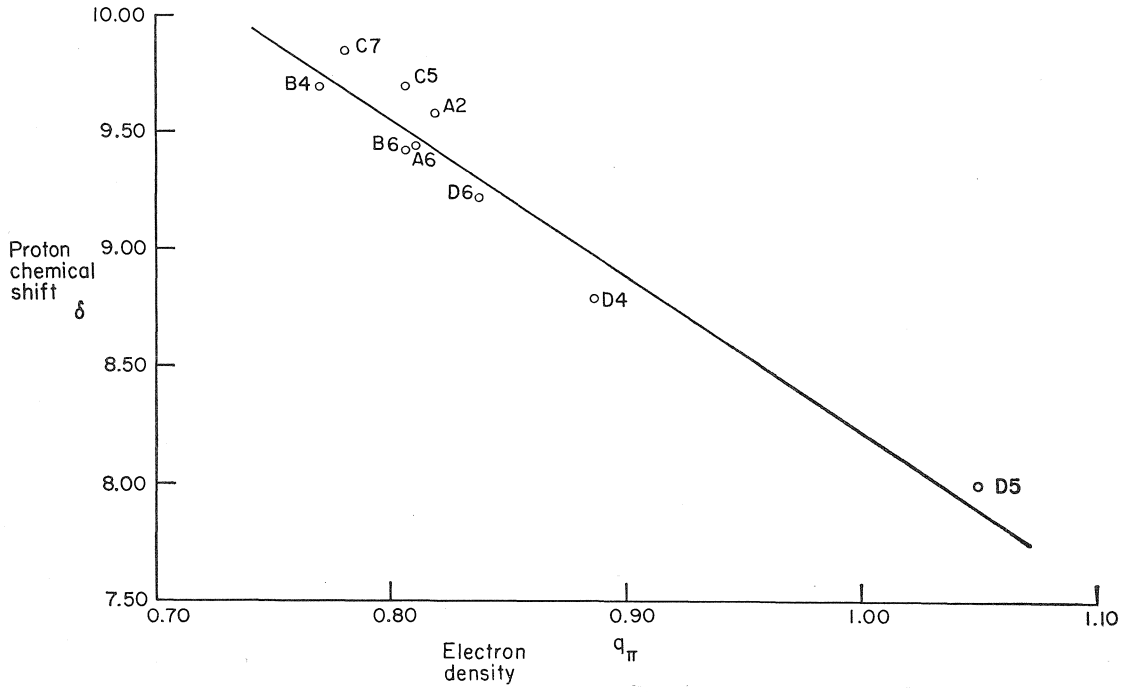

FIG. 1. Plot of π-electron density vs. corrected proton chemical shift. A, Purine; B, 1-methylpyrazolo(3,4-*d*)pyrimidine; C, 3*H*-v-Triazolo(4,5-*d*)pyrimidine; D, 1-methylpyrazolo(3,4-*b*)pyridine. Numerical suffixes refer to positions of protons.

value: although there is a significant correlation between the relative ionization potential and pK_a for purine and some aminopurines ($r = 0.984$) (29), use of the regression line to predict the pK_as of the cations of 4-aminopyrazolo(3,4-*d*)pyrimidine (cf. 9), v-triazolo(4,5-*d*)pyrimidine (30), and its 7-amino derivative results in spectacular failure (the respective values (predicted, found) are: 3.14, 4.59; 1.31, −0.10; 3.05, 2.84). Although the aminopyrazolo pyrimidine and the aminotriazolopyrimidine are predicted to have almost identical pK_a values (their relative ionization potentials are quoted as −1.67 and −1.65 e.V. (29)), the actual values differ by almost two units (see Table V, also (9)).

Further, although it is quite probable that all three basic sites in purine are protonated to some extent (9, 21), the Nakajima–Pullman treatment uses the existence of very small differences in relative ionization potentials to predict preferential basic centers, although as Table V demonstrates, very small differences in relative ionization potentials are accompanied by large variations in actual basic strength.

In view of the failure of the Nakajima–Pullman approach in these examples, we must conclude that calculations in terms of the π-electron approximation do not enable us to predict the base strengths of purines or their analogues (cf. 32).

MO Quantities and Nucleophilic Substitutions

As Pullman (33) has pointed out, π-electron densities in heterocyclic rings often give no indication of the relative reactivities of different positions, and it might be expected that calculations of localization energies would be of greater significance. Pullman and Pullman's calculations of these quantities for the neutral molecules of purine, pyrazolo(3,4-*d*)pyrimidine, and v-triazolo(4,5-*d*)pyrimidine might therefore be expected to be of correlative value for the rates of nucleophilic substitution in such molecules.

One difficulty in a direct correlation has been pointed out by Sutcliffe and Robins (4), since the nature of the reacting species may change with the pH of the reaction medium, and realistic localization energies should take these

Can. J. Chem. Downloaded from www.nrcresearchpress.com by 210.87.254.5 on 09/05/12
For personal use only.

TABLE I

Calculated π-electron densities in purine and some analogues

No.	Method of calculation	Input parameters	Corresponding model	π-Electron density, q_π						
				Position						
				1	2	3	6	7	8	9
A: Purine										
1	HMO	$h_9 = 1$ $h_{1,3,7} = 0.5$	Neutral molecule (9H isomer)	1.233	0.876	1.247	0.884	1.362	0.883	1.539
2	ω-technique	output from No. 1	Neutral molecule (9H isomer)	1.154	0.975	1.154	0.968	1.270	1.013	1.404
3	HMO	$h_{1,9} = 1$ $h_{3,7} = 0.5$	1-Protonated conjugate acid	1.402	0.820	1.248	0.811	1.356	0.878	1.533
				Position						
				1	2	3	4	5	6	7
B: 1H-Pyrazolo(3,4-d)pyrimidine										
4	HMO	$h_1 = 1$ $h_{2,5,7} = 0.5$	Neutral molecule	1.538	1.211	1.050	0.848	1.239	0.859	1.252
5	ω-technique	output from No. 4	Neutral molecule	1.399	1.177	1.107	0.959	1.155	0.971	1.153
6	HMO	$h_{1,5} = 1$ $h_{2,7} = 0.5$	5-Protonated conjugate acid	1.531	1.209	1.039	0.770	1.407	0.807	1.253
				Position						
				1	2	3	4	5	6	7
C: 3H-v-Triazolo(4,5-d)pyrimidine										
7	HMO	$h_3 = 1$ $h_{1,2,4,6} = 0.5$	Neutral molecule	1.256	1.095	1.494	1.245	0.860	1.228	0.860
8	ω-technique	output from No. 7	Neutral molecule	1.227	1.132	1.374	1.147	0.966	1.147	0.958
9	HMO	$h_{3,6} = 1$ $h_{1,2,4} = 0.5$	6-Protonated conjugate acid	1.247	1.090	1.490	1.246	0.807	1.397	0.781
D: 1H-Pyrazolo(3,4-b)pyridine										
10	HMO	$h_1 = 1$ $h_{2,7} = 0.5$	Neutral molecule	1.544	1.213	1.062	0.942	1.046	0.919	1.248
11	HMO	$h_{1,7} = 1$ $h_2 = 0.5$	7-Protonated conjugate acid	1.541	1.216	1.054	0.887	1.050	0.838	1.428

variations into account. Robins and Sutcliffe were able to give excellent qualitative explanations of apparent inconsistencies in the order of reactivity of the 2-, 6-, and 8-positions in chloropurines and their 7- or 9-alkyl derivatives by postulating cation or anion formation at the appropriate pH as reactivity-controlling factors. Recent kinetic studies of nucleophilic substitutions in 9-alkylchloropurines and chloropurines by Barlin and Chapman (12*a*) and by Barlin (12*b*) show that these explanations are well founded.

The localization energies for nucleophilic attack at the 6- and 8-positions in neutral purine were evaluated by Pullman (3, 33), and these results (suggesting virtually equivalent reactivities for these positions) are consistent with Barlin and Chapman's findings for the piperidinodechlorinations of 9-methyl-6- and 8-chloropurines (12*a*). It is likely that this agreement is an artifact of the parameters used in the calculation (the localization energy will depend upon the choice of resonance integral for the C_8—N_9 bond), and direct comparison of localization energies for five- and six-membered rings is a risky procedure. Evidence regarding this point is available from Barlin's study (34) of nucleophilic piperidinodebrominations of

Can. J. Chem. Downloaded from www.nrcresearchpress.com by 210.87.254.5 on 09/05/12
For personal use only.

TABLE II

Localization energies for ionic species of purine and some analogues

Species	Position:	Localization energy (−β units) for nucleophilic substitution 2	6	8
A: Purine				
Neutral molecule (9H isomer)		2.269	2.121	2.249
Neutral molecule (7H isomer)			2.138	
1-Protonated conjugate acid		2.146	1.960	2.235
3-Protonated conjugate acid		2.069	2.011	2.222
7-Protonated conjugate acid		2.269	2.136	2.075
Anion		2.300	2.110	2.572
B: 1H-Pyrazolo(3,4-d)pyrimidine				
	Position:	3	4	6
Neutral molecule		2.599	2.049	2.219
5-Protonated conjugate acid		2.464	1.896	2.112
C: 3H-v-Triazolo(4,5-d)pyrimidine				
	Position:		7	
Neutral molecule			2.053	

bromoazoles. There is a reasonable correspondence between calculated HMO localization energies (35) and observed activation energies (the ratio is 0.16 ± 0.02), but the ratio for the analogous 2-substitution in pyridine is 0.11. Further, the localization energy for nucleophilic 4-substitution in 2-methyltetrazole is −2.65β and the activation energy 18.7 Kcal, while the localization energy for 2-substitution in pyridine is −2.35β, and the activation energy 21.8 Kcal.

It is therefore probable that direct comparisons in calculated localization energies for 6- and 8-positions are not meaningful.

The changes in relative localization energies accompanying anion formation (see Table II) are as expected, with the value at the 8-position increasing by 0.3β, with little effect at the 2- and 6-positions. Thus, the experimental activation energies for nucleophilic ethoxydechlorination of 9-methyl chloropurines and for the chloropurines (which will exist entirely as anions under the reaction conditions) differ by 11.5 Kcal for the 2-isomer, by 9.8 Kcal for the 6-isomer, but by 17.2 Kcal for the 8-isomer.

TABLE III

Delocalization energies (11) for nucleophilic piperidinodechlorinations*

Compound	Delocalization energy (units of −β)
2-Chloropurine	1.839
6-Chloropurine	1.734
8-Chloropurine	1.826
4-Chloro-1*H*-pyrazolo(3,4-*d*)pyrimidine	1.689
6-Chloro-1*H*-pyrazolo(3,4-*d*)pyrimidine	1.811
7-Chloro-3*H*-v-triazolo(4,5-*d*)pyrimidine	1.680
5-Chloro-3*H*-v-triazolo(4,5-*d*)pyrimidine	1.807

*The following parameters were employed: $h_{NH} = +1$, $h_N = +\frac{1}{2}$, $h_{Cl} = +1$, h for pseudoatom $= -0.4$. All resonance integrals are equal to β_{CC} except $\beta_{C-Cl} = 0.45\ \beta_{CC}$.

Localization energies corresponding to various protonated species (Table II) are relevant to Robins' findings (cf. 2) of selective nucleophilic replacement of 6,8-dichloropurine at the 8-position in aqueous acid solution (where 7-protonation is postulated), and also of 6-amino-2,8-dichloropurine under similar conditions to yield 6-amino-8-chloro-2-hydroxypurine (where 1-protonation seems probable by analogy with adenine).

Within the pyrimidine ring of purine and its aza-analogues, direct comparison of reactivities towards nucleophilic substitution with calculated localization energies should be acceptable. Barlin and Chapman (12*a*) have examined the kinetics of piperidinodechlorinations of 9-methyl-2- and 6-chloropurines in 99.8% ethanol, using classical titrimetry, and we have examined analogous reactions with 1-substituted 4-chloropyrazolo(3,4-*d*)pyrimidine and 3-phenyl-7-chloro-v-triazolo(4,5-*d*)pyrimidine in 99.9% methanol, where we have used ultraviolet spectrophotometry to follow the rates (36). The

Can. J. Chem. Downloaded from www.nrcresearchpress.com by 210.87.254.5 on 09/05/12
For personal use only.

TABLE IV

π-Electron densities and corrected proton chemical shifts

Compound	Position of proton	π-Electron density*	Proton chemical shift (observed) δ obs.	Proton chemical shift (corrected)† δ corr.
Purine	2	0.820	9.57	9.57
Purine	6	0.811	9.92	9.42
1-Methylpyrazolo(3,4-*d*)pyrimidine	4	0.770	9.88	9.68
1-Methylpyrazolo(3,4-*d*)pyrimidine	6	0.807	9.40	9.40
3*H*-v-triazolo(4,5-*d*)pyrimidine	5	0.807	9.68	9.68
3*H*-v-triazolo(4,5-*d*)pyrimidine	7	0.781	10.33	9.83
1-Methylpyrazolo(3,4-*b*)pyridine	4	0.887	8.98	8.78
1-Methylpyrazolo(3,4-*b*)pyridine	5	1.050	7.97	7.97
1-Methylpyrazolo(3,4-*b*)pyridine	6	0.838	9.20	9.20

*These refer to protonated species (see Table I).
†See text for details of correction procedure.

solvents should be closely comparable in their effects, and Table VI shows that the effects of *N*-methyl and *N*-phenyl groups are similar. The effects of substituents in the *N*-phenyl moiety, and the rate-retarding influence of a 6-methyl group, are as expected for a normal nucleophilic substitution. These reactions, therefore, provide a series establishing the effects of annelation of five-membered rings on the reactivity of the pyrimidine ring. The enthalpies of activation for these reactions and the free energies of activation were compared with the following HMO quantities for the relevant positions in the neutral molecules of the three annelated pyrimidines: (*a*) the HMO π-electron

TABLE V

Ionization behavior of corresponding pyrazolo(3,4-*d*)pyrimidines* and v-triazolo(4,5-*d*)pyrimidines*

R_1	R_4	Pyrazolopyrimidine	Triazolopyrimidine
H	NH_2	4.59	—
H	$NHCH_3$	4.53	2.84
H	NHC_2H_5	4.60	2.82
H	$N(CH_3)_2$	4.53	2.67
CH_3	NH_2	4.32	2.76
CH_3	$NHCH_3$	4.24	2.73

*Compounds of type 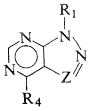 where Z = —CH: pyrazolopyridine) or —N: (triazolopyrimidine).

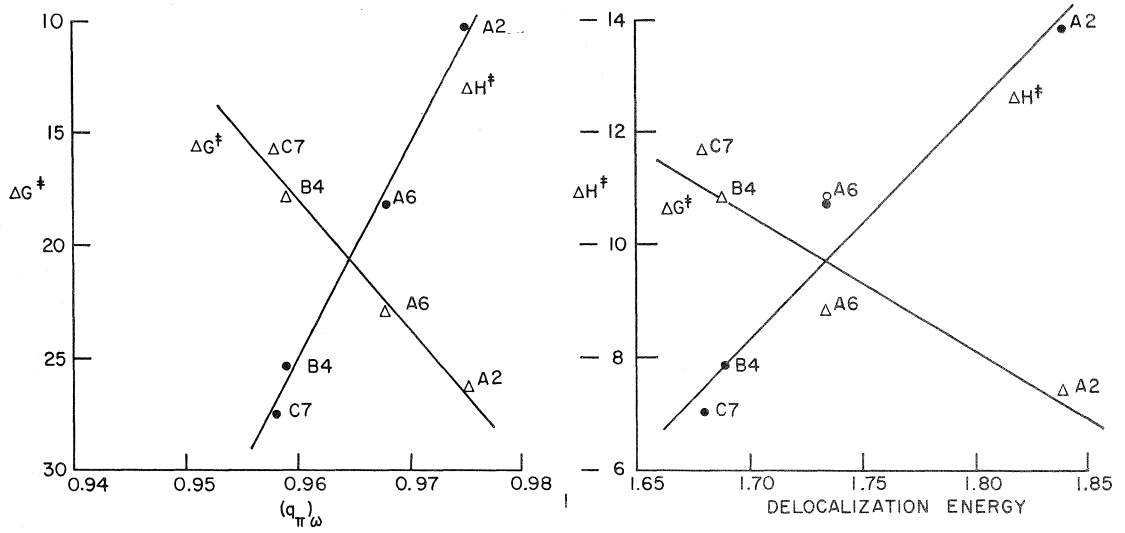

FIG. 2. Plot of activation parameters vs. MO quantities for purines and analogues (see Tables I–III). A, Purine; B, 1-methylpyrazolo(3,4-*d*)pyrimidine; C, 3*H*-v-Triazolo(4,5-*d*)pyrimidine; D, 1-methylpyrazolo(3,4-*b*)pyridine. Numerical suffixes refer to positions of protons.

Can. J. Chem. Downloaded from www.nrcresearchpress.com by 210.87.254.5 on 09/05/12
For personal use only.

TABLE VI

Kinetic results for piperidinodehalogenations*

Compound	k_2, $M^{-1}s^{-1}$ (at 25 °C)	$\Delta H^{\neq}$ (kcal·mole^{-1})	$\Delta G^{\neq}$ (kcal·mole^{-1})	$\Delta S^{\neq}$ (cal·deg^{-1}mole^{-1})
Pyrazolo(3,4-d)pyrimidines				
1-Phenyl-4-chloro	4.61×10^{-1}	7.82	17.90	33.8
1-Methyl-4-chloro	3.45×10^{-1}	7.70	18.12	34.9
1-Phenyl-4-bromo	6.14×10^{-1}	7.14	17.71	35.5
1-*p*-Nitrophenyl-4-chloro	8.68×10^{-1}	6.30	17.57	37.6
1-*p*-Tolyl-4-chloro	4.17×10^{-1}	7.87	17.94	33.8
1-Phenyl-4-chloro-6-methyl	2.16×10^{-1}	7.88	18.40	35.2
v-Triazolo(4,5-d)pyrimidine				
3-Phenyl-7-chloro	12.06	7.05	15.96	29.9
Purines†				
9-Methyl-2-chloro	1.6×10^{-5}	13.8	26.4	42.2
9-Methyl-6-chloro	5.0×10^{-3}	10.7	23.0	41.2
9-Methyl-8-chloro	4.0×10^{-3}	9.0	23.1	45.4

*Parameters of activation are calculated at 25 °C.
†From ref. 46.

TABLE VII

Regression equations linking activation parameters to molecular-orbital quantities*

			Slope	Intercept	Correlation coefficient, r
$\Delta G^{\neq}$	vs.	q_π (HMO)	223	−173	0.764
		q_π (ω)	587	−546	0.991
		Localization energy	43.1	−70.7	0.931
		Delocalization energy	61.4	−85.7	0.940
$\Delta H^{\neq}$	vs.	q_π (HMO)	136	−108	0.723
		q_π (ω)	381	−357	0.997
		Localization energy	29.1	−51.9	0.973
		Delocalization energy	41.2	−61.7	0.978

*Activation parameters refer to 1-phenyl-4-chloropyrazolo(3,4-*d*)pyrimidine, 3-phenyl-7-chloro-v-triazolo(4,5-*d*)pyrimidine, 9-methyl-2-chloro- and 9-methyl-6-chloropurine. Slopes are in kcal/electron or kcal/|β|.

densities q_π (HMO), (*b*) ω-technique π-electron densities (Table I), (*c*) localization energies for nucleophilic substitution (Table II), and (*d*) delocalization energies (11) (Table III) for piperidinodechlorination. Least-squares regression lines were drawn relating the experimental energy parameters to these quantities; slopes, intercepts, and correlation coefficients are given in Table VII, and illustrated in Fig. 2. Significant correlations are found between the free energies of activation or enthalpies of activation and the ω-technique electron densities, and also the localization and delocalization energies. The delocalization energy calculations and the ω-technique electron densities would predict the experimentally observed order of reactivities.

We conclude that simple HMO calculations can mirror reality in nucleophilic substitution reactions in purines and their analogues, providing that comparisons of the same fundamental ring system are being made.

Experimental

General

Melting points were determined using a Fisher–Johns block or a Kofler Heizbank, and are uncorrected. Proton magnetic resonance spectra were recorded for dilute solutions (2% w/w) using a Varian A-60A spectrometer; signals are expressed in parts per million downfield from

Can. J. Chem. Downloaded from www.nrcresearchpress.com by 210.87.254.5 on 09/05/12
For personal use only.

TABLE VIII

1,4-Substituted pyrazolo(3,4-*d*)pyrimidines

R_1	R_4	Melting point (°C)*	Ultraviolet absorption in methanol (nm)	
			λ_{max}	log ε
CH_3	Cl	96(98)	258	3.71
CH_3	NC_5H_{10}	120	293	4.22
C_6H_5	Cl	126(128)	243	4.51
C_6H_5	Br	135	244	4.50
C_6H_5	NC_5H_{10}	112	243, 300	4.35, 4.28
p-CH_3·C_6H_4	Cl	124	245.5	4.47
p-CH_3·C_6H_4	NC_5H_{10}	118	244, 301	4.49, 4.31
p-NO_2·C_6H_4	Cl	206	224, 263, 310	4.33, 3.93, 4.23
p-NO_2·C_6H_4	NC_5H_{10}	214	281, 327	4.36, 4.30
C_6H_5	Cl (6-CH_3)	89	245	4.50
C_6H_5	NC_5H_{10}(6-CH_3)	139	298	4.25

*Literature values are given in parentheses.

tetramethylsilane, present as internal reference; signal positions were unaffected by fivefold dilution. Trifluoroacetic acid-*d* was supplied by Merck, Sharp, and Dohme, Montreal. Ultraviolet spectroscopic measurements were made using a Beckman DK-2A ratio-recording spectrophotometer (for pK_a determinations) or a Hitachi Perkin–Elmer model 139 spectrophotometer (for kinetic measurements). A Radiometer model 4 pH meter was used for standardization of buffer solutions.

Sources of Materials

1-Methylpyrazolo(3,4-d)pyrimidine, m.p. 125°, was prepared by desulfurization of the corresponding thio-compound using Raney nickel (37).

1-Substituted-4-halopyrazolo(3,4-d)pyrimidines were prepared *via* cyclization of 1-substituted-5-amino-4-pyrazolo-carboxamides to 1-substituted-4-hydroxypyrazolo(3,4-*d*) pyrimidines followed by treatment with the appropriate phosphorus oxyhalide, using the general method developed by Robins and Cheng (37). The corresponding 1-substituted-4-piperidinopyrazolo (3,4-*d*) pyrimidines were prepared by a standard nucleophilic displacement reaction using an excess of piperidine in methanol solvent, following the general conditions used previously (37, 38). The reaction products were crystallized from methanol. Physical constants for these compounds are given in Table VIII. Proton magnetic resonance signals (in two solvents, deuteriochloroform and trifluoroacetic acid-*d*) were completely consistent with the assigned structures (39), and revealed no impurities. The intensity ratios of the various proton signals, established by electronic integration, were also in agreement with the assigned structures. It is considered that the spectroscopic evidence provides more satisfactory confirmation of structures than conventional element analyses, in view of difficulties in analysis often encountered with polyaza-heterocyclic compounds.

3-Phenyl-7-chloro-v-triazolo(4,5-d)pyrimidine was prepared as follows: 4,6-dichloro-5-aminopyrimidine (Aldrich Chemical Co.) (10 g) was dissolved in acetic acid (75 ml), aniline (6.5 g) was added, and the mixture was heated under reflux for 30 min. After cooling, water (100 ml) was added and the reaction mixture was cooled to 0°. A solution of sodium nitrite (10 g) in water (100 ml), also at 0°, was added rapidly (2 min) and the resulting precipitate was collected and twice crystallized from petroleum (b.p. 27–55°), yielding 3-phenyl-7-chloro-v-triazolo(4,5-*d*)pyrimidine (5.0 g), m.p. 117–118° (lit. 118–119° (40)) (ultraviolet absorption in methanol: λ_{max} 235.5 nm, log ε 4.51).

3-Phenyl-7-piperidino-v-triazolo(4,5-d)pyrimidine, m.p. 85° (ultraviolet absorption in methanol: λ_{max} 246, 308.5 nm; log ε 4.35, 4.28), was obtained by displacement of chlorine from the chloro precursor using piperidine in methanol (cf. 37, 38), and was crystallized from methanol.

Substituted-amino-v-triazolo(4,5-d)pyrimidines listed in Table V were provided through the courtesy of the Cancer Chemotherapy National Service Center.

3H-v-triazolo(4,5-d)pyrimidine, m.p. 174°, was prepared from 4,5-diaminopyrimidine and butyl nitrite (Albert (3)). The proton magnetic resonance spectra of the triazolopyrimidines (39) were consistent with their postulated structures.

1-Methyl-pyrazolo(3,4-b)pyridine, m.p. ca. −10°, was prepared by dediazoniation (41) of the diazonium salt from 1-methyl-3-aminopyrazolo (3,4-*b*) pyridine, prepared by treatment of 2-chloronicotinonitrile with methylhydrazine (42). Its proton magnetic resonance spectrum in trifluoroacetic acid-*d* and in deuteriochloroform was in complete accord with the assigned structure (42).

Molecular Orbital Calculations

Detailed results are available on request, as are listings of the standard HMO programs and the ω-technique program (the averaging method suggested by Ettinger (43) was used).

pK_a Determinations of (substituted amino)triazolopyrimidines

A method based on differential ultraviolet spectrophotometry was used (Lynch *et al.* (9)). Measurements were made at 20°. Although the ionization steps of the triazolopyrimidines overlap significantly, the absorption spectra of the neutral and the anionic species are virtually

Can. J. Chem. Downloaded from www.nrcresearchpress.com by 210.87.254.5 on 09/05/12
For personal use only.

Can. J. Chem. Downloaded from www.nrcresearchpress.com by 210.87.254.5 on 09/05/12
For personal use only.

identical, and differ from those of the cationic species. The spread of pK_a values obtained using buffers of varying pH was 0.20 (i.e. ± 0.10 from the mean). Full details of the ultraviolet absorption spectra of the various ionic species are available on request. The results are assembled in Table V.

Kinetics of Piperidinodehalogenations

The reactions between the various halogen derivatives of pyrazolo(3,4-*d*)pyrimidine and v-triazolo(4,5-*d*)pyrimidine with excess piperidine in methanol (99.9%; Fisher Scientific Co.) were followed by ultraviolet spectrophotometry. The increase in absorbance of the solutions in the region of maximum ultraviolet absorbance of the reaction products was followed as a function of time.

All reactions were carried out in standardized 500 ml flasks immersed in a constant temperature bath regulated to $\pm 0.02°$ using a Bronwill constant temperature circulator–controller. Samples were withdrawn at various times, rapidly diluted to an appropriate concentration and their ultraviolet absorbance was measured. Since all reactions were carried out above 25° and the cell compartment temperature was 20°, cooling accompanied the dilution procedure and reactions were arrested while the absorbance measurements were in progress. For each reaction and reaction temperature, at least ten samples were taken, and in almost all cases reactions were followed to 85% of completion. The "infinite-time" readings (ten half-lives) coincided within 3% with the values expected from the known ultraviolet absorption spectra of the reaction products.

Rate constants were determined from the concentrations of reactants and products (as deduced from their known ultraviolet absorptions) and time measurements using the appropriate second-order reaction expression (12), employing a Fortran II program. The correlation coefficients linking the time and the appropriate term involving the concentrations of the reactants and products exceeded 0.99 in all examples. Typical initial concentrations were: pyrazolopyrimidine, $2 \times 10^{-4} M$; piperidine, $1 \times 10^{-3} M$. Reactions were carried out either in duplicate at three temperatures, or as individual measurements at five temperatures ranging from 25° to 45°.

A Fortran II program was used to establish the activation energies from the linear regression equations linking the logarithms of the rate constants to the reciprocal of the Kelvin temperatures. The correlation coefficients for these regressions exceeded 0.99. The activation parameters $\Delta G^{\neq}$, $\Delta H^{\neq}$, and $\Delta S^{\neq}$ were calculated from the rate constants at 25° and the activation energies, and the values of these parameters, together with the rate constants at 25°, are listed in Table VI. Detailed results, listing the rate constants at various temperatures, are available on request.

Conclusions

Simple HMO calculations are very successful in correlating proton chemical shifts in the conjugate acids of purine and its analogues, and we are currently engaged in further synthetic work to test the scope of these correlations. Further examples of linear relationships linking π-electron densities to corrected chemical shifts have been found for the neutral molecules of several azaindenes prepared in recent years by the research groups of Potts (44) and W. W. Paudler (45) and we hope to present a complete analysis of these results in a later paper in the present series.

In nucleophilic substitution reactions of purine analogues, the correlation coefficients linking activation parameters to the ω-technique electron densities and to the delocalization energies are highly significant, suggesting, for example, that the regression equations could be used with some confidence to predict the rates of nucleophilic piperidinodehalogenations of 1-substituted-6-halopyrazolo(3,4-*d*)pyrimidines and of 3-substituted-5-halo-v-triazolo(4,5-*d*)pyrimidines.

Acknowledgments

We are grateful for support from the National Research Council of Canada through operating and equipment grants to B.M.L., and for a Scholarship to J.G.K.W., and also for grants-in-aid to this university for computing facilities. Supplies of triazolopyrimidines from the Cancer Chemotherapy National Service Center of the National Institutes of Health, Bethesda, Maryland are gratefully acknowledged. It is a pleasure to acknowledge many valuable discussions with Professor Roland K. Robins (University of Utah).

1. R. K. ROBINS. J. Med. Chem. **7**, 186 (1964).
2. R. K. ROBINS. *In* Heterocyclic compounds. Vol. 8. *Edited by* R. C. Elderfield. John Wiley and Sons, Inc. New York. 1967.
3. B. PULLMAN and A. PULLMAN. Quantum biochemistry. John Wiley and Sons, Ltd. London. 1963.
4. E. Y. SUTCLIFFE and R. K. ROBINS. J. Org. Chem. **28**, 1663 (1963).
5. B. PULLMAN. Tetrahedron Letters, 231 (1963).
6. B. PULLMAN. J. Org. Chem. **29**, 508 (1964).
7. B. M. LYNCH and H. J. M. DOU. Tetrahedron Letters, 2627 (1966).
8. B. M. LYNCH, B. C. MACDONALD, and J. G. K. WEBB. Tetrahedron, **24**, 3595 (1968).
9. B. M. LYNCH, R. K. ROBINS, and C. C. CHENG. J. Chem. Soc. 2973 (1958).
10. A. STREITWIESER. Molecular orbital theory for organic chemists. John Wiley and Sons, Inc., New York. 1961. p. 335.
11. P. BELTRAME, P. L. BELTRAME, and M. SIMONETTA. Tetrahedron, **24**, 3043 (1968).
12. (*a*) G. B. BARLIN and N. B. CHAPMAN. J. Chem. Soc. 3017 (1965); (*b*) G. B. BARLIN. J. Chem. Soc. B, 954 (1967).

13. A. STREITWIESER. Molecular orbital theory for organic chemists. John Wiley and Sons, Inc. New York. 1961. Chap. 2.
14. C. L. WILKINS and C. E. KLOPFENSTEIN. J. Chem. Educ. **43**, 10 (1966).
15. B. M. LYNCH and L. POON. Can. J. Chem. **45**, 1431 (1967).
16. A. STREITWIESER. Molecular orbital theory for organic chemists. John Wiley and Sons, Inc. New York. 1961. p. 120.
17. A. STREITWIESER. J. Am. Chem. Soc. **82**, 4123 (1960).
18. P. J. BLACK, R. D. BROWN, and M. L. HEFFERNAN. Australian J. Chem. **20**, 1305 (1967).
19. F. J. BULLOCK and O. JARDETZKY. J. Org. Chem. **29**, 1988 (1964).
20. S. MATSUURA and T. GOTO. Tetrahedron Letters, 1499 (1963).
21. J. M. READ and J. H. GOLDSTEIN. J. Am. Chem. Soc. **87**, 3440 (1965).
22. R. J. PUGMIRE, D. M. GRANT, R. K. ROBINS, and G. W. RHODES. J. Am. Chem. Soc. **87**, 2225 (1965).
23. B. M. LYNCH and J. G. K. WEBB. To be published.
24. H. H. JAFFE. Chem. Rev. **53**, 191 (1953).
25. J. CLARK and D. D. PERRIN. Quart. Rev. London, **18**, 295 (1964).
26. J. J. ELLIOTT and S. F. MASON. J. Chem. Soc. 2352 (1959).
27. H. C. LONGUET-HIGGINS. J. Chem. Phys. **18**, 275 (1950).
28. T. NAKAJIMA and A. PULLMAN. J. Chim. Phys. 793 (1958).
29. T. NAKAJIMA and B. PULLMAN. Bull. Soc. Chim. France, 1502 (1958).
30. A. ALBERT. J. Chem. Soc. B, 427 (1966).
31. D. D. PERRIN. J. Chem. Soc. 5590 (1965).
32. P. G. LYKOS and R. L. MILLER. Tetrahedron Letters, 1743 (1963).
33. B. PULLMAN. J. Chem. Soc. 1621 (1959).
34. G. B. BARLIN. J. Chem. Soc. B, 641 (1967).
35. B. M. LYNCH. To be published.
36. A. J. ROBERTSON. Studies in purine analogs. M.Sc. Thesis. St. Francis Xavier University. Antigonish, Nova Scotia. 1967.
37. R. K. ROBINS and C. C. CHENG. J. Org. Chem. **21**, 1240 (1956).
38. R. K. ROBINS. J. Am. Chem. Soc. **78**, 786 (1956).
39. B. M. LYNCH and A. J. ROBERTSON. To be published.
40. D. J. BROWN and M. N. PADDON-ROW. J. Chem. Soc. C, 1856 (1967).
41. J. F. BUNNETT and H. TAKAYAMA. J. Org. Chem. **33**, 1924 (1968).
42. B. M. LYNCH, M. A. KHAN, and J. G. K. WEBB. To be published.
43. R. ETTINGER. Tetrahedron, **20**, 1579 (1964).
44. K. T. POTTS, H. R. BURTON, T. H. CRAWFORD, and S. W. THOMAS. J. Org. Chem. **31**, 3522 (1966).
45. W. W. PAUDLER and J. E. KUDER. J. Heterocyclic Chem. **3**, 33 (1966).

Can. J. Chem. Downloaded from www.nrcresearchpress.com by 210.87.254.5 on 09/05/12
For personal use only.

Isolation and characterization of (+)-sesamin and β-cyclopyrethrosin from pyrethrum flowers

RAYMOND W. DOSKOTCH AND FAROUK S. EL-FERALY
College of Pharmacy, The Ohio State University, Columbus, Ohio 43210
Received September 30, 1968

Two compounds isolated from the alcoholic extract of pyrethrum flowers (*Chrysanthemum cinerariaefolium* Visiani) have been characterized as the lignan, (+)-sesamin (**2**) by physical methods and by direct comparison with a known sample and the sesquiterpene, β-cyclopyrethrosin (**3**) by physical methods and conversion to the known ketone **6**.

Canadian Journal of Chemistry, 47, 1139 (1969)

Can. J. Chem. Downloaded from www.nrcresearchpress.com by 210.87.254.42 on 09/05/12
For personal use only.

To date, the only reported sesquiterpene from the flowering heads of *Chrysanthemum cinerariaefolium* Visiani is pyrethrosin (**1**) whose gross structure was determined by Barton *et al.* (1) and whose stereochemical assignments were given by Iriuchijima and Tamura (2). We wish to report the isolation and identification of a new natural occurring sesquiterpene that has been known as one of two inseparable isomers obtained from pyrethrosin (**1**) by chemical means. Our study originated in connection with another investigation for which pyrethrosin was required and a fractionation method was devised for its isolation from the natural source. One particular lot of plant material did not yield any of the desired substance but instead gave two crystalline fractions, which are the subject of this note.

The ethanolic residue from the percolation of the flowers was partitioned between chloroform and water, and the chloroform solubles were partitioned between petroleum ether and 10% aqueous methanol. The residue from the methanolic phase was chromatographed on silicic acid with chloroform as the eluting agent. The first crystalline fraction yielded a substance which showed an ultraviolet (u.v.) absorption spectrum typical of an oxygenated benzene derivative and a nuclear magnetic resonance (n.m.r.) spectrum identical to that of (+)-sesamin (**2**) (3). A direct comparison with a sample of (+)-sesamin previously isolated in our laboratory from *Zanthoxylum martinicense* DC. (4) showed them to give superimposable infrared (i.r.) and u.v. spectra and an undepressed mixture m.p. Although (+)-sesamin (**2**) had been isolated from the roots of *Chrysanthemum frutescens* L. (5) it has not been previously obtained from pyrethrum flowers. It is of interest to note that the source of the pyrethrum insecticides also contains a compound known to have an important activity as a pyrethrum synergist (6).

The second crystalline fraction gave a compound, m.p. 166–167° that was shown by the physical and chemical evidence to follow to be β-cyclopyrethrosin (**3**). In the i.r. region it exhibited peaks (see Experimental) for an alcohol, an α,β′-unsaturated-γ-lactone, an acetate, and an unconjugated exocyclic olefin. The n.m.r. spectrum (Fig. 1) showed the presence of a pair of doublets at δ 6.12 (H_e) and 5.45 (H_d) coupled to H_c with constants $J = 3.1$ and 2.9 Hz, respectively. A triplet at δ 5.52 was assigned to the axial H_b proton coupled to two axial protons H_a and H_c (J = 10.3 and 10.3 Hz). The two protons of the isolated exocyclic methylene are found at δ 4.89 and 4.62 as broadened singlets due to allylic coupling. The sextet at δ 4.10 for the axial H_f proton results from interaction with the neighboring two axial and one equatorial hydrogens (J = 11.6, 11.6, and 3.7 Hz). The quartet at δ 3.60 (J = 10.2 and 5.0 Hz) was designated for the axial H_g proton coupled to an axial and an equatorial hydrogen. The alcoholic group must therefore have the β (equatorial) assignment.

The H_c proton located at about δ 2.8 shows clearly only one triplet of a trio of triplets as other protons mask it in that region. The removal of the alcoholic proton absorption at δ 2.59 by exchange with deuterium oxide revealed more clearly the H_c pattern. A first-order analysis of the pattern showed it to be an ABMN type resulting from interactions with the H_b, H_d, H_e, and H_f protons. An acetate methyl at δ 2.06 and a tertiary methyl at δ 0.87 completed the information derivable from the n.m.r. spectrum. The assignments were assisted by double irradiation

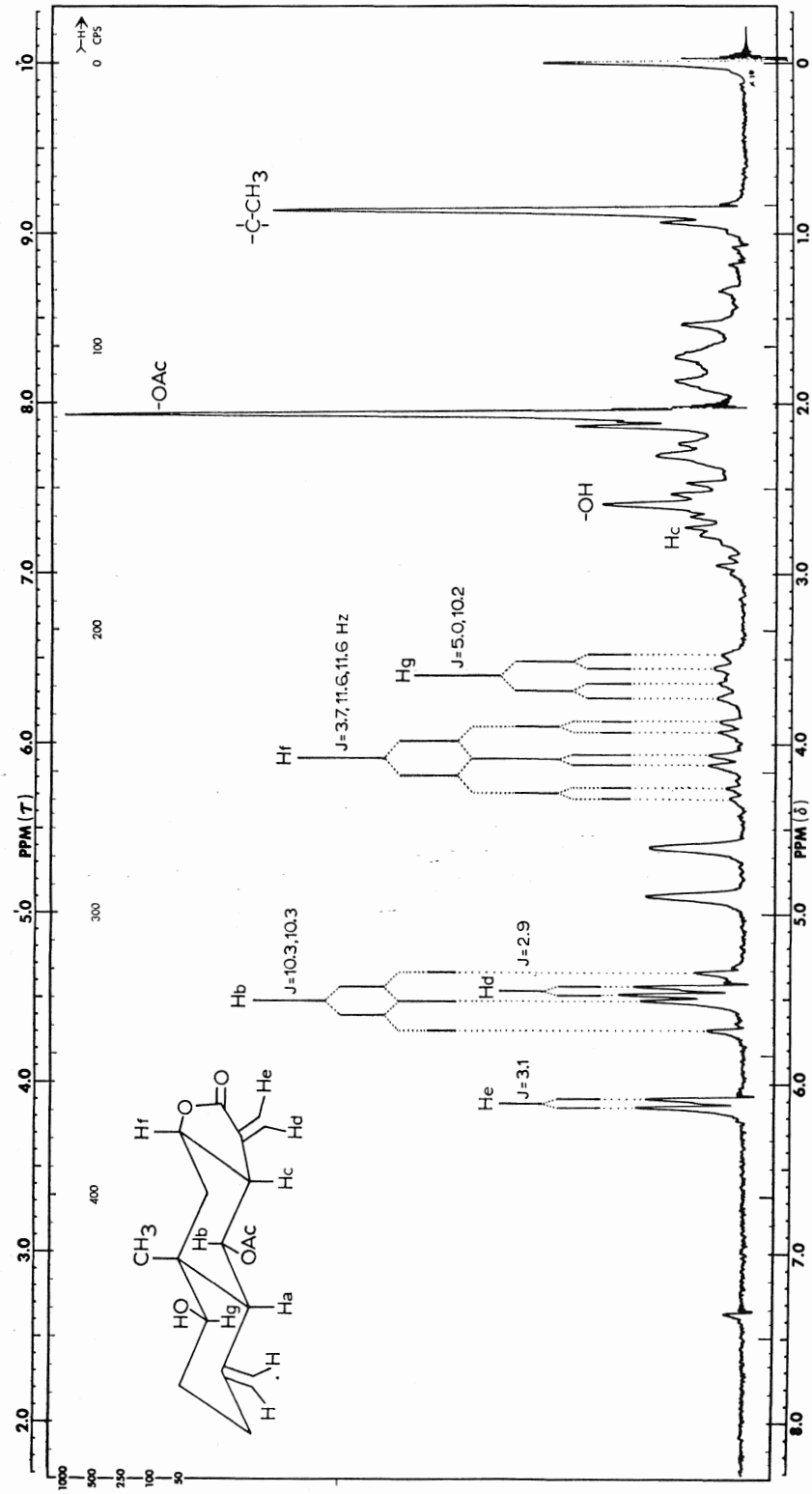

FIG. 1. The nuclear magnetic resonance spectrum of β-cyclopyrethrosin (3).

Can. J. Chem. Downloaded from www.nrcresearchpress.com by 210.87.254.42 on 09/05/12
For personal use only.

Can. J. Chem. Downloaded from www.nrcresearchpress.com by 210.87.254.42 on 09/05/12
For personal use only.

experiments and previously reported results (2), as well as changes in the spectrum for the derivatives.

The acetate **4** of **3** showed in the n.m.r. spectrum a six-proton singlet at δ 2.08 for the two acetate methyls and also the loss of the alcoholic proton from δ 2.59 and the shift of the quartet for H_g from δ 3.60 downfield to δ 4.84. The H_c trio of triplets became clearly visible in this derivative.

Hydrogenation of **3** over palladium on charcoal as catalyst yielded dihydro-β-cyclopyrethrosin (**5**). The pair of doublets for H_d and H_e were no longer present in the n.m.r. spectrum but a three-proton doublet at δ 1.17 (J = 7.0 Hz) for a secondary methyl appeared. The remainder of the spectrum was relatively unchanged except for the H_c pattern which because of masking by other peaks could not be clearly interpreted.

Oxidation of **5** with Jones' reagent (7) produced the known ketone **6** (2). A comparison of the i.r. and n.m.r. spectra, the optical rotation, and the m.p. of the two, confirmed their identity and established conclusively that the isolated substance was β-cyclopyrethrosin (**3**).

The possibility that the sesquiterpene **3** was an artifact resulting from the cyclization of pyrethrosin (**1**) had to be eliminated. The mixture of α-, β-, and possibly γ-cyclopyrethrosins that is obtained by cyclization with acid was subjected to the same column chromatographic separation as the fraction of the flower extract. No separation of the isomers was observed. β-Cyclopyrethrosin (**3**) is therefore the second reported sesquiterpene elaborated by *C. cinerariaefolium*.

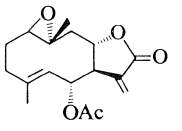

1

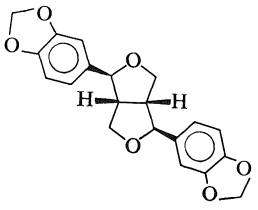

2

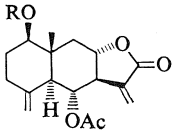

3, R = H
4, R = Ac

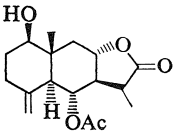

5

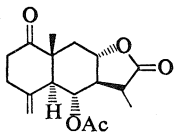

6

Experimental

Melting points are uncorrected. Elemental analyses were determined by Joseph F. Alicino, Metuchen, New Jersey. Infrared (i.r.) spectra were determined at about 8–10% concentration in chloroform on a Perkin–Elmer Infracord 237 or 257 spectrophotometer. Ultraviolet spectra were obtained in methanol on a Cary model 15 spectrophotometer. The nuclear magnetic resonance (n.m.r.) spectra were obtained in deuteriochloroform with tetramethylsilane as internal standard, signals reported in δ (p.p.m.), and J in Hz units, using a Varian A-60A spectrometer equipped with the model V-6058A spin decoupler. Optical rotations were measured on a Zeiss–Winkel polarimeter or on a Jasco model ORD/UV-5 optical rotatory dispersion recorder in methanol.

Ethanol (95%) was U.S.P. grade; petroleum ether (b.p. 60–68°) was Skellysolve B and other solvents were A.R. grade. Silicic acid (100 mesh) was from Mallinckrodt Chemical Works, St. Louis; Celite 545 from Johns-Manville Corp., New York, and Silica Gel G from E. Merck, Darmstadt, Germany.

Isolation of (+)-Sesamin (2) and β-Cyclopyrethrosin (3)

The flowering heads (2.1 kg) of *Chrysanthemum cinerariaefolium* (Lot. no. LHC 2048, S. B. Penick and Co.) were percolated at room temperature with ethanol to exhaustion. The residue (290 g) remaining after removal of the solvent at reduced pressure and at 40° was partitioned between 1750 ml of chloroform and 500 ml of water. The interfacial solid was discarded and the chloroform phase shaken with 400 ml of water, dried (Na_2SO_4), and evaporated at reduced pressure. The chloroform residue (143 g) was partitioned between 2 l of 10% aqueous methanol and four 500 ml portions of petroleum ether. The combined petroleum ether extract was back-washed with 100 ml of 10% aqueous methanol and the pooled methanolic phase evaporated at reduced pressure to yield 90 g of residue.

A chromatographic column, 7 cm × 52 cm from 1 kg of silicic acid – Celite 545 (4:1), poured as a slurry in chloroform, was loaded with 45 g of the 10% aqueous methanol residue. Elution was with chloroform at a flow rate of 20 ml/h and 80 ml fractions were taken to dryness and weighed.

Fractions 36–38 (110 mg) on crystallization from ethanol gave 43 mg of (+)-sesamin (**2**), m.p. 122–123°; $[\alpha]_D^{25}$ +57.4° (*c*, 0.74 in chloroform); λ_{max}(MeOH) 236 mμ (log ε 4.09), 287 mμ (4.04), (lit. (4) m.p. 124–125°; $[\alpha]_D^{25}$ +57°; λ_{max}(MeOH) 236 mμ (log ε 4.09), 2.87 mμ (log ε 4.04)).

Fractions 65–72 (1.04 g) on crystallization from isopropyl ether – ethanol then 80% aqueous ethanol gave 720 mg of β-cyclopyrethrosin (**3**), m.p. 166–167°; $[\alpha]_D^{25}$ +58.2° (*c*, 0.49); $\lambda_{end\ abs.}$ 210 mμ (log ε 3.94); ν_{max} 3600 and 3490 cm^{-1} (hydroxyl), 1768 and 1674 cm^{-1} (α,β′-unsaturated-γ-lactone), 1734 cm^{-1} (acetate), 1657 and 914 cm^{-1} (olefinic methylene). The C—O—C stretching

Can. J. Chem. Downloaded from www.nrcresearchpress.com by 210.87.254.42 on 09/05/12
For personal use only.

for the lactone and acetate appears as a broad band between 1200–1260 cm^{-1}. The n.m.r. spectrum is shown in Fig. 1.

Anal. Calcd. for $C_{17}H_{22}O_5$: C, 66.65; H, 7.24. Found: C, 66.35; H, 7.21.

β-Cyclopyrethrosin Acetate 4

β-Cyclopyrethrosin (**3**) (100 mg) was dissolved in 1 ml of pyridine and 2 ml of acetic anhydride and allowed to stand overnight at room temperature. The excess acetic anhydride was decomposed by the addition of water and slight warming. Chloroform was added and the pyridine and acetic acid removed by extraction with water, dilute acid, base, and finally with water. Removal of the chloroform (Na_2SO_4 dried) by evaporation at reduced pressure left a residue (101 mg) which gave from 90% ethanol, 91 mg of colorless needles, m.p. 185–186°, $[\alpha]_D^{25}$ +45.7° (*c*, 0.405). The i.r. spectrum showed a double intensity peak at 1735 cm^{-1} (acetate) and no hydroxyl bands.

Anal. Calcd. for $C_{19}H_{24}O_6$: C, 65.50; H, 6.94. Found: C, 65.40; H, 7.03.

Dihydro-β-cyclopyrethrosin 5

β-Cyclopyrethrosin (**3**) (100 mg) was dissolved in 10 ml of absolute ethanol and added to a suspension of 60 mg of 5% Pd on charcoal presaturated with hydrogen in 10 ml of absolute ethanol. At room temperature and atmospheric pressure the uptake of one mole equivalent of hydrogen was rapid and the reaction was stopped. Removal of the catalyst by filtration and evaporation of the solvent left a crystalline residue (105 mg) that on recrystallization from isopropyl ether – ethanol gave colorless needles, m.p. 212–213°; $[\alpha]_D^{25}$ +72.4° (*c*, 0.235); ν_{max} 3600 and 3485 cm^{-1} (hydroxyl), 1772 cm^{-1} (γ-lactone), 1730 cm^{-1} (acetate), and 1650, 910 cm^{-1} (exocyclic olefin).

Anal. Calcd. for $C_{17}H_{24}O_5$: C, 66.21; H, 7.85. Found: C, 66.00; H, 7.97.

Oxidation of Dihydro-β-cyclopyrethrosin (5) to Ketone 6

Dihydro-β-cyclopyrethrosin (**5**) (80 mg) dissolved in 5 ml of acetone was treated with 1 ml of Jones' reagent (7) for 5 min at room temperature. Methanol was added to destroy the excess reagent and the reaction mixture filtered. The filtrate was treated with 25 ml of 5% $NaHCO_3$ and extracted three times with 50 ml portions of ether. The combined ether extract was washed with water, dried (Na_2SO_4), and evaporated to give an oil (70 mg) that crystallized from 80% ethanol as colorless needles (59 mg). These gave a positive Zimmerman's test (8), m.p. 166–167°, (lit. (2), m.p. 168–168.5°); $[\alpha]_D^{25}$ +135.0° (*c*, 0.10); λ_{max}(MeOH) 270 mμ (ε 62) (as shoulder); ν_{max} 1780 cm^{-1} (γ-lactone), 1735 cm^{-1} (acetate), 1712 cm^{-1} (cyclohexanone), and 1660 and 910 cm^{-1} (exocyclic olefin). A comparison of the i.r. spectrum with the known spectrum[1] (both in Nujol) showed no differences. The n.m.r. spectra were likewise comparable.

Anal. Calcd. for $C_{17}H_{22}O_5$: C, 66.65; H, 7.24. Found: C, 66.66; H, 7.15.

Acid Cyclization of Pyrethrosin 1

Five drops of concentrated hydrochloric acid were added to 70 mg of pyrethrosin (**1**) dissolved in 1 ml of chloroform and diluted with 10 ml of ether and the mixture was stirred 5 min. The solution when analyzed on Silica Gel G t.l.c. plates, employing 5% acetone in chloroform as developing solvent and then spraying with dilute aqueous $KMnO_4$, showed that pyrethrosin (R_f 0.05) was absent. A new single spot at R_f 0.3 (same as β-cyclopyrethrosin) was present. The n.m.r. spectrum of this material showed it to be a mixture. The contribution of β-cyclopyrethrosin to the spectrum was taken as evidence for its presence. Chromatography of the mixture on 10 g of silicic acid – Celite 545 (4:1) with chloroform as eluting solvent resulted in recovery of the unresolved mixture.

[1]Personal communication from Dr. S. Iriuchijima.

Acknowledgments

This investigation was supported by Public Health Service Research Grant No. CA-08133 from the National Cancer Institute. We wish to thank Dr. Robert W. Price of S. B. Penick and Company, New York, for the generous supply of pyrethrum flowers and Dr. S. Iriuchijima, University of Tokyo, for the i.r. and n.m.r. spectra and physical constants for ketone **6**.

1. D. H. R. Barton, O. C. Böckman, and P. de Mayo. J. Chem. Soc. 2263 (1960).
2. S. Iriuchijima and S. Tamura. Tetrahedron Letters, No. **21**, 1965 (1967).
3. W. A. Jones, M. Beroza, and E. D. Becker. J. Org. Chem. **27**, 3232 (1962).
4. J. Tomko, A. T. Awad, J. L. Beal, and R. W. Doskotch. Lloydia, **30**, 231 (1967).
5. E. Winterfeldt. Chem. Ber. **96**, 3349 (1963).
6. H. L. Haller, F. B. LaForge, and W. N. Sullivan. J. Org. Chem. **7**, 185 (1942); W. A. Gersdorff, N. Mitlin, and M. Beroza. J. Econ. Entomol. **47**, 839 (1954).
7. B. Tursch, I. S. de Souza Guimaraes, B. Gilbert, R. T. Aplin, A. M. Duffield, and Carl Djerassi. Tetrahedron, **23**, 761 (1967).
8. R. Neher. Steroid chromatography. Elsevier Press, Inc., New York. 1964. p. 125.

Can. J. Chem. Downloaded from www.nrcresearchpress.com by 210.87.254.6 on 09/05/12
For personal use only.

Thermal and photolytic decomposition of *N*-benzhydrylidene azidobenzhydrylamine

N. KOGA, G. KOGA, AND J.-P. ANSELME[1]
Department of Chemistry, University of Massachusetts, Boston, Massachusetts 02116

Received November 1, 1968

The thermal and photolytic decomposition of *N*-benzhydrylidene azidobenzhydrylamine (**2**) in aromatic solvents gave *N*-phenyl-*N'*-benzhydrylidene benzamidine (**5**); no benzophenone azine could be isolated. Photolysis in methanol gave no **5** but instead benzophenone dimethylketal and ammonium azide were obtained. Attempts to trap the presumed nitrene intermediate with cyclohexene gave only **5**. Thermal decomposition in decalin gave *N*-benzhydryl benzophenone imine (**9**). The possible mechanisms of these transformations are presented.

Canadian Journal of Chemistry, 47, 1143 (1969)

The formation of *N*-benzhydrylidene azidobenzhydrylamine (**2**) from the reaction of lithio benzophenone imine and tosyl azide has been reported recently (1). This result involves the dimerization of the lithium salt followed by the *diazo transfer* reaction (2) to the resulting dianion (**1**) to give **2**.

The assignment of structure **2** was based on its elemental analysis, its molecular weight, and its reactions (1). We would like to report now its photolytic and thermal decompositions, the results of which confirm further the assigned structure.

Triarylmethyl azides, upon the loss of nitrogen, undergo the Stieglitz rearrangement (3) to give the corresponding imines, possibly via a discrete nitrene intermediate (**3**) or through a concerted displacement (3, 4). Two products **5** and **6** could arise from the rearrangement of **2**. However, when a solution of **2** in benzene was irradiated with a 200 W high-pressure mercury lamp in a quartz apparatus, the only product isolated in 83% yield was a canary yellow solid, m.p. 138–140°. Its identity as *N*-phenyl-*N'*-benzhydrylidene benzamidine (**5**) was proved by its elemental analysis, its infrared (i.r.) spectrum, and by comparison with an authentic sample prepared from *N*-phenyl benzimidoyl chloride and benzophenone imine.

The addition of benzophenone had no effect on the nature or the yield of the products. No evidence for the formation of benzophenone azine

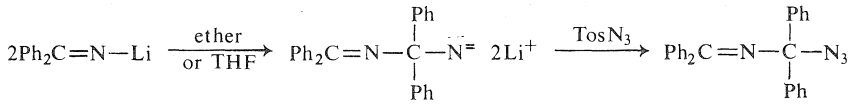

1 **2**

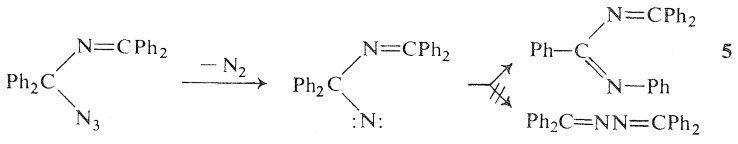

2 **3** **6** **5**

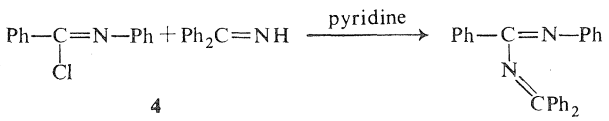

4 **5**

[1]To whom all correspondence should be addressed.

Can. J. Chem. Downloaded from www.nrcresearchpress.com by 210.87.254.6 on 09/05/12
For personal use only.

(**6**) could be obtained. The absence of the product resulting from nitrogen migration (hetero rearrangement (5)) recalls the similar behavior of the so-called "rigid" azides (6). An attempt to trap the presumed nitrene intermediate was made by carrying out the photolysis in cyclohexene as solvent. However, **5** was the only product isolated in 79% yield. None of the anticipated bicyclic aziridine could be detected.

When methanol was used as a solvent, the photo-induced decomposition of **2** followed a completely different course. No **5** was formed; instead, benzophenone dimethylketal (**7**) and ammonium azide were formed. Both compounds were identified by the comparison of their i.r. spectra with those of authentic samples. The reaction of **2** with methanol, under identical conditions (time and temperature), in the absence of light gave **7** but in much lower yield; no ammonium azide could be detected. Thus, the effect of light on the course of the reaction is unquestionable although it is difficult at this time to decide in which step it is involved. The absence of ammonium azide in the control run indicates that the light-induced decomposition of hydrazoic acid is the source of ammonium azide (7). The irradiation of benzophenone imine with methanol did not give any appreciable amount of the ketal. A solution of **5** in methanol heated to 40–45° for 6 h did not give any benzophenone dimethylketal (**7**). Irradiation of this solution under the same conditions failed to give any **7**. Irradiation of benzophenone imine (**10**) in methanol also failed to produce any **7**, even in the presence of hydrazoic acid; ammonium azide, traces of benzophenone, and unreacted benzophenone imine were obtained. The formation of **7** and ammonium azide may be summarized as shown in the following equations:

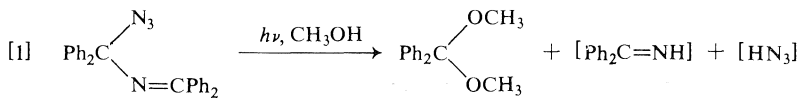

[1] $Ph_2C(N_3)(N{=}CPh_2) \xrightarrow{h\nu,\ CH_3OH} Ph_2C(OCH_3)_2 + [Ph_2C{=}NH] + [HN_3]$

7 **10**

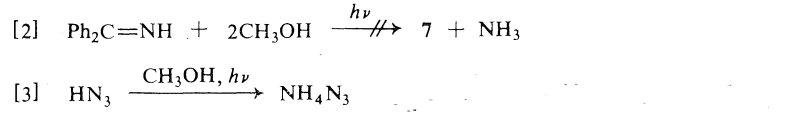

[2] $Ph_2C{=}NH + 2CH_3OH \xrightarrow{h\nu} 7 + NH_3$

[3] $HN_3 \xrightarrow{CH_3OH,\ h\nu} NH_4N_3$

The thermal decomposition of **2** in naphthalene at 190° was not as clean as the photolysis. A black tarry mass was obtained after removal of the naphthalene and only **5** could be isolated in 23% yield; none of the azine (**6**) could be detected. The pyrolysis of **2** in benzophenone azine (**6**) at 190° gave a tarry residue from which **5** and **6** were obtained by chromatography on alumina. The tarry product of the pyrolysis of **2** in **5** did not yield any benzophenone azine. In decalin, the thermal decomposition at 190° followed a different path and from the black tarry pyrolyzate, a 20% yield of a solid was obtained. It was identified as *N*-benzhydryl benzophenone imine (**9**) by comparison with an authentic sample. The formation of **9** may be viewed as arising via the formation of the azo compound **8** or less likely via the homolytic cleavage of the C—N_3 bond of **2** (8). Although the rearrangement product (**5**) is stable thermally up to 200°, the reaction of **5** with **2** at 200° gave a black mass. This may account for the absence of **5** in the thermolysis in decalin and its low yield from the thermolysis in naphthalene.

The fact that *no* benzophenone azine (**6**) was detected from the products of the decomposition of **2** is reminiscent of the failure of *N*,*N*-dialkylcarbonyl azides and of azidoformates to undergo Curtius-type rearrangement (9). In all these cases, the migrating groups are anchored by hetero atoms such as nitrogen or oxygen. The transition state for the migration of a phenyl group to an electron-deficient center such as a carbonium ion has been described (10). A similar picture can be used to rationalize the migration of the phenyl group in the rearrangement of **2** to give **5**. However, a major difference becomes apparent when the transition state for the migration of —N=CPh_2 is visualized. The presence of a nonbonded pair of electrons on the nitrogen may result in the electrostatic repulsion with the non-

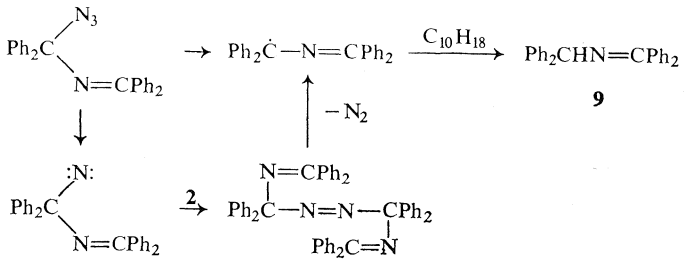

8

bonded electrons of the migration terminus. This could slow down the rearrangement and would explain the absence of benzophenone azine.[2]

Experimental

All melting points are uncorrected. Infrared (i.r.) spectra were obtained on a Perkin–Elmer Infracord. The photolyses were carried out under nitrogen in a quartz apparatus similar to that described by De Boer *et al.* (11). A Hanovia 200 W high-pressure mercury lamp was used as the light source.

Photolysis of 2 in Benzene

A solution of 2.0 g (5 mmoles) of **2** in 175 ml of benzene was photolyzed for 6 h. The maximum temperature during the photolysis was 40–45°. Removal of the solvent left a crude oil which crystallized. Recrystallization from cyclohexane gave 1.5 g (83%) of a fine yellow powder, m.p. 138–140°. Its i.r. spectrum exhibited aromatic absorptions at normal positions and a cluster of four closely spaced bands at 1645, 1610, 1585, and 1570 cm^{-1}. It was identical to the spectrum of an authentic sample of **5** (see below) and the mixture m.p. was not depressed.

Anal. Calcd. for $C_{26}H_{20}N_2$: C, 86.66; H, 5.55; N, 7.76. Found: C, 86.76; H, 5.64; N, 7.55.

N-Phenyl-N′-benzhydrylidene Benzamidine (5)

A mixture of 2.1 g (10 mmoles) of benzimidoyl chloride, 1.8 g (10 mmoles) of benzophenone imine, and 5 ml of dry pyridine was heated on a steam-bath for 2h. The reaction mixture was poured into 100 ml of ice water and the organic layer was extracted with two 30 ml portions of ether. The dried ether extract was evaporated to dryness and 3.0 g of crude yellow solid were obtained. One recrystallization from cyclohexane gave 2.4 g (66%) of a yellow powder, m.p. 138–140°. It was identical in all respects with the product obtained from the photolysis of **2** in benzene.

Photolysis of 2 in Cyclohexene

A solution of 3.0 g (7.7 mmoles) of **2** in 175 ml of cyclohexene was photolyzed for 6 h at 40–45°. Work-up of the photolyzate as previously described gave 2.2 g (79%) of **5**, m.p. 137–138°. All attempts to detect the presence of the bicyclic aziridine failed.

[2]The arguments presented here would hold equally well (with minor differences) for a transition state involving the azide (concerted displacement) instead of a nitrene.

Photolysis of 2 in Methanol

A solution of 2.0 g (5 mmoles) of **2** in 200 ml of methanol was photolyzed for 6 h. After removal of the solvent, the residue was extracted with 100 ml of ether. Evaporation of the ether gave 2.0 g (mixture of **7** and **10**) of an oil. Crystallization from methanol gave 0.5 g (45% based on eq. [1] of **7**, m.p. 105.5–106°. Its i.r. spectrum was superimposable on that of an authentic sample of benzophenone dimethylketal. The ether insoluble fraction (0.2 g) was identified as ammonium azide by comparison of its i.r. spectrum with that of an authentic sample.

When **2** was kept for 6 h in methanol, only 40% of **7** was isolated and no ammonium azide was obtained. The irradiation of benzophenone imine in methanol for 6 h did not give **7** in any appreciable amounts.

Thermal Decompositions of 2

(a) In Decalin

A solution of 1.0 g (2.5 mmoles) of **2** in 20 ml of decalin was heated at 190° for 2 h. Removal of the solvent *in vacuo* left a black tar which was chromatographed on Fisher A-540 alumina. Elution with benzene gave 0.17 g (20%) of benzhydryl benzophenone imine (**9**), identical with an authentic sample (12).

(b) In Naphthalene

A mixture of 1.0 g (2.5 mmoles) of **2** in 3 g of naphthalene was heated at 190° for 2 h. The naphthalene was sublimed and the tarry residue was chromatographed as above. Elution with 1:3 *n*-hexane – benzene gave 0.2 g (23%) of **5**, m.p. 136–137°.

Acknowledgment

The generous support of this work by the National Institutes of Health of the United States Department of Health, Education, and Welfare under grant Nos. 13689–02 and 13689–03 is hereby acknowledged with deep appreciation.

1. J. -P. Anselme, W. Fischer, and N. Koga. Tetrahedron. To be published.
2. W. Fischer and J. -P. Anselme. J. Am. Chem. Soc. **89**, 5284 (1967); J. -P. Anselme and W. Fischer. Tetrahedron. To be published; G. Koga and J. -P. Anselme. Chem. Commun. 446 (1968).
3. P. A. S. Smith. *In* Molecular rearrangements. Vol. 1. *Edited by* P. de Mayo. Interscience Publishers, Inc,. New York. 1963. pp. 462, 479, 481.
4. (*a*) W. H. Saunders and J. C. Ware. J. Am. Chem. Soc. **80**, 3328 (1958). (*b*) W. H. Saunders and E. A.

Can. J. Chem. Downloaded from www.nrcresearchpress.com by 210.87.254.6 on 09/05/12
For personal use only.

CARESS. J. Am. Chem. Soc. **85**, 861 (1964); F. D. LEWIS and W. H. SAUNDERS. J. Am. Chem. Soc. **89**, 645 (1967).
5. J. E. LEFFLER. The reactive intermediates of organic chemistry. Interscience Publishers, Inc., New York. 1956. p. 156.
6. A. BERTHO. J. Prakt. Chem. [2], **120**, 89 (1929).
7. E. KOCH. Tetrahedron, **23**, 1747 (1967).
8. F. D. LEWIS and W. H. SAUNDERS. J. Am. Chem. Soc. **90**, 3828 (1968).
9. W. LWOWSKI, R. DEMAURIAC, T. W. MATTINGLY, and E. SCHEIFFELE. Tetrahedron Letters, 3285 (1964).
10. A. STREITWIESER. Molecular orbital theory for organic chemists. John Wiley and Sons, Inc., New York. 1961. p. 383.
11. C. D. DE BOER, N. J. TURRO, and G. S. HAMMOND. Organic syntheses. *Edited by* W. D. Emmons. John Wiley and Sons, Inc., New York. 1967. p. 65.
12. G. CHARLES. Bull. Soc. Chim. France, 1576 (1963).

Can. J. Chem. Downloaded from www.nrcresearchpress.com by 210.87.254.6 on 09/05/12
For personal use only.

Studies in terpenoids. XII.[1] Optical rotatory dispersion and circular dichroism studies on some cyclobutanones derived from α-pinene[2]

L. R. SUBRAMANIAN AND G. S. KRISHNA RAO
Department of Organic Chemistry, Indian Institute of Science, Bangalore-12, India
Received October 23, 1968

The optical rotatory dispersion and circular dichroism studies on the cyclobutanones (**1–5**) are discussed.
Canadian Journal of Chemistry, **47**, 1147 (1969)

Can. J. Chem. Downloaded from www.nrcresearchpress.com by 210.87.254.5 on 09/05/12
For personal use only.

The octant rule, at first applied to cyclohexanones (1) and later to other systems (2), was successfully extended to cyclobutanones by Conia and Gore (3). The absolute configurations and the preferred conformations of various substituted cyclobutanones were established by these authors from a study of their circular dichroism (c.d.) curves, which clearly demonstrated the puckering of the cyclobutanones investigated by them. Low-temperature c.d. study (4) has also been made use of to investigate the conformational mobility of cyclobutanones (4*a*). The most recent application of the c.d. and the extension of the octant rule for deducing the stereochemistry of optically active cyclobutanones is in the assignment of the absolute configuration of the naturally occurring cyclobutanones, D- and L-filifolones (5).

In the course of our work on the transformation reactions of α-pinene (6), optically active cyclobutanones **1–4** became available. (−)-2,2,3(R)-Trimethylcyclobutanone (**5**) was prepared (*vide* Experimental) from *cis*-(+)-pinonic acid (**6**) (7) by the route: **6** → **7** → **8** → **9** → **5** (Scheme I).

(+)-2,2,3(S)-Trimethylcyclobutanone (**5E**) prepared by Conia and Gore (3) exhibited a positive Cotton effect in c.d. and was also prone to conformational mobility as revealed by the low-temperature c.d. measurement (4*a*). (−)-2,2,3(R)-Trimethylcyclobutanone (**5**) prepared in this study exhibited a single well-defined negative Cotton effect in c.d. (Table I) confirming its antipodal configuration. Since **5** was prepared from *cis*-(+)-pinonic acid (**6**, *ex*.(+)-α-pinene), which in turn was the starting material for the synthesis of methyl (−)-2,2-dimethyl-3-ketocyclobutyl-1(S)-acetate (**2**) (6), the absolute configuration of **2** is correlated with that of **5** and is shown as depicted.

A study of the c.d. curve of the cyclobutanone ester (**2**), however, gave results in contrast with those of the cyclobutanone (**5**) with which it was correlated *via* **6**. In cyclohexane and methanol the cyclobutanone methyl ester (**2**) exhibited multiple Cotton effects in the c.d. curve (a positive extremum at 319–322 mμ, a negative extremum at 302–304 mμ (Table I), and again a positive extremum at 240–248 mμ[3]). Multiple extrema of opposite signs and the change in amplitude with change of solvent from cyclohexane to methanol, as observed from the molecular ellipticity values of the cyclobutanone ester (**2**), (Table I), have been attributed to conformational/solvational equilibria (8). Consider conformers (**2***a* and **2***b*) (Scheme 1) for **2** with the ester side chain equatorial in **2***a* and axial in **2***b*. By the application of the octant rule, conformer **2***a* should exhibit an overall negative Cotton effect and conformer **2***b* a positive Cotton effect and an equilibrium mixture of the two can be expected to show multiple Cotton effects and also an alteration in amplitude from a change of nonpolar to polar solvent.

In the optical rotatory dispersion (o.r.d.) curves the cyclobutanone ethyl ester[4] (**1**, from (+)-α-pinene) exhibited a single positive Cotton effect, the antipodal ester[4] (**1***e*, from (−)-α-pinene) exhibiting a single negative Cotton effect. The negative Cotton effect for **5** (c.d.) and the positive Cotton effect for **1** (o.r.d.) with identical

[1]For Part XI see ref. 18.
[2]Taken from the Ph.D. Thesis of L. R. Subramanian (Indian Institute of Science, 1968).

[3]This positive extremum, also observed in compound **3** (Table I), may be attributed to the $n \rightarrow \pi^*$ transition of the ester carbonyl, the pronounced bathochromic shift observed in the c.d. curve being due to a proximity effect exerted on the ester carbonyl by the cyclobutanone.
[4]The o.r.d. data recorded in Table I for the ethyl esters **1** and **1E** were obtained by us much earlier, while the c.d. data (Table I) for the methyl ester **2**, extending to shorter wavelengths, which enabled us to detect the multiple Cotton effect exhibited by **2**, were obtained recently.

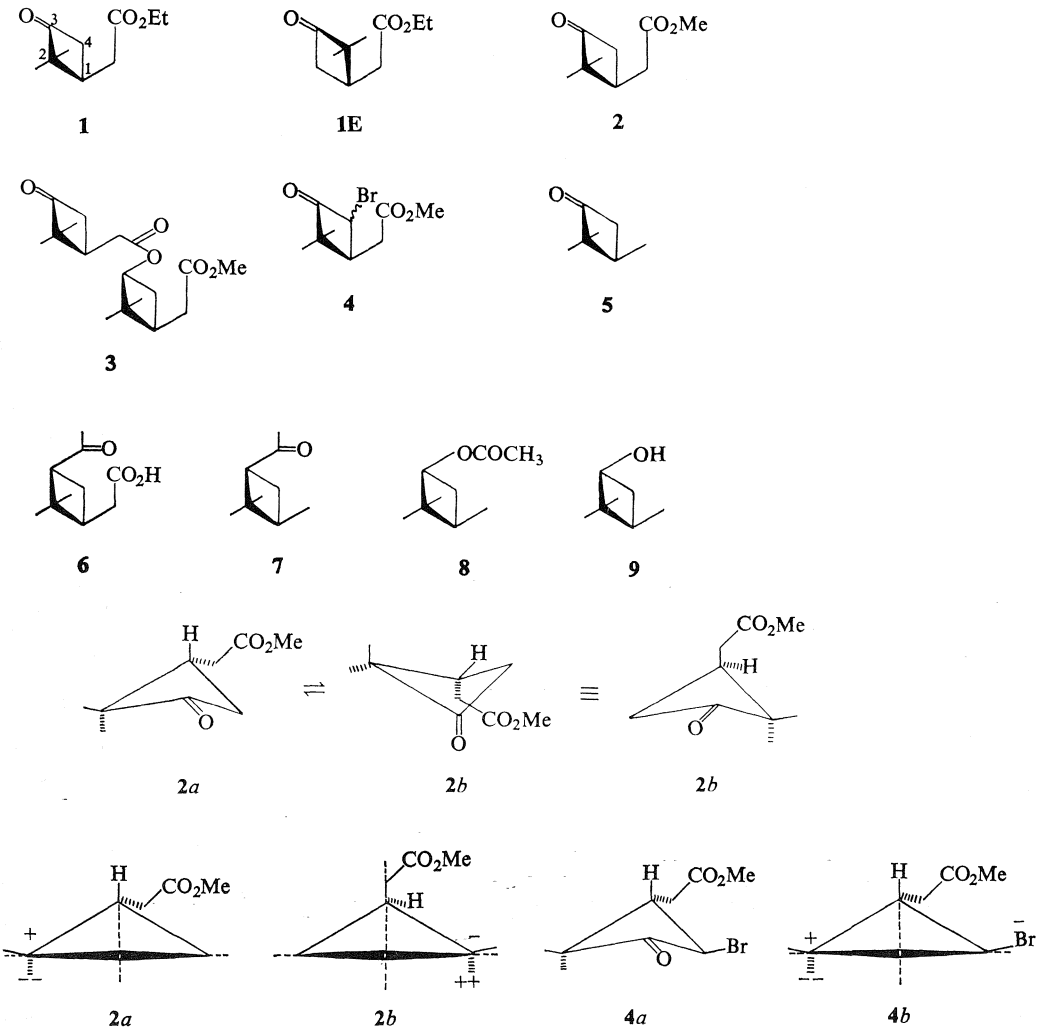

SCHEME I Cyclobutanones **1**–**5** and related compounds.

configurations in both **5** and **1** at the asymmetric center appear to be at variance at first sight. However, the observed reversal in Cotton effects may be ascribed to the preference shown by the freely rotating —CO_2Et group (compound **1**) to one quadrant over the other in a situation of possible steric restriction. The special effect of a β,γ-unsaturated double bond in a cyclobutanone was noted earlier (9). What the effect of a δ-carbonyl (of an ester in a compound like **1**) might be is unknown, but it could be significant.[5]

The dimeric cyclobutanone ester (6) (**3**) exhibited a remarkably similar c.d. curve profile (in dioxan) to that of **2** (in methanol) with positive extrema at 320 and 244 mμ and a negative extremum at 292 mμ (Table I) in conformity with their structural similarity. Methyl (−)-2,2-dimethyl-3-keto-4-bromocyclobutyl acetate (**4**) exhibited c.d. data in agreement with those observed for similar bromocyclobutanones by Conia and Gore (3). Since the bromocyclobutanone ester used in this study consisted of 80% *trans*-isomer,[6] the predominant conformer **4***a* with equatorial bromine (negative octant) satisfies the observed negative Cotton effect for **4**.

[5]We are grateful to one of the referees for this suggestion to explain the observed difference in the Cotton effects.

[6]Deduced from the nuclear magnetic resonance spectrum of **4** (10).

Can. J. Chem. Downloaded from www.nrcresearchpress.com by 210.87.254.5 on 09/05/12
For personal use only.

TABLE I

Optical rotatory dispersion and circular dichroism studies of cyclobutanones

Compound	Cyclohexane			Methanol		
	λ_{max} (mμ)	Δε	[Θ]	λ_{max} (mμ)	Δε	[Θ]
5	302–308	−0.37	−122			
2	319–322	+0.0235	+77	319	+0.027	+89
	302–304	−0.0720	−238	291–293	−0.031	−102
3*	320	+0.04618	+152			
	292	−0.0714	−235			
4	315	−1.287	−4250	312	−0.45	−1485

o.r.d. in methanol (L = 0.1)

	Concentration	Long wavelength extremum, mμ and specific rotation
1	0.146	318 (+27°)
1E	0.350	319 (−28°)

*Solvent: dioxan.

Experimental[7]

(−)-2,2,3(R)-Trimethylcyclobutanone (5)

(i) Hunsdiecker Brominative Decarboxylation (11) of Pinonic Acid

To *cis*-(+)-pinonic acid (**6**, 40.5 g) (7) in anhydrous CCl_4 (240 ml) was added red oxide of mercury (47.7 g) and the mixture stirred slowly while heating it to gentle reflux for 5 min. The heating was stopped and bromine (13.2 ml) in CCl_4 (80 ml) was added cautiously. The exothermic reaction maintained the reaction mixture boiling for a few min. After addition of bromine was over, the vigor of the reaction subsided. Refluxing was continued for another 3 h. The reaction mixture was cooled and filtered. The filtrate was shaken thrice with 10% $NaHCO_3$ solution and the solvent removed under suction. The crude brownish product (24 g) partially decomposed on distillation, b.p. 105–106°/16 mm; i.r. (neat): 1701 cm^{-1} (>C=O).

(ii) 1-Acetyl-2,2,3-trimethylcyclobutane (Pinonone) (7)

The crude bromide (24 g) was refluxed with water (500 ml) and zinc powder (240 g) (12) for 10 h and the product was steam-distilled to give the ketone **7** (10 g), b.p. 160–162°/690 mm; i.r. (neat): 1706 cm^{-1} (>C=O); nuclear magnetic resonance (n.m.r.) (60 MHz, TMS = 0) 117, CO—*CH*$_3$; 166, *CH*—C(=O)—CH$_3$ (for other proton signals see ref. 10).

Anal. Calcd. for $C_9H_{16}O$: C, 77.1; H, 11.4. Found: C, 77.4; H, 11.2.

The *semicarbazone* had m.p. 210–211° (aqueous MeOH) (lit. (13–15) for the *cis*-, *trans*-isomer mixture, m.p. 197–198°).

Anal. Calcd. for $C_{10}H_{19}ON_3$: C, 60.9; H, 9.7; N, 21.3. Found: C, 60.9; H, 9.6; N, 21.5.

The *2,4-dinitrophenylhydrazone* was prepared by refluxing the above semicarbazone (100 mg) with 2,4-dinitrophenylhydrazine (110 mg) and HCl (2–4 drops) in ethanol for 5 h. The crude product on recrystallization from methanol had m.p. 202.5–204°, (lit. (15), m.p. 202–203°).

Anal. Calcd. for $C_{15}H_{20}O_4N_4$: N, 17.5. Found: N, 17.1.

(iii) 2,2,3-Trimethylacetoxycyclobutane (8)

The ketone (**7**, 14 g) was mixed with standardized, moist $CHCl_3$ solution containing perbenzoic acid (approximately 0.12 mole, 200 ml), and the resulting cloudy solution was swirled at intervals and allowed to stand in the dark at room temperature (16). After the theoretical amount of perbenzoic acid had been consumed (ca. 15 days), the $CHCl_3$ solution was shaken with 10% $NaHCO_3$ solution until free of acid. Distillation after removal of solvent gave the acetoxy compound **8** (13.5 g), b.p. 86–88°/65 mm; n_D^{29} 1.4262; α_D −34.8° (neat): i.r. (neat): 1742 (ester >C=O) and 1242 cm^{-1} (ester —C—O).

Anal. Calcd. for $C_9H_{16}O_2$: C, 69.2; H, 10.3. Found: C, 69.3; H, 10.1.

(iv) 2,2,3-Trimethylcyclobutanol (9)

To a suspension of $LiAlH_4$ (10 g) in ether (100 ml) was slowly added with stirring an ethereal solution of the acetoxycyclobutane (**8**, 36.1 g). After the addition was over, it was gently refluxed for 3 h, cooled, and decomposed with saturated NH_4Cl solution. It was then filtered and the organic matter was extracted with ether. Removal of solvent and distillation furnished 2,2,3-trimethylcyclobutanol (**9**, 23 g), b.p. 108–110°/185 mm; i.r. (neat): 3450 cm^{-1} (O—H).

[7]All m.p.s and b.p.s are uncorrected. The infrared (i.r.) spectra were recorded on a Perkin–Elmer 137 spectrophotometer. All organic extracts were washed neutral and dried (Na_2SO_4) prior to removal of the solvent, unless otherwise stated.

Can. J. Chem. Downloaded from www.nrcresearchpress.com by 210.87.254.5 on 09/05/12
For personal use only.

Anal. Calcd. for $C_7H_{14}O$: C, 73.7; H, 12.3. Found: C, 73.8; H, 12.4.

(−)-2,2,3(R)-Trimethylcyclobutanone (5)

To a stirred solution of the hydroxy compound (**9**, 13.5 g) in ether (50 ml) was added dropwise chromic acid solution, prepared from $Na_2Cr_2O_7 \cdot 2H_2O$ (12 g) in 96% H_2SO_4 (9 ml) diluted to 60 ml with water, in about 15 min at 20° (17). After stirring the solution for 2 h, the ether layer was separated and the aqueous layer extracted thrice with ether. On removal of solvent from the combined ether layer and distillation, two fractions were obtained. Fraction 1, b.p. 128°/690 mm was redistilled, b.p. 124–126°/690 mm, to give (−)-2,2,3(R)-trimethylcyclobutanone (**5**, 4 g); n_D^{25} 1.4278; α_D −21.6° (neat); i.r. (neat): 1783 cm^{-1} (cyclobutanone). The i.r. spectrum was superimposable with that of the enantiomeric (+)-2,2,3(S)-trimethylcyclobutanone (**5E**) prepared by Conia and Gore (3).

Anal. Calcd. for $C_7H_{12}O$: C, 74.8; H, 10.7. Found: C, 74.8; H, 10.7.

Fraction 2, b.p. 168°/690 mm proved to be β,γ,γ-*trimethylbutyrolactone* (cf. ref. 6), b.p. 160°/690 mm, n_D^{25} 1.4388; i.r. (neat): 1779 (γ-lactone) and 1418 cm^{-1} (O=C—CH_2—).

Anal. Calcd. for $C_7H_{12}O_2$: C, 65.6; H, 9.4. Found: C, 65.2; H, 9.2.

Acknowledgments

We are indebted to Dr. Sukh Dev for the n.m.r. spectrum of **7**; to Professor Conia for the c.d. curves of **2**, **3**, **4**, and **5** and the i.r. spectrum of **5E**; and to Professor Djerassi for the o.r.d. curves of **1** and **1E**. We thank Professor D. K. Banerjee of this Department for his interest in this work. One of us (L. R. S.) thanks the authorities of the Indian Institute of Science for the award of a scholarship.

1. W. Moffit, R. B. Woodward, A. Moscowitz, W. Klyne, and C. Djerassi. J. Am. Chem. Soc. **83**, 4013 (1961).
2. P. Crabbe. Optical rotatory dispersion and circular dichroism in organic chemistry. Holden-Day, San Francisco. 1965. pp. 83–147.
3. J. -M. Conia and J. Gore. Bull. Soc. Chim. France, 1968 (1964).
4. (*a*) J. -M. Conia, J. Gore, and C. Djerassi. Bull. Soc. Chim. France, 950 (1967); (*b*) G. Snatzke. Angew. Chem. Intern. Ed. Engl. **7**, 14 (1968).
5. R. B. Bates, M. Onore, S. K. Paknikar, C. Steelink, and E. P. Blanchard. Chem. Commun. 1037 (1967).
6. L. R. Subramanian and G. S. Krishna Rao. Tetrahedron, **23**, 4167 (1967).
7. M. Delepine. Bull. Soc. Chim. France, 1369 (1936).
8. A. Moscowitz, K. M. Wellman, and C. Djerassi. Proc. Natl. Acad. Sci. U. S. **50**, 799 (1963); K. M. Wellman, P. H. A. Laur, W. S. Briggs, A. Moscowitz, and C. Djerassi. J. Am. Chem. Soc. **87**, 66 (1965).
9. A. Moscowitz, K. Mislow, M. A. W. Glass, and C. Djerassi. J. Am. Chem. Soc. **84**, 1945 (1962).
10. L. R. Subramanian and G. S. Krishna Rao. Tetrahedron. To be published.
11. K. B. Wiberg, G. M. Lampman, R. P. Ciula, D. S. Connor, P. Schertler, and J. Lavanish. Tetrahedron, **21**, 2749 (1965).
12. N. L. Allinger and L. A. Tushaus. J. Org. Chem. **30**, 1945 (1965).
13. H. E. Eschinazi. U. S. Patent No. 3,019,263. April 2, 1959; Chem. Abstr. **57**, 696 (1962).
14. J. -M. Conia and C. Faget. Bull. Soc. Chim. France, 1963 (1964).
15. H. E. Eschinazi. J. Am. Chem. Soc. **81**, 2905 (1959).
16. C. H. Hassall. *In* Organic reactions. Vol. 9. *Edited by* R. Adams. John Wiley and Sons, Inc., New York. 1957. pp. 73–106.
17. H. C. Brown and C. P. Garg. J. Am. Chem. Soc. **83**, 2952 (1961).
18. J. Alexander and G. S. Krishna Rao. Chem. Ind. London. To be published.

Can. J. Chem. Downloaded from www.nrcresearchpress.com by 210.87.254.5 on 09/05/12
For personal use only.

Effect of *N*-acylamino groups on the chemical shift of the *ortho* proton in biphenyls

F. K. HESS
Pharma-Research Canada Ltd., 250 Hymus Blvd., Pointe-Claire, Quebec

AND

K. H. POOK
C. H. Boehringer Sohn, Ingelheim a. Rhein, Germany

Received November 1, 1968

The proton magnetic resonance spectra of several acylamino biphenyls were determined. Evidence was obtained that the proton adjacent to the acylamino group was shifted to lower field relative to the remaining ring protons.

Canadian Journal of Chemistry, 47, 1151 (1969)

Can. J. Chem. Downloaded from www.nrcresearchpress.com by 210.87.254.42 on 09/05/12
For personal use only.

In a recent paper, Ribera and Rico (1) described the deshielding of the *ortho* proton in the nuclear magnetic resonance (n.m.r.) spectra of *N*-(2-substituted-phenyl)amides. A low-field shift of the signal corresponding to the *ortho* proton was observed only for those compounds which simultaneously had one free (H) and one occupied (F, Cl, Br, I) position. The magnitude of the chemical shift in this series varied from 0.86 to 1.04 p.p.m. relative to benzene.

The deshielding effect of a proton adjacent to an *N*-acetyl group had been described previously in a number of publications. For instance, it was shown by Carter (2) that the resonance for the *ortho* protons in the spectrum of acetanilide was shifted 0.89 p.p.m. downfield from the corresponding resonance in the spectrum of aniline, by determining the residual proton spectra of the partially deuterated compounds. The low-field shift was attributed primarily to the fact that the anisotropic carbonyl group in acetanilide points towards the aromatic ring, with the plane of the acetamido group and the benzene ring making an angle of approximately 38° (3). A lowering for the *ortho* proton signal was also reported for several *para*-substituted acetanilides (4).

A low-field shift arising from the anisotropic shielding of a neighboring *N*-acetyl group was observed in a number of pyridine derivatives. Brügel (5) showed that acetylation of 2-aminopyridine markedly influenced the resonance of the 3-proton. The chemical shift difference expressed as $\Delta\nu_3 - \nu_4$ relative to pyridine between 2-aminopyridine and 2-acetamidopyridine was approximately 1.1 p.p.m.

Similar effects have been observed for other heterocyclic acylamines in which the *N*-acylamino group is adjacent to a ring hydrogen atom. In the n.m.r. spectra of the *N*-acetyl derivatives of benzimidazoles and purines (6), a constant downfield shift of about 19 c.p.s. (40 Mc.p.s.) of the proton adjacent to the acetyl position had been noted. In 4-*N*-acetylpyrimidine all the remaining ring protons are shifted to lower field relative to the signals for the corresponding 4-amino derivative; however, by far the most striking effect was noticed for the adjacent proton (H-5), which was shifted by 1.5 p.p.m. to low-field (7).

The situation where one of the *ortho* positions is occupied exists also in *N*-acylindoline and compounds related to it. Some years ago it was shown by Anet (8) that the aromatic proton in strychnospermine nearest to the *N*-acyl grouping (H-12)[1] appeared as a doublet at 2.35 τ when the spectrum was taken at about −20°; this corresponded to that conformation in which the carbonyl group was preferentially oriented towards the phenyl ring. The band of the same proton in the opposite conformation was at about 3.25 τ. The low-field position was ascribed to the strong, magnetic anisotropy of the carbonyl group. A similar effect was observed in the n.m.r spectrum of fruticosin (9), and depended on the steric arrangement of the N_a-carbomethoxy group. At −30° two doublets of different intensity at 8.00 p.p.m. and 7.55 p.p.m. (100 Mc.p.s.) for H-17[1] were observed. In fruticosamin the *N*-$COOCH_3$ group is conformationally fixed through hydrogen

[1]This corresponds to H-7 in indoline.

Can. J. Chem. Downloaded from www.nrcresearchpress.com by 210.87.254.42 on 09/05/12
For personal use only.

bonding; this compound shows a normal doublet at 7.54 p.p.m. More recently a detailed study by Nagarajan *et al.* (10) on the configuration of the amide bond in *N*-acylindolines and *N*-acyltetrahydroindolines, clearly indicated that the carbonyl group was oriented towards the phenyl ring as in the case of the low temperature n.m.r. spectrum of strychnospermine; the proton at C-7 was seen as a broad doublet at 8.22 p.p.m. as compared to 6.45 p.p.m. in indoline ($\Delta\delta = 1.77$ p.p.m.!). In compounds in which the carbonyl group is rigidly held in the vicinity of a nearby proton, as in hexahydropyrrolo[1,2-*a*]quinoxaline (11, 12), a pronounced low-field shift was again observed.

In connection with some other studies we had prepared a number of acylamino biphenyl derivatives:

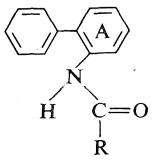

1*a*, R = CH_2—N⟨O⟩ **1***f*, R = CCl_3

1*b*, R = CH_2—N⟨ ⟩ **1***g*, R = CH_2F

1*c*, R = CH_3 **1***h*, R = CH_2I

1*d*, R = CH_2Cl **1***i*, R = CH_2Br

1*e*, R = $CHCl_2$

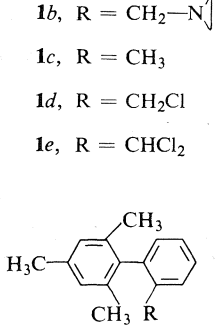

2, R = $NHCOCH_2Cl$

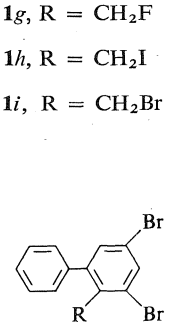

3, R = $NHCOCH_2Cl$

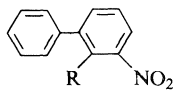

4, R = $NHCOCH_3$

The n.m.r. spectra of the various amides were determined at 60 Mc.p.s. in chloroform-*d* solution. It was found, that the resonance for one of the protons in compounds (**1***a–i*) was shifted downfield from the corresponding spectrum in 2-amino biphenyl, ranging from 1.40–1.95 p.p.m., (corrected for the diamagnetic anisotropy effect of the vicinal phenyl ring, see below), representing a downfield shift of 1.23–0.68 p.p.m. relative to benzene. Our results are summarized in Table I. The partial n.m.r. spectrum of compound **1***a* is shown in Fig. 1.

TABLE I

Nuclear magnetic resonance data for the *ortho* proton in *N*-acyl biphenyls*

Compound	τ_H†	τ'_H‡	Δ§
1*a*	1.28	1.40	1.23
1*b*	1.39	1.51	1.12
1*c*	1.45	1.57	1.06
1*d*	1.45	1.57	1.06
1*e*	1.56	1.68	0.95
1*f*	1.54	1.66	0.97
1*g*	1.70	1.82	0.81
1*h*	1.73	1.85	0.78
1*i*	1.83	1.95	0.68

*Spectra were determined at 60 M c.p.s., using 0.66 *M* solutions in $CDCl_3$.
†With reference to internal TMS, (τTMS 10 p.p.m.).
‡Adjusted for adjacent ring current effect: $\tau'_H = \tau_H + 0.12$.
§Shift to low field with reference to the chemical shift of benzene, (τ p.p.m. 2.63).

Except for compounds **3** and **4**, all derivatives have one free and one occupied *ortho* position. With regard to the orientation of the carbonyl group, it is clear from our results that this group is oriented towards the aromatic ring as in acetanilide (3), but not necessarily coincident with it and that the adjacent proton lies in the deshielding zone of this group. The *a priori* possibility that the *ortho* position in the neighboring ring might be deshielded because its proximity (cf. 13), was ruled out by the following facts:

a) The spectrum of the mesityl derivative (**2**) clearly showed that the position and the intensity of the low-field signal had not been altered.

b) In the spectrum of **3** the low-field C—H proton signal was absent.

c) In 2-nitro-1-acetamidobiphenyl (**4**) the *N*-acetyl carbonyl group is probably oriented towards the neighboring phenyl ring because of intramolecular hydrogen-bonding between the amido proton and the nitro group.[2] However, the characteristic low-field signal observed for com-

[2]The deshielding of aromatic protons in *ortho*-nitro substituted acetanilides was recently described in great detail (14, 15).

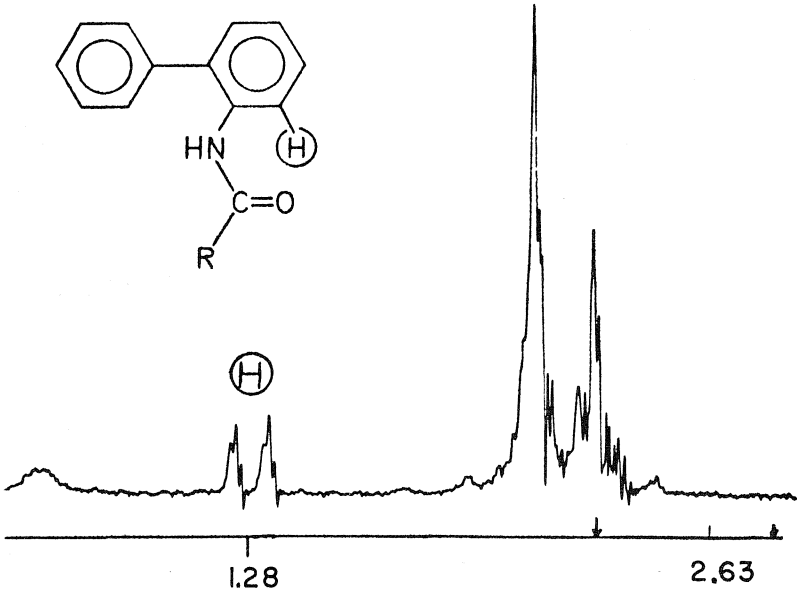

FIG. 1. Partial nuclear magnetic resonance spectrum of **1***a*, R = CH_2-N⟨O⟩, in $CDCl_3$ at 60 Mc.p.s. (numbers are in p.p.m. (τ)).

pounds (**1***a–i*) was absent in the n.m.r. spectrum ($CDCl_3$ and $(CD_3)_2SO$).

It may be concluded, therefore, that it is the proton next to the *N*-acetyl group which resonates at lower field.

In order to correct for the influence of the phenyl substituent on the chemical shift of the protons in ring A we have used the data given in the literature. A correction for the contribution of the halogen atoms to the chemical shift of the *ortho* proton was made by Ribera and Rico (1) using the ^{S}*meta* values given by Diehl (16). Mayo and Goldstein (17), who have carried out a detailed proton resonance investigation of biphenyl, showed that the anisotropic shielding of a given proton is a function of the dihedral angle between the two benzene rings. From their work as well as from a variety of independent evidence cited in their paper these authors suggested, that "the chemical shifts in biphenyl are most plausibly accounted for by a model involving free, or nearly free, rotation of the rings (in solution) and very weak interactions between the phenyl groups". The diamagnetic anisotropic shielding at each position was calculated as a function of the dihedral angle; the corrections were +19.1, +7.2, and +6.0 c.p.s. at 60 Mc.p.s. (determined in $CHCl_3$) for the *o-*, *m-*, and *p*-positions, respectively.[3]

The freely rotating model may not be strictly applicable in our series of biphenyl derivatives since one of the *ortho* positions is occupied by a relatively large group. However, since the shielding of the *meta* protons varies only slightly with the change in dihedral angle as shown by Mayo and Goldstein (17), we have taken the average values of 7.2 c.p.s. for our biphenyl derivatives (**1***a–i*). The correction was not applied for the mesityl compound (**2**), since the values for biphenyl are not necessarily applicable for this case. However, the general trend for the low-field shift was clearly observable (cf. Fig. 2).

The methyl protons in compound **2** give rise to two signals at 2.35 p.p.m. (3 protons) and 2 p.p.m. (6 protons) respectively. The introduction of three large *ortho* substituents in **2** widens the dihedral angle to 70° or greater (18). The effect of twisting the two phenyl rings almost out of plane brings the protons of the *ortho* methyl groups under the influence of the induced field of the adjacent ring which accounts for the observed

[3]An ^{S}*m*-value of -11 ± 2 p.p.h.m. (40 Mc.p.s., CCl_4) was given by Smith (4).

Can. J. Chem. Downloaded from www.nrcresearchpress.com by 210.87.254.42 on 09/05/12
For personal use only.

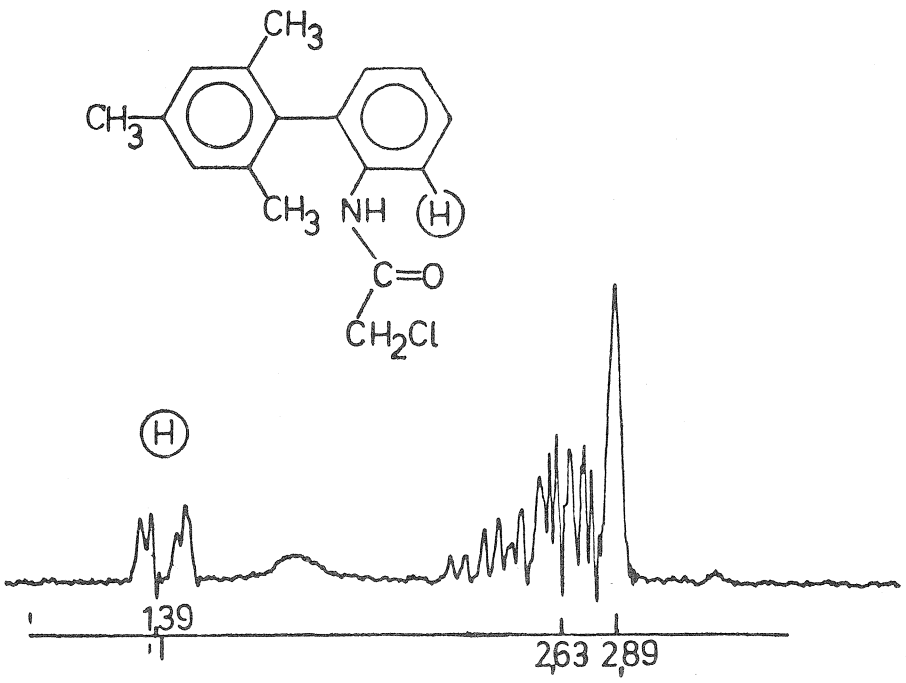

FIG. 2. Partial nuclear magnetic resonance spectrum of **2** in $CDCl_3$ at 60 Mc.p.s. (numbers are in p.p.m. (τ)).

upfield shift of approximately 0.3 p.p.m. For comparison, the signals for the methyl protons in 2,2′,4,4′-tetramethyl biphenyl, occur at 2.37 and 2.03 p.p.m., respectively (19). On the other hand, in 4,5-dimethyl-9,10-tetrahydrophenanthrene the methyl protons give rise to only one signal at 2.29 p.p.m. (20).

From an inspection of Table I, it can be seen that there is a noticeable change in chemical shift values within this series of compounds. This is diagrammatically shown below:

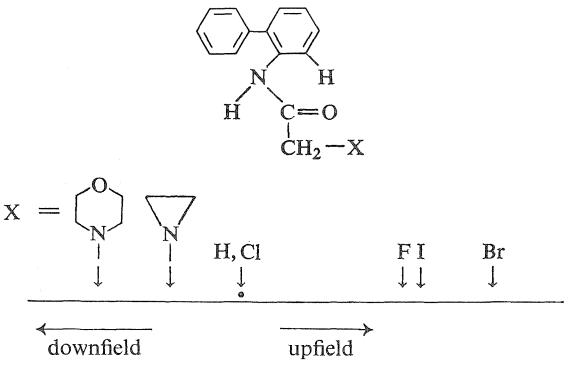

The observed downfield shift of the *ortho* proton is due to a combination of the anisotropic deshielding by the *N*-acetyl carbonyl group as well as to electric and field effects of the amide group, in accord with the general observations cited in this text. This effect is then further modified as shown above. Although there is no observable change for the mono-chloro derivative (**1***d*), additional α-halogenation causes an upfield shift. However, a direct correlation between this upfield shift and the size or the number of the halogen atoms does not exist as shown in Table I; substitution by fluorine, bromine, or iodine results in a noticeable shift to higher frequencies. On the other hand, a shift to lower fields was observed for the two compounds with nitrogen-containing substituents, (**1***a*) and (**1***b*).[4] This variation in chemical shift is rather difficult to assess. Transmission solely through bonds cannot alone account for it; both inductive effects and changes in the magnetic anisotropy of the C—X bond as well as steric differences and

[4]Zanger and co-workers, in a recent publication on the nuclear magnetic resonance spectra of *N*-acylanilines, (21 and cf. ref. 1) also found no change for the monochloroacetyl derivative, and concluded that the nature of the group attached to the acyl carbon atom has relatively little effect on the chemical shift of the aromatic protons.

Can. J. Chem. Downloaded from www.nrcresearchpress.com by 210.87.254.42 on 09/05/12
For personal use only.

Can. J. Chem. Downloaded from www.nrcresearchpress.com by 210.87.254.42 on 09/05/12
For personal use only.

TABLE II

Characterization of *N*-acylamino biphenyls

Compound	Melting point* °C	Analysis calculated							Analysis found						
		C	H	N	F	Cl	Br	I	C	H	N	F	Cl	Br	I
1*a*	148–149	72.95	6.80	9.45	—	—	—	—	72.90	6.93	9.39	—	—	—	—
1*b*	96–98	76.16	6.39	11.11	—	—	—	—	75.91	6.59	11.02	—	—	—	—
1*c*	120–122	79.59	6.20	6.63	—	—	—	—	79.81	6.32	6.76	—	—	—	—
1*d*	98–100	68.43	4.93	5.70	—	14.43	—	—	68.26	5.04	5.69	—	14.46	—	—
1*e*	106–107	60.02	3.96	5.00	—	25.31	—	—	60.09	3.77	5.11	—	25.38	—	—
1*f*	95–96	53.45	3.20	4.45	—	33.81	—	—	53.65	3.28	4.59	—	33.76	—	—
1*g*	91–93	73.35	5.27	6.11	8.29	—	—	—	73.35	5.46	6.20	8.44	—	—	—
1*h*	122–123	49.87	3.59	4.16	—	—	—	37.64	49.98	3.49	4.15	—	—	—	37.64
1*i*	96–98	57.95	4.15	4.83	—	—	27.54	—	57.92	4.45	4.88	—	—	27.45	—
2	95–96	70.95	6.29	4.87	—	12.32	—	—	70.21	6.25	4.91	—	12.46	—	—
3	196	41.67	2.50	3.47	—	8.79	39.61	—	41.56	2.10	3.45	—	8.94	39.82	—
4	184–186†	—	—	—	—	—	—	—	—	—	—	—	—	—	—

*Melting points (in °C) are uncorrected.
†Lit., 185–187 °C (25).

changes in bond angles are likely contributing factors and are probably interdependent.[5]

Experimental

Elemental microanalyses were provided by Dr. C. Daesslé, Montreal, Quebec, and Dr. A. B. Gygli, Toronto, Ontario. The nuclear magnetic resonance (n.m.r.) spectra were determined as 0.66 *M* solutions in $CDCl_3$ using a Varian Associates model A60-A.

Materials

Compounds (**1***c–f*) and (**1***i*) were obtained by reacting 2-aminobiphenyl (Aldrich Chemical Company) with the corresponding acetyl halides in DMF at 5–10 °C in the presence of K_2CO_3. The mono-iodo compound, (**1***h*), was prepared from the mono-chloro derivative, (**1***d*), by halogen exchange (NaI–acetone).

Monofluoroacetyl chloride was prepared by the method of Truce (22). The fluoroacetyl compound (**1***g*), was then prepared by the method indicated above.

We used the method of Smolinsky (23) for the preparation of 2,4,6-trimethyl-2′-aminobiphenyl; the latter was converted into the monochloroacetyl derivative (**2**) by the previous procedure.

According to the procedure of Scarborough and Waters (24) we obtained 3,5-dibromo-2-aminobiphenyl, which was subsequently converted into the monochloroacetyl compound (**3**) in the usual manner.

For the preparation of 2-nitro-1-acetamidobiphenyl we employed the procedure given by Stepan and Hamilton (25).

The morpholino- and aziridino-compounds (**1***a*) and (**1***b*) were prepared by reacting the monochloroacetyl derivative (**1***d*) with the respective amines.

Characterization data for all compounds are given in Table II.

[5]A correlation with other substituent parameters was not established, because the data are too limited to evaluate the relative importance of these factors accurately.

1. A. Ribera and M. Rico. Tetrahedron Letters, 535 (1968).
2. R. E. Carter. Acta Chem. Scand. **21**, 75 (1967).
3. C. J. Brown and D. E. C. Corbridge. Acta Cryst. **7**, 711 (1954).
4. G. W. Smith. J. Mol. Spectry. **12**, 146 (1964).
5. W. Brügel. Z. Elektrochem. **66**, 159 (1962).
6. G. S. Reddy, L. Mandell, and J. H. Goldstein. J. Chem. Soc. 1414 (1963).
7. S. Gronowitz, B. Norrman, B. Gestblom, B. Mathiasson, and R. A. Hoffman. Arkiv Kemi, **22**, 65 (1963).
8. F. A. L. Anet. Can. J. Chem. **41**, 883 (1963).
9. A. Guggisberg, M. Hesse, W. von Philipsborn, K. Nagarajan, and H. Schmid. Helv. Chim. Acta, **49**, 2321 (1966).
10. K. Nagarajan, M. D. Nair, and P. M. Pillai. Tetrahedron, **23**, 1683 (1967).
11. E. C. Taylor and A. McKillop. J. Am. Chem. Soc. **87**, 1968 (1965).
12. S. C. Bell and G. Conklin. J. Heterocyclic Chem. **5**, 179 (1968).
13. S. Brownstein. J. Am. Chem. Soc. **80**, 2300 (1958).
14. R. F. C. Brown, L. Random, S. Sternhell, and I. D. Rae. Can. J. Chem. **46**, 2577 (1968).
15. J. R. Bartels-Keith and R. F. W. Cieciuch. Can. J. Chem. **46**, 2593 (1968).
16. P. Diehl. Helv. Chim. Acta, **44**, 829 (1961).
17. R. E. Mayo and J. H. Goldstein. Mol. Phys. **10**, 301 (1965).
18. M. S. Newman. Steric effects in organic chemistry. John Wiley and Sons, Inc., New York. 1956. p. 511.
19. N. S. Bhacca, L. F. Johnson, and J. N. Shoolery. NMR Spectra Catalog. Varian Associates, Palo Alto. 1962. Spectrum No. 659.
20. N. S. Bhacca, L. F. Johnson, and J. N. Shoolery. NMR Spectra Catalog. Varian Associates, Palo Alto. 1962. Spectrum No. 654.
21. M. Zanger, W. W. Simmons, and A. R. Gennaro. J. Org. Chem. **33**, 3673 (1968).
22. W. E. Truce. J. Am. Chem. Soc. **70**, 2828 (1948).
23. G. Smolinsky. J. Am. Chem. Soc. **82**, 4717 (1960).
24. H. A. Scarborough and W. A. Waters. J. Chem. Soc. 89 (1927).
25. A. H. Stepan and C. S. Hamilton. J. Am. Chem. Soc. **71**, 2438 (1949).

Can. J. Chem. Downloaded from www.nrcresearchpress.com by 210.87.254.42 on 09/05/12
For personal use only.

Conformations and configurations of some chlorosulfated α- and β-D-pentopyranosyl chlorides[1]

H. J. JENNINGS
Division of Biosciences, National Research Council of Canada, Ottawa, Canada
Received November 5, 1968

The conformations of the fully chlorosulfated α- and β-D-xylopyranosyl and lyxopyranosyl chlorides in deuteriochloroform solution have been studied by proton magnetic resonance spectroscopy. The analysis of the spectra indicated that the anomeric effect is a factor in determining the conformational preference of the pentopyranosyl chlorides, as each existed predominantly in the conformation in which the chlorine was axial. A number of factors involving the synthesis of these chlorides have also been elucidated.

Canadian Journal of Chemistry, **47**, 1157 (1969)

Can. J. Chem. Downloaded from www.nrcresearchpress.com by 210.87.254.105 on 09/05/12
For personal use only.

Introduction

Previous studies on the proton magnetic resonance (p.m.r.) spectra of the acylpentopyranosyl halides (1–4) have indicated that their conformational preference in solution is influenced to a large extent by the anomeric effect (5). This has been found to be the case with both the thermodynamically more stable and less stable anomers of these halides. The thermodynamically more stable anomers of the acetylpentopyranosyl bromides (1) have been shown by Horton and Turner to exist predominantly in the conformation in which the bromine is axial, and comparisons of both anomers of the tri-*O*-benzoyl-D-ribopyranosyl fluorides, chlorides, and bromides (2) have also shown that in each case, the halogen is predominantly axial. Similar comparisons have been made using the α- and β-anomers of tri-*O*-acetyl-D-xylopyranosyl chlorides (3), and fluorides (4) and again these compounds adopt the conformation in which the halogen substituent is predominantly axial. For the β-D-xylopyranosyl halides this requires that every large substituent group on the pyranose ring be axial and demonstrates the large contribution made by the anomeric effect. We now report an analogous situation for the chlorosulfated α- and β-D-xylopyranosyl and lyxopyranosyl chlorides. The present work reports on the synthesis of these chlorides in both their α-D and β-D configurations and the analysis of their p.m.r. spectra in deuteriochloroform solution. Configurational assignments made previously on both α- and β-D-xylopyranosyl chloride 2,3,4-tri(chlorosulfate) have also been confirmed by p.m.r. spectroscopy.

Discussion

The method of synthesis of β-D-xylopyranosyl chloride 2,3,4-tri(chlorosulfate) (**1**) has been previously described (6), but it has now been established that the conditions of the reaction are such that pure crystalline α-D-xylopyranose yields crystalline **1** in a high degree of purity. This was established by comparison of the p.m.r. spectrum of the crude product with that of pure **1**. The spectra were identical and none of the signals associated with the α-D-chloride (**2**) could be detected. This was also the case when crystalline β-D-lyxopyranose was treated with sulfuryl chloride under identical conditions (6). Only the signals corresponding to those of α-D-lyxopyranosyl chloride 2,3,4-tri(chlorosulfate) (**4**) could be detected in the crude reaction product. This would suggest strongly that 1-chloro substitution occurs via an intermediate 1-chlorosulfate ester, resulting in overall inversion of configuration at the anomeric center. It also demonstrates that anomerization does not occur to any significant extent using these reaction conditions, thus providing a controlled synthesis of the pure anomeric chlorides even in the case of the thermodynamically less stable anomers (**1** and **3**). Further support for this hypothesis was obtained when treatment of an equilibrium mixture of D-xylose with sulfuryl chloride yielded a mixture of chlorides (**1** and **2**) essentially in the same ratio as the original anomeric mixture of reducing pyranoses but with reversed configurations (by p.m.r.). Similar evidence

[1]Issued as NRCC No. 10537.

Can. J. Chem. Downloaded from www.nrcresearchpress.com by 210.87.254.105 on 09/05/12
For personal use only.

could not be obtained from the p.m.r. spectrum of the crude reaction product of an equilibrium mixture of D-lyxose with sulfuryl chloride because of the overlap of the anomeric signals of **3** and **4**, but the specific rotation of the crude syrupy mixture in comparison with the specific rotations of pure **3** and **4** did indicate a comparable situation. The synthesis of α-D-xylopyranosyl chloride 2,3,4-tri(chlorosulfate) (**2**) had been previously achieved by the anomerization of **1** using aluminium chloride (6). However, the reported yield was not good and successive repetitions of this reaction have recently indicated that the yields are also very variable. A preferable method is to effect the anomerization of **1** with titanium tetrachloride which gives consistently higher yields of **2**. β-D-Lyxopyranosyl 2,3,4-tri(chlorosulfate) (**3**) was obtained by crystallization from the crude product of the reaction of sulfuryl chloride with an equilibrium mixture of D-lyxose.

Coupling constants were obtained by first-order analysis of the spectra of **1**, **2**, **3**, and **4** and are shown in Table I. The data clearly indicate that all the compounds, regardless of anomeric configuration, exist predominantly in that conformation which places the chlorine at C-1 in an axial position. This requires a predominance of the 1C(D) conformation for **1** and **3** and of the C1(D) conformation for **2** and **4**.

The spectrum of **1** (Fig. 1*a*) gave a narrow unresolved signal at τ 3.74 which was assigned to the anomeric proton (H-1). The fact that the signal was not a simple doublet was due to long-range coupling with H-3 (assigned to the complex multiplet at τ 4.56). This was substantiated when irradiation of H-3 (δ = +48 Hz) resulted in the collapse of the anomeric signal to a doublet ($J_{1,2}$ = 1.4 Hz). This small value of the $J_{1,2}$ coupling constant is consistent with a *gauche* orientation (7) of the H-1 and H-2 protons and a much larger value of $J_{1,2}$ would be required to assign **1** to the C1(D) conformation as in this case the H-1 and H-2 protons would be diaxially oriented (7). The H-5a and H-5e protons were assigned to the quartet and sextet at high field. Irradiation of H-3 (δ = −68 Hz) caused the sextet to collapse to a quartet indicating long-range coupling ($J_{3,5e}$ = 1.4 Hz) of H-3 with one of the H-5 protons. The highest field sextet was thus assigned to the H-5e proton as this type of coupling occurs most frequently when the two protons involved have a diequatorial orientation (8). Similar long-range couplings of the H-3 proton with both H-1 and H-5e have been reported in related pyranose ring compounds (2,3,4,9) and this evidence strongly supports the 1C(D) conformation of **1**. The small values of $J_{4,5e}$ (1.8 Hz) and $J_{4,5a}$ (2.0 Hz) are also in agreement with the *gauche* orientation (7) of H-4 with both H-5e and H-5a.

TABLE I

First-order coupling constants (Hz) of the chlorosulfated α- and β-D-pentopyranosyl chlorides of D-xylose and D-lyxose

Compound	$J_{1,2}$	$J_{2,3}$	$J_{3,4}$	$J_{4,5e}$	$J_{4,5a}$	$J_{5a,5e}$	$J_{3,5e}$
1	1.4*	—	—	1.8	2.0	14.4	1.4*
2	3.8	9.0	9.0	6.0	10.6	11.6	—
3	3.9	—	—	2.3	1.7†	14.2	1.4†
4	1.8	—	10.0	6.0	10.2	12.0	—

*Obtained by spin decoupling.
†Not unambiguously assigned.

The spectrum of **3** is shown in Fig. 2*a* and although the H-2, H-3, and H-4 signals were superimposed, there were sufficient similarities between the spectra of **3** and **1** to indicate a β-D-pyranose structure for **3** (see below). Additional proof of this structure was also obtained when **3** was methanolyzed in the presence of silver carbonate to give a syrupy methyl glycoside which on dechlorosulfation, (6) yielded crystalline methyl α-D-lyxopyranoside. The anomeric proton of **3** was assigned to the low-field doublet at τ 3.74 and the small value of the coupling constant ($J_{1,2}$ = 3.9 Hz) is consistent with a *gauche* orientation (7) of the H-1 and H-2 protons. The H-5 protons of **3** gave almost identical signals to the H-5 protons of **1**. The small values of $J_{4,5e}$ and $J_{4,5a}$ are in agreement with the *gauche* orientation (7) of H-4 with both H-5e and H-5a, and the appearance of the H-5e signal of **3** as a high-field sextet indicated a similar situation to **1** with long-range coupling between the diequatorial protons H-3 and H-5e. This evidence supports the 1C(D) conformation of **3** as the alternate C1(D) conformation would require one large coupling constant indicative of the vicinal diaxial H-4 and H-5a protons, and would not be favorable for this type of long-range coupling (8). The $J_{4,5e}$ and $J_{3,5e}$ couplings of **3** were assigned by analogy with those of **1** and could not be confirmed by spin decoupling

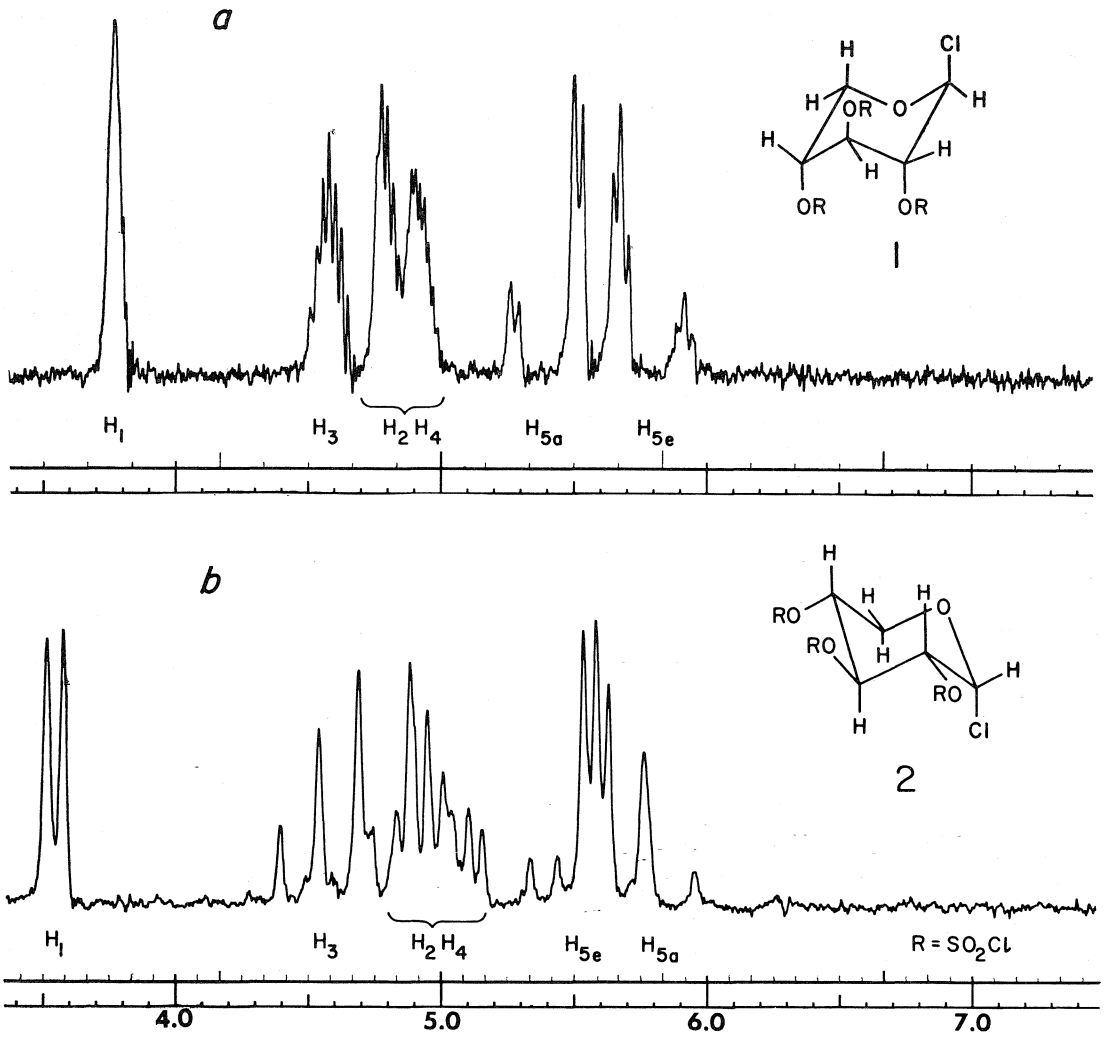

FIG. 1. Proton magnetic resonance spectra at 60 MHz in deuteriochloroform of: *a*) β-D-xylopyranosyl chloride 2,3,4-tri(chlorosulfate) (**1**); *b*) α-D-xylopyranosyl chloride 2,3,4-tri(chlorosulfate) (**2**).

experiments due to the complex overlap of the H-2, H-3, and H-4 signals. However, their small numerical values even if reversed would not affect the conformational deductions.

The p.m.r. spectra of **2** (Fig. 1*b*) and **4** (Fig. 2*b*) are consistent with the existence of both compounds predominantly in the C1(D) conformation. The first-order coupling constants of **2** ($J_{3,4}$ = 9.0 Hz, $J_{4,5e}$ = 6.0 Hz, and $J_{4,5a}$ = 10.6 Hz) are similar to those of **4** ($J_{3,4}$ = 10.0 Hz, $J_{4,5e}$ = 6.0 Hz, and $J_{4,5a}$ = 10.2 Hz) and are consistent with the vicinal diaxial orientation (7) of the H-3, H-4, and H-5a protons of both **2** and **4**. This evidence was also supported in the case of **2** by the fact that equal coupling of the axial H-3 proton with both the axial H-2 and H-4 protons resulted in the appearance of the H-3 signal as a triplet centered on τ 4.52 with $J_{2,3}$ = $J_{3,4}$ = 9.0 Hz. The anomeric protons of **2** and **4** were assigned to the low-field doublets at τ 3.54 and τ 3.69 respectively and the respective coupling constants ($J_{1,2}$ = 3.9 Hz and 1.8 Hz) are

Can. J. Chem. Downloaded from www.nrcresearchpress.com by 210.87.254.105 on 09/05/12
For personal use only.

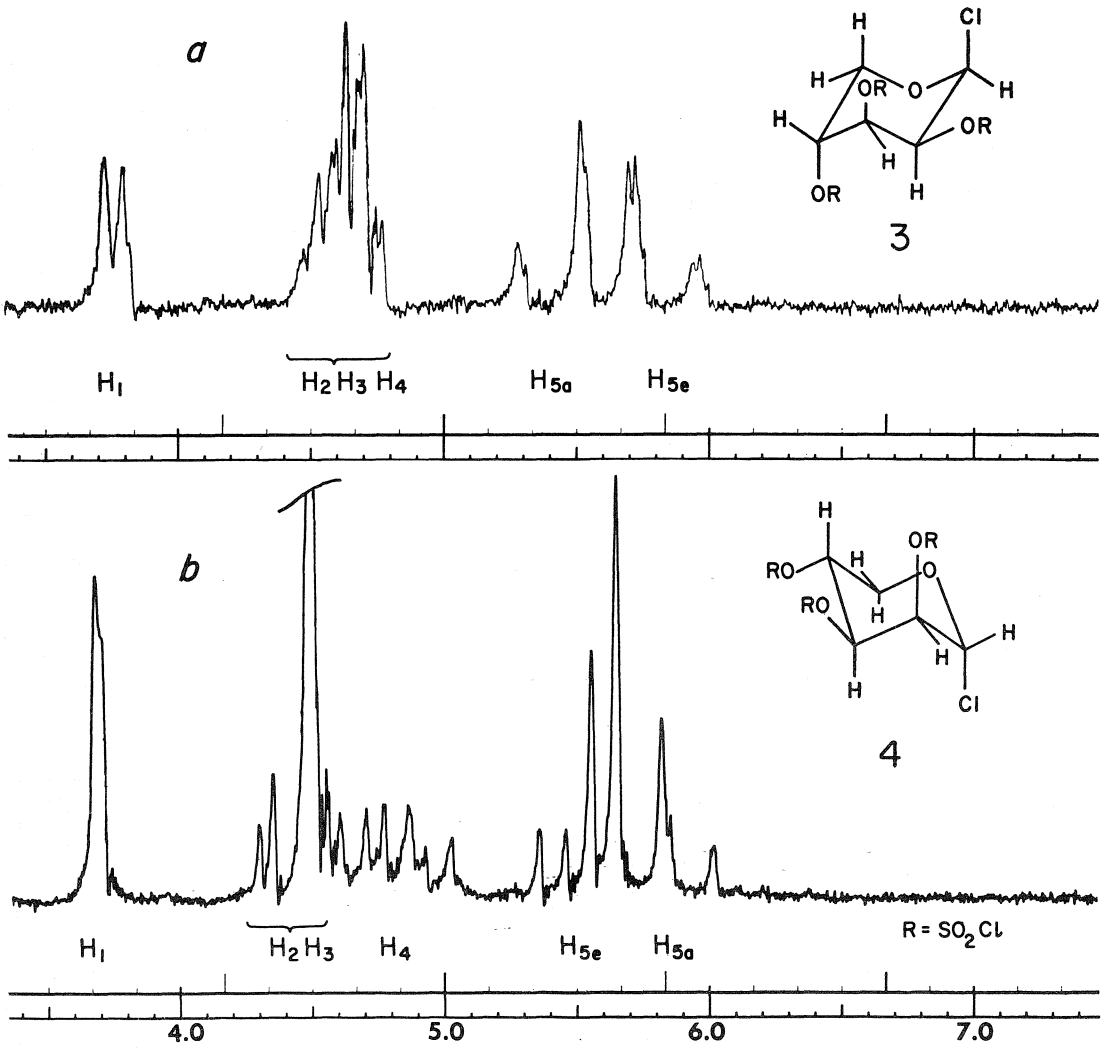

FIG. 2. Proton magnetic resonance spectra at 60 MHz in deuteriochloroform of: *a*) β-D-lyxopyranosyl chloride 2,3,4-tri(chlorosulfate) (**3**); *b*) α-D-lyxopyranosyl chloride 2,3,4-tri(chlorosulfate) (**4**).

consistent with the *gauche* orientation (7) of their H-1 and H-2 protons.

Although the small $J_{1,2}$ values of **1**, **2**, **3**, and **4** are all consistent with a *gauche* orientation (7) of their respective H-1 and H-2 protons, they can be further differentiated as the range of $J_{1,2}$ values of **1** and **4** (1.4–1.8 Hz) are appreciably smaller than those of **2** and **3** (3.8–3.9 Hz). This effect has been previously encountered in pyranose ring systems (9, 10) and in agreement with previous results, these values are typical of J_{ee} coupling for **1** and **4** and J_{ea} coupling for **2** and **3**. A comparison of the geminal coupling constants of **1**, **2**, **3**, and **4** shows that both **1** and **3** have a larger range of values of $J_{5a,5e}$ (14.2–14.4 Hz) than those of compounds **2** and **4** (11.6–12.0 Hz). It has been suggested that the numerical value of $J_{5a,5e}$ is in part dependent on the relative orientation of the vicinal electronegative substituent to the geminal protons (11) the coupling being larger when the electronegative substituent is *gauche* to only one of the geminal protons. The conformations assigned to **1** and **3** (1C(D)) and **2** and **4** (C1(D)) are con-

Can. J. Chem. Downloaded from www.nrcresearchpress.com by 210.87.254.105 on 09/05/12
For personal use only.

sistent with this suggestion which is also supported by observations made from the spectra of other pyranose ring compounds (2, 4, 10).

Experimental

Melting points were obtained on a Kofler hot stage and are uncorrected, and optical rotations were measured at 21 ± 3°. The proton magnetic resonance (p.m.r.) spectra were obtained from a Varian A-60A spectrometer at ambient temperature (approximately 30°). The crystalline compounds **1**, **2**, **3**, and **4** were examined as 10–20% solutions in deuteriochloroform using tetramethylsilane (τ 10.0) as the internal standard. Chemical shifts and coupling constants were obtained by first-order analysis and field swept spin decoupling (δ = ±frequency separation in Hz) was carried out using a Varian V-6058A spin decoupler. An equilibrium mixture of each sugar was obtained by concentrating its fully mutarotated aqueous solution to a syrup. The syrup was subsequently treated directly with sulfuryl chloride.

β-D-Xylopyranosyl Chloride 2,3,4-Tri(chlorosulfate) (1)

Crystalline α-D-xylopyranose when treated with sulfuryl chloride as previously described (6) gave a comparable yield of crystalline **1** which had m.p. 84°, undepressed on admixture with authentic **1** (6). The p.m.r. spectrum of **1** (Fig. 1*a*) indicated that **1** was the pure β-D-anomer, and the spectrum remained unchanged after the deuteriochloroform solution had been kept for 24 h at room temperature. The p.m.r. spectrum of the crude reaction product was found to be virtually identical to that of pure **1**.

α-D-Xylopyranosyl Chloride 2,3,4-Tri(chlorosulfate) (2)

Compound **2** was previously synthesized by the anomerization of **1** using aluminium chloride (6). Repetitions of this reaction have indicated that the yields of **2** are poor and unreliable due to the formation of a complex reaction product (p.m.r.). This situation can be improved by using titanium tetrachloride.

Crystalline **1** (3.0 g) was refluxed with titanium tetrachloride (10.2 g) in absolute chloroform (100 ml) solution for 2 h. The mixture was then poured onto crushed ice, and the resultant chloroform phase was separated and washed with sodium bicarbonate solution and water. The chloroform solution was then dried over anhydrous sodium sulfate, filtered, and concentrated to a syrup which rapidly crystallized. Recrystallization from chloroform – light petroleum (b.p. 30–60°) gave crystalline **2** (2.0 g, 60%) of m.p. 98°, undepressed on admixture with authentic **2** (6). The p.m.r. spectrum of **2** (Fig. 1*b*) indicated that **2** was anomerically pure.

An equilibrium mixture of D-xylose (6.0 g) was treated with sulfuryl chloride (6) and yielded a syrupy chloroform soluble mixture (12.0 g) of **1** and **2** (p.m.r.) from which **2** could not be crystallized. Integration of the signals at τ 3.74 and τ 3.54 (anomeric protons of **1** and **2** respectively) indicated that the ratio of α- to β-anomers was 1.6:1 which corresponds roughly to the ratio of β- to α-anomers (D-xylopyranoses) present in the original equilibrium mixture of D-xylose (12).

β-D-Lyxopyranosyl Chloride 2,3,4-Tri(chlorosulfate) (3)

A syrupy equilibrium mixture of D-lyxose (5.0 g) was treated with sulfuryl chloride (6) and the chloroform soluble product was isolated as before (6). The resultant syrup (10.2 g) of $[\alpha]_D$ −60° (*c*, 4.0 in chloroform) slowly crystallized, and recrystallization from chloroform – light petroleum (b.p. 30–68°) gave colorless needles (4.0 g, 26%) of m.p. 78° and $[\alpha]_D$ = −82.8° (*c*, 1.6 in chloroform).

Anal. Calcd. for $C_5H_6Cl_4S_3O_{10}$: C, 13.03; H, 1.30; Cl, 30.55; S, 20.70. Found: C, 13.08; H, 1.53; Cl, 30.41; S, 20.40.

The p.m.r. spectrum of **3** (Fig. 2*a*) indicated that **3** was anomerically pure and the spectrum remained unchanged after the deuteriochloroform solution had been kept for 24 h at room temperature.

The methanolysis of **3** (2.0 g) using silver carbonate was carried out using identical conditions previously described for the methanolysis of **1** (6). The methanolysis produced a syrup (1.8 g) which did not crystallize and which was subsequently dechlorosulfated in aqueous acetone solution with sodium iodide in the presence of excess barium carbonate (6). The aqueous acetone solution was then filtered, and the filtrate was deionized by passage of it through Amberlite I.R. 120 (H^+ form) and Duolite A.4 (OH^- form) ion-exchange resins. Concentration of the deionized solution yielded a syrup which crystallized and recrystallization (two times) from ethyl acetate gave colorless needles (0.21 g, 30%) of $[\alpha]_D$ +57° (1.1 in methanol) and m.p. 109–110°, undepressed on admixture with authentic methyl α-D-lyxopyranoside (13).

α-D-Lyxopyranosyl Chloride 2,3,4-Tri(chlorosulfate) (4)

Crystalline β-D-lyxopyranose (5.0 g) when treated with sulfuryl chloride (6) yielded a syrup which rapidly crystallized. Recrystallization from chloroform – light petroleum (b.p. 30–60°) gave large crystals (9.5 g, 61.3%) of m.p. 92–93° and $[\alpha]_D$ +20.6° (*c*, 1.1 in chloroform).

Anal. Calcd. for $C_5H_6Cl_4S_3O_{10}$: C, 13.03; H, 1.30; Cl, 30.55; S, 20.70. Found: C, 12.80; H, 1.14; Cl, 30.52; S, 20.31.

The p.m.r. spectrum of **4** (Fig. 2*b*) indicated that **4** was anomerically pure and the p.m.r. spectrum of the crude reaction product was virtually identical to that of pure **4**. Compound **4** has been previously isolated in a yield of 52% but the anomeric configuration was not assigned (14); lit. (14) m.p. 94–96° and $[\alpha]_D$ = +20.4° (chloroform).

Acknowledgments

The author wishes to thank Mrs. B. McLean for technical assistance and Mr. A. E. Castagne for determination of the microanalyses and the proton magnetic resonance spectra.

1. D. Horton and W. N. Turner. J. Org. Chem. **30**, 3387 (1965).
2. B. Coxon. Tetrahedron, **22**, 2281 (1966).
3. C. V. Holland, D. Horton, and J. S. Jewell. J. Org. Chem. **32**, 1818 (1967).
4. L. D. Hall and J. F. Manville. Carbohydrate Res. **4**, 512 (1967).

Can. J. Chem. Downloaded from www.nrcresearchpress.com by 210.87.254.105 on 09/05/12
For personal use only.

5. R. U. LEMIEUX. *In* Molecular rearrangements. Part II. *Edited by* P. de Mayo. Interscience Publishers Inc., New York. 1964.
6. H. J. JENNINGS. Can. J. Chem. **46**, 2799 (1968).
7. R. U. LEMIEUX, R. K. KULLNIG, H. J. BERNSTEIN, and W. G. SCHNEIDER. J. Am. Chem. Soc. **80**, 6098 (1958).
8. L. D. HALL and L. HOUGH. Proc. Chem. Soc. 382 (1962).
9. B. COXON. Tetrahedron, **21**, 3481 (1965).
10. R. U. LEMIEUX, E. FRAGA, and K. A. WATANABE. Can. J. Chem. **46**, 61 (1968).
11. J. A. POPLE and A. A. BOTHNER-BY. J. Chem. Phys. **42**, 1339 (1965).
12. F. J. BATES. Polarimetry, Saccharimetry, and the Sugars. Natl. Bur. of Std. Washington, 481 (1942).
13. F. P. PHELPS and C. S. HUDSON. J. Am. Chem. Soc. **48**, 503 (1926).
14. A. G. COTTRELL, E. BUNCEL, and J. K. N. JONES. Can. J. Chem. **44**, 1483 (1966).

Can. J. Chem. Downloaded from www.nrcresearchpress.com by 210.87.254.105 on 09/05/12
For personal use only.

Can. J. Chem. Downloaded from www.nrcresearchpress.com by 210.87.254.5 on 09/05/12
For personal use only.

Cyclic organophosphorus compounds. III. Reactions of nitrosyl chloride with cyclic and open-chain hydrogen thiophosphites[1]

ANDRZEJ ZWIERZAK AND JAN MICHALSKI
Department of Organic Synthesis, Technical University (Politechnika), Łódź 40, Poland

Received September 19, 1968

2-Thiono-5,5-dimethyl-1,3,2-dioxaphosphorinan **1** treated with nitrosyl chloride yields a mixture of asymmetric **2** and symmetric **3** dithiopyrophosphates. Reinvestigation of the reaction of nitrosyl chloride with diethyl thiophosphite showed that, in addition to tetraethyl thiopyrophosphate, the corresponding dithiopyrophosphates are also formed. A mechanism is suggested for the reactions investigated, with nitrosyl chloride as an ambident nucleophile.

Canadian Journal of Chemistry, **47**, 1163 (1969)

Cyclic esters of phosphoric acid with a neopentyl glycol skeleton have recently been extensively applied as model compounds for studying reaction mechanisms (1–4), primarily owing to their relatively high—as compared with acyclic esters—stability and tendency to crystallization. The reaction of dialkyl phosphites with nitrosyl chloride affording pyrophosphate systems was discovered in this laboratory (5). Its mechanistic scheme was supplemented and verified in the elegant studies by Samuel and Silver (6). Almasi and Paskucz (7) claimed that, contrary to the expectations based on the full analogy with dialkyl phosphites, tetraalkyl monothiopyrophosphates are formed in the reaction between dialkyl thiophosphites and nitrosyl chloride. However, no suggestions concerning the reaction mechanism were proposed. The purpose of the present work was to apply the cyclic thiophosphite, 2-thiono-5,5-dimethyl-1,3,2-dioxaphosphorinan **1**, for more detailed studies on the reactions of nitrosyl chloride with thiophosphites.

It was found that **1** reacts with nitrosyl chloride readily in benzene solution at 35–40° to yield a

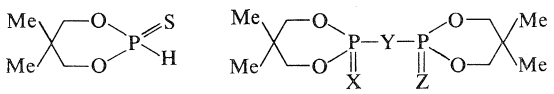

1

2; X=Y=S, Z=O **4**; X=Z=O, Y=S
3; X=Z=S, Y=O **5**; X=Y=O, Z=S

mixture of asymmetric **2** and symmetric **3** cyclic dithiopyrophosphates.

The reaction proceeds in the presence or absence of pyridine. The overall yield of dithiopyrophosphates **2** and **3** amounts to 60–70%, the **2**:**3** ratio ranging from 1.6:1 in the presence of pyridine to 2.3:1 in the absence of amine, when a ca. 20% benzene solution of nitrosyl chloride was used in the reaction. The **2**:**3** ratio of 3.5:1 was achieved in the presence of pyridine when a ca. 12% solution of nitrosyl chloride in benzene was employed. Compounds **2** and **3** were isolated and purified by crystallization. Their melting points, R_f values (Table I), and infrared (i.r.) spectra, were identical with those of authentic specimens obtained by individual routes. Thin-layer chromatography (t.l.c.) and i.r. spectroscopy revealed that absolutely no monothiopyrophosphates **4** and **5** had formed, a fact in apparent conflict with the results reported by Almasi and Paskucz (7), who claimed that tetraalkyl thiopyrophosphates constitute the major products in the reactions between acyclic thiophosphites and nitrosyl chloride. This observation prompted us to reinvestigate the products of the latter reactions.

The crude[2] and distilled products (R_f values given in Table I) obtained in the reaction between diethyl thiophosphite and nitrosyl chloride, run in the presence as well as in the absence of pyridine, were demonstrated by t.l.c. to be mixtures containing, in addition to *asym* tetraethyl thiopyrophosphate, considerable amounts of the *sym* compound as well as *sym* and *asym* tetraethyl dithiopyrophosphates. Moreover, it was found that the resulting monothiopyrophosphates cannot be the products of subsequent

[1]Paper CXXXVIII on organophosphorus compounds. For Part II see ref. 4.

[2]In this laboratory *sym* tetraethyl thiopyrophosphate was demonstrated to be detectable by t.l.c. On distillation it isomerizes completely to yield the thermodynamically more stable *asym* compound (8).

oxidation of the primarily formed dithiopyrophosphates. Independent experiments revealed that such oxidation does not take place under the conditions of the reaction of dialkyl thiophosphites with nitrosyl chloride.

Kinetic investigations by Samuel and Silver (6) proved that nitrosyl chloride behaves as a typical nucleophile in reactions with dialkyl phosphites. Such behavior may also reasonably be assumed to take place in the reactions with thiophosphites; it is therefore possible to postulate a mechanism for these transformations which would explain the formation of all the products detected. As an ambident nucleophile, nitrosyl chloride can attack the electrophilic phosphorus atom of the thiophosphite, with its softer nucleophilic center located at the nitrogen atom or the harder center situated on the oxygen atom. The two possible reaction sequences are represented by Schemes 1 and 2:

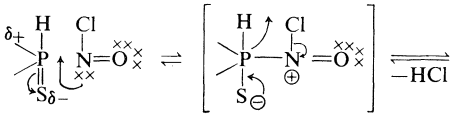

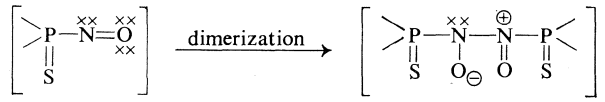

6 7

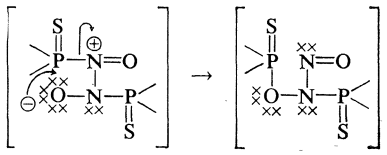

7 8

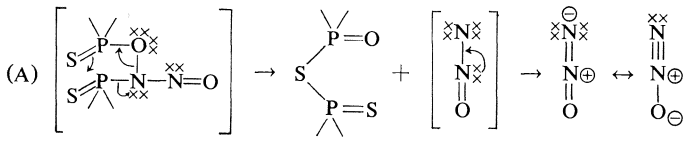

8

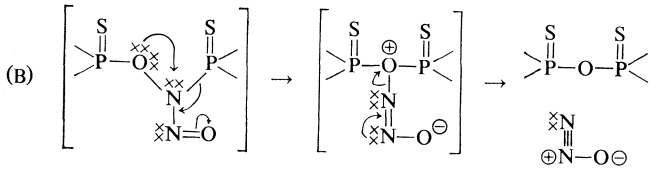

8

SCHEME 1

Can. J. Chem. Downloaded from www.nrcresearchpress.com by 210.87.254.5 on 09/05/12
For personal use only.

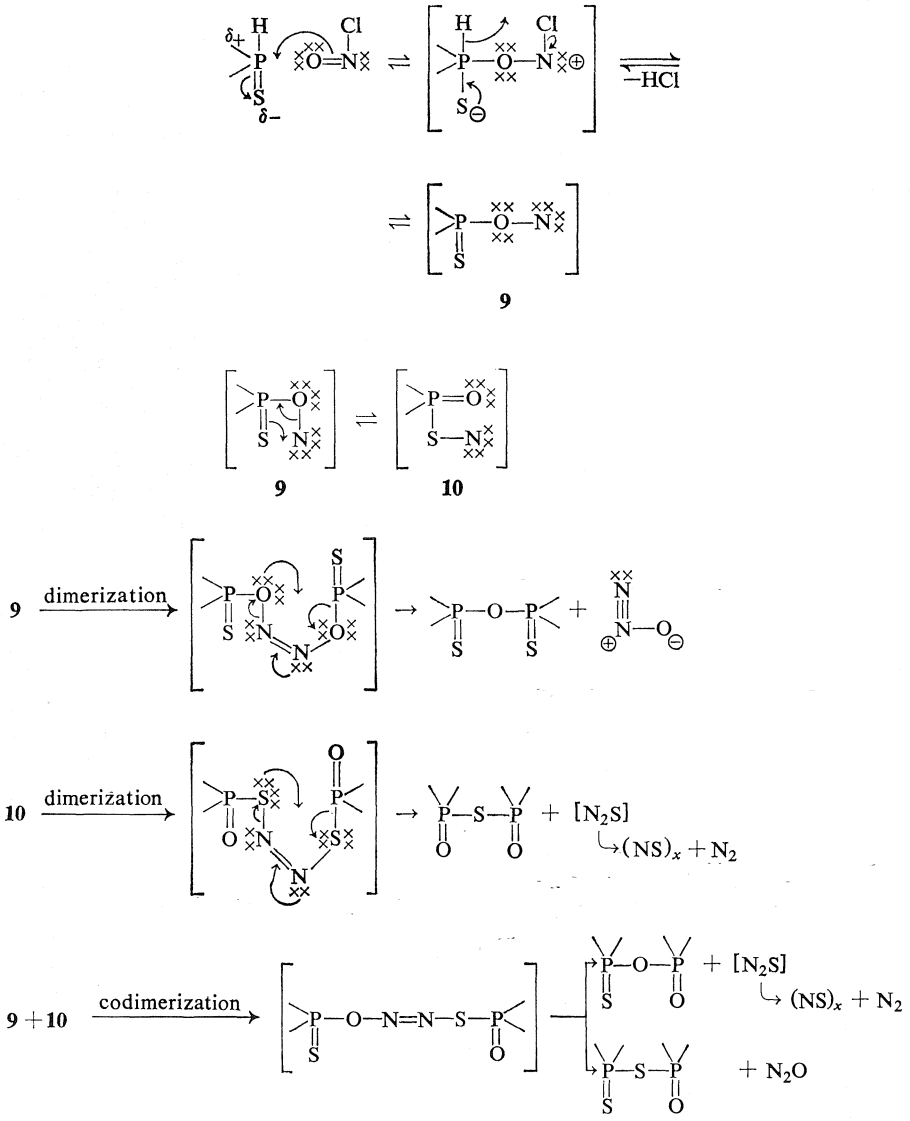

SCHEME 2

While attacking with the nucleophilic nitrogen atom, nitrosyl chloride yields a P-nitroso compound **6**. Its dimer **7**[3] is then intramolecularly rearranged to yield **8** with a phosphorus oxygen bond formed. Samuel and Silver have emphasized (6) that compounds with structures similar to **7** tend to rearrange in order to increase the number of bonds with oxygen. Cyclic rearrangements of oxygen to phosphorus were found in the thermal decomposition of *N*-benzylphosphorimidic trichloride (9) and suggested in the nitrosation of phosphoramides (10). They were also postulated in many reactions of the "Wittig" type (11). A subsequent collapse of the new dimer **8** can account for the formation of asymmetric dithiopyrophosphate (path A) as well as symmetric dithiopyrophosphate (path B). A similar scheme has already been suggested (6) as one of the alternative possibilities of formation of tetraalkyl pyrophosphates in the reactions of nitrosyl chloride with dialkyl phosphites.

[3]Compound **7** is one of the resonance structures of the mesomeric dimer.

Can. J. Chem. Downloaded from www.nrcresearchpress.com by 210.87.254.5 on 09/05/12
For personal use only.

TABLE I

R_f Values of thio- and dithiopyrophosphates

Compound	Solvent system: benzene – chloroform – acetone (11:8:1)	Solvent system: benzene–acetone (4:1)	Observations*
1	0.62	—	Black spot
2	0.34	0.54	Yellow spot
3	0.70	0.74	Orange spot
4	0.12	0.32	Yellow spot, strong "tailing effect"
5	0.30	0.54	Yellow, round spot
$(EtO)_2P(O)SP(O)(OEt)_2$	0.20	—	Orange spot, strong "tailing effect"
$(EtO)_2P(O)OP(S)(OEt)_2$	0.40	—	Yellow, round spot
$(EtO)_2P(S)OP(S)(OEt)_2$	0.77	—	Orange spot, characteristic moderate "tailing effect"
$(EtO)_2P(O)SP(S)(OEt)_2$	0.45	—	Orange spot, weak "tailing effect"

*Chromatograms were developed by spraying them with 5% aqueous $AgNO_3$ followed by 2% ethanolic bromothymol blue.

Scheme 2, depicting the consequences of nucleophilic attack by the oxygen atom of the nitrosyl on the electrophilic phosphorus atom of the thiophosphite, attempts to explain the path of formation of tetraalkyl thiopyrophosphates.

The resulting primary unstable compound **9**[4] of a mixed thiophosphoro–hyponitrous anhydride type can dimerize and subsequently split intramolecularly, yielding a *sym* dithiopyrophosphate. The formation of monothiopyrophosphates may be explained only by assuming **9** to exist at equilibrium with the rearrangement product **10**. Such a rearrangement is likely to occur because of the strong p_π—d_π interaction which stabilizes the resulting phosphoryl group. Dimerization of **10**, or codimerization of **9** and **10**, and subsequent intramolecular collapse of the resulting dimers leads to monothiopyrophosphates or possibly to an *asym* dithiopyrophosphate.

The above quoted experimental evidence indicates that the reactions of **1** proceed according to Scheme 1, because no monothiopyrophosphates were found among the products. Such an assumption complies with the predictions, because in this case the softer nucleophilic center on the nitrogen atom of the nitrosyl attacks the relatively soft electrophilic center on the dioxaphosphorinan ring phosphorus atom. Although no direct experimental evidence concerning the electrophilic character of cyclic and open-chain hydrogen thiophosphites is available at present, the latter compounds can be expected to possess a harder electrophilic center at the phosphorus atom. ^{31}P Nuclear magnetic resonance (n.m.r.) data indicate greater electronic shielding of phosphorus in the 1,3,2-dioxaphosphorinan ring ($\delta + 8.13 \pm 1.1$ p.p.m.) (12), than in acyclic phosphate triesters ($\delta + 0.5 \pm 1.5$ p.p.m.) (13). This points to an enhancement in the p_π—d_π double-bond character of the cyclic P—O bonds in the six-membered ring and offers an explanation for the diminished electrophilic reactivity of six-membered phosphate esters as compared with their acyclic analogues. Experimental data bear out this suggestion. The formation of monothiopyrophosphates in the reactions of dialkyl thiophosphites with nitrosyl chloride is explicable only in terms of Scheme 2 which assumes the hard nucleophilic center on the oxygen atom of the nitrosyl to be involved in the attack. However, in terms of the present evidence, the reaction of dialkyl thiophosphites according to Scheme 1 cannot be ruled out as a possibility.

The above presented data reveal a lack of full analogy in the behavior of cyclic and acyclic thiophosphites towards nitrosyl chloride, consequent upon the essential structural differences caused by electronic and steric factors. This indicates that cyclic esters of phosphoric acid

[4]Samuel and Silver (6) have also postulated the formation of intermediates analogous in structure to **9** as one of the alternative possibilities of tetraalkyl pyrophosphates formation in the reactions of dialkyl phosphites with nitrosyl chloride.

Can. J. Chem. Downloaded from www.nrcresearchpress.com by 210.87.254.5 on 09/05/12
For personal use only.

Can. J. Chem. Downloaded from www.nrcresearchpress.com by 210.87.254.5 on 09/05/12
For personal use only.

are only partially useful as models for mechanistic studies and that the conclusions arrived at should be verified and treated with caution.

Experimental

Solvents were purified by conventional methods. All extracts were dried over $MgSO_4$. Melting points and boiling points are uncorrected. All evaporations were carried out under reduced pressure. Petroleum ether refers to the fraction boiling at 60–80°. Infrared spectra were recorded on a UR-10 spectrophotometer (C. Zeiss). All samples were examined as thin films or Nujol mulls. Thin-layer chromatography (t.l.c.) was carried out on standard glass plates covered with 0.25 mm of Kieselgel G (E. Merck). Samples were analyzed as ca. 5% solutions in benzene or acetone. Two solvent systems (benzene – chloroform – acetone (11:8:1) and benzene–acetone (4:1)) were employed. All chromatograms were developed by spraying them with 5% aqueous $AgNO_3$ followed by 2% ethanolic bromothymol blue solution.

Materials

Nitrosyl chloride was prepared according to Morton and Wilcox (14) by the action of concentrated HCl on an aqueous solution of sodium nitrite, yield 50–60%; benzene solutions (ca. 10 or 20%) of the reagent were used.

2-Thiono-5,5-dimethyl-1,3,2-dioxaphosphorinan **1** was synthesized as described previously (15), yield 90%, m.p. 83.5–84.5°.

Diethyl thiophosphite was prepared by the action of hydrogen sulfide on diethyl phosphorochloridite in the presence of pyridine (16), yield 80%, b.p. 84–86° at 25 mm, n_D^{20} −1.4608.

Reaction of 2-Thiono-5,5-dimethyl-1,3,2-dioxaphosphorinan (1) with Nitrosyl Chloride in the Presence of Pyridine

Nitrosyl chloride (5.9 g, 0.09 mole) in ca. 12% benzene solution was added dropwise for ½ h with stirring and cooling (20–25°) to a mixture of 2-thiono-5,5-dimethyl-1,3,2-dioxaphosphorinan (12.45 g, 0.075 mole), pyridine (5.9 g, 0.075 mole), and benzene (100 ml). Stirring was continued for a further 4 h at 35–40°; the precipitate was then filtered off and washed successively with benzene (2 × 50 ml) and water (2 × 50 ml). The remaining insoluble material (1.9 g, 15%) was dried over P_2O_5 and crystallized from acetone – ethylene chloride (1:1) yielding colorless, long needles of *sym* dithiopyrophosphate **3**, m.p. 228–230°, undepressed on admixture with the specimen prepared by an independent procedure (4) (lit. (4), m.p. 228–230°; (17), m.p. 233°). The infrared (i.r.) spectrum of **3** was identical with that of an authentic sample.

The combined benzene layer and washings were washed successively with water (2 × 100 ml), 5% $NaHCO_3$ solution (2 × 100 ml), and water (2 × 100 ml), before being dried and evaporated. The orange, crystalline residue (9.85 g) was analyzed by the t.l.c. method described and was shown to contain *asym* dithiopyrophosphate **2** contaminated with some amounts of *sym* dithiopyrophosphate **3** and unreacted thiophosphite **1**. *Sym*-monothiopyrophosphate **4** was not found in the mixture, neither did the product contain *asym* monothiopyrophosphate **5** as proved by the absence of the characteristic peak at 733 cm^{-1} in its i.r. spectrum. The spectrum showed bands at 683s, 788s, 824s, 837s, and 864s cm^{-1}, characteristic of **2** and also at 778s and 797s cm^{-1} which indicated the presence of **3**. The crude product was crystallized from benzene – ethyl acetate (1:1) to give slightly yellow prisms (6.75 g, 52%) of *asym* dithiopyrophosphate **2**, m.p. 174–176° (lit. (17), m.p. 171–173°), identical (mixture m.p., i.r. spectrum) with an authentic specimen of **2**.

When a ca. 20% benzene solution of nitrosyl chloride was used in this reaction, more *sym* dithiopyrophosphate **3** (25%) was formed and the yield of *asym* dithiopyrophosphate **2** dropped to 40%.

Reaction of 2-Thiono-5,5-dimethyl-1,3,2-dioxaphosphorinan 1 with Nitrosyl Chloride in the Absence of Pyridine

The reaction was run as described immediately above, starting from **1** (6.23 g, 0.0375 mole) in benzene (50 ml) and nitrosyl chloride (2.95 g, 0.045 mole) in ca. 20% benzene solution. After the mixture had been stirred for 4 h at 35–40°, it was left overnight at room temperature and then degassed and filtered. The solid (1.25 g, 19%) which was washed with benzene (2 × 25 ml) and crystallized from benzene–chloroform (5:2) had m.p. 225–227°. It was identified (i.r. spectrum, mixture m.p.) as *sym* dithiopyrophosphate **3**. Evaporation of the solvent left an orange, crystalline residue (2.8 g, 43%), which was shown (t.l.c., i.r. spectrum) to contain *asym* dithiopyrophosphate **2** contaminated with **3**, unreacted thiophosphite **1**, and two unidentified compounds, possibly decyclization products.

Reaction of Diethyl Thiophosphite with Nitrosyl Chloride in the Presence of Pyridine

A solution of nitrosyl chloride (7.2 g, 0.11 mole) in benzene (30 ml) was added dropwise for ½ h, with stirring and occasional cooling (30–35°) to a solution of diethyl thiophosphite (15.4 g, 0.1 mole) and pyridine (7.9 g, 0.1 mole) in petroleum ether (75 ml). Pyridine hydrochloride precipitated immediately and the mixture acquired a yellow coloration. After the addition had been completed, stirring was continued for 1 h at room temperature; pyridine hydrochloride was then filtered off and washed with benzene. Thin-layer chromatography of the filtrate revealed the presence of *sym* tetraethyl thiopyrophosphate (8). Evaporation of the filtrate and flash distillation of the residue *in vacuo* yielded two fractions: (*a*) 3.0 g, b.p. 52–55° at 0.05 mm (bath temp. 100–105°), n_D^{20} −1.4620 and (*b*) 5.5 g, (36% as calculated for the main component), b.p. 100–102° at 0.01 mm (bath temp. 140–145°), n_D^{20} −1.4614. Fraction (*a*) was identified (t.l.c., i.r. spectrum) as pure, unreacted diethyl thiophosphite. Fraction (*b*) analyzed by t.l.c. was shown to contain *asym* tetraethyl thiopyrophosphate as the main component and *sym* and *asym* tetraethyl dithiopyrophosphates as contaminants.

Reaction of Diethyl Thiophosphite with Nitrosyl Chloride in the Absence of Pyridine

The reaction was carried out as described immediately above, but without pyridine. The same amounts of starting materials were used. A pale-yellow precipitate

(possibly polymeric sulfur nitride) collected on the walls of the reaction vessel during the addition of nitrosyl chloride solution. After the addition had been completed, stirring was continued for 2 h at room temperature. The solution was then filtered, degassed, and evaporated. The residue distilled *in vacuo* afforded two fractions: (*a*) 5.5 g, b.p. 50–60° at 0.05 mm (bath temp. 100–105°), n_D^{20} −1.4614 and (*b*) 4.2 g (28% as calculated for the main component), b.p. 100–103° at 0.01 mm (bath temp. 140–150°), n_D^{20} −1.4694. Fraction (*a*) was identified (t.l.c., i.r. spectrum) as pure, unreacted diethyl thiophosphite. Fraction (*b*) was found (t.l.c.) to contain *asym* tetraethyl thiopyrophosphate contaminated with *sym* and *asym* tetraethyl dithiopyrophosphates. Authentic mixtures of these three components could be resolved and satisfactorily analyzed by the t.l.c. method. The undistilled reaction product (examined by t.l.c.) also revealed the presence of *sym* tetraethyl thiopyrophosphate (8).

Attempted Oxidative Desulfurization of sym and asym Tetraethyl Dithiopyrophosphates by means of Nitrosyl Chloride

Nitrosyl chloride (0.003 mole) in ca. 20% benzene solution was added to *asym* tetraethyl dithiopyrophosphate (0.97 g, 0.003 mole) in petroleum ether (2.5 ml) and the mixture was left for 24 h at 20–25°. After removal of the solvent the residue was shown (t.l.c., i.r. spectrum) to contain only unchanged *asym* tetraethyl dithiopyrophosphate.

No appreciable change was observed when *sym* tetraethyl dithiopyrophosphate was treated with nitrosyl chloride under analogous conditions.

1. R. S. Edmundson and J. O. L. Wrigley. Tetrahedron, **23**, 283 (1967).
2. R. S. Edmundson. J. Chem. Soc. C, 1635 (1967).
3. J. Michalski, M. Mikolajczyk, B. Mlotkowska, and A. Zwierzak. Angew. Chem. **79**, 1069 (1967).
4. W. Stec and A. Zwierzak. Can. J. Chem. **45**, 2513 (1967).
5. J. Michalski and A. Zwierzak. Roczniki Chem. **35**, 619 (1961).
6. D. Samuel and B. L. Silver. J. Chem. Soc. 3582 (1963).
7. L. Almasi and L. Paskucz. Chem. Ber. **96**, 2024 (1963).
8. J. Michalski, M. Mikolajczyk, and B. Mlotkowska. Chem. Ber. **102**, 90 (1969).
9. A. Lapidot and D. Samuel. J. Chem. Soc. 2110 (1962).
10. P. J. Bunyan and J. I. G. Cadogan. J. Chem. Soc. 1304 (1962).
11. U. Schöllkopf. Angew. Chem. **71**, 260 (1959).
12. G. M. Blackburn, J. S. Cohen, and Lord Todd. Tetrahedron Letters, 2873 (1964).
13. R. A. Y. Jones and A. R. Katritzky. Angew. Chem. **74**, 60 (1962).
14. J. R. Morton and H. W. Wilcox. Inorg. Syn. **4**, 48 (1953).
15. A. Zwierzak. Can. J. Chem. **45**, 2501 (1967).
16. C. Krawiecki and J. Michalski. J. Chem. Soc. 881 (1960).
17. R. S. Edmundson. Tetrahedron, **21**, 2379 (1965).

Can. J. Chem. Downloaded from www.nrcresearchpress.com by 210.87.254.5 on 09/05/12
For personal use only.

Can. J. Chem. Downloaded from www.nrcresearchpress.com by 210.87.254.40 on 09/05/12
For personal use only.

Reaction of dibromocarbene with aromatic ethers

S. D. SARAF
Defence Science Organisation, Chaklala, West Pakistan

Received September 25, 1968

The reaction of dibromocarbene with 1-methoxynaphthalene, 2-methoxynaphthalene, and anisole is discussed. Bromotropones were isolated in good yields in the case of 1- and 2-methoxynaphthalenes. Anisole, on treatment with bromoform and potassium *t*-butoxide gave 4-bromotropone, whereas, on heating with phenyl(tribromomethyl)mercury, *p*-anisic acid and 4,4′-dimethoxybenzophenone were the main products.

Canadian Journal of Chemistry, **47**, 1169 (1969)

Parham and Reiff (1) have reported that dichlorocarbene reacts with indenes to give cyclopropyl adducts which subsequently afford chloronaphthalenes in high yields by ring expansion and elimination of hydrogen chloride. Birch and Graves (2) have shown that 2,5-dihydroanisole affords tropone and substituted tropones with dichlorocarbene. Parham *et al.* (3) have also reported the formation of chlorobenztropones from 1- and 2-methoxynaphthalenes.

Seyferth *et al.* (4–6) have extensively studied the reaction of phenyl(trihalomethyl)mercury with a large number of carbene acceptors. The yields obtained were good and the neutral conditions could be maintained, since on heating phenyl(trihalomethyl)mercury compounds in benzene, phenylmercury halide is formed.

Using this method as a source of carbene, a number of aromatic ethers were studied in the hope of isolating bromotropones, which, on subsequent hydrolysis, would lead to the corresponding tropolones.

1-Methoxynaphthalene on heating with phenyl(tribromomethyl)mercury in dry benzene afforded 7-bromo-2,3-benztropone (**1**, 33%). The ketone was characterized by conversion to the corresponding dinitrophenylhydrazone and by comparison of its infrared (i.r.) and ultraviolet (u.v.) spectra to those of known 7-chloro-2,3-benztropone. The reaction of 2-methoxynaphthalene was effected in the same manner as above. In addition to recovered ether (80%), there was obtained a bromotropone (**2**) in 37% yield. The ketone was characterized by conversion to the corresponding oxime and by its i.r. and u.v. spectra.

Bromotropones proved resistant to acid hydrolysis and were recovered essentially unchanged after reaction with aqueous hydrochloric acid at 120–140° and concentrated sulfuric acid at 0–15°. Similarly, no useful products could be isolated with aqueous potassium hydroxide at 100°.

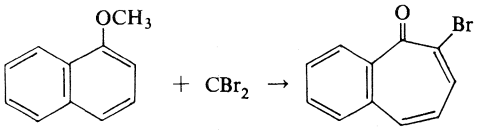

1

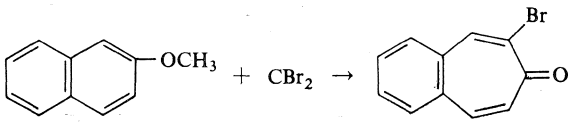

2

Anisole showed no reactivity towards dichlorocarbene derived from chloroform and a base (7). Similarly, anisole was recovered unchanged on heating with sodium trichloroacetate in diglyme and with phenyl(trichloromethyl)-mercury in benzene; however, reaction of anisole with bromoform and potassium *t*-butoxide gave 4-bromotropone in low yield. Reaction of anisole with phenyl(tribromomethyl)mercury in benzene at 80° gave none of the tropone but instead, *p*-anisic acid (**4**) and 4,4′-dimethoxybenzophenone (**5**) along with a host of other products.

The formation of 4-bromotropone (**3**) probably involves a similar mechanism to that

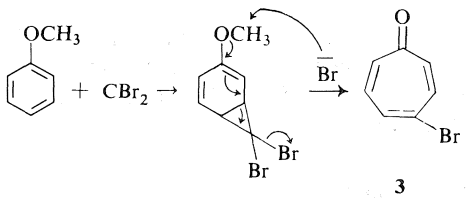

3

Can. J. Chem. Downloaded from www.nrcresearchpress.com by 210.87.254.40 on 09/05/12
For personal use only.

involved in the formation of 7-chloro-2,3-benztropone (3) from 1-methoxynaphthalene, i.e. addition of the carbene to the aromatic ring followed by a nucleophilic displacement of a bromide ion, subsequent to a nucleophilic attack on the methyl group.

The formation of *p*-anisic acid (**4**) is difficult to explain. Seyferth and Burlitch (8) have isolated, besides other products, cyclohexyl bromide from a reaction of cyclohexane and phenyl(bromodichloromethyl)mercury, which suggests the possibility of a radical mechanism (9). On that basis the following mechanism may be suggested:

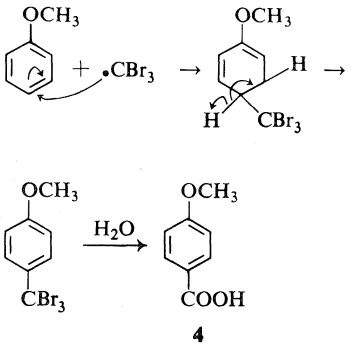

Alternatively, *p*-anisic acid may be formed by an ionic mechanism as shown in Schemes 1 and 2.

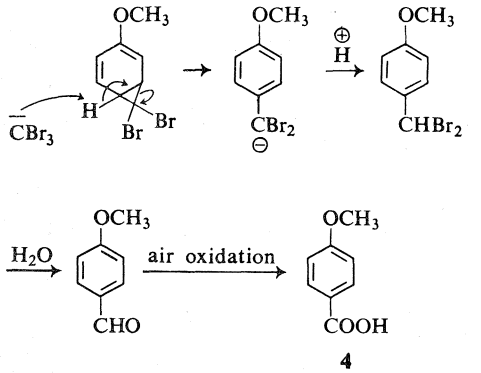

SCHEME 1

The isolation of diphenylmercury, haloforms, and metallic mercury in such reactions by various research groups (6, 10)[1] supports the above mechanisms.

[1]S. D. Saraf. Unpublished results.

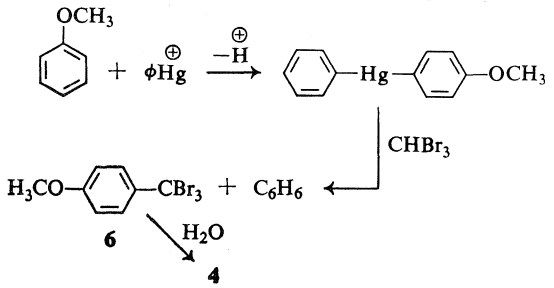

SCHEME 2

The formation of 4,4′-dimethoxybenzophenone may be rationalized by Scheme 3.

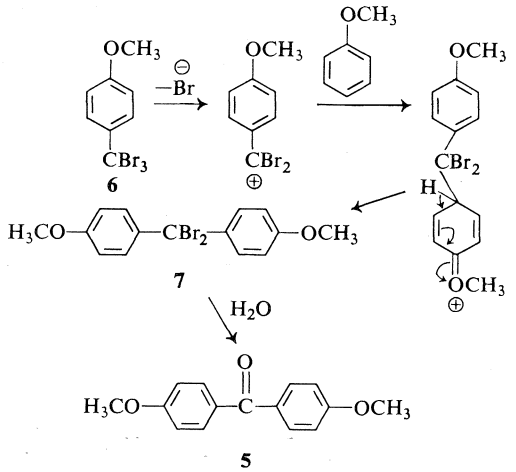

SCHEME 3

The above mechanism postulates the formation of **6** as shown in Scheme 2. This may ionize to give an electrophile which would react with anisole to give **8** followed by hydrolysis to the observed product.

Experimental

Reaction of 1-Methoxynaphthalene

A solution of 1-methoxynaphthalene (7 g) and phenyl(tribromomethyl)mercury (8 g) was refluxed with stirring in dry benzene (100 ml) under nitrogen for 2.5 h. The mixture was cooled, filtered, and the residue washed several times with benzene. The filtrate and the washings were combined and distilled *in vacuo* to remove the solvent and the unreacted starting ether (3.5 g). The residue was extracted with boiling petroleum ether (b.p. 40–60°) until no unreacted 1-methoxynaphthalene was recovered and then with 1:1 petroleum ether (b.p. 40–60°) – benzene mixture to give dirty yellow crystals of 7-bromo-2,3-benztropone (**1**) m.p. 94–102°. Recrystallization of this product from petroleum ether (b.p. 60–80°) after sublimation gave white crystals, m.p. 108–109° (1 g,

Can. J. Chem. Downloaded from www.nrcresearchpress.com by 210.87.254.40 on 09/05/12
For personal use only.

33%). Ultraviolet spectrum (95% ethanol): E_{max} 226 mμ ($\log_e$ 4.2), E_{max} 315 mμ ($\log_e$ 4.1), E_{max} 325 mμ ($\log_e$ 4.1). Infrared spectrum (Nujol): included bands at 1626, 1609, 1594, and 1577 cm^{-1}.

Anal. Calcd. for $C_{11}H_7BrO$: C, 56.17; H, 3.0; Br, 34.0. Found: C, 56.17; H, 2.9; Br, 34.3.

The dinitrophenylhydrazone was prepared in the usual manner and recrystallized from ethyl acetate as red needles, m.p. 232–233°.

Anal. Calcd. for $C_{17}H_{12}N_4O_4Br$: C, 49.15; H, 2.65; Br, 19.3; N, 13.5. Found: C, 49.10; H, 2.90; Br, 19.2; N, 13.5.

Reaction of 2-Methoxynaphthalene

The reaction of 2-methoxynaphthalene (10 g) with phenyl(tribromomethyl)mercury (10 g) in dry benzene (200 ml) was carried out as described above for 1-methoxynaphthalene. Work-up in the usual manner, followed by chromatography on neutral alumina, gave 2-methoxynaphthalene (8 g) and 2-bromo-4,5-benztropone (**2**). The ketone was purified by vacuum sublimation followed by crystallization from petroleum ether (b.p. 60–80°) to give white needles, m.p. 142–143° (1.1 g, 37%). Ultraviolet spectrum (95% ethanol): E_{max} 237 mμ ($\log_e$ 4.4), E_{max} 276 mμ ($\log_e$ 4.6), E_{max} 341 mμ ($\log_e$ 3.6), E_{max} 358 mμ ($\log_e$ 3.3). Infrared spectrum (Nujol): included bands at 1632, 1607, 1558, and 1550 cm^{-1}.

Anal. Calcd. for $C_{11}H_7BrO$: C, 56.17; H, 3.0; Br, 34.0. Found: C, 56.2; H, 3.2; Br, 33.5.

The oxime of **2** was prepared in the usual manner and crystallized from ethanol–water. Light yellow needles were obtained which melted at 201–202°.

Anal. Calcd. for $C_{11}H_8NBrO$: C, 52.3; H, 3.3; N, 5.8; Br, 31.5. Found: C, 52.3; H, 3.2; N, 5.6; Br, 32.0.

Reaction of Anisole with Dibromocarbene

Method A

A stirred solution of anisole (10 g) and potassium *t*-butoxide (20 g) in dry benzene was cooled to −10° and bromoform (15 ml) added dropwise. After 2 h at room temperature, the mixture was filtered, anisole (8 g) recovered by distillation, and the residue was chromatographed on neutral alumina. It was eluted with ether–benzene mixture (1:2) to give a brown solid (132 mg). Repeated crystallizations of this product gave 4-bromotropone (**3**) as colorless needles, m.p. 111–112° (lit. (11) m.p. 112–113°). Ultraviolet spectrum (95% ethanol): E_{max} 230 mμ($\log_e$ 4.12) E_{max} 308 mμ ($\log_e$ 3.72).

Anal. Calcd. for C_7H_5BrO: C, 45.4; H, 2.7. Found: C, 45.6; H, 3.0.

Method B

A stirred solution of freshly distilled anisole (30 g) and phenyl(tribromomethyl)mercury (35 g) in dry benzene (200 ml) was heated at 80° under nitrogen for 2.5 h and the reaction mixture was worked up in the usual manner. Unreacted anisole was distilled and the residue was extracted with boiling petroleum ether (b.p. 40–60°). This extract deposited a solid, which was crystallized from aqueous ethanol to give *p*-anisic acid (110 mg), yield 2%, m.p. 182–184°, undepressed on admixture with an authentic specimen (lit. (12) m.p. 182–183°).

The filtrate was concentrated and chromatographed on neutral alumina with petroleum ether (b.p. 40–60°). The first fraction from the column gave a light-yellow liquid (*a*, 3.2 g). Further elution with benzene gave two solids (*b*, 445 mg) and (*c*, 100 mg).

Fraction a

Thin-layer chromatography showed it to be a mixture of ten compounds but repeated chromatography on alumina resulted in the isolation of only one compound (25 mg) which crystallized from ethanol as colorless needles, m.p. 95–96°. Ultraviolet spectrum (95% ethanol): E_{max} 225 and 312 mμ. The product could not be identified. Fractional distillation of the rest failed to separate the products.

Fraction b

This fraction was rechromatographed on alumina with benzene. The product 4,4′-dimethoxybenzophenone crystallized from petroleum ether (b.p. 60–80°) as long colorless needles, m.p. 145–146.5°, undepressed on admixture with an authentic specimen (lit. (13) m.p. 145–146.5°).

Fraction c

This fraction was rechromatographed on alumina to give a colorless solid, m.p. 151–152.5°, ultraviolet spectrum (95% ethanol): E_{max} 272 and 279 mμ. The molecular weight (Rast) was 226 and an analysis gave: C, 78.6; H, 6.8; OCH_3, 27.6. The product could not be identified.

Acknowledgments

The author is grateful to E. J. Forbes for his guidance and to Birmingham University, England for providing the facilities to carry out this work.

1. W. E. Parham and H. E. Reiff. J. Am. Chem. Soc. **77**, 1177 (1955).
2. A. J. Birch and J. M. H. Graves. Proc. Chem. Soc. **282** (1962).
3. W. E. Parham, D. A. Bolon, and E. E. Schweiser. J. Am. Chem. Soc. **83**, 603 (1961).
4. D. Seyferth, J. M. Burlitch, and J. K. Heeren. J. Org. Chem. **27**, 1491 (1962).
5. D. Seyferth, R. J. Minasz, A. J. Treiber, J. M. Burlitch, and S. R. Dowd. J. Org. Chem. **28**, 1163 (1963).
6. D. Seyferth, H. E. Gordon, and R. Damraner. J. Org. Chem. **32**, 469 (1967).
7. A. Ledwith and R. M. Bell. Chem. Ind. London, 459 (1959).
8. D. Seyferth and J. M. Burlitch. J. Am. Chem. Soc. **85**, 2667 (1963).
9. W. Kirmse. Organic chemistry. Vol. 1. Carbene chemistry. Academic Press, Inc., New York. 1964, p. 162.
10. W. E. Parham and J. R. Potoski. Tetrahedron Letters, **21**, 2311 (1966).
11. T. Nozoe. Sci. Rept. Tohoku Univ. First Ser. **36**, 166 (1952).
12. A. Oppenheim and S. Pfaff. Ber. **8**, 890 (1875).
13. Bader *et al.* Chem. Abstr. 3365 (1948).

Reaction of dihalocarbene with *N,N*-dimethylaniline

S. D. SARAF
Defence Science Organisation, Chaklala, West Pakistan

Received September 25, 1968

The reaction of dihalocarbenes with *N,N*-dimethylaniline is discussed. α,α-Dihaloacetanilides and 4,4′-dimethylaminodiphenylmethane were the products isolated.

Canadian Journal of Chemistry, 47, 1173 (1969)

Can. J. Chem. Downloaded from www.nrcresearchpress.com by 210.87.254.105 on 09/05/12
For personal use only.

Previous studies of reaction of aliphatic tertiary amines with dichlorocarbene (generated from chloroform and potassium *t*-butoxide) have been reported by Saunders and Murray (1). Dialkyl formamides along with some halogenated amides were the main products isolated.

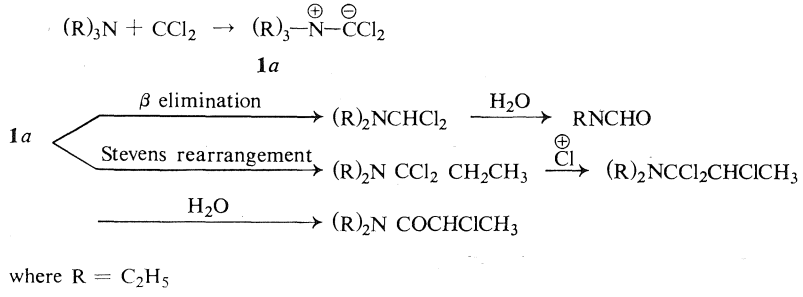

where R = C_2H_5

Seyferth *et al.* (2) in his studies with phenyl(trihalomethyl)mercury and triethylamine, isolated *N,N*-diethyltrichlorovinylamine in varying yields depending on the reaction conditions. The formation of the product was rationalized by Scheme 1.

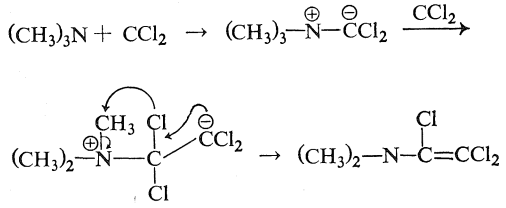

SCHEME 1

The object of the present work was to determine the nature of the products resulting from the reaction of dihalocarbenes (from $PhHgCX_3$) with aromatic tertiary amines. *N,N*-Dimethylaniline was heated with phenyl(trihalomethyl)-mercury in benzene at 80° in the hope that ring expansion might lead to the formation of halotropones. However, no tropone like substance was isolated, but instead, *N*-methyldihaloacetanilides, 4,4′-dimethylaminodiphenylmethane and *N*-methylformanilide were the main products of the reaction.

The amide formation can be explained by a mechanism suggested by Seyferth *et al.* (2) as shown in Scheme 2.

The ylid postulated in the above mechanism reacts with one equivalent of dihalocarbene to give **5** followed by the loss of methyl halide to give **6**, which in turn is hydrolyzed to the observed product (**4**).

Trihalovinylamines have been shown to be unstable at room temperature and are hydrolyzed in the presence of moisture to the corresponding halogenated amides (3). Water required to hydrolyze **4** may come from the moisture adsorbed on the alumina.

Scheme 4 postulates the formation of *N*-methylanilines as one of the products of this reaction. Parham and Potoski (4) have shown that *N*-methylaniline reacts with phenyl(trichloromethyl)mercury under similar conditions to give *N*-methyl-α,α-dichloroacetanilide as shown in Scheme 3.

This alternative mechanism is probably the most likely one for the formation of **4** and *N*-methylformanilide.

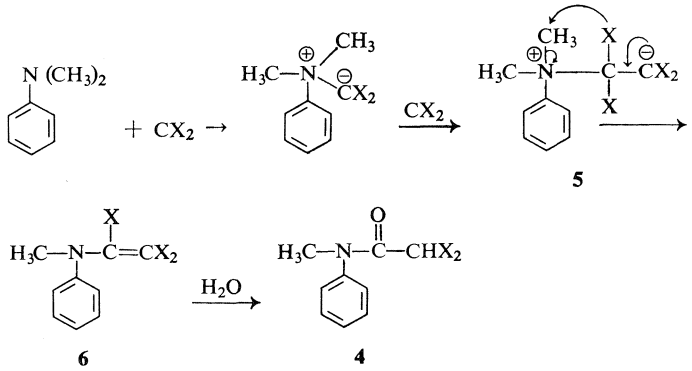

SCHEME 2

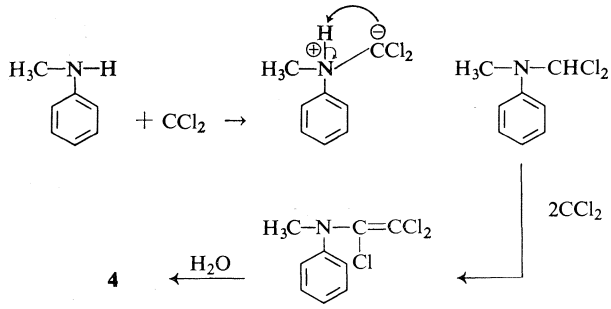

SCHEME 3

The formation of 4,4′-dimethylaminodiphenylmethane could easily be explained by Scheme 4.

The above mechanism postulates the formation of an intermediate **7**, which reacts with one equivalent of dimethylaniline to give **8**. Protonation followed by a further reaction with dimethylaniline would lead to the observed product (**9**). This mechanism is similar to that postulated by Parham and Groen (5) for the reaction $\phi S\ CH_3 + CCl_2$.

Experimental

Reaction of N,N-Dimethylaniline with Dibromocarbene

A solution of *N,N*-dimethylaniline (40 g) and phenyl-(tribromomethyl)mercury (45 g) in 200 ml of dry benzene was heated at reflux with stirring under nitrogen for 2.5 h. The mixture was cooled, filtered, and the residue washed several times with benzene. The filtrate and the washings were combined and distilled *in vacuo* to give unreacted *N,N*-dimethylaniline (32 g). The residue was extracted with boiling petroleum ether (b.p. 40–60°) and the extract was chromatographed on neutral alumina. It was first eluted with petroleum ether (b.p. 40–60°) until no unreacted dimethylaniline was recovered, followed by benzene to give slightly yellowish solid (A, 100 mg). Further elution with 25% ether–benzene gave slightly brownish crystals (B, 4.8 g), and a liquid (C, 100 mg).

Fraction A

This fraction was rechromatographed on alumina to give a colorless solid of 4,4′-dimethylaminodiphenylmethane (80 mg), m.p. 89–90° from ethanol, undepressed on admixture with an authentic specimen (lit (6) m.p. 89–90°).

Anal. Calcd. for $C_{17}H_{22}N_2$: C, 80.3; H, 8.6; N, 11.0. Found: C, 80.3; H, 8.4; N, 10.8.

It formed a bis-picrate, which crystallized from methanol as yellow plates, m.p. 183–184°.

Anal. Calcd. for $C_{29}H_{28}N_8O_{14}$: C, 48.9; H, 3.9; N, 15.7. Found: C, 48.9; H, 3.9; N, 15.5.

Fraction B

This fraction was rechromatographed on neutral alumina with 25% ether–benzene to give a colorless solid, m.p. 98–104°. Crystallization of this crude product from petroleum ether (b.p. 60–80°) gave *N*-methyl-α,α-dibromoacetanilide as colorless needles, m.p. 104–105°, undepressed on admixture with an authentic specimen, yield 4.5 g, 26%.

Anal. Calcd. for $C_9H_9Br_2NO$: C, 35.1; H, 3.0; N, 4.6; Br, 52.4. Found: C, 35.0; H, 3.0; N, 4.4; Br, 52.1.

Hydrogenation of this product (**4**) (200 mg) in ethanol

Can. J. Chem. Downloaded from www.nrcresearchpress.com by 210.87.254.105 on 09/05/12
For personal use only.

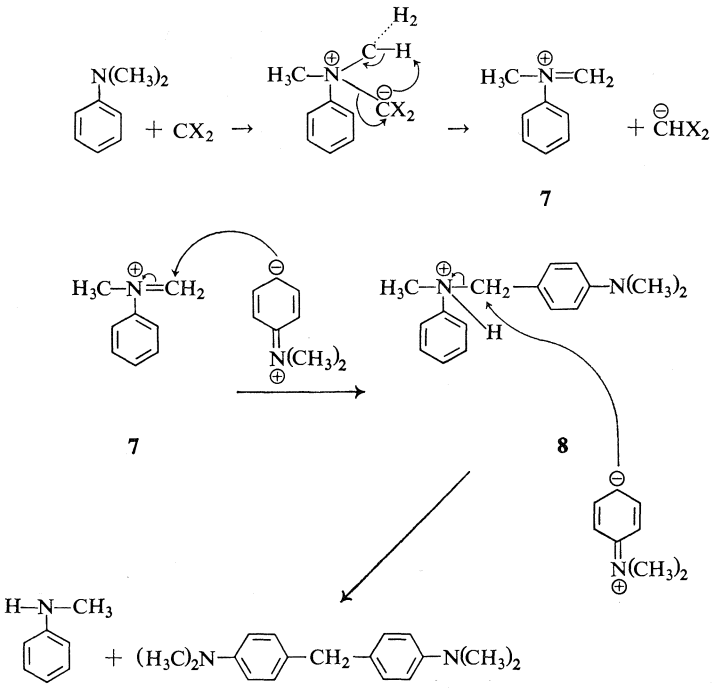

SCHEME 4

(10 ml) with palladium/charcoal (10%, 15 mg) and sodium acetate (120 mg) gave *N*-methylacetanilide (**3**) as a colorless solid, which crystallized from petroleum ether (b.p. 40–60°) and melted at 98–99°, undepressed on admixture with an authentic specimen, yield 82 mg, 85%, (lit. (7) m.p. 100–101°).

Anal. Calcd. for $C_9H_{11}NO$: C, 72.4; H, 7.4; N, 9.4. Found: C, 72.3; H, 7.5; N, 9.5.

N-Methyl-α,α-dibromoacetanilide—To a solution of *N*-methylaniline (2 g) in benzene (10 ml) containing potassium carbonate (2 g) was added dibromoacetyl bromide (1 ml). The mixture was warmed on a water bath for 1 h. Work-up in the usual manner gave a colorless solid, m.p. 100–102°. Crystallization of this product from petroleum ether (b.p. 40–60°) gave *N*-methyl-α,α-dibromoacetanilide as colorless plates, m.p. 105–106°, yield 5 g, 85%.

Fraction C

This fraction was shown to be *N*-methylformanilide by comparison of its infrared (i.r.) spectrum, with that of an authentic specimen.

Reaction with Dichlorocarbene

A solution of *N*,*N*-dimethylaniline (20 g) and phenyl-(trichloromethyl)mercury (8 g) was refluxed with stirring in dry benzene under nitrogen for 44 h. Work-up as described above, left a residue (4 g) which was chromatographed on neutral alumina. It was eluted with benzene to give a brown semi solid (A, 2.3 g). Further elution with 25% ether–benzene mixture gave a yellow solid (B, 900 mg), and a liquid (C, 300 mg).

Fraction A

Crystallization of this fraction from petroleum ether (b.p. 60–80°) gave 4,4′-dimethylaminodiphenylmethane as colorless plates, m.p. 89–90°, yield 1.9 g, 30%.

Fraction B

This fraction on crystallization from petroleum ether (b.p. 60–80°) gave *N*-methyl-α,α-dichloroacetanilide as colorless plates, m.p. 67–68°, undepressed on admixture with an authentic specimen, yield 540 mg, 5%.

Anal. Calcd. for $C_9H_9Cl_2O$: C, 49.5; H, 4.1; N, 6.4; Cl, 32.5. Found: C, 49.7; H, 3.9; N, 6.6; Cl, 32.2.

Hydrogenation of this product in the presence of palladium/charcoal and sodium acetate gave *N*-methylacetanilide (**3**) as a colorless solid, m.p. 98–99°.

N-Methyl-α,α-dichloroacetanilide—A mixture of dichloroacetic acid (1 g) *N*-methylaniline (1 g), and phosphorous pentoxide (5 g) was warmed on a steam bath for 2 h. Work-up in the usual manner gave *N*-methyl-α,α-dichloroacetanilide as a colorless solid, m.p. 67–68°, yield 1.5 g, 75%.

Fraction C

This fraction was shown to be *N*-methylformanilide by comparison of its i.r. spectrum, with that of an authentic specimen.

Acknowledgments

The author is grateful to E. J. Forbes for his guidance and to the Birmingham University,

Can. J. Chem. Downloaded from www.nrcresearchpress.com by 210.87.254.105 on 09/05/12
For personal use only.

England for providing the facilities to carry out this work.

1. M. SAUNDERS and R. W. MURRAY. Tetrahedron, **11**, 1 (1960).
2. D. SEYFERTH, H. E. GORDON, and R. DAMRANER. J. Org. Chem. **32**, 469 (1967).
3. A. J. SPEZIALE and R. C. FREEMAN. J. Am. Chem. Soc. **82**, 902 (1960).
4. W. E. PARHAM and J. R. POTOSKI. Tetrahedron Letters, **21**, 2311 (1966).
5. W. E. PARHAM and S. H. GROEN. J. Org. Chem. **30**, 3181 (1965).
6. G. COHN. Chem. Ztg. **24**, 564 (1900).
7. A. KAUFMANN. Ber. **42**, 3480 (1909).

Can. J. Chem. Downloaded from www.nrcresearchpress.com by 210.87.254.105 on 09/05/12
For personal use only.

Can. J. Chem. Downloaded from www.nrcresearchpress.com by 210.87.254.40 on 09/05/12
For personal use only.

Synthesis of isomers of acetylcarnitylcholine and other carnitine derivatives

GABOR KATO[1] AND E. A. HOSEIN
Department of Biochemistry, McGill University, Montreal, Quebec

Received April 17, 1968

Carnitine, γ-trimethylammonium-β-hydroxy butyric acid, was synthesized from γ-chloro-β-hydroxy butyronitrile. Acetylcarnitylcholine was prepared either by the esterification of acetylcarnitine or by the acetylation of carnitylcholine.

Canadian Journal of Chemistry, **47**, 1177 (1969)

There is some evidence that acetyl-1-carnitylcholine can be synthesized *in vitro* on the esterification of choline by acetyl-1-carnityl CoA (isolated from fresh rat brain) and choline acetyltransferase (E.C.2.3.1.6) (1). Since acetyl-1-carnitylcholine and/or its precursors *in vivo* would at best be present only in extremely minute amounts (< 1 μg/g fresh brain) the need of larger quantities of such compounds for testing with various chemical, biochemical, physiological, and/or pharmacological systems is apparent. We describe methods for the synthesis of acetylcarnitylcholine, its isomers and various other carnitine derivatives.

Experimental

*Preparation of (±) Carnitine Nitrile Chloride (**1**)*

This material was prepared by the method of Strack *et al.* (2). The infrared spectrum of this compound in Nujol showed the following bands: 3200 cm^{-1} (—OH); 2250 cm^{-1} (—C≡N); 1095 cm^{-1} and 1008 cm^{-1} ($—CH_3$); 964 cm^{-1} and 974 cm^{-1} ($—N^+(CH_3)_3$). The proton nuclear magnetic resonance (n.m.r.) spectrum of **1** consisted of 5 peaks, having areas in the ratio of 1:1:9:1:1 and τ ($≡N^+CH_2—$) – 6.40 and 6.50 p.p.m., τ $(CH_3)_3N^+—$ =6.74 p.p.m., and τ ($—CH_2C≡N$) =7.10 and 7.18 p.p.m. relative to dilute tetramethylsilane (TMS, τ = 10.0 p.p.m.) as external standard.

*Preparation of (−) Carnitine Nitrile Chloride (−**1**) and (+) Carnitine Nitrile Chloride (+**1**)*

Separation of a racemic mixture of **1** was accomplished by the following modification of a procedure by Strack *et al.* (3).

Twenty grams of **1** were changed to the basic form with silver oxide. The aqueous solution was concentrated *in vacuo* to 50 ml with an equimolar amount of *d*-10-camphor-sulfonic acid (**3**) (29.0 g) whereby the crystals came out of solution. These crystals were filtered by suction and washed with absolute alcohol. This will be referred to as *Fraction 1* and contains essentially *d*-carnitine nitrile-*d*-camphorsulfonate, with some contamination of *l*-carnitine nitrile-*d*-camphorsulfonate. The yield was 16.4 g, $[\alpha]_D$ +24.0°.

The mother liquor of *Fraction 1* was concentrated *in vacuo* to dryness, the residue dissolved in boiling 90% ethanol and mixed with sixfold volume of 30% ethanol – HCl mixture, at 0°. The solution was then mixed with an equal volume of anhydrous ether, and allowed to cool at 0°. After 12 h, impure (−**1**) crystallized out of solution, was filtered, and washed with absolute alcohol. The yield was 10.6 g, $[\alpha]_D$ −24.8° (94% optically pure). To obtain optically pure material either one of the following procedures was followed:

(*a*) (−**1**) (10.6 g) obtained above was made into a paste with 75 ml of absolute ethanol at 0°, and converted into the hydroxide with silver oxide previously washed free of water with absolute ethanol. The filtrate and the absolute ethanol extracts of the silver oxide residues were mixed with an equimolar amount of dibenzoyl-*d*-tartaric acid. The total volume was about 150–200 ml from which *l*-carnitine nitrile dibenzoyl-*d*-hydrogentartrate slowly crystallized out. Further fractions were obtained after 24 and 48 h on concentrating the mother liquor. Total yield of *l*-carnitine nitrile-dibenzoyl-*d*-hydrogentartrate was 24.4 g.

The dibenzoyl hydrogentartrate was then converted to the chloride (60% yield) with ethanolic HCl as described earlier. *d*-10-Camphorsulfonic acid and dibenzoyl-*d*-tartaric acid were recovered from the acidic alcohol solution almost quantitatively. Crystallization from absolute ethanol gave 3.9 g of pure (−**1**), melting at 261°, $[\alpha]_D$ −26.2°.

(*b*) An alternative step used in the purification of the optically impure nitrile was to recrystallize this compound ten to fifteen times from absolute ethanol to constant m.p. 261° and constant $[\alpha]_D$ −26.2°. Greater losses were encountered with this process. The final yield of (−**1**) was usually between 2.5 and 4.0 g, $[\alpha]_D$ −26.2°, and m.p. 261°. Infrared bands: 3200 cm^{-1} (—OH); 2254 cm^{-1} (—C≡N); 964 cm^{-1} and 977 cm^{-1} ($—N^+(CH_3)_3$). Its proton n.m.r. spectrum was identical to **1**.

Fraction 1 was converted to the chloride form with ethanolic HCl, and the (+)carnitine nitrile (+**1**) further purified as described above for (−**1**), employing either procedure (*a*) or (*b*). Procedure (*b*) was preferred and typical yield of optically pure (+**1**) was between 4 and 5 g, $[\alpha]_D$ +26.2°, and m.p. 261°. Infrared bands showed identical peaks as **1** and −**1**. Its proton n.m.r. spectrum was also identical with **1** and −**1**.

*Preparation of (±) Carnitine Amide Chloride (**4**)*

This compound was prepared by mild hydrolysis of **1** in HCl. **1** was dissolved in concentrated HCl and stored at room temperature for 2 to 3 weeks. NH_4Cl

[1]Present address: Wellcome Department of Research in Anaesthesia, McGill University, Montreal, Quebec.

TABLE I

Elemental analysis of various carnitine derivatives shown in Chart 1

Compound	Isomer		Analysis % Carbon	Hydrogen	Nitrogen
Carnitine nitrile chloride	(±)	Found	46.96	8.21	15.33
	(−)		47.00	8.32	15.66
	(+)		47.01	8.12	15.34
		Calcd. for $C_7H_{15}N_2O\cdot Cl$	47.06	8.40	15.69
Acetylcarnitine nitrile chloride	(±)	Found	48.71	7.62	12.61
	(−)		—	—	—
	(+)		—	—	—
		Calcd. for $C_9H_{17}N_2O_2\cdot Cl$	48.98	7.71	12.70
Carnitine amide chloride	(±)	Found	—	—	—
	(−)		41.62	8.62	14.36
	(+)		41.79	8.55	14.30
		Calcd. for $C_7H_{17}N_2O_2\cdot Cl$	42.75	8.65	14.25
Acetylcarnitine amide chloride	(±)	Found	—	—	—
	(−)		44.34	7.82	11.69
	(+)		—	—	—
		Calcd. for $C_9H_{19}N_2O_3\cdot Cl$	45.28	7.97	11.74
Carnitine chloride	(±)	Found	—	—	—
	(−)		42.51	8.01	7.08
	(+)		—	—	—
		Calcd. for $C_7H_{16}NO_3\cdot Cl$	42.53	8.10	7.09
Acetylcarnitine chloride	(±)	Found	—	—	—
	(−)		45.08	7.39	5.81
	(+)		45.10	7.60	5.84
		Calcd. for $C_9H_{18}NO_4\cdot Cl$	45.09	7.52	5.85

was filtered off, the filtrate evaporated *in vacuo* and the residue recrystallized several times from absolute ethanol to give pure **4** melting at 206°. The iodide was obtained by refluxing the chloride in 10% methyl iodide in methanol for 2 h. (±)Carnitine amide iodide melted at 160–162°. The infrared spectrum of **4** showed the following bands: 3300 cm^{-1} (—OH); 1680 cm^{-1} (—C=O); 1620 cm^{-1} (—NH). The n.m.r. spectrum in D_2O showed signals at 6.70 τ (singlet for $-N^+(CH_3)_3$), 6.40 and 6.52 τ ($=N^+CH_2-$), and 7.37 and 7.27 τ ($-CH_2C=O$).

Preparation of (±)Acetyl Carnitine Nitrile Chloride (5)

1 (10 g) was dissolved in minimal amount of glacial acetic acid and an excess of acetyl chloride added. The solution was refluxed for 4 h, cooled, and the solvent mixture evaporated *in vacuo* at 40°. The solid was recrystallized from acetone–ethanol (1:3) mixture to give 8.3 g pure **5** melting with decomposition at 200°. Acetyl carnitine nitrile iodide melted at 180°. Its infrared spectrum in Nujol showed the following bands: 2254 cm^{-1} (—C=N); 1760 cm^{-1} (—C=O); 1015 cm^{-1} and 1240 cm^{-1} (—COC=); 1650 cm^{-1} and 3200–3400 cm^{-1} (H_2O).

Preparation of (±)Acetyl Carnitine Amide Chloride (6)

Compound **4** was acetylated as described above for **1**. The solid product was recrystallized several times from acetone–ethanol (1:3) to yield **6** which melted at 180°. Its infrared spectrum in Nujol showed the following bands: 1750 cm^{-1} (—C=O); 1625 cm^{-1} (—NH).

Preparation of (±)Carnitine Iodide Ethyl Ester (7)

A mixture of 10 g of **10** and 100 ml of ethanol was refluxed with 10 ml of 50% HI for 5 h, cooled and concentrated *in vacuo*. A mixture of 100 g of acetone and 50 g of ether was added slowly to precipitate 6 g of **7** melting at 140°. Its infrared spectrum in Nujol showed the following bands: 3320 cm^{-1} (—OH); 1738 cm^{-1} (—C=O). The n.m.r. spectrum in D_2O showed signals at 6.77 τ ($-N^+(CH_3)_3$), 6.46 and 6.58 τ ($=N^+CH_2$), 7.28 and 7.39 τ ($-CH_2COO-$), 5.62, 5.73, 5.86, 5.96 τ (methylene group in $-CO_2CH_2CH_3$) and 8.63, 8.76, and 8.88 τ (methyl group in $-CO_2CH_2CH_3$).

Preparation of (±)Carnitine Iodide Methyl Ester (8)

The same procedure was employed as above for **7** using methanol instead of ethanol. **8** melted at 120°. Infrared bands were at: 3322 cm^{-1} (—OH); 1740 cm^{-1} (—C=O).

Hydrolysis of (±)Carnitine Nitrile Chloride (1) in Concentrated HCl. Preparation of (±)Carnitine Chloride (10) and Product G_1 (9)

A quantity (17.8 g, 0.1 mole) of **1** was dissolved in 200 ml concentrated HCl and refluxed for 4 h. The reaction mixture was cooled, whereupon a heavy precipitate of NH_4Cl was formed. The slurry was cooled overnight at 5°, the excess NH_4Cl was filtered off and the supernatant kept at room temperature from 5 to 10 days until crystal formation was maximum. Crystallization from absolute ethanol gave 11.5 g of pure **10** which melted at 196°. Its infrared spectrum showed the following major bands: 3255 cm^{-1} (—OH); 1725 cm^{-1} (—COO—); 1056 cm^{-1}, 1069 cm^{-1}, 1097 cm^{-1}, ($-CH_3$); 962 cm^{-1}, 972 cm^{-1} ($-N^+(CH_3)_3$). The proton n.m.r. spectrum

Can. J. Chem. Downloaded from www.nrcresearchpress.com by 210.87.254.40 on 09/05/12
For personal use only.

TABLE II

Optical rotation and melting points of some carnitine derivatives shown in Chart 1

Derivative		*dl* (±)	*d* (+)	*l* (−)	Natural *l* (−)
Carnitine nitrile chloride	m.p.	232°	259–261°	259–261°	—
	$[\alpha]_D$	0.00°	+26.3°	−26.3°	—
Carnitine nitrile *d*-camphorsulfonate	m.p.	—	202°	195°	—
	$[\alpha]_D$	+14.5°	+27.1°	+1.60°	—
Carnitine nitrile tetrachloroaurate	m.p.	126°	111°	111°	—
Carnitine nitrile Reineckate	m.p.	201°	168°	168°	—
Carnitine amide chloride	m.p.	206°	238°	238°	—
	$[\alpha]_D$	0.00°	+27.0°	−27.0°	—
Acetylcarnitine amide chloride	m.p.	180°	202°	202°	—
Carnitine chloride	m.p.	196°	142°	142°	142°
	$[\alpha]_D$	0.00°	+23.6°	−23.7°	−23.7°
Carnitine tetrachloroaurate	m.p.	145°	156°	156°	156°
Carnitine Reineckate	m.p.	148°	147°	147°	147°
Carnitine ethyl chloride	m.p.	—	148°	148°	148°
	$[\alpha]_D$	0.00°	+17.1°	−17.1°	−17.2°
Carnitine ethyl tetrachloroaurate	m.p.	122°	105°	105°	105°
Acetylcarnitine chloride	m.p.	188°	188°	188°	188°
	$[\alpha]_D$	0.00°	+27.7°	−27.7°	−27.0°
Acetylcarnitine tetrachloroaurate	m.p.	168°	129°	129°	130°

in D_2O showed a singlet at 6.76 τ ($—N^+(CH_3)_3$), 6.45 and 6.56 τ ($=N^+CH_2$), 7.28 and 7.38 τ ($—CH_2COO^-$). When the mother liquor of the NH_4Cl supernatant yielded no more crystalline product (usually after 10 days), the supernatant was evaporated *in vacuo* for 24 h. The oil which separated (3 g), solidified on cooling. This oily solid was called Product G_1 (**9**). It was stored in a desiccator ($MgSO_4$) under reduced pressure. Its infrared spectrum in Nujol showed the following bands: 3250 cm^{-1} (—OH); 1735 cm^{-1} ($—COO^-$); 1050 cm^{-1}, 1069 cm^{-1}, 1099 cm^{-1}, ($—CH_3$); 968 cm^{-1}, 978 cm^{-1} ($—N^+(CH_3)_3$).

*Acetylation of (±) Carnitine Chloride (**10**) and Product G_1 (**9**). Preparation of (±) Acetyl Carnitine Chloride (**12**) and Product G_2 (**11**)*

10 (19.7 g) was acetylated in minimum amount of warm glacial acetic acid and excess acetyl chloride as described for the preparation of **5** and **6**. The solution was refluxed for 4 h, cooled and kept for two days at room temperature when a heavy precipitate (13.2 g) of **12** was formed. Two more crops of crystals of 2.8 and 1.2 g were collected later from the mother liquor. Crystallization from ethanol gave 1.1 g of **10** and 14.8 g of pure **12** (as determined by m.p. and infrared) from ethanol–acetone (3:1) mixture. **12** melted at 188° and showed the following infrared bands: 1720 cm^{-1}, 1745 cm^{-1} (—C=O); 1050 cm^{-1}, 1081 cm^{-1} ($—CH_3$); 1020 cm^{-1} and 1240 cm^{-1} (—COC=); 947 cm^{-1}, 970 cm^{-1} ($—N^+(CH_3)_3$). The proton n.m.r. spectrum in D_2O showed peaks at 6.80 τ ($—N^+(CH_3)_3$), 6.10 and 6.24 τ ($=N^+CH_2—$), 7.12 and 7.23 τ ($—CH_2COO^-$), and 7.86 τ ($—COCH_3$).

The original mother liquor was then evaporated to dryness *in vacuo* in a desiccator for 24 h. Removal of the solvent *in vacuo* led to a colorless thick semisolid gum (4.2 g). Occasionally, the reaction mixture turned pale-yellow. In this instance, the dry gum was dissolved in a minimal amount of ethanol and decolorized with Norit. The product G_2 (**11**) was a clear, colorless sticky material and appeared to be polymeric in nature. Acetylation of **9** by the method described above also gave **11** as determined by infrared. The ester exhibited the following infrared absorption bands: 1725 cm^{-1}, 1745 cm^{-1} (—C=O); 1050 cm^{-1}, 1081 cm^{-1} ($—CH_3$); 1020 cm^{-1} (—COC=); 947 cm^{-1}, 970 cm^{-1} ($—N^+(CH_3)_3$) but several attempts to crystallize this substance were unsuccessful. Consequently the oily ester was employed without further purification in later experiments.

Preparation of the Optical Isomers

The levorotatory and dextrarotatory isomers of most of the compounds shown on Chart 1 from **4** to **12** were also prepared, but since their synthesis were identical to those of their corresponding racemates, only some of their pertinent chemical properties will be given in Table II. Their infrared and proton n.m.r. spectra were virtually identical to their corresponding racemates.

There was, however, a small but significant difference in the absorption of the acetate peaks as shown in Table II.

Isolation of (−)carnitine was accomplished by the method of Friedman *et al.* (4). The total yield from 500 g Difco beef extract was 4.31 g. Its infrared and proton n.m.r. spectra were identical to synthetic (−)carnitine and showed an optical rotation $[\alpha]_D$ −23.7°. It melted at 142°.

*Chemical Properties of (−) Product G_1 (−**9**) and (−) Product G_2 (−**11**)*

It was found in the present investigation that on

Can. J. Chem. Downloaded from www.nrcresearchpress.com by 210.87.254.40 on 09/05/12
For personal use only.

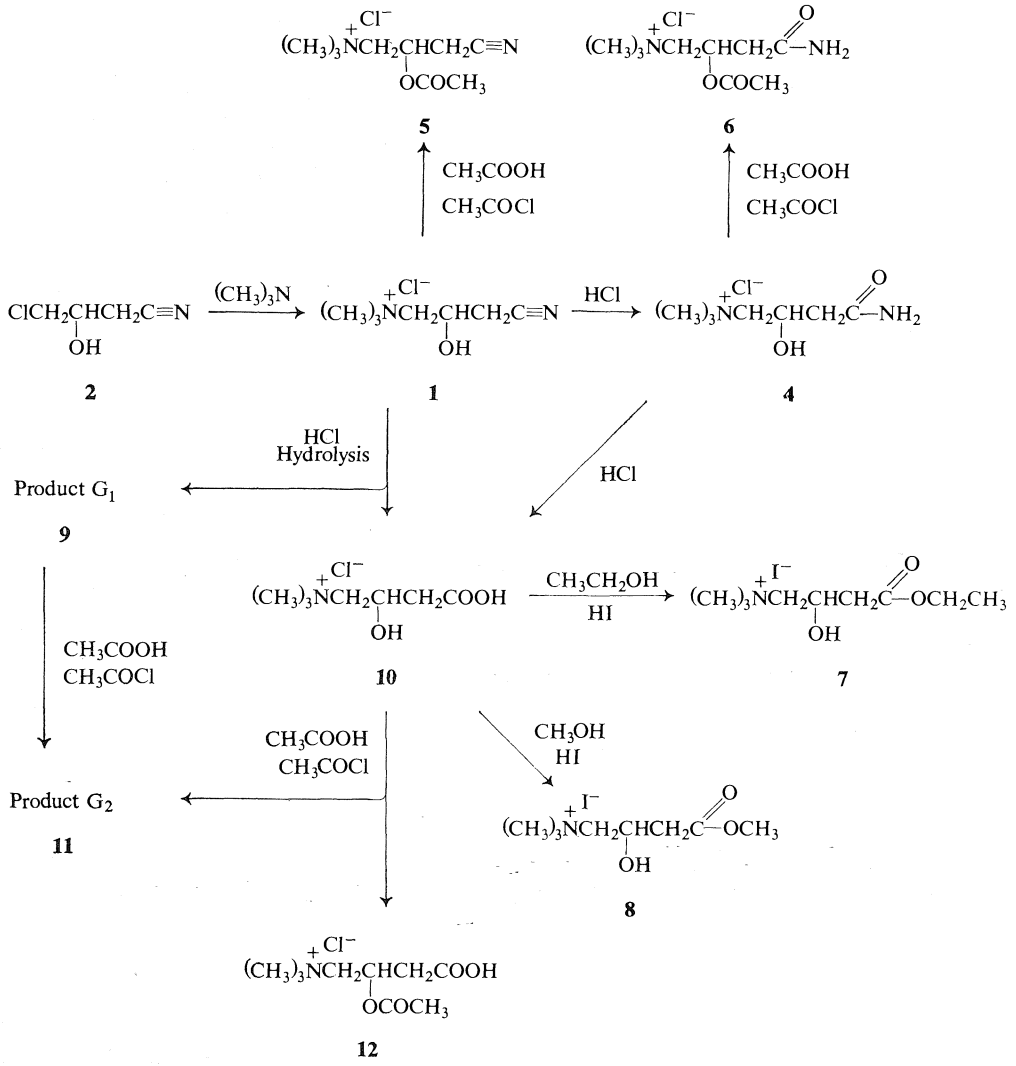

Chart 1

Preparation of certain carnitine derivatives.

reacting −**1** with concentrated HCl two major components (Chart 1) were obtained. One crystalline product was identified as −**10** while the other (−) Product G_1 (−**9**) existed in a gum form, and appeared polymeric. Acetylation of **10** with acetic acid – acetyl chloride mixture also gave two products, one in the crystalline state was identified as −**12** and a second fraction in the gum form referred to as (−)Product G_2(−**11**). Products G_1 and G_2 could not be crystallized and were always obtained as gums. Their n.m.r. and infrared spectra were superimposable upon those of the crystalline products in the same reaction and they appeared to be polymeric as judged by viscosity and dialysis data. Although these products remain to be identified and may be non-homogeneous, it seems that products G_1 and G_2 are apparently polymers of **10** and **12** respectively.

*Preparation of Acetylcarnitylcholine (**18**, Chart 2)*

Method 1

Preparation of 2-Chloroethyl-β-hydroxy-γ-chlorobutyrate

Dry HCl gas (Matheson) was bubbled through a solution containing 250 g of **2**, 180 ml of ethylene chlorohydrin, and 250 ml dry ether for 20 h at −15° according to Braun (5). The thick syrupy product was evacuated overnight at room temperature to eliminate the ether and some of the excess HCl. The imido ester (**13**) was suspended in 500 ml water and allowed to stand at

Can. J. Chem. Downloaded from www.nrcresearchpress.com by 210.87.254.40 on 09/05/12
For personal use only.

Can. J. Chem. Downloaded from www.nrcresearchpress.com by 210.87.254.40 on 09/05/12
For personal use only.

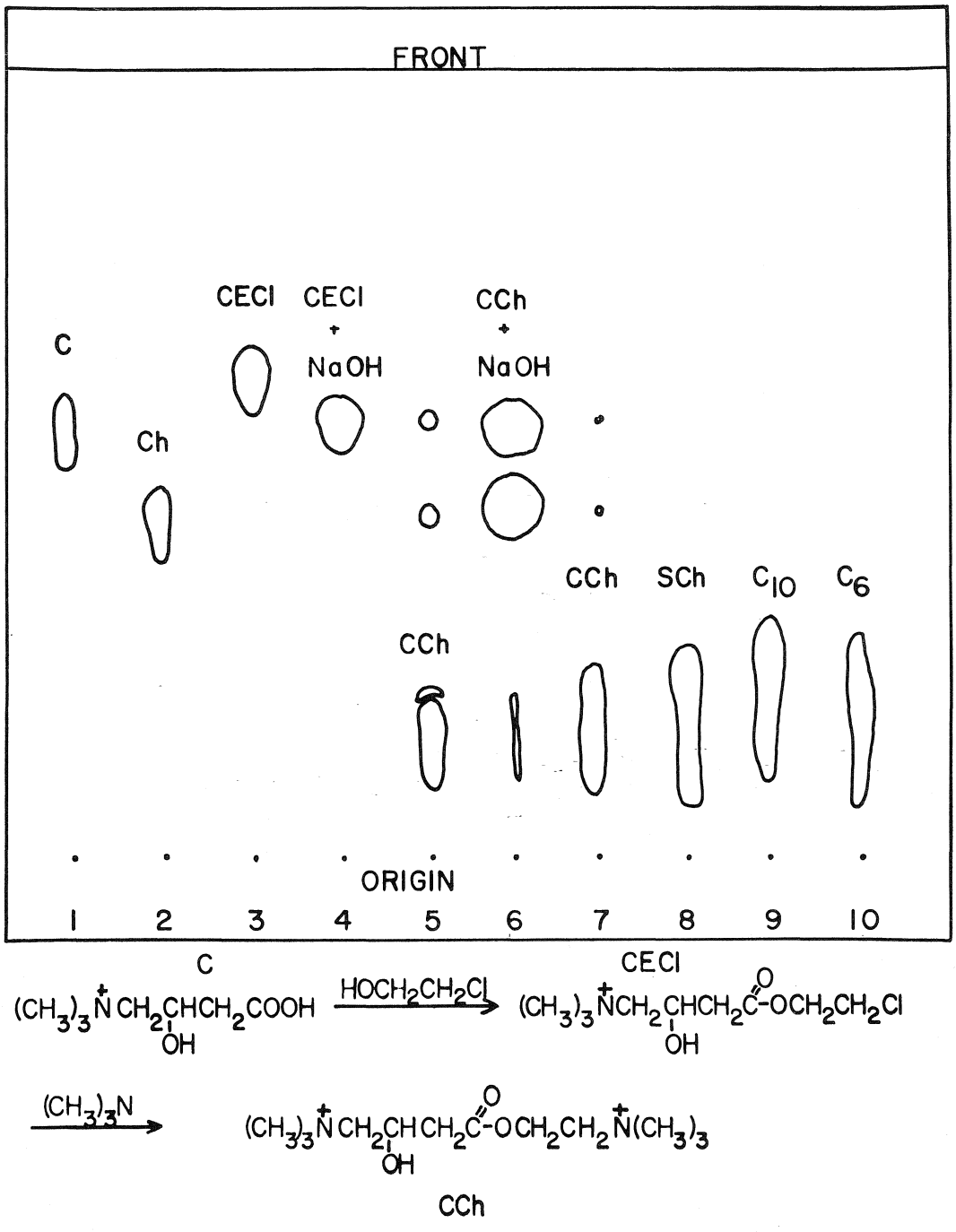

FIG. 1. Thin-layer chromatogram of some related quaternary ammonium compounds: 1, Carnitine (C); 2, choline (Ch); 3, carnitine ethylchloride (CECl); 4, 3 + 1*N* NaOH; 5, carnitylcholine (CCh); 6, 5 + 1*N* NaOH; 7, 5 rechromatographed; 8, succinylcholine (SCh); 9, decamethonium (C_{10}); 10, hexamethonium (C_6). Chromatography was carried out on a 20 × 20 cm plate with a Silica Gel G base, thickness 100 μ.

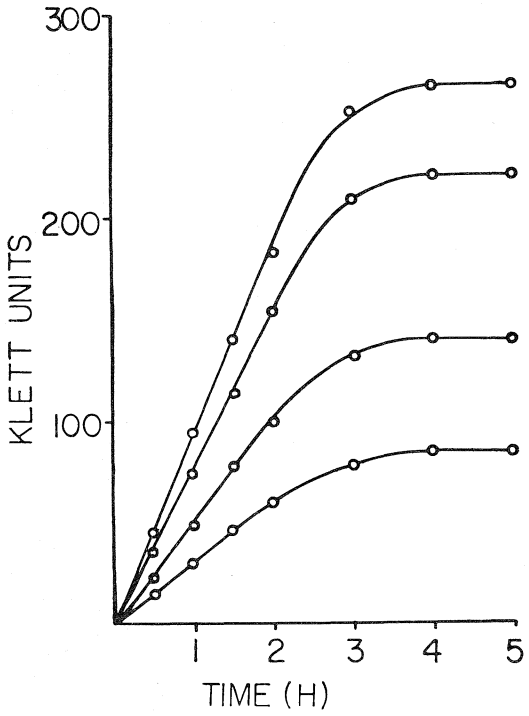

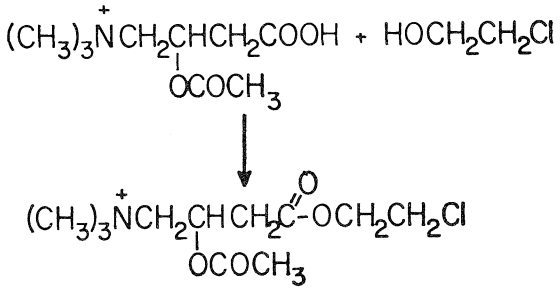

FIG. 2. The curve of ester formation by the reaction of acetyl-*dl*-carnitine chloride with ethylene chlorohydrin at 128°. Aliquots were taken at various intervals for ester determination by the Hestrin method (6). Plots obtained are for increasing initial acetyl-*dl*-carnitine concentrations of 5, 10, and 15 and 20 g/100 ml ethylene chlorohydrin.

45° for 1 h, after which the ester was separated and combined with the etheral extract of the aqueous solution. The combined etheral solution was washed with saturated sodium bicarbonate solution, dried over ammonium sulfate and fractionated by vacuum distillation gave a final yield of 120 g of a colorless sweet smelling ester (**14**) boiling at 140–144° at 7–9 mm Hg.

Anal. Calcd. for $C_6H_{10}O_3Cl_2$: C, 35.82; H, 4.98; Cl, 35.32. Found: C, 36.82; H, 4.37; Cl, 35.72.

The infrared spectrum of **14** showed an alcohol group at 3350 cm^{-1}, an ester group at 1750 cm^{-1} and a chloride group at 667 cm^{-1}.

Preparation of (±) Carnitylcholine Dichloride (17)

Fifty grams of **14** were dissolved in 160 ml of absolute ethanol and treated with 45 g anhydrous trimethylamine in a metallic bomb. After cooling the mixture in a dry ice – acetone bath for 20 min, the bomb was sealed with a clamping device and heated to 60° for 4 h in a water bath. At the end of the reaction, the bomb was cooled in a dry ice – acetone bath, then carefully opened, the excess trimethylamine and ethanol evaporated *in vacuo*, and the solid residue washed with dry ether. Thin-layer chromatography on Silica Gel G of a small quantity (80 mg) of the product in methanol, acetone, HCl (90, 10, 10 v/v) gave two minor bands at R_f 0.48 and one major band at R_f 0.23. Careful removal of the two upper bands and extraction with methanol gave 22 mg of the faster moving material (R_f 0.58) and 14 mg of the slower moving derivative (R_f 0.48). Three recrystallizations of the slower moving component (R_f 0.48) from ethanol–acetone gave crystals melting at 305°. Infrared analysis revealed this substance to be choline. The upper band (R_f 0.58) was recrystallized from ethanol and was found to be carnitine from its melting point (196°) and its infrared spectrum.

The main band (R_f 0.23) was eluted with methanol and converted into its iodo derivative. Three recrystallizations from ethanol gave 12 mg of pure **17** iodide melting at 185°. Upon mild alkaline hydrolysis of **17** with 0.3 *N* NaOH only two major spots were revealed corresponding to carnitine and choline and one minor spot corresponding to unhydrolyzed **17**. Rechromatography of **17** in the same system gave one spot at R_f 0.23. This thin-layer chromatogram along with a number of other bis-quaternary ammonium compounds is shown in Fig. 1. Its infrared spectrum (Fig. 3) showed absorption at 3300 cm^{-1} (—OH); 1735 cm^{-1} (—C=O); 1240 cm^{-1} and 1268 cm^{-1} (—CH_2—); 945 cm^{-1}, 950 cm^{-1}, 962 cm^{-1} (—$N^+(CH_3)_3$). Its proton n.m.r. spectrum in D_2O showed signals at 6.78 τ (—$N^+(CH_3)_3$), 6.45 and 6.55 (=N^+CH_2—), 7.20 and 7.30 τ (—CH_2COO) and 6.16, 6.25, and 6.32 τ (—$COOCH_2CH_2$—).

Preparation of (±) Acetylcarnitylcholine Dichloride (18)

This compound was prepared by the acetylation of **17** in acetic anhydride or acetic acid – acetyl chloride mixture. Excess acetic anhydride (50 ml) was added to 3.2 g of **17** and heated, whereby the crystals dissolved.

Can. J. Chem. Downloaded from www.nrcresearchpress.com by 210.87.254.40 on 09/05/12
For personal use only.

Can. J. Chem. Downloaded from www.nrcresearchpress.com by 210.87.254.40 on 09/05/12
For personal use only.

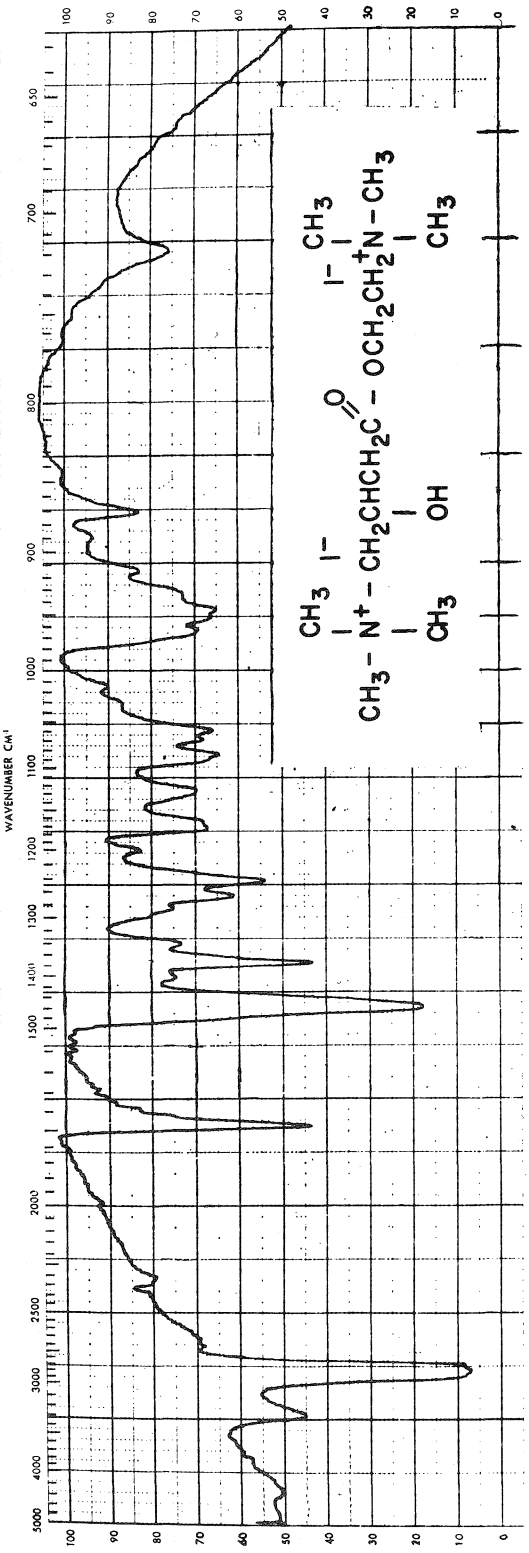

FIG. 3. The infrared spectrum of carnitylcholine iodide.

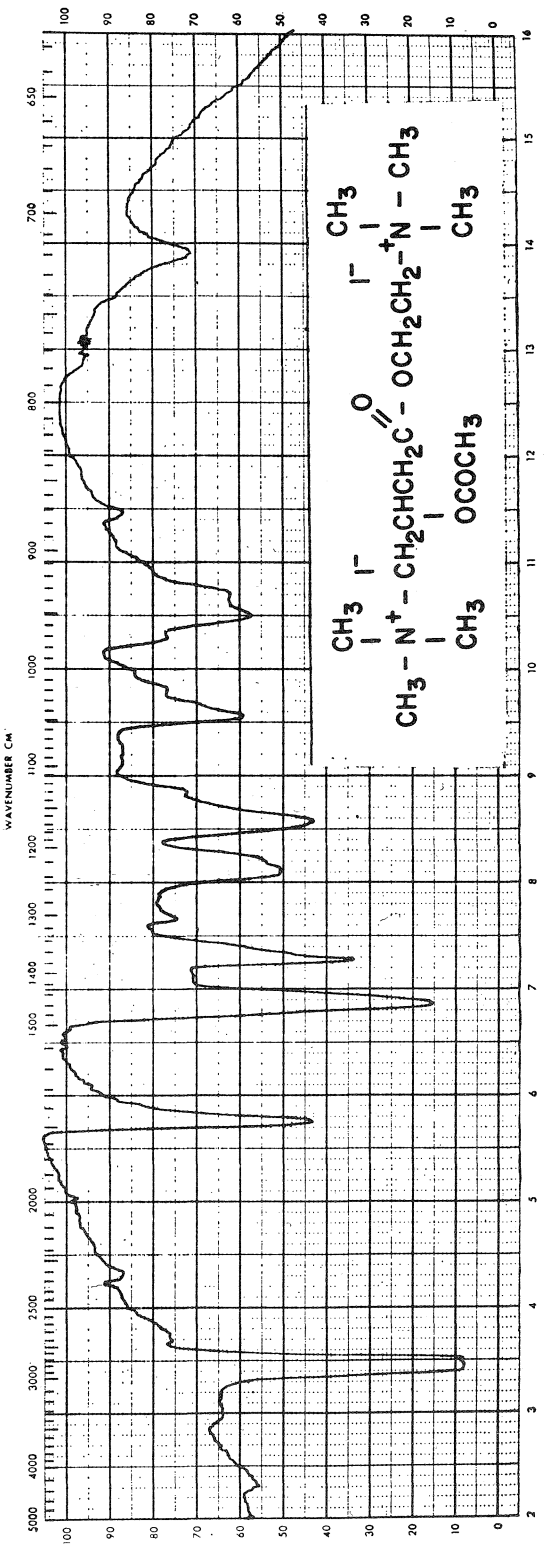

FIG. 4. The infrared spectrum of acetyl-l-carnitylcholine iodide.

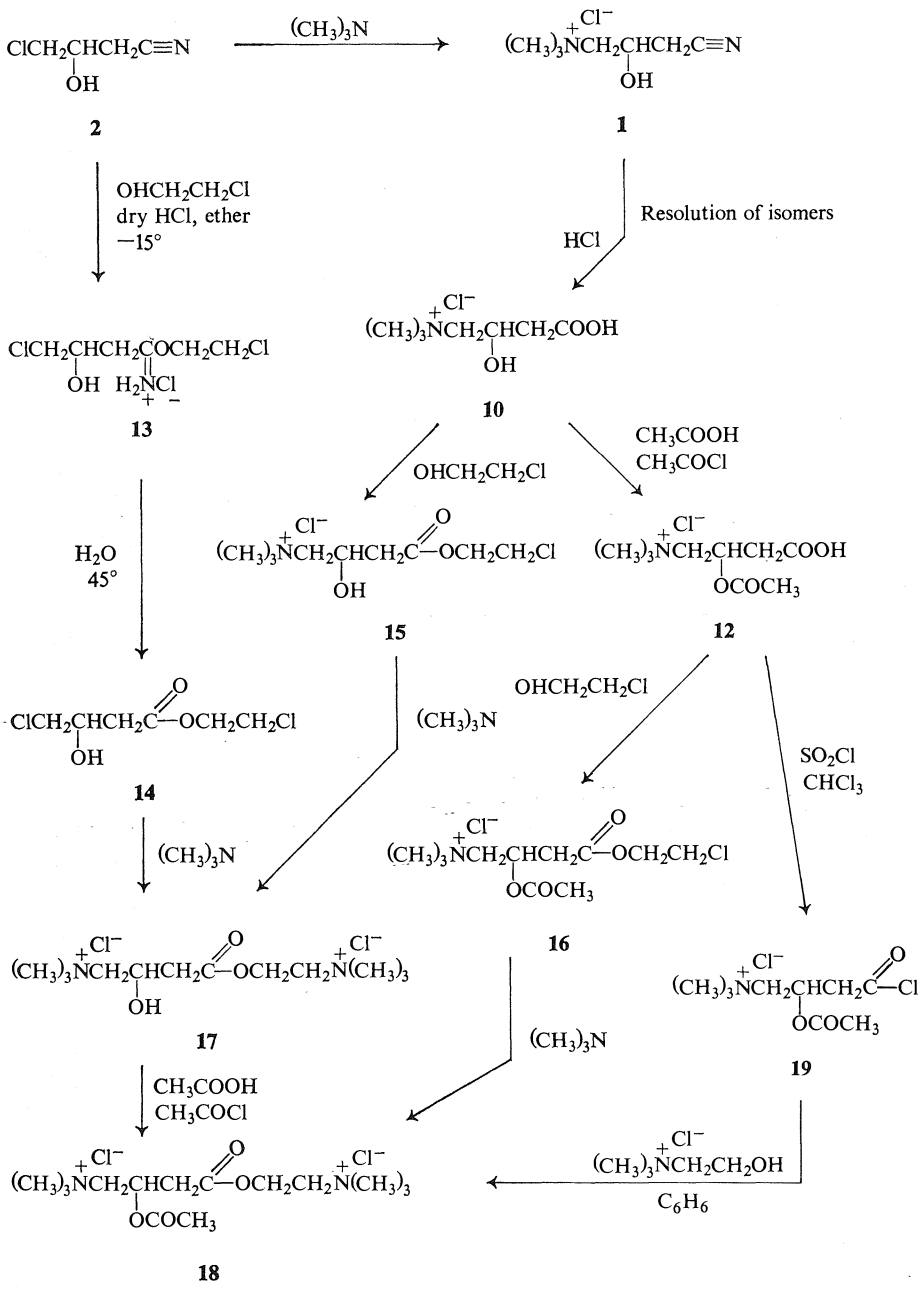

Chart 2
Preparation of certain bis-quaternary ammonium carnitine derivatives.

Can. J. Chem. Downloaded from www.nrcresearchpress.com by 210.87.254.40 on 09/05/12
For personal use only.

TABLE III

Infrared carbonyl and carboxyl absorption peaks of some carnitine derivatives taken in the solid state and in ethanol

Compound		Crystals: cm^{-1} C=O Solid*	Crystals: cm^{-1} C=O in C_2H_5OH
$+Cl^-$ $(CH_3)_3NCH_2CH_2OCOCH_3$ Acetylcholine chloride		1760	1763
$+Cl^-$ $(CH_3)_3NCH_2CHCH_2CN$ | $OCOCH_3$	(±)	1760	1768
	(+)	1753	1761
Acetylcarnitine nitrile chloride	(−)	1751	1761
$+Cl^-$ $(CH_3)_3NCH_2CHCH_2CONH_2$ | $OCOCH_3$	(±)	1750	1758
	(+)	1745	1755
Acetylcarnitine amide chloride	(−)	1745	1753
$+Cl^-$ $(CH_3)_3NCH_2CHCH_2COOH$ | OH	(±)	1725	1730
	(+)	1730	1738
Carnitine chloride	(−)	1730	1738
$+Cl^-$ $(CH_3)_3NCH_2CHCH_2COOH$ | $OCOCH_3$	(±)	1720+1745	1730+1750
	(+)	1725+1750	1733+1752
Acetylcarnitine chloride	(−)	1723+1751	1731+1754

*KBr pellet.

TABLE IV

Elemental analysis of various carnitine derivatives shown in Chart 2

Compound	Isomer		Analysis % Carbon	Hydrogen	Nitrogen
Carnitine ethylchloride chloride	(±)		48.00	8.30	6.13
	(−)		48.09	8.41	6.20
	(+)	Found	—	—	—
		Calcd. for $C_9H_{19}NO_3 \cdot Cl$	48.11	8.46	6.24
Carnitylcholine iodide	(±)		28.51	5.51	5.56
	(−)		28.60	5.51	5.50
	(+)	Found	—	—	—
		Calcd. for $C_{12}H_{28}N_2O_3 \cdot 2I$	28.69	5.58	5.58
Acetylcarnitylcholine iodide	(±)		30.21	5.40	5.10
	(−)		30.10	5.61	4.96
	(+)	Found	—	—	—
		Calcd. for $C_{14}H_{30}N_2O_4 \cdot 2I$	30.88	5.51	5.15

The reaction mixture was refluxed for an additional 3 h, then cooled and evaporated *in vacuo*. The precipitate was further dried under P_2O_5, converted to the iodo salt, taken up in absolute ethanol and precipitated with ether. Three recrystallizations from ethanol–acetone (3:1) mixture gave pure **18** iodide melting at 208°. Its infrared spectrum (Fig. 4) had the following bands: 1735 cm^{-1} (—C=O); 1307 cm^{-1}, 1228 cm^{-1}, 1165 cm^{-1}, 1045 cm^{-1} (—CH_3); 971 cm^{-1}, 952 cm^{-1}, 932 cm^{-1} (—$N^+(CH_3)_3$). The proton n.m.r. spectrum of **18** in D_2O showed signals at 6.74 τ (—$N^+(CH_3)_3$), 6.16, 6.22 and 6.29 τ (—$CH_2CH_2N^+$=), 6.96 and 7.06 τ (—CH_2COO—) and 7.81 τ (—$OCOCH_3$).

Method 2

Preparation of (±) Carnitine Ethylchloride Chloride (15)

6 g of **10** were dissolved in 100 ml ethylene chlorohydrin and refluxed at 120°. The progress of the reaction was followed by removing aliquots and reading OD of a ferric hydroxamate complex at 560 mu.

Can. J. Chem. Downloaded from www.nrcresearchpress.com by 210.87.254.40 on 09/05/12
For personal use only.

TABLE V

Optical relations and melting points of some carnitine derivatives shown in Chart 2

Derivative		*dl* (±)	*d* (+)	*l* (−)
Carnitine ethylchloride chloride	$[\alpha]_D$	0.00	+19.85	−19.85
Carnitine ethylchloride tetrachloroaurate	m.p.	112°	94°	94°
Carnitylcholine iodide	m.p.	185°	—	—
	$[\alpha]_D$	0.00	+9.32	−9.32
Carnitylcholine tetrachloroaurate	m.p.	122°	—	—
Acetylcarnitylcholine iodide	m.p.	206°	186°	186°
	$[\alpha]_D$	0.00	+9.16	−9.16

In this reaction the excess ethylene chlorohydrin was evaporated *in vacuo* at 45° and the remaining solids were dissolved in boiling ethanol. The solution was cooled and crystals of unreacted carnitine appeared. These were removed by filtration. The supernatant fluid was then evaporated to dryness and recrystallized from an ethanol–ether (3:1) mixture to yield 4.2 g of pure **15**. This product was converted to its tetrachloroaurate derivative which melted at 112°. The n.m.r. spectrum in D_2O showed signals at 6.72 τ ($(CH_3)_3N^+$—), 7.16 and 7.26 τ (—CH_2COO—), 6.40 and 6.50 τ (=CH_2CHOH), 6.04, 6.10, 6.14 and 6.21 τ (—$COOCH_2$—) and 5.42, 5.50, 5.53, and 5.59 τ (—CH_2Cl).

Preparation of (±) Carnitylcholine Iodide

One hundred grams of anhydrous trimethylamine were cooled in an acetone – dry ice bath and carefully poured into a 200 ml capacity metallic container. An amount (usually between 10–15 g) of finely ground **15** was slowly added to the container which was then closed and completely sealed by a clamp. The container was placed on a steam bath for 3 days after which time it was opened and the trimethylamine allowed to evaporate in a fume hood. The hygroscopic residue was washed with ether and converted to its iodo salt and recrystallized three times from ethanol to yield pure (**17**) iodide melting at 185°. Its infrared and proton n.m.r. spectra were identical to (±)carnitylcholine (**17**) prepared by method 1.

Preparation of (±) Acetylcarnitylcholine Iodide

A sample (4.8 g) of acetyl (±)carnitine was dissolved in approximately 150 ml of ethylene chlorohydrin. This solution was then refluxed for 5 h, cooled and the solvent removed under reduced pressure at room temperature. Esterification was again confirmed by removing aliquots and reading OD at 560 mμ. The plot of OD in Klett units (ester concentration) against time for the esterification of acetyl (±)carnitine with ethylene chlorohydrin is shown in Fig. 4.

The crystalline product was dissolved in boiling ethanol and approximately one-third of this volume of acetone was added. After 2 days, the unreacted acetyl (±)carnitine which crystallized out was removed by filtration and the supernatant was removed under reduced pressure. **16** was not isolated but was immediately treated with an excess of anhydrous trimethylamine in a pressure bomb as described earlier for **17**. At the end of the reaction (3 days) the excess trimethylamine was volatilized in a fume hood and any remaining traces were removed by repeated washings with ether. The hygroscopic product was dissolved in distilled water and immediately converted to its iodo salt by conventional methods. After the water was evaporated *in vacuo* at room temperature, a powder was obtained which was recrystallized from ethanol–ether (3:1) to yield 2.3 g of pure **18** iodide which melted at 206°. Its infrared and proton n.m.r. spectra were again identical with **18** iodide prepared by method 1.

Method 3

Preparation of (±) Acetylcarnitylcholine Iodide

The acid chloride (**19**) was prepared by adding 15 ml of thionyl chloride to a suspension of 4.8 g (**12**) in excess chloroform. The solution was heated under gentle reflux on a water bath for 5–10 min until all the crystals

TABLE VI

Paper chromatographic R_f values, thin-layer chromatographic R_f values and electrophoretic mobilities (R_m) of acetylcholine and related substances

	Descending paper chromatography*	Thin-layer chromatography†	High voltage electrophoresis‡
	Butanol–water	Methanol/Acetone/ HCl(90/10/10 v/v)	Ammonium acetate Buffer pH 4.6
Substance	R_f	R_f	R_m
Acetylcholine chloride	0.09	0.55	1
Choline chloride	0.05	0.45	1.15
Acetylcarnitine chloride	0.07	0.65	0.15
Carnitine chloride	0.05	0.60	0.18
Acetylcarnitylcholine chloride	0.04	0.20	1.25
Carnitylcholine chloride	0.03	0.18	1.18

*Whatman No. 1 paper (running time 17–18 h).
†Silica Gel G base (thickness about 100 μ).
‡Whatman No. 1 paper (running time 1.5 h, 1500 v).
$R_m = \frac{\text{distance the compound moved}}{\text{distance ACh moved}}$.

Can. J. Chem. Downloaded from www.nrcresearchpress.com by 210.87.254.40 on 09/05/12
For personal use only.

dissolved. The solution was cooled and evaporated under vacuum. The residue was washed several times with dry ether, and the solvent removed. An equimolar amount (2.4 g) of choline chloride was added and the mixture suspended in 100 ml benzene. The reaction mixture was heated under gentle reflux on water bath for 30 min, cooled, and the solvent removed by evaporation under vacuum. The crystalline residue was converted to its iodo salt by interaction with equimolar quantities of KI and recrystallized several times from ethanol–ether (3:1) to yield 3.6 g pure **18** in the iodo form. It melted at 206°.

Preparation of the Optical Isomers

The optically active compounds **15**, **16**, **17**, and **18** were prepared by methods 2 and 3 as for the racemates described above. Since the procedure was identical for their racemates, only certain relevant chemical properties are listed in Tables III, IV, and V. Their infrared and proton n.m.r. spectra were also identical to their corresponding racemates.

Acknowledgments

This work was supported by grants from the Medical Research Council of Canada (MT-904), the Multiple Sclerosis Society of Canada and the United Cerebral Palsy Research and Educational Foundation, Inc., New York (Project R-201-66).

1. E. A. Hosein and J. M. Smoly. Arch. Biochem. Biophys. **114**, 102 (1966).
2. E. Strack, M. Röhnert, and I. Lorenz. Ber. **86**, 525 (1953).
3. E. Strack and I. Lorenz. Z. Physiol. Chem. **318**, 129 (1960).
4. S. Friedman, J. E. McFarlane, P. K. Bhattacharyya, and G. Fraenkel. Biochem. Prep. **6** (1958).
5. G. Braun. J. Am. Chem. Soc. **52**, 3167 (1930).
6. S. Hestrin. J. Biol. Chem. **180**, 249 (1949).

Can. J. Chem. Downloaded from www.nrcresearchpress.com by 210.87.254.40 on 09/05/12
For personal use only.

Cationic cyclization of deuterated manool[1]

O. E. EDWARDS AND B. S. MOOTOO[2]
Division of Biochemistry and Molecular Biology, National Research Council of Canada, Ottawa, Canada

Received December 10, 1968

A test of the mechanism of acid-catalyzed cyclization of manool to 14α-hydroxyhibane was achieved by synthesis and cyclization of 7,7,9,17,17-pentadeuteriomanool. The reaction involves initial formation of a cyclooctenyl cation, an unusual *in vitro* step. The mass spectrum of the deuterated manool in relation to that of manool was used to analyze its fragmentation.

Canadian Journal of Chemistry, 47, 1189 (1969)

Can. J. Chem. Downloaded from www.nrcresearchpress.com by 210.87.254.5 on 09/05/12
For personal use only.

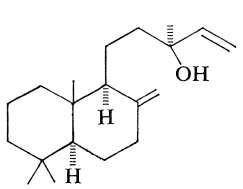

1

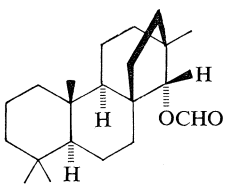

2

In our recent study (1) of the action of formic acid on manool (**1**), the hoped-for cyclization to a tetracyclic skeleton was observed. However, a completely unexpected feature was the formation of 14α-formyloxyhibane (**2**) rather than 16-formyloxyhibane, hibaene, or kaurane derivatives. This product was also observed by Wenkert and Kumazawa (2). Two mechanisms (*a*) and (*b*) have been considered (1, 2) for the formation of **2**:

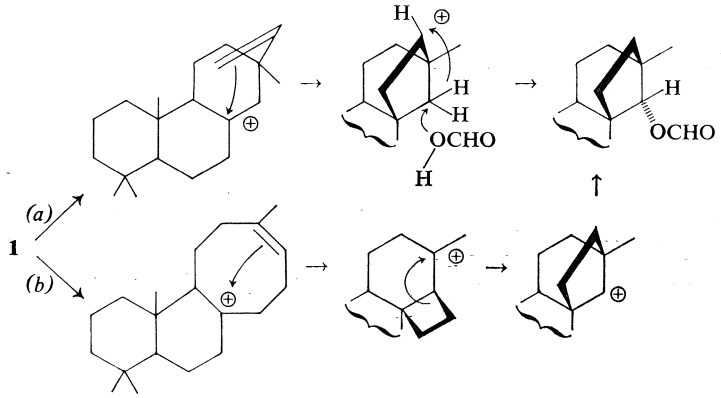

A simple way to distinguish these mechanisms appeared to be the preparation and cyclization of 17,17-dideuteriomanool (**3**). The expected location of deuterium in the product is illustrated in **4** and **5**.

A specifically deuterated manool **9** was prepared as shown on page 1190.

The selective epoxidation has already been described by Jeger and co-workers (3), and by Mousseron-Canet and Mani (4). The epoxide opening to the acetoxy diol **7** (R = Ac) was achieved using anhydrous lithium acetate in dry dimethyl sulfoxide. Traces of water in the dimethyl sulfoxide resulted in opening to the triol **7** (R = H).

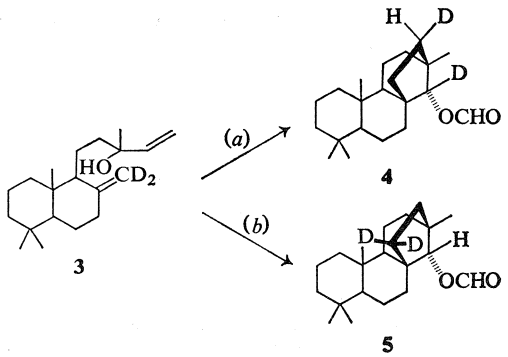

3 **4** **5**

[1]Issued as NRCC No. 10574.
[2]NRCC Postdoctoral Fellow, 1966–1968.

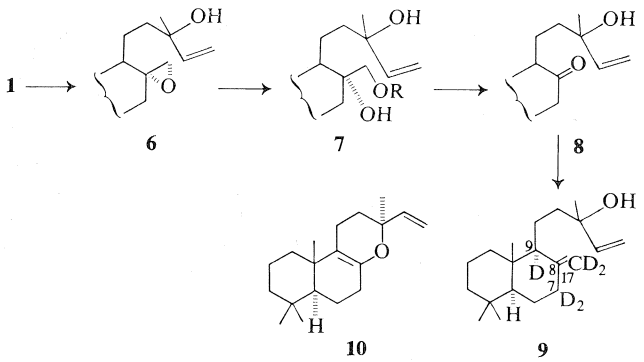

Hydrolysis of the acetoxy-diol gave the triol (**7**, R = H) which was cleaved by periodate under very weakly acidic conditions. At acidities below pH 4 the ketone **8** was largely converted to the enol ether **10**. Ketone **8** had probably previously been prepared in low yield by Wenkert and co-workers (5) by osmium tetroxide – periodate oxidation of manool; however, the cited rotation was of opposite sign.

We were unable to prepare dideuteromanool from **8** using dideuteriomethylenetriphenylphosphorane in hexadeuteriodimethylsulfoxide.[3] The hydrogens α to the carbonyl exchanged more rapidly than the Wittig reaction took place. As a consequence the major product was 7,7,9,17,17-pentadeuteriomanool (**9**).

The deuterated manool was treated with formic acid as in our previous work (1). Deuterated 14-hydroxyhibane was produced in ca. 12% yield. Its mass spectrum showed retention of the five deuterium atoms. Its nuclear magnetic resonance (n.m.r.) spectrum had a sharp one-hydrogen signal at δ 2.92 as in the case of the deuterium-free molecule (1). Thus carbon-14 carried a hydrogen instead of the deuterium predicted by mechanism (*a*).

This result eliminates mechanism (*a*) from consideration. Mechanism (*b*) could not readily be confirmed chemically since the deuterium atoms could not be precisely located. However, mass spectrometry provided strong support for it. Two important fragment ions from 14α-hydroxyhibane involved loss of water and ethylene. The composition of these ions and the parent–daughter relations shown below were established by high resolution mass spectrometry:[4]

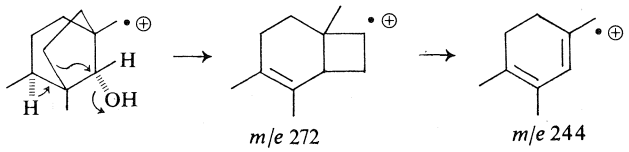

The pentadeuterio-14α-hydroxyhibane gave ions corresponding exactly with the labelling predicted for mechanism (*b*):

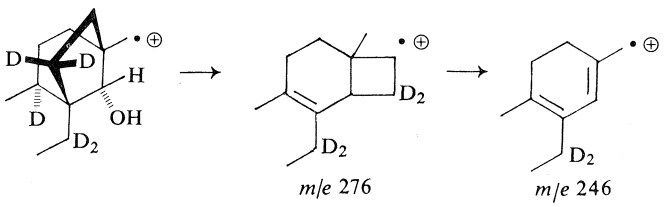

[3]As observed by Atkinson *et al.* (6) this ylid exchanged deuterium rapidly in dimethyl sulfoxide, so that in this solvent only ordinary manool was produced.

[4]We are grateful to Dr. W. D. Jamieson, Atlantic Regional Laboratory, National Research Council of Canada, Halifax, Nova Scotia for these determinations.

Can. J. Chem. Downloaded from www.nrcresearchpress.com by 210.87.254.5 on 09/05/12
For personal use only.

Can. J. Chem. Downloaded from www.nrcresearchpress.com by 210.87.254.5 on 09/05/12
For personal use only.

Thus, in the absence of any alternative mechanism consistent with the above facts, we conclude the mechanism (*b*) is correct.

To the best of our knowledge, this is the first *in vitro* cationic cyclization to an eight-membered ring to be observed. However, Marshall and Andersen (7) have recently formed a seven-membered ring by cationic cyclization of an unsaturated aldehyde (**11** → **12**).

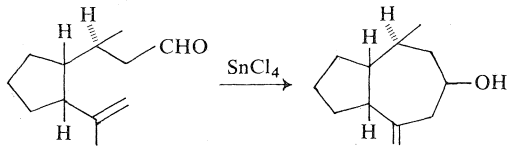

11 **12**

An interesting parallel to mechanism (*b*) is to be found in the postulated route from humulene to α-caryophyllene alcohol (8).

In view of the above results our arguments (1) against the probability of mechanism (*b*) need reexamination. We had assumed that the transition state for formation of the 6–4 ring-fused intermediate would resemble product (nearly tetrahedral C-8). Repulsive interaction developing between the cyclobutane ring and the 10-methyl group (see **13**) would then impede the formation of the hibane skeleton, while the transition state for formation of the isohibane skeleton is quite favorable (see **14**). However, if mechanism (*b*) is correct the transition state must resemble the starting cation (planar C-8). Then the folding leading to **2** (see **15**) would be more favorable than that leading to the isohibane skeleton (**16** → **17**).

It is intriguing that to date no *in vitro* cationic cyclization of the pimarane to hibane systems has been demonstrated, despite the fact that this is such a plausible biosynthetic route to the tetracyclic diterpenes (9). Hence, if this is the *in vivo* route, enzymatic control is vital both for this cyclization step and for the placing of the double bonds of the naturally occurring pimaradienes (ref. 1, page 1115).

The mass spectrum of pentadeuteriomanool (**9**) confirmed some of the assignments made to fragments by Enzell and Ryhage (10). However, others, notably those corresponding to the ions with *m/e* 177, 189, and 204 from manool, require

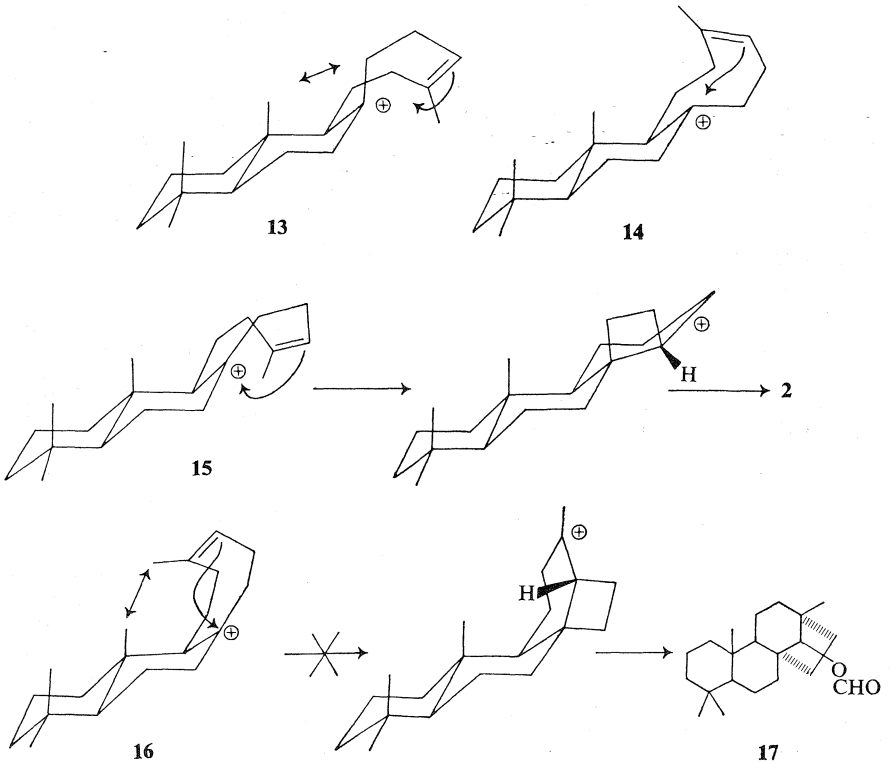

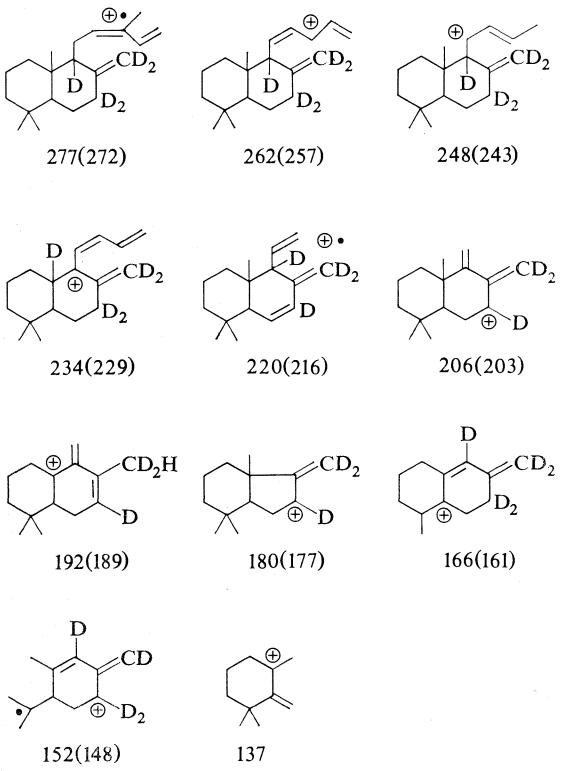

CHART 1

modification. Chart 1 gives our tentative assignments[5] to the most abundant of each of the clusters of ions above *m/e* 137. The least certain of these is the ion with *m/e* 180. The corresponding ions from manool itself are given in parentheses. The main ions below *m/e* 137 contained no deuterium and hence came from the side chain (*m/e* 71) or from ring A.

The most intense peaks below *m/e* 123 in the mass spectrum of 14-hydroxyhibane and the pentadeuterio analogue coincided. Hence these ions originated in ring A. For example, the ion at *m/e* 123 is probably **18** ($C_9H_{15}^+$).

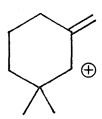

18

[5]The assumption was made that the most abundant ion or the "center of gravity" of each cluster of ions corresponded to the same fragmentation in the deuterated and undeuterated cases.

Experimental

Rotations were of solutions in absolute ethanol. Infrared (i.r.) spectra were of chloroform solutions, measured on a Perkin–Elmer model 257 grating spectrometer, and n.m.r. spectra were of deuteriochloroform solutions with tetramethylsilane as internal reference.

Manool Epoxide

A solution of *m*-chloroperbenzoic acid (9.61 g containing 74% peracid as determined by iodimetry) in chloroform (75 ml) was added dropwise at 0° to a stirred solution of manool (10.99 g) in chloroform (70 ml). Stirring was continued overnight at room temperature. The reaction mixture (containing precipitated *m*-chlorobenzoic acid) was washed thrice with 10% Na_2CO_3 solution. The aqueous washings were grouped and re-extracted with chloroform. The chloroform extracts were washed with water, dried over anhydrous magnesium sulfate, and evaporated to dryness to give 11.2 g of product. Thin-layer chromatography (t.l.c.) (SiO_2, acetone–hexane, 4:1) indicated the presence of a trace of manool and a small amount of a second impurity (possibly β-epoxide; see ref. 3). It was used without further purification.

Reaction of Manool Epoxide with Lithium Acetate

A solution of crude manool epoxide (18 g) and 25 g of anhydrous lithium acetate in 200 ml of dry dimethyl sulfoxide was heated under nitrogen for 35 h at 140–145°. The bulk of the solvent was then removed under 1 mm pressure, the residue diluted with 150 ml of water, and the product extracted into ether (4 × 50 ml). The dried ether solution gave 17.4 g of oil. This was adsorbed on 400 g of neutral alumina, activity 4 from benzene. Methylene chloride – benzene (20:80, 300 ml) eluted the unchanged manool and epoxide (8.17 g). A further 200 ml of this solvent eluted 1.4 g of epoxide and acetoxy diol **7** (R = Ac). Three hundred ml of 50% CH_2Cl_2 in benzene, 100 ml each of 60% and 80% methylene chloride in benzene, followed by 100 ml of methylene chloride, eluted 2.90 g of acetoxy-diol **7** (R = Ac). Methanol in methylene chloride (20:70) eluted a mixture of acetoxy diol and a component with lower R_f on a t.l.c. plate (possibly triol **7**, R = H).

Acetoxy-diol (7, R = Ac)

This crystallized from hexane. After two recrystallizations it had m.p. 106–109° and $[\alpha]_D$ −14.5° (*c*, 1.16). It was sublimed at 100°, 5 × 10^{-4} mm for analysis.

Anal. Calcd. for $C_{22}H_{38}O_4$: C, 72.09; H, 10.45. Found: C, 71.94; H, 10.41.

Its n.m.r. spectrum had peaks at δ 0.81, 0.87, and 1.27 (C—CH_3 groups), 2.11 ($OCOCH_3$), 2.27 (OH), 3.99, 4.07, and 4.26 (CH_2O), 4.91, 4.93, 5.05, 5.12, 5.32, 5.35, 5.73, 5.90, and 6.02 (three vinyl hydrogens).

Triol 7 (R = H)

A solution of 2.9 g of acetoxy-diol **7** (R = Ac) in 60 ml of ethanol was left at room temperature for 5 h, after addition of 10 ml of 10% sodium hydroxide solution. The ethanol was removed under reduced pressure, the mixture diluted with water, and the product extracted into ether. After removal of the ether the triol crystallized. After recrystallization from acetone it formed fine needles, m.p. 145–146°, $[\alpha]_D$ −17° (*c*, 1.27). It was sublimed at 120°, 6 × 10^{-4} mm for analysis.

Can. J. Chem. Downloaded from www.nrcresearchpress.com by 210.87.254.5 on 09/05/12
For personal use only.

Can. J. Chem. Downloaded from www.nrcresearchpress.com by 210.87.254.5 on 09/05/12
For personal use only.

Anal. Calcd. for $C_{20}H_{36}O_3$: C, 74.02; H, 11.18. Found: C, 74.14; H, 11.08.

Its n.m.r. spectrum had peaks at δ 0.75, 0.81, and 0.87 (C—CH_3 groups) 3.36 (3 OH), 3.7 (CH_2O), 4.91, 4.93, 5.07, 5.11, 5.27, 5.32, 5.36, 5.75, 5.92, 6.04, and 6.11 (three vinyl hydrogens).

Acetylation of the triol at room temperature in 1:1 pyridine – acetic anhydride gave an acetate identical (m.p. and mixed m.p.) with the acetoxy-diol **7** (R = Ac).

*Keto-alcohol **8***

A solution of 2.1 g of sodium periodate in 25 ml of water was brought to pH 6.5 by addition of sodium bicarbonate solution. An ethanol solution of triol **7** (R = H) (2.01 g, in 25 ml) was added slowly with stirring. The pH rose to 7.5 then returned to 7 for the duration of the reaction. After 45 min the reaction mixture was diluted with 25 ml of water then extracted with 4 × 30 ml of ether. The ether yielded 1.66 g of quite pure ketone. This was adsorbed from hexane on to 33 g of neutral alumina, activity 2. A 1:1 hexane–benzene mixture eluted 660 mg of ketone, contaminated with a trace of enol ether **10**. Benzene and methylene chloride eluted 900 mg of pure ketone. Methanol in methylene chloride eluted 83 mg of crystalline impurity.

The ketone would not crystallize. It had ν_{max} 1702 cm^{-1} and n.m.r. signals at δ 0.71, 0.85, 0.97, and 1.26 (CH_3 groups), and a multiplet at δ 4.9–6.2 (three vinyl hydrogens) (see ref. 5 for an alternative preparation). It was distilled for analysis over a short path at 105°, 5 × 10^{-4} mm in ammonia-washed Pyrex bulbs.

Anal. Calcd. for $C_{19}H_{32}O_2$: C, 78.03; H, 11.03. Found: C, 77.88; H, 11.14.

It had $[\alpha]_D$ −43° (*c*, 1.43).

*Enol-ether **10***

To a solution of 120 mg of keto-alcohol **8** in 3 ml of chloroform (¾% ethanol) was added 11 mg of *p*-toluenesulfonic acid hydrate. After 10 min shaking the crystals of acid had nearly completely disappeared, and small liquid droplets had settled on the walls. The i.r. spectrum of the solution now showed no ketone to be present, and a sharp band at 1677 cm^{-1} (enol-ether) had appeared. Solid sodium carbonate was added to the solution, which was then filtered and dried. The oil remaining after removal of the solvent crystallized. After two recrystallizations from methanol it formed stout needles with m.p. 47–48°. It was distilled for analysis at 80°, 5 × 10^{-4} mm. It then had $[\alpha]_D$ +50° (*c*, 0.82).

Anal. Calcd. for $C_{19}H_{30}O$: C, 83.15; H, 11.02. Found: C, 82.91; H, 11.09.

It had ν_{max} 1681 cm^{-1} (vinyl ether) and 1650 cm^{-1} (vinyl group). Its n.m.r. spectrum had peaks at δ 0.85, 0.90, 0.98, and 1.28 (CH_3 groups), 4.87, 4.90, 4.94, 5.11, 5.17, 5.54, 5.70, 5.82, and 6.00 (three vinyl hydrogens). This product proved identical with the readily eluted by-product in the periodate cleavage of triol **7** (R = H).

Manool-d_5

An oil dispersion of sodium hydride (56% hydride) (392 mg) was washed with ether under dry nitrogen to remove the oil. To the hydride was added 10 ml of dry dimethyl sulfoxide-d_6. As soon as the hydride had dissolved, 3.79 g of dry trideuteriomethyltriphenyl phosphonium iodide was added. An orange solution resulted. A solution of 488 mg of keto-alcohol **8** in 6 ml of dimethyl sulfoxide-d_6 was added. The reaction mixture was stirred under nitrogen at room temperature for 14 h, then heated at 65° for 1 h. The cooled mixture was diluted with 20 ml of water, and the product extracted into hexane. The hexane solution was washed with water, dried, and distilled. The residue was adsorbed on 15 g of neutral alumina, activity 2 from hexane. Hexane (20 ml) eluted 4 mg of triphenylphosphine oxide; benzene (10 ml) eluted 53 mg of deuterated manool containing a small amount of triphenylphosphine oxide; benzene, benzene – ether mixtures and ether eluted 395 mg of pure deuterated manool, m.p. after sublimation 50.5–51.5°. Its mass spectrum had intense peaks at *m/e* 277 (12), 262 (30), 248 (2), 235 (2.6), 220 (6), 206 (6), 192 (9), 180 (13), 165 (10), 164 (10), 152 (17), 151 (16), 137 (62), 123 (45), 109 (45), 95 (65), 81 (100), 69 (100), and 55 (80).

Action of Formic Acid on Manool-d_5

To 395 mg of finely divided deuterated manool was added 10 ml of 100% formic acid (dried over boric anhydride). The mixture was shaken vigorously for 20 min, then poured onto a mixture of 90 ml of crushed ice and a concentrated aqueous solution of 15 g of sodium hydroxide. The product was extracted into methylene chloride. The dried solution was concentrated. Its i.r. spectrum had a strong formate ester band at 1715 cm^{-1}.

The methylene chloride was distilled, finally under reduced pressure, giving 385 mg of product. This was dissolved in 5 ml of absolute ethanol. After addition of 200 mg of potassium hydroxide and heating to effect solution, the mixture was left overnight at room temperature. The solution was then boiled for 10 min, then the bulk of the solvent removed under reduced pressure. Water was added and the product extracted into methylene chloride. Evaporation of the methylene chloride left 364 mg of oil. Its i.r. spectrum showed the presence of hydroxyl, but no ester. A hexane solution of 350 mg of the oil was added to a column of 8 g of neutral alumina, activity 3. Hexane (40 ml) eluted 252 mg of pimaradienes; 25% benzene in hexane (20 ml) eluted 4 mg of oil followed by 32 mg of crystals; 50% benzene–hexane (10 ml) eluted 20 mg which crystallized spontaneously. Further elution with 10 ml of 50% benzene–hexane gave 21 mg of oil. Benzene eluted 26 mg which crystallized and ether eluted 26 mg which also crystallized. The 52 mg of less strongly adsorbed crystalline solid was recrystallized from aqueous methanol giving 28 mg of prisms, m.p. 114°. A second crystallization gave pure deuterated 14-hydroxyhibane, m.p. 114–115°. Its mass spectrum had strong peaks at *m/e* 295 (49), 280 (19), 276 (14), 262 (17), 261 (17), 246 (53), 210 (18), 191 (17), 182 (29), 177 (8), 165 (19), 152 (21), 136 (37), 123 (100), 109 (50), 95 (73), 82 (74), 81 (71), 69 (92), and 55 (76).

14α-Hydroxyhibane

Its mass spectrum had prominent peaks at *m/e* 290 (25), 275 (11), 272 (12), 257 (22), 244 (47), 229 (23), 216 (3), 215 (3), 205 (16), 187 (19), 177 (28), 175 (17), 173 (13), 161 (22), 160 (20), 159 (19), 149 (28), 136 (29), 133 (34), 123 (88), 109 (61), 95 (86), 81 (100), 69 (87), 67 (86), and 55 (94). Accurate mass to charge ratios for the ions with *m/e* 290, 272, and 244 were 290.2612 (calcd. for $C_{20}H_{34}O$,

290.26097); 272.2495 (calcd. for $C_{20}H_{32}$, 272.25040); and 244.2188 (calcd. for $C_{18}H_{28}$, 244.21910) respectively.

Acknowledgments

We are grateful to Dr. W. D. Jamieson for accurate *m/e* ratios and parent ion – daughter ion relationships. We thank Mr. A. Knoll and Miss F. Johnson for technical assistance, and Mr. H. Seguin for microanalyses.

1. O. E. Edwards and R. S. Rosich. Can. J. Chem. **46**, 1113 (1968).
2. E. Wenkert and Z. Kumazawa. Chem. Commun. 140 (1968).
3. U. Scheidegger, K. Schaffner, and O. Jeger. Helv. Chim. Acta, **45**, 400 (1962).
4. M. Mousseron-Canet and J. C. Mani. Bull. Soc. Chim. France, 481 (1965).
5. E. Wenkert, J. R. Mahajan, M. Nussim, and F. Schenker. Can. J. Chem. **44**, 2575 (1966).
6. J. G. Atkinson, M. H. Fisher, D. Horley, A. T. Morse, R. S. Stuart, and E. Synnes. Can. J. Chem. **43**, 1614 (1965).
7. J. A. Marshall and N. H. Andersen. Tetrahedron Letters, 1219 (1967).
8. E. J. Corey and S. Nozoe. J. Am. Chem. Soc. **87**, 5733 (1965).
9. E. Wenkert. Chem. Ind. London, 282 (1955).
10. A. R. Enzell and R. Ryhage. Arkiv. Kemi, **23**, 367 (1965).

Can. J. Chem. Downloaded from www.nrcresearchpress.com by 210.87.254.5 on 09/05/12
For personal use only.

Hydrogenolysis of carbohydrate acetals, ketals, and cyclic orthoesters with lithium aluminium hydride – aluminium trichloride[1]

S. S. Bhattacharjee and P. A. J. Gorin
Prairie Regional Laboratory, National Research Council of Canada, Saskatoon, Saskatchewan

Received August 19, 1968

The reduction of hexofuranose and hexopyranose acetals with $LiAlH_4$–$AlCl_3$ (1:1, probably AlH_2Cl) to the corresponding ethers proceeds in similar fashion as that of simple acetals and ketals (Scheme I) (refs. 1–7). Certain *O*-methyl and *O*-benzyl derivatives, not readily obtainable otherwise, are conveniently synthesized from appropriate acetals in this way. Cyclic orthoesters of glucofuranose may be selectively reduced to acetals; the steric course of such reduction has been shown unequivocally in the case of orthoformates (Scheme II). Of several cleavable groups, the ease of hydrogenolysis is (*a*) cyclic orthoester > isopropylidene ketal, cyclohexylidene ketal > benzylidene acetal > ethylidene acetal > formal and (*b*) 5,6-*O*-linked or 3,5-*O*-linked acetal or ketal > 1,2-*O*-linked acetal or ketal.

Canadian Journal of Chemistry, **47**, 1195 (1969)

Can. J. Chem. Downloaded from www.nrcresearchpress.com by 210.87.254.42 on 09/05/12
For personal use only.

The reductive cleavage of 1,3-dioxolanes, 1,3-dioxanes, 1,3-oxathiolanes, *O*-tetrahydropyran-2-yl, and *O*-tetrahydrofuran-2-yl derivatives to ethers with $LiAlH_4$–$AlCl_3$ has been investigated in detail by several workers, especially in the groups of Eliel (1–3) and Brown (4–7). The effects of various substituents at C-2 and C-4 (Scheme I) on the position of cleavage have been established (4). Although polar effects have been found to predominate, steric factors can also play a role. For example, in **1** electron donor substituents at C-4 result mainly in C_2–O_1 bond cleavage due to the formation of an intermediate ion (**2**) which is partially stabilized, in contrast to the other possible intermediate (**3**). Steric effects arise (8) in the cleavage of compounds that are di-substituted at both C-2 and C-4. In this case scission of the C_2—O_3 bond occurs since the intermediate species is destabilized by non-bonded interactions between the C-2 and C-4 substituents. A rarer type of effect has been observed by Brown and co-workers (9) in hydrogenolysis of compounds in which the approach of reducing species is sterically impeded.

In the light of the existing knowledge of the reductive cleavage with $LiAlH_4$–$AlCl_3$, we were interested in hydrogenolyzing various carbohydrates with the reagent in order to evaluate its synthetic utility and also to test the validity of the reported mechanistic principles in somewhat more complex systems. Various carbohydrates containing cyclic orthoester, *O*-isopropylidene, *O*-cyclohexylidene, *O*-propylidene, *O*-ethylidene, *O*-methylene, and *O*-benzylidene groups were prepared by conventional procedures and each treated with an equimolar mixture of lithium aluminium hydride and aluminium chloride. The condition of hydrogenolysis was generally similar to that used by Brown *et al.* (4–7). The crude reaction products were examined by thin-layer chromatography (t.l.c.) and in some cases by gas–liquid chromatography (g.l.c.) in order to ascertain the number and proportion of various components. The principal reaction product(s) (Table I) obtained from various compounds were isolated and characterized.

The routes of cleavage of *O*-methylene derivatives to methyl ethers are readily predictable, since steric effects should be absent. Hydrogenolysis of methyl 2,3-4,6-di-*O*-methylene-α-D-mannopyranoside (**41**) to methyl 2,6-di-*O*-methyl-α-D-mannopyranoside (**42**) occurs via intermediates which are stabilized by the electron donating environments of C-2 and C-6.[2] The reactions of two moles of the reagent with one mole of 1,2-5,6-di-*O*-substituted glucofuranose ketals or acetal were examined. The main product, in all cases, had the 6-*O*-alkyl group as anticipated by de Belder (10). The 1,2-*O*-isopropylidene or 1,2-*O*-cyclohexylidene group remained intact. The preferential mode of cleavage of the 5,6-*O*-isopropylidene, 5,6-*O*-cyclohexylidene, or 5,6-benzylidene ring follows the

[1]Issued as NRCC No. 10482. Presented at the 51st Meeting of the Chemical Institute of Canada, Vancouver, British Columbia, June 1968.

[2]This method appears to hold promise for preparation of hitherto unsynthesized di-*O*-methyl mannoses, which may be utilized in identification of products obtained by methylation–fragmentation analysis of branched-chain yeast mannans.

TABLE I

Hydrogenolyses of carbohydrates using $LiAlH_4$–$AlCl_3$ (1:1)

Starting material	Molar equivalent of reagent	Reaction time (h)	Unreacted material (%)	Yield %	Principal products
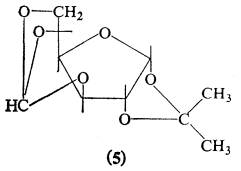 (5)	1	1.25	0	73	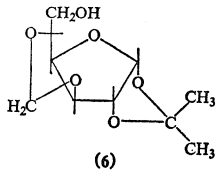 (6)
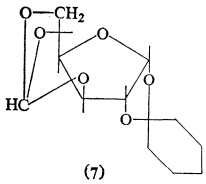 (7)	1	1.25	0	67	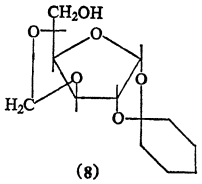 (8)
	1, ($LiAlH_4$–$AlCl_3$ 1:3)	1.25	0	Not isolated	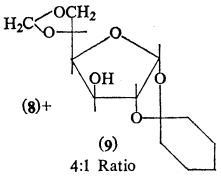 (8)+ (9) 4:1 Ratio
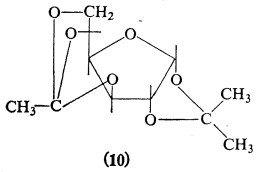 (10)	1	1.25	0	70	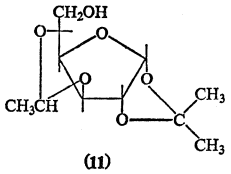 (11)
		0.5	0	63	
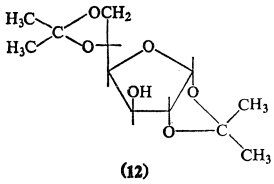 (12)	2	2.0	0	49	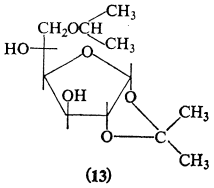 (13)
		0.75	0	60	
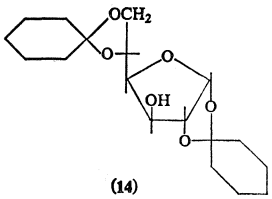 (14)	2	2.0	0	60	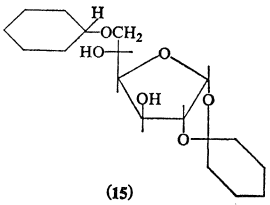 (15)
		0.75	0	55	
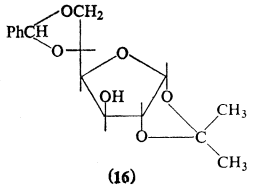 (16)	2	3	0	52	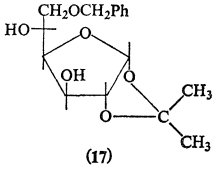 (17)

Can. J. Chem. Downloaded from www.nrcresearchpress.com by 210.87.254.42 on 09/05/12
For personal use only.

TABLE I (*Continued*)

Starting material	Molar equivalent of reagent	Reaction time (h)	Unreacted material (%)	Yield %	Principal products
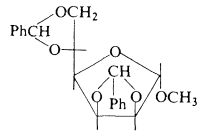 (18)	2	5	0	51	Methyl di-*o*-benzyl α-D-manno-furanoside
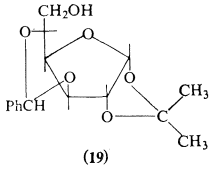 (19)	1	3	Trace	42	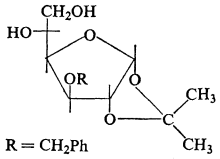 R = CH_2Ph (20)
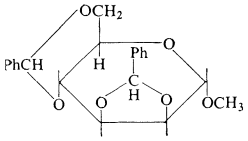 (21)	2	3.5	0	56	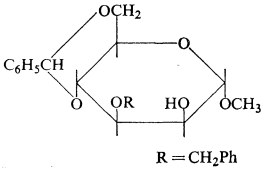 R = CH_2Ph (22) + 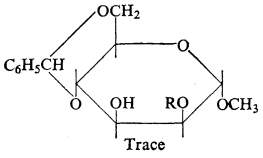 Trace (23)
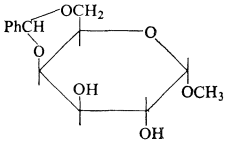 (24)	1	3	32	27	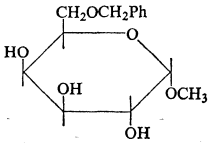 (25)
		20	27	29	
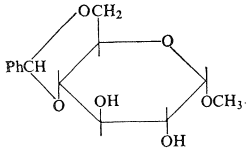 (26)	1	6	38	36	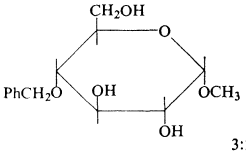 + 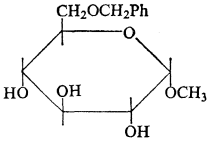 3:2 Ratio (27) (28)
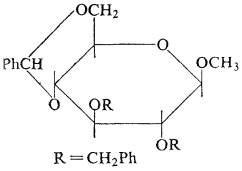 R = CH_2Ph (29)	1	3	36	36	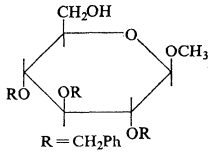 R = CH_2Ph (30)
		40	0	64	
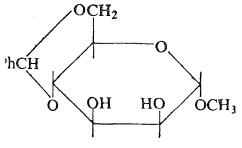 (31)	1	6	34	38	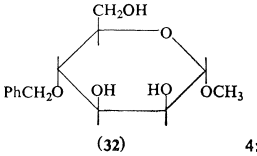 (32) 4:1 Ratio 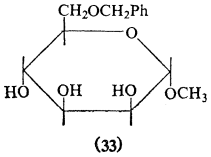 (33)

Can. J. Chem. Downloaded from www.nrcresearchpress.com by 210.87.254.42 on 09/05/12
For personal use only.

TABLE I (*Concluded*)

Starting material	Molar equivalent of reagent	Reaction time (h)	Unreacted material (%)	Yield %	Principal products
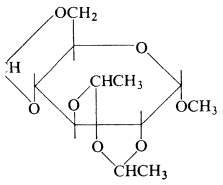 (34)	3	3	0	68	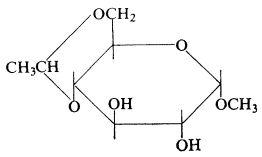 (35) 8:9 Ratio 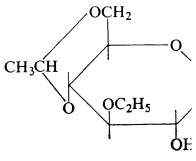 (36)
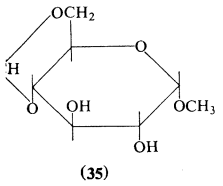 (35)	1	3	65	4	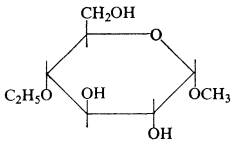 (37) + 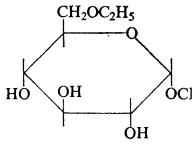 (38)
		24	56	7	
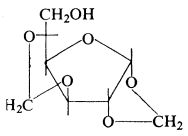 (39)	2	96	60	6	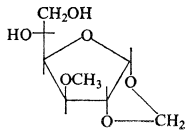 (40)
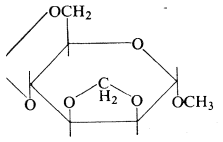 (41)	2	168	40	20	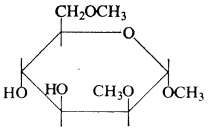 (42)

polar rule (3, 4), since electrons are likely more available from C-6 than C-5 substituents. Hydrogenolysis of 1,2-5,6-*O*-isopropylidene-α-D-glucofuranose (**12**) and 1,2-5,6-di-*O*-cyclohexylidene-α-D-glucofuranose (**14**) in the presence of copper chromite catalyst gave a similar cleavage pattern (11).

However, hydrogenolysis of methyl 4,6-*O*-benzylidene derivatives of α-galactopyranoside (**24**), α-glucopyranoside (**26**), and α-mannopyranoside (**31**) are less predictable than that of the 5,6-*O*-substituted derivative. The 6-*O*-benzyl derivative (**25**) was obtained preferentially in the case of galactoside; whereas preferential formation of 4-*O*-benzyl derivatives of glucoside (**27**) and mannoside (**32**) was observed. Taking into consideration the yield of the main products and the time of reaction, it is evident that six-membered acetals are more resistant to hydrogenolysis compared to the five-membered ones. This is in accord with previous observations (12, 13) on substituted 1,3-dioxanes and 1,3-dioxolanes.

The hydrogenolysis studies were extended to include the 3,5,6-*O*-substituted orthoesters of α-glucofuranose. The 3,5,6-*O*-orthoformyl derivatives of 1,2-*O*-isopropylidene-α-D-glucofuranose (**5**) and 1,2-*O*-cyclohexylidene-α-D-glucofuranose (**7**) were converted selectively to the corresponding 3,5-*O*-methylene derivatives (**6** and **8**) respectively. Similarly, the corresponding 3,5,6-*O*-orthoacetate (**10**) was converted to the 3,5-*O*-ethylidene (**11**) derivative. The mechanisms of orthoacetate and orthoformate cleavage were studied using proton magnetic resonance (p.m.r.) spectroscopy. 1,2-*O*-isopropylidene-3,5-

Can. J. Chem. Downloaded from www.nrcresearchpress.com by 210.87.254.42 on 09/05/12
For personal use only.

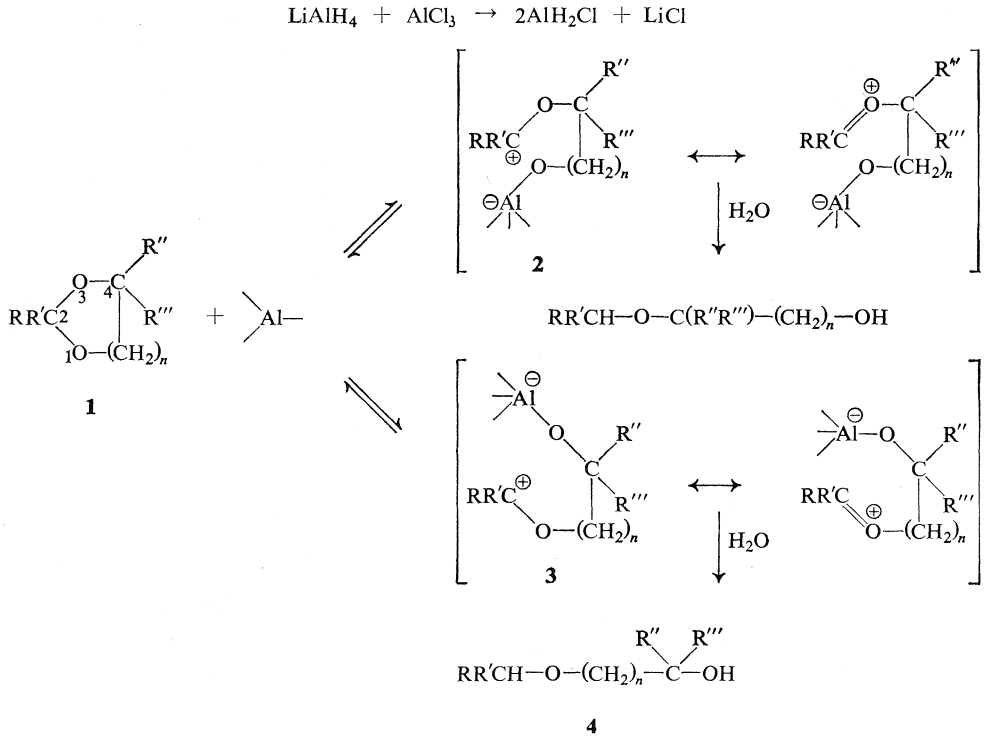

1 2 3 4

SCHEME I. Cleavage of acetals and ketals with $LiAlH_4$–$AlCl_3$.

O-methylene-α-D-glucofuranose contains doublets at τ 5.03 (J = 6 c.p.s.) and τ 5.19 (J = 6 c.p.s.), which are assigned to equatorial and axial *O*-methylene protons, respectively, by analogy with the assignments of Delmau and Duplan (14) in the substituted 1,3-dioxane series. When the orthoformyl derivative was treated with $LiAlD_4$–$AlCl_3$, both the crude reaction product and derived crystals gave one signal at τ 5.18, thus indicating deuteration in the equatorial position (**43**). Interestingly, the product was not equilibrated with approximately 0.1 *N* HCl in chloroform to yield its stereoisomer, and is thus more stable than many other types of acetal and ketal (15, 16, and references therein, 17).

Similar observations on the incorporation of deuterium were made on conversion of 1,2-*O*-cyclohexylidene-3,5,6-*O*-orthoformyl-α-D-glucofuranose (**7**) to a 3,5-*O*-deuteromethylene derivative. Since AlH_2Cl is likely the predominant reactive species in the hydrogenolysis reaction (18), a four-center transition state (19) can be visualized in formation of the specifically labelled 3,5-*O*-deuteromethylene derivatives (Reaction 1, Scheme II).

The hydrogenolysis of 1,2-*O*-cyclohexylidene-3,5,6-*O*-orthoformyl-α-D-glucofuranose (**7**) was less stereospecific when the ratio of $LiAlH_4$–$AlCl_3$ was changed to 1:3. Proton magnetic resonance spectroscopy of the crude reaction product revealed a doublet (τ 4.97: J = 2 c.p.s.; 20% of total methylene signals) with a splitting corresponding to a 5,6-*O*-methylene derivative (**9**) in addition to the quartet of the 3,5-*O*-methylene derivative (**8**). Significantly, isomerization of the 3,5-*O*-methylene derivative to its 5,6-isomer could not be effected using $LiAlH_4$–$AlCl_3$ (1:3) or $AlCl_3$ alone. The mechanism of formation of the 5,6-*O*-methylene derivative appears to involve introduction of a *cis*-hydrogen atom into the 1,3-dioxolane ring since treatment of the orthoester with $LiAlD_4$–$AlCl_3$ (1:3) results in disappearance of the methylene proton at low field.[3]

[3]The position of deuterium labelling of the concomitantly formed 3,5-*O*-deuteromethylene group is the same as the compound formed with $LiAlD_4$–$AlCl_3$ in a 1:1 ratio.

Can. J. Chem. Downloaded from www.nrcresearchpress.com by 210.87.254.42 on 09/05/12
For personal use only.

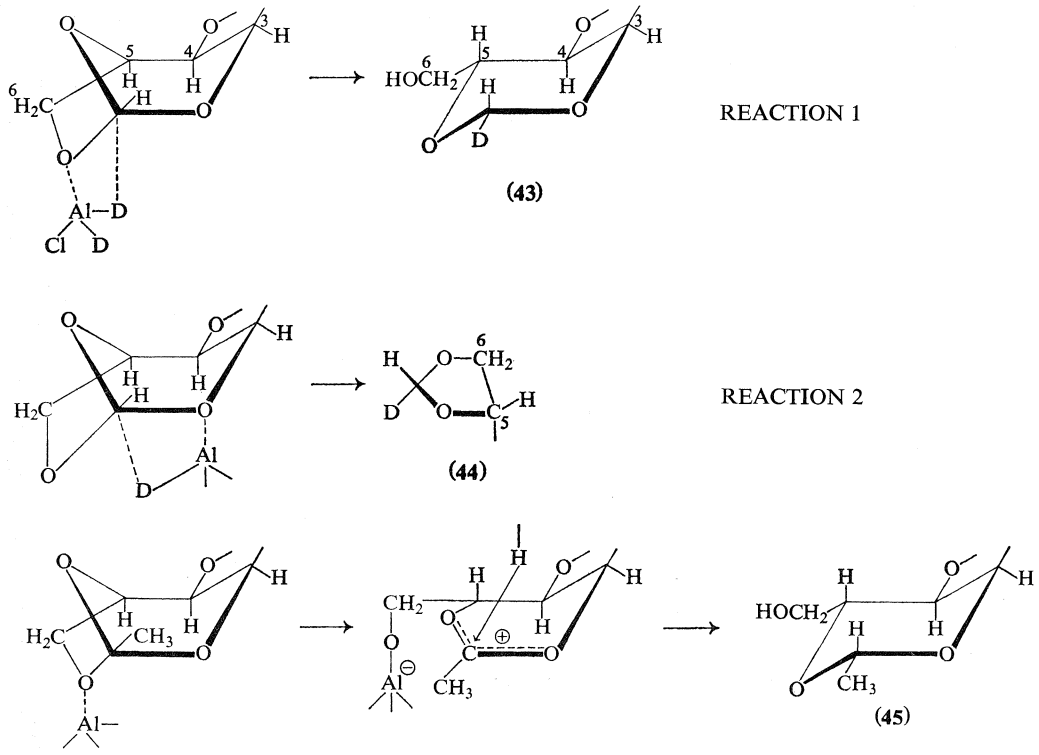

SCHEME II. Conversion of cyclic orthoesters to acetals using $LiAlH_4$–$AlCl_3$.

This proton should be *cis* to the substituent at C-5 since *cis*-ethylidene proton signals in 1,2-*O*-ethylidene glycerol (and its analogues) are at lower field than those of the *trans*-isomer (15). A concerted mechanism involving a four-center transition state (19) similar to that occurring in formation of the 3,5-*O*-deuteromethylene derivative (**44**) therefore occurs (Reaction 2; Scheme II).

Hydrogenolysis of 1,2-*O*-isopropylidene-3,5,6-*O*-orthoacetyl-α-D-glucofuranose using equimolar amounts of $LiAlH_4$ and $AlCl_3$ gave 3,5-*O*-ethylidene-1,2-*O*-isopropylidene-α-D-glucofuranose, which is the thermodynamically stable isomer (**45**, also **11**) since isomerization of acetals may be caused by the reagent when the molar proportion of aluminium trichloride approaches that of lithium aluminium hydride (7). The reaction was repeated using a 1:3 ratio of reagents, respectively. Again the thermodynamically stable isomer was obtained. Unfortunately the possibility of isomeration could not be completely eliminated since we were not able to synthesize the thermodynamically unstable *O*-ethylidene isomer and then test its stability in the hydrogenolysis mixture. The following conclusions should be regarded therefore as tentative. If introduction of an axial hydrogen into the 3,5-*O*-ethylidene group in fact occurred, the four-point attack of the AlH_2Cl species reported in the cleavage of the orthoformates is thus precluded. Instead, the attacking hydride species approaches from the opposite side of the ring from the departing oxygen atom and the reaction is S_N1 in nature (Reaction 3; Scheme II).

In addition to the results reported above on the hydrogenolysis of carbohydrates with $LiAlH_4$–$AlCl_3$, the following observations can be made. The case of hydrogenolysis is comparable to the case of acid hydrolysis of acetals and ketals (10). It occurs in the following order (*a*) cyclic orthoester > *O*-isopropylidene > *O*-cyclohexylidene > *O*-benzylidene > *O*-ethylidene > *O*-propylidene > *O*-methylene, (*b*) 5,6-*O*-

Can. J. Chem. Downloaded from www.nrcresearchpress.com by 210.87.254.42 on 09/05/12
For personal use only.

Can. J. Chem. Downloaded from www.nrcresearchpress.com by 210.87.254.42 on 09/05/12
For personal use only.

linked or 3,5-*O*-linked acetal or ketal > 1,2-*O*-linked acetal or ketal. No change was observed at the anomeric centers under the described reaction conditions, although minor products in the above reactions were not investigated. Investigations on this topic are proceeding since it is known that anomerization can be effected by using Lewis acid alone (20).

Experimental

Proton magnetic resonance spectra were obtained with a Varian HA-100 spectrometer, using tetramethylsilane as standard and chemical shifts were expressed in τ values. Hydroxyl proton signals were detected in their disappearance on D_2O addition or by variation of chemical shifts with temperature. Characterization of primary, secondary, or tertiary hydroxyls was made according to the method of Chapman and King (21). The g.l.c. unit was of conventional design, with thermal conductivity detectors. The helium pressure was 40 p.s.i. and 2% nitrile silicone gum XE-60 on Chromosorb W (80–100 mesh) (175°) or 2% neopentylglycol succinate on Chromosorb W (190°) in $\frac{1}{4}$ in. × 12 ft columns were used. Thin-layer chromatography was carried out on silica gel G (sulfuric acid spray). Evaporations were performed under reduced pressure and specific rotations were determined at 25°. Infrared spectra were recorded on a Perkin–Elmer instrument. Paper chromatography was carried out on Whatman No. 1 filter paper, solvent: ethyl acetate – acetic acid – water (9:2:2, v/v/v); spray, *p*-anisidine hydrochloride.

General Procedure for Hydrogenolysis with $LiAlH_4$–$AlCl_3$

The starting material (0.5–1.0 g) was added to a stirred suspension of the required amount of lithium aluminium hydride in CH_2Cl_2 – diethyl ether (20 ml). The resulting suspension was stirred magnetically and an ethereal solution of aluminium trichloride, equimolar quantity with respect to lithium aluminium hydride, was added (final ratio of CH_2Cl_2 – ether was generally 1:3, v/v). The reaction mixture was stirred under reflux (anhydrous conditions were maintained) for a definite period as shown in Table I. The reaction was arrested by addition of cold water, the ether layer separated, and the aqueous suspension extracted several times with ether, and then with chloroform. The combined extract was dried (K_2CO_3), filtered, and evaporated to dryness. The mixed product was examined by t.l.c. and in some cases a small aliquot of the product was acetylated and examined by g.l.c. Generally, the principal reaction product crystallized, either directly or after purification by silicic acid column chromatography using an appropriate solvent. The principal reaction products were characterized, but trace components were not further examined. The reaction time, molar equivalents of reagent and yields of principal products are presented in Table I.

Hydrogenolysis of 1,2-O-Isopropylidene-3,5,6-O-orthoformyl-α-D-glucofuranose (5)

Examination of the crude reaction product by t.l.c. (solvent:chloroform–acetone, 1:1, v/v) and g.l.c. (2% nitrile silicone gum) of the acetate showed the presence of one predominant component. Crystallization from chloroform – *n*-hexane, with or without prior chromatography on silicic acid (solvent: chloroform–acetone, 1:1, v/v) gave 1,2-*O*-isopropylidene-3,5-*O*-methylene-α-D-glucofuranose (**6**), m.p. 70–72°; $[\alpha]_D$ +25° (*c*, 1.0 EtOH).

Anal. Calcd. for $C_{10}H_{16}O_6$: C, 51.72; H, 6.89. Found: C, 51.91; H, 6.84.

Proton magnetic resonance data (in $CDCl_3$): 4.00 (doublet, $J_{1,2}$ = 4 c.p.s., anomeric H), 5.03 (doublet, J = 6 c.p.s. equatorial H of —OCH_2O—), 5.19 (doublet, J = 6 c.p.s., axial H of —OCH_2O—), 8.12 (triplet, J = 5 c.p.s., primary OH), 8.48 (singlet, CH_3), 8.64 (singlet, CH_3).

Treatment of the *O*-methylene derivative (50 mg) with trityl chloride in pyridine gave a product (15 mg) which was identical (t.l.c. and mixture m.p.) with 1,2-*O*-isopropylidene-3,5-*O*-methylene-6-*O*-trityl-α-D-glucofuranose prepared in the following manner (22). Potassium *t*-butoxide (1.2 g) was added to a mixture of *t*-butanol (7.5 ml) and toluene (7.5 ml). Subsequent addition of 1,2-*O*-isopropylidene-6-*O*-trityl-α-D-glucofuranose (500 mg), dichloromethane (2 ml), and benzene (50 ml) was made and the mixture refluxed for 72 h under anhydrous conditions. Further addition of potassium *t*-butoxide (1 g) and dichloromethane (2 ml) was made during this period. The reaction mixture was cooled and washed with excess water. The non-aqueous layer was dried (K_2CO_3) and concentrated to a syrup which was chromatographed on a silicic acid column (solvent: chloroform). The faster moving fraction was collected and crystallized from chloroform, m.p. 121°; p.m.r. data (in $CDCl_3$): 2.48–2.80 (multiplet, 15 aromatic H), 4.00 (doublet, $J_{1,2}$ = 3.5 c.p.s., anomeric H), 4.90 (doublet, J = 5.5 c.p.s.; H of —OCH_2O—), 5.18 (doublet, J = 5.5, a H of —OCH_2O—), 8.48, 8.64 (singlets, 2 CH_3).

Preparation of 1,2-O-Cyclohexylidene-3,5,6-O-orthoformyl-α-D-glucofuranose (7)

The procedure for the preparation of 1,2-*O*-isopropylidene-3,5,6-*O*-orthoformyl-α-D-glucofuranose (23) was followed. To a mixture of 1,2-5,6-*O*-cyclohexylidene-α-D-glucofuranose (2.5 g), ethyl orthoformate (3.5 ml), and methanol (1.5 ml), one drop of concentrated hydrochloric acid was added and the mixture stirred for 45 min. Benzene (50 ml) was then added to the resulting mixture, which was shaken with K_2CO_3, filtered, and on concentration 1,2-*O*-cyclohexylidene-3,5,6-*O*-orthoformyl-α-D-glucofuranose (1 g) crystallized. After crystallization from benzene it had m.p. 191° and $[\alpha]_D$ −30° (*c*, 1.0 $CHCl_3$).

Anal. Calcd. for $C_{13}H_{18}O_6$: C, 57.77; H, 6.66. Found: C, 57.97; H, 6.63.

Proton magnetic resonance data (in $CDCl_3$): 3.94 (doublet, $J_{1,2}$ = 4 c.p.s., anomeric H), 4.04 (singlet,

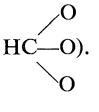

Hydrogenolysis of 1,2-O-Cyclohexylidene-3,5,6-O-orthoformyl-α-D-glucofuranose (7)

The hydrogenolysis product of the orthoformate consisted of mainly one component (t.l.c. and g.l.c. of the

Can. J. Chem. Downloaded from www.nrcresearchpress.com by 210.87.254.42 on 09/05/12
For personal use only.

acetate). The reaction product was chromatographed on a silicic acid column (solvent: chloroform–acetone 1:1 v/v) to give (from *n*-hexane) 1,2-*O*-cyclohexylidene-3,5-*O*-methylene-α-D-glucofuranose (**8**) with m.p. 68–70° and $[\alpha]_D$ +22° (*c*, 1.0 EtOH).

Anal. Calcd. for $C_{13}H_{20}O_6$: C, 57.35; H, 7.35. Found: C, 57.26; H, 7.27.

Proton magnetic resonance data (in $CDCl_3$): 3.99 (doublet, $J = 4$ c.p.s. anomeric H), 5.02 (doublet, $J = 6$ c.p.s., equatorial H of —OCH_2O—), 5.20 (doublet, $J = 6$ c.p.s., axial H of —OCH_2O—), 7.16 (triplet, $J = 5$ c.p.s., primary —OH).

*Preparations of 1,2-O-Isopropylidene-3,5,6-O-orthoacetyl-α-D-glucofuranose (**10**)*

A mixture of 1,2-*O*-isopropylidene-α-D-glucofuranose (5 g), ethyl orthoacetate (20 ml), and concentrated hydrochloric acid (3 drops) was shaken for 15 min. On addition of benzene (20 ml) and shaking for another 10 min, complete dissolution occurred. The solution was shaken with K_2CO_3, filtered, and concentrated to a crystalline residue. Recrystallization from benzene gave 1,2-*O*-isopropylidene-3,5,6-*O*-orthoacetyl-α-D-glucofuranose (**10**; 3.5 g) with m.p. 132–134°; $[\alpha]_D$ −41° (*c*, 1.0 in $CHCl_3$).

Anal. Calcd. for $C_{11}H_{16}O_6$: C, 54.09; H, 6.55. Found: C, 54.01; H, 6.46.

Proton magnetic resonance data (in $CDCl_3$): 3.94 (doublet, $J_{1,2}$ = 3.5 c.p.s., anomeric H), 5.48 (doublet, J = 3.5 c.p.s., H_2) 8.38 (singlet, $CH_3C(O)O$—), 8.50, 8.66 (singlets, 2 CH_3).

1,2-*O*-Isopropylidene-3, 5, 6-*O*-orthoacetyl-α-D-glucofuranose was converted to 6-*O*-acetyl-1,2-*O*-isopropylidene-α-D-glucofuranose by treatment with aqueous acid. The orthoester (200 mg) was dissolved in chloroform (15 ml) and 4 drops of 4 *N* HCl added. A crystalline precipitate appeared after 15 min and the reaction was complete in about 30 min (t.l.c.). The crystalline precipitate was dissolved in chloroform, shaken with K_2CO_3, filtered, and concentrated. After recrystallization from chloroform–ether, 6-*O*-acetyl-1,2-*O*-isopropylidene-α-D-glucofuranose (150 mg) with m.p. 146° and $[\alpha]_D$ −5.1° (*c*, 1.0 EtOH) was obtained, (lit. m.p. 146° and $[\alpha]_D$ −6.3° (24).

Anal. Calcd. for $C_{11}H_{18}O_7$: C, 50.38; H, 6.87. Found: C, 50.28; H, 6.98.

The infrared spectrum of this product shows hydroxyl and carbonyl absorptions at 3500 and 1810 cm^{-1}, respectively. Proton magnetic resonance data (DMSO-d_6): 3.85 (doublet, $J = 4$ c.p.s., anomeric H); 4.46, 4.68 (2 doublets, 2 secondary hydroxyls); 7.59 (singlet, CH_3CO—); 8.23, 8.38 (singlets, 2 CH_3).

*Hydrogenolysis of 1,2-O-Isopropylidene-3,5,6-O-orthoacetyl-α-D-glucofuranose (**10**)*

The crude hydrogenolysis product obtained from the orthoacetate consisted of two components (t.l.c. in chloroform–acetone 1:1, v/v, and g.l.c. (silicone nitrile gum) of the acetate). The syrupy minor component comprising about 15% of the mixture is an *O*-ethoxyl derivative of 1,2-*O*-isopropylidene-α-D-glucofuranose as indicated by its p.m.r. spectrum. The major component (80–85%) obtained after silicic acid column chromatography (solvent: chloroform–acetone, 1:1, v/v) was crystallized from chloroform–*n*-hexane and was identified as 3,5-*O*-ethylidene-1,2-*O*-isopropylidene-α-D-glucofuranose (**11**; **45**) with m.p. 101–102° and $[\alpha]_D$ +21° (*c*, 1.0 in ethanol).

Anal. Calcd. for $C_{11}H_{18}O_6$: C, 53.65; H, 7.38. Found: C, 53.87; H, 7.47.

Proton magnetic resonance data (in DMSO-d_6): 3.74 (doublet $J = 4$ c.p.s., anomeric H), 4.62 (quartet, CH of —$OCH(CH_3)O$—), 4.78 (triplet, primary OH) at 70°, 8.20 (singlet, CH_3), 8.34 (singlet, CH_3), 8.49 (doublet, CH_3 of —$OCH(CH_3)O$—).

Treatment of the product with 50% HI (20 min, 100°) gave glucose. The p.m.r. spectrum of the product is identical with that of 3,5-*O*-ethylidene-1,2-*O*-isopropylidene-α-D-glucofuranose prepared by shaking 1,2-*O*-isopropylidene-6-*O*-formyl-α-D-glucofuranose (500 mg) with paraldehyde (10 ml) and 1 drop of concentrated H_2SO_4 for 45 min. Chloroform was added to this mixture, which was then shaken with K_2CO_3, filtered, evaporated to a syrup, and treated with $LiAlH_4$ in ether. The resulting product was purified by silica gel column chromatography (solvent: chloroform–acetone, 1:1, v/v) and crystallization from chloroform–hexane gave 3,5-*O*-ethylidene-1,2-*O*-isopropylidene-α-D-glucofuranose (50 mg).

The 6-acetate was prepared, m.p. 75–76°; p.m.r. data (in $CDCl_3$): 4.00 (doublet, anomeric H); 5.05 (quartet, CH of —$OCH(CH_3)O$—); 7.92 (singlet, —$OCCH_3$); 8.52, 8.68 (singlets, 2 CH_3); 8.72 (doublet, $J = 5$ c.p.s., CH_3 of $CH_3CH(O)O$).

*Hydrogenolysis of 1,2-5,6-Di-O-isopropylidene-α-D-glucofuranose (**12**)*

The crude reaction products obtained by treating the di-*O*-isopropylidene derivative with $LiAlH_4$–$AlCl_3$ had one main component (t.l.c. and g.l.c. of the acetate) which comprised 60–75% of the mixture. It was obtained by fractionation of the reaction product by silica gel column chromatography (solvent: $CHCl_3$–acetone, 1:1, v/v), crystallized from hexane, and identified as 1,2-*O*-isopropylidene-6-*O*-isopropyl-α-D-glucofuranose (**13**) with m.p. 60–63°. After two recrystallizations from hexane the m.p. was 65–66° (lit. 65–67° (25)); $[\alpha]_D$ +5° (*c*, 1.0 $CHCl_3$); lit. +6.6° (25).

Anal. Calcd. for $C_{12}H_{22}O_6$: C, 54.96; H, 8.39. Found: C, 54.68; H, 8.43.

Proton magnetic resonance data (in DMSO-d_6): 4.26 (doublet, $J = 4$ c.p.s., anomeric H), 4.96 and 5.42 (2 doublets, 2 OH), 8.65 and 8.79 (2 singlets, 2 CH_3), 8.91 (doublet 2 CH_3).

A small quantity (50 mg) of the principal product on hydrolysis with *N* sulfuric acid (6 h, 100°) afforded a crystalline compound (20 mg) with m.p. 120–122° (lit. 123° (25)), which was indistinguishable from 6-*O*-iso-

Can. J. Chem. Downloaded from www.nrcresearchpress.com by 210.87.254.42 on 09/05/12
For personal use only.

propyl-D-glucose (11) on a paper chromatogram. Treatment of 1,2-*O*-isopropylidene-6-*O*-isopropyl-α-D-glucofuranose with 50% HI (20 min, 100°) gave glucose.

*Hydrogenolysis of 1,2-5,6-Di-O-cyclohexylidene-α-D-glucofuranose (**14**)*

Silicic acid column chromatography (solvent: chloroform–acetone, 1:1, v/v) of the crude hydrogenolysis product gave a syrupy major component 1,2-*O*-cyclohexylidene-6-*O*-cyclohexyl α-D-glucofuranose (**15**); 70–80% of the crude product) with $[\alpha]_D$ −3.7° (*c*, 0.5 EtOH).

Anal. Calcd. for $C_{18}H_{30}O_6$: C, 63.15; H, 8.76. Found: C, 62.88; H, 8.86.

The syrupy material (80 mg) was hydrolyzed with *N* H_2SO_4 (5 h, 100°), neutralized ($BaCO_3$), filtered, and evaporated to 6-*O*-cyclohexyl-D-glucose (45 mg) which, from methanol–water, had m.p. 111–113° (lit. 115–117° (11)). On oxidation with sodium metaperiodate in D_2O for 16 h, p.m.r. examination indicated 4 formic acid protons (1.16) and 11 cyclohexyl protons (7.4–8.4).

Syrupy 1,2-*O*-cyclohexylidene-6-*O*-cyclohexyl-α-D-glucofuranose was converted to crystalline 1,2-*O*-cyclohexylidene-6-*O*-cyclohexyl-3,5-*O*-methylene-α-D-glucofuranose. A portion (200 mg) was mixed with a solution of anhydrous potassium *t*-butoxide (600 mg) in *t*-butanol (5 ml) and toluene (5 ml). This was followed by the addition of dichloromethane (2 ml) and benzene (50 ml). The resulting mixture was refluxed under anhydrous conditions for 3 days, during which another 5 ml of dichloromethane and potassium *t*-butoxide (800 mg) were added. The mixture was then cooled, washed with excess of water, dried (K_2CO_3), filtered, and evaporated to dryness. The product was chromatographed on a column of silicic acid (solvent: chloroform) and the fast-moving fraction (30 mg) crystallized from chloroform – *n*-hexane. 1,2-*O*-Cyclohexylidene-6-*O*-cyclohexyl-3,5-*O*-methylene-α-D-glucofuranose, thus obtained, had m.p. 86° and $[\alpha]_D$ +23° (*c*, 0.6 $CHCl_3$).

Anal. Calcd. for $C_{19}H_{30}O_6$: C, 64.40; H, 8.47. Found: C, 64.36; H, 8.57.

Proton magnetic resonance data (in $CDCl_3$): 4.00 (doublet, $J_{1,2}$ = 4 c.p.s., anomeric H), 4.83 (doublet, J = 6 c.p.s., H of —OCH_2O—), 5.23 (doublet, J = 6 c.p.s., H of —OCH_2O—), 5.48 (doublet, J = 4 c.p.s. H_2), 8.00–8.80 (21 cyclohexyl protons).

*Hydrogenolysis of 5,6-O-Benzylidene-1,2-O-isopropylidene-α-D-glucofuranose (**16**)*

Reaction with $LiAlH_4$–$AlCl_3$ gave a crude product, which on silicic acid column chromatography (solvent: chloroform–acetone, 1:1, v/v) afforded a fastest-moving fraction (**17**; 55–65% of the crude reaction product). Proton magnetic resonance data (in DMSO-d_6): 2.30 (multiplet, aromatic H), 3.84 (doublet, $J_{1,2}$ = 4 c.p.s., anomeric H), 4.50 (doublet, secondary OH), 4.80 (doublet, secondary OH), 5.10 (singlet, *O*-benzyl), 8.26 (singlet, CH_3), 8.40 (singlet, CH_3).

*Preparation of Methyl 2,3-4,6-Di-O-methylene-α-D-mannopyranoside (**41**)*

To a suspension of methyl α-D-mannopyranoside (4 g) in acetic acid (20 ml), paraformaldehyde (5 g) and concentrated H_2SO_4 (4 drops) were added and the mixture heated at 100° for 1 h. The resulting solution was cooled, mixed with chloroform and cold water, and the aqueous portion extracted with chloroform. The combined extract was washed several times with water, dried (K_2CO_3), and concentrated to a crystalline residue. Three recrystallizations from methanol gave 600 mg of pure di-*O*-methylene derivative. Alternately, silicic acid column chromatography (solvent: chloroform) of the crude reaction product (3 g) afforded a fastest-moving fraction which was crystallized from methanol. The methyl 2,3-4,6-di-*O*-methylene-α-D-mannopyranoside (**41**; 1 g) had m.p. 144–146°, $[\alpha]_D$ +19° (*c*, 1.0 EtOH).

Anal. Calcd. for $C_9H_{14}O_6$: C, 49.54; H, 6.47. Found: C, 49.64; H, 6.54.

Its i.r. spectrum does not show hydroxyl absorption, and g.l.c. (2% neopentyl glycol succinate column) gave a single peak. Proton magnetic resonance data (in $CDCl_3$): 4.75 (singlet, anomeric H), 4.92 and 5.34 (2 doublets, —OCH_2O— protons of six-membered ring). 4.98 (doublet, —OCH_2O— protons of five-membered ring), 6.60 (singlet, OCH_3).

*Preparation of Methyl 2,6-Di-O-methyl-α-D-mannopyranoside (**42**) from Methyl 2,3-4,6-Di-O-methylene-α-D-mannopyranoside (**41**)*

Reaction with $LiAlH_4$–$AlCl_3$ was carried out according to the general procedure. After 3 days another addition of the same amount of reagents was made. The reaction was discontinued after 7 days and worked up in the usual way. Silicic acid column chromatography (solvent: chloroform; followed by chloroform–acetone, 1:1, v/v) on a 1.3 g sample gave three fractions.

Fraction A (500 mg), the fastest moving component, crystallized from methanol and was identified as the unreacted material.

Fraction B (syrup, 300 mg) appeared to be a mixture of two mono-*O*-methylene-mono-*O*-methyl derivatives of methyl α-D-mannopyranoside on the basis of g.l.c. (2% neopentyl glycol succinate column) and its p.m.r. spectrum.

Fraction C (syrup, 330 mg) was homogeneous on t.l.c. and g.l.c. (2% neopentyl glycol succinate at 190°). The consumption of periodate and its p.m.r. spectrum are consistent with a methyl 2,6-di-*O*-methyl-α-D-mannopyranoside structure.

Anal. Calcd. for $C_9H_{18}O_6$: C, 48.64; H, 8.16. Found: C, 48.12; H, 8.16.

Proton magnetic resonance data ($CDCl_3$): 5.23 (doublet, $J_{1,2}$ = 2 c.p.s., anomeric H); 6.56, 6.62, and 6.65 (singlets 3 —OCH_3). The product had $[\alpha]_D$ +71° (*c*, 1.0 EtOH) and on treatment with 50% HI (100°, 20 min) gave mannose.

Hydrogenolysis of Several Methyl O-Benzylidene-hexoside Derivatives

*(1) Methyl 4,6-O-Benzylidene-α-D-galactopyranoside (**24**)*

Reductive cleavage of methyl 4,6-*O*-benzylidene-α-D-galactopyranoside afforded a crude mixture which consisted of one major component and a minor fraction in addition to some unreacted material, as revealed by t.l.c. (solvent: chloroform–acetone, 1:1, v/v). The major component, methyl 6-*O*-benzyl-α-D-galactopyranoside (**25**), was fractionally crystallized from chloroform–acetone (1:1). Two further recrystallizations from

chloroform–hexane gave a product with m.p. 138–140° and $[\alpha]_D$ +116° (*c*, 1.0 EtOH), lit. m.p. 142–144° and $[\alpha]_D$ +113° (26).

Anal. Calcd. for $C_{14}H_{20}O_6$: C, 59.15; H, 7.00. Found: C, 58.81; H, 6.77.

Its p.m.r. data (in DMSO-d_6): 2.25 (multiplet, 5 aromatic H), 5.04 (doublet, J = 3 c.p.s., anomeric H), 5.08 (singlet, 2H, *O*-benzyl), 6.30 (singlet, anomeric OCH_3), OH signals obscured by other signals. Oxidation with sodium metaperiodate in D_2O liberated formic acid (p.m.r. spectrum) consistent with a methyl 6-*O*-benzyl-α-D-galactopyranoside structure.

*(2) Methyl 2,3-Di-O-benzyl-4,6-O-benzylidene-β-D-glucopyranoside (**29**)*

Methyl 2,3-di-*O*-benzyl-4,6-*O*-benzylidene-β-D-glucopyranoside, on treatment with $LiAlH_4$–$AlCl_3$ reagent, gave mainly one reaction product and only traces of another component. The principal component obtained after purification of the crude reaction product by silicic acid column chromatography (solvent: chloroform–acetone, 1:1, v/v) was crystallized from chloroform–hexane to give methyl 2,3,4-tri-*O*-benzyl-β-D-glucopyranoside (**30**) with m.p. 74–76°. After being recrystallized from 90% methanol it had m.p. 83–85° and $[\alpha]_D$ +8.5° (*c*, 1.0 $CHCl_3$), lit. m.p. 90–91° and $[\alpha]_D$ +10° (27).

Anal. Calcd. for $C_{28}H_{32}O_6$: C, 72.40; H, 6.94. Found: C, 72.40; H, 6.74.

Proton magnetic resonance data (in $CDCl_3$): 2.70 (multiplet, 15 aromatic H), 5.64 (doublet, J = 7 c.p.s. anomeric H), 6.43 (singlet, anomeric OCH_3), 8.10 (triplet, J = 6 c.p.s., primary OH).

*(3) Methyl 4,6-O-Benzylidene-α-D-mannopyranoside (**31**)*

Hydrogenolysis of methyl 4,6-*O*-benzylidene-α-D-mannopyranoside gave a reaction product containing mainly one component in addition to the unreacted material. After removal of starting material by silicic acid column chromatography (solvent: chloroform–acetone, 1:1, v/v), the main reaction product (syrup) could not be further resolved. Its p.m.r. spectrum (in DMSO-d_6) at room temperature and at 70° showed two doublets and one triplet assigned to three hydroxyl groups. However, the spectrum indicated the presence of a minor component in this syrup. Sodium metaperiodate was added to this sample in D_2O and after 14 h a trace signal at 1.24 for formic acid was observed. Integration and correlation with the aromatic protons with the signal due to formic acid indicates that at least 80% of the syrup was methyl 4-*O*-benzyl-α-D-mannopyranoside (**32**).

*(4) Methyl 2,3-5,6-Di-O-benzylidene-α-D-mannofuranoside (**18**)*

Hydrogenolysis of methyl 2,3-5,6-di-*O*-benzylidene-α-D-mannofuranoside gave a syrup free from any unreacted material. Thin-layer chromatography (solvent: chloroform–acetone, 1:1, v/v) showed the presence of trace amounts of other components which were removed by silicic acid column chromatography. The purified syrupy material did not have any *O*-benzylidene group, as revealed by its p.m.r. spectrum. A portion (30%) crystallized out from the syrup and was recrystallized twice from chloroform – *n*-hexane. The uncharacterized crystalline methyl di-*O*-benzyl-α-D-mannofuranoside had m.p. 74–76° and $[\alpha]_D$ +100° (*c*, 1.0 EtOH).

Anal. Calcd. for $C_{21}H_{26}O_6$: C, 67.37; H, 6.95. Found: C, 67.08; H, 6.90.

*(5) Methyl 2,3-4,6-Di-O-benzylidene-α-D-mannopyranoside (**21**)*

Hydrogenolysis of methyl 2,3-4,6-di-*O*-benzylidene-α-D-mannopyranoside gave a mixture of two compounds which was chromatographed on a silicic acid column (solvent: chloroform–acetone 1:1). The faster moving syrupy component, which comprised 80% of the mixture had $[\alpha]_D$ +38° (*c*, 1.0 EtOH) and p.m.r. data (in DMSO-d_6): 2.1–2.4 (multiplet, 10 aromatic H), 3.86 (singlet, *O*-benzylidene H), 4.40 (doublet, J = 5 c.p.s., secondary OH), 5.00 (superimposed signals, 3H, *O*-benzyl and anomeric H), 6.36 (singlet, anomeric OCH_3). Treatment of the above compound (100 mg) with 3% methanolic hydrogen chloride (reflux 7 h) afforded a syrup (60 mg) which was resistant to periodate oxidation. Proton magnetic resonance data (in DMSO-d_6): 2.1–2.4 (multiplet, 10 aromatic H), 4.74 (doublet, J = 5 c.p.s., secondary OH), 4.88 (doublet, J = 5 c.p.s., secondary OH), 5.18 (triplet, J = 6 c.p.s., primary OH), 5.00 (doublet, *O*-benzyl), 5.07 (doublet, J = 2 c.p.s., anomeric), 6.38 (singlet, anomeric OCH_3). Hydrolysis of the hydrogenolyzed material (N H_2SO_4, 6 h, 100°) gave a product which consumed 0.9 mole/mole of lead tetraacetate after 2, 5, and 10 min reaction (28) thus showing the principal hydrogenolysis product to be methyl 4,6-*O*-benzylidene-3-*O*-benzyl-α-D-mannopyranoside (**22**).

*(6) Methyl 4,6-O-Benzylidene-α-D-glucopyranoside (**26**)*

After removal of the unreacted starting material by silicic acid column chromatography (solvent: chloroform–acetone, 2:1, v/v) the crude reaction product could not be further resolved. On periodate oxidation, the mixture gave 0.4 mole of formic acid per mole of methyl mono-*O*-benzyl-α-D-glucopyranoside corresponding to a 3:2 mixture of the 4-*O*- (**27**) and 6-*O*-benzyl (**28**) isomers, respectively.

*(7) Hydrogenolysis of 3,5-O-Benzylidene-1,2-O-isopropylidene-α-D-glucofuranose (**19**)*

The crude reaction product consisted of one main component (ca. 75%) which was purified through silicic acid column chromatography (solvent: chloroform–acetone 1:1, v/v). Proton magnetic resonance data (in DMSO-d_6) of the purified syrup: 2.15–2.40 (multiplet, aromatic H), 3.78 (doublet, J = 4 c.p.s., anomeric H), 4.84 (*O*-benzyl H), 5.00–5.40 (a doublet and a triplet appeared at 70° corresponidng to a secondary and primary OH respectively), 8.18 (singlet, CH_3), 8.32 (singlet, CH_3). The syrupy material was oxidized completely by periodate indicating a 3-*O*-benzyl-1,2-*O*-isopropylidene-α-D-glucofuranose structure (**20**).

*Hydrogenolysis of Methyl 4,6-O-Ethylidene-2,3-O-oxydiethylidene-α-D-glucopyranoside (**34**)*

Two equal fractions were obtained by silicic acid column chromatography (solvent: chloroform–acetone, 1:1, v/v) of the mixed hydrogenolysis product. Fraction *A* could be identified as methyl 4,6-*O*-ethylidene-α-D-glucopyranoside (**35**). The fastest-moving fraction *B*, methyl 3-*O*-ethyl-4,6-*O*-ethylidene-α-D-glucopyranoside (**36**) could be crystallized from chloroform – *n*-hexane, m.p. 136–138° and $[\alpha]_D$ +140° (*c*, 1.0 EtOH).

Can. J. Chem. Downloaded from www.nrcresearchpress.com by 210.87.254.42 on 09/05/12
For personal use only.

Can. J. Chem. Downloaded from www.nrcresearchpress.com by 210.87.254.42 on 09/05/12
For personal use only.

Anal. Calcd. for $C_{11}H_{20}O_6$: C, 53.22; H, 8.06. Found: C, 53.13; H, 8.01.

Proton magnetic resonance data (in DMSO-d_6): 4.68 (doublet, $J = 6$ c.p.s., secondary OH), 5.08 (doublet, $J = 3$ c.p.s., anomeric H), 4.94 (quartet, CH of $CH_3CH\begin{smallmatrix}O\\O\end{smallmatrix}$), 6.24 (singlet, anomeric OCH_3), 8.44 (doublet, $J = 5$ c.p.s., CH_3), 8.54 (triplet, $J = 7$ c.p.s CH_3).

Treatment of the compound with 3% methanolic hydrogen chloride (reflux 100°, 7 h) afforded methyl 3-*O*-ethyl-α-D-glucopyranoside, crystallized from acetone, m.p. 139–141° and $[\alpha]_D$ +56° (*c*, 1.2 EtOH).

Anal. Calcd. for $C_9H_{18}O_6$: C, 48.64; H, 8.16. Found: C, 49.06; H, 8.55.

It did not consume periodate and the p.m.r. spectrum is consistent with the designated structure. Hydrolysis of methyl 3-*O*-ethyl-α-D-glucopyranoside with *N* H_2SO_4 (6 h, 100°) gave 3-*O*-ethyl-D-glucose which crystallized from acetone with m.p. 134–135° and $[\alpha]_D$ +25 → +60° (*c*, 0.6 H_2O); lit. m.p. 137–138° and $[\alpha]_D$ +26.1 → +55.2° (29). Oxidation of this compound with lead tetraacetate (28) for 5 min and examination by paper chromatography showed a faster-moving pink spot without any starting material.

*Hydrogenolysis of Methyl 4,6-O-Ethylidene-α-D-glucopyranoside (**35**) and of Methyl 4,6-O-Propylidene-α-D-glucopyranoside*

In each case, two components were obtained (approximately in equal amounts) as revealed by t.l.c. No satisfactory fractionation could be achieved in either case, since they had almost identical R_f values. However, small quantities of products were isolated (each was slightly contaminated by the other) by silicic acid column chromatography (chloroform–acetone 1:1, v/v). Tentative structural assignments were made as shown in Table I.

*Hydrogenolysis of 1,2-3,5-Di-O-methylene-α-D-glucofuranose (**39**)*

Thin-layer chromatography (solvent: chloroform–acetone, 1:1, v/v) of the crude reaction mixture after hydrogenolysis revealed the presence of mainly one component along with about 80% of the unreacted material. After being fractionated by silicic acid column chromatography (solvent: chloroform–acetone, 2:1, v/v) the reaction product could be crystallized from hexane with m.p. 90–92°. Proton magnetic resonance data (in DMSO-d_6): 3.82 (doublet, $J = 4$ c.p.s., anomeric H), 4.66 (doublet, $J = 4$ c.p.s., —OCH_2O), 5.02 (doublet, $J = 5$ c.p.s., secondary OH), 5.24 (triplet, $J = 6$ c.p.s., primary OH), 6.24 (singlet, OCH_3). On oxidation with periodate it gave formaldehyde, thus indicating a 3-*O*-methyl-1,2-*O*-methylene-α-D-glucofuranose structure (**40**).

Reaction of 1,2-O-Cyclohexylidene-3,5,6-O-orthoformyl-α-D-glucofuranose with $LiAlD_4$–$AlCl_3$ (1:1)

The crude reaction product consisted of mainly one component as revealed by t.l.c. and g.l.c. The product crystallized from chloroform – *n*-hexane had m.p. 68–70° and $[\alpha]_D$ +23° (*c*, 1.0 EtOH).

Anal. Calcd. for $C_{13}H_{19}DO_6$: C, 57.14; H + D, 7.69. Found: C, 56.96; H + D, 7.23.

Proton magnetic resonance data ($CDCl_3$): 4.00 (doublet, $J_{1,2} = 4$ c.p.s., anomeric H); 5.20 (singlet, *O*-deuteromethylene H); 6.80 (triplet, $J = 5$ c.p.s., primary OH).

Reaction of 1,2-O-Isopropylidene-3,5,6-O-orthoformyl-α-D-glucofuranose with $LiAlD_4$–$AlCl_3$ (1:1)

Equimolar quantities of the starting material, $LiAlD_4$, and $AlCl_3$ were reacted according to the general procedure for 75 min (Table II). Thin-layer chromatography and g.l.c. showed only one principal product (**43**) which was crystallized from chloroform – *n*-hexane with m.p. 66–68° and $[\alpha]_D$ +26° (*c*, 1.0 EtOH).

Anal. Calcd. for $C_{10}H_{15}DO_6$: C, 51.50; H + D, 7.29. Found: C, 51.49; H + D, 6.96.

Proton magnetic resonance data (in $CDCl_3$): 4.00 (doublet, $J_{1,2} = 4$ c.p.s., anomeric H); 5.18 (singlet, *O*-deuteromethylene H); 8.12 (triplet, primary OH); 8.48 and 8.64 (singlets, 2 CH_3).

Acknowledgments

The authors wish to thank Mr. M. Mazurek for preparation of p.m.r. spectra and Mr. W. C. Haid for microanalytical determinations.

1. E. L. Eliel, V. G. Badding, and M. N. Rerick. J. Am. Chem. Soc. **84**, 2371 (1962).
2. E. L. Eliel, L. A. Pilato, and V. G. Badding. J. Am. Chem. Soc. **84**, 2377 (1962).
3. E. L. Eliel, B. E. Nowak, R. A. Daignault, and V. G. Badding. J. Org. Chem. **30**, 2441 (1965).
4. B. E. Leggetter and R. K. Brown. Can. J. Chem. **42**, 990 (1964).
5. B. E. Leggetter and R. K. Brown. Can. J. Chem. **41**, 2671 (1963).
6. U. E. Diner and R. K. Brown. Can. J. Chem. **45**, 2547 (1967).
7. B. E. Leggetter and R. K. Brown. Can. J. Chem. **43**, 1030 (1965).
8. B. E. Leggetter and R. K. Brown. Can. J. Chem. **42**, 1005 (1964).
9. W. W. Ziajac, Jr., B. Rhee, and R. K. Brown. Can. J. Chem. **44**, 1547 (1966).
10. A. N. de Belder. Advan. Carbohydrate Chem. **20**, 219 (1965).
11. P. A. J. Gorin. J. Org. Chem. **24**, 49 (1959).
12. B. E. Leggetter, U. E. Diner, and R. K. Brown. Can. J. Chem. **42**, 2113 (1964).
13. U. E. Diner and R. K. Brown. Can. J. Chem. **45**, 1297 (1967).
14. J. Delmau and J. Duplan. Tetrahedron Letters, No. 6, 559 (1966).
15. P. A. J. Gorin and T. Ishikawa. Can. J. Chem. **44**, 1787 (1966).
16. P. A. J. Gorin and T. Ishikawa. Can. J. Chem. **45**, 521 (1967).
17. E. L. Eliel and M. C. Knoeber. J. Am. Chem. Soc. **90**, 3444 (1968).
18. U. E. Diner, H. A. Davis, and R. K. Brown. Can. J. Chem. **45**, 207 (1967).
19. E. C. Ashby and J. Prather. J. Am. Chem. Soc. **88**, 729 (1966).
20. B. Lindberg. Arkiv. Kemi Mineral. Geol. Ser. B, **18**, (9), 1 (1944).

21. O. L. CHAPMAN and R. W. KING. J. Am. Chem. Soc. **86**, 1256 (1964).
22. N. BAGGETT, J. M. DUXBURY, A. B. FOSTER, and J. M. WEBBER. Carbohydrate Res. **1**, 22 (1965).
23. K. FREUDENBERG and W. JACOB. Ber. **80**, 325 (1947).
24. E. FISHER and H. NOTH. Ber. **51**, 321 (1918).
25. H. OHLE and K. TESSMAR. Ber. **71**, 1843 (1938).
26. C. E. BALLOU and H. O. L. FISCHER. J. Am. Chem. Soc. **76**, 3188 (1954).
27. N. PRAVDIC and D. KEGLEVIC. Tetrahedron, **21**, (7), 1897 (1965).
28. A. J. CHARLSON and A. S. PERLIN. Can. J. Chem. **34**, 1200 (1956).
29. W. GLEN, G. MYERS, and G. GRANT. J. Chem. Soc. 2568 (1951).

Can. J. Chem. Downloaded from www.nrcresearchpress.com by 210.87.254.42 on 09/05/12
For personal use only.

Identification of di-*O*-, tri-*O*-, and tetra-*O*-methylmannoses by gas–liquid chromatography[1]

S. S. BHATTACHARJEE[2] AND P. A. J. GORIN
Prairie Regional Laboratory, National Research Council of Canada, Saskatoon, Saskatchewan

Received November 28, 1968

Some di-*O*- and tri-*O*-methylmannoses which are unknown or difficult to prepare have been synthesized. These and the other isomers, which can arise from methylation–fragmentation analyses of mannofuranose- and mannopyranose-containing polysaccharides can be used as gas–liquid chromatographic (g.l.c.) standards. A system has been devised in which methylation fragments are fractionated on a cellulose column into di-*O*-, tri-*O*-, and tetra-*O*-methylmannose fractions, which are then analyzed individually by g.l.c. following conversion to suitable derivatives.

Canadian Journal of Chemistry, 47, 1207 (1969)

Can. J. Chem. Downloaded from www.nrcresearchpress.com by 210.87.254.105 on 09/05/12
For personal use only.

In recent studies 88 structurally different mannose-containing polysaccharides have been isolated from 294 yeast species and their proton magnetic resonance (p.m.r.) spectra (1–4) used as an aid in identification of the parent organisms. Since it was felt that further biochemical studies on yeasts containing mannans and galactomannans would be of interest, some of these polysaccharides were selected for structural analysis. Frequent use was made of the methylation–fragmentation technique, in which *O*-methylmannoses were obtained and identified by gas–liquid chromatography (g.l.c.) of suitable derivatives. For this purpose the di-*O*-, tri-*O*-, and tetra-*O*-methyl methylmannosides were used as standards and when they were unknown or not readily available, syntheses were carried out. The syntheses, described in the present publication, make use of lithium aluminium hydride – aluminium trichloride hydrogenolyses in a number of cases. This reagent cleaves *O*-methylene acetals to *O*-methyl ethers and also converts *O*-benzylidene acetals to *O*-benzyl ethers (5, 6), which can be used as intermediates in preparation of partly methylated mannoses.

Preparation of Partly Methylated Methylmannosides

Methyl 2,4-Di-O-methyl-αβ-D-mannopyranoside

Crude 1,6-anhydro-β-D-mannopyranose (7) was converted to its 2,3-*O*-benzylidene derivative (**1**) which was methylated to give 1,6-anhydro-2,3-*O*-benzylidene-4-*O*-methyl-β-D-mannopyranose (**4**). Hydrogenolysis with 1.2 molar equivalents of $LiAlH_4$–$AlCl_3$ (1:1) caused selective cleavage of the *O*-benzylidene ring giving 1,6-anhydro-3-*O*-benzyl-4-*O*-methyl-β-D-mannopyranose (**5**). Successive methylation, debenzylation, and acid methanolysis provided methyl 2,4-di-*O*-methyl-αβ-D-mannopyranoside (**7**) with a retention time (r.t.) of 17.0 min on a neopentyl–glycol succinate g.l.c. column maintained at 190°. The glycoside was separated from a by-product by silicic acid chromatography and since the derived free aldose was not attacked by lead tetraacetate, the possibility of 3,4-di-*O*-substitution was eliminated. Also the glycoside had a different g.l.c. retention time from the 3,4-isomer (8).

The crystalline by-product was unaffected by hot aqueous acid and had an elemental composition and p.m.r. spectrum corresponding to a tri-*O*-methyl derivative of an anhydromannitol. A hydroxyl group at C-3 was indicated by consecutive spin decoupling experiments starting with H-1. In an analogous hydrogenolysis 1,6-anhydro-2,3-*O*-benzylidene-β-D-mannose (**1**) was cleaved by $LiAlH_4$–$AlCl_3$ to 1,6-anhydro-3-*O*-benzyl-β-D-mannopyranose (**2**) and a smaller proportion of 1,5-anhydro-3-*O*-benzyl-D-mannitol (**3**). Structure **2** was assigned since hydrolysis gave 3-*O*-benzyl-D-mannose, which had the same R_f as authentic material on a paper chromatogram (6), and consumed lead tetraacetate, in contrast to the possible 2-*O*-isomer. Compound **3** was not hydrolyzed by hot aqueous acid and was not oxidized with periodate. Since a 1,5-anhydromannitol derivative with this structure is formed on hydrogenolysis of 1,6-anhydro-2,3-*O*-benzylidene-β-D-mannopyranose derivatives the by-product from 1,6-anhydro-2,3-*O*-benzylidene-4-*O*-methyl-β-D-mannopyranose (**4**) is probably 1,5-anhydro-2,4,6-tri-*O*-methyl-D-mannitol (**8**).

[1]Issued as NRCC No. 10585.
[2]NRCC Postdoctorate Fellow, 1967–1969.

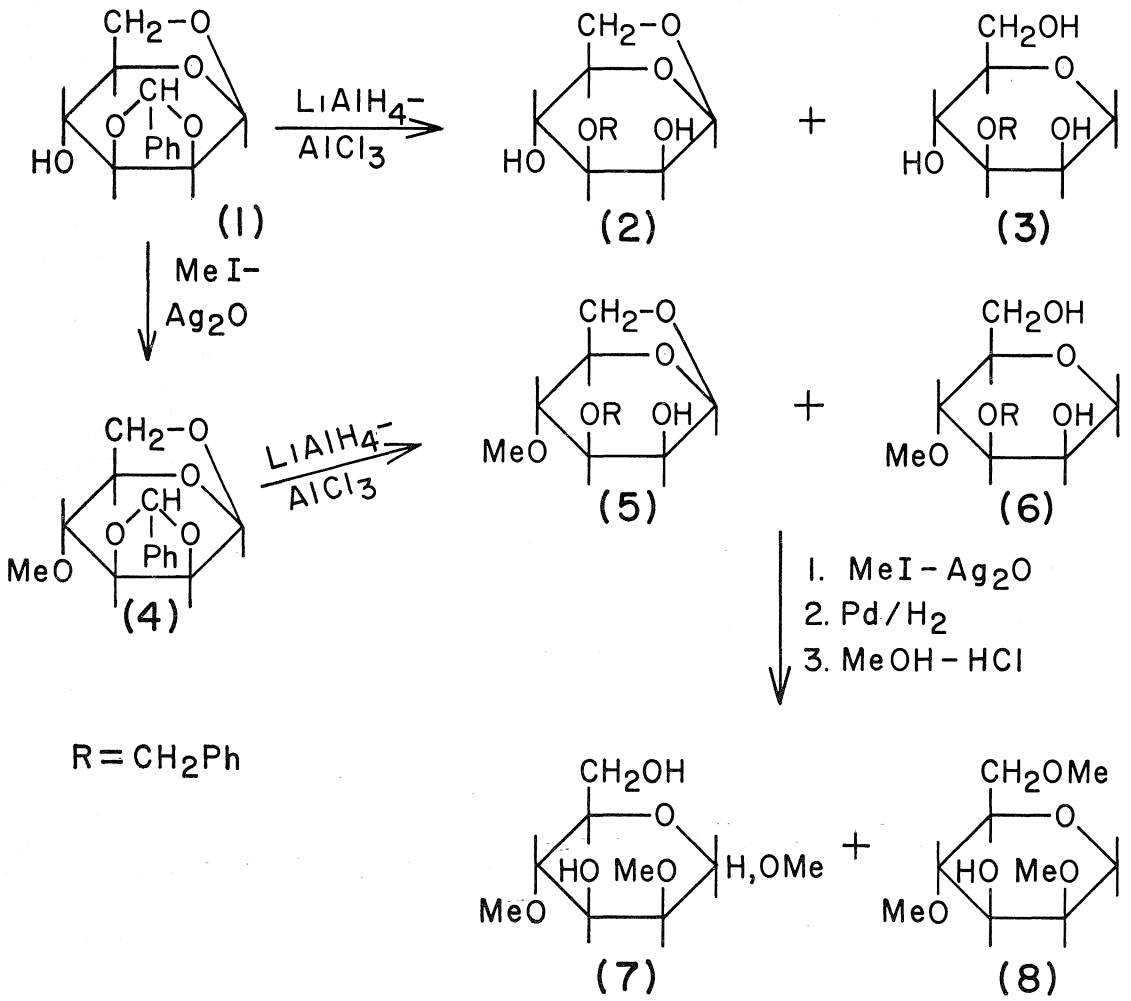

Methyl 5,6-Di-O-methyl-αβ-D-mannofuranoside

Methylation of D-mannose 2,3-carbonate (**9**, 9) with Purdie reagent gave crystalline methyl 2,3-*O*-carbonyl-5,6-di-*O*-methyl-α-D-mannofuranoside (**10**). It has an α-configuration since derived methyl 5,6-di-*O*-methyl-α-D-mannofuranoside has $[\alpha]_D$ +99°. The αβ-anomeric mixture (**11**; r.t. 15.3 min) was obtained from the glycoside by refluxing with methanolic hydrogen chloride. The possibility of 4,6-di-*O*-substitution is eliminated since the retention time of the glycosides on g.l.c. differs from that of methyl 4,6-di-*O*-methyl-αβ-D-mannopyranoside (r.t. 22.3 min).

3,5- and 2,5-Isomers of Methyl Di-O-methyl-αβ-D-mannofuranoside and Methyl 3,6-Di-O-methyl-αβ-D-mannopyranoside

Hydrogenolysis of methyl 2,3-5,6-di-*O*-benzylidene-α-D-mannofuranoside with $LiAlH_4$–$AlCl_3$ gives a crystalline methyl di-*O*-benzyl-α-D-mannofuranoside (**21**, 6). This compound has now been characterized as the 2,6-isomer since treatment with methanolic hydrogen chloride gave a methyl di-*O*-benzyl-αβ-D-mannopyranoside which consumed sodium periodate. The methyl 2,6-di-*O*-benzyl-αβ-D-mannopyranoside structure was confirmed by its conversion to methyl 3,4-di-*O*-methyl-αβ-D-mannopyranoside (g.l.c.

Can. J. Chem. Downloaded from www.nrcresearchpress.com by 210.87.254.105 on 09/05/12
For personal use only.

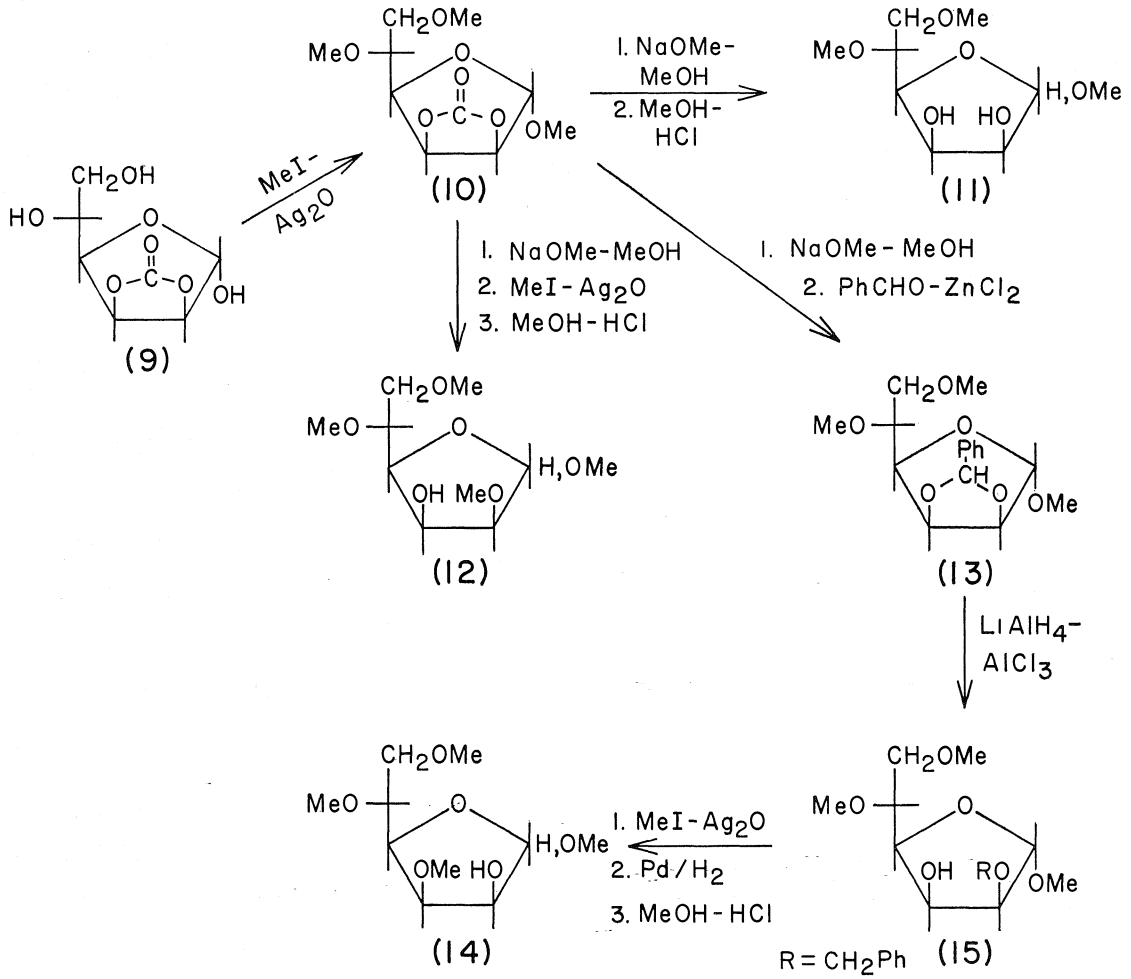

identification; r.t. 15.4 min) by methylation and subsequent debenzylation. Methyl 2,6-di-*O*-benzyl-α-D-mannofuranoside (**21**) was converted by the same procedure to methyl 3,5-di-*O*-methyl-α-D-mannofuranoside (α-anomer of **24**), which was then equilibrated to an αβ-anomeric mixture (**24**; r.t. 18.4 min) with methanolic hydrogen chloride.

The mother liquors, obtained following crystallization of methyl 2,6-di-*O*-benzyl-α-D-mannofuranoside, contained a mixture a portion of which (**21**, **22**, **23**) was treated with methanolic hydrogen chloride (to give **18**, **19**, **20**) and then subjected to methylation and subsequent debenzylation. Examination by g.l.c. showed 3 peaks, two of which corresponded to the 3,4- (**16**; r.t. 15.4 min) and 2,4-isomers (**7**; r.t. 17.0 min) of methyl di-*O*-methyl-αβ-D-mannopyranoside. No 2,6-isomer (r.t. 20.5 min; ref. 6) was detected. The material in the remaining peak (r.t. 14.0 min) was therefore methyl 3,6-di-*O*-methyl-αβ-D-mannofuranoside. The mixture of glycosides was treated with methanolic hydrogen chloride and one of the products, methyl 3,6-di-*O*-methyl-αβ-D-mannopyranoside (**17**; r.t. 19.3 min), could be differentiated from the other components, the 2,4- and 3,4-isomers, by g.l.c.

Another portion of the above mother liquors (**21**, **22**, **23**) was successively methylated and debenzylated yielding 3,6- (r.t. 14.0 min), 2,5- (r.t. 15.5 min), and 3,5-isomers (r.t. 18.4 min) of methyl di-*O*-methyl-α-D-mannofuranoside. The mixture, after reaction with methanolic hydrogen chloride, was resolved into 3 peaks on g.l.c. Two

Can. J. Chem. Downloaded from www.nrcresearchpress.com by 210.87.254.105 on 09/05/12
For personal use only.

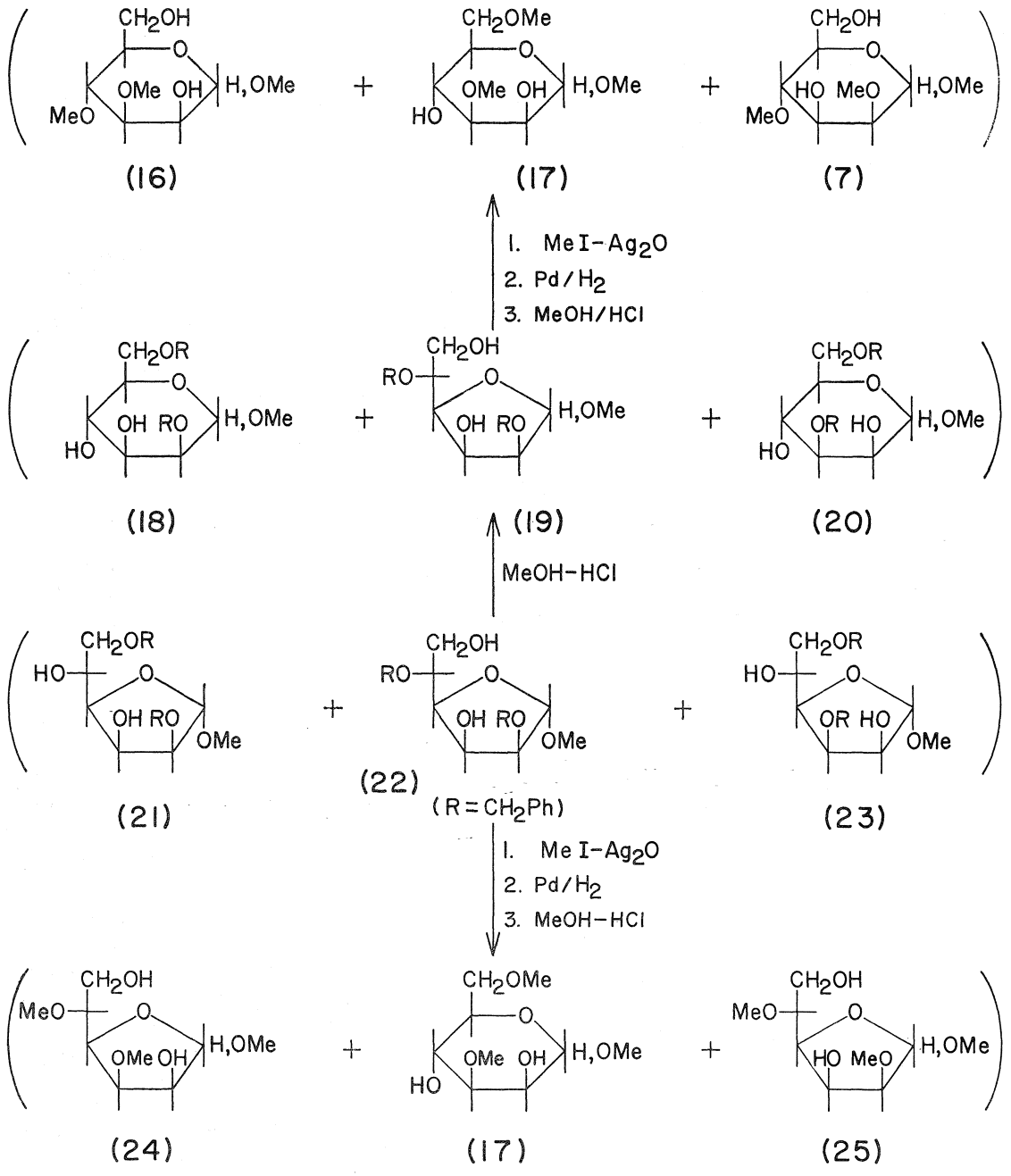

of the peaks were assigned to previously synthesized methyl 3,6-di-*O*-methyl-αβ-D-mannopyranoside (**17**; r.t. 19.3 min) and methyl 3,5-di-*O*-methyl-αβ-D-mannofuranoside (**24**; r.t. 18.4 min). The third peak (r.t. 15.5 min) thus corresponds to methyl 2,5-di-*O*-methyl-αβ-D-mannofuranoside (**25**).

Formation of the 2,6-, 2,4-, and 3,6-Isomers of Methyl Di-O-methyl-α-D-mannopyranoside

Hydrogenolysis of methyl 2,3,4,6-di-*O*-benzylidene-α-D-mannopyranoside (**26**; 6) with $LiAlH_4$–$AlCl_3$ gave a complex mixture from which three main fractions were obtained by silicic acid

Can. J. Chem. Downloaded from www.nrcresearchpress.com by 210.87.254.105 on 09/05/12
For personal use only.

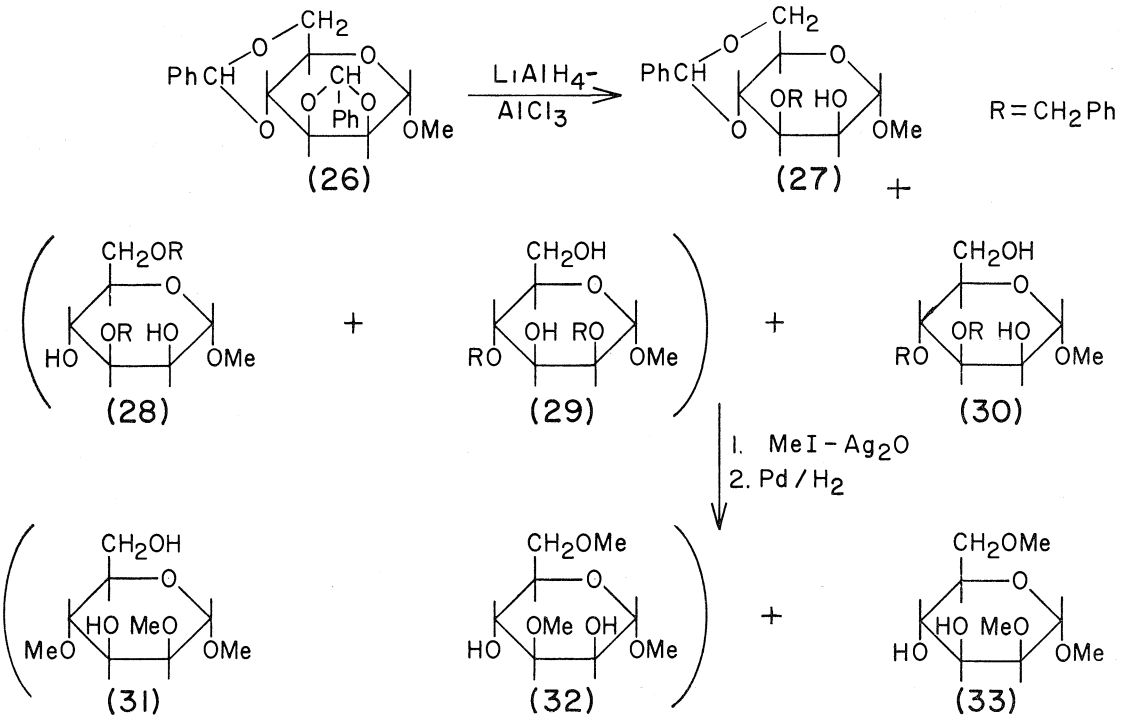

chromatography. The first fraction was identified as 3-*O*-benzyl-4,6-*O*-benzylidene-α-D-mannopyranoside (**27**) since successive methylation, methanolysis, and debenzylation gave methyl 2-*O*-methyl-α-D-mannopyranoside, which could be oxidized by sodium periodate. The second fraction contained two components, methyl 3,6-di-*O*-benzyl-α-D-mannopyranoside (**28**) and methyl 2,4-di-*O*-benzyl-α-D-mannopyranoside (**29**). Methylation of the mixture, followed by debenzylation gave methyl 2,4-di-*O*-methyl-α-D-mannopyranoside (**31**) and methyl 3,6-di-*O*-methyl-α-D-mannopyranoside (**32**) in a 2:1 ratio (g.l.c.). The last fraction contained methyl 3,4-di-*O*-benzyl-D-mannopyranoside (**30**) since methylation followed by debenzylation gave a product corresponding to methyl 2,6-di-*O*-methyl-α-D-mannopyranoside (**33**; 6) on g.l.c.

*Methyl 2,5,6-Tri-O-methyl-*αβ-D-*mannofuranoside*

Partial methylation of methyl 5,6-di-*O*-methyl-α-D-mannofuranoside (α-anomer of **11**) with Purdie reagent resulted in preferential substitution at OH-2. The product was hydrolyzed and the tri-*O*-methyl fraction separated from 5,6-di-*O*-methyl- and 2,3,5,6-tetra-*O*-methylmannoses by cellulose column chromatography. The tri-*O*-methylmannose fraction consumed 0.14 mole/mole of lead tetraacetate indicating that 2,5,6-tri-*O*- and 3,5,6-tri-*O*-methyl-D-mannose were present in a ratio of 6:1. The 2,5,6-isomer crystallized and was converted to its methyl glycosides (**12**; r.t. at 160°, 18.4 min) by treatment with methanolic hydrogen chloride.

*Methyl 3,5,6-Tri-O-methyl-*αβ-D-*mannofuranoside*

Methyl 5,6-di-*O*-methyl-D-mannofuranoside (α-anomer of **11**) was converted to its 2,3-*O*-benzylidene derivative (**13**) which was hydrogenolyzed with $LiAlH_4$–$AlCl_3$ to methyl 2-*O*-benzyl-5,6-di-*O*-methyl-α-D-mannofuranoside (**15**). This compound was resistant to methylation with the Purdie reagent, but the Kuhn procedure proved successful. The methylated product was debenzylated and the glycoside hydrolyzed giving a mixture of 2,5,6- and 3,5,6-tri-*O*-methyl-D-mannoses, which was fractionated by cellulose column chromatography. The methyl glycosides of the 3,5,6-isomer (**14**) had the same g.l.c. retention time as methyl 2,5,6-tri-*O*-methyl-αβ-D-mannofuranoside (**12**), both as the free glycoside and the trimethylsilyl (TMS) derivative. Fortunately,

Can. J. Chem. Downloaded from www.nrcresearchpress.com by 210.87.254.105 on 09/05/12
For personal use only.

TABLE I

Retention times of derivatives of partially methylated mannoses

Position of *O*-methyl substitution of methylmannoside	Reference to free aldose	Ring type*‡	Retention times (min) at column temperature		
			190°	160°	136° (TMS derivatives)
3,6-	—	f	14.0	—	32.2
5,6-	—	f	15.3	—	38.2
3,4-	17	p	15.4	—	18.4
2,5-	—	f	15.5	—	32.7
2,6-†	—	f	15.6	—	30.0
2,4-	—	p	17.0	—	24.6
3,5-	—	f	18.4	—	35.2
3,6-	—	p	19.3	—	23.0
2,6-	6	p	20.5	—	38.4
4,6-	18	p	22.3	—	21.8
2,3-	19	p	24.2	—	25.7
2,5,6-	—	f	7.1	18.4	29.0
3,5,6-	10	f	7.1	18.4	29.0
2,3,4-	20	p	7.8	20.7	24.2
3,4,6-	17	p	7.9	21.2	17.2
2,4,6-	17	p	8.7	25.3	17.2
2,3,5-	21	f	—	30.0	35.2
2,3,6-	22	p	10.6	32.2	33.6
2,3,4,6-	23	p	—	11.0	29.4
2,3,5,6-	24	f	—	10.8	—
Position of *O*-methyl substitution of mannose					
2,5,6-		f	—	—	28.5
3,5,6-		f	—	—	30.8(20%), 36.1(80%)
2,3,4,6-		p	—	—	28.0(80%),§ 30.7(20%)
2,3,5,6-		f	—	—	33.0§
2,4-		p	—	—	27.0
3,5-		f	—	—	41.6(80%), 50.0(20%)
3,4-		p	—	—	19.8
2,6-		p	—	—	37.4(85%), 49.0(15%)
5,6-		f	—	—	42.6(85%), 56.6(15%)
2,3,4,6-Tetra-*O*-methylhexose derivative					
of glucose		p	—	—	20.2(46%), 22.3(54%)
of galactose		p	—	—	24.3(53%), 31.5(47%)

*p = pyranoside, f = furanoside.

†The synthesis of methyl 2,6-di-*O*-methyl α-D-mannofuranoside has not yet been published by us.

‡In cases where the methyl α-mannopyranoside derivative was available, no change of retention time was observed on conversion to the αβ-methyl glycosides.

§Since the proportion of α- to β-TMS ether can vary from one experiment to another, it is difficult to detect the furanoside in the presence of the pyranoside isomer. In cases where the furanoside is suspected the formaldehyde produced on periodate oxidation of the parent mannan should be estimated.

however, the TMS derivatives of 2,5,6- and 3,5,6-tri-*O*-methyl-D-mannose could be separated by g.l.c. Our assignments of the g.l.c. peaks of 3,5,6-tri-*O*-methylmannose and its derivatives corresponded to those obtained from another sample of this compound, which has been synthesized by Siddiqui by another route (10).

Gas–Liquid Chromatography Characterization of Di-O-, Tri-O-, and Tetra-O-mannoses and Derivatives

Partially methylated mannoses and their derivatives were gas chromatographed on a column of neopentylglycol succinate (12 ft), a packing used previously in the separation of partially methylated methylmannosides (8). Retention times of (*a*) methyl di-*O*-methylmannosides (190°) and TMS derivatives (136°), (*b*) methyl tri-*O*-methylmannosides (160°) and TMS derivatives (136°), and (*c*) TMS derivatives of tri-*O*-methyl and tetra-*O*-methylmannoses (136°) are recorded in Table I. Using these values a methylation–fragmentation experiment can be carried out on a mannan or mannose-containing polysaccharide

Can. J. Chem. Downloaded from www.nrcresearchpress.com by 210.87.254.105 on 09/05/12
For personal use only.

Can. J. Chem. Downloaded from www.nrcresearchpress.com by 210.87.254.105 on 09/05/12
For personal use only.

by individual g.l.c. analysis of the di-*O*-, tri-*O*-, and tetra-*O*-methylmannose fractions (obtained by cellulose column chromatography) following their conversion to suitable derivatives. The di-*O*-methylmannoses can be characterized by g.l.c. of both their methyl glycosides and the TMS derivatives of the methyl glycosides.[3] 2,3,4,6- and 2,3,5,6-Tetra-*O*-methylmannoses, although not separated as their methyl glycosides, can be distinguished as their TMS derivatives. All the methyl tri-*O*-methylmannosides that could arise from mannofuranose and mannopyranose units in polysaccharides can be identified by g.l.c. of the methyl glycosides and the corresponding TMS ethers, except for the 2,5,6- and 3,5,6-isomers, which can be distinguished by g.l.c. of the TMS ethers of the free aldoses.

Experimental

Hydrogenolyses with $LiAlH_4$–$AlCl_3$ (in equimolar amounts) were carried out by the general procedure described earlier (6). Methylations were carried out with silver oxide in refluxing iodomethane (13) until the product did not show hydroxyl absorption in the infrared (i.r.) at ca. 3600 cm^{-1}. Infrared spectra were recorded using a Perkin–Elmer Infracord model 21. *O*-Benzyl groups were removed by hydrogenolysis using 5% Pd on charcoal catalyst with ethanol as solvent. Methanolysis was effected by refluxing with 3% methanolic hydrogen chloride for 2 h. Proton magnetic resonance spectra were obtained with a Varian HA-100 spectrometer using tetramethylsilane as external standard and chemical shifts are expressed as τ values. The g.l.c. unit was of conventional design, with thermal conductivity detectors. The helium pressure was 36 p.s.i. and 2% neopentyl glycol succinate on Chromosorb W (80/100 mesh) in $\frac{1}{4}$ in. × 12 ft columns was used. Unless otherwise mentioned, the retention times given in this section refer to the values obtained at 190° for methyl di-*O*-methylmannosides with a flow rate of 55 ml per min, 160° for methyl tri-*O*-methylmannosides, and at 136° for tetramethylsilyl (TMS) ethers, with a flow rate of 60 ml/min at both these temperatures. Thin-layer chromatography (t.l.c.) was carried out on silica gel G (sulfuric acid spray). Evaporations were performed under reduced pressure and specific rotations determined at 25°. Paper chromatography was carried out on Whatman No. 1 filter paper; solvent *n*-butanol – ethanol – water (40:11:19 v/v/v); spray *p*-anisidine hydrochloride. Tetramethylsilyl derivatives were prepared according to the procedure of Sweeley *et al.* (14).

Synthesis of Methyl 2,4-Di-O-methyl-αβ-D-mannopyranoside

Treatment of 1,6-anhydro-β-D-mannopyranose with benzaldehyde and zinc chloride in a conventional manner gave crystalline 1,6-anhydro-2,3-*O*-benzylidene-β-D-mannopyranose (**1**) with m.p. 188–189° (from EtOAc) and $[\alpha]_D$ −78.8° (*c*, 1.0 $CHCl_3$).

Anal. Calcd. for $C_{13}H_{14}O_5$: C, 62.39; H, 5.64. Found: C, 62.5; H, 5.8.

Methylation of the above compound (500 mg) with Purdie reagent gave 1,6-anhydro-2,3-*O*-benzylidene-4-*O*-methyl-β-D-mannopyranose (**4**; 500 mg) which was crystallized from hexane, m.p. 92–93° and $[\alpha]_D$ −92° (*c*, 1.0 EtOH).

Anal. Calcd. for $C_{14}H_{16}O_5$: C, 63.62; H, 6.10. Found: C, 63.3; H, 6.4.

Hydrogenolysis of 1,6-anhydro-2,3-*O*-benzylidene-4-*O*-methyl-β-D-mannopyranose (450 mg) with 1.2 molar equivalents of the $LiAlH_4$–$AlCl_3$ (1:1) reagent for 3 h gave a product (420 mg) which could not be resolved at this stage. Successive methylation, debenzylation, and methanolysis of this material afforded a mixture (180 mg) of two compounds as revealed by t.l.c. (solvent: chloroform–acetone 2:1 v/v). Silicic acid column chromatography (solvent: chloroform–acetone, 2:1 v/v, followed by methanol) gave initially a crystalline minor component (**8**; 25 mg) with m.p. 68–70°.

Anal. Calcd. for $C_9H_{18}O_5$: C, 52.41; H, 8.80. Found: C, 52.7; H, 8.9.

This compound was unchanged by treatment with *N* sulfuric acid (6 h, 100°) and did not react with the *p*-anisidine hydrochloride spray.

The second fraction contained syrupy methyl 2,4-di-*O*-methyl-αβ-D-mannopyranoside (**7**; 70 mg) with $[\alpha]_D$ +47.6° (*c*, 1.0 EtOH). It appeared to be homogeneous by t.l.c. and g.l.c. (r.t. 17.0 min; r.t. of the TMS derivative, 24.6 min). Proton magnetic resonance data (in DMSO-d_6); 5.01 (doublet, J = 2 c.p.s.), anomeric H); 6.26, 6.30, and 6.40 (3 singlets, 3 OCH_3); 4.85 (doublet, secondary OH); 5.10 (triplet, primary OH). A spin decoupling experiment, starting at H-1, showed the absence of hydroxyl group at C-2. On hydrolysis with *N* H_2SO_4 (6 h, 100°) it gave 2,4-di-*O*-methylmannose, which was resistant to lead tetraacetate oxidation (15). It crystallized from EtOAc on seeding with a sample of di-*O*-methyl-D-mannose (11, 12) and had m.p. 120° and $[\alpha]_D$ +13.5° (*c*, 0.6 H_2O). The m.p. was undepressed on admixture with 2,4-di-*O*-methyl-D-mannose, previously considered to be 3,5-di-*O*-methyl-D-mannose by Adams, Bishop, and associates (11, 12). (These workers report $[\alpha]_D$ +14.5°.)

Anal. Calcd. for $C_8H_{16}O_6$: C, 46.15; H, 7.75. Found: C, 46.2; H, 7.7.

Hydrogenolysis of 1,6-Anhydro-2,3-O-benzylidene-β-D-mannopyranose

1,6-Anhydro-2,3-*O*-benzylidene-β-D-mannopyranose (**1**; 50 mg) was treated with $LiAlH_4$–$AlCl_3$ (2.5 molar equivalents) in the usual manner. After 12 h the reaction

[3]During the course of g.l.c. examination of our standards, a crystalline sample of di-*O*-methyl-D-mannose, considered to be 3,5-di-*O*-methyl-D-mannose by Adams, Bishop, and associates (11, 12) was supplied to us. On g.l.c. examination of the methyl glycoside and the TMS derivative of the methyl glycoside, however, it corresponded to 2,4-di-*O*-methylmannose. On further investigation other physical characteristics proved identical to our synthetic material. Our results therefore indicate that the structures of the polysaccharides of birch sap (11) and mannans from several *Candida* spp. (12) should be re-evaluated.

Can. J. Chem. Downloaded from www.nrcresearchpress.com by 210.87.254.105 on 09/05/12
For personal use only.

product (40 mg) was isolated and refluxed with 3% methanolic hydrogen chloride for 3 h. After neutralization, the resulting material could not be oxidized by periodate and on hydrolysis with *N* H_2SO_4 (100°, 6 h) two spots were obtained on t.l.c. (solvent: chloroform–acetone 2:1 v/v). The faster moving component (approximately 1 part) was resistant to periodate and did not give any color with *p*-anisidine hydrochloride spray. The slow moving fraction (approximately 4 parts) was identical with 3-*O*-benzyl mannose (6) (paper chromatogram) and could be oxidized by lead tetraacetate.

Hydrogenolysis of Methyl 2,3-4,6-Di-O-benzylidene-α-D-mannopyranoside

Methyl 2,3-4,6-di-*O*-benzylidene-α-D-mannopyranoside (**26**; 1.0 g) was treated with 2.1 molar equivalents of the $LiAlH_4$–$AlCl_3$ (1:1) reagent for 6 days in the usual manner and the resulting product fractionated by silicic acid column chromatography (solvent: chloroform–acetone, 2:1 v/v). Fractions 1 to 4 were obtained consecutively. *Fraction 1* (250 mg) was identified as methyl 3-*O*-benzyl-4,6-*O*-benzylidene-α-D-mannopyranoside (**27**; 6). Successive methylation, methanolysis, and debenzylation of this material afforded methyl 2-*O*-methylmannopyranoside which consumed periodate. *Fraction 2* (200 mg) showed two overlapping spots (**28** and **29**; t.l.c.), which could not be further fractionated. This mixture did not consume periodate. Methylation and subsequent debenzylation afforded a product (92 mg) which was also resistant to periodate. By g.l.c. it was found to contain methyl 2,4-di-*O*-methyl-α-D-mannopyranoside (**31**; r.t. 17.0 min; r.t. of its TMS derivative 24.6 min) and methyl 3,6-di-*O*-methyl-α-D-mannopyranoside (**32**; r.t. 19.3 min; r.t. of its TMS derivative 23.0 min) in a ratio of 2:1 respectively. *Fraction 3* (**30**; 300 mg) with $[\alpha]_D$ +34° (*c*, 1.2 EtOH) was resistant to periodate. Methylation and subsequent debenzylation of a 200 mg portion gave a compound (85 mg) identical (g.l.c. and p.m.r.) with methyl 2,6-di-*O*-methyl-α-D-mannopyranoside (**33**; 6). On hydrolysis with *N* sulfuric acid at 100° 2,6-di-*O*-methylmannose was obtained (paper chromatogram). *Fraction 4* (46 mg) was a mixture of mono-*O*-benzyl derivatives of methyl-α-D-mannopyranoside since a mixture of methyl 2,3,6-, 2,4,6-, and 2,3,4-tri-*O*-methylmannoside (ratio 26:37:2; g.l.c. identification and estimation) was obtained on successive methylation, debenzylation, and methanolysis.

Hydrogenolysis of Methyl 2,3-5,6-Di-O-benzylidene-α-D-mannofuranoside

This reaction was performed in the same way as described earlier (6). The crystalline material with m.p. 74–76° and $[\alpha]_D$ +100°, comprised about 30% of the principal reaction product and was identified as methyl 2,6-di-*O*-benzyl-α-D-mannofuranoside (**21**) since the mannopyranoside obtained by treating the former with methanolic hydrogen chloride (3%, reflux, 2 h) was oxidized by periodate. Methyl 2,6-di-*O*-benzyl-αβ-D-mannopyranoside (**18**) was converted to methyl 3,4-di-*O*-methyl αβ-D-mannopyranoside (**16**; identical with an authentic sample by g.l.c.), by the application of methylation, debenzylation, and methanolysis techniques. 3,4-Di-*O*-methylmannose obtained on hydrolysis was oxidized by lead tetraacetate. By consecutive methylation and debenzylation methyl 2,6-di-*O*-benzyl-α-D-mannofuranoside was converted to methyl 3,5-di-*O*-methyl-α-D-mannofuranoside (α-anomer of **24**) with r.t. 18.4 min (r.t. of its TMS derivative 35.2 min) and $[\alpha]_D$ +63.5° (*c*, 0.5 EtOH).

A portion of the mother liquor, which contained methyl di-*O*-benzyl-mannofuranoside derivatives, was treated with 3% methanolic hydrogen chloride (reflux 2 h) and then subjected to methylation and debenzylation. Gas–liquid chromatography of the reaction product showed three peaks with retention values 14.0, 15.4, and 17.0 min which could be assigned to methyl 3,6-di-*O*-methyl-αβ-D-mannofuranoside, methyl 3,4-di-*O*-methyl-αβ-D-mannopyranoside (**16**), and methyl 2,4-di-*O*-methyl-αβ-D-mannopyranoside (**7**), respectively, in an approximate ratio 1.5:1:1. Methanolysis of the methyl di-*O*-methylmannosides afforded a material which was resistant to periodate and consisted of methyl 3,4-(**16**), 2,4-(**7**), and 3,6-di-*O*-methylmannopyranosides (**17**) with retention values of 15.4, 17.0, and 19.3 min respectively. Another portion of the mother liquor was methylated and then debenzylated. A mixture of methyl 3,6- (r.t. 14.0 min), 2,5- (r.t. 15.5 min), and 3,5- (r.t. 18.4 min) di-*O*-methyl-αβ-D-mannofuranoside, in a ratio of 1.5:1:1, respectively, resulted. On treatment with methanolic hydrogen chloride this mixture gave a periodate-resistant material composed of methyl 2,5-(**25**) and 3,5-di-*O*-methylmannofuranosides (**24**), and methyl 3,6-di-*O*-methylmannopyranoside (**17**; r.t. 19.3 min).

Preparation of Methyl 5,6-Di-O-methyl-αβ-D-mannofuranoside and Methyl 2,5,6-Tri-O-methyl-αβ-D-mannofuranoside

D-Mannose 2,3-carbonate (**9**; 0.30 g, ref. 9) was refluxed overnight in iodomethane (10 ml) containing silver oxide (3 g) and Drierite (3 g). The reaction mixture was filtered, evaporated, and methyl 2,3-*O*-carbonyl-5,6-di-*O*-methyl α-D-mannofuranoside (**10**; 0.19 g) crystallized from ether–*n*-hexane. It had m.p. 85–86° and $[\alpha]_D$ +34° (*c*, 3.2 EtOH).

Anal. Calcd. for $C_{10}H_{16}O_7$: C, 48.38; H, 6.50. Found: C, 48.5; H, 6.6.

Deesterification with methanolic sodium methoxide gave methyl 5,6-di-*O*-methyl-α-D-mannofuranoside (α-anomer of **11**) with $[\alpha]_D$ +99° (*c*, +99° *c*, 1.0 EtOH). The equilibrium αβ-anomeric mixture, obtained with refluxing methanolic hydrogen chloride, had a r.t. of 15.3 min, compared with 22.3 min of methyl 4,6-di-*O*-methyl-αβ-D-mannopyranoside.

Methyl 5,6-di-*O*-methyl-α-D-mannofuranoside (80 mg) was shaken for 6 h in iodomethane (2.5 ml) containing silver oxide (0.5 g). Analysis by g.l.c. showed that the ratio of tri-*O*- to unchanged di-*O*-methyl methyl glycoside was 9:1. The mixture was hydrolyzed (0.1 *N* H_2SO_4, 1 h at 100°) and the product fractionated on a cellulose column using benzene – ethanol – water (500:50:1 v/v/v) as eluant. The tri-*O*-methylmannose fraction (61 mg) consumed 0.14, 0.17, and 0.25 mole/mole of lead tetraacetate (15) after 2, 5, and 15 min, respectively. 2,5,6-Tri-*O*-methyl-D-mannose crystallized from ether–*n*-hexane and had m.p. 92–93° and $[\alpha]_D$ +54° (*c*, 0.6 H_2O; constant value).

Anal. Calcd. for $C_9H_{18}O_6$: C, 48.64; H, 8.16. Found: C, 48.8; H, 8.3.

It was not oxidized by lead tetraacetate. A portion was converted to the methyl glycosides (**12**) with methanolic hydrogen chloride.

*Preparation of 3,5,6- and 2,5,6-Tri-O-methyl-*D*-mannoses*

Methyl 5,6-di-*O*-methyl-α-D-mannofuranoside (200 mg) was shaken with benzaldehyde (2 ml) and anhydrous zinc chloride (150 mg) overnight. The derived methyl 2,3-*O*-benzylidene-5,6-di-*O*-methyl-α-D-mannofuranoside (**15**; 150 mg) was hydrogenolyzed using one molar equivalent of $LiAlH_4$–$AlCl_3$ (1:1) for 5 h. The product was methylated by the Kuhn method (16) and then debenzylated. Hydrolysis with *N* sulfuric acid (100°, 1 h) gave a spot corresponding to tri-*O*-methylmannose and a minor spot corresponding to 5,6-di-*O*-methylmannose. The tri-*O*-methylmannose fraction (25 mg) was purified by cellulose column chromatography using eluants described above. Analysis by g.l.c. of the TMS derivative of the tri-*O*-methylmannose fraction showed that it was a mixture of 3,5,6-tri-*O*-methylmannose (1.5 parts; r.t.'s 36.1 and 30.8 min) and 2,5,6-tri-*O*-methylmannose (1 part, r.t. 28.5 min).

Acknowledgments

The authors would like to thank Mr. R. J. Magus for technical assistance, Mr. M. Mazurek for obtaining p.m.r. spectra, and Mr. W. C. Haid for performing elemental analyses. Also thanks are due to Dr. C. T. Bishop for a sample of 2,4-di-*O*-methyl-D-mannose and Dr. I. R. Siddiqui for 3,5,6-tri-*O*-methyl-D-mannose.

1. P. A. J. Gorin and J. F. T. Spencer. Can. J. Chem. **46**, 2299 (1968).
2. P. A. J. Gorin and J. F. T. Spencer. Can. J. Chem. **46**, 2305 (1968).
3. J. F. T. Spencer and P. A. J. Gorin. J. Bacteriol. **96**, 180 (1968).
4. J. F. T. Spencer and P. A. J. Gorin. Antonie van Leeuwenhoek. To be published.
5. B. E. Leggetter and R. K. Brown. Can. J. Chem. **42**, 990 (1964).
6. S. S. Bhattacharjee and P. A. J. Gorin. Can. J. Chem. This issue.
7. A. E. Knauf, R. M. Hann, and C. S. Hudson. J. Am. Chem. Soc. **63**, 1447 (1941).
8. Y-C Lee and C. E. Ballou. Biochemistry, **4**, 257 (1965).
9. A. S. Perlin. Can. J. Chem. **42**, 1365 (1964).
10. I. R. Siddiqui. Private communication.
11. B. Urbas, G. A. Adams, and C. T. Bishop. Can. J. Chem. **42**, 2093 (1964).
12. R. J. Yu, C. T. Bishop, F. P. Cooper, H. Hasenclever, and F. Blank. Can. J. Chem. **45**, 2205 (1967).
13. T. Purdie and J. C. Irvine. J. Chem. Soc. 1021 (1903).
14. C. C. Sweeley, R. Bentley, M. Makita, and W. W. Wells. J. Am. Chem. Soc. **85**, 2497 (1963).
15. A. J. Charlson and A. S. Perlin. Can. J. Chem. **34**, 1200 (1956).
16. R. Kuhn, H. Trischmann, and I. Löw. Angew. Chem. **67**, 32 (1955).
17. W. N. Haworth, R. L. Heath, and S. Peat. J. Chem. Soc. 833 (1941).
18. R. G. Ault, W. N. Haworth, and E. L. Hirst. J. Chem. Soc. 1012 (1935).
19. G. J. Robertson. J. Chem. Soc. 330 (1934).
20. W. N. Haworth, E. L. Hirst, F. A. Isherwood, and J. K. N. Jones. J. Chem. Soc. 1878 (1934).
21. D. Heslop and F. Smith. J. Chem. Soc. 574 (1944).
22. F. Klages. Ann. **512**, 185 (1934).
23. J. C. Irvine and A. M. Moodie. J. Chem. Soc. 1462 (1905).
24. W. N. Haworth, E. L. Hirst, and J. I. Webb. J. Chem. Soc. 651 (1930).

Can. J. Chem. Downloaded from www.nrcresearchpress.com by 210.87.254.105 on 09/05/12
For personal use only.

Synthetic reactions by complex catalysts. XII. Copper-catalyzed reaction of isocyanide with alcohol

TAKEO SAEGUSA, YOSHIHIKO ITO, SHIRO KOBAYASHI, KIWAMI HIROTA, AND NOBUYUKI TAKEDA
Department of Synthetic Chemistry, Faculty of Engineering, Kyoto University, Kyoto, Japan

Received September 16, 1968

The reaction of alkyl isocyanide with alcohol to produce alkyl formimidate requires catalysis by metal compounds. The catalysts are classified into two groups. The first group includes metallic copper, and the oxides of copper (Cu (I) and Cu (II)), silver, and mercury, which induce the isocyanide reactions of various alcohols including saturated and unsaturated alcohols and amino-alcohol. The second group catalysts are the chlorides of copper (Cu (I)), silver, zinc, and cadmium, which cause the reactions of isocyanide only with special alcohols having strong coordinating tendencies toward the catalyst, as being exemplified by allyl alcohol and β-*N*,*N*-dimethylaminoethanol. Among these catalysts, metallic copper and copper oxides are the most effective and give the products almost quantitatively. The difference in catalyst activity between the two groups of catalysts has been explained by assuming a ternary complex consisting of the catalyst, isocyanide, and alcohol as the site of reaction.

Canadian Journal of Chemistry, **47**, 1217 (1969)

Can. J. Chem. Downloaded from www.nrcresearchpress.com by 210.87.254.5 on 09/05/12
For personal use only.

In previous communications (1), we preliminarily reported a new reaction of an isocyanide with an alcohol to produce a formimidate, which was accomplished for the first time by means of catalysts of metallic copper and some copper compounds. This reaction provides a convenient,

$$[1]\quad ROH + :C{\leftrightharpoons}N{-}R' \xrightarrow{\text{Cu catalyst}} \underset{\mathbf{1}}{ROCH{=}N{-}R'}$$

highly selective method for the preparation of formimidates. The product formimidate may be regarded as being derived by the insertion of the isocyanide carbon bearing lone pair electrons between the oxygen and the hydrogen of the alcohol. In the absence of the copper catalyst, alcohol is quite inert toward isocyanides. Alcohol has been employed as an inert solvent in several reactions of isocyanides (2). The activity of copper catalysts is much affected by the valency of copper and the nature of the ligand. Metallic copper and cuprous and cupric oxides are excellent catalysts, which induce the reactions of isocyanides with various alcohols (1*b*). On the other hand, cuprous chloride and cyanide catalyze the reactions with specific alcohols such as β-dimethylaminoethanol and β,γ-unsaturated alcohols (1*a*) including allyl alcohol.

It is well known that isocyanides form complexes with various transition metal salts, especially copper compounds. Therefore, it is suggested that the isocyanide–copper complex plays an essential role in the function of the copper catalyst. In addition, the coordination of alcohol onto copper catalyst is also assumed to be quite important for the reaction. Thus, it seems likely that the reaction has taken place within the ligand sphere of the so-called mixed ligand complex consisting of copper, isocyanide, and alcohol.

The present paper describes the details of the copper-catalyzed reaction of isocyanides with alcohol, as well as some results of infrared spectral studies upon the interactions between copper catalyst and the reaction components.

Results

Reactions of Isocyanides with Alcohols Catalyzed by Metallic Copper and Copper Oxides

Metallic copper and copper oxides (Cu (I) and Cu (II)) catalyzed quite effectively the reactions of cyclohexyl isocyanide with various alcohols (Tables I and II).

TABLE I

Metallic copper-catalyzed reactions of cyclohexyl isocyanide with alcohols*

	Product yield (%)	
ROH	**1**	**2**
EtOH	99†	1
n-BuOH	99‡	—
sec-BuOH	98§	2
$CH_2{=}CHCH_2OH$	95‖	3

*Reaction conditions: cyclohexyl isocyanide, 30 mmoles; alcohol, 34 mmoles; Cu, 3 mmoles; 120°; 5 h.
†Boiling point, 54.5° (8 mm).
‡Boiling point, 81° (21 mm).
§Boiling point, 90° (21 mm).
‖Boiling point, 90° (26 mm).

TABLE II

Copper oxide catalyzed reaction of cyclohexyl isocyanide with alcohols*

ROH	Catalyst	Product yield (%) 1	2	3
EtOH	Cu_2O	95	2	1
n-BuOH		95	1	
sec-BuOH		94	2	Trace
t-BuOH		94		
CH_2=$CHCH_2OH$		92	5	
EtOH	CuO	87	1	
n-BuOH		81	—	
sec-BuOH		88	—	
t-BuOH		91†	1	Trace
CH_2=$CHCH_2OH$		89	3	

*Reaction conditions: cyclohexyl isocyanide, 30 mmoles; alcohol, 34 mmoles; CuO (or Cu_2O), 3 mmoles; 120°; 5 h.
†Boiling point, 93° (19 mm).

Several alkyl *N*-cyclohexylformimidates were produced in almost quantitative yields. In the reactions catalyzed by cuprous and cupric oxides, small amounts of two by-products, *N*-cyclohexylformamide (**2**) and alkyl *N*-cyclohexylcarbamates (**3**) were formed. Compound **2** may possibly have been produced by the hydrolysis of the isocyanide or formimidate (**1**) with water which either was present as an impurity in the initial reaction mixture or was produced *in situ* by the etherification of alcohol. Compound **2** may also be derived from the formimidate according to

$$ROCH{=}N{-}R' + ROH \rightarrow (RO)_2CHNHR' \rightarrow R'NHCHO + ROR$$

The formation of **3** is ascribed to the oxidation of isocyanide to isocyanate by the copper oxide catalysts. The reduction–oxidation between mercuric oxide and isocyanide is known, in which isocyanide is oxidized into isocyanate (3).

As expected, **3** was not formed in the reaction when metallic copper was the catalyst. As to the catalyst activity of metallic copper, it is very important to note that a small amount of metallic copper dissolved in cyclohexyl isocyanide to form a soluble complex. The complex formation from metallic copper and isocyanide will be described later. From these observations, it appears possible that copper oxide catalysts are reduced by isocyanide to form a copper (O)-isocyanide complex which is the actual active species responsible for their catalytic activities. The exact characterization of active species of the metallic copper and copper oxides catalysts is the subject of a future study.

Cuprous Chloride Catalyst in the Isocyanide–Alcohol Reaction

The catalysis of cuprous chloride in the alcohol–isocyanide reaction was somewhat different from that of metallic copper and of copper oxides. Cuprous chloride did not induce the isocyanide reactions with the usual saturated alcohols such as ethanol and *n*-butanol. It catalyzed only the reactions involving β-dimethylaminoethanol and β,γ-unsaturated alcohols such as allyl alcohol. As will be discussed later, these alcohols are characterized by a strong tendency of coordination onto cuprous chloride. The complexes of cuprous chloride and these alcohols are stable and can be isolated. These findings suggest that the coordination of isocyanide as well as alcohol onto cuprous chloride are essential for this reaction.

The reactions of cyclohexyl isocyanide with β,γ-unsaturated alcohols, and β-dimethylaminoethanol by cuprous chloride catalyst are shown in Table III. Benzyl alcohol is among the alcohols which react with isocyanide in the presence of cuprous chloride. Perhaps the phenyl group plays a role similar to that of β,γ-unsaturated group.

In these reactions, *N*-cyclohexylformamide (**2**) and *N*-alkenyl-*N*-cyclohexylformamide (**4**) were produced as the by-products. The amount of **2**, the product of the hydrolysis of cyclohexyl isocyanide, was much higher than that in the reactions with metallic copper and copper oxides

TABLE III

Cuprous chloride catalyzed reaction of cyclohexyl isocyanide with alcohol*

ROH	Product yield (%) 1	2	4
CH_2=$CHCH_2OH$	67	25	6
CH_2=$C(CH_3)CH_2OH$	50	32	‖
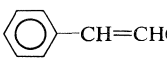 —CH=$CHCH_2OH$	45†	20	‖
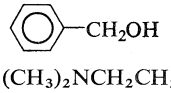 —CH_2OH	20‡	10	63
$(CH_3)_2NCH_2CH_2OH$	67§	16	‖
$C_nH_{2n+1}OH$	No reaction		

*Reaction conditions: cyclohexyl isocyanide, 40 mmoles; alcohol, 70 mmoles; CuCl, 8 mmoles; 120°; 5 h.
†Boiling point, 130° (3 mm).
‡Boiling point, 155° (3 mm).
§Boiling point, 85–86° (5 mm).
‖Not determined.

Can. J. Chem. Downloaded from www.nrcresearchpress.com by 210.87.254.5 on 09/05/12
For personal use only.

Can. J. Chem. Downloaded from www.nrcresearchpress.com by 210.87.254.5 on 09/05/12
For personal use only.

catalysts. It may be attributed to a higher concentration of water formed *in situ* by the etherifications of these alcohols. It is known that β,γ-unsaturated alcohols are easily etherified by cuprous chloride catalyst (4). The by-product **4** was probably produced by the thermal rearrangement (5) of **1** (Chapman rearrangement) which took place, at least partly, during the distillation of the reaction mixture. A higher yield of **4** in the reaction with benzyl alcohol may be due in part to the higher distillation temperature.

In the cuprous chloride catalyzed reaction of cyclohexyl isocyanide with allyl alcohol, the decrease of isocyanide and the increases of the yields of products are plotted against the reaction time (Fig. 1).

There is observed an induction period of 4 h for the formation of **1**. The nature of the induction period has not yet been elucidated. As to the induction period, a possibility that the reaction is autocatalytic may be excluded. The addition of formamide or formimidate to the reaction system did not shorten the induction period. Cuprous chloride catalyst itself was not changed throughout the reaction. The hydrolysis of isocyanide to produce a by-product of **2** starts at the beginning of the reaction. Another by-product of **4**, however, is produced only after the main product of **1** is accumulated in the reaction system.

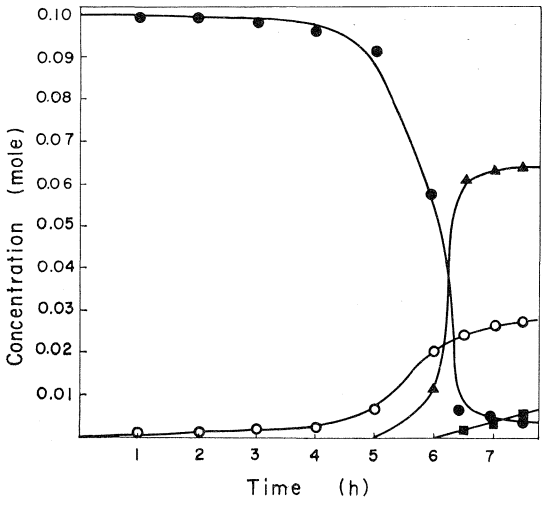

FIG. 1. CuCl catalyzed reaction of cyclohexyl isocyanide with allyl alcohol; ——●——, cyclohexyl isocyanide; ——○——, *N*-cyclohexylformamide; ——▲——, allyl *N*-cyclohexylformimidate; ——■——, *N*-cyclohexyl-*N*-allylformamide.

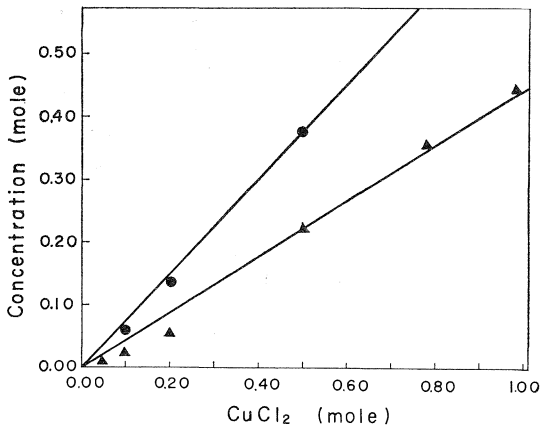

FIG. 2. $CuCl_2$ – cyclohexyl isocyanide reaction in ethanol; ——●——, CuCl (formed by reduction of $CuCl_2$); ——▲——, ethyl *N*-cyclohexylcarbamate.

Catalytic Behavior of Other Copper Compounds

In the cupric chloride catalyzed reaction of isocyanide with saturated alcohols, only small amounts of *N*-substituted carbamate (**3**) and *N*-substituted formamide (**2**) were produced. The carbamate formation suggests the reduction–oxidation reaction between isocyanide and cupric chloride. A series of reactions of cyclohexyl isocyanide with increasing amounts of cupric chloride in the presence of excess ethanol was carried out (Fig. 2).

It was found that cupric chloride was reduced to cuprous chloride, and the molar ratio of cuprous chloride and carbamate was about two. A separate study by us[1] has shown that the isocyanide – cupric chloride reaction in the absence of alcohol produces cuprous chloride and *N*-substituted imidocarbonyl chloride, the precursor of

[2] $2CuCl_2 + RN{\geq}C: \rightarrow 2CuCl + RN{=}CCl_2$

carbamate. The catalytic activity of cuprous cyanide was similar to that of cuprous chloride in the isocyanide–alcohol reaction. Cuprous cyanide induces the isocyanide – allyl alcohol reaction to form allyl formimidate but it does not promote the isocyanide reactions with the usual saturated alcohols.

Catalytic Activities of Other Metal Compounds

Silver oxide and mercuric oxide also catalyzed the reaction of isocyanide with saturated alcohol. Two runs of the cyclohexyl isocyanide–ethanol

[1]T. Saegusa, Y. Ito, and S. Tomita. To be published.

Can. J. Chem. Downloaded from www.nrcresearchpress.com by 210.87.254.5 on 09/05/12
For personal use only.

reaction in the presence of silver oxide and mercuric oxide respectively were carried out under the same conditions as Table I, in which ethyl *N*-cyclohexylformimidate was formed in yields of 89 and 51%, respectively. However, oxides of zinc, cadmium, and iron were inactive. Oxides of cobalt and nickel caused only the homopolymerization of isocyanide to produce brown colored, insoluble, and infusible polymers.

Chlorides of silver, zinc, and cadmium caused the reaction of isocyanide with allyl alcohol, but they did not induce that with the usual saturated alcohol. Mercuric chloride did not show catalytic activity even for the isocyanide – allyl alcohol reaction. Chlorides of nickel, cobalt, and palladium did not induce the insertion reaction but caused the homopolymerization of isocyanide.

Mechanisms of Copper Catalysis

According to the catalysis behavior, copper catalysts are divided into two groups. The first group includes metallic copper and cuprous and cupric oxides, which catalyze the reactions of isocyanide with saturated and unsaturated alcohols. The second group of catalysts are cuprous chloride and cyanide which induce the reactions of isocyanide only with β,γ-unsaturated alcohol and β-aminoalcohol. The infrared (i.r.) spectra of mixtures of cyclohexyl isocyanide and copper catalysts showed a new band at a frequency higher than 2140 cm^{-1} of $\nu_{N\equiv C}$ of free isocyanide. The new band has been assigned to $\nu_{N\equiv C}$ of isocyanide coordinating to metal compound (6). From a Hammett relationship of the argentation constant of styrene derivatives (7), it is assumed that the contribution of the back-donation in the complex of d^{10} metal ion is small. The shift of $\nu_{N\equiv C}$ to a shorter wavelength is due to the donation of the electrons of isocyanide to d^{10} metal ion. Therefore, the magnitude of shift of $\nu_{N\equiv C}$ caused by coordination may be utilized as a measure of the strength of the coordination of isocyanide onto copper catalysts. It follows that the coordination of isocyanide with the first group catalysts is weaker than that with the members of the second group.

The cyclohexyl isocyanide – metallic copper system for i.r. diagnosis was prepared at room temperature by the addition of metallic copper powder to liquid cyclohexyl isocyanide under nitrogen. Metallic copper was prepared by the reduction of cupric sulfate with zinc powder in aqueous solution. The copper–isocyanide mixture was centrifuged. The i.r. spectrum of the liquid phase of copper–isocyanide showed a fairly strong absorption at 2180 cm^{-1} as well as the band of $\nu_{N\equiv C}$ of free isocyanide at 2140 cm^{-1}. This finding indicates the formation of a soluble complex from metallic copper and isocyanide. On treating the centrifuged solution with alcohol, the formimidate was produced. This indicates that the metallic copper-catalyzed reaction proceeds in a homogeneous solution phase, and the solid phase is merely the source of soluble catalyst complexes. The band of coordinating species of cyclohexyl isocyanide appeared at 2181 cm^{-1} in the system of cuprous oxide with isocyanide.

On the other hand, the i.r. spectrum of the 1:1 complex of cuprous chloride with cyclohexyl isocyanide showed the band of coordinating isocyanide group at 2192 cm^{-1}. Thus, the magnitude of the shift of $\nu_{N\equiv C}$ caused by cuprous chloride is larger than that caused by metallic copper and cuprous oxide. These findings are taken to indicate that isocyanide coordinates more tightly with cuprous chloride than with the first group catalysts.

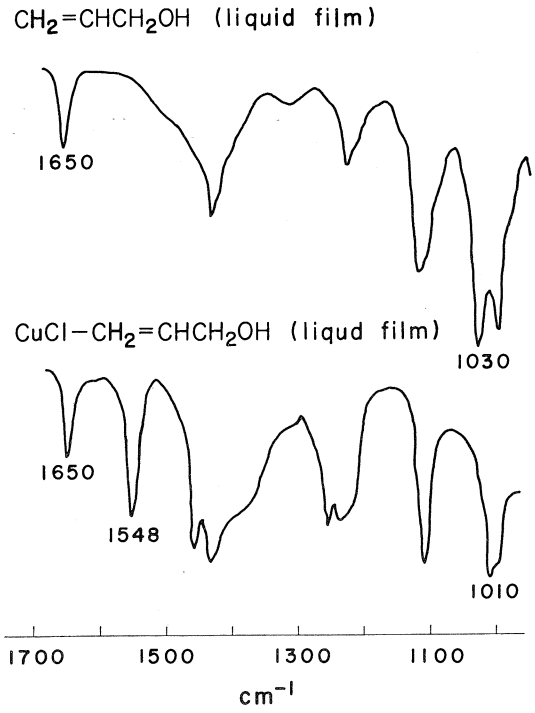

FIG. 3. Infrared spectra of allyl alcohol and CuCl allyl alcohol complex.

Can. J. Chem. Downloaded from www.nrcresearchpress.com by 210.87.254.5 on 09/05/12
For personal use only.

The coordination of alcohol with copper catalysts depends upon the nature of the alcohol and of the copper catalysts. Cuprous chloride is almost insoluble in the usual saturated alcohols, whereas it is quite soluble in allyl alcohol and in β-dimethylaminoethanol. This observation suggests a specific interaction between cuprous chloride and these particular alcohols. The complexing of cuprous chloride with these alcohols was indicated by i.r. spectroscopy. In comparison with the i.r. spectrum of allyl alcohol, the spectrum of cuprous chloride dissolved in allyl alcohol had additional bands at 1548 and 1010 cm^{-1}, which are assigned to the olefin and alcohol groups, respectively, of the allyl alcohol – cuprous chloride complex (Fig. 3) (8). The strong complexing tendency of β-dimethylaminoethanol with cuprous chloride was also demonstrated by i.r. spectroscopy. From cuprous chloride and β-dimethylaminoethanol, a 1:1 complex was successfully isolated, whose i.r. spectrum showed the shift of ν_{C-O} band from 1039 to 1020 cm^{-1} (Fig. 4).

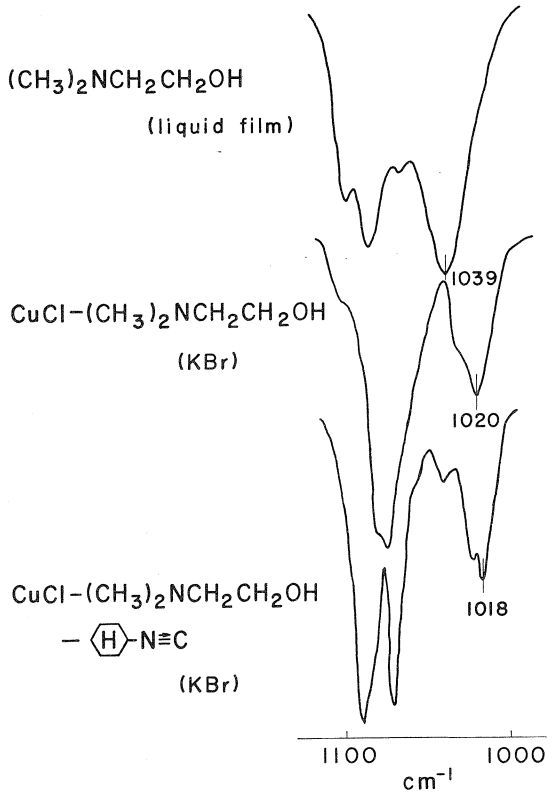

FIG. 4. Infrared spectra of β-*N*-dimethylaminoethanol and its complexes.

On the basis of these i.r. spectroscopic studies, the difference in catalyst activity between the first group catalysts and those of the second group is explained by a hypothesis of mixed ligand complex. Isocyanide is held rather loosely by the first group catalysts, and hence a part of the isocyanide ligand will be replaced by alcohols including saturated alcohols of weak complexing tendency as well as the particular alcohols mentioned above. The first group catalysts will form a ternary, mixed ligand complex consisting of copper, isocyanide, and various alcohols. On the other hand, isocyanide is held tightly by the second group catalyst, and the isocyanide ligand is partly replaced only by the special alcohols of strong coordinating tendencies. The ternary, mixed ligand complexes of the second group catalysts are feasible only for the special alcohols. It is assumed that the reaction between alcohol and isocyanide will take place in the ligand sphere of the mixed ligand complex. Thus, the formation of the mixed ligand complex is a prerequisite for the occurrence of the reaction.

Experimental

(a) Metallic Copper-catalyzed Reaction of Cyclohexyl Isocyanide with Ethanol

Metallic copper was prepared by treating an excess of aqueous solution of cupric sulfate maintained below 70° with zinc powder under a nitrogen atmosphere. The metallic copper precipitate was collected and washed successively with water and dry acetone, and then dried.

A mixture of cyclohexyl isocyanide 3.27 g (0.030 mole), ethanol 1.56 g (0.034 mole), and metallic copper 0.43 g (0.003 g-atom) was heated at 120° for 5 h. After the insoluble catalyst was removed by filtration, the filtrate was subjected to gas–liquid chromatography (g.l.c.) analysis (PEG 20000 on Celite). Two products, **1***a* and **2***a*, were detected. The product **1***a* was also isolated by distillation *in vacuo*, b.p. 54.5° (8mm).

On the basis of the following analyses, **1***a* was identified as ethyl *N*-cyclohexylformimidate.

Nuclear magnetic resonance (CCl_4) of **1***a*: δ 1.21 (3H, triplet), 1.00–2.00 (10H, complex multiplet), 2.70–3.10 (1H, broad singlet), 3.98 (2H, quartet), 7.43 (1H, singlet). Infrared (i.r.) (neat): 1650 (s), 1200 cm^{-1} (s). The structure of **1***a* was further confirmed by comparisons of the g.l.c. retention time and i.r. spectrum with the authentic sample. The authentic sample of **1***a* was prepared as follows (9). *N*-Cyclohexylformamide (0.5 mole) was added dropwise to triethyloxonium fluoroborate (0.5 mole) (10) in ether at room temperature. Ethyl *N*-cyclohexylformimidate hydrogen fluoroborate, which separated as a viscous liquid in the lower layer, was treated with triethylamine to give ethyl *N*-cyclohexylformimidate.

Can. J. Chem. Downloaded from www.nrcresearchpress.com by 210.87.254.5 on 09/05/12
For personal use only.

Compound **2***a*, b.p. 103° (3mm) was identified as *N*-cyclohexylformamide by comparison with the authentic sample prepared from cyclohexylamine and ethyl formate.

(b) Cuprous Oxide Catalyzed Reaction of Cyclohexyl Isocyanide with sec-Butanol

A mixture of cyclohexyl isocyanide 3.27 g (0.030 mole), *sec*-butanol 2.52 g (0.034 mole), and cuprous oxide 0.43 g (0.003 mole) was heated at 120° for 5 h. After working up the mixture as described above, *sec*-butyl *N*-cyclohexylformimidate, b.p. 90° (21mm) (**1***b*), *N*-cyclohexylformamide, and *sec*-butyl *N*-cyclohexylcarbamate (**3***b*), were detected by g.l.c. and identified.

Nuclear magnetic resonance (CCl_4) of **1***b*: δ 0.87 (3H, triplet), 1.15 (3H, doublet), 1.00–2.00 (12H, complex multiplet), 2.70–3.10 (1H, broad singlet), 4.73 (1H, multiplet), 7.33 (1H, singlet). Infrared (neat) : 1650 (s), 1205 cm^{-1} (s). The authentic sample of **3***b* was prepared by the reaction of cyclohexyl isocyanate with *sec*-butyl alcohol.

(c) Cupric Oxide Catalyzed Reaction of Cyclohexyl Isocyanide with t-Butanol

A mixture of cyclohexyl isocyanide 3.27 g (0.030 mole), *t*-butanol 2.52 g (0.034 mole), and cupric oxide 0.24 g (0.003 mole) was heated at 120° for 5 h. According to the same procedure, *t*-butyl *N*-cyclohexylformimidate, b.p. 93° (10mm) (**1***c*), *N*-cyclohexylformamide, and *t*-butyl *N*-cyclohexylcarbamate (**3***c*) were identified.

Nuclear magnetic resonance (CCl_4) of **1***c*: δ 1.40 (9H, singlet), 1.00–2.00 (10H, complex multiplet), 2.70–3.10 (1H, broad singlet), 7.36 (1H, singlet). Infrared (neat): 1650 (s), 1220 (s), 1170 (s) cm^{-1}.

(d) Cuprous Chloride Catalyzed Reaction of Allyl Alcohol with Cyclohexyl Isocyanide

A solution of cyclohexyl isocyanide 4.36 g (0.040 mole), allyl alcohol 4.06 g (0.070 mole), and cuprous chloride 0.80 g (0.008 mole) was heated at 120° for 5 h. Then the reaction mixture was subjected to g.l.c. analysis and the products were identified. Allyl *N*-cyclohexylformimidate (**1***d*), b.p. 90° (26mm), cyclohexylformamide, and *N*-allyl-*N*-cyclohexylformamide (**4***d*) were the products.

Nuclear magnetic resonance (CCl_4) of **1***d*: δ1.00–2.00 (10H, complex multiplet), 2.70–3.20 (1H, broad singlet), 4.49 (2H, doublet), 4.90–6.20 (3H, multiplet), 7.53 (1H, singlet). Infrared (neat) : 1650 (s), 1190 (s), 990 (m), 910 cm^{-1} (s). The authentic sample of **1***d* was synthesized by the reaction of triallyloxonium fluoroborate with *N*-cyclohexylformamide.

Nuclear magnetic resonance ($CDCl_3$) of **4***d*: 1.00–2.00 (10H, complex multiplet), 2.90–3.50 (1H, broad singlet), 3.84 (2H, doublet), 4.80–6.10 (3H, multiplet), 8.04 and 8.20 (1H, two singlets).

(e) Cuprous Chloride Catalyzed Reaction of Cyclohexyl Isocyanide with Benzyl Alcohol

A solution of cyclohexyl isocyanide 4.36 g (0.040 mole), benzyl alcohol 7.56 g (0.070 mole), and cuprous chloride 0.80 g (0.008 mole) was heated at 120° for 5 h. The whole product could not be analyzed by g.l.c. Distillation of the reaction mixture gave benzyl *N*-cyclohexylformimidate (**1***e*), b.p. 155° (3mm), *N*-cyclohexylformamide, and *N*-benzyl-*N*-cyclohexylformamide (**4***e*), b.p. 133° (3mm).

Nuclear magnetic resonance ($CDCl_3$) of **1***e*: δ 1.00–2.00 (10H, complex multiplet), 2.80–3.20 (1H, broad singlet), 4.49 (2H, singlet), 7.24 (5H, singlet), 7.60 (1H, singlet).

Nuclear magnetic resonance (CCl_4) of **4***e*: δ 1.00–2.00 (10H, complex multiplet), 2.90–3.30 (1H, broad singlet), 4.28 and 4.40 (2H, two singlets), 7.15 (5H, singlet), 8.02 and 8.15 (1H, two singlets).

(f) Cupric Chloride Catalyzed Reaction of Cyclohexyl Isocyanide with Ethanol

A solution of cyclohexyl isocyanide 4.36 g (0.040 mole), ethanol 5.52 g (0.120 mole), and cupric chloride 2.69 g (0.020 mole) was heated at 120° for 5 h. The insoluble matter was separated by filtration, and the filtrate was analyzed by g.l.c. Ethyl *N*-cyclohexylcarbamate (0.0084 mole) was obtained in a yield of 42% (based on $CuCl_2$). CuCl in the insoluble portion was analyzed according to the thiocyanate method. It was found that 76% of $CuCl_2$ was reduced to CuCl (0.0152 mole).

(g) Complex of Cyclohexyl Isocyanide – Cuprous Chloride (1:1)

Cuprous chloride was added slowly to excess cyclohexyl isocyanide at room temperature, and the precipitation was collected by filtration. The white crystalline product was recrystallized from chloroform–ether, m.p. 95–96°. Elemental analysis revealed that the crystalline product consisted of 1 mole cyclohexyl isocyanide and 1 mole cuprous chloride.

Anal. Calcd. for $C_7H_{11}NClCu$: C, 40.40; H, 5.22; N, 6.60; Cl, 17.01. Found : C, 40.40; H, 5.29; N, 6.73; Cl, 17.07.

(h) Complex of β-Dimethylaminoethanol – Cuprous Chloride (1:1)

A dark blue solution of cuprous chloride (0.01 mole) in β-dimethylaminoethanol (0.04 mole) was treated with excess petroleum ether, and the precipitating green crystalline mass was collected and dried, m.p. 144–145°.

Anal. Calcd. for $(C_4H_{11}NOClCu)_2$: C, 25.53; H, 5.86; N, 7.45; Cl, 18.88. Found : C, 25.93; H, 5.42; N, 7.27; Cl, 18.78.

1. (*a*) T. Saegusa, Y. Ito, S. Kobayashi, and K. Hirota. Tetrahedron Letters, 521 (1967). (*b*) T. Saegusa, Y. Ito, S. Kobayashi, N. Takeda, and K. Hirota. Tetrahedron Letters, 1273 (1967).
2. T. L. Cairns, A. W. Larchar, and B. C. McKusick. J. Org. Chem. **17**, 1497 (1952).
3. P. A. S. Smith and N. W. Kalenda. J. Org. Chem. **23**, 1599 (1958).
4. T. Ogura, N. Furuno, and S. Kawaguchi. Shokubai, Tokyo, **9**, 22 (1967).
5. J. W. Schulenberg and S. Archer. Organic reactions. Vol. 14. John Wiley and Sons, Inc., New York. p. 1.
6. F. A. Cotton and F. Zingales. J. Am. Chem. Soc. **83**, 351 (1961).
7. T. Fueno, T. Okuyama, T. Deguchi, and J. Furukawa. J. Am. Chem. Soc. **87**, 170 (1965).
8. T. Ogura, N. Furuno, and S. Kawaguchi. Bull. Chem. Soc. Japan, **40**, 1171 (1967).
9. S. Petersen and E. Tietze. Ann. **623**, 166 (1959).
10. H. Meerwein, W. Florian, N. Schon, and G. Stopp. Ann. **641**, 1 (1961).

Can. J. Chem. Downloaded from www.nrcresearchpress.com by 210.87.254.40 on 09/05/12
For personal use only.

NOTES

Metabolites of pathogenic fungi. VII. On the structure and stereochemistry of xanthomegnin, vioxanthin, and viopurpurin, pigments from *Trichophyton violaceum*[1,2]

A. S. NG[3] AND G. JUST
Department of Chemistry, McGill University, Montreal, Quebec

AND

F. BLANK
The Skin and Cancer Hospital, Temple University Health Sciences Center, Philadelphia, Pennsylvania

Received August 30, 1968

Recently, we proposed structure **1** for xanthomegnin (1) and tentatively assigned structures **2** and **3** for vioxanthin and viopurpurin respectively (2). We should now like to present evidence which confirms the structure of vioxanthin (**2**), adds weight to the structure proposed for viopurpurin, and which defines the stereochemistry of the lactone ring in **1** and **3**.

Canadian Journal of Chemistry, 47, 1223 (1969)

Lithium aluminium hydride reduction of **4**, an oxidation product of **1** (1), followed by ozonolysis and oxidation with silver oxide (3), gave β-hydroxybutyric acid, $[\alpha]_D -22.8°$. R-β-hydroxybutyric acid has $[\alpha]_D -24°$ (4). The configuration of the asymmetric center in **4**, and therefore in the lactone ring of xanthomegnin, is R.

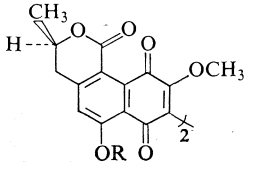

1, Xanthomegnin, R = H
1*a*, R = Ac

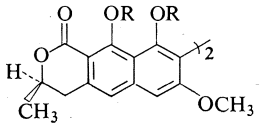

2, Vioxanthin, R = H
2*a*, R = CH_3
2*b*, R = Ac

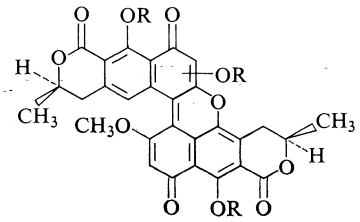

3, Viopurpurin, R = H
3*a*, R = CH_3
3*b*, R = Ac

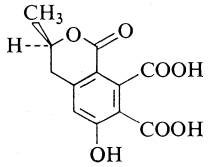

4

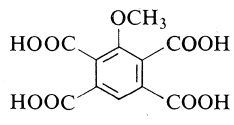

5

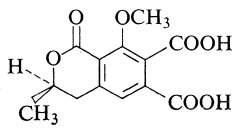

6

[1]This work was supported by United States Public Health Service research grants AI-04050 and 5 ROI AI 05378 from the National Institute of Allergy and Infectious Diseases, and a grant from the John A. Hartford Foundation, Inc., New York.

[2]For part VI in this series, see ref. 9.

[3]Abstracted from part of the Ph.D. Thesis of A. S. Ng, McGill University, 1968.

Oxidation of trimethylviopurpurin (**3***a*) with alkaline hydrogen peroxide gave lactone **6**, identical in all respects with the known lactone obtained by oxidation of floccosin (5). The optical rotatory dispersion (o.r.d.) curves of **4** and **6** are

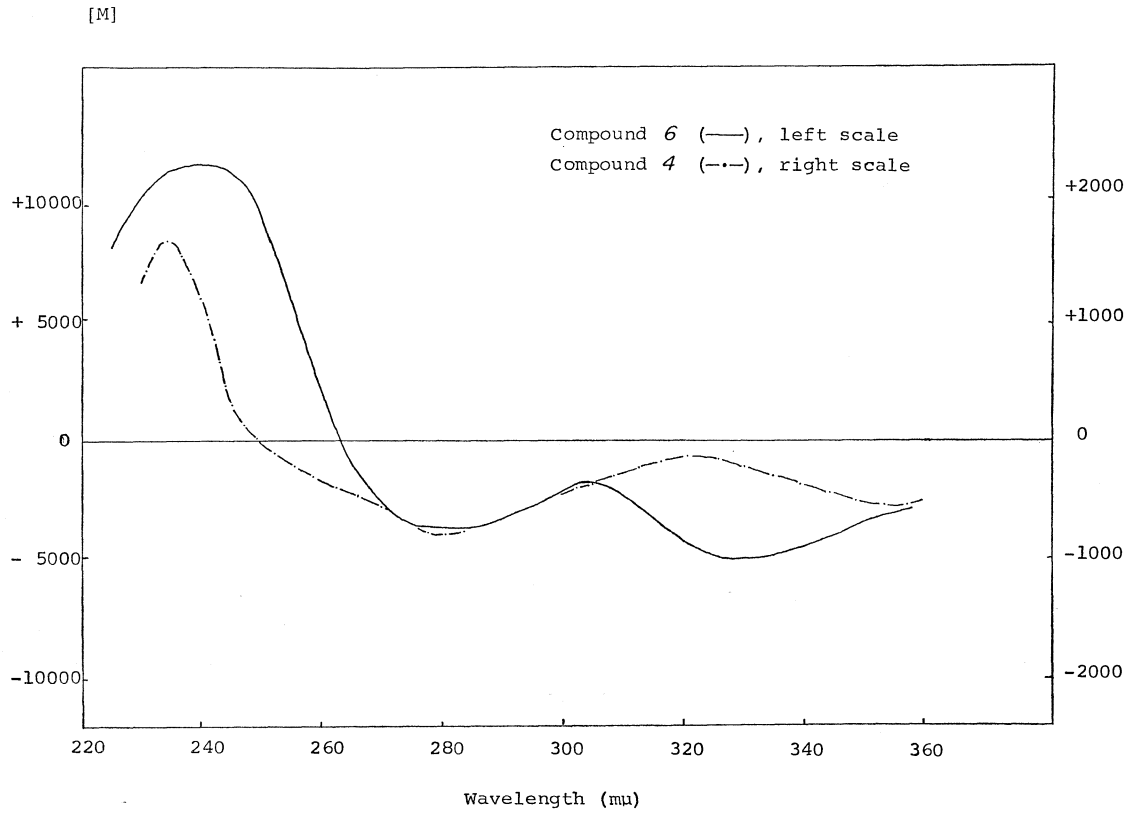

FIG. 1. The optical rotatory dispersion curves of **4** and **6**.

very similar (Fig. 1). It may therefore be concluded that the lactone rings in **4** and **6**, and therefore in **1** and **3**, have the same absolute configuration. This is not unreasonable, especially since both pigments were obtained from the same organism. No degradation product of **2** containing the intact lactone ring could be obtained. It is, however, quite probable that it too has the same absolute stereochemistry.

In our original paper on xanthomegnin (1), we had proposed the S-configuration for the lactone ring, based on an apparently unwarranted extension of the Hudson–Klyne rule (6). It is conceivable that the o.r.d. curve of the acid (or sodium salt) of **1** (see Fig. 3) is sufficiently different from **1** to simulate an apparent reversal of the ΔM_D, (which is taken to reflect the absolute stereochemistry at the asymmetric center) upon opening of the lactone ring.

Vioxanthin has been assigned structure **2**, based mainly on spectroscopic data (2). The linear arrangement of the three rings has now been confirmed by oxidation of **2***a* with alkaline permanganate to the known anisole-2,3,5,6-tetracarboxylic acid[4] and the dimeric nature has been corroborated by mass spectrometry (molecular ion of **2***a*: *m/e* 602).

Biogenetic considerations had governed the assignment of the positions of the dimer linkage and of the methoxy groups in vioxanthin (2). This assignment has now been confirmed by o.r.d. of vioxanthin (**2**) and its tetramethyl ether **2***a* and tetraacetate **2***b* (Fig. 2), which shows a very large Cotton effect (M_D = 480 000) associated with the hindered rotation at the dimer linkage. This large effect cannot be associated with the dissymmetry of the lactone ring (see Fig. 1), and excludes the alternative arrangement in which the

[4]We should like to thank Dr. J. S. E. Holker, Department of Organic Chemistry, University of Liverpool, England, for the infrared spectra of an authentic sample.

Can. J. Chem. Downloaded from www.nrcresearchpress.com by 210.87.254.40 on 09/05/12
For personal use only.

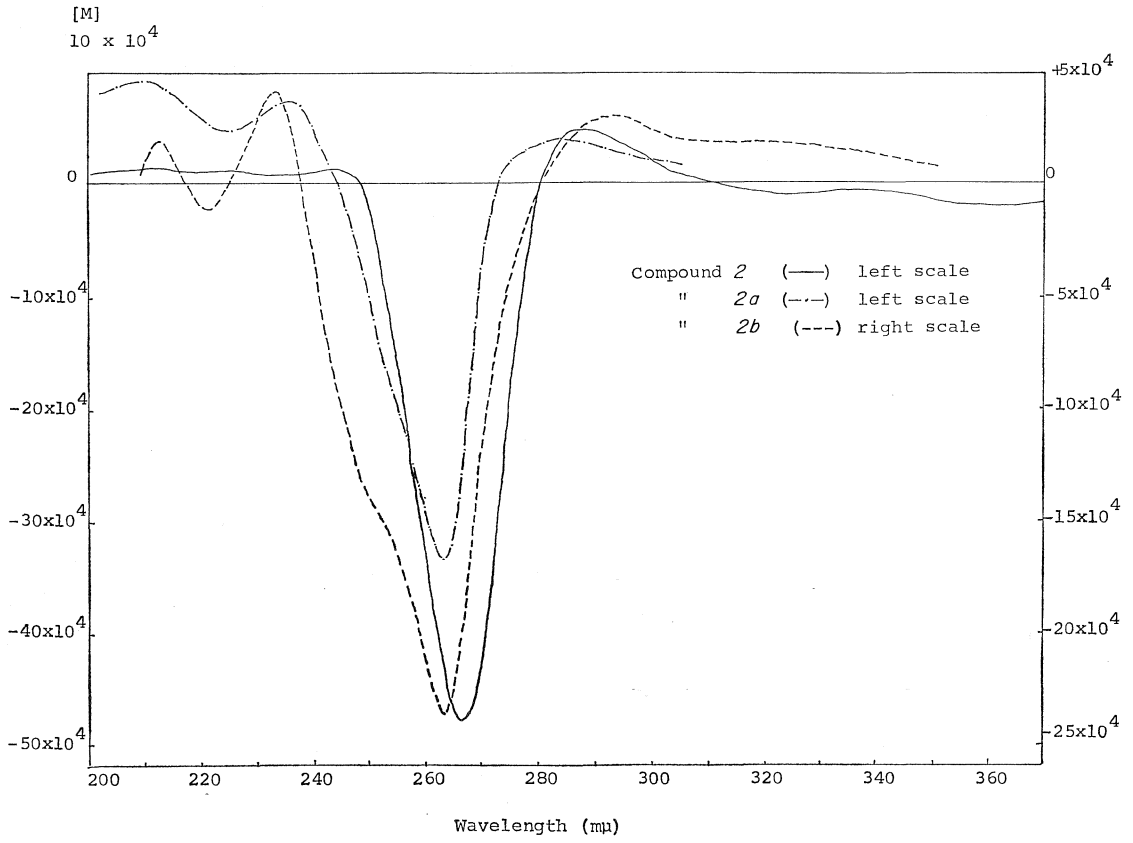

FIG. 2. The optical rotatory dispersion curves of **2**, **2***a*, and **2***b*.

positions of the methoxy group and the dimer linkage are switched, and in which no optical activity due to hindered rotation around the dimer-linkage should be observed.

Not enough model compounds of types **1** and **2** have been described to permit the assignment of the absolute stereochemistry of the binaphthyl linkage in xanthomegnin and vioxanthin (7).

An alternative structure for viopurpurin, which cannot be excluded at the present time, is represented by **7**.

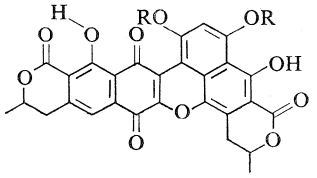

7, R = H,CH_3

Experimental

β-*Hydroxybutyric Acid from Xanthomegnin (**1**)*

Xanthomegnin (500 mg) was dissolved in 50 ml 1% aqueous potassium hydroxide. To the alkaline solution, 10 ml 50% hydrogen peroxide was dropped in slowly with stirring and the solution was stirred for 5 h. The solution was then acidified with concentrated hydrochloric acid to pH 4, and extracted with ether in a liquid–liquid extractor for 48 h.

The oxidation product **4** was then dried *in vacuo*, and dissolved in 50 ml anhydrous tetrahydrofuran. To the tetrahydrofuran solution, 1 g of lithium aluminium hydride was added cautiously, and the mixture stirred for 24 h. The excess reagent was decomposed with 1.6 ml 10% sodium hydroxide and 2 ml of distilled water. After the decomposition was completed, the solution was filtered, the filtrate was taken to dryness, and an oil was obtained. It showed one major spot on thin-layer chromatography (t.l.c.). The crude reduced product was dissolved in 40 ml of chloroform and ozonized at room temperature for 2 h. After the solvent was removed, 20 ml of distilled water and 500 mg of silver oxide were added to the ozonide. The mixture was warmed on a water bath for 20 min at 70°, the oxide was filtered off, and the filtrate acidified

Can. J. Chem. Downloaded from www.nrcresearchpress.com by 210.87.254.40 on 09/05/12
For personal use only.

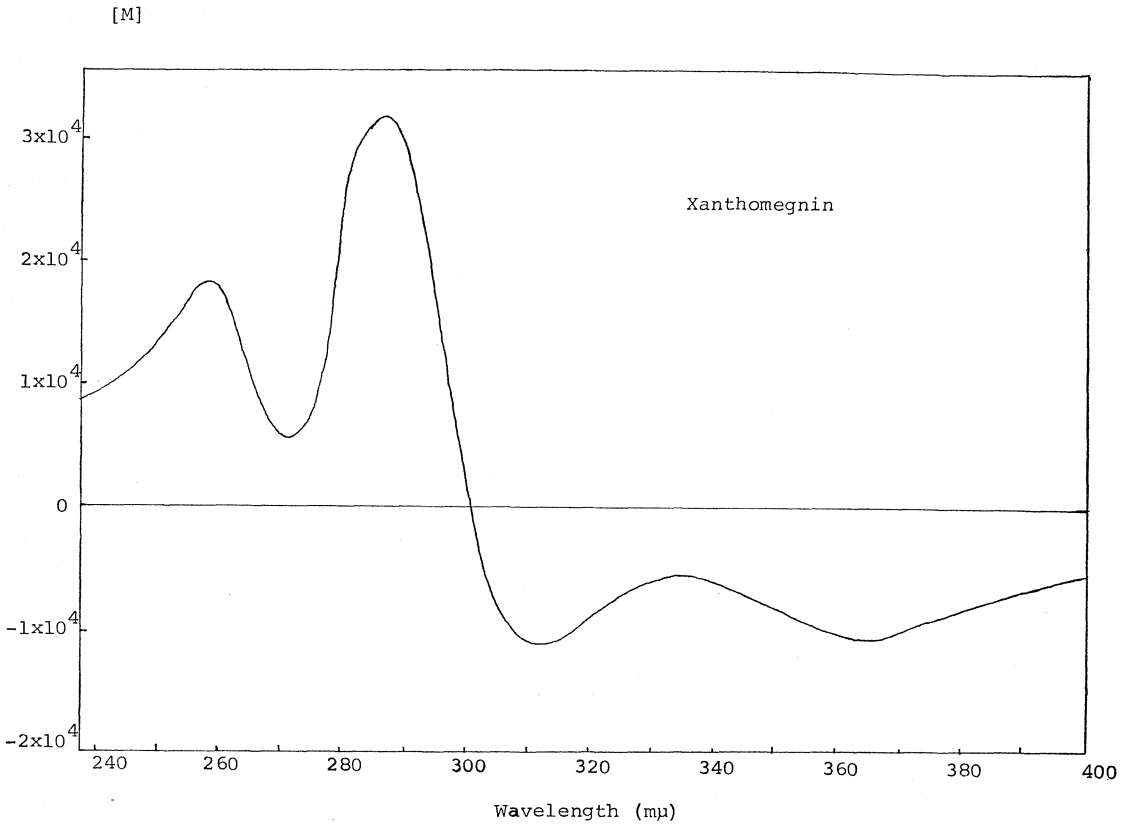

FIG. 3. The optical rotatory dispersion curve of the acid (or sodium salt) of **1**.

with concentrated hydrochloric acid. After removal of silver chloride, the filtrate was extracted with ether; β-hydroxybutyric acid was obtained and identified by t.l.c. The chromatogram was sprayed with methyl orange indicator after developing in acetone. A red spot having the same R_f value as authentic β-hydroxybutyric acid was observed. The acid was further identified by comparison of its retention time with that of an authentic sample on vapor-pressure chromatography (v.p.c.). Optical rotation of the acid was $[\alpha]_D - 22.8°$ ($CHCl_3$).

Tetramethyl Vioxanthin (2a)

To an acetone (20 ml) solution of vioxanthin (50 mg), were added 5 ml of dimethyl sulfate and 2 g of anhydrous potassium carbonate. The mixture was refluxed with stirring for 5 h, cooled, and the solid removed. Acetone was removed by evaporation *in vacuo*. The excess dimethyl sulfate was hydrolyzed with 5% aqueous sodium hydroxide solution. The alkaline solution was acidified with concentrated hydrochloric acid and extracted with chloroform. The chloroform solution was washed with distilled water until free from acid. The pale-colored tetramethyl vioxanthin obtained from the chloroform solution was purified by using t.l.c. (silicagel plates; benzene: hexane, 3:7); 40 mg of pure tetramethyl vioxanthin, m.p. 170–171°, was obtained as a powder and could not be crystallized.

λ_{max} (EtOH) 350 mμ (ε 5380), 320 mμ (ε 8840), 307 mμ ε 9250), 264 mμ (ε 53 000).

Anal. Calcd. for $C_{34}H_{34}O_{10}$ (mol. wt., 602): C, 67.76; H, 5.46; O, 26.60. Found[5] (mol. wt. (osmometric), 583): C, 66.82; H, 5.41; O, 27.69.

Mass spectrum: parent peak at *m/e* 602. The nuclear magnetic resonance (n.m.r.) spectrum differed from that of **2** mainly by the absence of the hydroxyl hydrogens and the presence of methoxy signals at 3.55 and 3.9 p.p.m.

Oxidation of Tetramethyl Vioxanthin

Tetramethyl vioxanthin (20 mg) was suspended in 20 ml of 5% aqueous sodium hydroxide solution. About 20 ml of 5% aqueous potassium permanganate was added portionwise and the solution was heated to reflux for 18 h. Manganese dioxide was removed and the filtrate acidified with dilute sulfuric acid. Sodium bisulfite was added to destroy the remaining manganese dioxide. The acidic solution was then extracted with ether in a liquid–liquid extractor for 48 h. The material obtained (2 mg) from the ether extract showed a spot corresponding to authentic anisole-2,3,5,6-tetracarboxylic acid (8) on t.l.c. Its infrared (i.r.) spectrum was also identical to that of the authentic sample. Crystallization was not possible because of the scarcity of the sample.

[5]Not enough sample to repeat the analysis.

Can. J. Chem. Downloaded from www.nrcresearchpress.com by 210.87.254.40 on 09/05/12
For personal use only.

Can. J. Chem. Downloaded from www.nrcresearchpress.com by 210.87.254.40 on 09/05/12
For personal use only.

Anisole-2,3,5,6-tetracarboxylic Acid Methyl Ester

The crude anisole-2,3,5,6-tetracarboxylic acid (2 mg) was dissolved in 1 ml of methanol. The solution was methylated with ethereal diazomethane for 30 min. The methylated product was dissolved in ether and injected into a DC 710 v.p.c. column (Model F & M 700, temperature 200 °C). Three peaks appeared with retention times at 0.95, 1.45, and 3.75 min. The retention time of an authentic sample of anisole-2,3,5,6-tetracarboxylic acid methyl ester (8) was 3.75 min.

Trimethyl Viopurpurin (3a)

Viopurpurin triacetate (**3***b*) (40 mg) was dissolved in absolute methanol. A methanol solution of sodium methoxide was added with stirring. The orange colored solution turned blue slowly. After stirring for 2 h, the solvent was removed and methyl iodide added to destroy the excess sodium methoxide. The resulting blue solid was suspended in 20 ml of spectrograde acetone, and 2 g of anhydrous potassium carbonate and 5 ml of dimethyl sulfate were added to the acetone solution. The mixture was refluxed for 8 h. After cooling, the solid was removed. The solvent was taken off by evaporating *in vacuo*. The excess dimethyl sulfate was hydrolyzed by stirring with 5% aqueous sodium hydroxide for 3 h. After the hydrolysis was complete, the alkaline solution was acidified with concentrated hydrochloric acid and extracted with chloroform; 30 mg of red crystalline trimethyl viopurpurin were obtained.[6] Recrystallization from methanol gave blood-red crystals, m.p. 173–174 °C.

λ_{max} (EtOH) 355 mμ (ε 1220), 278 mμ (ε 24 600), 270 mμ (ε 24 000), 218 mμ (ε 14 000); λ_{max} ($CHCl_3$) 455 mμ (ε 1030).

The mass spectrum showed a molecular ion peak at *m/e* 586 (calcd: 586). The n.m.r. of **3***a* showed the following peaks: δ 1.58 (6H, d), 3.10 (4H, d), 4.70 p.p.m. (2H, multiplet), corresponding to $CH_3CH(O)CH_2$—Ar; 7.8 (1H, s), 7.88 p.p.m. (1H, s) corresponding to two aromatic hydrogens; 4.11 (6H, s), 4.15 (3H, s), 4.2 p.p.m. (3H, s) corresponding to four methoxy groups.

[6]The material was used for degradation work. No analysis was obtained.

Alkaline Hydrogen Peroxide Oxidation of Trimethyl Viopurpurin (3a)

Trimethyl viopurpurin (20 mg) was dissolved in 5 ml of methanol and 5 ml of 20% sodium hydroxide was added. To the solution, 10 ml of 50% hydrogen peroxide was added slowly with stirring. Stirring was continued for 5 h, when the intense orange color faded to pale amber. The solution was then acidified with concentrated hydrochloric acid and extracted with ether in a liquid–liquid extractor for 24 h. The ether solution was evaporated to dryness: 3 mg of lactone **6** were obtained which on recrystallization from ether had a m.p. 192–194°. The m.p. was not depressed upon admixture of an authentic sample, and the i.r. spectrum and R_f value (t.l.c.) were identical with those of an authentic sample (5).

Acknowledgments

We would like to thank Dr. Ulrich Weiss, Laboratory of Physical Biology, National Institute of Arthritis and Metabolic Diseases, for taking the optical rotatory dispersion measurements, and Professor K. Mislow, Princeton University, for valuable suggestions.

1. G. Just, W. Day, and F. Blank. Can. J. Chem. **41**, 74 (1963).
2. F. Blank, A. S. Ng, and G. Just. Can. J. Chem. **44**, 2873 (1966).
3. K. J. Van der Merwe, P. S. Steyn, and D. L. Fourie. J. Chem. Soc. 7083 (1965).
4. R. S. Cahn and C. K. Ingold. J. Chem. Soc. 612 (1951); R. S. Cahn, C. K. Ingold, and V. Prelog. Experientia, **12**, 81 (1956).
5. J. Tudor. Ph.D. Thesis. McGill University, Montreal, Quebec. 1966.
6. C. S. Hudson. J. Am. Chem. Soc. **32**, 338 (1910). W. Klyne. Chem. Ind. London, 1198 (1954).
7. K. Mislow, M. A. W. Glass, R. E. O'Brien, P. Rutkin, D. H. Steinberg, J. Weiss, and C. Djerassi. J. Am. Chem. Soc. **84**, 1455 (1962).
8. J. C. Roberts. J. Chem. Soc. 2989 (1955).
9. C. Pace-Asciak, G. Just, and F. Blank. Can. J. Microbiol. **14**, 90 (1968).

Some derivatives of 1-benzazepine

A. H. Rees and K. Simon
Department of Chemistry, Trent University, Peterborough, Ontario

Received September 12, 1968

A new rearrangement of a substituted 5*H*-1-benzazepine-5-one is described. A new route to certain dimethyl-1-benzazepines has been developed and linked up with a known synthesis. Several new derivatives of 1-benzazepine are reported.

Canadian Journal of Chemistry, 47, 1227 (1969)

A number of 1-benzazepines based on the ketolactam **1**, (R = R′ = Me) have been described (1) and screened for pharmacological activity (2). Continuing our studies of this heterocyclic system, although we were unable to prepare analogues **1**, (RR′ = $(CH_2)_3$) and **1**, (R = Cl, R′ = Me) based on 5-acetylaminoindane and 3-methyl-4-chloroacetanilide respectively, we

Anisole-2,3,5,6-tetracarboxylic Acid Methyl Ester

The crude anisole-2,3,5,6-tetracarboxylic acid (2 mg) was dissolved in 1 ml of methanol. The solution was methylated with ethereal diazomethane for 30 min. The methylated product was dissolved in ether and injected into a DC 710 v.p.c. column (Model F & M 700, temperature 200 °C). Three peaks appeared with retention times at 0.95, 1.45, and 3.75 min. The retention time of an authentic sample of anisole-2,3,5,6-tetracarboxylic acid methyl ester (8) was 3.75 min.

Trimethyl Viopurpurin (3a)

Viopurpurin triacetate (**3***b*) (40 mg) was dissolved in absolute methanol. A methanol solution of sodium methoxide was added with stirring. The orange colored solution turned blue slowly. After stirring for 2 h, the solvent was removed and methyl iodide added to destroy the excess sodium methoxide. The resulting blue solid was suspended in 20 ml of spectrograde acetone, and 2 g of anhydrous potassium carbonate and 5 ml of dimethyl sulfate were added to the acetone solution. The mixture was refluxed for 8 h. After cooling, the solid was removed. The solvent was taken off by evaporating *in vacuo*. The excess dimethyl sulfate was hydrolyzed by stirring with 5% aqueous sodium hydroxide for 3 h. After the hydrolysis was complete, the alkaline solution was acidified with concentrated hydrochloric acid and extracted with chloroform; 30 mg of red crystalline trimethyl viopurpurin were obtained.[6] Recrystallization from methanol gave blood-red crystals, m.p. 173–174 °C.

λ_{max} (EtOH) 355 mμ (ε 1220), 278 mμ (ε 24 600), 270 mμ (ε 24 000), 218 mμ (ε 14 000); λ_{max} ($CHCl_3$) 455 mμ (ε 1030).

The mass spectrum showed a molecular ion peak at *m/e* 586 (calcd: 586). The n.m.r. of **3***a* showed the following peaks: δ 1.58 (6H, d), 3.10 (4H, d), 4.70 p.p.m. (2H, multiplet), corresponding to $CH_3CH(O)CH_2$—Ar; 7.8 (1H, s), 7.88 p.p.m. (1H, s) corresponding to two aromatic hydrogens; 4.11 (6H, s), 4.15 (3H, s), 4.2 p.p.m. (3H, s) corresponding to four methoxy groups.

[6]The material was used for degradation work. No analysis was obtained.

Alkaline Hydrogen Peroxide Oxidation of Trimethyl Viopurpurin (3a)

Trimethyl viopurpurin (20 mg) was dissolved in 5 ml of methanol and 5 ml of 20% sodium hydroxide was added. To the solution, 10 ml of 50% hydrogen peroxide was added slowly with stirring. Stirring was continued for 5 h, when the intense orange color faded to pale amber. The solution was then acidified with concentrated hydrochloric acid and extracted with ether in a liquid–liquid extractor for 24 h. The ether solution was evaporated to dryness: 3 mg of lactone **6** were obtained which on recrystallization from ether had a m.p. 192–194°. The m.p. was not depressed upon admixture of an authentic sample, and the i.r. spectrum and R_f value (t.l.c.) were identical with those of an authentic sample (5).

Acknowledgments

We would like to thank Dr. Ulrich Weiss, Laboratory of Physical Biology, National Institute of Arthritis and Metabolic Diseases, for taking the optical rotatory dispersion measurements, and Professor K. Mislow, Princeton University, for valuable suggestions.

1. G. Just, W. Day, and F. Blank. Can. J. Chem. **41**, 74 (1963).
2. F. Blank, A. S. Ng, and G. Just. Can. J. Chem. **44**, 2873 (1966).
3. K. J. Van der Merwe, P. S. Steyn, and D. L. Fourie. J. Chem. Soc. 7083 (1965).
4. R. S. Cahn and C. K. Ingold. J. Chem. Soc. 612 (1951); R. S. Cahn, C. K. Ingold, and V. Prelog. Experientia, **12**, 81 (1956).
5. J. Tudor. Ph.D. Thesis. McGill University, Montreal, Quebec. 1966.
6. C. S. Hudson. J. Am. Chem. Soc. **32**, 338 (1910). W. Klyne. Chem. Ind. London, 1198 (1954).
7. K. Mislow, M. A. W. Glass, R. E. O'Brien, P. Rutkin, D. H. Steinberg, J. Weiss, and C. Djerassi. J. Am. Chem. Soc. **84**, 1455 (1962).
8. J. C. Roberts. J. Chem. Soc. 2989 (1955).
9. C. Pace-Asciak, G. Just, and F. Blank. Can. J. Microbiol. **14**, 90 (1968).

Some derivatives of 1-benzazepine

A. H. Rees and K. Simon
Department of Chemistry, Trent University, Peterborough, Ontario

Received September 12, 1968

A new rearrangement of a substituted 5*H*-1-benzazepine-5-one is described. A new route to certain dimethyl-1-benzazepines has been developed and linked up with a known synthesis. Several new derivatives of 1-benzazepine are reported.

Canadian Journal of Chemistry, 47, 1227 (1969)

A number of 1-benzazepines based on the ketolactam **1**, (R = R′ = Me) have been described (1) and screened for pharmacological activity (2). Continuing our studies of this heterocyclic system, although we were unable to prepare analogues **1**, (RR′ = $(CH_2)_3$) and **1**, (R = Cl, R′ = Me) based on 5-acetylaminoindane and 3-methyl-4-chloroacetanilide respectively, we

Can. J. Chem. Downloaded from www.nrcresearchpress.com by 210.87.254.6 on 09/05/12
For personal use only.

were able to make various modifications to the heterocyclic ring.

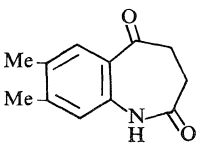

1

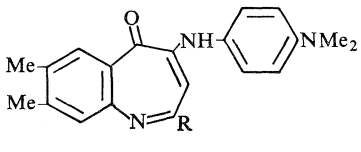

2

7,8-Dimethyl-2-hydroxy-4-(4′-dimethylamino)phenylamino-5*H*-1-benzazepine-5-one (**2**, R = OH) (1) was converted by phosphorus oxychloride into the corresponding 2-chloro-derivative (**2**, R = Cl). Reduction of the latter has so far given only a ring dihydro-derivative still containing the chlorine atom. During removal of the basic sidechain by acid hydrolysis (1), ring contraction occurred (3) to give the known 2-chloro-6,7-dimethylquinoline-4-carboxylic acid (4), presumably via the ion **3**. This is a new reaction of the sensitive "azatropone" system (5).

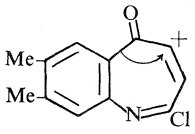

3

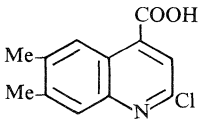

4

We have also developed a new route to 6,7-dimethyl-1-benzazepines based on β-3,4-xyloyl-propionic acid via reduction, cyclization to the tetralone, and Beckmann rearrangement of the ketoxime to give the lactam **5**.

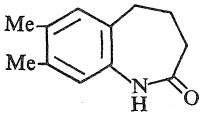

5

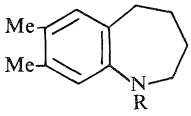

6

Subsequent hydride reduction gave the amine **6**, (R = H). Dehydration of the known alcohol **7** (1), followed by hydrogenation, gave a product shown to be the amine **6**, (R = H) by m.p., mixture m.p., and infrared (i.r.) spectrum, thus proving that both routes led to the same series of compounds.

The ketolactam **1**, (R = R′ = Me) was reduced by borohydride to the alcohol **8** providing a potential route to still further compounds.

Among variations of our original synthesis (1) of 1-benzazepines, we investigated the use of

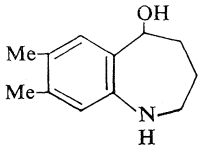

7

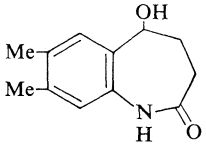

8

methylsuccinic anhydride and of *N*-methyl-*N*-acetyl-3,4-xylidine. To our surprise, the nuclear magnetic resonance (n.m.r.) spectra of compounds from these series showed the two aromatic protons as AB quartets, (J = 7 c.p.s.), suggesting structures **9** and **10** for the amino-acids isolated. The n.m.r. spectra of lactams **1**, (R = R′ = Me) and **5**, showed the aromatic protons as uncoupled (para-) singlets, confirming their orientation.

Although the amino-acids **9** and **10** might ultimately lead to 1-benzazepines, these were not prepared as they would be 6,7-dimethyl-1-benzazepines, whereas our thesis is (2) that maximum pharmacological activity would lie in the 7,8-dimethyl series.

Further work in this field continues.

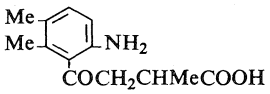

9

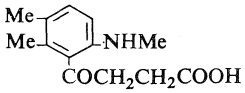

10

Experimental

7,8-Dimethyl-2-chloro-4-(4′-dimethylamino)phenylamino-5H-1-benzazepine-5-one (2, R = Cl)

The red 2-hydroxy compound **2**, (R = OH), (9.8 g) (1) was heated for 1 h on a steam bath with phosphorus oxychloride (25 ml). The solution was cooled and poured onto ice to decompose excess acid chloride, then filtered to remove a brown substance (0.3 g). On neutralization, the deep-red 2-chloro derivative was precipitated. It was collected and washed with 0.5 *N* carbonate solution, then water, and dried, to give a yield of 8.3 g, m.p. 230° from toluene.

Anal. Calcd. for $C_{20}H_{20}ClN_3O$: C, 67.9; H, 5.7; Cl, 10.0; N, 11.9. Found: C, 68.2; H, 5.8; Cl, 10.2; N, 11.6.

The carbonate washings, on acidification, gave 0.4 g of 7,8-dimethyl-3-hydro-1*H*-1-benzazepine-2,4,5(3*H*)-trione (1).

Catalytic hydrogenation or chromous chloride reduction of compound **2**, (R = Cl), gave the same yellow compound, m.p. 180–200° from aqueous acetic acid. This compound was difficult to purify but analyzed roughly for the acetate monohydrate of the dihydro derivative.

Acid Hydrolysis of the Chloro Compound (2, R = Cl)

The above chloro compound had λ_{max} 395, 280, and 225 mμ, log ε 4.06, 4.34, and 4.71 respectively, in ethanol

Can. J. Chem. Downloaded from www.nrcresearchpress.com by 210.87.254.6 on 09/05/12
For personal use only.

Can. J. Chem. Downloaded from www.nrcresearchpress.com by 210.87.254.6 on 09/05/12
For personal use only.

but gave an unstable spectrum in acid. On a preparative scale, the chloro compound was boiled with dilute hydrochloric acid until the color had faded. The filtered solution was neutralized, giving a carboxylic acid m.p. 217° from acetic acid, spectroscopically identical with and undepressed in mixed melt by 2-chloro-6,7-dimethylquinoline-4-carboxylic acid, prepared according to the literature (4).

7,8-Dimethyl-3,4,5-trihydro-1H-1-benzazepine-2(H)-one (5)

6,7-Dimethyl-1-tetralone (6) was treated with hydroxylamine hydrochloride in ethanolic pyridine at reflux. Addition of water gave the oxime, m.p. 179°.

Anal. Calcd. for $C_{12}H_{15}NO$: C, 76.15; H, 8.0; N, 7.4. Found: C, 75.75; H, 7.85; N, 7.35.

Beckmann rearrangement (7) of the oxime gave the azepinone (**5**), m.p. 175° from ligroin.

Anal. Calcd. for $C_{12}H_{15}NO$: C, 76.15; H, 8.0; N, 7.4. Found: C, 76.55; H, 8.3; N, 7.4.

7,8-Dimethyl-2,3,4,5-tetrahydro-1H-1-benzazepine (6, R = H)

The azepinone (**5**) gave on hydride reduction (8), the amine **6**, (R = H), m.p. 82° after sublimation.

Anal. Calcd. for $C_{12}H_{17}N$: C, 82.2; H, 9.8; N, 8.0. Found: C, 82.0; H, 9.8; N, 8.0.

The amine was characterized as its picrolonate, m.p. 205°, crystallized from dioxan.

Anal. Calcd. for $C_{22}H_{25}N_5O_5$: C, 60.1; H, 5.7; N, 15.95. Found: C, 60.0; H, 5.7; N, 15.9.

The *N*-acetyl derivative **6**, (R = CH_3CO) had m.p. 90° when crystallized from aqueous ethanol.

Anal. Calcd. for $C_{14}H_{19}NO$: C, 77.4; H, 8.8; N, 6.45. Found: C, 77.05; H, 8.9; N, 6.5.

Dehydration and Subsequent Hydrogenation of 5-Hydroxy-7,8-dimethyl-2,3,4,5-tetrahydro-1H-1-benzazepine (7)

The above azepine (**7**) (1 g) (1) was refluxed with concentrated hydrochloric acid (6 ml). On cooling, crystals of the hydrochloride of the dehydrated base appeared, m.p. 196°.

Anal. Calcd. for $C_{12}H_{16}ClN$: C, 68.7; H, 7.7; N, 6.7; Cl^-, 16.9. Found: C, 68.65; H, 7.5; N, 6.6; Cl^-, 17.0.

This salt was alkalized and a benzene extract washed until neutral, then evaporated, giving the free base, 7,8-dimethyl-2,3-dihydro-1*H*-1-benzazepine (1). This in turn was hydrogenated in ethanol using Adam's catalyst, giving the tetrahydrobenzazepine **6**, (R = H), m.p. 82°, which was undepressed in mixed melt, and the infrared (i.r.) spectrum was superimposable with that of the sample made by the other route.

5-Hydroxy-7,8-dimethyl-3,4,5-trihydroxy-1H-1-benzazepine-2(H)-one (8)

The ketolactam **1**, (R = R′ = Me) in tetrahydrofuran was treated with excess sodium borohydride in water. The mixture was neutralized with dilute acetic acid and extracted with hot benzene giving on cooling, the hydroxy compound (**8**), m.p. 192°. The i.r. spectrum confirmed the structure.

Anal. Calcd. for $C_{12}H_{15}NO_2$: C, 70.2; H, 7.4; N, 6.8. Found: C, 70.5; H, 7.35; N, 6.6.

Friedel–Crafts Reaction of N-Acetyl-3,4-xylidine with Methylsuccinic Anhydride

The above amide (81.7 g) gave (1) the keto-acid (55.4 g) assumed to be the α-methyl isomer (9), m.p. 206°, crystallized from ethanol.

Anal. Calcd. for $C_{15}H_{19}NO_4$: C, 64.95; H, 6.9; N, 5.05. Found: C, 64.85; H, 7.0; N, 5.05.

Hydrolysis with 6 *N* hydrochloric acid yielded the amino-acid hydrochloride, m.p. 143°, crystallized from 2 *N* acid.

Anal. Calcd. for $C_{13}H_{17}NO_3 \cdot HCl \cdot H_2O$: Cl^-, 12.4. Found: Cl^-, 12.1.

Recrystallization from aqueous ethanol resulted in hydrolysis of the salt, giving the free amino-acid, m.p. 173°, crystallized from toluene.

Anal. Calcd. for $C_{13}H_{17}NO_3$: C, 66.4; H, 7.3; N, 6.0. Found: C, 66.4; H, 7.3; N, 6.5.

The nuclear magnetic resonance (n.m.r.) spectrum of the *N*-acetyl derivative showed *ortho* protons indicating structure **9**.

N-Acetyl-N-methyl-3,4-xylidine

N-Formyl-3,4-xylidine (10), b.p. 134°/0.4 mm was reduced by lithium aluminium hydride (8) to *N*-methyl-3,4-xylidine, b.p. 170°/110 mm, n_D^{22} 1.553, lit.(11) 1.558; picrate m.p. 139°, lit. 133–136°. The picrolonate had m.p. 205° decomp., crystallized from ethanol.

Anal. Calcd. for $C_9H_{21}N_5O_5$: N, 17.5. Found: N, 17.6.

The above methylxylidine (20 g), after refluxing for 2 h with acetic anhydride (20 ml) then distilling, gave the *N*-acetyl derivative (23.7 g) b.p. 202°/83 mm which had m.p. 76°, crystallized from cyclohexane.

Anal. Calcd. for $C_{11}H_{15}NO$: C, 74.55; H, 8.55; N, 7.9. Found: C, 74.65; H, 8.65; N, 7.95.

The above methyl-xylidine, after reflux for 1 h with succinic anhydride (1 equivalent) in dioxan, gave on precipitation with water, the *N*-succinoyl derivative, m.p. 102°, crystallized from benzene/cyclohexane.

Anal. Calcd. for $C_{13}H_{17}NO_3$: C, 66.4; H, 7.3; N, 5.95. Found: C, 66.6; H, 7.6; N, 5.8.

Friedel–Crafts Reaction of N-Methyl-N-acetyl-3,4-xylidine with Succinic Anhydride

The above amide (24.3 g) gave (1) the crude keto-acid in benzene solution. After extraction with dilute alkali, starting amide (10 g) remained in the benzene. The alkaline extract was acidified, precipitating the keto-acid as an oil which was triturated with ether leaving insoluble material (2 g). The ether solution was washed with water, dried, and the solvent evaporated leaving a golden brown oil (10.8 g) which did not crystallize. It was therefore hydrolyzed with 6 *N* hydrochloric acid (40 ml) at the reflux (3 h), then concentrated to 20 ml. Neutralization gave an oil which was stored in vacuum until partly solid. After pressing this on a porous plate, a tacky solid remained which was triturated with methanol to give pure amino-acid (1.85 g), m.p. 118°, crystallized from aqueous ethanol.

Anal. Calcd. for $C_{13}H_{17}NO_3$: C, 66.35; H, 7.3; N, 5.95. Found: C, 66.0; H, 7.3; N, 5.85.

The n.m.r. spectrum of the amino-acid revealed *ortho* protons, indicating structure **10**.

Acknowledgments

We wish to thank the Department of University Affairs for a Province of Ontario Graduate Studentship (to K. Simon) and the National Research Council of Canada for general support and funds for a Summer Student (1967).

1. A. H. Rees. J. Chem. Soc. 3111 (1959).
2. D. M. James and A. H. Rees. J. Med. Pharm. Chem. **5**, 1234 (1962).
3. G. Jones. J. Chem. Soc. C, 1808 (1967).
4. H. King and J. Wright. Proc. Roy. Soc. London, Ser. B, **135**, 271 (1948).
5. W. C. Peaston and G. R. Proctor. J. Chem. Soc. C, 2481 (1968), and preceding papers.
6. E. deBarry Barnett and F. G. Sanders. J. Chem. Soc. 434 (1933).
7. E. C. Horning and V. L. Stromberg. J. Am. Chem. Soc. **74**, 2680 (1952).
8. V. M. Micovic and M. LJ. Mihailovic. J. Org. Chem. **18**, 1190 (1953).
9. E. Berliner. Organic reactions. Vol. V. John Wiley and Sons, Inc., New York. 1949. p. 242.
10. L. Limpach. Chem. Ber. **21**, 646 (1888).
11. P. Hemmerich, S. Fallab, and H. Erlenmeyer. Helv. Chim. Acta, **39**, 1242 (1956).

Metallation of 5- and 6-membered ring sultones

T. Durst and J. du Manoir

Department of Chemistry, University of Ottawa, Ottawa, Canada

Received September 18, 1968

Treatment of 1,3-propane and 1,4-butane sultone with *n*-butyllithium in tetrahydrofuran at −78° has been shown to result in metallation α to the sulfonyl group. This is in contrast to ring opening which has been observed when the reaction was carried out at room temperature (1, 2). The products obtained from the interaction of the lithio derivatives **3** and **4** with carbonyl compounds and alkyl halides are described.

Canadian Journal of Chemistry, 47, 1230 (1969)

The reaction of 5- and 6-membered ring sultones with a wide variety of nucleophilic reagents such as alcohols, amines, alkoxides, and metal alkyls has been reported to lead invariably to derivatives of sulfonic acids, see eq. [1] (1, 2). This type of reaction has been of considerable industrial importance since it has allowed the introduction of a water-solubilizing group into a variety of organic molecules.

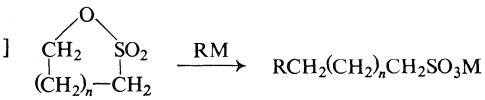

[1] $\xrightarrow{RM}$ $RCH_2(CH_2)_nCH_2SO_3M$

1, $n = 1$
2, $n = 2$

The reactions of **1** and **2** with the organometallic reagents were generally carried out at temperatures above 0° (2). We have found that if the treatment of the sultones with alkyllithiums, e.g. *n*-butyllithium, is carried out at acetone – dry ice temperature in tetrahydrofuran solution, the ring opening reaction is suppressed and metallation occurs α to the sulfonyl group, thereby yielding the lithio salts **3** and **4** as shown by quantitative deuterium incorporation upon hydrolysis with D_2O. The success of the metallation procedure at the low temperature apparently stems from the fact that the ring opening reaction is considerably more temperature dependent than metallation. Metallation α to the sulfonyl groups of aliphatic sulfonic acid esters has recently been reported by Corey and Durst (3).

The lithio derivatives appeared to be stable for at least 3 h in tetrahydrofuran solution at −78°. Decomposition occurred rapidly upon warming to −20° as evidenced by the formation of a colorless water-soluble precipitate. The infrared (i.r.) spectrum (KBr) of this material showed only a few ill-defined bands; its structure has not been further investigated.

Reaction of **3** and **4** with carbonyl derivatives afforded, after hydrolysis, the adducts **5** and **6** in 65–85% yield. The structures of the adducts were assigned on the basis of elemental analyses and spectroscopic properties. The i.r. spectrum of each adduct showed a moderately strong band at about 3550 cm^{-1} due to the newly formed hydroxyl group and strong bands between 1340–1360, 1160–1170, and 980–995 cm^{-1} which indicated that the sultone grouping had been retained. Nuclear magnetic resonance (n.m.r.) data (see Experimental) fully supported the above conclusions.

Can. J. Chem. Downloaded from www.nrcresearchpress.com by 210.87.254.6 on 09/05/12
For personal use only.

Acknowledgments

We wish to thank the Department of University Affairs for a Province of Ontario Graduate Studentship (to K. Simon) and the National Research Council of Canada for general support and funds for a Summer Student (1967).

1. A. H. Rees. J. Chem. Soc. 3111 (1959).
2. D. M. James and A. H. Rees. J. Med. Pharm. Chem. **5**, 1234 (1962).
3. G. Jones. J. Chem. Soc. C, 1808 (1967).
4. H. King and J. Wright. Proc. Roy. Soc. London, Ser. B, **135**, 271 (1948).
5. W. C. Peaston and G. R. Proctor. J. Chem. Soc. C, 2481 (1968), and preceding papers.
6. E. deBarry Barnett and F. G. Sanders. J. Chem. Soc. 434 (1933).
7. E. C. Horning and V. L. Stromberg. J. Am. Chem. Soc. **74**, 2680 (1952).
8. V. M. Micovic and M. LJ. Mihailovic. J. Org. Chem. **18**, 1190 (1953).
9. E. Berliner. Organic reactions. Vol. V. John Wiley and Sons, Inc., New York. 1949. p. 242.
10. L. Limpach. Chem. Ber. **21**, 646 (1888).
11. P. Hemmerich, S. Fallab, and H. Erlenmeyer. Helv. Chim. Acta, **39**, 1242 (1956).

Metallation of 5- and 6-membered ring sultones

T. Durst and J. du Manoir

Department of Chemistry, University of Ottawa, Ottawa, Canada

Received September 18, 1968

Treatment of 1,3-propane and 1,4-butane sultone with *n*-butyllithium in tetrahydrofuran at −78° has been shown to result in metallation α to the sulfonyl group. This is in contrast to ring opening which has been observed when the reaction was carried out at room temperature (1, 2). The products obtained from the interaction of the lithio derivatives **3** and **4** with carbonyl compounds and alkyl halides are described.

Canadian Journal of Chemistry, 47, 1230 (1969)

The reaction of 5- and 6-membered ring sultones with a wide variety of nucleophilic reagents such as alcohols, amines, alkoxides, and metal alkyls has been reported to lead invariably to derivatives of sulfonic acids, see eq. [1] (1, 2). This type of reaction has been of considerable industrial importance since it has allowed the introduction of a water-solubilizing group into a variety of organic molecules.

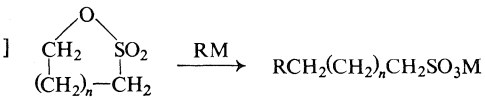

[1] $\xrightarrow{RM}$ $RCH_2(CH_2)_nCH_2SO_3M$

1, $n = 1$
2, $n = 2$

The reactions of **1** and **2** with the organometallic reagents were generally carried out at temperatures above 0° (2). We have found that if the treatment of the sultones with alkyllithiums, e.g. *n*-butyllithium, is carried out at acetone – dry ice temperature in tetrahydrofuran solution, the ring opening reaction is suppressed and metallation occurs α to the sulfonyl group, thereby yielding the lithio salts **3** and **4** as shown by quantitative deuterium incorporation upon hydrolysis with D_2O. The success of the metallation procedure at the low temperature apparently stems from the fact that the ring opening reaction is considerably more temperature dependent than metallation. Metallation α to the sulfonyl groups of aliphatic sulfonic acid esters has recently been reported by Corey and Durst (3).

The lithio derivatives appeared to be stable for at least 3 h in tetrahydrofuran solution at −78°. Decomposition occurred rapidly upon warming to −20° as evidenced by the formation of a colorless water-soluble precipitate. The infrared (i.r.) spectrum (KBr) of this material showed only a few ill-defined bands; its structure has not been further investigated.

Reaction of **3** and **4** with carbonyl derivatives afforded, after hydrolysis, the adducts **5** and **6** in 65–85% yield. The structures of the adducts were assigned on the basis of elemental analyses and spectroscopic properties. The i.r. spectrum of each adduct showed a moderately strong band at about 3550 cm^{-1} due to the newly formed hydroxyl group and strong bands between 1340–1360, 1160–1170, and 980–995 cm^{-1} which indicated that the sultone grouping had been retained. Nuclear magnetic resonance (n.m.r.) data (see Experimental) fully supported the above conclusions.

Can. J. Chem. Downloaded from www.nrcresearchpress.com by 210.87.254.6 on 09/05/12
For personal use only.

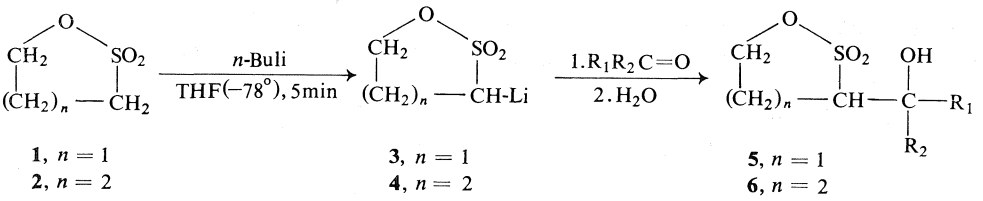

1, $n = 1$
2, $n = 2$

3, $n = 1$
4, $n = 2$

5, $n = 1$
6, $n = 2$

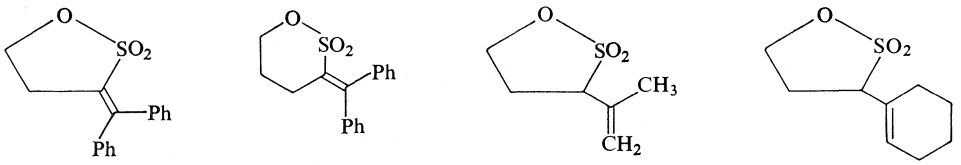

7 **8** **9** **10**

Dehydration of the hydroxy sultones (benzene-*p*-toluenesulfonic acid) led to the formation of the α,β-unsaturated derivatives **7** and **8** in the case of the benzophenone adducts, and to β,γ-unsaturated sultones **9** and **10** for the acetone and cyclohexanone adducts respectively. The preference of the double bond in the β,γ- rather than α,β-position in the latter two sultones is not unexpected. Similar observations have been made for unsaturated sulfoxides and sulfones (4, 5). The yields of the various dehydrated derivatives were of the order of 75–90%. Analytical and spectroscopic data fully supported the individual assignments.

Reaction of **3** with methyl iodide and benzyl chloride resulted in the formation of the expected alkylation products in 62 and 49% yield respectively. With less reactive alkylating agents, e.g. ethyl bromide or isopropyl iodide, the yields were considerably less. With these reagents no alkylation occurred at −78°. At −20° the decomposition of **3** as judged by formation of the colorless precipitate is apparently more rapid than the alkylation reaction.

It is thus likely that only a limited number of 3-alkylated sultones can be synthesized by the direct alkylation procedure. However, a much larger variety may be obtained in quite reasonable yields by the 3-step sequence involving reaction of the lithio derivatives with the appropriate carbonyl compound, followed by dehydration and hydrogenation.

Experimental

Melting points were determined with a Thomas Hoover apparatus and are not corrected. Infrared spectra were recorded on a Beckman (model IR8) infrared (i.r.) spectrophotometer and nuclear magnetic resonance (n.m.r.) spectra were obtained on a Varian Associates model HA-100 spectrophotometer.

Generation of the Lithio Derivatives 3 and 4

To a rapidly stirred solution of approximately 1 g sultone in 30 ml tetrahydrofuran at −78° under a nitrogen atmosphere, were added dropwise 1.1 equivalents of *n*-butyllithium (1.6 *M* in hexane). The clear solution was stirred for 5 min and then treated with the appropriate reagent. The lithio salt **3** was stable at −78° for at least 3 h. When warmed to −20° decomposition occurred within 10 min and a colorless water-soluble precipitate was deposited. The i.r. spectrum (KBr) of this material showed strong bands at 1280 and 1040 cm^{-1}. Similar stability behavior was noted for **4**.

Reaction of Lithio Derivatives 3 and 4 with Ketones and Aldehydes

The lithio derivatives were prepared as described above. To a solution kept at −78° was added the carbonyl compound, neat if liquid, or as a tetrahydrofuran solution if solid. The reaction mixture was stirred at −78° for a further 10 min and then poured into water and extracted with methylene chloride. The organic extracts were dried over magnesium sulfate and the solvent was evaporated under reduced pressure. Yields were not significantly altered if the reaction mixture was allowed to warm to room temperature prior to the addition of water.

Deuteration of 3

A solution of **3** in tetrahydrofuran at −78° was allowed to react with excess D_2O for 2 min. The reaction mixture was poured into water and extracted with ether. The

Can. J. Chem. Downloaded from www.nrcresearchpress.com by 210.87.254.6 on 09/05/12
For personal use only.

recovery of mono-deuterated 1,3-propane sultone was generally between 65–70%. The n.m.r. spectrum ($CDCl_3$) showed peaks at 2.5–2.8 (m, 2H), 3.1–3.4 (m, 1H), and 4.48 p.p.m. (t, J = 5.5 c.p.s., 2H). In separate experiments it was shown that only approximately 70% of 1,3-propane sultone was recovered under the work-up conditions employed above.

Benzophenone

A solution of 6.6 mmoles of **3** in 30 ml tetrahydrofuran and 1.20 g (6.6 mmoles) of benzophenone gave 1.30 g (65%) of adduct as colorless granules, m.p. 169–171° (decomp.). The i.r. spectrum ($CHCl_3$) showed bands at 3550 (m), 1340 (s), 1162 (s), and 990 (m) cm^{-1}. The n.m.r. absorption ($CDCl_3$) occurred at 2.0–2.4 (m, 1H), 2.6–3.0 (m, 1H), 4.0–4.7 (m, 4H), and 7.2–7.8 p.p.m. (m, 10H).

Anal. Calcd. for $C_{16}H_{16}O_4S$: C, 63.15; H, 5.30; S, 10.52. Found: C, 63.37; H, 5.38; S, 10.90.

The above adduct (2.15 g) and 150 mg of *p*-toluenesulfonic acid in 50 ml of benzene were refluxed for 6 h. The reaction mixture was washed with water. The benzene layer was dried and the solvent evaporated. Recrystallization from methylene chloride – pentane gave 1.76 g (87%) of the unsaturated sultone **7**, m.p. 133–134°. The i.r. spectrum ($CHCl_3$) showed bands at 1620 (w), 1348 (s), 1175 (s), and 997 (m) cm^{-1}. The n.m.r. absorption ($CDCl_3$) occurred at 3.20 (t, J = 7.0 c.p.s., 2H), 4.41 (t, J = 7.0 c.p.s., 2H), and 7.2–7.5 p.p.m. (m, 10H).

Anal. Calcd. for $C_{16}H_{14}O_3S$: C, 67.12; H, 4.93; S, 11.18. Found: C, 67.33; H, 5.27; S, 11.23.

Benzaldehyde

A solution of 11.0 mmoles of **3** in 40 ml of tetrahydrofuran and 1.17 g (11.0 mmoles) of benzaldehyde gave 2.40 g of crude adduct whose i.r. spectrum indicated less than 5% benzaldehyde. The crude product solidified when triturated with 1:1 ether–pentane to yield 2.21 g (88%) of colorless solid. Recrystallization from ether–pentane gave colorless granules, m.p. 83–88°. The i.r. spectrum ($CHCl_3$) showed peaks at 3550 (m), 1348 (s), 1162, and 984 (m) cm^{-1}. The n.m.r. absorption occurred at 2.2–2.5 (m, 1H), 2.6–2.9 (m, 1H), 3.03 (s, 1H), 3.5–3.8 (m, 1H), 4.2–4.7 (m, 2H), 5.50 (d, J = 3 c.p.s., 1H), and 7.40 p.p.m. (s, 5H).

Anal. Calcd. for $C_{10}H_{12}O_4S$: C, 52.63; H, 5.30; S, 14.02. Found: C, 52.81; H, 5.38; S, 14.17.

Cyclohexanone

Addition of 0.60 g cyclohexanone to a solution of 6.0 mmoles of the lithio derivative **3** gave 1.07 g (81%) of crude adduct, m.p. 98–101°. Recrystallization from methylene chloride – pentane furnished colorless plates, m.p. 102–104°. The n.m.r. spectrum ($CDCl_3$) showed a singlet at 2.60 (1H), a pair of doublets at 3.34 (J = 10, 11 c.p.s., 1H), and multiplets at 1.2–2.2 (10H), 2.2–3.1 (2H), and 4.2–4.6 p.p.m. (2H). The i.r. peaks ($CHCl_3$) occurred at 3550 (m), 1342 (s), 1170 (s), 995 (m), and 982 (m) cm^{-1}.

Anal. Calcd. for $C_9H_{16}O_4S$: C, 49.08; H, 7.32; S, 14.53. Found: C, 48.86; H, 7.38; S, 14.73.

Dehydration of the above adduct under the conditions described for the benzophenone adduct gave a 75% yield of **10**, m.p. 66–67°. Three recrystallizations from ether–pentane gave fluffy needles, m.p. 70–71°. Infrared absorptions (CCl_4) occurred at 1357 (s), 1168 (s), and 996 (m) cm^{-1}. The n.m.r. peaks ($CDCl_3$) occurred at 1.5–1.9 (m, 4H), 2.0–2.3 (m, 4H), 2.4–2.9 (m, 2H), 3.85 (t, J = 11.0 c.p.s., 1H), 4.2–4.6 (m, 2H), and 5.9 p.p.m. (broad singlet, 1H).

Anal. Calcd. for $C_9H_{14}O_3S$: C, 53.46; H, 6.98; S, 15.82. Found: C, 53.34; H, 6.93; S, 16.10.

Acetone

Reaction of 10.0 mmoles of **3** in 35 ml tetrahydrofuran at −78° with 580 mg of acetone furnished after recrystallization from ether, 1.11 g (61%) of adduct, m.p. 53–55°. The i.r. spectrum ($CHCl_3$) showed absorption at 3550 (m), 1342 (s), 1162 (s), and 990 (m) cm^{-1}. The n.m.r. peaks ($CDCl_3$) occurred at 1.30 (s, 3H), 1.57 (s, 3H), 2.4–2.9 (m, 2H), 2.99 (s, 1H), 3.35 (doublet of doublets, J = 8.0, 9.0 c.p.s., 1H), and 4.2–4.6 p.p.m. (m, 2H).

Anal. Calcd. for $C_6H_{12}O_4S$: C, 40.00; H, 6.71; S, 17.77. Found: C, 40.50; H, 6.82; S, 17.90.

Dehydration of the acetone adduct in the usual manner furnished a colorless oil (81%) which was homogeneous on thin-layer chromatography (t.l.c.). Spectroscopic properties of this oil were in agreement with its formulation as **9**. Infrared peaks (CCl_4) occurred at 1635 (w), 1355 (s), 1168 (s), 990 (m), and 905 (m) cm^{-1}. The n.m.r. peaks ($CDCl_3$) were at 1.96 (s, 3H), 2.5–2.8 (m, 2H), 3.92 (t, J = 9.0 c.p.s., 1H), 4.3–4.6 (m, 2H), and 2 slightly broadened singlets at 5.18 (1H) and 5.24 p.p.m. (1H).

Reaction of 3 with Benzyl Bromide

To a solution of 7.0 mmoles of **3** in 30 ml of tetrahydrofuran were added 1.20 g (7.0 mmoles) of benzyl bromide. The reaction mixture was stirred at −78° for 30 min and at −20° for 1 h. Work-up yielded 1.42 g of crude product which was purified by preparative t.l.c. The yield of 5-benzyl-1,3-propane sultone was 0.73 g (49%), m.p. 54–55° (colorless needles from ether–pentane). The i.r. spectrum showed bands at 1355 (s), 1168 (s), and 995 (m) cm^{-1}.

Anal. Calcd. for $C_{10}H_{12}O_3S$: C, 56.60; H, 5.70; S, 15.08. Found: C, 56.72; H, 5.70; S, 15.06.

Reaction of 3 with Methyl Iodide

Methyl iodide 1.42 g (10.0 mmoles) was added to a solution of 10.0 mmoles of **3** in tetrahydrofuran at −78°. The reaction mixture was stirred at −78° for 5 min and at −20° for 10 min. The slightly turbid reaction mixture was poured into water and extracted with methylene chloride. The organic phase was dried and the solvent evaporated, yielding 900 mg (67%) of an oil which upon distillation gave 822 mg (62%) of 5-methyl-1,3-propane sultone, $n_D^{25} = 1.4532$; lit.(1, 6) $n_D^{25} = 1.4525$. The n.m.r. spectrum (CCl_4) showed the methyl doublet at 1.48 p.p.m. (J = 7 c.p.s.).

Reaction of 3 with Ethyl Bromide and Isopropyl Iodide

A solution of **3** in tetrahydrofuran was allowed to react with an equimolar amount of alkyl halide, first at −78° for 10 min then at −20° for 2 h. A large amount of colorless precipitate was formed at −20°. The reaction mixture was diluted with water and extracted with ether. The organic layer was dried and the solvent evaporated yielding approximately 25% of crude product which was mainly the 3-alkylated sultone (by n.m.r.).

Can. J. Chem. Downloaded from www.nrcresearchpress.com by 210.87.254.6 on 09/05/12
For personal use only.

In other experiments it was shown that virtually no alkylation occurred at −78° and that the precipitate formed at −20° was identical to that formed from **3** at −20° in the absence of alkyl halide.

Reaction of the Lithio Derivative 4 with Benzophenone

To a solution of **4**, generated from 1.00 g (7.35 mmoles) of butane-1,4-sultone in 30 ml of tetrahydrofuran at −78° were added 1.30 g (7.2 mmoles) of solid benzophenone. The reaction mixture was stirred at −78° for 10 min and then worked up as described above. Recrystallization of the crude solid adduct from methylene chloride – pentane gave 1.44 g (63%) colorless needles, m.p. 182–182.5°. The i.r. spectrum ($CHCl_3$) showed peaks at 3550 (m), 1350 (s), 1165 (s), and 955 (m) cm^{-1}. The n.m.r. peaks ($CDCl_3$) occurred at 1.6–2.6 (m, 4H), 4.12 (s, 1H), 4.2–4.7 (m, 2H), and 7.1–7.7 p.p.m. (10H).

Anal. Calcd. for $C_{17}H_{18}O_4S$: C, 64.14; H, 5.70; S, 10.06. Found: C, 64.23; H, 5.87; S, 10.11.

Dehydration of 315 mg of the above adduct under the usual conditions furnished 263 mg (89%) of unsaturated sultone **8**, m.p. 172–173.5° (needles from methylene chloride – pentane). The i.r. spectrum ($CHCl_3$) showed peaks at 1360 (s), 1170 (s), and 970 (m) cm^{-1}. The n.m.r. bands ($CDCl_3$) occurred at 1.9–2.2 (m, 2H), 2.8–3.0 (m, 2H), 4.60 (t, J = 5.5 c.p.s., 2H), and 7.1–7.5 p.p.m. (m, 10H).

Anal. Calcd. for $C_{17}H_{16}O_3S$: C, 67.99; H, 5.37; S, 10.66. Found: C, 68.31; H, 5.45; S, 10.91.

Acknowledgment

Financial support of this work by the National Research Council of Canada is gratefully acknowledged.

1. D. S. Breslow and H. Skolnik. *In* The chemistry of heterocyclic compounds. Vol. 21. Part I. *Edited by* A. Weissberger. Interscience Publishers, Inc., New York. 1966. pp. 87–95; Vol. 21. Part II. pp. 780–783.
2. W. E. Truce and D. F. Hoerger. J. Am. Chem. Soc. **77**, 2496 (1955).
3. E. J. Corey and T. Durst. J. Am. Chem. Soc. **88**, 5656 (1966); **90**, 5548 (1968).
4. C. D. Broaddus. Acc. Chem. Res. **1**, 231 (1968).
5. D. E. O'Connor and W. I. Lyness. J. Am. Chem. Soc. **86**, 3840 (1964).
6. J. H. Hellberger. Ann. **588**, 71 (1959).

S-[(*N*-Terpenoid carboxamidinium)methyl] thiosulfates (Bunte salts) as potential antiradiation agents

Jerry M. Barton and Ludwig Bauer[1]

Department of Chemistry, College of Pharmacy, University of Illinois (Medical Center), P.O. Box 6998, Chicago, Illinois 60680

Received November 26, 1968

The synthesis of a number of α-acetamidinium Bunte salts, substituted on one of the nitrogen atoms by a terpenoid moiety, is reported.

Canadian Journal of Chemistry, **47**, 1233 (1969)

It has been shown that a number of *S*-[(*N*-substituted carboxamidinium)methyl] thiosulfates, $^{-}O_3SSCH_2C(=NH_2^{+})NHR$, **1**, are promising radiation-protective compounds in mice (1, 2). This paper describes the synthesis of derivatives of **1** in which one of the amidine nitrogen atoms bears a highly condensed aliphatic structure. It has been observed in a series of *N*-(ω-cycloalkane)-alkyl derivatives of **1** [R = *cyclo*-C_nH_{2n-1}—$(CH_2)_m$] that good activity was retained up to R = 4-(cyclohexyl)butyl, (3). In a recent report, it was disclosed that those *S*-2-aminoethyl thiosulfates, $HO_3S_2CH_2CH_2NHR$, bearing similarly constituted (cycloalkane)alkyl substituents on nitrogen, were among the best radiation-protective substances (4). The project described at present was designed to modify the polar character of **1** by introducing highly condensed aliphatic systems into the molecule. By attaching bi- and tricyclic aliphatic ring systems to the amidine function of **1**, it was hoped to impart additional lipid solubility and possibly facilitate transport of these substances through living systems. Toward this end, derivatives of **1** bearing either terpenoid or adamantane substituents were synthesized and their structures are listed in Table I.

The synthesis employed to prepare these compounds was as described previously (1–3). Methyl α-chloroacetimidate is generated *in situ*

[1]The authors gratefully acknowledge support for this project from the Office of the Surgeon General, United States Army Medical Research and Development Command (Contract No. DA-49-193-MD-2047).

Can. J. Chem. Downloaded from www.nrcresearchpress.com by 210.87.254.6 on 09/05/12
For personal use only.

In other experiments it was shown that virtually no alkylation occurred at −78° and that the precipitate formed at −20° was identical to that formed from **3** at −20° in the absence of alkyl halide.

Reaction of the Lithio Derivative 4 with Benzophenone

To a solution of **4**, generated from 1.00 g (7.35 mmoles) of butane-1,4-sultone in 30 ml of tetrahydrofuran at −78° were added 1.30 g (7.2 mmoles) of solid benzophenone. The reaction mixture was stirred at −78° for 10 min and then worked up as described above. Recrystallization of the crude solid adduct from methylene chloride – pentane gave 1.44 g (63%) colorless needles, m.p. 182–182.5°. The i.r. spectrum ($CHCl_3$) showed peaks at 3550 (m), 1350 (s), 1165 (s), and 955 (m) cm^{-1}. The n.m.r. peaks ($CDCl_3$) occurred at 1.6–2.6 (m, 4H), 4.12 (s, 1H), 4.2–4.7 (m, 2H), and 7.1–7.7 p.p.m. (10H).

Anal. Calcd. for $C_{17}H_{18}O_4S$: C, 64.14; H, 5.70; S, 10.06. Found: C, 64.23; H, 5.87; S, 10.11.

Dehydration of 315 mg of the above adduct under the usual conditions furnished 263 mg (89%) of unsaturated sultone **8**, m.p. 172–173.5° (needles from methylene chloride – pentane). The i.r. spectrum ($CHCl_3$) showed peaks at 1360 (s), 1170 (s), and 970 (m) cm^{-1}. The n.m.r. bands ($CDCl_3$) occurred at 1.9–2.2 (m, 2H), 2.8–3.0 (m, 2H), 4.60 (t, J = 5.5 c.p.s., 2H), and 7.1–7.5 p.p.m. (m, 10H).

Anal. Calcd. for $C_{17}H_{16}O_3S$: C, 67.99; H, 5.37; S, 10.66. Found: C, 68.31; H, 5.45; S, 10.91.

Acknowledgment

Financial support of this work by the National Research Council of Canada is gratefully acknowledged.

1. D. S. Breslow and H. Skolnik. *In* The chemistry of heterocyclic compounds. Vol. 21. Part I. *Edited by* A. Weissberger. Interscience Publishers, Inc., New York. 1966. pp. 87–95; Vol. 21. Part II. pp. 780–783.
2. W. E. Truce and D. F. Hoerger. J. Am. Chem. Soc. **77**, 2496 (1955).
3. E. J. Corey and T. Durst. J. Am. Chem. Soc. **88**, 5656 (1966); **90**, 5548 (1968).
4. C. D. Broaddus. Acc. Chem. Res. **1**, 231 (1968).
5. D. E. O'Connor and W. I. Lyness. J. Am. Chem. Soc. **86**, 3840 (1964).
6. J. H. Hellberger. Ann. **588**, 71 (1959).

S-[(*N*-Terpenoid carboxamidinium)methyl] thiosulfates (Bunte salts) as potential antiradiation agents

Jerry M. Barton and Ludwig Bauer[1]

Department of Chemistry, College of Pharmacy, University of Illinois (Medical Center), P.O. Box 6998, Chicago, Illinois 60680

Received November 26, 1968

The synthesis of a number of α-acetamidinium Bunte salts, substituted on one of the nitrogen atoms by a terpenoid moiety, is reported.

Canadian Journal of Chemistry, **47**, 1233 (1969)

It has been shown that a number of *S*-[(*N*-substituted carboxamidinium)methyl] thiosulfates, $^{-}O_3SSCH_2C(=NH_2^{+})NHR$, **1**, are promising radiation-protective compounds in mice (1, 2). This paper describes the synthesis of derivatives of **1** in which one of the amidine nitrogen atoms bears a highly condensed aliphatic structure. It has been observed in a series of *N*-(ω-cycloalkane)-alkyl derivatives of **1** [R = *cyclo*-C_nH_{2n-1}—$(CH_2)_m$] that good activity was retained up to R = 4-(cyclohexyl)butyl, (3). In a recent report, it was disclosed that those *S*-2-aminoethyl thiosulfates, $HO_3S_2CH_2CH_2NHR$, bearing similarly constituted (cycloalkane)alkyl substituents on nitrogen, were among the best radiation-protective substances (4). The project described at present was designed to modify the polar character of **1** by introducing highly condensed aliphatic systems into the molecule. By attaching bi- and tricyclic aliphatic ring systems to the amidine function of **1**, it was hoped to impart additional lipid solubility and possibly facilitate transport of these substances through living systems. Toward this end, derivatives of **1** bearing either terpenoid or adamantane substituents were synthesized and their structures are listed in Table I.

The synthesis employed to prepare these compounds was as described previously (1–3). Methyl α-chloroacetimidate is generated *in situ*

[1]The authors gratefully acknowledge support for this project from the Office of the Surgeon General, United States Army Medical Research and Development Command (Contract No. DA-49-193-MD-2047).

Can. J. Chem. Downloaded from www.nrcresearchpress.com by 210.87.254.40 on 09/05/12
For personal use only.

Can. J. Chem. Downloaded from www.nrcresearchpress.com by 210.87.254.40 on 09/05/12
For personal use only.

TABLE I

S-[*N*-(Substituted carboxamidinium)methyl] thiosulfates, $^{-}O_3S_2CH_2C(=NH_2^{+})NHR$, **1**

R in **1**	Yield %	Melting point (°C)	Formula	C% Calcd.	C% Found	H% Calcd.	H% Found	N% Calcd.	N% Found	S% Calcd.	S% Found
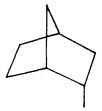 *endo*-2-Norbornyl	27	165	$C_9H_{16}N_2O_3S_2$	40.91	40.79	6.10	6.30	10.60	10.48	24.23	24.09
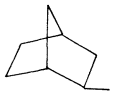 *exo*-2-Norbornyl	28	168–170	$C_9H_{16}N_2O_3S_2$	40.91	40.89	6.10	6.07	10.60	10.65	24.23	24.40
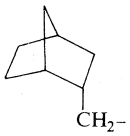 *endo*-2-Norbornanemethyl	36	150–153	$C_{10}H_{18}N_2O_3S_2$	43.16	43.21	6.52	6.66	10.07	10.21	23.00	22.98
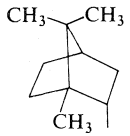 Bornyl	40	168	$C_{12}H_{22}N_2O_3S_2$	47.05	47.36	7.24	7.10	9.15	9.25	20.89	21.02

Can. J. Chem. Downloaded from www.nrcresearchpress.com by 210.87.254.40 on 09/05/12
For personal use only.

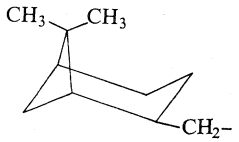 *cis*-Myrtanyl	80	162–165	$C_{12}H_{22}N_2O_3S_2$	47.05	47.44	7.24	7.38	9.15	9.45	20.89	20.83
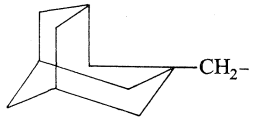 1-Adamantanemethyl	79	175–179	$C_{13}H_{22}N_2O_3S_2$	49.05	49.36	6.97	6.90	8.80	8.80	20.10	19.53
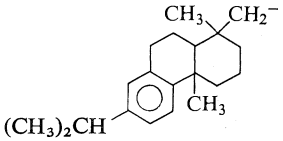 Dehydroabietyl	57	202–205	$C_{22}H_{34}N_2O_3S_2$	60.24	60.28	7.81	7.73	6.39	6.24	14.62	14.70

Can. J. Chem. Downloaded from www.nrcresearchpress.com by 210.87.254.40 on 09/05/12
For personal use only.

from the base-catalyzed addition of methanol to chloroacetonitrile. Addition of a primary amine hydrochloride leads to the intermediate α-chloroacetimidinium chloride, $ClCH_2C(=NH_2^+)NHR\ Cl^-$. In the present series, only two of these chloroacetamidinium chlorides could be isolated as crystalline solids (see Experimental). The rest were transformed directly by thiosulfate ion to the corresponding Bunte salt. The crystalline *N*-(1-adamantanemethyl)-α-chloroacetamidinium chloride was converted *via* the phosphorothioate method (5) to the corresponding α-mercaptoacetamidinium chloride.

The procedure for ascertaining *in vivo* activity of these compounds in mice was described in detail previously (2, 4, 6). Of the compounds tested, the *N*-bornyl and *N*-(*cis*-myrtanyl) derivatives of **1**, when administered orally or intraperitoneally 15 min prior to irradiation (800–1000 R, X-rays) showed a high survival rate at one-half to one-quarter of the toxic (LD_{50}) dosage.

Experimental

Melting and boiling points are uncorrected. Microanalyses were performed by Micro-Tech Laboratories, Skokie, Illinois. Some nitrogen analyses were obtained by (the late) Mr. Leo Horner in this Department, using a Coleman model D-29. Proton magnetic resonance (p.m.r.) spectra were recorded by means of a Varian A-60 spectrometer, with tetramethylsilane and sodium 3-(trimethylsilyl)-1-propanesulfonate as internal standards in organic and aqueous media, respectively. Chemical shifts are recorded in p.p.m. (δ) downfield from these internal references and multiplicities are indicated by the usual abbreviations.

Starting Materials

The following chemicals were purchased from Aldrich Chemical Co.: chloroacetonitrile, norbornylene, (−)-β-pinene, 2-norbornanecarbonitrile, 1-adamantanecarbonitrile, 2-norboranamine hydrochloride and dehydroabietylamine. 2-Bornanamine [m.p. 159–169°, lit. (7) m.p. 163°] was purchased from K & K Laboratories and converted to the hydrochloride by passing HCl gas through a chilled solution of the amine in dry ether.

exo-2-Norbornanamine Hydrochloride

The procedure to prepare the amine was adapted from a recent literature method (8), except that hydroboration of norbornylene was accomplished here by generating diborane *in situ* (9). The hydrochloride was obtained by adding a slight excess of concentrated HCl to a solution of the free base in methanol, followed by evaporation to dryness. The yield was 25%; p.m.r. (D_2O) δ 3.29 (m, 1, *endo* H), 2.44 (broad s, 2, bridgehead H), 0.97–2.12 (m, 8, methylene H). The *N*-acetyl derivative of the amine melted at 138–140° [lit. (10) m.p. 139°].

The p.m.r. spectrum of commercial 2-norbornanamine hydrochloride (D_2O) was as follows: δ 3.63 (m, 1, *exo* H), 2.42 (m, 2, bridgehead H), 0.87–2.17 (m, 8, methylene H). Since the α-methine and bridgehead hydrogens showed distinct signals from those of the synthetic *exo* compound, it was concluded that the purchased material is the *endo* isomer. There is no indication that either sample was a mixture of isomers.

cis-Myrtanylamine

This amine was prepared by a combination of the literature procedures for hydroboration of (−)-β-pinene (9) and amination of the resulting dialkylborane (8). The free base had b.p. 60–70° at 2–3 mm [lit. (8) b.p. 60–61° at 2 mm]; p.m.r. ($CDCl_3$) δ 2.67 (broad d, 2, J = 6.1 Hz, CH_2N), 1.25–2.50 (m, 9), 1.17 (s, 3, CH_3), 1.05 (s, NH), 0.97 (s, 3, CH_3). The yield was 15%.

The *N*-benzoyl derivative had m.p. 103.5–104.5° [lit. (8) m.p. 105–106°].

endo-2-Norbornanemethylamine Hydrochloride

This compound has previously been obtained from the corresponding phthalimido derivative (11, 12).

A solution of 2-norbornanecarbonitrile (24 g) in dry tetrahydrofuran (40 ml) was added during 1 h to a stirred suspension of $LiAlH_4$ (7.6 g) in dry tetrahydrofuran (350 ml) under a nitrogen atmosphere. The mixture was heated under reflux for 1 h and cooled. The excess hydride was decomposed by the dropwise addition of water (10 ml), and 10% NaOH solution (30 ml) was added with vigorous stirring. The mixture was filtered and the filtrate was dried over anhydrous Na_2SO_4, decanted, and evaporated *in vacuo* at 40–50°. The residual amine was dissolved in methanol and treated with a slight excess of concentrated HCl. Evaporation of the solvents *in vacuo* and recrystallization of the residue from 2-propanol gave 21.3 g of the hydrochloride (64%).

The *N*-benzoyl derivative was prepared directly from the hydrochloride using pyridine as solvent and melted at 99–101.5° [lit. (12) m.p. 99.5–101.5°; the *exo N*-benzoyl isomer reportedly has m.p. 116–117°]. From the m.p. of the derivative it was concluded that the commercially available nitrile used for this reduction was the *endo* isomer.

1-Adamantanemethylamine

This compound has previously been prepared by reduction of 1-adamantanecarboxamide (13).

A suspension of $LiAlH_4$ (4.2 g, 0.11 mole) in dry tetrahydrofuran (200 ml) was stirred in a nitrogen atmosphere and a solution of 1-adamantanecarbonitrile (16.1 g, 0.1 mole) in dry tetrahydrofuran (45 ml) was added during 0.5 h. The mixture was heated under reflux for 2.5 h, cooled, and treated dropwise with water (15 ml) and then 20% NaOH (25 ml). The mixture was filtered, and the filtrate was dried over anhydrous Na_2SO_4, decanted, and evaporated *in vacuo* at 40–50°. The residual amine was distilled to yield 11.6 g (70%) of product, $b.p._{.4}$ 95–97° [lit. (13) $b.p._3$ 83–85°], p.m.r. ($CDCl_3$) δ 2.30 (s, 2, CH_2—N), 1.97 (broad s, 3, bridgehead H), 1.73 (6 H), 1.47 (6 H), 1.10 (s, NH).

The *N*-benzoyl derivative had m.p. 144–145° [lit. (13) m.p. 142°].

S-(Carboxamidinium)methyl Thiosulfates 1

A 1 *M* solution of methyl α-chloroacetimidate was

prepared by adding distilled chloroacetonitrile to the required amount of a stock solution of $NaOCH_3$ (0.1 *N* in methanol), e.g., 20 mmole to 20 ml. Formation of the imidate is readily followed by p.m.r. (14) and was found to be complete in 15 min under these conditions.

One equivalent of the appropriate amine hydrochloride was then added, and stirring was continued for 30–45 min (see below for exception). A solution of one equivalent of $Na_2S_2O_3 \cdot 5H_2O$ in an equal volume of water was then added, and methanol was evaporated *in vacuo* at 25° or under a gentle stream of filtered air at 25°. Some dark tar generally separated, and evaporation was continued until solids began to separate. The supernatant liquid was then decanted and chilled to obtain the product. The tar was extracted once with hot water to recover any product trapped therein, and the combined product was recrystallized either from water, ethanol or a mixture thereof. Details are listed in Table I. Yields are based on chloroacetonitrile.

N-(1-Adamantanemethyl)-α-chloroacetamidine Hydrochloride

1-Adamantanemethylamine (3.3 g, 0.02 mole) was converted to the hydrochloride by treatment with excess concentrated HCl in methanol followed by evaporation of the solvent. Chloroacetonitrile (1.5 g, 0.02 mole) was then stirred for 25 min with $NaOCH_3$ solution (20 ml), and the amine hydrochloride was added. The mixture was stirred for 2 h at room temperature. Some of the product (2.5 g) which had precipitated, was filtered off and the filtrate was diluted with dry ether (100 ml) to yield another 1.4 g of product, m.p. 274–276°. The p.m.r. spectra of the two samples were identical, and the product was recrystallized from absolute ethanol. The total yield was 3.9 g (70%), and the product proved to be sparingly soluble in water; p.m.r. (CF_3CO_2H) δ 4.38 (s, 2, $ClCH_2$), 3.13 (broad d, 2, J = 5.0 Hz, CH_2N), 2.06 (broad d, 2, bridgehead H), 1.80, 1.67 (broad singlets, 12 total, methylene H.)

Anal. Calcd. for $C_{13}H_{22}Cl_2N_2$: C, 56.28; H, 7.97; N, 10.20. Found: C, 56.50; H, 8.06; N, 10.27.

S-[N-(Dehydroabietyl)carboxamidinium)methyl] Thiosulfate

Dehydroabietylamine hydrochloride was precipitated by passing dry HCl through a solution of the free amine (mixed isomers) in dry ether. A solution of the amine hydrochloride (12.2 g) in methanol (50 ml) was added to 40 ml of 1 *M* methyl α-chloroacetimidate (see above). After 45 min, concentrated HCl (1 ml) was added, and most of the solvent was evaporated. Ether was added to precipitate inorganic solids, which were removed by filtration. The solvents were again evaporated, the residue was dissolved in methanol (15 ml), and water was added in small portions until solids began to separate. After several hours, 9.4 g were collected, m.p. 138–146°. The intermediate defied recrystallization from H_2O, organic solvents, and mixtures thereof.

A 2.0 g sample of the solid was dissolved in warm mixture of water (25 ml) and 95% ethanol (5 ml), and $Na_2S_2O_3 \cdot 5H_2O$ (1.25 g) in water (5 ml) was added with stirring. The mixture was cooled, and the precipitate was collected and washed with hot water. The dry weight was 2.0 g. Additional details are listed in Table I.

N-(1-Adamantanemethyl)-α-mercaptoacetamidine Hydrochloride

N-(1-Adamantanemethyl)-α-chloroacetamidine hydrochloride (5.54 g) was suspended in a solution of Na_3SPO_3 (5) (4.0 g) in water (60 ml). The mixture was stirred vigorously for 30 min. The flask was then flushed with nitrogen, and 6*N* HCl (35 ml) and 2-propanol (30 ml) were added. The mixture was stirred, heated to 80–90° for 20 min, and cooled. The product was collected, 5.0 g (91%), m.p. 220.5–222.5° (decomp.). Recrystallization from water did not alter the decomposition range.

Anal. Calcd. for $C_{13}H_{23}ClN_2S$: C, 56.79; H, 8.43; N, 10.19; S, 11.66. Found: C, 56.35; H, 8.36; N, 10.25; S, 11.04.

Acknowledgments

Sincere thanks are extended to Drs. D. Jacobus, T. Sweeney, and E. Steck of the Walter Reed Army Institute of Research for their interest, biological test results, and suggestions during the course of this investigation.

1. L. Bauer and T. L. Welsh J. Org. Chem. **27**, 4382 (1962).
2. L. Bauer and K. R. Sandberg. J. Med. Chem. **7**, 766 (1964).
3. T. T. Conway, Ph.D. Dissertation. University of Illinois at the Medical Center, Chicago, Illinois, June 1967.
4. R. D. Westland, J. L. Holmes, M. L. Mouk, D. D. Marsh, R. A. Cooley, and J. R. Dice. J. Med. Chem. **11**, 1190 (1968).
5. T. T. Conway, A. Shoeb, and L. Bauer. J. Pharm. Sci. **57**, 455 (1968); J. R. Piper and T. P. Johnston. J. Org. Chem. **32**, 1261 (1967).
6. T. P. Johnston, C. R. Stringfellow, and J. R. Piper. J. Med. Chem. **11**, 1256 (1968).
7. K. Alder and G. Stein. Ann. **525**, 222 (1936).
8. H. C. Brown, W. R. Heydkamp, E. Breuer, and W. S. Murphy. J. Am. Chem. Soc. **86**, 3565 (1964).
9. G. Zweifel and H. C. Brown. Organic reactions. John Wiley and Sons, New York. Vol. **13**, 1963, Ch. 1.
10. K. Alder. Ann. **514**, 226 (1934).
11. K. Alder, K. Heimbach, and R. Reubke. Chem. Ber. **91**, 1516 (1958).
12. J. A. Berson, J. S. Walia, A. Remanick, S. Suzuki, P. Reynolds-Warnhoff, and D. Willner. J. Am. Chem. Soc. **83**, 3986 (1961).
13. H. Stetter and P. Goebel. Chem. Ber. **96**, 550 (1963).
14. A. P. Parulkar and L. Bauer. J. Heterocyclic Chem. **3**, 472 (1966).

Can. J. Chem. Downloaded from www.nrcresearchpress.com by 210.87.254.40 on 09/05/12
For personal use only.

Coupling of allylic halides promoted by iron metal dispersed in dimethyl formamide

DAVID W. HALL[1] AND EDWARD HURLEY, JR
Denver Research Center, Marathon Oil Company, 7400 South Broadway, Littleton, Colorado 80121

Received July 18, 1968

The coupling reaction of allylic halides to produce non-conjugated dienes was investigated. It was found that iron powder could be utilized, without any special pretreatment, to promote the coupling reaction when a dipolar aprotic solvent was employed as the reaction medium.

Effects of variables such as the nature of the halogen atom in the reactive position of the substrate, substituents on the substrate, presence or absence of organic or inorganic halide catalysts, and solvent type were explored briefly.

Non-conjugated dienes can be prepared in yields which exceed 90% in the more favorable cases. The present procedure avoids many of the difficulties inherent in such previous methods as the Grignard reaction or the nickel carbonyl-promoted reaction.

Canadian Journal of Chemistry, **47**, 1238 (1969)

Can. J. Chem. Downloaded from www.nrcresearchpress.com by 210.87.254.6 on 09/05/12
For personal use only.

Introduction

The coupling reaction of allylic halides in the presence of magnesium metal in ether is a well-known side reaction which occurs when one attempts to prepare allylic Grignard reagents (1, 2). The nature of the magnesium-promoted coupling reaction has been investigated by Henne and Chanan (3). These workers utilized the reaction to prepare a series of non-conjugated dienes. The yields were in general around 50%.

Coupling of allylic halides via their reaction with nickel carbonyl has been the subject of considerable study (4–6). A decided inconvenience of this procedure is the care in handling nickel carbonyl which is necessitated by its high toxicity, flammability, and volatility (4*b*).

Though synthetic routes to dimers and polymers of benzylic-type halides by their reactions with free transition metals have been explored in some detail (7–10), relatively little has been done to utilize allylic halides in this manner. Fainberg and Miller have reported that perfluoroallyl iodide reacts with zinc dust in dioxane to give perfluoro-1,5-hexadiene in 83% yield (11). A vapor phase reaction employing allyl chloride and copper deposited on various supporting agents which produces 1,5-hexadiene in 80% yield has been reported (12). Dupont and Zuber obtained 1,5-hexadiene in 70% yield by the reaction of allyl chloride with copper in ethanol (13).

The patent literature contains several reports that coupled products were obtained from allylic halides when iron metal was used as the coupling agent (14–16). A variety of solvents was stated to be effective media for the coupling reaction.

Results and Discussion

Judging from examples given in the patent literature (14–16), the nature of the solvent employed as the reaction medium appeared to us to be a critical variable in the reactions of allylic halides with iron metal, contrary to claims made in the patents. Accordingly, we reinvestigated the effects of using hydrocarbon and alcohol solvents in this reaction. Careful evaluation of the previous studies suggested that acetonitrile, a dipolar aprotic solvent, was superior. Results for these solvent-screening experiments, including data for the dipolar aprotic solvent dimethyl formamide (DMF), are given in Table I.

The data in Table I clearly show that inferior results are obtained when either *n*-heptane or ethanol is used as the solvent for this reaction. Use of the dipolar aprotic solvent DMF leads to high conversions and yields under comparable conditions. The last experiment in Table I shows that addition of benzene to DMF results in decreased reaction rate. This strongly suggests, in contrast to previous reports (14–16) that aromatic hydrocarbons are also poor solvents for this reaction. Presumably, dipolar aprotic solvents other than DMF or acetonitrile would also be suitable for promoting the reaction between allylic halides and iron powder.

Although Dupont and Zuber (13) reported

[1]To whom correspondence should be directed; Department of Chemistry, University of British Columbia, Vancouver 8, British Columbia.

TABLE I

Solvent effects on the reaction of allyl chloride or bromide with iron powder

Solvent (g)	Allyl halide (moles)	Iron (g-atoms)	Reaction time (h)	Reaction temperature (°C)	Substrate conversion (%)*	Yield (%)*
n-Heptane (77.2)	Chloride (0.55)	0.60	1.0	150†	<5	Trace
n-Heptane (210)	Bromide (0.50)	0.25	9.0	80‡	<2	Zero
Ethanol (150.0)	Chloride (1.0)	1.1	14.0	50‡	Zero	Zero
Ethanol (80.5)	Chloride (0.52)	0.55	1.0	150†,§	56	27
Dimethyl formamide (190)	Chloride (0.50)	0.25	1.0	150†	99+	95.5‖
Dimethyl formamide (95) and benzene (34.5)	Chloride (0.43)	0.22	1.0	150†	66	56.7

*Conversions and yields were based on semiquantitative v.p.c. analyses (see Experimental) done on the reaction mixtures immediately upon the termination of an experiment. Hence, the reported yields are for crude 1,5-hexadiene.
†Conducted in a stirred stainless steel autoclave; reaction time does not include about 1/2 h heat up time and about 1½ h cooling time.
‡Conducted in a baffled glass flask of the Morton type, using a Teflon paddle-blade stirrer.
§Solvent was partially oxidized under the conditions employed.
‖The recovered yield of 99 + % pure 1,5-hexadiene, after a water washing and distillation, was 81%. Iron salts in the DMF residue analyzed 70% Fe^{+2} and 30% Fe^{+3}; the latter presumably was found due to subsequent air oxidation of Fe^{+2} formed initially.

TABLE II

Relative reactivities of allyl chloride and allyl bromide towards iron powder suspended in dimethyl formamide, and catalytic effect of added halides*

Allyl halide	Added halide (g)	Reaction time (h)	Reaction temperature (°C)	Yield of crude 1,5-hexadiene (%)†
Allyl bromide	Zero	24.0	25.0	Zero
Allyl bromide	Zero	2.0	90.0	88.6
		4.0		96.5
Allyl chloride	Zero	4.5	90.0	7.3
		11.5		46.7
		18.5		62.2
Allyl chloride	Sodium bromide (1.0)	2.0	90.0	10.3
		4.0		31.8
Allyl chloride	Allyl bromide (3.3)	2.0	90.0	9.4
		4.0		30.0
Allyl chloride	Sodium iodide (0.7)	2.0	90.0	18.3
		4.0		57.9

*These experiments were conducted in a baffled glass flask of the Morton type, fitted with a Teflon paddle-blade stirrer assembly. In all runs 0.5 moles of benzene was added to the 200 ml of DMF solvent to serve as an internal standard for analysis; 0.50 moles of the allyl halide and 1/4 g-atom of iron were employed. The reaction temperature was maintained within ± 5° of the values listed.
†These yield data have a relative accuracy of about 1%.

that 1,5-hexadiene was formed in 70% yield using pretreated copper powder in ethanol, we found that oxidation of the ethanol occurred with iron at temperatures sufficiently high to promote the coupling reaction. We repeated the work of Dupont and Zuber and found that a long reaction time was required and that a low yield was obtained if the copper powder was not pretreated. At higher temperatures, oxidation of the ethanol became a problem, just as in the case where iron was used. In view of the results we obtained using DMF, there would appear to be little point in employing alcohols as solvents for the coupling reaction.

In most of the experiments conducted in the present investigation the stoichiometry of the coupling reaction was determined by following the conversion of the metal as well as that of the allylic halide. Within a range of about plus or minus 10%, iron was consumed to the extent of about 0.5 g-atom/mole of the allylic halide.

Experiments were carried out to determine the relative reactivities of allyl chloride and allyl bromide towards iron powder suspended in DMF. Effects of several materials added in low concentrations as catalysts were also studied. The results are given in Table II.

The data in Table II show that an added

Can. J. Chem. Downloaded from www.nrcresearchpress.com by 210.87.254.6 on 09/05/12
For personal use only.

TABLE III

Reaction of substituted allyl chlorides with iron in dimethyl formamide*

Allyl chloride (moles)	Conversion (%)	Products	Crude yield (%)
Allyl chloride (0.69)	65†	1,5-Hexadiene	61.5†
β-methallyl chloride (0.52)	77†,‡	2,5-Dimethyl-1,5-hexadiene	60.0†
Allyl chloride (0.25) plus β-methallyl chloride (0.25)	98§	1,5-Hexadiene	21.0§
		2-Methyl-1,5-hexadiene	44.8§
		2,5-Dimethyl-1,5-hexadiene	24.1§
2,3-Dichloropropene‖ (0.50)	55§	2,5-Dichloro-1,5-hexadiene + Polymer	35.0§

*These experiments were conducted in a 300 ml stainless steel stirred autoclave using 100 ml dimethyl formamide solvent and 1/2 g-atom of iron per mole of organic substrate. The reaction temperature was 150 °C and the reaction time was 1 h; see footnote † of Table I.

†Benzene equimolar with the allyl chloride substrate, was added as an internal standard for vapor phase chromatographic analysis.

‡Recovered iron corresponded with a substrate conversion of 71%.

§Conversion and yield were determined by vapor phase chromatographic analysis of the crude product after filtration and water washing to remove unchanged iron and most of the dimethyl formamide.

‖A preliminary study with this substrate showed that addition of benzene as an internal standard for vapor phase chromatographic analysis resulted in such a low conversion under the standard conditions that insufficient product could be obtained for characterization.

inorganic bromide or iodide salt, or a labile organic bromide, greatly decreases the required reaction time for coupling allyl chloride, even when a low concentration is employed. Dupont and Zuber found a similar catalytic effect for sodium or zinc bromide on the reaction of allyl chloride with copper in ethanol (13).

Effects of simple substituents such as methyl or halogen in the β position on the course of the reaction of allyl chlorides with iron dispersed in DMF were explored briefly. Table III lists results for experiments on these substrates carried out under standard conditions in a stirred stainless steel autoclave. An experiment employing allyl chloride is included for comparison. Benzene added as an internal standard for vapor phase chromatographic (v.p.c.) analysis in the experiments on allyl chloride and β-methallyl chloride reduced the yield of coupling product formed in the 1 h reaction time at 150 °C.

The yield of 2,5-dimethyl-1,5-hexadiene from β-methallyl chloride is essentially the same as the yield of 1,5-hexadiene from allyl chloride. These data suggest that the substitution of a β-methyl group on allyl chloride changes its reactivity towards iron dispersed in DMF rather little. Additional evidence for this was obtained from mixed-coupling experiments in which equimolar amounts of allyl chloride and β-methallyl chloride were treated with iron in DMF. Two such experiments conducted under quite different reaction conditions gave the following weight percent distributions (weight % in the crude product mixture, as determined by v.p.c. analysis, were normalized to consider only the three coupling products on a 100% basis): 1,5-hexadiene, 21.7 ± 3.0%, 2-methyl-1,5-hexadiene, 49.1 ± 1.2%; and 2,5-dimethyl-1,5-hexadiene, 29.3 ± 1.7%. Theoretical weight percentages for the three products from coupling, presuming equal reactivities for allyl chloride and β-methallyl chloride and an absence of any side reactions, are: 1,5-hexadiene, 21.4%; 2-methyl-1,5-hexadiene, 50.0%; and 2,5-dimethyl-1,5-hexadiene, 28.6%. In the experiment listed in Table III, the combined yields of the three coupling products totalled about 90%. In the second experiment, carried out in glassware at 80 °C using sodium iodide catalyst, the sum of the combined yields was in excess of 95%.

Henne and co-workers (17) reported that equimolar amounts of allyl chloride and β-methallyl chloride reacted with magnesium in ether to give coupling products in the following weight % distributions: 1,5-hexadiene, 13.5%; 2-methyl-1,5-hexadiene, 52.8%; and 2,5-

Can. J. Chem. Downloaded from www.nrcresearchpress.com by 210.87.254.6 on 09/05/12
For personal use only.

dimethyl-1,5-hexadiene, 33.7%. Their yield data were normalized to put the relative percents of the three dienes on a 100% basis for comparison with our own data. The yield of coupled products found by Henne and co-workers was only 40–50%.

Substitution of a halogen atom in the β-position of allyl chloride markedly decreased the reactivity towards iron dispersed in DMF. The last experiment in Table III shows that 2,3-dichloropropene coupled to give 2,5-dichloro-1,5-hexadiene in only 35% yield under the standard conditions of 1 h at 150 °C. A considerable amount of polymer was also produced.

Experimental

Solvents employed in this investigation were commercially available reagent grade materials. They were used as received; no special care was taken to prevent their absorbing atmospheric moisture during storage and handling. Similarly, iron used was commercially available reagent grade of mesh size 200. The only precaution taken was to store the iron under conditions such that undue oxidation of the surface did not occur. Inorganic catalysts were granular reagent grade. All the organic substrates were reagent grade and were readily available from the major suppliers.

The progress of the reactions was followed in many cases by a semiquantitative v.p.c. analysis, and in selected cases by quantitative v.p.c. analysis. In the semiquantitative procedure calibration curves were made up by determining relative response factors of the substrate and product relative to the solvent over concentration ranges corresponding to from 10% up to 90% conversion of the substrate. This method is termed semiquantitative since it presumed no solvent decomposition or mechanical loss occurred during a run. It further presumed that any complexes formed between the metal halides produced and the solvents decomposed very rapidly in the injection port of the chromatograph so that all the solvent value appeared as a single peak in the chromatogram. This latter assumption appears valid when the yield data obtained in this way are compared with isolated yields or yields determined by the quantitative method.

In the quantitative analysis response factors for the substrate, product and solvent were determined over a range, but relative to the added internal standard, benzene. The internal standard was added directly to the reaction mixture at the beginning of an experiment so that any sampling problems arising because of the inhomogeneity of the mixture would affect all components equally. This procedure was followed only after determining that the internal standard was inert under the reaction conditions employed.

Peaks in the chromatograms were assigned by spiking aliquots to be analyzed with authentic samples of the materials in question. Where such standards for comparison were not commercially available, the products of the reaction were carefully purified and their physical properties compared with published values. Retention times under the standard set of v.p.c. analysis conditions were then obtained and compared with the retention times of the various component peaks in the chromatogram obtained from the original analysis of the crude reaction mixture.

Products from all the experiments listed in Tables I–III were isolated and purified in at least one run among a set of related runs so that their identities could be established with certainty. Conversions and yields are reported on a molar basis.

Nuclear magnetic resonance (n.m.r.) spectra were determined on a Varian Associates model A60 spectrometer using tetramethylsilane (TMS) as an internal standard.

Cross-coupling of allyl chloride and β-methallyl chloride

Allyl chloride (2.0 moles), β-methallyl chloride (2.0 moles), iron powder (2.0 g-atom), and sodium iodide (10.1 g) were added to DMF (1000 g) in a conventional glassware apparatus with the reflux condenser open to the atmosphere. The mixture was stirred at 80 °C for 7 h; semiquantitative analysis showed complete conversion of both organic substrates. Volatile components were distilled until the overhead temperature reached that of DMF. Analysis of the crude distillate by the semiquantitative v.p.c. method showed the following weight percentage distribution of coupling products: 1,5-hexadiene, 23.5%; 2-methyl-1,5-hexadiene, 45.8%; and 2,5-dimethyl-1,5-hexadiene, 26.3%. The first and third of these products were identified by spiking with authentic standards. The peak corresponding with 2-methyl-1,5-hexadiene was identified by comparison of its retention time with that of the material subsequently isolated and purified. The sum of the combined yields of the three crude products was 97%.

The distillate was washed with water to remove the small amount of DMF present, dried, and then subjected to a second, more precise, distillation. A center cut (10 g) of the 2-methyl-1,5-hexadiene fraction was collected at 81 °C at a pressure of 623 mm Hg. Analysis (v.p.c.) of this cut showed only a single component present. This very pure material had n_D^{25} 1.4169 and d_{25} 0.7155. Literature values (17) are n_D^{20} 1.4184 and d_4^{20} 0.7198. The infrared and n.m.r. spectra were in accord with the structure and further served to confirm the purity.

Coupling 2,3-Dichloropropene

The conditions for this experiment are outlined in Table III. The product, 2,5-dichloro-1,5-hexadiene, was isolated in the manner described above and purified by distillation through a spinning band apparatus. A center fraction of water-white product was collected at 66 °C at 43 mm Hg. This material had n_D^{25} 1.4695. The n.m.r. spectrum (TMS internal standard) showed a resonance peak for the methylene hydrogens at 7.44 τ and for the vinyl hydrogens at 4.88 τ. The peaks showed no fine structure and were, within the limits of the measurement, in a 1:1 ratio. The n.m.r. spectrum of 2,5-dichloro-1,5-hexadiene was in accord with those of the comparable chloropropenes studied by DeWolf and Baldeschwieler (18).

A molecular weight determination and elemental analysis were not as satisfactory as desired, but in view of

Can. J. Chem. Downloaded from www.nrcresearchpress.com by 210.87.254.6 on 09/05/12
For personal use only.

the spectral data and the fact that v.p.c. analysis showed only a single component, these do suffice to characterize the material adequately.

Anal. Calcd. for $C_6H_8Cl_2$ (mol. wt., 151.04): C, 47.71; H, 5.34; Cl, 46.95. Found (Elek Laboratories mol. wt., 142.4–143.8.): C, 47.22; 47.24; H, 5.34, 5.39; Cl, 46.51.

Acknowledgments

We are grateful to R. Hughes and R. Schill for the chromatographic analyses and to Dr. A. L. Schalge and D. Conway for the spectral determinations. We are particularly indebted to J. T. Kelly for his many helpful suggestions throughout this investigation.

1. L. F. Fieser and M. Fieser. Organic chemistry, 3rd ed. D. C. Heath and Co., Boston. 1957. p. 151.
2. M. Tamele, C. J. Ott, K. E. Marple, and G. Hearne. Ind. Eng. Chem. **33**, 115 (1941).
3. A. L. Henne and H. H. Chanan. J. Am. Chem. Soc. **66**, 392 (1944).
4. *a*) I. D. Webb. Belgian Patent 448,884 (1943) to E. I. duPont de Nemours and Company; Chem. Abstr. **41**, 6576 (1947). *b*) I. D. Webb and G. T. Borcherdt. J. Am. Chem. Soc. **73**, 2654 (1951). *c*) I. D. Webb. U.S. Patent 2,654,787 (1953) to E. I. duPont de Nemours and Company; Chem. Abstr. **48**, 10048*g* (1954).
5. *a*) G. P. Chiusoli and G. Cometti. Chimica e Industria (Milan) **45**, 401 (1963). *b*) M. Dubini, G. P. Chiusoli, and F. Montino. Tetrahedron Letters, No. 24, 1591 (1963).
6. *a*) E. J. Corey and M. F. Semmelhack. J. Am. Chem. Soc. **89**, 2755 (1967). *b*) E. J. Corey and E. K. W. Wat. J. Am. Chem. Soc. **89**, 2757 (1967). *c*) E. J. Corey, M. F. Semmelhack, and L. S. Hegedus. J. Am. Chem. Soc. **90**, 2416 (1968). *d*) E. J. Corey, L. S. Hegedus, and M. F. Semmelhack. J. Am. Chem. Soc. **90**, 2417 (1968).
7. *a*) Y. Ogata, T. Tsuruta, and R. Oda. Bull. Inst. Phys. Chem. Research Tokyo, **21**, 616 (1942); Chem. Abstr. **43**, 2194 (1949). *b*) Y. Ogata and H. Nakamura. J. Org. Chem. **21**, 1170 (1956).
8. Ng. Ph. Buu-Hoï and Ng. Hoan. J. Org. Chem. **14**, 1023 (1949).
9. K. Sisido, Y. Udô, and H. Nozaki. J. Am. Chem. Soc. **82**, 434 (1960).
10. K. Sisido, N. Kusano, R. Noyori, Y. Nozaki, M. Simosaka, and H. Nozaki. J. Polymer Sci. Part A, **1**, 2101 (1963).
11. A. H. Fainberg and W. T. Miller, Jr. J. Am. Chem. Soc. **79**, 4170 (1957).
12. Shell Internationale Research Maatschappij N. V., British Patent 913,278 (1962).
13. G. Dupont and G. Zuber. Bull. Soc. Chim. France, 342 (1959); Chem. Abstr. **54**, 24329*b* (1960).
14. R. S. Urban. U.S. Patent 2,658,922 to Rohm and Haas Company (1953).
15. G. Boffa and A. Quilico. German Patent 1,156,818 to Montecatini (1963).
16. *a*) M. J. Hurwitz and E. M. Beavers. German Patent 1,155,105 to Rohm and Haas Company. 1963. *b*) M. J. Hurwitz and E. M. Beavers. U.S. Patent 3,201,479 to Rohm and Haas Company. 1965. *c*) M. J. Hurwitz and E. M. Beavers. U.S. Patent 3,262,980 to Rohm and Haas Company (1966).
17. A. L. Henne, H. Chanan, and A. Turk. J. Am. Chem. Soc. **63**, 3474 (1941).
18. M. Y. DeWolf and J. D. Baldeschwieler. Journal of Molecular Spectroscopy, **13**, 344 (1964).

Can. J. Chem. Downloaded from www.nrcresearchpress.com by 210.87.254.6 on 09/05/12
For personal use only.

Partial asymmetric synthesis of methylenecyclopropanes and spiropentanes

R. Noyori and H. Takaya
Department of Chemistry, Nagoya University, Nagoya, Japan

AND

Y. Nakanisi and H. Nozaki
Department of Industrial Chemistry, Kyôto University, Kyôto, Japan

Received September 23, 1968

Reaction of substituted allenes and diazomethane gives rise to optically active methylenecyclopropane and spiropentane derivatives in the presence of dissymmetric copper chelates, bis[*N*-(*R* and *S*)-α-phenethylsalicylaldiminato]copper(II).

Canadian Journal of Chemistry, **47**, 1242 (1969)

Interest in homogeneous catalysis motivated our previous investigation on the decomposition of some diazo compounds by means of *soluble, dissymmetric* copper chelates. The observed asymmetric carbenoid reactions have been ascribed to intermediary chiral carbene–copper complexes (1, 2). The present paper as a continuation of this work refers to the synthesis of certain optically active methylenecyclopropane and spiropentane derivatives which were prepared with great difficulty.

Methylenation of substituted allenes (**1**) with

the spectral data and the fact that v.p.c. analysis showed only a single component, these do suffice to characterize the material adequately.

Anal. Calcd. for $C_6H_8Cl_2$ (mol. wt., 151.04): C, 47.71; H, 5.34; Cl, 46.95. Found (Elek Laboratories mol. wt., 142.4–143.8.): C, 47.22; 47.24; H, 5.34, 5.39; Cl, 46.51.

Acknowledgments

We are grateful to R. Hughes and R. Schill for the chromatographic analyses and to Dr. A. L. Schalge and D. Conway for the spectral determinations. We are particularly indebted to J. T. Kelly for his many helpful suggestions throughout this investigation.

1. L. F. Fieser and M. Fieser. Organic chemistry, 3rd ed. D. C. Heath and Co., Boston. 1957. p. 151.
2. M. Tamele, C. J. Ott, K. E. Marple, and G. Hearne. Ind. Eng. Chem. **33**, 115 (1941).
3. A. L. Henne and H. H. Chanan. J. Am. Chem. Soc. **66**, 392 (1944).
4. *a*) I. D. Webb. Belgian Patent 448,884 (1943) to E. I. duPont de Nemours and Company; Chem. Abstr. **41**, 6576 (1947). *b*) I. D. Webb and G. T. Borcherdt. J. Am. Chem. Soc. **73**, 2654 (1951). *c*) I. D. Webb. U.S. Patent 2,654,787 (1953) to E. I. duPont de Nemours and Company; Chem. Abstr. **48**, 10048*g* (1954).
5. *a*) G. P. Chiusoli and G. Cometti. Chimica e Industria (Milan) **45**, 401 (1963). *b*) M. Dubini, G. P. Chiusoli, and F. Montino. Tetrahedron Letters, No. 24, 1591 (1963).
6. *a*) E. J. Corey and M. F. Semmelhack. J. Am. Chem. Soc. **89**, 2755 (1967). *b*) E. J. Corey and E. K. W. Wat. J. Am. Chem. Soc. **89**, 2757 (1967). *c*) E. J. Corey, M. F. Semmelhack, and L. S. Hegedus. J. Am. Chem. Soc. **90**, 2416 (1968). *d*) E. J. Corey, L. S. Hegedus, and M. F. Semmelhack. J. Am. Chem. Soc. **90**, 2417 (1968).
7. *a*) Y. Ogata, T. Tsuruta, and R. Oda. Bull. Inst. Phys. Chem. Research Tokyo, **21**, 616 (1942); Chem. Abstr. **43**, 2194 (1949). *b*) Y. Ogata and H. Nakamura. J. Org. Chem. **21**, 1170 (1956).
8. Ng. Ph. Buu-Hoï and Ng. Hoan. J. Org. Chem. **14**, 1023 (1949).
9. K. Sisido, Y. Udô, and H. Nozaki. J. Am. Chem. Soc. **82**, 434 (1960).
10. K. Sisido, N. Kusano, R. Noyori, Y. Nozaki, M. Simosaka, and H. Nozaki. J. Polymer Sci. Part A, **1**, 2101 (1963).
11. A. H. Fainberg and W. T. Miller, Jr. J. Am. Chem. Soc. **79**, 4170 (1957).
12. Shell Internationale Research Maatschappij N. V., British Patent 913,278 (1962).
13. G. Dupont and G. Zuber. Bull. Soc. Chim. France, 342 (1959); Chem. Abstr. **54**, 24329*b* (1960).
14. R. S. Urban. U.S. Patent 2,658,922 to Rohm and Haas Company (1953).
15. G. Boffa and A. Quilico. German Patent 1,156,818 to Montecatini (1963).
16. *a*) M. J. Hurwitz and E. M. Beavers. German Patent 1,155,105 to Rohm and Haas Company. 1963. *b*) M. J. Hurwitz and E. M. Beavers. U.S. Patent 3,201,479 to Rohm and Haas Company. 1965. *c*) M. J. Hurwitz and E. M. Beavers. U.S. Patent 3,262,980 to Rohm and Haas Company (1966).
17. A. L. Henne, H. Chanan, and A. Turk. J. Am. Chem. Soc. **63**, 3474 (1941).
18. M. Y. DeWolf and J. D. Baldeschwieler. Journal of Molecular Spectroscopy, **13**, 344 (1964).

Can. J. Chem. Downloaded from www.nrcresearchpress.com by 210.87.254.40 on 09/05/12
For personal use only.

Partial asymmetric synthesis of methylenecyclopropanes and spiropentanes

R. Noyori and H. Takaya
Department of Chemistry, Nagoya University, Nagoya, Japan

AND

Y. Nakanisi and H. Nozaki
Department of Industrial Chemistry, Kyôto University, Kyôto, Japan

Received September 23, 1968

Reaction of substituted allenes and diazomethane gives rise to optically active methylenecyclopropane and spiropentane derivatives in the presence of dissymmetric copper chelates, bis[*N*-(*R* and *S*)-α-phenethylsalicylaldiminato]copper(II).

Canadian Journal of Chemistry, **47**, 1242 (1969)

Interest in homogeneous catalysis motivated our previous investigation on the decomposition of some diazo compounds by means of *soluble, dissymmetric* copper chelates. The observed asymmetric carbenoid reactions have been ascribed to intermediary chiral carbene–copper complexes (1, 2). The present paper as a continuation of this work refers to the synthesis of certain optically active methylenecyclopropane and spiropentane derivatives which were prepared with great difficulty.

Methylenation of substituted allenes (**1**) with

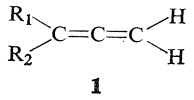

1

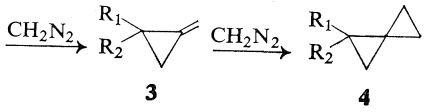

3 4

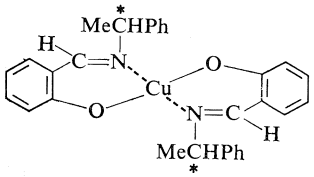

2

a: R_1 = Ph, R_2 = H
b: R_1 = Ph, R_2 = Me
c: R_1 = *n*-C_6H_{13}, R_2 = H

TABLE I

Partial asymmetric synthesis of methylenecyclopropanes and spiropentanes

Allene	Product	Catalyst*	α_D† Observed	*c* g/100 ml	$[\alpha]_D$ (deg)
1*a*	**3***a*‡	*S*-**2**	−0.269	2.32	−23.2
	4*a*§	*S*-**2**	−2.73	10.3	−53.0
	4*a*§	*R*-**2**	+2.66	10.2	+52.2
1*b*	**3***b*‡	*S*-**2**	−0.314‖	5.82	−10.8
	4*b*§	*S*-**2**	−0.589‖	7.58	−15.5
	4*b*§	*R*-**2**	+0.544‖	6.88	+15.8
1*c*	**4***c*§	*S*-**2**	+0.041	21.1	+ 0.39

*More than 60% of the catalysts used were recovered unchanged.
†Unless otherwise stated, the value was obtained in chloroform solution at 20° using a cell of 5 cm length.
‡Isolated by g.l.c. at 70° (high-vacuum silicone grease 30%, 2m). The magnitude depends on the isolation conditions, and samples isolated at 135° exhibited no measurable specific rotation.
§Isolated at 135° (Apiezon L 30%, 2m).
‖Measured at 15°.

diazomethane occurred smoothly in benzene solution at 0° in the presence of a catalytic amount of copper chelates, bis[*N*-(*R*)-α-phenethylsalicylaldiminato]copper(II) (*R*-**2**) or its enantiomer (*S*-**2**) to afford mono- and dimethylenated products (**3** and **4**) in good yields. Products were isolated by distillation and purification by gas–liquid chromatography (g.l.c.), and identified on the basis of spectral data (infrared (i.r.) and nuclear magnetic resonance (n.m.r.)). As shown in Table I, all the methylene adducts were obtained in optically active form. The enantiomeric catalysts yielded products with comparable magnitude but opposite sign of rotation. Because of lack of an appropriate resolving group in the hydrocarbon products, the optical yield and absolute configuration have not been determined. In order to transform **3***a* to *trans*-1-methyl-2-phenylcyclopropane whose absolute configuration has been established (2, 3), the reduction was attempted by means of potassium azodicarboxylate. However, the preferential attack of diimide from the sterically less hindered side of the double bond resulted in the formation of the *cis* isomer instead of the desired product.[1]

Monitoring the reaction by g.l.c. indicated that the initial attack of the copper carbenoid occurred almost exclusively at the inner double bond of the allenes as observed in the reaction of other carbenoids (4–7). Thus the asymmetric synthesis of spiropentanes should be attained at the stage of precursory methylenecyclopropane formation.

Finally it should be noted that methylenecyclopropanes **3***a* and **3***b* underwent facile thermal racemization, the half-lives (in $CHCl_3$, 100°) being 22 and 10 min, respectively. However, no signs of rearrangement into benzylidenecyclopropanes could be detected under these conditions.[2] Although further investigations will be required to elucidate the racemization mechanism,

[1]To our knowledge, diimide reduction presents the most effective method for double bond saturation of methylenecyclopropane without concurrent cleavage of the adjacent cyclopropane ring.

[2]For competitive rearrangement and racemization of methylenecyclopropane derivatives, see refs. 8 and 9.

Can. J. Chem. Downloaded from www.nrcresearchpress.com by 210.87.254.40 on 09/05/12
For personal use only.

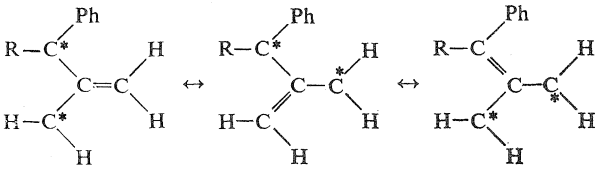

5

The asterisk represents an odd electron or ± charge.

it may proceed *via* certain concerted bond forming – bond rupture process rather than through distinct planar trimethylene species or corresponding zwitterion (**5**) (8–11).

Experimental

Microanalyses were performed at the Elemental Analyses Center of Kyôto University. All nuclear magnetic resonance (n.m.r.) spectra were taken in 10% CCl_4 solution using tetramethylsilane as an internal standard. Infrared spectra were obtained in neat liquid film.

Reaction of Diazomethane and Allenes in the Presence of Dissymmetric Copper Chelate (2)

Catalysis of diazomethane with copper chelate (*R*-**2** or *S*-**2**) was performed in the previously described manner (2). In the absence of the copper chelate practically no reaction was observed between diazomethane and allenes at 0°.

Gaseous diazomethane generated separately from *N*-methyl-*N*-nitrosourea (27.0 g, 260 mmoles) and KOH in decalin was diluted with dry N_2 and introduced into a solution of phenylallene (**1***a*) (12) (7.0 g, 60 mmoles) and benzene (40 ml) containing a small amount of *S*-**2** (350 mg, 0.69 mmole). The reaction temperature was maintained at 0°. After the introduction was completed, an N_2 stream was bubbled into the mixture for an additional hour. The reaction mixture was fractionated *in vacuo* below 40° at 0.05 mm to give a volatile fraction (3.7 g) which consisted mainly of 2-phenylmethylenecyclopropane (**3***a*) and phenylspiropentane (**4***a*) along with some starting allene. Each component was separated by preparative gas–liquid chromatography (g.l.c.) to yield the analytical samples in optically active form (Table I).

2-Phenylmethylenecyclopropane (**3***a*) (35% yield at 84% conversion): b.p. 35–40° (1 mm); infrared (i.r.) spectrum: 3080, 1750, 890 (=CH_2), 3060 and 1015 cm^{-1} (cyclopropane); n.m.r. spectrum: δ 1.2 (1H, H_2 C-3 *cis* to Ph, multiplet), 1.7 (1H, H_2 C-3 *trans* to Ph, multiplet), 2.5 (1H, PhC*H*, multiplet), 5.6 (2H, =CH_2, multiplet), and 7.2 p.p.m. (5H, Ph, multiplet).

Anal. Calcd. for $C_{10}H_{10}$: C, 92.3; H, 7.7. Found: C, 92.5; H, 7.9.

Phenylspiropentane (**4***a*) (54% yield), b.p. 45–50° (1 mm). Spectral data including i.r. and n.m.r. spectra were quite identical with reported ones (13).

Anal. Calcd. for $C_{11}H_{12}$: C, 91.6; H, 8.4. Found: C, 91.8; H, 8.4.

Formation of benzylidenecyclopropane was not observed.

Decomposition of diazomethane in 1-methyl-1-phenylallene (**1***b*) (12) and *n*-hexylallene (**1***c*) (12) was carried out in the similar manner. The optical data are summarized in Table I. Physical properties of the products are as follows:

2-Methyl-2-phenylmethylenecyclopropane (**3***b*) (44% yield at 97% conversion), b.p. 45–50° (1 mm); i.r. spectrum: 3080, 1735, 880 (=CH_2), 3050, and 1020 cm^{-1} (cyclopropane); n.m.r. spectrum: δ 1.3 (2H, cyclopropane CH_2, multiplet), 1.50 (3H, Me, singlet), 5.5 (2H, =CH_2, multiplet), and 7.2 p.p.m. (5H, Ph, multiplet).

Anal. Calcd. for $C_{11}H_{12}$: C, 91.6; H, 8.4. Found: C, 91.4; H, 8.4.

1-*Methyl*-1-*phenylspiropentane* (**4***b*) (54% yield), b.p. 55–58° (1 mm); i.r. spectrum: 3050, 1025, and 995 cm^{-1} (cyclopropane); n.m.r. spectrum: δ 0.8 (4H, H_2 C-4 and H_2 C-5, multiplet), 1.16 (2H, H_2 C-2, AB quartet, J = 4.5 Hz), 1.45 (3H, Me, singlet), and 7.1 p.p.m. (5H, Ph, multiplet).

Anal. Calcd. for $C_{12}H_{14}$: C, 91.1; H, 8.9. Found: C, 91.3; H, 9.2.

2-*n*-*Hexylmethylenecyclopropane* (**3***c*) (8% yield at 89% conversion), b.p. (bath temperature) 35–40° (1 mm); i.r. spectrum: 3070, 1746, 883 (=CH_2), 3040, and 1018 cm^{-1} (cyclopropane); n.m.r. spectrum: δ 0.5–1.5 (3H, cyclopropane, multiplet), 0.9 (3H, Me, multiplet), 1.3 (10H, CH_2 of *n*-hexyl, multiplet), and 5.3 p.p.m. (2H, =CH_2, multiplet). Reliable optical value could not be obtained because of the low yield, which was ascribed to rapid formation of **4***c*.

Anal. Calcd. for $C_{10}H_{18}$: C, 86.9; H, 13.1. Found: C, 87.0; H, 13.4.

n-Hexylspiropentane (**4***c*) (48% yield), b.p. 38–42° (1 mm); i.r. spectrum: 3070 and 995 cm^{-1} (cyclopropane); n.m.r. spectrum: δ 0.3–1.1 (7H, cyclopropane, multiplet), 0.9 (3H, Me, multiplet), and 1.3 p.p.m. (10H, CH_2 of *n*-hexyl, multiplet).

Anal. Calcd. for $C_{11}H_{20}$: C, 86.8; H, 13.2. Found: C, 86.9; H, 13.3.

Another minor component was detected by g.l.c. (ca. 1%), but not isolated pure. On the basis of the relative retention time and the i.r. spectrum (3070, 3000, 2975, 2950, 2870, 1470, 1380, 1090, 998, 959, 930, 775, 750, 704, and 660 cm^{-1}) it was tentatively assigned to *n-heptylidenecyclopropane*.

Diimide Reduction of **3***a*

To a mixture of **3***a* (1.5 g, 12 mmoles) and potassium azodicarboxylate (14) (4.5 g, 23 mmoles) in methanol (100 ml) was added acetic acid (43 ml) in the course of 3 h under an N_2 atmosphere at room temperature. The mixture was stirred for an additional 12 h and then treated with water, extracted with ether, and dried on Na_2SO_4.

Can. J. Chem. Downloaded from www.nrcresearchpress.com by 210.87.254.40 on 09/05/12
For personal use only.

Distillation *in vacuo* followed by g.l.c. purification gave a pure sample of *cis*-1-methyl-2-phenylcyclopropane (74% yield). The i.r. and n.m.r. data were quite identical with those of the authentic one (15).

Acknowledgments

The authors are indebted to Professor K. Sisido for his help and encouragement. This work was supported in part by Grant-in-aid administered by the Ministry of Education, Japanese Government.

1. H. NOZAKI, S. MORIUTI, H. TAKAYA, and R. NOYORI. Tetrahedron Letters, 5239 (1966).
2. H. NOZAKI, H. TAKAYA, S. MORIUTI, and R. NOYORI. Tetrahedron, **24**, 3655 (1968).
3. T. SUGITA and Y. INOUYE. Bull. Chem. Soc. Japan, **39**, 1075 (1966).
4. E. F. ULLMAN and W. J. FANSHAWE. J. Am. Chem. Soc. **83**, 2379 (1961).
5. D. SEYFERTH, J. M. BURLITCH, R. J. MINASZ, J. Y.-P. MUI, H. D. SIMMONS, JR., A. J. H. TREIBER, and S. R. DOWD. J. Am. Chem. Soc. **87**, 4259 (1965).
6. A. BEZAQUET and M. BERTRAND. Compt. Rend. Ser. C, **262**, 428 (1966).
7. W. RAHMAN and H. G. KUIVILA. J. Org. Chem. **31**, 772 (1966).
8. E. F. ULLMAN. J. Am. Chem. Soc. **81**, 5386 (1959).
9. E. F. ULLMAN. J. Am. Chem. Soc. **82**, 505 (1960).
10. J. P. CHESICK. J. Am. Chem. Soc. **85**, 2720 (1963).
11. J. K. CRANDALL and D. R. PAULSON. J. Am. Chem. Soc. **88**, 4302 (1966).
12. L. SKATTEBØL and S. SOLOMON. Acta Chem. Scand. **17**, 1683 (1963).
13. C. L. BUMGARDNER. J. Org. Chem. **29**, 767 (1964).
14. J. THIELE. Ann. **271**, 127 (1892).
15. W. L. DILLING. J. Org. Chem. **29**, 960 (1964).

Synthesis of 2-acetamido-2-deoxy-D-gulose, 2-acetamido-2-deoxy-D-idose, and 2-deoxy-D-*xylo*-hexose from 3,4,5,6-tetraacetoxy-D-*xylo*-1-nitro-1-hexene[1]

M. B. PERRY AND ANN C. WEBB

Division of Biochemistry and Molecular Biology, National Research Council of Canada, Ottawa 2, Canada

Received August 23, 1968

3,4,5,6-Tetraacetoxy-D-*xylo*-1-nitro-1-hexene with methanolic ammonia afforded a mixture of 2-acetamido-1,2-dideoxy-1-nitro-D-gulitol and 2-acetamido-1,2-dideoxy-1-nitro-D-iditol which were converted *via* a Nef reaction to 2-acetamido-2-deoxy-D-gulose and 2-acetamido-2-deoxy-D-idose.

Reduction of 3,4,5,6-tetraacetoxy-D-*xylo*-1-nitro-1-hexene afforded 3,4,5,6-tetra-*O*-acetyl-1,2-dideoxy-1-nitro-D-*xylo*-hexitol which was converted *via* the Nef reaction to 2-deoxy-D-*xylo*-hexose.

Canadian Journal of Chemistry, **47**, 1245 (1969)

2-Acetamido-2-deoxy-D-gulose and 2-acetamido-2-deoxy-D-idose were prepared in 32 and 4% yields respectively from 3,4,5,6-tetraacetoxy-D-*xylo*-1-nitro-1-hexene by the general procedure in which polyacetoxy-1-nitro-1-alkenes are treated with ammonia to yield epimeric 2-acetamido-1,2-dideoxy-1-nitroglycitols which may be converted *via* a modified (1) Nef (2) reaction to the corresponding 2-acetamido-2-deoxyglycoses (3–7). This procedure had previously been applied to the preparation of 2-amino-2-deoxy-D-gulose in about 15% yield from the intermediate acetoxylated nitroalkene (8); 2-amino-2-deoxyidose was detected chromatographically in the reaction products.

2-Amino-2-deoxy-D-gulose and 2-amino-2-deoxy-D-idose have been synthesized from D-xylose in 8 and 38% yields respectively by the condensation of D-xylose with hydrogen cyanide and aniline or *p*-toluidine followed by controlled hydrogenation of the products (9). 2-Amino-2-deoxy-D-gulose has been synthesized from 2-amino-2-deoxy-D-galactose by configurational inversion at C-3 (10) and 2-amino-2-deoxy-D-idose has been made by ammonolysis of methyl 4,6-*O*-benzylidene-2,3-di-*O*-*p*-tolylsulfonyl-α-D-galactopyranoside in the presence of sodium methoxide and subsequent *N*-acetylation to yield methyl 2-acetamido-4,6-*O*-benzylidene-2-deoxy-α-D-idopyranoside from which 2-amino-2-deoxy-D-idose could be obtained (11).

3,4,5,6-Tetraacetoxy-D-*xylo*-1-nitro-1-hexene (12) with saturated methanolic ammonia solution gave a mixture of 2-acetamido-1,2-dideoxy-1-nitro-D-gulitol and 2-acetamido-1,2-dideoxy-1-nitro-D-iditol which could not be separated by fractional crystallization. The mixed 2-acetamido-1,2-dideoxy-1-nitroglycitols on treatment with sulfuric acid afforded a mixture of 2-acetamido-2-deoxy-D-gulose and 2-acetamido-2-deoxy-D-idose and a small proportion of the corresponding free aminoglycoses. The product after

[1]Issued as NRCC No. 10509.

Can. J. Chem. Downloaded from www.nrcresearchpress.com by 210.87.254.40 on 09/05/12
For personal use only.

Distillation *in vacuo* followed by g.l.c. purification gave a pure sample of *cis*-1-methyl-2-phenylcyclopropane (74% yield). The i.r. and n.m.r. data were quite identical with those of the authentic one (15).

Acknowledgments

The authors are indebted to Professor K. Sisido for his help and encouragement. This work was supported in part by Grant-in-aid administered by the Ministry of Education, Japanese Government.

1. H. NOZAKI, S. MORIUTI, H. TAKAYA, and R. NOYORI. Tetrahedron Letters, 5239 (1966).
2. H. NOZAKI, H. TAKAYA, S. MORIUTI, and R. NOYORI. Tetrahedron, **24**, 3655 (1968).
3. T. SUGITA and Y. INOUYE. Bull. Chem. Soc. Japan, **39**, 1075 (1966).
4. E. F. ULLMAN and W. J. FANSHAWE. J. Am. Chem. Soc. **83**, 2379 (1961).
5. D. SEYFERTH, J. M. BURLITCH, R. J. MINASZ, J. Y.-P. MUI, H. D. SIMMONS, JR., A. J. H. TREIBER, and S. R. DOWD. J. Am. Chem. Soc. **87**, 4259 (1965).
6. A. BEZAQUET and M. BERTRAND. Compt. Rend. Ser. C, **262**, 428 (1966).
7. W. RAHMAN and H. G. KUIVILA. J. Org. Chem. **31**, 772 (1966).
8. E. F. ULLMAN. J. Am. Chem. Soc. **81**, 5386 (1959).
9. E. F. ULLMAN. J. Am. Chem. Soc. **82**, 505 (1960).
10. J. P. CHESICK. J. Am. Chem. Soc. **85**, 2720 (1963).
11. J. K. CRANDALL and D. R. PAULSON. J. Am. Chem. Soc. **88**, 4302 (1966).
12. L. SKATTEBØL and S. SOLOMON. Acta Chem. Scand. **17**, 1683 (1963).
13. C. L. BUMGARDNER. J. Org. Chem. **29**, 767 (1964).
14. J. THIELE. Ann. **271**, 127 (1892).
15. W. L. DILLING. J. Org. Chem. **29**, 960 (1964).

Synthesis of 2-acetamido-2-deoxy-D-gulose, 2-acetamido-2-deoxy-D-idose, and 2-deoxy-D-*xylo*-hexose from 3,4,5,6-tetraacetoxy-D-*xylo*-1-nitro-1-hexene[1]

M. B. PERRY AND ANN C. WEBB

Division of Biochemistry and Molecular Biology, National Research Council of Canada, Ottawa 2, Canada

Received August 23, 1968

3,4,5,6-Tetraacetoxy-D-*xylo*-1-nitro-1-hexene with methanolic ammonia afforded a mixture of 2-acetamido-1,2-dideoxy-1-nitro-D-gulitol and 2-acetamido-1,2-dideoxy-1-nitro-D-iditol which were converted *via* a Nef reaction to 2-acetamido-2-deoxy-D-gulose and 2-acetamido-2-deoxy-D-idose.

Reduction of 3,4,5,6-tetraacetoxy-D-*xylo*-1-nitro-1-hexene afforded 3,4,5,6-tetra-*O*-acetyl-1,2-dideoxy-1-nitro-D-*xylo*-hexitol which was converted *via* the Nef reaction to 2-deoxy-D-*xylo*-hexose.

Canadian Journal of Chemistry, **47**, 1245 (1969)

2-Acetamido-2-deoxy-D-gulose and 2-acetamido-2-deoxy-D-idose were prepared in 32 and 4% yields respectively from 3,4,5,6-tetraacetoxy-D-*xylo*-1-nitro-1-hexene by the general procedure in which polyacetoxy-1-nitro-1-alkenes are treated with ammonia to yield epimeric 2-acetamido-1,2-dideoxy-1-nitroglycitols which may be converted *via* a modified (1) Nef (2) reaction to the corresponding 2-acetamido-2-deoxyglycoses (3–7). This procedure had previously been applied to the preparation of 2-amino-2-deoxy-D-gulose in about 15% yield from the intermediate acetoxylated nitroalkene (8); 2-amino-2-deoxyidose was detected chromatographically in the reaction products.

2-Amino-2-deoxy-D-gulose and 2-amino-2-deoxy-D-idose have been synthesized from D-xylose in 8 and 38% yields respectively by the condensation of D-xylose with hydrogen cyanide and aniline or *p*-toluidine followed by controlled hydrogenation of the products (9). 2-Amino-2-deoxy-D-gulose has been synthesized from 2-amino-2-deoxy-D-galactose by configurational inversion at C-3 (10) and 2-amino-2-deoxy-D-idose has been made by ammonolysis of methyl 4,6-*O*-benzylidene-2,3-di-*O*-*p*-tolylsulfonyl-α-D-galactopyranoside in the presence of sodium methoxide and subsequent *N*-acetylation to yield methyl 2-acetamido-4,6-*O*-benzylidene-2-deoxy-α-D-idopyranoside from which 2-amino-2-deoxy-D-idose could be obtained (11).

3,4,5,6-Tetraacetoxy-D-*xylo*-1-nitro-1-hexene (12) with saturated methanolic ammonia solution gave a mixture of 2-acetamido-1,2-dideoxy-1-nitro-D-gulitol and 2-acetamido-1,2-dideoxy-1-nitro-D-iditol which could not be separated by fractional crystallization. The mixed 2-acetamido-1,2-dideoxy-1-nitroglycitols on treatment with sulfuric acid afforded a mixture of 2-acetamido-2-deoxy-D-gulose and 2-acetamido-2-deoxy-D-idose and a small proportion of the corresponding free aminoglycoses. The product after

[1]Issued as NRCC No. 10509.

Can. J. Chem. Downloaded from www.nrcresearchpress.com by 210.87.254.42 on 09/05/12
For personal use only.

Can. J. Chem. Downloaded from www.nrcresearchpress.com by 210.87.254.42 on 09/05/12
For personal use only.

treatment with aqueous acetic anhydride, was shown by paper chromatography, to contain only the 2-acetamido-2-deoxygulose and 2-acetamido-2-deoxyidose derivatives in the visual ratio of about 10:1. The mixture was fractionated by cellulose column chromatography to yield pure samples of 2-acetamido-2-deoxy-D-gulose and 2-acetamido-2-deoxy-D-idose. This preparative procedure gives a simple and direct route to the synthesis of the 2-acetamido-2-deoxyglycoses from readily available and inexpensive precursors and should be of practical value.

2-Deoxy-D-*xylo*-hexose was prepared in 25% yield from 3,4,5,6-tetraacetoxy-D-*xylo*-1-nitro-1-hexene by reduction with hydrogen to give 3,4,5,6-tetra-*O*-acetyl-1,2-dideoxy-1-nitro-D-*xylo*-hexitol which underwent the Nef reaction to yield the 2-deoxy-D-*xylo*-hexose. 2-Deoxy-D-*xylo*-hexose which has been reported to be a constituent of a glycoside isolated from *Erysimum perowskianum* (13) has been synthesized from methyl 2,3-anhydro-4,6-*O*-benzylidene-β-D-gulopyranoside by reduction with lithium aluminium hydride to methyl 4,6-*O*-benzylidene-2-deoxy-D-*xylo*-hexopyranoside, which on mild hydrolysis afforded 2-deoxy-D-*xylo*-hexose (14).

Experimental

Paper chromatography was performed by the descending method (15) on Whatman No. 1 filter paper using pyridine – ethyl acetate – water (2:5:5 v/v, top layer) as the mobile phase. The glycoses were detected with (*A*) 2% silver nitrate in acetone followed by 2% sodium hydroxide in ethanol (16), (*B*) 2% *p*-anisidine hydrochloride in ethanol (17), or (*C*) 0.02 *M* sodium metaperiodate followed by ethylene glycol – acetone – sulfuric acid (50:50:0.3 v/v) and 6% sodium 2-thiobarbiturate (18). The rates of movement of the glycoses on the chromatograms are quoted relative to D-galactose (R_{gal}).

Gas–liquid partition chromatography (g.l.c.) was carried out using a Hewlett–Packard 402 chromatograph with a hydrogen flame detector and fitted with glass U tubes (4ft × 6mm × 3mm internal diameter) packed with 10% neopentylglycol sebacate polyester on 80–100 mesh acid-washed Chromosorb W, maintained at 225 °C. Dry helium was used as the carrier gas and retention times of the compounds are quoted relative to 2-acetamido-2-deoxy-1,3,4,5,6-penta-*O*-(trimethylsilyl)-D-glucitol (T_{GN}) or 1,2,3,4,5,6-hexa-*O*-acetyl-D-glucitol (T_G).

Melting points were determined on a Fisher–Johns apparatus and are corrected. Solutions were concentrated under reduced pressure, below 40 °C. Optical rotations were determined at 20 °C using a Perkin–Elmer 141 polarimeter.

2-Acetamido-2-deoxy-D-idose and 2-Acetamido-2-deoxy-D-gulose

A solution of 3,4,5,6-tetraacetoxy-D-*xylo*-1-nitro-1-hexene (20 g) (12), in methanol (150 ml) cooled to 0 °C, was saturated with dry ammonia (about 1 h) and the mixture was then allowed to stand at room temperature for 20 h. The reaction mixture was concentrated to a syrup which was triturated with warm chloroform (4 × 100 ml) to remove acetamide. The residual syrup (13 g) was then dissolved in a solution of $Ba(OH)_2 \cdot 8H_2O$ (16 g) in water (240 ml). This solution was added dropwise with vigorous stirring to a cold mixture of sulfuric acid (14 ml) in water (240 ml) and, after stirring at 10 °C for 2 h the mixture was left at 20 °C for 18 h. The neutralized ($BaCO_3$) reaction mixture was filtered and the filtrate after concentration to about 100 ml was treated with Dowex-1($CO_3^=$) ion-exchange resin (30 ml), methanol (10 ml), and acetic anhydride (0.8 ml). The mixture was then shaken for 30 min. The filtered solution was concentrated to a syrup (11 g) and paper chromatographic examination of the product showed two spots having R_{gal} 1.87 and 2.19 in the visual ratio of 10:1 which corresponded in rates of movement with 2-acetamido-2-deoxygulose and 2-acetamido-2-deoxyidose respectively.

The mixed 2-acetamido-2-deoxyhexoses were separated by cellulose column (4.5 × 85 cm) chromatography using butan-1-ol half saturated with water as the mobile phase. Chromatographically pure 2-acetamido-2-deoxy-D-idose (0.48 g) was eluted first and was followed by 2-acetamido-2-deoxy-D-gulose (3.90 g).

2-Acetamido-2-deoxy-D-idose

The product from the column which could not be crystallized showed a single spot on paper chromatography (R_{gal} 2.19) and had $[\alpha]_D$ −38° (*c*, 2 in water) (lit. (9) $[\alpha]_D$ −45°).

Anal. Calcd. for $C_8H_{15}O_6N$: C, 43.43; H, 6.84; N, 6.33. Found: C, 43.3; H, 6.8; N, 6.3.

The trimethylsilylated (19) 2-acetamido-2-deoxy-D-idose on gas chromatography gave four peaks having T_{GN} 0.58 (4%), 0.87 (48%), 1.06 (18%), and 1.13 (30%).

2-Acetamido-2-deoxy-D-iditol

2-Acetamido-2-deoxy-D-idose (0.1 g) in water (5 ml) was reduced with sodium borohydride (50 mg) for 3 h at room temperature and the isolated 2-acetamido-2-deoxy-D-iditol (65 mg) after recrystallization from ethanol had m.p. 139 °C and $[\alpha]_D$ +25° (*c*, 0.6 in water) and gave a single spot on paper chromatography (R_{gal} 1.13).

Anal. Calcd. for $C_8H_{17}O_6N$: C, 43.05; H, 7.68; N, 6.27. Found: C, 43.1; H, 7.8; N, 6.3.

The fully acetylated hexitol (20) on g.l.c. gave a single peak having T_G 3.23 corresponding in retention time with authentic 1,3,4,5,6-penta-*O*-acetyl-2-acetamido-2-deoxy-D-iditol.

2-Acetamido-2-deoxy-D-gulose

The product obtained crystalline from ethanol solution had m.p. 125–126 °C and $[\alpha]_D$ −66° (*c*, 2.5 in water) (lit. (9) $[\alpha]_D$ −59°) and gave a single spot on paper chromatography (R_{gal} 1.87).

Anal. Calcd. for $C_8H_{15}O_6N$: C, 43.43; H, 6.84; N, 6.33. Found: C, 43.4; H, 6.7; N, 6.4.

The trimethylsilylated crystalline 2-acetamido-2-deoxy-D-gulose on gas chromatography gave two peaks having T_{GN} 1.04 (26%) and 1.16 (74%) and the trimethylsilylated glycose after equilibration in water gave the same two peaks (29 and 71% respectively).

2-Acetamido-2-deoxy-D-gulitol

2-Acetamido-2-deoxy-D-gulose (0.15 g) was reduced as

described above for the preparation of 2-acetamido-2-deoxy-D-iditol to yield 2-acetamido-2-deoxy-D-gulitol which after recrystallization from methanol had m.p. 169–170 °C and $[\alpha]_D$ +6.2° (*c*, 0.5 in water) and gave a single spot on paper chromatography (R_{gal} 1.18).

Anal. Calcd. for $C_8H_{17}O_6N$: C, 43.05; H, 7.68; N, 6.27. Found: C, 43.0; H, 7.8; N, 6.2.

The fully acetylated hexitol on gas chromatography gave a single peak having T_G 3.59.

*2-Deoxy-*D*-xylo-hexose*

*(a) 3,4,5,6-Tetra-O-acetyl-1,2-dideoxy-1-nitro-*D*-xylo-hexitol*

3,4,5,6-Tetraacetoxy-D-*xylo*-1-nitro-1-hexene (10 g) in ethanol (200 ml) was shaken with hydrogen at atmospheric pressure in the presence of palladium black (0.4 g). One mole of hydrogen was absorbed in 20 min. The reaction mixture was filtered and the filtrate was concentrated to a syrup which crystallized. The 3,4,5,6-tetra-*O*-acetyl-1,2-dideoxy-1-nitro-D-*xylo*-hexitol (7.8 g) after recrystallization from ethanol had m.p. 81 °C and $[\alpha]_D$ −5.9° (*c*, 1.5 in chloroform).

Anal. Calcd. for $C_{14}H_{21}O_{10}N$: C, 46.28; H, 5.83; N, 3.86. Found: C, 46.3; H, 6.0; N, 3.8.

*(b) 2-Deoxy-*D*-xylo-hexose*

3,4,5,6-Tetra-*O*-acetyl-1,2-dideoxy-1-nitro-D-*xylo*-hexitol (7.5 g) was dissolved in *N* sodium hydroxide (100 ml) and after 1 h at 20 °C the mixture was added dropwise with stirring to a solution of sulfuric acid (12 ml) in water (20 ml). The neutralized ($BaCO_3$) reaction mixture after filtration, was passed down columns of Rexyn 101(H^+) (200 ml) and Duolite A4(OH^-) (25 ml) ion-exchange resins and the eluate and washings were concentrated to a syrup (2.6 g) which was fractionated on a cellulose column (4 × 35 cm), using butan-1-ol half saturated with water as the mobile phase, to yield chromatographically pure 2-deoxy-D-*xylo*-hexose (1.1 g).

The 2-deoxy-D-*xylo*-hexose on paper chromatography had R_{gal} 2.70 and gave the characteristic red color with the periodate – thiobarbiturate spray reagents. It had $[\alpha]_D$ +9.4° (*c*, 0.5 in water) (lit. (14) $[\alpha]_D$ +12 ± 2°).

Anal. Calcd. for $C_6H_{12}O_5$: C, 43.90; H, 7.37. Found: C, 44.0; H, 7.4.

The 2-deoxy-D-*xylo*-hexose (100 mg) on bromine oxidation gave 2-deoxy-D-*xylo*-hexonolactone (90 mg) having $[\alpha]_D$ −56° (*c*, 1.9 in acetone) (lit. (14) $[\alpha]_D$ −57°) which on treatment with phenylhydrazine afforded 2-deoxy-D-*xylo*-hexonic acid phenylhydrazide (38 mg) having m.p. 125–126 °C (lit. (14) m.p. 124–125 °C).

1. C. Satoh and A. Kiyomoto. Chem. Pharm. Bull. Tokyo, **12**, 615 (1964).
2. J. U. Nef. Ann. **280**, 263 (1894).
3. A. N. O'Neill. Can. J. Chem. **37**, 1747 (1959).
4. J. C. Sowden and M. L. Oftedahl. J. Am. Chem. Soc. **82**, 2303 (1960).
5. S. D. Gero and J. Defaye. Compt. Rend. Acad. Sci. Paris, **261**, 1555 (1965).
6. M. B. Perry and A. C. Webb. Can. J. Chem. **46**, 2481 (1968).
7. M. B. Perry and J. Furdova. Can. J. Chem. **46**, 2859 (1968).
8. J. C. Sowden and M. L. Oftedahl. J. Org. Chem. **26**, 2153 (1961).
9. R. Kuhn and W. Bister. Ann. **617**, 92 (1958).
10. Z. Tarasiejska and R. W. Jeanloz. J. Am. Chem. Soc. **79**, 4215 (1957).
11. R. W. Jeanloz, Z. Tarasiejska Glazer, and D. A. Jeanloz. J. Org. Chem. **26**, 532 (1961).
12. J. C. Sowden and H. O. L. Fischer. J. Am. Chem. Soc. **69**, 1048 (1947).
13. Z. Kowalewski, O. Schindler, H. Jäger, and T. Reichstein. Helv. Chim. Acta, **43**, 1280 (1960).
14. T. Golab and T. Reichstein. Helv. Chim. Acta, **68**, 616 (1961).
15. S. M. Partridge. Biochem. J. **42**, 238 (1948).
16. W. E. Trevelyan, D. P. Procter, and J. S. Harrison. Nature, **166**, 444 (1950).
17. L. Hough, J. K. N. Jones, and W. H. Wadman. J. Chem. Soc. 1702 (1950).
18. L. Warren. Nature, **186**, 237 (1960).
19. M. B. Perry. Can. J. Biochem. **42**, 451 (1964).
20. M. B. Perry and A. C. Webb. Can. J. Biochem. **46**, 1163 (1968).

Formation of a C_{22} dihydroxyketo acid by a yeast

Ronald F. Vesonder and Frank H. Stodola

Northern Regional Research Laboratory, Agricultural Research Service, United States Department of Agriculture, Peoria, Illinois 61604

Received December 4, 1968

Saponification of extracellular lipids from the yeast NRRL YB-2501 yielded 8,9,13-trihydroxydocosanoic acid and a new keto dihydroxy acid of melting point 131–132 °C. The keto acid was shown to be 8,9-dihydroxy-13-oxodocosanoic acid by conversion to 5-ketotetradecanoic acid and suberic acid. By means of the method of Ames and Bowman (3), it was established that the vicinal hydroxyls of the new acid have the *erythro* configuration.

Canadian Journal of Chemistry, **47**, 1247 (1969)

In 1965 we reported (1) that 8,9,13-triacetoxydocosanoic acid is produced by a yeast closely related to *Torulopsis fujisanensis*. More recently, in a review (2) on the extracellular lipids of yeasts, we mentioned that this organism also forms at the same time a smaller amount of

Can. J. Chem. Downloaded from www.nrcresearchpress.com by 210.87.254.42 on 09/05/12
For personal use only.

described above for the preparation of 2-acetamido-2-deoxy-D-iditol to yield 2-acetamido-2-deoxy-D-gulitol which after recrystallization from methanol had m.p. 169–170 °C and $[\alpha]_D$ +6.2° (*c*, 0.5 in water) and gave a single spot on paper chromatography (R_{gal} 1.18).

Anal. Calcd. for $C_8H_{17}O_6N$: C, 43.05; H, 7.68; N, 6.27. Found: C, 43.0; H, 7.8; N, 6.2.

The fully acetylated hexitol on gas chromatography gave a single peak having T_G 3.59.

*2-Deoxy-*D*-xylo-hexose*

*(a) 3,4,5,6-Tetra-O-acetyl-1,2-dideoxy-1-nitro-*D*-xylo-hexitol*

3,4,5,6-Tetraacetoxy-D-*xylo*-1-nitro-1-hexene (10 g) in ethanol (200 ml) was shaken with hydrogen at atmospheric pressure in the presence of palladium black (0.4 g). One mole of hydrogen was absorbed in 20 min. The reaction mixture was filtered and the filtrate was concentrated to a syrup which crystallized. The 3,4,5,6-tetra-*O*-acetyl-1,2-dideoxy-1-nitro-D-*xylo*-hexitol (7.8 g) after recrystallization from ethanol had m.p. 81 °C and $[\alpha]_D$ −5.9° (*c*, 1.5 in chloroform).

Anal. Calcd. for $C_{14}H_{21}O_{10}N$: C, 46.28; H, 5.83; N, 3.86. Found: C, 46.3; H, 6.0; N, 3.8.

*(b) 2-Deoxy-*D*-xylo-hexose*

3,4,5,6-Tetra-*O*-acetyl-1,2-dideoxy-1-nitro-D-*xylo*-hexitol (7.5 g) was dissolved in *N* sodium hydroxide (100 ml) and after 1 h at 20 °C the mixture was added dropwise with stirring to a solution of sulfuric acid (12 ml) in water (20 ml). The neutralized ($BaCO_3$) reaction mixture after filtration, was passed down columns of Rexyn 101(H^+) (200 ml) and Duolite A4(OH^-) (25 ml) ion-exchange resins and the eluate and washings were concentrated to a syrup (2.6 g) which was fractionated on a cellulose column (4 × 35 cm), using butan-1-ol half saturated with water as the mobile phase, to yield chromatographically pure 2-deoxy-D-*xylo*-hexose (1.1 g).

The 2-deoxy-D-*xylo*-hexose on paper chromatography had R_{gal} 2.70 and gave the characteristic red color with the periodate – thiobarbiturate spray reagents. It had $[\alpha]_D$ +9.4° (*c*, 0.5 in water) (lit. (14) $[\alpha]_D$ +12 ± 2°).

Anal. Calcd. for $C_6H_{12}O_5$: C, 43.90; H, 7.37. Found: C, 44.0; H, 7.4.

The 2-deoxy-D-*xylo*-hexose (100 mg) on bromine oxidation gave 2-deoxy-D-*xylo*-hexonolactone (90 mg) having $[\alpha]_D$ −56° (*c*, 1.9 in acetone) (lit. (14) $[\alpha]_D$ −57°) which on treatment with phenylhydrazine afforded 2-deoxy-D-*xylo*-hexonic acid phenylhydrazide (38 mg) having m.p. 125–126 °C (lit. (14) m.p. 124–125 °C).

1. C. Satoh and A. Kiyomoto. Chem. Pharm. Bull. Tokyo, **12**, 615 (1964).
2. J. U. Nef. Ann. **280**, 263 (1894).
3. A. N. O'Neill. Can. J. Chem. **37**, 1747 (1959).
4. J. C. Sowden and M. L. Oftedahl. J. Am. Chem. Soc. **82**, 2303 (1960).
5. S. D. Gero and J. Defaye. Compt. Rend. Acad. Sci. Paris, **261**, 1555 (1965).
6. M. B. Perry and A. C. Webb. Can. J. Chem. **46**, 2481 (1968).
7. M. B. Perry and J. Furdova. Can. J. Chem. **46**, 2859 (1968).
8. J. C. Sowden and M. L. Oftedahl. J. Org. Chem. **26**, 2153 (1961).
9. R. Kuhn and W. Bister. Ann. **617**, 92 (1958).
10. Z. Tarasiejska and R. W. Jeanloz. J. Am. Chem. Soc. **79**, 4215 (1957).
11. R. W. Jeanloz, Z. Tarasiejska Glazer, and D. A. Jeanloz. J. Org. Chem. **26**, 532 (1961).
12. J. C. Sowden and H. O. L. Fischer. J. Am. Chem. Soc. **69**, 1048 (1947).
13. Z. Kowalewski, O. Schindler, H. Jäger, and T. Reichstein. Helv. Chim. Acta, **43**, 1280 (1960).
14. T. Golab and T. Reichstein. Helv. Chim. Acta, **68**, 616 (1961).
15. S. M. Partridge. Biochem. J. **42**, 238 (1948).
16. W. E. Trevelyan, D. P. Procter, and J. S. Harrison. Nature, **166**, 444 (1950).
17. L. Hough, J. K. N. Jones, and W. H. Wadman. J. Chem. Soc. 1702 (1950).
18. L. Warren. Nature, **186**, 237 (1960).
19. M. B. Perry. Can. J. Biochem. **42**, 451 (1964).
20. M. B. Perry and A. C. Webb. Can. J. Biochem. **46**, 1163 (1968).

Formation of a C_{22} dihydroxyketo acid by a yeast

Ronald F. Vesonder and Frank H. Stodola

Northern Regional Research Laboratory, Agricultural Research Service, United States Department of Agriculture, Peoria, Illinois 61604

Received December 4, 1968

Saponification of extracellular lipids from the yeast NRRL YB-2501 yielded 8,9,13-trihydroxydocosanoic acid and a new keto dihydroxy acid of melting point 131–132 °C. The keto acid was shown to be 8,9-dihydroxy-13-oxodocosanoic acid by conversion to 5-ketotetradecanoic acid and suberic acid. By means of the method of Ames and Bowman (3), it was established that the vicinal hydroxyls of the new acid have the *erythro* configuration.

Canadian Journal of Chemistry, **47**, 1247 (1969)

In 1965 we reported (1) that 8,9,13-triacetoxydocosanoic acid is produced by a yeast closely related to *Torulopsis fujisanensis*. More recently, in a review (2) on the extracellular lipids of yeasts, we mentioned that this organism also forms at the same time a smaller amount of

Can. J. Chem. Downloaded from www.nrcresearchpress.com by 210.87.254.6 on 09/05/12
For personal use only.

erythro-8,9-dihydroxy-13-oxodocosanoic acid (**1**), presumably in the acylated form; the evidence for the structure of **1** is now presented.

Acid **1** (m.p. 131–132 °C; $[\alpha]_D^{20}$ − 2.8°) was isolated from mother liquors left after the crystallization of 8,9,13-trihydroxydocosanoic acid, obtained by the saponification of the crude lipid excreted by the yeast. The structure and configuration of **1** were established by the following reactions:

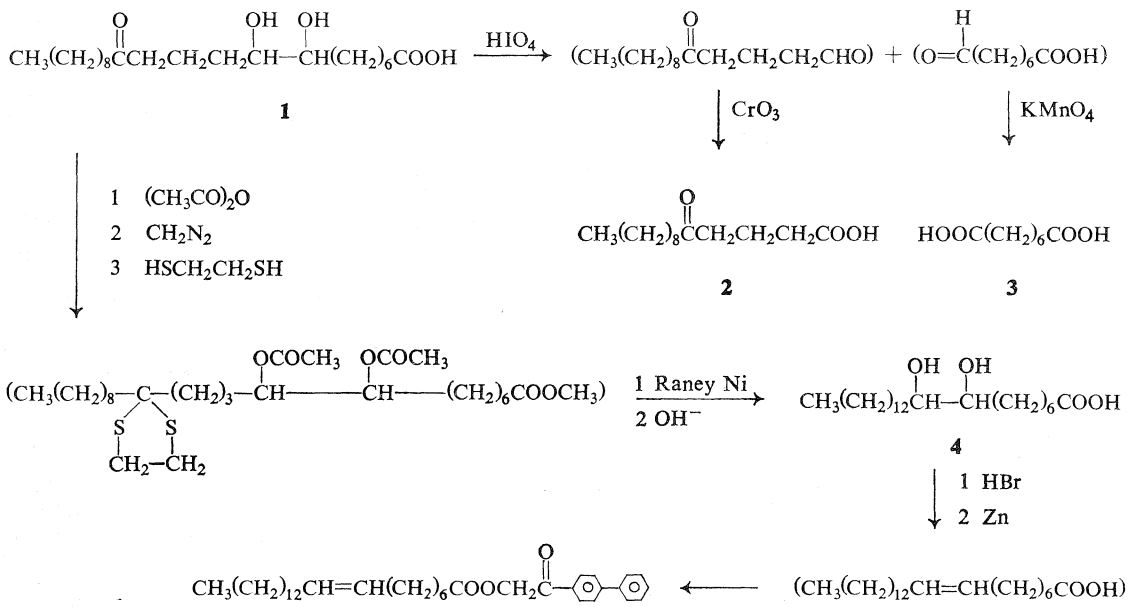

Cleavage of **1** with periodic acid gave aldehydes that yielded 5-ketotetradecanoic acid (**2**) and suberic acid (**3**) on oxidation. Configuration of the vicinal hydroxyl groups in **1** was established in the following manner: the diacetyl methyl ester of **1** was converted to 8,9-dihydroxydocosanoic acid (**4**) by way of the thioketal; hydrobromination of **4** according to the method of Ames and Bowman (3), and subsequent debromination yielded a *cis* acid, which indicated an *erythro* configuration of the hydroxyl groups.

In our review (2) we reported the oxidation of 8,9,13-trihydroxydocosanoic acid to acid **1** after protection of the vicinal hydroxyls as an acetonide. A number of unsuccessful attempts to repeat this work, however, have since led us to the conclusion that this oxidation is no value as a structure proof because of very low yields.

Acid **1** is characterized by the following derivatives: methyl ester, m.p. 107–108 °C; *p*-bromophenacyl ester, m.p. 141–142 °C; and the semicarbazone, m.p. 129–130.5 °C.

Experimental

Melting points were determined with a Fisher–Johns apparatus[1] and were not corrected.

*Isolation of erythro-8,9-Dihydroxy-13-oxodocosanoic Acid (**1**)*

Crude lipid (48.3 g), obtained from the yeast NRRL YB-2501 by the procedure already described (1), was heated for 1 h at 95 °C with *N*-methylpyrrolidone (300 ml), *t*-butyl alcohol (250 ml), and 180 ml of water containing 43 g KOH. Acidification of the hot solution with 6 *N* HCl (360 ml), gave 34.0 g of crude 8,9,13-trihydroxydocosanoic acid, which on crystallization from acetic acid yielded 25.2 g of almost pure trihydroxy acid, m.p. 157–158 °C. Dilution of the mother liquor with water gave 7.49 g of crude crystalline acid **1** (m.p. 118–123 °C). Three crystallizations from ethyl acetate gave pure acid **1** with a constant melting point of 131–132 °C; yield, 4.83 g; $[\alpha]_D^{20}$ −2.8° (*c*, 10 in dimethyl sulfoxide).

Acid **1** liquefies in a few days on standing in an evacuated sulfuric acid desiccator, presumably due to ring closure between the hydroxyl and keto groups. Similar

[1]Mention of firm names or trade products does not constitute endorsement by the United States Department of Agriculture over other firms or products not mentioned.

Can. J. Chem. Downloaded from www.nrcresearchpress.com by 210.87.254.6 on 09/05/12
For personal use only.

behavior was observed when the acid was boiled for a few hours in petroleum ether (b.p. 93–97 °C).

Anal. Calcd. for $C_{22}H_{42}O_5$: C, 68.35; H, 10.95. Found: C, 68.6; H, 11.0.

Methyl 8,9-Dihydroxy-13-oxodocosanate

Acid **1** (100 mg) was treated with excess diazomethane in methanol–ether. The crude ester was crystallized from methanol-saturated petroleum ether (b.p. 65–68 °C), 75 mg, m.p. 107–108 °C.

Anal. Calcd. for $C_{23}H_{44}O_5$: C, 68.96; H, 11.07. Found: C, 69.1; H, 11.2.

p-Bromophenacyl-8,9-dihydroxy-13-oxodocosanate

Acid **1** (38.6 mg) was converted to the phenacyl ester in a mixture of acetone and *N*-methylpyrrolidone, according to the dicyclohexylethylamine (DICE) procedure (4). The crude product (89%, m.p. 125–130 °C) on crystallization from ethanol gave 38 mg of *p*-bromophenacyl ester, m.p. 141–142 °C.

Anal. Calcd. for $C_{30}H_{47}BrO_6$: C, 61.74; H, 8.12. Found: C, 61.8; H, 8.20.

Semicarbazone of Acid 1

Crude semicarbazone (25 mg) from 31.5 mg of acid **1** was crystallized from ethyl acetate, 16 mg, m.p. 129–130.5 °C.

Anal. Calcd. for $C_{23}H_{45}N_3O_5$: C, 62.27; H, 10.22; N, 9.47. Found: C, 62.6; H, 10.3; N, 9.22.

Periodic Acid Cleavage of Acid 1

A mixture of acid **1** (90 mg), periodic acid (106 mg), water (0.06 ml), and acetonitrile (1 ml) was kept in the dark for 1 h at room temperature. Water (0.5 ml) containing 85 mg $NaHCO_3$ was added, and the reaction mixture was extracted with ether. Removal of ether gave 57.5 mg of pale-yellow solid, which was oxidized with 1.55 ml of 0.91 *M* CrO_3 in acetic acid to 5-ketotetradecanoic acid, m.p. 77.5–79 °C (*p*-bromophenacyl ester, m.p. 83–84 °C).

The aqueous fraction yielded suberic acid after $KMnO_4$ treatment, as described in our earlier work (1).

8,9-Dihydroxydocosanoic Acid (4)

Acid **1** (1 g) was converted to the diacetate with acetic anhydride – pyridine (24 h; room temperature), and the crude diacetate was methylated with diazomethane. The methyl ester was dissolved in a mixture of acetic acid (1.25 ml), BF_3 etherate (0.66 ml), and $HSCH_2CH_2SH$ (0.25 ml). After 20 h at room temperature, the reaction mixture was added to 4 *N* NH_4OH (45 ml). An oil (1.33 g), recovered by ether extraction, was heated at 80 °C for 5 h with Raney nickel in ethanol. Filtration and removal of solvent gave 787 mg of product melting at 128–131 °C, which on crystallization from ethyl acetate yielded 592 mg pure acid **4** (m.p. 132–133 °C).

Anal. Calcd. for $C_{22}H_{44}O_4$: C, 70.92; H, 11.90. Found: C, 70.8; H, 11.8.

p-Phenylphenacyl cis-8-Docosenoate

Acid **4** (50 mg) was dissolved in 25% HBr – CH_3COOH (25 ml) containing 0.2 ml of concentrated sulfuric acid. After standing at room temperature for 20 h, the reaction mixture was heated at 95 °C for 3.5 h. Heating was continued for 4 h more after addition of 0.4 ml of 25% HBr – CH_3COOH. The dibromo compound was isolated by petroleum ether extraction and was esterified with diazomethane. The ester was refluxed under nitrogen for 1 h with ethanol (3 ml) and 30-mesh activated zinc (600 mg). The mixture of *cis* and *trans* esters was recovered by petroleum ether extraction and was shown by infrared absorption to be 93% *cis*. Saponification gave 43.8 mg of colorless crystals, which were converted by the DICE method (4) to crude *p*-phenylphenacyl ester (64.1 mg, m.p. 40–60 °C). Recrystallization from alcohol gave an analytical sample (45.1 mg, m.p. 67–68 °C).

Anal. Calcd. for $C_{36}H_{52}O_3$: C, 81.16; H, 9.84. Found: C, 81.0; H, 9.62.

1. F. H. Stodola, R. F. Vesonder, and L. J. Wickerham. Biochemistry, **4**, 1390 (1965).
2. F. H. Stodola, M. H. Deinema, and J. F. T. Spencer. Bacteriol. Rev. **31**, 194 (1967).
3. D. E. Ames and R. E. Bowman. J. Chem. Soc. 1079 (1951).
4. F. H. Stodola. Microchem. J. **7**, 389 (1963).

Monomer and dimer formation in esters of dihydroxyacetone

Lorrin R. Garson, Ronald P. Quintana, and Andrew Lasslo
Department of Medicinal Chemistry, College of Pharmacy, University of Tennessee Medical Units, Memphis, Tennessee 38103

Received January 13, 1969

The monomer (1-undecanoyloxy-3-hydroxyacetone) and dimer (2,5-diundecanoyloxymethyl-2,5-dihydroxy-1,4-dioxane) of dihydroxyacetone monoundecanoate have been characterized, and the conditions associated with their interconversion have been determined. The respective molecular constitutions have been unequivocally documented with ultraviolet and infrared spectral characteristics.

Canadian Journal of Chemistry, **47**, 1249 (1969)

In our preceding communication (1), we reported the synthesis of 1-undecanoyloxy-3-hydroxyacetone (**1**), a compound with potential perdurable insect-repellent efficacy. The data available at that time, however, did not permit us to establish unequivocally whether the compound existed as a monomer or dimer (or as a mixture of these two forms). In order to prepare the substantial quantities of **1** required for the evaluation of its repellent properties, we employed a direct

Can. J. Chem. Downloaded from www.nrcresearchpress.com by 210.87.254.6 on 09/05/12
For personal use only.

behavior was observed when the acid was boiled for a few hours in petroleum ether (b.p. 93–97 °C).

Anal. Calcd. for $C_{22}H_{42}O_5$: C, 68.35; H, 10.95. Found: C, 68.6; H, 11.0.

Methyl 8,9-Dihydroxy-13-oxodocosanate

Acid **1** (100 mg) was treated with excess diazomethane in methanol–ether. The crude ester was crystallized from methanol-saturated petroleum ether (b.p. 65–68 °C), 75 mg, m.p. 107–108 °C.

Anal. Calcd. for $C_{23}H_{44}O_5$: C, 68.96; H, 11.07. Found: C, 69.1; H, 11.2.

p-Bromophenacyl-8,9-dihydroxy-13-oxodocosanate

Acid **1** (38.6 mg) was converted to the phenacyl ester in a mixture of acetone and *N*-methylpyrrolidone, according to the dicyclohexylethylamine (DICE) procedure (4). The crude product (89%, m.p. 125–130 °C) on crystallization from ethanol gave 38 mg of *p*-bromophenacyl ester, m.p. 141–142 °C.

Anal. Calcd. for $C_{30}H_{47}BrO_6$: C, 61.74; H, 8.12. Found: C, 61.8; H, 8.20.

Semicarbazone of Acid 1

Crude semicarbazone (25 mg) from 31.5 mg of acid **1** was crystallized from ethyl acetate, 16 mg, m.p. 129–130.5 °C.

Anal. Calcd. for $C_{23}H_{45}N_3O_5$: C, 62.27; H, 10.22; N, 9.47. Found: C, 62.6; H, 10.3; N, 9.22.

Periodic Acid Cleavage of Acid 1

A mixture of acid **1** (90 mg), periodic acid (106 mg), water (0.06 ml), and acetonitrile (1 ml) was kept in the dark for 1 h at room temperature. Water (0.5 ml) containing 85 mg $NaHCO_3$ was added, and the reaction mixture was extracted with ether. Removal of ether gave 57.5 mg of pale-yellow solid, which was oxidized with 1.55 ml of 0.91 *M* CrO_3 in acetic acid to 5-ketotetradecanoic acid, m.p. 77.5–79 °C (*p*-bromophenacyl ester, m.p. 83–84 °C).

The aqueous fraction yielded suberic acid after $KMnO_4$ treatment, as described in our earlier work (1).

8,9-Dihydroxydocosanoic Acid (4)

Acid **1** (1 g) was converted to the diacetate with acetic anhydride – pyridine (24 h; room temperature), and the crude diacetate was methylated with diazomethane. The methyl ester was dissolved in a mixture of acetic acid (1.25 ml), BF_3 etherate (0.66 ml), and $HSCH_2CH_2SH$ (0.25 ml). After 20 h at room temperature, the reaction mixture was added to 4 *N* NH_4OH (45 ml). An oil (1.33 g), recovered by ether extraction, was heated at 80 °C for 5 h with Raney nickel in ethanol. Filtration and removal of solvent gave 787 mg of product melting at 128–131 °C, which on crystallization from ethyl acetate yielded 592 mg pure acid **4** (m.p. 132–133 °C).

Anal. Calcd. for $C_{22}H_{44}O_4$: C, 70.92; H, 11.90. Found: C, 70.8; H, 11.8.

p-Phenylphenacyl cis-8-Docosenoate

Acid **4** (50 mg) was dissolved in 25% HBr – CH_3COOH (25 ml) containing 0.2 ml of concentrated sulfuric acid. After standing at room temperature for 20 h, the reaction mixture was heated at 95 °C for 3.5 h. Heating was continued for 4 h more after addition of 0.4 ml of 25% HBr – CH_3COOH. The dibromo compound was isolated by petroleum ether extraction and was esterified with diazomethane. The ester was refluxed under nitrogen for 1 h with ethanol (3 ml) and 30-mesh activated zinc (600 mg). The mixture of *cis* and *trans* esters was recovered by petroleum ether extraction and was shown by infrared absorption to be 93% *cis*. Saponification gave 43.8 mg of colorless crystals, which were converted by the DICE method (4) to crude *p*-phenylphenacyl ester (64.1 mg, m.p. 40–60 °C). Recrystallization from alcohol gave an analytical sample (45.1 mg, m.p. 67–68 °C).

Anal. Calcd. for $C_{36}H_{52}O_3$: C, 81.16; H, 9.84. Found: C, 81.0; H, 9.62.

1. F. H. Stodola, R. F. Vesonder, and L. J. Wickerham. Biochemistry, **4**, 1390 (1965).
2. F. H. Stodola, M. H. Deinema, and J. F. T. Spencer. Bacteriol. Rev. **31**, 194 (1967).
3. D. E. Ames and R. E. Bowman. J. Chem. Soc. 1079 (1951).
4. F. H. Stodola. Microchem. J. **7**, 389 (1963).

Monomer and dimer formation in esters of dihydroxyacetone

Lorrin R. Garson, Ronald P. Quintana, and Andrew Lasslo

Department of Medicinal Chemistry, College of Pharmacy, University of Tennessee Medical Units, Memphis, Tennessee 38103

Received January 13, 1969

The monomer (1-undecanoyloxy-3-hydroxyacetone) and dimer (2,5-diundecanoyloxymethyl-2,5-dihydroxy-1,4-dioxane) of dihydroxyacetone monoundecanoate have been characterized, and the conditions associated with their interconversion have been determined. The respective molecular constitutions have been unequivocally documented with ultraviolet and infrared spectral characteristics.

Canadian Journal of Chemistry, **47**, 1249 (1969)

In our preceding communication (1), we reported the synthesis of 1-undecanoyloxy-3-hydroxyacetone (**1**), a compound with potential perdurable insect-repellent efficacy. The data available at that time, however, did not permit us to establish unequivocally whether the compound existed as a monomer or dimer (or as a mixture of these two forms). In order to prepare the substantial quantities of **1** required for the evaluation of its repellent properties, we employed a direct

Can. J. Chem. Downloaded from www.nrcresearchpress.com by 210.87.254.40 on 09/05/12
For personal use only.

Can. J. Chem. Downloaded from www.nrcresearchpress.com by 210.87.254.40 on 09/05/12
For personal use only.

acylation method (2, 3) rather than the method of Schlenk *et al.* (4). The former procedure yielded the desired monoester in considerably higher yield, and with greater facility than the one using the diazoketone intermediate (4).

When compound **1**—prepared by direct acylation—was carefully recrystallized from hexane or chloroform, it afforded a product melting at 96.8–98.3°; recrystallization from ethanol, subsequent to prolonged heating of the solution, yielded a product melting at 44.8–46.1°. Furthermore, when the lower-melting compound was allowed to stand in the crystalline state at room temperature, it slowly reverted to the higher-melting compound; an increase in the melting-point range could be detected even after 24 h.

The data reported below unambiguously indicate that the lower-melting compound is 1-undecanoyloxy-3-hydroxyacetone (monomer, **1***a*) and the higher-melting product is 2,5-diundecanoyloxymethyl-2,5-dihydroxy-1,4-dioxane (dimer, **1***b*).

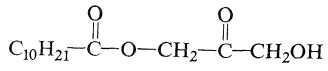

1*a*

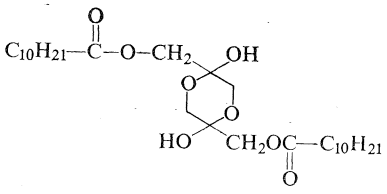

1*b*

The ultraviolet spectrum of a solution of **1***a* in *p*-dioxane reflects the presence of two chromophores; maximum absorption at 274.5 mμ (ε 19.8) is characteristic of a ketone carbonyl function (5), and that at 224 mμ (ε 39.7) is indicative of the ester carbonyl. The ultraviolet spectrum of **1***b* exhibits only a single maximum at 224 mμ (ε 74.5) consistent with the presence of two ester moieties. In the infrared region, apparent molecular absorption coefficients (ε^a) at 1736 cm^{-1} for solutions of **1***a* and **1***b* in chloroform are 330 and 550, respectively, which also substantiate the structural assignments. This observation is consistent with the fact that esters exhibit a higher absorption coefficient than ketones (6); i.e., **1***a* embodying one keto and one ester function has a lower ε^a value than **1***b* with two ester functions.

In addition, the OH stretching frequencies for **1***a* (3509 cm^{-1}) and **1***b* (3571 and 3425 cm^{-1}) are markedly different. The concentration of **1***a*, in carbon tetrachloride, did not affect band intensity at 3509 cm^{-1}; the latter and the relatively low wavenumber reflect an intramolecularly hydrogen-bonded hydroxyl function. Because of the limited solubility of **1***b* in carbon tetrachloride, the latter could not be correspondingly evaluated. Examined in chloroform, however, the band at 3571 cm^{-1} can be attributed to free hydroxyl groups indicative of the dimer (**1***b*); the moderately weak OH vibrational bands 3571 (sharp) and 3425 cm^{-1} (broad) being specifically characteristic of a sterically hindered alcohol (7), evident only in the dimer.

The structure assignments for **1***a* and **1***b* are supported by the findings of Schlenk *et al.* (4); they reported that 1-palmitoyloxy-3-hydroxyacetone can exhibit monomeric (m.p. 63°) and dimeric (m.p. 93°) forms; however, no structure was even suggested for the dimer. Dihydroxyacetone itself is known to exist as a monomer and dimer (8), the latter being 2,5-dihydroxymethyl-2,5-dihydroxy-1,4-dioxane (9, 10).

Experimental

Melting points are corrected; they were determined with a Büchi melting point apparatus. Ultraviolet (u.v.) and infrared (i.r.) spectra were obtained with the Perkin–Elmer model 202 and 137B spectrophotometers, respectively. Combustion analyses were performed by Drs. G. Weiler and F. B. Strauss, Oxford, England.

*1-Undecanoyloxy-3-hydroxyacetone [monomer (**1a**) and dimer (**1b**)]*

A solution of undecanoyl chloride (56.8 g, 0.277 mole) in 555 ml of chloroform (freshly distilled from P_2O_5) was added dropwise, over a period of 2 h, to a stirred solution of 100 g (1.110 mole) of dry 1,3-dihydroxypropanone in 555 ml of dry, freshly distilled pyridine. The temperature of the reaction mixture was maintained at −2 to −6°. After stirring an additional 1.2 h while warming to 18°, the pyridine–chloroform solution was slowly added to 500 ml of cold (−10°) 3 *N* HCl and 1000 g of ice; during the addition, 1 l of 6 *N* HCl was simultaneously added. The aqueous phase was extracted with chloroform (3 × 400 ml) and the combined chloroform phases were dried over anhydrous Na_2SO_4. Removal of the solvent *in vacuo* afforded 78 g of oily crude product. This was dissolved in 95% ethanol, and upon standing, a total of 12.5 g of crystalline material was collected.[1] Ethanol was then removed by distillation

[1]This consisted primarily of 1,3-diundecanoyloxyacetone, the properties of which we described in our preceding paper (1).

in vacuo, the oily residue was treated with benzene (3 × 70 ml), and the solvent was removed *in vacuo* after each addition.

The residue was dissolved in hexane and, upon standing, a crystalline product (23.6 g, m.p. 91.3–93.3°) was collected; a second crop (14.0 g, m.p. 60.3–83.2°) was also obtained. Recrystallization of the first crop from chloroform yielded **1***b*: m.p. 96.8–98.3°;[2] λ_{max} (*p*-dioxane) 224 mμ (ε 74.5); ν_{max} (chloroform) 3571, 3425 (O—H stretching),[2] 1736 cm^{-1} (ester carbonyl).

Anal. Calcd. for $C_{28}H_{52}O_8$: C, 65.09; H, 10.14. Found: C, 65.25; H, 10.27.

After refluxing **1***b* in 95% ethanol for 2 h, and two recrystallizations from the same solvent, **1***a* was obtained: m.p. 44.8–46.1°; λ_{max} (*p*-dioxane) 224 (ε 39.7), 274.5 mμ (ε 19.8); ν_{max} (chloroform) 3509 (O—H stretching), 1736 cm^{-1} (ester and ketone carbonyl).

Anal. Calcd. for $C_{14}H_{26}O_4$: C, 65.09; H, 10.14. Found: C, 65.18; H, 10.27.

Acknowledgments

This investigation was supported by the United States Army Medical Research and Development Command, Washington, D.C., through Research Contract No. DA-49-193-MD-2636. The authors wish to thank Miss B. D. Bramham for the infrared and ultraviolet spectra.

[2]The melting point and the O—H stretching frequencies reported for **1** in our preceding paper (1) are indicative of a monomer–dimer mixture.

1. R. P. Quintana, L. R. Garson, and A. Lasslo. Can. J. Chem. **47**, 853 (1969).
2. A. K. Hajra and B. W. Agranoff. J. Biol. Chem. **243**, 1617 (1968).
3. A. K. Hajra and B. W. Agranoff. J. Biol. Chem. **242**, 1074 (1967).
4. H. Schlenk, B. G. Lamp, and B. W. DeHaas. J. Am. Chem. Soc. **74**, 2550 (1952).
5. H. H. Jaffé and M. Orchin. Theory and applications of ultraviolet spectroscopy. John Wiley and Sons, New York. 1962. pp. 178–182.
6. K. Nakanishi. Infrared absorption spectroscopy. Holden–Day, San Francisco. 1962. pp. 42, 44.
7. C. N. R. Rao. Chemical applications of infrared spectroscopy. Academic Press, New York. 1963. p. 180.
8. G. Bertrand. Compt. Rend. **129**, 341 (1899).
9. R. P. Bell and E. C. Baughan. J. Chem. Soc. 1947 (1937).
10. L. Goldman, J. Barkoff, D. Blaney, T. Nakai, and R. Suskind. J. Invest. Dermatol. **35**, 161 (1960).

Nucleophilic displacement of vinylic halogen in fluorinated cycloalkenes. II. Reaction with triphenylphosphine

S. E. Ellzey, Jr.

Southern Regional Research Laboratory, Southern Utilization Research and Development Division, Agricultural Research Service, United States Department of Agriculture, New Orleans, Louisiana 70119

Received October 28, 1968

1,2-Dichloroperfluorocyclobutene and the corresponding cyclopentene react with triphenylphosphine under hydrolytic conditions in wet acetic acid to yield novel triphenyl(fluorocycloalkenyl)phosphonium betaines. Structural assignments are made on the basis of elemental analysis, ^1H and ^{19}F nuclear magnetic resonance spectra, infrared spectra, and degradation studies. Triphenylphosphine and 1,2-dichloroperfluorocyclohexene yield triphenylphosphine oxide and a product which appears to be 1-chloro-2-hydrooctafluorocyclohexene.

Canadian Journal of Chemistry, **47**, 1251 (1969)

Displacement of both vinyl chlorines from the olefins **1***a–c* with trialkyl phosphites, phosphonites, and phosphinites yields products substituted in the 1- and 2-positions with phosphorus (1). Depending on the type of nucleophile used, certain secondary phosphines or diphosphines were reported to yield either mono- or disubstitution products (2).

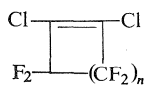

1*a*, $n = 1$
b, $n = 2$
c, $n = 3$

It has now been found that reaction of triphenylphosphine with **1***a* and **1***b* in acetic acid–water yields the triphenylphosphonium betaines **2***a* and **2***b*, respectively, in low yield (3). These are the phosphorus analogues of the quaternary ammonium betaines **3** obtained when the nucleophile is tertiary amino nitrogen (4*a–c*). The structures **2** are assigned on the basis of elemental analysis, molecular weight, infrared, ^1H and ^{19}F

Can. J. Chem. Downloaded from www.nrcresearchpress.com by 210.87.254.40 on 09/05/12
For personal use only.

in vacuo, the oily residue was treated with benzene (3 × 70 ml), and the solvent was removed *in vacuo* after each addition.

The residue was dissolved in hexane and, upon standing, a crystalline product (23.6 g, m.p. 91.3–93.3°) was collected; a second crop (14.0 g, m.p. 60.3–83.2°) was also obtained. Recrystallization of the first crop from chloroform yielded **1***b*: m.p. 96.8–98.3°;[2] λ_{max} (*p*-dioxane) 224 mμ (ε 74.5); ν_{max} (chloroform) 3571, 3425 (O—H stretching),[2] 1736 cm^{-1} (ester carbonyl).

Anal. Calcd. for $C_{28}H_{52}O_8$: C, 65.09; H, 10.14. Found: C, 65.25; H, 10.27.

After refluxing **1***b* in 95% ethanol for 2 h, and two recrystallizations from the same solvent, **1***a* was obtained: m.p. 44.8–46.1°; λ_{max} (*p*-dioxane) 224 (ε 39.7), 274.5 mμ (ε 19.8); ν_{max} (chloroform) 3509 (O—H stretching), 1736 cm^{-1} (ester and ketone carbonyl).

Anal. Calcd. for $C_{14}H_{26}O_4$: C, 65.09; H, 10.14. Found: C, 65.18; H, 10.27.

Acknowledgments

This investigation was supported by the United States Army Medical Research and Development Command, Washington, D.C., through Research Contract No. DA-49-193-MD-2636. The authors wish to thank Miss B. D. Bramham for the infrared and ultraviolet spectra.

[2]The melting point and the O—H stretching frequencies reported for **1** in our preceding paper (1) are indicative of a monomer–dimer mixture.

1. R. P. Quintana, L. R. Garson, and A. Lasslo. Can. J. Chem. **47**, 853 (1969).
2. A. K. Hajra and B. W. Agranoff. J. Biol. Chem. **243**, 1617 (1968).
3. A. K. Hajra and B. W. Agranoff. J. Biol. Chem. **242**, 1074 (1967).
4. H. Schlenk, B. G. Lamp, and B. W. DeHaas. J. Am. Chem. Soc. **74**, 2550 (1952).
5. H. H. Jaffé and M. Orchin. Theory and applications of ultraviolet spectroscopy. John Wiley and Sons, New York. 1962. pp. 178–182.
6. K. Nakanishi. Infrared absorption spectroscopy. Holden–Day, San Francisco. 1962. pp. 42, 44.
7. C. N. R. Rao. Chemical applications of infrared spectroscopy. Academic Press, New York. 1963. p. 180.
8. G. Bertrand. Compt. Rend. **129**, 341 (1899).
9. R. P. Bell and E. C. Baughan. J. Chem. Soc. 1947 (1937).
10. L. Goldman, J. Barkoff, D. Blaney, T. Nakai, and R. Suskind. J. Invest. Dermatol. **35**, 161 (1960).

Nucleophilic displacement of vinylic halogen in fluorinated cycloalkenes. II. Reaction with triphenylphosphine

S. E. Ellzey, Jr.

Southern Regional Research Laboratory, Southern Utilization Research and Development Division, Agricultural Research Service, United States Department of Agriculture, New Orleans, Louisiana 70119

Received October 28, 1968

1,2-Dichloroperfluorocyclobutene and the corresponding cyclopentene react with triphenylphosphine under hydrolytic conditions in wet acetic acid to yield novel triphenyl(fluorocycloalkenyl)phosphonium betaines. Structural assignments are made on the basis of elemental analysis, ^1H and ^{19}F nuclear magnetic resonance spectra, infrared spectra, and degradation studies. Triphenylphosphine and 1,2-dichloroperfluorocyclohexene yield triphenylphosphine oxide and a product which appears to be 1-chloro-2-hydrooctafluorocyclohexene.

Canadian Journal of Chemistry, **47**, 1251 (1969)

Displacement of both vinyl chlorines from the olefins **1***a–c* with trialkyl phosphites, phosphonites, and phosphinites yields products substituted in the 1- and 2-positions with phosphorus (1). Depending on the type of nucleophile used, certain secondary phosphines or diphosphines were reported to yield either mono- or disubstitution products (2).

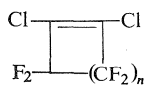

1*a*, $n = 1$
b, $n = 2$
c, $n = 3$

It has now been found that reaction of triphenylphosphine with **1***a* and **1***b* in acetic acid–water yields the triphenylphosphonium betaines **2***a* and **2***b*, respectively, in low yield (3). These are the phosphorus analogues of the quaternary ammonium betaines **3** obtained when the nucleophile is tertiary amino nitrogen (4*a–c*). The structures **2** are assigned on the basis of elemental analysis, molecular weight, infrared, ^1H and ^{19}F

Can. J. Chem. Downloaded from www.nrcresearchpress.com by 210.87.254.105 on 09/05/12
For personal use only.

nuclear magnetic resonance spectra, and oxidation of **2***b* to the expected dicarboxylic acid with CrO_3.

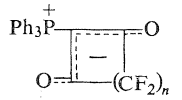

2*a*, $n = 1$
b, $n = 2$

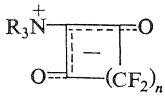

3*a*, R = alkyl, $n = 1$
b, R_3N = , $n = 1,2$

The infrared spectra of the betaines **2** in the 1540–1820 cm^{-1} region were quite similar to those of **3***b* of the same ring size (**4***a*). Strong bands were present in **2***a* at 1779, 1669, and 1637 cm^{-1} for the O⁻C⁻C⁻C⁻O system, while in **2***b* a strong band was present at 1653 cm^{-1}, with much weaker absorption at 1721 and 1686 cm^{-1}.

Absorptions due only to aromatic protons at δ 7.56–7.95 and 7.52–7.95 p.p.m., respectively, were present in the ^1H spectra of **2***a* and **2***b* (acetone-d_6, TMS as internal reference). The ^{19}F spectrum of **2***a* in dimethyl formamide (relative to internal $CFCl_3$) consisted of a doublet at δ +118.1 p.p.m., J_{PF} = 20.5 Hz; the chemical shift for **2***b* in the same solvent was at δ +127.2 p.p.m., J_{PF} = 1.1 Hz. These chemical shifts are very close to those of the corresponding **3***b*[1] and a related system studied by Stockel and co-workers (5). The larger J_{PF} in **2***a* relative to that in **2***b* may result from strong through-space coupling, reflecting the highly strained nature of the four-membered ring (6).

Neither **2***a* nor **2***b* decolorized bromine in CCl_4 or permanganate in acetone, and neither reacted with *m*-nitrobenzaldehyde after 18 h in refluxing tetrahydrofuran. With methyl iodide for 7 h in refluxing acetone **2***a* and **2***b* were unreactive, as was **2***b* with refluxing 50% sulfuric acid for 15 h.

Upon refluxing **2***a* with concentrated HCl for 15 h and recrystallizing the product from ethanol – acetone – water, there was obtained a material of empirical formula $C_{21}H_{17}F_2OP$, to which the structure **4** is assigned on the basis of its infrared and ^1H nuclear magnetic resonance spectra. A pair of strong bands at 1587 and 1562 cm^{-1} is indicative of the proposed betaine structure (7); no absorption due to OH or C=O stretch was evident. In the nuclear magnetic resonance spectrum (dimethyl sulfoxide-d_6), absorption was present at δ 4.12 (PCH, doublet, J_{PH} = 22 Hz) (8), 5.98 (CF_2H, triplet, J_{FH} = 56 Hz), and at 7.38–7.93 p.p.m. (aryl H). The peaks of the doublet and triplet were broad, possibly because of allylic couplings. Integration of the spectrum was in fair agreement with that expected for **4**. Stereochemistry about the C=C bond was not assigned.

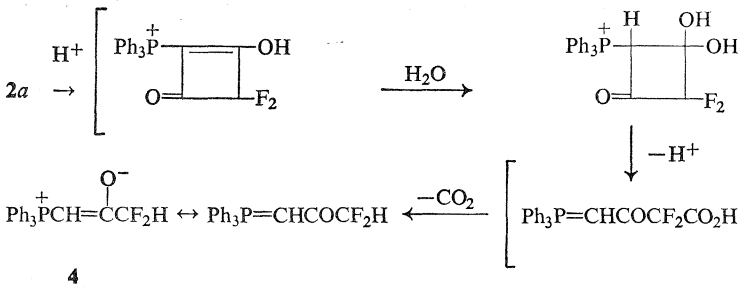

4

In contrast to the behavior of **1***a* and **1***b* with triphenylphosphine, **1***c* gave an 81% yield of triphenylphosphine oxide but no product analogous to **2** was isolated. Distillation of the reaction mixture prior to phosphine oxide isolation gave a mixture of acetic acid, unchanged **1***c*, and a material having infrared absorption at 1658 cm^{-1} in CCl_4 and a complex multiplet at δ 6.45 p.p.m. in its ^1H nuclear magnetic resonance spectrum. Although difficulties in separation prevented full characterization, spectral data for the latter compound are in accord with 1-chloro-2-hydrooctafluorocyclohexene, **5**, which reportedly

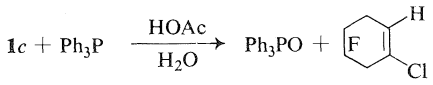

5

[1]D. F. Keeley, private communication.

Can. J. Chem. Downloaded from www.nrcresearchpress.com by 210.87.254.105 on 09/05/12
For personal use only.

has C=C absorption at 1660 cm^{-1} (9). A reason for the apparent change in mode of attack by phosphorus is not known at this time.

Experimental

The olefins **1***a* and **1***c* were obtained from Peninsular ChemResearch, Inc.[2] **1***b* was from either the latter source or Hooker Chemical Corporation. Triphenylphosphine was a product of Eastman Kodak.

Infrared spectra were obtained from KBr disks with a Perkin–Elmer model 137 spectrophotometer (NaCl optics). The nuclear magnetic resonance spectra were recorded on Varian spectrometer models A-60A and HR-60 (56.4 MHz).

Triphenyl(3,3-difluoro-2-hydroxy-4-oxo-1-cyclobuten-1-yl)phosphonium Hydroxide, Inner Salt (2a)

A mixture of 5.85 g (0.03 mole) of **1***a* and 8.66 g (0.033 mole) of triphenylphosphine in 50 ml of acetic acid and 2 ml of water was refluxed for 3 h. The gaseous products gave positive tests for F^- and Cl^-. After refluxing, about 10 ml of the mixture were distilled at 100–116° but gas–liquid partition chromatography (g.l.p.c.) analysis indicated only solvent and traces of other compounds. The remainder of the reaction mixture was poured into about 150 ml of water and ice and the precipitate was filtered and washed with water, 6.71 g, m.p. ca. 120–200°. The solid was washed with two 25 ml portions of ethanol, followed by 25 ml of ether, to give 3.27 g (29%) of **2***a*, m.p. 228–233°. Recrystallization from acetone–water gave an analytical sample, m.p. 230–231°.

Anal. Calcd. for $C_{22}H_{15}F_2O_2P$ (mol. wt., 380): C, 69.47; H, 3.98; F, 9.99; P, 8.14. Found (mol. wt., 375 osmometric in acetone): C, 69.67; H, 3.97; F, 9.59; P, 8.18.

The combined ethanol and ether washes were evaporated and the residue washed with petroleum ether, b.p. 30–60°. The soluble fraction yielded 1.13 g (13% recovery) of triphenylphosphine (mixture m.p. and infrared spectrum); the insoluble fraction yielded 0.56 g of the crude betaine and 0.75 g (9%) of crude triphenylphosphine oxide (m.p. and infrared spectrum).

2*a* could be distilled unchanged (92% recovery) in a sublimation apparatus at 3–3.5 mm, bath temperature 285–295°.

Triphenyl (3,3,4,4-tetrafluoro-2-hydroxy-5-oxo-1-cyclopenten-1-yl)phosphonium Hydroxide, Inner Salt (2b)

A mixture of 7.08 g (0.027 mole) of triphenylphosphine and 6.12 g (0.025 mole) of **1***b* was refluxed for 20 h in 50 ml of acetic acid containing 1 ml of water. Distillation of the reaction mixture until the vapor temperature was about 117° gave no starting material; on g.l.p.c. analysis only acetic acid and an impurity originally present in the olefin were noted. After pouring the distillation residue into water and ice, a dark emulsion formed and was coagulated by heating on a steam cone. The tarry semisolid was recrystallized twice from ethanol–water to yield 3.75 g (35%) of product, m.p. 173–174°. Further recrystallization gave a product melting mostly at 176–178°, but with some melting at 166°. If the melted material was cooled rapidly with ice and then placed in the bath preheated to 165°, it melted at 181–182°. Allowing the melt to cool slowly to room temperature in the bath gave a solid, m.p. 175–176°. The infrared spectra of all the forms were identical.

Anal. Calcd. for $C_{23}H_{15}F_4O_2P$ (mol. wt., 430): C, 64.19; H, 3.51; F, 17.66; P, 7.20. Found (mol. wt., 422 osmometric in acetone): C, 64.34; H, 3.62; F, 17.81; P, 7.34.

The tarry, semisolid residue obtained from the filtrate of the first recrystallization of **2***b* was chromatographed in benzene on a column of Alcoa F-20 alumina and eluted with ethanol and acetone. From the eluate there was obtained 2.15 g of a solid, m.p. 148–153°, which yielded 0.51 g (7%) of triphenylphosphine oxide (infrared spectrum), m.p. 156–157°, and some tar.

Evaporation of the original reaction mixture filtrate gave a few grams of tarry material.

Oxidation of 2b with CrO_3

A solution of 3.01 g (0.007 mole) of **2***b* in acetic acid at 75–80° was treated with a solution of 2.00 g (0.02 mole) of CrO_3 in acetic acid and water and held at 75–80° for 30 min. From this solution was obtained 1.14 g (38%) of recovered **2***b* and 0.54 g (40%) of perfluorosuccinic acid, m.p. 88–90° (from benzene). Identification of this acid was by means of infrared spectrum and neutralization equivalent.

Reaction of 2a with HCl

A stirred slurry of 1.14 g (0.003 mole) of **2***a* in 30 ml of concentrated HCl was refluxed 15 h, cooled, filtered, and the product was washed with tetrahydrofuran and acetone, 0.63 g. It had no sharp melting point and gave a positive test for Cl^- with silver nitrate, but upon recrystallization from ethanol – acetone – water, colorless needles of a chlorine-free product, m.p. 210–211° (decomp.), were obtained.

Anal. Calcd. for $C_{21}H_{17}F_2OP$: C, 71.18; H, 4.84; F, 10.72; P, 8.74. Found: C, 70.89; H, 4.83; F, 10.50; P, 8.63.

The infrared spectrum of the tetrahydrofuran- and acetone-washed product was quite different from that of the recrystallized material. Strong bands at 1587 and 1562 cm^{-1} in the latter were absent in the former; very broad and strong absorption at about 3226 cm^{-1} in the initial product was absent in the recrystallized solid.

Reaction of 1c with Triphenylphosphine

A mixture of 7.38 g (0.025 mole) of **1***c* and 7.08 g (0.027 mole) of triphenylphosphine in 50 ml of acetic acid containing 1 ml of water was refluxed for 43 h. Positive tests for F^- and Cl^- were obtained on the effluent gases. About 20 ml were distilled from the mixture and the distillate was dried over sodium sulfate and redistilled. A fraction weighing 5.68 g was collected at 83–84°. Gas–liquid partition chromatographic analysis indicated about 21% starting olefin and about 75% of an unknown component, in addition to minor peaks. An infrared spectrum of this mixture in CCl_4 showed C=O at 1721 (acetic acid), C=C at 1658 (**5**), and C=C at 1626 cm^{-1} (**1***c*). Further washing with water and redistillation removed the acetic acid; the ^1H nuclear magnetic resonance spectrum (CCl_4) showed a broad multiplet at δ 6.45 p.p.m., in addition to signals due to ether used in the work-up.

[2]Mention of a product or company name does not imply endorsement by the Department to the exclusion of others which may also be suitable.

Can. J. Chem. Downloaded from www.nrcresearchpress.com by 210.87.254.105 on 09/05/12
For personal use only.

The residue from the first distillation was diluted with water to give 6.88 g of solid which yielded 5.63 g (81%) of triphenylphosphine oxide and 0.79 g (11% recovery) of crude triphenylphosphine, both of which were identified by comparison of their infrared spectra with those of authentic samples.[3]

Acknowledgments

^{1}H nuclear magnetic resonance spectra were recorded by Gordon J. Boudreaux of this Laboratory and the ^{19}F spectra were obtained through the courtesy of Dr. Dean F. Keeley and Judith A. O'Connor, University of Southwestern Louisiana, Lafayette, Louisiana. Elemental analyses were by Galbraith Laboratories, Inc., Knoxville, Tennessee.

[3]*Note Added in Proof*: While this note was in press a report (10) appeared which substantially confirmed the present results, although the transformation of **1***c* into **5** went unnoticed. In the present work the formation of **5** was confirmed by analysis of a sample obtained by preparative gas–liquid chromatography.

Anal. Calcd. for C_6HClF_8: Cl, 13.61; F, 58.34. Found: Cl, 13.39; F, 57.80.

1. A. W. FRANK. J. Org. Chem. **30**, 3663 (1965).
2. W. R. CULLEN, D. S. DAWSON, and P. S. DHALIWAL. Can. J. Chem. **45**, 683 (1967). R. F. STOCKEL. Can. J. Chem. **46**, 2625 (1968).
3. S. E. ELLZEY, JR. U. S. Patent No. 3,359,321 (1967).
4. (*a*) S. E. ELLZEY, JR. and W. A. GUICE. J. Org. Chem. **31**, 1300 (1966). (*b*) R. F. STOCKEL and F. H. MEGSON. Can. J. Chem. **45**, 1998 (1967). (*c*) R. L. PRUETT, C. T. BAHNER, and H. A. SMITH. J. Am. Chem. Soc. **74**, 1633 (1952).
5. R. F. STOCKEL, M. T. BEACHEM, and F. H. MEGSON. J. Org. Chem. **30**, 1629 (1965).
6. V. W. GASH and D. J. BAUER. J. Org. Chem. **31**, 3602 (1966).
7. A. J. SPEZIALE and K. W. RATTS. J. Am. Chem. Soc. **85**, 2790 (1963).
8. F. J. RANDALL and A. W. JOHNSON. Tetrahedron Letters, 2841 (1968).
9. D. E. M. EVANS, W. J. FEAST, R. STEPHENS, and J. C. TATLOW. J. Chem. Soc. 4828 (1963).
10. R. F. STOCKEL, F. MEGSON, and M. T. BEACHEM. J. Org. Chem. **33**, 4395 (1968).

New nitrochalcones. IX[1]

T. SZÉLL AND I. SOHÁR

Department of Applied Chemistry, University of Szeged, Szeged, Hungary

Received September 5, 1968

A number of new nitrohydroxychalcones are reported. Electron-donating groups in the aldehyde favor condensation by HCl, and electron-withdrawing substituents favor condensation by NaOH.

Canadian Journal of Chemistry, **47**, 1254 (1969)

A number of chalcones have been synthesized from acetophenones and benzaldehydes and the yields compared. Table I lists the results of condensations carried out in the presence of NaOH. The substituents in the aldehyde component increase the yield of chalcone formation in aqueous ethanol in the following way:

2,3-diOMe $\gtrsim$ 2,5-diOMe > H > 2-OMe > 2,4-diOMe

Table II records the results of experiments carried out in ethanol in the presence of HCl. The order of effectiveness of reactants with substituents other than *ortho* can be established as follows:

4-OH $\gtrsim$ 4-OMe $\gtrsim$ 3-OMe-4-OH > 3,4-diOMe $\approx$ 3,4-diOEt $\gtrsim$ 4-Me > H > 4-Cl > 4-NO_2 > 2,4-diNO_2

and for *ortho* substituents:

2,4-diOMe $\gtrsim$ 2-OMe > H > 2,3-diOMe = 2,5-diOMe

The yields show a rough parallelism with Hammett's substituents constants (1), and with basicities (pK_{BH^+}) (2). These results are in accordance with earlier observations (3–5). It can be concluded that electron-donating substituents favor condensation by acid catalysts and that electron-withdrawing groups favor condensation by bases. The choice of condensing agent for the synthesis of chalcones can generally be decided on this basis.

Experimental

Aldehydes and acetophenones were obtained from Aldrich Chemical Co. Inc.; Columbia Organic Chemical Co.; and from Distillation Products. After having checked their purity most of them were used without further purification. Nitrohydroxyacetophenones were prepared as described earlier (4). Syntheses of chalcones in the presence of NaOH were the same as previously reported (4). The acidic condensation was carried out as follows.

An ethanolic solution of the appropriate acetophenone and aldehyde was kept ice-cold while being saturated with HCl gas for 30 min. It was kept in a thermostat at 30° for 1 h, and after allowing it to stand at room temperature

[1]For Part VII see ref. 4*a* and for Part VIII see ref. 10.

On page 1254, in the left-hand column, the order of effectiveness of reactants with substituents should read 4-Cl > H and not H > 4-Cl.

FOR ERRATA SEE
V.48 1970 P.2643

Can. J. Chem. Downloaded from www.nrcresearchpress.com by 210.87.254.105 on 09/05/12
For personal use only.

The residue from the first distillation was diluted with water to give 6.88 g of solid which yielded 5.63 g (81%) of triphenylphosphine oxide and 0.79 g (11% recovery) of crude triphenylphosphine, both of which were identified by comparison of their infrared spectra with those of authentic samples.[3]

Acknowledgments

^{1}H nuclear magnetic resonance spectra were recorded by Gordon J. Boudreaux of this Laboratory and the ^{19}F spectra were obtained through the courtesy of Dr. Dean F. Keeley and Judith A. O'Connor, University of Southwestern Louisiana, Lafayette, Louisiana. Elemental analyses were by Galbraith Laboratories, Inc., Knoxville, Tennessee.

[3]*Note Added in Proof*: While this note was in press a report (10) appeared which substantially confirmed the present results, although the transformation of **1***c* into **5** went unnoticed. In the present work the formation of **5** was confirmed by analysis of a sample obtained by preparative gas–liquid chromatography.

Anal. Calcd. for C_6HClF_8: Cl, 13.61; F, 58.34. Found: Cl, 13.39; F, 57.80.

1. A. W. FRANK. J. Org. Chem. **30**, 3663 (1965).
2. W. R. CULLEN, D. S. DAWSON, and P. S. DHALIWAL. Can. J. Chem. **45**, 683 (1967). R. F. STOCKEL. Can. J. Chem. **46**, 2625 (1968).
3. S. E. ELLZEY, JR. U. S. Patent No. 3,359,321 (1967).
4. (*a*) S. E. ELLZEY, JR. and W. A. GUICE. J. Org. Chem. **31**, 1300 (1966). (*b*) R. F. STOCKEL and F. H. MEGSON. Can. J. Chem. **45**, 1998 (1967). (*c*) R. L. PRUETT, C. T. BAHNER, and H. A. SMITH. J. Am. Chem. Soc. **74**, 1633 (1952).
5. R. F. STOCKEL, M. T. BEACHEM, and F. H. MEGSON. J. Org. Chem. **30**, 1629 (1965).
6. V. W. GASH and D. J. BAUER. J. Org. Chem. **31**, 3602 (1966).
7. A. J. SPEZIALE and K. W. RATTS. J. Am. Chem. Soc. **85**, 2790 (1963).
8. F. J. RANDALL and A. W. JOHNSON. Tetrahedron Letters, 2841 (1968).
9. D. E. M. EVANS, W. J. FEAST, R. STEPHENS, and J. C. TATLOW. J. Chem. Soc. 4828 (1963).
10. R. F. STOCKEL, F. MEGSON, and M. T. BEACHEM. J. Org. Chem. **33**, 4395 (1968).

New nitrochalcones. IX[1]

T. SZÉLL AND I. SOHÁR

Department of Applied Chemistry, University of Szeged, Szeged, Hungary

Received September 5, 1968

A number of new nitrohydroxychalcones are reported. Electron-donating groups in the aldehyde favor condensation by HCl, and electron-withdrawing substituents favor condensation by NaOH.

Canadian Journal of Chemistry, **47**, 1254 (1969)

A number of chalcones have been synthesized from acetophenones and benzaldehydes and the yields compared. Table I lists the results of condensations carried out in the presence of NaOH. The substituents in the aldehyde component increase the yield of chalcone formation in aqueous ethanol in the following way:

2,3-diOMe $\gtrsim$ 2,5-diOMe > H > 2-OMe > 2,4-diOMe

Table II records the results of experiments carried out in ethanol in the presence of HCl. The order of effectiveness of reactants with substituents other than *ortho* can be established as follows:

4-OH $\gtrsim$ 4-OMe $\gtrsim$ 3-OMe-4-OH > 3,4-diOMe $\approx$ 3,4-diOEt $\gtrsim$ 4-Me > H > 4-Cl > 4-NO_2 > 2,4-diNO_2

and for *ortho* substituents:

2,4-diOMe $\gtrsim$ 2-OMe > H > 2,3-diOMe = 2,5-diOMe

The yields show a rough parallelism with Hammett's substituents constants (1), and with basicities (pK_{BH^+}) (2). These results are in accordance with earlier observations (3–5). It can be concluded that electron-donating substituents favor condensation by acid catalysts and that electron-withdrawing groups favor condensation by bases. The choice of condensing agent for the synthesis of chalcones can generally be decided on this basis.

Experimental

Aldehydes and acetophenones were obtained from Aldrich Chemical Co. Inc.; Columbia Organic Chemical Co.; and from Distillation Products. After having checked their purity most of them were used without further purification. Nitrohydroxyacetophenones were prepared as described earlier (4). Syntheses of chalcones in the presence of NaOH were the same as previously reported (4). The acidic condensation was carried out as follows.

An ethanolic solution of the appropriate acetophenone and aldehyde was kept ice-cold while being saturated with HCl gas for 30 min. It was kept in a thermostat at 30° for 1 h, and after allowing it to stand at room temperature

[1]For Part VII see ref. 4*a* and for Part VIII see ref. 10.

On page 1254, in the left-hand column, the order of effectiveness of reactants with substituents should read 4-Cl > H and not H > 4-Cl.

FOR ERRATA SEE
V.48 1970 P.2643

Can. J. Chem. Downloaded from www.nrcresearchpress.com by 210.87.254.42 on 09/05/12
For personal use only.

Can. J. Chem. Downloaded from www.nrcresearchpress.com by 210.87.254.42 on 09/05/12
For personal use only.

TABLE I§

Physical constants and yields for nitr ohydroxychalcones obtained in the presence of NaOH

Ketone	Aldehyde	Chalcone	Yield (%)	Melting point (°C)	Nitrogen analysis		Σσ of the substituents of the aldehyde portion
					Calcd.	Found	
1. 3-NO_2-4-OH-acetophenone	Piridin-3- *	$C_{14}H_{10}O_4N_2$	70	211–212	10.4	10.4	
2.	Benz- †	$C_{15}H_{11}O_4N$	58	158–160	5.2	5.5	0.0
3.	2-OMe-benz- †	$C_{16}H_{13}O_5N$	47	170–171	4.7	4.7	
4.	2,3-di-OMe-benz- ‡	$C_{17}H_{15}O_6N$	75	195–197	4.25	4.1	
5.	2,4-di-OMe-benz- ‡	$C_{17}H_{15}O_6N$	18	156–158	4.25	4.4	
6.	2,5-di-OMe-benz-	$C_{17}H_{15}O_6N$	64	173	4.25	4.4	
7.	3,4-diCl-benz- *	$C_{15}H_9O_4NCl_2$	80	195–197	4.1	4.2	+0.67
8. 4-NO_2-2-OH-acetophenone	Piridin-3- *	$C_{14}H_{10}O_4N_2$	86	193–194	10.4	10.2	
9.	Benz- †	$C_{15}H_{11}O_4N$	64	190–191	5.2	5.4	0.0
10.	9-anthr- ‡	$C_{23}H_{15}O_4N$	60	200–202	—	—	
11.	2-OMe-benz- †	$C_{16}H_{13}O_5N$	75	171–172	4.7	4.5	
12.	2,3-di-OMe-benz- ‡	$C_{17}H_{15}O_6N$	85	182–184	4.25	4.1	
13.	2,4-di-OMe-benz- ‡	$C_{17}H_{15}O_6N$	42	206–207	4.25	4.5	
14.	2,5-di-OMe-benz- ‡	$C_{17}H_{15}O_6N$	83	193–195	4.25	4.0	
15. 5-NO_2-2-OH-acetophenone	Piridin-3- *	$C_{14}H_{10}O_4N_2$	83	219–221	10.4	10.4	
16.	Benz- †	$C_{15}H_{11}O_4N$	63	182–183	5.2	5.3	0.0
17.	2-OMe-benz- ‖	$C_{16}H_{13}O_5N$	60	159–160	4.7	4.8	
18.	2,3-di-OMe-benz- ‡	$C_{17}H_{15}O_6N$	61	162–164	4.25	4.2	
19.	2,4-di-OMe-benz- ‡	$C_{17}H_{15}O_6N$	40	186–188	4.25	4.5	
20.	2,5-di-OMe-benz- ‡	$C_{17}H_{15}O_6N$	66	161–162	4.25	4.1	

*New compounds.
†See ref. 4.
‡C.f. with the same chalcones listed in Table II.
§In runs no. 1, 8, and 15, the concentration of the ketone was 0.1 mole l^{-1}, that of the aldehyde 0.15 mole l^{-1} and the base concentration 1.0 mole l^{-1}. In run 7, the concentrations were 0.17, 0.17, and 1.7 and in all other runs 0.04, 0.04, and 0.5 mole l^{-1} respectively. Yields are reported for crude products, and melting points for the recrystallized materials. Recrystallization was carried out from ethyl acetate, ethanol, or acetic acid. The melting points of the crude products were generally 1–4° below those of the purified materials. The sodium salt of the chalcone was precipitated during the course of each run.
‖See ref. 6.

Can. J. Chem. Downloaded from www.nrcresearchpress.com by 210.87.254.42 on 09/05/12
For personal use only.

FOR ERRATA SEE
1.48....1970....P.2643..

In Table II on p. 1256, for compound 12 the yield should read 73 and not 39%, and the melting point 184–185 and not 215–216°.

TABLE II*

Physical constants and yields for nitrohydroxychalcones obtained in the presence of HCl

	Ketone	Aldehyde	Chalcone	Yield (%)	Melting point (°C)	Analysis Calcd. C	Calcd. H	Calcd. N	Found C	Found H	Found N	Σσ of the substituents of the aldehyde portion
1.	3-NO_2-4-OH-acetophenone	4-OH-benz- †	$C_{15}H_{11}O_5N$	86	225	63.2	3.9	—	63.3	3.7	—	−0.37
2.		4-OMe-benz- †	$C_{16}H_{13}O_5N$	83	153	64.2	4.4	—	64.5	4.2	—	−0.27
3.		3-OMe-4-OH ‡	$C_{16}H_{13}O_6N$	81	224–225	—	—	4.4	—	—	4.1	−0.25
4.		4-Me-benz- §	$C_{16}H_{13}O_4N$	75	154–156	67.8	4.6	—	67.6	4.4	—	−0.17
5.		3,4-di-OMe-benz- ‡	$C_{17}H_{15}O_6N$	77	154–156	—	—	4.2	—	—	4.2	−0.15
6.		3,4-di-OEt-benz- ‡	$C_{19}H_{19}O_6N$	78	139–140	—	—	3.9	—	—	3.8	−0.15
7.		Benz- ‡	$C_{15}H_{11}O_4N$	70	167–169	66.9	4.1	5.2	66.7	4.2	5.3	0
8.		2,4-di-OMe-benz- §	$C_{17}H_{15}O_6N$	91	156–158 (110)	—	—	4.2	—	—	4.1	—
9.		2-OMe-benz- ‡	$C_{16}H_{13}O_5N$	82	167–170	64.2	4.4	4.7	64.3	4.2	4.5	—
10.		2,3-di-OMe-benz- §	$C_{17}H_{15}O_6N$	86	195–197	—	—	4.2	—	—	4.2	—
11.		2,5-di-OMe-benz- §	$C_{17}H_{15}O_6N$	86	171–173	—	—	4.2	—	—	4.1	—
12.		4-Cl-benz- ‖	$C_{15}H_{10}O_4NCl$	39	215–216	—	—	—	—	—	—	+0.23
13.		4-NO_2-benz- ¶	$C_{15}H_{10}O_6N_2$	19	228–230	57.3	3.2	—	58	3.2	—	+0.78
14.		2,4-di-NO_2-benz- §	$C_{15}H_9O_8N_3$	7.9	206–209	50.1	2.5	—	50.5	2.5	—	—
15.		9-anthr- §	$C_{23}H_{15}O_4N$	93	162–164	74.8	4.1	—	75.0	3.9	—	—
16.		Phenanthrene-9- §	$C_{23}H_{15}O_4N$	92	218–220	74.8	4.1	—	75.1	4.0	—	—
17.		Naphthalene-1- ‡	$C_{19}H_{13}O_4N$	92	216–218	71.5	4.1	—	71.8	4.2	—	—
18.	4-NO_2-2-OH-acetophenone	2-OEt-3-OMe §	$C_{18}H_{17}O_6N$	Uncertain	187–189	63.0	5.0	4.1	63.1	5.0	4.0	—
19.		9-anthr- §	$C_{23}H_{15}O_4N$ (red.)	71	200–202	74.8	4.1	—	74.7	4.0	—	—
20.		Phenanthrene-9- §	$C_{23}H_{15}O_4N$	78	234–236	74.8	4.1	—	75.0	3.9	—	—
21.		Naphthalene-1- ‡	$C_{19}H_{13}O_4N$	70.5	223–226	71.5	4.1	—	71.8	4.2	—	—
22.		Benz- ‡	$C_{15}H_{11}O_4N$	38	188–190	66.9	4.1	—	67.2	4.3	—	—
23.		2,4-diOMe-benz- §	$C_{17}H_{15}O_6N$	77	206–207 (140)	—	—	4.2	—	—	4.1	—
24.		2-OMe-benz- ‡	$C_{16}H_{13}O_5N$	75	171–172	—	—	4.7	—	—	4.6	—
25.		2,3-di-OMe-benz- §	$C_{17}H_{15}O_6N$	34	182–184	—	—	4.2	—	—	4.2	—
26.		2,5-di-OMe-benz- §	$C_{17}H_{15}O_6N$	38	193–195	—	—	4.2	—	—	4.1	—
27.		2-OEt-3-OMe §	$C_{18}H_{17}O_6N$	31	184–185	63.0	5.0	4.1	62.9	4.0	4.0	—

Can. J. Chem. Downloaded from www.nrcresearchpress.com by 210.87.254.42 on 09/05/12
For personal use only.

TABLE II*—(*Concluded*)

Ketone	Aldehyde	Chalcone	Yield (%)	Melting point (°C)	Analysis Calcd. C	Calcd. H	Calcd. N	Found C	Found H	Found N	Σσ of the substituents of the aldehyde portion
28. 5-NO_2-2-OH-acetophenone	9-anthr- §	$C_{23}H_{15}O_4N$	81.5	218–220	74.8	4.1	—	74.7	4.08	—	—
29.	Phenanthrene-9- §	$C_{23}H_{15}O_4N$	80.8	240–242	74.8	4.1	—	75.1	4.01	—	—
30.	Naphthalene-1- ‡	$C_{19}H_{13}O_4N$	62	255–257	71.5	4.1	—	71.7	4.1	—	—
31.	Benz- ‡	$C_{15}H_{11}O_4N$	36	178–179	—	—	5.2	—	—	5.3	—
32.	2,4-diOMe-benz- §	$C_{17}H_{15}O_6N$	65	186–188 (110)	—	—	4.2	—	—	4.3	—
33.	2-OMe-benz- **	$C_{16}H_{13}O_5N$	65	159–160 (140)	—	—	4.7	—	—	4.7	—
34.	2,3-di-OMe-benz- §	$C_{17}H_{15}O_6N$	23	160–162	—	—	4.2	—	—	4.4	—
35.	2,5-di-OMe-benz- §	$C_{17}H_{15}O_6N$	55	161–162 (180)	—	—	4.2	—	—	4.3	—
36.	4-Me-benz- §	$C_{16}H_{13}O_4N$	48	173–175	67.8	4.6	—	67.7	4.7	—	−0.17
37.	3,4-CH_2-benz- **	$C_{16}H_{11}O_6N$	35	201–202	—	—	4.5	—	—	4.7	—

*The acetophenone and aldehyde took part in the condensation in a 0.054 mole l^{-1} concentrated ethanolic solution. Yields are for washed crude products, corrected for the solubility of chalcones; melting points are for recrystallized (using EtOAc, EtOH, or AcOH) materials. The melting points of the crude products were generally 1–4° below those of the purified materials but in some cases the difference was higher and the crude melting point is given in parentheses. In the case of runs 1 and 2 the melting points given in the literature are 220 and 151°, somewhat different from those obtained in this work. In other cases the melting points were practically the same as those given in the literature.

†See ref. 7.
‡See ref. 4.
§New compounds.
‖See ref. 8.
¶See ref. 9.
**See ref. 6.

for a day, the product was precipitated by twofold dilution with water, filtered, and washed with 2 × 1.5 ml of ice-cold ethanol and 2 × 2 ml of water. In runs 8, 23, and 32 the crude products were strongly contaminated with high melting greenish materials and were not easy to purify. These by-products are obtainable alone from the mixture of aldehydes and ketones so that they are not self-condensation products.

Acknowledgments

The generous gift of a number of benzaldehydes from the National Research Council of Canada is gratefully acknowledged. Thanks are due to Mrs. K. Lakos-Láng and Mrs. G. Bartók-Bozóki (University of Szeged) for the microanalyses. The authors are indebted to the Hungarian Ministry of Education for the grant.

1. J. CLARK and D. D. PERRIN. Quart. Rev. **18**, 295 (1964).
2. K. YATES and R. STEWART. Can. J. Chem. **37**, 664 (1959); G. CULBERTSON and R. PETTIT. J. Am. Chem. Soc. **85**, 741 (1963).
3. J. F. MICQUEL. Bull. Soc. Chim. France, **61**, 1369 (1961).
4. (*a*) T. SZÉLL, A. M. EASTHAM, and GY. SIPOS. Can. J. Chem. **42**, 2417 (1964); (*b*) T. SZÉLL. Ber. **91**, 2609 (1958).
5. D. S. NOYCE and W. L. REED. J. Am. Chem. Soc. **80**, 5539 (1958).
6. G. S. CHHAYA, P. L. TRIVEDI, and G. V. JADHAV. J. Univ. Bombay, **26A**, 16 (1957).
7. GY. SIPOS. Thesis submitted for the degree: Candidate of Chemical Sciences. Szeged, Hungary. 1963.
8. GY. SIPOS, Á. FURKA, and T. SZÉLL. Monatsh. Chem. **91**, 643 (1960).
9. T. SZÉLL. Ber. **92**, 1672 (1959).
10. GY. SIPOS and T. SZÉLL. Acta Phys. Chem. Szeged. **11**, 43 (1965).

Reaction of dialkyl phosphorothioic acids with cyanogen bromide

ROBERT R. ENGEL

Department of Chemistry, Queens College of the City University of New York, Flushing, New York 11367

Received November 5, 1968

Dialkyl phosphorothioic acids (**1**) in benzene solution and in the presence of a tertiary amine react with cyanogen bromide to form the corresponding dialkyl phosphoroisothiocyanatidates (**2**). Under the reaction conditions these are partially decomposed to yield the alkylthiocyanates (**3**) and the alkylmetaphosphates (**4**).

Canadian Journal of Chemistry, **47**, 1258 (1969)

Several years ago Schrader obtained a German patent (1) for the preparation of thiophosphorylcarbimides by the action of cyanogen bromide on *O,O'*-dialkyl thionophosphoric acids. Although Schrader refers to the products as thiocarbimides and writes the structure as containing a P—N=C=S linkage, no evidence is presented which either supports the proposal, or excludes the presence of a P—S—C≡N type linkage. In the present work the reaction of cyanogen bromide with dialkyl phosphorothioic acids (**1**) has been studied under conditions similar to those used by Schrader with the resulting formation of the dialkyl phosphoroisothiocyanatidates (**2**).

$$(RO)_2\overset{\overset{O}{\|}}{P}\text{—SH} + CNBr \xrightarrow{Et_3N} (RO)_2\overset{\overset{O}{\|}}{P}\text{—NCS} + Et_3NHBr$$

(**1**) (**2**)

a, R = Et
b, R = Bu

When diethyl phosphorothioic acid (**1***a*) in benzene solution and in the presence of triethylamine is treated with cyanogen bromide, a violent reaction occurs attended by a series of color changes (yellow→green→red→brown) and the formation of a precipitate. Upon removal of the precipitate (triethylamine hydrobromide) and the solvent, ethylthiocyanate (**3***a*), a nondistillable viscous liquid, presumably ethylmetaphosphate (**4***a*), (soluble in benzene and carbon tetrachloride) and diethyl phosphoroisothiocyanatidate (**2***a*) are isolated. Considering the decomposition material isolated, the primary reaction of diethyl phosphorothioic acid with cyanogen bromide proceeded to the extent of at least 60%.

The formation of ethylthiocyanate was confirmed by comparison of infrared (i.r.) and nuclear magnetic resonance (n.m.r.) spectra with those of an authentic sample prepared by the action of potassium thiocyanate on ethyl iodide in acetone solution.

The structure of the viscous residue was deduced as ethylmetaphosphate (**4***a*) from its n.m.r. spectrum (symmetrical triplet at 1.42 δ,

Can. J. Chem. Downloaded from www.nrcresearchpress.com by 210.87.254.42 on 09/05/12
For personal use only.

for a day, the product was precipitated by twofold dilution with water, filtered, and washed with 2 × 1.5 ml of ice-cold ethanol and 2 × 2 ml of water. In runs 8, 23, and 32 the crude products were strongly contaminated with high melting greenish materials and were not easy to purify. These by-products are obtainable alone from the mixture of aldehydes and ketones so that they are not self-condensation products.

Acknowledgments

The generous gift of a number of benzaldehydes from the National Research Council of Canada is gratefully acknowledged. Thanks are due to Mrs. K. Lakos-Láng and Mrs. G. Bartók-Bozóki (University of Szeged) for the microanalyses. The authors are indebted to the Hungarian Ministry of Education for the grant.

1. J. CLARK and D. D. PERRIN. Quart. Rev. **18**, 295 (1964).
2. K. YATES and R. STEWART. Can. J. Chem. **37**, 664 (1959); G. CULBERTSON and R. PETTIT. J. Am. Chem. Soc. **85**, 741 (1963).
3. J. F. MICQUEL. Bull. Soc. Chim. France, **61**, 1369 (1961).
4. (*a*) T. SZÉLL, A. M. EASTHAM, and GY. SIPOS. Can. J. Chem. **42**, 2417 (1964); (*b*) T. SZÉLL. Ber. **91**, 2609 (1958).
5. D. S. NOYCE and W. L. REED. J. Am. Chem. Soc. **80**, 5539 (1958).
6. G. S. CHHAYA, P. L. TRIVEDI, and G. V. JADHAV. J. Univ. Bombay, **26A**, 16 (1957).
7. GY. SIPOS. Thesis submitted for the degree: Candidate of Chemical Sciences. Szeged, Hungary. 1963.
8. GY. SIPOS, Á. FURKA, and T. SZÉLL. Monatsh. Chem. **91**, 643 (1960).
9. T. SZÉLL. Ber. **92**, 1672 (1959).
10. GY. SIPOS and T. SZÉLL. Acta Phys. Chem. Szeged. **11**, 43 (1965).

Reaction of dialkyl phosphorothioic acids with cyanogen bromide

ROBERT R. ENGEL

Department of Chemistry, Queens College of the City University of New York, Flushing, New York 11367

Received November 5, 1968

Dialkyl phosphorothioic acids (**1**) in benzene solution and in the presence of a tertiary amine react with cyanogen bromide to form the corresponding dialkyl phosphoroisothiocyanatidates (**2**). Under the reaction conditions these are partially decomposed to yield the alkylthiocyanates (**3**) and the alkylmetaphosphates (**4**).

Canadian Journal of Chemistry, **47**, 1258 (1969)

Several years ago Schrader obtained a German patent (1) for the preparation of thiophosphorylcarbimides by the action of cyanogen bromide on *O,O'*-dialkyl thionophosphoric acids. Although Schrader refers to the products as thiocarbimides and writes the structure as containing a P—N=C=S linkage, no evidence is presented which either supports the proposal, or excludes the presence of a P—S—C≡N type linkage. In the present work the reaction of cyanogen bromide with dialkyl phosphorothioic acids (**1**) has been studied under conditions similar to those used by Schrader with the resulting formation of the dialkyl phosphoroisothiocyanatidates (**2**).

$$(RO)_2\overset{\overset{O}{\|}}{P}\text{—SH} + CNBr \xrightarrow{Et_3N} (RO)_2\overset{\overset{O}{\|}}{P}\text{—NCS} + Et_3NHBr$$

(**1**) (**2**)

a, R = Et
b, R = Bu

When diethyl phosphorothioic acid (**1***a*) in benzene solution and in the presence of triethylamine is treated with cyanogen bromide, a violent reaction occurs attended by a series of color changes (yellow→green→red→brown) and the formation of a precipitate. Upon removal of the precipitate (triethylamine hydrobromide) and the solvent, ethylthiocyanate (**3***a*), a nondistillable viscous liquid, presumably ethylmetaphosphate (**4***a*), (soluble in benzene and carbon tetrachloride) and diethyl phosphoroisothiocyanatidate (**2***a*) are isolated. Considering the decomposition material isolated, the primary reaction of diethyl phosphorothioic acid with cyanogen bromide proceeded to the extent of at least 60%.

The formation of ethylthiocyanate was confirmed by comparison of infrared (i.r.) and nuclear magnetic resonance (n.m.r.) spectra with those of an authentic sample prepared by the action of potassium thiocyanate on ethyl iodide in acetone solution.

The structure of the viscous residue was deduced as ethylmetaphosphate (**4***a*) from its n.m.r. spectrum (symmetrical triplet at 1.42 δ,

Can. J. Chem. Downloaded from www.nrcresearchpress.com by 210.87.254.6 on 09/05/12
For personal use only.

Can. J. Chem. Downloaded from www.nrcresearchpress.com by 210.87.254.6 on 09/05/12
For personal use only.

J = 7 c.p.s., area of 3 protons; quintet centered at 4.23 δ, J = 7 c.p.s., area of 2 protons)[1] and its i.r. spectrum which exhibited a phosphoryl band at 1297 cm^{-1} (calculated position: 1308 cm^{-1}) (2). The diethyl phosphoroisothiocyanatidate structure (**2***a*) was assigned to the remaining product after comparison of its spectral and chemical properties with those of an authentic sample prepared by a modification of the method of Kulka (3, 4) in which potassium thiocyanate in acetone solution was allowed to react with diethyl phosphorochloridate. Kulka (3) has shown the compound prepared under his experimental conditions to contain the P—N=C=S linkage by its formation of a thiourea in reaction with a secondary amine. Likewise, the material (**2***a*) reacted violently with secondary amines even at 0°.

The i.r. spectrum of the compound prepared by both routes were identical exhibiting a broad band at 2005 cm^{-1} with a strong shoulder at 2065 cm^{-1}. This type of absorption has been noted (5) for —N=C=S linkages as opposed to the sharp bands for —S—C≡N systems. Also, both exhibited a phosphoryl band at 1290 cm^{-1} and had identical n.m.r. spectra (symmetrical triplet at 1.42 δ, J = 7 c.p.s., area of 3 protons; multiplet centered at 4.20 δ, area of 2 protons).

The diethyl phosphoroisothiocyanatidate is presumably the primary reaction product which undergoes subsequent decomposition under the reaction conditions to yield ethylthiocyanate (**3***a*) and ethylmetaphosphate (**4***a*). This decomposition route has previously been observed for the compound (3). Indeed, further heating of the compound (**2***a*) isolated from the cyanogen bromide reaction yielded additional ethylthiocyanate and ethylmetaphosphate.

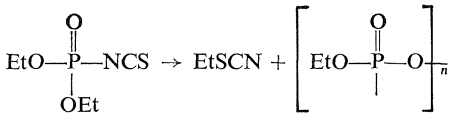

(**2***a*) (**3***a*) (**4***a*)

Similarly, upon treatment of dibutyl phosphorothioic acid (**1***b*) with triethylamine and cyanogen bromide, butylthiocyanate (**3***b*), butylmetaphosphate (**4***b*), and the dibutyl phosphoroisothiocyanatidate (**2***b*) were obtained.

Butylthiocyanate (**3***b*) was identified by comparison of i.r. and n.m.r. spectra with those of an authentic sample prepared as above in the ethyl case.

The butylmetaphosphate (**4***b*) was identified by its n.m.r. spectrum (triplet centered at 1.05 δ, J = 6 c.p.s., area of 3 protons; multiplet centered at 1.63 δ, area of 4 protons; multiplet centered at 4.13 δ, area of 2 protons) and the position of the phosphoryl band in its i.r. spectrum (1298 cm^{-1}).

As with the ethyl case, the dibutyl phosphoroisothiocyanatidate (**2***b*) structure was assigned on the basis of its spectral and chemical properties compared with those of an authentic sample prepared by a modification of the method of Kulka (3, 4). Both materials in the i.r. spectrum exhibited a phosphoryl band at 1285 cm^{-1} and a broad band at 2002 cm^{-1} with a strong shoulder at 2065 cm^{-1}. The n.m.r. spectrum showed a triplet centered at 1.05 δ, J = 6 c.p.s., area of 3 protons; a multiplet centered at 1.57 δ, area of 4 protons; and a multiplet centered at 4.04 δ, area of 2 protons.

A mechanism analogous to that proposed by Douglas and Burditt (6) for the reaction of cyanogen bromide with salts of aliphatic acids is presumed to be operating here as shown in the following reaction:

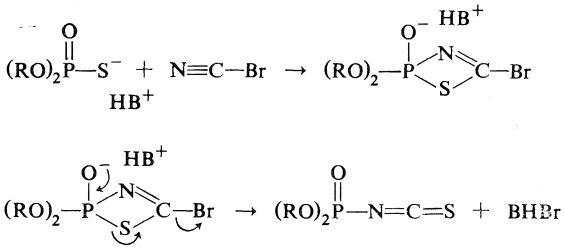

Experimental

Reagents

The dialkyl phosphorothioic acids used were prepared according to the method described by Hoffmann *et al.* (7, 8). The cyanogen bromide was commercial material (Aldrich) and was used without further purification. Benzene solvent was dried by storage over sodium metal.

The Reaction of Cyanogen Bromide with Diethyl Phosphorothioic Acid

To a stirred solution of 4.60 g (0.037 mole) of diethyl phosphorothioic acid and 3.71 g (0.037 mole) of triethylamine in 30 ml of benzene cooled in an ice bath, was added dropwise, over a period of 1 h, 3.93 g (0.037 mole)

[1]All positions given relative to tetramethylsilane observed on a Varian A-60A instrument purchased under NSF Grant GP6926.

of cyanogen bromide, dissolved in 30 ml of benzene. The reaction mixture was allowed to come to room temperature over a period of 1½ h, after completion of the addition of cyanogen bromide. After the precipitate of triethylamine hydrobromide had been removed by filtration, the solvent was removed using a rotary evaporator at room temperature and reduced pressure. Vacuum distillation of the liquid residue yielded 1.73 g (0.010 mole, 28%) of pure diethyl phosphoroisothiocyanatidate and 0.53 g (0.006 mole, 16%) of ethylthiocyanate. Also recovered was 1.22 g (0.011 mole, 31%) of ethylmetaphosphate.

The Reaction of Cyanogen Bromide with Dibutyl Phosphorothioic Acid

To a stirred solution of 10.0 g (0.042 mole) of dibutyl phosphorothioic acid and 4.3 g (0.042 mole) of triethylamine in 40 ml of benzene cooled in an ice bath, was added dropwise, over a period of 1 h, 4.5 g (0.042 mole) of cyanogen bromide, dissolved in 30 ml of benzene. The reaction mixture was allowed to come to room temperature over a period of 2 h, after completion of the addition of cyanogen bromide. After the removal of the triethylamine hydrobromide by filtration the solvent was removed using a rotary evaporator at room temperature and reduced pressure. Vacuum distillation of the residue yielded 2.13 g (0.0085 mole, 20%) of pure dibutyl phosphoroisothiocyanatidate and 0.63 g (0.0055 mole, 13%) of butylthiocyanate. Also recovered was 1.20 g (0.0088 mole, 21%) of butylmetaphosphate.

1. G. SCHRADER. German Patent No. 952,085. Nov. 8, 1956; Chem. Abstr. **51**, 12958*e* (1957).
2. L. C. THOMAS and R. A. CHITTENDEN. Spectrochim. Acta, **20**, 467 (1964).
3. M. KULKA. Can. J. Chem. **37**, 525 (1959).
4. Z. M. IVANOVA, E. A. STUKALO, and G. I. DERKACH. Zh. Obshch. Khim. **37**, 1144 (1967).
5. E. LIEBER, C. N. R. RAO, and J. RAMACHANDRAN. Spectrochim. Acta, **13**, 296 (1959).
6. D .E. DOUGLAS and A. M. BURDITT. Can. J. Chem. **36**, 1256 (1958).
7. F. W. HOFFMANN, D. H. WADSWORTH, and H. D. WEISS. J. Am. Chem. Soc. **80**, 3945 (1958).
8. F. W. HOFFMANN, B. KAGAN, and J. H. CANFIELD. J. Am. Chem. Soc. **81**, 148 (1959).

Hexahalocyclopentadienes. I. A reinvestigation of the reaction of hexachlorocyclopentadiene with fluoro- and chlorosulfonic acids

R. G. PEWS

Hydrocarbons and Monomers Research Laboratory, The Dow Chemical Company, Midland, Michigan 48640

Received August 26, 1968

The reaction of hexachlorocyclopentadiene with chlorosulfonic acid has been reinvestigated and the product found by spectral methods to be the chlorosulfate ester of undecachloropentacyclo[5.3.0.$0^{2,6}$.$0^{3,9}$-.$0^{4,8}$]decan-5-ol. With fluorosulfonic acid, the analogous fluorosulfate ester is formed and not octachloro-3*a*,4,7,7*a*-tetrahydro-4-7-methanoindene-1,8-dione as reported by McBee and Newcomer. A mechanism is proposed for the reaction.

Canadian Journal of Chemistry, 47, 1260 (1969)

McBee and Newcomer (1, 2) have reported that hexachlorocyclopentadiene (**1**) when allowed to react with chlorosulfonic acid yielded a compound (m.p. 146–147°) of molecular formula "$C_{10}H_2OSCl_{12}$" whereas fluorosulfonic acid under similar conditions gave octachloro-3*a*,4,7,-7*a*-tetrahydro-4,7-methanoindene-1,8-dione (**2**). The formation (3) of pentacyclo[5.3.0.$0^{2,6}$.$0^{3,9}$.-$0^{4,8}$] dodecan-5-one (**3**) on hydrolysis of "$C_{10}H_2O_3SCl_{12}$" suggests that the latter had the same pentacyclodecane carbon skeleton. In this note we report, firstly, spectral data which are in agreement[1] with the recently reported X-ray determination (7) of "$C_{10}H_2O_3SCl_{12}$" as the chlorosulfate ester of undecachloropentacyclo-[5.3.0.$0^{2,6}$.$0^{3,9}$.$0^{4,8}$] decan-5-ol (**4***a*), and secondly, results which show that **1** and fluorosulfonic acid yield **4***b* and not compound **2** as reported by McBee and Newcomer.

The mass spectrum of **4***a* showed a parent peak *m/e* 620 and the presence of twelve chlorine atoms. Other ion peaks which support structure **4***a* were found at *m/e* 251 ($C_5Cl_5O^+$) and *m/e* 451 ($C_{10}Cl_9O^+$). In further support of **4***a* no hydrogens were discernible in the nuclear magnetic resonance (n.m.r.) spectrum and the ultraviolet spectrum of the compound was transparent above 215 mμ. In the infrared, the symmetric and antisymmetric stretching vibrations of the sulfonyl group were found at 1431 and 1209 cm^{-1} respectively.

[1]X-Ray crystallographic studies are generally accepted as the ultimate in structural elucidations. The method, however, is not infallible. See for examples the work on triphenylene (4), β-selenium (5), and octaphenylcubane (6).

Can. J. Chem. Downloaded from www.nrcresearchpress.com by 210.87.254.6 on 09/05/12
For personal use only.

of cyanogen bromide, dissolved in 30 ml of benzene. The reaction mixture was allowed to come to room temperature over a period of 1½ h, after completion of the addition of cyanogen bromide. After the precipitate of triethylamine hydrobromide had been removed by filtration, the solvent was removed using a rotary evaporator at room temperature and reduced pressure. Vacuum distillation of the liquid residue yielded 1.73 g (0.010 mole, 28%) of pure diethyl phosphoroisothiocyanatidate and 0.53 g (0.006 mole, 16%) of ethylthiocyanate. Also recovered was 1.22 g (0.011 mole, 31%) of ethylmetaphosphate.

The Reaction of Cyanogen Bromide with Dibutyl Phosphorothioic Acid

To a stirred solution of 10.0 g (0.042 mole) of dibutyl phosphorothioic acid and 4.3 g (0.042 mole) of triethylamine in 40 ml of benzene cooled in an ice bath, was added dropwise, over a period of 1 h, 4.5 g (0.042 mole) of cyanogen bromide, dissolved in 30 ml of benzene. The reaction mixture was allowed to come to room temperature over a period of 2 h, after completion of the addition of cyanogen bromide. After the removal of the triethylamine hydrobromide by filtration the solvent was removed using a rotary evaporator at room temperature and reduced pressure. Vacuum distillation of the residue yielded 2.13 g (0.0085 mole, 20%) of pure dibutyl phosphoroisothiocyanatidate and 0.63 g (0.0055 mole, 13%) of butylthiocyanate. Also recovered was 1.20 g (0.0088 mole, 21%) of butylmetaphosphate.

1. G. SCHRADER. German Patent No. 952,085. Nov. 8, 1956; Chem. Abstr. **51**, 12958*e* (1957).
2. L. C. THOMAS and R. A. CHITTENDEN. Spectrochim. Acta, **20**, 467 (1964).
3. M. KULKA. Can. J. Chem. **37**, 525 (1959).
4. Z. M. IVANOVA, E. A. STUKALO, and G. I. DERKACH. Zh. Obshch. Khim. **37**, 1144 (1967).
5. E. LIEBER, C. N. R. RAO, and J. RAMACHANDRAN. Spectrochim. Acta, **13**, 296 (1959).
6. D .E. DOUGLAS and A. M. BURDITT. Can. J. Chem. **36**, 1256 (1958).
7. F. W. HOFFMANN, D. H. WADSWORTH, and H. D. WEISS. J. Am. Chem. Soc. **80**, 3945 (1958).
8. F. W. HOFFMANN, B. KAGAN, and J. H. CANFIELD. J. Am. Chem. Soc. **81**, 148 (1959).

Hexahalocyclopentadienes. I. A reinvestigation of the reaction of hexachlorocyclopentadiene with fluoro- and chlorosulfonic acids

R. G. PEWS

Hydrocarbons and Monomers Research Laboratory, The Dow Chemical Company, Midland, Michigan 48640

Received August 26, 1968

The reaction of hexachlorocyclopentadiene with chlorosulfonic acid has been reinvestigated and the product found by spectral methods to be the chlorosulfate ester of undecachloropentacyclo[5.3.0.$0^{2,6}$.$0^{3,9}$-.$0^{4,8}$]decan-5-ol. With fluorosulfonic acid, the analogous fluorosulfate ester is formed and not octachloro-3*a*,4,7,7*a*-tetrahydro-4-7-methanoindene-1,8-dione as reported by McBee and Newcomer. A mechanism is proposed for the reaction.

Canadian Journal of Chemistry, 47, 1260 (1969)

McBee and Newcomer (1, 2) have reported that hexachlorocyclopentadiene (**1**) when allowed to react with chlorosulfonic acid yielded a compound (m.p. 146–147°) of molecular formula "$C_{10}H_2OSCl_{12}$" whereas fluorosulfonic acid under similar conditions gave octachloro-3*a*,4,7,-7*a*-tetrahydro-4,7-methanoindene-1,8-dione (**2**). The formation (3) of pentacyclo[5.3.0.$0^{2,6}$.$0^{3,9}$.-$0^{4,8}$] dodecan-5-one (**3**) on hydrolysis of "$C_{10}H_2O_3SCl_{12}$" suggests that the latter had the same pentacyclodecane carbon skeleton. In this note we report, firstly, spectral data which are in agreement[1] with the recently reported X-ray determination (7) of "$C_{10}H_2O_3SCl_{12}$" as the chlorosulfate ester of undecachloropentacyclo-[5.3.0.$0^{2,6}$.$0^{3,9}$.$0^{4,8}$] decan-5-ol (**4***a*), and secondly, results which show that **1** and fluorosulfonic acid yield **4***b* and not compound **2** as reported by McBee and Newcomer.

The mass spectrum of **4***a* showed a parent peak *m/e* 620 and the presence of twelve chlorine atoms. Other ion peaks which support structure **4***a* were found at *m/e* 251 ($C_5Cl_5O^+$) and *m/e* 451 ($C_{10}Cl_9O^+$). In further support of **4***a* no hydrogens were discernible in the nuclear magnetic resonance (n.m.r.) spectrum and the ultraviolet spectrum of the compound was transparent above 215 mμ. In the infrared, the symmetric and antisymmetric stretching vibrations of the sulfonyl group were found at 1431 and 1209 cm^{-1} respectively.

[1]X-Ray crystallographic studies are generally accepted as the ultimate in structural elucidations. The method, however, is not infallible. See for examples the work on triphenylene (4), β-selenium (5), and octaphenylcubane (6).

Can. J. Chem. Downloaded from www.nrcresearchpress.com by 210.87.254.42 on 09/05/12
For personal use only.

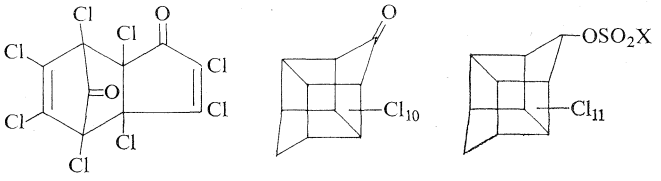

2 **3** **4***a*, X = Cl
4*b*, X = F

In order to clarify the products of the reaction of **1** with halosulfonic acids, fluorosulfonic acid and **1** were allowed to react under conditions identical with those for the preparation of **4***a* from **1** and chlorosulfonic acid. The product, a white crystalline solid, m.p. 222–224°, was characterized by the spectral methods (see Experimental) described for **4***a* and found to be the expected fluorosulfate ester **4***b*. In our laboratory, the reaction of **1** with fluorosulfonic acid, under identical conditions as described by McBee and Newcomer (2) for the synthesis of **2** gave only **4***b* and some unreacted **1**. With a molar excess of fluorosulfonic acid, the yield of **4***b* was 72% with no apparent formation of **2**. The results of the present study suggest that the results of McBee and Newcomer on the reaction of **1** with fluorosulfonic acid may have been due to impurities in the starting materials.

Mechanistically, the formation of **4** can be envisioned as proceeding by the abstraction of a chlorine by the halosulfonium ion to give the pentachlorocyclopentadienyl cation[2] (**5**). Electrophilic addition of the latter to another molecule of **1** would give a new cation **6** which could then undergo cage formation through cationic intermediates **7**–**9** which eventually react with solvent anion to give product (see Scheme 1). Such a mechanism could also apply to the dimerization of **1** to dodecachloropentacyclo[5.3.0.$0^{2,6}$.$0^{3,9}$.$0^{4,8}$] decane (Prins dimer).

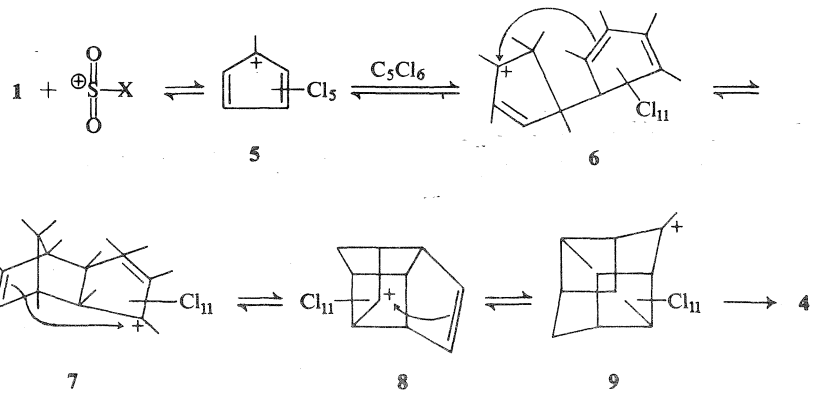

SCHEME 1

Experimental

Ultraviolet spectra were determined with a Cary recording spectrophotometer, model 15, and are reported in millimicrons. Infrared spectra were obtained with a Beckmann IR-9 spectrometer. The mass spectra were obtained on a CEC 21-110B (direct probe) instrument. The isotope peaks observed match the relative abundances calculated for the naturally occurring isotopes. The melting points were taken on a Thomas–Hoover melting point apparatus and are uncorrected.

Material

Hexachlorocyclopentadiene was redistilled *in vacuo* and a middle fraction was collected b.p. 92° (5 mm), n_D^{25} 1.5623 [lit. (9) b.p. 92° (5 mm), n_D^{25} 1.5626].

Chlorosulfonic Acid: *Undecachloropentacyclo-*[5·3·0·$0^{2,6}$·$0^{3,9}$·$0^{4,8}$]*decan-5-yl ester (4a)*.

This compound was prepared as described by McBee and Newcomer (1).

[2]Breslow, Hill, and Wasserman (8) have concluded that the ground state of the pentachlorocyclopentadienyl cation is either a triplet or at most 6–8 cal/mole from the singlet ground state in SbF_5 solution. The triplet was not detected with **1** and other Lewis acids in SO_2 solution. For simplicity of discussion, **5** is represented as a classical species.

Can. J. Chem. Downloaded from www.nrcresearchpress.com by 210.87.254.42 on 09/05/12
For personal use only.

*Reaction of **1** with Fluorosulfonic Acid*

The procedure was identical to that described by McBee and Newcomer (2), except that the temperature was controlled at 90° after the addition of the fluorosulfonic acid to **1** at 120°. The white solid obtained after purification had m.p. 222–224°.

Anal. Calcd. for $C_{10}Cl_{11}SO_3F$: C, 19.72; H, 0.00; Cl, 64.02; S, 5.26; O, 7.88; F, 3.12. Found: C, 19.90; H, 0.18; Cl, 64.15; S, 5.02; O, 8.50; F, 3.22.

The mass spectrum gave a molecular ion *m/e* 604, as well as the following: *m/e* 251 ($C_5Cl_5O^+$) and *m/e* 451 ($C_{10}Cl_9O^+$). The compound was transparent in the ultraviolet about 215 mμ and failed to show any absorption in the proton magnetic resonance experiment. The fluorine resonance in CH_2Cl_2 showed a singlet at −51.5 p.p.m. from $CFCl_3$ which is consistent with the proposed —OSO_2F group. The antisymmetric and symmetric sulfonyl stretching vibrations were observed at 1466 cm^{-1} and 1235 cm^{-1} respectively.

Acknowledgments

The author is grateful to Dr. J. Heeschen, Mr. R. Nyquist, and Dr. L. Shadoff for determining the nuclear magnetic resonance, infrared, and mass spectral data respectively. I am also indebted to Mr. J. Simek for the ultraviolet spectra and to Mr. L. Swim and his associates for the elemental analyses reported herein.

1. E. T. McBee and J. S. Newcomer. U. S. Patent 2,516,404; Chem. Abstr. **45**, 647 (1951).
2. J. S. Newcomer and E. T. McBee. J. Am. Chem. Soc. **71**, 946 (1949).
3. K. V. Scherer, Jr., G. A. Ungefug, and R. S. Lunt, III. J. Am. Chem. Soc. **88**, 2860 (1966).
4. V. Vand and R. Pepinsky. Acta Cryst. **7**, 595 (1954).
5. R. E. Marsh and L. Pauling. Acta Cryst. **6**, 71 (1953).
6. G. S. Pawley, W. N. Lipscomb, and H. H. Freedman. J. Am. Chem. Soc. **86**, 4725 (1964).
7. Y. Okaya and A. Bednowitz. Acta Cryst. **22**, 111 (1967).
8. R. Breslow, R. Hill, and E. Wasserman. J. Am. Chem. Soc. **86**, 5349 (1964).
9. H. E. Ungnade and E. T. McBee. Chem. Rev. **58**, 249 (1958).

Can. J. Chem. Downloaded from www.nrcresearchpress.com by 210.87.254.42 on 09/05/12
For personal use only.

Can. J. Chem. Downloaded from www.nrcresearchpress.com by 210.87.254.5 on 09/05/12
For personal use only.

Canadian Journal of Chemistry

Published by THE NATIONAL RESEARCH COUNCIL OF CANADA

VOLUME 47 APRIL 15, 1969 NUMBER 8

Nucleophilic substitution at silicon: the reaction of triphenylsilyl chloride with 2-propanol in CCl_4

A. D. ALLEN AND S. J. LAVERY

Lash Miller Chemical Laboratories, University of Toronto, Toronto, Ontario

Received August 29, 1968

The reaction of triphenylsilyl chloride with 2-propanol in CCl_4 has been reinvestigated and a mechanism proposed. The HCl produced in the reaction is catalytic. The rate of the uncatalyzed reaction, as determined by extrapolations to zero time, increases more rapidly with 2-propanol concentration than would be required for an order of one in the alcohol. The rate of the HCl-catalyzed path is independent of the 2-propanol concentration in the range studied (5 to 15 volume %) but first order in the HCl concentration, suggesting that the reactive alcohol species in this case is of the form ROH...ClH.

Canadian Journal of Chemistry, 47, 1263 (1969)

The reactions of triphenylsilyl chloride with H_2O in dioxan (1) and with 2-propanol in CCl_4 (2) are autocatalytic. The reactions may be represented generally by

$$(C_5H_6)_3SiCl + ROH \rightarrow (C_5H_6)_3SiOR + HCl$$

The HCl and chloride ions have been shown to be catalytic species (1, 2).

Petersen and Ross (2) concluded that there was little or no reaction of triphenylsilyl chloride and 2-propanol in the absence of HCl and that the order in the alcohol was one. They interpreted their results as support for a mechanism involving formation of a pentacovalent silicon intermediate followed by HCl-catalyzed decomposition to products.

Allen and Modena (1) assumed that no HCl was present initially in their reaction mixtures and obtained pseudo first-order rate constants for the uncatalyzed reaction of triphenylsilyl chloride and water in dioxan by extrapolation to zero time of plots of log $[R_3SiCl]$ against time. The initial slopes of these plots were constant at any one water concentration. The order in water was greater than one. Multiple orders in alcohol or water have been noted in a number of other systems (3–6) involving substitution at silicon in non-hydroxylic solvents. Allen and Modena proposed that in alcoholysis and hydrolysis, the reactive nucleophilic species is of the form ROH . . . B, where B is any entity that can act as a base and assist proton removal from the OH group.

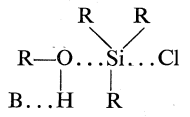

Transition state

This type of mechanism has been used to explain the action of certain catalysts, the high order in the nucleophile, and temperature effects in a number of systems (1, 3–7).

Analyses of samples of triphenylsilyl chloride, combined with the observation that CCl_4 solutions of the silicon halide failed to show any detectable acid, led us to conclude that the samples used in this work did not contain HCl impurity. This suggested that, contrary to the arguments of Petersen and Ross, it should be possible to determine rate constants for the uncatalyzed reaction of triphenylsilyl chloride and 2-propanol in CCl_4 by extrapolations to zero time, and to determine the order in 2-propanol from the rate constants obtained. We have reinvestigated this reaction using a direct titrimetric method to determine the HCl produced in the reaction.

Can. J. Chem. Downloaded from www.nrcresearchpress.com by 210.87.254.5 on 09/05/12
For personal use only.

Results and Discussion

The reaction of 2-propanol and triphenylsilyl chloride in CCl_4 solvent is catalyzed by the HCl produced in the reaction, but HCl need not be present to initiate the reaction. The first-order plot shown in Fig. 1 is typical. Extrapolations to zero time on such plots for runs to which no HCl has been added give pseudo first-order rate constants, k_u, applicable to the uncatalyzed reaction. The results are summarized in Table I. All data were obtained at 25.2°.

From the data in Table I it can be seen that at any one alcohol concentration, k_u is reasonably constant. The rate increases with 2-propanol concentration more rapidly than would be required for an order of one in the alcohol. A plot of log k_u against log (volume % of ROH) is linear with slope equal to 2.4 in the range studied. The multiple order in 2-propanol is consistent with the mechanism proposed by Allen and Modena (1); B is another alcohol molecule. It is known that 2-propanol exists to a large extent as a polymer in CCl_4 (8, 9), and that the pseudo first-order rate constants for the 2-propanolysis of acetyl chloride in CCl_4 are proportional to the concentration of associated alcohol (9).

When HCl is added to the reaction mixtures, the pseudo first-order rate constants obtained by extrapolation, k_1, are higher than the k_u value at the same alcohol concentration. The increments, $k_1 - k_u$, are linear in HCl concentration, but appear to be independent of the alcohol concentration in the range studied (5 to 15 volume % 2-propanol), as can be seen from the k_c entries in column 6 of Table II. Catalysis by HCl is explained in terms of the increased basicity towards silicon of the oxygen of an alcohol molecule hydrogen-bonded through its proton to the chloride of the HCl. If this association of alcohol and HCl is virtually complete, so that the concentration of the reactive alcohol species is equal to the analytical concentration of HCl, then the independence of alcohol concentration shown by k_c is explained.

TABLE I

Pseudo first-order rate constants for the uncatalyzed reaction of $(C_6H_5)_3SiCl$ and 2-propanol at 25.2°

$[R_3SiCl]_0 \times 10^3$ (M)	$[ROH]_0$ (volume %)	$k_u \times 10^5$ (s^{-1})
4.31	5.0	0.64
8.59	5.0	0.74
11.48	5.0	0.77
12.17	5.0	0.67
13.88	5.0	0.69
17.84	5.0	0.65
	Mean:	0.69
7.69	10.0	2.6
9.55	10.0	2.8
11.33	10.0	2.6
13.74	10.0	2.3
33.07	10.0	2.6
	Mean:	2.6
6.03	12.0	5.9
8.17	12.0	5.5
15.26	12.0	6.2
	Mean:	5.9
5.94	15.0	10.2
8.82	15.0	9.6
14.79	15.0	9.3
	Mean:	9.7

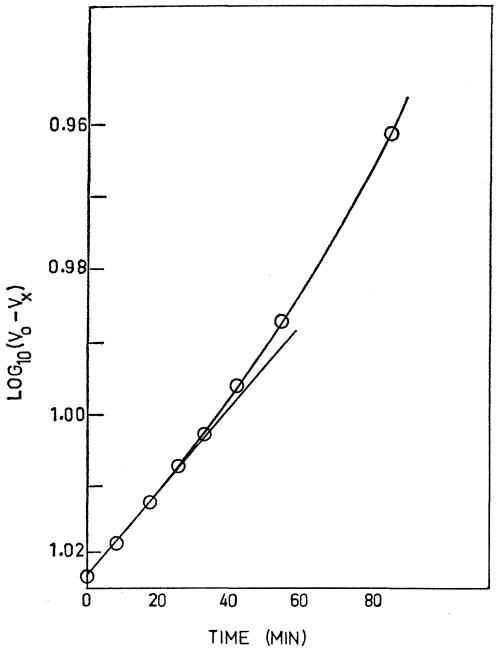

FIG. 1. First-order plot for 2-propanolysis $(C_6H_5)_3SiCl$ in CCl_4 at 25.2°; $[R_3SiCl]_0 = 1.374 \times 10^{-2}$ M, $[ROH]_0 = 10$ volume %, V_0 = volume of Et_3N solution corresponding to the initial silyl chloride concentration, V_x = volume of Et_3N solution corresponding to the HCl produced in the reaction.

The rate equation appears to have the form

$$dx/dt = k_u[R_3SiCl] + k_c[HCl]\,[R_3SiCl]$$
$$= k_u(a_0 - x) + k_c(p_0 + x)\,(a_0 - x)$$

where k_u varies with alcohol concentration but k_c does not. The first term refers to the uncatalyzed path, the second to the HCl-catalyzed path. For runs to which no HCl is added initially, p_0 equals zero. The integrated form of this rate law is

TABLE II

Rate constants for the HCl-catalyzed reaction of $(C_6H_5)_3SiCl$ and 2-propanol at 25.2°

$[R_3SiCl]_0 \times 10^3$ (M)	$[ROH]_0$ (volume %)	$[HCl]_0 \times 10^3$ (M)	$k_1 \times 10^5$ (s^{-1})	$(k_1 - k_u) \times 10^5$ (s^{-1})	$\frac{(k_1 - k_u) \times 10^5}{[HCl]_0 \times 10^3} = k_c \times 10^2$ ($M^{-1}\ s^{-1}$)
11.50	5.0	0.742	1.65	0.96	1.3
10.19	5.0	0.742	1.62	0.93	1.3
16.87	5.0	1.29	2.25	1.56	1.2
10.83	5.0	3.31	5.07	4.38	1.3
16.73	5.0	5.02	6.30	5.61	1.1
10.72	5.0	5.33	6.84	6.15	1.2
10.04	10.0	3.21	6.6	4.0	1.3
18.14	10.0	3.63	8.3	5.7	1.6
8.13	10.0	3.89	7.2	4.6	1.2
10.30	10.0	4.23	7.3	4.7	1.1
10.43	10.0	6.33	11.7	9.1	1.4
10.58	12.0	1.60	7.7	1.8	1.1
17.35	12.0	2.19	9.7	3.8	1.7
9.37	12.0	5.78	12.4	6.5	1.1
8.29	15.0	2.68	14.6	4.9	1.8
11.89	15.0	7.20	22.1	12.4	1.7
16.74	15.0	11.80	29.6	19.9	1.7

$$\log_e\left[\frac{1-M}{1+M}\right] = (k_c a_0 + k_c p_0 + k_u)t + \log_e\left[\frac{1-B}{1+B}\right]$$

where

$$M = \frac{k_c a_0 - k_c p_0 - k_u - 2k_c x}{k_c a_0 + k_c p_0 + k_u}$$

and

$$B = \frac{k_c a_0 - k_c p_0 - k_u}{k_c a_0 + k_c p_0 + k_u}$$

If values for k_u and k_c are assumed, values of $\log_e [(1 - M)/(1 + M)]$ can be plotted against time for any run. Then the linearity of the plot can be checked and the slope of the least squares straight line through the points compared with the theoretical slope $(k_c a_0 + k_c p_0 + k_u)$. This was done for a wide range of k_c values at each of several k_u values for each run. In general, for each value of k_u there exists a value of k_c at which the theoretical and least squares slopes are essentially equal, and the deviation of points from the least squares straight line is very small. Other values of k_c with this k_u result in much greater deviations. However, for any one run several sets of k_u and k_c with different k_u values meet the requirements given above equally well. Despite this complication, the following points are evident (*a*) for k_u values within ±10% of the values obtained by extrapolation, the best k_c values are close to those calculated from the extrapolation data, (*b*) sets of k_u and k_c values for runs with and without added HCl at the same alcohol concentration show best agreement in the neighborhood of the values obtained by extrapolation, (*c*) the k_c values at any one alcohol concentration are reasonably constant, and (*d*) the k_c values appear to be independent of the alcohol concentration.

Data at various percentages of reaction are, therefore, consistent with the rate law deduced from extrapolations to zero time. Typical results are shown in Table III and a typical plot of $\log_e [(1 - M)/(1 + M)]$ is shown in Fig. 2.

When tetraethylammonium chloride is added to the reaction mixtures, the pseudo first-order rate constants obtained by extrapolation, k_1, are higher than those for the uncatalyzed reaction. The increments to the rate constant appear to be linear in salt concentration, as evidenced by the values of k_s at any one alcohol concentration in column 5 of Table IV. As in all other cases, runs containing Et_4NCl eventually showed autocatalysis by the HCl produced in the reaction.

Pseudo first-order rate constants obtained by extrapolation for runs with both HCl and Et_4NCl added show that the effect of one catalyst is not diminished in the presence of the other. This observation does not agree with the rate law for the

Can. J. Chem. Downloaded from www.nrcresearchpress.com by 210.87.254.5 on 09/05/12
For personal use only.

TABLE III

k_u (s^{-1})	k_c ($M^{-1}\,s^{-1}$)	Required slope (s^{-1})	Slope of least squares line (s^{-1})	$\log_e \frac{1-B}{1+B}$	Intercept of least squares line	% reaction followed
0.64×10^{-5}	0.82×10^{-2}	4.17×10^{-4}	4.16×10^{-4}	−1.71	−1.68	24
0.65×10^{-5}	0.90×10^{-2}	1.67×10^{-4}	1.67×10^{-4}	−3.21	−3.18	6.5
0.77×10^{-5}	1.18×10^{-2}	1.72×10^{-4}	1.72×10^{-4}	−3.06	−3.06	13
0.69×10^{-5}	1.38×10^{-2}	1.76×10^{-4}	1.76×10^{-4}	−2.23	−2.21	20
0.69×10^{-5}	1.18×10^{-2}	1.74×10^{-4}	1.74×10^{-4}	−1.03	−1.01	45
0.69×10^{-5}	0.93×10^{-2}	2.09×10^{-4}	2.08×10^{-4}	−1.07	−1.06	26
2.44×10^{-5}	1.03×10^{-2}	1.41×10^{-4}	1.41×10^{-4}	−1.57	−1.57	17
2.60×10^{-5}	0.83×10^{-2}	2.99×10^{-4}	2.99×10^{-4}	−2.35	−2.35	13
2.60×10^{-5}	1.27×10^{-2}	2.11×10^{-4}	2.11×10^{-4}	−0.495	−0.498	37
2.60×10^{-5}	1.24×10^{-2}	2.97×10^{-4}	2.97×10^{-4}	−1.15	−1.12	47
2.60×10^{-5}	1.42×10^{-2}	2.14×10^{-4}	2.14×10^{-4}	−0.689	−0.693	35
2.60×10^{-5}	1.40×10^{-2}	1.95×10^{-4}	1.95×10^{-4}	−0.346	−0.360	31
6.20×10^{-5}	1.18×10^{-2}	2.43×10^{-4}	2.43×10^{-4}	−1.07	−1.08	24
6.02×10^{-5}	1.51×10^{-2}	1.84×10^{-4}	1.84×10^{-4}	−0.717	−0.720	13
5.90×10^{-5}	1.30×10^{-2}	2.56×10^{-4}	2.56×10^{-4}	+0.096	+0.089	39
5.90×10^{-5}	1.36×10^{-2}	3.25×10^{-4}	3.24×10^{-4}	−0.978	−0.945	36
5.90×10^{-5}	1.38×10^{-2}	2.27×10^{-4}	2.27×10^{-4}	−0.589	−0.593	32
10.2×10^{-5}	1.38×10^{-2}	1.84×10^{-4}	1.84×10^{-4}	−0.216	−0.209	50
9.6×10^{-5}	1.17×10^{-2}	1.99×10^{-4}	1.99×10^{-4}	−0.072	−0.073	44
9.7×10^{-5}	1.32×10^{-2}	2.42×10^{-4}	2.42×10^{-4}	+0.191	+0.197	49
9.7×10^{-5}	1.29×10^{-2}	4.66×10^{-4}	4.66×10^{-4}	+0.143	+0.167	34
9.7×10^{-5}	1.29×10^{-2}	3.44×10^{-4}	3.44×10^{-4}	+0.212	+0.230	44

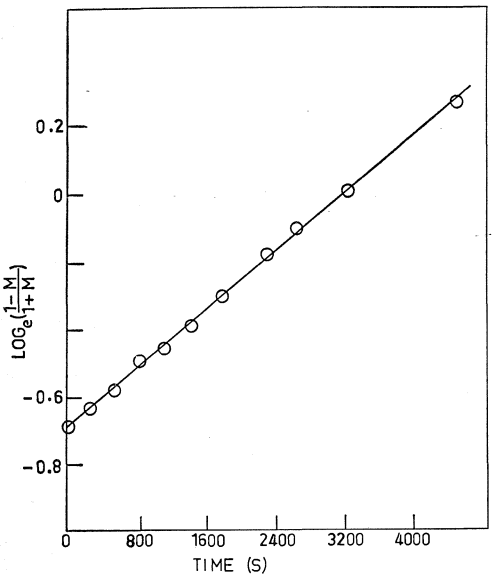

FIG. 2. Plot of $\log_e [(1 - M)/(1 + M)]$ against time with least squares line shown; $[R_3SiCl]_0 = 1.040 \times 10^{-2}\ M = a_0$, $[ROH]_0 = 10$ volume %, $[HCl]_0 = 3.21 \times 10^{-3}\ M = p_0$.

salt-catalyzed reaction proposed by Petersen and Ross (2). The results for samples containing both catalysts are shown in Table V.

Since $k_s > k_c$, Et_4NCl is more effective as a catalyst than HCl. It seems reasonable to conclude that the Cl in both catalysts acts by association with the proton of the alcohol OH group. Such association is known to occur between quaternary ammonium halides and alcohols in CCl_4 (10). The HCl may not be appreciably dissociated (2), while the tetraethylammonium chloride may be present as ion pairs (11).

It is impossible to tell from our kinetic data whether the reaction of the silyl chloride and ROH . . . B proceeds by an S_N2 mechanism or by formation of a pentacovalent silicon intermediate. We favor the former after considering collectively the information dealing with substitution of chloride at silicon by more basic groups as presented in refs. 1, 3, 7, 12–14.

Experimental Details

A. Solvents

Carbon Tetrachloride. Reagent grade CCl_4 was used without further purification or drying. Numerous blanks containing only triphenylsilyl chloride and CCl_4 were run, and in all cases no more than 1% reaction occurred over a 24 h period; there was no detectable acidity produced in the length of time for which normal kinetic runs were followed.

2-Propanol. Molecular sieves were used for drying. The water content was reduced to 0.008% or less (Karl Fisher titration) in 3 to 4 days.

Dioxan. Reagent grade dioxan was refluxed with sodium until formation of resin ceased and the sodium remained shiny. It was then distilled.

Can. J. Chem. Downloaded from www.nrcresearchpress.com by 210.87.254.5 on 09/05/12
For personal use only.

TABLE IV

Rate constants for the Et_4NCl-catalyzed reaction of $(C_6H_5)_3SiCl$ with 2-propanol at 25.2°

$[R_3SiCl]_0 \times 10^3$ (M)	$[ROH]_0$ (volume %)	[Salt] $\times 10^4$ (M)	$k_1 \times 10^5$ (s^{-1})	$\frac{(k_1 - k_u) \times 10^5}{[\text{Salt}] \times 10^4} = k_s \times 10$ ($M^{-1}\ s^{-1}$)
11.74	5.0	0.422	2.69	4.7
12.51	10.0	0.712	5.4	3.9
12.37	10.0	0.929	6.6	4.3
10.07	10.0	1.85	9.1	3.5
8.02	10.0	4.04	16.6	3.5
11.97	15.0	1.04	13.7	3.8
9.19	15.0	3.87	22.1	3.2
12.56	15.0	5.44	25.0	2.8

TABLE V

Rate constants for the Et_4NCl-catalyzed reaction of $(C_6H_5)_3SiCl$ with 2-propanol as determined from runs containing added HCl

$[R_3SiCl]_0 \times 10^3$ [M]	$[ROH]_0$ (volume %)	$[HCl]_0 \times 10^3$ (M)	[Salt] $\times 10^4$ (M)	$k_1 \times 10^5$ (s^{-1})	$\frac{(k_1 - k_u - k_c p_0) \times 10^5}{[\text{Salt}] \times 10^4} = k_s \times 10$ ($M^{-1}\ s^{-1}$)
8.82	10.0	2.08	1.77	12.6	4.1
10.76	12.0	1.64	3.03	14.4	3.2
8.32	15.0	0.684	2.06	20.2	4.7

Benzene. Reagent grade benzene was dried by distillation from sodium.

Diethyl Ether. Anhydrous diethyl ether was distilled from sodium or used as obtained from Mallinckrodt (A.R., A.C.S., 0.01% H_2O).

B. Preparation of Triphenylsilyl Chloride

$(C_6H_5)_3SiCl$ was prepared by chlorination of $(C_6H_5)_3SiH$ in CCl_4.

The reaction vessel was immersed in an ice-water bath. The CCl_4, Cl_2, and dissolved HCl were pumped off following completion of the reaction. The crude product was recrystallized from benzene and petroleum ether and then distilled at reduced pressure (boiling point 147 °C at 0.01 mm Hg).

Anal. Calcd. for $(C_6H_5)_3SiCl$: C, 73.33; H, 5.12; Cl, 12.03. Found: C, 73.41; H, 5.21; Cl, 11.92.

C. Procedure Followed in Kinetic Runs

Separate solutions of $(C_6H_5)_3SiCl$ and 2-propanol in CCl_4 were made up quantitatively at 25.2° and then mixed. Aliquots were removed from the reaction mixture at intervals, quenched in dry benzene or ether, and titrated immediately for HCl with a dioxan solution of Et_3N. Neutral red dissolved in 2-propanol was used as the indicator. Total acid values were obtained by titration of an aliquot run into 95% ethanol; production of HCl was complete and rapid in the ethanol.

Solutions of HCl in CCl_4 were prepared with HCl which had been passed through a H_2SO_4 drying train.

Tetraethylammonium chloride was dried over P_2O_5 under vacuum at the temperature of boiling methanol for several hours.

1. A. D. Allen and G. Modena. J. Chem. Soc. 3671 (1957).
2. R. C. Petersen and S. D. Ross. J. Am. Chem. Soc. **85**, 3164 (1963).
3. A. D. Allen, J. C. Charlton, C. Eaborn, and G. Modena. J. Chem. Soc. 3668 (1957).
4. G. Modena and P. Todesco. Boll. Sci. Fac. Chim. Ind. Bologna, **18**, 109 (1960).
5. G. Schott, H. Kelling, and R. Schild. Chem. Ber. **99**, 291 (1966).
6. R. H. Prince and R. E. Timms. Inorg. Chim. Acta, **1**, 133 (1967).
7. J. R. Chipperfield and R. H. Prince. J. Chem. Soc. 3567 (1963).
8. E. G. Hoffmann. Z. Physik. Chem. Leipzig, B, **53**, 211 (1942–1943).
9. R. F. Hudson and I. Stelzer. Trans. Faraday Soc. **54**, 213 (1958).
10. A. Allerhand and P. von R. Schleyer. J. Am. Chem. Soc. **85**, 1233 (1963).
11. H. S. Harned and B. B. Owen. The physical chemistry of electrolytic solutions. Reinhold Publishing Corp., New York. 1963.
12. L. H. Sommer. Stereochemistry, mechanism and silicon. McGraw-Hill Book Co., Inc., New York. 1965.
13. C. G. Swain, R. M. Esteve, Jr., and R. H. Jones. J. Am. Chem. Soc. **71**, 965 (1949).
14. C. A. Burkhard, E. G. Rochow, H. S. Booth, and J. Hartt. Chem. Rev. **41**, 120 (1947).

Can. J. Chem. Downloaded from www.nrcresearchpress.com by 210.87.254.5 on 09/05/12
For personal use only.

Can. J. Chem. Downloaded from www.nrcresearchpress.com by 210.87.254.6 on 09/05/12
For personal use only.

Reaction of metallic nitrilotriacetates with histamine

A. L. BEAUCHAMP, J. ISRAELI, AND H. SAULNIER
Département de Chimie, Université de Montréal, Montréal, Québec

Received August 15, 1968

Cu(II), Ni(II), Co(II), and Zn(II) nitrilotriacetates (MeX^-) react with histamine nitrate (LH^+) to form a protonated mixed complex MeXLH where the metal appears to be bound only to the tertiary imidazolic nitrogen of histaminium ion. At higher pH values the proton dissociates to yield a mixed complex ion $MeXL^-$ in which both the imidazolic nitrogen and the terminal amino group are coordinated. The formation constants of these species were calculated from the potentiometric titration curves.

Canadian Journal of Chemistry, 47, 1269 (1969)

Introduction

The reaction of nitrilotriacetate complexes with bidentate ligands was studied previously in this laboratory (1). Mixed complexes of metallic nitrilotriacetates with various mono- and bidentate ligands were also investigated by Mergerum (2) and Angelici (3).

Perrin (4) recently reported on mixed complexes containing histamine. Although this molecule is believed to act in most cases as a bidentate ligand by coordination of both the tertiary imidazolic nitrogen and the terminal amino group (5), coordination through a single nitrogen atom cannot be a priori ruled out. In fact, the present work shows that metallic nitrilotriacetates (MeX^-) of copper(II), nickel(II), cobalt(II), and zinc(II), react with histamine nitrate (LH^+) to form a protonated mixed complex MeXLH in which the metallic nitrilotriacetate is likely to be bound only to the tertiary imidazolic nitrogen atom. At higher pH values, the proton is liberated to yield a mixed complex anion $MeXL^-$ in which coordination of both nitrogen atoms is very probably involved.

Experimental

The metal ions were introduced in solution as perchlorates and standardized by complexometric methods (6, 7). Potentiometric titrations were made with a Radiometer 26 pH meter, with the calomel electrode connected to the solution to be titrated by means of a Fisher bridge 13–639–55 filled with 0.5 *M* $NaNO_3$. Calibration was made to give directly $-\log (H^+)$ (8). All experiments were performed at ionic strength 0.10 ($NaClO_4$) and 25.0 ± 0.1 °C.

Results

Aqueous solutions containing equimolecular amounts of $Me(ClO_4)_2$, Na_2HX, and $LHNO_3$ (where Me = Zn, Cu, Ni, Co) were titrated potentiometrically with sodium hydroxide. Experiments were carried out at three concentration levels (5×10^{-3}, 1×10^{-2}, and 2×10^{-2} *M*) for each metal ion and the results obtained at 2.0×10^{-2} *M* are given in Fig. 1. All curves show two inflection points at $a = 1$ and $a = 2$, respectively, where a is the number of moles of base added per mole of metal ion. The following reaction pathway turned out to explain satisfactorily the essential features of these results.

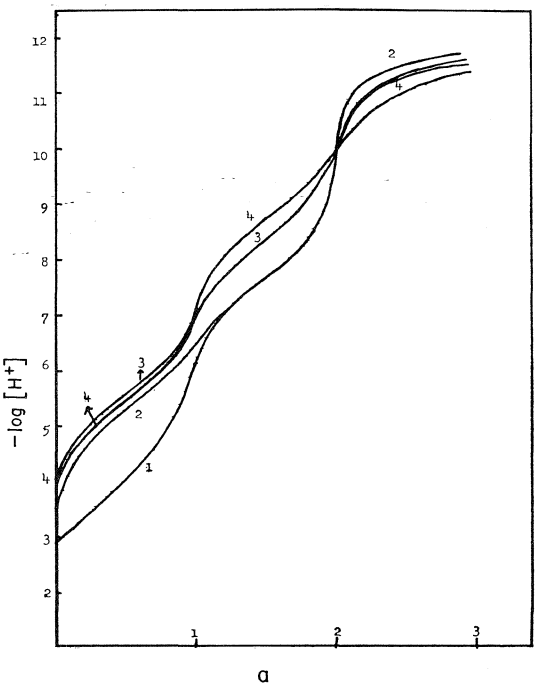

FIG. 1. Potentiometric titration of nitrilotriacetic acid disodium salt (HX^{-2}) 0.02 *M* and histamine nitrate (LH^+) 0.02 *M* in presence of metal ion (Me^{2+}) 0.02 *M*; a = number of moles of sodium hydroxide added per mole of metal; $T = 25.0 \pm 0.1$ °C; $\mu = 0.1$ ($NaClO_4$); 1, Me = Cu; 2, Me = Ni; 3, Me = Co; 4, Me = Zn.

TABLE I

The formation constants* of the complexes MeXLH

Me	log K_{f1}^0	log K_{f1} $C_{Me} = 5\times10^{-3}$	log K_{f1} $C_{Me} = 1\times10^{-2}$	log K_{f1} $C_{Me} = 2\times10^{-2}$	log K_{f1} (average)
Cu	3.98±0.04	4.00±0.03	3.96±0.02	3.96±0.04	3.97±0.04
Ni	2.54±0.05	2.59±0.05	2.51±0.03	2.54±0.03	2.55±0.05
Co	2.07±0.09	1.88±0.09	1.95±0.03	2.08±0.09	1.97±0.09
Zn	2.27±0.05	2.31±0.10	2.26±0.04	2.34±0.04	2.30±0.04

*K_{f1} = [MeXLH]/[MeX$^-$][LH$^+$], μ = 0.1 ($NaClO_4$), T = 25 °C.

The pH value of the first point of each curve shows that histamine nitrate is converted nearly quantitatively to the biprotonated histamine LH_2^{2+} and the formation constants reported elsewhere (9) indicate that the formation of the nitrilotriacetate complex MeX^- is virtually complete. Consequently, mixing equimolecular amounts of the reactants results in the following overall reaction

[1] $Me^{2+} + XH^{2-} + LH^+ \rightarrow MeX^- + LH_2^{2+}$

which involves a proton transfer to the histaminium ion. The first portion of the curve, till a = 1, might then correspond to the neutralization of one proton of LH_2^{2+}.

[2] $$LH_2^{2+} \rightarrow LH^+ + H^+$$

$$K_{a2} = \frac{[H^+][LH^+]}{[LH_2^{2+}]}$$

Although this process actually takes place, the reaction scheme above could only explain the first few points of each curve. It was then assumed that the increasing amount of LH^+ produced by addition of hydroxide would promote the formation of a protonated mixed complex MeXLH, by the reaction

[3] $$MeX^- + LH^+ \rightleftarrows MeXLH$$

$$K_{f1} = \frac{[MeXLH]}{[MeX^-][LH^+]}$$

This reaction would progress till a = 1, after which neutralization of MeXLH takes place to give $MeXL^-$

[4] $$MeXLH \rightleftarrows MeXL^- + H^+$$

$$K_i = \frac{[MeXL^-][H^+]}{[MeXLH]}$$

The formation constant of the unprotonated complex is denoted K_{f2} and defined as follows

[5] $$MeX^- + L \rightleftarrows MeXL^-$$

$$K_{f2} = \frac{[MeXL^-]}{[MeX^-][L]}$$

The constants K_{f1} were obtained from the points in the range a = 0–1 by a graphical method described by Schwarzenbach (10) and Martell (11). The following equations should be valid for the case $C_{Me} = C_X = C_L$, where these symbols denote the total concentrations of metal ion, nitrilotriacetate, and histamine, respectively.

[6] $$C_{Me} \simeq [MeX^-] + [MeXLH]$$

[7] $$C_L = [LH_2^{2+}] + [LH^+] + [MeXLH]$$

[8] $$(1 - a)C_{Me} = [LH_2^{2+}] + [H^+] - [OH^-]$$

From eq. [8], one easily obtains

[9] $$[LH^+] = \frac{K_{a2}}{[H^+]}[(1 - a)C_{Me} - [H^+] + [OH^-]]$$

and from eqs. [6], [7], and [3]

[10] $$K_{f1}[LH^+] + 1 = \frac{C_{Me}}{[LH^+]\left(1 + \frac{[H^+]}{K_{a2}}\right)} = y$$

The dissociation constants of histamine were redetermined and found equal to $pK_{a1} = 9.72 \pm 0.01$ and $pK_{a2} = 6.00 \pm 0.01$. The expected straight lines $y = K_{f1}[LH^+] + 1$ were obtained from the data till $a \sim 0.7$. Severe deviations were obtained at $0.7 < a < 1.0$, due to the fact that reaction [4] cannot be neglected in these conditions. The average values of the formation constants obtained by the graphical method are denoted K_{f1}^0 in Table I.

Can. J. Chem. Downloaded from www.nrcresearchpress.com by 210.87.254.6 on 09/05/12
For personal use only.

TABLE II

The formation constants* of the complexes $MeXL^-$

Me	log K_{f2}^0	log K_{f2} $C_M = 5\times10^{-3}$	log K_{f2} $C_M = 1\times10^{-2}$	log K_{f2} $C_M = 2\times10^{-2}$	log K_{f2} (average)
Cu	6.15±0.04	6.14±0.03	6.10±0.03	6.08±0.05	6.11±0.04
Ni	4.88±0.04	4.93±0.04	4.86±0.03	4.86±0.03	4.89±0.04
Co	3.70±0.06	3.75±0.04	3.72±0.04	3.81±0.05	3.76±0.05
Zn	3.57±0.08	3.69±0.08	3.55±0.08	3.58±0.04	3.61±0.08

*$K_{f2} = [MeXL^-]/[MeX^-][L]$, $\mu = 0.1$ ($NaClO_4$), $T = 25$ °C.

The constants K_{f2}^0 were determined from the data after $a = 1$, using the following equations, valid for $C_{Me} = C_X = C_L$

$$[11]\quad C_{Me} = [MeXLH] + [MeXL^-] + [MeX^-]$$

$$[12]\quad C_L = [MeXLH] + [MeXL^-] + [LH^+] + [L]$$

$$[13]\quad (2-a)C_{Me} = [MeXLH] + [LH^+] + [H^+] - [OH^-]$$

Equations [11] and [12] lead to

$$[14]\quad [MeX^-] = [LH^+]\left(1 + \frac{K_{a1}}{[H^+]}\right)$$

while eqs. [3] and [13] give

$$[15]\quad (2-a)C_{Me} = K_{f1}[LH^+]^2\left(1 + \frac{K_{a1}}{[H^+]}\right) + [LH^+] + [H^+] - [OH^-]$$

For each point, the values of $[LH^+]$, $[MeX^-]$, [MeXLH], $[MeXL^-]$, and [L] can be calculated after stepwise substitution from eqs. [15], [14], [3], [11], and [2], respectively, and introducing into eq. [5], we obtained the values of K_{f2}^0 given in Table II.

Computer programs were used to show that the reaction scheme above holds for the entire curves and to refine the results obtained graphically. A program SICOUTIT, adapted by one of us (A.L.B.) from SCOGS (see below), was used to compute a calculated curve $V_c = f(pH)$ for each experiment. In addition to K_{f1}^0 and K_{f2}^0 obtained graphically, three acidity constants for XH_3 and two for LH_2^{2+} were included in the calculation, together with the formation constants of the simple complexes MeL, MeL_2, MeL_3, and MeX^-, assuming the values given in the literature (9).

All equilibrium constants are modified to correspond to the general formula

$$\beta = \frac{[Me_mX_xL_lH_h]^{(3x-2h-2m)-}}{[Me^{2+}]^m[X^{3-}]^x[L]^l[H^+]^h}$$

and the following material balance was used:

$$C_{Me} = [Me^{2+}] + \sum_i m_i\,[Me^{2+}]^{m_i}\,[X^{3-}]^{x_i}\,[L]^{l_i}\,[H^+]^{h_i}\,\beta_i$$

$$C_X = [X^{3-}] + \sum_i x_i\,[Me^{2+}]^{m_i}[X^{3-}]^{x_i}[L]^{l_i}[H^+]^{h_i}\,\beta_i$$

$$C_L = [L] + \sum_i l_i\,[Me^{2+}]^{m_i}[X^{3-}]^{x_i}[L]^{l_i}[H^+]^{h_i}\,\beta_i$$

The experimental value of $[H^+]$ is treated as the independent variable and the roots $[Me^{2+}]$, $[X^{3-}]$, and [L] in the system of material balance equations are obtained by the Raphson–Newton iterative process, the convergence criterion being that the calculated values of C_{Me}, C_X, and C_L are equal to the experimental ones within 10^{-5} %. The values of $[Me^{2+}]$, $[X^{3-}]$, and [L] are then substituted in the electroneutrality equation from which the calculated volume V_c is obtained. The computed curves $V_c = f(pH)$ were found to agree quite satisfactorily with the experimental results and confirmed the proposed reaction scheme.

The formation constants K_{f1}^0 and K_{f2}^0 obtained graphically were then refined by a least-squares technique, using a computer program SCOGS by Perrin and Sayce. This particular program has not been described by the authors but seems to be an adaptation of another program GAUSS by the same authors (12), particularly suitable for the treatment of alkali titration data. The function minimized during the least-squares refinement is $\sum(V_c - V_{exp})^2$.

Can. J. Chem. Downloaded from www.nrcresearchpress.com by 210.87.254.6 on 09/05/12
For personal use only.

Can. J. Chem. Downloaded from www.nrcresearchpress.com by 210.87.254.6 on 09/05/12
For personal use only.

Since precipitation occurs shortly after the second inflection point for some systems, the data corresponding to $a \leqslant 2$ ($\sim$ 50 points) were used and each titration curve was treated independently. All equilibria mentioned above were included in the calculation and the corresponding constants were fixed to the values of the literature (9), except $K_{f1}{}^0$ and $K_{f2}{}^0$ which were allowed to refine simultaneously. After three or four cycles of refinement, convergence was attained and the refined values of K_{f1} and K_{f2} are given in Tables I and II, together with the initial values. The standard deviation on titre varied between 0.02 and 0.05 ml for a total titre of 5.00 ml. The error given is equal to 4.5 times the standard deviations (σ_{esd}) estimated from the diagonal elements of the least-squares inverse matrix from the last cycle.

The results of Table I and II show that the refined values obtained at three different concentrations for each system are equal within 4.5 times their respective σ_{esd}. Although this appears to be slightly more than the usual criterion ($3 \times \sigma_{esd}$) for a 99% confidence level, the latter criterion implicitly assumes that the fixed constants of the systems (obtained from the literature) are exact, which of course is highly unrealistic in the present case. Average values for each constant are also given in the last column of the tables.

Figure 2 shows the distribution curve for the system cobalt-nitrilotriacetate–histidine. It was calculated from the concentration table computed by the program SCOGS at the end of the last least-squares refinement cycle. This curve shows clearly that the calculation of $K_{f1}{}^0$ from the data corresponding to $a < 0.7$ is fully justified, since the only metallic species present in appreciable concentrations are MeX^- and MeXLH.

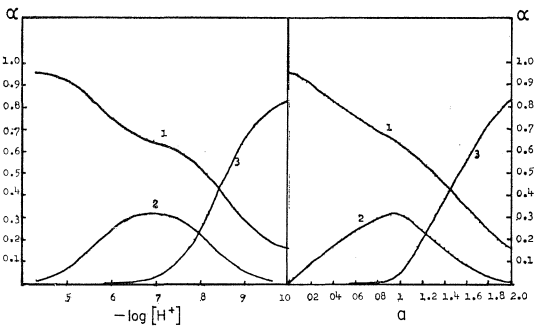

FIG. 2. Distribution curve of metal for the system cobalt-nitrilotriacetate–histamine, each at a total concentration of 0.02 *M*. Curves 1, 2, and 3 correspond to $\alpha_{MeX} = [MeX^-]/C_{Me}$, $\alpha_{MeXLH} = [MeXLH]/C_{Me}$, and $\alpha_{MeXL} = [MeXL^-]/C_{Me}$, respectively.

Discussion

As in previous cases (13, 14), both formation constants K_{f1} and K_{f2} follow the Irving–Williams stability series (15). It is noteworthy that a slight decrease in the relative stability of $CuXL^-$/$NiXL^-$ compared to CuL^{2+}/NiL^{2+} is observed. K_{f2} also conforms to various generalizations frequently observed: for example log K_{f2} is a linear function of log K_1, where K_1 is the formation constant of MeL^{2+}. The overall formation constants $K_s = K_{MeX}K_{f2}$ of the mixed nitrilotriacetate–histamine complex $MeXL^-$ also obey the following empirical relationship observed in previous works (13, 14), K_{MeX} being the formation constant of MeX^-,

$$\log K_s = \alpha \log K_{MeX}K_1 + c$$

In the present case, α assumes a value of 0.70.

It is interesting to note that log K_{f2} is generally greater than log K_{f1} by $\sim$2 log units. In Angelici's work (3) on the reaction of metallic nitrilotriacetates with glycine and glycine esters, similar differences were observed between both types of mixed complexes where the ligands are bi- and monodentate respectively. Although equilibrium constants alone cannot afford direct structural conclusions, the same difference of $\sim$ 2 log units between K_{f1} and K_{f2} might suggest that histamine acts as a monodentate ligand in the protonated mixed complex MeXLH, while the chelate ring is closed in $MeXL^-$.

Furthermore, the tertiary imidazolic nitrogen appears to be the atom actually coordinated to the metal ion in the "open" protonated complex MeXLH; values only slightly higher than those of the present work were obtained for the 1:1 mixed complexes of the same metallic nitrilotriacetates with imidazole which is a monodentate ligand (16). Indeed slightly higher values are expected for the latter system, since the tertiary imidazolic nitrogen of imidazole ($pK_a = 7.0$) is more basic than the one of histamine ($pK_a = 6.0$).

Acid dissociation constants K_i (eq. [4]) of the protonated mixed complex MeXLH can easily be obtained from the results of Tables I and II

$$K_i = K_{f2}\, K_{a1}/K_{f1}$$

TABLE III

Acid dissociation constants* of protonated complexes MeXLH

Me	pK_i
Cu	7.58 ± 0.08
Ni	7.38 ± 0.09
Co	7.93 ± 0.14
Zn	8.41 ± 0.12

*$\mu = 0.1$ ($NaClO_4$), $T = 25$ °C.

The values of pK_i are given in Table III. Assuming the model above, this indicates that the acidity strength of the $-NH_3^+$ group in MeXLH is considerably enhanced by coordination of the tertiary imidazolic nitrogen to the metal nitrilotriacetate. Similar effects on the acidity of unbound groups have been observed for several types of ligands (17, 18) and have been attributed to resonance and inductive effects within the ligands. Although this might act to a certain extent in the present case, we believe that these effects should be small since the amino group is separated from the rest of the molecule by two methylene groups. Therefore the relatively high acidity of the terminal NH_3^+ group would originate to a greater extent from the additional stabilization of the conjugated base $MeXL^-$ by closure of the chelate ring and formation of the mixed complex where both the tertiary imidazolic nitrogen and the terminal amino group are coordinated.

Acknowledgments

We wish to thank the National Research Council of Canada for research grants from which one of us (J.I.) awarded a fellowship to H. Saulnier. We are very thankful to Professor D. D. Perrin who kindly supplied a copy of the computer program SCOGS and for his helpful advice for its utilization, and to Professor R. S. Tobias for detailed information on the least-squares refinement treatment. The use of the CDC 3400 computer of the "Centre de Calcul de l'Université de Montréal" is also acknowledged.

1. J. Israeli. Can. J. Chem. **41**, 2710 (1963).
2. N. E. Jackobs and D. W. Margerum. Inorg. Chem. **6**, 2038 (1967).
3. D. Hopgood and R. Angelici. J. Am. Chem. Soc. **90**, 2508 (1968).
4. D. D. Perrin, I. G. Sayce, and V. S. Sharma. J. Chem. Soc. A, 1755 (1967).
5. A. Chakravorty and F. A. Cotton. J. Phys. Chem. **67**, 2878 (1963).
6. F. J. Welcher. The analytical use of EDTA. D. Van Nostrand Co., Inc., Toronto. 1958.
7. H. Flaschka. EDTA titrations. The Pergamon Press, Ltd., London. 1959.
8. A. Beauchamp and R. L. Benoit. Can. J. Chem. **42**, 2161 (1964).
9. Stability constants of metal-ion complexes. Chemical Society, London. 1964.
10. G. Schwarzenbach, A. Willi, and R. O. Bach. Helv. Chim. Acta, **30**, 1303 (1947).
11. A. E. Martell and S. Chaberek. J. Am. Chem. Soc. **74**, 5053 (1952).
12. D. D. Perrin and I. G. Sayce. J. Chem. Soc. A, 82 (1967).
13. J. Israeli and M. Cecchetti. Can. J. Chem. **48**, 3821 (1968).
14. J. Israeli and M. Cecchetti. Talanta, **15**, 1031 (1968).
15. H. Irving and R. J. P. Williams. J. Chem. Soc. 3192 (1953).
16. J. Israeli and H. Saulnier. Inorg. Chim. Acta, **2**, 482 (1968).
17. A. Corsini, Q. Fernando, and H. Freiser. Inorg. Chem. **2**, 224 (1963).
18. R. W. Green, P. S. Hallman, and F. Lions. Inorg. Chem. **3**, 376 (1964).

Can. J. Chem. Downloaded from www.nrcresearchpress.com by 210.87.254.6 on 09/05/12
For personal use only.

Can. J. Chem. Downloaded from www.nrcresearchpress.com by 210.87.254.6 on 09/05/12
For personal use only.

Coordination of silicon tetrafluoride with pyridine and other nitrogen electron-pair donor molecules[1]

JACQUES P. GUERTIN[2] AND MARIO ONYSZCHUK
Department of Chemistry, McGill University, Montreal, Quebec

Received August 22, 1968

Silicon tetrafluoride reacts with pyridine, pyrrolidine, and piperidine forming solid 1:2 complexes. With ethylenediamine, the stable 1:1 complex results. These compounds are easily hydrolyzed and sublimed and have no measurable vapor pressure at 25°. Hydrolysis of $SiF_4 \cdot 2C_5H_5N$ with aqueous HF produces pyridinium hexafluorosilicate (**4**), $(C_5H_5NH^+)_2SiF_6^{2-}$. Ethylenediamine readily displaces pyridine from $SiF_4 \cdot 2C_5H_5N$, forming $SiF_4 \cdot NH_2(CH_2)_2NH_2$. Infrared spectra of the complexes are compared in the 900–280 cm^{-1} region, but it was not possible to decide whether the pyrrolidine and piperidine complexes are *cis*- or *trans*-octahedral.

Canadian Journal of Chemistry, **47**, 1275 (1969)

Introduction

Campbell-Ferguson and Ebsworth (1) recently confirmed that $SiF_4 \cdot 2py$ is the only complex formed between silicon tetrafluoride and pyridine (abbreviated py in formulae), contrary to previous reports of $SiF_4 \cdot py$ (2, 3) and $2SiF_4 \cdot 3py$ (4) complexes. We had also found that under a variety of experimental conditions silicon tetrafluoride and pyridine produce only $SiF_4 \cdot 2py$ (5). Our results are now reported in detail together with data for complexes of silicon tetrafluoride with pyrrolidine, piperidine, and ethylenediamine.

Results and Discussion

Preparation and Properties of $SiF_4 \cdot 2py$

Various methods of preparation always yielded only the 1:2 complex, $SiF_4 \cdot 2py$, when silicon tetrafluoride was mixed with pyridine at 25°, as summarized in Table I. The white solid complex melted at 170–180° (with decomposition), had no measurable vapor pressure at 25°, but could be sublimed in vacuum at 60–80° (without decomposition).

Although the authors' methods were followed carefully, $2SiF_4 \cdot 3py$ (4) and $SiF_4 \cdot py$ (2, 3) could not be synthesized. Schnell (6) and, more recently, Campbell-Ferguson and Ebsworth (1) obtained only the 1:2 complex. The reports of combining ratios other than 1:2 are likely incorrect with the error probably due to loss of pyridine by $SiF_4 \cdot 2py$ on hydrolysis (1).

TABLE I

A summary of analytical data obtained for $SiF_4 \cdot 2py$ prepared by various methods

Method of synthesis	Product mole ratio, py/SiF_4	Fluorine elemental analysis (%)*
Direct gas–liquid, vacuum,		
(*i*) with excess SiF_4 present initially	2.00	28.60
(*ii*) with excess py present initially	2.00	28.60
(*iii*) after sublimation of solid product	†	29.01
py-Diethyl ether solution, stirred in a vacuum	†	28.58
Bubbling SiF_4 into py-diethyl ether solution	†	29.17
Tensimetric titrations,		
(*i*) SiF_4 with py	2.01	28.90
(*ii*) py with SiF_4	2.01	28.85

*Anal. Calcd. for $SiF_4 \cdot 2py$: F, 28.95. Anal. Calcd. for $SiF_4 \cdot py$: F, 41.50.
†In these cases it was not possible to determine combining ratios directly.

Crystalline $SiF_4 \cdot 2py$ reacted with aqueous HF (48%) to produce a colorless solution. Gentle boiling of the resultant solution to dryness yielded a white solid, which after vacuum sublimation at 165° was pure pyridinium hexafluorosilicate (**4**), $(C_5H_5NH^+)_2SiF_6^{2-}$, in 100% yield. This compound was not hygroscopic and melted without decomposition at 154–157°, with some sublimation.

The reaction of $SiF_4 \cdot 2py$ with aqueous HF is similar to a simple hydrolysis using only water, except that in the latter case SiO_2 and pyridine are formed as well as $(C_5H_5NH^+)_2SiF_6^{2-}$. The overall reaction with aqueous HF may be written as follows

[1]This work was supported by a grant from the Defence Research Board of Canada (Grant number 9530-20, Project D-46-95-30-20).
[2]Present address: Bell Telephone Laboratories, Reading, Pennsylvania.

$$SiF_4 \cdot 2py + 2H_3O^+ + 2F^- \longrightarrow 2pyH^+ + SiF_6^{2-} + 2H_2O$$
$$\downarrow -2H_2O$$
$$(pyH^+)_2SiF_6^{2-}$$

The complex $SiF_4 \cdot 2py$ was insoluble in the following solvents: methanol, carbon tetrachloride, benzonitrile, pyridine, benzene, nitrobenzene, monochlorobenzene, chloroform, methyl iodide, thiophene, methylene chloride, methylene bromide, mesitylene, acetonitrile, and a few fluorinated aromatic solvents such as perfluorodecalin, 2-chloro-5-nitrobenzotrifluoride, trichlorobenzotrifluoride, dichlorobenzotrifluoride, meta-nitrobenzotrifluoride, and benzotrifluoride[3]. It appeared to be soluble to the extent of about 5 g/l in nitromethane and bis(2-methoxyethyl)ether. Due to the low volatility of this ether at 25°, it was not possible to evaporate the solvent in order to examine whether the complex would precipitate from solution unchanged; moreover, heating the solution above 25° resulted in the decomposition of the complex.

A careful investigation of the $SiF_4 \cdot 2py$ – nitromethane system revealed that as little as 0.01% water in the nitromethane, present even after it was treated with calcium hydride, could account for the observed "solubility". The solid remaining after evaporation of the solvent contained $SiF_4 \cdot 2py$, $(C_5H_5NH^+)_2SiF_6^{2-}$, and a little SiO_2, indicative of hydrolysis.

Ethylenediamine (abbreviated en in formulae) converted $SiF_4 \cdot 2py$ almost quantitatively into $SiF_4 \cdot en$. The stoichiometry of the reaction was shown by analysis of the amount of pyridine liberated to be

$$SiF_4 \cdot 2py + en \rightarrow SiF_4 \cdot en + 2py$$

The fact that the amount of ethylenediamine consumed was greater than the theoretical value was attributed to some degradation of ethylenediamine during the reaction, as evidenced by a slight yellowing of the product mixture.

Preparation and Properties of $SiF_4 \cdot 2(CH_2)_4NH$, $SiF_4 \cdot 2(CH_2)_5NH$, and $SiF_4 \cdot en$

Direct vacuum synthesis of the complexes at 25° invariably yielded slightly impure pale yellow solids although combining ratios were satisfactory. With pyrrolidine and piperidine the 1:2 complexes, $SiF_4 \cdot 2(CH_2)_4NH$ and $SiF_4 \cdot 2(CH_2)_5NH$, respectively, were obtained; with ethylenediamine, a bidentate ligand, the 1:1 complex, $SiF_4 \cdot en$, resulted. Vacuum sublimation gave analytically pure white solids.

The purest complexes were obtained by bubbling silicon tetrafluoride through precooled solutions of the base in acetonitrile. The precipitated solids were always white, although the solvent had a tinge of yellow, and the solids analyzed to the pure complexes without further purification.

Infrared Spectra of the Complexes

Tables containing infrared (i.r.) absorption band peak positions and suggested assignments in the range 4000–280 cm^{-1} for $SiF_4 \cdot 2py$, $(pyH^+)_2SiF_6^{2-}$, $SiF_4 \cdot en$, $SiF_4 \cdot 2(CH_2)_4NH$, and $SiF_4 \cdot 2(CH_2)_5NH$, all in Nujol and KBr disk form, have been filed with the Depository of Unpublished Data[4]. Spectra in the regions 900–600 cm^{-1} and 600–280 cm^{-1} are reproduced in Fig. 1 in order that band contours and number of bands may be compared.

Previously, Beattie and Webster (7) and Hickie (8) decided that $SiF_4 \cdot 2py$ was *trans*-octahedral on the basis that only a single band was observed in the Si—F bond stretching region, consistent with D_{4h} symmetry of the complex. Although this approach was criticized for valid reasons (9), Bain *et al.* (10) have determined by a three-dimensional X-ray analysis of single crystal $SiF_4 \cdot 2py$ that the complex is molecular with a centrosymmetric *trans* configuration. An X-ray analysis has also confirmed that $SiCl_4 \cdot 2py$ is *trans* octahedral, contrary to earlier i.r. data which, because there were three bands in the Si—Cl stretching region, had been interpreted in terms of *cis* (C_{2v}) configuration (11, 8). After a more complete analysis of the i.r. and Raman spectra of $SiCl_4 \cdot 2py$, Beattie *et al.* (12) were unable to assign the structure decisively even though "the spectroscopic evidence in the 500 cm^{-1} region still looks remarkably *cis*". Coupling of vibrational modes and removal of degeneracies gives the multiple bands in the 300 to 500 cm^{-1} region. This clearly illustrates the danger of

[3]We are very grateful to Professor W. F. Forbes of the Department of Chemistry, University of Waterloo, for having kindly provided purified samples of the fluorinated aromatic solvents.

[4]Photocopies of these Tables may be obtained free of charge, upon request, from: Depository of Unpublished Data, National Science Library, National Research Council of Canada, Ottawa, Canada.

Can. J. Chem. Downloaded from www.nrcresearchpress.com by 210.87.254.6 on 09/05/12
For personal use only.

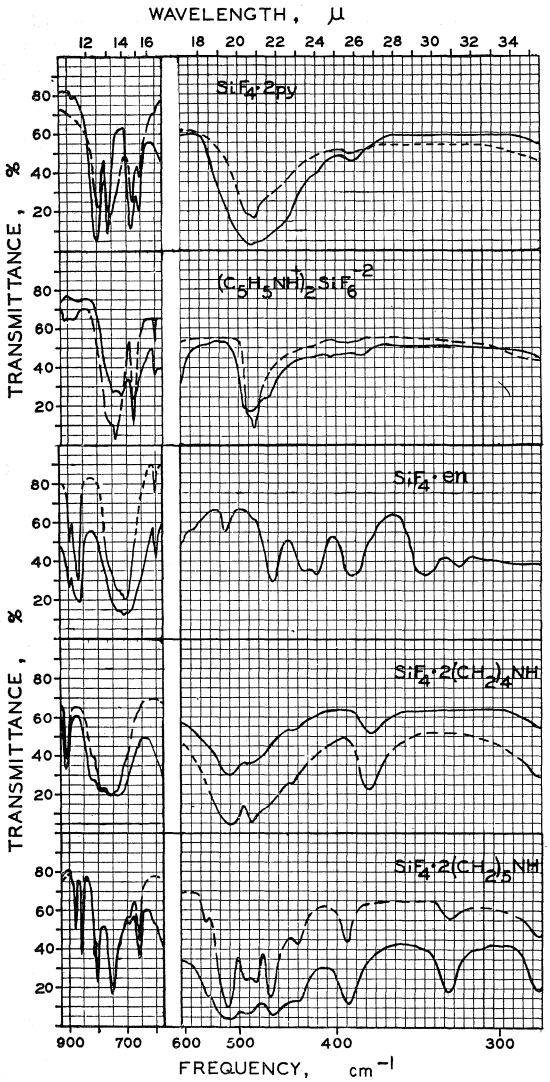

FIG. 1. Infrared spectra of the complexes in Nujol mull (——) and KBr disk (– – – –).

making structural assignments on the basis of the number of bands observed in the solid state spectra of $MX_4 \cdot 2L$ complexes. Accordingly, it is not possible to decide whether the pyrrolidine and piperidine complexes are *cis* or *trans* even though the measured spectra look *cis*.

Experimental

Volatile materials were manipulated in a standard Pyrex glass high-vacuum system which had stopcocks and joints lubricated with No. 90 Kel-F grease. Hygroscopic solids and nonvolatile liquids were manipulated in the dry nitrogen atmosphere of a glove box. Bubbling silicon tetrafluoride through a precooled solution of a base in an inert solvent proved to be the most convenient preparatory method for the complexes. The purity of the volatile compounds was determined by measurements of their vapor pressure, molecular weights, i.r. spectra, and melting points.

Infrared spectra in the range 4000–650 cm^{-1} were recorded on a Perkin–Elmer Model 137 Infracord spectrophotometer equipped with sodium chloride optics. When greater resolution was required, spectra were measured on a grating Perkin–Elmer Model 421 spectrophotometer. This instrument was also used for measurements in the 650–265 cm^{-1} range by replacing the grating with a CsBr prism interchange unit.

Spectra of solids were taken in KBr disks and in Nujol or Fluorolube mulls. The spectra of liquids were taken using fixed or variable space NaCl liquid cells or more simply using a thin film between two NaCl plates. The spectra of gases were taken at known pressures using a cylindrical gas cell (10 cm length and 2.5 cm radius) equipped with Viton O-rings and screw caps for the 7.5 mm thick NaCl windows.

Measurements in the 650–265 cm^{-1} range were made on samples in pure liquid (or in Nujol mull-form) placed between CsBr plates, the delicate surfaces of which were protected by 7.0 μ polyethylene film (Dow Chemical Company "Handi-Wrap"). This film does not absorb in the 650–265 cm^{-1} region. It was found that thin KBr pellets could also be used for measurements to 300 cm^{-1}.

Ultraviolet (u.v.) spectra used in the displacement reaction were recorded on a Perkin–Elmer Model 350 spectrophotometer.

Anhydrous pyridine, nitromethane, acetonitrile, ethylenediamine, pyrrolidine, piperidine (all Fisher reagent grade), and bis-(2-methoxyethyl)ether (Matheson, Coleman and Bell, practical grade) were obtained by refluxing the commercial product over CaH_2 for a few hours and collecting the distillates boiling at 116°/754 mm; 101.5°/757 mm; 82°/760 mm; 117°/751 mm; 86°/748 mm; 106°/756 mm; 163°/750 mm respectively; these compare well with the published normal boiling points (13). Hydrofluoric acid, 48% (Fisher, reagent grade), diethyl ether (Mallinckrodt, reagent grade), and absolute ethyl alcohol (Gooderham and Worts, U.S.P.) were used without further purification. Commercial silicon tetrafluoride (Matheson, 99.5%) was purified by several low-temperature vacuum distillations.

Preparation of $SiF_4 \cdot 2py$

(i) In the direct vacuum synthesis, SiF_4 (35.45 mmoles) was condensed over C_5H_5N (27.12 mmoles) and the mixture slowly warmed to 25°. Distillation at −78° yielded SiF_4 (21.90 mmoles), indicating a combining ratio, 1:2.00, corresponding to the complex, $SiF_4 \cdot 2py$. Fluorine analysis showed that the complex was pure.

Anal. Calcd. for $SiF_4 \cdot 2py$: F, 28.95. Found: F, 28.60.

(ii) The same complex resulted when excess C_5H_5N was used initially. Thus, C_5H_5N (40.40 mmoles), when condensed over SiF_4 (15.00 mmoles) and slowly warmed to 25°, produced unreacted C_5H_5N (10.38 mmoles) recovered by distillation at 25°, and a white solid which contained SiF_4 and C_5H_5N in a mole ratio, 1:2.00, as required for the complex, $SiF_4 \cdot 2py$. Found: F, 28.60.

(iii) Silicon tetrafluoride (15.10 mmoles) was condensed over a 10.5% (by weight) solution of C_5H_5N

Can. J. Chem. Downloaded from www.nrcresearchpress.com by 210.87.254.6 on 09/05/12
For personal use only.

Can. J. Chem. Downloaded from www.nrcresearchpress.com by 210.87.254.6 on 09/05/12
For personal use only.

(12.10 mmoles) in diethyl ether (183.0 mmoles) and the mixture was warmed slowly to 25° and stirred magnetically. The resulting insoluble white precipitate was freed of solvent by vacuum distillation at 25° and an analysis for fluorine confirmed that it was pure $SiF_4 \cdot 2py$. Found: F, 28.58.

(iv) Silicon tetrafluoride was bubbled through solutions of C_5H_5N in diethyl ether (1.5, 3.0, and 6.0% by weight) and C_5H_5N in acetonitrile (10% by weight) with the resultant production of copious quantities of white insoluble precipitates which also proved to be the complex $SiF_4 \cdot 2py$. Found: F, 29.40, 29.09, 29.00 for the diethyl ether solution preparation, and 28.64 for the acetonitrile solution preparation. Extensive pumping under vacuum did not change the composition of the samples.

Tensimetric Titration

In the tensimetric titration of SiF_4 (17.52 mmoles) with C_5H_5N, the plots of which are given in (5), pressures were measured after the temperature of the mixture had been decreased from 25 to −78°. The pressure decreased linearly to zero at a mole ratio, 1:2.01 (corresponding to the addition of 35.25 mmoles C_5H_5N) indicating the formation of only the 1:2 complex, $SiF_4 \cdot 2py$.

In the case of the reverse titration of C_5H_5N (31.02 mmoles) with SiF_4, using the above temperature conditions, the pressure remained zero until the mole ratio had decreased to 2.01 (corresponding to the addition of 15.45 mmoles SiF_4), when it increased rapidly as more SiF_4 was added. This confirmed the formation of only the 1:2 complex.

Displacement Reaction with Ethylenediamine

Under dry conditions, a previously prepared sample of $SiF_4 \cdot 2py$ (0.9103 g) was mixed with $NH_2(CH_2)_2NH_2$ (1.8198 g) and the mixture was kept at 25° for 1 h. The volatile components (2.0845 g) were then distilled from the remaining yellowish nonvolatile residue and condensed into a weighing tube. An i.r. spectrum confirmed that the solid residue was $SiF_4 \cdot en$ free from $SiF_4 \cdot 2py$.

Before the volatile components were analyzed for pyridine by quantitative u.v. spectroscopy, u.v. spectra of ethyl alcohol solutions of pyridine (4.680×10^{-4} g/l, $A = 1.620$) and ethylenediamine (4.028×10^{-2} g/l) were recorded separately and when equal volumes of the two solutions were mixed together. There was no interference between pyridine and ethylenediamine.

An ethyl alcohol solution of the volatile components from the reaction gave a satisfactory absorbance (4.364×10^{-4} g/l, $A = 0.395$) and it contained 1.142×10^{-4} g/l of C_5H_5N, corresponding to an almost quantitative displacement of C_5H_5N from the original sample of $SiF_4 \cdot 2py$.

Anal. Calcd. for 100% displacement: 0.549 g. Found: 0.546 g C_5H_5N.

Calculations were also made of the $NH_2(CH_2)_2NH_2$ consumed but the value found was greater than the theoretical value.

Anal. Calcd. for 100% displacement: 0.2085 g. Found: 0.2798 g.

Reactions of $SiF_4 \cdot 2py$ with Aqueous HF

The complex, $SiF_4 \cdot 2py$ (3.21 mmoles) was mixed with excess HF (48%) in a Pt crucible and the resultant colorless solution boiled gently to dryness. Heating the white solid in an oven at 105° for 2 h did not remove all the unreacted HF.

Anal. Calcd. for $(C_5H_5NH)_2SiF_6$: F, 37.7. Found: F, 39.2.

Vacuum distillation at 165° gave pure $(C_5H_5NH)_2SiF_6$. Found: F, 37.3; in 100% yield (3.21 mmoles).

"Solubility" of $SiF_4 \cdot 2py$ in Nitromethane

A colorless solution and a little insoluble, grey, jelly-like material resulted when $SiF_4 \cdot 2py$ (19.05 mmoles) was mixed with nitromethane (100 ml). After filtering the insoluble material, the i.r. of which showed that it was SiO_2 (0.02 g) (broad ν(Si—O) at 1095 cm^{-1}), the solution was evaporated to dryness at 25° and a white solid remained. Infrared measurement and elemental analysis showed that it was $(C_5H_5NH)_2SiF_6$ (11.88 mmoles) containing a trace of $SiF_4 \cdot 2py$ and/or SiO_2.

Anal. Calcd. for $(C_5H_5NH)_2SiF_6$: F, 37.7; Si, 9.3; N, 9.25; C, 39.7; H, 4.0. Found: F, 36.9; Si, 10.3; N, 8.2; C, 39.1; H, 4.1.

Therefore, the mole ratio of $(C_5H_5NH)_2SiF_6$ formed to $SiF_4 \cdot 2py$ consumed was 1:1.60.

Preparation of $SiF_4 \cdot en$

A mixture of SiF_4 (64.20 mmoles) and $NH_2(CH_2)_2NH_2$ (60.20 mmoles) was slowly warmed from −195 to 25°. Distillation at −78° of the unreacted SiF_4 (5.36 mmoles) indicated that the reaction had occurred in a mole ratio, 1:1.02, corresponding to the complex, $SiF_4 \cdot en$.

The complex was further purified by vacuum sublimation at 120°. Analysis indicated that it was pure.

Anal. Calcd. for $SiF_4 \cdot en$: F, 46.2. Found: F, 46.0.

Since $NH_2(CH_2)_2NH_2$ was found to react with stopcock grease, it was measured and introduced by a syringe (14).

Preparation of $SiF_4 \cdot 2(CH_2)_4NH$

When SiF_4 (5.99 mmoles) was condensed over $(CH_2)_4NH$ (8.63 mmoles) and the mixture slowly warmed from −195 to 25°, a yellow-white solid formed. It was apparent from the amount of unreacted SiF_4 (1.72 mmoles) distilled at −78° that SiF_4 and $(CH_2)_4NH$ had reacted in a mole ratio, 1:2.02, forming the complex, $SiF_4 \cdot 2(CH_2)_4NH$. Further purification by vacuum sublimation at 80° gave the pure, white, 1:2 complex.

Anal. Calcd. for $SiF_4 \cdot 2(CH_2)_4NH$: F, 30.85. Found: F, 30.86.

Using the same "bubbling technique" as that used to prepare $SiF_4 \cdot 2py$, SiF_4 was bubbled through a 10% solution of $(CH_2)_4NH$ in acetonitrile maintained at 0°. Analysis of the resultant white product indicated the formation of pure $SiF_4 \cdot 2(CH_2)_4NH$. Found: F, 30.85.

Preparation of $SiF_4 \cdot 2(CH_2)_5NH$

Again, using the "bubbling technique" and identical conditions as those used for the preparation of $SiF_4 \cdot 2(CH_2)_4NH$, the white solid complex, $SiF_4 \cdot 2(CH_2)_5NH$ was prepared and needed no further purification.

Anal. Calcd. for $SiF_4 \cdot 2(CH_2)_5NH$: F, 27.65. Found: F, 27.56.

Sublimation at 80° did not change its composition. Found: F, 27.60.

Acknowledgments

We thank the National Research Council of Canada and the Defence Research Board for financial assistance in the form of annual grants (to M.O.). We are grateful to G. H. Hickie for his contributions in the interpretation of the infrared measurements.

1. H. J. CAMPBELL-FERGUSON and E. A. V. EBSWORTH. J. Chem. Soc. A, 1508 (1966).
2. J. GOUBEAU and H. GROSSE-RUYKEN. Z. Anorg. Allgem. Chem. **264**, 230 (1951).
3. E. L. MUETTERTIES. J. Am. Chem. Soc. **82**, 1082 (1960).
4. U. WANNAGAT, R. SCHWARZ, R. VOSS, and K. G. KNAUFF. Z. Anorg. Allgem. Chem. **277**, 75 (1954).
5. J. P. GUERTIN. Ph.D. Thesis, McGill University, Montreal. 1964.
6. E. SCHNELL. Monatsh. Chem. **93**, 65 (1962).
7. I. R. BEATTIE and M. WEBSTER. J. Chem. Soc. 3672 (1965).
8. G. H. HICKIE. M.Sc. Thesis, McGill University, Montreal. 1964.
9. H. J. CAMPBELL-FERGUSON and E. A. V. EBSWORTH. J. Chem. Soc. A, 705 (1967).
10. V. A. BAIN, R. C. G. KILLEAN, and M. WEBSTER. To be published.
11. I. R. BEATTIE, T. GILSON, M. WEBSTER, and (in part) G. P. MCQUILLAN. J. Chem. Soc. 238 (1964).
12. I. R. BEATTIE, T. R. GILSON, and G. A. OZIN. J. Chem. Soc. A, 2772 (1968).
13. Handbook of chemistry and physics. 48th ed. Chemical Rubber Publishing Co., Cleveland, Ohio. 1967.
14. F. FEHER, G. KUHLBORSCH, and H. LUHLEICH. Z. Anorg. Allgem. Chem. **303**, 294 (1960).

Can. J. Chem. Downloaded from www.nrcresearchpress.com by 210.87.254.6 on 09/05/12
For personal use only.

Infrared spectra of the interactions of aniline and porous glass surfaces

M. J. D. Low and V. V. Subba Rao
Department of Chemistry, New York University, New York 10453

Received August 15, 1968

Infrared spectra were recorded of aniline sorbed on highly dehydroxylated, deuterated, and on fluoridated porous glass as well as on pure and boria-impregnated silica. The results suggest that two types of weak interactions involving the surface SiOH and B—OH groups occurred; the nitrogen atom of the amine was hydrogen bonded to surface OH and there was an interaction between OH groups and the π system of the aromatic ring. Some aniline chemisorbed on surface boron via the nitrogen atom of the amine group. Some aniline chemisorbed dissociatively to form secondary amine structures bonded through the nitrogen to surface boron atoms and new B—OH groups formed. Surface boron impurity acted as an adsorption and dissociation center.

Canadian Journal of Chemistry, 47, 1281 (1969)

Can. J. Chem. Downloaded from www.nrcresearchpress.com by 210.87.254.40 on 09/05/12
For personal use only.

Recent studies have provided evidence that much of the reactivity of porous glass surfaces could be attributed to the presence of impurities (1–7). With NH_3 sorption on highly dehydrated porous glass (4), infrared spectra indicated that residual boron played a role in physical adsorptions, dissociative chemisorption, as well as in an undissociative chemisorption involving the coordination of NH_3 to boron present on the glass. The surface $\equiv B{:}NH_3$ complex was weakly bonded, but may have been the precursor of dissociated, more tightly held species. In order to determine if similar surface complexes were formed with molecules larger than NH_3, we have studied the sorption of aniline on highly degassed, deuterated, and fluoridated porous glass as well as on pure and boria-impregnated silicas.

Experimental

The glass adsorbents were 10 × 25 × 1 mm pieces of Code 7930 porous glass purchased from Corning Glass Works. Silica and 3% $B_2O_3 - SiO_2$ samples were prepared from Cab-O-Sil silica (G. Cabot Co., Boston, Mass.). Most experimental details including the dehydration, deuteration, and fluoridation of specimens have been described elsewhere (1–5). Reagent grade (Matheson Co.) aniline was dried over Na_2SO_4 and distilled 4 times; the final purification was done by repeated freezing and thawing in vacuo. A thermocouple gauge was used to measure the pressure of adsorbate. Spectra were recorded with Perkin–Elmer models 521 and 621 spectrophotometers. The ordinates of spectra shown in the various Figures are displaced to avoid overlapping of traces. The number at the left of each spectrum shows the % transmittance for the particular spectrum at 4000 cm^{-1}.

Results

Trace A of Fig. 1 is a typical "background" spectrum of highly-degassed porous glass; the prominent features are a band at 3748 cm^{-1} due to surface silanols and a smaller but sharp band at 3703 cm^{-1} due to surface B—OH groups (1–5), hereafter termed SiOH and B—OH bands. When such a glass specimen was exposed to aniline vapor at room temperature at increasingly higher pressures from 10 to 200 μ and was then degassed, the surface hydroxyl bands were altered and a series of absorptions caused by sorbed aniline were observed. A typical sorption–desorption cycle is illustrated by the alphabetical sequence of spectra A to L of Figs. 1 and 2 (spectra X and Y were taken from a different sequence and are presented to illustrate intermediate stages). The salient points of the interactions can be summarized as follows.

(*a*) The first bands to appear when a freshly degassed specimen was exposed to aniline were small, sharp bands at 3361 and 3301 cm^{-1} in the N—H region and a small, sharp band at 3050 cm^{-1} in the C—H region. These grew with increasing pressure, and a band near 3440 cm^{-1} with a shoulder near 3420 cm^{-1} appeared. The 3361 cm^{-1} band became slightly asymmetric and a shoulder appeared near 3350 cm^{-1}; similarly, shoulders were observed near 3280 and 3230 cm^{-1} on the 3301 cm^{-1} band, e.g. spectrum B, Fig. 1. The 3050 cm^{-1} band broadened and shifted to 3060 cm^{-1}, and smaller bands appeared at 3030, 3185, 3110, and 3137 cm^{-1}.

(*b*) With increasing pressure, bands grew at 3480–3490, 3410, 3340, and 3245 cm^{-1}; the 3060 cm^{-1} band grew and then the smaller bands near it became difficult to define. The 3361 and 3301 cm^{-1} bands did not shift but were swamped by the broad and strong 3340 and 3245 cm^{-1} bands. Eventually, the entire region from 3500 to

Can. J. Chem. Downloaded from www.nrcresearchpress.com by 210.87.254.40 on 09/05/12
For personal use only.

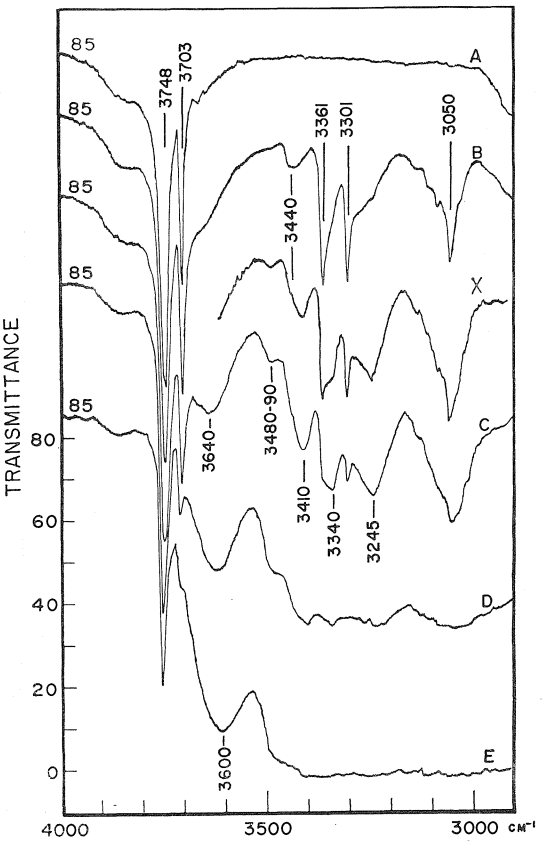

FIG. 1. Aniline sorption: porous glass. After the degassing at 750° for 24 h (spectrum A), the specimen was exposed to aniline at room temperature at the following pressures in μ: B, 13; C, 35; D, 65; E, 150. Spectrum X is taken from a different sequence after exposure to 20 μ aniline.

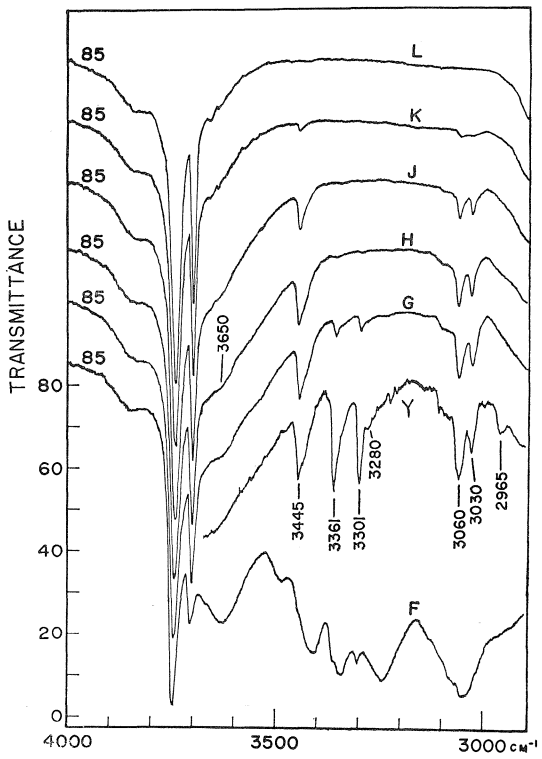

FIG. 2. Aniline desorption: porous glass. Continuation of the sequence of Fig. 1. The temperature (°C) at which the sample was degassed and the time (h) were: F: room temperature, 15; G: 100, 15; H: 150, 15; J: 200, 6; K: 300, 10; L: 400, 3. Spectrum Y was taken from a different sequence after degassing at 100° for 1 h.

3000 cm^{-1} became opaque, there being an intense absorption from 3500 to 2000 cm^{-1}.

(*c*) Pumping at room temperature restored some transmittance below 3500 cm^{-1} but even after long times intense absorptions remained, e.g. spectrum F, Fig. 2. However, degassing at 50 or 100° removed much of the adsorbed aniline. The bands at 3480, 3410, 3340, and 3245 cm^{-1} declined. Bands remained at 3445 and 3361 cm^{-1}, (both asymmetric on the low wavenumber side), and at 3301 cm^{-1} with a shoulder near 3280 cm^{-1}. In the C—H region, the broad and almost structureless 3360 cm^{-1} band declined and split into two bands at 3060 and 3030 cm^{-1}; there were weak absorptions near 3130, 3110–3070, 2965, and 2920 cm^{-1}, e.g. spectrum Y, Fig. 2. All absorptions in the N—H and C—H regions decreased on degassing at higher temperatures. The 3061 and 3030 cm^{-1} bands decreased more rapidly than the 3445 cm^{-1} band and disappeared above 200°. All bands disappeared above 300°, e.g. spectra G–L, Fig. 2.

(*d*) Initial aniline sorption brought about an absorption in the range 3700–3500 cm^{-1}. A definite band formed, grew in intensity, and the band center shifted from about 3650 to 3600 cm^{-1}, e.g. spectra A–E, Fig. 1. The broad absorption, hereafter termed the 3600 cm^{-1} band, decreased in intensity and shifted towards higher wavenumbers on mild degassing (spectrum F, Fig. 2), and declined abruptly along with the removal of much of the sorbed aniline on degassing at higher temperature, e.g. spectra Y, G, Fig. 2. However, even after most of the sorbed aniline had been removed, a weak but definite band remained near 3650 cm^{-1}, e.g. spectra G, H, Fig. 2. The band was hardly noticeable after a 200° degassing and was not detected above 200°.

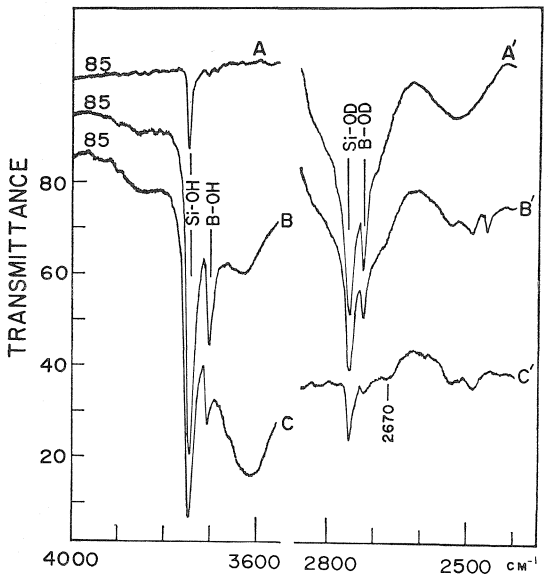

FIG. 3. Aniline sorption: deuterated porous glass. A,A′: after deuteration and degassing; B,B′: after exposure to 27 μ aniline; C,C′: after exposure to 62 μ aniline.

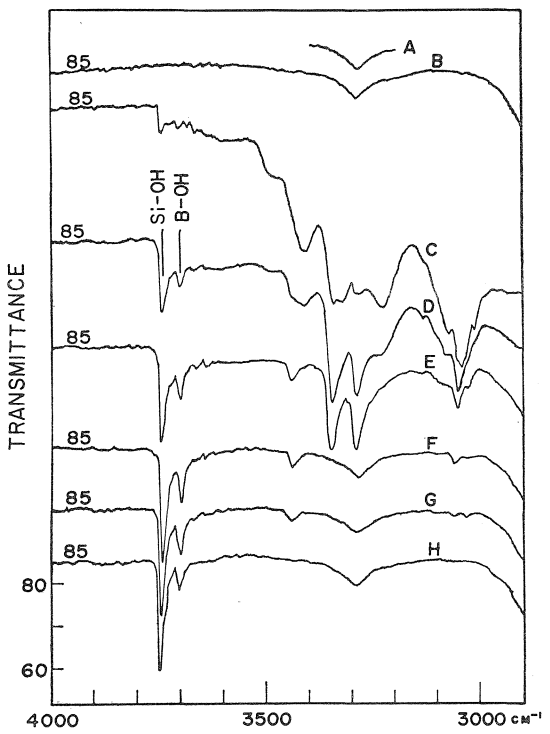

FIG. 4. Reactions on fluoridated porous glass. A: cell windows contaminated by NH_4F; B: fluoridated and degassed specimen; C: after exposure to 170 μ aniline at room temperature. The sample was then degassed at the following temperatures (°C) and times (h): D: room temperature, 12; E: 100, 1; F: 150, 6; G: 200, 15; H: 300, 10.

(*e*) During the sorption part of a cycle the B—OH band broadened, declined, and shifted to lower wavenumbers. At the highest pressures the band frequently disappeared completely. On desorption, the band reappeared near 3700 cm^{-1} and, with progressive degassing, shifted towards 3703 cm^{-1} and increased in intensity. The B—OH band was larger at the completion than at the beginning of a cycle. The SiOH band similarly declined in intensity and shifted to 3745 cm^{-1} with increasing adsorbate pressure, and then regained its original position and intensity upon degassing. However, the increase in transmittance of the sample at wavenumbers higher than the SiOH band and the decrease brought about by the 3600 cm^{-1} band make it difficult to evaluate small changes in the OH bands during a cycle.

Spectra were recorded of the interactions of aniline and deuterated porous glass. Some results are shown in Fig. 3. A deuterated specimen showed bands at 2756 and 2723 cm^{-1} due to surface OD groups (2) and weak bands at 3744 and 3702 cm^{-1} due to residual OH groups. When aniline was sorbed, the OH bands increased and the OD bands declined rapidly. A broad band formed near 2670 cm^{-1}, analogous to the 3600 cm^{-1} band. Small bands formed near 2335, 2490, 2460, and 2400 cm^{-1}, attributed to deuteroaniline. Bands in the N—H and C—H regions were entirely like those found with hydroxylated specimens. On desorption, the small bands in the 2700–2400 cm^{-1} region disappeared and the OD bands declined slightly; other changes in the N—H and C—H regions were similar to those found with hydroxylated specimens.

Figure 4 shows some results obtained with fluoridated porous glass. Spectrum B shows that of the specimen after fluoridation and degassing; all OH groups had been removed. The cell windows were irreversibly contaminated by NH_4F during the fluoridation procedure, leading to a stable band in the 3400–3200 cm^{-1} region. During an adsorption–desorption cycle, the bands and changes in bands below 3500 cm^{-1} found with fluoridated glass were similar to those occurring with hydroxylated specimens. However, the amount of aniline taken up by the fluoridated surface, estimated from the intensity

Can. J. Chem. Downloaded from www.nrcresearchpress.com by 210.87.254.40 on 09/05/12
For personal use only.

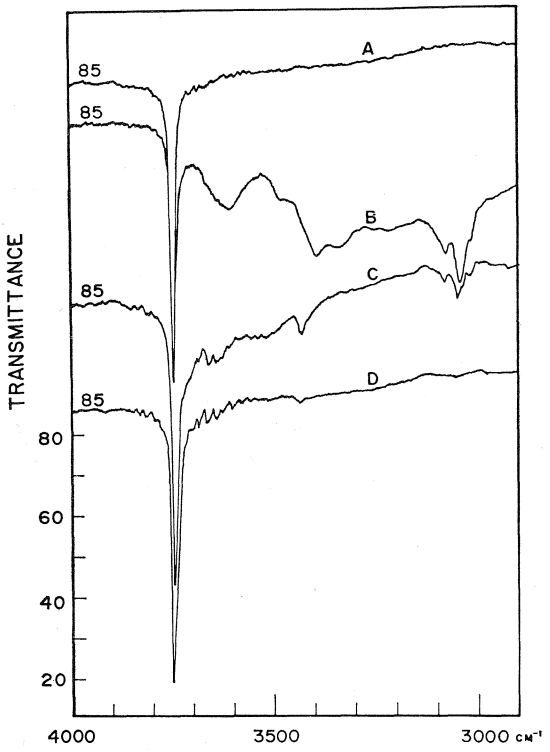

FIG. 5. Aniline sorption: Cab-O-Sil. A: after degassing; B: after exposure to 200 μ aniline at room temperature; C: after degassing at room temperature for 15 h; D: after degassing at 300° for 15 h.

of the bands, was less than that sorbed by a hydroxylated surface. The 3600 cm^{-1} band was not observed. Also, small bands at 3744 and 3700 cm^{-1} were built up.

Some experiments were also carried out with pure Cab-O-Sil silica and with boria-impregnated Cab-O-Sil. Exposure of pure Cab-O-Sil to aniline diminished the 3747 cm^{-1} OH band and caused absorption at 3600, 3470, 3390, 3325, 3070, and 3010 cm^{-1}, e.g. Fig. 5. Evacuation at room temperature restored the OH band and removed other absorptions; small bands remained at 3435 and 3050 cm^{-1}. The two sharp bands at 3361 and 3301 cm^{-1} found with porous glass were not observed.

The results obtained with a Cab-O-Sil – 3% B_2O_3 specimen were quite similar to those obtained with porous glass. Some results are shown in Fig. 6. The sharp 3361 and 3301 cm^{-1} bands were observed, and there was an increase in the B—OH band.

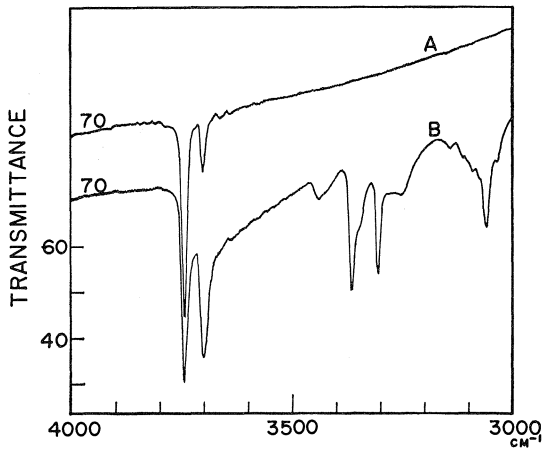

FIG. 6. Aniline sorption: 3% $B_2O_3 \cdot SiO_2$. A: base spectrum; B: after exposure to 15 μ aniline, followed by degassing at room temperature for 15 h.

Discussion

Infrared spectra taken in the overtone region of aniline adsorbed on porous glass have been reported by Yaroslavskii and Terenin (8) and on silica–alumina gel by Filimonov (9). Hydrogen bonding to surface hydroxyls and shifts of N—H bands were found. However, as pointed out by Kiselev and Lygin (ref. 10, p. 213), spectra of the overtone region are limited and difficult to analyze, so that a comparison of overtone spectra with the present data is not attempted. Abramov, Kiselev, and Lygin (11) found the OH groups on Aerosil silica to be strongly perturbed by adsorbed aniline, and that the N—H and C—H stretching frequencies of adsorbed aniline were at 3395, 3330, 3044, and 3078 cm^{-1}, in comparison to 3480, 3394, 3038, and 3075 cm^{-1}, respectively, for aniline in CCl_4 solution. The shift in the N—H bands was ascribed to hydrogen bonding to surface hydroxyls via the nitrogen atom of the amine group. The smaller shift in the C—H bands was taken as an indication that π electrons of the aromatic ring interacted with the surface hydroxyls to a smaller extent than the amine group. More recently (12), spectra recorded in situ of aniline adsorbed on Cab-O-Sil from CCl_4 solution showed N—H bands at 3395 and 3300 cm^{-1}, similarly suggesting hydrogen bonding via the amine group. Also a broad band occurred near 3600 cm^{-1} and was attributed to an interaction of the π system of the adsorbed aniline with SiOH groups. Such π–OH inter-

Can. J. Chem. Downloaded from www.nrcresearchpress.com by 210.87.254.40 on 09/05/12
For personal use only.

Can. J. Chem. Downloaded from www.nrcresearchpress.com by 210.87.254.40 on 09/05/12
For personal use only.

actions were recently described by Galkin *et al.* (13) for a variety of aromatic compounds adsorbed on silica and are reviewed elsewhere (see ref. 10, p. 309). The present data on porous glass show similar effects.

The broad absorption termed the 3600 cm^{-1} band, which appears in conjunction with the intense N—H and C—H bands of adsorbed aniline and can easily be diminished by mild degassing of the adsorbent, e.g. Figs. 1–3, is attributed to a weak hydrogen bonding involving an interaction of the π system of the aromatic ring of adsorbed aniline and surface OH groups (ref. 10, pp. 213 and 309 and ref. 13). Further evidence indicating that hydroxyls were involved in this comes from the experiments with fluoridated glass (Fig. 4), which showed that the 3600 cm^{-1} band was not produced in the absence of OH groups. With hydroxylated surfaces the 3600 cm^{-1} band was broad and structureless, so that it is not possible to discern individual interactions of the benzene moiety with SiOH or B—OH groups. However, both types of OH groups were diminished by aniline adsorption, so that it is reasonable to assume that each OH species was involved in the same type of interaction.

The spectrum of aniline adsorbed on Aerosil showed a broad absorption near 3600 cm^{-1} which was attributed to bound and intraglobular OH groups; a second, broader absorption near 3200 cm^{-1} was attributed to perturbed hydroxyls (see ref. 11, Fig. 1, spectrum 3). However, the spectrum indicates that the Aerosil sample was hydroxylated to a considerable extent; the 3600 cm^{-1} absorption may well have been caused by the π–OH interaction. A distinct absorption band below 3600 cm^{-1} ascribable to the type of OH perturbation reported for the Aerosil was not found in the present data. However, a series of spectra recorded at increasing aniline pressures, e.g. Figs. 1 and 2, showed that although individual bands did not increase greatly, all bands broadened and the entire region below 3500 cm^{-1} decreased markedly in transmittance, much as if the discrete bands were superimposed on a much broader absorption. In view of the large shifts produced by strongly hydrogen bonded adsorbates (11, 13, and 10, p. 309), the strong absorption below 3500 cm^{-1} can be attributed to SiOH and B—OH perturbed by the hydrogen bonded aniline. However, when appreciable amounts of aniline were adsorbed, the transmittance decreased appreciably not only in the range where a "perturbed OH band" would be expected, but over the entire range from 3500 to 2000 cm^{-1}. This might suggest that a continuous absorption occurred in addition to the absorption produced by direct hydrogen bonding. A similar effect was found with the adsorption of NH_3 on porous glass (4, 14). Cant and Little (14) attributed a continuous absorption to a rapid exchange of the surface hydroxyl proton with the adsorbed NH_3, in analogy to a similar effect found with the polystyrene – sulfonic acid – water system where the continuous absorption was shown to originate in the high exchange probability of a proton in the strongly hydrogen-bonded system (15). Such a mechanism might account for a portion of the intense absorption found with aniline – porous glass. The rapid exchange of adsorbed aniline with surface OD groups, e.g. Fig. 3, would support such a mechanism.

Spectra of aniline adsorbed on pure Cab-O-Sil show bands at 3390 and 3325 cm^{-1} in close agreement with earlier work (11, 12). These bands are assigned to the N—H stretching vibration of adsorbed aniline, shifted because of hydrogen bonding between the hydrogen of SiOH groups and the nitrogen atom of the amine group (8–12). With porous glass, however, comparable bands are observed at 3410 and 3340 cm^{-1} (the absorption at 3245 cm^{-1} is a combination band). The difference in the N—H band positions on pure silica and on porous glass is attributed to the presence of B—OH groups on porous glass. It is considered that absorptions due to hydrogen bonding to B—OH groups contribute to the 3390 and 3325 cm^{-1} absorptions, so that each of the 3410 and 3340 cm^{-1} bands found with porous glass corresponds to two strongly overlapping bands. Support for this view comes from the fact that the 3390 and 3325 cm^{-1} bands with pure silica can be shifted to 3410 and 3340 cm^{-1} by impregnating the silica with boria, thereby producing surface B—OH groups, e.g. Fig. 6. The results thus suggest the existence of 3 types of weak interactions between aniline and surface OH groups. There appear to be somewhat stronger interactions also. Sharp bands occurred at 3361 and 3301 cm^{-1} with porous glass, but not with pure silica. The bands were observed after those due to hydrogen-bonded aniline had been removed, so that the species responsible for the

Can. J. Chem. Downloaded from www.nrcresearchpress.com by 210.87.254.40 on 09/05/12
For personal use only.

sharp bands was more strongly bonded than most of the adsorbed aniline. The pair of bands agrees well with Bellamy and Williams' relation between asymmetric and symmetric stretching frequencies (16), apparently does not shift with changes in intensity, and is not far from the positions of the N—H stretching frequencies of hydrogen bonded aniline. Also, the bands can be induced with silica by impregnating the silica with boria. The 3361 and 3301 cm^{-1} bands are consequently assigned to the asymmetric and symmetric N—H vibrations of the amine group of aniline, coordinated to surface boron, structure **1**. The slight asymmetry on the low wavenumber side of each band in the absence of physically adsorbed aniline may be caused by interaction with neighboring OH groups.

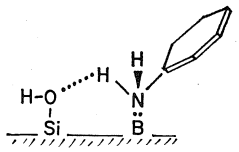

1

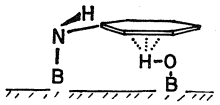

2

A band occurred at 3445 cm^{-1} with porous glass and boria-impregnated silica, but not with pure silica. The 3445 cm^{-1} band appeared at low aniline pressures and remained after other bands had been caused to disappear by degassing, so that the species responsible for the band was more tightly bound to the surface than the hydrogen-bonded species or the chemisorbed structure **1**. The single band is associated with the occurrence of boron on the surface, and its frequency falls in the range found for the single N—H vibrations of secondary amines (17). In analogy to the assignment of a band at 3455 cm^{-1} to a B—NH—B structure found with the reaction of NH_3 with boron-containing surfaces (4), the 3445 cm^{-1} band is assigned to the N—H stretching vibration of a secondary amine, **2**. Such a structure could form through the reaction of aniline with a B—O—B bridge to yield **2** and a B—OH group, leading to an increase of the B—OH band. Such increases occurred with porous glass and boria-impregnated silica but not with pure silica. Also, OH groups formed when aniline reacted with fluoridated glass. The various results thus suggest that surface boron acted as adsorption and dissociation center for aniline in the same fashion found with H_2O (5), NH_3 (4), or HCN (7). It is interesting to note that some traces of the 3600 cm^{-1} band were observed after the weakly held species, which would contribute to the formation of the 3600 cm^{-1} band, had been desorbed, e.g. spectra G, H, J, Fig. 2. As previous work had shown that it is difficult to remove the adsorbed water (2, 3, 5) and the 3600 cm^{-1} band could be removed relatively easily, it is unlikely that the 3600 cm^{-1} remnant was caused by water contamination. Rather, it seems plausible that the aromatic ring of **2** was oriented in such a fashion that some π–OH interaction was possible, thus producing a weak 3600 cm^{-1} band.

Two small bands at 3435 and near 3050 cm^{-1} were observed during the desorption of aniline from silica. The bands are similar, although not identical, to the bands observed with porous glass and may indicate the formation of a surface structure similar to **2**. This could come about through a reaction of aniline with a siloxane bridge or with a SiOH to produce H_2O and the silicon analogue of **2**. Alternatively, there could have been some contamination of the silica by boria evaporated from the all walls (6), but the sharp bands due to **1** were not observed and the single band due to **2** was at a different frequency, so that this alternative seems unlikely.

Acknowledgments

Support by grants from the Communicable Disease Center and the National Center for Air Pollution Control of the Department of Health, Education, and Welfare, and N.S.F. GP1434, is gratefully acknowledged, as are fruitful discussions with Norman Madison.

1. M. J. D. Low and N. Ramasubramanian. Chem. Commun. **20**, 1965.
2. M. J. D. Low and N. Ramasubramanian. J. Phys. Chem. **70**, 2740 (1966).
3. M. J. D. Low and N. Ramasubramanian. J. Phys. Chem. **71**, 730 (1967).
4. M. J. D. Low, N. Ramasubramanian, and V. V. Subba Rao. J. Phys. Chem. **71**, 1726 (1967).
5. M. J. D. Low and N. Ramasubramanian. J. Phys. Chem. **71**, 3077 (1967).
6. M. J. D. Low, N. Ramasubramanian, and P. Ramamurthy. J. Vacuum Sci. Technol. **4**, 111 (1967).
7. M. J. D. Low, N. Ramasubramanian, P. Ramamurthy, and A. V. Deo. J. Phys. Chem. **72**, 2371 (1968).
8. N. G. Yaroslavskii and A. N. Terenin. Dokl. Akad. Nauk SSSR, **66**, 885 (1949).
9. V. N. Filimonov. Opt. i Spektroskopiya, **1**, No. 4, 490 (1956).
10. A. V. Kiselev and V. I. Lygin. *In* Infrared spectra

of adsorbed species. Academic Press, Inc., New York. 1966.
11. V. N. ABRAMOV, A. V. KISELEV, and V. I. LYGIN. Russian J. Phys. Chem. English Transl. **38**, No. 4, 575 (1964).
12. M. J. D. LOW and M. HASEGAWA. J. Colloid Interface Sci. **26**, 95 (1968).
13. G. A. GALKIN, A. V. KISELEV, and V. I. LYGIN. Trans. Faraday Soc. **60**, 431 (1964).
14. N. W. CANT and L. H. LITTLE. Can. J. Chem. **42**, 802 (1964).
15. G. ZUNDEL and G. M. SCHWAB. J. Phys. Chem. **67**, 771 (1963).
16. L. J. BELLAMY and R. L. WILLIAMS. Spectrochim. Acta, **9**, 341 (1957).
17. L. J. BELLAMY. The infrared spectra of complex molecules. 2nd ed. John Wiley and Sons, Inc., New York. 1954. p. 215.

Can. J. Chem. Downloaded from www.nrcresearchpress.com by 210.87.254.40 on 09/05/12
For personal use only.

Microwave spectrum and conformation of tetrahydropyran

V. M. RAO[1] AND R. KEWLEY
Department of Chemistry, Queen's University, Kingston, Ontario
Received October 4, 1968

The microwave spectrum of tetrahydropyran has been recorded in the region 8–40 GHz. The rotational constants of the molecule in its ground vibrational state are, in MHz, $A = 4673.48 \pm 0.05$, $B = 4495.02 \pm 0.11$, and $C = 2601.31 \pm 0.05$. The dipole moment components are, in Debye units, $\mu_a = 1.53 \pm 0.02$, $\mu_c = 0.82 \pm 0.02$, and $\mu = 1.74 \pm 0.03$. The direction of μ with respect to the principal axes of rotation together with the rotational constants show that the observed spectrum is due to the chair form of tetrahydropyran.

Canadian Journal of Chemistry, **47**, 1289 (1969)

Can. J. Chem. Downloaded from www.nrcresearchpress.com by 210.87.254.105 on 09/05/12
For personal use only.

Introduction

Tetrahydropyran is a cyclic ether of structure

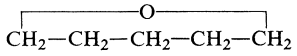

Other compounds of similar structure for which microwave spectra are known are sym-trioxane (1), which is an oblate symmetric top, piperidine (2), and cyclohexanone (3). All three molecules were shown to have the chair form structure for the ring atoms.

A study of the rotational spectrum of tetrahydropyran was undertaken in order to establish the conformation of the molecule and also to discover whether or not the spectrum showed any unusual effects due to excited vibrational states involving distortion of the ring.

Experimental

The spectrum was recorded using a Stark modulation spectrometer.

Varian klystrons type X13 and X12 were selected to cover the frequency range 8–16 GHz and OKI tubes 17V10, 20V10, 24V10, and 30V11 for the range 16–31 GHz, using an FXR model Z815B power supply. The klystron sawtooth sweep voltage was obtained by amplification of a signal from a Tektronix model 502A dual beam oscilloscope. The oscilloscope was also the display unit for the spectrum and frequency markers. Both the klystron and crystal detector were coupled to the main microwave system through ferrite isolators, giving an improved signal-to-noise ratio.

The 100 kHz Stark modulation and detection was achieved with an Industrial Components Incorporated square-wave generator, preamplifier, and receiver, the latter operating in its phase sensitive detection mode.

Frequency measurements were made by taking the output of a Micronow model 101D frequency standard followed by a Micronow model 301 frequency multiplier, and beating this output with the klyston frequency in the appropriate Micronow model 600 series side arm. The difference in frequency was then fed to a Hallicrafters model SX-62A receiver operating at one of its calibration points. The receiver output was delivered to the oscilloscope, thus providing the frequency marker trace. The marker position was varied by altering the frequency of the model 101D. All frequency measurements were made using both forward and reverse sawtooth sweeps. The 5 MHz fundamental frequency, variable ± 15 kHz, of the model 101D frequency standard was measured by difference using a Micronow model 501 frequency converter. The beat frequency was determined by a Hewlett Packard model 521C 100 kHz counter. The model 501 frequency converter could be checked against the WWV standard 5 MHz signal. Frequency measurements are considered accurate to ± 0.10 MHz.

Sample pressures in the range 10–100 μ were used when recording the spectrum. On account of the very small vapor pressure of tetrahydropyran at dry-ice temperature the measurements were made at temperatures in the range 230–300 °K.

The sample used was obtained from K and K laboratories and was used without further purification.

Results

Rotational Spectrum

Although the spectrum contains many unassigned, presumably high J, lines, it was possible to pick out series of Q-branch absorption peaks with series heads occurring about every 4000 MHz. Each such series is formed from transitions of the ${}^aQ_{0,1}$ and ${}^aQ_{2,-1}$ sub-branches. From these frequencies, given in Table I, approximate values of $(A - C)/2$ and the asymmetry parameter κ were obtained which assisted in the assignment of low J R-branch transitions. The latter were confirmed by their Stark patterns. Both a- and c-type R-branch transitions were observed, as shown in Table II.

The spectrum is that of slightly asymmetric oblate top with the unusual feature that μ_c is the

[1]Present address: Physics Department, Aligarh Muslim University, Aligarh, Uttar Pradesh, India.

Can. J. Chem. Downloaded from www.nrcresearchpress.com by 210.87.254.105 on 09/05/12
For personal use only.

TABLE I

Q-branch transitions of tetrahydropyran (ground vibrational state)

Transition	ν_{obsd} (MHz)	$\nu_{obsd} - \nu_{calcd}$ (MHz)
5_{15}–5_{14}	17821.80	0.27
6_{15}–6_{34}	17811.00	−0.13
7_{25}–7_{44}	17794.20	−0.66
7_{35}–7_{34}	17792.30	0.38
8_{35}–8_{54}	17771.20	−0.54
8_{45}–8_{44}	17763.40	0.47
9_{45}–9_{64}	17741.40	0.08
6_{16}–6_{15}	21784.40	0.22
7_{26}–7_{25}	21775.20	0.08
8_{36}–8_{35}	21761.00	−0.53
9_{46}–9_{45}	21741.90	−0.12
10_{46}–10_{65}	21716.90	−0.34
10_{56}–10_{55}	21714.66	−0.21

TABLE II

R-branch transitions of tetrahydropyran (ground vibrational state)

Transition	ν_{obsd} (MHz)	$\nu_{obsd} - \nu_{calcd}$ (MHz)
a-type		
1_{11}–2_{12}	12299.00	0.04
1_{01}–2_{02}	12465.20	−0.18
1_{10}–2_{11}	16086.40	0.02
2_{12}–3_{13}	17583.40	−0.12
2_{02}–3_{03}	17594.70	−0.34
2_{21}–3_{22}	21289.10	0.10
2_{11}–3_{12}	21764.40	−0.19
3_{22}–4_{23}	26729.30	−0.12
3_{12}–4_{13}	26785.50	−0.15
3_{31}–4_{32}	30191.90	0.00
c-type		
1_{01}–2_{11}	18158.80	0.25
1_{10}–2_{20}	18349.40	0.36
1_{11}–2_{21}	18515.80	0.33
2_{12}–3_{22}	27505.60	0.09
2_{20}–3_{30}	27553.60	0.34
2_{21}–3_{31}	27780.40	−0.07

lesser component of the dipole moment, so that the *a*-type rather than the *c*-type transitions are predominant, see Fig. 1. There is no *b*-component of μ.

The rotational constants were calculated by applying a least squares fit to the 29 lines in Tables I and II, neglecting the effects of centrifugal stretching. The fit was achieved with a standard deviation of 0.29 MHz. The resulting rotational constants are given in Table III.

Dipole Moment

Stark measurements were carried out on both *a*- and *c*-type lines of the $J = 1$–2 transition. The squared dipole moment components μ_a^2 and μ_c^2 were obtained from a least squares fit of the observed coefficients $\Delta\nu/E^2$. The Stark cell was calibrated with carbonyl sulfide using the value of $\mu_{OCS} = 0.7124 \pm 0.0002$ D (4). The Stark measurement data and the dipole moment components are given in Table IV.

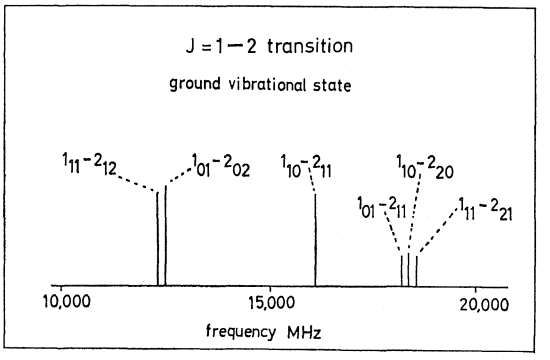

FIG. 1. The $J = 1$–2 transition of tetrahydropyran showing the relative intensities of the *a*-type and *c*-type transitions.

Conformation

To determine the complete r_s structure of tetrahydropyran, it would be necessary to carry out isotopic substitution on the oxygen, three of the carbons, and six of the hydrogen atoms. Since only one isotopic form has been investigated in the present work, detailed structural information cannot be obtained from the observed rotational constants.

The observed constants may, however, be compared with those calculated from reasonable bond lengths and angles assuming that the molecule could exist in either the boat or chair conformation. Taking Hendrickson's values for C—H and C—C of 1.108 and 1.533 Å respectively (5), assuming that all bond angles at carbon are 109° 28′ and that the C—O distance and C—O—C angle are 1.410 Å and 111° 43′ respectively, as in dimethyl ether (6), the calculated rotational constants are as given by Table V.

Comparison of these figures with the observed ones does not allow a clear decision to be made as to which of the two forms gives rise to the observed spectrum, although the chair form is favored. A more detailed consideration of the dipole moment components does enable this to be done. The observed total dipole moment of 1.74 D is very close to the value 1.75 D found for tetrahydrofuran from its microwave spectrum (7), and it can, therefore, be concluded that the main contribution to the molecular dipole moment arises

TABLE III

Rotational constants and principal moments of inertia of tetrahydropyran* in the ground vibrational state

Rotational constant	Value (MHz)	Principal moments of inertia	Value (u Å²)	κ
A	4673.48±0.05	I_a	108.136	0.82776±0.00007
B	4495.02±0.11	I_b	112.429	
C	2601.31±0.05	I_c	194.276	

*Conversion factor 5.05371 MHz u Å², mass of C^{12} = 12.0000.

TABLE IV

Stark effect coefficients and dipole moment components of tetrahydropyran

Transition	M	$10^4 \times \Delta\nu/E^2$ (MHz cm² V⁻²) Observed	Calculated	Dipole moment	Value(D)
1_{01}–2_{02}	0	−0.1306	−0.1283	μ_a	1.53±0.02
1_{10}–2_{11}	1	−0.7601	−0.7625	μ_c	0.82±0.02
1_{10}–2_{11}	0	0.0547	0.0567	μ	1.74±0.03
1_{11}–2_{12}	0	0.1246	0.1269		
1_{10}–2_{20}	1	−0.4271	−0.4266		

TABLE V

Calculated rotational constants of tetrahydropyran

Conformation	Rotational constants A (MHz)	B (MHz)	C (MHz)	κ
Chair	4676.82	4558.71	2643.64	0.88382
Boat	4739.02	4517.20	2759.64	0.76816

TABLE VI

Vibrational satellite lines from the $v = 1$ state of lowest frequency ring deformation mode

Transition	ν_{obsd} (MHz)	$\nu_{obsd} - \nu_{calcd}$ (MHz)
R-branch, *a*-type		
1_{11}–2_{12}	12264.2	0.1
1_{01}–2_{02}	12433.9	0.3
1_{10}–2_{11}	16061.2	0.1
2_{02}–3_{03}	17542.2	0.0
2_{12}–3_{13}	17530.2	−0.1
R-branch, *c*-type		
1_{01}–2_{11}	18141.8	0.3
1_{10}–2_{20}	18335.7	−0.2
1_{11}–2_{21}	18506.0	0.7
Q-branch, *a*-type		
5_{15}–5_{14}	17878.9	−0.4
6_{25}–6_{24}	17867.4	−0.2
7_{35}–7_{34}	17848.9	0.4
9_{55}–9_{54}	17771.8	−0.3
6_{16}–6_{15}	21854.1	−0.7
7_{26}–7_{25}	21845.4	0.0

from the C—O bond moment. Assuming that the total dipole lies along the bisector of the C—O—C angle in the C—O—C plane and using the same assumed structural parameters as above, then it is calculated that for the chair form the μ vector should be inclined at 35° 30′ to the molecular principal *a*-axes, but that in the boat form μ makes an angle 56° with the *b*-axis and that only *b*- and *c*-type transitions would be expected to occur for the boat form, as illustrated in Fig. 2.

The observed angle between μ and μ_a of 28° 22′ is, therefore, in good agreement with the chair structure of tetrahydropyran. Although a search was carried out for a spectrum due to the boat form, no lines could be found due to this isomer.

Excited Vibrational States

Each of the transitions 1_{11}–2_{12}, 1_{01}–2_{02}, and

Can. J. Chem. Downloaded from www.nrcresearchpress.com by 210.87.254.105 on 09/05/12
For personal use only.

TABLE VII

Rotational constants for $v = 1$ states of four of the ring deformation modes

State	Rotational constants			
	A (MHz)	B (MHz)	C (MHz)	κ
I	4671.8±0.1	4489.9±0.2	2591.4±0.1	0.8251±0.0002
II	4665.2	4494.2	2608.6	0.8337
III	4661.3	4493.8	2611.4	0.8366
IV	4678.4	4493.2	2592.8	0.8224

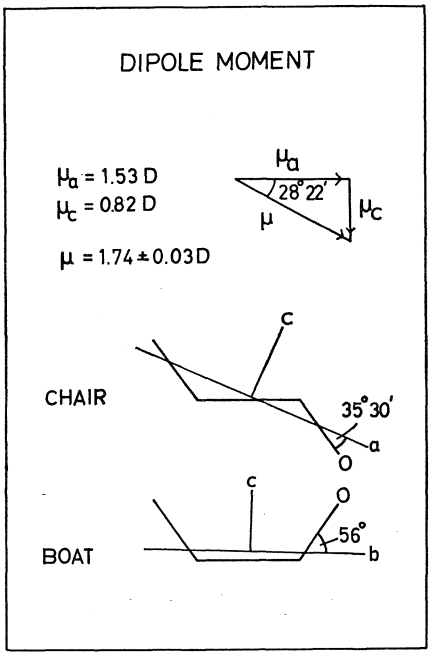

FIG. 2. The relationship between the direction of the total dipole moment vector and the principal axes of tetrahydropyran; 28° 22′ is the observed angle. The figure shows also calculated angles using Hendrickson's values of C—C and C—H (5), tetrahedral carbons and the C—O—C angle, and C—O distance as in dimethyl ether (6).

1_{10}–2_{11} has, associated with the absorption peak due to the ground vibrational state of the molecule, 4 weak satellite lines. No intense satellites of the type characteristic of pseudorotation were present. This phenomenon would not be expected to occur for a molecule that has the relatively rigid chair form structure.

The vibrational satellites can be attributed to 4 of the 6 of the ring deformation frequencies, which are all known to be below 800 cm^{-1} (8). The lowest frequency ring deformation mode occurs in the region of 256 cm^{-1} (8, 9). The first excited state of this vibration is very likely responsible for the lines given in Table VI.

The rotational constants for this state (I) and the other three excited states (II, III, IV) are given in Table VII. For states II, III, and IV the rotational constants were obtained using only lines in the $^aR_{0,1}$ $J = 1$–2 transition.

The next lowest ring deformation frequencies after 256 cm^{-1} are 276, 403, and 434 cm^{-1} (8, 9) which, from the intensities, probably correspond to the states II, III, and IV respectively.

A further ring deformation which might affect the spectrum is the motion

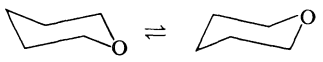

for which nuclear magnetic resonance data (10) give an activation energy or barrier height of 10.5 kcal/mole. This inversion motion causes a reversal of the dipole moment component μ_c and might be expected to cause splitting of the *c*-type transitions. Very few *c*-type lines were recorded and, of those that were, only the 1_{01}–2_{11} and 1_{11}–2_{21} transitions were observed to have pairs of lines, with separations 0.8 Mc. The lines making up these doublets did not show the same intensity relationship for the two transitions and quite possibly could be the unsplit rotational transitions accidentally situated near unidentified high J Q-branch transitions. A doublet was not found for the 1_{10}–2_{20} transition or for any of the other *c*-type R-branch transitions in Table II.

Conclusion

The rotational spectrum of tetrahydropyran shows the molecule to be in the chair form as are the related molecules sym-trioxan (1), piperidine (2), and also cyclohexanone (3). No spectrum from the boat form or any effect that could be definitely attributed to pseudorotation or to inversion of the chair form was found. The observed vibrational satellites are considered to be due solely to deformation modes of the ring with frequencies in the range 250–500 cm^{-1}.

Can. J. Chem. Downloaded from www.nrcresearchpress.com by 210.87.254.105 on 09/05/12
For personal use only.

1. T. OKA, K. TSUCHIYA, S. IWATA, and Y. MORINO. Bull. Chem. Soc. Japan, **37**, 4 (1964).
2. P. J. BUCKLEY, C. C. COSTAIN, and J. E. PARKIN. Chem. Commun. 668 (1968).
3. Y. OHNISHI and K. KOZIMA. Bull. Chem. Soc. Japan, **41**, 1323 (1968).
4. S. A. MARSHALL and J. WEBER. Phys. Rev. **105**, 1502 (1957).
5. J. B. HENDRICKSON. J. Am. Chem. Soc. **83**, 4537 (1961).
6. U. BLUKIS, P. H. KASAI, and R. J. MYERS. J. Chem. Phys. **38**, 2753 (1963).
7. G. G. ENGERHOLM. Dissertation Abstr. **26**, 7060 (1966).
8. H. PICKETT. Private communication.
9. P. A. AKISHIN, N. G. RAMBIDI, I. K. KOROBITSYNA, G. YA. KONDRAT'EVA, and YU. K. YUR'EV. Vestnik Moskov. Univ. **10**, No. 12, Ser. Fiz. Mat. i Estestven. Nauk. No. 8, 103 (1955). See also Chem. Abstr. **56**, 8330d (1956).
10. G. GATTI, A. L. SEGRE, and C. MORANDI. J. Chem. Soc. B, 1203 (1967).

Can. J. Chem. Downloaded from www.nrcresearchpress.com by 210.87.254.105 on 09/05/12
For personal use only.

Erratum Pg 1289

When recalibrating the Stark cell during the determination of the dipole moment of 1,3-dioxane, an error was discovered in the earlier calibration, which had been used in the calculations of the dipole moments of tetrahydropyran (1) and morpholine (2). Correcting this calculation error and using the same experimental data (1, 2) the corrected values are:

	μ_a(D)	μ_c(D)	μ(D)
Tetrahydropyran	1.39(0.02)	0.74(0.02)	1.58(0.03)
Morpholine	1.53(0.01)	0.27(0.01)	1.55(0.02)

The μ values agree well with those measured in benzene solution of 1.55 (3) and 1.52 D(4), respectively.

Also in Table IX of the morpholine publication (2), the transition given as 2_{12}—3_{22} is actually 2_{21}—3_{22}.

1. V. M. Rao and R. Kewley. Can. J. Chem. 47, 1289 (1969).
2. J. J. Sloan and R. Kewley. Can. J. Chem. 47, 3453 (1969).
3. C. W. N. Cumper and A. I. Vogel. J. Chem. Soc. 3521 (1959).
4. M. Aroney and R. J. W. Lefèvre. J. Chem. Soc. 3002 (1958).

Can. J. Chem. Downloaded from www.nrcresearchpress.com by 210.87.254.105 on 09/05/12
For personal use only.

Effect of solvent and temperature upon the rotationally averaged vicinal coupling constants of some substituted 1,2-dibromoethanes

W. F. Reynolds and D. J. Wood
Department of Chemistry, University of Toronto, Toronto 5, Ontario
Received September 3, 1968

The solvent dependence of vicinal coupling constants has been investigated for (1,2-dibromoethyl)-benzene and three of its 4-substituted derivatives and for threo- and erythro(1,2-dibromopropyl)benzene. The temperature dependence of the vicinal coupling constants of three of the compounds has also been investigated. The difference between the two vicinal coupling constants of (1,2-dibromoethyl)benzene is dependent upon solution dielectric constant (in non-aromatic solvents) while the sum of coupling constants remains constant. The relative stabilities of its three rotamers are deduced from this information. A polar substituent in the 4-position does not affect the rotational equilibrium in any predictable manner. The vicinal coupling constant of threo(1,2-dibromopropyl)benzene is strongly solvent dependent. The relative stabilities of its three rotamers are deduced from the observation that the vicinal coupling constant is temperature independent. The most stable rotamer of erythro(1,2-dibromopropyl)-benzene is deduced from the observation that the vicinal coupling constant is large and independent of solvent. Factors affecting conformational preference are deduced. It is concluded that dipolar interactions are as important as steric interactions.

Canadian Journal of Chemistry, 47, 1295 (1969)

Can. J. Chem. Downloaded from www.nrcresearchpress.com by 210.87.254.40 on 09/05/12
For personal use only.

Introduction

Rotational isomerism in substituted ethanes has been widely investigated by nuclear magnetic resonance (n.m.r.) spectroscopy (1). In the most commonly applied technique (2), energy differences, ΔE, between rotational isomers (rotamers) are estimated from the temperature dependence of averaged vicinal coupling constants, $\langle J_{ij} \rangle$, and chemical shifts. Values of ΔE and the coupling constants for the "frozen" rotamers are determined by a least squares fitting technique. However, it has recently been shown that the value of ΔE and coupling constants for the frozen rotamers of 1,1,2,2-tetrabromofluoroethane measured directly at low temperatures are much different than those obtained from $\langle J_{HF} \rangle$ at high temperatures (3). This was attributed to the insensitivity of the least squares fitting technique. It has also been pointed out that the values of ΔE are temperature dependent (4). Consequently, the above-discussed technique is of doubtful accuracy.

It is well established that for substituted ethanes containing two or more polar groups, the more polar rotamers increase in fractional population upon going from the gas phase to a polar medium (5). Solvent dependent changes in rotationally averaged coupling constants have been noted and interpreted in terms of population changes with change in solvent dielectric constant (6). Recently, Abraham and co-workers have developed a theory which allows one to predict the change in energy difference between rotamers upon going from the gas phase to a solution of dielectric constant ε (4). Then if ΔE is known in the gas phase, ΔE can be determined in the liquid phase. This approach has been successfully applied to a number of simple substituted ethanes (7) and has been extended to include compounds containing three or more polar groups (8).

It is much more difficult to apply this technique quantitatively to the investigation of conformational preference in complex substituted ethanes. Firstly, one generally has no knowledge of the energy differences either in gas phase or in solution; in fact, this is the information one would like to obtain. Secondly, one must also know the molecular volume, polarizability, etc. These quantities are often unavailable. However, it was decided to investigate whether at least semiquantitative information concerning conformational preference could be obtained from an investigation of the effect of ε and, where necessary, temperature upon $\langle J_{ij} \rangle$ for complex substituted ethanes.

A previous investigation of this type had been carried out by Snyder (9). He investigated the effect of a limited number of solvents upon chemical shifts and coupling constants of 12 trisubstituted ethanes (9*a*). He also developed semiempirical relationships which allowed one to estimate ΔE from $\langle J_{ij} \rangle$ (9*c*). It was concluded that changes in energy differences between

Can. J. Chem. Downloaded from www.nrcresearchpress.com by 210.87.254.40 on 09/05/12
For personal use only.

rotamers were only weakly related to the solvent dielectric constant. However, we felt that this conclusion might be incorrect because it was based upon results in a limited number of solvents and because the solutions investigated were very concentrated (40 wt./vol. %).

The initial compounds chosen for this investigation were (1,2-dibromoethyl)benzene and three 4-substituted (1,2-dibromoethyl)benzenes. These compounds were chosen for two main reasons. Firstly, the most stable rotamer of (1,2-dibromoethyl)benzene had been determined by specific deuteration experiments (9*b*). Therefore, it was possible to check the conclusions from the solvent effect investigation. Secondly, it was considered important to determine the effect of the remote dipolar groups. 4-Substituted (1,2-dibromoethyl)benzenes were chosen since the effect of a remote dipole could be determined by direct comparison with the results for the parent compound. In addition, the orientation of the remote dipole with respect to the substituted ethane group would be unaffected by rotation about the carbon–phenyl bond and no additional steric hindrance would be added to the system.

Erythro- and threo(1,2-dibromopropyl)benzene were investigated as examples of substituted ethanes in which there is only one vicinal coupling constant.

In this paper, results are presented for the six compounds mentioned above.

Experimental

(1,2-Dibromoethyl)benzene was prepared by the bromination of styrene in methylene chloride. The corresponding 4-substituted derivatives were prepared by bromination of 4-substituted styrenes in carbon tetrachloride. Erythro(1,2-dibromoethyl)benzene was prepared by bromination of *trans*-propenylbenzene in methylene chloride while the threo isomer was prepared by bromination of *cis*-propenylbenzene in carbon tetrachloride. All reactions were carried out in the dark. The starting materials were obtained commercially and were used without purification. Solid products were purified by recrystallization from methanol–water. The only liquid product, threo(1,2-dibromopropyl)benzene, contained approximately 20–25% of the erythro isomer as an impurity. Attempts to purify this compound by vapor phase chromatography and by low temperature recrystallization were unsuccessful and it was used unpurified.

Spectra were recorded on a Varian HA-100 spectrometer operating in frequency sweep mode at a probe temperature of 30 °C (except for variable temperature experiments). The variable temperature controller was calibrated using standard calibration samples before each variable temperature experiment.

Spectra were recorded at a sweep rate of 0.05 Hz/s. The spectra were recorded twice in each direction for all coupling constant measurements. Spectra were calibrated by measuring the frequency difference between the lock and sweep oscillators, using a Hewlett–Packard 5253B frequency counter in period average mode.

Samples were usually 0.30 *M* in solute. Samples were deoxygenated by bubbling N_2 through them. Five percent tetramethylsilane was added as a lock and reference signal. Any solvents which were not analytical reagent grade were distilled prior to use.

Solution dielectric constants were measured with a W.T.W. DKO3 dekameter.

Results

Spectral analyses of the ABC spectra of the 1,2-dibromoethyl groups of (1,2-dibromoethyl)-benzene and its para substituted derivatives were carried out by the exact method (10), using the computer program EXAN. Iterative analyses were also attempted, using the computer program LAOCN3 (11). The former method was found to be superior for this system. It provided all possible solutions while the iterative method provided only one solution in each case. The latter solution depended upon the choice of approximate input parameters. This is extremely important in this system since in several cases two solutions were obtained with the correct signs for the coupling constant (9*b*), i.e., with both vicinal coupling constants positive and the geminal coupling constant negative. This can be understood by considering that the spectrum is an approximate ABX spectrum. The AB part consists of two quartets or subspectra (12) (see Fig. 1). The two solutions correspond to the two possible signs of the apparent chemical shift (12) of the nearly collapsed quartet. In most cases, the correct solution was chosen on the basis that the vicinal coupling constant in erythro(1,2-dibromoethyl-2-*d*)benzene has a value of 10.5 to 11.0 Hz (9*b*). The correct solution for (1,2-dibromoethyl)benzene in benzene was chosen on a basis which will be discussed later. Results for (1,2-dibromoethyl)benzene are given in Table I while results for its para substituted derivatives are given in Table II.

The 1,2-dibromopropyl groups of erythro- and threo(1,2-dibromopropyl)benzene gave ABC_3 spectra. A complete ABC_3 spectral analysis was carried out for the erythro isomer in carbon tetrachloride, using the computer program LAOCN3. It was found that the doublet splittings of the A proton and the C_3 methyl

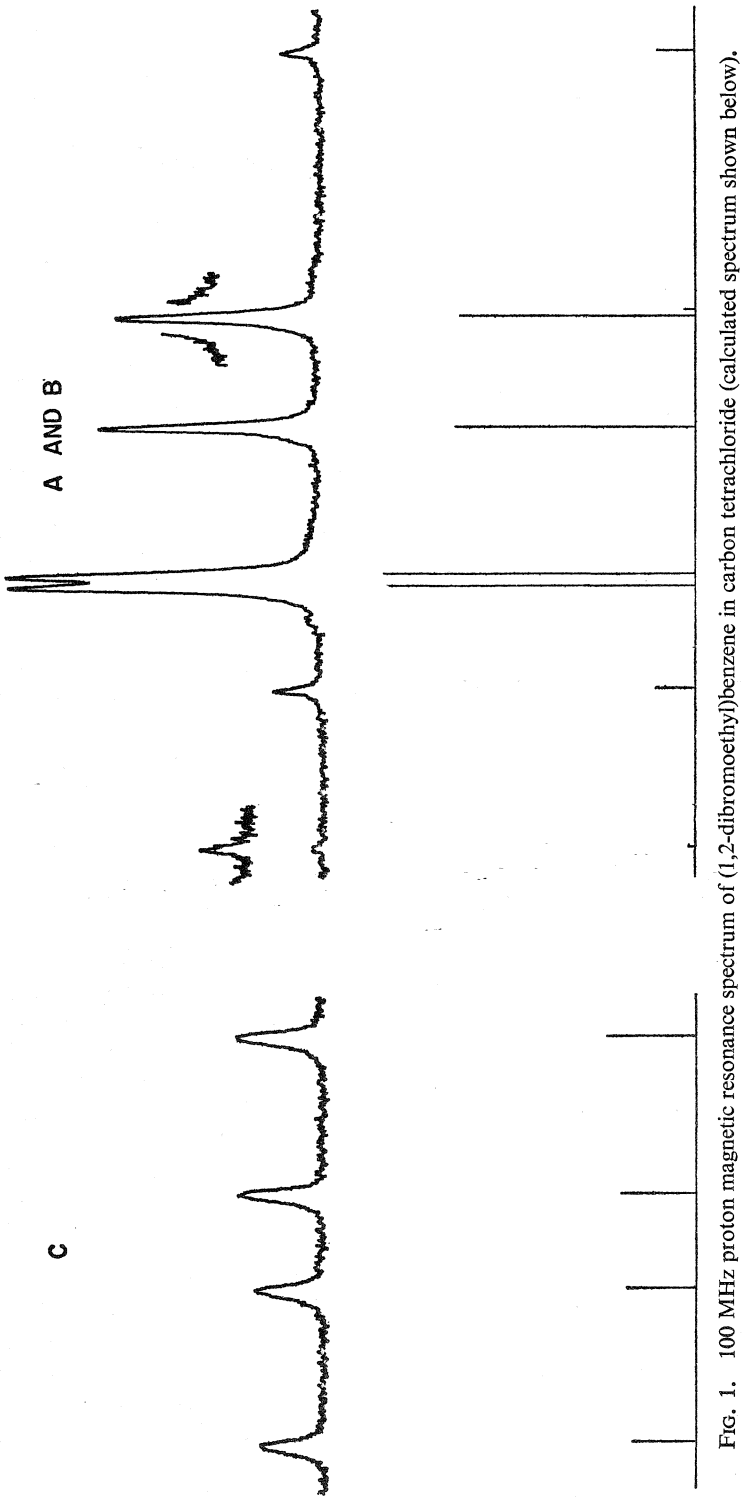

FIG. 1. 100 MHz proton magnetic resonance spectrum of (1,2-dibromoethyl)benzene in carbon tetrachloride (calculated spectrum shown below).

Can. J. Chem. Downloaded from www.nrcresearchpress.com by 210.87.254.40 on 09/05/12
For personal use only.

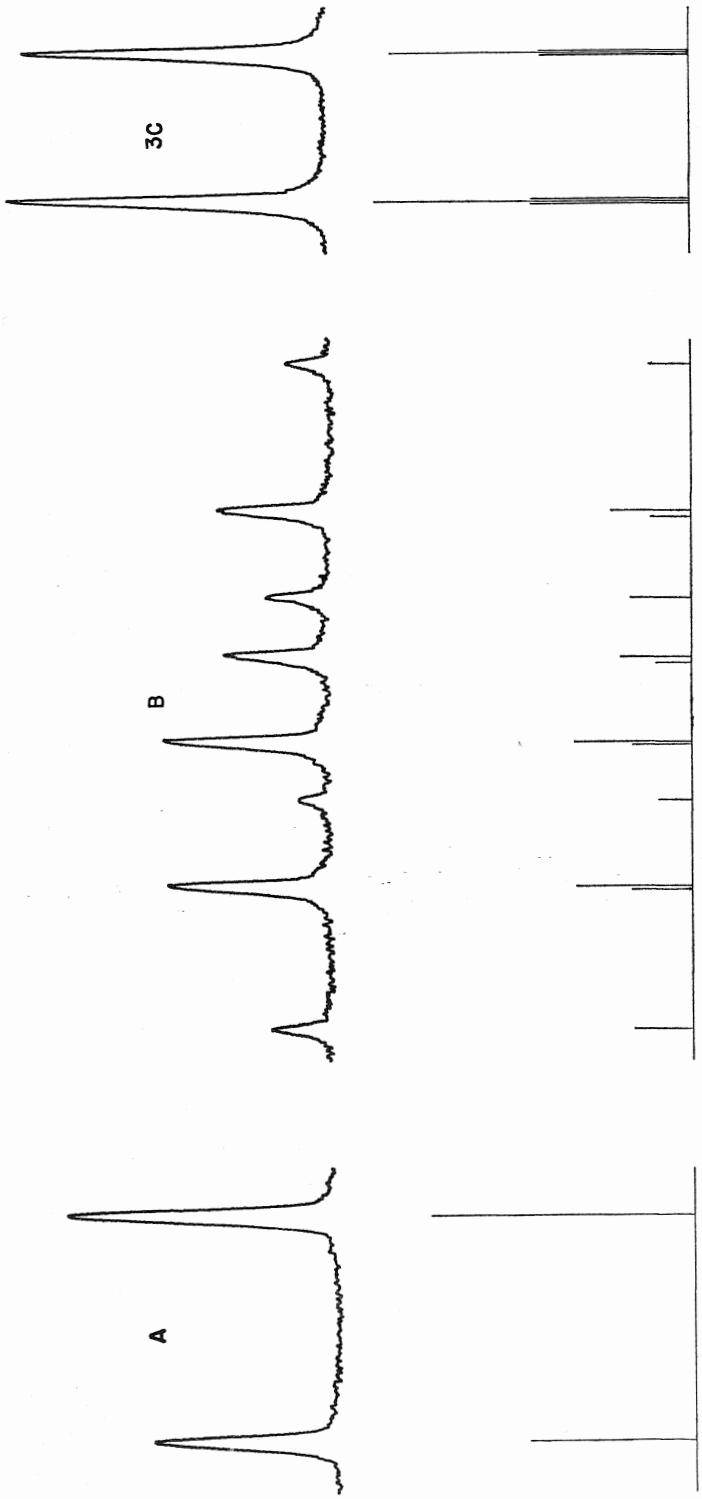

FIG. 2. 100 MHz proton magnetic resonance spectrum of erythro(1,2-dibromopropyl)benzene in carbon tetrachloride. Spectrum amplitude is reduced by a factor of two for methyl protons. (Calculated spectrum shown below.) The calculated spectrum of the A proton actually consists of two multiplets. The multiplet line positions are too close to coincidence to represent separately.

Can. J. Chem. Downloaded from www.nrcresearchpress.com by 210.87.254.40 on 09/05/12
For personal use only.

Can. J. Chem. Downloaded from www.nrcresearchpress.com by 210.87.254.40 on 09/05/12
For personal use only.

TABLE I

Chemical shifts (in p.p.m. to low field of tetramethylsilane) and coupling constants (in Hz) for (1,2-dibromoethyl)benzene

Solvent	ε	$\langle J_{AB} \rangle$	$\langle J_{AC} \rangle$	$\langle J_{BC} \rangle$	$\langle J_{AC} \rangle + \langle J_{BC} \rangle$	$\langle J_{AC} \rangle - \langle J_{BC} \rangle$	δ_A	δ_B	δ_C	$\delta_A - \delta_B$	Root-mean-square error (Hz)
Hexane	1.98	−10.14	10.95	5.03	15.98	5.92	3.859	3.926	4.979	−0.067	0.05*
Cyclohexane	2.07	−10.14	11.04	4.98	16.02	6.06	3.857	3.924	4.974	−0.067	0.05
Carbon tetrachloride	2.30	−10.12	11.07	5.00	16.07	6.07	3.950	4.015	5.055	−0.065	0.02
Benzene	2.31	−10.28	10.53	5.42	15.95	5.11	3.544	3.573	4.685	−0.029	0.03
	†	(−10.28)	(10.95)	(5.00)	(15.95)	(5.95)	(3.546)	(3.571)	(4.685)	(−0.025)	(0.03)
Carbon disulfide	2.59	−10.14	10.97	4.96	15.93	6.01	3.918	3.979	5.010	−0.061	0.02
Chloroform-*d*	4.26	−10.23	10.90	5.16	16.06	5.74	4.007	4.057	5.128	−0.050	0.03
t-Butyl chloride	8.40	−10.26	10.82	5.15	15.97	5.67	3.976	4.017	5.115	−0.041	0.02
Acetone	18.1	−10.33	10.55	5.39	15.94	5.16	4.245	4.191	5.396	+0.054	0.03
Dimethylsulfoxide	42.4	−10.19	10.41	5.62	16.03	4.79	4.358	4.238	5.526	+0.120	0.01

*Root-mean-square deviation between experimental and calculated peak positions.
†Alternate solution.

Can. J. Chem. Downloaded from www.nrcresearchpress.com by 210.87.254.40 on 09/05/12
For personal use only.

TABLE II

Chemical shifts (in p.p.m. to low field of tetramethylsilane) and coupling constants (in Hz) for 4-substituted (1,2-dibromoethyl)benzene

Substituent	Solvent	ε	$\langle J_{AB} \rangle$	$\langle J_{AC} \rangle$	$\langle J_{BC} \rangle$	$\langle J_{AC} \rangle + \langle J_{BC} \rangle$	$\langle J_{AC} \rangle - \langle J_{BC} \rangle$	δ_A	δ_B	δ_C	Root-mean-square error (Hz)
4-Chloro	Carbon tetrachloride	2.25	−10.28	11.40	4.80	16.20	6.60	3.906	4.012	5.030	0.05*
4-Chloro	Benzene	2.28	−10.32	10.94	5.14	16.08	5.80	3.388	3.475	4.513	0.01
4-Chloro	*t*-Butyl chloride	8.50	−10.28	10.87	5.11	15.98	5.76	3.940	4.017	5.101	0.05
4-Chloro	Dimethylsulfoxide	†	−10.20	10.59	5.56	16.15	5.03	4.368	4.239	5.570	0.02
4-Methoxy	Carbon tetrachloride	2.41	−10.26	11.22	4.90	16.12	6.32	3.936	4.010	5.065	0.08
4-Methoxy	Benzene	2.38	−10.22	10.75	5.28	16.03	5.47	3.616	3.656	4.785	0.01
4-Methoxy	*t*-Butyl chloride	9.27	−10.17	10.87	5.17	16.04	5.70	3.970	4.017	5.132	0.03
4-Methoxy	Acetone	†	−10.21	10.54	5.57	16.11	4.97	4.223	4.169	5.389	0.02
4-Nitro	Carbon tetrachloride	2.67	−10.38	11.52	4.74	16.26	6.78	3.962	4.069	5.134	0.02
4-Nitro	Benzene	2.66	−10.35	11.06	5.19	16.25	5.87	3.297	3.397	4.407	0.06
4-Nitro	*t*-Butyl chloride	9.48	−10.36	11.14	4.88	16.02	6.26	3.991	4.065	5.205	0.03
4-Nitro	Dimethylsulfoxide	46.8	−10.18	10.59	5.45	16.04	5.14	4.435	4.292	5.717	0.01

*Root-mean-square deviation between experimental and calculated peak positions.
†Cell malfunction prevented measurement of the dielectric constants of these solutions.

TABLE III

Chemical shifts (in p.p.m. to low field of tetramethylsilane) and coupling constants (in Hz) for threo- and erythro(1,2-dibromopropyl)benzene

Isomer	Solvent	ε	$\langle J_{AB} \rangle$	$\langle J_{BC} \rangle$	δ_A	δ_B	δ_C
Threo	Carbon tetrachloride	2.32	5.28	6.81	5.19_0	4.53_9	1.69_6
Threo	Benzene	2.38	5.75	6.74	4.87_6	4.20_0	1.36_1
Threo	Chloroform-*d*	4.33	5.68	6.73	5.22_1	4.59_0	1.69_8
Threo	*cis*-Dichloroethylene	7.95	5.85	6.78	5.18_4	4.56_0	1.66_5
Threo	*t*-Butyl chloride	8.78	5.66	*	5.20_7	4.55_0	*
Threo	Acetone	18.90	6.15	6.71	5.41_6	4.72_5	1.68_5
Threo	Dimethylsulfoxide	†	6.13	6.67	5.56_7	4.81_7	1.63_5
Erythro	Carbon tetrachloride	2.23	10.25	6.41	4.94_4	4.50_1	2.02_7
Erythro	Benzene	2.28	10.12	6.51	4.70_9	4.19_7	1.72_1
Erythro	Chloroform-*d*	4.18	10.16	6.42	5.02_9	4.58_6	2.03_0
Erythro	*cis*-Dichloroethylene	7.88	10.18	6.42	4.99_8	4.56_2	1.99_1
Erythro	*t*-Butyl chloride	8.25	10.08	*	5.01_9	4.55_8	*
Erythro	Acetone	18.60	10.10	6.42	5.30_2	4.83_6	2.00_1
Erythro	Acetonitrile	32.20	10.32	*	5.23_3	4.78_2	*
Erythro	Dimethylsulfoxide	†	10.19	6.41	5.48_5	4.99_1	1.95_2

*Interference with solvent peak prevented measurement.
†Cell malfunction prevented measurement of the dielectric constants of these solutions.

protons (see Fig. 2) correspond within 0.01 Hz to the calculated values of $\langle J_{AB} \rangle$ and $\langle J_{BC} \rangle$. Consequently $\langle J_{AB} \rangle$ and $\langle J_{BC} \rangle$ were determined by measuring these splittings. Results are given in Table III.

Values of coupling constants for erythro- and threo(1,2-dibromopropyl)benzene are estimated to be accurate within 0.05 Hz. It is more difficult to estimate the accuracy of the coupling constants for the (1,2-dibromoethyl)benzene compounds since the coupling constants do not correspond to first order splittings. "Probable errors" determined by LAOCN3 ranged from 0.01 to 0.1 Hz with the largest errors found when the chemical shift difference of the methylene protons approached zero.

Results of variable temperature experiments are given in Table IV. Results for concentration dependence experiments are given in Table V.

Discussion

A. (1,2-Dibromoethyl)benzene

The three staggered rotamers for (1,2-dibromoethyl)benzene are shown in Fig. 3. There is a bromine–phenyl steric interaction in rotamer **1**, a bromine–bromine steric and a dipolar interaction in rotamer **2**, and two steric and one dipolar interaction in rotamer **3**. On this basis one would expect rotamer **3** to be the least stable. It is difficult to predict the relative stabilities of rotamers **1** and **2**. However, one can make certain predictions concerning the effect of the dielectric constant, ε, upon the vicinal coupling constants. The more polar rotamers (**2** and **3**) should be relatively more stable in solutions of high ε. If rotamer **1** is the most stable rotamer in solutions of low ε, then $\langle J_{AC} \rangle$ should be large but should decrease as ε increases (since protons A and C are *trans* in rotamer **1** and *gauche* in the other rotamers). Correspondingly $\langle J_{BC} \rangle$ should be small but should increase with ε (since protons B and C are *gauche* in rotamer **1** and *trans* in rotamer **2**), i.e., the difference between the coupling constants should decrease as ε increases. On the other hand, the reverse effect would be noted if rotamer **2** is the most stable rotamer. $\langle J_{BC} \rangle$ should be larger than $\langle J_{AC} \rangle$ and the former should increase and the latter should decrease as ε increases, i.e., the difference in coupling constants should increase as ε increases. In rotamer **3** both coupling constants are *gauche*. Consequently any increase in the population of rotamer **3** with ε should lead to a decrease in $(\langle J_{AC} \rangle + \langle J_{BC} \rangle)$[1]. The fractional population of rotamer **3**, p_3, is expected to increase with increasing ε. However, this increase would be negligible if rotamer **3** is considerably less stable than the non-polar rotamer **1**, since p_3 would then be small in all solvents.

[1]This and preceding arguments depend upon the assumption that *trans* proton coupling constants are larger than *gauche* proton coupling constants. Small variations of *gauche* or *trans* coupling constants between different rotamers will not significantly affect these arguments.

Can. J. Chem. Downloaded from www.nrcresearchpress.com by 210.87.254.40 on 09/05/12
For personal use only.

TABLE IV

Temperature dependence of vicinal coupling constants (in Hz) for (1,2-dibromoethyl)-benzene and threo- and erythro(1,2-dibromopropyl)benzene

(1,2-Dibromoethyl)benzene

Solvent	ε*	Temp. (°C)	$\langle J_{AC} \rangle$	$\langle J_{BC} \rangle$	$\langle J_{AC} \rangle + \langle J_{BC} \rangle$	$\langle J_{AC} \rangle - \langle J_{BC} \rangle$
Acetone	18.1	30	10.55	5.39	15.94	5.16
Acetone	21.0	0	10.77	5.37	16.14	5.40
Acetone	23.4	−25	11.05	5.26	16.31	5.79

Threo- and erythro(1,2-dibromopropyl)benzene

Isomer	Solvent	ε*	Temp. (°C)	$\langle J_{AB} \rangle$
Threo	Carbon tetrachloride	2.31	+35	5.34
Threo	Carbon tetrachloride	2.32	+30	5.28
Threo	Carbon tetrachloride	2.39	−5	5.19
Threo	Carbon tetrachloride	2.46	−24	5.14
Threo	Chloroform-*d*	4.33	+30	5.68
Threo	Chloroform-*d*	4.92	−5	5.73
Threo	Chloroform-*d*	5.52	−30	5.70
Threo	Chloroform-*d*	6.09	−50	5.70
Threo	Acetone	18.9	+30	6.15
Threo	Acetone	22.3	−5	6.29
Threo	Acetone	26.6	−40	6.41
Erythro	Chloroform-*d*	4.18	+30	10.16
Erythro	Chloroform-*d*	4.77	−5	10.39
Erythro	Chloroform-*d*	5.37	−30	10.63
Erythro	Acetone	18.6	+30	10.10
Erythro	Acetone	22.0	−5	10.46
Erythro	Acetone	26.3	−40	10.73

*Dielectric constant measured at 30 °C and calculated at other temperatures assuming the same temperature dependence of ε as for the pure solvent.

The fractional populations of the three rotamers approach equality if the temperature is increased sufficiently. Therefore, the difference between $\langle J_{AC} \rangle$ and $\langle J_{BC} \rangle$ should decrease with increasing temperature regardless of the relative stabilities of rotamers **1** and **2**. Consequently, the temperature dependence of the averaged vicinal coupling constants will not directly give information concerning the relative stabilities of these rotamers. A significant decrease in $(\langle J_{AC} \rangle + \langle J_{BC} \rangle)$ with temperature would suggest that the fractional population of rotamer **3** is not negligible.

From the above discussion it can be seen that it should be possible to determine the relative stabilities of rotamers of (1,2-dibromoethyl)-benzene and similar tri-substituted, dipolar ethanes from solvent effect studies, while variable temperature experiments should yield limited information unless one uses a complicated and probably insensitive curve-fitting procedure.

As can be seen from Table I and Fig. 4, the difference between $\langle J_{AC} \rangle$ and $\langle J_{BC} \rangle$ is significantly smaller in solutions of high ε than in solutions of low ε. The results show a slight anomaly for hexane (although this is barely larger than experimental error) and a major deviation for benzene. Otherwise, a very definite trend is noted. The results strongly suggest that rotamer **1** is the most stable rotamer (since $(\langle J_{AC} \rangle - \langle J_{BC} \rangle)$ decreases as ε increases). This is in agreement with the conclusion reached by Snyder and Buza from their specific deuteration experiments (*9b*). $(\langle J_{AC} \rangle + \langle J_{BC} \rangle)$ remains constant. This indicates that the population of rotamer **3** is small, as expected. It is obvious that measurements of the effect of ε upon averaged vicinal coupling constants can be used to obtain correct predictions of the relative stabilities of the three rotamers of (1,2-dibromoethyl)benzene. Therefore, it is probable that relative stabilities of rotamers of other tri-substituted, dipolar ethanes can be estimated by the same method. A number of compounds of this type are being investigated.

Rotamer **1** will be even more stable with respect to rotamer **2** in the gas phase. The more polar rotamer **2** is apparently significantly more sta-

Can. J. Chem. Downloaded from www.nrcresearchpress.com by 210.87.254.40 on 09/05/12
For personal use only.

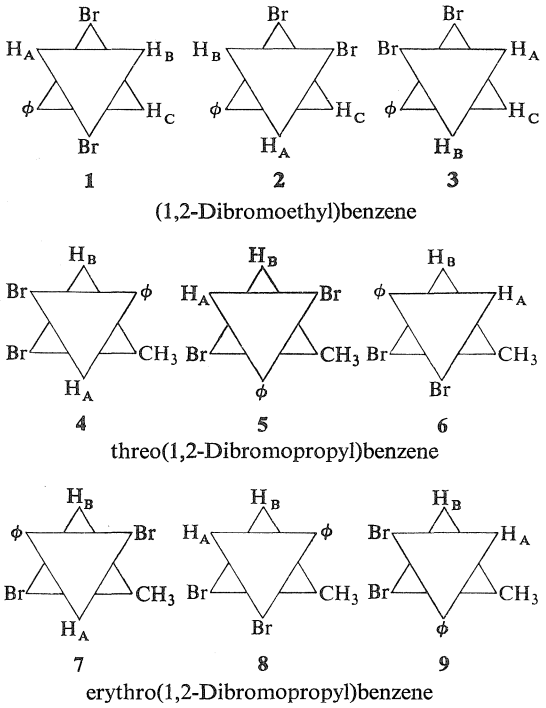

FIG. 3. Staggered rotamers of (1,2-dibromoethyl)-benzene and erythro- and threo(1,2-dibromopropyl)-benzene.

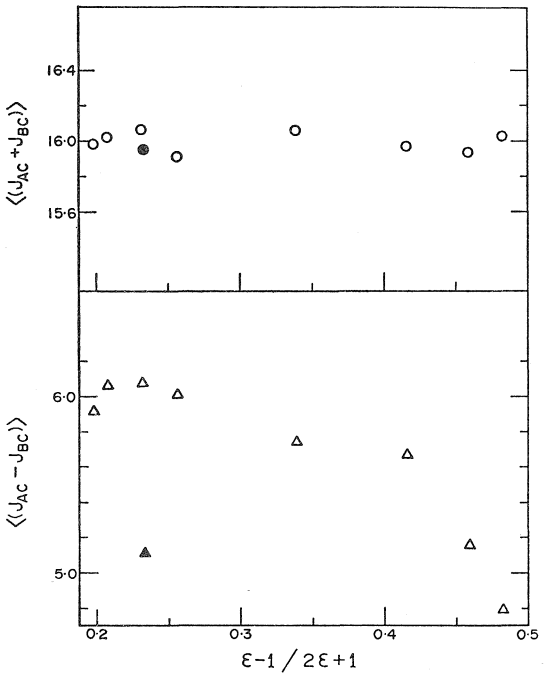

FIG. 4. Plot of $\langle J_{AC}\rangle + \langle J_{BC}\rangle$ and $\langle J_{AC}\rangle - \langle J_{BC}\rangle$ for (1,2-dibromoethyl)benzene versus the dielectric function $(\varepsilon - 1)/(2\varepsilon + 1)$. Filled point represents the benzene solutions.

ble in benzene than in carbon tetrachloride. Similar "benzene" effects have been noted by other investigators, both from vicinal coupling constant measurements (7) and from dipole moment measurements (13). It should be noted that the alternate solution (see Results) gives results which are apparently more consistent with other solvents. However, the first solution was chosen because in the 4-substituted derivatives, the change in $(\langle J_{AC}\rangle - \langle J_{BC}\rangle)$ on going from carbon tetrachloride to benzene was 0.8 to 0.9 Hz. This is more consistent with the first than with the alternate solution.

The conclusion of Snyder that energy differences between rotamers of substituted ethanes are only weakly related to ε was based upon results in a limited number of solvents including benzene. For several of the compounds which he investigated, the apparent discrepancies can be rationalized when it is realized that benzene may give anomalous results. We have noted a very good correlation between ε and $(\langle J_{AC}\rangle - \langle J_{BC}\rangle)$ for (1,2-dibromoethyl)benzene in eight non-aromatic solvents. However, it is only fair to point out that this correlation is probably better than one can normally expect in an investigation of this type. For erythro- and threo(1,2-dibromopropyl)benzene and for the compounds investigated by Abraham and co-workers (4, 7, 8), the variation of vicinal coupling constants with ε is less regular. However, in all cases definite trends can be noticed, provided that enough non-aromatic solvents are used. The most reasonable conclusion appears to be that there is a general relationship between ε and the energy differences of rotamers of substituted ethanes in non-aromatic solvents, but that for any one solvent this relationship may be partially obscured by specific interactions.

The vicinal coupling constants for (1,2-dibromoethyl)benzene are constant over the concentration range 0.15 to 0.60 *M* in both carbon tetrachloride and dimethylsulfoxide (see Table V). Consequently, the coupling constants are assumed to be very close to their infinite dilution values. However, the coupling constants in carbon tetrachloride, deuterochloroform, and acetone differ significantly from those reported by Snyder for 40 wt./vol. % solutions

Can. J. Chem. Downloaded from www.nrcresearchpress.com by 210.87.254.40 on 09/05/12
For personal use only.

Can. J. Chem. Downloaded from www.nrcresearchpress.com by 210.87.254.40 on 09/05/12
For personal use only.

TABLE V

Concentration dependence of chemical shifts (in p.p.m. to low field of tetramethylsilane) and coupling constants (in Hz)

(1,2-Dibromoethyl)benzene and 4-nitro(1,2-dibromoethyl)benzene

Substituent	Solvent	Concentration (M)	ε	$\langle J_{AB} \rangle$	$\langle J_{AC} \rangle$	$\langle J_{BC} \rangle$	$\langle J_{AC} \rangle + \langle J_{BC} \rangle$	$\langle J_{AC} \rangle - \langle J_{BC} \rangle$	δ_A	δ_B	δ_C	Root-mean-square error (Hz)
None	Carbon tetrachloride	0.15	2.21	−10.18	11.12	4.98	16.10	6.14	3.954	4.021	5.056	0.01
None	Carbon tetrachloride	0.30	2.30	−10.12	11.07	5.00	16.07	6.07	3.950	4.015	5.055	0.02
None	Carbon tetrachloride	0.60	2.36	−10.19	11.13	4.98	16.11	6.15	3.942	4.005	5.049	0.02
None	Dimethylsulfoxide	0.15	*	−10.15	10.38	5.63	16.01	4.75	4.368	4.245	5.533	0.02
None	Dimethylsulfoxide	0.30	42.4	−10.19	10.41	5.62	16.03	4.79	4.358	4.238	5.526	0.01
None	Dimethylsulfoxide	0.60	*	−10.15	10.40	5.62	16.02	4.78	4.358	4.240	5.526	0.02
4-Nitro	Carbon tetrachloride	0.15	2.42	−10.31	11.58	4.71	16.29	6.87	3.957	4.070	5.126	0.01
4-Nitro	Carbon tetrachloride	0.30	2.67	−10.38	11.52	4.74	16.26	6.78	3.962	4.069	5.134	0.02
4-Nitro	Carbon tetrachloride	0.45	2.85	−10.36	11.47	4.73	16.20	6.74	3.964	4.068	5.139	0.01
4-Nitro	Dimethylsulfoxide	0.15	*	−10.18	10.63	5.47	16.10	5.16	4.443	4.298	5.721	0.01
4-Nitro	Dimethylsulfoxide	0.30	46.8	−10.18	10.59	5.45	16.04	4.16	4.435	4.292	5.717	0.01

Erythro- and threo(1,2-dibromopropyl)benzene

Isomer	Solvent	Concentration (M)	ε	$\langle J_{AB} \rangle$	$\langle J_{BC} \rangle$	δ_A	δ_B	δ_C
Erythro	Carbon tetrachloride	0.30	2.23	10.25	6.41	4.94_4	4.50_1	2.02_7
Erythro	Carbon tetrachloride	0.45	2.26	10.27	6.38	4.94_4	4.50_1	2.02_5
Erythro	Carbon tetrachloride	0.60	2.30	10.25	6.49	4.94_5	4.50_1	2.02_0
Erythro	Dimethylsulfoxide	0.30	*	10.19	6.41	5.48_5	4.99_1	1.95_2
Erythro	Dimethylsulfoxide	0.45	*	10.15	6.41	5.47_8	4.98_2	1.95_3
Erythro	Dimethylsulfoxide	0.60	*	10.14	6.37	5.47_6	4.97_8	1.95_4
Threo	Dimethylsulfoxide	0.30	*	6.13	6.67	5.56_7	4.81_7	1.63_5
Threo	Dimethylsulfoxide	0.60	*	6.20	6.64	5.55_4	4.79_6	1.64_0

*Cell malfunction prevented measurements of dielectric constants for these solutions.

Can. J. Chem. Downloaded from www.nrcresearchpress.com by 210.87.254.40 on 09/05/12
For personal use only.

in the same solvents (9*a*). The value of ε should be significantly different in the more polar solvents and this could lead to population changes. Solute dimerization could also affect the coupling constants at high concentrations. The latter effect has been shown to be important for β-bromopropionitrile at much lower concentrations (7*c*).

($\langle J_{AC}\rangle - \langle J_{BC}\rangle$) decreases with increasing temperature, as expected. ($\langle J_{AC}\rangle + \langle J_{BC}\rangle$) decreases slightly, suggesting that the population of rotamer **3**, while small, is not negligible.

On the basis of the results presented (see Table I), there appears to be a very good correlation between the chemical shift difference for the methylene protons and solvent dielectric constant (except for benzene). However, this is misleading. Measurements were also made in acetonitrile. In this solvent, ($\delta_A - \delta_B$) is very nearly zero and, therefore, would not fit the above mentioned correlation. The coupling constants had approximately the expected values. However, these results have not been reported in detail since the "probable errors" in the vicinal coupling constants were sufficiently large (0.4 Hz) to make the results meaningless. As previously mentioned, this appears to be characteristic of this system as ($\delta_A - \delta_B$) approaches zero.

The observed changes in ($\delta_A - \delta_B$) with solvent appear to be much too large to be explained solely in terms of conformation changes. It appears more probable that they are due to specific solvent effects.

B. 4-Substituted (1,2-Dibromoethyl)benzene

The results for the 4-substituted derivatives are similar to those for the parent compound. The differences between vicinal coupling constants are generally larger in less polar solvents. There is a small but possibly significant concentration dependence for 4-nitro-(1,2-dibromoethyl)benzene. This might be due to the change in solution dielectric constant with solute concentration. Two conclusions can be reached.

Firstly, a remote dipole does not affect relative populations in any predictable fashion. For example, in the case of the 4-nitro derivative, rotamer **1** might be expected to be destabilized with respect to the parent compound, because of an additional dipolar interaction. In fact, the coupling constant difference is larger, indicating an apparent stabilization of rotamer **1**. It is quite possible, however, that the observed difference is due to electronic rather than conformational effects.

Secondly, the remote dipole does not significantly alter the effect of solvent upon rotamer populations. According to the theory for compounds containing three or more polar groups (8), the effect of ε upon energy differences between two rotamers is determined by the difference in net dipole moments and, to a lesser extent, quadrupole moments of the two rotamers. Assuming tetrahedral angles and dipole moments of 4.0 D for the 4-nitro–phenyl group and 2.0 D for C–Br groups, then for the 4-nitro derivative the net dipole moments for rotamers **1** and **2** are, respectively, 4.0 and 2.3 D. Consequently rotamer **1** should be stabilized with increasing ε. In actual fact, the reverse trend is found, suggesting that the remote dipole has little effect[2]. Since the theory assumes a point dipole in the center of a polarizable sphere, a breakdown in the theory for a bulky molecule such as 4-nitro-(1,2-dibromoethyl)benzene would hardly be surprising. The solvent probably tends to solvate the 1,2-dibromoethyl group quite independently of any solvation of the remote dipole, i.e., the effect of ε upon the conformation about the carbon–carbon bond depends only upon the polar groups directly bonded to the carbon atoms.

This conclusion, if correct, considerably extends the usefulness of the technique. For example, it may be possible to investigate conformational preference in low molecular weight polymers which contain many polar groups. It is obviously desirable to determine how close remote dipoles must be before they exert a significant influence. Unfortunately, it is difficult to find a suitable system. 2-Substituted or 3-substituted (1,2-dibromoethyl)benzenes would not be very suitable since the location of the remote dipole would depend upon the orientation of the phenyl group and since a substituent in the 2 or 3 position may cause additional steric hindrance.

---

[2]One might attempt to explain these results by suggesting that the quadrupolar term is more important than the dipolar term. However, nearly identical solvent effects upon vicinal coupling constants are noted for (1,2-dibromoethyl)benzene and its 4-substituted derivatives, in spite of the large differences in dipole and quadrupole moments for these compounds. Therefore, we feel that the explanation presented above is more logical.

Can. J. Chem. Downloaded from www.nrcresearchpress.com by 210.87.254.40 on 09/05/12
For personal use only.

C. *Erythro- and Threo(1,2-dibromopropyl)-benzene*

In each of these compounds there are only two protons in the substituted ethyl group and consequently only one vicinal coupling constant which should be solvent dependent owing to conformational changes. It is more difficult to deduce information concerning conformational preference from solvent effect studies on compounds of this type than on compounds with two solvent-dependent vicinal coupling constants. For example, for the threo compound, p_4 and p_6 should increase with increasing ε since rotamers **4** and **6** are polar (see Fig. 3). The protons are *trans* in rotamer **4** and *gauche* in the other two rotamers. Consequently $\langle J_{AB} \rangle$ should increase with increasing ε regardless of the relative energies of the three rotamers. Also, one cannot determine the relative populations of rotamers **5** and **6** since the protons are *gauche* in both rotamers. However, by observing the magnitude of the change in $\langle J_{AB} \rangle$ with ε and temperature, one can deduce much of the desired information.

$\langle J_{AB} \rangle$ for the threo compound increases irregularly with ε (see Table III and Fig. 5). However, a definite trend is noted. The overall change in $\langle J_{AB} \rangle$ is large (nearly twice as large as the changes in the vicinal coupling constants in (1,2-dibromoethyl)benzene for the same range in ε). From this observation one can only deduce that rotamers **4** and **5** must be relatively close in energy. If rotamer **4** is either very stable or very unstable with respect to rotamer **5**, then a small change in ΔE_{4-5} will have little effect upon p_4 (in the limiting case of infinite energy difference there would be no measurable effect). However, if the energy difference is small, then p_4 should be very sensitive to changes in ΔE_{4-5}.

More definite information can be deduced from the variable temperature results (see Table IV). In $CDCl_3$, J_{AB} is constant over a temperature range from −50 to +30 °C. Since the protons are *trans* in rotamer **4** and *gauche* in the other rotamers, one would expect a change in $\langle J_{AB} \rangle$ if there is any change in p_4. Conversely, the constancy of $\langle J_{AB} \rangle$ suggests that p_4 remains essentially constant over this temperature range. This fortuitous constancy can only occur if rotamer **4** is intermediate in energy relative to the other two rotamers. In rotamer **4**, there are two steric interactions and one dipolar interaction. There are three steric interactions in both rotamers **5** and **6** but only the latter has a dipolar interaction. On this basis it is believed that the energy order $E_6 > E_4 > E_5$ is much more probable than the alternate order $E_5 > E_4 \geqslant E_6$.

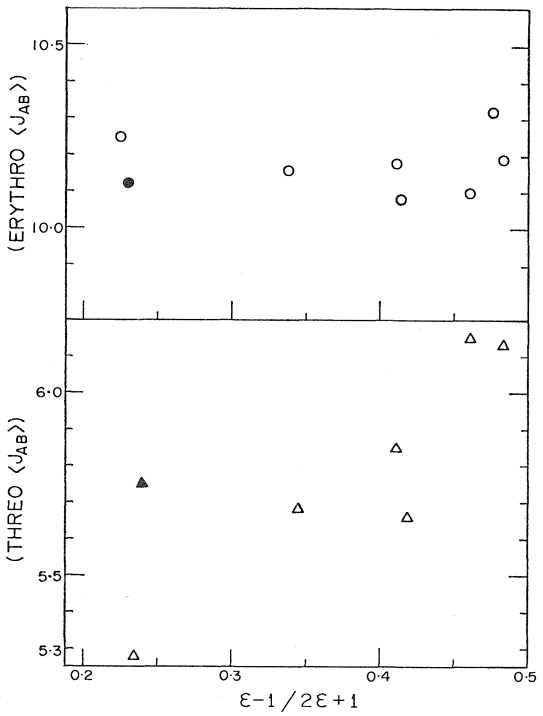

FIG. 5. Plot of $\langle J_{AB} \rangle$ for erythro- and threo(1,2-dibromopropyl)benzene versus the dielectric function $(\varepsilon - 1)/(2\varepsilon + 1)$. Filled points represent benzene solutions.

The conclusion that rotamer **4** must be intermediate in energy can be confirmed by simple calculations. For example, if $E_4 - E_5 = 150$, $E_6 - E_4 = 600$ cal/mole, $J_4 = 12.0$, and $J_5 = J_6 = 1.9$ Hz, then $\langle J_{AB} \rangle = 5.71$ Hz at 30 °C and 5.70 Hz at −50 °C[3]. A similar result can be obtained even if one allows for a slight temperature dependence of ΔE_{4-5} and ΔE_{5-6} (due to the decrease in ε with increasing temperature) and for the fact that J_5 is probably larger than J_6 (a vicinal coupling constant is believed

[3]The normal assumption is made that the entropy difference between rotamers is zero (2). It has been shown that there are small entropy differences between the rotamers of 1,1,2,2-tetrabromo-1-fluoroethane but that if one ignored the entropy difference, one obtained an apparent energy difference between rotamers which is only slightly different from the true energy difference (3).

Can. J. Chem. Downloaded from www.nrcresearchpress.com by 210.87.254.40 on 09/05/12
For personal use only.

to be smaller when one of the protons is *trans* to an electronegative group than when it is *gauche* to that group (7, 14)). For example, if ΔE_{4-5} is 275 cal/mole at -30 °C and 300 cal/mole at $+30$ °C, ΔE_{6-4} is constant at 500 cal/mole, $J_4 = 12.0$, $J_5 = 3.0$, and $J_6 = 1.5$ Hz, then $\langle J_{AB} \rangle = 5.71$ Hz at -30 °C and 5.71 Hz at $+30$ °C. One can obtain the same result for other reasonable choices of ΔE and J. It is impossible to determine from the available data which is the correct choice of parameters. However, any choice of parameters in which rotamer **4** is not intermediate in energy would require that the *trans* coupling constant be smaller than at least one of the *gauche* coupling constants. This would be contrary to all evidence concerning the effect of conformation upon vicinal proton coupling constants. The intermediate size of $\langle J_{AB} \rangle$ is also consistent with the conclusion that rotamer **4** is intermediate in energy.

The relative stability of rotamer **5** should be even greater in the gas phase since this rotamer is non-polar. Consequently, the order of energy levels should be the same in deuterochloroform, in solvents of lower ε, and in the gas phase. However, ΔE_{4-5} should decrease with increasing ε and could possibly change sign at high ε. In any case, relative to rotamer **5**, rotamer **4** should be less stable in carbon tetrachloride and more stable in acetone than in deuterochloroform. Since p_4 is essentially independent of temperature in deuterochloroform, p_4 and $\langle J_{AB} \rangle$ should decrease with decreasing temperature in carbon tetrachloride and increase with decreasing temperature in acetone. This reversal of the sign of the temperature is actually observed (see Table IV).

The above observations are significant since they strongly suggest that the observed solvent dependence of the vicinal coupling constants is due to changes in energy differences and rotamer populations with ε rather than to reaction field effects upon the coupling constants of the individual rotamers. The latter effect has been shown to be important for the ^1H–^{19}F coupling constant in 1-fluoro-1,1,2,2-tetrabromoethane (15). However, it is probable that the reaction field effect is more important for ^1H–^{19}F coupling constants than for ^1H–^1H vicinal coupling constants in substituted alkanes. Previous results support this contention. For example, it has been shown that the averaged vicinal coupling constants for 1-iodo-3,3-dimethylbutane are solvent independent (14). Since this molecule has only one polar group, no change in rotamer population with ε would be expected. Since the coupling constants do not change, it is improbable that there is a significant reaction field effect.

An increased stabilization of rotamer **4** in benzene was noted. It has been suggested that the increased stabilization of the polar forms of 1,2-dihaloethanes in benzene might be due to specific hydrogen bonding of two adjacent benzene protons with the two halogen atoms in a *gauche* conformation (16). An alternate possibility would involve the interaction of the *gauche* halogens with the π electron system of benzene. In an attempt to choose between the two possibilities, we ran the threo compound in *cis*-1,2-dichloroethylene. If the specific interaction is of the former type, one might expect it to occur with *cis*-1,2-dichloroethylene as well. Unfortunately, the results are not entirely conclusive. However, $\langle J_{AB} \rangle$ does have approximately the value which one would expect if no specific interaction occurred. Consequently, it appears probable that the specific interaction with benzene involves the π electron system.

$\langle J_{AB} \rangle$ is, within experimental error, independent of concentration. It was also found that adding pure erythro compound to the impure threo compound did not significantly alter $\langle J_{AB} \rangle$. Consequently, it is believed that our results are not affected by the presence of the erythro compound as an impurity.

$\langle J_{AB} \rangle$ for the erythro compound is independent of ε (see Table III and Fig. 5). There is a considerable scatter of values of $\langle J_{AB} \rangle$ but no trend which could be related to ε. One would expect $\langle J_{AB} \rangle$ to be independent of ε only if one of the rotamers was very much more stable than the other two, or possibly if both rotamers with *gauche* protons were much more stable than the rotamer with *trans* protons. Since $\langle J_{AB} \rangle$ is large (10.2 Hz), the compound must exist predominantly in the rotamer with *trans* protons, i.e., rotamer **7** is much more stable than the other two rotamers. The same order should be found in the gas phase since rotamer **7** is non-polar while the other two rotamers are polar. It is impossible to deduce the relative stabilities of rotamers **8** and **9** from the available information.

Can. J. Chem. Downloaded from www.nrcresearchpress.com by 210.87.254.40 on 09/05/12
For personal use only.

The above conclusion is not at all surprising since rotamer **7** has only two steric interactions and no dipolar interaction while both other rotamers have three steric interactions and one dipolar interaction.

The temperature dependence of $\langle J_{AB} \rangle$ is similar to the temperature dependence of the vicinal coupling constants in (1,2-dibromoethyl)-benzene. This suggests that the compound does not exist entirely in the conformation of rotamer **7**. However, this does not necessarily imply that there are appreciable fractional populations for rotamers **8** and **9**. Whitesides *et al.* have noted a similar temperature dependence of averaged vicinal coupling constants for a series of 1-substituted 3,3-dimethylbutanes (14). The larger vicinal coupling constant at room temperature had a value of 10.2 Hz for the cyano derivative and 12.9 Hz for the phenyl derivative, while the corresponding calculated values for J_{trans} were 13.9 and 13.7 Hz. Clearly the simple observation of temperature dependence of an averaged vicinal coupling constant does not provide unequivocal information concerning how close this coupling constant is to a pure *trans* coupling constant.

It is informative to consider the difference in the total number of steric and dipolar interactions for the two most stable rotamers for each of the compounds and to compare this with the observed solvent dependence of the vicinal coupling constants. In threo(1,2-dibromopropyl)-benzene there is a total of three steric and (or) dipolar interactions for each of rotamers **4** and **5**. In (1,2-dibromoethyl)benzene, rotamer **1** has one less (dipolar) interaction than rotamer **2**. In erythro(1,2-dibromopropyl)benzene, rotamer **7** has two less interactions than each of the other two rotamers. The changes in coupling constants (using the larger coupling constant for (1,2-dibromoethyl)benzene) upon going from carbon tetrachloride to acetone are respectively 0.83, 0.49, and 0.15 Hz. Provided that the protons were *trans* in one of the two most stable rotamers, one would expect the largest change in the vicinal coupling constant when the energy difference is smallest and populations are closest to equality. It is apparent that this inverse relationship does exist for the three compounds discussed above. Consequently, it appears that the relative solvent dependence of vicinal coupling constants for a series of closely related compounds can provide meaningful information about relative conformational preference in these compounds.

The value of $\langle J_{AB} \rangle$ for the erythro compound is significantly smaller than the value of the larger vicinal coupling constant in (1,2-dibromoethyl)benzene. This is surprising. On the basis of the previous discussion, one would expect that erythro(1,2-dibromopropyl)benzene would exist predominantly as rotamer **7** while for (1,2-dibromoethyl)benzene there should be appreciable populations of both rotamers **1** and **2**. Therefore, one would anticipate that $\langle J_{AB} \rangle$ for the former compound would be larger than $\langle J_{AC} \rangle$ for the latter compound. We believe that the most probable explanation for this apparent discrepancy is that the *trans* coupling constant in the former compound is significantly smaller than in the latter compound. If this is true, then estimates of conformational preference based only upon the size of a single vicinal coupling constant (17) must be regarded as suspect.

D. Factors Affecting Conformational Preference

Snyder believed that it was surprising that rotamer **1** was significantly more stable than rotamer **2** of (1,2-dibromoethyl)benzene (9). He first considered only steric interactions. Since the phenyl group has a much larger "A" factor (18) than the bromo group, he believed that there should be a much greater steric interaction in rotamer **1** than in rotamer **2**. He then postulated that the additional stability of rotamer **1** might be due to a stabilizing interaction between the phenyl group and the bromine on the β carbon atom. However, it has since been shown that "A" factors (which were determined from substituted cyclohexanes) are not an accurate measure of steric interactions in substituted ethanes (14). In actual fact, bromine has only a slightly smaller steric effect than a phenyl group in substituted ethanes (the energy differences between *gauche* and *trans* rotamers of 1-bromo- and 1-phenyl-3,3-dimethylbutane have been estimated as, respectively, 1.30 and 1.70 kcal/mole (14)). The lower stability of rotamer **2** can then be explained as due to the destabilizing effect of the dipolar repulsion of the *gauche* bromine atoms (if this effect was not important, there would not be any solvent dependence of rotamer population). However, one cannot entirely exclude the possibility of a stabilizing bromine–

Can. J. Chem. Downloaded from www.nrcresearchpress.com by 210.87.254.40 on 09/05/12
For personal use only.

phenyl interaction in rotamer **1** although it is no longer necessary to postulate an interaction of this kind. Indirect support for a stabilizing interaction is provided by the observation of stabilization of polar rotamers by benzene.

As previously discussed, the relative stabilities of rotamers for other compounds can also be rationalized if one assumes that dipolar repulsions are as important as steric interactions in solutions of low ε. Once again, conformational preference might also be affected by stabilizing bromine–phenyl interactions.

There should be considerable decrease of dipolar repulsion by the medium even for solutions of low ε. For example, if the dependence of ΔE upon ε has the form $(\varepsilon - 1)/(2\varepsilon + 1)$ (4), then a medium with $\varepsilon = 2$ will decrease dipolar repulsions 40% as effectively as a hypothetical medium of $\varepsilon = \infty$. Since dipolar interactions are apparently still important in solution, they will obviously be of greater importance in the gas phase.

Summary and Conclusions

The relative stability of the rotamers of (1,2-dibromoethyl)benzene can be deduced from the dependence of the sum and difference of the two vicinal coupling constants upon solution dielectric constant. It should be possible to deduce the relative stabilities of rotamers of other similar tri-substituted dipolar ethanes by a similar technique. A polar substituent in the 4-position of the phenyl group does not affect conformational equilibrium or the effect of solvent upon conformational equilibrium in any predictable manner.

It was not possible to develop a general procedure to deduce the relative stabilities of rotamers of erythro- and threo(1,2-dibromopropyl)benzene. These are examples of substituted ethanes with only one vicinal coupling constant. However, much of the desired information could be determined by specific observations of the sign and magnitude of the change of the coupling constant with solvent and temperature. There appears to be a definite relationship between the magnitude of change of vicinal coupling constants with solvent and the expected energy difference between the two most stable rotamers for a series of closely related substituted dipolar ethanes.

It is possible to rationalize the deduced relative stability of rotamers for the compounds investigated if one assumes that both dipolar and steric interactions determine energy differences. The former appears to be at least as important as the latter in solution and is probably of greater importance in the gas phase.

Acknowledgments

Financial support from the National Research Council of Canada and the Department of University Affairs of the Province of Ontario is gratefully acknowledged. We thank Professor A. A. Bothner-By for providing a listing of LAOCN3 and Professor H. M. Hutton for providing a listing of EXAN written in Fortran IV.

1. J. W. Emsley, J. Feeney, and L. H. Sutcliffe. High resolution nuclear magnetic resonance spectroscopy. Vol. 1. The Pergamon Press, Ltd., Oxford, England. 1965. Chap. 9.
2. H. S. Gutowsky, G. G. Bedford, and P. E. McMahon. J. Chem. Phys. **36**, 3353 (1962).
3. G. Govil and H. J. Bernstein. J. Chem. Phys. **47**, 2818 (1967).
4. R. J. Abraham, L. Cavalli, and K. G. R. Pachler. Nuclear magnetic resonance in chemistry. *Edited by* B. Pesce. Academic Press, Inc., New York. 1965. p. 111.
5. S. Mizushima. Structure of molecules and internal rotation. Academic Press, Inc., New York. 1954.
6. H. Finegold. J. Chem. Phys. **41**, 1808 (1964).
7. (*a*) R. J. Abraham and M. A. Cooper. Chem. Commun. 588 (1966). (*b*) R. J. Abraham, L. Cavalli, and K. G. R. Pachler. Mol. Phys. **11**, 471 (1966). (*c*) K. K. Deb and R. J. Abraham. J. Mol. Spectry. **23**, 393 (1967).
8. R. J. Abraham and M. A. Cooper. J. Chem. Soc. B, 202 (1967).
9. (*a*) E. I. Snyder. J. Am. Chem. Soc. **88**, 1155 (1966). (*b*) M. Buza and E. I. Snyder. J. Am. Chem. Soc. **88**, 1161 (1966). (*c*) E. I. Snyder. J. Am. Chem. Soc. **88**, 1165 (1966).
10. (*a*) S. Castellano and J. S. Waugh. J. Chem. Phys. **35**, 1900 (1961). (*b*) J. R. Cavanaugh. J. Chem. Phys. **39**, 2378 (1963).
11. S. Castellano and A. A. Bothner-By. LAOCN3. Mellon Institute, Pittsburgh. 1966.
12. J. A. Pople and T. Schaefer. Mol. Phys. **3**, 547 (1960).
13. C. Altona and H. J. Hageman. Rec. Trav. Chim. **87**, 279 (1968).
14. G. M. Whitesides, J. P. Sevenair, and R. W. Goetz. J. Am. Chem. Soc. **89**, 1135 (1967).
15. G. Govil and H. J. Bernstein. J. Chem. Phys. **48**, 285 (1968).
16. S. Kondo, E. Tagami, K. Iimura, and M. Takeda. Bull. Chem. Soc. Japan, **41**, 790 (1968).
17. C. A. Kingsbury and W. B. Thornton. J. Org. Chem. **31**, 1000 (1966).
18. E. L. Eliel. Stereochemistry of carbon compounds. McGraw-Hill Book Co., Inc., New York. 1962.

Can. J. Chem. Downloaded from www.nrcresearchpress.com by 210.87.254.6 on 09/05/12
For personal use only.

Kinetic studies of the substitution reactions of the *cis*-dihalotetracarbonylmanganate(I) ions [1,2]

FRANK E. SMITH AND IAN S. BUTLER
Department of Chemistry, McGill University, Montreal, Quebec

Received August 23, 1968

The substitution reactions of $(C_2H_5)_4$[*cis*-$Mn(CO)_4X_2$], where X = Br or I, with a variety of ligands, L, were observed to take place with the loss of halide ion, X^-, to form *cis*-$Mn(CO)_4LX$ and $(C_2H_5)_4NX$. The reaction rates in *s*-tetrachloroethane were first order in substrate, independent of both the nature and the concentration of L, and decreased with increasing atomic weight of the halogen. A dissociative mechanism involving the breaking of a manganese–halogen bond as the rate-determining step is proposed. It is postulated that the order of reactivity of the substrates is most probably the result of an entropy rather than an enthalpy effect. The substitution reactions of $(C_2H_5)_4N$[*cis*-$Mn(CO)_4BrI$] in *s*-tetrachloroethane were also studied kinetically and found to be first order in substrate and independent of the nature and concentration of L. The products of these reactions, however, were mixtures of *cis*-$Mn(CO)_4LBr$ and *cis*-$Mn(CO)_4LI$, and $(C_2H_5)_4NBr$ and $(C_2H_5)_4NI$. A solvent study of the reaction between $(C_2H_5)_4N$[*cis*-$Mn(CO)_4Br_2$] and $P(C_6H_5)_3$ indicated that the rate of reaction tended to increase with increasing polarity of the solvent.

Canadian Journal of Chemistry, 47, 1311 (1969)

Introduction

A large number of detailed kinetic studies have been reported concerning the substitution reactions of neutral metal carbonyl complexes (1). In contrast there have been only two such reports dealing with charged complexes. Hieber and Wollmann (2) investigated the ^{14}CO exchange reactions of $[Mn(CO)_6][AlCl_4]$, $[Re(CO)_6][AlCl_4]$, and $Na[Mn(CO)_5]$; and Allen and Barrett (3) recently published data for the reactions of $(C_2H_5)_4N[M(CO)_5X]$ and $(C_2H_5)_4N$[*cis*-$PR_3M(CO)_4X$] (M = Cr, Mo, and W; X = Cl, Br, and I), with aryl phosphines, PR_3. The Group VII complexes showed no evidence of CO exchange. The $(C_2H_5)_4N[M(CO)_5X]$ complexes apparently reacted by both an S_N1 and an S_N2 mechanism to form $(C_2H_5)_4N$[*cis*-$PR_3M(CO)_4X$] and $PR_3M(CO)_5$, respectively, while the $(C_2H_5)_4N$[*cis*-$PR_3M(CO)_4X$] complexes were believed to react by an S_N1 mechanism to form $(PR_3)_2M(CO)_4$. The effect of solvent on these reactions was not investigated nor were any activation data presented in support of the proposed mechanisms.

The d^6, diamagnetic complexes, $(C_2H_5)_4N$[*cis*-$Mn(CO)_4X_2$] and $(C_2H_5)_4N$[*cis*-$Re(CO)_4X_2$], have been reported (4–6). When the manganese complexes were reacted with phosphines, L, replacement of the halide ion, X^-, occurred (5, 7), see reaction [1].

[1] $(C_2H_5)_4N$[*cis*-$Mn(CO)_4X_2$] + L → *cis*-$Mn(CO)_4LX$ + $(C_2H_5)_4NX$

Angelici estimated the rates of reaction when $L = P(C_6H_5)_3$ and tentatively proposed an S_N1 dissociative mechanism (5). He also discussed the probable importance of the solvent on the reaction rates.

The present study reports kinetic data for the substitution reactions of $(C_2H_5)_4N$[*cis*-$Mn(CO)_4X_2$] and $(C_2H_5)_4N$[*cis*-$Mn(CO)_4BrI$] with a variety of ligands in *s*-tetrachloroethane. Activation parameters have been determined for certain of the reactions, and the reaction of $(C_2H_5)_4N$[*cis*-$Mn(CO)_4Br_2$] with $P(C_6H_5)_3$ was studied in four different solvents.

Experimental

Preparation and Purification of Materials

Chemicals were obtained from the following sources: dimanganese decacarbonyl and triphenylphosphine (Alfa Inorganics, Inc.); tetraethylammonium chloride and bromide, and tri-*n*-butylphosphite (Eastman Kodak Co.); tetraethylammonium iodide (Fluka); trimethylphosphite, triphenylphosphite, tri-*n*-butylphosphine, triphenylarsine, triphenylstibine, triallylphosphite, and triisopropylphosphite (Aldrich Chemical Co.); pyridine, *s*-tetrachloroethane, chloroform, 1,2-dichloroethane, and nitromethane (Fisher Chemical Co.).

The tetraethylammonium salts and all ligands except tri-*n*-butylphosphine were used without further purification. The latter was purified by fractional distillation, under reduced pressure. Solvents were distilled under

[1]Taken from the M.Sc. thesis of F.E.S.

[2]This work was presented in part at the 156th National Meeting of the American Chemical Society, Atlantic City, New Jersey, September, 1968.

Can. J. Chem. Downloaded from www.nrcresearchpress.com by 210.87.254.6 on 09/05/12
For personal use only.

nitrogen from calcium hydride. Before distillation, *s*-tetrachloroethane was shaken with concentrated sulfuric acid and washed with water, and nitromethane was washed twice with aqueous sodium hydrogen carbonate.

The methods described in the literature were used to prepare $Mn(CO)_5Cl$ (8), $Mn(CO)_5Br$ (8), $Mn(CO)_5I$ (9), and $(C_2H_5)_4N[cis\text{-}Mn(CO)_4X_2]$ (5). $(C_2H_5)_4N[cis\text{-}Mn(CO)_4BrI]$, first reported in ref. (4), was prepared by refluxing a mixture of $Mn(CO)_5Br$ (0.2 g, 0.73 mmole) and $(C_2H_5)_4NI$ (0.18 g, 0.7 mmole) in methanol (10 ml) under nitrogen for 1 h. After cooling, the methanol was evaporated off with a water pump. The orange residue was dissolved in CH_2Cl_2 (20 ml) and the solution filtered under nitrogen. The filtrate was slowly added to *n*-hexane (250 ml) and the mixture allowed to stand at room temperature for 24 h. The orange crystals which formed were separated by filtration, washed with *n*-hexane, and dried under vacuum; yield, 0.23 g (65%). All of the anions were recrystallized from CH_2Cl_2 – *n*-hexane mixtures immediately before use.

Determination of Rates

The rates were determined by monitoring the absorbance changes of the reaction mixtures at 450 mμ. Pseudo-first-order conditions were employed in all cases, the substrate concentrations being kept at about 2×10^{-3} *M*. For $(C_2H_5)_4N[cis\text{-}Mn(CO)_4I_2]$ and $(C_2H_5)_4N[cis\text{-}Mn(CO)_4BrI]$, reaction mixtures were prepared in foil-wrapped round bottom (50 ml) flasks fitted with teflon-barrelled stopcocks and neoprene serum caps. This arrangement kept solvent-loss by evaporation to a minimum. The flasks were thermostated in a constant temperature bath (±0.1°). Samples were withdrawn at intervals with a syringe, introduced into an absorption cell, and the spectrum scanned in the region of 450 mμ. A solution containing the same concentration of ligand as in the reaction mixture was used as reference. The presence of a single isosbestic point in every case suggested (10) that the absorbances were due to two species and that the main reactions were proceeding without side-effects. This technique proved too slow to follow the reactions of $(C_2H_5)_4N[cis\text{-}Mn(CO)_4Br_2]$. For these, a single sample was prepared in an absorption cell located in a thermostated block. This block could be mounted in the spectrophotometer and a constant-wavelength scanning device enabled continuous monitoring of the absorbance at 450 mμ. From the absorbance changes, linear plots of $\log(A_t - A_\infty)$ against time were obtained and the pseudo-first-order rate constants were calculated from the slopes of these lines. A_t is the absorbance at time t and A_∞ the absorbance at $t = \infty$. The reactions were assumed to go to completion since the experimental A_∞ values were in agreement with those calculated, and infrared spectra taken at the ends of the runs indicated total disappearance of the substrates.

The reaction of $(C_2H_5)_4N[cis\text{-}Mn(CO)_4Cl_2]$ with $P(C_6H_5)_3$ in *s*-tetrachloroethane was too fast to study kinetically by our methods. Attempts to follow the same reaction in 1,2-dichloroethane by infrared spectroscopy also failed owing to the large number of overlapping bands in the spectrum. The spectrum indicated that the reaction product, $cis\text{-}Mn(CO)_4P(C_6H_5)_3Cl$, was rapidly reacting further with $P(C_6H_5)_3$ to form $cis\text{-}Mn(CO)_3[P(C_6H_5)_3]_2Cl$ (11).

The rate constants were generally reproducible to within 10% or better. A least squares computer program was used to calculate values of the activation parameters. The uncertainties in $\Delta H^\ddagger$ are estimated to be ±2 kcal mole^{-1} and in $\Delta S^\ddagger$, ±4 e.u. mole^{-1}. These uncertainties are somewhat larger for the bromo-iodo complex, viz., $\Delta H^\ddagger$, ±3 kcal mole^{-1} and $\Delta S^\ddagger$, ±5 e.u. mole^{-1}. The calculations were performed on an IBM 7044 computer.

Identification of Products of Reaction [1]

It was not possible to isolate the products from the kinetic runs owing to the dilute solutions used and the very large excess of ligand, L, present. The metal carbonyl products were identified by the similarity of their spectra to those reported for the $cis\text{-}Mn(CO)_4LX$ compounds (12, 13). In the reactions where L was a phosphite, the infrared spectra taken at the end of the kinetic runs indicated that the replacement of a CO group to form the disubstituted product, $cis\text{-}Mn(CO)_3L_2X$, had already begun. In a few cases the reaction products were isolated on a preparative scale.

An equimolar mixture of $(C_2H_5)_4N[cis\text{-}Mn(CO)_4I_2]$ and $P(C_6H_5)_3$ in *s*-tetrachloroethane (20 ml) was allowed to stand at room temperature for 24 h. The solvent was then removed under vacuum and a brown solid remained. This was washed several times with distilled water (taking care to keep the washings) and dried under vacuum. The brown solid was dissolved in *n*-hexane and the solution cooled in a dry-ice – acetone bath. The orange crystals of $cis\text{-}Mn(CO)_4P(C_6H_5)_3I$ which formed were filtered off and dried under vacuum.

Anal. Calcd. for $C_{22}H_{15}O_4PIMn$: C, 47.5; H, 2.7; P, 5.6; I, 22.9. Found: C, 47.9; H, 3.08; P, 5.6; I, 20.6.

The washings were evaporated to dryness on a hot-plate leaving a white residue of $(C_2H_5)_4NI$ which was quickly washed with CH_2Cl_2 (3 × 10 ml) and dried under vacuum.

Anal. Calcd. for $C_8H_{20}NI$: C, 37.4; H, 7.8; I, 49.5. Found: C, 37.5; H, 8.3; I, 49.3.

A similar procedure was used to isolate $cis\text{-}Mn(CO)_4P(C_6H_5)_3Br$ from $(C_2H_5)_4N[cis\text{-}Mn(CO)_4Br_2]$ and $P(C_6H_5)_3$.

Anal. Calcd. for $C_{22}H_{15}O_4PBrMn$: C, 52.0; H, 2.95; P, 6.1. Found: C, 51.9; H, 3.16; P, 5.74.

Reaction of $(C_2H_5)_4N[cis\text{-}Mn(CO)_4Br_2]$ with Pyridine

An orange oil was obtained when $(C_2H_5)_4N[cis\text{-}Mn(CO)_4Br_2]$ was reacted with pyridine in *s*-tetrachloroethane at room temperature. The infrared spectrum corresponded to that reported for $cis\text{-}Mn(CO)_3(C_5H_5N)_2Br$ (12).

Anal. Calcd. for $C_{13}H_{10}N_2O_3BrMn$: C, 41.4; N, 7.4. Found: C, 39.8; N, 7.2.

Reaction of $(C_2H_5)_4N[cis\text{-}Mn(CO)_4BrI]$ with $P(C_6H_5)_3$

The products isolated from preparative scale reactions between $(C_2H_5)_4N[cis\text{-}Mn(CO)_4BrI]$ and $P(C_6H_5)_3$ in *s*-tetrachloroethane at room temperature contained both bromine and iodine. Found for the manganese carbonyl derivative: Br, 4.72 and 4.08; I, 20.09 and 15.08. Found for the tetraethylammonium salt: Br, 24.66; I, 22.61. The infrared spectrum of the carbonyl product showed that it was a mixture of $cis\text{-}Mn(CO)_4P(C_6H_5)_3Br$ and $cis\text{-}Mn(CO)_4P(C_6H_5)_3I$. The near-ultraviolet spectra of the reaction mixtures taken at the end of the kinetic runs

Can. J. Chem. Downloaded from www.nrcresearchpress.com by 210.87.254.6 on 09/05/12
For personal use only.

for this system indicated that the product was *cis*-$Mn(CO)_4P(C_6H_5)_3Br$. The infrared spectra of these reaction mixtures recorded somewhat later showed the presence of both *cis*-$Mn(CO)_4P(C_6H_5)_3Br$ and *cis*-$Mn(CO)_4P(C_6H_5)_3I$.

Mixed manganese carbonyl products were also formed when $(C_2H_5)_4N$[*cis*-$Mn(CO)_4BrI$] was reacted with other ligands.

Reaction of cis-$Mn(CO)_4P(C_6H_5)_3Br$ with $(C_2H_5)_4NI$

Excess solid $(C_2H_5)_4NI$ was added to a solution of *cis*-$Mn(CO)_4P(C_6H_5)_3Br$ in *s*-tetrachloroethane and the mixture was allowed to stand at room temperature for a few hours. The products were worked up in a manner similar to that described above. Infrared spectra of the manganese carbonyl product indicated the presence of both *cis*-$Mn(CO)_4P(C_6H_5)_3Br$ and *cis*-$Mn(CO)_4P(C_6H_5)_3I$. This was confirmed by halogen analyses. Found for *cis*-$Mn(CO)_4P(C_6H_5)_3X$: Br, 3.82; I, 15.16. The tetraethylammonium salt isolated also contained both bromine and iodine. Found for $(C_2H_5)_4NX$: Br, 8.22; I, 30.5. Since the reaction was carried out in the presence of a large excess of $(C_2H_5)_4NI$, a high iodine analysis would be expected for the tetraethylammonium salt.

The near-ultraviolet spectra of the above reaction mixture was monitored for a number of hours and it was observed that the band maximum gradually began to shift to lower energy and the spectrum corresponded more to that of *cis*-$Mn(CO)_4P(C_6H_5)_3I$ than *cis*-$Mn(CO)_4P(C_6H_5)_3Br$.

Spectra

The infrared spectra were obtained with a Perkin–Elmer 337 grating spectrophotometer equipped with a Texas Servo/Riter Model II expanded-scale recorder. The spectra were calibrated with polystyrene film and are considered to be accurate to at least ± 2.0 cm^{-1}. The near-ultraviolet spectra were recorded on a Unicam SP 800 spectrophotometer using 1 cm quartz cells and are accurate to ± 1.0 mμ.

Results

The substitution reactions of $(C_2H_5)_4N$[*cis*-$Mn(CO)_4Br_2$] in a variety of solvents and those of $(C_2H_5)_4N$[*cis*-$Mn(CO)_4I_2$] and $(C_2H_5)_4N$[*cis*-$Mn(CO)_4BrI$] in *s*-tetrachloroethane were all first order in substrate. The observed pseudo-first-order rate constants for these reactions are listed in Tables I and II. Since the reactions of $(C_2H_5)_4N$[*cis*-$Mn(CO)_4Cl_2$] with $P(C_6H_5)_3$ in *s*-tetrachloroethane were complete in less than 2 min, they were too fast to be measured quantitatively.

Data on the activation parameters for some of the reactions are given in Table III.

The C—O stretching frequencies of the reaction products in *s*-tetrachloroethane are shown in Table IV. The spectra of some of the compounds have been reported previously, but in different solvents (12). Since our measurements show significant differences from these, and the effect of solvent on C—O stretching frequencies in metal carbonyl compounds is well known (14), we feel that their inclusion in the Table is warranted. There is a general increase in the C—O stretching frequencies of the *cis*-$Mn(CO)_4LBr$ compounds with changes in L as, $P(C_6H_5)_3 \sim As(C_6H_5)_3 < P(OCH(CH_3)_2)_3 < P(n\text{-}OC_4H_9)_3 < P(OCH_2CH{:}CH_2)_3 < P(OC_6H_5)_3$. A similar order was given in ref. (12). It is tempting to try and correlate the position of a ligand in the order with its π-bonding ability. However, recent work (15) seems to indicate that C—O stretching frequency shifts may not be as reliable a measure of the π-bonding abilities of ligands in substituted metal carbonyl complexes as was previously believed and such correlations should be viewed with caution.

The near-ultraviolet spectra of the substrates and the reaction products are given in Table V. The near-ultraviolet spectra of *cis*-$Mn(CO)_4LX$ consist of one broad absorption band, the position of which is dependent on both L and X. The absorption maximum in *cis*-$Mn(CO)_4LBr$ moves towards lower energies with changes in L in the order

$$P(OCH_3)_3 > P(n\text{-}OC_4H_9)_3 \sim P(OCH_2CH{:}CH_2)_3 > P(OCH(CH_3)_2)_3 \sim P(OC_6H_5)_3 > P(n\text{-}C_4H_9)_3 > CO > P(C_6H_5)Cl_2 > P(C_6H_5)_3 > As(C_6H_5)_3 > Sb(C_6H_5)_3$$

This is an extension of the order given by Basolo and Angelici (13) who suggested that the higher the energy of the absorption maximum, the better the π-bonding ability of L. A similar, though much less complete series is found for *cis*-$Mn(CO)_4LI$, viz., $P(OCH_3)_3 > P(C_6H_5)_3 > As(C_6H_5)_3$. Keeping L constant and changing X from Br to I causes the band maximum to shift to lower energies. In the case of $P(C_6H_5)_3$ the energy of the band maximum decreases in the order Cl > Br > I. One broad absorption band is also found in the near-ultraviolet spectra of the $(C_2H_5)_4N$[*cis*-$Mn(CO)_4X_2$] and $(C_2H_5)_4N$[*cis*-$Mn(CO)_4BrI$] complexes. The energy of the band maximum decreases as $Cl_2 > Br_2 > BrI > I_2$.

TABLE I

Rates of reaction of $(C_2H_5)_4N[cis\text{-}Mn(CO)_4X_2]$* and $(C_2H_5)_4N[cis\text{-}Mn(CO)_4BrI]$ with various ligands, L, in *s*-tetrachloroethane at 25.5°

L	[L] (*M*)	$k_{obsd} \times 10^4$† (s^{-1})
Rates for $(C_2H_5)_4N[cis\text{-}Mn(CO)_4Br_2]$		
$P(C_6H_5)_3$	0.033	51[a]
	0.05	53
	0.066	45.5[a]
	0.33	52.5[a]
	0.66	50.5[a]
	0.33	170[a,b]
	0.33	330[a,c]
$P(OCH_2CH{:}CH_2)_3$	0.033	52
	0.05	60
	0.067	53
	0.33	60
	0.67	55
$P(OCH_3)_3$	0.033	53
	0.05	56
	0.067	56
	0.33	55
	0.67	54
	0.33	170[a,b]
	0.33	290[a,c]
$P(n\text{-}C_4H_9)_3$	0.165	44.5
	0.33	49[a]
	0.5	47
	0.66	54.5[a]
	1.33	56.5
	0.33	280[a,d]
	0.33	580[a,e]
$P(n\text{-}OC_4H_9)_3$	0.033	49
	0.05	46
	0.067	51.5
	0.33	54
	0.67	55
$P(OC_6H_5)_3$	0.033	45
	0.067	46
	0.33	48
	0.67	49
$P(OCH_2(CH_3)_2)_3$	0.033	58
	0.05	52.5
	0.067	52
	0.33	55.5
	0.67	53
C_5H_5N	0.033	50
	0.067	50
	0.33	51
	0.67	59
$As(C_6H_5)_3$	0.041	28
	0.05	30
	0.066	30[a]
	0.33	37
	0.66	36
	0.33	130[a,b]
	0.33	250[a,c]
$Sb(C_6H_5)_3$	0.025	11
	0.033	10
	0.041	10[a]
	0.05	11
	0.058	12
	0.066	11
Rates for $(C_2H_5)_4N[cis\text{-}Mn(CO)_4I_2]$		
$P(C_6H_5)_3$	0.033	0.71
	0.067	0.74
	0.33	0.77
	0.67	0.74
	0.33	2.9[f]
	0.33	7.2[g]
$P(OCH_3)_3$	0.033	0.80
	0.067	0.88
	0.33	0.88
	0.67	0.91
	0.33	2.3[f]
	0.33	5.6[g]
$As(C_6H_5)_3$	0.033	0.85
	0.067	0.97
	0.33	1.05
	0.67	1.05
	0.33	2.7[f]
	0.33	7.1[g]
Rates for $(C_2H_5)_4N[cis\text{-}Mn(CO)_4BrI]$		
$P(C_6H_5)_3$	0.033	3.2
	0.066	3.1
	0.33	3.2
	0.66	3.3
	0.066	14[h]
	0.33	13[h]
	0.066	28[i]
	0.263	28[i]
$P(OCH_3)_3$	0.033	2.9
	0.066	2.9
	0.33	2.8
	0.66	2.9
	0.066	15[h]
	0.33	17[h]
	0.066	33[i]
	0.33	32[i]
$As(C_6H_5)_3$	0.33	3.1
	0.66	3.1

*$t_{\frac{1}{2}}$ for $(C_2H_5)_4N$ $[cis\text{-}Mn(CO)_4Cl_2]$ and $P(C_6H_5)_3 \ll 1$ min.
†[a]Average value of several runs; [b]at 35.5°; [c]at 40.5°; [d]at 36.5°; [e]at 44.5°; [f]at 35.0°; [g]at 42.5°; [h]at 36.3°; [i]at 45.0°.

Can. J. Chem. Downloaded from www.nrcresearchpress.com by 210.87.254.6 on 09/05/12
For personal use only.

Can. J. Chem. Downloaded from www.nrcresearchpress.com by 210.87.254.6 on 09/05/12
For personal use only.

Discussion

Reactions of Tetraethylammonium cis-Dihalotetracarbonylmanganate(I) Complexes

The results of this investigation show that the $(C_2H_5)_4N[cis\text{-}Mn(CO)_4X_2]$ complexes, where X = Br, or I, react with ligands, L, to form $cis\text{-}Mn(CO)_4LX$ and $(C_2H_5)_4NX$. The kinetic data in Tables I and II demonstrate that the rates of substitution of X^- by L are independent of both the nature and concentration of L but decrease with increasing atomic weight of X. This suggests an S_N1 dissociative mechanism involving the slow loss of halide ion in the rate-determining step to form a five-coordinate intermediate, followed by the rapid entry of L (eq. [2])

[2] 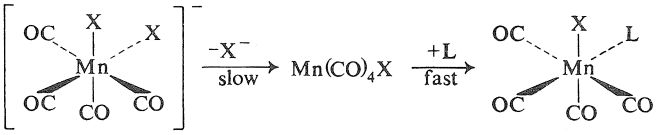

TABLE II

Rates of reaction of $(C_2H_5)_4N[cis\text{-}Mn(CO)_4Br_2]$ with $P(C_6H_5)_3$ in solvents other than *s*-tetrachloroethane at 25.5°

Solvent	$[P(C_6H_5)_3]$ (*M*)	$k_{obsd} \times 10^4$ (s^{-1})
1,2-Dichloroethane*	0.08	65
	0.17	64
	0.20	66
	0.33	70
	0.33	74
	0.40	71
	0.60	79
	0.80	71
Chloroform	0.017	70
	0.033	71
	0.067	77
	0.33	76
	0.67	73
Nitromethane	0.05	150
	0.10	150
	0.30	155

*Reactions at 24.5°.

TABLE III

Activation parameters for the substitution reactions of $(C_2H_5)_4N[cis\text{-}Mn(CO)_4X_2]$ with various ligands, L, in *s*-tetrachloroethane

X_2	L	$\Delta H^{\ddagger}$ (kcal $mole^{-1}$)	$\Delta S^{\ddagger *}$ (e.u. $mole^{-1}$)
Br_2	$P(C_6H_5)_3$	23	6
	$P(OCH_3)_3$	20	
	$P(n\text{-}C_4H_9)_3$	24	
I_2	$P(C_6H_5)_3$	24	−4
	$P(OCH_3)_3$	20	
	$As(C_6H_5)_3$	21	
BrI	$P(C_6H_5)_3$	21	−1
	$P(OCH_3)_3$	23	

*The activation entropies were calculated from the mean value of the activation enthalpy for each substrate and the mean rate constant at 25.5° for all of the ligands studied with that particular substrate.

Similar S_N1 dissociative mechanisms involving the breaking of a metal–halogen bond as the rate-determining step have been proposed by Allen and Barrett for the substitution reactions of $[cis\text{-}PR_3M(CO)_4X]^-$ (M = Cr, Mo, or W) with phosphines (3), and by Hieber and Wollmann for the halogen exchange reactions of $Mn(CO)_5Br$ and $Mn(CO)_5I$ (16).

Table III shows the activation parameters determined for several of the substitution reactions of $(C_2H_5)_4N[cis\text{-}Mn(CO)_4Br_2]$ and $(C_2H_5)_4N[cis\text{-}Mn(CO)_4I_2]$. The activation enthalpies for the loss of Br^- and I^- are the same within experimental error (mean values of $\Delta H^{\ddagger}$ are 22.3 and 21.7 kcal $mole^{-1}$ for $[cis\text{-}Mn(CO)_4Br_2]^-$ and $[cis\text{-}Mn(CO)_4I_2]^-$ respectively). The activation entropies given were calculated from the mean values of the activation enthalpies for each substrate. They are in the range expected for a dissociative mechanism (1). The activation entropy for the dibromo complex is greater than that for the di-iodo complex.

Correlating the activation data with the relative reaction rates of the two substrates presents some problems. That $[cis\text{-}Mn(CO)_4Br_2]^-$ should lose Br^- almost 100 times faster than $[cis\text{-}Mn(CO)_4I_2]^-$ loses I^- under the same conditions would immediately suggest that the Mn—Br bond is weaker than the Mn—I bond. Such a difference in bond strength would seem entirely reasonable since Mn(I) is classified as a *soft* acid and would be expected to form a weaker bond with the *harder* bromine atom than with the *softer* iodine atom (17). Furthermore, the C—O stretching modes in $[cis\text{-}Mn(CO)_4Br_2]^-$ occur at higher frequencies than those in $[cis\text{-}Mn(CO)_4I_2]^-$ (4, 5) implying a greater C—O

TABLE IV

C—O stretching frequencies of reaction products in *s*-tetrachloroethane*

Compound	L	$\nu_{CO}(cm^{-1})$			
cis-$Mn(CO)_4LCl$	$P(C_6H_5)_3$	2095	2022 (sh)	2010	1960
cis-$Mn(CO)_4LBr$	$P(C_6H_5)_3$	2090	2014 (sh)	2012	1965
	$As(C_6H_5)_3$	2090	2017 (sh)	2010	1957
	$P(OCH_3)_3$	2092		2010	1973
	$P(OCH(CH_3)_2)_3$	2094		2004	1963
	$P(n\text{-}OC_4H_9)_3$	2095		2002	1969
	$P(OCH_2CH{:}CH_2)_3$	2097		2012	1972
	$P(OC_6H_5)_3$	2101		2022	1988
cis-$Mn(CO)_4LI$	$P(C_6H_5)_3$	2082	2012 (sh)	2002	1962
	$As(C_6H_5)_3$	2083	2014 (sh)	2004	1962
	$P(OCH_3)_3$	2089		2034	1973
cis-$Mn(CO)_3L_2Br$	C_5H_5N	2022	1940	1910	
	$P(OCH(CH_3)_2)_3$	2028	1961	1921	
	$P(n\text{-}OC_4H_9)_3$	2036	1969	1926	
	$P(OCH_3)_3$	2040	1978	1929	
	$P(OCH_2CH{:}CH_2)_3$	2041	1976	1931	
	$P(OC_6H_5)_3$	2050	1993	1939	

*Relative intensities of absorptions in the order given are: *cis*-$Mn(CO)_4LX$, (m), (s), (s) and *cis*-$Mn(CO)_3L_2Br$, (s), (s), (s).

TABLE V

Near-ultraviolet absorption spectra of substrates and reaction products in *s*-tetrachloroethane

L	λ_{max}* (mμ) for *cis*-$Mn(CO)_4LX$, X is			
	Cl	Br		I
$P(OCH_3)_3$		380		391
$P(n\text{-}OC_4H_9)_3$		381	(382)	
$P(OCH_2CH{:}CH_2)_3$		381		
$P(OCH(CH_3)_2)_3$		383		
$P(OC_6H_5)_3$		383	(386)	
$P(n\text{-}C_4H_9)_3$			(385)	
CO			(386)	
$P(C_6H_5)Cl_2$			(392)	
$P(C_6H_5)_3$	386	396†	(396)	409
$As(C_6H_5)_3$		400	(403)	412
$Sb(C_6H_5)_3$		404	(409)	
Cl^-	402			
Br^-		429‡		438
I^-		438		441§

*Data from ref. (13) shown in parentheses.
†ε_{max} = 660 l mole^{-1} cm^{-1}.
‡ε_{max} = 640 l mole^{-1} cm^{-1}.
§ε_{max} = 980 l mole^{-1} cm^{-1}.

bond strength in the former. This can be interpreted to mean that the bromine atoms give a lower electron density to the central manganese ion than the less electronegative iodine atoms do, and so the Mn—Br bonds should be weaker than the Mn—I bonds. In view of the errors on the activation enthalpies it is, of course, possible that the activation enthalpy for the dibromo complex is significantly lower than that for the di-iodo complex, and this is the reason for the difference in their reactivity. Another possibility is that the bond strengths are comparable and that the difference in the reaction rates arises because of the difference in the activation entropies of the two substrates. An analogous situation has recently been reported for the substitution reactions of the $Re(CO)_5X$ compounds (18). Activation entropies have also been shown to be important in determining the relative rates of the substitution reactions of the Group VI metal hexacarbonyls, $M(CO)_6$, and substituted metal hexacarbonyls such as $M(CO)_4$(*o*-phen) (1).

Why the activated complex formed from $[cis\text{-}Mn(CO)_4Br_2]^-$ should show a greater gain in entropy over its ground state than that formed from $[cis\text{-}Mn(CO)_4I_2]^-$ remains to be explained. It might be expected that since the di-iodo complex is presumably the more constrained in the ground state, it would benefit more in the formation of an activated complex by a dissociation process. The fact that it does not, presumably means that its activated complex is more constrained than that from the dibromo complex. Two possible explanations to account for such a situation come to mind. Firstly, because of the larger halogen atom, the five groups in the intermediate, $Mn(CO)_4I$, have less freedom of movement around the central manganese ion than do those in the other intermediate,

Can. J. Chem. Downloaded from www.nrcresearchpress.com by 210.87.254.6 on 09/05/12
For personal use only.

Can. J. Chem. Downloaded from www.nrcresearchpress.com by 210.87.254.6 on 09/05/12
For personal use only.

$Mn(CO)_4Br$. Secondly, and more likely, the activated complex consists of a five-coordinated intermediate involved in a weak interaction with the leaving halide ion. The stronger this interaction, the less likelihood of two discrete entities being formed and the lower the activation entropy expected. Since I^- is the larger and more easily polarized of the two halide ions, it might be expected to interact with the intermediate, $Mn(CO)_4I$, to a greater extent than Br^- would interact with $Mn(CO)_4Br$ and hence the di-iodo complex would exhibit the lower activation entropy. The solvent would be expected to play an important part in stabilizing such activated complexes. It should also be pointed out that, from the above discussion, $(C_2H_5)_4N[cis\text{-}Mn(CO)_4Cl_2]$ would be expected to give rise to a larger activation entropy than $(C_2H_5)_4N[cis\text{-}Mn(CO)_4Br_2]$ and therefore to react faster, as was observed. It is planned to determine the activation parameters for the dichloro complex by studying the substitution reactions at low temperatures, to see if the dramatic difference in the reactivity of the substrates is truly the result of the differences in their activation entropies rather than an undetected difference in their activation enthalpies.

The $[Mn(CO)_4X_2]^-$ ions are isoelectronic and iso-structural with the neutral $Fe(CO)_4X_2$ molecules. The latter exchange X with $*X_2$ at a rate which is independent of $*X_2$ (16). The mechanism suggested involves the simultaneous dissociation of both X groups and concomitant X—X bond formation. Unfortunately, the difference in mechanism means that it is impossible to compare the reaction rates of the two systems. The $Mn(CO)_5X$ complexes exchange X with $*X_2$ by an S_N1 dissociative mechanism and at a much slower rate than the substitution reactions of the anions (16). This suggests that the Mn—X bonds are weaker in the anions. In the Introduction it was mentioned that the anionic complexes, $[M(CO)_5X]^-$ (M = Cr, Mo, W), react with phosphines by both an S_N1 and an S_N2 mechanism (3). The relative fraction of the reaction which proceeds by the S_N2 path versus the S_N1 path is larger for the Mo(0) and W(0) complexes than for the Cr(0) complexes. Similar observations have been made for the substitution reactions of the parent hexacarbonyls, $M(CO)_6$, and a variety of substituted hexacarbonyls (1). The occurrence of an S_N2 mechanism in these cases is particularly interesting as there are very few octahedral complexes known to undergo ligand substitution reactions *via* such a mechanism and, from a theoretical standpoint, d^6 metal complexes with filled t_{2g} orbitals would be considered the least likely of all to do so (1). The size of the central atom appears to be a very important factor for d^6, diamagnetic systems. Since Mn(I) is smaller than Cr(0), it comes as no surprise to find that the $[cis\text{-}Mn(CO)_4X_2]^-$ complexes react only by an S_N1 mechanism. We are currently investigating the substitution reactions of the $(C_2H_5)_4N[cis\text{-}Re(CO)_4X_2]$ complexes since, by analogy with Mo(0) and W(0), the much larger Re(I) should react by both an S_N1 and an S_N2 mechanism. Recently it has been reported that the CO substitution reactions of $cis\text{-}Re(CO)_4LX$ take place by both mechanisms (19).

The effect of solvent on the reaction rates has not yet been considered. Because of the ionic nature of the substrates and the release of X^- during the reactions, it was expected that the polarity of the solvent would greatly influence the rates. The reaction of $(C_2H_5)_4N[cis\text{-}Mn(CO)_4Br_2]$ with $P(C_6H_5)_3$ was studied in four different solvents. Unfortunately, the solubility properties of the substrate and ligand precluded the use of solvents covering a wide range of dielectric constants. Table VI indicates that, in general, the rate increases with increasing polarity of solvent. That the solvent has only a slight effect on the rate presumably means that there is very little difference in polarity between the ground state and the activated complex. This might be expected if the activated complex involves the leaving Br^- ion.

The results in Table I show that the reactions of $(C_2H_5)_4N[cis\text{-}Mn(CO)_4Br_2]$ with $As(C_6H_5)_3$ and $Sb(C_6H_5)_3$ in *s*-tetrachloroethane are slower than the reactions with the other ligands under the

TABLE VI

Rates of reaction of $(C_2H_5)_4N[cis\text{-}Mn(CO)_4Br_2]$ with $P(C_6H_5)_3$ in a variety of solvents at 25.5°

Solvent	$k_{obsd} \times 10^3$ (s^{-1})	Dielectric constant*
s-Tetrachloroethane	5.0	8.0 (20°)
1,2-Dichloroethane	7.0†	10.4 (25°)
Chloroform	7.3	4.8 (20°)
Nitromethane	15.0	34.8 (25°)

*From ref. 20.
†At 24.5°.

Can. J. Chem. Downloaded from www.nrcresearchpress.com by 210.87.254.6 on 09/05/12
For personal use only.

same conditions. However, the rates are also independent of ligand concentration. The activation enthalpy for the reaction with $As(C_6H_5)_3$ is 25 kcal mole^{-1}. This is slightly higher than that found for the other ligands and may be responsible for the slower reaction. Another possibility is that the slower rates for $As(C_6H_5)_3$ and $Sb(C_6H_5)_3$ are the result of some specific solvent effects. Similar anomalies were found in the substitution reactions of $Mn(CO)_5Br$ (12).

The reaction of $(C_2H_5)_4N[cis\text{-}Mn(CO)_4Br_2]$ with pyridine went directly to the disubstituted product, $cis\text{-}Mn(CO)_3(C_5H_5N)_2Br$, without giving any evidence for the monosubstituted intermediate. Since the rate constant for the reaction was the same as that found with the other ligands, it is assumed that reaction [2] was rapidly followed by loss of CO and entry of a second pyridine molecule. The same effect was observed when $Mn(CO)_5Br$ reacted with pyridine and other ligands which coordinate through nitrogen (12).

Reactions of Tetraethylammonium cis-Bromoiodotetracarbonylmanganate(I)

It was hoped that by studying the rates of the substitution reactions of the mixed halide complex, $(C_2H_5)_4N[cis\text{-}Mn(CO)_4BrI]$, it might be possible to determine the relative strengths of the Mn—Br and Mn—I bonds, since, if the Mn—Br bond is weaker than the Mn—I bond, reaction [6] would be expected to occur in preference to reaction [7]

[6] $(C_2H_5)_4N[cis\text{-}Mn(CO)_4BrI] + L \rightarrow cis\text{-}Mn(CO)_4LI + (C_2H_5)_4NBr$

[7] $(C_2H_5)_4N[cis\text{-}Mn(CO)_4BrI] + L \rightarrow cis\text{-}Mn(CO)_4LBr + (C_2H_5)_4NI$

The rate of disappearance of $(C_2H_5)_4N[cis\text{-}Mn(CO)_4BrI]$ was found to be independent of the nature and concentration of L. The reactions proceeded with pseudo-first-order rate constants in between the rates for $(C_2H_5)_4N[cis\text{-}Mn(CO)_4Br_2]$ and $(C_2H_5)_4N[cis\text{-}Mn(CO)_4I_2]$ but closer to those of the latter (Table I). The dilute solutions used in the kinetic runs prevented the isolation and analytical identification of the reaction products. The near-ultraviolet spectra of the reaction mixtures taken at the end of the kinetic runs indicated the presence of *cis*-$Mn(CO)_4LBr$. Infrared spectra recorded later showed the presence of both *cis*-$Mn(CO)_4LBr$ and *cis*-$Mn(CO)_4LI$. Preparative scale reactions were carried out with $P(C_6H_5)_3$. The manganese carbonyl derivative and the tetraethylammonium halide isolated proved to be mixtures of *cis*-$Mn(CO)_4P(C_6H_5)_3Br$ and *cis*-$Mn(CO)_4P(C_6H_5)_3I$, and $(C_2H_5)_4NBr$ and $(C_2H_5)_4NI$, respectively. No attempt was made to determine the exact composition of either of these mixtures. The formation of mixed products during these reactions would seem to indicate that both the Mn—Br and the Mn—I bonds are being broken. This would imply that the manganese–halogen bonds are of comparable strength. However, whilst these studies were in progress, the following halogen exchange reaction was observed

[8] *cis*-$Mn(CO)_4P(C_6H_5)_3Br + (C_2H_5)_4NI \rightarrow cis\text{-}Mn(CO)_4P(C_6H_5)_3I + (C_2H_5)_4NBr$

Although no kinetic investigation of this reaction was made, spectroscopic evidence indicated that it was approaching completion at a rate somewhat slower than the substitution reactions of the bromo-iodo complex. The near-ultraviolet spectra taken at the end of the kinetic runs showed the presence of only *cis*-$Mn(CO)_4P(C_6H_5)_3Br$. However, infrared spectra of these reaction mixtures recorded later indicated that both *cis*-$Mn(CO)_4P(C_6H_5)_3Br$ and *cis*-$Mn(CO)_4P(C_6H_5)_3I$ were present. This must mean that the bromo-iodo complex reacts only *via* reaction [7] and that the halogen exchange reaction [8] is responsible for the formation of mixed products. Furthermore, if reaction [8] reaches completion, mixed products would not be expected. It is possible, however, that the spectral studies and product isolation were carried out before the halogen exchange had had chance to reach completion. Another possible explanation for the mixed products is that the exchange reaction reaches an equilibrium rather than going to completion. The halogen exchange reaction is being further investigated at the present time.

It appears then that the rate-determining step in the substitution reactions of the bromo-iodo complex is the rupture of the Mn—I bond. The reactions are faster than those with the di-iodo complex which also take place by the breaking of an Mn—I bond. Recalling our previous discussion, since the mean activation enthalpies for the two substrates are very similar, the faster rate for the bromo-iodo complex is presumably because of the greater activation entropy expected for an

activated complex involving the five-coordinated intermediate, $Mn(CO)_4Br$, than for that involving $Mn(CO)_4I$. Within the experimental errors quoted, the activation entropies for the bromo-iodo and the di-iodo complexes are in agreement with this interpretation. It should be pointed out, however, that it was difficult to obtain satisfactory A_∞ values for the substitution reactions of the bromo-iodo complex at temperatures above 25°, owing to interference from the subsequent reactions of the *cis*-$Mn(CO)_4LBr$ compounds. This interference led to large errors in the activation parameters.

In conclusion, it appears that the substitution reactions of $(C_2H_5)_4N$[*cis*-$Mn(CO)_4BrI$] take place by the breaking of the Mn—I bond and not the Mn—Br bond. The initial products of the reaction appear to be *cis*-$Mn(CO)_4LBr$ and $(C_2H_5)_4NI$. As the result of a halogen exchange reaction, the compounds *cis*-$Mn(CO)_4LI$ and $(C_2H_5)_4NBr$ are also formed. In these substitution reactions and in the analogous reactions of the dibromo and di-iodo complexes there was no evidence of CO substitution by L to form ions of the type $[Mn(CO)_3LX_2]^-$.

Acknowledgments

This research was generously supported by a National Research Council of Canada Grant. We thank Mr. W. Dawson for technical assistance.

1. R. J. Angelici. Organometal. Chem. Rev. **3**, 173 (1968).
2. W. Hieber and K. Wollmann. Chem. Ber. **95**, 1552 (1962).
3. A. D. Allen and P. F. Barrett. Can. J. Chem. **46**, 1655 (1968).
4. E. W. Abel and I. S. Butler. J. Chem. Soc. 434 (1964).
5. R. J. Angelici. Inorg. Chem. **3**, 1099 (1964).
6. E. W. Abel, I. S. Butler, M. C. Ganorkar, C. R. Jenkins, and M. H. B. Stiddard. Inorg. Chem. **5**, 25 (1966).
7. I. S. Butler. Ph.D. thesis, University of Bristol, Bristol, England. 1964.
8. E. W. Abel and G. Wilkinson. J. Chem. Soc. 1501 (1959).
9. E. O. Brimm, M. A. Lynch, and W. J. Sesny. J. Am. Chem. Soc. **76**, 3831 (1954).
10. R. S. Drago. Physical methods in inorganic chemistry. Reinhold Publishing Corp., New York. 1965. p. 131.
11. E. W. Abel and G. Wilkinson. J. Chem. Soc. 1501 (1959).
12. R. J. Angelici and F. Basolo. J. Am. Chem. Soc. **84**, 2495 (1962).
13. R. J. Angelici and F. Basolo. Inorg. Chem. **2**, 728 (1963).
14. D. M. Adams. Metal-ligand and related vibrations. Edward Arnold Ltd., London. 1967. pp. 107–111.
15. R. J. Angelici. J. Inorg. Nucl. Chem. **28**, 2627 (1966).
16. W. Hieber and K. Wollmann. Chem. Ber. **94**, 305 (1961).
17. R. G. Pearson. J. Am. Chem. Soc. **85**, 3533 (1963).
18. F. Zingales, M. Graziani, F. Faraone, and U. Belluco. Inorg. Chim. Acta, **1**, 172 (1967).
19. F. Zingales, A. Trovati, and U. Belluco. Personal communication, R. E. Kirk and D. F. Othmer (*Editors*). Cited in ref. (18).
20. R. E. Kirk and D. F. Othmer (*Editors*). Encyclopedia of Chemical Technology. Interscience Publishers, Inc., New York. 1961.

Can. J. Chem. Downloaded from www.nrcresearchpress.com by 210.87.254.6 on 09/05/12
For personal use only.

^{14}N nuclear magnetic resonance: amines and ammonium ions

M. WITANOWSKI AND H. JANUSZEWSKI
Institute of Organic Chemistry, Polish Academy of Sciences, Warszawa, Poland

Received September 19, 1968

The ^{14}N nuclear magnetic resonance (n.m.r.) signals of alkylamines and ammonium ions are shifted to lower magnetic fields with the increasing number of alkyl groups at the carbon atom directly bonded to the nitrogen atom, and at the nitrogen atom itself. The resonance of an ammonium ion always occurs at a field lower than that for the corresponding amine. It seems that high-lying excited states, not only those corresponding to lowest-wavelength transitions, are important for an explanation of the observed resonance shifts. A downfield shift of the ^{14}N resonance and a substantial increase in signal width, as compared with the spectra of neat amines, are observed for aqueous solutions of amines. There is a very characteristic chemical shift for the $R—CH_2—NH_2$ molecules (R = alkyl, phenyl, vinyl) in the ^{14}N n.m.r. spectra.

Canadian Journal of Chemistry, 47, 1321 (1969)

Can. J. Chem. Downloaded from www.nrcresearchpress.com by 210.87.254.40 on 09/05/12
For personal use only.

Introduction

Correlations between ^{14}N chemical shifts and molecular structure have already been found (1, 2, 4, 5) for various classes of organic compounds that contain sp- or sp^2-hybridized nitrogen atoms. A theoretical explanation of the shifts has been postulated (5, 6) in terms of the linear combination of atomic orbitals (l.c.a.o.), molecular orbitals, and the mean excitation energy approximation. However, there have so far been no satisfactory observations and explanation of the ^{14}N shifts for the nitrogen atoms in saturated systems. The available data (7) for amines and ammonium ions, based on external reference measurements under non-uniform experimental conditions, did not show any obvious dependence of the shift on the structure and the number of alkyl groups at the nitrogen atom. The only exception was the observation of a downfield shift for symmetric ammonium ions, in order NH_4^+, $N(CH_3)_4^+$, $N(C_2H_5)_4^+$. The attempt (7) at finding a relationship between the longest-wavelength transition of the inert electron pair and the ^{14}N chemical shift gave rather unsatisfactory results for saturated amines, while a general correlation of this kind could be observed for large chemical shifts in the spectra of unsaturated molecules.

In this paper, the principal concern is the effect of alkyl groups R in structures $:N(R_1)(R_2)(R_3)$ and $^+N(R_1)(R_2)(R_3)(R_4)$ on the ^{14}N resonances, as can be inferred from a systematic study by internal reference methods (3). Such effects may have diagnostic value for interpretation of ^{14}N n.m.r. spectra. They should also contribute to a better understanding of nitrogen chemical shifts, since only σ-bond and lone-pair effects are involved here. Even if it should not be possible to obtain a complete description of the origin of spectral changes, the observations may be helpful in eliminating non-decisive factors in the theory of ^{14}N chemical shifts.

Experimental

The substances investigated were chemically pure commercial grade. A Varian HA-60 spectrometer operating at 4.33 Mc/s (14 100 G) in the HR mode was used for the measurements of ^{14}N n.m.r. spectra. The samples were placed in 15 mm outer diameter tubes, sealed if neccessary. Both the centerband and the 2 kc/s sideband from the base-line stabilizing system were recorded for calibration purposes, and for optimizing the signal-to-noise ratio of broad and sharp resonance peaks. The latter, particularly those of ammonium ions which showed fine multiplet structure, were measured in the sideband mode. The internal reference methods of calibration followed those suggested in earlier work (3) The results of measurements, given in Tables I and II, are averages of 4–6 runs; maximum experimental deviation is indicated in the Tables. If one or two results happened to differ significantly from the rest, six measurements were carried out, and the average was calculated of the four closest results. The half-height widths were measured under conditions where the power of the radiofrequency was far below the saturation level of the signal. Slight coloration of the samples containing nitromethane was observed after several hours, but the shifts and widths of the resonance signals did not change, at least outside the experimental error.

Results and Discussion

The ^{14}N chemical shifts and signal widths of amines and ammonium ions are given in Tables I and II, respectively. The ^{14}N n.m.r. signals of the aliphatic amines (2–19) occur between +320 and +380 p.p.m., while the amino groups at an

Can. J. Chem. Downloaded from www.nrcresearchpress.com by 210.87.254.40 on 09/05/12
For personal use only.

TABLE I

^{14}N Nuclear magnetic resonance spectra of amines*

Compound	Neat + trace CH_3NO_2		In dioxane + trace CH_3NO_2			In 5% $NaOH_{aq.}$ + KNO_3			Chemical shift† (p.p.m.)
	δ_N (p.p.m.)	Half-height width (c.p.s.)	δ_N (p.p.m.)	Half-height width (c.p.s.)	Concentration v/v	δ_N (p.p.m.)	Half-height width (c.p.s.)	Concentration v/v	
1 NH_3	+383±0.5	22±2	—	—	—	+375±1	110±3	30%	+376 (neat)
2 CH_3NH_2	+378±1	65±5	+378±2	75±10	5%	+370±2	350±10	30%	+353 (H_2O)
3 $CH_3CH_2NH_2$	+355±1	70±5	+355±1	90±5	30%	+351±2	350±10	30%	+338 (H_2O)
4 $CH_3CH_2CH_2NH_2$	+359±1	85±5	+360±1	110±5	50%	—	—	—	—
5 $CH_3CH_2CH_2CH_2NH_2$	+359±2	200±10	—	—	—	—	—	—	+314 (?)
6 $(CH_3)_2CHNH_2$	+334±1	100±5	+335±1	100±5	50%	—	—	—	—
7 Cyclohexylamine	+337±1	185±5	+340±2	185±10	50%	—	—	—	—
8 $(CH_3)_3CNH_2$	+319±1	98±5	+320±1	115±5	50%	+316±3	270±20	30%	—
9 $(CH_3)_2NH$	+371±1	98±5	+370±1	110±5	20%	+362±2	400±10	20%	+355 (H_2O)
10 $(CH_3)_3N$	+365±1	110±5	+366±2	150±10	30%	+340±3	650±20	15%	+356 (Et_2O)
11 $(CH_3CH_2)_2NH$	+332±1	180±5	+332±1	195±5	50%	—	—	—	+323 (H_2O)
12 $(CH_3CH_2)_3N$	+327±2	320±10	—	—	—	—	—	—	+329 (neat)
13 $(CH_3CH_2CH_2CH_2)_2NH$	+351±3	450±20	—	—	—	—	—	—	—
14 $CH_2{=}CHCH_2NH_2$	+360±1	100±5	—	—	—	—	—	—	—
15 Benzylamine	+356±2	220±10	—	—	—	—	—	—	—
16 $H_2NCH_2CH_2NH_2$	+363±1	160±5	+365±1	160±5	30%	—	—	—	—
17 $H_2N(CH_2)_4NH_2$	+360±1	235±5	—	—	—	—	—	—	—
18 $CH_3CH(NH_2)CH_2NH_2$	+354±2	285±10	+357±2	280±10	50%	—	—	—	—
19 $HOCH_2CH_2NH_2$	+364±5	900±30	—	—	—	—	—	—	—
20 Aniline	+319±3	700±20	—	—	—	—	—	—	+330 (Et_2O)
21 N-Methylaniline	+320±4	950±30	—	—	—	—	—	—	+328 (Et_2O)
22 2-Aminopyridine (in acetone)	+128±4 +315±4	650±20 680±20	—	—	—	—	—	—	+115 +313 (Et_2O)
23 3-Aminopyridine (in acetone)	+88±4 +326±4	680±20 680±20	—	—	—	—	—	—	+ 78 +328 (Et_2O)
24 4-Aminopyridine (in acetone)	+105±4 +317±4	680±20 620±20	—	—	—	—	—	—	+105 +321 (Me_2CO)

*Internal reference scale δ_N of chemical shifts ($\delta_N CH_3NO_2 = \delta_N NO_3^- = 0$ p.p.m.), see ref. 3.
†Referred to NO_3^- external standard; see ref. 7.

Can. J. Chem. Downloaded from www.nrcresearchpress.com by 210.87.254.40 on 09/05/12
For personal use only.

aromatic ring (**20–24**) are characterized by a rather narrow range, +315 to +320 p.p.m. The effect of an aprotic solvent, such as dioxane (Table I), is insignificant, but there is a definite downfield shift of the resonance in aqueous NaOH as well as a remarkable increase in signal width. The spectra of neat amines and their dioxane solutions are not affected by the varying proportion of nitromethane (1–10% v/v). The range of occurrence of ammonium ion resonance peaks overlaps with a large part of that for amines. The reliability of nitromethane as internal standard for concentrated acid solutions of alkylammonium salts was examined in the spectra of tetramethylammonium chloride in concentrated aqueous HCl with a trace of nitromethane, and in neutral aqueous solution with KNO_3 as the internal standard. The difference in the shifts was negligible (Table II).

Mono-alkylamines show a clear dependence of their ^{14}N shifts on the structure of the alkyl group, and a similar downfield shift with the increasing substitution at the α-carbon atom (decreasing electronegativity) is also observed for the corresponding ammonium ions, as shown below.

Compound	R	δ_N (p.p.m.)
$R—NH_2$ (neat)	CH_3	+378
	CH_2CH_3	+355
	$CH(CH_3)_2$	+334
	$C(CH_3)$	+319
$R—NH_3^+$	CH_3	+351
	CH_2CH_3	+336
	$C(CH_3)_3$	+314

Similar trends exist in the shifts of di- and trialkylamines as well as those of di-, tri-, and tetraalkylammonium ions.

The chemical shift of +360 ± 5 p.p.m. is very characteristic of the $R—CH_2—NH_2$ system where R = alkyl, aryl, or vinyl (**3–5**, **14–17**, **19**), since it is out of range of the shifts for di- and trialkylamines and ammonium ions.

A shift to lower field is also observed if the number of alkyl groups at the nitrogen atom increases,

$$RNH_2 \rightarrow R_2NH \rightarrow R_3N$$

$$RNH_3^+ \rightarrow R_2NH_2^+ \rightarrow R_3NH^+ \rightarrow R_4N^+$$

$$\longrightarrow \text{downfield } ^{14}\text{N shift}$$

but the effect is not so large and not so regular as for the substitution at the α-carbon atom. It is possible that steric hindrance and hybridization changes affect the spectra.

The resonance signal of an ammonium ion always occurs at a field lower by 5–30 p.p.m. than that for the corresponding amine. The origin of the low-field shift for aqueous solutions of amines (**1**, **2**, **3**, **8**, **9**, **10**), as compared with neat amines, may be of the same nature.

$$\underset{\text{weak hydrogen bond}}{R—\overset{H}{\underset{H}{N}}: \cdots H—\overset{H}{N}—} \rightarrow \underset{\text{stronger hydrogen bond}}{R—\overset{H}{\underset{H}{N}}: \cdots H—O—} \rightarrow \underset{\text{complete proton transfer}}{R—NH_3^+}$$

$$\longrightarrow \text{downfield } ^{14}\text{N shift}$$

The presence of hydroxyl groups which may be hydrogen-bonded to the amino group results in a large increase in signal width, as can be seen for the aqueous solutions of amines. The viscosity of the solution does not seem to be a dominant factor here, since the dioxane solutions do not show any appreciable broadening of the resonance signals in spite of the higher viscosity of dioxane as compared to water and neat amines.

One should note that the resonance shift between amines and the corresponding ammonium ions is diamagnetic, i.e. to lower fields with the decreasing electron density at the nitrogen atom, while shifts in the other direction are observed within the two groups of molecules. The former may simply be explained as due to a decrease in the diamagnetic term in the expression for the screening constant. However, caution is neccessary here, because of the latter shifts. An alternative explanation of the amine–ammonium ion shift may be found from a consideration of the paramagnetic term. In the mean excitation energy approximation, this is proportional (8) to the mean inverse cube of the 2p-orbital radius, the reciprocal mean excitation energy, and the $\sum Q_{AB}$ term

$$(Q_{AB})_{zz} = P_{x_Ax_B}(2\delta - P_{y_Ay_B}) + P_{y_Ay_B}(2\delta - P_{x_Ax_B}) + 2P_{x_Ay_B}P_{y_Ax_B}$$

with analogous other components of the tensor, where the P terms are p-bond orders and p-charge densities from the l.c.a.o. matrix. For structure $N(R_1)(R_2)(R_3)(R_4)$, where R = H,

TABLE II

^{14}N nuclear magnetic resonance spectra of ammonium ions*

Compound	Ammonium ion (saturated solution of the chloride in conc. HCl + trace nitromethane)	δ_N (p.p.m.)	Half-height† width (c.p.s.)	Literature data (p.p.m.)‡
25	NH_4^+	+354.5±0.5§	5±1	+353.5
26	$CH_3NH_3^+$	+351±1‖	30±4	+342
27	$(CH_3)_2NH_2^+$	+348±1¶	40±4	+336
28	$(CH_3)_3NH^+$	+334±1**	30±4	+350
29	$(CH_3)_4N^+$	+333.5±0.5††	6.5±1	+332
30	$CH_3CH_2NH_3^+$	+336±1‖	40±4	—
31	$(CH_3CH_2)_2NH_2^+$	+320±1¶	50±4	—
32	$(CH_3CH_2)_3NH^+$	+314±1**	50±4	—
33	$(CH_3CH_2)_4N^+$	+311±0.5	10±1	+312
34	$(CH_3)_3CNH_3^+$	+314±1	60±4	—
35	$(NH_3CH_2CH_2NH_3)^{++}$	+342±2	90±10	—
36	$HONH_3^+$	+293±5	500±30	+276
37	$NH_3^+SO_3^-$	+285±2	60±10	+285

*Internal reference scale δ_N of chemical shifts; see Table I and ref. 3.
†Measured directly or calculated from the apparent width, assuming $J_{NH} = 50$ c.p.s.
‡See ref. 7, shift from NO_3^- external reference.
§1:4:6:4:1 quintet, $J_{NH} = 50 \pm 1$ c.p.s.
‖1:3:3:1 quartet, $J_{NH} = 50$ c.p.s.
¶1:2:1 triplet.
**Doublet.
††The shift measured in aqueous solution with KNO_3 internal standard is +334.5 ± 0.5 p.p.m.

an alkyl, or an electron pair (one only), the molecular orbitals may be written as

$$\psi_{NR}^{\sigma} = \frac{1}{\sqrt{2}}[(1 + a)^{1/2}\phi_{N(sp^3)} + (1 - a)^{1/2}\phi_R]$$

where a is the σ-bond polarization parameter. Hence, $Q_{NR,H} = 0$ and $Q_{NN} = 2 - \frac{1}{3}(a_1a_2 + a_1a_3 + a_1a_4 + a_2a_3 + a_2a_4 + a_3a_4)$. This may be simplified, for structures with all groups R identical, to

Group	Q_{NN}
NR_4^+	$2 - a^2$
$:NR_3$	$2 - a - a^2$

The difference in Q_{NN} between NR_4^+ and $:NR_3$ is positive (thus suggesting a downfield shift for the former) if

$$a(NR_3) + a^2(NR_3) - 2a^2(NR_4^+) > 0$$

or else if $a(NR_3) = 0$; 0.05; or 0.10, then $a(NR_4^+) \leqslant 0$; 0.16; or 0.23, respectively. Thus the change in the Q_{NN} term and in the 2p-orbital radius may explain, at least in part, the resonance shift between amines and ammonium ions. However, the shifts within the two groups cannot be explained in this way. The remaining factor in the expression for the paramagnetic term (8) is the mean excitation energy. It is rather difficult to obtain a reliable estimate of the latter. Replacing the mean excitation energy with that of the longest-wavelength transition is a very crude method and gives poor correlation with the ^{14}N shifts of amines; it is better for the nitrogen-containing unsaturated systems (7). However, if the ^{14}N shifts of amines are compared with the available (9) data from vacuum ultraviolet absorption measurements (Table III), the correlation seems to improve for the second band. While the changes in the first band correspond roughly only to the downfield shift with the increasing number of alkyl groups at the nitrogen atom, the changes in the second band reciprocate the shift between the corresponding methyl and ethyl derivatives of ammonia. Nevertheless, the correlation is far from being linear. It is possible, that a still better relationship should be obtained if the next consecutive transition was included into the consideration of the mean excitation energy, but there were no data available.

The effect of delocalization of the lone electron pair at the nitrogen atom is observed on the ^{14}N n.m.r. spectra as a downfield shift (**20–24**) of the resonance. This effect is characteristic of the conjugated amines as a whole, but also shows variations consistent with the degree of delocali-

Can. J. Chem. Downloaded from www.nrcresearchpress.com by 210.87.254.40 on 09/05/12
For personal use only.

TABLE III

Vacuum ultraviolet absorption measurements of amines

Compound	Far ultraviolet absorption bands* (cm^{-1})		^{14}N chemical shift δ_N (p.p.m.)
	First band	Second band	
NH_3	51 500	66 000	+383
CH_3NH_2	46 500	57 500	+378
$(CH_3)_2NH$	45 000	52 500	+371
$(CH_3)_3N$	44 000	50 250	+365
$C_2H_5NH_2$	47 000	56 500	+355
$(C_2H_5)_2NH$	45 000	51 500	+332
$(C_2H_5)_3N$	—	47 250	+327

*Data from ref. 9.

zation of the lone pair (**22–24**). Most probably, the shift results from an increase in the paramagnetic term due to π-bonding between the nitrogen atom and the aromatic ring. It is analogous to the downfield shift of the ^{14}N resonance of amides (6), where the lone pair is also involved in a delocalized orbital system.

1. M. WITANOWSKI, T. URBAŃSKI, and L. STEFANIAK. J. Am. Chem. Soc. **86**, 2569 (1964).
2. M. WITANOWSKI and L. STEFANIAK. J. Chem. Soc. **B**, 1061 (1967).
3. M. WITANOWSKI and H. JANUSZEWSKI. J. Chem. Soc. **B**, 1062 (1967).
4. M. WITANOWSKI, L. STEFANIAK, and G. A. WEBB. J. Chem. Soc. **B**, 1065 (1967).
5. M. WITANOWSKI. Tetrahedron, **23**, 4299 (1967).
6. M. WITANOWSKI. J. Am. Chem. Soc. **90**, 5683 (1968).
7. D. HERBISON-EVANS and R. E. RICHARDS. Mol. Phys. **8**, 19 (1964), and references therein.
8. J. A. POPLE. Discussions Faraday Soc. **34**, 7 (1963).
9. E. TANNENBAUM, E. M. COFFIN, and A. J. HARRISON. J. Chem. Phys. **21**, 311 (1953).

Can. J. Chem. Downloaded from www.nrcresearchpress.com by 210.87.254.40 on 09/05/12
For personal use only.

Nuclear recoil reactions in organomanganese compounds. III. $Mn(CO)_5$

I. G. DE JONG, S. C. SRINIVASAN, AND D. R. WILES
Chemistry Department, Carleton University, Ottawa, Canada

Received October 1, 1968

Experimental evidence is presented which shows that upon neutron irradiation of the compounds $Mn_2(CO)_{10}$, $CpMn(CO)_3$, and $CH_3CpMn(CO)_3$ the recoiling ^{56}Mn atom gathers carbonyl radicals to stabilize itself in the group $Mn(CO)_5$, with about 10% radiochemical yield. Basically, the experiments involved addition of iodine to the irradiated compound and identification of the radioactive $IMn(CO)_5$ by carrier techniques. It is suggested that in $Mn_2(CO)_{10}$ targets, the species produced is the $\cdot Mn(CO)_5$ radical itself. Some experimental data are given to show that this radical is stable for over 1 h in the solid at room temperature, but decomposes rapidly above about 60°. The radical decomposes in 20–30 s in solution. In both other target compounds, the species produced is chemically more stable, although it reacts rapidly with iodine. This species is found to be $HMn(CO)_5$, which occurs to the extent of 10–12% in $CpMn(CO)_3$. $CH_3Mn(CO)_5$ was also detected in $CH_3CpMn(CO)_3$ targets, and its yield was found to be a function of the concentration of isooctane used as diluent in the targets.

Results from other studies are discussed in the light of the present data, and it is concluded that in general, in neutron-irradiated metal carbonyl compounds, the recoil atom is able to accumulate carbonyl radicals to a greater extent than is consistent with the composition of the target compound.

Canadian Journal of Chemistry, 47, 1327 (1969)

Can. J. Chem. Downloaded from www.nrcresearchpress.com by 210.87.254.40 on 09/05/12
For personal use only.

Introduction

The various phenomena resulting from the capture of a neutron by a nucleus can be divided into three groups. First, and most obvious, is the nuclear transition itself—in this case we shall consider only radiative capture, or the (n,γ) process.

Second, and much more obscure experimentally, is a group of essentially physical phenomena, which depends mostly on the nature of the nuclear de-excitation process and on the state of aggregation of the target material. These phenomena include high energy (up to several hundred eV) recoil of the product nucleus, or ejection of several (up to 10 or 15) of the atomic electrons, or combinations of these. As a result of this sudden deposition of energy, the region around the product nucleus is presumed to be heated very rapidly to temperatures which are very difficult to estimate but which may be several hundred degrees. The size and duration of this hot zone are also very difficult to evaluate, but current estimates suggest a diameter of some few Å and a lifetime of perhaps 10^{-10} s. A study of these phenomena is made extremely difficult by the short duration of the action and by the fact that invariably the results are severely altered by subsequent reactions.

The third group is one of essentially chemical reactions which depend strongly on the chemical nature of the medium. These reactions include electron capture, electron transfer, ionic diffusion, ligand transfer and exchange, and other reactions in ionic solids, radical diffusion, radical recombination, atom abstraction, group migration, and other reactions in molecular compounds.

It is clear, of course, that the reactions cannot be so neatly categorized in reality, although the reactions which have been studied seem to group themselves roughly along the lines just stated.

Although practical difficulties often interfere, this last group of phenomena is in principle amenable to chemical study. It is these phenomena which we have been studying, in an attempt ultimately to shed light on the nature of the second group of physical processes which precedes and causes the third group.

In previous papers of this series (1, 2) we have discussed studies of recoil reactions in cyclopentadienylmanganese tricarbonyl ($CpMn(CO)_3$) and its homologue methylcyclopentadienylmanganese tricarbonyl ($CH_3CpMn(CO)_3$). While several as yet unexplained phenomena were reported in these and other papers (3) it was established that the important reactions were radical reactions. Perhaps of equal significance, and less predictable, was the discovery and identification (4, 2) of $CH_3Mn(CO)_5$ as one of the products of recoil reactions in $CH_3CpMn(CO)_3$. While not without precedent, since Baumgärtner and Zahn (5) had found considerable chromium hexacarbonyl in neutron-irradiated

Can. J. Chem. Downloaded from www.nrcresearchpress.com by 210.87.254.40 on 09/05/12
For personal use only.

benzenechromium tricarbonyl, this discovery raised the question as to how five carbonyl groups could be collected by a manganese atom, in a milieu of only three carbonyls per molecule. Baumgärtner and Zahn had noted the same anomaly, and attributed the results to the mobility of the carbonyl radical. We conjectured similarly (2, 4) that the molecule was formed largely in the hot zone, but by reactions of a primarily chemical nature. The stepwise nature of such reactions has been suggested by work on the carbonyls of chromium and other Group VI metals (6). Thus, it became possible to pose the question (2) as to which was the final step:

[1] $$\cdot CH_3 + \cdot Mn(CO)_5 \rightarrow CH_3Mn(CO)_5$$

or

[2] $$CH_3\dot{M}n(CO)_4 + \cdot CO \rightarrow CH_3Mn(CO)_5$$

It was evident that the methyl group is the ring substituent, rather than a group reconstituted from ring fragments, since no $CH_3Mn(CO)_5$ was detected in irradiated $CpMn(CO)_3$ (7). Similarly, irradiation of $Mn_2(CO)_{10}$ in benzene solution gave rise to small amounts of phenylmanganese pentacarbonyl, ($C_6H_5Mn(CO)_5$), showing the importance of the available phenyl radicals (7, 8).

Recently, strong evidence was found for the existence of the $Mn(CO)_5$ radical in neutron-irradiated $Mn_2(CO)_{10}$, and the suggestion was made (8) that this radical might provide the mechanism for the formation of $CH_3Mn(CO)_5$ and the other observed manganese pentacarbonyls. Thus, it seemed that reaction [1] was chosen in preference to reaction [2]. This same $Mn(CO)_5$ group is commonly found as an entity forming part of a variety of organometal compounds (9), taking part in photochemical (10) and other reactions. It has been considered as a possible catalytic intermediate (11). Studies of its behavior in a mass spectrometer have been able to lead to determination of some thermodynamic (12) and kinetic (13) properties of $Mn(CO)_5$ in the gas phase. The present paper reports on various studies of the occurrence and behavior of the $Mn(CO)_5$ group in recoil reactions.

Experimental

This work involves experiments which are basically straightforward: a purified target material is irradiated with neutrons, it is dissolved in a purified solvent, macro quantities (e.g. 20 mg) of carriers are added for any suspected products, and the carriers are carefully separated and purified. The purified products are analyzed to determine chemical recovery, and the radioactivity of ^{56}Mn is measured to determine radiochemical yield. The result, after appropriate correction, is expressed as the retention (of the parent compound) or the yield (of all other identifiable products) which is in each case the % of the radioactive ^{56}Mn which is recovered in each of the respective forms.

Target Materials

$Mn_2(CO)_{10}$ was obtained from Strem Chemicals Inc. It was purified before use by chromatography, followed by vacuum sublimation. $CpMn(CO)_3$ was obtained from Ethyl Corporation, and was purified before use by vacuum sublimation. $CH_3CpMn(CO)_3$ was obtained from Ethyl Corporation, and was distilled under reduced pressure before use. In the handling of these materials, care was taken at all stages to avoid strong light, even fluorescent room light, whenever possible. Purified samples were stored in the dark until use.

Carrier Compounds

$IMn(CO)_5$ was prepared by direct reaction of $Mn_2(CO)_{10}$ with I_2 (14) and was purified by column chromatography on silica gel in petroleum ether. $CH_3Mn(CO)_5$ and $HMn(CO)_5$ were prepared by the reactions of CH_3I and of phosphoric acid with $NaMn(CO)_5$ (15). They were purified by high vacuum methods before use.

Chemical Processing

Separation and purification of the various products is done largely by column chromatography on silica gel. $CH_3Mn(CO)_5$ was separated by vapor–phase chromatography (v.p.c.) on Silicone 550 oil, supported on fire brick. $HMn(CO)_5$ was separated in some experiments by v.p.c. and in other experiments by high vacuum transfer techniques. In all cases, it was immediately converted to $IMn(CO)_5$, which was subsequently purified by column chromatography. Except for a few initial experiments, all chemical processing was done under nitrogen, using carefully purified solvents, so as to exclude oxygen and moisture since, as is shown below, some of the compounds are sensitive to the presence of atmospheric oxygen. In all cases the utmost care was taken to avoid severe treatment of the target compound, especially prior to the addition of carriers, since it has been shown (16) that the apparent retention may be affected by such treatment. One frequently used procedure was to dissolve the target compound in a solution of iodine in petroleum ether (8). The iodine was subsequently removed by extraction with an aqueous sulfite solution after the addition of carriers. No evidence has been found to suggest bulk reaction with the target materials, even under conditions much more severe than those actually used in our experiments.

Analysis

Chemical recovery of the carriers was determined by direct weighing whenever possible. Otherwise, spectrophotometric analysis was used, with care taken to minimize photolytic or thermal decomposition within the spectrophotometer.

Irradiations

Irradiations were performed in the Sb–Be neutron facilities of A.E.C.L., Commercial Products Division, in

Can. J. Chem. Downloaded from www.nrcresearchpress.com by 210.87.254.40 on 09/05/12
For personal use only.

Ottawa (17) and in the thermal column of the reactor at the Western New York Nuclear Research Center, Buffalo. The thermal neutron fluxes were $\sim 2 \times 10^8$ and $\sim 3 \times 10^9$ cm^{-2} s^{-1}, respectively. The irradiation conditions differed more significantly in the γ flux, which amounted to about 2 Mrads h^{-1} in the Ottawa source, and was very much lower in the thermal column.

Counting Procedure

The 0.84 MeV γ ray from ^{56}Mn was measured using various NaI scintillation counters. The sample geometry was kept constant through all measurements of each experiment. Correction was made for decay of the activity during the experiment.

Results

$Mn_2(CO)_{10}$

The results of various experiments on neutron-irradiated $Mn_2(CO)_{10}$ are shown in Figs. 1–3. The yield of $IMn(CO)_5$ shows a distinct dependence on the presence of atmospheric oxygen, and we accept the data from the nitrogen experiments as representing the more correct value. (The $IMn(CO)_5$ data given in ref. 8 were obtained from experiments done in air, and are thus less accurate than the present data.) The fact that the yield of $IMn(CO)_5$ is insensitive to the concentration of I_2 from very low concentrations, suggests that the scavenging reaction occurs in the solution rather than immediately at the dissolving interface. The evident insensitivity of the retention of $Mn_2(CO)_{10}$ to the iodine concentration, including no iodine at all, shows that the scavenged species does not recombine or exchange to form

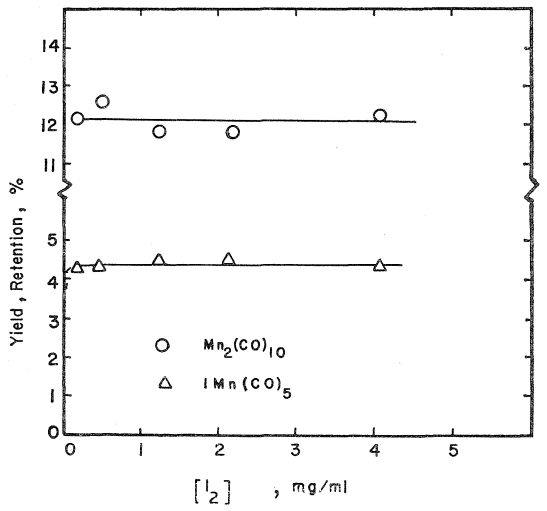

FIG. 1. Retention and yield data in $Mn_2(CO)_{10}$ as a function of iodine concentration.

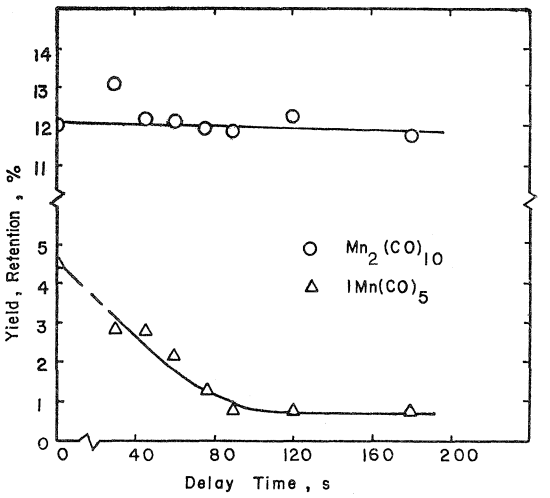

FIG. 2. Retention and yield data in $Mn_2(CO)_{10}$ as a function of the time of delayed addition of iodine (1.2 mg I_2 ml^{-1}). The zero of time is uncertain by about 0.3 min, but the timing of the experiments is consistent to within 2–3 s.

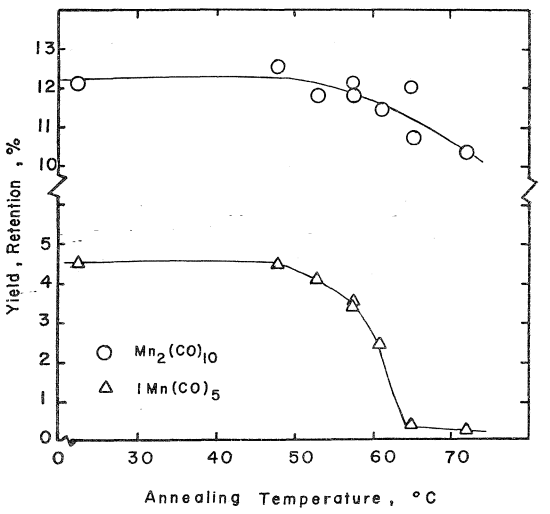

FIG. 3. Retention and yield data in $Mn_2(CO)_{10}$ as a function of temperature of isochronal (6.0 min) annealing.

$Mn_2(CO)_{10}$ in the absence of the scavenger. We have claimed earlier (8) that this species is the $\cdot Mn(CO)_5$ radical. We shall present later in this paper further arguments bearing on this identification.

The stability of the $\cdot Mn(CO)_5$ radical in solution is shown by the data in Fig. 2. The data are somewhat scattered, as one might expect from such an experiment. Nonetheless, it is clear that

the half-time of the radical under these conditions is some seconds—the exact value is not important to this present work. Once again, one sees no effect on the $Mn_2(CO)_{10}$ retention, so it is evident that, whatever their fate, these radicals do not combine or exchange to give $Mn_2(CO)_{10}$.

A very common experiment in the study of recoil reactions in ionic systems is the observation of the effects of heating the solid target material before its chemical processing, so as to learn about reactions which occur in the solid state before the chemical dissolution can have any destructive effect on the various unstable species. Such an experiment was done on the neutron-irradiated $Mn_2(CO)_{10}$, with the results shown in Fig. 3. Here it is quite apparent that the radical is being destroyed—once again without combination or exchange to re-form the target compound. There was no detectable bulk decomposition of the target compound. The fact that the decomposition occurs so abruptly at 55–60° suggests that a single-step reaction is involved. Thus the decomposition is evidently

[3] $$\cdot Mn(CO)_5 \rightarrow Mn(CO)_4 + CO \rightarrow \cdots$$

(We wish to point out here that the usual methods of studying radicals—notably by electron spin resonance—cannot be applied here because of the very small number of these radicals present. We estimate that at the time of our radioactivity measurements we have present about 10^7 $\cdot Mn(CO)_5$ radicals. To scale up the experiments to give a detectable number of radicals would involve the production of very intense radioactivity, which would be awkward to handle. Furthermore, the intense radiation necessary to produce this large an activity would likely cause severe damage to the material, and so obliterate any traces of the radical under study.)

$CpMn(CO)_3$

The results of studies on $CpMn(CO)_3$ are shown in Fig. 4. Only the iodine scavenging experiment was done on this target compound, with heat treatment of the samples prior to their dissolution. Here the behavior is quite different, in that we observe that the species giving rise to $IMn(CO)_5$ is no longer sensitive to the thermal treatment. To be sure, there is a small decrease in the yield of $IMn(CO)_5$, and a corresponding increase in the yield of $Mn_2(CO)_{10}$. If this is not merely coincidence, it may then be that a small

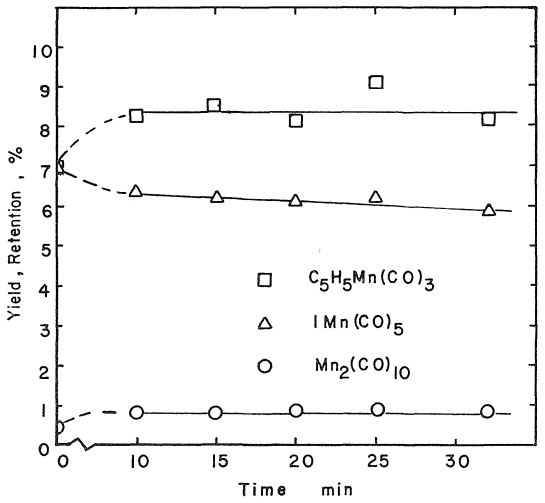

FIG. 4. Retention and yield data in $CpMn(CO)_3$ as a function of time of isothermal (70 °C) annealing.

amount of the species giving rise to $IMn(CO)_5$ is converted to $Mn_2(CO)_{10}$. However, in any case the change is very small, and the bulk of the species remains, at a temperature far higher, and for a time far longer than was the case for the $\cdot Mn(CO)_5$ radical in $Mn_2(CO)_{10}$ targets. This leads us to the conclusion that already in the solid target, long before heat treatment, and thus presumably in the hot or still warm zone, the $\cdot Mn(CO)_5$ radical is scavenged by some internal scavenger to give a stable compound. Again, the retention in the parent compound seems not to be substantially changed in the heating. Specific separation of $HMn(CO)_5$ has been done on samples of $CpMn(CO)_3$ irradiated in the A.E.C.L. neutron source, with the result that 10–12% of the ^{56}Mn was found to be in the form of $HMn(CO)_5$. We take this as satisfactory evidence that the 'stable compound' referred to above is indeed $HMn(CO)_5$. The quantitative discrepancy between these results and those of the iodine scavenging experiments remains unexplained, although it is possible that the reaction of iodine with $HMn(CO)_5$ may not be nearly 100% efficient.

$CH_3CpMn(CO)_3$

In addition to ambient-temperature neutron irradiations carried out in the Sb–Be facility in Ottawa, we have done low-temperature irradiations (using dry ice and liquid nitrogen) and ambient-temperature irradiations in the Western

Can. J. Chem. Downloaded from www.nrcresearchpress.com by 210.87.254.40 on 09/05/12
For personal use only.

Can. J. Chem. Downloaded from www.nrcresearchpress.com by 210.87.254.40 on 09/05/12
For personal use only.

TABLE I

Retention and yield data in $CH_3CpMn(CO)_3$ as a function of isooctane concentration in the irradiated sample*

Isooctane,	$CH_3Mn(CO)_5$	
% by volume	Retention, %	Yield, %
0	4.2	0.14
5	3.8	0.13
10	4.6	0.15
15	—	0.41
20	—	0.83
25	4.4	0.71
30	4.0	0.40
35	3.2	—
50	1.9	0.36

*Neutron irradiation was done at room temperature in the A.E.C.L. Sb–Be source.

New York Nuclear Research Center's reactor in Buffalo. The results are given in Tables I and II respectively, and are shown in Fig. 5. Here we find that the $CH_3Mn(CO)_5$ yield is a sensitive function of the irradiation conditions and of the physical state of the target. Experiments in which the manganese compound contained added isooctane during the irradiation, showed an increase in the $CH_3Mn(CO)_5$ yield in the Ottawa irradiations and a general decrease in the Buffalo irradiations, when the targets were in the liquid state. This difference of behavior shows a dependence of the yield on the γ dose rate which, in turn, presumably indicates that the reaction leading to the formation of $CH_3Mn(CO)_5$ is dependent on the presence of radiolysis products. However, irradiations at low temperatures show generally higher yields (1–3%) of the same compound. In further experiments, the $CH_3Mn(CO)_5$ yields were lower when iodine was added to the dissolving medium after the irradiations, suggesting that a chemical reaction had taken place between the $CH_3Mn(CO)_5$ produced and the iodine added. This reaction was confirmed in milligram tests which showed that a reaction occurs rapidly in these solutions according to eq. [4]

[4] $$CH_3Mn(CO)_5 + I_2 \rightarrow IMn(CO)_5 \ (+CH_3I \ ?)$$

These iodine scavenging experiments also showed a yield of $IMn(CO)_5$ to the extent of about 10% at low temperatures.

Experiments in which the addition of iodine was delayed by up to 30 min showed no significant variation of the $IMn(CO)_5$ yield, unlike the case of neutron-irradiated $Mn_2(CO)_{10}$ under similar conditions. This suggests once again the presence in the solvent of a stable chemical species which must have undergone reaction with the added iodine to give the ultimate product, $IMn(CO)_5$, but which does not decompose in solution under nitrogen. The general similarity between the two arene target systems is evident. The retentions are similar, the formation of an additional stable species occurs in both, and the only significant

TABLE II

Retention and yield data in $CH_3CpMn(CO)_3$ under various conditions of irradiation*

Temperature, °C	Isooctane, % by volume	Retention, %	Yield, %	
			$CH_3Mn(CO)_5$	$IMn(CO)_5$
20	0	5.5	0.57	—
	20	2.5	0.08†	—
	25	1.3	0.03†	—
	30	—	0.1†	—
	60	0.1	0.05†	—
−78	0	7.6	1.7	—
	10	11.2	2.5	—
	20	9.6	3.1	—
	30	8.0	1.5	—
	0	9.4	0.32	10.0
−190	0	8.1‡	—	12.7
	0	8.0‡	—	12.9
	0	7.6‡	—	13.9
	0	8.3‡	—	10.9
	0	8.4	—	—

*Neutron irradiations were done in the thermal columns at the Western New York Nuclear Research Center, Buffalo.
†The counting rates in these samples were very low, so that the yield values are very imprecise.
‡Iodine was added to these samples at times of 0, 10, 20, and 30 min after melting of the target compound.

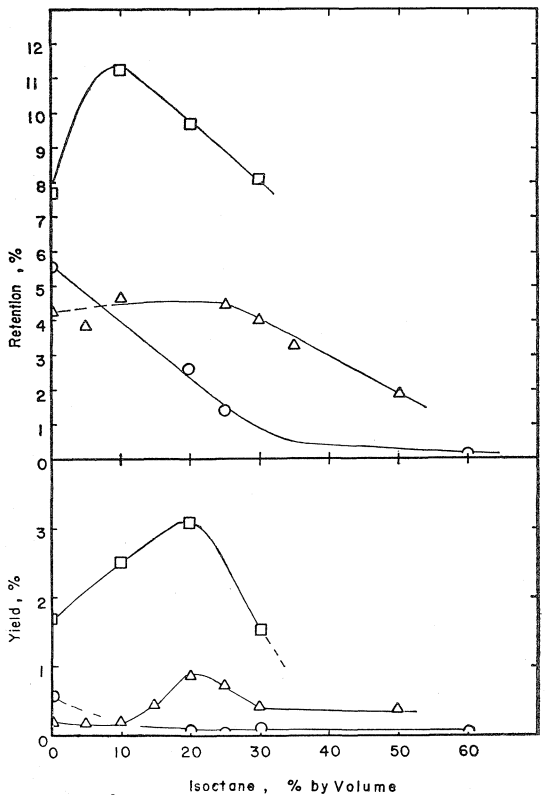

FIG. 5. Retention and yield of $CH_3Mn(CO)_5$ in $CH_3CpMn(CO)_3$ as a function of isooctane concentration. □, Irradiation done at Buffalo, −78 °C; △, irradiation done at Ottawa, ~20 °C; ○, irradiation done at Buffalo, ~20 °C (cf. Tables I and II).

difference appears to be the identity of the additional species, which is $HMn(CO)_5$ in one case and both $HMn(CO)_5$ and $CH_3Mn(CO)_5$ in the other.

Discussion

The identity of the species scavenged in the iodine experiments is perhaps the first thing to discuss. It was suggested earlier (8) that this must be the $\cdot Mn(CO)_5$ radical. From the data shown in Fig. 3, it is evident that in $Mn(CO_2)_{10}$ experiments, the scavenged species is thermally quite unstable, while from Fig. 2 it is apparent that the species has a short but measurable lifetime—some 20 s or so. This is in keeping with its being the $\cdot Mn(CO)_5$ radical, since none of the other expectable compounds of $—Mn(CO)_5$ would decompose so rapidly under such gentle conditions. This conclusion is supported by the data shown in Figs. 4 and 6, showing that in $CpMn(CO)_3$ and $CH_3CpMn(CO)_3$, in which a greater range of reactions are available, the yield of $IMn(CO)_5$ is unaffected by heating and by decomposition in solution. It is evident that in these latter two cases a stable compound is formed already in the solid target—identified as is described above. Thus we conclude that the radical $\cdot Mn(CO)_5$ is indeed formed in $Mn_2(CO)_{10}$ targets, and $HMn(CO)_5$ is produced when hydrogen atoms are available. $CH_3Mn(CO)_5$ is clearly formed only when methyl groups are available, and then not to as great an extent as $HMn(CO)_5$.

It is significant that in $Mn_2(CO)_{10}$ targets, heating does not cause the parent retention to increase in an amount proportional to the decrease in $\cdot Mn(CO)_5$ yield. This shows that the radical cannot combine with other nearby radicals, as in eq. [5], nor does there occur any exchange with nearby $Mn_2(CO)_{10}$ molecules, according to eq. [6].

$$[5] \quad \cdot{}^*Mn(CO)_5 + \cdot Mn(CO)_5 \rightarrow {}^*MnMn(CO)_{10}$$

$$[6] \quad \cdot{}^*Mn(CO)_5 + Mn_2(CO)_{10} \rightarrow {}^*MnMn(CO)_{10} + \cdot Mn(CO)_5$$

Reactions analogous to both of these have been postulated recently to occur in neutron-irradiated iron and ruthenium carbonyls (16).

Perhaps one of the most interesting results is the uniformly high yield of the $—Mn(CO)_5$ products which, in all cases, are *in toto* equal to or greater than the retention in the parent form. These results can be compared with the data from Baumgärtner and Zahn (5) who, on irradiating $C_6H_6Cr(CO)_3$, found a substantially higher yield of ^{51}Cr in $Cr(CO)_6$ than in the parent form. Likewise, it has been shown recently (16) that $Fe(CO)_5$ is formed in quite high yield in neutron-irradiated $Fe_3(CO)_{12}$. All of these results lead us to suggest the following rule (18): *in neutron-irradiated metal carbonyl compounds, the recoil atom is able to accumulate carbonyl radicals to a greater extent than is consistent with the composition of the target compound.* That is to say, the reaction

$$[7] \quad M + nCO \rightarrow M(CO)_x \qquad x = 5, 6$$

is kinetically favored over simultaneous competing reactions.

Several years ago, a paper by Baumgärtner and Zahn (19) showed that in various organochromium systems thermodynamic factors have

Can. J. Chem. Downloaded from www.nrcresearchpress.com by 210.87.254.40 on 09/05/12
For personal use only.

Can. J. Chem. Downloaded from www.nrcresearchpress.com by 210.87.254.40 on 09/05/12
For personal use only.

little effect in governing the distribution of recoil atoms among the various products. If that principle is generally valid, it is apparent that kinetic factors must be dominant, as is implied in our postulated rule. Although this postulate requires much wider experimental study than the few systems for which it now appears valid, it seems probable that it carries important implications about the nature of the hot zone surrounding the recoil atom.

Although the evidence is incomplete, it appears that the difference between the $IMn(CO)_5$ and $CH_3Mn(CO)_5$ yields in neutron-irradiated $CH_3CpMn(CO)_3$ (Table II) is entirely accounted for by the presence of $HMn(CO)_5$, and is thus the result of another kinetic competition—between H atoms and CH_3 radicals, competing for the $\cdot Mn(CO)_5$ radicals:

$$[8] \qquad \cdot Mn(CO)_5 \begin{cases} + \cdot H \rightarrow HMn(CO)_5 \\ + \cdot CH_3 \rightarrow CH_3Mn(CO)_5 \end{cases}$$

although one must not ignore the possibility that these reactions involve abstraction rather than radical combination.

The increase in $CH_3Mn(CO)_5$ yield in $CH_3CpMn(CO)_3$ with increasing isooctane concentration (Table I), is evidently the result of increased availability of methyl groups, although the two are not related in a simple way. The difference between these results, obtained at a high γ dose rate, and those of Table II, obtained in a very low γ dose rate, suggests that in these solutions the CH_3 radicals involved are produced radiolytically, not by the recoil action. The ensuing decrease in $CH_3Mn(CO)_5$ yield (Table I) may be attributed, without direct evidence, to the onset of competitive radical reactions which likely affect the availability of CO radicals for the reconstruction of $—Mn(CO)_5$. The decrease in parent retention shown in Table I seems to be related again to the availability of carbonyl radicals.

At this point, when the reactions leading to the observed and identified products are becoming clear, one is impelled to ask about the unidentified 80% of the recoil atoms. It has been common to label this intractable fraction as the 'inorganic' fraction, with the recognition that the only way in which it can be handled is after its conversion to Mn^{++} in aqueous solutions. We are coming to the opinion that this material may more likely be large polymeric species, of perhaps poorly definable composition, which are neither volatile nor soluble in organic solvents. It would be consistent with our observations and with our stated rule for these species to be polymeric carbonyls, $Mn_x(CO)_y$, where $x > 2$. We have no evidence on this point, but hope to make an experimental study of this fraction in the near future.

Acknowledgments

We wish to express our gratitude to Dr. K. E. Collins for extending the hospitality of his laboratory and facilities to one of us for several weeks. We are grateful to the staff of the A.E.C.L. neutron facility for frequent and willing assistance. We also express our thanks to Imperial Oil Ltd., and to the National Research Council of Canada for financial support, and to Carleton University for a Graduate Fellowship to S.C.S.

1. T. Costea, I. Negoescu, P. Vasudev, and D. R. Wiles. Can. J. Chem. **44**, 885 (1966).
2. I.-C. Yang and D. R. Wiles. Can. J. Chem. **45**, 1357 (1967).
3. U. Zahn. Radiochim. Acta, **7**, 170 (1967).
4. S. C. Srinivasan, D. R. Wiles, and I.-C. Yang. Inorg. Nucl. Chem. Letters, **2**, 399 (1966).
5. F. Baumgärtner and U. Zahn. Radiochim. Acta, **1**, 51 (1963).
6. U. Zahn, C. H. Collins, and K. E. Collins. To be published.
7. S. C. Srinivasan. Unpublished work.
8. I. G. de Jong and D. R. Wiles. Chem. Commun. 519 (1968).
9. R. W. Cattrall and R. J. H. Clark. J. Organometall. Chem. **6**, 167 (1966); W. Jetz, P. Simons, J. Thompson, and W. A. G. Graham. Inorg. Chem. **5**, 2217 (1966).
10. E. O. Fischer and M. Herberhold. *In* Essays in coordination chemistry. Experimentia, Suppl. IX. Birkhäusen Verlag, Basel. 1964. p. 259.
11. C. H. Bamford and R. Denyer. Trans. Faraday Soc. **62**, 1567 (1966).
12. D. R. Bidinosti and N. S. McIntyre. Chem. Commun. 555 (1966).
13. M. J. Mays and R. N. F. Simpson. J. Chem. Soc. 1936 (1967).
14. E. O. Brimm, M. A. Lynch, Jr., and W. J. Sesny. J. Am. Chem. Soc. **76**, 3831 (1954).
15. Organometallic syntheses. Vol. I. *Edited by* J. J. Eisch and R. B. King. Academic Press, Inc., New York. 1965. pp. 147, 158.
16. S. R. Narayan and D. R. Wiles. Can. J. Chem. In press.
17. R. Courtemanche and S. A. Kushneriak. Can. Nucl. Technol. **5**, (2) 32 (1966).
18. S. C. Srinivasan and D. R. Wiles. To be published.
19. F. Baumgärtner and U. Zahn. Z. Elektrochem. **64**, 1046 (1960).

Can. J. Chem. Downloaded from www.nrcresearchpress.com by 210.87.254.6 on 09/05/12
For personal use only.

Reactions of thiyl radicals. VI. Photolysis of ethanethiol[1]

R. P. Steer and A. R. Knight
Department of Chemistry and Chemical Engineering, University of Saskatchewan, Saskatoon, Saskatchewan

Received September 18, 1968

The photolysis of ethanethiol vapor in the pressure range 10 to 350 Torr and the effect of % decomposition, wavelength, and of added inert gas and ethylene on the rate of formation of the products has been determined. In addition, the effect of temperature on the photolysis of methanethiol – ethylene – inert gas and ethanethiol – ethylene – inert gas systems has been studied.

For the pure substrate, the primary process is S—H bond cleavage and the hydrogen atom produced abstracts the sulfyhydryl hydrogen of the substrate. The quantum yield of molecular hydrogen formation is unity, independent of pressure. C_2H_5S radicals, formed either in the primary process or as a result of abstractive attack by H atoms or radicals on the substrate, combine to form an excited disulfide molecule. The major condensable product, $C_2H_5SSC_2H_5$, arises via collisional deactivation of this excited species which can also sensitize the decomposition of the substrate to give C_2H_4, C_2H_6, and H_2S, the other products observed. With added inert gas the rates of formation of the minor products decrease whereas hydrogen and disulfide remain unchanged.

With added ethylene, the major products are H_2, $C_2H_5SSC_2H_5$, and $C_2H_5SC_2H_5$, the addition product. Diethyl sulfide is formed in a chain reaction by the attack of C_2H_5S on the olefinic double bond to form the composite radical, followed by H abstraction from the substrate. The hydrogen rate decreases due to the addition of H atoms to ethylene. The rate constant ratio, k_{22}/k_4, for the reactions [22] and [4], respectively,

$$H + RSH \rightarrow H_2 + RS \qquad H + C_2H_4 \rightarrow C_2H_5$$

is pressure dependent, indicative of the formation of hot hydrogen atoms in the primary process of the photolysis of methanethiol and ethanethiol. The Arrhenius parameters A_{22}/A_4 and $E_{22} - E_4$ for the methanethiol–ethylene and ethanethiol–ethylene systems have been determined. Kinetic treatments of the proposed mechanisms have been undertaken.

Canadian Journal of Chemistry, 47, 1335 (1969)

Introduction

Early investigations (1, 2) of the photolysis of ethanethiol have indicated that the products of the complete photolysis of this compound in the vapor phase are diethyl disulfide and hydrogen, together with a smaller amount of ethane and a trace of unidentified olefin, whereas the only significant gaseous product of the photolysis of liquid ethanethiol at low % conversion is hydrogen. The major products were suggested to arise from the reactions

[1] $$C_2H_5SH + h\nu \rightarrow C_2H_5S + H$$

[2] $$H + C_2H_5SH \rightarrow H_2 + C_2H_5S$$

[3] $$2C_2H_5S \rightarrow C_2H_5SSC_2H_5$$

The photolysis of ethanethiol vapor in the presence of ethylene has been shown (3) to result in a decrease in the rate of hydrogen formation due to the addition of hydrogen atoms to the olefin according to the reaction

[4] $$H + C_2H_4 \rightarrow C_2H_5$$

Using the method of Darwent and Roberts (4), a value of $k_2/k_4 = 1.9 \pm 0.1$ at 24 °C was calculated but was found to be inexplicably pressure-dependent at high total reactant pressures.

Recent work by several groups (5–7) has indicated that hot hydrogen atoms may be produced in the photolysis of H_2S. Preliminary work in this laboratory (8) has shown that hot hydrogen atoms may also be produced in the photolysis of simple alkanethiols. The results of a detailed study of the photolysis of ethanethiol and of the reactions of hot hydrogen atoms in this sytem and in the methanethiol system are presented in this paper as part of a continuing series of investigations (9–12) into the photochemical decomposition of low molecular weight sulfur-containing compounds.

Experimental

Experiments were carried out in a grease- and mercury-free high vacuum system previously described (12). Standard high vacuum techniques were used for handling and storing reactants and products and, when necessary, products were separated by low temperature, high vacuum distillations. Details of these procedures have been given elsewhere (12, 13).

Ethanethiol (Matheson, Coleman and Bell) was purified in the following manner. The thiol (50 ml) was

[1]From the Ph.D. Thesis of R. P. Steer, University of Saskatchewan, Saskatoon, 1968.

TABLE I

Effect of time of exposure on the rates of formation of the products of the photolysis of ethanethiol vapor

Exposure time (min)	Rate of formation of (μmoles/min exposure)				
	H_2	C_2H_4	C_2H_6	H_2S	$C_2H_5SSC_2H_5$
5.0	0.77	0.034	0.16	0.18	0.85
10.0	0.76	—	0.17	0.15	—
10.0	0.71	0.027	0.16	0.16	0.76
10.0	0.76	0.028	0.15	0.17	0.75
30.0	0.70	0.026	0.16	0.18	0.83
60.0	0.67	0.025	0.14	0.16	0.80

fractionally distilled at atmospheric pressure through a 2 ft column of glass helices (b.p. 34.3–34.6 °C/715 Torr), rejecting the first 10 ml of distillate and collecting the next six successive 5 ml fractions. Analysis by gas chromatography showed that fractions 4 and 5 contained the least amount of impurity and these were admitted to the vacuum line for further purification. After degassing, the thiol was vacuum distilled repeatedly from −84 °C (ethyl acetate slush) to −117 °C (ethanol slush), retaining the middle fraction each time. This procedure resulted in material which contained only small amounts of impurities, estimated to be about 0.05%, which were more volatile (on the basis of their gas chromatographic elution times) than ethanethiol but which could not be removed by further distillation. Carbon dioxide was obtained from three sources. Assayed reagent grade carbon dioxide (J. T. Baker Chemical Co. and Air Reduction Corp.) was stated to have no more than 4 p.p.m. impurity (air) and was used without further purification. Cylinder carbon dioxide (Matheson) was distilled once from −130 to −196 °C and was thoroughly degassed before use. Other materials were purified by methods previously given (12).

Light intensities were determined by measuring the rate of CO production from the photolysis of gaseous acetone at 150 °C. For experiments in which the quantum yields of the products of the photolysis of ethanethiol were measured, the absorbed light intensity was $(4.96 \pm 0.08) \times 10^{-2}$ μeinsteins min^{-1}, determined with an interference filter, which passed only the mercury 2537 Å line, in place.

Results

The products of the photolysis of ethanethiol vapor with the mercury 2537 Å line at room temperature were found to be hydrogen, diethyl disulfide, ethane, ethylene, and hydrogen sulfide. In the first series of runs, the rates of formation of these products were measured as a function of the pressure of ethanethiol vapor in the reaction cell. The results are given in Fig. 1.

The rates of formation of the hydrocarbon products, ethane and ethylene, increase rapidly at low ethanethiol pressures, then level off at pressures at which the absorption of 2537 Å light is complete. Hydrogen sulfide exhibits similar behavior, although the yields of this product are somewhat more scattered. The rate of hydrogen production also increases with increasing substrate pressure and levels off in the high pressure region. This behavior is unlike that of the methanethiol system (12) in which the hydrogen rate continues to increase with increasing substrate pressure even after light absorption is complete. Due to mechanical losses of diethyl disulfide in the vacuum line, the yields of this product are extremely scattered. However, within the limits of experimental error, it also increases with increasing substrate pressure and levels off at higher pressures when light absorption is complete.

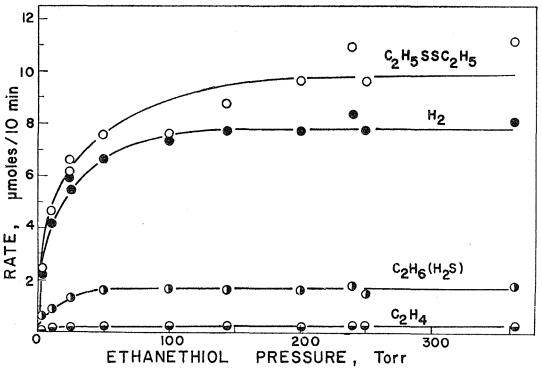

FIG. 1. Rates of formation of H_2, ●; $C_2H_5SSC_2H_5$, ○; C_2H_4, ◒; and C_2H_6 or H_2S, ◑; as a function of substrate pressure for the photolysis of ethanethiol at room temperature. The yields of C_2H_6 and H_2S are so similar that on this scale they can be represented by a single point at a particular thiol pressure.

The effect of increasing exposure time on the rates of formation of the products of the photolysis of 100 Torr of ethanethiol vapor at 25 ± 3 °C was next determined. The results are very similar to those obtained in the methanethiol system (12) and are presented in Table I. The rates of forma-

Can. J. Chem. Downloaded from www.nrcresearchpress.com by 210.87.254.6 on 09/05/12
For personal use only.

Can. J. Chem. Downloaded from www.nrcresearchpress.com by 210.87.254.6 on 09/05/12
For personal use only.

tion of all the products decrease with increasing exposure time due to increasing absorption by the disulfide product as the % decomposition of the substrate increases. However, the *relative* rates of formation of the products do not change significantly with increasing exposure time, indicating that none of the products measured are produced by secondary photolysis.

To determine whether ethylene in this system is produced by the disproportionation of ethyl radicals, a search for *n*-butane from a reaction in which 26 Torr of ethanethiol was photolyzed for 30 min was conducted. Gas chromatographic analysis of the −117 °C non-condensable product of this reaction indicated that *n*-butane was absent. Because *n*-butane is a product of the bimolecular reaction involving two ethyl radicals, its absence would indicate that neither combination nor disproportionation reactions of ethyl radicals are occurring in this system.

TABLE II

Hydrogen quantum yields for the photolysis of ethanethiol at 2537 Å and 22 °C

$P(C_2H_5SH)$ (Torr)	$\Phi(H_2)$
252.0	0.95
175.0	0.98
132.0	1.01
90.0	0.94
	Average 0.97 ± 0.03

The quantum yields of hydrogen, determined as a function of substrate pressure, are given in Table II. Within experimental error, the quantum yield of hydrogen is unity and, unlike the methanethiol system (12), is independent of pressure in the region of complete light absorption. Using the measured value of $\Phi(H_2) = 0.97$, the quantum yields of the other products may be calculated from their yields relative to that of hydrogen. The results are: $\Phi(C_2H_4) = 0.037$, $\Phi(C_2H_6) = 0.22$, $\Phi(H_2S) = 0.23$, and $\Phi(C_2H_5SSC_2H_5) = 1.26$, assuming that the rates of formation of all these products are independent of substrate pressure for pressures greater than 100 Torr. The mass balances $\Phi(H_2S) = \Phi(C_2H_4) + \Phi(C_2H_6)$ and $\Phi(C_2H_5SSC_2H_5) = \Phi(H_2) + \Phi(C_2H_6)$ hold within experimental error.

The addition of increasing pressures of carbon dioxide produces an effect on the photolysis of

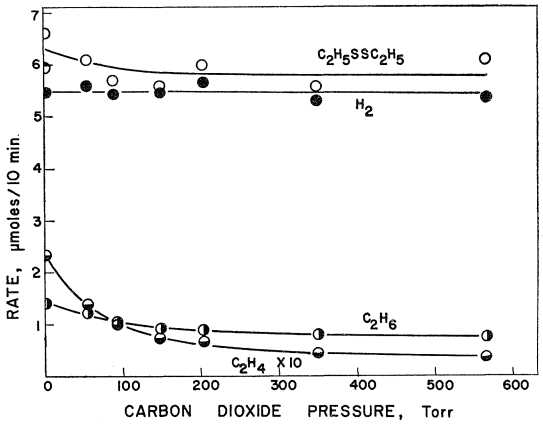

FIG. 2. Rates of formation of H_2, ●; $C_2H_5SSC_2H_5$, ○; C_2H_6, ◑; and C_2H_4, ◒; as a function of the pressure of added CO_2 for the photolysis of 25 Torr of ethanethiol at room temperature.

25 Torr of ethanethiol, which is similar to that observed in the CH_3SH system when CF_4 was used as a deactivating gas (12). The results are presented in Fig. 2. No significant change in the rate of hydrogen production is observed. The yields of the minor products, C_2H_4, C_2H_6, and H_2S (not shown), decrease with increasing inert gas pressure, ethylene decreasing at a faster rate than the others. As the pressure of inert addend is increased it becomes increasingly difficult to determine the yields of these products. Under these conditions, quantitative separation of the large amount of addend from the products and unreacted substrate cannot be easily accomplished. Thus the error in reported yields is highest at the largest pressures of addend used.

Diethyl disulfide also appears to decrease slightly, but again the errors involved in quantitative determination of the yields of this relatively non-volatile product are too large to permit a more definitive statement of its behavior.

To ensure that the pressure effects observed in the presence of CO_2 were actually due to the addend, varying pressures of C_2H_5SH were photolyzed in the presence of a constant CO_2 pressure of 715 ± 5 Torr. The results are given in Fig. 3. A comparison of these results with those for the pure substrate photolysis confirms that the rates of hydrogen and disulfide formation are independent of addend pressure. The rate of formation of minor products, however, apparently depends on the partial pressure of the substrate.

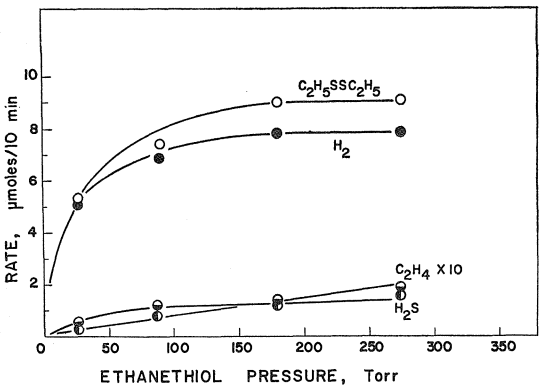

FIG. 3. Rates of formation of H_2, ●; $C_2H_5SSC_2H_5$, ○; C_2H_4, ◒; and H_2S, ◐; as a function of the partial pressure of substrate for the photolysis of ethanethiol in the presence of 715 ± 5 Torr of added CO_2.

The major products of the photolysis of ethanethiol in the presence of ethylene are hydrogen, diethyl disulfide, and diethyl sulfide, the addition product. Their rates of formation in the photolysis of 25 Torr of ethanethiol as a function of ethylene pressure are given in Fig. 4. As with similar experiments with methanethiol (12), an increase in ethylene pressure results in a rapid decrease in the rate of hydrogen formation and a rapid increase in the rate of formation of the addition product, diethyl sulfide. Disulfide decreases only slightly in rate.

From the data of Fig. 4 one may calculate, using the method of Darwent and Roberts (4), that the rate constant ratio, k_2/k_4 for the pure ethanethiol system is 2.03 ± 0.10 independent of ethylene pressure up to 100 Torr. This compares favorably with a value of 1.9 ± 0.1 obtained by Kuntz (3).

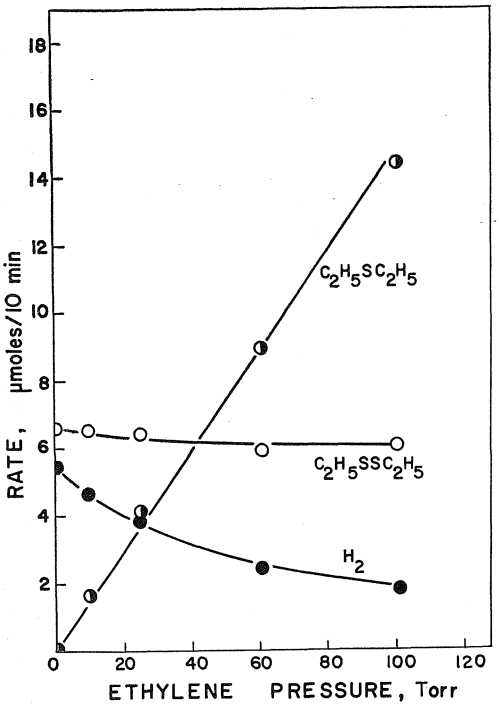

FIG. 4. Rates of formation of H_2, ●; $C_2H_5SSC_2H_5$, ○; and $C_2H_5SC_2H_5$, ◑; as a function of the pressure of added C_2H_4 for the photolysis of 25 Torr of ethanethiol at room temperature.

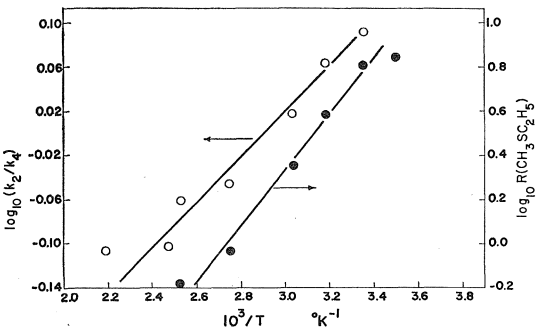

FIG. 5. Graph to determine the Arrhenius parameters of the hydrogen-, ○; and sulfide-, ●; forming reactions for the photolysis of 25 Torr of methanethiol with 25 Torr of ethylene added.

The effects of photolyzing equimolar mixtures of methanethiol or ethanethiol and ethylene in the presence of increasing pressures of inert gas have been previously reported (8). The results are indicative of the formation of hot hydrogen atoms in the primary processes. In order to determine activation energies (or activation energy differences) of reactions in which hydrogen and sulfide are formed, under conditions which would result in the reactions of thermal species only, the effects of varying the temperature of reaction mixtures containing 25 Torr of thiol, 25 Torr of ethylene, and an atmosphere of deactivating gas were studied. Arrhenius activation energy graphs are given in Fig. 5 for the methanethiol–ethylene–deactivator mixture and in Fig. 6 for the ethanethiol–ethylene–deactivator system. The significance of the activation energies obtained will be discussed presently.

The effect of increasing the energy of the photolysis light was briefly studied in a series of experiments in which ethanethiol vapor was photo-

Can. J. Chem. Downloaded from www.nrcresearchpress.com by 210.87.254.6 on 09/05/12
For personal use only.

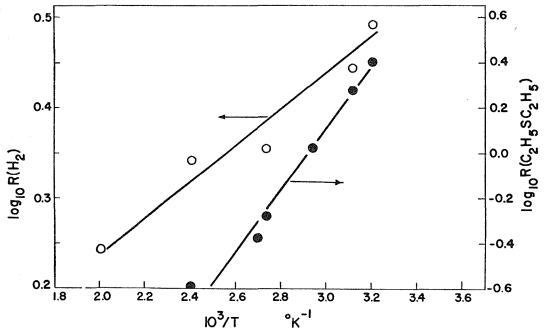

FIG. 6. Graph to determine the Arrhenius parameters of the hydrogen-, ○; and sulfide-, ●; forming reactions for the photolysis of 25 Torr of ethanethiol with 25 Torr of ethylene added.

lyzed with 2288 Å light. The photolysis of the pure thiol at this wavelength gave products whose relative yields are almost identical with the relative yields of products formed by photolysis at 2537 Å, as shown in Table III.

TABLE III

Comparison of the product yields from the photolysis of ethanethiol vapor at 2537 and 2288 Å

Product	Φ (2537 Å)	Rate (2288 Å)*	Relative rate (2288 Å)†
H_2	0.97±0.03	6.11	1.0
$C_2H_5SSC_2H_5$	1.26	8.05	1.32
C_2H_4	0.037	0.25	0.041
C_2H_6	0.22	1.36	0.22
H_2S	0.23	1.47	0.24

*Rates are in μmoles/120 min exposure.
†Relative to $R(H_2) = 1.00$.

Discussion

Nature of the Primary Process and Fates of the Hydrogen Atom

As in the methanethiol system (12), the only important primary photochemical process in the photolysis of ethanethiol at both 2537 and 2288 Å appears to be S—H bond cleavage,

[1] $$C_2H_5SH + h\nu \rightarrow C_2H_5S + H$$

Hydrogen atoms produced in this process apparently exclusively abstract the sulfyhydryl hydrogen atom of the substrate,

[2] $$H + C_2H_5SH \rightarrow C_2H_5S + H_2$$

as is also the case in the methanethiol system. Thus, the quantum yield of hydrogen is 0.97 ± 0.03, or unity within experimental error. Unlike the methanethiol case, however, the quantum yield of hydrogen in the ethanethiol system is independent of the substrate pressure and the absorbed light intensity.

Direct evidence in support of the suggestions that reaction [1] is the exclusive primary process and that reaction [2] is the sole fate of the hydrogen atoms produced in the ethanethiol system is somewhat sparse. Nonetheless, analogies drawn between the photochemical behavior of methanethiol and ethanethiol are probably quite valid, and thus evidence in favor of processes in the photolysis of methanethiol (12) also lends weight to analogous processes in the ethanethiol system. One should note in this connection that $D(CH_3S—H)$ and $D(C_2H_5S—H)$ are very similar; 88 ± 5 and 88.5 ± 5 kcal mole^{-1}, respectively (14).

The observation that only C_2H_5S radicals are formed on photolysis of ethanethiol in a rigid glass at 77 °K (15) or in a water clathrate at temperatures as high as −20 °C (16) lends support to both reactions [1] and [2], although radicals such as CH_2CH_2SH or CH_3CHSH might not have been found by the spectrophotometric techniques used in these studies. More convincing, however, is the observation by electron spin resonance spectroscopy that only the C_2H_5S radical is formed by ultraviolet irradiation of pure, solid ethanethiol at 77 °K (17). No evidence for any other radical was found in the latter work.

The only possible reaction that hydrogen atoms might undergo in the ethanethiol system that could not occur in the methanethiol system is abstraction of a methylene hydrogen atom from C_2H_5SH,

[4] $$H + CH_3CH_2SH \rightarrow H_2 + CH_3CHSH$$

However, the fact that neither 1,2-dimethyl-1,2-ethanedithiol, the dimer of the radical product of this reaction, nor the mercapto-sulfide from the reaction of C_2H_5S with CH_3CHSH, were observed in the reaction products, even at long exposure times, indicates that reaction [4] is probably not occurring to an appreciable extent.

The fact that ethane, hydrogen sulfide, and ethylene are found as reaction products suggests that alternative primary processes

[5] $$C_2H_5SH + h\nu \rightarrow C_2H_5 + SH$$

[6] $$C_2H_5SH + h\nu \rightarrow C_2H_4 + H_2S$$

might be occurring. However, assuming that hydrogen atoms and ethyl radicals both abstract

Can. J. Chem. Downloaded from www.nrcresearchpress.com by 210.87.254.6 on 09/05/12
For personal use only.

Can. J. Chem. Downloaded from www.nrcresearchpress.com by 210.87.254.6 on 09/05/12
For personal use only.

hydrogen from the substrate efficiently, reactions [5] and [1] cannot both be primary processes, since $\Phi(H_2) + \Phi(C_2H_6)$ is greater than unity. Reaction [6] might be responsible for the production of the small amount of ethylene ($\Phi(C_2H_4) = 0.037$) since $\Phi(H_2) + \Phi(C_2H_4)$ is also unity within experimental error. However, the observations that $\Phi(C_2H_4)$ is dependent on the pressure of added inert deactivating gas but not on the pressure of substrate, would seem to be inconsistent with the formation of an excited ethanethiol molecule in this system. Thus the reaction,

[7] $C_2H_5SH + h\nu \rightarrow C_2H_5SH^* \rightarrow H_2S + C_2H_4$

which would have to be postulated to account for the observed dependence of $\Phi(C_2H_4)$ on the pressure of inert gas, is probably not occurring.

Source of Ethane, Ethylene, and Hydrogen Sulfide

The minor products, C_2H_6, C_2H_4, and H_2S, all appear to be primary products of the photolysis since the rate of their formation does not decrease with decreasing exposure time. If these products do not arise from the initial decomposition process, then reactions involving the decomposition of additional ethanethiol must be occurring.

The observation that the rate of formation for these products decreases with increasing inert addend pressure indicates that they have their origin in reactions involving a species which can be collisionally deactivated. As indicated previously, this species is not involved in the formation of H-atoms. By analogy with the methanethiol system (12), this excited intermediate is proposed to be an excited disulfide molecule, $C_2H_5SSC_2H_5^*$, formed in the reaction

[8] $2C_2H_5S \rightleftarrows C_2H_5SSC_2H_5^*$

The excited molecule will have initially excess energy of at least the bond dissociation energy of the S—S linkage, 69 ± 6 kcal mole^{-1}. This is a minimum value since a fraction of the C_2H_5S radicals formed in the primary process may retain some of the energy excess in that step. As will be demonstrated below, the hydrogen atoms formed in this step have greater than thermal energies.

Considering the relatively large inert addend pressure required for significant deactivation effects, it is highly improbable that the excitation in $C_2H_5SSC_2H_5^*$ is vibrational in nature. Very little information about the excited state of disulfide molecules is known, and their spectroscopy has received only very limited attention. One possibility for $C_2H_5SSC_2H_5^*$ would be a nonspectroscopic electronic excited state. However, until more information is available on the excitation possibilities in disulfide molecules, further speculation is unwarranted. There is, however, experimental evidence that an excited disulfide molecule is also important in the photolysis of pure disulfides (10).

It is suggested that the $C_2H_5SSC_2H_5^*$ molecule participates in the following reactions.

[9] $C_2H_5SSC_2H_5^* + C_2H_5SH \rightarrow C_2H_5SSC_2H_5 + C_2H_5 + SH$

[10] $C_2H_5SSC_2H_5^* + C_2H_5SH \rightarrow C_2H_5SSC_2H_5 + C_2H_4 + H_2S$

[11] $C_2H_5SSC_2H_5^* + C_2H_5SH \rightarrow C_2H_5SSC_2H_5 + C_2H_5SH^*$

[12] $C_2H_5SSC_2H_5^* + M \rightarrow C_2H_5SSC_2H_5 + M$

[13] $C_2H_5 + C_2H_5SH \rightarrow C_2H_6 + C_2H_5S$

[14] $HS + C_2H_5SH \rightarrow H_2S + C_2H_5S$

[15] $C_2H_5SH^*(+M) \rightarrow$ deactivation

Since $D(C_2H_5S—H) = 71 \pm 5$ kcal mole^{-1} (15), reaction [9] should be thermoneutral or slightly exothermic if $C_2H_5S^*$ radicals from the primary process are important. Reaction [10] is highly exothermic with $\Delta H = -50 \pm 6$ kcal. Thus both processes in which $C_2H_5SSC_2H_5^*$ leads to substrate decomposition are energetically possible. The fact that in the absence of deactivator, only ca. 23% of the disulfide molecules formed in the system cause further decomposition may be a manifestation of the rather stringent requirements for this sequence.

Because the yield of ethylene is small compared with that of ethane, reaction [9] must be faster than reaction [10], with $\Phi(C_2H_6)/\Phi(C_2H_4) = k_9/k_{10} = 6$, assuming that no other processes are yielding either ethyl radicals or ethylene and that all of the ethyl radicals produce ethane by reaction [13]. This is not too surprising since the formation of ethylene and hydrogen sulfide via reaction [10] requires a much more drastic rearrangement of the ethanethiol molecule than does simple C—S bond cleavage, and thus reaction [10] might be expected to be somewhat

Can. J. Chem. Downloaded from www.nrcresearchpress.com by 210.87.254.6 on 09/05/12
For personal use only.

slower than reaction [9]. This may also be consistent with the fact that the rate at which $\Phi(C_2H_4)$ is decreased by the addition of inert gas is greater than the rate of decrease of $\Phi(C_2H_6)$, as shown in Fig. 2.

Combination–Disproportionation Reactions of C_2H_5S Radicals

If the reactions of CH_3S radicals (12) may be used as a model, the relative rates of the combination–disproportionation reactions of C_2H_5S radicals should be pressure dependent, with the combination mode becoming more important with increasing pressure. Unfortunately, the error in the rate of formation of diethyl disulfide is sufficiently large that a definite statement of the behavior of C_2H_5S radicals in the ethanethiol system cannot be made.

It is obvious, however, that the combination reaction of C_2H_5S radicals is much more important than disproportionation at the pressures studied. The mass balance, $H_2 + C_2H_6 = C_2H_5SSC_2H_5$, predicted by the mechanism presented, is satisfied within experimental error at almost all substrate pressures studied, although a deficiency in disulfide *might* be present at lower pressure. Thus, if anything, combination is an even more important mode of reaction of C_2H_5S radicals than for CH_3S radicals.

Reactions of C_2H_5S Radicals with the Substrate

Because the hydrogen quantum yield for the photolysis of ethanethiol is almost equal to unity and is independent of the pressure of substrate and the absorbed light intensity, reactions of C_2H_5S radicals with the substrate to yield hydrogen and disulfide, such as those previously postulated (12) for the methanethiol system, are apparently not occurring to any significant extent. The hydrogen exchange reaction,

$$[16] \quad C_2H_5S + C_2H_5SH \rightarrow C_2H_5SH + C_2H_5S$$

is probably occurring but this process will have no net effect. Thus, unlike the methanethiol photolysis, the quantum yields of hydrogen and disulfide show no apparent pressure or intensity dependence.

Kinetic Treatment of the Mechanism

A kinetic treatment of the mechanism of the photolysis of pure ethanethiol has been attempted, based on reactions [1], [2], [8] to [11], and [13] to [15].

Several assumptions have been made. First, it has been assumed that the only primary process is reaction [1], and that hydrogen atoms react only by reaction [2] even though they may have excess energy. It is also assumed that C_2H_5 or HS radicals react only by reactions [13] and [14], respectively, and that cross-combination or disproportionation reactions of these species are not important. Finally, it is assumed that the self-disproportionation of C_2H_5S radicals is much slower than the self-combination reaction.

Using steady state treatment of the mechanism, the following expressions may be obtained.

$$[I] \qquad \Phi(H_2) = 1.0$$

$$[II] \qquad \Phi(C_2H_6) = \frac{k_9}{k_{10} + k_{11}}$$

$$[III] \qquad \Phi(C_2H_4) = \frac{k_{10}}{k_{10} + k_{11}}$$

$$[IV] \qquad \Phi(H_2S) = \frac{k_9 + k_{10}}{k_{10} + k_{11}}$$

$$[V] \qquad \Phi(C_2H_5SSC_2H_5) = 1 + \frac{k_9}{k_{10} + k_{11}}$$

The mass balances, $\Phi(C_2H_5SSC_2H_5) = \Phi(H_2) + \Phi(C_2H_6)$ and $\Phi(H_2S) = \Phi(C_2H_6) + \Phi(C_2H_4)$ are therefore readily derived. From [II] and [III], $\Phi(C_2H_6)/\Phi(C_2H_4) = k_9/k_{10} = 6$, as previously noted. It is also apparent from these expressions that if the stated assumptions are valid, none of the quantum yields should be dependent on substrate pressure (in the complete absorption pressure range) or on the intensity, as observed.

A kinetic treatment of the mechanism including deactivation by inert addend in reaction [12] indicates that plots of the reciprocal of the quantum yields of ethane, ethylene, and hydrogen sulfide should be linear functions of the ratio $P(CO_2)/P(C_2H_5SH)$. The data from Figs. 2 and 3 have been used to calculate $1/\Phi$ for the minor products, assuming that the quantum yield of hydrogen is unity at all pressures. The results are presented in Fig. 7. The graph of $1/\Phi(C_2H_4)$ vs. $P(CO_2)/P(C_2H_5SH)$ yields the predicted straight line, with slope $k_{12}/k_{10} = 7.5$. Although as predicted qualitatively by the mechanism the yields of ethane and hydrogen sulfide decrease as $P(CO_2)$ increases, Fig. 7 shows that the reciprocal

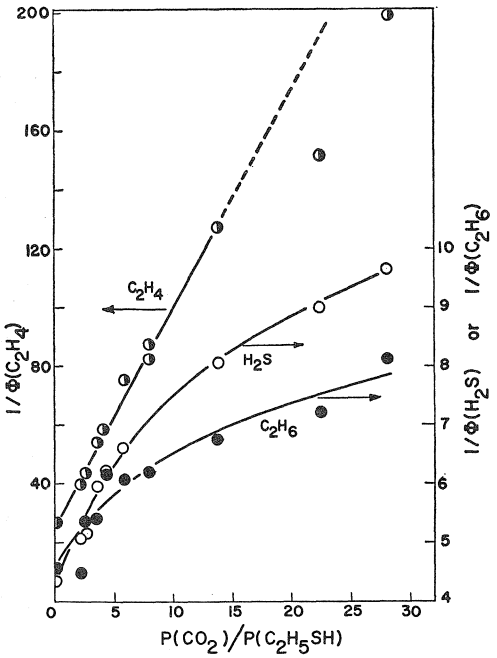

FIG. 7. Graph of $1/\Phi(C_2H_4)$, ◑; $1/\Phi(C_2H_6)$, ●; and $1/\Phi(H_2S)$, ○; versus $P(CO_2)/P$ (C_2H_5SH) for the photolysis of ethanethiol – carbon dioxide mixtures at room temperature.

plots are not linear. This may indicate that additional deactivation reactions involving $C_2H_5SSC_2H_5$* should be included in the mechanism, for example, two excited disulfide states which are deactivated at differing rates. Unfortunately, because of the uncertainties in the small yields of these products at high addend pressures, the data are not sufficient to permit the detailed analysis necessary to examine this possibility. It may be pointed out that in the methanethiol system, the rates of CH_4 and H_2S formation do yield a linear plot when presented in the form of Fig. 7.

Photochemical Addition to Ethylene

The major features of the photochemical addition of ethanethiol to ethylene in the absence of deactivating gas may be explained by the following reaction sequence.

[1] $C_2H_5SH + h\nu \rightarrow C_2H_5S + H$

[2] $H + C_2H_5SH \rightarrow H_2 + C_2H_5S$

[4] $H + C_2H_4 \rightarrow C_2H_5$

[13] $C_2H_5 + C_2H_5SH \rightarrow C_2H_6 + C_2H_5S$

[3] $2C_2H_5S \rightarrow C_2H_5SSC_2H_5$

[17] $C_2H_5S + C_2H_4 \rightleftarrows C_2H_5SC_2H_4$

[18] $C_2H_5SC_2H_4 + C_2H_5SH \rightarrow C_2H_5SC_2H_5 + C_2H_5S$

Here, it has been assumed (*a*) that chain terminations other than reaction [3] are not occurring, (*b*) that the polymerization reaction in which $C_2H_5SC_2H_4$ radicals add to ethylene is unimportant, (*c*) that excited disulfide molecules are deactivated with unit efficiency and without the production of C_2H_5 and HS radicals or ethylene and hydrogen sulfide, and (*d*) that hot ethyl radicals formed in reaction [4] will be efficiently deactivated (18) so that the use of the detailed reaction sequence,

[19] $H + C_2H_4 \rightleftarrows C_2H_5*$

[20] $C_2H_5* \rightarrow C_2H_5$

is unnecessary. The addition to ethylene of ethyl radicals formed in reaction [4] has been ignored, although this reaction is undoubtedly occurring to a significant extent. However, the formation of higher molecular weight alkanes by the process

[21] $C_2H_5 + n C_2H_4 + C_2H_5SH \rightarrow \text{alkanes} + C_2H_5S$

will be kinetically indistinguishable from reaction [13] being the sole fate of C_2H_5 radicals in so far as the rates of formation of hydrogen, diethyl sulfide, and diethyl disulfide are concerned. Each alkyl radical whether it is consumed in reaction [13] or [21] will eventually produce a C_2H_5S radical by reaction with ethanethiol so that the total number of C_2H_5S radicals will remain constant.

Reaction [17] is likely reversible since the analogous reaction of CH_3S radicals with ethylene has been previously shown to be reversible (19, 20). This reversibility is manifested by a negative overall activation energy, $E_{17} + E_{18} - E_{-17}$ for reactions forming diethyl sulfide, as will be shown presently.

The addition product, diethyl sulfide, is formed in the chain propagating reactions [17] and [18]. The order of the sulfide-forming reaction with respect to ethylene may be obtained from the slope of a graph of $\log_{10} R(C_2H_5SC_2H_5)$ versus $\log_{10} P(C_2H_4)$. The formation of diethyl sulfide is observed to have an order of 0.95, or unity within experimental error, with respect to ethylene, in agreement with the analogous reaction in the methanethiol–ethylene system (12).

Can. J. Chem. Downloaded from www.nrcresearchpress.com by 210.87.254.6 on 09/05/12
For personal use only.

Can. J. Chem. Downloaded from www.nrcresearchpress.com by 210.87.254.6 on 09/05/12
For personal use only.

The fact that the rate constant ratio, k_{22}/k_4, for the competitive reactions,

[22] $\quad H + RSH \rightarrow H_2 + RS$

[4] $\quad H + C_2H_4 \rightarrow C_2H_5$

is dependent on the pressure of added inert gas (3, 8) may be explained by postulating that hot hydrogen atoms are produced in the primary photochemical process. The following reactions are suggested.

[23] $\quad RSH + h\nu \rightarrow RS + H^*$

[22′] $\quad H^* + RSH \rightarrow H_2 + RS$

[4′] $\quad H^* + C_2H_4 \rightarrow C_2H_5$

[24] $\quad H^* + M \rightarrow H + M^*$

[22] $\quad H + RSH \rightarrow H_2 + RS$

[4] $\quad H + C_2H_4 \rightarrow C_2H_5$

Thus, the rate constant ratios, k_{22}'/k_4', which were found to be 2.03 ± 0.11 for ethanethiol and 2.32 ± 0.11 for methanethiol at 25 °C in the absence of deactivating gases are those associated with hot hydrogen atoms. These values may be compared with values of 1.9 ± 0.1 and 1.7 ± 0.2, respectively, obtained by Kuntz (3) under experimental conditions similar to those used in the present study. On the other hand, the values of k_{22}/k_4 equal to 0.96 ± 0.08 for ethanethiol and 1.15 ± 0.10 for methanethiol (8), determined in the presence of a large excess of deactivating gas, are for the reactions of thermal hydrogen atoms.

Values of $E_{22} - E_4$ and A_{22}/A_4 may be obtained from a measurement of the temperature variation of k_{22}/k_4 in the presence of excess inert gas. The values of these parameters may be calculated from the Arrhenius activation energy graphs given in Figs. 5 and 6. The value $E_{22} - E_4$ is -1.0 ± 0.3 kcal mole^{-1} for ethanethiol and -0.94 ± 0.09 kcal mole^{-1} for methanethiol. In each case the error quoted is that estimated by taking the average of the differences between the largest and smallest possible slopes and the actual slope, determined by the least squares method. The points on the graphs are rather scattered and therefore the errors in $E_{22} - E_4$ are somewhat larger than desirable. Nonetheless, within experimental error the difference between the activation energy of abstraction from thiol (reaction [22]) and the activation energy of addition of hydrogen atoms to ethylene (reaction [4]) is the same for both methanethiol and ethanethiol. This should not be surprising since $D(CH_3S—H)$ and $D(C_2H_5S—H)$ are very nearly equal (14). The ratios of the pre-exponential factors, A_{22}/A_4, are found to be 0.18 ± 0.06 for ethanethiol, slightly smaller than the value of 0.24 ± 0.01 for the reactions of thermal hydrogen atoms in the methanethiol system. This is to be expected since ethanethiol should offer somewhat more steric hindrance to an approaching hydrogen atom than methanethiol.

An activation energy difference, $E_{22} - E_4$, of 0.54 ± 0.12 kcal mole^{-1} and a ratio of pre-exponential factors, A_{22}/A_4, of 3.85 ± 0.25 have been obtained by Inaba and Darwent (21) for the undeactivated methanethiol–ethylene system. It may thus be noted that A_{22}/A_4 and $E_{22} - E_4$ decrease from 3.85 ± 0.25 and 0.54 ± 0.12 kcal mole^{-1}, respectively, for hot hydrogen atom reactions to 0.24 ± 0.01 and -0.94 ± 0.09 kcal mole^{-1}, respectively, for reactions involving thermal hydrogen atoms in the methanethiol–ethylene system.

This data would seem to resolve the apparent discrepancy between the observations that thermalizing hot hydrogen atoms by the addition of inert gas (8), and increasing the temperature of the thermalized reaction mixture, both result in a *decrease* in k_{22}/k_4. Using the Arrhenius parameters obtained in the present work and by Inaba and Darwent (21) for the methanethiol–ethylene system, one may calculate that the factor f in the expression

$$[VI] \qquad f = \frac{(k_{22}/k_4)_{\text{hot H}}}{(k_{22}/k_4)_{\text{thermal H}}}$$

is equal to 1.4 ± 0.6, where the error limits are those calculated by using the extremes in the Arrhenius parameters. (Maximum and minimum values of f, 2.0 and 0.8, respectively, vary greatly because of the extreme sensitivity of f to errors in the activation energies.) The data of ref. 8 may then be used to calculate the experimental value of f. Since k_{22}/k_4 is observed to decrease from 2.32 ± 0.11 with no added inert gas to a limiting value of 1.15 ± 0.10 at high pressures, the experimental value of f will be 2.0 ± 0.2. Thus, within the limits imposed by the errors involved in calculating and measuring the theoretical and experimental values of k_{22}/k_4, the observed and theoretical values of f agree. It is, therefore, likely that the observed variation in k_{22}/k_4 with inert gas pressure for the methanethiol–ethylene system

Can. J. Chem. Downloaded from www.nrcresearchpress.com by 210.87.254.6 on 09/05/12
For personal use only.

can be ascribed to variations in the Arrhenius parameters of reactions [22] and [4] due to hot hydrogen atom effects.

An explanation of why the Arrhenius parameters vary in the observed fashion is hampered by the fact that one may only observe alterations in the *ratio* of A_{22}/A_4 or the *difference*, $\Delta E_a = E_{22} - E_4$. How the individual parameters, A_{22}, A_4, E_{22}, and E_4 change with changing hydrogen atom energy is largely unknown at present. The fact that the value of ΔE_a actually does change with changing energy of the hydrogen atom should not be too surprising, although one might expect that the value of ΔE_a should approach zero as the energy of the hydrogen atoms becomes large relative to the activation energies of reactions [22] and [4]. In fact ΔE_a apparently increases from -0.94 ± 0.09 kcal mole^{-1} for reactions involving thermal hydrogen atoms to $+0.54 \pm 0.12$ kcal mole^{-1} for energetic hydrogen atoms.

The reasons for the change in the pre-exponential factors are somewhat more difficult to envisage, although the observed effects are not unique to thiol–olefin systems. Variations in the pre-exponential factors of reactions involving hot hydrogen atoms from the photolysis of HI and HBr have also been found by Ogg and Russell (22) and by Schwarz, Williams, and Hamill (23). In the HI system, the ratio of the pre-exponential factors, A_{25}/A_{26} for the reactions

[25] $\quad H + I_2 \rightarrow HI + I$

[26] $\quad H + HI \rightarrow H_2 + I$

decreases from a value of 3.8 ± 0.4 for hot hydrogen atoms to a value of about 3×10^{-2} for thermal atoms.

In the methanethiol–ethylene system, A_{22}/A_4 decreases from a value of 3.85 ± 0.25 for hot hydrogen atom reactions to a value of 0.24 ± 0.01 for the corresponding thermal reactions. An explanation of these effects will have to await more information about the general characteristics of hot atom reactions.

A kinetic treatment of the proposed mechanism for the photochemical addition of simple alkanethiols to ethylene has been attempted, based on reactions [4], [4′], [22], [22′], [23], and [24] and

[27] $\quad C_2H_5 + RSH \rightarrow C_2H_6 + RS$

[28] $\quad 2RS \rightarrow RSSR$

[29] $\quad RS + C_2H_4 \rightarrow RSC_2H_4$

[30] $\quad RSC_2H_4 + RSH \rightarrow RSC_2H_5 + RS$

As a simplification, reactions involving excited disulfide molecules have been excluded from this reaction scheme and, as such, only the kinetics of the formation of hydrogen and sulfide will be dealt with here. Also, it has been assumed that the reactions of hot hydrogen atoms may be treated kinetically in the same way as the reactions of thermal hydrogen atoms.

Using a steady state treatment, the following expressions may be derived.

$$[\text{VII}] \quad \Phi(H_2) = \frac{k_{22}'[RSH]}{k_{22}'[RSH] + k_4'[C_2H_4] + k_{24}[M]} + \frac{k_{24}k_{22}[RSH][M]}{\{k_{22}'[RSH] + k_4'[C_2H_4] + k_{24}[M]\}\{k_{22}[RSH] + k_4[C_2H_4]\}}$$

$$[\text{VIII}] \quad \Phi(RSC_2H_5) = \left\{\frac{1}{I_a^{1/2}}\right\}\left\{\frac{k_{29}k_{30}[RSH][C_2H_4]}{k_{28}^{1/2}(k_{-29} + k_{30}[RSH])}\right\}$$

Equation [VII] may be simplified for two special cases. First, for the undeactivated photoaddition of thiol to ethylene $[M] = 0$ and thus,

$$[\text{IX}] \quad \left\{\frac{1}{\Phi(H_2)}\right\}_{[M]=0} = 1 + \frac{k_4'[C_2H_4]}{k_{22}'[RSH]}$$

This equation is identical with that used by Kuntz (3) and Inaba and Darwent (21) for determining the rate constant ratio, k_4'/k_{22}', under experimental conditions which would have resulted in the production and reaction of hot hydrogen atoms.

Second, for the case in which $k_{24}[M] \gg k_{22}' \times [RSH] + k_4'[C_2H_4]$, that is, at very high pressures of deactivator, eq. [VII] may be simplified to give

$$\left\{\frac{1}{\Phi(H_2)}\right\}_{[M]\text{large}} = 1 + \frac{k_4[C_2H_4]}{k_{22}[RSH]}$$

This expression is that which must be used to calculate k_4/k_{22} for thermal hydrogen atoms.

It has been shown previously by Graham *et al.* (19, 20) that for the addition of CH_3S radicals to ethylene, the rate of decomposition of the adduct radical is much faster than its rate of abstraction of hydrogen from the thiol. If this holds true for both methyl and ethyl thiyl radicals, then $k_{-29} \gg k_{30}[RSH]$ and eq. [VIII] may be simplified to give

$$[X] \quad \Phi(RSC_2H_5) = \left\{\frac{1}{I_a^{1/2}}\right\}\left\{\frac{k_{29}k_{30}[RSH][C_2H_4]}{k_{28}^{1/2}k_{-29}}\right\}$$

Thus, measurement of the slopes of the graphs of $\log_{10} R(RSC_2H_5)$ versus $1/T$ for sulfide, given in Figs. 5 and 6 may be used to calculate values of $E_{29} + E_{30} - E_{-29}$, assuming $E_{28} = 0$. Values of -6.5 ± 0.3 kcal mole^{-1} and -6.1 ± 0.3 kcal mole^{-1} for methanethiol and ethanethiol are obtained. Because these values are almost equal, the reaction profiles of the two systems are probably very similar. The value of $E_{29} + E_{30} - E_{-29} = -6.1 \pm 0.3$ kcal mole^{-1} obtained in the methanethiol–ethylene–deactivator system is in reasonable agreement with a value of -5.3 ± 0.1 kcal mole^{-1} obtained by Graham *et al.* (19, 20).

Acknowledgments

The authors are grateful to the National Research Council of Canada for financial support of this work.

1. M. Meissner and H. W. Thompson. Trans. Faraday Soc. **34**, 1238 (1938).
2. W. E. Haines, G. L. Cook, and J. S. Ball. J. Am. Chem. Soc. **78**, 5213 (1956).
3. R. R. Kuntz. J. Phys. Chem. **71**, 3343 (1967).
4. B. de B. Darwent and R. Roberts. Discussions Faraday Soc. **14**, 55 (1953).
5. R. G. Gann and J. Dubrin. J. Chem. Phys. **47**, 1867 (1967).
6. R. L. Wadlinger and B. de B. Darwent. J. Phys. Chem. **71**, 2057 (1967).
7. B. de B. Darwent, R. L. Wadlinger, and M. J. Allard. J. Phys. Chem. **71**, 2346 (1967).
8. R. P. Steer and A. R. Knight. Can. J. Chem. **46**, 2878 (1968).
9. R. P. Steer, B. L. Kalra, and A. R. Knight. J. Phys. Chem. **71**, 783 (1967).
10. P. M. Rao, J. A. Copeck, and A. R. Knight. Can. J. Chem. **45**, 1369 (1967).
11. K. Sayamol and A. R. Knight. Can. J. Chem. **46**, 999 (1968).
12. R. P. Steer and A. R. Knight. J. Phys. Chem. **72**, 2145 (1968).
13. R. P. Steer. Ph.D. Thesis, University of Saskatchewan, Saskatoon. 1968.
14. H. Mackle. Tetrahedron, **19**, 1159 (1963).
15. Kj. Rosengren. Acta Chem. Scand. **16**, 1418 (1962).
16. P. Goldberg. J. Chem. Phys. **40**, 427 (1964).
17. D. H. Volman, J. Wolstenholme, and S. G. Hadley. J. Phys. Chem. **71**, 1798 (1967).
18. J. N. Bradley, H. W. Melville, and J. C. Robb. Proc. Roy. Soc. London, Ser. A, **236**, 318 (1956).
19. D. M. Graham, R. L. Mieville, R. H. Pallen, and C. Sivertz. Can. J. Chem. **42**, 2250 (1964).
20. D. M. Graham, R. L. Mieville, and C. Sivertz. Can. J. Chem. **42**, 2239 (1964).
21. T. Inaba and B. de B. Darwent. J. Phys. Chem. **64**, 1431 (1960).
22. R. A. Ogg and R. R. Williams. J. Chem. Phys. **13**. 586 (1945).
23. H. A. Schwarz, R. R. Williams, and W. H. Hamill. J. Am. Chem. Soc. **74**, 6007 (1952).

Can. J. Chem. Downloaded from www.nrcresearchpress.com by 210.87.254.6 on 09/05/12
For personal use only.

Methyl and trifluoromethyl radical attack on ethers[1]

N. L. ARTHUR[2], PETER GRAY, AND A. A. HEROD[3]
School of Chemistry, Leeds University, Leeds 2, England

Received August 28, 1968

The reactions of CF_3 radicals with dimethylether and diethylether and of CH_3 radicals with dimethylether and diisopropylether have been studied. The photolyses of acetone and hexafluoroacetone were used as radical sources; all rate constants are based on the rate constants for radical dimerization. The Arrhenius parameters measured are as follows

Reactions	$\log_{10} A$ (cm^3 $mole^{-1}$ s^{-1})	E (kcal $mole^{-1}$)
$CH_3 + CH_3OCH_3 \rightarrow CH_4 + CH_2OCH_3$	11.6	10.0
$CH_3 + (CH_3)_2CHOCH(CH_3)_2 \rightarrow CH_4 + C_3H_6OCH(CH_3)_2$	11.2	7.9
$CF_3 + CH_3OCH_3 \rightarrow CF_3H + CH_2OCH_3$	11.7	6.8
$CF_3 + C_2H_5OC_2H_5 \rightarrow CF_3H + C_2H_4OC_2H_5$	11.9	5.5

Canadian Journal of Chemistry, 47, 1347 (1969)

Introduction

Previous investigations of the hydrogen atom abstraction reactions from ethers by methyl radicals have centered on dimethylether (1–4), with one investigation of diethylether (5), and one of diisopropylether (2). The several dimethylether studies give rate constants which are in fair agreement ($\log_{10} k$ (182 °C) in the range 6.8–6.5 cm^3 $mole^{-1}$ s^{-1}), while the activation energies lie in the range 8.4–10 kcal $mole^{-1}$. The present work on dimethylether and diisopropylether was undertaken to clarify the earlier work and to provide accurate rate constants for comparison with the CF_3 radical work.

The reactions of CF_3 radicals with dimethyl- and diethyl-ethers have not been investigated previously and were studied for two reasons. First, a comparison between CH_3 and CF_3 radical attack on the ethers can be made. Second, although the attack of CF_3 radicals on methanol has been studied (6, 7), the two investigations are in poor agreement (activation energies for attack on the CH_3 group were 4.7 and 8.3 kcal $mole^{-1}$ while $\log_{10} k$ (182 °C) was 7.8 and 8.2 cm^3 $mole^{-1}$ s^{-1}). Since the alkyl groups of ethers and alcohols show the same reactivity to CH_3 radical attack (8, 9) and thus probably also to CF_3 radical attack, this work may shed some light on the conflict over methanol.

Experimental

Materials

Dimethylether

This was obtained from Matheson Co. Ltd. and was fractionated through traps at −78, −96, −150, and −196°. The fraction condensing at −150 °C was collected and stored in a blackened bulb.

Diethylether (A.R. grade)

This was refluxed over sodium, then distilled. A middle fraction was subjected to trap to trap fractionation and stored in a blackened bulb.

Diisopropylether

This was obtained from British Drug Houses Ltd. and was distilled with rejection of large head and tail fractions.

Acetone (A.R. grade)

This was obtained from British Drug Houses Ltd. and was distilled with rejection of large head and tail fractions.

Hexafluoroacetone

This was a gift from Du Pont and was fractionated through traps at −78, −96, −150, and −196°. The fraction collecting at −150° was stored in a blackened bulb.

Apparatus and Procedure

The apparatus and procedure involved in the methyl radical reactions have been described previously (9). With trifluoromethyl radicals, photolysis experiments were carried out in a silica reaction vessel (volume illuminated = 123 ml), fitted with plane parallel windows and housed in an aluminium block furnace fitted with quartz end plates. The furnace temperature was controlled by a platinum resistance thermometer and was measured by three chromel–alumel thermocouples. Photolyzing light (> 3000 Å) was obtained from a Mazda medium pressure mercury lamp and a Chance–Pilkington OX9A filter. Reactants were admitted to the reaction vessel separately.

[1]Complete tables of data upon which the present conclusions are based have been deposited in the Depository of Unpublished Data, National Science Library, National Research Council of Canada, Ottawa, Canada.

[2]Present address: Mellon Institute, 4400 Fifth Avenue, Pittsburgh, Pennsylvania.

[3]Present address: Lash Miller Chemical Laboratories, University of Toronto, Toronto 5, Ontario.

The analysis of reaction products has been described previously (10).

Interpretation

In experiments using CH_3 radicals, acetone was used as the radical source. The photolysis mechanism has been given before (9) and need not be repeated.

The mechanism of the photolysis of hexafluoroacetone may be described by the reactions

$$[1] \qquad CF_3COCF_3 \xrightarrow{h\nu} 2CF_3 + CO$$

$$[2] \qquad 2CF_3 \rightarrow C_2F_6$$

When acetone or hexafluoroacetone is photolyzed in the presence of a substrate RH, the additional reactions [3] and [4] occur

$$[3] \qquad CF_3 + RH \rightarrow CF_3H + R$$

$$[4] \qquad CH_3 + RH \rightarrow CH_4 + R$$

Expressing rate constants relative to those for reactions [2] and [5], ref. (11)

$$[5] \qquad 2\,CH_3 \rightarrow C_2H_6$$

we can write for CF_3 radical reactions

$$k_3/k_2^{1/2} = R_{CF_3H}/R_{C_2F_6}^{1/2}\,[RH]$$

and for CH_3 radical reactions

$$k_4/k_5^{1/2} = R_{CH_4}[4]/R_{C_2H_6}^{1/2}\,[RH]$$

where $R_{CH_4}[4]$ represents that methane formed by reaction [4] alone (allowance must be made to the total methane formed for that arising by attack of CH_3 radicals on acetone itself). The concentrations denote average values.

By carrying out photolyses over a range of initial conditions (temperature, concentration, etc.) the validity of the rate constant expressions may be checked and Arrhenius parameters evaluated.

Kinetic Parameters for Hydrogen Abstraction by CF_3 Radicals

Dimethyl- and Diethyl-Ethers

The temperature dependence of the rate constants (k_3) over the range 60–180 °C can be represented by the equations

$$\log_{10} k\ (\text{cm}^3\ \text{mole}^{-1}\ \text{s}^{-1}) = (11.71 \pm 0.03) - (6780 \pm 60)/2.303RT$$

for dimethylether, and

$$\log_{10} k\ (\text{cm}^3\ \text{mole}^{-1}\ \text{s}^{-1}) = (11.88 \pm 0.03) - (5550 \pm 60)/2.303RT$$

for diethylether. There are no earlier determinations of these rate constants for comparison.

Kinetic Parameters for Hydrogen Abstraction by CH_3 Radicals

(i) Dimethylether

The temperature dependence of k_4 over the temperature range 135–250 °C may be expressed as

$$\log_{10} k_4\ (\text{cm}^3\ \text{mole}^{-1}\ \text{s}^{-1}) = (11.62 \pm 0.08) - (9990 \pm 170)/2.303RT$$

Previous determinations of k_4 are in reasonable agreement; $\log_{10} k$ at 182 °C is 6.80 $\text{cm}^3\ \text{mole}^{-1}\ \text{s}^{-1}$ while the previous values (1, 2, 3, 4) are 6.76, 6.74, 6.80, and 6.53, respectively. The Arrhenius parameters agree within experimental errors.

(ii) Diisopropylether

The results for the rate constant between 135–250 °C may be expressed by the equation

$$\log_{10} k\ (\text{cm}^3\ \text{mole}^{-1}\ \text{s}^{-1}) = (11.16 \pm 0.01) - (7870 \pm 70)/2.303RT$$

A previous determination of the rate constant (2) is in good agreement with this work.

(iii) Diethylether

The reaction of methyl radicals with diethylether was not studied since a previous determination (5) is available which is in good agreement with our work on ethanol (9). The alkyl groups in each molecule show identical behavior.

Discussion

It is convenient to divide the discussion into three short sections: *(i)* comparing the reactivities of ethers to methyl radicals, *(ii)* comparing the reactivities to CF_3 radicals, and *(iii)* comparing the behavior of the two radicals.

(i) Methyl Radical Attack on Ethers

The order of reactivity of the three ethers is as expected, with diisopropylether the most reactive and dimethylether the least reactive; the relative overall reactivities are 1:3.4:3.7 at 182 °C. The similar reactivities of diethyl- and diisopropylethers is a result of a steric hindrance of the reactive α-CH group of diisopropylether compared with the alcohol (8), an effect noted in the hydrocarbons (13) $(CH_3)_3CH$, $(CH_3)_2CHCH(CH_3)_2$, and $(CH_3)_2CHCH(CH_3)CH(CH_3)_2$ where the rate constant at 182 °C fails to increase, being

TABLE I

CH_3 radical reactions

Substrate	$\log_{10} A$ (cm^3 $mole^{-1}$ s^{-1})	E (kcal $mole^{-1}$)	$\log_{10} k$ (182 °C)	Reference
CH_3OCH_3	11.6	10.0	6.80	This work
$C_2H_5OC_2H_5$	12.0	9.7	7.34	5
CH_3OD*	11.3	10.0	6.43	8
C_2H_5OD*	11.6	9.7	6.97	9
$C_3H_7OC_3H_7$	11.2	7.9	7.37	This work
C_3H_7OD*	11.2	7.9	7.36	8
C_2H_6	11.7	11.7	6.07	12
$C_2H_5C_2H_5$	11.4	9.5	6.73	12
$(CH_3)_2CHCH(CH_3)_2$	11.1	7.8	7.34	13

*Abstraction from the alkyl group.

TABLE II

CF_3 radical reactions

Substrate	$\log_{10} A$ (cm^3 $mole^{-1}$ s^{-1})	E (kcal $mole^{-1}$)	$\log_{10} k$ (182 °C)	Reference
CH_3OCH_3	11.7	6.8	8.46	This work
$C_2H_5OC_2H_5$	11.9	5.5	9.22	This work
CH_3OD*	12.2	8.3	8.2	7
CH_3OH*	10.0	4.7	7.8	6
C_2H_6	11.6	7.5	8.06	14
C_2H_6	11.0	6.5	7.84	16
n-C_4H_{10}	11.2	5.1	8.74	15
n-C_4H_{10}	11.4	5.3	8.90	17
n-C_4H_{10}	10.8	5.5	8.20	18
n-C_4H_{10}	11.8	6.2	8.80	6

*Abstraction from the alkyl group.

about $10^{7.3}$ cm^3 $mole^{-1}$ s^{-1} for all three compounds. The relative reactivities of the alkyl groups of the alcohols (8) CH_3OD, C_2H_5OD, and i-C_3H_7OD are 1:3.4:8.5. In the alcohols and ethers the activation energies for attack on the alkyl groups are the same (8) and except in diisopropylether where steric hindrance occurs, the rate constant for attack on an alkyl group is identical in the ether and alcohol.

In the series of hydrocarbons (12, 13) C_2H_6, n-C_4H_{10}, and $(CH_3)_2CHCH(CH_3)_2$, the relative reactivities are 1:4.6:18.6; the difference between the ratios for ethers or alcohols and hydrocarbons reflects the activating effect of the oxygen atom on the first members, dimethyl- and diethylethers, of the series compared with ethane and n-butane. This is indicated by the activation energies (Table I) which are the same for diisopropylether and 1,4-dimethylbutane (7.9 kcal $mole^{-1}$), similar for diethylether and n-butane (9.7 and 9.5 kcal $mole^{-1}$ respectively), but different for dimethylether and ethane (10.0 and 11.7 kcal $mole^{-1}$ respectively). The A-factors for the pairs of compounds dimethylether–ethane and diisopropylether–1,4-dimethylbutane are the same within experimental error. For diethylether and n-butane the A-factors are not similar; this may be a result of experimental error.

(ii) Trifluoromethyl Radical Attack on Ethers

No previous work has been done on any of the ethers. In the present work, dimethylether is less reactive than diethylether by a factor 5.7 in the rate constant at 182 °C. The greater reactivity of diethylether is a result of a lower activation energy and a higher A-factor than in dimethylether (see Table II).

The several determinations of the rate constants for attack on ethane and n-butane (6, 14–18) are in poor agreement (see Table II) for either paraffin. One ethane determination (16) may be unreliable (19), while the use of hexafluoroazomethane as a radical source with n-butane (17, 18) may be expected to yield low Arrhenius parameters (20).

Despite the disagreement in the hydrocarbon

TABLE III

Relative reactivity of CF_3 and CH_3 radicals

Substrate	(k_{CF_3}/k_{CH_3}) 182 °C	(A_{CF_3}/A_{CH_3})	$E_{CH_3} - E_{CF_3}$ (kcal mole^{-1})
CH_3OCH_3	46	1.23	3.2
$C_2H_5OC_2H_5$	76	1.32	4.2
C_2H_6	98	0.9	4.2
n-C_4H_{10}	117	2.5	3.3

work, the data indicate that *n*-butane is more reactive than ethane to CF_3 attack by about a factor 6 at 182 °C. Also dimethylether is more reactive than ethane (14) (by a factor of about 3 at 182 °C) while diethylether is more reactive than *n*-butane (6) (by a factor of 2.6 at 182 °C).

Since the alkyl groups of alcohols and ethers show identical behavior to CH_3 attack (8), they might be expected to show identical behavior to CF_3 attack. The attack of CF_3 radicals on methanol has been studied (6, 7), but the rate constants and Arrhenius parameters are not in agreement with expectations. In one case (7) a factor of 2 is apparent between the rate constants for ether and alcohol at 182 °C, but the agreement between this work and the methanol results is not sufficient to support either determination (6, 7).

(iii) Relative Reactivity of CF_3 and CH_3 Radicals

The quotients of *A*-factors and rate constants at 182 °C with activation energy differences for CF_3 and CH_3 radical attack on dimethylether and diethylether and the hydrocarbons ethane and *n*-butane are presented in Table III. It is clear that CF_3 radicals are more reactive than CH_3 radicals with all four compounds. With the exception of *n*-butane the ratio of *A*-factors is close to unity and the greater reactivity of the CF_3 radical is due to an activation energy difference of 3 or 4 kcal mole^{-1}. The CF_3 radical is more reactive than the CH_3 radical by 50–120 times. This is as expected for non-polar molecules (21), whereas for polar molecules, the reactivities of the two radicals are expected to be similar.

In the attack of CH_3 radicals on ethanol it has been shown (9) that the main reaction is with the α-CH_2 group and this is no doubt the case with diethylether. The CH_2 group is presumably also the main center of attack by CF_3 radicals.

Acknowledgments

We thank the Commonwealth Scientific and Industrial Research Organization of Australia and the Natural Rubber Producers' Research Association for financial support.

1. M. K. PHIBBS and B. DE B. DARWENT. Can. J. Res. B, **28**, 395 (1950).
2. A. F. TROTMAN-DICKENSON and E. W. R. STEACIE. J. Chem. Phys. **19**, 329 (1951).
3. R. A. MARCUS, B. DE B. DARWENT, and E. W. R. STEACIE. J. Chem. Phys. **16**, 987 (1948).
4. L. F. LOUCKS and K. J. LAIDLER. Can. J. Chem. **45**, 2775 (1967).
5. J. LONG and G. SKIRROW. Trans. Faraday Soc. **58**, 1403 (1962).
6. E. R. MORRIS and J. C. J. THYNNE. Trans. Faraday Soc. **64**, 414 (1968).
7. T. S. CARLTON, J. R. STEEPER, and R. L. CHRISTENSEN. J. Phys. Chem. **70**, 3222 (1966).
8. A. A. HEROD. Ph.D. Thesis, The University of Leeds, England. 1967.
9. P. GRAY and A. A. HEROD. Trans. Faraday Soc. **64**, 1568 (1968).
10. N. L. ARTHUR and T. N. BELL. Can. J. Chem. **44**, 1445 (1966).
11. A. SHEPP. J. Chem. Phys. **24**, 939 (1956); P. B. AYSCOUGH. J. Chem. Phys. **24**, 944 (1956).
12. W. M. JACKSON, J. R. MCNESBY, and B. DE. B. DARWENT. J. Chem. Phys. **37**, 1610 (1962).
13. A. F. TROTMAN-DICKENSON, J. R. BIRCHARD, and E. W. R. STEACIE. J. Chem. Phys. **19**, 163 (1951).
14. P. B. AYSCOUGH, J. C. POLANYI, and E. W. R. STEACIE. Can. J. Chem. **33**, 743 (1955).
15. P. B. AYSCOUGH and E. W. R. STEACIE. Can. J. Chem. **34**, 103 (1956).
16. L. A. OKSENT'EVICH and A. N. PRAVEDNIKOV. Dokl. Akad. Nauk SSSR, **169**, 541 (1966).
17. G. O. PRITCHARD, H. O. PRITCHARD, H. I. SCHIFF, and A. F. TROTMAN-DICKENSON. Trans. Faraday Soc. **52**, 849 (1956).
18. G. O. PRITCHARD, H. O. PRITCHARD, and A. F. TROTMAN-DICKENSON. Chem. Ind. London, 564 (1955).
19. R. D. GILES, L. M. QUICK, and E. WHITTLE. Trans. Faraday Soc. **63**, 662 (1967).
20. W. G. ALCOCK and E. WHITTLE. Trans. Faraday Soc. **62**, 664 (1966).
21. B. G. TUCKER and E. WHITTLE. Trans. Faraday Soc. **61**, 866 (1965).

An investigation of some iron halide complexes by Mössbauer spectroscopy

T. BIRCHALL
Department of Chemistry, McMaster University, Hamilton, Ontario
Received November 25, 1968

The products of the reaction between iron carbonyls and various ligands have been examined by Mössbauer spectroscopy. With triphenylphosphine and triphenylarsine, complexes of Fe(III) in a tetrahedral configuration are produced. In all other cases the complexes contain Fe(II), and it is suggested that these are not monomeric, but are chlorine bridged complexes.

Canadian Journal of Chemistry, **47**, 1351 (1969)

Can. J. Chem. Downloaded from www.nrcresearchpress.com by 210.87.254.5 on 09/05/12
For personal use only.

Relatively few tetrahedral complexes of iron(II) are known. The $[FeX_4]^{2-}$ ions exist with large cations where X = Cl^-, Br^-, NCS^-, etc. (1–3). Complexes of the type FeX_2L_2 and $[FeL_4]^{2+}$ are also known (3, 4). The $[FeX_4]^{2-}$ ion in a tetrahedral ligand field has a non-degenerate set of 3d orbitals, with a lower doublet d_γ (d_{z^2}, $d_{x^2-y^2}$) and a higher triplet d_ε (d_{xy}, d_{xz}, d_{yz}). The energy separation (10 *Dq*) between these sets of levels is typically of the order of 4000 cm^{-1} (3). The sixth electron in the Fe(II) 3d orbitals populates essentially only the d_γ levels. When the field at the iron is exactly cubic, then the d_{z^2} and $d_{x^2-y^2}$ energy levels are degenerate. If a tetragonal distortion is introduced, the degeneracy of the d_γ orbitals is removed and a small splitting of these levels occurs. This distortion, while not detected by X-ray crystallography (2), has been detected spectroscopically (3).

More recently, tetrahedral iron(II) compounds have been studied by Mössbauer spectroscopy (5, 6). The quadrupole splitting parameter is an extremely sensitive test for distortions from cubic symmetry, and a study of the variation of this parameter with temperature can lead to more accurate values for the energy separation than can be obtained by other spectroscopic techniques. The recent report by Singh and Rivest (7) on the preparation of some tetrahedral iron(II) complexes was therefore of much interest, and the results of a Mössbauer study of these complexes are reported here.

Experimental

Materials

All solvents were reagent grade and were dried and distilled before use. Iron pentacarbonyl and diiron nonacarbonyl were obtained from Alfa Inorganics and were used without further purification. All of the ligands used were purified by distillation or recrystallization from a suitable solvent.

Preparation

The complexes were prepared according to the method of Singh and Rivest (7), except that no special precautions were taken to exclude air except for the initial deoxygenation of the chloroform. It appears that the CO liberated in the reaction is sufficient to maintain a non-oxidizing atmosphere for the duration of the reaction. With $Fe_2(CO_9)$ as starting material the reaction was complete in approximately 1 h. In the case of $Fe(CO)_5$ the reaction was stopped after 12 h. The products, as finely divided precipitates, were subsequently separated by filtration in an oxygen free dry-box, washed with solvent, and dried in vacuum.

$FeCl_3 \cdot (C_6H_5)_3P$ and $FeCl_3 \cdot (C_6H_5)_3As$ were prepared in an identical manner to that of Singh and Rivest (7). Chloride analyses, infrared spectra, and melting point served to identify the compounds as being identical to those prepared previously (7), except for the benzamide and aniline complexes. The benzamide complex was obtained as a white (not brown) solid, m.p. > 210 °C (not 158 °C), with Cl = 27.8% (not 36.99). The yellow aniline complex (m.p. > 220°) was found to contain 31.68% Cl. The analyses for these compounds do not fit the $FeCl_3L$ formulation but are close to $FeCl_2L$ and are formulated as such in Table I. The fact that different products should be obtained from a preparation essentially the same as that used by the previous workers, seems somewhat surprising. The Mössbauer spectra of the compounds indicated that they contained only 1 kind of iron. No impurity peaks were detected (see Figs. 1–3).

Mössbauer Spectra

Mössbauer spectra were recorded with an Austin Science Associates drive system, used in conjunction with a Victoreen PIP400A multichannel analyzer operating in multiscalar mode. The source was ^{57}Co in a palladium matrix, and the 14.4 keV γ-ray was detected by a thin (1/32 in.) NaI(Tl) activated crystal with matching photomultiplier tube manufactured by the Harshaw Chemical Company. The velocity scale was calibrated with a sodium nitroprusside absorber and all chemical shifts are quoted with respect to the centroid of the sodium nitroprusside spectrum. Samples contained approximately 10 mg cm^{-2} of iron. Spectra were recorded at 295 and 77 °K (liquid nitrogen temperature). The Mössbauer data summarized

TABLE I

Mössbauer data for iron halide complexes

Compound*	Temperature (°K)	Isomer shift δ (mm s^{-1})	Quadrupole splitting ΔE (mm s^{-1})	% Absorption
$FeCl_2 \cdot 2AM$	295	1.39	2.64	5.4
	77	1.55	2.80	7.7
$FeCl_2 \cdot 2FA$	295	1.42	2.65	4.6
	77	1.59	3.00	8.7
$FeCl_2 \cdot BM$	295	1.41	2.57	3.3
	77	1.54	2.87	6.5
$FeCl_2 \cdot AN$	295	1.37	1.69	3.9
	77	1.49	2.18	7.1
$FeCl_3 \cdot TPP$	295	0.46	0.17	0.8
	77	0.54	0.21	4.7
$FeCl_3 \cdot TPA$	295		Negligible absorption	
	77	0.57	0.23	3.2

*AM = acetamide; FA = formamide; BM = benzamide; AN = aniline; TPP = triphenylphosphine; TPA = triphenylarsine.

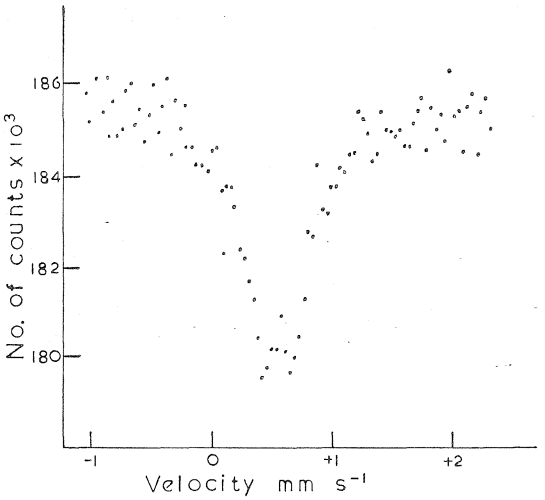

FIG. 1. Mössbauer spectrum of $FeCl_3 \cdot TPA$ at 77 °K.

in Table I are thought to be accurate to ± 0.02 mm s^{-1} and typical spectra are shown in Figs. 1–3.

Discussion

The data in Table I clearly separate the complexes examined into 2 classes: those with large isomer shift and quadrupole splitting, and those with small isomer shift and quadrupole splitting. The parameters for the triphenylphosphine and triphenylarsine complexes are typical of high spin iron(III) complexes. Isomer shift values for Fe(III) range generally from ~ 0.5–0.8 mm s^{-1} with the δ value for the $[FeCl_4]^-$ ion being 0.55 mm s^{-1} at liquid nitrogen temperature (8). Since a complex containing Fe(III) in the high spin state would have each d orbital singly occupied, the electric field gradient at the nucleus would be zero and the Mössbauer spectrum would consist of a single unsplit absorption. This is the situation in the $[FeCl_4]^-$ complexes (8). If the cubic field at the iron atom is distorted by replacement of one of the ligands, an electric field gradient will be produced, the degeneracy of the $I = 3/2$ state will be removed, and a quadrupole split doublet will be observed. Distortions arising from non-equivalence of ligands around a high spin d^5 ion are generally small, with the result that ΔE values are small. This is the situation for the $FeCl_3 \cdot TPP$

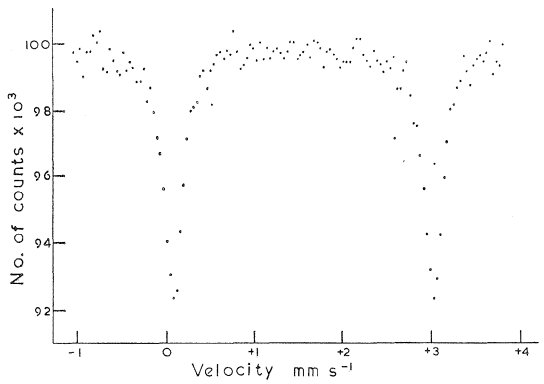

FIG. 2. Mössbauer spectrum of $FeCl_2 \cdot 2FA$ at 77 °K.

Can. J. Chem. Downloaded from www.nrcresearchpress.com by 210.87.254.5 on 09/05/12
For personal use only.

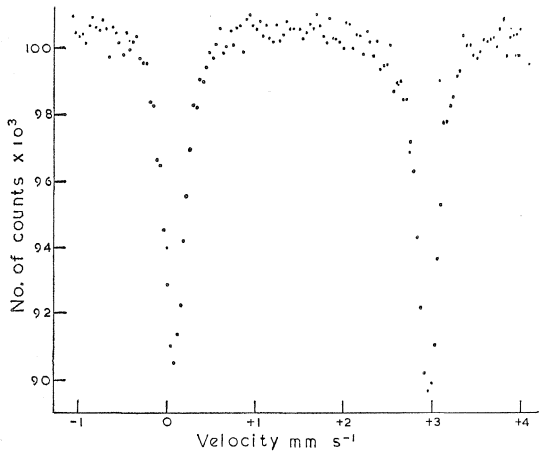

FIG. 3. Mössbauer spectrum of $FeCl_2 \cdot BM$ at 77 °K.

and $FeCl_3 \cdot TPA$ complexes. Support for the tetrahedral arrangement is found in the strong temperature dependence of the Mössbauer absorption. At room temperature, a very weak or negligible absorption is observed which increases in intensity as the temperature is lowered. Tetrahedral compounds of iron generally exhibit weak or undetectable absorption at room temperature (5, 6, 8). All of the Mössbauer evidence, therefore, supports the conclusions of Singh and Rivest (7), that $FeCl_3 \cdot TPP$ and $FeCl_3 \cdot TPA$ are high spin tetrahedral iron(III) complexes.

In sharp contrast are the data for the other complexes listed in Table I. Isomer shifts which are a measure of "s" electron density are markedly influenced by the occupation of d orbitals. An increase in the number of 3d electrons will result in a more efficient screening of the "s" electrons from the nucleus, with the resultant expansion of the 4s electron shell. This reduces the "s" electron density at the nucleus and gives more positive isomer shift values. Iron(II) isomer shifts range from 1.09–1.75 mm s^{-1} (9, 10). The values of $\sim$ 1.4 mm s^{-1} for the amide and aniline complexes fall clearly within this range and all without doubt are complexes of iron(II).

Quadrupole splitting values for d^6 iron in the high spin state vary considerably. The $[FeBr_4]^{2-}$ ion at room temperature has $\Delta E = 0.58$ mm s^{-1} (6), while $FeSO_4 \cdot 7H_2O$ has $\Delta E = 3.20$ mm s^{-1} (11, 12). The magnitude of the quadrupole splitting will be largely determined by the sixth d electron, and the orbital which it occupies. For a tetrahedral arrangement of ligands, the d_γ orbitals lie lowest in energy, with the d_{z^2} and $d_{x^2-y^2}$ being degenerate in an exactly cubic ligand field. Since the contribution to the electric field gradient of an electron in either of these orbitals is equal but of opposite sign (13), the quadrupole splitting would in this case be zero. A small tetragonal distortion lifts the degeneracy of the d_γ pair. The sixth d electron will have a preference for the orbital of lowest energy, an electric field gradient will result, and a quadrupole split absorption will be observed. Distortions of this kind are not large, e.g., 180–135 cm^{-1} for $[FeCl_4]^{2-}$ (5, 6). This is the same order of magnitude as the thermal energy, and the spectrum will therefore show a strong temperature dependence ($(Et_4N)_2FeBr_4$, $\Delta E = 0.52$ at 293 °K and 3.23 at 4.2 °K) (6). The large quadrupole splittings observed for the complexes studied here could, therefore, arise from a tetrahedral arrangement considerably distorted from cubic symmetry.

In an octahedral field the d_ε and d_γ sets are reversed in energy with d_ε lying lowest. As with the tetrahedral case, distortion from cubic symmetry would lift the degeneracy of the lowest lying set of orbitals, which would give rise to a quadrupole split absorption. Some typical parameters for high spin octahedrally coordinated iron(II) compounds are given in Table II. The first 4 compounds in Table I have ΔE values which fall into this range. The quadrupole splitting values for these complexes could, therefore, arise from either a tetrahedral or an octahedral arrangement of ligands.

TABLE II

Mössbauer spectra of some iron(II) compounds

Compound	δ (mm s^{-1})	ΔE (mm s^{-1})	Reference
$FeCl_2$	1.34	0.80	14
$FeCl_2 \cdot 2H_2O$	1.28	2.50	15
$FeCl_2 \cdot 4H_2O$	1.53	3.00	11
$FeSO_4 \cdot 7H_2O$	1.58	3.20	11

Chemical shifts for tetrahedrally coordinated iron(II) complexes are generally less positive than those for iron(II) in an octahedral environment with similar ligands (6). The shifts reported here are significantly more positive than those for the tetrahedral iron(II) complexes reported by Edwards and co-workers, after correcting

Can. J. Chem. Downloaded from www.nrcresearchpress.com by 210.87.254.5 on 09/05/12
For personal use only.

Can. J. Chem. Downloaded from www.nrcresearchpress.com by 210.87.254.5 on 09/05/12
For personal use only.

their shifts to sodium nitroprusside as zero (6). Complexes of iron(II) in octahedral environments, such as those listed in Table II, have very similar chemical shifts to those reported here. Anhydrous ferrous chloride has the polymeric $CdCl_2$ structure with all chlorines being shared, while $FeCl_2 \cdot 2H_2O$ has 4 chlorines and 2 water molecules surrounding each iron, with the chlorines bridging to another iron atom (16). A similar structure would be possible for the formamide and acetamide complexes to give the linear polymer **1** having a $FeCl_2L_2$ unit. The polymeric

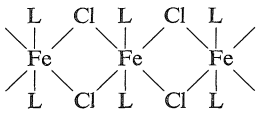

1

structure is also supported by the relatively strong absorption ($\sim 5\%$) observed at room temperature. Tetrahedral Fe(II) compounds, as stated above, have relatively low Debye temperatures and the absorption is generally $< 1\%$ (6). The Mössbauer nucleus in polymeric compounds will be more rigidly held in the lattice, have a higher Debye temperature, and hence a much stronger absorption.

The structures for the benzamide and aniline complexes are much less certain. While the Mössbauer parameters are similar to those for the acetamide and formamide complexes, the analyses indicate a formulation $FeCl_2 \cdot BM$ and $FeCl_2 \cdot AN$. A chlorine bridged dimer **2** with tetrahedral arrangement about each iron, is one

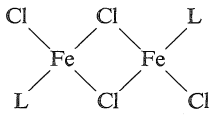

2 (*cis* or *trans*)

possible structure. One might expect the Debye temperature for such a unit to be higher than for a monomeric species, giving a somewhat more intense absorption. Other arrangements, such as a 5 coordinate polymeric species, can not of course be discounted.

Singh and Rivest (7), on the basis of analytical, infrared, and magnetic evidence, conclude that they are dealing with monomeric, tetrahedrally coordinated compounds of Fe(II) and Fe(III). The triphenylphosphine and triphenylarsine complexes give Mössbauer spectra which are in agreement with the $FeCl_3L$ formulation. Our analytical data for the benzamide and aniline complexes are not in agreement with the results of the above workers, though the mode of preparation was virtually the same. We find no evidence for either $FeCl_3 \cdot BM$ or $FeCl_3 \cdot AN$, and only complexes containing Fe(II) are produced under our reaction conditions with the amide and aniline ligands. The reasons for the different structures found, i.e. $FeCl_2L_2$ and $FeCl_2L$, are not clear, and further work on these and related complexes is continuing.

Acknowledgments

Miss M. Haley is thanked for technical assistance. Financial support from the National Research Council of Canada and the Ontario Department of University Affairs is gratefully acknowledged.

1. C. Furlani, E. Cervone, and V. Valenti. J. Inorg. Nucl. Chem. **25**, 159 (1963).
2. N. S. Gill. J. Chem. Soc. 3512 (1961).
3. D. Forster and D. M. L. Goodgame. J. Chem. Soc. 262, 268, 454 (1965).
4. J. T. Donoghue and R. S. Drago. Inorg. Chem. **2**, 1158 (1963).
5. T. G. Gibb and N. N. Greenwood. J. Chem. Soc. 6985 (1965).
6. P. R. Edwards, C. E. Johnson, and R. J. P. Williams. J. Chem. Phys. **47**, 2074 (1967).
7. P. P. Singh and R. Rivest. Can. J. Chem. **46**, 1773 (1968).
8. G. M. Bancroft, A. G. Maddock, W. K. Ong, and R. H. Prince. J. Chem. Soc. A, 723 (1966).
9. T. Fujita, A. Ito, and K. Ono. J. Phys. Soc. Japan, **21**, 1734 (1966).
10. C. E. Johnson, W. Marshall, and G. J. Perlow. Phys. Rev. **126**, 1503 (1962).
11. S. Debenedetti, G. Lang, and R. Ingalls. Phys. Rev. Letters, **6**, 60 (1961).
12. R. W. Grant, H. Wiedensich, A. H. Muir, Jr., U. Gonser, and W. N. Delgass. J. Chem. Phys. **45**, 1015 (1966).
13. R. Ingalls. Phys. Rev. **128**, 1155 (1962).
14. K. Ono, A. Ito, and T. Fujita. J. Phys. Soc. Japan, **19**, 2119 (1964).
15. S. Chandra and G. R. Hoy. Phys. Letters, **22**, 254 (1966).
16. A. F. Wells. Structural inorganic chemistry. 3rd ed. Oxford Univ. Press, London. 1967. p. 344.

Can. J. Chem. Downloaded from www.nrcresearchpress.com by 210.87.254.42 on 09/05/12
For personal use only.

Electrochemiluminescence of carbazole

K. S. V. SANTHANAM[1], R. N. O'BRIEN[2], AND A. D. KIRK
University of Victoria, Victoria, British Columbia

Received June 6, 1968

Effect of supporting electrolytes in the electrochemiluminescence of carbazole has been studied with a view to understanding more about the mechanism of the chemiluminescence process. Comparison of the emission spectrum with its fluorescence and phosphorescence spectra suggests that the excited state is not carbazole. The intense chemiluminescence observed with tetra-*n*-butyl ammonium iodide as supporting electrolyte has been examined.

Canadian Journal of Chemistry, **47**, 1355 (1969)

Bard *et al.* (1) recently reported the electrochemiluminescence of carbazole in N,N-dimethylformamide (DMF) containing tetra-*n*-butyl ammonium perchlorate as supporting electrolyte, which involved the reduction of carbazole at a mercury electrode apparently followed by a fast chemical reaction resulting in the luminescence process. The chemical reaction may involve the supporting electrolyte or the solvent (DMF), and in the present paper, the reduction of carbazole in different supporting electrolytes is reported.

Experimental

Experiments were conducted by using controlled potential or constant current techniques. The working electrode in both sets of experiments was a mercury electrode. A platinum or silver coil served as the auxiliary electrode. This electrode was placed in a sintered glass disc compartment when a separation from the working electrode was warranted. The reference electrode was an aqueous saturated calomel electrode (s.c.e.) connected through a salt bridge.

The experimental procedure for the controlled potential experiments was essentially the same as that described by Santhanam and Bard (2). Constant current electrolysis was performed in a cell provided with a joint so that it could be connected to a vacuum line. A volume of carbazole solution containing the appropriate supporting electrolyte ($\approx$ 2 ml) was transferred into the cell with a mercury pool at the bottom and a side mounted platinum electrode. After removing dissolved oxygen by evacuation, a constant current was applied to the cell.

A Wenking potentiostat model 61TR was used in all controlled potential experiments. Additional outside currents were superimposed on the built-in static control potential to enable reductions to be carried out at -2.7 V vs. s.c.e. In some cases involving light decay studies, square wave pulses of 5 ms or longer were obtained using a circuit similar to that described by Epstein and Kuwana (3).

Light emission was monitored using an RCA IP28 photomultiplier tube (maximum spectral sensitivity at $\sim$ 3400 Å). Photocurrents were recorded on a Tektronix oscilloscope model 549, by monitoring the potential drop across a 750 kΩ (0.1%) resistor connected between the photoanode and ground. Emission spectra were recorded using a Hilger D292 monochromator with a suitable wavelength drive system.

Carbazole was obtained from the Aldrich Chemical Company and was recrystallized three times in hexane. The purified sample had a melting point of 245 °C. Tetra-*n*-propyl ammonium bromide was obtained from Eastman Organic Chemicals. Tetra-*n*-butyl ammonium iodide and tetra-*n*-butyl ammonium perchlorate were supplied by Southwestern Analytical Chemicals. Tetra-*n*-butyl ammonium perchlorate was dried under vacuum for over 6 h before use. N,N-dimethylformamide (DMF), supplied by Fisher, was purified according to a well established procedure (2).

Results

Carbazole undergoes reduction at a hanging mercury drop electrode (h.m.d.e.) with E_p at -2.71 V vs. an aqueous s.c.e. in N,N-dimethylformamide containing tetra-*n*-butyl ammonium iodide as supporting electrolyte, when the reduction is examined by linear sweep cyclic voltammetry. A typical cyclic voltammogram is shown in Fig. 1. During the reduction process, a faint blue light is given out at the electrode.

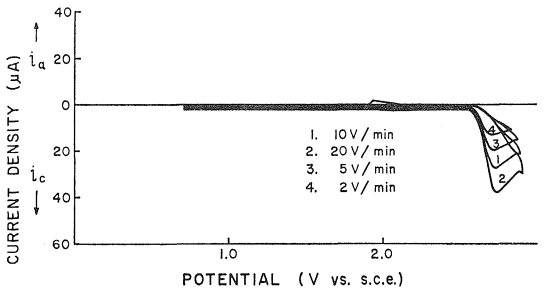

FIG. 1. Cyclic voltammograms.

[1]Present address: Tata Institute of Fundamental Research, Colaba, Bombay 5, India.

[2]To whom reprint requests should be addressed.

Can. J. Chem. Downloaded from www.nrcresearchpress.com by 210.87.254.42 on 09/05/12
For personal use only.

Since the electrochemical reduction was irreversible (even up to scan rates of 20 V s^{-1}), the E_p or peak potential, value was dependent on the scan rate (4) and the results are shown in Table I. The peak current, i_p, for a diffusion controlled irreversible electron transfer, is given by (4):

$$i_p = 3.01 \times 10^5 n(\alpha n_a)^{\frac{1}{2}} C^\circ v^{\frac{1}{2}}$$

where n is the number of electrons transferred per molecule, α is the transfer coefficient, n_a is the number of electrons in the rate determining step, A is the area of the electrode in cm^2, D is the diffusion coefficient in cm^2/s, C° is the bulk concentration of the electroactive species in mmoles per l, and v is the scan rate in V/s. The value of i_p is directly proportional to the square root of the scan rate and concentration of the electroactive species. The near constancy of the $i_p/v^{\frac{1}{2}}$ values in Table I indicates the absence of any chemical reaction preceding the electron transfer step. Cyclic voltammetric results in other supporting electrolytes such as tetra-*n*-propyl ammonium bromide or perchlorate are essentially the same. Previous work on carbazole has been done with tetra-*n*-butyl ammonium perchlorate (1).

TABLE I

Current function and peak potentials for carbazole at a hanging mercury drop electrode*

E_p (V vs. s.c.e.)	$i_p/v^{\frac{1}{2}}$ μA min V^{-1}	Scan rate V min^{-1}
−2.71	8.4	2.0
−2.72	8.2	5.0
−2.73	8.0	10.0
−2.75	8.1	20.0

*Supporting electrolyte: tetra-*n*-butyl ammonium iodide in DMF.

In order to determine the number of electrons involved in the reduction of carbazole, and to understand more about the electrochemical reduction process, controlled potential coulometric experiments were undertaken using a large mercury pool working electrode (20 cm^2) with its potential controlled at −2.75 V vs. s.c.e. In the absence of any chemical reaction, it has been established (5) that current i_t varies with time as

$$i_t = i_0 e^{-pt}$$

where p represents a constant which is a function of the area of the electrode, solution volume, mass transport, and thickness of the diffusion layer. However, when a chemical reaction occurs leading to the generation of another or the same electroactive species, deviations from the exponential behavior occur. Controlled potential coulometric experiments on carbazole with iodide as supporting electrolyte showed a deviation from the exponential behavior. The current during this reduction decayed with time and reached a constant value higher than the background. For example, in one experiment the value of the current decreased from an initial value of about 32 mA (the solution contained 0.012 g of carbazole in 27.5 ml dimethylformamide) to a steady state constant value of about 1.25 mA. When the electrolysis was resumed after interrupting it for 5 min, the value of the current increased to 3.5 mA (from its steady state value) and subsequently showed a decay to the same steady state value. Interruptions for longer periods gave higher values of the current on resumption of electrolysis. Examination of the solution at the steady state by cyclic voltammetry showed a peak at −2.71 V vs. s.c.e. which agreed with the original carbazole peak. This peak height increased with time, indicating that more carbazole was being generated by a chemical reaction.

Both the results during controlled potential coulometric experiments and the cyclic voltammetric data taken after the electrolysis, suggest that carbazole is being regenerated from the reduced species by a chemical reaction.

When the rate of the chemical reaction is equal to the rate of the electrochemical reduction, a steady state is reached in controlled potential electrolysis. Geske and Bard (6) have studied the case of regeneration by pseudo first order chemical reaction, according to which

$$\frac{k_2}{p} = \frac{C}{C_i - C}$$

where k_2 represents the rate constant for the chemical reaction, p the rate constant for the electrode reaction, C_i the initial concentration, and C the steady state concentration. Using this approach, the rate constant for the regeneration reaction is calculated as 4.8×10^{-4} s^{-1}. It has been shown (6) that the apparent number of electrons involved in the reduction in the presence of a chemical reaction is related to the true number of electrons *(n)* by the equation

$$n_{app} = n\left[\frac{1}{1+\gamma^1} + \frac{p\gamma^1 t}{1-e^{-p(1+\gamma^1)t}}\right]$$

where $\gamma^1 = k_2/p$ and t is the duration of electrolysis. The value of n for carbazole is calculated to be 0.9, which is convincingly close to 1.0.

Electrolysis conducted with a platinum auxiliary electrode in the same compartment where the working electrode was placed, showed a much higher steady state current value of 22 mA.

Electrochemiluminescence and Spectral Properties

During the reduction of carbazole at a mercury electrode, a faint blue light was produced in the solution immediately adjacent to the electrode. The emission spectrum was examined under controlled potential and constant current electrolysis conditions and is shown in Fig. 2. The oscillations

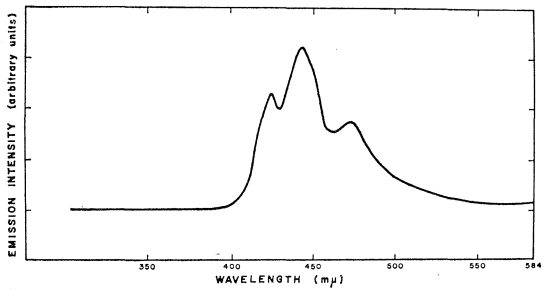

FIG. 2. Emission spectrum at constant current.

of mercury during the electrolysis, and consequently of the emitting zone, limit the precision of measurement of the emission maxima and the relative intensity distributions. Nevertheless, the wavelengths at which intensity maxima occur may be located at about 420, 450, and 470 mμ. Under controlled potential coulometric conditions, using a silver coil as the auxiliary electrode separated from the working electrode in a sintered glass disc compartment, the light intensity showed a decrease with a levelling off at the steady state current. However, under the same conditions, the use of a platinum auxiliary electrode without the sintered glass disc separation gave an increase in the light intensity for the first 20 min (see Fig. 3), decaying to a much higher steady value. Examination of the emission spectrum showed no appreciable change in the relative intensity of the three peaks (1.1:2.0:1) during the development of the emission to full intensity.

Similar results are obtained under constant

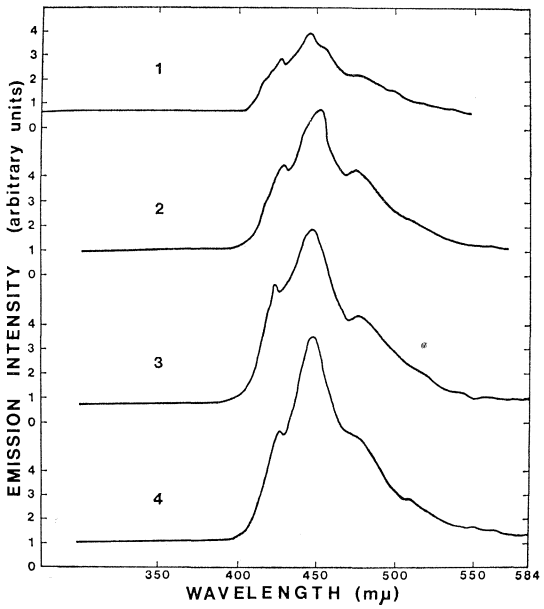

FIG. 3. Increase in emission intensity with electrolysis time.

current electrolysis conditions, realized by applying a current of 15 mA between the mercury pool electrode and a coiled platinum wire in a solution containing tetra-*n*-butyl ammonium iodide. Again, the emission spectrum had maxima around 420, 450, and 470 mμ. With tetra-propyl ammonium bromide as the supporting electrolyte, the light intensity was lower, but the spectrum had the same features. The chemiluminescence of a 5.4 m*M* carbazole solution in iodide medium is visible in an illuminated room with no appreciable decrease in intensity for a period of over 2 h. The emission spectrum does not change during this period. If only carbazole were being irreversibly reduced with this applied current, the electrolysis of the carbazole should have been complete in about 40 s. Spectrophotometric examination of the electrolyzed solution after 4 h of electrolysis showed absorption maxima at 268, 288, 293, 326, and 337 mμ, agreeing well with the carbazole spectrum. Cyclic voltammetric examination of the electrolyzed solution showed the carbazole peak at −2.71 V vs. s.c.e.

Results obtained in experiments conducted with different concentrations of iodide and carbazole are presented in Table II. It is clear that higher concentrations of iodide quench the chemiluminescence process. A similar quenching

Can. J. Chem. Downloaded from www.nrcresearchpress.com by 210.87.254.42 on 09/05/12
For personal use only.

TABLE II

Intensity (relative) studies in the reduction of carbazole

$[(C_4H_9)_4NI]$ (M)	[Carbazole] (mM)	Relative intensity
0.096	7.79	2.2
0.46	7.79	2.2
2.7	7.79	1.0
0.096	2.39	0.4
0.096	13.40	3.6
0.096	32.9	1.2

of fluorescence of fluorescein ions by iodide ion has previously been reported (7).

The relative intensities of emission using tetra-*n*-butyl ammonium bromide or perchlorate as supporting electrolytes were approximately equal and were 15 times less than that in iodide medium. Again, however, the luminescence was visible after 2 h of electrolysis. Electrolysis of the supporting electrolyte alone at 15 mA produced either a negligible luminescence or no luminescence. Oxygen (as mentioned) was eliminated on a vacuum line, and when it was bled in, it quenched the luminescence.

Light-Decay Studies

To evaluate the kinetics of the light emission following the reduction of carbazole in I^-, the decay of light intensity was examined after electrolysis was stopped. Such a decay of light intensity is shown in Fig. 4. It is seen that the decay is first order with a rate constant of 3×10^4 s. In controlled potential electrolysis experiments, although the light intensity showed the same type of decay after the termination of electrolysis at the steady state, the regeneration of carbazole continued in solution. Since the emission zone is visibly separated from the electrode, double layer discharge effects could be of only secondary importance in the process.

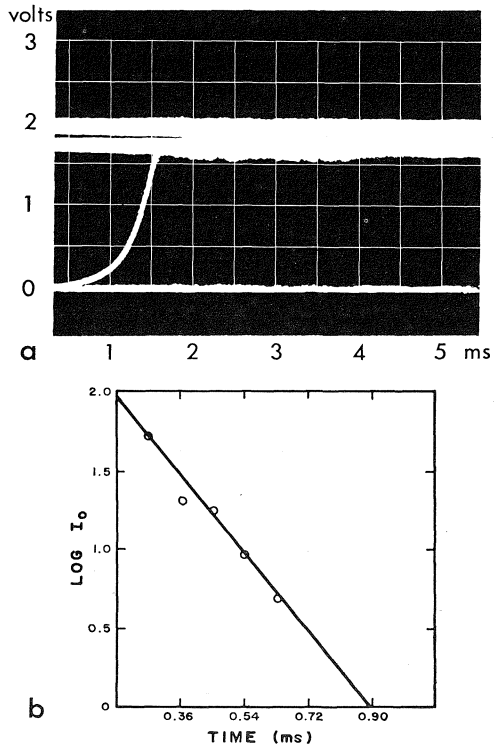

FIG. 4. Decay of light intensity.

Discussion

In the case of several aromatic hydrocarbons, the formation of an electronically excited species proceeds through a radical cation – anion annihilation (8, 9) or annihilation of an anion with an oxidizing agent (10), the reactants being generated by switching the potential from a negative region to a positive region or vice versa. Chemiluminescence of carbazole occurs in the reduction process itself and is more intense than is observed through annihilation processes. The formation of carbazole or carbazole anion in an electronically excited state by processes occurring directly at the electrode surface seems unlikely when one compares the molecular orbital diagram of carbazole with the energy (−2.71 eV) of the electrons available at the electrode surface (11). Both bonding and antibonding levels are full. Furthermore it has already been pointed out that the emission zone is visibly separated from the electrode surface.

It has been shown that carbazole reduces irreversibly at the hanging mercury drop electrode at a potential of −2.71 V vs. s.c.e. The absence of an oxidation wave on reversal of the potential sweep even at fast sweep rates (20 V/s) suggests that the anion produced has a lifetime in the solution of less than a few ms; the lifetime was independent of the nature of the supporting electrolyte.

The coulometric work demonstrates that carbazole is regenerated with a much slower first order rate constant of 4.8×10^{-4} s^{-1}. This result is confirmed by the studies of the recovery

Can. J. Chem. Downloaded from www.nrcresearchpress.com by 210.87.254.42 on 09/05/12
For personal use only.

Can. J. Chem. Downloaded from www.nrcresearchpress.com by 210.87.254.42 on 09/05/12
For personal use only.

of carbazole concentration after terminating the electrolysis. The carbazole regeneration is accelerated by the increased steady state current when the auxiliary electrode is in proximity to the mercury pool and also by the marked growth of luminescence intensity as I_2 accumulates in the electrolyzed solution.

Examination of the structure of the chemiluminescence spectrum has shown it to be independent of the nature of the supporting electrolyte. Further, the emission spectrum differed from the fluorescence (maxima at 345 and 373 mμ) or phosphorescence (maxima at 407, 420, and 440 mμ) (12) of carbazole. The lifetime of the chemiluminescent emission is 3×10^{-5} s, which is much shorter than the half-life for regeneration of carbazole. This evidence forces us to recognize that carbazole, while being the species initially reduced, is not the emitting species, but is rapidly converted to a second substance which is either not oxidizable or oxidizes at a potential more positive than Hg. This species leads to light emission with the half-life of 3×10^{-5} s to give the species which returns to carbazole with the much longer half-life of 2×10^{3} s. This latter step is also catalyzed by I_2. To account for all this evidence, we are forced to propose a mechanism of the type

[1]	$R + e^- \rightarrow R^-$	(Electro reduction)
[2]	$R^- + (x) \rightarrow F^*(+x^-)$	Apparent half life ms
[3]	$F^* \rightarrow (F + h\gamma)$	Life time 3×10^{-5} s (not necessarily the radiative life time)
[4]	$F \rightarrow R$	Half life 3×10^{3} s
[5]	$F + I_2 \rightarrow R$	

The data do not enable us to determine the molecularity of step [2]. It may involve the solvent or supporting electrolyte. The latter is unlikely in view of the absence of observable effects due to supporting electrolyte. The nature of the species F is not known definitely. As carbazole is weakly basic (13), it is likely that the carbazole anion would be protonated more easily than carbazole itself. Previous work has shown that anions of this type rapidly protonate even in aprotic solvents such as dimethylformamide (10). Thus, F* may be the protonated carbazole anion in an excited state and F its ground state. It would be surprising, however, if this ground state returned to carbazole as slowly as found here. An alternative possibility is that F* is an excited dimeric carbazole species and F is its ground state. It is hoped to continue this work in an effort to decide between some of these possibilities.

Acknowledgments

This work was supported by the National Research Council of Canada and the University of Victoria faculty research fund, to whom our thanks are due.

1. A. J. Bard, K. S. V. Santhanam, S. A. Cruiser, and L. R. Faulkner. *In* Symposia on fluorescence. Marcel Dekker, New York. 1967.
2. K. S. V. Santhanam and A. J. Bard. J. Am. Chem. Soc. **88**, 2669 (1966).
3. B. Epstein and T. Kuwana. Photochem. Photobiol. **4**, 1157 (1965).
4. R. S. Nicholson and I. Shain. Anal. Chem. **36**, 706 (1964).
5. L. Meites. *In* Technique of organic chemistry. Vol. I. Interscience Publishers, Inc., New York. 1960.
6. D. H. Geske and A. J. Bard. J. Phys. Chem. **63**, 1062 (1959).
7. Umberger and LaMer. J. Am. Chem. Soc. **67**, 1099 (1945).
8. D. M. Hercules. Science, **143**, 808 (1964).
9. E. A. Chandross and R. E. Visco. J. Am. Chem. Soc. **86**, 5350 (1964).
10. K. S. V. Santhanam and A. J. Bard. J. Am. Chem. Soc. **87**, 139 (1965).
11. C. A. Coulson and A. Streitwiser, Jr. Supplemental tables of m.o. calculations. Vol. II. The Pergamon Press, Ltd., New York. p. 344.
12. G. N. Lewis and M. Kasha. J. Am. Chem. Soc. **66**, 2100 (1944).
13. R. C. Elderfield. Heterocyclic compounds. Vol. 4. John Wiley and Sons, Inc., New York. 1952. p. 294.
14. A. M. Maki and D. H. Geske. J. Chem. Phys. **30**, 1356 (1959).

Can. J. Chem. Downloaded from www.nrcresearchpress.com by 210.87.254.6 on 09/05/12
For personal use only.

Infrared studies of water in crystalline hydrates: gypsum, $CaSO_4 \cdot 2H_2O$[1]

V. SEIDL[2] AND OSVALD KNOP
Department of Chemistry, Dalhousie University, Halifax, Nova Scotia

AND

MICHAEL FALK
Atlantic Regional Laboratory, National Research Council of Canada, Halifax, Nova Scotia

Received November 5, 1968

Infrared spectra of partially deuterated hydrates yield the fundamental frequencies of isotopically dilute H_2O, D_2O, and HDO molecules. Isotopic dilution eliminates vibrational coupling and allows the determination of the total number of crystallographically distinct water molecules in the crystal. It also yields the number of distinct symmetric (C_{2v}) and asymmetric (C_s) water molecules. The results for gypsum show that all the water molecules are equivalent and that they are asymmetric, in agreement with crystallographic results. The extent of asymmetry is measured by the difference between the two OH stretching frequencies of HDO molecules, which is 90 cm^{-1}. This corresponds to an estimated difference of 0.02 Å in the O···O distances of the two hydrogen bonds. The spectra of partially deuterated gypsum show clearly that spectral features previously explained by the presence of two sets of distinct water molecules or by proton tunnelling, are in fact due to vibrational coupling.

Canadian Journal of Chemistry, **47**, 1361 (1969)

The crystal structure of gypsum has been reported to have the space-group symmetry $C2/c$ $(I2/c)-C_{2h}^6$, with four $CaSO_4 \cdot 2H_2O$ per unit cell (1, 2). The oxygen atoms O_w of the water molecule have been placed in the $8(f)$ equipoint, which has a site symmetry $1-C_1$ (3). The 16 hydrogen atoms must then belong to two non-equivalent sets $8H_1 + 8H_2$. As a consequence there are 8 symmetrically equivalent water molecules in the unit cell, but the two O_w—H distances in each water molecule are non-equivalent and thus, at least in principle, of different length. This asymmetry is connected with the existence of hydrogen bonds between the water molecule and the oxygen atoms O_I of two SO_4 groups (Fig. 1); the sulfate groups are related by a center of symmetry, but the two O_I atoms that are engaged in the hydrogen bonding are not.

The extent of the asymmetry has never been estimated with confidence. An attempt to locate the hydrogen atoms by the most direct method, neutron diffraction, has resulted in these interatomic distances (2)[3]: O_w—H_1, 1.002 ± 0.030 Å; O_w—H_2, 0.981 ± 0.024 Å; Δ, 0.021 ± 0.038 Å; O_w—O_I, 2.816 ± 0.014 Å; O_w—O_I', 2.824 ± 0.015 Å; Δ, 0.008 ± 0.021 Å. It is seen that the differences Δ are absorbed in the corresponding uncertainty intervals, particularly if 3σ limits are used, so that *numerically* the differences have no statistical significance.

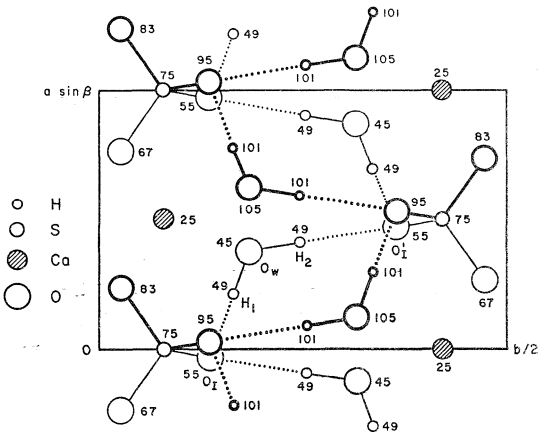

FIG. 1. Schematic projection of one-half of the unit cell of gypsum on the (001) plane (orientation $I2/c$; after ref. 2). The fractional coordinates z have been multiplied by 100.

Raman and infrared (i.r.) *frequencies* of natural (i.e. undeuterated) gypsum[4] cannot establish the

[1]Issued as NRCC No. 10 538.
[2]Killam Post-doctoral Fellow, 1967–1968.
[3]The standard deviations of these distances are based on the 1σ values of the positional parameters given in ref. 2. The distances have not been corrected for thermal motion; isotropic temperature factors were used in the structure refinement.

[4]The i.r. spectrum of undeuterated gypsum has been studied by many investigators (5–12). The spectrum of fully deuterated gypsum has also been reported (8, 9, 11), but not that of partially deuterated gypsum.

Can. J. Chem. Downloaded from www.nrcresearchpress.com by 210.87.254.6 on 09/05/12
For personal use only.

extent, or even confirm the existence, of the asymmetry. The number of normal vibrations and their activities in the i.r. and Raman spectra are the same for an unperturbed (C_{2v}) and a perturbed (C_s) water molecule. Raman and i.r. *intensities* of undeuterated gypsum are of equally little help. If an unperturbed water molecule is assumed, as was done by Cabannes *et al.* (4) in their analysis of the Raman spectrum, and by Hass and Sutherland (5) in their analysis of the i.r. spectrum, gross discrepancies arise between the expected and the observed intensities of the fundamental bands. Whether these discrepancies are due to an unrealistic model or to the contributions of combination modes to the intensities of the fundamentals, is difficult to decide.

When, however, the H_2O molecule in the crystal is replaced by HDO, the existing perturbation from the C_{2v} symmetry caused by asymmetric environment leads to the doubling of all three fundamentals. This doubling, if observed, demonstrates the existence of asymmetry, and its magnitude measures the extent of it. A spectroscopic study of partially deuterated gypsum can thus provide information on the details of geometry of water molecules in gypsum which are not otherwise obtainable.

With this as our main objective we have investigated the spectra of partially deuterated gypsum, paying special attention to the bending and stretching fundamentals of H_2O, D_2O, and HDO dispersed at low isotopic concentrations.

Experimental

A large, colorless, completely transparent crystal of natural gypsum (selenite) from East Milford, Nova Scotia, provided material for some of the experiments. Additional specimens of $CaSO_4 \cdot 2H_2O$ were prepared by precipitation from aqueous solutions of reagent-grade calcium nitrate and sodium sulfate, and in a few experiments commercial reagent-grade $CaSO_4 \cdot 2H_2O$ was also used. The i.r. spectra and X-ray powder diffraction patterns of all these specimens were identical.

Spectra were recorded on a Perkin–Elmer model 521 grating spectrophotometer thoroughly purged with dry nitrogen. Use of an automatic frequency marker and frequent re-calibration of the frequency scale made it possible to measure the frequencies of sharp peaks to within 0.5 cm^{-1}. The effective slit width was about 1 cm^{-1}. Spectra at low temperatures were recorded using a model VLT-2 variable temperature cell (Research and Industrial Instruments Company, London).

Most samples were studied by both the mull and the KBr pellet techniques. The spectra were compensated for absorption by the matrix material by placing suitable films of Nujol or halocarbon oil, or pellets of pure KBr, in the reference beam. The mulls were spread in a 0.1 mm thick layer between NaCl or KBr windows of a demountable cell. The pellets were prepared by pressing mixtures of the finely ground sample and freshly dried KBr in an evacuable die at about 90 000 p.s.i. The pellets had an area of 1.1 cm^2.

The mulls had the advantage that almost no H_2O was introduced in their preparation. On the other hand, sample concentration could not be controlled and the slow agglomeration of the suspended gypsum particles made it necessary to prepare a new mull for each spectrum to be recorded. Also, halocarbon bands completely block the D—O—D bending region of the spectrum, and Nujol bands block the H—O—D bending region. KBr pellets are free from these disadvantages, but small amounts of atmospheric moisture were invariably introduced into the pellets.

Preparation of Deuterated Specimens

Finely ground natural gypsum was soaked in 99.8% D_2O at room temperature or refluxed under exclusion of atmospheric moisture. The rate of exchange at room temperature was very slow and even after two days at the boiling point the deuteration was incomplete. The following two methods proved more satisfactory.

Precipitation

Solutions of calcium nitrate and sodium sulfate in D_2O–H_2O mixtures were prepared and mixed in such a way that the room-temperature solubility of $CaSO_4 \cdot 2H_2O$ was exceeded by a factor of about five. The precipitate consisted of needle-shaped crystals of very good quality. It was filtered, and washed successively with D_2O–H_2O of the desired D:H ratio, acetone, and anhydrous ether. Spectra showed that the precipitates were pure gypsum, without detectable traces of hemihydrate or anhydrous salt[5]. Deuterations up to about 93% were obtained[6].

Rehydration of Anhydrous $CaSO_4$

Reagent-grade $CaSO_4 \cdot 2H_2O$ was dehydrated by heating at 150° *in vacuo* for 24 h and then soaked in D_2O or in D_2O–H_2O mixtures of the desired D:H ratios. The sealed flask was agitated overnight. The samples were filtered, washed with acetone and anhydrous ether, and dried over magnesium perchlorate. Deuterations over 99% were conveniently obtained. Occasionally the spectrum of the product showed traces of hemihydrate.

For low deuterations, precipitation was the only method used. Rehydration was convenient for high degrees of deuteration.

Deuterium Content of Specimens

The D:H ratios were taken to equal twice the ratio of the integrated intensity in the OD stretching region to that in the OH stretching region. This assumes that the

[5]Spectra of $CaSO_4 \cdot \frac{1}{2}H_2O$ and anhydrous $CaSO_4$ have been reported by Morris (11). Our own spectra of these phases were closely similar.

[6]D:H ratios achieved in each deuteration were determined from spectra of mulls. The corresponding spectra of pellets gave considerably lower D:H ratios because of atmospheric moisture introduced in the preparation of the pellets and subsequent H–D exchange.

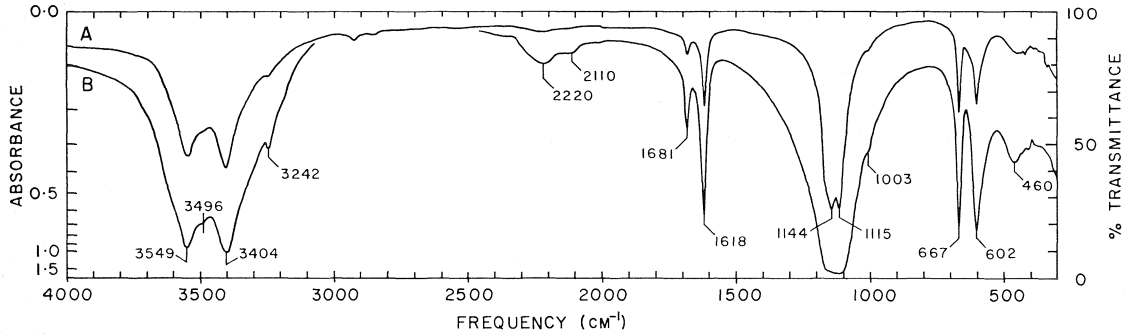

FIG. 2. Spectra of undeuterated gypsum in KBr pellets. *A*, 0.24 mg/200 mg KBr; *B*, 1.00 mg/200 mg KBr.

OD stretching bands have half the integrated intensity of the OH stretching bands (13). For samples of very low deuteration the D:H ratios were taken as those of the parent solution.

The concentrations of the three isotopic species of water were estimated from the molar fractions of hydrogen, x, and deuterium, y

$$[H_2O] : [HDO] : [D_2O] = x^2 : 2xy : y^2$$

This assumes a statistical distribution of deuterium over all the H sites of the crystal. An independent check on whether random distribution had in fact been attained was provided by the relative intensities of the H—O—H, H—O—D, and D—O—D bending bands. These gave a rough measure of the relative concentrations of the three species.

Results

Spectrum of Undeuterated Gypsum

The spectra of gypsum in Nujol and halocarbon oil were identical with those of gypsum in KBr pellets (Fig. 2). The frequencies of the main peaks were averaged from about a dozen spectra and rounded off to the nearest cm^{-1}. The standard deviation was 1.0 cm^{-1} for sharp peaks and 2–5 cm^{-1} for broad peaks and shoulders.

The present peak frequencies agree to within a few cm^{-1} with those reported by Morris (11) and by Wiegel and Kirchner (12). Many published infrared spectra of gypsum indicate the peak frequencies incompletely (8–10) or not at all (6, 7). The extensive set of frequencies obtained by Hass and Sutherland (5) with plane-polarized radiation and single crystals of gypsum is not directly comparable with values such as ours, obtained with unpolarized radiation and polycrystalline material.

The O—H and O—D Stretching Fundamentals of HDO

Figure 3 shows the spectrum in the O—H stretching region for different degrees of deuteration. The broad, complex band in undeuterated gypsum (Fig. 3*E*) becomes simpler and sharper with increasing deuteration (Figs. 3*D*, *C*). The two highest deuterations (Figs. 3*B*, *A*) yield the O—H stretching spectrum of HDO at sufficiently high isotopic dilution to eliminate all contribution from H_2O molecules and HDO–HDO nearest-neighbor pairs. This spectrum consists of two bands of equal intensity, with a separation of 90 cm^{-1}.

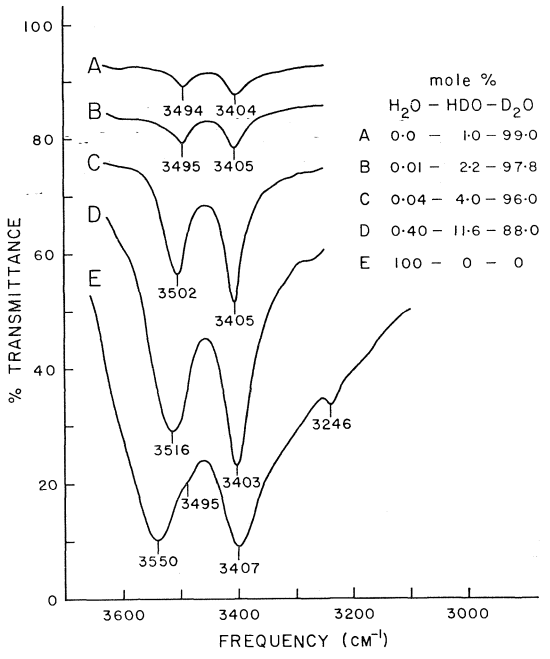

FIG. 3. Spectra of partially deuterated gypsum in Nujol in the OH stretching region. Spectrum *C* has been displaced downward by 15% transmittance, *D* by 18%, and *E* by 4%.

Can. J. Chem. Downloaded from www.nrcresearchpress.com by 210.87.254.6 on 09/05/12
For personal use only.

Can. J. Chem. Downloaded from www.nrcresearchpress.com by 210.87.254.6 on 09/05/12
For personal use only.

Similarly the O—D stretching band at high deuteration is complex and broad (Fig. 4*F*) but becomes simpler and sharper as the degree of deuteration decreases (Figs. 4*E*, *D*). The lowest deuterations (Figs. 4*B*, *A*) yield a spectrum which, like its O—H counterpart, consists of two bands of nearly equal intensity; their separation is 65 cm^{-1}.

The Bending Fundamental of HDO

At high HDO contents a complex pattern of peaks in the H—O—D bending region occurs (Fig. 5*F*). At lower HDO contents the outer components of this pattern are eliminated. A doublet, with a separation of about 14 cm^{-1}, remains (Fig. 5*C*) and does not change on further dilution (Figs. 5*B*, *A*). An identical doublet appears in the spectra of dilute HDO in highly deuterated samples.

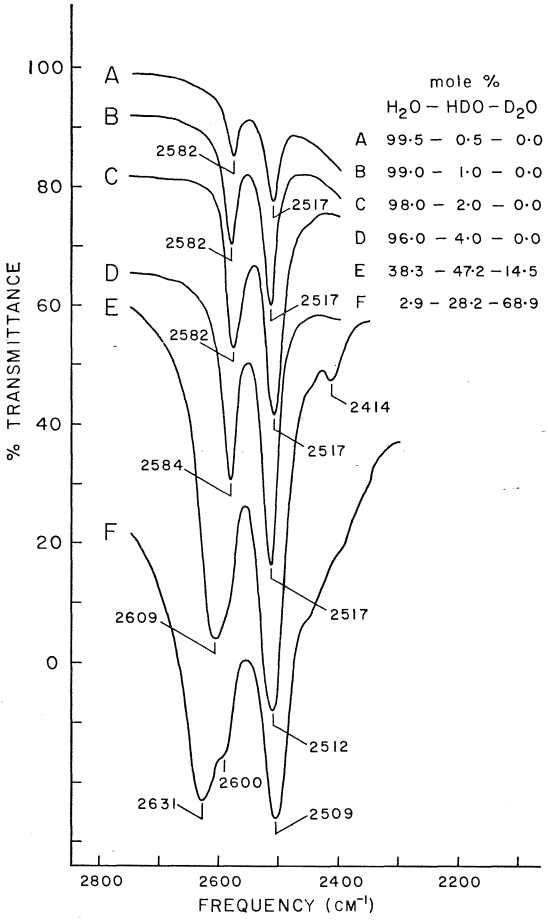

FIG. 4. Spectra of partially deuterated gypsum in KBr pellets in the OD stretching region. The amounts of gypsum used, in mg, were (from *A* to *F*), 4.59, 4.62, 5.00, 2.21, 0.99, and 0.75, respectively. Spectrum *B* has been displaced downward by 6% transmittance, *C* by 13%, *D* by 13%, *E* by 31%, and *F* by 40%.

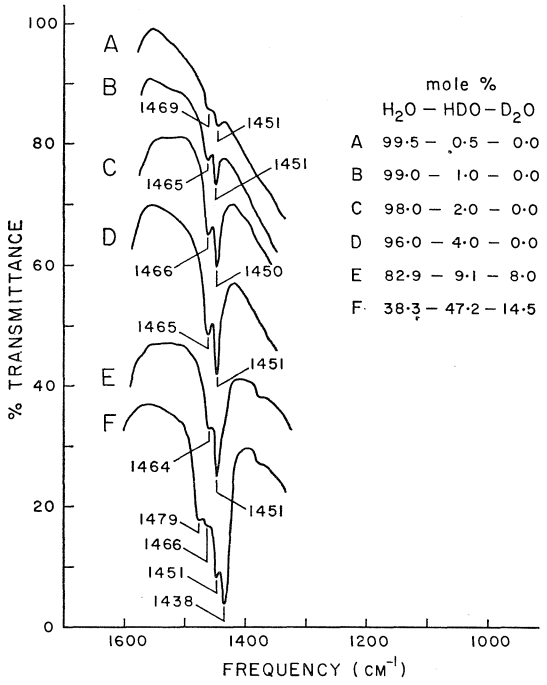

FIG. 5. Spectra of partially deuterated gypsum in KBr pellets in the H—O—D bending region. The amounts of gypsum used, in mg, were (from *A* to *F*) 4.59, 4.62, 5.00, 2.21, 1.02, and 0.99 respectively. Spectrum *A* has been displaced upward by 53% transmittance, *B* upward by 42%, *C* downward by 9%, *E* downward by 35%, and *F* downward by 50%.

The Bending Fundamentals of Isotopically Dilute H_2O and D_2O

At very high deuteration (Fig. 6*A*) the spectrum in the H—O—H bending region has no appreciable contribution from H_2O molecules. The absorption at about 1620 cm^{-1} arises from a weak D_2O band, usually assigned to the combination $\nu_2 + \nu_R$ of the bending vibration ν_2 and restricted rotation ν_R (14). As the deuterium content of the sample decreases, the band due to the bending vibrations of isotopically dilute H_2O molecules appears (Fig. 6*B*). This is a sharp, single band situated at 1654 cm^{-1}. At still lower deuterium contents higher concentrations of H_2O give rise to a more complex spectrum. Undeuterated samples yield the well-known doublet at 1681 and 1618 cm^{-1} (Fig. 6*C*).

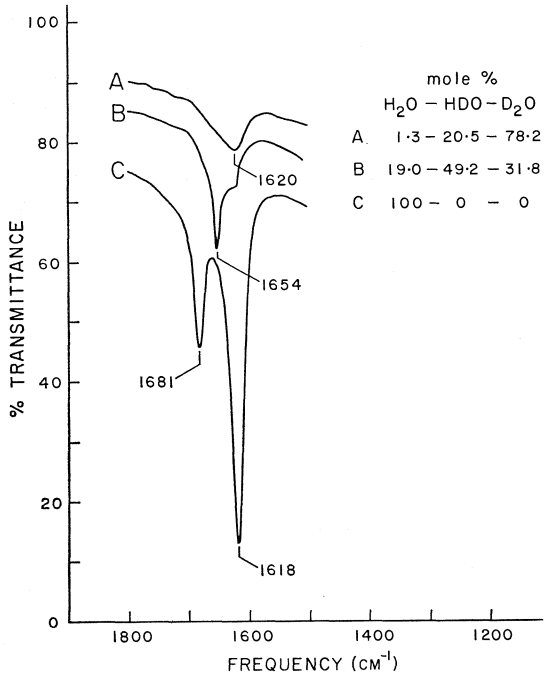

FIG. 6. Spectra of partially deuterated gypsum in KBr pellets in the H—O—H bending region. The amounts of gypsum used, in mg, were (from *A* to *C*) 1.00, 1.01, and 1.00. Spectrum *C* has been displaced downward by 10% transmittance.

The absorption from D—O—D vibrations in gypsum lies on the side of a very intense sulfate band (Figs. 7*B*, *E*). At high deuterium concentrations there are two D_2O peaks in this region, at 1238 and 1194 cm^{-1} (Figs. 7*D*). At lower deuterium concentrations (Fig. 7*A*) the spectrum of dilute D_2O molecules consists of one peak at 1215 cm^{-1}. The D_2O peaks can be seen more clearly in the difference spectra 7*C* and 7*F*, which are compensated for the sulfate group absorption.

Effect of Temperature

The temperature dependence of the frequencies of isotopically dilute HDO molecules is shown in Table I. Temperature shifts are remarkably small. The maximum shift observed was only 7 cm^{-1} for a temperature change of 250°. The half-widths at room temperature were about 30 cm^{-1} for the O—H stretching peaks, 20 cm^{-1} for the O—D stretching peaks, and about 13 cm^{-1} for the H—O—D bending peaks. The half-widths of the stretching peaks decreased on cooling by about 50% over 250°.

TABLE I

Fundamental frequencies, in cm^{-1}, of isolated HDO in gypsum

Vibration	Frequencies at temperatures†				
	−175	−75	0	30	75
OH stretching				3494* 3404*	
OD stretching	2577 2516	2579 2513	2580 2515	2582* 2517*	2584 2516
H—O—D bending	1466 1453			1465* 1451*	

*Average values from ten or more spectra.
†Temperatures in °C.

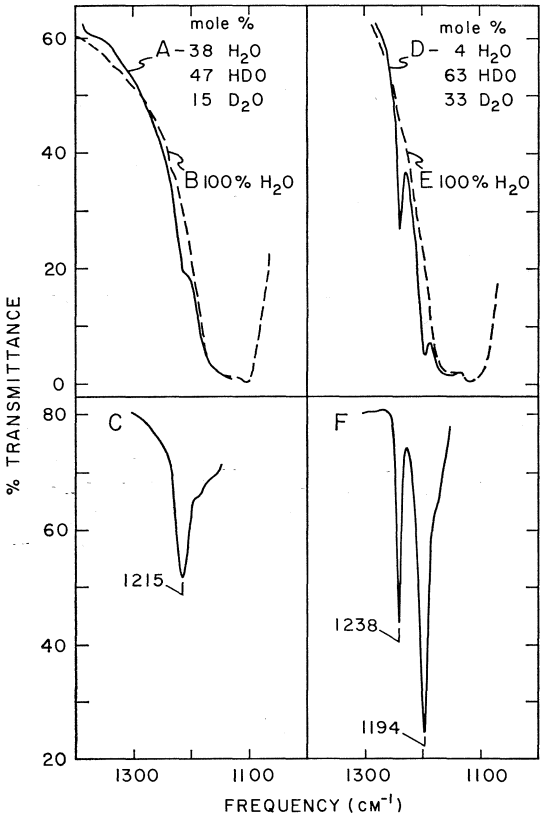

FIG. 7. Spectra of partially deuterated gypsum in KBr pellets in the D—O—D bending region. The amounts of gypsum used, in mg, were 0.99 in *A* and *B*, and 1.20 in *D* and *E*. Spectra *C* and *F* are difference spectra; *C* is the difference spectrum of *A* and *B*; *F* is the difference spectrum of *D* and *E*.

Discussion

The water molecules in a unit cell of a crystalline hydrate will be distributed over *n* crystallographically non-equivalent sets; in each of these

Can. J. Chem. Downloaded from www.nrcresearchpress.com by 210.87.254.6 on 09/05/12
For personal use only.

TABLE II

Numbers of fundamental vibrations of isotopically isolated H_2O, D_2O, and HDO molecules in crystalline hydrates

Molecule	Vibration	Approximate frequency (cm^{-1})	Single molecule		n sets of molecules (of which m are C_s)
			C_{2v}	C_s	
H_2O	OH stretching	3450*	2	2	$2n$
	HOH bending	1650	1	1	n
D_2O	OD stretching	2550*	2	2	$2n$
	DOD bending	1215	1	1	n
HDO	OH stretching	3450	1	2	$n+m$
	OD stretching	2550	1	2	$n+m$
	HOD bending	1460	1	2	$n+m$

*The stretching vibrations of isolated H_2O and D_2O molecules cannot be observed (see text).

sets the molecules are related by symmetry and therefore equivalent[7]. These n sets will give rise to n bending and $2n$ stretching fundamental H_2O vibrations, all of them i.r. active. Partial deuteration will replace some of the H_2O molecules by D_2O molecules and others by HDO molecules. Always assuming that the deuterium atoms are distributed at random throughout the crystal, the D_2O molecules will produce additional $3n$ fundamental vibrations, but the number of HDO fundamentals will depend on the symmetry of the H_2O molecules that the HDO molecules have replaced. A symmetric H_2O molecule on half-deuteration will generate 3 fundamentals, while an asymmetric one will yield either of the two possible distinct HDO species and thus 3 *pairs* of fundamentals. The total number of fundamentals in the partially deuterated hydrate will then be $3n$ from the H_2O molecules plus $3n$ from the D_2O molecules plus $3n + 3m$ from the HDO molecules, m being the number of sets of *asymmetric* H_2O molecules in the undeuterated hydrate. The approximate frequencies at which the absorption bands corresponding to these fundamentals will occur are indicated in Table II.

In principle, n and m can be determined from the study of any one of the H_2O or D_2O fundamentals *and* any one of the HDO fundamentals. In practice, the enumeration of these fundamentals will be complicated by the existence of coupling between vibrations of neighboring molecules which will tend to increase the number of observed bands. To eliminate this complication the fundamentals must be isolated by suitable isotopic dilution. Thus in a highly deuterated crystal the HDO molecules will be surrounded entirely by D_2O molecules as their nearest (water-molecule) neighbors, and the O—H stretching and H—O—D bending vibrations of HDO will be observed in their uncoupled form. Similarly a very low degree of deuteration will yield the frequencies of the O—D stretching and H—O—D bending vibrations of isolated HDO molecules, while intermediate degrees of deuteration may yield bending frequencies of isolated H_2O and D_2O. The *stretching* vibrations of isolated H_2O and D_2O molecules are masked by the stretching bands of HDO and cannot be observed.

Gypsum affords an example of a hydrate in whose spectrum all five observable fundamentals of isolated H_2O, D_2O, and HDO are actually observed. The spectrum of highly deuterated gypsum contains two distinct O—H stretching bands of isolated HDO, while at low deuterations there are two O—D stretching bands. At high and low deuterations there are two bending bands of dilute HDO. Each of these observations corresponds to $n + m = 2$. At intermediate deuterations, only one bending band each is found for isolated H_2O and isolated D_2O, either observation yielding $n = 1$. Consequently all water molecules in undeuterated (or fully deuterated) gypsum are crystallographically equivalent and asymmetric. This conclusion is in complete agreement with the expectations from the space-group symmetry $C2/c$ assigned to gypsum on the basis of X-ray and neutron diffraction studies.

That the asymmetry of the water molecules is appreciable is indicated by the large splittings of the three isolated HDO frequencies: 90 cm^{-1} for O—H stretching, 65 cm^{-1} for O—D stretching, and 14 cm^{-1} for the bending. The hydrogen bonds of the two OH groups must thus differ

[7]Zeolitic water molecules are not being considered here.

Can. J. Chem. Downloaded from www.nrcresearchpress.com by 210.87.254.6 on 09/05/12
For personal use only.

Can. J. Chem. Downloaded from www.nrcresearchpress.com by 210.87.254.6 on 09/05/12
For personal use only.

considerably in length and strength. The hydrogen-bond lengths can be estimated from the Lord–Merrifield correlation of O—H stretching frequencies and the O···O distances in crystals (15) or from one of its modified versions (16). These correlations are, in the region of interest, at best approximations, and so the two hydrogen-bond lengths in gypsum calculated from them, 2.82 and 2.84 Å, have no claim to accuracy. But they do give the order of magnitude of the *difference* of the two O···O distances, 0.02 Å, and show that the effect of temperature on factors responsible for the asymmetry of the water molecule is small. If a reliable correlation of O—H stretching frequencies with observed O—H distances were available, a similar estimate could be made of the difference of the two O—H bond lengths[8].

The spectroscopic estimate of the difference of two O···O distances in a crystal gives an idea of the accuracy with which such distances would have to be determined by diffraction methods to improve on the reliability of the Lord–Merrifield correlation. In gypsum the difference of the OH frequencies corresponding to the two O···O distances is quite large by spectroscopic standards of resolution, and an accurate determination of the positional parameters of two oxygen atoms in such a crystal ought not to present difficulties. Yet the O_w—O_I and O_w—O_I' distances of ref. 2 differ by 0.008 ± 0.021 Å (or, using 3σ limits, 0.01 ± 0.06 Å) compared with the above estimate, 0.02 Å. Admittedly the accuracy of the determination of the crystal structure of gypsum by neutron diffraction can be improved, but for the results to be useful in the present context the estimated standard deviations of the two distances would have to be of the order of 0.001 Å, i.e. ten times smaller than in ref. 2.

The present results also occasion comment on some of the previous spectroscopic studies of gypsum. Komarov *et al.* (10) interpreted the doublet in the H—O—H bending region at 1620 and 1667 cm^{-1} (1618 and 1681 cm^{-1} in our spectra) as indicating the presence of two types of water molecules in the ratio 3:1. Our spectra show that the H—O—H (and D—O—D) bending doublet reduces to a single peak of intermediate frequency in the spectrum of isolated H_2O (and D_2O). The doublet is thus due to two coupled vibrations of the water molecules present in the unit cell, as correctly assigned by Hass and Sutherland (5).

Stekhanov (18) suggested that the doublet in the O—H stretching region at 3405 and 3495 cm^{-1} in the Raman spectrum is due to the splitting of the energy levels caused by the tunnelling of hydrogen in a double-well potential. Such splitting of energy levels is known to be highly sensitive to the mass of the tunnelling atom; it would be expected to decrease drastically for the O—D stretching vibrations, for which the tunnelling mass doubles (19). Our stretching frequency ratios for isolated O—H and O—D frequencies in gypsum are 3494/2582 = 1.353 and 3404/2517 = 1.352. These ratios are very close to those observed in ice (20) and in $NaCl \cdot 2H_2O$ (21) and show that the two isolated O—H (and O—D) stretching bands originate in distinct OH groups in the crystal. The more complicated pattern of bands in undeuterated (and completely deuterated) gypsum is due to the coupling of these vibrations with those of the neighboring water molecules. There is no anomaly to indicate appreciable tunnelling.

Conclusion

A method is presented for determining the total number n of crystallographically distinct H_2O molecules, and the number m of crystallographically distinct *asymmetric* H_2O molecules, from the spectra of partially deuterated crystalline hydrates. The method is of general applicability. Its limit is set by the ability to resolve closely spaced fundamental bands of the isotopically dilute species of non-equivalent water molecules in the crystal. Whether the method will give the correct values of n and m, or only their minimum estimates, depends on how completely all the fundamentals required by the actual symmetry of the crystal structure are enumerated. There is no difficulty in recognizing as distinct, OH stretching bands 10 cm^{-1} apart ($NaCl \cdot 2H_2O$ at $-170°$; ref. 21). This separation corresponds to a difference of about 0.002 Å in the O···O length. In favorable circumstances, bands lying even closer together should be distinguishable. It is thus possible to detect spectroscopically differences in hydrogen-bonded O···O distances

[8]Mr. R. W. Green of the Department of Chemistry, University of British Columbia, used our frequencies to calculate the approximate ratio of the two O—H distances in gypsum (17). Using a harmonic approximation he found $d(O_w—H') : d(O_w—H) = 0.966$.

which would be difficult to establish by diffraction methods.

Among the experimental difficulties that may arise are (*a*) slow rate of deuteration; (*b*) masking of some of the water-molecule fundamentals by other bands; and (*c*) uncertainty whether vibrational coupling has been reduced to a level where it does not interfere. For gypsum it was possible to deal successfully with each of these problems.

The usefulness of the method is now being tested on several other crystalline hydrates[9].

Acknowledgments

We thank Miss Gwen Thomas for her capable assistance with some of the experimental work and Mr. P. F. Seto for help with the computations; Dr. K. B. Harvey and Mr. R. W. Green for the opportunity to discuss this problem with them; and National Gypsum (Canada) Ltd. for providing a large sample of selēnite.

1. W. A. Wooster. Z. Krist. **94**, 375 (1936).
2. M. Atoji and R. E. Rundle. J. Chem. Phys. **29**, 1306 (1958).
3. International Tables for X-Ray Crystallography. Vol. I. Kynoch Press, Birmingham. 1952.
4. J. Cabannes, L. Couture, and J. P. Mathieu. J. Chim. Phys. **50**, C89 (1953).
5. M. Hass and G. B. B. M. Sutherland. Proc. Roy. Soc. London, Ser. A, **236**, 427 (1956).
6. K. Omori and P. F. Kerr. Bull. Geol. Soc. Am. **74**, 709 (1963).
7. A. T. Logvinenko, D. K. Arkhipenko, M. A. Savinkina, and G. A. Golubova. Izv. Sibirsk. Otd. Akad. Nauk SSSR, 137 (1963).
8. C. Pain, C. Duval, and J. Lecomte. Compt. Rend. **237**, 238 (1953).
9. C. Duval and J. Lecomte. J. Chim. Phys. **50**, C64 (1953).
10. B. F. Komarov, E. S. Sakharov, and G. A. Ball. Zh. Vses. Khim. Obshchestva im. D. I. Mendeleeva, **7**, 692 (1962).
11. R. J. Morris. Anal. Chem. **35**, 1489 (1963).
12. E. Wiegel and H. H. Kirchner. Ber. Deut. Keram. Ges. **43**, 718 (1966).
13. C. A. Swenson. Spectrochim. Acta, **21**, 987 (1965).
14. P. A. Giguère and K. B. Harvey. Can. J. Chem. **34**, 798 (1956).
15. R. C. Lord and R. E. Merrifield. J. Chem. Phys. **21**, 166 (1953).
16. H. Ratajczak and W. I. Orville-Thomas. J. Mol. Structure, **1**, 449 (1967–1968).
17. R. W. Green. Private communication to M. Falk.
18. A. I. Stekhanov. Dokl. Akad. Nauk SSSR, **106**, 433 (1956); Izv. Akad. Nauk SSSR, Ser. Fiz. **21**, 311 (1957); **22**, 1109 (1958).
19. R. L. Somorjai and D. F. Hornig. J. Chem. Phys. **36**, 1980 (1962).
20. T. A. Ford and M. Falk. Can. J. Chem. **46**, 3579 (1968).
21. T. A. Ford and M. Falk. J. Mol. Structure. In print (1969).
22. J. Schiffer. Ph.D. Thesis, Princeton University, Princeton, New Jersey. 1963.
23. J. Schiffer and D. F. Hornig. *In* Molecular dynamics and structure of solids. Natl. Bur. Standards Monograph. 1968.
24. R. Kling and J. Schiffer. Abstract L7. 23rd Symp. on Mol. Struct. and Spectry. The Ohio State University, Columbus, Ohio. September 3–7, 1968. p. 58.

[9]It has come to our attention that a similar approach to the study of water in crystalline hydrates has been proposed by Schiffer (22). The conclusions from his recent work on gypsum (23, 24) appear largely to coincide with the conclusions of the present study. We thank Professor Schiffer for sending us a preprint of ref. 23.

Can. J. Chem. Downloaded from www.nrcresearchpress.com by 210.87.254.6 on 09/05/12
For personal use only.

Can. J. Chem. Downloaded from www.nrcresearchpress.com by 210.87.254.105 on 09/05/12
For personal use only.

Effect of pressure on the rates of hydrolysis of allyl chlorides

A. B. LATEEF AND J. B. HYNE
Department of Chemistry, The University of Calgary, Calgary, Alberta

Received October 11, 1968

The pressure dependence of the rates of hydrolysis of allyl chloride and α-, β-, and γ-methyl allyl chlorides has been examined. The significance of the activation volumes, ΔV^*, and their pressure dependence, $d\Delta V^*/dP$, is discussed. These activation parameters indicate an S_N2 mechanism for allyl and β-methyl allyl chloride and an S_N1 or intermediate character mechanism for the other methyl substituted allyl chlorides investigated. The results are compared with the corresponding ΔH^* and ΔC_P^* measurements of Robertson and co-workers. The temperature dependence of the activation volume, $d\Delta V^*/dT$, for the solvolysis of the parent allyl chloride has been measured and found to be small and negative.

Canadian Journal of Chemistry, **47**, 1369 (1969)

Introduction

DeWolfe and Young (1) have reviewed the extensive investigations of various workers on the solvolysis of allylic type halides. It has been suggested (2) that solvolysis reactions of this type represent a continuous spectrum of mechanism, ranging from bimolecular S_N2 to the limiting unimolecular S_N1 type ionization process.

Although the effect of pressure on the rates of reaction in solution has been under investigation for some time, the significance of the activation volume as a mechanistic probe has been recognized only recently (3–5). Whalley (4) has reviewed the significance of activation volumes in the determination of reaction mechanism, and has suggested that the volume of activation is probably easier to rationalize in terms of reaction mechanism than the other important parameters of activation, i.e. the free energy, enthalpy, and entropy. Improvements in the precision with which the pressure dependence of reaction rates can be determined has also permitted the evaluation of the second pressure differential of the rate, namely the pressure dependence of the activation volume, $d\Delta V^*/dP$. Robertson (6) has demonstrated the value of the second temperature differential of the rate, ΔC_P^*, as a measure of reaction mechanism type and it will be shown in this paper that $d\Delta V^*/dP$ may be an equally important and informative activation parameter. Table I summarizes the various activation parameters that may be obtained for a given system by a combination of pressure and temperature effect studies.

There are very few solvolysis reactions for which all of these pseudo thermodynamic activation parameters are available. In order to examine the relative significance of these various activation parameters, as far as reaction mechanism is concerned, it is important to have a complete set for a given system. Robertson *et al.* (7) have examined the solvolysis of methyl substituted allyl chlorides and reported the activation parameters with respect to temperature. The primary purpose of this work was to determine the activation parameters with respect to pressure for this same system, and to illustrate the inter-relationship of all of these activation parameters in indicating the variation of mechanism as the structure of the reacting substrate changes.

TABLE I
Thermodynamic parameters of activation

Variable	First derivative	Second derivative
Temperature	ΔH^* (ΔS^*)	ΔC_P^*
Pressure	ΔV^*	$d\Delta V^*/dP$

Experimental

Kinetic Method

The rate of production of HCl resulting from the hydrolysis of the various allyl chlorides was followed conductimetrically. Details of the in situ conductimetric technique have been reported previously (8). In this work an automatic balancing a.c. conductance bridge with digital print out (GR Type 1680-A) was used, providing improved accuracy and reproducibility, particularly with faster reactions. The high pressure vessel, pressure control, and conductance cell have been described in earlier papers (8). Temperature control was maintained to better than ± 0.01 °C by oil bath thermostating. At temperatures below ambient, an auxiliary refrigerated cooling coil immersed in the oil bath was employed. The temperature sensing device controlled both the cooling unit and the heating element. Pseudo first order rate constants were extracted from conductance/time data by the Guggenheim method (9).

TABLE II

Rate constants for the hydrolysis of substituted allyl chlorides as a function of pressure

Allyl chloride 50.25 °C		β-Methyl allyl chloride 50.25 °C		*trans*-γ-Methyl allyl chloride 12.02 °C	
Pressure (atm)	$10^5 \times k$ (s^{-1})	Pressure (atm)	$10^5 \times k$ (s^{-1})	Pressure (atm)	$10^4 \times k$ (s^{-1})
1.0	2.540[a]	1.0	5.706[a]	1.0	1.140±0.002
680.5	3.355±0.008	313.0	6.478±0.018	340.0	1.386±0.016
1360.9	4.340±0.024	680.5	7.546±0.060	510.3	1.518±0.018
2041.4	5.346±0.021	1360.9	9.296±0.065	680.5	1.696±0.020
2721.8	6.557±0.073	2041.4	11.560±0.22	850.6	1.811±0.017
		2721.8	14.350±0.100	1020.7	1.949±0.030
ΔV^* ml/mole	−11.40±0.13		−10.16±0.21		−14.83±0.05
$d\Delta V^*/dP \times 10^4$ ml/atm mole	16.11±1.44		9.85±1.03		46.66±4.69

[a]Calculated from the data of Robertson and co-workers (12, 7). N.B. The rate constants reported in Robertson's paper (7) are correct. However the values for the coefficients A, B, and C in the temperature dependence equation for β-methyl allyl chloride are in error. The correct values are $A = -8006.0996$, $B = -23.3571$, and $C = 79.13099$, as obtained from Robertson in a private communication.

Materials

Water

House distilled water was first passed through Ilco-way de-ionizing resin and then redistilled in Pyrex apparatus from which atmospheric carbon dioxide was excluded; storage was in polyethylene containers.

Allyl Chloride

Matheson, Coleman, and Bell material was redistilled at 10^{-3} mm, and the center cut stored for later use. Purity was checked by gas–liquid chromatography (g.l.c.).

β-Methyl Allyl Chloride

Eastman Organic Chemicals sample redistilled in small quantities at 10^{-3} mm, as required. Gas–liquid chromatography indicated no significant impurities.

trans-γ-Methyl Allyl Chloride

The crotyl chloride purchased from Aldrich Chemical Co. was found to be a mixture of *cis*- and *trans*-γ-methyl allyl chloride. The *trans*-γ-methyl allyl chloride was separated by preparative g.l.c. as described by Robertson *et al.* (7). The preparative column used was 9 ft × ⅜ in., packed with 15% β,β′-oxydipropionitrile on Chromosorb P(80–100 mesh), which is capable of separating the *cis* and *trans* isomers. The separation was carried out under the following conditions: injector 100 °C, oven 45 °C, detector 140 °C, flow rate 90 cc nitrogen per min. The purity of the sample of *trans*-γ-methyl allyl chloride was checked on an analytical column of 6 ft × ¼ in. packed with the same material, under the following conditions: injector 100 °C, oven 41 °C, detector 197 °C, nitrogen flow 28 cc per min. The sample of *trans*-γ-methyl allyl chloride was found to have less than 0.3% impurity.

α-Methyl Allyl Chloride

A pure sample of this substrate was kindly provided by R. E. Robertson. The purification method was as described in ref. 7.

Preparation of Working Solutions

All reaction solutions were prepared by weighing required amounts of the various allyl chlorides and dilution in standard flasks to yield 10^{-4} M concentrations. Solutions were degassed by repetitive freezing and melting before being loaded into conductance cells.

Results

Pseudo first order rate constants for the hydrolysis of allyl chloride, β-methyl allyl chloride, and *trans*-γ-methyl allyl chloride at various pressures to 2700 atm are reported in Table II. Attempts to measure the pressure dependence of the rate of hydrolysis of α-methyl allyl chloride were unsuccessful, due to the relatively rapid intramolecular rearrangement of this substrate to a mixture of *cis*- and *trans*-γ-methyl allyl chloride (10). Rearrangements of this kind have been shown (4, 11) to be particularly pressure sensitive and to have rates in excess of the rate of hydrolysis of the parent halide. Accordingly, any attempt to observe the rate of hydrolysis of α-methyl allyl chloride, particularly at elevated pressures, rapidly becomes an observation of the combined rate of hydrolysis of a rearranged mixture of methyl substituted allyl chlorides. The complication is clearly demonstrated by failure to obtain linear first order kinetic behavior in the case of α-methyl allyl chloride.

Allyl chloride and β-methyl allyl chloride were studied at 50.25 °C; at this temperature the reaction proceeded at a rate which permitted considerable pressure variation without increas-

Can. J. Chem. Downloaded from www.nrcresearchpress.com by 210.87.254.105 on 09/05/12
For personal use only.

TABLE III

Rate constants for the solvolysis of allyl chloride as a function of pressure at various temperatures

Pressure (atm)	Rate constant, $10^5 \times k$ (s^{-1}), at temperatures			
	29.34 °C	40.00 °C	50.25 °C	60.50 °C
1.0	0.210[a]	0.793[a]	2.540[a]	7.440±0.100
680.5		1.043±0.023	3.355±0.008	10.31 ±0.300
1360.9	0.343±0.012	1.329±0.012	4.340±0.024	13.060±0.250
2041.4			5.346±0.021	
2721.8	0.488±0.014	2.027±0.016	6.557±0.073	21.050±0.360
ΔV^* ml/mole	−10.20±0.74	−10.69±0.19	−11.40±0.13	−12.58±0.25
$d\Delta V^*/dP \times 10^4$ ml/atm mole	18.46±1.50	13.49±1.22	16.11±1.44	16.30±1.87

[a]Calculated from ref. 12.

ing the rate beyond a measurable value. *trans*-γ-Methyl allyl chloride, however, hydrolyzes at a considerably faster rate even at room temperature and atmospheric pressure. Accordingly, it was necessary to study the effect of pressure on the hydrolysis of this substrate at 12.02 °C. Since the purpose of this study was to compare the pseudo thermodynamic parameters of activation of the complete set of allyl chlorides, this experimentally dictated temperature difference required that a check of the temperature dependence of the pressure-derived activation parameters be carried out. This was done in the case of allyl chloride. Table III reports the dependence of the rate of hydrolysis of allyl chloride on pressure at four temperatures over the range of 30–60 °C. The activation volume and its pressure dependence derived from these results for each temperature shows a remarkable constancy as the temperature is varied. While this observation in itself is interesting, its main value is to serve as a good indication of the magnitude of any correction that should be applied when comparing the pressure-derived activation parameters obtained from kinetic data at different temperatures.

In any study in which the derivation of the measured rate constants with respect to pressure or temperature is extracted, the error associated with these derived parameters is strictly dependent on the accuracy of the rate determinations themselves. Selected rate data determined at atmospheric pressure in the apparatus used in this work were in excellent agreement with the previously reported values of Robertson and co-workers (7, 12). The values shown at atmospheric pressure in Tables II and III are those calculated from the rate/temperature dependence equation published by Robertson (6). All rate constants reported at elevated pressures are the average values of at least four separate rate determinations. The uncertainties associated with each value were obtained by the method previously described by Golinkin *et al.* (13), and are normally better than ±1.0%. Activation volumes and their pressure dependence were extracted from the rate/pressure data reported in Table II by obtaining a computer best fit to the rate/pressure quadratic equation.

$$\log k = A + BP + CP^2$$

This method has been described in detail in a previous paper (13). Figure 1 is a typical plot of log k vs. pressure for data reported in this paper. The error bars shown on each point illustrate the typical uncertainty associated with the rate

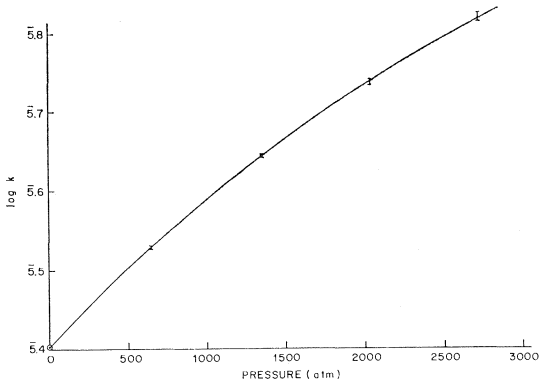

FIG. 1. Plot of log k vs. pressure for the hydrolysis of allyl chloride at 50.25 °C.

Can. J. Chem. Downloaded from www.nrcresearchpress.com by 210.87.254.105 on 09/05/12
For personal use only.

TABLE IV

Activation parameters derived from pressure and temperature dependence of rate for the solvolysis of various allyl chlorides

Substrate chloride	Pressure parameters		Temperature parameters[a]	
	ΔV^* (ml/mole)	$(d\Delta V^*/dP) \times 10^4$ (ml/atm mole)	ΔH^* (kcal/mole)	$(d\Delta H^*/dT)\Delta C_P^*$ (cal mole deg)
Allyl-	-11.40 ± 0.13 (50.25°) -8.0 (approx.) (12.0°)	16.11 ± 1.44	21.99 ± 0.01 (50.0°)	-49.6 ± 1.2
β-Methyl allyl-	-10.16 ± 0.21 (50.25°)	9.85 ± 1.03	20.98 ± 0.08 (50.0°)	-48.39 ± 4.5
α-Methyl allyl-			23.87 ± 0.01 (15°)	-91.6 ± 3.1
trans-γ-Methyl allyl-	-14.83 ± 0.05 (12.02°)	46.66 ± 4.69	23.93 ± 0.01 (15°)	-81.6 ± 3.3

[a]Robertson's data, ref. 7.

determinations at pressures above atmospheric, and the plot clearly establishes the non-linearity of the log k vs. pressure relationship. This curvature is reflected in the non-zero valued C coefficient in the quadratic equation used to describe the pressure dependence and yields the $d\Delta V^*/dP$ values shown in Tables II and III.

Discussion

All volumes of activation measured for the allyl halides studied in this work are negative. This observation is in keeping with the fact that where an S_N1 or S_N2 type mechanism is operative, the transition state is normally a more polar species than the initial state. Accordingly, volume reduction by electrostriction of solvent will tend to outweigh any volume increase due to bond extension in the activation process. Furthermore, it might be expected that the ΔV^* associated with the more ion-like transition state of an S_N1 mechanism would be more negative than in the case of an S_N2 mechanism.

Robertson and co-workers (7) have suggested, on the basis of their ΔH^* and ΔC_P^* values (see Table IV), that *trans*-γ-methyl allyl chloride hydrolyzes by a more S_N1 like mechanism while the parent allyl and β-methyl allyl chlorides are more S_N2 type reactions. The ΔV^* values reported in Table II for these three compounds suggest that the two S_N2 type reactions do indeed have volumes of activation somewhat less negative than that for the S_N1 type *trans*-γ-methyl allyl chloride. It is important at this point to recall the temperature dependence of ΔV^* as illustrated in Table III. If the ΔV^* value for allyl chloride is corrected to 12.02 °C a value of approximately -8 ml/mole is obtained, to be compared with a corresponding value for *trans*-γ-methyl allyl chloride of -14.8 ml/mole at the same temperature. Accordingly, the temperature difference between the data reported in Table II tends to obscure the differences in the ΔV^* values rather than accentuate them. Whether or not the ΔV^* values for allyl and β-methyl allyl chlorides reflect a true S_N2 type mechanism cannot be established conclusively. However, le Noble (11) has reviewed the volumes of activation of a number of bimolecular reactions for which other evidence suggests a simultaneous bond-making and bond-breaking reaction mechanism and has suggested that for such limiting S_N2 reaction types, a ΔV^* value between -5 and -10 ml/mole is to be expected. The ΔV^* values reported here suggest that allyl and β-methyl allyl chloride hydrolyze by a mechanism that might be termed non-limiting S_N2. In reactions for which the rate is controlled by an S_N1 type ionization process, the ΔV^* is expected to be of the order of -15 ml/mole (14). Hence the -14.8 ml/mole value of ΔV^* for the hydrolysis of *trans*-γ-methyl allyl chloride suggests an S_N1 type mechanism.

By far the most instructive presentation of the available data on the allyl chloride system is that presented in Table IV. Here are presented in summary form all of the activation parameters for allyl, β-methyl, and *trans*-γ-methyl allyl chlorides. It was on the basis of ΔC_P^* values shown, that Robertson and co-workers (7) classified the allyl and β-methyl allyl chlorides as S_N2 like and α-methyl and *trans*-γ-methyl allyl chlorides as

Can. J. Chem. Downloaded from www.nrcresearchpress.com by 210.87.254.105 on 09/05/12
For personal use only.

Can. J. Chem. Downloaded from www.nrcresearchpress.com by 210.87.254.105 on 09/05/12
For personal use only.

S_N1. While a classification of this type could be based on ΔH^* values, the relative differences in these parameters was not great. The more sensitive of the two temperature-derived activation parameters was the second differential ΔC_P^*. While it is unfortunate that rate/pressure data for α-methyl allyl chloride proved to be unobtainable in this work, the remaining three allyl chloride substrates provide sufficient data to compare ΔV^* and $d\Delta V^*/dP$ with ΔH^* and ΔC_P^* values. A very similar picture emerges. As discussed above, a classification into S_N1 and S_N2 type mechanisms is possible on the basis of ΔV^* alone, but a much clearer separation of types becomes apparent when the second derivative $d\Delta V^*/dP$ values are examined. It is, therefore, clear from Table IV that first derivatives of the rate with respect to pressure (ΔV^*) and temperature (ΔH^*) are considerably inferior to second derivatives, $d\Delta V^*/dP$ and ΔC_P^*, as activation parameters for use as mechanistic probes.

The main reason for examining the temperature dependence of activation volume in the case of the allyl chloride was to permit appropriate compensation to be made for the considerable temperature difference between the pressure studies of the three allyl systems. However, the observed small value for $d\Delta V^*/dT$ is, in itself, an interesting observation. Walling and Schugar (15) have previously commented on the apparent lack of temperature sensitivity of ΔV^* although Laidler and Chen (16) reported that ΔV^* for the hydrolysis of ethyl acetate changed from -9.9 ml/mole at 25 °C to -4.8 ml/mole at 2.4 °C. Even in the latter case, however, $d\Delta V^*/dT$ is less than 0.25 ml/mole deg compared with a value of less than 0.1 ml/mole deg in the case of allyl chloride hydrolysis. It is worth noting that in the ethyl acetate case, although the reaction mechanism differs from solvolysis, the temperature range involved includes the temperature of maximum density of water and, if ΔV^* in any way reflects solvent reorganization, it might be expected to show its maximum temperature dependence passing through the Td(max) of water. Whatever the explanation of the lack of temperature sensitivity of ΔV^* may be, it can at least be said, that since ΔV^* is the difference in volume between the initial and the transition states, the volumes of both of these states respond in a remarkably similar manner to temperature change. This observation is noteworthy since if the solvent is deemed to be more highly electrostricted around the more polar transition state, it might be reasoned that the volume of the transition state entity would be significantly less sensitive to temperature than the more "loosely solvated" initial state. The apparent lack of sensitivity of ΔV^* to temperature might, therefore, be interpreted as suggesting that the solvent cage around the initial state is a good deal more rigid and temperature stable than has heretofore been believed.

Conclusions

The heat capacity and pressure dependence of volume of activation appear to be more sensitive to variations in the reaction mechanism for the allyl chloride solvolyses studied than are the first derivative parameters, enthalpy and volume of activation. The temperature dependence of the enthalpy and volume of activation makes it advisable to determine these parameters at comparable temperatures before using their relative values as indicators of likely mechanistic types.

Acknowledgment

The authors wish to thank the National Research Council of Canada for financial assistance in support of this work.

1. R. H. DeWolfe and W. G. Young. Chem. Rev. **56**, 753 (1956).
2. S. Winstein, E. Grunwald, and H. W. Jones. J. Am. Chem. Soc. **73**, 2700 (1951).
3. S. D. Hamman. Physico-chemical effects of pressure. Academic Press, Inc., New York. 1964. Chap. 8 and 9.
4. E. Whalley. Advances in physical organic chemistry. Vol. 2. *Edited by* V. Gold. Academic Press, Inc., New York. 1964.
5. S. D. Hamman. Ann. Rev. Phys. Chem. **15**, 349 (1964).
6. R. E. Robertson. Progr. Phys. Org. Chem. **M4**, 213 (1967).
7. L. J. Brubacher, L. Treindl, and R. E. Robertson. J. Am. Chem. Soc. **90**, 4611 (1968).
8. J. B. Hyne, H. S. Golinkin, and W. G. Laidlaw. J. Am. Chem. Soc. **88**, 2104 (1966).
9. E. A. Guggenheim. Phil. Mag. [7], **2**, 538 (1926).
10. W. G. Young, S. H. Sharman, and S. Winstein. J. Am. Chem. Soc. **82**, 1376 (1960).
11. W. J. le Noble. J. Phys. Chem. **67**, 2451 (1963).
12. R. E. Robertson and J. M. W. Scott. J. Chem. Soc. 1596 (1961).
13. H. S. Golinkin, W. G. Laidlaw, and J. B. Hyne. Can. J. Chem. **44**, 2193 (1966).
14. W. J. le Noble. Progr. Phys. Org. Chem. **5**, 207 (1967).
15. C. Walling and H. J. Schugar. J. Am. Chem. Soc. **85**, 607 (1963).
16. K. J. Laidler and D. Chen. Trans. Faraday Soc. **54**, 1026 (1958).

An electron spin resonance study of ultraviolet photolyzed methanol adsorbed on porous high-silica glass[1]

MICHIE SHIMIZU AND H. D. GESSER
Department of Chemistry, University of Manitoba, Winnipeg, Manitoba

AND

M. FUJIMOTO[2]
Department of Physics, University of Manitoba, Winnipeg, Manitoba

Received September 13, 1968

The electron spin resonance (e.s.r.) spectra of $\cdot CH_3$, $\cdot CHO$, H and/or D, and possibly $\cdot CH_2OH$ or $\cdot CH_2OD$ were found by the ultraviolet (u.v.) photolysis of methanol —OH or —OD on porous high-silica glass at 77 °K. These e.s.r. spectra resemble the results of the u.v. photolysis of X-irradiated methanol indicating that some perturbation and/or sensitization occurred in the molecules by the glass surface. The absence of e.s.r. spectra from the same systems on the acid-leached glass, on the totally fluorinated glass, or on the totally —OH covered glass suggests that (*i*) the co-existence of surface contaminants, such as Al and Zr and not B, and some of surface —OH could be responsible for producing these free radicals, and (*ii*) the methanols adsorbed on these glass surfaces are stabilized against u.v. photolysis.

Canadian Journal of Chemistry, 47, 1375 (1969)

Introduction

In previous work (1, 2), we reported that porous high-silica glass was a good host for methyl radicals which had been formed from CH_3I by u.v. photolysis. On the other hand, these porous glasses have been well studied as catalysts for alcohol dehydration and some hydrocarbon crackings (3–6).

Sullivan and Koski (7) found (by e.s.r. measurements) free radicals identified as $\cdot CH_3$, $\cdot CH_2OH$, and $\cdot CHO$ trapped in a frozen methanol matrix during u.v. irradiation at 77 °K, and Yang *et al.* (8) found (by vapor pressure chromatography (v.p.c.)) that H_2, CO, CH_4, HCHO, $(CH_2OH)_2$, and glycerine were produced by u.v. photolysis of liquid methanol. As a result of these findings we undertook to examine the trapping of these radicals on the surface of porous glass by the method previously described (9), and to explore the general usefulness of porous glass as a free radical host and/or the relationship between the nature as catalyst and free radical host.

Experimental

Adsorbents

The adsorbents, rods of 2 mm diameter × 20 mm length Corning Code #7930 porous Vycor® glass, were treated in the same manner as in our previous work (9), except, in the present study, some of them were "not acid-leached"[3] with hot 18*N* HNO_3. After washing, some of the glasses were thermo-leached in air at 500 °C for 5–16 h until they had no infrared (i.r.) spectra in the C—H bonding region from 3100 to 2500 cm^{-1}, and they were then degassed or fluorinated (10, 11). The adsorbents were denoted as V, VFp, or VF for the original, partially, or totally fluorinated glasses, respectively, and are further characterized by informations in brackets. For example, VFp (700 °C, 5 h, OH = $\frac{1}{2}$) means a partially fluorinated glass degassed at 700 °C for 5 h and which retained about $\frac{1}{2}$ of the OH of the original glass. The original glass was degassed at 800 °C for 5 h. In this example, therefore, the glass was a half-fluorinated.

The surface areas of these glasses, determined by the B.E.T.-method (12) using the effective cross-sectional area of methanol molecule of 17.8 $Å^2$ at 0 °C, were approximately 120 m^2/g for V(700 °C); 110 m^2/g for V(800 °C); 100 m^2/g for VFp(700 °C); 48 m^2/g for VFp(800 °C); and VF(800 °C). In this report, the amounts adsorbed were represented by the surface coverage $\%\theta$ related to each B.E.T.-monolayer of methanol for convenience.

Ultraviolet photolysis of all these adsorbents produced no e.s.r. signals.

Adsorbates

Methanol-OH, spectroscopic grade of Fischer Scientific Co., was distilled over Drierite at 68 °C in dried air. It was further purified by bulb-to-bulb distillation in vacuo with the middle one-third portion retained. The methanol-OD obtained from Merck and Co., Inc. was redistilled in vacuo. The i.r. spectra of the methanols in gas phases from 4000 to 400 cm^{-1} showed that the CH_3—OH had no absorption due to water and B—O bondings, while the CH_3—OD had some absorption at 3683, 1495, and

[1]Presented at the 50th Conference of The Chemical Institute of Canada held at Toronto, Ontario, June 6, 1967.

[2]Present address: University of Guelph, Guelph, Ontario.

[3]Denoted as "nonacid-leached" in this text.

Can. J. Chem. Downloaded from www.nrcresearchpress.com by 210.87.254.105 on 09/05/12
For personal use only.

TABLE I

Appearances of e.s.r. spectra of free-radicals from water and methanol adsorbed on porous high-silica glass produced by u.v. irradiation at 77 °K

		Systems	
e.s.r.-Signals	Group*	Adsorbates	Adsorbents
None	A-*a*	None	All glasses† (450 °C, 16 h)
	b	Water	
	c	Methanols‡	
	d	None	V(800 °C, 5h, OH = 1)**
	e	None	VFp(700 °C, 5 or 16 h, OH = ½)§
	f	None	VFp(800 °C, 1, 3, or 5 h, OH < 1/20)‖
	g	None	VF(800 °C, 1.5 h, OH = 0)¶
	h	Methanols	VF(800 °C, 1.5 h, OH = 0)
	j	Water	All glasses(800 °C, 5h)
	k	Methanols	All glasses(800 °C), stored at room temperature over 2 weeks
Poor	B-*p*	Methanols	V(800 °C, 5h) acid-leached
	q	Methanols	VFp(700 °C, 5h) acid-leached
	r	Methanols	VFp(800 °C, 5h) acid-leached
Good	C-*x*	Methanols	V(800 °C, 5h) nonacid-leached
	y	Methanols	VFp(700 °C, 5h) nonacid-leached
	z	Methanols	VFp(800 °C, 5h) nonacid-leached

*The Groups are explained by the following example: Group A-*a* denotes the system of none adsorbate – all glasses (450 °C, 16h).
†"All glasses" means "V, VFp, or VF with acid-leaching or nonacid-leaching".
‡"Methanols" means "CH_3—OH and —OD".
§Prepared by dipping glass in 12.5% of NH_4F aqueous solution for 0.5h. The samples were then dried at 110 °C for 20 min and then degassed.
‖Prepared by dipping glass in 30% slightly basic solution for 1 h. The samples were then dried at 110 °C for 20 min and then degassed.
¶Prepared by dipping glass in 30% neutral solution for 1.5 h. The samples were then dried at 110 °C for 20 min and then degassed.
**As reference standard for OH retained.

1365 cm^{-1} indicating the presence of a small amount (less than 1%)[4] of CH_3—OH and trimethylborate (9). These impurities in CH_3—OD could not be removed by repeating the distillation. However, these i.r. spectra did not change notably during the course of this work. Ultraviolet photolysis of these methanols, CH_3—OH or —OD, generated very small e.s.r. signals with full strength of arc[5] for 1 h, indicating that the effects seen are due to the photolysis of the methanols which are adsorbed on the glasses and are not due to the bulk materials.

Methods

The experimental methods were similar to those used in our previous work (9), that is, the sample cells, which were made of "Infrasil" quartz tubing, were connected to a standard vacuum line to prepare the surface, to add adsorbate, or to degas.

The e.s.r. signals were observed with a Varian E-3 e.s.r. spectrometer at 77 °K at surface coverages of less than 1% and about 5%, 30%, and 80%. Before and after the e.s.r. measurements, the i.r. spectra of the sample were taken at room temperature with a Perkin–Elmer Model-337 spectrometer using an external recorder. The full beam of a 100 W medium pressure mercury arc, Hanovia S-100 Alpine Burner, was focused on the sample, which was kept in fresh liquid nitrogen in a quartz Dewar. The detailed experimental techniques have been described elsewhere (1, 2, 6, 9).

Results

Electron Spin Resonance

The e.s.r. results could be divided into three groups as listed in Table I. Group A gave no e.s.r. signals with u.v. irradiation for 1 h in the e.s.r. cavity[6]. Group B gave poor e.s.r. signals with u.v. photolysis out of the cavity[6] for 1 h or more. Group C showed good e.s.r. spectra, as shown in Figs. 1 and 2 with u.v. irradiation in the cavity almost immediately (within a few min).

The major experimental features are as follows:

(*a*)[7] All u.v. photolysis with a Pyrex filter gave no e.s.r. signals. The difference between direct photolysis and that with a Vycor filter was only a small time delay in signal development and implied a small change in effective intensity.

(*b*) The adsorption systems belonging to Group C were common to those of Group B. The

[4]Estimated by infrared spectra.
[5]These results agreed with those of Yang *et al.* (8) and Milliken and Johnsen (13).
[6]The intensity of u.v. irradiation out of the cavity was almost twice that in the cavity.
[7]These paragraphs will be referred to in the discussion.

Can. J. Chem. Downloaded from www.nrcresearchpress.com by 210.87.254.105 on 09/05/12
For personal use only.

Can. J. Chem. Downloaded from www.nrcresearchpress.com by 210.87.254.105 on 09/05/12
For personal use only.

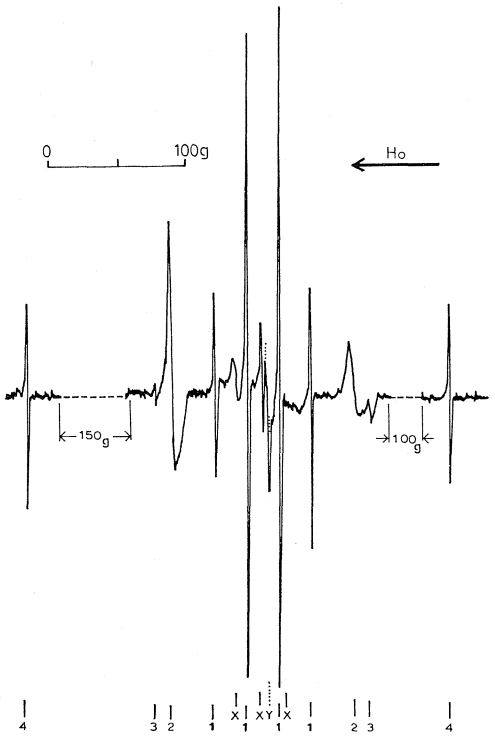

FIG. 1. Electron spin resonance spectra of VFp(800 °C)—CH_3OD system (about 80% θ); u.v.-photolyzed for 10 min at 77 °K. *1* denotes $\cdot CH_3$; *2*, $\cdot CHO$; *3*, D; *4*, H; ×, an unknown substance ($\cdot CH_2OH$ and/or $\cdot CH_2OD$?); Y (dotted line), Dewar and empty cell.

only difference between them was the leaching methods of the glasses. All glasses in Group B were acid-leached, whereas in Group C, the glasses were only thermo-leached.

(*c*) The e.s.r. spectra in Group C were similar in appearance, despite the different surface coverages, the different adsorbents of V or VFp, and even the different adsorbates of CH_3—OH or —OD, except for the spectra of D.

(*d*) In Group B, the e.s.r. spectra were similar in appearance to those in Group C, but were about 100 times less intense.

(*e*) The assignments in Figs. 1 and 2 for $\cdot CH_3$, $\cdot CHO$, H, D, and an unknown substance X have been made from the e.s.r. spectra results of Sullivan and Koski (7) and many workers (14). The spectra of D appeared only in the CH_3—OD systems. The unknown X may be $\cdot CH_2OH$ and/or $\cdot CH_2OD$, although this is not definite because of the weakness of the signals. An interesting phenomenon is the resemblance of these spectra to those from u.v. photolysis of X-irradiated methanol in bulk, determined by Milliken and Johnsen (13).

(*f*) The e.s.r. spectra grew very slowly indicating that the major reactions had ended within a few min with u.v. irradiation. It was, therefore, not possible to get enough data to clarify the mechanism of free radical formation.

Infrared Spectra

The i.r. spectra of methanol adsorbed on glasses

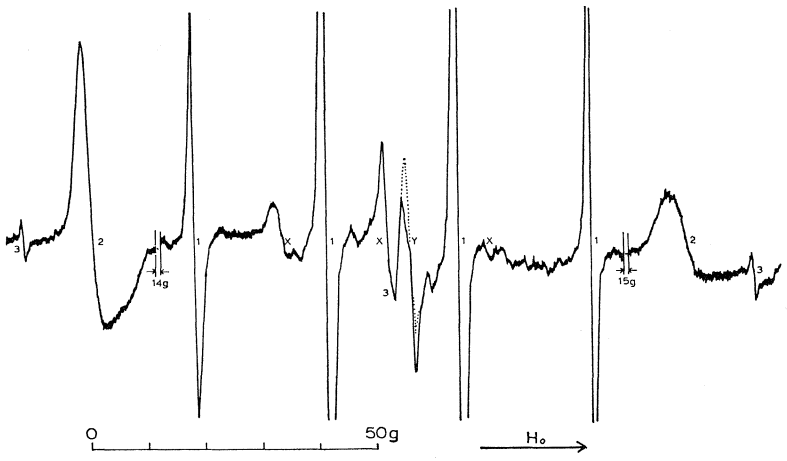

FIG. 2. Electron spin resonance spectra of VFp(800 °C)—CH_3OD system (about 80% θ); u.v.-photolyzed for 1 h at 77 °K (expanded). The notions are the same as those used in Fig. 1.

Can. J. Chem. Downloaded from www.nrcresearchpress.com by 210.87.254.105 on 09/05/12
For personal use only.

acid-leached or nonacid-leached, and before and after e.s.r. measurements, were all similar to each other. The detailed results of i.r. spectra of these systems will be reported in another paper (6).

Discussion

On the basis of the experimental results mentioned above, (i.e., methanols adsorbed on the porous glass showed no photo-inhibition effect with a Vycor filter, although Yang *et al.* (8) have shown that photolysis of liquid methanol was completely inhibited when a Vycor filter removed the 1847 Å-line and restricted photolysis to 2537 Å. See also section (*e*) of the results and Group A-*d* to -*f* in Table I) it is clear that some perturbation and/or sensitization occurred in the methanol molecules by some parts of the glass surfaces. The recent paper by Pariiskii *et al.* (15), where silica sensitized the photodecomposition of H_2, seems to support this.

It is well established that the adsorbent porous high-silica glass surfaces have hydroxyl $\equiv$Si—OH, siloxane bridge $\equiv$Si—O—Si$\equiv$, and analogous groups of B, Al, etc. (3–6, 9, 16). Of these functional groups, the surface hydroxyls are not u.v. photolyzed as shown in Group A-*a*, -*b*, and -*j*, and seem to inhibit the u.v. photolysis of adsorbed methanol of Group A-*c* when present in large surface concentration, and according to Low and Ramasubramanian (16) may extend over the monolayer. However, VF(800 °C, 1.5 h) of Group A-*h*, which has no OH according to the i.r. spectra (6, 11), has lost the activity for u.v. photosensitization while V(800 °C) and VFp(700 or 800 °C) of Group C seem to retain the activity. This implies that the co-existence of some surface —OH is required for such a sensitized reaction to occur on the surface.

It is reasonable to conclude that the surface siloxanes and fluorines both have little or no roles to play in the u.v. production of free radicals which bring about e.s.r. signals. This conclusion can be drawn because the acid-leached glasses (800 °C) of Groups A and B gave very poor e.s.r. signals, despite the existences of $\equiv$Si—O—Si$\equiv$ and $\equiv$Si—F on their surfaces which were confirmed by our i.r. studies (6, 9).

Considering the results of our works (6, 9) (i.e., the surface methoxides on the glass were very stable against u.v. photolysis at 77 °K, and the reaction of methanol molecules with the surface —OH of glasses to form the methoxides was slow), it might be suggested that the surface methoxides are stabilized during the storage of samples of Group A-*k* and destroy the u.v. photosensitization.

The effect of acid-leaching on such glass was reported by Little *et al.* (17). They showed that there was (*i*) no loss of boron, and (*ii*) a loss of Al and Zr from the surface which was estimated at about 0.4%. This was responsible for the isomerization and polymerization of adsorbed butene.

From our results, it might also be suggested that the similarity of i.r. spectra between the samples Groups B and C indicated no loss of boron, and, therefore, the surface boron has no effect on the photosensitization of methanol under these conditions, even though $=$B—OCH_3 is considered as a starter for methanol cracking during thermotreatment by Low and Harano (5). The results also suggest that siloxane-like bridges of the surface impurities, (Al and Zr, but not B) with the co-existence of some surface —OH (as mentioned above) could be responsible for this photosensitization of CH_3—OH or —OD molecules. Because of their low concentration, these could be independent of the surface coverages. The trace quantities of these surface impurities remaining on the glass surfaces after acid-leaching could account for the poor e.s.r. signals of Group B.

Despite the loss of Al and Zr, the absence of a notable change in i.r. spectra between these sample groups may be explained as follows: (*i*) the quantities of surface contaminants, mainly Al and Zr, on the glass were too small to identify any differences, and/or (*ii*) based on the results of Greenler (18), the surface $=$Al—OCH_3 may have so similar a structure to surface $\equiv$Si—OCH_3 and/or $=$B—OCH_3, that it could not be distinguished from them.

The stabilization tendency must also be accounted for. From the remarkable decrease and loss of photosensitization during the storage of all samples in Group A-*k*, it may be speculated that there were some less stable states of methanol at the early stage of adsorption, e.g., on siloxane-like surface bridges of Al and Zr which should be photosensitive. For example, H in CH_3 might be caught on metal-sites directly, and then transfered to a more stable form with aging. There is also a possibility that distillation of stop-cock

grease to the surface might mask and poison the active sites (19). This should be examined in an ultra-high vacuum grease free system.

The absence of a notable change of i.r. spectra before and after u.v. irradiation can be explained as follows: (*i*) the change in quantity was too small to be detectable with i.r. spectra, and/or (*ii*) most of the reactions would be reversible on the surface under these conditions.

Greenler (18) has suggested that the reaction of methanol on alumina occurs as follows:

$$CH_3—OH + —Al—O—Al—O— \rightarrow —\underset{\displaystyle OCH_3}{\underset{|}{Al}}—O—Al— + H$$

with H presumably forming =Al—O..H. However, this reaction cannot be considered to be the entire source of H or D in view of the relatively weak D-signals.

Acknowledgments

This work was supported by the Directorate of Chemical Sciences, The U.S. Air Force Office of Scientific Research, Grant No. AF-AFOSR 642-66, and by the National Research Council of Canada.

1. M. Fujimoto, H. D. Gesser, B. Garbutt, and A. Cohan. Science, **154**, 381 (1966).
2. M. Fujimoto, H. D. Gesser, B. Garbutt, and M. Shimizu. Science, **156**, 1105 (1967).
3. L. H. Little. Infrared spectra of adsorbed species. Academic Press, Inc., New York. 1966.
4. M. L. Hair. Infrared spectroscopy in surface chemistry. Marcell Dekker, Inc., New York. 1967.
5. M. J. D. Low and Yoshio Harano. Anniversary Issue. J. Res. Inst. Catalysis, Hokkaido Univ. Sapporo, Japan. In press. 1968.
6. M. Shimizu and H. D. Gesser. Unpublished results.
7. Sr. Patritia J. Sullivan, and W. S. Koski. J. Am. Chem. Soc. **85**, 384 (1963).
8. N. C. Yang, Donna P. C. Tang, Do-Minh Thap, and Jerome S. Sallo. J. Am. Chem. Soc. **88**, 2851 (1966).
9. M. Shimizu and H. D. Gesser. Can. J. Chem. **46**, 3517 (1968).
10. I. D. Chapman and M. L. Hair. J. Catalysis, **2**, 145 (1963).
11. T. H. Elmer, I. D. Chapman, and M. E. Nordberg. J. Phys. Chem. **67**, 2219 (1963).
12. S. Brunauer. The adsorption of gases and vapors. Vol. 1. Princeton Univ. Press, Princeton, New Jersey. 1942.
13. S. B. Milliken and R. H. Johnsen. J. Phys. Chem. **71**, 2116 (1967).
14. B. H. J. Bielski and J. M. Gebichi. Atlas of ESR-spectra. Academic Press, Inc., New York. 1967. pp. 121, 224, 263, 264, 329–331, 340, 341, 410, and 411.
15. G. B. Pariiskii, I. D. Mikheikin, A. I. Rez, and V. B. Kazanskii. Dokl. Acad. Nauk SSSR, **180**, 123 (1968).
16. M. J. D. Low and N. Ramasubramanian. J. Phys. Chem. **70**, 2740 (1966).
17. L. H. Little, H. E. Klauser, and C. H. Amberg. Can. J. Chem. **39**, 42 (1961).
18. H. G. Greenler. J. Chem. Phys. **37**, 2094 (1962).
19. J. H. de Boer. The dynamical character of adsorption. 2nd ed. The Clarendon Press, Oxford, England. 1968.

Can. J. Chem. Downloaded from www.nrcresearchpress.com by 210.87.254.105 on 09/05/12
For personal use only.

Reactions of alcohols adsorbed on MgO. Part I. Heterogeneous reactions with hydrogen atoms and trapped electrons at room temperature: a new technique in surface chemistry

D. R. SMITH[1] AND A. J. TENCH
Chemistry Division, Atomic Energy Research Establishment, Harwell, Berkshire, England

Received October 23, 1968

A series of alcohols, adsorbed on MgO powder, have been bombarded by a stream of hydrogen atoms at room temperature and the radicals thus formed are detected by electron spin resonance. Methanol, ethanol, *n*-propanol, iso-propanol, *n*-butanol, *sec*-butanol, and allyl alcohol have been studied. The radical species produced have been identified and radical lifetimes varying from minutes to hours at 300 °K have been observed. For methanol, the first monolayer appears to be chemisorbed as methoxy groups whereas the ethanol data indicate that some of the molecules in the first monolayer are physically adsorbed. The higher alcohols form secondary radicals via hydrogen elimination from the primary radical; the isopropyl alcohol radical appears to isomerize before losing hydrogen. Allyl alcohol undergoes hydrogen atom abstraction in preference to addition to the double bond and yields the α-hydroxy-allyl radical. Methanol and ethanol have also been reacted with electrons trapped on a MgO surface to form stable alkoxide ion radicals trapped at oxygen ion vacancies on the surface of the lattice.

Canadian Journal of Chemistry, **47**, 1381 (1969)

Can. J. Chem. Downloaded from www.nrcresearchpress.com by 210.87.254.5 on 09/05/12
For personal use only.

Introduction

In recent years there has been an increasing amount of evidence that free radicals can be stabilized on the surface of insulators. The observation of such intermediate species is of considerable relevance to problems in catalysis. However, in many cases where high energy radiation has been used to form the radicals, the situation is complicated by the number of paramagnetic fragments formed in the solid and by poorly understood energy-transfer processes that take place from the solid. These difficulties can be overcome, if the radicals are produced by a chemical reaction from the gas phase. In this present study our objective was to investigate the radicals formed when molecules adsorbed on a surface are bombarded with H-atoms.

There have been various studies of heterogeneous reactions of atoms or hydroxyl radicals with organic compounds. Solids investigated at room temperature are polymer "fluffs" (1, 2), suspensions on quartz wool (3), or pure finely divided powders (4–7); some compounds which are liquid at room temperature have been bombarded with atoms in the frozen state (8–10). Heterogeneous reactions with adsorbed molecules have been very few. Kokes (11) mentions the reaction of hydrogen atoms with oxygen adsorbed on ZnO, but the interpretation of the results is difficult; oxygen atoms have been reacted with NO_2 adsorbed on 13X molecular sieve to give what is thought to be NO_3 (12).

The formation of radicals stabilized on surfaces using atom bombardment has several advantages over conventional methods. Firstly, compounds that are volatile liquids may be adsorbed at room temperature and may form radicals which are stabilized on the surface even at room temperature. Secondly, usually only one kind of radical species is formed, thus simplifying the spectra. Thirdly, the radicals are formed in an exposed position and are readily available for further reactions; this is in contrast to studies in crystals and glasses where the radicals are buried in the matrix.

Tench and Smith (13) have shown that the heterogeneous reaction of hydrogen atoms with MgO leads to the formation of reactive surface centers. In this present work, a series of alcohols was adsorbed to form approximately a monolayer on the surface which was then reacted with H-atoms at room temperature. Alcohols were chosen because they are strongly adsorbed, and because important catalytic reactions involving dehydrogenation and dehydration are known to occur over oxide catalysts (14–17). The radicals formed are detected and identified by electron spin resonance (e.s.r.) techniques and their reactions studied.

[1]Attached from Atomic Energy of Canada Ltd., and to whom reprint requests should be sent at: Research Chemistry Branch, Atomic Energy of Canada Ltd., Chalk River Nuclear Laboratory, Chalk River, Ontario.

Can. J. Chem. Downloaded from www.nrcresearchpress.com by 210.87.254.5 on 09/05/12
For personal use only.

This work is closely related to the field of heterogeneous radiation chemistry and in a later paper (Part II), results for the irradiated systems will be reported for comparison.

Experimental

In an initial experiment a conventional hydrogen gas flow system through the TE_{102} e.s.r. cavity was constructed. Hydrogen atoms formed by a 2450 MHz microwave discharge were monitored by their e.s.r. signal. This was used to determine the optimum experimental conditions for obtaining the maximum concentration of hydrogen atoms, free from contamination by other atoms. Oxygen impurity was converted to water in a "Deoxo" unit. When this water was not removed, the hydrogen atom concentration increased by a factor of 20; however, there was then a significant concentration of oxygen atoms. Typical conditions in a pure dry H_2 flow were: 8 Torr pressure, 300 cm s^{-1} linear flow rate, and 60 W microwave discharge. Ample hydrogen atoms were obtained without having to poison the walls of the apparatus.

The apparatus for sample bombardment was made of Pyrex except for silica tubing in the discharge zone and where specified in Fig. 1. Preparation of MgO and adsorption of alcohols is performed in a silica side-tube. This sample is kept "safe" in this side-tube at 77 °K while the rest of the apparatus is "cleaned" by a stream of hydrogen atoms for 10 min. Then, after warming the sample to room temperature, the apparatus is rotated 180° about a greased joint, allowing the sample to fall into a 350 ml Kjeldahl flask. The hydrogen atom stream flows through a focussing nozzle inside the flask and reacts with the sample as it falls into the flask and while lying on the bottom.

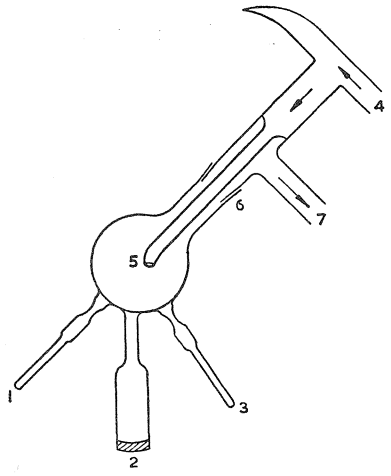

FIG. 1. (1) and (3), silica e.s.r. sample tubes; (2), silica sample preparation tube containing a 2 mm layer of powder; (4), hydrogen atom flow from the microwave discharge zone; (5), 0.5 cm nozzle to focus the hydrogen atom stream; (6), B 29/32 greased joint to permit rotation of the flask; (7), to the pumps and to the adsorbate inlet port.

After 5 or 10 s of atom bombardment, the flask is rotated further so that the powder falls into a silica e.s.r. sample tube. This tube is promptly immersed in liquid nitrogen to preserve any unstable radicals. The sample tube is then sealed off at a constriction. Prior to starting the flow of hydrogen atoms, "blank" samples were poured into a second silica e.s.r. sample tube on each run and sealed off.

When necessary, this apparatus permits atom bombardments at 77 °K by cooling the bottom of the flask and the e.s.r. sample tube in a polystyrene liquid nitrogen Dewar. This Dewar is "keyhole" shaped and deep enough to permit rotation of the apparatus in the Dewar. Such techniques have been found useful in some atom bombardments of pure oxides reported elsewhere. The technique is felt to be simpler than that described by Herak (18).

MgO was made by decomposing the carbonate in air at 900 °C. About 0.6 g of the oxide was placed in the sample preparation side tube and was gradually heated in vacuum to 800 °C in 2 h. This oxide has been previously found to have a surface area of about 25 m^2g^{-1} by B.E.T. adsorption methods. After the powder had cooled to room temperature, 3×10^{-3} ml (except when specified otherwise) of deaerated alcohol was admitted. The adsorption, monitored by a silicone oil manometer, was complete in 30 s. Half the sample was then taken off for comparison as a "blank" and the other half treated as described above. Samples were stored under liquid nitrogen (usually for no more than 10 min) until e.s.r. measurements could be made.

The alcohols were used as received from the supplier. They were deaerated by conventional freeze, pump, and thaw techniques, no effort being made to remove dissolved CO_2. The alcohols used were: methanol (B.D.H. Aristar), ethanol (B.D.H. Analar), *n*-propanol (B.D.H. Reagent), *i*-propanol (B.D.H. Analar), and B.D.H. Reagent grade *n*- and *sec*-butanol, and allyl alcohol. The MgO purity, determined by spectrographic analysis was, in p.p.m. (wt./wt.): Mn (< 2), Fe (< 20), Cr (< 5), Al (20), Si (< 30).

The e.s.r. spectra were obtained at $\sim$9.2 GHz using 100 kHz field modulation. In the diagrams the spectra are displayed as a first derivative and the field increases from left to right. Various field modulation amplitudes were used during this work and the splitting constants quoted, unless otherwise indicated, are those measured directly from the spectra and can be compared with spectra obtained in glasses or polycrystalline materials; the quoted values for the splitting constant are measured to $\sim \pm 0.5$ G.

Results

1. Reaction with Hydrogen Atoms

The first derivative spectra of the radicals are shown in Figs. 2–5, the magnetic field increasing from left to right. A field modulation of approximately 3 G at 100 kHz was used in each figure. In general, the spectra were obtained at 77 °K but room temperature spectra are shown if there is a significant difference. The narrow line on the

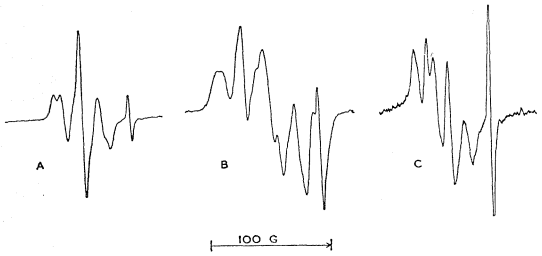

FIG. 2. A, methanol at 77 °K; B, ethanol at 77 °K; C, ethanol at 77 °K after 2 min at room temperature.

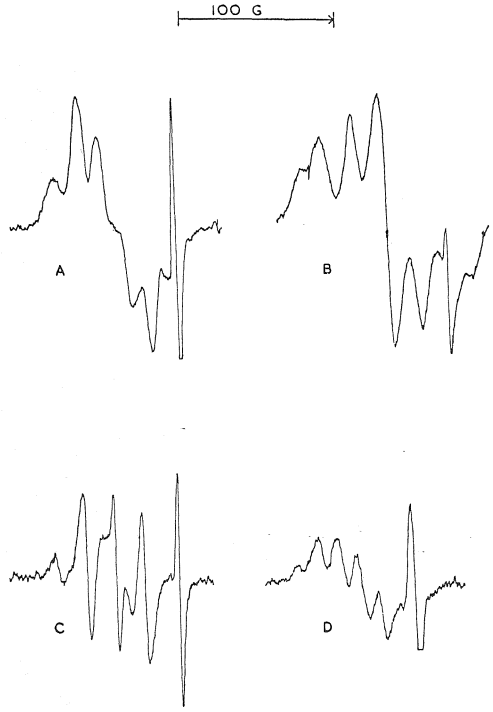

FIG. 3. A, *n*-propanol at 77 °K; B, isopropanol at 77 °K; C, isopropanol at room temperature, 2.5 min after warming up from 77 °K; D, isopropanol at room temperature 19 min after warm-up.

high field side of each spectrum is due to < 5 p.p.m. Cr^{3+} impurity with $g = 1.9796$; at high gain, 4 hyperfine lines are apparent from ^{53}Cr ($I = \frac{3}{2}$) natural abundance 9.54%. The e.s.r. spectrum obtained from each blank is shown in Fig. 4D; the low field lines are due to Fe^{3+} impurity ions (< 20 p.p.m.) and make a negligible contribution to the spectra at the normal amplifier gains used, except for the spectrum in Fig. 3D.

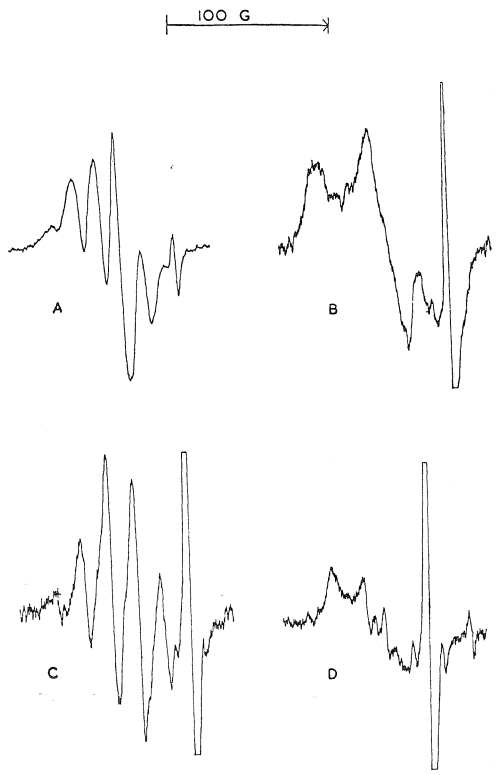

FIG. 4. A, *n*-butanol at 77 °K; B, *sec*-butanol at 77 °K; C, *sec*-butanol at room temperature; D, a typical "blank".

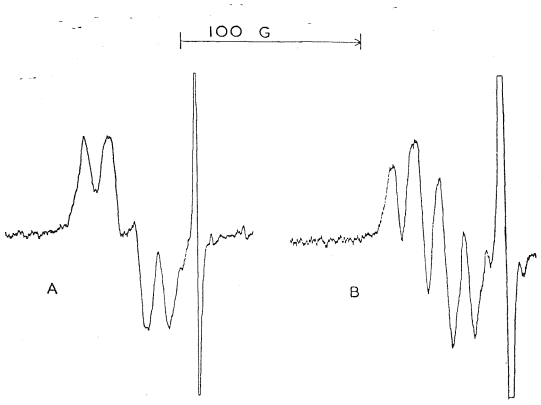

FIG. 5. A, allyl alcohol at 77 °K; B, allyl alcohol at room temperature.

Within experimental error, all the radicals observed below have $g = 2.0030 \pm 0.0005$.

Methanol

At 77 °K the triplet e.s.r. spectrum in Fig. 2A was obtained from methanol. A similar, though

Can. J. Chem. Downloaded from www.nrcresearchpress.com by 210.87.254.5 on 09/05/12
For personal use only.

Can. J. Chem. Downloaded from www.nrcresearchpress.com by 210.87.254.5 on 09/05/12
For personal use only.

less intense spectrum was observed at room temperature, though no line narrowing or reduction of anisotropy in the two outer lines occurred. This triplet is assigned to a $\cdot CH_2X$ radical where the identity of X will be discussed later. The asymmetry of the two outer lines can be interpreted in terms of an axially symmetric hyperfine interaction (19) and analysis of the spectrum gives $A_{\parallel} = 24.0$ and $A_{\perp} = 13.7$ G ($A_{\text{average}} = 17.1$ G). At room temperature this radical decayed bimolecularly with an initial second order half life of 3 min.

Two experiments were carried out to study the effect of surface coverage. In the first, the usual quantity (3×10^{-3} ml CH_3OH on 0.6 g MgO) of methanol was adsorbed, followed by 30 min of pumping at room temperature. Hydrogen atom bombardment gave an identical e.s.r. spectrum, with intensity similar to that obtained when no pumping was performed after adsorption. Furthermore, the radicals decayed at the same rate with second order kinetics. The second experiment involved the same procedure but this time only one-half as much methanol was adsorbed initially. The yield of radicals was about the same but the decay kinetics were different. The decay of radicals now followed first order kinetics and the half life had increased to 11 or 12 min.

When CH_3OD (1.5×10^{-3} ml on 0.6 g MgO) was treated similarly, the central line of the e.s.r. triplet had a width between derivative maxima of 3.3 G compared to 4.2 G when CH_3OH was used.

When hydrogen atoms were reacted with magnesium methoxide powder, the resultant e.s.r. spectrum was similar to Fig. 2A, though only one-third as intense. The spectrum can be interpreted as arising from $(\dot{C}H_2O)^-Mg^{2+}$ radicals and gives $A_{\parallel} = 25.1$, $A_{\perp} = 12.6$, and $A_{\text{average}} = 16.8$ G. The width between derivative maxima of the central line was 4.0 G. The room temperature decay of these radicals was second order with an initial half life of about 8 min. Allowing for the lower concentration, this decay rate is the same as for $\cdot CH_2X$ radicals formed after absorption of 3×10^{-3} ml CH_3OH on 0.6 g of MgO.

Ethanol

This initially gave the e.s.r. spectrum in Fig. 2B. It is basically a quintet with an average proton hyperfine coupling $A_H = 21.3$ G. After 2 min at room temperature the radical giving this spectrum had decayed. There remained a second spectrum, Fig. 2C, predominantly a 1:3:3:1 quartet with an average $A_H = 13.9$ G. This spectrum remained after several days at room temperature. Poorly resolved peaks in the initial spectrum suggest that the 1:3:3:1 radical was also present, and remained after the main radical decayed away. In experiments where 3×10^{-3} and 1.5×10^{-3} ml of C_2H_5OH were adsorbed, followed by pumping for 30 min at room temperature, the initial yield of radicals was reduced to about a quarter of the number obtained without subsequent evacuation. Only the 21.3 G quintet was formed and when this disappeared by thermal decay, the 13.9 G quartet was not observed. The decay curves were not sufficiently precise to establish the kinetic order but the half lives increased to about 2 and 5 min respectively, with decreasing coverage. Such short half lives cause difficulty with measurement of the decay curve for these powders, because of an unknown time lag in the warm-up time of the sample.

Higher Alcohols

Normal propanol gave a poorly resolved sextet, Fig. 3A, with $A_H = 13.9$ G; the spectrum was only slightly better resolved at room temperature. This decayed in about 20 min. iso-Propanol gave a septet with $A_H = 19.3$ G at 77 °K, Fig. 3B. At room temperature, 2.5 min after removing the sample from the liquid nitrogen Dewar, the unusual spectrum in Fig. 3C was obtained. It seems to consist mainly of a quintet with $A_H = 19.3$ G and the three central lines have equal intensity. After 19 min at room temperature, a poorly resolved sextet, Fig. 3D, with $A_H \simeq 13.6$ G remained. This decayed by only 10% in the following 30 min. The spectrum looks like a septet because of an underlying absorption due to iron impurity.

At 77 °K, *n*-butanol gave a 13.7 G sextet with an underlying singlet, Fig. 4A. At room temperature the singlet disappeared and the symmetrical sextet remained, with only slightly improved resolution. The width between derivative maxima for the 2 most intense lines was about 7.5 G. This radical decayed slowly with an initial half life of 2.5 h. *sec*-Butanol gave a poorly resolved triplet at 77 °K, Fig. 4B, with $A_H = 34$ G. At room temperature this had changed irreversibly to a sextet, Fig. 4C, with $A_H = 17$ G. On

Can. J. Chem. Downloaded from www.nrcresearchpress.com by 210.87.254.5 on 09/05/12
For personal use only.

recooling to 77 °K the sextet remained, though less well resolved. At room temperature the sextet decayed bimolecularly with an initial half life of 10 min.

Allyl alcohol gave the poorly resolved quartet in Fig. 5A at 77 °K while at room temperature the resolution improved, Fig. 5B; in each case the hyperfine coupling A_H was 13.7 G. At room temperature the radical decayed bimolecularly with an initial half life of 13 min.

It is of interest to know the fraction of the absorbed molecules converted to radicals and the concentration of the radicals (N_R). These data are summarized in Table I for those experiments where 3×10^{-3} ml of an alcohol was absorbed on 0.6 g MgO, without subsequent pumping.

TABLE I

Radicals formed from ROH adsorbed on MgO

ROH	N_R (spins/g $\times 10^{-16}$)	N_R/N_{ROH} ($\times 10^3$)	Initial $t_{\frac{1}{2}}$ (min)
MeOH	4.4	0.6	3
EtOH	19.6	3.9	<1
n-PrOH	5.2	1.3	—
i-PrOH	14.0	3.6	—
n-BuOH	7.0	2.1	150
sec-BuOH	5.2	1.6	10
Allyl OH	3.7	0.9	13

2. Reaction with Electrons

It has been established in separate experiments (13) that hydrogen atoms will react directly with MgO to form electrons trapped at an anion vacancy:

[1] $$H + O^{2-} \rightarrow e^- + OH^-$$

This was carried out, forming the blue colored powder characteristic of the trapped electrons on the surface. In separate experiments, the usual quantity of MeOH or EtOH was then admitted to the powder; in each case, the blue color disappeared instantly. The e.s.r. spectrum due to the trapped electrons was replaced by that of alcohol radicals. The intensity in each case was low because of the low starting concentration of electrons. Methanol and ethanol formed the same e.s.r. spectra as in Fig. 2A and 2B. The hyperfine couplings from the methanol radical were slightly lower, however, $A_{\parallel} = 23.4$, $A_{\perp} = 12.4$, and $A_{average} = 16$ G. The methanol radical was more stable than before but this may be due in part to its low concentration. Half of the ethanol radicals decayed in 5 min, leaving a radical which was completely stable at room temperature. The spectrum of this radical at room temperature contained much narrower lines (~ 3 G) and it was resolved into two quartets. The quartet splitting was 20.6 G and the splitting between quartets was 13.5 G. This spectrum is shown in a later paper on the radiolysis of these systems. The other alcohols also decolorized the blue powder but the e.s.r. signals were too weak for useful examination, probably because of the large line width.

Discussion

1. Radical Identification

Many of the spectra mentioned in the results are characterized by e.s.r. hyperfine couplings in the range 13.5–14.0 G compared to the normal range for β-protons of 20–22 G found for alcohol radicals in solution (20). Such low hyperfine constants must be associated with a considerable delocalization of the unpaired electron density from a single carbon 3p orbital. The proton hyperfine coupling in alcohol radicals is already considerably lower than that observed for alkyl radicals (21), and this further decrease could arise from (*1*) some delocalization of the electron into the surface or (*2*) the formation of unsaturated alkene species. The first of these seems unlikely because the *g* value would be expected to have a positive shift, and no change is observed. The second possibility appears most likely since the formation of unsaturated compounds from alcohols on some oxides at high temperatures is a well known process (14–17) and it is likely that the alcohol radicals might undergo a similar loss of hydrogen. The discussion in the subsequent pages follows this hypothesis except for the initial radicals from methanol, ethanol, and isopropanol.

Methanol and Ethanol

The triplet e.s.r. structure and hyperfine coupling for the methanol radical indicate that it is either the radical $\dot{C}H_2OH$ formed by hydrogen abstraction from physisorbed CH_3OH, or the radical $(\dot{C}H_2O)^-Mg^{2+}$ formed from methanol chemisorbed as a methoxy compound. We favor the latter because the hyperfine coupling agrees with that obtained by reaction with magnesium methoxide, and because the yield is not decreased

by pumping at room temperature. One would expect $(CH_3O)^-$ to be tightly held, but physisorbed CH_3OH should be pumped off and the yield of radical decreased, contrary to the results. In support, adsorption of less than a monolayer of methanol on MgO results in infrared (i.r.) absorption features, attributed to $(CH_3O)^-$, which are not diminished by pumping (22). Similar results have been obtained on Al_2O_3(23). The hydroxyl proton must be nearby and chemisorption probably occurs according to the schematic reaction [2]. Presumably, most of the first monolayer becomes chemisorbed.

[2] $$\begin{matrix} CH_3OH & & CH_3^- \\ \downarrow & \rightarrow & O \quad H^- \\ \ldots Mg^{2+}O^{2-}\ldots & & \ldots Mg^{2+}O\ldots \end{matrix}$$

The e.s.r. parameters for the initial radical (Fig. 2B) from ethanol, and the decrease in yield caused by pumping, indicate that this is the $CH_3\dot{C}HOH$ radical formed by hydrogen abstraction from physisorbed alcohol molecules. After pumping for 30 min, only a quarter as many radicals were formed. A small fraction of the first monolayer of ethanol must be very strongly physisorbed or has become bonded to the surface by a reaction analogous to [2]. The stable radical (Fig. 2C) was eliminated by pumping. This indicates that the radical was formed by reaction with a weakly adsorbed molecule, rather than by decomposition of $CH_3\dot{C}HOH$. It is difficult to assign the 13.9 G quartet to other than the acetyl $(CH_3\dot{C}O)$ radical even though the hyperfine coupling is slightly less than the 16.7 ± 1.8 G given by Morton and Falconer (24). Our g value of 2.003 is also in disagreement with their value of 2.0055 ± 0.0008 but their spectrum is poorly resolved from that of $\dot{C}H_3$ radicals. When ethanol is adsorbed on Al_2O_3 and heated at 170 °C, the acetate ion is formed according to the i.r. measurements of Greenler (21) and it seems likely that a similar reaction occurs on MgO at room temperature (22). It is possible that a small proportion of acetaldehyde can also be formed on the surface and when the hydrogen atom stream flows over the sample, reaction [3] would lead to the formation of acetyl radicals (25).

[3] $$CH_3CHO + H\cdot \rightarrow CH_3\dot{C}O + H_2$$

The acetaldehyde would not be strongly adsorbed and thus, on pumping, it would desorb and the radical could not be formed.

Propanols

The radical giving a 13.9 G sextet (Fig. 3A) from *n*-propanol is difficult to identify positively. We speculate that hydrogen abstraction forms the $CH_3CH_2\dot{C}HOH$ radical and that this promptly eliminates H_2 to give $CH_3\dot{C}HCHO$ or $CH_2 \cdots CH \cdots CH(OH)$. The α-hydroxy-allyl radical gives a 13.7 G hyperfine splitting, but the spectrum consists of 4 lines (see below). It is certainly similar to the central 4 lines in Fig. 3A (cf. Fig. 5A). On the other hand, the spectrum of $CH_3\dot{C}HCHO$ would normally be a quintet with 4 equivalent protons, the aldehydic proton having a very small coupling (26), and this does not fit the data. The identification is not certain but it seems likely that the observed spectrum arises from a mixture of radicals, probably involving the formation of the α-hydroxy-allyl radical.

The initial radical from isopropanol (Fig. 3B) gives a 19.3 G e.s.r. septet. This is undoubtedly the $(CH_3)_2\dot{C}(OH)$ radical. At room temperature, another radical exists for a few minutes, giving a 19.3 G quintet with three equal intensity lines in the middle, Fig. 3C. Probably the isopropyl alcohol radical has isomerized to give the $CH_3CH_2\dot{C}HOH$ radical. In the solid phase this has been known to give a 1:2:2:2:1 spectrum (27). Differing line widths cause the intensity ratio to appear greater than 2:1 in our spectrum. Finally, the 13.6 G sextet is left. This is believed to be the same radical as was obtained from propanol, formed by elimination of H_2 from $CH_3CH_2\dot{C}HOH$, since it seems to be a descendant of $CH_3CH_2\dot{C}HOH$ and has similar hyperfine coupling, structure, and lifetime to the radical from *n*-propanol.

Butanols

The *n*-butanol result (Fig. 4A) may be similarly explained. A hydrogen atom abstracts from the parent molecule to form $CH_3(CH_2)_2\dot{C}HOH$; this splits off H_2 to give $CH_3CH \cdots CH \cdots CHOH$ or $CH_3CH_2\dot{C}HCHO$; in this case, only the allylic radical could possibly give a 13.7 G sextet with line intensities such as those observed. It would give a 1:5:10:10:5:1 sextet and the hyperfine coupling would be close to that observed. The α-hydroxy-allyl radical $CH_2 \cdots CH \cdots CHOH$, discussed below has $A_H = 13.7$ G for comparison. Dehydration of the radical does not occur since this would lead to a spectrum consisting of a septet and not the sextet observed.

At 77 °K, *sec*-butanol gives three very wide

Can. J. Chem. Downloaded from www.nrcresearchpress.com by 210.87.254.5 on 09/05/12
For personal use only.

Can. J. Chem. Downloaded from www.nrcresearchpress.com by 210.87.254.5 on 09/05/12
For personal use only.

lines separated by 34 G (Fig. 4B) and at room temperature gives a 17 G sextet of well resolved lines. One would expect that the primary radical formed would be $CH_3\dot{C}(OH)CH_2CH_3$. However, this radical would neither give the structure nor the hyperfine splitting observed in the e.s.r. spectrum. We believe that, like most of the cases discussed above, this radical has eliminated H_2 to form a secondary radical. This reaction could form either the substituted allylic radical $CH_3C(OH) \cdots CH \cdots CH_2$ or one of the ketone radicals $CH_3CO\dot{C}HCH_3$ and $CH_3COCH_2\dot{C}H_2$. The allylic radical would give a sextet with $A_H \simeq 13.5$–14 G and $CH_3CO\dot{C}HCH_3$ would give a quintet, so these two may be ruled out. However, $CH_3COCH_2\dot{C}H_2$ fits all the observations and we assign both the 77 °K and the room temperature e.s.r. spectra to this radical. These spectra may be interpreted in terms of previous observations on the *n*-propyl radical $CH_3CH_2\dot{C}H_2$ (19, 25). Cochran *et al.* (19) have given a theoretical discussion of the case which fits the 77 °K spectrum. The 34 G triplet is due to a 34 G interaction from the two β-protons with the lines corresponding to $I = \pm 1$ for the two α-protons being so broadened by hyperfine anisotropy that they are not resolved and cause considerable broadening of the lines in the 34 G triplet. Cochran *et al.* obtained $A_H = 35$ G for the two β-protons in the *n*-propyl radical, in support of our assignment. The room temperature 17 G sextet can arise from the same radical, if one of the β-protons has $A_H = 34$ G and the other plus the two α-protons have $A_H = 17$ G. This was observed for the *n*-propyl radical by Ayscough and Thomson (28). Thus two cases exist in the literature in which the same radical gives different β-proton couplings when trapped in two different environments. This suggests that the $CH_3COCH_2\dot{C}H_2$ radical on an MgO surface can be trapped in different environments.

Allyl Alcohol

The 13.7 G quartet from allyl alcohol has been observed by others, for example Chachaty and Schmidt (8) and Maas and Volman (29) in the solid phase and Livingston and Zeldes (20) in the liquid phase. This spectrum is thought to arise from the α-hydroxy-allyl radical $CH_2 \cdots CH \cdots CHOH$. Evidently, abstraction of the α-proton is preferred to addition to the double bond.

2. Electron Reactions

When methanol and ethanol are reacted with electrons trapped on the surface of MgO, the situation is entirely different compared to the case where they are first adsorbed and then reacted with hydrogen atoms. This is discussed below in the section on surface effects since we prefer to limit this section to radical identification. The stable radical formed by reaction of ethanol with an electron seems to be the ethoxide ion radical $(CH_3\dot{C}HO)^-$ with the α-proton giving $A_\alpha = 13.5$ G and the methyl protons giving $A_{CH_3} = 20.6$ G. We base this assignment on spectroscopic and mechanistic arguments. Bennett (30) has observed the e.s.r. spectrum of $(CH_3\dot{C}HO)^-$ in sodium and potassium ethoxide. He found $A_\alpha = 13$ and $A_{CH_3} = 19.2$ G. Our parameters are close to those of Bennett and less than the corresponding values of 15.4 and 22.2 G for the isotropic couplings of $CH_3\dot{C}HOH$ in solution (20). In addition, one would expect reactions [4]–[6] to occur.

$$[4] \quad e^- + CH_3CH_2OH \rightarrow CH_3CH_2O^- + H$$

$$[5] \quad H + CH_3CH_2OH \rightarrow CH_3\dot{C}HOH + H_2$$

$$[6] \quad e^- + CH_3CH_2OH \rightarrow CH_3CHO^- + H_2$$

Reactions [4] and [5] would explain the formation of relatively unstable $CH_3\dot{C}HOH$ radicals and reaction [6] would account for the formation of $(CH_3\dot{C}HO)^-$. A concerted reaction has been postulated by Bennett *et al.* (31) to explain the formation of alcohol radicals during thermal and photolytic bleaching of electrons trapped in various alcohol matrices at low temperature. Our spectrum obtained from the reaction of electrons with methanol gave $A_{average} = 16$ G, which is midway between Bennett's value of 15 G for $(\dot{C}H_2O)^-$ in sodium and potassium methoxide (30) and our value of 16.8 G for $(\dot{C}H_2O)^-Mg^{2+}$ in $Mg(OCH_3)_2$. This, coupled with reactions analogous to [4]–[6], leads us to suppose that a mixture of $(\dot{C}H_2O)^-Mg^{2+}$ and $(\dot{C}H_2O)^-$ is present, the latter being trapped at an oxygen ion vacancy.

3. Effect of Surface

Radicals trapped on a surface may have properties which differ from those of similar radicals trapped, say, in a matrix of the parent compound. Bond and molecular rotations may be slowed down or oriented with respect to the surface and bond symmetries may be altered. Electron spin density might be decreased due to delocalization into the matrix (32). The possibility of different trapping sites, restricted

Can. J. Chem. Downloaded from www.nrcresearchpress.com by 210.87.254.5 on 09/05/12
For personal use only.

movement, and differing radical–molecule, radical–radical distances on a two-dimensional surface can alter the radical stability and the rate and mechanism of decay. A new phenomenon, which seems to have been observed for the first time in this work, is the formation of secondary radicals via elimination of a hydrogen molecule from the parent radical, evidently catalyzed by the surface or an impurity ion on the surface.

Electron spin delocalization into the MgO matrix would be indicated by lower than normal proton hyperfine couplings, positive g shifts if the delocalization is onto a matrix oxygen nucleus, or the observation of a hyperfine interaction with the 10% abundant $I = 5/2$ Mg^{25} nuclei. The latter is not observed but would not be expected due to the low abundance and high nuclear spin of Mg^{25} coupled with the low signal to noise ratio and relatively high line width in most of the e.s.r. spectra observed. All the radicals had a g value close to 2.003, which is normal for the saturated alcohol radicals and the allylic radicals (20). There is a discrepancy in our value of $g = 2.003$ for $CH_3\dot{C}O$ compared to 2.006 (24) but in view of the uncertainty of identification, no significance can be attached to this. To the best of our knowledge, the proton hyperfine couplings are also normal, though even a 5% decrease might not be detected, due to the line widths of our spectra. The $(\dot{C}H_2O)^-Mg^{2+}$ radical on MgO gives $A_{average} = 17.1$ compared to 16.8 G for $(\dot{C}H_2O)^-Mg^{2+}$ in $Mg(OCH_3)_2$. $CH_3\dot{C}HOH$, $CH_3\dot{C}(OH)CH$, and $CH_2 \cdots CH \cdots CHOH$ give A_H values of 21.3, 19.3, and 13.7 G compared to average values of 20.5, 19.7, and 13.7 G for the same radicals in solution (20). This is good agreement considering the line widths involved.

Some evidence of rotational freedom and orientation on the surface can be obtained from the axially symmetric hyperfine anisotropy shown by the two outer lines in the e.s.r. spectrum of the $(\dot{C}H_2O)^-$ radical. The hyperfine tensor for α-protons has three different principal values, and the line shape corresponding to an axial symmetry could be observed only if the radical was rotating. It seems likely that the radical is rotating about the C—O bond giving rise to ⊥ and ∥ components of the hyperfine tensor. Such a rotation would be considerably hindered if the radical were lying flat on the surface and the C—O bond of the radical probably lies in a plane perpendicular to the surface. This is in agreement with the orientation of the methoxy groups inferred from i.r. data (22).

Different trap environments have shown three effects. At 77 °K the two β-protons in the radical $CH_3COCH_2\dot{C}H_2$ (formed from *sec*-butanol) both gave $A_H = 34$ G. At room temperature, this radical has presumably reoriented or moved to a different type of trapping site, since now one β-proton gives $A_H = 34$ and the other 17 G. These numbers indicate different relative orientations of the β-carbon hydrogen bonds with respect to the p orbital containing the unpaired electron (see, for example, ref. 28). The second effect is most dramatically shown by the $(CH_3\dot{C}HO)^-$ ion radical, formed by reaction of ethanol with an electron. Since this electron was trapped at a surface oxygen ion vacancy (33) it is reasonable to presume that the ethoxide ion radical is also trapped there, with the oxygen fixed at this site and the rest of the radical pointing outwards. This ion radical is completely stable at room temperature so it must be fixed in position. This trapping site will be somewhat "buried" in the lattice and is evidently protected against even a chain transfer radical migration mechanism. The third phenomenon due to trap environment involves surface concentration, and hence spatial separation of radicals and parent molecules. This is reflected in the kinetics and rate of radical decay. When $(\dot{C}H_2O)^-Mg^{2+}$ radicals are formed in the presence of a monolayer of $(CH_3O)^-$ on the surface of MgO, the $(\dot{C}H_2O)^-Mg^{2+}$ radicals decay bimolecularly, with a half life of 3 min. In this case, we suggest that the migration required to achieve combination is via a series of atom transfer reactions

[7]
$$\begin{array}{ccccccccccc} \dot{C}H_2 & CH_3 & CH_3 & & CH_3 & \dot{C}H_2 & CH_3 & & CH_3 & CH_3 & \dot{C}H_2 & \\ O & HO & HO & \rightarrow & O & HO & HO & \rightarrow & O & HO & HO & \rightarrow \text{ etc.} \\ Mg & O\,Mg & O\,Mg & & Mg & O\,Mg & O\,Mg & & Mg & O\,Mg & O\,Mg & \end{array}$$

However, when the same number of $(\dot{C}H_2O)^-Mg^{2+}$ radicals is formed, with the rest of the surface having approximately half a monolayer of $(CH_3O)^-Mg^{2+}$, this mechanism cannot occur. The radicals then decay more slowly in a unimolecular reaction, with a half

life of 10 min. The nature of this unimolecular decay is not known.

Conclusion

A new method has been developed for forming and studying free radicals on surfaces. It has the merit that the radicals are formed without perturbing the matrix, unlike heterogeneous radiation chemistry. Identification of the radicals formed, sheds light on the nature of the adsorption of the parent compound in some cases, and in other cases indicates the occurrence of secondary reactions on the surface. A major observation is that, for *n*-propanol, iso-propanol, *n*-butanol, and *sec*-butanol, once the initial radical is formed by hydrogen atom abstraction from the carbon adjacent to the hydroxyl group, it eliminates H_2 to form a secondary radical. This type of reaction presumably is able to occur on the surface because combination and disproportionation reactions have been slowed down. In solution, the latter reactions are rapid and H_2 elimination is not observed. However, when another hydroxyl group or a halogen is present on the β-carbon atom, the situation is reversed and elimination of H_2O or HX occurs (26) under suitable conditions. Effects of trapping site and surface coverage on stability and mode of free radical disappearance have also been demonstrated.

Acknowledgments

D. R. Smith wishes to thank the Atomic Energy Research Establishment at Harwell for support during his attachment from Atomic Energy of Canada Ltd., Chalk River, 1967–1968 and Dr. C. B. Amphlett for his encouragement.

1. R. Ingalls and L. Wall. J. Chem. Phys. **35**, 370 (1961).
2. L. Wall and R. Ingalls. J. Chem. Phys. **41**, 1112 (1964).
3. D. E. Holmes, L. S. Myers, and R. B. Ingalls. Nature, **209**, 1017 (1966).
4. T. Cole and H. C. Heller. Nature, **42**, 1668 (1965).
5. H. Heller, S. Schlick, and T. Cole. Nature, **47**, 1874 (1967).
6. H. Heller, S. Schlick, and T. Cole. J. Phys. Chem. **71**, 97 (1967).
7. J. N. Herak and W. Gordy. Science, **153**, 1649 (1966); Proc. Natl. Acad. Sci. U.S. **54**, 1287 (1965); **56**, 1354 (1966).
8. C. Chachaty and M. C. Schmidt. J. Chim. Phys. **62**, 527 (1965).
9. A. Forchioni and C. Chachaty. Compt. Rend. **264**, 637 (1967).
10. H. Fisher. Z. Naturforsch. **17A**, 693 (1962).
11. R. J. Kokes. Proc. 3rd. Intern. Congress Catalysis. Vol. 1. Amsterdam, 1964. North-Holland Publishing Co., Amsterdam. 1965. p. 484.
12. D. E. Wood and J. M. Pietrzak. J. Chem. Phys. **46**, 2973(1967).
13. A. J. Tench and D. R. Smith. Chem. Commun. **18**, 1113 (1968).
14. K. Hauffe. Advan. Catalysis, **7**, 250 (1955).
15. M. E. Winfield. Catalysis, **7**, 93 (1960).
16. F. F. Volkenshtein. Electronic theory of catalysis on semiconductors. The Pergamon Press, Ltd., London. 1963. pp. 4, 66.
17. H. Pines and J. Manassen. Advan. Catalysis, **16**, 49 (1966).
18. J. N. Herak. Rev. Sci. Instr. **38**, 1669 (1967).
19. E. L. Cochran, F. J. Adrian, and V. A. Bowers. J. Chem. Phys. **34**, 1161 (1961).
20. R. Livingston and H. Zeldes. J. Chem. Phys. **44**, 1245 (1966).
21. R. W. Fessenden and R. H. Schuler. J. Chem. Phys. **39**, 2147 (1963).
22. A. J. Tench and J. Kibblewhite. Private communication.
23. R. G. Greenler. J. Chem. Phys. **37**, 2094 (1962).
24. J. R. Morton and W. E. Falconer. Nature, **197**, 1103 (1963).
25. C. McKnight, H. Niki, and B. Weinstock. J. Chem. Phys. **47**, 5219 (1967).
26. A. L. Buley, R. O. C. Norman, and R. J. Pritchett. J. Chem. Soc. B, 849 (1966).
27. F. S. Dainton, G. A. Salmon, P. Wardman, and U. Zucker. Proc. 2nd Tihany Symp. Radiation Chem. Budapest, 1967. p. 247.
28. P. B. Ayscough and C. Thomson. Trans. Faraday Soc. **58**, 1477 (1962).
29. D. A. Maas and D. H. Volman. Trans. Faraday Soc. **60**, 1202 (1964).
30. J. E. Bennett. Nature, **203**, 514 (1964).
31. J. E. Bennett, B. Mile, and A. Thomas. J. Chem. Soc. A, 1399 (1967).
32. V. B. Kazanskii, G. B. Pariiskii, I. V. Aleksandrov, and G. M. Zhidomirov. Soviet Phys.—Solid State, English Transl. **5**, 473 (1963).
33. A. J. Tench and R. L. Nelson. J. Colloid Interface Sci. **26**, 364 (1968).

Can. J. Chem. Downloaded from www.nrcresearchpress.com by 210.87.254.5 on 09/05/12
For personal use only.

Free radicals by mass spectrometry. XL. Primary processes and transient intermediates in the mercury ($^3P_1$) photosensitization of hydrazine[1]

A. JONES[2] AND F. P. LOSSING

Division of Pure Chemistry, National Research Council of Canada, Ottawa, Canada

Received November 25, 1968

The low pressure mercury ($^3P_1$) photosensitized decomposition of hydrazine has been studied at 55 °C in a fast flow reactor coupled to a mass spectrometer. Direct evidence was obtained for the participation of N_2H_2, N_2H_3, NH_2, and NH in the decomposition, and two primary decomposition modes were established

$$Hg(^3P_1) + N_2H_4 \rightarrow NH_2 + NH_2 + Hg(^1S_0) \quad \text{and} \quad Hg(^3P_1) + N_2H_4 \rightarrow N_2H_3 + H + Hg(^1S_0)$$

Canadian Journal of Chemistry, 47, 1391 (1969)

Can. J. Chem. Downloaded from www.nrcresearchpress.com by 210.87.254.105 on 09/05/12
For personal use only.

Introduction

Although the direct photolysis of N_2H_4 has been studied, there appear to have been no investigations of the mercury photosensitized decomposition. The earlier direct photochemical work was summarized in 1963 by Husain and Norrish (1) who discussed the photodecomposition in terms of the two primary processes

[1] $$N_2H_4 \rightarrow NH_2 + NH_2$$

[2] $$N_2H_4 \rightarrow N_2H_3 + H$$

In later work (2–5) on the vacuum ultraviolet photolysis, other primary processes have been postulated including

[3] $$N_2H_4 \rightarrow NH + NH_3$$

[4] $$N_2H_4 \rightarrow N_2H_2 + H_2$$

$Hg(^3P_1)$ has an excitation energy of 112.2 kcal mole^{-1} and reactions [1]–[4] above have enthalpy changes ΔH^0 of 56 ± 2, 78 ± 3, 57.3 ± 3, and 26.0 ± 5 kcal mole^{-1}, respectively. Thus all these reactions are thermochemically possible in the reaction of hydrazine with $Hg(^3P_1)$. Interest in an investigation of the mercury ($^3P_1$) photosensitized decomposition of hydrazine, therefore, centers on determining which of these possible primary decomposition modes occur.

Experimental

The apparatus and experimental procedure have been described previously (6). Briefly, the mercury photosensitized reactions were investigated using a fast flow system coupled to a mass spectrometer. The reactant and mercury vapor at partial pressures of a few microns are carried in a stream of helium at 8 mm pressure through a tubular reactor (maintained at 55 °C) which is illuminated by a low-pressure mercury lamp of high intensity. The residence time in the illuminated zone is about 1×10^{-3} s. Following the illuminated zone, the reaction stream passes over a small orifice through which a representative sample flows directly into the ionization chamber of a mass spectrometer. Observation of free radical products as well as stable products can be made. The length of the reaction zone can be varied by insertion of a metal sleeve to shield a part of the reactor from the incident light.

Results and Discussion

Initial experiments showed that under the conditions employed it was possible to decompose up to 80% of the hydrazine in the reactor. This would indicate a very large quenching cross section for N_2H_4 towards triplet mercury atoms. Addition of carbon monoxide to the reaction stream caused an increase in the rate of decomposition suggesting (7, 8) that the reaction proceeds, at least in part, by the formation of an electronically excited state of N_2H_4.

When a few microns of hydrazine vapor were added to the reaction stream with the lamp off, the mass spectrometer recorded the mass spectrum of the pure hydrazine. On illumination of the reactor, a composite mass spectrum was obtained consisting of the mass spectrum of the undecomposed hydrazine plus the spectra of the reaction products. Subtraction of the hydrazine spectrum then gave the mass spectrum of the reaction products. The product mass spectrum at 50 eV obtained in this way was consistent with the formation of nitrogen, hydrogen, and ammonia together with a compound having peaks at $m/e = 29$ and 30. This has been identified as diimide, N_2H_2, (see below). No products of mass greater than 32 were detected.

---

[1]NRCC Contribution No. 10 557.

[2]NRCC Postdoctorate Fellow 1965–1967. Present address: Department of Physical Chemistry, University of Leeds, Leeds, England.

Can. J. Chem. Downloaded from www.nrcresearchpress.com by 210.87.254.105 on 09/05/12
For personal use only.

A quantitative estimation of the products formed under these conditions could not be made owing to the fact that the mass spectral sensitivity of N_2H_2 could not be measured, since this compound is unstable under ordinary conditions, nor could any allowance be made for its fragment peaks at m/e 28 and 2 since its mass spectrum at 50 eV is not known.

Formation of Transient Intermediates

Although the formation of diimide is often invoked as a reaction intermediate (9), direct observations in the gas phase are few. It was first observed, mass spectrometrically, by Foner and Hudson (10) in the reactions occurring when HN_3 or N_2H_4 is subjected to an electrodeless discharge in a fast flow system. A study of the thermal decomposition of anthracene-9,10-diimine (11) in a mass spectrometer established N_2H_2 as a reaction product. More recently, Willhoft and Robertson (12) have observed its formation in the catalytic decomposition of hydrazine at low pressure on platinum. The latter authors report a ratio of 1.32 for the mass spectrometric peaks 29/30 (parent − 1)/(parent) using 70 eV electrons. The value found in this work, 29/30 = 1.30 (at 50 eV electron energy) is in excellent agreement with this value. The evidence for the formation of diimide in our system thus appears conclusive.

It was thought possible, in view of the results obtained in the direct photolysis, that the free radicals N_2H_3, NH_2, and NH may play a part in the decomposition. A search for these was made by adding to the reaction stream a small partial pressure of mercury dimethyl which is photodecomposed in the reactor to form methyl radicals. In this way, methyl addition products of free radicals present can be detected by the mass spectrometer. Although no dimethylamine $(CH_3)_2NH$ (which could have been formed by the successive additions of CH_3 to NH) was detected, the presence of N_2H_3 and NH_2 radicals was established by the detection of monomethylhydrazine, CH_3NHNH_2, and methylamine CH_3NH_2.

Using low energy electrons for direct detection of radicals, a large increase at $m/e = 16$ (NH_2^+) was observed, supporting the detection as above by methyl addition. Under the same conditions an increase at $m/e = 15$ (NH^+) was also observed. It was first thought that this might be a fragment ion of some other species present. However, an examination of the energetics of possible ionization fragmentation processes leading to the formation of NH^+ gave the following calculated minimum appearance potentials (see below for thermochemical values used)

NH^+ from N_2H_3 (16.7 eV), N_2H_2 (18.9 eV), NH_3 (17.5 eV), NH_2 (17.6 eV).

Since the electron energy (about 15 eV) used in this experiment was lower than any of these thresholds, the observed increase at $m/e = 15$ appears to be attributable to the free radical NH. The ionization potential (13) of NH, 13.1 eV, is consistent with this observation.

Primary Decomposition Reactions

On addition of successively increasing amounts of mercury dimethyl to the reaction stream, a plateau is reached in the "titration" curve when the radical being titrated is formed in a primary decomposition step. Results for the titrations of N_2H_3 and NH_2 radicals are shown in Fig. 1 and are consistent with the occurrence of the two primary decomposition reactions

[5] $Hg(^3P_1) + N_2H_4 \rightarrow N_2H_3 + H + Hg(^1S_0)$
$\Delta H^0 = -34 \pm 3$ kcal mole^{-1}

[6] $Hg(^3P_1) + N_2H_4 \rightarrow NH_2 + NH_2 + Hg(^1S_0)$
$\Delta H^0 = -56 \pm 2$ kcal mole^{-1}

From the measured sensitivities of CH_3NH_2 and CH_3NHNH_2, the limiting yields showed that for every molecule of CH_3NHNH_2, ca. 4.6 molecules of CH_3NH_2 are formed. This would suggest that reaction [6] is some 2.3 times faster

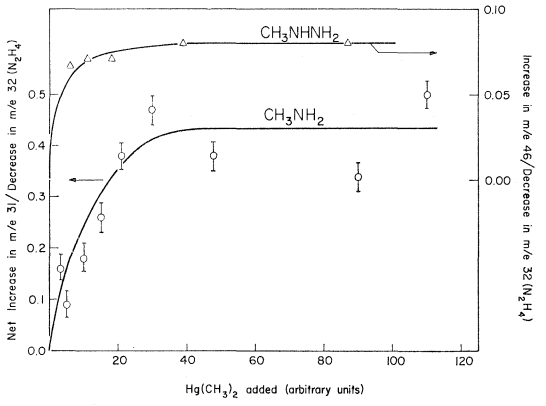

FIG. 1. Formation of CH_3NHNH_2 and CH_3NH_2 by titration of N_2H_3 and NH_2 radicals with added CH_3 radicals.

Can. J. Chem. Downloaded from www.nrcresearchpress.com by 210.87.254.105 on 09/05/12
For personal use only.

than reaction [5]. However, encounters between methyl radicals and NH_2 and N_2H_3 can also lead to disproportionation products by the reactions

[7] $$CH_3 + N_2H_3 \rightarrow CH_4 + N_2H_2$$
$$\Delta H^0 = -52 \pm 6 \text{ kcal mole}^{-1}$$

[8] $$CH_3 + NH_2 \rightarrow CH_4 + NH$$
$$\Delta H^0 = 0 \pm 3 \text{ kcal mole}^{-1}$$

If, as is likely, reaction [7] is faster than reaction [8] (it is some 50 kcal more exothermic), the factor of 2.3 can be regarded as an upper limit for k_6/k_5. An attempt was made to measure the sensitivity of N_2H_4 and so determine what fraction of the decomposition could be attributed to reactions [5] and [6]. It was found, however, that hydrazine undergoes a rapid surface decomposition at low pressures in the sample line, and no reliable measurement of the mass spectral sensitivity could be made.

In view of the products obtained, two other primary decomposition steps (both thermochemically feasible) are possible

[9] $$Hg(^3P_1) + N_2H_4 \rightarrow N_2H_2 + H_2 + Hg(^1S_0)$$
$$\Delta H^0 = -86 \pm 5 \text{ kcal mole}^{-1}$$

[10] $$Hg(^3P_1) + N_2H_4 \rightarrow NH_3 + NH + Hg(^1S_0)$$
$$\Delta H^0 = -55 \pm 3 \text{ kcal mole}^{-1}$$

Attempts to detect diimide and hydrogen in the presence of a large excess of methyl radicals, which would indicate the occurrence of reaction [9], resulted in inconclusive results due to interference from the mass spectra of other species present. Although no dimethylamine was found on addition of methyl radicals, some support for reaction [10] comes from experiments in which the peak at $m/e = 17$ (NH_3) was monitored during a methyl radical titration. These experiments showed that this peak decreased by only about 50% in the presence of an excess of CH_3, indicating that at least part of the ammonia is formed directly and not via free radical intermediates.

It is of interest to contrast the mercury photosensitized decomposition of hydrazine with that of the isoelectronic molecule ethane in which no C—C bond rupture occurs, and only the C—H bond is split. This difference may be understood in terms of formation of an electronically excited N_2H_4 molecule leading to fragmentation by two, or possibly more, modes of reaction, while ethane decomposes by a direct attack of $Hg(^3P_1)$ on a C—H bond. In ethane no appropriate excited state appears to be available.

Thermochemical values (kcal mole^{-1}) employed are as follows: $\Delta H_f^0(N_2H_4) = 22.7$ (14), $\Delta H_f^0(N_2H_2) = 48.7 \pm 5$ (10), $\Delta H_f^0(NH_3) = -11.0$, $\Delta H_f^0(CH_4) = -17.9$ (15), $\Delta H_f^0(CH_3) = 34.0 \pm 1$, $\Delta H_f^0(H) = 52.1$, $\Delta H_f^0(N) = 113.0$, $D(NH_2—NH_2) = 56 \pm 2$ (16), $D(N_2H_3—H) = 78 \pm 3$ (17, 10), and $D(N—H) = 74 \pm 3$ (18).

1. D. Husain and R. G. W. Norrish. Proc. Roy. Soc. London, Ser. A, **273**, 145 (1963).
2. L. J. Stief, V. J. DeCarlo, and R. N. Mataloni. J. Chem. Phys. **46**, 592 (1967).
3. K. H. Becker and K. H. Welge. Z. Naturforsh. **19a**, 1006 (1964).
4. L. J. Stief and V. J. DeCarlo. Nature, **205**, 889 (1965).
5. L. J. Stief and V. J. DeCarlo. J. Chem. Phys. **44**, 4638 (1966).
6. P. Kebarle and F. P. Lossing. Can. J. Chem. **37**, 389 (1959).
7. A. Jones and F. P. Lossing. Can. J. Chem. **45**, 1685 (1967).
8. J. B. Homer and F. P. Lossing. Can. J. Chem. **44**, 143 (1966).
9. S. Hünig, H. R. Müller, and W. Thier. Angew. Chem. Intern. Ed. **4**, 271 (1965).
10. S. N. Foner and R. L. Hudson. J. Chem. Phys. **28**, 719 (1958).
11. E. J. Corey and W. L. Mock. J. Am. Chem. Soc. **84**, 685 (1962).
12. E. M. A. Willhoft and A. J. B. Robertson. Chem. Commun. 385 (1967).
13. S. N. Foner and R. L. Hudson. J. Chem. Phys. **45**, 40 (1966).
14. L. F. Audrieth and R. A. Ogg. The chemistry of hydrazine. John Wiley and Sons, Inc., New York. 1951. p. 76.
15. Selected values of chemical thermodynamic properties. Natl. Bur. Stds. U.S. Circ. No. 500. Washington, D.C. 1952.
16. J. A. Kerr. Chem. Rev. **66**, 465 (1966).
17. I. P. Fisher and G. A. Heath. Nature, **208**, 1199 (1965).
18. K. E. Seal and A. G. Gaydon. Proc. Phys. Soc. **89**, 459 (1966).

Tensorial properties of an electronic Raman effect of the thulium ion[1]

J. A. KONINGSTEIN AND TOA-NING NG
E. W. R. Steacie Building, Department of Chemistry, Carleton University, Ottawa, Canada

Received November 5, 1968

The low temperature laser excited Raman spectrum of the compound thulium gallium garnet reveals the presence of an electronic transition of the thulium ion. The tensor associated with this transition can contain some asymmetry. Polarization measurements show, however, that the amount of asymmetry is too small to be detectable.

Canadian Journal of Chemistry, **47**, 1395 (1969)

Can. J. Chem. Downloaded from www.nrcresearchpress.com by 210.87.254.42 on 09/05/12
For personal use only.

Introduction

Recently the phonon spectrum of a single crystal of thulium gallium garnet ($Tm_3Ga_5O_{12}$) was investigated by means of laser Raman spectroscopy (1). The scattering tensors for the phonon modes are relatively simple because the garnet crystals belong (2) to the cubic space group O_h^{10} (*Ia3d*). Although there are as many as 80 atoms in the primitive cell, the factor group analysis suggests that a maximum number of 21 Raman lines can be expected (3). The Raman lines are of symmetry A_{1g}, E_g, T_{2g}, or of combinations of these species because the non-vanishing components of the scattering tensor for the vibrational Raman effect are divided over these three representations of the factor group O_h. For TmGaG a satisfactory assignment of the phonon spectrum could be made from polarized Raman spectra of an oriented crystal.

An interesting property of the Tm^{3+} ion is that its electronic ground state is one of the crystal field components of the $^3H_6$ manifold. The $2J + 1$-fold degeneracy of this manifold is completely removed for the thulium ion in the garnet crystal because the symmetry at the site of the rare earth ions belongs to the group D_2. The labelling of the crystal field levels can thus be such that the lowest lying level does not belong to the totally symmetric representation of the group D_2. This of course is nearly always the case in the vibrational Raman effect. Attention should thus be given to the integral

$$\int \psi_n^* \alpha_{\rho\sigma} \psi_m \, d\tau$$

which reflects the selection rules for the electronic transitions. ψ_n and ψ_m represent the wave functions of the initial and terminal states and $\alpha_{\rho\sigma}$ is an element of the scattering tensor. This integral is not equal to zero if the product of the irreducible representations $\Gamma_m \times \Gamma_\alpha \times \Gamma_m$ contains the totally symmetric representation of the group D_2. Γ_α can thus belong to all species occuring in the product $\Gamma_n \times \Gamma_m$. Another complication is that the scattering tensor for the electronic transition can be asymmetric (4). For the vibrational Raman effect it is not necessary to consider the transformation properties of the antisymmetric combination $\alpha_{\rho\sigma} - \alpha_{\sigma\rho}$ (where ρ and σ stand for x, y, and z). It was recently demonstrated that antisymmetry for rare earth transitions is quite important and results in profound changes in the polarization properties of Raman lines (5–7). Finally, interactions of rare earth ions in the unit cell are very small and although the symmetry of the crystal has to be adopted for the selection rules, this does not result in extra splitting effects. Of the 12 possible electronic Raman transitions of TmGaG, only one could be detected. Its intensity is, however, strong enough to measure the various elements of the scattering tensor. The tensor is symmetric and the components of this tensor are in agreement with the symmetry of the crystal field.

Theory

The trivalent thulium has the electronic configuration $Xe(4f)^{12}(5s)^2(5p)^6$. This configuration gives rise to a large number of Russell–Saunders terms. The lowest lying multiplet is ^3H and the ground manifold is $^3H_6$. This state is for the free ion 13-fold degenerate; however, for TmGaG this degeneracy is completely removed because the symmetry of the crystal field is orthorhombic. The thulium ion is surrounded by 8 oxygen ions located on the corners of a distorted cube (2) and the actual site symmetry is that given by the group D_2. The garnet crystals are, however, cubic and the space group is O_h^{10} (*Ia3d*).

[1]Supported in part by grants of the National Research Council and Defence Research Board of Canada.

Can. J. Chem. Downloaded from www.nrcresearchpress.com by 210.87.254.42 on 09/05/12
For personal use only.

Rare earth ions in garnet crystal experience a rather strong crystal field and the ground manifold can have an overall splitting of as much as 500 cm^{-1}. Raman scattering to the electronic levels thus occurs at low shifts and coincidences with the phonons are apt to occur. There are 80 atoms in the primitive cell giving rise to 21 Raman lines and all of them occur (3) with shifts $< 800\ cm^{-1}$.

The electronic Raman lines are allowed because the $^3H_6$ manifold levels have the same parity. A priori calculation of the absolute intensities revealed (8) that the transitions are weak and may well be obscured by the phonon spectrum.

For detailed study of the polarization properties, it is necessary to consider the symmetry labelling of the crystal field levels in terms of the species A, B_1, B_2, and B_3 of the group D_2. It follows that the non-vanishing elements of the scattering tensor between any of these levels belong to the same species. The product of the totally symmetric species with the other species equals the representation of these species and the product of $B_1 \times B_2 = B_3$ etc. The transformation properties of the antisymmetric combinations $\alpha_{xy} - \alpha_{yx}$, $\alpha_{xz} - \alpha_{zx}$, and $\alpha_{yz} - \alpha_{zy}$ are identical to the species B_1, B_2, and B_3, respectively. To these species belong also the symmetric combinations $\alpha_{xy} + \alpha_{yx}$, $\alpha_{xz} + \alpha_{zx}$, and $\alpha_{yz} + \alpha_{zy}$. Exact calculation of the antisymmetric combination can only be made if the wave functions of the states are known in great detail (5). The wave functions can only be calculated if the strength and symmetry of the crystal field is known and for TmGaG a reliable crystal field analysis has not been made.

The experimental data are obtained from measurements on the cubic garnet crystals and only combined effects are seen, not site group spectra. In fact, there are in the unit cell 12 sites of symmetry D_2 but the interactions of the rare earth ions in the unit cell are known to be extremely small and in employing correlation tables, the correct labelling of the levels and the transformation properties of the scattering tensor in the group O_h are directly obtained. The symmetry of the levels and the possible tensors are given in Tables I and II. One notes that in some cases more than one combination transforms according to the same species, and in such instances it is convenient to define a scattering matrix. The elements of this matrix are computed by taking the sum of the squares of identical elements of the individual contributing tensors (4). Intensities of the polarized Raman spectra can now be related to the elements of the matrix if the direction of propagation of the incident excitation radiation is along the cubic a axis and the direction of observation along the cubic b or c axis.

TABLE I

Transformation properties of crystal field levels of the thulium ion in site and space group

Symmetry properties of crystal field levels	
Site group (D_2)	Space group (O_h)
A	A_{1g}
B_1	T_{1g}
B_2	$T_{1g}+T_{2g}$
B_3	$T_{1g}+T_{2g}$

TABLE II

Scattering tensors for various representations of the group O_h

Representation	Elements of the tensor
A_{1g}	$\alpha_{xx}+\alpha_{yy}+\alpha_{zz}$
E_g	$\alpha_{xx}-\alpha_{yy}$; $2\alpha_{zz}-\alpha_{xx}-\alpha_{yy}$
T_{2g}	$\alpha_{xz}+\alpha_{zx}$; $\alpha_{xy}+\alpha_{yx}$; $\alpha_{yz}+\alpha_{zy}$
T_{1g}	$\alpha_{xz}-\alpha_{zx}$; $\alpha_{xy}-\alpha_{yx}$; $\alpha_{yz}-\alpha_{zy}$

Unfortunately this condition could not be met in our experiments on TmGaG. The incident laser beam was in fact parallel to the [111] direction and the direction of the scattered light perpendicular to the (101) plane. Under these experimental conditions, the observed intensities are not directly related to the elements of the scattering matrices. However, if the individual contributing tensors mentioned above are subjected to specific rotations, then new matrices are obtained whose elements are related to the observed intensities. The specific rotations are rather simple. First a rotation is carried out over an angle of 45° around one of the cubic axes (say y-axis) of the crystal and second, the same operation is performed again but now with the newly created x'-axis as axis of rotation (1). The new axes are now parallel to the experimental X, Y, and Z axes. The radiation of a He–Ne laser was parallel to the experimental Z-axis and the direction of observation of the scattered light was along the X-axis. By a suitable choice of polarization of the incident laser beam and, by employing an analyzer

in front of the slit of the monochromator, the following elements of the scattering matrix can be measured: YY, YZ, XY, and XZ. The computation of the scattering matrices for the experimental axis is a relatively straightforward matter and the result of the calculation is given in Table III.

TABLE III

Scattering matrices for various representations of the group O_h for the experimental case

Species	Matrix
A_{1g}	$\begin{bmatrix} \alpha_{xx}^2 & & \\ & \alpha_{yy}^2 & \\ & & \alpha_{zz}^2 \end{bmatrix}$
E_g	$\begin{bmatrix} 4\alpha_{xx}^2 & 10\alpha_{xy}^2 & 10\alpha_{xz}^2 \\ 10\alpha_{yx}^2 & \alpha_{yy}^2 & 9\alpha_{yz}^2 \\ 10\alpha_{zx}^2 & 9\alpha_{zy}^2 & \alpha_{zz}^2 \end{bmatrix}$
T_{2g}	$\begin{bmatrix} 4\alpha_{xx}^2 & 2\alpha_{xy}^2 & 2\alpha_{xz}^2 \\ 2\alpha_{yx}^2 & 5\alpha_{yy}^2 & \alpha_{yz}^2 \\ 2\alpha_{zx}^2 & \alpha_{zy}^2 & 5\alpha_{zz}^2 \end{bmatrix}$
T_{1g}	$\begin{bmatrix} 0 & 4\alpha_{xy}^2 & 4\alpha_{xz}^2 \\ 4\alpha_{yx}^2 & 0 & 4\alpha_{yz}^2 \\ 4\alpha_{zx}^2 & 4\alpha_{zy}^2 & 0 \end{bmatrix}$

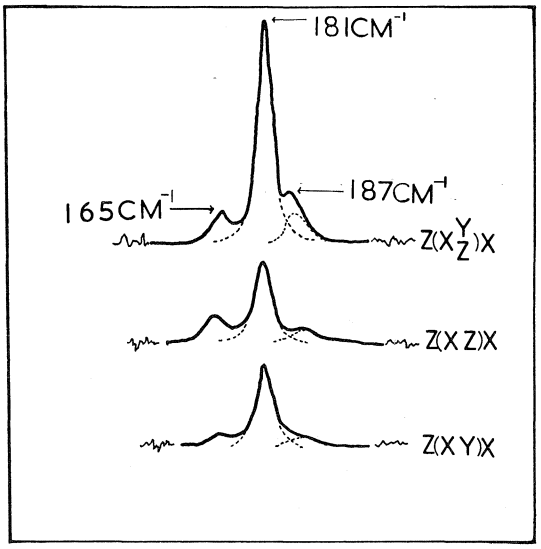

FIG. 1. The 80 °K laser excited Raman spectra of the compound thulium gallium garnet. Z is the direction of propagation of the incident laser beam and X is the direction of observation. XZ and XY refer to the elements of the scattering matrices given in Table III.

Results and Discussion

The phonon spectrum of TmGaG has been discussed in a recent publication and of importance here is the Raman spectrum with shifts around 180 cm^{-1}. Polarized low temperature Raman spectra of the crystal in that spectral region are shown in Figs. 1 and 2. Absorption and fluorescence measurements revealed that a crystal field level of the $^3H_6$ manifold of TmGaG is situated at 187 cm^{-1} above the ground state (9). In the Raman spectrum of this compound a band is observed at the same frequency and a comparison of the Raman spectrum of TmGaG with the spectrum of a single crystal of YbGaG or YGaG shows that the line at 187 cm^{-1} is unique. In accordance with the findings of the absorption and fluorescence spectra, we assign this weak transition to an electronic effect of the Tm^{3+} ion. According to theory one expects a maximum number of 12 electronic transitions but a search for the other transitions was negative. The absolute values of electronic Raman intensities can be

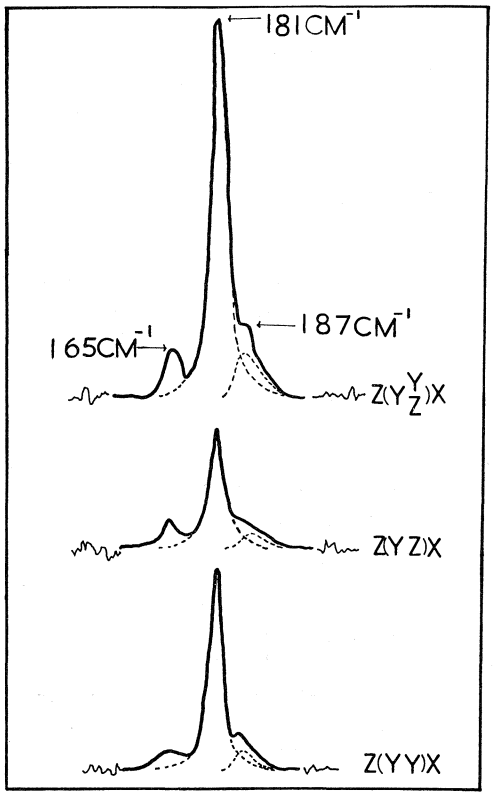

FIG. 2. The polarized Raman spectrum of the single crystal but now showing the components $YY + YZ$, YY, and YZ. The power of the laser beam was 50 mW and the spectra were photoelectrically recorded. The lines on 165 and 181 cm^{-1} are phonon modes and the line on 187 cm^{-1} is the electronic Raman line.

Can. J. Chem. Downloaded from www.nrcresearchpress.com by 210.87.254.42 on 09/05/12
For personal use only.

Can. J. Chem. Downloaded from www.nrcresearchpress.com by 210.87.254.42 on 09/05/12
For personal use only.

calculated and this calculation for the Tm ion suggests (8) that the cross sections can be as low as 10^{-34} cm^2. From Fig. 1 it is concluded that the intensity of the electronic transition is an order of magnitude smaller than the intensities associated with the phonon modes. A comparison with the intensity of the line of benzene at 992 cm^{-1} shows that the intensity of the phonon lines is approximately two orders of magnitude smaller than the intensity of the benzene line. The experimentally (10) determined cross section of this line is $\sim 10^{-29}$ cm^2. Consequently the estimated cross section of the electronic line is $\sim 10^{-32}$ cm^2. It is thus not surprising that some of the other electronic transitions are not observed.

Also, the antisymmetry of the scattering tensor of this ion has been computed (5). Theory predicts that the amount of asymmetry should be small. From Tables I and II it is seen that the tensors of the electronic transitions are those belonging to the species A_{1g}, T_{1g} or the combination of $T_{1g} + T_{2g}$. Transitions associated with a tensor belonging to the species T_{1g} are thus extremely weak because the amount of asymmetry is small. Also, all other transitions are related to a tensor which is nearly completely symmetric. Values of integrated intensities of some phonon modes of symmetry E_g and T_{2g} are given in Table IV. Also the intensity pattern is compared with appropriate elements of the scattering matrices in Table IV. Reasonable agreement exists between the two sets of values. Integrated intensities of the electronic line are given in Table V. Here again a comparison is made with the intensity matrices and the conclusion is reached that within experimental error the line of Tm^{3+} ion in TmGaG is of symmetry T_{2g}. For this transition, the antisymmetric tensor could contribute

TABLE IV

Relative intensities of some polarization measurements of phonon modes of TmGaG

Frequency phonon mode (cm^{-1})	Symmetry	Relative intensity I_{YY}	I_{YZ}	I_{XY}	I_{XZ}	
260	E_g	2	10	9	8	(found)
		1	9	10	10	(calcd.)
244	T_{2g}	4	2	2	2	(found)
		5	1	2	2	(calcd.)
274	T_{2g}	3	1.5	2	2	(found)
		5	1	2	2	(calcd.)

TABLE V

Relative intensities of some polarization measurements of the electronic transition

Frequency	Symmetry	Relative intensity I_{YY}	I_{YZ}	I_{XY}	I_{XZ}	
187 cm^{-1}						
	T_{1g}	0	4	4	4	(calcd.)
	T_{2g}	5	1	2	2	(calcd.)
		5	2	1.5	2	(found)

and the experimental data are thus in agreement with the theory which predicts that the amount of asymmetry should be small.

The energy level diagram of the thulium ion in the host lattice yttrium aluminium garnet has been studied (11) up to energies of 37 000 cm^{-1}. At low temperature, absorptions do not take place at the wavelengths of the principal lines of the argon ion laser. For TmGaG a similar situation can be expected and one might think that more information can be obtained in employing the argon ion laser. Nevertheless, the procedures presented here are valid for all rare earth ions in the garnet host lattices and in future work, use will be made of this type of calculation to relate the crystal field to the polarization properties of electronic Raman transitions.

Concluding Remarks

There is no difference in the electric dipole matrix element $\langle\psi_m|e\rho|\psi_n\rangle$ (where ρ is x, y, or z) for rare earth ion transitions if these ions are imbedded in cubic crystals. The symmetry characterization of the crystal field components of the split LSJ manifolds—in terms of the irreducible representations of the group which describes the appropriate symmetry at the site of the lanthanide ion—cannot directly be made from the fluorescence or absorption spectra. Such assignments can be made from polarization measurements of electronic Raman transitions. For TmGaG one transition has been observed employing the He–Ne laser as an exciting source. The Raman band is of symmetry T_{2g}. This suggests that the transition occurs between the levels of symmetry A and B_2, A and B_3, or B_1 and B_2, B_1 and B_3. The exact labelling of the level of the ground state can thus in principle be found by a process of elimination if the electronic transitions to other levels could be observed. This unfortunately is not the case for TmGaG, but for TbAlG, at least

10 electronic transitions have been observed between the crystal field levels of the $^4F_6$ manifold (12).

Many electronic Raman transitions of rare earth ions have been observed, and presently it can be said that the absolute intensity of these transitions depends strongly on the electronic configuration of the rare earth ions. Fortunately, excitation radiation at different wavelengths is now available for Raman spectroscopy and it thus seems possible to relate crystal field calculations with polarized electronic Raman spectra of rare earth ions.

Acknowledgment

The authors are thankful to Dr. B. A. Buchanan for supplying the single crystal of thulium gallium garnet.

1. J. A. KONINGSTEIN and TOA-NING NG. J. Opt. Soc. Am. **50**, 1462 (1968).
2. S. GELLER and M. A. GILLES. Phys. Chem. Solids, **3**, 30 (1957).
3. J. A. KONINGSTEIN and O. SONNICH MORTENSEN. J. Mol. Spectry. **27**, 343 (1968).
4. G. PLACZEK. Handbuch der Radiologie. Vol. 6. Leipzig. 1934. p. 205.
5. J. A. KONINGSTEIN and O. SONNICH MORTENSEN. Nature, **217**, 445 (1968).
6. O. SONNICH MORTENSEN and J. A. KONINGSTEIN. J. Chem. Phys. **48**, 3971 (1968).
7. J. A. KONINGSTEIN and O. SONNICH MORTENSEN. J. Opt. Soc. Am. **58**, 1208 (1968).
8. J. A. KONINGSTEIN and O. SONNICH MORTENSEN. Phys. Rev. **168**, 75 (1968).
9. J. G. SKINNER and W. NILSEN. J. Opt. Soc. Am. **58**, 113 (1968).
10. R. A. BUCHANAN. Private communication.
11. J. A. KONINGSTEIN. Theoret. Chim. Acta, **5**, 327 (1966).
12. J. A. KONINGSTEIN. Chem. Phys. Letters, **2**, 213 (1968).

Can. J. Chem. Downloaded from www.nrcresearchpress.com by 210.87.254.42 on 09/05/12
For personal use only.

Solvation thermodynamics of ions: free energies in water, ammonia, and fused LiCl–KCl eutectic

JAMES A. PLAMBECK
Department of Chemistry, University of Alberta, Edmonton, Alberta
Received August 21, 1968

Conventional free energies of solvation of ions are calculated from appropriate thermodynamic data in water, liquid ammonia, and fused LiCl–KCl eutectic. These are fitted to a modified Born-charging equation, whose origin and significance are discussed. Statistical tests are applied to certain aspects of the form of the equation. Parameters obtained from the equation can be used to calculate the free energies of solvation of single ions.

Canadian Journal of Chemistry, **47**, 1401 (1969)

Can. J. Chem. Downloaded from www.nrcresearchpress.com by 210.87.254.5 on 09/05/12
For personal use only.

Introduction

In the simplest approach (1), the free energy of charging a sphere of radius r to charge ze in vacuum is given by

$$\Delta G_{\mathrm{BC\ g}} = z^2e^2/2r$$

while in a solvent of dielectric constant ε the corresponding free energy is

$$\Delta G_{\mathrm{BC\ s}} = z^2e^2/2r\varepsilon$$

so that the free energy of transfer of a spherical ion from vacuum to such a medium is

$$[1] \quad \Delta G_{\mathrm{BC}} = \Delta G_{\mathrm{BC\ s}} - \Delta G_{\mathrm{BC\ g}} = \frac{-z^2e^2}{2r}(1 - 1/\varepsilon)$$

This will be referred to as the Born-charging free energy of solvation.

It is well known (2) that free energies calculated from the above equation are generally much greater than those calculated from experimental thermodynamic data. The reconciliation of theory and experiment has been approached in two ways. The first, exemplified by the work of Latimer, Pitzer, and Slansky (3), argues that the ionic radii used in eq. [1] should not be crystallographic radii but larger values, which would give a better fit to the data. These larger radii are justified as being more characteristic of a noncrystalline environment, and various empirical radii and correction factors for crystal radii have been employed in this approach. This approach has been criticized by Laidler and Pegis (4). The second approach, exemplified by the work of Noyes (5, 6) is to assume that the ionic sizes are known and constant (crystallographic radii) but that, in view of the large electrostatic potential gradient near the surface of an ion, the solvent in its vicinity is highly polarized. Under these circumstances the bulk dielectric constant of the solvent can no longer be assumed to be correct in the immediate neighborhood of ions, and agreement between theory and experiment is achieved by using an "effective dielectric constant" or dielectric saturation parameters.

The approach of the present paper to the reconciliation is almost identical in mathematical form, but not in physical interpretation, to the second approach mentioned above.

Theory

An appropriate formulation of the problem for aqueous solutions is that given by Noyes (5). Generalizing this formulation we obtain, for any solvent,

$$[2] \quad \Delta G_{\mathrm{SOLV}}{}^0 = \Delta G_{\mathrm{CON}}{}^0 + z\Delta G_{\mathrm{R}}{}^0$$

where z is the ionic charge and $\Delta G_{\mathrm{SOLV}}{}^0$ (Noyes: $\Delta F_{\mathrm{HYD}}{}^0$) is the free energy of solvation of the ion in question, $\Delta G_{\mathrm{CON}}{}^0$ (Noyes: $\Delta F_{\mathrm{CON}}{}^0 - \Delta F_{\mathrm{NEUT}}{}^0$) is the conventional free energy of solvation of the ion, and $\Delta G_{\mathrm{R}}{}^0$ (Noyes: $\Delta F_{\mathrm{H}}{}^0$) is a reference free energy of solvation. The value of the *conventional* free energy of solvation of any ion in any solvent is calculable unambiguously if sufficient thermodynamic data are available. These data must include at least ionization potentials, dissociation energies, sublimation energies, and electromotive force (e.m.f.) values. Such calculations are available in the literature (5, 7).

The solvation energy, $\Delta G_{\mathrm{SOLV}}{}^0$, can be considered as being strictly electrostatic, $\Delta G_{\mathrm{EL}}{}^0$, if the solvation process is considered as the sum of

Can. J. Chem. Downloaded from www.nrcresearchpress.com by 210.87.254.5 on 09/05/12
For personal use only.

three steps: discharging the gaseous ion, solvating the then-neutral species, and recharging the solvated neutral species. Noyes (5) has discussed the approaches to the second of these steps and we accept his conclusion that there is zero free energy of hydration for neutral species. There is still a free energy term for this step, arising wholly from the change from gaseous (1 atm) to liquid (1 molar) standard states (Noyes: $\Delta F_{NEUT}{}^0$) which is incorporated in the $\Delta G_{CON}{}^0$ values given here. We can, therefore, write

$$[3] \qquad -\Delta G_{CON}{}^0 = z\Delta G_R{}^0 - \Delta G_{EL}{}^0$$

where the terms on the right-hand side of the equation are unknown but $\Delta G_{CON}{}^0$ is known. The Born-charging equation unquestionably gives $\Delta G_{EL}{}^0$ correctly for any sphere of macroscopic dimensions, and for such spheres the macroscopic dielectric properties of the solvent are applicable. Thus, in the limit as the ionic radius r approaches infinity, $\Delta G_{EL}{}^0$ approaches $\Delta G_{BC}{}^0$.

For ions of real size in real solvents, however, the Born-charging equation cannot hold, because real solvent molecules are about the same size as real ions. To entities of ionic size, water or any other solvent will appear not as a continuum but as a collection of discrete molecular entities. It is only as the size of an ion approaches infinity on a molecular scale that the Born-charging equation should hold. It will hold in the limit of large ions, however, regardless of the actual sizes of ions or of the dielectric saturation effects, if any, in their vicinity because such effects become negligible at large radius. Thus, in the limit of $1/r \rightarrow 0$,

$$\Delta G_{EL}{}^0 = z^2K/r$$

where $K = \frac{1}{2}e^2(1 - 1/\varepsilon)$ and it is reasonable to represent the actual electrostatic charging energy as a power series expansion in reciprocal radius

$$[4] \quad \Delta G_{EL}{}^0 = -z^2K/r - z^2A/r^2 - z^2B/r^3 - z^2C/r^4 - \ldots$$

since the limit of such a series at infinite radius will be the same as that of the first term. The constants $A, B, C, \ldots$ are empirical and may have either positive or negative values.

From the above argument we now obtain

$$[5] \quad -\Delta G_{CON}{}^0/z = \Delta G_R{}^0 + zK/r + zA/r^2 + zB/r^3 + \ldots$$

in which $-\Delta G_{CON}{}^0/z$ is known and $\Delta G_R{}^0$, A, $B, \ldots$ are unknown. This equation should apply to all ions in any solvent if the appropriate value of K for that solvent is used.

The empirical constants $A, B, C, \ldots$ need have no specific physical significance as apparently assumed by Noyes (5, 6) and de Ligny and Alfenaar (8). They are deviations from the continuous dielectric medium model inherent in the Born equation which can be interpreted as arising from specific ion–solvent interaction, dielectric saturation, ion–quadrupole interactions, or simply the fact that ions see solvent molecules as discrete entities. What is significant is that in the limit of infinite ionic size these deviations all go to zero, and by this method a value of $\Delta G_R{}^0$ for a solvent can be obtained.

The calculation of $\Delta G_R{}^0$ requires values for the empirical constants $A, B, C, \ldots$; these and $\Delta G_R{}^0$ itself can be calculated by the method of least squares in any solvent for which sufficient experimental data are available. In this calculation, it cannot *a priori* be assumed that the deviations from the Born model, and hence the empirical constants, will be the same for anions and cations or that any particular number of empirical constants will be necessary; statistical tests must be applied to determine these aspects of the form of the equation. The results of this paper differ from previous calculations (5, 6, 8, 10) primarily in the use of data for ions of *all* charges (but only of inert-gas electronic structure, for reasons given below), thus giving a more soundly based value.

The value of $\Delta G_R{}^0$ obtained by this procedure can be used to calculate the free energies of solvation of single ions, as will be shown below, but is not itself the free energy of solvation of any ion. The value of $\Delta G_R{}^0$ is in principle neither measurable nor calculable by strictly thermodynamic procedures. This is because measurement of the potential of a single electrode is not possible.

The potential of the reference electrode system in any solvent is therefore arbitrarily assigned the value zero and all other potentials measured with respect to it (e.g., the aqueous hydrogen electrode). This is equivalent to defining the conventional free energy of solvation of the reference ion (ion of the reference electrode couple; hydrogen ion in aqueous solutions) as a fixed quantity whose numerical value is completely determined by the choice of standard states for

Can. J. Chem. Downloaded from www.nrcresearchpress.com by 210.87.254.5 on 09/05/12
For personal use only.

the system but cannot be calculated by strictly thermodynamic procedures. Thus, the values of $-\Delta G_{CON}^0/z$ given in Table I for hydrogen ion in water and liquid ammonia, and for Pt(II) in fused LiCl–KCl eutectic, incorporate this assumption explicitly while the values for all other ions do so implicitly. The assumption is removed on the subtraction of ΔG_R^0 from the values of $-\Delta G_{CON}^0/z$ given in Table I, and the absolute free energy of solvation (or free energy of transfer from vacuum to solvent) of any ion in kcal/mole is obtained by multiplying that sum by $-z$.

The exact physical meaning of ΔG_R^0 is not at present clear, and probably depends on the nature of the solvation mechanism assumed although the numerical value of ΔG_R^0 does not. Thus ΔG_R^0 includes any deviation from the zero energy assumption such as that suggested by Noyes (6), using the three-step approach; if the solvation occurs in a one-step procedure as the ion moves across the phase boundary as suggested by Stokes (9), an interpretation on the basis of interfacial potentials would appear preferable.

One of the advantages of the present method is that it is applicable to any solvent and that the value of ΔG_R^0 for that solvent is determined from data taken only in that solvent. Values of ΔG_R^0 can be compared between any pair of solvents for which reasonably extensive electromotive force series exist, without the necessity of assumptions regarding the free energy of transfer of any specific ions from one solvent to another. In this context, it should be pointed out that the most common such assumption (11) is that the free energy of transfer for a large ion of low charge, such as rubidium ion, between two solvents is zero, and hence the conventional free energy of transfer is to be wholly ascribed to the difference between the reference free energies of solvation of the two solvents. In the light of the present approach, this assumption appears reasonable because for such ions the deviation from the Born equation is minimal. Moreover, the Born-charging free energy of solvation for the ion in the two solvents will be nearly the same if their dielectric constants are similar.

Data and Calculations

Free Energies

Values of conventional free energies of solvation have been calculated previously (2, 5, 7). In the light of more recent data and the necessity of using as many experimental values as possible, a recalculation was considered necessary for this work. Aqueous data were taken from circular 500 (12) except for the halogens. The conventions used were those of Noyes (5, 6, 13). Values of ΔG_f^0 for monatomic gas elements were taken from Stull and Sinke (14) and free energies of formation of ions were calculated from the recent ionization potential data of Moore (15) or, in the case of the halogens, from Wagman *et al.* (16).

Minor entropic contributions to the free energies were calculated from the data of Moore (15) or Kelley and King (17); such contributions are of the order of a few kcal/mole and in no case seriously affect the arguments of this work. Data were lacking for the Pt(II) and Rh(III) ionic energy levels (15) and entropic contributions for these species were assumed zero. Liquid ammonia data were taken from compilations of Jolly (18). For aqueous ions, the values of ΔG_{CON}^0 given in Table I correspond closely to those calculated previously (5, 7). The calculation of ΔG_{CON}^0 values in fused LiCl–KCl eutectic at 450 °C was more complex. The values of ΔG_f^0 for the fused salt-solvated ions were calculated from the e.m.f. data tabulated by Plambeck (19, 20). It must be noted that the reference ion in this solvent is not solvated H^+ but solvated Pt(II). Additional corrections for changes in standard states were necessary for lithium and chloride ions, which are solvent constituents, and were made on the assumption of Henrian behavior. The data and conventional free energies of solvation calculated from them are given in Table I for all three solvents.

All free energy calculations were carried out to the nearest cal/mole. This was done to avoid introducing rounding errors into the computer calculation procedure and is not meant to imply that all such figures are significant. The usual significant figures convention is *not* used in this paper and should not be applied to any tabulated data given here; some of the problems in its use have been discussed (21). For most ions, the accuracy of the free energies is probably a few kcal/mole, probably arising primarily in the ionization potentials; a more elaborate discussion is considered to be beyond the scope of this paper. Estimates of error in data compilations are conspicuous by their absence, and the errors involved are more likely to be systematic than random.

Can. J. Chem. Downloaded from www.nrcresearchpress.com by 210.87.254.5 on 09/05/12
For personal use only.

An error in ref. 19 has led to some incorrect values of $\Delta G_{CON}{}^0/z$ in LiCl–KCl in Table I. The correct values are: V^{3+}, 452.447; Cr^{3+}, 467.736; Fe^{3+}, 463.174.

See Fig. 5

TABLE I

Conventional ionic free energies of solvation

Ion	r(Å)	$-\Delta G_{CON}{}^0/z$ H_2O (25°)	NH_3 (25°)	LiCl–KCl (450°)
		Cations of inert gas structure		
H^+	—	363.005	363.005	376.225
Li^+	0.60	226.002	209.589	220.000
Na^+	0.95	200.585	181.596	—
K^+	1.33	183.030	162.564	—
Rb^+	1.48	177.584	158.034	—
Cs^+	1.69	170.276	150.866	—
Be^{2+}	0.31	395.087	378.986	394.612
Mg^{2+}	0.65	330.281	315.786	331.104
Ca^{2+}	0.99	291.128	275.038	—
Sr^{2+}	1.13	275.592	262.992	—
Ba^{2+}	1.35	260.168	244.168	—
Ra^{2+}	1.40	261.324	—	—
Al^{3+}	0.50	471.030	455.030	468.461
Sc^{3+}	0.81	411.777	—	417.692
Y^{3+}	0.93	386.959	—	393.339
La^{3+}	1.15	366.927	—	371.285
Zr^{4+}	0.80	515.370	—	517.710
		Anions of inert gas structure		
H^-	2.08	−17.768	—	−2.316
F^-	1.36	+0.812	−13.908	—
Cl^-	1.81	29.548	16.798	52.628
Br^-	1.95	36.382	21.056	60.738
I^-	2.16	41.433	24.783	64.141
S^{2-}	1.84	−63.212	—	−44.216
Se^{2-}	1.98	−60.006	—	—
Te^{2-}	2.21	−40.851	—	—

Ion	r (Å)	$-\Delta G_{CON}{}^0/z$ H_2O (25°)	NH_3 (25°)	LiCl–KCl (450°)
		Ions of other electronic structure		
Ti^{2+}	0.90	324.278	—	320.928
V^{2+}	0.88	330.567	—	332.332
Cr^{2+}	0.84	332.247	—	338.704
Mn^{2+}	0.80	321.667	307.967	332.178
Fe^{2+}	0.76	332.568	323.918	343.191
Co^{2+}	0.74	339.511	334.361	350.302
Ni^{2+}	0.72	348.558	346.008	354.985
Cu^{2+}	0.74	352.051	350.716	365.580
Zn^{2+}	0.74	344.965	339.873	359.183
Ti^{3+}	0.76	430.022	—	434.896
V^{3+}	0.74	447.558	—	440.661
Cr^{3+}	0.69	462.476	—	456.780
Mn^{3+}	0.66	462.292	—	—
Fe^{3+}	0.64	451.187	446.014	454.156
Co^{3+}	0.63	469.341	474.208	—
Ga^{3+}		470.880	—	474.862
Cu^+	0.96	238.664	242.464	262.009
Ag^+	1.26	216.264	217.199	241.426
Au^+	1.37	249.754	—	273.328
Tl^+	1.40	184.166	170.711	201.821
Pd^{2+}	0.86	340.934	—	364.714
Cd^{2+}	0.97	317.779	311.989	334.842
Sn^{2+}	1.12	288.955	272.818	306.586
Pt^{2+}		353.080	—	374.405
Hg^{2+}	1.10	341.249	325.439	—
Pb^{2+}	1.20	281.810	272.405	300.544
Mo^{3+}		441.092	—	446.548
Rh^{3+}		457.614	—	476.477
In^{3+}	0.81	432.130	—	437.084
Sb^{3+}		—	—	416.431
Tl^{3+}	0.95	428.176	—	—
Bi^{3+}		—	—	404.930

FOR ERRATA SEE Vol. 47, 2219 (1969) ... p. 4293

TABLE II*

Least squares constants for best fit

ΔG_R^0	A	B	C	D	Standard error
		H_2O, 25 °C, 20 ions			
59.100	−40.505				56.2
95.586	−78.189	13.020			8.8
98.615†	−91.850	25.967	−2.737		6.1†
98.488	−83.048	10.613	5.383	−1.304	6.1
		NH_3, 25 °C, 15 ions			
60.482	−36.798				42.2
80.009†	−67.603	10.402			4.9†
80.334	−69.626	12.143	−0.348		5.1
80.083	−78.304	28.435	−9.248	1.452	5.2
		LiCl–KCl, 450 °C, 11 ions			
105.957	−21.694				19.6
115.789	−28.554	2.271			15.7
111.800	−6.514	−18.462	4.359		6.9
114.776†	37.048	−93.654	43.537	−6.222	3.7†

*Units of ΔG_R^0 and standard error are kcal/mole; the constants give kcal/mole when multiplied by r to appropriate power.

†Addition of constants does not improve fit beyond this point; see text.

Other Data

The crystallographic radii given are those of Pauling (22). The radius of Cu^{2+} was assumed equal to that of Zn^{2+} on the basis of their Goldschmidt radii since no Pauling radius was available. Values of dielectric constants of water were taken from Owen *et al.* (23) and of liquid ammonia from Grubb, Chittum, and Hunt (24). No measured value for the dielectric constant of fused LiCl–KCl eutectic is available; the value of 3.0 used was suggested by Van Artsdalen and Jaffe (25). These dielectric constants give the following values of K: H_2O, 25°, 163.908; NH_3, 25°, 156.202; LiCl–KCl, 450°, 110.684 kcal Å/mole.

Calculations

The conventional free energies of solvation and radii for the ions of inert gas electronic structure given in Table I were fitted to eq. [5] by a double-precision least-squares multiparameter computer program (26) used on the University of Alberta IBM 360 computer. The results of these fits are given in Table II. The standard error cited is the square root of the sum of the squares of the deviations of the experimental values of $\Delta G_{CON}^0/z$ divided by the number of degrees of freedom (number of experimental points less number of adjustable parameters). The "best" form of eq. [5], denoted by asterisks in Table II, is shown with the data for each solvent in Figs. 1–3. The "best" equation form was that giving the least

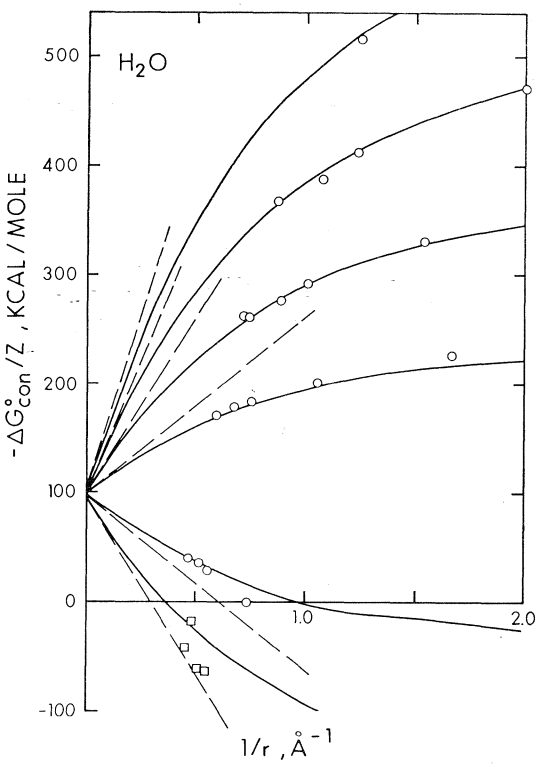

FIG. 1. Plot of $-\Delta G_{CON}^0/z$ against reciprocal radius for water at 25 °C. Dashed lines are those given by the Born equation, solid lines those given by the best form of eq. [5]. Circles, points used in least square fit; squares, other points. Beryllium point omitted for greater horizontal expansion.

Can. J. Chem. Downloaded from www.nrcresearchpress.com by 210.87.254.5 on 09/05/12
For personal use only.

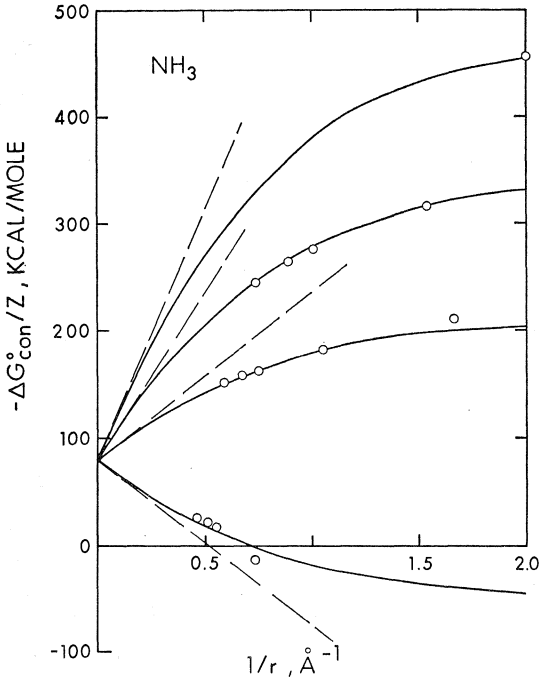

FIG. 2. Plot of $-\Delta G_{CON}{}^{0}/z$ against reciprocal radius for liquid ammonia at 25 °C; as Fig. 1.

standard error in fitting to the inert-gas ion data in that solvent, *provided* that the successively higher terms were actually required as shown by partial F test (27). This was necessary to avoid confusion of the decrease in standard error due to the decrease in degrees of freedom of the system with an actual improvement in fit.

Several alternative forms of eq. [5] have been suggested in the literature, and it appeared desirable to examine them. The present form, in which the free energy of solvation varies with the square of the ionic charge z, is to be preferred to a form in which the free energy of solvation varies directly with ionic charge, because with the present form the empirical constants calculated using only data for ions of unit charge also fitted the data for ions of greater charge, while if a direct dependence on charge were assumed, the data for ions of greater charge could not be fitted using such constants. This is in agreement with the conclusion reached by Laidler (28) that the entropy of solvated ions varies with the square of the ionic charge; the limit approach of the present paper leads to an equation for ionic entropy of solvation of the same form as that for free energy.

In view of the previous use of separate empirical constants for anions and cations (5), it was felt desirable to examine this alternative form of equation. The use of separate anion and cation constants produced less improvement in fit than the introduction of additional terms; e.g., the improvement in fit on the addition of the same term in $1/r^3$ for both was much greater than that produced by using separate anion and cation terms in $1/r^2$. The same result was obtained upon weighting the values for the three largest anions so as to compensate for the disparity in numbers of anion and cation points. If *no* deviation terms were applied to the anions, i.e. the free energies of solvation of anions were calculated using only the Born term and the empirical value of $\Delta G_R{}^0$, a slight improvement in fit appeared for water. However, when the assumption of different anionic and cationic behavior was treated as a decrease of one in the degrees of freedom of the system, a partial F test showed that the improvement is not significant at the 95% confidence level.

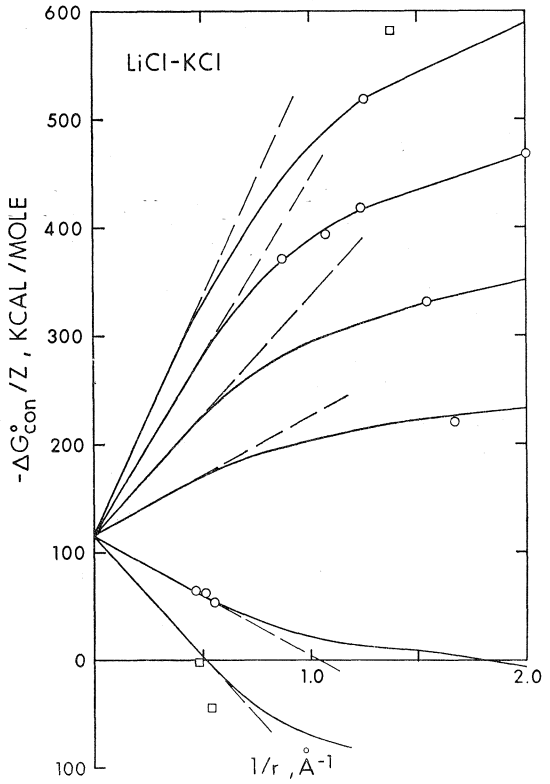

FIG. 3. Plot of $-\Delta G_{CON}{}^{0}/z$ against reciprocal radius for fused LiCl–KCl at 450 °C; as Fig. 1.

Can. J. Chem. Downloaded from www.nrcresearchpress.com by 210.87.254.5 on 09/05/12
For personal use only.

Can. J. Chem. Downloaded from www.nrcresearchpress.com by 210.87.254.5 on 09/05/12
For personal use only.

Use of different forms of eq. [5] for anions and cations appears to be unjustified.

A final possibility is that an equation which is a series in charge/radius ratio might fit the data better than one in radius alone. Attempts were therefore made to fit the data to the equation

$$[6] \quad -\Delta G_{CON}^{0}/z = \Delta G_R^{0} + zK/r \pm z^2A/r^2 \pm z^3B/r^3 \pm \cdots$$

in the same manner as to eq. [5]. The fit was in all cases much worse than that of eq. [5] with the same number of parameters. It is, therefore, concluded that the deviations from the Born term can best be expressed as a series in radius alone. A similar conclusion, expressed in different terms, was reached by Noyes (5). This implies, but does not prove, that the deviation of experimental data from the Born equation can be ascribed solely to the breakdown of the continuum aspect of the model inherent in that equation.

It was also considered desirable to compare the fit of the present model to that obtained from the additive-radius approach of Latimer, Pitzer, and Slansky (3). In the notation of the present paper, such a model is expressed in the equation

$$[7] \quad -\Delta G_{CON}^{0}/z = \Delta G_R^{0} + zK(r + A)$$

where A was considered an empirical constant. The same sets of data used for the fits in Table II were fitted to this equation with the following results. H_2O: ΔG_R^{0}, 100.000 kcal/mole, A, 0.78 Å, (standard error (s.e.), 9.0 kcal/mole). NH_3: ΔG_R^{0}, 82.842 kcal/mole, A, 0.72 Å, (s.e., 10.1 kcal/mole). LiCl–KCl: ΔG_R^{0}, 118.711 kcal/mole, A, 0.40 Å, (s.e., 26.3 kcal/mole). The values of ΔG_R^{0} obtained by this approach are in agreement with those in Table II, but the fit is in all cases poorer than that obtained using the best form of eq. [5]. Use of separate constants for anion and cation radii did not improve the fit beyond the improvement expected for a decrease of one degree of freedom in any of the three solvents. It is, therefore, concluded that attempts to reconcile theory and experiment by adding empirical constants to ionic radii will produce a worse fit than the use of a reciprocal-radius series in the form of eq. [5] and should be avoided.

Discussion

General

As shown in Figs. 1–3, eq. [5] fits the values of conventional free energies of solvation well for each of the three solvent systems investigated. Since these solvents are of widely divergent character it is probable that this approach is applicable to any solvent. In all three solvents the value of ΔG_R^{0} given by the "best" form of the equation is well within one standard error of the value given by the equation with one additional term. Except in the case of liquid ammonia where the "best" equation contains only two empirical power terms, the same is true of the value given by the equation with one fewer term, indicating the relative insensitivity of the calculated ΔG_R^{0} to the number of empirical terms.

Although the ionic radii used throughout this work were Pauling radii, several other sets of ionic radii have been advocated. Identical calculations were therefore made using the Goldschmidt radii, van der Waals radii (9), and an extended set of the Gourary and Adrian radii (29) whose use in ionic solvation has been advocated by Blandamer and Symons (30). In most cases the values of ΔG_R^{0} calculated using any of these sets of radii were well within one standard error of that calculated using the Pauling radii; the values calculated using Gourary and Adrian radii were usually slightly more than one standard error greater than those calculated using any other set. No set of radii consistently gave lower standard errors in all three solvents. On the basis of this work there appears to be no specific set of ionic radii which is particularly applicable to solution thermodynamics of ions.

The points used to establish the empirical constants for each solvent were those for all ions of inert gas structure for which reliable data were available. The electron affinities of the chalcogens are not accurately known (31, 32) and hence these ions were not used in the calculation; nevertheless, they fit the calculated curves quite well, as appears in Figs. 1 and 3. Considerable efforts were made to obtain additional points for ions in the LiCl–KCl system. Unfortunately, Na–Cs, Ca–Ra, and F_2 react with this solvent. The Ti(IV) point shown in Fig. 3 is estimated using the e.m.f. data of Flengas (33) taken in NaCl–KCl at 700 °C, but reported formation of K_2TiCl_6 makes the estimation unreliable. The point for S^{2-} is calculated from e.m.f. data recently obtained in this laboratory, but was not used to establish the parameters due to the inaccurate electron affinity

FOR ERRATA SEE
V. 47 N. 22 1969 P. 4293

Can. J. Chem. Downloaded from www.nrcresearchpress.com by 210.87.254.5 on 09/05/12
For personal use only.

mentioned above; e.m.f. data for O^{2-}, Se^{2-}, and Te^{2-} are not available.

Reference Free Energy of Solvation

For fused LiCl–KCl, the reference ion is Pt(II), and for liquid ammonia and water the reference ion is the hydrogen ion, solvated as they are in infinitely dilute solutions. Although the hydrogen–hydrogen ion standard potential has been measured in the fused salt system (34), the standard state of the ion in this medium is quite different from that in liquid ammonia and water and hence cannot be directly compared among the three media. The standard states for hydrogen ion in water and liquid ammonia are the same, however, and a direct comparison is possible. The difference between the values of the reference free energy of solvation, ΔG_R^0, in water and liquid ammonia is 18.6 kcal/mole from the data of Table II, that in liquid ammonia being less. This is in good agreement with the difference of 22.8 kcal/mole calculable from the e.m.f. series tabulated by Strehlow (11), and in even better agreement with the value of 19.6 kcal/mole calculable from the data in Table I; these are obtained on the basis of his assumption that the free energies of solvation of the rubidium ion are the same in both media. This agreement, well within the error of the present approach, is good but not surprising, since the free energy of solvation for larger ions should approach the reference free energy of solvation in any solvent. The assumption of Strehlow is thus seen to be an approximation to the limit approach of the present paper.

The value of ΔG_R^0 for water can be combined with that given in Table I for the aqueous hydrogen ion to give the free energy of solvation of the hydrogen ion as -264.4 ± 6.1 kcal/mole; the corresponding value for liquid ammonia is -283.0 ± 4.9 kcal/mole. No value for liquid ammonia is available for comparison with this calculation, but the value for the free energy of solvation of hydrogen ion in water of -260.5 ± 0.5 kcal/mole obtained by Randles (35) is in good agreement with the value obtained here.

Ions of Transition Metals

Ions of inert-gas electronic structure can all be considered, to a first approximation, as charged spheres. Their interaction with solvents should then differ only as their charges and/or radii. This cannot *a priori* be assumed for ions whose electronic structure is not that of an inert gas, however, and an examination of such ions is therefore desirable. Sufficient data (Table I) appear to be available to permit a systematic investigation only of the first-row transition elements in water and fused LiCl–KCl eutectic, although the fragmentary available data indicate similar behavior for the second-row transition elements and in liquid ammonia. The difference between the conventional (Table I) free energies of solvation of these ions and those predicted by the "best" least-squares equation for inert-gas ions of the same radii were calculated; in all cases the true free energy of solvation is greater than that predicted by the inert-gas equation, as shown in Figs. 4 and 5. These differences are clearly related to the d electron structure of the ion rather than to the radius, since the double-peaked curve is also obtained for a similar plot obtained on the assumption of constant radius. It must therefore be concluded that the greater energy of solvation of transition metal ions arises from interaction between their d orbitals and the surrounding

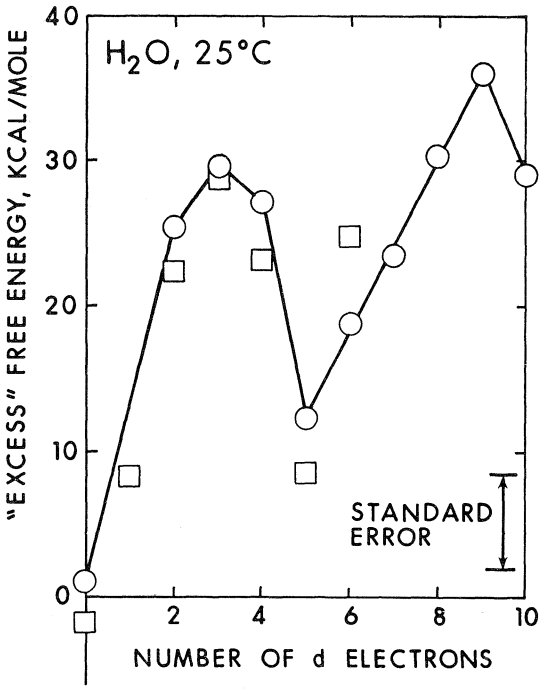

FIG. 4. Plot of "excess" free energy of solvation for first-row transition metal ions in water at 25 °C (see text) against d electronic structure. Circles, dipositive ions; squares, tripositive ions. Ions of d^0 structure used with other inert-gas ions to determine deviation parameters.

ERRATUM

The points for these ions in Fig. 5 should be raised by the difference between th values just given and those in Table I. The pap is not otherwise affected.

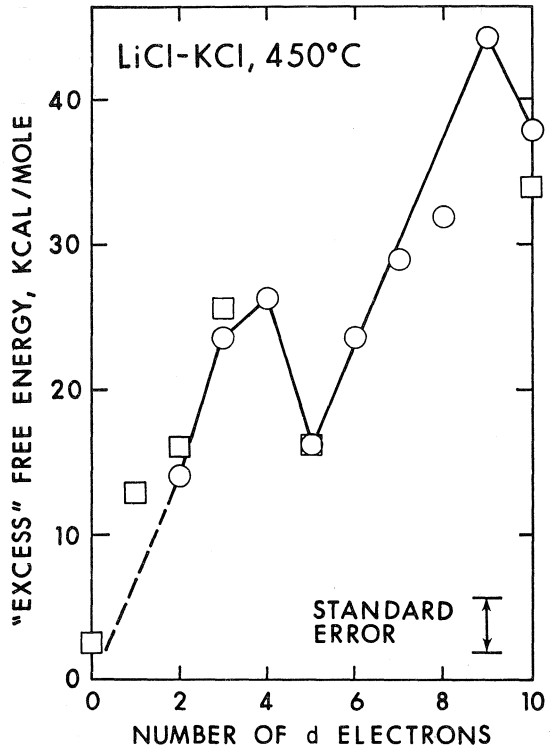

FIG. 5. Plot similar to Fig. 4 except in fused LiCl–KCl eutectic at 450 °C.

solvent molecules. The relation between thermodynamic properties of these ions and their d orbitals has been extensively reviewed (36).

Conclusion

It is concluded that the method of extrapolation to infinite ionic size, previously used in aqueous solution for ions of unit charge, is applicable to two quite different solvents and to polyvalent ions as well. The single-ion free energies of solvation obtained are in good agreement with literature values. Alternative forms of the equation, and the approach of empirically increasing the ionic radius, are examined and shown to be less desirable. Empirical constants included in the equation are interpreted simply as breakdown of the continuum solvent model inherent in the Born equation rather than as having specific physical significance.

Acknowledgments

The author is grateful to the National Research Council of Canada for an Operating Grant in support of this research, to W. D. Ellis for programing assistance, and to K. R. Betty for assistance in hand calculations.

1. M. BORN. Z. Physik, **1**, 45 (1920).
2. D. R. ROSSEINSKY. Chem. Rev. **65**, 467 (1965).
3. W. M. LATIMER, K. S. PITZER, and C. M. SLANSKY. J. Chem. Phys. **7**, 108 (1959).
4. K. J. LAIDLER and C. PEGIS. Proc. Roy. Soc. London, Ser. A, **21**, 80 (1957).
5. R. M. NOYES. J. Am. Chem. Soc. **84**, 513 (1962).
6. R. M. NOYES. J. Am. Chem. Soc. **86**, 971 (1964).
7. L. BENJAMIN and V. GOLD. Trans. Faraday Soc. **50**, 797 (1954).
8. C. L. DE LIGNY and M. ALFENAAR. Rec. Trav. Chim. **84**, 81 (1965).
9. R. H. STOKES. J. Am. Chem. Soc. **86**, 979 (1964).
10. N. A. IZMAILOV. Dokl. Akad. Nauk SSSR, **126**, 1033 (1959).
11. H. STREHLOW. Z. Elektrochem. **56**, 827 (1952); The chemistry of nonaqueous solvents. Vol. I. *Edited by* J. J. Lagowski. Academic Press, Inc., New York. 1966. p. 129.
12. F. D. ROSSINI, D. D. WAGMAN, W. H. EVANS, S. LEVINE, and I. JAFFE. Natl. Bur. Stds. v.s. Circ. 500. v.s. Govt. Printing Office, Washington, D.C. 1952.
13. R. M. NOYES. J. Chem. Educ. **40**, 2 (1963).
14. D. R. STULL and G. C. SINKE. Thermodynamic properties of the elements. Am. Chem. Soc. Washington, D.C. 1956.
15. C. E. MOORE. Atomic energy levels. Natl. Bur. Stds. U.S. Circ. No. 467. U.S. Govt. Printing Office, Washington, D.C. 1947–1958.
16. D. D. WAGMAN, W. H. EVANS, I. HALOW, V. B. PARKER, S. M. BAILEY, and R. H. SCHUMM. Natl. Bur. Stds. U.S. Techn. Note 270–1, 270–2, U.S. Govt. Printing Office, Washington, D.C. 1965, 1967.
17. K. K. KELLEY and E. G. KING. Entropies of the elements and inorganic compounds. Bureau of Mines Bulletin 592. U.S. Govt. Printing Office, Washington, D.C. 1961.
18. W. L. JOLLY. Private communication; J. Chem. Educ. **33**, 512 (1956); U.C.R.L. Report 2201, May, 1953; Chem. Rev. **51**, 351 (1951).
19. J. A. PLAMBECK. J. Chem. Eng. Data, **12**, 77 (1967).
20. J. A. PLAMBECK. Can. J. Chem. **46**, 929 (1968).
21. D. F. DETAR. J. Chem. Educ. **44**, 759 (1967).
22. L. PAULING. The nature of the chemical bond. 3rd ed. Cornell Univ. Press, Ithaca, New York. 1960.
23. B. B. OWEN, R. C. MILLER, C. E. MILNER, and H. L. COGAN. J. Phys. Chem. **65**, 2065 (1961).
24. H. M. GRUBB, J. F. CHITTUM, and H. HUNT. J. Am. Chem. Soc. **58**, 776 (1936).
25. E. R. VAN ARTSDALEN and I. S. YAFFE. J. Phys. Chem. **59**, 118 (1955).
26. D. M. MARQUARDT. Nonlinear least squares program, SDA 3094. Copy modified for IBM 360 available on request to present author.
27. E. S. KEEPING. Introduction to statistical inference. D. Van Nostrand, Co., Inc., Toronto. 1962. pp. 337–341.
28. K. J. LAIDLER. Can. J. Chem. **34**, 1107 (1956).
29. B. S. GOURARY and F. J. ADRIAN. Solid State Phys. **10**, 127 (1960).
30. M. J. BLANDAMER and M. C. R. SYMONS. J. Phys. Chem. **67**, 1304 (1963).
31. D. F. C. MORRIS. Proc. Roy. Soc. London, Ser. A, **242**, 116 (1937).

Can. J. Chem. Downloaded from www.nrcresearchpress.com by 210.87.254.5 on 09/05/12
For personal use only.

32. M. L. HUGGINS and Y. SAKAMOTO. Proc. Phys. Soc. Japan, **12**, 241 (1957).
33. S. N. FLENGAS. Ann. N.Y. Acad. Sci. **79**, 853 (1960).
34. H. A. LAITINEN and J. A. PLAMBECK. J. Am. Chem. Soc. **87**, 1202 (1965).
35. J. E. B. RANDLES. Trans. Faraday Soc. **52**, 1573 (1965).
36. P. GEORGE and D. S. MCCLURE. Progress in inorganic chemistry. Vol. I. *Edited by* F. A. Cotton. Interscience Publishers, Inc., New York. 1959. p. 381 *et seq.*

Can. J. Chem. Downloaded from www.nrcresearchpress.com by 210.87.254.5 on 09/05/12
For personal use only.

Can. J. Chem. Downloaded from www.nrcresearchpress.com by 210.87.254.42 on 09/05/12
For personal use only.

Study of isotopic effects and determination of the quadrupole coupling constant from the nuclear magnetic resonance spectra of monodeuterobenzene in a nematic phase

P. DIEHL AND C. L. KHETRAPAL[1]
Department of Physics, University of Basel, Switzerland

Received October 21, 1968

The proton and the deuteron magnetic resonance spectra of monodeuterobenzene have been studied in the nematic phase of a mixture of 50% 4-methoxybenzylidene-4-amino-α-methyl cinnamic acid-*n*-propyl ester and 50% anisole – azophenyl-*n*-capronate at room temperature.

The proton spectrum is studied as a superposition of three 5-spin sub-spectra due to coupling with one deuteron (spin $I = 1$) and analyzed iteratively as a 7-spin system, treating the deuteron as two spin $\frac{1}{2}$ particles.

The values of the dipole–dipole couplings show minor but significant deviations due to isotopic substitution, from those expected for the regular hexagonal geometry. Two parameters are necessary to define molecular orientation. The ratio of the two orientation parameters is reported.

The ratios $(r_{HD}/r_{HH})_{ortho}$ and $(r_{CH} - r_{CD})/(r_{HH})_{ortho}$ are obtained. They indicate a reduction in the time average value of the C—D bond length compared to the C—H one.

It is suggested that the orientation parameters from the proton spectrum of the molecule are used in order to determine the deuteron quadrupole coupling constant from deuteron magnetic resonance (d.m.r.) spectra of partially deuterated molecules dissolved in the nematic phase. The method is applied to the present case. Its limitations and the sources of errors are discussed.

Canadian Journal of Chemistry, **47**, 1411 (1969)

Introduction

The analysis of the proton magnetic resonance spectra of partially oriented molecules in the nematic phases usually provides information about the molecular geometry. Such studies have attracted the attention of several workers. No work, however, seems to have been reported on the influence of isotopic substitution on such spectra and hence on the molecular geometry. Also, the literature on the d.m.r. spectra of molecules dissolved in the nematic phase is limited (1). On the other hand, since the interaction of the deuteron quadrupole moment with the electric field gradients of the bond through which the deuteron is attached to the molecule, are manifested in the d.m.r. spectra in the nematic phases, such studies are extremely informative. The spectrum of a deuteron in a C—D bond is a doublet, the spacing (Δ) of which is given by

$$[1] \qquad \Delta = \frac{3}{2}\left(\frac{e^2qQ}{\mu_D}\right) \cdot |S_{C-D}|$$

where q is the electric field gradient experienced by the deuteron quadrupole moment Q and S_{C-D} is the degree of orientation of the C—D bond axis. The degree of orientation S_{ij} along the axis joining the two nuclei i, and j is given as follows

$$[2] \qquad D_{ij} = -\frac{h\gamma_i\gamma_j}{4\pi^2 r_{ij}^3} \cdot S_{ij}$$

where D_{ij} is the direct coupling between the two nuclei separated by a distance r_{ij}, and γ is the magnetogyric ratio.

If S is determined from the proton spectrum of the molecule, one can determine the deuteron quadrupole coupling constant $(e^2qQ)/\mu_D$ from the spacing of the d.m.r. spectrum in the nematic phase.

The present paper describes the proton and the deuteron magnetic resonance spectra of monodeuterobenzene oriented in the nematic phase of a mixture of 50% 4-methoxy benzylidene-4-amino-α-methyl cinnamic acid-*n*-propyl ester (**1**) and 50% anisole-azophenyl-*n*-capronate (**2**) at room temperature. The study has been made with a view to understand the effect of one deuterium substitution on the proton spectrum and hence on the molecular geometry, as well as to determine the deuteron quadrupole coupling constant.

Experimental

A 24 mole % solution of monodeuterobenzene obtained from Stohler isotope chemicals was studied in the nematic phase of (**1**) + (**2**) at 27 °C.

[1]Post-doctoral Fellow; on leave from Tata Institute of Fundamental Research, Bombay-5, India.

Can. J. Chem. Downloaded from www.nrcresearchpress.com by 210.87.254.42 on 09/05/12
For personal use only.

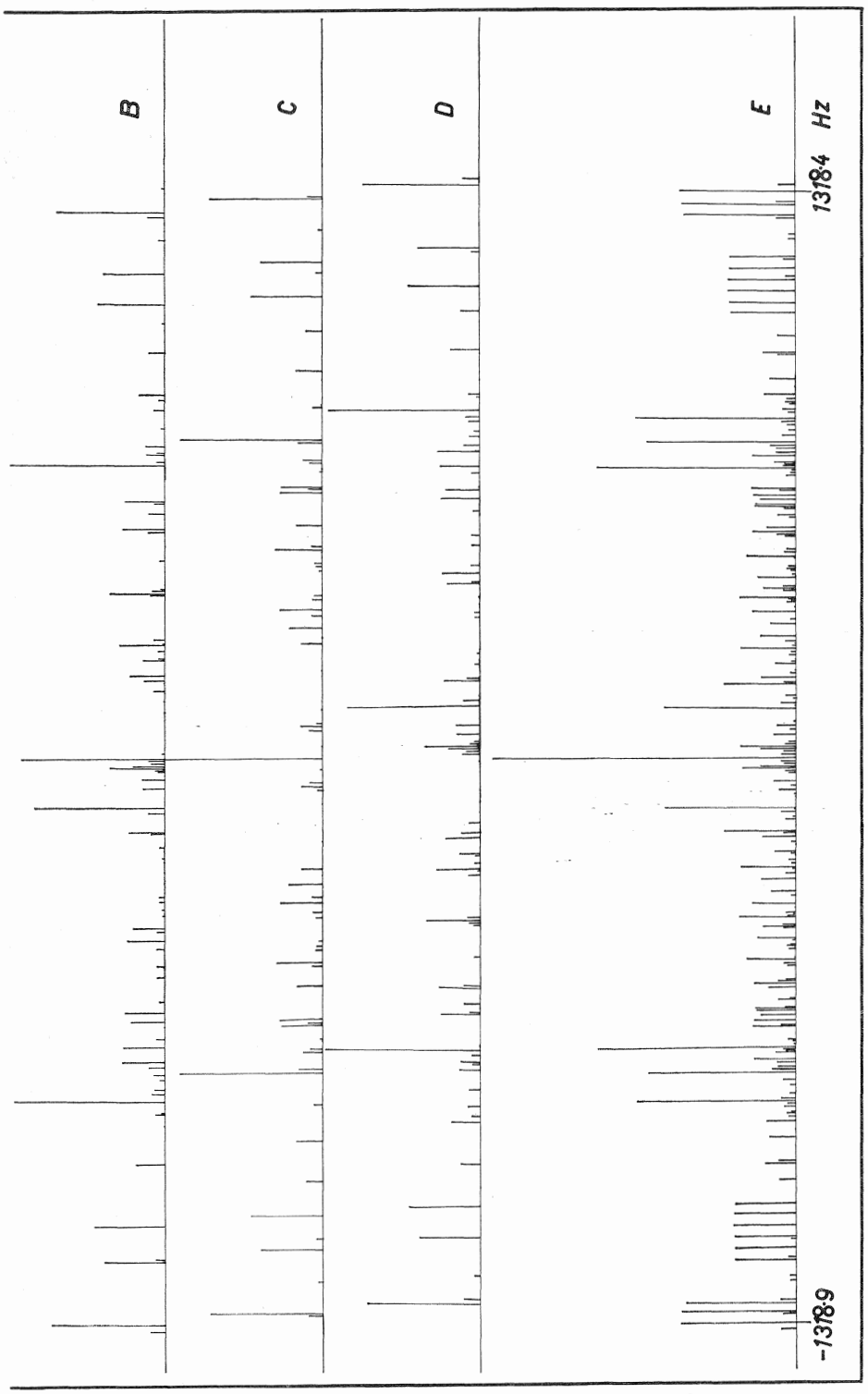

FIG. 1*b*. Proton magnetic resonance spectra of a 24 mole % solution of monodeuterobenzene at 27 °C in the nematic phase (1) and (2). A, the observed spectrum; B, the 5 spin sub-spectrum corresponding to $m(D) = 1$; C, the 5 spin sub-spectrum due to $m(D) = 0$; D, the 5 spin sub-spectrum involving the state $m(D) = -1$; and E, the calculated spectrum (superposition of B, C, and D).

Can. J. Chem. Downloaded from www.nrcresearchpress.com by 210.87.254.42 on 09/05/12
For personal use only.

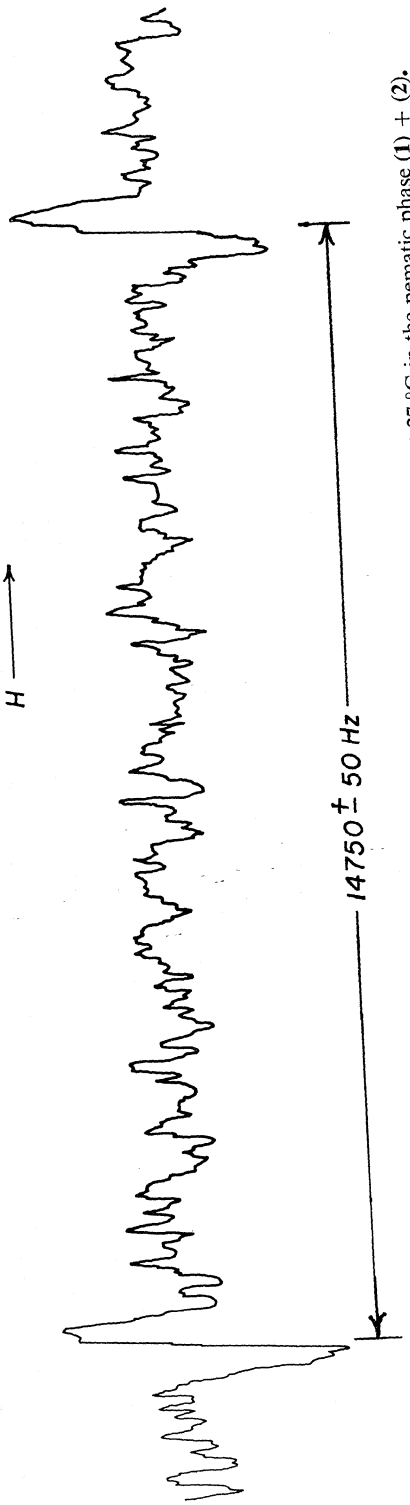

FIG. 2. Deuteron magnetic resonance spectrum of the 24 mole % solution of monodeuterobenzene at 27 °C in the nematic phase (1) + (2).

Can. J. Chem. Downloaded from www.nrcresearchpress.com by 210.87.254.42 on 09/05/12
For personal use only.

TABLE I

The direct couplings, the chemical shifts, the ratios S_{22}/S_{11}, r_{16}/r_{12}, $(r_{CH} - r_{CD})/r_{12}$, and the quadrupole coupling constant in monodeuterobenzene

Parameter	Value* (Hz)	Parameter	Value*
$D_{12} = D_{45}$	-393.7 ± 0.7	$\nu_2 - \nu_1$	0.1 ± 0.3 Hz
$D_{23} = D_{34}$	-396.1 ± 0.4	$\nu_3 - \nu_1$	0.4 ± 0.4 Hz
$D_{16} = D_{56}$	-61.5 ± 0.7	S_{22}/S_{11}	0.992 ± 0.004
$D_{13} = D_{35}$	-76.4 ± 0.4	r_{16}/r_{12}	0.996 ± 0.004
$D_{26} = D_{46}$	-11.6 ± 0.3	$(r_{CH} - r_{CD})/r_{12}$	0.008 ± 0.008
$D_{14} = D_{25}$	-50.3 ± 0.5	(e^2qQ/μ_D)	196.5 ± 1.3 kHz
D_{24}	-75.5 ± 0.5		
D_{15}	-76.3 ± 2.1		
D_{36}	-6.9 ± 0.3		

*The errors of the parameters given are larger than the most probable values. They are defined under section Analysis of the proton spectrum.

The proton spectrum was recorded on a Varian spectrometer HA60 operating in the field sweep mode without lock. The statistical error in the measurement of line positions (side band technique) was ± 1.5 Hz. The average line width was 8 Hz.

The d.m.r. spectrum was studied in the same sample and at the same temperature at 7.65 MHz in the absorption mode with 40 Hz modulation.

Results and Discussion

Analysis of the Proton Spectrum

The proton spectrum is shown in Fig. 1.

The spectrum is a superposition of three 5-spin sub-spectra due to coupling with one deuteron ($I = 1$) with equal coupling constants but different effective Larmor frequencies. The various effective Larmor frequencies are $(2D_{HD} + J_{HD})$, 0, and $-(2D_{HD} + J_{HD})$ corresponding to the states with $m(D) = +1$, 0, and -1 of the deuteron, on the assumption that a deuterium substitution does not produce a detectable chemical shift between the ortho, meta, and para protons. The various sub-spectra were first computed on the basis of a 6-fold symmetry in the molecule, i.e. with only one S-value. It was then possible to identify lines corresponding to each sub-spectrum. An iterative analysis of the whole spectrum was then carried out as a 7-spin system treating the deuteron as two spin $\frac{1}{2}$ particles. The known J-values (2) ($J_{HD} = (\gamma_D/\gamma_H)J_{HH}$) and the LAOCOONOR program (3) on a UNIVAC 1107 computer were used for the analysis. The intensity of each line of the zero spin state sub-spectrum had to be halved in order to obtain the real spectrum. The root-mean-square error between the observed and the calculated line positions was 1.5 Hz. The calculated spectrum is shown (E) in Fig. 1*b* and the values of the parameters are given in Table I. Using these parameters the sub-spectra were calculated and are reproduced in B, C, and D of Fig. 1.

The signs of the direct and the indirect couplings are found to be opposite to each other. Since the indirect couplings in benzene are known to be positive, the sign of the direct ones must be negative. This corresponds to the fact that the molecule orients preferentially with its plane along the direction of the magnetic field.

The errors of the various parameters, reported in Table I, are not the most probable ones given by the computer program, but are larger. They were estimated by changing all the observed line positions by ± 1.5 Hz, the accuracy of the measurement, in such a way that the position of each line deviated from the calculated by the maximum possible amount. Using these values, the spectrum was again iteratively calculated. The difference between the values of the parameters thus obtained and those obtained before was taken as the error.

Influence of Deuterium Substitution

Table I indicates that the value of D_{12} is not equal to that of D_{23}, and both of these are smaller than $D_{16} \cdot (\gamma_H/\gamma_D)$ $(-400.6 \pm 4.5$ Hz) where $\gamma_H/\gamma_D = 6.5144$. This corresponds to deviations from a regular hexagonal geometry of the molecule. As a consequence of the effective C_{2v} symmetry, two orientation parameters S_{11} and S_{22} (Fig. 1) are necessary to specify the molecular orientation. They are related to D_{12}, D_{23}, and the ortho proton–proton distance in benzene by eqs. [3] and [4]

$$[3] \qquad D_{12} = -\frac{h\gamma_H^2}{4\pi^2 r_{12}^3} S_{22}$$

Can. J. Chem. Downloaded from www.nrcresearchpress.com by 210.87.254.42 on 09/05/12
For personal use only.

$$[4] \quad (D_{23} - \tfrac{1}{4}D_{12}) = -\frac{3}{4}\frac{h\gamma_H{}^2}{4\pi^2 r_{12}{}^3} S_{11}$$

$$[5] \quad (S_{22}/S_{11}) = \frac{3}{4}\frac{D_{12}}{(D_{23} - \tfrac{1}{4}D_{12})}$$

S_{11} and S_{22} can be determined individually but with relatively low precision from the known $[(r_{HH})_{ortho}]$ in benzene (2.481 ± 0.005 Å) (4). However, S_{22}/S_{11} is independent of $(r_{HH})_{ortho}$ (eq. [5]) and can, therefore, be determined quite precisely. The value is included in Table I. S_{22}/S_{11} is significantly different from unity (1%). The results indicate that the deuterium substitution reduces the orientation.

If it is assumed that a deuterium substitution does not change the carbon ring geometry and the geometry of the remaining 5 protons in deuterobenzene, the relations between the ratios of the various H—D distances to r_{12} and the direct couplings are given by eqs. [6] and [7].

$$[6] \quad (\gamma_H/\gamma_D)D_{i6}(r_{i6}/r_{12})^5 = \left\{\left(\frac{r_{i6}}{r_{12}}\right)^2 - 0.75\right\} \times D_{12} + (D_{23} - \tfrac{1}{4}D_{12})$$

where $i = 1$ or 2

$$[7] \quad (\gamma_H/\gamma_D)D_{36}(r_{36}/r_{12})^3 = D_{12}$$

Equation [8] allows one to obtain $(r_{CH} - r_{CD})/r_{12}$ as a function of H—D and H—H distances

$$[8] \quad \frac{(r_{CH} - r_{CD})}{r_{12}} = \left\{0.5 - \left[\left(\frac{r_{16}}{r_{12}}\right)^2 - 0.75\right]^{\frac{1}{2}}\right\}$$

The derivation of eqs. [6]–[8] is straightforward from eqs. [4] and [5] and the angles θ and φ (defined in Fig. 1). These angles, in turn, can be expressed in terms of r_{12} and r_{i6}.

Equations [6] and [7] do not provide the values of r_{26}/r_{12} and r_{36}/r_{12}, respectively, with any reasonable precision because of the larger uncertainties of D_{26} and D_{36}. However, eqs. [6] and [8] give (r_{16}/r_{12}) and $(r_{CH} - r_{CD})/r_{12}$ values with reasonable accuracy (Table I). The results indicate a slight reduction of the time average value of the C—D bond length compared to C—H. This is in agreement with results obtained from different spectroscopies (4–6).

Deuteron magnetic resonance spectrum

The spectrum is shown in Fig. 2. It is essentially a doublet caused by the quadrupole interaction (Δ = 14 750 ± 50 Hz). Each component of the doublet is broadened due to the unresolved H—D couplings and is actually an envelope of several lines. Using eq. [1] and the S_{22} value calculated on the basis of $r_{12} = 2.481 \pm 0.005$ Å (4), a value of the quadrupole coupling constant equal to 196.5 ± 1.3 KHz is obtained. The value is more accurate than the one determined from spin–lattice relaxation studies and from d.m.r. of polycrystalline benzene-d_6 (7, 8). The above uncertainty of 1.3 KHz arises mainly from the uncertainty of r_{12}. If r_{12} can be measured more precisely, the accuracy of the quadrupole coupling constant measurement can be increased.

An obvious limitation of the present method of determination of the quadrupole coupling constant is the condition that the molecule must contain a sufficient number of protons so that the orientation parameters can be determined. The limitation can be overcome at the cost of precision. The present example demonstrates that the isotopic substitution reduces the orientation by about 1% only. One can, therefore, use a mixture of fully deuterated and undeuterated molecules for such a study. The proton spectrum in the mixture will provide the orientation parameters which can be used for the calculation of the quadrupole coupling constants from the d.m.r. spectra. If, in future, more is known about the isotopic effects on the molecular orientation, it may be possible to improve the accuracy of the measurements by taking into account these effects.

Acknowledgments

The authors are grateful to the Swiss National Foundation for the Advancement of Science for financial support.

1. J. C. Rowell, W. D. Phillips, L. R. Melby, and M. Panar. J. Chem. Phys. **43**, 3442 (1965).
2. J. M. Read, R. E. Mayo, and J. H. Goldstein. J. Mol. Spectry. **21**, 235 (1966).
3. P. Diehl, C. L. Khetrapal, and H. P. Kellerhals. Mol. Phys. **15**, 333 (1968).
4. A. Langseth and B. P. Stoischeff. Can. J. Phys. **34**, 350 (1956).
5. L. Nygaard, I. Bojesen, T. Pedersen, and J. R. Andersen. J. Mol. Structure, **2**, 209 (1968).
6. V. W. Laurie and D. R. Herschbach. J. Chem. Phys. **37**, 1687 (1962).
7. D. E. Woessner. J. Chem. Phys. **40**, 2341 (1964).
8. E. R. Andrew and R. G. Eades. Proc. Roy. Soc. London, Ser. A, **218**, 537 (1953).

Can. J. Chem. Downloaded from www.nrcresearchpress.com by 210.87.254.42 on 09/05/12
For personal use only.

Proton magnetic resonance investigation of the system zinc perchlorate – methanol: evidence for the association of zinc and perchlorate ions

S. A. AL-BALDAWI AND T. E. GOUGH[1]
Department of Chemistry, University of Waterloo, Waterloo, Ontario
Received May 22, 1968

The proton magnetic resonance spectrum of the system zinc perchlorate – methanol is reported for a range of sample concentrations and temperatures. The results are interpreted in terms of association between the zinc and perchlorate ions, and the various features of the spectrum discussed in terms of this interaction. From the temperature-dependence of line-widths, $E_a = 14 \pm 2$ kcal mole^{-1} and $\log_{10} A = 16 \pm 3$ are estimated for the molecular exchange of methanol from the solvation shell of zinc into the bulk solvent.

Canadian Journal of Chemistry, 47, 1417 (1969)

Can. J. Chem. Downloaded from www.nrcresearchpress.com by 210.87.254.42 on 09/05/12
For personal use only.

Introduction

Nuclear magnetic resonance (n.m.r.) has been used by many workers in the study of electrolyte solutions, and recent reviews (1, 2) may be used as a key to the existing literature. Of particular interest is the fact that, under suitable conditions, it is possible to observe a separate resonance for solvent molecules bound into the primary solvation shell of various cations, and hence to determine the primary solvation number of these cations. With one exception (3) the reported primary solvation numbers are close to 6 (4–9); a value of 5 has been reported for the magnesium ion in liquid ammonia (3), but the authors discount ionic association as the factor responsible for this result. We report here the results of such studies performed on solutions of zinc perchlorate in methanol.

The stereochemistry of zinc is complicated; coordination numbers of 4 (10–12), 5 (13, 14), and 6 (10, 11, 15) have been reported. However, it appears that the aquo-zinc ion is octahedral both in the solid state (16) and in solution (17); accordingly, it is reasonable to expect a primary solvation number of 6 for the zinc ion in methanol.

Raman spectra of aqueous solutions of several perchlorates give no indication of perchlorate complexes (18), while the Raman spectra of aqueous solutions of zinc nitrate show that contact ion-pair formation does not occur unless the molar ratio of water to zinc is less than 6:1 (19). However, conductivity vs. concentration plots for zinc perchlorate in 50–50 methanol–acetone are non-linear and at reduced temperatures exhibit a maximum (20), suggesting that zinc perchlorate ion-pairs may be detectable in anhydrous media.

[1]To whom correspondence should be addressed.

Experimental

Preparation of Solutions

Anhydrous methanol was prepared by the method of Grunwald, Jumper, and Meiboom (21); anhydrous zinc perchlorate was prepared by heating zinc perchlorate hexadioxanate (22) *in vacuo* at 120 °C for a few hours. Solutions of zinc perchlorate in methanol were prepared on the vacuum line and a portion sealed into an n.m.r. tube; the remainder of the sample was quantitatively analyzed for zinc using EDTA and Eriochrome Black indicator (23).

As a check on the anhydrous nature of the zinc perchlorate hexadioxanate, n.m.r. spectra of a 0.6 *M* solution of this compound in acetone were recorded. The addition of the salt caused no detectable increase in the intensity of the resonance attributed to residual water in the acetone; however, the addition did cause a marked downfield shift of this resonance confirming its assignment as being due to residual water. We estimate an upper limit of 0.1 molecule of water per zinc to be present in the zinc perchlorate hexadioxanate.

Recording of n.m.r. Spectra

Nuclear magnetic resonance spectra were recorded on a J.E.O.L. C-60 spectrometer and were individually calibrated using audio-frequency side-bands generated by a JNM-SD-20B spin decoupler. The resonance of the methyl protons was used as an internal reference. The temperature of the sample was controlled by a JES VT2 unit modified by the inclusion of a Thermovolt relay operated by a thermocouple placed adjacent to the sample. Sample temperatures were determined by measuring the chemical shift between the methyl and hydroxyl protons of a sample of pure methanol, prepared as above. This shift, δ c.p.s., was converted to temperature, T °C, by means of the equation $T = 1.95\ (106 - \delta)$.

Results

Proton magnetic resonance spectra of solutions of zinc perchlorate in methanol were recorded for

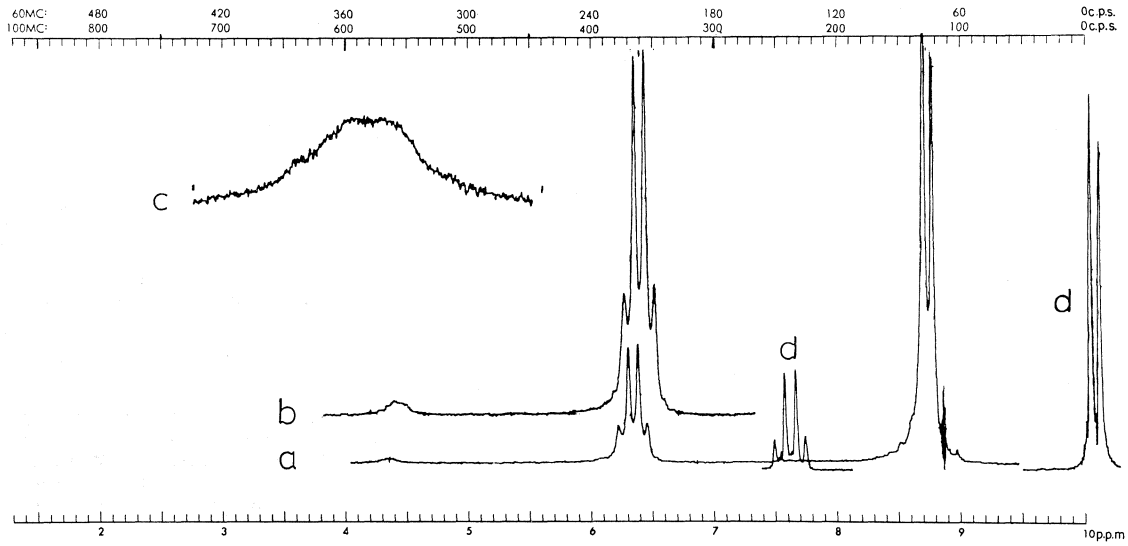

FIG. 1. (*a*) Proton magnetic resonance spectrum at 60 Mc/s of a 0.25 *M* solution of zinc perchlorate in methanol at −83 °C; (*b*) magnified spectrum of the hydroxyl region; (*c*) expanded (×5) spectrum of the bound hydroxyl resonance; (*d*) reference spectrum of pure methanol.

15 solute concentrations, up to 1.8 *M*, at sample temperatures from −90 to +30 °C.

At the highest sample temperature studied, both the methyl and hydroxyl proton resonances were singlets. Decreasing the sample temperature to −50 °C sufficiently slowed down proton exchange reactions for spin–spin splitting between the methyl and hydroxyl protons to be observed, although the high viscosity of the more concentrated samples precluded the resolution of these splittings. Further decrease in temperature caused the hydroxyl proton resonance to broaden asymmetrically to low fields and finally to split into two discrete absorptions; for the most dilute sample, spin–spin splitting with the methyl protons could be seen for both hydroxyl proton resonances (see Fig. 1).

The relative area of the lower field hydroxyl proton resonance increased with increase in the concentration of zinc perchlorate, and we therefore attribute this resonance to methanol molecules participating in the solvation shell of the zinc ion. For convenience, we refer to these solvating methanol molecules as "bound". From measurements of the relative areas of the two hydroxyl proton resonances and of the concentration of zinc perchlorate, estimates were made of the average number of methanol molecules bound to each zinc ion. In Fig. 2, this solvation

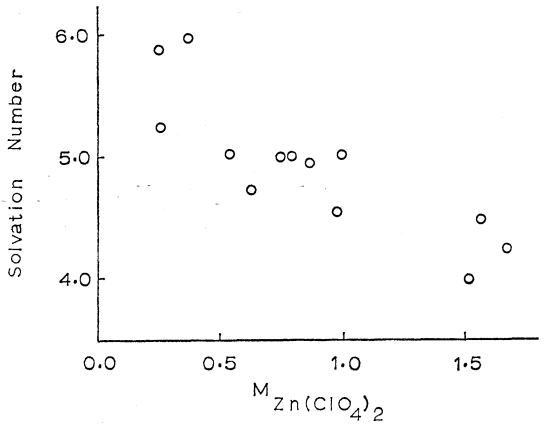

FIG. 2. The dependence of the solvation number of zinc upon solute molarity for solutions of zinc perchlorate in anhydrous methanol. Sample temperature −82 °C.

number is plotted against the concentration of zinc perchlorate. In Fig. 3, the chemical shift of the bound hydroxyl protons is also plotted as a function of the concentration of zinc perchlorate, the sample temperature (−82 °C) being the same as that for the results in Fig. 2. Both this chemical shift and the solvation number were found to show considerable, and similar dependence upon the concentration of zinc perchlorate. In Fig. 4, once again for the same sample temperature of

Can. J. Chem. Downloaded from www.nrcresearchpress.com by 210.87.254.42 on 09/05/12
For personal use only.

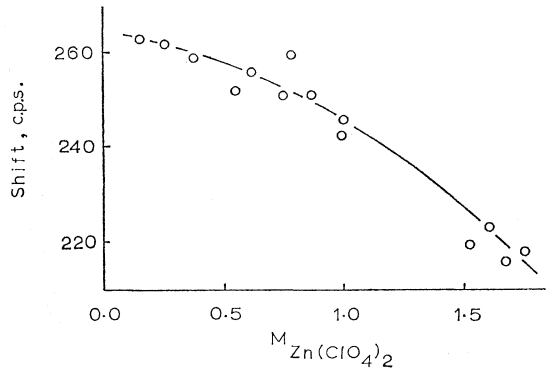

FIG. 3. The dependence of the chemical shift of cationically-bound hydroxylic protons upon solute molarity for solutions of zinc perchlorate in anhydrous methanol. Shifts are in c.p.s. downfield from the methyl proton's resonance. Sample temperature −82 °C.

−82 °C, the chemical shift of the remaining hydroxyl protons is plotted as a function of the concentration of zinc perchlorate.

In Fig. 5, the average chemical shift of the hydroxylic protons is plotted as a function of the concentration of zinc perchlorate for a range of sample temperatures. For the plot at −82 °C the results were obtained by calculating the weighted average of the two observed hydroxyl resonances; at the remaining temperatures exchange reactions performed this averaging and only one hydroxyl resonance was observed. At high temperatures,

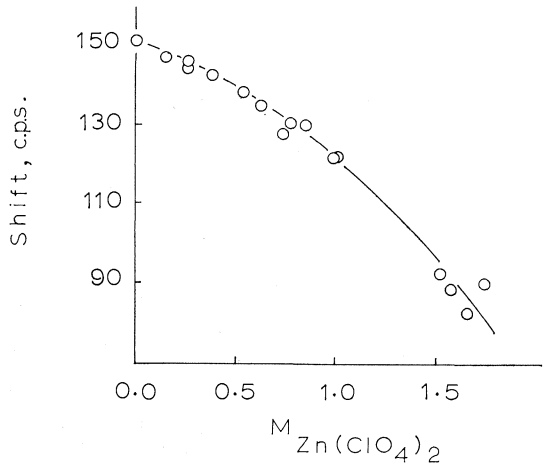

FIG. 4. The dependence of the chemical shift of bulk hydroxylic protons upon solute molarity for solutions of zinc perchlorate in anhydrous methanol. Shifts are in c.p.s. downfield from the methyl proton's resonance. Sample temperature −82 °C.

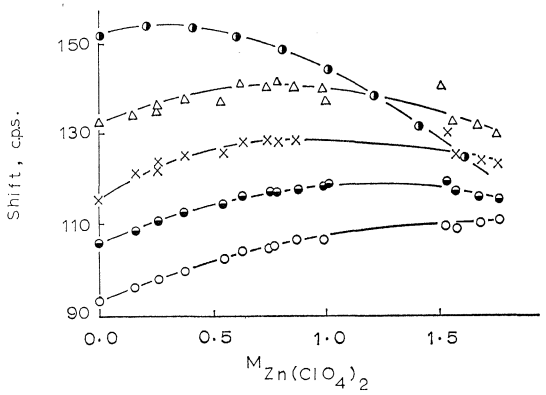

FIG. 5. The dependence of the average chemical shift of hydroxylic protons upon solute molarity for solutions of zinc perchlorate in anhydrous methanol. Shifts are in c.p.s. downfield from the methyl proton's resonance. Sample temperatures: ○, 27 °C; ◒, 0 °C; ×, −25 °C; △, −50 °C; ◑, −82 °C.

the addition of zinc perchlorate to methanol shifts the hydroxyl resonance to low fields. However, at higher concentrations and lower temperatures the addition of zinc perchlorate causes a high field shift of this resonance.

Correlation times for the exchange of methanol from the solvation shell of zinc into the bulk solvent were obtained by comparing the line shapes of the experimental spectra with the spectra computed using the expression of Gutowsky and Saika (24). In computing these spectra it was assumed that each methanol exchanged molecularly (5) with no change in its nuclear spin quantum numbers. Hence, each hydroxyl resonance was simulated as a quartet even though this structure was not always resolvable. It was further assumed that the transverse relaxation times of the methyl and of both kinds of hydroxyl protons were all equal; for each set of experimental conditions the value of this parameter was then evaluated by comparison of the observed line shape of the methyl protons with those calculated for a doublet of Lorentzian lines using several trial values of the transverse relaxation time. The reciprocals of the exchange correlation times obtained at several temperatures were fitted to the Arrhenius equation, and hence values of the energy of activation and the frequency factor for the removal of a methanol molecule from the solvation shell of zinc were obtained (Table I). The average values obtained were $E_a = 14 \pm 2$ kcal/

Can. J. Chem. Downloaded from www.nrcresearchpress.com by 210.87.254.42 on 09/05/12
For personal use only.

TABLE I

Activation energies and frequency factors for the removal of a methanol molecule from the solvation shell of the zinc ion

Solute molarity	E_a	$\log_{10} A$
0.25	12.1	13.1
0.62	16.0	18.1
0.78	13.3	15.4
1.10	15.7	19.0

mole, $\log_{10} A = 16 \pm 3$; the large scatter in $\log_{10} A$ is caused by the small range of temperatures over which significant line-width effects were observable, coupled with the long extrapolation required to evaluate this parameter.

Discussion

From Fig. 2 it can be seen that as the concentration of zinc perchlorate is increased, the primary solvation number of zinc decreases, approximately from 6 to 4. The concentration of zinc perchlorate in these samples is too low for this decrease to be interpreted in terms of competition between zinc ions for the available methanol molecules; therefore, the decrease is attributed to the progressive displacement of methanol, by perchlorate from the solvation shell of zinc. This modification of the environment of the zinc ion is also reflected in the dependence of the chemical shift of the bound hydroxylic protons upon concentration (Fig. 3). If the zinc ion were not to experience any interaction with the perchlorate ion, then the chemical shift of hydroxyl groups bound to the zinc ion should be independent of the concentration of zinc perchlorate; such is not the case. As the concentration of zinc perchlorate is increased, the resonance of the bound hydroxylic protons shifts to higher fields. This shift is compatible with a decrease in the cationic character of the zinc ion brought about by association between it and perchlorate ions. The resonance of the non-bound hydroxylic protons also shifts to higher fields as the concentration of zinc perchlorate is increased (Fig. 4).

The plots in Fig. 5 show the concentration dependence of the average value of the chemical shift of all the hydroxylic protons in the sample, and are thus equivalent to previous studies performed on aqueous solutions of electrolytes (25–27). The curvature of these plots also indicates the presence of associated zinc species in methanol, and the concentration at which the plots begin to break may be taken as the concentration at which association becomes appreciable. As might be expected, a decrease in temperature decreases the concentration at which significant association occurs.

Values obtained for E_a of the removal of methanol from the solvation shell of zinc were not sufficiently precise for the evaluation of any trend in this parameter with changes in concentration. Hence, we are unable to determine the effect on E_a of the introduction of a perchlorate ion into the solvation shell of zinc. The value of 14 ± 2 kcal/mole is similar to the 16.7 kcal/mole previously observed for the removal of methanol from the solvation shell of magnesium (5). This similarity may be taken as supporting evidence for the applicability of the postulated exchange model and the associated Bloch equations.

The value obtained for $\log_{10} A$, 16 ± 3, is extremely high and would seem to rule out a bimolecular rate determining step in the mechanism whereby methanol is exchanged between the bulk and bound regions. Thus the mechanism of this exchange, like that of the magnesium perchlorate – methanol system (5), must involve a unimolecular, rather than a pseudo-unimolecular, rate-determining step. Similar unimolecular mechanisms have been postulated to interpret the kinetics of solvent and ligand exchange reactions studied in aqueous solution by relaxation techniques (28).

To interpret our experimental data, we are led to postulate the existence, in solutions of zinc perchlorate in anhydrous methanol, of the species $[Zn(MeOH)_6]^{2+}$ and $[Zn(MeOH)_4(ClO_4)_2]$; in addition, the presence of $[Zn(MeOH)_5(ClO_4)]^{+}$ would seem reasonable, though this species is not essential to our interpretation.

Acknowledgments

We thank the National Research Council of Canada for operating funds, and the Gulbenkian Foundation, through the Iraqui Government, for a scholarship to S. A. Al-B.

1. J. F. Hinton and E. S. Amis. Chem. Rev. **67**, 367 (1967).
2. J. Burgess and M. C. R. Symons. Quart. Rev. London, **22**, 276 (1968).
3. T. J. Swift and H. H. Lo. J. Am. Chem. Soc. **89**, 3988 (1967).

Can. J. Chem. Downloaded from www.nrcresearchpress.com by 210.87.254.42 on 09/05/12
For personal use only.

4. J. H. SWINEHART and H. TAUBE. J. Chem. Phys. **47**, 1579 (1962).
5. S. NAKAMURA and S. MEIBOOM. J. Am. Chem. Soc. **89**, 1765 (1967).
6. Z. LUZ and S. MEIBOOM. J. Chem. Phys. **40**, 1058, 1066, 2682 (1964).
7. A. FRATIELLO and D. P. MILLER. Mol. Phys. **11**, 37 (1966).
8. A. FRATIELLO and D. P. MILLER. Mol. Phys. **12**, 111 (1967).
9. A. FRATIELLO, R. E. LEE, V. M. NISHIDA, and R. E. SCHUSTER. J. Chem. Phys. **47**, 4951 (1967).
10. I. LINDQUVIST and B. STRANDBERG. Abstracts. Proc. Intern. Conf. Coord. Chem. Stockholm and Upsala, Sweden, 47 (1962).
11. C. C. ADDISON and D. SUTTON. Prog. Inorg. Chem. **8**, 25 (1967).
12. B. J. HATHAWAY and D. G. HOLAH. Abstracts. Proc. Intern. Conf. Coord. Chem. Stockholm and Upsala, Sweden, 47 (1962).
13. P. L. ORIOLI, M. DIVAIRA, and L. SACCONI. Chem. Commun. 103 (1965).
14. D. A. BRISBIN and R. J. BALAHURA. Can. J. Chem. **44**, 2157 (1966).
15. M. NORDALLI, G. FAVA, and G. GIRALDI. Abstracts. Proc. Intern. Conf. Coord. Chem. Stockholm and Upsala, Sweden, 211 (1962).
16. A. FERRARI, A. BRIABANTI, A. M. MANOTTI LANFREDI, and A. TIRIPICCHIO. Acta Cryst. **22**, 240 (1967).
17. D. E. IRISH, B. MCCARROLL, and T. F. YOUNG. J. Chem. Phys. **39**, 3436 (1963).
18. R. E. HESTER and R. A. PLANE. Inorganic Chem. **3**, 769 (1964).
19. D. E. IRISH, A. R. DAVIS, and R. A. PLANE. J. Chem. Phys. In press.
20. P. G. SEARS, W. W. WHARTON, and L. R. DAWSON. J. Electrochem. Soc. **102**, 430 (1955).
21. E. GRUNWALD, C. F. JUMPER, and S. MEIBOOM. J. Am. Chem. Soc. **84**, 4664 (1962).
22. L. I. CHUDNOVA. Zh. Neorgan. Khim. **10**, 1300 (1965).
23. A. I. VOGEL. Textbook of quantitative inorganic analysis. John Wiley and Sons, Inc., New York. 1967.
24. H. S. GUTOWSKY and A. SAIKA. J. Chem. Phys. **21**, 1688 (1953).
25. J. N. SHOOLERY and B. J. ALDER. J. Chem. Phys. **23**, 805 (1955).
26. B. P. FABRICAND and S. GOLDBERG. J. Chem. Phys. **34**, 1624 (1961).
27. J. C. HINDMAN. J. Chem. Phys. **36**, 1000 (1962).
28. M. EIGEN and L. DEMAEYER. Technique of organic chemistry. Vol. VIII. Part II. *Edited by* A. Weissberger. Interscience Publishers, Inc., New York. 1961. Chap. 18.

Can. J. Chem. Downloaded from www.nrcresearchpress.com by 210.87.254.42 on 09/05/12
For personal use only.

Organoantimony compounds. I. Infrared spectra of some trimethyl- and triphenyl-antimony derivatives[1]

R. G. GOEL[2], AND (IN PART) P. N. JOSHI[3], D. R. RIDLEY[4], AND R. E. BEAUMONT[4]
Departments of Chemistry, St. Francis Xavier University, Antigonish, Nova Scotia
AND
University of Guelph, Guelph, Ontario

Received September 12, 1968

Organoantimony compounds of the type R_3SbX and $(R_3Sb)_2OX$, where R is methyl or phenyl, and X is a bivalent anionic group such as SeO_4, CrO_4, or C_2O_4, have been prepared. Structural characteristics of these compounds have been determined by studying their infrared spectra in the solid state between 4000 and 250 cm^{-1}. The spectral results indicate that in both types of compounds the anion X is co-ordinated to the R_3Sb or (R_3Sb—O—SbR_3) group resulting in non-ionic, five coordinate, polymeric structures.

Canadian Journal of Chemistry, 47, 1423 (1969)

Can. J. Chem. Downloaded from www.nrcresearchpress.com by 210.87.254.6 on 09/05/12
For personal use only.

Introduction

Structural aspects of trialkyl- and triphenyl-antimony(V) derivatives, R_3SbY_2, such as halides, nitrates, and carboxylates have been investigated by several workers (1–8). These compounds are covalently constituted, with trigonal bipyramidal structures in which the organic groups occupy equatorial positions. They are monomeric when dissolved in non-polar organic solvents. A few trimethylantimony derivatives of the type R_3SbX, where X is a bivalent anion, have also been studied by Clark and one of the present authors (1). Unlike the corresponding dihalides, dinitrates, or dicarboxylates, these compounds do not dissolve in non-polar solvents. However, infrared (i.r.) spectral studies (1) indicate that these compounds also have non-ionic five coordinate structures possibly involving bridging anion groups and planar trimethylantimony groups. Similar conclusions have been drawn by Doak *et al.* (4) for triphenylantimony sulfate and oxybis(triphenylantimony)sulfate. In continuation of our studies on organoantimony compounds we have prepared several new derivatives of the type R_3SbX and $(R_3Sb)_2OX$ and have examined their structural aspects by i.r. spectroscopy in the 4000 to 250 cm^{-1} region.

[1]Presented in part at 51st Annual Conference of Chemical Institute of Canada, Vancouver, June 5, 1968.
[2]To whom enquiries should be addressed at the Department of Chemistry, University of Guelph, Guelph, Ontario.
[3]Summer Research Assistant, St. Francis Xavier University, 1967.
[4]Summer Research Assistant, University of Guelph, 1968.

Experimental

Compounds of the type R_3SbX were prepared by reacting trimethyl- or triphenyl-antimony dichloride or dibromide with the appropriate silver salt in the solvent indicated in Table I. $(R_3Sb)_2OX$ derivatives were prepared in a similar manner by the reaction of oxybis(trimethyl- or triphenyl-antimony)dichloride or dibromide and the silver salt. The solvent was removed under vacuum except where preparations were performed in aqueous solutions. In each case the final product was dried under vacuum. Trimethyl- or triphenyl-antimony dichloride or dibromide and corresponding oxybis dihalides were prepared according to methods described in the literature (1, 2, 4). Elemental analyses were performed by Dr. A. B. Gygli, Microanalytical Laboratory, Toronto, or by the Schwarzkopf Microanalytical Laboratory, New York. Analytical data are recorded in Table I.

Infrared spectra were recorded on a Perkin–Elmer model 521 spectrophotometer. Samples were prepared as mulls in Nujol, hexachlorobutadiene, or halocarbon oil, and then placed between plates of cesium iodide or cesium bromide. Several spectra of each compound were recorded at different concentrations. Melting points were measured on a Gallenkamp melting point apparatus in glass tubes with one end open.

Results and Discussion

R_3SbX compounds studied in this investigation include trimethyl- and triphenyl-antimony selenates, and triphenylantimony chromate and oxalate. The latter two compounds were sought to provide a comparison between analogous trimethyl- and triphenyl-antimony(V) compounds. Oxybis(trimethyl- or triphenyl-antimony) derivatives, $(R_3Sb)_2OX$, studied include the selenates, chromates, oxalates, and oxybis-(trimethylantimony)sulfate.

TABLE I
Analytical data

Compound	Solvent	Calculated (%) C	Calculated (%) H	Found (%) C	Found (%) H	Melting point (°C)
$(CH_3)_3SbSeO_4$	Water	11.62	2.90	11.98	3.03	380‡
$(C_6H_5)_3SbSeO_4$	Methanol	43.57	3.02	42.95	3.16	308–309
$(C_6H_5)_3SbCrO_4$*	Nitrobenzene	46.08	3.20	44.92	2.91	180‡
$(C_6H_5)_3SbC_2O_4$	Methanol	54.44	3.41	54.18	3.76	160–161§
$[(CH_3)_3Sb]_2OSeO_4$†	Water, methanol, or 95% alcohol	14.62	3.65	14.79	4.18	204§
$[(CH_3)_3Sb]_2OSO_4$†	Water, methanol, or 95% alcohol	16.16	4.04	15.55	4.09	222–224§
$[(CH_3)_3Sb]_2OCrO_4$	Water	15.46	3.86	15.37	4.12	172§
$[(CH_3)_3Sb]_2OC_2O_4$	Water	21.96	4.15	21.74	4.34	247–248§
$[(C_6H_5)_3Sb]_2OSeO_4$	Methanol	49.97	3.47	49.72	3.95	248§
$[(C_6H_5)_3Sb]_2OCrO_4$	Tetrahydrofuran	51.59	3.60	51.15	3.89	
$[(C_6H_5)_3Sb]_2OC_2O_4$	Methanol	56.34	3.71	55.60	3.72	208–209

*Product was precipitated by adding excess of petroleum ether.
†Product appears to be a mixture of $[(CH_3)_3Sb]_2OX$ and $[(CH_3)_3Sb(OH)]_2X$. Anal. Calcd. for $[(CH_3)_3Sb(OH)]_2SeO_4$: C, 14.10; H, 3.50. Anal. Calcd. for $[(CH_3)_3Sb(OH)]_2SO_4$: C, 15.53; H, 4.31.
‡Decomposed without melting.
§Decomposed on melting.

R_3SbX Derivatives

The observed i.r. absorption frequencies due to the anion groups in the R_3SbX compounds are given in Table II. The results show that in each case the spectrum of the anion part, X, differs significantly from that of the free anion. In any of these compounds the symmetry of the anion group does not appear to be higher than C_{2v}. Moreover, the symmetric stretching frequencies which are forbidden in the i.r. spectrum of the free anion are observed as strong bands. Marked shifts are also observed in some of the vibrational frequencies. The spectroscopic observations can best be explained in terms of coordination of the X group to the R_3Sb group. In the solid state the symmetry of an anion of high symmetry can also be reduced due to the lower site symmetry of the ion in the crystal lattice. However, in view of previous spectroscopic studies of Clark and Goel on a variety of organotin (9, 10) and organoantimony (1) acid derivatives, we do not consider that the spectroscopic observations can be attributed entirely to the solid state effects. In fact, the i.r. spectra due to the anion groups in some of the R_3SbX compounds can be compared with the spectra of related covalent species. An examination of the i.r. spectra (11) of numerous coordination compounds of oxyanions, and the results of the vibrational analysis of some oxyanion–metal complexes (12), show that when the anion is involved in coordination, the intensity of the symmetric stretching vibrations is greatly increased as compared with the effects caused by low site symmetry of the anion. Similarly, the splitting of the degenerate modes and the frequency shifts are also related to the degree of covalency of the metal–oxygen bond.

The SeO_4^{2-} ion belongs to the point group T_d and has four fundamental vibrational frequencies arising from symmetric and asymmetric stretching and bending modes. Only the asymmetric modes are i.r. active. The symmetric and asymmetric stretching frequencies for the free SeO_4^{2-} have been reported (11) at 833 and 875 cm^{-1}, respectively, and the corresponding bending frequencies are 335 and 432 cm^{-1} (11), respectively. In the i.r. spectra of trimethyl- and triphenylantimony selenates there are four strong well resolved bands near 950, 900, 800, and 750 cm^{-1} which can be attributed to the selenate absorption. In the low frequency region the selenate absorption bands occur near 475–485, 438–445, 388, and 350–355 cm^{-1}. Although i.r. spectral data on coordinated selenates are not available, the observed frequencies of the selenate group in both the compounds indicate that the selenate group is involved in coordination through two of its oxygen atoms.

The chromate absorption frequencies in triphenylantimony chromate are more or less similar to those observed in trimethylantimony chromate (1), and dimethyltin chromate (9).

Can. J. Chem. Downloaded from www.nrcresearchpress.com by 210.87.254.6 on 09/05/12
For personal use only.

TABLE II

Infrared absorption bands* due to X group in R_3SbX compounds

$(CH_3)_3SbSeO_4$	$(C_6H_5)_3SbSeO_4$	$(C_6H_5)_3SbCrO_4$	$(C_6H_5)_3SbC_2O_4$
955 s	950 s	960 s	1740 s
908 s	900 s	940 s	1655 s
805 s	802 s	830 sh	1360 s
780–720 vs	760–740 vs	780 vs	1200 s
485 s	475 m	420 w	970 m
438 m	445 s	385 m	780 m
388 s	388 s	325 sh	760 s
350 sh	365 m		345 m

*In cm^{-1}; m, medium; s, strong; sh, shoulder; vs, very strong; w, weak.

The absorption frequencies of the oxalate group in triphenylantimony oxalate agree very well with those of trimethylantimony oxalate (1), and metal–oxalato complexes (11). The oxalate absorption bands at 1740, 1655, 1360, and 1200 cm^{-1} in triphenylantimony oxalate correspond to the C—O stretching frequencies reported for *cis*-dimethyl oxalate (13).

With respect to the absorption bands due to the trimethyl- or triphenyl-antimony group, the spectra of R_3SbX compounds do not show any significant change when compared to the spectra of trimethyl- or triphenyl-antimony dihalides (5, 4). In the case of trimethylantimony selenate, weak absorption bands are observed in the C—H symmetric and asymmetric stretching (3000–2900 cm^{-1}), and C—H symmetric and asymmetric bending (1400–1200 cm^{-1}), and CH_3 rocking (862 cm^{-1}) regions. Only the asymmetric Sb—C stretching frequency is observed at 590 cm^{-1}. The presence of only one Sb—C stretching vibration indicates that the trimethylantimony group is planar. All the triphenylantimony compounds studied show absorption bands associated with monosubstituted phenyl groups. In the low frequency region, absorption bands due to the triphenylantimony group occur near 450 and 290 cm^{-1}. Metal–carbon stretching frequencies in heavy metal–phenyl compounds have not been established unequivocally. In the case of triphenylantimony dinitrate and oxybis(triphenylantimony)dinitrate, Doak *et al.* (4) consider the absorption at 450 cm^{-1} to be due to the Sb—C asymmetric stretch, while Tranter *et al.* (14) assign the band near 290 cm^{-1} to the Sb—C asymmetric stretch. Both bands occur in all the triphenylantimony(V) compounds including the dichloride (which is trigonal bipyramidal) and triphenylantimony (which would probably be pyramidal). No conclusions can therefore be reached concerning the geometry of the triphenylantimony group on the basis of its i.r. spectrum. However, in view of the almost identical spectra of the X groups in trimethyl- and triphenyl-antimony derivatives, we suggest that the analogous trimethyl- and triphenylantimony compounds have similar structures.

$(R_3Sb)_2OX$ Derivatives

Investigations on a few oxybis(trimethyl- and triphenyl-antimony) derivatives such as halides, nitrates, and perchlorates (2, 4, 5, 14, 15) have been reported. From i.r. studies, Doak *et al.* (4) consider that oxybis(trimethylantimony)diperchlorate and dichloride are ionic and contain the ion $[(CH_3)_3Sb]O_2^{2+}$. On the other hand, oxybis(triphenylantimony)dichloride (15) and dinitrate (14) are reported to be non-ionic, on the basis of electrical conductance and i.r. spectral data. Among the oxybis derivatives of dibasic acids only oxybis(triphenylantimony)sulfate has been studied (4), and it was reported to be non-ionic. In this investigation we have prepared several oxybis(trimethyl- and triphenyl-antimony) derivatives of dibasic acids and examined their i.r. spectra.

The significant difference between the i.r. spectrum of the oxybis(trimethylantimony) group and that of the trimethylantimony group is the occurrence of a very strong band near 775 cm^{-1} (due to the Sb—O—Sb group) and a weak band near 530 cm^{-1} (possibly due to Sb—C symmetric stretch), in the former case. In the phenyl series the Sb—O—Sb group gives rise to a strong band near 750 cm^{-1}. However, in most of the compounds we have examined, the Sb—O—Sb absorption is masked by strong bands due to the anionic groups. The observed i.r. absorption frequencies

Can. J. Chem. Downloaded from www.nrcresearchpress.com by 210.87.254.6 on 09/05/12
For personal use only.

Can. J. Chem. Downloaded from www.nrcresearchpress.com by 210.87.254.6 on 09/05/12
For personal use only.

TABLE III

Infrared absorption bands* due to X group in $(R_3Sb)_2OX$ compounds

$[(CH_3)_3Sb]_2OSO_4$	$[(CH_3)_3Sb]_2OSeO_4$	$[(C_6H_5)_3Sb]_2OSeO_4$	$[(CH_3)_3Sb]_2OCrO_4$	$[(C_6H_5)_3Sb]_2OCrO_4$†	$[(CH_3)_2Sb]_2OC_2O_4$	$[(C_6H_5)_3Sb]_2OC_2O_4$
1200 s	918 s	935 s	930 s	950 s	1625 s	1655 s
1115 s	870 s	885 s	910 s	928 s	1605 s	1570 m
1000 s	795 s	810 s	840–810 s	830 s	1420 m	1360 m
960 m	745 vs	735 vs	690 vs	690 vs	1250 s	1215 s
635 m	445 s	442 s	410 w	420 w	775 sh	965 w
590 s	425 s	415 m	375 m	380 m	738 s	780 sh
470 m	400 m	385 m	345 w		370 m	730 s
	350 w	340 w	310 m			370 w

*In cm^{-1}; m, medium; s, strong; sh, shoulder; vs, very strong; w, weak.
†A well resolved spectrum could not be obtained due to poor dispersion of the compound in Nujol.

Can. J. Chem. Downloaded from www.nrcresearchpress.com by 210.87.254.6 on 09/05/12
For personal use only.

which can be attributed to the anion groups in oxybis(trimethyl- and triphenyl-antimony)selenates, chromates, and oxalates, and oxybis(trimethylantimony)sulfate are listed in Table III. Considering the spectral features of the anion group, none of the above compounds can be described as ionic, in the solid state. In $[(CH_3)_3Sb—O—Sb(CH_3)_3]^{2+}$ cation, each of the antimony atoms would be bonded by four covalent bonds and both the symmetric and asymmetric Sb—C stretching vibrations would be expected to give rise to i.r. absorption bands of medium intensity. Infrared spectra of all the oxybis(trimethylantimony) derivatives studied show a band of medium intensity (580 cm^{-1}) due to Sb—C asymmetric stretch, but only a weak band (near 530 cm^{-1}) in the region of Sb—C symmetric stretch (16). Since the i.r. spectra of the anion groups in analogous R_3SbX and $(R_3Sb)_2OX$ compounds show similar features, a similar structural function for the anion group is indicated in both types of compounds.

Infrared spectra of oxybis(trimethylantimony)-selenate and sulfate also show two additional bands of medium intensity near 3350 and 1050 cm^{-1}. These bands could not be removed even after prolonged pumping and drying of the samples. The samples were also washed with acetone to remove trimethylantimony hydroxide which might be formed. Since no absorption is observed between 1700–1500 cm^{-1}, the above mentioned bands cannot be due to the presence of either free or coordinated water. The formulation of the products as hydrogen selenate or hydrogen sulfate can be ruled out from the analytical data. The two bands may be associated with the Sb—OH bond. In hydroxo complexes of ruthenium (17) O—H stretching and Ru—OH bending frequencies are observed at 3500–3200 and 1000–970 cm^{-1}, respectively. Although there are conflicting reports (4) about the existence of compounds of the type $R_3Sb(OH)Y$ or $[R_3Sb(OH)_2]X$, we consider that the products most likely contain trimethylantimonyhydroxy sulfate or selenate, $[(CH_3)_3SbOH]_2SeO_4$ or $[(CH_3)_3SbOH]_2SO_4$. However, the formulation of the hydroxy species as adducts of the type $[(CH_3)_3SbO]_2H_2SO_4$ or $[(CH_3)_3SbO]_2H_2SeO_4$ cannot be ruled out.

Summarizing, the results of this investigation further support the conclusions derived earlier by Clark and Goel (1), from the i.r. studies of trimethylantimony(V) compounds. Compounds of the type R_3SbX are indicated to be non-ionic solids possessing five coordinate structures, most likely involving bridging X (through two of its oxygen atoms) and R_3Sb groups. The interaction between R_3Sb and X is not significantly affected by changing R from methyl to phenyl, suggesting structural similarities between analogous methyl and phenyl derivatives. The $(R_3Sb)_2OX$ compounds also appear to have the above structural features.

Acknowledgments

We gratefully acknowledge the financial assistance of the National Research Council of Canada for the support of this work.

We are also thankful to the Analytical Division of the Uniroyal Research Laboratories, Guelph, for the use of a Perkin–Elmer model 521 spectrophotometer.

1. H. C. Clark and R. G. Goel. Inorg. Chem. **5**, 998 (1966).
2. M. Shindo and R. Okawara. J. Organometal. Chem. Amsterdam, **5**, 537 (1966).
3. T. N. Polinova and M. A. Porai-Koshits. Zh. Strukt. Khim, **7**, 742 (1966).
4. G. O. Doak, G. G. Long, and L. D. Freedman. J. Organometal. Chem. Amsterdam, **4**, 82 (1965).
5. G. G. Long, G. O. Doak, and L. D. Freedman. J. Am. Chem. Soc. **86**, 209 (1964).
6. T. N. Polynova and M. A. Porai-Koshits. J. Struct. Chem. USSR, Engl. Transl. **1**, 146 (1960).
7. K. A. Jensen. Z. Anorg. Allgem. Chem. **250**, 268 (1943).
8. A. F. Wells. Z. Krist. **99**, 367 (1938).
9. H. C. Clark and R. G. Goel. Inorg. Chem. **4**, 1428 (1965).
10. H. C. Clark and R. G. Goel. J. Organometal. Chem. Amsterdam, **7**, 263 (1967).
11. K. Nakamoto. Infrared spectra of inorganic and coordination compounds. John Wiley and Sons, Inc., New York. 1963, and the references therein.
12. H. Brintzinger and R. E. Hester. Inorg. Chem. **6**, 980 (1966).
13. M. J. Schmelz, T. Miyazawa, S. Mizushima, T. J. Lane, and J. V. Quagliano. Spectrochim. Acta, **9**, 51 (1957).
14. G. C. Tranter, C. C. Addison, and D. B. Sowerby. J. Organometal. Chem. Amsterdam, **12**, 369 (1968).
15. L. Kolditz, M. Gilter, and E. Rosel. Z. Anorg. Allgem. Chem. **316**, 270 (1962).
16. A. J. Downs and I. A. Steer. J. Organometal. Chem. Amsterdam, **8**, 21 (1967).
17. D. Scargill. J. Chem. Soc. 4440 (1961).

Can. J. Chem. Downloaded from www.nrcresearchpress.com by 210.87.254.40 on 09/05/12
For personal use only.

Some new diphosphine-bridged nickel carbonyl and cyclopentadienyl compounds

A. J. CARTY, A. EFRATY, AND T. W. NG
Chemistry Department, University of Waterloo, Waterloo, Ontario

Received October 25, 1968

The binuclear diphosphine bridged monocarbonyl compound $[Ni(CO)]_2(DPPA)_3$ has been obtained by reaction of $Ni(CO)_4$ with bis(diphenylphosphino)acetylene (DPPA) under mild conditions and by displacement of π-cyclopentadienyl groups from $[\pi\text{-}C_5H_5Ni(CO)]_2$ at room temperature. The latter reaction suggests a possible route to other monocarbonyl nickel phosphine compounds not available by direct reaction of $Ni(CO)_4$ with phosphines. The preparation and characterization of the binuclear compounds $[Ni(CO)_2]_2(DPPA)_2$, $[Ni(CO)_3]_2(DPPA)$, and $(\pi\text{-}C_5H_5NiI)_2(DPPA)$ are also described.

Canadian Journal of Chemistry, 47, 1429 (1969)

Introduction

Although tertiary phosphines readily displace one or two carbonyl groups from $Ni(CO)_4$ to give substitution products of the types $Ni(CO)_3(PR_3)$ and $Ni(CO)_2(PR_3)_2$, compounds containing only one residual carbonyl group are rare and difficult to obtain (1). Trialkyl and Triarylphosphites (2) as well as certain triphosphines (3) will, however, give monocarbonyl products under appropriate conditions. In several recent publications (4) we have described the preparation and characterization of a series of binuclear complexes of the ligand bis(diphenylphosphino)acetylene **1**. We now find that this ligand reacts with $Ni(CO)_4$ and

$$Ph_2PC{\equiv}CPPh_2$$

1

$[\pi\text{-}C_5H_5Ni(CO)]_2$ under very mild conditions to give a diphosphine bridged product $[Ni(CO)]_2(DPPA)_3$, DPPA = bis(diphenylphosphino)acetylene, having only one terminal carbonyl group per nickel atom. These and related reactions are the subject of this note.

Results and Discussion

The ligand **1** readily displaces two carbonyl groups from $Ni(CO)_4$ in diethyl ether to give a binuclear compound analyzing as $Ni_2(CO)_4(DPPA)_2$. The infrared spectrum in the region 1600–650 cm^{-1} closely resembles that of the free ligand except for certain changes in frequency and intensity similar to those noted previously (4*c*). A carbon tetrachloride solution spectrum in the ν(CO) region shows two peaks at 2005, 1944 cm^{-1} consistent with the two modes ($a_1 + e$) expected for the C_{2v} local symmetry of a disubstituted $Ni(CO)_2L_2$ species. ν(C≡C) of the coordinated ligand appears in the Raman[1] at 2117 cm^{-1}, 20 cm^{-1} higher than in the free ligand, confirming unambiguously that the triple bond is uncoordinated (4). Since the linear P—C—C—P skeleton of **1** prevents chelation the most likely

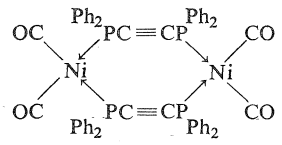

2

structure is **2** having two bridging bis(diphenylphosphino)acetylene groups. The only other example of a stable diphosphine-bridged carbonyl compound of this type is $[Ni(CO)_2]_2(DEPE)_2$, DEPE = 1,2-bis(diethylphosphino)ethane, isolated as a by-product in the preparation of $Ni(CO)_2(DEPE)$ by Chatt and Hart (3), although Meriwether and Leto (6) have found nuclear magnetic resonance (n.m.r.) evidence for $[Ni(CO)_2]_2(DPPE)_2$, DPPE = 1,2-bis(diphenylphosphino)ethane, in solution, and other workers (7, 9, 10) have prepared monobridged compounds of the type $[Ni(CO)_3]_2(P_2R_4)$ (R = Ph, Me, CF_3).

Compound **2** reacts smoothly with **1** in ethanol affording a yellow, air-stable compound. Microanalysis and molecular weight data are consistent with a binuclear species $[Ni(CO)]_2(DPPA)_3$. A

[1]Raman measurements were made on the solid compounds using helium–neon laser excitation.

single ν(CO) band (a_1) at 1938 cm^{-1} in carbon tetrachloride solution suggests a C_{3v} environment of one carbonyl group and three phosphorus atoms per nickel atom and the appearance of ν(C≡C) at 2120 cm^{-1} in the Raman confirms structure **3** for this compound. The compound is, therefore,

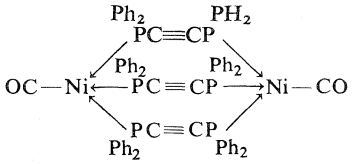

3

structurally analogous to $(CuCl)_2(DPPA)_3$ and $(AuI)_2(DPPA)_3$ (4). A further point of interest is the unexpected appearance of two ν(CO) bands at 1940, 1925 cm^{-1} in a mull spectrum of $[Ni(CO)]_2(DPPA)_3$. This feature has been noted previously for monocarbonyl compounds (3) and may in this case be due to interaction between carbonyl groups on different nickel atoms. Direct reaction of $Ni(CO)_4$ and **1** in ethanol also gives **3** in good yields. This represents the first preparation of a monocarbonyl nickel phosphine complex by direct reaction under mild conditions, and implies that **1** is at least as effective as phosphites in labilizing the CO groups of $Ni(CO)_4$.

In pentane at −10°, $Ni(CO)_4$ reacts with **1** to yield a product having ν(CO) at 2078, 2004 cm^{-1}. This is the spectrum expected for a monobridged tricarbonyl species but the material is impure and difficult to separate from the dicarbonyl.

Few substitution reactions of $[(\pi\text{-}C_5H_5)Ni(CO)]_2$ with phosphines have been reported (1). Tetraalkyldiphosphines replace both carbonyl groups and are cleaved in the process giving the dimeric phosphido bridged species $[(\pi\text{-}C_5H_5)Ni]_2(PR_2)_2$ (8). By contrast $[(\pi\text{-}C_5H_5)Ni(CO)]_2$ reacts with **1** at 25 °C in benzene to give a 20% yield of a product having no $\pi\text{-}C_5H_5$ groups and identical with **3** obtained from $Ni(CO)_4$ and **1**. This is an unusual reaction since carbonyl groups are preferentially removed in substitution reactions of $[(\pi\text{-}C_5H_5)Ni(CO)]_2$ and other π-cyclopentadienyl carbonyls (1), although recent work (11) has shown that π-cyclopentadienyl groups can be removed from $[\pi\text{-}C_5H_5Fe(CO)_2]_2$ by phosphines under extreme conditions. Apparently the reduction Ni(I) → Ni(0) occurs in order to retain the inert gas configuration for nickel, since the bridging properties of **1** and the long P—P distance clearly prevent retention of the metal–metal bond present in $[(\pi\text{-}C_5H_5)Ni(CO)]_2$.

However, reaction of iodine with a solution of $[(\pi\text{-}C_5H_5)Ni(CO)]_2$ and **1** in benzene gives dark red, diamagnetic $[(\pi\text{-}C_5H_5)NiI]_2$(DPPA) having no carbonyl groups but showing a sharp single cyclopentadienyl resonance at δ = 5.27 in the n.m.r. Molecular weight data and the absence of ν(C≡C) in the infrared again confirm the presence of a bridging diphosphine. If the π-cyclopentadienyl group is considered as a tridentate ligand, this compound has structure **4** containing a single diphosphine bridge.

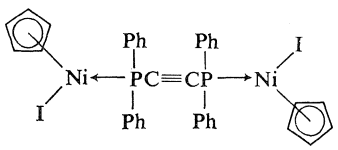

4

X-Ray structural determinations of compounds **2** and **3** are now in progress and we are currently exploring the reaction of $[(\pi\text{-}C_5H_5)Ni(CO)]_2$ with other phosphines as a possible route to other monocarbonyl substitution products.

Experimental

Microanalyses and molecular weight determinations were by Alfred Bernhard, Mulheim, Germany and A.B. Gygli, Toronto. Melting points were determined in evacuated capillaries and were uncorrected. Infrared spectra were obtained using Beckmann IR-9 and -10 spectrometers. Proton magnetic resonance spectra were measured with Varian A60 and HA-100 spectrometers using tetramethylsilane as an internal reference. For all the cyclopentadienyl compounds described, sharp n.m.r. spectra were obtained and the compounds were thus presumed to be diamagnetic.

All reactions were carried out under a blanket of nitrogen.

Bis(diphenylphosphino)acetylene was prepared as previously described (4*c*). Cyclopentadienylnickel carbonyl dimer was prepared by a reported method (12).

[Di-μ-bis(diphenylphosphino)acetylene]-tetracarbonyldinickel

A solution of $Ni(CO)_4$ (1.7 g, 10.0 mmoles) in ether (50 ml) was added dropwise to **1** (4.0 g, 10.0 mmoles) in ether (100 ml). The reaction mixture was refluxed for 1 h. On cooling to room temperature white crystals of the product were formed. Recrystallization from dichloromethane/ethanol gave the pure material, m.p. 180–200°, decomp.

Anal. Calcd. for $Ni_2(CO)_4(DPPA)_2$, mol. wt. 1018: C, 66.1; H, 4.0. Found: mol. wt. 995; C, 66.0; H, 3.91.

Can. J. Chem. Downloaded from www.nrcresearchpress.com by 210.87.254.40 on 09/05/12
For personal use only.

[Tri-μ-bis(diphenylphosphino)acetylene]-dicarbonyldinickel

$[CpNi(CO)]_2$ (1.0 g, 3.3 mmoles) and **1** (3.3 g, 8.4 mmoles) were refluxed in benzene (60 ml) for 2 h. The hot reaction mixture was filtered and ethanol added to give a pale yellow crystalline product which was recrystallized from dichloromethane–ethanol. The same product can be obtained at room temperature with longer reaction times, m.p. 264–265°, decomp.

Anal. Calcd. for $Ni_2(CO)_2(DPPA)_3$, mol. wt. 1357: C, 70.8; H, 4.5. Found: mol. wt. 1304; C, 70.4; H, 4.4.

Direct reaction of $Ni(CO)_4$ with **1** in refluxing ethanol gave $Ni_2(CO)_2(DPPA)_3$ in 75% yield. $Ni_2(CO)_4(DPPA)_2$ also reacted with **1** in boiling ethanol to give the same product.

Diiodo-μ-bis(diphenylphosphino)acetylene-di-π-cyclopentadienyldinickel

$[CpNi(CO)]_2$ (1.5 g, 4.9 mmoles), **1** (2.0 g, 5.0 mmoles), and iodine (1.5 g, 5.9 mmoles) were stirred at room temperature in benzene (60 ml) for 10 h. The reaction mixture was filtered, and ethanol added to the filtrate. On reducing the volume of the solution, red crystals of the product were obtained. Recrystallization was from dichloromethane/ethanol, m.p. 172–173°.

Anal. Calcd. for $(C_5H_5)_2Ni_2I_2(DPPA)$, mol. wt. 896: C, 48.3; H, 3.4; I, 28.3. Found: mol. wt. 943; C, 48.6; H, 3.5; I, 28.2.

Acknowledgment

We acknowledge the financial support of the National Research Council of Canada.

1. I. Wender and P. Pino. Organic syntheses via metal carbonyls. Interscience Publishers, Inc., New York. 1968. pp. 74–77.
2. L. Malatesta and A. Sacco. Ann. Chim. Rome, **44**, 134 (1954).
3. J. Chatt and F. A. Hart. J. Chem. Soc. 812 (1965).
4. (*a*) A. J. Carty and A. Efraty. Can. J. Chem. **46**, 1598 (1968). (*b*) A. J. Carty and A. Efraty. Inorg. Nucl. Chem. Letters, **4**, 427 (1968). (*c*) A. J. Carty and A. Efraty. Inorg. Chem. In press.
5. J. Chatt and F. A. Hart. J. Chem. Soc. 1378 (1960).
6. L. S. Meriwether and J. R. Leto. J. Am. Chem. Soc. **83**, 3192 (1961).
7. R. G. Hayter. Inorg. Chem. **3**, 711 (1964).
8. R. G. Hayter. Inorg. Chem. **2**, 1031 (1963).
9. A. B. Burg and W. Mahler. J. Am. Chem. Soc. **80**, 2334 (1958).
10. W. Schweckendiek. German Patent No. 1 072 244 (1959).
11. H. Behrens and W. Aquila. Z. Naturforsch. **22b**, 454 (1967).
12. J. F. Tilney-Bassett. J. Chem. Soc. 577 (1961).

Can. J. Chem. Downloaded from www.nrcresearchpress.com by 210.87.254.40 on 09/05/12
For personal use only.

Dehydrochlorination of chlorodihydridocarbonylbis(triphenylphosphine)Ir(III) in the presence of strong bases

J. F. Harrod, D. F. R. Gilson, and R. Charles
Chemistry Department, McGill University, Montreal, Quebec
Received October 21, 1968

The dehydrochlorination of dihydridochlorocarbonylbis(triphenylphosphine)iridium(III) by organic and inorganic bases is described. The manner in which this reaction provides a formal link between the homolytic activation of hydrogen at a single metal center and the heterolytic activation of hydrogen is discussed.

Canadian Journal of Chemistry, 47, 1431 (1969)

In the course of attempts to synthesize hydridocarbonylbis(triphenylphosphine)iridium(I) (compound **1**), we have investigated the reaction of chlorodihydridocarbonylbis(triphenylphosphine)iridium(III) (**2**) with a variety of bases. The rationale for such a synthesis, depicted in eq. [1], derives from the relationship between the activation of molecular hydrogen through homolytic oxidative addition, and the heterolytic activation path frequently observed in aqueous solution (1). The two types of activation process may be schematically represented as in eqs. [2] and [3].

[1] 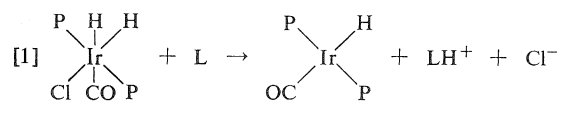

2 **1**

L = base, P = $(C_6H_5)_3P$

[2] $M + H_2 \rightarrow MH^- + H^+$

[3] $M + H_2 \rightarrow H—M—H$

The essential difference between these two processes is that, axiomatically, in eq. [2] there is some other species in the system which is a stronger base than MH^-, whereas in eq. [3] there is not.

[Tri-μ-bis(diphenylphosphino)acetylene]-dicarbonyldinickel

$[CpNi(CO)]_2$ (1.0 g, 3.3 mmoles) and **1** (3.3 g, 8.4 mmoles) were refluxed in benzene (60 ml) for 2 h. The hot reaction mixture was filtered and ethanol added to give a pale yellow crystalline product which was recrystallized from dichloromethane–ethanol. The same product can be obtained at room temperature with longer reaction times, m.p. 264–265°, decomp.

Anal. Calcd. for $Ni_2(CO)_2(DPPA)_3$, mol. wt. 1357: C, 70.8; H, 4.5. Found: mol. wt. 1304; C, 70.4; H, 4.4.

Direct reaction of $Ni(CO)_4$ with **1** in refluxing ethanol gave $Ni_2(CO)_2(DPPA)_3$ in 75% yield. $Ni_2(CO)_4(DPPA)_2$ also reacted with **1** in boiling ethanol to give the same product.

Diiodo-μ-bis(diphenylphosphino)acetylene-di-π-cyclopentadienyldinickel

$[CpNi(CO)]_2$ (1.5 g, 4.9 mmoles), **1** (2.0 g, 5.0 mmoles), and iodine (1.5 g, 5.9 mmoles) were stirred at room temperature in benzene (60 ml) for 10 h. The reaction mixture was filtered, and ethanol added to the filtrate. On reducing the volume of the solution, red crystals of the product were obtained. Recrystallization was from dichloromethane/ethanol, m.p. 172–173°.

Anal. Calcd. for $(C_5H_5)_2Ni_2I_2(DPPA)$, mol. wt. 896: C, 48.3; H, 3.4; I, 28.3. Found: mol. wt. 943; C, 48.6; H, 3.5; I, 28.2.

Acknowledgment

We acknowledge the financial support of the National Research Council of Canada.

1. I. Wender and P. Pino. Organic syntheses via metal carbonyls. Interscience Publishers, Inc., New York. 1968. pp. 74–77.
2. L. Malatesta and A. Sacco. Ann. Chim. Rome, **44**, 134 (1954).
3. J. Chatt and F. A. Hart. J. Chem. Soc. 812 (1965).
4. (*a*) A. J. Carty and A. Efraty. Can. J. Chem. **46**, 1598 (1968). (*b*) A. J. Carty and A. Efraty. Inorg. Nucl. Chem. Letters, **4**, 427 (1968). (*c*) A. J. Carty and A. Efraty. Inorg. Chem. In press.
5. J. Chatt and F. A. Hart. J. Chem. Soc. 1378 (1960).
6. L. S. Meriwether and J. R. Leto. J. Am. Chem. Soc. **83**, 3192 (1961).
7. R. G. Hayter. Inorg. Chem. **3**, 711 (1964).
8. R. G. Hayter. Inorg. Chem. **2**, 1031 (1963).
9. A. B. Burg and W. Mahler. J. Am. Chem. Soc. **80**, 2334 (1958).
10. W. Schweckendiek. German Patent No. 1 072 244 (1959).
11. H. Behrens and W. Aquila. Z. Naturforsch. **22b**, 454 (1967).
12. J. F. Tilney-Bassett. J. Chem. Soc. 577 (1961).

Can. J. Chem. Downloaded from www.nrcresearchpress.com by 210.87.254.5 on 09/05/12
For personal use only.

Dehydrochlorination of chlorodihydridocarbonylbis(triphenylphosphine)Ir(III) in the presence of strong bases

J. F. Harrod, D. F. R. Gilson, and R. Charles
Chemistry Department, McGill University, Montreal, Quebec
Received October 21, 1968

The dehydrochlorination of dihydridochlorocarbonylbis(triphenylphosphine)iridium(III) by organic and inorganic bases is described. The manner in which this reaction provides a formal link between the homolytic activation of hydrogen at a single metal center and the heterolytic activation of hydrogen is discussed.

Canadian Journal of Chemistry, 47, 1431 (1969)

In the course of attempts to synthesize hydridocarbonylbis(triphenylphosphine)iridium(I) (compound **1**), we have investigated the reaction of chlorodihydridocarbonylbis(triphenylphosphine)iridium(III) (**2**) with a variety of bases. The rationale for such a synthesis, depicted in eq. [1], derives from the relationship between the activation of molecular hydrogen through homolytic oxidative addition, and the heterolytic activation path frequently observed in aqueous solution (1). The two types of activation process may be schematically represented as in eqs. [2] and [3].

[1] 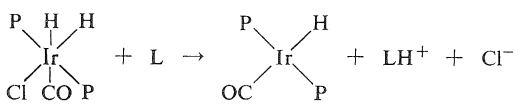

2 **1**

L = base, P = $(C_6H_5)_3P$

[2] $M + H_2 \rightarrow MH^- + H^+$

[3] $M + H_2 \rightarrow H—M—H$

The essential difference between these two processes is that, axiomatically, in eq. [2] there is some other species in the system which is a stronger base than MH^-, whereas in eq. [3] there is not.

Can. J. Chem. Downloaded from www.nrcresearchpress.com by 210.87.254.5 on 09/05/12
For personal use only.

The first known example of eq. [3] was the reaction of hydrogen with chlorocarbonylbis-(triphenylphosphine)iridium(I) (**3**) to produce **2** (2). This synthesis is normally effected at room temperature in organic solvents of low basicity, e.g. benzene, methylene chloride, a condition which would favor oxidative addition rather than heterolytic splitting. We have treated **2** under a variety of basic conditions using both organic bases, e.g. tetramethylethylenediamine, pyridine, and inorganic bases, e.g. Na_2CO_3, KOH, in both benzene and ethanol. In all cases dehydrochlorination occurred, but not according to the stoichiometry of eq. [1]. The product of the reaction consisted of ca. 50% hydridocarbonyltris(triphenylphosphine)iridium(I) (**4**) and an uncharacterized mixture of carbonyl–phosphine-iridium complexes. The presence of **4** as a major component of the mixture was confirmed by observation of a 1:3:3:1 quartet (τ = 20.9; J(P—H) = 24 Hz in CH_2Cl_2) in the proton magnetic resonance and by infrared absorptions at 2070 cm^{-1} (ν_{Ir-H}) and 1925 cm^{-1} (ν_{CO}). The CO band of the other fraction was at 1985 cm^{-1} (strong).

Dehydrochlorination of **2** by KOH in ethanol, in the presence of excess triphenylphosphine, led to the exclusive formation of **4**, in high yield. The stoichiometry of this reaction is thus

[4] 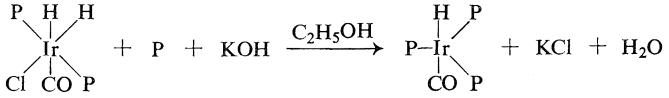

4

That reaction [4] goes via dehydrochlorination rather than some other route involving hydride abstraction from solvent was proven unequivocally by dedeuteriochlorination of the dideuterido analogue of **2** under the same conditions. The reaction product gave two intense carbonyl bands at 1945 cm^{-1} (CO *trans* to deuterium (3)) and 1920 cm^{-1} (CO *trans* to protium), the former being about three times the intensity of the latter. Assuming the extinction coefficients for the two complexes to be identical, at least 75% of the product was produced directly by dedeuteriochlorination, in spite of the fact that the reaction occurred in a vast excess of normal ethanol.

The possibility that thermal dissociation of **2**, with loss of H_2, occurs during this reaction is discounted on the evidence that only infrared bands of **2** and **4** were observed during the reaction. In addition, loss of hydrogen would be irreversible under the conditions of reflux under N_2 and the effectively quantitative yields of **4** would not be achievable.

Several syntheses of **1** have been reported by Malatesta (4). We have repeated one of these, namely carbonylation of iridium(IV) iodide, followed by reflux with triphenylphosphine in ethanolic KOH. This reaction yielded a product indistinguishable from the product of our dehydrochlorination reaction, consisting of a mixture of **4** and other unidentified carbonyl containing species. The infrared spectrum of this mixture was the same as that reported by Malatesta for compound **1** (4). It is our opinion that **1** is not stable under the conditions of the reactions described above and apparently it disproportionates readily to **4**, and other species containing carbonyl groups and only a single phosphine ligand. This would also provide an explanation for the anomalous observation of two carbonyl bands in the infrared spectrum of **1** reported by Malatesta (4). No other complex of the type $P_2(CO)IrX$ has been shown to exhibit more than a single carbonyl stretch.

Although the above dehydrochlorination reaction appears to represent the first example of a *heterolytic* splitting of H_2 *via* a stable dihydrido intermediate, the use of dehydrohalogenation of monohydridoiridium(III) complexes as a general synthetic route to iridium(I) complexes has recently been reported by Shaw (5). A similar principle may be operative in the base promotion of reaction [5], described by Wilkinson (6), although the existence of a stable seven-coordinate dihydride of Ru(IV) seems most unlikely[1] (8).

[5] $P_3RuCl_2 + H_2 \rightarrow P_3RuClH + HCl$

[1]A ruthenium(IV) dihydride does not seem so unlikely in view of the recent synthesis of P_3RuH_4.

Experimental

Chlorocarbonylbis(triphenylphosphine)iridium(I) was prepared by the method of Collman and Kang (7). The hydrogen and deuterium adducts were prepared as described by Vaska and DiLuzio (2).

Preparation of Hydridocarbonyltris(triphenylphosphine)-iridium(I) by Dehydrochlorination of the Dihydride **2**

The following is the preferred synthesis of the complex **4** in our laboratory. It allows preparation of **4** in high overall yield, proceeding in simple steps from iridium trichloride trihydrate.

A suspension of the dihydride **2** (3 g), triphenyl phosphine (3 g), and ethanolic KOH (4 ml; 0.9 *M*) in ethanol (30 ml) was boiled for 2 h under nitrogen. After the mixture had cooled to room temperature, the yellow solid was filtered and washed with ethanol. The precipitate was triturated with benzene and the residue of potassium chloride filtered off. The benzene solution was evaporated to dryness *in vacuo* and the solid residue recrystallized from benzene/hexane. Yield after recrystallization: 3.3 g (86%). The reaction with the dideuteride was carried out under conditions identical with those described above.

The above reaction was carried out in the absence of added triphenylphosphine under N_2, H_2, or CO. Under N_2 or H_2 it was necessary to avoid exposure of the yellow solid to air before the removal of KCl was completed. The products under N_2 and H_2 were the same. Under CO the initial product obtained was different, giving two strong, almost coincident, broad CO bands at 1930 and 1955 cm^{-1} in the infrared. Over a period of about an hour in methylene chloride at room temperature this product reverted to the same mixture of compounds obtained under N_2, or H_2. This change was manifest by the gradual appearance of the characteristic quartet due to **4** in the nuclear magnetic resonance spectrum and the appearance of infrared bands identical with those of the products obtained under N_2 or H_2.

Spectroscopic Measurements

Nuclear magnetic resonance spectra were measured with a Varian A60 spectrometer using a C-1024 CAT attachment. The samples were saturated solutions in methylene chloride.

Infrared spectra were measured in methylene chloride and in benzene. The latter solvent obscures the carbonyl absorption of **4**, which probably accounts for the fact that Malatesta reported two carbonyl absorptions for **1** in methylene chloride, but only one in benzene (4). Spectra were also recorded of thin films spread from solution by evaporation. These spectra were identical with those obtained with methylene chloride within the resolution of the instrument used (Perkin–Elmer 257).

Acknowledgment

The authors gratefully acknowledge support for this work by grants from the National Research Council of Canada.

1. J. Halpern. Ann. Rev. Phys. Chem. **16**, 103 (1965).
2. L. Vaska and J. W. DiLuzio. J. Am. Chem. Soc. **84**, 679 (1962).
3. L. Vaska. J. Am. Chem. Soc. **88**, 400 (1966).
4. L. Malatesta, G. Caglio, and M. Angeletta. J. Chem. Soc. 6974 (1965).
5. A. J. Deeming and B. L. Shaw. J. Chem. Soc. A, 1887 (1968).
6. F. Charentenay, J. A. Osborn, and G. Wilkinson. J. Chem. Soc. A, 787 (1968).
7. J. P. Collman and J. W. Kang. J. Am. Chem. Soc. **89**, 844 (1967).
8. W. H. Kanoth. J. Am. Chem. Soc. **90**, 7172 (1968).

Polarographic reduction of D-mannurono-γ-lactone

J. R. Johnston and R. J. Thibert
Department of Chemistry, University of Windsor, Windsor, Ontario

Received December 2, 1968

The polarographic reduction of D-mannuronolactone is a diffusion controlled process, and is analytically applicable over the concentration range 20–100 μg lactone per ml. The addition of KH_2PO_4 gives similar results to those obtained with D-glucuronolactone, but the results suggest that the D-mannuronolactone ring is less reactive.

Canadian Journal of Chemistry, **47**, 1433 (1969)

Introduction

In conjunction with a detailed study of the polarography of D-glucuronolactone (1), a preliminary investigation was conducted with D-mannurono-γ-lactone. Because of the structural similarities of D-glucurono-γ-lactone and D-mannurono-γ-lactone, it was assumed that their polarographic behavior would be much the same. Since it had been found that D-glucuronolactone could not be reduced at the dropping mercury electrode in buffered solutions, but was reducible in unbuffered solutions (2), D-mannuronolactone was also studied in unbuffered solutions.

Can. J. Chem. Downloaded from www.nrcresearchpress.com by 210.87.254.5 on 09/05/12
For personal use only.

Experimental

Chlorocarbonylbis(triphenylphosphine)iridium(I) was prepared by the method of Collman and Kang (7). The hydrogen and deuterium adducts were prepared as described by Vaska and DiLuzio (2).

Preparation of Hydridocarbonyltris(triphenylphosphine)-iridium(I) by Dehydrochlorination of the Dihydride **2**

The following is the preferred synthesis of the complex **4** in our laboratory. It allows preparation of **4** in high overall yield, proceeding in simple steps from iridium trichloride trihydrate.

A suspension of the dihydride **2** (3 g), triphenyl phosphine (3 g), and ethanolic KOH (4 ml; 0.9 *M*) in ethanol (30 ml) was boiled for 2 h under nitrogen. After the mixture had cooled to room temperature, the yellow solid was filtered and washed with ethanol. The precipitate was triturated with benzene and the residue of potassium chloride filtered off. The benzene solution was evaporated to dryness *in vacuo* and the solid residue recrystallized from benzene/hexane. Yield after recrystallization: 3.3 g (86%). The reaction with the dideuteride was carried out under conditions identical with those described above.

The above reaction was carried out in the absence of added triphenylphosphine under N_2, H_2, or CO. Under N_2 or H_2 it was necessary to avoid exposure of the yellow solid to air before the removal of KCl was completed. The products under N_2 and H_2 were the same. Under CO the initial product obtained was different, giving two strong, almost coincident, broad CO bands at 1930 and 1955 cm^{-1} in the infrared. Over a period of about an hour in methylene chloride at room temperature this product reverted to the same mixture of compounds obtained under N_2, or H_2. This change was manifest by the gradual appearance of the characteristic quartet due to **4** in the nuclear magnetic resonance spectrum and the appearance of infrared bands identical with those of the products obtained under N_2 or H_2.

Spectroscopic Measurements

Nuclear magnetic resonance spectra were measured with a Varian A60 spectrometer using a C-1024 CAT attachment. The samples were saturated solutions in methylene chloride.

Infrared spectra were measured in methylene chloride and in benzene. The latter solvent obscures the carbonyl absorption of **4**, which probably accounts for the fact that Malatesta reported two carbonyl absorptions for **1** in methylene chloride, but only one in benzene (4). Spectra were also recorded of thin films spread from solution by evaporation. These spectra were identical with those obtained with methylene chloride within the resolution of the instrument used (Perkin–Elmer 257).

Acknowledgment

The authors gratefully acknowledge support for this work by grants from the National Research Council of Canada.

1. J. Halpern. Ann. Rev. Phys. Chem. **16**, 103 (1965).
2. L. Vaska and J. W. DiLuzio. J. Am. Chem. Soc. **84**, 679 (1962).
3. L. Vaska. J. Am. Chem. Soc. **88**, 400 (1966).
4. L. Malatesta, G. Caglio, and M. Angeletta. J. Chem. Soc. 6974 (1965).
5. A. J. Deeming and B. L. Shaw. J. Chem. Soc. A, 1887 (1968).
6. F. Charentenay, J. A. Osborn, and G. Wilkinson. J. Chem. Soc. A, 787 (1968).
7. J. P. Collman and J. W. Kang. J. Am. Chem. Soc. **89**, 844 (1967).
8. W. H. Kanoth. J. Am. Chem. Soc. **90**, 7172 (1968).

Polarographic reduction of D-mannurono-γ-lactone

J. R. Johnston and R. J. Thibert
Department of Chemistry, University of Windsor, Windsor, Ontario

Received December 2, 1968

The polarographic reduction of D-mannuronolactone is a diffusion controlled process, and is analytically applicable over the concentration range 20–100 μg lactone per ml. The addition of KH_2PO_4 gives similar results to those obtained with D-glucuronolactone, but the results suggest that the D-mannuronolactone ring is less reactive.

Canadian Journal of Chemistry, **47**, 1433 (1969)

Introduction

In conjunction with a detailed study of the polarography of D-glucuronolactone (1), a preliminary investigation was conducted with D-mannurono-γ-lactone. Because of the structural similarities of D-glucurono-γ-lactone and D-mannurono-γ-lactone, it was assumed that their polarographic behavior would be much the same. Since it had been found that D-glucuronolactone could not be reduced at the dropping mercury electrode in buffered solutions, but was reducible in unbuffered solutions (2), D-mannuronolactone was also studied in unbuffered solutions.

Can. J. Chem. Downloaded from www.nrcresearchpress.com by 210.87.254.5 on 09/05/12
For personal use only.

This paper reports the results of this preliminary investigation and compares them to the corresponding results found for D-glucuronolactone (1).

Experimental

Materials

Gelatin (purified, calfskin) was obtained from Eastman Organic Chemicals; D-mannuronolactone from General Biochemicals, Inc.; mercury (triply distilled) from Engelhard Industries of Canada, Ltd.; and KCl and KH_2PO_4 from Fisher Scientific Co., Ltd. (Fisher certified reagents). Deionized water, obtained by passing distilled water through a column containing Rexyn I-300 Research Grade resin (a mixed bed resin), was used throughout.

Methods

The calibration procedure was exactly the same as that reported for D-glucuronolactone over the range 0–100 μg per ml (1). Polarograms were run over the voltage range −1.0 to −2.0 V with the appropriate sensitivity setting, using the Sargent (E. H. Sargent and Co.) model XXI polarograph. The polarographic cell was an H-cell with a saturated calomel electrode (s.c.e.) as the reference electrode. All $E_{1/2}$ values are reported with respect to the s.c.e. The capillary characteristics were: $m = 1.101$ mg s^{-1}, $t = 4.87$ s, $m^{2/3}t^{1/6} = 1.388$ $mg^{2/3}s^{-1/2}$. All polarograms were run at 25 °C with a mercury column height of 50 cm. No damping was used.

pH measurements were made with a Radiometer type TTTlc titrator (used as a pH meter), and a Radiometer model PHA630T scale expander. The meter was standardized with buffers of pH 4.01 (potassium acid phthalate) and pH 6.48 (Radiometer buffer solution S1001).

Phosphate was added by pipetting the desired amount of KH_2PO_4 from a stock solution of 1 mg PO_4^{3-} (as KH_2PO_4) per ml.

Results and Discussion

Over the concentration range 50–100 μg D-mannuronolactone per ml, there is a linear relationship between i_D and the concentration of the lactone, as is shown in Table I. The value of i_D at a lactone concentration of 20 μg per ml does not fall on this line, but is reproducible. The half-wave potential for the reduction was found to be −1.49 V.

As can be seen from Table I, there is only a slight change in pH with increasing D-mannuronolactone concentration. This behavior is similar to that noted with D-glucuronolactone solutions.

A plot of diffusion (i_D) vs. the square root of the height of the mercury column (the height of the mercury column was varied from 30–50 cm) showed that the reduction process is diffusion controlled. This is in marked contrast to the results obtained in this concentration range for D-glucuronolactone (1), where the reduction process was found to be kinetic or catalytic in nature.

TABLE I

Variation of the diffusion current of D-mannuronolactone*

μg Lactone per ml	i_D (μA)†	μg PO_4^{3-} per ml‡	pH
0	0	0	5.10
20	0.150	0	5.07
50	1.14	0	5.07
80	1.99	0	5.05
100	2.51	0	5.05
100	2.37	10	5.04
100	0	30	5.03

*All solutions are 0.2 *M* KCl and 0.005% with respect to gelatin.
†When no phosphate was present, these i_D values are the average of triplicate values.
‡Phosphate added as KH_2PO_4.

Upon the addition of KH_2PO_4, solutions containing 100 μg D-mannuronolactone per ml behaved in a similar manner to D-glucuronolactone solutions of this concentration. There was very little change in the pH, and increasing the phosphate concentration caused the polarographic wave height to be depressed until the wave was obliterated.

The reduction of D-glucuronolactone is a kinetic or catalytic process, indicating that the lactone undergoes a reaction prior to its reduction at the dropping mercury electrode. The fact that the reduction of D-mannuronolactone is a diffusion controlled process indicates that either D-mannuronolactone reacts very quickly on being dissolved, or does not react to any appreciable extent prior to its reduction. In the aqueous gelatin – KCl medium, the most probable reaction would be hydrolysis of the lactone to the acid. Should this reaction occur rapidly, the D-mannuronic acid ($pK_a = 3.38$) produced would completely overwhelm the buffer capacity of the gelatin – KCl solution, and the pH should decrease markedly on increasing the lactone concentration. The pH data in Table I show that D-mannuronolactone does not undergo such a reaction immediately on dissolution. Therefore, it would appear that D-mannuronolactone does not undergo a reaction prior to its reduction, while D-glucuronolactone does. This difference indicates that the D-mannuronolactone ring is less reactive than the D-glucuronolactone ring.

When KH_2PO_4 was added, 10 μg PO_4^{3-} per

Can. J. Chem. Downloaded from www.nrcresearchpress.com by 210.87.254.5 on 09/05/12
For personal use only.

ml caused a perceptible decrease in the diffusion current of D-mannuronolactone (100 μg per ml), and 30 μg PO_4^{3-} per ml eliminated the wave entirely. This is considerably more $H_2PO_4^-$ than was the case with D-glucuronolactone where 7.5 μg PO_4^{3-} per ml sufficed to depress the wave to the residual current (1). This is taken as further evidence that the D-mannuronolactone ring is less reactive than the D-glucuronolactone ring.

Acknowledgment

The authors gratefully acknowledge the financial support of the National Research Council of Canada.

1. R. J. THIBERT and J. R. JOHNSTON. Can. J. Chem. **47**, 265 (1969).
2. R. J. THIBERT and A. J. BOYLE. Talanta, **7**, 175 (1961).

Can. J. Chem. Downloaded from www.nrcresearchpress.com by 210.87.254.5 on 09/05/12
For personal use only.

Thermal reaction of the U(VI) and Th(IV) 8-hydroxyquinoline adducts

A. CORSINI AND J. ABRAHAM[1]

Department of Chemistry, McMaster University, Hamilton, Ontario

Received September 18, 1968

The use of [^{14}C]-8-hydroxyquinoline has shown that when the 8-hydroxyquinoline adducts, $UO_2(C_9H_6NO)_2 \cdot C_9H_7NO$ and $Th(C_9H_6NO)_4 \cdot C_9H_7NO$, are thermally converted to the normal compounds, $UO_2(C_9H_6NO)_2$ and $Th(C_9H_6NO)_4$, intermolecular ligand exchange in the solid phase occurs. The extent to which the exchange equilibrium proceeds suggests that the thermal energy absorbed is sufficient to promote considerable metal–ligand bond rupture.

Canadian Journal of Chemistry, **47**, 1435 (1969)

The 8-hydroxyquinoline "addition" compounds (adducts), $UO_2(C_9H_6NO)_2 \cdot C_9H_7NO$ and $Th(C_9H_6NO)_4 \cdot C_9H_7NO$, are structurally interesting compounds (1–3) that have been exploited for analytical purposes for many years (4). A significant analytical reaction is the thermal conversion of the adducts to 8-hydroxyquinoline and the normal complexes, $UO_2(C_9H_6NO)_2$ and $Th(C_9H_6NO)_4$ (4–10).

The complete mechanism of each thermal reaction has not been unambiguously determined, although proposals concerning mechanism have been made (5, 10–12).

In the present study, the use of [^{14}C]-8-hydroxyquinoline has provided evidence that during the thermal reaction, extensive bond rupture between the central metal [U(VI) or Th(IV)] and the ligand occurs, resulting in an appreciable amount of solid-phase intermolecular ligand exchange.

Experimental

The uranyl and thorium nitrate hexahydrates (ANALAR, British Drug Houses) were used without further purification. Unlabelled 8-hydroxyquinoline (certified grade, Fisher Scientific Co.) was purified by sublimation.

[1]Present address: Department of Chemistry, Dalhousie University, Halifax, Nova Scotia.

The [^{14}C]-8-hydroxyquinoline was prepared by diluting about 50 mg of [^{14}C]-glycerol (0.5 mC, Volk Radiochemical Co., Chicago) with 28.7 mg of unlabelled glycerol and thereafter following the procedure of Manske *et al.* (13) for the preparation of unlabelled 8-hydroxyquinoline. The crude material (yield 70%) was steam distilled and recrystallized from aqueous ethanol, m.p. 73.5–74.0 °C, specific activity 3.58 ± 0.02 mV/s mg (see below).

The [^{14}C]-8-hydroxyquinoline was used to prepare the U(VI) and Th(IV) adducts. The U(VI) compound was synthesized by Moeller and Wilkins' method (14) for the preparation of the unlabelled compound. The Th(IV) compound was prepared as follows: 25.0 ml of a Th(IV) solution (1.4 mg Th/ml) was diluted to 50 ml with water and heated to about 70 °C. In turn, the following solutions (warmed to 70 °C) were added dropwise with stirring: 8.0 ml of a 1.8% solution of [^{14}C]-8-hydroxyquinoline (1.8 g dissolved in 6 ml of glacial acetic acid and diluted to 100 ml with water), and 15 ml of an aqueous solution containing 2 g of ammonium acetate. The pH was adjusted to 6.5–7.0 with 1.0 *M* aqueous ammonia, the volume adjusted to about 90 ml with water, and the mixture digested for 1 h at 70 °C. The orange precipitate was filtered by suction, washed with 100 ml of hot water, adjusted to pH 7.5 ± 0.5 with dilute ammonia, and dried for 3 h by suction and about 15 h over P_2O_5. The compound is deficient in 8-hydroxyquinoline, having a composition close to $Th(C_9H_6NO)_4 \cdot 0.9C_9H_7NO$ (unpublished results).

The normal bis and tetrakis compounds were prepared thermally from the respective *unlabelled* adducts. The apparatus and the preparation of $UO_2(C_9H_6NO)_2$ were as described previously (12). $Th(C_9H_6NO)_4$ was prepared

ml caused a perceptible decrease in the diffusion current of D-mannuronolactone (100 μg per ml), and 30 μg PO_4^{3-} per ml eliminated the wave entirely. This is considerably more $H_2PO_4^-$ than was the case with D-glucuronolactone where 7.5 μg PO_4^{3-} per ml sufficed to depress the wave to the residual current (1). This is taken as further evidence that the D-mannuronolactone ring is less reactive than the D-glucuronolactone ring.

Acknowledgment

The authors gratefully acknowledge the financial support of the National Research Council of Canada.

1. R. J. THIBERT and J. R. JOHNSTON. Can. J. Chem. **47**, 265 (1969).
2. R. J. THIBERT and A. J. BOYLE. Talanta, **7**, 175 (1961).

Can. J. Chem. Downloaded from www.nrcresearchpress.com by 210.87.254.40 on 09/05/12
For personal use only.

Thermal reaction of the U(VI) and Th(IV) 8-hydroxyquinoline adducts

A. CORSINI AND J. ABRAHAM[1]

Department of Chemistry, McMaster University, Hamilton, Ontario

Received September 18, 1968

The use of [^{14}C]-8-hydroxyquinoline has shown that when the 8-hydroxyquinoline adducts, $UO_2(C_9H_6NO)_2 \cdot C_9H_7NO$ and $Th(C_9H_6NO)_4 \cdot C_9H_7NO$, are thermally converted to the normal compounds, $UO_2(C_9H_6NO)_2$ and $Th(C_9H_6NO)_4$, intermolecular ligand exchange in the solid phase occurs. The extent to which the exchange equilibrium proceeds suggests that the thermal energy absorbed is sufficient to promote considerable metal–ligand bond rupture.

Canadian Journal of Chemistry, **47**, 1435 (1969)

The 8-hydroxyquinoline "addition" compounds (adducts), $UO_2(C_9H_6NO)_2 \cdot C_9H_7NO$ and $Th(C_9H_6NO)_4 \cdot C_9H_7NO$, are structurally interesting compounds (1–3) that have been exploited for analytical purposes for many years (4). A significant analytical reaction is the thermal conversion of the adducts to 8-hydroxyquinoline and the normal complexes, $UO_2(C_9H_6NO)_2$ and $Th(C_9H_6NO)_4$ (4–10).

The complete mechanism of each thermal reaction has not been unambiguously determined, although proposals concerning mechanism have been made (5, 10–12).

In the present study, the use of [^{14}C]-8-hydroxyquinoline has provided evidence that during the thermal reaction, extensive bond rupture between the central metal [U(VI) or Th(IV)] and the ligand occurs, resulting in an appreciable amount of solid-phase intermolecular ligand exchange.

Experimental

The uranyl and thorium nitrate hexahydrates (ANALAR, British Drug Houses) were used without further purification. Unlabelled 8-hydroxyquinoline (certified grade, Fisher Scientific Co.) was purified by sublimation.

[1]Present address: Department of Chemistry, Dalhousie University, Halifax, Nova Scotia.

The [^{14}C]-8-hydroxyquinoline was prepared by diluting about 50 mg of [^{14}C]-glycerol (0.5 mC, Volk Radiochemical Co., Chicago) with 28.7 mg of unlabelled glycerol and thereafter following the procedure of Manske *et al.* (13) for the preparation of unlabelled 8-hydroxyquinoline. The crude material (yield 70%) was steam distilled and recrystallized from aqueous ethanol, m.p. 73.5–74.0 °C, specific activity 3.58 ± 0.02 mV/s mg (see below).

The [^{14}C]-8-hydroxyquinoline was used to prepare the U(VI) and Th(IV) adducts. The U(VI) compound was synthesized by Moeller and Wilkins' method (14) for the preparation of the unlabelled compound. The Th(IV) compound was prepared as follows: 25.0 ml of a Th(IV) solution (1.4 mg Th/ml) was diluted to 50 ml with water and heated to about 70 °C. In turn, the following solutions (warmed to 70 °C) were added dropwise with stirring: 8.0 ml of a 1.8% solution of [^{14}C]-8-hydroxyquinoline (1.8 g dissolved in 6 ml of glacial acetic acid and diluted to 100 ml with water), and 15 ml of an aqueous solution containing 2 g of ammonium acetate. The pH was adjusted to 6.5–7.0 with 1.0 *M* aqueous ammonia, the volume adjusted to about 90 ml with water, and the mixture digested for 1 h at 70 °C. The orange precipitate was filtered by suction, washed with 100 ml of hot water, adjusted to pH 7.5 ± 0.5 with dilute ammonia, and dried for 3 h by suction and about 15 h over P_2O_5. The compound is deficient in 8-hydroxyquinoline, having a composition close to $Th(C_9H_6NO)_4 \cdot 0.9C_9H_7NO$ (unpublished results).

The normal bis and tetrakis compounds were prepared thermally from the respective *unlabelled* adducts. The apparatus and the preparation of $UO_2(C_9H_6NO)_2$ were as described previously (12). $Th(C_9H_6NO)_4$ was prepared

by heating the adduct (150–200 mg) in vacuo (0.1 mm Hg) at 165–170 °C for 1½ h.

The apparatus for the wet-oxidation of [^{14}C]-containing compounds and the collection of radioactive carbon dioxide has been described elsewhere (15). Measurements of [^{14}C]-radioactivity were made by the "rate-of-drift" method (16), which yields units of mV/s mg. It was not necessary in this work to convert to the more customary units of disintegrations/s mg.

Thermal Ligand Exchange

Known amounts of the [^{14}C]-adduct and of the unlabelled normal complex were ground and mixed thoroughly by mortar and pestle and carried through the thermal-conversion procedure. The specific activity of the residual normal complex and of the sublimed 8-hydroxyquinoline was determined and used to estimate the extent of intermolecular ligand exchange during the thermal reaction (Tables I and II).

TABLE I

Intermolecular ligand exchange in thermal reaction of $UO_2(C_9H_6NO)_2 \cdot C_9H_7NO$*

Specific activity (mV/s mg)			Exchange equilibrium (%)
Measured	Complete exchange†	No exchange†	
	Sublimed 8-hydroxyquinoline		
3.16	2.03	3.58	27
	Residual bis compound		
1.79	2.03	1.67	33
		Average	30 ± 3

*Unlabelled bis compound taken: 58.7 mg. Labelled addition compound taken (initial specific activity of C_9H_7NO, 3.58 mV/s mg): 64.6 mg.

†Calculated from the initial specific activity of C_9H_7NO and the amounts of the species taken.

TABLE II

Intermolecular ligand exchange in thermal reaction of $Th(C_9H_6NO)_4 \cdot C_9H_7NO$*

Specific activity (mV/s mg)			Exchange equilibrium (%)
Measured	Complete exchange†	No exchange†	
	Sublimed 8-hydroxyquinoline		
2.74	1.96	3.58	52
	Residual tetrakis compound		
1.90	1.96	1.78	67
		Average	60 ± 8

*Unlabelled tetrakis compound taken: 110 mg; labelled addition compound taken (initial specific activity of C_9H_7NO, 3.58 mV/mg s): 126.5 mg.

†Calculated from the initial specific activity of C_9H_7NO and the amounts of the species taken, using the formula $Th(C_9H_6NO)_4 \cdot 0.9\text{-}C_9H_7NO$.

Results and Discussion

Since the specific activity of the 8-hydroxyquinoline used to synthesize the adduct compounds was 3.58 mV/s mg, the specific activity of the 8-hydroxyquinoline sublimed in the thermal reactions should, in the absence of intermolecular exchange, have the same value. The data of Tables I and II show that the value in each case is significantly lower. The difference between 3.58 and the measured value is well beyond the precision error of ±0.06[2]. Similarly, in the absence of intermolecular exchange, the specific activity of the residual bis and tetrakis compounds should have the calculated values listed in the tables. The measured values, however, are higher[3].

These results could be obtained only if the labelled adduct and the unlabelled normal compound were involved in an intermolecular exchange of ligands during the thermal reaction. The large precision error in the extent of exchange, for the Th(IV) adduct particularly, arises because the difference between the specific activity for complete and no exchange for the residual normal compounds is small and subject to a considerable error (20–30%) in measurement. Therefore, the extent of exchange equilibrium based on the data for the sublimed 8-hydroxyquinoline is more reliable.

The larger extent of exchange for the Th(IV) adduct compared to that for the U(VI) compound reflects the greater overall lability of the Th(IV) adduct, which, for example, requires a lower temperature for the thermal reaction and is more extensively dissociated in organic solvents.

The energy of the thermal reaction is sufficient to cause appreciable bond rupture and intermolecular ligand transfer in the solid phase. The transfer involves the mono- *and* bi-dentate ligands, both of which have been shown (1–3) to be present in the U(VI) and Th(IV) adducts. The exchange mechanism could involve the transfer of the monodentate ligand in the labelled adduct to the normal compound to produce a labelled intermediate adduct (reaction [1] below), followed by intramolecular ligand exchange in this intermediate (reaction [2]) which involves, basi-

[2]The standard deviation for the combustion and counting method is ±0.04, as determined on 16 samples. The precision error for the difference between two such measurements is thus ±0.06.

[3]It can readily be shown for both the U(VI) and Th(IV) compounds that within experimental error, a radiobalance exists between the decrease in specific activity of the sublimed 8-hydroxyquinoline and the increase in specific activity of the residual bis and tetrakis compounds.

Can. J. Chem. Downloaded from www.nrcresearchpress.com by 210.87.254.40 on 09/05/12
For personal use only.

cally, only a proton transfer. These reactions would account for the distribution of [^{14}C]-activity found experimentally[4].

[1] $MQ^*_n \cdot H^*Q + MQ_n \rightleftharpoons MQ^*_n + MQ_n \cdot H^*Q$

where H*Q = [^{14}C]-8-hydroxyquinoline.

[2] $MQ_n \cdot H^*Q \rightleftharpoons MQ_{n-1}Q^* \cdot HQ$

The occurrence of reactions [1] and [2] would make possible reactions [3] and [4]. Reaction [3] would not alter the effect of reaction [2] on the

[3] $MQ_{n-1}Q^* \cdot HQ + MQ^*_n \rightleftharpoons MQ_{n-1}Q^* + MQ^*_n \cdot HQ$

[4] $MQ^*_n \cdot HQ \rightleftharpoons MQ^*_{n-1}Q \cdot H^*Q$

specific activity of the sublimed 8-hydroxyquinoline and the residual normal compound, although reaction [4] would somewhat offset this effect.

No direct evidence for intramolecular ligand exchange was obtained in the experiments but it must be presumed that this exchange occurs, since it would operate through transfer of the proton on the monodentate ligand: a low energy process compared to intermolecular ligand exchange.

Finally, we could not prepare the adduct in which only the monodentate ligand is labelled[5]. The occurrence of exchange could be detected using such a compound, although it would not be possible to distinguish intermolecular from intramolecular exchange.

[4]Complete equilibration of the activity is not obtained since the monodentate ligand is eliminated before such equilibration can occur.

[5]The addition of a solution of H*Q to MQ_n yielded $MQ^*_n \cdot H^*Q$, even for short reaction times.

Acknowledgment

We wish to thank the National Research Council of Canada for the financial support of this study.

1. D. Hall, A. D. Rae, and T. N. Waters. Acta Cryst. **22**, 258 (1967).
2. A. Corsini, J. Abraham, and M. Thompson. Chem. Commun. 1101 (1967).
3. A. Corsini and J. Abraham. Chem. Commun. 856 (1968).
4. R. G. W. Hollingshead. Oxine and its derivatives. Vols. II and IV. Butterworths Scientific Publications, London. 1954–1956.
5. J. H. Van Tassel and W. W. Wendlandt. J. Am. Chem. Soc. **81**, 813 (1959).
6. K. Yakiyama, E. D. Salesin, and L. Gordon. Talanta, **5**, 231 (1960).
7. C. E. Crouthamel and C. E. Johnson. Talanta, **8**, 377 (1961).
8. J. Bordner and L. Gordon. Talanta, **9**, 1003 (1962).
9. G. R. Horton and W. W. Wendlandt. J. Inorg. Nucl. Chem. **25**, 241 (1963).
10. G. R. Horton and W. W. Wendlandt. J. Inorg. Nucl. Chem. **25**, 247 (1963).
11. M. Borrel and R. Pâris. Anal. Chim. Acta, **4**, 267 (1950).
12. A. Corsini and J. Abraham. Talanta, **15**, 562 (1968).
13. R. H. F. Manske, A. E. Ledingham, and W. R. Ashford. Can. J. Research, **27F**, 359 (1949).
14. T. Moeller and D. H. Wilkins. Inorganic syntheses. Vol. IV. McGraw-Hill Book Co., Inc., New York. 1953. p. 101.
15. J. G. Burr, Jr. Anal. Chem. **26**, 1395 (1954).
16. V. F. Raaen and G. A. Ropp. Anal. Chem. **25**, 174 (1953).

Anilinium chloride as a model for the transition state for benzyl chloride solvolysis

Ikchoon Lee and J. B. Hyne

Department of Chemistry, The University of Calgary, Calgary, Alberta

Received August 10, 1967

The solvent composition dependence of the partial molal volume of the transition state of benzyl chloride solvolysing in water–ethanol mixtures is compared with that of anilinium chloride and a number of quaternary alkyl ammonium chlorides. It is concluded that anilinium chloride is not a good electrostatic model for the benzyl chloride transition state even though it may be a fair structural model. The partial molal volume of tetraethylammonium chloride is very similar to that of the transition state suggesting that charge development in the activation process is far from being fully ionic.

Canadian Journal of Chemistry, **47**, 1437 (1969)

We have recently reported the dependence of the partial molal volume, $\bar{V}_t$, of the transition state for benzyl chloride solvolysis on the composition of the ethanol–water solvolysing medium (1) and also the behavior of the partial molal volumes of a series of tetraalkylammonium salts,

Can. J. Chem. Downloaded from www.nrcresearchpress.com by 210.87.254.40 on 09/05/12
For personal use only.

cally, only a proton transfer. These reactions would account for the distribution of [^{14}C]-activity found experimentally[4].

[1] $MQ^*_n \cdot H^*Q + MQ_n \rightleftharpoons MQ^*_n + MQ_n \cdot H^*Q$

where H*Q = [^{14}C]-8-hydroxyquinoline.

[2] $MQ_n \cdot H^*Q \rightleftharpoons MQ_{n-1}Q^* \cdot HQ$

The occurrence of reactions [1] and [2] would make possible reactions [3] and [4]. Reaction [3] would not alter the effect of reaction [2] on the

[3] $MQ_{n-1}Q^* \cdot HQ + MQ^*_n \rightleftharpoons MQ_{n-1}Q^* + MQ^*_n \cdot HQ$

[4] $MQ^*_n \cdot HQ \rightleftharpoons MQ^*_{n-1}Q \cdot H^*Q$

specific activity of the sublimed 8-hydroxyquinoline and the residual normal compound, although reaction [4] would somewhat offset this effect.

No direct evidence for intramolecular ligand exchange was obtained in the experiments but it must be presumed that this exchange occurs, since it would operate through transfer of the proton on the monodentate ligand: a low energy process compared to intermolecular ligand exchange.

Finally, we could not prepare the adduct in which only the monodentate ligand is labelled[5]. The occurrence of exchange could be detected using such a compound, although it would not be possible to distinguish intermolecular from intramolecular exchange.

[4]Complete equilibration of the activity is not obtained since the monodentate ligand is eliminated before such equilibration can occur.

[5]The addition of a solution of H*Q to MQ_n yielded $MQ^*_n \cdot H^*Q$, even for short reaction times.

Acknowledgment

We wish to thank the National Research Council of Canada for the financial support of this study.

1. D. Hall, A. D. Rae, and T. N. Waters. Acta Cryst. **22**, 258 (1967).
2. A. Corsini, J. Abraham, and M. Thompson. Chem. Commun. 1101 (1967).
3. A. Corsini and J. Abraham. Chem. Commun. 856 (1968).
4. R. G. W. Hollingshead. Oxine and its derivatives. Vols. II and IV. Butterworths Scientific Publications, London. 1954–1956.
5. J. H. Van Tassel and W. W. Wendlandt. J. Am. Chem. Soc. **81**, 813 (1959).
6. K. Yakiyama, E. D. Salesin, and L. Gordon. Talanta, **5**, 231 (1960).
7. C. E. Crouthamel and C. E. Johnson. Talanta, **8**, 377 (1961).
8. J. Bordner and L. Gordon. Talanta, **9**, 1003 (1962).
9. G. R. Horton and W. W. Wendlandt. J. Inorg. Nucl. Chem. **25**, 241 (1963).
10. G. R. Horton and W. W. Wendlandt. J. Inorg. Nucl. Chem. **25**, 247 (1963).
11. M. Borrel and R. Pâris. Anal. Chim. Acta, **4**, 267 (1950).
12. A. Corsini and J. Abraham. Talanta, **15**, 562 (1968).
13. R. H. F. Manske, A. E. Ledingham, and W. R. Ashford. Can. J. Research, **27F**, 359 (1949).
14. T. Moeller and D. H. Wilkins. Inorganic syntheses. Vol. IV. McGraw-Hill Book Co., Inc., New York. 1953. p. 101.
15. J. G. Burr, Jr. Anal. Chem. **26**, 1395 (1954).
16. V. F. Raaen and G. A. Ropp. Anal. Chem. **25**, 174 (1953).

Anilinium chloride as a model for the transition state for benzyl chloride solvolysis

Ikchoon Lee and J. B. Hyne

Department of Chemistry, The University of Calgary, Calgary, Alberta

Received August 10, 1967

The solvent composition dependence of the partial molal volume of the transition state of benzyl chloride solvolysing in water–ethanol mixtures is compared with that of anilinium chloride and a number of quaternary alkyl ammonium chlorides. It is concluded that anilinium chloride is not a good electrostatic model for the benzyl chloride transition state even though it may be a fair structural model. The partial molal volume of tetraethylammonium chloride is very similar to that of the transition state suggesting that charge development in the activation process is far from being fully ionic.

Canadian Journal of Chemistry, **47**, 1437 (1969)

We have recently reported the dependence of the partial molal volume, $\bar{V}_t$, of the transition state for benzyl chloride solvolysis on the composition of the ethanol–water solvolysing medium (1) and also the behavior of the partial molal volumes of a series of tetraalkylammonium salts,

Can. J. Chem. Downloaded from www.nrcresearchpress.com by 210.87.254.5 on 09/05/12
For personal use only.

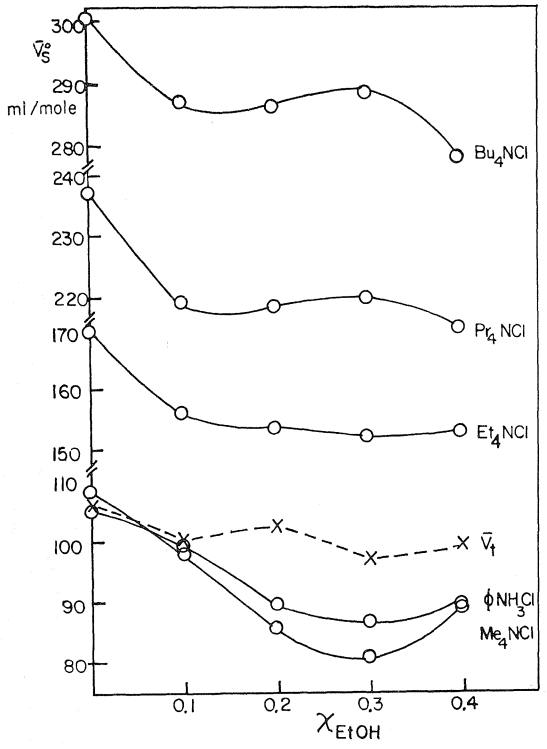

FIG. 1. Dependence of partial molal volumes of tetraalkylammonium chlorides, anilinium chloride, and benzyl chloride transition state on mole fraction ethanol.

$\bar{V}_s^0$, in the same solvents (2) (see Fig. 1). The general similarity in behavior between the transition state and the salts prompted us to use the partial molal volume behavior as an experimental probe to determine whether anilinium chloride was a reasonable model for the transition state of benzyl chloride solvolysing in ethanol–water solvent mixtures. Anilinium chloride is a reasonable structural model for the transition state of benzyl chloride but the question remains as to whether it represents a reasonable charge distribution model.

That there is charge development in the C—Cl bond of benzyl chloride during the activation process has never been denied; the as yet unanswered question is whether this charge development more nearly approximates the classical S_N1 type of transition state, which implies incipient ion formation along the reaction path towards an intermediate benzyl carbonium and chloride ion, or the less charge developed S_N2 transition state. Since partial molal volumes of solute species are strongly dependent on electrostriction phenonema and these in turn reflect charge density on the solute species, it is not unreasonable to expect that a comparison of partial molal volume behavior of the transition state with model compounds of known charge type might yield information on the charge type of the transition state.

Experimental Results

The partial molal volume data for the series of quaternary alkylammonium salts used in Fig. 1 have been reported previously (2). The method previously described was used without modification to obtain the results shown below for anilinium chloride.

Eastman reagent grade aniline hydrochloride was twice recrystallized from acetone and dried *in vacuo* at 80° for at least 24 h before use. Magnesium dried ethanol and double distilled water mixtures were prepared by weight.

Procedure and accuracy of density measurements were the same as described previously (2). Apparent molal volumes ϕ were calculated using the equation

$$\phi = \frac{M_2}{d_0} - \frac{1000}{d_0}\frac{(d - d_0)}{C}$$

where M_2 is the molecular weight of aniline hydrochloride, C is the concentration in moles per liter, and d and d_0 are the density of solution and solvent respectively. Values of ϕ and densities are summarized in Table I. Partial molal volumes $\bar{V}^0$ were then obtained from ϕ and its concentration dependence using the relation

$$\phi = \bar{V}^0 + SC^{1/2}$$

where S is the limiting slope. The values of $\bar{V}^0$ and S for each solvent composition are

water ; $\phi = 105.1 + 2.4\,C^{1/2}$

0.10 mole fraction ethanol ; $\phi = 99.5 + 16.7\,C^{1/2}$

0.20 " " " ; $\phi = 89.7 + 49.5\,C^{1/2}$

0.30 " " " ; $\phi = 86.7 + 54.5\,C^{1/2}$

0.40 " " " ; $\phi = 89.0 + 41.0\,C^{1/2}$

Discussion

The data presented in Fig. 1 show that the behavior of $\bar{V}_t$ for benzyl chloride from pure

Can. J. Chem. Downloaded from www.nrcresearchpress.com by 210.87.254.5 on 09/05/12
For personal use only.

TABLE I

Densities and apparent molal volumes of anilinium chloride in ethanol–water mixtures at 50.25°

Solvent (mole fraction EtOH)	$C^{1/2}$ (mole $l^{-1})^{1/2}$	d (g ml^{-1})	ϕ (ml $mole^{-1}$)
0.00	0.570	0.99584	106.6
	0.499	0.99404	106.5
	0.402	0.99194	106.2
	0.379	0.99149	106.2
	0.307	0.99033	105.7
	0.226	0.98924	105.8
	0.219	0.98916	105.7
0.10	0.501	0.95242	106.3
	0.403	0.94997	105.6
	0.351	0.94882	105.3
	0.300	0.94793	104.3
	0.249	0.94708	103.8
	0.200	0.94643	102.7
0.20	0.546	0.92352	107.0
	0.451	0.92083	105.8
	0.351	0.91835	104.4
	0.304	0.91739	103.4
	0.277	0.91698	101.5
	0.247	0.91646	100.4
	0.199	0.91572	98.6
0.30	0.500	0.89296	105.2
	0.399	0.88983	103.7
	0.355	0.88850	103.3
	0.299	0.88713	102.5
	0.276	0.88676	101.8
	0.246	0.88631	99.9
	0.226	0.88596	98.7
	0.193	0.88542	97.3
0.40	0.499	0.86812	104.9
	0.349	0.86325	103.1
	0.300	0.86214	101.1
	0.250	0.86098	100.2
	0.226	0.86060	97.9
	0.201	0.86015	97.1
	0.175	0.85980	95.7

water up to 0.1 mole fraction ethanol is remarkably similar to the behavior of the volumes of both $Me_4N^+Cl^-$ and $C_6H_5NH_3{}^+Cl^-$. Beyond this point, however, there is marked divergence and the shape of the $\overline{V}_t$ curve is much more similar to that for the partial molal volume of $Et_4N^+Cl^-$. The marked reduction in volume for anilinium chloride up to 0.3 mole fraction is not observed for $\overline{V}_t$. This can only mean that the charge density and hence the electrostriction caused by the transition state of benzyl chloride is considerably less than in anilinium chloride, but it is still somewhat greater than the surface charge associated with $Et_4N^+Cl^-$.

We can conclude, therefore, that while anilinium chloride is a fair structural model for the solvolysis transition state of benzyl chloride there is less charge development in the transition state than is represented by anilinium chloride. The surface charge density on the transition state, however, is not by any means small, since the volume behavior establishes that it is at least as great as that characteristic of $Et_4N^+Cl^-$. It must be remembered, however, that what is being observed in these studies is the *sum* of the electrostriction effects of both the anion and the cation.

The similarity in behavior of the transition state and $Et_4N^+Cl^-$, therefore, merely implies that the sum of the electrostriction effects at 0.3 mole fraction are comparable. Nothing is implied about the relative charge densities on the individual ions; for example, the degree of charge development in the transition state may well be much less than the full ionic character of $Et_4N^+Cl^-$, but the charge that has developed in the transition state may be much more accessible to the solvent than is the case in the bulkier tetraethylammonium cation.

There is obviously a temptation to use the evidence presented here to comment on the question as to whether benzyl chloride solvolysis is S_N1 or S_N2! This temptation will be resisted if for no other reason than the fact that we have already described the transition state, through comparison with models, in much greater detail than the S_N1–S_N2 categorization is capable of doing. Charge is developed in passing from the initial to the transition state and the accessibility of solvent to that charge is intermediate between that for anilinium chloride and tetraethylammonium chloride. Whether solvent interaction with the transition state is describable as "covalent interaction" or "ion–dipole electrostriction" is not a resolvable question at present.

Acknowledgments

We are grateful to the National Research Council of Canada for general financial assistance and to The University of Calgary for a Post-doctoral Fellowship to one of us (I.L.).

1. H. S. Golinkin, I. Lee, and J. B. Hyne. J. Am. Chem. Soc. **89**, 1307 (1967).
2. I. Lee and J. B. Hyne. Can. J. Chem. **46**, 2333 (1968).

Can. J. Chem. Downloaded from www.nrcresearchpress.com by 210.87.254.5 on 09/05/12
For personal use only.

Distortions in tetrahedral copper(I)–phosphine complexes : bis(triphenylphosphine)copper(I) nitrate

G. G. MESSMER AND GUS J. PALENIK
Department of Chemistry, University of Waterloo, Waterloo, Ontario

Received October 30, 1968

The crystal structure of bis(triphenylphosphine)copper(I) nitrate has been determined by a three-dimensional X-ray diffraction study. The copper(I) atom is bonded to the two phosphines and two oxygen atoms of the nitrate group. However, the molecule is distorted from that of an ideal tetrahedron, with the P—Cu—P angle being 131.1°.

Canadian Journal of Chemistry, **47**, 1440 (1969)

Can. J. Chem. Downloaded from www.nrcresearchpress.com by 210.87.254.42 on 09/05/12
For personal use only.

The molecular structure of bis(triphenylphosphine)copper(I) nitrate has been in question since the compound was first prepared by Cotton and Goodgame (1). The various structures suggested include a tricoordinate monomer (1), a nitrate bridged dimer (1), and a monomer involving a bidentate nitrate group (2). We undertook an X-ray crystal structure determination to resolve these conflicts. The results of our study have raised a number of questions regarding the nature of the copper–phosphorus bond and dπ–dπ bonding.

Bis(triphenylphosphine)copper(I) nitrate was prepared following the method reported by Cotton and Goodgame (1). Long acicular crystals were grown by slowly cooling a hot saturated ethanol solution. The crystals are monoclinic with $a = 22.254$, $b = 9.197$, $c = 15.440$ Å, $\beta = 101.56°$, and 4 molecules per unit cell, with the space group $I2/a$ or Ia. The intensities were measured using a General Electric Diffractometer, automated by the Datex Corporation. A total of 4197 measurements were made employing molybdenum radiation ($K\alpha_1 = 0.70926$ Å) and the stationary crystal – stationary counter technique. After averaging the equivalent reflections and correcting for the background, a total of 1343 reflections were considered as observed and used in the analysis.

The three dimensional Patterson yielded trial coordinates for both the copper and phosphorus. The symmetry appeared to be $I2/a$ which is in agreement with the statistical distribution of intensities. The positions for the light atoms were determined from electron density calculations. The trial structure was refined by full-matrix least-squares methods, first with isotropic thermal parameters, then with anisotropic thermal parameters to an R of 0.074.

The molecular structure of bis(triphenylphosphine)copper(I) nitrate is that of a bidentate nitrate monomer. However, the angular distortions are among the largest observed for the nominally tetrahedral copper(I) atom. The P—Cu—P angle is 131.1°, which is larger than the P—Cu—P angle of 123.3° reported by Lippard and Melmed (3) in borohydridobis(triphenylphosphine)copper(I), or the angle of 123.8° reported by Corfield and Shearer (4) in phenylethynyl(trimethylphosphine)copper(I). The large P—Cu—P bond angles in the three complexes cannot be rationalized on the basis of steric repulsions since the trimethylphosphine ligand is smaller than the triphenylphosphine ligand. Furthermore, the P–metal–P angles in four other coordinate complexes involving triphenylphosphine as a ligand are smaller than in the present case. For example, the P—Ni—P angle in $Br_2Ni[(C_6H_5)_3P]_2$ (5) is 110.4°, where Ni—P is 2.333 Å, and the P—Pt—P angle is 98.2° in $[(C_6H_5)_3P]_2PtCO_3$ (6), where the P—Pt distance is 2.24 Å. The metal–P distances in the Ni and Pt complexes are reasonably close to the Cu—P distances (2.222 to 2.276 Å) found in the three Cu(I)–phosphine complexes. The larger angle found in the nitrate complex relative to that in the borohydride case may indicate increased dπ–dπ bonding in the latter structure. Further structural studies are in progress on other phosphine copper(I) complexes to aid in understanding the distortions in these compounds.

The nitrate group is bidentate with N—O distances of 1.24 Å for N—O (bridging) and 1.16 Å for N—O (terminal). The shorter N—O

distance is uncorrected for thermal motion, which would increase the N—O length by 0.03 to 0.06 Å. The analysis of the thermal parameters will be carried out after our refinement is concluded.

Acknowledgment

We wish to thank the National Research Council of Canada for financial support.

1. F. A. COTTON and D. M. L. GOODGAME. J. Chem. Soc. 5267 (1960).
2. C. C. ADDISON and D. SUTTON. Progress in inorganic chemistry. Vol. 8. Interscience Publishers, Inc., New York. 1967. p. 258.
3. S. J. LIPPARD and K. M. MELMED. Inorg. Chem. **6**, 2223 (1967).
4. P. W. R. CORFIELD and H. M. M. SHEARER. Acta Cryst. **21**, 957 (1966).
5. J. A. J. JARVIS, R. H. B. MAIS, and P. G. OWSTON. J. Chem. Soc. A, 1473 (1968).
6. F. CARIATI, R. MASON, G. B. ROBERTSON, and R. UGO. Chem. Commun. 408 (1967).

Some comments on the Wigner tunneling formula[1]

J. C. NASH[2] AND W. G. LAIDLAW
Chemistry Department, University of Calgary, Calgary, Alberta

Received August 26, 1968

Tunneling through a barrier is calculated with the Wigner distribution function. The use of a simple height-to-width formula for various potential types is illustrated. The effect of higher order terms is also investigated.

Canadian Journal of Chemistry, **47**, 1441 (1969)

Can. J. Chem. Downloaded from www.nrcresearchpress.com by 210.87.254.42 on 09/05/12
For personal use only.

The transmission of a species of mass m over a one-dimensional barrier can be estimated from the Wigner (1) current formula

$$[1]\quad \text{Current} = e^{-\beta V_0}\left(\frac{1}{\beta} - \frac{\hbar^2\beta}{24m}V_2 - \frac{\hbar^2}{96m}\frac{V_4}{V_2}\right)$$

where $\hbar$ = Planck's Constant/2π, and $\beta = 1/kT$, with k = the Boltzmann constant and T = the absolute temperature.

Usually the first term in $\hbar^2$ is considered as providing an adequate measure of tunneling so that

$$[2]\quad \text{Tunneling} = T_1 = -e^{-\beta V_0}\left(\frac{\hbar^2\beta}{24m}V_2\right)$$

$V_2/2$ can be taken as the coefficient of the quadratic term in a parabolic representation of the potential for small x as

$$[3]\quad V(x) = V_0 + x^2\frac{V_2}{2}$$

If V_0 is fixed as the height of the barrier, V_2 can be found by a least squares fit to either a discrete set of $V(x)$ and x, or the $V(x)$ generated by an appropriate analytical form. The value obtained for V_2 and the accuracy of the representation of the potential by eq. [3] will, of course, depend on the potential and how closely it is approximated by the parabola [3]. The values of V_2 obtained, when some of the more common types of potential are represented by eq. [3], are given in the second column of Table I. The ratio of the current for a parabola with a given height and width to the current for a different type of potential with the same height and width is given in the last column as the "shape factor". This clearly shows that different barrier types, having the same height-to-width characteristics, yield currents differing by as much as a factor of 2 from one another. Obviously care should be exercised in assessing barrier characteristics, e.g. width, from a knowledge of tunneling current only. Conversely any calculated tunneling contribution will depend on the shape assumed for the potential.

The equation for T_1 may be converted to an expression in terms of height and width. This is done quite simply by first defining that width = $W = 2|x_n|$ where x_n is the value of the argument when the potential $V(x_n) = V_0/n$. Here n is an

[1]Submitted in partial fulfillment of the requirements for the B.Sc. (Honours) degree by J. C. Nash.
[2]Present address: The Mathematical Institute, 24–29 St. Giles, Oxford, England.

distance is uncorrected for thermal motion, which would increase the N—O length by 0.03 to 0.06 Å. The analysis of the thermal parameters will be carried out after our refinement is concluded.

Acknowledgment

We wish to thank the National Research Council of Canada for financial support.

1. F. A. COTTON and D. M. L. GOODGAME. J. Chem. Soc. 5267 (1960).
2. C. C. ADDISON and D. SUTTON. Progress in inorganic chemistry. Vol. 8. Interscience Publishers, Inc., New York. 1967. p. 258.
3. S. J. LIPPARD and K. M. MELMED. Inorg. Chem. **6**, 2223 (1967).
4. P. W. R. CORFIELD and H. M. M. SHEARER. Acta Cryst. **21**, 957 (1966).
5. J. A. J. JARVIS, R. H. B. MAIS, and P. G. OWSTON. J. Chem. Soc. A, 1473 (1968).
6. F. CARIATI, R. MASON, G. B. ROBERTSON, and R. UGO. Chem. Commun. 408 (1967).

Some comments on the Wigner tunneling formula[1]

J. C. NASH[2] AND W. G. LAIDLAW
Chemistry Department, University of Calgary, Calgary, Alberta

Received August 26, 1968

Tunneling through a barrier is calculated with the Wigner distribution function. The use of a simple height-to-width formula for various potential types is illustrated. The effect of higher order terms is also investigated.

Canadian Journal of Chemistry, **47**, 1441 (1969)

The transmission of a species of mass m over a one-dimensional barrier can be estimated from the Wigner (1) current formula

$$[1]\quad \text{Current} = e^{-\beta V_0}\left(\frac{1}{\beta} - \frac{\hbar^2\beta}{24m}V_2 - \frac{\hbar^2}{96m}\frac{V_4}{V_2}\right)$$

where $\hbar$ = Planck's Constant/2π, and $\beta = 1/kT$, with k = the Boltzmann constant and T = the absolute temperature.

Usually the first term in $\hbar^2$ is considered as providing an adequate measure of tunneling so that

$$[2]\quad \text{Tunneling} = T_1 = -e^{-\beta V_0}\left(\frac{\hbar^2\beta}{24m}V_2\right)$$

$V_2/2$ can be taken as the coefficient of the quadratic term in a parabolic representation of the potential for small x as

$$[3]\quad V(x) = V_0 + x^2\frac{V_2}{2}$$

If V_0 is fixed as the height of the barrier, V_2 can be found by a least squares fit to either a discrete set of $V(x)$ and x, or the $V(x)$ generated by an appropriate analytical form. The value obtained for V_2 and the accuracy of the representation of the potential by eq. [3] will, of course, depend on the potential and how closely it is approximated by the parabola [3]. The values of V_2 obtained, when some of the more common types of potential are represented by eq. [3], are given in the second column of Table I. The ratio of the current for a parabola with a given height and width to the current for a different type of potential with the same height and width is given in the last column as the "shape factor". This clearly shows that different barrier types, having the same height-to-width characteristics, yield currents differing by as much as a factor of 2 from one another. Obviously care should be exercised in assessing barrier characteristics, e.g. width, from a knowledge of tunneling current only. Conversely any calculated tunneling contribution will depend on the shape assumed for the potential.

The equation for T_1 may be converted to an expression in terms of height and width. This is done quite simply by first defining that width = $W = 2|x_n|$ where x_n is the value of the argument when the potential $V(x_n) = V_0/n$. Here n is an

[1]Submitted in partial fulfillment of the requirements for the B.Sc. (Honours) degree by J. C. Nash.
[2]Present address: The Mathematical Institute, 24–29 St. Giles, Oxford, England.

Can. J. Chem. Downloaded from www.nrcresearchpress.com by 210.87.254.6 on 09/05/12
For personal use only.

TABLE I

Tunneling as a function of barrier shape*

Barrier type	V_2	Second Wigner term $e^{+\beta V_0} \times T_1 \times 10^{16}$	T_1(parabola)/T_1(curve) = shape factor
Parabola	-1.042×10^5	14.57	1.0
Gaussian	-1.676×10^5	23.44	0.62
Eckart	-1.837×10^5	25.69	0.57
exp $(-a\|x\|)$	-2.392×10^5	33.45	0.45

*Barrier height = $V_0 = 1.7368 \times 10^{-12}$ ergs/molecule (25 kcal/mole), temperature = 300 °K, particle mass = $m = 8 \times 10^{-23}$ g, barrier width at 1/4 height = $W = 1$ Å.

integer, for example, $n = 2$ for a width defined as "width at half-height". Solving eq. [3] for x_n gives

$$x_n = \pm \left[\frac{-2V_0}{V_2} \left(\frac{n-1}{n} \right) \right]^{1/2}$$

But

$$W = 2|x_n| = 2 \left[\frac{-2V_0}{V_2} \left(\frac{n-1}{n} \right) \right]^{1/2}$$

and since V_0 = height = H this gives

$$V_2 = -8 \frac{H}{W^2} \left(\frac{n-1}{n} \right)$$

Hence, the tunneling current can be expressed in terms of more familiar height and width parameters as

$$T_1 = \left(\frac{\hbar^2 \beta}{3m} \right) \frac{H}{W^2} \left(\frac{n-1}{n} \right) e^{-\beta H}$$

so that

[4] Current =

$$e^{-\beta H} \left[\frac{1}{\beta} + \frac{\hbar^2 \beta}{3m} (H/W^2) \left(\frac{n-1}{n} \right) \right]$$

Equation (4) is the same numerically as T_1 in the first row of Table I and, as indicated in Table I, is different, by a factor, from T_1 obtained for the other types of potentials. When the height and width are evaluated for the different potential types given in Table I, the value of T_1 obtained by eq. [4] is very nearly the same as the value given by the product of the shape factor and T_1, as obtained by the more tedious curve fitting method, i.e., T_1(by curve fitting)·(shape factor) = T_1 (by simple height-to-width formula, eq. [4]). Consequently, if the shape factor appropriate to the potential of interest is read from Table I, then eq. [4] can be used to quickly obtain the tunneling current for a large variety of values of H and W for various potential types.

In all of the foregoing, only the first two terms of eq. [1], resulting from the parabolic potential [3], were used in obtaining the current. Certainly potentials which differ markedly in shape from that of a parabola would be better represented by

$$[5] \qquad V(x) = V_0 + \frac{V_2}{2!} x^2 + \frac{V_4}{4!} x^4$$

and consequently both the second and third terms of eq. [1] would be used to generate the quantum mechanical tunneling current.

$$[6] \quad T = -e^{-\beta V_0} \frac{\hbar^2 \beta}{24m} V_2 - e^{-\beta V_0} \frac{\hbar^2}{96m} \frac{V_4}{V_2}$$

$$= T_1 + T_2$$

Again V_2 and V_4 can be obtained by a least squares fit to a set of $V(x)$ and x and will differ somewhat depending on the shape of the potential. However, this variation will be less since the fourth order term allows better accommodation of the variations in shape. What appears to be more important is the range of x over which the fitting is carried out. In Wigner's derivation, the potential in [5] was assumed to be valid over the "transition region", i.e., the region in which the distribution function was significantly different than that obtained classically. Specifically, since tran-

TABLE II

The effect of the "transition region" size*

Range of x for transition region (Å)	$\|T_2/T_1\|$†
1.0	0.001– 0.01
0.1	0.01 – 0.1
0.01	1.0 –10.0

*Barrier height = $V_0 = 1.7368 \times 10^{-12}$ ergs/molecule (25 kcal/mole), temperature = 300 °K, particle mass = $m = 8 \times 10^{-23}$ g, barrier width at 1/4 height = $W = 1$ Å.

†The variation in $|T_2/T_1|$ results from fitting different types of potentials.

Can. J. Chem. Downloaded from www.nrcresearchpress.com by 210.87.254.6 on 09/05/12
For personal use only.

sition over the barrier was considered, the "transition region" of interest was for small values of x. Consequently eq. [5] must be made to fit the potential only over the appropriate small range of x encompassing the "transition region". Table II indicates the ratio T_2 to T_1 for different transition regions. The third term, T_2, is very dependent on the magnitude of the transition region. Consequently any estimation of the significance of the third term in the calculation of the tunneling current can lead to serious errors unless care is taken in estimating the dimensions of the "transition region".

Acknowledgment

The support of the National Research Council of Canada for this work is acknowledged.

1. E. WIGNER. Phys. Rev. **40**, 749 (1932). E. WIGNER. Z. Physik. Chem. **B19**, 203 (1932). R. P. BELL. Proc. Roy. Soc. London, Ser. A, **139**, 446 (1933). R. P. BELL. Trans. Faraday Soc. **55**, 1 (1959).

Erratum: Tris(ethylenediamine)ruthenium(III) iodide

GEORGE W. WATT AND C. V. SENOFF
Department of Chemistry, The University of Texas at Austin, Austin, Texas 78712

Received February 13, 1969

(Ref.: Can. J. Chem. **47**, 359 (1969))

Canadian Journal of Chemistry, **47**, 1443 (1969)

In the first line of the text, $[Ru(en)_3]^{3+}$ should read $[Ru(en)_3]^{2+}$.

Can. J. Chem. Downloaded from www.nrcresearchpress.com by 210.87.254.6 on 09/05/12
For personal use only.

Can. J. Chem. Downloaded from www.nrcresearchpress.com by 210.87.254.105 on 09/05/12
For personal use only.

Canadian Journal of Chemistry

Published by THE NATIONAL RESEARCH COUNCIL OF CANADA

VOLUME 47 MAY 1, 1969 NUMBER 9

Stereochemistry of bimolecular nucleophilic opening of a dioxolenium ring fused to an anchored cyclohexane system[1]

J. F. KING[2] AND A. D. ALLBUTT

Department of Chemistry, University of Western Ontario, London, Ontario

Received November 18, 1968

This paper describes the characterization of certain dioxolenium salts in which the heterocyclic ring is fused (via positions-4 and -5) to an anchored cyclohexane ring, and the steric course of their bimolecular cleavage with nucleophilic reagents. It was found that diaxial opening is normally favored strongly over diequatorial; this is accounted for in terms of differences in angle strain in the transition states. The presence of an axial (angular) methyl group gave a preference for diequatorial opening; on the other hand an analogous investigation of the diaxial : diequatorial opening ratio with epoxides showed the stereochemistry of the reaction to be virtually insensitive to an angular methyl group. These observations are interpreted in terms of the different non-bonded interactions arising from the different geometrical arrangements of epoxides and dioxolenium ions. The variation in the diaxial : diequatorial opening ratio is shown to be of significance in the interpretation of rates of diaxial → diequatorial rearrangement.

Canadian Journal of Chemistry, 47, 1445 (1969)

Introduction

Dioxolenium or acyloxonium ions (**1**) have comparatively recently achieved the status of species whose existence, both as transitory intermediates and isolable products, has been rigorously proved (1). Amongst the characteristic reactions of such species is nucleophilic displacement at one of the uncharged carbon atoms, e.g. **1** → **2**, a reaction known to take place with inversion of configuration. When a dioxolenium ring is fused to an anchored six-membered ring[3] as in **3**, the two oxygen atoms differ in their stereochemistry and attack of **3** by an unspecified nucleophile Z^- could lead in principle to either the diaxial product **4**, or its diequatorial isomer **5**. For reasons connected with our study of the diaxial → diequatorial rearrangement (2) and which are dealt with more fully elsewhere in this paper, we wished to know the ratio of the amount (or rate) of diaxial opening to that for diequatorial; throughout this paper this is referred to as the diaxial:diequatorial opening ratio. Contemplation of the question led to the realization that it was part of the larger problem of the stereochemical course of S_N2 reactions in six-membered ring systems and warranted study in its own right.

An attempt to predict the diaxial:diequatorial opening ratio of dioxolenium ions was unsuccessful because it revealed the existence of opposing influences of uncertain magnitude (cf. ref (2)). From the work of Eliel and co-workers on S_N2 reactions of 4-*t*-butylcyclohexyl derivatives (3), one might expect that displacement of the axial oxygen (diequatorial opening) might be the easier reaction. But bimolecular nucleophilic attack on *three-membered* rings fused to six-membered systems almost invariably takes place with displacement of the quasi-equatorial function — i.e. diaxial opening; included within the scope of this "diaxial opening rule" at present are epoxides (4), three-membered ring halonium ions (5),

[1]Part of the work described in this paper has been published in preliminary form: J. F. King and A. D. Allbutt. Chem. Commun. 14 (1966).

[2]Fellow of the Alfred P. Sloan Foundation, 1966–1968.

[3]We use the term *anchored* in this paper to denote a six-membered ring in the chair conformation which is sterically constrained so that conformational inversion to the other chair form is either impossible or of such high energy as to be of no importance. Such a system is not truly rigid (though we have used this description previously), since it may flip into boat forms (either twist or symmetrical).

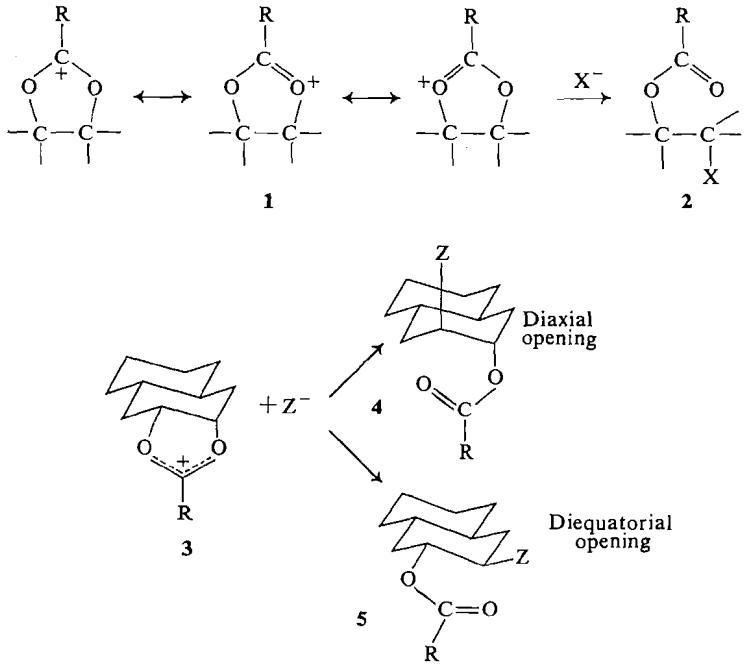

ethylenimmonium ions (6), and episulfonium ions (7). Because of the ring strain introduced by the presence of the three-membered ring in these systems, it is evident that any extensions to predict the behavior of five-membered ring systems would have to be made with caution, but examination of molecular models suggested (2) that the opening of dioxolenium ions may also show signs of ring strain in the diequatorial opening not present in the diaxial cleavage. It was evident that at the outset of this study there was not sufficient basis for making any sort of a quantitative prediction of the diaxial:diequatorial opening ratio and we thereupon set out to investigate the question experimentally.

Results and Discussion

Synthesis and Proof of Structure of the Dioxolenium Ions

Winstein and Buckles (8) first provided evidence that treatment of vicinal halohydrin esters with silver salts gave the dioxolenium ion as a transitory intermediate, and Meerwein *et al.* (9) showed that if the anion were sufficiently inert the dioxolenium salt could be isolated. Accordingly we treated 2β-bromo-5α-cholestan-3α-yl anisate (**6**) with silver hexafluoroantimonate and obtained the dioxolenium hexafluoroantimonate (**7**) as white crystals melting at 196–198°.

The infrared spectrum of **7** shows no absorption from 1610 to 2000 cm^{-1}, but the 1400–1600 cm^{-1} region displays four prominent bands, at 1600(m), 1540(m), 1465(s), and 1435(m), respectively. These four bands are found with the other two anisoxonium hexafluoroantimonates **3***a* and **10***a*, whereas the benzoxonium species **3***b* and **10***b* show bands at 1600(m), 1520(s), and 1460(s) cm^{-1}. Magnuson, *et al.* (10) reported that 2,4,4,-5,5-pentamethyldioxolenium perchlorate absorbs strongly at 1536 and 1511 cm^{-1}. As a consistent interpretation we suggest that the stretching modes of the O—C—O system in the dioxolenium ions are 1520 and 1460 cm^{-1} for the 2-phenyl substituted (benzoxonium) compounds, and 1460 and 1435 cm^{-1} for the *p*-methoxyphenyl (anisoxonium) species. The lower frequency of the *p*-methoxyphenyl- vs. phenyl-, as well as phenyl- vs. methyl-substituted compounds, is ascribable to conjugation. The bands at 1600 cm^{-1} and 1540 cm^{-1}, are probably due to the aromatic system. All of the hexafluoroantimonates showed strong absorption at 660 cm^{-1} characteristic of the SbF_6^- anion.

The nuclear magnetic resonance (n.m.r.) spectrum of **7** was also consonant with the dioxol-

458945

Can. J. Chem. Downloaded from www.nrcresearchpress.com by 210.87.254.105 on 09/05/12
For personal use only.

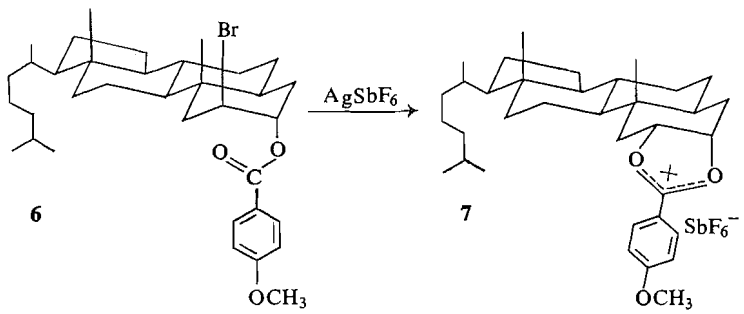

6 7

enium ion structure, with a singlet at 4.0 p.p.m. due to the methoxyl group, a broad multiplet around 5.8 p.p.m. arising from the hydrogens on C-2 and C-3. The aromatic absorption might be described either as a widely spaced quartet or a slightly perturbed pair of doublets at respectively 8.26 and 7.17 p.p.m., (J = 9 c.p.s.). These bands are in excellent agreement with the presence of a strongly electron-withdrawing group para to the methoxyl function. The other hydrogens of the steroidal skeleton absorbed between 0.5 and 2.0 p.p.m., the C-19 hydrogens evidently appearing at 0.83 p.p.m. (for further information see the more detailed account elsewhere (11)).

Carbon and hydrogen analyses were in good agreement with the oxonium ion structure **7**, which was further supported by the chemical reactions of the material. Treatment with tetraethylammonium bromide gave the expected mixture of the diaxial and diequatorial bromohydrin anisates; the relative amounts of the two isomers is, of course, the subject of prime interest of this account and is discussed more fully below. Reaction of **7** with dilute acetic acid, which was virtually instantaneous, gave a half ester which on alkaline hydrolysis gave the known glycol 5α-cholestan-2α,3α-diol (12). Of the two possible half esters, that in which the anisoxyl group is axial was formed in much greater amount, this remarkable stereoselectivity has already been reported in a brief communication (13), and will be discussed more fully in a subsequent publication.

It is clear that the physical and chemical data unambiguously establish **7** as the structure of the product obtained by reaction of **6** with silver hexafluoroantimonate. A number of other dioxolenium hexafluoroantimonates (**3***a*, **3***b*, **10***a*, and **10***b*) were obtained similarly. In all instances the spectroscopic and chemical properties were analogous to those already described for **7** and were clearly compatible only with the dioxolenium ion formulations, though in certain instances the carbon analysis was somewhat low, perhaps because the samples may have taken up water prior to analysis.

Bimolecular Nucleophilic Cleavage of the Dioxolenium Ions

Each of the dioxolenium salts was treated in solution with tetraethylammonium bromide. The reaction was practically instantaneous and gave a good yield of the mixed halohydrin esters. The total yields of the ester mixtures and the relative amounts of diaxial and diequatorial products in each mixture are listed in Table I. No particular attempt was made to optimize the reaction conditions, as the diaxial:diequatorial opening ratio appeared completely insensitive to the total yield. Methylene chloride was used as the reaction solvent in comparing the different substrates. Reaction of **7** in nitromethane and acetonitrile solutions gave little or no change from methylene chloride.

It is evident that the salt derived from decalin (**3**) most closely approximates the simple cyclohexane system, whereas the steroidal derivatives because of the presence of angular methyls and other perturbing groups might be expected to deviate to a greater or lesser degree from the norm. The "norm" as manifest by the reaction of **3**, is that diaxial opening is favored to the extent of about 20:1. The β-oxonium salts **10***a* and **10***b* behave very similarly, an observation which is not surprising since the stereochemical changes on proceeding from the initial to the transition state would be expected to be much the same as in the decalin derivative. Similarly, variation of the nature of the attacking nucleophile did not affect the reaction very much, chloride ion giving

Can. J. Chem. Downloaded from www.nrcresearchpress.com by 210.87.254.105 on 09/05/12
For personal use only.

TABLE I

The reaction of the dioxolenium salts with nucleophilic anions

Dioxolenium salt	Nucleophilic anion	Solvent	Yield of mixed diaxial and diequatorial esters (%)	Diaxial:diequatorial opening ratio*
9β,10α-Decalin-2β,3β-*p*-anisoxonium hexafluoroantimonate (**3***a*)	Br^-	CH_2Cl_2	99	19:1
9β,10α-Decalin-2β,3β-*p*-anisoxonium hexafluoroantimonate (**3***a*)	Cl^-	CH_2Cl_2	92	16:1
9β,10α-Decalin-2β,3β-*p*-anisoxonium hexafluoroantimonate (**3***a*)	CF_3COO^-†	CH_2Cl_2	64	(evidently mostly diaxial)‡
9β,10α-Decalin-2β,3β-benzoyloxonium hexafluoroantimonate (**3***b*)	$PhCOO^-$†	CH_2Cl_2	69	7:1
5α-Cholestan-2β,3β-*p*-anisoxonium hexafluoroantimonate (**10***a*)	Br^-	CH_2Cl_2	83	49:1
5α-Cholestan-2β,3β-benzoyloxonium hexafluoroantimonate (**10***b*)	Br^-	CH_2Cl_2	72	(evidently mostly diaxial)‡
5α-Cholestan-2α,3α-*p*-anisoxonium hexafluoroantimonate (**7**)	Br^-	CH_2Cl_2	94	0.5:1
5α-Cholestan-2α,3α-*p*-anisoxonium hexafluoroantimonate (**7**)	Br^-	CH_3CN	78	0.5:1
5α-Cholestan-2α,3α-*p*-anisoxonium hexafluoroantimonate (**7**)	Br^-	CH_3NO_2	90	0.7:1

*Determined with the steroids by a combination of optical rotation and infrared measurements, with the decalin halohydrin esters by semi-quantitative comparative thin-layer chromatography, and with the decalin dibenzoate by weighing of products separated by t.l.c. See Experimental for details.

†Reaction carried out by mixing the carboxylic acid with *N,N*-diisopropylethylamine in methylene chloride and adding a solution of the dioxolenium salt to the mixture.

‡Only one product was isolated from the reaction mixture. The yield refers to yield of isolated product.

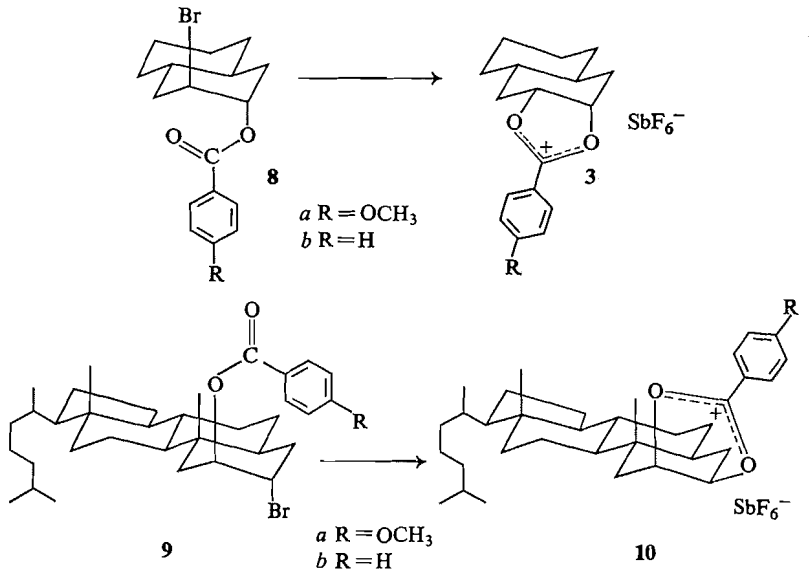

Can. J. Chem. Downloaded from www.nrcresearchpress.com by 210.87.254.105 on 09/05/12
For personal use only.

Can. J. Chem. Downloaded from www.nrcresearchpress.com by 210.87.254.105 on 09/05/12
For personal use only.

almost exactly the same diaxial:diequatorial opening ratio. That found with the benzoate anion is somewhat lower, though still strongly favoring the diaxial product. This is similar to an observation made by Meakins and co-workers (14) who found a diaxial:diequatorial opening ratio of 9 under the conditions of the Prevost reaction in benzene at room temperature.

Reaction of the α-oxonium salt **7**, however, might be expected (cf. ref. (2)) to be different, because in the transition state for diaxial opening the attacking nucleophile must certainly be close enough to the angular methyl group (C-19) to experience strong repulsion that is without counterpart in the diequatorial cleavage. The experimental results are clearly in accord with these considerations, the major product being the *diequatorial* isomer, though only by a factor of two.

This observation is to be contrasted with that made with the corresponding epoxide, 5α-cholestan-2α,3α-epoxide (**11**). This compound like its β-isomer (**14**), when cleaved with hydrobromic acid has been reported to give the diaxial isomer as the only isolated product (15). After some reflection it seemed to us that there could be two distinct situations which could lead to the difference in sensitivity to introduction of the angular methyl group shown by 2α,3α-dioxolenium species and the 2α,3α-epoxide. On the one hand it is possible that the methyl group increases the activation energy for diaxial opening by the same amount in both the dioxolenium and epoxide reactions, and that there is simply a much

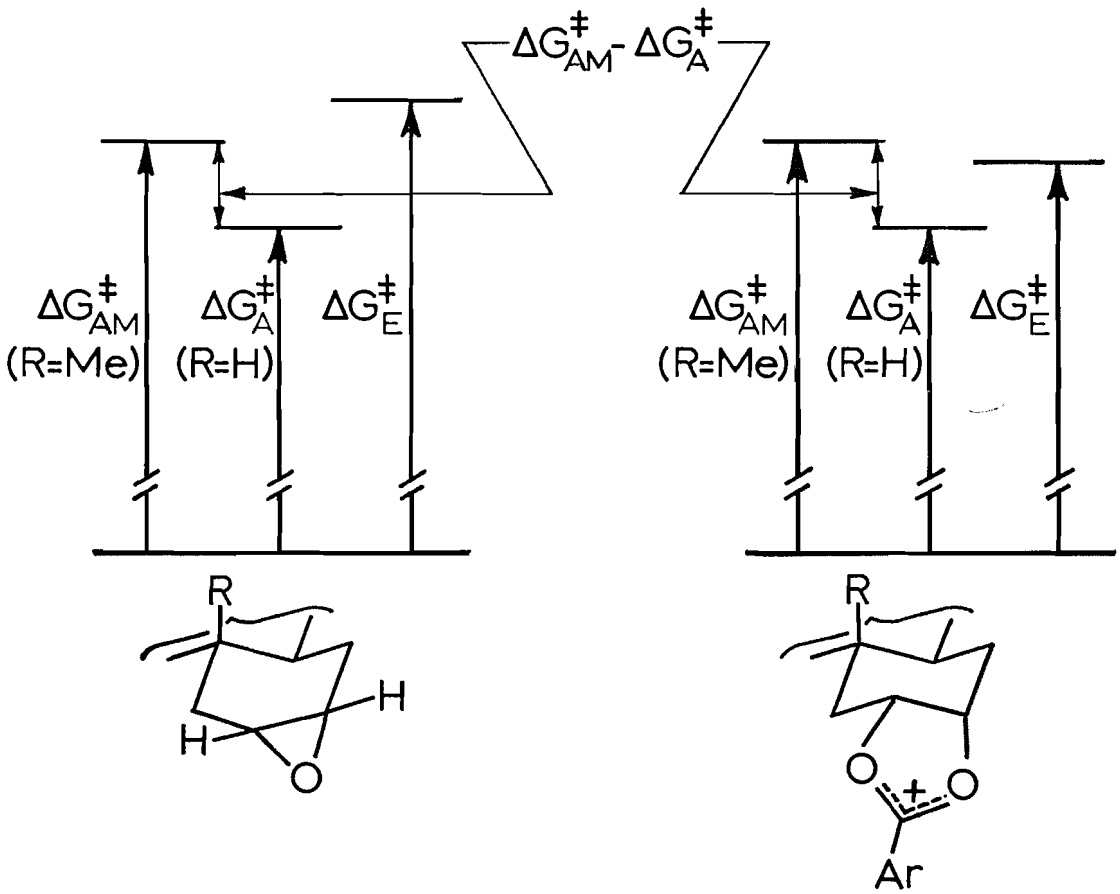

FIG. 1. Schematic energy diagram for the effect of angular methyl groups on the cleavage of epoxide and dioxolenium systems in which $(\Delta G^{\ddagger}_{E} - \Delta G^{\ddagger}_{A})_{epoxide} > (\Delta G^{\ddagger}_{AM} - \Delta G^{\ddagger}_{A})_{epoxide} = (\Delta G^{\ddagger}_{AM} - \Delta G^{\ddagger}_{A})_{dioxolenium\ ion} > (\Delta G^{\ddagger}_{E} - \Delta G^{\ddagger}_{A})_{dioxolenium\ ion}$.

Can. J. Chem. Downloaded from www.nrcresearchpress.com by 210.87.254.105 on 09/05/12
For personal use only.

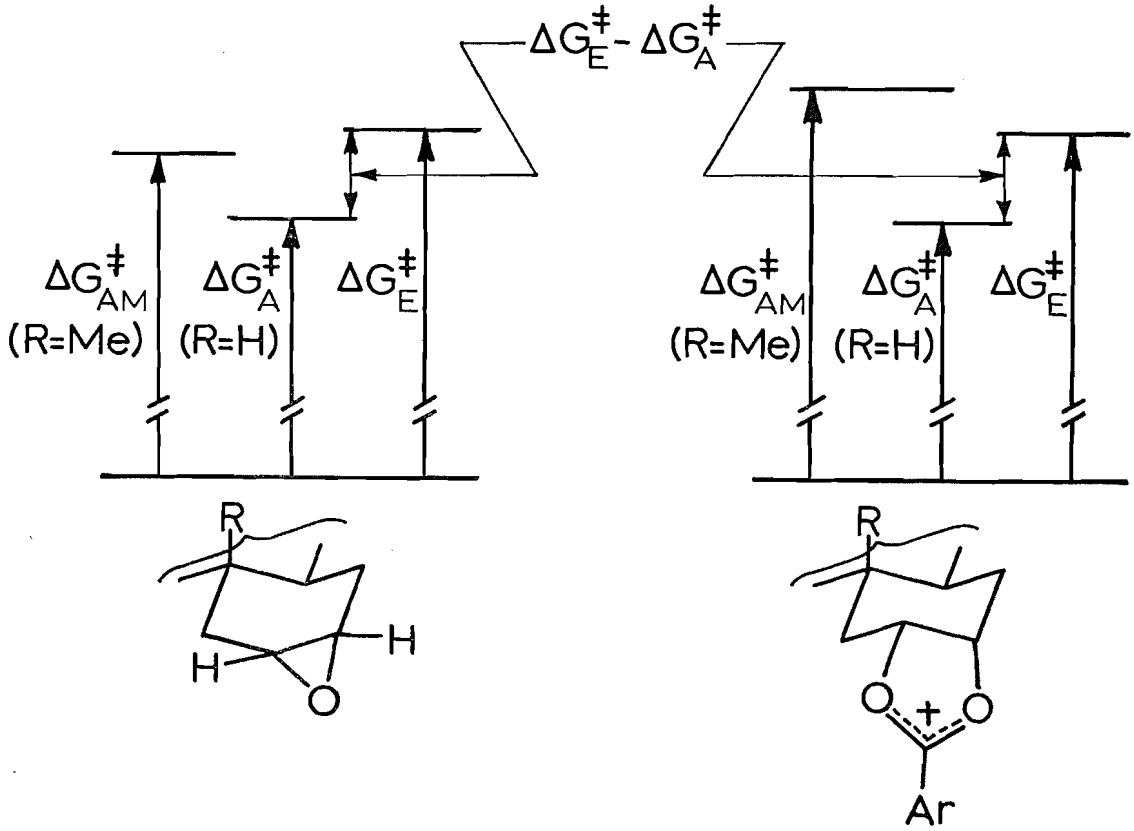

FIG. 2. Schematic energy diagram for the effect of angular methyl groups on the cleavage of epoxide and dioxolenium systems in which $(\Delta G_{EM}^{\ddagger} - \Delta G_A^{\ddagger})_{\text{dioxolenium ion}} > (\Delta G_E^{\ddagger} - \Delta G_A^{\ddagger})_{\text{dioxolenium ion}} = (\Delta G_E^{\ddagger} - \Delta G_A^{\ddagger})_{\text{epoxide}} > (\Delta G_{AM}^{\ddagger} - \Delta G_A^{\ddagger})_{\text{epoxide}}$.

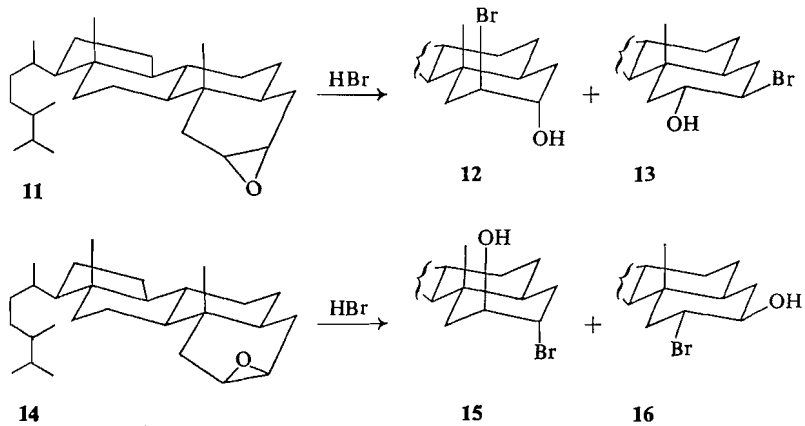

greater tendency for the epoxide to open diaxially. The energy relationships for such a situation are summarized schematically in Fig. 1. The effect of introducing the angular methyl group leads to an activation energy increase of $\Delta G_{AM}^{\ddagger} - \Delta G_A^{\ddagger}$ which is the same for both the epoxide and dioxolenium ion cleavages, but which is less than $\Delta G_E^{\ddagger} - \Delta G_A^{\ddagger}$ in the epoxide case (and hence

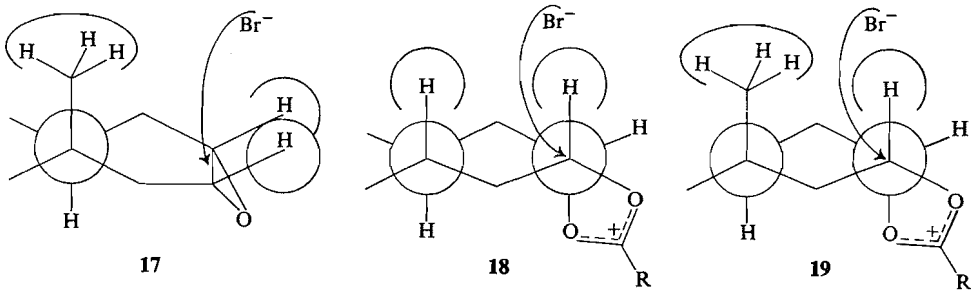

diaxial opening predominates) and greater than $\Delta G_E^{\ddagger} - \Delta G_A^{\ddagger}$ in the dioxolenium ion opening. The latter circumstance leads to the major reaction being diequatorial opening. On the other hand the same experimental consequence would result from the circumstances summarized in Fig. 2. In this case the unperturbed epoxide and dioxolenium ion have the same diaxial:diequatorial opening ratio and the effect of the methyl group is greater with the dioxolenium ion opening — sufficiently so as to make diequatorial opening preferred. It is evident that each of these two possible situations is, in fact, an extreme case in which the observed result derives entirely from one cause; it is, of course, entirely possible that the actual circumstance has its origins partly from one effect partly from the other.

To obtain a semi-quantitative estimate of the relative importance of these factors it is merely necessary to acquire data for the opening of the corresponding epoxides analogous to those listed in Table I for the dioxolenium ion reactions. Estimation of the composition of the product of the reaction of *trans*-decalin-2,3-epoxide with hydrobromic acid proved impracticable by the thin-layer chromatographic procedures that had been of such value in obtaining the data in Table I, though the presence of the diaxial bromohydrin as the major product and the diequatorial bromohydrin in small amount was indicated. With the steroidal epoxides **11** and **14**, however, the diaxial:diequatorial opening ratios were found to be 97:3 and 95:5 for the β-epoxide **14** and α-epoxide **11**, respectively. These correspond to $\Delta G_E^{\ddagger} - \Delta G_A^{\ddagger}$ values at room temperature of 2.1 and 1.7 kcal/mole, and are very close to the value of 2.3 kcal/mole found for the opening of the β-anisoxonium salt **9***a* (and also to the 1.7 kcal/mole found with the decalin dioxolenium salt **3**). Introduction of the angular methyl group in the epoxide case thus has little if any effect, whereas in the dioxolenium ion reaction it makes diaxial opening more difficult by roughly 2 kcal/mole. These results indicate that the reality corresponds remarkably closely to the situation depicted in Fig. 2.

The probable origin of this circumstance is perhaps most simply explained with reference to structures **17–19**. It is apparent that because of the relative openness of the epoxide system, attack on C-2 as indicated by the arrow in **17** ought to be comparatively facile. With the dioxolenium ion, the introduction of the angular methyl group places a large obstacle directly in what would be the path of any group about to initiate diaxial opening of the dioxolenium ring, and the reaction path indicated by the arrow in **19** will have severe non-bonded interactions in the transition state not present in the process shown in **18**.

Origin of the Normal Preference for Diaxial S_N2 Opening of Dioxolenium Ions

As a preliminary to understanding how the normal preference for diaxial opening of dioxolenium ions by bimolecular nucleophilic attack arises, it is instructive to examine the geometry of the transition state of the S_N2 reaction of a simple cyclohexane derivative. Structures **20–23** illustrate, albeit in somewhat oversimplified form, the change in geometry between the starting material and the transition state for displacement by a nucleophile N^- of a substituent X which is respectively equatorial and axial. The simplest case, in which the substituents on both carbons α to the reacting center are hydrogen atoms, has been the subject of a penetrating analysis by Eliel (3, 16). When N^- is larger than X^- it is found that the axial isomer reacts faster than the equatorial; for $N^- = PhS^-$ and X = tosylate, in 87% ethanol at 25°, $\Delta G_{Eq}^{\ddagger} - \Delta G_{Ax}^{\ddagger} = 2.1$ kcal/mole. Part of the difference in activation energy is ascribed to the difference in free energy of the

Can. J. Chem. Downloaded from www.nrcresearchpress.com by 210.87.254.105 on 09/05/12
For personal use only.

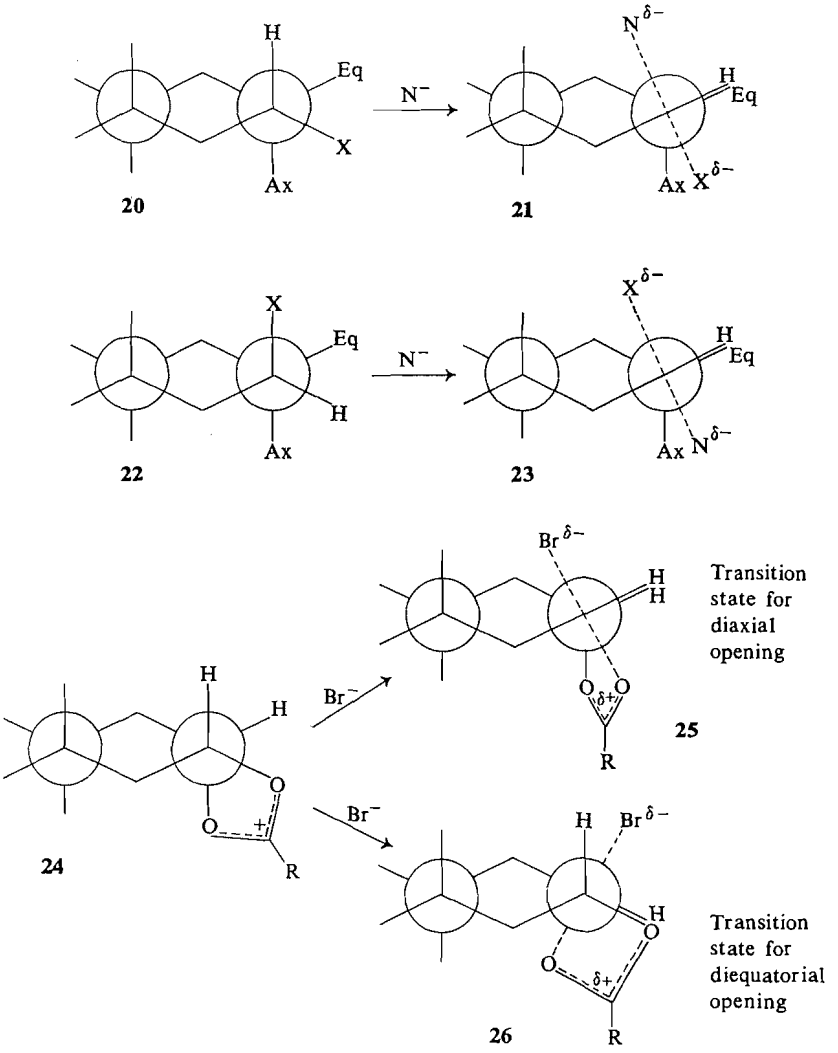

starting materials, $-\Delta G^{\circ}_{OTs}$ (the "*A* value") being about 0.7 kcal/mole. The remainder (1.4 kcal/mole) is believed to be largely due to the non-bonding interactions of the quasi-axial group in the transition state; i.e. when N is larger than X, these interactions are greater in **21** than in **23**.

If one of the α-carbon atoms bears a substituent then other factors must be added to those already considered by Eliel. Relevant to the present discussion are the circumstances which arise when this substituent is *cis* to the leaving group. When the leaving group is equatorial the α-*cis* substituent is axial, and in the transition state (**21**) the dihedral angle between the α-*cis* substituent (Ax) and the leaving group (X) is 30°. On the other hand when the leaving group is axial, the α-*cis* substituent is equatorial; in the transition state the dihedral angle is 90°, and the hydrogen attached to the carbon undergoing exchange of substituents and the α-*cis* function become eclipsed.

In the event that the α-*cis* group and the leaving group form a ring, as in the dioxolenium ion system described in this paper, the effect of this alteration in the dihedral angle is to flatten the substituent ring when the leaving group is equatorial and to pucker the same ring when the leaving group is axial. Structures **24–26** display in somewhat idealized fashion this effect for the dioxolenium ion system. It would seem very

Can. J. Chem. Downloaded from www.nrcresearchpress.com by 210.87.254.105 on 09/05/12
For personal use only.

Can. J. Chem. Downloaded from www.nrcresearchpress.com by 210.87.254.105 on 09/05/12
For personal use only.

likely that the preferred conformation of a free dioxolenium ion is a flat or very nearly flat ring, but fusion with a cyclohexane ring probably requires the dioxolenium ring to be somewhat puckered as indicated in **24**, and (though not shown in **24**) the cylohexane ring probably to be somewhat flattened. Displacement of the axial oxygen (diequatorial opening), which would be preferred in the simpler system described by Eliel, would lead to greater puckering of the heterocyclic system (as in **26**), that is to say, to a considerable increase in the angle strain. Diaxial opening, on the other hand, results in a diminishment of the puckering in the ring (as in **25**) and hence to a lessening of the angle strain. It would appear that this effect of angle strain, perhaps with an eclipsing interaction between oxygen and hydrogen added, is sufficient to completely overshadow the non-bonding interaction effects which presumably control the stereochemistry in the absence of α-substituents.

It is perhaps illuminating to compare this rationale with the currently accepted interpretation of the diaxial preference in the opening of epoxides and other three-membered ring species. Inspection of molecular models readily leads to the expectation that diaxial opening of an epoxide would be expected to be facile, but the corresponding direct diequatorial opening is difficult to visualize. It is probably easier to consider the reverse process, i.e. the formation of an epoxide, for example, by internal displacement. The formation of the epoxide from the diaxial starting material **27** is sterically favorable, but from the diequatorial anion **28** the formation of the ring would require a remarkable distortion of the normal bond angles in order to follow the arrows. For comparison, the formation of a dioxolenium ion is illustrated analogously by **29** and **30**. Again with the diaxial substrate **29** the reaction is straightforward, but with **30** the angular distortions are not so great that one can dismiss the possibility out of hand. For the diequatorial opening (or formation from diequatorial starting materials) of epoxides and other three-membered ring species, it has been postulated that the reaction proceeds via a diaxial boat or flexible conformation which then flips into (or has previously flipped from) the diequatorial chair form (17, 18). It is possible that the diequatorial opening of the dioxolenium species is also taking place through a boat conformation. In our view neither examination of molecular models nor the experimental evidence available at present demands such an interpretation. The above discussion of diequatorial opening (and closing) may be summarized in the following way. With epoxides direct diequatorial opening is sterically absurd and any diequatorial product arises from the boat-diaxial compound followed by conformational inversion. With dioxolenium ions direct diequatorial opening must at the very least be considered as a possible route. There is good reason to believe that such opening would produce increased angle strain, but whether or not this is sufficient to make the activation energy for this process greater than that through the diaxial boat is unknown.

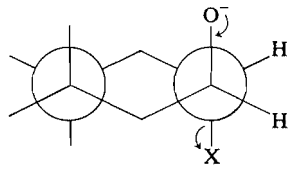

27

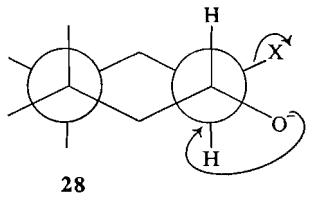

28

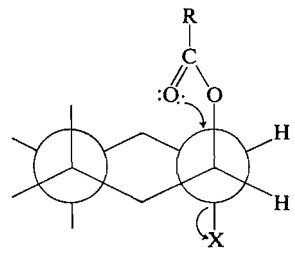

29

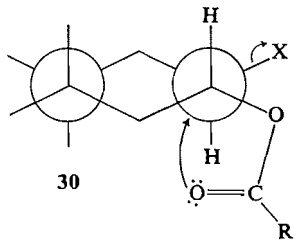

30

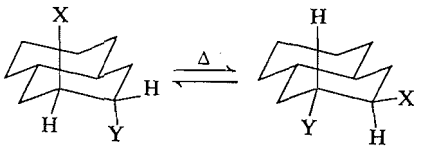

31 32

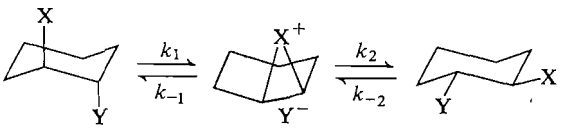

33 34 35

Returning to structures **20**–**23**, it is of interest to speculate on the possible influence of an α-substituent that is not part of a ring with the leaving group (e.g. a methyl group). If such an α-methyl group were equatorial as in **20** (or **22**), and the gauche Me:X interaction significant, then in the transition state **21** (or **23**) the Me:X interaction would be smaller than in the starting material. It is at least conceivable that this lowering of the non-bonded interaction energy would be sufficient to outweigh the eclipsing Me:H interaction and any non-bonded repulsion between the attacking nucleophile N and the equatorial methyl group. Under such circumstances the effect of introducing an equatorial α-methyl group would be to *accelerate* the S_N2 displacement with respect to the unsubstituted compound. An axial α-methyl substituent, on the other hand, would be expected to slow the reaction owing to a 30° interaction in the transition state (**21** or **23**) between the methyl group and N or X.

The Diaxial:Diequatorial Opening Ratio and the Diaxial → Diequatorial Rearrangement

As mentioned in the Introduction, the present research was instigated by questions arising from our study of the diaxial → diequatorial rearrangement (2), a reaction which may be illustrated in a general way by **31** ⇄ **32**. It has become evident that in the more polar media, at least, the diaxial → diequatorial rearrangement is in all likelihood taking place by internal return from intermediate ion pairs, e.g. **33** ⇄ **34** ⇄ **35**. It is further evident that any detailed investigation of the mechanism using the kinetic method will at some stage require some knowledge of the relative rates of the individual steps. In more specific terms, if one uses the steady state assumption (and if k_{-2} is very small), then k_a the measured rate constant for the overall reaction **33** → **35** is given by $k_a = k_1/(1+k_{-1}/k_2)$. That is, a change in k_a accompanying a change in structure (e.g. a change in X or Y), could be due to a change in either k_1 or the diaxial:diequatorial opening ratio, k_{-1}/k_2.

In investigating the diaxial → diequatorial rearrangement of **6** and **9** (in nitromethane at 99°), we found (2) that k_a for **6** was 6 times greater than that for **9**. We were reluctant to attempt any interpretation of this difference at that stage because it seemed that k_{-1}/k_2 might well be different for the two isomers, but, as mentioned at the beginning of this paper, by a magnitude which we could not predict. If one takes as a rough first approximation of k_{-1}/k_2 in nitromethane at 99°, the values of the diaxial:diequatorial opening ratio listed in Table I, then one finds that k_1 for **9** is about 5 times faster than k_1 for **6**. In other words, because of a more than 70-fold difference in k_{-1}/k_2 the relative values of k_a and k_1 for **6** and **9** are inverted. This would seem to be an instructive illustration of how the overall rate of a multistep reaction is not always an accurate indicator of the rate of the slow step.

In the context of this paper it is attractive to assign the origin of the smaller value of k_1 for **6** vs. **9**, in part at least, to non-bonding interactions in the transition state for the ionization step, and which are illustrated for the reverse process by structure **19**.

Experimental

Vacuum capillary melting points were determined with a Gallenkamp melting point apparatus, other melting points on a Köfler hot stage; they are uncorrected. Infrared spectra were obtained with Beckman IR-5 or IR-10 instruments using sodium chloride cells, except for those run in the region 600–750 cm^{-1} to analyze mixtures of bromohydrin esters, which were run on a Beckman IR-5A instrument equipped with CsBr optics and using KBr cells. Infrared spectra and rotations were run in chloroform (Fisher Spectranalyzed grade, containing 0.75% ethanol) except where another solvent is specified. Nuclear magnetic resonance (n.m.r.) spectra were run on a Varian A-60 spectrometer in $CDCl_3$, unless otherwise specified. Thin-layer chromatography (t.l.c.) was carried out using Camag silica gel DF 5, if not otherwise indicated.

Petroleum ether refers to the fraction of boiling range 30–60°. Drying of organic extracts was carried out with anhydrous magnesium sulfate. Tetraethylammonium bromide and chloride (Eastman) were recrystallized from methylene chloride – petroleum ether and dried under vacuum prior to use.

Preparation of Acyloxonium Hexafluoroantimonates

The general procedure used was similar to that des-

Can. J. Chem. Downloaded from www.nrcresearchpress.com by 210.87.254.105 on 09/05/12
For personal use only.

Can. J. Chem. Downloaded from www.nrcresearchpress.com by 210.87.254.105 on 09/05/12
For personal use only.

cribed by C.B. Anderson (19): A known amount of diaxial bromoester in nitromethane was treated with an equimolar quantity of silver hexafluoroantimonate (Alfa Inorganics Inc., Beverly, Massachussetts). After standing overnight at room temperature the reaction mixture was filtered and the filtrate evaporated under reduced pressure at room temperature. The residue was dissolved in a minimum quantity of methylene chloride and crystallization effected by the addition of anhydrous ether. The product was collected by filtration and dried under high vacuum. All of the above steps were carried out in a dry box containing phosphorus pentoxide and filled with nitrogen; in all the experiments involving these acyloxonium salts all weighings and transfers were carried out in a dry box. With the steroid bromoesters, because of their low solubility, it was found necessary to heat the reaction mixture at 50°.

5α-Cholestan-2α,3α-p-anisoxonium Hexafluoroantimonate (7)

2β-Bromo-5α-cholestan-3α-yl-*p*-anisate (**6**, 1.0 g) was treated overnight with silver hexafluoroantimonate (0.57 g) in nitromethane (10 ml) at 50°. The product was isolated as described above. Crystallization from methylene chloride : ether gave 5α-cholestan-2α,3α-*p*-anisoxonium hexafluoroantimonate (0.7 g), m.p. 196–198° (sealed capillary tube), $[\alpha]_D$ +21° (CH_2Cl_2). The n.m.r. spectrum showed signals at 0.83 (singlet), 4.0 (singlet), a broad multiplet centered at 5.77, and a signal interpreted as an AB quartet, δ_A 7.17, δ_B 8.26 p.p.m., J_{AB} 9 c.p.s. These peaks were assigned to the C-19 methyl group,[4] the methoxyl group, the C-2 and C-3 hydrogens (axial and equatorial) and to the phenyl hydrogens respectively.

Anal. Calcd. for $C_{35}H_{53}O_3SbF_6$: C, 55.40; H, 7.0. Found: C, 55.42; H, 7.0.

5α-Cholestan-2β,3β-p-anisoxonium Hexafluoroantimonate (10a)

3α-Bromo-5α-cholestan-2β-yl *p*-anisate (**9***a*, 1.82 g) was treated with silver hexafluoroantimonate (1.07 g) in nitromethane (10 ml) as described above. Crystallization from methylene chloride : ether gave 5α-cholestan-2β,3β-*p*-anisoxonium hexafluoroantimonate (**10***a*, 1.31 g), m.p. 188–189° (sealed capillary tube), $[\alpha]_D$ −74° (CH_2Cl_2). The n.m.r. spectrum showed peaks at 0.87 (singlet) and 4.03 (singlet), a broad unresolved multiplet centered at 5.82 and a quartet at 7.20 and 8.30 p.p.m., J_{AB} 9 c.p.s. These bands were assigned to the C-19 methyl group, the methoxyl group, the C-2 and C-3 hydrogens (equatorial and axial) and to the phenyl hydrogens respectively.

Anal. Calcd. for $C_{35}H_{53}O_3SbF_6$: C, 55.40; H, 7.0. Found: C, 54.95; H, 6.87.

5α-Cholestan-2β,3β-benzoyloxonium Hexafluoroantimonate (10b)

A solution of 3α-bromo-5α-cholestan-2β-yl benzoate (**9***b*, 1.07 g) in nitromethane (15 ml) was treated with silver hexafluoroantimonate (0.57 g) for 12 h at 50°. Crystallization from methylene chloride : ether gave 5α-cholestan-2β,3β-benzoyloxonium hexafluoroantimonate (**10***b*, 0.85 g), m.p. 140–141°, $[\alpha]_D$ −28° (CH_2Cl_2).

Anal. Calcd. for $C_{34}H_{51}O_2SbF_6$: C, 56.12; H, 7.07. Found: C, 55.45; H, 6.68.

9β,10α-Decalin-2β,3β-p-anisoxonium Hexafluoroantimonate (3a)

2β-Bromo-9β,10α-decalin-3β-yl *p*-anisate (**8***a*, 1.93 g) was treated with silver hexafluoroantimonate (1.8 g) in nitromethane (10 ml) as above. Crystallization from methylene chloride : ether gave 9β,10α-decalin-2β,3β-*p*-anisoxonium hexafluoroantimonate (**3***a*, 2.15 g), m.p. 178–179° (sealed capillary tube). The n.m.r. spectrum (CD_2Cl_2) had a peak at 4.02 (singlet), an unresolved multiplet at 5.78 and a quartet at 7.20 and 8.30 p.p.m., J_{AB} 9 c.p.s. These bands were assigned to the methoxyl group, the C-2 and C-3 hydrogens (equatorial and axial) and the phenyl hydrogens respectively.

Anal. Calcd. for $C_{18}H_{23}O_3SbF_6$: C, 41.32; H, 4.43. Found: C, 40.92; H, 4.61.

9β,10α-Decalin-2β,3β-benzoyloxonium Hexafluoroantimonate (3b)

2β-Bromo-9β,10α-decalin-3α-yl benzoate (**8***b*, 1.0 g) was treated with silver hexafluoroantimonate (1.0 g) in nitromethane (10 ml), as described above. Crystallization from methylene chloride : ether gave 9β,10α-decalin-2β,3β-benzoyloxonium hexafluoroantimonate (**3***b*, 1.24 g), m.p. 142–144° (sealed capillary tube). The n.m.r. spectrum (CD_2Cl_2) had an unresolved multiplet centered at 5.89 and a complex multiplet centered at 8.08 p.p.m., assigned to the C-2 and C-3 hydrogens (equatorial and axial) and the phenyl hydrogens respectively.

Anal. Calcd. for $C_{17}H_{21}O_2SbF_6$: C, 41.41; H, 4.30. Found: C, 41.49; H, 4.32.

Reaction of 5α-Cholestan-2α,3α-p-anisoxonium Hexafluoroantimonate (7) with Bromide Ion in Methylene Chloride

A solution of the salt (250 mg) in methylene chloride (10 ml) was treated with tetraethylammonium bromide (670 mg). After standing for 1 h at room temperature the reaction mixture was diluted with ether and washed several times with water, dried, and the solvent removed under reduced pressure. The product (197 mg), $[\alpha]_D$ 0°, was shown by t.l.c. (benzene) to consist of two compounds corresponding to the diaxial (R_f 0.53) and the diequatorial (R_f 0.56) bromoanisates.

The infrared spectrum showed also that a mixture had been obtained. The diaxial bromoester, 2β-bromo-5α-cholestan-3α-yl *p*-anisate (**6**) had absorption at 695 cm^{-1} (m) while the diequatorial bromoester, 3β-bromo-5α-cholestan-2α-yl *p*-anisate, had absorption at 695 (w) and 714 cm^{-1} (m). The product from the reaction above was dissolved in CS_2 to give a suitable concentration and the infrared spectrum taken between 800 and 600 cm^{-1}. Mixtures of the diaxial and diequatorial bromoanisates were prepared and dissolved in CS_2 to give the same concentration as that of the product, and their infrared spectra in the same region were determined. From a comparison of the peak heights at 714 and 695 cm^{-1} it was

[4]The assignment of the C-19 methyl peak position followed from the observation that it was only methyl peak whose position changed in the various ring A derivatives. The other methyl peaks appeared at 38, 48, and 54 c.p.s. downfield from the tetramethylsilane signal, and since these peaks did not change with the ring A substituents, they are not recorded.

concluded that the product contained approximately 68% diequatorial and 32% diaxial bromoanisate.

*Reaction of 5α-Cholestan-2β,3β-p-anisoxonium Hexafluoroantimonate (**10a**) with Bromide Ion in Methylene Chloride*

A solution of the salt (154 mg) in methylene chloride (10 ml) was treated with tetraethylammonium bromide (500 mg) for 30 min as described above. Thin-layer chromatography (benzene) showed the product to be almost entirely bromoanisate with a small amount of material at the origin (most likely hydrolysis product). The product was purified by t.l.c., using benzene as the developing solvent. The product (101 mg), $[\alpha]_D + 34°$, had an infrared spectrum almost identical with that of 3α-bromo-5α-cholestan-2β-yl *p*-anisate (**9***a*). Crystallization from methylene chloride : pentane gave 3α-bromo-5α-cholestan-2β-yl *p*-anisate (**9***a*) identified by m.p., mixture m.p., and infrared spectrum.

The two bromoesters could not be separated very easily by t.l.c. In most solvent compositions used the product showed only one spot, but, multiple elution in benzene (seven times) showed the product to consist of two materials corresponding to the diaxial and diequatorial bromoanisates, with only a trace of the diequatorial compound being present.

In a second experiment the anisoxonium salt (297 mg) gave, on treatment with tetraethylammonium bromide in methylene chloride, 229 mg of product, which was dissolved in CS_2 and its infrared spectrum around 700 cm^{-1} determined. In the infrared spectrum of the diequatorial bromoanisate, 2α-bromo-5α-cholestan-3β-yl *p*-anisate, there was a peak at 716 cm^{-1} (w) which did not appear in the spectrum of the diaxial bromoester, 3α-bromo-5α-cholestan-2β-yl *p*-anisate (**9***a*). Mixtures of the diaxial and diequatorial bromoanisates were prepared and dissolved in CS_2 to give the same concentration as that of the reaction product. From the intensity of the peak at 716 cm^{-1} in the infrared spectra of the mixtures of diaxial and diequatorial bromoanisates and in the spectrum of the product, it was estimated that there was less than 3% of the diequatorial bromoanisate present in the reaction product.

*Reaction of 5α-Cholestan-2α,3α-p-anisoxonium Hexafluoroantimonate (**7**) with Bromide Ion in Acetonitrile*

The anisoxonium salt (7, 225 mg) was treated with tetraethylammonium bromide (630 mg) in acetonitrile (10 ml) for 1 h as described above. The product, $[\alpha]_D$ 0°, had an infrared spectrum (CS_2), in the region 800 to 600 cm^{-1} which corresponded to the same product composition as obtained in methylene chloride, i.e. 68% diequatorial and 32% diaxial bromoanisates.

*Reaction of 5α-Cholestan-2α,3α-p-anisoxonium Hexafluoroantimonate (**7**) with Bromide Ion in Nitromethane*

The salt (0.23 g) was treated with tetraethylammonium bromide (0.59 g) in nitromethane (10 ml) for 23 h at room temperature as previously described, and gave 164 mg of bromoanisate mixture $[\alpha]_D + 5°$. The infrared spectrum (CS_2) corresponded to a product composition of 60% diequatorial and 40% diaxial bromoanisate.

Reaction of 9β,10α-Decalin-2β,3β-p-anisoxonium Hexafluoroantimonate (3a) with Bromide Ion in Methylene Chloride

A solution of the salt (**3***a*, 0.26 g) in methylene chloride (10 ml) was treated with tetraethylammonium bromide (1.05 g) for 1 h at room temperature as described above. The product (0.18 g) had an infrared spectrum almost identical with that of 2β-bromo-9β,10α-decalin-3α-yl *p*-anisate (**8***a*). Thin-layer chromatography [benzene : cyclohexane (1:1)], after two elutions, showed two compounds, corresponding to the diaxial (R_f 0.44) and diequatorial (R_f 0.35) bromoanisates, with only a trace of the diequatorial bromoester being present. Crystallization from petroleum ether gave 2β-bromo-9β,10α-decalin-3α-yl *p*-anisate, identified by m.p., mixture m.p., and infrared spectrum.

The crude product from above was dissolved in chloroform (0.7 ml). Mixtures of the diaxial and diequatorial bromoanisates were prepared and dissolved in chloroform to give the same concentration as that of the product. A standard number of drops of each solution were applied to t.l.c. plates which were then eluted twice with benzene : cyclohexane (1:1). The plates were sprayed with 30% sulfuric acid and charred, and the intensities of the spots compared. By this method it was estimated that the amount of diequatorial bromoanisate was approximately 5%.

Reaction of 9β,10α-Decalin-2β,3β-p-anisoxonium Hexafluoroantimonate (3a) with Chloride Ion in Methylene Chloride

A solution of the salt (**3***a*, 95 mg) in methylene chloride (10 ml) was treated with tetraethylammonium chloride (350 mg) for 30 min at room temperature. Thin-layer chromatography [benzene : cyclohexane (1:1)] after two elutions, showed the product (54 mg) to consist of almost entirely diaxial chloroanisate together with a small amount of the diequatorial compound. Crystallization from methylene chloride: methanol gave 2β-chloro-9β,10α-decalin-3α-yl *p*-anisate (38 mg) identified by m.p., mixture m.p., and infrared spectrum.

The crude product (54 mg) from the above reaction was dissolved in chloroform (0.5 ml). Mixtures of the diaxial and diequatorial chloroanisates were prepared and also dissolved in chloroform to give the same concentration as that of the product. A standard number of drops of each solution (from the same dropping pipette) were applied to t.l.c. plates, which were then eluted with benzene : cyclohexane (1:1) four times. From the intensities of the spots, after charring, it was estimated that the amount of diequatorial chloroanisate was about 6% of the product.

*Reaction of 5α-Cholestan-2β,3β-benzoyloxonium Hexafluoroantimonate (**10b**) with Bromide Ion in Methylene Chloride*

A solution of the benzoyloxonium salt (**10***b*, 250 mg) in methylene chloride (15 ml) was treated with tetraethylammonium bromide (1.0 g) for 1 h at room temperature. The product (182 mg) showed one spot upon thin-layer chromatography (benzene) and had an infrared spectrum almost identical with that of the diaxial bromobenzoate, **9***b*. Crystallization from ether : methanol

Can. J. Chem. Downloaded from www.nrcresearchpress.com by 210.87.254.105 on 09/05/12
For personal use only.

Can. J. Chem. Downloaded from www.nrcresearchpress.com by 210.87.254.105 on 09/05/12
For personal use only.

gave 3α-bromo-5α-cholestan-2β-yl benzoate (140 mg), m.p. 115–116°, mixture m.p. with authentic sample 114–115°; $[\alpha]_D$ +51°. The infrared spectrum was identical to that of an authentic sample.

Reaction of 9β,10α-Decalin-2β,3β-benzoyloxonium Hexafluoroantimonate (3b) with Benzoic Acid and N,N-Diisopropylethylamine

N,N-Diisopropylethylamine (131 mg) (Fluka AG, Buchs SG, Switzerland) was dissolved in methylene chloride (2.5 ml) and added to a solution of benzoic acid (128 mg) in methylene chloride (2.5 ml). To the resulting mixture was added the decalin benzoyloxonium salt (*3b*, 100 mg) and the solution allowed to stand at room temperature for 24 h. The reaction was washed several times with water, dried, and the solvent evaporated. Thin-layer chromatography (benzene) showed two spots corresponding in R_f values to the diaxial and diequatorial dibenzoates with only a small amount of the diequatorial compound being present. These two materials were separated by t.l.c., eluting with benzene. 9β,10α-Decalin-2α,3β-diyl dibenzoate (7 mg) crystallized from ether : methanol and was identified by m.p., mixture m.p. with authentic sample, and infrared spectrum. 9β,10α-Decalin-2β,3α-diyl dibenzoate (48 mg) crystallized from ether : methanol and was identified by m.p., mixture m.p. with authentic sample, and infrared spectrum.

Reaction of 9β,10α-Decalin-2β,3β-p-anisoxonium Hexafluoroantimonate (3a) with N,N,-Diisopropylethylamine and Trifluoroacetic Acid

N,N-Diisopropylethylamine (125 mg) in methylene chloride (2.5 ml) was added to a solution of trifluoroacetic acid (113 mg) in methylene chloride (2.5 ml). To the resulting solution the decalin anisoxonium salt (*3a*, 100 mg) was added and the reaction allowed to stand at room temperature for 36 h. The solution was washed several times with water, dried and the solvent evaporated. Thin-layer chromatography (benzene) showed the product (49 mg) to consist of almost entirely one compound together with a trace of a second compound, both being visible under ultraviolet light. Crystallization from pentane gave 9β,10α-decalin-2β-yl *p*-anisate-3α-yl trifluoroacetate, m.p. 66–68°; ν_{max} 1780, 1710 cm^{-1}. The n.m.r. spectrum showed peaks at 3.83, 5.25 (2*H*, multiplet, half-width 5 c.p.s.) and a quartet 7.95 and 6.91 p.p.m., J_{AB} 9 c.p.s. These absorptions were assigned to the methoxyl group, C-2 and C-3 hydrogens (both diequatorial) and the phenyl ring hydrogens respectively.

Anal. Calcd. for $C_{20}H_{23}O_5F_3$: C, 59.99; H, 5.79. Found: C, 59.81; H, 5.87.

Reaction of Epoxides with Hydrobromic Acid

(i) 2,3-Epoxy-9β,10α-decalin

A solution of the epoxide (20) (198 mg) in methylene chloride (20 ml) was shaken with 48% aqueous hydrobromic acid (5 ml) for 5 min. The methylene chloride solution was washed with dilute solutions of sodium bisulfite and sodium bicarbonate, water, dried and then evaporated. The residue (279 mg) was dried under vacuum.

On silica gel thin-layer chromatography [benzene : ether (1:1)] it was found that the diaxial and diequatorial bromohydrins had the same R_f value. If the t.l.c. plate was developed with iodine vapor, the diequatorial bromohydrin showed up, but the diaxial did not develop. With the product from the reaction a small amount of the diequatorial material was detected using this method. Thin-layer chromatography using Merck aluminium oxide G and ether : methanol (98:2), separation of the bromohydrins was achieved, with the diequatorial compound moving slower than the diaxial material. In the product from the epoxide opening reaction a small amount of the diequatorial bromohydrin was again detected, but owing to poor development on charring, no estimate of the amount of this compound could be made.

(ii) 5α-Cholestan-2α,3α-epoxide (11)

The epoxide (99 mg) in methylene chloride (30 ml) was treated with aqueous hydrobromic acid as described in (*i*). Thin-layer chromatography [benzene : ether (9:1)] showed the product (115 mg) to consist of a mixture of the corresponding diaxial and diequatorial bromohydrins, (**12**) and (**13**) (R_f 0.38 and 0.55) with only a small amount of the diequatorial material being present.

(iii) 5α-Cholestan-2β,3β-epoxide (14)

The epoxide (104 mg) in methylene chloride was treated as above (*i*). The residue (122 mg) was shown by t.l.c. [benzene : ether (9:1)] to be a mixture of the two possible bromohydrins, again only a small amount of the diequatorial compound being detected. In this case the diequatorial bromohydrin (2α-bromo-5α-cholestan-3β-ol, **16**) ran slower (R_f 0.39) than the diaxial bromohydrin (**15**) (R_f 0.49).

The analyses of the products from (*ii*) and (*iii*) were carried out by quantitative thin-layer chromatography in a similar manner to that described for the analysis of the decalin bromoanisate mixtures. For 5α-cholestan-2α,3α-epoxide the product mixture was estimated to consist of 95% of diaxial and 5% diequatorial bromohydrins. For 5α-cholestan-2β,3β-epoxide the product was estimated to contain 97% diaxial and 3% diequatorial bromohydrins.

Preparation of the Decalin Halohydrins

(i) 2β-Bromo-9β,10α-decalin-3α-ol

Treatment of 2,3-epoxy-9β,10α-decalin (20) with aqueous hydrobromic acid (48%) following the analogous procedure (15) for the steroidal bromohydrins gave 2β-bromo-9β,10α-decalin-3α-ol, which was purified by recrystallization from petroleum ether; m.p. 77–78°; ν_{max} 3600 cm^{-1}. The n.m.r. spectrum showed signals at 2.08 (singlet) and 4.23 (multiplet), assigned to the hydroxyl group and the protons at C-2 and C-3.

Anal. Calcd. for $C_{10}H_{17}OBr$: C, 51.50; H, 7.35; Br, 34.27. Found: C, 51.61; H, 7.32; Br, 34.44.

(ii) 2α-Bromo-9β,10α-decalin-3β-ol

A solution of 2α-bromo-9β,10α-decalin-3β-yl *p*-anisate (180 mg) plus 35% perchloric acid (2 ml) in dioxan (10 ml) was refluxed for 96 h. The reaction was diluted with water and extracted with ether; the ether extracts being then washed with dilute sodium bicarbonate solution and water, dried and evaporated. Thin-layer chromatography [benzene : ether (9:1)] showed the product to consist of two compounds (R_f 0.63 and 0.38). The faster running material had the same R_f value as the starting material and was visible under ultraviolet light. The second compound was not visible under ultraviolet light. These two

Can. J. Chem. Downloaded from www.nrcresearchpress.com by 210.87.254.105 on 09/05/12
For personal use only.

materials were separated by t.l.c., the plates being developed with iodine vapor. The slower moving band gave 70 mg of 2α-bromo-9β,10α-decalin-3β-ol which was recrystallized from ether : pentane; m.p. 86–87°; ν_{max} 3480 cm^{-1}. The n.m.r. spectrum had a band at 2.57 (singlet, OH), and a broad multiplet centered at 3.75 p.p.m. (C-2 and C-3 hydrogens).

Anal. Calcd. for $C_{10}H_{17}OBr$: C, 51.50; H, 7.35; Br, 34.27. Found: C, 51.56; H, 6.93; Br, 34.40.

(iii) 2β-Chloro-9β,10α-decalin-3α-ol

Prepared by treating a solution of 2,3-epoxy-9β,10α-decalin (20) in methylene chloride (20 ml) with hydrogen chloride gas for 5 min. The reaction solution was washed with dilute sodium bicarbonate solution, water, dried, and the solvent evaporated under reduced pressure. The product was crystallized from ether : pentane; m.p. 72–73°; ν_{max} 3600 cm^{-1}. The n.m.r. spectrum had bands at 2.18 (singlet, O—H) and 4.08 p.p.m. (2*H*, half-width 11 c.p.s.).

Anal. Calcd. for $C_{10}H_{17}ClO$: C, 63.63; H, 9.08; Cl, 18.79. Found: C, 63.64; H, 8.98; Cl, 18.75.

General Procedure for the Preparation of the Halohydrin Esters from the Alcohols

About 1 to 2 equivalents of the acid chloride were added to a solution of the alcohol in 5 to 10 times its weight in pyridine. After standing at room temperature overnight, the reaction mixture was poured into ether and washed with dilute hydrochloric acid solution, dilute sodium bicarbonate solution and water, dried and the solvent evaporated. Further purification was effected by column chromatography on silica gel (British Drug Houses chromatographic grade).

(i) 3α-Bromo-5α-cholestan-2β-yl Benzoate (9b)

The alcohol was obtained as previously described (15). The ester was recrystallized from ether : methanol; m.p. 114–115°, $[\alpha]_D$ +50°; ν_{max} 1715 cm^{-1}. The n.m.r. spectrum had absorption at 4.53 (multiplet), 5.48 (multiplet), 7.57 and 8.07 (both multiplets). These bands were assigned to the C-3 hydrogen (equatorial), the C-2 hydrogen (equatorial) and to the phenyl hydrogens respectively.

Anal. Calcd. for $C_{34}H_{51}O_2Br$: C, 71.43; H, 8.99. Found: C, 71.15; H, 9.04.

(ii) 3α-Bromo-5α-cholestan-2β-yl p-anisate (9a) was prepared as described previously (2); m.p. 117–120°, $[\alpha]_D$ +36°. The n.m.r. spectrum showed signals at 1.07 (singlet), 3.88 (singlet), 4.50 (half-width 8 c.p.s.), 5.43 (half-width 8 c.p.s.), and 6.93 and 8.02 p.p.m. J_{AB} 9 c.p.s. assigned to the C-19 methyl group, the methoxyl group, the C-3 hydrogen (equatorial), the C-2 hydrogen (axial) and to the phenyl hydrogens, respectively.

(iii) 2β-Bromo-5α-cholestan-3α-yl p-anisate (6) was prepared as before (21); m.p. 107–109°, $[\alpha]_D$ +82°; reported m.p. 136–138°, $[\alpha]_D$ +83°; m.p. on admixture with an authentic specimen 134–136°. Comparison of infrared spectra and thin-layer chromatographic behavior confirmed the identity. The n.m.r. spectrum showed absorption at 1.17 (singlet), 3.87 (singlet), 4.45 (half-width 7 c.p.s.), 5.40 (half-width 7 c.p.s.), and 6.98 and 8.00 p.p.m., J_{AB} 9 c.p.s., assigned to the C-19 methyl group, the methoxyl group, the C-2 hydrogen (equatorial) the C-3 hydrogen (equatorial) and to the phenyl hydrogens respectively.

(iv) 2α-Bromo-5α-cholestan-3β-yl p-anisate was prepared as before (2); m.p. 173–175°; reported m.p. 174–176°. The n.m.r. spectrum showed bands at 0.90 (singlet), 3.88 (singlet), 4.4 and 5.1 (both broad diffuse bands) and 6.95 and 8.05 p.p.m. (J_{AB} 9 c.p.s.), attributed to C-19, C-2 and C-3 (both axial), and phenyl hydrogens, respectively.

(v) 2β-Bromo-9β,10α-decalin-3α-yl p-anisate (8a) was recrystallized from petroleum ether, m.p. 61–63°; ν_{max} 1705 cm^{-1}. The n.m.r. spectrum had signals at 3.78 (singlet), 4.50 (half-width 6 c.p.s.), 5.38 (narrow multiplet), and 6.96 and 8.00 p.p.m. J_{AB} 9 c.p.s., assigned in the same way as above.

Anal. Calcd. for $C_{18}H_{23}O_3Br$: C, 58.86; H, 6.31; Br, 21.49. Found: C, 58.99; H, 6.46; Br, 21.60.

(vi) 2β-Chloro-9β,10α-decalin-3α-yl p-anisate was recrystallized from methylene chloride : methanol, m.p. 57–59°; ν_{max} 1705 cm^{-1}. Then. m.r. spectrum showed absorption at 3.85 (singlet), 4.35 (half-width 8 c.p.s.), 5.28 (half-width 7 c.p.s.) and 6.97 and 7.99 p.p.m. J_{AB} 9 c.p.s., assigned as above.

Anal. Calcd. for $C_{18}H_{23}O_3Cl$: C, 66.95; H, 7.18; Cl, 10.98. Found: C, 66.73; H, 7.03; Cl, 11.04.

(vii) 2β-Bromo-9β,10α-decalin-3α-yl benzoate (8b) was recrystallized from methylene chloride : petroleum ether, m.p. 110–111°; ν_{max} 1710 cm^{-1}. The n.m.r. spectrum had signals at 4.47 (half-width 7 c.p.s.), 5.37 (narrow multiplet), 7.43 (multiplet) and 8.0 (multiplet), assigned to the C-2 and C-3 hydrogens and the phenyl hydrogens respectively.

Anal. Calcd. for $C_{17}H_{21}BrO_2$: C, 60.53; H, 6.28; Br, 23.69. Found: C, 60.57; H, 6.28; Br, 24.01.

(viii) 9β,10α-Decalin-2α,3β-diyl dibenzoate

The alcohol was obtained by the method of Ali and Owens (22). The ester was purified by t.l.c. (benzene) and then recrystallized from ether : methanol, m.p. 113–115°; ν_{max} 1710 cm^{-1}. The n.m.r. had bands at 5.30 (broad band), 7.33, and 7.70 p.p.m. (both complex multiplets).

Anal. Calcd. for $C_{24}H_{26}O_4$: C, 76.14; H, 6.92. Found: C, 76.24; H, 6.70.

(ix) 9β,10α-Decalin-2β,3α-diyl dibenzoate

9β,10α-Decalin-2β,3α-diol (23) was treated as described above. The product was purified by t.l.c. [ether : benzene (5:95)] and recrystallized from methylene chloride : petroleum ether; m.p. 148–150°; ν_{max} 1710 cm^{-1}. The n.m.r. spectrum had bands at 5.35 (multiplet, half-width 4 c.p.s.), 7.42 and 8.02 p.p.m. (multiplets), assigned to the C-2 and C-3 hydrogens and the phenyl hydrogens respectively.

Anal. Calcd. for $C_{24}H_{26}O_4$: C, 76.14; H, 6.92. Found: C, 75.80; H, 6.62.

3β-Bromo-5α-cholestan-2α-yl p-anisate

This was prepared by the diaxial → diequatorial rearrangement of 2β-bromo-5α-cholestan-3α-yl *p*-anisate as previously described (21); m.p. 112–115°, $[\alpha]_D$ −35°; reported m.p. 114–115°, $[\alpha]_D$ −37°.

2α-Bromo-9β,10α-decalin-3β-yl p-anisate

This was prepared from 2β-bromo-9β,10α-decalin-3α-yl *p*-anisate (**8***a*, 0.4 g) by heating at 130° for 18 h under nitrogen. Thin-layer chromatography, eluting four times with benzene : cyclohexane (1:1), showed two spots, very close together, with R_f values of 0.63 and 0.54 respec-

tively, the faster moving material corresponding to the diaxial bromoanisate (**8***a*). The pyrolysis product was separated by t.l.c. as above; under ultraviolet light a broad band was observed on the t.l.c. plates, with no apparent separation. The lower half of this band was removed from the plates and extracted with chloroform (+1% methanol). After filtration, evaporation of the extract yielded 2α-bromo-9β,10α-decalin-3β-yl *p*-anisate, which was recrystallized from ether : petroleum ether, m.p. 122–124°; ν_{max} 1730 cm^{-1}. The n.m.r. spectrum had bands at 3.80 (singlet), 4.0 (multiplet), 5.08 (broad band) and 6.87 and 7.97 p.p.m. (J_{AB} 9 c.p.s.).

Anal. Calcd. for $C_{18}H_{23}O_3Br$: C, 58.86; H, 6.31; Br, 21.49. Found: C, 58.76; H, 6.20; Br, 21.72.

Rearrangement of 2β-Chloro-9β,10α-decalin-3α-yl p-anisate to 2α-Chloro-9β,10α-decalin-3β-yl p-anisate

The diaxial chloroanisate (500 mg) in a test tube, flushed with nitrogen and stoppered by a plug of cotton wool, was heated at 140° for 96 h. Thin-layer chromatography [benzene : cyclohexane (1:1)] of the product (a dark brown oil) showed two spots running very close together. These two materials were separated by eluting with benzene : cyclohexane (1:1) five times; under ultraviolet light the materials showed up as a wide spread band on the plates. This band was cut in half and each half extracted, the upper half gave 390 mg which was almost entirely diaxial chloroanisate, and the lower half (108 mg) gave the diequatorial chloroanisate, recrystallized from methylene chloride : methanol; m.p. 106–107°, ν_{max} 1705 cm^{-1}. The n.m.r. had absorption at 3.80 (singlet), 4.0 (broad multiplet), 5.0 (broad band) and 6.87 and 7.97 p.p.m. (J_{AB} 9 c.p.s.).

Anal. Calcd. for $C_{18}H_{23}O_3Cl$: C, 66.95; H, 7.18; Cl, 10.98. Found: C, 66.74; H, 7.02; Cl, 10.98.

Acknowledgments

We gratefully acknowledge the financial support of the National Research Council of Canada and the Alfred P. Sloan Foundation.

1. H. MEERWEIN. *In* Houben-Weyl Methoden der Organischen Chemie. 4th ed. *Edited by* E. Müller. Vol. 6. Part 3. Georg Thieme Verlag, Stuttgart, 1965. pp. 344 ff.; C. B. ANDERSON, E. C. FRIEDRICH, and S. WINSTEIN. Tetrahedron Letters, 2037 (1963), and references cited.
2. J. F. KING and R. G. PEWS. Can. J. Chem. **43**, 847 (1965).
3. E. ELIEL and R. S. RO. J. Am. Chem. Soc. **79**, 5995 (1957); E. ELIEL and R. G. HABER. J. Am. Chem. Soc. **81**, 1249 (1959).
4. A. FÜRST and P. A. PLATTNER. Intern. Congr. Pure Appl. Chem. 12th Congr. New York. 1951. Abstracts of papers, p. 409.
5. D. H. R. BARTON and R. C. COOKSON. Quart. Rev. London, **10**, 44 (1956).
6. A. HASSNER and C. HEATHCOCK. Tetrahedron Letters, 393 (1963); A. HASSNER and C. HEATHCOCK. J. Org. Chem. **30**, 1748 (1965).
7. J. F. KING, K. ABIKAR, D. M. DEAKEN, and R. G. PEWS. Can. J. Chem. **46**, 1 (1968).
8. S. WINSTEIN and R. E. BUCKLES. J. Am. Chem. Soc. **64**, 2780 (1942).
9. H. MEERWEIN and K. WUNDERLICH. Angew. Chem. **69**, 481 (1957); H. MEERWEIN, K. BODENBENNER, P. BORNER, F. KUNERT, and K. WUNDERLICH. Ann. **632**, 38 (1960).
10. J. A. MAGNUSON, C. A. HIRT, and P. J. LAUNER. Chem. and Ind. London. 691 (1965).
11. A. D. ALLBUTT. Ph.D. Thesis, University of Western Ontario, London, Ontario. 1967. pp. 93–95 and p. 149.
12. H. HENBEST and M. SMITH. J. Chem. Soc. 926 (1957).
13. J. F. KING and A. D. ALLBUTT. Tetrahedron Letters, 49 (1967).
14. P. S. ELLINGTON, D. G. HEY, and G. D. MEAKINS. J. Chem. Soc. (C), 1327 (1966).
15. G. H. ALT and D. H. R. BARTON. J. Chem. Soc. 4284 (1954).
16. E. L. ELIEL. Stereochemistry of carbon compounds. McGraw–Hill, New York, 1962. pp. 224–226.
17. J. VALLS and E. TOROMANOFF. Bull. Soc. Chim. France, 758 (1961).
18. D. H. R. BARTON, D. A. LEWIS, and J. F. MCGHIE. J. Chem. Soc. 2907 (1957); L. F. FIESER and M. FIESER. Steroids, Reinhold, New York, 1959. p. 251; J. LEVISALLES. Bull. Soc. Chim. France, 551 (1960).
19. C. B. ANDERSON. Ph.D. Thesis. University of California. Los Angeles, 1963.
20. W. S. JOHNSON, V. J. BAUER, J. L. MARGRAVE, M. A. FRISCH, L. H. DREGER, and W. N. HUBBARD. J. Am. Chem. Soc. 83, 606 (1961).
21. D. H. R. BARTON and J. F. KING. J. Chem. Soc. 4398 (1958).
22. M. E. ALI and L. N. OWEN. J. Chem. Soc. 2119 (1958).
23. H. B. HENBEST, M. SMITH, and A. THOMAS. J. Chem. Soc. 3293 (1958).

Can. J. Chem. Downloaded from www.nrcresearchpress.com by 210.87.254.105 on 09/05/12
For personal use only.

Can. J. Chem. Downloaded from www.nrcresearchpress.com by 210.87.254.42 on 09/05/12
For personal use only.

Structure of the product obtained in the base-catalyzed condensation of acetone and indanedione-1,3

STEPHEN J. KUHN
Exploratory Research Laboratory, Dow Chemical of Canada, Limited, Sarnia, Ontario[1]
Received December 27, 1967[2]

It has been found that acetone and indanedione-1,3 gives 1,1-dimethyl-3-oxo-1,2,3,9*a*-tetrahydro-9-indanedionylene fluorene in the presence of a base, instead of 1,1-dimethyl-3-oxo-1,2,3,4-tetrahydro-9-indanedionylene fluorene or other products claimed in the literature. The nuclear magnetic resonance spectra of the product and some of its derivatives have been recorded.

Canadian Journal of Chemistry, 47, 1461 (1969)

Introduction

The base-catalyzed condensation of acetone and indanedione-1,3 has been studied by a number of investigators.

Radulescu and Georgescu (1) have suggested that one molecule of acetone condenses with two molecules of indanedione-1,3 through the carbonyl group of the acetone and the methylene group of the indanedione. They postulated structure **1** for their product. Cirulis (2) has suggested

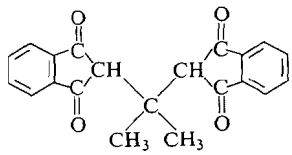

1

that the condensation takes place between the methyl groups of the acetone and the carbonyl group of the indanedione (**2**). Kalnins (3) assigned

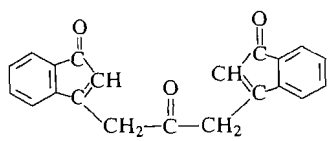

2

a pyrane type of structure **3** for the product, which is formed by the further condensation of **1**.

Geita and Vanags (4) have shown that the product forms by the condensation of 2 moles of acetone with 2 moles of indanedione-1,3 by splitting off 3 moles of water. They postulated the product as 1,1-dimethyl-3-oxo-1,2,3,4-tetrahydro-9-indanedionylene fluorene (**4**) formed as shown in Scheme 1.

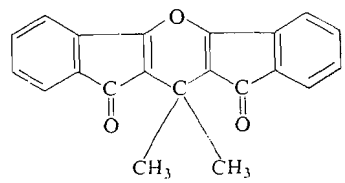

3

They have concluded from the infrared (i.r.) spectrum that the indanedione group is present in the molecule.

For some time we have been interested in the base-catalyzed condensation of ketones and indanedione-1,3 and it occurred to us that the condensation may take a course other than that suggested by Geita and Vanags, leading to a compound isomeric with theirs (Scheme 2).

Experimental

Many of these compounds were prepared by using slightly modified methods of Cirulis (2) and Geita and Vanags (4).

1,1-Dimethyl-3-oxo-1,2,3,9a-tetrahydro-9-indanedionylene Fluorene (5)

A mixture of 140 ml of acetone, 15 g of indanedione-1,3, and 7 g of piperidine was heated under reflux on a water bath for 1 h then allowed to stand at room temperature for 5 h. The dark-blue solution was added in small portions to 1.5 l of well stirred 10% aqueous acetic acid. The brownish-yellow precipitate was collected on a filter, washed with water, and then washed several times with alcohol. After the alcohol treatment, the solid was washed with 10% Na_2CO_3 solution, then with 10% aqueous acetic acid solution. After drying, the yellow

[1]Contribution No. 158.
[2]Revision received July 17, 1968.

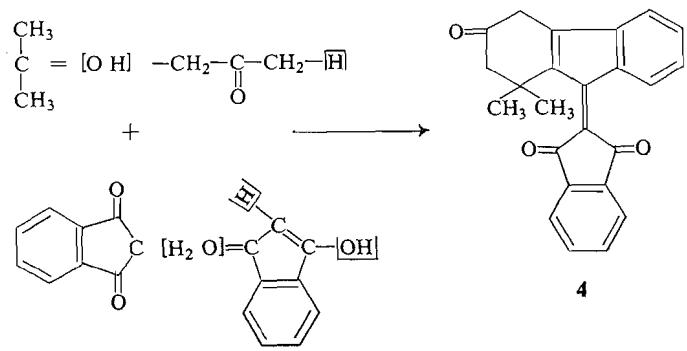

4

SCHEME 1

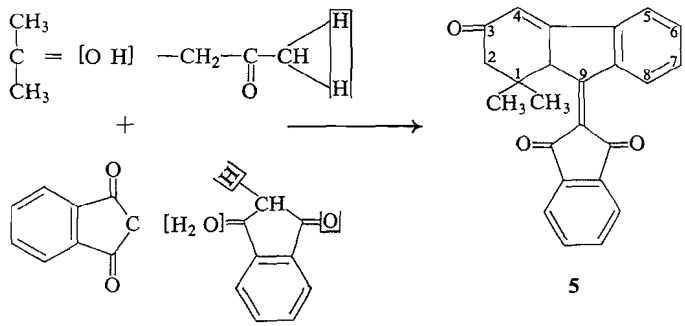

5

SCHEME 2

product was crystallized from glacial acetic acid, yielding 9.7 g of product, m.p. 198–200 °C.

Anal. Calcd. for $C_{24}H_{18}O_3$ (mol. wt., 354.0): C, 81.35; H, 5.08. Found (mol. wt., 360.0): C, 81.3; H, 5.07.

1,1-Dimethyl-2,9a-dibromo-3-oxo-1,2,3,9a-tetrahydro-9-indanedionylene Fluorene (6)

Compound **5**, (5 g) was dissolved in 50 ml of glacial acetic acid, 1.5 ml of bromine was added and the mixture was heated on a water bath for 4 h. After cooling and standing for 5 h, a brownish-yellow solid precipitated. It was filtered and purified by dissolving it in warm chloroform and reprecipitated by ether. The pure product (6.5 g) was yellow with m.p. 216–217°C.

Anal. Calcd. for $C_{24}H_{16}Br_2O_3$: C, 56.24; H, 3.12; Br, 31.25. Found: C, 56.4; H, 3.12; Br, 30.95.

1,1-Dimethyl-3-oxo-9a-methyl-1,2,3,9a-tetrahydro-9-indanedionylene Fluorene (7)

Compound **5**, (5 g) was dissolved in 50 ml 1% solution of $NaOCH_3$ in dry methanol, then 10 g of methyl iodide was added to the reaction mixture. The reaction mixture was refluxed for 5 h. Upon cooling a brownish-yellow solid precipitated (5.1 g). The solid product was crystallized from glacial acetic acid, m.p. 251 °C. The product was a mixture of **5** (30%) and 7 (70%). A small amount of pure 7 was isolated from the mixture (5g) by washing it on a glass filter 10 times with 100 ml hot, aqueous 10% K_3PO_4 solution. It was then crystallized from hot acetic acid, dimethyl sulfoxide, *N,N*-dimethyl formamide, hexamethyl phosphoramide, and finally from acetic acid. The product was obtained with m.p. 265 °C, yield 0.3 g.

Anal. Calcd. for $C_{25}H_{20}O_3$: C, 84.2; H, 5.4. Found: C, 84.1; H, 5.3.

3-Oxime of 1,1-Dimethyl-3,9-dioxo-1,2,3,9a-tetrahydrofluorene (10)

Compound **5**, (12 g) and 16 g hydroxylamine hydrochloride were added to 200 ml of ethyl alcohol and the mixture was heated to the boiling point, then 10 g sodium bicarbonate was added in small portions. After the addition of the bicarbonate the reaction mixture was refluxed for 1 h, then filtered hot. Upon cooling more indanedione dioxime precipitated. This was filtered off and the mother liquor was diluted with 1 l of cold water. The solid which precipitated upon dilution of the mother liquor was filtered, then mixed with 1 l of water, boiled for 10 min and filtered hot, then crystallized from a small amount of ethyl alcohol. Yellow crystals 5 g were obtained, m.p. 199–201 °C.

1,1-Dimethyl-3,9-dioxo-1,2,3,9a-tetrahydrofluorene (11)

Compound **10**, (3 g) was dissolved in 80 ml of 18% HCl, 8 ml of glacial acetic acid was added, and the mixture was refluxed for 3 h. The hot solution was filtered and the mother liquor was diluted with a little cold water. Upon standing yellow crystals (1 g) separated from the

Can. J. Chem. Downloaded from www.nrcresearchpress.com by 210.87.254.42 on 09/05/12
For personal use only.

Can. J. Chem. Downloaded from www.nrcresearchpress.com by 210.87.254.42 on 09/05/12
For personal use only.

mother liquor. The product was crystallized from ethyl alcohol, m.p. 146–148 °C.

Anal. Calcd. for $C_{15}H_{14}O_2$: C, 79.66; H, 6.19. Found: C, 79.7; H, 6.16.

1,1-Dimethyl-3,9-dioxo-9a-deuterio-1,2,3,9a-tetrahydrofluorene (13)

Potassium phosphate (4.24 g, 0.02 mole) was dissolved in 30 ml of heavy water and 2.26 g (0.01 mole) of **11** were added to the solution. Upon shaking the mixture a homogeneous dark blue solution was obtained, which was acidified with CH_3—COOD. The yellow precipitate was filtered, washed with water, dried, and crystallized from ethyl alcohol (2.1 g), m.p. 146–147 °C.

Anal. Calcd. for $C_{15}H_{13}DO_2$: C, 79.3; D + H, 6.6. Found: C, 79.21; D + H, 6.5.

Nuclear Magnetic Resonance

The nuclear magnetic resonance spectra were recorded on a Varian A-60 spectrometer operating at room temperature. The chemical shifts were measured relative to internal tetramethylsilane.

Results and Discussion

Molecular weight measurement and analytical results agree equally with formula **4** or **5**.

The nuclear magnetic resonance (n.m.r.) spectrum of the product **5** in $CDCl_3$ (Fig. 1) shows peaks in the methyl, methylene, aromatic, aliphatic single proton, and olefinic proton regions. The signals have been tentatively assigned as follows: the peaks at 0.78 and 1.61 p.p.m. (internal TMS) to different sets of methyl protons; the two doublets centered at 2.59 and 4.06 p.p.m. respectively to two different methylene protons on the same carbon with a coupling constant of 19 c.p.s.; the doublet centered at 3.13 p.p.m. to an aliphatic proton and another doublet centered at 8.78 p.p.m. to an olefinic proton, these two protons having a coupling constant of 2 c.p.s., and the pattern centered around 7.78 p.p.m. to the aromatic protons. Integration of the peaks shows there are six methyl protons, two single protons, two methylene protons, and eight aromatic protons in the molecule. These results indicate that **5** is the right structure for the product. The proton at position-4 resonates at unusually low field.[3] However, Hayashi (5) has reported that the vinyl protons in substituted α-cyanocinnamic esters can resonate as low as 8.75 p.p.m. Double irradiation experiments have shown that proton-9*a* and proton-4 are coupled (Fig. 2). When proton-9*a* was replaced by deuterium (**5***a*) the signal for proton-4 coalesced to a broad singlet. Using the double resonance technique the methylene protons were also decoupled.

The doublet centered at 2.59 p.p.m. assigned to one of the methylene protons appears to have some fine structure. A careful inspection of the spectrum reveals that there is a small coupling between this proton and the olefinic proton at position-4 ($J \approx 0.5$ c.p.s.).

Structures **5***a* and **5** would give similar n.m.r. spectra; however, it is unlikely that the condensation would follow the path involving reaction of an indanedione carbonyl with an acetone carbonyl producing **5***a*.

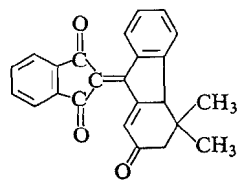

5*a*

Bromination of **5** in hot acetic acid gave a dibromo product **6**. The n.m.r. spectrum of **6** (in $SOCl_2$, internal TMS) shows peaks at 1.08 p.p.m. (3 Me protons), at 1.95 p.p.m. (3 Me protons), at 6.5 p.p.m. (aliphatic single proton), and at 8.78 p.p.m. (olefinic proton). The eight aromatic protons center at 7.63 p.p.m. The olefinic proton and the other single proton are coupled (0.7 c.p.s.). Based on this spectrum the following structure has been assigned to **6**.[4]

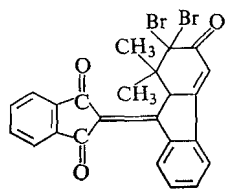

6

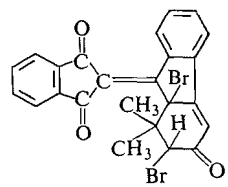

6*a*

To obtain more information on the structure

[3]One of the referees has suggested that this unique proton in **5** is that in the aromatic nucleus in proximity to the carbonyl group and that Fig. 1 is equally difficult to reconcile with **4** unless it is a mixture of isomers.

[4]One of the referees has suggested that allylic bromination rather than *gem*-dibromination appears more probable.

Can. J. Chem. Downloaded from www.nrcresearchpress.com by 210.87.254.42 on 09/05/12
For personal use only.

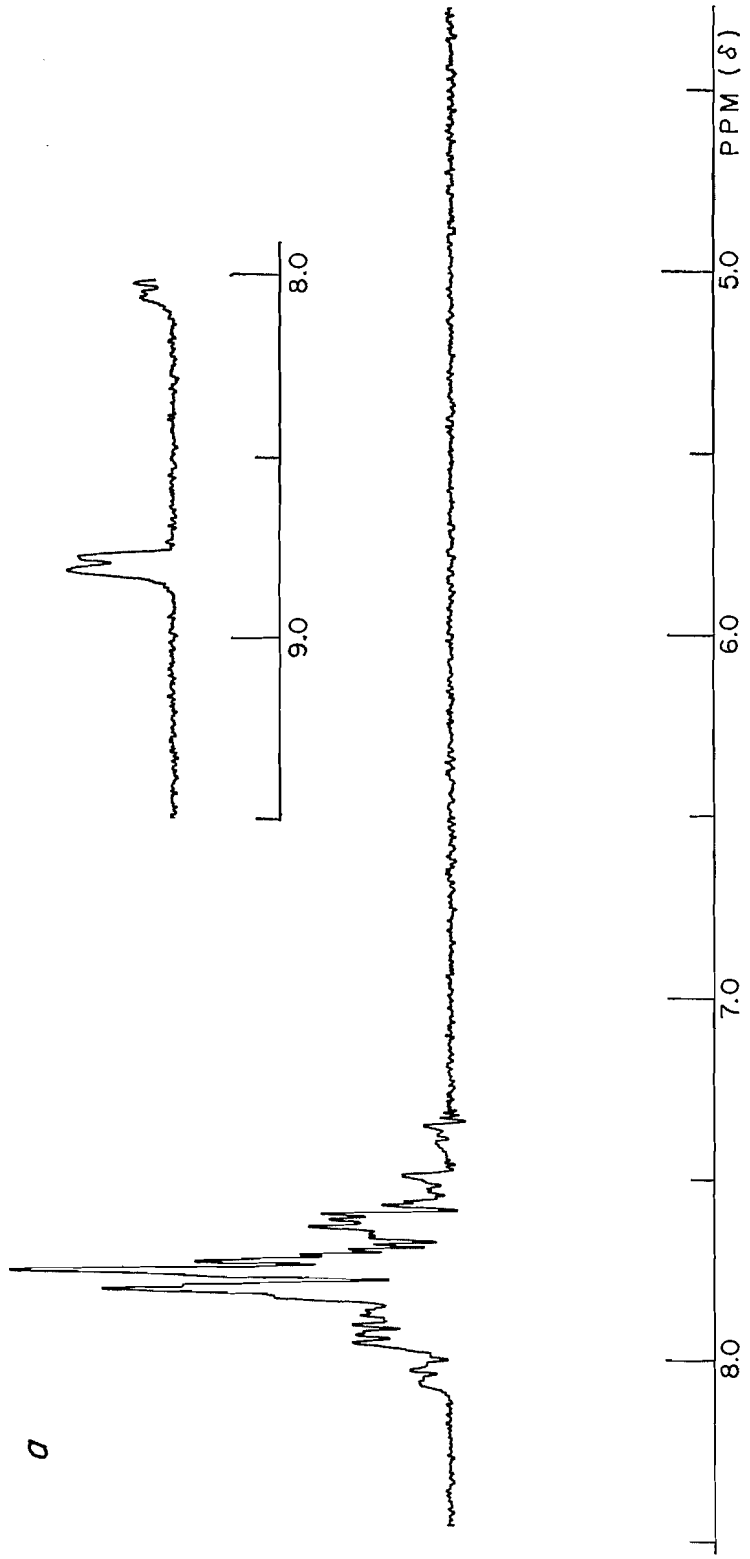

Can. J. Chem. Downloaded from www.nrcresearchpress.com by 210.87.254.42 on 09/05/12
For personal use only.

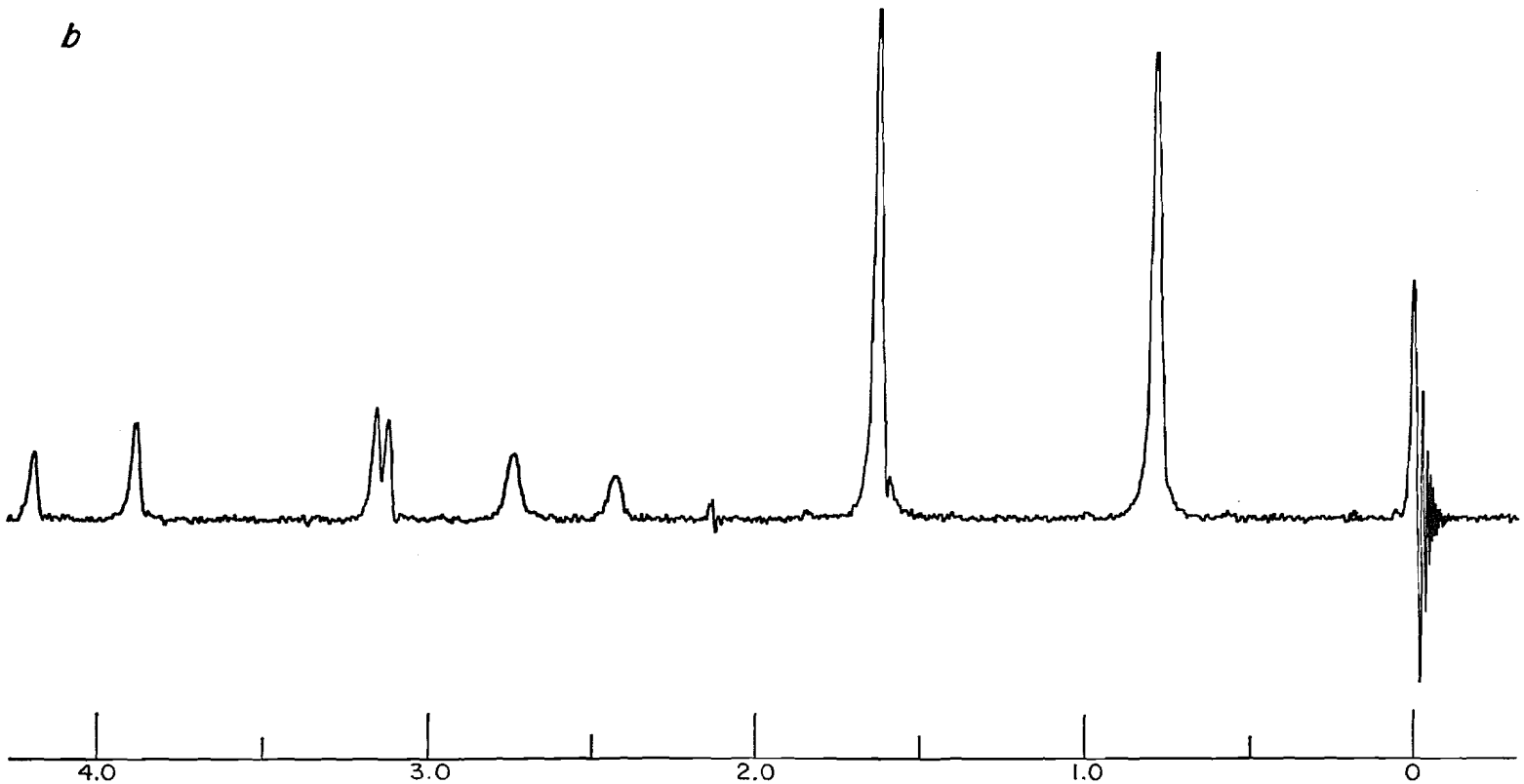

FIG. 1. Nuclear magnetic resonance spectrum of compound **5** in $CDCl_3$ solution, internal TMS as reference.

Can. J. Chem. Downloaded from www.nrcresearchpress.com by 210.87.254.42 on 09/05/12
For personal use only.

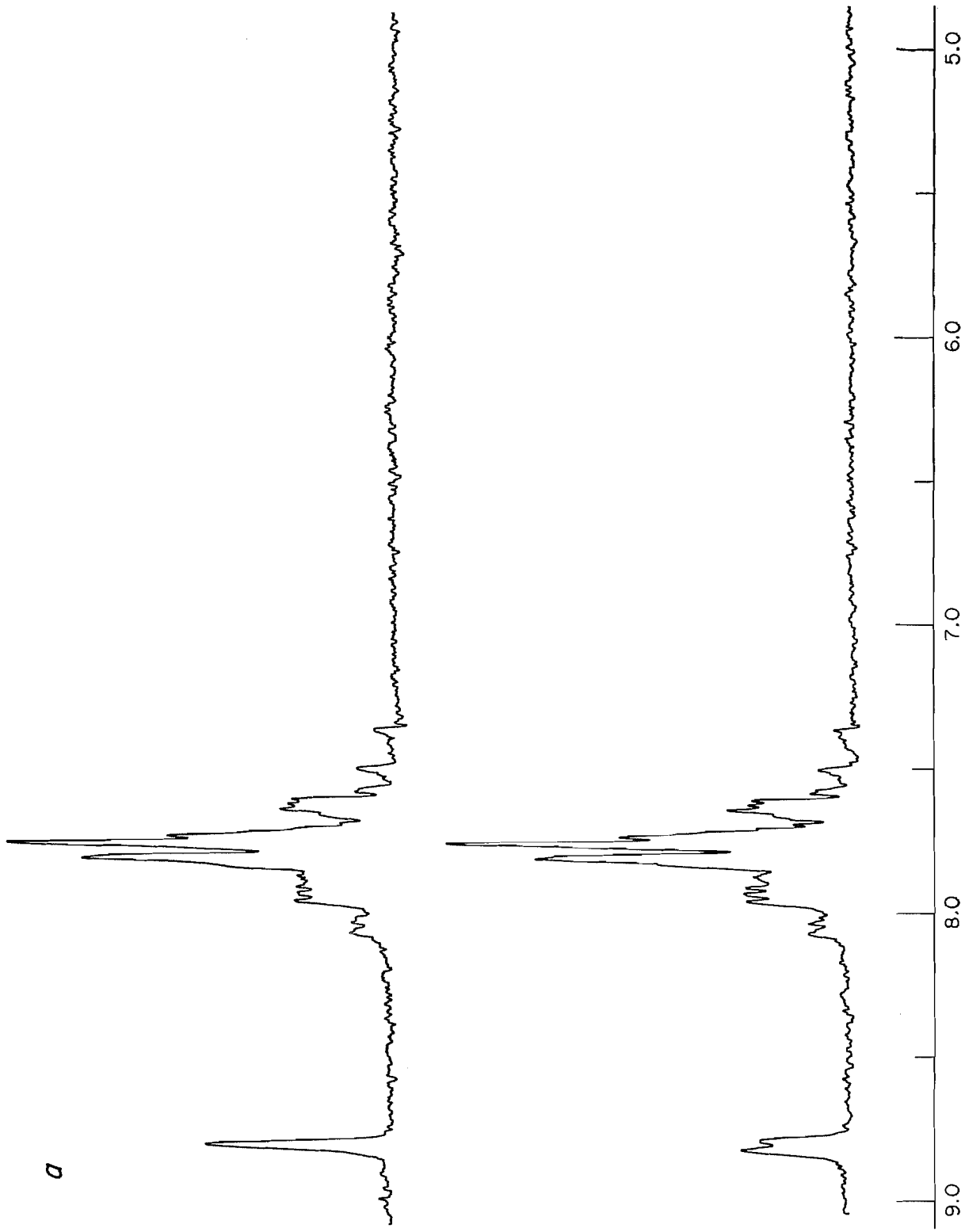

Can. J. Chem. Downloaded from www.nrcresearchpress.com by 210.87.254.42 on 09/05/12
For personal use only.

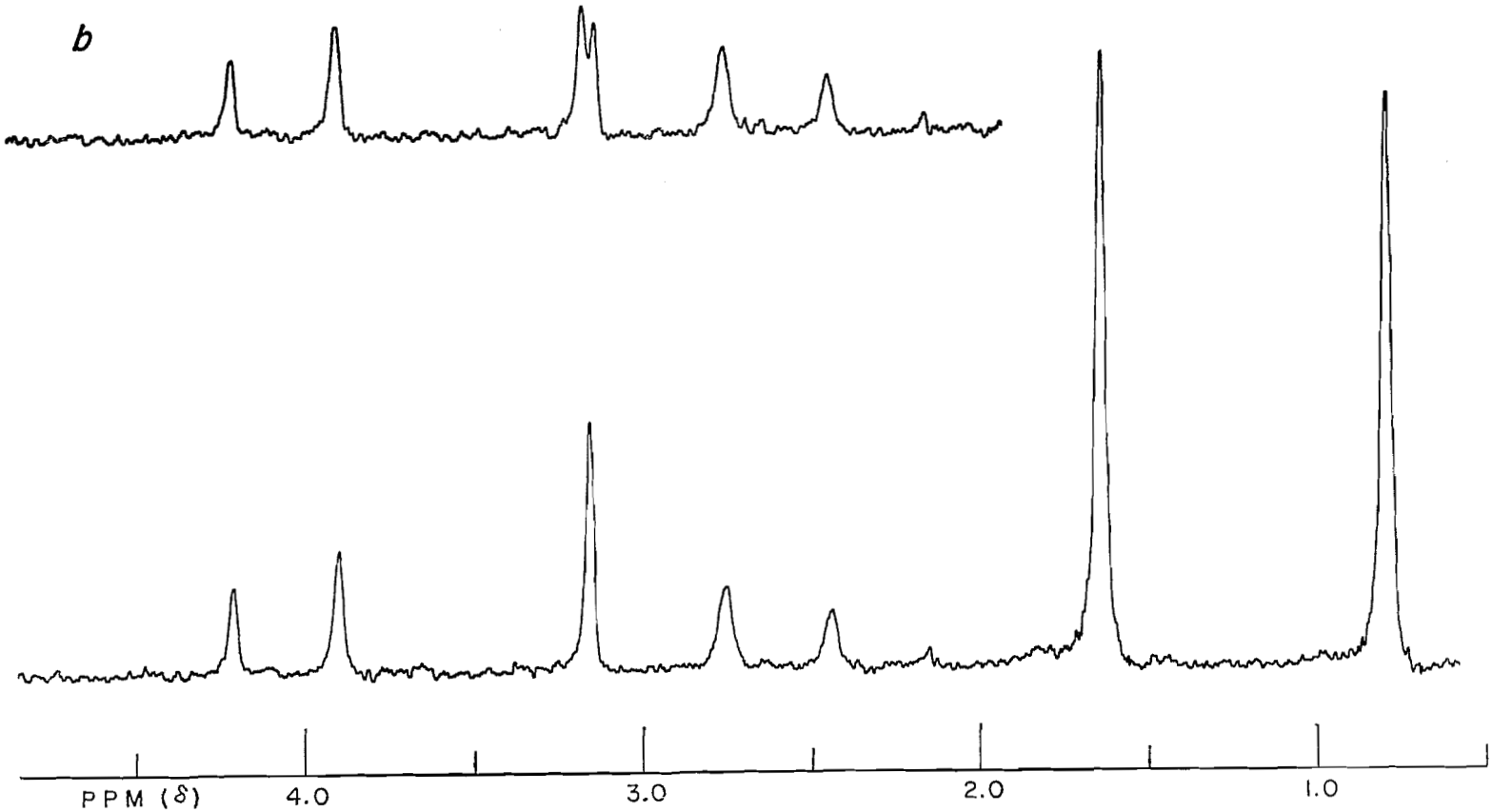

FIG. 2. Double irradiation of compound **5** in $CDCl_3$ with reference TMS.

Can. J. Chem. Downloaded from www.nrcresearchpress.com by 210.87.254.42 on 09/05/12
For personal use only.

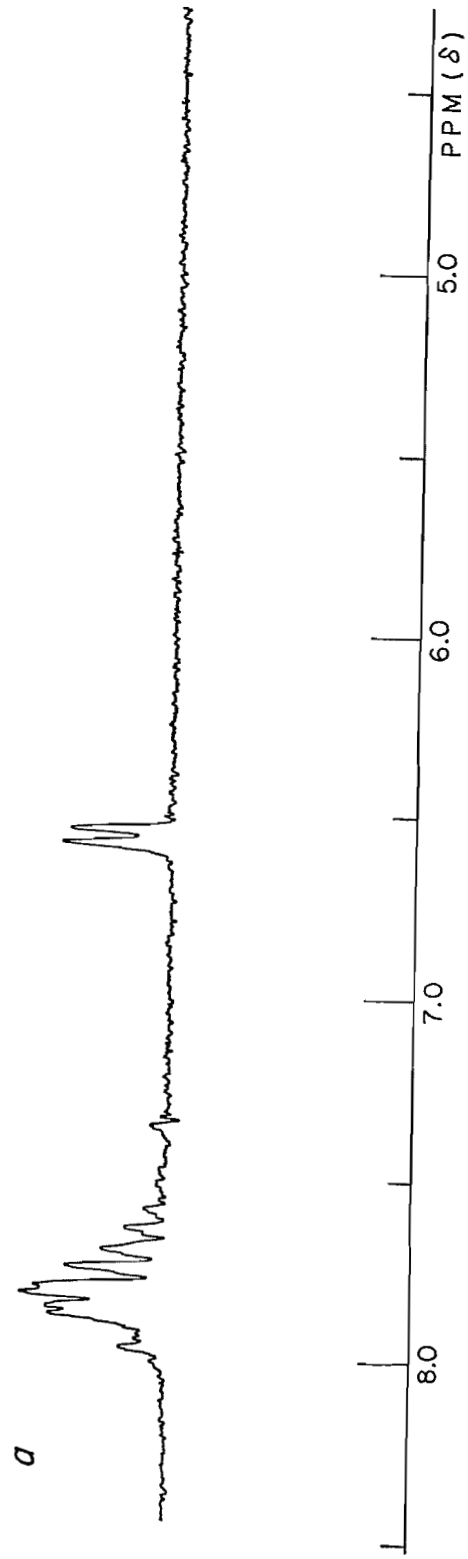

Can. J. Chem. Downloaded from www.nrcresearchpress.com by 210.87.254.42 on 09/05/12
For personal use only.

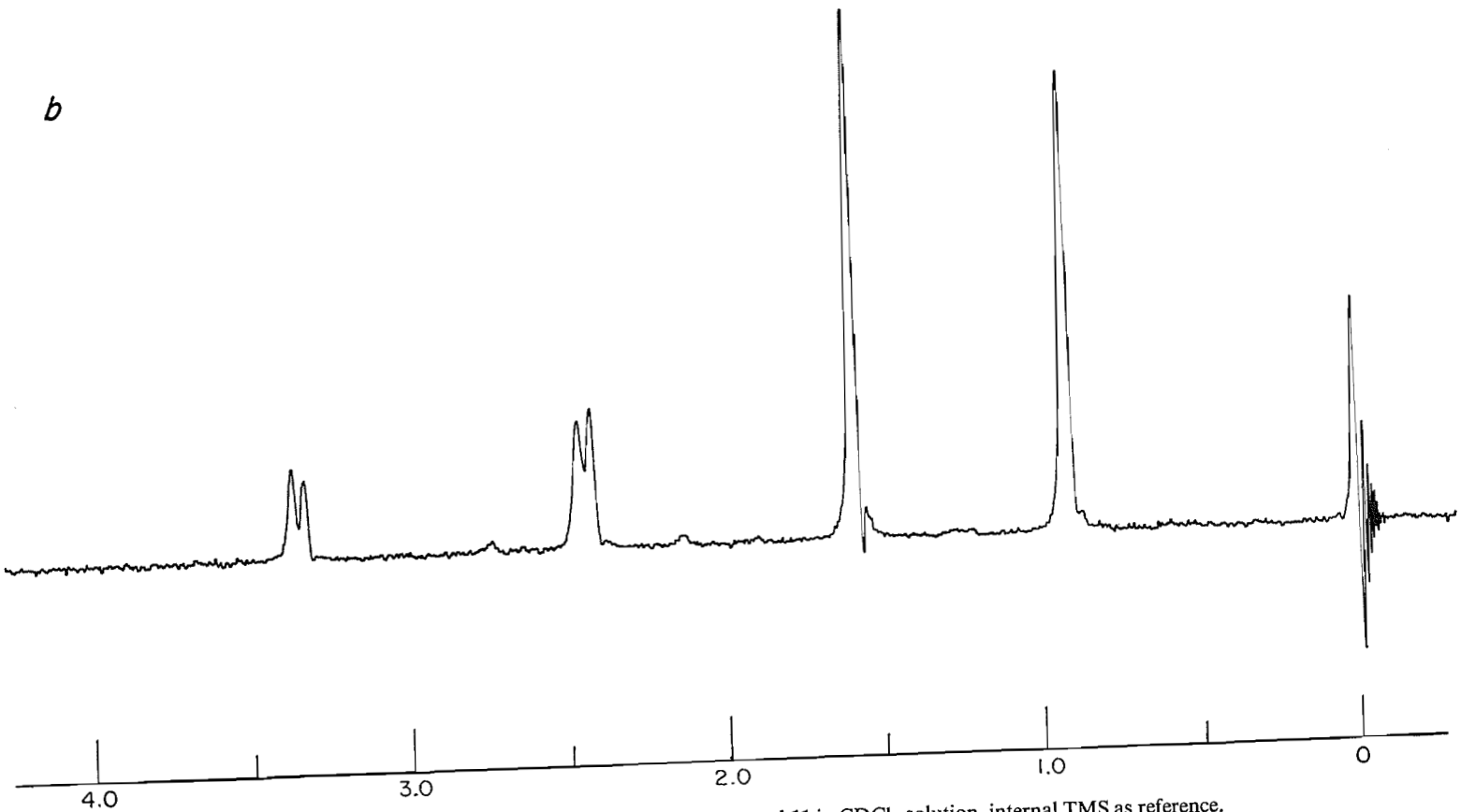

FIG. 3. Nuclear magnetic resonance spectrum ofcompound **11** in $CDCl_3$ solution, internal TMS as reference.

Can. J. Chem. Downloaded from www.nrcresearchpress.com by 210.87.254.42 on 09/05/12
For personal use only.

of the dibromo product, **5** was deuterated at position-9*a*, by dissolving it in a hexadeuterated dimethyl sulfoxide solution of K_3PO_4 followed by acidification with CH_3—COOD and brominated in hot acetic acid. If *gem*-dibromination takes place, both of the doublets assigned to the methylene protons should disappear from the spectrum of the compound. If the bromination takes place at positions-2 and -9*a*, a signal for proton-2 should be present in the spectrum. The signal for proton-2 is still present in the spectrum of the dibromo product indicating that **6***a* best represents the structure for the dibromo compound. Protons-2 and -4 are still coupled (0.7 c.p.s.) and this unusual coupling was misinterpreted in the original manuscript for coupling between the -4 and -9*a* protons. Cirulis (2) methylated the condensation product by treating it with $NaOCH_3$ and refluxing the Na salt with excess methyl iodide. He isolated a product which he claimed was a dimethylated derivative. Upon repeating his experiment and investigating the n.m.r. spectrum of the product (in $CDCl_3$) it was found that it consisted of approximately 30% of unchanged **5** and 70% of a new monomethylated product. While the monomethylated product (**7**) has a similar spectrum to **5**, all the peaks have shifted, the signal assigned to the 9*a*-proton has disappeared, the olefinic proton gives only a single peak, and in the methyl proton region a new signal has appeared. Integration of the peaks shows that there are nine methyl protons, two methylene protons, one olefinic proton, and eight aromatic protons in the compound. The peaks were assigned as follows: peaks at 0.63 and 1.51 p.p.m. to the methyl protons attached to C-1; the peak at 1.30 p.p.m. to the new methyl group at the 9*a*-position; the two doublets centered at 2.74 and 3.75 p.p.m. respectively (J_{AB} 20.5 c.p.s.), to the methylene protons; single peak at 8.73 p.p.m. to the olefinic proton; and the pattern centered around 7.76 p.p.m. to the aromatic protons. Based on the n.m.r. spectrum the following structure has been assigned to **7**. Pure **7** can be isolated

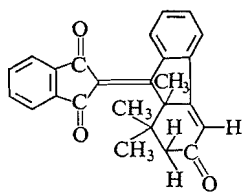

7

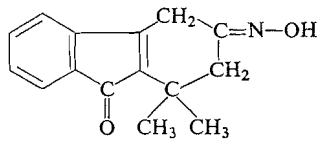

8

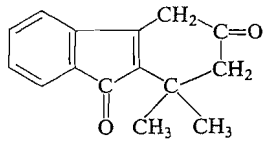

9

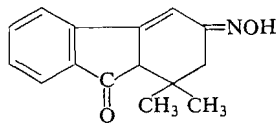

10

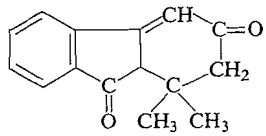

11

by base extraction and repeated crystallization of the mixture.

To obtain more experimental proof for the structure of **5** it was treated with hydroxylamine. Geita and Vanags (4) have claimed that **5** and hydroxylamine gave the dioxime of indanedione-1,3 and **8**. Upon hydrolysis **8** should give **9**. The n.m.r. spectrum of this product has shown, as it was expected, that **11** represents the correct structure for the compound (Fig. 3), and **10** is its precursor.

The spectrum still shows the presence of two different methyl proton peaks (at 0.88 and 1.56 p.p.m. respectively). The methylene protons are centered at 3.26 p.p.m. and appear as a pair of doublets in which the chemical shift difference of AB (10.5 c.p.s.) is smaller than J_{AB} (17 c.p.s.). The olefinic proton and the aliphatic single proton are coupled (2 c.p.s.) and centered at 6.53 and 3.31 p.p.m. respectively. The aromatic protons are centered at 7.75 p.p.m. The large upfield shift

of proton-4 in **11** compared to proton-4 in **5** is striking and may be due to change in the extent of conjugation of the molecule.

Compound **11** dissolves in aqueous NaOH or aqueous K_3PO_4 (but not in Na_2CO_3 solution) forming a dark-blue solution, indicating the formation of a carbanion **12**.

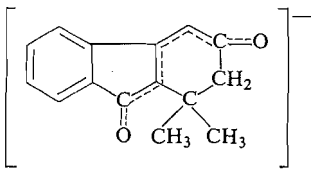

12

The n.m.r. spectrum of this solution shows only one signal for the methyl protons and one signal for the methylene protons, indicating that the cyclohexene ring is either coplanar, or that there is a rapid inversion of configuration at position-9*a*. The signal for proton-9*a* has disappeared from the spectrum and the proton in the 4-position gives only a single peak.

When **11** was treated with K_3PO_4 in D_2O solution followed by acidification with CH_3—COOD, the 9*a*-deuterated compound was obtained (**13**). The n.m.r. spectrum of **13** in $CDCl_3$

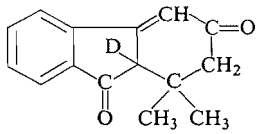

13

is similar to the spectrum of **11**. However, there is no signal for proton-9*a* and the proton in position-4 gives only a broad single peak.

The mass spectrum and infrared (i.r.) spectrum of **5** have also been recorded. The molecule–ion (M^+) was observed and the fragmentation pattern is consistent with structure **5**. The i.r. spectrum shows two carbonyl stretching bands at 1682 and 1720 cm^{-1} which can be assigned to the carbonyls of the indanedionyl part of the molecule. Another carbonyl band at 1675 cm^{-1} may be due to C=O stretching of the cyclohexenone part of the molecule. Both aromatic and aliphatic hydrogens were observed. The i.r. spectrum is in general consistent with structure **5**.

One can conclude from these results that **5** represents the structure of the product formed in the base-catalyzed condensation of acetone and indanedione-1,3. Radulescu and Georgescu (1) and Kalnins (3), however, may have isolated an intermediate in the condensation reaction or were dealing with the impure **5**. Cirulis (2), Kalnins (3), and Geita and Vanags (4), have isolated **5**, but have assigned the wrong structure to it. These results do not prove, however, the mechanism of the condensation. Compound **5** may form as we suggest in Scheme 2 or it is possible that **4** forms first according to the scheme of Geita and Vanags (4), (Scheme 1) and then is isomerized to **5** during the reaction. It is interesting to note, that mesityloxide and indanedione-1,3 did not give **5** in a similar condensation. The condensation of bindone (bisindanedione) and acetone also gave a different product.

Attempts have also been made to carry out similar condensations between indanedione-1,3 and 3-pentanone or 1,3-diphenylacetone respectively; however, no product similar to **5** could be isolated from these reactions.

Acknowledgments

The writer is grateful to C. G. Carlson and J. S. McIntyre for the helpful discussion and suggestions, and to H. D. Mak and J. P. Heeschen for recording the nuclear magnetic resonance spectra, and to S. T. King and J. C. Tou for the mass and infrared spectra. The author is also thankful to the referees for many valuable suggestions and comments. The microanalyses and molecular weight determinations were carried out in the Microanalyses Laboratory, Toronto.

1. D. Radulescu and V. Georgescu. Bull. Soc. Chim. France, **37**, 1077 (1925).
2. A. Cirulis. Ann. **522**, 278 (1936).
3. P. Kalnins. Latvijas PSR Zinatnu Akad. Vestis, **9**, 129 (1954).
4. L. Geita and G. Vanags. Latvijas PSR Zinatnu Akad. Vestis, Kim. Ser. 57–63 (1964).
5. T. Hayashi. J. Org. Chem. **31**, 3253 (1966).

Can. J. Chem. Downloaded from www.nrcresearchpress.com by 210.87.254.42 on 09/05/12
For personal use only.

Can. J. Chem. Downloaded from www.nrcresearchpress.com by 210.87.254.42 on 09/05/12
For personal use only.

1,3-Dipolar cycloaddition of nitrile oxides. II. Reactions with *o*-quinoid structures

WILLIAM IBRAHIM AWAD AND MICHEAL SOBHY
Chemistry Department, Faculty of Science, Ain Shams University, Abbassia, Cairo, United Arab Republic

Received May 24, 1968

o-Chloro-, 2-chloro-4-methoxy-, and 5-chloro-3,4-methylenedioxy-benzonitrile oxides react with phenanthrenequinone, chrysenequinone, phenanthrenequinonimine, chrysenequinonimine, and phenanthrenequinone monoxime to give a 1:1 adduct. Tetrabromo-*o*-quinone gives an adduct with benzonitrile *N*-oxide in ratio of 1:2.

When benzoyl chloride or benzyl chloride was allowed to react with benzonitrile oxide, dibenzohydroxamic acid, *o*-benzohydroxamic benzyl ether were obtained respectively.

The constitution of the products is discussed.

Canadian Journal of Chemistry, 47, 1473 (1969)

In continuation of our previous work (1, 2), *o*-chloro-benzonitrile oxide, 2-chloro-4-methoxybenzonitrile oxide, and 5-chloro-3,4-methylenedioxybenzonitrile oxide were reacted with phenanthrenequinone to give 9(10)-phenanthrone-10(9)-spiro-5′-aryl-1′,3′,4′-dioxazoles (**1**).

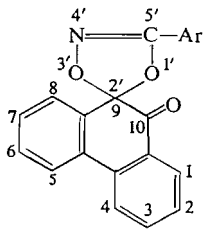

1

1 *a*, Ar = $C_6H_4Cl(o-)$
b, Ar = $C_6H_3(OCH_3)(Cl)(4\text{–}2)$
c, Ar = $C_6H_2(O_2CH_2)(Cl)(3,4\text{–}5)$

During the preparation of the hydroxamic acid chloride by passing chlorine gas into piperonaldoxime a chlorine atom enters the aromatic ring, as well, to give **2**. A similar reaction was previously observed (2, 3). Oxidation of **2** gave an acid, m.p. 238° which proved to be different from 6-chloro-3,4-methylenedioxybenzoic acid (m.p. 208°) (4), the latter being the only known chloromethylenedioxybenzoic acid. Thus we can conclude that the nuclear chlorine is in the 2- or 5-position. Since the 2-position can be considered as sterically deactivated as compared with the 5-position, the product is most probably chlorinated in the latter position.

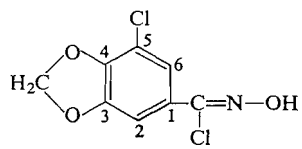

2

The dioxazoles **1** are stable to both acids and alkalies and give 2,4-dinitrophenylhydrazone derivatives. Oxidation of these compounds with chromic anhydride gives phenanthrenequinone. The dioxazoles **1** show $\nu_{C=O}$ and ν_{N-O-}, and their ultraviolet spectra show close similarity (cf. Experimental).

Phenanthrenequinonimine gives, with the above mentioned nitrile oxides, 9(10)-phenanthrone-10(9)-spiro-(1′,5′-dihydro-3′-aryl)-1′,2′,4′-oxadiazoles (**3**).

These compounds give 2,4-dinitrophenylhydrazone derivatives which are different from the corresponding phenanthrenequinone ones. This fact led to the conclusion that the addition of the nitrile oxides takes place on $\diagdown C{=}N{-}H$ rather than on $\diagdown C{=}O$ of the monoimine. The infrared spectra of these products showed besides $\nu_{C=O}$, ν_{N-O}, and ν_{N-H}.

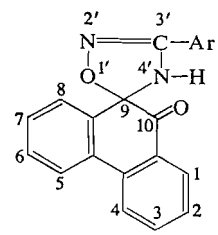

3

3 *a*, Ar = $C_6H_4Cl(o-)$
b, Ar = $C_6H_3(OCH_3)(Cl)(4\text{–}2)$
c, Ar = $C_6H_2(O_2CH_2)(Cl)(3,4\text{–}5)$

Can. J. Chem. Downloaded from www.nrcresearchpress.com by 210.87.254.42 on 09/05/12
For personal use only.

TABLE I

Action of benzonitrile and substituted benzonitrole *N*–oxides on *o*-quinones

Quinone	Benzonitrile oxide and its derivative	Product	Solvent	Melting point °C	Yield %	Formula	Analyses C Calcd	C Found	H Calcd	H Found	Analyses N Calcd	N Found	Cl Calcd	Cl Found	Dinitrophenylhydrazone melting point °C	Ultraviolet spectra λ_{max} mμ	ε_{max}	λ_{max} mμ	ε_{max}	Infrared spectra (cm^{-1}) $\nu_{C=O}$	ν_{NO}
Phenanthraquinone	B	1*a*	Benzene–methanol	135–136	90	$C_{21}H_{12}O_3NCl$	69.71	69.73	3.31	3.19	3.86	3.60	9.82	9.52	295*	250	39411	275	13590	1730	1345
	C	1*b*	Benzene	175–176	80	$C_{22}H_{14}O_4NCl$	67.43	68.25	3.57	3.78	3.57	3.58	9.06	9.52	295*	255	44859	275	21021	1690	1345
	D	1*c*	Toluene	167	77	$C_{22}H_{12}O_5NCl$	65.14	65.44	3.20	3.16	3.44	3.18	8.62	8.66	255*	252	43952	277	16887	1710	1360
Chrysenequinone	B	5*a*	Toluene	190–194	75	$C_{25}H_{14}O_3NCl$	72.90	72.57	3.40	3.33	3.40	3.41	8.50	8.35	258*	270 288	23660 28460	278 355	27432 5795	1680	1345
	C	5*b*	Toluene	202–203	83	$C_{26}H_{16}O_4NCl$	—	—	—	—	3.62	3.38	—	—	230*	264 360	26933 9249	282	36508	1680	1340
	D	5*c*	Toluene	209	86	$C_{26}H_{14}O_3NCl$	68.34	68.85	3.07	3.13	3.07	3.13	7.77	7.88	220†	265 355	34648 5837	290	33428	1700	1360
													Br								
Tetrabromo-*o*-benzoquinone	A	8*a*	Benzene–benzine (b.p. 40–60°)	216–217	85	$C_{20}H_{10}O_4N_2Br_4$	36.25	36.28	1.51	1.31	4.33	4.44	48.33	47.86							
	B	8*b*	Benzene–benzine (b.p. 40–60°)	194–195	93	$C_{20}H_8O_4N_2Cl_2Br_4$	32.89	32.88	1.09	1.13	3.83	3.83	Halogen 53.52	51.18							
	D	8*c*	Benzene	226–227	87	$C_{22}H_8O_8N_2Cl_2Br_4$	32.19	32.93	0.97	0.97	3.41	3.41	47.73	46.58							

NOTE: A: Benzonitrile *N*-oxide; B: *o*-Chloro-benzonitrile *N*-oxide; C: 2-Chloro-4-methoxybenzonitrile *N*-Oxide; D: 5-Chloro-3,4-methylenedioxybenzonitrile *N*-oxide.
*Crystallized from toluene.
†Crystallized from methanol.

TABLE II

Action of substituted benzonitrile *N*-oxides on quinonimines

Quinonimine	Substituted benzonitrile oxide	Product	Solvent	Melting point °C	Yield %	Formula	Analyses C Calcd	C Found	H Calcd	H Found	Analyses N Calcd	N Found	Cl Calcd	Cl Found	Dinitrophenylhydrazone melting point °C	Ultraviolet spectra λ_{max} mμ	ε_{max}	λ_{max} mμ	ε_{max}	Infrared spectra (cm^{-1}) $\nu_{C=O}$	ν_{NH}	ν_{N-O}
Phenanthraquinonimine	A	3*a*	Benzene	155	66	$C_{21}H_{13}O_2N_2Cl$	69.92	69.08	3.60	3.53	7.76	7.15	9.85	9.98	Above 300*	265	29000	290	27400	1689	3425	1335
	B	3*b*	Toluene	188	55	$C_{22}H_{15}O_3N_2Cl$	67.60	67.71	3.84	3.84	7.17	7.17	9.09	8.86	225†	—	—	277	20500	1700	3425	1345
	C	3*c*	Toluene	194–195	61	$C_{23}H_{14}O_4N_2Cl$	65.16	65.60	3.21	3.28	6.90	6.96	8.57	8.57	185*					1700	3400	1350
Chrysenequinonimine	A	7*a* '	Toluene	195	82	$C_{21}H_{13}O_2N_2Cl$	73.08	72.93	3.65	3.65	6.82	6.72	8.55	8.06		265	33764	360	9504	1700	3333	1360
	B	7*b*	Toluene	204–205	70	$C_{28}H_{17}O_3N_2Cl$	70.60	69.85	3.85	4.04	6.35	6.03	8.05	8.36		268 260	44000 8470	288	47300	1700	3333	1330
	C	7*c*	Benzene	222	76	$C_{28}H_{15}O_4N_2Cl$	68.49	69.04	3.29	3.12	6.26	6.12	7.79	7.65	285§	264 360	33700 6000	290	3000	1670	3330	1350

NOTE: A: *o*-Chloro-benzonitrile *N*-oxide; B: 2-Chloro-4-methoxybenzonitrile *N*-oxide; C: 5-Chloro-3,4-methylenedioxybenzonitrile *N*-oxide.
*Crystallized from toluene–methanol.
†Crystallized from toluene.

Can. J. Chem. Downloaded from www.nrcresearchpress.com by 210.87.254.42 on 09/05/12
For personal use only.

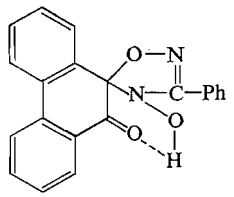

4

Benzonitrile *N*-oxide gives with phenanthrenequinone monoxime a product to which structure **4** is assigned.

It is a 1:1 adduct (deduced by analytical data) with $\nu_{C=O}$ at 1690 cm^{-1} and a clear hydrogen bonded ν_{O-H} between 3060–2800 cm^{-1} (broad band). It also gives a dinitrophenylhydrazone derivative.

Chrysenequinone reacts similarly with the previously mentioned nitrile oxides to give 1,2-benz-9(10)-phenanthrone-10(9)-spiro-5′-aryl-1′,-3′,4′-dioxazoles (**5**).

Structure **5** is preferred to **6** on steric grounds (5). These compounds are stable to both acids and alkalies and give dinitrophenylhydrazone derivatives and upon oxidation chrysenequinone is obtained. Their infrared spectra showed $\nu_{C=O}$ and ν_{N-O}. Their ultraviolet spectra show clear similarity with those previously described (1).

Chrysenequinonimine behaves similarly to give 1,2-benz-9(10)-phenanthrone-10(9)-spiro-(1′,5′-dihydro-3′-aryl)-1′,2′,4′-oxadiazoles (**7**). For a discussion of chrysenequinonimine structure see ref. (5).

Their 2,4-dinitrophenylhydrazone derivatives are different from those of the corresponding quinone derivatives and their infrared spectra showed ν_{N-H} besides $\nu_{C=O}$ and ν_{N-O-}. The ultraviolet spectra of these compounds are indentical with the corresponding ones previously described (1).

When arylnitrile oxides are allowed to react

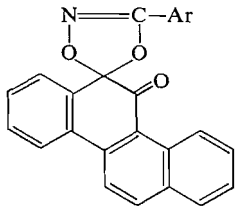

5

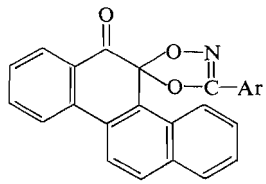

6

a, Ar = $C_6H_4Cl(o\text{–})$
b, Ar = $C_6H_3(OCH_3)(Cl)(4\text{–}2)$
c, Ar = $C_6H_2(O_2CH_2)(Cl)(3,4\text{–}5)$

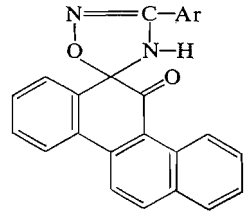

7

a, Ar = $C_6H_4Cl(o\text{–})$
b, Ar = $C_6H_3(OCH_3)(Cl)(4\text{–}2)$
c, Ar = $C_6H_2(O_2CH_2)(Cl)(3,4\text{–}5)$

with *o*-tetrabromobenzoquinone, almost colorless products are obtained. Analytical data show that two molecules of the nitrile oxide add to one molecule of the quinone, a fact which is different from the case of phenanthrenequinone or chrysenequinone derivatives. We believe that one carbonyl and one carbon–carbon double bond are involved in the reaction since the infrared spectra show $\nu_{C=O}$. Structure **8** is assigned.

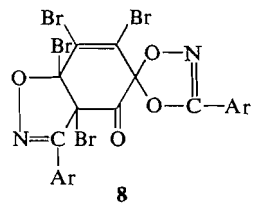

8

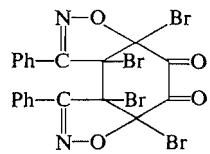

8′

8 *a*, Ar = C_6H_5
b, Ar = $C_6H_4Cl(o\text{–})$
c, Ar = $C_6H_2(O_2CH_2)(Cl)(3,4\text{–}5)$

The addition to activated double bond has been previously observed (6). The availability of the carbon–carbon double bond for this reaction is more obvious in the case of *o*-tetrabromoquinone than in the case of phenanthrenequinone and its derivatives. This may be the reason why the former adds two molecules of arylnitrile oxides while the latter reacts only with one molecule.

Structure **8′**[1] is also compatible with the known data. However, the authors are more inclined to structure **8** since the product does not give the test for 1,2-dioxocompounds (7).

Attempts to extend the possibility of 1,3-dipolar addition to the carbonyl group of acid chlorides did not lead to the expected dioxazole (**9**). However, the infrared spectrum of the product showed two bands for carbonyl stretching frequency, one at 1754 cm^{-1} and the other at 1660 cm^{-1}, together with an ν_{NH} at 3333 cm^{-1}, and the product

[1]This structure was proposed by one of the referees.

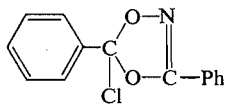

9

was chlorine free. These data are in conformity with dibenzhydroxamic acid (**10**). This was proved

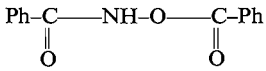

10

by melting and mixture melting point with an authentic sample (8). This product can be formed according to the following scheme.

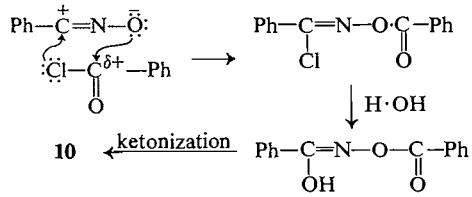

Moisture is expected to be present in the benzonitrile oxide as it is prepared here. The intermediate chloro-compound, which has been isolated in other cases (9), was not isolated in this case. Benzyl chloride was also allowed to react with benzonitrile oxide and the product proved to be *O*-benzohydroxamic benzyl ether (**11**) by melting and mixture melting point with an authentic specimen (10).

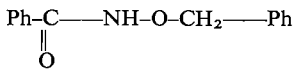

11

Experimental

Melting points are not corrected. Analyses were carried out by Alfred Bernhardt, Max Planck Institute, Mülheim, Ruhr, Germany. Infrared spectra were measured on a Perkin–Elmer Infracord Model 137 spectrophotometer in KBr wafers. Ultraviolet spectra were measured on a Perkin–Elmer spectracord Model 4000A spectrophotometer in ethyl alcohol solutions.

Preparation of 5-Choloro-3,4-methylenedioxybenzohydroxamic Acid Chloride (2)

Piperonaldoxime (10 g) dissolved in chloroform – carbon tetrachloride mixture (1:1) (20 ml) was cooled to about 0° and chlorine gas was passed into the solution slowly. The solution turned green and the chloride separated as fine greenish powder after 90 min. It was filtered off and used without purification in the preparation of 2-chloro-3,4-methylenedioxybenzonitrile oxide.

Oxidation of 5-Chloro-3,4-methylenedioxybenzohydroxamic Acid Chloride

The hydroxamic acid chloride (1 g) (in acetone) was treated dropwise with aqueous potassium permanganate solution (2%) till the color of the permanganate dominates. The excess of the permanganate was destroyed. The precipitate formed was filtered off. The latter was extracted with sodium carbonate solution (20%). The alkaline extract was cooled and acidified with dilute HCl. The acid obtained was crystallized from acetic acid into colorless crystals, m.p. 238° (poor yield).

Anal. Calcd. for $C_8H_5O_4Cl$: C, 47.88; H, 3.49; Cl, 17.70. Found: C, 48.22; H, 3.10; Cl, 17.52.

Action of Benzonitrile N-Oxide and its Derivatives on o-Quinones. General Procedure

An ethereal solution of benzonitrile *N*-oxide or its derivatives (from 10 g of the corresponding benzohydroxamic acid chloride) was refluxed with the quinone (1 g) suspended in dry benzene for 2 h on a water bath. the reaction mixture was kept overnight at room temperature. The reaction product was filtered off, washed with ether, and crystallized from a suitable solvent (cf. Table I).

The 2,4-dinitrophenylhydrazone derivatives were crystallized from a suitable solvent.

Reaction of Benzonitrile N-Oxide with Phenanthraquinone Monoxime

Phenanthraquinone monoxime (1 g) was treated with an ethereal solution of benzonitrile *N*-oxide (from 5 g benzohydroximic acid chloride). The reaction mixture was left at room temperature for 30 min and then refluxed gently for another 30 min. The yellowish oil separated after removing the solvent was solidified by trituration with light petroleum ether (b.p. 40–60°). Crystallization from light petroleum ether (b.p. 60–80°) gave **4** in colorless crystals, m.p. 161–162° (0.5 g, yield 35%).

Anal. Calcd. for $C_{21}H_{14}N_2O_3$: C, 73.38; H, 4.09; N, 8.18. Found: C, 73.68; H, 4.12; N, 8.23.

The 2,4-dinitrophenylhydrazone derivative was prepared as usual and crystallized from benzene, m.p. 190°.

Anal. Calcd. for $C_{27}H_{18}N_5O_6$: C, 63.78; H, 3.56; N. 13.76. Found: C, 64.38; H, 3.78; N, 12.80.

Action of Substituted Benzonitrile N-Oxide on Quinonimines. General Procedure

Quinonimine (1 g) in dry ether or benzene was treated with the ethereal solution of benzonitrile *N*-oxide derivative (from 7 g of the corresponding benzohydroxamic acid chloride). The reaction was completed as mentioned before. The solid product obtained after removal of most of the solvent was filtered off, washed with ether, and crystallized from a suitable solvent (cf. Table II).

The 2,4-dinitrophenylhydrazone derivatives were prepared as usual and crystallized from a suitable solvent (cf. Table II).

Action of Benzonitrile N-Oxide on Benzoyl Chloride

The ethereal solution of benzonitrile *N*-oxide (from 10 g of PhCCl-NOH) was added to benzoyl chloride (1 g) dissolved in ether. The reaction mixture was kept at room temperature for 30 min. On cooling and treating with excess light petroleum ether (b.p. 40–60°) colorless

Can. J. Chem. Downloaded from www.nrcresearchpress.com by 210.87.254.42 on 09/05/12
For personal use only.

crystalline compound separated out. Crystallization from petroleum ether (b.p. 40–60°) gave dibenzhydroxamic acid (**10**), m.p. 162°, undepressed on admixture with an authentic sample (8).

Preparation of O-Benzohydroxamic Benzyl Ether

Benzyl chloride (2 g) was treated with the ethereal solution of benzonitrile *N*-oxide (from 10 g of PhCCl-NOH). The reaction mixture was left at room temperature for a few hours and then boiled gently for 1 h on a water bath. After removal of most of the ether, petroleum ether (b.p. 40–60°) was added and the solution was left at room temperature for two days during which colorless plates separated out, were filtered, washed with petroleum ether, and crystallized from petroleum ether (b.p. 40–60°) to give *O*-benzohydroxamic benzyl ether (**11**), m.p. 105°, undepressed when mixed with an authentic sample (10), (0.6 g, yield 33%).

1. W. I. AWAD, S. M. A. R. OMRAN, and M. SOBHY. J. Org. Chem. **31**, 331 (1966).
2. W. I. AWAD, S. M. A. R. OMRAN, and M. SOBHY. J. Chem. U. A. R. **10**, 1 (1967).
3. R. H. WILEY and B. J. WAKEFIELD. J. Org. Chem. **25**, 547 (1960).
4. O. R. R. ROBINSON and M. WILLIAMS. J. Chem. Soc. **111**, 948 (1917).
5. W. I. AWAD and A. R. A. RAOUF. J. Am. Chem. Soc. **77**, 1013 (1955).
6. R. HUISGEN and W. MACK. Tetrahedron letters, 583 (1961); R. HUISGEN. Angew. Chem. **75**, 614 (1963).
7. F. FEIGL. Spot tests in organic analysis. Elsevier Publishing Company, Amsterdam, 1966. p. 328.
8. T. W. GREGORY, and W. H. PERKIN. J. Chem. Soc. **83**, 788 (1903).
9. P. RAJAGOPALAN and C. N. TALATY. Tetrahedron Letters, 2101 (1966).
10. R. M. BEESLY, C. K. INGOLD, and J. F. THORPE. J. Chem. Soc. **107**, 1080 (1915).

Can. J. Chem. Downloaded from www.nrcresearchpress.com by 210.87.254.42 on 09/05/12
For personal use only.

Can. J. Chem. Downloaded from www.nrcresearchpress.com by 210.87.254.42 on 09/05/12
For personal use only.

Synthesis of epimeric 2-acetamido-2-deoxyheptoses from D-mannose, D-galactose, and D-talose[1]

C. F. GIBBS,[2] D. T. WILLIAMS,[2] AND M. B. PERRY
Division of Biochemistry and Molecular Biology, National Research Council of Canada, Ottawa, Canada

Received September 3, 1968

D-Mannose, D-galactose, and D-talose were converted *via* the action of nitromethane to their corresponding 3,4,5,6,7-pentaacetoxy-1-nitro-1-heptene derivatives which on treatment with ammonia afforded the epimeric 2-acetamido-1,2-dideoxy-1-nitroheptitol derivatives. The 2-acetamido-1,2-dideoxy-1-nitroheptitols were converted *via* the Nef reaction to the corresponding 2-acetamido-2-deoxyheptoses. The configuration of the 2-acetamido-2-deoxyheptoses was established by their degradation to known 2-acetamido-2-deoxyhexitol derivatives. The properties of the 2-acetamido-2-deoxyheptoses are described.

Canadian Journal of Chemistry, 47, 1479 (1969)

2-Amino-2-deoxyhexuronic acid derivatives, related to compounds found in microbial products (1–5) were required in order to study their biological and analytical chemistry. An approach to their synthesis was considered in which glycosides of 2-acetamido-2-deoxyheptopyranosides were oxidized by one mole of periodate, in the manner previously described for neutral heptose derivatives (6–8), resulting in almost exclusive scission of the exocyclic C_6–C_7 glycol system to yield C_6-aldehydo derivatives which are oxidized to the corresponding hexuronosides. This paper records the synthesis of six 2-acetamido-2-deoxyheptoses used as precursors for the above work.

D-Mannose, D-galactose, and D-talose were converted to the corresponding 3,4,5,6,7-pentaacetoxy-1-nitro-1-heptenes and after treatment with ammonia, the resulting epimeric 2-acetamido-1,2-dideoxy-1-nitroheptitols were converted to 2-acetamido-2-deoxyheptoses *via* the Nef (9) reaction. The epimeric 2-acetamido-1,2-dideoxy-1-nitroheptitols derived from D-mannose and D-galactose were each obtained in pure form and were used separately for the preparation of the individual 2-acetamido-2-deoxyheptoses, however, the epimeric 2-acetamido-1,2-dideoxy-1-nitroheptitols derived from D-talose could not be resolved and the mixture was therefore converted to the corresponding 2-acetamido-2-deoxyheptoses which were separated by column chromatography.

The identity of the 2-acetamido-2-deoxyheptoses and their 2-acetamido-1,2-dideoxy-1-nitroheptitol precursors was established by degradation of each 2-acetamido-2-deoxyheptose to a 2-acetamido-2-deoxyhexitol. Oxidation of each 2-acetamido-2-deoxyheptose with one mole of periodate resulted in the major glycol scission (ca. 90–98%, measured by H.CHO production) taking place at the C_6–C_7 glycol system and the product, without isolation, was reduced with borohydride to yield a 2-acetamido-2-deoxyhexitol which was identified by gas–liquid chromatographic (g.l.c.) analysis of its penta-*O*-acetyl-2-acetamido-2-deoxyhexitol derivative (10).

Since the completion of the work, Satoh and Kiyomoto (11) have described the synthesis of the epimeric 2-acetamido-1,2-dideoxy-1-nitroheptitols from D-galactose and D-mannose by the direct action of ammonia on the derived 2,3,4,5,6,7-hexa-*O*-acetyl-1-deoxy-1-nitroheptitols and proved the structure of 2-acetamido-2-deoxy-D-*glycero*-D-*talo*-heptitol and 2-acetamido-2-deoxy-D-*glycero*-L-*manno*-heptitol by degradation to D-serine and L-serine respectively. The physical properties of the compounds described by Satoh and Kiyomoto are in reasonable agreement with our results and the assignments of the configurations based on degradation to 2-acetamido-2-deoxyhexitol derivatives are in complete agreement.

The prepared 2-acetamido-2-deoxyheptoses were pure by paper chromatography but all were extremely hygroscopic and gave variable melting points. Gas–liquid chromatographic analysis of the trimethylsilylated powdered 2-acetamido-2-deoxyheptoses (12) gave one major peak, however, the trimethylsilylated heptoses, after equilibration in water, showed several peaks indicating

[1]NRCC No. 10510.
[2]NRCC Postdoctorate Fellow 1967–1969.

Can. J. Chem. Downloaded from www.nrcresearchpress.com by 210.87.254.42 on 09/05/12
For personal use only.

the presence of anomeric forms. The gas chromatograms of the powdered heptoses, trimethylsilylated after exposure to the room atmosphere, were almost identical to the water-equilibrated samples indicating that the observed absorption of atmospheric water results in rapid anomerization of the products and thus explains the difficulties experienced in determining satisfactory melting points.

Experimental

Paper chromatography was performed by the descending method (13) on Whatman No. 1 filter paper using pyridine – ethyl acetate – water (2:5:5 v/v, top layer) as the mobile phase. Glycoses were detected with 1% silver nitrate in acetone, followed by 2% sodium hydroxide in ethanol (14) and their rates of movement are quoted relative to D-galactose (R_{gal}).

Gas–liquid chromatography was carried out at 220 °C using a Hewlett–Packard model 402 chromatograph with a hydrogen flame detector and fitted with glass U tubes (4 ft × 6 mm × 3 mm internal diameter) packed with 10% neopentylglycol sebacate polyester on 80–100 mesh acid washed Chromosorb W. Retention times of compounds are quoted relative to 2-acetamido-2-deoxy-1,3,4,5,6-penta-*O*-(trimethylsily)-D-glucitol (T_{GN}) or 1,2,3,4,5,6-hexa-*O*-acetyl-D-glucitol (T_G).

Melting points were determined on a Fisher–Johns apparatus and are corrected. Solutions were concentrated under reduced pressure, below 40 °C. Optical rotations were determined at 20 °C using a Perkin–Elmer 141 polarimeter.

(A) Synthesis of 2-Acetamido-2-deoxy-D-glycero-D-talo-heptose and 2-Acetamido-2-deoxy-D-glycero-D-galacto-heptose

(1) 2-Acetamido-1,2-dideoxy-1-nitro-D-glycero-D-talo-heptitol and 2-Acetamido-1,2-dideoxy-1-nitro-D-glycero-D-galacto-heptitol

3,4,5,6,7-Pentaacetoxy-D-*manno*-1-nitro-1-heptene (25 g) prepared from D-mannose (15), was suspended in methanol (250 ml) at 0 °C and dry ammonia was added to saturation. The mixture was brought to room temperature and after 16 h it was concentrated to a syrup and, following the addition of ethanol (50 ml), crystalline 2-acetamido-1,2-dideoxy-1-nitro-D-*glycero*-D-*talo*-heptitol was obtained which after recrystallization from an ethanol–methanol mixture (2:1) gave the pure product (8 g, 49%) which had m.p. 184–185 °C and $[\alpha]_D$ +20.4° (*c*, 3.4 in water), (lit. (11) m.p. 180–181 °C and $[\alpha]_D$ + 21.4°).

Anal. Calcd. for $C_9H_{18}N_2O_8$: C, 38.30; H, 6.43; N, 9.92. Found: C, 38.0; H, 6.5; N, 9.8.

The original ethanolic mother liquors were concentrated to a thin syrup which on keeping afforded crystalline 2-acetamido-1,2-dideoxy-1-nitro-D-*glycero*-D-*galacto*-heptitol which after recrystallization from an ethanol–acetone mixture (1:1) gave the pure product (1.2 g, 7.4%) having m.p. 166–167 °C and $[\alpha]_D$ −28.8° (*c*, 1.3 in water) (lit. (11), m.p. 159–160.5 °C and $[\alpha]_D$ −26.4°).

Anal. Calcd. for $C_9H_{18}N_2O_8$: C, 38.30; H, 6.43; N, 9.92. Found: C, 38.2; H, 6.6; N, 9.8.

(2) 2-Acetamido-2-deoxy-D-glycero-D-talo-heptose

2-Acetamido-1,2-dideoxy-1-nitro-D-*glycero*-D-*talo*-heptitol (6.7 g), dissolved in 2 *N* sodium hydroxide solution (16 ml), was added dropwise with vigorous stirring to concentrated hydrochloric acid (13 ml) and after boiling the mixture for 5 min it was cooled to 0 °C and saturated with hydrogen chloride gas. The precipitated sodium chloride was removed and after concentration to a syrup it was dried *in vacuo* over potassium hydroxide to yield 2-amino-2-deoxy-D-*glycero*-D-*talo*-heptose hydrochloride (5 g). The product which failed to crystallize was *N*-acetylated by shaking its solution in water (100 ml) containing methanol (15 ml) and acetic anhydride (2 ml) in the presence of Dowex-1 ($CO_3^=$) ion-exchange resin (60 ml) for 30 min at room temperature and, after filtration, the filtrate was passed down a column of mixed Rexyn 101 (H^+) and Rexyn RG6 (OH^-) ion-exchange resins (60 ml). The eluate was concentrated to a syrup (5.3 g) which was fractionated by cellulose column chromatography (16) using butan-1-ol half saturated with water as the mobile phase, to yield pure 2-acetamido-2-deoxy-D-*glycero*-D-*talo*-heptose (2.7 g). The product gave crystals from an ethanol – ethyl acetate mixture which were extremely hygroscopic and did not give a satisfactory melting point, $[\alpha]_D$ −15° (*c*, 1.7 in water). A single spot was obtained on paper chromatography having R_{gal} 1.63.

Anal. Calcd. for $C_9H_{17}NO_7$: C, 43.03; H, 6.82; N, 5.58. Found: C. 42.8; H, 6.8; N, 5.5.

Gas–liquid chromatographic analysis of the trimethylsilylated (12) crystalline 2-acetamido-2-deoxy-D-*glycero*-D-*talo*-heptose gave a major peak (T_{GN} 1.60) and minor peak (T_{GN} 3.36) whereas the trimethylsilylated glycose after equilibration in water showed four peaks having T_{GN} 1.56, 1.60 (major), 2.67, and 3.36.

(3) Degradation of 2-Acetamido-2-deoxy-D-glycero-D-talo-heptose to 2-Acetamido-2-deoxy-D-talitol

2-Acetamido-2-deoxy-D-*glycero*-D-*talo*-heptose (50 mg) in water (5 ml) was oxidized by the addition of sodium metaperiodate (43 mg) in water (2 ml) and after 1 h at room temperature the mixture was passed through mixed Rexyn 101 (H^+) and Duolite A4 (OH^-) ion-exchange resins (15 ml) and the eluate was treated with sodium borohydride (35 mg). After 3 h the mixture was acidified with acetic acid and after passing down a column of Rexyn 101 (H^+) ion-exchange resin (10 ml) the eluate was concentrated to dryness and then further concentrated after the addition of methanol (4 × 20 ml). Paper chromatography of the product showed a major component (R_{gal} 1.26) corresponding to 2-acetamido-2-deoxytalitol and very minor components having R_{gal} 0.98, 1.56, and 1.80. The major component isolated by preparative paper chromatography afforded crystalline 2-acetamido-2-deoxy-D-talitol which had m.p. 146–148° undepressed on admixture with an authentic sample. The fully acetylated glycitol (10) on g.l.c. gave a single peak (T_G 2.69) having the same retention time as penta-*O*-acetyl-2-acetamido-2-deoxy-D-talitol.

(4) 2-Acetamido-2-deoxy-D-glycero-D-galacto-heptose

2-Acetamido-1,2-dideoxy-1-nitro-D-*glycero*-D-*galacto*-heptitol (3 g) was subjected to the series of reactions

Can. J. Chem. Downloaded from www.nrcresearchpress.com by 210.87.254.42 on 09/05/12
For personal use only.

used for the synthesis of 2-acetamido-2-deoxy-D-*glycero*-D-*talo*-heptose (expt. *A* (*2*)) to give 2-acetamido-2-deoxy-D-*glycero*-D-*galacto*-heptose (1.3 g) which after recrystallization from an ethanol – ethyl acetate mixture had m.p. 164.5–165.5 °C and $[\alpha]_D$ +81.5° → +75.5° (40 min equilib. value; *c*, 1.7 in water).

Anal. Calcd. for $C_9H_{17}NO_7$: C, 43.03; H, 6.82; N, 5.58. Found: C, 42.8; H, 6.6; N, 5.5.

Paper chromatographic analysis of the 2-acetamido-2-deoxy-D-*glycero*-D-*galacto*-heptose showed a single spot having R_{gal} 1.05. Gas–liquid chromatography of the trimethylsilylated crystalline heptose showed peaks having T_{GN} 3.39 (major) and 6.32 and the trimethylsilylated heptose after equlibration in water showed peaks having T_{GN} 2.30, 2.42, 3.39, and 6.32.

*(5) Degradation of 2-Acetamido-2-deoxy-*D*-glycero-*D*-galacto-heptose to 2-Acetamido-2-deoxy-*D*-galactitol*

2-Acetamido-2-deoxy-D-*glycero*-D-*galacto*-heptose (50 mg) was oxidized with periodate as described above (expt. *A*(*3*)) to yield 2-acetamido-2-deoxy-D-galactitol (43 mg) which after recrystallization from aqueous acetone had m.p. and mixture m.p. 174–175 °C. Gas–liquid chromatography of the fully acetylated derived 2-acetamido-2-deoxy-D-galactitol gave a single peak (T_G 3.32) corresponding to authentic 1,3,4,5,6-penta-*O*-acetyl-2-acetamido-2-deoxy-D-galactitol.

*(B) Synthesis of 2-Acetamido-2-deoxy-*D*-glycero-*L*-manno-heptose and 2-Acetamido-2-deoxy-*D*-glycero-*L*-gluco-heptose*

*(1) 2-Acetamido-1,2-dideoxy-1-nitro-*D*-glycero-*L*-manno-heptitol and 2-Acetamido-1,2-dideoxy-1-nitro-*D*-glycero-*L*-gluco-heptitol*

3,4,5,6,7-Pentaacetoxy-D-*galacto*-1-nitro-1-heptene (42 g) prepared from D-galactose (17) was treated in the way described for 3,4,5,6,7-pentaacetoxy-D-*manno*-1-nitro-1-heptene (expt. *A* (*1*)). The concentrated product, dissolved in ethanol, on cooling gave 2-acetamido-1,2-dideoxy-1-nitro-D-*glycero*-L-*manno*-heptitol (22 g, 80%), m.p. 191 °C which after recrystallization from ethanol had m.p. 197 °C and $[\alpha]_D$ +13° (*c*, 0.8 in water) (lit. (11), m.p. 189–190 °C and $[\alpha]_D$ +12.9°).

Anal. Calcd. for $C_9H_{18}N_2O_8$: C, 38.30; H, 6.43; N, 9.92. Found: C, 38.5; H, 6.6; N, 9.9.

The concentrated ethanolic mother liquors were extracted with chloroform to remove acetamide and the residue, moistened with ethanol, gave 2-acetamido-1,2-dideoxy-D-*glycero*-L-*gluco*-heptitol (2.2 g, 8%), m.p. 140–146 °C which after recrystallization from ethanol gave the pure product which had m.p. 149–150 °C and $[\alpha]_D$ +9° (*c*, 1.6 in water) (lit. (11), 144.5–145.5 °C and $[\alpha]_D$ +10.7°).

Anal. Calcd. for $C_9H_{18}N_2O_8$: C, 38.30; H, 6.43; N, 9.92. Found: C, 38.7; H, 6.7; N, 9.8.

*(2) 2-Acetamido-2-deoxy-*D*-glycero-*L*-manno-heptose*

(*a*) 2-Acetamido-1,2-dideoxy-1-nitro-D-*glycero*-L-*manno*-heptitol (3 g) was converted to 2-acetamido-2-deoxy-D-*glycero*-L-*manno*-heptose (0.8 g) (m.p. 180–183 °C) using the previously described experimental procedure (expt. *A* (2)).

(*b*) An improved yield of 2-acetamido-2-deoxy-D-*glycero*-L-*manno*-heptose was obtained as follows (18). 2-Acetamido-1,2-dideoxy-1-nitro-D-*glycero*-L-*manno*-heptitol (12.5 g) was dissolved in a solution of $Ba(OH)_2 \cdot 8H_2O$ (13.8 g) in water (220 ml) and the mixture was (added dropwise with stirring to a solution of sulfuric acid (23 g) in water (96 ml). After 30 min at room temperature the reaction mixture was neutralized ($BaCO_3$), filtered, and the filtrate after concentration was fractionated by cellulose column chromatography using butan-1-ol half saturated with water as the mobile phase to yield pure 2-acetamido-2-deoxy-D-*glycero*-L-*manno*-heptose (5.5 g, 50%) obtained from ethanol solution as an amorphous powder which had m.p. 174–185 °C and $[\alpha]_D$ −33° → −17° (equilib. value; *c*, 1.4 in water).

Anal. Calcd. for $C_9H_{17}NO_7$: C, 43.03; H, 6.82; N, 5.58. Found: C, 43.2; H, 7.0; N, 5.5.

Paper chromatographic analysis of the 2-acetamido-2-deoxy-D-*glycero*-L-*manno*-heptose showed a single spot having R_{gal} 1.34 and the trimethylsilylated product on g.l.c. showed a major peak (T_{GN} 1.48, ca. 98%) and a minor peak (T_{GN} 2.06) whereas the trimethylsilylated heptose after equlibration in water showed peaks having T_{GN} 1.48, 2.06, 2.62, and 3.4.

*(3) Degradation of 2-Acetamido-2-deoxy-*D*-glycero-*L*-manno-heptose to 2-Acetamido-2-deoxy-*L*-mannitol*

2-Acetamido-2-deoxy-D-*glycero*-L-*manno*-heptose (142 mg) was degraded with periodate under the previously described conditions (expt. *A* (*3*)) to yield crystalline 2-acetamido-2-deoxy-L-mannitol (82 mg) which had m.p. and mixed m.p. 140 °C and $[\alpha]_D$ +7.7° (*c*, 1 in water).

Anal. Calcd. for $C_8H_{17}NO_6$: C, 43.05; H, 7.68; N, 6.27. Found: C, 43.1; H, 7.4; N, 6.2.

The derived 2-acetamido-2-deoxy-L-mannitol (60 mg) was acetylated (10) to yield 1,3,4,5,6-penta-*O*-acetyl-2-acetamido-2-deoxy-L-mannitol which after recrystallization from methanol had m.p. and mixture m.p. 189 °C and $[\alpha]_D$ −12.4° (*c*, 0.8 in chloroform), and gave a single peak on g.l.c. (T_G 3.54) having the same retention time as an authentic sample.

Anal. Calcd. for $C_{18}H_{27}NO_{11}$: C, 49.88; H, 6.28; N, 3.23. Found: C, 49.7; H, 6.2; N, 3.3.

*(4) 2-Acetamido-2-deoxy-*D*-glycero-*L*-gluco-heptose*

2-Acetamido-1,2-dideoxy-1-nitro-D-*glycero*-L-*gluco*-heptitol (0.8 g) treated by the modified (18) Nef reaction described above (expt. *B* (*2b*)) afforded 2-acetamido-2-deoxy-D-*glycero*-L-*gluco*-heptose as an amorphous powder (187 mg) which had m.p. 152–156 °C and $[\alpha]_D$ −56° → −41° (24 h equilib. value; *c*, 0.8 in water).

Anal. Calcd. for $C_9H_{17}NO_7$: C, 43.03; H, 6.82; N, 5.58. Found: C, 43.0; H, 6.7; N, 5.5.

The heptose gave a single spot on paper chromatography (R_{gal} 1.05) and the trimethylsilylated powder, and product of equilibration in water, on g.l.c. gave two peaks having T_{GN} 3.8 and 5.2.

*(5) Degradation of 2-Acetamido-2-deoxy-*D*-glycero-*L*-gluco-heptose to 2-Acetamido-2-deoxy-*L*-glucitol*

2-Acetamido-2-deoxy-D-*glycero*-L-*gluco*-heptose (10 mg) was degraded by one mole of periodate (expt. *A* (*3*)) and, following reduction and acetylation of the product, g.l.c. analysis revealed a major peak (90%) having T_G 2.87 corresponding in retention time with 1,3,4,5,6-penta-*O*-acetyl-2-acetamido-2-deoxyglucitol.

*(C) Synthesis of 2-Acetamido-2-deoxy-*D*-glycero-*L*-allo-heptose and 2-Acetamido-2-deoxy-*D*-glycero-*L*-altro-heptose*

*(1) 3,4,5,6,7-Pentaacetoxy-*D*-talo-1-nitro-1-heptene*

To a vigorously stirred solution of D-talose (6 g) in methanol (75 ml) and nitromethane (75 ml) was added a solution of sodium (2.7 g) in methanol (60 ml) and after 8 h at room temperature the mixture was kept at 0 °C for 12 h. The precipitated product was collected and its solution in water (60 ml) was passed down a column of Rexyn 101 (H^+) ion-exchange resin (100 ml). The eluate and washings were concentrated to a syrup which was dissolved in acetic anhydride (70 ml) and, following the addition of sulfuric acid (0.1 ml), the mixture was heated on a boiling water bath for 30 min. The cooled reaction mixture was poured onto crushed ice (11) and the product, after extraction with chloroform in the usual way, was concentrated to a syrup (12.5 g) containing the acetate derivatives of the epimeric 1-deoxy-1-nitroheptitols (19).

The above syrup (12 g) in ethyl benzene (150 ml) was boiled for 1 h in the presence of sodium bicarbonate (25 g) and the filtered solution after concentration was fractionated on a column of silica gel using a benzene–acetone (4:1) mixture to yield pure 3,4,5,6,7-pentaacetoxy-D-*talo*-1-nitro-1-heptene (3 g, 21%) which had m.p. 88–89 °C and $[\alpha]_D$ +24° (*c*, 0.4 in chloroform).

Anal. Calcd. for $C_{17}H_{23}NO_{12}$: C, 47.12; H, 5.35; N, 3.23. Found: C, 47.1; H, 5.2; N, 3.1.

*(2) Reaction of 3,4,5,6,7-Pentaacetoxy-*D*-talo-1-nitro-1-heptene with Ammonia*

3,4,5,6,7-Pentaacetoxy-D-*talo*-1-nitro-1-heptene (3 g) was treated with ammonia as previously described (expt. *A* (*1*)) to yield a mixture of 2-acetamido-1,2-dideoxy-1-nitro-D-*glycero*-L-*allo*-heptitol and 2-acetamido-1,2-dideoxy-1-nitro-D-*glycero*-L-*altro*-heptitol (2.8 g) (ca. 1:1 by silica gel thin-layer chromatography using pyridine – ethyl acetate – water (2:5:5)) which could not be resolved by fractional crystallization or chromatography.

The mixed 2-acetamido-1,2-dideoxy-1-nitroheptitols (2.6 g) were converted to the corresponding 2-acetamido-2-deoxyheptoses by the modified Nef reaction (expt. *B* (*2b*)) and following their fractionation by cellulose column chromatography (160 × 3 cm), using butan-1-ol half saturated with water as the mobile phase, pure 2-acetamido-2-deoxy-D-*glycero*-L-*altro*-heptose (103 mg) and 2-acetamido-2-deoxy-D-*glycero*-L-*allo*-heptose (172 mg) were, in order of elution, obtained.

*(3) 2-Acetamido-2-deoxy-*D*-glycero-*L*-altro-heptose*

The heptose was obtained from ethanol as a hygroscopic amorphous powder having m.p. 78–82 °C and $[\alpha]_D$ −11° → −8.5° (24 h equilib. value; *c*, 1 in water).

Anal. Calcd. for $C_9H_{17}NO_7$: C, 43.03; H, 6.82; Found: C, 42.1; H, 7.2.

The heptose gave a single spot on paper chromatograms (R_{gal} 1.66) and the trimethylsilylated glycose on g.l.c. gave four peaks having T_{GN} 1.14, 1.97, 2.10, and 2.66.

The heptose on degradation (expt. *A* (*3*)) gave 2-acetamido-2-deoxy-L-altritol and the derived 1,3,4,5,6-penta-*O*-acetyl-2-acetamido-2-deoxy-L-altritol on g.l.c. gave a single peak (T_G 2.60) having the same retention time as an authentic derivative.

*(4) 2-Acetamido-2-deoxy-*D*-glycero-*L*-allo-heptose*

The heptose had m.p. 70–90 °C and $[\alpha]_D$ +19° → +25° (24 h equilib. value; *c*, 1 in water).

Anal. Calcd. for $C_9H_{17}NO_7$: C, 43.03; H, 6.82; N, 5.58. Found: C, 42.9; H, 6.6; N, 5.5.

On paper chromatography the heptose gave a single spot (R_{gal} 1.23) and the trimethylsilylated glycose on g.l.c. gave peaks having T_{GN} 1.12, 1.44, 2.08, 2.35, and 2.54.

The heptose on degradation (expt. *A* (*3*)) gave 2-acetamido-2-deoxy-L-allitol and the acetate derivative on g.l.c. gave a single peak (T_G 2.26) having the same retention time as 1,3,4,5,6-penta-*O*-acetyl-2-acetamido-2-deoxy-L-allitol.

1. K. Heyns, G. Kiessling, W. Lindenberg, H. Paulsen, and M. Webster. Chem Ber. **92**, 2435 (1959).
2. H. R. Perkins. Biochem. J. **86**, 457 (1963).
3. W. R. Clark, J. McLaughlin, and M. E. Webster. J. Biol. Chem. **230**, 81 (1958).
4. A. R. Williamson and S. Zamenhoff. J. Biol. Chem. **238**, 2255 (1963).
5. T. H. Haskell and S. Hanessian. Biochim. Biophys. Acta, **83**, 35 (1964).
6. M. B. Perry and T. Pietak. Periodate oxidation of aldoheptoses. Royal Society of Canada, Kingston, Ontario. June, 1960.
7. N. J. Antia and M. B. Perry. Can. J. Chem. **38**, 1917 (1960).
8. J. K. N. Jones, M. B. Perry, and R. J. Stoodley. Can. J. Chem. **40**, 1798 (1962).
9. J. U. Nef. Ann. Chem. **280**, 263 (1894).
10. M. B. Perry and A. C. Webb. Can. J. Biochem. **46**, 1163 (1968).
11. C. Satoh and A. Kiyomoto. Carbohydrate Res. **7**, 138 (1968).
12. M. B. Perry. Can. J. Biochem. **42**, 451 (1964).
13. S. M. Partridge. Biochem. J. **42**, 238 (1948).
14. W. E. Trevelyan, D. P. Procter, and J. S. Harrison. Nature, **166**, 444 (1950).
15. J. C. Sowden and R. Schaffer. J. Am. Chem. Soc. 73, 4662 (1950).
16. L. Hough, J. K. N. Jones, and W. H. Wadman. J. Chem. Soc. 2511 (1949).
17. J. C. Sowden and D. R. Strobach. J. Am. Chem. Soc. **82**, 954 (1960).
18. C. Satoh and A. Kiyomoto. Chem. Pharm. Bull. Tokyo, **12**, 615 (1964).
19. R. Young and G. A. Adams. Can. J. Chem. **44**, 32 (1966).

Can. J. Chem. Downloaded from www.nrcresearchpress.com by 210.87.254.42 on 09/05/12
For personal use only.

Further studies on the Stobbé condensation with 2-methyl cyclohexanone

A. M. El-Abbady, M. El-Ashry, and S. H. Doss
Department of Chemistry, University College for Girls, Ain Shams University, Cairo, United Arab Republic
Received April 22, 1968

2-Methyl cyclohexanone is condensed with dimethyl succinate in the presence of potassium tertiary butoxide giving a solid mixture of isomers of the corresponding alkylidene and alkenyl half-esters. On alkaline hydrolysis this gives β-carboxy-β-(2-methyl cyclohex-1-enyl)propionic acid. The keto-ester obtained by cyclization of the half-ester yielded the corresponding unsaturated ketone after acid hydrolysis and decarboxylation. Reduction of the keto-ester affords the corresponding α,β-unsaturated ester. Both the unsaturated ketone and ester are easily hydrogenated in the presence of platinum oxide to the corresponding saturated ketone and ester.

Canadian Journal of Chemistry, 47, 1483 (1969)

Can. J. Chem. Downloaded from www.nrcresearchpress.com by 210.87.254.6 on 09/05/12
For personal use only.

Cook and Phillip (1), and Chatterjee and Bhattacharyya (2) reported the Stobbé condensation of 2-methyl cyclohexanone with diethyl and dimethyl succinate respectively in the presence of potassium *t*-butoxide. They obtained the half-ester, β-carbethoxy-β-(2-methyl cyclohex-1-enyl)propionic acid (**1***c*; R = C_2H_5) as a solid, and β-carbmethoxy-β-(2-methyl cyclohex-1-enyl)propionic acid (**1***c*; R = CH_3) as an oil.

In the present investigation the above reaction was repeated for further study and for the preparation of a methyl perhydroindane nucleus which can be regarded as an intermediate for the synthesis of steroid-like compounds.

2-Methyl cyclohexanone was condensed with dimethyl succinate in the presence of potassium *t*-butoxide (3) to yield the corresponding half-ester as an oil. The yield was found to be greatly increased (from 71% (2) to 90%) by increasing the molality of potassium *t*-butoxide. This oil solidified and was found to be a mixture of isomers (**1***a*, **1***b*, and **1***c*; R = CH_3). The ultraviolet (u.v.) absorption spectrum showed one strong band at 225 mμ (ε 10 000), characteristic of α,β-unsaturated esters (see ref. 4, p. 32). This indicated the presence of the half-ester (**1***a*; R = CH_3) as one isomer of the mixture. It seems that this isomer is present in a small amount as indicated by the low value of the molecular extinction coefficient. Moreover, no 2-methyl cyclohexanone could be isolated from a mild oxidation of the half-ester mixture using alkaline permanganate at room temperature, but instead a neutral carbonyl compound was obtained which gave a 2,4-dinitrophenyl hydrazone. This substance is still under investigation. Repeating the oxidation at 0° failed to give any neutral carbonyl substance. The infrared (i.r.) spectrum of the half-ester showed bands at 2800–2500 (w), 1750 (s), 935 (v), and 810 (s) cm^{-1}, characteristic of the stretching frequencies of hydroxyl and carbonyl groups of saturated acids and esters, the hydroxyl deformation (out of plane) of acids, and the CH (out of plane) deformation vibrations of trisubstituted alkenes respectively (5). These vibrations strongly suggest the presence of the isomer (**1***b*; R = CH_3). Finally the nuclear magnetic resonance (n.m.r.) spectrum showed signals at 1.6 and 5.1 p.p.m. (δ), characteristic of a methyl group attached to an unconjugated double bond and a vinyl proton respectively (see ref. 4, p. 175). This indicated the presence of the two isomers (**1***b* and **1***c*; R = CH_3).

The half-ester mixture on alkaline hydrolysis gave one homogeneous crystalline dibasic acid, m.p. 157°, which probably has the structure of one of the three possible isomers (**1***a*, **1***b*, and **1***c*; R = H). This acid showed no u.v. absorption in the characteristic region of the α,β-unsaturated acids (220–260 mμ), thus excluding structure (**1***a*; R = H). Its i.r. spectrum showed bands at 2800–2500 (w), 1740 (s), and 930 (v) cm^{-1}, characteristic of the stretching frequencies of hydroxyl and carbonyl groups of saturated acids and the hydroxyl deformation (out of plane) of acids respectively (5). The disappearance of the strong band at 810 cm^{-1} characteristic of γ CH of trisubstituted alkenes (shown by the half-ester) excluded structure (**1***b*; R = H) and confirmed structure (**1***c*; R = H) for this unsaturated dibasic acid. The presence of the olefinic linkage was chemically proved by

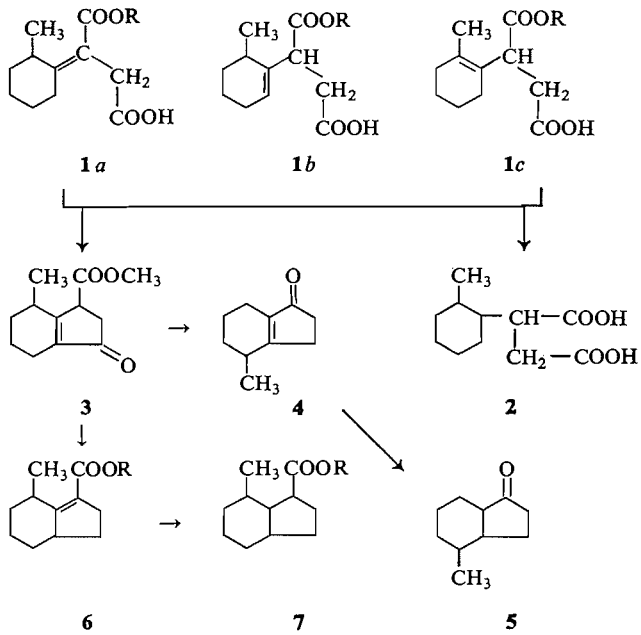

catalytic hydrogenation giving the known 2-methyl cyclohexyl succinic acid (**2**), m.p. 163–164° (lit. 2, m.p. 155–156°).

The crude half-ester was converted into its acid chloride (6) which was then cyclized (7). The neutral oily product thus obtained was found to be the keto-ester (**3**). It gave a 2,4-dinitrophenyl hydrazone and a semicarbazone.

Acid hydrolysis and decarboxylation of the keto-ester was effected by refluxing with a mixture of glacial acetic acid, constant boiling hydrobromic acid, and water to give the corresponding unsaturated ketone (**4**) in a good yield. It gave a 2,4-dinitrophenyl hydrazone in addition to the known semicarbazone (1).

The u.v. spectra of the keto-ester and the unsaturated ketone in ethanol had maxima at 237 mμ (ε 6162) and 236 mμ (ε 11 000) respectively. These values confirm the presence of α,β-unsaturated ketone grouping (see ref. 4, p. 139).

The unsaturated ketone (**4**) was then hydrogenated at a platinum oxide catalyst, absorbing one mole of hydrogen to give 4-methyl-*cis*-perhydro-indan-1-one (**5**) as a colorless oil. The n.m.r. spectrum showed mainly signals at 0.9 and 1.05 p.p.m. (δ), characteristic of a methyl group attached to a secondary carbon atom. This oil gave a 2,4-dinitrophenyl hydrazone and the known semicarbazone (1).

Clemmensen's reduction of the keto-ester (**3**) afforded mainly a neutral oil, which is probably the α,β-unsaturated ester (**6**; R = CH_3) since its observed absorption band λ_{max}(ethanol) 230 mμ (ε 6021) agrees with those reported for α,β-unsaturated esters in alcoholic solution (8, and ref. 4, p. 143). Alkaline hydrolysis of the unsaturated ester gave the corresponding α,β-unsaturated acid (**6**; R = H) as a colorless oil.

The unsaturated ester was then hydrogenated in the presence of platinum oxide to yield the corresponding saturated ester (**7**; R = CH_3) as a colorless oil. The n.m.r. spectrum showed mainly signals at 0.9, 1.05, and 3.6 p.p.m. (δ) corresponding to a methyl group attached to a secondary carbon atom and to a methyl ester group. Alkaline hydrolysis of this oil gave 7-methyl perhydroindan-1-carboxylic acid (**7**; R = H) as a colorless solid.

Experimental

Infrared spectra were recorded on a Beckmann IR4 double beam spectrometer using a sodium chloride cell. The ultraviolet absorption spectra were determined with a Unicam 700 spectrophotometer.

Strobbé Condensation

A solution of 2-methyl cyclohexanone (22.4 g, 0.2 mole) and dimethyl succinate (44 g, 0.3 mole) in *t*-butanol (40 ml) was added with stirring to a hot solution of potassium *t*-butoxide (from potassium metal, 11.7 g, 0.3 mole, in dry *t*-butanol 200 ml). The experiment was

Can. J. Chem. Downloaded from www.nrcresearchpress.com by 210.87.254.6 on 09/05/12
For personal use only.

Can. J. Chem. Downloaded from www.nrcresearchpress.com by 210.87.254.6 on 09/05/12
For personal use only.

continued as usual (3) and the resulting viscous oil (about 41 g, 90%) solidified on keeping and cooling as glittering colorless crystals (a mixture of isomers **1**; R = CH_3), m.p. 126–129° (from aqueous methanol).

Anal. Calcd. for $C_{12}H_{18}O_4$: C, 63.71; H, 7.96. Found: C, 63.92; H, 7.73.

Oxidation of the Half-ester

The half-ester (1 g) was dissolved in a 20% sodium carbonate solution (10 ml). Aqueous potassium permanganate solution (10%) was added dropwise with stirring till the color of permanganate became permanent. The solution was kept at room temperature for 2 h then extracted with ether. The ethereal layer afforded a brown oil. This gave a 2,4-dinitrophenyl hydrazone as glittering yellow crystals, m.p. 161–162° (from ethanol).

Anal. Found: C, 43.39; H, 3.72; N, 24.57.

β-*Carboxy-*β-*(2-methyl cyclohex-1-enyl)propionic Acid (1c; R = H)*

The half-ester (2 g) was refluxed in 10% sodium hydroxide solution (20 ml) for 3 h. On acidification this precipitated the unsaturated dibasic acid (**1***c*; R = H), 1.7 g, m.p. 157° (from benzene).

Anal. Calcd. for $C_{11}H_{16}O_4$: C, 62.26; H, 7.54. Found: C, 62.07; H, 7.78.

2-Methyl Cyclohexyl Succinic Acid (2)

The unsaturated dibasic acid (1 g), dissolved in glacial acetic acid (15 ml), was shaken with hydrogen in the presence of platinum oxide (0.1 g) until uptake of hydrogen (one mole) was complete (3½ h). This afforded the known saturated diacid (**2**), m.p. 163–164° (from water) (lit. 2, m.p. 155–156° from ether – petroleum ether).

Anal. Calcd. for $C_{11}H_{18}O_4$: C, 61.68; H, 8.41. Found: C, 61.90; H, 8.29.

Cyclization of the Half-ester

The half-ester (5 g) in dry benzene (50 ml) was treated with pyridine (2.3 ml) and redistilled thionyl chloride (2 ml) at 0° for ½ h. The benzene solution of the acid chloride was decanted from the solid cake, which was then pulverized and washed by decantation with dry benzene. The acid chloride solution and washings were treated with stannic chloride (2 ml) for 15 h at 0°; the benzene solution was then poured on ice and concentrated hydrochloric acid (15 ml) and shaken. This was worked up as usual (7) giving 3-carbmethoxy-4-methyl-4,5,6,7-tetrahydroindan-1-one (**3**) as a pale-yellow liquid, b.p. 110° at 0.6 mm.

Anal. Calcd. for $C_{12}H_{16}O_3$: C, 69.23; H, 7.69. Found: C, 69.98; H, 7.65.

Recrystallization from ethanol yielded a semicarbazone as pale-yellow crystals, m.p. 227–228° (decomp.).

Anal. Calcd. for $C_{13}H_{19}O_3N_3$: C, 58.86; H, 7.17; N, 15.84. Found: C, 58.70; H, 7.12; N, 15.73.

Its 2,4-dinitrophenyl hydrazone melted at 201–202° (decomp., from ethanol).

Anal. Calcd. for $C_{18}H_{20}O_6N_4$: C, 55.67; H, 5.15; N, 15.6. Found: C, 55.45; H, 5.12; N, 15.33.

4-Methyl-4,5,6,7-tetrahydroindan-1-one (4)

The keto-ester (3.4 g) was refluxed with glacial acetic acid (45 ml), constant-boiling hydrobromic acid (26 ml), and water (13 ml) for 1 h. The mixture was poured carefully on crystalline sodium carbonate (125 g) in sufficient water to form a slurry. The product was extracted with ether and dried (Na_2SO_4). This yielded 4-methyl-4,5,6,7-tetrahydroindan-1-one as a pale-yellow liquid (2 g), b.p. 84° at 0.4 mm.

Anal. Calcd. for $C_{10}H_{14}O$: C, 79.95; H, 9.39. Found: C, 79.72; H, 9.12.

It gave a semicarbazone, m.p. 240° (decomp.) from ethanol (1).

Anal. Calcd. for $C_{11}H_{17}ON_3$: C, 63.74; H, 8.27; N, 20.27. Found: C, 63.46; H, 8.25; N, 19.27.

Its 2,4-dinitrophenyl hydrazone melted at 208° (from acetic acid).

Anal. Calcd. for $C_{16}H_{18}O_4N_4$: C, 58.17; H, 5.49; N, 16.96. Found: C, 58.07; H, 5.56; H, 16.96.

4-Methyl-cis-perhydroindan-1-one (5)

A solution of the unsaturated ketone (1.2 g) in glacial acetic acid (10 ml) was shaken with hydrogen in the presence of Adams platinum oxide (0.15 g) until the absorption of hydrogen was ceased. After filtration, the acetic acid was neutralized with sodium carbonate solution. This yielded the saturated ketone as a colorless liquid (0.8 g), b.p. 65–67° at 0.5 mm.

Anal. Calcd. for $C_{10}H_{16}O$: C, 78.95; H, 10.59. Found: C, 78.70; H, 10.42.

It gave a semicarbazone as colorless crystals, m.p. 210–212° (decomp.) from ethanol (1).

Anal. Calcd. for $C_{11}H_{19}ON_3$: C, 63.20; H, 9.10; N, 20.10. Found: C, 63.41; H, 8.92; N, 19.88.

Its 2,4-dinitrophenyl hydrazone recrystallized as orange crystals from methanol, and melted at 205–206°.

Anal. Calcd. for $C_{16}H_{20}O_4N_4$: C, 57.83; H, 6.02; N, 17.39. Found: C, 57.97; H, 5.93; N, 17.18.

7-Methyl-$^1\Delta^{(8)}$*-hexahydroindan-1-carboxylic Acid (6; R = H) and its Methyl Ester (6; R = CH_3)*

To amalgamated zinc wool (20 g) in water (20 ml) and concentrated hydrochloric acid (40 ml) was added the keto-ester (5 g) in toluene (35 ml). The mixture was refluxed for 30 h with addition of concentrated hydrochloric acid (10 ml) every 6 h. The toluene layer was separated and the aqueous layer extracted with ether. The combined toluene and ether extracts, after washing with sodium bicarbonate solution, water, and drying (Na_2SO_4), afforded mainly the unsaturated ester (**6**; R = CH_3) as a pale-yellow oil (3.1 g), b.p. 85° at 0.04 mm.

Anal. Calcd. for $C_{12}H_{18}O_2$: C, 74.23; H, 9.28. Found: C, 74.43; H, 9.54.

A mixture of this oil (1 g) and 5% sodium hydroxide solution (20 ml) was refluxed for 3 h. The alkaline solution, after washing with ether, was cooled in ice and acidified to give the unsaturated acid (**6**, R = H) as a colorless oil, b.p. 92° at 0.05 mm.

Anal. Calcd. for $C_{11}H_{16}O_2$: C, 73.33; H, 8.90. Found: C, 72.97; H, 9.35.

7-Methyl Perhydroindan-1-carboxylic Acid (7; R = H) and its Methyl Ester (7; R = CH_3)

A solution of the unsaturated ester (**7**; R = CH_3) (2 g) in absolute ethanol (30 ml) was shaken with hydrogen in the presence of Adams platinum oxide (0.2 g), until the absorption of hydrogen ceased. Filtration and removal of the solvent afforded the saturated ester (**7**; R = CH_3) as a colorless oil, b.p. 142° at 0.05 mm (1.8 g).

Anal. Calcd. for $C_{12}H_{20}O_2$: C, 73.47; H, 10.20. Found: C, 73.22; H, 10.09.

The saturated ester (1 g) was refluxed for 6 h with 10% sodium hydroxide solution (10 ml) and ethanol (10 ml). Removal of the alcohol, washing the aqueous residue with ether, then acidification gave the saturated acid (**7**; R = H) as a colorless oil (0.8 g), b.p. 88–90° at 0.03 mm, which solidified on keeping, m.p. 157–158° (from benzene).

Anal. Calcd. for $C_{11}H_{18}O_2$: C, 72.52; H, 9.89. Found: C, 72.22; H, 9.91.

Acknowledgment

The authors thank Dr. Leigh C. Anderson, Professor of Organic Chemistry, University of Michigan, for measuring the nuclear magnetic resonance spectra.

1. J. W. Cook and R. Phillip. J. Chem. Soc. 162 (1948).
2. R. C. Chatterjee and B. K. Bhattacharyya. J. Indian Chem. Soc. **34**, 515 (1957).
3. W. S. Johnson, W. Petersen, and W. P. Schneider. J. Am. Chem. Soc. **64**, 74 (1947).
4. J. C. P. Schwarz. Physical methods in organic chemistry. Oliver and Boyd, Ltd., London. 1965.
5. L. J. Bellamy. The infrared spectra of complex molecules. Methuen & Co. Ltd., London. 1958. pp. 140, 152, 31.
6. J. W. Cook and C. A. Lawrence. J. Chem. Soc. 1637 (1935).
7. M. Elliott. J. Chem. Soc. 2231 (1956).
8. H. E. Ungnade and I. Ortega. J. Am. Chem. Soc. **73**, 1565 (1951).

Can. J. Chem. Downloaded from www.nrcresearchpress.com by 210.87.254.6 on 09/05/12
For personal use only.

Can. J. Chem. Downloaded from www.nrcresearchpress.com by 210.87.254.5 on 09/05/12
For personal use only.

A mechanistic study of the base-catalyzed methanolysis and hydrolysis of the hydrogen phthalate ester of 4-bromo-4′-nitrobenzhydrol

K. G. RUTHERFORD, O. A. MAMER,[1] AND B. K. TANG
Department of Chemistry, University of Windsor, Windsor, Ontario

Received October 8, 1968

The hydrogen phthalate ester of 4-bromo-4′-nitrobenzhydrol has been subjected to base-catalyzed methanolysis and hydrolysis. In both cases the $B_{AC}2$ mechanism has been observed. There is no evidence of ortho-carboxylate anion participation ($B_{AC}1$ mechanism). The results have been substantiated by kinetics, stereochemistry, and ^{18}O isotope studies.

Canadian Journal of Chemistry, 47, 1487 (1969)

The base-catalyzed solvolysis of hydrogen phthalate esters is especially interesting because of the following mechanistic possibilities for such systems: (*1*) alkyl–oxygen fission involving: (*a*) prior ionization ($B_{AL}1$); (*b*) nucleophilic displacement ($B_{AL}2$); (*2*) acyl–oxygen fission involving: (*a*) ortho-carboxylate anion participation ($B_{AC}1$); (*b*) normal ester solvolysis ($B_{AC}2$).

Paths *1a* and *2a* should exhibit first order kinetics (in ester only) while paths *1b* and *2b* should be characterized by second order kinetics (first order in both ester and base). In the case of the alkaline hydrolysis of these esters, ^{18}O isotopically enriched hydroxide ion will appear ultimately in the alcohol fragment through an alkyl–oxygen fission mechanism, and in the phthalic acid if an acyl–oxygen mechanism prevails. From the stereochemical standpoint, path *1a* should lead to racemization of an optically active center, *1b* should result in an inversion of configuration, and both *2a* and *2b* should lead to the retention of configuration. Thus, by observing the kinetics, the ^{18}O isotopic distribution among the reaction products and the stereochemistry of a given solvolysis, one should be able to deduce which path is operative.

In the benzhydryl hydrogen phthalate series, path *1a* has been observed to be quite general when the 4-position of one of the benzene rings is substituted by electron releasing groups. Thus, Davies (1) showed that when optically active 4-methylbenzhydryl hydrogen phthalate was treated for 24 h with boiling methanol, a 20% yield of racemic 4-methylbenzhydryl methyl ether was obtained along with 74% of the original ester. Similarly, 4-alkylthio- (2) and 4-dialkylamino- (3) substituted benzhydryl esters lead to racemized products on solvolysis. Path *1b* to our knowledge has not been observed in hydrogen phthalate ester solvolysis and is indeed extremely rare in the case of base solvolysis of other carboxylic esters.

Path *2a* was first observed by Bender (4) who showed that the ortho-carboxylate anion has an intramolecular catalytic effect on the hydrolysis of methyl hydrogen phthalate. More recently, Thanassi and Bruice (5) have shown ortho-carboxylate anion participation in the hydrolysis of phenyl- and 2′,2′,2′,-trifluoroethyl hydrogen phthalate. Such was not the case with poorer leaving groups, however, and the authors concluded that hydrogen phthalate esters with good leaving groups hydrolyze with catalysis of the ortho-carboxylate anion, while those with poor leaving groups (methoxy and 2′-chloroethoxy) hydrolyze with catalysis of the neutral carboxylic acid function.

Puckowski and Ross (6) reported that optically active 2-, 3-, and 4-nitro, 3,5-dinitro-, and 3-bromobenzhydryl hydrogen phthalate esters yielded optically active benzhydrols on treatment with 0.2 *N* aqueous sodium hydroxide or with 10% aqueous sodium carbonate (presumably by either path *2a* or *2b*). In view of the work of Thanassi and Bruice, one might expect that the nitro-substituted benzhydryl hydrogen phthalates would undergo acyl–oxygen fission according to path *2a* since nitro-substituted benzhydroxy moieties would be classified as good leaving groups.

In a recent study in our laboratory on the sodium methoxide catalyzed methanolysis of a series of benzhydryl hydrogen phthalate esters, results similar to those of Puckowski and Ross were obtained for those esters which were

[1]Present address: Division of Pure Chemistry, National Research Council of Canada, Ottawa 7, Canada.

Can. J. Chem. Downloaded from www.nrcresearchpress.com by 210.87.254.5 on 09/05/12
For personal use only.

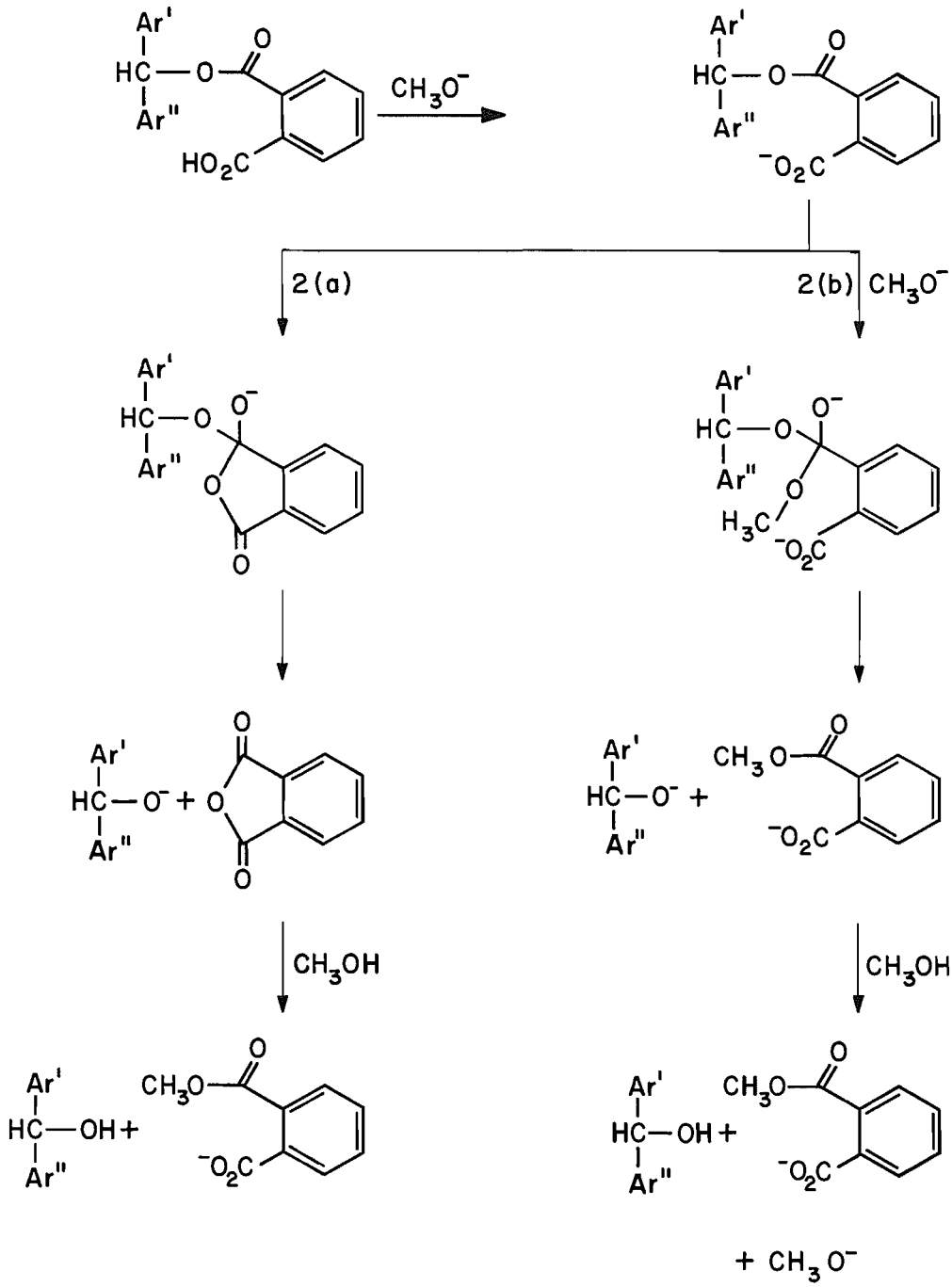

FIG. 1. Reaction paths leading to acyl–oxygen fission in the methoxide ion catalyzed methanolysis of 4-bromo-4′-nitrobenzhydryl hydrogen phthalate.

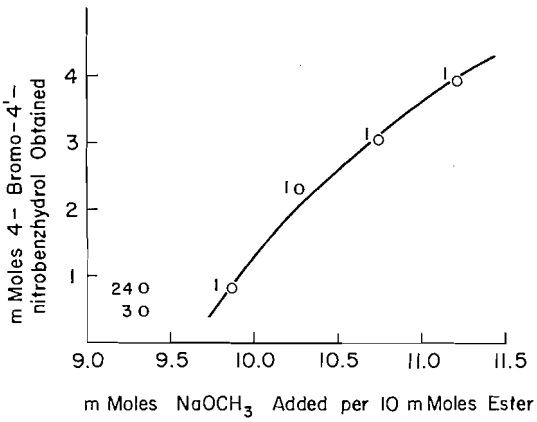

FIG. 2. Methoxide ion catalyzed methanolysis of 4-bromo-4′-nitrobenzhydryl hydrogen phthalate in moles hydrol obtained vs. mmoles methoxide added to 10 mmoles ester. Numbers accompanying datum points indicate reaction time in h.

substituted in one of the benzene rings by even the weaker electron-seeking atoms (4-Cl, $\sigma = +0.227$). We chose to study in more detail the base-catalyzed methanolysis and hydrolysis of 4-bromo-4′-nitrobenzhydryl hydrogen phthalate. The presence of the nitro group and bromine atom should make the benzhydroxy group an excellent leaving group and thus path *2a* should be observed to some extent. Figure 1 shows the two accepted mechanisms for these solvolyses involving acyl–oxygen fission (*2a* and *2b*).

Results and Discussion

Methoxide Ion Catalyzed Methanolysis Studies

Figure 2 shows the effect of adding increasing amounts of sodium methoxide to a solution of 4-bromo-4′-nitrobenzhydryl hydrogen phthalate. It can be seen that as the methoxide is added progressively to the ester solution, no appreciable methanolysis occurs even after the lapse of 24 h at 25° until the equivalent point is reached. Further addition of methoxide (i.e. in excess of equivalency) results in a progressive increase in the amount of 4-bromo-4′-nitrobenzhydrol produced after 1 h of reaction time. Thus when 11.2 mmoles of methoxide are added to 10 mmoles of the ester, approximately 40% methanolysis is realized at the end of 1 h. It is to be noted at the lower left portion of the graph that when 9.34 mmoles of methoxide are added to 10 moles of ester, no significant difference in yields of the benzhydrol is observed at the end of 3 and 24 h. The solvolysis obtained before equivalency probably arose from local high base concentrations existing briefly during the initial mixing. It would appear from the above that the intramolecular catalyzed methanolysis of this ester by the ortho-carboxylate anion is relatively insignificant, and that mechanism *2a* can be essentially discounted as a reaction path.

It was decided to substantiate this indirect stoichiometric evidence with a kinetic study of the reaction. If the reaction proceeds via path *2b*, the addition of base in excess of equivalency should cause a rate enhancement paralleling that observed in normal ester solvolysis. Such kinetic studies for methoxide catalyzed methanolysis present a problem. Since the concentration of methoxide does not change after equivalency regardless of the mechanistic path, the normal acid–base titrimetric methods usually followed in normal ester hydrolysis cannot be employed. It was decided then to follow the rate of reaction using gravimetric means. The ester was dissolved in tetrahydrofuran (THF) and a standard sodium methoxide solution was added. Aliquots of the reaction mixture were removed at intervals and rapidly acidified with hydrochloric acid. The methyl hydrogen phthalate formed from the reaction was found to be soluble under the conditions used. Thus only 4-bromo-4′-nitrobenzhydrol and unchanged hydrogen phthalic ester were precipitated after rapid acidification. From the weights (w) of the precipitates obtained, the concentration of the unchanged ester was calculated from the following relationship.

By mass balance

$$N_A + N_B = N_A \quad [1]$$

and

$$N_A M_A + N_B M_B = W \quad [2]$$

where N_A and N_B are the number of moles of the ester and benzhydrol respectively in the precipitate, and M_A and M_B are the corresponding molecular weights. N_{Ao} is the number of moles of ester expected to be in the aliquot taken at time zero and is calculated as

$$N_{Ao} = V_{aliq.} \times [\text{ester}]_{t=0} \quad [3]$$

The aliquot volume is 50 ml, and the reaction solution is made up to 0.020 moles ester per 275 ml reaction volume.

Can. J. Chem. Downloaded from www.nrcresearchpress.com by 210.87.254.5 on 09/05/12
For personal use only.

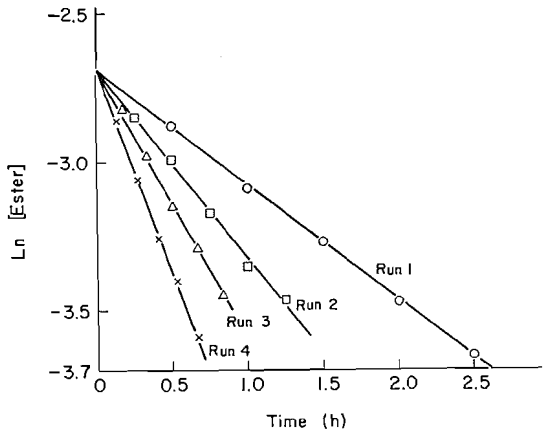

FIG. 3. Methoxide ion catalyzed methanolysis of 4-bromo-4′-nitrobenzhydryl hydrogen phthalate. Rate first-order in ester concentration. Excess methoxide ion concentration: run 1, 1.0; run 2, 2.0; run 3, 3.0; run 4, 4.0 mmoles methoxide ion per 20 mmoles ester in 275 ml reaction volume.

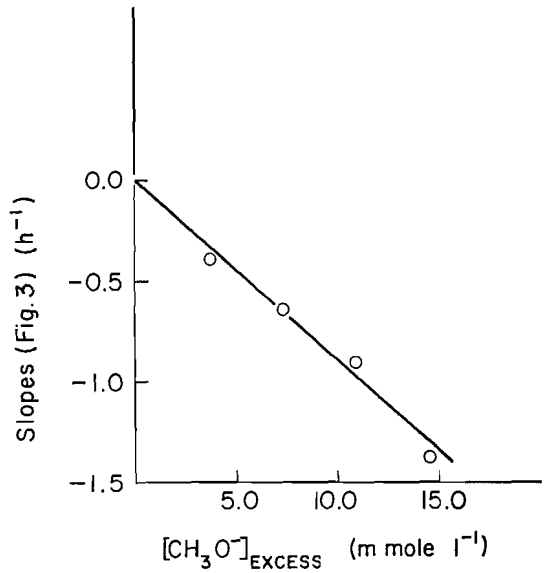

FIG. 4. Slopes from Fig. 3 vs. concentration of excess methoxide ion showing first-order dependency of rate on methoxide ion concentration in excess of equivalency.

Therefore

$$[4] \qquad N_{Ao} = 0.050 \times \frac{0.020}{0.275} = 0.00364 \text{ moles}$$

By arranging [1] and substituting in [2] we have for a 50 ml aliquot:

$$[5] \qquad N_A = \frac{W - N_{Ao}M_B}{M_A - M_B} = \frac{W - 1.121}{148}$$

Therefore

$$[6] \qquad [\text{ester}] = \frac{N_A}{0.050\,1} = \frac{W - 1.121}{7.40}$$

Thus expression [6] provides for the convenient determination of the concentration of the unreacted ester (in mole l^{-1}) in the solvolyzing solutions from the weight of the precipitate (in g) obtained from each aliquot.

Figure 3 shows the first-order dependency of the reaction rate on the ester anion concentration. Each line represents an experiment different from the others only in the concentration of methoxide ion existing in excess of equivalency. A linear relationship (Fig. 4) is shown to exist between the slopes of the first-order plots of Fig. 3 and the concentration of methoxide ion remaining in excess of equivalency. This indicates that the solvolytic rate is proportional to that quantity of methoxide ion that is in excess of equivalency and not consumed by the reaction (Fig. 1). This observed proportionality dismisses path *2a* as being of importance as this path suggests that the rate should be independent of the concentration of excess methoxide ion. On the other hand, path *2b* predicts the experimentally observed first-order dependency in both ester anion and methoxide ion concentrations.

Thus the second-order rate law for the reaction is then:

$$[7] \qquad \frac{d[\text{ester}]}{dt} = -k_2[\text{ester}][CH_3O^-]_{\text{excess}}$$

where k_2 (l mole^{-1} h^{-1}) is the slope of the line in Fig. 4.

Therefore

$$[8] \qquad k_2 = 89.0$$

Hydroxide Ion Catalyzed Hydrolysis Studies

The hydroxide ion catalyzed hydrolysis of the same hydrogen phthalate ester was found to follow a kinetic scheme similar to that for the methoxide ion study. Figures 5 and 6 show the dependency of the hydrolytic rate on the concentration of both the ester and the excess hydroxide ion. A similar mathematical treatment based on aliquot precipitate weights was employed to calculate the concentrations of unreacted ester remaining in each aliquot.

In order to effect a reaction on a convenient time scale, the concentrations of the basic ion were increased approximately ten-fold over those

Can. J. Chem. Downloaded from www.nrcresearchpress.com by 210.87.254.5 on 09/05/12
For personal use only.

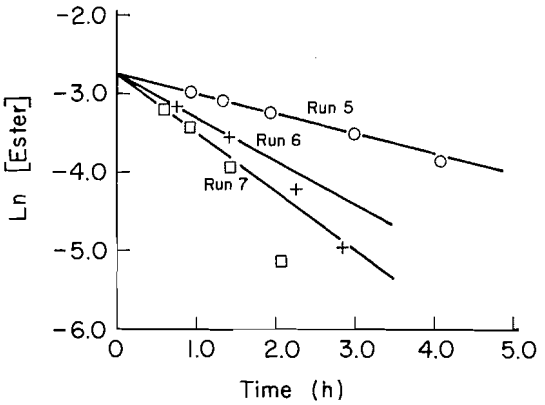

FIG. 5. Hydroxide ion catalyzed hydrolysis of 4-bromo-4′-nitrobenzhydryl hydrogen phthalate. First-order in ester concentration. Excess hydroxide ion concentration: run 5, 13.4; run 6, 25.2; run 7, 36.8 mmoles hydroxide ion per 10 mmoles ester in 137.5 ml reaction volume.

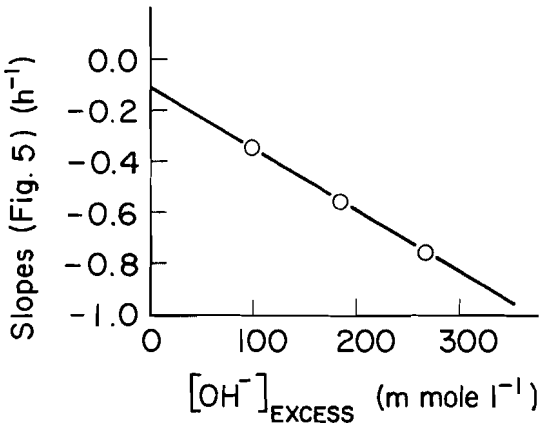

FIG. 6. Slopes from Fig. 5 vs. concentration of excess hydroxide ion. First-order rate dependency on excess hydroxide ion concentration.

used in the methanolysis study. The lines in Fig. 6 are straight at least in the range of conversions found in the methanolysis study. The apparent increase in the hydrolytic rate with increasing conversion is probably not a kinetic effect but only a mechanical handling error caused by incomplete precipitation of the reaction products or incomplete transfer of the products to the weighing crucibles. This gravimetric method becomes increasingly sensitive to errors arising from incomplete collection of the products as the hydrolysis nears completion. A loss or gain of 3 mg of precipitate for example at 92% completion (last datum point in run 7, Fig. 5) causes an uncertainty of 0.4 logarithm units at that point.

Another method of analysis was used in the first few samples as a check on the gravimetric procedure. This was a titrimetric method involving the measurement of an apparent neutralization equivalent of a quenched aliquot, from which the concentration of the unsolvolyzed ester in the reaction mixture was calculated (7). It was found early in the experiments that the two methods gave results agreeing to within 7% of each other, with the conversions determined through the titrimetric method being consistently lower. From the point of view of convenience, the titrimetric method was abandoned and the kinetics studied by only the gravimetric method.

The initial slopes (Fig. 5) are directly proportional to the concentration of hydroxide ion in excess of equivalency (Fig. 6). Thus for the hydrolysis

$$[9] \qquad \frac{d[\text{ester}]}{dt} = -k_2[\text{ester}][OH^-]_{\text{excess}}$$

where k_2 (l mole^{-1} h^{-1}) is the slope of the line in Fig. 6.
Therefore

$$[10] \qquad k_2 = 2.40$$

It is to be noted from Fig. 6 that at equivalency (i.e. $[OH^-]_{\text{excess}} = 0$) there appears to be a slight hydrolytic rate. It is not clear whether this is due to hydrolysis occurring via path *2a* or an overall displacement of the line downwards, caused by localized and transient high base concentrations generated on mixing.

The second-order nature of the alkaline hydrolysis of this ester indicates that the ester anion and the hydroxide ion are both involved in the rate-determining step. In the interpretation of these kinetic results, a problem arises here which did not arise in the methanolysis studies. Thus the absence of 4-bromo-4′-nitrobenzhydryl methyl ether in the methanolysis of the benzhydryl ester discounts any argument that the kinetics could be explained by path *1b*. Although intuitively one might not expect any variation in mechanism, it is necessary to eliminate *1b* as a reaction path.

The same conclusion can be drawn from a stereochemical study of this same ester. The methoxide ion catalyzed methanolysis of optically active 4-bromo-4′-nitrobenzhydryl hydrogen

Can. J. Chem. Downloaded from www.nrcresearchpress.com by 210.87.254.5 on 09/05/12
For personal use only.

Can. J. Chem. Downloaded from www.nrcresearchpress.com by 210.87.254.5 on 09/05/12
For personal use only.

phthalate ($[\alpha]_D^{25}$ +0.87°) yielded optically active 4-bromo-4′-nitrobenzhydrol ($[\alpha]_D^{25}$ +0.23°). Since the methanolysis reaction was shown to result in acyl–oxygen cleavage, the configuration of the hydroxyl group was then established. When the same optically active ester was subjected to hydroxide ion catalyzed hydrolysis, similar optical activity for the "hydrol" ($[\alpha]_D^{25}$ +0.50°) was noted. It must be concluded then that hydrolysis as well as methanolysis by the benzhydryl ester in this study proceeds by the attack of the base at the ester carbonyl (path *2b*).

It is difficult to rationalize the failure of the ortho-carboxylate anion to participate in the removal of the 4-bromo-4′-nitrobenzhydroxy group without resorting to an argument based on a steric effect preventing the formation of the five-membered ring intermediate. Certainly, any electrical influences affecting the ester carbonyl would be the same whether or not this group was attacked by carboxylate, methoxide, or hydroxide.

Since the ring substituents are in the 4-position of the benzhydryl portion, only electrical effects can be realized from these sources. It might be deduced then that benzhydryl hydrogen phthalate esters, in which the overall effect of substituent groups is to withdraw electrons from the carbinyl carbon atom, undergo base-catalyzed solvolysis according to the $B_{AC}2$ mechanism.

Experimental

4-Bromo-4′-nitrobenzhydryl Hydrogen Phthalate

A solution of 4-bromo-4′-nitrobenzhydrol (8)[2] (31 g, 0.10 mole) phthalic anhydride (16.3 g, 0.11 mole), and pyridine (100 ml) was added to a 300 ml conical flask. Sodium hydride (5.28 g, 0.11 mole, of a 50% dispersion in mineral oil) was added with stirring at a rate adjusted to keep the temperature of the solution below 35°. When the addition was completed, the flask was loosely stoppered and the mixture was magnetically stirred for a period of 6 h. The mixture was then poured slowly into 1 l of 2 *N* hydrochloric acid. The organic material was extracted twice with two 100 ml portions of chloroform which was then washed three times with 0.1 *N* hydrochloric acid, dried over anhydrous sodium sulfate, and the solvent removed *in vacuo*. The remaining gum was dissolved in 0.2 *N* sodium hydroxide (750 ml) and the resultant solution filtered through a fine sintered glass plate. The solution was slowly acidified with dilute hydrochloric acid thus yielding the crude ester (42 g, 92%) m.p. 171–180°. Recrystallization from a chloroform – petroleum ether (b.p. 30–60°) solvent pair produced the pure ester (38 g) m.p. 184–185°. The infrared spectrum of the compound showed the following bands: a broad OH band beginning at 3500 cm^{-1} and merging with CH stretching at 3000 cm^{-1} (characteristic of carbonyl OH stretching), an ester carbonyl stretching at 1736 cm^{-1}, and an acid carbonyl stretching at 1702 cm^{-1}, aromatic skeletal vibrations at 1602 and 1490 cm^{-1}, and nitro group stretching at 1524 and 1350 cm^{-1}.

Anal. Calcd. for $C_{21}H_{14}BrNO_6$ (neutralization equivalent, 456.24): C, 55.30; H, 3.60. Found (neutralization equivalent, 455.7): C, 55.70; H, 3.23.

(+)-Bromo-4′-Nitrobenzhydryl Hydrogen Phthalate

A solution of the racemic ester (20 g, 0.044 mole), brucine (16 g, 0.041 mole), and acetone (250 ml) was heated at reflux for 10 min. Removal of the solvent at reduced pressure yielded the brucine salt as a bright-yellow spongy glass. Three successive recrystallizations of the salt from 2:1 toluene–methylcyclohexane yielded the salt as a brilliant yellow powder (10.5 g), m.p. 138–140°. The salt was too highly colored to allow determination of its specific rotation. The melting point range could not be improved by further recrystallization. A solution of the salt in acetone (200 ml) was poured into ice-cold 0.2 *N* hydrochloric acid (400 ml) which yielded the ester. The resolved ester was obtained as a white crystalline material (5.1 g, 23% on resolution) m.p. 180–181°, $[\alpha]_D^{25}$ + 0.87° (l, 2; *c*, 4.0 in acetone) after one recrystallization from chloroform – petroleum ether.

Solvolytic Reactions of 4-Bromo-4′-Nitrobenzhydryl Hydrogen Phthalate

(a) With Sodium Methoxide

The ester (4.5 g, 0.01 mole) was dissolved in anhydrous THF (30 ml), and to this was added a methanol solution of sodium methoxide (1.0 g, 0.044 mole sodium; 30 ml anhydrous methanol). The solution was stirred for 5 min and then poured over a slurry of ice (20 g) and concentrated hydrochloric acid (5 ml), yielding 4-bromo-4′-nitrobenzhydrol (3.0 g, 97%), m.p. 150–154°. Saturation of the cold mother liquor with potassium chloride and extraction with ether yielded methyl hydrogen phthalate (0.2 g, 12%) m.p. 82–83°. When this procedure was repeated with the optically active ester (4.0 g, 0.0088 mole), (+)-4-bromo-4′-nitrobenzhydrol (2.15 g, 80%), m.p. 157–159°, was obtained having $[\alpha]_D^{25}$ +0.23° (l, 2; *c*, 2.15 in acetone).

(b) With Methanol

The racemic ester was recovered unchanged (92%) after heating at reflux in methanol for 24 h.

(c) With Aqueous Sodium Hydroxide

A solution of (+)-4-bromo-4′-nitrobenzhydryl hydrogen phthalate (2.25 g, 0.0049 mole) in THF (25 ml) was mixed with 2 *N* sodium hydroxide (400 ml). After standing for 30 min, the mixture was rendered neutral with dilute hydrochloric acid. The 4-bromo-4′-nitrobenzhydrol (1.2 g, 80%) so obtained had m.p. 156–158°, $[\alpha]_D^{25}$ +0.50° (l, 2; *c*, 6 in acetone).

A sample of the racemic ester (1.0 g, 0.0022 moles) was similarly treated with ^{18}O labeled aqueous sodium hydroxide (0.2 g, 0.0050 moles NaOH; 1 ml 20% ^{18}O enriched H_2O; 1 ml THF). The benzhydrol obtained

[2]For preparation and characterization of this alcohol, see reference 8.

from this reaction was found by mass spectrometry[3] not to be enriched in ^{18}O over natural abundance. On the other hand, the phthalic acid contained 4.58% ^{18}O enrichment (99.8% of the theoretically required amount).

Kinetic Study of the Solvolysis of 4-Bromo-4'-Nitrobenzhydryl Hydrogen Phthalate

(a) With Methoxide

Stoichiometric study—Known amounts of the ester (4.56 g, 0.010 mole) were dissolved in anhydrous THF (40 ml volumes). To each ester solution was added a carefully pipetted quantity of a standard methanolic sodium hydroxide solution (0.934 *N*) prepared from anhydrous methanol (500 ml) and freshly cut sodium (11.5 g, 0.5 mole). The resulting solutions were tightly stoppered and kept in a constant temperature bath at 25 °C for varying lengths of time. The samples were then poured quantitatively into ice-cold water (300 ml) and the resulting solutions were rapidly made acidic (pH 2) with 2 *N* hydrochloric acid. The precipitates were allowed to remain in contact with the mother liquor for ½ h to ensure high yields of the insoluble material. The crystalline precipitates were collected in preweighed sintered glass crucibles (medium porosity), washed with distilled water, air dried for 6 h, and finally dried *in vacuo* for 12 h. The weights of the precipitates were then noted, and the extents of conversion were calculated for each sample (Fig. 2).

Kinetic study—A different method of conducting the kinetic study of the solvolysis with sodium methoxide was used in determining the reactant orders. The ester samples (9.12 g, 0.020 moles) were dissolved in volumes of THF (150 ml). Varying amounts (22.5–25.7 ml) of the methanolic sodium methoxide stock solution (0.934 *N*) were pipetted into volumes of anhydrous methanol (100 ml). The methanol solutions were then poured rapidly and quantitatively into the rapidly stirred ester solutions to start the experiment. Immediately the reaction solutions were diluted to exactly 275 ml with anhydrous methanol (less than 5 ml being sufficient), and tightly stoppered. The solutions were kept in a constant temperature bath (25°). At intervals during the length of the reaction period, aliquots (50 ml) were removed from the reaction flasks and were quenched and weighed exactly as described above. The concentrations of unreacted ester were then calculated as described previously.

(b) With Hydroxide

The kinetics of the alkaline hydrolysis of 4-bromo-4'-nitrobenzhydryl hydrogen phthalate were followed by gravimetric technique similar to that described above. In all the kinetic experiments with aqueous hydroxide, the following method was used. Samples of the ester (4.56 g, 0.010 mole) were dissolved in volumes of anhydrous THF (30 ml) and these solutions were quantitatively added to volumes of aqueous potassium hydroxide solution (100 ml) of different concentrations. The solutions were immediately diluted to 137.5 ml (less than 10 ml being sufficient). The solutions were kept in a constant temperature bath (25° ± 0.5°). At intervals during the length of the reaction period, aliquots (25 ml) were withdrawn from the reaction flasks and were quenched and the precipitates weighed in exactly the manner described previously.

[3]Limiting sensitivity $^{18}O/(^{18}O + ^{16}O) < 0.05\%$. Analysis was performed by Morgan and Schaffer Corp., Montreal, Quebec.

Acknowledgment

The authors wish to thank the National Research Council of Canada for generous support of this project.

1. A. G. Davies. J. Chem. Soc. 3473 (1954).
2. M. P. Balfe, R. E. Darby, and J. Kenyon. J. Chem. Soc. 382 (1951).
3. M. P. Balfe. J. Chem. Soc. 790 (1952).
4. M. L. Bender, F. Cloupek, and M. Neveu. J. Am. Chem. Soc. **80**, 5384 (1958).
5. J. W. Thanassi and T. C. Bruice. J. Am. Chem. Soc. **88**, 747 (1966).
6. R. T. Puckowski and W. A. Ross. J. Chem. Soc. 3555 (1959).
7. O. A. Mamer. Ph.D. Thesis. University of Windsor, Windsor, Ontario. 1966. pp. 121–122.
8. K. G. Rutherford and O. A. Mamer. J. Org. Chem. **31**, 2708 (1966).

Can. J. Chem. Downloaded from www.nrcresearchpress.com by 210.87.254.5 on 09/05/12
For personal use only.

Can. J. Chem. Downloaded from www.nrcresearchpress.com by 210.87.254.6 on 09/05/12
For personal use only.

Stereochemistry of hydrogenation of 19-substituted 5α-cholestan-3-ones[1]

Y. WATANABE AND Y. MIZUHARA[2]
Chemical Laboratory, School of Medicine, Keio University, Hiyoshi, Yokohama, Japan

AND

M. SHIOTA
Chemical Laboratory, Ochanomizu University, Otsuka, Tokyo, Japan

Received September 27, 1968

The effect of 19-substituents on the stereochemistry of hydrogenation of 19-substituted 5α-cholestan-3-ones was examined. It has been shown that hydroxyl, acetoxyl, and methoxyl groups have some effect in increasing 3α-alcohols on hydrogenation over platinum in ethanol compared with the case of the unsubstituted ones.

Canadian Journal of Chemistry, 47, 1495 (1969)

The stereochemistry of the alcohols resulting from the catalytic hydrogenation of steroidal ketones has been known to be very sensitive to the reaction medium (1–3), and the reason for this is a debated point (3, 4). On the other hand, the substituent effect on the stereochemistry of hydrogenation of ketones has not yet been well examined, and an investigation of the effect of some substituents in a rather rigid steroidal system seems to be of interest. Previously, we reported on the catalytic hydrogenation of 3β-acetoxy-19-hydroxy- and 3α,19-dihydroxycholest-5-enes and showed that the 19-hydroxyl group in the above compounds is effective in increasing the proportion of 5β-dihydro compounds (5, 6). It appeared that the lone paired electrons of the oxygen atom of the 19-hydroxyl group made it easier for the catalyst to approach the β-side of the molecule. As part of the investigation of the effect of 19-substituents on stereochemistry of hydrogenation we examined the influence of 19-substituents on the proportion of 3α- and 3β-alcohols obtained in the catalytic hydrogenation of 19-substituted 5α-cholestan-3-ones.

The proportion of the 3α-alcohol obtained in hydrogenation of 5α-cholestan-3-one over platinum has been reported to vary with acidity of the solvent used (1, 2), and the 3α-alcohol became the main product of hydrogenation by adding small amounts of hydrochloric acid to the solvent (3). As the stereochemistry of the hydrogenation of steroidal 3-ketones appears very susceptible to the influence of the condition of the reaction, for instance, the catalyst used, solvent, temperature and other factors, the proportion of 3α-alcohols obtained in hydrogenation of several ketones under the same condition was compared with that of 5α-cholestan-3-one in the present experiments.

We synthesized the 19-substituted 5α-cholestan-3-one derivatives listed below.

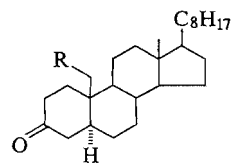

1*a* R = H
1*b* R = OH
1*c* R = OAc
1*d* R = OCH_3
1*e* R = Cl

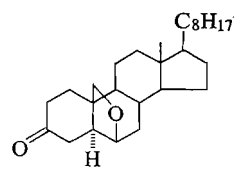

2

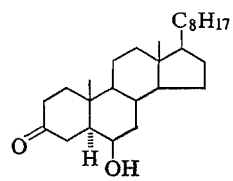

3

Optical rotatory dispersion (o.r.d.) curves of the above ketones were measured and the results are shown in Table I. All 3-ketones measured showed

[1]Presented in part at the 21st Annual Meeting of the Chemical Society of Japan in Osaka, Japan. April 1968.
[2]To whom all correspondence should be addressed.

TABLE I

Optical rotatory dispersion molecular amplitude (in dioxane)

Compound	Molecular amplitude
1*a*	+49
1*b*	+14
1*c*	+37
1*d*	+31
1*e*	+27
2	+114

positive Cotton effect curves such as that of 5α-cholestan-3-one, but some differences in amplitude were observed. Especially in 19-hydroxy-3-one (**1***b*) a considerable decrease of the positive amplitude was seen, and this phenomenon has been interpreted by Crabbé (7, 8) to be due to the possibility that the compound exists as the free and intramolecular hemiketal form. It has also been shown that the introduction of 6β,19-epoxide causes the considerable increase in molecular amplitude compared with that of 5α-cholestan-3-one.

The above ketones were hydrogenated over platinum in acetic acid and in ethanol solution, and the proportion of 3α- and 3β-alcohols was determined by gas–liquid chromatography. The results are reported in Table II. The experimental results of the reduction of the compound **1**, **2**, and **3** with sodium borohydride in methanol are also mentioned for comparison. The configurations of the epimeric alcohols obtained in the hydrogenation of **1***a*, **1***b*, **1***c*, **1***e*, **2**, and **3** have already been established (5, 6). The configurations of the products from the 19-methoxy derivative (**1***d*) have been assigned on the basis of nuclear magnetic resonance (n.m.r.) spectra. The differences in the chemical shift and in the half-widths of the peaks of the epimeric C-3 protons were used (3), namely, the 3α-alcohol had a C-3 proton peak centered at 5.05 p.p.m. (half-width 8 c.p.s.), while in the 3β-one it was centered at 4.7 p.p.m. (23 c.p.s.), as the 3-acetoxy derivative.

When reduced with sodium borohydride, all hydrogenated compounds gave about 10% of 3α-alcohols as in the case of 5α-cholestan-3-one and it was shown that 19-substituents have little effect on the steric course of the reaction. The catalytic hydrogenation in ethanol gave proportions of 3α-alcohols varying with the change of 19-substituent and it was observed that the presence of the 19-substituents such as hydroxyl, acetoxyl, and methoxyl groups caused the increase of the proportions of 3α-alcohols by 10–20% in ethanol. In acetic acid, the proportion of 3α-alcohol was shown to decrease a little in all 19-substituted derivatives compared with that in the unsubstituted one.

TABLE II

The proportions of 3α- and 3β-alcohols obtained in reduction*

Compound (19-substituent)	$NaBH_4$		H_2/Pt–EtOH		H_2/Pt–AcOH	
	3α-	3β-	3α-	3β-	3α-	3β-
1*a* (H)	13	87	17	83	16	84
1*b* (OH)	10	90	40	60	6	94
1*c* (OAc)	8	92	32	68	1	99
1*d* (OCH_3)	11	89	26	74	4	96
1*e* (Cl)	6	94	7	93	3	97
2	12	88	17	83	2	98
3	9	91	6	94	1	99

*Proportions expressed as percentages.

From the above experimental results, the effect of 19-substituents on hydrogenation in ethanol appears to be due to electronic interaction between substituents and catalyst rather than steric effect. In acetic acid, this interaction appears to be weakened by protonation, and the steric course of the hydrogenation seems to be more controlled by steric factors. On the hydrogenation of the 5,6-double bond, the effect of the 19-hydroxyl group in increasing the 5β-dihydro compound was shown to be weakened in acetic acid, but 3β-acetoxy-19-hydroxycholest-5-ene gave 36.5% of the 5β-dihydro compound even when it was hydrogenated over platinum in acetic acid, while 3β-acetoxycholest-5-ene afforded only 10% of the 5β-dihydro compound under the same conditions. On the other hand the effect of the 19-hydroxyl group completely disappeared in acetic acid on the reduction of the 3-keto group. On the basis of these results, it was supposed that the hydrogen bonding between the 19-hydroxyl group and the π-electrons of the 5,6-double bond contributed to the determination of the steric course of hydrogenation together with the lone paired-electrons of the oxygen atom. Not only hydroxyl but also acetoxyl and methoxyl groups appear to have some effect on the stereochemistry of hydrogenation of the 3-keto group in ethanol. Though the effect of acetoxyl and methoxyl groups as above has scarcely been reported, it

Can. J. Chem. Downloaded from www.nrcresearchpress.com by 210.87.254.6 on 09/05/12
For personal use only.

Can. J. Chem. Downloaded from www.nrcresearchpress.com by 210.87.254.6 on 09/05/12
For personal use only.

has been suggested that the lone paired-electrons of the oxygen atoms in these groups may play some role to promote the β-side hydrogenation. On the hydrogenation of the 5,6-double bond the 19-acetoxyl group has no effect in increasing the 5β-dihydro compound both in ethanol and in acetic acid. But in the case of the reduction of the 3-keto group an acetylation of the 19-hydroxyl group did not cause a large change in the proportion of the 3α-alcohol. This difference in the effect of the 19-acetoxyl group and the 3-keto group on the reduction of the 5,6-double bond seems to be related to the difference in the distance between the 19-substituent and the unsaturated bond to be hydrogenated, or may be due to a steric effect.

Numerous intramolecular reactions of A/B-*trans*- and Δ^5-steroids possessing functional groups at C-3 and C-19 have been reported (9–13). As the flexibility of ring A allows the interaction of the functional groups at C-3 and C-19, it is not clear that the larger effect of 19-hydroxyl group than that of others is partially attributed to the formation of the intramolecular hemi-ketal. From a consideration of the o.r.d. and n.m.r. results, it is suggested that the steric course of hydrogenation depends much more from the nature of the substituent at C-19 than from the possible changes of conformation occurring in ring A.

Experimental

All melting points are uncorrected. Nuclear magnetic resonance spectra were obtained at 60 Mc.p.s. on $CDCl_3$ solution containing TMS as an internal standard; the chemical shifts are expressed in p.p.m.; s = singlet, q = quartet.

3β-Acetoxy-19-benzoyloxy-5α-cholestane (4a)

Benzoylation of 3β-acetoxy-19-hydroxy-5α-cholestane (5) with pyridine and benzoyl chloride at room temperature gave **4a**, which was recrystallized from methanol, m.p. 125–126°; $[\alpha]_D^{26}$ +30.6° ($CHCl_3$, *c*, 1.625); ν_{max} (KBr) 1733, 1720, 1603, 1585, 1273, 1247, 1117, 1028, and 720 cm^{-1}; λ_{max} (EtOH) 231 mμ (ε 13 900), 274 mμ (ε 1 100).

Anal. Calcd. for $C_{36}H_{54}O_4$: C, 78.50; H, 9.88. Found: C, 78.62; H, 9.72.

3β-Hydroxy-19-benzoyloxy-5α-cholestane (4b)

Hydrolysis of **4a** with 0.5% KOH–ethanol gave **4b**, which was recrystallized from acetone–methanol, m.p. 154.5–155.2°; $[\alpha]_D^{26}$ +41.7° ($CHCl_3$, *c*, 1.440); ν_{max} (KBr) 3420, 1717, 1603, 1585, 1270, 1118, 1033, 1029, and 715 cm^{-1}; λ_{max} (EtOH) 231 mμ (ε 13 100), 274 mμ (ε 950).

Anal. Calcd. for $C_{34}H_{52}O_3$: C, 80.26; H, 10.30. Found: C, 79.96; H, 10.53.

19-Benzoyloxy-5α-cholestan-3-one (1f)

A solution of 300 mg of 3β-hydroxy compound (**4b**) in 30 ml of acetone was oxidized with 0.7 ml of 8 *N* chromic–sulfuric acid solution at 0° for 30 min. The crude product (270 mg) was recrystallized from acetone–methanol; yield, 230 mg, m.p. 152–152.5°; ν_{max} (KBr) 1718, 1603, 1585, 1273, 1115, 1030, and 719 cm^{-1}; λ_{max} (EtOH) 231 mμ (ε 13 600), 274 mμ (ε 910); n.m.r. (δ): 4.72 (s, 19-CH_2), 7.4–8.15 (aromatic H); o.r.d. (*c*, 0.0057, dioxane, 20°): $[\phi]_{450}$ +360°, $[\phi]_{315}$ +2430°, $[\phi]_{288}$ 0°, $[\phi]_{283}$ −320°.

Anal. Calcd. for $C_{34}H_{50}O_3$: C, 80.58; H, 9.95. Found: C, 80.78; H, 10.19.

19-Hydroxy-5α-cholestan-3-one (1b)

19-Benzoyloxy compound (**1f**) was hydrolyzed with 5% KOH–ethanol solution at room temperature. The crude product was recrystallized from methanol, m.p. 143.5–144.5°; ν_{max} (KBr) 3420, 1720 (weak), and 1045 cm^{-1}; n.m.r. (δ): 4.18 and 4.00 (AB type q, J = 10.5 c.p.s., 19-CH_2); o.r.d. (*c*, 0.0071, dioxane, 20°): $[\phi]_{450}$ +380°, $[\phi]_{313}$ +1730°, $[\phi]_{275}$ +330°, $[\phi]_{260}$ +590°.

Anal. Calcd. for $C_{27}H_{46}O_2$: C, 80.54; H, 11.52. Found: C, 80.67; H, 11.52.

19-Acetoxy-5α-cholestan-3-one (1c)

Acetylation of **1b** with pyridine and acetic anhydride overnight at room temperature gave the acetate (**1c**). Recrystallization of the crude product from methanol gave a pure product, m.p. 99.5–100.5°; ν_{max} (KBr) 1735, 1710, 1249, 1240, and 1050 cm^{-1}; n.m.r. (δ): 4.49 (s, 19-CH_2), 2.10 ($OCOCH_3$); o.r.d. (*c*, 0.006, dioxane, 20°): $[\phi]_{450}$ +270°, $[\phi]_{315}$ +2180°, $[\phi]_{293}$ 0°, $[\phi]_{274}$ −1560°, $[\phi]_{260}$ −1250°.

Anal. Calcd. for $C_{29}H_{48}O_3$: C, 78.32; H, 10.88. Found: C, 78.49; H, 10.96.

3-Ethylenedioxy-19-benzoyloxy-5α-cholestane (5a)

19-Benzoyloxy-3-ketone (**1f**) was converted into the ethylenedioxy derivative by exchange dioxolonation (14). The mixture of 250 mg of 3-ketone (**1f**) and 7 mg of *p*-toluenesulfonic acid in 4 ml of 2-methyl-2-ethyl-1,3-dioxolane was refluxed for 6 h. After cooling, the reaction mixture was diluted with benzene and the resulting solution was washed with sodium bicarbonate solution and with water, and dried over sodium sulfate. Evaporation of the solvent *in vacuo* gave the crude product, which was recrystallized from acetone–methanol; yield, 200 mg, m.p. 138.5–139.5°; $[\alpha]_D^{26}$ +42.9° ($CHCl_3$, *c*, 1.625); ν_{max} (KBr) 1715, 1274, 1115, 1104, 1073, 1028, 946, and 710 cm^{-1}; λ_{max} (EtOH) 231 mμ (ε 13 600), 274 mμ (ε 910); n.m.r. (δ): 3.95 (s, 3-ethylenedioxy), 4.52 (s, 19-CH_2), 7.4–8.15 (aromatic H).

Anal. Calcd. for $C_{36}H_{54}O_4$: C, 78.50; H, 9.88. Found: C, 78.37; H, 9.79.

3-Ethylenedioxy-19-hydroxy-5α-cholestane (5b)

19-Benzoyloxy compound (**5a**) was hydrolyzed with 5% KOH–ethanol under reflux for 45 min. The crude product was recrystallized from *n*-hexane, m.p. 146.1–146.7°; $[\alpha]_D^{26}$ +48.1° ($CHCl_3$, *c*, 2.075); ν_{max} (KBr) 3530, 1112, 1103, 1097, 1040, and 946 cm^{-1}; n.m.r. (δ):

3.95 (s, 3-ethylenedioxy), 3.75, and 4.00 (AB type q, J = 12 c.p.s., 19-CH_2).

Anal. Calcd. for $C_{29}H_{50}O_3$: C, 77.97; H, 11.28. Found: C, 77.74; H, 11.16.

3-Ethylenedioxy-19-methoxy-5α-cholestane (5c)

Potassium metal (55 mg) was added to a solution of 100 mg of 19-hydroxy compound (**5b**) in 5 ml of dry benzene, and the mixture was refluxed for 2 h with vigorous stirring. Then methyl iodide (2 ml) was added and the refluxing was continued for 3 h (15). After cooling, methanol was added, the reaction mixture was diluted with ether, and the solution was washed with water and dried over sodium sulfate. Evaporation of the solvent gave the crude product (92 mg), which was purified by chromatography on alumina eluting with *n*-hexane–chloroform (10:1). Recrystallization of the product purified by chromatography gave 70 mg of the pure methoxy compound (**5c**), m.p. 128–129°; $[\alpha]_D^{26}$ +30.0° ($CHCl_3$, *c*, 1.340); ν_{max} (KBr) 1110, 1096, 1070, 978, and 810 cm^{-1}; n.m.r. (δ): 3.32 (s, OCH_3), 3.51 (s, 19-CH_2), 3.97 (s, 3-ethylenedioxy).

Anal. Calcd. for $C_{30}H_{52}O_3$: C, 78.20; H, 11.38. Found: C, 78.38; H, 11.52.

19-Methoxy-5α-cholestan-3-one (1d)

A solution of 140 mg of **5c** and 14 mg of *p*-toluenesulfonic acid in 20 ml of anhydrous acetone was refluxed for 15 h. After cooling, the solution was diluted with ether and washed with sodium bicarbonate solution and water, and dried over sodium sulfate. The crude product obtained was recrystallized from acetone–methanol; yield, 90 mg, m.p. 104–105°; ν_{max} (KBr) 1723, 1110, and 960 cm^{-1}; n.m.r. (δ): 3.33 (s, OCH_3), 3.62 (s, 19-CH_2); o.r.d. (*c*, 0.0059, dioxane, 20°): $[\phi]_{450}$ +170°, $[\phi]_{315}$ +1970°, $[\phi]_{291}$ 0°, $[\phi]_{273}$ −1100°, $[\phi]_{260}$ −850°.

Anal. Calcd. for $C_{28}H_{48}O_2$: C, 80.71; H, 11.61. Found: C, 80.62; H, 11.92.

19-Chloro-5α-cholestan-3-one (1e)

Oxidation of 3β-hydroxy-19-chloro-5α-cholestane with 8 *N* chromic–sulfuric acid solution at 0–5° for 30 min gave **1e**, which was recrystallized from methanol, m.p. 107.2–108°; ν_{max} (KBr) 1717, 778, and 730 cm^{-1}; n.m.r. (δ): 3.86 and 4.02 (AB type q, J = 13 c.p.s., 19-CH_2); o.r.d. (*c*, 0.0053, dioxane, 20°): $[\phi]_{450}$ +240°, $[\phi]_{315}$ +1810°, $[\phi]_{291}$ 0°, $[\phi]_{273}$ −930°, $[\phi]_{260}$ −710°.

Anal. Calcd. for $C_{27}H_{45}OCl$: C, 77.01; H, 10.77. Found: C, 76.98; H, 11.05.

6β,19-Epoxy-5α-cholestan-3-one (2)

The epoxy compound (**2**) was synthesized by usual oxidative cyclization of 3β-acetoxy-6β-hydroxy-5α-cholestane with lead tetraacetate – iodine (16, 17) followed by hydrolysis and oxidation. Recrystallization of the crude product from methanol gave a pure product, m.p. 131–132.5°; ν_{max} (KBr) 1725, 1490, 1034, 1022, and 960 cm^{-1}; n.m.r. (δ): 3.95 (s, 19-CH_2); o.r.d. (*c*, 0.0019, dioxane, 20°): $[\phi]_{450}$ +760°, $[\phi]_{315}$ +6290°, $[\phi]_{307}$ +5650° (shoulder), $[\phi]_{292}$ 0°, $[\phi]_{270}$ −5140°, $[\phi]_{260}$ −4700°.

Anal. Calcd. for $C_{27}H_{44}O_2$: C, 80.94; H, 11.07. Found: C, 81.11; H, 11.13.

Reduction of 5α-Cholestan-3-one Derivatives with Sodium Borohydride

A solution of 20 mg of 5α-cholestan-3-one in 2 ml of methanol was treated with 20 mg of sodium borohydride at room temperature for 30 min. After addition of a small amount of acetic acid, the reaction mixture was treated with water and ether, and the ethereal extract was washed with water to neutrality. The reduction product was analyzed by gas–liquid chromatography (g.l.c.) as the trimethylsilyl ether.

Catalytic Hydrogenation of 5α-Cholestan-3-one Derivatives over Platinum Catalyst

(*A*) A solution of 10 mg of **1a** in 1 ml of acetic acid was hydrogenated in the presence of 3 mg of pre-reduced platinum oxide under atmospheric pressure at room temperature for 2 h. After the catalyst was removed by decantation, ether and water were added. The ethereal solution was washed with sodium bicarbonate solution and with water, dried, and evaporated. The residue was analyzed by g.l.c. as above.

(*B*) A solution of 10 mg of **1a** in 1 ml of ethanol was hydrogenated with 5 mg of pre-reduced platinum oxide for 2 h. After addition of ether, the catalyst was removed by filtration. Evaporation of the solvent *in vacuo* gave a product, which was analyzed by g.l.c. as above.

Acknowledgments

The authors wish to express their appreciation to Teikoku Hormone Manufacturing Company, Ltd., for the elemental analyses. Part of the expenses have been covered by the Grant in Aid for Fundamental Scientific Research of the Ministry of Education.

1. G. Vavon and B. Jakubowicz. Bull. Soc. Chim. France, **53**, 581 (1933).
2. L. Ruzicka, H. Brüngger, E. Eichenberger, and J. Meyer. Helv. Chim. Acta, **17**, 1407 (1934).
3. J. T. Edward and J. M. Ferland. Can. J. Chem. **44**, 1311 (1966).
4. J. H. Brewster. J. Am. Chem. Soc. **76**, 6361 (1954).
5. Y. Watanabe, Y. Mizuhara, and M. Shiota. J. Org. Chem. **31**, 3785 (1966).
6. Y. Watanabe, Y. Mizuhara, and M. Shiota. J. Org. Chem. **33**, 468 (1968).
7. P. Crabbé. Optical rotatory dispersion and circular dichroism in organic chemistry. Holden-Day, San Francisco. 1965. p. 110.
8. L. H. Knox, E. Blossey, H. Carpio, L. Cervantes, P. Crabbé, E. Verlarde, and J. A. Edwards. J. Org. Chem. **30**, 2198 (1965).
9. B. Berkoz, E. Denot, and A. Bowers. Steroids, **1**, 251 (1963).
10. J. F. Bagli, P. E. Morand, and R. Gaudry. J. Org. Chem. **28**, 1207 (1963).
11. R. M. Moriarty and T. D. J. D'Silva. Tetrahedron Letters, **21**, 547 (1965).
12. D. Hauser, K. Heusler, J. Kalvoda, K. Schaffner and O. Jeger. Helv. Chim. Acta, **47**, 1961 (1964).
13. E. Caspi and J. Wicha. Chem. Commun. 209 (1966).
14. H. J. Dauben, Jr., B. Löken, and H. J. Ringold. J. Am. Chem. Soc. **76**, 1359 (1954).
15. C. R. Narayanan and K. N. Iyer. J. Org. Chem. **30**, 1734 (1965).
16. J. Kalvoda, K. Heusler, H. Ueberwasser, G. Anner, and A. Wettstein. Helv. Chim. Acta, **46**, 1361 (1963).
17. M. Akhtar and D. H. Barton. J. Am. Chem. Soc. **86**, 1528 (1964).

Can. J. Chem. Downloaded from www.nrcresearchpress.com by 210.87.254.6 on 09/05/12
For personal use only.

Can. J. Chem. Downloaded from www.nrcresearchpress.com by 210.87.254.5 on 09/05/12
For personal use only.

Structures of yeast mannans containing both α- and β-linked D-mannopyranose units[1]

P. A. J. GORIN, J. F. T. SPENCER, AND S. S. BHATTACHARJEE[2]
Prairie Regional Laboratory, National Research Council of Canada, Saskatoon, Saskatchewan

Received December 18, 1968

Several mannans from yeasts give proton magnetic resonance spectra with distinctive H-1 signals at higher field than τ 4.55. A number of these mannans were investigated polarimetrically and each has a specific rotation corresponding to a mixture of α- and β-D-linkages. Four were partially hydrolyzed and shown to have most of the α-linkages in the main chains and the β-linkages in the side chains. Detailed structural investigations showed that the *Pichia pastoris* mannan probably has an α-(1→6)-D-mannopyranosyl main-chain substituted in the 2-positions with a substantial proportion of *O*-α-D-mannopyranosyl-(1→2)-*O*-β-D-mannopyranosyl-(1→2)-*O*-β-D-mannopyranosyl-(1→2)-*O*-α-mannopyranosyl side-chains (**1**). The related mannan from *Citeromyces matritensis* has a similar main-chain, which is substituted in the 2-positions by α-D-mannopyranosyl units and β-(1→2)-pyranose-linked D-mannotriosyl and perhaps mannobiosyl side-chains (**2**).

Canadian Journal of Chemistry, 47, 1499 (1969)

The proton magnetic resonance (p.m.r.) spectra of yeast mannans and galactomannans in D_2O at 70° have been studied and used in structural and taxonomic studies (1–4). The spectra obtained from 28 out of the 189 species examined contained a substantial proportion of H-1 signals at higher field than τ 4.55 (Table I[3]), in contrast with the majority of yeast mannan and galactomannan spectra which have H-1 signals at τ 4.0–4.55. The high field signals were of interest to us since they suggested β-D-pyranoside units on consideration of the relative chemical shifts of H-1 signals of the α- and β-anomers of the methyl D-mannosides. Methyl β-D-mannopyranoside H-1 has τ 4.92 compared with the H-1 signals of its α-anomer (τ 4.71), methyl α-D-mannofuranoside (τ 4.50) and its β-anomer (τ 4.58). To check our conclusion, the specific rotations of a few of the yeast mannans giving high field signals were measured (Table II) and found to be intermediate between those of mannans containing α-D-linkages (baker's yeast mannan, +88° (5)) and β-D-linkages (*Rhodotorula glutinis* mannan, −78° (6)). Since each of the examined mannans (Table II) gave only one peak on ultracentrifugation, it appeared likely that each molecular species contained both α- and β-D-linkages;[3] a hitherto unreported structural feature in yeast mannans. A number of mannans

TABLE I

Yeast* containing mannans with H-1 signals at higher field than τ 4.55

Mannan-producing yeast	Yield of mannan based on dry cell-weight (%)
Brettanomyces anomalus NCYC 449	3
Brettanomyces bruxellensis NCYC 362	2
Brettanomyces dublinensis NCYC 615	3
Brettanomyces lambicus NCYC 395	2
Candida obtusa UC 60-17	4
Candida lusitaniae CBS 4413	6
Citeromyces matritensis CBS 2764	3
Debaryomyces castelli CBS 2923	2
Debaryomyces hansenii CBS 767	3
Debaryomyces kloeckeri NCYC 8	1
Debaryomyces phaffii PRL 199-64	2
Debaryomyces subglobosus PRL RS4	2
Hanseniaspora osmophila JPV 72	4
Kloeckera africana CBS 277	4
Kloeckera magna CBS 105	5
Pichia farinosa HO E 3b	6
Pichia ohmeri CBS 2557	9
Pichia pastoris PRL 63-208	9
Pichia toletana UC 66-1015	6
Pichia vanrijii JPV 143	6
Saccharomyces lodderi JPV 193	2
Saccharomyces microellipsodes NRRL Y-1549	4
Saccharomyces pretoriensis JPV 111	6
Saccharomyces rosei PRL 16B5	7
Saccharomyces vafer NCYC 678	4
Schwanniomyces alluvius UC 54-83	7
Schwanniomyces castelli CBS 2863	7
Torulopsis colliculosa NCYC 608	3

*The yeasts were obtained from the following sources: NCYC—National Collection of Yeast Cultures, Brewing Industry Research Foundation, Nutfield, Surrey, England; CBS—Centraalbureau voor Schimmelcultures, Yeast Division, Delft, The Netherlands; UC—Collection of Dr. H. J. Phaff, University of California, Davis, California; JPV—Collection of Dr. J. P. van der Walt, Pretoria, South Africa; HO—Collection of Dr. H. Onishi, Noda Institute of Scientific Research, Japan; PRL—Prairie Regional Laboratory, National Research Council, Saskatoon, Sask.

[1]NRCC No. 10620.
[2]NRCC Postdoctorate Fellow, 1967–1969.
[3]*Rhodotorula* spp. with mannans containing β-(1→3)- and β-(1→4)-D-mannopyranosyl units (6) are excluded from the Table.

TABLE II

Specific rotations of yeast mannans with H-1 signals at relatively high field, and the mannans formed on partial hydrolysis

Source of mannan	High field signals, τ	Specific rotation	Specific rotation of acid-degraded mannan with yield
Brettanomyces anomalus	4.60, 4.67	+1°	+55°, 31%
Citeromyces matritensis	4.55, 4.61	−12°	+44°, 11.5%
Pichia pastoris	4.56, 4.60	+12°	+50°, 22%
Saccharomyces lodderi	4.68	−34°	—
Saccharomyces rosei	4.60	−16°	+20°, 27%

were therefore selected for further structural examination.

The mannans of *Pichia pastoris*, *Citeromyces matritensis* (the perfect form of *Torulopsis globosa* (7)), *Bretannomyces anomalus*, and *Saccharomyces rosei* were subjected to a preliminary structural investigation. The β-linkages appeared to be mainly in the side chains since partial acid hydrolysis with 0.33 *N* H_2SO_4 at 100° (8) provided polymers with higher specific rotations than the parent mannans (Table II). The p.m.r. spectra of each of the degraded mannans contained a strong signal at about τ 4.57, which corresponds to the chemical shift of H-1 of a linear mannan containing α-(1→6)-D-mannopyranosyl units (Fig. 1). Such a polymer has been obtained by partial acid hydrolysis of the galactomannan from *Schizosaccharomyces octosporus* and identified by its periodate oxidation characteristics. The H-1 signal patterns in the spectra of the degraded mannans have a strong resemblance to that of degraded baker's yeast mannan, obtained under comparable acid hydrolysis conditions (Fig. 1). The material contains an α-(1→6)-linked D-mannopyranosyl main-chain with some of the units substituted in the 2-positions by α-D-mannopyranosyl units (2, 8).

The structures of the side chains in the mannans of *Pichia pastoris* and *Citeromyces matritensis* were investigated in more detail. The results obtained from the *Pichia* mannan are presented first since they have a bearing on the *Citeromyces* mannan.

Side-chain fragments containing (1→2)-linkages were obtained from *Pichia pastoris* mannan by partial acetolysis which cleaves α-(1→6)-linkages in preference to (1→2)- and (1→3)-D-mannopyranose linkages (9, 10). The product was deacetylated and resolved into di-, tri-, tetra-, and penta-saccharides by cellulose column chromatography. Proton magnetic resonance spectroscopy of each fraction (H-1 region) indicated that only the disaccharide (16% yield) and pentasaccharide (26% yield) were homogeneous. The former has a spectrum and specific rotation corresponding to 2-*O*-α-D-mannopyranosyl-D-mannose, but the latter required further investigation to elucidate its structure. The penta-

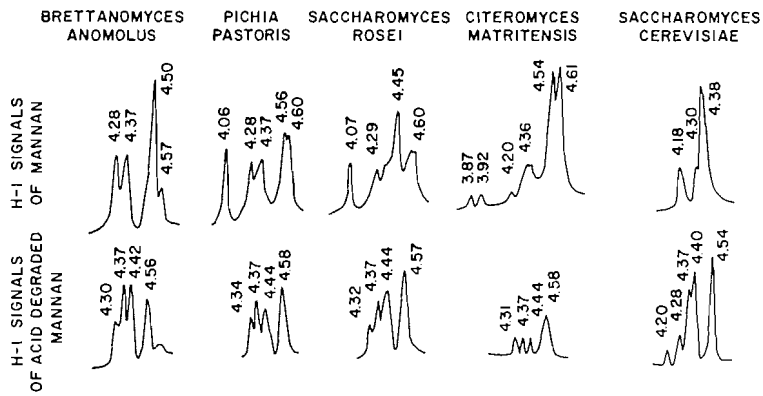

FIG. 1. H-1 signals of proton magnetic resonance spectra of yeast mannans and acid-degraded mannans.

Can. J. Chem. Downloaded from www.nrcresearchpress.com by 210.87.254.5 on 09/05/12
For personal use only.

Can. J. Chem. Downloaded from www.nrcresearchpress.com by 210.87.254.5 on 09/05/12
For personal use only.

saccharide is linear and contains (1→2)-linked mannopyranosyl units, since methylation–fragmentation gave 2,3,4,6-tetra-*O*-methylmannose (1 part) and 3,4,6-tri-*O*-methylmannose (3.8 parts), identified and estimated by gas–liquid chromatography (g.l.c.) of the methyl glycosides and the trimethylsilyl ethers of the methyl glycosides (10, 11). The presence of both α- and β-linkages was indicated by a specific rotation of −3°. The sequence of the linkages was determined as follows. Fragments were obtained from the pentasaccharide by a Smith degradation (12) involving oxidation by lead tetraacetate in acetic acid, followed by sodium borohydride reduction and partial hydrolysis (pH 2, 100°) of the resulting alditols. Following use of 3 moles/mole of oxidant for 3 h, mannotetraosyl mannitol, mannotriosyl mannitol, and mannobiosyl mannitol were formed and isolated. With a higher proportion of oxidant over a longer period of time, 2-*O*-α-D-mannopyranosyl-D-mannitol was obtained and tentatively identified by the chemical shift of the H-1 proton and its mobility on a paper chromatogram. The degradation occurs according to the scheme shown in Fig. 2 and assignments of configuration were made by comparing the specific rotations of consecutively related pairs of compounds that were formed during the degradation. For example, the reduced trisaccharide must contain a β-linkage since it has a lower specific rotation (−14°) than 2-*O*-α-D-mannopyranosyl-D-mannitol (+40°). By consideration of the consecutive increases or decreases in specific rotation on going from reduced trisaccharide to reduced tetrasaccharide to reduced pentasaccharide, the latter compound must be *O*-α-D-mannopyranosyl-(1→2)-*O*-β-D-mannopyranosyl-(1→2)-*O*-β-D-mannopyranosyl-(1→2)-*O*-α-D-mannopyranosyl-(1→2)-D-mannitol.

Since insufficient 2-*O*-α-D-mannopyranosyl-D-mannitol was obtained for a measurement of specific rotation, another approach was used to prove the configuration of the α-linkage adjacent to the reducing end-unit of the pentasaccharide. The reducing end-unit of the pentasaccharide was removed by the following method (13). Bromine oxidation, followed by saponification gave the sodium salt of the aldonic acid, which was oxidized with lead tetraacetate to the mannotetraosyl tartronic acid semialdehyde derivative, and partial hydrolysis gave *O*-α-D-mannopyranosyl-(1→2)-*O*-β-D-mannopyranosyl-(1→2)-*O*-β-D-mannopyranosyl-(1→2)-D-mannose which was purified by cellulose column chromatography. The alditol obtained by sodium borohydride reduction was homogeneous since it gave 3 H-1 signals of equal magnitude. Its specific rotation, −27°, is lower than that of the alditol (−5°) obtained by reduction of the pentasaccharide, indicating that the glycosidic linkage attached to the reducing end-unit of the pentasaccharide has an α-configuration.

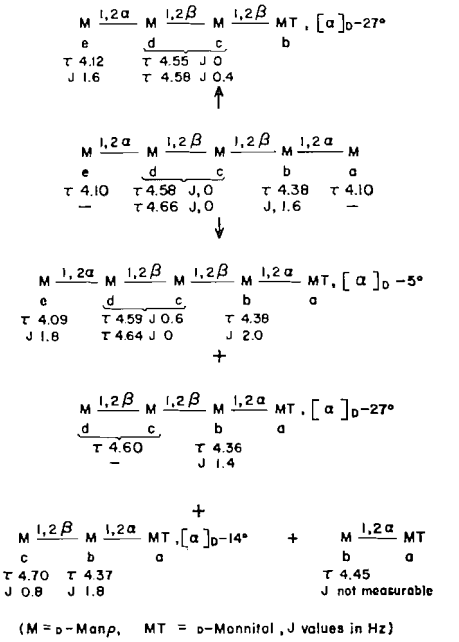

FIG. 2. Specific rotations, τ and *J* values of H-1 signals of fragments obtained from the *Pichia pastoris* pentasaccharide.

The mannan of *P. pastoris* was analyzed by the methylation–fragmentation technique, and the resulting partly methylated mannoses were characterized by g.l.c. of the methyl glycosides and the trimethylsilyl derivatives of the methyl glycosides. These fragments were 2,3,4,6-tetra-*O*-methylmannose, 3,4,6-tri-*O*-methylmannose, and 3,4-di-*O*-methylmannose, in accord with the probable structure of **1** containing an α-(1→6)-linked D-mannopyranosyl main-chain substituted in the 2-positions with a substantial proportion of (1→2)-linked D-mannopyranosyl side-chains. An average side-chain length of 3 is indicated by the formation of 0.25 mole of formic acid per mole of anhydromannose unit on periodate oxidation.

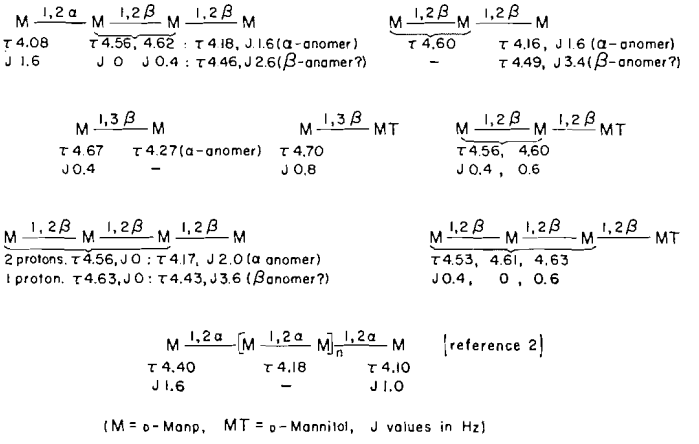

FIG. 3. τ and *J* values of H-1 signals of mannose oligosaccharides.

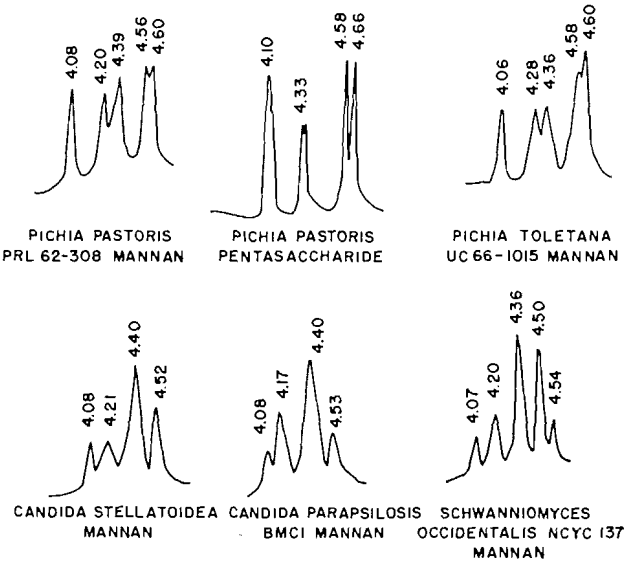

FIG. 4. Proton magnetic resonance spectra containing a signal at ca. τ 4.08.

The low field H-1 p.m.r. signal of the pentasaccharide at τ 4.10 corresponds to 2 protons and is of interest because signals of this chemical shift occur in spectra of a number of yeast mannans. The signal arises partly from the reducing end *a* (Fig. 2) by analogy with the reducing end-unit signal of α-(1→2)-linked D-mannopyranosyl oligosaccharides at τ 4.10 (2). In the case of mannose oligosaccharides containing a β-(1→2)-linkage in this position, signals of higher chemical shift are observed (Fig. 3). The other proton contributing to the signal at τ 4.10 is that of the non-reducing end-unit *e* since a low field signal is absent from mannotriosyl mannitol derived by the Smith degradation. Of 88 types of spectra from yeast mannans and galactomannans examined, 16 contain a signal close to τ 4.08, which may be due to (1→2)-linked side-chains with the terminal unit α-linked to the adjacent unit which is then followed by consecutive β-linkages. This signal is strongest in the spectra of *Pichia pastoris*, *Pichia toletana*, and *Candida* sp. CBS 5389 mannans. Weaker signals at τ 4.08 are present in spectra of mannans from *Candida parapsilosis*

Can. J. Chem. Downloaded from www.nrcresearchpress.com by 210.87.254.5 on 09/05/12
For personal use only.

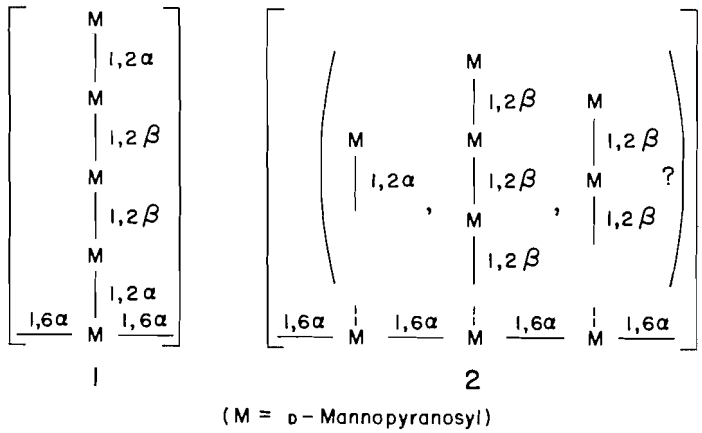

FIG. 5. Structures of mannans of *Pichia pastoris* (1) and *Citeromyces matritensis* (2).

(BMC 1), *Candida stellatoidea*, *Hansenula fabianii*, *Torulopsis halophila*, *Torulopsis famata*, *Torulopsis* sp. 62-304, *Schwanniomyces occidentalis* (Fig. 4). Low field signals are prominent in the p.m.r. spectra of galactomannans from *Candida lipolytica*, *Dipodascus albidus*, *Nadsonia fulvescens*, and *Trichosporon fermentans*, but these appear to arise from structures associated with D-galactopyranosyl units (1).

The nature of the side chains in *Citeromyces matritensis* mannan was determined by partial acetolysis over a shorter period of time than that described for the *P. pastoris* mannan. 2-*O*-α-D-Mannopyranosyl-D-mannose (10% yield), a trisaccharide (4% yield), and a tetrasaccharide fraction (5% yield) were isolated. The trisaccharide fraction contained only (1→2)-linkages, as shown by the methylation–fragmentation technique, but its homogeneity could not be determined from the H-1 region of its p.m.r. spectrum. This was complex and it appeared that an appreciable proportion of β-anomer existed in addition to the α-anomer. However, reduction with sodium borohydride gave an alditol with 2 equal H-1 signals, as would be expected from a single compound. In addition, its specific rotation of −36° indicates the presence of 2 β-D-linkages since *O*-β-D-mannopyranosyl-(1→2)-*O*-α-D-mannopyranosyl-(1→2)-D-mannitol obtained on Smith degradation of the *Pichia pastoris* pentasaccharide, has a higher rotation of −10°. The tetrasaccharide fraction was characterized as containing β-(1→2)-linked D-mannopyranose units by similar considerations of its methylation–fragmentation products and specific rotation. The derived alditol gave 3 equal H-1 signals and its specific rotation of −58° is lower than the −25° of *O*-β-D-mannopyranosyl-(1→2)-*O*-β-D-mannopyranosyl-(1→2)-*O*-α-D-mannopyranosyl-(1→2)-D-mannitol, obtained by the Smith degradation of the *P. pastoris* pentasaccharide. *O*-α-D-Mannopyranosyl-(1→2)-*O*-β-D-mannopyranosyl-(1→2)-*O*-β-D-mannopyranosyl-(1→2)-D-mannitol, described earlier in this section, has a similar specific rotation of −27°.

Methylation–fragmentation of *Citeromyces matritensis* mannan gave 2,3,4,6-tetra-*O*-methylmannose, 3,4,6-tri-*O*-methylmannose, and 3,4-di-*O*-methylmannose. The mannan probably contains an α-(1→6)-D-mannopyranose main-chain, substituted in the 2-positions by side chains. The side chains consist of single mannopyranosyl units attached α-D-(1→2)- to the main chain, and β-D-(1→2)-pyranosidically-linked mannotriosyl units attached by β-linkages to the main chain (**2**). 2-*O*-β-D-Mannopyranosyl-D-mannosyl side-chains are not necessarily present since the β-D-(1→2)-linked trisaccharide obtained in the acetolysis experiment could have arisen by partial degradation of the homologous tetrasaccharide. The formation of 0.40 mole of formic acid per mole of anhydromannose unit on periodate oxidation shows that the average side-chain length is 1.5 units, shorter than that of the *Pichia pastoris* mannan.

The chemical shifts of the H-1's of the mannose-containing oligosaccharides obtained during the course of this investigation are recorded in Figs.

Can. J. Chem. Downloaded from www.nrcresearchpress.com by 210.87.254.5 on 09/05/12
For personal use only.

Can. J. Chem. Downloaded from www.nrcresearchpress.com by 210.87.254.5 on 09/05/12
For personal use only.

2 and 3. It can be seen that the H-1's of mannopyranosyl units with β-linkages are at higher field than those of corresponding α-linked analogues, and with the exception of reducing end-units the J values of the β-linked units are smaller. It can also be observed that oligosaccharides with a β-linkage attached to the 2-position of the reducing end give complex p.m.r. spectra since, in contrast to oligosaccharides with an α-linkage in this position, both the α- and β-forms of the reducing sugar can be detected.

Experimental

The cultural methods used in production of yeast cells and the method of isolation of mannans from the cells are summarized in a previous publication (1). The yields of mannans based on dry cell-weight are recorded in Table I. The mannans were tested for homogeneity by sedimentation at 59 000 r.p.m. as 0.15, 0.30, and 0.60% solutions in 0.5% aqueous sodium chloride. The p.m.r. spectra of the mannans were obtained using a 100 Mc.p.s. Varian spectrometer from 20% solutions in D_2O at 70° with tetramethylsilane as the external standard. The p.m.r. spectra of oligosaccharides were obtained under identical conditions, except for the use of lower sugar concentrations. The mannans from *P. pastoris* and *C. matritensis* were hydrolyzed to D-mannose which was crystallized and identified. Paper chromatography was used to identify mannose from the other mannans. Paper chromatography of oligosaccharides was carried out using *n*-butanol – ethanol – water (2:1:1 v/v/v) as solvent and ammoniacal silver nitrate as spray reagent.

Methylation–Fragmentation of Mannans and Mannose-Containing Oligosaccharides

The mannans and mannose-containing oligosaccharides were methylated by the Haworth procedure (14) and the partially methylated products were further methylated by the Kuhn method (15) for a week. The fully methylated materials did not show hydroxyl absorption in the infrared (i.r.) at 3600 cm^{-1} on examination of 0.8% chloroform solutions in a cell with a path length of 5 mm.

The methylated mannans were partially methanolyzed in refluxing 3% methanolic hydrogen chloride overnight and the product hydrolyzed in N H_2SO_4 at 100° overnight. The partially methylated mannose derivatives were fractionated into di-*O*-, tri-*O*-, and tetra-*O*-methyl fractions on cellulose columns by the previously described method (2) from both mannans. These components were shown to be 3,4-di-*O*-, 3,4,6-tri-*O*-, and 2,3,4,6-tetra-*O*-methylmannose by a g.l.c. method (10, 11).

Periodate Oxidation Characteristics of Mannans from P. pastoris and C. matritensis

After 1, 2, and 3 days the *P. pastoris* mannan consumed 1.13, 1.20, and 1.21 moles/mole of anhydromannose unit with formation of 0.20, 0.24, and 0.25 mole/mole of acid, respectively. For the *C. matritensis* mannan the respective consumption figures were 1.20, 1.25, and 1.34, and acid production of 0.35, 0.40, and 0.41 mole/mole. Each of the polyalcohols obtained on sodium borohydride reduction of the polyaldehydes gave glycerol (paper chromatogram) on hydrolysis.

Partial Hydrolysis of Mannans

The mannans were partially hydrolyzed as 10% solutions in 0.33 N H_2SO_4 at 100° (2, 8). After 20 h samples were abstracted and residual polysaccharide precipitated by addition of 10 volumes of ethanol. The products were isolated by centrifugation followed by filtration. The specific rotations and yield of degraded mannans are recorded in Table II and their p.m.r. spectra in Fig. 1.

Partial Acetolysis of the P. pastoris Mannan

The mannan (2.0 g) was shaken for 5 days in acetic anhydride (12 ml) – acetic acid (12 ml) containing H_2SO_4 (1.2 ml) at 25°. The reaction mixture was added to excess ice-cold aqueous sodium bicarbonate and after 3 h the acetates were extracted with chloroform, which was evaporated to dryness. The acetates were deacetylated in chloroform–methanol (25:25 ml) containing 0.1 N methanolic sodium methoxide (30 ml). Examination on a paper chromatogram showed mannose-containing disaccharide and oligosaccharides running at 1.4 and 0.31, 0.46, 0.60 and 0.83 the rate of lactose (R_{lact}). The sugars were fractionated on a cellulose column (40 cm × 4.5 cm diameter) using the following acetone–water (v/v) mixture. Four liters of a 6:1 v/v mixture eluted mannose (0.15 g) and a disaccharide fraction (0.34 g) with $[\alpha]_D$ +35° (*c*, 0.9 H_2O) and R_{lact} 1.4, equal H-1 signals at τ 4.12 and 4.42. It consisted predominantly of 2-*O*-α-D-mannopyranosyl-D-mannose although a much smaller signal at τ 4.70 could arise from the non-reducing end H-1 of 2-*O*-β-D-mannopyranosyl-D-mannose. A 4:1 v/v mixture (3 l) eluted trisaccharides (190 mg, R_{lact} 0.83) which gave a complex p.m.r. spectrum indicating a mixture. Similarly the tetrasaccharide fraction (160 mg, R_{lact} 0.72 and a trace at 0.46) eluted with a 7:2 v/v ratio (3 l) was a mixture. Finally a 3:1 v/v mixture (2 l) was used to obtain a pentasaccharide (0.53 g, R_{lact} 0.31), which had H-1 signals at τ 4.10 (2 protons) and 1 proton signals at τ 4.33, 4.58, and 4.66, and $[\alpha]_D$ −3° (*c*, 0.9 H_2O). It was shown to contain only (1→2)-linkages by the methylation–fragmentation technique.

Smith Degradation of the Pichia pastoris Pentasaccharide to Oligosaccharide Alditols

The pentasaccharide (150 mg) was dissolved in water (1 ml) and acetic acid (50 ml) added. Lead tetraacetate (3 moles/mole of pentasaccharide) was dissolved by shaking, and after 3 h excess reagent was destroyed by addition of ethylene glycol (0.5 ml) and oxalic acid (2.9 moles/mole) in acetic acid. Water (200 ml) was added, the solution filtered, and the filtrate evaporated to dryness. Salts were removed by an aqueous suspension of mixed-bed resins followed by filtration. Sodium borohydride (0.2 g) was added to the filtrate and after 1 h Amberlite IR120 (H^+ form) was added, the solution filtered off, and evaporated to a residue which was freed from boric acid by repeatedly dissolving in methanol and evaporating the solution. The products were partially hydrolyzed at 100° for 1 h in an aqueous solution (10 ml) adjusted to pH 2 with H_2SO_4. The solution was neutralized, filtered, and evaporated and on paper chromatography the product gave spots with R_{lact} 0.45, 0.75, and

Can. J. Chem. Downloaded from www.nrcresearchpress.com by 210.87.254.5 on 09/05/12
For personal use only.

1.07 corresponding to mannotetraosyl mannitol, mannotriosyl mannitol, and mannobiosyl mannitol, respectively. The mixture was fractionated on a cellulose column and acetone–water (4:1 v/v) eluted the trisaccharide alditol (18 mg) with R_{lact} 1.07, $[\alpha]_D$ −14° (*c*, 0.6 H_2O) and equal H-1 signals at τ 4.70 and 4.37. A 3:1 v/v mixture eluted the tetrasaccharide alditol (31 mg) with R_{lact} 0.75, $[\alpha]_D$ −27° (*c*, 1.0 H_2O) and H-1 signals at τ 4.60 (2 protons) and 4.36 (1 proton) and a 2:1 v/v mixture eluted the pentasaccharide alditol (23 mg) with R_{lact} 0.45, $[\alpha]_D$ −5° (*c*, 0.8 H_2O) and equal H-1 signals at τ 4.09, 4.38, 4.59, and 4.64. The signal at τ 4.09 was moved downfield on addition of sodium tetraborate and thus arises from an α-linked non-reducing end-unit (2).

An experiment similar to above, but using 6 moles of lead tetraacetate per mole of pentasaccharide over 9 h, was carried out. From the pentasaccharide (200 mg) a product (5 mg) was formed and isolated and corresponded to 2-*O*-α-D-mannopyranosyl-D-mannitol on a paper chromatogram. It had an H-1 signal at τ 4.45.

Conversion of the Pichia pastoris Pentasaccharide to a Reduced Mannotetraose

The pentasaccharide (200 mg) was dissolved in water (20 ml) containing bromine (1 ml). After 6 days excess bromine was removed by evaporation, the solution neutralized (Ag_2CO_3), filtered, treated with Amberlite IR120 (H^+ form), and evaporated to a small volume. The sodium salt of the aldonic acid was obtained by addition of sodium hydroxide and heating at 100°. The solution was evaporated to approximately 3 ml and acetic acid (100 ml) added, followed by lead tetraacetate (4 moles/mole of aldonate). After 2 h the excess oxidant was destroyed and removed by the procedure described above. The mannotetraosyl tartronic acid semialdehyde derivative, thus formed, was converted to a mannotetraose by hydrolysis in 50% aqueous acetic acid (20 ml) at 100° for 1 h. Fractionation of the product on a cellulose column using acetone–water (3:1 v/v) as eluant gave the mannotetraose (71 mg) with $[\alpha]_D$ −23° (*c*, 0.9 H_2O) and single proton H-1 signals at τ 4.08, 4.56, 4.62, and others at τ 4.18 (0.6 proton) and τ 4.46 (0.5 proton). The alditol derived by sodium borohydride reduction had $[\alpha]_D$ −27° (*c*, 0.7 H_2O) and equal H-1 signals at τ 4.12, 4.55, and 4.58.

Partial Acetolysis of the C. Matritensis Mannan

The mannan was acetolyzed for 3 days using the same reagents and quantities as in the acetolysis of the *P. pastoris* mannan. The acetates were converted to the free sugars which were fractionated on a cellulose column using the eluants described previously. Mannose (1.1 g), 2-*O*-α-D-mannopyranosyl-D-mannose (194 mg), with $[\alpha]_D$ +37° (*c*, 0.7 H_2O) and equal H-1 signals at τ 4.12 and 4.42, *O*-β-D-mannopyranosyl-(1→2)-*O*-β-D-mannopyranosyl-(1→2)-D-mannose (92 mg) with R_{lact} 0.97, $[\alpha]_D$ −31° (*c*, 0.6 H_2O) and H-1 signals at τ 4.60 (2 protons), 4.49 (0.2 proton), and 4.16 (0.7 proton), and *O*-β-D-mannopyranosyl-(1→2)-*O*-β-D-mannopyranosyl-(1→2)-*O*-β-D-mannopyranosyl-(1→2)-D-mannose (103 mg) with R_{lact} 0.85, $[\alpha]_D$ −49° (*c*, 0.4 H_2O) and H-1 signals at τ 4.56 (2 protons), 4.63 (1 proton), 4.43 (0.3 proton), and 4.17 (0.7 proton) were obtained. The tri- and tetrasaccharide were shown to contain only (1→2)-linked D-mannopyranosyl linkages by the methylation–fragmentation g.l.c. technique. The respective alditols derived by sodium borohydride reduction of the tri- and tetrasaccharide had $[\alpha]_D$ −36° (*c*, 0.7 H_2O) with equal H-1 signals at τ 4.60 and 4.56 and $[\alpha]_D$ −58° (*c*, 0.3 H_2O) with equal H-1 signals at τ 4.53, 4.61, and 4.63.

Acknowledgments

The authors thank Mr. M. Mazurek for preparation of proton magnetic resonance spectra. Thanks are also due to Mr. R. J. Magus and Mr. N. Gardner for technical assistance, and Mr. W. C. Haid for microanalytical and infrared determinations. The illustrations were drawn by Mr. E. Knapp and Mr. A. Lutzko.

1. P. A. J. Gorin and J. F. T. Spencer. Can. J. Chem. **46**, 2299 (1968).
2. P. A. J. Gorin, M. Mazurek, and J. F. T. Spencer. Can. J. Chem. **46**, 2305 (1968).
3. J. F. T. Spencer and P. A. J. Gorin. J. Bacteriol. **96**, 180 (1968).
4. J. F. T. Spencer and P. A. J. Gorin. Antonie van Leeuwenhoek. J. Microbiol. Serol. **35**, 33 (1969).
5. W. N. Haworth, R. L. Heath, and S. Peat. J. Chem. Soc. 833 (1941).
6. P. A. J. Gorin, K. Horitsu, and J. F. T. Spencer. Can. J. Chem. **43**, 950 (1965).
7. J. Lodder, W. Ch. Slooff, and N. J. W. Kreger van Rij. *In* The chemistry and biology of yeasts. *Edited by* A. H. Cook. Academic Press, Inc., New York. 1958.
8. S. Peat, W. H. Whelan, and T. E. Edwards. J. Chem. Soc. 29 (1961).
9. P. A. J. Gorin and A. S. Perlin. Can. J. Chem. **34**, 1796 (1956).
10. Y-C Lee and C. E. Ballou. Biochem. **4**, 257 (1965).
11. S. S. Bhattacharjee and P. A. J. Gorin. Can. J. Chem. **47**, 1207 (1969).
12. I. J. Goldstein, G. W. Hay, B. A. Lewis, and F. Smith. Abstr. Paper Am. Chem. Soc. Meeting 135, 3D (1959).
13. P. A. J. Gorin and A. S. Perlin. Can. J. Chem. **35**, 262 (1957).
14. W. N. Haworth. J. Chem. Soc. 8 (1915).
15. R. Kuhn, H. Trischmann, and I. Löw. Angew. Chem. **67**, 32 (1955).
16. P. A. J. Gorin and A. S. Perlin. Can. J. Chem. **39**, 2474 (1961).

Can. J. Chem. Downloaded from www.nrcresearchpress.com by 210.87.254.6 on 09/05/12
For personal use only.

Signs of proton–proton and proton–fluorine spin–spin coupling constants in 2-fluoro-3-methylpyridine. Sigma and pi contributions to coupling in a nitrogen heterocycle[1]

T. SCHAEFER,[2,4] S. S. DANYLUK, AND C. L. BELL[2,3]

Division of Biological and Medical Research, Argonne National Laboratory, Argonne, Illinois 60439

Received November 13, 1968

The signs of all proton–proton and proton–fluorine spin–spin coupling constants in 2-fluoro-3-methylpyridine have been determined by double and triple resonance experiments. The signs of the long-range coupling constants, J^{H,CH_3} and J^{F,CH_3} are the same as in fluorotoluene derivatives. Their magnitudes are consistent with the assumption that the nitrogen atom primarily polarizes the σ bonds in the molecule, leaving the π contribution to the long-range coupling relatively unaffected.

Canadian Journal of Chemistry, 47, 1507 (1969)

Introduction

Hoffman's (1, 2) methyl group replacement technique (=C—H → =C—CH_3) has been used to measure π electron contributions, $J(\pi)$, to ring proton – ring proton coupling constants, J^{HH}, in toluene derivatives (3–5), as well as to ring proton – ring fluorine couplings, J^{HF}, in fluorotoluene derivatives (6). Since $J_{o,p}^{H,CH_3} < 0 < J_{o,p}^{F,CH_3}$ it follows (2) that $J_o^{HF}(\pi) < 0$ while $J_{o,p}^{H,H}(\pi) > 0$. These results are in agreement with theory and experiment (7–14), which give the hyperfine interaction constants Q_{CH}, Q_{CCH}, and Q_{CF} as negative, positive, and positive, respectively.

In general, the π contributions to J_o^{HH} and J_o^{HF} in benzene derivatives are much smaller than σ contributions (7) and, therefore, substituent effects upon these couplings can be rationalized most easily in terms of an inductive, alternating model (14, 15) primarily involving the polarization of σ bonds by the substituent. These effects are expected to decrease rapidly with an increase in the number of intervening bonds between the substituent and the carbon atoms to which H or F are attached. In pyridine derivatives the electronegative nitrogen atom is directly bonded to the carbon atoms in question. Consequently, the changes in magnitude of J^{HH} and J^{HF} are strikingly greater than in benzene derivatives (15–17), reflecting the relatively large polarization of the σ core by the nitrogen atom. The polarization of the σ core is also apparent in the chemical shifts of ^{13}C and ^{1}H in pyridine (18, 19).

The question therefore arises of how strongly the polarized σ core influences the π electrons. A strong influence should result in changes in J^{H,CH_3} and J^{F,CH_3} since they are presumably dominated by a π electron mechanism. In this paper we determine the signs and magnitudes of $J_{o,m,p}^{H,CH_3}$ and of J_o^{F,CH_3} in 2-fluoro-3-methylpyridine and compare them to those found in benzene derivatives.

Experimental

2-Fluoro-3-methylpyridine from Peninsular Chem-Research, Inc. was examined as dilute solutions in tetramethylsilane (TMS) and benzene-d_6. The resonance from proton-6 (H_6) consisted of a broad (10 c.p.s.) peak. Addition of sufficient trifluoroacetic acid (TFA) to the TMS solution to serve as an alternate locking signal also relaxed the ^{14}N spin states (20). The effect of the ^{14}N–H_6 coupling was still observable as a slight broadening of the H_6 resonance peaks but did not now obscure the splittings due to the coupling between H_6 and the other nuclei in the molecule. Decomposition of 2-fluoro-3-methylpyridine was noted in concentrated hydrochloric acid and in TFA solutions with the most likely products being pyridones (21).

Solutions were degassed by the freeze–pump–thaw technique. Proton magnetic resonance spectra were recorded on a DA-60-I spectrometer in the frequency sweep mode. Double and triple resonance experiments were performed in the usual manner (22–25). When decoupling the methyl protons it was necessary to lock to the TFA signal. Double resonance experiments were also carried out in benzene-d_6 solutions in order to check that the presence of small amounts of TFA in the TMS solution had not noticeably affected the magnitudes or signs of the coupling constants.

[1]This work was performed under the auspices of the U.S. Atomic Energy Commission.

[2]Visiting summer scientist, 1968.

[3]Permanent address: University of Illinois Medical Center, Chicago, Illinois 60612.

[4]Permanent address: University of Manitoba, Winnipeg, Manitoba.

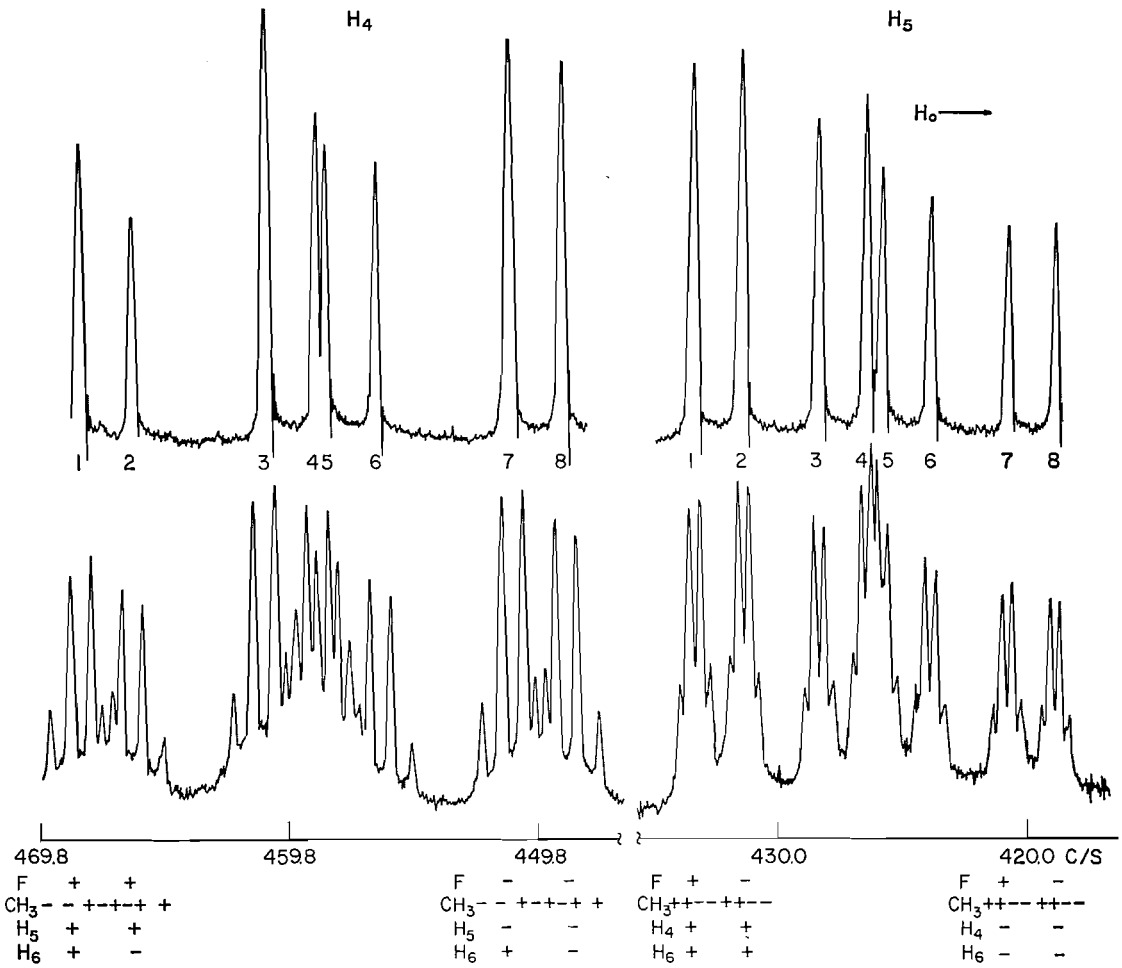

FIG. 1. The lower part shows the proton resonance spectrum of H_4 and H_5 in 2-fluoro-3-methylpyridine (**1**) in TMS at 60 Mc.p.s. As in all figures the scale is to low field of internal TMS. The spin states of coupled nuclei are given with the convention that the plus sign under the low-field resonance peak of a proton refers to a positive coupling between it and the coupled nucleus. The upper part shows the eight resonance peaks of each of H_4 and H_5 when the methyl protons are decoupled. These peaks, each of which refers to a quartet in the single resonance spectrum, are numbered from low to high field and are referred to in later figures.

Results

1. Relative Signs of Coupling Constants

The proton resonance spectrum of H_4 and H_5 of **1** is presented in the lower part of Fig. 1. As in all the figures, the external magnetic field increases from left to right. The upper part of Fig. 1 shows the eight resonance peaks of each proton when the methyl protons are decoupled. The spin states of the coupled nuclei are labeled at the bottom of Fig. 1 with the convention that the plus sign under the low-field resonance peak of a proton refers to a positive coupling between that proton and the labeled nucleus. This convention is followed throughout the paper.

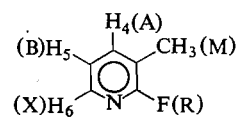

1

In Fig. 2*c*, the resonance of H_6 indicates the presence of residual broadening caused by incomplete relaxation of the coupling to ^{14}N. In Fig. 2*b*, the methyl protons have been decoupled, while in Fig. 2*a* an additional weak irradiation of peak

Can. J. Chem. Downloaded from www.nrcresearchpress.com by 210.87.254.6 on 09/05/12
For personal use only.

Can. J. Chem. Downloaded from www.nrcresearchpress.com by 210.87.254.6 on 09/05/12
For personal use only.

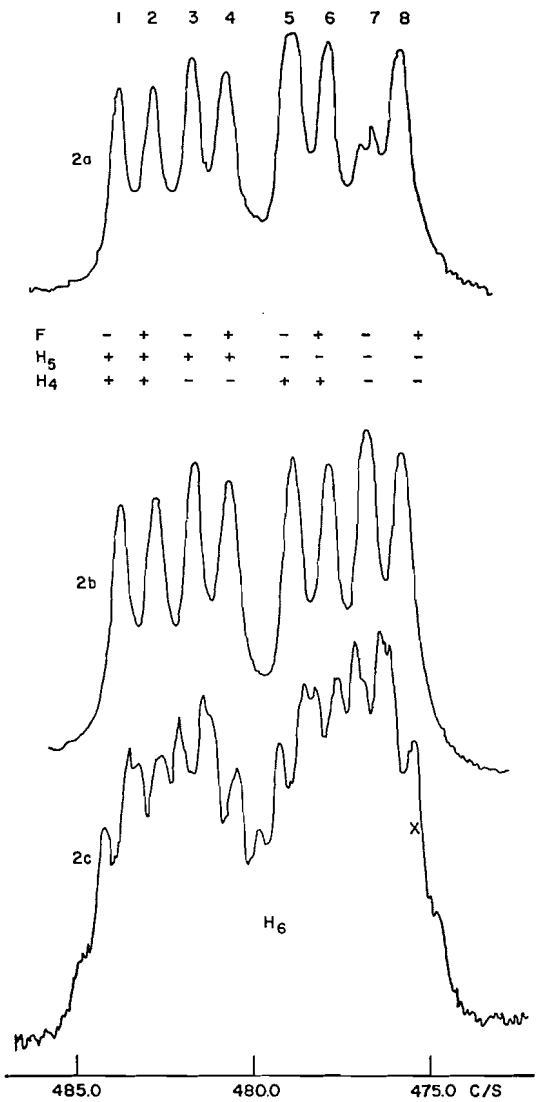

FIG. 2. The proton resonance spectrum of H_6 in **1**. In (*c*) the single resonance spectrum can be compared with the relatively well resolved eight peak pattern obtained in (*b*) by decoupling the methyl protons. In (*a*) peak 7 is affected by weak irradiation of peak 8 of H_4. The peak marked X in (*c*) is referred to in Fig. 3.

8 of H_4 (see Fig. 1) affects peak 7 of H_6. It follows that $J_m^{F,H_4}/J_m^{F,H_6} < 0$ and that $J_o^{H_4,H_5}/J_o^{H_5,H_6} > 0$.

In Fig. 3*a*, the peak marked X in the resonance of H_6 in Fig. 2*c* is being weakly irradiated by a second radio frequency field. The zero beat between the first and second radio frequency fields at the position of X is clearly noticeable. Peak X corresponds to the more intense, high-field peak of the quartet into which peak 8 (Fig. 2*b*) is split by the methyl protons. Observation of the quartets, numbered 7 and 8, of H_5 clearly shows that a low-field transition in quartet 7 is affected (Fig. 3*a*). Consequently, $J_m^{H,CH_3}/J_p^{H,CH_3} < 0$, $J_m^{F,H_6}/J_p^{F,H_5} < 0$, and $J_o^{H_4,H_5}/J_m^{H_4,H_6} > 0$.

In Fig. 3*b*, the more intense, low-field peak of the quartet corresponding to peak 1 of H_5 (Fig. 1) is weakly irradiated while observing the low-field quartets (1 and 2) of H_4. The more intense, high-field peak of the low-field quartet (peak 1) is affected. Hence, $J_o^{H,CH_3}/J_m^{H,CH_3} < 0$, $J_o^{H_5,H_6}/J_m^{H_4,H_6} > 0$, and $J_p^{F,H_5}/J_m^{F,H_4} > 0$.

In Fig. 4*a*, the 16 peaks of the methyl proton resonance are displayed. Below it in Fig. 4*d* the H_6 protons are decoupled, resulting in what is very nearly a first-order octet due to coupling with H_4, H_5, and F. Other experiments in which H_5 was decoupled, together with the observation of the single resonance spectra of the ring protons, allowed the spin labeling of the methyl peaks in Fig. 4*a* as shown.

In Fig. 4*b*, the methyl proton single resonance spectrum is shown under somewhat lower resolution (the smaller splittings amount to less than 0.20 c.p.s. and cannot always be resolved as well as in Fig. 4*a*). In Fig. 3*c* the high-field quartet (peak 8 in Fig. 1) of H_5 is being decoupled. Peaks 7 and 9 of the methyl proton resonance collapse and coincide with peak 8. In Fig. 4*e* the methyl single resonance spectrum is again given and can be compared with Fig. 4*f*, where peaks 1 and 2 collapse when the quartet 7 of H_5 is decoupled. Therefore $J_o^{H,CH_3}/J_o^{H_4,H_5} < 0$, $J_p^{H,CH_3}/J_o^{H_5,H_6} < 0$, and $J_o^{F,CH_3}/J_p^{H,F} > 0$. All of the sign determinations were supported by many additional experiments not described here.

2. *Spectral Analysis*

The ring proton resonance, with the methyl protons decoupled, was analyzed as the ABX part of an ABXR spectrum (see **1**). The analysis is valid because $J_{AX}/\nu_A - \nu_X$ and $J_{BX}/\nu_B - \nu_X$ are both less than 0.1. The ring proton shifts were corrected for effects analogous to Bloch–Siegert shifts (26, 27). The final shift parameters should not be treated as standard values because of the relatively high concentration (ca. 30%) of the solute and because of the presence of some trifluoroacetic acid.

The small couplings from the ring protons to the methyl protons were obtained from the

Can. J. Chem. Downloaded from www.nrcresearchpress.com by 210.87.254.6 on 09/05/12
For personal use only.

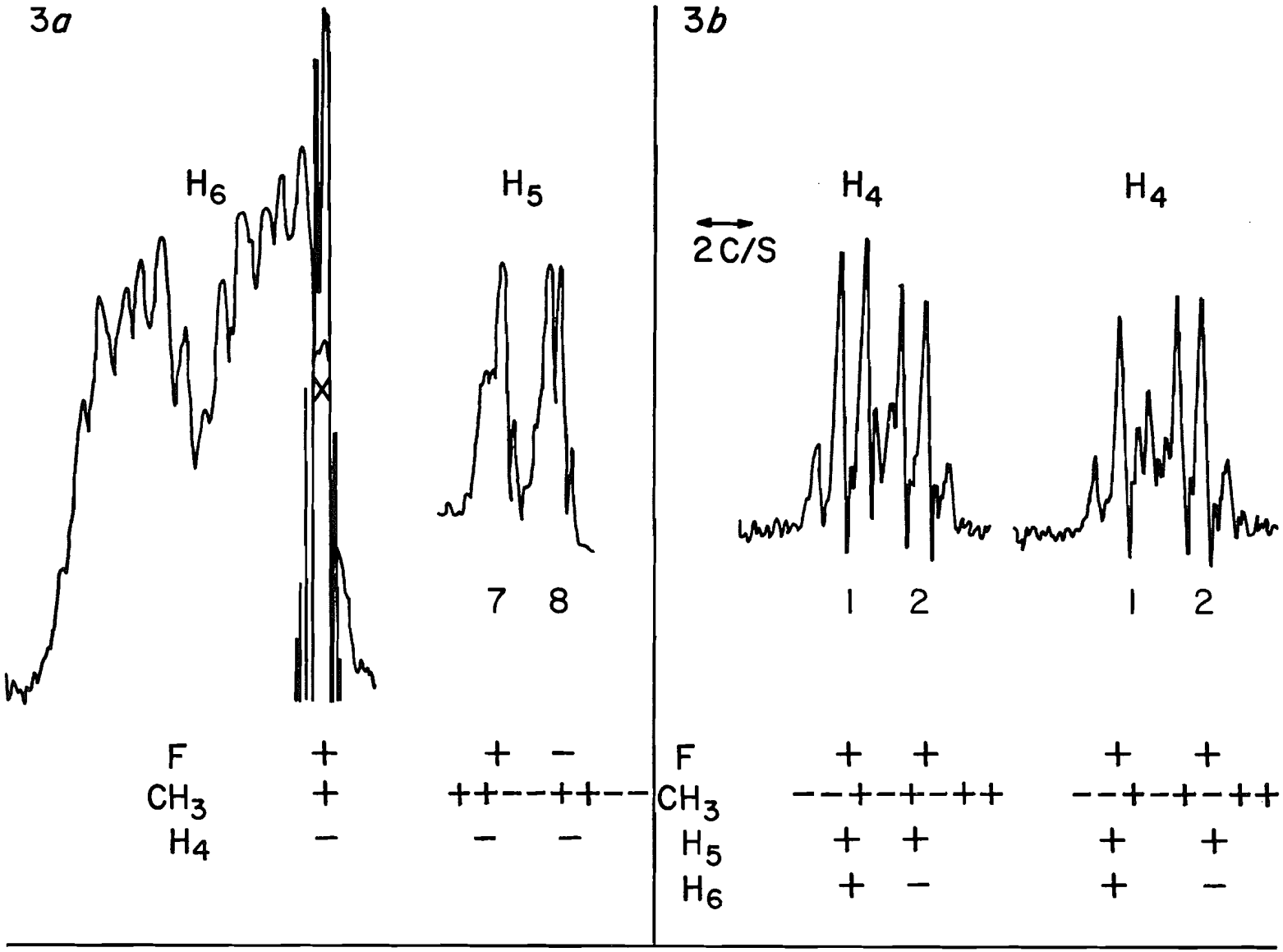

FIG. 3. In (*a*) the peak marked X in the resonance of H_6 is weakly irradiated while observing the pair of high-field quartets in the resonance of H_5. Note the zero beat pattern between the observing r.f. field and the irradiating field. The frequency scale of 2 c.p s./cm in this figure is twice as large as in the other figures.

Can. J. Chem. Downloaded from www.nrcresearchpress.com by 210.87.254.6 on 09/05/12
For personal use only.

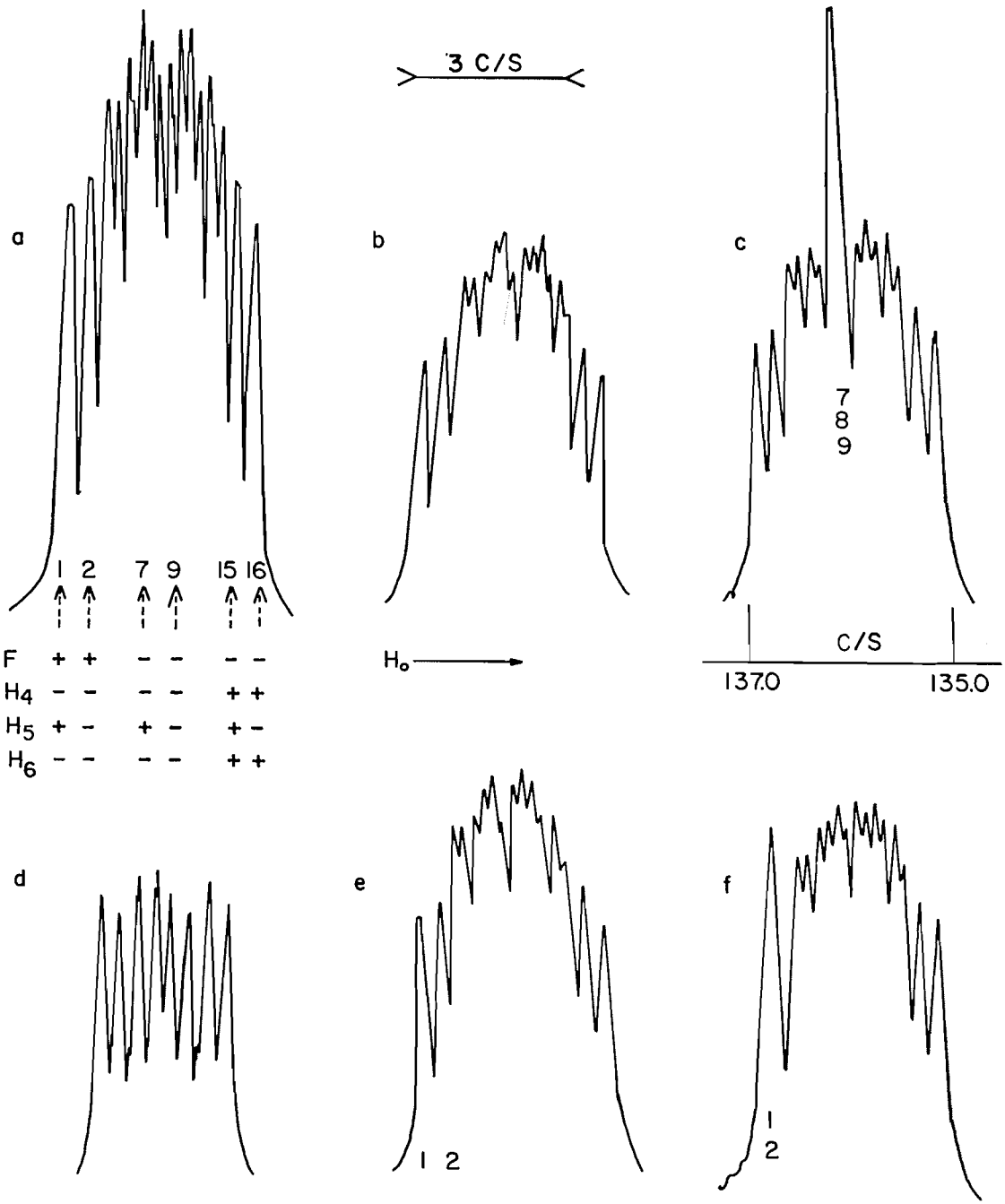

FIG. 4. In (*a*) the 16 peaks of the single resonance of the methyl protons in **1** are displayed. In (*b*) a lower resolution single resonance spectrum is compared with (*c*) in which the high-field quartet of H_5 (peak 8) is being decoupled. In (*e*) the single resonance spectrum is juxtaposed to the pattern obtained in (*f*) where quartet 7 of H_5 is weakly irradiated. In (*d*) is shown the approximately first-order octet obtained while decoupling H_6.

observed splittings in the ring proton resonance. Decoupling of H_5 resulted in an AXM_3R proton spectrum from which J_o^{F,CH_3} could be determined.

Deck (16) has shown that $J_m^{F,H_4}/J_o^{HH} > 0$ in 2-fluoropyridine derivatives. Since J_o^{HH} is positive (28) and since J_m^{F,H_4} in 2-fluoro-3-methylpyridine is undoubtedly of the same sign as in 2-fluoro-3-bromopyridine (16), it can be concluded that J_m^{F,H_4} in the former compound is also positive. A summary of the constants, in c.p.s., and the chemical shifts v, in p.p.m. relative to internal TMS, is given below

$$\nu_{CH_3} = -2.212 \pm 0.002$$
$$\nu_{H_4} = -7.643 \pm 0.005$$
$$\nu_{H_5} = -7.102 \pm 0.005$$
$$\nu_{H_6} = -7.997 \pm 0.005$$
$$J_m^{F,H_4} = 9.93 \pm 0.06$$
$$J_m^{F,H_6} = -1.02 \pm 0.05$$
$$J_p^{F,H_5} = 1.83 \pm 0.04$$
$$J_o^{H_4,H_5} = 7.50 \pm 0.08$$
$$J_o^{H_5,H_6} = 5.01 \pm 0.07$$
$$J_m^{H_4,H_6} = 1.98 \pm 0.06$$
$$J_o^{H,CH_3} = -0.85 \pm 0.05$$
$$J_m^{H,CH_3} = 0.40 \pm 0.03$$
$$J_p^{H,CH_3} = -0.7 \pm 0.1$$
$$J_o^{F,CH_3} = 1.45 \pm 0.06$$

Discussion

1. *The Methyl Proton – Ring Proton Coupling Constants*

The signs of J^{H,CH_3} in **1** are the same as those found in toluene derivatives (3). Molecular orbital theory predicts, that for alternant hydrocarbons and freely rotating methyl groups,

$$[1] \qquad J^{H,CH_3} \propto Q_{CH}\, Q_{CCH}\, P^2/\Delta E$$

where Q_{CH} and Q_{CCH} have values near -23 and $+25$ G, respectively; ΔE is a mean excitation energy to triplet states; and P is the mobile bond order between the carbon atoms to which the proton and methyl group are attached. In a recent study of radical anions of methylpyridines, Talcott and Myers (29) give Q values very near those found in anions of toluene derivatives. The signs of $J_{o,p}^{H,CH_3}$ are thus in agreement with the electron spin resonance data.

The magnitude of J_p^{H,CH_3} could only be determined to within 0.1 c.p.s. but the magnitude of J_o^{H,CH_3} (0.85 c.p.s.) is nearly 0.2 c.p.s. greater than that found in many toluene derivatives (5, 3031); however, $J_o^{H,CH_3} = -0.87$ c.p.s. in 2-fluoro-4-chloro-5-nitrotoluene (6). The resonance structures **2** and **3** suggest an increase in P^2 in eq. [1]

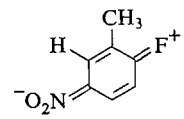

2

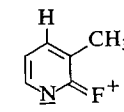

3

and therefore cause an increase in the magnitude of J_o^{H,CH_3}. It is interesting to note that fluorine is one of the stronger resonance electron donors while the nitro group is a strong electron acceptor by resonance (32).

Evidence for the importance of structure **3** is available from ^{14}N pure quadrupole resonance spectra of pyridine derivatives (33, 34). Methyl substituents in the *meta* position affect neither the σ nor the π populations on nitrogen. *Ortho* or *para* chlorine substituents substantially increase the π population on nitrogen (33). Because fluorine is a considerably better π donor than chlorine (32) the large magnitude of J_o^{H,CH_3} in 2-fluoro-3-methylpyridine can best be explained in terms of an increase of P^2.

A final piece of evidence in favor of this interpretation is the magnitude of J_o^{H,CH_3} (0.65 c.p.s.) in 2-amino-5-methylpyridine (35). Resonance structure **4** does not increase P^2 between C_4 and

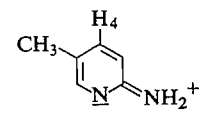

4

C_5, resulting in a "normal" value of J_o^{H,CH_3}.

The magnitude of J_m^{H,CH_3} in **1** is within the range observed in toluene derivatives (6, 30). Simple molecular orbital theory (7) predicts $J_m^{H,CH_3} = 0$, but a valence bond calculation (36) suggests that $J_m^{H,CH_3} > 0$. The stereospecificity of $J_m^{H,CHCl_2}$ in $\alpha,\alpha,2,6$-tetrachlorotoluene (37) further indicates the existence of σ contributions (38)

Can. J. Chem. Downloaded from www.nrcresearchpress.com by 210.87.254.6 on 09/05/12
For personal use only.

Can. J. Chem. Downloaded from www.nrcresearchpress.com by 210.87.254.6 on 09/05/12
For personal use only.

to J_m^{H,CH_3}. We find $|J_m^{CH_3,CH_3}| = 0.25 \pm 0.02$ c.p.s. in 2,4,6-trimethylbenzaldehyde, 0.1 to 0.2 c.p.s. less than the observed range of J_m^{H,CH_3} (30). On the basis of the methyl group replacement technique (1), σ contributions to J_m^{H,CH_3} are therefore about 0.15 c.p.s., amounting to approximately one-third of its magnitude. Consequently, J_m^{H,CH_3} cannot be discussed exclusively in terms of eq. [1].

2. The Methyl Proton – Fluorine Coupling

The sign of J_o^{F,CH_3} is the same as in fluorotoluene derivatives (6). Its magnitude is about 0.5 c.p.s. smaller than in *o*-fluorotoluene (39) or in 2-fluoro-4-chloro-5-nitrotoluene (6). On the assumption that π contributions dominate J_o^{F,CH_3}, the positive sign implies a positive Q_{CF}. The latter is a composite term, consisting of positive and negative contributions from diagonal and off-diagonal terms in the π electron spin density matrix (9). It is not obvious how the nitrogen atom in **1** will affect these terms. A decrease in the positive contributions to Q_{CF}, an increase in the negative contributions, or both, could cause the observed decrease in J_o^{F,CH_3}. The present results strongly suggest that the π contribution dominates J_o^{F,CH_3} even in the presence of a directly bonded heteroatom.

It would be expected therefore that 3-fluoro and 4-fluoromethylpyridines will also display positive $J_{o,p}^{F,CH_3}$ values. On the other hand, J_m^{F,CH_3} is small (6, 39) and its sign needs to be determined in a series of fluoromethylpyridines.

3. Ring Proton and Ring Proton – Fluorine Couplings

The substituent dependence of the coupling constants between ring protons and between ring protons and fluorine nuclei can be rationalized on the basis of the inductive, alternating model (15) as follows. Consider molecules **5** and **6**. Experimentally (15, 16, 40, and 41) the relevant changes, ΔJ, induced by a substituent of electronegativity $E_X > E_H$, are summarized in the columns below.

J	ΔJ_X	ΔJ_N	J	ΔJ_X	ΔJ_N
F_2,H_3	±	−	F_2,H_6	+	−
F_2,H_4	−	+	H_5,H_6	+	−
F_2,H_5	−	+	H_3,H_4	v. small	v. small

If ΔJ is caused by an alternation of charge (42) along the σ bonds then $|\Delta J_N| > |\Delta J_X|$ and ΔJ_X is of opposite sign to ΔJ_N. The experimental results for derivatives of **5** and **6** agree, in the main, with these predictions. However, several points can be noted; the experimental ΔJ_o^{HF} values are accurately known mainly for X = halogen (40). There is also the probability of strong van der Waals interactions between X and F (43). Furthermore, substituents *ortho* to F in **5** may cause changes in π contributions to J_o^{HF} which are comparable in magnitude to changes induced through the σ system (6). For purposes of discussing ΔJ_o^{HF} it is probably better to compare **6** and **7**.

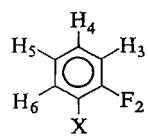

5

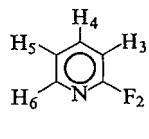

6

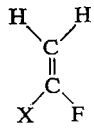

7

In **7**, J^{HF}_{cis} decreases from 20.1 c.p.s. in vinyl fluoride (44) to 7.7 c.p.s. when X = Cl (45) and to 0.6 c.p.s. when X = F (46). Comparison of ΔJ^{HF}_{cis} with ΔJ^{HH}_{cis} in vinyl derivatives (47) emphasizes that $\Delta J^{HF} \gg \Delta J^{HH}$. In view of these results, the change in J_o^{HF} from 8.90 c.p.s. in fluorobenzene (48) to −2.8 c.p.s. in 2-fluoropyridine (16, 17) is not entirely unexpected. In fact, in 2-fluoropyrazine, $J_o^{HF} = -8.17$ c.p.s. (49). In contrast, no negative J_o^{HH} values are found even in pyrazines (49).

The positive J_o^{F,CH_3} in 2-fluoro-3-methylpyridine therefore implies that to a good approximation the π contribution to J_o^{HF} is relatively unaffected even though the total J_o^{HF} changes in sign. In this sense it is reasonable to distinguish between σ and π contributions to J_o^{HF} in heterocyclic molecules.

J_p^{HF} is positive in 2-fluoropyridine but is negative in substituted fluorobenzenes (6, 40). On the reasonable assumption that the unknown J^{F,CH_3} in 2-fluoro-5-methylpyridine is positive, comparable σ and π contributions to J_p^{HF} may be inferred. Further measurements are needed to confirm this point.

J_m^{F,H_6} in **1** is negative, as it also is in 2-fluoropyrazine (16, 49). The small, negative $J_m^{H_2,H_6}$ in pyridine (50) is consistent with these data and with the inductive, alternating model. It would be of interest to measure the sign of J_m^{F,CH_3} in 2-fluoro-6-methylpyridine. $J_m^{F,H_4} = 9.9$ c.p.s. in **1** is the largest known *meta* proton–fluorine coupling. It is larger than most *ortho* proton–fluorine

couplings in fluorobenzene derivatives and approaches the largest known value of J_o^{HF} = 10.4 c.p.s. in 1,2-difluorobenzene (51).

$J_{o,m}^{HH}$ values in 2-fluoro-3-methylpyridine lie within 0.15 c.p.s. of those in pyridine (50, 52), as expected on the basis of the inductive, alternating model of substituent effects.

Conclusions

The π contributions to $J_{o,p}^{H,CH_3}$ and to J_o^{F,CH_3} in 2-fluoro-3-methylpyridine have the same signs and comparable magnitudes as in benzene derivatives. This is so even though J_o^{HF} in 2-fluoropyridines is negative, in contrast to its large positive value in fluorotoluene derivatives. These results are consistent with a model of substituent effects on J^{HH} and J^{HF} in which the substituent acts primarily through the σ framework in benzene and pyridine derivatives. Further measurements on a series of fluoromethylpyridines are indicated.

1. R. HOFFMAN. Arkiv Kemi, **17**, 1 (1961).
2. R. HOFFMAN and S. GRONOWITZ. Arkiv Kemi, **16**, 471 (1960).
3. G. KOTOWYCZ and T. SCHAEFER. Can. J. Chem. **44**, 2743 (1966).
4. D. T. WITIAK, D. P. PATEL, and Y. LIN. J. Am. Chem. Soc. **89**, 1908 (1967).
5. W. C. RIPKA and E. APPLEQUIST. J. Am. Chem. Soc. **89**, 4035 (1967).
6. D. J. BLEARS, S. S. DANYLUK, and T. SCHAEFER. J. Chem. Phys. **47**, 5037 (1967).
7. H. M. MCCONNELL. J. Mol. Spectry. **1**, 11 (1957).
8. M. J. S. DEWAR and R. C. FAHEY. J. Am. Chem. Soc. **85**, 2704 (1963).
9. A. HINCHLIFFE and J. N. MURRELL. Mol. Phys. **14**, 147 (1968).
10. A. D. MCLACHLAN. Mol. Phys. **1**, 233 (1958).
11. A. FORMAN, J. N. MURRELL, and L. E. ORGEL. J. Chem. Phys. **31**, 1129 (1960).
12. D. R. EATON, A. D. JOSEY, W. D. PHILLIPS, and R. E. BENSON. Mol. Phys. **5**, 407 (1962).
13. R. J. COOK, J. R. ROWLANDS, and D. H. WHIFFEN. Mol. Phys. **7**, 31 (1963).
14. A. D. COHEN and T. SCHAEFER. Mol. Phys. **10**, 209 (1965).
15. S. CASTELLANO and R. KOSTELNIK. J. Am. Chem. Soc. **90**, 141 (1968).
16. J. C. DECK. Ph.D. Thesis. University of Illinois. 1966.
17. W. BRÜGEL. Z. Elektrochem. **66**, 159 (1962).
18. T. TOKUHIRO, N. K. WILSON, and G. FRAENKEL. J. Am. Chem. Soc. **90**, 3622 (1968).
19. J. W. EMSLEY. J. Chem. Soc. A, 1387 (1968).
20. J. P. KINTZINGER and J. M. LEHN. Mol. Phys. **14**, 133 (1968).
21. H. L. BRADLOW and C. A. VANDERWERF. J. Org. Chem. **14**, 509 (1949).
22. J. P. MAHER and D. F. EVANS. Proc. Chem. Soc. **208**, (1961).
23. R. FREEMAN and D. H. WHIFFEN. Mol. Phys. **4**, 321 (1961).
24. R. FREEMAN and W. A. ANDERSON. J. Chem. Phys. **37**, 2053 (1962).
25. J. D. BALDESCHWIELER and E. W. RANDALL. Chem. Rev. **63**, 81 (1963).
26. W. A. ANDERSON. Phys. Rev. **103**, 151 (1956).
27. T. M. CONNOR, D. H. WHIFFEN, and K. A. MCLAUCHLAN. Mol. Phys. **13**, 221 (1967).
28. A. SAUPE. Z. Naturforsch. **19a**, 161 (1964); **20**, 572 (1965).
29. C. L. TALCOTT and R. J. MYERS. Mol. Phys. **12**, 549 (1967).
30. G. KOTOWYCZ. Ph.D. Thesis. University of Manitoba. 1967.
31. D. J. BLEARS, S. S. DANYLUK, and T. SCHAEFER. Can. J. Chem. **46**, 654 (1968).
32. C. G. SWAIN and E. C. LUPTON, JR. J. Am. Chem. Soc. **90**, 4328 (1968).
33. L. GUIBÉ and E. A. C. LUCKEN. Mol. Phys. **14**, 79 (1968).
34. R. IKEDA, S. ONADA, D. NAKAMURA, and M. KUBO. J. Phys. Chem. **72**, 2501 (1968).
35. Unpublished work, this laboratory.
36. H. M. MCCONNELL. J. Chem. Phys. **30**, 126 (1959).
37. T. SCHAEFER, R. SCHWENK, C. J. MACDONALD, and W. F. REYNOLDS. Can. J. Chem. **46**, 2187 (1968).
38. H. FRISCHLEDER and G. BÄR. Mol. Phys. **11**, 359 (1966).
39. R. E. RICHARDS and T. SCHAEFER. Trans. Faraday Soc. **54**, 1447 (1958).
40. J. E. LOEMKER, J. M. READ, JR., and J. H. GOLDSTEIN. J. Phys. Chem. **72**, 991 (1968).
41. H. M. HUTTON, B. RICHARDSON, and T. SCHAEFER. Can. J. Chem. **45**, 1795 (1967).
42. J. A. POPLE and M. GORDON. J. Am. Chem. Soc. **89**, 4253 (1967).
43. G. L. CALDOW. Mol. Phys. **11**, 71 (1966).
44. C. N. BANWELL and N. SHEPPARD. Proc. Roy. Soc. London, Ser. A, **263**, 136 (1961).
45. H. M. HUTTON and T. SCHAEFER. Can. J. Chem. **45**, 1111 (1967).
46. C. J. MACDONALD and T. SCHAEFER. Can. J. Chem. **45**, 3157 (1967).
47. T. SCHAEFER. Can. J. Chem. **40**, 1 (1962).
48. J. E. LOEMKER, J. M. READ, JR., and J. H. GOLDSTEIN. Mol. Phys. **13**, 433 (1967).
49. R. H. COX and A. A. BOTHNER-BY. J. Phys. Chem. **72**, 1646 (1968).
50. S. CASTELLANO, C. SUN, and R. KOSTELNIK. J. Chem. Phys. **46**, 327 (1967).
51. J. E. LOEMKER, J. H. GOLDSTEIN, and J. M. READ, JR. Chem. Commun. 745 (1968).
52. P. DIEHL and R. J. CHUCK. Mol. Phys. **14**, 183 (1968).

Can. J. Chem. Downloaded from www.nrcresearchpress.com by 210.87.254.6 on 09/05/12
For personal use only.

Can. J. Chem. Downloaded from www.nrcresearchpress.com by 210.87.254.105 on 09/05/12
For personal use only.

Preparation, absolute configuration, and thermolysis of (*3R*:*5R*)-(+)-*trans*-3,5-dimethyl-1-pyrazoline

ANUPAMA MISHRA AND ROBERT J. CRAWFORD
Department of Chemistry, University of Alberta, Edmonton, Alberta

Received September 30, 1968

Thermolysis of (*3R*:*5R*)-(+)-*trans*-3,5-dimethyl-1-pyrazoline produces 25.6% of *trans*-1,2-dimethylcyclopropane of 23% optical purity having the *S*:*S* configuration. Thermolysis mechanisms which explain the racemization and the double inversion process are discussed. The absolute configuration of *active*-2,4-pentanediol and 2,4-dibromopentane is correlated with that of 4-hydroxy-1-pentene.

Canadian Journal of Chemistry, 47, 1515 (1969)

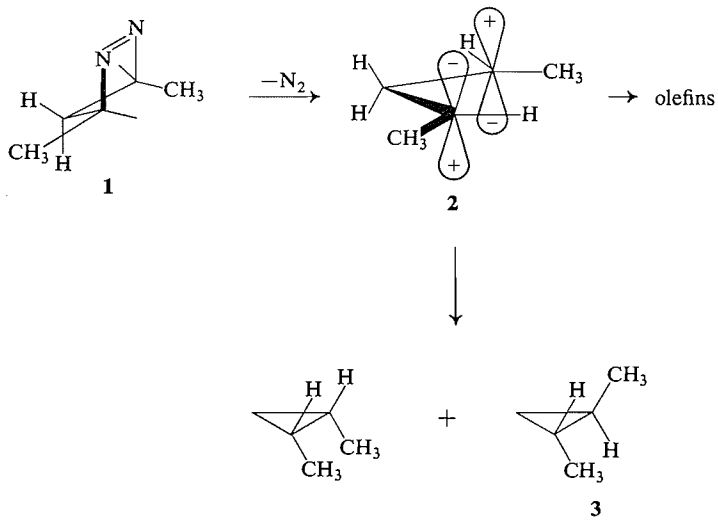

SCHEME 1

Introduction

The gas-phase thermolysis of 1-pyrazoline has been shown to proceed by cleavage of both carbon–nitrogen bonds (1) to produce a hydrocarbon intermediate which in turn produces propylene and cyclopropane (2). The intermediate suggested for the thermolysis is such that the two hydrogen atoms attached to each end of the trimethylene species are in the plane defined by the three trimethylene carbon atoms. This has been referred to as the O,O-trimethylene configuration and extended Hückel molecular orbital calculations support the suggestion that it represents an energy minimum (3).

The thermolysis of *trans*-3,5-dimethyl-1-pyrazoline (**1**) produces 73% *cis*-1,2-dimethylcyclopropane, 25% of the *trans* isomer (**3**), and 1% each of *cis*- and *trans*-2-pentene. These products were rationalized as in Scheme 1 (2). The stereochemistry of the intermediate (**2**) is such that optically active **1** on thermolysis should generate racemic **3** if **2** is an intermediate. Recently alternative mechanisms have been proposed which may account for the minor product. Roth and Martin (4) have observed what is essentially inversion at both carbons (to which the azo nitrogens are attached) in the thermolysis of *exo*,*exo*-5,6-dideuterio-2,3-diazabicyclo[2·2·1]hept-2-ene, and by analogy the **3** produced upon thermolysis of active **1** should be optically active and involve inversion at each of its asymmetric centers (Scheme 2). Allred and Smith (5) using a similar bicyclic system have proposed a recoil mechanism by which **1** would be expected to produce a pyramidal diradical intermediate (**4**) which could close to produce **3**.

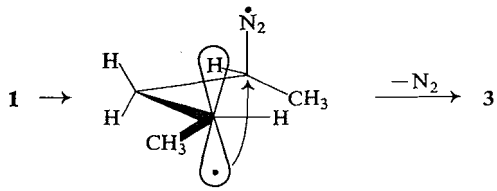

SCHEME 2

Again optically active **1** would be expected to produce **3** by inversion at both asymmetric centers (Scheme 3).

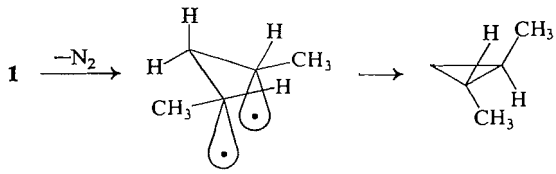

SCHEME 3

Correlations of Configurations

Chart 1 shows the method of synthesis, rotations, and absolute configurations of each of the compounds used in the sequence from (*R*)-(−)-4-hydroxy-1-pentene (6) to (*3R*:*5R*)-(+)-*trans*-3,5-dimethyl-1-pyrazoline. The 4-hydroxy-1-pentene was resolved via the brucine salt of the phthalate half ester (6*b*). Oxymercuration (7) of the hydroxy-1-pentene followed by borohydride reduction gave an 80% yield of 2,4-pentanediol consisting of a 30:70 mixture of *meso* and *active* forms. This mixture was not separated but converted directly to the dibromide using the procedure of Pritchard and Vollmer (8). The ratio of *active* to *meso* remained essentially that of the reactant, suggesting that the dibromide was produced by inversion of both centers in a clean manner (8, 9). The dibromide was then converted to the pyrazolidine and oxidized to the pyrazoline without characterization of rotation at the pyrazolidine stage (the latter is air sensitive and generally contains some of the 1-pyrazoline). The magnitude of rotation of each of these compounds was put on a firm basis by the resolution of *rac-trans*-3,5-dimethylpyrazolidine using (+)-10-camphorsulfonic acid, the pyrazolidine thus resolved was oxidized to give **1** with $[\alpha]_D^{25}$ +605°.

Thermolysis of 1

The resolved pyrazoline **1** on thermolysis produced *cis*- and *trans*-2-butene (1% each), *cis*-1,2-dimethylcyclopropane (73%) and *trans*-1,2-dimethylcyclopropane (25%); only the latter product has an asymmetric center and thus, to minimize losses, the hydrocarbon products were isolated and the total hydrocarbon fraction examined. The proportion of *cis* and *trans* isomers was then determined by gas–liquid chromatography (g.l.c.) and upon correction for the percentage of *cis*-3,5-dimethyl-1-pyrazoline in the starting material the optical activity of the **3** produced from *active*-**1** was calculated. Table I gives the results of several runs carried out in this manner. The percentage of *cis*-3,5-dimethyl-1-pyrazoline in the initial mixture was determined by 100 MHz nuclear magnetic resonance (n.m.r.) spectroscopy. This ratio was verified by the g.l.c. analysis of the cyclopropane

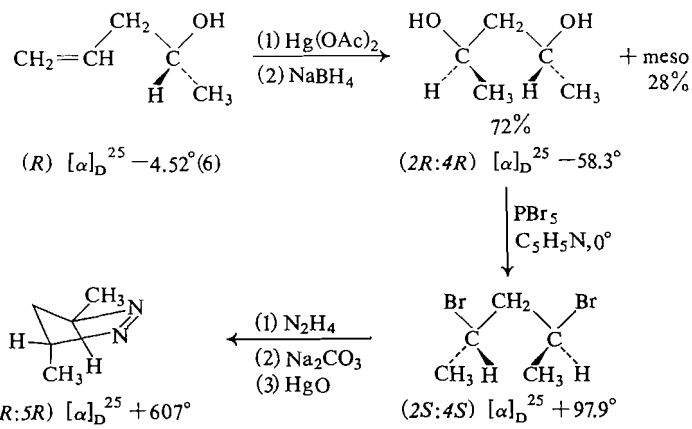

CHART 1: Preparation of (*3R*,*5R*)-(+)-*trans*-3,5-dimethyl-1-pyrazoline with maximum observed rotations.

Can. J. Chem. Downloaded from www.nrcresearchpress.com by 210.87.254.105 on 09/05/12
For personal use only.

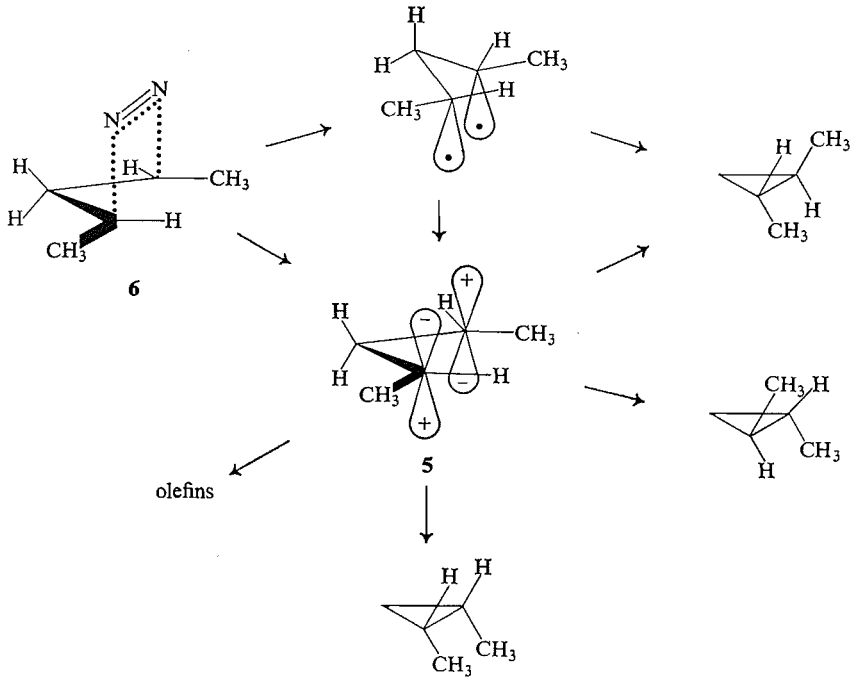

SCHEME 4

and olefin products obtained upon thermolysis, and agreement to within 1% was obtained for the amount of *cis*- and *trans*-3,5-dimethyl-1-pyrazoline. Because the rotation of the hydrocarbon product was the same in sign as that of the reactant, and because of the magnitude of the rotation of **1** relative to that of **3**, it was necessary to be sure that unreacted **1**, or its tautomer, was not a contaminant. This was achieved by passing the whole product mixture through a 20 ft Carbowax 20M column and by collection of only the hydrocarbon fraction.

The results from Table I indicate an excess of double inversion to retention of absolute configuration of 23.6 ± 1.7% for the *trans*-1,2-dimethylcyclopropane (10) produced from *active*-**1**. The most concise scheme that fits the kinetic and stereochemical data is that shown as Scheme 4. This incorporates the pyramidal diradical suggested by Allred and Smith (5) to account for the optically active portion of the **3** produced, which is 6% of the total product. The racemic **3**, *cis*-1,2-dimethylcyclopropane and olefins are believed to arise from the trimethylene intermediate **5**. The present data cannot distinguish between **5** being formed directly from **1** via the transition state **6**, and a small fraction going via the pyramidal diradical or whether all of the material goes via the pyramidal diradical, 94% of which in turn produces **5**. Similarly the possibility exists that the 6% optically active *trans*-1,2-dimethylcyclopropane is produced via a mechanism similar to that suggested by Roth and Martin (4).

Experimental

The nuclear magnetic resonance spectra were obtained using a Varian A-60 and a Varian HA 100 spectrometer. Optical rotations were measured using a 1.00 dm cell in a Perkin–Elmer Model 141 spectropolarimeter and a Jasco ORD-UV5 spectrophotometer. A Wilkens Aerograph Autoprep was used for the preparative g.l.c. and a Gow-Mac Model TR-11-B,w thermal conductivity cell with a Gow-Mac Model 40-05C power supply was used on a vacuum line for analytical g.l.c. and the trapping of hydrocarbon samples (11).

Resolution of trans-3,5-Dimethylpyrazolidine and its Conversion to trans-3,5-Dimethyl-1-pyrazoline (1)

trans-3,5-Dimethylpyrazolidine was originally resolved through its *N,N'*-bishydroxymethylene-(+)-camphor derivative (2). However, regeneration of the pyrazolidine from this derivative proved to give too low a yield to be useful in this work. Among the different acids employed for an attempted salt formation, (+)-10-camphorsulfonic acid was found to be the most suitable.

Can. J. Chem. Downloaded from www.nrcresearchpress.com by 210.87.254.105 on 09/05/12
For personal use only.

TABLE I

Stereochemistry of the thermolysis product **3**

Source	Reactant		Time at 200° (h)	Hydrocarbon product			% optical purity of **3**
	Optical purity*	Weight (mg)		Weight† (mg)	α_D^{25}	Calcd. max.‡	
1. Direct resolution	10·2% (*R*:*R*) $[\alpha]_D^{25}$ +61·5°‖	115	5	75	+0·018° ±0·002°	0·089°	20·3§
2. 84·3% *trans*	93·4% (*S*:*S*)	160	10	101·6	−0·240°¶ ±0·002° ±0·002°	0·940°	25·5
3. 84·3% *trans*	93·4% (*S*:*S*)	167	15	99·0	−0·212°¶ ±0·002°	0·910°	23·2
4. 88·4% *trans*	50·6% (*S*:*S*)	128·4	10	74·0	+0·085°¶ ±0·002°	0·385°	22·1

*Calculated on the basis of $[\alpha]_D^{25}$ +607°.
†Represents 95, 94, 87, and 84% of theoretical amount of C_5H_{10}.
‡Calculated using $[\alpha]_D^{25}$ for 3 of 46°, if all 3 from optically pure 1 was active (see Experimental).
§Rotation taken in methanol; value 46° from diglyme assumed.
‖Diluted with racemic material.
¶Diglyme used as solvent.

Crude *trans*-3,5-dimethylpyrazolidine (6 g, 0.06 mole) was dissolved in ether (50 ml) and then added to a solution of (+)-10-camphorsulfonic acid (25 g, 0.11 mole) in ether (1500 ml). The reaction mixture containing the salt was stirred at room temperature for 2 h and the solids were separated by filtration (about 20 g). The salt was dissolved in methanol (300 ml) and ether (1500 ml) was added to precipitate an impurity having a wide melting point range, from 195–210°. The bulky filtrate was evaporated to dryness on a rotary evaporator and the residue was dissolved in a minimum volume of methanol, and ether (400 ml) was added to precipitate the salt (6 g, m.p. 120–125°). Dissolution of this substance in methanol (10 ml) and reprecipitation by ether gave 3.5 g of the salt m.p. 128–132°. Recrystallizations were repeated until the m.p. was found to be constant at 135–137°. The n.m.r. spectrum of the salt in deuteriochloroform indicated that the pyrazolidine and the sulfonic acid were present in the ratio 1:2 respectively.

The salt was decomposed with aqueous potassium carbonate solution until the solution became basic and it was then extracted three times with ether. The ether extracts were combined and dried over anhydrous sodium sulfate. The product was oxidized by mercuric oxide to the 1-pyrazoline, which was separated by g.l.c. on a 20 ft column of 10% Uconinsoluble on Fluoropak; $[\alpha]_D^{25}$ +605° (CH_3OH, *c*, 7.5 × 10^{-3} g/ml).

Larger quantities of **1** were prepared from the active glycol as described below.

R(−)-4-Hydroxy-1-pentene and S(+)-4-Hydroxy-1-pentene

4-Hydroxy-1-pentene was prepared by the method of Whitmore (12) from allyl bromide and acetaldehyde. This compound was converted to its acid phthalate ester and resolved through its brucine salt according to the procedure of Levene (6*c*).

The acid phthalate ester (crude, 130 g) was dissolved in warm acetone (50 ml) and then added to a suspension of brucine (200 g) in warm acetone (700 ml). The solution thus obtained was filtered and slow crystallization was allowed to occur at room temperature after it was seeded with the proper diastereomeric crystal. The crystals thus obtained had a m.p. of 144–146°; yield 140 g. Three more recrystallizations in progressively larger volumes of acetone gave a product having m.p. 148–149°, yield 125 g. The alcohol was recovered from the salt in about 90% yield.

The *S*(+)-alcohol corresponded to an optical purity of 93.4% (6). The *R*(−)-alcohol obtained from the mother liquor had an optical purity of 50.6%.

2,4-Pentanediol

This compound was prepared from 4-hydroxy-1-pentene, following the method of Brown and Geoghegan (7).

Starting with 4-hydroxy-1-pentene (17.2 g, 200 mmole) and mercuric acetate (64 g, 200 mmole) dissolved in a mixture of water (200 ml) and tetrahydrofuran (THF) (200 ml), the oxymercuration was conducted for 12 min at room temperature. A sodium hydroxide solution (200 ml, 3 *M*) was added, followed by a sodium borohydride solution (200 ml of 0.5 *M* $NaBH_4$ in 3 *M* sodium hydroxide). The reaction mixture was saturated with sodium chloride and the THF layer separated. The aqueous layer was extracted three times with THF (100 ml) and the combined THF solutions were dried over anhydrous potassium carbonate. Removal of the solvent and distillation gave the glycol (16 g, 80%), b.p. 70–74°/3mm. Analysis of the diol by g.l.c. on a polyethyleneimine column gave the ratio of the *active* to *meso* isomers.

R(−)-4-hydroxy-1-pentene of 50.6% optical purity gave the diol mixture of α_D^{25} −21.1° (methanol; *c*, 4.43 × 10^{-2} g/ml). Since the percentage of the *active* form was 71.6 ± 0.2%, the minimum rotation of (*2R*:*4R*)-(−)-2,4-pentanediol is $[\alpha]_D^{25}$ −58.3°.

S(+)-4-hydroxy-1-pentene of 93.4% optical purity gave the diol mixture of $[\alpha]_D^{25}$ +35.8° (methanol; *c*, 2.5 × 10^{-2} g/ml). Since the *active* form in the mixture was 64.8 ± 0.3%, the minimum rotation of (*2S*:*4S*)-(+)-2,4-pentanediol is +59.1°.

Can. J. Chem. Downloaded from www.nrcresearchpress.com by 210.87.254.105 on 09/05/12
For personal use only.

Can. J. Chem. Downloaded from www.nrcresearchpress.com by 210.87.254.105 on 09/05/12
For personal use only.

2,4-Dibromopentane

This compound was prepared by the method of Pritchard and Vollmer (6) by the action of phosphorus pentabromide on 2,4-pentanediol. A sample of *(2S:4S)*-(+)-2,4-pentanediol of 93.4% optical purity gave the 2,4-dibromopentane $[\alpha]_D^{25}$ +65.1° (CCl_4; *c*, 1.5×10^{-2} g/ml).

Analysis of the dibromide by g.l.c. using a Carbowax 20M column indicated the *active* form to be 71.2 ± 0.5%, thus *(2R:4R)*-(+)-2,4-dibromopentane has $[\alpha]_D^{25}$ +97.9°.

3,5-Dimethyl-1-pyrazoline (1)

This compound was prepared as previously described (2). The ratio of the *trans* to *cis* isomers was determined by measuring the absorptions due to the methyne protons at C-3 and C-5 in the 100 MHz n.m.r. spectrum of the sample.

This ratio was verified by the analysis of cyclopropane and olefin products obtained by the thermal decomposition of the mixture. Since the product ratios from each of pure *cis*- and *trans*-3,5-dimethyl-1-pyrazolines are known, the ratio actually obtained can be used to solve the percentage of individual components present in the mixture. The values from n.m.r. and g.l.c. agreed within 1%. The value from n.m.r. was used to calculate the stereospecifity of the thermal decomposition and optical rotation. The *active* dihalide reacts more readily than the *meso* compound and thus there is a slight enrichment in the percent *trans*.

(*a*) The dihalide sample derived from *(S)*-(+)-4-hydroxy-1-pentene of 93.4% optical purity produced a sample of 3,5-dimethyl-1-pyrazoline (84.3 ± 0.5% *trans* by n.m.r.; 84.8 ± 1.0% by g.l.c.) α_D^{25} −0.851° (CH_3OH; *c*, 1.83×10^{-3} g/ml); $[\alpha]_D^{25}$ −588°.

(*b*) The dihalide sample derived from *(R)*-(−)-4-hydroxy-1-pentene of 50.6% optical purity produced a sample of 3,5-dimethyl-1-pyrazoline (88.4 ± 0.8% *trans* by n.m.r.; 88.3 ± 0.3% by g.l.c.) α_D^{25} +0.623° (CH_3OH; *c*, 1.83×10^{-3} g/ml); $[\alpha]_D^{25}$ +630°.

(*c*) The dihalide sample derived from *(R)*-(−)-4-hydroxy-1-pentene of 31% optical purity produced a sample of 3,5-dimethyl-1-pyrazoline (85% *trans* by n.m.r.) $\alpha_D^{25°}$ +0.366° (CH_3OH; *c*, 2.21×10^{-3} g/ml); $[\alpha]_D^{25}$ +603°.

The average value of 607 ± 21° agrees with the value of 605° obtained by direct resolution from the pyrazolidine.

Thermal Decomposition of Optically Active trans-3,5-Dimethyl-1-pyrazoline

Decomposition of the optically active compound was affected by transferring it to a glass bulb with a break-seal and then degassing the system thoroughly before sealing. The pressure at the temperature of decomposition varied from 1–2 atm. After the decomposition was over, the container was connected to a vacuum line and the seal broken. Nitrogen was pumped off and the other products trapped by liquid nitrogen. This was later transferred to a system suitable for g.l.c. analysis. The whole mixture was passed through a 20 ft column of Carbowax 20M to ensure that only the hydrocarbon products were collected. Hydrocarbon products collected were later weighed and transferred into 1 ml of diglyme and their optical rotation measured.

The column marked calculated maximum for the hydrocarbon product in Table I was calculated using $[\alpha]_D^{25}$ +46° for *trans*-1,2-dimethylcyclopropane (10). The theoretical maximum of *active-trans*-1,2-dimethylcyclopropane present was calculated from the known amount of optically pure **1** that was present in the sample on the basis that all of the 25.6% of **3** produced would be optically active.

Controls

A sample of *(3S:5S)*-(−)-3,5-dimethyl-1-pyrazoline, containing 15.6% of the *cis* isomer, was heated to 205° for 10 min (63% reaction for the *trans* isomer and 48.4% reaction for the *cis* isomer (2)) then quenched. The n.m.r. spectrum of the unreacted material indicated 81 ± 1% *trans* and 19 ± 1% *cis*. The values calculated from the rate data are 80% *cis* and 20% *trans*. The original sample had a rotation of $[\alpha]_D^{25}$ −588°, the recovered sample had a rotation of $[\alpha]_D^{25}$ −592°. Thus the reactants do not isomerize under the reaction conditions. *Active-trans*-1,2-dimethylcyclopropane was similarly recovered unchanged.

Acknowledgments

The authors acknowledge support from the National Research Council of Canada and from the Petroleum Research Fund of the American Chemical Society. We also wish to acknowledge helpful discussions with Dr. J. A. Mills and Professor K. R. Kopecky.

1. B. Al-Sader and R. J. Crawford. Can. J. Chem. **46**, 3301 (1968).
2. R. J. Crawford and A. Mishra. J. Am. Chem. Soc. **88**, 3963 (1966).
3. R. Hoffmann. J. Am. Chem. Soc. **90**, 1475 (1968).
4. W. R. Roth and M. Martin. Tetrahedron Letters, 4695 (1967).
5. E. L. Allred and R. L. Smith. J. Am. Chem. Soc. **89**, 7133 (1967).
6. (*a*) E. R. Novack and D. S. Tarbell. J. Am. Chem. Soc. **89**, 73 (1967). (*b*) P. A. Levene and H. L. Haller. J. Biol. Chem. **81**, 425 (1929). (*c*) P. A. Levene and A. Rothen. J. Chem. Phys. **41**, 982 (1937).
7. H. C. Brown and P. Geoghegan, Jr. J. Am. Chem. Soc. **89**, 1522 (1967).
8. J. G. Pritchard and R. L. Vollmer. J. Org. Chem. **28**, 1545 (1963).
9. W. Gerrard, J. Kenyon, and H. Phillips. J. Chem. Soc. 153 (1937).
10. W. von E. Doering and W. Kirmse. Tetrahedron, **11**, 272 (1960).
11. R. Moore, A. Mishra, and R. J. Crawford. Can. J. Chem. **46**, 3305 (1968).
12. W. H. Yanko, H. S. Mosher, and F. C. Whitmore. J. Am. Chem. Soc. **67**, 664 (1945).

Can. J. Chem. Downloaded from www.nrcresearchpress.com by 210.87.254.5 on 09/05/12
For personal use only.

Reduction of trichloromethylcarbinols.[1] Hydrogenolysis of phenyl(trichloromethyl)carbinol and 1,1,1-trichloro-2-hydroxy-6-methyl-4-heptanone on metal surfaces

EBERHARD KIEHLMANN, ROBERT J. BIANCHI, AND WILKINS REEVE
Departments of Chemistry, Simon Fraser University, Burnaby 2, British Columbia

AND

University of Maryland, College Park, Maryland

Received September 13, 1968

Reduction with zinc in neutral or acidic medium or catalytic hydrogenation of phenyl(trichloromethyl)-carbinol (**1**) gives β,β-dichlorostyrene (**2**), β-chlorostyrene (**3**), and phenyl(dichloromethyl)carbinol (**4**). β,β-Dichlorostyrene is the sole product of reduction of phenyl(trichloromethyl)carbinyl methyl ether with zinc and acetic acid. Lithium in liquid ammonia reduces the trichloromethyl group of **1** to give α-phenethyl alcohol (**5**) in low yield; acetophenone and β-phenethyl alcohol have been identified as by-products of this reaction.

Clemmensen reduction of 1,1,1-trichloro-2-hydroxy-6-methyl-4-heptanone (**6**) does not yield the expected 1,1,1-trichloro-6-methyl-2-heptanol; instead, 1,1-dichloro-6-methyl-1-hepten-4-one (**7**) and 1,1-dichloro-6-methyl-1-heptene (**8**) are formed as the main reaction products. Long reflux time, efficient stirring, and the employment of a large excess of amalgamated zinc and concentrated hydrochloric acid favor the formation of **8** while **7** is obtained in high yield when sulfuric acid is used instead of hydrochloric acid.

A mechanism for the reduction of trichloromethylcarbinols (**1** and **6**) with zinc has been proposed, **7** being postulated as an intermediate in the formation of **8**.

Canadian Journal of Chemistry, 47, 1521 (1969)

Introduction

In the course of investigations on the mechanism of nucleophilic displacement reactions of phenyl(trichloromethyl)carbinol (**1**) and on synthetic methods for the preparation of aliphatic trichloromethylcarbinols, it became desirable to reduce the trichloromethyl group of **1** to a methyl group without changing the structure and configuration of the adjacent asymmetric carbon, and to reduce selectively the carbonyl function of 1,1,1-trichloro-2-hydroxy-6-methyl-4-heptanone (**6**) to a methylene group without causing structural changes in the terminal trichloromethylcarbinol residue (—CHOH—CCl_3). Since it was observed that in most reactions of **1** and **6** several functional groups undergo structural changes simultaneously, we decided to investigate the mechanism of interaction between a trichloromethyl group and an adjacent hydroxyl group when these compounds are treated with metallic reducing agents.

Although the literature contains several reports on the hydrogenolysis of haloalkanes containing isolated trihalomethyl groups, little is known about the reduction of trihalomethylcarbinols. Nagao and Sato (1) have described an electrolytic method for the conversion of a CCl_3 group to a $CHCl_2$ or CH_2Cl group; Dinesman (2) observed the formation of β,β-dichlorostyrene from phenyl(trichloromethyl)carbinol and zinc in acetic acid; and Kaspar and Wiechert (3) have reported the complete reduction of a tribromomethyl group by catalytic hydrogenolysis over Raney nickel. Studies on the reduction of haloalkanes and -alkenes over palladium (4) have shown that hydrogen chloride inhibits the hydrogenolysis of ethyl chloride at 120° in proportion to its concentration, and that $CF_2{=}CCl_2$ suffers hydrogenolysis more readily than hydrogenation yielding $CF_2{=}CHCl$ (82%) and $CF_2{=}CH_2$ (18%) but not $CHF_2{-}CH_3$ when treated with an insufficient amount of hydrogen (5). On the basis of this information we selected palladium, platinum oxide, Raney nickel, zinc, lithium, and sodium as catalysts and reducing agents for our investigations.

Experimental

All melting points are corrected. Analyses were performed by Dr. Franz Kasler. The infrared (i.r.)

[1]Taken in part from the Ph.D. theses of Eberhard Kiehlmann and Robert J. Bianchi, University of Maryland, 1964 and 1967.

Can. J. Chem. Downloaded from www.nrcresearchpress.com by 210.87.254.5 on 09/05/12
For personal use only.

spectra were recorded on a Beckman IR-5 spectrometer using a thin film of neat liquid between sodium chloride plates. Nuclear magnetic resonance (n.m.r.) spectra were run on a Varian A-56/60 spectrometer using TMS as internal standard and $CDCl_3$ as solvent (unless specified otherwise). Chemical shifts are reported in τ units (10.00 p.p.m. downfield from TMS). Vapor-phase chromatographic (v.p.c.) analyses were performed on a Varian Aerograph model 1200-1 HY-FI III gas chromatograph using a 5 ft × $\frac{1}{8}$ in. column packed with 5% Carbowax 20M on Aeropak 30.

All quantitative estimates of the composition of product mixtures by gas–liquid chromatographic (g.l.c.) and n.m.r. spectroscopic analysis are based on comparison of integrated peak areas obtained for the various components of a reaction mixture with those obtained for standard mixtures prepared from the pure components. The v.p.c. peak areas were measured planimetrically. For the purpose of analysis and identification, small samples of all the components of a product mixture were isolated in >95% purity by fractional distillation or preparative gas chromatography. Preparative separations were performed on a Varian Aerograph A-90-P3 using a 30% QF-1 column 20 ft × $\frac{3}{8}$ in.

Phenyl(trichloromethyl)carbinol (*1*)

Compound **1** was prepared from benzaldehyde, chloroform, and powdered potassium hydroxide as described in the literature (6). The desired product was obtained in 31% yield, b.p. 141–143°/15 mm.

Reduction of 1 with Zinc and Acetic Acid

A solution of 45.1 g (0.20 mole) of **1** in 300 ml of glacial acetic acid was cooled to 0°. After the addition of 50 g (0.765 g-atoms) of zinc dust, the mixture was stirred for 1 h at ice-bath temperature. There was no visible evidence of reaction. Excess zinc was filtered off and water was added. Extraction with ether, washing with water and aqueous sodium carbonate solution, and distillation gave 33 g of crude product, b.p. 91–102°/12 mm. The product mixture was shown by g.l.c. and n.m.r. spectroscopic analysis to consist of 66% β,β-dichlorostyrene (**2**), b.p. 98–101°/15 mm, 10% *cis*-β-chlorostyrene (**3***a*), 8% *trans*-β-chlorostyrene (**3***b*), b.p. 91–93°/15 mm, and 12% starting material (**1**).

Nuclear magnetic resonance absorption peaks:
2, ν_{max} ($CDCl_3$) τ 3.28 singlet (1 proton, —CH=CCl_2), 2.75 multiplet (5 protons, C_6H_5—);
3*a*, ν_{max} ($CDCl_3$) τ 3.87 doublet (1 proton, $\rangle C{=}CH_a-$Cl), 3.47 doublet (1 proton, $C_6H_5-CH_b{=}C\langle$), 2.65 multiplet (5 protons, C_6H_5—); J_{ab} = 8.0 c.p.s.;
3*b*, ν_{max} ($CDCl_3$) τ 3.52 doublet (1 proton, $\rangle C{=}CH_a-$Cl), 3.22 doublet (1 proton, $C_6H_5-CH_b{=}C\langle$), 2.82 multiplet (5 protons, C_6H_5—); J_{ab} = 13.7 c.p.s.

Reduction of 1 with Zinc Amalgam under Standard Clemmensen Reduction Conditions (7)

A mixture of 100 g (1.53 g-atoms) of mossy zinc, 7.5 g of mercuric chloride, 5 ml of concentrated hydrochloric acid, and 125 ml of water was shaken for 5 min in a stoppered 1-l flask. The aqueous solution was decanted and 54.0 g (0.24 mole) of phenyl(trichloromethyl)-carbinol, 75 ml of water, and 175 ml of concentrated hydrochloric acid were added to the amalgamated zinc The reaction mixture was vigorously refluxed for 11 h during which period three 50-ml portions of concentrated hydrochloric acid were added at 3-h intervals. Dilution with water, extraction with ether, drying ($MgSO_4$), and evaporation of the solvent gave 27.0 g of crude product, b.p. 106–109°/21 mm, which was found by v.p.c. and n.m.r. spectroscopic analysis to have the following composition: 55% **2**, 16% **3***a*, 12% **3***b*, and 17% unidentified by-products.

1,1,1-Trichloro-2-hydroxy-6-methyl-4-heptanone (6)

This compound was prepared from methyl isobutyl ketone and chloral as described in the literature (8); **6** was obtained in 58% yield, m.p. 86–87° (lit. (8) 86–87°).

Reduction of 6 with Zinc Amalgam (Standard Conditions)

Following the procedure outlined for the reduction of **1** with zinc amalgam, 64.4 g (0.26 mole) of **6** gave 40.4 g of crude product. Vacuum distillation through a modified Widmer column at 12 mm pressure gave the following three fractions: forerun, 1.3 g, b.p. 40–77°; 1,1-dichloro-6-methyl-heptene (**8**), 16.5 g, b.p. 80–83°; 1,1-dichloro-6-methyl-1-hepten-4-one (**7**), 20.3 g, b.p. 105–110°.

Anal. Calcd. for $C_8H_{14}Cl_2$ (**8**): C, 53.05; H, 7.79; Cl, 39.15. Found: C, 53.02; H, 8.00; Cl, 38.90.

Anal. Calcd. for $C_8H_{12}Cl_2O$ (**7**): C, 49.25; H, 6.20; Cl, 36.34. Found: C, 49.71; H, 6.35; Cl, 35.98.

The yields obtained were 35% (**8**) and 40% (**7**), respectively. Spectroscopic analysis:

8; i.r.: ν_{max} (neat) 1615 cm^{-1} (C=C), no absorption at the frequencies characteristic for OH and C=O; n.m.r.: ν_{max} (CCl_4) τ 4.30 triplet (1 proton, —CH=CCl_2), 7.97 multiplet (2 protons, —CH_2—CH=CCl_2), τ 8.5 to 8.8 multiplet (5 protons, $\rangle$CH—CH_2—CH_2—), 9.15 doublet (6 protons, $(CH_3)_2C$).

7; i.r.: ν_{max} (neat) 1630 cm^{-1} (C=C), and 1720 cm^{-1} (C=O), no OH absorption; n.m.r.: ν_{max} (CCl_4) τ 3.74 triplet (1 proton, —CH=CCl_2), 6.61 doublet (2 protons, —CO—CH_2—CH=CCl_2), 7.66 multiplet (3 protons, $\rangle$CH—CH_2—CO—), and 9.10 doublet (6 protons, $(CH_3)_2C$).

The structure assignments were further verified by qualitative functional group tests ($KMnO_4$, Br_2/CCl_4, 2,4-DNPh, and Na fusion).

1,1-Dichloro-6-methyl-1-hepten-4-one (7)

1,1,1-Trichloro-2-hydroxy-6-methyl-4-heptanone (**6**) (64.4 g, 0.26 mole) was reduced with zinc amalgam and sulfuric acid by the procedure outlined for the reduction of **1** (for details, see Table II, No. 2). The usual work-up procedure gave 46.5 g of crude product which was fractionated at 17 mm pressure to give 32.5 g (64% yield) of 1,1-dichloro-6-methyl-1-hepten-4-one (**7**), b.p. 110–120°/17 mm.

Anal. Calcd. for $C_8H_{12}Cl_2O$: C, 49.25; H, 6.20; Cl, 36.34. Found: C, 49.31; H, 6.48; Cl, 36.10.

In addition to this main product, 2.8 g (6% yield) of 1,1-dichloro-6-methyl-1-heptene (**8**), b.p. 80–104°/17 mm,

Can. J. Chem. Downloaded from www.nrcresearchpress.com by 210.87.254.5 on 09/05/12
For personal use only.

and 7.0 g (11% recovery) of unreacted 1,1,1-trichloro-2-hydroxy-6-methyl-4-heptanone, b.p. 144–164°/17 mm, were isolated by fractional distillation.

1,1-Dichloro-6-methyl-1-heptene (8)

Following the procedure outlined for the reduction of **1**, 64.4 g (0.26 mole) of **6** was reduced with zinc amalgam and hydrochloric acid (for details, see Table II, No. 4). The crude reaction product (35 g) was distilled through a modified Widmer column to give 28 g (60% yield) of 1,1-dichloro-6-methyl-1-heptene (**8**), b.p. 75–82°/14 mm. No 1,1-dichloro-6-methyl-1-hepten-4-one was found in the v.p.c. (decyl phthalate column at 170°) of the crude product.

Reduction of 1,1-Dichloro-6-methyl-1-hepten-4-one (7)

Reduction of 76.7 g (0.394 mole) of **7** with 250 g of amalgamated zinc in hydrochloric acid (27 h reflux time, other procedural details as described before) and fractional distillation of the crude product obtained after extraction with methylene chloride, drying ($MgSO_4$), and evaporation of the solvent gave 12.3 g (17% yield) of 1,1-dichloro-6-methyl-1-heptene (**8**), b.p. 83–88°/15 mm, and 28.0 g (37% recovery) of unreacted 1,1-dichloro-6-methyl-1-hepten-4-one (**7**), b.p. 113–120°/15 mm.

Reduction of 1,1,1-Trichloro-2-hydroxy-6-methyl-4-heptanone (6) with Zinc and Acetic Acid

Following the procedure outlined for the reduction of **1** with zinc and acetic acid, 49.6 g (0.20 mole) of **6** gave 38.6 g of crude product which was found by v.p.c. and n.m.r. spectroscopic analysis to have the following composition: 65% 1,1-dichloro-6-methyl-1-hepten-4-one (**7**), b.p. 104–105°/15 mm, 24% 1-chloro-6-methyl-1-hepten-4-one, b.p. 85–90°/15 mm, and 3% unidentified, low-boiling products. Spectroscopic identification of 1-chloro-6-methyl-1-hepten-4-one: i.r.: ν_{max} (neat) 1635 cm^{-1} (C=C), 1715 cm^{-1} (C=O); n.m.r.: ν_{max} ($CDCl_3$) τ 9.07 doublet (6 protons, $(CH_3)_2C$), 7.68 multiplet (3 protons, $\rangle CH—CH_2—$), 6.67 doublet (2 protons, $—CH_2—CH=C$), 3.93 multiplet (2 protons, —CH=CH—Cl).

Catalytic Hydrogenation of Phenyl(trichloromethyl)-carbinol (1)

A solution of 5.0 g (0.022 mole) of **1** in 95% ethanol was hydrogenated over 20% palladium/carbon catalyst at room temperature and 40 p.s.i. of hydrogen pressure. Filtration of the reaction mixture and evaporation of the solvent gave 1.3 g of crude product which was shown by v.p.c. and spectroscopic analysis to consist of 25% starting material and 75% phenyl(dichloromethyl)-carbinol (**4**). A sample of pure **4**, m.p. 54–55° (lit. (9) 56°) was isolated from this mixture by preparative g.l.c. and identified by n.m.r. spectroscopy. The rest of the products are believed to be lower-boiling components which evaporated with the solvent. There were indications of ethylbenzene having formed during the reaction.

Reduction of (+)Phenyl(trichloromethyl)carbinol (1) with Lithium in Liquid Ammonia

To a stirred solution of 5.0 g (0.022 mole) of **1** in 1 l of liquid ammonia (taken from an ammonia cylinder without further purification) was added 1.0 g (0.14 mole) of lithium metal (small pieces). At the appearance of the blue color, after approximately 90 s, a solution of 24 g (0.30 mole) of ammonium nitrate in 200 ml of liquid ammonia was added to destroy lithium amide and unreacted lithium metal. Evaporation of the solvent, addition of 200 ml of 2 *N* hydrochloric acid, extraction with ether, drying ($MgSO_4$), and distillation gave 0.25 g of crude product, b.p. 84–85°/8 mm. The product mixture was shown by n.m.r. spectroscopy to consist of 85% α-phenethyl alcohol, 11% β-phenethyl alcohol, and 4% acetophenone. The specific rotation of this mixture was measured using a polarimeter (Franz Schmidt and Haensch, Berlin S.) with sodium lamp as light source and a two-decimeter tube. The measured value of $[\alpha]_D^{25}$ +18.6° (*c*, 5.0 g of solute per 100 ml of toluene solution) corresponded to 37% optical purity (lit.(10)$[\alpha]_D^{25}$ +50.6° for optically pure L-α-phenethyl alcohol).

Results

As shown in Table I, β,β-dichlorostyrene (**2**) has been found as the major product of reduction of phenyl(trichloromethyl)carbinol (**1**) with zinc, zinc–copper couple or zinc amalgam in neutral or acidic solution. In all but one of these reactions β-chlorostyrene (**3**) was formed as minor product. The reductions with zinc–copper in ethanol and with amalgamated zinc in hydrochloric acid were accompanied by the formation of small amounts of phenyl(dichloromethyl)carbinol (**4**) and β-phenethyl chloride, respectively. Reduction with Raney nickel or hydrogenation over 5% palladium/carbon results in the replacement of only one chlorine atom of **1** by hydrogen while simultaneous hydrogenolysis of one carbon–chlorine bond and ring hydrogenation was observed with platinum oxide as catalyst.

No α-phenethyl alcohol (**5**) was detected in any of these experiments, and no olefinic products were formed when the reduction of **1** was carried out in neutral alcoholic solution with catalysts and reducing agents other than zinc.

The reaction of 1,1,1-trichloro-2-hydroxy-6-methyl-4-heptanone (**6**) with zinc in acetic acid or aqueous mineral acid leads to the same structural changes as the corresponding reactions of **1** except that under the standard conditions of the Clemmensen reduction, i.e. reflux with amalgamated zinc in strong hydrochloric acid, the carbonyl group of **6** is also reduced. The data summarized in Table II show that the formation of **8** is facilitated by long reflux time and high concentration of hydrochloric acid, and that **7** becomes the major product when the reduction is carried out in sulfuric acid. The

TABLE I

Reduction of phenyl(trichloromethyl)carbinol

Number	Reducing agent	Solvent and reaction conditions	Major product	Minor products
1	Zn + HOAc	HOAc, 0°	C_6H_5—CH=CCl_2	C_6H_5—CH=CH—Cl
2	Zn + HCl	CH_3OH, 25°	C_6H_5—CH=CCl_2	—
3	Zn + $CuSO_4$	EtOH, 25°	C_6H_5—CH=CCl_2	C_6H_5CH=CHCl, C_6H_5CHOH—$CHCl_2$
4	Zn_xHg_y + HCl	H_2O, reflux	C_6H_5CH—CCl_2	C_6H_5CH=CHCl, $C_6H_5CH_2CH_2Cl$
5	Raney nickel	CH_3OH, reflux	C_6H_5CHOH—$CHCl_2$	—
6	H_2 + 5% Pd/C	EtOH, 25°, 35 p.s.i.	C_6H_5CHOH—$CHCl_2$	—
7	H_2 + 20% Pd/C	EtOH, 150°, 700 p.s.i.	Hydrocarbons	
8	H_2 + PtO_2	EtOH, 25°, 35 p.s.i.	$C_6H_{11}CHOH$—$CHCl_2$	
9	Li + NH_3	NH_3, −34°	C_6H_5CHOH—CH_3	$C_6H_5COCH_3$, $C_6H_5CH_2CH_2OH$
10	Na + NH_3	NH_3, −34°	C_6H_5—CO—CH_3	C_6H_5—CHOH—CH_3

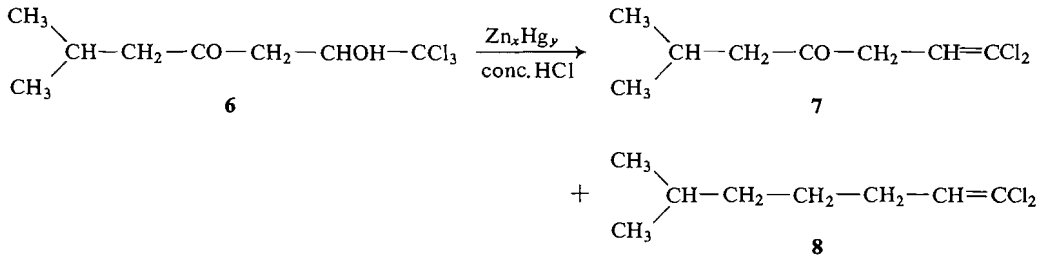

6

7

+

8

TABLE II

Clemmensen reduction of 1,1,1-trichloro-2-hydroxy-6-methyl-4-heptanone (6)

Number	Moles 6	Zn amalgam (g-atoms)	Amount of acid	Reflux time (h)	Unreacted Zn (g-atoms)	Percentage yield: Fore-run*	7	8
1	0.26	1.53	400 ml 9.8 *N* HCl	11	0.28	4	40	35
2	0.26	1.53	400 ml 9.8 *N* H_2SO_4	11	1.00	3	64	6
3	0.30	3.06	500 ml 4.8 *N* HCl‡	11	2.26	12	59	20
4	0.26	3.06	550 ml 10.4 *N* HCl	36	0.83	20	0	60
5	0.30	3.06	500 ml 10.2 *N* HCl	26	1.22	12	5	51
6†	0.20	0.765	300 ml glacial HOAc	—	—	30§	65	0

*Percentage yield of forerun is based on the molecular weight 128 for *n*-propyl isobutyl ketone which is believed to be the major component of the forerun.
†Compound 6 stirred for 1 h with zinc dust at 0–10° in glacial acetic acid.
‡Containing 100 ml ethanol.
§$(CH_3)_2CH$—CH_2—CO—CH_2—CH=CH—Cl.

intermediacy of **7** in the formation of **8** has been demonstrated by Clemmensen reduction of pure **7**. In glacial acetic acid as solvent, zinc dust reduces phenyl(trichloromethyl)carbinyl methyl ether ($C_6H_5CHOCH_3$—CCl_3) to β,β-dichlorostyrene (**2**), and **6** to 1,1-dichloro-6-methyl-1-hepten-4-one (**7**) and 1-chloro-6-methyl-1-hepten-4-one.

Alkali metals in liquid ammonia were found to convert phenyl(trichloromethyl)carbinol (**1**) to α-phenethyl alcohol (**5**) in low yield with partial racemization at the CHOH carbon and formation of acetophenone and β-phenethyl alcohol as by-products. When sodium or potassium was used as reducing agent instead of lithium, the reduction proceeded more rapidly and the yield of acetophenone increased at the expense of α-phenethyl alcohol. This indicates that hydrogenolysis of the CCl_3 group occurs at the metal surface and is not accomplished by the solvated electrons. Confirming this conclusion, acetophenone was formed as the main product

Can. J. Chem. Downloaded from www.nrcresearchpress.com by 210.87.254.5 on 09/05/12
For personal use only.

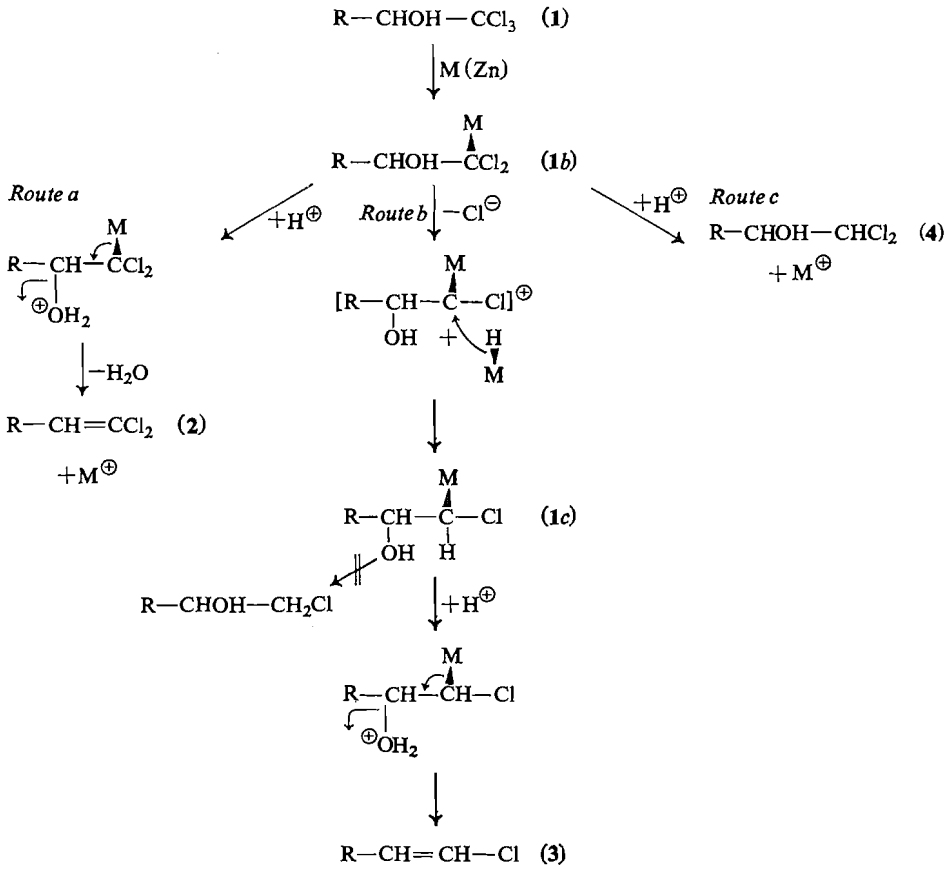

SCHEME 1 (R = C_6H_5)

when sodium was first dissolved in liquid ammonia to produce solvated electrons (blue) and **1** was subsequently added to the stirred solution.

Discussion

Reductions with Zinc and Catalytic Hydrogenolyses

On the basis of the experimental results summarized in Table I and of our present knowledge on electrochemical reduction processes and on the mechanism of the Clemmensen reduction (7, 11), it is proposed that the reduction of trichloromethylcarbinols with zinc in neutral or acidic solution is due to a heterogeneous reaction on the metal surface. It is the polar character of the carbonyl group, i.e., the high electrophilicity of the carbonyl carbon, which makes the Clemmensen reduction possible for aldehydes and ketones but not for carboxylic acids or esters, since the partial positive charge on the carbonyl carbon of the latter compounds is reduced by resonance interaction with the second oxygen atom. Due to the inductive effect of three chlorine atoms, the trichloromethyl carbon of **1** is sufficiently electrophilic to undergo adsorption and reduction on the zinc surface, but the cationic character of the mono- or dichloromethyl carbon is not sufficient to allow for replacement of all three chlorine atoms of **1** by hydrogen. In addition, the presence of a good leaving group (OH) in α-position to the trichloromethyl group, the acidity of the reaction medium, and the magnitude of the overvoltage of hydrogen on the metal surface have a marked effect on the course of the reaction and the structure of the products.

In the first step, the organic molecule diffuses to the metal surface where it is chemisorbed forming a carbon–metal bond. Since the metal

Can. J. Chem. Downloaded from www.nrcresearchpress.com by 210.87.254.5 on 09/05/12
For personal use only.

acts as an electron source pumping electrons into the molecule, the intermediate organometallic complex may be represented by structure **1***a* (in analogy to Grignard reagents) or more generally by **1***b* where M represents the metal surface (the latter presentation is used throughout this paper):

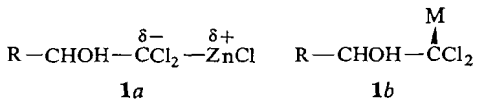

1*a* **1***b*

A wedge-shaped bond is used between carbon and metal to indicate the electron density distribution. This chemisorbed species (**1***b*) may undergo further reaction to form the observed products (see Table I) by any one of the three routes (*a*, *b*, and *c*) shown in Reaction Scheme 1.

Which of these routes is followed depends on the free energies of activation and on the nature of the transition states involved in the various reaction steps under different experimental conditions. Route *a*, stabilization of the chemisorbed molecule by formation of a double bond and elimination of water, apparently requires the lowest activation energy and is particularly favored in strongly acidic solution after preliminary protonation of the OH group. Thus, the presence of a good leaving group in the α-position accounts for the formation of β,β-dichlorostyrene (**2**) as the major product of reduction of **1** with zinc (Table I, Nos. 1–4). The same elimination of electronegative α-substituents due to the "pressure" of the electron gas of the metal on adjacent bonds has been observed for the Clemmensen reduction of various α-hydroxy ketones (12, 13). Desorption and combination of **1** with a proton (route *c*) is unfavorable because this process requires a relatively high activation energy due to the overvoltage of hydrogen on the zinc surface. Thus, phenyl(dichloromethyl)carbinol (**4**) is formed only in low yield when a zinc–copper couple is used as reducing agent.

In close similarity to the final steps of the Clemmensen reduction (11), the formation of β-chlorostyrene (**3**) may be explained by the "push" of the electron gas of the metal. Elimination of a chloride ion from the carbon bonded to the metal surface generates an electron-deficient carbon, and stabilization takes place by migration of a neighboring hydride ion (surface hydride), elimination of water, and desorption of the organic molecule from the metal surface (route *b*). The metal hydride is believed to be formed by discharge and dehydration of protonated solvent molecules on the metal surface and chemisorption of the resulting hydrogen atoms:

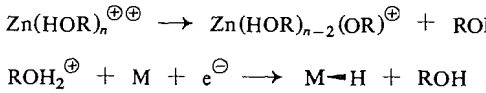

It is again the overvoltage of hydrogen on the metal surface which inhibits rapid combination of the hydride ion or the new organometallic intermediate (**1***c*) with protons to form H_2 or β-hydroxy-β-phenethyl chloride, respectively.

The mechanism of catalytic hydrogenolysis of **1** over Raney nickel, palladium, or platinum oxide is not well understood. In analogy to the preceding discussion and to the heterogeneous reaction of hydrogen with alkenes on catalytic surfaces, it may be assumed that on these metals "bonding" by chemisorption is partially replaced by weaker adsorption forces, and that the CCl_3 carbon of **1** but not the $CHCl_2$ carbon of **4** is sufficiently electrophilic for adsorption (or chemisorption) and hydrogenolysis to occur (via route *c*, Reaction Scheme 1). Thus phenyl-(dichloromethyl)carbinol (**4**) is rapidly desorbed from the catalyst surface before the reduction can proceed any further.

The reduction of 1,1,1-trichloro-2-hydroxy-6-methyl-4-heptanone (**6**) by zinc amalgam has been shown to be a two-step process. First, the trichloromethylcarbinol (—CHOH—CCl_3) is converted to a dichlorovinyl compound (—CH=CCl_2) by the mechanism outlined for route *a* (Reaction Scheme 1, R = *i*-Bu$COCH_2$). This step requires a lower activation energy than the regular Clemmensen reduction thus accounting for the absence of 1,1,1-trichloro-2-hydroxy-6-methylheptane in the product mixture. The second, slow step is the Clemmensen reduction of the carbonyl group (11). Route *b* (Reaction Scheme 1, R = *i*-Bu$COCH_2$) accounts for the formation of 1-chloro-6-methyl-1-hepten-4-one when **6** is reduced with zinc in glacial acetic acid.

It should be pointed out that the steric requirements for chemisorption of chlorinated carbon on metal surfaces are largely unknown; further studies will be needed on the factors

Can. J. Chem. Downloaded from www.nrcresearchpress.com by 210.87.254.5 on 09/05/12
For personal use only.

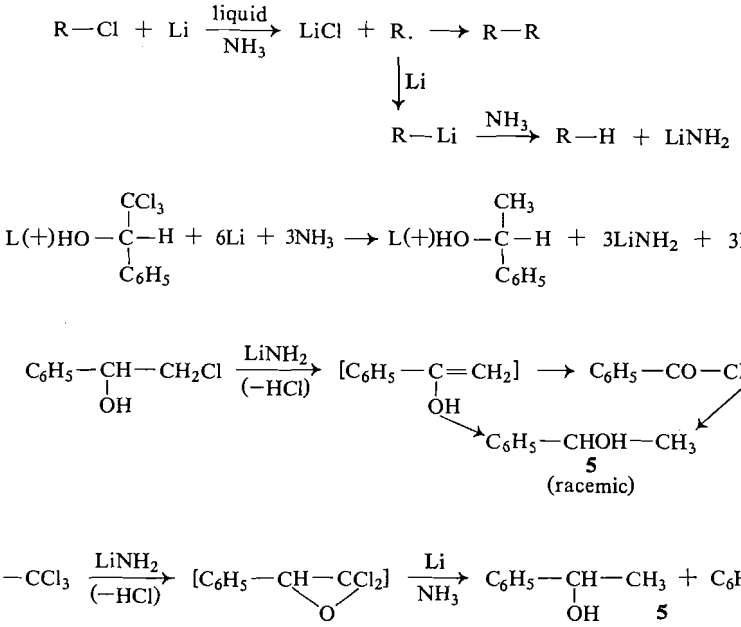

determining the strengths of the carbon–metal bonds of the various chemisorbed complexes postulated in Scheme 1 (and thus determining the activation energies required for desorption and stabilization of the desorbed molecules).

Reduction with Lithium

The mechanism of the reaction of phenyl-(trichloromethyl)carbinol (**1**) with lithium in liquid ammonia is probably closely related to the formation of organometallic derivatives (or dimeric products) when alkyl halides are allowed to react with alkali metals (14).

Three consecutive reaction steps of this kind would convert a trichloromethyl group to a methyl group with retention of configuration at the adjacent —CHOH— carbon.

The formation of acetophenone may be explained by dehydrohalogenation of the intermediate β-hydroxy-β-phenethyl chloride, and the racemic α-phenethyl alcohol may be due to subsequent reduction of acetophenone by excess lithium.

Both β-phenethyl alcohol and α-phenethyl alcohol may also be formed via a *gem*-dichloroepoxide intermediate (6).

Acknowledgments

The authors wish to express their gratitude to Harris Research Laboratories, Celanese Corporation (E. K.), American Cyanamid Company (R. J. B.), and to the National Research Council of Canada (E. K.) for providing the financial support for these investigations.

1. M. NAGAO and N. SATO. J. Am. Chem. Soc. **88**, 3447 (1966).
2. A. DINESMAN. Compt. Rend. **141**, 202 (1905).
3. E. KASPAR and R. WIECHERT. Ber. **91**, 2664 (1958).
4. G. C. BOND. Catalysis by metals. Academic Press, Inc., London. 1962. p. 401.
5. J. R. LACHER, A. KIANPOUR, F. OETTING, and J. D. PARK. Trans. Faraday Soc. **52**, 1500 (1956).
6. W. REEVE and L. W. FINE. J. Org. Chem. **29**, 1148 (1964).
7. E. L. MARTIN. Organic reactions. Vol. 1. John Wiley and Sons, Inc., New York. 1942. p. 155.
8. W. REEVE and E. KIEHLMANN. J. Org. Chem. **31**, 2164 (1966).
9. F. BERGMANN, A. KALMUS, and E. BREUER. J. Am. Chem. Soc. **80**, 4540 (1958).
10. W. VON E. DOERING and T. C. ASCHNER. J. Am. Chem. Soc. **71**, 838 (1949).
11. D. STASCHEWSKI. Angew. Chem. **71**, 726 (1959).
12. N. L. ALLINGER and D. J. CRAM. J. Am. Chem. Soc. **76**, 2362 (1954).
13. W. T. SMITH. J. Am. Chem. Soc. **73**, 1883 (1951).
14. H. O. HOUSE. Modern synthetic reactions. W. A. Benjamin, Inc., New York. 1965. p. 76.

Can. J. Chem. Downloaded from www.nrcresearchpress.com by 210.87.254.5 on 09/05/12
For personal use only.

Can. J. Chem. Downloaded from www.nrcresearchpress.com by 210.87.254.105 on 09/05/12
For personal use only.

Acylation and alkylation of 1,3-dimethoxybenzene in polyphosphoric acid

T. R. KASTURI AND K. M. DAMODARAN
Department of Organic Chemistry, Indian Institute of Science, Bangalore-12, India

Received August 20, 1968

Products of the reaction of 3-halo- and 3-ethoxypropionic acids with 1,3-dimethoxybenzene (**4**) in polyphosphoric acid have been shown to be 2′,4′-dimethoxy-3-(2,4-dimethoxyphenyl)-propiophenone (**6**) and 1,5-bis[3-(2,4-dimethoxyphenyl)-3-keto-propyl]-2,4-dimethoxybenzene (**15**) and these have been prepared by unambiguous syntheses. 2′,4′-Dimethoxy-3-ethoxypropiophenone (**3***a*) and 2′,3,4′-trimethoxypropiophenone (**3***d*) have been synthesized by the reaction of 3-chloro-2′,4′-dimethoxypropiophenone (**3***c*) with ethanol and methanol respectively.

Canadian Journal of Chemistry, **47**, 1529 (1969)

Friedel–Crafts acylation of aromatic compounds with bifunctional reagents (1) like halo- or alkoxypropionic acids in polyphosphoric acid (PPA) is rather difficult (2). Musgrave and coworkers (3) have reported unsuccessful attempts at acylations of 3,4-dimethoxyphenyl-, as well as 3,5-dimethoxyphenylacetic esters with substituted octanoic acids (**1***a*,*b*,*c*). One example wherein acylation employing 3-chloropropionic acid in PPA is successful, is that of Davis and Watkins (4) who have prepared the 3-chloropropionyl ketone **2***a* by the reaction of 3-chloropropionic acid with the ester **2***b*.

In connection with a synthetic project on hand, we needed 2′,4′-dimethoxy-3-ethoxypropiophenone (**3***a*) as a starting material. We thought of preparing compound **3***a* by acylation of 1,3-dimethoxybenzene (**4**) with 3-ethoxypropionic acid using PPA. First, PPA was chosen as the reagent as, unlike aluminium chloride, it is known to effect Friedel–Crafts acylations without causing aryl–alkyl ether cleavage (2, 5–8). We also anticipated that at lower reaction temperatures, the alkyl–alkyl ether linkage will remain unaffected.

Adopting Dev's general procedure (8) for PPA acylations with minor modifications, we treated 1,3-dimethoxybenzene with 3-ethoxypropionic acid in the presence of PPA at 40° for about 3–5 min.[1] The neutral product of the reaction was chromatographed on alumina to give two[2] ketonic substances, designated **A** and **B**, in 1:4 ratio. The occurrence of the M^+ peak at *m/e* 330 in the mass spectrum[3] of ketone **A** substantiated the molecular formula $C_{19}H_{22}O_5$. This ketone showed λ_{max} at 226, 269, and 300 mμ (ε 22 000, 14 500, and 8600) indicating the presence of a 2,4-dimethoxybenzoyl chromophore (10) in the molecule. The presence of a benzoyl group was indicated by peaks at 1661 (C=O of conjugated carbonyl), 1605, and 1575 cm^{-1} (aromatic C=C) in the infrared (i.r.) spectrum. Further, it gave the following signals in the nuclear magnetic resonance (n.m.r.) spectrum: 3.10 (m, 8 H), 3.81 (s, 6 H, two aromatic methoxyls), 3.87 (s, 6 H, two aromatic methoxyls), 6.33–6.70 (m, 4 H), 7.09 (d, 1 H, J = 9.5 Hz), and 7.83 δ (d, 1 H, J = 9.5 Hz).

Sodium borohydride reduction of ketone **A** gave a carbonyl-free hydroxylic substance, while its hydrogenolysis with diborane (11) gave the desoxo compound **5***a*. On the basis of the above data, ketone **A** was assigned the structure, 2′,4′-dimethoxy-3-(2,4-dimethoxyphenyl)-propiophenone (**6**). The mass spectral fragments *m/e* 165 (strong, **7**), 151 (strong, **8**), and 138 (weak, **9**) further substantiated this structure, which was proved by its unambiguous synthesis (*vide infra*).

Ketone **B**, which had an M^+ peak at *m/e* 522 in its mass spectrum showed λ_{max} at 227, 268, and 304 mμ (ε 40 800, 27 600, and 17 900), characteristic of a 2,4-dimethoxybenzoyl chromophore (10). The presence of carbonyl group and aromatic ring was indicated by peaks at 1661 (C=O of conjugated carbonyl), 1605, and 1575 cm^{-1} (aromatic C=C) in the i.r. spectrum. The

[1]In acylations employing PPA, reaction temperature and time are found to be critical factors (9).

[2]Thin-layer chromatography showed the presence of small amounts of other substances, which are under investigation.

[3]We are thankful to Dr. J. S. Shannon, Division of Entomology, C.S.I.R.O., Chatswood, New South Wales, Australia, for his help in obtaining the mass spectra reported herein and their interpretation.

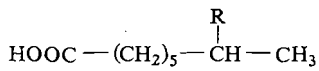

1 *a*, R = OAc
b, R = OMe
c, R = Br

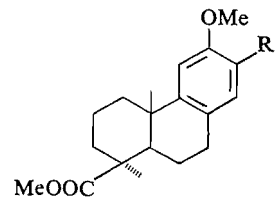

2 *a*, R = $COCH_2CH_2Cl$
b, R = H

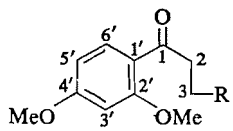

3 *a*, R = OEt
b, R = Br
c, R = Cl
d, R = OMe

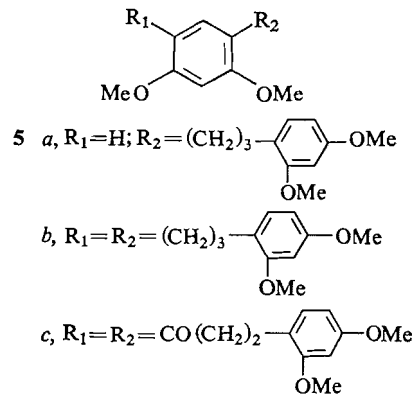

5 *a*, R_1=H; R_2=$(CH_2)_3$-(OMe)(OMe)
b, R_1=R_2=$(CH_2)_3$-(OMe)(OMe)
c, R_1=R_2=$CO(CH_2)_2$-(OMe)(OMe)
d, R_1=H; R_2=CH_2CH_2COOH
e, R_1=H; R_2=CH_2CH_2COOMe
f, R_1=R_2=CH_2CH_2COOH

complex n.m.r. spectrum showed peaks at 2.75–3.37 (m, 8 H), 3.81, 3.83, and 3.85 (18 H, probably six aromatic methoxyls), 6.37–6.60 (m, 5 H), 6.93 (s, 1 H), and 7.83 δ (d, 2 H, J = 9.5 Hz). Sodium borohydride reduction of ketone **B** gave a carbonyl-free hydroxylic substance, while diborane reduction gave a carbonyl-free desoxo compound **5***b*, indicating its benzylic nature.

The molecular weight as well as the presence of the fragments *m/e* 357 (weak, **10**), 343 (strong, **11**), 177 (weak, **12**), 165 (strong, **7**), and 151 (weak, **13**) in its mass spectrum led us to consider structures **14** or **15** for this ketone. The mass spectrum clearly ruled out the third alternative structure **5***c*, as it is not possible to derive the ion at *m/e* 343 from it. Further, structure **5***c* could be precluded on mechanistic grounds also (12).

In order to differentiate between structures **14** and **15**, these compounds were prepared by unambiguous methods as follows:

[1] **4** + **5***d* → **6** + **14**

[2] **4** + **5***f* → **15**

Preparation of the acid **5***d* has already been reported (13, 14). However, we tried alternative methods for preparing this acid. For example, treatment of 7-methoxydihydrocoumarin, obtained by high pressure hydrogenation (15) of 7-methoxycoumarin over Raney nickel catalyst, with cold alkali, followed by methylation with dimethyl sulfate in the presence of potassium carbonate in refluxing acetone, and saponification gave the acid **5***d* in good yields. The best and easiest method for the preparation of **5***d* was by the addition of methyl acrylate to 1,3-dimethoxybenzene in pyrophosphoric acid,[4] followed by saponification.

Reaction of the acid **5***d* with a fourfold excess of 1,3-dimethoxybenzene in PPA gave in good yield, according to eq. [1], the monoketone **6** and the unsymmetrical diketone **14** in 2:1 ratio. Compound **6** was identical with the aforementioned ketone **A**. The n.m.r. spectrum of the unsymmetrical diketone **14** was significantly

[4]Cf. Gardner *et al.* (16).

Can. J. Chem. Downloaded from www.nrcresearchpress.com by 210.87.254.105 on 09/05/12
For personal use only.

Can. J. Chem. Downloaded from www.nrcresearchpress.com by 210.87.254.105 on 09/05/12
For personal use only.

different from that of ketone **B** in the aromatic region (see Experimental).

Acylation of 1,3-dimethoxybenzene with the diacid **5***f* (16) in PPA according to eq. [2] led to the exclusive formation of the symmetrical diketone **15**, which was identical with the previously mentioned ketone **B**.

Having failed to obtain the required propiophenone **3***a* by the reaction of 1,3-dimethoxybenzene with 3-ethoxypropionic acid, we carried out the acylation of 1,3-dimethoxybenzene with 3-bromopropionic acid in PPA with a view to getting the bromoketone **3***b* which could easily be converted to the ethoxyketone **3***a* by known procedures. Chromatography of the neutral product from this reaction gave only the aforementioned ketones **6** and **15** in 3:1 ratio.

Acylation of 1,3-dimethoxybenzene with either 3-ethoxypropionyl chloride (cf. ref. 17) in the presence of aluminium chloride (7, 18) in carbon disulfide medium or with 3-chloropropionic acid in PPA, resulted only in the formation of the ketones **6** and **15**.

In the present work, the formation of monoketone **6** can be visualized by initial acylation (7) of 1,3-dimethoxybenzene with one molecule of 3-halo- or alkoxy-propionic acid, and subsequent electrophilic attack on a second molecule of the highly reactive aromatic ether **4** (7). The alkylation reaction might proceed by either of the following mechanisms:

(*a*) Elimination of 3-halo or alkoxy group to give the corresponding α,β-unsaturated carbonyl derivative followed by alkylation (7), or

(*b*) Formation of the intermediate complexes such as **16**, or **17** (1, 19, 20), which *in situ* might attack the aromatic ether **4**.

In order to get a clear picture of this mechanism, we carried out the reaction of the chloroketone **3***c* (*vide infra*) with 1,3-dimethoxybenzene in PPA. Thin-layer chromatography (t.l.c.) of the neutral product showed the presence of the starting chloroketone[5] as well as ketones **6** and **15**. In the light of this result and that of Davis and Watkins (4), mechanism (*a*) could be ruled out.

Since acylation of 1,3-dimethoxybenzene as the first step might result in the exclusive formation of the intermediate complex **16** or **17**, there is no possibility for the formation of the unsymmetrical ketone **14** in these reactions by further acylation of the monoketone **6**. However, the symmetrical ketone **15** may be formed by further alkylation of the ketone **6** or by simultaneous dialkylation of 1,3-dimethoxybenzene by the intermediate complex **16** or **17**. This is evident from the aforementioned alkylation reaction of 1,3-dimethoxybenzene with the chloroketone **3***c*. This is further substantiated by the reaction of either of the alkoxy ketones **3***a* or **3***d*[6] with 1,3-dimethoxybenzene in PPA, when the same ketones **6** and **15** were formed.

Finally, the required ethoxypropiophenone **3***a* was prepared by acylation of 1,3-dimethoxybenzene with 3-chloropropionyl chloride in the presence of aluminium chloride in carbon disulfide medium (cf. ref. 18), followed by heating the resulting chloroketone **3***c* with either ethanolic potassium hydroxide (17, 21) or sodium iodide in ethanol (17). Similarly, the corresponding methoxypropiophenone **3***d* was also synthesized. The structures of ketones **3***a* and **3***d* were confirmed by their ultraviolet (u.v.), i.r., and n.m.r. spectra.

Experimental

Melting points (hot stage) and boiling points reported herein are uncorrected. Ultraviolet (ethanol solution) and infrared (i.r.) spectra were recorded on a Beckmann DU and a Perkin–Elmer model 137B Infracord spectrophotometers respectively. Nuclear magnetic resonance spectra were taken in $CDCl_3$ or CCl_4 solution on a Varian A-60 spectrometer using tetramethylsilane as internal standard. All organic extracts were dried over anhydrous sodium sulfate. Neutral alumina and silica gel were used for column chromatography and thin-layer chromatography (t.l.c.) respectively. Light petrol refers to fraction boiling 45–65°. Microanalyses were carried out by Messrs. B. R. Seetharamia and H. S. Thyagarajan of this department.

Reaction of 1,3-Dimethoxybenzene

(a) With 3-Ethoxypropionic Acid

A mixture of 1,3-dimethoxybenzene (6.9 g, 0.05 mole) and 3-ethoxypropionic acid (5.9 g, 0.05 mole) was added in one lot to PPA (phosphorus pentoxide (35 g) and *ortho*-phosphoric acid (15 ml)) at 40° and stirred vigorously for 3–5 min. The pale-red viscous reaction mixture was decomposed with ice-cold water and the resulting oily organic material was extracted with benzene. The benzene extract was washed successively with water, saturated aqueous sodium bicarbonate, and water. The solvent was distilled off and the residue (8 g) was chromatographed. The benzene – light petrol fraction (1 g) gave, on crystallization from ethanol, ketone **6**, m.p. 88–89°.

[5]However, the chloroketone could not be isolated after chromatography over neutral alumina, as it probably underwent decomposition.

[6]These experiments were suggested by one of the referees.

Can. J. Chem. Downloaded from www.nrcresearchpress.com by 210.87.254.105 on 09/05/12
For personal use only.

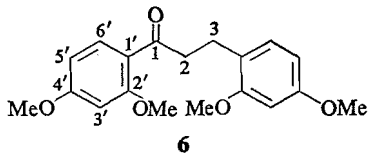

6

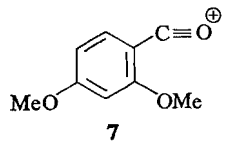

7

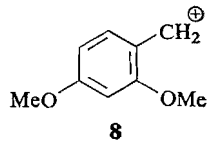

8

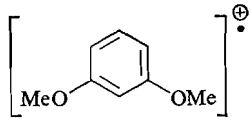

9

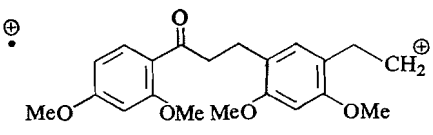

10

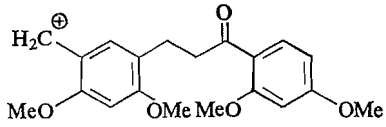

11

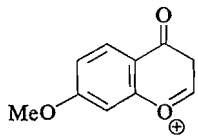

12

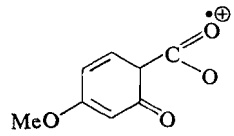

13

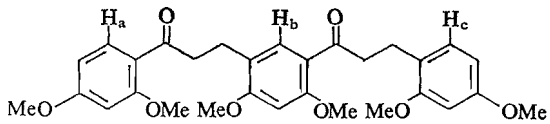

14

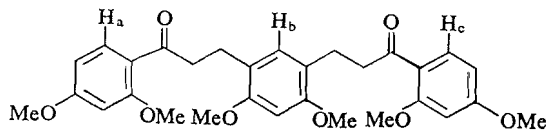

15

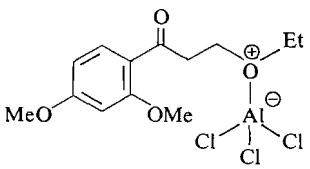

16

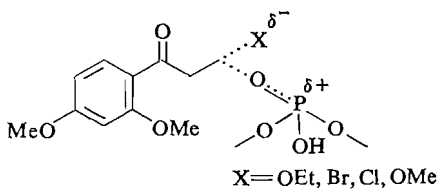

17

Anal. Calcd. for $C_{19}H_{22}O_5$: C, 69.07; H, 6.71. Found: C, 68.73; H, 6.52.

The 2,4-dinitrophenylhydrazone was recrystallized from ethanol, m.p. 121–123°.

Anal. Calcd. for $C_{25}H_{26}N_4O_8$: N, 10.97. Found: N, 11.16.

The fraction (4.2 g) eluted with benzene–ether was crystallized from ethanol to afford 1,5-bis[3-(2,4-dimethoxyphenyl)-3-ketopropyl]-2,4-dimethoxybenzene (**15**), m.p. 125–127°.

Anal. Calcd. for $C_{30}H_{34}O_8$: C, 68.95; H, 6.56. Found: C, 69.08; H, 6.6.

The bis-2,4-dinitrophenylhydrazone was recrystallized from ethyl acetate, m.p. 200–202°.

Can. J. Chem. Downloaded from www.nrcresearchpress.com by 210.87.254.105 on 09/05/12
For personal use only.

Anal. Calcd. for $C_{42}H_{42}N_8O_{14}$: N, 12.7. Found: N, 13.01.

(b) With 3-Bromopropionic Acid

A mixture of 1,3-dimethoxybenzene (3.5 g, 0.025 mole) and 3-bromopropionic acid (3.9 g, 0.025 mole) was poured in one lot into PPA (phosphorus pentoxide (16.25 g) and *ortho*-phosphoric acid (9.8 ml)) kept at 0°. The mixture was stirred vigorously and the temperature gradually raised to 20° during 15 min. Stirring was continued for a further 30 min at 40° during which time evolution of hydrogen bromide was observed. The reaction mixture was worked up as before to yield an oily residue (4.5 g) which, on chromatography, gave two fractions; the benzene fraction (2.9 g), on crystallization from ethanol, afforded ketone **6**, m.p. 88–89°, while recrystallization of the ether fraction (0.9 g) from ethanol furnished diketone **15**, m.p. 125–127°.

(c) With 3-Ethoxypropionyl Chloride

Powdered aluminium chloride (16 g) was added during 1 h to a stirred mixture of 1,3-dimethoxybenzene (16 g) and 3-ethoxypropionyl chloride (15 g) in carbon disulfide (32 ml) at 0°. The mixture was stirred at room temperature and let stand overnight. The supernatant liquid was decanted and the dark-red complex decomposed with crushed ice. The organic material was extracted with ether; the extract was washed successively with water, 5% aqueous sodium hydroxide, and water. The residue (20 g), obtained after evaporation of the solvent, was chromatographed; the light petrol – benzene fraction (2 g), on crystallization from ethanol, gave ketone **6**, m.p. 88–89°; the benzene–ether fraction (14 g), on crystallization from ethanol, yielded diketone **15**, m.p. 125–127°.

(d) With 3-Chloropropionic Acid

A mixture of 1,3-dimethoxybenzene (3.45 g) and 3-chloropropionic acid (2.71 g) was added in one lot to PPA (phosphorus pentoxide (17.5 g) and *ortho*-phosphoric acid (7.5 ml)) at 35° and stirred for 30 min. After work-up, the residue (4 g), on chromatography followed by crystallization from ethanol, gave ketone **6** (1.5 g), m.p. 88–89°, and diketone **15** (0.5 g), m.p. 125–127°.

(e) With 3-Chloro-2',4'-dimethoxypropiophenone (3c)

The chloroketone **3***c* (5.7 g, 0.025 mole) was added in one lot to a mixture of 1,3-dimethoxybenzene (3.45 g, 0.025 mole) and PPA (phosphorus pentoxide (17.5 g) and *ortho*-phosphoric acid (7.5 ml)) at 45° and stirred vigorously for 30 min. After work-up, the residue was chromatographed to give two fractions; the benzene fraction (3.8 g), on crystallization from ethanol, afforded ketone **6**, m.p. 88–89°, and the chloroform fraction (2 g) yielded diketone **15**, m.p. 125–127°.

(f) With 2',3,4'-Trimethoxypropiophenone (3d)

The methoxypropiophenone **3***d* (1.12 g) was added to a mixture of 1,3-dimethoxybenzene (0.69 g) and PPA (phosphorus pentoxide (3.5 g) and *ortho*-phosphoric acid (1.5 ml)) at 45° and stirred vigorously for 10 min. After work-up, the residue was chromatographed into two fractions; crystallization from ethanol gave monoketone **6** (0.4 g), m.p. 88–89°, and the diketone **15** (0.2 g), m.p. 125–127°.

(g) With 2',4'-Dimethoxy-3-ethoxypropiophenone (3a)

The ethoxypropiophenone **3***a* (0.6 g) was added to a mixture of 1,3-dimethoxybenzene (0.35 g) and PPA (phosphorus pentoxide (1.75 g) and *ortho*-phosphoric acid (0.75 ml)) at 45° and stirred vigorously for 10 min. After work-up, the residue was chromatographed to give two fractions; the benzene fraction (0.22 g), on crystallization from ethanol, afforded ketone **6**, m.p. 88–89°, and the chloroform fraction (0.15 g) yielded diketone **15**, m.p. 125–127°.

*Hydrogenolyses of Ketones **6** and **15** with Diborane*

(*i*) A solution of borontrifluoride–etherate (5 ml) and diglyme (13 ml) was added to ketone **6** (0.30 g) and sodium borohydride (0.95 g). After 3 h at room temperature, the reaction mixture was heated at 40–50° for 2 h, and cooled. Methanol was added to destroy the excess of diborane, the mixture diluted with ice-cold water, and extracted with benzene. The extract was washed with water. Removal of benzene followed by purification gave 2',4'-dimethoxy-3-(2,4-dimethoxyphenyl)propylbenzene (**5***a*) as an oil (0.29 g), b.p. 120°/1–2 mm (bath temperature); ν_{max} (neat): 1613 and 1587 cm^{-1}; λ_{max}: 226 and 279 mμ (ε 17 250 and 6300).

Anal. Calcd. for $C_{19}H_{24}O_4$: C, 72.15; H, 7.59. Found: C, 72.28; H, 7.18.

(*ii*) Similarly, hydrogenolysis of diketone **15** afforded 1,5-bis[3-(2,4-dimethoxyphenyl)propyl]-2,4-dimethoxybenzene (**5***b*) as an oil, b.p. 175–180°/1–2 mm (bath temperature); ν_{max} (neat): 1613 and 1587 cm^{-1}; λ_{max}: 227 and 280 mμ (ε 30 000 and 11 500).

Anal. Calcd. for $C_{30}H_{38}O_6$: C, 72.85; H, 7.74. Found: C, 72.81; H, 7.71.

7-Methoxydihydrocoumarin and its Conversion into 2,4-Dimethoxyphenylpropionic Acid (5d)

A solution of 7-methoxycoumarin (22) (10 g) in ethanol (80 ml) was hydrogenated over Raney nickel catalyst (3 g) at 90–100° at 200 atm of hydrogen for 45 min. After cooling the solution, the catalyst was filtered off, and the ethanol evaporated. The residue (10.5 g) yielded, on distillation, 7-methoxydihydrocoumarin (13) as an oil, b.p. 158–160°/0.5–1 mm; ν_{max} ($CHCl_3$): 1770, 1631, and 1590 cm^{-1}. Treatment of 7-methoxydihydrocoumarin with 5% aqueous sodium hydroxide followed by acidification afforded 2-hydroxy-4-methoxyphenylpropionic acid, m.p. 138–139°; (lit. (13), m.p. 138–139.5°).

A solution of 2-hydroxy-4-methoxyphenylpropionic acid (0.10 g) and dimethyl sulfate (0.1 ml) in acetone (10 ml) was refluxed in the presence of anhydrous potassium carbonate (0.30 g) for 20 h. The mixture was cooled, filtered, and the solvent removed *in vacuo* in the cold. The residue was treated with water, extracted with ether, and the solvent distilled off. A benzene solution of the residue was filtered through alumina (3 g) and distilled to give **5***e* (0.10 g), b.p. 135–140°/1–2 mm (bath temperature); (lit. (14), b.p. 160°/10 mm); $n_D^{25.7}$ 1.5170; ν_{max} (neat): 1757, 1610, and 1585 cm^{-1}.

Anal. Calcd. for $C_{12}H_{16}O_4$: C, 64.27; H, 7.19. Found: C, 64.32; H, 7.04.

Saponification (16) of the ester **5***e* gave the acid **5***d*, m.p. 103–104°; (lit. (13, 14), m.p. 102.5–103.5°).

Methyl 2,4-Dimethoxyphenylpropionate (5e)

Methyl acrylate (18.8 g) was added during 20 min to a

Can. J. Chem. Downloaded from www.nrcresearchpress.com by 210.87.254.105 on 09/05/12
For personal use only.

stirred mixture of pyrophosphoric acid (150 g) and 1,3-dimethoxybenzene (90 g), maintained at 65°. Stirring was continued for an additional 30 min. The reaction mixture was poured onto crushed ice and water (400 ml), and let stand for a while. The resulting oily product was extracted with ether, and the extract washed successively with water, saturated aqueous sodium bicarbonate, and water. Removal of ether and distillation of the residue yielded the ester **5***e* (30 g), b.p. 154–155°/1–2 mm.

*2′,4′-Dimethoxy-3-(2,4-dimethoxyphenyl)-propiophenone (**6**) and 2,4-Dimethoxy-1-[1-keto-3-(2,4-dimethoxyphenyl)-propyl]-5-[3-keto-3-(2,4-dimethoxyphenyl)-propyl]-benzene (**14**)*

A mixture of 1,3-dimethoxybenzene (13.80 g) and the acid **5***d* (5.25 g) was poured in one lot into PPA (phosphorus pentoxide (35 g) and *ortho*-phosphoric acid (15 ml)) maintained at 50–53° and stirred vigorously for 15 min. The residue was chromatographed; the benzene fraction (5 g), on crystallization from ethanol, afforded ketone **6**, m.p. 88–89°; crystallization of the benzene–chloroform fraction (2.5 g) from ethanol furnished the diketone **14**, m.p. 143–144°; λ_{max}: 227, 267, and 304 mμ (ε 39 100, 26 000, and 16 800); ν_{max} (Nujol): 1661, 1597, and 1575 cm^{-1}; n.m.r.: 2.71–3.41 (m, 8 H), 3.80, 3.89 (s, 18 H, six aromatic methoxyls), 6.41–6.59 (m, 5 H, aromatic protons), 7.08 (d, 1 H, J = 9.5 Hz, proton H_c), 7.67 (s, 1 H, proton H_b), and 7.81 δ (d, 1 H, J = 9.5 Hz, proton H_a).

Anal. Calcd. for $C_{30}H_{34}O_8$: C, 68.95; H, 6.56. Found: C, 69.29; H, 6.97.

The bis-2,4-dinitrophenylhydrazone was recrystallized from ethyl acetate, m.p. 209–210°.

Anal. Calcd. for $C_{42}H_{42}N_8O_{14}$: N, 12.7. Found: N, 12.6.

*1,5-bis[3-Keto-3-(2,4-dimethoxyphenyl)-propyl]-2,4-dimethoxybenzene (**15**)*

A mixture of the diacid **5***f* (4.2 g) and 1,3-dimethoxybenzene (15 g) was added in one lot into PPA (phosphorus pentoxide (35 g) and *ortho*-phosphoric acid (15 ml)) kept at 50–52° and stirred vigorously for 10 min. The dark-red reaction mixture after work-up gave a viscous oil (8 g) which, on trituration with light petrol followed by recrystallization from ethanol, afforded diketone **15**, m.p. 126–128°.

*3-Chloro-2′,4′-dimethoxypropiophenone (**3***c*)*

A solution of 1,3-dimethoxybenzene (7.2 g) in carbon disulfide (10 ml) was added during 30 min to a stirred mixture of 3-chloropropionyl chloride (5.9 g) and powdered aluminium chloride (6.9 g) in carbon disulfide (10 ml) at 0–5°. Stirring was continued at room temperature for further 8 h and the reaction mixture was allowed to stand overnight. After work-up, a crystalline solid (10.5 g) was obtained, which, on recrystallization from methanol, yielded white needles of chloroketone **3***c* (8 g), m.p. 101–102°; ν_{max} (Nujol): 1658, 1603, and 1572 cm^{-1}; λ_{max}: 229, 268, and 305 mμ (ε 13 400, 12 100, and 8 500).

Anal. Calcd. for $C_{11}H_{13}ClO_3$: C, 57.77; H, 5.69. Found: C, 57.32; H, 5.30.

*2′,4′-Dimethoxy-3-ethoxypropiophenone (**3***a*)*

(*i*) A solution of the chloroketone **3***c* (1 g) in ethanolic potassium hydroxide (2 g in 60 ml) was stirred at room temperature for 5 min followed by heating on a steam bath for 5 min. The reaction mixture, after cooling, was neutralized with 4 *N* acetic acid, ethanol was removed *in vacuo* in the cold, and the residual oil was extracted with benzene. The extract was washed successively with water, saturated aqueous sodium bicarbonate, and water. Removal of benzene gave a crystalline solid (1 g) which, on recrystallization from light petrol, afforded white plates of ketone **3***a*, m.p. 42–43°; ν_{max} (Nujol): 1658, 1605, and 1572 cm^{-1}; λ_{max}: 228, 267, and 302 mμ (ε 14 000, 12 400, and 8 150); n.m.r.: 1.12 (t, 3 H), 2.87–3.70 (m, 6 H), 3.78 (s, 3 H), 3.85 (s, 3 H), 6.31–6.50 (m, 2 H), and 7.60 δ (d, J = 9.5 Hz, 1 H).

Anal. Calcd. for $C_{13}H_{18}O_4$: C, 65.53; H, 7.61. Found: C, 65.38; H, 7.58.

(*ii*) A mixture of the chloroketone **3***c* (1.5 g) and anhydrous sodium iodide (10 g) in dry ethanol (50 ml) was refluxed on a steam bath for 36 h. About half of the solvent was removed *in vacuo*, and ether (200 ml) was added to the mixture. The ether solution was washed with 5% aqueous sodium thiosulfate and water. Ether was distilled off and the residue (1.5 g) crystallized from light petrol to give ketone **3***a* (1.2 g), m.p. 42–43°.

*2′,3,4′-Trimethoxypropiophenone (**3***d*)*

A solution of the chloroketone **3***c* (1 g) in methanolic potassium hydroxide (2 g in 60 ml) was stirred for 5 min at room temperature followed by heating on a steam bath for 5 min. The cooled reaction mixture was neutralized with 4 *N* acetic acid. Methanol was removed *in vacuo* in the cold, and the crystalline residue was filtered off, washed with water, and dried. Recrystallization from light petrol yielded white needles of the ketone **3***d* (0.8 g), m.p. 56–57°; ν_{max} (Nujol): 1658, 1605, and 1572 cm^{-1}; λ_{max}: 228, 267, and 303 mμ (ε 14 000, 12 400, and 8 200); n.m.r.: 2.84–3.70 (m, 4 H), 3.21 (s, 3 H), 3.73 (s, 3 H), 3.81 (s, 3 H), 6.17–6.42 (m, 2 H), and 7.51 δ (d, J = 9.5 Hz, 1 H).

Anal. Calcd. for $C_{12}H_{16}O_4$: C, 64.27; H, 7.19. Found: C, 64.18; H, 7.04.

Acknowledgments

We are thankful to Professor D. K. Banerjee for his keen interest in this work, to Professor George R. Pettit, Arizona State University, Tempe, Arizona, U.S.A., for kindly furnishing the n.m.r. spectra, and to Dr. G. Subrahmanyam for useful discussions. Thanks are also due to the authorities of the Indian Institute of Science and the Council of Scientific and Industrial Research, New Delhi, for the award of research fellowships to one of us (K.M.D.).

1. Friedel–Crafts and related reactions. Vol. II. Alkylation and related reactions. *Edited by* G. A. Olah. Interscience Publishers, Inc., New York. 1964.
2. F. D. Popp and W. E. McEwen. Chem. Rev. **58**, 321 (1958).
3. O. C. Musgrave, R. Templeton, and H. D. Munro. J. Chem. Soc. 250 (1968).

4. B. R. DAVIS and W. B. WATKINS. Tetrahedron, **24**, 2165 (1968).
5. F. UHLIG. Angew. Chem. **66**, 435 (1954).
6. F. UHLIG and H. R. SNYDER. *In* Advances in organic chemistry. Vol. I. Methods and Results. Polyphosphoric acid as a reagent in organic chemistry. *Edited by* R. A. Raphael, E. C. Taylor, and H. Wynberg. Interscience Publishers, Inc., New York. 1960. p. 35.
7. F.-H. MARQUARDT. Helv. Chim. Acta, **48**, 1476, 1486, 1490 (1965).
8. S. DEV. J. Indian Chem. Soc. **33**, 703 (1956).
9. H. R. SNYDER and F. X. WERBER. J. Am. Chem. Soc. **72**, 2965 (1950).
10. R. HUISGEN, G. SEIDL, and I. WIMMER. Ann. Chem. **677**, 21 (1964).
11. G. P. THAKAR and B. C. SUBBA RAO. J. Sci. Ind. Res. India, Sect. B, **21**, 583 (1962).
12. W. L. MOSBY. J. Org. Chem. **19**, 294 (1954).
13. W. D. LANGLEY and R. ADAMS. J. Am. Chem. Soc. **44**, 2320 (1922).
14. D. NASIPURI and G. PYNE. J. Chem. Soc. 3105 (1962).
15. P. L. DE BENNEVILLE and R. CONNOR. J. Am. Chem. Soc. **62**, 283, 3067 (1940).
16. M. NARAYANA, J. F. DASH, and P. D. GARDNER. J. Org. Chem. **27**, 4704 (1962).
17. A. B. CRAMER, M. J. HUNTER, and H. HIBBERT. J. Am. Chem. Soc. **61**, 509 (1939).
18. K. FREUDENBERG and H. FIKENTSCHER. Ann. Chem. **440**, 36 (1924).
19. G. M. BADGER and J. W. CLARK-LEWIS. *In* Molecular rearrangements. Part 1. Molecular rearrangement in some heterocyclic compounds. *Edited by* P. de Mayo. Interscience Publishers, Inc., New York. 1963. p. 653.
20. R. L. BURWELL, JR. Chem. Rev. **54**, 615 (1954).
21. E. P. KOHLER. Am. Chem. J. **42**, 375 (1909).
22. B. B. DEY, R. H. RAMACHANDRA RAO, and T. R. SESHADRI. J. Indian Chem. Soc. **11**, 743 (1934).

Can. J. Chem. Downloaded from www.nrcresearchpress.com by 210.87.254.105 on 09/05/12
For personal use only.

Can. J. Chem. Downloaded from www.nrcresearchpress.com by 210.87.254.5 on 09/05/12
For personal use only.

Secondary kinetic isotope effects in bimolecular nucleophilic substitutions. III. Deuterium effects in the Bunte salt reaction of methyl halides and sulfonates

G. E. JACKSON AND K. T. LEFFEK
Department of Chemistry, Dalhousie University, Halifax, Nova Scotia

Received December 16, 1968

Secondary kinetic deuterium isotope effects have been measured for the reaction between thiosulfate ion and methyl-d_3 halides and sulfonates in 50% v/v ethanol–water. The results are used to extend the correlation of Seltzer of k_H/k_D with the difference between the polarizabilities of the attacking nucleophile and the leaving group.

Dissociation constants for the $[NaS_2O_3]^-$ ion have been determined by conductivity measurements for the reaction conditions and used to calculate the concentration of free thiosulfate ions present in the reaction mixture. The activation parameters $\Delta H^{\ddagger}$ and $\Delta S^{\ddagger}$, based on second order rate constants calculated with respect to the concentration of thiosulfate ion, are reported.

Canadian Journal of Chemistry, 47, 1537 (1969)

Introduction

Secondary deuterium isotope effects in non-solvolytic S_N2 reactions, although generally smaller than analogous effects in S_N1 or solvolytic S_N2 reactions, are, nevertheless, large enough to warrant systematic study. An earlier paper (1) in this series showed that for the Bunte salt reaction

$$S_2O_3^{2-} + RBr \rightarrow RS_2O_3^- + Br^-$$

of certain alkyl bromides in 50% v/v ethanol–water, α-deuterium isotope effects were normal ($k_H/k_D > 1$) and could be as large as 7%. The direction of this effect was opposite to that expected from the solvolytic studies of Hartman and Robertson (2) and the magnitude was, at that time, greater than any previous measurements (3, 4). Since then several reports have confirmed the frequent occurrence of normal secondary deuterium isotope effects in S_N2 reactions; e.g., Wu and Robertson (5) found normal effects for the attack of phenoxide and ethoxide ion on deuterated trimethylsulfonium ion, Östman (6) obtained ratios (k_H/k_D) between 1.05 and 1.09 for the chloride-36 exchange of α-deuterated benzyl chloride and both 2-thenyl and 3-thenyl chloride. Recently, Seltzer and Zavitsas (7) have measured the iodide-131 exchange of methyl-d_3 iodide ($k_H/k_D = 1.05$ in methanol and 1.10 in water) and also proposed a correlation of isotope effects with the polarizabilities of the attacking nucleophile and leaving group. For a given alkyl group the rate ratio was correlated with the difference between the Edwards E-value (8–10) for the entering and leaving groups ($E_n - E_1$).

This paper further explores the deuterium isotope effect in Bunte salt reactions and, in particular, tests Seltzer's correlation for this system in which the value of ($E_n - E_1$) is large and positive, outside of the range of ($E_n - E_1$) previously available.

Results and Discussion

Solutions of sodium thiosulfate in 50% v/v ethanol–water are not fully ionized (11) and it has been shown for the case of magnesium thiosulfate and *n*-propylbromide that the reaction takes place entirely via the thiosulfate ion (12). Thus the second order rate constant calculated with respect to the concentration of thiosulfate ion does not vary with the ionic concentration, whereas that calculated with respect to the stoichiometric sodium thiosulfate concentration does vary with the stoichiometric concentration. However, the latter rate constants may be used in isotopic studies since

$$k_{2(\text{ionic})} = \frac{k_{2(\text{stoich.})}}{\alpha}$$

where α is the fraction of thiosulfate present as $S_2O_3^{2-}$ ions. All values of k quoted in this paper are second order rate constants calculated with respect to the stoichiometric sodium thiosulfate concentration.

Isotope Effects

Since extensive selective solvation takes place

TABLE I

Secondary α-deuterium isotope effects for the reaction of sodium thiosulfate with ethyl-1,1d_2 bromide at 25 °C

Solvent (% v/v ethanol)	$[Na_2S_2O_3]$ (M)	No. of runs	10^4k_H (1 mole^{-1} s^{-1})	10^4k_D (1 mole^{-1} s^{-1})	$k_H/k_D \pm$ Std. error
56	0.075	3	10.22	9.53	$1.07_2 \pm 0.01$
50	0.075	4	11.19	10.36	$1.08_0 \pm 0.01$
42	0.075	2	14.78	13.65	$1.08_3 \pm 0.01$
50	0.050	3	12.07	11.23	$1.07_5 \pm 0.01_6$
50	0.050	3	12.23	11.45	$1.06_8 \pm 0.01$*
50	0.030	3	13.10	12.35	$1.06_1 \pm 0.01$

*Reference (1).

TABLE II

Secondary deuterium isotope effect for the reaction of sodium thiosulfate with methyl esters in 50% v/v ethanol–water at 25 °C

Compound	No. runs	$10^4k_2 \pm$ Std. error (1 mole^{-1} s^{-1})	$k_H/k_D \pm$ Std. error
Methyl bromide	5	872±7	$1.03_1 \pm 0{\cdot}01$*
Methyl-d_3 bromide	3	846±6	
Methyl iodide	4	1078±5	$1.05_8 \pm 0{\cdot}01$
Methyl-d_3 iodide	3	1017±5	
Methyl methanesulfonate	5	285.1±1.7	$1.11 \pm 0{\cdot}01$
Methyl-d_3 methanesulfonate	4	257.2±0.9	
Methyl p-toluenesulfonate	3	231.2±1.0	$1.12 \pm 0{\cdot}01$
Methyl-d_3 p-toluenesulfonate	3	205.8±1.0	

*Reference (1).

when sodium thiosulfate is dissolved in alcohol–water mixtures, it is necessary to be sure that no significant changes in isotopic rate ratio can be produced by variation of the solvent medium. Table I contains results obtained for several solvent mixtures and concentrations of sodium thiosulfate. Ethyl-1,1,d_2 bromide was used as the substrate as this compound was known to give an isotope effect of about 7% (1).

The experimental requirements preclude large variations in the medium, but it can be seen that no distinct changes in rate ratio occur, and that none is likely to occur from accidental variations in the medium or reagent concentration which is large compared to the experimental error.

The correlation of Seltzer and Zavitsas of k_H/k_D with $(E_n - E_1)$ (7), although strictly valid only for solvent water, works well with the Bunte salt isotope effects previously reported (1).

Since $E = 2.52$ for thiosulfate, a large normal isotope effect would be expected for the Bunte salt reactions of alkyl sulfonates. Some results for a series of methyl compounds are shown in Table II.

Qualitatively, the sulfonate rate ratios are as predicted by the correlation. The plot k_H/k_D versus $(E_n - E_1)$, including the results presented in Table II, is given in Fig. 1. Drawing a line with a slightly steeper gradient than that used by Seltzer gives a reasonably good correlation of the effect, except for a few points already discussed by Seltzer and Zavitsas (7).[1]

In the above correlation the fact that the rate measurements were made at temperatures varying between 25° and 100 °C has been ignored. The justification for this is that a number of secondary deuterium isotope effects have been found to be independent of temperature (13, 14).[2]

However, none of the rate ratios included in the above plot has been tested experimentally because of the difficulty of determining the temperature dependence of a small effect over the experimentally accessible range of tempera-

[1]Another anomalous result has been found for the attack of cyanide ion on methyl-d_3 iodide in aqueous solution by A. Willi (private communication). For this reaction $k_H/k_D = 0.926$.

[2]R. E. Robertson. Private communication.

Can. J. Chem. Downloaded from www.nrcresearchpress.com by 210.87.254.5 on 09/05/12
For personal use only.

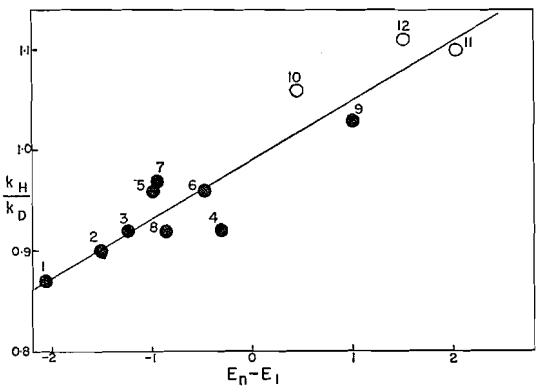

FIG. 1. Correlation of the isotopic rate ratio with the difference between the polarizabilities of the attacking nucleophile and the leaving group. Open circles—This work; closed circles—earlier work. Circles refer to: Solvolysis in water of: 1, CH_3I; 2, CH_3Br; 3, CH_3Cl; 4, CH_3ONO_2; 5, $CH_3OSO_2CH_3$; 6, $CH_3OSO_2C_6H_4CH_3$; 7, $(CH_3O)_2SO_2$; 8, CH_3I + C_5H_5N in C_6H_6 solvent; attack of $S_2O_3^{2-}$ in 50% v/v ethanol–water on 9, CH_3Br; 10, CH_3I; 11, $CH_3OSO_2C_6H_4CH_3$; 12, $CH_3OSO_2CH_3$.

ture, although a closely related reaction to No. 8 of Fig. 1 has been investigated (14). As the 12% effect found with methyl-d_3 *p*-toluensulfonate is the largest of this type observed to date, an attempt to determine its temperature dependence was made. The results are given in Table III. Although the rate ratios are not precise enough to separate the isotope effect into its enthalpic and entropic contributions, it is clear that the rate ratio is not markedly dependent on temperature so that no serious error in the correlation plot is likely to arise from this source. Robertson *et al.* (15) have suggested that the relation between these secondary isotope effects and temperature may be a further means of distinguishing between S_N1 and S_N2 mechanisms. Arguing from the theoretical treatment of Wolfsberg and Stern (16), they suggested that temperature-independent isotope effects are more likely to occur in an S_N2 reaction than in an S_N1 reaction. As far as the results in Table III show no clear change with temperature, they agree with Robertson's proposal.

Activation Parameters

Calculation of activation parameters from the rate constants would yield values which were correct only for one particular sodium thiosulfate concentration. To obtain true parameters, it is necessary to use k_2/α. Conductivity measurements were carried out using the procedure

TABLE III

Secondary deuterium isotope effect for the reaction of sodium thiosulfate with methyl *p*-toluenesulfate in 50% v/v ethanol–water

Temperature (°C)	No. runs	$10^4 k_H$ (1 mole^{-1} s^{-1})	$10^4 k_D$ (1 mole^{-1} s^{-1})	k_H/k_D*
14.95	3	92.7	84.7	1.09_5
19.98	3	150.3	138.2	1.09
25.00	3	231.2	205.8	1.12
29.98	3	364.7	325.1	1.12
35.02	3	562.1	512.4	1.10
40.02	4	812.3	743.2	1.09

*Standard error in each ratio is 0.01.

described by Bevan and Monk (11) to determine the fraction of sodium thiosulfate, α, which was present in the 50% ethanol–water solution as free thiosulfate ion at temperatures between 20° and 40 °C.

For the system

$$[NaS_2O_3]^- \rightleftarrows Na^+ + [S_2O_3]^{2-}$$

the dissociation constant K_{diss} is related to α by the expression

$$K_{diss} = \frac{\alpha^2 C \cdot f_{S_2O_3}{}^{2-}}{(1 - \alpha)}$$

where C is the stoichiometric sodium thiosulfate concentration and $f_{[S_2O_3]}{}^{2-}$ is the activity coefficient of the thiosulfate ion. Table IV shows the average values of K_{diss} obtained at the various temperatures using solutions of concentration less than 10^{-3} M, together with those of α calculated for the actual reaction conditions of the rates quoted in Table III. Bevan and Monk (11) measured K_{diss} for sodium thiosulfate at 25 °C and obtained a value of 1.45×10^{-2}, about 10% lower than our result.

When the apparent rate constants are divided by α, the true second order rate constants, i.e.,

TABLE IV

K_{diss} values and α for the reaction conditions

Temperature (°C)	$10^2 K_{diss}$(mole l^{-1})	α
40.0	4.46	0.847
35.0	3.59	0.818
30.0	2.21	0.736
25.0	1.62	0.673
20.0	1.305	0.625
15.0	—	0.57*

*Obtained by extrapolation.

Can. J. Chem. Downloaded from www.nrcresearchpress.com by 210.87.254.5 on 09/05/12
For personal use only.

Can. J. Chem. Downloaded from www.nrcresearchpress.com by 210.87.254.5 on 09/05/12
For personal use only.

those which do not change with change of the sodium thiosulfate concentration, are obtained. Figure 2 shows plots of k_H/α and k_D/α vs. $10^3/T$, for methyl and methyl-d_3 *p*-toluenesulfonate: from which the following true activation parameters were obtained by least squares computations:

$$CH_3OTs\ \Delta H_H^{\ddagger} = 12.6_5 \pm 0.07\ \text{kcal}\cdot\text{mole}^{-1}$$
$$\Delta S_H^{\ddagger} = -22.7_6 \pm 0.25\ \text{cal}\cdot\text{mole}^{-1}\cdot\text{deg}^{-1}$$
$$CD_3OTs\ \Delta H_D^{\ddagger} = 12.6_4 \pm 0.13\ \text{kcal}\cdot\text{mole}^{-1}$$
$$\Delta S_D^{\ddagger} = -23.02 \pm 0.4_4\ \text{cal}\cdot\text{mole}^{-1}\cdot\text{deg}^{-1}$$

Hammett *et al.* (17, 18) determined apparent activation parameters for several Bunte salt reactions, one of which was re-determined by Bevan and Monk (11) with magnesium thiosulfate as reagent, from which true activation parameters were calculated using k_2/α values. It is now possible to recalculate Hammett's results (17, 18) with k_2/α values using our conductivity measurements to calculate the values of α for the reaction conditions used by Hammett. These revised activation parameters, recorded in Table V, were obtained graphically since rate constants are available at only three temperatures in most cases. The temperature range 12.5° to 37.5° was used, except for methyl bromide for which two, at 10° and 20° were used.

The changes in enthalpy and entropy of activation with change in alkyl group remain almost the same as those originally reported by Hammett *et al.* (17, 18), but the absolute values are markedly different (compare with the figures quoted by Streitwieser (19)). These reactions are now seen to be characterized by low enthalpies of activation which are balanced by large negative entropies of activation. The recalculated values are qualitatively very similar to those for Menschutkin reactions in nitro-

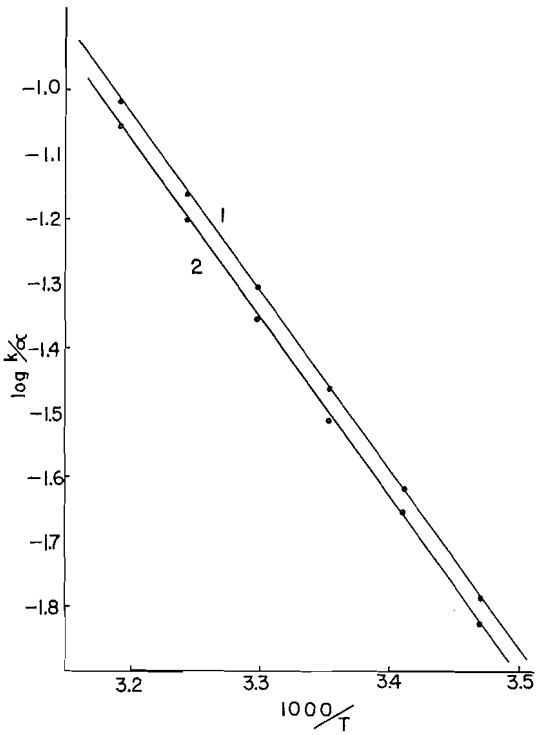

FIG. 2. Temperature dependence of the corrected rate constants for the reactions between methyl *p*-toluenesulfonate (1) and methyl-d_3 *p*-toluenesulfonate (2) and thiosulfate ions in 50% v/v ethanol–water solvent.

TABLE V

Activation parameters for the attack of thiosulfate ion on alkyl esters in 50% v/v ethanol–water solvent*

Compound	$\Delta H^{\ddagger}$ (kcal·mole^{-1})	$\Delta S^{\ddagger}$ (cal·mole^{-1}·deg^{-1})
CH_3Br	8.5±1	−39±3
C_2H_5Br	11.6	−32
n-C_3H_7Br	11.1	−35
n-C_3H_7Br†	17.5	−14
iso-C_3H_7Br	13.0	−34
iso-C_4H_9Br	13.4	−34
$CH_3OSO_2C_6H_4CH_3$‡	12.6	−22.8

*Original data from Hammett (17, 18), except as noted. Errors are probably less than one unit in $\Delta H^{\ddagger}$ and two units in $\Delta S^{\ddagger}$, except for methyl bromide.
†Using MgS_2O_3 (12).
‡This work.

benzene and benzene solvent (19). The low enthalpies of activation are to be expected from a large polarizable nucleophile such as the thiosulfate ion, since the energy required to place the electrons into a bond forming position would be small. Negative entropies of activation are characteristic of S_N2 reactions where two entities in the initial stage are merging into one in the transition state. However, the size of the parameters in these Bunte salt reactions requires further discussion. The doubly charged thiosulfate ion is strongly and preferentially solvated by water molecules when dissolved in 50% aqueous ethanol. Concentrated solutions separate into two immiscible layers. On the other hand alkyl compounds will not be expected to be nearly as efficient in solvent sorting until the bromine takes on a fractional negative charge in the transition state. This fractional negative charge has been transferred from the thiosulfate ion which still carries more than one unit of negative charge. Thus, the amount of solvent sorting may well be increased in the transition state relative to the initial state, which would introduce another negative contribution to the entropy of activation.

Experimental

Materials

Ethyl-1,1,d_2 bromide (99.5% isotopic purity) was supplied by Merck, Sharp and Dohme Ltd., and methyl-d_3 iodide (99.5%) by Stohler Isotope Chemicals. The normal compounds were reagent grade chemicals which were dried and fractionally distilled before use.

Methyl-d_3 methanesulfonate was prepared by reaction of silver methanesulfonate (1 g) in pure acetonitrile (40 ml) with methyl-d_3 iodide (0.31 ml) at 50° for 8 h. The suspension was filtered to remove silver iodide and the solvent was removed under vacuum. Recovery of the silver iodide showed that the reaction had gone to completion. The product, after purification by distillation under reduced pressure, was obtained in about 75% yield.

Methyl-d_3 *p*-toluenesulfonate was prepared by a similar procedure. The protium analogues were purchased from Eastman Organic Chemicals.

The solvent was prepared and analyzed as described previously (1).

Kinetic Methods

The method used was that described in Part I of this series (1). The initial concentration of the ethyl bromides was 0.020–0.025 *M*. For the ethyl compounds the thiosulfate concentration was initially about 0.05 *M* (except for the runs quoted in Table I) and for the methyl compounds about 0.02 *M*.

Conductance Measurements

The conductance measurements were made with a Wayne Kerr Universal Bridge B221 and stirred cells, which were the cells used by Robertson *et al.* (15) for ethanol–water mixtures. The dissociation constants of the ion pair (K) and the degrees of dissociation (α) were calculated by the method described by Bevan and Monk (11, 12).

Acknowledgments

The authors are grateful for financial support of this work by the National Research Council of Canada and, in particular, thank Dr. R. E. Robertson (National Research Council) for the loan of conductivity cells.

1. K. T. Leffek. Can. J. Chem. **42**, 851 (1964).
2. S. Hartman and R. E. Robertson. Can. J. Chem. **38**, 2033 (1960).
3. V. J. Shiner, Jr. J. Am. Chem. Soc. **74**, 5285 (1952).
4. R. R. Johnson and E. S. Lewis. Proc. Chem. Soc. **52**, (1958).
5. C-Y. Wu and R. E. Robertson. Chem. & Ind. 1803 (1964).
6. B. Östman. J. Am. Chem. Soc. **87**, 3163 (1965).
7. S. Seltzer and A. A. Zavitsas. Can. J. Chem. **45**, 2023 (1967).
8. J. O. Edwards. J. Am. Chem. Soc. **76**, 1540 (1954).
9. J. O. Edwards. J. Am. Chem. Soc. **78**, 1819 (1956).
10. R. E. Davis. J. Am. Chem. Soc. **87**, 3010 (1965).
11. J. R. Bevan and C. B. Monk. J. Chem. Soc. 1392 (1956).
12. J. R. Bevan and C. B. Monk. J. Chem. Soc. 1396 (1956).
13. K. T. Leffek, R. E. Robertson, and S. E. Sugamori. Can. J. Chem. **39**, 1989 (1961).
14. K. T. Leffek and J. W. MacLean. Can. J. Chem. **43**, 40 (1965).
15. L. Hakka, A. Queen, and R. E. Robertson. J. Am. Chem. Soc. **87**, 161 (1965).
16. M. Wolfsberg and M. J. Stern. Pure Appl. Chem. **8**, 325 (1964).
17. T. I. Crowell and L. P. Hammett. J. Am. Chem. Soc. **70**, 3444 (1948).
18. P. M. Dunbar and L. P. Hammett. J. Am. Chem. Soc. **72**, 109 (1950).
19. A. Streitwieser, Jr. Solvolytic displacement reactions. McGraw–Hill, Inc., New York. 1962. p. 22.

Can. J. Chem. Downloaded from www.nrcresearchpress.com by 210.87.254.5 on 09/05/12
For personal use only.

Can. J. Chem. Downloaded from www.nrcresearchpress.com by 210.87.254.6 on 09/05/12
For personal use only.

Ortho lithiation of *N,N*-dimethylbenzenesulfonamide by *n*-butyllithium. Condensation with electrophilic compounds[1]

HAMAO WATANABE, RICHARD A. SCHWARZ, AND CHARLES R. HAUSER
Department of Chemistry, Duke University, Durham, North Carolina

AND

J. LEWIS AND D. W. SLOCUM
Department of Chemistry, Southern Illinois University, Carbondale, Illinois

Received October 30, 1968

N,N-Dimethylbenzenesulfonamide was converted by *n*-butyllithium to the *ortho*-lithiosulfonamide, which was condensed with benzophenone, benzonitrile, phenylisocyanate, and carbon dioxide to form a carbinol, an imine, an amide, and an acid, respectively. The carbinol was cyclized thermally to give a sultone. The imine was converted to the corresponding ketone, oxime, and phenylhydrazone. The oxime underwent a Beckmann rearrangement to afford the same amide that was obtained in the reaction of the *ortho*-lithiosulfonamide with phenylisocyanate.

Canadian Journal of Chemistry, 47, 1543 (1969)

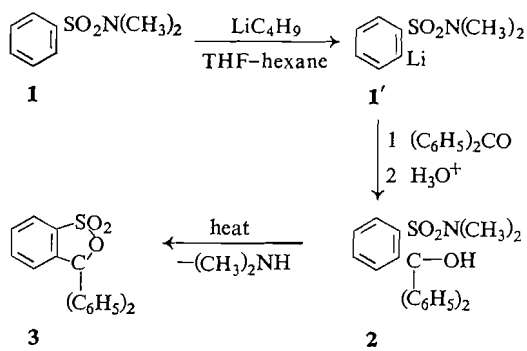

SCHEME 1

Although the carbonyl group of *N,N*-dimethylbenzamide is attacked by *n*-butyllithium leading to formation of valerophenone (1), the sulfonyl group of *N,N*-dimethylbenzenesulfonamide (**1**) should be less susceptible to attack by this reagent so that ring lithiation of **1** to form *ortho*-lithiosulfonamide **1′** appeared feasible. This was verified in the present investigation by condensation with electrophilic compounds in tetrahydrofuran (THF)–hexane to give *ortho* derivatives. Thus, **1′** underwent an addition reaction with benzophenone to afford carbinol-sulfonamide **2**, which underwent thermal cyclodeamination to produce sultone **3** (Scheme 1).

Similarly, lithiosulfonamide **1′** underwent addition reactions with benzonitrile, phenyl isocyanate, and carbon dioxide to form imine-sulfonamide **4**, carboxamide-sulfonamide **5**, and acid-sulfonamide **6**, respectively. The imine **4** was hydrolyzed to form ketone **7**, and condensed with hydroxylamine and phenylhydrazine to give oxime **8** and phenylhydrazone **9**, respectively; incidentally, the ketone **7** failed to afford oxime **8** or phenylhydrazone **9** under similar conditions.

The yields of these products were good to excellent (57–93%), except that for sultone **3**. Their structures were supported by analyses and/or absorption spectra (see Experimental).

Although the yield of sultone **3** was only 30%, this is better than that (18%) obtained previously by the action of hot sulfuric acid on carbinol-sulfonamide **11** (R = C_6H_5), which was prepared by condensation of dilithiosulfonamide **10** with benzophenone (2). The more characteristic reaction of carbinol-sulfonamides of type **11** involves

[1]Supported by the Army Research Office (Durham, North Carolina).

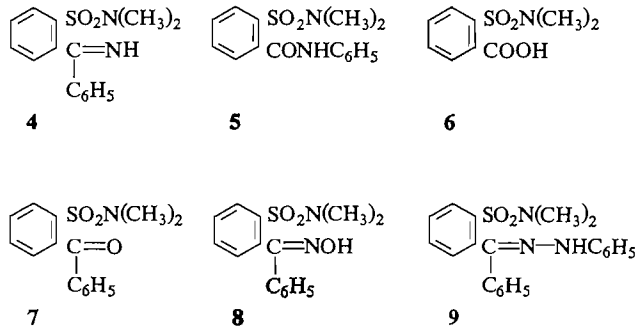

4 5 6

7 8 9

cyclodehydration to form sultams of type **12** (2); this reaction has generally been effected by treatment of **11** with cold sulfuric acid, followed by water (2). Similar treatment of carbinol-sulfonamide **2** has now resulted only in recovery of **2**.

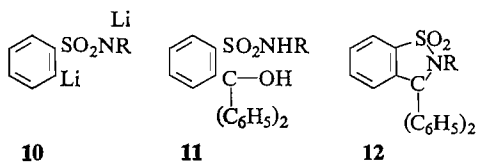

10 11 12

Oxime-sulfonamide **8** underwent a Beckmann rearrangement with phosphorus pentachloride to form amide-sulfonamide **5**, which was shown to be identical with that obtained from lithiosulfonamide **1′** and phenylisocyanate, (Scheme 2).

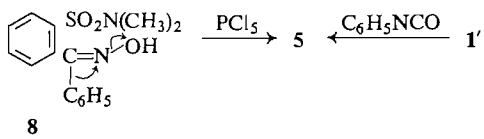

8

SCHEME 2

Although this result would ordinarily be considered to establish the indicated configuration of the oxime in which phenyl and hydroxyl are *trans* (see Scheme 2), there appears to be a possibility that the other isomer of the oxime might have given the same result by isomerization prior to rearrangement. This might have occurred because of the expected reluctance of the aryl group in oxime **8**, which has the strongly electron attracting sulfonyl substituent, to undergo migration. An attempt to test this possibility by isolation and rearrangement of the other isomer of the oxime, however, was unsuccessful.

An attempt to extend the present method of lithiation and condensation to *N,N*-diphenylbenzenesulfonamide was unsuccessful. Incidently, this sulfonamide was obtained in excellent yield (92%) when benzenesulfonyl chloride and diphenylamine were treated with pyridine (3), but not when this chloride and amine were treated with aqueous alkali or with excess amine in ether according to other earlier methods (4).

Experimental[2]

Ortho-Lithiation of N,N-Dimethylbenzenesulfonamide (1)

A solution of 0.025 mole of *N,N*-dimethylbenzenesulfonamide (**1**, m.p. 47–48°; lit (4, 5) 47–48°) in 50 ml of tetrahydrofuran (THF)[3] in a dry flask under nitrogen was cooled to 0°, and 20 ml (0.030 mole) of a solution of 1.59 *M* *n*-butyllithium in hexane[4] was added during 5–6 min. After stirring for 30 min at 0°, the brown suspension was considered to contain 0.025 mole of monolithiosulfonamide **1′**. The suspension was employed at 0° as described below.

Condensation of Lithiosulfonamide 1′ with Benzophenone to Form Carbinol-sulfonamide 2

To a stirred, cold suspension of 0.025 mole of lithiosulfonamide **1′** was added under nitrogen, during 4 min, a solution of 5.47 g (0.030 mole) of benzophenone in 30 ml of THF,[3] and the stirring was continued for 30 min at 0°. To the resulting clear, dark-brown solution (cooled in an ice bath) was added, with stirring, 20 ml of water followed by 30 ml of 5% hydrochloric acid. The two layers were separated. After saturation with sodium chloride, the

[2]Melting points are uncorrected. Elemental analyses were performed by Janssen Pharmaceutica, Beerse, Belgium, and by M-H-W Laboratories, Garden City, Michigan, and by Alfred Bernhardt, West Germany. Infrared spectra (KBr method) were produced on Perkin–Elmer Infracord Model 137 and 237 spectrophotometers. Nuclear magnetic resonance spectra were obtained with a Varian A-60 spectrometer and signals are reported in p.p.m. downfield from an internal tetramethylsilane standard.

[3]Freshly distilled from lithium aluminium hydride.

[4]Foote Mineral Company, Route 100, Exton, Pennsylvania.

Can. J. Chem. Downloaded from www.nrcresearchpress.com by 210.87.254.6 on 09/05/12
For personal use only.

Can. J. Chem. Downloaded from www.nrcresearchpress.com by 210.87.254.6 on 09/05/12
For personal use only.

aqueous layer was extracted three times with ether, and the extracts were combined with the organic layer. After washing twice with a saturated solution (30 ml) of sodium chloride and drying ($MgSO_4$), the solvent was removed under reduced pressure on the steam bath. The crystalline residue was stirred with a little methanol, and the mixture was filtered. The solid was washed with a little methanol, and dried in air to give 7.46 g (82%) of α,α-diphenyl-*o*-(*N*,*N*-dimethylsulfamyl) benzyl alcohol (**2**), m.p. 162–164° and 164–165° (fine crystals) after recrystallization from acetone–methanol; i.r. 3380 (OH), 1303 and 1140 cm^{-1} (SO_2); n.m.r. ($CDCl_3$) 8.15–6.78 (m, 14.1, aromatic), 6.78 (s, 1.0, OH), and 2.57 p.p.m. (s, 6.0, N-CH_3).

Anal. Calcd. for $C_{21}H_{21}NSO_3$: C, 68.64; H, 5.76; N, 3.81; S, 8.73. Found: C, 68.29; H, 5.76; N, 3.88; S, 8.62.

Cyclization of Carbinol-sulfonamide **2**

Cyclization of 1.0 g of **2** was effected by heating it under a slow stream of nitrogen in a Wood's metal bath at 185–195° for 6 h. After cooling, the molten mass was dissolved in a little hot methanol, and the solution was allowed to stand overnight. The resulting crystals were collected, and recrystallized from methanol to afford 0.26 g (30%) of 3,3-diphenyl-2,1-benzoxathiole-1,1-dioxide (**3**) (fine leaflets), m.p. 162–164°, undepressed on admixture with an authentic sample (2) of **3** (m.m.p. 163–165°); the i.r. spectra of the two samples were identical.

When the cyclization of **2** was effected at 205–215° in the presence of 20 mg of benzoyl peroxide, sultone **3**, m.p. 162–164°, was obtained in 10% yield.

Condensation of Lithiosulfonamide **1′** *with Benzonitrile to Form Imine-sulfonamide* **4**

This reaction was effected as described above for benzophenone to give a brown-red suspension which was cooled in an ice bath and stirred with 20 ml of water followed by 30 ml of 10% hydrochloric acid. The resulting two layers were separated. The acidic, aqueous layer, which was combined with acidic extracts of the organic layer, was made basic with potassium carbonate powder. After standing in a current of air under a hood for several hours, the crystalline solid was collected, washed with water, and dried in air to give 5.69 g (79%) of *o*-(*N*,*N*-dimethylsulfamyl)benzophenone imine (**4**), m.p. 153–156° and 155.5–156.5° (as prismatic crystals) after recrystallization from methanol; i.r. 3255 (NH), 1600 (C=N), 1345 and/or 1335 (SO_2), and 1155 cm^{-1} (SO_2); n.m.r. ($CDCl_3$) 8.22–7.17 (m, 9.1, aromatic and NH), and 2.57 p.p.m. (s, 6.0, N—CH_3).

Anal. Calcd. for $C_{15}H_{16}N_2SO_2$: C, 62.47; H, 5.60; N, 9.72. Found: C, 62.69; H, 5.20; N, 9.47.

Hydrolysis of imine-sulfonamide **4** (1.0 g) was effected by refluxing it with 40 ml of 5% sulfuric acid for 1 h. After cooling, the mixture was filtered. The solid was washed with water, and dried to give 0.85 g (85%) of *o*-(*N*,*N*-dimethylsulfamyl)benzophenone (**7**), m.p. 146–147.5°. Recrystallization from methanol afforded 0.76 g (76%) of **7** (fine crystals), m.p. 147–148°; i.r. 1660 (CO), 1330 and 1155 cm^{-1} (SO_2); n.m.r. ($CDCl_3$) 8.08–7.22 (m, 9.1, aromatic), and 2.72 p.p.m. (s, 6.0, N-CH_3).

Anal. Calcd. for $C_{15}H_{15}NSO_3$: C, 62.26; H, 5.23; N, 4.84. Found: C, 62.11; H, 5.19; N, 4.74.

Oximation of imine-sulfonamide **4** (2.50 g) was effected by refluxing it with 1.21 g of hydroxylamine hydrochloride and 3.54 g of sodium acetate (hydrate) in 80 ml of 70% (by weight) aqueous ethanol for 24 h. After cooling, the solution was allowed to stand overnight in a current of air under a hood. The resulting prismatic crystals were collected and recrystallized from methanol to give 2.55 g (97%) of *o*-(*N*,*N*-dimethylsulfamyl)benzophenone oxime (**8**) (large prismatic cluster), m.p. 156–158°. Another recrystallization from methanol gave 2.25 g (85%) of **8**, m.p. 158–160° and 156.5–158.5° i.r. 3420 (broad) and 3250 (broad, OH), 1630 (very weak, C=N), 1320 and 1150 cm^{-1} (SO_2); n.m.r. (acetone-d_6) 10.38 (s, 0.8, OH), 8.17–6.95 (m, 9.4, aromatic), and 2.63 p.p.m. (s, 6.0, N-CH_3).

Anal. Calcd. for $C_{15}H_{16}N_2SO_3$: C, 59.19; H, 5.30; N, 9.20. Found: C, 59.05; H, 5.19; N, 9.14.

Condensation of imine-sulfonamide **4** (2.0 g) with phenylhydrazine (2.25 g) was effected in 100 ml of 50% acetic acid by refluxing the solution for 24 h. After standing overnight at room temperature, the resulting prismatic yellow crystals were collected to give 1.65 g (63%) of *o*-(*N*,*N*-dimethylsulfamyl)benzophenone phenylhydrazone (**9**), m.p. 167–168.5° and 168.5–169° after recrystallization from acetone–methanol; i.r. 3280 (NH), 1580 (C=N), 1315 and 1105 cm^{-1} (SO_2); n.m.r. ($CDCl_3$) 8.45–8.07 (m, 0.9, NH), 7.85–6.60 (m, 14.8, aromatic), and 2.42 p.p.m. (s, 6.0, N-CH_3).

Anal. Calcd. for $C_{21}H_{21}N_3SO_2$: C, 66.46; H, 5.58; N, 11.07. Found: C, 66.54; H, 5.88; N, 10.99.

Condensation of Lithiosulfonamide **1′** *with Phenylisocyanate to Form Sulfobenzanilide* **5**

This reaction was effected as described above for benzophenone to give a dark-brown, clear solution, which was cooled in an ice bath and stirred with 20 ml of water followed by 25 ml of 5% hydrochloric acid. The mixture, which consisted of two layers and suspended solid, was partly evaporated in a current of air under a hood. The mixture was filtered. The solid was washed with water, a little ether, and then dried in air to give 4.35 g (57%) of carboxamide-sulfonamide **5** (fine crystals), m.p. 202–204° and 204.5–205.5° after recrystallization from acetone–methanol; i.r. 3280 and 3258 (NH), 1650 (CO), 1340 and 1160 cm^{-1} (SO_2).

Anal. Calcd. for $C_{15}H_{16}N_2SO_3$: C, 59.19; H, 5.30; N, 9.20. Found: C, 59.49; H, 5.34; N, 9.09.

The two layers of the filtrate (see above) were separated, and the organic layer was worked up to give 1.26 g of fine crystals, m.p. 175–195°, which seemed to consist partly of **5**.

Carbonation of Lithiosulfonamide **1′** *to Form Carboxysulfonamide* **6**

Method A

A solution of **1′** was prepared by slowly adding 47 ml (0.0752 mole) of 1.6 *M* *n*-butyllithium in hexane[4] to a stirred solution of 11.71 g (0.0632 mole) of **1** in 250 ml of dry ether under argon at room temperature. Stirring was continued for 1 h and then carbon dioxide (from a CO_2 generator) was bubbled through the reaction mixture for 30 min. A saturated solution of sodium carbonate was added, the aqueous and ether–hexane layers were separated, and the aqueous layer was made acidic with dilute hydrochloric acid. The cloudy acidic solution was extracted with ether. The ethereal extract was dried ($MgSO_4$)

and the solvent was removed under reduced pressure to give a yellowish oil which crystallized overnight to yield 8.60 g (63%) of *o*-(*N*,*N*-dimethylsulfamyl)benzoic acid (**6**), m.p. 98–102°; i.r. (Nujol mull) 2630 and 2540 (OH) (6), 1710 (C=O), 1370 (SO_2), 1300 (C—O or OH) (6), 1165 and 1155 (SO_2), 735 cm^{-1} (ortho disubstitution); n.m.r. ($CDCl_3$) 11.28 (s, 1.0, CO_2H), 7.70 (m, 4.0, aromatic), and 2.85 p.p.m. (s, 5.8, N-CH_3).

Anal. Calcd. for $C_9H_{11}NSO_4$: C, 47.15; H, 4.83; O, 27.92; N, 6.11; S, 13.99. Found: C, 47.14; H, 4.81; O, 28.05; N, 5.89; S, 13.94.

Method B

A solution of 0.05 mole of **1′** in 200 ml of THF[3] was prepared under nitrogen from 9.16 g (0.05 mole) of **1** and 35 ml (0.055 mole) of 1.59 *M* *n*-butyllithium in hexane.[4] After 1 h, the solution of **1′** was poured onto 500 g of dry ice in a 1 l Erlenmeyer flask which had been swept with dry nitrogen. After the excess dry ice had evaporated, 200 ml of water and 100 ml of ether were added. The layers were separated. The organic phase was extracted twice with saturated sodium bicarbonate solution and the extracts were combined with the aqueous layer. After washing with ether, the aqueous solution was acidified with 3 *N* hydrochloric acid. The resulting acidic solution was extracted with ether and the extracts were combined. After washing with saturated sodium chloride solution, the ethereal solution was dried ($MgSO_4$). The solvent was removed under reduced pressure on the steam bath to yield 8.59 g (75%) of **6** as a pale-yellow oil which crystallized slowly (48 h) to give light-yellow needles, m.p. 96–98° and 97–101° when the sample was placed in the bath at 94° and the temperature then raised.

*Beckmann Rearrangement of Oxime-sulfonamide **8** to Form Sulfobenzanilide **5***

A solution of 1.00 g of oxime **8** in 30 ml of THF[3] and 20 ml of anhydrous ether was cooled to 0° in an ice bath, and 1.00 g of phosphorus pentachloride was added. The mixture was magnetically stirred for 3 h at 0°, and then poured onto 30 g of ice. After making basic with sodium carbonate powder, the mixture was partly evaporated in a current of air under a hood (overnight). The white crystalline solid was collected, washed with water, and dried to give 0.77 g (77%) of carboxamide-sulfonamide **5** (fine bulky crystals), m.p. 203–205°, undepressed on admixture with the authentic sample of **5** prepared as described above (m.m.p. 204–205°), and the i.r. spectra of the two samples were identical.

*Attempt to Prepare Second Isomer of Oxime-sulfonamide **8***

A boiling solution of 0.70 g of oxime **8** in 70 ml of anhydrous ether was saturated with anhydrous hydrogen chloride gas (15 min) to form a white precipitate. After refluxing for 10 min, the mixture was poured onto excess of saturated sodium becarbonate solution in an ice bath. The resulting, basic mixture was partly evaporated in a current of air under a hood (overnight). The solid was collected, washed with water, and dried in air to give 0.67 g of recovered oxime **8**, m.p. and m.m.p. 156–158°; the i.r. spectrum was identical with that of the starting oxime.

Also, a solution of 0.8 g of oxime **8** in 8 ml of concentrated sulfuric acid at 0° was allowed to stand for 1 h, and then poured onto 50 g of ice. The resulting white precipitate was collected, washed with water, and dried in air to give 0.75 g of recovered oxime **8**, m.p. and m.m.p. 157.5–159.5°; the i.r. spectra of the two samples were identical.

Beckmann rearrangement of these samples of oxime **8** (recovered after treatment with the acids) with phosphorus pentachloride in THF–ether under the conditions described above afforded, on work-up, carboxamide-sulfonamide **5** in 73–74% yield.

1. W. H. PUTERBAUGH and C. R. HAUSER. J. Org. Chem. **29**, 853 (1964).
2. H. WATANABE, R. L. GAY, and C. R. HAUSER. J. Org. Chem. **33**, 900 (1968).
3. L. ALMASI and N. SERBAN. Acad. Rep. Poulare Romine, Filiala Cluj, Studii Cercetari Chem. **7**, 141 (1956); Chem. Abstr. **52**, 12871 h (1958).
4. A. GINZBERG. Chem. Ber. **36**, 2706 (1903).
5. L. W. JONES and H. F. WHALEN. J. Am. Chem. Soc. **47**, 1348 (1925).
6. L. J. BELLAMY. The infrared spectra of complex molecules. 2nd ed. John Wiley and Sons, Inc., New York. 1962. p. 162.

Can. J. Chem. Downloaded from www.nrcresearchpress.com by 210.87.254.6 on 09/05/12
For personal use only.

Can. J. Chem. Downloaded from www.nrcresearchpress.com by 210.87.254.5 on 09/05/12
For personal use only.

Alcaloïdes stéroïdiques. LXXXIX.[1] Transposition d'une *N*-chloroazétidine. Synthèse partielle du cyclo-18(*N*) méthoxy-17ξ aza-17*a* D-homo androstane-5α

CLAUDE BENEZRA[2] ET XAVIER LUSINCHI
CNRS, Institut de Chimie des Substances Naturelles, 91-Gif-sur-Yvette, France

Reçu le 12 décembre 1968

Traité dans les conditions de Ruschig [(*1*) hypochlorite de sodium; (*2*) méthanolate de sodium dans le méthanol], le cyclo-18(*N*) amino-17β androstane-5α, **5**, conduit à un produit transposé le cyclo-18(*N*) méthoxy-17ξ aza-17*a* D-homo androstane-5α, **7**. La structure de ce composé a été prouvée chimiquement: l'hydrogénolyse de **7**, suivie d'une formylation conduit au *N*-formyl aza-17*a* D-homo androstane-5α, **9**, préparé indépendamment à partir de l'androstane-5α ol-17β. Les spectres infrarouges, de résonance magnétique nucléaire et de masse sont interprétés et des transpositions apparentées sont brièvement passées en revue.

Treatment of 18(*N*)-cyclo-17β-amino-5α-androstane, **5** under Ruschig conditions [(*1*) sodium hypochlorite; (*2*) sodium methoxide in methanol] gave the rearranged 18(*N*)-cyclo-17ξ-methoxy-17*a*-aza-D-homo-5α-androstane, **7**. The structure of this compound has been proved chemically: hydrogenolysis of **7**, followed by formylation, gave *N*-formyl-17*a*-aza-D-homo-5α-androstane, **9** prepared independently from 5α-androstan-17β-ol. Infrared, nuclear magnetic resonance, and mass spectra are discussed and related rearrangements are briefly reviewed.

Canadian Journal of Chemistry, 47, 1547 (1969)

Conformément aux résultats établis par Kaminsky et Lamchen (2) pour des oxazirannes pyrrolidiniques simples, la transposition par irradiation ultraviolette (u.v.) de l'oxaziranne stéroïdique **3** (3) conduit avec un rendement de 60% à l'azétidine stéroïdique *N*-acétylée **4**, offrant ainsi une méthode de passage de la série du pregnane à la série de l'androstane. L'oxaziranne **3** étant facilement préparé à partir de la conessine **1** par l'intermédiaire de la pyrrolidine **2** (4), il est donc possible d'envisager l'obtention, par ouverture de l'hétérocycle azétidinique, de dérivés de l'androstane substitués sur les carbones 17 et 18.

La méthode de Ruschig *et al.* (5) peut formellement être envisagée comme un procédé d'ouverture de l'hétérocycle selon le schéma réactionnel suivant:

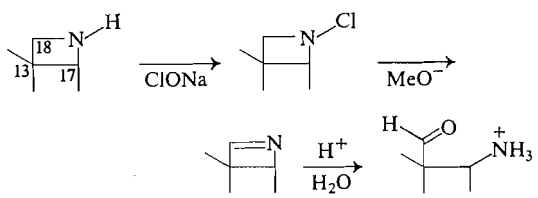

L'élimination d'acide chlorhydrique, impossible avec l'hydrogène porté par le carbone 17 (règle de Bredt), peut éventuellement s'effectuer avec un des hydrogènes en 18.

Cependant deux facteurs rendaient aléatoire a priori une telle élimination. Celle-ci n'a jamais encore été observée avec les hydrogènes du carbone en 18, même comme réaction secondaire. Généralement, pour des structures convenables, l'élimination s'effectue préférentiellement sur un autre carbone: carbone 20 pour la chloramine dérivée de la *N*-déméthylconanine (4); carbone benzylique pour les dérivés benzylamino-18 (6). Dans certains cas, la chloramine oxyde préférentiellement une fonction voisine. C'est ainsi que, traitée en milieu alcalin, la monochloramine d'un dérivé de l'amino-18 prégnanol-20β se cyclise pour conduire à un dérivé à structure pyrrolidinique analogue à **2** (6). Dans le cas de la chloramine du monométhylamino-18 prégnane, aucun produit défini n'a pu être isolé (7). Si ces exemples n'excluent pas rigoureusement la possibilité d'une élimination avec un des hydrogènes en 18, ils établissent que cette réaction est suffisamment inhibée pour que l'élimination s'effectue de préférence sur un autre point de la molécule ou qu'un autre type de réactivité des chloramines soit révélé. D'autre part, dans l'éventualité d'une élimination sur le carbone 18 celle-ci aboutirait à la formation d'une azétine. Celle-ci reste improbable. Il semble en effet que les azétines ne puissent exister que pour des substitutions très particulières de l'hétérocycle (8*a*, 9). Il n'était

[1]Alcaloïdes stéroïdiques. LXXXVIII, ref. 1.
[2]Adresse actuelle: Département de Chimie, Université d'Ottawa, Ottawa, Canada.

Can. J. Chem. Downloaded from www.nrcresearchpress.com by 210.87.254.5 on 09/05/12
For personal use only.

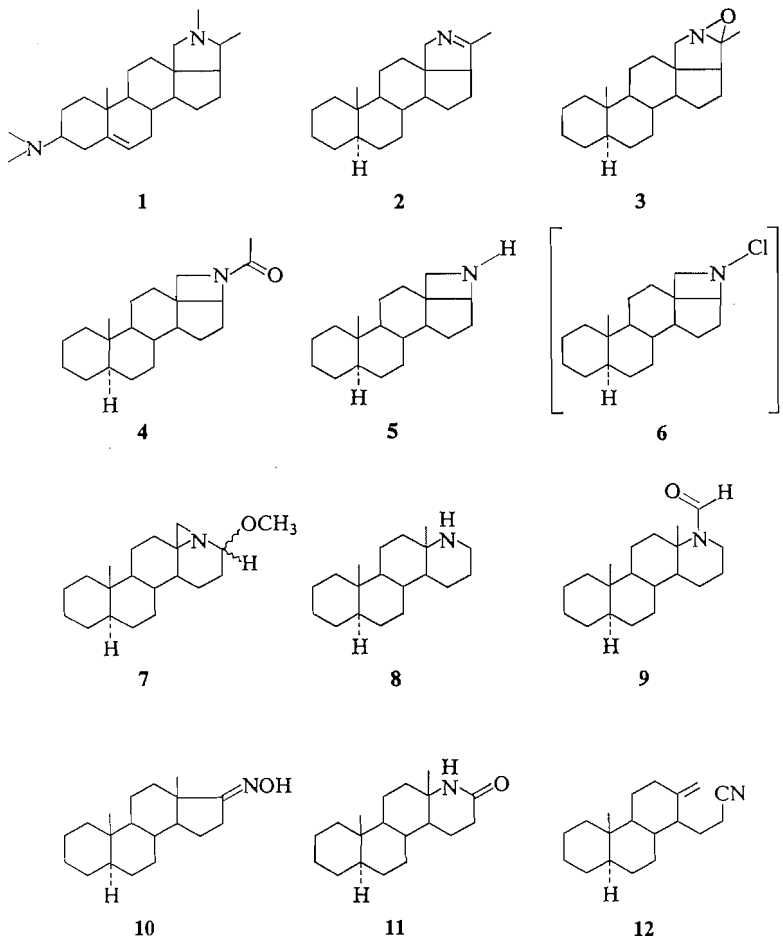

donc pas sans intérêt d'étudier la réactivité de la chloramine **6**.

L'azétidine libre **5** est préparée à partir du dérivé *N*-acétylé **4** (3) par hydrolyse dans un mélange d'acide chlorhydrique, d'éthanol et d'eau (10). L'ouverture de l'hétérocycle au cours de l'hydrolyse reste possible (8*b*). Une analyse élémentaire satisfaisante du dérivé **5** n'a pu être obtenue. Cependant l'obtention du pic moléculaire convenable en spectrographie de masse, la présence dans le spectre de résonance magnétique nucléaire (r.m.n.) d'un système AB caractéristique du méthylène en 18 et le retour à l'acétylazétidine **4** par acétylation montrent que, dans les conditions de l'hydrolyse, le cycle est conservé.

L'action de l'hypochlorite de sodium sur l'azétidine **5** conduit à la chloramine **6** qui a conservé la structure azétidinique. Le spectre de r.m.n. de cette chloramine présente en effet le système AB caractéristique du méthylène 18.

Si cette chloramine, **6**, est chauffée à reflux pendant $2\frac{1}{2}$ h dans une solution méthanolique de méthanolate de sodium, elle conduit à un mélange de produits dont est isolé par chromatographie, avec un rendement de 56%, un dérivé à structure aziridinique correspondant à la formule **7**, cyclo-18(*N*) méthoxy-17ξ aza-17*a* D-homo androstane-5α.

Le composé **7**, de masse moléculaire 303, absorbe dans l'infrarouge (i.r.) à 3020 cm^{-1}. Le spectre de r.m.n. ($CDCl_3$) correspond apparemment à un produit homogène. Il met en évidence un groupement méthoxy, présente par ailleurs un signal élargi à 1.53 p.p.m., qui persiste après deutériation, et un doublet de doublet à 3.82 p.p.m. dont les intensités des pics sont voisines. Ces données excluent une structure azétine. La

Can. J. Chem. Downloaded from www.nrcresearchpress.com by 210.87.254.5 on 09/05/12
For personal use only.

masse moléculaire 303 et la présence du groupe méthoxy pouvaient faire penser à un dérivé résultant de l'addition d'une molécule de méthanol sur la fonction imine de l'azétine. Cependant dans cette éventualité le spectre de r.m.n. aurait dû présenter un signal correspondant à un proton mobile et un singulet à champ faible dû à l'hydrogène en 18 qui serait alors sur un carbone portant un groupement méthoxy. En revanche, les données sont en accord avec la structure aziridinique proposée **7**. Le signal à 1.53 p.p.m. correspond dans ce cas aux deux hydrogènes du cycle aziridinique en 18. Ces protons sont signalés à 1.60 p.p.m. pour l'aziridine elle-même (11). Le doublet de doublet à champ faible correspond au proton en 17: partie X d'un système ABX ($J_{AX} \neq J_{BX}$). La bande à 3020 cm^{-1} du spectre i.r. peut être attribuée à la vibration des liaisons C—H du cycle aziridinique (12). Le spectre ne présente pas aux environs des 1220 cm^{-1} de bande particulière. Généralement donnée comme caractéristique d'une aziridine, cette bande n'est cependant pas signalée par tous les auteurs (12*e*). Il est à noter que sur le spectre de r.m.n. effectué dans le benzène le signal à 1.53 p.p.m. est remplacé par deux pics fins à 1.41 et 1.58 p.p.m. Les deux protons du cycle aziridinique ne couplent donc pas entre eux, résultat en accord avec les couplages géminaux généralement très faibles observés pour ce type de protons (13).

La structure **7** a été d'autre part vérifiée par une corrélation chimique. Cette corrélation a été effectuée au niveau du D-homo azastéroïde **8** facilement accessible à partir de l'androstanone-17. On pouvait en effet espérer obtenir ce composé en une seule étape par simple hydrogénolyse en présence de platine du dérivé **7**, avec élimination de la fonction éther (14) et ouverture simultanée du cycle aziridine sur la liaison *N*, C-18, conduisant ainsi à une pipéridine. Les hydrogénolyses d'aziridines cycliques décrites par Nagata *et al.* (12*a*) montrent en effet que l'ouverture de l'aziridine s'effectue très sélectivement sur la liaison C—N qui conduit à la formation d'hétérocycles azotés à 6 atomes. Traité par l'hydrogène en présence de platine Adams, le dérivé **7** conduit effectivement au D-homo aza-17*a* androstane **8** (42%) qui, difficilement cristallisable, a été formylé, **9**. Le spectre de r.m.n. montre la présence d'un méthyle angulaire en plus du méthyle-19. Le composé a été identifié au *N*-formyl aza-17*a* D-homo androstane-5α préparé par synthèse à partir de l'androstanolone.

La fonction cétonique en 3 de l'androstanolone est éliminée par réduction de Wolff–Kishner. L'androstanol-17β obtenu est oxydé dans les conditions de Jones pour conduire à l'androstanone-17. L'oxime de cette dernière, **10**, conduit par transposition de Beckmann à la lactame **11**. Le *N*-formyl aza-17*a* D-homo androstane-5α est obtenu par réduction à l'hydrure d'aluminium-lithium de cette dernière, suivie de formylation. Il est identique au dérivé obtenu par hydrogénolyse suivie de formylation du dérivé **7**.

La transposition de Beckmann de l'oxime d'un céto-17 androstane[3] a été effectuée de nombreuses fois (15). Le réactif généralement utilisé est le chlorure de l'acide *p*-acétamidobenzènesulfonique. L'oxime **10**, traitée dans des conditions analogues par ce réactif ne conduit pas à la lactame **11** qui est par contre obtenue avec un rendement de 40% au moyen de l'oxychlorure de phosphore (16). La réaction est effectuée par action du chlorure d'acide dans la pyridine, suivie de dilution à l'eau puis d'acidification. Nous avons observé qu'avec le chlorure de l'acide *p*-acétamidobenzènesulfonique un précipité se forme après addition d'eau alors que rien ne précipite avec l'oxychlorure de phosphore; ce n'est qu'après acidification du milieu que dans ce dernier cas la lactame précipite, immédiatement. Il a été vérifié, par analyse sur couche mince, que, dans le premier cas, le précipité formé, vraisemblablement l'ester de l'oxime, n'évoluait pratiquement pas au contact de l'acide et que, dans le second cas, la solution aqueuse avant acidification ne renfermait pas la lactame, même après un contact prolongé. La transposition n'a donc lieu qu'après acidification et elle semble alors très rapide. Nous avons accessoirement isolé le nitrile éthylènique **12**, produit de fragmentation qui accompagne généralement la transposition de Beckmann (15 *c,d*).

Les résultats obtenus pour le dérivé **7** ne permettent pas de préciser la stéréochimie autour du carbone 17. Le proton en 17 forme avec les deux protons en 16 un système ABX avec $J_{AX} \neq J_{BX}$. Ceci traduit pour des protons appartenant à un cycle à 6 atomes des positions relatives voisines d'axiales–axiales et axiales–équatoriales. Une des deux conformations possibles de chacun des

[3]La lactame **11** vient d'être décrite, très récemment (25). Les constantes pour ce dérivé sont en bon accord avec les nôtres.

Can. J. Chem. Downloaded from www.nrcresearchpress.com by 210.87.254.5 on 09/05/12
For personal use only.

épimères en 17 présente une telle relation. Conformation pseudo-chaise pour le dérivé méthoxy-17β **14**, et forme pseudo-bateau pour le dérivé méthoxy-17α **13**. Cette dernière conformation étant pour cet isomère vraisemblablement plus stable que la conformation pseudo-chaise pour laquelle un certain encombrement apparaît entre le groupe méthoxy et l'hydrogène β du pont méthylènique en 18.

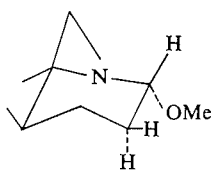

13

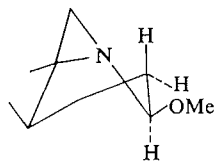

14

Le pic de base du spectre de masse du dérivé **7** est à $m/e = 273$ ($M^+ - 30$). Ce pic correspond à la perte des éléments du formol CH_2O. La formule proposée permet d'en donner une interprétation hypothétique. Il est à remarquer qu'une telle interprétation peut être formulée à partir de l'une ou de l'autre des configurations épimères en 17.[4]

Le rendement observé en produit de transposition **7** (56% isolé) et l'homogénéité stérique de ce produit montrent que la réaction de *trans*-position est largement prépondérante et qu'elle est vraisemblablement stéréospécifique. Cependant plusieurs produits secondaires résultant de l'action du méthanolate de sodium sur la chloramine **6** n'ont pû être isolés. L'éventualité de la formation de l'autre épimère en 17 n'est donc pas entièrement écartée ni la possibilité d'une réaction secondaire faisant intervenir les hydrogènes en 18.

Des exemples de transpositions de chloramines aliphatiques ont été récemment décrits par Gassman et Fox (17), et Gassman et Cryberg (18). Ces transpositions sont observées au cours de l'action d'un sel d'argent sur une solution méthanolique de la chloramine, donc dans des conditions différentes de celles que nous avons décrites: action du méthanolate de sodium dans le méthanol. C'est ainsi que la chloramine dérivée de l'isoquinuclidine se transpose avec intervention du méthanol:

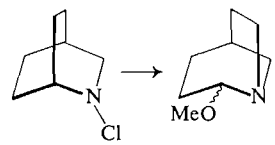

Un seul isomère est obtenu dont la stéréochimie n'a pû être précisée. Cependant, au cours de l'isomérisation dans les mêmes conditions du triméthyl-4,7,7 chloro-2 aza-2 bicyclo[2,2,1]-heptane (18), à côté du dérivé de transposition chloré, prépondérant, un dérivé transposé méthoxylé a été isolé avec un rendement de 8.5%, dont la structure correspond à une inversion de configuration sur le carbone transposé.

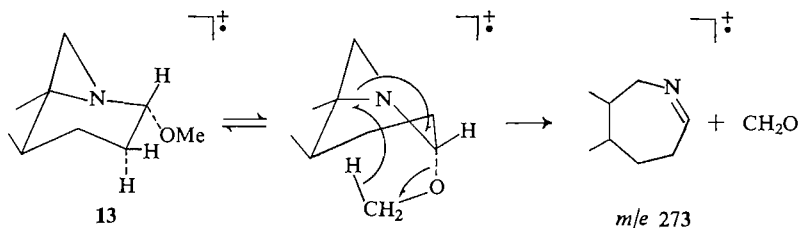

13 *m/e* 273

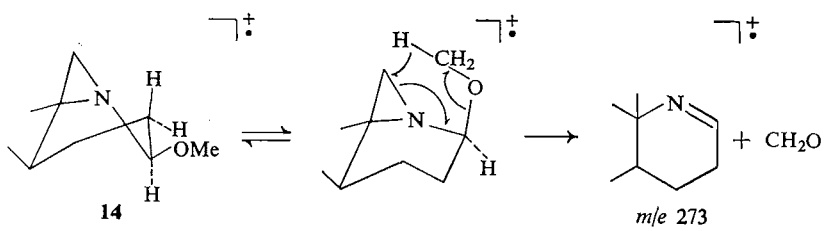

14 *m/e* 273

[4]Cette interprétation nous a été aimablement suggérée par le Dr. P. Longevialle que nous tenons à remercier.

Can. J. Chem. Downloaded from www.nrcresearchpress.com by 210.87.254.5 on 09/05/12
For personal use only.

Ces résultats s'interprètent au mieux (17) par l'hypothèse de la formation intermédiaire d'un ion mésomère analogue à celui invoqué dans les transpositions classiques du bicyclo[2,2,1]heptane, qui s'accompagnent également d'inversion de configuration (19). Dans le cas de la transposition que nous avons observée en milieu alcalin, il s'agit vraisemblablement d'un mécanisme concerté avec inversion de configuration sur le carbone 17 et formation de l'isomère méthoxy-17α.[5] La conformation **13** plus stable que **14**, semble en effet le mieux rendre compte du spectre de r.m.n. obtenu.

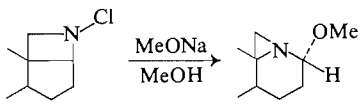

Il est à noter que des essais de transposition effectués avec la chloramine **6** dans le méthanol en présence de nitrate d'argent ont conduit à des mélanges complexes dont aucun produit défini n'a pû être isolé. Il n'est pas sans intérêt de remarquer que, parallèlement, des réactions de transfert d'hydrure observées pour certaines chloramines en présence de sels d'argent (20) ont été observées, en milieu alcalin, potasse dans le méthanol, par d'autres auteurs (21).

Il a été constaté au cours de cette étude que l'hydrogénolyse du groupe méthoxy du dérivé **7** (22) ne pouvait être effectuée par l'hydrure d'aluminium-lithium, même après action prolongée dans le tétrahydrofuranne à reflux. Cette inertie pourrait être due à l'impossibilité pour ce produit de s'équilibrer avec une forme immonium qui rendrait compte de la réductibilité des éthers de *gem*-aminocarbinols (23). Une telle structure immonium ne peut se former à partir du dérivé **7**, les liaisons autour de l'atome d'azote ne pouvant se mettre dans un même plan.

En conclusion, la réaction de Ruschig ne permet pas l'ouverture de l'hétérocycle de l'azétidine stéroïdique **5**, qui conduit dans ces conditions à un produit transposé. L'étude des dérivés obtenus par quaternarisation de l'azote du cycle azétidinique devrait vraisemblablement permettre d'obtenir cette ouverture.

[5]L'un des rapporteurs nous fait remarquer à juste titre que le passage du système aza-7 bicyclo[3,2,0]heptane **5** rattaché au squelette perhydrophénanthrénique au système aza-1 bicyclo[4,1,0]heptane **7** conduit certainement à une diminution de la contrainte stérique, ce qui permet une interprétation supplémentaire du comportement inhabituel de la chloramine **6** par rapport à celui de chloramines moins tendues.

Partie expérimentale

Les points de fusion sont pris en tube capillaire et corrigés. Les pouvoirs rotatoires sont déterminés dans le chloroforme (RP contenant 0.5% d'éthanol) avec le Quick-polarimètre électronique Jouan–Roussel. Les spectres de r.m.n. sont effectués en solution dans le deutérochloroforme sur un spectromètre Varian A-60. Les déplacements chimiques sont mesurés en δ par rapport au tétraméthylsilane (δ = 0). Les spectres de masse sont déterminés sur le spectrographe de masse MS-9. Les chromatographies sur couche mince (c.c.m.) sont faites sur des plaques neutres préparées à partir du silicagel G (Merck) et révélées soit par pulvérisations successives de réactif de Draggendorf puis d'acide sulfurique à 60%, soit par pulvérisation d'une solution éthérée d'acide sulfurique suivie de calcination.

Cyclo-18(N) amino-17β androstane-5α, 5

Une solution dans 125 ml d'éthanol absolu de 1.27 g de *N*-acétyl cyclo-18(*N*) amino-17β androstane-5α, **4** (3) est additionnée d'un mélange de 75 ml d'eau et 130 ml d'acide chlorhydrique concentré. Après un reflux de 16 h, la solution est concentrée sous vide jusqu'à 100 ml environ. Le précipité formé, essoré, lavé à l'eau et séché sous vide sur anhydride phosphorique correspond à 1.05 g de chlorhydrate de cyclo-18(*N*) amino-17β androstane-5α, 84%, homogène en c.c.m.

Un échantillon de ce précipité (92 mg) est agité avec une solution de soude dans l'eau (10%). L'extraction à l'éther fournit 75 mg de cyclo-18(*N*) amino-17β androstane-5α, **5**, p.f. 90–92°; $[\alpha]_D^{20}$ +12° (*c*, 0.25), après sublimation sous vide poussé.

Une analyse centésimale convenable n'a pû être obtenue pour $C_{19}H_{31}N$ = 273.45. Spectre de masse: pic moléculaire à *m/e* 273. Spectre de r.m.n.: à 0.69 p.p.m. un singulet (CH_3-19); à 3.12 p.p.m. un singulet correspondant à 1 proton, disparaissant par deutériation (N—H); centré à 3.30 p.p.m., un système AB, J = 9 c.p.s., $\delta_A - \delta_B$ = 0.35 p.p.m. (CH_2-18); à 3.76 p.p.m. un multiplet correspondant à 1 proton (H-17).

Une solution de 21 mg du dérivé **5** dissous dans 0.5 ml de pyridine est additionnée de 0.5 ml d'anhydride acétique et laissée une nuit à la température ambiante. Après dilution à l'eau, le milieu est extrait à l'éther. L'extrait éthéré, après lavage avec une solution d'acide chlorhydrique 2 *N*, puis avec une solution de bicarbonate de sodium puis à l'eau, est séché sur sulfate de sodium puis évaporé à sec. Le produit obtenu (22 mg) est identique au *N*-acétyl cyclo-18(*N*) amino-17β androstane-5α, **4**, (3).

Cyclo-18(N) méthoxy-17ξ aza-17a D-*homo androstane-5α, 7*

Une solution de 1.035 g du chlorhydrate de cyclo-18*(N)* amino-17β androstane-5α, **5**, dans 42 ml de chlorure de méthylène est agitée pendant 2 h en présence de 42 ml d'une solution d'hypochlorite de sodium (0.45 mole/l). La phase organique lavée à l'eau jusqu'à neutralité est séchée sur sulfate de sodium puis évaporée sous vide à la température ambiante. La laque obtenue, homogène en c.c.m., correspond à la chloramine **6**. Spectre de r.m.n.: à 0.66 p.p.m. un singulet (CH_3-19); à 3.65 p.p.m. un système AB, J = 10 c.p.s., $\delta_A - \delta_B$ = 0.11 p.p.m.; à 4.0 p.p.m. un multiplet correspondant à un proton (H-17).

La laque obtenue est dissoute dans une solution méthanolique de méthanolate de sodium (1.8 g de sodium

Can. J. Chem. Downloaded from www.nrcresearchpress.com by 210.87.254.5 on 09/05/12
For personal use only.

dans 120 ml de méthanol). Après 2½ h de reflux, le milieu refroidi est extrait avec un mélange d'éther et de chlorure de méthylène. Le résidu d'extraction, 0.95 g, est chromatographié sur 30 g d'alumine Merck standard diluée avec 3% d'eau. Après élution à l'hexane de 10 mg de produit de tête non identifié sont élués successivement à l'hexane, à l'hexane–benzène puis au benzène pur 573 mg (56%) de cyclo-18(*N*) méthoxy-17ξ aza-17*a* D-homo androstane-5α, **7**, homogène à la c.c.m. et dont le spectre de r.m.n. est pratiquement identique à celui de l'échantillon analytique. Celui-ci est obtenu par sublimation sous vide poussé, p.f. 91–92°, $[\alpha]_D^{20}$ +61° (*c*, 0.95).

Anal. Calc. pour $C_{20}H_{33}NO$: C, 79.15; H, 10.96; N, 4.62. Trouvé: C, 78.90; H, 10.99; N, 4.70.

Spectre de masse: pic moléculaire à *m/e* 303; pics à *m/e* 273 ($M^+ - 30$ pic de base) et à *m/e* 272 ($M^+ - 31$), perte de CH_3O. Spectre i.r. (Nujol): bande à 3020 cm^{-1}, faible (CH_2 aziridinique); entre 1050 et 1150 cm^{-1} bandes fines caractéristiques de la vibration C—O. Spectre de r.m.n.: ($CDCl_3$); à 0.75 p.p.m. un singulet (CH_3-19); à 1.53 p.p.m. un signal élargi (CH_2-18); à 3.47 p.p.m. un singulet correspondant à 3 protons (OCH_3); à 3.82 p.p.m. un quadruplet correspondant à un proton (—C*H*(OMe)—CH_2), (C_6H_6); à 0.70 p.p.m. un singulet (CH_3-19); à 1.40 et 1.58 p.p.m. deux singulets (CH_2-18), à 3.59 p.p.m. un singulet correspondant à 3 protons (OCH_3), à 3.78 p.p.m. un doublet de doublet correspondant à un proton (—C*H*(OMe)—CH_2).

La chromatographie poursuivie avec des mélanges de benzène–éther puis à l'éther et à l'éther–méthanol (9/1) fournit des mélanges de produits renfermant le dérivé **7**. L'élution au méthanol fournit 57 mg de matière de départ **5** (6%).

N-Formyl aza-17a D-*homo androstane-5α*, ***9***

(1) A Partir du N-Cyclo-18(N) méthoxy-17ξ aza-17a D-*homo androstane-5α*, ***7***

Une solution de 300 mg de **7** dans un mélange de 300 ml d'éthanol à 95° et 100 ml d'acide acétique, est hydrogénée à pression atmosphérique et température ambiante en présence de 250 mg de platine Adams, pendant 22 h. Après élimination du catalyseur par filtration, le milieu est évaporé à sec. Le résidu repris à l'eau, alcalinisé à l'ammoniaque et extrait à l'éther, fournit 275 mg d'un produit pulvérulent blanchâtre qui est chromatographié sur 9 g d'alumine standard. Sont isolés, par élution au benzène et au mélange benzène–éther (4/1, puis 1/1) 67 mg de produits non identifiés, puis à l'éther pur et à l'éther–méthanol (9/1, puis 8/2) 114 mg d'un produit pulvérulent pratiquement unitache à la c.c.m., correspondant à l'aza-17*a* D-homo androstane-5α, **8**.

Ce composé (30 mg) est traité pendant 45 min par un mélange acide formique (0.06 ml) – anhydride acétique (0.16 ml) à 80°. Après refroidissement et addition d'eau, le précipité gommeux qui se forme peut être cristallisé dans l'acétone fournissant 3 mg de *N*-formyl aza-17*a* D-homo androstane-5α, **9**. 15 mg de ce composé sont obtenus à partir du résidu d'évaporation des eaux-mères, par chromatographie sur couche épaisse. Plaque 20 × 20 cm préparée à partir de 5.5 g de silice G (Merck); élution par un mélange méthanol – chlorure de méthylène (3/97); pulvérisation par le réactif de Morin et examen en u.v. Elution de la bande révélée par un mélange méthanol – chlorure de méthylène (3/97). Le produit obtenu p.f. 182–183°; $[\alpha]_D^{20}$ −5° (*c*, 0.7) est identique au *N*-formyl aza-17*a* D-homo androstane-5α préparé à partir de l'androstane-5α oxime-17, **10** (p.f., p.f. mélange, $[\alpha]_D$, i.r., r.m.n. et c.c.m.).

(2) A Partir de l'Aza-17a D-*homo androstane-5α one-17*, ***11***

Une suspension de 710 mg de **11** dans 200 ml d'éther anhydre est additionnée de 730 mg d'hydrure d'aluminium-lithium et chauffée à reflux pendant 4 h. Après une nouvelle addition de 300 mg d'hydrure d'aluminium-lithium le reflux est poursuivi pendant 3 h. L'excès d'hydrure est détruit par addition d'éther humide puis d'eau. L'alumine formée est essorée et lavée à l'éther. Les filtrats éthérés, lavés à l'eau, séchés sur sulfate de sodium et évaporés à sec laissent 610 mg d'un résidu pulvérulent blanc dont l'analyse par c.c.m. révèle qu'il contient une certaine quantité du produit de départ. Une solution de ce résidu dans l'éther contenant quelques gouttes de méthanol est extraite à l'aide d'une solution aqueuse d'acide chlorhydrique 2*N*. La phase éthérée lavée à l'eau, séchée et évaporée à sec fournit 69 mg de matière de départ **11**. La phase chlorhydrique alcalinisée par de la lessive de soude est extraite à l'éther, puis avec un mélange éther – chlorure de méthylène. Les phases organiques réunies, lavées à l'eau, séchées et évaporées à sec laissent 444 mg de résidu correspondant à l'aza-17*a* D-homo androstane-5α, **8**, homogène à la c.c.m. (66% par rapport à la lactame transformée).

Les 444 mg de dérivé amine sont chauffés à 80° pendant 45 min dans un mélange de 2.25 ml d'acide formique et de 6.75 ml d'anhydride acétique. Après refroidissement et addition d'eau, le précipité gélatineux qui se forme est essoré et cristallisé dans l'acétone fournissant 250 mg de *N*-formyl aza-17*a* D-homo androstane-5α **9**, p.f. 180°. Un échantillon analytique est obtenu par cristallisation dans l'acétone; p.f. 183°; $[\alpha]_D^{20}$ −6° (*c*, 0.99).

Anal. Calc. pour $C_{20}H_{30}NO$: C, 79.15; H, 10.96; N, 4.62. Trouvé: C, 79.04; H, 10.98; N, 4.55.

Spectre i.r. (Nujol) : bande à 1660 cm^{-1} (O=C—N). Spectre de r.m.n.: à 0.765 p.p.m. un singulet (CH_3-19); à 1.23 p.p.m. un singulet (CH_3-18); à 4.45 p.p.m. un multiplet (CH_2-17); à 8.40 p.p.m. un singulet correspondant à 1 proton (H—C=O).

Androstanol-17β

Une solution de 3.5 g d'androstanol-17β one-3 dans 120 ml d'une solution résultant de l'action de 6.8 g de sodium sur 120 ml de glycol est additionnée de 16.8 ml d'hydrate d'hydrazine et chauffée à reflux pendant 5 h. Après refroidissement le milieu est versé dans un mélange eau-glace. L'extraction à l'éther fournit 3.2 g d'androstanol-17β (96%), p.f. 167°, litt. 164–166° (24).

Androstanone-17

3.2 g d'androstanol-17β oxydés dans les conditions de Jones fournissent 3.2 g d'androstanone-17, p.f. 120°, litt. 122° (24). Spectre i.r. (Nujol): bande à 1750 cm^{-1} (C=O).

Oxime de l'Androstanone-17

Une solution de 2.8 g d'androstanone-17 dans 450 ml d'éthanol à 95° est additionnée de 2.8 g de chlorhydrate d'hydroxylamine et 2.8 g d'acétate de sodium. Après 2 h de reflux et addition d'eau (500 ml), le précipité formé est

essoré et cristallisé dans le méthanol fournissant 2.24 g d'oxime de l'androstanone-17 (81%), homogène en c.c.m., p.f. 175°, $[\alpha]_D^{20}$ +19° (*c*, 1.1).

Anal. Calc. pour $C_{19}H_{31}NO$: C, 78.84; H, 10.80; N, 4.84. Trouvé: C, 78.84; H, 11.08; N, 4.81.

Aza-17a D-*homo androstane-5α one-17*, **11**. *Seco-13,17 androstane-5α ène-13,18 nitrile-17*, **12**

Une solution dans 250 ml de pyridine anhydre de 3 g de l'oxime de l'androstanone-17 est additionnée, goutte à goutte, a 0°, de 7 ml d'oxychlorure de phosphore. Après une nuit d'agitation à la température ambiante, 500 ml d'eau sont ajoutés puis de l'acide chlorhydrique 2 *N* jusqu'à pH 2–3. Le précipité qui se forme est essoré (1.73 g). Le filtrat est extrait au chlorure de méthylène. La solution organique est lavée à l'eau, séchée sur sulfate de sodium et évaporée à sec.

Le précipité, cristallisé dans le méthanol, fournit 0.73 g d'aza-17*a* D-homo androstane-5α one-17, **11**, homogène à la c.c.m. L'échantillon analytique est obtenu par recristallisation dans le méthanol. p.f. 298–303°, $[\alpha]_D^{20}$ +14° (*c*, 1.07).

Anal. Calc. pour $C_{19}H_{31}NO$: C, 78.84; H, 10.80; N, 4.84. Trouvé: C, 78.54; H, 10.66; N, 4.54.

Spectre i.r. (Nujol): bandes à 3160 et 3040 cm^{-1} (N—H); à 1668 et 1605 cm^{-1} (O=C—NH).

Les eaux-mères de cristallisation évaporées à sec sont réunies au résidu de l'extraction au chlorure de méthylène (1.04 g). Un échantillon de 120 mg est chromatographié sur couche épaisse: plaque 20 × 20, préparée avec 20 g de silicagel G (Merck); élution avec un mélange chlorure de méthylène–méthanol (96/4); pulvérisation au réactif de Morin et repérage des bandes par u.v.; extraction au chloroforme. Sont isolés de cette façon: 30 mg de la lactame **11** (rendement global en lactame 42%) et 63 mg (19%) de seco-13,17 androstane-5α ène-13,18 nitrile-17, **12**. Un échantillon pour analyse de ce dérivé est obtenu par sublimation sous vide poussé, p.f. 58–60°, $[\alpha]_D^{20}$ 21° (*c*, 0.37).

Anal. Calc. pour $C_{19}H_{29}N$: C, 84.07; H, 10.77; N, 5.16. Trouvé: C, 84.02; H, 10.71; N, 5.27.

Spectre i.r. (Nujol): bandes à 3080, 1643, 902 cm^{-1} (C=CH_2) et 2250 cm^{-1} (—CN). Spectre de r.m.n.: à 0.70 p.p.m. un singulet (CH_3-19) a 4.49 et 4.79 p.p.m., deux singulets correspondant chacun à un proton (C=CH_2).

Remerciements

Nous remercions le Professeur Janot et le Docteur Goutarel pour tout l'intérêt qu'ils ont porté à ce travail, le Docteur O. E. Edwards pour une lecture critique du manuscrit et la communication de ses résultats sur les *N*-chloramines avant publication ainsi que le Docteur R.R. Fraser pour d'utiles discussions. Les spectres de masse ont été effectués par le Docteur Longevialle, les spectres de r.m.n. par Madame Allais et les microanalyses dans le laboratoire de Microanalyse du CNRS à Gif-sur-Yvette.

1. P. Longevialle. Bull. Soc. Chim. France, sous presse.
2. L. S. Kaminsky et M. Lamchen. J. Chem. Soc. C, 2295 (1966).
3. J. Parello, R. Beugelmans, P. Milliet et X. Lusinchi. Tetrahedron Letters, 5087 (1968).
4. V. Cerny et F. Sorm. Collection Czech. Chem. Comm. **24**, 4015 (1959).
5. H. Ruschig, W. Fritsch, J. Schmidt-Thome et W. Haede. Chem. Ber. **88**, 883 (1955).
6. V. Cerny et F. Sorm. Collection Czech. Chem. Comm. **25**, 2841 (1960).
7. H. Favre, R. D. Haworth, J. McKenna, R. G. Powell et G. H. Whitfield. J. Chem. Soc. 1115 (1953).
8. J. A. Moore. Heterocyclic compounds. T. II. A. Weissberger (*éditeur*). Interscience Publishers, Inc., London. 1964. (*a*) p. 885, (*b*) p. 902.
9. G. Pifferi, P. Lonsonni, G. Pelizza et E. Testa. J. Heterocyclic Chem. **4**, 619 (1968).
10. E. Testa, L. Fontanella, L. Mariani et G. F. Cristiani. Liebigs Ann. Chem. **633**, 56 (1960); **639**, 157 (1961).
11. P. L. Levins et Z. B. Papanastassiou. J. Am. Chem. Soc. **87**, 826 (1965).
12. (*a*) W. Nagata, S. Hirai, K. Kawata et T. Aoki. J. Am. Chem. Soc. **89**, 5045, 5046 (1967). (*b*) O. E. Paris et P. E. Fanta. J. Am. Chem. Soc. **74**, 3007 (1952). (*c*) J. B. Patrick, R. P. Williams, W. E. Meyer, W. Fulmor, D. B. Cosulich, R. W. Broschard, et J. S. Webb. J. Am. Chem. Soc. **86**, 1889 (1964). (*d*) H. T. Hofman Jr., G. E. Evans et G. Glockler. J. Am. Chem. Soc. **73**, 3028 (1951). (*e*) K. C. Tsou, K. Hoegerle et H. C. F. Su. J. Med. Chem. **6**, 434 (1963).
13. S. J. Brois. J. Org. Chem. **27**, 3532 (1962).
14. L. H. Briggs, W. E. Harvey, R. H. Locker, W. A. McGillivray et R. N. Seelye. J. Chem. Soc. 3013 (1950). A. T. Stewart et C. R. Hauser. J. Am. Chem. Soc. 77, 1098 (1955).
15. (*a*) St. Kaufmann. J. Am. Chem. Soc. **73**, 1779 (1951). (*b*) R. Anliker, M. Müller, J. Wohlfahrt et H. Heusser. Helv. Chim. Acta, **38**, 1404 (1955). (*c*) R. Anliker, M. Müller, M. Perelman, J. Wohlfahrt et H. Heusser. Helv. Chim. Acta, **42**, 1071 (1959). (*d*) W. Nagata, M. Narisada et T. Sugasawa. J. Chem. Soc. C, 648 (1967).
16. J. Schmidt-Thome. Chem. Ber. **88**, 895 (1955).
17. P. G. Gassman et B. L. Fox. J. Am. Chem. Soc. **89**, 338 (1967).
18. P. G. Gassman et R. L. Cryberg. J. Am. Chem. Soc. **90**, 1355 (1968).
19. J. A. Berson. *Dans* Molecular rearrangements. P. de Mayo (*éditeur*). Interscience Publishers, Inc., New York. 1964. p. 111.
20. O. E. Edwards, O. Vocelle, J. W. ApSimon et F. Haque. J. Am. Chem. Soc. **87**, 678 (1965).
21. G. Adams et K. Schreiber. Angew. Chem. **76**, 752 (1964).
22. N. G. Gaylord. Reduction with complex metal hydrides. Interscience Publishers, Inc., New York. 1956. p. 809.
23. Z. Welvart. Thèse de doctorat ès Sciences, Université de Paris, 1956. p. 69.
24. Dictionary of organic compounds. 4e édit. T. 1. Eyre and Spottiswoode, London. 1965. p. 234.
25. A. Cervantes, P. Crabbé, J. Iriarte et G. Rosenkranz. J. Org. Chem. **33**, 4294 (1968).

Can. J. Chem. Downloaded from www.nrcresearchpress.com by 210.87.254.5 on 09/05/12
For personal use only.

Can. J. Chem. Downloaded from www.nrcresearchpress.com by 210.87.254.40 on 09/05/12
For personal use only.

Kinetic isotope effect for the thermally-induced migration of hydrogen in cyclopentadienes

STEWART MCLEAN, C. J. WEBSTER, AND R. J. D. RUTHERFORD
Department of Chemistry, University of Toronto, Toronto 5, Ontario

Received November 28, 1968

The Arrhenius parameters have been obtained for the rearrangement of 5-methylcyclopentadiene by a 1,2-hydrogen migration and for the corresponding rearrangement of 5-methylpentadeuteriocyclopentadiene. The results, taken in conjunction with those reported previously, allow the effect of the methyl group on the rate of hydrogen migration to be assessed. The kinetic isotope effect is of particular interest because the hydrogen transfer takes place through a transition state that is unequivocally non-linear.

Canadian Journal of Chemistry, 47, 1555 (1969)

We have previously studied the migration of the C-5 hydrogen in certain appropriately substituted cyclopentadienes and we have shown that a pathway exists by which a thermally-induced, intramolecular 1,2-hydrogen shift can take place; a study of the kinetics of the rearrangement (e.g. **1** → **2**) showed that it had true first order characteristics, and the Arrhenius parameters for the migration process were determined in certain cases (1). Related studies have been made by others (2, 3), and the significance of these results as examples of 1,5-sigmatropic processes was pointed out by Woodward and Hoffmann (4).

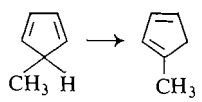

1 **2**

A determination of the kinetic isotope effect for the hydrogen migration process would be of considerable value for several reasons. We would like to determine the effect of various substituents on the rate of the migration process, and a knowledge of the rate of hydrogen migration in cyclopentadiene itself would be valuable in establishing a basis of comparison; the degenerate rearrangement in cyclopentadiene itself is, of course, unobservable by the techniques we have used, and it has not been experimentally possible to obtain dependable kinetic results for the derivative involving the smallest possible change, 5-deuteriocyclopentadiene[1] (1). However, Roth (3) has been able to study the rate of *deuterium* migration in 5-*H*-pentadeuteriocyclopentadiene, and a knowledge of the kinetic isotope effect for the process would allow his results and ours to be interrelated.

The kinetic isotope effect is also of theoretical interest because the intramolecularity of the hydrogen transfer process unambiguously places certain severe restrictions on the transition state for the reaction. The vast majority of kinetic isotope effects for hydrogen transfer reactions that have been investigated have involved linear transition states with respect to the bond making–bond breaking processes; the predominant contribution to the activation energy has then come from the C—H stretching components that are undergoing change, and although attempts have been made to incorporate bending force constants into calculations (5*a*) for linear transition states, non-linear transition states with a significant C—H bending component appear to have been considered in only a few special cases (5*b*). In contrast, the hydrogen migration in cyclopentadienes requires unequivocally a non-linear transition state in which the C—H bending component is important, and, in fact, the rearrangement can be viewed as the result of an exaggerated C—H bending vibration. For the rearrangement of cyclopentadiene itself, provided that no metastable intermediate is implicated, the transition state must be symmetrical, with the hydrogen equally bonded to the migration origin and the migration terminus. Furthermore, it appeared reasonable to assume at the start that the distortion of this symmetry in the 5-methylcyclopentadiene case, would have a minimal effect on the characteristics of the transition state.

[1]We are very grateful to Professor A. G. Harrison and Mr. D. Priddle for carrying out these measurements for us.

Can. J. Chem. Downloaded from www.nrcresearchpress.com by 210.87.254.40 on 09/05/12
For personal use only.

Unfortunately, one further modification had to be introduced into the system in order to make the study of the kinetic isotope effect for the 5-methylcyclopentadiene case experimentally feasible. It was not possible to develop a synthesis of 5-methyl-5-deuteriocyclopentadiene and we had to be content to use 5-methylpentadeuteriocyclopentadiene (**1**-D), which is readily available from cyclopentadiene-d_6. The second order effects of the 4 extra deuterium atoms could not be determined and the assumption was made that their combined effect would be small relative to the primary effect associated with the migrating atom.

In our first experiments we simply used the technique we have previously described (1) to monitor the decay of the methyl signal of 5-methylcyclopentadiene (**1**-H) and its deuterio derivative (**1**-D) while each was maintained at a fixed temperature in the probe of the nuclear magnetic resonance (n.m.r.) spectrometer. The k_H/k_D values obtained varied over a range that was greater than that of the expected experimental error and we decided that it would be necessary to have more precise temperature control and calibration than the variable temperature probe affords. We then used a technique in which the reaction was carried out in a thermostatted bath and then quenched by rapid cooling; the progress of the reaction was then determined from the area of the 5-methyl signal measured in an n.m.r. spectrometer with the probe temperature set low enough that no appreciable further rearrangement of the sample could take place. In this way we were able to study the rearrangement over the temperature range most suitable for each (5–25° for **1**-H and 20–40° for **1**-D). Table I shows the values obtained for k_H(migration), the average value for the (statistically-corrected) rate constant for the hydrogen migration process itself, and the rate constant, k_H(decay), for the process actually measured, the decay of the 5-methyl signal in **1**-H. The corresponding values for **1**-D are shown in Table II, and in Table III these values are corrected for the presence in **1**-D of incompletely deuteriated material. The correction was based on the isotopic dilution of the C_5D_6 precursor, determined mass spectrometrically, and assumed that the methyl group entered the molecule in a random fashion; the value obtained in this way for the isotopic dilution of 5-*D*-5-methyl species is probably an upper limit.

TABLE I

Rate constants for migration of hydrogen

T (°C)	k_H(decay) ($s^{-1} \times 10^5$)	Standard deviation*	k_H(migration) ($s^{-1} \times 10^5$)
6.1	3.785	0.032	1.90
	3.815	0.041	
9.8	6.044	0.035	3.01
	5.975	0.055	
14.4	10.61	0.13	5.24
	10.32	0.07	
19.5	21.33	0.78	10.6
	20.85	0.30	
25.1	36.82	0.41	18.4
	36.65	0.34	

*Based only on the slope obtained by a least squares treatment of the kinetic data and assuming first order kinetics.

TABLE II

Rate constants for migration of deuterium (uncorrected for effect of isotope dilution)

T (°C)	k_D(decay) ($s^{-1} \times 10^5$)	Standard deviation*	k_D(migration) ($s^{-1} \times 10^5$)
19.5	3.385	0.241	1.63
	3.139	0.073	
25.1	6.584	0.080	3.34
	6.780	0.064	
30.1	12.79	0.19	6.29
	12.37	0.07	
35.1	22.84	0.48	11.2
	22.15	0.28	
40.1	40.75	0.23	20.2
	39.89	0.30	

*Based only on the slope obtained by a least squares treatment of the kinetic data and assuming first order kinetics.

TABLE III

Rate constants for migration of deuterium (corrected for effect of isotope dilution)

T (°C)	k_D(decay) ($s^{-1} \times 10^5$)	Standard deviation*	k_D(migration) ($s^{-1} \times 10^5$)
19.5	3.179	0.203	1.55
	3.003	0.071	
25.1	6.322	0.063	3.20
	6.484	0.037	
30.1	12.26	0.15	6.05
	11.96	0.05	
35.1	21.82	0.32	10.8
	21.37	0.22	
40.1	39.21	0.20	19.4
	38.34	0.23	

*Based only on the slope obtained by a least squares treatment of the kinetic data and assuming first order kinetics.

Can. J. Chem. Downloaded from www.nrcresearchpress.com by 210.87.254.40 on 09/05/12
For personal use only.

Comparison of the results recorded in Table I with those we obtained previously (1) reveals a significant difference between the two sets of figures for the values of k_H(migration) at each temperature. This difference, which has caused us some concern, probably arises from a systematic error in one of the sets of figures; in our earlier work (1) we depended on the calibration of the variable temperature probe, while in the present investigation our technique has allowed a much higher degree of precision in the determination of the reaction temperature, and consequently we believe that our present results are the more dependable and the temperatures recorded previously were 4–5° too low. In agreement with this, the Arrhenius plot of our present results gave a good straight line, the slope of which was the same, within the expected limits of accuracy, as that obtained in the earlier study. Our present results correspond to:

$$k_H(\text{migration}) = (7.49 \times 10^{10}) \exp(-19\,930/RT)\ s^{-1}$$

$$E_a = 19.9 \text{ kcal/mole (standard deviation 0.3)}$$

$$\Delta S^{\ddagger}\ (300\ °K) = -10.8 \text{ e.u. (standard deviation 1.0)}$$

Comparison of the results in Tables II and III shows that slightly better first order kinetic plots were obtained when the correction for isotope dilution was applied. The differences between the two sets of figures are, in fact, within the expected limits of error for this technique, and this serves to confirm our supposition that our material was of sufficient isotopic purity. When each set of kinetic data was plotted separately, there was very little difference in the Arrhenius parameters obtained, but the standard deviations of slope and intercept were very slightly lower in the corrected case. We choose, therefore, to report the results obtained from Table III which are:

$$k_D(\text{migration}) = (7.58 \times 10^{11}) \exp(-22\,350/RT)\ s^{-1}$$

$$E_a = 22.35 \text{ kcal/mole (standard deviation 0.1)}$$

$$\Delta S^{\ddagger}\ (300\ °K) = -6.2 \text{ e.u. (standard deviation 0.3)}$$

It can be seen that the Arrhenius activation energy for deuterium migration is greater than that for hydrogen migration, but the entropy of activation is less negative for deuterium; from these results it follows that the free energy of activation for deuterium migration is higher by about 1.1 kcal mole^{-1} in the temperature range studied. The values for k_H/k_D, calculated from the Arrhenius plot, show a substantial temperature dependence, being 7.67 at 7 °C, 5.75 at 27 °C, and 4.45 at 47 °C; the isokinetic temperature is 253 °C, calculated by extrapolation and with the assumption that the Arrhenius plots are linear through the whole range.

It is clear from a comparison of our present results with those of Roth (3) that, as we had previously suggested (1), the 5-methyl group appreciably lowers the activation energy for the migration of the hydrogen from C-5, leading to an increase in the rate of rearrangement. The 1-methyl isomer (with methyl at sp^2 carbon) is appreciably more stable than the 5-methyl isomer (with methyl at sp^3 carbon) (1); it is probable that the methyl group in the first isomer has a stabilizing effect relative to the unsubstituted case and it is possible that the methyl group has the opposite effect in the second case. The lowering of the activation energy for the rearrangement of 5-methylcyclopentadiene may reflect both influences, one raising the ground state and the other lowering the transition state energy. It seems probable in any case that the transition state is appreciably affected by the stabilizing influence of the methyl group at the incipient sp^2 carbon center, and to this extent the approximation made earlier that the distortion of the symmetry of the transition state by the methyl substituent could be neglected is inaccurate, but it is difficult to place this on a quantitative basis with any confidence. The stabilization of the 1-methyl isomer with respect to the 5-methyl isomer (from equilibrium studies (1)) and the lowering by the methyl group of the activation energy for hydrogen migration (from the kinetic comparison of substituted and unsubstituted cyclopentadienes) are both about 2 kcal/mole, indicative that the major part of the effect that the methyl group has in the product is already felt in the transition state. However, the equilibrium values are recognized to be only very approximate and the activation energy figures are based on the difference between our results and those of Roth (3), both of which have probable error limits that are appreciable relative to the difference.

Can. J. Chem. Downloaded from www.nrcresearchpress.com by 210.87.254.40 on 09/05/12
For personal use only.

Because measurements were made on **1**-H and **1**-D under conditions that were as nearly identical as possible, the phenomenological aspects of the study of the kinetic isotope effects can, we feel, be accepted with some confidence. The range of k_H/k_D values is not unusual and the rate differences can be traced to both enthalpy and entropy factors. However, because we have not been able to separate primary and secondary isotope effects and because of the difficulties already outlined regarding the nature of the transition state, we do not feel that it is appropriate at this time to do more than comment briefly on the theoretical significance of the results. The important feature of this rearrangement is the non-linearity of the transition state; the difference in activation energy between the hydrogen and the deuterium cases could be attributed to the complete loss in the transition state of one bending mode (near 1360 cm^{-1} for C—H) and smaller contributions from other modes, but we have not followed this approach any further than the observation than any meaningful calculation will require consideration of a more extensive portion of the molecule and its associated vibrational modes. The extent of tunneling is another question of considerable interest here (and it may be noted that proton tunneling in "Woodward–Hoffmann forbidden" cases is a question of further interest); the ratio of pre-exponential factors we have determined ($A_H/A_D \sim 0.1$) has a value that has been considered evidence for an appreciable degree of tunneling (5*c*), but we recognize that our data have been obtained over a restricted temperature range only and the evidence is therefore suggestive rather than definitive.

Experimental

A Varian A-60 nuclear magnetic resonance (n.m.r.) spectrometer equipped with a variable-temperature probe was used. Analyses of isotopic composition were carried out directly by mass spectrometry using an AEI MS902.[1]

Cyclopentadiene-d_6

A solution of NaOD in D_2O, prepared by the reaction of Na_2O_2 (5.0 g) with D_2O (33.0 g), was vigorously stirred for 1 h at 0° in an atmosphere of nitrogen with cyclopentadiene (12.0 g) and 25 ml dimethyl sulfoxide. When the mixture was allowed to settle, three layers separated. The upper layer was partly deuteriated cyclopentadiene (62 atom % D) and the lower layers were dimethyl sulfoxide and partly exchanged D_2O (which could be recovered by distillation and used again in a preliminary treatment of another sample of cyclopentadiene). When the partly deuteriated cyclopentadiene was taken through another two cycles of this process, the composition of the product typically obtained was: C_5D_6, 82.3; C_5D_5H, 15.3; $C_5D_4H_2$, 1.9; less highly deuteriated species 0.5 (95.6 atom % D).[2] Material of at least this isotopic purity was converted to 5-methylpentadeuteriocyclopentadiene by the method described previously for cyclopentadiene itself (6).

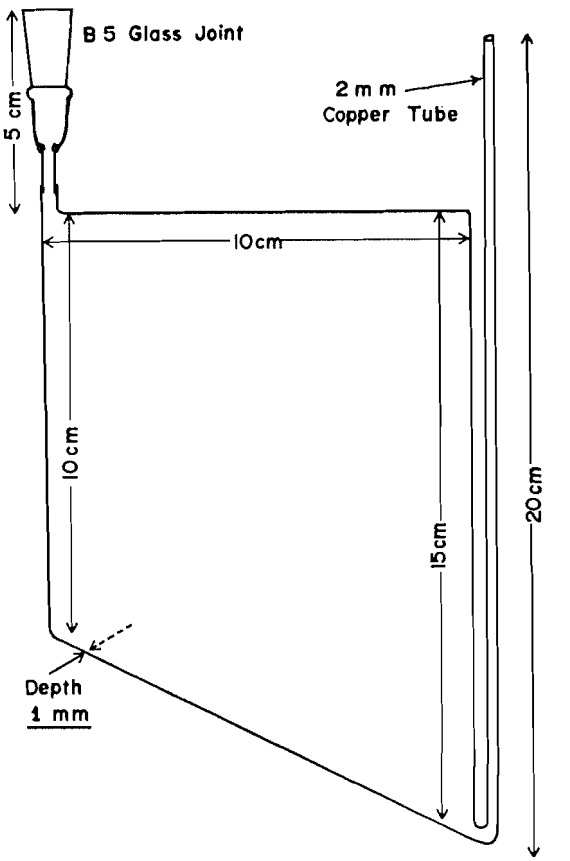

FIG. 1. The reaction vessel.

Kinetic Measurements

The reaction vessel shown in Fig. 1 was constructed from thin copper sheet. Reactants were introduced from a syringe which was adapted to fit the glass joint, and, when a sample was required, a measured volume could be forced through the copper tube, to which was connected

[2]This method was developed in this laboratory by Mr. T. F. W. McKillop and we are very appreciative of the experimental skill that he demonstrated in doing so. Under the conditions used here virtually no deuteriation of the DMSO takes place (on the basis of the mass spectrum of recovered DMSO); the rate of base-catalyzed hydrogen exchange in DMSO is known to be strongly dependent on the composition and nature of the reaction medium and it is interesting to note that, under prescribed conditions, the DMSO – D_2O – NaOD system can be used to prepare DMSO-d_6 rapidly and efficiently (7).

a piece of flexible Teflon tubing, by a pumping action of the syringe.

The reaction vessel containing 8 ml of a 4% solution of hexamethyldisiloxane in carbon tetrachloride was placed in a thermostatted bath (±0.02°) and, when thermal equilibrium was established, the substituted cyclopentadiene (2 ml) was added and thoroughly mixed with the solvent by agitation of the reaction vessel. Aliquots were withdrawn at measured intervals and collected in chilled n.m.r. sample tubes, which were then immediately placed in a mixture of dry ice and acetone and stored there until they could be examined in an n.m.r. spectrometer with a probe temperature of −20°. Peak areas were then measured by electronic integration after optimum instrumental conditions had been established. The area of the 5-methyl peak was measured relative to that of (*a*) the hexamethyldisiloxane signal and (*b*) the total methyl signal of all methylcyclopentadienes.

The data obtained were analyzed by a standard least squares routine using an IBM 7094 computer to obtain first order rate constants. The values obtained from areas as a fraction of the total methyl signal gave more consistent results and these are reported in Tables I and II. Arrhenius parameters were obtained by the corresponding least squares analysis. Corrections for the effects of isotope dilution were made on the assumption that the methylation reaction replaced hydrogen or deuterium in the precursor cyclopentadiene in a random manner; thus 5-methyl-5-H species would be formed from 1/6 of the C_5D_5H molecules, 1/3 of the $C_5D_4H_2$ molecules, and so on. The typical deuteriated cyclopentadiene described above would then lead to 3.5% 5-methyl-5-H species in the product. The actual concentration of 5-methyl-5-D species at time t, $D(t)$, was calculated from the apparent concentration $S(t)$ based on the 5-methyl n.m.r. signal and the concentration of 5-methyl-5-H species, $H(t)$, which in turn was calculated from the above fractions and the value of k_H(decay) obtained from the Arrhenius plot.

$$D(t) = S(t) - H(t) = S(t) - H(0) \exp(-k_H t)$$

Rate constants calculated from these corrected values are reported in Table III.

Acknowledgment

We thank the National Research Council of Canada for financial support of this research.

1. S. McLEAN and P. HAYNES. Tetrahedron Letters, 2385 (1964); Tetrahedron, **21**, 2329 (1965).
2. V. A. MIRONOV, E. V. SOBOLEV, and A. N. ELIZAROVA. Tetrahedron, **19**, 1939 (1963).
3. W. R. ROTH. Tetrahedron Letters, 1009 (1964).
4. R. B. WOODWARD and R. HOFFMANN. J. Am. Chem. Soc **87**, 2511 (1965)
5. (*a*) R. F. W. BADER. Can. J. Chem. **42**, 1822 (1964). R. A. M. O'FERRALL and J. KOUBA. J. Chem. Soc. B, 985 (1967).
   (*b*) M. F. HAWTHORNE and E. S. LEWIS. J. Am. Chem. Soc. **80**, 4296 (1958). V. J. SHINER, JR. and J. G. JEWETT. J. Am. Chem. Soc. **87**, 1382 (1965).
   (*c*) R. P. BELL. The proton in chemistry. Methuen and Co., Ltd., London. 1959. p. 211.
6. S. McLEAN and P. HAYNES. Tetrahedron, **21**, 2313 (1965).
7. E. BUNCEL, E. A. SYMONS, and A. W. ZABEL. Chem. Commun. 173 (1965).

Can. J. Chem. Downloaded from www.nrcresearchpress.com by 210.87.254.40 on 09/05/12
For personal use only.

Can. J. Chem. Downloaded from www.nrcresearchpress.com by 210.87.254.105 on 09/05/12
For personal use only.

Metabolites of pathogenic fungi. VIII.[1-3] Floccosin and floccosic acid, two metabolites from *Epidermophyton floccosum* (Harz) Langeron and Milochevitch, 1930

F. BLANK[4]
The Skin and Cancer Hospital, Temple University Health Sciences Center, Philadelphia, Pennsylvania

AND

C. BUXTORF,[5] O. CHIN, G. JUST,[4] and J. L. TUDOR
Department of Chemistry, McGill University, Montreal, Quebec

Received January 9, 1969

Floccosic acid, floccosin, its magnesium complex, and a green iron-containing pigment, floccoviridin, were isolated from *E. floccosum*. Structure **7** is proposed for floccosic acid, and degradative work defining some of the functions in floccosin as depicted in partial formula **C** is described.

Canadian Journal of Chemistry, 47, 1561 (1969)

Isolation

The chloroform and acetone extracts of dry, powdered mycelium of *Epidermophyton floccosum*, previously extracted with petroleum ether and diethyl ether, yielded the metabolites floccosin and floccosic acid. Floccosin was obtained in a yield of approximately 1% of the dry mycelium,[6] and floccosic acid in 0.02% yield on one occasion.[6] It could not be isolated from subsequent batches of mycelium. When the chloroform extract was worked up by preparative thin-layer chromatography (t.l.c.), a yellow major compound containing magnesium with the virtual exclusion of all other metals was obtained in 0.5% yield. Nuclear magnetic resonance (n.m.r.) and infrared (i.r.) spectra, in conjunction with analytical data, indicated that it consisted of floccosin complexed with magnesium. All attempts to remove the metal resulted in extensive decomposition, with recovery of approximately 5% of floccosin. When the neutral fraction of the chloroform extract of the mycelium was chromatographed on silica gel thin layers using chloroform – acetic acid (9:1) as eluent, a green band appeared immediately behind the solvent front. From this band, floccoviridin, a green iron-containing complex, was eluted. The iron content of this compound was found to be about 1.0%.[7] Since very little of this material was obtained (200 mg from 2 kg of mycelium), no work has been done on it.

Floccosin

Floccosin, a yellow crystalline magnesium-free pigment, had the molecular formula $C_{30}H_{26}O_{14}$. This formula was based on elemental analysis, n.m.r. proton count[8] (see Table II) and osmometric weight determination of the parent compound and some of its derivatives. The total proton count in the n.m.r. spectrum of floccosin was 13. Floccosin therefore possessed a molecular structure consisting of two identical halves, joined by an odd number of bonds. The dimeric nature of floccosin was confirmed by the mass spectrum of floccosin tetra-trimethylsilyl ether, which showed a peak at 811 (calculated molecular ion: 898). Floccosin formed a tetramethyl ether and two isomeric tetraacetates **A** and **B**. The spectral data of floccosin and its derivatives are summarized in Tables I–IV. No interpretable

[1]Part VII. A. S. Ng, G. Just, and F. Blank. Can. J. Chem. **47**, 1223 (1969).
[2]Abstracted from the Ph.D. Theses of J. L. Tudor and O. Chin, McGill University, 1966 and 1968.
[3]This work was supported by a grant from the John A. Hartford Foundation Inc., New York, and by United States Public Health Service research grants 5ROI AI 05378 and AI 04050 from the National Institute of Allergy and Infectious Diseases.
[4]To whom correspondence should be addressed.
[5]Holder of a NRCC Postdoctorate Fellowship, 1965–1966.
[6]See Experimental for details.
[7]Determined by X-ray fluorescence.
[8]All nuclear magnetic resonance spectra will be discussed in terms of the monomeric units, while names will be based on the dimeric formulae. Chemical shifts will be given in the p.p.m. scale, using tetramethylsilane (δ = 0.00 p.p.m.) as an external reference.

TABLE I

Infrared spectra of floccosin and some derivatives

Compound	OH (cm^{-1})	OAc (cm^{-1})	Unsaturated lactone (cm^{-1})	C=O (cm^{-1})	1500–1650 cm^{-1}
Floccosin	3560 3500		1670	1700	1625, 1576
Floccosin diacetate	3400	1735	1675	1700	1625, 1580
Floccosin tetraacetate **A**		1785 1770	1735	1715	1620, 1570
Floccosin tetraacetate **B**		1785 1735	1735	1715	1620, 1570
Tetramethylfloccosin			1730	1700	1600, 1570
Dimethylfloccosin diacetate		1735	1735	1715	1600, 1570

TABLE II

Chemical shifts* (δ p.p.m.) of the protons in floccosin and derivatives

Compound	Solvent	*a*	$\frac{b}{c}$	*d*	$\frac{e}{f}$	*g*	$\frac{h}{i}$	*j*
Floccosin	Pyridine-d_5	0.66	—	2.10	$\frac{3.16}{—}$	4.00	$\frac{5.38}{6.72}$	9.20
Floccosin	$CDCl_3$	1.57	—	3.05	3.85	4.80	$\frac{5.45}{7.47}$	$\frac{4.38}{12.02}$
Floccosin	DMSO-d_6	1.36	—	3.00	$\frac{3.55}{—}$	4.76	$\frac{5.16}{7.34}$	11.56
Floccosin diacetate	$CDCl_3$	1.46	$\frac{2.03}{—}$	2.95	$\frac{3.75}{—}$	4.68	$\frac{6.98}{7.35}$	11.56
Floccosin tetraacetate **A**	$CDCl_3$	1.52	$\frac{—}{2.33}$	3.04	$\frac{3.83}{—}$	4.70	$\frac{6.53}{7.90}$	—
Floccosin tetraacetate **B**	$CDCl_3$	1.42	$\frac{2.08}{2.18}$	3.00	$\frac{3.78}{—}$	4.69	$\frac{6.88}{7.90}$	—
Tetramethylfloccosin	$CDCl_3$	1.48	—	3.03	$\frac{3.77}{4.03}$	4.72	$\frac{5.05}{7.68}$	—
Dimethylfloccosin diacetate	$CDCl_3$	1.50	$\frac{—}{2.13}$	3.02	$\frac{3.80}{3.85}$	4.65	$\frac{7.05}{7.68}$	—

**a*: CH_3CH; *b,c*: AcO; *d*: CH_2Ph; *e,f*: $—OCH_3$; *g*: O—*CH*; *h,i*: vinyl H; *j*: —*OH*.

TABLE III

Ultraviolet spectra of floccosin and some derivatives

Floccosin	λ335	288	272	224 (inf.)	204.5
	ε8450	19 320	21 980	28 990	47 090
Floccosin diacetate	λ352	278	270	222 (inf.)	205
	ε8800	18 620	21 100	29 800	49 050
Floccosin tetraacetate **A**	λ315		259		208
	ε2980		22 500		44 960
Floccosin tetraacetate **B**	λ315		259		208
	ε3000		21 480		52 570
Tetramethylfloccosin	λ335		270	229 (inf.)	207.5
	ε6080		23 130	27 390	51 140
Dimethylfloccosin diacetate	λ337.5		270	229 (inf.)	212
	ε5970		23 180	27 390	49 160

Can. J. Chem. Downloaded from www.nrcresearchpress.com by 210.87.254.105 on 09/05/12
For personal use only.

TABLE IV

Specific and molecular rotations of some floccosin derivatives

Compound	$[\alpha]_D$	$[M]_D$
Floccosin	84.1°	513°
Floccosin diacetate	153.3°	1060°
Floccosin tetraacetate **A**	−126.9°	−985°
Floccosin tetraacetate **B**	62.4°	485°
Tetramethylfloccosin	−77.5°	−516
Dimethylfloccosin diacetate	−66.7°	−482°
3*a*	−112°	−435°
4	−171°	−482°

mass spectrum of floccosin or the above derivatives could be obtained.

Oxidation of tetramethylfloccosin with alkaline permanganate yielded anisole-2,3,5,6-tetracarboxylic acid **1***a* (1), which was identified by mixed m. p. and comparison of the i.r. spectrum with that of a synthetic sample.

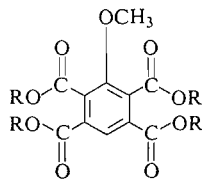

1*a*, R = H
1*b*, R = CH_3

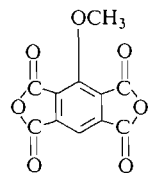

2

Methylation of **1***a* with diazomethane yielded the tetramethyl ester **1***b*, (2), which was also identified by mixed m. p. and comparison of the i.r. spectrum[9] with that of a synthetic sample. Nuclear magnetic resonance and mass spectrometry (M^+ = 340) also confirmed its structure. The anisole tetracarboxylic acid, **1***a*, was also converted to its dianhydride **2**, m.p. 215–217°, by sublimation.

From the n.m.r. spectrum of floccosin and its derivatives, and spin decoupling experiments on floccosin,[10] the following structural unit **A** could be derived. Taken in conjunction with the results of the oxidation of tetramethylfloccosin, partial structure **B** may be written for floccosin. The lactone function of floccosin absorbed in the i.r. at 1670 cm^{-1}. Upon acetylation or methylation

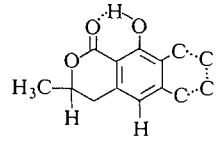

A

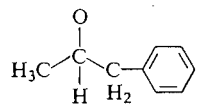

B

of floccosin, this carbonyl function reverted to its normal position at 1730–1735 cm^{-1}, proving that the lactone function in floccosin was strongly hydrogen-bonded.

Acetylation of floccosin with pyridine – acetic anhydride containing triethylamine for a short period of time gave floccosin tetraacetate **A**, ν 1785 and 1770 cm^{-1}, δ 2.33 p.p.m. (6H), $[\alpha]_D$ −126.9°. Recrystallization from methanol converted tetraacetate **A** to a mixture of tetraacetates **A** and **B**, a mixture also obtained by acetylation of floccosin with pyridine – acetic anhydride. Prolonged heating in methanol gave floccosin tetraacetate **B**, ν 1785 and 1735 cm^{-1}, δ 2.08 (3H), 2.18 (3H), p.p.m., $[\alpha]_D$ +62.4°. The conversion of tetraacetate **A** to tetraacetate **B** must have involved transformation of an acetate (ν 1770 cm^{-1}) to an aliphatic acetate (ν 1735 cm^{-1}), the absorption of which overlapped with the absorption due to the lactone function.

In an attempt to prove the nature of the oxygen functionality absorbing at 1700–1715 cm^{-1} (see Table I), floccosin tetraacetate **A** was treated with hydroxylamine hydrochloride and sodium acetate in aqueous methanol at room temperature. A crystalline product, floccosin diacetate, was obtained. Reacetylation gave floccosin tetraacetate **B**. The main spectral differences between tetraacetate **B**, ν 1785 and 1735 cm^{-1}, and the diacetate, ν 3400, 1735, and 1675 cm^{-1}, were consistent with the hydrolysis of the acetate group, which, as a hydroxy group, was hydrogen-bonded to the lactone function. Floccosin diacetate was further characterized by conversion to dimethylfloccosin diacetate.

When tetramethylfloccosin was heated under reflux with acetic anhydride and zinc dust for a few minutes, a naphthalene derivative **3***a*, $C_{14}H_8O_2(OCH_3)_2(OAc)_2$, was obtained in 43% yield. Using the same method, dimethylfloccosin diacetate was also transformed to **3***a*. The oxygen function lost during the zinc – acetic anhydride reduction was present in tetramethylfloccosin as a methoxy group and in dimethylfloccosin diacetate as an acetate group, and must therefore

[9]The infrared spectrum was kindly supplied by Dr. J. S. E. Holker, Department of Organic Chemistry, University of Liverpool, England.

[10]We wish to thank Miss M. Feser, Department of Chemistry, University of Alberta, Edmonton, Alberta, who performed this experiment.

Can. J. Chem. Downloaded from www.nrcresearchpress.com by 210.87.254.105 on 09/05/12
For personal use only.

Can. J. Chem. Downloaded from www.nrcresearchpress.com by 210.87.254.105 on 09/05/12
For personal use only.

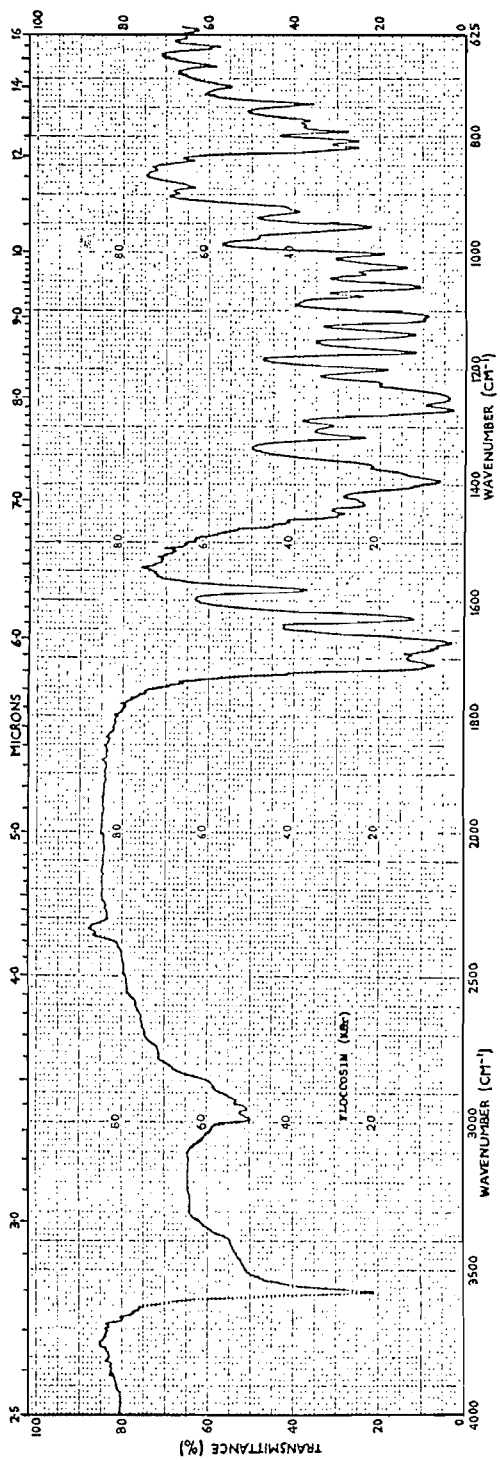

FIG. 1. The infrared spectrum of floccosin (KBr disk).

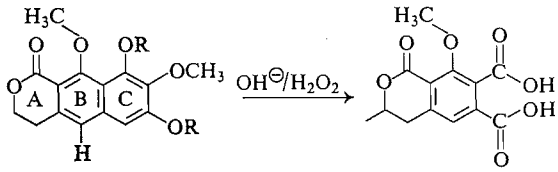

3a, R = Ac
3b, R = H

4

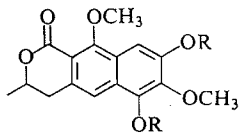

3'a, R = Ac
3'b, R = H

have been attached to ring **C** of floccosin as a hydroxy group.

Hydrolysis of **3a** in a nitrogen atmosphere gave diol **3b**, which could be reacetylated to **3a**. Both **3a** and **3b** showed the appropriate n.m.r. signals and i.r. absorption bands. Oxidation of **3a** with alkaline hydrogen peroxide gave 3-methoxy-5(2'-hydroxypropyl)trimellitic acid δ-lactone (**4**), the structure of which was derived from its origin and spectral data.[6] Oxidation of **3a** with alkaline hydrogen permanganate gave anisole tetracarboxylic acid **1a**.

Diol **3b** was readily oxidized by air to a dark, unidentified crystalline product. Reductive acetylation of this material did not regenerate **3a**, implying that the two hydroxy groups in **3b** did not bear an *ortho* or *para* relationship. No identifiable quinone could be obtained by oxidation of **3b** with silver oxide. Comparison of the ultraviolet (u.v.) spectrum of **3b** with those of catechol, resorcinol, and hydroquinone, made a *meta*-relation of the two hydroxy groups in **3b** very likely. Compound **3b** gave a positive Gibbs test (3), showing that the position *para* to a phenolic group was unsubstituted.

Compounds **3'a** and **3'b** are alternative formulations for **3a** and **3b**, and cannot be ruled out at the present time. However, the low value (1695 cm^{-1}) for the lactone absorption in **3b** suggested that a hydroxyl group may be present in a position permitting conjugation, thus favoring **3b** over **3'b**. When floccosin was heated under reflux in glacial acetic acid with potassium iodide for a short time, a naphthoquinone **5a**, $C_{15}H_{12}O_7$, ν 3300, 1690 cm^{-1} (hydrogen-bonded lactone) and 1660 cm^{-1} (quinone), λ_{max} 218 (ε 14 850), 230 (shoulder 12.650), 272 (9640), and 385 mμ (3990) was obtained in 48% yield. The n.m.r. spectrum in deuterated pyridine showed peaks which were consistent with structure **5a**: a singlet at 10.90 p.p.m. (2 protons, —OH); a peak at 6.85 p.p.m.

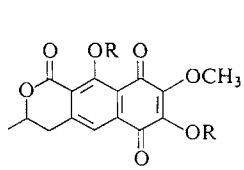

5a, R = H
5b, R = Ac
5c, R = CH_3

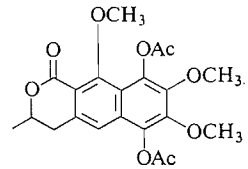

6

(1 proton, aromatic); a singlet at 3.44 p.p.m. (3 protons, —OCH_3); and the acyloxypropyl grouping, [0.65 p.p.m. (3 protons, doublet); 2.16 p.p.m. (2 protons of ABX system); and 3.90 p.p.m. (1 proton of ABX system, multiplet)] which is present in floccosin and its derivatives. The solvent peaks obscured the aromatic proton at 6.85 p.p.m. However, integration and comparison with pure solvent accounted for this proton. The low field signal (10.90 p.p.m.) disappeared on shaking with deuterium oxide. Neither a Rast nor an osmometric molecular weight determination could be obtained due to insolubility of **5a**.

Acetylation of compound **5a** with pyridine – acetic anhydride gave a diacetate **5b**, ν 1785 cm^{-1} (phenolic acetate) and 1735 cm^{-1} (lactone), λ_{max} 212 mμ (ε 14 000); 260 mμ (ε 12 800); inflexion at 284 mμ (ε 5430); and 344 mμ (ε 2130). The n.m.r. spectrum showed the same general features as in **5a** except that the hydroxyl peaks were replaced by two acetate peaks at 2.48 and 2.55 p.p.m. The above spectral data were consistent with the acetylation of two hydroxyl groups, one of which was hydrogen bonded to the lactone. Osmometric molecular weight determination indicated the monomeric nature of the diacetate **5b**. Treatment of compound **5a** with methyl iodide and silver oxide in chloroform gave the dimethyl ether **5c**, ν 1735 cm^{-1}, λ_{max} 214 mμ (ε 23 900); 267 mμ (ε 16 600); and 354 mμ (ε 4150). The n.m.r. spectrum indicated replacement of two hydroxyl groups in **5a** by methoxyl groups at 4.20 and 4.25 p.p.m.

Reductive acetylation of the dimethyl ether **5c** with zinc dust and acetic anhydride yielded a

Can. J. Chem. Downloaded from www.nrcresearchpress.com by 210.87.254.105 on 09/05/12
For personal use only.

Can. J. Chem. Downloaded from www.nrcresearchpress.com by 210.87.254.105 on 09/05/12
For personal use only.

napthalenic compound **6**, $C_{14}H_7O_2(OCH_3)_2(O_2CCH_3)_3$. The i.r. spectrum now showed no quinone bands but peaks at 1770 and 1740 cm^{-1}, attributable to phenolic acetate and lactone absorptions respectively. The u.v. spectrum showed maxima at 254 mμ (ε 35 300); 300 mμ (ε 3670); and 350 mμ (ε 2100). The spectrum, as expected, was similar to that of 1,7-dimethoxy-6,8-diacetoxy-3(2′-hydroxypropyl)-2-naphthoic acid δ-lactone (**3***a*). The n.m.r. spectrum showed methoxyl peaks at 3.95 p.p.m. (6 protons) and 3.85 p.p.m. (3 protons), and acetate peaks at 2.45 p.p.m. (3 protons) and 2.40 p.p.m. (3 protons). The change brought about by the reductive acetylation was then the conversion of the two quinone oxygens to two acetate groups.

In the naphthoquinone **5***c*, the three rings are arranged in a linear fashion, since oxidation gave anisole-2,3,5,6-tetracarboxylic acid, which was identified as its methyl ester. The structure of the quinone must therefore be represented as in **5***a*, with the methoxy and hydroxy groups on the quinone ring perhaps exchanged, if **3′** rather than **3** proves to be the correct formula of the naphthalene compound obtained from the zinc – acetic anhydride reduction of tetramethylfloccosin.

Catalytic reduction of tetramethylfloccosin with platinum oxide in ethyl acetate – acetic acid gave as one of many products **3***b*, identified by its i.r. and u.v. spectrum and mixed m.p. determination. All other experiments tried on floccosin did not lead to characterizable products.

Based on the data presented, the following partial structure **C** can be written for floccosin.

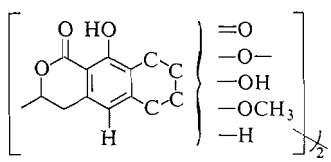

C

Floccosic Acid

Floccosic acid $C_{14}H_{12}O_7$, ν 3500–2500 and 1675 cm^{-1}, δ 11.66 p.p.m., formed a methyl ester, ν 1720 cm^{-1}, δ 4.04 p.p.m. Both floccosic acid and its methyl ester absorbed at 1795 (5-membered lactone) and 1755 cm^{-1} (aliphatic methyl ester). The n.m.r. spectrum of floccosic acid showed the appropriate signals for a $CH_3CH(O)CH_2Ph$ group (1.6 p.p.m., 3H, doublet, 3.15, 2H, ABX-system, 4.86, 1H, multiplet) similar to those observed for floccosin, xanthomegnin (4), vioxanthin, and viopurpurin (5), a methoxy group (3.86 p.p.m.) most likely associated with the ester function absorbing at 1755 cm^{-1}, an aromatic proton (7.36 p.p.m.), and a singlet at 5.97 p.p.m. (C-7 in **7**). The u.v. spectrum of floccosic acid and its methyl ester resembled that of benzoic acid derivatives. These spectral features suggested partial structure **D** for floccosic acid. Comparison of the u.v., i.r., and mass spectra of floccosic acid

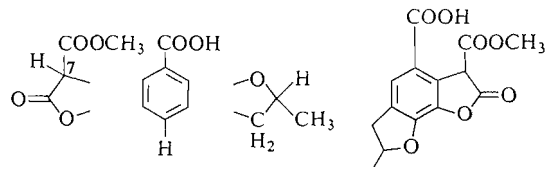

D **7**

and its methyl ester with those of appropriate model compounds suggested structure **7** for floccosic acid, without excluding any of the other possible isomeric structures, in which rings **A** and **C** are attached to the central ring in a different manner.[11] Floccosic acid melted over a 20° range. Since it appeared homogeneous by t.l.c. and n.m.r., it was very likely that the lack of sharpness of the m.p. was due to epimerization at the C-7 position.

Experimental

The i.r. spectra were recorded on a Perkin–Elmer model 337 spectrophotometer. The n.m.r. spectra were recorded on a Varian A-60 spectrometer. The u.v. spectra were measured in ethanol, on a Perkin–Elmer model 350, and a Beckman recording model DK spectrophotometer. The optical rotations were measured on a Carl Zeiss 367732 polarimeter, using chloroform as solvent. The mass spectra were recorded by the Morgan and Schaffer Corporation, 5110 Courtrai, Montreal, Quebec. The elemental analyses, and osmometric molecular weight determinations were performed by the Mikroanalytisches Laboratorium Beller, 34 Gottingen, Theaterstrasse 23, Germany. The melting points were determined on a Kofler hot stage.

Preparation of Mycelium

The fungus was grown in 500 ml Erlenmeyer flasks containing 200 ml medium at room temperature in the dark for 3 weeks. The medium consisted of 4% crude glucose (cerelose), 2% neopeptone Difco, 0.05% yeast extract Difco, 0.005% inositol, 0.001% thiamine, and 1.5% agar. The cultures were autoclaved, and the harvested mycelium washed free from adhering medium by

[11]For detailed discussion, see Ph.D. thesis of J. L. Tudor, McGill University, Montreal, Quebec.

TABLE V

Solvent	Time (days)	Code	Yield* (g)	Average yield (%) of dry mycelium
Hexane	7	H	13.36 (12.60)	3.37
Diethyl ether	7	E	5.63 (5.96)	1.5
Chloroform	7	C-1, C-1⁻†	14.38 (15.40)	3.87
Chloroform	7	C-2	2.50 (2.70)	0.67
Chloroform	7	C-3	1.00 (2.10)	0.40
Acetone	7	A-1	4.40 (4.40)	1.14
Acetone	7	A-2	2.60	0.68

*Bracketed values refer to the second run.
†C-1⁻ refers to the second run.

boiling three times in water. After pressing, the mycelium was freeze-dried, and milled in a ball-mill.

Isolation of Metabolites

Powdered mycelium of *Epidermophyton floccosum* (384 g, first run; 386 g, second run) was stirred twice with 4 l of various solvents at room temperature for one week each. The extraction results are summarized in Table V.

Floccosin

Fraction C-1 was dissolved in 2 l of methylene chloride and washed successively with (*a*) aqueous methanol (2:1, 3 × 1.5 l), (*b*) 1.6% hydrochloric acid in aqueous methanol (4:1, 3 × 1.25 l), (*c*) aqueous methanol (4:1, 3 × 1.25 l), (*d*) 1% sodium carbonate in aqueous methanol (1:1, 3 × 2 l), (*e*) aqueous methanol (1:1, 1 × 2 l), (*f*) 0.5% sodium hydroxide in aqueous methanol (1:1, 3 × 2 l), and (*g*) aqueous methanol (1:1, 1 × 2 l), yielding fractions C-1*a*, C-1*b*, etc. respectively. All washings were re-extracted with 2 × 2 l portions of methylene chloride.

Fraction C-1*e* was acidified with 60 ml of concentrated hydrochloric acid, and re-extracted with three 2 l portions of chloroform. After washing with water, the chloroform was evaporated to dryness. A pale-yellow powder (1.305 g) was obtained. The i.r. spectrum of this material indicated that it consisted of a fairly pure sample of floccosin. This material was introduced onto a column consisting of an inert support, (sand and cellulose), and washed with hexane, ether, methanol, and chloroform successively. The chloroform wash was crystallized, after evaporation from chloroform–methanol; floccosin (0.919 g), m.p. 261–263°, was obtained. Similarly, fraction C-1*g* gave floccosin (1.75 g), m.p. 263–265°. From the second run (C-1⁻), fraction C-1⁻ *g* gave floccosin (2.2 g), m.p. 263–264°, by the same procedure.

The washed, neutral powdery chloroform extract (5 g) was introduced onto a similar column, and washed with hexane, ether, methanol, chloroform, and chloroform – acetic acid (9:1). The combined chloroform and chloroform – acetic acid washings yielded floccosin (0.77 g), m.p. 256–259°, after removing acetic acid by repeated washing with water.

The neutral chloroform extract did not yield reproducible amounts of floccosin in subsequent runs. The acetone extracts were treated in the same fashion and also yielded floccosin, although in lesser amounts.

Floccosin was recrystallized from chloroform–methanol, m.p. 263–264° with decomposition. The average yield of floccosin was approximately 1% of dry mycelium.

Anal. Calcd. for $C_{30}H_{26}O_{14}$: C, 59.02; H, 4.29; O, 36.69. Found (osmometric mol. wt., 646): C, 59.00, 59.22; H, 4.08, 4.47; O, 36.98, 36.66.

Floccosic Acid

Dried mycelium of *Epidermophyton floccosum* (1 kg) was extracted with various solvents as described above. The combined chloroform and acetone extracts (C-1, C-2, C-3, A-1, and A-2 of two other runs), were submitted to a washing procedure similar to that described for floccosin. The sodium carbonate wash C-1*d* was acidified and re-extracted with chloroform. The chloroform extract was evaporated to dryness. The brown residue was introduced onto a column consisting of an inert support and washed with hexane, ether, methanol, and chloroform. The ether wash was evaporated to dryness and partially dissolved in benzene. The benzene soluble portion was chromatographed on silica gel (100 g). Elution was effected with benzene and benzene–ether mixtures. Benzene–ether (8:2) gave approximately 200 mg of crystalline floccosic acid, which was recrystallized from methanol, m.p. 156.5–178.5°, yield: 0.02% of dry mycelium.

Anal. Calcd. for $C_{14}H_{12}O_7$: C, 57.54; H, 4.14; O, 38.32. Found: C, 57.50; H, 3.89.

Yellow Magnesium–Floccosin Complex

Dry powdered mycelium (930 g) was extracted in a Soxhlet extractor successively with 4 l petroleum ether (b.p. 40–60°), 4 l diethyl ether, and 4 l chloroform for 7 days each. The chloroform extract upon evaporation to dryness yielded a dark-brown material (30 g), which was dissolved in 2 l chloroform, and washed extensively with water, 5% hydrochloric acid, 5% sodium bicarbonate, and 3% sodium hydroxide. The remaining neutral chloroform solution was evaporated to dryness, giving solid material (25 g). This material was placed in a Soxhlet extractor and extracted with solvents (600 ml) in the following sequence for 24 h each: hexane, diethyl ether, methanol, benzene, and methylene chloride. The benzene extract yielded solid material (9.2 g) upon evaporation to dryness. Part of this material (4.6 g) was dissolved in methylene chloride and chromatographed on silica gel thin layer plates using methylene chloride – methanol (9:1 v/v) as eluent. The developed chromatogram showed two main bands: a reddish brown band just above the start, and a yellow band which moved with the solvent front. The yellow band was cut out and eluted with a mixture of methanol and methylene chloride. Upon

Can. J. Chem. Downloaded from www.nrcresearchpress.com by 210.87.254.105 on 09/05/12
For personal use only.

Can. J. Chem. Downloaded from www.nrcresearchpress.com by 210.87.254.105 on 09/05/12
For personal use only.

evaporation of the solvent a yellow material (magnesium–floccosin complex) was obtained, yield: 0.5% of dry mycelium. The magnesium complex did not melt. Found: C, 56.02; H, 3.89; O, 32.95; ash, 0.351 mg in 4.141 mg.

Isolation of Floccoviridin

Dry powdered mycelium (463.6 g) was extracted in a Soxhlet extractor as described in the isolation of the yellow magnesium complex. The chloroform extract was evaporated to dryness, yielding 16.0 g of dark brown material, which was washed extensively with water, 5% hydrochloric acid, 5% aqueous sodium bicarbonate, and 3% sodium hydroxide solution.

The remaining neutral chloroform phase was evaporated to dryness, and the dry material was washed with 3 × 900 ml hexane and 2 × 600 ml diethyl ether. The neutral solid material (5 g) remaining was dissolved in chloroform and chromatographed on silica gel thin layers (½ mm thick) with methylene chloride – acetic acid (9:1 v/v) as eluent. A series of bands, brown, yellow, orange, and green (increasing R_f values), developed. The green band was removed and eluted with a methylene chloride – acetic acid mixture (approx. 9:1). The solvent was evaporated and traces of acetic acid were removed by azeotroping with benzene. The green pigment was further purified by rechromatography on silica gel thin layers, using methylene chloride – pyridine (9:1 v/v) as eluent. The green pigment (120 mg) was recovered by elution from the silica gel and evaporation to dryness, (yield 0.03% of dry mycelium). Found: C, 60.20; H, 4.90; ash: 0.397 mg brown residue in 4.293 mg. X-ray fluorescence analysis indicated that the sample contained 1% of iron. Optical spectroscopy indicated that together the metals copper, tin, calcium, silicon, and aluminium were present to the extent of less than 0.1%. No other metals were detected.

Floccosin Tetraacetate 'A'

Floccosin (100 mg) was dissolved in pyridine (3.0 ml). Triethylamine (0.25 ml) and acetic anhydride (1.5 ml) were added. The mixture was shaken and allowed to stand for 15 min at room temperature in the dark. The solution was poured onto crushed ice, and set aside until the ice melted. The white flocculent solid was filtered off and washed with water. A quantitative yield of floccosin tetraacetate '**A**' was obtained, m.p. 216–227°.

Anal. Calcd. for $C_{38}H_{34}O_{18}$: C, 58.61; H, 4.37; O, 37.02. Found: C, 58.90; H, 4.23; O, 36.92.

*Floccosin Tetraacetate '**B**'*

Floccosin tetraacetate '**A**' was refluxed in methanol for 4 days, and then crystallized from methanol, m.p. 246–248°.

Anal. Calcd. for $C_{38}H_{34}O_{18}$: C, 58.61; H, 4.37; O, 37.02. Found: C, 58.85; H, 4.26; O, 36.85.

Floccosin Diacetate

Floccosin tetraacetate '**A**' (100 mg) was dissolved in methanol (10 ml). Hydroxylamine hydrochloride (100 mg) and sodium acetate (180 mg) were dissolved in a minimum of water and methanol (10 ml) and this solution was added to that of the tetraacetate. After standing for about 18 h at room temperature, yellow needle-like crystals of the diacetate (45 mg) separated out, while the solution turned brown. The crystals were filtered off and recrystallized from methanol, m.p. 259–261°.

Anal. Calcd. for $C_{34}H_{30}O_{16}$: C, 58.79; O, 36.89; H, 4.32. Found (osmometric mol. wt., 675): C, 58.96, 59.10; O, 36.51, 37.08; H, 4.43, 3.94.

Tetramethylfloccosin

Floccosin (108 mg) was dissolved in dioxane (10 ml). Methyl iodide (10 ml) and silver oxide (375 mg) were added, and the mixture was stirred at room temperature for 48 h. The supernatant was filtered off and evaporated to dryness. Crude tetramethylfloccosin (127 mg) was recovered and crystallized several times from a methylene chloride – methanol mixture, m.p. 258–261° (with decomp.).

Anal. Calcd. for $C_{34}H_{34}O_{14}$: C, 61.26; H, 5.14; O, 33.60. Found (osmometric mol. wt., 650): C, 60.86; H, 4.84; O, 34.17.

Dimethylfloccosin Diacetate

Floccosin diacetate (83 mg) was dissolved in methyl iodide (6 ml). Silver oxide (200 mg) was added, and the mixture was stirred for 24 h at room temperature. The solution was filtered off and evaporated to dryness. Dimethylfloccosin diacetate was recovered as a white amorphous solid in quantitative yield, m.p. 180–184°.

Anal. Calcd. for $C_{36}H_{34}O_{16}$: C, 59.84; H, 4.74; O, 35.42. Found: C, 60.13; H, 4.40; O, 35.45.

*Anisole-2,3,5,6-tetracarboxylic Acid (**1a**) from Tetramethylfloccosin*

Aqueous potassium permanganate (120 ml, 5%) was added, in small portions over a period of 48 h, to a suspension of tetramethylfloccosin (100 mg) in 2 *N* sodium hydroxide solution (35 ml) under reflux. The manganese dioxide formed was filtered off and washed. The entire filtrate was acidified with concentrated hydrochloric acid, heated nearly to boiling, and again treated with 5% potassium permanganate until the oxidant was in slight excess. After 10 min, the excess reagent was reduced with sulfur dioxide. Crude anisole-2,3,5,6-tetracarboxylic acid (79 mg) was isolated from the resulting solution by continuous liquid–liquid extraction with ether, m.p. 248–250°; ν KBr 1730, 1705 cm^{-1}. The i.r. spectrum was identical with that of a synthetic sample.

*Anisole-2,3,5,6-tetracarboxylic Acid Tetramethyl Ester (**1b**)*

Anisole-2,3,5,6-tetracarboxylic acid (40 mg) was treated with diazomethane in an ether solution. The solvent was evaporated to dryness, and the resulting product was sublimed at 70° and 10^{-2} Torr yielding the pure ester (42 mg), m.p. 104–105°; ν KBr 1740, 1725 cm^{-1}. The i.r. spectrum was identical with that of a synthetic sample.

*Anisole-2,3,5,6-tetracarboxylic Acid Anhydride (**2**)*

Anisole-2,3,5,6-tetracarboxylic acid (6.5 mg) was heated at 165° for 4 h under atmospheric pressure in a narrow tube, and for 12 h at 165° and 10^{-2} Torr. The sublimate consisted of pale-yellow prisms, m.p. 215–217°; ν KBr 1845, 1825, 1780, and 1765 cm^{-1}.

*1,7-Dimethoxy-6,8-diacetoxy-3(2'-hydroxypropyl)-2-naphthoic Acid δ-Lactone (**3a**)*

Tetramethylfloccosin (410 mg) and sodium acetate (200 mg) were added to acetic anhydride (20 ml). The mixture was heated to boiling under reflux, and zinc

Can. J. Chem. Downloaded from www.nrcresearchpress.com by 210.87.254.105 on 09/05/12
For personal use only.

powder (1.8 g) was added. Boiling was continued for 7 min. The reaction mixture was immediately cooled and filtered. The zinc residue was washed with chloroform. The entire filtrate was reduced in volume, under low pressure, until all of the chloroform had been removed. Crushed ice was then added to the acetic anhydride solution, and the mixture was stirred until all of the anhydride was hydrolyzed. The yellowish white precipitate formed was extracted with three portions of chloroform, each of which was washed three times with water. The entire chloroform extract was evaporated to dryness. The solid residue was crystallized from methanol yielding 221 mg of white needle-like crystals, which were recrystallized several times from methanol, m.p. 169–170°, ν KBr 1770, 1720, 1630, 1610, and 1570 cm^{-1}, λ_{max} 350 mμ (ε 2190), 295 mμ (ε 6570), 252 mμ (ε 52 600), and 224 mμ (ε 20 450); δ ($CDCl_3$) 1.47 p.p.m., (3H, doublet); 2.38 and 2.48, (3H each, singlets); 3.06 (2H of *ABX* system); 3.94 and 4.10 (3H each, singlets); 4.62 (1H of AB*X* system); 7.32 (1H, doublet); and 7.96 (1H, singlet).

Anal. Calcd. for $C_{20}H_{20}O_8$: C, 61.85; H, 5.19; O, 32.96. Found (osmometric mol. wt., 386): C, 62.08, 61.76; H, 4.83, 5.06; O, 33.00, 33.20.

1,7-Dimethoxy-6,8-dihydroxy-3-(2'-hydroxypropyl)-2-napthoic Acid δ-Lactone (3b)

1,7-Dimethoxy-6,8-diacetoxy-3-(2-hydroxypropyl)-2-naphthoic acid δ-lactone (**3***a*) (200 mg) was dissolved in methanol (20 ml). Concentrated hydrochloric acid (5 ml) and water (5 ml) were added, and the mixture was stirred under nitrogen at room temperature for 3 days. The yellow solution was extracted with chloroform. The chloroform solution was evaporated to dryness and the yellow solid residue was crystallized from chloroform under nitrogen to yield yellow crystals of **3***b* quantitatively, m.p. 227–230° (with decomp.); ν KBr 3430, 3420, 1695, 1630, 1615, 1580, and 1530 cm^{-1}; λ_{max} 365 mμ (ε 1870), 298 (4800), 263 (31 770), 225 (15 970), δ (pyridine-d_5) 0.58 p.p.m. (3H, doublet); 2.16 (2H of *ABX* system); 3.32 and 3.38 (3H, each singlets); 3.78 (1H of AB*X* system), 6.98 and 7.38 (1H each, singlets); signals due to the hydroxyl protons were not seen because of the presence of water in the solvent.

Anal. Calcd. for $C_{16}H_{16}O_6$: C, 63.15; H, 5.30; O, 31.55. Found (osmometric mol. wt., 307)[14]: C, 62.25; H, 4.70; O, 31.55.

3-Methoxy-5-(2-hydroxypropyl) Trimellitic Acid δ-Lactone (4)

1,7-Dimethoxy-6,8-diacetoxy-3-(2-hydroxypropyl)-2-naphthoic acid δ-lactone (330 mg) was dissolved in methanol (40 ml). Sodium hydroxide (4 g) in water (20 ml) was added. Hydrogen peroxide (10 ml, 30%) was then added slowly, while the solution was stirred at room temperature for 0.5 h. An additional portion of hydrogen peroxide (10 ml) was added and stirring was continued for a total of 5 h. The light amber solution was acidified with concentrated hydrochloric acid and extracted in a continuous liquid–liquid extractor with ether. The ether solution was evaporated to dryness, and the white solid residue was crystallized from ether–hexane to yield crystalline 3-methoxy-5-(2-hydroxypropyl) trimellitic acid δ-lactone (150 mg), m.p. 193–194°.

Anal. Calcd. for $C_{13}H_{12}O_7$: C, 55.72; H, 4.32; O, 39.97. Found: C, 55.12, 56.13; H, 4.90, 3.62; O, 39.91, 40.22.[15]

3-Methoxy-5(2'-hydroxypropyl) Trimellitic Anhydride δ-Lactone (5)

3-Methoxy-5-(2-hydroxypropyl) trimellitic acid δ-lactone was heated at 150° in a tube (12 in. long, ¼ in. diameter), sealed at one end, under vacuum for 24 h. A yellow melt solidified on the cool portion of the tube; ν KBr 1860, 1770, 1730, and 1620 cm^{-1}.

Oxidation of 1,7-Dimethoxy-6,8-diacetoxy-3-(2-hydroxypropyl)-2-naphthoic Acid δ-Lactone (3a)

Compound **3***a* (20 mg) was dissolved in 2 *N* sodium hydroxide (15 ml) and oxidized with 5% aqueous potassium permanganate (15 ml) using the method described above for the oxidation of tetramethylfloccosin. Liquid–liquid extraction with diethyl ether for 24 h gave a crystalline material whose i.r. spectrum and t.l.c. behavior were identical to **1***a*. Methylation with diazomethane in ether gave an ester which had the same retention time (7 min, 5% DC-710 on chromosorb W, acid washed, 45/60, 240 °C) as **1***b*.

Silylation of Floccosin (8)

To a solution of floccosin (10 mg) in anhydrous pyridine (0.2 ml) was added hexamethyldisilazane (0.2 ml) and bis(trimethylsilyl)acetamide (0.1 ml). The mixture was shaken for 30 s and allowed to stand at room temperature for overnight.

The mixture was then separated by t.l.c. (silica gel G)[16] using anhydrous ether as the developing solvent. The u.v. active band (R_f 0.9) was scraped off and dissolved with anhydrous ether. After stripping the solvent with a stream of nitrogen, a creamish crystalline material was obtained. Recrystallization from anhydrous ether gave colorless needles, m.p. 130–133° (decomp.), ν (KBr) 1250, 850, 755 [$Si(CH_3)_3$], and 1040 cm^{-1} (Si—O—C).

1,6-Dihydroxy-5,8-diketo-7-methoxy-3(2'-hydroxypropyl)-2-naphthoic Acid δ-Lactone (5a)

A mixture of floccosin (256 mg), potassium iodide (724 mg), and glacial acetic acid (25 ml) was refluxed for 10 min. After cooling, the mixture was diluted to 250 ml with water. The red precipitate (180 mg) was filtered and collected. The filtrate was titrated against sodium thiosulfate. Calcd. (for one active oxygen): 13.56 ml of 0.01 *N* $Na_2S_2O_3$. Found: 11.40 ml.[17]

The aqueous solution was then extracted with methylene chloride, washed with water, dried over anhydrous sodium sulfate, and the solvent evaporated to yield 68 mg of a red crystalline material. This was combined with the

[14]This compound could not be completely purified, because of the ease with which it is oxidized by air, when in solution.

[15]The inexact analysis is probably due to the fact that thorough drying could not be achieved, without the formation of the anhydride.

[16]The plates, after standing at room temperature for 2 days, were heated at 120° for ½ h immediately before use.

[17]The low value is probably due to the difficulty in determining the end point since the solution was orange in color.

red precipitate above and crystallized from methylene chloride to give 123 mg (48%) of red needle-like crystals, m.p. 262° (with decomp.); $[\alpha]_D^{25}$ −42° (*c*, 0.1, chloroform).

Anal. Calcd. for $C_{15}H_{12}O_7$: C, 59.21; H, 3.98; O, 36.81. Found: C, 58.90; H, 4.20; O, 37.10.

1,6-Diacetoxy-5,8-diketo-7-methoxy-3-(2′-hydroxypropyl)-2-naphthoic Acid δ-Lactone (5b)

Compound **5***a* (50 mg) was dissolved in pyridine (1 ml) and acetic anhydride (6 ml) added. The mixture was stirred overnight at room temperature and then poured on ice chips to destroy excess acetic anhydride. The yellow precipitate (45 mg) was filtered and crystallized from a methylene chloride – methanol mixture to give yellow needles, m.p. 169–170°; $[\alpha]_D^{25}$ −256° (*c*, 0.1, chloroform).

Anal. Calcd. for $C_{19}H_{16}O_9$: C, 58.76; H, 4.15; O, 37.08. Found (osmometric mol. wt., 395): C, 58.97; H, 4.35; O, 36.90.

1,6,7-Trimethoxy-5,8-diketo-3-(2′-hydroxypropyl)-2-naphthoic Acid δ-Lactone (5c)

A mixture of compound **5***a* (56 mg), methyl iodide (10 ml), silver oxide (531 mg), and chloroform (20 ml) was refluxed for 30 min. After cooling, the silver oxide was filtered and the filtrate taken to dryness to give a quantitative yield of the dimethyl ether. Crystallization from a chloroform–methanol mixture afforded yellow needles, m.p. 166–168°; $[\alpha]_D^{25}$ −362° (*c*, 0.1, chloroform).

Anal. Calcd. for $C_{17}H_{16}O_7$: C, 61.44; H, 4.85; O, 33.70. Found (osmometric mol. wt., 340): C, 61.32; H, 4.86; O, 33.75.

1,6,7-Trimethoxy-5,8-diacetoxy-3-(2′-hydroxypropyl)-2-naphthoic Acid δ-Lactone (6)

A mixture of the dimethyl ether (**5***c*) (12.5 mg), acetic anhydride (4.5 ml), pyridine (0.5 ml), and zinc dust (236 mg) was stirred at room temperature for 5 h. The solution was filtered and the precipitate washed with methylene chloride. The filtrate and washings were combined and after removing the methylene chloride *in vacuo*, ice chips were added. When the ice had melted the resulting aqueous solution was extracted with methylene chloride. The organic phase was washed with 5% aqueous hydrochloric acid and water. After the solvent was evaporated the crude extract was separated by t.l.c. on silica gel G, (benzene–acetone, 4:1). The major band (R_f 0.50) was eluted with chloroform and crystallized from an ether–chloroform mixture, m.p. 168–170° (decomp.); $[\alpha]_D^{25}$ −198° (*c*, 0.1, chloroform).

Anal. Calcd. for $C_{21}H_{22}O_9$: C, 60.28; H, 5.30. Found: C, 60.32; H, 5.48.

Oxidation of 1,6,7-Trimethoxy-5,8-diketo-3-(2′-hydroxypropyl)-2-naphthoic Acid δ-Lactone (5c)

The dimethyl ether **5***c* (20 mg) was oxidized with potassium permanganate using the method described for the oxidation of **3***a*. After the usual work-up, methylation of the crude extract with diazomethane gave anisole-2,3,5,6-tetra-carboxylic acid tetramethyl ester which was identified by comparison of its g.l.c. and t.l.c. behavior with an authentic sample.

Methyl Ester of Floccosic Acid

Floccosic acid (100 mg) was dissolved in methanol (10 ml), and a slight excess of diazomethane in ether was added. The mixture was allowed to stand for 10 min and was then evaporated to dryness. The methyl ester was obtained in quantitative yield; it was crystallized from methanol, m.p. variable, 160–180°.

Anal. Calcd. for $C_{15}H_{14}O_7$: C, 58.82; H, 4.58; O, 36.30. Found: C, 58.72; H, 4.80.

1. J. C. Roberts. J. Chem. Soc. 2989 (1955).
2. E. J. Haws and J. S. E. Holker. J. Chem. Soc. 3820 (1961).
3. F. E. King, T. J. King, and L. C. Manning. J. Chem. Soc. 563 (1957).
4. G. Just, W. C. Day, and F. Blank. Can. J. Chem. **41**, 74 (1963).
5. F. Blank, A. S. Ng, and G. Just. Can. J. Chem. **44**, 2873 (1966).
6. G. L. Schmir, L. A. Cohen, and B. Witkop. J. Am. Chem. Soc. **81**, 2228 (1959).
7. L. Jurd. Arch. Biochem. Biophys. **63**, 376 (1956).
8. T. Furuya. J. Chromatog. **19**, 607 (1965).

Can. J. Chem. Downloaded from www.nrcresearchpress.com by 210.87.254.105 on 09/05/12
For personal use only.

Can. J. Chem. Downloaded from www.nrcresearchpress.com by 210.87.254.6 on 09/05/12
For personal use only.

Distribution of substituent groups in *O*-(2-aminoethyl)cellulose

E. J. ROBERTS AND S. P. ROWLAND

Southern Regional Research Laboratory, Southern Utilization Research and Development Division, Agricultural Research Service, United States Department of Agriculture, New Orleans, Louisiana

Received June 17, 1968

O-(2-Aminoethyl)cellulose (degree of substitution 0.14), prepared by reaction of sodium 2-aminoethyl sulfate with cotton fabric, was hydrolyzed to glucose and mono-*O*-(2-aminoethyl)-D-glucopyranoses which were identified by gas–liquid chromatography (g.l.c.). Complications arise from reactions between the functional group at C-1 of the glucose unit and the amine function of a substituent. The distribution of 2-aminoethyl substituents in the 3-*O*- and 6-*O*-positions of the D-glucopyranosyl units of cotton cellulose was estimated to be 0.20:1.00 from direct analysis of the hydrolyzate of *O*-(2-aminoethyl)cellulose, but the total substitution in the 2-*O*-position could not be estimated in this manner. The ratio of substituents in the 2-*O*-, 3-*O*-, and 6-*O*-positions was found to be 0.64:0.14:1.00 when the amino groups were converted to hydroxyl groups by diazotization, and the distribution was estimated in terms of the 2-hydroxyethyl substituents. It has been observed that a substantial fraction (57.5%) of the 2-*O*-(2-hydroxyethyl)-D-glucose from the chemically modified cellulose exists in the form of the inner glucosides. Several new monosubstituted glucoses have been prepared and characterized by g.l.c. for this purpose.

Canadian Journal of Chemistry, 47, 1571 (1969)

Introduction

Development of an understanding of the chemistry of the hydroxyl groups of the D-glucopyranosyl units of cotton cellulose is dependent upon a knowledge of the relative reactivities of these hydroxyl groups toward a variety of reagents. In this regard, but also in connection with the characterization of the products from reaction of cellulose with *tris*-(1-aziridinyl)phosphine oxide, we have been interested in the reaction of cellulose with sodium 2-aminoethyl sulfate and the distribution of the resulting substituents at the 2-*O*-, 3-*O*-, and 6-*O*-positions of the D-glucopyranosyl units.

In previous publications, we have delineated the distribution of *O*-[2-(diethylamino)ethyl] substituents in the D-glucopyranosyl residues of chemically modified cellulose (1, 2) and starch (2). This paper describes the relative distribution of substituent groups resulting from the related rate-controlled reaction of sodium 2-aminoethyl sulfate with cotton cellulose. The unambiguous approach to the identification of the hydrolysis products of the modified cotton by chromatographic comparison with authentic glucose derivatives has been employed.

Experimental

Gas–Liquid Chromatography

The gas–liquid chromatograms (g.l.c.) were obtained with an Aerograph model 1520 instrument equipped with a hydrogen flame ionization detector. The column was based on a solid phase of acid-washed, dimethyldichlorosilane-treated Chromosorb W of 60–80 mesh obtained from Johns-Manville Corporation. The liquid phase consisted of SE-30 from Wilkins Instrument and Research Incorporated. The column was prepared in a $\frac{1}{8}$ in. outer diameter tube, 5 ft in length; it carried a 5% liquid phase and was operated isothermally at 185 and 190° with a carrier gas flow of 20 ml/min and an inlet pressure of 65 p.s.i. Similar columns with liquid phases of QF-1 and XE-60 were investigated but these did not give as good separations of *O*-(2-aminoethyl)-D-glucopyranoses and the *O*-(2-hydroxyethyl)-D-glucopyranoses as the SE-30 column. All samples to be analyzed were equilibrated overnight in dry pyridine before conversion to the trimethylsilyl ethers (3).

Preparation of O-(2-Aminoethyl)cellulose

Scoured and bleached 48 × 48 cotton sheeting was padded with a solution prepared by dissolving 20 parts by weight of 2-aminoethylsulfuric acid in 80 parts of a 37.5% solution of sodium hydroxide. The wet pick-up was adjusted to 159%. The fabric was heated at 130° for 15 min on steam-heated rotating cans. The treated fabric was washed with cold water and then with hot (85°) water; this was followed by rinsing with dilute acetic acid, dilute ammonium hydroxide, and finally with water. The fabric was dried on a tenter frame; it contained 0.64% nitrogen corresponding to a degree of substitution of 0.075, at this stage. The fabric was subjected to a second treatment in exactly the same manner; the finished product contained 1.20% nitrogen, corresponding to a degree of substitution of 0.14.

Diazotization of O-(2-Aminoethyl)cellulose

Ten grams of *O*-(2-aminoethyl)cellulose ground in the Wiley Mill to pass a 20-mesh screen was suspended in 150 ml of a 20% solution of sodium hydroxide and stirred for 30 min. The swollen chemically modified cellulose was removed by filtration and was washed several times with water to remove the sodium hydroxide. It was then suspended in 300 ml of 20% acetic acid; 10 g of sodium nitrite were added slowly and stirring was maintained for

Can. J. Chem. Downloaded from www.nrcresearchpress.com by 210.87.254.6 on 09/05/12
For personal use only.

1.5 h. The diazotized modified cellulose was isolated by filtration and was washed free of acidity with water prior to air drying. The sample of diazotized cellulose contained 0.34% nitrogen.

Hydrolysis of O-(2-Aminoethyl)cellulose or Diazotized O-(2-Aminoethyl)cellulose

Five grams of the chemically modified cellulose were hydrolyzed with sulfuric acid by the three-step process of Hägglund (4) as modified by Zollinger (5). The sulfuric acid was removed with barium hydroxide and the solution was concentrated and freeze-dried. The nitrogen content of the hydrolyzate was 1.10%; the yield was 4.9 g. The nitrogen content of the hydrolyzate from diazotized *O*-(2-aminoethyl)cellulose was 0.2%; the yield was 4.8 g.

Synthesis of 2-O- , 3-O- , and 6-O-(2-Aminoethyl)-D-glucopyranoses, 3-O-[N-(2-Aminoethyl)-2-aminoethyl]-D-glucopyranose, and 2-O- , 3-O- , and 6-O-(2-Hydroxyethyl)-D-glucopyranoses

The glucose derivatives were prepared by the conventional method of blocking all hydroxyl groups except that for the desired substituent. Since the *O*-aminoethyl substituents were introduced under alkaline conditions, the blocking groups had to be stable to alkali and to be easily removable after introduction of the substituent groups.

The sulfuric acid used in the hydrolysis of the blocking groups was removed by adding barium hydroxide to pH 10–11 to insure the presence of free basic amine groups in the *O*-(2-aminoethyl)-D-glucopyranoses. The excess barium ions were precipitated by carbon dioxide and the solutions were decolorized with Darco carbon G-60. The filtrates were concentrated under reduced pressure and the products were freeze-dried.

All of the *O*-(2-aminoethyl)-D-glucopyranoses and some of the intermediate compounds were amorphous solids that did not crystallize. The intermediates were therefore purified by crystallization at the last possible step in the synthesis before removal of the blocking groups. Some of the derivatives contain impurities due to small amounts of side reaction or slightly incomplete reaction in the last stage of the syntheses. However, the compounds are considered to be authentic derivatives since they were prepared by unambiguous methods.

Methyl 3-O-Benzyl-4,6-O-benzylidene-2-O-carbethoxymethyl-α-D-glucopyranoside

To 25 g (0.067 mole) of chromatographically pure methyl 3-*O*-benzyl-4,6-*O*-benzylidene-α-D-glucopyranoside (1) in 500 ml of dry dioxane were added 2.4 g (0.1 mole) of sodium hydride. After a 16-h period at room temperature (with stirring), 13 g (0.067 mole) of ethyl bromoacetate were added. An additional 13 g (0.067 mole) of ethyl bromoacetate was added after 4 h of stirring. Gas–liquid chromatographic analysis of the reaction mixture after 16 h at room temperature showed that the reaction was complete. The solid was removed by filtration and was washed with dioxane. The combined filtrate and washings were evaporated to a syrup. The syrup was dissolved in 200 ml of ether and washed twice with water. The ether solution was dried with sodium sulfate and evaporated, yielding 27 g (87% of theory) of white needles. After three crystallizations from methanol, 22.5 g of the pure product, m.p. 99–101°, were obtained. The product showed a single peak in g.l.c. with the SE-30 column operated isothermally at 250°.

Anal. Calcd. for $C_{25}H_{30}O_8$: C, 65.48; H, 6.58. Found: C, 65.39; H, 6.47.

Methyl 3-O-Benzyl-4,6-O-benzylidene-2-O-carbamoylmethyl-α-D-glucopyranoside

Methyl 3-*O*-benzyl-4,6-*O*-benzylidene-2-*O*-carbethoxymethyl-α-D-glucopyranoside, 20 g (0.044 mole) were dissolved in 800 ml of absolute ethanol which was saturated with ammonia. The solution was stirred at room temperature for 4 h and the alcohol was evaporated under reduced pressure, yielding 18 g (98% of theory) of white microscopic needles melting at 176–180°. After two crystallizations from methanol the m.p. was 180–183°. Neither the amide nor its trimethylsilyl derivative could be eluted from the SE-30 column at 250°.

Anal. Calcd. for $C_{23}H_{26}O_7N$: C, 64.33; H, 6.29; N, 3.26. Found: C, 64.10; H, 6.27; N, 3.21.

Methyl 2-O-(2-Aminoethyl)-3-O-benzyl-4,6-O-benzylidene-α-D-glucopyranoside

To a solution of 15 g (0.036 mole) of methyl 3-*O*-benzyl-4,6-benzylidene-2-*O*-carbamoylmethyl-α-D-glucopyranoside in 300 ml of dry tetrahydrofuran were slowly added 2.8 g (0.072 mole) of lithium aluminium hydride. After stirring overnight at room temperature, the excess lithium aluminium hydride was destroyed by cautious addition of wet tetrahydrofuran. The solid was removed by filtration and was washed with tetrahydrofuran. The combined filtrate and washings were evaporated, yielding 14 g (95% of theory) of a white waxlike solid.

2-O-(2-Aminoethyl)-D-glucopyranose

Methyl 2-*O*-(2-aminoethyl)-3-*O*-benzyl-4,6-*O*-benzylidene-α-D-glucopyranoside, 14 g (0.034 mole), was dissolved in 200 ml of ethanol and 1.5 g of 10% palladium/carbon, together with 25 ml of 2 *N* sulfuric acid (essential for hydrogenolysis), were added. The solution was shaken under a slight positive hydrogen pressure at room temperature until the theoretical amount of hydrogen (3 moles) was absorbed (about 4 h). This removed the benzyl and benzylidene groups. The catalyst was removed by filtration and the solution was evaporated under reduced pressure to a residual volume of 30 ml. Sulfuric acid (75 ml, 2 *N*) was added and the solution was refluxed for 16 h. The sulfuric acid was removed with barium hydroxide; the solution was decolorized with Darco G-60 carbon and was evaporated to a volume of about 25 ml. This solution was freeze-dried, yielding 6.4 g (85% of theory) of tan, highly viscous syrup. Gas–liquid chromatography of the trimethylsilylated product on the SE-30 column operated isothermally at 185° showed two peaks (designated 2 in Fig. 1) as expected for the two anomers of 2-*O*-(2-aminoethyl)-D-glucopyranose. Three additional peaks, one designated 2″ and two designated 2′, were also present. These are considered to be the inner *N*-glucosyl derivative of the 2-*O*-(2-aminoethyl)-α-D-glucofuranose and the two anomeric forms of the inner *N*-glucosyl derivative of 2-*O*-(2-aminoethyl)-D-glucopyranose by analogy to the results obtained for 2-*O*-(2-hydroxyethyl)-D-glucose (6, 7).

3-O-(2-Aminoethyl)-D-glucopyranose

3-*O*-(2-Aminoethyl)-1,2;5,6-di-*O*-isopropylidene-α-D-glucofuranose, 2 g (0.0066 mole), prepared by the pro-

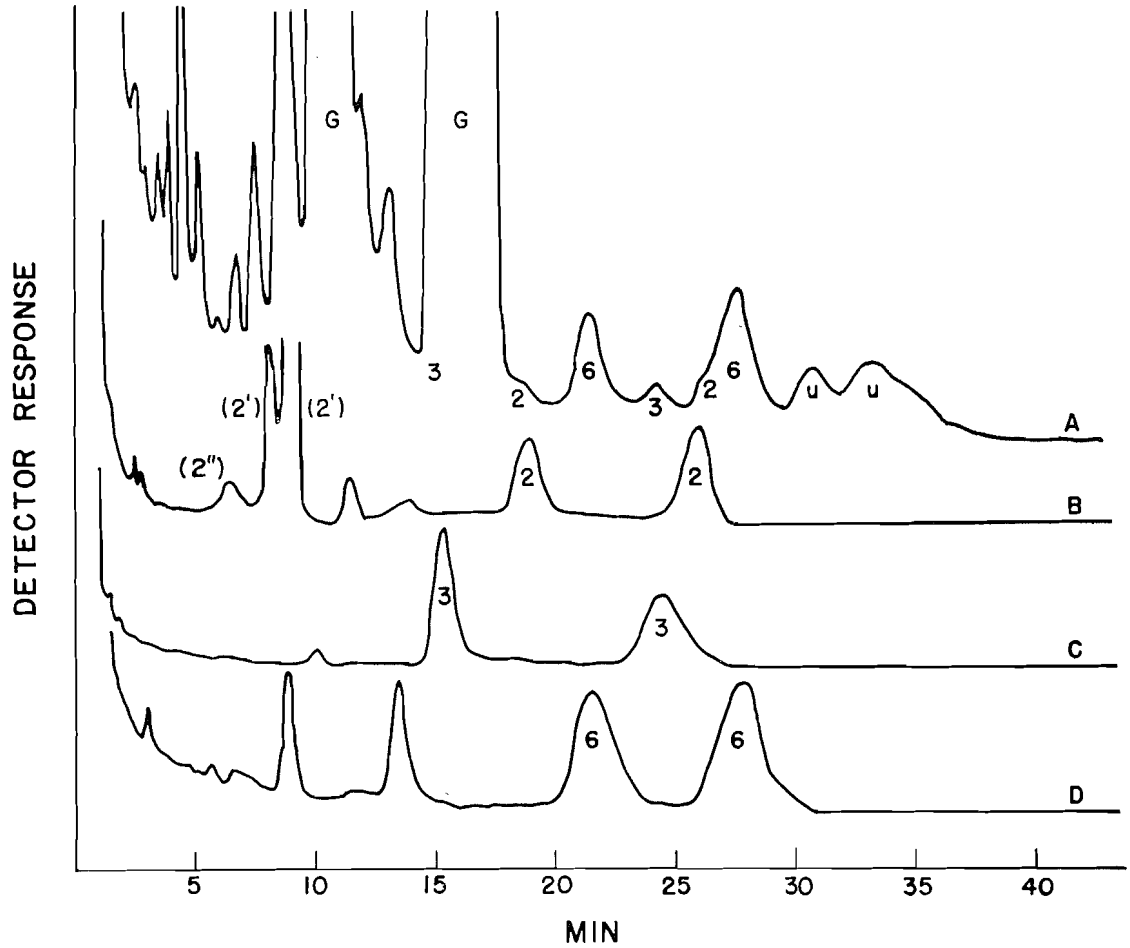

FIG. 1. Chromatograms of trimethylsilyl derivatives on an SE-30 column operated isothermally at 185°. Curve A is the hydrolyzate of *O*-(2-aminoethyl)cellulose; Curve B is 2-*O*-(2-aminoethyl)-D-glucopyranose; Curve C is 3-*O*-(2-aminoethyl)-D-glucopyranose; and Curve D is 6-*O*-(2-aminoethyl)-D-glucopyranose. Peaks labeled G are the anomers of glucose. The peaks designated 2″ and 2′ are believed to be the inner *N*-glucosyl forms of the 2-*O*-(2-aminoethyl)-D-glucose. Peaks designated U are unknowns.

cedure described by Corbett (8) was refluxed in 50 ml of 1 *N* sulfuric acid for 16 h. The sulfuric acid was removed with barium hydroxide and the solution was concentrated and freeze-dried, yielding 1.4 g (70% of theory) of tan, hygroscopic, amorphous solid. Gas–liquid chromatography of the trimethylsilylated derivative on the SE-30 column operated isothermally at 185° showed only the anomeric peaks for the 3-*O*-(2-aminoethyl)-D-glucopyranose (Fig. 1).

6-O-Carbamoylmethyl-1,2;3,5-di-O-methylene-α-D-glucofuranose

6-*O*-Carbomethoxymethyl-1,2;3,5-di-*O*-methylene-α-D-glucofuranose, 15 g (0.061 mole), (chromatographically pure) prepared by the procedure of Shyluk and Timell (9) was suspended in 400 ml of concentrated ammonium hydroxide and was stirred for 4 h at room temperature. The solution was then evaporated under reduced pressure; the product crystallized, yielding 12.8 g (88% of theory) of white needles melting at 127–130°. After recrystallization from methanol, the m.p. was 130–132°. Neither the amide nor its trimethylsilyl derivative could be eluted from the SE-30 column operated isothermally at 185°.

Anal. Calcd. for $C_{10}H_{15}O_7N$: C, 45.97; H, 5.74; N, 5.36. Found: C, 45.90; H, 5.77; N, 5.29.

6-O-(2-Aminoethyl)-1,2;3,5-di-O-methylene-α-D-glucofuranose

6-*O*-Carbamoylmethyl-1,2;3,5-di-*O*-methylene-α-D-glucofuranose, 10 g (0.033 mole), was dissolved in 300 ml of dry tetrahydrofuran and 2.5 g (0.066 mole) of lithium aluminium hydride was added slowly. The mixture was stirred at room temperature for 16 h. The excess lithium aluminium hydride was destroyed by the cautious addition of a 10% solution of water in tetrahydrofuran. The

Can. J. Chem. Downloaded from www.nrcresearchpress.com by 210.87.254.6 on 09/05/12
For personal use only.

Can. J. Chem. Downloaded from www.nrcresearchpress.com by 210.87.254.6 on 09/05/12
For personal use only.

solid was removed by filtration and washed with tetrahydrofuran. The combined filtrate and washings were evaporated, yielding 8.4 g (91% of theory) of colorless syrup which did not crystallize.

6-O-(2-Aminoethyl)-D-*glucopyranose*

6-*O*-(2-Aminoethyl)-1,2;3,5-di-*O*-methylene-α-D-glucofuranose, 8.4 g (0.033 mole), were refluxed for 16 h in 100 ml of 1 *N* sulfuric acid. The acid was removed with barium hydroxide. The solution was concentrated and freeze-dried yielding 4.8 g (74% of theory) of tan, amorphous solid. Gas–liquid chromatography of the trimethylsilylated derivative on the SE-30 column operated isothermally at 185°, showed two expected anomeric peaks for the 6-*O*-(2-aminoethyl)-D-glucose (Fig. 1). Two small peaks were also present. These peaks did not correspond to glucose in retention time and were not identified.

*3-O-[N-(2-Aminoethyl)carbamoylmethyl]-1,2;5,6-di-O-isopropylidene-α-*D-*glucofuranose*

3-*O*-Carbomethoxymethyl-1,2;5,6-di-*O*-isopropylidene-α-D-glucofuranose, 5 g (0.015 mole) (chromatographically pure) prepared by the method of Shyluk and Timell (9), were dissolved in 5 g (0.083 mole) of freshly distilled ethylenediamine. The solution was allowed to stand at room temperature and after 4 h, g.l.c. showed that the reaction was complete as indicated by the disappearance of the starting compound. The solution was heated at 135° and 50 μ pressure to remove the unreacted ethylenediamine. The product, 5.2 g (94% of theory), was a clear amorphous solid.

*3-O-[N-(2-Aminoethyl)-2-aminoethyl]-1,2;5,6-di-O-isopropylidene-α-*D-*glucofuranose*

To 5.2 g (0.014 mole) of 3-*O*-[*N*-(2-aminoethyl)carbamoylmethyl]-1,2;5,6-di-*O*-isopropylidene-α-D-glucofuranose in 200 ml of dry ether was added 1.0 g (0.028 mole) of lithium aluminium hydride. After a 16-h period at room temperature with stirring, the excess lithium aluminium hydride was destroyed by the cautious addition of wet ether. The solid was removed by filtration and was washed with ether. The combined filtrate and washings were evaporated yielding 4.5 g (90% of theory) of slightly yellow, clear amorphous solid.

3-O-[N-(2-Aminoethyl)-2-aminoethyl]-D-*glucopyranose*

3-*O*-[*N*-(2-Aminoethyl)-2-aminoethyl]-1,2;5,6-di-*O*-isopropylidene-α-D-glucofuranose, 4.2 g (0.012 mole), was refluxed for 16 h in 100 ml of 1 *N* sulfuric acid. The sulfuric acid was removed with barium hydroxide. The solution was concentrated to a volume of 20 ml and freeze-dried, yielding 2.2 g (70% of theory) of tan, amorphous solid. Gas–liquid chromatography of the trimethylsilylated derivative, on the SE-30 column operated isothermally at 185°, showed only the two expected anomeric peaks for the glucose derivative.

*Methyl 3-O-Benzyl-4,6-O-benzylidene-2-O-(2-hydroxyethyl)-α-*D-*glucopyranoside*

Methyl 3-*O*-benzyl-4,6-*O*-benzylidene-2-*O*-carbethoxymethyl-α-D-glucopyranoside, 2.5 g (0.0055 mole), described above and chromatographically pure, were dissolved in 200 ml of dry ether; 0.4 g (0.011 mole) of lithium aluminium hydride was added and the mixture was stirred for 5 h. The excess lithium aluminium hydride was destroyed by the cautious addition of wet ether. The solid was removed by filtration and was washed with ether. The combined filtrate and washings were evaporated yielding 2.2 g (96% of theory) of white needles. After crystallization from methanol the m.p. was 108–110°.

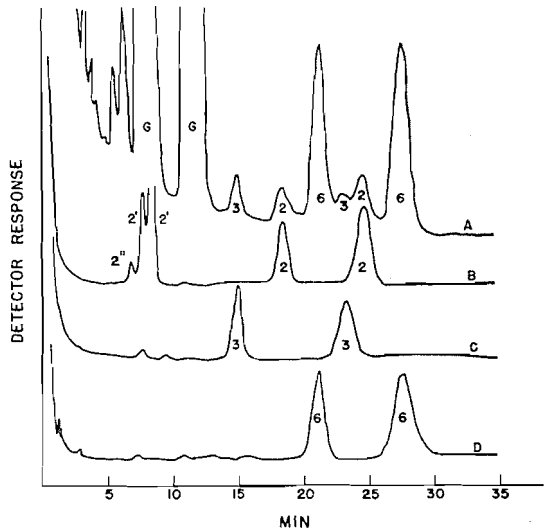

FIG. 2. Chromatograms of trimethylsilyl derivatives on an SE-30 column operated isothermally at 190°. Curve A is the hydrolyzate of diazotized *O*-(2-aminoethyl)cellulose; Curve B is 2-*O*-(2-hydroxyethyl)-D-glucopyranose; Curve C is 3-*O*-(2-hydroxyethyl)-D-glucopyranose; and Curve D is 6-*O*-(2-hydroxyethyl)-D-glucopyranose. Peaks labeled G are the anomers of glucose, and the peaks labeled 2″ and 2′ represent the inner glucosides of 2-*O*-(2-hydroxyethyl)-D-glucose.

2-O-(2-Hydroxyethyl)-D-*glucopyranose*

Methyl 3-*O*-benzyl-4,6-*O*-benzylidene-2-*O*-(2-hydroxyethyl)-α-D-glucopyranoside, 2.0 g, was dissolved in 150 ml of ethanol; 1 g of 10% palladium/carbon and 50 ml of 2 *N* sulfuric acid (necessary for hydrogenolysis) were added. The solution was shaken under a slight positive hydrogen pressure until the amount of hydrogen (3 moles) required to remove the benzyl and benzylidene groups was absorbed. The catalyst was removed by filtration and the alcohol was evaporated to a volume of 50 ml. The solution was refluxed for 16 h to hydrolyze the glucoside. The sulfuric acid was removed with barium hydroxide and the solution was concentrated and freeze-dried, yielding 1.0 g (85% of theory) of white amorphous solid. Gas–liquid chromatography of the trimethylsilylated derivative on the SE-30 column operated isothermally at 190° showed two anomeric peaks for the 2-*O*-(2-hydroxyethyl)-D-glucopyranose (designated 2 in Fig. 2). Three additional peaks, one designated 2″ and two designated 2′, with shorter retention times than the anomers of 2-*O*-(2-hydroxyethyl)-D-glucopyranose were also present. The peak designated 2″ was shown to be 1,2-*O*-ethylene-α-D-glucofuranose, the first peak labelled 2′ was shown to be 1,2-*O*-ethylene-β-D-glucopyranose, and the second peak labelled 2′ was

Can. J. Chem. Downloaded from www.nrcresearchpress.com by 210.87.254.6 on 09/05/12
For personal use only.

shown to be 1,2-*O*-ethylene-α-D-glucopyranose (6). Hook and Lindberg (7) showed that the anomeric 2-*O*-(2-hydroxyethyl)-D-glucopyranoses are converted to the three inner glucosides noted above by heating in dilute acid solution.

3-O-(2-Hydroxyethyl)-D-glucopyranose

This derivative was prepared by lithium aluminium hydride reduction of 4.0 g of chromatographically pure 3-*O*-carbomethoxymethyl-1,2;5,6-di-*O*-isopropylidene-α-D-glucofuranose by the procedure of Shyluk and Timell (9). The isopropylidene groups were removed by hydrolysis. Gas–liquid chromatography of the trimethylsilyl derivatives of the freeze-dried sample on the SE-30 column operated isothermally at 190° showed only the anomeric peaks for 3-*O*-(2-hydroxyethyl)-D-glucopyranose (Fig. 2).

6-O-(2-Hydroxyethyl)-D-glucopyranose

This derivative was prepared by reduction of 4 g of chromatographically pure 6-*O*-carbomethoxymethyl-1,2;3,5-di-*O*-methylene-α-D-glucofuranose with lithium aluminium hydride by the method of Shyluk and Timell (9). The methylene groups were removed by hydrolysis and the product was freeze-dried. Gas–liquid chromatography of the trimethylsilylated derivative on the SE-30 column operated isothermally at 190° showed only the two anomeric peaks of 6-*O*-(2-hydroxyethyl)-D-glucopyranose (Fig. 2).

Conversion of 6-O-(2-Aminoethyl)-D-glucopyranose to 6-O-(2-Hydroxyethyl)-D-glucopyranose by Diazotization

6-*O*-(2-Aminoethyl)-D-glucopyranose, 1.0 g (0.0045 mole) was dissolved in 100 ml of 20% acetic acid; 5.0 g (0.072 mole) of sodium nitrite was added slowly and stirring was maintained for 1.5 h. The solution was then concentrated below 50° and was freeze-dried. Silylation and g.l.c. of the freeze-dried product showed only a trace of the peaks corresponding to the original 6-*O*-(2-aminoethyl)-D-glucopyranose and showed pronounced peaks corresponding to 6-*O*-(2-hydroxyethyl)-D-glucopyranose. The new peaks represented a 79.5% conversion of the starting material to product, assuming the detector response of the two compounds to be equal. No additional peaks resulting from the diazotization were detected.

Removal of Glucose from Hydrolyzed O-(2-Hydroxyethyl)cellulose by Fermentation

One gram of the hydrolyzate of diazotized *O*-(2-aminoethyl)cellulose was dissolved in 25 ml of water. The pH was adjusted to 4.5 with acetic acid and 0.5 g of brewers yeast was added. After 24 h, the glucose had been consumed. The yeast was removed by filtration. The filtrate was concentrated below 50°. Silylation and g.l.c. of a sample of the freeze-dried product showed three peaks (one designated 2″ and two designated 2′ in Fig. 2) corresponding to the inner glucosides of 2-*O*-(2-hydroxyethyl)-α-D-glucofuranose and 2-*O*-(2-hydroxyethyl)-D-glucopyranose (α+β) in addition to peaks for 2-*O*-, 3-*O*-, and 6-*O*-(2-hydroxyethyl)-D-glucopyranoses. The three peaks representing the inner glucosides amounted to 57.5% of the total 2-*O*-(2-hydroxyethyl)-D-glucoses. The peaks for the inner glucosides are hidden under the first glucose peak in the original hydrolyzate (i.e., prior to removal of the glucose).

Results

Syntheses of 2-O-, 3-O-, and 6-O-Substituted-D-glucopyranoses

The identification of the various components in the hydrolyzates from *O*-(2-aminoethyl)cellulose necessitated the preparation of three types of monosubstituted-glucopyranoses: (*a*) 2-*O*-, 3-*O*-, and 6-*O*-(2-aminoethyl)-D-glucopyranoses, (*b*) 3-*O*-[*N*-(2-aminoethyl)-2-aminoethyl]-D-glucopyranose, and (*c*) 2-*O*-, 3-*O*-, and 6-*O*-(2-hydroxyethyl)-D-glucopyranoses. Three of these compounds, 2-*O*-(2-aminoethyl)-D-glucopyranose, 6-*O*-(2-aminoethyl)-D-glucopyranose, and 3-*O*-[*N*-(2-aminoethyl)-2-aminoethyl]-D-glucopyranose, were prepared for the first time but the routes and the reactions are conventional. The preparation of the known derivatives is illustrated in the case of the 3-*O*-substituted-D-glucopyranoses in Fig. 3. With few exceptions, the intermediates as well as the final products were hygroscopic and amorphous. Recoveries of crude products from each step were above 70%; in spite of our inability to purify the intermediates at each step in the synthesis, the final products have generally been remarkably free of impurities as measured by g.l.c.

Chromatograms of the trimethylsilyl derivatives of the mono-*O*-(2-aminoethyl)-D-glucopyranoses are shown in Fig. 1, and the curves for the trimethylsilyl derivatives of mono-*O*-(2-hydroxyethyl)-D-glucopyranoses are shown in Fig. 2. Both of the 2-*O*-substituted-D-glucopyranoses contained extra components. These components of the 2-*O*-(2-aminoethyl)-D-glucopyranose, by analogy to the results from the corresponding 2-hydroxyethyl compound (6, 7), are considered to be the inner *N*-glucosyl amines resulting from the reactions of the functional groups at C-1 with the amine group of the 2-aminoethyl substituent at C-2.

The relative retention values for the mono-*O*-substituted-D-glucopyranoses in g.l.c. are summarized in Table I. The ratios of anomers of the individual glucose derivatives (in the form of the trimethylsilyl ethers) are summarized in Table II. For a specific substitution isomer of glucose, these ratios are essentially constant for these substituted glucoses and for the *O*-[2-(diethyl-

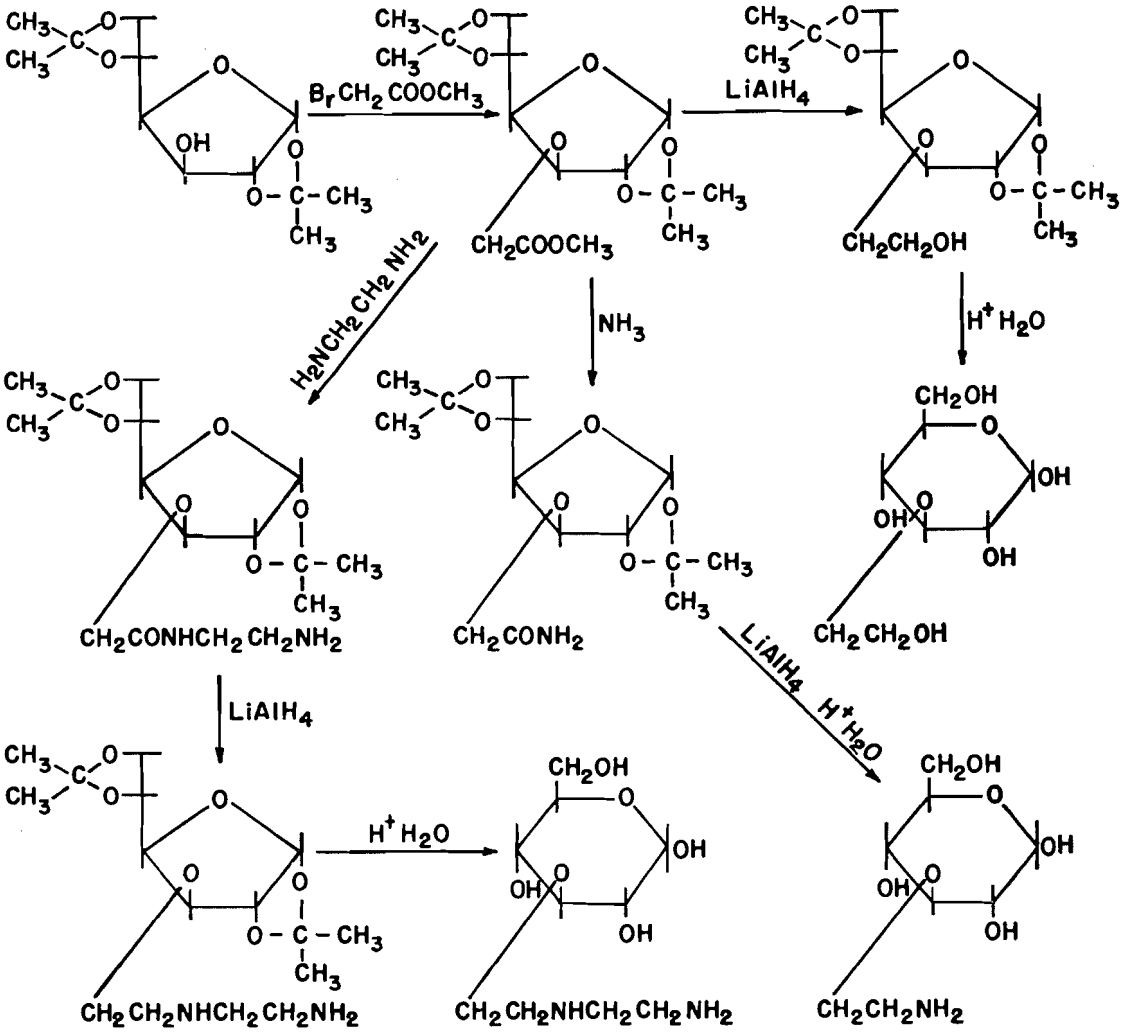

FIG. 3. Schematic illustration of the preparation of the three types of substituted glucoses using the 3-*O*-derivatives as an example.

amino)ethyl]-D-glucopyranoses[1] (1) and are quite similar to those of the *O*-(methylsulfonylethyl)-D-glucopyranoses (10) which have been reported earlier.

Determination of Aminoethyl Substituents in O-(2-Aminoethyl)cellulose

O-(2-Aminoethyl)cellulose, which was prepared by double treatment of cotton fabric with sodium 2-aminoethyl sulfate in the presence of excess base at 130°, was hydrolyzed with sulfuric acid to a mixture of glucose and *O*-(2-aminoethyl)-D-glucopyranoses. This hydrolyzate was converted to the corresponding trimethylsilyl ethers and was analyzed by g.l.c. which showed the presence of the 2-*O*- , 3-*O*- , and 6-*O*-(2-aminoethyl)-D-glucopyranoses (see Fig. 1). These were identified by comparison of retention times and by peak enhancement with the corresponding known derivatives. The first anomers of the 2-*O*- and 3-*O*-isomers were hidden beneath the second peak of glucose; the second peak of the 2-*O*-isomer was not well separated from the second peak of the 6-*O*-isomer. Several columns were investi-

[1]See Table II for correction of a typographical error in a previous paper, (1).

Can. J. Chem. Downloaded from www.nrcresearchpress.com by 210.87.254.6 on 09/05/12
For personal use only.

Can. J. Chem. Downloaded from www.nrcresearchpress.com by 210.87.254.6 on 09/05/12
For personal use only.

TABLE I

Relative retention values for the *O*-(2-aminoethyl)-D-glucopyranoses (*O*-AEG) and *O*-(2-hydroxyethyl)-D-glucopyranoses (*O*-HEG)

Isomer	*O*-AEG*	*O*-HEG†
2-*O*-	0.24‡	0.24§
	0.28‖	0.28¶
	0.31‖	0.31¶
	0.68	0.66
	0.91	0.89
3-*O*-	0.53	0.54
	0.88	0.83
6-*O*-	0.77	0.77
	1.00	1.00

*The *O*-(2-aminoethyl)-D-glucopyranoses were run isothermally at 185°.
†The *O*-(2-hydroxyethyl)-D-glucopyranoses were run isothermally at 190°.
‡This value refers to the peak which is assumed to be due to the inner *N*-glucosyl amine form of 2-*O*-(2-aminoethyl)-D-glucofuranose.
§This value refers to 1,2-*O*-ethylene-α-D-glucofuranose.
‖These values refer to the peaks which are assumed to be due to the inner *N*-glucosyl amine forms of 2-*O*-(2-aminoethyl)-D-glucopyranose.
¶These values refer to the inner glucosides of 2-*O*-(2-hydroxyethyl)-D-glucopyranose.

TABLE II

Anomer ratios of the isomers of *O*-(2-aminoethyl)-D-glucopyranoses (*O*-AEG), *O*-(2-hydroxyethyl)-D-glucopyranoses (*O*-HEG), and *O*-[2-(diethylamino)-ethyl]-D-glucopyranoses (*O*-DEAEG)*

Isomer	*O*-AEG	*O*-HEG	*O*-DEAEG†
2-*O*-	1.00‡	1.00§	
	0.35‖	0.25¶	
	0.65‖	0.75¶	
	0.39**	0.38**	0.34
	0.61**	0.62**	0.66
3-*O*-	0.50	0.50	0.48
	0.50	0.50	0.52
6-*O*-	0.43	0.43	0.43
	0.57	0.57	0.57

*The numbers indicate the fraction of anomer appearing in the peak.
†These values for the 2-*O*-[2-(diethylamino)ethyl]-D-glucopyranoses correct a typographical error which appeared in a previous paper, (1).
‡This value is for the peak which is assumed to be due to the inner *N*-glucosyl amine form of 2-*O*-(2-aminoethyl)-α-D-glucofuranose.
§This value is for 1,2-*O*-ethylene-α-D-glucofuranose. None of the anomeric form has been observed.
‖These values are for the peaks which are assumed to be due to the inner *N*-glucosyl amine forms of 2-*O*-(2-aminoethyl)-D-glucopyranose.
¶These values are for the inner glucosides of 2-*O*-(2-hydroxyethyl)-D-glucopyranose.
**These values refer to the normal forms.

gated; the SE-30 column gave the most satisfactory separations.

Two peaks, designated U in Curve A of Fig. 1, with greater retention times than the second peak of the 6-*O*-isomer were present in the hydrolyzate. The possibility that these peaks represented *O*-[*N*-(2-aminoethyl)-2-aminoethyl]-D-glucopyranoses was examined by comparison of the mobility of 3-*O*-[*N*-(2-aminoethyl)-2-aminoethyl]-D-glucopyranose with that of the components of hydrolyzed *O*-(2-aminoethyl)cellulose on paper electrophoresis in 0.75 *M* formic acid (2). Individual position isomers are not separated by electrophoresis under these conditions. No evidence was found for the presence of *O*-[*N*-(2-aminoethyl)-2-aminoethyl]-D-glucopyranoses in the hydrolyzate. The nonidentity was further verified by g.l.c.

Paper electrophoresis of the hydrolyzate showed the presence of a component which exhibited characteristics of a reducing sugar and an amine and which had a lower mobility than *O*-(2-aminoethyl)-D-glucopyranose. This suggests that we are dealing with a molecule which is larger than *O*-(2-aminoethyl)-D-glucopyranose but which contains no more amino groups. It is believed that this component corresponds to the peaks designated U in Curve A of Fig. 1 and that it represents a mixture of *N*-glucosyl-(2-aminoethyl)-D-glucopyranoses. Compounds of this type arise from facile reaction of sugars with amines (11, 12).

Three difficulties were encountered in attempts to determine the ratio of 2-aminoethyl substituents in the 2-*O*-, 3-*O*-, and 6-*O*-positions of the D-glucopyranosyl units. The first difficulty, already noted above, was the inability to realize better separation in g.l.c. than those illustrated in Fig. 1. Removal of the preponderance of free glucose, the second difficulty, could not be achieved by fermentation without simultaneous destruction of the substituted glucoses; however, *O*-[2-(diethylamino)ethyl]-D-glucopyranoses were not attacked by fermentation. The third difficulty concerned reproducibility of results from one to another hydrolyzate of the *O*-(2-aminoethyl)cellulose. The question of stability of the ether linkage between the aminoethyl substituent and the glucose unit was settled by showing in electrophoresis (0.75 *M* formic acid) that 3-*O*-(2-aminoethyl)-D-glucopyranose was recovered and that no trace of glucose or ethanolamine was formed when the substituted glucose was subjected to the same conditions employed for hydrolysis of the *O*-(2-aminoethyl)cellulose. A significant change did occur, however, as a result of the strenuous conditions of hydrolysis applied to 3-*O*-(2-aminoethyl)-D-glucopyranose. There

Can. J. Chem. Downloaded from www.nrcresearchpress.com by 210.87.254.6 on 09/05/12
For personal use only.

was formed a component whose mobility in electrophoresis was greater than that of the substituted glucose and which was not eluted in g.l.c. These data are consistent with the formation of material of higher molecular weight, i.e., reaction of the functional group at C-1 of an *O*-(2-aminoethyl)-D-glucopyranose with the amino function of another unit. Reactions of this type are known (11, 12) and occur to extents which are dependent upon the specific conditions of reaction and concentrations of the media (13). In connection with this third difficulty, it is concluded that the inconsistencies in the results obtained with different hydrolyzates resulted from varying degrees of reaction of glucose with the amino functions of substituent groups.

One of the more satisfactory chromatograms of a hydrolyzate of an *O*-(2-aminoethyl)cellulose (in the form of its trimethylsilyl ether) is reproduced in Fig. 1. By taking full advantage of (*a*) the resolution of a single anomer of each of the 2-*O*- and 3-*O*-substituted glucoses into distinctly separate peaks, (*b*) the established ratio of anomers in the individual substituted glucoses (Table II), and (*c*) a computer-curve analyzer, the ratio of peaks for substitution in the 2-*O*- , and 3-*O*- , and 6-*O*-positions was estimated to be 0.25:0.20:1.00. This ratio takes only the normal form of the 2-*O*-(2-aminoethyl)-D-glucopyranose into consideration, since the peaks which are believed to represent the inner *N*-glucosyl forms are hidden under the glucose peaks. Assuming that the ratio of inner *N*-glucosyl forms to normal form of the 2-*O*-(2-aminoethyl)-D-glucopyranose is the same in the hydrolyzate of *O*-(2-aminoethyl)cellulose as in the synthesized 2-*O*-(2-aminoethyl)-D-glucopyranose, this ratio becomes 0.83:0.20:1.00.

Determination of Hydroxyethyl Substituents in Diazotized O-(2-Aminoethyl)cellulose

It was found that diazotization of the alkali-swollen, Wiley-milled *O*-(2-aminoethyl)cellulose eliminated most of the nitrogen from the chemically modified cellulose and converted the 2-aminoethyl groups to 2-hydroxyethyl groups. Due to the questionable results obtained with hydrolyzed *O*-(2-aminoethyl)cellulose, it was expedient to determine the distribution of 2-aminoethyl groups in terms of 2-hydroxyethyl groups.

Diazotization of a sample of 6-*O*-(2-aminoethyl)-D-glucopyranose under conditions identical to those employed in the diazotization of the *O*-(2-aminoethyl)cellulose showed that the 6-*O*-(2-aminoethyl)-D-glucopyranose was converted to 6-*O*-(2-hydroxyethyl)-D-glucopyranose in 79.5% yield as determined by g.l.c.

The nitrogen content of 1.20% in *O*-(2-aminoethyl)cellulose was reduced to 0.34% by diazotization. Hydrolysis of the diazotized *O*-(2-aminoethyl)cellulose yielded a product containing 0.20% nitrogen. The residual nitrogen remaining after diazotization and hydrolysis is believed to result from the reaction of carbonyl groups (formed during the reaction of the cellulose with the sodium 2-aminoethyl sulfate) with amino groups. The Schiff bases which are formed (14) are not eliminated by diazotization. This will be described in detail in a subsequent paper.

Gas–liquid chromatography of the trimethylsilyl derivatives of the hydrolyzate from diazotized *O*-(2-aminoethyl)cellulose showed the presence of the 2-*O*- , 3-*O*- , and 6-*O*-(2-hydroxyethyl)-D-glucopyranoses. Good separations were realized on the SE-30 column without removal of the large amount of glucose present (Fig. 2). The glucose derivatives in the hydrolyzate were identified by comparison of retention times and peak enhancement with authentic known derivatives. The second peak of the 3-*O*-isomer was not completely separated from the first peak of the 6-*O*-isomer. The ratio of the anomers of the 3-*O*-isomer (see Table II) was utilized to calculate the area of the second peak of this isomer. The ratios of the areas of the peaks of the 2-*O*- , 3-*O*- , and 6-*O*-isomers in the hydrolyzate were calculated by triangulation on three chromatograms and were found to be 0.27, 0.26, 0.28:0.13, 0.13, 0.15:1.00, 1.00, 1.00 for the 2-*O*- , 3-*O*- , and 6-*O*-isomers. Average values are 0.27:0.14:1.00; this ratio takes into consideration only the normal form of the 2-*O*-(2-hydroxyethyl)-D-glucopyranose since the peaks of the inner glucosides are hidden under the peaks of glucose.

It was necessary to remove the glucose from the hydrolyzate (by fermentation) in order to obtain a measure of the inner glucosides of the 2-*O*-substituted glucose. Gas–liquid chromatography of the product (after fermentation, freeze-drying, and silylation) showed that 57.5% of the 2-*O*-(2-hydroxyethyl)-D-glucopyranose was in the form of the inner glucosides. By considering all forms of the 2-*O*-(2-hydroxyethyl)-D-glucose in the hydrolyzate-fermentate, the distribution of

Can. J. Chem. Downloaded from www.nrcresearchpress.com by 210.87.254.6 on 09/05/12
For personal use only.

substituent groups was estimated to be 0.64:0.14:1.00 for the 2-*O*-, 3-*O*-, and 6-*O*-isomers.

Discussion

The etherification of cellulose with sodium 2-aminoethyl sulfate is a rate-controlled (irreversible) reaction. This is one of the few rate-controlled reactions of cellulose in which the substitution predominates at the 6-*O*-position. In this regard, the distribution of 2-aminoethyl substituents lies between those of the allyl group and the 2-hydroxyethyl group.[2] It has been pointed out that the preferential reaction of the hydroxyl group at C-2 decreases as the size of the reagent molecule increases (21, 22). The data of Table III show a progressive decrease in the relative amount of substitution at the 2-*O*-position in proceeding from methyl chloride to ethyl chloride to 2-diethylaminoethyl chloride. Comparison of the results from the reactions of cellulose with methyl chloride and dimethyl sulfate suggests that the distribution is affected by the size of the leaving group of the reagent as well as that of the entering group. These and other considerations of the data in Table III emphasize that steric factors play an important role in these reactions.

TABLE III

Distribution of substituents in cellulose ethers prepared by rate-controlled reactions

Reagent	Ratio of substituents 2-*O*-	3-*O*-	6-*O*-	Reference
Sodium 2-aminoethyl sulfate	0.64	0.14	1.00	—
2-Diethylaminoethyl chloride	1.27	0.35	1.00	1
Methyl chloride	2.50	0.50	1.00	15
Dimethyl sulfate	1.75	0.50	1.00	16
Ethyl chloride	2.25	0.50	1.00	17
Sodium allyl sulfate	0.70	0.20	1.00	18
Sodium chloroacetate	0.80	0.40	1.00	19
Ethylene oxide	0.30	0.10	1.00	20

The aminoethylation of cellulose via sodium 2-aminoethyl sulfate and the methylation of cellulose via sodium methyl sulfate occur with similar sluggishness, both reactions requiring strong base and elevated temperature (23). In contrast, the diethylaminoethylation of cellulose via 2-(diethylamino)ethyl chloride proceeds readily with strong base at room temperature (1). The latter reaction is considered to be facilitated by intermediate formation of the diethylenimmonium ion (1, 24). While ethylenimine is formed under the conditions employed for aminoethylation of cellulose, our attempts and those of others (23, 25, 26) to realize reaction between ethylenimine and cellulose (under conditions comparable to those involving sodium 2-aminoethyl sulfate) in the presence of strong base have been generally unsuccessful. Under pressure at elevated temperature in the presence of cellulose, ethylenimine undergoes a reaction; it has been suggested that polyethylenimine is deposited in the fibers under these conditions (much of the pertinent work has been summarized briefly by Segal and Eggerton (25) and by Einsele (26)). The similarity between reactions of cellulose with sodium 2-aminoethyl sulfate and sodium methyl sulfate is basis for belief that these are bimolecular substitution reactions proceeding by a similar mechanism; i.e., little or no participation of the amino group in the case of the reaction of sodium 2-aminoethyl sulfate.

The foregoing mechanistic consideration is consistent with the substantially different distributions of substituents at the 2-*O*-, 3-*O*-, and 6-*O*-positions which resulted from aminoethylation and diethylaminoethylation. The former reaction would be subject to the greater steric effect and would be expected to show increased preference for substitution at the 6-*O*-position.

[2]It should be noted, however, that the distribution of 2-hydroxyethyl substituents resulting from reaction of cellulose with ethylene oxide may need revision if the inner glucosides were present and were not measured in the analysis of product.

Acknowledgment

The authors gratefully acknowledge the constructive suggestions of Professor Bengt Lindberg of the University of Stockholm.

1. E. J. Roberts and S. P. Rowland. Can. J. Chem. **45**, 261 (1967).
2. E. J. Roberts and S. P. Rowland. Carbohydrate Res. **5**, 1 (1967).
3. C. C. Sweeley, R. Bentley, M. Makita, and W. W. Wells. J. Am. Chem. Soc. **85**, 2497 (1963).
4. E. Hägglund. *In* Chemistry of wood. Academic Press, Inc., New York. 1951. p. 100.
5. H. Zollinger. Private communication.
6. E. J. Roberts and S. P. Rowland. Can. J. Chem. This issue.
7. J. E. Hook and Bengt Lindberg. Acta Chem. Scand. To be published.
8. W. M. Corbett. J. Chem. Soc. 2966 (1961).

9. W. P. SHYLUK and T. E. TIMELL. Can. J. Chem. **34**, 575 (1956).
10. S. P. ROWLAND, V. O. CIRINO, and A. L. BULLOCK. Can. J. Chem. **44**, 1051 (1966).
11. J. HODGE and C. E. RIST. J. Am. Chem. Soc. **74**, 1494 (1952).
12. W. PIGMAN. The carbohydrates. Academic Press, Inc., New York. 1957. pp. 406–476.
13. J. P. DUSTIN, C. CZAJKOWSKA, S. MOORE, and E. J. BIGWOOD. Anal. Chim. Acta, **9**, 256 (1953).
14. M. F. MARGAVIO and J. D. GUTHRIE. Am. Dyestuff Reptr. **54**, 71 (1965).
15. I. CROON. Svensk Papperstid. **61**, 919 (1958).
16. I. CROON and B. LINDBERG. Svensk Papperstid. **60**, 843 (1957).
17. I. CROON and E. FLAMM. Svensk Papperstid. **61**, 963 (1958).
18. D. E. HOINESS, C. P. WADE, and S. P. ROWLAND. Can. J. Chem. **46**, 667 (1968).
19. I. CROON and C. B. PURVES. Svensk Papperstid. **62**, 876 (1959).
20. I. CROON and B. LINDBERG. Svensk Papperstid. **59**, 794 (1956).
21. I. CROON. Svensk Papperstid. **63**, 247 (1960).
22. R. W. LENZ. J. Am. Chem. Soc. **82**, 182 (1962).
23. J. D. GUTHRIE. Private communication.
24. N. J. LEONARD. Record Chem. Progr. Kresge-Hooker Sci. Lib. **26**, 211 (1965).
25. L. SEGAL and F. V. EGGERTON. Textile Res. J. **33**, 739 (1963).
26. U. EINSELE. Melliand Textileber. **45**, 641 (1964).

Can. J. Chem. Downloaded from www.nrcresearchpress.com by 210.87.254.6 on 09/05/12
For personal use only.

Can. J. Chem. Downloaded from www.nrcresearchpress.com by 210.87.254.5 on 09/05/12
For personal use only.

NOTES

Reactions of hydrazines with phosphate esters

JAN H. VIS AND PHYLLIS MEINKE

The Standard Oil Company (Ohio), Research and Development Department, Broadway Laboratory, Cleveland, Ohio

Received July 15, 1968

Phosphate esters with the general formula $(RO)_2P(O)OR'$, with R = methyl or phenyl, and R′ = H, methyl, or phenyl, but with a maximum of two phenyls per molecule, react with hydrazines to form hydrazinium phosphates. Continued substitution of hydrazine protons by methyl groups appears to be a combination of methylation by phosphate esters and proton abstraction by part of the hydrazine present.

Canadian Journal of Chemistry, 47, 1581 (1969)

The reactions of phosphate esters with various types of compounds, including alkyl- and arylhalides, alcohols, and amines have been studied extensively (1–4). However, little attention has been paid to their reactions with hydrazines. Klages *et al.* (5) reported the formation of a quaternary hydrazine salt from the exothermic reaction of *unsym*-dimethylhydrazine and trimethyl phosphate. Similar salts were obtained in low yield by reacting *unsym*-dimethylhydrazine and some organic esters under special temperature and pressure conditions (6). Normally the reaction products from organic esters and hydrazines are acylhydrazines. With phosphate esters, however, hydrazines formed hydrazine salts exclusively, as illustrated by the example we wish to report.

The selection of hydrazines and phosphate esters was based on their availability, and was restricted to compounds containing hydrogen atoms, methyl, and phenyl groups, because of their simple and easily detectable nuclear magnetic resonance (n.m.r.) signals. A schematic representation of the reactions and products is given in Table I.

In order to explain the formation of some unexpected reaction products we investigated the possibilities of exchange reactions between hydrazine salts and hydrazines or phosphate esters. These reactions are schematically represented in Table II.

Experimental

Materials and Apparatus

The selected hydrazines and phosphate esters were: hydrazine, methylhydrazine, *unsym*-dimethylhydrazine, *sym*-dimethylhydrazine, *unsym*-diphenylhydrazine, *sym*-diphenylhydrazine, trimethyl phosphate, dimethyl phenyl phosphate, methyl diphenyl phosphate, triphenyl phosphate, diphenyl phosphate.

Dimethyl phenyl phosphate was prepared from dimethyl phosphite (7). *sym*-Dimethylhydrazine and *unsym*-diphenylhydrazine were prepared from their HCl salts by treatment with NaOH. These salts, dimethyl phosphite, and all other chemicals were commercially available. Elemental analyses were carried out in this laboratory and by Crobaugh Laboratories, Cleveland, Ohio. Infrared (i.r.) spectra were obtained using a Perkin–Elmer 521 instrument. The spectra were taken from both KBr disks and Nujol mulls. Integrated nuclear magnetic resonance spectra were recorded on a Varian DP-60 spectrometer from deuteriodimethylsulfoxide (DMSO-d_6) solutions with TMS as internal standard.

Procedure

All reactions were performed in the following manner:

A slight excess of the hydrazine in ether was slowly added to a solution of the phosphate ester in ether, with stirring and at room temperature. After the addition the mixture was stirred for 1–3 h. During the reaction, oils or solids separated from the solution. These products were separated, washed with ether to remove starting materials, and subsequently recrystallized. When the reactants were mixed without solvent, the reactions were strongly exothermic after a short induction period. The only exceptions were triphenyl phosphate which did not react with *unsym*-dimethylhydrazine, and the diphenylhydrazines which did not react with methyl diphenyl phosphate.

1,1,1-Trimethylhydrazinium[1] *Dimethyl Phosphate (1)*

This was prepared from 6.6 g (0.11 mole) *unsym*-dimethylhydrazine and 14 g (0.1 mole) trimethyl phosphate as white hygroscopic crystals, yield, 16.6 g (83%),

[1]For discussion of the nomenclature of quaternized hydrazine salts, see ref. 9.

Can. J. Chem. Downloaded from www.nrcresearchpress.com by 210.87.254.5 on 09/05/12
For personal use only.

TABLE I

Reaction products from hydrazines and phosphate esters

	$H_2N—NH_2$	$(CH_3)HN—NH_2$	$(CH_3)_2N—NH_2$	$(CH_3)HN—NH(CH_3)$	$(C_6H_5)_2N—NH_2$	$(C_6H_5)HN—NH(C_6H_5)$
Diphenyl phosphate	$H_3N^+—NH_2$ P⁻ * (7)	$(CH_3)H_2N^+—NH_2$ P⁻ (5) or $(CH_3)H_2N^+—^+NH_3$ 2P⁻ (8)	$(CH_3)_2N—N^+H_3$ P⁻ (6)	$(CH_3)H_2N^+—NHCH_3$ P⁻ (4)	$(C_6H_5)_2N—^+NH_3$ P⁻ (10)	$(C_6H_5)H_2N^+—N^+H_2(C_6H_5)$ 2P⁻ (9)
Methyl diphenyl phosphate	$(CH_3)_3N^+—NH_2$ P⁻ (3) $(CH_3)_2N—^+NH_3$ P⁻ (6) $(CH_3)H_2N^+—NH_2$ P⁻ (5) $H_3N^+—NH_2$ P⁻ (7)	$(CH_3)_3N^+—NH_2$ P⁻ (3) $(CH_3)H_2N^+—NH_2$ P⁻ (5)	$(CH_3)_3N^+—NH_2$ P⁻ (3)	$(CH_3)H_2N^+—NHCH_3$ P⁻ (4)	No reaction	No reaction
Dimethyl phenyl phosphate	—	$(CH_3)_3N^+—NH_2$ Q⁻ † (2)				
Trimethyl phosphate	—	$(CH_3)_3N^+—NH_2$ R⁻ ‡ (1)				
Triphenyl phosphate	—	No reaction				

*P⁻ = 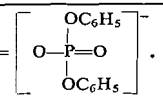

†Q⁻ = 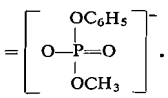

‡R⁻ = 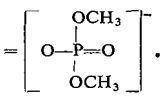

Can. J. Chem. Downloaded from www.nrcresearchpress.com by 210.87.254.5 on 09/05/12
For personal use only.

TABLE II

Exchange reactions between hydrazines or phosphates and hydrazinium diphenyl phosphates

	$H_2N—NH_2$	$(CH_3)HN—NH_2$	$(CH_3)_2N—NH_2$	$(C_6H_5)HN—NH(C_6H_5)$	Methyl diphenyl phosphate
$(CH_3)H_2{}^+N—NH_2$ P^-	$H_3{}^+N—NH_2$ P^- * (7)	—	—	—	—
$(CH_3)_2N—{}^+NH_3$ P^-	$H_3{}^+N—NH_2$ P^- (7)	$(CH_3)H_2{}^+N—NH_2$ P^- (5)	—	—	No reaction
$(C_6H_5)H_2{}^+N—N^+H_2(C_6H_5)$ P^-	—	—	$(CH_3)_2N—{}^+NH_3$ P^- (6)	No reaction	—

*For P^- see footnote * of Table I.

Can. J. Chem. Downloaded from www.nrcresearchpress.com by 210.87.254.5 on 09/05/12
For personal use only.

m.p. 88–90° (ethyl acetate (EtOAc)/hexane). The i.r. spectrum showed significant absorption at 3210 and 3103 cm^{-1} (*asym*- and *sym*-NH_2 stretch). The n.m.r. spectrum exhibited singlets at 3.22 τ (NH) and 6.62 τ (NCH_3), and a doublet at 6.64 τ(P-OCH_3, $J_{P\text{-}OCH_3}$ = 10.5 c.p.s.).

Anal. Calcd. for $C_5H_{17}N_2O_4P$: C, 30.00; H, 8.50; N, 14.00. Found: C, 29.10; H, 8.50; N, 13.50.

1,1,1-Trimethylhydrazinium Methyl Phenyl Phosphate (2)

This was prepared from 0.7 g (0.012 mole) *unsym*-dimethylhydrazine and 2.02 g (0.01 mole) dimethyl phenyl phosphate as colorless needles, yield, 1.8 g (70%), m.p. 82° (EtOAc/hexane). The i.r. spectrum showed significant absorption at 3210 and 3106 cm^{-1} (*asym*- and *sym*-NH_2 stretch). The n.m.r. spectrum showed singlets at 3.30 τ (NH) and 6.70 τ (NCH_3), a multiplet at 2.28 (phenyl), and a doublet at 6.57 τ (P-OCH_3, $J_{P\text{-}OCH_3}$ = 11 c.p.s.).

Anal. Calcd. for $C_{10}H_{19}N_2O_4P$: C, 45.80; H, 7.25; N, 10.69. Found: C, 45.50; H, 7.50; N, 10.90.

1,1,1-Trimethylhydrazinium Diphenyl Phosphate (3)

This was prepared from 1.5 g (0.025 mole) *unsym*-dimethylhydrazine and 5.2 g (0.02 mole) methyl diphenyl phosphate as white crystals, yield 4.8 g (72%), m.p. 118° (EtOH/hexane). The i.r. spectrum showed significant absorption at 3243 and 3128 cm^{-1} (*asym*- and *sym*-NH_2 stretch). The n.m.r. spectrum exhibited singlets at 3.60 τ (NH) and 6.77 τ (NCH_3), and a multiplet at 2.82 τ (phenyl) in an area ratio of respectively 1.8:9:10.

Anal. Calcd. for $C_{15}H_{21}N_2O_4P$: C, 55.50; H, 6.48; N, 8.63. Found: C, 55.25; H, 6.42; N, 8.42.

1,2-Dimethylhydrazinium Diphenyl Phosphate (4)

The product was obtained from 0.7 g (0.011 mole) *sym*-dimethylhydrazine and 2.6 g (0.01 mole) methyl diphenyl phosphate as white crystals; yield, 1.1 g. It was to be expected that in analogy with the reaction of methylhydrazine with methyl diphenyl phosphate, a 1,1,1-trimethyl, 2-methyl hydrazinium salt should also have been formed. Such a salt, however, could not be isolated. Compound **4** was also obtained from 0.03 g (0.001 mole) *sym*-dimethylhydrazine and 0.5 g (0.002 mole) diphenyl phosphate, as white crystals, yield, 0.3 g (60%), m.p. 90° (EtOAc/hexane). The composition of the reaction product was independent of the ratio of the starting materials. The i.r. spectrum showed significant absorption at 3242 cm^{-1} (NH stretch), as well as at 2675 and 2510 cm^{-1} (*asym*- and *sym*-NH_2^+ stretch). The n.m.r. spectrum exhibited a broad singlet at 1.50 τ (NH), a singlet at 7.48 τ (NCH_3), and a multiplet at 2.82 τ (phenyl).

Anal. Calcd. for $C_{14}H_{19}N_2O_4P$: C, 54.20; H, 6.12; N, 9.04. Found: C, 53.67; H, 6.13; N, 9.20.

Methylhydrazinium Diphenyl Phosphate (5)

The product was obtained from 1.1 g (0.025 mole) methylhydrazine and 5.2 g (0.02 mole) methyl diphenyl phosphate. Fractionated crystallization from EtOAc/hexane gave 2 g of **3** at room temperature and subsequently 2.5 g of **5** (m.p. 52–54°) by chilling to −20°. The white waxy crystalline product was identical to the product from 0.1 g (0.002 mole) methylhydrazine and 0.5 g (0.002 mole) diphenyl phosphate, yield, 0.4 g (66%). The i.r. spectrum showed significant absorption at 3271 and 3171 cm^{-1} (*asym*- and *sym*-NH_2), and at ±2750 and 2500 cm^{-1} (*asym*- and *sym*-NH_2^+). The n.m.r. spectrum exhibited singlets at 3.30 τ (broad, NH) and 7.44 τ (NCH_3), and a multiplet at 2.80 τ (phenyl). The area ratio (phenyl + NH):NCH_3 = 15.4:3. Purification problems reduced the significance of analysis. However, the structural possibilities of the compound are limited and both n.m.r. and analysis indicate the presence of only one phosphate anion per molecule. (Compare compound **8**.)

1,1-Dimethylhydrazinium Diphenyl Phosphate (6)

The product was obtained from 0.7 g (0.023 mole) hydrazine and 5.2 g (0.02 mole) methyl diphenyl phosphate. The result was a mixture of products from which 0.6 g of **3** could be isolated by fractionated crystallization from EtOAc/ether at −20°. The rest consisted of an oily mixture of three components which could not be separated. The i.r. spectrum of this oil proved to be composed of the spectra of **5**, **6**, and hydrazinium diphenyl phosphate. Pure **6** was prepared from 0.35 g (0.006 mole) *unsym*-dimethylhydrazine and 1 g (0.004 mole) diphenyl phosphate as white crystals; yield, 1.15 g (95%); m.p. 104° (EtOAc/hexane). The i.r. spectrum showed significant absorption between 3200 and 2350 cm^{-1} (NH_3^+ stretch), and at 2147 cm^{-1} (NH_3^+ combination). No absorptions were present which could be assigned to NH_2 or NH_2^+. The n.m.r. spectrum exhibited singlets at 1.90 τ (NH) and 7.40 τ (NCH_3), and a multiplet at 2.80 τ (phenyl) with an area ratio of respectively 3:10:5.9.

Anal. Calcd. for $C_{14}H_{19}N_2O_4P$: C, 54.19; H, 6.13; N, 9.05. Found: C, 54.11; H, 6.08; N, 8.55.

Hydrazinium Diphenyl Phosphate (7)

Like compound **6**, this was one of the products from the reaction between hydrazine and methyl diphenyl phosphate.

Pure **7** was prepared by adding 0.07 g (0.0022 mole) hydrazine in 2 ml EtOH to 0.5 g (0.002 mole) diphenyl phosphate in 15 ml ether. A viscous oil was obtained, yield, 0.3 g. Recrystallization from EtOAc/hexane gave 0.2 g (40%) of flaky, white crystals, m.p. 70°. The composition of the product was independent of the ratio of the starting materials. The i.r. spectrum showed significant absorptions at 3358 and 3297 cm^{-1} (*asym*- and *sym*-NH_2 stretch), 3225–2500 cm^{-1} (broad, NH_3^+ stretch), and 2085 cm^{-1} (NH_3^+ combination). The n.m.r. spectrum exhibited a singlet at 3.50 τ (broad, NH) and a multiplet at 2.80 τ (phenyl) in an area ratio of 1.1:2 respectively.

Anal. Calcd. for $C_{12}H_{15}N_2O_4P$: C, 51.10; H, 5.32; N, 9.93. Found: C, 51.02; H, 5.60; N, 9.81.

Methylhydrazinium bis(Diphenyl Phosphate) (8)

The product was obtained from 0.1 g (0.002 mole) methylhydrazine and 1 g (0.004 mole) diphenyl phosphate as white crystals, yield, 0.8 g (72%), m.p. 88.5° (EtOAc/hexane). The same product was obtained from 0.3 g (0.001 mole) **5** and 0.25 g (0.001 mole) diphenyl phosphate, yield, 0.5 g (81%) **8**. The i.r. spectrum showed significant absorption between 3200 and 1800 cm^{-1} as a broad and rather unresolved band indicating both NH_2^+ and NH_3^+. There was no indication of NH_2. The n.m.r. spectrum exhibited singlets at 3.65 τ (broad, NH) and 7.42 τ (NCH_3), and a multiplet at 2.80 τ (phenyl). Area ratio phenyl:NCH_3 = 23:3.

Can. J. Chem. Downloaded from www.nrcresearchpress.com by 210.87.254.5 on 09/05/12
For personal use only.

Anal. Calcd. for $C_{25}H_{28}N_2O_8P_2$: C, 54.90; H, 5.13; N, 5.13. Found: C, 54.60; H, 5.07; N, 4.86.

Both n.m.r. and analysis indicated the presence of two phosphate anions per molecule. (Compare compound **5**.)

1,2-Diphenylhydrazinium bis(Diphenyl Phosphate) (9)

The product was obtained from 0.37 g (0.002 mole) *sym*-diphenylhydrazine and 0.5 g (0.002 mole) diphenyl phosphate as white crystals, yield, 0.3 g (48%), m.p. 225° (decomp.) (EtOH). The i.r. spectrum showed significant absorption at 2850 and 2600 cm^{-1} (*asym*- and *sym*-NH_2^+ stretch). There was no evidence of uncharged —NH. The n.m.r. spectrum exhibited a singlet at 1.25 τ (NH) and a multiplet at 2.82 τ (phenyl) in an area ratio of 4.4:30.

Anal. Calcd. for $C_{36}H_{34}N_2O_8P_2$: C, 63.10; H, 4.98; N, 4.09. Found: C, 63.00; H, 5.01; N, 3.94.

1,1-Diphenylhydrazinium Diphenyl Phosphate (10)

A white cotton-like product was obtained from 0.37 g (0.002 mole) *unsym*-diphenylhydrazine and 0.5 g (0.002 mole) diphenyl phosphate, yield, 0.8 g (92%), m.p. 126–129° (EtOAc/hexane). The i.r. spectrum showed a broad band at 3140 to 2300 cm^{-1} (NH_3^+ stretch) and a band at 2170 cm^{-1} (NH_3^+ combination). There was no evidence of NH_2. The n.m.r. spectrum showed a singlet at 0.80 τ (NH) and a multiplet at 2.82 τ (phenyl) in an area ratio of 3.3:20.

Anal. Calcd. for $C_{24}H_{23}N_2O_4P$: C, 66.40; H, 5.30; N, 6.46. Found: C, 66.88; H, 5.42; N, 6.40.

Reaction between Methylhydrazinium Diphenyl Phosphate (5) and Hydrazine

A sample of 0.6 g (0.002 mole) hydrazinium salt was stirred with 0.07 g (0.0021 mole) hydrazine in 10 ml ether and 1 ml EtOH for 1 h. The resulting oil was separated from the mixture and recrystallized from EtOAc/hexane, giving 0.2 g (36%) of **7**.

Reaction between 1,1-Dimethylhydrazinium Phosphate (6) and Hydrazine

A solution of 0.04 g (0.0012 mole) hydrazine in 2 ml ether and 0.5 ml EtOH was added to a slurry of 0.3 g hydrazinium salt in 5 ml ether. Immediately an oil was formed. After stirring for $\frac{1}{2}$ h the oil was separated and recrystallized from EtOAc/hexane giving 0.18 g (64%) **7**.

Reaction between 1,1-Dimethylhydrazinium Phosphate and Methylhydrazine

A solution of 0.5 g (0.0011 mole) methylhydrazine in 2 ml ether was added to a slurry of 0.3 g (0.001 mole) hydrazinium salt in 5 ml ether. After stirring for $\frac{1}{2}$ h, an oil was formed. The oil was worked up to give 0.2 g (70%) (EtOAc/hexane) methylhydrazinium diphenyl phosphate **5**.

Reaction between 1,2-Diphenylhydrazinium bis(Diphenyl Phosphate) (9) and unsym-Dimethylhydrazine

A slurry of 0.34 g (0.0004 mole) hydrazinium salt in 5 ml ether was treated with 0.06 g (0.001 mole) hydrazine in 1 ml ether. After stirring for 3 h, the mixture was filtered and the residue was recrystallized from EtOAc/hexane giving 0.18 g (60%) **6**.

Reaction between 1,2-Diphenylhydrazinium bis(Diphenyl Phosphate) and sym-Diphenylhydrazine

Mixing equimolar amounts of the compounds did not result in a reaction. After stirring for 24 h the hydrazinium salt was recovered quantitatively.

Reaction between 1,1-Dimethylhydrazinium Diphenyl Phosphate and Methyl Diphenyl Phosphate

Stirring a mixture of equimolar amounts of the hydrazinium salt and the phosphate ester in an EtOH/ether solution for 3 h yielded only starting materials.

Discussion

Hydrazinium salts, commonly prepared from hydrazines and alkylhalides, are usually formed in such a way that the most highly substituted nitrogen atom is quaternized (8). It has been suggested that this is caused by a more basic character of that nitrogen atom (9).

Klages *et al.* (5) suggest that the reason for quaternization is a kinetic one: Hydrazines are basically hydrophilic, and methyl halides are lipophilic. The more highly substituted the hydrazine, the more lipophilic it becomes, thus facilitating the approach between the methyl halide and the hydrazine, especially that side of the hydrazine which is most highly substituted. This way asymmetric and complete substitution is promoted.

Hinman (10) suggests that continued substitution on the same nitrogen atom is favored by a better ability of the substituted nitrogen to stabilize the positive charge in the transition state. In our experiments we found that in the reactions between hydrazines and phosphate esters containing at least one methyl group, continued substitution is also favored. Reaction of methyl diphenyl phosphate with hydrazine, methylhydrazine, or *unsym*-dimethylhydrazine resulted each time in the formation of a 1,1,1-trimethylhydrazinium salt. However, in the case of hydrazine and methylhydrazine the formation of 1-methyl-, and 1,1-dimethylhydrazinium salts was also observed.

This could not be due to incomplete reaction between the hydrazine and the phosphate ester, because these partly substituted salts did not react with methyl diphenyl phosphate. Partly substituted salts did, however, react with certain hydrazines, as shown in Table II. The data in Table II show that the hydrazines can be placed in the following order of ability to displace other hydrazines from their salts:

$$H_2N—NH_2 > (CH_3)HN—NH_2 > (CH_3)_2N—NH_2 > (C_6H_5)HN—NH(C_6H_5)$$

For hydrazine and the methylhydrazines this

sequence is identical to the one found by Hinman with respect to their base strengths (10).

This suggests that the reaction of methylhydrazine and methyl diphenyl phosphate (See Table I) takes place according to the following scheme:

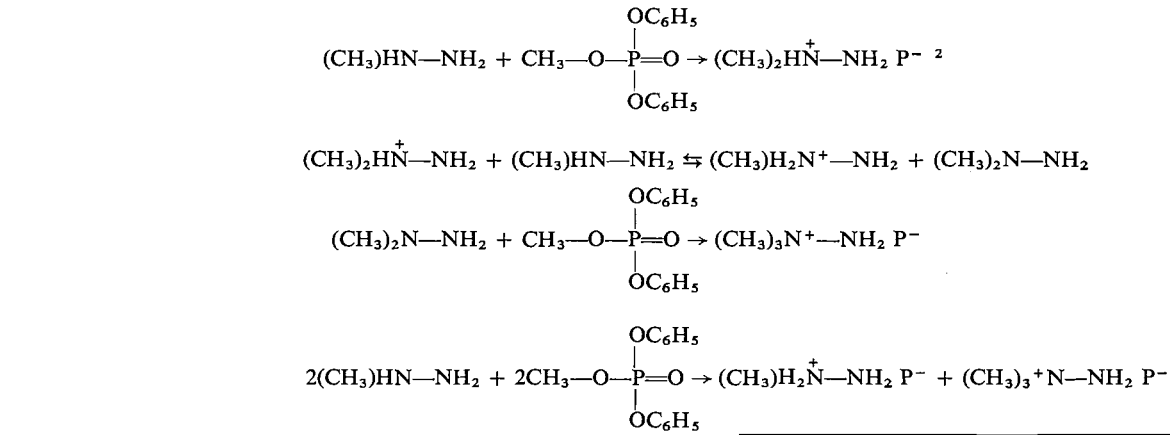

Methylhydrazine being a stronger base than *unsym*-dimethylhydrazine will liberate it from its salt to form *unsym*-dimethylhydrazine and methylhydrazinium diphenyl phosphate. Similar schemes can be devised for the reactions of diphenyl methyl phosphate with hydrazine and with *sym*-dimethylhydrazine. This suggests that the driving force for continued substitution is not just the ability of the nitrogen atom to accommodate still another methyl group. Continued substitution can only take place when the free hydrazine is basic enough to abstract protons from the intermediate hydrazinium salts.

The methylated hydrazine has to be liberated from its salt before it can be methylated further, as is demonstrated by the fruitless attempt to methylate 1,1-dimethylhydrazinium diphenyl phosphate with methyl diphenyl phosphate.

The i.r. spectra were taken from the crystalline material and showed distinctive differences in NH absorption frequencies for the different salts. The *asym*- and *sym*-NH_2 stretching absorptions displayed in the i.r. spectra of compounds **1**, **2**, **3**, **5**, and **7** in the ranges of 3358–3190 cm^{-1}, and 3297–3080 cm^{-1} respectively are in accord with NH_2 stretching vibrations found in the literature for hydrazinium salts (11–13). These bands are absent in compound **6**, which indicates the structure $(CH_3)_2N—{}^+NH_3$ instead of the expected $(CH_3)_2HN^+—NH_2$. This indication is strengthened by the presence of *asym*- and *sym*-NH_3^+ stretching bands as well as a NH_3^+ combination band, which according to the literature generally range from 3225–2300 cm^{-1} (12) and 2170–2085 cm^{-1} (14) respectively. A similar situation exists in **10**.

Thus we find that methylation of *unsym*-dimethylhydrazine by methyl diphenyl phosphate gives a quaternary nitrogen, whereas reaction with diphenyl phosphate gives a charged non-substituted nitrogen. Similar protonation of the non-substituted nitrogen in 1-methyl,1-phenylhydrazine by picric acid was observed by Aubagnac *et al.* (15).

NH_3^+ stretching and combination bands were also observed in **7**. In **8**, both NH_3^+ and NH_2^+ appear as an extremely broad and unresolved band.

NH_2^+ *asym*- and *sym*-stretch displays itself as two bands in compounds **4**, **5**, and **9**. The wavenumbers are slightly lower than those found for secondary amine salts, which range between 3000 and 2700 cm^{-1} (16).

Acknowledgments

The authors wish to thank Dr. R. J. DeGray for his continuous and stimulating interest. They thank Mr. Frank Knoll and Mr. Herb Grossman for determination of the n.m.r. spectra in this work, and Mr. Richard Wander for his assistance in C, H, and N analyses.

[2]For P^- see footnote * of Table I.

Can. J. Chem. Downloaded from www.nrcresearchpress.com by 210.87.254.5 on 09/05/12
For personal use only.

1. H. J. HARWOOD, M. L. BECKER, and R. R. SMITH. J. Org. Chem. **32**, 3882 (1967).
2. J. R. COX, JR. and O. B. RAMSAY. Chem. Rev. **64**, 317 (1964).
3. J. CHEYMOL, P. CHABRIER, M. SELIN, and P. CRELEC. Compt. Rend. **249**, 2573 (1959).
4. F. R. ATHERTON. Quart. Rev. London, **3**, 146 (1949).
5. F. KLAGES, G. NOBER, F. KIRCHER, and M. BOCK. Ann. **547**, 1 (1941).
6. R. F. SMITH, A. C. BATES, A. J. BATTISTI, P. C. BYRNES, C. T. MROZ, T. J. SMEARING, and F. X. ALBRECHT. J. Org. Chem. **33**, 851 (1968).
7. H. D. ORLOFF, C. J. WORREL, and F. X. MARKLEY. J. Am. Chem. Soc. **80**, 727 (1958).
8. O. WESTFAL. Chem. Ber. **74**, 759 (1941).
9. H. H. SISLER, G. M. OMIETANSKI, and B. RUDNER. Chem. Rev. **57**, 1027 (1957).
10. R. L. HINMAN. J. Org. Chem. **23**, 1587 (1958).
11. M. C. HARVEY and D. E. KRAMM. Appl. Spectry. **18**, 140 (1964).
12. J. C. DECIUS and D. P. PEARSON. J. Am. Chem. Soc. **75**, 2436 (1953).
13. J. C. DECIUS and E. C. GILBERT. J. Am. Chem. Soc. **80**, 3872 (1958).
14. C. BRISETTE and C. SANDORFY. Can. J. Chem. **38**, 34 (1960).
15. JEAN-LOUIS AUBAGNAC, JOSE ELGUERO, and ROBERT JACQUIER. Compt. Rend. Ser. C, 263, 739 (1966).
16. N. B. COLTHUP, L. H. DALY, and S. E. WIBERLEY. Introduction to infrared and Raman spectroscopy. Academic Press, Inc., New York. 1964.

Hydrogen bonding in some *t*-amino-alcohols related to methadone

A. F. CASY AND M. M. A. HASSAN
Faculty of Pharmacy, University of Alberta, Edmonton, Alberta

Received May 7, 1968

Hydroxyl stretching frequency data upon 1-dimethylamino-3,3-diphenylhexan-4-ol and related amino-alcohols are reported which give evidence of unusually strong intramolecular hydrogen bonding between the hydroxy and *t*-amino functions of these compounds. In corresponding salts, concentration independent ν_{OH} bands, typical of hydrogen bonded species, also occur and a bonded system comprising anion, OH, and N^+H functions is proposed together with probable methadol base and salt conformations.

Canadian Journal of Chemistry, 47, 1587 (1969)

Can. J. Chem. Downloaded from www.nrcresearchpress.com by 210.87.254.5 on 09/05/12
For personal use only.

This paper reports some spectroscopic properties of 1-dimethylamino-3,3-diphenylhexan-4-ols related to methadone, work undertaken as part of a conformational study of analgesics (1–3). The main point of infrared (i.r.) interest regarding the conformation of α- and β-methadol (**1***a*), the diastereoisomeric alcohols derived from methadone, lies in the detection of intermolecular and/or intramolecular hydrogen bonding of type **2** for the bases and **3** (or some variant) for

$$Me_2NCHRCH_2CPh_2CH(OH)Et$$

1

R = (*a*) Me; (*b*) H

the hydrohalide salts, through a study of ν_{OH} bands.

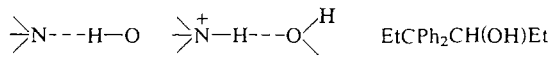

2 **3** **4**

The non-basic analogue, 4,4-diphenylhexan-3-ol, **4** showed both free and bonded ν_{OH} bands as a film and in solutions above 5% in CCl_4 while more dilute solutions displayed single, free[1] ν_{OH} bands (Table I). In sharp contrast, solutions of the isomeric methadols (α- and β-**1***a*) and normethadol **1***b* showed no distinct ν_{OH} bands; these appeared as broad shoulders superimposed upon the ν_{CH} bands as is clearly apparent on comparing the 3μ region of the α-methadol spectrum with that of the hydrocarbon analogue, 3-dimethylamino-1, 1-diphenylbutane (Table I, nos. 2–3 and Fig. 1). No change in the ν_{OH} band appearance occurred upon dilution of the methadol solution to 0.03% (i.e. to well below the concentration of 0.005 mole/l generally regarded as sufficiently low to exclude intermolecular association (4)), and this result indicates that very strong intramolecular hydrogen

[1] ν_{OH} Bands near 3600 cm^{-1} are regarded as free throughout this paper although most have positions indicative of weak π...HO bonding, intramolecular in character (4).

1. H. J. HARWOOD, M. L. BECKER, and R. R. SMITH. J. Org. Chem. **32**, 3882 (1967).
2. J. R. COX, JR. and O. B. RAMSAY. Chem. Rev. **64**, 317 (1964).
3. J. CHEYMOL, P. CHABRIER, M. SELIN, and P. CRELEC. Compt. Rend. **249**, 2573 (1959).
4. F. R. ATHERTON. Quart. Rev. London, **3**, 146 (1949).
5. F. KLAGES, G. NOBER, F. KIRCHER, and M. BOCK. Ann. **547**, 1 (1941).
6. R. F. SMITH, A. C. BATES, A. J. BATTISTI, P. C. BYRNES, C. T. MROZ, T. J. SMEARING, and F. X. ALBRECHT. J. Org. Chem. **33**, 851 (1968).
7. H. D. ORLOFF, C. J. WORREL, and F. X. MARKLEY. J. Am. Chem. Soc. **80**, 727 (1958).
8. O. WESTFAL. Chem. Ber. **74**, 759 (1941).
9. H. H. SISLER, G. M. OMIETANSKI, and B. RUDNER. Chem. Rev. **57**, 1027 (1957).
10. R. L. HINMAN. J. Org. Chem. **23**, 1587 (1958).
11. M. C. HARVEY and D. E. KRAMM. Appl. Spectry. **18**, 140 (1964).
12. J. C. DECIUS and D. P. PEARSON. J. Am. Chem. Soc. **75**, 2436 (1953).
13. J. C. DECIUS and E. C. GILBERT. J. Am. Chem. Soc. **80**, 3872 (1958).
14. C. BRISETTE and C. SANDORFY. Can. J. Chem. **38**, 34 (1960).
15. JEAN-LOUIS AUBAGNAC, JOSE ELGUERO, and ROBERT JACQUIER. Compt. Rend. Ser. C, 263, 739 (1966).
16. N. B. COLTHUP, L. H. DALY, and S. E. WIBERLEY. Introduction to infrared and Raman spectroscopy. Academic Press, Inc., New York. 1964.

Hydrogen bonding in some *t*-amino-alcohols related to methadone

A. F. CASY AND M. M. A. HASSAN
Faculty of Pharmacy, University of Alberta, Edmonton, Alberta

Received May 7, 1968

Hydroxyl stretching frequency data upon 1-dimethylamino-3,3-diphenylhexan-4-ol and related amino-alcohols are reported which give evidence of unusually strong intramolecular hydrogen bonding between the hydroxy and *t*-amino functions of these compounds. In corresponding salts, concentration independent ν_{OH} bands, typical of hydrogen bonded species, also occur and a bonded system comprising anion, OH, and N^+H functions is proposed together with probable methadol base and salt conformations.

Canadian Journal of Chemistry, 47, 1587 (1969)

Can. J. Chem. Downloaded from www.nrcresearchpress.com by 210.87.254.105 on 09/05/12
For personal use only.

This paper reports some spectroscopic properties of 1-dimethylamino-3,3-diphenylhexan-4-ols related to methadone, work undertaken as part of a conformational study of analgesics (1–3). The main point of infrared (i.r.) interest regarding the conformation of α- and β-methadol (**1***a*), the diastereoisomeric alcohols derived from methadone, lies in the detection of intermolecular and/or intramolecular hydrogen bonding of type **2** for the bases and **3** (or some variant) for

$$Me_2NCHRCH_2CPh_2CH(OH)Et$$

1

R = (*a*) Me; (*b*) H

the hydrohalide salts, through a study of ν_{OH} bands.

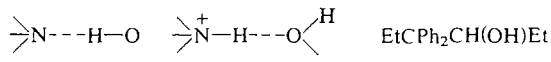

2 **3** **4**

The non-basic analogue, 4,4-diphenylhexan-3-ol, **4** showed both free and bonded ν_{OH} bands as a film and in solutions above 5% in CCl_4 while more dilute solutions displayed single, free[1] ν_{OH} bands (Table I). In sharp contrast, solutions of the isomeric methadols (α- and β-**1***a*) and normethadol **1***b* showed no distinct ν_{OH} bands; these appeared as broad shoulders superimposed upon the ν_{CH} bands as is clearly apparent on comparing the 3μ region of the α-methadol spectrum with that of the hydrocarbon analogue, 3-dimethylamino-1, 1-diphenylbutane (Table I, nos. 2–3 and Fig. 1). No change in the ν_{OH} band appearance occurred upon dilution of the methadol solution to 0.03% (i.e. to well below the concentration of 0.005 mole/l generally regarded as sufficiently low to exclude intermolecular association (4)), and this result indicates that very strong intramolecular hydrogen

[1] ν_{OH} Bands near 3600 cm^{-1} are regarded as free throughout this paper although most have positions indicative of weak π...HO bonding, intramolecular in character (4).

Can. J. Chem. Downloaded from www.nrcresearchpress.com by 210.87.254.105 on 09/05/12
For personal use only.

TABLE I

The O—H stretching frequencies of some aryl-substituted amino-alcohols and related compounds

Number	Compound	Form	Solvent (conc.), film or Nujol mull	ν_{OH} cm^{-1} Free	ν_{OH} cm^{-1} Bonded
1	$EtCPh_2CH(OH)Et$	—	Film	3580(s)	3480(s)
			CCl_4(10%),	3595(s)	3470(s)
			(5–0.05%)	3600(s)	—
2	α-Methadol (*1a*)	Base	Nujol mull	—	Broad shoulder between 3100 and 3500
			CCl_4(10–0.03%)		
	(β-Methadol gave near-identical ν_{OH} values)	HCl	Nujol mull	—	3330(s)
			$CHCl_3$(10–0.1%)	3580(w shoulder)	3360(s)
		MeI	Nujol mull	—	3340(s)
3	Normethadol (*1b*)	Base	Nujol mull	—	Broad shoulder between 3100 and 3500
			CCl_4(10–0.1%)		
		HCl	Nujol mull	—	3300(s)
			$CHCl_3$(10–0.1%)	3580(w)	3370(s)
		MeI	Nujol mull	—	3310(s)
			$CHCl_3$(10–0.1%)	3580(w)	3380(s)
		HI	Nujol mull	—	3360(s)
			$CHCl_3$(5–0.1%)	3570(w)	3420(s)
		HNO_3	Nujol mull	—	3380(s)
			$CHCl_3$(1–0.1%)	3570(w)	3460(s)
		Camphor-10-sulfonate	Nujol mull	—	3300(s)
			$CHCl_3$(5–0.1%)	—	3420(s)
		p-Toluene sulfonate	Nujol mull	—	3300(s) 3400(s)
			$CHCl_3$	—	3420(s)
4	$Me_2N(CH_2)_2OH$	Base	Film	—	3200, 3400
			CS_2(10–1%)	—	3200, 3400–3490
			(0.5–0.3%)	3630(w)	3200(w), 3500(s)
			(0.1–0.05%)	3630(w)	3500(s)
5	1-Methyl-3-piperidinol	Base	Film	—	3200, 3350
			CCl_4(10%)	3640(w)	3200, 3400(s)
			(5–0.5%)	3640(w)	3300–3350(s)
			(0.3–0.05%)	3636(m)	3545(m)
		HCl	Nujol mull	—	3320(s)
6	Tropine	HCl	Nujol mull	—	3330(s)
			$CHCl_3$(10–0.03%)	3600(vw)	3350–3400(s)
		MeI	Nujol mull	—	3400(s)
7	1-Methyl-4-phenyl-4-piperidinol	Base	Nujol mull	—	3200(w),3390(m)
			$CHCl_3$(10%)	3600(s)	3200 (broad)
			(5–0.03%)	3600(s)	doubtful at lower dilutions
		HCl	Nujol mull	—	3300
			$CHCl_3$(5–3%)	3600(w)	3400(s)
			(1–0.03%)	3600(m)	3360–3400(m)
8	1,3-Dimethyl-4-phenyl-4-piperidinol (*trans* 4 Ph/3 Me)	Base	Nujol mull	—	3140 (broad)
			$CHCl_3$(10%)	3610(s)	3140 (broad)
			(5–0.1%)	3600(s)	doubtful at lower dilutions
		HCl	Nujol mull	—	3270
			$CHCl_3$(3%)	3600(w)	3360–3390(s)
			(3–0.03%)	3600(s)	3400(s)

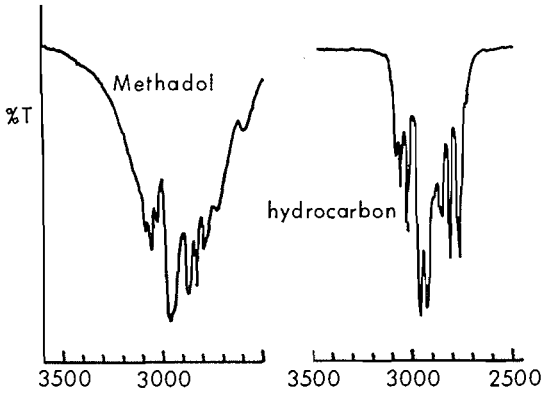

FIG. 1. Infrared spectrum (3 μ region) of α-methadol and its hydrocarbon analogue, 3-dimethylamino-1,1-diphenylbutane (both 10% in CCl_4).

bonding occurs in these compounds.[2] If such be the case, the bonding must be of type **2** because the effect is not seen in the non-basic analogue **4**. There was no significant difference in the ν_{OH} bands of the three amino-alcohols (Table I, nos. 2 and 3) examined at comparable dilutions. The O*H* proton magnetic resonance signals of the α- and β-methadols in $CDCl_3$ had low-field positions (5) anticipated for strongly hydrogen bonded hydroxyls (α, broad band τ 1.43; β, signal fell within aromatic signal τ 2.5–3.1) but these data do not provide evidence of intramolecular effects because they relate to strong solutions.

Intramolecular hydrogen bonding is well documented in non-aromatic amino-alcohols such as β-dimethylaminoethanol and 1-methyl-3-piperidinol (4, 6) which have the correct geometry for an N – HO interaction, but the order of the effects is much less in these two compounds than in the methadols. Thus a weak solution of β-dimethylaminoethanol in CS_2 showed a broad but distinct ν_{OH} (b) band well removed from the ν_{CH} absorption plus a small ν_{OH} (f) band, while a dilute solution of the 3-piperidinol in CCl_4 similarly displayed distinct free and bonded ν_{OH} bands (Table I, nos. 4 and 5). The unusually strong N — HO bonding seen in the methadols appears to be characteristic of phenyl substituted amino-alcohols because simi-

[2]There is a possibility of the bands arising from "abnormal" intermolecular association (mainly dimerization) but this rare phenomenon has not been reported for amino-alcohols (4).

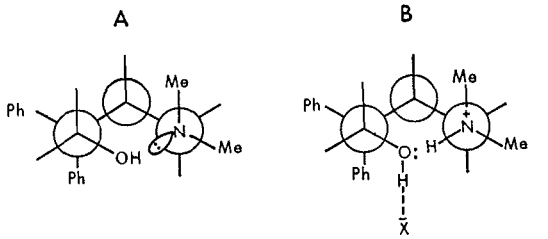

FIG. 2. Representation of probable methadol and normethadol conformations: **A**, base; **B**, protonated base. Some substituents on carbons α- to N and OH have been omitted. In **A** the N-lone-pair orbital is represented.

lar ν_{OH} shoulders were also noted in the related *vic* and *gem* diphenyl *t*-alcohols, **5** and **6** respectively. These alcohols must therefore adopt solute conformations in which the hydroxyl and

$Me_2NCH_2CHMeCPh(OH)CH_2Ph$

5

α β
$MeNCH_2CHMeCPh_2OH$
(and α-Me isomer)

6

amino functions lie close enough together to permit intramolecular hydrogen bonding, as illustrated for the methadols in Fig. 2.

Hydrohalide salts of the two methadols and of normethadol were examined as Nujol mulls and solutions in $CHCl_3$ (the salts were insoluble in CCl_4 and CS_2). This solvent had the disadvantage of (*a*) preventing the use of cells larger than 2 mm because of compensation problems, and (*b*) introducing possible solvent effects. The latter factor is probably only of small significance since the proton donor properties of $CHCl_3$ appear to be small as judged from the near-identical ν_{OH} shoulders obtained for normethadol base as solute in CCl_4 and $CHCl_3$. All spectra of the salts exhibited broad but distinct ν_{OH} bands (Table I, nos. 2 and 3) which were clearly apparent even in solutions more dilute than 0.5% where resolution was not optimum because of cell width restrictions; very weak free ν_{OH} bands near 3580 cm^{-1} appeared in 1% and weaker solutions. The intense broad bands were typical of strongly bonded species and their positions were unaltered on dilution; hence, it is probable that intramolecular effects are again in force. Similarly placed, but sharper bands (also concentration independent) were seen in corresponding methiodides (Table I, no. 3), thus the

Can. J. Chem. Downloaded from www.nrcresearchpress.com by 210.87.254.105 on 09/05/12
For personal use only.

Can. J. Chem. Downloaded from www.nrcresearchpress.com by 210.87.254.105 on 09/05/12
For personal use only.

interactions responsible for bonded ν_{OH} bands in these compounds do not require an acidic proton on nitrogen as in **3** and involvement of the anion (viz. O—H.....$\bar{X}$) is more probable. In support, ν_{OH} for crystalline choline chloride is reported[3] as 3289 cm^{-1} while tropine hydrochloride, of geometry which precludes an intramolecular $\overset{+}{N}H$/OH association, displays a concentration independent ν_{OH} bonded band near 3350 cm^{-1} plus a weak free band (Table I, no. 6).

In the present series, the influence of the anion upon the O—H stretching frequency is apparent from data upon normethadol salts (Table I, no. 3), ν_{OH} band positions varying from salt to salt. Anions are generally concluded to bond to the acidic proton of amine salts and hence to be responsible for the lower wavenumbers of ν^{+}_{NH} compared with ν_{NH} bands (7, 8). Thus the ν^{+}_{NH} positions of amino-alcohol salts in which OH and $\overset{+}{N}H$ protons compete for the anion, would be expected to fall at higher wavenumbers than those of analogues lacking free OH functions. The dilute solution spectra of most methadol salts, however, displayed broad complex bands between 2200 and 2800 cm^{-1} with maxima near 2300 and/or 2600 cm^{-1}, typical of bonded $R_3\overset{+}{N}H$ protons. Similar bands were seen, for example, in hydrochlorides of α-acetylmethadol **7** and the hydrocarbon analogue **8** in which exclusive $\overset{+}{N}H....\bar{X}$ bonding may occur.

$Me_2NCHMeCH_2CPh_2C(OCOMe)Et$

7

$Me_2NCHMeCH_2CPh_2H$

8

It is therefore concluded that a hydrogen bonded system comprising anion, OH, and $\overset{+}{N}H$ functions obtains in most methadol salts. Bonding of this type could take the form $O—H....\bar{X}....H—\overset{+}{N}$ or $\bar{X}....H—O:....H\overset{+}{N}$ either of which require the two proton groups to be fairly close together. Hence, it is to be expected that salts of amino-alcohols of geometry which precludes proximate OH and $\overset{+}{N}H$ groups will be populated by separate $OH....\bar{X}$ and $\overset{+}{N}—H....\bar{X}$ species. It is significant, in this respect, that spectra of the salts of tropine **9** and the 4-phenylpiperidinols **10** display both bonded and free ν_{OH} bands (Table I, nos. 6–8) while the ν^{+}_{NH} band

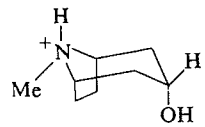

9

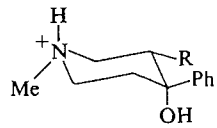

10 R = H or Me

of tropine hydrochloride has higher wavenumber maxima than those of the methadol salts. The OH and $\overset{+}{N}H$ stretching frequency characteristics of hydrochlorides of the more flexible phenyl substituted amino-alcohols **5** and **6** were similar to those of methadol salts.

The three-component hydrogen bonded system proposed for methadol salts rests upon the assumption of the ν^{+}_{NH} bands, present in their spectra, being due to bonded functions. Evidence for $\overset{+}{N}H....\bar{X}$ bonding, and in particular for assigning bands in the 2200–2800 cm^{-1} region to bonded rather than free $\overset{+}{N}H$ groups, is not extensive and is mostly indirect, e.g. movement of the ν^{+}_{NH} band of certain *t*-amine hydrochlorides to higher wavenumbers when water of crystallization is present, is attributed to a weakening of $\overset{+}{N}H.....\bar{X}$ bonding through formation of water–anion bonds (7), and its further study is desirable. We have noted poorly defined ν^{+}_{NH} bands in the Nujol mull spectra of base salts involving bulky anions, e.g. iodides, iodates, nitrates, and nitrites, the more characteristically placed bands reappearing in dilute solution spectra.[4] It appears, therefore, that $\overset{+}{N}H....\bar{X}$ bonding is weak in the solid state forms of these salts. Normally placed ν^{+}_{NH} bands are also absent in the spectrum (mull) of the perchlorate of 3-dimethylamino-1,1-diphenylbutyl cyanide; instead, a strong band at 3080 cm^{-1} (i.e. close to the secondary amine N—H range) is present (Fig. 3). The normethadol perchlorate spectrum (mull) similarly lacks

[3]M. E. Senko and D. H. Templeton. Private communication (quoted by Pimental and McClellan (8)).

[4]A. F. Casy and M. A. A. Hassan. Unpublished results.

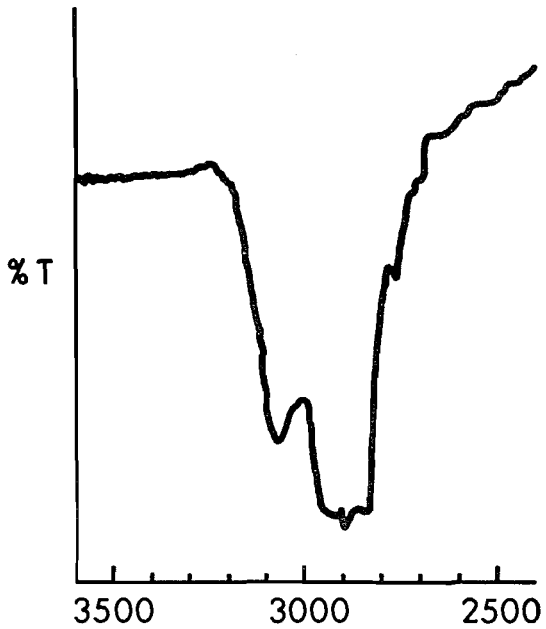

FIG. 3. Infrared spectrum (3 μ region) of the perchlorate of 3-dimethylamino-1,1-diphenylbutyl cyanide (Nujol mull).

the usual ν^{+}_{NH} features and has bands at 3160 and 3570 cm^{-1} tentatively assigned to ν^{+}_{NH} and ν_{OH} (both weakly bonded) respectively, plus a broad bonded absorption near 3350 cm^{-1} due, in part at least, to water of crystallization. Solution data upon this perchlorate, unique amongst normethadol salts examined in showing a pronounced free ν_{OH} band, could not be obtained because the salt was insoluble in $CHCl_3$.

If the operation of intramolecular bonding between chloride ion, OH, and $\overset{+}{N}H$ functions in methadol salts be accepted as a reasonable assumption on the basis of the i.r. evidence presented here, favored salt conformations similar to those of the free bases may be proposed, e.g. Fig. 2B in which anion bonding to OH is represented. Possible pharmacological implications of these conclusions will be discussed elsewhere.

Experimental

Infrared spectra were recorded with a Beckman IR-10 spectrophotometer. Cells of path length 0.05 mm (10–5%), 0.5 mm (5–3%), 2 mm (1.0–0.5%), and 12 mm (<0.5%) were used for solution studies in CCl_4. A 2 mm cell was the largest usable when $CHCl_3$ was solvent. Most of the compounds have been described previously (9–12) or were commercially available. New compounds are described below.

4,4-Diphenylhexan-3-ol

Ethyl bromide (5.45 g) in dry benzene (10 ml) was added to a mixture of diphenylacetonitrile (9.65 g), powdered sodamide (2 g), and benzene (50 ml) which had previously been stirred at 30–40° for 1 h, and the product heated under reflux for 12 h. The benzene solution was then washed with water, dried over anhydrous sodium sulfate, evaporated to dryness, and the oily residue distilled to give 1,1-diphenylpropylcyanide (10 g), b.p. 120°/0.2 mm.

Anal. Calcd. for $C_{16}H_{15}N$: C, 86.8; H, 6.8. Found: C, 86.6; H, 6.7.

This cyanide (6.63 g) in dry toluene (100 ml) was added to ethyl magnesium bromide in ether (40 ml) prepared from ethyl bromide (9.7 g) and magnesium (2.2 g). The ether was removed, the mixture heated under reflux for 3 h, and then added to ice and concentrated hydrochloric acid (40 ml). The basic ketimine (6.5 g), ν_{max} 1709, 1636 cm^{-1} (C=NH) recovered from the aqueous phase, with hydrogen chloride gave 1,1-diphenylpropyl ethyl ketimine hydrochloride, m.p. 203–205° from ethanol ether, ν_{max} 1679 cm^{-1} (C=N).

Anal. Calcd. for $C_{18}H_{22}ClN$ (equiv. wt., 287): C, 75.1; H, 7.7; N, 4.9. Found (equiv. wt., 285): C, 74.4; H, 7.8; N, 4.75.

The ketimine (6 g) was heated under reflux with concentrated hydrochloric acid (25 ml) for 8 h and the oil which separated was isolated by ether extraction and distilled to give 4,4-diphenylhexan-3-one (4.5 g), b.p. 114–118°/0.25 mm.

Anal. Calcd. for $C_{18}H_{20}O$: C, 85.7; H, 8.0. Found: C, 86.3; H, 7.8.

4,4-Diphenylhexan-3-one (5.04 g) in ether (50 ml) was added dropwise to $LiAlH_4$ (0.76 g) in ether (50 ml). After a period of stirring (2 h at R°, 1 h at reflux temperature) the mixture was treated with water (15 ml) and filtered. The residue from the dried filtrate was distilled to give 4,4-diphenylhexan-3-ol, b.p. 134–136°/2–5 mm.

Anal. Calcd. for $C_{18}H_{22}O$: C, 85.0; H, 8.7. Found: C, 84.8; H, 8.5.

Salts of 6-Dimethylamino-4,4-diphenylhexan-3-ol (Normethadol)

These were all recrystallized from ethanol–ether.

Camphor-10-sulfonate, m.p. 200–202°

Anal. Calcd. for $C_{30}H_{43}NO_5S$: C, 68.0; H, 8.2. Found: C, 67.7; H, 8.3.

Hydriodide, m.p. 183–185°

Anal. Calcd. for $C_{20}H_{28}INO$: C, 56.5; H, 6.6. Found: C, 56.3; H, 6.3.

Methiodide, m.p. 183–185°

Anal. Calcd. for $C_{21}H_{30}INO$: C, 57.4; H, 6.9; N, 3.2. Found: C, 57.0; H, 6.7; N, 3.25.

Nitrate, m.p. 159–161° (decomp.)

Anal. Calcd. for $C_{20}H_{28}N_2O_4$: C, 66.6; H, 7.8. Found: C, 66.2; H, 7.5.

Perchlorate, m.p. 140–141°

Anal. Calcd. for $C_{20}H_{28}NO_4Cl \cdot H_2O$: C, 60.1; H, 7.6. Found: C, 59.8; H, 7.3.

p-Toluene Sulfonate, m.p. 140–142°

Anal. Calcd. for $C_{27}H_{35}NO_4S$: C, 69.0; H, 7.5. Found: C, 68.7; H, 7.55.

Can. J. Chem. Downloaded from www.nrcresearchpress.com by 210.87.254.105 on 09/05/12
For personal use only.

1. A. F. CASY. J. Chem. Soc. B, 1157 (1966).
2. A. F. CASY and M. M. A. HASSAN. J. Pharm. Pharmac. **19**, 114 (1967).
3. A. F. CASY. J. Med. Chem. **11**, 188 (1968).
4. M. TICHY. *In* Advances in organic chemistry. Vol. 5. *Edited by* R. A. Raphael, E. C. Taylor, and H. Wynberg. Interscience Publishers, Inc., New York. 1965. p. 115.
5. P. S. PORTOGHESE and D. A. WILLIAMS. J. Pharm. Sci. **55**, 990 (1966).
6. R. E. LYLE, D. H. MCMAHON, W. E. KRUEGER, and C. K. SPICER. J. Org. Chem. **31**, 4164 (1966).
7. R. J. WARREN, W. E. THOMPSON, and J. E. ZAREMBO. J. Pharm. Sci. **54**, 1554 (1965). I. B. EISDORFER, R. J. WARREN, and J. E. ZAREMBO. J. Pharm. Sci. **57**, 195 (1968).
8. G. C. PIMENTAL and A. L. MCCLENNAN. The hydrogen bond. W. H. Freeman and Co., San Francisco. 1960.
9. M. M. A. HASSAN. Ph.D. Thesis, University of London. England. 1967.
10. P. A. J. JANSSEN. Synthetic analgesics. Part I. Diphenylpropylamines. See also refs. cited therein. The Pergamon Press, Ltd., Oxford. 1960.
11. A. F. CASY and M. M. A. HASSAN. J. Med. Chem. **11**, 601 (1968).
12. A. POHLAND and H. R. SULLIVAN. J. Am. Chem. Soc. **75**, 4458 (1953).

Inner glucosides of the anomeric 2-*O*-(2-hydroxyethyl)-D-glucoses

E. J. ROBERTS AND S. P. ROWLAND

Southern Regional Research Laboratory, Southern Utilization Research and Development Division, Agricultural Research Service, United States Department of Agriculture, New Orleans, Louisiana

Received October 16, 1968

It has been found that 2-*O*-(2-hydroxyethyl)-D-glucopyranose is partially converted to 1,2-*O*-ethylene-α-D-glucofuranose, 1,2-*O*-ethylene-α-D-glucopyranose, and 1,2-*O*-ethylene-β-D-glucopyranose when heated in dilute acid solution. The ratio of the furanose derivative to the pyranose derivatives is dependent upon the concentration of the acid (3, 5). The three inner glucosides of 2-*O*-(2-hydroxyethyl)-D-glucose have been characterized by gas–liquid chromatography. The interrelationship of 2-*O*-(2-hydroxyethyl)-D-glucose and its inner glucosides is also reported.

Canadian Journal of Chemistry, 47, 1592 (1969)

Introduction

Studies of the distribution of substituents in *O*-(2-hydroxyethyl)starch (1) and *O*-(2-hydroxyethyl)cellulose (2) have been reported. In recent studies of the distribution of substituents in *O*-(2-hydroxyethyl)starch, Bollenback *et al.* (3) and Srivastava *et al.* (4) reported the presence of a small quantity of 1,2-*O*-ethylene-α-D-glucofuranose resulting from the hydrolysis of *O*-(2-hydroxyethyl)starch with 0.75 *M* sulfuric acid. They concluded that the inner glucoside is formed by the dehydration of 2-*O*-(2-hydroxyethyl)-D-glucopyranose during the acid hydrolysis of the modified starch. No 1,2-*O*-ethylene-β-D-glucofuranose or the corresponding pyranose derivatives were reported.

Hook and Lindberg (5) have shown that 1,2-*O*-ethylene-α-D-glucofuranose and the corresponding α- and β-pyranose derivatives are formed upon heating 2-*O*-(2-hydroxyethyl)-D-glucopyranose in dilute hydrochloric acid.

This note reports the characterization of 2-*O*-(2-hydroxyethyl)-D-glucopyranose, 1,2-*O*-ethylene-α-D-glucofuranose, and the inner glucosides of α- and β-2-*O*-(2-hydroxyethyl)-D-glucopyranose by gas–liquid chromatography (g.l.c.). The interrelationship of 2-*O*-(2-hydroxyethyl)-D-glucopyranose and its inner glucosides is also reported.

Experimental

Gas–Liquid Chromatography

The gas–liquid chromatograms (g.l.c.) were obtained on an Aerograph model 1520 instrument. The samples to be analyzed were silylated, and the SE-30 column was operated isothermally at 190° as described by Roberts and Rowland (6).

1,2-O-Ethylene-α-D-glucofuranose

In an attempt to synthesize 2-*O*-(2-aminoethyl)-D-glucopyranose, methyl 3-*O*-benzyl-2-*O*-carbomethoxymethyl-4,6-*O*-benzylidene-α-D-glucopyranoside was prepared by the procedure described by Roberts and Rowland (6) for the preparation of the corresponding 2-*O*-carbethoxymethyl derivative. The product (10 g) was obtained as a syrup which did not crystallize. The syrupy methyl 3-*O*-benzyl-2-*O*-carbomethoxymethyl-4,6-*O*-benzylidene-α-D-glucopyranoside (10 g, 0.023 mole) was stirred into 400 ml of concentrated ammonium hydroxide in which it was insoluble. The mixture was stirred, and after 6 h the syrup had solidified. The solid was removed by filtration and was crystallized from methanol, yielding 10 g of white crystals melting at 130–135°.

Can. J. Chem. Downloaded from www.nrcresearchpress.com by 210.87.254.105 on 09/05/12
For personal use only.

1. A. F. CASY. J. Chem. Soc. B, 1157 (1966).
2. A. F. CASY and M. M. A. HASSAN. J. Pharm. Pharmac. **19**, 114 (1967).
3. A. F. CASY. J. Med. Chem. **11**, 188 (1968).
4. M. TICHY. *In* Advances in organic chemistry. Vol. 5. *Edited by* R. A. Raphael, E. C. Taylor, and H. Wynberg. Interscience Publishers, Inc., New York. 1965. p. 115.
5. P. S. PORTOGHESE and D. A. WILLIAMS. J. Pharm. Sci. **55**, 990 (1966).
6. R. E. LYLE, D. H. MCMAHON, W. E. KRUEGER, and C. K. SPICER. J. Org. Chem. **31**, 4164 (1966).
7. R. J. WARREN, W. E. THOMPSON, and J. E. ZAREMBO. J. Pharm. Sci. **54**, 1554 (1965). I. B. EISDORFER, R. J. WARREN, and J. E. ZAREMBO. J. Pharm. Sci. **57**, 195 (1968).
8. G. C. PIMENTAL and A. L. MCCLENNAN. The hydrogen bond. W. H. Freeman and Co., San Francisco. 1960.
9. M. M. A. HASSAN. Ph.D. Thesis, University of London. England. 1967.
10. P. A. J. JANSSEN. Synthetic analgesics. Part I. Diphenylpropylamines. See also refs. cited therein. The Pergamon Press, Ltd., Oxford. 1960.
11. A. F. CASY and M. M. A. HASSAN. J. Med. Chem. **11**, 601 (1968).
12. A. POHLAND and H. R. SULLIVAN. J. Am. Chem. Soc. **75**, 4458 (1953).

Inner glucosides of the anomeric 2-*O*-(2-hydroxyethyl)-D-glucoses

E. J. ROBERTS AND S. P. ROWLAND

Southern Regional Research Laboratory, Southern Utilization Research and Development Division, Agricultural Research Service, United States Department of Agriculture, New Orleans, Louisiana

Received October 16, 1968

It has been found that 2-*O*-(2-hydroxyethyl)-D-glucopyranose is partially converted to 1,2-*O*-ethylene-α-D-glucofuranose, 1,2-*O*-ethylene-α-D-glucopyranose, and 1,2-*O*-ethylene-β-D-glucopyranose when heated in dilute acid solution. The ratio of the furanose derivative to the pyranose derivatives is dependent upon the concentration of the acid (3, 5). The three inner glucosides of 2-*O*-(2-hydroxyethyl)-D-glucose have been characterized by gas–liquid chromatography. The interrelationship of 2-*O*-(2-hydroxyethyl)-D-glucose and its inner glucosides is also reported.

Canadian Journal of Chemistry, 47, 1592 (1969)

Introduction

Studies of the distribution of substituents in *O*-(2-hydroxyethyl)starch (1) and *O*-(2-hydroxyethyl)cellulose (2) have been reported. In recent studies of the distribution of substituents in *O*-(2-hydroxyethyl)starch, Bollenback *et al.* (3) and Srivastava *et al.* (4) reported the presence of a small quantity of 1,2-*O*-ethylene-α-D-glucofuranose resulting from the hydrolysis of *O*-(2-hydroxyethyl)starch with 0.75 *M* sulfuric acid. They concluded that the inner glucoside is formed by the dehydration of 2-*O*-(2-hydroxyethyl)-D-glucopyranose during the acid hydrolysis of the modified starch. No 1,2-*O*-ethylene-β-D-glucofuranose or the corresponding pyranose derivatives were reported.

Hook and Lindberg (5) have shown that 1,2-*O*-ethylene-α-D-glucofuranose and the corresponding α- and β-pyranose derivatives are formed upon heating 2-*O*-(2-hydroxyethyl)-D-glucopyranose in dilute hydrochloric acid.

This note reports the characterization of 2-*O*-(2-hydroxyethyl)-D-glucopyranose, 1,2-*O*-ethylene-α-D-glucofuranose, and the inner glucosides of α- and β-2-*O*-(2-hydroxyethyl)-D-glucopyranose by gas–liquid chromatography (g.l.c.). The interrelationship of 2-*O*-(2-hydroxyethyl)-D-glucopyranose and its inner glucosides is also reported.

Experimental

Gas–Liquid Chromatography

The gas–liquid chromatograms (g.l.c.) were obtained on an Aerograph model 1520 instrument. The samples to be analyzed were silylated, and the SE-30 column was operated isothermally at 190° as described by Roberts and Rowland (6).

1,2-O-Ethylene-α-D-glucofuranose

In an attempt to synthesize 2-*O*-(2-aminoethyl)-D-glucopyranose, methyl 3-*O*-benzyl-2-*O*-carbomethoxymethyl-4,6-*O*-benzylidene-α-D-glucopyranoside was prepared by the procedure described by Roberts and Rowland (6) for the preparation of the corresponding 2-*O*-carbethoxymethyl derivative. The product (10 g) was obtained as a syrup which did not crystallize. The syrupy methyl 3-*O*-benzyl-2-*O*-carbomethoxymethyl-4,6-*O*-benzylidene-α-D-glucopyranoside (10 g, 0.023 mole) was stirred into 400 ml of concentrated ammonium hydroxide in which it was insoluble. The mixture was stirred, and after 6 h the syrup had solidified. The solid was removed by filtration and was crystallized from methanol, yielding 10 g of white crystals melting at 130–135°.

Can. J. Chem. Downloaded from www.nrcresearchpress.com by 210.87.254.5 on 09/05/12
For personal use only.

Can. J. Chem. Downloaded from www.nrcresearchpress.com by 210.87.254.5 on 09/05/12
For personal use only.

Ten grams of this compound was reduced with lithium aluminium hydride (6) yielding 8.5 g of white crystals melting at 125–129°. The benzyl and benzylidene groups were removed by hydrogenolysis (7), and the glucosidic methyl group was removed by refluxing in 100 ml of 1 *N* sulfuric acid for 16 h. The sulfuric acid was removed with barium hydroxide. The barium sulfate was removed by filtration. The filtrate was concentrated to a dark syrup, and upon cooling, 400 mg of crystals separated. After two recrystallizations from methanol, 300 mg of white crystals melting at 221–223° were obtained; $[\alpha]_D^{25} - 57°$(*c*,1,water), lit. (3) m.p. 222–223° and $[\alpha]_D^{25} - 58°$(*c*,1,water) and lit. (5) m.p. 218–220° and $[\alpha]_{578} - 56°$(water).

Anal. Calcd. for $C_8H_{14}O_6$: C, 46.60; H, 6.80. Found: C, 46.54; H, 6.92.

It is therefore apparent that the methyl 3-*O*-benzyl-2-*O*-carbomethoxymethyl-4,6-*O*-benzylidene-α-D-glucopyranoside underwent hydrolysis of the ester in the ammonium hydroxide rather than the expected amide formation. The resulting ammonium salt, upon reduction, was partially converted to the 2-*O*-hydroxyethyl derivative which was cyclized to 1,2-*O*-ethylene-α-D-glucofuranose during the hydrolysis step.

The nuclear magnetic resonance spectrum of this compound showed a doublet at $\tau = 4.55$ p.p.m., (3-(trimethylsilyl)-1-propanesulfonic acid, sodium salt as internal standard) $J_{1,2} = 2.5$ Hz, identical to the spectrum reported by Hook and Lindberg (5).

Hydrolysis of 1,2-O-Ethylene-α-D-glucofuranose

1,2-*O*-Ethylene-α-D-glucofuranose (100 mg, 0.00049 mole) was dissolved in 100 ml of 2 *N* sulfuric acid and was refluxed overnight. The sulfuric acid was removed with barium hydroxide. The barium sulfate was removed by filtration, and the filtrate was concentrated and freeze-dried. Silylation and g.l.c. of the freeze-dried product showed that the 1,2-*O*-ethylene-α-D-glucofuranose was converted to a mixture consisting of 49.4% 1,2-*O*-ethylene-α-D-glucopyranose, 26.5% 1,2-*O*-ethylene-β-D-glucopyranose, 24.1% 2-*O*-(2-hydroxyethyl)-D-glucopyranose, and a trace of the original 1,2-*O*-ethylene-α-D-glucofuranose.

1,2-O-Ethylene-β-D-glucopyranose

This compound was prepared by a procedure similar to that described by Helferich and Werner (8), who dehydrohalogenated the iodo analogue with sodium hydroxide. To 25 g (0.10 mole) of amorphous 2-chloroethyl-β-D-glucopyranoside (9) dissolved in 250 ml of water were added 40 g of barium hydroxide. The solution was stirred under reflux for 16 h. The solution was cooled and the excess barium hydroxide was precipitated with carbon dioxide. The barium carbonate was removed by filtration. The filtrate was evaporated to dryness, and the residue was extracted with methanol. Upon cooling, 10.5 g (81% of theory) of white crystals melting at 215–217° were obtained. After two crystallizations from methanol, the m.p. was unchanged; $[\alpha]_D^{25} + 60.5°$(*c*, 1.7104, water), lit. (8) m.p. 210–211°, $[\alpha]_D^{21} + 56°$(water).

Anal. Calcd. for $C_8H_{14}O_6$: C, 46.60; H, 6.80. Found: C, 46.61; H, 6.89.

Hydrolysis of 1,2-O-Ethylene-β-D-glucopyranose

1,2-*O*-Ethylene-β-D-glucopyranose (1 g, 0.0049 mole) was refluxed for 16 h in 100 ml of 2 *N* sulfuric acid in the same manner as described for the hydrolysis of 1,2-*O*-ethylene-α-D-glucofuranose. The hydrolyzate was freeze-dried yielding 1 g of amorphous solid. Silylation and g.l.c. analysis of a sample of the hydrolyzate showed a mixture of products consisting of 67.4% 1,2-*O*-ethylene-β-D-glucopyranose, 17.4% 1,2-*O*-ethylene-α-D-glucopyranose, 15.2% 2-*O*-(2-hydroxyethyl)-D-glucopyranose, and a trace of 1,2-*O*-ethylene-α-D-glucofuranose.

1,2-O-Ethylene-α-D-glucopyranose

To 500 ml of 2-chloroethanol containing 5% hydrogen chloride were added 36 g (0.20 mole) of α-D-glucose and 200 ml of benzene. The mixture was stirred under reflux with a water trap connected to the apparatus until no further water was liberated (about 3 h). The hydrogen chloride remaining was removed with an excess of lead carbonate. The lead salts were removed by filtration. The filtrate was decolorized with Darco carbon G-60 and concentrated in a rotary evaporator at 90° and 12 mm pressure, yielding 45 g (93% of theory) of a thick syrup which did not crystallize. Silylation and g.l.c. analysis of the product showed that 74% of the 2-chloroethyl-D-glucoside was the α-anomer (first peak) and 26% was the β-anomer. Only a trace of glucose was present.

The syrupy mixture of glucosides (45 g, 0.18 mole) was converted to a mixture of α- and β-1,2-*O*-ethylene-D-glucopyranoses in the same manner as described for the preparation of 1,2-*O*-ethylene-β-D-glucopyranose. The yield was 30.4 g (80% of theory) of a thick syrup. After several unsuccessful attempts to crystallize the product, it was dissolved in water and freeze-dried.

Silylation and g.l.c. of a sample of the freeze-dried mixture showed that the product was 70% 1,2-*O*-ethylene-α-D-glucopyranose (second peak) and 30% β-anomer.

Results and Discussion

During a study of the distribution of 2-aminoethyl groups (after conversion to 2-hydroxyethyl groups) in *O*-(2-aminoethyl)cellulose (6), it was necessary to prepare the 2-*O*-, 3-*O*-, and 6-*O*-(2-hydroxyethyl)-D-glucopyranoses. Gas–liquid chromatography of the silylated 2-*O*-(2-hydroxyethyl)-D-glucopyranose showed three peaks (designated 2″, 2′, and 2′ in curve A, Fig. 1) in addition to those representing the anomeric forms of 2-*O*-(2-hydroxyethyl)-D-glucopyranose (designated 2 and 2 in curve A, Fig. 1).

The retention time of the peak designated 2″ (curve A, Fig. 1) was identical to that of 1,2-*O*-ethylene-α-D-glucofuranose (curve D, Fig. 1). For this reason it was suspected that the two peaks designated 2′ (curve A, Fig. 1) might be the anomeric 1,2-*O*-ethylene-D-glucopyranoses.

Gas–liquid chromatography of the trimethylsilyl ether of 1,2-*O*-ethylene-β-D-glucopyranose showed a retention time (curve B, Fig. 1) identical to that of the first peak designated 2′ (curve A, Fig. 1).

Can. J. Chem. Downloaded from www.nrcresearchpress.com by 210.87.254.5 on 09/05/12
For personal use only.

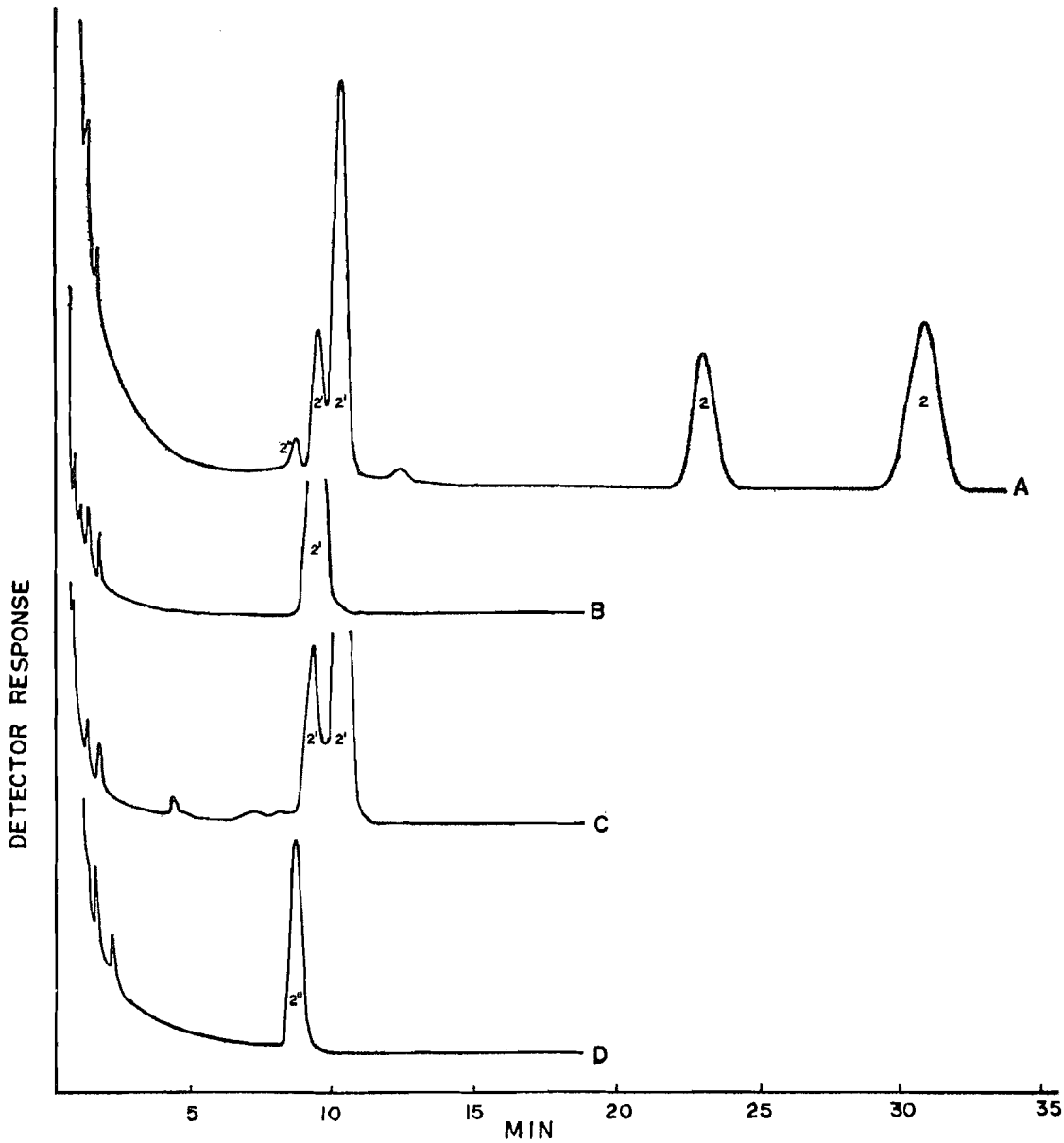

FIG. 1. Chromatograms of trimethylsilyl derivatives on SE-30 column operated isothermally at 190°. Curve A is 2-*O*-(2-hydroxyethyl)-D-glucoses and the inner glucosides. Curve B is 1,2-*O*-ethylene-β-D-glucopyranose (2′). Curve C is a mixture of (predominantly) 1,2-*O*-ethylene-α-D-glucopyranose and 1,2-*O*-ethylene-β-D-glucopyranose (2′ and 2′). Curve D is 1,2-*O*-ethylene-α-D-glucofuranose (2″).

The 1,2-*O*-ethylene-α-D-glucopyranose contained some of the β-anomer. Gas–liquid chromatography of the mixture showed that the second peak, designated 2′ (curve A, Fig. 1), corresponded to that of 1,2-*O*-ethylene-α-D-glucopyranose (second peak designated 2′, curve C, Fig. 1). The 2-*O*-(2-hydroxyethyl)-D-glucopyranose preparation was found to contain 3.0% 1,2-*O*-ethylene-α-D-glucofuranose, 13.0% 1,2-*O*-ethylene-β-D-glucopyranose, 38.4% 1,2-*O*-ethyl-

ene-α-D-glucopyranose, and 45.6% 2-*O*-(2-hydroxyethyl)-D-glucopyranose based on peak areas.

Bollenback *et al.* (3) have pointed out that by inspection of molecular models, *cis* (α)-fused ring formation is favored over the *trans* (β). This conclusion is consistent with the results reported in this paper. However, no strains were observed in the model of the *trans* pyranose configuration.

Bollenback *et al.* (3) did not report the detection of either α- or β-1,2-*O*-ethylene-D-glucopyranose. This suggests that the mild conditions employed in the hydrolysis of starch favor the formation of the furanose form, while the more strenuous conditions necessary for the hydrolysis of cellulose favor the pyranose form. Hook and Lindberg (5) also reported a predominance of the furanose form of 1,2-*O*-ethylene-α-D-glucose resulting from the treatment of 2-*O*-(2-hydroxyethyl)-D-glucopyranose and methyl 2-*O*-(2-hydroxyethyl)-β-D-glucopyranoside with 1 *N* hydrochloric acid.

The inner glucosides are obviously formed by dehydration of 2-*O*-(2-hydroxyethyl)-D-glucopyranose during acid hydrolysis of the blocking groups.

These results suggest that previous reports on the distribution of 2-hydroxyethyl groups in *O*-(2-hydroxyethyl)starch and *O*-(2-hydroxyethyl)cellulose should be reexamined since the inner glucosides must be considered as part of the 2-*O*-(2-hydroxyethyl)-D-glucopyranose.

Acknowledgment

The authors gratefully acknowledge the advice of Professor Bengt Lindberg of Stockholm University and his assistance in making available a prepublication copy of his paper "Intramolecular glucosidation of 2-*O*-hydroxyethyl-D-glucose."

1. C. E. Lott and K. M. Brobst. Anal. Chem. **38**, 1767 (1966).
2. I. Croon and B. Lindberg. Svensk Papperstid. **59**, 794 (1956).
3. G. N. Bollenback, R. S. Golik, and F. W. Parrish. Private communication. To be published in Cereal Chemistry.
4. H. C. Srivastava, K. V. Ramalingam, N. M. Doshi, and A. S. Chaudhari. Am. Chem. Soc. Absr. 156th Natl. Meeting, Sept. 8–13, 1968. P. Carb. 34.
5. J. E. Hook and Bengt Lindberg. Acta Chem. Scand. To be published.
6. E. J. Roberts and S. P. Rowland. Can. J. Chem. This issue.
7. E. J. Roberts and S. P. Rowland. Can. J. Chem. **45**, 261 (1967).
8. B. Helferich and J. Werner. Ber. **75**, 949 (1942).
9. L. P. Miller. Contribs. Boyce Thompson Inst. **11**, 25 (1940).

Fluoranthene studies. IV. Nitration of 2-nitro-, 3-nitro-, and 2-acetamido-fluoranthene

E. H. Charlesworth and Caroline U. Lithown
Department of Chemistry, The University of Manitoba, Winnipeg, Manitoba

Received November 27, 1968

Nitration of 3-nitrofluoranthene yields 3,9-dinitrofluoranthene, and nitration of 2-acetamidofluoranthene yields 2-acetamido-3-nitrofluoranthene. The orientation of both these compounds has been proved. Nitration of 2-nitrofluoranthene has given a dinitro product, but its orientation has not been established. A number of other new fluoranthene derivatives are described.

Canadian Journal of Chemistry, 47, 1595 (1969)

In 1964 Charlesworth and Blackburn (1) showed that 3-amino and 3-acetamidofluoranthene were brominated in pyridine solution in the 2-position. This was in agreement with the postulate of Kloetzel *et al.* (2) that a strongly activating substituent in the A ring would cause further substitution to occur in the same ring. Blackburn (3), in his experimental work and not mentioned in the above paper, describes a bromination of 3-acetamidofluoranthene (**3**) in acetic acid which gave a rather poor yield of a product, m.p. 265–266 °C. This product gave a large depression on mixing with 3-acetamido-2-bromofluoranthene and was not studied further at the time. Blackburn's concluding sentence reads "the possibility exists that this compound

Can. J. Chem. Downloaded from www.nrcresearchpress.com by 210.87.254.5 on 09/05/12
For personal use only.

ene-α-D-glucopyranose, and 45.6% 2-*O*-(2-hydroxyethyl)-D-glucopyranose based on peak areas.

Bollenback *et al.* (3) have pointed out that by inspection of molecular models, *cis* (α)-fused ring formation is favored over the *trans* (β). This conclusion is consistent with the results reported in this paper. However, no strains were observed in the model of the *trans* pyranose configuration.

Bollenback *et al.* (3) did not report the detection of either α- or β-1,2-*O*-ethylene-D-glucopyranose. This suggests that the mild conditions employed in the hydrolysis of starch favor the formation of the furanose form, while the more strenuous conditions necessary for the hydrolysis of cellulose favor the pyranose form. Hook and Lindberg (5) also reported a predominance of the furanose form of 1,2-*O*-ethylene-α-D-glucose resulting from the treatment of 2-*O*-(2-hydroxyethyl)-D-glucopyranose and methyl 2-*O*-(2-hydroxyethyl)-β-D-glucopyranoside with 1 *N* hydrochloric acid.

The inner glucosides are obviously formed by dehydration of 2-*O*-(2-hydroxyethyl)-D-glucopyranose during acid hydrolysis of the blocking groups.

These results suggest that previous reports on the distribution of 2-hydroxyethyl groups in *O*-(2-hydroxyethyl)starch and *O*-(2-hydroxyethyl)cellulose should be reexamined since the inner glucosides must be considered as part of the 2-*O*-(2-hydroxyethyl)-D-glucopyranose.

Acknowledgment

The authors gratefully acknowledge the advice of Professor Bengt Lindberg of Stockholm University and his assistance in making available a prepublication copy of his paper "Intramolecular glucosidation of 2-*O*-hydroxyethyl-D-glucose."

1. C. E. Lott and K. M. Brobst. Anal. Chem. **38**, 1767 (1966).
2. I. Croon and B. Lindberg. Svensk Papperstid. **59**, 794 (1956).
3. G. N. Bollenback, R. S. Golik, and F. W. Parrish. Private communication. To be published in Cereal Chemistry.
4. H. C. Srivastava, K. V. Ramalingam, N. M. Doshi, and A. S. Chaudhari. Am. Chem. Soc. Absr. 156th Natl. Meeting, Sept. 8–13, 1968. P. Carb. 34.
5. J. E. Hook and Bengt Lindberg. Acta Chem. Scand. To be published.
6. E. J. Roberts and S. P. Rowland. Can. J. Chem. This issue.
7. E. J. Roberts and S. P. Rowland. Can. J. Chem. **45**, 261 (1967).
8. B. Helferich and J. Werner. Ber. **75**, 949 (1942).
9. L. P. Miller. Contribs. Boyce Thompson Inst. **11**, 25 (1940).

Fluoranthene studies. IV. Nitration of 2-nitro-, 3-nitro-, and 2-acetamido-fluoranthene

E. H. Charlesworth and Caroline U. Lithown
Department of Chemistry, The University of Manitoba, Winnipeg, Manitoba

Received November 27, 1968

Nitration of 3-nitrofluoranthene yields 3,9-dinitrofluoranthene, and nitration of 2-acetamidofluoranthene yields 2-acetamido-3-nitrofluoranthene. The orientation of both these compounds has been proved. Nitration of 2-nitrofluoranthene has given a dinitro product, but its orientation has not been established. A number of other new fluoranthene derivatives are described.

Canadian Journal of Chemistry, 47, 1595 (1969)

In 1964 Charlesworth and Blackburn (1) showed that 3-amino and 3-acetamidofluoranthene were brominated in pyridine solution in the 2-position. This was in agreement with the postulate of Kloetzel *et al.* (2) that a strongly activating substituent in the A ring would cause further substitution to occur in the same ring. Blackburn (3), in his experimental work and not mentioned in the above paper, describes a bromination of 3-acetamidofluoranthene (**3**) in acetic acid which gave a rather poor yield of a product, m.p. 265–266 °C. This product gave a large depression on mixing with 3-acetamido-2-bromofluoranthene and was not studied further at the time. Blackburn's concluding sentence reads "the possibility exists that this compound

Can. J. Chem. Downloaded from www.nrcresearchpress.com by 210.87.254.40 on 09/05/12
For personal use only.

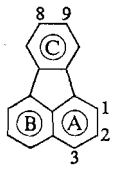

1

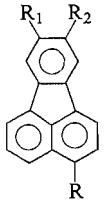

2 R = NO_2, $R_1 = R_2 = H$
3 R = $NHCOCH_3$, $R_1 = R_2 = H$
4 R = $NHCOCH_3$, R_1 = Br, $R_2 = H$
5 R = $NHCOCH_3$, $R_1 = H$, R_2 = Br
13 R = $R_2 = NO_2$, $R_1 = H$
14 R = $R_2 = NHCOCH_3$, $R_1 = H$
15 R = $R_2 = COCH_3$, $R_1 = H$

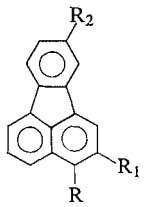

6 R = $R_2 = H$, $R_1 = NHCOCH_3$
7 R = NO_2, $R_1 = NHCOCH_3$, $R_2 = H$
8 R = NO_2, $R_1 = NH_2$, $R_2 = H$
10 R = NH_2, $R_1 = NHCOCH_3$, $R_2 = H$
11 R = $R_1 = NHCOCH_3$, $R_2 = H$
12 R = $NHCOCH_3$, $R_1 = NO_2$, $R_2 = H$

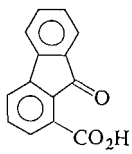

9

is an isomer of 3-acetamido-2-bromofluoranthene".

Kaminska and Mazonski (4) report the preparation of 3-acetamide-8-bromofluoranthene (**4**), m.p. 260–262 °C, by a bromination of the 3-acetamido derivative in a mixture of glacial acetic acid and carbon tetrachloride. We have repeated their bromination and find no melting point depression on mixing with Blackburn's product. Isolation of two different bromination compounds proves that not only directing substituents must be considered, but the solvents and conditions used in the bromination as well.

We have prepared a third bromo isomer, namely 3-acetamido-9-bromofluoranthene (**5**). This has been obtained by the reduction and acetylation of 3-nitro-9-bromofluoranthene prepared by the method of Campbell and Keir (5).

As the bromination of 2-nitro and 2-acetamidofluoranthene had been studied by Charlesworth and Dolenko (6), it now seemed desirable to undertake nitration studies of these two products. An attempt at nitration of 2-nitrofluoranthene was reported by Wilshire (7), but the orientation of the product was not established. Unfortunately we have not been able to obtain sufficient chromatographed product to work extensively with it. Mass spectral studies do not prove the position of the second nitro group, but the 8- or 9-position seems most probable.

Nitration of 2-acetamidofluoranthene (**6**) gave a mononitration product **7** and hydrolysis gave the 2-aminonitro product **8.** Deamination by diazotization and treatment with hypophosphorous acid gave the well-known 3-nitrofluoranthene (**2**), indicating that the nitro group had entered position-3. Oxidation of 2-amino-3-nitrofluoranthene (**8**) gave 1-fluorenone carboxylic acid (**9**), which is further proof that the nitro group had entered the A ring. Catalytic reduction of 2-acetamido-3-nitrofluoranthene (**7**) gave the rather crude 2-acetamido-3-aminofluoranthene (**10**). Acetylation gave 2,3-diacetamidofluoranthene (**11**) identical with that prepared by Kloetzel, King, and Menkes (2) from 3-acetamido-2-nitrofluoranthene (**12**).

Further nitration of 3-nitrofluoranthene (**2**) was attempted by Wilshire (7), but gave only a very crude product of m.p. 180–280° which was not studied further. By nitration at 70–80° in acetic anhydride with fuming nitric acid, we obtained dinitro product (**13**) which after several purifications by thin–layer chromatography (t.l.c.) and finally sublimation *in vacuo*, appeared to be reasonably pure. The corresponding diamine obtained by reduction was isolated in the form of its diacetamido derivative (**14**). No depression in melting point occurred on mixing with an authentic sample of 3,9-diacetamidofluoranthene (**14**), prepared from 3,9-diacetyl-

Can. J. Chem. Downloaded from www.nrcresearchpress.com by 210.87.254.40 on 09/05/12
For personal use only.

fluoranthene (**15**) by a Schmidt reaction with sodium azide, as described by Campbell *et al.* (9). Both samples of diacetamidofluoranthene also gave identical infrared (i.r.) and ultraviolet (u.v.) spectra. This evidence proves the 3,9-orientation of the dinitro compound. This 3,9-dinitrofluoranthene was extremely stable to oxidation and no dinitro fluorenone carboxylic acid was isolated.

Experimental

Melting points are corrected and have been determined on a Fisher–Johns melting point apparatus. The following instruments have been used, a Perkin–Elmer 450 spectrophotometer for u.v., a Perkin–Elmer 137 spectrophotometer for i.r., and a Hitachi Perkin–Elmer RMU 6 D mass spectrometer.

3-Nitrofluoranthene (**2**) was prepared from fluoranthene (**1**) by the method of Garascia *et al.* (8), reduced to 3-aminofluoranthene, and acetylated to the 3-acetamido derivative (**3**) by following the directions of Kloetzel *et al.* (2).

2-Nitrofluoranthene was produced from fluoranthene in seven steps, as also described by Kloetzel *et al.* (2). In three further steps also described by them the 2-nitrofluoranthene was changed to 2-acetamidofluoranthene (**6**).

3-Acetamido-8-bromofluoranthene (4)[1]

Bromine (1.0 ml) in glacial acetic acid (25 ml) was added dropwise over a period of 20 min to a stirred solution of 3-acetamidofluoranthene (2.0 g) in glacial acetic acid (190 ml) at 80 °C. The mixture was stirred at 80 °C for a further 35 min during which time a small amount of precipitate separated. This crude product was filtered and crystallized from chlorobenzene (charcoal). It melted at 249–250 °C. On further crystallization from pyridine it melted at 265–266 °C. There was no depression of melting point on mixing with a sample of 3-acetamido-8-bromofluoranthene, m.p. 260–262 °C, prepared by the bromination directions of Kaminska and Mazonski (4). The i.r. and u.v. spectra of the two samples also confirmed their identity. Infrared peaks (Nujol) are at 3.13, 6.01, 6.52, and 7.84 μ.

There is a large melting point depression on mixing with a sample of 3-acetamido-2-bromofluoranthene, m.p. 266–267 °C as prepared by Charlesworth and Blackburn (1).

3-Acetamido-9-bromofluoranthene (5)

3-Amino-9-bromofluoranthene obtained by Campbell and Keir (5) by reduction of 3-nitro-9-bromofluoranthene with iron powder was prepared by us, by reduction with platinum as described by Charlesworth and Dolenko (6) for the corresponding 2-acetamido-9-bromofluoranthene. Acetylation of Campbell and Keir's amine gave the apparently hitherto unprepared 3-acetamido-9-bromofluoranthene. It was obtained as light-yellow needles, m.p. 280–281 °C from chlorobenzene.

Anal. Calcd. for $C_{18}H_{12}ONBr$: N, 4.1; Br, 23.6. Found: N, 4.0, Br, 23.9.

Infrared peaks for this compound (Nujol mull) are at 3.23, 6.15, 5.60, and 7.90 μ. Admixture with 3-acetamido-8-bromofluoranthene gave a melting point depression of at least 30°.

Nitration of 2-Nitrofluoranthene

Fuming (95%) nitric acid (1 ml) was added dropwise with stirring to a solution of 2-nitrofluoranthene (0.5 g) in freshly distilled acetic anhydride (15 ml). The solution was refluxed for 3 h, cooled to room temperature, and allowed to stand overnight. The solid (0.15 g) which precipitated out of solution was filtered, washed with water, dried, and dissolved in benzene. The benzene solution was chromatographed on a column (12 in. × ½ in.) filled with alumina (Brockman, neutral, activity I) and the dinitrofluoranthene was eluted in the first portion. The pure 2,(?)-dinitrofluoranthene (0.08 g) was isolated from acetone as bright-yellow needles, m.p. 345–347 °C (sublimation).

Anal. Calcd. for $C_{16}H_8O_4N_2$: N, 9.59. Found: N, 9.60.

Infrared peaks (Nujol) are at 6.55 and 7.43 μ. Mass spectra: M^+/e; 292, 276, 262, 246, 234, 216, 202, 200.

2-Acetamido-3-nitrofluoranthene (7)

2-Acetamidofluoranthene (1.3 g) was dissolved at 80–85 °C in glacial acetic acid (130 ml) to which acetic anhydride (10 drops) had been added. Concentrated nitric acid (0.66 ml) was added dropwise and the solution stirred at the aforementioned temperature for 3 h. The reaction mixture was then allowed to stand at room temperature in an open vessel for 2 days. During this time, most of the solvent evaporated and black crystals (0.8 g) of m.p. 150–153 °C were formed. On recrystallization from glacial acetic acid (charcoal) the 2-acetamido-3-nitrofluoranthene separated as golden-yellow micro crystals of m.p. 190–193 °C. It can also be obtained as bright yellow flocculent needles by crystallization from ethanol–water.

Anal. Calcd. for $C_{18}H_{12}O_3N$: N, 9.21. Found: N, 9.17.

Infrared peaks of this compound (Nujol) occur at 3.02, 5.97, 6.22, 6.57, and 7.27 μ.

2-Amino-3-nitrofluoranthene (8)

2-Acetamido-3-nitrofluoranthene (0.6 g) was hydrolyzed by refluxing for 3 h with a mixture of ethanol (33 ml, 95%) and concentrated hydrochloric acid (33 ml). After the reaction mixture had cooled it was neutralized with 10% aqueous sodium hydroxide solution, and the crude amine (0.5 g) collected. It was recrystallized from ethanol–water, dried in a vacuum desiccator, and then in a drying pistol over P_2O_5. It melted at 244–246 °C.

Anal. Calcd. for $C_{16}H_{10}O_2N_2$: N, 10.68. Found: N, 10.97.

Infrared peaks occur at 2.90, 3.02, 6.00, 6.27, 7.34, and 7.95 μ.

Deamination of 2-Amino-3-nitrofluoranthene

Sodium nitrite (0.09 g) was dissolved at room temperature in a solution of concentrated sulfuric acid (3.1 ml) and water (0.2 ml). The solution was cooled to −5 °C and powdered 2-amino-3-nitrofluoranthene (0.25 g) was carefully added at this temperature. The reaction mixture

[1]This was prepared with the assistance of B. J. Blackburn.

Can. J. Chem. Downloaded from www.nrcresearchpress.com by 210.87.254.40 on 09/05/12
For personal use only.

Can. J. Chem. Downloaded from www.nrcresearchpress.com by 210.87.254.40 on 09/05/12
For personal use only.

was stirred at the stated temperature for 30 min. Precooled 50% hypophosphorous acid (6.53 ml) was added over a period of 30 min such that the temperature did not exceed 5 °C. The reaction mixture was allowed to stand for 6 days at 2–3 °C, after which it was diluted with 3 volumes of water. The precipitate formed was filtered, washed with sodium hydroxide solution (10%) and water. After drying, it was recrystallized from glacial acetic acid and gave pure 3-nitrofluoranthene (0.12 g) m.p. 156–158 °C.

Anal. Calcd. for $C_{16}H_9O_2N$: N, 5.76. Found: N, 5.57.

A mixed m.p. with an authentic sample of 3-nitrofluoranthene prepared by direct nitration of fluoranthene gave no depression. Infrared and u.v. spectra of the two specimens also confirmed their identity. Infrared peaks (Nujol) are at 6.24, 6.62, and 7.56 μ.

Oxidation of 2-Amino-3-nitrofluoranthene

A solution of chromic anhydride (1.5 g) in water (2 ml) and glacial acetic acid (2 ml) was added over a period of 10 min to a boiling suspension of 2-amino-3-nitrofluoranthene (0.4 g) in glacial acetic acid (20 ml). The mixture was refluxed for 4 h and then poured into dilute sulfuric acid solution (50 ml, 1:4 v/v) and allowed to stand at room temperature overnight. The separated solid was filtered, washed with dilute acid, then water and allowed to dry. It was purified by dissolving in 5% sodium carbonate solution, filtering out a small amount of insoluble material. The acid was reprecipitated by acidification with 25% sulfuric acid, collected, and dried. On crystallization from acetic acid, fluorenone-1-carboxylic acid (**9**) was obtained as orange needles (0.12 g) which melted at 191–193 °C.

Admixture with an authentic sample of fluorenone-1-carboxylic acid prepared by the oxidation of fluoranthene gave no melting point depression. Infrared spectra of the two specimens were also identical.

*2-Acetamido-3-aminofluoranthene (**10**)*

2-Acetamido-3-nitrofluoranthene (0.5 g) and palladium–charcoal catalyst (0.056 g) were suspended in absolute ethanol (21 ml). The suspension was hydrogenated at a pressure of 21 p.s.i. for 24 h. The product was brought into solution by adding pyridine (25 ml) and heating. The catalyst was filtered and most of the solvent evaporated under vacuum. Crude 2-acetamido-3-aminofluoranthene (0.38 g) precipitated on dilution with water. It was recrystallized from pyridine as a bright yellow solid (0.28 g) which melted at 204–206 °C.

Anal. Calcd. for $C_{18}H_{14}ON_2$: N, 10.21. Found: N, 8.85.

As this analysis indicates a rather crude amine it was purified by t.l.c. on silica gel. The plate was developed five times using (*a*) chloroform – 1%methanol; (*b*) chloroform – 3%methanol, (*c*) chloroform – 5%methanol, (*d*) chloroform – 7%methanol, and (*e*) chloroform – 10% methanol. The lowest band on extraction gave yellow needles, m.p. 235–236 °C.

Anal. Calcd. for $C_{18}H_{14}ON_2$: N, 10.21. Found: N, 10.97.

*2,3-Diacetamidofluoranthene (**11**)*

Impure 2-acetamido-3-aminofluoranthene (0.15 g) was dissolved in pyridine (25 ml) and acetic anhydride (4 drops) was added. The solution was stirred at room temperature for 90 min and allowed to stand for 2 h to allow some of the pyridine to evaporate. A bright yellow solid precipitated and was crystallized from glacial acetic acid as cream colored microcrystals (0.13 g). These melted at 262–263 °C and the m.p. was not depressed by admixture with 2,3-diacetamidofluoranthene of m.p. 267–268 °C prepared as described by Kloetzel, *et al.* (2). Comparison of i.r. and u.v. spectra of the two samples confirmed the identity of the two samples.

*3,9-Dinitrofluoranthene (**13**)*

Fuming (95%) nitric acid (2 ml) was added dropwise, over a period of 10 min, to a mixture of 3-nitrofluoranthene (2.0 g) in acetic anhydride (60 ml) maintained at 65–71 °C. The nitration mixture was stirred at 70–80 °C for 30 min and then allowed to stand at room temperature for a further 90 min. The solid (1.5 g) was filtered and washed with water. After two crystallizations from glacial acetic acid (charcoal) it was obtained as yellow-orange crystals (0.75 g), of m.p. 275–276 °C.

Anal. Calcd. for $C_{10}H_8N_2O_4$: N, 9.60. Found: N, 10.26.

The somewhat high nitrogen suggested the presence of a little trinitrofluoranthene, so the product was developed twice by t.l.c. on silica gel and finally sublimed at 150° *in vacuo*.

Anal. Calcd. for $C_{16}H_8N_2O_4$: C, 65.7; H, 2.76; N, 9.60. Found: C, 64.7; H, 2.73; N, 9.56.

Oxidative treatment of the dinitro compound with chromic anhydride in the conventional manner in an attempt to isolate a substituted fluorenone was unsuccessful. Unchanged starting product only was isolated.

*3,9-Diacetamidofluoranthene (**14**)*

3,9-Dinitrofluoranthene (1.5 g), and palladium–charcoal (0.25 g) were suspended in ethanol (100 ml). The dinitro compound was reduced with hydrogen under pressure (26–23 p.s.i.) for 6 h. The catalyst was filtered off and the solvent evaporated to about 10 ml. The solution of the diamine was unstable and darkened quickly, so it was isolated as its diacetyl derivative, by adding pyridine (25 ml) and acetic anhydride (5 ml). The mixture was stirred at room temperature for 10 h. The excess solvent was evaporated *in vacuo* and the cream colored solid which separated was filtered and crystallized from benzene. The 3,9-diacetamidofluoranthene (0.9 g) was isolated as a light-yellow solid, m.p. ~ 360 °C (lit. ref. 9, 370 °C).

Admixture with an authentic sample of 3,9-diacetamidofluoranthene prepared from 3,9-diacetylfluoranthene by a Schmidt reaction with sodium azide according to the directions of Campbell, *et al.* (9), did not depress the melting point. These workers established the orientation by conversion of the 3,9-diamino dihydrobromide by a Sandmeyer reaction into 3,9-dibromofluoranthene. Our own attempts to pass from the crude 3,9-diamine to the 3,9-dibromo compound were unsuccessful.

Comparison of i.r. and u.v.s pectra of the two samples of the diacetamidofluoranthene confirmed their identity.

Acknowledgments

The authors are grateful to the National Research Council of Canada for a grant-in-aid

of this research and to the University of Manitoba for a graduate student Fellowship awarded to one of us (C. U. L.). We extend our thanks to Mr. C. Reichert and Dr. J. Westmore of this department for the mass spectra and interpretation thereof.

1. E. H. CHARLESWORTH and B. J. BLACKBURN. Can. J. Chem. **42**, 353 (1964).
2. M. C. KLOETZEL, W. KING, and J. H. MENKES. J. Am. Chem. Soc. **78**, 1165 (1956).
3. B. J. BLACKBURN. M.Sc. Thesis, University of Manitoba, Winnipeg, Manitoba. 1963.
4. B. KAMINSKA and T. MAZONSKI. Roczniki Chem. **40**, 65 (1966); Chem. Abstr. **65**, 3809 *g* (1965).
5. N. CAMPBELL and N. H. KEIR. J. Chem. Soc. 1233 (1955).
6. E. H. CHARLESWORTH and A. J. DOLENKO. Can. J. Chem. **45**, 96 (1967).
7. J. F. L. WILSHIRE. Ph.D. Thesis, University of Edinburgh, Edinburgh, Scotland. 1952.
8. R. J. GARASCIA, E. F. FRIES, and C. CHING. J. Org. Chem. **17**, 226 (1952).
9. N. CAMPBELL, W. K. LEADILL, and J. F. K. WILSHIRE. J. Chem. Soc. 1404 (1951).

Electron impact-induced rearrangements of acetylenic compounds[1]

R. T. APLIN
Dyson Perrins Laboratory, Oxford, England

AND

S. SAFE
Atlantic Regional Laboratory, National Research Council of Canada, Halifax, Nova Scotia

Received September 18, 1968

The mass spectra of all-*trans*-hepta-2,4-dien-6-yn-1-ol (**3**) and all-*trans*-hepta-2,4-dien-6-yn-1-al (**6**) are remarkably similar to benzyl alcohol and benzaldehyde respectively. Comparison of α-*d*-all-*trans*-hepta-2,4-dien-6-yn-1-ol (**5**) and α-*d*-benzyl alcohol shows that the deuterium in the $C_7H_7^+$ tropylium ion is randomized in both compounds.

Canadian Journal of Chemistry, 47, 1599 (1969)

A problem of mass spectrometry concerns the formation of the $C_7H_7^+$ tropylium ion and other stable aromatic species. Acetylenic compounds of the type (**1**) undergo extensive rearrangement to give the $C_{11}H_9^+$ ion (**2**), as a major fragment (1). The C_7 acetylenic alcohol (**3**) possesses the yne-diene chromophore which is often contained in more complex polyacetylenes and upon electron impact affords a spectrum which resembles

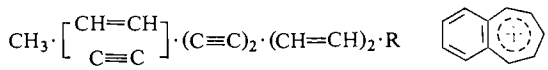

1 **2**

R = —CH_2OH, —CH_2OAc, —$CH_2CH_2CH_2OH$, —$(CH_2)_4 \cdot CH{=}CH_2$, —$CH(OH)(CH_2)_3 \cdot CH{=}CH_2$

that of benzyl alcohol (**4**). A comparison of the fragmentation patterns is shown in Fig. 1. In addition it has been previously shown (3, 4) that the mass spectra of toluene and several of

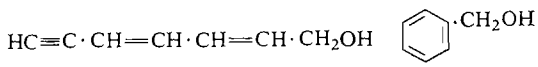

3 **4**

its acyclic C_7H_8 isomers are also similar, each giving a strong $C_7H_7^+$ tropylium ion. The formation of the $C_7H_7^+$ ion from benzyl alcohol (**4**) and several of its deuterated derivatives occurs with complete hydrogen (or deuterium) and carbon scrambling (5–8). Recently, however, Meyerson *et al.* (9) have shown that the statistics for diphenylmethane-α-d_2 fragmentation support tropylium-1,2-d_2 as the precursor for the $C_5H_5^+$ ion. Bohlmann and his co-workers (2) have examined the spectra of several acetylenic compounds in which both the $C_{11}H_9^+$ and $C_7H_7^+$ ions are assigned linear structures in which hydrogen scrambling has not occurred.

We have now determined the mass spectrum of the deuterated alcohol (**5**) and compared it with that of α-*d*-benzyl alcohol. Examination of the $C_5H_5^+$ and $C_5H_4D^+$ ions indicates that for

[1]NRCC No. 10529.

Can. J. Chem. Downloaded from www.nrcresearchpress.com by 210.87.254.40 on 09/05/12
For personal use only.

of this research and to the University of Manitoba for a graduate student Fellowship awarded to one of us (C. U. L.). We extend our thanks to Mr. C. Reichert and Dr. J. Westmore of this department for the mass spectra and interpretation thereof.

1. E. H. CHARLESWORTH and B. J. BLACKBURN. Can. J. Chem. **42**, 353 (1964).
2. M. C. KLOETZEL, W. KING, and J. H. MENKES. J. Am. Chem. Soc. **78**, 1165 (1956).
3. B. J. BLACKBURN. M.Sc. Thesis, University of Manitoba, Winnipeg, Manitoba. 1963.
4. B. KAMINSKA and T. MAZONSKI. Roczniki Chem. **40**, 65 (1966); Chem. Abstr. **65**, 3809 *g* (1965).
5. N. CAMPBELL and N. H. KEIR. J. Chem. Soc. 1233 (1955).
6. E. H. CHARLESWORTH and A. J. DOLENKO. Can. J. Chem. **45**, 96 (1967).
7. J. F. L. WILSHIRE. Ph.D. Thesis, University of Edinburgh, Edinburgh, Scotland. 1952.
8. R. J. GARASCIA, E. F. FRIES, and C. CHING. J. Org. Chem. **17**, 226 (1952).
9. N. CAMPBELL, W. K. LEADILL, and J. F. K. WILSHIRE. J. Chem. Soc. 1404 (1951).

Electron impact-induced rearrangements of acetylenic compounds[1]

R. T. APLIN
Dyson Perrins Laboratory, Oxford, England

AND

S. SAFE
Atlantic Regional Laboratory, National Research Council of Canada, Halifax, Nova Scotia

Received September 18, 1968

The mass spectra of all-*trans*-hepta-2,4-dien-6-yn-1-ol (**3**) and all-*trans*-hepta-2,4-dien-6-yn-1-al (**6**) are remarkably similar to benzyl alcohol and benzaldehyde respectively. Comparison of α-*d*-all-*trans*-hepta-2,4-dien-6-yn-1-ol (**5**) and α-*d*-benzyl alcohol shows that the deuterium in the $C_7H_7^+$ tropylium ion is randomized in both compounds.

Canadian Journal of Chemistry, 47, 1599 (1969)

A problem of mass spectrometry concerns the formation of the $C_7H_7^+$ tropylium ion and other stable aromatic species. Acetylenic compounds of the type (**1**) undergo extensive rearrangement to give the $C_{11}H_9^+$ ion (**2**), as a major fragment (1). The C_7 acetylenic alcohol (**3**) possesses the yne-diene chromophore which is often contained in more complex polyacetylenes and upon electron impact affords a spectrum which resembles

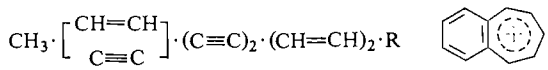

1 **2**

R = —CH_2OH, —CH_2OAc, —$CH_2CH_2CH_2OH$, —$(CH_2)_4 \cdot CH{=}CH_2$, —$CH(OH)(CH_2)_3 \cdot CH{=}CH_2$

that of benzyl alcohol (**4**). A comparison of the fragmentation patterns is shown in Fig. 1. In addition it has been previously shown (3, 4) that the mass spectra of toluene and several of

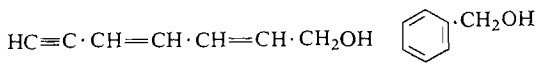

3 **4**

its acyclic C_7H_8 isomers are also similar, each giving a strong $C_7H_7^+$ tropylium ion. The formation of the $C_7H_7^+$ ion from benzyl alcohol (**4**) and several of its deuterated derivatives occurs with complete hydrogen (or deuterium) and carbon scrambling (5–8). Recently, however, Meyerson *et al.* (9) have shown that the statistics for diphenylmethane-α-d_2 fragmentation support tropylium-1,2-d_2 as the precursor for the $C_5H_5^+$ ion. Bohlmann and his co-workers (2) have examined the spectra of several acetylenic compounds in which both the $C_{11}H_9^+$ and $C_7H_7^+$ ions are assigned linear structures in which hydrogen scrambling has not occurred.

We have now determined the mass spectrum of the deuterated alcohol (**5**) and compared it with that of α-*d*-benzyl alcohol. Examination of the $C_5H_5^+$ and $C_5H_4D^+$ ions indicates that for

[1]NRCC No. 10529.

Can. J. Chem. Downloaded from www.nrcresearchpress.com by 210.87.254.5 on 09/05/12
For personal use only.

Can. J. Chem. Downloaded from www.nrcresearchpress.com by 210.87.254.5 on 09/05/12
For personal use only.

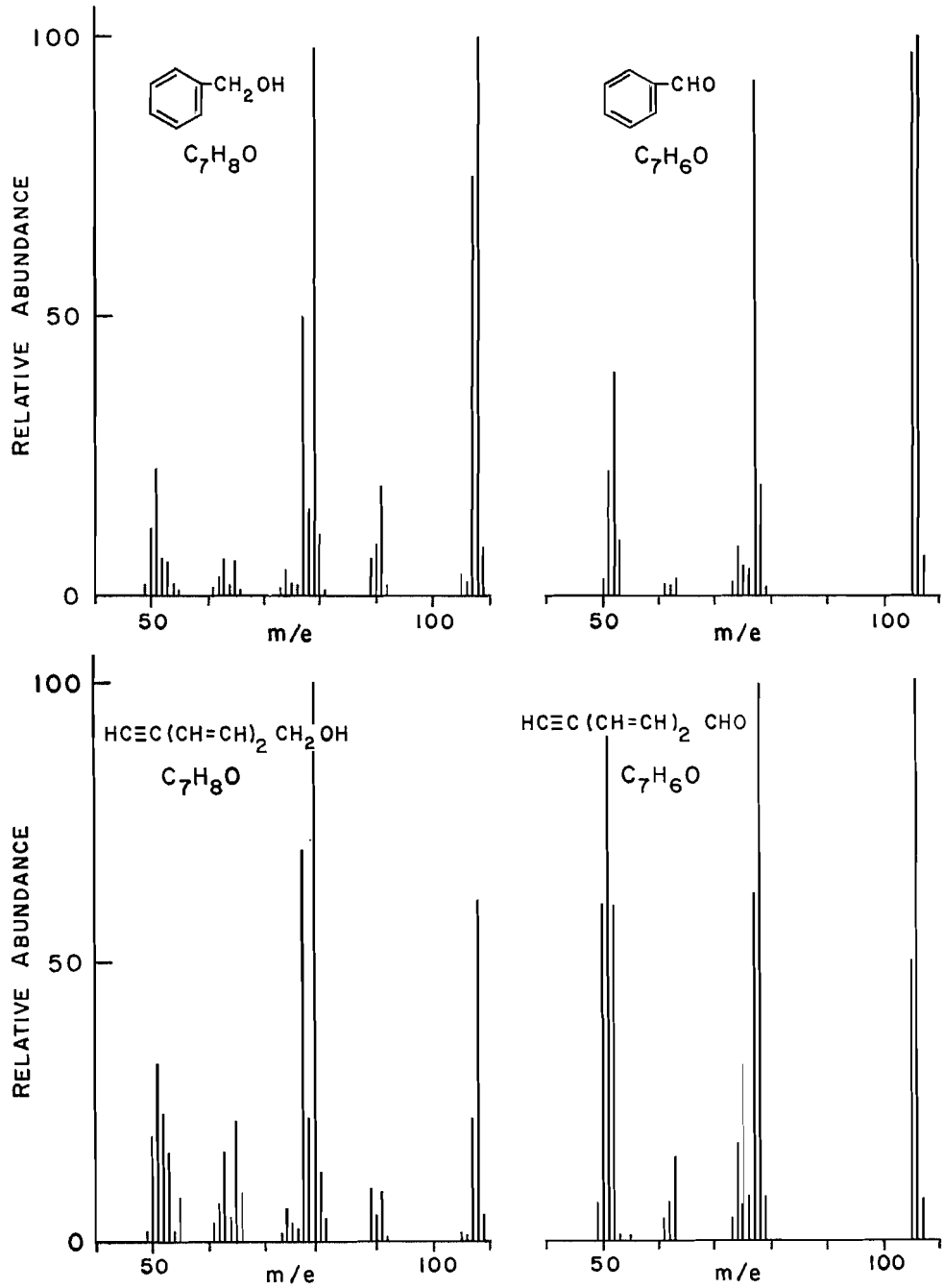

FIG. 1. A comparison of mass spectral fragmentation patterns.

the deuterated acetylenic alcohol (**5**), 74% of the deuterium is retained in the latter ion; the spectrum for α-*d*-benzyl alcohol shows 69% of the label retention (6) in the $C_5H_4D^+$ ion. These data are in agreement with 71% calculated for complete equilibration of the hydrogen atoms in the $C_7H_7^+$ precursor. The results obtained for the deuterated alcohol (**5**) and α-*d*-benzyl alcohol clearly indicate a common ion fragmentation pathway but the nature of the $C_7H_7^+$ ion, commonly designated as the tropylium moiety, is still not certain. The hydrogen atoms in the acetylenic

alcohols (**6**) and (**7**) are also equilibrated (12) in their decomposition to $C_9H_7^+$ (*m/e* 115) represented as the indene ion (1).

$$HC{\equiv}C\cdot CH{=}CH\cdot CH{=}CH\cdot CHDOH$$
5

$$CH_3\cdot(C{\equiv}C)_3\cdot CH{=}CH\cdot CH_2OH$$
6

$$CH_3\cdot CH{=}CH\cdot(C{\equiv}C)_2\cdot CH{=}CH\cdot CH_2OH$$
7

A comparison of the mass spectra of the acyclic C_7 aldehyde (**8**) and benzaldehyde (**9**) is shown in Fig. 1. In both spectra metastable ions at m* 104 (106 $\xrightarrow{-H\cdot}$ 105), m* 76 (78 $\xrightarrow{-H\cdot}$ 77), and m* 56.4 (105 $\xrightarrow{-CO}$ 77) are observed. Since some evidence has been reported that acetylenic compounds give prominent linear ions (2) this result raises some doubt about the cyclic nature

$HC{\equiv}C\cdot CH{=}CH\cdot CH{=}CH\cdot CHO$ **8**

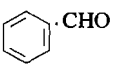

9

of the $C_6H_5^+$ ion (10) which is reported to be a prominent fragment in the mass spectra of benzaldehyde and several other monosubstituted phenyl derivatives.

Experimental

Mass spectra were measured with a Consolidated Electrodynamics Corporation 21-110B instrument using electrical detection. Samples were introduced by effusion of vapor from a glass reservoir at 80 °. Several spectra in sequence showed constancy of the mass spectral patterns and absence of thermal reactions in the inlet system.

All-trans-hepta-2,4-dien-6-yn-1-ol (3)

The alcohol (**3**) was prepared by the method of Bohlmann *et al.* (11) in which Zincke aldehyde (all-*trans*-5-methylanilinopentadienal) is converted into all-*trans*-hepta-2,4-dien-6-yn-1-al (**6**) by the action of lithium acetylide in liquid ammonia; the alcohol is readily obtained by sodium borohydride reduction of the corresponding aldehyde.

All deuterated derivatives were prepared by sodium borodeuteride reduction of the corresponding aldehydes.

1. R. T. Aplin and S. Safe. Chem. Commun. 140 (1967).
2. F. Bohlmann, C. Zdero, H. Bethke, and D. Schumann. Chem. Ber. **101**, 1553 (1968).
3. S. Meyerson, J. D. McCollum, and P. N. Rylander. J. Am. Chem. Soc. **83**, 1401 (1961).
4. V. Hanus and Z. Dolejsek. Kernenergie, **3**, 836 (1960).
5. S. Meyerson, P. N. Rylander, E. L. Eliel, and J. D. McCollum. J. Am. Chem. Soc. **81**, 2606 (1959).
6. H. M. Grubb and S. Meyerson. *In* Mass spectrometry of organic ions. *Edited by* F. W. McLafferty. Academic Press, Inc., New York. 1963. p. 453.
7. K. L. Rinehart, Jr., A. C. Buchholz, G. E. van Lear, and H. L. Cantrill. J. Am. Chem. Soc. **90**, 2983 (1968).
8. P. N. Rylander, S. Meyerson, and H. M. Grubb. J. Am. Chem. Soc. **79**, 842 (1957).
9. S. Meyerson, H. Hart, and L. C. Leitch. J. Am. Chem. Soc. **90**, 3419 (1968).
10. J. D. McCollum and S. Meyerson. J. Am. Chem. Soc. **85**, 1739 (1963).
11. F. Bohlmann, U. Hinz, A. Seyberlich, and J. Repplinger. Chem. Ber. **97**, 809 (1964).
12. R. T. Aplin, S. Safe, and M. Wright. Unpublished results.

Conformation of the esters of steroid hydroxyl groups by infrared spectroscopy

C. R. Narayanan, M. R. Sarma, T. K. K. Srinivasan, and M. S. Wadia[1]

National Chemical Laboratory, Poona, India[2]

Received September 30, 1968

Infrared spectral studies show that the carbonyl group of the esters of steroid hydroxyl groups are stabilized near the adjacent alkyl hydrogen atoms; this energy of stabilization appears to be more than that of hydrogen bonding between the carbonyl and a nearby hydroxyl group.

Canadian Journal of Chemistry, 47, 1601 (1969)

In their extensive studies on the infrared (i.r.) spectra of steroids, Jones and co-workers (1) had found as early as 1951 from the spectra of a number of isomeric steroid C_3-acetates, that the equatorial C_3-acetate shows a single strong band in the region 1200–1260 cm^{-1}, whereas the axial one shows two or three strong bands in the same region. This empirical correlation has been of

[1]Present address: Department of Chemistry, University of Poona, Poona 7, India.

[2]Communication No. 1226, National Chemical Laboratory, Poona 8, India.

Can. J. Chem. Downloaded from www.nrcresearchpress.com by 210.87.254.5 on 09/05/12
For personal use only.

alcohols (**6**) and (**7**) are also equilibrated (12) in their decomposition to $C_9H_7^+$ (*m/e* 115) represented as the indene ion (1).

$$HC{\equiv}C\cdot CH{=}CH\cdot CH{=}CH\cdot CHDOH$$
5

$$CH_3\cdot(C{\equiv}C)_3\cdot CH{=}CH\cdot CH_2OH$$
6

$$CH_3\cdot CH{=}CH\cdot(C{\equiv}C)_2\cdot CH{=}CH\cdot CH_2OH$$
7

A comparison of the mass spectra of the acyclic C_7 aldehyde (**8**) and benzaldehyde (**9**) is shown in Fig. 1. In both spectra metastable ions at m* 104 (106 $\xrightarrow{-H\cdot}$ 105), m* 76 (78 $\xrightarrow{-H\cdot}$ 77), and m* 56.4 (105 $\xrightarrow{-CO}$ 77) are observed. Since some evidence has been reported that acetylenic compounds give prominent linear ions (2) this result raises some doubt about the cyclic nature

$HC{\equiv}C\cdot CH{=}CH\cdot CH{=}CH\cdot CHO$ **8**

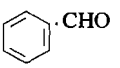

9

of the $C_6H_5^+$ ion (10) which is reported to be a prominent fragment in the mass spectra of benzaldehyde and several other monosubstituted phenyl derivatives.

Experimental

Mass spectra were measured with a Consolidated Electrodynamics Corporation 21-110B instrument using electrical detection. Samples were introduced by effusion of vapor from a glass reservoir at 80 °. Several spectra in sequence showed constancy of the mass spectral patterns and absence of thermal reactions in the inlet system.

All-trans-hepta-2,4-dien-6-yn-1-ol (3)

The alcohol (**3**) was prepared by the method of Bohlmann *et al.* (11) in which Zincke aldehyde (all-*trans*-5-methylanilinopentadienal) is converted into all-*trans*-hepta-2,4-dien-6-yn-1-al (**6**) by the action of lithium acetylide in liquid ammonia; the alcohol is readily obtained by sodium borohydride reduction of the corresponding aldehyde.

All deuterated derivatives were prepared by sodium borodeuteride reduction of the corresponding aldehydes.

1. R. T. Aplin and S. Safe. Chem. Commun. 140 (1967).
2. F. Bohlmann, C. Zdero, H. Bethke, and D. Schumann. Chem. Ber. **101**, 1553 (1968).
3. S. Meyerson, J. D. McCollum, and P. N. Rylander. J. Am. Chem. Soc. **83**, 1401 (1961).
4. V. Hanus and Z. Dolejsek. Kernenergie, **3**, 836 (1960).
5. S. Meyerson, P. N. Rylander, E. L. Eliel, and J. D. McCollum. J. Am. Chem. Soc. **81**, 2606 (1959).
6. H. M. Grubb and S. Meyerson. *In* Mass spectrometry of organic ions. *Edited by* F. W. McClafferty. Academic Press, Inc., New York. 1963. p. 453.
7. K. L. Rinehart, Jr., A. C. Buchholz, G. E. van Lear, and H. L. Cantrill. J. Am. Chem. Soc. **90**, 2983 (1968).
8. P. N. Rylander, S. Meyerson, and H. M. Grubb. J. Am. Chem. Soc. **79**, 842 (1957).
9. S. Meyerson, H. Hart, and L. C. Leitch. J. Am. Chem. Soc. **90**, 3419 (1968).
10. J. D. McCollum and S. Meyerson. J. Am. Chem. Soc. **85**, 1739 (1963).
11. F. Bohlmann, U. Hinz, A. Seyberlich, and J. Repplinger. Chem. Ber. **97**, 809 (1964).
12. R. T. Aplin, S. Safe, and M. Wright. Unpublished results.

Conformation of the esters of steroid hydroxyl groups by infrared spectroscopy

C. R. Narayanan, M. R. Sarma, T. K. K. Srinivasan, and M. S. Wadia[1]

National Chemical Laboratory, Poona, India[2]

Received September 30, 1968

Infrared spectral studies show that the carbonyl group of the esters of steroid hydroxyl groups are stabilized near the adjacent alkyl hydrogen atoms; this energy of stabilization appears to be more than that of hydrogen bonding between the carbonyl and a nearby hydroxyl group.

Canadian Journal of Chemistry, 47, 1601 (1969)

In their extensive studies on the infrared (i.r.) spectra of steroids, Jones and co-workers (1) had found as early as 1951 from the spectra of a number of isomeric steroid C_3-acetates, that the equatorial C_3-acetate shows a single strong band in the region 1200–1260 cm^{-1}, whereas the axial one shows two or three strong bands in the same region. This empirical correlation has been of

[1]Present address: Department of Chemistry, University of Poona, Poona 7, India.

[2]Communication No. 1226, National Chemical Laboratory, Poona 8, India.

Can. J. Chem. Downloaded from www.nrcresearchpress.com by 210.87.254.42 on 09/05/12
For personal use only.

TABLE I

Carbonyl frequencies of steroid hydroxyl esters

	Compound	Carbonyl frequencies (cm^{-1}) in CS_2	CCl_4	$CHCl_3$	Dioxan
4‡	Cholestan-3α-ol-acetate			1733	
5‡	Cholestan-3β,5α,6β-triol-3-methyl ether-6-acetate	1732 1718	1733 1721	1734 1726	1728
6‡	Cholestan-5α,6β-diol-6-acetate	1736 1710	1733 1723		1728
7‡	Cholestan-3β,5α,6β-triol-3-methyl ether 6-formate			1719 1710	
8*	Cholestan-3β,5α,6β-triol-3-methyl ether 6-benzoate	1710 1691	1718 1700		1712
9‡	Cholestan-4β,5α-diol-4-acetate		1735 1724		
10‡	Cholestan-3β,5α,6β-diol-3-methyl ether 5-acetate		1727 1713		1725
11†	Cholestan-6α-ol-acetate	1732	1732		
12‡	Cholestan-3β,5α,6α-triol-3-methyl ether 6-acetate	1732	1737		

*See experimental.
†Reference (5).
‡See ref. 4.

considerable use in determining the conformation of the hydroxyl group concerned in the formation of the acetate (2). The origin of these multiple bands was suggested by these authors, as due to the presence of an equilibrium mixture of labile rotational isomers resulting from hindrance to the rotation about one or both of the C—O bonds of the axial acetate group. No indication was given, however, for the actual conformation of these isomers. It was also implied in these arguments that the strong single band of the equatorial acetate was due to free rotation around the C—O bonds.

Recent optical rotatory dispersion (o.r.d.) studies have, however, shown that both the axial and the equatorial acetates of secondary hydroxyl groups in rigid systems as the steroids, have no free rotation in solution, but assume a preferred conformation (3). Nuclear magnetic resonance (n.m.r.) spectral studies of different esters of steroid hydroxyl groups also lead to the same conclusion and extend it to the esters of tertiary and primary hydroxyl groups (4). We now wish to report that i.r. spectral studies fully support the above conclusions.

The preferred conformation of the esters of steroid C_6 α- and C_6 β-hydroxyl groups can now be represented by **1** and **2** respectively (wherein the carbonyl group nearly eclipses the secondary hydrogen atom concerned), and that of the C_5 α-ester by **3** (wherein the carbonyl group is situated near to, and at an equal distance from, the C_4 α-H and the C_6 α-H) (4). Models would then show that in the steroid 5α,6β-diol monoesters of type **2** or **3** intermolecular hydrogen bonds would be possible between the ester carbonyl of one, and the free hydroxyl group of the other molecule. But intramolecular hydrogen bonds would not be possible as the minimum distance between the two would be over 3.5 Å. In the case of 5α,6α-diol-6-monoacetates of type

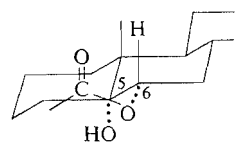

1

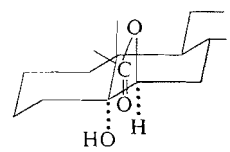

2

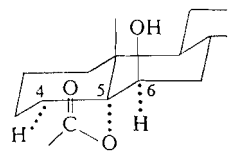

3

Can. J. Chem. Downloaded from www.nrcresearchpress.com by 210.87.254.42 on 09/05/12
For personal use only.

Can. J. Chem. Downloaded from www.nrcresearchpress.com by 210.87.254.42 on 09/05/12
For personal use only.

1 also, no intramolecular hydrogen bond would be possible if the acetate group is in conformation **1**, since the distance between the two is then over 4 Å. Intermolecular hydrogen bonds would also be difficult, because the other steroid molecule has to be near the highly hindered β-face of one molecule. Data collected from 9 steroid esters and given in Table I, fully support the above arguments.

The axial secondary acetate **4** which cannot form any hydrogen bond displays a single carbonyl absorption at about 1733 cm^{-1} in $CHCl_3$ solution, but **5** and **6** which have in addition a 5α-OH show an additional carbonyl band at a lower frequency in all the solvents tried, except dioxan. Similarly in the other esters **7** and **8** formate and benozate, an additional carbonyl band is found at a lower frequency. Compound **9**, which has its acetate at C_4, but with the same conformation as those at C_6, also behaves similarly. Compound **10** also (type **3**), as would be expected, shows an additional absorption at a lower frequency. The fact that the ratio of the intensity of the higher frequency band to that of the lower frequency band (it varies from 1.32 to 5.35 for compound **5**) is dependent on concentration (0.05–0.005 *M* solutions were used), with the corresponding changes in the OH absorption region, and the fact that, in dioxan solution, the lower frequency band completely disappears, clearly shows that the lower frequency band is due to intermolecular hydrogen bonding.

The 5α,6α-diol 6-equatorial monoacetate **12** shows only a single carbonyl absorption at the higher frequency, and that it is due to a non-bonded carbonyl is vouched for by the spectrum of the 6α-acetate, **11**. By rotating the carbonyl group of **1** through 180° along the C_6—O axis (when it would ultimately become 1,3-*cis*-diaxial with the C_5 α-OH), conformations can be obtained in which the carbonyl can readily form intermolecular or intramolecular hydrogen bonds. But the molecule does not appear to do so, in spite of the possible energy release by hydrogen bonding. Also in compounds of type **2**, intermolecular hydrogen bonding would have been difficult if the carbonyl had assumed other conformations in which it goes near the hindered β-face of the molecule. Thus, it would appear that the conformation of the ester carbonyl group of secondary hydroxyl groups are stabilized near the methine hydrogen atoms (and probably those of esters of tertiary and primary alcohol groups near the methine and methylene protons concerned), perhaps due to some intramolecular forces, which are not yet very clear (6). The energy of this stabilization of conformation, or that required to move it from the preferred conformation appears to be more than that gained by hydrogen bonding of the carbonyl with a favorably placed hydroxyl group, since the 6α-acetate carbonyl does not get hydrogen bonded to the 5α-OH.

This preferred conformation of the carbonyl group would at least partly account for the absence of hydrogen bonding noted in the ground state, between the carbonyl and hydroxyl groups, in the i.r. spectra of 1,3-*cis*-diol monoacetates (7).

Experimental

The spectra were determined in the solvents given, on a Perkin–Elmer Model 221 spectrophotometer, using a sodium chloride prism and grating. Concentrations varying from 0.05 to 0.005 *M* solutions were used. The intensities of peaks were measured by the areas enclosed by them.

8,Cholestan-3β,5α,6β-triol-3-methyl Ether-6-benzoate

Benzoyl chloride (2 ml) was added to a solution of cholestan-3β,5α,6β-triol-3-methyl ether (300 mg) in pyridine (2 ml) and left at room temperature overnight. The reaction mixture was then poured into ice cold water, extracted with ether, worked up in the usual way, and crystallized from methanol. Yield, 200 mg, m.p. 154°, $(\alpha)_D$ −26° (*c*, 1.0 in chloroform), ν_{max}, 3400 (hydroxyl) 1718, and 1700 cm^{-1} (ester carbonyl in CCl_4).

Anal. Calcd. for $C_{35}H_{54}O_4$: C, 78.02; H, 10.1. Found: C, 78.0; H, 10.2.

1. R. N. Jones, P. Humpheries, F. Herling, and K. Dobriner. J. Am. Chem. Soc. 73, 3215 (1951).
2. C. R. Narayanan and K. N. Iyer. Tetrahedron Letters, 285 (1966); C. R. Narayanan and M. R. Sarma. Tetrahedron Letters, 5695 (1966).
3. J. P. Jennings, W. P. Mose, and P. M. Scopes. J. Chem. Soc. C, 1102 (1967).
4. C. R. Narayanan and M. R. Sarma. Tetrahedron Letters, 1553 (1968).
5. C. W. Shoppe and G. H. R. Summers. J. Chem. Soc. 3361 (1952).
6. A. McL. Mathieson. Tetrahedron Letters, 4137 (1965).
7. H. B. Henbest and B. J. Lowell. J. Chem. Soc. 1965 (1957); R. West, J. J. Korst, and W. S. Johnson. J. Org. Chem. **25**, 1976 (1960).

Can. J. Chem. Downloaded from www.nrcresearchpress.com by 210.87.254.6 on 09/05/12
For personal use only.

Canadian Journal of Chemistry

Published by THE NATIONAL RESEARCH COUNCIL OF CANADA

VOLUME 47 MAY 15, 1969 NUMBER 10

Carbonyl ammine complexes of ruthenium(II)

A. D. ALLEN, T. ELIADES, R. O. HARRIS, AND P. REINSALU

Lash Miller Chemical Laboratories, University of Toronto, Toronto 5, Ontario

Received September 6, 1968

A series of carbonyl tetrammine and pentammine complexes of ruthenium(II) has been prepared. The compounds have been characterized by analytical techniques and by the reactions they undergo. Some carbonyl triammine and nitrogen tetrammine compounds are also reported.

Canadian Journal of Chemistry, 47, 1605 (1969)

Introduction

There have been several reports of substituted carbonyl complexes of ruthenium(II). These are generally of the type $[RuXYCOA_3]$ (1) and *cis*- and *trans*-$[RuXY(CO)_2A_2]$ (2) where X = Cl^-, Br^-, NCS^-; Y = H^-, Cl^-, Br^-, NCS^-; and A = PR_3, AsR_3 (R = alkyl or aryl), and $[RuS_2CO]$ and $[RuS_2(CO_2)]$ (3) where S = $R_2NCS_2^-$. No simple ammine carbonyls of ruthenium have been reported, but a number of similar complexes such as nitrosyl-pentammines (4) and -tetrammines (5), sulfur dioxide-tetrammines (6) and -pentammines (7), and nitrogen-pentammines (8) are known. We now report the preparation and characterization of some carbonyl–ammine–ruthenium(II) complexes and nitrogenaquotetrammine–ruthenium(II) complexes.

Experimental

The instruments used in this work were a Perkin–Elmer 521 infrared (i.r.) spectrophotometer (Nujol mull between KBr plates), a B and L 505 spectrophotometer (1 cm fused silica cells), and a Varian HA 100 nuclear magnetic resonance (n.m.r.) spectrometer. A Gouy balance was used for the magnetic susceptibilities. Micro-analyses were performed by A. B. Gygli, Toronto (see Table I).

Preparations

1. Chloropentammineruthenium(III) Dichloride, $[Ru(NH_3)_5Cl]Cl_2$

This was prepared by the method of Gleu (10) except that the oxidation of the hexammineruthenium(II) to hexammineruthenium(III) was carried out using bromine vapor instead of concentrated nitric acid (unpublished results). This method of oxidation has the advantage of excluding nitrate from the solution which, if not removed completely, tends to give insoluble brown products.

2. cis-Dichlorotetrammineruthenium(III) Chloride, cis-$[Ru(NH_3)_4Cl_2]Cl$

This was prepared by the method of Gleu and Cuntze (11) through the oxalatotetrammine.

3. trans-Chloro(sulfur dioxide)tetrammineruthenium-(II) Chloride, trans-$[Ru(NH_3)_4SO_2Cl]Cl$

This was prepared by the method of Gleu *et al.* (6).

4. Carbonylpentammineruthenium(II) Dihalide, $[Ru(NH_3)_5CO]X_2$ where X = Cl^-, Br^-, I^-

Chloropentammineruthenium(III) dichloride (1 g, 0.0034 mole) was dissolved in 0.1 *M* sulfuric acid (or 0.1 *M* formic acid). Freshly prepared amalgamated granulated zinc (2 g) was added. Carbon monoxide was passed through the stirred mixture for 2–3 h at room temperature. The appropriate anion was then added to the pale yellow filtrate. The colorless to pale yellow precipitate of $[Ru(NH_3)_5CO]X_2$ that formed on cooling was washed with cold water, alcohol, and ether, and air dried, yield 0.6 g (61.5%) for X = Cl^-. The product can be recrystallized from dilute ammonia.

5. cis-Aquocarbonyltetrammineruthenium(II) Dihalide, cis-$[Ru(NH_3)_4H_2OCO]X_2$ where X = Br^-, I^-

cis-Dichlorotetrammineruthenium(III) dichloride (1 g, 0.0036 mole) was dissolved in water and enough sulfuric acid (or formic acid) was added to bring the pH to 4.5–5.5. Freshly prepared amalgamated zinc (2 g) was added. Carbon monoxide was passed through the stirred solution at room temperature for 5 h while the pH of the solution was kept at about 4.5–5.5 by dropwise addition of dilute acid. Addition of the appropriate anion to the yellow filtrate gave, on cooling, a pale yellow precipitate of *cis*-$[Ru(NH_3)_4H_2OCO]X_2$, which was washed with alcohol and ether and air dried, yield 0.42 g (25%) for

Can. J. Chem. Downloaded from www.nrcresearchpress.com by 210.87.254.6 on 09/05/12
For personal use only.

TABLE I
Analytical results

Complex	% C		% H		% N		% X (halide)	
	Calculated	Found	Calculated	Found	Calculated	Found	Calculated	Found
$[Ru(NH_3)_5CO]Cl_2$	4.21	4.33	5.26	5.32	24.6	24.2	24.8	25.0
$[Ru(NH_3)_5CO]Br_2$	3.21	3.95	4.01	4.09	18.7	19.3	42.8	42.1
$[Ru(NH_3)_5CO]I_2$	2.56	2.53	3.21	3.01	15.0	14.6	54.2	53.6
cis-$[Ru(NH_3)_4COH_2O]Cl_2$							24.8	25.1
cis-$[Ru(NH_3)_4COH_2O]Br_2$	3.20	3.92	3.74	4.07	14.9	15.8	42.7	39.9
cis-$[Ru(NH_3)_4COH_2O]I_2$	2.56	3.03	2.99	2.99	11.9	12.8	54.2	52.2
trans-$[Ru(NH_3)_4COH_2O]Cl_2$	4.20	4.26	4.93	4.92	19.6	19.5	24.8	24.9
trans-$[Ru(NH_3)_4COH_2O]Br_2$	3.20	3.49	3.74	3.54	14.9	15.2	42.7	42.4
trans-$[Ru(NH_3)_4COH_2O]I_2$	2.56	2.61	2.99	2.97	11.9	12.6	54.2	53.6
trans-$[Ru(NH_3)_4(CO)NCS]NCS$	11.5	12.0	3.83	4.49	26.8	26.0	—	—
$[Ru(NH_3)_4H_2ON_2]Cl_2$	—	—	4.90	5.18	29.4	30.7	24.8	23.5
$[Ru(NH_3)_4H_2ON_2]Br_2$	—	—	3.73	3.96	22.4	23.8	42.7	40.2
$[Ru(NH_3)_4H_2ON_2]I_2$	—	—	2.99	3.06	17.9	18.0	54.1	52.9
$[Ru(NH_3)_3COCl_2]$	4.78	4.67	3.59	3.65	16.7	16.9	28.3	27.1
$[Ru(NH_3)_3COBr_2]$	3.53	3.70	2.65	2.65	12.3	11.9	47.1	45.8
$[Ru(NH_3)_3COI_2]$	2.77	2.81	2.06	1.94	9.6	9.6	58.5	56.2

Can. J. Chem. Downloaded from www.nrcresearchpress.com by 210.87.254.6 on 09/05/12
For personal use only.

X = I^-. The product can be recrystallized from dilute HX.

6. trans-Aquocarbonyltetramminеruthenium(II) Dihalide, trans-[Ru(NH$_3$)$_4$H$_2$OCO]X$_2$ where X = Cl$^-$, Br$^-$, I$^-$

trans - Chloro (sulfur dioxide) tetramminеruthenium (II) chloride (1 g, 0.0033 mole) was made into a slurry with 20 ml 0.1 *M* formic acid. Carbon monoxide gas was passed through the stirred mixture at 70° for 2–3 h. After about 1 h the starting material had dissolved to give a pale red solution, and as the reaction neared completion, the color slowly changed to yellow. Addition of the appropriate anion to the cooled filtrate gave a colorless to yellow precipitate of *trans*-[Ru(NH$_3$)$_4$H$_2$OCO]X$_2$ which was washed with ice-cold water, alcohol, and ether, and air dried, yield 0.8 g (84%) for X = I^-. The product may be recrystallized from hot dilute HX.

7. trans-Thiocyanatocarbonyltetramminеruthenium(II) Thiocyanate, trans-[Ru(NH$_3$)$_4$NCSCO]NCS

trans-Aquocarbonyltetramminеruthenium(II) dichloride (0.5 g, 0.0017 mole) was dissolved in 10 ml of warm water. To the clear colorless solution 5 ml of a saturated solution of sodium thiocyanate was added and the mixture was kept at 50° for 30 min. Colorless needle-like crystals of *trans*-[Ru(NH$_3$)$_4$NCSCO]NCS which formed on cooling to 0° were recrystallized from hot methanol, washed with ethanol and ether, and air dried, yield 0.4 g (70%).

8. Nitrogenaquotetramminеruthenium(II) Dihalide, [Ru(NH$_3$)$_4$H$_2$ON$_2$]X$_2$ where X = Cl, Br, I

cis-Dichlorotetramminеruthenium(III) chloride[1] (1 g, 0.0036 mole) was dissolved in 20 ml of water and excess sodium azide (2 g) was added to the solution, which was stirred at room temperature for 15 min. The resulting red solution was cooled to 10°. Acidification with methanesulfonic acid to pH 2, gave a vigorous reaction with evolution of gas and loss of color. Addition of the appropriate anion gave a colorless to pale yellow precipitate of [Ru(NH$_3$)$_4$H$_2$ON$_2$]I$_2$ which was recrystallized from dilute HX, washed with alcohol and ether, and air dried, yield 0.68 g (40%) for X = I. Nitrogenoaquotetrammine can also be prepared in poor yield from *cis*-dichlorotetramminеruthenium(III), by treatment with amalgamated zinc under nitrogen. A dimeric ion is first formed which on treatment with ammonia yields nitrogenoaquotetramminеruthenium(II).

Results and Discussion

Typical i.r. spectra are shown in Figs. 1–4 and summarized in Table II. By comparison with similar ruthenium complexes (8, 9), all bands can be assigned to coordinated ammonia vibrations, except for the following. In the carbonyl complexes a strong band in the region 1970–1890 cm^{-1}, is assigned to ν_{C-O} (Table III), and another two bands in the region 500–600 cm^{-1}, δ_{C-O} and ν_{M-C} (12–14). In the nitrogen complexes a strong band in the region 2120–2080 cm^{-1} is assigned to ν_{N-N} and another in the region 450–550 cm^{-1} to ν_{M-N} (8). A high energy shoulder on the ρ_{NH_3} band in the region 850–780 cm^{-1} for all aquotetrammine complexes is assigned to coordinated water (15).

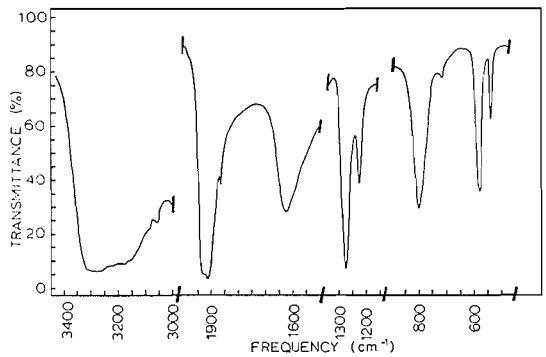

FIG. 1. Infrared spectrum of [Ru(NH$_3$)$_5$CO]Cl$_2$.

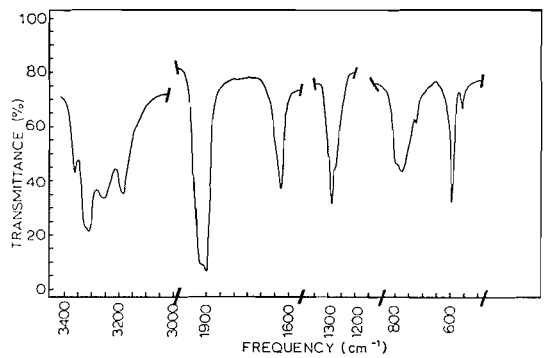

FIG. 2. Infrared spectrum of *cis*-[Ru(NH$_3$)$_4$H$_2$OCO]Cl$_2$.

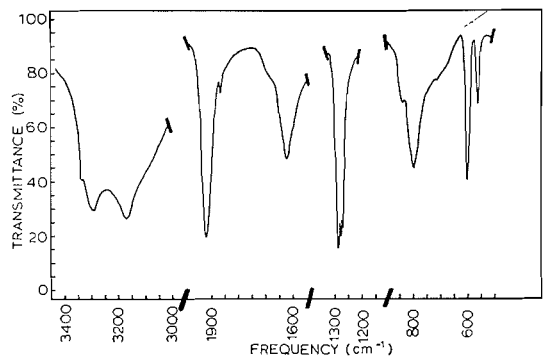

FIG. 3. Infrared spectrum of *trans*-[Ru(NH$_3$)$_4$H$_2$OCO]Cl$_2$.

[1] [Ru(NH$_3$)$_4$O$_x$]$_2$S$_2$O$_6$ may also be used as a starting material.

Can. J. Chem. Downloaded from www.nrcresearchpress.com by 210.87.254.6 on 09/05/12
For personal use only.

TABLE II

Vibrational frequencies (cm^{-1})* and assignments for the absorption bands for some ruthenium(II) and -(III) ammine complexes

Complex	ν_{N-H}	ν_{C-O}	δ_{NH_3asym}	δ_{NH_3sym}	ρ_{NH_3}	δ_{C-O}	ν_{M-C}	Others
$[Ru(NH_3)_5Cl]Cl_2$†	3405m 3208s,b	—	1610m	1290s	790m	—	—	—
cis-$[Ru(NH_3)_4Cl_2]Cl$‡	3400–3100vs,b	—	1620m	1292s	785m			
trans-$[Ru(NH_3)_4SO_2Cl]Cl$§	3300s,b	—	1625m	1280s	779m,b			ν_{S-Osym} 1100
	3170s			1304s				$\nu_{S-Oasym}$ 1248s δ_{S-O} 552m
trans-$[Ru(NH_3)_4H_2OCO]Cl_2$	3330s,b 3288vs,b 3165vs,b	1919vs 1868sh	1626m	1290s 1282s 1274s	797m	603m	562m	
trans-$[Ru(NH_3)_4H_2OCO]Br_2$	3277vs,b 3225vs,b 3165s,b	1924vs 1877sh	1620m	1291s 1282s 1274s	785m	596m	554m	
trans-$[Ru(NH_3)_4H_2OCO]I_2$	3275vs,b 3220vs,b 3168s,b	1938vs 1890sh	1606m	1292s 1286s 1281s	773m	587m	543m	
cis-$[Ru(NH_3)_4H_2OCO]Cl_2$	3344vs,b 3246vs,b 3180s,b	1921vs	1618m	1295sh 1277s 1265sh	780m	590w	551w	806sh
cis-$[Ru(NH_3)_4H_2OCO]Br_2$	3329vs,b 3235vs,b 3166s,b	1930vs	1610m	1290m 1269s 1258sh	782m	578m	539w	802sh
cis-$[Ru(NH_3)_4H_2OCO]I_2$	3285vs,b 3218s,b 3160s,b	1942vs	1601m	1288sh 1278s 1255sh	777m	569m	521w	800sh
$[Ru(NH_3)_5CO]Cl_2$•	3280s,b 3215s,b 3170s,b	1925vs 1876sh	1608m	1278s 1234m	790m	578m	532w	
$[Ru(NH_3)_5CO]Br_2$	3280s,b 3215s,b 3170s,b	1932vs 1878sh	1608m	1278s 1250m	790m	578m	532w	
$[Ru(NH_3)_5CO]I_2$	3290s,b 3220s,b 3175s,b	1943vs 1888sh	1606m	1285s 1250m	778m	572m	521w	

Can. J. Chem. Downloaded from www.nrcresearchpress.com by 210.87.254.6 on 09/05/12
For personal use only.

TABLE II (*concluded*)

Vibrational frequencies (cm^{-1})* and assignments for the absorption bands for some ruthenium(II) and -(III) ammine complexes

Complex	ν_{N-H}	ν_{C-O}	$\delta_{NH_3 asym}$	$\delta_{NH_3 sym}$	ρ_{NH_3}	δ_{C-O}	ν_{M-C}	Others
trans-$[Ru(NH_3)_4NCSCO]NCS$	3292s,b	1931vs	1620s	1315m	772m	606m	519w	ν_{C-N} 2118 2050
	3233s,b	1923vs		1294vs				ν_{C-S} 800
	3175s,b	1887sh		1276m				745
$[Ru(NH_3)_3COCl_2]$	3352s	1896s	1619m	1290sh	760w,b	592m	552w	
	3311s,b	1914sh		1278s				
	3252s			1266sh				
	3176s,b							
$[Ru(NH_3)_3COBr_2]$	3344s	1905s	1611m	1275sh	760w,b	571m	546w	
	3303s,b	1918sh		1240s				
	3241s			1212sh				
	3174s							
$[Ru(NH_3)_3COI_2]$	3332s	1914vs	1601m	1285sh	750w,b	561m	538w	582
	3300s,b			1265s				
	3226s							
	3168s,b							
		ν_{N-N}						ν_{M-N} sh
$[Ru(NH_3)_4H_2ON_2]Cl_2$	3290s,b	2088s	1618m	1288s	798m			506 820
	3250s,b							
	3130s,b							
		ν_{N-N}						ν_{M-N} sh
$[Ru(NH_3)_4H_2ON_2]Br_2$	3290vs,b	2102vs	1607m	1282s	782m			498 813
	3230s,b							
	3110s,b							
		ν_{N-N}						ν_{M-N} sh
$[Ru(NH_3)_4H_2ON_2]I_2$	3280vs,b	2115vs	1604m	1275s	777m			491 820
	3240s,b							
	3110s,b							

*Abbreviations: s = strong; v = very; m = medium; b = broad; sh = shoulder; w = weak; asym = asymmetric; sym = symmetric.

†See ref. 9.

‡Unpublished results.

§The infrared spectrum of this compound was reported by Vogt *et al.* (18), who assigned the bands at 1304 and 1280 cm^{-1} to SO stretching vibrations and the band at 1245 cm^{-1} to the δ_{NH_3} symmetric vibration. We have found that the bands at 1340 and 1280 cm^{-1} shift to 1062 and 998 cm^{-1} on deuteration, the band at 1248 cm^{-1} being unshifted. We have, therefore, assigned the bands at 1304 and 1280 cm^{-1} to δ_{NH_3} symmetric vibrations and the band at 1248 cm^{-1} to SO stretching vibrations. We also found that ν_{NH_3} vibrations (3300, 3170 cm^{-1}) were at lower frequency than reported by Vogt *et al.*

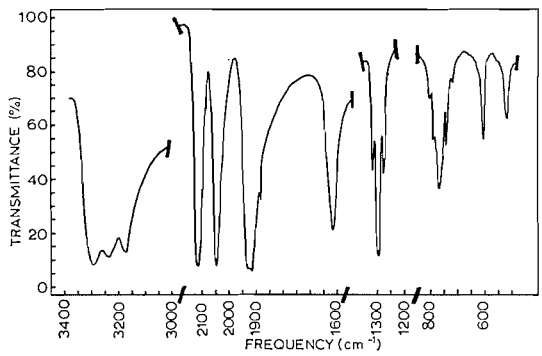

FIG. 4. Infrared spectrum of *trans*-$[Ru(NH_3)_4NCSCO]NCS$.

In the case of the thiocyanato carbonyl complex, two additional bands at 2118 and 2050 cm^{-1} are assigned to coordinated ν_{C-N} and free (ionic) ν_{C-N} respectively, and two bands at 800 and 745 cm^{-1} are assigned to coordinated ν_{C-S} and ionic ν_{C-S}. On the basis of the i.r. spectrum (Fig. 4) it appears that the thiocyanate is coordinated through the nitrogen rather than the sulfur (16). Replacement of ionic thiocyanate by iodide (by ion exchange) removes the two bands assigned to the free thiocyanate (2050, 745 cm^{-1}).

The electronic spectra of these complexes in aqueous solution have been examined in the region 200–600 mμ. Spectra of all the carbonyl complexes are similar, with absorption maxima in the region 275–290 mμ, $\varepsilon_{max} \simeq 200$–300. The nitrogen complex shows a strong absorption at 220 mμ with $\varepsilon_{max} \simeq 13\,000$.

The p.m.r. spectra were taken in D_2O. The *trans*-aquocarbonyl complex (**1**) should show a single band, corresponding to 4 equivalent ammonia ligands. The carbonylpentammine (**2**) should show two bands, in the ratio 1:4, one for the ammonia *trans* to the carbonyl and one for the four ammonias *cis* to the carbonyl. The *cis*-aquocarbonyl isomer (**3**) should exhibit three bands, in the ratio 1:1:2, one from the ammonia *trans* to the carbonyl, one from the ammonia *trans* to the aquo group, and one for the two ammonia ligands *trans* to each other.

TABLE III

C—O Stretching frequencies (cm^{-1}) of some ruthenium carbonyls in Nujol mulls

Complex	ν_{C-O}
$[Ru\{(CH_3)_2NCS_2\}CO]$*	1916
$[Ru(NCS)_2CO(PMe_2Ph)_3]$†	1968
$[RuCl_2(CO)(PMe_2Ph)_3]$†	1961
$[RuHCl(CO)(PEt_2Ph)_3]$‡	1910
$[Ru(NH_3)_5CO]Cl_2$	1919
trans-$[Ru(NH_3)_4NCSCO]NCS$	1923,1931
trans-$[Ru(NH_3)_4H_2OCO]I_2$	1938
cis-$[Ru(NH_3)_4H_2OCO]I_2$	1932
$[Ru(NH_3)_3COI_2]$	1916

*See ref. 3.
†See ref. 1.
‡See ref. 2.

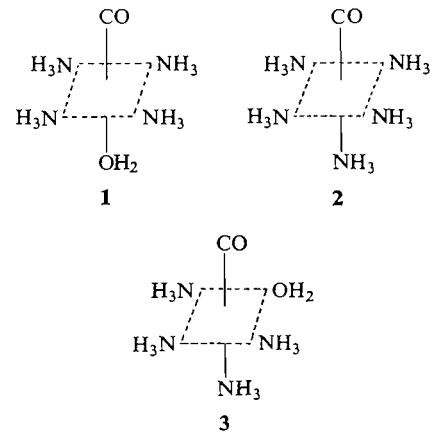

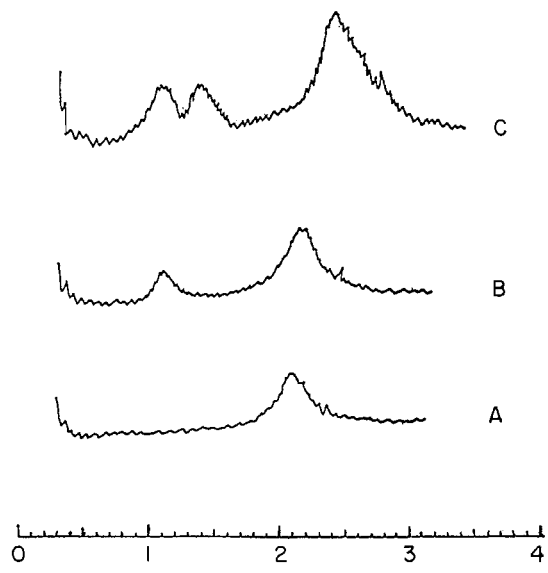

FIG. 5. Nuclear magnetic resonance spectra: *A*, *trans*-$[Ru(NH_3)_4H_2OCO]Cl_2$; *B*, $[Ru(NH_3)_5CO]Cl_2$; *C*, *cis*-$[Ru(NH_3)_4H_2OCO]Cl_2$.

Figure 5 shows the n.m.r. spectra obtained. The required bands are observed in approximately the correct ratios (the *cis*-aquocarbonyl isomer ratio is closer to 1:1:3). Exchange between the com-

Can. J. Chem. Downloaded from www.nrcresearchpress.com by 210.87.254.6 on 09/05/12
For personal use only.

plexes and the deuterated solvent reduced the quality of these spectra, and may account for the poor quantitative result, but the presence of the right number of bands supports other strong evidence in favor of the formulations given for these isomers.

Magnetic Measurements

All the complexes are diamagnetic at room temperature, consistent with spin-paired d^6 ruthenium(II).

Conductivity Measurements

Conductivities were measured in dimethyl sulfoxide in the concentration range 10^{-5} to 10^{-4} *M* at 24°. The results obtained (Fig. 6) indicate that all of the complexes are 2:1 electrolytes except the *trans*-$[Ru(NH_3)_4CONCS]NCS$, which is a 1:1 electrolyte. Halide analysis of the iodide salt of the carbonyl thiocyanato complex gave the required one equivalent of iodide.

Mass Spectra

Analysis of the gas obtained by thermal decomposition of $[Ru(NH_3)_4H_2OCO]I_2$ complex in vacuo gave a substantial band at mass 28 indicating CO or N_2 or both. At high resolution the mass 28 band analyzed to give a $CO:N_2$ ratio of 4:1, confirming the liberation of carbon monoxide from the complex. Similar analysis of the $[Ru(NH_3)_4H_2ON_2]I_2$ complex gave a substantial band at mass 28 and 14 confirming the liberation of nitrogen.

Reactions with Ammonia and Acid

Both the *cis*- and the *trans*-aquocarbonyl and the aquonitrogentetramminеruthenium(II) ions react with aqueous ammonia to give an almost quantitative yield of the carbonyl (or nitrogen) pentammine complex. Treatment of the carbonyl pentammine complex with dilute hydrochloric acid gives the *trans*-aquocarbonyltetrammine. This isomer is unaffected by dilute hydrochloric acid, but the *cis*-aquocarbonyl complex loses one ammonia on warming in dilute (3 *N*) acid giving insoluble products which analyze for dihalocarbonyltriammineruthenium(II). The aquonitrogentetrammine complex gives with acid the unidentified blue solutions which are characteristic of ruthenium(II) (17). The reactions are summarized below

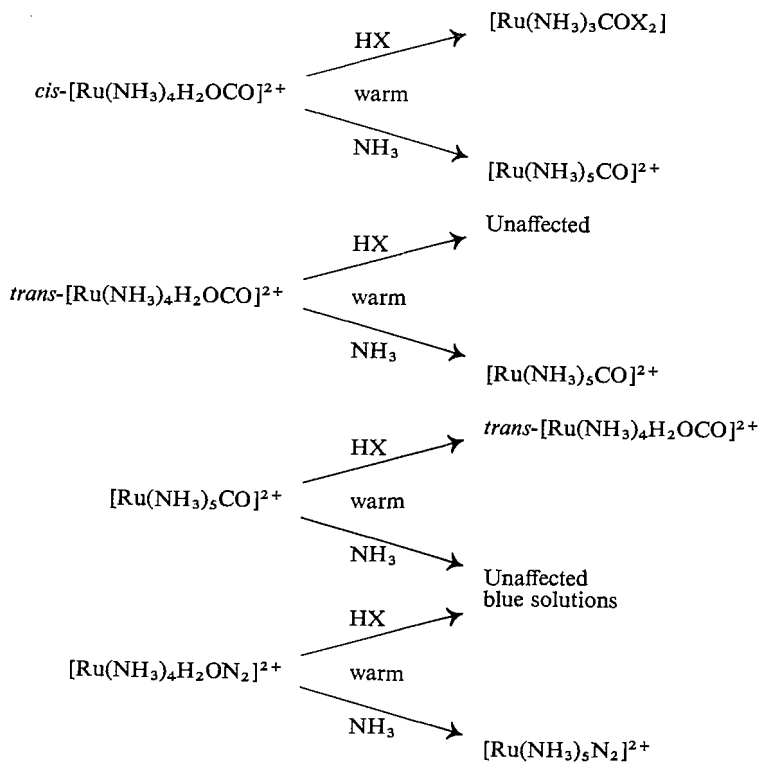

Can. J. Chem. Downloaded from www.nrcresearchpress.com by 210.87.254.6 on 09/05/12
For personal use only.

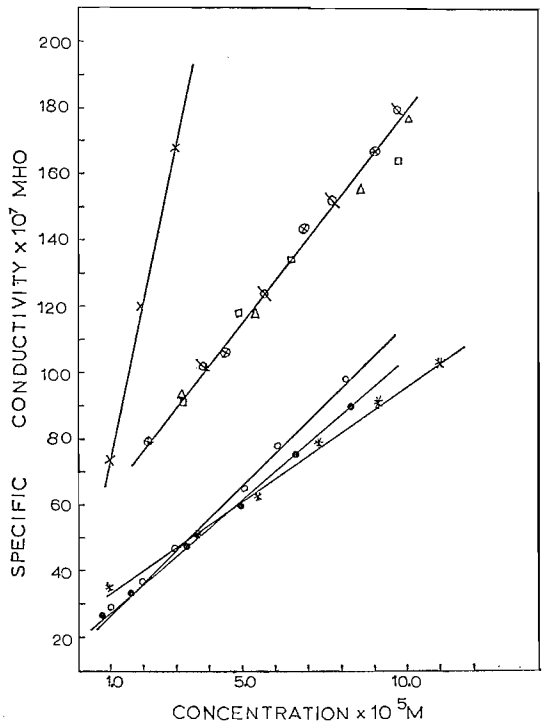

FIG. 6. Conductivity of some complexes of ruthenium in dimethyl sulfoxide at 24°: ×, $[Ru(NH_3)_6]I_3$; *, tertiarybutylammonium iodide; ○, NH_4SCN; ●, *trans*-$[Ru(NH_3)_4CONCS]NCS$; △, *trans*-$[Ru(NH_3)_4H_2OCO]I_2$; ⊕, *cis*-$[Ru(NH_3)_4H_2OCO]I_2$; □, $[Ru(NH_3)_5CO]I_2$; ⊗, $[Ru(NH_3)_4H_2ON_2]I_2$.

The lability of the ammonia *trans* to a carbonyl group is similar to that in nitrosylruthenium(II) complexes, indicating the high *trans* effect of the carbonyl group. These carbonyl complexes are very resistant to oxidation. For example, bromine in hydrobromic acid seems to have no effect at room temperature and on heating, some ammonia is replaced but the carbon monoxide remains attached. The complex products obtained are always diamagnetic, indicating no oxidation. This behavior is similar to that observed with nitrosylruthenium complexes (4) but not with the corresponding nitrogen complexes (8) where oxidation to ruthenium(III) occurs more readily. The carbonyl group can, however, be replaced by nitric oxide by treatment with aqueous nitric acid.

Acknowledgment

The authors are grateful to the National Research Council of Canada for financial assistance during this work.

1. J. M. JENKINS, M. S. LUPIN, and B. L. SHAW. J. Chem. Soc. A, 1787 (1966).
2. J. CHATT, B. L. SHAW, and A. E. FIELD. J. Chem. Soc. 3466 (1964).
3. J. R. KINGSTON and G. WILKINSON. J. Inorg. Nucl. Chem. **28**, 2709 (1966).
4. K. GLEU and I. BUDDECKER. Z. Anorg. Allgem. Chem. **268**, 208 (1952).
5. K. GLEU and I. BUDDECKER. Z. Anorg. Allgem. Chem. **268**, 202 (1952).
6. K. GLEU, K. REHM, and W. BREUEL. Z. Anorg. Allgem. Chem. **235**, 201 (1938).
7. K. GLEU, W. BREUEL, and K. REHM. Z. Anorg. Allgem. Chem. **235**, 211 (1938).
8. A. D. ALLEN, F. BOTTOMLEY, R. O. HARRIS, V. P. REINSALU, and C. V. SENOFF. J. Am. Chem. Soc. **89**, 5595 (1967).
9. A. D. ALLEN and C. V. SENOFF. Can. J. Chem. **45**, 1337 (1967).
10. K. GLEU and K. REHM. Z. Anorg. Allgem. Chem. **227**, 237 (1936).
11. K. GLEU and W. CUNTZE. Z. Anorg. Allgem. Chem. **237**, 197 (1938).
12. J. CHATT, P. L. PAULSON, and L. M. VENANZI. Organometallic chemistry. A.C.S. Monogram No. 147. Reinhold Publishing Corp., New York. 1960. p. 476.
13. R. POILBLANC and M. BIGORGUE. Bull. Soc. Chim. France, 1301 (1962).
14. L. VASKA. J. Am. Chem. Soc. **86**, 1943 (1964).
15. J. FUJITA, K. NAKAMOTO, and M. KOBAYASHI. J. Am. Chem. Soc. **78**, 3963 (1956).
16. M. M. CHAMBERLAIN and J. C. BAILAR, JR. J. Am. Chem. Soc. **81**, 6412 (1959).
17. I. E. STARIK and YU. A. BARBANEL. Russ. J. Inorg. Chem. English Transl. **6**, 109 (1961).
18. L. H. VOGT, J. L. KATZ, and S. E. WIBERLEY. Inorg. Chem. **4**, 1157 (1965).

Can. J. Chem. Downloaded from www.nrcresearchpress.com by 210.87.254.6 on 09/05/12
For personal use only.

Can. J. Chem. Downloaded from www.nrcresearchpress.com by 210.87.254.42 on 09/05/12
For personal use only.

Fragmentation and rearrangement processes in the mass spectra of perhalogenoaromatic compounds. Part II.[1] Pentafluorophenyl derivatives of Group IV[2,3]

J. M. MILLER
Department of Chemistry, Brock University, St. Catharines, Ontario

Received October 8, 1968

The mass spectra of compounds of the type $(C_6F_5)_4M$ (M = Si, Ge, Sn, and Pb) have been studied. Bond forming rearrangements were detected, involving fluorine abstraction by the central atom, forming perfluorophenylene ions and neutral metal fluoride species. The heavier metals give simpler spectra and fragmentation schemes. The bulk of the ion current is carried by fluorocarbon ions for the silicon derivative and by organometallic or metal fluoride ions in the other three cases, SnF^+ and PbF^+ forming the base peaks in their spectra. When M is carbon in the compounds $(C_6F_5)_3COH$ and $(C_6F_5)_2CO$, there is little evidence for rearrangements and transfer of fluorine to the central carbon atom.

Canadian Journal of Chemistry, 47, 1613 (1969)

Introduction

The mass spectra of some pentafluorophenyl derivatives of phosphorus, germanium, silicon, and phosphido-bridged iron carbonyls were shown to exhibit not only normal fragmentation, but also molecular rearrangements involving elimination of central atom-fluoride species formed by fluorine transfer, leaving perfluorophenylene type ions (1). King (2*a*, *b*) and Bruce (2*c*) also have established, by metastable ion analysis, the formation of neutral metal fluorides in mass spectra of a series of aliphatic and aromatic fluorocarbon derivatives of iron and cobalt. Similar results are also reported for manganese derivatives (3). Cavell and Dobbie have reported on fragmentations and rearrangements for a series of trifluoromethyl derivatives of arsenic (4, 7) and phosphorus (5–7).

In this paper the mass spectra of pentafluorophenyl derivatives of Group IV elements are discussed along with postulated mechanisms for the observed rearrangements.

Experimental

Tetrakis(pentafluorophenyl)germane was prepared as described previously (1). Tris(pentafluorophenyl)carbinol was supplied by Filler[4]. The compounds $(C_6F_5)_4M$ (M = Si, Sn, and Pb) were supplied by Tamborski[5]. Decafluorobenzophenone was purchased from Pierce Chemical Company. All samples with the exception of the carbinol and benzophenone were purified by a further sublimation before use.

Mass spectra were recorded on an A.E.I. Model MS9 instrument at 70 eV using the heated inlet system (200°) and on a Hitachi RMU-6E instrument, also at 70 eV but using a direct inlet probe. Spectra obtained on the two instruments were similar. Problems arose with the tin and lead compounds which deposited a conducting metallic film on the insulators in the source, necessitating frequent cleaning. For comparisons, several portions of the spectra were also examined using a Bendix Model 12 time-of-flight mass spectrometer. This instrument, with its lower resolution and difficulty in observing metastable ions, is more suitable for the studies of reaction energetics, rather than for fragmentation and rearrangement pathways.

Results and Discussion

Table I contains a listing of the most important ions in the spectra of the compounds $(C_6F_5)_4M$ (M = Si, Ge, Sn, and Pb)[6]. To facilitate comparisons, since the central atoms are polyisotopic in nature, the ion abundances are taken as a sum of all isotopic contributions and are expressed as a % of the total positive ion current. Part A of Table I shows the metal containing ions while Part B is a list of the major ions containing only carbon and fluorine. Table II summarizes the observed metastable ions.

---

[1]For Part I, see ref. 1.

[2]Presented in part at the 50th Conference of the Chemical Institute of Canada, Toronto, Ontario, June 4–7, 1967.

[3]Photocopies of the original mass spectra of the compounds dealt with here may be obtained free of charge upon request, from Depository for Unpublished Data, National Science Library, National Research Council of Canada, Ottawa, Canada.

[4]Professor R. Filler, address: Department of Chemistry, Illinois Institute of Technology, Chicago.

[5]Dr. C. Tamborski, address: Air Force Materials Lab., Wright Patterson Air Force Base, Ohio.

[6]An asterisk in a reaction scheme indicates a transition supported by metastable ion evidence.

Can. J. Chem. Downloaded from www.nrcresearchpress.com by 210.87.254.42 on 09/05/12
For personal use only.

TABLE I

Mass spectra of $(C_6F_5)_4M$*

Ion	Abundances† as % of total positive ion current for M = Si	Ge	Sn	Pb
A. Metal containing ions				
$(C_6F_4)_4M^+$	11.1	20.3	7.2	1.5
$(Parent–F)^+$	0.1	0.1	—	0.1
$(C_6F_5)_3M^+$	0.4	25.5‡	20.6	22.3
$(C_6F_5)_2MC_5F_3^+$	1.5	1.0	—	—
$(C_6F_5)_2MF^+$	—	3.4	10.5	—
$(C_6F_5)_2M^+$	1.1	—	—	—
$(C_6F_5)_4M^{2+}$	0.2	1.2	0.2	0.1
$C_{11}F_9M^+$	2.0	—	—	—
$C_6F_5MF_2^+$	—	3.6	2.8	—
$C_6F_5MF^+$	1.3	—	0.2	0.1
$C_6F_5M^+$	—	—	1.3	19.1
$C_5F_5M^+$	3.3	—	—	—
MF_3^+	1.3	—	—	—
MF^+	0.3	7.7	34.9‡	28.1‡
B. Ions without metal atoms				
$(C_6F_4)_4^+$	0.1	—	—	—
$(C_6F_4)_3^+$	2.6	5.9	0.8	<0.1
$C_{18}F_{11}^+$	2.8	0.3	0.2	—
$C_{17}F_{11}^+$	0.6	0.9	0.8	<0.1
$C_{18}F_{10}^+$	7.5	0.1	0.1	—
$C_{17}F_9^+$	7.9	0.9	0.1	—
$(C_6F_5)_2^+$	—	0.3	0.5	0.2
$(C_6F_4)_2^+$	4.6	12.7	3.4	0.1
$C_{12}F_7^+$	11.7‡	1.6	0.5	—
$C_{12}F_6^+$	4.1	—	0.2	—
$C_{11}F_5^+$	6.5	0.2	0.4	Masked by PbF
$C_6F_5^+$	—	3.8	2.0	0.4
$C_6F_4^+$	1.7	1.0	1.0	0.3
$C_6F_3^+$	6.6	1.0	0.3	<0.1
$C_5F_3^+$	1.6	1.4	1.8	2.0
$C_5F_2^+$	0.9	—	1.0	0.9
$C_3F_3^+$	1.3	Masked by GeF	0.7	0.7
CF_3^+	0.4	0.9	—	0.2

*M in this paper designates a metal atom, not the molecular ion. Here M = Si, Ge, Sn, or Pb.
†Sum of isotopic contributions.
‡Most abundant species when the sum of isotopic contributions is taken into account.

TABLE II

Fragmentations supported by metastable ions*

Fragmentation	*m** Observed	*m** Calculated
$(C_6F_5)_4Si^+ \rightarrow (C_6F_5)_2Si^+ + (C_6F_5)_2$	188.2	188.3
$(C_6F_5)_2Si^+ \rightarrow (C_6F_4)_2^+ + SiF_2$	242.0	242.0
$(C_6F_5)_4Sn^+ \rightarrow (C_6F_5)_3Sn^+ + C_6F_5$	~490	489.4
$(C_6F_5)_3Sn^+ \rightarrow (C_6F_5)_2SnF^+ + C_6F_4$	~360	360.3
$(C_6F_5)_2SnF^+ \rightarrow C_6F_5SnF_2^+ + C_6F_4$	~223	223.3
$(C_6F_5)_2SnF^+ \rightarrow C_{12}F_9^+ + SnF_2$	~209	208.4
$(C_6F_5)_3Pb^+ \rightarrow C_6F_5Pb^+ + (C_6F_5)_2$	~198	198.3
$(C_6F_5)_3Pb^+ \rightarrow Pb^+ + (C_6F_5)_3$	~61	61.0
$C_6F_5Pb^+ \rightarrow PbF^+ + C_6F_4$	~137	137.4
$C_{18}F_{11}^+ \rightarrow C_{18}F_{10}^+ + F$	387.8	387.8

*For polyisotopic species the metastable ion is calculated for the most abundant isotope. For these very broad peaks it is impossible to accurately determine the *m/e* of the maximum.

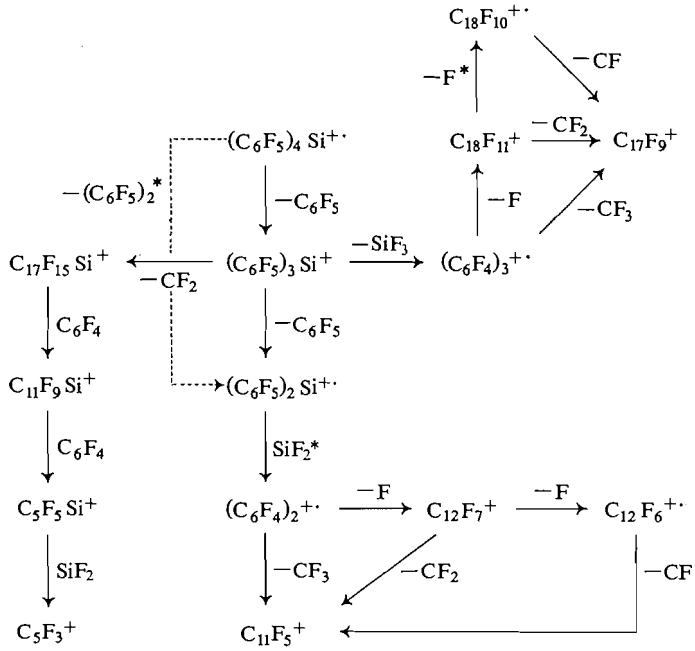

FIG. 1. Breakdown of $(C_6F_5)_4Si$.

Unlike the phosphorus compounds studied previously (1), the Group IV derivatives show few metastable transitions in their mass spectra, making assignment of fragmentation and rearrangement pathways more difficult.

(a) $(C_6F_5)_4Si$

The spectrum of the silane differs from the other three in several respects. There are many more peaks assignable to fluorocarbon fragments and it is the only example in this series, except for the $C_{17}F_{13}Ge^+$ ion, in which the metal atom is found attached to fluorocarbon fragments after the cleavage of an aromatic ring, e.g. $C_{17}F_{13}Si^+$, $C_{11}F_9Si^+$, and $C_5F_5Si^+$. Since Tamborski *et al.* (8) have reported that the thermal stability of the silane is less than that of the germane and stannane, a higher degree of fragmentation might be expected, but this fragmentation is a result of electron bombardment and certainly not due to thermal breakdown in the inlet system. Although the fraction of the total ionization carried by fluorocarbon fragments is highest for the silane, under the conditions of these experiments the yields of $(C_6F_4)_3^{+\cdot}$ and $(C_6F_4)_2^{+\cdot}$ are less than for the germane, contrary to earlier predictions (1).

The fluorocarbon peaks bear strong resemblance to the fragmentation pattern of the three perfluorophenylenes, ($C_{12}F_8$, $C_{18}F_{12}$, and $C_{24}F_{16}$), reported by Cohen and Massey (9). This indicates that many of the fluorocarbon species may have as their precursor ions $C_{12}F_8^{+\cdot}$, $C_{18}F_{12}^{+\cdot}$, and $C_{24}F_{16}^{+\cdot}$. In particular, the former two ions are quite abundant.

These phenylene ions likely are formed by loss of SiF_2, $SiF_3\cdot$, and SiF_4 from $(C_6F_5)_2Si^{+\cdot}$, $(C_6F_5)_3Si^+$, and $(C_6F_5)_4Si^{+\cdot}$, respectively. In contrast to the other three compounds studied in this work, and their hydrogen analogues (10, 11), the ion $(C_6F_5)_3Si^+$ is exceedingly weak. The more complex nature of the mass spectrum of $(C_6F_5)_4Si$ when compared to its Group IV homologues is paralleled by similar behavior for the $(C_6H_5)_4M$ series (M = Group IV elements), for which Enrione and Warren (12) have reported that the spectrum and processes become more complicated as one proceeds to lighter central atoms. The scheme in Fig. 1 illustrates the breakdown of the silane.

(b) $(C_6F_4)_4Ge$

The spectrum of the germane bears some resemblance to that of $(C_6H_5)_4Ge$ (1, 10). The most intense peaks (after taking into account the various isotopes of germanium) are $(C_6F_5)_3Ge^+$

Can. J. Chem. Downloaded from www.nrcresearchpress.com by 210.87.254.42 on 09/05/12
For personal use only.

Can. J. Chem. Downloaded from www.nrcresearchpress.com by 210.87.254.42 on 09/05/12
For personal use only.

and $(C_6H_5)_3Ge^+$ respectively. The intensity of these peaks are in marked contrast to the weak R_3M^+ peak of the silane. Characteristic of the germane fragmentation is the rearrangement which leads to the formation of two phenylene radical ions, $(C_6F_4)_3^{+\cdot}$ and $(C_6F_4)_2^{+\cdot}$ in high yield, whereas $(C_6H_4)_2^{+\cdot}$ and $(C_6H_4)_3^{+\cdot}$ were not observed in the spectrum of $(C_6H_5)_4Ge$ (1). Certainly fluorine abstraction by germanium is more prevalent than is hydrogen abstraction from the phenyl analogue, as is indicated by the presence of species such as $(C_6F_5)_2GeF^+$, $G_6F_5GeF_2^+$, GeF^+, and the presence of ions such as the biphenylenes which are undoubtedly formed by fluorine shifts to the central atom. Although metastable ions were not observed for the biphenylene rearrangement in the case of Group IV fluoroaromatics, mechanisms have been clearly established by metastable ions for phosphorus compounds (1). A fragmentation scheme for the germane is shown in Fig. 2. Some of the pathways are by analogy with $(C_6F_5)_4Sn$ for which metastable ions were observed.

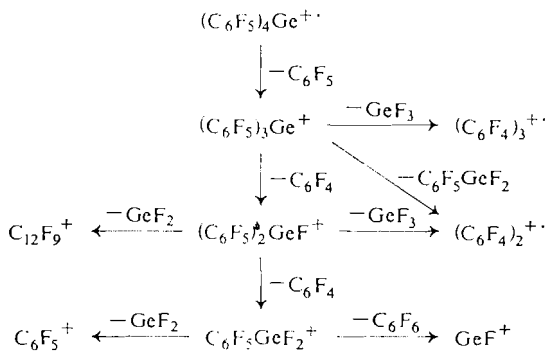

FIG. 2. Breakdown of $(C_6F_5)_4Ge$.

Formation of octafluorobiphenylene ions, $(C_6F_4)_2^{+\cdot}$, appears to result from the elimination of $GeF_3\cdot$ from $(C_6F_5)_2GeF^+$ compared to what appears to be SiF_2 elimination from $(C_6F_5)_2Si^{+\cdot}$, the analogue of this latter ion being absent in the spectrum of the germane. Alternatively, a $C_6F_5GeF_2\cdot$ radical could be eliminated from the abundant ion $(C_6F_5)_3Ge^+$, to produce the biphenylene ion. Dodecafluorotriphenylene ions, $(C_6F_4)_3^{+\cdot}$ could result from $GeF_3\cdot$ elimination from $(C_6F_5)_3Ge^+$. Transfer of three fluorines in a single elimination step has been established previously for Group V derivatives (1, 4, 6).

(c) $(C_6F_5)_4Sn$

The nature of fragmentation and rearrangement processes continues to change on going to heavier central atoms. The spectrum of the stannane shows a much weaker molecular ion than that of the germane, but the R_3M^+ ion retains a prominent place in the spectrum. However, unlike the spectrum of $(C_6H_5)_4Sn$, the $(C_6F_5)_3Sn^+$ ion is not the most intense in the spectrum. The ion SnF^+ is now most intense, indicative perhaps of the gradual weakening of the metal carbon bonds on descending the group. Intensities of the phenylene ions also drop off compared to the germane. For the first time, $C_6F_5M^+$ ions are observed, presumably as one stage leading to the formation of SnF^+ and $Sn^{+\cdot}$ ions. The bare metal ion, not present in the spectrum of the silane and germane is apparent for the stannane.

Apart from these few new ions and changes in intensities, the breakdown scheme (Fig. 3) is similar to that of the germane. Metastable ions were observed, verifying the mode of formation of $(C_6F_5)_2SnF^+$ and $C_6F_5SnF_2^+$ ions through elimination of uncharged C_6F_4 species. In contrast,

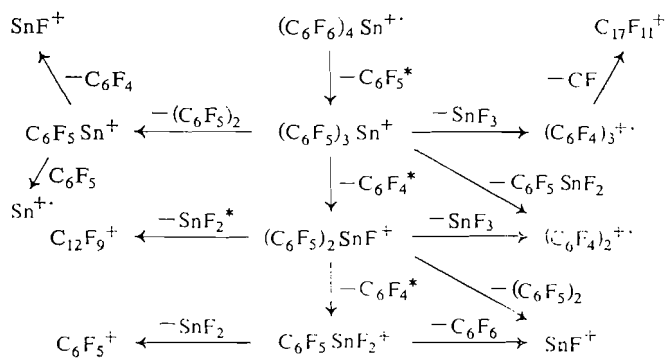

FIG. 3. Breakdown of $(C_6F_5)_4Sn$.

Can. J. Chem. Downloaded from www.nrcresearchpress.com by 210.87.254.42 on 09/05/12
For personal use only.

no major formation of tin–hydrogen bonds was detected in the spectrum of $(C_6H_5)_4Sn$, not surprising since the tin–hydrogen bond is quite weak. Such species are most abundant in the spectra of ethyl–tin derivatives where $Sn–H^+$ abundance parallels the ethyl content of the compound. No evidence is found for any partial fragmentation of the fluoroaromatic rings of any tin containing ions in contrast to the situation observed for phenyl–tin derivatives. This does not rule out such reactions as ring opening and expansion to a seven-membered ring by metal insertion.

(d) $(C_6F_5)_4Pb$

Simplification of the spectra continues to the last member of the series $(C_6F_5)_4Pb$. The parent ion and species such as $C_6F_5PbF_2^+$ are now much weaker, or absent. There are essentially only four strong ions, $(C_6F_5)_3Pb^+$, $C_6F_5Pb^+$, PbF^+, and $Pb^{+\cdot}$ giving a much abbreviated reaction scheme (Fig. 4). Like the tin spectrum the strongest peak is due to MF^+ with the other three major ions being of similar intensity. The increased intensity of $Pb^{+\cdot}$ is not unexpected because of the relatively weak nature of the lead–carbon bond. The observed drastic increase of the RM^+ ion has also been noted for phenyl–lead relative to phenyl–tin compounds (11) although the difference is much smaller than that observed in this case.

Metastable ions clearly show that the route outlined in the scheme (Fig. 4) is a major source of the large PbF^+ peak. For tin the weakness of the precursor ion $C_6F_5Sn^+$ may indicate that SnF^+ is formed via a different pathway, or simply that $C_6F_5Sn^+$ is unstable yielding SnF^+ virtually as soon as it is formed. Going one stage farther back in the sequence, the metastable established loss of $(C_6F_5)_2$ from $(C_6F_5)_3Pb^+$ could not be verifled for tin, but cannot be eliminated until further studies have been carried out. Bi-

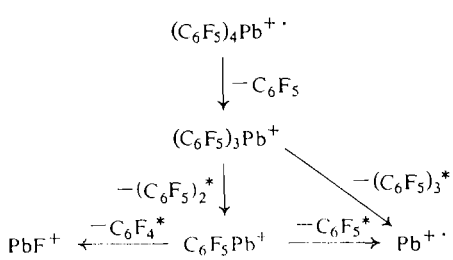

FIG. 4. Breakdown of $(C_6F_5)_4Pb$.

phenyl elimination has been established as a major process for phenyl derivatives of germanium, tin, and lead (11). A weak metastable ion suggests a reaction

$$(C_6F_5)_3Pb^+ \rightarrow Pb^{+\cdot} + C_{18}F_{15}$$

but it is more likely to be a rapid two step elimination of $(C_6F_5)_2$ and $C_6F_5\cdot$ as outlined in (Fig. 4) and suggested by Chambers *et al.* (11) for an analogous loss of $C_{18}H_{15}$ from $(C_6H_5)_3Sn^+$. Species of the type $C_6F_5MF_2^+$ and $(C_6F_5)_2MF^+$, important in the spectra of the germane and stannane, are notably absent for the lead derivative.

TABLE III

Nature of the charge carrying species in the mass spectra of compounds of the type $(C_6F_5)_4M$

	% of total positive ion current for M =			
Ion type	Si	Ge	Sn	Pb
N^{+*}	27	62	80	88
$MC_mF_n^+$	25	55	43	43
MF_n^+	2	7	35	28
M^+	0	0	2	17
$C_mF_n^+$	73	38	20	12
$C_mF_nMF_a^{+}$†	~1	7	14	<1

*Total metal containing ions.
†Fluorocarbon attached to a metal–fluorine species.

(e) Modes of Fragmentation

Major variations in the mode of breakdown of tetrakis(pentafluorophenyl) derivatives of Group IV under electron bombardment are apparent simply from the nature of the species carrying the ion current (Table III). There is a large change in the % of ion current carried by metal containing species, especially between the silane (27%) and stannane and plumbane (80 and 88%). These latter two are similar to their phenyl analogues in this respect. Metal–fluorocarbon ions carry about half of the current when M = Ge, Sn, or Pb, but only a quarter of the current for the silane. The bulk of this difference arises because of the lack of $(C_6F_5)_3Si^+$ ions (0.4%) compared to the other three compounds for which the analogous ions account for 20–25% of the total ion current. Ions of the R_3M^+ type have been found to be the most abundant ions in the spectra of hydrogen analogues of these compounds (10, 11), but only for the germane is this observed for pentafluorophenyl derivatives. The molecular ions are quite strong for all except the

Can. J. Chem. Downloaded from www.nrcresearchpress.com by 210.87.254.42 on 09/05/12
For personal use only.

lead compound. For both tin and lead the most abundant ion is MF^+, a species which is 4 to 5 times weaker for the germane and virtually nonexistant for the silane. Only for silicon was a MF_3^+ ion observed. Its relative intensity was 4 times that of the SiF^+ peak. $Sn^{+\cdot}$ and $Pb^{+\cdot}$ were the only metal ions observed but these were less abundant than in spectra of $(C_6H_5)_4M$ derivatives for which $Ge^{+\cdot}$ was also observed. This may be indicative of the greater stability of fluoroaromatic derivatives. The weakening of C—M bonds as M becomes heavier can in part explain the increase in metal and metal–fluoride ions. However, there is also the change from general reactions of type [1]

$$[1] \qquad RM^+ \rightarrow R^+ + M$$

which are more common for the lighter metals, to reactions of type [2]

$$[2] \qquad RM^+ \rightarrow M^+ + R$$

which predominates for the heavier metals. This change in charge distribution is also apparent in the change from 73% of the ion current carried by fluorocarbon fragments for the silane to only 12% for the plumbane. Only for the silane does the most abundant ion, $C_{12}F_7^+$, lack a metal atom. The germane, and more particularly the stannane, have a significant % of the ion current (7 and 14%, respectively) carried by species in which fluorine transfer to the metal has occurred while a fluoroaromatic entity remains attached. Ions such as $(C_6F_5)_2MF^+$ and $C_6F_5MF_2^+$ play a significant role in their breakdown mechanism.

Comparisons with mass spectra of the phenyl analogues show as many differences as similarities. No evidence has been reported for the elimination of M—H species leading to phenylene formation. However, loss of $(C_6H_5)_2$ is quite common. The corresponding analogous process with the fluorinated derivative was verified by metastables in evidence for the following cases

$$(C_6F_5)_3Pb^+ \rightarrow C_6F_5Pb^+ + (C_6F_5)_2$$

$$(C_6F_5)_4Si^{+\cdot} \rightarrow (C_6F_5)_2Si^{+\cdot} + (C_6F_5)_2$$

This latter reaction is analogous to similar eliminations from odd electron ions $(C_6H_5)_4M^{+\cdot}$ (M = Ge or Sn). However, when M = Ge or Sn such behavior is not detected for $(C_6F_5)_4M^{+\cdot}$. The lack of any biphenylene ion formation in the spectra of Group IV tetraphenyls is somewhat surprising. In the mass spectra of various phosphines (1, 13) biphenylene ion formation is observed, but arises via a different mechanism than the formation of $(C_6F_4)_2^{+\cdot}$ ions. Biphenylene ions are also found in the spectrum of 2,2′-diiododiphenyl mercury (14), but these are obviously due to the presence of halogen atoms.

The fluoroaromatic derivatives did not show ions corresponding to successive acetylene eliminations found for tetraphenyl derivatives of germanium, tin, and lead (10, 11).

Even electron ions predominate in the spectra of the fluoroaromatics as is the case for their phenyl analogues, and for both series, the molecular ion usually eliminates an odd electron neutral fragment. The abundant R_3M^+ ion eliminates an even electron neutral fragment. Exceptions to this behavior may occur in reactions of the following type

$$(C_6F_5)_3M^+ \rightarrow (C_6F_5)_3^{+\cdot} + MF_3$$

and

$$(C_6F_5)_3M^+ \rightarrow (C_6F_4)_2^{+\cdot} + C_6F_5MF_2$$

although these might possibly be two step eliminations. Apart from the molecular ions, $Sn^{+\cdot}$ and $Pb^{+\cdot}$, the only significant metal containing odd electron ions were $(C_6F_5)_2Si^{+\cdot}$ and $C_6F_5SiF^{+\cdot}$, again illustrating the different behavior of

TABLE IV

Mass spectra of tris(pentafluorophenyl)carbinol and decafluorobenzophenone

Ions	Abundances as % of total positive ion current for $(C_6F_5)_3COH$	Abundances as % of total positive ion current for $(C_6F_5)_2C{=}O$
$(C_6F_5)_3COH^+$	0.2	—
$(C_6F_5)_3C^+$	0.5	—
$(C_6F_4)_3C^+$	0.1	—
$(C_6F_5)_2CO^+$	6.7	10.9
$(C_6F_4)_2^+$	0.3	0.3
$C_{11}F_5^+$	0.2	1.0
$C_{10}F_4^+$	0.4	1.4
$C_6F_5CO^+$	30.7*	31.5*
$(C_6F_5)_2CO^{2+}$	0.3	0.5
$C_6F_5H^+$	12.6	—
$C_6F_5^+$	10.1	18.6
$C_6F_4H^+$	1.0	—
$C_6F_4^{2+}$	1.4	1.9
$C_6F_3^+$	0.3	0.4
$C_5F_3H^+$	1.3	—
$C_5F_3^+$	8.2	16.9
$C_5F_2H^+$	6.6	—
$C_5F_5^+$	2.0	2.0
$C_3F_3^+$	3.2	4.5
C_5F^+	1.2	1.8
$C_3F_2H^+$	1.0	—
CF_3^+	0.8	0.3
CF^+	3.1	2.0

*Most abundant ion in the spectrum.

TABLE V
Fragmentation supported by metastable ions

Fragmentation	m^* Observed	m^* Calculated
$C_6F_5CO^+ \rightarrow C_6F_5^+ + CO$	143.1	143.0
$C_6F_5^+ \rightarrow C_5F_3^+ + CF_2$	82.1	81.9
$C_6F_5H^+ \rightarrow C_5F_2H^+ + CF_3$	58.5	58.3
$(C_6F_5)_2CO^+ \rightarrow C_{10}F_4^+ + C_3F_6O$	106.2	106.1

the silane. The remaining odd electron ions are fluorocarbon species such as the phenylene radical ions.

(f) $(C_6F_5)_3COH$ and $(C_6F_5)_2C{=}O$

Since tetrakis(pentafluorophenyl)methane was not available, the mass spectra of tris(pentafluorophenyl)carbinol and decafluorobenzophenone were obtained in an attempt to compare the behavior of fluoroaromatic derivatives of carbon to fluoroaromatic–organometallics of Group IV. Table IV summarizes the abundances of major peaks in the spectra as a % of the total ion current and Table V summarizes the observed metastable ions. Both spectra have in common the base peak at *m/e* 195 corresponding to $C_6F_5CO^+$, and carrying about one third of the total ion current, but whereas the benzophenone has a strong molecular ion, that for the carbinol is very weak, the first stage of breakdown being loss of $H^\cdot$ and $C_6F_5^\cdot$ forming the $(C_6F_5)_2C{=}O^{+\cdot}$ ion of similar intensity to the molecular ion of the benzophenone. With the exception of peaks attributable to hydrogen transfer from the carbinol, remaining parts of the spectra are very similar. There is evidence, supported by a metastable transition in the bezophenone spectrum, for the elimination of C_3F_6O

$$(C_6F_5)_2CO^{+\cdot} \rightarrow C_{10}F_4^{+\cdot} + C_3F_6O$$

There is essentially no elimination of the central carbon to form phenylenes as only very weak peaks were observed (0.3% of the total ion current in both spectra) for $C_{12}F_8^{+\cdot}$ ions and a trace of $C_{18}F_{12}^{+\cdot}$ was detected in the carbinol spectrum. In both cases 13 and 19 carbon ions were more abundant, and the carbon lost in the weak C-12 and C-18 peaks could also be a result of ring cleavage. Carbon monoxide is not lost from $(C_6F_5)_2CO^{+\cdot}$ ions but metastable ions show that CO is ejected from $C_6F_5CO^+$.

(g) Mechanism of Fragmentation

The absence of fluorine migrations and rearrangements leading to phenylene ions and neutral central atom–fluoride species when the central atom is carbon is consistent with evidence obtained when another first row element, namely nitrogen, was involved. Fluorine atom transfers were not observed in the mass spectra of trifluoromethylamines (15). Cavell and Dobbie (5) have suggested that rearrangement processes in trifluoromethylphosphines arise because of interactions of non-bonding fluorine p orbitals with vacant d orbitals on phosphorus, nitrogen lacking the appropriate orbitals. An explanation involving d orbitals is applicable to the pentafluorophenyl derivatives of silicion, germanium, tin, and lead which possess vacant d orbitals, whereas carbon lacks these orbitals. The involvement of d orbitals can also explain the existance of fluorine transfer to transition metals (1–3). Hawthorne, Mays, and Simpson (3) have suggested that when there are unsaturated σ-bonded organic ligands, the rearrangement ions can be rationalized by assuming that the ligand becomes π-bonded to the metal during fragmentation. Their conclusion is based on fluorine migrations which occur from all three ortho-, meta-, and para-substituted fluorophenyl manganese pentacarbonyls to the metal, although the ortho migration is most favored. However, well established scrambling of substituents or aromatic rings could account for this observation. In the nonaromatic case of chlorohexafluorocyclopentenyl manganese and rhenium pentacarbonyls no evidence was found for fluorine or chlorine migration to the metal (16). For Group IV elements such a σ–π rearrangement could explain reactions of the type

$$(C_6F_5)_3M^+ \rightarrow (C_6F_5)MF^+ + C_6F_4$$

$$(C_6F_5)_2MF^+ \rightarrow C_6F_5MF_2^+ + C_6F_4$$

Can. J. Chem. Downloaded from www.nrcresearchpress.com by 210.87.254.42 on 09/05/12
For personal use only.

and perhaps formation of the phenylenes, although satisfactory stereochemistry exists for simple σ-bonded intermediates, especially if d orbitals participate in the transition structure. The σ–π scheme is less satisfactory, however, in explaining the loss of neutral metal fluoride species and the formation of charged fluoroaromatic fragments.

The rearrangement reactions and fluorine transfers observed in the mass spectra of the Group IV fluoroaromatic derivatives are certainly not due to thermal decompositions in the inlet system, since the high thermal stability of these compounds has been established by Tamborski *et al.* (8). Biphenylene ions are unlikely to be formed by fragmentation of the previously formed decafluorobiphenyl since the abundance of this species is low and its mass spectrum (17) shows only small yields of $(C_6F_4)_2^{+\cdot}$ ions. It is necessary to conclude that, despite a lack of metastable ion evidence, the phenylene ions are formed by rearrangements including fluorine transfers and elimination of neutral metal–fluoride containing species.

A mass spectral study of the energetics of this type of reaction is now underway along with pyrolysis studies.

Acknowledgments

The author wishes to thank the National Research Council of Canada for financial support and Professor R. Filler and Dr. C. Tamborski for the donation of some of the compounds used in this study.

1. J. M. Miller. J. Chem. Soc. A, 828 (1967).
2. (*a*) R. B. King. J. Am. Chem. Soc. **89**, 6368 (1967). (*b*) R. B. King and T. F. Korenowski. Chem. Commun. 771 (1966). (*c*) M. I. Bruce. J. Organometal. Chem. Amsterdam, **10**, 495 (1967).
3. J. D. Hawthorne, M. J. Mays, and R. N. F. Simpson. J. Organometal. Chem. Amsterdam, **12**, 407 (1968). M. J. Mays and R. N. F. Simpson. J. Chem. Soc. A, 1936 (1967).
4. C. Dobbie and R. G. Cavell. Inorg. Chem. **6**, 1450 (1967).
5. R. G. Cavell and R. C. Dobbie. Inorg. Chem. **7**, 101 (1968).
6. R. G. Cavell and R. C. Dobbie. Inorg. Chem. **7**, 690 (1968).
7. R. G. Cavell and R. C. Dobbie. J. Chem. Soc. A, 1406 (1968).
8. C. Tamborski, E. J. Soloski, and S. M. Dea. J. Organometal. Chem. Amsterdam, **4**, 446 (1965).
9. S. C. Cohen and A. G. Massey. J. Organometal. Chem. Amsterdam, **10**, 471 (1967).
10. F. Glockling and J. R. C. Light. J. Chem. Soc. A, 717 (1968).
11. D. B. Chambers, F. Glockling, and M. Weston. Chem. Commun. 281 (1966); J. Chem. Soc. A, 1759 (1967).
12. R. Enrione and T. Warren. Abstracts Division Inorg. Chem. Am. Chem. Soc. 156th ACS Meeting. Atlantic City, September, 1968. Paper 112.
13. D. H. Williams, R. S. Ward, and R. G. Cooks. J. Am. Chem. Soc. **90**, 966 (1968).
14. H. F. Gruetzmacher and J. Lehmann. Liebigs Ann. Chem. **705**, 81 (1967).
15. R. C. Dobbie and H. J. Emeléus. J. Chem. Soc. A, 933 (1966). R. C. Dobbie. J. Chem. Soc. A, 1555 (1966). D. P. Babb and J. M. Shreeve. Inorg. Chem. **6**, 351 (1967).
16. M. I. Bruce. J. Organometal. Chem. Amsterdam, **10**, 95 (1967).
17. D. E. Fenton and A. G. Massey. Tetrahedron, **21**, 3009 (1965).

Can. J. Chem. Downloaded from www.nrcresearchpress.com by 210.87.254.42 on 09/05/12
For personal use only.

Diethyl lead dinitrate

D. POTTS AND A. WALKER
Chemistry Department, Scarborough College, University of Toronto, Toronto 5, Ontario
Received October 25, 1968

The reaction, at 0 °C, between tetra-ethyl lead and dinitrogen tetroxide in both nitromethane and diethyl ether as solvents has been studied. The product in both solvents is always diethyl lead dinitrate, the properties of which have been investigated and compared with both dimethyl tin dinitrate and triethyl lead nitrate. The infrared spectrum is consistent with covalent unidentate nitrate groups, while molecular weight and conductivity measurements indicate that the compound behaves essentially as a 1:2 electrolyte in water and dimethyl sulfoxide. Decomposition of diethyl lead dinitrate in solution and in the solid state is discussed with the aid of ultraviolet spectroscopy and thermogravimetric analysis.

Canadian Journal of Chemistry, 47, 1621 (1969)

Can. J. Chem. Downloaded from www.nrcresearchpress.com by 210.87.254.6 on 09/05/12
For personal use only.

Following the work on $Me_2Sn(NO_3)_2$ (1), it was of interest to us to investigate the organo-nitrate chemistry of lead, where it might be expected that the organic groups would be more easily replaced, possibly giving $Pb(NO_3)_4$ as a final product. The reaction between tetra-ethyl lead and dinitrogen tetroxide though vigorous (and sometimes explosive), always stops at the diethyl lead dinitrate stage. Further replacement of ethyl groups was not possible even when the product was treated with dinitrogen pentoxide.

We have consistently been unable to repeat the work of Hetnarski and Urbański (2), who claim that the product of the reaction when carried out in diethyl ether as solvent at 0 °C is $[(NO)_2PbEt_4]^{2+}(NO_3)_2^-$, with no replacement of the ethyl groups. Under these conditions we find the product to be the same as in nitromethane solution, namely, diethyl lead dinitrate.

Diethyl lead dinitrate has been previously made by Hurd and Austin (3) by the reaction of nitric acid on tetra-ethyl lead in hot chloroform, but they did not investigate its properties in detail. They did note that triethyl lead nitrate and lead(II) nitrate were present in the reaction mixture and our investigation shows that these products are the result of decomposition of diethyl lead dinitrate in solution.

This paper discusses the properties of diethyl lead dinitrate and in particular the decomposition reactions which it undergoes.

Results and Discussion

Diethyl lead dinitrate is a white amorphous solid and is non-deliquescent. On heating in a bunsen flame the compound explodes. The compound is only stable at temperatures below 0 °C. At room temperature significant decomposition occurs within two weeks and the compound turns progressively reddish brown in color, presumably due to lead dioxide, while the infrared (i.r.) spectrum of the solid indicates the formation of ionic nitrate.

Diethyl lead dinitrate is appreciably soluble in cold water and polar organic solvents but is insoluble in non-polar solvents.

Infrared Spectrum

The total i.r. spectrum observed for $Et_2Pb(NO_3)_2$ is, in cm^{-1}, as follows: 1495 s,sp; 1450 vw,sh; 1421 m; 1380 w,sh; 1309 s,sp; 1259 s,sp; 1169 s,sp; 1032 m,sp; 1018 s,sp; 972 w; 809 m,sp; 745 w; 731 s,sp; 714 m,sp; 498 w; and 430 vw (where s = strong, m = medium, w = weak, vw = very weak, sh = shoulder, sp = sharp).

In order to assign bands associated with the ethyl groups, the spectrum of Et_2PbCl_2 was taken, and by direct comparison, the following bands can definitely be assigned to vibrations of the nitrato groups: 1495, 1421, asymmetric NO_2 stretch; 1309, 1259, symmetric NO_2 stretch; 1032, 1018, NO stretch; and 809 cm^{-1}, NO_3 out-of-plane rock.

As was found with the spectrum of $Me_2Sn(NO_3)_2$ (1), the observed splitting of the (NO) and (NO_2) stretching modes is consistent with a tetrahedral structure for $Et_2Pb(NO_3)_2$ containing two unidentate nitrato groups. The smaller value of the splitting between the (NO_2) asymmetric and symmetric stretching frequencies and the higher frequency of the (NO) stretches as compared to $Me_2Sn(NO_3)_2$ is consistent with a less covalent metal–nitrato bond in the lead

TABLE I

Molar conductivities of aqueous solutions of diethyl lead dinitrate

Molar concentration	Molar conductivity (Ω^{-1} cm^2)		
	Fresh solution, 25 °C	Solution, boiled 5 min	Solution, boiled 2 days
0.0010	222	328	218
0.0025	217	324	214
0.0050	209	318	208
0.0075	202	311	201
0.0100	194	305	195

compound. The bands at 498 and 430 cm^{-1} are assigned to the two Pb—C stretching modes and are also in agreement with a tetrahedral model.

Infrared Spectrum of Et_3PbNO_3

A pure sample of Et_3PbNO_3 was prepared by the action of $AgNO_3$ on Et_3PbCl in methyl cyanide, and its i.r. spectrum is as follows: 1455 sh; 1438 m; 1420 m; 1375 m; 1280 s,b; 1225 m,sp; 1158 s,sp; 1039 m,sp; 1030 m,sp; 970 w; 952 w; 815 m,sp; 720 w,sp; 690 s,sp; 475 m; and 445 cm^{-1} vw.

By comparison with the spectrum observed for Et_3PbCl the following bands can be assigned to vibrations of the nitrato group: 1438, asymmetric NO_2 stretch; 1280, symmetric NO_2 stretch; 1039, NO stretch; and 815 cm^{-1}, NO_3 out-of-plane rock. The bands at 475 and 445 cm^{-1} are assigned to Pb—C stretching modes indicating a non-planar structure for the Et_3Pb group. The nitrate bands are consistent with a unidentate nitrato group, and as was the case with Me_3Sn-NO_3 (1), the nitrato group is less covalently bound to the lead atom than in $Et_2Pb(NO_3)_2$.

Molecular Weights

Using Analar lead nitrate as a reference 1:2 electrolyte in water, it was found that over the concentration range 0.01–0.06 *M* at 25 °C, a fresh solution of diethyl lead dinitrate behaves as a 1:2 electrolyte and is consistent with a molecular weight of 389.3.

Conductivities

Molar conductivities for solutions of diethyl lead dinitrate in water and dimethyl sulfoxide are given in Table I and Table II respectively. A fresh aqueous solution has values nearly consistent with a 1:2 electrolyte in water (ca. 240 Ω^{-1} cm^2, at 0.001 *M*), and on boiling under reflux for 5 min these conductivities rise sharply to around 330 Ω^{-1} cm^2; on prolonged boiling under reflux the conductivity drops to the initial value of the fresh cold solution.

TABLE II

Molar conductivities of solutions of diethyl lead dinitrate in dimethyl sulfoxide at 25 °C

Molar concentration	Molar conductivity (Ω^{-1} cm^2)	
	Fresh solution	Solution 24 h old
0.0025	64.3	66.8
0.0050	61.5	61.5
0.0075	58.3	58.3
0.0100	56.5	56.5
0.0125	55.0	55.0

In dimethyl sulfoxide a fresh solution also has values consistent with a 1:2 electrolyte in this

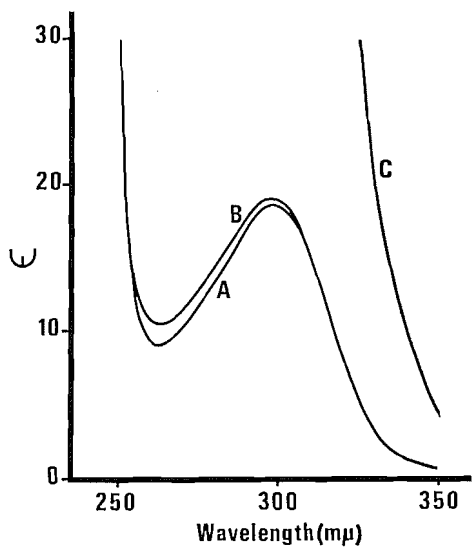

FIG. 1. Ultraviolet spectra of solutions of diethyl lead dinitrate in water: A, fresh solution at 25 °C; B, solution on standing 12 h at 25 °C; C, fresh solution boiled for 5 min.

Can. J. Chem. Downloaded from www.nrcresearchpress.com by 210.87.254.6 on 09/05/12
For personal use only.

Can. J. Chem. Downloaded from www.nrcresearchpress.com by 210.87.254.6 on 09/05/12
For personal use only.

solvent (1) and no change in conductivity was observed even upon standing for 24 h at 25 °C.

Ultraviolet Spectra

The spectrum of a freshly prepared aqueous solution of diethyl lead dinitrate at 25 °C is shown in Fig. 1, curve A.

The observed peak at 300 mμ (ε = 18.76) is consistent with the presence of two nitrate ions per mole. By comparison, the spectrum of lead nitrate in water at 25 °C has a peak at 300 mμ (ε = 16.50).

The solution is virtually unchanged on standing at 25 °C for a period of 12 h (Fig. 1, curve B). On refluxing a fresh solution for only 5 min the spectrum is that of curve C in Fig. 1. The appearance of an intense charge transfer band completely obscures the nitrate ion spectrum.

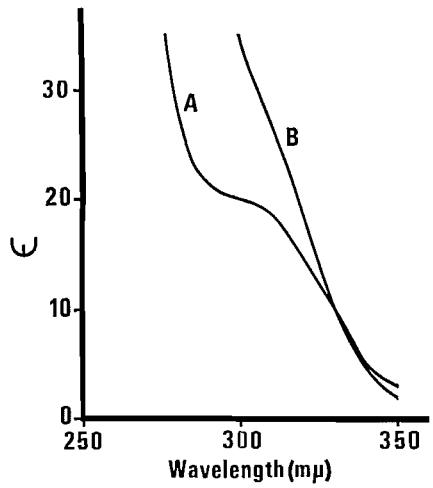

FIG. 2. Ultraviolet spectra of solutions of diethyl lead dinitrate in dimethyl sulfoxide: A, fresh solution at 25 °C; B, solution on standing 12 h at 25 °C.

A freshly prepared solution of diethyl lead dinitrate in dimethyl sulfoxide at 25 °C has the spectrum shown in Fig. 2, curve A. The nitrate ion in this solvent absorbs at 312 mμ (4). Curve A shows only an inflection at this wavelength, and on standing for 12 h at 25 °C the solution has the spectrum shown in Fig. 2, curve B.

Figure 3 shows the spectra obtained for solutions of diethyl lead dinitrate in methyl cyanide. Curve A is a fresh solution at 25 °C and shows a peak at 290 mμ (ε = 22.4); curve B shows the solution on standing for 12 h at 25 °C with a peak at 285 mμ (ε = 29.0), and this solution had

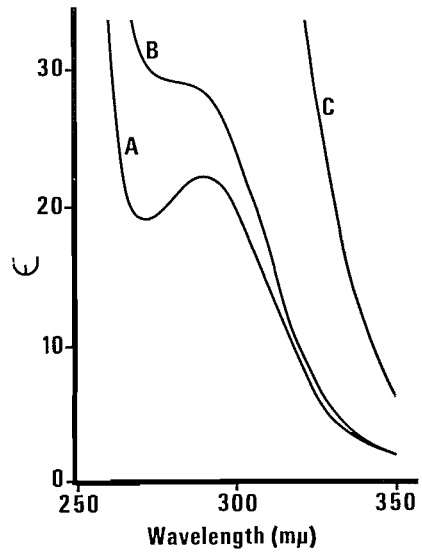

FIG. 3. Ultraviolet spectra of solutions of diethyl lead dinitrate in methyl cyanide: A, fresh solution at 25 °C; B, solution on standing 12 h at 25 °C; C, fresh solution boiled for 5 min.

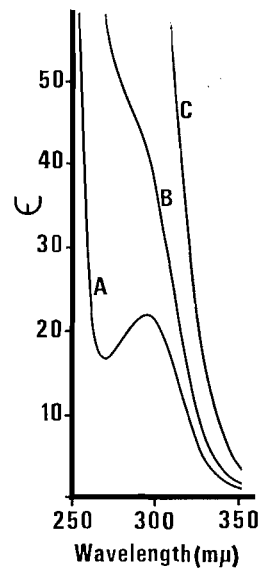

FIG. 4. Ultraviolet spectra of solutions of diethyl lead dinitrate in methyl alcohol: A, fresh solution at 25 °C; B, solution on standing 12 h at at 25 °C; C, fresh solution boiled for 5 min.

by then deposited crystals of lead(II) nitrate. Curve C is the fresh solution refluxed for 5 min and this solution immediately deposited a large amount of lead(II) nitrate.

Figure 4 shows similar spectra for solutions in

Can. J. Chem. Downloaded from www.nrcresearchpress.com by 210.87.254.6 on 09/05/12
For personal use only.

methyl alcohol. Curve A has a peak at 294 mμ ($\varepsilon = 21.9$), curve B is the spectrum on standing for 12 h, and curve C that of a fresh solution refluxed for 5 min.

While ionization is obviously occurring in fresh cold solutions of diethyl lead dinitrate in methyl alcohol and methyl cyanide, the wavelengths of the peak maxima indicate (1, 4) some degree of covalent metal nitrate interaction though not as much as for many metal nitrates in these solvents. The inflection observed in the fresh cold solution in dimethyl sulfoxide is not, however, consistent with simple dissociation into diethyl lead and nitrate ions, and a charge transfer spectrum is already evident. Discussion of the refluxed solutions and those obtained upon standing at 25 °C for 12 h will be deferred until the next section.

A diffuse reflectance spectrum of solid diethyl lead dinitrate has a peak maximum at 277 mμ which is consistent with covalent metal nitrate interaction.

Reactions in Solution

A fresh aqueous solution at 25 °C is neutral and on treatment with hydrogen sulfide yields a cream precipitate characteristic of the diethyl lead ion (5). On refluxing for 5 min the solution becomes quite acidic (pH = 3.5), thus explaining the high conductivities observed. This acidity probably results from hydrolysis of the diethyl lead ion following initial ionization

$$(C_2H_5)_2Pb(NO_3)_2 + 2H_2O \rightleftharpoons (C_2H_5)_2Pb(H_2O)_n^{2+} + 2NO_3^-$$

$$(C_2H_5)_2Pb(H_2O)_n^{2+} \rightleftharpoons (C_2H_5)_2Pb(H_2O)_{n-1}(OH)^+ + H^+$$

It should be noted that this hydrolysis only occurs on refluxing, as compared to the more acidic $(CH_3)_2Sn^{2+}$ ion which undergoes hydrolysis in cold solution (1).

On treating the refluxed solution with hydrogen sulfide, it became apparent that hydrolysis was not the only process occurring, since a black precipitate of lead(II) sulfide was obtained. On buffering the supernatant liquid (5), a non-characteristic brownish precipitate occurred, which is probably a mixture of organolead and lead(II) sulfides. After refluxing the solution 2 days, it finally became neutral again, and the conductivity dropped to that of the original cold solution. Treatment of this solution with hydrogen sulfide yielded a black precipitate of lead(II) sulfide, and the supernatant liquid upon buffering yielded a pure white precipitate, characteristic of the Et_3Pb^+ ion (5). It is known (5) that aqueous solutions of dialkyl lead salts tend to decompose into trialkyl lead salts and lead(II) salts, particularly upon heating. Such a decomposition can be represented by the equation

$$2Et_2Pb(NO_3)_2 \rightarrow Et_3PbNO_3 + EtNO_3 + Pb(NO_3)_2$$

It is also known (6) that trialkyl lead salts have a charge transfer spectrum which is continuous over the 200–350 mμ region. In keeping with this we found that a solution of triethyl lead nitrate in water had such a spectrum, in contrast to the diethyl lead dinitrate which does not. Thus the charge transfer spectrum observed in curve C of Fig. 1 can be attributed to the presence of some triethyl lead nitrate in solution. Complete decomposition of the diethyl lead species in aqueous solution obviously requires prolonged refluxing for two reasons. Firstly, we found that even a refluxed solution of triethyl lead nitrate, lead(II) nitrate, and ethyl nitrate is not acidic and yet the solution of diethyl lead dinitrate required 2 days refluxing before the acidity due to the hydrolysis products disappeared. Secondly, the conductivity of the diethyl lead dinitrate remained high for the same period before dropping to values consistent with the decomposition products.

The charge transfer spectra observed in curves B and C for both methyl alcohol and methyl cyanide and curves A and B for dimethyl sulfoxide (DMSO) can likewise be assigned to the formation of triethyl lead nitrate in solution. While it is not difficult to understand a rise in temperature effecting some decomposition of the diethyl lead dinitrate in the solvents after only 5 min, the behavior on standing at 25 °C does not follow a regular pattern. The rate of decomposition of fresh solutions at 25 °C as measured by the appearance of charge transfer bands, is in the decreasing order

$$DMSO >> MeOH > MeCN >>> H_2O$$

which follows the order of increasing dielectric constant with the exception of dimethyl sulfoxide in which the rate is by far the fastest. One might expect the mechanism of decomposition to involve the transfer of a charged ethyl species as has been suggested (5), and this process will be slowest in media of high dielectric constant due to extensive non-specific solvation (7). By

Can. J. Chem. Downloaded from www.nrcresearchpress.com by 210.87.254.6 on 09/05/12
For personal use only.

contrast dimethyl sulfoxide will enter into strong specific interaction (7) with the diethyl lead ion and presumably will thus facilitate the rupture of a lead–carbon bond.

Attempts to analyze quantitatively the decomposition products in the refluxed aqueous solution proved difficult due to separation of the products in this medium. However, the results in methyl cyanide proved much more conclusive. A solution of diethyl lead dinitrate in methyl cyanide was refluxed on a water bath for 30 min. During this period crystalline lead(II) nitrate was deposited quantitatively according to the proposed mechanism. The supernatant liquid was removed under vacuum and passed through a gas chromatograph showing only the presence of solvent and ethyl nitrate. The residual yellow solid analyzed as follows:

Anal. Calcd. for Et_3PbNO_3: C, 20.20; NO_3^-, 17.40. Found: C, 19.08; NO_3^-, 18.33.

A solution of this residual solid in water had a charge transfer ultraviolet spectrum and when treated with hydrogen sulfide gave a characteristic white precipitate of the Et_3Pb^+ ion. The i.r. spectrum was also identical with that obtained for Et_3PbNO_3 prepared as mentioned previously.

Pyrolysis

A sample of diethyl lead dinitrate was heated under a vacuum of 10^{-2} mm to 200 °C. During this period the sample remained white and did not melt. The residual solid had an i.r. spectrum identical with that of lead(II) nitrate and a nitrate analysis was as follows:

Anal. Calcd. for $Pb(NO_3)_2$: NO_3^-, 37.5. Found: NO_3^-, 36.8.

An aqueous solution of the residue gave only a black precipitate when treated with hydrogen sulfide. A colorless oil was collected in a liquid nitrogen trap during the period in which the sample was heated, but no oxides of nitrogen were observed. This oil had an i.r. spectrum identical to that of a mixture of tetra-ethyl lead and ethyl nitrate with the latter component predominant.

By comparison, when a sample of triethyl lead nitrate was similarly heated, the original yellow solid melted to a yellow liquid at 100 °C and resolidified to a white solid at 150 °C. During the liquid stage the sample spluttered considerably, leaving a residue of lead(II) nitrate.

The residual solid was identified as lead(II) nitrate and a colorless oil was again collected in the cold trap. This oil was also a mixture of tetra-ethyl lead and ethyl nitrate, as identified by its i.r. spectrum, but now the former component was predominant.

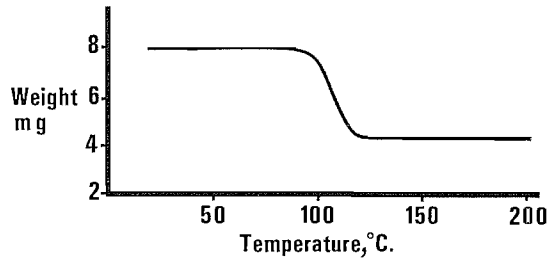

FIG. 5. Thermogravimetric analysis of diethyl lead dinitrate.

The spluttering of the liquid in the triethyl case precluded an investigation by thermogravimetric analysis, but this was done for diethyl lead dinitrate and is shown in Fig. 5. The weight loss observed is consistent with the decomposition

$$3Et_2Pb(NO_3)_2 \rightarrow 2Pb(NO_3)_2 + Et_4Pb + 2EtNO_3$$

and no intermediate stable product is detectable, such as the triethyl lead nitrate which is produced in the solution decompositions observed.

A possible equation for the decomposition of triethyl lead nitrate is

$$3Et_3PbNO_3 \rightarrow Pb(NO_3)_2 + 2Et_4Pb + EtNO_3$$

which results in relative concentrations of tetra-ethyl lead and ethyl nitrate which are the reverse of those obtained from the diethyl lead dinitrate. The observed i.r. spectra of the two oils produced qualitatively confirm this.

Finally, it is interesting to note that we found that triethyl lead chloride sublimes unchanged at 60 °C under vacuum, while diethyl lead dichloride decomposes to triethyl lead chloride and lead(II) chloride.

Experimental

Diethyl Lead Dinitrate

Tetra-ethyl lead (5 ml) was placed in a 250 ml two-necked flask fitted with a P_2O_5 guard tube and a dropping funnel. Dry nitromethane (15 ml) was added to the flask, forming a separate layer above the tetra-ethyl lead. Dinitrogen tetroxide (20 ml) was mixed with 25 ml of dry nitromethane and placed in the dropping funnel. The flask was cooled in an acetone – dry ice bath and the $N_2O_4 - CH_3NO_2$ mixture added a few drops at a time. Between each addition the flask was allowed to warm to about 0 °C. A white solid formed immediately above the tetra-ethyl lead layer, the solution became green, and much

gas was evolved. After the reaction was complete, an excess of dinitrogen tetroxide was added, and the product was filtered and washed with fresh dinitrogen tetroxide. The product was dried under vacuum to remove solvent traces and was isolated as a white amorphous powder, yield 7.33 g.

The reaction using diethyl ether as solvent was carried out following the procedure described (2).

Analyses for nitrate were done with nitron, for carbon by the Van Slyke wet oxidation technique, and for lead by evaporation to dryness with concentrated nitric acid followed by chromate determination.

Anal. Calcd. for $Et_2Pb(NO_3)_2$: C, 12.3; NO_3^-, 31.9; Pb, 53.2. Found: C, 12.3; NO_3^-, 31.5; Pb, 52.6.

Triethyl Lead Nitrate

A 1:1 mole ratio of triethyl lead chloride and silver nitrate was dissolved in dry methyl cyanide. The precipitated silver chloride was removed by filtration and the solvent was removed under vacuum. The product was purified by extraction with chloroform.

Anal. Calcd. for Et_3PbNO_3: C, 20.2; NO_3^-, 17.4. Found: C, 20.6; NO_3^-, 17.2.

All solvents were dried and purified by standard methods and organo-lead halides used were reagent grade chemicals.

Ultraviolet spectra were recorded using a Cary No. 14 spectrophotometer using fused silica cells and dried spectroscopic solvents.

Infrared spectra were recorded using a Beckman IR 12 spectrophotometer, with Nujol and halocarbon mulls between both KRS-5 and high density polyethylene windows.

Molecular weights were determined using a Hewlett–Packard vapor pressure osmometer model 302.

Conductivities were recorded using a Beckman model RC-18 bridge system, and a cell following the design of Greiner (8).

Thermogravimetric analysis was done using an R. L. Stone furnace and a Cahn electrobalance.

Acknowledgment

We thank the National Research Council of Canada for supporting this work and for a Studentship to D.P.

1. C. C. Addison, W. B. Simpson, and A. Walker. J. Chem. Soc. 2360 (1964).
2. B. Hetnarski and T. Urbański. Tetrahedron, **19**, 1319 (1963).
3. C. D. Hurd and P. R. Austin. J. Am. Chem. Soc. **53**, 1543 (1931).
4. C. C. Addison and D. Sutton. J. Chem. Soc. A, 1524 (1966).
5. R. Heap, B. C. Saunders, and G. J. Stacey. J. Chem. Soc. 658 (1951).
6. L. Riccoboni. Gazz. Chim. Ital. **71**, 696 (1941); Chem. Abstr. **36**, 6902 (1942).
7. R. S. Drago and K. F. Purcell. Non-aqueous solvent systems. *Edited by* T. C. Waddington. Academic Press, Inc., New York. 1965. p. 221.
8. R. H. Greiner. Fusion. Nov. 1960. p. 11

Can. J. Chem. Downloaded from www.nrcresearchpress.com by 210.87.254.6 on 09/05/12
For personal use only.

Can. J. Chem. Downloaded from www.nrcresearchpress.com by 210.87.254.6 on 09/05/12
For personal use only.

Abstraction of hydrogen atoms from bicyclo[2.1.1]hexane by methyl radicals and chlorine atoms: photochlorination of 1-methylbicyclo[2.1.1]hexane

R. SRINIVASAN AND F. I. SONNTAG

IBM Thomas J. Watson Research Center, Yorktown Heights, New York 10598

Received November 13, 1968

Photolysis of acetone has been used as a source of methyl radicals to study the abstraction of hydrogen atoms from bicyclo[2.1.1]hexane by methyl radicals. The reaction was found to have an activation energy of 10.3 kcal/mole and a pre-exponential factor that is typical of other abstraction reactions. The absolute rate of abstraction of hydrogen atoms from bicyclo[2.1.1]hexane by chlorine atoms at room temperature was measured to be 8.1×10^{10} l mole^{-1} s^{-1}. The photochlorination of 1-methylbicyclo-[2.1.1]hexane in solution gave both the 1-chloromethyl and 2- or 3-chloro-1-methylbicyclohexanes. The relative rates of attack at the methyl and the 2- or 3-position were determined to be 1:2.1. It is pointed out that the rate parameters for the abstraction of an H atom from bicyclo[2.1.1]hexane by a methyl radical are slower than for cyclopentane, as would be expected for a highly strained hydrocarbon, whereas the abstraction by chlorine is slightly faster than the rate for cyclopentane.

Canadian Journal of Chemistry, 47, 1627 (1969)

Introduction

The study of the chemistry of strained small-ring compounds is of considerable interest in understanding the nature of chemical bonding. Quantitative data, on the basis of which correlations between strain and reactivity may be made, are not extensive. In this work we have obtained quantitative data on the abstraction of a hydrogen atom from bicyclo[2.1.1]hexane (**1**) by a chlorine atom or a methyl radical, and

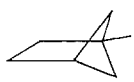

1

2

competitive rates of chlorination of 1-methylbicyclo[2.1.1]hexane (**2**).

Experimental

Materials

Bicyclo[2.1.1]hexane was prepared by the photoisomerization of 1,5-hexadiene (1). Following distillation, it was partially chlorinated in order to remove all the unsaturated impurities, and finally purified by vapor phase chromatography. Its m.p. was 26.5°. 1-Methylbicyclo-[2.1.1]hexane was prepared by the photoisomerization of 2-methyl-1,5-hexadiene (2). It was purified in the same way as the bicyclo[2.1.1]hexane. Acetone (Mallinckrodt TR grade) was dried over Drierite and distilled *in vacuo* before use. Chlorine gas (Matheson Co.) was used as obtained in the solution phase experiments.

Apparatus

The photolysis of acetone vapor at 3130 Å was used as the source of methyl radicals. The light source was a Hanovia S-100 medium pressure mercury arc which was energized through a Sola constant voltage transformer. The light beam was collimated, filtered with Pyrex glass (2 mm thickness), and admitted to the cylindrical quartz reaction cell of 9.3 cm length and 186.3 cc volume. The cell was placed in a furnace which was heated electrically. The temperature of the furnace was constant to ±1° during a run.

Procedure

Samples of acetone and bicyclo[2.1.1]hexane were measured in a calibrated part of the vacuum line and mixed together by condensation. The two compounds had boiling points which differed by only 15°. After photolysis, the mixture was separated into fractions by distillation. The fraction that was removed at liquid nitrogen temperature was found to consist of methane and CO. It was analyzed quantitatively by mass spectrometry. A second fraction which was removed at −156° was ethane only. The residue was analyzed by vapor phase chromatography. Three product peaks were invariably present in the C_7 region and were identified as C_7H_{12} compounds by mass spectrometry. Attempts to prepare them in substantial quantity for further identification proved fruitless.

Reaction of Cl(3/2) with Bicyclo[2.1.1]hexane

These experiments were carried out by Davis and Braun[1] by the technique which has been described in detail elsewhere[2]. The method involves the direct measurement of the concentration of chlorine atoms in the reaction system made up of chlorine gas and bicyclo-[2.1.1]hexane vapor by the change in the intensity of chlorine resonance fluorescence.

Photochlorination of 1-Methylbicyclo[2.1.1]hexane in Solution

The apparatus and procedure were exactly the same as in the earlier study (1) of the photochlorination of bicyclo[2.1.1]hexane in solution.

---

[1]National Bureau of Standards. U.S. Department of Commerce, Washington, D.C.

[2]D. Davis and W. Braun, to be published.

Can. J. Chem. Downloaded from www.nrcresearchpress.com by 210.87.254.6 on 09/05/12
For personal use only.

Results

1. Reaction of CH_3· with Bicyclo[2.1.1]hexane

The photolysis of acetone in the absence of addend yields methane and ethane by reactions [1] and [2] only. Conditions for which this

[1] $CH_3 + CH_3COCH_3 \rightarrow CH_4 + CH_2COCH_3$

[2] $2CH_3 \rightarrow C_2H_6$

mechanism is valid are quite well established (3). The usual treatment (3) applied to data obtained in the interval 150 to 225° led to

$$\log k_1/k_2^{\frac{1}{2}} = (4.2 \pm 0.9) - ((9200 \pm 500)/2.303RT)$$

in units of l mole^{-1} s^{-1}. The Arrhenius parameters agree reasonably well with those recently obtained (4), even though the present data were taken at less than 20 mm pressure of acetone, and thus are near the low end of the "high pressure" region discussed by Shaw and Toby (4). This pressure was chosen to permit the slow abstraction from bicyclo[2.1.1]hexane to compete when the hydrocarbon was present. Under those conditions, methane is also formed in reaction [3]

[3] $CH_3 + C_6H_{10} \rightarrow CH_4 + C_6H_9$

The usual treatment of the data gives $k_3[C_6H_{10}]/k_2^{\frac{1}{2}}$. These values at various temperatures have been plotted in the usual way in Fig. 1. The best line through the points, which was determined by least-squares analysis, corresponded to a value for $E_3 - \frac{1}{2}E_2$ of 10.3 ± 0.5 kcal/mole. Using the expression $k_2 = 2 \times 10^9 T^{\frac{1}{2}}$ l mole^{-1} s^{-1} (4), the value of log A_3 can be calculated to be 8.7 in the same units.

2. Reaction of Cl(3/2) Atoms with Bicyclo-[2.1.1]hexane

This reaction was studied at room temperature at 2 different pressures of bicyclo[2.1.1]hexane. The bimolecular rate constant was 8.13 × 10^{10} l mole^{-1} s^{-1}, with an uncertainty of ±10%.

3. Photochlorination of 1-Methylbicyclo[2.1.1]-hexane in Solution

In preparative experiments, it was found that photochlorination of 1-methylbicyclo[2.1.1]-hexane gave 2 monochloro products in about 20% yield. The products were separated by vapor phase chromatography. The first product, amounted to a third of the total monochloro compounds, was analyzed as follows.

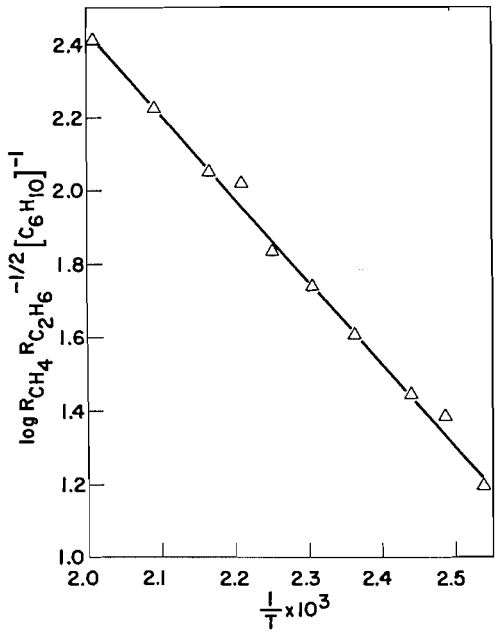

FIG. 1. Arrhenius plot for the abstraction of hydrogen atoms from bicyclo[2.1.1]hexane by methyl radicals. The ordinate should be multiplied by 8.00 × 10^{-5} to convert to units of l$^{\frac{1}{2}}$ mole$^{-\frac{1}{2}}$ s$^{-\frac{1}{2}}$.

Anal. Calcd. for $C_7H_{11}Cl$: C, 64.37; H, 8.49. Found: C, 64.61; H, 8.55.

It had an intense infrared absorption at 724 cm^{-1} (C—Cl) and no strong absorption between 1350 and 1400 cm^{-1}, showing the absence of a CH_3 group. Its nuclear magnetic resonance (n.m.r.) spectrum consisted of a singlet 6.31 τ (2H), a broad absorption at 7.58 τ (1H), and a complex absorption from 8.1 to 9.0 τ which accounted for the remaining protons. The material could be reduced with sodium and ethanol to regenerate 1-methylbicyclo[2.1.1]hexane. This showed that the chloro compound had the same carbon skeleton as 1-methylbicyclo[2.1.1]-hexane. The absence of a methyl absorption in the infrared, coupled with the unsplit absorption at 6.31 τ due to 2 protons, indicates that the chlorine was most probably in a CH_2Cl group adjacent to a carbon with no protons on it. The structure **3** would fit all of these observations. The remainder of the monochlorinated product is believed to be a mixture of possibly 2 com-

TABLE I

Ratio of rate of formation of (**4**+**5**) to **3** during photochlorination in solution*

Run no.	Temperature, °C	No. of determinations averaged	$\frac{R_{4+5}}{R_3}$	Remarks
1	5	5	2.1	Conversion at the end 14%
2	5	7	2.0	
3	32	4	2.2	Rate of chlorocyclohexane formation/$R_{(4+5)} \sim 2.3$

*Solvent: CCl_4; visible light (tungsten lamp).

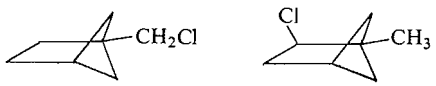

3

4

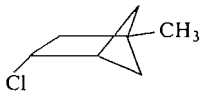

5

pounds, although it could not be resolved into 2 peaks on a gas chromatograph.

Anal. Calcd. for $C_7H_{11}Cl$: C, 64.37; H, 8.49; Cl, 27.14. Found: C, 64.34; H, 8.47; Cl, 27.37.

Its infrared spectrum showed a medium absorption at 1365 cm^{-1} (CH_3—) and an intense one at 710 cm^{-1} (C—Cl). There was no evidence of unsaturation. In the n.m.r. spectrum there was no absorption $> 5.5\ \tau$. There was an absorption at about 5.7 τ which had 1/11 of the total intensity of the spectrum. The remaining absorptions formed a complex pattern from 7.3 to 9.1 τ. In 2-chlorobicyclo[2.1.1]hexane, the proton on the 2-carbon occurs at 5.7 τ as a doublet with a splitting of 7 cycles (1). In the present case, the absorption at 5.7 τ was made up of a pair of doublets 17 cycles apart, each of which had a separation of 7 cycles. This material was most probably a mixture that was made up of nearly equal amounts of **4** and **5**, since extrapolation from earlier results on the photochlorination of bicyclo[2.1.1]hexane indicated that substitution in the ring in **2** would occur almost exclusively in the 2- and/or 3-positions (1).

The results of quantitative studies are given in Table I. The study was complicated by the fact that the $C_6H_{11}Cl$ compounds reacted much more rapidly with chlorine than with hydrocarbon so that the conversion had to be kept low. At the same time, only 16–20% of the hydrocarbon that disappeared was observed to lead to **3**, **4**, and **5**. The ratio of **3** to **4** + **5** (*i*) could be consistently reproduced, (*ii*) held constant over conversions which ranged from 0 to 20%, and (*iii*) was the same at 5 and 32°. Owing to experimental problems in separating 1-methylbicyclo[2.1.1]hexane from cyclohexane in the gas chromatograph, it was not possible to obtain accurate data on the relative rates of monochlorination of these two compounds. The result of only one run is included in Table I.

Discussion

In an earlier investigation on the photochlorination of bicyclo[2.1.1]hexane in solution (1), it was observed that (*i*) the chlorination was highly selective since better than 95% of the attack occurred at only one of 4 possible sites in the molecule, and (*ii*) the rate of monochlorination was comparable to the rate of monochlorination of cyclohexane, which meant that on a per atom basis, the C—H bond in the 2-position in bicyclo[2.1.1]hexane was slightly *more* reactive than a C—H bond in cyclohexane. Both these observations are considered unusual (5), in reference to what is known of the photochlorination of linear, aliphatic compounds. Bicyclo[2.1.1]-hexane should, strictly speaking, be compared to other strained, bicyclic systems. It has already been noted (1) that the data on the photochlorination of bicyclo[2.2.1]heptane (6) also show the trends that are observed in bicyclo-[2.1.1]hexane.

The experiments undertaken in this study were intended to examine if

(*i*) The abstraction of a hydrogen atom from

Can. J. Chem. Downloaded from www.nrcresearchpress.com by 210.87.254.6 on 09/05/12
For personal use only.

Can. J. Chem. Downloaded from www.nrcresearchpress.com by 210.87.254.6 on 09/05/12
For personal use only.

bicyclo[2.1.1]hexane by a radical other than chlorine (i.e. methyl) shows the trend that has been observed with the same radical and other strained hydrocarbons.

(*ii*) The absolute rate of reaction of chlorine atoms and bicyclo[2.1.1]hexane supports the contention that this rate is greater than that between chlorine atoms and a saturated, unstrained hydrocarbon.

(*iii*) In the photochlorination of 1-methylbicyclo[2.1.1]hexane, the chlorination in the 2- or 3-positions shows an acceleration in comparison to chlorination at the methyl group, which would serve as an internal reference for the reaction.

We shall analyze the present data in terms of these questions.

Accurate rate parameters for a large number of abstraction reactions of methyl radicals are known (7, 8). In a series of saturated hydrocarbons, which serve as the donor molecules, the activation energies increase as the C—H bonds go from tertiary to secondary and primary, while for similarly substituted C—H bonds, the activation energies increase with increasing strain in the molecules. The activation energies for abstraction from cyclopentane, cyclobutane, and cyclopropane (all of which contain only secondary C—H bonds) are 9.1, 10.1, and 12.9 kcal/mole, respectively (8). In bicyclo[2.1.1]hexane, it is reasonable to assume that abstraction of a hydrogen atom will occur only in the 2-position, since even such an unselective agent as a chlorine atom will abstract hydrogen from only that position 95% of the time. Although the 2-position is part of a cyclopentane ring, the fusion of a second ring should increase the strain in the 5-membered ring. One may expect the activation energy for the abstraction of a hydrogen atom to be considerably more than that for a cyclopentane ring (strain energy $\sim$ 6 kcal/mole), and comparable to that for a cyclobutane (strain energy 26.1 kcal/mole) or a cyclopropane (strain energy 27.5 kcal/mole) (9). The experimental value of 10.3 kcal/mole for [3] indicates the considerable influence of strain on the activation energy. The A factor for [3] when reduced to a per "active hydrogen" basis is comparable to those for similar abstractions from cyclopropane, cyclobutane, and cyclopentane (8). These data strongly suggest that the C—H bond in the 2-position in bicyclo[2.1.1]hexane behaves predictably as far as the abstraction reaction by methyl radicals is concerned[3].

The absolute rate of the abstraction reaction [4] in the gas phase when RH is cyclohexane is

$$[4] \qquad Cl + RH \rightarrow HCl + R$$

not known, but the rate with RH = cyclopentane has been found to be 8.35×10^{10} l mole^{-1} s^{-1} at 25 °C (10). The relative rates of abstraction of a hydrogen from cyclopentane and bicyclo[2.1.1]hexane would hence be 1:0.97. On an "active hydrogen" basis, this ratio would be cyclopentane:bicyclo[2.1.1]hexane = 1:2.4. From the rates of photochlorination of cyclopentane and cyclohexane in solution, it is known (11) that[4] abstraction from cyclopentane is 0.85 (relative to cyclohexane as 1.00) per hydrogen at 68° and 0.95 at 0°. If, at 25°, this value is taken to be 0.9, and assumed to be applicable to the gas phase reaction, the ratio cyclohexane:bicyclo[2.1.1]hexane (on a per "active hydrogen" basis) would be 1:2.2. This compares favorably with the value of 2.4 that was found (1) by competitive chlorination of cyclohexane and bicyclo[2.1.1]hexane in solution. There seems to be no doubt that on the basis of per "active hydrogen", bicyclo[2.1.1]hexane is more reactive towards chlorine atoms than cyclohexane.

The photochlorination of 1-methylbicyclo[2.1.1]hexane is obviously not a simple reaction as the yield of monochlorinated products is poor. A check of the consistency of the present values on chlorination, at two competitive sites within the molecule, against the earlier values on competitive attack on bicyclo[2.1.1]hexane and cyclohexane (if methylcyclohexane is used as a reference compound to provide a correlation between the two ring systems), showed that the

---

[3]The trend has been found to persist in the more highly strained bicyclic hydrocarbons. The activation energy for the abstraction of a hydrogen by methyl radicals from bicyclo[1.1.1]pentane has been measured to be 11.2 kcal/mole. It is likely that in the case of bicyclo[1.1.0]butane and bicyclo[2.2.0]hexane, the hydrocarbon may not survive the temperatures at which such competitive abstraction reactions can be studied.

[4]The reactivity of cyclopentane relative to cyclohexane is so nearly the same that there are other studies in the literature (5) that place cyclopentane ahead of cyclohexane on the reactivity scale. However, it seems to be agreed that the difference is no more than $\pm 10\%$, so that this is the correction that has to be applied in this investigation to the bicyclo[2.1.1]hexane value to take it from cyclopentane scale to the cyclohexane scale.

present results were not in quantitative agreement with the earlier work (1).

In conclusion, it is relevent to speculate on the cause of the increased reactivity of the hydrogen in the 2-position in bicyclo[2.1.1]hexane relative to cyclohexane. Since the experiments with methyl radicals show that the activation energy for abstraction does increase as would be expected, the activation energy for the abstraction process [5] may be expected to be about 200 cal/

[5] $Cl\cdot$ + 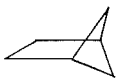 $\longrightarrow$ HCl + 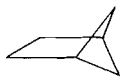

mole greater than the value of 600 cal/mole that has been measured for cyclopentane (10). There is a similar increase in going from cyclopentane to cyclobutane. The resultant value of log A_5 = 11.4 would be outside the observed range of 9.7–10.6 for the values of log A for such reactions (10). There is no doubt that more data on reaction [5] over a range of experimental conditions are needed before these unusual effects can be explained.

Acknowledgments

It is a pleasure to thank Mrs. J. M. Picone for her skillful assistance. R.S. also thanks Dr. M. Poutsma of the Union Carbide Research Institute for many helpful discussions.

1. R. Srinivasan and F. I. Sonntag. J. Am. Chem. Soc. **89**, 407 (1967).
2. R. Srinivasan and K. H. Carlough. J. Am. Chem. Soc. **89**, 4932 (1967).
3. E. W. R. Steacie. Atomic and free radical reactions. Vol. II. Reinhold Publishing Corp., New York. 1954. p. 497.
4. H. Shaw and S. Toby. J. Phys. Chem. **72**, 2337 (1968).
5. M. Poutsma. Free-radical chlorination of organic molecules. Marcel Dekker, New York. In press.
6. E. C. Kooyman and G. C. Vegter. Tetrahedron, **4**, 382 (1958).
7. S. W. Benson. The foundations of chemical kinetics. McGraw-Hill Book Co., Inc., New York. 1960. p. 296.
8. A. F. Trotman-Dickenson. Advances in free-radical chemistry. *Edited by* G. H. Williams. Logos Press, London. 1965. p. 21.
9. K. B. Wiberg and R. A. Fenoglio. J. Am. Chem. Soc. **90**, 3395 (1968).
10. Calculated from the rate parameters given by G. C. Fettis and J. H. Knox. Progr. Reaction Kinetics, **2**, 1 (1964).
11. C. Walling and P. S. Fredericks. J. Am. Chem. Soc. **84**, 3326 (1962).

Can. J. Chem. Downloaded from www.nrcresearchpress.com by 210.87.254.6 on 09/05/12
For personal use only.

Can. J. Chem. Downloaded from www.nrcresearchpress.com by 210.87.254.40 on 09/05/12
For personal use only.

Vibrational spectra and a force field for H_2S_3 and H_2S_4[1]

H. WIESER AND P. J. KRUEGER
Department of Chemistry, University of Calgary, Calgary, Alberta

AND

E. MULLER AND J. B. HYNE
Fundamental Sulphur Research Group, Alberta Sulphur Research Ltd., Department of Chemistry, University of Calgary, Calgary, Alberta

Received November 8, 1968

The infrared and Raman spectra of H_2S_3 and H_2S_4 in CCl_4 and CS_2 solutions are reported and a complete assignment is presented. On the basis of the spectra and their temperature and concentration dependence, H_2S_3 is considered to be in the GG and H_2S_4 in the GG'G conformation. A valence force field is derived which provides a least-squares fit between observed and calculated frequencies for both molecules simultaneously, with an average error of 1.5 cm^{-1} (or 0.4%) over all frequencies.

Canadian Journal of Chemistry, 47, 1633 (1969)

Introduction

Except for the work of Fehér *et al.* (1) the vibrational spectra of the hydrogen polysulfides have not been studied in any detail. Fehér's Raman spectra were those of the pure liquid, while no infrared (i.r.) spectra have been reported yet. Moreover, the vibrational assignments which have been made are incomplete, and conformational analysis has not been attempted (2).

In this communication the i.r. and Raman spectra of H_2S_3 and H_2S_4 in solution (CS_2 and CCl_4) are reported, together with complete assignments. At the same time an attempt was made to establish whether the two polysulfides exist in one or more conformations, and if so, to identify these alternatives. Assuming that the geometrical parameters of H_2S_2 (3) and S_8 (4) may also apply to the polysulfides (Fig. 1) and allowing only staggered conformations, there are 4 possible rotamers for H_2S_3 and 10 possible rotamers for H_2S_4. Since in H_2S_3 the 3 sulfur atoms lie in a plane, the various conformations differ only in terms of the angles of the S—H bonds with respect to this plane. In H_2S_4, on the other hand, the 4 S atoms need not lie in a single plane. Since polymeric sulfur chains are highly coiled (5), it was assumed in the first instance that the G conformation about the central S—S bond is the most stable. However, a similar decision could not be made with regard to the conformations of the S—H bonds without first considering the spectroscopic results. Figure 1 shows the two conformers which were finally chosen as the most probable ones (see Discussion). In addition, an attempt was made to find a refined force field (modified valence force field) which would provide the best possible fit between the calculated and observed frequencies of both molecules simultaneously (in the harmonic oscillator approximation).

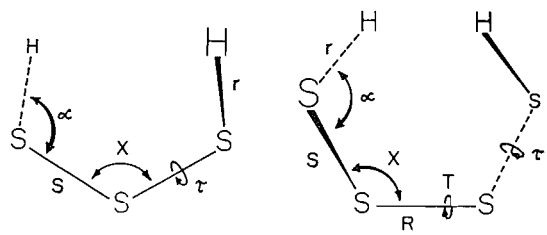

FIG. 1. Internal coordinates for H_2S_3 (GG conformer) and H_2S_4 (GG'G conformer); the geometrical parameters are those for H_2S_2(3) and S_8 (4). r_{S-S} = 2.048 Å, r_{S-H} = 1.352 Å, ∠SSS = 107° 55′, ∠SSH = 91° 57′, dihedral ∠SS–SS = 98° 39′, dihedral ∠SS–SH = 90° 37′.

Experimental

Compounds and Spectra

Solutions of H_2S_3 and H_2S_4 in CCl_4 and CS_2 (2 *M*) were prepared by the reaction of liquid H_2S with SCl_2 and S_2Cl_2 as reported previously (6). The purity of the polysulfides, as established by nuclear magnetic resonance (n.m.r.) (7), was found to be 90 ± 2 mole % for H_2S_3 and 95 ± 2 mole % for H_2S_4, the higher sulfanes being present only in small quantities. The solvents used (CCl_4 and CS_2) were spectrograde quality as supplied by Fisher Scientific Co.

The i.r. spectra were recorded on a Perkin–Elmer 621 spectrophotometer over the range of 4000–400 cm^{-1}

[1]Presented at the 15th Spectroscopy Symposium of Canada, Toronto, October 21–23, 1968.

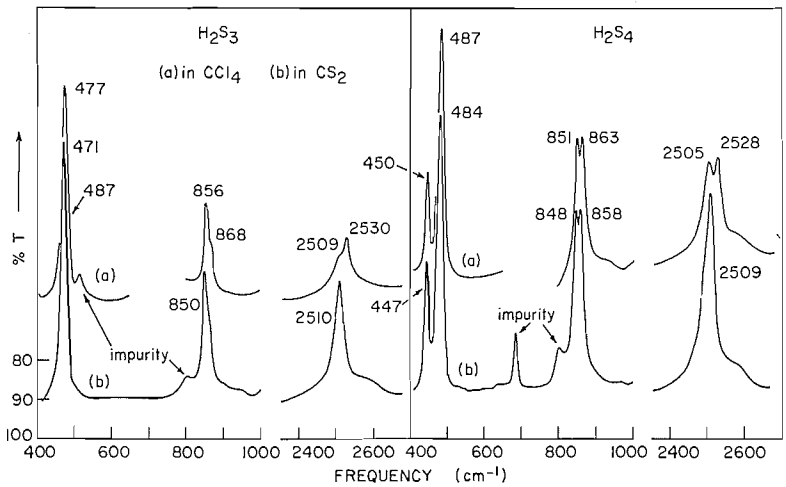

FIG. 2. Infrared spectra of H_2S_3 and H_2S_4 in CCl_4 and CS_2 solutions (2 *M*).

using 0.1 and 1.0 mm KBr or 2.0 cm Infrasil cells depending on the concentrations of the solutions. The Raman spectra were obtained with a Cary 81 spectrophotometer equipped with a He–Ne laser (6328 Å exciting line, 50 mW power output). Since the coaxial excitation mode was found to be the most convenient, the depolarization ratios had to be corrected by comparison with spectra of CCl_4 obtained with the same capillary cells. Accurate depolarization ratios therefore cannot be reported. Except where indicated otherwise, all measurements were made at room temperature.

Both instruments were calibrated in the conventional manner. The frequency values reported constitute averages of several runs. By comparing the spectra of several different preparations of the same polysulfide containing different percentages of the higher sulfanes, the absorptions could be assigned unambiguously and any interference from other sulfanes ruled out. The spectra are reproduced in Figs. 2 and 3.

Force Field Calculations

The force constants were determined by an iterative technique (8) which provided a least-squares fit between the observed and calculated frequencies. Seventeen observed frequencies were entered for GG H_2S_3 and GG'G H_2S_4 and weighted in a reciprocal manner. Convergence led to an average error of 1.5 cm^{-1} (or 0.4%) over the entire frequency range.

The internal coordinates and geometrical parameters are defined in Fig. 1. Table I defines the group and skeletal coordinates, and Table II lists and identifies the refined valence force constants. The initial values for the main constants for the calculations were taken as those for H_2S_2 (9) and S_8 (10) and these are listed in the last column of Table II. The H_2S_2 values were adjusted since our calculations made no provisions for anharmonicity. Initially all interaction force constants were set to zero. The force field as defined in Table II is modified so that interactions which probably would not contribute to the potential energy have been neglected arbitrarily. Transformation of the force field based on internal coordinates to a force field in terms of the symmetry coordinates as required by Wilson's **FG** method (11) shows that 9 of the 16 possible interaction constants have been considered for H_2S_3 and 15 of the 31 possible constants have been considered for H_2S_4. The observed and calculated frequencies for GG H_2S_3 and GG'G H_2S_4 are listed in Table III, together with the potential energy distributions based on the diagonal contributions from the group coordinates defined in Table I.

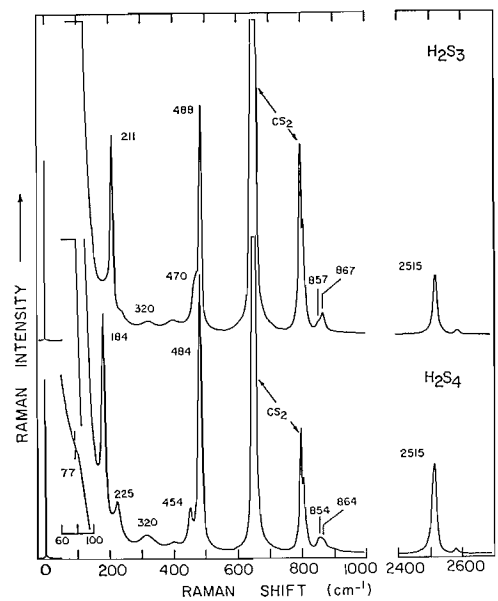

FIG. 3. Raman spectra of H_2S_3 and H_2S_4 in CS_2 solution (2 *M*).

Can. J. Chem. Downloaded from www.nrcresearchpress.com by 210.87.254.40 on 09/05/12
For personal use only.

TABLE I

Definition of coordinates used in potential energy distribution (Table III)

Coordinates	Definition
r^-	out-of-phase S—H stretch
r^+	in-phase S—H stretch
α^-	out-of-phase HSS bend
α^+	in-phase HSS bend
τ^-	out-of-phase HS—SS torsion
τ^+	in-phase HS—SS torsion
S^-	asymmetric S—S stretchin H_2S_3, and out-of-phase S—S stretch of terminal bonds in H_2S_4
S^+	symmetric S—S stretch in H_2S_3, and in-phase S—S stretch of terminal bonds in H_2S_4
R	S—S stretch of central bond in H_2S_4
X	SSS bend in H_2S_3
X^-	out-of-phase SSS bend in H_2S_4
X^+	in-phase SSS bend in H_2S_4
T	SS—SS torsion in H_2S_4

Discussion

Assignments

According to the n.m.r. proton shifts and the positions and shapes of the S—H stretching bands, H_2S_3 in CCl_4 forms intermolecularly hydrogen bonded polymers in concentrated solutions (2 *M*) and intramolecularly bonded monomers in dilute solution (0.02 *M*). In CS_2 the intramolecular bonds are competing with the intermolecular interaction with the solvent molecules, even at low concentration (7). The question arises whether the H_2S_3 monomer undergoes a conformational change upon forming intermolecular hydrogen bonds. In this work no significant shifts in the position of the absorptions of H_2S_3 upon dilution in CCl_4 have been noted except for the S—H stretching band as reported previously (7). Moreover, the doublet structure of the S—H bending absorption apparent in the i.r. spectrum of the CCl_4 solution persists in the Raman spectrum of the CS_2 solution. There are two ways in which the results may be interpreted; either H_2S_3 remains in the same conformation regardless of the environment, or the vibrations (except S—H stretching) are insensitive to conformational changes.

Our assignments and calculations are based on the GG conformer (Fig. 1), since in this conformation intramolecular hydrogen bonding may be achieved by both hydrogen atoms. This conformer has C_2 symmetry, giving rise to 5 vibrations of symmetry species *A* and 4 of *B*. The

TABLE II

Refined force constants for H_2S_3 and H_2S_4

Force constant	Group	Coordinate(s) involved	Atoms common to interacting coordinates	Calculated force constant (ϕ_i)	Error $\sigma(\phi_i)$*	Literature force constants
		Valence force constants				
K_r	H—SSS	H—S	—	3.700	0.0	3.70†
K_S	HS—SS	S—S	—	2.236	0.0	2.65†
K_R	SS—SS	S—S	—	1.721	0.0	2.37‡
H_α	H—SSS	∠HSS	—	0.746	0.0	0.78†
H_X	HS—SS	∠SSS	—	1.114	0.0	0.23‡
H_τ	HS—SS	$\angle_d$HS—SS	—	0.102	0.0012	0.08†
H_T	SS—SS	$\angle_d$SS—SS	—	0.117	0.0	0.04‡
		Interaction force constants				
F_S	HS—S—S	S—S,S—S	S	0.344	0.0	
F_R	SS—S—S	S—S,S—S	S	0.232	0.0	
F_{rS}	H—S—SS	H—S,S—S	S	0.0	0.0	
$F_{r\alpha}$	H—S—SS	H—S,∠HSS	H—S	0.0	0.0	
$F_{S\alpha}$	H—S—SS	S—S,∠HSS	S—S	−0.018	0.0	
F_{SX}	HS—S—S	S—S,∠SSS	S—S	0.040	0.0	
F_{RX}	SS—S—S	S—S,∠SSS	S—S	−0.057	0.0	
$f_{rr'}$	H—S...S—H	H—S,H—S	None	0.012	0.0	
$f_{SS'}$	S—S...S—S	S—S,S—S	None	−0.042	0.0	
$f_{\alpha\alpha'}$	H—S...S—H	∠HSS,∠HSS	None	0.012	0.0022	
$f_{\alpha X}$	H—S—S—S	∠HSS,∠SSS	S—S	0.119	0.0	
f_{XX}	S—S—S—S	∠SSS,∠SSS	S—S	0.031	0.023	
$f_{X\tau}$	HS—S—S	∠SSS,$\angle_d$HS—SS	S—S	0.037	0.0	
f_{XT}	S—S—SS	∠SSS,$\angle_d$SS—SS	S—S	0.009	0.016	

*$\sigma(\phi_i)$ is the standard error in ϕ_i estimated from the standard error in the frequency parameters and the variance-covariance matrix.
†From H_2S_2 (9).
‡From S_8 (10).

Can. J. Chem. Downloaded from www.nrcresearchpress.com by 210.87.254.40 on 09/05/12
For personal use only.

TABLE III

Observed and calculated frequencies for H_2S_3 and H_2S_4

Observed frequencies (cm^{-1})*				
Infrared		Raman	Calculated frequencies	
CCl_4 solution	CS_2 solution	CS_2 solution	(cm^{-1})	Approximate potential energy distribution (%)†
H_2S_3				
~2540 sh‡			2540	(*A*) r^+ (100)
2532 m‡			2532	(*B*) r^- (100)
(2509 sh)	(2510 m)	(2515 m p)		Intermolecular SH...S (another H_2S_3 molecule or CS_2)
868 sh		867 w p	863	(*A*) α^+ (95)
856 m	850 m	857 w d	856	(*B*) α^- (100)
487 sh		488 s p	485	(*A*) S^+ (79), X (10)
477 s	471 s	470 sh	477	(*B*) S^- (117)
		320 vw bd	323	(*B*) τ^- (100)
			310	(*A*) τ^+ (101)
		211 s p	211	(*A*) X (97)
H_2S_4				
~2540 sh‡			2540	(*A*) r^+ (100)
2532 m‡			2532	(*B*) r^- (100)
(2505 sh)	(2509 m)	(2515 m p)		Intermolecular SH...S (another H_2S_4 molecule or CS_2)
863 m	858 m	864 w d	869	(*A*) α^+ (96)
851 m	848 m	854 w d	851	(*B*) α^- (100)
487 s	484 s		489	(*B*) S^- (96)
		484 s p	483	(*A*) S^+ (80), X^+ (12)
450 m	447 m	454 w p	451	(*A*) R (83), S^+ (19)
		320 vw bd	322	(*A*) τ^+ (87)
			318	(*B*) τ^- (98)
		225 w d	225	(*B*) X^- (103)
		184 s p	183	(*A*) X^+ (75), R (13), τ^+ (11)
		77 sh	76	(*A*) T (92)

*Frequencies in italics entered into force field refinement. Abbreviations are: s, strong; m, medium; w, weak; vw, very weak; sh, shoulder; bd, broad; p, polarized; d, depolarized.

†Potential energy distributions are given in % contribution of the diagonal force constants for coordinates defined in Table I. Because of some off-diagonal negative contributions, the sum of the diagonal contributions may exceed 100%. Only contributions of 10% or more are listed.

‡Measurements in dilute solution.

vibrations of species *A* should give polarized Raman lines; they have been assigned accordingly. It is interesting to note the intensity reversal of the 477 and 487 cm^{-1} vibrations on going from the i.r. to the Raman spectrum.

H_2S_4 in CCl_4 solution shows the usual concentration dependent self-association, although the monomer does not appear to be as strongly intramolecularly bonded as H_2S_3 (7). In CS_2 solution, association between the sulfane and solvent molecules appears to be preferred even at low concentration (0.02 *M*) (7). As an extension of this work the temperature dependence of the "free" S—H stretching band in very dilute CCl_4 solution (0.02 *M*), and of all absorptions in 2 and 1 *M* CCl_4 solutions, was tested over a temperature range of 40 °C (+20 to −20 °C). No changes in the shapes of any bands as a function of the temperature could be observed, and concentration changes did not result in any significant shifts in the band positions (except for the S—H stretching absorption). Moreover, changing the solvent from CCl_4 to CS_2 (2 *M* solutions) resulted only in a general shift to lower frequencies for all absorptions (about 20 cm^{-1} for the S—H stretching band and about 5 cm^{-1} for all others). It appears therefore that essentially no conformational rearrangement is occurring, unless the band positions are the same for two or more conformers.

Our assignments and calculations have been based on the GG'G conformer (Fig. 1), since again in this conformation both hydrogen atoms are able to form hydrogen bonds. It is of interest to note that the crown form of the S_8 ring has exactly that arrangement of bonds. Due to the C_2 symmetry point group of this conformer, the 12 normal modes can be divided into 7 vibrations of symmetry *A* and 5 of *B*. Only the *A*-type vibrations should give rise to polarized Raman lines

Can. J. Chem. Downloaded from www.nrcresearchpress.com by 210.87.254.40 on 09/05/12
For personal use only.

which have been assigned accordingly. The S^- (*B*-type) and S^+ (*A*-type) vibrations are considered to overlap, with the prominent lines being measured at 487 and 484 cm^{-1} in the i.r. and Raman spectra, respectively.

Valence Force Field

In view of the spectral behavior of the CCl_4 and CS_2 solutions of H_2S_3 and H_2S_4, the choice of the GG and GG'G conformers, respectively, seems the most reasonable. It is in these conformers that the non-bonded interactions required to explain the doublet structure of the S—H stretching and bending and the S—S stretching vibrations, are most plausible. In the valence force field the non-bonded interactions have been taken into consideration by introducing $f_{rr'}$, $f_{SS'}$, and $f_{\alpha\alpha'}$. As shown in Table III, the force field so derived results in an excellent fit between the observed and calculated frequencies, whereas if the non-bonded interaction constants are neglected, a reasonable fit simply cannot be achieved. Using this refined force field, it was found that the frequencies calculated for other conformations were not significantly different. Consequently the calculated force field rests heavily on the validity of the arguments supporting the conformers selected.

Acknowledgments

We gratefully acknowledge financial support from the National Research Council of Canada and Alberta Sulphur Research Ltd.

1. F. FEHÉR, W. LAUE, and G. WINKHAUS. Z. Anorg. Allgem. Chem. **228**, 8 (1956).
2. M. L. JOSIEN and G. SOURISSEAU. *In* Nouveau traité de chimie minérale. Vol. 13. Masson et Cie., Paris. 1960.
3. M. WINNEWISSER and J. HAASE. Z. Naturforsch. **23A**, 56 (1968).
4. A. S. COOPER, W. L. BOND, and S. C. ABRAHAMS. Acta Cryst. **14**, 1008 (1961).
5. J. A. SEMLYEN. Trans. Faraday Soc. **63**, 743 (1967).
6. E. MULLER and J. B. HYNE. Can. J. Chem. **46**, 2341 (1968).
7. E. MULLER and J. B. HYNE. Can. J. Chem. **46**, 3587 (1968).
8. H. WIESER, W. G. LAIDLAW, P. J. KRUEGER, and H. FUHRER. Spectrochim. Acta, **24A**, 1055 (1968).
9. B. P. WINNEWISSER and M. WINNEWISSER. Private communication.
10. D. W. SCOTT, J. P. MCCULLOUGH, and F. H. KRUSE. J. Mol. Spectry. **13**, 313 (1964).
11. E. B. WILSON, J. C. DECIUS, and P. C. CROSS. Molecular vibrations. McGraw-Hill Book Co., Inc., New York. 1955. p. 309.

Can. J. Chem. Downloaded from www.nrcresearchpress.com by 210.87.254.40 on 09/05/12
For personal use only.

Can. J. Chem. Downloaded from www.nrcresearchpress.com by 210.87.254.5 on 09/05/12
For personal use only.

Anion–molecule complexes in solution. III.[1] Nuclear magnetic resonance studies of halide ion – alcohol association

R. D. GREEN AND JOHN S. MARTIN
Department of Chemistry, University of Alberta, Edmonton, Alberta

AND

W. B. MCG. CASSIE AND J. B. HYNE
Department of Chemistry, University of Calgary, Calgary, Alberta

Received September 24, 1968

Certain alkyl-, aryl-, and arene-substituted alcohols form linear, hydrogen bonded complexes with bromide and other halide ions in tetrachloromethane. The hydroxyl proton shifts ca. 4 p.p.m. downfield in the complex, regardless of the degree or type of substitution. The interaction is enhanced by inductive electron withdrawal by substituents on the C—O—H moiety. A comparison of the present results with infrared spectroscopy shows that the absorption at ca. 3300 cm^{-1} is entirely due to 1:1 alcohol–anion complexes. The a coefficient in Buckingham's equation for electrostatic interaction of a molecule with an ion, $\delta\sigma_E = aE_z - bE^2$, is found to be 5.5 for alcohol O—H bonds.

Canadian Journal of Chemistry, 47, 1639 (1969)

Introduction

Nuclear magnetic resonance (n.m.r.) and infrared (i.r.) spectroscopy have been used extensively in the detection and characterization of the hydrogen bonding of alcohols and other hydroxyl bearing compounds to a variety of bases (1–3). Characteristically, hydrogen bond formation results in a decrease in shielding of the hydrogen nucleus. The extent of this deshielding has been regarded as a measure of hydrogen bond strength, in much the same way as have hydrogen bond shifts and intensities in the i.r. (1, 3, 4). Both the i.r. frequency shift and the n.m.r. shielding change have been correlated with the enthalpy of hydrogen bond formation (5).

Pursuant to our studies of specific complexes to anions in weakly interacting solvents, we have observed deshielding of hydroxyl protons in methanol, primary, secondary, and tertiary alcohols, and a phenol, of magnitude up to 4.5 p.p.m., on addition of a tetrabutylammonium salt to a dilute solution of the alcohol in tetrachloromethane. We interpret the monotonic salt concentration dependence of the hydroxyl proton shifts as arising from specific hydrogen bonded interaction of the alcohols with the anions. Conditions have been chosen to favor one to one complex formation; the alcohol concentration was kept as low as possible (0.1 M) to minimize alcohol to alcohol hydrogen bonding, and the proton shielding observed as a function of the halide ion concentration.

[1]For Paper I see ref. 23, and for Paper II see ref. 24.

Experimental

Materials

Methanol

This was Shawinigan reagent grade, and contained less than 0.2% water when received. This material was dried by storing over 4A molecular sieves (m.s.) for several days; the initial vigorous effervescence ceased after about 24 h. The tightly stoppered vial was kept in the dry-box. Samples containing methanol and tetrabutylammonium bromide decomposed slowly, the n.m.r. spectrum showing a change after 1 day, but no observable change within 1 h of sample preparation. All spectra were obtained within 1 h of preparation of the sample.

Ethanol

This was 98%, as received, and showed no benzene in the n.m.r. and, at most, traces of water. This material was distilled, and a center fraction totalling ca. 75% collected on m.s. The fraction collected was refluxed over the m.s. for 1 h. The material was then redistilled with a center fraction totalling ca. 50% being collected on m.s. (boiling range 0.4 °C). The tightly-stoppered flask was immediately transferred to the dry-box, where the ethanol was placed in a storage vial over fresh m.s. A subsequent Karl Fischer titration of a portion of this material showed no detectable water (less than 0.01% by volume) in the ethanol.

2-Propanol

Fisher reagent grade material was dried over m.s. for several days before being used.

2-Methyl-2-propanol

British Drug Houses reagent grade material was received as a colorless liquid. This was dried over m.s., the container being kept warm in a water bath. On cooling, the material crystallized.

Can. J. Chem. Downloaded from www.nrcresearchpress.com by 210.87.254.5 on 09/05/12
For personal use only.

Phenylmethanol, 1-Phenylethanol, and 4-Methoxyphenylmethanol

These materials, all Eastman "white label", were dried over m.s. before use.

2-Phenyl-2-propanol

This was kindly supplied by L. B. Green, and was dried over m.s. Its n.m.r. spectrum showed no significant impurities.

4-Nitrophenylmethanol

This was Eastman "white label" grade, and was used as received, since the n.m.r. signal of the OH proton (dissolved in CH_3CN) was a sharp triplet.

Tetra-n-butylammonium Bromide, Tetra-n-butylammonium Iodide

The Eastman "white label" salts were pumped under vacuum in a desiccator (over P_2O_5) for several weeks, then stored in the dry-box.

Tetra-n-butylammonium Chloride

This was from Eastern Chemical Corportion and contained benzene which was not easily removed by pumping. The salt was dissolved in a small volume of CCl_4, then precipitated by adding cyclohexane. The salt so obtained was then dried by pumping as above and found by n.m.r. to be free of benzene. It, too, was stored in the dry-box.

Tetrachloromethane

This was Shawinigan reagent grade, and was passed through a column of alumina (activity grade I); tetramethylsilane was added to serve as an n.m.r. internal reference before storing in the dry-box over m.s.

Tetramethylsilane (TMS)

This was obtained from NMR Specialties and was refrigerated over m.s. before using.

Procedures

All samples were prepared inside a sealed dry-box which was kept under a slight positive pressure of dry nitrogen. Volumetric tubes (2 ml) were weighed before and after solid materials (usually salt) were placed in them. Enough solvent was added to dissolve the solids, then the liquids were added using a 10 or 50 μl syringe. The solutions were made up to the mark with solvent, thoroughly mixed, and ca. 0.5 ml transferred to n.m.r. sample tubes fitted with auxilliary stopcocks to exclude air, connected to a vacuum rack, degassed by freezing and pumping, and sealed.

The concentrations of the solid materials were calculated from their weights and the volumes of the volumetric tubes. Concentrations of liquids were calculated from their volumes and densities.

The n.m.r. spectra were obtained, for the most part on Varian HA-60 and A-60 spectrometers, with a few on a Varian HA-100 fitted with a C-1024 time-averaging computer. The internal reference was always TMS. The line positions were measured from the chart calibrations (1 Hz = 1 mm) in the case of A-60 spectra; HA-60 spectra were measured by setting the sweep oscillator at the resonance, and measuring the difference between its frequency and that of the lock-in oscillator.

The operation of the C-1024 with the HA-100 was modified by installing auxiliary microswitches to limit the travel of the recorder carriage to about one fifth of the full chart width. The modification allowed single peaks in dilute samples to be accumulated efficiently. Accumulated spectra were calibrated by measuring frequency differences at the limit switches and interpolating to find the peak positions.

Results

Analysis of n.m.r. Shielding vs. Concentration

The hydroxyl proton shift dependence on salt concentration was analyzed to yield the limiting shift in the 1:1 complex and the association constant by an iterative Benesi–Hildebrand–Scott (B–H–S) method, described in Paper I of this series (see ref. 23). Uncertainties quoted in derived quantities include contributions from the uncertainties in measurement of shifts and concentrations, and generally are about twice as large as uncertainties based on standard deviation of fit alone.

In this study, the association constant, K, falls in the range 10 to 125 M^{-1}. Consequently, in many cases, at salt concentrations of about 1 M, essentially all of the salt was complexed and the shielding became independent of concentration. This directly-observed complex shift in all cases verified the value derived from the B–H–S analysis.

Tables I and II give the ambient-temperature (ca. 27 °C) equilibrium constants (K), and limiting complex shifts (Δ_c) for a number of alkyl- and arene-substituted carbinols complexed with halide ion in tetrachloromethane.

Complicating the treatment of these systems as involving simple 1:1 complex formation, is the well-known self-association of alcohols (6, 7), even at very low concentrations. Figure 1 shows the concentration dependence of the OH-proton shielding of phenylmethanol from 0.002 to 0.2 M; the three points of the most dilute solutions were obtained from spectra accumulated on the C-1024 computer, using as many as 300 scans per spectrum. The region below about 0.1 M is very nearly linear with the possible exception of a small "dip" near 0.05 M. It is evident that extrapolation to infinite dilution gives a δ_{OH} for "free" phenylmethanol of -1.05 p.p.m., whereas at the 0.1 M concentration used in this study, the δ_{OH} is -1.50_5 p.p.m., that is, 0.45 p.p.m. to low field of the "free" OH resonance.

We have performed a "dummy" calculation on a set of parameters typical of an alcohol in order to arrive at an estimate of the amount of error introduced into our results by the assump-

Can. J. Chem. Downloaded from www.nrcresearchpress.com by 210.87.254.5 on 09/05/12
For personal use only.

TABLE I

Experimentally determined quantities for alcohol – bromide ion* complex formation in tetrachloromethane at 27 °C

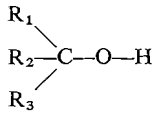

R_1	R_2	R_3	$K(M^{-1})$	Δ_c(raw) p.p.m.	$\Delta_{dil'n}$ p.p.m.	Δ_c(corr.) p.p.m.
H	H	H	70±18	−3.40±0.07	0.30	−3.70
CH_3	H	H	40±16	−3.32±0.13	0.38	−3.70
CH_3	CH_3	H	21±6	−3.42±0.20	0.36	−3.78
CH_3	CH_3	CH_3	15±4	−3.24±0.17	0.58	−3.82
C_6H_5	H	H	71±40	−3.92±0.04	0.45	−4.37
C_6H_5	CH_3	H	39±14	−3.70±0.07	0.30	−4.00
C_6H_5	CH_3	CH_3	15±2	−3.76±0.09	0.15	−3.91
$C_6H_5CH_2$	H	H	43±24	−3.47±0.06	0.21	−3.68
4-$MeOC_6H_5$	H	H	49±10	−3.82±0.12	0.58	−4.40
4-$NO_2C_6H_5$	H	H	10±3†	−2.50±0.14†	Not determined	
4-Methylphenol			32±8	−4.50±0.10	0.25	−4.75

*Anion provided by tetrabutylammonium bromide.
†Solvent: acetonitrile.

TABLE II

Effect of anion size on alcohol–anion complex formation in CCl_4 at 27 °C*

Donor (anion)	$K(M^{-1})$	Δ_c (p.p.m.)
Cl^-	130±110	−4.50±0.17
Br^-	39±14	−3.70±0.07
I^-†	12±3	−2.89±0.26

*Donor anion provided by tetrabutylammonium salt. Alcohol is 1-phenylethanol.
†Donor anion provided by tetraheptylammonium iodide.

tion that our measured shifts are not influenced by alcohol self-association.

We take as numbers representative of alcohol–anion complexing $\Delta_c = -4$ p.p.m.; $K_c = 25$. For simplicity we assume that at low concentrations the dimer, in which one of the two OH protons is hydrogen bonded, is the only polymer present (8, 9). Consistent with previous studies (7) we assume a typical dimerization constant, K_D, of 0.75 M^{-1}. We estimate the shielding in the dimer using the slope of the dilution curve at zero concentration, using the relation (10)

$$[1] \qquad \left(\frac{\partial\Delta}{\partial C}\right)_{C\to 0} = 2K_D\Delta_D$$

This yields $\Delta_D = -3.1$ p.p.m.

At each of 4 typical salt concentrations, the concentrations of all species were computed and iterated to self-consistency. Duplicate calculations were performed, with and without self-association. The results of these two sets of computations are given in Table III. It is evident that self-association effects practically no measurable change in the n.m.r. observations.

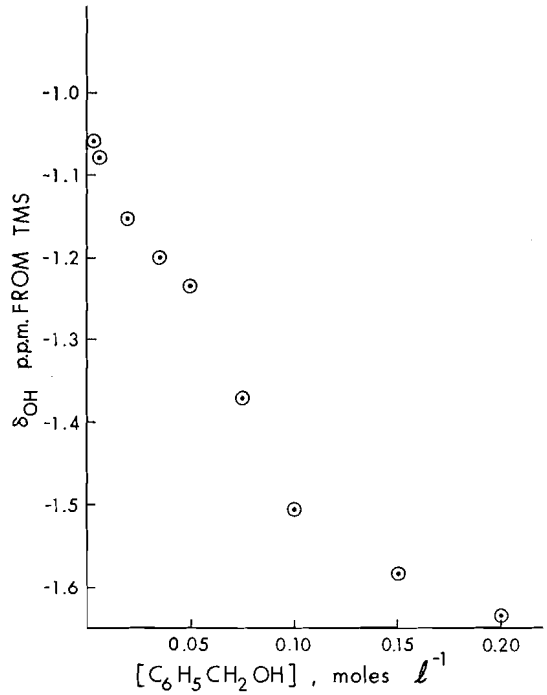

FIG. 1. Dilution curve for O—H shift of phenylmethanol in tetrachloromethane.

TABLE III

Computed shieldings, for typical case, including contribution from alcohol self-association*

[Salt] *M*	Complex shift (p.p.m.)	Dimer shift (p.p.m.)	Total shift (p.p.m.)	
			With dimers	Without dimers
0.1	2.08	0.06	2.14	2.20
0.2	3.00	0.02	3.02	3.00
0.4	3.54	0.01	3.55	3.54
0.6	3.68	0.00	3.68	3.68

*Total alcohol concentration assumed: 0.1 *M*.

Consequently, we consider that our treatment of the data in terms of only the one alcohol–anion complexing process is justified; all the more so in that the points at high concentration, which are least influenced by dimerization, are most heavily weighted in the analysis (see Appendix, Paper I). Hence, in Table I, equilibrium constants are given as obtained directly from the B–H–S analysis. By adding the dilution shift of the alcohol from 0.1 *M* to zero concentration, Δ_{diln}, to the limiting shift obtained from the B–H–S analysis, Δ_c(raw), obtained in the usual way, the resulting Δ_c(corrected) (see Fig. 2) should be quite a precise measure of the difference in shielding of the hydroxyl proton in an isolated alcohol molecule, and in the complex with the anion.

As may be seen in Table I, this correction for

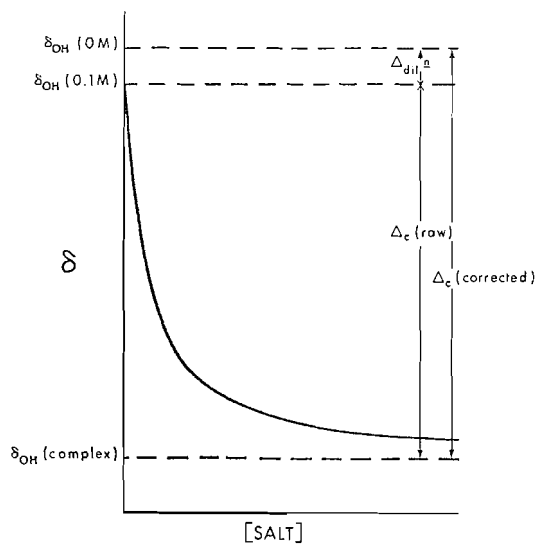

FIG. 2. Derivation of O—H complex shifts.

self-association, Δ_{diln}, is typically only about 2–3 times the experimental uncertainty, the average standard error being 0.11 p.p.m., and the average correction 0.33 p.p.m.

Three-point dilution curves (0.03, 0.06, 0.10 *M*) were obtained for all the other alcohols; these were all linear and were used to obtain each dilution shift individually, although all were found to fall within quite a narrow range of values.

It is apparent that, within the experimental uncertainty, the complex shifts are the same no matter what the degree of substitution by alkyl (methyl) groups. However, an arene substituent consistently accompanies shifts approximately 0.2 to 0.5 p.p.m. greater.

Infrared vs. Nuclear Magnetic Resonance

Several studies (11, 12) have been made on this type of system using i.r. spectroscopy. These have, of necessity, assumed that the new band at about 3300 cm^{-1} is due to OH hydrogen bonded to the anion; however, it has also been suggested (11) that this band may be due to aggregations of polymeric alcohol, with the anion as a center of nucleation.

Our n.m.r. results are obtained under conditions which tend to favor 1:1 complex formation over larger aggregates. Complexes of the type 1:*n* (more than one ion per alcohol) are unlikely, since the alcohol has only one electrophilic site (this may not be true of some aryl alcohols: *vide infra*). The 1:*n* aggregates also bring ions of like charge together. Some *n*:1 complexes may occur, although the alcohol concentration is kept as low as possible to avoid this. In any case, it is not readily apparent why the presence of one alcohol on an ion should have a large effect on its interaction with a second molecule. The analysis weights most strongly the points at high salt concentration, where *n*:1 complexes are least

Can. J. Chem. Downloaded from www.nrcresearchpress.com by 210.87.254.5 on 09/05/12
For personal use only.

TABLE IV

Infrared data and results for 1-phenylethanol and bromide ion*

[Bu_4NBr] (M)	Absorbance		K (M^{-1})	
	A_{3610}	A_{3300}	Method (*1*)	Method (*2*)
0	0.179	0	—	—
0.0248	0.113	0.161	91	44
0.0586	0.077	0.265	44	(44)
0.085	0.068	0.309	30	37
0.171	0.023	0.398	54	46

*[1-Phenylethanol] = 0.05 M.

likely. In any case, no systematic deviation from the B–H–S straight lines was observed.

We have examined the i.r. spectrum of one of these systems, 1-phenylethanol and tetrabutylammonium bromide, under conditions essentially identical to those of the n.m.r. study. If the band at 3300 cm^{-1} is due entirely to 1:1 ion–molecule complexes, then the i.r. absorption intensity should vary in the same way as the n.m.r. shift, and yield the same equilibrium constant.

In Table IV are given the absorbances of 5 solutions at 3610 and 3300 cm^{-1}, measured by reading the absorbance relative to a baseline defined as a straight line connecting the two minima closest to the band measured.

The spectrum of the sample containing no salt exhibited two absorptions, at ca. 3470 and 3390 cm^{-1}, which have been assigned to associated forms of alcohols (6, 8, 11). These absorptions are either absent or obscured by the band at 3300 cm^{-1} when salt is present (see Fig. 3).

Table IV also contains estimates of K obtained at each salt concentration by two methods: (*1*) taking the decrease in absorbance at 3610 cm^{-1} as a measure of the decrease in free alcohol concentration; (*2*) taking the result for one sample (the third in the table) as exact, and computing the complex concentrations at other concentrations using it as a standard. It matters little which sample is taken as the standard: for example, using the fourth sample, and its value of $K = 30$, instead of the third sample and its $K = 44$, the average value of K derived by method (*2*) becomes 39 instead of 43, an insignificant difference.

The average value of K from Table IV is $49 \pm 20\ M^{-1}$. In view of the crudity of the i.r. measurements, this is in reasonable agreement with the n.m.r. determination, $39 \pm 14\ M^{-1}$.

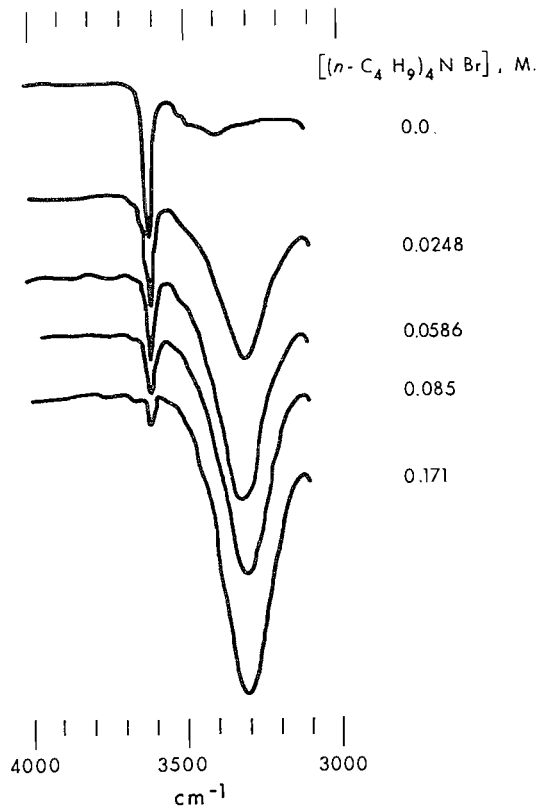

FIG. 3. O—H stretch region of 1-phenylethanol vs. concentration of $(n\text{-}C_4H_9)_4NBr$.

If the i.r. determination with the largest deviation from the mean, 91 M^{-1}, is rejected, the i.r. average is $43 \pm 9\ M^{-1}$. The deviant point may reasonably be disregarded, since it is derived from the smallest difference between two large numbers. We consider this to be reasonable evidence that the absorption band at 3300 cm^{-1}

Can. J. Chem. Downloaded from www.nrcresearchpress.com by 210.87.254.5 on 09/05/12
For personal use only.

is entirely due to 1:1 complexes between the alcohol and the anion.

Discussion

Effect of Alcohol Structure

The equilibrium constants for complexes with bromide ion show marked dependence on the degree of alkyl substitution at the α-carbon atom (Table I). K decreases by 30 to 50% for each additional methyl or benzyl group; on the other hand, it is hardly affected by substitution of a phenyl group for hydrogen (70 vs. 71; 40 vs. 39; 21 vs. 15). These observations correlate with the inductive character of the substituents; alkyl groups are known to be more electron donating than phenyl groups or hydrogen; increasing alkyl substitution leads to an accumulation of negative charge in the hydroxyl group, rendering it less acidic and less attractive to a negative ion.

Subject to the usual reservations concerning linear free energy relationships (13), it is possible to correlate the relative free energies of bromide complex formation (as log K) with the Taft inductive substituent constants, σ* (14). These have been shown to be reasonably additive. By regarding the —COH moiety as the core of all the alcohols, only 4 values of σ* are required, normalized for convenience to H: H, 0.0; CH_3, −0.49; C_6H_5, +0.11; $C_6H_5CH_2$, −0.27.

Figure 4 is a graph of log K as a function of Σσ*, for the complexes in Table I, not including the last 3 entries. The relationship is linear, consistent with our assertion that the variation of K reflects inductive properties of the substituents. The only point falling badly off the line is the one for $C_6H_5C(CH_3)_2OH$, a highly-substituted alcohol; this may reflect an effect of crowding.

Inductive charge withdrawal from the electrophilic site should affect primarily the enthalpy of complex formation. The validity of the foregoing free energy correlation rests, as all such correlations do, on the assumption that the entropy of complex formation either does not change, or varies in the same manner as the enthalpy, in the set of complexes studied.

The most apparent influence on the strength of complex formation of alcohols to bromide ions *via* their hydroxyl groups is thus the inductively determined electrophilicity of the binding site.

Effect of Anion Size

Table II shows the effect of changing the size

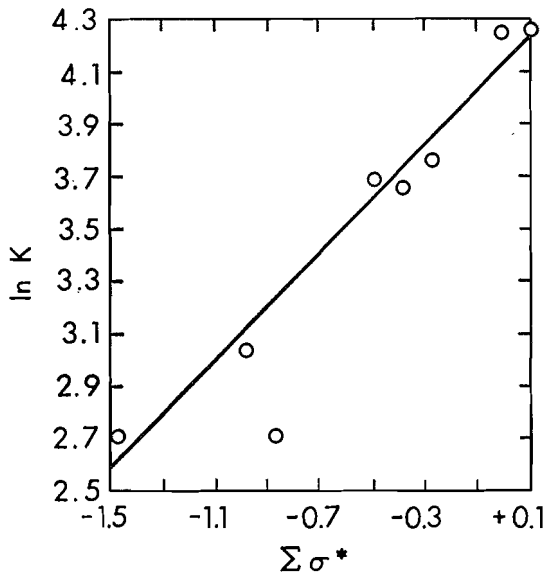

FIG. 4. Dependence on substituent inductive parameters of alcohol – bromide ion equilibrium constant.

of the anion on the complex formation with 1-phenylethanol. Since tetrabutylammonium iodide is insoluble in CCl_4, the tetraheptylammonium salt was used. Consistent with the model of purely electrostatic interactions in hydrogen bonding to anions, as developed in Paper I, the complex shifts are largest for the smallest anion. In addition, the equilibrium constant increases in roughly three-fold steps in the progression $I^- < Br^- < Cl^-$, consistent with a complex energy dominated by electrostatic interaction with the anion field.

Interaction with the Aromatic Ring

It was observed during the course of this investigation that the addition of tetrabutylammonium bromide to a CCl_4 solution of an arene alcohol resulted in a change in the n.m.r. spectrum of the phenyl protons; whereas, in the absence of salt, these were all essentially equivalent and gave rise to a single narrow band, the spectrum broadened into a very complex multiplet having, at the highest salt concentrations, a total width of about 20–25 Hz.

In an endeavor to find out what part or parts of the ring were being affected, and to simplify the spectral analysis involved, the complexing behavior of 4-nitrophenylmethanol and 4-methoxyphenylmethanol with bromide ion was studied.

Can. J. Chem. Downloaded from www.nrcresearchpress.com by 210.87.254.5 on 09/05/12
For personal use only.

TABLE V

Comparison of hydroxyl- and *ortho*-proton behavior in 4-substituted phenylmethanols on addition of bromide ion

4-Substituent	Δ_c(OH) (p.p.m.)	Δ_c(*ortho*) (p.p.m.)	K(OH) (M^{-1})	K(*ortho*) (M^{-1})
OCH_3*	−3.82	−0.13	49	19
NO_2†	−2.50	−0.16	10	4

*Solvent: CCl_4.
†Solvent: CH_3CN.

It was found that, in both cases, the ring protons *meta* to the CH_2OH group were unaffected by the addition of salt, while those *ortho* to the group shifted downfield monotonically with salt concentration. Both K and Δ_c values were evaluated from the shift of the *ortho* ring protons in the same manner as reported previously for the OH proton shifts. These values are given in Table V and compared with the corresponding values for the OH proton constants. Since, for reasons of solubility, the 4-nitro compound was run in acetonitrile as solvent, the results are not directly comparable to those run in CCl_4. Nonetheless, for both the 4-MeO and 4-NO_2 compounds, the equilibrium constant is found to be a factor of three smaller for "complexing" of the *ortho* protons than for the OH protons. Figure 5, which is a plot of OH shift vs. *ortho*-proton shift for each of the 4-methoxy- and 4-nitrophenylmethanol, shows clearly that there is not a simple proportionality between the salt concentration dependent shift of the *ortho* hydrogens and that of the hydroxyl hydrogen. Thus these two shifts cannot both reflect formation of a single complex, either through inductive transmission of a deshielding effect from the primary binding site to the other hydrogen, or through formation of a chelated complex:

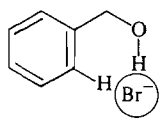

The case where only bromide ion already bound at the hydroxyl could then complex a ring site would also lead to simple proportionality between the two shifts, and thus must be rejected.

On the other hand, the presence of a hydroxyl group near the ring does appear to be necessary for anion–ring interaction. The methyl ether of phenylmethanol exhibits no ring perturbation on addition of bromide ion. The ring protons of 4-methylphenol shift downfield on addition of bromide ion; the ring protons of methoxybenzene are unaffected by the presence of bromide ion.

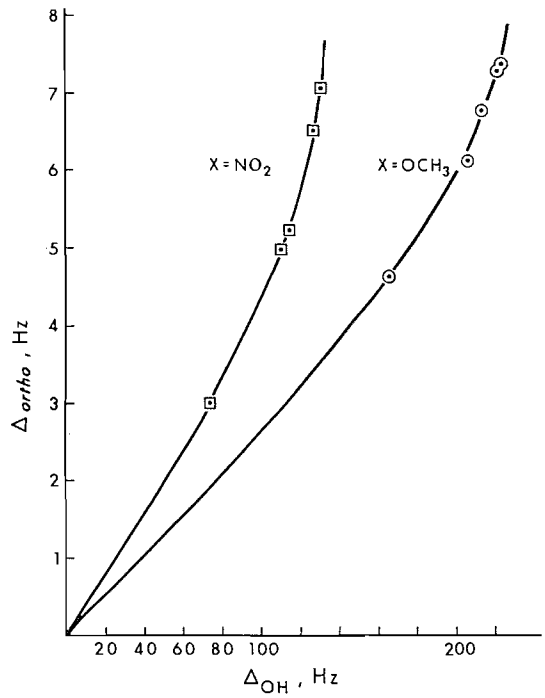

FIG. 5. Comparison of shifts of O—H and *ortho*-phenyl proton signals in 4-substituted phenylmethanols.

Moving the hydroxyl group to a position β- to the ring, as in 2-phenylethanol, results in the ring being unperturbed by formation of bromide complex by the hydroxyl group.

Interaction of bromide ion with aromatic rings has been observed in other cases. The *ortho* hydrogens in the phenoxy substituent of certain β-D-glucopyranosides were observed to shift downfield on formation of halide ion complexes with the pyranose ring (Paper II). The *meta* and

Can. J. Chem. Downloaded from www.nrcresearchpress.com by 210.87.254.5 on 09/05/12
For personal use only.

Can. J. Chem. Downloaded from www.nrcresearchpress.com by 210.87.254.5 on 09/05/12
For personal use only.

para hydrogens of nitrobenzene are deshielded on addition of bromide ion (15).

It is apparent that a more systematic study of the interactions between aromatic systems and halide ions will be necessary before the mechanism of the interaction can be understood. The results reported here do, however, indicate that both the nature and orientation of the interacting sites are significant.

Chemical Shift in the Complex

The complex shifts in Table I, for bromide complexes to hydroxyl hydrogens in a variety of aliphatic and aromatic structures, are consistently about twice as large as those reported in Paper I for bromide complexes to C—H hydrogens. The total range of complex shifts is about 30% of the average shift. It appears reasonable, therefore, to attempt to account for the hydrogen deshielding, on formation of a complex to the hydroxyl group, as a property of the O—H bond.

An electrostatic field model of the deshielding may be devised, analogous to that used for C—H bonds in Paper I. There is no body of theoretical or experimental results concerning electrostatic deshielding of O—H hydrogens comparable to that for C—H; however, assuming that the interaction with the ion is entirely electrostatic, an equation governing electrostatic perturbation of the O—H bond analogous to the Buckingham equation (16) for C—H may be assumed

$$[2] \quad \delta\sigma_E = a \times 10^{-12} E_z - b \times 10^{-18} E^2$$

The z-axis is directed from O to H. The coefficient of E^2, b, may be assumed to have the hydrogen atom value (17); this results in the contribution from the E^2 term being about 10% of the total observed shift.

We postulate that the electrostatic field may be regarded as originating at the center of the ion. If the distance from the ion center to the hydrogen nucleus is ρ Å, and the angle between the O—H and H—ion vectors is θ, the complex shift, in p.p.m., is predicted to be

$$[3] \quad \Delta_c = -4.803\, a\, (1/\rho^2) \cos\theta - 23.07\, b\, (1/\rho^4)$$

Assuming a collinear complex ($\cos\theta = 1$), the complex shift was a quadratic in $(1/\rho^2)$. The internuclear distance observed in many H bonded complexes is typically 0.3–0.6 Å less than the sum of the appropriate van der Waals radii. We have chosen, as before, to represent ρ as

$$[4] \quad \rho = r_- + r_H - 0.5$$

where r_H is the hydrogen van der Waals radius, 1.2 Å, and r_- is the crystal radius (18) of the ion.

It is now possible to evaluate the a coefficient using experimentally obtained complex shifts, Δ_c. A plot of $(\Delta_c + 23.07\, b/\rho^4)$ vs. $(4.803/\rho^2)$ should yield a straight line through the origin, of slope a. The data for complexes in Tables I and II, excepting the phenol, are plotted in Fig. 6. The experimental uncertainty does not permit evaluation of the straight line postulate. From the slope of the best straight line through the origin, we obtain $a = 5.5 \pm 0.3$ e.s.u.$^{-1}$. The magnitude of this coefficient relative to the value of 3.0 determined in Paper I for C—H is reasonably certain. Its absolute magnitude must be regarded as a lower limit, since counter-ion effects, the actual degree of hydrogen bond shortening, and dielectric polarization effects may contribute (see discussion of these in Paper I).

The systematic trend of the points in Fig. 6, tending towards a negative intercept, is difficult to understand. The van der Waals shifts, which are

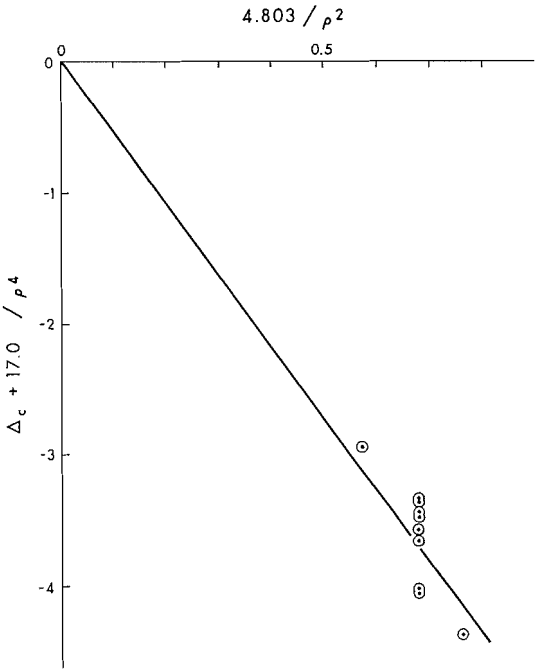

FIG. 6. Buckingham's a — coefficient for alcohols.

Can. J. Chem. Downloaded from www.nrcresearchpress.com by 210.87.254.5 on 09/05/12
For personal use only.

likely to be about the same for the three ions, would tend to produce a positive intercept. One possible explanation might be that there is a variation in the degree of hydrogen bond shortening: greatest for Cl^- and least for the most weakly interacting I^-. If the bond shortenings were taken as Cl^-, 0.6 Å; Br^-, 0.5 Å; I^-, 0.4 Å; instead of 0.5 Å for all ions, then the Cl^- and I^- would be on the line shown. This is not to argue that the bond shortenings have the values postulated, but that reasonable variation of the shortening could account for the observed discrepancy.

In view of the fact that the deviations of the points for Cl^- and I^- from the line are less than the range found for Br^-, concern over these deviations would presently appear unwarranted.

It is apparent that the O—H proton shielding is more sensitive to the electrostatic field than the C—H proton shielding, by a factor of nearly two. Our coefficient of the linear field term a_{OH}, is 5.5; the coefficient a_{CH}, measured in trichloromethane by the same method, was 3.0 (Paper I). This value was in agreement with several other determinations (19).

Buckingham's derivation of the linear field dependence of the shielding (16) treats the covalently bound hydrogen as a hydrogen atom, perturbed by a charge λ at a distance R. The coefficient of the linear term is then,

$$[5] \quad a = (\lambda/R^2) \times 1.5 \times 10^{-18} \text{ e.s.u.}^{-1}$$

Although it is unrealistic to expect that λ or R should represent observable molecular properties, it is evident that a positive charge is analogous to an electronegative atom covalently bonded to hydrogen. The effective λ, and thus a should reasonably increase with increasing electronegativity of the atom to which the hydrogen is bonded. This is consistent with the observation that a_{OH} is larger than a_{CH}.

Evaluation of a_{OH} is of considerable importance, since the electrostatic contribution to the chemical shift is needed in studies of ionic hydration (20). In the past, a_{OH} has been estimated (21) or assumed to be equal to a_{CH}; it appears that this may have led to an underestimate of the polarization contribution to hydration shifts.

Conclusions

Halide ions appear to interact specifically with the hydroxyl proton of an alcohol, in dilute solutions in a relatively inert solvent. This is consistent with the accepted view that the strong solvation of small anions by alcohols is primarily *via* hydrogen bonding (22). In addition, weak interaction occurs with the *ortho* protons of phenyl substituents located α- to, or directly bonded to the hydroxyl group. No significant interaction of the anion with any other site in the alcohols was observed.

The correlation of the association constant with the inductive properties of substituents, and the dependence of both association constant and complex shift on the ionic radius, suggest that the interaction with the hydroxyl group is primarily electrostatic, and is controlled by the electrophilicity of the hydroxyl hydrogen.

The hydroxyl hydrogen complex shifts are substantially independent of the nature of the group to which the hydroxyl group is bonded, and suggest that the susceptibility of a hydrogen to electrostatically induced shielding change is essentially a bond property.

The coefficient, a, of the linear field term in the "Buckingham" equation [2] is significantly larger for O—H than for C—H, in accordance with the bond polarities. Assuming that trihalomethanes and alcohols form halide complexes of similar (presumably linear) structure with respect to the hydrogen, we have determined that $a_{OH}/a_{CH} = 1.8$. A reasonable estimate of a_{OH} is 5.5 e.s.u.$^{-1}$, subject to the same reservations which applied to the previous determination of a_{CH}.

Acknowledgments

We wish to express our gratitude to Mr. A. Redpath for untiring preparation of samples. R.D.G. acknowledges a studentship from the National Research Council of Canada. This work was supported in part by NRCC Grant No. A-2051.

1. L. W. Reeves, E. A. Allen, and K. L. Strømme. Can. J. Chem. **38**, 1249 (1960).
2. C. Reid and T. M. Connor. *In* Hydrogen bonding. *Edited by* D. Hadzi. The Pergamon Press, Ltd., London. 1959. pp. 77–93.
3. R. M. Badger and S. H. Bauer. J. Chem. Phys. **5**, 839 (1937).
4. G. C. Pimentel and A. L. McClellan. The hydrogen bond. W. F. Freeman and Co., San Francisco. 1960.
5. D. P. Eyman and R. S. Drago. J. Am. Chem. Soc. **88**, 1617 (1966); T. D. Epley and R. S. Drago. J.

Am. Chem. Soc. **89**, 5770 (1967), and references cited therein.
6. N. D. COGGESHALL. J. Chem. Phys. **18**, 978 (1950).
7. M. SAUNDERS and J. B. HYNE. J. Chem. Phys. **29**, 1319 (1958).
8. R. H. HAMMAKER, R. M. CLEGG, L. K. PATTERSON, P. E. RIDER, and S. L. ROCK. J. Phys. Chem. **72**, 1837 (1968).
9. A. N. FLETCHER and C. A. HELLER. J. Phys. Chem. **72**, 1839 (1968).
10. E. D. BECKER. J. Chem. Phys. **31**, 269 (1959).
11. J. B. HYNE and R. M. LEVY. Can. J. Chem. **40**, 692 (1962).
12. J. BUFALINI and K. H. STERN. J. Am. Chem. Soc. **83**, 4362 (1961).
13. K. B. WIBERG. Physical organic chemistry. John Wiley and Sons, Inc., New York. 1964. pp. 278–279.
14. R. W. TAFT, JR. *In* Steric effects in organic chemistry. *Edited by* M. S. Newman. John Wiley and Sons, Inc., New York. 1956. Chap. 13.
15. J. B. HYNE and A. R. FABRIS. Can. J. Chem. **46**, 73 (1968).
16. A. D. BUCKINGHAM. Can. J. Chem. **38**, 300 (1960).
17. T. W. MARSHALL and J. A. POPLE. Mol. Phys. **1**, 199 (1958).
18. V. M. GOLDSCHMIDT. Geochemische Verteilungsgesetze der Elemente. Skrifter Norske Videnskaps-Akad. Oslo, i, Math.-Natur. Kl. 1926.
19. J. I. MUSHER. J. Chem. Phys. **37**, 34 (1962); P. J. BERKELEY and M. W. HANNA. J. Am. Chem. Soc. **86**, 2990 (1964).
20. J. F. HINTON and E. S. AMIS. Chem. Rev. **67**, 367 (1967).
21. J. C. HINDMAN. J. Chem. Phys. **36**, 1000 (1962).
22. R. ALEXANDER and A. J. PARKER. J. Am. Chem. Soc. **89**, 5549 (1967).
23. R. D. GREEN and J. S. MARTIN. J. Am. Chem. Soc. **90**, 3659 (1968).
24. J. S. MARTIN, J.-I. HAYAMI, and R. U. LEMIEUX. Can. J. Chem. **46**, 3263 (1968).

Can. J. Chem. Downloaded from www.nrcresearchpress.com by 210.87.254.5 on 09/05/12
For personal use only.

Can. J. Chem. Downloaded from www.nrcresearchpress.com by 210.87.254.6 on 09/05/12
For personal use only.

Oxidations involving silver. II. The oxidation of alcohols and aldehydes with silver(II) picolinate

T. G. CLARKE, N. A. HAMPSON, J. B. LEE[1], J. R. MORLEY, AND B. SCANLON
Department of Chemistry, University of Technology, Loughborough, Leicestershire, England

Received March 29, 1968

The oxidation of alcohols by argentic picolinate has been studied and has been shown to give high yields of aldehyde and ketone. Examination of the oxidation of aldehydes shows that smooth conversion to the acid occurs in most cases, but in some cases, an anomalous reaction occurs, which probably involves attack upon the aromatic ring of substituted benzaldehydes. The oxidation of aldehydes occurs much more slowly than alcohol-oxidation under similar conditions.

Canadian Journal of Chemistry, **47**, 1649 (1969)

In connection with the use of solid silver anodes (1) for the oxidation of organic compounds, we examined the effect of some complexing agents upon the course of oxidations at these electrodes. Since oxidation may proceed by formation of some species which diffuse into the mass of the electrolyte (2) before reacting, it was important to know the behavior of these species. One such species in our studies was silver(II) picolinate.

The argentic oxides produced at a silver anode, or in persulfate oxidations of silver salts, are stoichiometrically AgO. Study shows them to be in fact lattice compounds of Ag(I) and Ag(III), (3). In contrast, complexing agents such as picolinic acid permit the isolation of definite Ag(II) compounds (4), thus offering the possibility of studying the oxidizing activity of the Ag(II) state[2] uncomplicated by Ag(III); likewise derivatives of Ag(III) may be obtained and studied (5)[3].

One measure of the relative oxidizing power of these compounds is their relative oxidation potential. We measured the electrode potentials of the systems H^+ $pic^-/Ag(I)$ $pic_{(s)}/Ag$ and H^+ $pic^-/Ag(II)pic_{2(s)}/Ag$ at 25 °C and pH 5, and found them to be respectively 0.694 and 0.720 V. The corresponding (extrapolated) electrode potentials for the $Ag/Ag_2O/OH^-$ and $Ag/AgO/OH^-$ systems are 0.60 and 0.86 V respectively. Although these figures represent free energy changes for reversible equilibria, and most organic oxidations are not reversible processes in this sense, the figures indicate the approximate oxidizing power of the reagents. We have found one immediate difference between the oxide and picolinate, namely that, while the latter usually (but not always) undergoes the equivalent of a one-electron change giving silver(I) picolinate as product, under similar (neutral) conditions AgO usually undergoes a two-electron change, metallic silver being the main inorganic product in most of the cases we have examined. Differences in selectivity of action and products formed might be expected from this, but, while differences have been noted, they are surprisingly few. Thus, for example, both reagents convert benzylic alcohols to aldehydes (some acid also is obtained using AgO), toluene and *p*-cymene to benzaldehyde and *p*-cumaldehyde respectively, and 2-ethylhexanol to 2-ethylhexanal. With each reagent, alcohols are oxidized more slowly than amines, which oxidize more slowly than phosphines and phosphites. (The oxidation of triphenylphosphite by AgO at room temperature, for instance, is almost explosive.)

Our experiments show, in those cases we have examined, that product-wise there is a close parallel with oxidations at the electrode, under similar conditions[4].

We here discuss the oxidizing action of silver(II) picolinate in isolation from the electrode system. The action of AgO will be discussed separately[4].

---

[1]Author to whom all correspondence should be addressed.

[2]Details of the preparation and reactivity of some new Ag(II) complexes will be presented shortly in Part VI (in preparation).

[3]The oxidation of organic compounds by these reagents proceeds in many ways more parallel to the action of Cu(III) derivatives; J. B. Lee, unpublished results.

[4]For a preliminary survey of the oxidizing actions of Ag(II) picolinate and AgO see ref. 18 and Parts III and IV of this series, which are in preparation.

Can. J. Chem. Downloaded from www.nrcresearchpress.com by 210.87.254.6 on 09/05/12
For personal use only.

Oxidation of alcohols proceeds rapidly in neutral conditions at moderate temperatures. The overall reaction may be written

$$2Ag(pic)_2 + R_2CHOH \rightarrow 2Ag(pic) + R_2C{=}O + 2\ pic\text{-}H$$

(pic = picolinate)

While the rate of reaction is influenced by the nature of the solvent, (use of dimethyl sulfoxide (DMSO), for example, generally leads to more rapid reaction) we find that reaction proceeds quite satisfactorily in water, despite the heterogeneous nature of the system, and isolation of products is simplified. Volatile products may be swept out in a nitrogen stream; less volatile products are isolated by extraction with a suitable solvent. Reaction is rapid in the 30–70 °C range.

Secondary alcohols are converted in high yield into ketones. More interestingly, high yields of aldehydes are obtained from primary alcohols with negligible over-oxidation to acids. Table I lists some products and yields obtained. No attempt has been made to maximize these yields. The identity of the products has been confirmed in each case by physical properties, chromatographic comparison, formation of derivatives, and/or examination of infrared (i.r.) and proton magnetic resonance (p.m.r.) spectra, as appropriate.

TABLE I

Reaction of alcohols with silver(II) picolinate

Alcohol	Product	% Yield*
CH_3	Formaldehyde	80
Ethyl	Acetaldehyde	77
n-Propyl	Propionaldehyde	71
iso-Propyl	Acetone	80
n-Butyl	Butyraldehyde	76
iso-Butyl	iso-Butyraldehyde	57
sec-Butyl	Ethylmethyl ketone	68
n-Amyl	*n*-Valeraldehyde	74
iso-Amyl	iso-Valeraldehyde	61
n-Hexyl	*n*-Hexaldehyde	69
2-Ethylhexyl	2-Ethylhexaldehyde	55
n-Heptyl	*n*-Heptaldehyde	54
n-Decyl	*n*-Decaldehyde	68
DL-Phenylethyl	Acetophenone	73
2-Phenylethyl	Phenylacetaldehyde	61
Bornyl	Camphor	66
Cyclohexyl	Cyclohexanone	70
Benzyl	Benzaldehyde	80
p-Nitrobenzyl	*p*-Nitrobenzaldehyde	83
Anisyl	Anisaldehyde	87
Veratryl	Veratraldehyde	83
Piperonyl	Piperonaldehyde	77
Tetrahydrofurfuryl	Tetrahydrofurfuraldehyde	62
2-Ethoxyethyl	2-Ethoxyacetaldehyde	53

*No attempt was made to maximize yields.

These results indicate the wide applicability of the reagent. Many methods are available for the preparation of aldehydes from primary alcohols, but nearly all suffer from limitations in one or other respect, giving low yields, involving severe conditions, or product-isolation difficulties. Recently Syper (6) has described the use of AgO as an oxidant but the conditions he employed (hot concentrated acids) are rather severe. In our experience AgO is a useful oxidant in neutral or mildly alkaline conditions[4].

Chromic acid oxidations (7) may give good yields, but involve acid conditions, and formation of esters etc. often reduces yields, unless the aldehyde can be removed quickly from the mixture (8). *t*-Butyl chromate and chromium trioxide in pyridine are more successful (9), but may occasionally prove hazardous. Manganese dioxide[5] has been often applied for benzylic and allylic alcohols (10) and may in certain cases oxidize saturated systems if a large excess of oxidant is used (11). The strongly basic conditions of the Oppenauer oxidation are conducive to condensation and polymerization of the aldehyde (12). A variety of other reagents including selenium dioxide (13), nickel peroxide (14, 16), nitrogen tetroxide (15), lead(IV), thallium(III), and mercury(II) complexes (16), and *N*-halo-compounds (17), etc. have been used for these conversions, but often usefully only with benzylic alcohols.

The influence of structure on rate of oxidation is illustrated in Tables II–V. Table II lists the approximate rates of oxidation of some aliphatic alcohols under comparable conditions relative to ethanol, as standard. It can be seen that the rate decreases with increasing chain length for primary and secondary alcohols; primary alcohols are oxidized more rapidly than secondary alcohols. Applications of these differences to selective oxidation of single hydroxyl groups in polyhydroxy compounds and sugars will form the subject of a later publication. Benzyl alcohol is oxidized somewhat more readily than ethanol,

[5]We (J.B.L. and T.G.C.) have used a method for the preparation of highly active MnO_2, sufficiently active to inflame alcohols on contact in some cases, but even in this case a large excess of reagent is required, and losses occur unless excess oxidant is carefully destroyed with SO_2.

Can. J. Chem. Downloaded from www.nrcresearchpress.com by 210.87.254.6 on 09/05/12
For personal use only.

TABLE II

Approximate relative oxidation rates of aliphatic alcohols with silver(II) picolinate

Alcohol	Rate*
Ethanol	100
Propanol-1	83
Propanol-2	71
Butanol-1	45
2-Methyl-propanol-1	43
Butanol-2	32
Pentanol-1	42
3-Methyl-butanol-1	38
Benzyl alcohol	125

*Relative to ethanol as 100.

TABLE III

Approximate relative oxidation rates of benzyl alcohols

Alcohol	Rate*
3,4-(Methylenedioxy)benzyl	950
3,4-Dimethoxybenzyl	1330
p-Nitrobenzyl	43
p-Methoxy benzyl	266
Benzyl	100

*Relative to benzyl alcohol as 100.

TABLE IV

Approximate relative oxidation rates of some β-alkoxy alcohols

Alcohol	Rate*
Ethanol	100
2-Ethoxyethanol	80
2-Butoxyethanol	71
2-Acetoxyethanol	31
Tetrahydropyran-2-carbinol	59
Tetrahydrofuran-2-carbinol	76

*Relative to ethanol as 100.

and Table III illustrates the effect of various substituents upon the rate of oxidation of benzylic alcohols relative to benzyl alcohol itself. It is clear that the reaction is facilitated by electron-releasing groups, retarded by electron-attracting substituents. It is interesting to note that the effect of a β-oxygen function is to markedly increase the rate of oxidation over that which one might expect for a molecule of similar steric size. Table IV lists the approximate oxidation rates of some β-alkoxy alcohols, and one β-acyloxy alcohol, compared with ethanol as standard, and it may be seen that 2-ethoxyethanol, for example, is oxidized considerably more quickly than *n*-amyl alcohol which is approximately equivalent sterically. The influence of substituents in cyclohexanols, on the oxidation rate relative to the rate of oxidation of cyclohexanol itself, is shown in Table V. Since these materials were mixtures of *cis* and *trans* isomers, little more can be concluded beyond noting the obvious reduction in rate with steric crowding of the hydroxyl group.

Although the reagent converts primary alcohols into aldehydes in good yield, the oxidation of aldehydes to acids also proceeds smoothly in most cases. Aliphatic, aromatic, and heterocyclic aldehydes are oxidized rapidly in neutral aqueous solution at 50 °C. Aliphatic aldehydes (e.g. 2-ethylbutanal and 2-ethylhexanal) are oxidized more quickly than for example furfural, which again oxidizes more quickly than benzaldehyde. The rate of oxidation of aromatic aldehydes is increased by electron-releasing substituents, and decreased by electron-attracting substituents, as can be seen by reference to Table VI, which indicates the approximate rates relative to furfuraldehyde (taken as 100).

TABLE V

Approximate relative oxidation rates of some cyclohexanols

Alcohol	Rate*
Cyclohexanol	100
4-Methylcyclohexanol	35
3,5-Dimethylcyclohexanol	33
2,5-Dimethylcyclohexanol	31
2,2-Dimethylbutanol-3†	10

*Relative to cyclohexanol as 100.
†Included for comparison.

TABLE VI

Approximate relative oxidation rates of some aldehydes

Aldehyde	Rate*
Piperonaldehyde	2000
2-Ethylbutyraldehyde	855
2-Ethylhexaldehyde	375
Veratraldehyde	363
Anisaldehyde	125
(Furfuraldehyde	100
p-Tolualdehyde	75
Benzaldehyde	42
Benzyl alcohol†	910
p-Nitrobenzyl alcohol†	384

*Relative to furfuraldehyde as 100.
†Included for comparison.

Can. J. Chem. Downloaded from www.nrcresearchpress.com by 210.87.254.6 on 09/05/12
For personal use only.

The yields of acid obtained were often less satisfactory (*p*-nitrobenzoic acid, for example was isolated in only 31% yield), and in two cases highly anomalous reactions occurred. Thus with piperonal and veratraldehyde very rapid reduction of the silver(II) picolinate occurred, but in neither case could any trace of the corresponding acids be found. Furthermore, the aldehydes were largely (approx. 80%) recovered unchanged. Although no definite product has been isolated, it would appear that the oxidant is consumed, in these two cases, in attack upon the aromatic ring, with cleavage occurring rapidly to the exclusion of the expected mode of action, and with consumption of several moles of oxidant per mole of aldehyde.

Silver in the Ag(I) state is well known to complex with olefines and aromatic rings, and the oxidation of benzene to benzoquinone by AgO (6) may involve a similar (unstable) coordination compound. Our results with a number of other systems are in agreement with the possible formation of (unstable) Ag(II) olefine- and aryl-complexes. In contrast, the successful oxidation of piperonyl alcohol and veratryl alcohol to the corresponding aldehydes without complication must depend upon the more powerful coordination of the alcoholic oxygen to the silver in these two cases. Since the other aromatic aldehydes examined react more normally, we consider that the electron-releasing effect of the substituent groups is sufficient to favor aryl–silver rather than oxygen–silver coordination for piperonal and veratraldehyde.

The successful oxidation of alcohols to aldehydes depends upon the lower reactivity of the latter. Thus benzyl alcohol is oxidized at approximately 20 times the rate for benzaldehyde under similar conditions; the rates for both benzyl alcohol and paranitrobenzyl alcohol have been included in Table VI for comparison.

The oxidation of hydroquinone was examined. 1,4-Benzoquinone was obtained in 89% yield. The use of the reagent with this type of compound is probably restricted by the great instability of the products.

Silver(II) picolinate is a square planar complex isomorphous with the analogous copper(II) derivative and probably having a *trans* planar structure like the latter.

Oxidation could proceed through an outer-sphere mechanism, with electron-transfer via an OH^- or a water ligand, or the relative rates observed for aliphatic alcohols may represent the steric requirements for formation of an Ag—O linked intermediate, before the actual oxidation process. On this basis the effect of changing substituents on the reactivity of benzyl alcohol would reflect the changing nucleophilicity of the alcohol oxygen atom.

Further experiments, including kinetic and labelling studies, are under way to clarify the mechanism.

Experimental

Infrared spectra were recorded using Perkin–Elmer 237 and 257 spectrophotometers. Nuclear magnetic resonance spectra were measured upon a Perkin–Elmer R 10 (60 megacycle) instrument. Ultraviolet (u.v.) spectra were recorded using a Unicam S.P. 800 instrument. Where available, analytical grade materials were used. Otherwise reagent grade materials were suitably purified. Gas–liquid chromatographic (g.l.c.) examination of materials was carried out using Pye 104 Chromatographs, single and dual columned, isothermal, or temperature programed models, and one or more stationary phases including silicone oil, dinonyl phthalate, tricresyl phosphate, PEGA, carbowax, and apiezon L, usually 5% or 10% upon celite. (Nitrogen gas carrier; flame-ionization detector.)

Picolinic Acid

α-Picoline (50 g, 0.54 mole) and potassium permanganate (90 g, 0.57 mole) in water (2.5 l) were heated on a steam bath until no purple coloration remained. A further 90 g portion of potassium permanganate in water (500 ml) was added and heating was continued until again no purple coloration remained. The mixture was cooled slightly and then filtered at the pump through a thin layer of Kieselguhr. The precipitated manganese dioxide was washed with boiling water (1 l). The combined filtrate and washings were concentrated under reduced pressure to give about 200 ml of solution. The solution was acidified to congo red with concentrated hydrochloric acid. Solvent was removed at the pump and the residue was repeatedly extracted with portions (250 ml) of 95% aqueous ethanol. Evaporation of the extract gave α-picolinic acid (40 g, 60% of theoretical yield) m.p., 128–129 °C, raised to 136–138 °C on recrystallization from ethanol. The p.m.r. spectrum showed a multiplet at 1.0–2.0 τ (in D_2O), with no other signals. The i.r. spectrum (KBr discs) showed bands at 3420 (b, s), 3100 (w), 1720 (w), 1654 (m), 1600 (s), 1563 (w), 1516 (w), 1446 (w), 1378 (s), 1388 (w), 1286 (m), 743 (s), and 672 (s) cm^{-1}.

Argentic Picolinate

The method of Cox *et al.* (4) proved unsatisfactory in our hands, and the following modification was developed. To a solution of picolinic acid (61.5 g, 0.5 mole) in water (2 l) was added a solution of silver nitrate (42.5 g, 0.25 mole). Aqueous potassium persulfate (33.8 g, 0.125 mole) was added to the vigorously stirred suspension. Stirring was continued for 48 h. The red precipitate was separated,

Can. J. Chem. Downloaded from www.nrcresearchpress.com by 210.87.254.6 on 09/05/12
For personal use only.

washed with distilled water, and dried in darkness at room temperature in vacuo to constant weight; yield 75 g. This material was stable on storage in the dark at room temperature over several months.

Silver(II) Oxide (AgO)

A solution of sodium hydroxide (36 g) in water (500 ml) was brought to 80 °C, and maintained at this temperature while potassium persulfate (37.5 g) and silver nitrate (25.5 g) were added successively with stirring, the latter substance being added in small portions. Stirring was continued for 5 min, and the solution was maintained at 80 °C for a further 45 min. The cooled solution was filtered at the pump, and the residue was washed successively with sodium hydroxide (5 g) in water (500 ml), and then distilled water (500 ml). The dark brown argentic oxide was dried in vacuo; yield 18.3 g (almost quantitative).

Oxidations with Argentic Picolinate

The following are typical procedures.

Oxidation of Methanol

Methanol (1 ml) was stirred at 40 °C with argentic picolinate (2.1 g) in DMSO (15 ml) and water (15 ml), while a stream of N_2 swept the surface. The N_2 was passed into aqueous 2,4-dinitrophenylhydrazine (19) and the yellow precipitate was separated, washed, dried, and weighed (0.48 g, 80%); m.p. 165–166 °C, (lit. (19) m.p. 166 °C).

Oxidation of C_2–C_{10} Alcohols

Using a similar technique with N_2 blown *through* the solution, the aldehydes (or ketones) up to C_{10} could be swept from the mixture, although it was necessary to raise the temperature, after reaction was complete, to recover all the highest boiling members.

To confirm that no skeletal rearrangement had occurred, the p.m.r. spectra of the 2,4-dinitrophenylhydrazones were routinely examined. All these showed resonances at 0.88 τ (1 proton, doublet, very slightly split further, $J_{H_3H_5}$ = 2.8 c.p.s.), $H_{(3)}$: 1.65 τ (1 proton double doublet $J_{H_3H_5}$ = 2.8 c.p.s. and $J_{H_5H_6}$ = 9.8 c.p.s.), $H_{(5)}$: 2.05 τ (1 proton doublet $J_{H_6H_5}$ = 9.8 c.p.s.), $H_{(6)}$: 1.0 τ (broad singlet, NH). The signal due to the $H_{(1')}$ proton (i.e. —CH=N—) in aldehyde 2,4-dinitrophenylhydrazones regularly appeared at 2.4 τ (triplet usually, quartet for acetaldehyde) where no β-branching was present. β-Branched compounds gave doublets centered at 2.45 to 2.55 τ. Remaining signals were as expected in the 7.4–9.1 τ region, and no evidence of any skeletal change was observed.

Oxidation of Isoborneol

A mixture of isoborneol (0.01 mole, 1.54 g) and argentic picolinate (0.02 mole, 7.0 g) in DMSO (10 ml, containing a little water) was warmed to 40 °C for 15 min with gentle stirring, by which time the red coloration had disappeared. The mixture was poured into water (250 ml), filtered, and the residue and filtrate extracted with chloroform. The chloroform layers were combined and washed several times with water, dried over magnesium sulfate, filtered, and evaporated. Camphor (66% yield) was obtained, identical in i.r. spectrum with authentic material (m.p. 170–171 °C), on precipitation as 2,4-dinitrophenylhydrazone. It was identical in retention time on g.l.c. with authentic camphor, and had the expected p.m.r. spectrum.

Oxidation of DL-*Phenylethanol*

Phenylethanol (0.01 mole, 1.2 g) and argentic picolinate (0.02 mole, 7.0 g) were warmed together in DMSO (10 ml) for 10 min at 40 °C. The mixture was poured into water (300 ml) and extracted with petroleum–ether (60–80°). The petrol extract was washed, dried, and evaporated to give acetophenone (73%) identical in i.r. spectrum with authentic material m.p., 246–247 °C (lit. 250 °C) (2,4-dinitrophenylhydrazone). It was identical in retention time on g.l.c. with authentic material.

Oxidation of Hydroquinone

A mixture of hydroquinone (0.31 g) and argentic picolinate (2.0 g) in water (10 ml) was heated using a magnetic stirrer at 50 °C until the red coloration was discharged. The mixture was extracted with ether (2 × 50 ml) and the extract filtered and evaporated to give 1,4-benzoquinone (89%) as a yellow powder which gradually darkened on storage. This material was identical in i.r. spectrum, and in retention time on g.l.c. with authentic material.

Oxidation of Anisyl Alcohol

Anisyl alcohol (0.79 g) and argentic picolinate (4.0 g) were heated with stirring in water (50 ml) at 70 °C. After 25 min the mixture was cooled and extracted with ether. The dried ether layer was examined by g.l.c. (S.E. 30 on Celite: 210°), which showed only ether and anisaldehyde to be present. Evaporation of the extract gave anisaldehyde (0.7 g; 87%, identical in i.r. spectrum with authentic material).

Oxidation of Anisaldehyde

Anisaldehyde (0.4 g) and argentic picolinate (2.0 g) were heated with stirring in water (30 ml) at 70 °C. Stirring was continued until the reaction was complete (9.6 h). The mixture was acidified with dilute HCl and extracted with ether and chloroform. Evaporation of the extracts gave anisic acid.

Measurement of Relative Rates of Oxidation

Approximate measurements of relative reaction rates were made by taking appropriate quantities of materials at a selected thermostat temperature and measuring *either* the decrease in absorbance with time at 325 mμ *or* the disappearance of the red coloration against time. Whilst not suitable for accurate determination of absolute rates, the relative order of rates was found to be reasonably reproducible.

Oxidation of p-Nitrobenzaldehyde

A mixture of *p*-nitrobenzaldehyde (0.43 g) and argentic picolinate (2.0 g) was stirred vigorously in water (10 ml) at 70 °C. After 26 h the reaction was complete. The mixture was acidified with slightly more than the calculated amount of dilute hydrochloric acid, extracted, and the solution was examined by thin-layer chromatography (silica, eluted with ether). The major component corresponded in R_f (0.74) to authentic *p*-nitrobenzoic acid. After isolation, the acid was obtained (0.15 g, 31%) identical in physical constants (m.p., 240–241 °C, i.r. spectrum) with authentic material.

Oxidation of Piperonaldehyde

Piperonaldehyde (0.43 g) and argentic picolinate (2.0 g) were stirred in water (10 ml) at 70 °C. After 25 min no

argentic picolinate remained. The mixture was acidified (dilute HCl, calculated quantity) and extracted with ether and chloroform. From the extracts, piperonaldehyde (0.3 g) was recovered but no acid was found. Repetition of the reaction several times led in each case to rapid reduction of argentic picolinate, but in no case was the expected acid found, and in each case a good recovery of aldehyde was obtained.

Electrode Potentials

The electrode potentials of the systems Ag(pic)/Ag and $Ag(pic)_2/Ag$ were measured (at pH 5 and 25 ± 0.1 °C) against a calomel reference electrode (saturated) using a potentiometer (Tinsley Type 4363E). Solution junctions were made at an asbestos wick, the junction potential being eliminated using saturated KCl. Full details of results will be communicated later.

Acknowledgments

We thank Boots Pure Drug Co. Ltd., the Science Research Council, and Loughborough University of Technology for financial assistance (to T.G.C., B.S., and J.R.M., respectively). We thank Professor R. F. Phillips for continued encouragement and interest.

1. N. A. HAMPSON, D. LARKIN, and J. R. MORLEY. J. Electrochem. Soc. **114**, 817 (1967). N. A. HAMPSON, P. C. JONES, and R. F. PHILLIPS. Can. J. Chem. **45**, 2039 (1967). T. G. CLARKE, N. A. HAMPSON, J. B. LEE, J. R. MORLEY, and B. SCANLON. Can. J. Chem. **46**, 3437 (1968); Tetrahedron Letters, to be published.
2. H. S. ISBELL. Bur. Stds. J. Res. **6**, 1145 (1931); **14**, 359 (1935); **17**, 331 (1936). U.S. Patent 1 976 731 (1934); Chem. Abstr. **28**, 7263 (1934); Ind. Eng. Chem. **24**, 1 (1932).
3. V. SCATTURIN and P. BELLON. J. Electrochem. Soc. **108**, 819 (1961).
4. G. A. BARBIERI. Atti Acad. Lincei, **17**, 1708 (1933). E. G. COX, W. WARDLAW, and K. C. WEBSTER. J. Chem. Soc. 775 (1936).
5. G. L. COHEN and G. ATKINSON. Inorg. Chem. **3**, 1741 (1964).
6. L. SYPER. Tetrahedron Letters, 4193 (1967); J. Org. Chem. **32**, 3865 (1967).
7. W. A. WATERS. Quart. Rev. London, **12**, 277 (1958).
8. E. WERTHEIM. J. Am. Chem. Soc. **44**, 2658 (1922). A. L. HENNE. J. Am. Chem. Soc. **72**, 3370 (1950).
9. G. L. POOS, L. H. SARETT, G. E. ARTH, and R. E. BEYLER. J. Am. Chem. Soc. **75**, 422, 427 (1953). L. H. HERZOG. J. Am. Chem. Soc. **75**, 5751 (1953). R. M. LUKES, G. L. POOS, R. E. BEYLER, W. F. JONES, and L. H. SARETT. J. Am. Chem. Soc. **75**, 1710, 2116 (1953). W. J. HICKINBOTTOM, D. R. HOGG, D. PETERS, and D. G. M. WOOD. J. Chem. Soc. 4402 (1954). H. W. BERSCH and A. V. MLETZKO. Arch. Pharm. **291**, 91 (1958). T. SUGA, K. KIHARA, and T. MATSURU. Bull. Chem. Soc. Japan, **38**, 893 (1965); **38**, 1503 (1965).
10. R. M. EVANS. Quart. Rev. London, **13**, 61 (1959).
11. L. T. HARRISON. Proc. Chem. Soc. London, 110 (1964). R. J. GRITTER and T. J. WALLACE. J. Org. Chem. **24**, 1051 (1959).
12. C. DJERASSI. Org. Reactions, **6**, 207 (1961).
13. H. P. KAUFMANN and D. B. SPANNUTH. Chem. Ber. **91**, 2127 (1958).
14. K. NAKAGAWA, R. KONAKA, and T. NAKATA. J. Org. Chem. **27**, 1597 (1962).
15. B. O. FIELD and J. GRUNDY. J. Chem. Soc. 1110 (1955). P. GRAY and A. WILLIAMS. Chem. Rev. **59**, 283 (1959).
16. J. B. LEE and J. M. PRYCE. Unpublished results.
17. J. BLAIR, W. R. LOGAN, and G. T. NEWBOLD. J. Chem. Soc. 2443 (1956).
18. T. G. CLARKE and J. B. LEE. Tetrahedron Letters, **5**, 415 (1967).
19. F. WILD. Estimation of organic compounds. The University Press, Cambridge, England. 1953. p. 142.

Can. J. Chem. Downloaded from www.nrcresearchpress.com by 210.87.254.6 on 09/05/12
For personal use only.

Can. J. Chem. Downloaded from www.nrcresearchpress.com by 210.87.254.6 on 09/05/12
For personal use only.

A ^{19}F nuclear magnetic resonance investigation of the formation of $Sb_2F_{11}^-$ and $Sb_nF_{5n+1}^-$ in the CsF–SbF_5, *t*-butyl halide – SbF_5, and tetraalkylammonium hexafluoroantimonate – SbF_5 systems

J. BACON, P. A. W. DEAN, AND R. J. GILLESPIE
Department of Chemistry, McMaster University, Hamilton, Ontario

Received September 23, 1968

Fluorine nuclear magnetic resonance spectra have been obtained for the *t*-butyl fluoride – SbF_5, *t*-butyl chloride – SbF_5, tetraethylammonium hexafluoroantimonate – SbF_5, and cesium fluoride – SbF_5 systems, both with and without SO_2 solvent. In SO_2 solution the anion is $Sb_2F_{11}^-$ for all the systems, any remaining SbF_5 being converted to $SbF_5 \cdot SO_2$. It is concluded that in the systems that do not contain SO_2, higher polymeric anions $Sb_nF_{5n+1}^-$, where $n > 2$, are present. *t*-Butyl chloride and *t*-butyl fluoride give the *t*-butyl carbonium ion, as has been previously reported. Tetrabutylammonium and benzyltrimethylammonium cations appear to decompose to a carbonium ion and an adduct $SbF_5 \cdot NR_3$ in the presence of SbF_5.

Canadian Journal of Chemistry, 47, 1655 (1969)

Introduction

By reacting alkyl fluorides with antimony pentafluoride or antimony pentafluoride dissolved in liquid sulfur dioxide, Olah and coworkers (1) were able to obtain a colored[1] liquid which they formulated as a solution of the alkylcarbonium hexafluoroantimonate in SbF_5 (or SO_2), e.g.

$$(CH_3)_3CF + SbF_5 \rightarrow (CH_3)_3C^+ \cdot SbF_6^-$$

They obtained proton magnetic resonance spectra consistent with the production of the dimethylcarbonium, trimethylcarbonium, and dimethylethylcarbonium ions from solutions of propyl fluorides, butyl fluorides, and amyl fluorides, respectively, the proton–fluorine coupling disappearing and the proton chemical shifts and the proton–proton and carbon–proton coupling constants being in agreement with a planar sp^2-hybridized structure for the carbonium ion. While they reported that the ^{19}F spectra of these complexes showed the absence of covalent C—F bonds, no fluorine spectra were given, nor was the anion identified. The definite identification of the anionic species in these complexes is of considerable interest, particularly as evidence that the complex is ionic and not a rapidly exchanging donor–acceptor complex. We have, therefore, used ^{19}F nuclear magnetic resonance (n.m.r.) spectroscopy to investigate the nature of the anion in various fluoride–SbF_5 systems.

[1]Recent work by Olah *et al.* (2) shows that carbonium ions themselves are colorless, the colored solutions arising from the presence of polymeric impurities.

Results and Discussion

The CsF–SbF_5 System

Neither cesium fluoride nor cesium hexafluoroantimonate is appreciably soluble in liquid sulfur dioxide. However, an exothermic reaction occurs between SbF_5 and CsF in the presence of this solvent. When $SbF_5/CsF = 2.0$, the product of the reaction is quite soluble and the ^{19}F n.m.r. spectrum of the solution at $-60°$ is that of the $Sb_2F_{11}^-$ anion, previously reported by Gillespie and Moss (3) for solutions of SbF_5 in HF. The spectrum is shown in Fig. 1. It consists of a multiplet at 89.4, a doublet of doublets at 109.1, and a quintet at 131.2 p.p.m. from external $CFCl_3$. This is essentially the same spectrum as was observed previously for a 20.9% solution of SbF_5 in hydrogen fluoride (3) and attributed to the $Sb_2F_{11}^-$ ion, **1**.

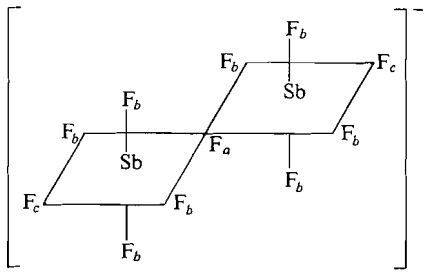

1

The low field multiplet is assigned to the bridging fluorine F_a, the doublet of doublets to the eight equivalent fluorines F_b, and the quintet to the two equivalent fluorines F_c. A weak doublet is present at 100.1 p.p.m., and may be attributed to

TABLE I

^{19}F chemical shifts* for various complexes in liquid SO_2

Complex	Chemical shift				
	F_a	F_b	$F_c + F_e$	F_d	F_f
$CsSb_2F_{11}$	89.4	109.1	131.2	100.1	—
$SbF_5 \cdot SO_2$	—	—	133.7	100.9	—
t-BuF/3.8SbF_5	90.3	110.2	132.2	101.0	106.6
t-BuCl/5.5SbF_5	90.1	110.2	132.2	101.0	106.7
Et_4NSbF_6/4.6SbF_5	90.5	110.9	134.3	101.5	105.4
Et_4NSbF_6/7.9SbF_5	91.2	110.9	135.1	101.3	—

*In p.p.m. relative to $CFCl_3$. Complexes externally referenced by sample interchange: F_a, $Sb_2F_{11}^-$ bridging fluorine (9-line multiplet); F_b, $Sb_2F_{11}^-$, F_b (doublet of doublets); F_c, SbF_{11}^-, F_c (quintet); F_d, $SbF_5 \cdot SO_2$ doublet; F_e, $SbF_5 \cdot SO_2$ (quintet); F_f, unassigned peak (see text).

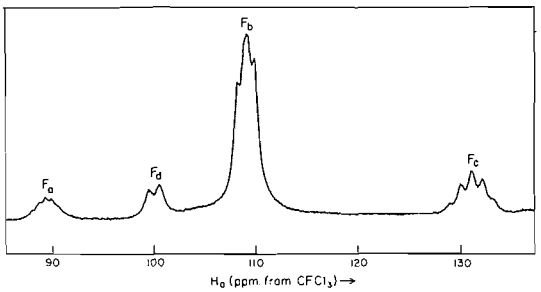

FIG. 1. ^{19}F (94.077 MHz) spectrum of $CsSb_2F_{11}$ in SO_2 at −60 °C.

the presence of a small amount of $SbF_5 \cdot SO_2$; this compound in liquid SO_2 at low temperatures gives rise to a doublet at 100.9 and a quintet at 133.7 p.p.m. (Table I). (Moore *et al.* (4) have previously reported 105 and 137 p.p.m. for these values.) The $SbF_5 \cdot SO_2$ quintet is not seen in the present case; it probably lies under the right hand side of the $Sb_2F_{11}^-$ quintet at 131.2 p.p.m. Sulfur dioxide can be recovered quantitatively from this solution leaving a white solid of composition $CsF \cdot 2SbF_5$ which may be recrystallized from sulfur dioxide. In a solution having $SbF_5/CsF > 2.0$ the $Sb_2F_{11}^-$ spectrum remains essentially unchanged while the peaks attributed to $SbF_5 \cdot SO_2$ increase in intensity. There is no indication of the formation of $Sb_3F_{16}^-$ or higher polyanions. Even for the composition $SbF_5/CsF = 1.0$, the solution appears to contain only the $Sb_2F_{11}^-$ anion and not the SbF_6^- anion as might have been expected. It appears that although $CsSbF_6$ is rather insoluble in SO_2, $CsSb_2F_{11}$ is relatively soluble. If higher polymeric anions exist they clearly undergo complete solvolysis (to $Sb_2F_{11}^-$) in solution in sulfur dioxide.

t-Butyl Halide/SbF_5 Solutions in SO_2

We prepared the "trimethylcarbonium hexafluoroantimonate" compound reported by Olah *et al.* (1) by allowing *t*-butyl fluoride vapor to react with antimony pentafluoride on a vacuum line until the product had the composition *t*-BuF/SbF_5 = 1/3.8. Under our experimental conditions this is the smallest amount of SbF_5 required for complete reaction with the *t*-butyl fluoride. Slightly larger amounts of SbF_5 can be used, but when *t*-BuF/SbF_5 = 1/5, an almost colorless layer separates out, as previously reported (1). This colorless layer appears to be almost entirely SbF_5; the ^{19}F resonance at low temperatures shows only the SbF_5 spectrum (5), while the room temperature ^1H spectrum shows a very weak single line resonance in the $(CH_3)_3C^+$ region. Hence *t*-butyl fluoride and SbF_5 are miscible in the range $3.8 \leqslant SbF_5/t\text{-BuF} < 5$ only, and any further addition of SbF_5 causes an SbF_5 layer containing a very small amount of alkylcarbonium ion to separate out. The SbF_5 layer is slightly less viscous than purified SbF_5 while the colored layer is much less viscous. The colored layer, neat or dissolved in liquid SO_2, gives the same room temperature proton spectrum as that reported by Olah *et al.* (1), namely the strong single resonance assigned to $(CH_3)_3C^+$.

When the *t*-BuF/3.8SbF_5 mixture was dissolved in SO_2, the ^{19}F n.m.r. spectrum shown in Fig. 2 was obtained at −80°. Clearly both the $Sb_2F_{11}^-$ (F_a, F_b, F_c) anion and $SbF_5 \cdot SO_2$ (F_d, F_e) are present, the quintet resonances of both species overlapping. The stoichiometry implies $Sb_2F_{11}^-/SbF_5 \cdot SO_2$ = 1/1.8 assuming these are the only two species present. Spectral areas are in the ratios $F_a/F_b/(F_c+F_e)/F_d$ = 1.4/8.0/3.7/5.7, which are close to the values of 1/8/3.4/5.6 expected for $Sb_2F_{11}^-/SbF_5 \cdot SO_2$ = 1/1.4; a small amount of $SbF_5 \cdot SO_2$ appears to separate out of the solution. We have not definitely assigned the remaining

Can. J. Chem. Downloaded from www.nrcresearchpress.com by 210.87.254.6 on 09/05/12
For personal use only.

Can. J. Chem. Downloaded from www.nrcresearchpress.com by 210.87.254.6 on 09/05/12
For personal use only.

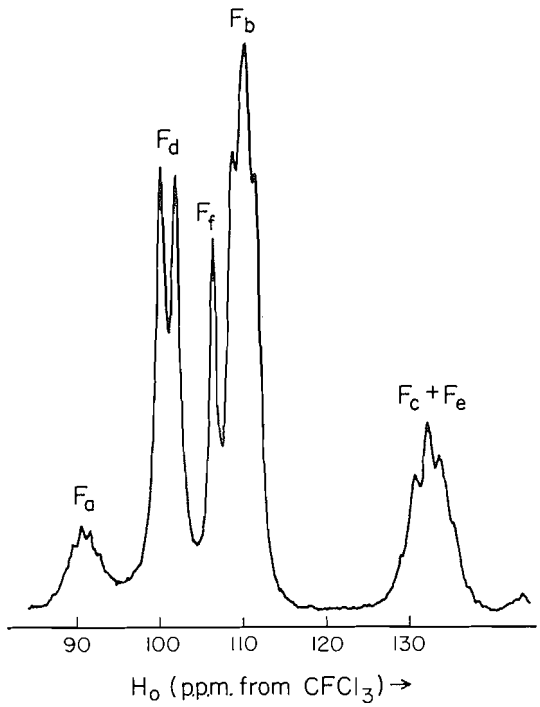

FIG. 2. ^{19}F (56.445 MHz) spectrum of *t*-BuF/3.8-SbF_5 in SO_2 at −80 °C.

resonance, the single peak at 106.6 p.p.m., F_f. It can possibly be attributed to some fluorine-containing species of antimony(III) such as SbF_3 complexed with SbF_5. We noted a slight charring of these solutions with time, hence some of the carbonium ion may be oxidized by SbF_5, accounting for the presence of antimony(III).

Alkyl chlorides also give rise to alkylcarbonium ions on reaction with SbF_5 (1). From the low temperature ^{19}F spectrum of *t*-BuCl/5.5SbF_5 in SO_2 solution (Table I), it appears quite definitely that the anion is again $Sb_2F_{11}^-$ and not the previously suggested SbF_5Cl^-.

We conclude, therefore, that the anion of both the "alkylcarbonium hexafluoroantimonate" and "alkylcarbonium chloropentafluoroantimonate" complexes in SO_2 solution is actually $Sb_2F_{11}^-$. In the latter case the chlorine is presumably present in some neutral species such as $SbF_4Cl \cdot SO_2$ which precipitates from solution.

The $Et_4NSbF_6/SbF_5/SO_2$ System

Et_4NSbF_6 is very soluble in liquid SO_2. The low temperature ^{19}F n.m.r. spectra of mixtures of this salt and SbF_5 in SO_2 (Table I) indicate that for $SbF_5/SbF_6^- \leqslant 1$, the $Sb_2F_{11}^-$ ion is formed quantitatively from SbF_5 within the limits of observation. When $SbF_5/SbF_6^- > 1$ the ^{19}F n.m.r. shows the $Sb_2F_{11}^-$ spectrum and the spectrum of $SbF_5 \cdot SO_2$. When tetrabutylammonium or benzyltrimethylammonium hexafluoroantimonate are dissolved in SO_2 together with SbF_5, the solutions are colored and some solid separates out in each case. It seems likely that carbonium ions are produced from the NR_4^+ cation and that the solid is an adduct of the form $SbF_5 \cdot NR_3$. This explanation is in accord with the absence of a corresponding reaction with the Et_4N^+ cation which would not be expected to give a stable carbonium ion.

We note from Table I the close similarity of the ^{19}F chemical shifts of $Sb_2F_{11}^-$ in SO_2 solutions of $CsSb_2F_{11}$, alkyl halide/SbF_5 mixtures, and Et_4NSbF_6/SbF_5 mixtures. Since interactions between Cs^+ or NR_4^+ and the $Sb_2F_{11}^-$ anion are almost certainly quite small, we can conclude that there is also no strong interaction between the carbonium ion and the $Sb_2F_{11}^-$ anion.

The t-Butyl Fluoride–SbF_5 and Et_4NSbF_6–SbF_5 Systems

We have obtained the ^{19}F spectra of both the *t*-butyl fluoride and Et_4NSbF_6 mixtures with SbF_5 in the absence of SO_2 solvent as a function of temperature.

The low temperature spectrum of the neat *t*-BuF/3.8SbF_5 mixture shown in Fig. 3 consists of a very broad line (δ = 110 p.p.m. relative to external $CFCl_3$) which has superimposed on it the spectrum of SbF_5 (5). As the temperature is lowered, the broad peak increases in width ($\approx$ 2000 Hz at −40 °C) and the area of the SbF_5 peaks increases but at no time exceeds 10% of the main spectrum. This SbF_5 appears to be present as a suspension in the *t*-BuF/SbF_5 (see below).

Et_4NSbF_6 is soluble in SbF_5 in the absence of any other solvent in the approximate range $5 \leqslant SbF_5/SbF_6^- \leqslant 11$ at room temperature. The ^{19}F spectrum of these solutions is a single

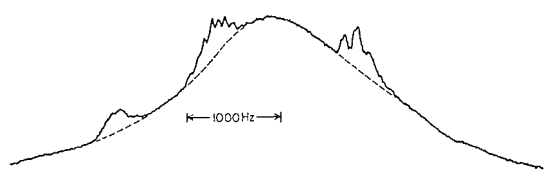

FIG. 3. ^{19}F (56.445 MHz) spectrum of *t*-BuF/3.8-SbF_5 at −40 °C.

broad line ($\approx$ 800 Hz half width at 0 °C; δ = 113.2 relative to external $CFCl_3$) at all temperatures. A solution having $SbF_5/SbF_6^- = 11.6$ was homogenous at room temperature, but on lowering the temperature it became turbid. The spectrum of this solution below room temperature showed a broad line with the spectrum of SbF_5 superimposed upon it. This and the observed turbidity suggests that some of the SbF_5 now exists as a suspension in Et_4NSbF_6/SbF_5. As the temperature was lowered, the area of the SbF_5 spectrum increased relative to that of the broad line, reaching 36% of the total area at −40 °C. These changes in area were reversible. With $SbF_5/SbF_6^- > 12$, homogenous solutions could not be prepared even at room temperature; two layers were formed. The lower layer gave the SbF_5 spectrum while the spectrum of the upper layer showed only the broad line observed for the homogenous solutions.

If the homogeneous liquids were in fact solutions of $(CH_3)_3C^+Sb_2F_{11}^-$ and $Et_4N^+Sb_2F_{11}^-$ in SbF_5 it seems quite unlikely that SbF_5 should separate out under certain conditions of temperature and concentration as we have observed.

The above results are consistent with all the SbF_5 in the homogeneous systems being incorporated into a polynuclear anion which disproportionates with increasing length or decreasing temperature into a smaller anion and polymeric SbF_5. (In this interpretation *t*-BuF/3.8-SbF_5 would be regarded as a mixture of $(CH_3)_3C^+Sb_3F_{16}^-$, $(CH_3)_3C^+Sb_4F_{21}^-$, and possibly $(CH_3)_3C^+Sb_5F_{26}^-$.) The proposed long, unstable anion might be expected to break up and reform readily, giving the broad temperature dependent line observed and the decomposition of such an anion by the SO_2 solvent is not surprising. The liquids may, therefore, be regarded as room temperature fused salts.

Conclusions

Polynuclear anions $Sb_nF_{5n+1}^-$ have previously been postulated by Aubrey and Van Wazer (6) who studied solutions of $SbCl_5$ in SbF_5 using ^{19}F n.m.r., conductivity, and viscosity measurements. They suggested the reaction

$$4SbCl_5 + (5n + 1)SbF_5 \rightleftarrows 5SbCl_4^+ + 5Sb_nF_{5n+1}^-$$

but were unable to identify the anion with any certainty. Gillespie and Moss (3) found that at high concentrations of SbF_5 in HF ($\geqslant$ 30 mole % SbF_5), changes occurred in the n.m.r. spectrum which could be attributed to some formation of higher polyanions such as $Sb_3F_{16}^-$, but these could not be definitely identified. Ruff (7) has prepared the crystalline complex $N_2F_4 \cdot 3SbF_5$, m.p. 74–78°, which may contain the $Sb_3F_{16}^-$ anion, since the complex $N_2F_4 \cdot 2SbF_5$, m.p. 116–119°, dissolved in SO_2 as $N_2F_3^+$ and $Sb_2F_{11}^-$ (7).

In addition to $N_2F_4 \cdot 2SbF_5$, a number of 1:2 SbF_5 complexes also exist: $BrF_5 \cdot 2SbF_5$, m.p. $\approx$ 60° (8); $XeF_2 \cdot 2SbF_5$, m.p. 63° (9); $KrF_2 \cdot 2SbF_5$, m.p. $\approx$ 50° (10); and $XeF_6 \cdot 2SbF_5$, m.p. 108° (11). Some or all of these complexes may contain the $Sb_2F_{11}^-$ anion[2].

The present work shows that the $Sb_2F_{11}^-$ ion is stable as the simple cesium salt and that it is stable in sulfur dioxide solution. Attempts to make sulfur dioxide solutions of the higher polyanions in sulfur dioxide were not successful as the complex $SbF_5 \cdot SO_2$ is formed preferentially. In other words the higher polyanions, if they are formed, undergo essentially complete solvolysis in sulfur dioxide whereas the $Sb_2F_{11}^-$ anion is reasonably stable and undergoes only a limited amount of solvolysis to SbF_6^- and $SbF_5 \cdot SO_2$. It appears that higher polyanions are formed in the absence of sulfur dioxide, for example, in mixtures of alkyl fluorides or tetraalkylammonium fluorides with SbF_5. Indeed over the range where single phase homogenous systems are formed, they appear to be room temperature fused salts with the formulae $R^+Sb_nF_{5n+1}^-$ or $R_4N^+Sb_nF_{5n+1}^-$. We note that the 1:2 complexes cited above are all relatively low melting (50° $\leqslant$ m.p. $\leqslant$ 116°) and that $N_2F_4 \cdot 3SbF_5$, has a m.p. 42° below that of the 1:2 complex with N_2F_4. It seems reasonable, therefore, that a salt containing $Sb_nF_{5n+1}^-$, where $n \geqslant 4$, would be liquid at room temperature.

Experimental

Fluorine n.m.r. spectra were obtained using either a Varian DA-60 spectrometer operating in the HR centerband mode or a Varian HA-100 spectrometer. Low temperature spectra were obtained using a Varian V4540 temperature controller and a variable temperature analytical probe.

[2]Professor Peacock informs us in a private communication that an X-ray diffraction study of $XeF_2 \cdot 2SbF_5$ shows this to be the case for this compound.

Can. J. Chem. Downloaded from www.nrcresearchpress.com by 210.87.254.6 on 09/05/12
For personal use only.

Can. J. Chem. Downloaded from www.nrcresearchpress.com by 210.87.254.6 on 09/05/12
For personal use only.

Antimony pentafluoride was obtained from Ozark Mahoning Company and distilled twice in glass apparatus immediately before use. *t*-Butyl fluoride was prepared by the reaction (12) of *t*-butyl alcohol and 48% hydrofluoric acid at 60–70 °C in plastic apparatus. *t*-Butyl chloride was obtained commercially. Isobutylene impurities were removed from both halides by treatment with bromine and distillation.

Benzyltrimethylammonium hexafluoroantimonate was from Alfa Inorganics Inc., and was used without purification.

Tetraethylammonium hexafluoroantimonate was prepared by mixing solutions of SbF_5 and Et_4NOH in excess 48% hydrofluoric acid; the precipitate was washed with anhydrous ether and dried in vacuo. The product was purified by precipitation from dichloromethane solution using carbon tetrachloride. The tetrabutylammonium salt was prepared similarly; the starting material was tetrabutylammonium chloride.

Cesium hexafluoroantimonate was prepared by the method of Kolditz and Rehak (13).

All mixtures were made up under moisture free conditions in a dry box. The R_4NSbF_6/SbF_5 and CsF/SbF_5 mixtures were made up by weighing the salt into an n.m.r. tube followed by addition of a weighed amount of antimony pentafluoride from a glass hypodermic syringe. The tubes were closed with detachable taps and attached to a vacuum line where the sulfur dioxide (which had been dried by standing the gas over P_2O_5) was condensed in. The tubes were sealed and weighed. For the alkyl halides a small amount (about 0.03 mole) of SbF_5 was placed in a 100 ml round bottomed flask equipped with a detachable tap. The flask was then attached to the vacuum line and evacuated; the *t*-butyl halide was allowed to evaporate very slowly into the SbF_5 flask and react over the period of 1 h. Nuclear magnetic resonance samples were made up by transferring small amounts from the reaction flask to n.m.r. tubes equipped with detachable taps in the dry box. The n.m.r. tubes, with taps, were then attached to the vacuum line, any SO_2 required distilled in, and sealed.

Cesium μ-Fluoro-bis(pentafluoroantimonate)

Cesium fluoride (1 mole) and antimony pentafluoride (2 moles) were weighed into a glass reaction vessel having a side arm and a receiver. Sulfur dioxide (about 5 moles) was condensed onto the solids at liquid nitrogen temperature and the vessel sealed. As the reaction mixture warmed up, a vigorous exothermic reaction began, with local boiling of the solvent; cooling was necessary and when boiling ceased, the temperature was kept at 50° for 12 h to ensure completion of the reaction. The sulfur dioxide was condensed into the receiver and the side arm sealed off. The portion having the solid was opened in the dry box and the solid recrystallized from sulfur dioxide.

The method of Johnson and Newman (14) was used to determine antimony; a slight excess of boric acid was added to complex the fluoride just before the titration with iodine. Fluoride was determined by potentiometric titration with La(III) using an Orion specific ion electrode. Cesium was determined as the tetraphenylborate (15).

Anal. Calcd. for $CsF_{11}Sb_2$: Cs, 22.70; F, 35.70; Sb, 41.61. Found: Cs, 21.5; F, 35.1; Sb, 41.9.

Acknowledgments

We thank the United States Air Force Office of Scientific Research for financial support of this work. One of us (J.B.) thanks the National Research Council of Canada for the award of a Studentship.

1. G. A. Olah, E. B. Baker, J. C. Evans, W. S. Tolgyesi, J. S. McIntyre, and I. J. Bastien. J. Am. Chem. Soc. **86**, 1360 (1964).
2. G. A. Olah, C. U. Pittman, R. Waack, and M. Doran. J. Am. Chem. Soc. **88**, 1488 (1966).
3. R. J. Gillespie and K. C. Moss. J. Chem. Soc. 1170 (1966).
4. J. W. Moore, H. W. Baird, and H. B. Miller. J. Am. Chem. Soc. **90**, 1358 (1968).
5. C. J. Hoffman, B. E. Holder, and W. L. Jolly. J. Phys. Chem. **62**, 364 (1958).
6. N. E. Aubrey and J. R. Van Wazer. J. Inorg. Nucl. Chem. **27**, 1761 (1965).
7. J. K. Ruff. Inorg. Chem. **5**, 1791 (1966).
8. M. Schmeisser and E. Pammer. Angew. Chem. **69**, 781 (1957).
9. A. J. Edwards, J. H. Holloway, and R. D. Peacock. Proc. Chem. Soc. 275 (1963).
10. H. Selig and R. D. Peacock. J. Am. Chem. Soc. **86**, 3895 (1964).
11. G. L. Gard and G. H. Cady. Inorg. Chem. **3**, 1745 (1964).
12. K. A. Cooper and E. D. Hughes. J. Chem. Soc. 1183 (1937).
13. L. Kolditz and W. Rehak. Z. Anorg. Allgem. Chem. **300**, 322 (1959).
14. E. A. Johnson and E. J. Newman. Analyst, **80**, 631 (1955).
15. W. Geilmann and W. Gebauhr. Z. Anal. Chem. **139**, 161 (1953).

Can. J. Chem. Downloaded from www.nrcresearchpress.com by 210.87.254.40 on 09/05/12
For personal use only.

Potentiostatic study of ferrous–ferric kinetics at bright gold and platinum electrodes

SIDNEY BARNARTT

Edgar C. Bain Laboratory For Fundamental Research, United States Steel Corporation, Monroeville, Pennsylvania

Received August 15, 1968

Ferrous–ferric reaction kinetics on gold in chloride and sulfate solutions, and on platinum in a sulfate solution, were studied potentiostatically. The data illustrate the importance of precise potential control and of automatic ohmic compensation. The standard exchange current density is $0.38/f$ A cm^{-2} (where f is the mean ionic activity coefficient) on platinum; it is an order of magnitude larger on gold.

Canadian Journal of Chemistry, 47, 1661 (1969)

In potentiostatic investigations of electrode kinetic mechanisms, the electrode potential is usually maintained constant within ± 1 to 5 mV. This is adequate for a slow electrode reaction, characterized by standard exchange current density $i_{0,s} < 10$ mA cm^{-2}, which can be studied at high overpotentials (in the Tafel region). More rapid reactions must be studied at low overpotentials (1–4), where closer potential control is required. This is particularly true if it is desirable to work within the linear current-potential region (4, 5). Also, rapid reactions at constant potential are associated with large currents which decrease with time (6, 7), because mass-transfer polarization builds up quickly. Therefore the ohmic drop in the electrolyte between the test electrode and reference probe causes the applied potential step to vary, unless accurate compensation is provided (8–12). Compensated potential control to ± 0.1 mV was the goal of the present work. Some of the problems involved were examined in a study of the ferrous–ferric reaction at gold and platinum electrodes. The standard exchange current density is found to be much higher on gold than on platinum. The data on gold emphasize that large errors can be incurred unless almost full ohmic compensation is continuously applied.

Experimental

Potentiostat

The essential features of the potentiostatic circuit employed are indicated schematically in Fig. 1. The circuit is shown in the mode required for a cathodic reaction at the test electrode; on–off and cathodic–anodic switches are omitted for simplicity. The circuit was designed around two units previously described (8), a transistorized voltage controller (v.c.) and a transistorized ohmic compensator (o.c.). It was necessary to change these units from a.c. to d.c. operation in order to reduce a.c. components of the control voltage to < 0.1 mV peak to peak.

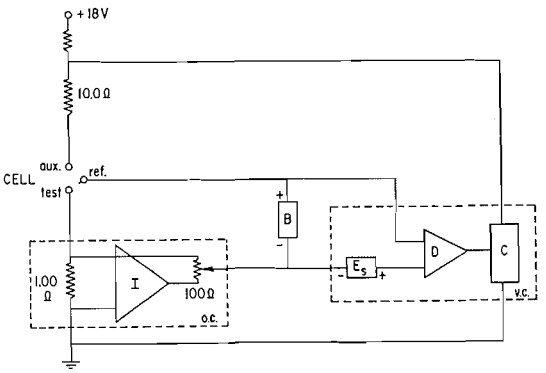

FIG. 1. Schematic diagram of potentiostatic circuit.

Current from the 18 V power supply had two parallel paths to ground, one through the cell and the other through the current regulator C of the voltage controller. The controller, containing also difference amplifier D and Zener reference potential E_s, exhibited stability within ± 0.1 mV but did not have very high internal impedance. At a given potential setting it drew a fixed current from the reference electrode, e.g. 10^{-6} A at $E_s = 5$ mV. A bias current supply B (battery operated, 0–10 μA) was inserted to supply most of this current and it was thus possible to eliminate errors from the reference-electrode current, as shown later. The ohmic compensator contained an inverter amplifier I (amplification $= -1$) which reproduced accurately the voltage drop across the 1.00 Ω resistor, changed its sign, and applied it across a ten-turn potentiometer. Setting the potentiometer to yield a fraction u of this voltage drop, where u is the known uncompensated resistance between the reference and the test electrodes (u varied from 0.13 to 0.21 Ω in this work), compensated for the ohmic voltage iu at any cell current i. In each experiment the test electrode was initially at its reversible potential before the potential step was applied. Current–time ($i-t$) curves, for times up to 50 ms after application of the potential step, were photographed on a storage oscilloscope (Tektronix type 564, with 3A3 and 3B3 plug-in units).

Cell

The simple cell used, Fig. 2, was designed to provide

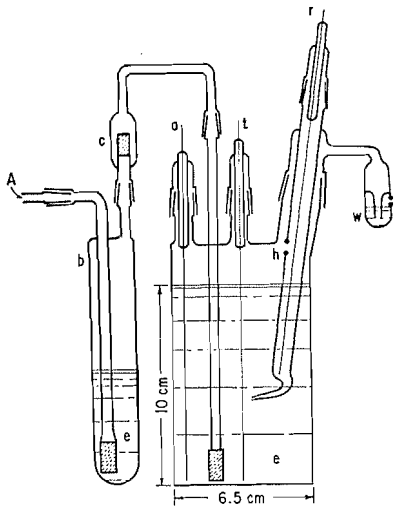

FIG. 2. Cylindrical cell.

essentially undistorted cylindrical symmetry. The central wire test electrode (t), of diameter 1.00 mm, was separated by a distance of 3 cm from the similar auxiliary electrode (a). Because of this large separation, the auxiliary electrode (which ideally should have been a coaxial cylinder) was expected to induce insignificant non-uniformity in the current density over the test electrode.

The reference-electrode (r) compartment terminated in a short capillary of tip diameter d (0.6–1 mm), the tip being placed a distance $2d$ from the test electrode to avoid shielding errors (13). The internal IR drop in the electrolyte between the capillary tip and a cylindrical test electrode of radius r_0 and length L is given by (14)

$$[1] \qquad V_{IR} = i\rho r_0 \ln \frac{r_0 + 2d - d/3}{r_0}$$

where i is the current density and ρ the electrolyte resistivity. The corresponding electrolyte resistance is therefore

$$[2] \qquad R_e = \frac{\rho}{2\pi L} \ln \frac{r_0 + 2d - d/3}{r_0}$$

Electrodes were positioned in the cell with standard-taper joints sealed with Teflon sleeves. An argon atmosphere was maintained by passing cylinder argon (99.995%) through metal and Teflon tubing into bubbler (b) containing some of the test electrolyte (e), then through a fritted-glass droplet trap (c) into the cell, and out of the cell through water trap (w); air initially trapped above the reference electrode diffused out through hole (h). Argon flow was turned off during electrochemical measurements.

The electrodes were made from 1 mm diameter platinum wires sealed into Pyrex tubes by a transition seal to Corning No. 3321 glass on the wire. The platinum test electrode (3.14 cm^2 geometrical working area) was polished to a bright finish, ending with abrasive of diameter 0.3 μm. The gold test electrode was made from a similar platinum electrode which was plated with gold to a thickness of 15 μm from the cyanide bath; $KAu(CN)_2$, 0.08 M; KCN, 0.03 M; K_2CO_3, 0.1 M; 60 °C; 3 mA cm^{-2}. The surface was repolished after plating. The platinum reference and auxiliary electrodes were polished and then platinized (15). Just before use all electrodes were cleaned in CrO_3–H_2SO_4 cleaning solution and in 11 M HCl, with prolonged rinsing in distilled water after each step. The test electrodes were given an additional cleaning step, being made cathode for 30 s in 1 M H_2SO_4 at 0.02 A cm^{-2}, using a new portion of the acid each time in order to minimize possible metal transfer from the platinum anode. This acid was purified by treatment with activated charcoal (see below).

Electrolytes

The ferrous–ferric reaction was studied at 25 °C in the following aqueous solutions:

I. 0.100 m $FeCl_2$, 0.100 m $FeCl_3$, 1.00 m NaCl, 0.10 m HCl; pH = 0.87; ρ = 7.8 Ω cm; ε_r = 0.464 V.

II. 0.020 m $FeCl_2$, 0.020 m $FeCl_3$, 1.00 m NaCl, 0.10 m HCl; pH = 0.92; ρ = 8.6 Ω cm; ε_r = 0.465 V.

III. 0.101 m $FeSO_4$, 0.050_5 m $Fe_2(SO_4)_3$, 0.91 m $NaHSO_4$; pH = 0.56; ρ = 6.6 Ω cm; ε_r = 0.423 V.

Here m is molality and ε_r is the reversible potential of the gold electrode at 25 °C with respect to saturated calomel (including any liquid junction potential). In each solution, bright gold, bright platinum, and platinized platinum electrodes exhibited the same potential within $\pm 10^{-5}$ V.

The solutions were prepared from reagent grade salt, redistilled hydrochloric acid, and water redistilled from alkaline permanganate. The chloride solutions were filtered by suction through a "Fine" porosity Pyrex fritted disk; without further treatment these yielded reproducible potentiostatic current–time curves for a period of several hours after immersion of the gold electrode.

The sulfate solution, unpurified, caused a pronounced deactivation of the gold surface with time (described later). This solution was purified by percolating it slowly through a bed of acid-washed activated charcoal, as recommended by James (16). A column of charcoal, volume 25 cm^3 and height 10 cm, supported by a 2 cm "Medium" Pyrex fritted disk, was set up using Pittsburgh Activated Carbon Co. type CPG acid-washed charcoal (14 × 40 mesh, B.E.T. surface area > 1000 m^2g^{-1}). The column was first acid-extracted with hot 6 N HCl (10 batches), then hot doubly-distilled water (10 batches) and hot 6 N H_2SO_4 (5 batches), each batch consisting of 50 cm^3 of liquid at 80–90 °C when poured into the column. Each liquid was drawn through the column initially at a rate of 1 cm/min, slowing gradually to 0.4 cm/min by the final batch. Next a 50 cm^3 batch of 1 N H_2SO_4, followed by a 50 cm^3 batch of the test solution, were drawn through the column and discarded. Finally 1 l of the test solution was passed through the column at 0.2 cm/min; it was collected in two 0.5 l portions, the second portion being used for kinetic studies. Some oxidation occurred during this treatment; to obtain a Fe^{2+}:Fe^{3+} concentration ratio of unity in the purified solution it was necessary to start with a ratio of 1.10.

Results and Discussion

Accuracy of Potential Control

An initial study of the problems involved in

Can. J. Chem. Downloaded from www.nrcresearchpress.com by 210.87.254.40 on 09/05/12
For personal use only.

Can. J. Chem. Downloaded from www.nrcresearchpress.com by 210.87.254.40 on 09/05/12
For personal use only.

obtaining a constant electrode potential was carried out with the gold electrode in solution I.

(a) Potential Stability

In the study of moderately fast reactions where mass-transfer polarization builds up rapidly, the preselected potential must be achieved very quickly. The mass-transfer effect causes the reaction rate to decrease, and the rate of decrease is greatest at time $t \rightarrow 0$ (6, 7, 17). Thus a relatively fast-rise potential step may be required. With the present cell-circuit combination at a setting of 95% ohmic compensation, potential steps of 4–20 mV were established to ± 0.1 mV in about 1 ms after switching in the cell. The rise time was measured by displaying the upper section of the potential rise on an oscilloscope at 1 mV/cm sensitivity; a mercury-wetted-contact relay (type HG-3A-1008, C.P. Clare Co.) was used in the switching. The rise time was found to decrease as the percentage of ohmic compensation was reduced, becoming 0.1 ms at zero compensation[1]. For reactions having large exchange currents, such slow response can prevent accurate determination of the charge-transfer current from a given $i-t$ curve, as illustrated later. With respect to long-term potential stability, the potentiostat setting drifted < 0.1 mV/h.

(b) Reference-electrode Current

In circuits of very high impedance reference-electrode current can be neglected, but in the present circuit it was not normally negligible and led to two possible sources of error: reference-potential drift, and an ohmic drop within the reference electrode (internal resistance < 1 kΩ). By means of the bias current supply, however, reference-electrode current was reduced to 10^{-7} A or less, and each of these errors remained less than 0.1 mV. Reference-potential drift was monitored by replacing the reference compartment with one containing two identical platinized platinum electrodes, one working and the other detached; potential drift ≪ 0.1 mV/h was observed.

(c) Uncompensated Resistance

If no correction is provided for the uncompensated resistance R_u which comprises electrolyte resistance (calculated from eq. [2]) plus the measured associated lead and contact resistances (0.02–0.03 Ω), then a change ΔV applied by the voltage controller will change the potential of the test electrode by $\Delta V \pm R_u I(t)$, where $I(t)$ is the time-dependent current produced. Here the positive sign applies to cathodic reactions (ΔV negative) and the negative sign to anodic (ΔV positive). Thus the test electrode experiences a potential change smaller than the desired potential step, giving rise to a negative error in the current. If we set the IR compensator to compensate a fraction ϕ of R_u, the electrode potential at time t is given by

$$[3] \qquad \varepsilon(t) - \varepsilon_r = \Delta V \pm (1 - \phi) R_u I(t)$$

Only for full IR compensation ($\phi = 1$) will a current- and time-independent potential be strictly attained. But when the compensator is set at $\phi \simeq 1$, oscillations may be induced (8, 9, 12) causing large fluctuations in cell current and in control voltage. In the present system, over the range $\phi = 0$ to 0.98, the control voltage exhibited no change in d.c. level (> 0.1 mV) and no a.c. components (> 0.1 mV peak to peak). Current oscillations were obtained, however, at ϕ just greater than unity.

Figure 3 presents typical $i-t$ curves for gold in chloride solution I. It illustrates that uncompensated-resistance effects can be very large. The plotted points represent the mean curve from seven oscilloscope traces; the maximum deviation from the mean currents was 3% and the curve was independent of time for a period of several

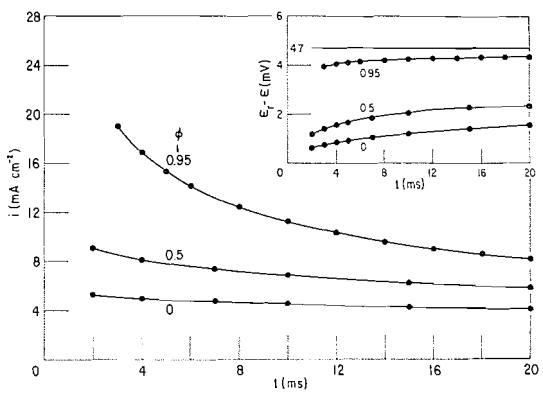

FIG. 3. Ferric ion reduction on gold in solution I, $\Delta V = -4.7$ mV.

[1]The operational characteristics of the present potentiostat have not been determined in sufficient detail for fundamental comparison with circuits recently described. Reference may be made particularly to improved circuits based on operational amplifiers, which are designed for fast response and high stability at 100% ohmic compensation (11, 12).

hours after the test electrode was placed in the cell. Uncertainty in the measurement of the distance of the capillary tip from the gold electrode led to a probable error of 3% in the degree of ohmic compensation. The current–time curves in Fig. 3 demonstrate that large inaccuracies can result from uncompensated resistance, both in the reaction rates (currents) and in the shape of the current–time curve. The uncompensated-resistance effect is illustrated also by the time variation of the electrode potential, shown inset in Fig. 3. These curves were obtained from the measured currents by use of eq. [3], with $R_u = 0.21_3$ Ω. When no ohmic compensation is applied, the electrode potential remains far from the desired value throughout the 0.02 s reaction time; hence the remarkably low currents. Even with 95% compensation, the potential still remains somewhat lower than the desired value.

Effect of Impurities in Sulfate Solutions

In the sulfate solution before activated-charcoal purification, a relatively rapid deactivation of the gold electrode occurred, as shown in Fig. 4. This pronounced deactivation was reduced by the activated-charcoal treatment to less than a $3\%\,h^{-1}$ current decrease; after prolonged use of the gold electrode, the latter could be cleaned again and replaced in the solution to regenerate the original current–time curve. The current levels of the initial (3 min) curve obtained in the unpurified solution were only 5% below the corresponding levels for the purified solution. Platinum test electrodes also exhibited this impurity effect in the sulfate solution.

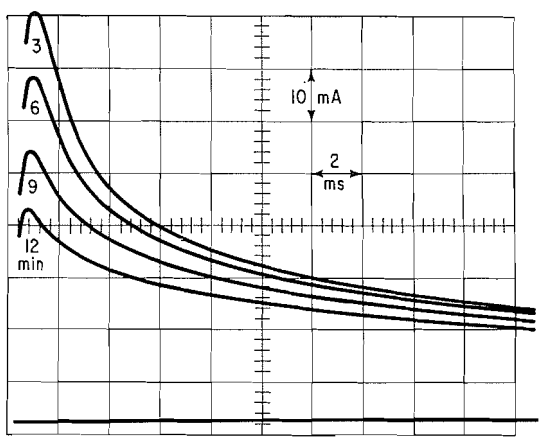

FIG. 4. Ferric ion reduction on gold in unpurified solution III, $\Delta V = -4.8$ mV. Time after electrode inserted into cell is shown.

Evaluation of Exchange Current Densities

The method of analysis used to obtain the charge-transfer current from a given $i - t$ curve is based upon the theoretical relation for planar electrodes

$$[4] \qquad i/i_{t=0} = \exp(\lambda^2 t)\,\mathrm{erfc}\,(\lambda\sqrt{t})$$

Here[2] i is the current density at time t and $i_{t=0}$ its initial value (the desired charge-transfer current density); λ is a constant directly proportional to the exchange current density i_0 and inversely proportional to the concentration (6). The planar-electrode relation is applicable to cylindrical electrodes if λ is sufficiently large (7); this condition is satisfied here as shown later. Because eq. [4] is valid, the "ratio method" of analysis previously described (7, 18) was utilized to evaluate the charge-transfer current. In this method the measured ratio of the current at time t to that at $4t$ gives the value of $\lambda\sqrt{t}$ corresponding to the selected time through the relation (18)

$$[5] \qquad \lambda\sqrt{t} = \frac{a_0(\mathscr{R} - 1) + a_1(\mathscr{R} - 1)^2}{1 + a_2(\mathscr{R} - 1)}$$

$$\mathscr{R} = i(t)/i(4t)$$

$$a_0 = 0.8827$$

$$a_1 = -0.4539$$

$$a_2 = -0.9071$$

Knowing λ, eq. [4] yields $i_{t=0}$, from which i_0 is obtained by the well-known relation for small overpotential (η)

$$[6] \qquad (i_{t=0}/i_0)_{\eta\to 0} = nF|\eta|/RT$$

where F is the Faraday, R the gas constant, T the temperature, and n is unity, the number of electrons involved in the ferrous–ferric reaction.

Considering first the ferrous–ferric reaction on bright gold, we applied this method of analysis to the 95% compensated current–time curve in Fig. 3, and to other such curves determined in solutions I – III over reaction times from 3 to 50 ms. In all cases the experimental ratio $i(t)/i(4t)$ consistently exceeded 1.80 at $t \Rightarrow 3$ ms and increased

[2] $\mathrm{erfc}\,(x) = 1 - \mathrm{erf}\,(x) = 1 - (2/\sqrt{\pi})\int_0^x e^{-z^2}\,dz$

Can. J. Chem. Downloaded from www.nrcresearchpress.com by 210.87.254.40 on 09/05/12
For personal use only.

TABLE I

Ferrous–ferric reaction on bright gold, 95% ohmic compensation, 25 °C

Solution	$c = c(Fe^{2+}) = c(Fe^{3+})$ (mole/1000 cm^3)	η (V)	i at 3 ms (A cm^{-2})	Lower limits (A cm^{-2})		
				$i_{t=0}$	i_0	$i_{0,s}f$
I	0.097	−0.0047	0.019_0	0.059	0.37	3.8
I	0.097	$+0.0050_5$	0.020_1	0.063	0.33	3.4
II	0.0195	−0.0049	0.0038_7	0.0121	0.063_5	3.3
II	0.0195	+0.0049	0.0040_2	0.0126	0.066	3.4
III	0.096	-0.0048_5*	0.016_3	0.051	0.027	2.8

*Anodic reaction at 4.8_5 mV gave same current–time curve.

smoothly with increasing t towards 2 (the theoretical maximum). Taking the ratio 1.80 as being a minimum value for $t = 3$ ms, whence $\lambda\sqrt{t} > 1.51$ and $\lambda > 27$ s$^{-1/2}$, we may compute lower limits to the values of $i_{t=0}$ and i_0. These are listed in Table I. It is true that $i_{t=0}$ cannot be derived with precision from a current ratio corresponding to such a large value of $\lambda\sqrt{t}$ (preferably $\lambda\sqrt{t} <$ unity (6, 19)), because at such long times the reaction rate is controlled mostly by diffusion and only in small part by the charge-transfer process; nevertheless it is felt from the consistency of the current–time curves examined that the exchange current densities listed in Table I all underestimate the true values. Note that incomplete ohmic compensation tends to make $i_{t=0}$ low, since the actual electrode potential deviates more from the nominal value at time t than at $4t$. Our use of eq. [4] is justified only if $\lambda \gg D^{\frac{1}{2}}/r_0$, where D is the average diffusivity of the ferrous and ferric ions (7); D may be given the rough value 10^{-5} cm^2 s^{-1} to obtain $D^{\frac{1}{2}}/r_0 \simeq 0.063$ s$^{-1/2}$, indeed much smaller than λ.

The quantity in the last column of Table I is an estimate of the standard exchange current density $i_{0,s}$. For the first-order (defined at constant potential) ferrous–ferric reaction, we may write (20)

$$[7] \quad i_0/i_{0,s} = [a_{Fe^{3+}}/(a_{Fe^{3+}})_s]^{1-\beta}[a_{Fe^{2+}}/(a_{Fe^{2+}})_s]^{\beta}$$

where a is activity and β the transfer coefficient. Subscript s refers to the electrode in the defined standard state where $(a_{Fe^{3+}})_s = (a_{Fe^{2+}})_s = 1$ mole/1000 cm^3. Equation [7] shows that $i_{0,s}$ is indeed a real current density, measurable in principle and with units of A cm^{-2}, although the same quantity is also a standard rate constant when expressed as $(i_{0,s}/nF)$ in the units cm s^{-1} (with concentration in mole cm^{-3}). When the two ions have the same concentration c, eq. [7] yields $i_0/c = i_{0,s}f$, where f is the mean activity coefficient .Assuming $f < 1$, we obtain the high value of $i_{0,s} > 3$ A cm^{-2} for the ferrous–ferric reaction on gold in the chloride and sulfate solutions.

A more favorable case for quantitative analysis of the potentiostatic $i - t$ curve was obtained with the ferrous–ferric reaction on bright platinum in solution III; $i_{0,s}$ is an order of magnitude smaller for platinum than it is for gold in this solution. Because of the smaller currents involved, ε_{Pt} remained closer to the nominal value as compared with ε_{Au} in Fig. 3 (95% compensation). Also, accurate analysis of the $i - t$ curve by the ratio method was possible because the observed values of $\mathscr{R}$ were sufficiently small (i.e., below 1.6). Typical analytical data are presented in Table II for cathodic Fe^{3+} reduction on platinum at −4.8 mV. The fact that constant values of λ and $i_{t=0}$ are established at $t \geqslant 5$ ms confirms that the $i - t$ curve obeys eq. [4] and that the ratio method of analysis is valid. It was assumed that distortion by the slow electronic transient persisted to 4 ms, hence the first two values in the table were omitted in determining the mean.

TABLE II

Analysis of the potentiostatic current–time curve at −4.8 mV. Ferrous–ferric reaction on bright platinum, solution III, 25 °C*

Time (ms)	i (mA cm^{-2})	$\frac{i(t)}{i(4t)}$	λ (s$^{-\frac{1}{2}}$)	$i_{t=0}$ (mA cm^{-2})
3	5.02	1.282	5.23	7.48
4	4.76	1.284	4.56	7.12
5	4.57	1.287	4.12	6.85
6	4.43	1.298	3.93	6.72
7	4.31	1.315	3.89	6.67
8	4.20	1.328	3.83	6.60
9	4.12	1.344	3.82	6.59
10	4.04	1.359	3.83	6.58
Mean (5–10 ms inclusive)			3.90	6.67

*$i_0 = 0.036$, $i_{0,s}f = 0.38$ (A cm^{-2}).

Can. J. Chem. Downloaded from www.nrcresearchpress.com by 210.87.254.40 on 09/05/12
For personal use only.

The standard exchange current density found here is about 1.5 times the value ($i_{0,s}f = 0.26$ A cm^{-2}) calculated from Anson's galvanostatic data (21) for the ferrous–ferric reaction on bright platinum in similar $NaHSO_4$ solutions. Since differences in surface activity and roughness can result from the particular electrode precleaning procedures used, the agreement may be considered satisfactory.

The result that the classically simple (22) ferrous–ferric reaction is at least an order of magnitude slower on platinum than on gold, two "inert" metals, is surprising. Such dependence on the metal can arise, however, in several different ways; one way is through specific anion adsorption on the platinum. We conclude that new diagnostic experiments on the ferrous–ferric electrode reaction are needed.

In summary, the Fe^{2+},Fe^{3+}(Au) system has been shown to have a high standard exchange current density ($i_{0,s} > 3$ A cm^{-2}), and therefore is an ideal one for illustrating quantitatively the effect of uncompensated (or partly compensated) resistance on potentiostatic kinetics. The effect is to prevent the attainment of a constant potential step, and to yield reaction rates which are too small and which have distorted time dependence. In the case of the Fe^{2+},Fe^{3+}(Pt) system, where $i_{0,s}$ is much smaller, the rather slow potentiostat used in this work was adequate for obtaining precise current–time curves. These curves were analyzed by the ratio method which was shown to yield the charge-transfer current with good precision.

Acknowledgments

The author is grateful to Robert B. Gosser and Paul R. Malmberg of the Westinghouse Research and Development Center, Pittsburgh, Pennsylvania, for several helpful circuit suggestions.

1. P. DELAHAY. Advan. Electrochem. Electrochem. Eng. **1**, 247 (1961).
2. P. DELAHAY. Double layer and electrode kinetics. Interscience Publishers, Inc., New York. 1965.
3. H. GERISCHER. Z. Elektrochem. **54**, 362, 366 (1950).
4. D. J. KOOYMAN, M. SLUYTERS-REHBACH, and J. H. SLUYTERS. Electrochim. Acta, **11**, 1197 (1966).
5. S. BARNARTT. Corrosion Sci. In press.
6. H. GERISCHER and W. VIELSTICH. Z. Physik. Chem. **3**, 16 (1955).
7. C. A. JOHNSON and S. BARNARTT. J. Phys. Chem. **71**, 1637 (1967).
8. S. BARNARTT, P. R. MALMBERG, and R. B. GOSSER. Electrochem. Technol. **3**, 327 (1965).
9. A. L. HODGKIN, A. F. HUXLEY, and B. KATZ. J. Physiol. **116**, 424 (1952).
10. H. GERISCHER and K. E. STAUBACH. Z. Elektrochem. **61**, 789 (1957).
11*a*. G. L. BOOMAN and W. B. HOLBROOK. Anal. Chem. **35**, 1793 (1963). *b*. E. R. BROWN, D. E. SMITH, and G. L. BOOMAN. Anal. Chem. **40**, 1411 (1968).
12*a*. G. LAUER and R. A. OSTERYOUNG. Anal. Chem. **38**, 1107 (1966). *b*. D. POULI. J. R. HUFF, and J. C. PEARSON. Anal. Chem. **38**, 382 (1966).
13. S. BARNARTT. J. Electrochem. Soc. **99**, 549 (1952).
14. S. BARNARTT. J. Electrochem. Soc. **108**, 102 (1961).
15. G. J. HILLS and D. J. G. IVES. J. Chem. Soc. 305 (1951).
16. S. D. JAMES. J. Electrochem. Soc. **114**, 1113 (1967).
17. K. B. OLDHAM. J. Electroanal. Chem. **11**, 171 (1966).
18. C. A. JOHNSON and S. BARNARTT. J. Electrochem. Soc. **114**, 1256 (1967).
19. K. B. OLDHAM and R. A. OSTERYOUNG. J. Electroanal. Chem. **11**, 397 (1966).
20. S. BARNARTT. J. Phys. Chem. **70**, 412 (1966).
21. F. C. ANSON. Anal. Chem. **33**, 939 (1961).
22. K. J. VETTER. Electrochemical kinetics. Academic Press, Inc., New York. 1965. p. 455.

Can. J. Chem. Downloaded from www.nrcresearchpress.com by 210.87.254.40 on 09/05/12
For personal use only.

Can. J. Chem. Downloaded from www.nrcresearchpress.com by 210.87.254.5 on 09/05/12
For personal use only.

Isomer ratios for the $^{44}Ca(p,n)^{44}Sc^{m,g}$ and $^{85}Rb(p,n)^{85}Sr^{m,g}$ reactions[1]

D. R. SACHDEV AND L. YAFFE

Radiochemistry Laboratory, Department of Chemistry, McGill University, Montreal, Quebec

Received December 19, 1968

Isomeric cross-section ratios for the $^{44}Ca(p,n)^{44}Sc^{m,g}$ and $^{85}Rb(p,n)^{85}Sr^{m,g}$ reactions have been measured over a proton energy range of 6–85 and 6–27 MeV, respectively. Experimental results are compared with calculations based on the Vandenbosch–Huizenga formalism (1, 2), while spin-cutoff parameter values were obtained from various models. For the isomeric pair of $^{44}Sc^{m,g}$, the parameters required to obtain a good fit with the experimental results are in agreement with those of Keedy *et al.* (6). On the other hand, the experimental results for the $^{85}Sr^{m,g}$ isomeric pair are unusually high compared with the calculated isomer ratios. Half-lives of $^{44}Sc^{g}$ and $^{85}Sr^{m}$ were redetermined to be 4.05 ± 0.03 h and 68.0 ± 0.2 min, respectively.

Canadian Journal of Chemistry, 47, 1667 (1969)

The formalism suggested by Vandenbosch and Huizenga (1, 2) for indirectly testing the spin dependence of nuclear level densities by determining isomer ratios has become a very useful method. The formalism is valid only in the low-energy region where the formation of a compound nucleus can, with some justification, be assumed. In order that the calculated and the experimental isomer ratios agree, effective moments of inertia much less than rigid body values, have invariably been required. This, along with some other factors, (like odd–even effects, etc.) strongly suggests that other interactions, particularly the pairing interaction, should be introduced into the calculation. More recent calculations (3–7) have introduced such refinements into the calculation.

In a recent communication (5), the isomer ratios obtained at various proton bombarding energies for the $^{88}Sr(p,2n)^{87}Y^{m,g}$ reaction were reported. The parameters required to fit the calculated values to those observed experimentally were compared with parameters obtained for the isomer ratios from the $^{85}Rb(\alpha,2n)^{87}Y^{m,g}$ and $^{87}Sr(d,2n)^{87}Y^{m,g}$ reactions (4). In all the foregoing cases the reaction proceeded via the same compound nucleus. With the same approach in mind, the isomer ratios for the $^{44}Ca(p,n)^{44}Sc^{m,g}$ reaction were measured and compared with the parameters obtained from isomer ratios found (6, 8–10) for the reaction $^{41}K(\alpha,n)^{44}Sc^{m,g}$. Our measurements have been carried out in the proton bombardment energy region of 6–85 MeV. Since in this energy region it is generally believed that the compound nucleus mechanism slowly changes to the direct interaction mechanism, it should be of interest to see how the isomer ratios are affected.

Isomer ratios have also been measured for the $^{85}Rb(p,n)^{85}Sr^{m,g}$ reaction in the proton bombardment energy region of 6–27 MeV. The results obtained are also compared with theoretical predictions.

Experimental

(a) Target and Irradiations

The target materials were calcium carbonate, enriched to 94.0% in ^{44}Ca and rubidium chloride, enriched to 99.54% in ^{85}Rb[2].

About 1–3 mg of the sample were loaded into a thin aluminium tube which was pinched shut at both ends, rolled flat, and irradiated in the internal circulating beam of the McGill Synchrocyclotron. Corrections for the energy degradation of the beam (though within the energy spread of ± 2 MeV) were made from Sternheimer's (11) range–energy relation. Duration of the bombardments was of the order of 10–15 min.

(b) Chemical Separation

The irradiated aluminium tubes were dissolved in a small amount of dilute hydrochloric acid and a drop of hydrogen peroxide. The procedure for the chemical separation of strontium has been described previously (12). Scandium was purified by tributyl phosphate extraction, essentially similar to the method used by Matsuo and Sugihara (9).

(c) Activity Measurements

$^{44}Sc^{m}$ decays essentially (98.6%) (13) by an isomeric transition to the ground state. The activities of both of these species were determined by following the decay of the 1.156 MeV γ-ray associated with $^{44}Sc^{g}$, by means of a 3 in. × 3 in. NaI (Tl) Harshaw Integral Assembly (resolution 7.5% for the 0.662 MeV γ-ray) coupled to a

[1]This research was supported by the National Research Council of Canada.

[2]The enriched materials were purchased from the Isotope Division, Oak Ridge National Laboratory.

Can. J. Chem. Downloaded from www.nrcresearchpress.com by 210.87.254.5 on 09/05/12
For personal use only.

400-channel pulse-height analyzer. At bombardment energies up to 12 MeV, since $^{44}Sc^{g}$ decays predominantly by positron emission, the associated annihilation radiation was also measured by two 1.5 in. × 1.5 in. NaI (Tl) Harshaw Integral Assemblies, gated to accept 0.511 MeV pulses in coincidence (12). At higher bombardment energies the latter technique was not used, since the production of ^{43}Sc (with very similar half-life) by the (p,2n) reaction made the results difficult to interpret.

Isomeric species of ^{85}Sr was also measured by two methods. The first consisted in measuring the γ-rays associated with each of the species. The metastable state was measured by following the decay of the 0.225 MeV γ-ray. To the normal abundance of 85%, one must add 1.3% (4) arising from the decay of the 0.2325 MeV γ-ray, also associated with the isomeric transition. The ground state was measured by its 0.514 MeV γ-ray. A branching ratio of 100% and a conversion coefficient of 0.007 were used (14). Experimental detection efficiencies for the counting assembly were determined by using standard sources.

The other procedure avoided the use of efficiency curves. $^{85}Sr^{m}$ decays by electron capture (13.7%) to an excited state of ^{85}Rb, while $^{85}Sr^{g}$ decays by electron capture (100%) to another excited state of the same residual nucleus. The K X-rays associated with ^{85}Rb were measured with a thin (2 mm) NaI (Tl) Harshaw Integral Assembly coupled to a multi-channel analyzer. Internal conversion coefficients (14) of $\alpha_k = 0.04$ for 0.150 MeV, $\alpha_k = 0.02$ for 0.225 MeV, and $\alpha_k = 0.007$ for the 0.514 MeV γ-rays were used, and an apparent branching ratio of 15.7%, instead of 13.7%, for the metastable state was obtained in this way. (The disadvantage of this method is that a small error in the branching ratio of internal conversion coefficients will greatly influence the measurement.)

The decay curves were all analyzed by the CLSQ decay curve analysis program (15) and this, as well as all the other calculations, was done on the McGill IBM 7044 Computer.

Results

(a) Half-lives

The half-life of $^{44}Sc^{m}$ was determined by following the decay of the 0.270 MeV γ-ray over a period of more than 6 half-lives. It was found to be 2.44 days, identical with the accepted value (14). The half-life of $^{44}Sc^{g}$, followed over a similar period of time, was found to be 4.05 ± 0.03 h, agreeing very well with that found by Tatarczuk and Medicus (16), 4.00 ± 0.02 h. The half-life was determined both by positron as well as γ-ray (1.156 MeV) measurement. The activity was produced by the $^{44}Ca(p,n)^{44}Sc$ reaction at proton bombardment energies of 6–9 MeV.

Similarly the half-life of $^{85}Sr^{m}$ was determined by following the decay of the 0.225 MeV γ-ray over a period of more than 6 half-lives. The activity was produced by the $^{85}Rb(p,n)^{85}Sr$ reaction from a sample of rubidium virtually monoisotopic in ^{85}Rb. The half-life of the ground state is very long (65 days), compared with the metastable state, and any expected interference from the Compton background from the 0.514 MeV γ-ray will be negligible. The same will apply to possible interference from the 0.388 MeV γ-ray from ^{87}Sr (half-life 2.83 h), since the abundance of ^{87}Rb in the enriched target was only 0.46%.

The half-life for $^{85}Sr^{m}$ was found to be 68.0 ± 0.2 min, to be compared with 70 ± 2 min as previously reported (14).

No attempt was made to re-determine the half-life of $^{85}Sr^{g}$. The data were in good agreement with the accepted value of 65.0 days.

(b) Isomer Ratios

The ratio of the formation cross sections of the high-spin species to that of the low-spin species is defined as the isomer ratio throughout this paper, i.e. $\sigma_{^{85}Sr^{g}}/\sigma_{^{85}Sr^{m}}$ and $\sigma_{^{44}Sc^{m}}/\sigma_{^{44}Sc^{g}}$. The experimental results of these ratios are given in Table I. The values obtained for ^{44}Sc by γ-ray and positron measurements are identical within experimental error. The values of the isomer ratios for ^{85}Sr obtained by γ-ray and X-ray measurements are shown separately. The former involves detection efficiencies which are prone to error, while the latter process, as indicated earlier, involves decay scheme data which may lend systematic errors to the results. Unless errors introduced into both methods lie in the same direction, and are of the same general magnitude, it would seem that they are within the errors quoted, which as shown, include only uncertainties in decay curve analysis, photopeak area measurements, and detection efficiencies. The isomer ratios are shown graphically in Figs. 1 and 2.

Calculations and Discussion

(a) Qualitative Considerations

The isomer ratio of ^{44}Sc (Fig. 1) increases rapidly with increasing energy to a proton bombardment energy of about 20 MeV, at which point it begins to decrease until a flat portion is reached at about 40 MeV. At still higher energies the data show a very slight increase with energy, although they are also, within experimental error, consistent with no variation with energy.

The isomer ratio of ^{85}Sr shows a similar behavior, although in this case the peak is reached at

TABLE I

Experimental isomer ratios ($\sigma_{\text{high spin}}/\sigma_{\text{low spin}}$)

Proton energy (MeV)	Isomer ratios			
	$^{44}Ca(p,n)^{44}Sc^{m,g}$		$^{85}Rb(p,n)^{85}Sr^{m,g}$	
	γ-Measurements (±8%)	Positron measurements (±8%)	γ-Measurements (±15%)	X-ray measurements (±10%)
6	0.015	0.014	1.4	1.5
9	0.063	0.064	1.9	2.1
12	0.090	0.085	3.0	3.1
15	0.140	—	3.9	4.5
18	0.20	—	4.0	4.7
21	0.24	—	3.5	4.2
24	0.23	—	3.4	3.9
27	—	—	3.3	—
30	0.19	—	—	—
40	0.16	—	—	—
50	0.14_5	—	—	—
60	0.15	—	—	—
72	0.16	—	—	—
85	0.17	—	—	—

about 17 MeV. The difference in the peak positions of the two curves can be attributed to the threshold of the next reaction, (p,2n), i.e., 14.5 and 10.5 MeV respectively for the $^{44}Ca(p,2n)^{43}Sc$ and $^{85}Rb(p,2n)^{84}Sr$ reactions, as calculated from the tables of Mattauch *et al.* (17).

It is also evident that the isomer ratios continue to increase with bombarding energy, beyond the peaks of the excitation function curves which would be close to the thresholds for the (p,2n) species. This rise beyond the peaks of the excitation function curves lends weight to the hypothesis (5) that competition between neutron and γ-ray emission favors the high-spin species in the present case.

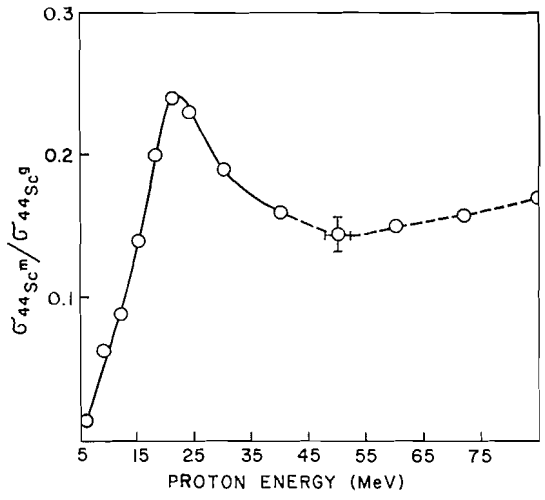

FIG. 1. Experimental isomer ratio ($\sigma_{44Sc^m}/\sigma_{44Sc^g}$) produced in the reaction $^{44}Ca(p,n)^{44}Sc^{m,g}$.

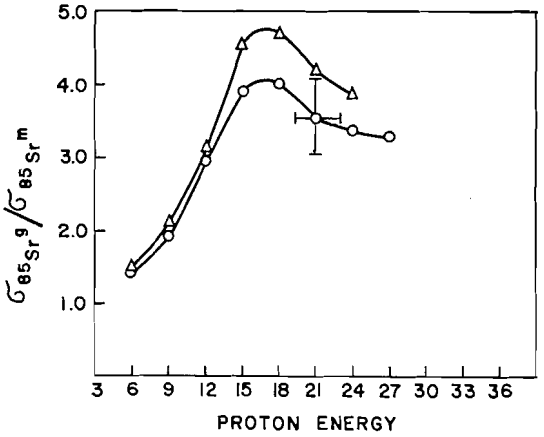

FIG. 2. Experimental isomer ratio ($\sigma_{85Sr^g}/\sigma_{85Sr^m}$) produced in the reaction $^{85}Rb(p,n)^{85}Sr^{m,g}$; ○, γ-ray measurements; Δ, X-ray measurements.

The isomer ratios for ^{85}Sr are much larger than those for ^{44}Sc. The following reasons can be advanced to explain this. The spin in the ground state of ^{85}Rb is 5/2. The spins of the metastable and ground states of ^{85}Sr are 1/2 and 9/2 respectively, with an intermediate state of 7/2. At the end of the de-excitation stage, the last γ-ray from states with spins of 5/2 or greater will populate the ground state (high-spin species), while those states with spins of 3/2 or less will contribute to

Can. J. Chem. Downloaded from www.nrcresearchpress.com by 210.87.254.5 on 09/05/12
For personal use only.

Can. J. Chem. Downloaded from www.nrcresearchpress.com by 210.87.254.5 on 09/05/12
For personal use only.

the low-spin state. On the other hand the spin of ^{44}Ca in the ground state is zero, while the spins of the metastable and ground states of ^{44}Sc are 6 and 2 respectively. The last γ-ray from states with spins of 5 or more will cause the metastable state to be populated, while those arising from states with spins of 3 or less will populate the ground state. States with intermediate spin of 4 will populate both states equally.

In Fig. 3 the experimental isomer ratio is plotted as a function of excitation energy of the compound nucleus ^{45}Sc, for the reaction ^{44}K(α,n)^{44}Sc^{m,g} from the data of Matsuo *et al.* (10), Riley *et al.* (8), and Keedy *et al.* (6). The data were compared with those obtained in the present work and show the effect (on isomer ratios) of greater amount of angular momentum associated with incoming α-particles as compared with protons. The excitation energy, E_c, was calculated from the equation $E_c = E_{cm} + Q$, where E_{cm} is the projectile energy in the center-of-mass system and Q is the energy liberated in the reaction to form the compound nucleus, as calculated from the mass tables of Mattauch *et al.* (17).

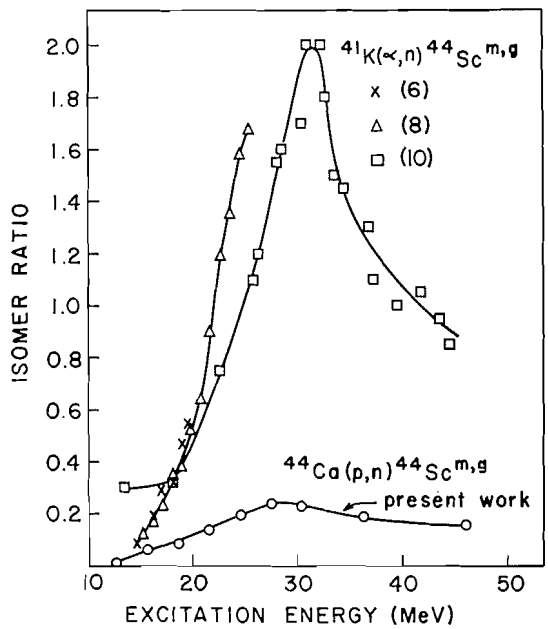

FIG. 3. Experimental isomer ratios as a function of excitation energy of the compound nucleus (^{45}Sc*), produced in the reactions, (*a*) ^{41}K + α → ^{45}Sc*; □, Matsuo *et al.* (10); Δ, Riley, *et al.* (8); ×, Keedy *et al.* (6). (*b*) ^{44}Ca + p → ^{45}Sc*; ○, present work.

(b) Calculations

These were performed with the original program of Hafner *et al.* (18). Keedy *et al.* (6) have shown that proton emission would not significantly affect isomer ratios, but implied that in the system studied by them, ^{41}K(α,n)^{44}Sc^{m,g}, α-particle emission might play a role. As before, we have not included competition due to protons or α-particles in our calculation. Details of the calculations have been described previously (5) and only a brief recapitulation is given here.

Three models were used for obtaining the excitation energy, U, and energy-dependent spin-cutoff parameter, σ, needed for the basic equation giving the spin-dependent level density, $\rho(U,J)$

$$\rho(U,J) = \rho(U,0)(2J + 1) \exp\left\{-\frac{J(J+1)}{2\sigma^2}\right\}$$

(*i*) Shifted Fermi Gas Model. With this model the excitation energy is measured from the mass surface of an odd–odd nuclide (19). Since ^{44}Sc is itself an odd–odd nuclide, no pairing correction is required. For ^{85}Sr the pairing energy Δ = 1.4 MeV (20) was subtracted from E to get the value of U. The variation of σ with energy was obtained from the relations

$$U = at^2 - t$$

and

$$\sigma^2 = \frac{It}{\hbar^2}$$

where t is the thermodynamic temperature, a is the usual level-density parameter, and I is the rigid body moment of inertia.

(*ii*) Independent Pairing Model. According to this model (21, 22) the excitation energy is measured from a fictitious mass surface, lying below even that of an even–even nuclide. The correction for the odd–even ^{85}Sr was made by adding Δ = 1.4 MeV, and that for ^{44}Sc by adding 2Δ = 4.0 MeV (20) to the normal excitation energy. All the other equations, including those linking the excitation energy with the spin-cutoff parameter have been given previously (5).

(*iii*) Superconductor Model. An attempt is made by use of this model to compare the nucleus to the superconducting state of a metal. Following Lang (22), Vonach *et al.* (3) used this model to interpret isomer ratios. According to this model, there is a critical energy above which

Can. J. Chem. Downloaded from www.nrcresearchpress.com by 210.87.254.5 on 09/05/12
For personal use only.

the superconductor behaves like a normal Fermi gas, except that its ground state is shifted by an amount equal to the condensation energy. Above this critical energy the moment of inertia values correspond to rigid body values, while below this energy the moment of inertia decreases strongly (3) with decrease in excitation energy.

In the present calculations with all these models the value of σ, as previously (5), was not allowed to decrease below certain limiting values. Also neutron emission was restricted to neutrons with kinetic energy of $2T$, where T is the nuclear temperature. Optical model transmission coefficients were used, with parameters due to Perey (23) for protons and those of Campbell *et al.* (24) for neutrons. Only dipole transitions were assumed for the γ-ray cascade. Calculations for the average γ-ray energy were made with the empirical formula given by Vonach *et al.* (3) and described previously (5). The prescription of Vonach *et al.* was also used to determine the isomer-deciding transition. When the excitation energy of the residual nucleus was greater than 2 MeV, the next γ-ray was not an "isomer-deciding" transition. When the excitation energy of the residual nucleus was between 1 and 2 MeV, the probability for the emission of an isomer-deciding transition was taken to be $(2 - E)$, and for not being the case as $(E - 1)$. For excitation energies less than 1 MeV the last γ-ray was assumed to be emitted.

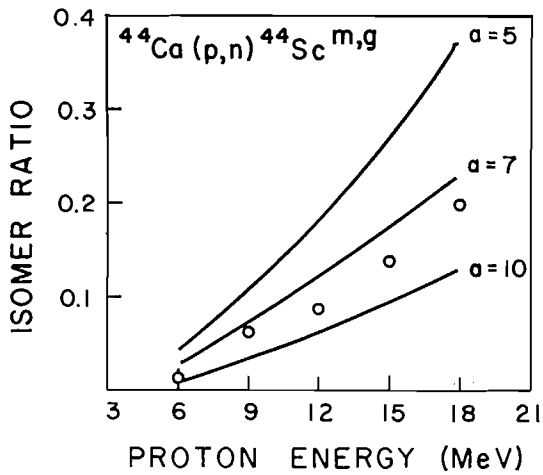

FIG. 4. Comparison of experimental isomer ratios ($\sigma_{^{44}Sc^m}/\sigma_{^{44}Sc^g}$) with calculations based on Shifted Fermi Gas Model and various values of the level-density parameter; ○, experimental; —, calculated.

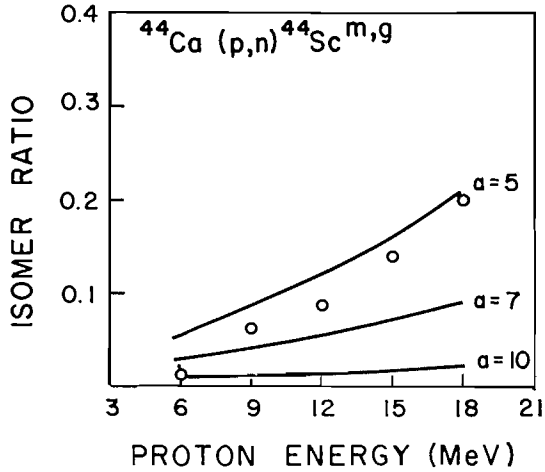

FIG. 5. Comparison of experimental isomer ratios ($\sigma_{^{44}Sc^m}/\sigma_{^{44}Sc^g}$) with calculations based on Independent Pairing Model and various values of the level-density parameter; ○, experimental; —, calculated.

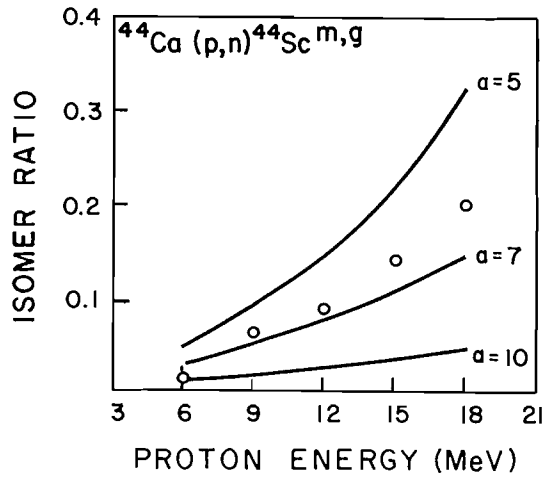

FIG. 6. Comparison of experimental isomer ratios ($\sigma_{^{44}Sc^m}/\sigma_{^{44}Sc^g}$) with calculations based on the Superconductor Model and various values of the level-density parameter; ○, experimental; —, calculated.

(c) *Comparison of Experimental Results with Calculations*

Figures 4, 5, and 6 show the experimental results for $^{44}Sc^{m,g}$ compared with the calculations based on the three models described. Figure 4 shows the results obtained by using spin-cutoff parameters obtained from the shifted Fermi Gas model calculations. A level-density parameter value of $a = 8$ or $A/5.5$ agrees with the results. It should be noted that, in the data of Keedy *et al.*

Can. J. Chem. Downloaded from www.nrcresearchpress.com by 210.87.254.5 on 09/05/12
For personal use only.

(Curve A, Fig. 1 of ref. (6)), when the value of a is taken as 5 and the neutron emission energy is limited to $2T$, the ratio of the calculated to experimental isomer ratios is the same as in the present work. This argues in favor of the same parameters applying to the two different systems proceeding via the same compound nucleus.

The Independent Pairing Model calculations shown in Fig. 5 suggest that $a = 6$ or $A/7.5$ agrees best with the experimental results, while the Superconductor Model (Fig. 6) gives values of $a = 6.5$ or $A/7$. For the latter case, Keedy *et al.* (6) found a level-density parameter value of $a = 5$, but their calculations took into account the effect due to competition of protons as well as α-particles, and the slightly higher value obtained by us is probably due to the neglect of these factors. The agreement obtained between the two systems proceeding via the same compound nucleus is gratifying.

In Figs. 7 and 8 the experimental isomer ratios for ^{85}Sr are compared with the calculations from the Shifted Fermi Gas and Superconductor Models, respectively. The calculated results are extremely low compared with the experimental values, and could not be matched, even for extremely low values of the level-density parameters. This is very difficult to explain and does not agree with the results obtained by other workers and us in this mass region. For example, calculations for $^{87}Y^{m,g}$ (5) required the extremely high value of $a = 21$ to match the experimental results for the Shifted Fermi Gas calculations. If one uses a value of $a = 21$ for $^{85}Sr^{m,g}$, the experimental results are a factor of at least 3 higher than the calculated values.

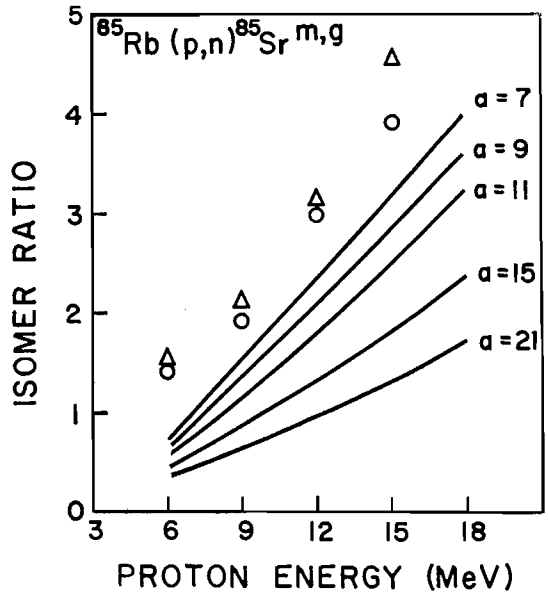

FIG. 7. Comparison of experimental isomer ratios ($\sigma_{^{85}Sr^g}/\sigma_{^{85}Sr^m}$) with calculations based on the Shifted Fermi Gas Model and various values of the level-density parameter; ○, experimental; —, calculated.

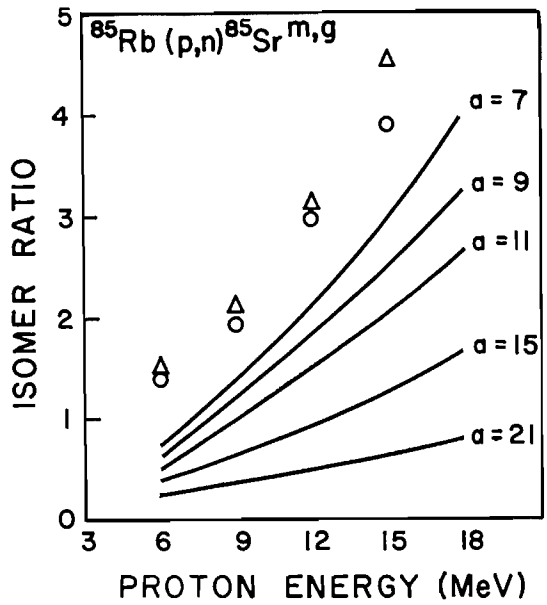

FIG. 8. Comparison of experimental isomer ratios ($\sigma_{^{85}Sr^g}/\sigma_{^{85}Sr^m}$) with calculations based on the Superconductor Model and various values of the level-density parameter; ○, experimental; —, calculated.

In the case of odd–odd nuclides where great discrepancies have also been found, Keedy *et al.* (6) suggested that the spin-cutoff parameter is sensitive to the type of single particle orbitals which are close to the Fermi surface, and as a result one should expect the spin-cutoff parameters to fluctuate from nucleus to nucleus. A more probable explanation in this case may well be the perturbation caused by the existence of an unknown state or states of intermediate spin, perhaps lying close to, but above the metastable state and decaying to the ground state by a crossover transition.

Acknowledgments

We would like to express our appreciation to Dr. R. E. Bell, Director of the Foster Radiation

Laboratory for ready permission to use the McGill Synchrocyclotron and to Mr. R. H. Mills who, as always, cheerfully performed the irradiations.

1. J. R. HUIZENGA and R. VANDENBOSCH. Phys. Rev. **120**, 1305 (1960).
2. R. VANDENBOSCH and J. R. HUIZENGA. Phys. Rev. **120**, 1313 (1960).
3. H. K. VONACH, R. VANDENBOSCH, and J. R. HUIZENGA. Nucl. Phys. **60**, 70 (1964).
4. R. VANDENBOSCH, L. HASKIN, and J. C. NORMAN. Phys. Rev. **137**, B1134 (1965).
5. D. R. SACHDEV and L. YAFFE. Can. J. Chem. **45**, 2711 (1967).
6. C. R. KEEDY, L. HASKIN, J. WING, and J. R. HUIZENGA. Nucl. Phys. **82**, 1 (1966).
7. C. T. BISHOP, J. R. HUIZENGA, and J. P. HUMMEL. Phys. Rev. **135**, B401 (1964).
8. C. RILEY, K. UNEO, and B. LINDER. Phys. Rev. **135**, B1340 (1964).
9. T. MATSUO and T. T. SUGIHARA. Can. J. Chem. **39**, 697 (1961).
10. T. MATSUO, J. M. MATUSZEK, JR., N. D. DUDEY, and T. T. SUGIHARA. Phys. Rev. **139**, B886 (1965).
11. R. M. STERNHEIMER. Phys. Rev. **115**, 137 (1959).
12. D. R. SACHDEV, N. T. PORILE, and L. YAFFE. Can. J. Chem. **45**, 1149 (1967).
13. C. M. LEDERER, J. M. HOLLANDER, and I. PERLMAN. Table of isotopes. 6th ed. John Wiley and Sons, Inc., New York. 1967.
14. Nuclear Data Sheets. Natl. Acad. Sci., Natl. Res. Council. Washington, D.C.
15. J. B. CUMMING. Natl. Acad. Sci., Natl. Res. Council, Nucl. Sci. Ser. NAS-NS-3107 1962.
16. J. R. TATARCZUK and H. A. MEDICUS. Phys. Rev. **143**, 818 (1966).
17. J. MATTAUCH, W. THIELE, and A. H. WAPSTRA. Nucl. Phys. **67**, 1 (1965).
18. W. L. HAFNER, J. R. HUIZENGA, and R. VANDENBOSCH. Argonne National Laboratory Report. ANL-6662. Dec. 1962 (unpublished).
19. H. HURWITZ and H. A. BETHE. Phys. Rev. **81**, 898 (1951).
20. P. E. NEMIROVOSKY and YU. V. ADAMCHUK. Nucl. Phys. **39**, 551 (1962).
21. D. W. LANG and K. E. LECOUTEUR. Nucl. Phys. **14**, 21 (1959).
22. D. W. LANG. Nucl. Phys. **42**, 353 (1963).
23. F. G. PEREY. Phys. Rev. **131**, 745 (1963).
24. E. J. CAMPBELL, H. FESHBACH, C. E. PORTER, and V. F. WEISSKOPF. MIT Technical Report No. 73, Feb. 1960 (unpublished).

Can. J. Chem. Downloaded from www.nrcresearchpress.com by 210.87.254.5 on 09/05/12
For personal use only.

Can. J. Chem. Downloaded from www.nrcresearchpress.com by 210.87.254.6 on 09/05/12
For personal use only.

Liquid hydrogen chloride solvent system. XII. Reactions of some sulfur, selenium, and tellurium compounds[1]

M. E. PEACH
Department of Chemistry, Acadia University, Wolfville, Nova Scotia

Received October 10, 1968

The ions Me_2SCl^+ and $MeSCl_2^+$ have been prepared in hydrogen chloride solution from the oxidation of dimethyl sulfide and methanesulfenyl chloride with chlorine, or from methyl sulfur trichloride ($MeSCl_2^+$), and characterized as their tetrachloroborates and hexafluorophosphates. $Et_2SCl^+BCl_4^-$ and $EtSCl_2^+BCl_4^-$ have been prepared analogously. Dimethyl selenium and dimethyl tellurium solutions were oxidized with chlorine to dimethyl selenium dichloride and dimethyl tellurium dichloride.

Methanesulfenyl chloride solution was ionized due to the protonation of sulfur, and not to the loss of a chloride ion. Methylchlorosulfonium hexafluorophosphate has been characterized. Methane- and ethane-sulfenyl chloride solutions reacted with boron trichloride giving $(RSCl)_2BCl_3$.

Sulfur tetrachloride, selenium tetrachloride, and tellurium tetrachloride were sparingly soluble and showed no acidic or basic properties in the solvent. Sulfur monochloride, sulfur dichloride, selenium monochloride, and tellurium dichloride were non-basic in solution.

The new compounds, $Me_2S_2.BCl_3$ and $Me_2Te.BCl_3$, have been prepared and characterized.

Canadian Journal of Chemistry, 47, 1675 (1969)

Introduction

The reactions of some sulfur compounds in solvent liquid hydrogen chloride have been described previously. Thiols and sulfides act as solvobases of varying strengths, and when treated with the solvoacid boron trichloride, form boron trichloride adducts in solution (1)

$$Me_2S + 2HCl \rightarrow Me_2SH^+ + HCl_2^-$$

$$Me_2SH^+ + BCl_3 \rightarrow Me_2S.BCl_3 + H^+$$

The properties of compounds containing a double sulfur oxygen bond, R_2SO, R_2SO_2, RSO_2Cl, SO_2Cl_2, $SOCl_2$, SO_2, H_2SO_4, $MeSO_3H$, CF_3SO_3H, and $ClSO_3H$ have been studied as potential acids and bases (2). This paper extends the previous work on divalent sulfur compounds by considering the oxidation of certain compounds in solution with chlorine and stabilization of the products as tetrachloroborates or hexafluorophosphates. Analogous reactions have been studied with some selenium and tellurium compounds. The properties of the sulfur, selenium, and tellurium chlorides in solution have also been examined.

Results and Discussion

The dialkylsulfonium ion, R_2SH^+, can only be isolated from hydrogen chloride solution as an unstable hexafluorophosphate (3). The S—H bond formed in solution by protonation of dialkyl sulfides and alkanesulfenyl chlorides has been oxidized with chlorine to form the dialkylchlorosulfonium and alkyldichlorosulfonium ions in solution.

$$R_2SH^+ + Cl_2 \rightarrow R_2SCl^+ + HCl$$

The use of the halogens as oxidizing agents in solvent liquid hydrogen chloride has been studied (4). Dialkyl sulfur dichlorides could not be isolated as stable materials from the oxidation of the sulfide solutions, but the reaction of a solution of the dialkylchlorosulfonium ion with boron trichloride or phosphorus pentafluoride resulted in the formation of dimethyl- and diethylchlorosulfonium tetrachloroborates and dimethylchlorosulfonium hexafluorophosphate. Phosphorus pentafluoride acts as a solvoacid and reacts with solvobases, such as tetramethylammonium hydrogendichloride, according to the equation

$$2Me_4N^+HCl^- + 3PF_5 \rightarrow 2Me_4N^+PF_6^- + PF_3Cl_2 + 2HCl$$

Methyl sulfur trichloride was formed in the chlorine oxidation of methanesulfenyl chloride. Methyl and ethyl sulfur trichlorides and trimethylsulfonium iodide acted as solvobases, forming stable tetrachloroborates, $RSCl_2^+BCl_4^-$ and $Me_3S^+BCl_4^-$, with boron trichloride and an unstable methyldichlorosulfonium hexafluorophosphate with phosphorus pentafluoride. Tri-*n*-butylsulfonium tetrachloroborate has been prepared from tri-*n*-butyl sulfur chloride and boron trichloride, and its properties investigated (5).

[1]For Part XI, see ref. 21.

Can. J. Chem. Downloaded from www.nrcresearchpress.com by 210.87.254.6 on 09/05/12
For personal use only.

The methods described here represent a good method of preparing the previously unknown ions R_2SCl^+ and $RSCl_2^+$.

Chlorine oxidation of solutions of alkanethiols or dialkyl disulfides caused a fracture of the S—S bond (formed initially in the alkanethiol reaction) and the formation of the alkanesulfenyl chloride in solution. Methane- and ethane-sulfenyl chlorides both act as solvobases, forming good conducting solutions. These compounds may ionize in either of two ways

[1] $$RSCl + 2HCl \rightarrow [R{-}\underset{\displaystyle H}{\underset{|}{S}}{-}Cl]^+ + HCl_2^-$$

[2] $$RSCl + HCl \rightarrow RS^+ + HCl_2^-$$

The scant evidence for the existence of the sulfenium ion, RS^+, in other media (6) and the observation that sulfenyl chlorides are protonated in strong sulfuric acid (7) both suggest that the ionization may be due to protonation, as in reaction [1]. The reactions of methanesulfenyl chloride in solution with phosphorus pentafluoride, which gave methylchlorosulfonium hexafluorophosphate and not methanesulfenyl hexafluorophosphate, and its oxidation with chlorine to methyl sulfur trichloride, are further evidence in favor of ionization caused by protonation.

Dimethyl selenium and dimethyl tellurium were found to be strong solvobases which were oxidized with chlorine in solution to dimethyl selenium dichloride and dimethyl tellurium dichloride. Dimethyl selenium dichloride reacted with boron trichloride in solution giving dimethylchloroselonium tetrachloroborate, previously prepared from dimethyl selenium dichloride and boron trichloride at $-25°$ in methylene dichloride (8). A solution of dimethyl tellurium dichloride reacted with boron trichloride to give a dimethyl tellurium dichloride boron trichloride adduct of unknown structure, which lost boron trichloride very readily on pumping at room temperature. Diphenyl selenium dichloride reacted with boron trichloride to form diphenylchloroselonium tetrachloroborate in solution, but this decomposed on warming to room temperature.

The reactions of solutions of diethyl sulfide, dimethyl selenium, and dimethyl tellurium with boron trichloride yielded the corresponding adducts at room temperature,

$$Me_2Se + 2HCl \rightarrow Me_2SeH^+ + HCl_2^-$$

$$Me_2SeH^+ + BCl_3 \rightarrow Me_2SeBCl_3 + H^+$$

although dimethyl telluronium tetrachloroborate was formed in solution. The diethyl sulfide – boron trichloride adduct has been prepared by the reaction of boron trichloride with diethyl sulfide in ligroin (9) and the dimethyl selenium – boron trichloride adduct prepared by the direct interaction of dimethyl selenium and boron trichloride (8). Dimethyl and diethyl disulfides reacted in solution with boron trichloride to form the somewhat unstable boron trichloride adducts, $R_2S_2 . BCl_3$. Methane- and ethane-sulfenyl chlorides reacted with boron trichloride to form an ionic compound in solution of stoichiometry $(RSCl)_2BCl_3$; the methanesulfenyl chloride compound has been characterized (10). Various structures have been suggested for the compound $(MeSCl)_2BCl_3$

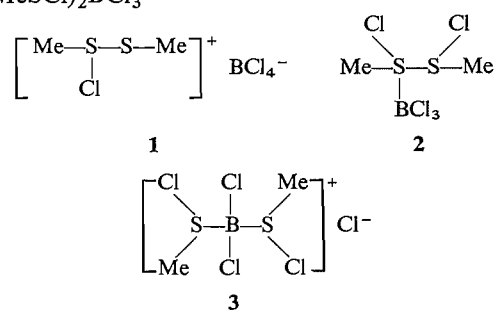

1 2

3

of which **3** is favored (10).

The potentially amphoteric chlorides $SeCl_4$ and $TeCl_4$, and SCl_4 were examined; ions of the type MCl_3^+ (11) and $SeCl_6^{2-}$ and $TeCl_6^{2-}$ (12) are all well known. It has very recently been shown that $SeCl_4$ and $TeCl_4$ both dissolve in chlorosulfuric acid to form the ions $SeCl_3^+$ and $TeCl_3^+$ (13). Sulfur, selenium, and tellurium tetrachlorides were all sparingly soluble and did not show any basic properties in solution, failing to react with boron trichloride, although sulfur tetrachloride is known to form an unstable adduct with boron trichloride in the absence of a solvent; this adduct decomposes at $-20°$ (14). Selenium and tellurium tetrachlorides did not react with boron trichloride in the absence of a solvent. The acidic properties, if any, of selenium and tellurium tetrachlorides, dimethyl and diphenyl selenium dichlorides, and dimethyl tellurium dichloride were investigated by mixing them with stoichiometric amounts of tetramethylammonium chloride in the solvent. From the increase in weight observed and the infrared (i.r.) spectrum of the product, it was inferred that tetramethylammonium hydrogen dichloride had

Can. J. Chem. Downloaded from www.nrcresearchpress.com by 210.87.254.6 on 09/05/12
For personal use only.

been formed, and that none of these chlorides had any acidic properties in liquid hydrogen chloride solution. Sulfur dichloride, sulfur monochloride, selenium monochloride, and tellurium dichloride did not react with boron trichloride in liquid hydrogen chloride or without a solvent.

Comparison of the conductivities of dimethyl sulfide, dimethyl selenium, and dimethyl tellurium shows that for solutions of approximately the same concentration, the basicities are of the same order of magnitude and that changing the Group VI element has little effect on the ease of protonation of Me_2M to form Me_2MH^+. A much greater change in conductivities is observed in changing the methyl group for chlorine; in the series $Me_xSCl_{3-x}^+$ it is observed that the basic strengths are

$$Me_3S^+ > Me_2SCl^+ > MeSCl_2^+$$

The derivatives of tetravalent sulfur, R_2SCl_2 and $RSCl_3$, are considerably less stable than R_2SeCl_2 and R_2TeCl_2 and are comparable to the relative stabilities of sulfur, selenium, and tellurium tetrachlorides. The ions $MeSCl_2^+$, Me_2SCl^+, and Me_2SeCl^+ could be stabilized as tetrachloroborates, but the ion Me_2TeCl^+ could not be stabilized analogously, suggesting that Me_2TeCl_2 may react with boron trichloride to form a non-ionized adduct $Me_2Cl_2Te.BCl_3$ containing a Te—B bond.

Experimental

The apparatus and techniques have been described previously (15). Volatile reactants were distilled into the conductivity cell from a calibrated volume at a known pressure and temperature; by the use of liquid nitrogen, quantitative transfer was possible. Measured volumes of liquids were obtained using a syringe and solids were weighed directly into the cell. The products were very hydrolytically sensitive and were therefore handled in a dry box. Chloride was analyzed gravimetrically and boron acidimetrically as the mannitol–borate complex. Infrared spectra were recorded on a Perkin–Elmer 457 spectrophotometer.

All the reagents were available commercially, unless their preparation is described.

The conductivities of the materials studied are shown in Table I.

Reactions with Chlorine (and Boron Trichloride)

Dimethyl and diethyl sulfide solutions were both separately titrated against chlorine, the titration showing a break when the mole ratio of R_2S:Cl_2 was 1.0:1.0, see Fig. 1. No stable products were isolated at room temperature, both products decomposing with partial chlorination of the alkyl groups. Titration of a solution of a mixture of 1 mole of dimethyl or diethyl sulfide and 1 mole of chlorine against boron trichloride showed end points when the mole ratios R_2SCl_2:BCl_3 were 1.0:1.05 (Me_2SCl_2) and 1.0:1.10 (Et_2SCl_2), see Fig. 1. The high conductivity at the end points in all these titrations indicates the formation of the ions R_2SCl^+ in solution.

White solids dimethylchlorosulfonium tetrachloroborate, m.p. 172–173° and diethylchlorosulfonium tetrachloroborate, m.p. 35–36° were isolated.

TABLE I

Specific and molar conductances of compounds in liquid hydrogen chloride at −95°

Compound	Concentration (mole/l)	Specific conductance ($\mu\Omega^{-1}$ cm^{-1})	Molar conductance (Ω^{-1} cm^2 mole^{-1})
Me_2S	0.29	3 165	10.8
Et_2S	0.39	6 430	16.6
$(C_6F_5)_2S$	Saturated	7.8	—
EtSH	0.34	68.0	0.200
Me_2S_2	0.40	168	0.415
Et_2S_2	0.42	285	—
MeSCl	0.43	3 778	8.80
EtSCl	0.59	7 010	11.9
$MeSCl_3$	0.46	4 780	10.5
$EtSCl_3$	0.40	4 360	10.9
Me_2SCl_2	0.29	6 180	21.1
Et_2SCl_2	0.42	12 800	30.8
Me_3SI	0.39	10 500	27.3
S_2Cl_2	Saturated	0.33	—
SCl_2	0.40	1.44	0.004
SCl_4	Saturated	1.97	—
Me_2Se	0.34	5 490	16.0
Me_2SeCl_2	0.34	30.7	0.090
Ph_2SeCl_2	0.26	1 500	5.71
$SeCl_4$	Saturated	1.30	—
Se_2Cl_2	Saturated	1.83	—
$SeOCl_2$	Saturated	0.75	—
Me_2Te	0.32	3 123	9.64
Me_2TeCl_2	Saturated	20.7	—
$TeCl_4$	Saturated	0.22	—
$TeCl_2$	Saturated	0.86	—

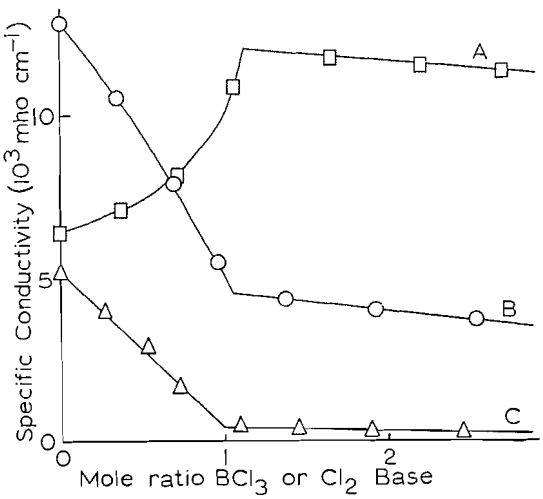

FIG. 1. Conductimetric titrations in liquid hydrogen chloride. A, 0.39 *M* Et_2S and Cl_2; B, 0.42 *M* Et_2SCl_2 and BCl_3; C, 0.34 *M* Et_2S and BCl_3.

Can. J. Chem. Downloaded from www.nrcresearchpress.com by 210.87.254.6 on 09/05/12
For personal use only.

Anal. Calcd. for $C_2H_6BCl_5S$: B, 4.32; Cl, 70.8. Found: B, 4.24: Cl, 70.3.

Anal. Calcd. for $C_4H_{10}BCl_5S$: B, 3.94; Cl, 64.6. Found: B, 3.92; Cl, 64.4.

The i.r. spectra of the products showed frequencies characteristic of the RS group, the BCl_4^- ion (16), and S—Cl frequencies at 521(m) cm^{-1} ($Me_2SCl.BCl_4$) and at 536(m) and 516(m) cm^{-1} ($Et_2SCl.BCl_4$).

A solution of methanesulfenyl chloride was oxidized with chlorine to methyl sulfur trichloride; on treatment with boron trichloride, methyldichlorosulfonium tetrachloroborate was formed, which was isolated and characterized by its m.p. and i.r. spectrum.

The reactions of solutions of dimethyl disulfide and ethanethiol with chlorine gave ill-defined products both of which were shown by their i.r. spectra to contain C—Cl and S—Cl bonds. The reaction of 1 mole of dimethyl disulfide solution, after equilibration at −95° and treatment with 1 mole of chlorine and then 1 mole of boron trichloride yielded the same product as the reaction of MeSCl and BCl_3.

Sulfur dichloride was not oxidized in solution with chlorine to sulfur tetrachloride.

Dimethyl selenide formed a colorless solution; titration with chlorine caused precipitation and the end point was not sharp. Dimethyl selenium dichloride was isolated, m.p. 60–62° (lit. 61° (8)). A suspension of dimethyl selenium dichloride was prepared in situ and treated with boron trichloride, to form dimethylchloroselenonium tetrachloroborate, m.p. 81–82° (lit. 58° decomp. (8)).

Anal. Calcd. $C_2H_6BCl_5Se$: B, 3.64; Cl, 59.7. Found: B, 3.56; Cl, 59.6, 58.6.

The i.r. spectrum differs from that reported previously in that distinct tetrachloroborate ion peaks are found at 695, 671, and 663 cm^{-1} (10).

Dimethyl tellurium formed a colorless solution which when titrated with chlorine showed a break at a mole ratio 1.0:1.0 and the very low conductivity indicated the formation of a non-conducting species. White dimethyl tellurium dichloride, m.p. 94–95°, was isolated.

Anal. Calcd. for $C_2H_6Cl_2Te$: Cl, 30.9. Found: Cl, 31.0.

Reaction of a suspension of dimethyl tellurium dichloride, prepared in situ, with boron trichloride, gave an adduct $Me_2TeCl_2.BCl_3$ which decomposed on warming from −80° to room temperature with the quantitative evolution of boron trichloride, leaving solid dimethyl tellurium dichloride.

Reactions of Sulfur Compounds with Boron Trichloride

Methane- and ethane-sulfenyl chlorides, prepared in situ by allowing 1 mole of dialkyl disulfide and 1 mole of chlorine to equilibrate at −20° for ½ h (17), when titrated against boron trichloride, showed sharp breaks at mole ratio RSCl:BCl_3 of 2.3:1.0 (MeSCl) and 2.0:1.0 (EtSCl), see Fig. 2, indicating the formation of an ionic species $(RSCl)_2BCl_3$. A white solid $(MeSCl)_2BCl_3$, m.p. 159° decomp., and a yellow liquid $(EtSCl)_2BCl_3$ were isolated at room temperature.

Anal. Calcd. for $C_2H_6BCl_5S_2$: B, 3.84; Cl, 62.8. Found: B, 3.81; Cl, 62.5.

Anal. Calcd. for $C_4H_{10}BCl_5S_2$: B, 3.48; Cl, 57.1. Found: B, 3.49; Cl, 57.0.

Both products decomposed on standing. In the i.r. spectra RS peaks, B—Cl peaks at 682(s), 655(s) cm^{-1} ($(MeSCl)_2BCl_3$); 656(s), 688(s) cm^{-1} ($(EtSCl)_2BCl_3$); and

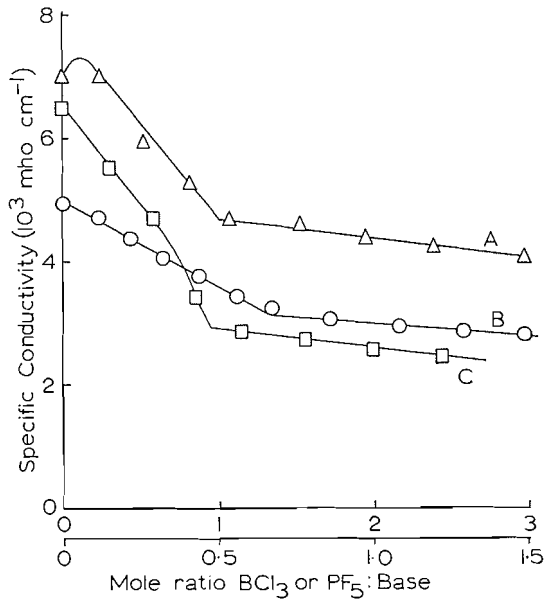

FIG. 2. Conductimetric titrations in liquid hydrogen chloride. A, 0.59 *M* EtSCl and BCl_3 (0–1.5 scale); B, 0.56 *M* MeSCl and PF_5 (0–3 scale); C, 0.51 *M* MeSCl and BCl_3 (0–1.5 scale).

S—Cl peaks at 494(m), 470(m), 460(m) cm^{-1} ($(MeSCl)_2$-BCl_3); and 509(m), 466(m), 452(sh) cm^{-1} ($(EtSCl)_2BCl_3$) were observed.

Methyl and ethyl sulfur trichlorides, prepared in situ from 1 mole of the dialkyl disulfide and 3 moles of chlorine at −20° (18), both reacted with boron trichloride to form the corresponding alkyldichlorosulfonium tetrachloroborate. White methyldichlorosulfonium tetrachloroborate, m.p. 155–156°, precipitated from solution.

Anal. Calcd. for CH_3BCl_6S: B, 3.99; Cl, 78.6. Found: B, 3.91; Cl, 79.6.

The conductiometric titration of ethyl sulfur trichloride against boron trichloride showed a break at mole ratio 1.0:1.0, $EtSCl_3$:BCl_3, see Fig. 3, indicating the formation of the ionic species $EtSCl_2^+BCl_4^-$ in solution, which was isolated as a white solid, m.p. 101–104°.

Anal. Calcd. for $C_2H_6BCl_6S$: B, 4.57; Cl, 69.6. Found: B, 4.17; Cl, 69.9.

The i.r. spectra showed peaks characteristic of the RS group, the BCl_4^- ion (10), and S—Cl frequencies at 522(m) and 496(m) cm^{-1} ($MeSCl_2^+$) and 541(m) and 508(m) cm^{-1} ($EtSCl_2^+$).

Solutions of dimethyl and diethyl disulfide reacted with boron trichloride to form the boron trichloride adducts; no sharp break was observed in the conductiometric titration, both products being colorless liquids which fumed readily in moist air. The diethyl disulfide boron trichloride adduct was also formed by mixing diethyl disulfide with an excess of boron trichloride in a sealed tube, which was opened after standing for 4 days at room temperature. From the amount of boron trichloride recovered it was deduced that an adduct of composition $Et_2S_2.BCl_3$ had been formed, but the colorless fuming

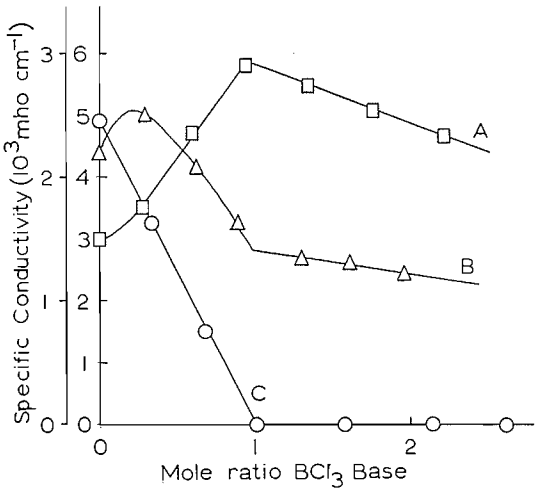

FIG. 3. Conductimetric titrations in liquid hydrogen chloride. A, 0.26 *M* Ph_2SeCl_2 and BCl_3 (0–3 scale); B, 0.40 *M* $EtSCl_3$ and BCl_3 (0–6 scale); C, 0.34 *M* Me_2Se and BCl_3 (0–6 scale).

liquid readily decomposed in a glove box to a brown liquid, and could not be analyzed satisfactorily.

Anal. Calcd. for $C_2H_6BCl_3S_2$: B, 5.11; Cl, 50.3. Found: B, 5.26; Cl, 50.6.

The i.r. spectra showed peaks characteristic of the RS group B—Cl frequencies at 760(vs), 751(vs), 691(m), and 584(s) cm^{-1} ($Me_2S_2.BCl_3$); 759(vs), 750(vs), 696(m), and 582(s) cm^{-1} ($Et_2S_2.BCl_3$); and B—S peaks at 960(m) cm^{-1} ($Me_2S_2.BCl_3$); 1054(m) cm^{-1} ($Et_2S_2.BCl_3$).

Titration of diethyl sulfide solution against boron trichloride showed a sharp break at mole ratio 1.0:1.0 (Et_2S:BCl_3), see Fig. 1, the low conductivity at the end point indicating the formation of the undissociated adduct in solution. Colorless liquid diethyl sulfide – boron trichloride adduct was isolated.

Anal. Calcd. for $C_2H_{10}BCl_3S$: B, 5.55; Cl, 51.7. Found: B, 5.29; Cl, 51.2.

The i.r. spectrum showed peaks characteristic of the EtS group, B—Cl peaks at 743(vs) and 616(s) cm^{-1}, and a possible B—S frequency at 1054(m) cm^{-1}.

Trimethylsulfonium iodide formed a highly conducting solution; titration with boron trichloride showed an end point at mole ratio Me_3SI:BCl_3 of 1.0:1.2. A white solid, trimethylsulfonium tetrachloroborate, decomp. 300°, was isolated.

Anal. Calcd. for $C_3H_9BCl_4S$: B, 4.70; Cl, 61.7. Found: B, 4.60; Cl, 60.4.

This formula was confirmed by the i.r. spectrum which contained only Me_3S^+ ion and BCl_4^- ion frequencies (19, 10).

The compounds sulfur monochloride, sulfur dichloride, sulfur tetrachloride (prepared by allowing 1 mole of sulfur dichloride and 1 mole of chlorine to equilibrate at −60°), and bis(pentafluorophenyl)sulfide formed very poorly conducting solutions and did not react with boron trichloride.

Reactions of Selenium Compounds with Boron Trichloride

Dimethyl selenium solution showed a break at mole ratio 1.0:1.0, Me_2Se:BCl_3, when titrated against boron trichloride, see Fig. 3, the low conductivity at the equivalence point indicating the formation of the undissociated dimethyl selenium – boron trichloride adduct in solution, which was isolated as a white solid, 93–95° (lit. 101–102° (5)).

Anal. Calcd. for $C_2H_6BCl_3Se$: B, 4.78; Cl, 47.0. Found: B, 4.79; Cl, 47.4.

The i.r. spectrum agrees with that reported previously (5).

Diphenyl selenium dichloride when titrated against boron trichloride gave an equivalence point when the ratio Ph_2SeCl_2:BCl_3 was 1.0:1.0, see Fig. 3, the high conductivity indicating the formation of an ionic species, probably $Ph_2SeCl^+BCl_4^-$. After removal of the solvent, the white solid product decomposed on warming to room temperature.

Selenium monochloride and selenium tetrachloride both formed poorly conducting solutions which did not react with boron trichloride.

Reactions of Tellurium Compounds with Boron Trichloride

The reaction of boron trichloride with a solution of dimethyl tellurium produced a white precipitate. After removal of the solvent and pumping at −80° for 2 h, 0.98 mole of hydrogen chloride per mole of dimethyl tellurium was evolved and the white dimethyl tellurium boron trichloride adduct, m.p. 231–233°, remained.

Anal. Calcd. for $C_2H_6BCl_3Te$: B, 3.93; Cl, 38.7. Found: B, 3.81; Cl, 38.6.

The almost quantitative evolution of hydrogen chloride suggests that dimethyl telluronium tetrachloroborate, $Me_2TeH^+BCl_4^-$, had precipitated from solution and decomposed on warming to room temperature, forming the dimethyl tellurium boron trichloride adduct. The dimethyl tellurium boron trichloride adduct decomposed to a black material, probably tellurium, in a dry box within a day. The i.r. spectrum showed frequencies characteristic of the MeTe group and B—Cl frequencies at 750(sh), 712(vs), and 662(s) cm^{-1}.

Tellurium dichloride and tellurium tetrachloride were both sparingly soluble and did not react with boron trichloride.

Reactions with Phosphorus Pentafluoride

A solution of dimethylchlorosulfonium chloride reacted with phosphorus pentafluoride and white dimethylchlorosulfonium hexafluorophosphate, m.p. 182–184°, was isolated.

Anal. Calcd. for $C_2H_6ClF_6PS$: Cl, 14.6. Found: Cl, 14.6.

The i.r. spectrum is consistent with its structure as $Me_2SCl^+PF_6^-$, showing only peaks characteristic of the Me_2SCl^+ and PF_6^- ions (3).

Methanesulfenyl chloride solution was titrated against phosphorus pentafluoride, see Fig. 2; the equivalence point was found at mole ratio 1.3:1.0, PF_5:MeSCl, indicating that the reaction,

$$2\left[\begin{array}{c}\mathrm{MeSCl}\\ |\\ \mathrm{H}\end{array}\right]^+ HCl_2^- + 3PF_5 \rightarrow 2\left[\begin{array}{c}\mathrm{MeSCl}\\ |\\ \mathrm{H}\end{array}\right]^+ PF_6^- + PF_3Cl_2 + 2HCl$$

probably had occurred. White methylchlorosulfonium hexafluorophosphate, m.p. 132–133° decomp., was isolated.

Can. J. Chem. Downloaded from www.nrcresearchpress.com by 210.87.254.6 on 09/05/12
For personal use only.

Anal. Calcd. for CH_4ClF_6PS: Cl, 15.5. Found: Cl, 15.5.

In the i.r. spectrum PF_6^- ion peaks (3), MeS group peaks and possible S—Cl frequencies at 496(m) and 479(m) cm^{-1} were observed. The S—H frequency would be expected to be very weak and no peak can be assigned with certainty, although there may be one at 2270(vw) cm^{-1}.

An unstable white methyldichlorosulfonium hexafluorophosphate could be isolated from the reaction of a solution of methyl sulfur trichloride and phosphorus pentafluoride. The solid decomposed with loss of PF_5; its i.r. spectrum showed the presence of the ions $MeSCl_2^+$ and PF_6^- (3).

Potential Acids

Solutions were prepared of approximately 2 moles of Me_4NCl and 1 mole of $SeCl_4$, Me_2SeCl_2, Ph_2SeCl_2, $TeCl_4$, and Me_2TeCl_2. After removal of the solvent the increase in weight showed that Me_4NCl had formed Me_4NHCl_2 and not $(Me_4N)_2MCl_6$. The i.r. spectra of the products of the reactions with Me_2SeCl_2, Ph_2SeCl_2, and Me_2TeCl_2 showed the presence of the HCl_2^- ion (20). When 2 moles of Me_4NHCl_2 and 1 mole of $SeCl_4$ or $TeCl_4$ were ground up in Nujol, the i.r. peaks corresponding to the HCl_2^- ion had disappeared, indicating that in the grinding process the HCl_2^- ion had decomposed and the hexachloroselenate and hexachlorotellurate ions had probably been formed. The HCl_2^- ion would not be expected in the i.r. spectra of the Me_4NCl and $SeCl_4$ or $TeCl_4$ reaction products. It can be concluded that none of these chlorides exhibit acidic properties in liquid hydrogen chloride solution.

Reactions with Boron Trichloride without a Solvent

Sulfur monochloride, sulfur dichloride, sulfur tetrachloride, selenium monochloride, selenium tetrachloride, tellurium dichloride, and tellurium tetrachloride were each sealed in a tube under vacuum with an excess of boron trichloride and shaken at room temperature for a week. In all cases, except for sulfur tetrachloride, no reaction occurred and the reactants were recovered. A white solid formed in the sulfur tetrachloride reaction, but after removal of the excess boron trichloride at $-60°$, it started to decompose at about $-20°$ and decomposed too rapidly at room temperature to be analyzed.

Acknowledgment

The National Research Council of Canada is thanked for generous financial assistance.

1. M. E. Peach and T. C. Waddington. J. Chem. Soc. 1238 (1961).
2. M. E. Peach and T. C. Waddington. J. Chem. Soc. 2680 (1962).
3. M. E. Peach and T. C. Waddington. J. Chem. Soc. 799 (1963).
4. J. A. Salthouse and T. C. Waddington. J. Chem. Soc. A, 1188 (1966).
5. M. F. Lappert. J. Chem. Soc. 2784 (1953).
6. G. K. Helmkamp and D. C. Owsley. Quart. Rep. Sulfur Chem. **2**, 303 (1967).
7. E. A. Robinson and S. A. A. Zaidi. Can. J. Chem. **46**, 3927 (1968).
8. K. J. Wynne and J. W. George. J. Am. Chem. Soc. **87**, 4750 (1965).
9. G. M. Phillips, J. S. Hunter, and L. E. Sutton. J. Chem. Soc. 145 (1945).
10. H. Nöth and G. Mikulaschek. Chem. Ber. **97**, 709 (1964).
11. I. R. Beattie and H. Chudzynska. J. Chem. Soc. A, 984 (1967).
12. N. N. Greenwood and B. P. Straugham. J. Chem. Soc. A, 962 (1966).
13. E. A. Robinson and J. A. Ciruna. Can. J. Chem. **46**, 3197 (1968).
14. D. R. Martin. J. Phys. Chem. **51**, 1400 (1947).
15. T. C. Waddington and F. Klanberg. J. Chem. Soc. 2329 (1960).
16. T. C. Waddington and F. Klanberg. J. Chem. Soc. 2339 (1960).
17. H. Brintzinger, K. Pfannstiel, H. Koddenbusch, and K. E. Klug. Chem. Ber. **83**, 87 (1950).
18. K. R. Brower and I. B. Douglass. J. Am. Chem. Soc. **73**, 5787 (1951).
19. J. A. Creighton, J. H. S. Green, D. J. Harrison, and S. M. Walker. Spectrochim. Acta, **23A**, 2973 (1967).
20. T. C. Waddington. J. Chem. Soc. 1708 (1958).
21. Z. Iqbal and T. C. Waddington. J. Chem. Soc. A, 2958 (1968).

Can. J. Chem. Downloaded from www.nrcresearchpress.com by 210.87.254.6 on 09/05/12
For personal use only.

Can. J. Chem. Downloaded from www.nrcresearchpress.com by 210.87.254.5 on 09/05/12
For personal use only.

Complexes of Co(II), Ni(II), and Zn(II) with pyrazolone ligands[1]

R. A. BAILEY
Department of Chemistry, Rensselaer Polytechnic Institute, Troy, New York 12181

AND

T. R. PETERSON
Imperial Color and Chemical Department, Hercules Incorporated, Glens Falls, New York 12801

Received November 12, 1968

Complexes of Co(II), Ni(II), and Zn(II) with 4-aminoantipyrine and 4-dimethylaminoantipyrine have been prepared and characterized. These contain chloride, bromide, thiocyanate, nitrate, and perchlorate anions. Magnetic, conductivity, and electronic spectral data show that all of the Ni(II) and Co(II) complexes have high spin configurations and octahedral geometries, with coordinated halide, thiocyanate, and probably nitrate anions in the respective examples. Infrared analysis indicates that all of the complexes containing Cl^-, NCS^-, and NO_3^- anions involve chelated 4-aminoantipyrine, whereas the bromide complexes are only bonded to the organic ligands through nitrogen.

Canadian Journal of Chemistry, 47, 1681 (1969)

Introduction

Complexes of 1-phenyl-2,3-dimethyl-5-pyrazolone (antipyrine) shown below and its 4-amino and 4-dimethylamino derivatives have been of considerable interest.

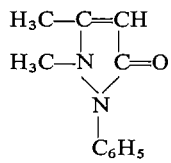

Antipyrine is expected to be unidentate, bonding through oxygen (other behavior, such as use of the ring nitrogens, is conceivable but unlikely). A large number of compounds of this ligand have been shown to be unidentate and oxygen coordinated from infrared (i.r.) spectral studies (1–5); a variety of coordination geometries are encountered.

A number of 4-aminoantipyrine and 4-dimethylaminoantipyrine compounds with Mn(II), Co(II), Ni(II), Cu(II), Zn(II), and Cd(II) ions were prepared but not characterized structurally by Souchay (6). Three modes of coordination must be considered for these; unidentate behavior with bonding through either the oxygen or the amino nitrogen, or chelation utilizing both these atoms. Infrared studies by Zaitsev *et al.* (7) on compounds of the type M(4-dimethylaminoantipyrine)$_2$(NCS)$_2$, (M = Zn(II), Co(II), and others) indicated chelation. This was confirmed by Dick *et al.* (8) who also showed that the thiocyanate groups in the above compounds were coordinated rather than free as supposed by Zaitsev *et al.* (7). Guru and Rao (9, 10), considering only the carbonyl region of the i.r. spectra, postulated that in Zn(4-aminoantipyrine)$_4$(ClO_4)$_2$ and in Zn(4-aminoantipyrine)$_2X_2$ (X = Cl^-, Br^-, I^-, NCS^-, NO_3^-), tetrahedral geometries are present with unidentate oxygen-bonded organic ligands. None of these i.r. interpretations is particularly convincing, as rigorous assignments of bands in the organic ligands have not been made. Knowledge of the coordination geometry is generally very uncertain.

In this report we have examined the structures of a variety of compounds containing 4-aminoantipyrine and 4-dimethylaminoantipyrine ligands with Co(II) and Ni(II), and have reconsidered some of the conclusions regarding the Zn(II) compounds.

Experimental Section

Materials

$NiBr_2$ (anhydrous), $CoBr_2$ (anhydrous), 4-aminoantipyrine, and 4-dimethylaminoantipyrine were obtained from K and K Laboratories, Inc., and were used without further purification. All other chemicals used were of reagent grade quality.

Syntheses

The nickel and cobalt complexes were prepared using anhydrous ethanol as solvent, following essentially the same procedures reported by Souchay (6). The analytical results are given in Table I. Although the earlier report

[1]Based on part of a thesis submitted by T. R. Peterson to the Graduate School of Rensselaer Polytechnic Institute in partial fulfillment of the requirements for the degree of Doctor of Philosophy, February, 1969.

TABLE I
Analytical results*

Compound†	Calculated					Found				
	C	H	N	S	Metal	C	H	N	S	Metal
$Ni(AM)_4Br_2$	51.23	5.08	16.29		5.69	51.08	5.18	16.48		5.71
$Ni(AM)_2(NCS)_2$	49.58	4.51	19.27	11.03	10.10	49.32	4.55	19.35	10.99	10.15
$Ni(DAM)_2(NCS)_2$	52.76	5.38	17.58	10.06	9.21	52.75	5.40	17.62	9.91	9.15
$Ni(DAM)_2(NO_3)_2(H_2O)_2$	45.83	5.62	16.45		8.62	45.77	5.56	16.41		8.69
$Co(AM)_4Br_2$	51.22	5.08	16.29		5.71	51.20	5.02	16.42		5.87
$Co(AM)_2(NCS)_2$	49.56	4.51	19.27	11.03	10.13	49.51	4.49	19.31	11.05	10.25
$Co(DAM)_2(NCS)_2$	52.74	5.37	17.57	10.06	9.24	52.75	5.31	17.65	9.95	9.20
$Co(DAM)_2(NO_3)_2(H_2O)_2$	45.82	5.62	16.44		8.65	45.59	5.52	16.24		8.50
$Zn(AM)_2(NCS)_2$	49.02	4.46			11.12	49.01	4.46			11.10
$Zn(AM)_2Cl_2$	(Cl, 13.1)		15.50		12.04	(Cl, 13.25)		15.15		12.08
$Zn(AM)_4(ClO_4)_2$	(ClO_4^-, 18.50)		15.60		6.07	(ClO_4^-, 18.25)		15.31		6.05

*Results expressed as %.
†AM = 4-aminoantipyrine; DAM = 4-dimethylaminoantipyrine.

(6) cited the preparation of anhydrous Co(4-dimethylaminoantipyrine)$_2(NO_3)_2$ and Ni(4-dimethylaminoantipyrine)$_2(NO_3)_2$, we were only successful in obtaining the corresponding dihydrate compounds. The zinc compounds were prepared by the method of Guru and Rao (9, 10).

Spectroscopic Measurements

Solid state electronic spectra were obtained by the reflectance technique from finely ground samples, using $MgCO_3$ as standard in a Beckman DU spectrophotometer. Infrared spectra in the region 4000–300 cm^{-1} were obtained by the KBr pellet technique using a Perkin–Elmer Model 621 spectrophotometer.

Magnetic Measurements

Magnetic data were obtained at room temperature by the Gouy technique using $Hg[Co(NCS)_4]$ as calibrant, and results were corrected for diamagnetism and temperature independent paramagnetism in the usual manner (11). The diamagnetism of the organic ligands was determined experimentally and found to be close to the values obtained using Pascal's constants (11). Measurements at a number of field strengths (4–10 000 G) all gave essentially identical results.

Conductivity Measurements

Conductivities were measured in ethanol using an Industrial Instruments Model RC-16 conductivity bridge and a cell having a cell constant of 0.1 cm^{-1}. Allowance was made for the conductivity of the solvent in the calculations.

Analytical Procedures

Analyses for C, H, and N were performed by Schwarzkopf Microanalytical Laboratory, Woodside, New York. Nickel, cobalt, and zinc were determined by EDTA titration (12). Sulfur was determined as $BaSO_4$ using Eschkas mixture to effect decomposition, nitrogen by the Kjeldahl technique, chloride by $AgNO_3$ titration, and perchlorate as the tetraphenylarsonium salt.

Results and Discussion

Conductivity Studies

The equivalent conductances, Λ, of some of the Ni(II) and Co(II) complexes in ethanol are shown in Fig. 1. The values obtained at a concentration of 10^{-3} *N* of ca. 25–40 cm^2 equivalents^{-1} Ω^{-1} are in all cases lower than the value of ca. 55 cm^2 equivalents^{-1} Ω^{-1} found under similar condi-

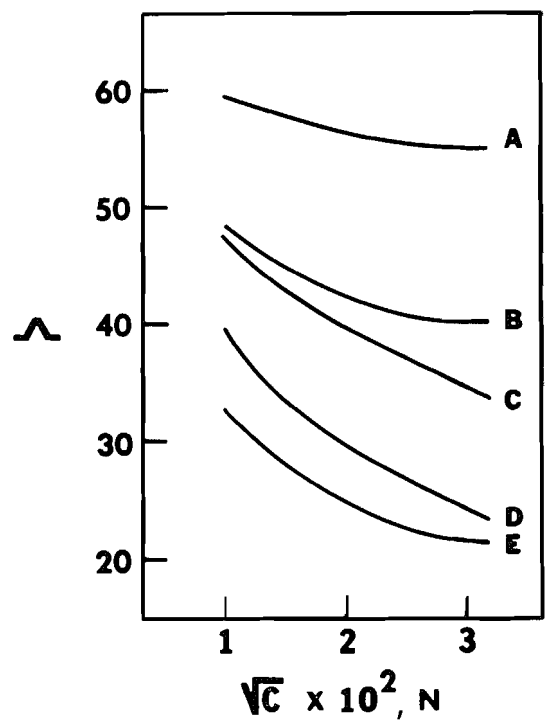

FIG. 1. Conductivity data in ethanol, 25 °C (Λ, equivalent conductivity, cm^2 equivalents^{-1} Ω^{-1}): A, tetraethylammonium bromide; B, Co(4-dimethylaminoantipyrine)$_2(NO_3)_2(H_2O)_2$; C, Co(4-aminoantipyrine)$_4Br_2$; D, Ni(4-aminoantipyrine)$_4Br_2$; E, Ni(4-dimethylaminoantipyrine)$_2(NO_3)_2(H_2O)_2$.

Can. J. Chem. Downloaded from www.nrcresearchpress.com by 210.87.254.5 on 09/05/12
For personal use only.

TABLE II
Magnetic data for Co(II) and Ni(II) pyrazolone complexes

Compound*	Diamagnetic correction $\times 10^6$ c.g.s.u.	χ_m† $\times 10^6$ c.g.s.u.	μ B.M.
$Ni(AM)_4Br_2$	−348	4 450	3.30
$Ni(AM)_2(NCS)_2$	−208	4 350	3.23
$Ni(DAM)_2(NCS)_2$	−230	3 940	3.06
$Ni(DAM)_2(NO_3)_2(H_2O)_2$	−233	3 890	3.05
$Co(AM)_4Br_2$	−348	9 600	4.88
$Co(AM)_2(NCS)_2$	−208	10 200	5.00
$Co(DAM)_2(NCS)_2$	−230	10 000	4.96
$Co(DAM)_2(NO_3)_2(H_2O)_2$	−233	9 950	4.95

*AM = 4-aminoantipyrine; DAM = 4-dimethylaminoantipyrine.
†Uncorrected molar susceptibility.

tions for tetraethylammonium bromide, a 1:1 electrolyte. The concentration dependence of Λ is typical of weak electrolytes. These results may be interpreted on the basis of partial dissociation of coordinated anions.

Magnetic Susceptibility Studies

The room temperature magnetic moments of all the paramagnetic complexes are given in Table II. The Ni(II) complexes exhibit moments of ca. 3.05–3.23 B.M., while the Co(II) compounds have moments of ca. 4.88–5.0 B.M. These are within the range normally found for both of these ions in octahedral fields (13), and may be compared to the room temperature values of 3.19 B.M. found previously for hexaantipyrine Ni(II) perchlorate and 4.99 B.M. for hexaantipyrine Co(II) perchlorate (4).

Electronic Spectral Studies

The solid state reflectance spectra of the Ni(II) and Co(II) compounds given in Table III and Figs. 2 and 3 are typical of these ions in O_h symmetry, confirming the magnetic susceptibility results. Assignments of the observed bands (Table III) were made on the basis of octahedral geometries using the energy level diagram of Liehr and Ballhausen (14) for the Ni(II) complexes and that of Tanabe and Sugano (15) for the Co(II) complexes. For the Ni(II) complexes the $^3A_{2g} \rightarrow {}^3T_{2g}(F)$ transition (Table III) gives the values of $10\,Dq_{oct}$ directly (15); these are observed to be on the order of ca. 8900–9500 cm^{-1}. The Racah parameter B for the Ni(II) complexes may be evaluated from the relation $B = (\nu_2 + \nu_3 - 3\nu_1)/15$, giving values for the Ni(II) complexes of ca. 875–975 cm^{-1}. These

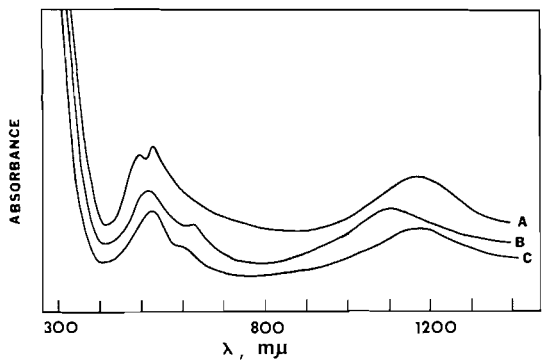

FIG. 2. Reflectance spectra of Co(II) pyrazolone complexes: A, $Co(4\text{-dimethylaminoantipyrine})_2(NO_3)_2(H_2O)_2$; B, $Co(4\text{-aminoantipyrine})_4Br_2$; C, $Co(4\text{-aminoantipyrine})_2(NCS)_2$.

represent reasonable reduction from the free ion value for Ni(II) of 1030 cm^{-1} (15). For the analogous Co(II) complexes, the best fit of the spectra with the energy level diagram could be obtained with values of $10Dq$ of ca. 8900–9400 cm^{-1} and with values of B of the order of 810 cm^{-1}, which may be compared to the free ion value of 971 cm^{-1} (15). As seen in Table III, and Fig. 2, the weak ν_2 band in the Co(II) complexes has been assigned to the spin-allowed transition, $^4T_{1g} \rightarrow {}^4A_{2g}(F)$. This transition, which involves two electrons, would be expected to be of very low intensity (16). It is not observed in Co(4-dimethylaminopyrine)$_2$(NO$_3$)$_2$(H$_2$O)$_2$ here, and is frequently missing in Co(II) spectra. It is to be noted, however, that the spin-forbidden transitions, $^4T_{1g}(F) \rightarrow {}^2T_{2g}(G)$ and $^4T_{1g}(F) \rightarrow {}^2T_{1g}(G)$, are in this region also. In some cases, splitting of the $^4T_{1g} \rightarrow {}^4T_{1g}(P)$ band (ν_3) is seen. This has

Can. J. Chem. Downloaded from www.nrcresearchpress.com by 210.87.254.5 on 09/05/12
For personal use only.

Can. J. Chem. Downloaded from www.nrcresearchpress.com by 210.87.254.5 on 09/05/12
For personal use only.

TABLE III

Electronic spectra of Ni(II) and Co(II) pyrazolone compounds

Compound*	Band position (cm^{-1})						Dq cm^{-1}	B cm^{-1}	β
	ν_1	Assignment	ν_2	Assignment	ν_3	Assignment			
$Ni(AM)_4Br_2$	9500	$^3A_{2g} \rightarrow {}^3T_{2g}(F)$	16 400	$^3A_{2g} \rightarrow {}^3T_{1g}(P)$	26 700	$^3A_{2g} \rightarrow {}^3T_{1g}(F)$	950	975	0.95
$Ni(AM)_2(NCS)_2$	9100	"	15 400	"	25 000	"	910	875	0.85
$Ni(DAM)_2(NCS)_2$	8900	"	15 200	"	25 000	"	890	900	0.87
$Ni(DAM)_2(NO_3)_2(H_2O)_2$	8900	"	15 400	"	25 650	"	890	955	0.93
$Co(AM)_4Br_2$	9000	$^4T_{1g} \rightarrow {}^4T_{2g}(F)$	16 000	$^4T_{1g} \rightarrow {}^4A_{2g}(F)$	19 400	$^4T_{1g} \rightarrow {}^4T_{1g}(F)$	940	780	0.81
$Co(AM)_2(NCS)_2$	8500	"	16 700	"	19 050	"	890	810	0.84
$Co(DAM)_2(NCS)_2$	8500	"	16 700	"	18 200 19 600	"	890	810	0.84
$Co(DAM)_2(NO_3)_2(H_2O)_2$	8500	"	—	"	18 900 20 000	"	890	816	0.84

*AM = 4-aminoantipyrine; DAM = 4-dimethylaminoantipyrine.

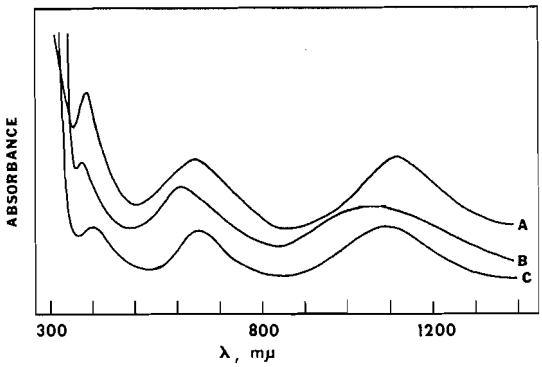

FIG. 3. Reflectance spectra of Ni(II) pyrazolone complexes: A, Ni(4-dimethylaminoantipyrine)$_2$(NO$_3$)$_2$(H$_2$O)$_2$; B, Ni(4-aminoantipyrine)$_2$Br$_2$; C, Ni(4-aminoantipyrine)$_2$(NCS)$_2$.

been explained as spin–orbit splitting of the $^4T_{1g}$(P) state (16).

For the case of Ni(4-aminoantipyrine)$_4$Br$_2$, with the reasonable assumption of unidentate organic ligands and coordinated bromide ions as indicated from the conductance data, application of the rule of average environments using the known value of 10 Dq_{oct} for Br^- (7600 cm^{-1}) (17) yields a value of 10 Dq_{oct} for unidentate 4-aminoantipyrine of 10 450 cm^{-1}. This value is clearly much higher than that observed for Ni–O$_6$ chromophores such as Ni(H$_2$O)$_6^{2+}$ (8900 cm^{-1}) (18), Ni(substituted urea)$_6^{2+}$ (8000–8500 cm^{-1}) (19), and hexaantipyrine Ni(II) perchlorate (7630 cm^{-1}) (4). The observed value is more nearly in the range observed for Ni–N$_6$ chromophores such as in Ni(NH$_3$)$_6^{2+}$ (10 800 cm^{-1}) (18), Ni(pyridine)$_6^{2+}$ (10 100 cm^{-1}) (20), and Ni(methylamine)$_6^{2+}$ (9930 cm^{-1}) (21). It appears that in Ni(4-aminoantipyrine)$_4$Br$_2$, the Ni(II) ion is bonded to the nitrogen atom of the organic ligand.

For Ni(L)$_2$(NCS)$_2$, where L = 4-aminoantipyrine or 4-dimethylaminoantipyrine, similar calculations using the average environment rule in conjunction with the known value of 10 Dq_{oct} for N-bonded thiocyanate groups of 9600 cm^{-1} (22), yield values of 10 Dq_{oct} for the organic ligands of ca. 8550–8850 cm^{-1}. These values are clearly too low for unidentate N-bonded groups as found for dibromotetrakis(4-aminoantipyrine)Ni(II), (10 450 cm^{-1}) and too high for unidentate O-bonded groups as are found in hexaantipyrine Ni(II) perchlorate, (7630 cm^{-1}) previously reported (4), but do agree with the value of ca. 9000 cm^{-1} calculated for this ligand as a chelate assuming the average of 10 Dq values from N- and O-bonded cases. Since the i.r. data (see below) show the thiocyanate ions to be coordinated and terminally bonded to the metal ion and the geometry has been established to be octahedral, bidentate behavior of this organic ligand is expected.

It is not possible to draw conclusions about the structures of either Ni(4-dimethylaminoantipyrine)$_2$(NO$_3$)$_2$(H$_2$O)$_2$ or Co(4-dimethylaminoantipyrine)$_2$(NO$_3$)$_2$(H$_2$O)$_2$ from similar arguments since the various possibilities give similar values of 10 Dq.

The results obtained from the spectra of Co(4-aminoantipyrine)$_4$Br$_2$, Co(4-aminoantipyrine)$_2$(NCS)$_2$, and Co(4-dimethylaminoantipyrine)$_2$(NCS)$_2$, see Table III and Fig. 2, are also straightforward, yielding values of 10 Dq_{oct} for unidentate N-bonded 4-aminoantipyrine in the bromo compound of ca. 10 800 cm^{-1}. This value is in line with 10 Dq_{oct} values found in N-bonded Co(II) complexes such as Co(NH$_3$)$_6^{2+}$ (10 100 cm^{-1}) (18). The 10 Dq value for oxygen bonded antipyrine is much lower, < 7000 cm^{-1} (23). For the thiocyanate complexes the observed value of 10 Dq_{oct} for the organic ligands of ca. 8300 cm^{-1} also indicates that chelation is present as in the corresponding Ni(II) complexes. For these calculations it was assumed that 10 Dq_{oct} was 9/4 the value of 10 Dq_{tet} (1, 23).

Infrared Spectra

The i.r. spectra of all the thiocyanate complexes prepared in this study are in excellent agreement with the earlier report of Dick *et al.* (8). The positions of the ν_{CN} frequency at ca. 2085–2104 cm^{-1}, ν_{CS} at ca. 792–786 cm^{-1}, and δ_{NCS} at ca. 462–480 cm^{-1} in these complexes clearly indicate the presence of only terminal N-bonded thiocyanate groups (24).

The i.r. spectra of the organic ligands are quite complex. In antipyrine and its 4-amino-derivatives, a strong band in the 1650 cm^{-1} region has been attributed to the C=O stretching frequency. This decreases on coordination in antipyrine, and its similar decrease in the amino compounds has been used as evidence for oxygen coordination. In 4-aminoantipyrine, evidence for coordination through nitrogen can be obtained from the N—H stretching frequencies, which should decrease. Chelation should lead to a decrease in both the

Can. J. Chem. Downloaded from www.nrcresearchpress.com by 210.87.254.5 on 09/05/12
For personal use only.

Can. J. Chem. Downloaded from www.nrcresearchpress.com by 210.87.254.5 on 09/05/12
For personal use only.

C=O stretching frequency and N—H stretching frequencies. As is illustrated in Fig. 4, the bands in the N—H stretching region decrease in all compounds (the $M(L)_2(NO_3)_2(H_2O)_2$ species show O—H bands in this region, so that the N—H bands are rather obscured). Interpretation of the behavior of bands in the 1600 cm^{-1} region is not straightforward, since besides the C=O stretching frequency, the C=C stretching and the H—N—H bending modes occur here. The first of these is usually below the C=O frequency while the second may be expected below 1600 cm^{-1}. Dick *et al.* (8) have suggested that on chelation the C=O band (assigned at 1645–1665 cm^{-1}) disappears and a new band appears at 1610–1635 cm^{-1} which is caused by the stretching mode of the C=N bond which can be written for one of the resonance structures. Assignment of this band to a shifted C=O frequency is probably more reasonable. Sauro and Moeller (25) have shown that this band shifts to about 1600 cm^{-1} in some chelated rare earth pyrazalone complexes.

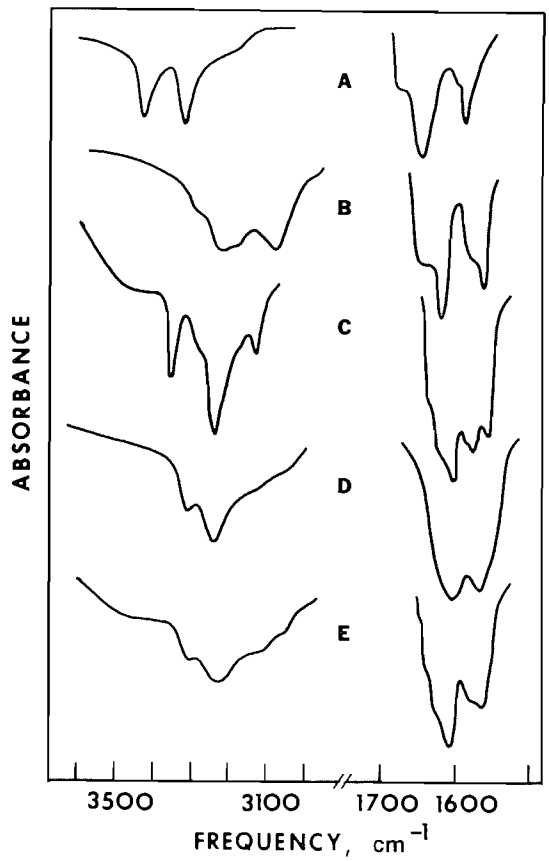

FIG. 4. Infrared spectra of metal 4-aminoantipyrine complexes in the N—H stretching and C=O stretching regions: A, 4-aminoantipyrine; B, Ni(4-aminoantipyrine)$_4Br_2$; C, Zn(4-aminoantipyrine)$_4(ClO_4)_2$; D, Ni(4-aminoantipyrine)$_2(NCS)_2$; E, Zn(4-aminoantipyrine)$_2$-$(NCS)_2$.

The spectra shown for the corresponding nickel and cobalt compounds (Fig. 4) are almost identical and fall into two types; those for the $M(L)_4Br_2$ compounds, which we have considered to be nitrogen bonded on the basis of ligand field data, and those for the nitrates and thiocyanates, where the latter was considered chelated on the above evidence. The bromide spectra show considerable decrease in the positions of the N—H stretching bands, but the bands in the carbonyl region, although somewhat shifted (to about 1620 cm^{-1}), have the same general character as in the free ligand. While the decreases in the 1600 cm^{-1} region are unexplained, they may arise from the fact that these bands are composites of several modes. The chelated thiocyanate spectra, on the other hand, show much more extensive shifts here, as would be expected for coordination through the carbonyl oxygen (to near 1600 cm^{-1}), as well as decreases in the N—H region. The 1600 cm^{-1} region profile is now greatly changed.

The spectrum of Zn(4-aminoantipyrine)$_2$-$(NCS)_2$ and Zn(4-aminoantipyrine)$_2Cl_2$ described by Guru and Rao (9, 10) are nearly identical in the N—H and C=O regions (Fig. 4) and are quite similar to the nickel and cobalt thiocyanate compounds in these ranges. From these data, it appears that the organic ligands are chelated rather than unidentate, and that the compounds are octahedral rather than tetrahedral as the anions are coordinated.

Zn(4-aminoantipyrine)$_4(ClO_4)_2$ is quite different, with a spectrum which is more similar to that of the cobalt and nickel bromides. The N—H stretching frequencies are decreased less, and the 1600 cm^{-1} bands more, than in the former compounds. We hesitate to draw any conclusions as to the mode of bonding in this compound from the i.r. spectrum. Certainly the previous suggestion of unidentate oxygen coordination is questionable, and it is apparent that great care must be taken in interpreting shifts in the spectrum of this ligand, particularly in the 1600 cm^{-1} region.

The i.r. spectra of Co(4-dimethylaminoantipyrine)$_2(NO_3)_2(H_2O)_2$ and Ni(4-dimethylaminoantipyrine)$_2(NO_3)_2(H_2O)_2$ are essentially the

same in the carbonyl stretching region as those of the Ni(II) and Co(II) thiocyanate complexes which appear to be chelated. The presence of either coordinated water or nitrate groups could not be established from their i.r. spectra due to interference from organic ligand bands, but conductance data on both these compounds in ethanol clearly suggest the presence of coordinated nitrate groups. A chelated octahedral structure with non-coordinated water molecules but coordinated anions appears most reasonable.

It is interesting that 4-aminoantipyrine may be either bidentate, or unidentate with bonding through the nitrogen. In the compounds studied here, the latter behavior is found only when Br^- is also coordinated to the metal. Chelation would appear to be expected on entropy grounds. While there is hardly sufficient data on which to draw conclusions, one may speculate that the major difference of Br^- is its greater ability to accept electrons from the metal (via back π-bonding, say), thereby reducing the electron density on the latter. This effect could better be counteracted by donation from nitrogen than from oxygen.

1. J. GOPALAKRISHNAN and C. C. PATEL. Indian J. Chem. **5**, 364 (1967).
2. J. GOPALAKRISHNAN, A. RAVI, and C. C. PATEL. Bull. Chem. Soc. Japan, **40**, 791 (1967).
3. V. N. KRISHNAMURTHY and S. SOUNDARARAJAN. Proc. Indian Acad. Sci. Sect. A, **65**, 148 (1967).
4. A. RAVI, J. GOPALAKRISHNAN, and C. C. PATEL. Indian J. Chem. **5**, 356 (1967).
5. D. N. SATHYANARAYANA and C. C. PATEL. Indian J. Chem. **5**, 360 (1967).
6. P. SOUCHAY. Bull. Soc. Chim. France, **7**, 797 (1940).
7. B. E. ZAITSEV, V. K. AKIMOV, A. I. BUSEV, and S. I. GUSEV. Zh. Obshch. Khim. **35**, 2119 (1965).
8. I. DICK, R. BACALOGLU, and A. MAURER. Rev. Roumaine Chimie, **12**, 607 (1967); **12**, 617 (1967).
9. S. GURU and D. V. RAO. Current Sci. India, **36**, 317 (1967).
10. S. GURU and D. V. RAO. J. Indian Chem. Soc. **45**, 160 (1968).
11. B. N. FIGGIS and J. LEWIS. *In* Modern coordination chemistry. *Edited by* J. Lewis and R. G. Wilkins. Interscience Publishers, Inc., New York. 1960. p. 415.
12. G. SCHWARZENBACH. Complexometric titrations. *Translated by* H. Irving. Interscience Publishers, Inc., New York. 1957, and references therein.
13. B. N. FIGGIS and J. LEWIS. *In* Progress in inorganic chemistry. Vol. 6. *Edited by* F. A. Cotton. Interscience Publishers, Inc., New York. 1964. Chap. 2.
14. A. D. LIEHR and C. J. BALLHAUSEN. Ann. Phys. N.Y., **6**, 134 (1959).
15. Y. TANABE and S. SUGANO. J. Phys. Soc. Japan, **9**, 753 (1954).
16. C. J. BALLHAUSEN. Introduction to ligand field theory. McGraw-Hill Book Co., Inc., New York. 1962. pp. 256–257.
17. S. L. HOLT and R. L. CARLIN. J. Am. Chem. Soc. **86**, 3017 (1964).
18. C. K. JORGENSEN. Absorption spectra and chemical bonding in complexes. The Pergamon Press, Ltd., Oxford. 1962. Chap. 7.
19. R. A. BAILEY, I. R. FEINS, and T. R. PETERSON. Can. J. Chem. **47**, 171 (1969).
20. W. E. BULL and L. E. MOORE. J. Inorg. Nucl. Chem. **27**, 1341 (1965).
21. R. S. DRAGO, D. W. MEEK, R. LONGHI, and M. D. JOESTEN. Inorg. Chem. **2**, 1056 (1963).
22. D. FORSTER and D. M. L. GOODGAME. Inorg. Chem. **4**, 823 (1965).
23. D. W. HERLOCKER and R. S. DRAGO. Inorg. Chem. **7**, 1479 (1968).
24. I. BERTINI and S. SABATINI. Inorg. Chem. **5**, 1025 (1966).
25. L. J. SAURO and T. MOELLER. J. Inorg. Nucl. Chem. **30**, 953 (1968).

Can. J. Chem. Downloaded from www.nrcresearchpress.com by 210.87.254.5 on 09/05/12
For personal use only.

Can. J. Chem. Downloaded from www.nrcresearchpress.com by 210.87.254.6 on 09/05/12
For personal use only.

Co(II) complexes with 2-pyrrolidinone

O. BOHUNOVSKY[1], S. C. JAIN, AND R. RIVEST
Department of Chemistry, University of Montreal, Montreal, Quebec

Received October 4, 1968

For the known complexes CoL_3X_2 (X = Cl, Br, and L = 2-pyrrolidinone) a more detailed infrared study was made. Together with the electronic spectra this study indicates dissociation of CoL_2X_3 into CoL_2X_2 + L in chloroform and acetone solution. The conductivity measurements and the molecular weight determinations also support dissociation. The probable structure in the solid state is $[CoL_3X]X$. The new 1:1 compound of 2-pyrrolidinone with boron trichloride was prepared to confirm the conclusions made from the infrared spectra of the cobalt complexes.

Les complexes connus CoL_3X_2 (X = Cl, Br, et L = 2-pyrrolidinone) ont été préparés. Une étude plus détaillée des spectres infrarouges et les données des spectres électroniques indiquent la dissociation en CoL_2X_2 + L en solution de chloroform et d'acétone. La structure en phase solide semble être $[CoL_3X]X$. La nouveau composé 1:1 de 2-pyrrolidinone avec le trichlorure de bore a été préparé pour vérifier les conclusions des spectres infrarouges des complexes de cobalt.

Canadian Journal of Chemistry, **47**, 1689 (1969)

Introduction

Madan and Sturr (1) recently reported complexes of Co(II) halides with 2-pyrrolidinone (**1**) (γ-butyrolactam) (L), CoL_3X_2 and concluded, that the structure is $[CoL_6][CoX_4]$ and that $[CoL_6]^{2+}$ and $[CoX_4]^{2-}$ are present in solution. Here we report the same complexes for X = Cl, Br, or I and a complex of the ligand with BCl_3. From the infrared (i.r.) and electronic spectra in chloroform solution and from the electronic spectral data reported by Madan we propose a different structure.

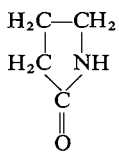

1

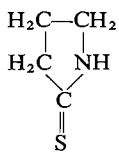

2

In an earlier article (2) the site of coordination of 2-thiazolidinethione (**2**) towards Co(II) was reported to be nitrogen. This conclusion was based besides other arguments, upon the shift of ν(N—H). On the other hand, 2-pyrrolidinone is coordinated through oxygen, but the ν(NH) is also shifted. This shift of ν(NH) in both cases is discussed.

[1]Present address: Research and Development Division, Sherritt Gordon Mines Limited, Fort Saskatchewan, Alberta.

Experimental

All manipulations were performed in a dry-box flushed with nitrogen. Cobalt halides were obtained from Alfa Inorganics and used without further purification; 2-pyrrolidinone was obtained from J. T. Baker Organic Chemicals and recrystallized twice from hexane. Analyses were carried out by Organic Microanalysis, Montreal.

$C_4H_7NO.BCl_3$

Into a solution of 2-pyrrolidinone in dry and alcohol-free chloroform, BCl_3 was bubbled at 0 °C, and a colorless precipitate was formed. To remove excess BCl_3, the mixture was boiled for a short period. The precipitate was then filtered off, washed with chloroform, and dried in vacuo. The compound so obtained was found to be insoluble in CH_2Cl_2 and CCl_4 but was soluble in acetone, m.p. 125°.

$[CoX_2(C_4H_7NO)_3]$

The dichloro- and dibromo-tris-(2-pyrrolidinone)cobalt(II)[2] were prepared by the method of Madan and Sturr (1). *Diido-tris-(2-pyrrolidinone)cobalt(II)* was prepared by refluxing 2.58 g CoI_2 and 2.37 g of 2-pyrrolidinone for 14 h in $CHCl_3$. A dark green solution formed, from which green prismatic crystals formed after a few days standing. These were filtered off and washed with ether. The analytical results are given in Table I.

Spectra

Vibration spectra were recorded on a Perkin-Elmer

[2]The preparation of a complex CoL_3Br_2 was already reported in a patent (3) in 1958. It was described as a red-violet compound with m.p. 125 °C. We observed that this red-violet compound contained more than three ligands per cobalt, but on continued washing with ether, the blue compound, described by Madan, was obtained.

TABLE I
Analytical results

Compound	Carbon (%)		Hydrogen (%)		Nitrogen (%)		Halogen (%)	
	Calcd.	Found	Calcd.	Found	Calcd.	Found	Calcd.	Found
$CoCl_2.3L$	37.45	37.30	5.51	5.54	10.90	10.91	18.44	18.71
$CoBr_2.3L$	30.39	29.55	4.47	4.59	8.86	8.65	33.66	32.68
$CoI_2.3L$	25.34	23.87	3.73	3.61	7.40	6.40	44.70	44.36
$BCl_3.L$	23.75	21.77	3.49	4.8*	6.91	6.18	52.58	51.9*

*The analysis of this very hygroscopic compound, for which the weighing was performed in the open air, differed remarkably from the theoretical value, especially for hydrogen and halogen. The halogen analysis was repeated with exclusion of humidity. This result is given here. Precaution was taken to prevent the loss of HCl during hydrolysis in water.

TABLE II
Comparison of the spectra of CoL_3X_2 in solutions with those of $[CoX_4]^{2-}$ in acetone solution

X	CoL_3X_2 in chloroform		CoL_3X_2 in acetone*				$[CoX_4]^{2-}$ in acetone†			
	ν_3 (cm^{-1})	ε_{max}	ν_3 (cm^{-1})	ε_{max}‡	ν_2 (cm^{-1})	ε_{max}	ν_3 (cm^{-1})	ε_{max}	ν_2 (cm^{-1})	ε_{max}
Cl	17 200	(330)	17 100	(502)	7 590	(83)	16 000	(353)	6 100	(57)
	16 100 (sh)	(420)			6 270	(101)	15 000	(557)	5 300	(59)
	15 400	(450)	15 200	(920)			14 400	(612)	4 800	(52)
Br	16 100 (sh)	(430)	14 900	(1 247)	6 610	(97)	15 600	(287)	5 400	(81)
	15 000	(490)					15 100	(630)	4 900	(83)
							14 400	(989)		
							13 800	(1 090)		
I	16 100	(490)	16 100	(625)	6 930	(111)	14 400	(522)	5 000	(154)
	15 200	(550)	16 600§	(900)	5 880	(133)	13 800	(710)		
	14 300	(530)	14 200	(875)			12 900	(1 120)		
			13 500	(280)						

*Results from ref. 1.
†Results from ref. 6.
‡ε_{max} values were calculated by Madan and Sturr (1) based on the assumption of $[CoL_6][CoX_4]$. Half of the values are applicable, if all the Co(II) is tetrahedrally coordinated.
§Because the bands are given in this order by Madan and Sturr (1), it might be that this was a typing mistake and should read 15 600 instead of 16 600.

621 spectrophotometer using cesium iodide optics. Sodium chloride cells were used for the region from 4000–600 cm^{-1} and polyethylene cells, for the region from 600–200 cm^{-1} for solutions. Electronic spectra were obtained on a Cary Model 14 spectrophotometer. Samples were in approximately 10^{-3} M solutions or in Nujol mulls and the technique described by Cotton *et al.* (4) was used.

Molecular Weight and Conductivity

The molecular weight determinations were carried out in nitrobenzene solution by a cryoscopic method. The conductivity was measured with a conductoscope type E 365B (Metrohm Ltd.) using EA 608 immersion cell with cell constant 0.84 cm^{-1}. Molecular weight and molar conductance results are reported in Table IV.

Results and Discussion

The i.r. spectra for CoL_3X_2 in chloroform solution indicate dissociation, showing bands for the uncoordinated as well as for the coordinated ligand (Table III). The visible spectra of these solutions are very similar to the spectra for $[CoX_2(DMA)_2]$ (DMA = N,N-dimethylacetamide) in N,N-dimethylacetamide solution (5). This indicates, that in solution, the species $[CoL_2X_2]$ and L are present, according to

[1] $CoL_3X_2(solid) \rightarrow CoL_2X_2 + L(solution)$

Madan and Sturr (1) concluded from the electronic spectra that the structure of the complexes is $[CoL_6][CoX_4]$. We obtained identical spectra in Nujol mulls and the spectra in chloroform solution were very similar to those obtained by Madan and Sturr in acetone solution with 100-fold excess of the ligand (Table II). Two facts, however, suggest that it is not correct to propose the structure $[CoL_6][CoX_4]$ for these complexes, from the data obtained in solution:

(*1*) The conductivity found by Madan and Sturr is too low to support complete ionization.

Can. J. Chem. Downloaded from www.nrcresearchpress.com by 210.87.254.6 on 09/05/12
For personal use only.

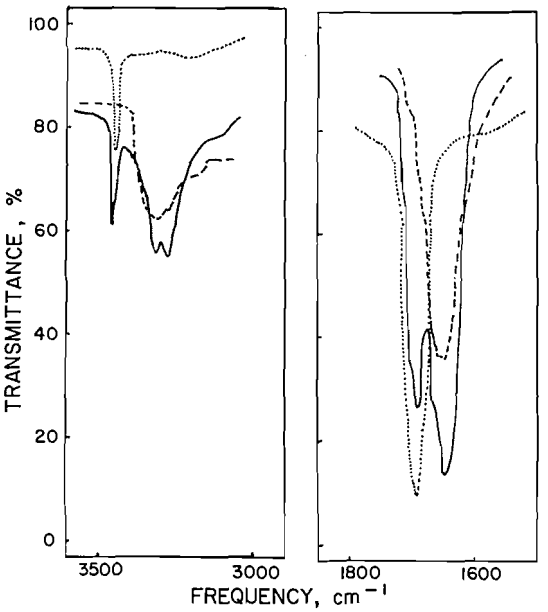

FIG. 1. Infrared spectra of $CoCl_2.3L$ compound in ν(N—H) and ν(C=O) regions; ---, in Nujol mull; ——, in $CHCl_3$ solution; ....., the ligand in $CHCl_3$ solution.

(*2*) Fine (6) reported the spectra of $[CoX_4]^{2-}$ in acetone solution. The spectra found by Madan and Sturr are different from these. The frequencies for the strongest bands for CoL_3X_2 are 800, 1100, and 3700 cm^{-1} higher than the strongest bands for $[CoCl_4]^{2-}$, $[CoBr_4]^{2-}$, and $[CoI_4]^{2-}$, respectively. The high excess of the ligand cannot be responsible for this shift, as Gutmann and Bohunovsky (5) found that spectra of $[CoX_4]^{2-}$ have a negligible variation in solvents of different donor strength. Furthermore, the extinction coefficient for the strongest band, found by Madan and Sturr for "$[CoL_6]$-$[CoX_4]$" is 50% higher than for $[CoCl_4]^{2-}$, which indicates that more than half of the Co(II) ions are tetrahedrally coordinated.

The arguments of Madan and Sturr seem to be valid only inasmuch as some sort of tetrahedrally coordinated Co(II) must be present. Equilibrium [1] explains the visible spectra and accounts for the presence of an uncoordinated ligand indicated by i.r. spectroscopy. Figure 1 is in accordance with the conductivity and does not conflict with the magnetic evidence provided by Madan and Sturr. The following equilibria should, however, be considered to some extent too

[2] $$[CoL_2X_2] + L \rightleftharpoons [CoL_3X]^+ + X^-$$

[3] $$2[CoL_2X_2] + 2L \rightleftharpoons [CoL_5X]^+ + [CoLX_3]^-$$

In acetone it is probably not possible to confirm the dissociation in the i.r. spectra, as the region for the ν(CO) is masked and the ν(NH) is influenced by hydrogen bonding to the solvent in the case of the coordinated and uncoordinated ligand.

The bands for octahedral species reported by Madan and Sturr for CoL_3X_2 at higher concentrations, could be easily explained by a small fraction of $[CoL_5X]^+$, according to equilibrium [3], which should have a band at the same position, but with higher extinction than $[CoL_6]^{2+}$ (10). For the spectra of the solid CoL_3X_2 in Nujol, it does not seem to be correct to suppose the presence of $[CoX_4]^{2-}$ ions. Cotton *et al.* (7) reported the spectra of $[CoX_4]^{2-}$ in different compounds in different mulls. The highest shift of any ν_3 band of $[CoX_4]^{2-}$ due to different environment is 450 cm^{-1}; normally they vary in a range of 300 cm^{-1} only. All the ν_3 bands of CoL_3X_2 in Nujol are about 600 cm^{-1} higher in frequency than the bands for the respective $[CoX_4]^{2-}$ in mulls. This again suggests that fewer than four halogens are coordinated to cobalt.

Molecular Weight and Conductivity

To further confirm whether the structure of $CoCl_2.3L$ is $[CoL_6]^{2+}[CoCl_4]^{2-}$ or CoL_2Cl_2 + L, molecular weight and conductivity measurements were carried out at different concentrations (Table IV). In the case of $[CoL_6][CoCl_4]$, a degree of association of 1 would be expected. We found a degree of association of 0.5 at 0.012 mole concentration which, together with the molar conductance values at various temperatures and concentrations, corresponds to the structure CoL_2Cl + L in solution. Moreover, if an ion $[CoX_4]^{2-}$ was present in solution, it could be precipitated by tetraphenylarsonium chloride. We found that no precipitate was obtained on mixing the two in acetone solutions.

The i.r. spectra (Table III) show, that the ν(NH) as well as the ν(CO) are lowered on complex formation. The shift in ν(CO) indicated coordination through oxygen (1). In our previous article (2) it was concluded from the shift of ν(NH) in the i.r. spectra of complexes of cobalt(II) halides with 2-thiazolidinethione, that the site of coordination was nitrogen. ν(NH) was lowered by 265, 225, and 175 cm^{-1} for the $CoCl_2$, $CoBr_2$, and CoI_2 complex of this ligand

Can. J. Chem. Downloaded from www.nrcresearchpress.com by 210.87.254.6 on 09/05/12
For personal use only.

TABLE III
Infrared spectra of 2-pyrrolidinone (L) and its complexes

Assignment	Literature*	Liquid	L ($CHCl_3$)	L.BCl_3 (Nujol)	CoL_3Cl_2 (Nujol)	CoL_3Br_2 (Nujol)	CoL_3I_2 (Nujol)	CoL_3Cl_2 ($CHCl_3$)	CoL_3Br_2 ($CHCl_3$)	CoL_3I_2 ($CHCl_3$)
ν(NH) free	3450		3440(s)					3444(m)	3446(s)	3443(m)
ν(NH) complex				3357(s)	3320(m,b)	3308(m)	3330(s,b)	3264(m,b)	3260(m,b)	3270(m,b)
ν(NH) H-bonded	3240	3235(s,b)	3230(s,b)							
$\nu(CH_2)$		2950(s)	2995(s)	Nujol	Nujol	Nujol	Nujol	3002(s)	2997(s)	3000(s)
$\nu(CH_2)$		2890(s)	2886(s)	Nujol	Nujol	Nujol	Nujol	2897(m)	2890(m)	2897(m)
ν(CO) free	1687		1691(s)					1691(s)	1688(s)	1691(s)
ν(CO) H-bonded		1680								
ν(CO) coordinated				1646(s)	1650(s)	1650(s)	1645(s)	1646(s)	1643(s)	1644(s)
(CH_2) sciss.	1494	1492(m)	1491(s)	1488(sh)	1490(w)	1492(s)	1490(s)	1491(s)	1491(m)	1491(s)
(CH_2) sciss.	1466	1462(s)	1459(s)	Nujol	Nujol	Nujol	Nujol	1470(m)	1462(m)	1470(m)
ν(NH)	1443	1437(s)	1440(sh)	Nujol	Nujol	Nujol	Nujol			1450(w)
(CH_2) sciss.	1427	1425(s)	1420(s)	1408(s)	1420(w)	1420(m)	1414(m)	1419(m)	1420(m)	1421(w)
ν(N—H) + ν(C—N)	1383	1377(m)	1380(s)	Nujol	Nujol	Nujol	Nujol	$CHCl_3$	$CHCl_3$	
		1303(sh)	1308(m)	1308(s)	1298(sh)	1298(s)	1302(s)	1310(m)	1307(m)	1312(m)
ν(C—N)	1287	1285(s)	1283(s)	1275(m)	1290(s)	1290(s)	1290(s)	1298(m)	1286(m)	1301(m)
(CH_2) wagging		1265(sh)	1259(m)			1272(sh)	1270(sh)	1262(sh)	1261(m)	
		1225(w)	$CHCl_3$	1220(sh)		1232(w)	1224(w)	$CHCl_3$	$CHCl_3$	
						1218(w)	1213(sh)	$CHCl_3$	$CHCl_3$	
$\nu(CH_2—N)$ + ν(NH)	1194	1170(m)	$CHCl_3$	1180(w)		1178(w)	1168(w)	$CHCl_3$	$CHCl_3$	
(CH_2) rocking		1067(s)	1059(s)	1058(m)	1059(m)	1059(m)	1057(m)	1059(m)	1059(m)	1060(m)
(CH_2) rocking		995(s)	991(s)	993(s)	995(m)	993(m)	991(m)	991(m)	990(m)	992(m)
(CH_2) rocking				945(s)						
ν(B—X)		912(w)	912(m)	908(s)		896(w)	888(w)	$CHCl_3$	$CHCl_3$	
				853(s,b)						
γ(N—H)	735		$CHCl_3$		803(w)	806(m)	805(w)	$CHCl_3$	$CHCl_3$	
			$CHCl_3$	753(s,vb)	740(s)	747(sh)	760			
						720(s)				
δ(CO)	683(s)	680(s)					690(s,b)			
γ(CO)	630(m)		622(s)	622(sh)	629(m)	634(m)	631(m)		627(m)	632(m)
								574(s)	570(s)	570(s)
	537(m)	539(m)		548(m)	539(m)	545(sh)	535(m)	528(s)	528(s)	526(s)
				526(w)						
	490(sh)			507(w)	512(w)	514(s)	512(m)			
Skeletal	474(s)	475(s)						473(m)	473(m)	472(m)
								336(s)	321(m)	316(m)
								300(s)		
ν(Co—X)					285(s)	240(s)	234(m)			
				280(w,b)						

*4000–700 cm^{-1} ref. 9; 700–200 cm^{-1} refs. 8, 10; s: strong, m: medium, w: weak, v: very, sh: shoulder, b: broad.

Can. J. Chem. Downloaded from www.nrcresearchpress.com by 210.87.254.6 on 09/05/12
For personal use only.

TABLE IV

Molecular weight and conductance results of $CoCl_2.3L$*

Concentration (mole)	Molecular weight	Degree of association	Concentration of adduct	Molar conductance ($cm^2\ \Omega^{-1}$/mole) at temperature: 25 °C	35 °C	45 °C
0.021	260	0.67	M/64	2.55	2.29	2.15
0.016	240	0.62	M/128	1.98	1.90	1.85
0.012	200	0.52	M/256	1.71	1.72	1.73
			M/512	1.45		
			M/1024	1.45		

*Compound in nitrobenzene solution.

respectively. We found shifts of 126, 138, and 116 cm^{-1} for the ν(NH) of the 2-pyrrolidinone complexes of $CoCl_2$, $CoBr_2$, and CoI_2. In order to obtain a complex of 2-pyrrolidinone, where the site of coordination is expected to be oxygen (11), we prepared the complex to the ligand with BCl_3. It was found to be a 1:1 compound and showed a lowering of ν(CO) of 45 cm^{-1} and a lowering of ν(NH) of 89 cm^{-1}.

The earlier conclusion, that coordination through nitrogen of cyclic thioamides is accompanied by a lowering of the ν(NH) of about 200 cm^{-1} does not, therefore, conflict with the present findings of a lowering of the ν(NH) of about 100 cm^{-1} in the case of coordination through oxygen.

As the i.r. spectra in Nujol, unlike those in solution, indicate that all ligand molecules are coordinated, and from the conclusion drawn from the electronic spectra, it seems reasonable to assume a structure $[CoL_3X]X$ for the complexes in the solid phase.

The assignments of other i.r. bands are given in Table III.

Acknowledgment

The authors gratefully acknowledge financial support from the National Research Council of Canada.

1. S. K. Madan and J. A. Sturr. J. Inorg. Nucl. Chem. 29, 1669 (1967).
2. P. P. Singh and R. Rivest. Can. J. Chem. **46**, 2361 (1968).
3. German Patent No. 1 033 207 (1958); Chem. Abstr. **54**, 17417g (1960).
4. F. A. Cotton, D. M. L. Goodgame, and A. Sacco. J. Am. Chem. Soc. **83**, 4157 (1961).
5. V. Gutmann and O. Bohunovsky. Monatsh. Chem. **99**, 740 (1968).
6. A. Fine. J. Am. Chem. Soc. **84**, 1139 (1962).
7. F. A. Cotton, D. M. L. Goodgame, and M. Goodgame. J. Am. Chem. Soc. **83**, 4690 (1961).
8. J. E. Katon, W. R. Feairheller, and J. V. Pustinger, Jr. Anal. Chem. **36**, 2126 (1964).
9. K. Kurosaki. Nippon Kagaku Zasshi, **82**, 1691 (1961); Chem. Abstr. **58**, 13312d (1962).
10. K. Mizutani and K. Stone. Z. Anorg. Allgem. Chem. **350**, 216 (1967).
11. W. Gerrard, M. F. Lappert, H. Pyszora, and J. W. Wallis. J. Chem. Soc. 2144 (1960).

Ferric benzoylacetanilides

A. Syamal

Department of Chemistry, Emory University, Atlanta, Georgia, U.S.A.

Received September 10, 1968

Ferric chelates with benzoylacetanilide and benzoyl-metanitroacetanilide have been prepared and characterized. The complexes are dark red in color and are paramagnetic (μ_{eff} = 5.8 B.M.). Electrolytic conductance, electronic spectra, and infrared spectra of the complexes are reported. Absorption spectra point to weak donor ability of the ligands in comparison to acetylacetone. The complexes are octahedral.

Canadian Journal of Chemistry, 47, 1693 (1969)

There has been appreciable interest in the ferric β-diketone complexes from the standpoint of syntheses, spectra, and structure (1–5). Though ferric complexes with β-diketones are well established, nothing has appeared so far in the literature concerning the ferric complexes of benzoylacetanilides, which are capable of keto–enol tautomerism shown by β-diketones. Little work has been

Can. J. Chem. Downloaded from www.nrcresearchpress.com by 210.87.254.6 on 09/05/12
For personal use only.

TABLE IV

Molecular weight and conductance results of $CoCl_2.3L$*

Concentration (mole)	Molecular weight	Degree of association	Concentration of adduct	Molar conductance ($cm^2\ \Omega^{-1}$/mole) at temperature: 25 °C	35 °C	45 °C
0.021	260	0.67	M/64	2.55	2.29	2.15
0.016	240	0.62	M/128	1.98	1.90	1.85
0.012	200	0.52	M/256	1.71	1.72	1.73
			M/512	1.45		
			M/1024	1.45		

*Compound in nitrobenzene solution.

respectively. We found shifts of 126, 138, and 116 cm^{-1} for the ν(NH) of the 2-pyrrolidinone complexes of $CoCl_2$, $CoBr_2$, and CoI_2. In order to obtain a complex of 2-pyrrolidinone, where the site of coordination is expected to be oxygen (11), we prepared the complex to the ligand with BCl_3. It was found to be a 1:1 compound and showed a lowering of ν(CO) of 45 cm^{-1} and a lowering of ν(NH) of 89 cm^{-1}.

The earlier conclusion, that coordination through nitrogen of cyclic thioamides is accompanied by a lowering of the ν(NH) of about 200 cm^{-1} does not, therefore, conflict with the present findings of a lowering of the ν(NH) of about 100 cm^{-1} in the case of coordination through oxygen.

As the i.r. spectra in Nujol, unlike those in solution, indicate that all ligand molecules are coordinated, and from the conclusion drawn from the electronic spectra, it seems reasonable to assume a structure $[CoL_3X]X$ for the complexes in the solid phase.

The assignments of other i.r. bands are given in Table III.

Acknowledgment

The authors gratefully acknowledge financial support from the National Research Council of Canada.

1. S. K. Madan and J. A. Sturr. J. Inorg. Nucl. Chem. 29, 1669 (1967).
2. P. P. Singh and R. Rivest. Can. J. Chem. **46**, 2361 (1968).
3. German Patent No. 1 033 207 (1958); Chem. Abstr. **54**, 17417g (1960).
4. F. A. Cotton, D. M. L. Goodgame, and A. Sacco. J. Am. Chem. Soc. **83**, 4157 (1961).
5. V. Gutmann and O. Bohunovsky. Monatsh. Chem. **99**, 740 (1968).
6. A. Fine. J. Am. Chem. Soc. **84**, 1139 (1962).
7. F. A. Cotton, D. M. L. Goodgame, and M. Goodgame. J. Am. Chem. Soc. **83**, 4690 (1961).
8. J. E. Katon, W. R. Feairheller, and J. V. Pustinger, Jr. Anal. Chem. **36**, 2126 (1964).
9. K. Kurosaki. Nippon Kagaku Zasshi, **82**, 1691 (1961); Chem. Abstr. **58**, 13312d (1962).
10. K. Mizutani and K. Stone. Z. Anorg. Allgem. Chem. **350**, 216 (1967).
11. W. Gerrard, M. F. Lappert, H. Pyszora, and J. W. Wallis. J. Chem. Soc. 2144 (1960).

Ferric benzoylacetanilides

A. Syamal

Department of Chemistry, Emory University, Atlanta, Georgia, U.S.A.

Received September 10, 1968

Ferric chelates with benzoylacetanilide and benzoyl-metanitroacetanilide have been prepared and characterized. The complexes are dark red in color and are paramagnetic (μ_{eff} = 5.8 B.M.). Electrolytic conductance, electronic spectra, and infrared spectra of the complexes are reported. Absorption spectra point to weak donor ability of the ligands in comparison to acetylacetone. The complexes are octahedral.

Canadian Journal of Chemistry, 47, 1693 (1969)

There has been appreciable interest in the ferric β-diketone complexes from the standpoint of syntheses, spectra, and structure (1–5). Though ferric complexes with β-diketones are well established, nothing has appeared so far in the literature concerning the ferric complexes of benzoylacetanilides, which are capable of keto–enol tautomerism shown by β-diketones. Little work has been

Can. J. Chem. Downloaded from www.nrcresearchpress.com by 210.87.254.40 on 09/05/12
For personal use only.

TABLE I

Analyses, molar conductance, and magnetic moment of iron(III) chelates

Complex†		Analyses %Fe	%N	%H_2O*	Molar conductance Ω^{-1} cm^2 mole^{-1}	Magnetic moment (B.M.) T = 298 °K
$[Fe(C_{15}H_{12}O_2N)_3]$	Found:	7.48	5.56	—	1.5	5.84
	Calcd:	7.27	5.45			
$[Fe(C_{15}H_{11}O_4N_2)_3]\cdot 2H_2O$	Found:	6.16	9.08	3.52	1.8	5.85
	Calcd:	5.95	8.92	3.82		

*The water molecules stay outside the coordination zone as is evident from their ready loss at 110 °C with no color change accompanying dehydration.

†Where $C_{15}H_{13}O_2N$ = benzoylacetanilide, $C_6H_5—\overset{\overset{O}{\|}}{C}—CH_2—\overset{\overset{O}{\|}}{C}—NHC_6H_5$, $C_{15}H_{12}O_4N_2$ = benzoyl-metanitroacetanilide.

reported concerning the complexing ability of benzoylacetanilides. Syntheses of oxo-vanadium(IV), dioxo-molybdenum(VI), dioxo-uranium(VI), Ti(IV),Cu(II) (6, 7), and reports concerning the estimation of titanium, vanadium, and mercury (8) are all that have appeared so far. This report describes the syntheses and characterization of ferric chelates with benzoylacetanilide and benzoylmetanitroacetanilide.

Experimental

Ferric sulfate hexahydrate was a product of E. Merck (Germany). Benzoylacetanilide and benzoyl-metanitroacetanilide were prepared according to the published procedures (6, 9).

General Method of Syntheses of the Complexes

Ferric sulfate hexahydrate (1.0 g, 2 mmoles) was dissolved in 30 ml of hot water and a few drops of concentrated H_2SO_4. The appropriate amount of the ligand used was weighed out for a 1:3, Fe^{3+}:ligand complex. This was dissolved in a minimum amount of hot ethanol and this solution was added to the Fe^{3+} solution. To the resulting violet solution, dilute sodium acetate was added dropwise with stirring. The separated dark red oily layer was taken up with ethanol. Water was added dropwise to the ethanol solution resulting in the formation of dark red crystals. These crystals were suction filtered and washed with hot water followed by a warm 50% water–ethanol solution. The product was dried in a desiccator over $CaCl_2$ and P_4O_{10}.

Methods

The electrolytic conductance was measured with the help of a conductivity bridge (fitted with magic eye) and a dip type cell. Room temperature magnetic susceptibility measurements were taken in a Gouy Balance using A.R. $CuSO_4\cdot 5H_2O$ as the calibrant. Electronic absorption spectra in the region of 12.5–50 kK were recorded in methanol solution (concentration varying from 0.5×10^{-3} to 1.0×10^{-3} M) with the help of a Perkin–Elmer spectrophotometer. Infrared (i.r.) spectra were measured in Nujol mulls on a Perkin–Elmer recording spectrophotometer, model 21.

The analyses, molar conductance, and magnetic moment of the compounds are recorded in Table I. The electronic spectral characteristics of the complexes are presented in Table II.

Results and Discussion

When alcoholic solution of benzoylacetanilides is added to an aqueous solution of Fe^{3+}, a fine purple color is formed. Formation of this purple color is characteristic of benzoylacetanilides and no other metals interfere in this color reaction. The analytical data show that the Fe^{3+}: ligand ratio in the complexes is 1:3. The complexes are in general insoluble in water and soluble in methanol, ethanol, chloroform, and carbontetrachloride. The electrical conductance measurements of the complexes in methanol ($\Lambda_M \sim 1$ Ω^{-1} at 25 °C) indicate nonelectrolytic nature of the complexes. The complexes are all paramagnetic and record a magnetic moment ($\mu_{eff} \sim 5.8$ B.M.) close to the spin-only value. This value is in close agreement with the high-spin octahedral structure with 5 unpaired electrons in $3d^5$ system and having Fe^{3+} in the ^6S ground state level (10). The u.v. and visible spectra of the complexes exhibit 2 intense bands around 20.6 and 27.5 kK. These two bands are electron transfer bands corresponding to the transitions $\pi \rightarrow \nu_5$ and $\nu_3 \rightarrow \pi^*$, respectively (4). The high molar absorptivity of these bands is indicative of electron transfer bands rather than the weak, spin-forbidden bands (3, 4). The latter are the only type of d $\leftrightarrow$ d transitions expected in an O_h symmetry Fe^{3+} environment. Probably the characteristic spin-forbidden bands are obscured by the low energy tails of the electron transfer bands and this observation is in line with other octahedral spin-free iron(III) complexes (10). The corresponding

Can. J. Chem. Downloaded from www.nrcresearchpress.com by 210.87.254.40 on 09/05/12
For personal use only.

TABLE II

Numerical values for the electron transfer transitions of Fe(III) complexes obtained by the choice of parameters†

Ligand	I. $\pi \rightarrow \nu_5$		II. $\pi \rightarrow \nu_3$		III. $\nu_5 \rightarrow \pi^*$		IV. $\nu_3 \rightarrow \pi^*$	
	Calcd.	Found	Calcd.	Found	Calcd.	Found	Calcd.	Found
Benzoylacetanilide	22	20.6(3.22)	40	—	46	—	28	27.5(3.69)
Benzoyl-metanitro-acetanilide	22	20.6(3.20)	40	—	46	—	28	27.2(3.50)
Acetylacetone‡	23	23.2(3.47)	41	—	45	—	27	28.5(3.55)

†$V_1 = 30$ kK, $V_2 = 18$ kK, $\Delta = 18$ kK, $D = 4.5$ kK, $E - A = 4$ kK (1 kK = 1000 cm^{-1}).
‡Taken from ref. 4 for comparison. Figures in the parentheses indicate log ε.

electron transfer bands in *tris*(acetylacetonato) iron(III) occur at 23.2 kK (log ε = 3.47) and 28.5 kK (log ε = 3.55) (3). The band positions suggest that the ligand field of *tris*(acetylacetonato) iron(III) is stronger than those of *tris*(benzoylacetanilido) iron(III) and *tris*(benzoyl-metanitroacetanilido) iron(III). In the uranyl complexes (6) of the present ligands, the OUO stretch frequency was also observed at lower energy than those of the OUO stretch frequency of *bis*(acetylacetonato) UO_2(VI). Thus the electronic absorption spectra undoubtedly identify the ligands benzoylacetanilides as weak donors in comparison to acetylacetone.

Generally 4 electron transfer transitions from or to the π levels of the ligand are expected for octahedral high-spin complexes of the type $Fe(acac)_3$ or $Fe(benzoylacetanilide)_3$. These 4 different electron transfer spectra are (4) I, $\pi \rightarrow \nu_5$; II, $\pi \rightarrow \nu_3$; III, $\nu_5 \rightarrow \pi^*$; and IV, $\nu_3 \rightarrow \pi^*$. For a high spin d^5 configuration the dependence on the parameters V_1, V_2, $E - A$, and D of the transitions I, II, III, and IV is given as $V_1 - 5(E - A) + 8/3\ D$, $V_1 + \Delta - 5(E - A) + 8/3\ D$, $V_2 + 4(E - A) + 8/3\ D$, and $V_2 - \Delta + 4(E - A) + 8/3\ D$, respectively, where V_1 and V_2 are related by the equation: $V_2 + V_1 - (E - A) = 44$ kK (4). D is roughly $7B$ for d electrons, and is known from internal transitions in the d shell of similar complexes to be approximately 4.5 kK. From the experimental results the value of V_1 is derived, noting that the strong band of $Fe(benzoylacetanilide)_3$ or $Fe(benzoyl\text{-}metanitroacetanilide)_3$ at 20.6 kK must belong to the category I. Δ, the ligand field splitting parameter, is assumed to be of the same value (18 kK) as in $Fe(acac)_3$ due to the very close positions of these two types of ligands in the spectrochemical series, and it allows the calculation to be made without prior knowledge of the spectrum. Thus good agreement between the calculated and observed energies of the electron transfer transitions was obtained by choice of suitable parameters (cf. Table II). The electron transfer bands II and III were not observed in these complexes as these bands were obscured by the intense charge-transfer spectra at the calculated frequencies. In the corresponding acetylacetonato complex also, these bands were not observed due to the same reason.

The i.r. spectra of the complexes were characterized by the presence of chelated carbonyl absorptions. In both the complexes the normal carbonyl vibration of the ligand is replaced by metal coordinated carbonyl absorptions at much lower frequencies. The carbonyl spectrum of the chelating ligands benzoylacetanilide and benzoyl-metanitroacetanilide occur at 1700 and 1670 cm^{-1}, respectively. *Tris*(benzoylacetanilido) iron(III) and *tris*(benzoyl-metanitroacetanilido) iron(III) exhibit chelated carbonyl absorptions at 1.66 and 1.625 kK, respectively. The frequency of the carbonyl band of the ligands is therefore shifted to lower frequency (∼ 0.04 kK) by coordination with ferric ion.

Acknowledgment

Thanks are due to Dr. R. L. Dutta of Department of Chemistry, Ohio State University, Columbus, Ohio, U.S.A., for his interest in the work.

1. A. COMBES. Compt. Rend. **105**, 868 (1887). G. T. MORGAN, H. D. K. DREW, and C. R. PORTER. Ber. **58**, 333 (1925).
2. B. C. GUHA. Proc. Roy. Soc. London, Ser. A, **206**, 353 (1931). R. H. HOLM and F. A. COTTON. J. Am. Chem. Soc. **80**, 5658 (1958). T. S. PIPER and R. L. CARLIN. Inorg. Chem. **2**, 260 (1963). D. T. FARREN and M. M. JONES. J. Phys. Chem. **68**, 1717 (1964).

Can. J. Chem. Downloaded from www.nrcresearchpress.com by 210.87.254.40 on 09/05/12
For personal use only.

3. D. W. BARNUM. J. Inorg. Nucl. Chem. **21**, 221 (1961); **22**, 183 (1961).
4. C. K. JORGENSEN. Acta Chem. Scand. **16**, 2406 (1962).
5. R. B. ROOF, JR. Acta Cryst. **9**, 781 (1956). B. MOROSIN and J. R. BRATHOVDE. Acta Cryst. **17**, 705 (1964).
6. A. SYAMAL. J. Inorg. Nucl. Chem. Letters, **4**, 543 (1968).
7. A. SYAMAL. J. Indian Chem. Soc. **44**, 656 (1967); **45**, 755 (1968).
8. A. K. SARKAR and J. DAS. Anal. Chem. **39**, 1608 (1967); Anal. Letters **1**, 325 (1968).
9. H. GILMAN and A. H. BLATT. Org. Syn. **39**, 2 (1954); **39**, 32 (1954).
10. F. A. COTTON and G. WILKINSON. Advanced inorganic chemistry. Interscience Publishers, Inc., New York. 1966. p. 861.

Can. J. Chem. Downloaded from www.nrcresearchpress.com by 210.87.254.40 on 09/05/12
For personal use only.

Reaction of atomic hydrogen with tetrafluoroethene[1]

LEI TENG AND W. E. JONES
Department of Chemistry, Dalhousie University, Halifax, Nova Scotia

Received August 20, 1968

Hydrogen atoms, generated in a Wood's electric discharge tube, were allowed to react with tetrafluoroethene. The products of the reaction were found to be HF, C_2F_3H, C_2H_2, $C_2F_2H_2$, $C_2F_4H_2$, C_2FH_3, C_2H_4, and CHF_3. The formation of the products with the exception of HF was studied quantitatively from 30–330 °C.

Canadian Journal of Chemistry, 47, 1696 (1969)

Introduction

The reactions of atomic hydrogen with fluorocarbons have received only summary attention in the past. Chadwell and Titani (1), using the discharge tube method at room temperature, found no reaction of hydrogen atoms with methyl fluoride. Later, Dacey and Hodgins (2) investigated the mercury photosensitized reactions of the mixture of tetrafluoromethane and hydrogen molecules but again no evidence was found for the occurrence of a reaction. Clark and Tedder (3–5) studied a series of free radical substitutions in aliphatic compounds. They found that the first step in the reactions of hydrogen atoms with bromotrichloromethane and fluorotrichloromethane was the abstraction of a halogen atom. The resulting trihalomethyl radical added H to form a vibrationally excited molecule, which either stabilized or decomposed by elimination of HX. If fluorocarbons were the reactant species, the elimination of HF always occurred in preference to stabilization.

The kinetics of the reaction of hydrogen atoms with tetrafluoroethene were investigated by Allen, Melville, and Robb (6). They did not study the products of the reaction and it thus seemed worthwhile to study the products of this reaction in an attempt to get an insight into the reaction mechanism.

[1]Presented at the 51st Conference of the Chemical Institute of Canada, Vancouver, June 1968.

Experimental

Hydrogen was supplied by Canadian Liquid Air Ltd. Ethane, ethene, hexafluoroethane, acetylene, and 1,1-difluoroethene were obtained from Matheson Company of Canada Ltd.; trifluoromethane and tetrafluoroethene were obtained from Pierce Chemical Company. Each of these gases was frozen in a liquid nitrogen trap and traces of non-condensable gases were pumped off.

The flow system for this work was a typical Wood–Bonhoffer system similar to those described by many workers. Dry hydrogen flowed into each end of the V-shaped discharge tube. The power from a 3000 V Hammond transformer was rectified and supplied to the discharge tube through a 5000 Ω resistor. With 80 V across the primary of the transformer, and a hydrogen pressure of 4.60 mm Hg, a stable discharge and a stable production of atomic hydrogen were obtained. A molecular hydrogen flow rate of 182×10^{-6} moles/s produced the above pressure when a Cenco HyperVac No. 23 was used as the vacuum pump. The hydrogen atom flow rate was estimated at 0.8×10^{-6} moles/s by reaction with 2-dimethylethylenimine (7).

The mixture of atomic and molecular hydrogen passed from the discharge tube into a cylindrical reaction vessel made from 25 mm o.d. Pyrex tubing. Tetrafluoroethene was admitted to the hydrogen stream through a jet centered in the reaction vessel. The wall of the reaction vessel was thoroughly poisoned with phosphoric acid.

Qualitative and quantitative analysis of the reactant and products was made by gas–liquid chromatography (g.l.c.) on a column of $\frac{1}{4}$ in. copper tubing packed with silica gel which had been coated with 3% squalane (8). Identification was made by comparison of retention times, and where necessary, from mass and infrared (i.r.)

3. D. W. BARNUM. J. Inorg. Nucl. Chem. **21**, 221 (1961); **22**, 183 (1961).
4. C. K. JORGENSEN. Acta Chem. Scand. **16**, 2406 (1962).
5. R. B. ROOF, JR. Acta Cryst. **9**, 781 (1956). B. MOROSIN and J. R. BRATHOVDE. Acta Cryst. **17**, 705 (1964).
6. A. SYAMAL. J. Inorg. Nucl. Chem. Letters, **4**, 543 (1968).
7. A. SYAMAL. J. Indian Chem. Soc. **44**, 656 (1967); **45**, 755 (1968).
8. A. K. SARKAR and J. DAS. Anal. Chem. **39**, 1608 (1967); Anal. Letters **1**, 325 (1968).
9. H. GILMAN and A. H. BLATT. Org. Syn. **39**, 2 (1954); **39**, 32 (1954).
10. F. A. COTTON and G. WILKINSON. Advanced inorganic chemistry. Interscience Publishers, Inc., New York. 1966. p. 861.

Can. J. Chem. Downloaded from www.nrcresearchpress.com by 210.87.254.6 on 09/05/12
For personal use only.

Reaction of atomic hydrogen with tetrafluoroethene[1]

LEI TENG AND W. E. JONES
Department of Chemistry, Dalhousie University, Halifax, Nova Scotia

Received August 20, 1968

Hydrogen atoms, generated in a Wood's electric discharge tube, were allowed to react with tetrafluoroethene. The products of the reaction were found to be HF, C_2F_3H, C_2H_2, $C_2F_2H_2$, $C_2F_4H_2$, C_2FH_3, C_2H_4, and CHF_3. The formation of the products with the exception of HF was studied quantitatively from 30–330 °C.

Canadian Journal of Chemistry, 47, 1696 (1969)

Introduction

The reactions of atomic hydrogen with fluorocarbons have received only summary attention in the past. Chadwell and Titani (1), using the discharge tube method at room temperature, found no reaction of hydrogen atoms with methyl fluoride. Later, Dacey and Hodgins (2) investigated the mercury photosensitized reactions of the mixture of tetrafluoromethane and hydrogen molecules but again no evidence was found for the occurrence of a reaction. Clark and Tedder (3–5) studied a series of free radical substitutions in aliphatic compounds. They found that the first step in the reactions of hydrogen atoms with bromotrichloromethane and fluorotrichloromethane was the abstraction of a halogen atom. The resulting trihalomethyl radical added H to form a vibrationally excited molecule, which either stabilized or decomposed by elimination of HX. If fluorocarbons were the reactant species, the elimination of HF always occurred in preference to stabilization.

The kinetics of the reaction of hydrogen atoms with tetrafluoroethene were investigated by Allen, Melville, and Robb (6). They did not study the products of the reaction and it thus seemed worthwhile to study the products of this reaction in an attempt to get an insight into the reaction mechanism.

[1]Presented at the 51st Conference of the Chemical Institute of Canada, Vancouver, June 1968.

Experimental

Hydrogen was supplied by Canadian Liquid Air Ltd. Ethane, ethene, hexafluoroethane, acetylene, and 1,1-difluoroethene were obtained from Matheson Company of Canada Ltd.; trifluoromethane and tetrafluoroethene were obtained from Pierce Chemical Company. Each of these gases was frozen in a liquid nitrogen trap and traces of non-condensable gases were pumped off.

The flow system for this work was a typical Wood–Bonhoffer system similar to those described by many workers. Dry hydrogen flowed into each end of the V-shaped discharge tube. The power from a 3000 V Hammond transformer was rectified and supplied to the discharge tube through a 5000 Ω resistor. With 80 V across the primary of the transformer, and a hydrogen pressure of 4.60 mm Hg, a stable discharge and a stable production of atomic hydrogen were obtained. A molecular hydrogen flow rate of 182×10^{-6} moles/s produced the above pressure when a Cenco HyperVac No. 23 was used as the vacuum pump. The hydrogen atom flow rate was estimated at 0.8×10^{-6} moles/s by reaction with 2-dimethylethylenimine (7).

The mixture of atomic and molecular hydrogen passed from the discharge tube into a cylindrical reaction vessel made from 25 mm o.d. Pyrex tubing. Tetrafluoroethene was admitted to the hydrogen stream through a jet centered in the reaction vessel. The wall of the reaction vessel was thoroughly poisoned with phosphoric acid.

Qualitative and quantitative analysis of the reactant and products was made by gas–liquid chromatography (g.l.c.) on a column of $\frac{1}{4}$ in. copper tubing packed with silica gel which had been coated with 3% squalane (8). Identification was made by comparison of retention times, and where necessary, from mass and infrared (i.r.)

Can. J. Chem. Downloaded from www.nrcresearchpress.com by 210.87.254.6 on 09/05/12
For personal use only.

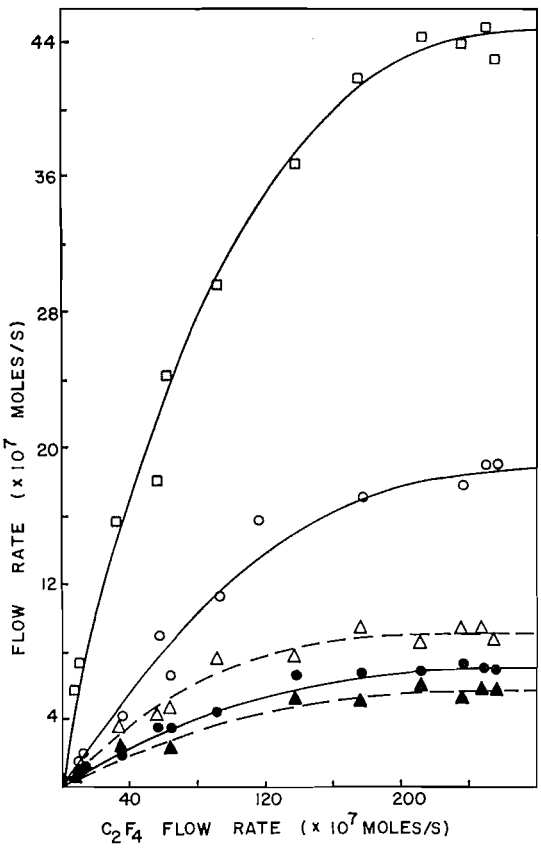

FIG. 1. Flow rates of major products at 30 °C. □, C_2F_4 reacted; product flow rates: ○, C_2F_3H; ●, $C_2F_2H_2$; △, C_2H_2; ▲, $C_2F_4H_2$.

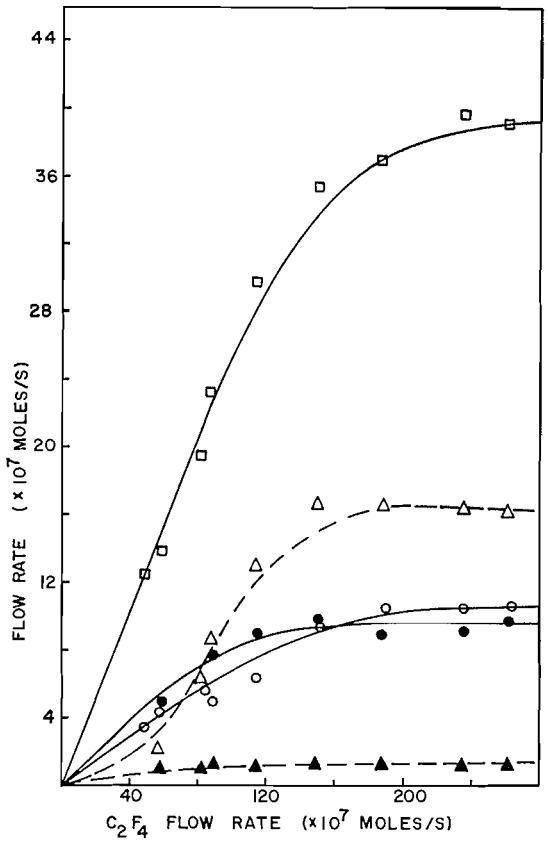

FIG. 2. Flow rates of major products at 230 °C. □, C_2F_4 reacted; product flow rates: ○, C_2F_3H; ●, $C_2F_2H_2$; △, C_2H_2; ▲, $C_2F_4H_2$.

spectra. Quantitative analysis was made by comparison of peak heights with peak height calibration curves prepared by using pure samples of each gas.

Results and Discussion

The products of the reaction of atomic hydrogen with tetrafluoroethene were identified as hydrogen fluoride, 1,1,2-trifluoroethene, acetylene, 1,1-difluoroethene, 1,1,1,2-tetrafluoroethane, vinyl fluoride, ethene, and fluoroform. The production of these products was studied quantitatively[2] for the three temperatures 30, 230, and 330 °C. The compounds C_2FH_3, C_2H_4, and CF_3H have not been included in the quantitative results since the amounts formed were barely detectable and not sufficient to measure quantitatively.

Figure 1 illustrates the flow rate of reacted C_2F_4 and product flow rates at 30 °C. At this temperature, the flow rate of C_2F_4 reacted appears to reach a limiting or plateau value of 4.4 μmoles/s. The major product at 30 °C is C_2F_3H, followed by lesser amounts of C_2H_2, $C_2F_2H_2$, and $C_2F_4H_2$.

At 230 °C similar curves are found, as shown in Fig. 2. At this temperature, the plateau value for the flow rate of C_2F_4 reacted is slightly less than at 30 °C, having a value of 3.9 μmoles/s. The major product now becomes C_2H_2, the flow rate of which has approximately doubled over that formed at 30 °C. It would appear that C_2H_2 has formed at the expense of C_2F_3H, since the flow rate of this product has decreased to approximately half its value at 30 °C. The flow rate

[2]Photocopies of the detailed data may be obtained free of charge, upon request, from: the Depository of Unpublished Data, National Science Library, National Research Council of Canada, Ottawa, Canada.

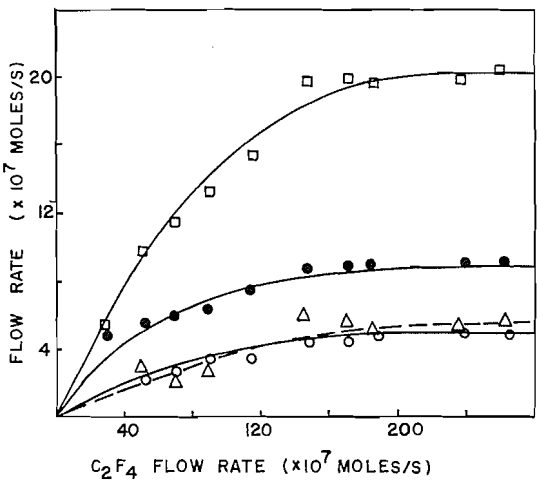

FIG. 3. Flow rates of major products at 330 °C. □, C_2F_4 reacted; product flow rates: ○, C_2F_3H; ●, $C_2F_2H_2$; △, C_2H_2.

of the product $C_2F_2H_2$ has increased slightly while that of $C_2F_4H_2$ has decreased to become almost negligible.

At 330 °C the maximum flow rate of C_2F_4 reacted has fallen to 2.0 μmoles/s as shown in Fig. 3. The major product is now $C_2F_2H_2$ while the production of C_2H_2 and C_2F_3H has dropped markedly and the flow rate of $C_2F_4H_2$ has become negligible.

The original purpose of this study, namely, the determination of the reaction mechanism, has now become extremely complicated by the large number and type of products formed. In order to assist in the formulation and substantiation of the mechanism for this reaction, the reactions of several related compounds are presently under study. These results and the mechanism will be presented in the near future.

Acknowledgments

The authors wish to express their thanks to the National Research Council of Canada and to the Faculty of Graduate Studies, Dalhousie University, for financial assistance.

1. H. M. CHADWELL and T. TITANI. J. Am. Chem. Soc. **55**, 1363 (1933).
2. J. R. DACEY and J. W. HODGINS. Can. J. Res. B, **28**, 173 (1933).
3. D. T. CLARK and J. M. TEDDER. Trans. Faraday Soc. **62**, 393 (1966).
4. D. T. CLARK and J. M. TEDDER. Trans. Faraday Soc. **62**, 399 (1966).
5. D. T. CLARK and J. M. TEDDER. Trans. Faraday Soc. **62**, 405 (1966).
6. P. E. M. ALLEN, H. W. MELVILLE, and J. C. ROBB. Proc. Roy. Soc. London, Ser. A, **218**, 311 (1953).
7. J. W. S. JAMIESON, G. R. BROWN, and W. K. HANCOCK. Can. J. Chem. **43**, 1973 (1965).
8. G. O. PRICHARD, J. R. DACEY, W. C. KENT, and C. R. SIMONDS. Can. J. Chem. **44**, 171 (1966).

Detection of the triple ion (durosemiquinone-Na_2)$^+$ by electron spin resonance spectroscopy

T. E. GOUGH AND P. R. HINDLE
Department of Chemistry, University of Waterloo, Waterloo, Ontario

Received November 25, 1968

Reduction of duroquinone by sodium in tetrahydrofuran and in 2-methyltetrahydrofuran in the presence of sodium tetraphenylboride yields the triple ion (durosemiquinone-Na_2)$^+$ which shows hyperfine interaction with twelve equivalent hydrogen and two equivalent sodium nuclei. When the reduction is performed in 1,2-dimethoxyethane, the triple ion is not formed, and the electron spin resonance spectra indicate the presence of an intermolecular cation exchange process.

Canadian Journal of Chemistry, 47, 1698 (1969)

The presence of triple ions in solution has been postulated in the interpretation of conductivity data (1–3); however, there appears to be no well authenticated case of their detection by electron spin resonance (e.s.r.) spectroscopy, in spite of the large number of investigations of ionic association using this technique (4). Triple ions of the formula M_2A^+, where A^- is a radical anion, should be characterized by the interaction of the unpaired electron with the nuclei of two counterions; care should be taken to ensure that the observed species is not an ionic quadrupole, because

Can. J. Chem. Downloaded from www.nrcresearchpress.com by 210.87.254.6 on 09/05/12
For personal use only.

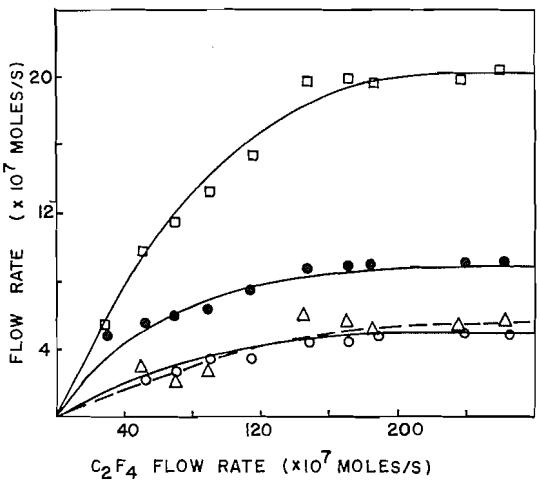

FIG. 3. Flow rates of major products at 330 °C. □, C_2F_4 reacted; product flow rates: ○, C_2F_3H; ●, $C_2F_2H_2$; △, C_2H_2.

of the product $C_2F_2H_2$ has increased slightly while that of $C_2F_4H_2$ has decreased to become almost negligible.

At 330 °C the maximum flow rate of C_2F_4 reacted has fallen to 2.0 μmoles/s as shown in Fig. 3. The major product is now $C_2F_2H_2$ while the production of C_2H_2 and C_2F_3H has dropped markedly and the flow rate of $C_2F_4H_2$ has become negligible.

The original purpose of this study, namely, the determination of the reaction mechanism, has now become extremely complicated by the large number and type of products formed. In order to assist in the formulation and substantiation of the mechanism for this reaction, the reactions of several related compounds are presently under study. These results and the mechanism will be presented in the near future.

Acknowledgments

The authors wish to express their thanks to the National Research Council of Canada and to the Faculty of Graduate Studies, Dalhousie University, for financial assistance.

1. H. M. CHADWELL and T. TITANI. J. Am. Chem. Soc. **55**, 1363 (1933).
2. J. R. DACEY and J. W. HODGINS. Can. J. Res. B, **28**, 173 (1933).
3. D. T. CLARK and J. M. TEDDER. Trans. Faraday Soc. **62**, 393 (1966).
4. D. T. CLARK and J. M. TEDDER. Trans. Faraday Soc. **62**, 399 (1966).
5. D. T. CLARK and J. M. TEDDER. Trans. Faraday Soc. **62**, 405 (1966).
6. P. E. M. ALLEN, H. W. MELVILLE, and J. C. ROBB. Proc. Roy. Soc. London, Ser. A, **218**, 311 (1953).
7. J. W. S. JAMIESON, G. R. BROWN, and W. K. HANCOCK. Can. J. Chem. **43**, 1973 (1965).
8. G. O. PRICHARD, J. R. DACEY, W. C. KENT, and C. R. SIMONDS. Can. J. Chem. **44**, 171 (1966).

Detection of the triple ion (durosemiquinone-Na_2)$^+$ by electron spin resonance spectroscopy

T. E. GOUGH AND P. R. HINDLE
Department of Chemistry, University of Waterloo, Waterloo, Ontario

Received November 25, 1968

Reduction of duroquinone by sodium in tetrahydrofuran and in 2-methyltetrahydrofuran in the presence of sodium tetraphenylboride yields the triple ion (durosemiquinone-Na_2)$^+$ which shows hyperfine interaction with twelve equivalent hydrogen and two equivalent sodium nuclei. When the reduction is performed in 1,2-dimethoxyethane, the triple ion is not formed, and the electron spin resonance spectra indicate the presence of an intermolecular cation exchange process.

Canadian Journal of Chemistry, 47, 1698 (1969)

The presence of triple ions in solution has been postulated in the interpretation of conductivity data (1–3); however, there appears to be no well authenticated case of their detection by electron spin resonance (e.s.r.) spectroscopy, in spite of the large number of investigations of ionic association using this technique (4). Triple ions of the formula M_2A^+, where A^- is a radical anion, should be characterized by the interaction of the unpaired electron with the nuclei of two counterions; care should be taken to ensure that the observed species is not an ionic quadrupole, because

Can. J. Chem. Downloaded from www.nrcresearchpress.com by 210.87.254.105 on 09/05/12
For personal use only.

Can. J. Chem. Downloaded from www.nrcresearchpress.com by 210.87.254.105 on 09/05/12
For personal use only.

the ionic quadrupoles formed by aliphatic (5) and aromatic (6) ketyls also show hyperfine splitting from two alkali metal nuclei. If the electron spin dipolar interaction between the two A^- systems of the quadrupole is strong, then the quadrupole may be recognized by its characteristic solid state e.s.r. spectrum (7). However, if the dipolar interaction is weak, it becomes difficult to distinguish between a triple ion and an ionic quadrupole; for these reasons no firm assignment has been made for the species obtained when naphthalene was reduced for long periods of time by sodium in tetramethylethylenediamine (6).

Reduction of quinones by alkali metals in ethereal solution forms mixtures of free and associated semiquinones (8, 9). Reduction of duroquinone by sodium in tetrahydrofuran was difficult because the sodium rapidly became coated with a coherent greenish film, presumably of the reduction product. An e.s.r. spectrum of the solution recorded at a sample temperature of $-20°$ is given in Fig. 1*a*; it may be analyzed in terms of six equivalent protons with a hyperfine splitting constant of 2.66 G, six equivalent protons with a splitting of 1.20 G, and one sodium with a splitting of 0.25 G. These values are in good agreement with those of a previous report (10). When a 1:1 molar mixture of duroquinone and sodium tetraphenylboride was similarly reduced, the reaction proceeded instantaneously, no protective film was formed on the sodium, and at a sample temperature of $-20°$ the e.s.r. spectrum given in Fig. 1*b* was obtained; this spectrum was analyzed in terms of twelve equivalent protons with a hyperfine splitting constant of 1.94 G, and two equivalent sodium nuclei with a splitting of 0.17 G. No signal was obtained when the reduction of duroquinone by sodium in 2-methyltetrahydrofuran was attempted; the addition of sodium tetraphenylboride allowed rapid reduction to a solution having an intense e.s.r. spectrum analogous to that of Fig. 1*b*. In Fig. 2 the measured sodium hyperfine splitting constants of the three systems are plotted as a function of temperature. For spectra such as that in Fig. 1*b*, the measured proton hyperfine splitting constant was always equal, within experimental error, to the accepted value for durosemiquinone (11) and to the value for the dihydroxydurene cation (12). The e.s.r. spectrum of frozen solutions of the species responsible for Fig. 1*b* was a single line, 12 G wide, at $g = 2$; no half-field resonance was detected.

We attribute the spectrum in Fig. 1*b* to a triple

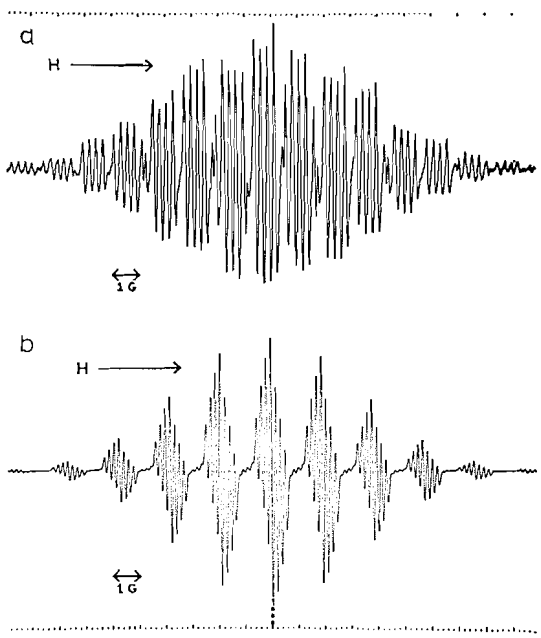

FIG. 1. (*a*) Electron spin resonance spectrum of the solution obtained after the reduction of duroquinone by sodium in tetrahydrofuran; sample temperature -20 °C. (*b*) Electron spin resonance spectrum of the solution obtained after a similar reduction in the presence of sodium tetraphenyl boride; sample temperature -20 °C; the low intensity lines between the main groups are caused by a C^{13} splitting of 1.42 G from the methyl groups.

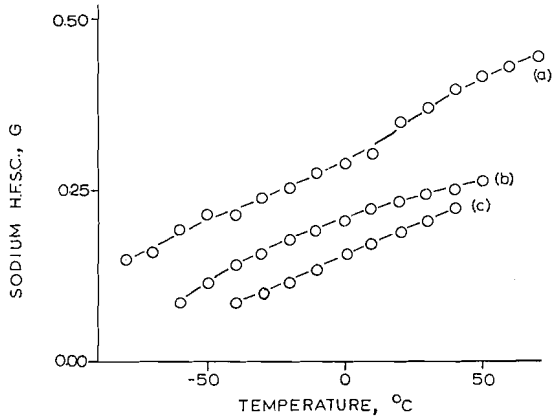

FIG. 2. The dependence upon temperature of the sodium hyperfine splitting constants of the ion-pair (durosemiquinone–Na) in tetrahydrofuran, plot (*a*); and of the triple ion (durosemiquinone-Na_2)$^+$ in tetrahydrofuran, plot (*b*); and in 2-methyltetrahydrofuran, plot (*c*).

ion rather than an ionic quadrupole, because the addition of sodium ions in excess of those introduced by the reduction process is necessary for the formation of this species. Of a substantial number of investigations of the reduction of quinones in ethereal solution (8–10, 13–16), none has given any indication of hyperfine splitting from more than one alkali metal nucleus. Furthermore, the marked increase in solubility (a factor of at least 10^3) of the semiquinone in the presence of added sodium tetraphenylboride indicates that an interaction takes place between the existing ion-pairs and the added salt. Structurally, the triple ion may be thought of as a durosemiquinone anion ionically associated with a sodium cation at each oxygen, a configuration which makes all four methyl groups equivalent. Since each cation of the triple ion will be attracted to a lesser extent than the cation of the ion-pair, the smaller sodium splitting observed when two cations interact supports the hypothesis that a triple ion is formed. Dimerization of the ion-pairs to form ionic quadrupoles should not affect the magnitude of the sodium hyperfine splitting constant.

The addition of a sodium salt does not necessarily bring about the formation of triple ions. Thus, when 1,2-dimethoxyethane was used as the solvent, complex spectra indicating the presence of intermolecular cation exchange processes analogous to those discussed for the *m*-dinitrobenzene anion (17) were obtained; similarly, triple ion formation was not observed (18) when sodium iodide was added to ion-pairs of sodium-9,10-anthrasemiquinone dissolved in 1,2-dimethoxyethane, or to ion-pairs of sodium-2,5-di-*t*-butyl parabenzosemiquinone dissolved in tetrahydrofuran. Semiquinone ion-pairs may also be generated in alcoholic solution in the presence of excess alkoxide (19, 20), but once again, the presence of excess cations does not lead to the formation of triple ions. We are at present conducting a systematic study of the factors which control the formation of triple ions.

Acknowledgment

Financial support of this work by the National Research Council of Canada is gratefully acknowledged.

1. R. M. Fuoss and C. A. Krauss. J. Am. Chem. Soc. **55**, 2387 (1933).
2. R. M. Fuoss. J. Am. Chem. Soc. **57**, 2604 (1935).
3. R. M. Fuoss. Chem. Rev. **17**, 227 (1935).
4. M. C. R. Symons. J. Phys. Chem. **71**, 172 (1967).
5. G. R. Luckhurst. Mol. Phys. **9**, 179 (1965).
6. A. H. Reddoch. J. Chem. Phys. **43**, 3411 (1965).
7. N. Hirota and S. I. Weissman. J. Am. Chem. Soc. **86**, 2538 (1964).
8. P. S. Gill and T. E. Gough. Can. J. Chem. **45**, 2112 (1967).
9. P. S. Gill and T. E. Gough. Trans. Faraday Soc. **64**, 1997 (1968).
10. M. P. Khakhar, B. S. Prabhananda, and M. R. Das. J. Am. Chem. Soc. **89**, 3100 (1967).
11. B. Venkataraman, B. G. Segal, and G. K. Fraenkel. J. Chem. Phys. **30**, 1006 (1959).
12. P. D. Sullivan. J. Am. Chem. Soc. **89**, 4294 (1967).
13. P. S. Gill and T. E. Gough. Can. J. Chem. **46**, 656 (1968).
14. M. P. Khakhar, B. S. Prabhananda, and M. R. Das. J. Chem. Phys. **45**, 2327 (1966).
15. D. H. Chen, E. Warhurst, and A. M. Wilde. Trans. Faraday Soc. **63**, 2561 (1967).
16. J. C. Chippendale and E. Warhurst. Trans. Faraday Soc. **64**, 2332 (1968).
17. R. F. Adams and N. M. Atherton. Trans. Faraday Soc. **64**, 7 (1968).
18. A. W. Rutter and E. Warhurst. Trans. Faraday Soc. **64**, 2338 (1968).
19. T. E. Gough and M. C. R. Symons. Trans. Faraday Soc. **62**, 269 (1966).
20. T. A. Claxton, J. Oakes, and M. C. R. Symons. Trans. Fraday Soc. **63**, 2125 (1967).

Can. J. Chem. Downloaded from www.nrcresearchpress.com by 210.87.254.105 on 09/05/12
For personal use only.

Can. J. Chem. Downloaded from www.nrcresearchpress.com by 210.87.254.42 on 09/05/12
For personal use only.

Hot molecules in radical combination

T. N. Bell and U. F. Zucker
Department of Chemistry, Simon Fraser University, Burnaby 2, British Columbia

Received February 25, 1969

1:1 Difluoroethylene is formed when CF_3 radicals react with alkyl silanes. We propose that the olefin results from the rearrangement and decomposition of a hot molecule arising from radical recombination

$$CF_3 + CH_2SiX_3 \rightarrow CF_3CH_2SiX_3^* \xrightarrow{M} CF_3CH_2SiX_3$$
$$\searrow CF_2CH_2 + FSiX_3$$

Canadian Journal of Chemistry, 47, 1701 (1969)

In the presence of the alkylsilanes $(CH_3)_4Si$, $(CH_3)_2SiF_2$, and CH_3SiF_3, the photolysis of hexafluoroacetone (HFA) leads to the expected radical products CF_3H and C_2F_6, but in addition, some CF_2CH_2 is formed. We suggest that this does not arise from a reaction involving excited HFA* with the silanes, from the following evidence: (*a*) The emission spectrum of HFA is not quenched but slightly enhanced by the silanes, in a manner similar to third bodies such as CO_2 (1). (*b*) Addition of sufficient oxygen to quench ^{3}HFA (2) does not suppress the CF_2CH_2 to zero, some 16 mm O_2 being required to eliminate this product. While this does not eliminate ^{1}HFA*, it does suggest that oxygen is acting as a radical scavenger. (*c*) CF_2CH_2 is still formed when the pyrolysis and photolysis of hexafluoroazomethane is used as a radical source.

The CF_2CH_2 is therefore considered to arise from some reaction involving CF_3 radicals. Hydrogen abstraction will lead to CH_2SiX_3 radicals, and the following recombination is possible.

[1] $$CF_3 + CH_2SiX_3 \rightarrow CF_3CH_2SiX_3$$
(X = Me and/or F)

F atoms in a position β to silicon are known to be labile (3*a*, *b*), leading to the thermal unimolecular elimination [2].

[2] $$CF_3CH_2SiX_3 \xrightarrow{\text{Heat}} CF_2CH_2 + FSiX_3$$

In Fig. 1 is plotted the amount of CF_2CH_2 formed when HFA, 60.5 mm, and CH_3SiF_3, 210 mm, were photolyzed for 1 min at 204°, and the reaction mixture then allowed to stand at 204° in the dark for varying periods. It is clear that $R_{CF_2CH_2}$ during photolysis is considerably greater than that formed in the dark reaction. The amount of CO, CF_3H, and C_2F_6 showed no change during this thermal reaction. SiF_4 was also found (infrared and mass spectra). No reaction products were formed on heating the reaction mixture without a period of photolysis.

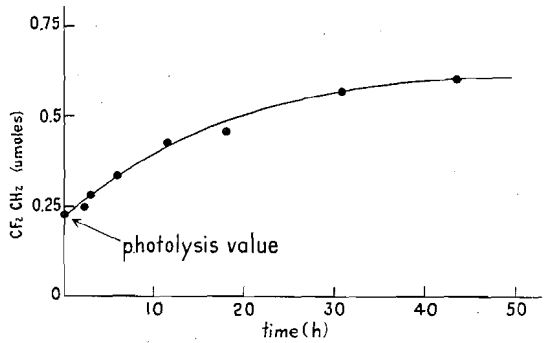

FIG. 1. Amount of CF_2CH_2 formed against time for a photolysis time of 60 s (P_{HFA} 60.5 mm; $P_{CH_3SiF_3}$, 210 mm; temperature, 204°).

In order to explain these results we suggest the formation of a hot molecule in the recombination reaction [3], which leads to the CF_2CH_2 formed during photolysis, reaction [4*b*].

[3] $$CF_3 + CH_2SiF_3 \rightarrow CF_3CH_2SiF_3^*$$

This may be stabilized or decomposed according to reactions [4*a*] and [4*b*],

[4*a*] $$CF_3CH_2SiF_3^* \xrightarrow{M} CF_3CH_2SiF_3$$
[4*b*] $$\searrow CF_2CH_2 + SiF_4$$

The dark reaction leading to the much slower $R_{CF_2CH_2}$ is ascribed to the thermolysis [5].

[5] $$CF_3CH_2SiF_3 \rightarrow CF_2CH_2 + SiF_4$$

The absence of products expected from methyl radicals, allows us to ignore elimination from CF_3CH_3* as a source of CF_2CH_2 (4*a*, *b*).

If the other reactions of CF_3 radicals are hydrogen abstraction, and recombination [6] and [7]

[6] $$CF_3 + CH_3SiF_3 \rightarrow CF_3H + CH_2SiF_3$$

[7] $$CF_3 + CF_3 \rightarrow C_2F_6$$

then, provided reaction [5] goes to completion, $CO = C_2F_6 + \frac{1}{2}CF_3H + \frac{1}{2}CF_2CH_2$. After 43.5 h, we have, as shown in Fig. 1

$$3.75_{(CO)} = 2.95_{(C_2F_6)} + 0.45_{(\frac{1}{2}C_2F_6)} + 0.30_{(\frac{1}{2}CF_2CH_2)} \quad \text{(amounts in μmole)}$$

The CF_3 discrepancy immediately after photolysis is thus recovered during the dark reaction.

A first order Guggenheim plot of the pyrolysis results in Fig 1 gives a good straight line from which $k_5 = 1.6 \times 10^{-5}\ s^{-1}$.

Assuming $A_5 \sim 10^{12}$ yields $E_5 \sim 37$ kcal in agreement with Arrhenius parameters for similar decompositions (3*b*). The hot molecule formed in reaction [3] thus has a large enough excess energy to decompose, assuming the new C—C bond to have a strength ~ 85 kcal.

From reactions [4*a*] and [4*b*], we obtain

[8] $$R_{4a}/R_{4b} = k_{4a}[M]/k_{4b}$$

$R_{4a}/R_{4b} \simeq CF_2CH_2$ (total from pyrolysis)/CF_2CH_2 (photolysis)

The pressure dependence of this ratio is shown below for experiments with photolysis times of 2 min at 200°. The dark decomposition was carried out at higher temperatures. The linear relationship predicted by eq. [8] is not observed. Using the arguments of Pritchard (5*a*, *b*) this could be ascribed to different collisional efficiencies of the two molecules, and multistep deactivation in reaction [4*a*].

TABLE I

Pressure dependence of R_{4a}/R_{4b}

Pressure of M (mm)		
HFA	CH_3SiF_3	R_{4a}/R_{4b}
60.5	210	1.74
116	69	0.76
49.5	70.5	0.67
38.2	48.7	0.30
30.0	30.0	0.15
10.0	20.0	0.06
4.9	10.6	0.09

Elimination reactions from hot molecules formed from radical recombination have been shown to be important (4*a*, *b*; 5*a*, *b*). In our case both rearrangement, presumably through the silicon d orbitals, and elimination occur, and exemplify a new type of process.

It is intended to make a full study of this reaction, and extend the work to systems containing boron, germanium, and tin.

Acknowledgment

We thank the National Research Council of Canada for financial support, and Mr. F. Wick for construction of apparatus.

1. H. Okabe and E. W. R. Steacie. Can. J. Chem. **36**, 137 (1958).
2. A. Gandini and K. O. Kutschke. Can. J. Chem. **44**, 1720 (1966).
3. (*a*) T. N. Bell, R. N. Haszeldine, M. J. Newlands, and J. B. Plumb. J. Chem. Soc. 2107 (1965). (*b*) G. Fishwick, R. N. Haszeldine, C. Parkinson, P. J. Robinson, and R. F. Simmons. Chem. Commun. 383 (1965); J. Chem. Soc. 1890 (1964).
4. (*a*) W. G. Alcock and E. Whittle. Trans. Faraday Soc. **61**, 244 (1965). (*b*) R. D. Giles and E. Whittle. Trans. Faraday Soc. **61**, 1424 (1965).
5. (*a*) G. O. Pritchard and R. L. Thommason. J. Phys. Chem. **71**, 1674 (1967). (*b*) J. T. Bryant and G. O. Pritchard. J. Phys. Chem. **71**, 3439 (1967).

Can. J. Chem. Downloaded from www.nrcresearchpress.com by 210.87.254.42 on 09/05/12
For personal use only.

Can. J. Chem. Downloaded from www.nrcresearchpress.com by 210.87.254.42 on 09/05/12
For personal use only.

Atmospheric electron–ion and ion–ion recombination processes[1]

MANFRED A. BIONDI
Physics Department, University of Pittsburgh, Pittsburgh, Pennsylvania 15213

Received December 17, 1968

The electron–ion and ion–ion recombination processes of importance in the upper atmosphere are considered, and available laboratory experimental and theoretical information concerning the relevant processes is discussed. For atomic ions the principal electron–ion recombination process is radiative, with theory indicating that the two-body coefficient at ~200 °K is $\sim 10^{-11}$ cm³/s and decreases with increasing electron temperature. Microwave afterglow/mass spectrometer studies of diatomic ionospheric ions (e.g. NO^+, O_2^+, and N_2^+) show a loss by dissociative recombination with a coefficient substantially in excess of 10^{-7} cm³/s at 250 °K and decreasing with increasing electron and ion temperature. There is some evidence from flame studies that H_3O^+ ions exhibit a very large coefficient (10^{-6}–10^{-5} cm³/s) at 300 °K. Ion–ion recombination evidently proceeds by mutual neutralization, with laboratory studies of ions such as NO^+ and NO_2^- indicating a two-body coefficient of the order of 10^{-7} cm³/s at 300 °K. In the lower D region, three-body Thomson recombination may be important, since laboratory studies of "air" ions indicate a three-body coefficient of $\sim 2 \times 10^{-25}$ cm⁶/s at 300 °K.

Canadian Journal of Chemistry, 47, 1711 (1969)

Introduction

The purpose of the present paper is to single out those processes of electron–ion and ion–ion recombination which are of importance in the upper atmosphere, and to discuss the available information from laboratory experiments and theoretical calculations concerning these processes. In order to make clear some of the limitations of current theoretical treatments, results of certain experiments involving non-atmospheric ions will also be discussed. The present paper, in part, brings up to date the reviews presented at the I.A.G.A. Aeronomy Symposium of 1963 (1) and at the COSPAR meeting in Vienna in 1966 (2).

Although conditions encountered in the upper atmosphere are somewhat variable and there is by no means complete agreement concerning the constituents, we have adopted the model given in Table I in order to make clear the regions of operation of the various recombination processes. Several features are apparent from the Table; atomic positive ions predominate in certain regions and molecular ions in others, the neutral density is sufficiently large to affect recombination rates only in the D region, and the electron temperature appreciably exceeds the ion temperature in certain regions (in addition, although not given in the Table, the charged particle densities are rather modest, $< 10^6$ cm^{-3}). The significance of these features will be made clear in the next section.

[1]Some of the research described in this paper has been supported by the Army Research Office (Durham) DA-ARO-D-124-G965, by the Defense Atomic Support Agency, and by the Advanced Research Projects Agency, DA-31-124-ARO-D-440.

Electron–Ion Recombination

The significant electron–ion recombination processes occurring in the ionosphere are dissociative and radiative recombination. These processes involve the capture of the electron by the positive ion without the assistance of a third body in the reaction. We rule out as unimportant three-body processes involving electrons or neutral molecules acting as the third bodies, since the electron-stabilized case theory (3) indicates that the three-body coefficient decreases rapidly with increasing electron temperature from a value of $< 10^{-18}$ cm⁶/s at 250 °K, leading to a maximum effective two-body coefficient, "α", of $< 10^{-13}$ cm³/s which occurs at E-layer altitudes. The available experimental information (see, for example, ref. 4) supports the results of the calculations.

In the neutral stabilized cases, calculations (5) of the three-body coefficient ($\lesssim 10^{-26}$ cm⁶/s for a monatomic third body and $\lesssim 10^{-25}$ cm⁶/s for diatomic third body at 250 °K) suggest that the maximum rate, which would occur in the E region, is equivalent to a two-body coefficient of "α" $< 10^{-12}$ cm³/s. As we shall see, dissociative recombination outweighs this process by a factor of $> 10^5$ and at higher altitudes, where the neutral concentration is lower, even radiative recombination is of greater importance.

A. Radiative Recombination

In the case of atomic positive ions in the

TABLE I

Approximate ionospheric conditions* (quiet, daytime, mid-solar cycle)

Region	Height	Principal ions	[M]	[A]	T_e	T_i	T_n
D	60	$H_3O^+\cdot(H_2O)_n$† NO^+ NO_2^-(?)	15	10	350	350	350
E	110	NO^+, O_2^+, e^-	13	11	$\geqslant 250$	250	250
Sporadic E	110	$Mg^+, Fe^+, Si^+, Ca^+, e^-$	13	11	$\geqslant 250$	250	250
F1	170	NO^+, O_2^+, O^+, e^-	10	10	1100	700	700
F2	300	$O^+ (O_2^+, NO^+), e^-$	8	9	2500	1800	1500
Magnetosphere‡	1000	H^+, He^+(?), e^-	—	5	1500	1500	1500
Protonosphere	2500	H^+, e^-	—	4	1500	1500	1500

*The heights are in km, temperatures in °K, and molecular [M] and atomic [A] densities are given as $\log_{10}$ [N (cm^{-3})].
†See comment by F. E. Niles at end of this paper; $n = 0, 1, 2$.
‡H^+ is the principal ion at solar minimum, while He^+ is believed to be the principal ion at solar maximum.

ionosphere, electron capture proceeds via two-body radiative recombination in which an electron makes a radiative transition from a free (continuum) state to a bound state of the resulting atom, i.e.

$$[1] \qquad X^+ + e \rightarrow X^* + h\nu$$

where X^+ and X^* denote ionized and excited states of the atom X. Probably the best information concerning the rates of radiative recombination comes from theoretical calculations (6, 7). It is found that the recombination coefficient is not particularly sensitive to the identity of the positive ion, varying by less than a factor of two in going from H^+ to K^+. The partial recombination coefficient for electron capture into the lower states of the excited atom varies as $T_e^{-0.5}$ (T_e is the electron temperature), while for capture into the highly excited states lying within $\sim kT_e$ of the continuum, it varies approximately as $T_e^{-1.5}$. The total recombination coefficient varies approximately as $T_e^{-0.7}$, starting from a value of $\sim 5 \times 10^{-12}$ cm^3/s at 250 °K. Few experimental studies of recombination have been carried out under conditions where radiative recombination is the predominant process; those that have (see, for example, ref. 8) yield α values in reasonable agreement with theory.

As we shall see shortly, dissociative electron–ion recombination exhibits α values $\gtrsim 10^{-7}$ cm^3/s at electron temperatures $\lesssim 1000$ °K; therefore radiative recombination will be the predominant electron loss process only in regions where the concentration ratio of atomic to molecular ions is $\gtrsim 10^4$. The required atomic ion excess is found in the magnetosphere and the protonosphere and possibly in the sporadic-E layer, and in the latter case the small rate of radiative recombination may account for the layer's persistence.

B. Dissociative Recombination

In those regions of the ionosphere containing molecular ions, electrons are removed by the highly efficient dissociative recombination process. The direct process may be represented in reaction form by

$$[2] \qquad XY^+ + e \rightleftharpoons (XY^*)_{unstable} \rightleftharpoons X + Y + \text{kinetic energy}$$

Here the large recombination coefficient ($\alpha_{diss} \geqslant 10^{-7}$ cm^3/s) results from the radiationless initial capture step (which involves no energy change) which forms the unstable excited molecule, followed by a high probability of dissociation before auto-ionization (first portion of reaction [2] going to the left).

At present the most detailed information concerning the recombination coefficients of molecular ionospheric ions has been obtained from a rather wide variety of experimental studies. We shall discuss these first, emphasizing those experiments in which the ion identity is clearly established, and then shall review recent progress in theoretical calculations of dissociative recombination. As will be seen from Table I, the ions involved are NO^+, O_2^+, N_2^+, H_3O^+, and its hydrated forms. In order to be of use in ionospheric calculations, it is important that the laboratory measurement establish clearly the identity of the ion undergoing recombination and specify as well as possible the electronic and vibrational state of the ion.

Studies of the recombination of electrons with NO^+ ions have been carried out over the temperature range 200–450 °K by Weller and Biondi (9)

Can. J. Chem. Downloaded from www.nrcresearchpress.com by 210.87.254.42 on 09/05/12
For personal use only.

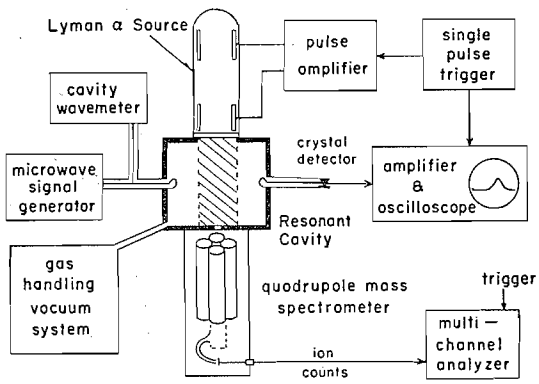

FIG. 1. Schematic diagram of a typical microwave afterglow apparatus employing mass analysis of the ions undergoing electron–ion recombination. In this case a photoionizing source is used to ionize the gas.

using the microwave afterglow apparatus shown in Fig. 1. The NO^+ ions are created in their ground electronic state and in the first few vibrational levels by a pulse of Lyman α radiation (a "single pulse-afterglow" technique is used to avoid negative ion accumulation effects). The recombination coefficient is determined by measuring the rate of decay of average electron density during the afterglow following the pulse (using microwave resonant cavity frequency shift techniques), and the ions undergoing recombination are identified by a mass spectrometer which simultaneously measures the ion currents diffusing to the cavity wall and effusing through a small hole. (Only those data in which the NO^+ ion wall current satisfactorily follows the volume decay of electron density are considered trustworthy.)

In order to obtain accurate recombination coefficients from the average electron density data, computer solutions (10) of the electron continuity equation

$$[3] \qquad \partial n_e/\partial t = -\alpha n_e^2 + D_a \nabla^2 n_e$$

where n_e is the electron concentration and D_a is the ambipolar diffusion coefficient, are used to account for the effect of diffusion on the electrons' spatial distribution within the cavity. By using very low partial pressures of NO($\sim 10^{-2}$ Torr) in neon buffer gas ($\sim$ 5 Torr), complex ion formation is avoided and diffusion loss sufficiently inhibited to provide recombination control of the afterglow. The results of the measurements yield values of $\alpha(NO^+)$ of $(7.4 \pm 0.7), (4.1 + 0.3 - 0.2)$, and $(3.1 \pm 0.2) \times 10^{-7}$ cm^3/s at T = 200, 300, and 450 °K, respectively. (Afterglow conditions are such that $T_e = T_i = T_n = T$.) These values are in good agreement with the results at $T \geqslant 300$ °K of Gunton and Shaw (11), who employed a similar type of apparatus but could not operate their mass spectrometer at the high buffer gas pressures required in their recombination studies. They obtained values $\alpha = (10+2, -4), (4.6+0.5, -1.3)$, and $(3.5+0.2, -0.5) \times 10^{-7}$ cm^3/s at T = 196, 298, and 358 °K, respectively. Weller and Biondi found that, at low temperatures ($\sim$ 200 °K), appreciable concentrations of the dimer ion $(NO)_2^+$ are very difficult to avoid. This ion exhibits a very large recombination coefficient; a value $\alpha[(NO)_2^+] = (1.7 \pm 0.4) \times 10^{-6}$ cm^3/s was obtained (9) at 300 °K. Thus, Gunton and Shaw's large and highly uncertain α value at 196 °K probably resulted from an appreciable concentration of $(NO)_2^+$ ions, illustrating the value of simultaneous mass analysis of the ionic species undergoing recombination.

An interesting study of the recombination of NO^+ ions produced by *chemi*-ionization in mixtures of N, O, and N_2 has been carried out by Young and St. John (12). Currents arriving at pulsed collector electrodes (no mass analysis was employed) were used to measure the rate of growth and the equilibrium value of the charge density produced by the chemi-ionization, leading to a value $\alpha(NO^+) = (4 \pm 1) \times 10^{-7}$ cm^3/s at 300 °K.

Measurements of the recombination of electrons and NO^+ ions at very high temperatures ($\sim$ 3000–5000 °K) are much less certain. Stein *et al.* (13) used microwave techniques to measure the electron density decay in shock-heated air at $\sim$ 2900 °K in which the principal ion is thought to be NO^+, obtaining a value, $\alpha \approx 4 \times 10^{-8}$ cm^3/s. Also, Lin *et al.* (14), from a complicated analysis of ionization behind shock waves in air, concluded that a value, $\alpha \approx 2 \times 10^{-8}$ cm^3/s at 5000 °K, is consistent with their electron density measurements. The measured values of $\alpha(NO^+)$ over the range 200–5000 °K are shown in Fig. 2. It will be seen that the temperature variation can be approximately represented by $\alpha \approx T^{-1}$ ($T_e = T_i = T_n = T$), although at low temperatures the data are sufficiently accurate to indicate noticeable deviations from this simple law.

Systematic studies of the recombination of

Can. J. Chem. Downloaded from www.nrcresearchpress.com by 210.87.254.42 on 09/05/12
For personal use only.

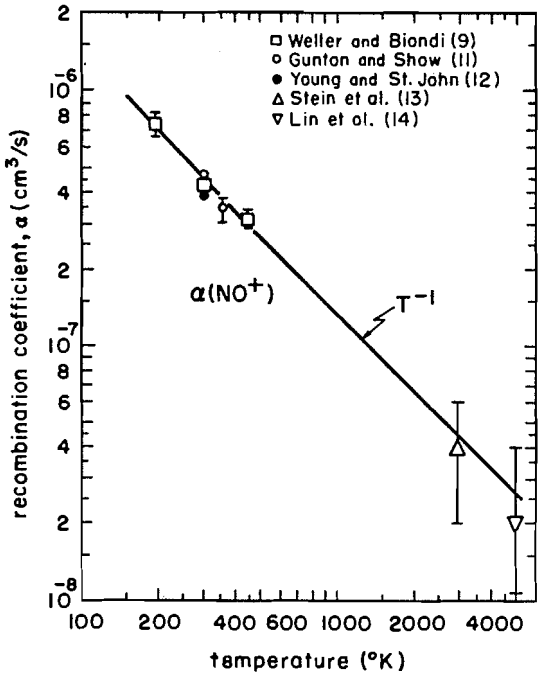

FIG. 2. Temperature dependence of the dissociative recombination coefficient $\alpha(NO^+)$ under conditions where $T_e = T_i = T_n = T$.

electrons with mass-identified O_2^+ ions have been carried out over the temperature range 200–700 °K by Kasner and Biondi (15). A microwave afterglow/mass spectrometer apparatus similar to that shown in Fig. 1 was used, except that a "single pulse" microwave discharge was used to produce O_2^+ ions in their ground electronic and a low vibrational state by a combination of Penning ionization and charge transfer reactions. Triple mixtures of O_2(~ 10^{-2} Torr), Kr(~ 1 Torr), and Ne(~ 20 Torr) were used, and the sequence of neon metastables ionizing krypton which then charge transferred with O_2 was used to prevent formation of O_2^+ ions in electronically excited states. An alternate sequence of neon metastables directly ionizing oxygen molecules can leave the O_2^+ ions in a highly excited vibrational state of the ground electronic state ($X^2\Pi_g$) or even in the metastable excited electronic state ($a^4\Pi_u$).

The recombination coefficient $\alpha(O_2^+)$ was determined from measurements of the decay of average electron density in recombination controlled afterglows. The measured decay curves were either compared with computer solutions (10) of eq. [3] or were corrected for diffusion effects using correction factors given by Gray and Kerr (16). As in the case of NO^+, at low temperatures difficulty with the measurements was encountered as a result of the appearance of significant concentrations of the dimer ion, O_4^+, under certain conditions. Kasner and Biondi obtained a value for the dimer ion recombination coefficient, $\alpha(O_4^+) \approx 2.3 \times 10^{-6}$ cm^3/s at 205 °K.

The values of $\alpha(O_2^+)$ obtained under conditions where the O_2^+ (the only significant ion) wall current satisfactorily follows the electron density decay are (3.0 ± 0.3), (2.2 ± 0.2), (1.7 ± 0.2), (1.37 ± 0.15), (1.25 ± 0.2), and $(1.0 \pm 0.2) \times 10^{-7}$ cm^3/s at 205, 300, 385, 488, 560, and 690 °K, respectively. These values are shown in Fig. 3.

Also shown in Fig. 3 are data obtained by Mentzoni (17) from microwave afterglow studies at high oxygen pressures (~ 2 Torr) which did not employ mass analysis. In view of the inability to identify the ion or its state in Mentzoni's studies, in Fig. 3 we have drawn the curve indicating the temperature dependence through the data of Kasner and Biondi. It will be seen that a single power law temperature dependence, of the form T^{-1}, is followed over the measured range.

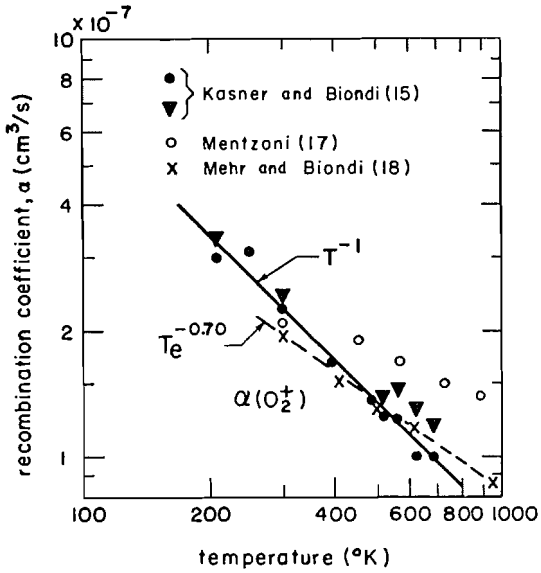

FIG. 3. Temperature dependence of the dissociative recombination coefficient $\alpha(O_2^+)$ under conditions where $T_e = T_i = T_n = T$ (solid line) and under conditions where $T_i = T_n = 300$ °K and T_e is varied (dashed line). The ● symbols indicate triple mixture (O_2, Kr, Ne) studies, while the ▼ and × symbols indicate the binary mixture (O_2, Ne) studies (see text for details).

Can. J. Chem. Downloaded from www.nrcresearchpress.com by 210.87.254.42 on 09/05/12
For personal use only.

Can. J. Chem. Downloaded from www.nrcresearchpress.com by 210.87.254.42 on 09/05/12
For personal use only.

Very recently, Mehr and Biondi (18) have used a microwave afterglow/mass spectrometer apparatus with microwave electron heating to study $\alpha(O_2^+)$ under conditions such that $T_e \geqslant T_i = 300\ °K$. For O_2^+ ions it is found that $\alpha = 1.95 \times 10^{-7}\ cm^3/s$ at $T_e = 300\ °K$ and decreases as $T_e^{-0.70}$ up to $T_e = 1200\ °K$ and then decreases as $T_e^{-0.56}$ up to $T_e = 5000\ °K$. In these studies excited electronic states of O_2^+ may be present (O_2–Ne mixtures were used); thus the data should be compared with the inverted triangles shown in Fig. 3. Within the combined experimental uncertainties, the variations of $\alpha(O_2)$ are the same when T_e alone is varied and when T_e, T_i, and T_n are all covaried.

Before leaving the subject of dissociative recombination of O_2^+ ions, it should be noted that recently Zipf (19) has used absolute intensity and microwave electron density determinations in oxygen afterglows at 300 °K to determine the partial dissociative recombination coefficients leading to formation of oxygen atoms in the ^1S and ^1D states. He finds that $\alpha'(^1S) \simeq 0.4 \times 10^{-7}\ cm^3/s$ and $\alpha'(^1D) \simeq 1.5 \times 10^{-7}\ cm^3/s$, indicating that a substantial number of the recombination events lead to formation of one of the oxygen atoms in an electronically excited state.

Detailed studies of the recombination of N_2^+ ions and electrons have been carried out by Kasner and Biondi (20) and by Kasner (21) using essentially the same apparatus as in the O_2^+ studies, except that a repetitive pulse-afterglow cycle was used because there was no problem of negative ion accumulation from pulse to pulse. The N_2^+ ions were produced in mixtures of nitrogen ($\lesssim 10^{-2}$ Torr) and neon (~ 20 Torr) by Penning ionization of N_2 by $Ne(^3P_2)$ metastable atoms, assuring that the ions were in their ground electronic and a low ($v \leqslant 4$) vibrational state.

At $T = 300\ °K$, Kasner and Biondi obtained a value $\alpha(N_2^+) = (2.9 \pm 0.3) \times 10^{-7}\ cm^3/s$. From studies at higher partial pressures of nitrogen, they were able to evaluate the dimer ion's recombination coefficient, $\alpha(N_4^+) \sim 2 \times 10^{-6}\ cm^3/s$, although the presence of some N_3^+ ions (which apparently have a rather smaller coefficient) makes this result somewhat uncertain. Kasner (21) extended the studies over the temperature range 200–480 °K and found very little dependence of $\alpha(N_2^+)$ on temperature, a variation as $T^{-0.02}$ providing the best fit to the data (see Fig. 4). Very recent results (10, 18) of microwave

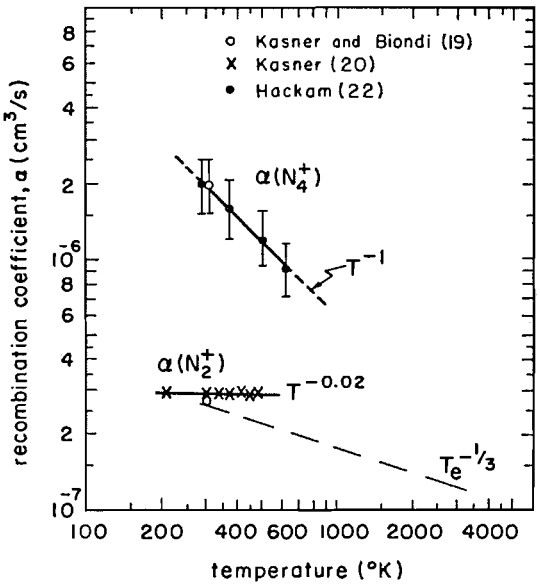

FIG. 4. Temperature dependence of the dissociative recombination coefficient $\alpha(N_2^+)$. The × symbols indicate conditions where $T_e = T_i = T_n = T$, while the dashed line indicates preliminary results obtained when T_e is varied while $T_i = T_n$ is held at 300 °K. The upper curve apparently applies to the variation of $\alpha(N_4^+)$ under conditions where $T_e = T_i = T_n = T$.

electron heating experiments indicate that when $T_+ = T_n = 300\ °K$ and T_e is independently varied, $\alpha(N_2^+)$ varies approximately as $T_e^{-1/3}$ over the range $300\ °K \leqslant T_e \leqslant 3000\ °K$. As we shall see shortly, the dissociative recombination process admits quite different "temperature dependences" when T_e and T_i are varied first together and then independently.

In the data shown in Fig. 4, we have included results of microwave studies of Hackam (22) at higher nitrogen pressures (2–6 Torr) which did not make use of mass analysis. In as much as his value for α at 300 °K agrees with the results of Kasner and Biondi for $\alpha(N_4^+)$, we tentatively conclude that his measured variation as $\sim T^{-1}$ over the range $300\ °K \leqslant T \leqslant 700\ °K$ applies to the N_4^+ ion.

There is little information concerning the magnitudes of the recombination coefficients of the recently discovered D-layer ions, H_3O^+ and its hydrated forms (masses 19, 37, 55). Hydrogen–oxygen–acetylene flame studies at $\sim 2100\ °K$ were carried out by Green and Sugden (23*a*), who used a mass spectrometer to monitor the decay of H_3O^+ ions (the only significant ion).

Can. J. Chem. Downloaded from www.nrcresearchpress.com by 210.87.254.42 on 09/05/12
For personal use only.

They found a value $\alpha(H_3O^+) \simeq 2 \times 10^{-7}$ cm^3/s. Wilson and Evans (23*b*) used microwave techniques to measure the decay of electron density behind shock fronts in argon containing small amounts of oxygen and hydrocarbon (e.g. acetylene). From recombination controlled decays, they found that α varies roughly as T^{-2} over the range 2400 °K $< T <$ 5600 °K, with a value $\alpha \approx 1.5 \times 10^{-7}$ cm^3/s at 3000 °K. Presumably these values refer to H_3O^+ ions. If an inverse temperature dependence of this order is maintained down to much lower temperatures, the coefficient at $\sim$ 300 °K may be in excess of 10^{-6} cm^3/s, perhaps even as large as 10^{-5} cm^3/s. (It has been suggested by Donahue that such a large recombination coefficient is required to offset the enhanced ionization rate implied by the larger D region NO concentrations recently measured in rocket sounding experiments.) Measurements of the recombination coefficients of the ions $H_3O^+ \cdot (H_2O)_n$ at low temperatures ($\sim$ 300 °K) are thus of considerable interest.

Finally, we include determinations of $\alpha(CO_2^+)$ in our discussion of experimental measurements of ionospheric ion recombination coefficients, since it is thought that the ionospheres of Mars and of Venus contain CO_2^+ ions. Using a modification of the microwave afterglow/mass spectrometer apparatus shown in Fig. 1, Weller and Biondi (24) obtained a value $\alpha = (3.8 \pm 0.5) \times 10^{-7}$ cm^3/s at 300 °K and a value $\sim 4 \times 10^{-7}$ at 210 °K for mass-identified CO_2^+ ions.

Recently, several theoretical calculations (25–27) of dissociative recombination coefficients have appeared. None can be said to represent true ab initio calculations, in which the wave functions for the various ion and excited molecule states of reaction [2] are computed and used to obtain the molecular potential curves, the resonance capture cross section, and the probability of auto-ionization as a function of the internuclear separation of the atoms. At present, the calculations employ simplifications and/or use of experimental information concerning the potential curves of the ionospheric ions in order to obtain values of the dissociative recombination coefficients.

It has been shown (27) that, in dissociative recombination, not only the direct process indicated by eq. [2] but also an *indirect* process may contribute significantly to the total recombination coefficient. The indirect process proceeds via resonance electron capture to form a vibrationally excited, stable Rydberg state of the excited molecule which predissociates as a result of a pseudo-crossing with the unstable molecule state indicated in eq. [2]. In addition, the energy dependences of the direct and indirect processes appear to be quite different (27).

Bardsley (27) has calculated the *direct* dissociative recombination coefficient $\alpha_d(NO^+)$ at 300 °K using spectroscopic data to obtain the shape of the ground electronic state of NO^+ and to estimate the resonance capture formation rate and the auto-ionization rate. His value $\alpha_d(NO^+) = 2.6 \times 10^{-7}$ cm^3/s is about 60% of the experimental value, and he argues that the indirect process (for which he is unable to obtain a quantitative estimate) may provide the remainder.

Warke (26) has used a semiclassical formalism to calculate the coefficient of the direct process for the ions O_2^+ and N_2^+ at 300 °K and obtains values $\alpha_d(O_2^+) = 1.1 \times 10^{-7}$ cm^3/s and $\alpha_d(N_2^+) = 2.0 \times 10^{-7}$ cm^3/s at 300 °K, both of which are smaller than the corresponding experimental values. In all three cases, for NO^+, O_2^+, and N_2^+, the theory applies to ions in the $v = 0$ vibration state, while in the experimental measurements the ions may be in a low vibration state as they undergo recombination.

The final point to consider is the energy dependence of the dissociative recombination process. Highly simplified theories (7, 28) of the direct process (reaction [2]) indicate that for a favorable potential curve crossing between the molecular ion and the unstable excited molecule, α varies as $T_e^{-1/2}$ if the initial resonance capture step (left hand portion of reaction [2]) is rate limiting. It is estimated (27) that the indirect process may vary as rapidly as $T_e^{-1.5}$.

Since in some regions of the ionosphere the electron and ion temperatures are equal, while in others they are not (refer to Table I), it is interesting to compare the observed temperature dependences under these differing conditions. Unfortunately, the useful data are comparatively limited. In addition to the recent O_2^+ and N_2^+ results mentioned above, the two cases (10, 29–31) most accurately studied to date are the temperature dependences of $\alpha(Ne_2^+)$ and of $\alpha(Ar_2^+)$ under conditions where on the one hand $T_e = T_i = T_n$ and on the other $T_i = T_n$ and T_e is independently varied.

We noted earlier that $\alpha(N_2^+)$ varies little (21) under conditions where T_e, T_i, and T_n are simultaneously varied over the range 200–480 °K,

Can. J. Chem. Downloaded from www.nrcresearchpress.com by 210.87.254.42 on 09/05/12
For personal use only.

while there is some evidence (18) that $\alpha(N_2^+)$ varies rather *strongly* (approximately as $T_e^{-1/3}$) when T_e alone is varied (see Fig. 4). By way of contrast, Kasner (29) finds that $\alpha(Ne_2^+)$ varies as $T^{-0.42}$ ($T_e = T_i = T_n = T$) over the range 300–500 °K, while Frommhold *et al.* (10) find an essentially identical power law variation with *electron* temperature ($\alpha \sim T_e^{-0.43}$) over the range 300 °K $\leqslant T_e \leqslant$ 11 000 °K with $T_i = T_n =$ 300 °K. Finally, Fox and Hobson (30) carried out shock tube studies of the variation of $\alpha(Ar_2^+)$ under conditions such that $T_e = T_i = T_n$ over the range 1000–3000 °K and obtained a variation as $T^{-1.3}$. In this case, corresponding electron temperature variation studies of $\alpha(Ar_2^+)$ by Mehr and Biondi (31) revealed a weaker temperature dependence (as $T_e^{-0.67}$) over the range 300 °K $\leqslant T_e \leqslant$ 10 000 °K with $T_i = T_n = 300$ °K.

It is possible to account qualitatively for these strikingly different behaviors in terms of the details of the potential curve crossings between the molecular ion and the unstable molecule states and in terms of the changing vibrational state populations of the molecular ion with changing T_i (31). We point out the problem to demonstrate that present theoretical treatments of the dissociative recombination process are essentially in their infancy and to stress the critical importance of being able to specify the ions' electronic and vibrational states in laboratory measurements before the results can be applied with confidence to ionospheric calculations.

Ion–Ion Recombination

As in the case of electron–ion recombination, ion–ion recombination in the ionosphere is evidently controlled predominantly by two-body rather than three-body processes, with the possible exception of the lower end of the D region. At present there is somewhat more theoretical and experimental information available concerning the three-body, neutral stabilized, recombination process than two-body ion–ion recombination processes. This situation is changing rapidly, with a number of experimental and theoretical investigations of two-body processes involving ionospheric ions in progress.

A. Neutral Stabilized (Thomson) Recombination

Many years ago Thomson (32) proposed a simple theory of recombination between positive and negative ions which involved either ion's suffering a collision with a neutral molecule while within a certain "trapping distance" of the other. In reaction form the process may be represented by

$$[4] \qquad X^+ + Y^- + M \rightarrow X + Y + M$$

where X^+, Y^-, and M represent atomic *or* molecular positive ions, negative ions, and neutrals, respectively. Recently, there have been several theoretical treatments of this process (33–37) which either introduced refinements of Thomson's original method of calculation or used novel techniques (e.g. Monte Carlo calculations to follow the histories of the ion pairs).

Thomson (32), Natason (33), and Bates and Moffett (36) predict a variation of the three-body recombination coefficient as $T_i^{-2.5}$, and for the ions of the masses expected in the D region (e.g. NO^+, NO_2^-) a value $K_{\text{Thomson}} \sim 10^{-25}$ cm^6/s is estimated at $T_i = 350$ °K. The available experimental information (38–41) concerning the three-body coefficient largely supports the predicted magnitude. In particular, older studies by Gardner (38) in oxygen and by Sayers (39) in air verify the three-body character of the process and yield a value $K \sim 3 \times 10^{-25}$ cm^6/s at 300 °K.

Mahan and Person (40) used pulsed charge collection in a parallel plate ionization chamber apparatus (without mass identification) to determine the three-body coefficients for a whole series of ions. Of particular interest is their study of what they believe to be the reaction

$$[5] \qquad NO^+ + NO_2^- + N_2 \rightarrow \text{neutrals}$$

for which they obtain a value $K \simeq 2 \times 10^{-25}$ cm^6/s at 300 °K, in satisfactory agreement with the older results. Unfortunately, none of the experimental studies has established the temperature dependence of the recombination process.

From these results, it will be seen that, at the nominal lower D region neutral density of $\sim 10^{15}$ cm^{-3}, the Thomson recombination process presents an *effective* two-body coefficient, "α" $\equiv K[M] \sim 2 \times 10^{-10}$ cm^3/s. As we shall see in the next subsection, true two-body processes such as mutual neutralization apparently provide a much greater ion–ion recombination rate.

B. Two-Body (Mutual Neutralization) Recombination

Probably the simplest and most efficient of the two-body ion–ion recombination processes is that of mutual neutralization, in which the electron is captured from the negative ion by the

TABLE II

Two-body ion–ion recombination coefficients at 300 °K

Investigators	α (cm^3/s)	Ions	Remarks	Reference
Hirsch *et al.*	$(4.4 \pm 1) \times 10^{-8}$	NO^+, NO_2^-, NO_3^-	Mass-identified ions	45
Mahan and Person	$(2.0 \pm 0.5) \times 10^{-7}$	NO^+(?), NO_2^-(?)	No mass analysis	40
Greaves	1×10^{-7}	I_2^+, I^- Br_2^+, Br^-	Mass analysis; variation as $T_i^{-1.5}$ over range 300–340 °K	43, 44
Baulknight and Bortner	5×10^{-8}	O^+, O^- N^+, O^-	Theoretical estimate; variation as $T_i^{-0.5}$ predicted	42

positive ion in a reaction of the form

[6] $$X^+ + Y^- \rightarrow X^* + Y$$

where, once again, the symbols X and Y may refer either to atomic or molecular species. The energetics of the reaction (i.e., the ionization potential of the positive ion and the electron affinity of the negative ion) are such that in many cases, one or both of the neutrals produced may be in excited states.

Theoretical calculations by Baulknight and Bortner (42) for atomic species, i.e. $O^+ + O^-$ and $N^+ + O^-$, suggest that at 300 °K a mutual neutralization coefficient, $\alpha_{mn} \sim 5 \times 10^{-8}$ cm^3/s is to be expected. Further, a variation as $T_i^{-0.5}$ is predicted. There are few experimental studies of mass-identified ionospheric ions with which to compare these predictions; therefore we shall also discuss information obtained for non-ionospheric species.

Greaves (43, 44) employed an afterglow technique making use of radio frequency ($\sim$ 10 MHz) determinations of the dielectric coefficient of the ions to determine the decay of ion concentration during the afterglow. Ion identification was supplied by a small, differentially pumped mass spectrometer appended to the experimental tube. Halogen ions were studied, and for the systems $I_2^+ + I^-$ and $Br_2^+ + Br^-$, a coefficient $\alpha_{mn} \approx 1 \times 10^{-7}$ cm^3/s was obtained from decay curves which clearly exhibited recombination control of the afterglow. Over the temperature range 300–340 °K a decrease of α_{mn} from 1.2×10^{-7} to 1.0×10^{-7} cm^3/s was noted in the case of iodine, suggesting an approximate variation as $T_i^{-1.5}$ over this *very* limited range.

Mahan and Person (40), using the technique described earlier (no mass analysis), have studied ionic recombination in photoionized NO – NO_2 – noble gas mixtures and have argued that the ions under study are probably NO^+ and NO_2^-. From recombination controlled afterglow decays they obtained a value $\alpha_{mn} = (2.0 \pm 0.5) \times 10^{-7}$ cm^3/s, at 300 °K. (The rather large error limit arises chiefly from uncertainties concerning the spatial distribution of the ions in the measuring chamber; refer to the discussion in Section B under heading Electron–Ion Recombination concerning eq. [3] for the corresponding electron–ion case.)

Very recently, Hirsch *et al.* (45) have carried out afterglow studies of ion–ion recombination using an r-f impedance probe to determine the decay of ion concentration in air-like, N_2–O_2 mixtures following ionization by a pulse of MeV electrons. A differentially pumped mass-spectrometer sampled the ions diffusing to the walls of the experimental chamber. For the case in which NO^+, NO_2^-, and NO_3^- were the principal ions in the afterglow they obtained a value $\alpha_{mn} = (4.4 \pm 1) \times 10^{-8}$ cm^3/s at 300 °K.

Thus, it appears that the various studies indicate that the two-body ion–ion recombination coefficient is of the order of 10^{-7} cm^3/s at 300 °K; however, much work is needed to establish more definitely the identities of the ions undergoing recombination and then to specify the particular electronic and vibrational states of the ions. The results of the various investigations are summarized in Table II.

We have omitted from our discussion other two-body ion–ion recombination processes which involve rearrangement of the atoms in the molecules during the reaction, in as much as estimates (46) of the rates of such processes suggest that they are orders of magnitude smaller than the simple mutual neutralization process. Thus, such processes would not be expected to play a

Can. J. Chem. Downloaded from www.nrcresearchpress.com by 210.87.254.42 on 09/05/12
For personal use only.

significant role in charge removal from the ionosphere.

Acknowledgments

The author wishes to thank his colleagues, especially W. H. Kasner, C. S. Weller, L. Frommhold, and F. J. Mehr for their important contributions to some of the researches described in this paper, and T. M. Donahue for his helpful discussions concerning current ideas of the ionospheric constituents and conditions.

1. M. A. Biondi. Ann. de Geophysique, **20**, 34 (1964).
2. M. A. Biondi. *In* Space research VII. *Edited by* R. L. Smith-Rose, in cooperation with S. A. Bowhill and J. W. King. North-Holland Publ. Co., Amsterdam. 1967.
3. D. R. Bates, A. E. Kingston, and R. W. P. McWhirter. Proc. Roy. Soc. London, Ser. A **267**, 297 (1962).
4. E. Hinnov and J. G. Hirschberg. Phys. Rev. **125**, 795 (1962).
5. D. R. Bates and S. P. Khare. Proc. Phys. Soc. **85**, 231 (1965). D. R. Bates and N. Young. Private communication.
6. M. J. Seaton. Monthly Notices Roy. Astron. Soc. **119**, 81 (1959).
7. D. R. Bates and A. Dalgarno. *In* Atomic and molecular processes. *Edited by* D. R. Bates. Academic Press, Inc., New York and London. 1962.
8. R. G. Fowler and W. R. Atkinson. Phys. Rev. **113**, 1268 (1959).
9. C. S. Weller and M. A. Biondi. Bull. Am. Phys. Soc. **13**, 199 (1968). C. S. Weller and M. A. Biondi. Phys. Rev. **172**, 198 (1968).
10. L. Frommhold, M. A. Biondi, and F. J. Mehr. Phys. Rev. **165**, 44 (1968). L. Frommhold and M. A. Biondi. Ann. Phys. N.Y. **48**, 407 (1968).
11. R. C. Gunton and T. M. Shaw. Phys. Rev. **140**, A756 (1965).
12. R. A. Young and G. St. John. Phys. Rev. **152**, 25 (1966).
13. R. P. Stein, M. Schiebe, M. W. Syverson, T. M. Shaw, and R. C. Gunton. Phys. Fluids, **7**, 1641 (1964).
14. S. C. Lin and J. D. Tease. Phys. Fluids, **6**, 355 (1963).
15. W. H. Kasner and M. A. Biondi. Bull. Am. Phys. Soc. **12**, 218 (1967). W. H. Kasner and M. A. Biondi. Phys. Rev. **174**, 139 (1968).
16. E. P. Gray and D. E. Kerr. Ann. Phys. N.Y. **17**, 276 (1962).
17. M. H. Mentzoni. J. Appl. Phys. **36**, 57 (1965).
18. F. J. Mehr and M. A. Biondi. Bull. Am. Phys. Soc. **13**, 189 (1968). F. J. Mehr and M. A. Biondi. Phys. Rev. To be published.
19. E. C. Zipf. Bull. Am. Phys. Soc. **11**, 494 (1966).
20. W. H. Kasner and M. A. Biondi. Phys. Rev. **137**, A317 (1965).
21. W. H. Kasner. Phys. Rev. **164**, 194 (1967).
22. R. Hackam. Planetary Space Sci. **13**, 667 (1965).
23. (*a*) J. A. Green and T. M. Sugden. Ninth symposium on combustion. The Combustion Institute, Pittsburgh, Pa., 1963. p. 607. (*b*) L. N. Wilson and E. W. Evans. J. Chem. Phys. **46**, 859 (1967).
24. C. S. Weller and M. A. Biondi. Phys. Rev. Letters, **19**, 59 (1967).
25. R. L. Wilkins. J. Chem. Phys. **44**, 1884 (1966).
26. C. S. Warke. Phys. Rev. **144**, 120 (1966).
27. J. N. Bardsley. J. Phys. B**1**, 365 (1968).
28. D. R. Bates. Phys. Rev. **77**, 718 (1950); **78**, 492 (1950); **82**, 103 (1951).
29. W. H. Kasner. Phys. Rev. **167**, 148 (1968).
30. J. N. Fox and R. M. Hobson. Phys. Rev. Letters, **17**, 161 (1966), and Contributed papers of the Eighth international conference on phenomena in ionized gases, Vienna. Springer-Verlag, Vienna. 1967. p. 5.
31. F. J. Mehr and M. A. Biondi. Phys. Rev. **176**, 322 (1968).
32. J. J. Thomson. Phil. Mag. [6], **47**, 337 (1924).
33. G. L. Natason. Zhur. Tekhn. Fiz. **29**, 1373 (1959). [English transl.: Soviet Phys. **4**, 1263 (1959).]
34. K. A. Brueckner. J. Chem. Phys. **40**, 439 (1964).
35. P. J. Feibelman. J. Chem. Phys. **42**, 2462 (1965).
36. D. R. Bates and R. J. Moffett. Proc. Roy. Soc. London, Ser. A **291**, 1 (1966).
37. I. S. Veselovskii. J. Exptl. Theoret. Phys. USSR. **52**, 1034 (1967), translated in Sov. Phys. JETP **25**, 687 (1967).
38. M. E. Gardner. Phys. Rev. **53**, 75 (1938).
39. J. Sayers. Proc. Roy. Soc. London, Ser. A **169**, 83 (1938).
40. B. H. Mahan and J. C. Person. J. Chem. Phys. **40**, 392, 3683 (1964).
41. S. McGowan. Can. J. Phys. **45**, 439 (1967).
42. C. W. Baulknight and M. H. Bortner. Report No. AFCRL-64-142, Air Force Cambridge Research Laboratories, Bedford, Mass., Jan. 1964, unpublished.
43. C. Greaves. J. Electronics and Control **17**, 171 (1964).
44. J. Sayers. *In* Atomic and Molecular Processes. *Edited by* D. R. Bates. Academic Press, Inc., New York and London. 1962.
45. M. N. Hirsch, G. M. Halpern, and N. S. Wolf. Bull. Am. Phys. Soc. **13**, 199 (1968).
46. M. H. Bortner. Report No. AFCRL-65-392. Air Force Cambridge Research Laboratories, Bedford, Mass., April, 1965. Unpublished.

Comments, Replies, and Summary

COMMENTS BY F. E. NILES

In view of the recent D region mass spectrometric measurements of Narcisi and others, the identity of the principal positive ion at 60 km as NO^+ as given in Table I is highly questionable. The measurements reveal that an ion with mass 37, probably $H_5O_2^+$, is the dominant positive ion for most of the D region. Other water-clustered ions were also detected.

Can. J. Chem. Downloaded from www.nrcresearchpress.com by 210.87.254.42 on 09/05/12
For personal use only.

significant role in charge removal from the ionosphere.

Acknowledgments

The author wishes to thank his colleagues, especially W. H. Kasner, C. S. Weller, L. Frommhold, and F. J. Mehr for their important contributions to some of the researches described in this paper, and T. M. Donahue for his helpful discussions concerning current ideas of the ionospheric constituents and conditions.

1. M. A. Biondi. Ann. de Geophysique, **20**, 34 (1964).
2. M. A. Biondi. *In* Space research VII. *Edited by* R. L. Smith-Rose, in cooperation with S. A. Bowhill and J. W. King. North-Holland Publ. Co., Amsterdam. 1967.
3. D. R. Bates, A. E. Kingston, and R. W. P. McWhirter. Proc. Roy. Soc. London, Ser. A **267**, 297 (1962).
4. E. Hinnov and J. G. Hirschberg. Phys. Rev. **125**, 795 (1962).
5. D. R. Bates and S. P. Khare. Proc. Phys. Soc. **85**, 231 (1965). D. R. Bates and N. Young. Private communication.
6. M. J. Seaton. Monthly Notices Roy. Astron. Soc. **119**, 81 (1959).
7. D. R. Bates and A. Dalgarno. *In* Atomic and molecular processes. *Edited by* D. R. Bates. Academic Press, Inc., New York and London. 1962.
8. R. G. Fowler and W. R. Atkinson. Phys. Rev. **113**, 1268 (1959).
9. C. S. Weller and M. A. Biondi. Bull. Am. Phys. Soc. **13**, 199 (1968). C. S. Weller and M. A. Biondi. Phys. Rev. **172**, 198 (1968).
10. L. Frommhold, M. A. Biondi, and F. J. Mehr. Phys. Rev. **165**, 44 (1968). L. Frommhold and M. A. Biondi. Ann. Phys. N.Y. **48**, 407 (1968).
11. R. C. Gunton and T. M. Shaw. Phys. Rev. **140**, A756 (1965).
12. R. A. Young and G. St. John. Phys. Rev. **152**, 25 (1966).
13. R. P. Stein, M. Schiebe, M. W. Syverson, T. M. Shaw, and R. C. Gunton. Phys. Fluids, **7**, 1641 (1964).
14. S. C. Lin and J. D. Tease. Phys. Fluids, **6**, 355 (1963).
15. W. H. Kasner and M. A. Biondi. Bull. Am. Phys. Soc. **12**, 218 (1967). W. H. Kasner and M. A. Biondi. Phys. Rev. **174**, 139 (1968).
16. E. P. Gray and D. E. Kerr. Ann. Phys. N.Y. **17**, 276 (1962).
17. M. H. Mentzoni. J. Appl. Phys. **36**, 57 (1965).
18. F. J. Mehr and M. A. Biondi. Bull. Am. Phys. Soc. **13**, 189 (1968). F. J. Mehr and M. A. Biondi. Phys. Rev. To be published.
19. E. C. Zipf. Bull. Am. Phys. Soc. **11**, 494 (1966).
20. W. H. Kasner and M. A. Biondi. Phys. Rev. **137**, A317 (1965).
21. W. H. Kasner. Phys. Rev. **164**, 194 (1967).
22. R. Hackam. Planetary Space Sci. **13**, 667 (1965).
23. (*a*) J. A. Green and T. M. Sugden. Ninth symposium on combustion. The Combustion Institute, Pittsburgh, Pa., 1963. p. 607. (*b*) L. N. Wilson and E. W. Evans. J. Chem. Phys. **46**, 859 (1967).
24. C. S. Weller and M. A. Biondi. Phys. Rev. Letters, **19**, 59 (1967).
25. R. L. Wilkins. J. Chem. Phys. **44**, 1884 (1966).
26. C. S. Warke. Phys. Rev. **144**, 120 (1966).
27. J. N. Bardsley. J. Phys. B**1**, 365 (1968).
28. D. R. Bates. Phys. Rev. **77**, 718 (1950); **78**, 492 (1950); **82**, 103 (1951).
29. W. H. Kasner. Phys. Rev. **167**, 148 (1968).
30. J. N. Fox and R. M. Hobson. Phys. Rev. Letters, **17**, 161 (1966), and Contributed papers of the Eighth international conference on phenomena in ionized gases, Vienna. Springer-Verlag, Vienna. 1967. p. 5.
31. F. J. Mehr and M. A. Biondi. Phys. Rev. **176**, 322 (1968).
32. J. J. Thomson. Phil. Mag. [6], **47**, 337 (1924).
33. G. L. Natason. Zhur. Tekhn. Fiz. **29**, 1373 (1959). [English transl.: Soviet Phys. **4**, 1263 (1959).]
34. K. A. Brueckner. J. Chem. Phys. **40**, 439 (1964).
35. P. J. Feibelman. J. Chem. Phys. **42**, 2462 (1965).
36. D. R. Bates and R. J. Moffett. Proc. Roy. Soc. London, Ser. A **291**, 1 (1966).
37. I. S. Veselovskii. J. Exptl. Theoret. Phys. USSR. **52**, 1034 (1967), translated in Sov. Phys. JETP **25**, 687 (1967).
38. M. E. Gardner. Phys. Rev. **53**, 75 (1938).
39. J. Sayers. Proc. Roy. Soc. London, Ser. A **169**, 83 (1938).
40. B. H. Mahan and J. C. Person. J. Chem. Phys. **40**, 392, 3683 (1964).
41. S. McGowan. Can. J. Phys. **45**, 439 (1967).
42. C. W. Baulknight and M. H. Bortner. Report No. AFCRL-64-142, Air Force Cambridge Research Laboratories, Bedford, Mass., Jan. 1964, unpublished.
43. C. Greaves. J. Electronics and Control **17**, 171 (1964).
44. J. Sayers. *In* Atomic and Molecular Processes. *Edited by* D. R. Bates. Academic Press, Inc., New York and London. 1962.
45. M. N. Hirsch, G. M. Halpern, and N. S. Wolf. Bull. Am. Phys. Soc. **13**, 199 (1968).
46. M. H. Bortner. Report No. AFCRL-65-392. Air Force Cambridge Research Laboratories, Bedford, Mass., April, 1965. Unpublished.

Comments, Replies, and Summary

COMMENTS BY F. E. NILES

In view of the recent D region mass spectrometric measurements of Narcisi and others, the identity of the principal positive ion at 60 km as NO^+ as given in Table I is highly questionable. The measurements reveal that an ion with mass 37, probably $H_5O_2^+$, is the dominant positive ion for most of the D region. Other water-clustered ions were also detected.

Can. J. Chem. Downloaded from www.nrcresearchpress.com by 210.87.254.5 on 09/05/12
For personal use only.

Can. J. Chem. Downloaded from www.nrcresearchpress.com by 210.87.254.5 on 09/05/12
For personal use only.

REPLY BY M. A. BIONDI

The point is well taken, and Table I and the text have been modified to consider these ions.

COMMENTS BY J. N. BARDSLEY

The well-established theory of dissociative recombination suggests that for a fixed ion temperature the recombination coefficient should vary with the electron temperature, T_e, approximately as $T_e^{-0.5}$. Several experimental investigations have shown variations significantly different from the predicted behavior. I have recently suggested an alternative mechanism for dissociative recombination which could lead to a different temperature dependence. However, this mechanism seems to be possible only at low temperatures, say below 1000 °K, and probably cannot account for deviations from a $T_e^{-0.5}$ law at higher temperatures.

A more likely explanation, as described by Dr. Biondi, is that the deviations are due to the presence of excited vibrational levels of the ion. Experiments carried out on the rare gases have revealed very different temperature variations, depending upon whether the whole gas is heated or the electrons alone. It would be interesting theoretically to check the consistency of these results, but this is not possible due to the paucity of information about the potential curves of rare gas ions. It would, therefore, be useful if the consequences of the two methods of heating could be measured in each of the atmospheric gases.

COMMENTS BY L. M. BRANSCOMB

Since the lifetime of a negative ion in the mesosphere against ion–ion recombination is $\tau = (\gamma N^+)^{-1}$ and even in disturbed (e.g. Polar Cap Absorption) atmospheres the ion density is only $\lesssim 10^5$ while $\gamma \sim 10^{-7}$–10^{-8} cm^3/s, τ is quite long, perhaps 50–100 s or longer, if the ions are "terminal ions" in the sense that they are not subject to photodetachment or associative detachment. Niles commented that in the mesosphere (when H_2O exceeds N^+ by 10^6 or so) hydration of the ions, both positive and negative, will proceed substantially more quickly.

What evidence, experimental or theoretical, is there concerning the effect on the two-body ion recombination rate of clustering? Has a process such as $X^+ + Y^- \cdot (H_2O) \rightarrow X + Y + H_2O$ been examined as a possible efficient stabilization mechanism for the recombination increasing its rate?

REPLY BY M. A. BIONDI

I am not aware of any experimental or theoretical evidence concerning ion–ion recombination rates where one or both of the partners are in a hydrated form.

COMMENTS BY MICHAEL B. McELROY

In reply to a question from the chair (Donahue) concerning recombination processes of interest in other planetary atmospheres, I mentioned the known importance of CO_2^+ on Venus and Mars and the probable importance of HCO_2^+ formed either by $H_2^+ + CO_2 \rightarrow HCO_2^+$ or $CO_2^+ + H_2$. In the outer planets H_3^+ recombination is of interest.

COMMENTS[1] BY WILLIAM ABERTH[2] AND JAMES R. PETERSON[2]

Ion–ion neutralization cross sections have been obtained for the reactants $N^+ + O^-$ (1), $O_2^+ + O_2^-$, and $N_2^+ + O_2^-$. The range of barycentric kinetic energies covered is between 0.1 and 98 eV for $N^+ + O^-$ and $N_2^+ + O_2^-$, and between 0.1 and 50 eV for $O_2^+ + O_2^-$ with about 0.1 eV resolution. The products of the neutralization cross section, Q, times the relative velocity, v, of the $N^+ + O^-$ and the $N_2^+ + O_2^-$ systems, are nearly independent of energy, with values close to 10^{-7} cm^3/s, except below 0.5 eV where a rapid increase of Qv with decreasing energy is observed. The $O_2^+ + O_2^-$ data can be described by the equation $Qv = -3.1 \times 10^{-14}v + 5.7 \times 10^{-8}$ cm^3/s. No rapid increase of Qv with decreasing v below 0.5 eV is observed. However, this system exhibits a greater degree of scatter in the data and such structure may consequently be unobservable.

The merging beams technique (2) involves superimposing particle beams of different speeds and observing their interactions over a known

[1]This work was sponsored by the Defense Atomic Support Agency Reaction Rate Program through contract with the Air Force Cambridge Research Laboratories.

[2]Address: Stanford Research Institute, Menlo Park, California 94025.

Can. J. Chem. Downloaded from www.nrcresearchpress.com by 210.87.254.5 on 09/05/12
For personal use only.

path length. In the present apparatus the positive and negative ion beams are deflected by a common magnetic field. Both beams have keV energies in the laboratory coordinate system but can have relative energies as low as 0.1 eV while merged. After traveling together about 33 cm, the beams are separated by electrostatic deflection and collected in two Faraday cups. The neutral particles formed by ion–ion neutralization (as well as a much larger "background" of neutrals formed by electron stripping and capture reactions of the beam ions with the ambient gas) continue along the superimposed beam direction. The neutrals are detected indirectly by the secondary electron emission produced when they collide with a stainless steel surface. The component of this current due to ion–ion neutralization is separated from the large background by a beam-chopping technique. The neutralization products are not identified.

1. W. ABERTH, J. R. PETERSON, D. C. LORENTS, and C. J. COOK. Phys. Rev. Letters, **20**, 979 (1968).
2. S. M. TRUJILLO, R. H. NEYNABER, and E. W. ROTHE. Rev. Sci. Instr. **37**, 1655 (1966).

COMMENTS BY FRANKLIN E. NILES

The merging beams experiment has revealed and will reveal interesting results; however, as presently constructed the experiment is deficient in that the products of the reaction are not identified. Unless the products of a reaction can be identified, it is better to ascribe a cross section or a rate constant to a reaction without writing down the products, e.g., $O_2^+ + O_2^- \rightarrow$ products and not $O_2^+ + O_2 \rightarrow 2O_2$. Whenever many reactions are occurring together, the products of the reactions are important. In particular, mutual neutralization with dissociation may be an important source of atomic nitrogen and atomic oxygen in the upper atmosphere. Consequently, rate constants for reactions such as $O_2^+ + O_2^- \rightarrow O + O + O_2$ and $NO^+ + O_2^- \rightarrow N + O + O_2$ need to be determined.

REPLY BY J. R. PETERSON

Dr. Niles' comment is certainly valid. The fact that molecular reaction products were printed on the slides was actually accidental rather than intentional. I would guess that a substantial number, say 25%, of the product molecules are in unbound final states in the $O_2^+ + O_2^-$ reaction, but it is virtually impossible to determine which of the many possible states are involved, at least in our experiment. In principle, it is possible to determine the excited final states in some atomic cases by observing the allowed radiation. We have considered trying to do this for $H^+ + H^-$, where presumably only the $n = 2$ and $n = 3$ states are excited to any extent. I suspect that the most promising method of determining the distribution of final states (including repulsive molecular states) may be through theory, and hopefully we can aid the development of a reliable theory by making good total cross section measurements, as a function of energy, for a number of species.

SUMMARY (1) BY CHAIRMAN, T. M. DONAHUE[3]

With one major exception, the state of agreement between ionospheric requirements and laboratory measurements for dissociative recombination coefficients is now excellent. The temperature dependences for $\alpha(NO^+)$ and $\alpha(O_2^+)$ reported here are very close to those required by the terrestrial ionosphere, nighttime and daytime from the E region to the F_2 peak.

The troubles lie in the D region below 80 km. Here recent measurements of nitric oxide densities by Pearce (1) give values so large that Lyman α ionization and charge transfer from O_2^+ produce NO^+ ten times as fast as dissociative recombination can remove it. This is supposing that

$$n_e = n(NO^+)$$

and

$$\alpha(NO^+) = 8 \times 10^{-7}\ \text{cm}^3\ \text{s}^{-1}$$

In this region, however, such ions as $(H_3O^+)\cdot(H_2O)_n$ are dominant. There is at least a chance that these ions are formed from NO^+ (Ferguson and Fehsenfeld, private communication). There is also a good possibility that negative ion to positive ion density ratios are large at 70 km. (L. Hale, private communication.) Still the problem remains that the source is so strong that recombination coefficients, whether dissociative or neutralization, must be very large for the ions present in the steady state. If, for

[3]Address: Physics Department, University of Pittsburgh, Pittsburgh, Pennsylvania 15213.

example, at 70 km

$$n(NO^+) = 3 \times 10^2 \text{ cm}^{-3}$$
$$n[H_3O^+ \cdot (H_2O)_n] = 1.5 \times 10^3 \text{ cm}^{-3}$$
$$n_e = 3 \times 10^2 \text{ cm}^{-3}$$
$$n^- = 1.5 \times 10^3 \text{ cm}^{-3}$$

the steady state requires that

$$(\alpha + 5\alpha_i)H_3O^+ \cdot (H_2O)_n + \alpha_i(NO^+) = 10^{-4} \text{ cm}^3 \text{ s}^{-1}$$

Hence it appears that recombination rates for hydrated hydronium ions below 200 °K ought to be measured.

The problem of the metal ion removal in sporadic E layers and near 95 km requires eventually that we know α's for species such as MgO^+ or $MgO_2{}^+$, although the ion chemistry of these species is completely mysterious.

Finally, as McElroy mentions, the other planets involve other ions. There is a possibility that $HCO_2{}^+$ is formed at high rates on Venus. The outer planets have atmospheres containing copious quantities of H_2. In their ionospheres $H_3{}^+$ should appear prominently, and at temperatures perhaps as low as 100 °K. Recombination rates for such ions are of current interest.

1. J. P. PEARCE. Ph.D. Thesis, University of Colorado, Colorado. 1968.

Can. J. Chem. Downloaded from www.nrcresearchpress.com by 210.87.254.5 on 09/05/12
For personal use only.

Inelastic collisions at low energies

A. DALGARNO
Harvard College Observatory and Smithsonian Astrophysical Observatory, Cambridge, Massachusetts
Received December 12, 1968

A summary is presented of the processes by which low energy electrons lose energy in moving through the atmosphere and estimates are given of the cross sections and energy loss rates. The mechanisms by which thermal electrons cool are described and the cooling efficiencies are listed.

Canadian Journal of Chemistry, 47, 1723 (1969)

Can. J. Chem. Downloaded from www.nrcresearchpress.com by 210.87.254.6 on 09/05/12
For personal use only.

Introduction

Low energy electrons, moving in the upper atmospheres of the planets, produce luminosity by electronic excitation of the atmospheric constituents and they modify the chemistry of the upper atmospheres through the production of metastable and vibrationally excited species. The low energy electrons also selectively heat the ambient electron and ion gases so that their temperatures tend to rise above that of the neutral atmosphere. A detailed description of the possible modes of energy loss is a fundamental part of the physics and chemistry of planetary atmospheres.

Elastic Collisions

An important energy loss mechanism for low energy electrons in the ionosphere is provided by the transfer of momentum in elastic collisions of the low energy electrons with the thermal electrons of the ionospheric plasma, the high efficiency arising from the equal masses and the long range of the Coulomb repulsion. According to Butler and Buckingham (1), the mean rate of energy loss due to elastic collisions of electrons of velocity v with charged particles of mass M, velocity V, and density n_e is given by

$$[1] \qquad \frac{1}{n_e}\frac{dE}{dx} = \frac{-8\pi^{\frac{1}{2}}}{M}\frac{e^4}{vV}F(v/V)\ln\Lambda$$

where Λ is a parameter characterizing the plasma and

$$[2] \quad F(x) = \frac{1}{x}\int_0^x \exp(-x^2)dx - \left(1+\frac{m}{M}\right)\exp(-x^2)$$

Values of [1] for collisions with electrons have been tabulated by Dalgarno, McElroy, and Moffett (2). Provided that the electron energy exceeds 3 eV, [1] simplifies in the case of collisions with electrons to

$$[3] \quad \frac{dE}{dx} = -n_e\frac{1.3\times10^{-13}}{E}\ln\Lambda \quad \text{eV cm}^{-1}$$

where E is the electron energy measured in eV. Values of $\ln\Lambda$ have been tabulated by Henry and McElroy (3). For plasmas typical of planetary ionospheres, $\ln\Lambda$ is of the order of 15 and [3] is approximately

$$[4] \quad \frac{dE}{dx} = -n_e\times\frac{2\times10^{-12}}{E} \quad \text{eV cm}^{-1}$$

Because of the mass M in the denominator of [1], energy loss through elastic collisions with positive ions is negligible in comparison to collisions with electrons.

Because of the greater neutral particle density, elastic collisions with neutral particles might be an important process of energy loss. For an electron energy substantially in excess of the mean thermal energy of the neutral particles, the mean rate of energy loss may be expressed as

$$[5] \qquad \frac{dE}{dx} = -n(\mathrm{A})\frac{2m}{M}E\,\sigma_m(E)$$

where $n(\mathrm{A})$ is the number density of neutral particles A of mass M and $\sigma_m(E)$ is the momentum transfer cross section, defined in terms of the differential cross section $I(\theta|E)$ for scattering through an angle θ by

$$[6] \quad \sigma_m(E) = 2\pi\int_{-1}^{+1} I(\theta|E)(1-\cos(\theta))\times d(\cos\theta)$$

Since σ_m is of the order of 10^{-15} cm^2, it is clear that the energy loss by momentum transfer in collisions with neutral particles is negligible

Can. J. Chem. Downloaded from www.nrcresearchpress.com by 210.87.254.6 on 09/05/12
For personal use only.

compared to [1] for the ambient electron and neutral particle densities occuring in planetary ionospheres.

Rotational Excitation

Slow electrons can lose energy by the excitation of the rotational levels of the molecular atmospheric constituents. If it is assumed that rotational excitation is caused largely by the long range interaction of the electron with the quadrupole moment q of the molecule, the Born approximation yields the simple formula for the cross section for excitation from rotational level j to rotational level $j+2$

$$[7] \quad \sigma(j,j+2|E) = 4.7 \times q^2 \frac{(j+1)(j+2)}{(2j+1)(2j+3)} \times 10^{-17} \quad \text{cm}^2$$

(4) where q is measured in atomic units. For N_2, $q = -1.1$ (5). More refined theoretical studies (6) have shown that long range polarization interactions, short range interactions, and distortion are significant effects. However, the low energy experiment data of Engelhardt, Phelps, and Risk (7) can be satisfactorily reproduced by postulating cross sections of the form [7]. In calculating the associated rate of energy loss, it is necessary to take account of rotational de-excitation processes also. Approximate values of the rate of energy loss have been computed by Takayanagi and Takahashi (8). For energies of about 0.5 eV

$$\frac{dE}{dx} = -n(N_2) \times 5 \times 10^{-19} \quad \text{eV cm}^{-1}$$

Molecular oxygen has a small quadrupole moment $q = -0.3$ (5) and the rotational excitation of oxygen may be strongly modified by short range interactions (9). Experimental studies by Mentzoni and Rao (10) showed that the earlier calculations (10, 11) underestimated the energy loss rate. No satisfactory theoretical description of the rotational excitation of oxygen has yet been presented and the most precise information is that derived from swarm data by Hake and Phelps (12). It appears from the analysis that a gross representation of the rotational cross sections for oxygen is provided by [7] with an empirical value of 1.8 for $|q|$. For energies of about 0.5 eV, the associated energy loss rate is approximately

$$\frac{dE}{dx} = -n(O_2) \times 10^{-18} \quad \text{eV cm}^{-1}$$

Rotational excitation of carbon dioxide may be important in the atmospheres of Mars and Venus. Hake and Phelps (12) were unable to derive rotational cross sections from swarm data. The quadrupole moment of carbon dioxide is large and [7] may prove a satisfactory description. Using $q = -3.2$, the energy loss rate is comparable to that for molecular nitrogen.

Fine Structure Transitions

In the upper atmosphere of the planet Earth, energy loss can occur through the excitation of the fine structure levels of atomic oxygen

$$[10] \quad e + O(^3P_J) \rightarrow e + O(^3P_{J'})$$

the cross sections for which have been calculated by Breig and Lin (13). For electrons of energy 0.5 eV, the energy loss rate is approximately

$$[11] \quad \frac{dE}{dx} = -n(O) \times 2 \times 10^{-18} \quad \text{eV cm}^{-1}$$

Vibrational Excitation

It is clear from a comparison of [8], [9], and [11] with [14] that except in regions of very low electron density, neither rotational excitation nor fine-structure excitation compares in efficiency with energy loss through elastic collisions with the ambient electron gas. With increasing energy, vibrational excitation becomes possible and it does provide a mode of energy loss which is competitive with elastic collisions (2).

The vibrational excitation of molecular nitrogen

$$[12] \quad e + N_2(v=0) \rightarrow > e + N_2(v')$$

has been studied experimentally by Haas (14), Schulz (15), Schulz and Koon (16), Boness and Hasted (17), Andrick and Ehrhardt (18), and Ehrhardt and Willmann (19), and theoretical interpretations of the process in terms of a resonating $^2\pi_g$ state of N_2^- have been developed by Schulz (15), Herzenberg and Mandl (20), Chen (21), Gilmore (22), and Bardsley, Mandl, and Wood (23). The associated energy loss rates have been calculated by Dalgarno, McElroy, and

Can. J. Chem. Downloaded from www.nrcresearchpress.com by 210.87.254.6 on 09/05/12
For personal use only.

Moffett (2) and Takayanagi and Takahashi (8). They pass through a maximum value, given by

$$[13] \quad \frac{dE}{dx} = -n(N_2) \times 3 \times 10^{-16} \quad \text{eVcm}^{-1}$$

at an energy E of 2.5 eV. The efficiency decreases rapidly both at low and at high energies. Vibrational excitation of molecular nitrogen is the dominant mode of energy loss for electrons with energies in the range from 6.5 to about 1 eV throughout most of the F region of the ionosphere.

Vibrational excitation cross sections for molecular oxygen have been derived by Hake and Phelps (12) from swarm data and from cross section measurements by Schulz and Dowell (24) and Boness and Hasted (17). The associated energy loss rates have been calculated by Henry and McElroy (3). They have a flat maximum for energies between 1 and 1.8 eV, given by

$$[14] \quad \frac{dE}{dx} = -n(O_2) \times 8 \times 10^{-18} \quad \text{eV cm}^{-1}$$

and the process is important in and below the ionospheric E region.

Henry and McElroy (3) have also used cross sections derived by Hake and Phelps (12) to calculate the energy loss rates associated with the vibrational excitation of carbon dioxide. The efficiency passes through a maximum given by

$$[15] \quad \frac{dE}{dx} = -n(CO_2) \times 1.5 \times 10^{-16} \quad \text{eV cm}^{-1}$$

at an energy near 0.7 eV and a second maximum, given by

$$[16] \quad \frac{dE}{dx} = -n(CO_2) \times 3.1 \times 10^{-16} \quad \text{eV cm}^{-1}$$

at an energy near 4 eV. Between 1.5 and 3.5 eV, the energy loss rate is given by

$$[17] \quad \frac{dE}{dx} = -n(CO_2) \times 2.5 \times 10^{-17} \quad \text{eV cm}^{-1}$$

Vibrational excitation of carbon dioxide is an important energy loss mechanism in the atmospheres of Mars and Venus. Vibrational excitation is important not only as a mechanism for extracting energy from the energetic electrons but also because the presence of vibrationally excited species can influence the chemistry of the atmospheres. Thus Schmeltekopf, Fehsenfeld, Gilman, and Ferguson (25) have found that the rate of the ion–molecule reaction

$$[18] \quad O^+ + N_2 \rightarrow NO^+ + O$$

increases rapidly with increasing vibrational temperature above 1500 °K (though the effect of the increased ion removal rate of [18] will be balanced in part by an increase in the ion production rate), and Walker (26) has suggested that vibrationally excited nitrogen may heat the electron gas in the E region through super-elastic collisions

$$[19] \quad N_2(v) + e \rightarrow N_2(v') + e$$

Rate coefficients for [19] may be derived from the model calculations of Chen (21).

Electron impact is not the only source of vibrational excitation. The deactivation process

$$[20] \quad O(^1D) + N_2 \rightarrow O(^3P) + N_2^*$$

may be a more abundant source (26, 27) as may be fluorescence processes such as

$$[21] \quad \begin{aligned} &O_2(X^3\Sigma_g^-, v = 0) + h\nu \rightarrow O_2(B^3\Sigma_u^-, v) \\ &O_2(B^3\Sigma_u^-, v) \rightarrow O_2(X^3\Sigma_g^-, v') + h\nu \end{aligned}$$

Electronic Excitation

Molecular oxygen has a number of low-lying metastable levels. The $a^1\Delta_g$ level has a threshold of 0.98 eV and the $b^1\Sigma_g^+$ level has a threshold of 1.63 eV. The cross sections for exciting the $a^1\Delta_g$ and $b^1\Sigma_g^+$ levels are not known with any certainty and their influence on the energy loss rates has been included approximately in the energy loss rates of the section associated with vibrational excitation.

The threshold of the $A^3\Sigma_u^+$ level of molecular oxygen occurs at 4.5 eV. Hake and Phelps (12) suggest that the cross section attains a maximum value of 2×10^{-17} cm^2 at an energy near 7 eV corresponding to an energy loss rate at 7 eV, given approximately by

$$[22] \quad \frac{dE}{dx} = -n(O_2) \times 10^{-16} \quad \text{eV cm}^{-1}$$

At 9.7 eV, the data of Schulz and Dowell (24) indicate another threshold. At this energy there exists a number of exit channels and indeed considerable structure occurs in the experimental

Can. J. Chem. Downloaded from www.nrcresearchpress.com by 210.87.254.6 on 09/05/12
For personal use only.

data above 8.5 eV. The associated energy loss rate is comparable to [22].

The lowest lying electronically excited state of N_2 is the $A^3\sum_u^+$ state with a threshold at 6.5 eV. It appears from the analysis of Engelhardt, Phelps, and Risk (7) that the associated energy loss rate for electrons of about 8 eV energy is given by

$$[23] \quad \frac{dE}{dx} = -n(N_2) \times 2 \times 10^{-16} \quad \text{eV cm}^{-1}$$

A comparable energy loss rate occurs for excitation to the $B^3\pi_g$ state which has a threshold near 7.4 eV. Above 8.4 eV, further excitation channels open and the energy loss rate increases.

Atomic oxygen has two low-lying metastable levels, the $O(^1D)$ level at 1.96 eV and the $O(^1S)$ level at 4.17 eV. The ^1D level is the upper level of the oxygen red lines at 6300 and 6364 Å and the ^1S level is the upper level of the oxygen green line at 5577 Å.

The cross sections have been computed by Smith, Henry, and Burke (28). At 5 eV, the energy loss rate associated with excitation to the ^1D level is given by

$$[24] \quad \frac{dE}{dx} = -n(O) \times 7 \times 10^{-17} \quad \text{eV cm}^{-1}$$

and the energy loss rate associated with excitation to the ^1S level is given by

$$[25] \quad \frac{dE}{dx} = -n(O) \times 4 \times 10^{-17} \quad \text{eV cm}^{-1}$$

Electron impact is a major source of excitation of the red and green lines in the day airglow.

It appears that excitation of electronic levels of positive ions is not a significant energy loss mechanism for low energy electrons. The cross sections for

$$[26] \quad e + O^+(^4S) \rightarrow e + O^+(^2D)$$

and

$$[27] \quad e + O^+(^4S) \rightarrow e + O^+(^2P)$$

have been calculated by Seaton and Osterbrock (29). Unlike the case of neutral species, the cross sections are finite at threshold. Above 3.3 eV, the energy loss rate is

$$[28] \quad \frac{dE}{dx} = -n(O^+) \times \frac{1.3 \times 10^{-15}}{E} \quad \text{eV cm}^{-1}$$

and above 5.0 eV, the energy loss rate is

$$[29] \quad \frac{dE}{dx} = -n(O^+) \times 2.2 \times 10^{-15} \quad \text{eV cm}^{-1}$$

These rates are negligible compared to [3].

Deactivation of the metastable states of O^+ by thermal electrons is an important process. Its influence on the day glow and twilight glow emission of the O^+ lines has been discussed by Dalgarno and McElroy (30).

Dissociative Attachment

Cross sections for the dissociative attachment processes

$$[30] \quad e + O_2 \rightarrow O + O^-$$

$$[31] \quad e + CO_2 \rightarrow CO + O^-$$

have been measured in several experiments (31). The cross section for O_2 has a maximum value of 1.4×10^{-18} cm^2 at an electron energy of 6.5 eV. The structure of the cross section for CO_2 is more complex. It has a maximum of 1.5×10^{-19} cm^2 at 4.3 eV and a second maximum of 4.3×10^{-19} at 8.1 eV. The processes are of minor importance in aeronomy.

Cooling Mechanisms

The electron gas which is selectively heated by the low energy electrons cools by various mechanisms. A precise evaluation of the cooling rates is valuable since measurements of the ambient electron temperatures can then be analyzed to yield the magnitude of the heat source responsible for the lack of kinetic thermal equilibrium.

Elastic Collisions

At high altitudes where the fractional ionization is large, the major cooling mechanisms are thermal conduction in the electron gas and elastic collisions with the positive ions. Averaging [1] over the Maxwellian velocity distributions of the electron and ion gases, characterized by temperatures T_e and T_i, respectively, the cooling rate corresponding to elastic collisions of electrons with positive ions X^+ is

$$[32] \quad \frac{dU_e}{dt} = \frac{-n_e n(X^+) \times 5 \times 10^{-7} \times (T_e - T_i)}{M(X^+) T_e^{3/2}} \times \ln \Lambda \quad \text{eV cm}^{-3}\,\text{s}^{-1}$$

where $M(X^+)$ is the mass of X^+, measured in

Can. J. Chem. Downloaded from www.nrcresearchpress.com by 210.87.254.6 on 09/05/12
For personal use only.

units of the proton mass (32). Typically $\ln \Lambda \sim 15$ so that for O^+ ions

$$[33]\quad \frac{dU_e}{dt} = -n_e n(O^+) \times 5 \times 10^{-7}(T_e - T_i) \times T_e^{-3/2} \quad \text{eV.cm}^{-3}\ \text{s}^{-1}$$

The electron–ion cooling rate passes through a maximum at $T_e = 3T_i$ so that for $T_e > 3T_i$ it may be necessary to include electron–neutral cooling even in strongly ionized regions.

The cooling due to elastic collisions may be evaluated from [5]. For molecular nitrogen, the momentum transfer cross sections have been derived from swarm data (7) and they lead to a cooling rate (33)

$$[34]\quad \frac{dU_e}{dt} = -n_e n(N_2) \times 1.8 \times 10^{-19} \times T_e(T_e - T_n)(1 - 1.21 \times 10^{-4} T_e) \quad \text{eV cm}^{-3}\ \text{s}^{-1}$$

where T_n is the neutral particle temperature. For molecular oxygen, momentum transfer cross sections have been derived also from swarm data (12) and they yield a cooling rate (33)

$$[35]\quad \frac{dU_e}{dt} = -n_e n(O_2) \times 1.2 \times 10^{-18} T_c^{1/2} \times (T_e - T_n)(1 + 3.6 \times 10^{-2} T_e^{1/2}) \quad \text{eV cm}^{-3}\ \text{s}^{-1}$$

There are no reliable experimental values at thermal velocities for atomic oxygen, but the most recent theoretical values (34) are consistent at higher velocities with most of the measurements. They give a cooling rate (3)

$$[36]\quad \frac{dU_e}{dt} = -n_e n(O) \times 5.3 \times 10^{-19} T_e^{1/2} \times (T_e - T_n)(1 + 5.7 \times 10^{-4} T_e) \quad \text{eV cm}^{-3}\ \text{s}^{-1}$$

Momentum transfer cross sections have been derived for carbon dioxide (12) and they yield (3)

$$[37]\quad \frac{dU_e}{dt} = -n_e n(CO_2) \times 3.0 \times 10^{-16}(T_e - T_n) \times (1 - 5 \times 10^{-5} T_e^{1/2}) \quad \text{eV cm}^{-3}\ \text{s}^{-1}$$

Cooling rates for elastic collisions with atomic hydrogen and helium have been computed by Banks (33).

Rotational Excitation

Elastic scattering by neutral atoms is rarely of significance in the evaluation of the cooling efficiency in the atmosphere. In regions where molecular species exist, cooling through rotational excitation is more rapid. Approximate formulae can be derived by adopting [7] for the variation of the cross section with velocity. It may be shown (35) from [7] that

$$[38]\quad \frac{dU_e}{dt} = -n_e n(M) \times 1.17 \times 10^{-10} B q^2 \times \frac{(T_e - T_n)}{T_e^{1/2}} \quad \text{eV cm}^{-3}\ \text{s}^{-1}$$

where B is the rotational constant measured in eV.

For N_2, $B = 2.49 \times 10^{-4}$ and $q = -1.0$ and [38] becomes

$$[39]\quad \frac{dU_e}{dt} = -n_e n(N_2) \times 2.9 \times 10^{-14} \times \frac{(T_e - T_n)}{T_e^{1/2}} \quad \text{eV cm}^{-3}\ \text{s}^{-1}$$

For O_2, $B = 1.81 \times 10^{-4}$, Hake and Phelps (12) recommend an effective $|q| = 1.8$, and we obtain accordingly

$$[40]\quad \frac{dU_e}{dt} = -n_e n(O_2) \times 6.9 \times 10^{-14} \times \frac{(T_e - T_n)}{T_e^{1/2}} \quad \text{eV cm}^{-3}\ \text{s}^{-1}$$

For CO_2, $B = 4.85 \times 10^{-5}$ and $q = -3.2$ so that

$$[41]\quad \frac{dU_e}{dt} = -n_e n(CO_2) \times 5.8 \times 10^{-14} \times \frac{(T_e - T_n)}{T_e^{1/2}} \quad \text{eV cm}^{-3}\ \text{s}^{-1}$$

Fine Structure Transitions

It has been pointed out recently (36) that energy loss caused by excitation of the fine structure transitions of atomic oxygen [10] is the dominant cooling mechanism in the F region of the ionosphere. Detailed estimates have been presented by

Can. J. Chem. Downloaded from www.nrcresearchpress.com by 210.87.254.6 on 09/05/12
For personal use only.

Dalgarno and Degges (36). A gross representation of their results is provided by the formula

$$[42]\quad \frac{dU_e}{dt} = -n_e n(O) \times \frac{3.4 \times 10^{-12}}{T_n} \times (T_e - T_n) \times (1 - 7 \times 10^{-5} T_e) \quad \text{eV cm}^{-3}\ \text{s}^{-1}$$

Vibrational Excitation

With increasing electron temperature, vibrational excitation becomes more efficient than rotational excitation. For molecular nitrogen, vibrational excitation is more efficient for temperatures above 1500 °K (37). Some of the nitrogen vibrational cooling rates, computed by Rees, Walker, and Dalgarno (38), are reproduced in Table I.

TABLE I
Cooling rates*

	Cooling rates at T_n (°K)			
$T_e - T_n$ (°K)	500	700	900	1500
500	2.5	4.8	7.0	10.7
700	5.5	8.7	11.5	25.3
1000	11.9	16.1	19.5	82.0
1500	25.8	49.0	93.1	332.4

*Cooling rates in units of 10^{-13} eV cm^{-3} s^{-1} for unit electron and nitrogen densities corresponding to vibrational excitation of molecular nitrogen.

The calculation assumes that the vibrational distribution of the ambient nitrogen is governed by the neutral particle kinetic temperature. Should this prove not to be the case (cf. Walker (26)), further calculations will be necessary.

Cooling rates through vibrational excitation of molecular oxygen have been calculated by Lane (private communication) from the cross section data of Hake and Phelps (12). If the high electron temperatures derived for the E region by probe measurements (39) are correct, oxygen vibrational cooling will be an important heat sink. Again the position is complicated by the possible departure of the oxygen vibrational distribution from thermal equilibrium.

Cooling by vibrational excitation of carbon dioxide is a very efficient process. Henry and McElroy (3) have computed cooling rates from the cross section data of Hake and Phelps (12). Their results can be represented approximately by the formula

$$[43]\quad \frac{dU_e}{dt} = -n_e n(CO_2) \times 8 \times 10^{-14} \times (T_e - T_n)\{1 + 2.5 \times 10^{-3} \times (T_e - T_n)\} \quad \text{eV cm}^{-3}\ \text{s}^{-1}$$

Electronic Excitation

The cooling efficiency resulting from electron impact excitation of the ^{1}D level of atomic oxygen can be derived immediately from the calculated cross sections (28). According to Rees, Walker, and Dalgarno (38)

$$[44]\quad \frac{dU_e}{dt} = -n_e n(O) \times 1.1 \times 10^{-10} T_e^{1/2} \exp(-2.27 \times 10^4/T_e)\{0.406 + 0.357 \times 10^{-4} T_e - (0.333 + 0.183 \times 10^{-4} T_e) \exp(-1.37 \times 10^4/T_e) - (0.456 + 0.174 \times 10^{-4} T_e) \times \exp(-2.97 \times 10^4/T_e)\} \quad \text{eV cm}^{-3}\ \text{s}^{-1}$$

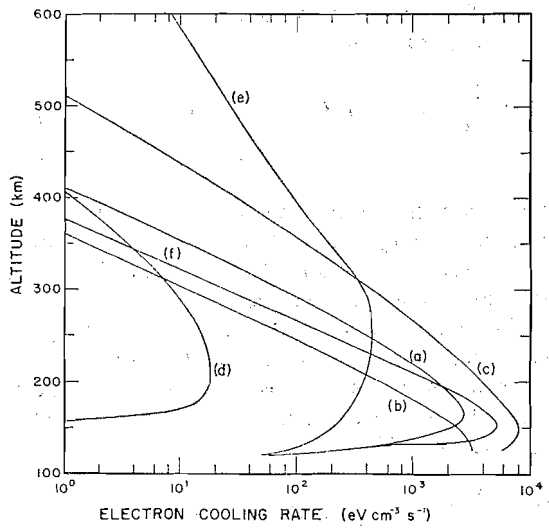

FIG. 1. The electron cooling rates appropriate to the atmosphere and ionosphere at noon, July, 1963. The curves show cooling resulting from excitation of (*a*) vibrational levels of molecular nitrogen, (*b*) rotational levels of molecular nitrogen, (*c*) fine structure levels of atomic oxygen, (*d*) metastable levels of atomic oxygen, (*e*) elastic collisions with positive ions, and (*f*) vibrational levels of molecular oxygen. The rates from elastic collisions with neutral particles and from rotational excitation of molecular oxygen are negligibly small.

Can. J. Chem. Downloaded from www.nrcresearchpress.com by 210.87.254.6 on 09/05/12
For personal use only.

Energy transfer from the thermal electrons to excitation energy of the ^1S level of atomic oxygen is unimportant. Energy transfer to excitation of the $a^1\Delta_g$ and $b^1\sum_g{}^+$ levels of molecular oxygen may be significant but the cross sections are largely unknown. Excitation to the higher electronic levels of atomic and molecular oxygen and molecular nitrogen can be neglected for the range of electron temperatures occuring in the ionosphere, as can excitation of the metastable levels of the positive ion of atomic oxygen.

A comparison of the efficiencies of the various cooling processes in the upper atmosphere of the Earth for noon in July 1963 has been given by Dalgarno, McElroy, Rees, and Walker (40). The comparison, supplemented by the addition of the cooling resulting from vibrational excitation of molecular oxygen, is reproduced in Fig. 1.

1. S. T. Butler and M. J. Buckingham. Phys. Rev. **126**, 1 (1962).
2. A. Dalgarno, M. B. McElroy, and R. J. Moffett. Planetary Space Sci. **11**, 463 (1963).
3. R. J. W. Henry and M. B. McElroy. The atmospheres of Mars and Venus. Gordon and Breach. New York. 1968.
4. E. Gerjuoy and S. Stein. Phys. Rev. **97**, 1671 (1955); **98**, 1848 (1955).
5. N. J. Bridge and A. D. Buckingham. Proc. Roy. Soc. London, Ser. A, **295**, 334 (1966).
6. A. Dalgarno and R. J. Moffett. Proc. Natl. Acad. Sci. India, **A33**, 511 (1963). R. C. Mjolness and D. H. Sampson. Phys. Rev. **140**, A1466 (1965). K. Takayanagi and S. Geltman. Phys. Letters, **13**, 135 (1964). K. Takayanagi and S. Geltman. Phys. Rev. **138**, A1003 (1965). S. Geltman and K. Takayanagi. Phys. Rev. **143**, 25 (1966). K. Takayanagi and T. Takahashi. Rept. Ionosphere Space Res. Japan, **20**, 357 (1966).
7. A. C. Engelhardt, A. V. Phelps, and C. G. Risk. Phys. Rev. **135**, A1566 (1964).
8. K. Takayanagi and T. Takahashi. Rept. Ionosphere Space Res. Japan, **20**, 357 (1966).
9. S. Geltman and K. Takayanagi. Phys. Rev. **143**, 25 (1966). D. H. Sampson and R. C. Mjolness. Phys. Rev. **144**, 116 (1966).
10. M. H. Mentzoni and K. V. N. Rao. Phys. Rev. Letters, **14**, 779 (1965).
11. A. Dalgarno and R. J. W. Henry. Proc. Roy. Soc. London, Ser. A, **288**, 521 (1965). K. Takayanagi. Rept. Ionosphere Space Res. Japan, **19**, 1 (1965).
12. R. D. Hake and A. V. Phelps. Phys. Rev. **158**, 70 (1967).
13. E. L. Breig and C. C. Lin. Phys. Rev. **151**, 67 (1966).
14. R. Haas. Z. Physik. **148**, 177 (1957).
15. G. J. Schulz. Phys. Rev. **116**, 1141 (1959); **125**, 229 (1962); **135**, A988 (1964).
16. G. J. Schulz and H. C. Koon. J. Chem. Phys. **44**, 1297 (1966).
17. M. J. W. Boness and J. B. Hasted. Phys. Letters, **21**, 526 (1966).
18. D. Andrick and H. Ehrhardt. Z. Physik, **192**, 99 (1966).
19. H. Ehrhardt and K. Willmann. Z. Physik, **204**, 462 (1967).
20. A. Herzenberg and F. Mandl. Proc. Roy. Soc. London, Ser. A, **270**, 48 (1962).
21. J. C. Y. Chen. J. Chem. Phys. **40**, 3513 (1964).
22. F. R. Gilmore. J. Quant. Spectry. Radiative Transfer, **5**, 369 (1965).
23. J. N. Bardsley, F. Mandl, and A. R. Wood. Chem. Phys. Letters, **1**, 359 (1967).
24. G. J. Schulz and J. T. Dowell. Phys. Rev. **128**, 174 (1962).
25. A. L. Schmeltekopf, F. C. Fehsenfeld, G. I. Gilman, and E. E. Ferguson. Planetary Space Sci. **15**, 401 (1967).
26. J. C. G. Walker. Planetary Space Sci. **16**, 321 (1968).
27. A. Dalgarno. Rev. Mod. Phys. **39**, 850 (1967).
28. K. Smith, R. J. W. Henry, and P. G. Burke. Phys. Rev. **157**, 51 (1967).
29. M. J. Seaton and D. E. Osterbrock. Astrophys. J. **125**, 66 (1957).
30. A. Dalgarno and M. B. McElroy. Planetary Space Sci. **11**, 727 (1963); **13**, 947 (1965).
31. J. D. Craggs, R. Thorburn, and B. A. Tozer. Proc. Roy. Soc. London, Ser. A, **240**, 473 (1957). B. A. Tozer, R. Thorburn, and J. D. Craggs. Proc. Phys. Soc. London, **72**, 1081 (1958). L. M. Chanin, A. V. Phelps, and M. Biondi. Phys. Rev. Letters, **2**, 344 (1959). I. S. Buchelnikova. Soviet Phys. JETP, **8**, 783 (1959). R. K. Asundi, J. D. Craggs, and M. V. Kurepa. Proc. Phys. Soc. **82**, 967 (1963). G. J. Schulz. Phys. Rev. **128**, 178 (1962). D. Rapp and D. D. Briglia. J. Chem. Phys. **43**, 1480 (1965).
32. L. Spitzer. Physics of fully ionized gases. Interscience Publishers, Inc., New York. 1956.
33. P. Banks. Planetary Space Sci. **14**, 1085 (1966).
34. R. W. J. Henry. Phys. Rev. **162**, 56 (1967).
35. M. H. Mentzoni and R. V. Rao. Phys. Rev. **130**, 2312 (1963).
36. A. Dalgarno and T. C. Degges. Planetary Space Sci. **16**, 125 (1968).
37. A. Dalgarno and R. J. W. Henry. Proc. Roy. Soc. London, Ser. A, **288**, 521 (1965).
38. M. H. Rees, J. C. J. Walker, and A. Dalgarno. Planetary Space Sci. **15**, 1097 (1967).
39. R. L. Boggess, L. H. Brace, and N. W. Spencer. J. Geophys. Res. **64**, 1627 (1959). N. W. Spencer, L. H. Brace, and G. R. Carignan. J. Geophys. Res. **67**, 157 (1962). L. H. Brace, N. W. Spencer, and G. R. Carignan. J. Geophys. Res. **68**, 5397 (1963). N. W. Spencer, L. H. Brace, G. R. Carignan, D. R. Taeusch, and H. Niemann. J. Geophys. Res. **70**, 2665 (1965). L. G. Smith, C. A. Accardo, L. H. Weeks, and P. J. McKinnon. J. Atmospheric Terrest. Phys. **27**, 803 (1965).
40. A. Dalgarno, M. B. McElroy, M. H. Rees, and J. C. G. Walker. Planetary Space Sci. **16**, 1371 (1968).

Comments and Summary

COMMENTS BY A. V. PHELPS

In connection with eqs. [9] and [40] it should be kept in mind that the effective quadrupole moment for rotational excitation of O_2 derived by Hake and Phelps from swarm experiments applies only for electron energies in the range from about 0.1 to 0.3 eV.

It should also be pointed out that the details of the energy dependence of the vibrational excitation cross sections in CO_2 for levels with thresholds above 0.08 eV as given in ref. 12 are based on tentative electron beam data. These cross sections are being reexamined by Schulz and coworkers. Only the behavior of the 0.08 eV cross section near threshold is given by analysis of swarm experiment data. At higher energies the swarm experiments should be regarded primarily as a measure of the sum of the vibrational excitation cross sections, weighted with the energy loss and averaged over an electron energy distribution with a rather large fractional energy width. Thus, the cross sections given in ref. 12 should be useful for energy loss calculations but are of uncertain accuracy for the individual vibrational states.

COMMENTS BY N. P. CARLETON

The electron energy distribution in the E region is well described by a Maxwellian distribution at low energy, with a sharp break to a more or less flat, long tail extending to high energies, thus justifying the classification of electrons as "thermal" and "photo" electrons. This inference comes from a numerical solution of a detailed Boltzmann–Fokker–Planck equation.

If one arbitrarily assigns an N_2 vibrational temperature higher than the gas temperature in the above equation, then the dip in the energy distribution occurring around 2 eV is somewhat filled in and the thermal distribution does not fall so far before breaking off into the high-energy tail.

COMMENTS BY A. V. PHELPS

In the calculation of energy losses in N_2 (or other gases) at high vibrational temperatures of the gas, account must be taken of the excitation of the vibrationally excited molecules and of the corresponding de-excitation processes. At present the only information regarding these cross sections is the theoretical calculation of refs. (1) and (2). As an example of the net effect of the excitation of vibrational excited N_2, the rate of cooling of electrons with energies near 2 eV will be relatively independent of vibrational temperature, for vibrational temperatures well below 2 eV. It is probable that the excitation cross sections for vibrational excitation of vibrationally excited states near threshold are considerably larger than for the $N_2(v = 0)$ level so that the cooling rates for low energy electrons may be significantly modified.

1. J. C. Y. CHEN. J. Chem. Phys. **40**, 3507 (1964).
2. J. C. Y. CHEN. Phys. Letters, **45**, 2710 (1966).

SUMMARY BY CHAIRMAN, L. BRANSCOMB

Since the upper atmosphere of the earth selectively absorbs the non-thermal component of the solar radiation in the hard ultraviolet region, the photoelectrons created in this manner have energies far above the energies of most of the "thermal" particles. As first studies by Dalgarno, McElroy, and Moffett showed, the photoelectrons exchange energy with other electrons, with ions, and with the kinetic and internal energy states of the neutrals. In the first approximation, the kinetic energy distributions of these three species can be taken as Maxwellian, with the coupling between species sufficiently weaker than the energy exchange between particles of similar type that the kinetic energy distributions of each, electrons, ions, and neutrals, can be described by a different temperature parameter. In this approximation the internal energy distributions of the neutrals, while not necessarily characterized by thermodynamic equilibrium at the local temperature of the neutrals, can nonetheless be taken as determined by factors other than energy exchange with the electrons.

Dalgarno's review provides a very convenient and comprehensive summation of present knowledge of all of the processes through which electrons cool by interaction with the atmosphere between their birth as photoelectrons and their final disappearance by recombination (or attachment). To provide estimates of these cooling

Can. J. Chem. Downloaded from www.nrcresearchpress.com by 210.87.254.6 on 09/05/12
For personal use only.

rates, Dalgarno appeals both to theoretical and experimental sources. Most of the latter data are provided by A.V. Phelps and his colleagues. The two comments by Phelps emphasize the caution with which the experimental data must be used.

The next level of sophistication in the treatment of this problem must involve examination of the actual steady state electron velocity distribution. It must also include examination of non-linear interactions between the electron cooling processes and the internal energy distributions of the neutral molecules. Much of the discussion is centered on the importance of electron cooling through the excitation of nitrogen vibration, followed by exchange of this vibrational energy with other molecules. The inefficiency with which vibration is deactivated from homonuclear molecules raises the possibility of non-thermal populations of molecular nitrogen vibrational states. Carleton pointed out that the resulting effect on the electron velocity distribution may be significant.

In addition, the energy loss processes for electrons in collision with excited vibrational states of nitrogen must be considered.

Finally, the discussion turned to a question that remained unresolved. To what extent does vibrational energy transfer from N_2 to CO_2, followed by infrared radiation, provide an energy drain from the N_2 vibrational "sink"? This mechanism, familiar in laboratory studies of the CO_2 infrared laser, has been considered by Gilmore (unpublished). The current state of knowledge about the rates involved has been reviewed by Taylor and Bitterman (Rev. Mod. Phys. In press). To the extent that this mechanism does remove an appreciable amount of electron energy in the E region, the net effect is the transformation of vacuum ultraviolet solar photons into infrared quanta.

Can. J. Chem. Downloaded from www.nrcresearchpress.com by 210.87.254.6 on 09/05/12
For personal use only.

Can. J. Chem. Downloaded from www.nrcresearchpress.com by 210.87.254.6 on 09/05/12
For personal use only.

Inelastic scattering of high energy electrons by atmospheric gases[1]

EDWIN N. LASSETTRE

Mellon Institute and the Department of Chemistry, Carnegie-Mellon University, 4400 Fifth Avenue, Pittsburgh, Pennsylvania 15213

Received December 4, 1968

Inelastic scattering of electrons by nitrogen, oxygen, carbon monoxide, carbon dioxide, water, argon, and helium is reviewed. Electron impact spectra at both high (less than 40 keV) and low (greater than 15 eV) kinetic energies are presented and discussed. Collision cross sections and generalized oscillator strengths are described, when data are available, and the connection with optical oscillator strengths is discussed. The limiting selection rules which hold in the excitation of atoms and molecules by electron impact are discussed and typical examples of forbidden transitions are described.

Canadian Journal of Chemistry, 47, 1733 (1969)

Introduction

Scope of Review

In preparing a review of the scattering of high energy electrons by atmospheric gases it seems essential to limit it in some fashion which will permit fairly complete but not merely superficial coverage. By confining it to the discussion of electron impact spectroscopy of atmospheric gases, including measurements of differential collision cross sections, we can hope to approach this objective. In order to get oriented on the orders of magnitude of the energies involved, it is useful to consider the results of some calculations of electronic excitation in gas mixtures.

Energy Degradation in the Excitation of Gases

The calculation (or measurement) of energy degradation in the excitation of gases by fast charged particles is important in many fields, especially radiological physics, radiation chemistry, and atmospheric physics. Some recent calculations by Green illustrate the magnitude of the energies and the problems involved. As a first step in Green's investigation, empirical formulas were developed for fitting differential collision cross sections (1). These were selected partly for convenience in the calculation of total cross sections and general simplification of the numerical calculations. The problem of obtaining a system of cross sections for helium was considered next (2). Empirical cross section equations were then formulated for many transitions in molecular nitrogen (3) and molecular oxygen (4). Cross sections for atomic oxygen were also estimated, mostly from theoretical calculations. These cross sections have been applied to the calculation of auroral intensities (5) and the treatment of the day-glow (6). Obviously many of the finer details of excitation cross sections were omitted in these calculations and extensive use was made of the Born approximation to extend measurements made at one kinetic energy to higher and lower kinetic energies. These surveys do, however, reveal quite clearly how sparse are the data from which meaningful calculations of energy degradation can be made. Moreover, the partition of energy among molecular and ionic species and the energies of secondary electrons are of substantial qualitative interest. Two tables from ref. 5 are of particular interest. Table I shows the percentage of the primary energy which goes into each species when the bombarded atmosphere is 45% N_2, 45% O, and 10% O_2, corresponding roughly to the atmosphere at great altitudes. The percentages change but little for E = 30, 10, 1 keV but excitation (in contrast to ionization) becomes relatively more important at 0.1 keV. The column labeled "remainder" is the percentage of the energy which is lost in the interval from zero to about 1 eV through the processes of rotation, vibration, and elastic scattering. Table II from ref. 5 shows the breakdown into secondary, tertiary, and quaternary spectra and also the average energies. Note in Table I that roughly equal proportions of energy go into excitation and ionization at primary energies of 30, 10, and 1 keV but the proportion producing excitation is considerably larger at a primary energy of 0.1 keV. Note also the low mean energy of secondaries in Table II. Because of this low energy the next collision of a secondary is more likely to excite than to ionize and hence the abrupt drop in the tertiary

[1]Some of the research described in this review was supported in part by the United States Air Force Office of Scientific Research under Grant No. AFOSR-68-1495.

TABLE I

Energy into species

Incident energy (keV)	Energy (%) into species						
	N_2	O	O_2	N_2^+	O^+	O_2^+	Remainder
30	32.8	6.1	7.3	27.1	16.2	6.6	3.9
10	33.3	6.1	7.4	27.7	16.5	6.7	2.3
1	34.0	6.1	7.7	27.7	16.6	6.3	1.6
0.1	40.5	11.4	9.1	21.4	13.9	3.4	0.3

TABLE II

Energy into ions and eV per ion pair

Incident energy, keV	Number of ion pairs	eV per ion pair	Number of			Average energy of		
			Secondaries	Tertiaries	Quaternaries	Secondaries	Tertiaries	Quaternaries
30	911	32.9	698	205	8	20.4	6.2	4.5
10	310	32.3	240	67	2	19.0	6.2	4.5
1	31	32.3	27	4	0.01	13.1	4.9	2.2
0.1	2.4	41.5	2.4	0.01	0	5.05	1.5	—

population compared to the secondary. It is not the purpose of this review to critically appraise the theory of Green and collaborators. However, in those calculations liberal use was made of the cross sections measured by the author and his collaborators and hence this affords a good opportunity to consider the current status of these cross sections. It should be noted that the development of electron impact spectroscopy is important to chemistry in ways not directly related to atmospheric phenomena and comments on points relevant to these objectives will be made occasionally. Before discussing electron impact spectra, some definitions and elementary theoretical results must be summarized. This is done in the following section.

The Born Approximation: Generalized Oscillator Strengths

In the discussion of transitions it is useful to employ generalized oscillator strengths which we designate by f. This quantity is defined (in atomic units) as

$$[1] \qquad f = (W/2)\,(k_1/k_2)K^2\sigma$$

where W is the excitation energy, σ is the differential collision cross section, k_1, k_2 are the magnitudes of the wave vectors of the incident and scattered electrons, and K is the magnitude of the change in wave vector of the incident electron on collision. ($(h/2\pi)K$ is the magnitude of the momentum change vector and $h/2\pi = 1$ in atomic units.) When the Born approximation holds we can substitute Bethe's modification of the Born formula into eq. [1] and obtain

$$[2] \qquad f = 2W\,\varepsilon\varepsilon^*/K^2$$

where ε is a matrix element

$$[3] \qquad \varepsilon = \langle\psi_1\,|\,\textstyle\sum_j N_j e^{iKz_j} - \sum_s e^{iKz_s}\,|\psi_2\rangle$$

Here ψ_1, ψ_2 are the eigenfunctions of the scatterer in the initial and final states, N_j is the atomic number of the jth nucleus, and z_j, z_s are the z coordinates of the jth nucleus and the sth electron of the scatterer. It is useful to expand eq. [3] in a power series in K

$$[4] \qquad \varepsilon = \textstyle\sum_{n=1}^{\infty}(iK)^n\varepsilon_n$$

where

$$[5] \qquad \varepsilon_n = (1/n!)\,\langle\psi_1\,|\,\textstyle\sum_j N_j z_j^n - \sum_s z_s^n\,|\psi_2\rangle$$

Then ε_1 is the matrix element of electric dipole moment. If a transition is allowed and K is very small then

$$[6] \qquad f = 2W\,|\varepsilon_1\,|^2$$

If $\varepsilon_1 = 0$ and $\varepsilon_2 \neq 0$, then at small values of K (neglecting higher order powers of K)

$$[7] \qquad f = 2W\,|\varepsilon_2\,|^2K^2$$

Can. J. Chem. Downloaded from www.nrcresearchpress.com by 210.87.254.6 on 09/05/12
For personal use only.

Can. J. Chem. Downloaded from www.nrcresearchpress.com by 210.87.254.6 on 09/05/12
For personal use only.

Since $z^2 = r^2/3 + (z^2 - r^2/3)$ the quantity ε_2 is expressible in the form

$$[8] \quad \varepsilon_2 = 1/3\langle\psi_1 | \sum_j N_j r_j^2 - \sum_s r_s^2 | \psi_2\rangle + \langle\psi_1 | \sum_j N_j (z_j^2 - r_j^2/3) - \sum_s (z_s^2 - r_s^2/3) | \psi_2\rangle$$

For the lack of a better word we have referred to ε_2 as the matrix element of electric quadrupole moment and any transition for which $\varepsilon_1 = 0$ and $\varepsilon_2 \neq 0$ has been referred to as an electric quadrupole transition. This is not the same as the terminology employed in spectroscopy. In optical spectra only the second term on the right of eq. [8] arises in considering the intensities of electric quadrupole transitions. There is no analogue of the first term on the right. The $1^1S \rightarrow 2^1S$ transition in helium is an example of a transition in which the second term on the right of eq. [8] vanishes but the first does not, while the Lyman–Birge–Hopfield bands of N_2 provide an example in which the first term vanishes and the second does not (7, 8). Garstang (9) has shown that when eq. [8] is substituted into eq. [7] the cross products vanish in summation over magnetic quantum numbers and he has obtained a formula in which Einstein's A replaces the term containing the square of the second matrix element in eq. [8]. The formula, which we omit, is developed in a sufficiently general fashion to include both atoms and diatomic molecules. An application of Garstang's formula will be discussed later.

For convenience in subsequent discussion we note how the cross sections depend on momentum change at small values of K. For transitions in which $\varepsilon_1 \neq 0$ we may assume that $f = 2W\varepsilon_1^2$ at small K and hence, designating the cross section by σ_d

$$[9] \quad \sigma_d \simeq (4\varepsilon_1^2)/K^2$$

We have assumed that $k_2/k_1 \simeq 1$. At zero scattering angle and high kinetic energy $\bar{E}$, $K^2 = W^2/2\bar{E}$ where $\bar{E} = E - W/2$. This relation holds accurately when $W/\bar{E} < 0.1$. Hence

$$[10] \quad \sigma_d \simeq (8\varepsilon_1^2\bar{E})/W^2$$

For quadrupole transitions $\varepsilon_1 = 0$, $\varepsilon_2 \neq 0$, we designate the cross section by σ_Q and find using eq. [7] when K is small

$$[11] \quad \sigma_Q \simeq 4\varepsilon_2^2$$

This is independent of kinetic energy. Hence the ration of σ_d to σ_Q is

$$[12] \quad \sigma_d/\sigma_Q = 2\bar{E}\,\varepsilon_1^2/(W^2\varepsilon_2^2)$$

Electron Impact Spectra: Relative Intensities

Apparatus

High resolution electron impact spectroscopy requires velocity selection before scattering. The first successful monochromatic electron source, based on the 127° analyzer, was developed by Marmet and Kerwin (10). The "electron" velvet used by them was replaced by platinum black by Schulz (11, 12) in his study of very low energy resonances. Ehrhardt (13), McGowan (14), and Brion (15) have also used this source, the latter without coatings (except for gold plate). Of these investigators only Schulz and Ehrhardt did velocity analysis on the scattered electrons (McGowan and Brion used the sources in mass spectrometers). Since the low kinetic energy range (used by Schulz and Ehrhardt) is being covered by another reviewer, we pass on to the consideration of spectrometers which have been used at higher kinetic energy.

Electron sources based on the spherical condenser (hemispheres) have been developed by Skerbele and Lassettre (16) and Simpson (17). High resolution electron spectrometers have been considerably refined and developed by Lassettre and collaborators (18–20) and by Simpson and Kuyatt (21, 22). These are based on hemispheres which are used both for velocity selection before scattering and for velocity analysis afterwards. Both apparatuses permit variation in scattering angle (from -16 to $+16°$ in the instrument of ref. 20 and from -20 to 90° in that of ref. 22). The apparatuses differ in size, in the manner of correction for chromatic aberration, and in the measurement of scattered current (a reed amplifier in refs. 21, 22 and an electron counter in refs. 18–20.) Boersch and collaborators (23–25) (especially Geiger) have achieved the highest resolution in electron impact spectroscopy at very high kinetic energies (most frequently at 25 keV). In their instrument the scattering angle cannot be varied. Crossed electric and magnetic fields (Wien filter) are used in the monochromator.

From an instrumental viewpoint the velocity analyzers used by Turner (26) (in the determination of photoelectron energy distributions) are of interest. In the case of oxygen, the broadening of

Can. J. Chem. Downloaded from www.nrcresearchpress.com by 210.87.254.6 on 09/05/12
For personal use only.

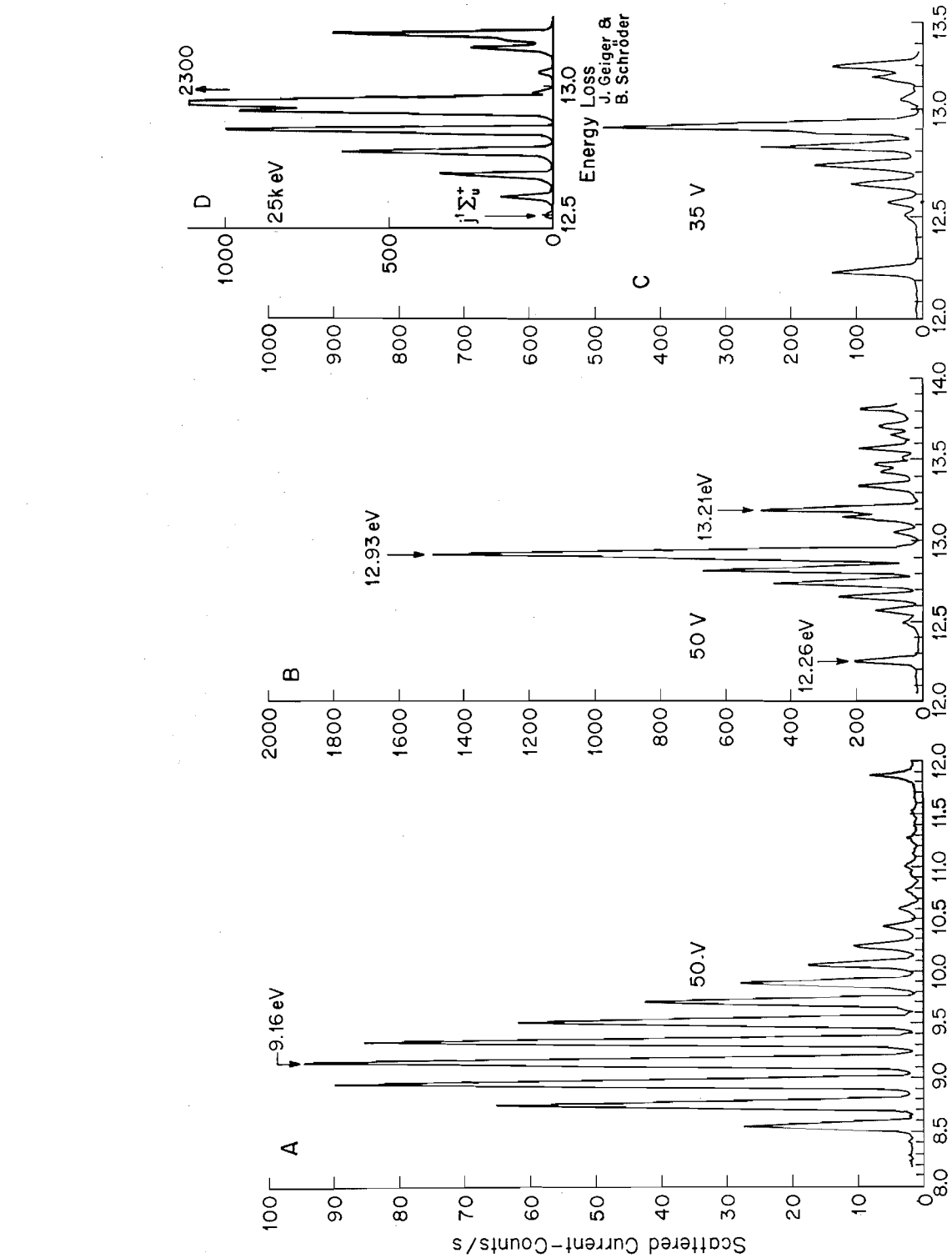

FIG. 1. Electron impact spectra of N_2. A and B; accelerating voltage 50, kinetic energy 48 eV, $\theta = 0°$. C: voltage 35, kinetic energy 33 eV, $\theta = 0°$. See ref. 20 for A, B, and C. D: inset at upper right N_2 spectrum at 25 keV, $\theta = 0°$, by Geiger and Schröder; see ref. 27.

Can. J. Chem. Downloaded from www.nrcresearchpress.com by 210.87.254.6 on 09/05/12
For personal use only.

bands (presumably thermal) has been observed in comparison to atomic line widths. In these experiments the instrumental line width is reduced by 40% since only one analyzer is employed. The electrostatic analyzers employed in Turner's experiments are based on the 127° analyzer but with intermediate elements to correct for aberration at high entrance angles.

Electron Impact Spectra

Relative Intensities

Since high resolution is now obtainable in electron impact spectroscopy it is useful to exhibit electron impact spectra of the principal atmospheric gases. Spectra at both high and low kinetic energies are included where available and spectra under additional conditions are also given when especially significant points are involved. Since the experimental technique is developing rapidly (a large percentage of all research in electron impact spectroscopy is still in the process of publication) the spectra obtained by investigators other than the present author may not be the best available. An attempt has been made to include at least a portion of each spectrum of the highest resolution in all cases where this is known.

Nitrogen

Electron impact spectra of nitrogen are shown in Fig. 1. The spectra labeled A, B, and C were obtained by Lassettre, Skerbele, Dillon, and Ross (20). The inset at the upper right is a portion of a nitrogen spectrum covering the same range as C, obtained by Geiger and Schröder (27). The complete spectrum is being published elsewhere (28) together with an extended discussion of its interpretation. Spectra A and B are on the same scale but spectrum C cannot be quantitatively compared in intensity with A and B. The resolution obtained by Geiger and Schröder is higher than that of spectrum C but not by a sufficient margin to conceal the striking similarity between the two, despite the fact that the kinetic energy in one case is 25 keV and in the other 33 eV. The most conspicuous exception is the j state at 12.5 eV. The relative intensity of this state is higher at 33 eV than at 25 keV.

At excitation energies less than 12.5 eV Geiger (29) finds no peak at 25 keV. Obviously, however, several such transitions appear in spectra A and B of Fig. 1. These are (electric dipole) forbidden transitions. Mulliken (30) has suggested term symbols and excitation energies for many states of nitrogen. Using his tables we note 24 transitions from the ground state to electronic states which have energies below that of the j state. We deduce from Mulliken's term symbols that only one of these is allowed and this seems not to have been observed in either absorption or emission. Of the remaining 23 transitions, however, a considerable number have been found in the ultraviolet absorption spectrum of nitrogen and several are shown in spectra A and B of Fig. 1. In particular, transition to the E state ($^3\Sigma_g^+$) at 11.87 eV is clearly visible. This transition was observed by Heideman, Kuyatt, and Chamberlain (31) in spectra obtained at 35 and 15.7 eV incident kinetic energy and independently by Meyer and Lassettre (32) in spectra obtained at 400 eV kinetic energy. We thought at first (32) that the E state could not be a triplet when the transition is obtained at such high kinetic energies and spin–orbit coupling cannot mix the proper configurations to make the transition electric dipole allowed. However, it was later recognized (19) that second order terms (see eq. [8]) in the cross section (or generalized oscillator strength) are sufficient to account for the transition. The electron impact spectra of Heideman, Kuyatt, and Chamberlain (31) at 33 and 15.7 eV are shown in Fig. 2. Note the rapid decrease in relative intensity of the 12.93 eV transition as the kinetic energy is reduced.

An array of forbidden transitions, more complete than that of Fig. 1, is shown in Fig. 3. The excitation to $C^3\Pi_u$ is observed (33) over the angle range 3 to 16° although it does not appear in the upper spectrum of Fig. 2 and it was not observed in an earlier investigation (19) at kinetic energies between 30 and 100 eV, presumably due to lower resolution and higher background. Forbidden transitions in N_2 will be discussed further after the introduction of one additional spectrum.

The electron impact spectra shown thus far contain transitions corresponding to the vacuum ultraviolet in a radiation absorption spectrum. In Fig. 4 the spectrum of nitrogen (34) is shown in the vicinity of the elastic peak. A carbon monoxide spectrum is included for comparison. The fundamental vibration is obviously excited together with one overtone. The ratio of the intensity, I, to that I_0, for the elastic peak is $I/I_0 = (4.3 \pm 0.3) \times 10^{-4}$. Between 2 and 15° this ratio is constant. Schulz (11) has observed vibrational excitation in N_2 at very low kinetic energies (2–3 eV) where excitation is attributable to negative

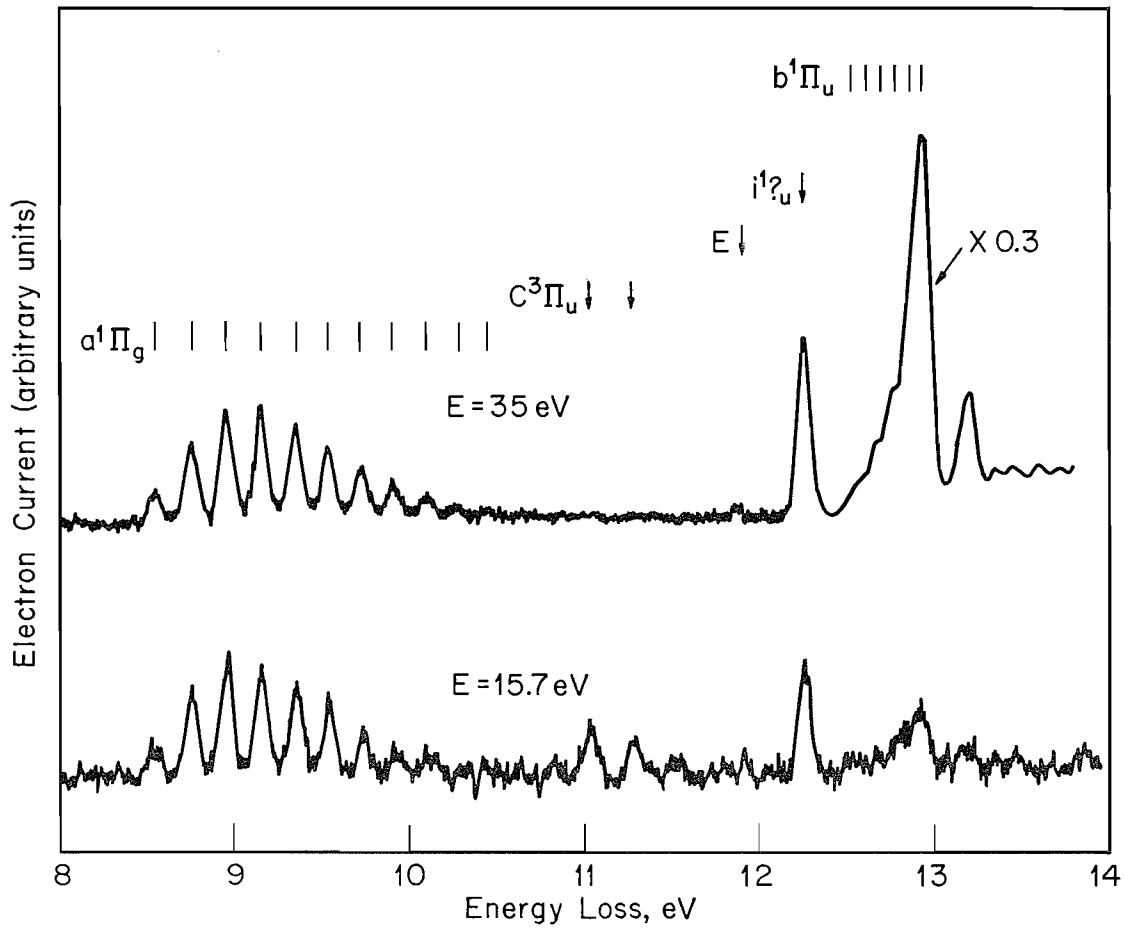

FIG. 2. Electron impact spectra of N_2 at 35 and 15.7 eV electron kinetic energies by Heideman, Kuyatt, and Chamberlain (31). $\theta = 0°$. Note decrease in intensity of 12.93 eV transition.

ion resonances. Figure 4 shows that vibrational excitations in homonuclear molecules are also detectable at much higher kinetic energy. The transitions are, of course, forbidden and are very weak.

Referring back to Fig. 1 the vibrational progression with peak at 9.16 eV is the analogue of the Lyman–Birge–Hopfield band system observed in in the vacuum ultraviolet. Until 1946 it was thought to be an electric dipole allowed system but very weak. In 1946, Herzberg (35) gave strong reasons for believing that the transition is forbidden (upper state $a^1\Pi_g$) and that it appears in the ultraviolet absorption spectrum due to a non-vanishing matrix element of magnetic dipole moment. Wilkinson and Mulliken (36) resolved the rotation lines in the band system well enough to detect not only the system of lines obeying the magnetic dipole selection rules but another system of weaker lines which obey the electric quadrupole selection rules. This observation definitely establishes $^1\Pi_g$ as the upper state term symbol and proves that two different processes are contributing to the band system. Moreover, by determining the relative intensities of the two different types of rotation lines, the proportion of the band intensity due to magnetic dipole and electric quadrupole transitions can be determined. The most recent studies by Vanderslice, Tilford, and Wilkinson (37) give 75% magnetic dipole and 25% electric quadrupole.

The cross section formulas of the previous section are not only based on the Born approximation but assume in addition that the interac-

Can. J. Chem. Downloaded from www.nrcresearchpress.com by 210.87.254.6 on 09/05/12
For personal use only.

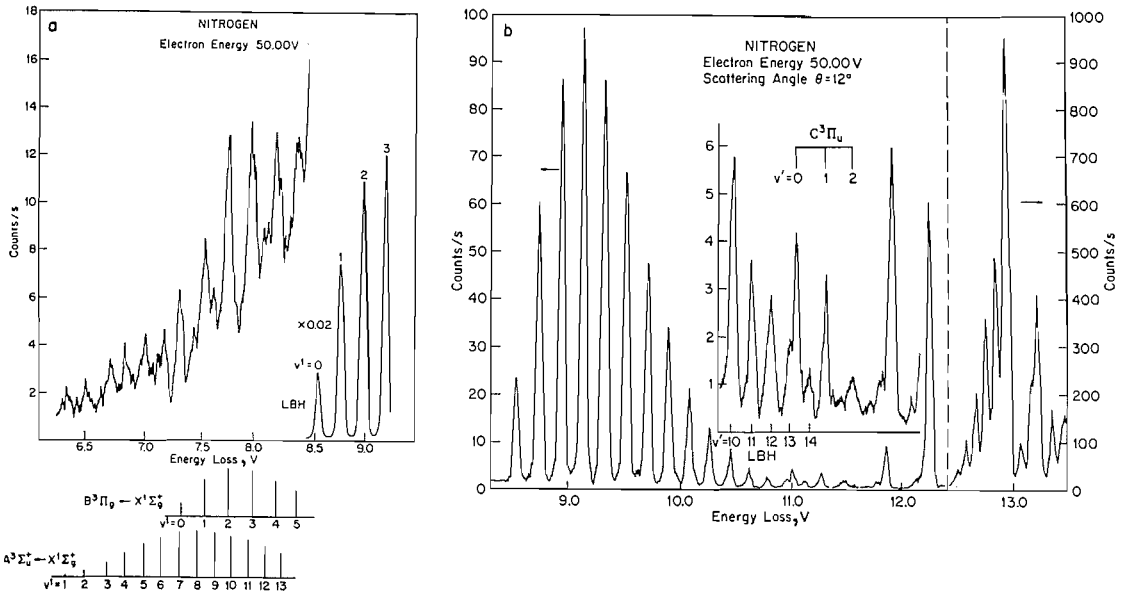

FIG. 3. Electron impact spectra of N_2 by Skerbele, Dillon, and Lassettre (33). Accelerating voltage 50, kinetic energy 48. Right hand spectrum at $\theta = 12°$, left hand spectrum at $\theta = 3°$. Note singlet–triplet transitions.

tion of the incoming electron with the scatterer is the coulomb (electrostatic) term in the Hamiltonian. Since magnetic interactions are neglected entirely, no magnetic dipole excitation mechanism can arise in that theory. Since the Lyman–Birge–Hopfield bands are a prominent part of the electron impact spectrum, it is possible to determine collision cross sections (and hence generalized oscillator strengths) and to determine independently whether the system is forbidden. This has been done by Lassettre and Krasnow (38) and the results are given in Fig. 5. The vibrational levels were not resolved in these experiments but this should not affect the intensity integrated over the band. In Fig. 5 we have used the momentum change ΔP rather than the wave vector K ($h/2\pi(K) = \Delta P$), but the two are numerically equal in atomic units. There is an obvious trend towards zero as the momentum change decreases in accord with the hypothesis that the transition is forbidden. Garstang (9) has analyzed these data further in the following fashion. Since the term symbol for the excited state differs from that for the ground state, the first term on the right of eq. [8] vanishes. Since the second term on the right involves the same matrix element as that appearing in intensity formulas for the absorption of radiation in electric quadrupole transitions, it should

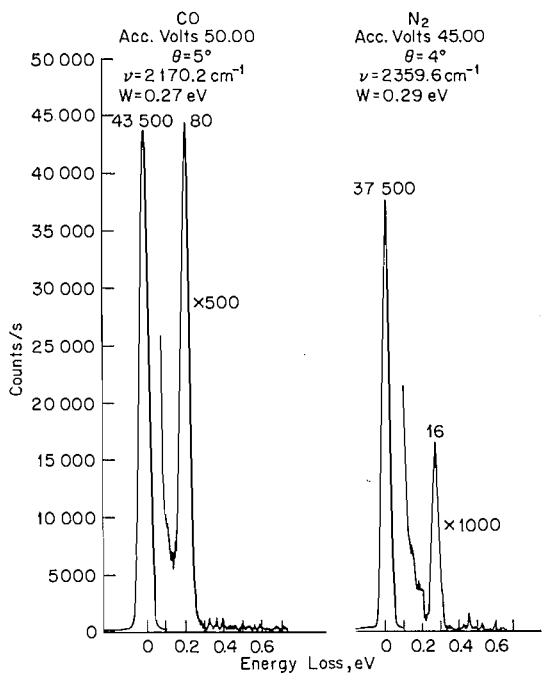

FIG. 4. Electron impact spectra of CO and N_2 showing vibrational excitation, by Skerbele, Dillon, and Lassettre (34). Transition in N_2 is forbidden. Subtract 2 V from accelerating voltage to obtain kinetic energy.

Can. J. Chem. Downloaded from www.nrcresearchpress.com by 210.87.254.6 on 09/05/12
For personal use only.

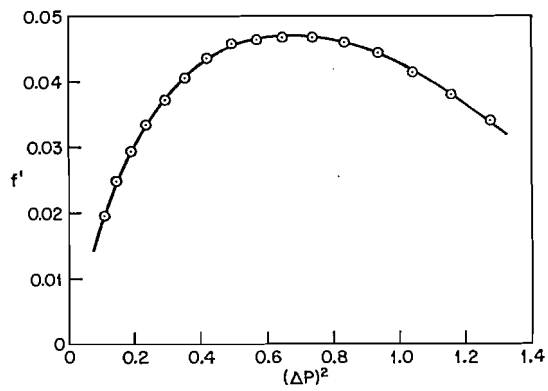

FIG. 5. Generalized oscillator strength vs. square of momentum change (atomic units) for the transition $a^1\Pi_g \leftarrow X^1\Sigma_g^+$ of N_2 (Lyman–Birge–Hopfield bands) by Lassettre and Krasnow (38). Kinetic energy ~ 500 eV.

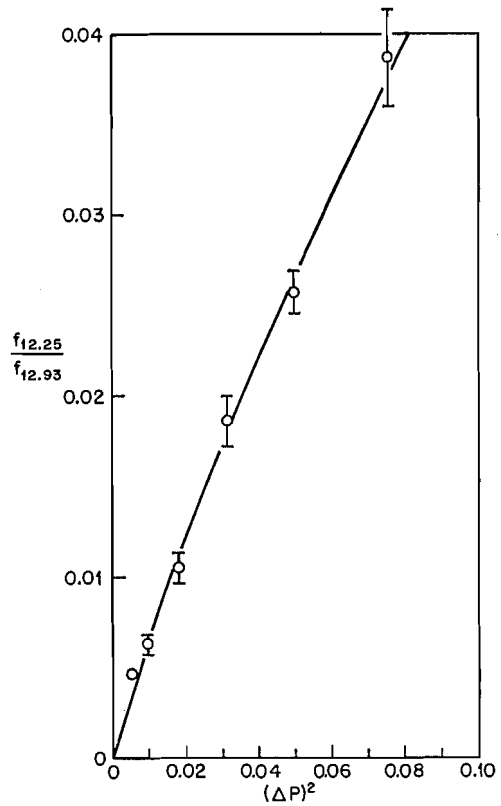

FIG. 6. Ratio of generalized oscillator strength of 12.26 to 12.93 eV transitions of N_2 vs. square of momentum change (atomic units) by Lassettre, Skerbele, and Meyer (19). Kinetic energy 500 eV.

be possible to recast this expression in terms of Einstein's A for the transition. This has been done by Garstang (9). The value of A calculated from the data of Fig. 5 is 2000 s^{-1}. Lichten (39) also measured the lifetime of the state by a molecular beam technique and obtained for A the value 5900 $\pm$ 1000 s^{-1}. This value involves transitions by both magnetic dipole and electric quadrupole mechanisms, hence only 25% of this value, 1500 $\pm$ 250 s^{-1}, is due to electric quadrupole transitions. As Garstang (9) pointed out, this agrees about as well with the value obtained from analysis of the electron impact data as could be expected.

The Lyman–Birge–Hopfield bands are an example of a forbidden system for which the second term on the right of eq. [8] is non-vanishing. We now discuss a transition for which the first term proves to be non-vanishing. The transition referred to is that at 12.26 eV. A transition at approximately this excitation potential was reported by Heideman, Kuyatt, and Chamberlain (31) working at incident kinetic energies of 33 and 15.7 eV and (independently) by Meyer and Lassettre (40) working at 400 eV. Both sets of investigators also reported an excitation potential at 11.87 eV. The first excitation potential (12.26 eV) seemed to agree with Worley's (41) *i* state and the second (11.87 eV) to involve excitation to the *E* state ($^3\Sigma_g^+$). To determine whether the 12.26 eV transition is (electric dipole) allowed, the ratio of the oscillator strengths of the 12.26 and 12.93 eV transitions has been determined (19) and is shown as a function of momentum change for the 12.26 eV transition in Fig. 6. Since the peak at 12.93 eV is the highest in the entire spectrum it is certainly electric dipole allowed, and hence the ratio $f_{12.26}/f_{12.93}$ will approach zero if the 12.26 eV transition is forbidden. From Fig. 6 it is obvious that the transition is forbidden and, moreover, the first non-vanishing power of the momentum change (in a Taylor series expansion) is the second, i.e. $f \propto (\Delta P)^2$ at small momentum changes. Since the ground state term symbol for N_2 is $^1\Sigma_g^+$ it follows from an elementary application of group theory that the term symbols for the excited state must be one of the following $^1\Sigma_g^+$, $^1\Pi_g$, $^1\Delta_g$. After consulting Mulliken's list of term symbols, only one, $^1\Sigma_g^+$, seemed probable and this was proposed in ref. (19). For a transition between two $^1\Sigma_g^+$ states the first term on the right of eq. [8] does not vanish, while the second term vanishes. This is in contrast to the Lyman–Birge–Hopfield bands.

Can. J. Chem. Downloaded from www.nrcresearchpress.com by 210.87.254.6 on 09/05/12
For personal use only.

Can. J. Chem. Downloaded from www.nrcresearchpress.com by 210.87.254.6 on 09/05/12
For personal use only.

The 12.26 eV transition is strongly forbidden in radiation absorption but Lutz and Dressler (42) have found it at high pressures due to a collision induced dipole moment. They also showed that the 12.26 eV transition is not the same as Worley's *i* state. The latter, although close in excitation energy, actually arises from a radiation absorption process in which the initial state is the excited vibrational level $v'' = 1$ of the ground electronic state.

It was also shown in ref. 19 that the 11.86 eV transition is electric quadrupole (i.e. $\varepsilon_1 = 0, \varepsilon_2 \neq 0$. See section on Born approximation). This was shown by determining the intensity ratio $I_{11.87}/I_{12.26}$ at several kinetic energies and zero scattering angle. The ratio is nearly independent of kinetic energy as it must be if the 11.87 and 12.26 eV transitions are both electric quadrupole in type. This is compatible with the term symbol $^3\Sigma_g^+$ assigned by Mulliken (30) provided that spin–orbit coupling has mixed additional (singlet) configurations such that the transition from the ground state acquires a small electric quadrupole component. It could also be that some different state with term symbol $^1\Sigma_g^+$ is being excited as suggested by Cermak (43) on the basis of the study of Penning ionization.

A third type of transition which can occur in electron impact experiments as well as radiation absorption is one which involves a change in multiplicity. Singlet–triplet transitions are a frequently encountered example. Singlet–triplet transitions in optical spectra are usually encountered under conditions where spin–orbit coupling is significant. If the actual molecular (or atomic) eigenfunction is expressed as a linear combination of eigenfunctions of a Hamiltonian without magnetic terms, then both singlet and triplet terms contribute to the sum when magnetic contributions are taken into account (44). These added terms may make the transition electric dipole allowed (but weak) and hence such transitions will be observed in radiation absorption. They should also be encountered in electron impact spectra. An especially interesting example is provided by the transition to the $C^3\Pi_u$ state of N_2. This transition is the most intense singlet–triplet transition in the ultraviolet absorption spectrum of N_2. It was mentioned earlier that the excitation to $C^3\Pi_u$ was difficult to detect in the kinetic energy range 30 to 100 eV. However, as the resolution was improved and background

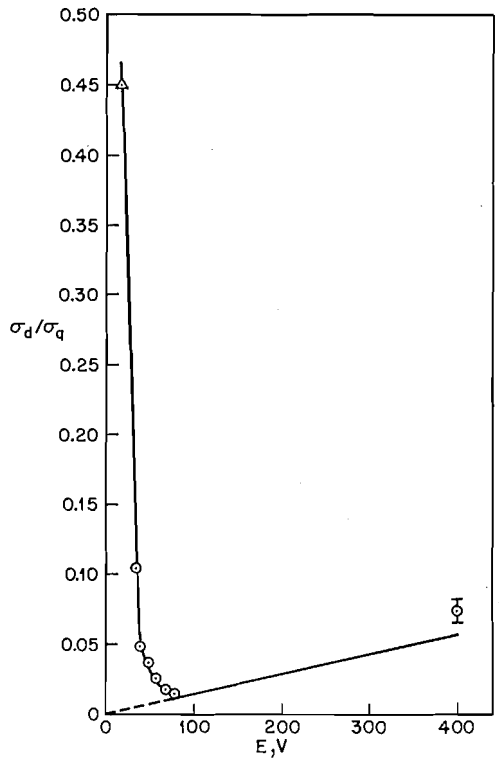

FIG. 7. Ratio of cross section for transition ($v' = 0$) $C^3\Pi_u \leftarrow X^1\Sigma_g^+$ to that for the transition ($v' = 3$) $a^1\Pi_g \leftarrow X^1\Sigma_g^+$ vs. kinetic energy. $\theta = 0°$. ⊙ from ref. 33, △ from ref. 31, Φ from ref. 19. Straight line calculated from ultraviolet absorption coefficients.

decreased, the transition could be detected (see e.g. Fig. 3). It is convenient to deal with the ratio of the intensity of the singlet–triplet transition to the Lyman–Birge–Hopfield (L.B.H.) bands at zero scattering angle. This is given by eq. [12]. Since the second term on the right of eq. [8] is non-vanishing for the L.B.H. bands, we can use Garstang's formula (9) to relate ε_2^2 to Einstein's *A* and hence the absorption coefficient and ε_1^2 can also be related to the absorption coefficient for the singlet–triplet transition. Hence the cross section ratio σ_d/σ_Q can be calculated from the ratio of absorption coefficients in the ultraviolet spectrum after a correction has been made which removes the magnetic dipole contribution to the absorption coefficient. This calculation has been made (32) and the calculated and observed cross section ratios compared (32, 33). The curve obtained in a recent research (33) is shown in Fig. 7. The solid line is calculated using the absorption

TABLE III

Comparison of relative intensities in electron impact and ultraviolet absorption, N_2

U (eV)	Excited state	v'	Relative intensity: Meyer, Skerbele, and Lassettre[a] (200 eV)	Geiger and Stickel[b] (33 000 eV)	Geiger and Schröder[c] (25 000 eV)	Lawrence, Mickey, and Dressler[d] (Ultraviolet)	Franck–Condon factor[e] (Theory)
—	$b^1\Pi_u$	0	—	—	—	—	0.017
12.58	$b^1\Pi_u$	1	0.17	0.13	0.16	—	0.13
12.66	$b^1\Pi_u$	2	0.36	0.32	0.35	—	0.38
12.75	$b^1\Pi_u$	3	0.68	0.62	0.64	0.36[g]	0.73
12.84	$b^1\Pi_u$	4	1.00	1.00	1.00	1.00[f]	1.00
12.91	$1^1\Pi_u$	5?	Unresolved	Unresolved	0.71	0.73	1.03?
12.935	$p'^1\Sigma_u^+$	0	2.3	2.9	2.3	2.5	—

[a]Reference 46.
[b]Reference 49.
[c]References 27 and 28.
[d]Reference 50.
[e]Reference 47.
[f]Lawrence *et al.* found 0.055 ± 0.011 as the oscillator strength for this transition and oscillator strengths for three other transitions were also determined. See ref. 50. Ultraviolet absorption spectra employed. Cases *a*, *b*, *c* refer to electron impact spectra (at zero angle) while *e* refers to calculated Franck–Condon factors.
[g]Measurements affected by source line. See ref. 50.

coefficients. Only one point has been found at high kinetic energies (19) from spectra of considerably poorer quality than those of Fig. 3. The data apply to forward scattering and show that the region 30–100 eV is not a favorable one for the study of singlet–triplet transitions because they tend to be obscured, not only by other more intense allowed transitions, but by electric quadrupole transitions as well.

An intensity anomaly (45) was encountered in the region between 12.5 and 12.93 eV. The first indication of its existence was the disagreement between the excitation potential for the most intense transition in the electron impact spectrum of N_2 (12.93 eV) and that found by others in the ultraviolet absorption spectrum (12.76 eV). The vibrational levels in the electron impact spectrum were not resolved and the discrepancy was initially attributed to a failure of the Born approximation (45). However, with improved spectrometer design, the spectrum was more completely resolved (at 200 eV kinetic energy) and the observed relative intensities (46) of the vibrational levels agreed well with the Franck–Condon factors calculated by Nicholls (47), provided that the vibrational quantum numbers are re-assigned as recommended by Ogawa, Tanaka, and Jursa (48). Geiger and Stickel (49) have independently studied the nitrogen spectrum at 25 keV kinetic energy and obtained intensity ratios in agreement with those of Meyer, Skerbele, and Lassettre (46). It is obvious, therefore, that no failure of the Born approximation is involved. Meyer, Skerbele, and Lassettre (46) suggested that line saturation in the absorption spectrum could account for the discrepancy between ultraviolet and electron impact spectra. Lawrence, Mickey, and Dressler (50) have re-investigated the absorption coefficients in the ultraviolet and have shown that the relative intensities at high resolution and very low pressures (where line saturation is unimportant) are in agreement with electron impact spectra. Relative intensities obtained in electron impact and in the ultraviolet are collected in Table III. The relative Franck–Condon factors are also included. The agreement is good. Lawrence, Mickey, and Dressler (50) have referred to a new analysis of the N_2 spectrum, involving especially the $b^1\Pi_u$ state, which takes into account the strong perturbations which affect the state. The Franck–Condon factors of Nicholls (47) were calculated from a Morse potential function and perturbations were not explicitly taken into account. A more refined theory which considers this point is obviously needed. Oscillator strengths are also reported in ref. (50). These will be discussed later.

At low kinetic energies (48 eV) the relative intensities of the vibrational levels of the $b^1\Pi_u$ state have been studied as a function of angle (20). The results are collected in Table IV. These data are to be compared with Table III. The agreement is obviously excellent except for the 12.93 eV transition. In the first place we note that the relative intensities do not change with angle except for

Can. J. Chem. Downloaded from www.nrcresearchpress.com by 210.87.254.6 on 09/05/12
For personal use only.

TABLE IV

Relative intensities as a function of the scattering angle $b^1\Pi_u \leftarrow X'\Sigma_g^+$ transition in N_2

v'	U (eV)	Relative intensity at scattering angle 0°	2°	4°	6°	8°	10°	12°	14°	16°	I_{av}	Franck–Condon factor
0												0.017
1	12.578	0.19	0.18	0.18	0.18	0.19	0.18	0.18	0.18	0.20	0.18	0.13
2	12.665	0.41	0.38	0.40	0.37	0.42	0.40	0.41	0.42	0.42	0.40	0.38
3	12.750	0.70	0.67	0.70	0.67	0.73	0.70	0.70	0.72	0.72	0.70	0.73
4	12.835	1.00	1.00	1.00	1.00	1.00	1.00	1.00	1.00	1.00	1.00	1.00
5	12.930	2.03	2.27	2.26	2.22	2.06	2.05	1.92	1.71	1.52	—	—

TABLE V

Relative intensities as a function of the scattering angle $a^1\Pi_g \leftarrow X'\Sigma_g^+$ transition in N_2

v'	U (eV)	Relative intensity at scattering angle 2°	5°	8°	11°	14°	I_{av}	Franck–Condon factor
0	8.550	0.25	0.26	0.24	0.24	0.22	0.24	0.24
1	8.755	0.62	0.64	0.62	0.61	0.55	0.61	0.63
2	8.958	0.91	0.93	0.92	0.92	0.87	0.91	0.93
3	9.156	1.00	1.00	1.00	1.00	1.00	1.00	1.00
4	9.357	0.88	0.90	0.88	0.85	0.85	0.87	0.87
5	9.544	0.70	0.69	0.65	0.71	0.64	0.68	0.66
6	9.739	0.50	0.48	0.46	0.48	0.47	0.48	0.45
7	9.926	0.33	0.32	0.31	0.33	0.31	0.32	0.29
8	10.104	0.18	0.19	0.18	0.20	0.17	0.18	0.17
9	10.280	0.13	0.12	0.11	0.11	0.11	0.11	0.10
10	10.462	0.063	0.067	0.063	0.064	0.074	0.066	0.054
11	10.633	0.038	0.031	0.036	0.038	0.046	0.038	0.028
12	10.800	0.026	0.021	0.025	0.026	0.031	0.026	0.015
13	10.971	0.020	0.015	0.018	0.020	0.023	0.019	0.008
14	11.129	0.015	0.008	0.011	0.015	0.013	0.012	0.004
	11.030	0.031	0.030	0.031	0.048	0.053		
	12.256	2.28	1.34	0.89	0.45	0.22		
$v' = 3$	L.B.H./12.930	0.055	0.064	0.080	0.112	0.172		
	12.256/12.930	0.126	0.086	0.071	0.050	0.038		

the 12.93 eV transition. This peak belongs to a different electronic state ($p'^1\Sigma_u^+$) from the remaining peaks ($b^1\Pi_u$), and hence a change in relative intensity with angle is not surprising. In the section entitled Energy Degradation in the Excitation of Gases, the energy degradation calculations of Green *et al.* were mentioned. These were based on cross sections for the entire electronic transitions and the question arises as to whether the vibrational components change in relative intensity with angle. From Table IV it is obvious that the relative intensities for different vibrational levels of the $^1\Pi_u$ state are not changing with angle even though the state is strongly perturbed by adjacent states. Constant relative intensities (as scattering angle is varied) should greatly simplify calculations of energy degradation and others of a similar nature. The Franck–Condon principle suggests that relative intensities should change but little with angle, but a direct experimental confirmation is well worthwhile. In contrast, there are pairs of *electronic* transitions in N_2 whose relative intensities change by a factor of 10 within the same range of angle.

The relative intensities in the vibrational progression of the transition $a^1\Pi_g \leftarrow X^1\Sigma_g^+$ have also been studied as a function of angle at 48 eV kinetic energy. The results are shown in Table V for 15 members of the progression and for several other electronic transitions by way of contrast. There is some trend for the first two members ($v' = 0, 1$) but the trend is small in comparison to changes in intensity ratios of different electronic transitions. The average relative intensities agree well with the Franck–Condon factors of Benesch *et al.* (51) except at very high vibrational quantum

Can. J. Chem. Downloaded from www.nrcresearchpress.com by 210.87.254.6 on 09/05/12
For personal use only.

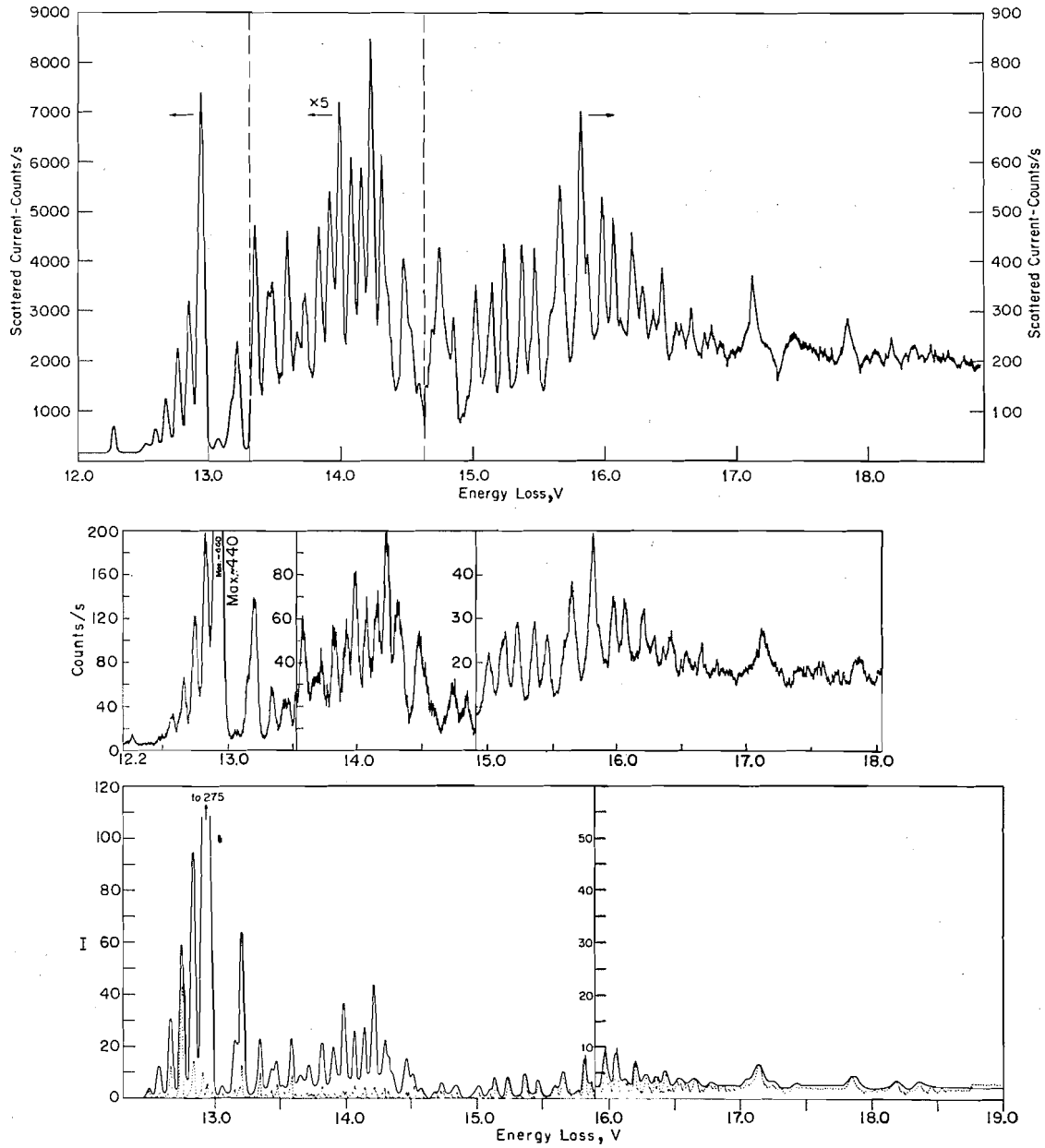

FIG. 7*a*. Electron impact spectra of nitrogen at zero scattering angle and different kinetic energies. Top spectrum 70 eV kinetic energy by Lassettre, Skerbele, and Dillon (unpublished). Note auto-ionized transitions. Middle spectrum, 200 eV kinetic energy by Lassettre, Skerbele, and Meyer (19). Lower spectrum, 33 keV, by Geiger and Stickel (49).

numbers. It is again obvious that calculations like those of the above mentioned section are greatly simplified because relative intensities in a vibrational progression change but little with angle.

Three members of the vibrational progression associated with the transition $C^3\Pi_u \leftarrow X^1\Sigma_g^+$ have been resolved (20). Relative intensities as a function of angle are given in Table VI. There is no significant change with angle but the average does not agree well with calculated Franck–Con-

Can. J. Chem. Downloaded from www.nrcresearchpress.com by 210.87.254.6 on 09/05/12
For personal use only.

TABLE VI

Relative intensities as a function of the scattering angle $C^3\Pi_u \leftarrow X'\Sigma_g^+$ transition in N_2

v'	U (eV)	Relative intensity at scattering angle 2°	5°	8°	11°	14°	I_{av}	Franck–Condon factor
0	11.030	1.00	1.00	1.00	1.00	1.00	1.00	1.00
1	11.281	0.68	0.70	0.74	0.65	0.77	0.71	0.56
2	11.522	0.45	0.37	0.26	0.35	0.40	0.37	0.19

don factors. The transition is so weak that the intensity measurements are subject to large random errors and an accurate background correction is difficult to make. It is probable, however, that the difference between theory and experiment is real.

Referring back to Table I we see that for a 30 keV incident electron, 32.8% of the energy contributes to excitation of N_2 and 27.1% produces ionization. We now inquire into the state of the ions produced. Much attention has been devoted to the determination of energy levels of positive ions. Limited information is obtained by extending electron impact spectra into the ionized continuum. When this is done auto-ionized transitions are encountered. The theory of line shapes of such transitions has been developed by Fano (52) and has been extensively tested by experiments on atoms, especially helium. This situation will be further discussed in the section on helium. Nitrogen has been studied at high resolution by Geiger and Stickel (49) and by Lassettre, Skerbele, and Meyer (19). Electron impact spectra have been extended into the ionized continuum and three spectra are shown in Fig. 7*a*. The bottom spectrum is that of Geiger and Stickel (49) at 25 keV, the middle figure is from ref. 19 at 200 eV, while the upper figure is a previously unpublished spectrum at 70 eV obtained by Lassettre, Skerbele, and Dillon. The auto-ionized transitions at excitation energies above 17 eV are obvious. Since auto-ionization is accompanied by substantial line broadening there is a loss of detail in the ionized continua which cannot be regained by increase in resolution. Nevertheless, this loss in detail is not inevitable because it results in part from the fact that in an ionized continuum, the energy of the ejected electron is not selected or controlled, and hence the collision (above the ionization limit) is not fully defined. This could be remedied, with an additional velocity analyzer, by counting coincident events. Thus far, this has been done only by Erhardt and Linder (53) at low resolution. However, the expected result at high resolution can be forecast in the following way. At small scattering angles the collision cross section is proportional to the oscillator strength (eq. [1]) and hence the energy spectrum of electrons ejected in a glancing collision should be the same as the energy spectrum of electrons ejected in the absorption of a photon whose energy is that transferred to the molecule in the electron collision. Turner and May have studied the kinetic energy distribution of electrons ejected from N_2 by absorption of helium resonance radiation (54) ($h\nu = 21.21$ eV). The spectrum of ejected electrons observed by Turner and May is shown in Fig. 8. A magnetic velocity analyzer was used. Since the ejected electrons have been completely separated from the ion (whose recoil energy is negligible) the spectrum, in an energetic sense, is that of the positive ion. The relative intensities

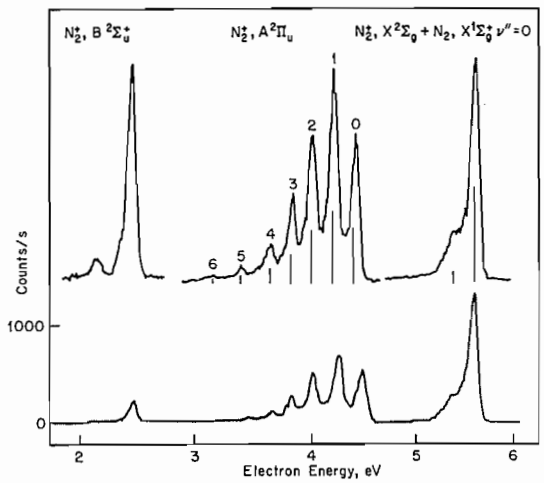

FIG. 8. Energy distribution of electrons ejected on absorption of helium resonance radiation ($h\nu = 21.21$ eV) by Turner and May (54). Top figure is a re-run at higher sensitivity. Vertical lines are Franck–Condon factors.

Can. J. Chem. Downloaded from www.nrcresearchpress.com by 210.87.254.6 on 09/05/12
For personal use only.

Can. J. Chem. Downloaded from www.nrcresearchpress.com by 210.87.254.6 on 09/05/12
For personal use only.

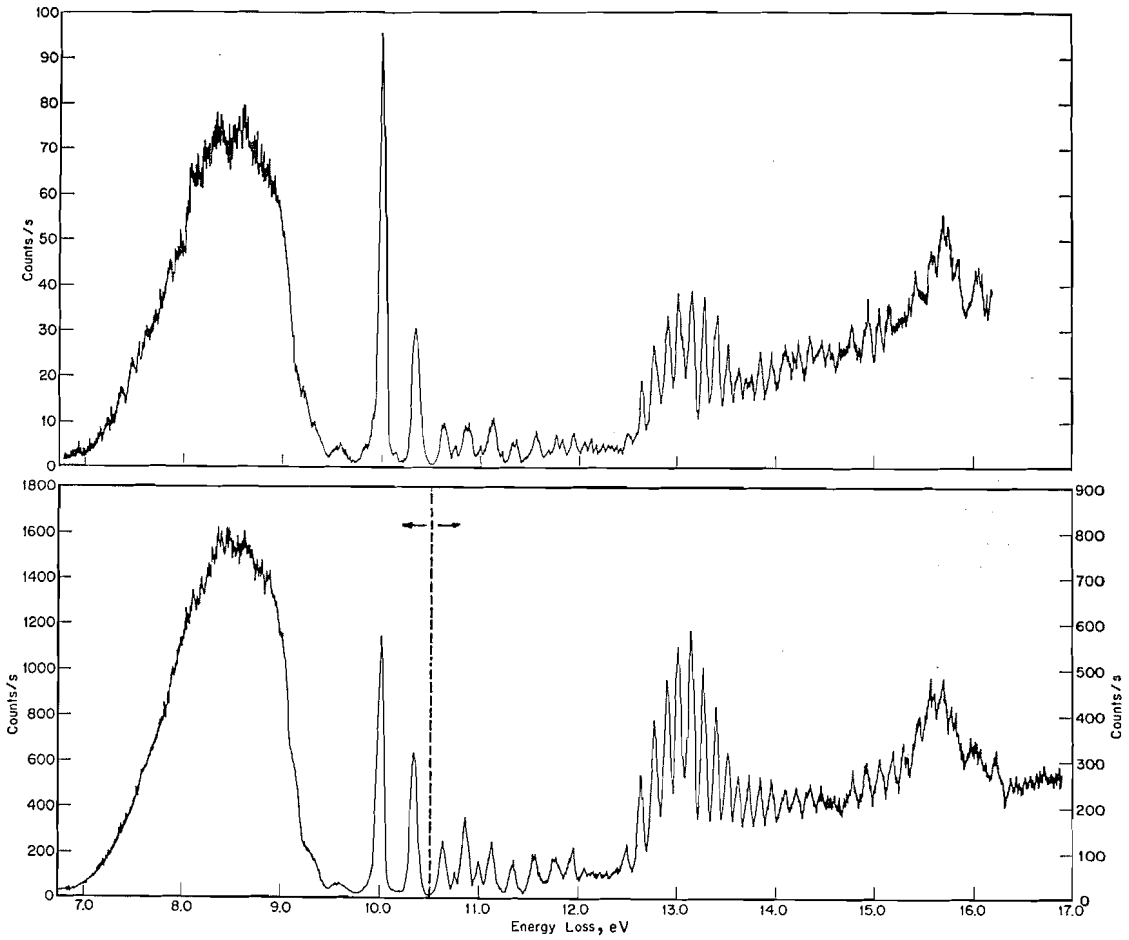

FIG. 9. Electron impact spectra of oxygen at 48 eV kinetic energy and scattering angles $\theta = 14°$ (top) and 4° (bottom) by Lassettre, Skerbele, Dillon, and Ross (20).

within a vibrational progression are given by the Franck–Condon factors with good accuracy. The relative intensities of different electronic states of the ion are determined by the probabilities of simultaneous two electron jumps (one electron excited, the other ejected). A theory of this process must take account of electron correlation. Approximations of the Hartree–Fock type are not adequate. Since the energies of electronic states of positive ions are of great chemical interest, this method has been widely developed and applied by Turner and collaborators under the designation "photoelectron spectroscopy". It would be of considerable interest to develop apparatus for the study of ejected electron spectra when the gas is ionized by electron impact with the transfer of a pre-selected amount of energy

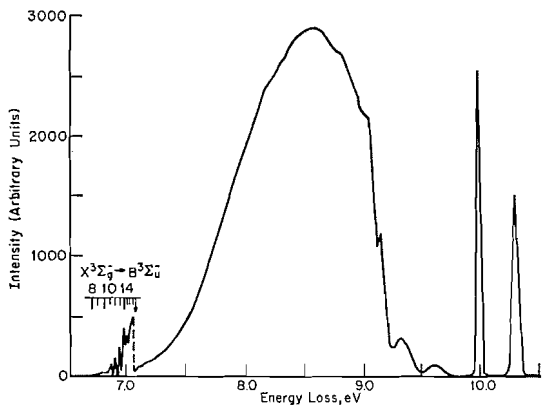

FIG. 10. Electron impact spectrum of O_2 at 25 keV by Geiger and Schröder (56). Note resolution of Schumann–Runge bands. See also ref. 27.

Can. J. Chem. Downloaded from www.nrcresearchpress.com by 210.87.254.6 on 09/05/12
For personal use only.

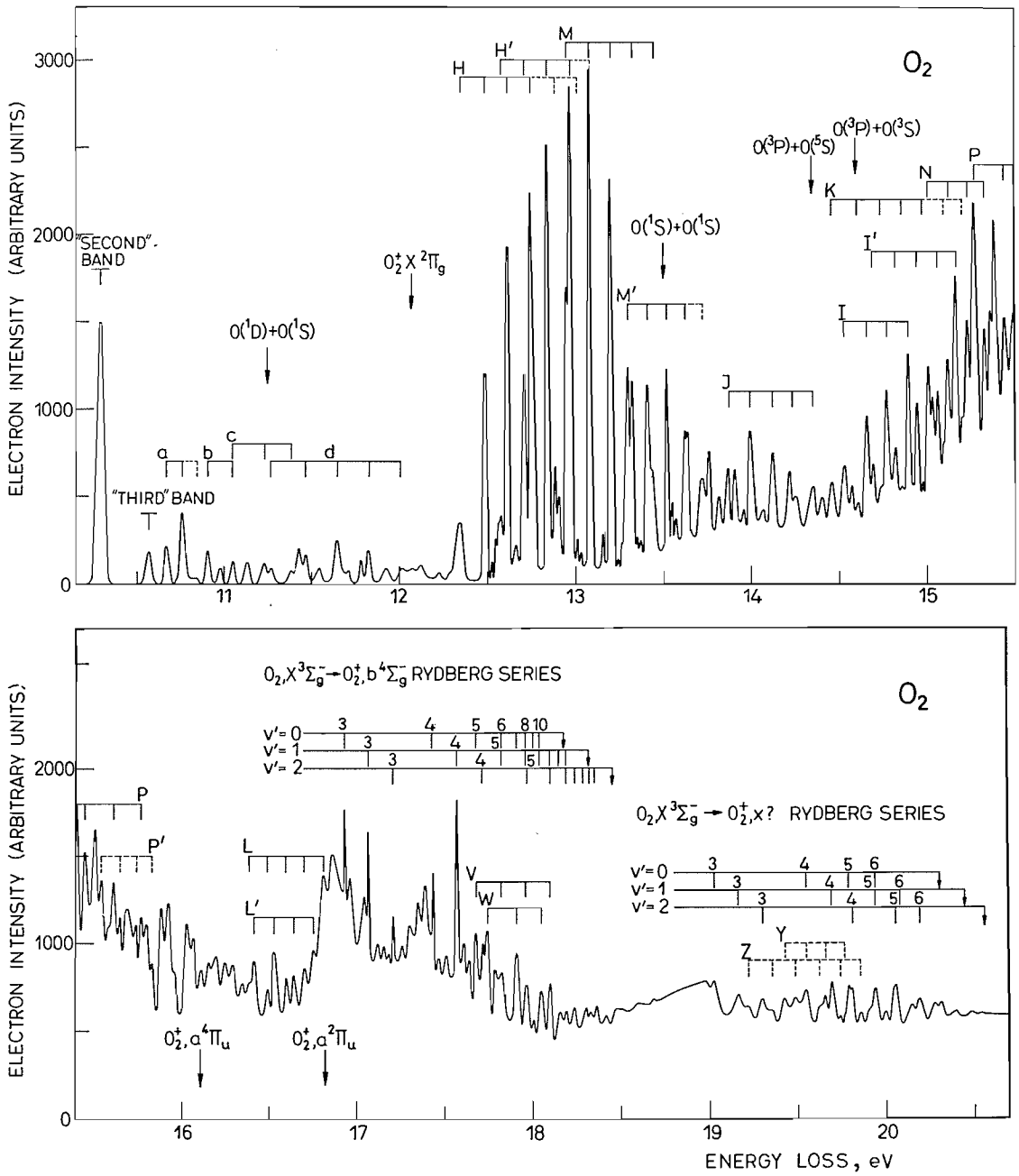

FIG. 11. Electron impact spectrum of O_2 by Geiger and Schröder (56). Kinetic energy = 25 keV, $\theta = 0°$.

to the scatterer. Spectra similar to Fig. 8 are expected, but it would be of interest to test this point by experiment. However, there are formidable difficulties involved in such experiments.

Mass spectrometric methods for the study of excited ionic states are also well developed and are being reviewed by a different author.

Electron impact spectra of N_2 at low kinetic energy and large scattering angles have been obtained by Doering and Williams (55). Singlet–triplet transitions are prominent under these conditions.

Can. J. Chem. Downloaded from www.nrcresearchpress.com by 210.87.254.6 on 09/05/12
For personal use only.

Oxygen

Electron impact spectra of oxygen at 48 eV kinetic energy (20) are shown in Fig. 9. The scattering angle in the upper spectrum is 14° and in the lower, 4°. The broad peak (7–9 eV) corresponding to the dissociation continuum of the Schumann–Runge bands dominates the spectrum. Changes in relative intensity with change in angle are obvious. Geiger and Schröder (56) have also studied the oxygen spectrum at a scattering angle of 0° and kinetic energy of 25 keV. The results are shown in Figs. 10 and 11. Figure 10 is very similar to the small angle spectrum of Fig. 9. The differences are attributable to the different angles and resolving powers. On the other hand there are distinct differences in relative intensity between Figs. 11 and 9. This is especially noticeable in the excitation energy range 10.5 to 12.0 eV and is not attributable either to differences in scattering angle or resolution. The transitions shown in Figs. 10 and 11 are all electric dipole allowed and in Fig. 9 no peak is definitely associated with a forbidden transition. However, the kinetic energy at which the spectra of Fig. 9 were obtained is low enough so that forbidden transitions should be excited. It seems very probable that the differences in relative intensity are due to optically forbidden transitions which are not resolved from the allowed transitions in Fig. 9. In less crowded regions of the spectrum, forbidden transitions are observed. In Fig. 12 the portion of the energy loss spectrum of oxygen from 0 to 2 eV is shown. Aside from the elastic peak (at energy loss 0) all of the remaining peaks arise from forbidden transitions. The fundamental vibration (at 0.196 eV) and one overtone, together with the peak corresponding to $a^1\Delta_g \leftarrow X^3\Sigma_g^-$, are obvious. An overtone of the latter transition is also observed although many spectra were needed to distinguish it from the background. The transition $b^1\Sigma_g^+ \leftarrow X^3\Sigma_g^-$ should be observed at 1.6 eV and there is a suggestion of a peak in Fig. 12. Additional spectra obtained at 60 eV suggest that the transition does occur but it exceeds the background by so little that its intensity cannot be reliably estimated. None of the excited states is new. All are known from previous research. The ratio of the intensity of the $a^1\Delta_g \leftarrow X^3\Sigma_g^-$ to the elastic peak has been determined over the angle range 2 to 15° at kinetic energy 45 eV and found to be constant and equal to $(1.3 \pm 0.2) \times 10^{-4}$.

It is convenient at this point to digress briefly

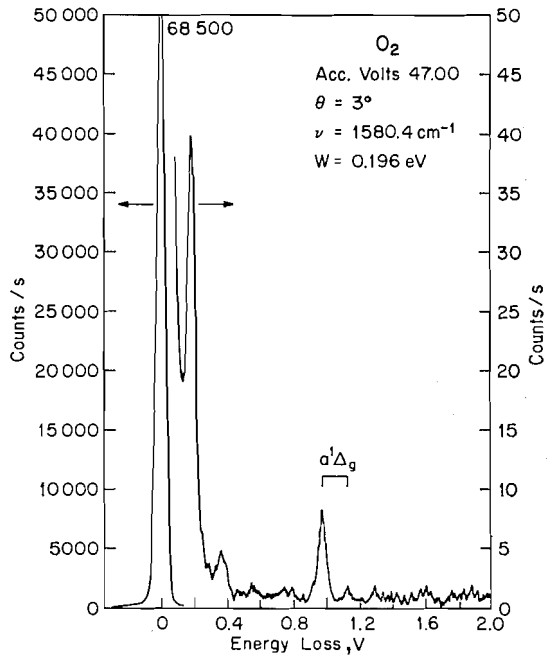

FIG. 12. Electron impact spectrum of O_2 by Skerbele, Dillon, and Lassettre (34).

for some comments on the resolution of velocity analyzers. To complete the basis for this discussion we show one additional electron impact spectrum of oxygen in Fig. 13. In this spectrum the electrons were scattered at a kinetic energy of 70 eV and then retarded to 20 eV, this being the kinetic energy at which electrons traverse the velocity analyzer. When this spectrum was taken, slits of width W equals 0.01 in. were installed in the focal plane and the orbit diameter in the analyzer is D, equals 10 in. Hence the resolving power, R, equals D/W, is 1000. If electrons of a given energy are incident on a velocity analyzer then the fraction transmitted at different energy settings is a triangular curve with half width $\Delta E = E/R$. Since both monochromator and analyzer are involved, a convolution will give the overall fraction transmitted. If electrons pass through both monochromator and analyzer at the same energy then the resultant transfer function is a bell shaped curve with half width $1.4\Delta E = 1.4E/R$. As used in Fig. 13 the half width is 0.028 eV. Turner (26) has analyzed the performance of velocity analyzers in photoelectron spectroscopy and pointed out that the breadth of molecular bands due to unresolved rotational structure is of the order of kT

Can. J. Chem. Downloaded from www.nrcresearchpress.com by 210.87.254.6 on 09/05/12
For personal use only.

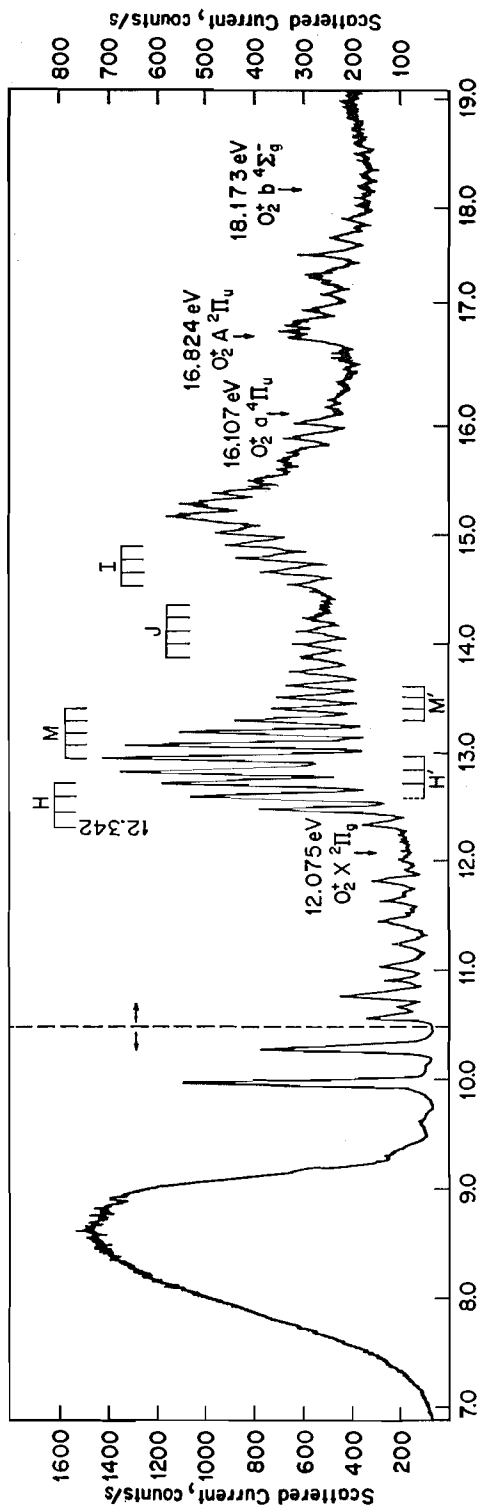

FIG. 13. Electron impact spectrum of O_2 at 68 eV kinetic energy and zero scattering angle by Lassettre, Skerbele, Dillon, and Ross (20). Instrumental half width (0.028 eV), i.e. velocity analysis after retarding to 20 eV through an analyzer with resolution of 1000.

TABLE VII
Vibrational spectrum of H_2O

Upper state[a]				Intensity		
Species	Designation	ν (cm^{-1})	U (eV)	Infrared[b]	Infrared[c]	Electron impact
A_1	ν_2	1595.0	0.198	1.00	1.00	1.00
A_1	$2\nu_2$	3151.4	0.391	—	0.006	—
A_1	ν_1	3651.7	0.453	0.72	0.625	0.77
B_1	ν_3	3755.8	0.466			
B_1	$\nu_2+\nu_3$	5332.0	0.661	0.058	0.081	0.046
B_1	$\nu_1+\nu_3$	7251.6	0.899	0.047	0.063	0.034
B_1	$\nu_1+\nu_2+\nu_3$	8807.1	1.092	0.002	—	—
B_1	$2\nu_1+\nu_3$	10613.1	1.316	—	—	—

[a]Reference 137.
[b]Reference 138.
[c]Reference 139.

$\sim$ 0.028 eV, this quantity being largely independent of the structure of the molecule. In Fig. 13 we have a spectrum in which the instrumental band width is equal to the thermal, rotational spread, while in Fig. 11 there is given a spectrum in which the band width is considerably smaller ($\sim$ 0.01 eV). Obviously in Fig. 11 more detail is resolved but the half width of the narrowest peaks is comparable with the 0.028 eV expected for the thermal width. The band width used in Fig. 13 is not the smallest employed in our research. In Fig. 1, spectrum C at 33 eV was obtained with a band width of approximately 0.014 eV. The path length through our scattering cell is 5 cm and the pressures employed range from 0.2 to 1.0 μ. Hence pressure times path length is between 10^{-3} and 5×10^{-3} Torr cm. At these small values (and high angular resolution) the scattered currents become too small for reliable measurement when the band width is less than 0.014 eV. This, however, may be only a temporary block.

Turner (26) has shown that in photoelectron spectroscopy the widths of peaks of molecular ions are distinctly larger than atomic ions. This is illustrated in Fig. 14 which shows the peak widths of lines from an atomic ion (Xe^+) in the right hand part and that due to O_2^+ in the left hand part. Note the peak due to Xe^+ in the left hand spectrum. The peak widths of the atomic lines are 0.015 eV. The O_2^+ peaks are broadened more than the doublet splitting, 0.024 eV. In these experiments electron kinetic energies were only a few volts. More complete O_2^+ spectra have also been obtained by Turner and May (54). A spectrum is shown in Fig. 15. This figure provides the states of the ion and can be considered as an electron ejection spectrum brought about by a

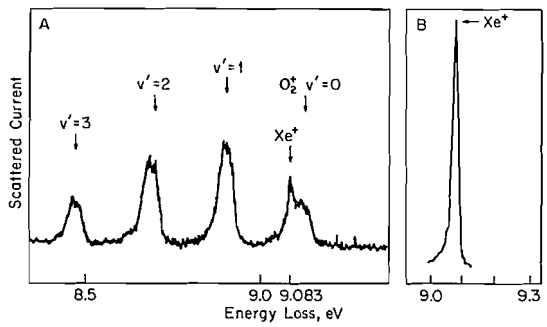

FIG. 14. Energy distribution of electrons ejected from O_2 (left) and Xe (right) on illumination with helium resonance radiation ($h\nu = 21.21$) by Turner (26). The left hand spectrum is due to the excited state $^2\Pi_g$ of the O_2^+ ion while the right hand peak is due to $^2P_{3/2}$ state of Xe^+. Xe mixed with O_2 in left hand spectrum. Note difference in peak widths.

glancing collision in which the incident electron transfers 21.21 eV to the O_2 molecule. A precisely similar case is discussed for N_2.

Water Vapor

An electron impact spectrum of H_2O at low resolution was reported by Lassettre and Francis (57). At higher resolution a spectrum was obtained by Skerbele and Lassettre (58) and at still higher resolution by Skerbele, Meyer, and Lassettre (59). The intensity was studied as a function of angle by Skerbele and Lassettre (60). A spectrum obtained recently (20) at 100 eV is shown in Fig. 16. Term symbols, taken from the compilation of Herzberg (61), are shown on the figure for several transitions.

Very recently, background has been reduced in the vicinity of the elastic peak to such a degree that vibrational transitions can be found. Examples have already been given for N_2 and O_2. In Fig.

Can. J. Chem. Downloaded from www.nrcresearchpress.com by 210.87.254.6 on 09/05/12
For personal use only.

Can. J. Chem. Downloaded from www.nrcresearchpress.com by 210.87.254.6 on 09/05/12
For personal use only.

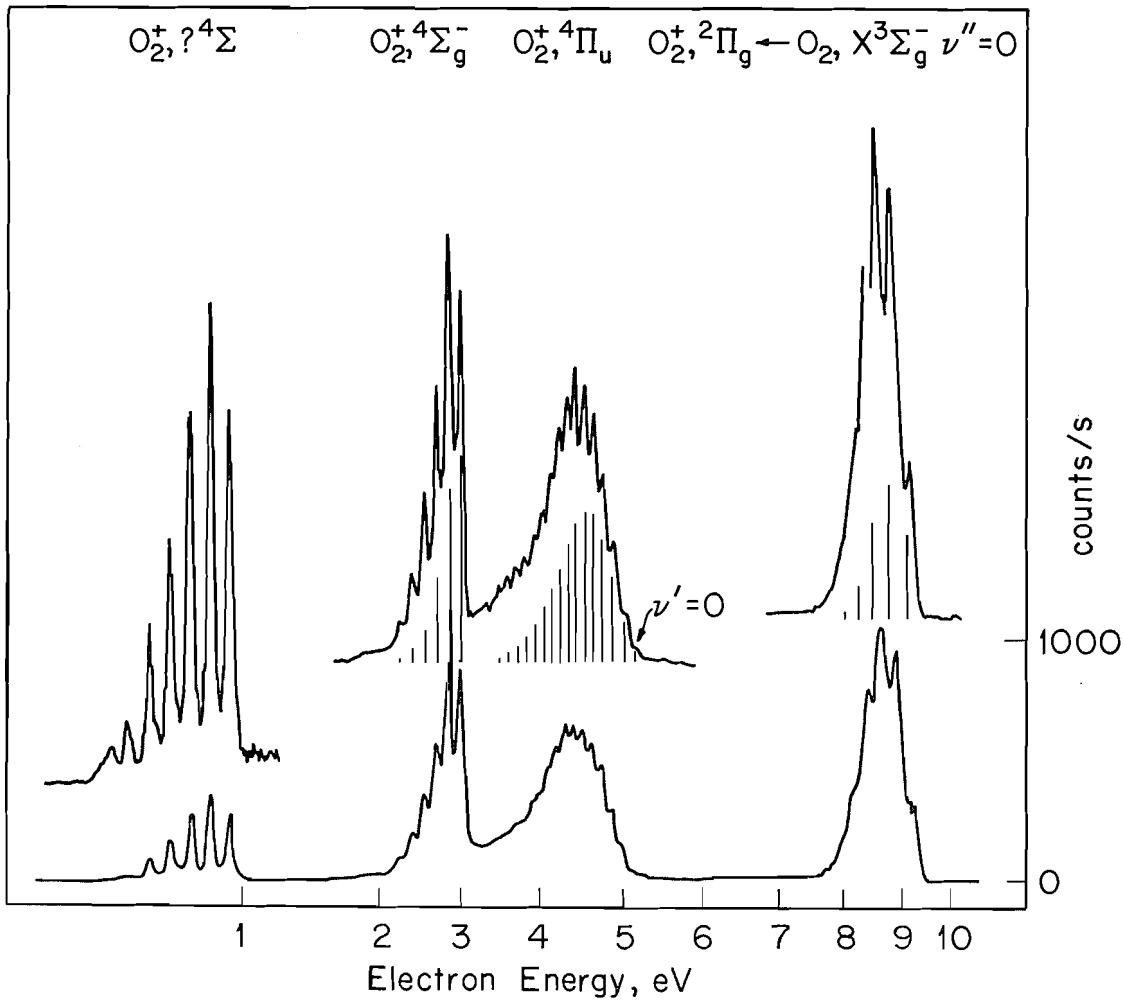

FIG. 15. Energy distribution of electrons ejected by absorption of helium resonance radiation ($h\nu$ = 21.21 eV) by Turner and May (54). Top spectrum at higher sensitivity. Vertical lines are Franck–Condon factors. Magnetic analyzer was used.

17 is shown a rather complete spectrum (62) of water vapor at 55 eV and a scattering angle of 5°. The fundamental vibrations and several overtones are apparent. A portion of the spectrum at a smaller angle (and hence higher scattered current) is shown in the inset. Additional overtones are found. Table VII identifies the frequencies, and gives the observed relative intensities from electron impact spectra and also from the infrared absorption coefficients of others. Note also the weak scattering beginning at 4.5 eV and extending to 6.5 eV. Schulz (63) found such scattering at very low kinetic energies (threshold) and the observation was confirmed by Compton *et al.* (64). In Fig. 17 the excitation is detected at much higher energies. See ref. 65 for positive ion spectra.

Figure 17 is of special interest because of the wide spectral range (infrared to vacuum ultraviolet) covered in a single spectrum. Elastic cross sections are being determined by Bromberg at Mellon Institute. Once these are available, collision cross sections can be determined over the complete spectral range of Fig. 17 with comparative ease.

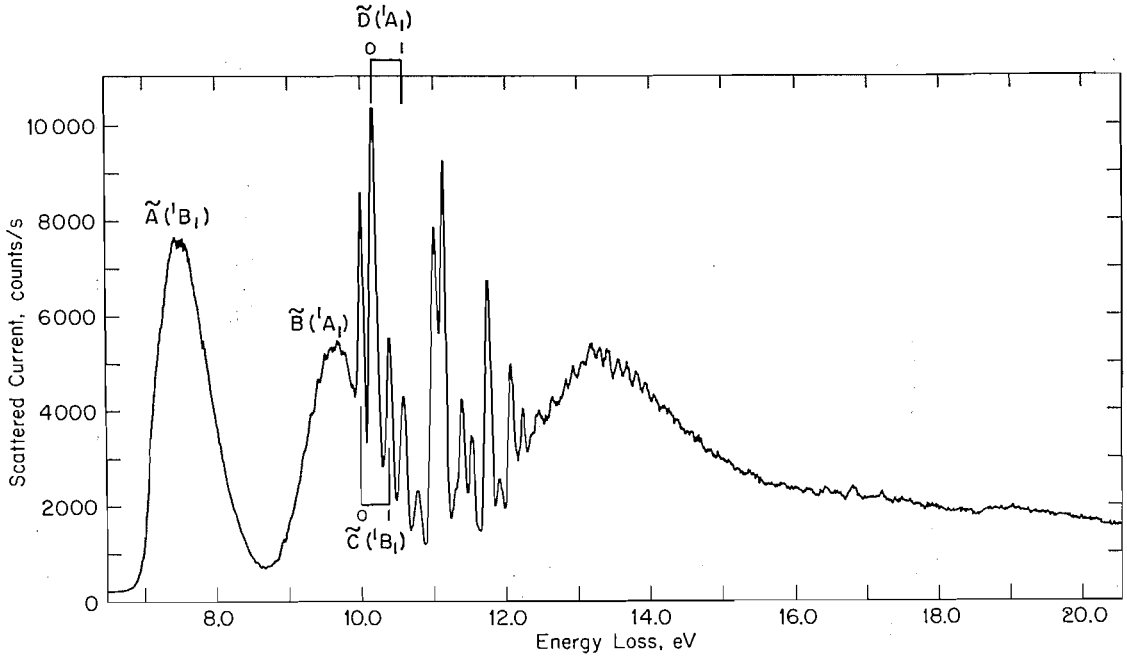

FIG. 16. Electron impact spectrum of H_2O at 100 eV and zero scattering angle by Lassettre, Skerbele, Dillon, and Ross (20).

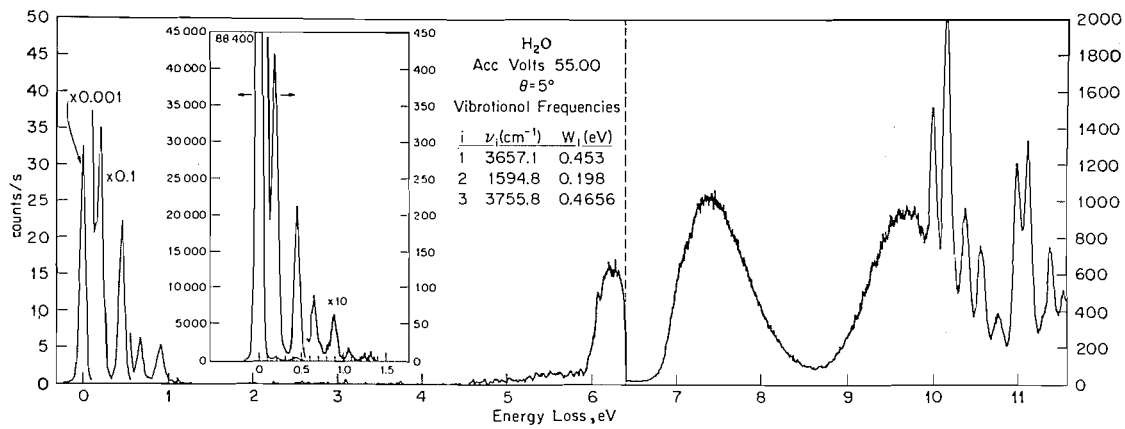

FIG. 17. Electron impact spectrum of H_2O by Skerbele, Dillon, and Lassettre (62). Note vibrational excitations near elastic peak in main spectrum (θ = 5°) and in the inset (θ = 4°). Kinetic energy, 53 eV. In optical equivalent, the spectrum covers the full range from infrared to vacuum-ultraviolet. Note weak scattering from 4.5 to 6 eV, and scale change at 6.4 eV.

Carbon Dioxide

Electron impact spectra of carbon dioxide (20) are shown in Fig. 18. The 7–10 eV region is one in which vibronically allowed transitions are occurring. There is a general change in envelope shape as the kinetic energy decreases but no new lines (attributable to forbidden, perhaps electric quadrupole, transitions) are found. At kinetic energies up to 200 eV, there is very little change in the spectrum outside the 7–10 eV region and no major change in that range.

Near the elastic peak, vibrational excitations are observed (62), as shown on the right in Fig. 19. Geiger and Wittmaack (66) have also observed

Can. J. Chem. Downloaded from www.nrcresearchpress.com by 210.87.254.6 on 09/05/12
For personal use only.

Can. J. Chem. Downloaded from www.nrcresearchpress.com by 210.87.254.6 on 09/05/12
For personal use only.

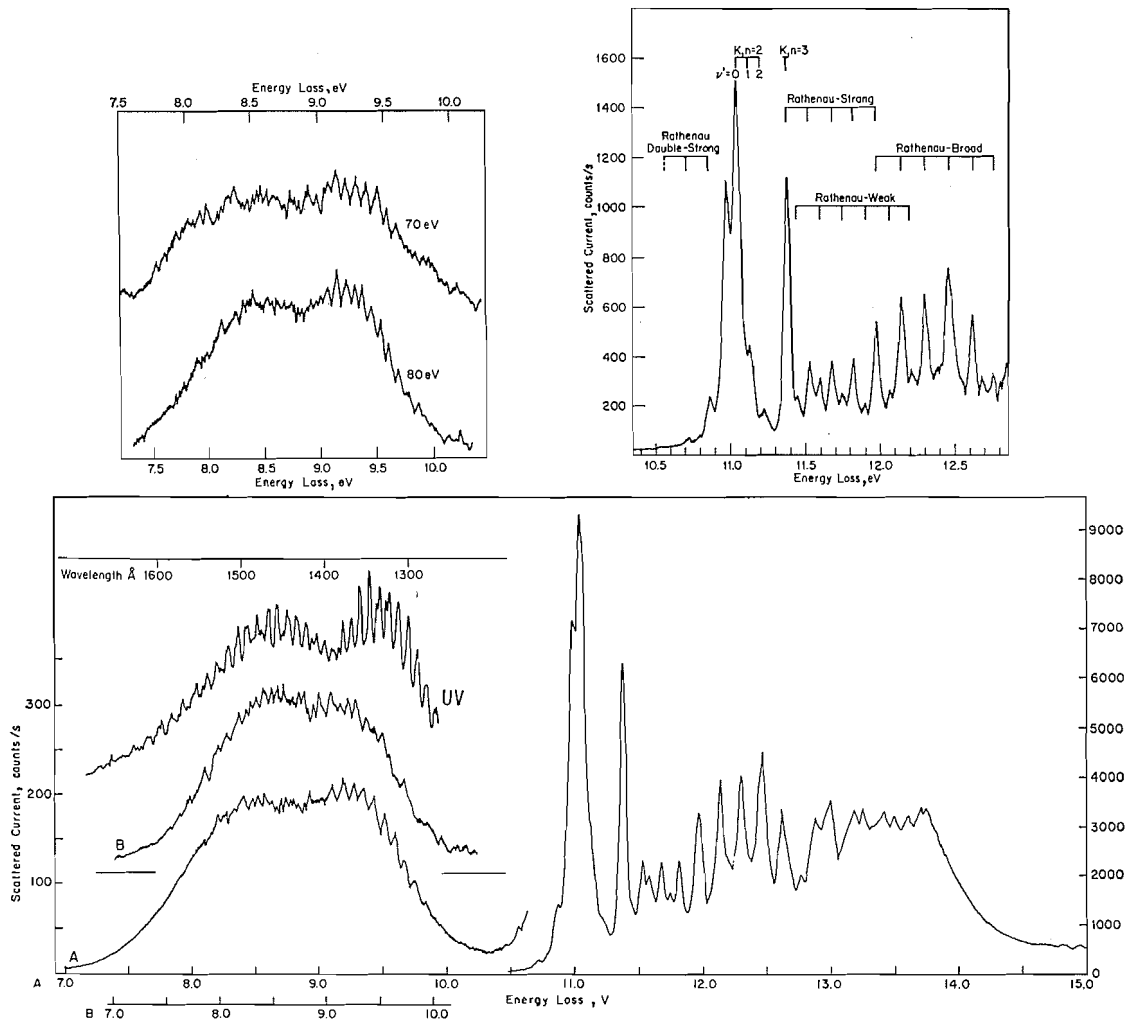

FIG. 18. Electron impact spectra of CO_2 at $\theta = 0°$ and kinetic energies 48 (lower) and 58 eV (upper right) by Lassettre *et al.* (20). Curve A is continuation of 48 eV spectrum while B is a new spectrum at 28 eV kinetic energy. Spectrum labeled UV is ultraviolet spectrum. Note spectra at 70 and 80 eV at upper left.

vibrational transitions at high kinetic energies and their spectra at 25 keV are shown on the left of Fig. 19. The spectra on the right contain the symmetric stretching (forbidden) transition while the spectra on the left do not. This is to be expected in view of the great difference in kinetic energy.

The unsymmetrical stretching vibration is much more intense, relative to elastic scattering, than any of the transitions of N_2 or O_2. The ratio of scattered current at the peak to the elastic peak current is shown in Fig. 20 as a function of scattering angle. For N_2 and O_2 this ratio was essentially constant. Cross section determinations at these kinetic energies would be of considerable interest but have not yet been done.

Argon

Electron impact spectra of argon have been studied at high incident electron energies by Boersch, Geiger, and Hellwig (23) and Boersch (67). An electron impact spectrum (20) is shown in Fig. 21. Chamberlain, Heideman, Simpson, and Kuyatt (68) have studied the spectrum at low kinetic energies. One of their spectra is shown in

Can. J. Chem. Downloaded from www.nrcresearchpress.com by 210.87.254.6 on 09/05/12
For personal use only.

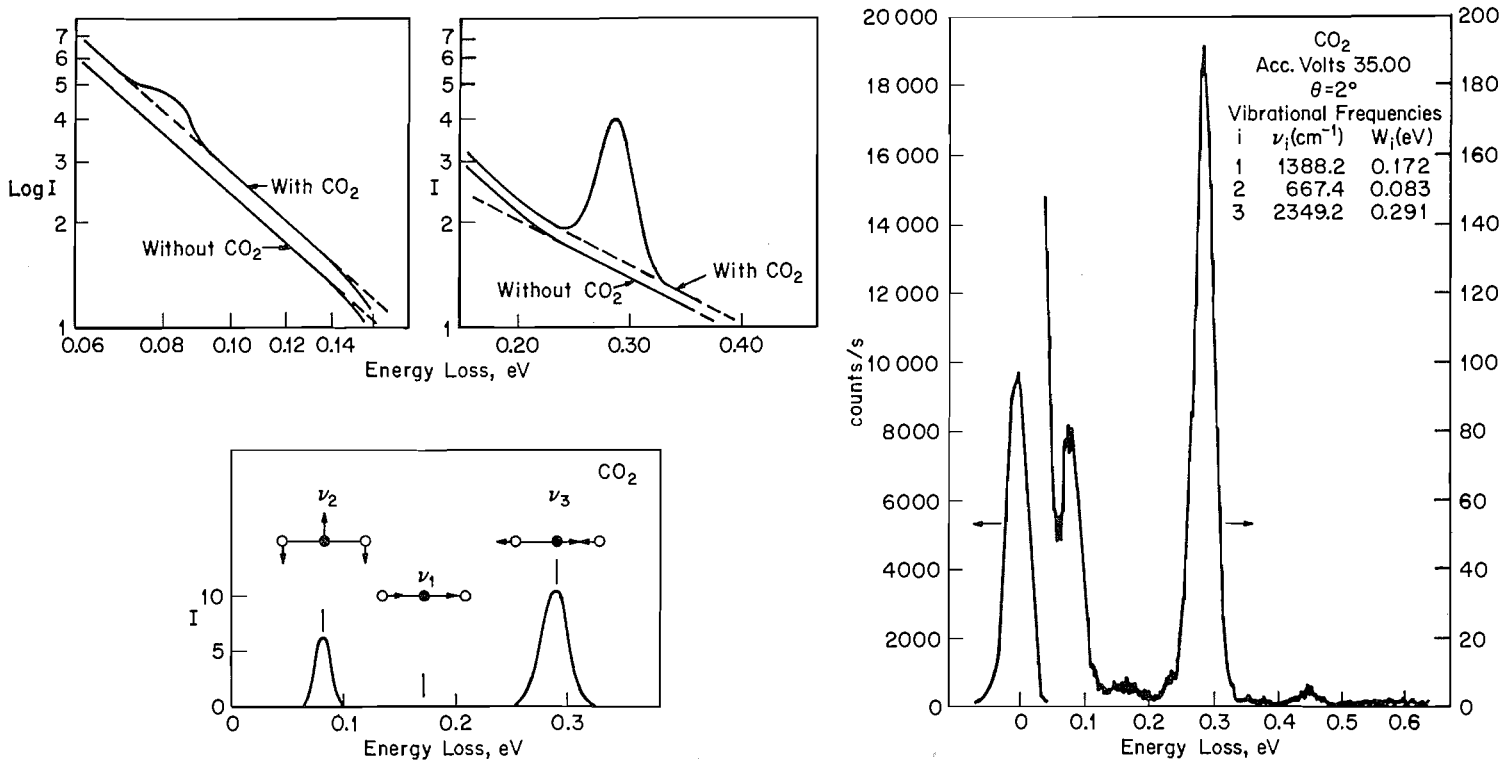

FIG. 19. Electron impact spectrum of CO_2, near elastic peak, containing vibrational transitions. Spectrum at right by Skerbele, Dillon, and Lassettre (62) at 33 eV kinetic energy and that at left by Geiger and Wittmaack (66) at kinetic energy 25 keV. Note forbidden transition at 0.172 eV in spectrum at right. This is missin~ in spectrum at left.

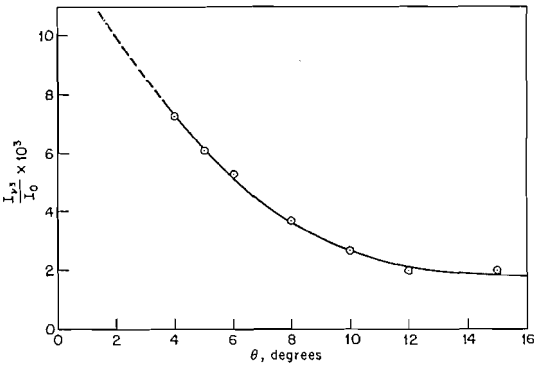

FIG. 20. Ratio of scattered current due to excitation of ν_3 vibration ($h\nu_3$ = 0.291 eV) to that for elastic scattering (see Fig. 19) of CO_2 as a function of scattering angle by Skerbele, Dillon, and Lassettre (62). Kinetic energy 48 eV.

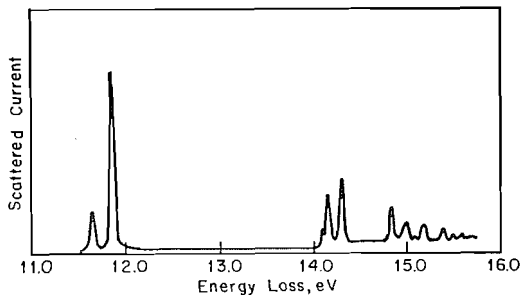

FIG. 21. Electron impact spectrum of argon at kinetic energy 25 keV and zero scattering angle by Boersch (67).

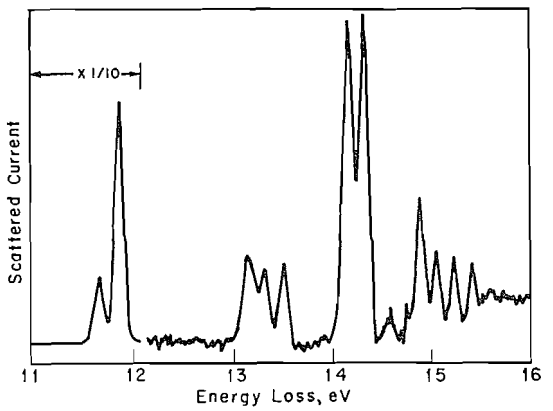

FIG. 22. Electron impact spectrum of argon at kinetic energy 40.7 eV and zero scattering angle by Chamberlain, Heideman, Simpson, and Kuyatt (68). Note forbidden transitions from 13.0 to 13.7 eV.

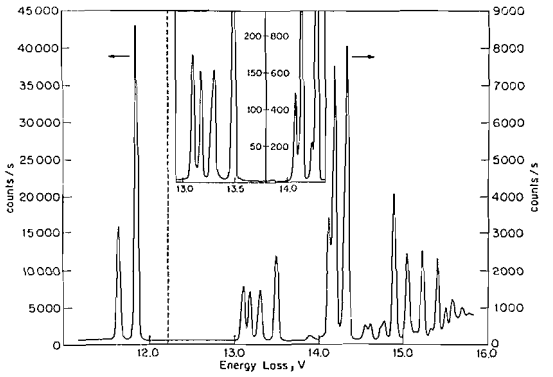

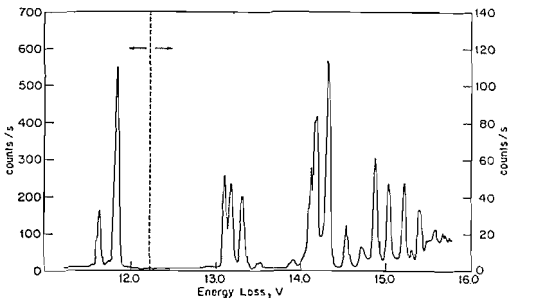

FIG. 23. Argon spectra at an accelerating voltage of 60 for the inset and 50 for the others by Lassettre, Skerbelle, Dillon, and Ross (20). Scattering angle in the top spectrum 0° and at the bottom 15°. Note changes in relative intensity of the four peaks between 13.0 and 13.7 eV.

Fig. 22. More highly resolved spectra at 50 eV have also been obtained (20) and spectra at two angles are shown in Fig. 23. In Figs. 22 and 23 a group of forbidden transitions occurs between 13.0 and 13.7 eV. Note the differences in relative intensities at the two angles of Fig. 23. Theoretical calculations for this group of states would be well worthwhile.

Helium

Helium has been very extensively studied. The substance is widely used as a comparison gas in the determination of collision cross sections (section following) and has considerable theoretical interest as well. Electron impact spectra obtained by four different groups are of interest. High resolution spectra were obtained at zero scattering angle and low kinetic energies by Chamberlain, Heideman, Simpson, and Kuyatt (68). Their spectrum at 30.7 eV is shown in Fig. 24.

An interesting series of electron impact spectra has been obtained by Kupperman and collaborators (69) and the spectra are reproduced in Fig.

Can. J. Chem. Downloaded from www.nrcresearchpress.com by 210.87.254.6 on 09/05/12
For personal use only.

TABLE VIII
Cross section ratios in helium spectra

	Ratios at E value				
	48 eV			300 eV[a]	400 eV[b]
n	I_{n1P}/I_{21P}	I_{n1S}/I_{21S}	I_{n3S}/I_{23S}	I_{n1P}/I_{21P}	$\sigma_{n1P}/\sigma_{21P}$
3	0.205±0.004	0.204±0.010	0.22±0.01	0.210±0.019	0.206
4	0.081±0.005	0.084±0.009	0.10±0.02	0.079±0.005	0.078
5	0.043±0.003	—	—	0.037±0.001	—
6	0.024±0.002	—	—	—	—

[a]Reference 116, Table II.
[b]Reference 140.

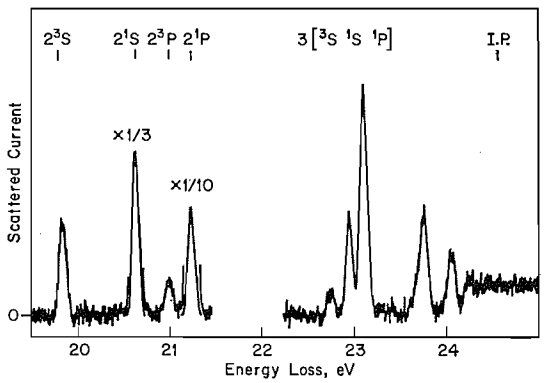

FIG. 24. Helium spectrum at kinetic energy 30.7 eV and zero scattering angle by Chamberlain, Heideman, Simpson, and Kuyatt (68). Note forbidden transitions.

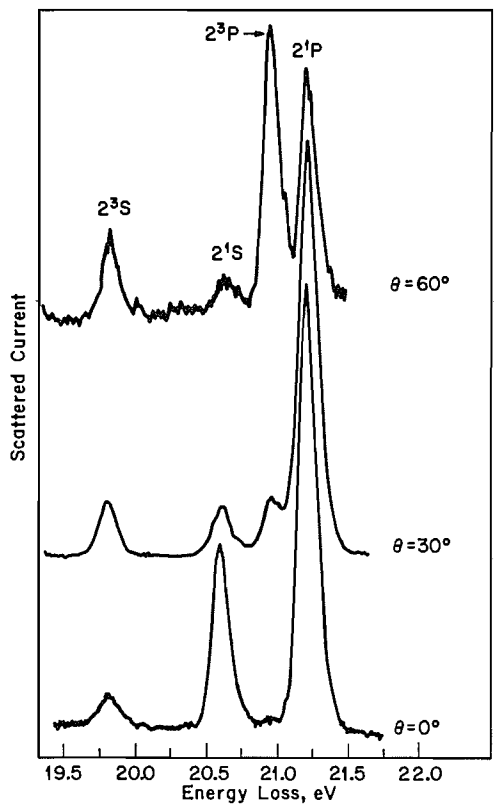

FIG. 25. Helium spectra at different scattering angles by Rice, Kupperman, and Trajmar (69). Kinetic energy 36 eV. Note reversal in relative heights of 2^1P and 2^3P peaks.

25. Note the reversal in relative intensity of the excitations to 2^3P and 2^1P. This (ref. 69) is the first of a series of papers by Kupperman and his coworkers aimed at the development of a new method for the detection and identification of singlet–triplet transitions. It is known from the theory of Ochkur (71) and Bonham (72) that the cross sections of singlet–triplet transitions decrease with increase in momentum change (and hence angle) more slowly than allowed transitions. By studying the relative intensity over an extensive range of angles one can frequently select those transitions which involve changes in multiplicity from the manifold of others which do not involve any such change. The methods seem especially promising for polyatomic molecules.

The spectrum has been studied at 50 eV and small angles by Skerbele and Lassettre (70) (see Fig. 26). The ratios of intensities in Rydberg series exhibit surprising regularities as shown in Table VIII. These observations are of considerable interest in view of the methods used by Green and collaborators in estimating collision cross sections (see section on Energy Degradation in the Excitation of Gases in the Introduction).

Finally Boersch, Geiger, and Schröder (73) have studied the spectrum of helium at 25 keV

Can. J. Chem. Downloaded from www.nrcresearchpress.com by 210.87.254.6 on 09/05/12
For personal use only.

Can. J. Chem. Downloaded from www.nrcresearchpress.com by 210.87.254.6 on 09/05/12
For personal use only.

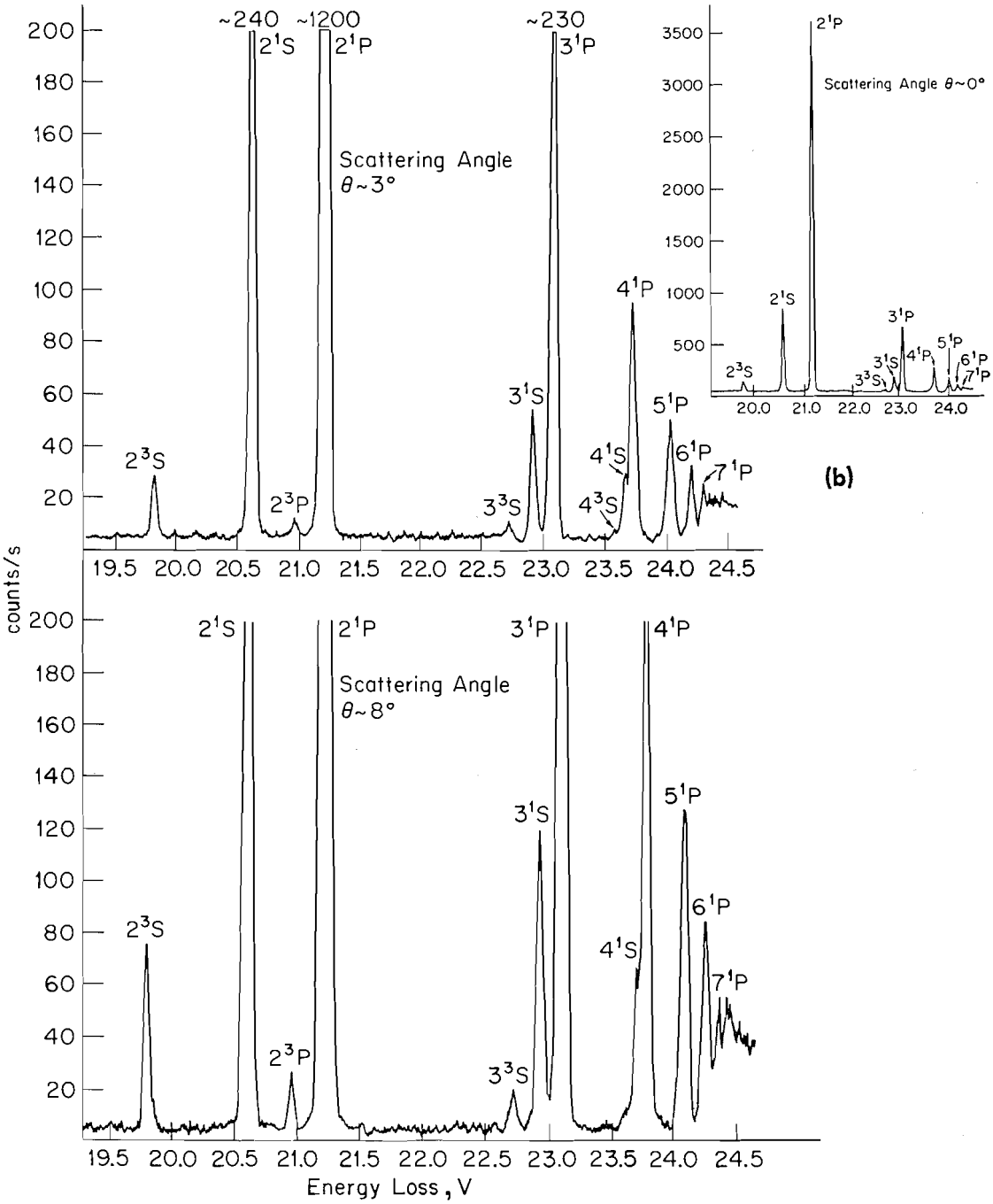

FIG. 26. Electron impact spectra of helium at 48 eV kinetic energy (accelerating voltage 50) by Skerbele and Lassettre (70). Spectra are shown at scattering angles 0, 3, and 8°. Note weak singlet–triplet transitions.

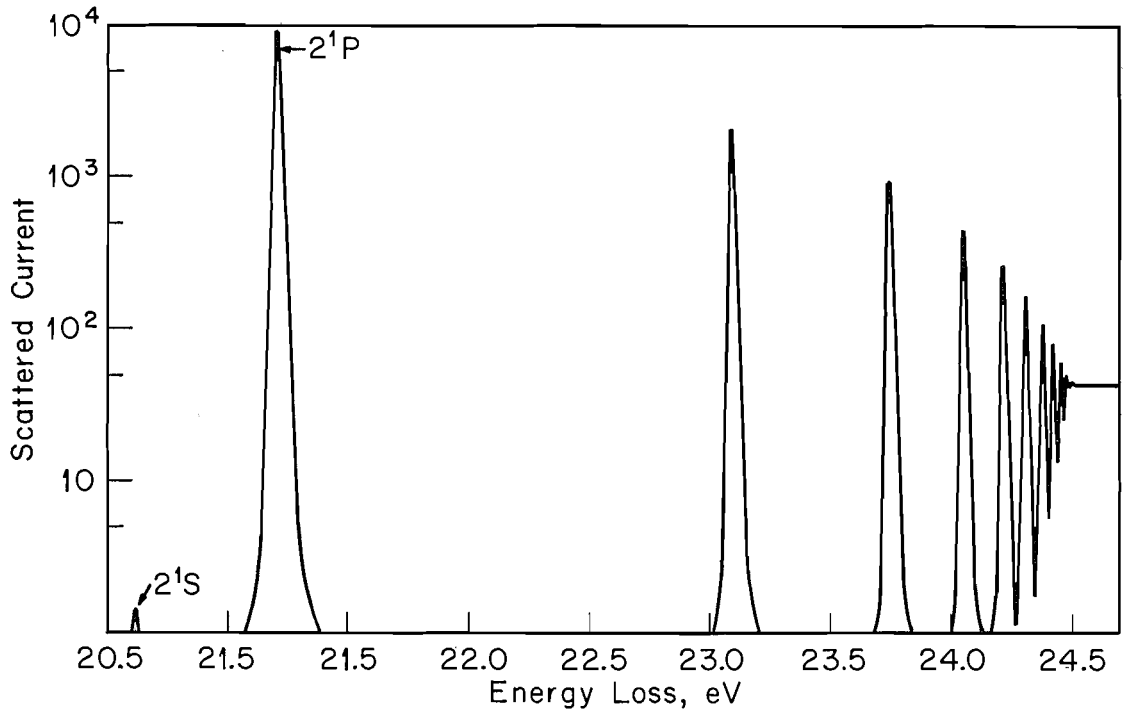

FIG. 27. Electron impact spectrum of helium at zero scattering angle and 25 keV kinetic energy by Boersch, Geiger, and Schröder (73). Note weak excitation to 2^1S state with intensity four orders of magnitude less than that to 2^1P.

kinetic energy and very high resolution. The spectrum is shown in Fig. 27. These experiments were done at high pressures (6–8 Torr) and multiple collisions were encountered in some spectra. Assuming that the scattering cell was the same as that of Geiger and Wittmaack (66) (2.5 cm) we obtain a pressure – path length product between 15 and 20 Torr cm. This is to be compared with pressure – path length products between 0.001 and 0.005 employed by Lassettre and collaborators. Higher pressures can be tolerated at high kinetic energy since electronic free paths are longer.

Collision Cross Sections of Atmospheric Gases

In the discussion of collision cross sections attention will be confined entirely to differential collision cross sections. This excludes the discussion of cross sections determined by the study of emission spectra which is unfortunate but unavoidable.

An extensive discussion of helium is given in the following section. Although helium is not a major atmospheric constituent, the helium cross sections have been extensively used for comparison purposes and have provided a very searching test of the accuracy with which relative cross sections and oscillator strengths can be determined. The comparison of a continuum with an excitation of the discrete spectrum is of special interest and importance. The recent discrepancies with other investigators are also discussed in detail.

In the case of nitrogen and oxygen the discussion is brief. In these sections references to the literature are given with a minimum amount of discussion. The electron impact spectra of both N_2 and O_2 have already been discussed at length in the previous sections and further elaboration seems unnecessary.

Electron impact spectra of carbon monoxide were not described in the above section because collision cross sections and relative intensity distributions in the fourth positive bands have aroused considerable interest and can best be discussed along with electron impact spectra.

Can. J. Chem. Downloaded from www.nrcresearchpress.com by 210.87.254.6 on 09/05/12
For personal use only.

Can. J. Chem. Downloaded from www.nrcresearchpress.com by 210.87.254.6 on 09/05/12
For personal use only.

Although the collision cross section measurements on CO are less extensive, and less precise, than those on N_2 and O_2, it is necessary to discuss the data at greater length since questions of accuracy in data analysis have arisen. It is convenient to illustrate these points (which arise in other investigations as well) with the fourth positive bands of carbon monoxide. This is done in the section entitled Carbon Monoxide.

References to other cross section determinations are given in the section entitled Other Substances of Atmospheric Interest, and a comparison of optical and electron impact oscillator strengths is given in the following section.

Helium

Collision cross sections for helium have been studied by several groups. The most thoroughly investigated transition is $1^1S \rightarrow 2^1P$. Since this transition has also been used for comparison purposes a special section is directed to it.

$1^1S \rightarrow 2^1P$ Transition

The pioneering theoretical calculation of the collision cross section is due to Massey and Mohr (74) who used the Born approximation and approximate eigenfunctions for the ground and excited states of helium. Early experimental and theoretical investigations have been reviewed by Massey (75). Scattering of electrons as a function of angle was studied by Lassettre, Krasnow, and Silverman (76). Their relative intensity measurements were normalized to the cross section calculated by Lassettre and Jones (77). The measurements were extended by Silverman and Lassettre (78). Since relative cross sections (and generalized oscillator strengths) are obtained, the experiment provides a test of the *shape* of the calculated curve of oscillator strength vs. momentum change. The agreement is good but not perfect (see ref. 78). Small systematic differences between theory and experiment are found especially at intermediate values of the momentum change.

In a recent publication, Vriens, Simpson, and Mielczarek (79) (V.S.M.) have studied the $1^1S \rightarrow 2^1P$ transition in helium. The data were fitted with a semi-theoretical formula and normalized by requiring that the limit of the generalized oscillator strength (at zero momentum change) be equal to the optical oscillator strength calculated by Schiff and Pekeris (80). Several kinetic energies were employed in the range (100–400 eV) and curves of oscillator strength vs. square of momentum change were coincident at kinetic energies of 200 eV and higher. Hence it was concluded that the Born approximation holds but at the same time there is a systematic disagreement (which becomes larger at higher momentum changes) with the results of Lassettre and collaborators (76, 78). Since this work was published, Kim and Inokuti at Argonne National Laboratory (81) have completed a calculation of generalized oscillator strengths using the Born approximation but with accurate approximations to the ground and excited state eigenfunctions. (Hylleraas type combinations containing more than 50 terms for both ground and excited states.) Aside from the use of the Born approximation, the generalized oscillator strength should be accurate to at least 1%. The calculated oscillator strengths agree better with the results of Lassettre and collaborators (76, 78) than with those of Vriens, Simpson, and Mielczarek (79). This is illustrated by Tables IX and X where f's calculated by Kim and Inokuti (column 3) are compared with values reported in refs. 76 (Table I, column 2) and 78 (Table IX, column 2). The % difference is given in column 4. The values calculated from the empirical formula of Vriens, Simpson, and Mielczarek are shown in column 5 and the deviations from column 3 are given in column 6. If we omit the values at the largest momentum changes (where the backgrounds are high) the mean difference between the data of ref. 78 and the calculations of Kim and Inokuti is 2.2%. The average deviation in Table X (again omitting the values at highest momentum change) is 2.8% and the grand average is 2.5% (4.2% if nothing is omitted). Note that the values in column 2 have not been re-normalized. This was not necessary since the normalizations were done in the region $0.3 \leq (\Delta P)^2 \leq 1.0$, and within this range the results of Kim and Inokuti (81) differ but little from those of Lassettre and Jones (77). In Table X the first experimental value of f (0.186) differs considerably from the calculated value. This is undoubtedly due to an error in the experimental f. The average of 6 determinations (calculated from data used in an apparatus calibration (82)) gives the value 0.195 which agrees better with the calculated value (0.202) but which is still too low. In a recent study (83) using the apparatus of ref. 20, we have determined relative oscillator

TABLE IX

Generalized oscillator strengths for helium

$(\Delta P)^2$	f	$f_{K.I.}$	$\Delta\%$	$f_{V.S.M.}$	$\Delta\%$
0.5080	0.133[a]	0.127[b]	+ 4.7	0.122[c]	− 3.9
0.4511	0.144	0.138	+ 4.3	0.132	− 4.3
0.6651	0.103	0.102	+ 1.0	0.096	− 5.8
0.5996	0.117	0.112	+ 4.5	0.105	− 5.9
0.8442	0.081	0.0801	+ 1.3	0.0742	− 7.4
0.9620	0.068	0.0687	− 1.0	0.0631	− 8.2
1.0448	0.062	0.0619	+ 0.2	0.0565	− 8.7
1.1754	0.051	0.0526	− 3.0	0.0475	− 9.7
1.4106	0.039	0.0396	− 1.5	0.0352	−11.1
1.6672	0.029	0.0296	− 2.0	0.0258	−12.8
1.9451	0.022	0.0219	+ 0.5	0.0188	−14.2
2.2446	0.013	0.0161	−19.2*	0.0136	−15.5
2.5650	0.010	0.0118	−15.2*	0.0098	−16.9
		Average, omit starred values	2.2		

[a]Reference 78.
[b]Reference 81.
[c]Calculated from an empirical formula of ref. 79.

strengths at 500 eV and scattering angles from 2.5 to 6.0°. The data were fitted using the formula of V.S.M.

$$[13] \quad f = (b/(1 + x)^6)(1 + cx/(1 + x))$$

where $x = (\Delta P)^2/\alpha^2$, and $\alpha^2 = 3.391$. Normalizing the data so that $b = 0.2762$ (as V.S.M. did) we find from a least squares analysis that $c = 0.87$. When V.S.M. fitted this equation to the data in column 2 of Tables IX and X they obtained $c = 0.86$, in excellent agreement with our more recent determination. This suggests that the low values in Table X are in error. Vriens, Simpson, and Mielczarek suggested low angular resolution as the source of error but this gives an error in the wrong direction. The reason for the discrepancy is not definitely known. Incidentally, when V.S.M. fitted their own data the value 0.1 was obtained for c. (When V.S.M. fitted the data of refs. 76 and 78 in the range $0.3 \leq (\Delta P)^2 \leq 1.0$, they obtained $c = 0.2$, in contrast to 0.86 when all data were used.) The limiting oscillator strength at zero momentum change has been studied theoretically by Lassettre, Skerbele, and Dillon. They showed that the limit is equal to the optical oscillator strength whether the Born approximation is satisfied or not. A paper describing these results has been submitted for publication in J. Chem. Phys.

Chamberlain, Simpson, Mielczarek, and Kuyatt (84) have studied the apparent cross section as a function of the pressure and pointed out the importance of multiple collisions. Vriens, Simpson, and Mielczarek (79) suggested that the data of Lassettre and co-workers (76, 78) are in error due to multiple scattering in which an elastic collision is responsible for the main change in direction, while an inelastic collision causes the incident electron to lose energy with little change in direction. Lassettre and John (85) have estimated the proportion of such collisions and concluded that at 500 eV and scattering angle 13° (covering the range of Tables IX and X), multiple collisions contribute less than 1% to the scattered current for the $1^1S \rightarrow 2^1P$ transition. At smaller angles the proportion is less. This study also shows that the percentage error is strongly dependent on apparatus design. Two different apparatuses for which the pressure – path length products are the same (path length being the total distance from source to analyzer entrance aperture) are not necessarily affected to the same extent by multiple scattering. That portion of the path which follows the elastic collision is much less important than that which precedes it, because the target areas for the two collisions are much smaller when the elastic collision occurs first. In view of these results, and the good agreement between experiment and theory at large values of $(\Delta P)^2$ (Tables IX and X), it is believed that multiple scattering is negligible in the experiments of refs. 76 and 78. If the data of V.S.M. are renormalized to the Kim and Inokuti curve, the agreement is fairly good, although there are small systematic deviations. As far as the data of

Can. J. Chem. Downloaded from www.nrcresearchpress.com by 210.87.254.6 on 09/05/12
For personal use only.

TABLE X

Generalized oscillator strengths for helium

$(\Delta P)^2$	f	$f_{K.I.}$	$\Delta\%$	$f_{V.S.M.}$	$\Delta\%$
0.1969	0.186[a]	0.202[b]	− 7.9	0.198[c]	− 2.0
0.2447	0.185	0.187	− 1.0	0.183	− 2.1
0.2982	0.175	0.173	+ 1.2	0.167	− 3.5
0.3573	0.163	0.158	+ 3.2	0.153	− 3.2
0.4221	0.152	0.144	+ 5.5	0.138	− 4.2
0.4923	0.136	0.130	+ 4.6	0.124	− 4.6
0.5682	0.122	0.117	+ 4.3	0.111	− 5.1
0.6496	0.107	0.104	+ 2.9	0.098	− 5.8
0.7369	0.094	0.0924	+ 1.7	0.0864	− 6.5
0.8295	0.081	0.0816	− 0.8	0.0758	− 7.1
0.9277	0.072	0.0718	+ 0.3	0.0662	− 7.8
1.0315	0.064	0.0629	+ 1.8	0.0575	− 8.6
1.1410	0.054	0.0549	− 1.6	0.0497	− 9.5
1.2557	0.047	0.0476	− 1.3	0.0428	−10.1
1.3763	0.043	0.0413	+ 4.1	0.0368	−10.9
1.5022	0.039	0.0356	+ 9.5*	0.0314	−11.8
1.6337	0.036	0.0307	+17.3*	0.0269	−12.4
Average, omit starred values			2.8		
Grand average, both sets (Tables IX and X)			2.5		
Grand average, omit nothing			4.2		

[a]Reference 76.
[b]Reference 81. Calculated using the Born approximation and ground and excited state functions with 53 and 52 terms, respectively.
[c]Reference 79.

Lassettre and collaborators are concerned, it agrees in shape with the theoretical f curve of Kim and Inokuti to within an average of 2.5%. In the region $0.3 < (\Delta P)^2 \leq 0.7$ there are small systematic deviations. On the whole, the data agree with the Born approximation although small differences cannot be excluded[2].

Other Discrete Excitations

The $1^1S \rightarrow 2^1S$ transition has been previously studied (76, 78, 86) and the cross section for the transition was also studied by V.S.M. (79). In refs. 76 and 78 the $1^1S \rightarrow 2^1S$ transition was not fully resolved from $1^1S \rightarrow 2^1P$ and the data tend to be scattered since it is difficult to completely subtract out the latter transition. Oscillator strengths obtained in refs. 76 and 78 were fitted with a semi-theoretical formula obtained in a previous research (87). The relation is

$$[14] \quad f = [bx/(1 + x)^6][1 + cx/(1 + x)]$$

where b and c are constants and $x = (\Delta P)^2/\alpha^2$, where $\alpha^2 = 3.551$. The data of refs. 76 and 78 at 500 eV are fitted adequately with $c = 0$ and $b = 0.329$; V.S.M. found $b = 0.271$ and $c = 0$ at 400 eV. The data of Lassettre *et al.* are higher by about 20%. This is due largely to the difference in f for the $1^1S \rightarrow 2^1P$ transition (see preceding section). The data of refs. 76 and 78 are in better agreement with the calculations of Kim and Inokuti. Additional cross sections at kinetic energies to 100 eV have been determined (79). Different values of b and c are needed at each kinetic energy, an indication of failure of the Born approximation, since that theory shows that f should depend only on $(\Delta P)^2$ and not on incident energy. Differential cross sections for excitation to 2^3S were also determined by V.S.M. (79). Although the above cross sections might be re-normalized using the $1^1S \rightarrow 2^1P$ cross section calculated by Kim and Inokuti, this seems premature until the absolute cross section determinations are complete.

Fragmentary values of the cross section for

[2]Absolute cross section determinations (private communication from Chamberlain) are in progress at the National Bureau of Standards and results to date point (tentatively) to a small departure from the Born approximation (measured values ~ 10% less than theoretical with a 5% error). At Mellon Institute an absolute determination is also in progress (by Bromberg) via the determination of absolute elastic cross sections. Two unsuspected errors (one pointed out by Kuyatt) have recently been recognized and additional experiments will be necessary before the results are final. Re-normalization of our relative data by as much as 10% would be difficult to reconcile with a deviation from the Born approximation, since a roughly constant difference between theory and experiment would be involved. The theory of limiting oscillator strengths is being studied.

Can. J. Chem. Downloaded from www.nrcresearchpress.com by 210.87.254.6 on 09/05/12
For personal use only.

TABLE XI

Comparison of optical and electron impact oscillator strengths for helium

(*a*) Discrete states

		f_0					
n	U (eV)	Delgarno and Stewart[a]	Schiff and Pekeris[b]	Skerbele and Lassettre[c]	Boersch, Geiger, and Schröder[d]	Miller and Platzman[e]	Δ%
2	21.21	0.275	0.27616	0.268[f]	0.2762[g]	0.2770	2.9
3	23.08	0.0746	0.0734	0.073	0.0784	0.0755	0.5
4	23.74	0.0304	—	0.030	0.0367	0.0311	1.3
5	24.04	0.0153	—	0.0145	0.0188	0.0158	5.2
6	24.21				0.0110	0.0081	—
7	24.30				0.0069	0.0057	Average 2.5
8	24.37				0.0044	0.0038	
9	24.41				0.0032	0.0027	
10	24.45				0.0023	0.0020	
11	24.47				(0.0018)	0.0015	
12	24.49				(0.0018)	0.0011	

(*b*) Continuum

	f'_0 (electrons V^{-1})				
U (eV)	Stewart and Webb[h] theoretical average	Baker *et al.*[i] optical	Samson[j] optical	Silverman and Lassettre[k] electron impact	Δ%
24.6	0.0715	0.070	0.068	0.066	5.8
28.0	0.0580	0.055	0.056	0.055	0.0
31.4	0.0465	0.043	0.045	0.047	9.3
38.2	0.0313	0.030	0.030	0.032	6.7
51.8	0.0160	0.016	—	0.014	12.2
65.4	0.0092	0.0088	—	—	—
					Average 6.9

[a]Reference 90.
[b]Reference 80.
[c]Reference 116.
[d]Reference 73. Authors report I_{n^1P}/I_{2^1P} with a possible error of 10%. See also ref. 80.
[e]Reference 90*b*.
[f]Normalized to the calculated value of ref. 77.
[g]Normalized to the value of ref. 80.
[h]Reference 92.
[i]Reference 91.
[j]The values interpolated from Fig. 2 of Samson's paper (see ref. 91) using the solid line through the data points. Deviation of experimental points from curve is 2.5%. Estimated error in absorption coefficients is 5%. These values are more accurate than those of Baker *et al.*
[k]Reference 78.

excitation to the 3^1P state are reported in refs. 76 and 78. These are in error due to contamination by 3^1S (3^1P and 3^1S were not resolved). The cross sections calculated by Kim and Inokuti are certainly more accurate than the experimental values. The total cross sections for excitation to 3^1P calculated by Silverman and Lassettre (88) are also adversely affected by the unresolved (and unrecognized) 3^1S transition.

Helium Continuum

Generalized oscillator strengths in the helium continuum have been reported by Lassettre, Krasnow, and Silverman (76) and by Silverman and Lassettre (78). The limiting oscillator strengths, obtained by extrapolating to zero momentum change, have been reviewed by Silverman and Lassettre (89) as a means of estimating error in *relative* oscillator strength measurements. The results for both discrete and continuum states are given in Table XI (see ref. 89). The oscillator strengths, f_0, for the transitions $1^1S \rightarrow n^1P$ are compared with the values calculated from experimental data by Dalgarno and Stewart (90). The values obtained by Boersch *et al.* are also included, together with values calculated by Miller in a manner similar to that used by Dalgarno and Stewart. The continuum oscillator strengths, f'_0 (in electrons per volt), are given in Table XI*b*. They are compared with the experimental determinations of Baker *et al.* (91) (column 3) and those of Sampson (91) (column 4) and with the theoretical calculations

Can. J. Chem. Downloaded from www.nrcresearchpress.com by 210.87.254.6 on 09/05/12
For personal use only.

Can. J. Chem. Downloaded from www.nrcresearchpress.com by 210.87.254.6 on 09/05/12
For personal use only.

of Stewart and Webb (92). In Table XI*b*, column 6 gives the percentage differences between columns 3 and 5. The deviations in Table XI*a* are between columns 3 and 5 where values are available, otherwise between columns 2 and 5. The weighted deviation (1/4 for discrete states, 3/4 for continuum) is 6%. There is an auto-ionized transition at 60.1 ± 0.1 eV whose line shape has been treated by Fano (52) who also deduced the auto-ionization probability from the electron impact spectrum. The value found, 6×10^{13} s^{-1} has been checked by Madden and Codling (93) who found (in a spectroscopic study) 5.8×10^{13} s^{-1}. Since the auto-ionized transitions attracted widespread attention and have been the subject of several reviews, we shall not further consider these transitions. The data on helium, summarized in Table XI, are important because they provide a test of the experimental technique. It is obviously important that the collision cross sections in continuous spectra should be *experimentally comparable* with the collision cross sections for excitation to discrete states. Since every transition in Table XI (including continuum states) was investigated by comparing the scattering with that due to $1^1S \rightarrow 2^1P$ excitation in helium, the accuracy of the continuum oscillator strengths is a direct test of the precision with which this comparison can be made. The outcome is obviously favorable. The instrument of ref. 82 has been used in all cases.

Nitrogen

The trend of oscillator strength with momentum change for the Lyman–Birge–Hopfield bands has been discussed in the section entitled Electron Impact Spectra, the determinations being those of Lassettre and Krasnow (38). The remainder of the spectrum has also been studied at low resolution (89). The experimental technique is explained in detail in this reference. Oscillator strengths as functions of momentum change are shown in Fig. 28. The spectra are unresolved. Figure 28*a* refers to the peaks and Fig. 28*b* to the continua or, more accurately, the unresolved sections of the spectra without peaks. Extrapolated generalized oscillator strengths, together with those of O_2 and H_2O, will be further discussed in a subsequent section, Other Substances of Atmospheric Interest. They are also given in Table XII.

Oxygen

Oscillator strengths for the dissociation continuum of the Schumann–Runge bands have been determined (94) and oscillator strengths through the remainder of the spectrum have also been studied in a later research (95). Extrapolated oscillator strengths are given in Table XII. The trend in oscillator strength with momentum change is qualitatively similar to those found for N_2. Figures are shown in ref. 96. Total cross sections were calculated through the spectrum and the fraction of inelastic collisions which excite the Schumann–Runge bands and dissociation continuum was calculated and found to be one tenth. This is a very large fraction and emphasizes again that the transition dominates the spectrum. (See also Fig. 13.) These data are further

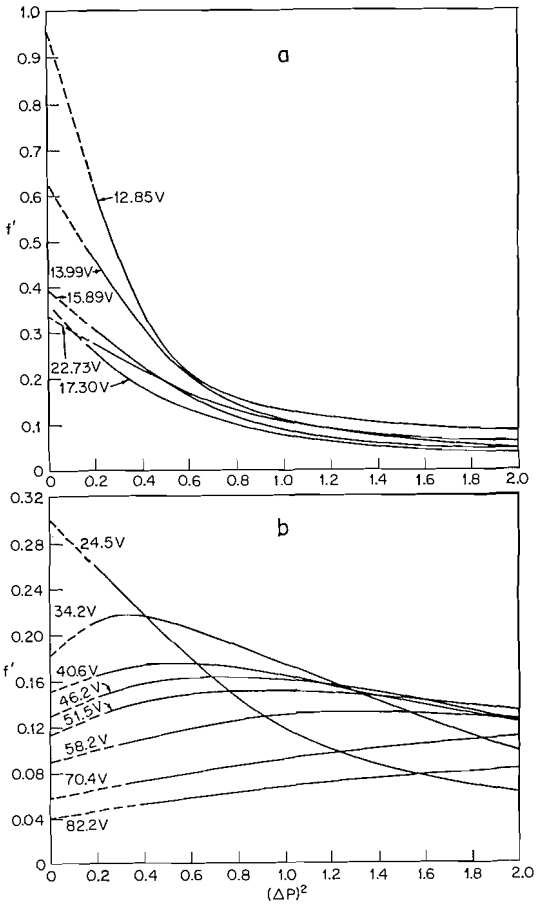

FIG. 28. Oscillator strengths, f', vs. square of momentum change for N_2 at approximately 500 eV by Lassettre and Silverman (89). (*a*) Portion of unresolved spectrum containing peaks. (*b*) Portion of spectrum containing no peaks. Momentum changes in atomic units. Excitation energies (eV) shown for each curve.

TABLE XII

Extrapolated oscillator strengths[a]

O_2 (ref. 96)		N_2 (ref. 89)		H_2O (ref. 104)	
U	f_0	U	f_0	U	f_0
8.4	0.230	9.1	0	7.37	0.061
9.9	0.025	12.85	0.872	10.09	0.123
12.9	0.188	13.99	0.602	11.02	0.0853
15.3	0.474	15.89	0.492	13.32	0.764
16.8	0.541	17.30	0.760	15.25	0.209
19.7	0.769	22.73	0.889	25.25	0.241
21.7	0.150	25	0.293	35.25	0.141
25	0.289	35	0.180	45.25	0.100
35	0.211	45	0.133	55.25	0.080
45	0.149	55	0.099	65.25	0.057
55	0.113	65	0.073	75.25	0.042
65	0.086	75	0.052		
75	0.064				

[a]Oscillator strengths above the horizontal lines refer to peaks in the spectra and have been integrated over the corresponding peaks. Below the horizontal lines there are no peaks and no integration over the spectrum has been performed, i.e. these are differential oscillator strengths. $f'_0 = (df_0)/(dU)$ expressed in electrons V^{-1}.

discussed in the section entitled Comparison of Electron Impact and Optical Oscillator Strengths.

Carbon Monoxide

Carbon monoxide has been less extensively studied than either N_2 or O_2. One transition ($A^1\Pi \leftarrow X^1\Sigma^+$), the fourth positive bands of optical spectra, is of considerable interest since very large discrepancies have been found between the extrapolated oscillator strength obtained by electron impact and that calculated from lifetime measurements. Because of these discrepancies the substance is discussed in considerable detail. The intensity distribution in the vibrational progression is also of interest.

Oscillator Strengths

Collision cross sections for carbon monoxide were studied by Lassettre and Silverman (96) at low resolution (no velocity selection before scattering). The oscillator strength, integrated over the band system, was studied at three kinetic energies. The extrapolated oscillator strength is 0.24. The generalized oscillator strengths vs. $(\Delta P)^2$ are shown in Fig. 29. The data are probably less precise for this transition than those mentioned in preceding sections for N_2 and O_2 because comparison of helium and CO scattering was not made immediately before and after each run on carbon monoxide (see ref. 82, p. 1239 for a discussion). Cross section determinations for nitrogen were made at the same time and a later, more thorough, investigation gave cross sections for N_2 which are lower by the factor

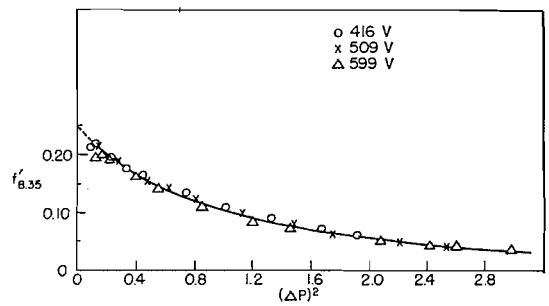

FIG. 29. Generalized oscillator strength of 8.35 eV transition of carbon monoxide vs. square of momentum change (atomic units) at three kinetic energies, by Lassettre and Silverman (96).

0.887 (see ref. 38, p. 1249). Unpublished research by Meyer and Lassettre suggests that the limiting cross section for CO (0.24) and the data of Fig. 29 should also be multiplied by this factor. The data have not been corrected, however, because an absolute determination is in progress at Mellon Institute and a final appraisal must await the completion of these experiments. In the meantime, it is of interest to consider the relative intensities in the fourth positive bands. Oscillator strengths are compared with optical and other determinations in the section entitled Comparison of Electron Impact and Optical Oscillator Strengths.

Born Approximation

Lassettre and Silverman (96) noted that the shape of the peak (consisting of unresolved vibrational levels) corresponding to the fourth

Can. J. Chem. Downloaded from www.nrcresearchpress.com by 210.87.254.6 on 09/05/12
For personal use only.

Can. J. Chem. Downloaded from www.nrcresearchpress.com by 210.87.254.6 on 09/05/12
For personal use only.

positive bands did not change with angle. Silverman and Lassettre (97) showed that the envelope shape is satisfactorily accounted for by Franck–Condon factors calculated by Jarmain *et al.* (98). As soon as an electron spectrometer was developed which could resolve the fourth positive bands, the system was re-investigated and relative intensities determined (18). The relative intensities seemed to change with angle, although the uncertainties were large. The data were analyzed using the formula of Craggs and Massey (99) in which the dependence of cross section on internuclear distance is neglected. The dependence on angle is accounted for in this way but when a quantity proportional to the Franck–Condon factor is deduced from the data, it is not in fact equal to the Franck–Condon factor calculated by Jarmain *et al.* The disagreement might be due either (*a*) to approximations in the Craggs and Massey formula, e.g. neglecting the dependence of cross section on internuclear distance, or (*b*) error in the Franck–Condon factors due to the assumption of a Morse potential function. The latter possibility was eliminated by Wentink *et al.* (100) who calculated the Franck–Condon factors using the Rydberg–Klein–Rees method (and computer programs developed by Spindler). These more accurate Franck–Condon factors are in even worse agreement with those deduced from the data than the factors calculated by Jarmain *et al.* Obviously, a more accurate theory is needed and one possibility is to take into account the dependence of collision cross sections (for vertical excitations) on internuclear distance. Wentink *et al.* (100) suggested this interpretation and it is indeed possible to account for the deviations in the extrapolated oscillator strength by using the approximation proposed by Nicholls (101) which relates the electronic transition moment to the r centroid, defined as

$$[15] \qquad \bar{r} = \int_0^\infty R_{v'} r R_{v''} \mathrm{d}r$$

where r is the internuclear distance and $R_{v'}$, $R_{v''}$ are vibrational eigenfunctions for the excited and ground electronic states. Nicholls (101) has also given a very convenient approximate formula for the collision cross section which can be put into the following form

$$[16] \qquad \sigma = \sigma_0(\bar{r})\left(\int_0^\infty R_{v'} R_{v''}\right)^2 = \sigma_0(\bar{r}) q_{v'v''}$$

Here $\sigma_0(\bar{r})$ is the collision cross section calculated for a vertical excitation at an internuclear distance equal to $\bar{r}$ and the second factor $q_{v'v''}$ is the Franck–Condon factor. In addition to $\bar{r}$, σ_0 also depends on scattering angle or, more accurately, on the momentum change appropriate to the excitation energy and the scattering angle. Since $\bar{r}$ varies from one vibrational state to another, the same will generally be true of σ_0. If eq. [16] is accurate, then it is apparent that dividing $q_{v'v''}$ into the experimentally observed cross section will give σ_0. This analysis of the data is only applicable at high kinetic energy where the Born approximation holds, but recent studies at lower kinetic energies have revealed a close relation between relative intensities and Franck–Condon factors, and it would be desirable to analyze the data in a different way which does not depend on the Born approximation. Before considering this point further, it will be useful to describe the intensity distributions observed for the fourth positive bands at different kinetic energies.

Relative Intensities

An electron impact spectrum of carbon monoxide is shown in Fig. 30. (Note the weak singlet–triplet transitions.) The fourth positive bands extend from 8 to 10 eV. Relative intensities as functions of angle at 48 eV are shown in Table XIII and at 98 eV in Table XIV. The trends with angle are so small that relative intensities have been averaged over all angles. The averages are compared with Franck–Condon factors calculated by Jarmain *et al.* (98) and Wentink *et al.* (100) in Table XV which also includes previous determinations (103) at 400 eV. Determinations (18) at 200 eV are included although the data are less accurate and are being redetermined. Data at 400 eV have been checked (in an unpublished investigation) and agreement is good except for $v' = 9$ where 0.021 is obtained instead of 0.026. Note that relative intensities at 48 eV and especially at 98 eV are in better agreement with Franck–Condon factors than at 400 eV. This has been confirmed in repeated experiments which show, however, that even at 400 eV agreement gets better at higher vibrational quantum numbers ($v' > 8$). Note that, unlike ref. 18, the relative intensities change but little with angle.

We cannot assume that the Born approximation holds at kinetic energies as low as 48 eV and hence eq. [16] cannot be used to discuss the data.

TABLE XIII

Relative intensities as a function of the scattering angle $A^1\Pi \leftarrow X'\Sigma^+$ transition in CO ($E = 48$ eV)

v'	U (eV)	Relative intensities at scattering angle 0°	3°	8°	12°	16°	I_{av}	Franck–Condon factor
0	8.028	0.54	0.52	0.50	0.47	0.45	0.50	0.49
1	8.212	0.97	0.91	0.92	0.91	0.87	0.92	0.94
2	8.390	1.00	1.00	1.00	1.00	1.00	1.00	1.00
3	8.566	0.83	0.82	0.81	0.80	0.79	0.81	0.79
4	8.737	0.57	0.54	0.55	0.55	0.55	0.55	0.52
5	8.903	0.35	0.33	0.32	0.31	0.32	0.33	0.30
6	9.064	0.18	0.18	0.18	0.18	0.16	0.17	0.16
7	9.223	0.093	0.091	0.088	0.092	0.089	0.091	0.080
8	9.375	0.047	0.045	0.039	0.041	0.037	0.042	0.039
9	9.525	0.020	0.022	0.018	0.020	0.019	0.020	0.018
10	9.671	0.0080	0.011	0.0076	0.0085	0.0086	0.0087	0.0084
11	9.812	0.0042	0.0035	0.0032	0.0041	(0.0065)	0.0037	0.0037
12	9.949	0.0031	0.0025	0.0030	(0.0042)	(0.0048)	0.0030	0.0018
13	10.080	0.0012	0.0005	0.0012	0.0026	0.0035	0.0018	0.0008

TABLE XIV

Relative intensities as a function of the scattering angle $A^1\Pi \leftarrow X^1\Sigma^+$ transition in CO ($E = 98$ eV)

v'	Relative intensities at scattering angle 0°	2°	4°	6°	8°	I_{av}	Franck–Condon factor
0	0.47	0.47	0.49	0.47	0.51	0.48	0.49
1	0.90	0.93	0.88	0.91	0.93	0.91	0.94
2	1.00	1.00	1.00	1.00	1.00	1.00	1.00
3	0.81	0.79	0.79	0.81	0.82	0.80	0.79
4	0.53	0.53	0.53	0.55	0.55	0.54	0.52
5	0.31	0.31	0.31	0.32	0.33	0.32	0.30
6	0.16	0.15	0.16	0.17	0.17	0.16	0.16
7	0.077	0.072	0.076	0.075	0.074	0.075	0.080
8	0.036	0.037	0.036	0.036	0.045	0.037	0.039
9	0.017	0.017	0.018	0.020	0.022	0.019	0.018
10	0.009	0.009	0.008	0.010	0.015	0.008	0.008
11	0.004	0.004	0.005	0.005	—	0.004	0.004
12	0.002	—	—	—	—	0.002	0.002
13	0.001	—	—	—	—	0.001	0.001

TABLE XV

Relative intensities in CO fourth positive bands at different kinetic energies

v'/E (eV)	Relative intensities at kinetic energy 48	98	200[a]	400	Calcd. Reference 98	Reference 100
0	0.50	0.48	0.48	0.45	0.49	0.49
1	0.92	0.91	0.92	0.87	0.94	0.94
2	1.00	1.00	1.00	1.00	1.00	1.00
3	0.81	0.80	0.86	0.83	0.79	0.78
4	0.55	0.54	0.58	0.56	0.52	0.50
5	0.33	0.32	0.36	0.34	0.30	0.28
6	0.17	0.16	0.22	0.19	0.16	0.15
7	0.091	0.075	0.11	0.10	0.080	0.070
8	0.042	0.037	(0.06)	0.047	0.039	0.032
9	0.020	0.019	—	0.026	0.018	—
10	0.0087	0.008	—	—	0.0084	—
11	0.0037	0.004	—	—	0.0037	—
12	0.0030	0.002	—	—	0.0018	—
13	0.0018	0.001	—	—	0.0008	—

[a]Average of relative intensities in Table III*a* of ref. 18.

Can. J. Chem. Downloaded from www.nrcresearchpress.com by 210.87.254.6 on 09/05/12
For personal use only.

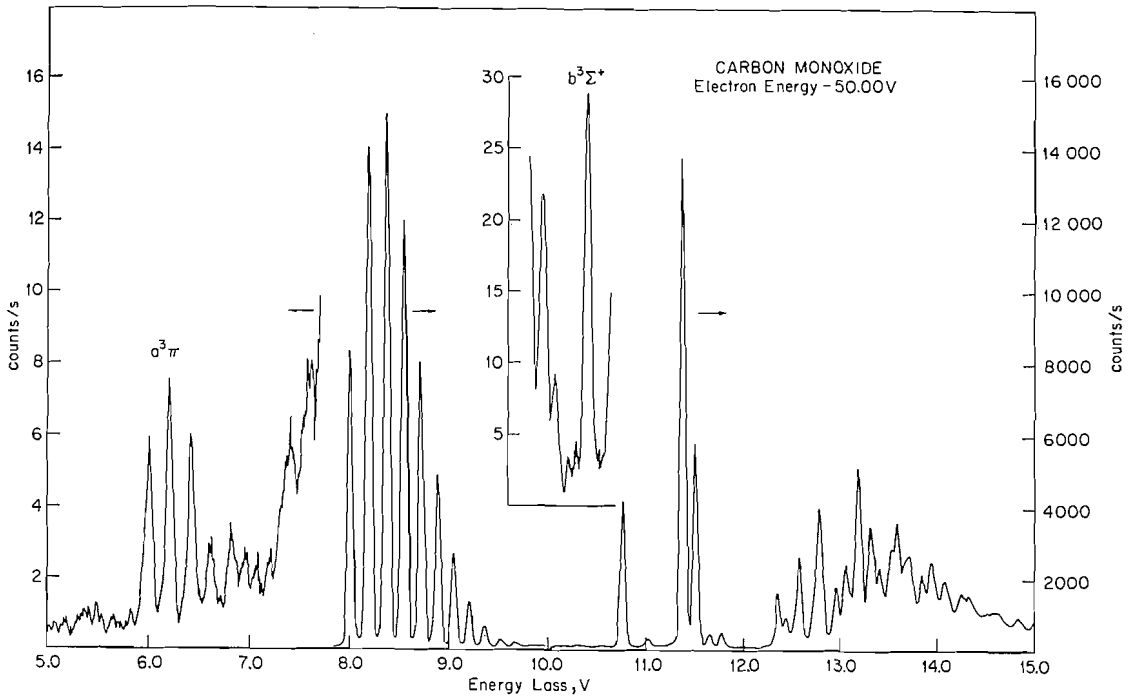

FIG. 30. Carbon monoxide spectrum at zero scattering angle and 48 eV kinetic energy by Skerbele, Dillon, and Lassettre (102). Note singlet–triplet transitions. Fourth positive bands extend from 8–10 eV.

Therefore the problem has been considered from a different viewpoint (see ref. 20) which does not depend on the Born approximation. These results are briefly described in the next section.

Excitation Probabilities

If we consider the excitation of a molecule as a time dependent process, we can then visualize the electronic excitation as occurring in a very short time to produce an excited state in which the state function (not an eigenfunction) describing the nuclear motion is ϕ. If we expand ϕ in a series of vibrational eigenfunctions of the excited state ψ_v, then the square of the v expansion coefficient gives the probability P_{Ev} that the system ends in a vibrational state with quantum number v when we know in advance that an electronic state E has been excited, i.e.

$$[17] \qquad P_{Ev} = |\int \phi \psi_v^* d\tau|^2$$

The quantity P_{Ev} is a conditional probability. Let P_E be the probability per unit time that the electronic state E is excited regardless of v. Then the probability per unit time that the molecule is excited to electronic state E and vibrational level v is

$$[18] \qquad P_E P_{Ev}$$

If the collision lifetime is small in comparison to a nuclear vibration period ($\sim 10^{-13}$ s) the nuclei have no time to redistribute and it is plausible that ϕ is approximately equal to the ground state vibrational function ψ and eq. [17] is the Franck–Condon factor. An exception to this may arise if the incident electron energy is such that resonance occurs to give a temporary negative ion. In that case lifetimes comparable with or greater than 10^{-13} s may be encountered. Under these conditions the nuclei can redistribute within the collision lifetime and ϕ may differ drastically from the ground state vibration function. A resonance can be tested for by determining scattered current as a function of kinetic energy. The data of Tables XIII and XIV were collected under non-resonant conditions.

The above argument is obviously *not* a rigorous demonstration that the relative intensity is independent of angle. We must regard this as a

Can. J. Chem. Downloaded from www.nrcresearchpress.com by 210.87.254.6 on 09/05/12
For personal use only.

Can. J. Chem. Downloaded from www.nrcresearchpress.com by 210.87.254.6 on 09/05/12
For personal use only.

hypothesis which deserves an experimental test. The data of Tables XIII and XIV provide a beginning of such a test. Note in Table XIII that the relative intensities at $v' = 0$ and 1 exhibit a small but noticeable (and reproducible) change with angle. We have ignored this trend and averaged the relative intensities at all angles in comparing with Franck–Condon factors. A more comprehensive investigation at other kinetic energies and scattering angles is in progress.

Other Substances of Atmospheric Interest

Collision cross section determinations on H_2O similar to those on N_2 and O_2 have been done by Lassettre and White but are not yet published (104). Less complete determinations are also available on CO_2 (105) (see next section for discussion). Geiger (106) and Geiger and Topchowsky (107) have studied oscillator strengths for several transitions in H_2, and obtained results which agree well with theory and with the recent spectroscopic investigation of Hesser, Brooks, and Lawrence (108). The research on hydrogen has not been discussed in detail because it seemed doubtful that this substance qualifies as being of direct aeronomic interest. These researches are, however, quite significant contributions to molecular physics and astrophysics. Extrapolated oscillator strengths for H_2O are given in Table XII.

Comparison of Electron Impact and Optical Oscillator Strengths

Oscillator strengths obtained by Lassettre and collaborators are compared with optical determinations in the section following. In the section entitled Experiments of Geiger, two transitions (in helium and hydrogen, respectively) studied by Geiger and collaborators are compared with experiment or theory.

Experiments of Lassettre and Collaborators

Initially we consider two regions of continuous spectrum, one in N_2 and the other in O_2. In the spectral range 580 to 660 Å the absorption coefficients of nitrogen are essentially constant and the spectrum seems to be continuous (109). Inspection of the spectrum given by Huffman, Tanaka, and Larrabee shows that the average absorption coefficient over this range is 950 cm^{-1} which corresponds to an oscillator strength $f' = (df)/(dW)$ of 0.32 electrons V^{-1}. By interpolating in the electron impact spectrum Silverman and Lassettre found a limiting oscillator strength which was very nearly constant and equal to 0.315 electrons V^{-1} This agrees extremely well with the measurements of Huffman, Tanaka, and Larrabee. Later, Cook and Metzger re-investigated the spectrum and reviewed the determinations made at 584 Å. The results for 6 determinations are shown in Table XVI, the second value being that of Cook and Metzger (110) and the first being that of Huffman, Tanaka, and Larrabee (109). These two values are most likely to be accurate but they differ by 20%. This cannot be attributed to line saturation since a continuum is involved. Huffman, Tanaka, and Larrabee corrected their measurements for fluorescence of the N_2^+ ion. Fluorescence was observed by Cook and Metzger but no correction was needed since their detector was not affected by the fluorescent radiation. In an accompanying review, Huffman has accepted the value 620 cm^{-1} as the probable value of the absorption coefficient at 584 Å. This gives an oscillator strength of 0.210 electrons V^{-1}. Obviously the uncertainty is substantial.

TABLE XVI

Absorption coefficients of N_2 at 584 Å

Absorption coefficient (cm^{-1})	Reference
980	109
800	110
700	111
620	Huffman[a]
400	112
480	113
351 (at 580 Å)	114

[a]See Table I in accompanying review by R. E. Huffman.

The second continuum, which has been much studied, is the dissociation continuum of the Schumann–Runge bands. A series of determinations covering the period since 1932 is summarized in Table XVII. The electron impact value is 0.230. The accepted optical value (see Huffman's review) is the first entry, 0.161, which is 30% less than the electron impact value.

The relation between refractive index and oscillator strength for a gaseous substance is well known and can be put into the following form

$$n - 1 = 0.01858 \sum (f_i)/(W_i^2 - (h\nu)^2)$$

where f_i is the oscillator strength, n is the refrac-

TABLE XVII

Oscillator strengths of Schumann–Runge continuum in O_2

Oscillator strength	Method	Δ%	Reference
0.161	Absorption	30	115, 121
0.177	Absorption	23	116
0.193	Absorption	16	117
0.20	Absorption	13	118
0.202	Dispersion	12	119
0.215	Absorption	6	120
0.230	Electron impact	—	94

tive index, W_i is the excitation potential, and ν is the frequency. The numerical constant has been calculated in such a way that W_i and $h\nu$ are in eV. Using the data of Table XII the value of $n - 1$ for N_2 at zero frequency has been calculated and found to be 394×10^{-6} while that measured (see ref. 90 for references to literature) at microwave frequencies is 294.1×10^{-6}. The experimental value is 25% less than that calculated from the oscillator strengths. For O_2 the value of $n - 1$ calculated from the oscillator strengths of Table XII at $\lambda = 2479$ Å is 392×10^{-6} while that interpolated from the measurements of Ladenburg and Wolfsohn (119) is 305×10^{-6}. The experimental value is 22% less than the calculated value. For H_2O the value of $n - 1$ calculated at $\lambda = 5460.7$ Å using the oscillator strengths of Table XII is 329×10^{-6} compared with the experimental value (122) of 253×10^{-6}. The experimental value is 23% less than the calculated. In all cases the oscillator strengths of Table XII have been linearly extrapolated to zero in the continuum and the extrapolated values obtained have been used in calculating the refractive indices. These contributions cannot explain the discrepancies between theory and experiment. Since refractive indices can be determined with high accuracy, these discrepancies must be taken seriously, especially since the percentages are all nearly the same for three different substances. Moreover, in the calculation of refractive indices it is not important to have high resolution since a summation over the spectrum is involved.

The cross section determinations on nitrogen (89), oxygen (96), and water (104) were done by comparing the scattering with that due to the $1^1S \rightarrow 2^1P$ transition in helium. An apparatus constant, K, was determined by scattering runs on helium, both before and after investigating the gas (N_2, O_2, or H_2O). This value of K was then used in calculating cross sections for the gas under investigation. An attempt was made, in the paper on nitrogen (89), to place an error bound on the cross section determinations. Assuming that errors from all known sources combine unfavorably, an error of 13% could be accounted for. This includes an estimate of possible error in comparing a sharp peak ($1^1S \rightarrow 2^1P$ in helium) with an unresolved or continuous spectrum. The estimate does not include an estimated extrapolation error. Some additional comments on the pressure measurements are pertinent at this point. Pressure measurements were made with a Knudsen gauge which had been calibrated against a McLeod gauge. The determinations were made before the discovery by Ishii and Nakayama of the streaming error in the McLeod gauge (123). By the time this error was announced, the present author had moved from Ohio State University to Mellon Institute and the gauge could not be re-calibrated. On the basis of the diameters of glass lines connecting the McLeod gauge to its cold trap, a streaming correction was estimated and the earlier conclusion that the Knudsen gauge was independent of gas seemed to be valid (124). Subsequent experience with McLeod gauges by Bromberg and Meyer at Mellon Institute are in approximate accord with this. Such ad hoc estimates are never completely satisfactory but nothing better is available at present. Absolute elastic collision cross sections are being determined at Mellon Institute by Bromberg. Once these measurements are complete an entirely independent check will be possible by comparing the areas of inelastic and elastic peaks using the high resolution spectrometer. Since these measurements are nearing completion it does not seem worthwhile to speculate further except for one point. In ref. 89 the discrepancy was attributed to a failure of the Born approximation. At the time, the intensity anomaly in the nitrogen spectrum seemed to point in this direction (45). However, when the vibration spectrum was resolved (46) it immediately became clear that no failure of the Born approximation was involved and this was confirmed by the work of Geiger and Stickel (49) as discussed in the section entitled Electron Impact Spectra, under the subheading Nitrogen. If we could be certain that the

Can. J. Chem. Downloaded from www.nrcresearchpress.com by 210.87.254.6 on 09/05/12
For personal use only.

TABLE XVIII
Oscillator strengths for fourth positive bands of CO

	Oscillator strength obtained by			
			Electron impact	
v'	Lifetime (ref. 127)	Shock tube (ref. 128)	Uncorrected (ref. 18)	Corrected[a]
0	0.0111	—	0.0219	0.0194
1	0.0195	0.027 ± 0.006	0.0444	0.0394
2	0.0222	0.033 ± 0.006	0.0508	0.0451
3	0.0184	—	0.0456	0.0404
4	0.0088	—	0.0327	0.0290
5	0.0068	—	0.0211	0.0187
6	—	—	0.0131	0.0116
7	—	—	0.0070	0.0062
8	—	—	(0.0035)	(0.0031)

[a]Obtained from column four on multiplication by 0.887. This factor is indicated by cross section determinations on nitrogen and by the unpublished research of Meyer and Lassettre. See section under Oscillator strength.

Born approximation was satisfied by both helium and nitrogen and the extrapolations were correct, then we would multiply our previous cross sections by 0.75. This factor would also bring our oscillator strengths into line with the probable optical values for the Schumann–Runge continuum of O_2 and the 584 Å region of the N_2 spectrum. In 1959 these cross section measurements were reviewed (125) (before publication) and this discrepancy was pointed out. It was unresolved then and remains so at present.

One of the biggest discrepancies between oscillator strengths obtained by electron impact and other methods is that for the fourth positive bands in carbon monoxide. Hesser and Dressler (126) investigated the life-times of excited states of CO and found that the calculated oscillator strengths are smaller by a factor of 2.6 than those obtained by Meyer, Skerbele, and Lassettre (18), using the value of f_0 for the whole band (0.24) obtained by Lassettre and Silverman (96). This is a much larger factor than anything suggested by comparison with refractive indices. A little improvement is introduced by correcting the electron impact results for a new determination of apparatus constant, K. The value 7.56×10^{10} was used in the original determination (ref. 82, p. 1239) but the value 6.71×10^{10} was found in a later determination on N_2 under conditions which strongly suggest that the earlier value was in error (ref. 38, p. 1249). Generalized oscillator strengths are given in Table XVIII. Column 4 contains the values found in ref. 18 and column 5 contains values corrected to take account of the revised apparatus constant. Column 2 contains values found by Hesser (127) in a recent investigation. The large discrepancies are obvious. Two values obtained by Rich (128) are given in column 3. Rich (128) states that his values agree with the determinations of Hesser and Dressler and when all values for transitions between states are considered this is probably true, but for the only two values which can be compared with our determinations, this is not true. The values are half-way between those of columns 2 and 5. At $v' = 0$ the value obtained by Rich (0.033 ± 0.006) does not differ from that of column 5 (0.0451) by more than the factor 0.75 indicated by refractive indices and the Schumann–Runge bands. The values obtained by Hesser, however, do differ by considerably more than this factor. In the experiments of both Rich and Hesser the transitions studied were from excited to ground state (radiation emitted) while ours are in the opposite direction. A dependence of transition moment on internuclear distance could be found which accounts for the difference, but Rich found no dependence and we cannot be certain that this is the true reason. Thus far the differences are unexplained.

Lawrence, Mickey, and Dressler (50) have determined (by absorption coefficient measurements) the oscillator strength of the band at 965 Å in N_2 and obtained the value 0.055 ± 0.011. From Geiger's N_2 spectrum they obtained 0.14 as the fractional intensity contributed by the

Can. J. Chem. Downloaded from www.nrcresearchpress.com by 210.87.254.6 on 09/05/12
For personal use only.

Can. J. Chem. Downloaded from www.nrcresearchpress.com by 210.87.254.6 on 09/05/12
For personal use only.

12.84 eV peak (λ = 965 Å) to the entire region from 11.4 to 13.6 eV of the nitrogen spectrum. Hence 0.055/0.14 = 0.40 is the estimated oscillator strength for this interval compared to 0.872 obtained by Silverman and Lassettre (89). (See Table XII.) Again a much larger factor than 0.75 is obtained. The origin of the fraction 0.14 is not completely clear. Geiger's spectrum gives scattered current. To obtain the oscillator strength each intensity must be multiplied by the cube of the excitation energy and corrected for angular resolution. It is not clear whether this was done.

Experiments of Geiger

Geiger and collaborators have studied oscillator strengths by electron impact at very high kinetic energies by determining the ratio of inelastic to elastic scattering and using the calculated elastic cross section to obtain oscillator strengths for the transition to the state excited in the inelastic scattering process. The helium transition $1^1S \rightarrow 2^1P$ has been studied in this way (129). The experimental value obtained in this way at 25 keV is 0.312 $\pm$ 0.040. This is to be compared to the theoretical value 0.2762 which is known to be accurate (80). An experimental value (131) of 0.27 $\pm$ 0.02 has recently been determined. Kim and Inokuti (130) have also calculated elastic cross sections for helium and have indicated the need to use relativistic kinematics and to make other relativistic corrections. These will no doubt be small (a few %).

Geiger and Topchowsky (107) have determined oscillator strengths for three electronic bands in hydrogen by a method similar to that for helium. The ratio of inelastic to elastic scattering was determined and the oscillator strength for the inelastic excitation determined using the calculated (Born approximation) elastic cross section obtained from an approximate eigenfunction for the H_2 ground state. The oscillator strength agreed well with theoretical values calculated in various ways. Hesser, Brooks, and Lawrence (108) have measured the oscillator strengths of the Lyman bands by resolving the rotation spectrum and measuring line intensities. The measured value for the whole band is 0.29 while Geiger and Topchowsky find a value of 0.30. Relativistic corrections were not made.

It is apparent that comparison of elastic and inelastic scattering within the same spectrum can be successfully used to determine oscillator strengths if reliable elastic cross sections are available. However, Geiger's method cannot be used at low kinetic energies because elastic cross sections calculated using the Born approximation are seriously in error. For example, Bromberg finds that at 500 eV the measured elastic cross section for He at 2° scattering angle exceeds the value calculated from the Born approximation by a factor of 2. Once measured elastic cross sections are available, however, the method should be very useful since it is much simpler to compare two peaks (elastic and inelastic) in the same spectrum than to compare the peaks in different gases.

The good agreement obtained for helium and hydrogen provide no clue to the large discrepancies obtained in N_2, O_2, H_2O, and CO. The data obtained by Lassettre *et al.* on helium are also self consistent (see section entitled Helium Continuum). Moreover, Lassettre and Jones (132) measured oscillator strengths through the hydrogen spectrum. The spectrum was unresolved and the precision was not high but the calculated refractive index agrees with the measured value and the oscillator sum rule is satisfied to within 5%. Hence no discrepancies like those on N_2, O_2, H_2O, and CO arise.

Additional Research of Aeronomic Interest

A program of research on electron impact spectra (and generalized oscillator strengths) of metal vapors is in progress under the direction of Ross. An initial paper on potassium has been published (133). Additional experiments on other alkali atoms are in progress and other metal vapors will be studied.

Collision cross sections for CO_2 at very low kinetic energies (at resonances) have recently been reported by Boness and Schulz (134). Although these energies are below the range covered by this review we note that the measurements have been done. It is interesting to compare their results with those of Fig. 19.

Turner (135) has published a detailed description of his photoelectron spectrometer and a more complete spectrum of O_2^+ at higher resolution than that of Fig. 15 but comparable with that of Fig. 14.

Kim, Inokuti, Chamberlain, and Mielczarek (136) have reported that collision cross sections for atomic substances can be zero at certain momentum changes. A case is encountered in the xenon spectrum where the observed cross section has a pronounced minimum which is nearly zero.

Can. J. Chem. Downloaded from www.nrcresearchpress.com by 210.87.254.6 on 09/05/12
For personal use only.

1. A. E. S. GREEN and S. K. DUTTA. J. Geophys. Res. **72**, 3933 (1967).
2. A. T. JUSICK, C. E. WATSON, L. R. PETERSON, and A. E. S. GREEN. J. Geophys. Res. **72**, 3943 (1967).
3. R. S. STOLARSKI, V. A. DULOCK, JR., C. E. WATSON, and A. E. S. GREEN. J. Geophys. Res. **72**, 3953 (1967).
4. C. E. WATSON, V. A. DULOCK, JR., R. S. STOLARSKI, and A. E. S. GREEN. J. Geophys. Res. **72**, 3961 (1967).
5. R. S. STOLARSKI and A. E. S. GREEN. J. Geophys. Res. **72**, 3967 (1967).
6. A. E. S. GREEN and C. A. BARTH. J. Geophys. Res. **72**, 3975 (1967).
7. E. N. LASSETTRE, V. D. MEYER, and M. S. LONGMIRE. J. Chem. Phys. **41**, 2952 (1964).
8. E. N. LASSETTRE, V. D. MEYER, and M. S. LONGMIRE. J. Chem. Phys. **42**, 807 (1965).
9. R. H. GARSTANG. J. Chem. Phys. **44**, 1308 (1966).
10. P. MARMET and L. KERWIN. Can. J. Phys. **38**, 787 (1960).
11. G. J. SCHULZ. Phys. Rev. **125**, 229 (1962).
12. G. J. SCHULZ. Phys. Rev. **135**, A988 (1964).
13. D. ANDRICK and H. EHRHARDT. Z. Physik, **192**, 99 (1966).
14. J. W. MCGOWAN and M. A. FINEMAN. *In* Proceedings, IVth International Conference on the Physics of Electronic and Atomic Collisions, Quebec. 1965. p. 429. See also J. W. McGowan. Rev. Sci. Instr. **38**, 285 (1967).
15. C. E. BRION. J. Chem. Phys. **40**, 2995 (1964).
16. A. SKERBELE and E. N. LASSETTRE. J. Chem. Phys. **40**, 1271 (1964).
17. J. A. SIMPSON. Rev. Sci. Instr. **35**, 1698 (1964).
18. V. D. MEYER, A. SKERBELE, and E. N. LASSETTRE. J. Chem. Phys. **43**, 805 (1965).
19. E. LASSETTRE, A. SKERBELE, and V. D. MEYER. J. Chem. Phys. **45**, 3214 (1966).
20. E. N. LASSETTRE, A. SKERBELE, M. A. DILLON, and K. J. ROSS. J. Chem. Phys. **48**, 5066 (1968).
21. J. A. SIMPSON and C. E. KUYATT. J. Appl. Phys. **37**, 3805 (1966).
22. J. A. SIMPSON and C. E. KUYATT. Rev. Sci. Instr. **38**, 103 (1968).
23. H. BOERSCH, J. GEIGER, and H. HELLWIG. Phys. Letters, **3**, 64 (1962).
24. H. BOERSCH, J. GEIGER, and W. STICKEL. Z. Physik, **180**, 415 (1964).
25. H. BOERSCH, J. GEIGER, and M. TOPCHOWSKY. Phys. Letters, **17**, 266 (1965).
26. D. W. TURNER. Nature, **167**, 795 (1967).
27. J. GEIGER and B. SCHRÖDER. *In* Proceedings, Vth International Conference on the Physics of Electronic and Atomic Collisions, Leningrad. 1967. p. 563.
28. J. GEIGER and B. SCHRÖDER. J. Chem. Phys. **50**, 7 (1969).
29. J. GEIGER. Private communication.
30. R. S. MULLIKEN. The threshold of space. The Pergamon Press, Ltd., New York. 1957.
31. H. G. M. HEIDEMAN, C. E. KUYATT, and G. E. CHAMBERLAIN. J. Chem. Phys. **44**, 355 (1966).
32. V. D. MEYER and E. N. LASSETTRE. J. Chem. Phys. **44**, 2535 (1966).
33. A. SKERBELE, M. A. DILLON, and E. N. LASSETTRE. J. Chem. Phys. **46**, 4161 (1967).
34. A. SKERBELE, M. A. DILLON, and E. N. LASSETTRE. J. Chem. Phys. **49**, 3543 (1968).
35. G. HERZBERG. Phys. Rev. **69**, 362 (1946).
36. P. G. WILKINSON and R. S. MULLIKEN. Astrophys. J. **126**, 10 (1957).
37. J. T. VANDERSLICE, P. G. WILKINSON, and S. G. TILFORD. J. Chem. Phys. **42**, 2681 (1965).
38. E. N. LASSETTRE and M. E. KRASNOW. J. Chem. Phys. **40**, 1248 (1964).
39. W. LICHTEN. J. Chem. Phys. **26**, 306 (1957).
40. V. D. MEYER and E. N. LASSETTRE. J. Chem. Phys. **44**, 2535 (1966).
41. R. E. WORLEY. Phys. Rev. **64**, 204 (1943).
42. B. LUTZ and K. DRESSLER. Phys. Rev. Letters, **19**, 1219 (1967).
43. V. CERMAK. J. Chem. Phys. **44**, 1318 (1966).
44. R. S. MULLIKEN. Phys. Rev. **57**, 500 (1940).
45. E. N. LASSETTRE, F. M. GLASER, V. D. MEYER, and A. SKERBELE. J. Chem. Phys. **42**, 3429 (1965).
46. V. D. MEYER, A. SKERBELE, and E. N. LASSETTRE. J. Chem. Phys. **43**, 3769 (1965).
47. R. W. NICHOLLS. J. Quant. Spectry. Radiative Transfer, **2**, 433 (1962).
48. M. OGAWA, Y. TANAKA, and A. J. JURSA. Can. J. Phys. **42**, 1716 (1964).
49. J. GEIGER and W. STICKEL. J. Chem. Phys. **43**, 4535 (1965).
50. G. M. LAWRENCE, D. L. MICKEY, and K. DRESSLER. J. Chem. Phys. **48**, 1989 (1968).
51. W. BENESCH, J. T. VANDERSLICE, S. G. TILFORD, and P. G. WILKINSON. Astrophys. J. **143**, 236 (1966).
52. U. FANO. Phys. Rev. **124**, 1866 (1961).
53. H. EHRHARDT and F. LINDER. Z. Naturforsch. **22a**, 444 (1967).
54. D. W. TURNER and D. P. MAY. J. Chem. Phys. **45**, 471 (1966).
55. J. P. DOERING and A. J. WILLIAMS III. J. Chem. Phys. **47**, 864 (1967).
56. J. GEIGER and B. SCHRÖDER. J. Chem. Phys. **49**, 740 (1968).
57. E. N. LASSETTRE and S. A. FRANCIS. J. Chem. Phys. **40**, 1208 (1964).
58. A. SKERBELE and E. N. LASSETTRE. J. Chem. Phys. **42**, 395 (1965).
59. A. SKERBELE, V. D. MEYER, and E. N. LASSETTRE. J. Chem. Phys. **43**, 817 (1965).
60. A. SKERBELE and E. N. LASSETTRE. J. Chem. Phys. **44**, 4066 (1966).
61. G. HERZBERG. Electronic spectra of polyatomic molecules. D. Van Nostrand Co., Inc., New York. 1966.
62. A. SKERBELE, M. A. DILLON, and E. N. LASSETTRE. J. Chem. Phys. **49**, 5042 (1968).
63. G. J. SCHULZ. J. Chem. Phys. **33**, 1661 (1960).
64. R. N. COMPTON, R. H. HUEBNER, P. W. REINHARDT, and L. G. CHRISTOPHOROU. J. Chem. Phys. **48**, 901 (1968).
65. C. R. BRUNDLE and D. W. TURNER. Proc. Roy. Soc. London, Ser. A, **307**, 27 (1968).
66. J. GEIGER and K. WITTMAACK. Z. Physik, **187**, 433 (1965).
67. H. BOERSCH. *In* Proceedings IVth International Conference on the Physics of Electronic and Atomic Collisions, Quebec. Abstracts of Papers. Science Bookcrafters, Inc., Hastings-on-Hudson, New York. 1965. p. 351.
68. G. E. CHAMBERLAIN, H. G. M. HEIDEMAN, J. A. SIMPSON, and C. E. KUYATT. *In* Proceedings IVth International Conference on the Physics of Electronic and Atomic Collisions, Quebec. Abstracts of Papers. Science Bookcrafters, Inc., Hastings-on-Hudson, New York. 1965. p. 378.
69. J. K. RICE, A. KUPPERMAN, and S. TRAJMAR. J. Chem. Phys. **48**, 945 (1968).
70. A. SKERBELE and E. N. LASSETTRE. *In* Proceedings Vth International Conference on the Physics of

Electronic and Atomic Collisions, Leningrad. Abstracts of Papers. Publishing House "Nauka." 1967. p. 495. See also ref. 20.
71. V. I. OCHKUR. Soviet Phys. JETP, **18**, 503 (1964).
72. R. A. BONHAM. J. Chem. Phys. **36**, 3260 (1962).
73. H. BOERSCH, J. GEIGER, and B. SCHRÖDER. *In* Abhandlungen der Deutsche Akad. der Wissenschaften zu Berlin, Klassefür Mathematische, Physik und Tech. No. 1 (1967). Akademic-Verlag, Berlin. p. 15.
74. H. S. W. MASSEY and C. B. O. MOHR. Proc. Roy. Soc. London, Ser. A, **13**, 605 (1931).
75. H. S. W. MASSEY. Handbuch der Physik. *Edited by* S. Flügge. Springer-Verlag, Berlin. 1956. pp. 307–408.
76. E. N. LASSETTRE, M. E. KRASNOW, and S. M. SILVERMAN. J. Chem. Phys. **40**, 1242 (1964).
77. E. N. LASSETTRE and E. A. JONES. J. Chem. Phys. **40**, 1218 (1964).
78. S. M. SILVERMAN and E. N. LASSETTRE. J. Chem. Phys. **40**, 1265 (1964).
79. L. VRIENS, J. A. SIMPSON, and S. R. MIELCZAREK. Phys. Rev. **165**, 7 (1968).
80. B. SCHIFF and C. L. PEKERIS. Phys. Rev. **134**, A638 (1964).
81. Y. K. KIM and M. INOKUTI. Phys. Rev. **175**, 176 (1968).
82. E. N. LASSETTRE, A. S. BERMAN, S. M. SILVERMAN, and M. E. KRASNOW. J. Chem. Phys. **40**, 1232 (1964).
83. E. N. LASSETTRE, A. SKERBELE, and M. A. DILLON. Unpublished.
84. G. E. CHAMBERLAIN, J. A. SIMPSON, S. R. MIELCZAREK, and C. E. KUYATT. J. Chem. Phys. **47**, 4266 (1967).
85. E. N. LASSETTRE and G. S. JOHN. Unpublished.
86. A. SKERBELE and E. N. LASSETTRE. J. Chem. Phys. **45**, 1077 (1966).
87. E. N. LASSETTRE. J. Chem. Phys. **43**, 4479 (1965).
88. S. M. SILVERMAN and E. N. LASSETTRE. J. Chem. Phys. **44**, 2219 (1966).
89. S. M. SILVERMAN and E. N. LASSETTRE. J. Chem. Phys. **42**, 3420 (1965).
90. *a*. A. DALGARNO and A. L. STEWART. Proc. Phys. Soc. London, **76**, 49 (1960). A complete set of oscillator strengths has also been derived by Miller and Platzman. *b*. W. N. MILLER. Ph.D. Thesis. Dept. Physics, Purdue Univ. 1955.
91. D. J. BAKER, D. E. BEDO, and D. H. TOMBOULIAN. Phys. Rev. **124**, 1471 (1961). J. A. R. SAMSON. J. Opt. Soc. Am. **54**, 876 (1964).
92. A. L. STEWART and T. G. WEBB. Proc. Phys. Soc. London, **82**, 532 (1963).
93. R. P. MADDEN and K. CODLING. Astrophys. J. **141**, 364 (1965).
94. E. N. LASSETTRE, S. M. SILVERMAN, and M. E. KRASNOW. J. Chem. Phys. **40**, 1261 (1964). The extrapolated oscillator strength was reported at a Physical Society meeting in 1954; see abstract in Phys. Rev. **95**, 635A (1954).
95. E. N. LASSETTRE and S. M. SILVERMAN. J. Chem. Phys. **40**, 1256 (1964).
96. S. M. SILVERMAN and E. N. LASSETTRE. J. Chem. Phys. **40**, 2922 (1964).
97. S. M. SILVERMAN and E. N. LASSETTRE. J. Chem. Phys. **41**, 3727 (1964).
98. W. R. JARMAIN, R. EBISUZAKI, and R. W. NICHOLLS. Can. J. Phys. **38**, 510 (1960).
99. J. D. CRAGGS and H. S. W. MASSEY. Handbuch der Physik. Vol. 37. *Edited by* S. Flügge. Springer-Verlag, Berlin. 1959. p. 314.
100. T. WENTINK, E. P. MARRAM, L. ISSAACSON, and R. J. SPINDLER. Avco Corp. Research and Technology Laboratories, Space Systems Division. Technical Report No. AFWL-TR-67-30, Vol. 1. Experimental Determination of Oscillator Strengths. Contract AF29(601)-7117. Nov. 1967.
101. R. W. NICHOLLS. J. Quant. Spectry. Radiative Transfer, **2**, 433 (1962).
102. A. SKERBELE, M. A. DILLON, and E. N. LASSETTRE. J. Chem. Phys. **46**, 4162 (1967).
103. A. SKERBELE, V. D. MEYER, and E. N. LASSETTRE. J. Chem. Phys. **44**, 4069 (1966).
104. E. N. LASSETTRE and E. R. WHITE. Scientific Report No. 12, Contract No. AF19(122)-642 with Air Force Cambridge Research Laboratories. AFCRC-TN-58-560 AD No. 152643, March 1958.
105. E. N. LASSETTRE and J. C. SHILOFF. J. Chem. Phys. **43**, 560 (1965).
106. J. GEIGER. Z. Physik, **181**, 413 (1964).
107. J. GEIGER and M. TOPCHOWSKY. Z. Naturforsch. **21a**, 626 (1966).
108. J. E. HESSER, N. H. BROOKS, and G. M. LAWRENCE. Astrophys. J. **153**, L65 (1968).
109. R. E. HUFFMAN, Y. TANAKA, and J. C. LARRABEE. J. Chem. Phys. **39**, 910 (1963).
110. G. R. COOK and P. H. METZGER. J. Chem. Phys. **41**, 321 (1964).
111. G. L. WEISSLER, P. LEE, and E. I. MOHR. J. Opt. Soc. Am. **42**, 84 (1952).
112. N. ASTOIN and J. GRANIER. Compt. Rend. **244**, 1350 (1957).
113. K. C. CLARK. Phys. Rev. **87**, 271 (1952).
114. J. P. CURTIS. Phys. Rev. **94**, 908 (1954).
115. K. WATANABE, E. C. Y. INN, and M. ZELIKOFF. J. Chem. Phys. **21**, 1026 (1953).
116. W. A. RENSE and R. MERCURE. Bull. Am. Phys. Soc. **30** (Jan. 27, 1955).
117. R. LADENBURG and C. C. VAN VOORHIS. Phys. Rev. **43**, 315 (1933).
118. J. F. JAMES. Thesis. Reading 1957. Quoted by D. W. O. HEDDLE. J. Chem. Phys. **32**, 1889 (1960).
119. R. LADENBURG and G. WOLFSOHN. Z. Physik, **79**, 42 (1932).
120. R. W. DITCHBURN and D. W. O. HEDDLE. Proc. Roy. Soc. London, Ser. A, **220**, 61 (1953).
121. K. WATANABE and F. F. MARMO. J. Chem. Phys. **25**, 965 (1956).
122. See ref. 104 for source of refractive indices.
123. H. ISHII and K. NAKAYAMA. Trans. Natl. Vacuum Symp. (8th, 1961) **1**, 319 (1962).
124. F. M. GLASER and E. N. LASSETTRE. Rev. Sci. Instr. **36**, 1658 (1965).
125. E. N. LASSETTRE. Radiation Research, Suppl. **1**, 530–546 (1959).
126. J. E. HESSER and K. DRESSLER. J. Chem. Phys. **45**, 3149 (1966).
127. J. E. HESSER. J. Chem. Phys. **48**, 2518 (1968).
128. J. C. RICH. Astrophys. J. **153**, 327 (1968).
129. J. GEIGER. Z. Physik, **175**, 530 (1963).
130. Y. K. KIM and M. INOKUTI. Phys. Rev. **165**, 39 (1968).
131. W. L. WILLIAMS and E. S. FRY. Phys. Rev. Letters, **20**, 1335 (1968).
132. E. N. LASSETTRE and E. A. JONES. J. Chem. Phys. **40**, 1222 (1964).
133. I. V. HERTEL and K. J. ROSS. J. Phys. Series 2, **1**, 697 (1968).
134. M. J. W. BONESS and G. J. SCHULZ. Phys. Rev. Letters, **21**, 1031 (1968).
135. D. W. TURNER. Proc. Roy. Soc. London, Ser. A, **307**, 15 (1968).

Can. J. Chem. Downloaded from www.nrcresearchpress.com by 210.87.254.6 on 09/05/12
For personal use only.

136. Y.-K. KIM, M. INOKUTI, G. E. CHAMBERLAIN, and S. R. MIELCZAREK. Phys. Rev. Letters, **21**, 1146 (1968).
137. G. HERZBERG. Molecular spectra and molecular structure. II. Infrared and Raman spectra of polyatomic molecules. D. Van Nostrand Co., Inc., Princeton, New Jersey. 1945.
138. S. S. PENNER. Quantitative molecular spectroscopy and gas emissivities. Addison–Wesley Publishing Co., Inc., Reading, Mass. 1959.
139. C. C. FERRISO, C. B. LUDWIG, and A. L. THOMSON. J. Quant. Spectry. Radiative Transfer, **6**, 241 (1966).
140. N. F. MOTT and H. S. W. MASSEY. The theory of atomic collisions. 3rd ed. Oxford University Press, London. 1965. p. 481.

Semi-empirical electron impact cross sections for atmospheric gases[1]

L. R. PETERSON, S. S. PRASAD, AND A. E. S. GREEN
Department of Physics and Astronomy, University of Florida, Gainesville

Received December 8, 1968

The present paper summarizes conveniently the electron-impact cross sections for N_2, O_2, and O used in recent aurora and dayglow studies at the University of Florida. The cross section parameters in their present form are a natural outgrowth of (*a*) the availability of an increasing number of cross section measurements in the laboratory as well as field observations of spectral intensities, and (*b*) more realistic calculations.

The values presented should serve as a useful interim reference list pending the full analyses of current extensive data. Their usefulness for practical applications to problems in aeronomy is enhanced by their integrable functional forms.

Canadian Journal of Chemistry, 47, 1774 (1969)

Introduction

The studies of semi-empirical cross sections for He, N_2, and O_2 (1–4) were attempts to use fragmentary experimental data in conjunction with simple rules derived from both theory and phenomenology to infer complete sets of approximate cross sections. The semi-empirical cross sections developed in these papers for electron impact are based on the Born approximation, which permits one to normalize the high energy limit by the use of optical oscillator strengths, and also are based on a semi-empirical modification to encompass low energy data. The resulting cross sections are then fitted with simple forms of the type given in the present paper for greater convenience in applications. Such complete sets are needed to provide some basis on which to study phenomena of aeronomical interest such as aurora and dayglow (5, 6).

This program, because of new information sources, can now be extensively refined for He, N_2, and O_2, as well as for several other species. First, there is a wealth of new data coming from laboratory measurements, which enable one to be much more realistic than previously. Improvements in resolution, extensions of the energies at which data are available, and additional theoretical sophistications enable one now to better identify states, to profitably consider individual Franck–Condon factors, and to get at the low energy aspects of the cross sections where the Born approximation must be appropriately modified. Second, there are now available increasing numbers of field measurements on spectral intensities which, when compared with realistic calculations, suggest how to modify the cross sections themselves. This is especially true for certain types of cross sections which are very difficult to measure in a laboratory and others which are clearly responsible for spectral lines without interference from chemical, radiative transfer, or similar effects.

The present paper is intended to list in an analytic form the cross sections for N_2, O_2, and O used in our most recent studies (7, 8). These cross sections are basically those of the original studies with some modifications as discussed later. They are meant as a convenient summary to clear the table for the next generation of cross section work, much more ambitious in nature, now in progress at the University of Florida.

All excitation cross sections have been expressed in the form

$$[1] \qquad \sigma_j(E) = \frac{q_0 f_0 c_0}{W_j^2}\left(\frac{W_j}{E}\right)^{\Omega}\sum_s a_s\left(\frac{W_j}{E}\right)^{\Gamma_s}$$

with the restrictions $(a_1,\Gamma_1) = (1,0)$ and $\sum_s a_s = 0$.

[1]Supported in part by the U.S. National Aeronautics and Space Administration, NsG-599.

Can. J. Chem. Downloaded from www.nrcresearchpress.com by 210.87.254.6 on 09/05/12
For personal use only.

136. Y.-K. KIM, M. INOKUTI, G. E. CHAMBERLAIN, and S. R. MIELCZAREK. Phys. Rev. Letters, **21**, 1146 (1968).
137. G. HERZBERG. Molecular spectra and molecular structure. II. Infrared and Raman spectra of polyatomic molecules. D. Van Nostrand Co., Inc., Princeton, New Jersey. 1945.
138. S. S. PENNER. Quantitative molecular spectroscopy and gas emissivities. Addison–Wesley Publishing Co., Inc., Reading, Mass. 1959.
139. C. C. FERRISO, C. B. LUDWIG, and A. L. THOMSON. J. Quant. Spectry. Radiative Transfer, **6**, 241 (1966).
140. N. F. MOTT and H. S. W. MASSEY. The theory of atomic collisions. 3rd ed. Oxford University Press, London. 1965. p. 481.

Semi-empirical electron impact cross sections for atmospheric gases[1]

L. R. PETERSON, S. S. PRASAD, AND A. E. S. GREEN
Department of Physics and Astronomy, University of Florida, Gainesville

Received December 8, 1968

The present paper summarizes conveniently the electron-impact cross sections for N_2, O_2, and O used in recent aurora and dayglow studies at the University of Florida. The cross section parameters in their present form are a natural outgrowth of (*a*) the availability of an increasing number of cross section measurements in the laboratory as well as field observations of spectral intensities, and (*b*) more realistic calculations.

The values presented should serve as a useful interim reference list pending the full analyses of current extensive data. Their usefulness for practical applications to problems in aeronomy is enhanced by their integrable functional forms.

Canadian Journal of Chemistry, 47, 1774 (1969)

Introduction

The studies of semi-empirical cross sections for He, N_2, and O_2 (1–4) were attempts to use fragmentary experimental data in conjunction with simple rules derived from both theory and phenomenology to infer complete sets of approximate cross sections. The semi-empirical cross sections developed in these papers for electron impact are based on the Born approximation, which permits one to normalize the high energy limit by the use of optical oscillator strengths, and also are based on a semi-empirical modification to encompass low energy data. The resulting cross sections are then fitted with simple forms of the type given in the present paper for greater convenience in applications. Such complete sets are needed to provide some basis on which to study phenomena of aeronomical interest such as aurora and dayglow (5, 6).

This program, because of new information sources, can now be extensively refined for He, N_2, and O_2, as well as for several other species. First, there is a wealth of new data coming from laboratory measurements, which enable one to be much more realistic than previously. Improvements in resolution, extensions of the energies at which data are available, and additional theoretical sophistications enable one now to better identify states, to profitably consider individual Franck–Condon factors, and to get at the low energy aspects of the cross sections where the Born approximation must be appropriately modified. Second, there are now available increasing numbers of field measurements on spectral intensities which, when compared with realistic calculations, suggest how to modify the cross sections themselves. This is especially true for certain types of cross sections which are very difficult to measure in a laboratory and others which are clearly responsible for spectral lines without interference from chemical, radiative transfer, or similar effects.

The present paper is intended to list in an analytic form the cross sections for N_2, O_2, and O used in our most recent studies (7, 8). These cross sections are basically those of the original studies with some modifications as discussed later. They are meant as a convenient summary to clear the table for the next generation of cross section work, much more ambitious in nature, now in progress at the University of Florida.

All excitation cross sections have been expressed in the form

$$[1] \qquad \sigma_j(E) = \frac{q_0 f_0 c_0}{W_j^2}\left(\frac{W_j}{E}\right)^{\Omega}\sum_s a_s\left(\frac{W_j}{E}\right)^{\Gamma_s}$$

with the restrictions $(a_1,\Gamma_1) = (1,0)$ and $\sum_s a_s = 0$.

[1]Supported in part by the U.S. National Aeronautics and Space Administration, NsG-599.

Can. J. Chem. Downloaded from www.nrcresearchpress.com by 210.87.254.40 on 09/05/12
For personal use only.

Can. J. Chem. Downloaded from www.nrcresearchpress.com by 210.87.254.40 on 09/05/12
For personal use only.

The constant q_0 is 6.514×10^{-14} eV^2 cm^2, f_0 and c_0 are constants giving the strength, W_j is the excitation threshold, Ω is the cross section fall-off parameter, and a_s, Γ_s determine the overall shape. This equation is used to describe Rydberg states by replacing f_0 with $f^*/(n-\delta)^3$, where n is the principal quantum number and δ is the quantum defect. We note in this regard that it is often convenient for $n > 4$ to sum the Rydberg states using $\sum_{n>n'} 1/(n-\delta)^3 \simeq 1/2(n'-\delta+0.5)^2$. All ionization cross sections are expressed similarly to eq. [1] as

$$[2] \qquad \frac{d\sigma_i(E)}{dW} = \frac{q_0 A_0}{W^2}\left(\frac{I_i}{W}\right)^p \left(\frac{W}{E}\right)^\Omega \sum_s a_s \left(\frac{W}{E}\right)^{\Gamma_s}$$

$$[3] \qquad \sigma_i(E) = \int_{I_i}^{(E+I_i)/2} \frac{d\sigma_i}{dW}\, dW$$

where now W is of course continuous and I_i is the ionization threshold. The parameter p controls the energy-loss behavior of the differential cross section. These forms are convenient in that in applications, where they are usually integrated, the calculations are analytic.

Changes in Ionization Cross Sections and Related Rydberg Series

From the work of Peterson and Green (7) ionization cross sections for N_2 and O_2 are now assumed to have values $p = 1.2$ and 1.1, respectively. In this regard it has been found by further study that the shape parameters (a_s, Γ_s) for O_2 can be made the same as for N_2 and in fact fit the data somewhat better at low energies. For atomic oxygen we have set $p = 1.2$. An additional feature not included by Stolarski *et al.* (3) and Watson *et al.* (4) was dissociative ionization. We have included fits to the dissociative ionization cross sections of N_2 and O_2 assuming that they behave similarly to simple ionization cross sections in the way they produce secondary electrons.

When the ionization cross sections are modified, one must also modify their attached Rydberg series, which means changing the auto-ionization contributions as well. For this purpose we compare the new to the old ionization cross sections at an energy of a few hundred volts and modify the strength of the Rydberg states accordingly.

The situation in N_2 appears on the whole to be reasonable. Guided by the results of McConkey and Latimer (9), Zapesochnyi and Skubenich (10), McConkey *et al.* (11), Stair and Gauvin (12), Srivastava and Mirza (13), and Holland (14), as well as by continuing auroral and dayglow studies by this group (8), we have readjusted the ionization cross sections of Stolarski *et al.* (3) after subtracting the dissociative ionization contribution (15) from the total. The new estimated cross sections are parameterized in Table I.

TABLE I

Parameters for transitions to the various ionization states

Species	State[1]	I_i (eV)	A_0	Ω
	(1,0) $(-1,1)^2$			
N_2	$A^2\Pi_u$	16.73	0.160	0.83
	(1,0) $(-2,1)$ (1,2)			
	$X^2\Sigma_g^+$	15.58	0.370	0.80
	$B^2\Sigma_u^+$	18.75	0.073	0.83
	$D^2\Pi_g$	22.0	0.056	0.83
	$C^2\Sigma_u^+$	23.6	0.060	0.83
	d.i.	25.0	0.380	0.95
O_2	$X^2\Pi_g$	12.1	0.058	0.80
	$a^4\Pi_u$	16.1	0.150	0.80
	$A^2\Pi_u$	16.9	0.150	0.80
	$b^4\Sigma_g^-$	18.2	0.130	0.80
	B	23.0	0.064	0.80
	(1,0) $(-3,1)$ (3,2) $(-1,3)$			
	d.i.($O^+{}^4S$)	18.0	0.400	0.93
	d.i.($O^+{}^2D$)	22.0	0.250	0.93
	(1,0) $(-1,0.3)$			
O	^4S	13.6	0.290	0.85
	^2D	16.9	0.360	0.85
	^2P	18.5	0.190	0.85

[1]The states labeled d.i. represent dissociative ionization.
[2](a_1, Γ_1) $(a_2, \Gamma_2) \ldots (a_s, \Gamma_s) \ldots$

The $B^2\Sigma_u^+$ state has been raised by a factor of about 1.5; the $A^2\Pi_u$ has been changed such that, although the high energy part of the cross section is relatively unchanged, the region below 100 eV is higher by a factor of about 2; and finally, the $X^2\Sigma_g^+$ state is lowered by a factor of about 0.65 overall to be consistent with the total ionization cross section. The strengths of the Rydberg states were changed to reflect these adjustments. The allowed electronic transitions to $b^1\Pi_u$ and $h^1\Sigma_u^+$, however, were left unchanged.

It is of interest to point out that these changes appear to be in the right direction based on other experimental evidence. For example, the work of Geiger and Stickel (16) suggests that about 40% of the 12.85 peak is associated with the $b^1\Pi_u$ state. Lowering R_X (3), which contributes to the 12.85 peak, raises the relative importance of $b^1\Pi_u$ to a value approaching 40%.

TABLE II

Parameters for transitions involving electronic states

Species	State	W_j (eV)	f_0c_0	Ω	(a_s,Γ_s)
N_2	$A^3\Sigma_u^+$	6.14	1.0	4.0	(1,0) (−2,1) (1,2)
	$B^3\Pi_g$	7.30	1.8	4.0	
	$a^1\Pi_g$	9.10	0.14	1.0	
	$C^3\Pi_u$	11.03	0.97	3.0	
	$b^1\Pi_u$	12.85	0.44	0.75	(1,0) (−3,1) (3,2) (−1,3)
	$h^1\Sigma_u^+$	14.00	0.39	0.75	
O_2	9.9 peak	9.9	0.080	0.85	
	$a^1\Delta_g$	0.98	0.000033	0.9	(1,0) (−1,1)
	$b^1\Sigma_g^+$	1.64	0.000037	0.9	
	$A^3\Sigma_u^+$	4.50	0.021	0.9	
	$B^3\Sigma_u^-$	8.4	0.23	0.75	(1,0) (−2,1) (1,2)
O	^1D	1.9	0.013	1.00	
	^1S	4.17	0.0061	1.00	(1,0) (−1,0.5)

The forbidden states of N_2 are still rather uncertain and we have chosen for the time being to retain the old cross sections because of the lack of enough evidence to the contrary. It is worth pointing out, however, that new measurements are available (14, 17, 10, 18) which suggest changes in the next generation work. The forbidden triplet states of N_2 are responsible for the first and second positive as well as the Vegard–Kaplan emissions in the aurora and airglow. These states then are of special interest in that the auroral and dayglow calculation can help us to fix limits on the cross sections. Tables II and III summarize the cross sections and their parameters.

The situation for O_2 is somewhat weaker than for N_2 because of the lack of data at the time of the original work of Watson *et al.* (4). For simplicity, then, with the realization that future work should be especially fruitful for O_2, we have kept the old relative values but have reduced the ionization and Rydberg cross section strengths to accommodate dissociative ionization. In addition the 8.4 eV Schumann–Runge peak is reinterpreted by assuming it to be composed of $R_X(3)$ and $B^3\Sigma_u^-$ with the latter carrying most of the strength rather than the former. Tables I, II, and III give the cross section parameters.

Finally we wish to present a tentative set of cross sections for atomic oxygen. The parameters for the ^1D and ^1S states are estimated from the recent calculations of Smith *et al.* (19) and appear in Table II. However, in an almost complete absence of further data, we have adopted the approach of assigning a shape function to each cross section according to its spin and orbital angular momentum quantum numbers. The assumed shapes are similar to those for helium given by Jusick *et al.* (2) except that we have made the forbidden transitions more sharply peaked. The general approach in estimating cross sections is to first obtain the optical oscillator strengths for the allowed transitions (type 1 in Table IV) leading to a particular ionization continuum. The cross sections for these transitions are then obtained from eq. [1] using $c_0 = 1.5$, and using $f^*/(n-\delta)^3$ to account for the n dependence in the higher members. The value of f^* found for an allowed transition, along with the c_0's given in Table IV, and proper values for δ, are then used for the other transition types leading to the same ionization continua. The comparison of realistic calculations of the resulting spectral lines with field observations indicates

TABLE III

Parameters for Rydberg states leading to the various ionization continua[1]

Species	Rydberg limit	δ	c_0f^*	W_j ($n=3$)
N_2	$X^2\Sigma_g^+$	0.7	6.6	13.0
	$A^2\Pi_u$	1.04	2.2	13.17
	$B^2\Sigma_u^+$	0.87	1.0	15.75
	$D^2\Pi_g$	1.53	0.7	15.7
	$C^2\Sigma_u^+$	0.8	0.7	14.0
O_2	$X^2\Pi_g$	1.08	1.2	8.4
	$a^4\Pi_u$	1.0	2.5	12.7
	$A^2\Pi_u$	1.07	2.1	13.2
	$b^4\Sigma_g^-$	0.69	1.8	15.7
	B	1.0	0.7	19.6

[1]In each case the shape parameters are the same with $\Omega = 0.75$ and with the set of (a_s, Γ_s) being (1,0) (−3,1) (3,2) (−1,3).

Can. J. Chem. Downloaded from www.nrcresearchpress.com by 210.87.254.40 on 09/05/12
For personal use only.

TABLE IV

General parameters for estimating cross sections in atomic oxygen

Type	$\|\Delta l\|$	$\|\Delta s\|$	Ω	c_0	Set of (a_s,Γ_s)
1	1	0	0.75	1.5	(1,0) (−3,1) (3,2) (−1,3)
2	0	0	0.75	0.06	(1,0) (−1,2)
3	1	1	3.0	1.4	(1,0) (−2,1) (1,2)
4	0	1	3.0	0.4	(1,0) (−1,1)

that these cross sections are not unreasonable on average.

For the ionization cross sections in O, we use the same estimates as Stolarski and Green (5) with ^4S and ^2D each contributing 40% and ^2P contributing 20% at 100 eV. Some contributions will also come from auto-ionization, but we have not included them. The total ionization cross section is about one half that of O_2 at 10 keV and fits the results of Fite and Brackmann (20) and Rothe *et al.* (21) below 1 keV.

Conclusions

It is hoped that the cross sections presented here will be of assistance to workers in aeronomy by providing a rather complete set. It is comforting that the use of these cross sections leads to good correlation with auroral and dayglow observations, to consistent loss functions in the keV range, and to reasonable values of ionization yield. However, in the face of rather large uncertainties in much of the data, it must be emphasized that continued recycling of these constants will be necessary until atomic cross section experiments or theory become an exact science.

1. A. E. S. Green and S. K. Dutta. J. Geophys. Res. **72**, 3933 (1967).
2. A. T. Jusick, C. E. Watson, L. R. Peterson, and A. E. S. Green. J. Geophys. Res. **72**, 3943 (1967).
3. R. S. Stolarski, V. A. Dulock, Jr., C. E. Watson, and A. E. S. Green. J. Geophys. Res. **72**, 3953 (1967).
4. C. E. Watson, V. A. Dulock, Jr., R. S. Stolarski, and A. E. S. Green. J. Geophys. Res. **72**, 3961 (1967).
5. R. S. Stolarski and A. E. S. Green. J. Geophys. Res. **72**, 3967 (1967).
6. A. E. S. Green and C. A. Barth. J. Geophys. Res. **72**, 3975 (1967).
7. L. R. Peterson and A. E. S. Green. Proc. Phys. Soc. **1B**, 1131 (1968).
8. A. E. S. Green, L. R. Peterson, and S. S. Prasad. *In* Aurora and airglow, Proceedings of the NATO advanced study institute. Ås, Norway. 1968. *Edited by* B. M. McCormac. Reinhold Publishing Corporation, New York.
9. J. W. McConkey and I. D. Latimer. Proc. Phys. Soc. **86**, 463 (1965).
10. I. P. Zapesochnyi and V. V. Skubenich. Opt. Spectry. USSR, **21**, 83 (1966).
11. J. W. McConkey, J. M. Woolsey, and D. J. Burns. Planetary Space Sci. **15**, 1332 (1967).
12. A. T. Stair and H. P. G. Gauvin. *In* Aurora and airglow. *Edited by* B. M. McCormac. Reinhold Publishing Corporation, New York. 1967.
13. B. N. Srivastava and I. M. Mirza. Phys. Rev. **168**, 168 (1968).
14. R. F. Holland. Cross sections for electron excitation of 3914 Å (0,0) band of the N_2^+ first negative system. No. LA-3783. Los Alamos Scientific Laboratory. Las Alamos, New Mexico. 1967.
15. L. J. Keiffer and G. H. Dunn. Rev. Mod. Phys. **38**, 1 (1966).
16. J. Geiger and W. Stickel. J. Chem. Phys. **43**, 4535 (1965).
17. A. Skerbele, M. A. Dillon, and E. N. Lassettre. J. Chem. Phys. **46**, 4162 (1967).
18. H. H. Brongersma, Johanna A. v. d. Hart, and L. J. Oosterhoff. *In* Nobel symposium V, Södergen. *Edited by* Stig Claesson. Interscience Publishers Inc., New York. 1967.
19. W. L. Fite and R. T. Brackmann. Phys. Rev. **113**, 815 (1959).
20. K. Smith, R. J. W. Henry, and P. G. Burke. Phys. Rev. **157**, 51 (1967).
21. E. W. Rothe, L. L. Marina, R. H. Neynaber, and S. M. Trujillo. Phys. Rev. **125**, 582 (1962).

Comments, Replies, and Summary

COMMENTS BY D. M. HUNTEN

The optical absorption coefficient of CO_2 near 2000 Å (6.4 eV) is of great interest for possible application to the Venus atmosphere. Cross sections as small as 10^{-24} cm^2 would be significant, but would be extremely difficult to measure optically, being only 10^{-7} of the peak value. From Fig. 18 of the paper by Lassettre, it appears that it might be possible to infer the required absorption coefficient by careful observation of

Can. J. Chem. Downloaded from www.nrcresearchpress.com by 210.87.254.40 on 09/05/12
For personal use only.

TABLE IV

General parameters for estimating cross sections in atomic oxygen

Type	$\|\Delta l\|$	$\|\Delta s\|$	Ω	c_0	Set of (a_s,Γ_s)
1	1	0	0.75	1.5	(1,0) (−3,1) (3,2) (−1,3)
2	0	0	0.75	0.06	(1,0) (−1,2)
3	1	1	3.0	1.4	(1,0) (−2,1) (1,2)
4	0	1	3.0	0.4	(1,0) (−1,1)

that these cross sections are not unreasonable on average.

For the ionization cross sections in O, we use the same estimates as Stolarski and Green (5) with ^4S and ^2D each contributing 40% and ^2P contributing 20% at 100 eV. Some contributions will also come from auto-ionization, but we have not included them. The total ionization cross section is about one half that of O_2 at 10 keV and fits the results of Fite and Brackmann (20) and Rothe *et al.* (21) below 1 keV.

Conclusions

It is hoped that the cross sections presented here will be of assistance to workers in aeronomy by providing a rather complete set. It is comforting that the use of these cross sections leads to good correlation with auroral and dayglow observations, to consistent loss functions in the keV range, and to reasonable values of ionization yield. However, in the face of rather large uncertainties in much of the data, it must be emphasized that continued recycling of these constants will be necessary until atomic cross section experiments or theory become an exact science.

1. A. E. S. Green and S. K. Dutta. J. Geophys. Res. **72**, 3933 (1967).
2. A. T. Jusick, C. E. Watson, L. R. Peterson, and A. E. S. Green. J. Geophys. Res. **72**, 3943 (1967).
3. R. S. Stolarski, V. A. Dulock, Jr., C. E. Watson, and A. E. S. Green. J. Geophys. Res. **72**, 3953 (1967).
4. C. E. Watson, V. A. Dulock, Jr., R. S. Stolarski, and A. E. S. Green. J. Geophys. Res. **72**, 3961 (1967).
5. R. S. Stolarski and A. E. S. Green. J. Geophys. Res. **72**, 3967 (1967).
6. A. E. S. Green and C. A. Barth. J. Geophys. Res. **72**, 3975 (1967).
7. L. R. Peterson and A. E. S. Green. Proc. Phys. Soc. **1B**, 1131 (1968).
8. A. E. S. Green, L. R. Peterson, and S. S. Prasad. *In* Aurora and airglow, Proceedings of the NATO advanced study institute. Ås, Norway. 1968. *Edited by* B. M. McCormac. Reinhold Publishing Corporation, New York.
9. J. W. McConkey and I. D. Latimer. Proc. Phys. Soc. **86**, 463 (1965).
10. I. P. Zapesochnyi and V. V. Skubenich. Opt. Spectry. USSR, **21**, 83 (1966).
11. J. W. McConkey, J. M. Woolsey, and D. J. Burns. Planetary Space Sci. **15**, 1332 (1967).
12. A. T. Stair and H. P. G. Gauvin. *In* Aurora and airglow. *Edited by* B. M. McCormac. Reinhold Publishing Corporation, New York. 1967.
13. B. N. Srivastava and I. M. Mirza. Phys. Rev. **168**, 168 (1968).
14. R. F. Holland. Cross sections for electron excitation of 3914 Å (0,0) band of the N_2^+ first negative system. No. LA-3783. Los Alamos Scientific Laboratory. Las Alamos, New Mexico. 1967.
15. L. J. Keiffer and G. H. Dunn. Rev. Mod. Phys. **38**, 1 (1966).
16. J. Geiger and W. Stickel. J. Chem. Phys. **43**, 4535 (1965).
17. A. Skerbele, M. A. Dillon, and E. N. Lassettre. J. Chem. Phys. **46**, 4162 (1967).
18. H. H. Brongersma, Johanna A. v. d. Hart, and L. J. Oosterhoff. *In* Nobel symposium V, Södergen. *Edited by* Stig Claesson. Interscience Publishers Inc., New York. 1967.
19. W. L. Fite and R. T. Brackmann. Phys. Rev. **113**, 815 (1959).
20. K. Smith, R. J. W. Henry, and P. G. Burke. Phys. Rev. **157**, 51 (1967).
21. E. W. Rothe, L. L. Marina, R. H. Neynaber, and S. M. Trujillo. Phys. Rev. **125**, 582 (1962).

Comments, Replies, and Summary

COMMENTS BY D. M. HUNTEN

The optical absorption coefficient of CO_2 near 2000 Å (6.4 eV) is of great interest for possible application to the Venus atmosphere. Cross sections as small as 10^{-24} cm^2 would be significant, but would be extremely difficult to measure optically, being only 10^{-7} of the peak value. From Fig. 18 of the paper by Lassettre, it appears that it might be possible to infer the required absorption coefficient by careful observation of

Can. J. Chem. Downloaded from www.nrcresearchpress.com by 210.87.254.40 on 09/05/12
For personal use only.

the 6.4 eV region. I should like to direct attention to this in the hope of stimulating some experimental attempts.

REPLY BY E. N. LASSETTRE

The spectral region near 6.4 eV has been studied at an incident kinetic energy of 50 eV but scattering in excess of the background could not be found. It would be of interest to re-investigate this spectral region at higher kinetic energies and reduced resolution. However, this has not yet been done.

QUESTION BY F. A. WOLF[1]

How do you distinguish between exchange and direct excitation processes, i.e., those which result in a change in multiplicity and those which do not?

How much reliability can one ascribe to the threshold behavior of these cross sections?

REPLY BY L. R. PETERSON

Cross sections for exchange and direct excitation processes have a very different form from one another in that exchange cross sections, in contrast to direct cross sections, rise quickly from threshold to peak and then fall off again very rapidly. This behavior can be well represented by our fits by choosing the parameters appropriately.

When speaking of threshold behavior, one must define whether we are talking about how the cross section fit varies with E at very small increments above threshold or how well the peak is represented by the fit when the peak occurs close to threshold. While our fits tend to reproduce the latter definition quite well, we do not worry at all about the former.

COMMENTS BY A. I. STEWART[2]

It is important to realize that in the dayglow, and to a somewhat lesser extent in the aurorae, it is the behavior of the cross section close to threshold which determines the rate of excitation of radiating states by electron impact. Cross sections deduced solely from high-energy scattering data are unlikely to be accurate in this most important region. Attempts to find curve fits to excitation cross sections should, therefore, use parameters which may be adjusted to give agreement at and near threshold with such experimental evidence as is available.

REPLY BY L. R. PETERSON

Consistent with the meaning of threshold behavior as we use it, we feel that the cross section near the peak or perhaps the integrated cross section, as approximated by the peak and width at half maximum, is the dominant feature in the majority of cases.

With respect to the second part of the question, we do agree that the cross sections deduced solely from high energy data are unlikely to be accurate in the region of importance, namely, the peak. For that reason in fitting our cross sections we make use of the many phenomenologically derived subsidiary conditions regarding the shape and magnitude scaling factors.

COMMENTS BY R. W. NICHOLLS[3]

I should like to compliment Dr. Peterson on the work which he, Professor Green, and associates are doing in Florida in an attempt to deal quantitatively with the gross phenomenology associated with the energy degradation of particles and photons which enter the earth's atmosphere. My question relates to the rationale for and the physical meaning of the terms in the empirical expressions they use for cross sections. Some years ago (1–3) when considering the excitation kinetics of N_2 in discharges, I had an occasion to seek plausible empirical expressions for excitation cross sections of the various electronic states of N_2, and found that expressions of the form

$$S(E) = CE^{\frac{1}{2}} \exp(-LE)$$

where C is a constant, fitted the sparse experimental data then available fairly well. I wonder if the Florida group experimented with similar empirical expressions?

1. R. W. NICHOLLS. Nature, **162**, 487 (1948).
2. R. W. NICHOLLS. Nature, **167**, 31 (1951).
3. R. W. NICHOLLS. The kinetics of excitation of molecular nitrogen and other molecules. *In* Proceedings of the Conference on Auroral Physics, Geophysical Research Papers No. 30, Air Force Cambridge Research Center. 1954. pp. 291–319.

[1]Address: San Diego College, San Diego, California.
[2]Address: University of Colorada, Boulder, Colorado.
[3]Address: York University, Downsview, Ontario.

Can. J. Chem. Downloaded from www.nrcresearchpress.com by 210.87.254.40 on 09/05/12
For personal use only.

Can. J. Chem. Downloaded from www.nrcresearchpress.com by 210.87.254.40 on 09/05/12
For personal use only.

REPLY BY A. E. S. GREEN

First, let us return the compliment by remarking that Professor Nicholls was far ahead of his time in using a phenomenological approach to the low energy degradation problem. The function mentioned, however, would fall off too sharply at the high energies involved in auroral and some dayglow applications. Our own functional forms for cross sections have been chosen with these applications in mind, and in view of the analytic forms which are suitable for loss functions.

COMMENTS BY F. R. GILMORE

In interpreting energy-loss measurements in nitrogen, it is important to keep in mind that N_2 has many electronic states which may be excited by electron impact. For example, within 3 eV of the $A^3\Sigma_u^+$ state there are four similar states: $W^3\Delta_u$, $B'^3\Sigma_u^-$, $a'^1\Sigma_u^-$, and $w^1\Delta_u$ (4–6). In the molecular-orbital approximation (1) these states have the same electronic configuration as the A state, so that their formation cross sections are probably comparable (except for varying statistical weight factors). Of course, since their vibrational levels overlap with each other and with other states (especially the strongly-excited $a^1\Pi_g$ state), competition will decrease the contribution of any one state.

Optical emission measurements can help greatly in determining the cross sections for production of specific excited states. However, such measurements are more difficult in N_2 because many of the stronger bands are in the infrared, while their interpretation is also more difficult because of the many possibilities for cascading. In addition to the usual type of cascade, such as $C \rightarrow B \rightarrow A$ (second positive and first positive bands) and $w \rightarrow a \rightarrow a'$, a type involving several vibrational levels of two neighboring electronic states may occur. An important example of the latter should occur when the A state is produced by electron impact. According to Franck–Condon factors (7), a considerable fraction of the A state will be formed in vibrational levels around $v = 10$. These can make radiative transitions to the lowest levels of B state, which then drop back to the A state with emission of first-positive bands. The "reversed" first-positive transitions A (high v) $\rightarrow$ B (low v) might be denoted "last positive" bands[4], since they have not yet been observed experimentally, but should be observable in the positive column of a nitrogen discharge at long wavelengths. The relevant Franck–Condon factors (4) indicate that the strongest bands should lie in the middle infrared.

Preliminary calculations by the writer of relative N_2 and N_2^+ band intensities in the aurora show that the "last positive" bands should be among the strongest emissions in the middle and far infrared regions. They also show that the $A \rightarrow B \rightarrow A$ cascade redistributes the vibrational population of the A state to give reasonable agreement with auroral measurements (8) on the Vegard–Kaplan system ($A \rightarrow X$), so that direct production of the C and B states, followed by cascading to the A state (5), no longer needs to be invoked.

4. R. S. MULLIKEN. The threshold of space. *Edited by* M. Zelikoff. The Pergamon Press, Ltd., New York. 1957. p. 169.
5. F. R. GILMORE. J. Quant. Spectry. Radiative Transfer, **5**, 369 (1965).
6. H. L. WU and W. BENESCH. Phys. Rev. **172**, 31 (1968).
7. D. L. ALBRITTON, A. L. SCHMELTEKOPF, and R. N. ZARE. To be published.
8. A. L. BROADFOOT and D. M. HUNTEN. Can. J. Phys. **42**, 1212 (1964).

COMMENTS BY J. W. McGOWAN

Another possible excitation mechanism for the Vegard–Kaplan bands is the charge transfer reaction

$$N_2^+(X^2\Sigma_g^+) + NO(X^2\Pi, v = 0) \rightarrow N_2(A^3\Sigma_u^+, v = 1) + NO^+(X^1\Sigma^+)$$
$$\Delta E \approx 0$$

That this mechanism might be of importance comes from the fact that the rate of reaction of N_2^+ with NO is fast, $\sim 5 \times 10^{-10}$ cm^3/s, which usually implies a near energy-resonant process like the one above. Moreover, the measured rotational temperature associated with the Vegard–Kaplan bands tends to be higher than that of the ambient atmosphere. A high rotational temperature is often associated with charge transfer. Finally, the density of NO in the D region is found to be higher than originally thought.

[4] A modification of R. W. Nicholls' impromptu suggestion, "last negative bands".

SUMMARY BY CHAIRMAN, F. R. GILMORE[5]

A large fraction of all published measurements of energy loss in fast electron collisions have been made by Professor E. N. Lassettre and his co-workers, so it was very appropriate that Professor Lassettre began the session by reviewing this field. His comprehensive review showed how greatly our knowledge has increased in the last three or four years. In the incident energy range from tens of eV to tens of keV, energy-loss measurements are now available for most of the atmospheric gases with sufficient resolution to show the vibrational structure, and thus clearly identify the final states produced. For each electronic state, it is usually found that the relative intensities of the different vibrational levels agree with the theoretical Franck–Condon factors, even at incident energies so low that the Born approximation does not hold.

For a number of electronic transitions, data are available on the absolute cross section and its variation with scattering angle. When these are extrapolated to zero momentum loss (corresponding to high incident energies and small scattering angles), the Born approximation predicts a simple relation to the optical f number. Experimentally, good agreement with this relation is found in several cases, but unexplained differences of up to a factor of 3 are found in other cases.

Following Lassettre's review, a paper by Peterson, Prasad, and Green was presented which conveniently summarized in analytic form the cross sections for electronic excitation, dissociation, and ionization of N_2, O_2, and O. This paper nicely complemented the preceding review because it emphasized overall cross sections without regard for vibrational or angular distribution, and it referenced the recent work using optical detection of excited products, which was not covered by Lassettre.

The discussion which followed this paper served to emphasize that the applications of electron-impact data to aeronomic problems attempted so far are quite preliminary and approximate, and much more work will be needed before definitive results are obtained.

---

[5]Address: The Rand Corporation, Santa Monica, California 90406.

Can. J. Chem. Downloaded from www.nrcresearchpress.com by 210.87.254.40 on 09/05/12
For personal use only.

Can. J. Chem. Downloaded from www.nrcresearchpress.com by 210.87.254.40 on 09/05/12
For personal use only.

Laboratory studies of electron attachment and detachment processes of aeronomic interest

A. V. PHELPS
Westinghouse Research Laboratories, Pittsburgh, Pennsylvania 15235

Received December 18, 1968

Techniques for the study of electron attachment and detachment are reviewed. The rate coefficients for the various processes of aeronomic interest are then discussed. The rates of three-body and dissociative attachment by thermal electrons have been successfully determined by swarm techniques and by high frequency studies of electrons produced by high energy particles and by photoionization. Collisional and associative detachment rates for thermal energy negative ions have been measured using the swarm and flowing afterglow techniques. Radiative attachment rates for some atmospheric negative ions have been calculated from measurements of photodetachment cross sections using crossed photon and ion beam techniques. Electron beam studies and measurements of ion kinetic energy have provided much useful information regarding the dissociative attachment process and the structure of molecular negative ions. Rate coefficients for low energy processes such as the three-body attachment to O_2, the radiative attachment to O, and the associative detachment of O^- in collisions with various atmospheric gases are reasonably well known. Other possibly important low energy processes, such as dissociative attachment to O_3, radiative attachment to O_2, and the associative detachment of O_2^- are less well known.

Canadian Journal of Chemistry, 47, 1783 (1969)

Introduction

Laboratory measurements of the rates of loss of free electrons by collisional attachment to molecular oxygen and radiative attachment to atomic oxygen under conditions of electron energy and gas temperature appropriate to the earth's atmosphere were first reported about 10 years ago. Measurements of photodetachment rates for O^- and O_2^- were made at about the same time. Information concerning such processes as of 1963 were reviewed by Branscomb (1). Although progress has been made in refining and understanding these processes, it was not until 1966 that really significant new laboratory data in the area of electron attachment and detachment processes became available in the form of associative detachment coefficients for O^- and O_2^- in collisions with atomic oxygen (2). These results, along with the accompanying studies of negative ion – molecule reaction rates (2–4) have made possible much more realistic models of the electron – negative ion balance at altitudes where atomic oxygen is present (3–5). In keeping with the purposes of this Symposium we will limit our discussion to some of the laboratory techniques and results which form a basis for atmospheric models.

Electron attachment and detachment processes which are considered to be of aeronomic interest are: three-body attachment, with a ground state molecule or an electron as the third body, and its inverse, collisional detachment; dissociative attachment and its inverse, associative detachment; and radiative attachment and its inverse, photodetachment. The photodetachment process is being reviewed by Schoen (6) and will not be considered here. Similarly, the negative ion – molecule reactions which largely determine the negative ion species which are present in the atmosphere and undergo detachment are being reviewed by Ferguson (7).

The experimental techniques used to study electron attachment and detachment processes are reviewed in Section II. The primary purpose of this review is to provide a basis for a critical discussion of the laboratory data. The results of the laboratory experiments for gases and ions of aeronomic interest are discussed and tabulated in Section III. Section IV contains a discussion of some of the outstanding problems which should be examined in the laboratory.

Laboratory Techniques

Laboratory techniques used for the study of attachment and detachment processes include (*a*) swarm techniques, (*b*) high frequency studies of electrons produced by high energy particles and by photoionization, (*c*) low energy electron beam techniques, (*d*) flowing afterglow techniques, and (*e*) ion beam techniques.

(a) Swarm Techniques

The name swarm techniques is used to designate those experiments in which very low densities

Can. J. Chem. Downloaded from www.nrcresearchpress.com by 210.87.254.40 on 09/05/12
For personal use only.

of electrons (less than about 10^3 electrons/cc) are introduced into a gas where they drift and diffuse through the gas under the action of a weak electric field. As the electrons drift through an attaching gas they form negative ions which in turn may undergo ion–molecule reactions, such as collisional detachment. The electron source may be a photocathode, an α particle source, or a shielded, low temperature filament. The partial pressure of the attaching gas is usually chosen such that a significant fraction of the electrons attach before they reach the most positive electrode of the drift region.

Reviews of electron attachment measurements using the swarm technique are given by Loeb (8), Prasad and Craggs (9), and McDaniel (10). Recent studies have determined the attachment coefficient for low energy electrons from the time variation of the ion current waveform (11, 12), the variation in the magnitude of electron current pulse reaching the anode with the concentration of the attaching gas (13), or the variation in the diffusive spread of negative charge (electrons and ions) with distance along the electric field (14, 15). Drift tubes have been coupled with mass spectrometers in order to identify the negative ions produced by attachment (16, 17).

The processes of collisional and associative detachment of electrons from negative ions can also be studied by the swarm technique. This is accomplished by using an electron filter (8) to separate the electron and ion components of the current. The detached electrons are distinguishable from the electrons which cross the drift tube without attaching because of the differences in time of arrival at the collector electrodes (18, 19).

Advantages of the swarm technique are that (*a*) because of the very low degree of ionization there should be negligible production of excited and dissociated molecules which could cause electron detachment or interfering ionization, (*b*) the temporal behavior of both the electrons and ions can be studied, and (*c*) the loss of electrons and ions due to recombination can be neglected. A disadvantage of the swarm technique is that the electric field used to produce the drift of the electrons and ions also raises the electron energy above the thermal values of principal aeronomic interest. Thermal attachment coefficients can be obtained by extrapolation from higher energies (12) and the energy over which extrapolation is necessary can be made small by the use of thermalizing gases such as CO_2 (18). An important source of error in all experimental studies of attachment using gas mixtures is the possible adsorption of the minority component on the walls with the resultant errors in partial pressures.

(b) High Frequency Studies

The term high frequency studies is used to designate those experiments in which the gas is ionized sufficiently to produce a measurable change in the dielectric properties of the gas. The measurements may be made (*a*) during the decay of electron density following a period of irradiation by a pulsed source (20–27), (*b*) during irradiation of the gas by a steady state source (20, 28, 39), or (*c*) during the decay of density following a pulsed discharge (30–38). A variant of these studies is to use Langmuir probes to measure the time variation of the electron density (21). The radiation used to produce the ionization has been high energy electrons (20, 33, 25, 26, 29), X-rays (28), or Lyman-α photons which ionize NO molecules (21, 23, 24, 27). The transient measurements, (*a*) and (*c*), are relatively easy to interpret when the electron and positive ion densities are so low that recombination can be neglected and the gas pressures are so high that diffusion effects are unimportant (39), i.e. the decay of electron density is exponential with a decay constant equal to the reciprocal of the lifetime of the electron against attachment. The response time of the electronic circuits and of the high frequency system set an upper limit to the decay constant (and gas pressure) which can be studied with the transient decay technique (20, 26). This limit is not present in the steady state measurements provided one corrects the measured change in the dielectric constant for the effects of electron collisions with the gas and the effect of negative ions, if significant (20, 29). The steady state experiments require a knowledge of the rate of electron production by irradiation, since the electron lifetime is equal to the measured electron density divided by the production rate at high pressures.

The advantages of the high frequency techniques are that (a) under conditions where attachment is the dominant electron loss mechanism and the pressure is not too high (less than atmospheric in pure O_2), the electrons are expected to thermalize before they attach (40–42)

Can. J. Chem. Downloaded from www.nrcresearchpress.com by 210.87.254.40 on 09/05/12
For personal use only.

and (b) measurements can be made at much higher attaching gas densities than in the swarm technique. A source of error in these experiments is the presence of excited species which may cause detachment and a reduction in the apparent attachment rate (12, 43, 44). This problem is most serious when the electrons are produced by an electrical discharge (30–38), i.e., when the fraction of the electrons with sufficient energy to ionize the gas is small compared to the fraction which can produce excited and dissociated molecules (8, 10). Until the effects of excited species, etc. are understood and measured, high frequency attachment and detachment studies using pulsed discharge produced ionization should be regarded as unreliable sources of data to be applied to aeronomic problems. Although some difficulties have been encountered in irradiation experiments using high energy electrons (20, 29), the high ionization efficiency of high energy particles results in a much lower degree of excitation and dissociation than in a discharge. Properly filtered Lyman-α radiation should produce little excitation and dissociation, although some changes in the electron transient due to frequent and intense irradiation have been reported (23, 24).

(c) Low Energy Electron Beam Techniques

Low energy electron beam techniques for the study of electron attachment employ a beam of nearly monoenergetic electrons which pass through the gas at low densities under conditions which allow collection of the negative ions and/or mass analysis of the ions (9, 10). Because of the difficulties in the control of low energy electrons, only a few electron beam studies have been carried out at low enough energies to yield cross sections of direct applicability to aeronomic problems (45, 46). However, studies of the details of the dissociative attachment process, e.g. temperature dependence of the attachment cross section (47, 48) and kinetic energy of the product ions (49), are possible only with electron beam techniques and have led to a much better understanding of molecular negative ion structure and of the associative detachment process. The associative detachment process is the inverse of the dissociative attachment process and is of considerable aeronomic interest (1–5).

(d) Flowing Afterglow Technique

The flowing afterglow technique is being discussed by Ferguson (7) at this Symposium in connection with ion–molecule reactions. We will simply point out that this technique was used in the first laboratory observation of associative detachment (2) and that the technique is particularly useful when the neutral partner in the associative detachment reaction is a free radical, such as O, or a relatively unstable species, such as O_3 (3). Although the technique has been applied to studies of electron loss by recombination with positive ions (50, 51), an attempt (3) to apply the technique to measurements of electron attachment to O_3 has yielded coefficients which appear to be too large (4, 52). Apparent observations of attachment–detachment effects in a nitrogen flowing afterglow seeded with various attaching gases have been reinterpreted in terms of attachment and recombination (53). The technique has been used to observe the effects of very high temperatures on attachment (53).

(e) Ion Beam Techniques

Negative ion beam techniques have been used to study photodetachment (1, 54, 55), electron induced collisional detachment (56, 57), and neutral particle induced collisional detachment (58). Since the photodetachment experiments and results are being reviewed by Schoen (6) at this Symposium, we will limit our discussion to pointing out that the use of measured photodetachment cross sections and detailed balancing arguments (1, 54) is the only method used thus far for determining radiative attachment cross sections from laboratory data for systems of aeronomic interest. Unfortunately, these techniques cannot be used to obtain accurate cross sections for the radiative attachment of low energy electrons to molecules such as O_2 and OH, because of the uncertainties in the threshold behavior of the photodetachment cross section (54, 55).

Laboratory studies of electron induced collisional detachment have been carried out by crossing a negative ion beam with an electron beam and measuring the rate of production of neutral atoms (56, 57). These experiments are very difficult because of the possibility of space charge interaction of the ion and electron beams, the presence of sources of extraneous signals, and the high ion – neutral atom energies required for efficient neutral atom detection. Thus far, the minimum incident electron energy for which measurements have been reported is about 10 eV.

Can. J. Chem. Downloaded from www.nrcresearchpress.com by 210.87.254.40 on 09/05/12
For personal use only.

TABLE I

Recommended rate coefficients

(*a*) Three-body attachment with neutral third body

Reaction	k_1(cm^6/s)	Reference
$e + O_2 + O_2 \rightarrow O_2^- + O_2$	$(1.4\pm0.2) \times 10^{-29}(300/T)e^{-600/T}$ $(195<T<600\ °K)$	(18)
$e + O_2 + N_2 \rightarrow O_2^- + N_2$	$(1\pm0.5) \times 10^{-31}$ $(300<T<500\ °K)$	(12, 30, 39)
$e + O_2 + H_2O \rightarrow O_2^- + H_2O$*	$(1.4\pm0.2) \times 10^{-29}$ $(300<T<400\ °K)$	(70)
$e + O_2 + CO_2 \rightarrow O_2^- + CO_2$	$(3.3\pm0.7) \times 10^{-30}$ $(300<T<525\ °K)$	(70)
$e + NO + NO \rightarrow NO^- + NO$*	$(1.3\pm0.2) \times 10^{-31}$ (300 °K)	(24)
$e + 2N_2O \rightarrow N_2O^- + N_2O$*	$(6\pm1) \times 10^{-23}$ (300 °K)	(67, 68)
$e + NO_2 + N_2 \rightarrow NO_2^- + N_2$	4×10^{-11} cm^3/s† (300 °K)	(27)

(*b*) Collisional detachment with neutrals

Reaction	k_2(cm^3/s)	Reference
$O_2^- + O_2 \rightarrow 2O_2 + e$	$(2.7\pm0.3) \times 10^{-10}(T/300)^{1/2}e^{-(5590/T)}$ $(375<T<600\ °K)$	(18)
$O_2^- + N_2 \rightarrow O_2 + N_2 + e$	$(1.9+0.4) \times 10^{-12}(T/300)^{3/2}e^{(-4990/T)}$	(18)
$O^- + O_2 \rightarrow O + O_2 + e$	$2.3 \times 10^{-9}e^{(-26000/T_i)}$‡ $(4000<\text{“}T_i\text{”}<20\,000\ °K)$	(78)
$O^- + N_2 \rightarrow O + N_2 + e$	Same as $O^- + O_2$	(78)
$O_2^- + O_2(^1\Delta_g) \rightarrow O_2 + O_2 + e$	2×10^{-10} (300 °K)	(77)

(*c*) Dissociative attachment at 300 °K

Reaction	k_3(cm^3/s)	Reference
$e + O_3 \rightarrow O^- + O_2$	$(1-10) \times 10^{-12}$	(52)

(*d*) Associative detachment at 300 °K

Reaction	k_4(cm^3/s)	Reference
$O^- + O \rightarrow O_2 + e$	1.4×10^{-10}	(4)
$O^- + N \rightarrow NO + e$	1.6×10^{-10}	(4)
$O^- + H_2 \rightarrow H_2O + e$	8.0×10^{-10}	(4, 19)
$O^- + NO \rightarrow NO_2 + e$	3.0×10^{-10}	(4, 19)
$O^- + N_2 \rightarrow N_2O + e$	$\sim1\times10^{-19}$	(19, 67)
$O_2^- + O \rightarrow O_3 + e$	2.5×10^{-10}	(4)
$O_2^- + N \rightarrow NO_2 + e$	3.0×10^{-10}	(4)
$O^- + O_2(^1\Delta_g) \rightarrow O_3 + e$	3×10^{-10}	(77)

(*e*) Radiative attachment

Reaction	k_6(cm^3/s)	Reference
$e + O \rightarrow O^- + h\nu$	$(1.3\pm0.1) \times 10^{-15}$ $(150<T<500\ °K)$	(54, 97)
$e + O_2 \rightarrow O_2^- + h\nu$	$10^{-19\pm1}$ (300 °K)	(54, 98)
$e + OH \rightarrow OH^- + h\nu$	$10^{-15\pm1}$ (300 °K)	(55)

*Product ions not mass spectrometrically identified.
†In units of cm^3/s since it is a saturated three-body process (27).
‡Here the ion "temperature" T_i is a value calculated using the Wannier relation (76).

Can. J. Chem. Downloaded from www.nrcresearchpress.com by 210.87.254.40 on 09/05/12
For personal use only.

Laboratory studies of detachment as the result of collisions between beams of negative ions and neutral gas atoms and molecules prior to 1964 have been reviewed by Hasted (58). These measurements are usually made by collecting the detached electrons with an electric field which is perpendicular to the motion of the incident ions. However, in gases where charge transfer is possible, it is necessary to separate the slow ions produced by charge transfer from the detached electrons (59, 60).

Electron Attachment and Detachment Processes

The results of laboratory studies of electron attachment and detachment are discussed in this section on the basis of the type of attachment or detachment process. The results for various gases of aeronomic interest will be discussed under the appropriate process.

(a) Three-Body Attachment with Neutral Third-Body

The three-body attachment process results from a collision between an electron, an electronegative gas molecule, and a third-body which stabilizes the negative ion and can be represented by the reaction

$$[1] \qquad e + X + M \rightarrow X^- + M$$

This reaction occurs at a rate of $k_1[e][X][M]$, where [e], [X], and [M] are the concentrations of electrons, the electronegative gas, and the stabilizing gas. Recommended values of k_1 for atmospheric gases are given in Table I. This type of reaction is usually considered to be of the pseudo three-body type proposed by Bloch and Bradbury (61) in which the electron and the electronegative gas molecule form an excited negative ion which may be stabilized in a collision with a third body M. The lifetime of the excited negative ion against autodetachment is expected to be short (12, 44, 61, 62). A second possibility is a dissociative attachment process involving an electron and a temporary or weakly bound XM complex. Dissociative attachment from a bound molecular complex would lead to an increasing rate coefficient with decreasing gas temperature at fixed electron energy (12).

The three-body attachment process has been found to be the dominant electron attachment process for low energy electrons in O_2 (12, 13, 15, 18, 20, 22, 25, 26, 29, 36, 45, 63), NO (23, 24, 64, 65, 66), and N_2O (67, 68). In view of the differences between recent results (23, 24) for NO, the apparent rapid variation of k_1 with temperature (23) should be reinvestigated. Data obtained in mixtures of NO_2 and other gases (27, 69) give an apparent two-body behavior, i.e., the lifetime of the excited NO_2^- appears to be long enough so that stabilization always occurred. Unpublished data obtained in pure NO_2 indicate a three-body dependence (20). Attachment is not observed in other atmospheric constituents such as N_2 (8–10), CO_2 (70), and H_2O (70–72). Although, gases such as CO_2 and H_2O have a high efficiency as stabilizing molecules during the three-body attachment to O_2 (63, 70, 72), only the stabilization by N_2 (12, 13, 18, 20, 22, 25, 26, 29, 36) and O_2 is likely to be of aeronomic interest. The results of temperature dependent studies (12, 18, 20) of the three-body attachment coefficient in O_2 are shown in Fig. 1. It is to be noted that the uncertainty in k_1 increases with decreasing temperature. No data are available for air-like mixtures at temperatures below room temperature.

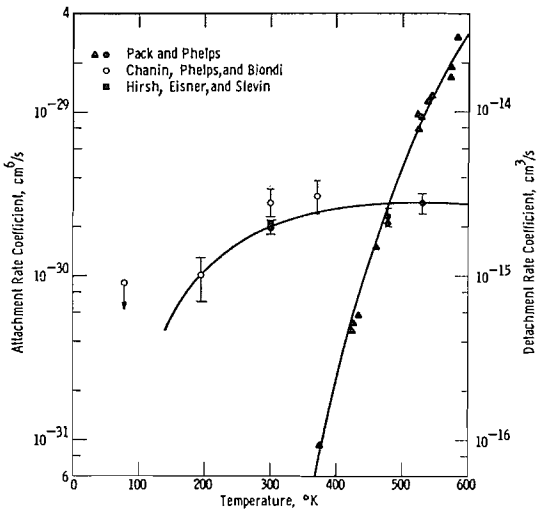

FIG. 1. Electron attachment and detachment in O_2.

On the basis of the numerous laboratory experiments which agree as to the nature and magnitude of the attachment process for thermal electrons in O_2 and O_2–N_2 mixtures at low pressures (< 10 Torr of O_2), experiments that appear to give significantly different attachment

Can. J. Chem. Downloaded from www.nrcresearchpress.com by 210.87.254.40 on 09/05/12
For personal use only.

coefficients (30–35, 37) must represent experimental situations in which there are interfering processes such as electron detachment. One aspect of the three-body attachment process in O_2 concerning which there is conflicting evidence, is whether or not one has observed effects due to the finite lifetime of the excited O_2^- ion in the Bloch–Bradbury attachment mechanism (61). The results of these experiments are conveniently expressed in terms of the apparent rate coefficient k_a for the formation of the excited O_2^- ion, i.e. the high pressure limit of the measured attachment frequency per unit oxygen density. Values of k_a in cm^3/s of 7×10^{-12} (62), 1.7×10^{-12} (25), and 4×10^{-12} (26) have been reported. The first of these values has been shown (63, 70) to be based on incorrect data, while the last has been found (private communication from the authors) to have been subject to errors because of the finite response time of the microwave cavity when filled with low collision frequency gases (42) at low pressures. Lower limits to k_a of 1.5×10^{-11} (20) and 2.5×10^{-11} (29) have been obtained in pure oxygen using high frequency measurements of the electron density produced by steady state irradiation of O_2 and O_2–N_2 mixtures. These values are somewhat uncertain because of uncertainties (42) as to electron collision frequencies in O_2. Even higher values for the lower limit for k_a have been found when C_2H_4 and CO_2 are used as the stabilizing gases, i.e. 7×10^{-11} cm^3/s from refs. 63 and 70. Although it has been suggested (62) that the Bloch–Bradbury mode for attachment to O_2 may not be applicable in these mixtures, and that negative ion formation occurs via the formation of long lived excited states of CO_4^- and $C_2H_4O_2^-$, the observed pressure dependence of the $[CO_4^-]/[O_2^-]$ ratio (17) is consistent with O_2^- formation followed by conversion to CO_4^- rather than a very efficient stabilization of excited CO_4^- formed in a three-body collision. These arguments are of aeronomic significance because of the differences in the predicted rate of electron attachment in air at pressures approaching atmospheric. Obviously, further work on this point is needed.

At present there are no quantitative theories available regarding the three-body attachment process in molecular gases although theories have been proposed for three-body attachment of electrons in atomic gases (73). In the case of excited negative ions containing large numbers of molecules, such as might be formed in the first step of the Bloch–Bradbury process in polyatomic gases, an attempt has been made to relate the lifetime against autodetachment to the electron affinity (74). In the case of diatomic negative ions, such as O_2^-, the only potentially relevant theoretical calculations are of the equilibrium separation and vibrational constant (75).

(b) Collisional Detachment by Neutrals

The collisional detachment reaction may be written as

$$[2] \qquad X^- + M \rightarrow X + M + e$$

and occurs at a rate of $k_2[M][X^-]$. Recommended values of k_2 are given in Table I. Laboratory measurements of the rate coefficients for the collisional detachment k_2 of electrons from thermal O_2^- ions in collisions with O_2 and N_2 have been made using the swarm technique (18). The measured values of k_2 for O_2^- and O_2 collisions are shown in Fig. 1. Although collisional detachment was not observed at temperatures below 350 °K, it is expected that an extrapolation of these results to lower temperatures should be valid, i.e., that $k_2 \approx 2.2 \times 10^{-18}$ and 1.6×10^{-22} cm^3/s at 300 and 200 °K, respectively. It would appear that other reported measurements of this rate coefficient are too large because of the presence of excited species or dissociated molecules (36) or too small (53) because of the recombination effects. An independent measurement of the adiabatic electron affinity of O_2 would be a valuable test of the consistency of the swarm measurements of the detachment and attachment rate coefficients (18).

The collisional detachment of electrons from O_2^- by O_2 molecules in the $^1\Delta_g$ state has been proposed as an important reaction in the ionosphere (76) and in afterglow studies of electron attachment (43, 44). The rate coefficient for this reaction has recently been measured (77) and is listed in Table I.

Collisional detachment cross sections for O^- and O_2^- ions and N_2 or O_2 molecules have been measured for ion energies as low as 3.6 eV (58–60). Unfortunately, these results are not readily extrapolated to the thermal energies of aeronomic interest. Also, the fixed internal energy of the molecules in these experiments means that the results of the ion beam studies cannot be used to infer temperature dependences of collisional

Can. J. Chem. Downloaded from www.nrcresearchpress.com by 210.87.254.40 on 09/05/12
For personal use only.

detachment rate coefficients. Collisional detachment from non-thermal O^- ions in O_2 and air has been observed using swarm techniques (78) and the measured rate coefficients are consistent with the results of the beam experiments. Evidence for collisional detachment has been observed in NO at elevated temperatures (64). However, the identity of the negative ions is not known (23, 24).

Theories of collisional detachment are available which give cross sections of the correct order of magnitude for collisions between atoms (79, 80) and between H^- and various molecules (81). These theories have not been tested against data obtained with molecular negative ions but are not expected to be applicable in systems where the Bloch–Bradbury model (61) of attachment is appropriate.

(c) Electron Induced Three-Body Attachment and Collisional Detachment

In order to decide whether or not there are aeronomic situations in which the electron density is high enough to result in a significant rate of electron induced three-body attachment or collisional detachment, we will summarize the present state of experiment and theory. Experimental studies of electron induced detachment for H^- (56, 57) agree with the later theories (82, 83) to within experimental uncertainties. However, the O^- results (55) appear to show significantly larger cross sections than predicted for low energy electrons (56, 84). Since the actual rate coefficients are expected to be less than the values given by classical theory, it would appear that electron induced attachment will be negligible compared to neutral particle induced attachment, unless the ratio of the electron to the molecular oxygen concentrations is greater than about one part in 10^5. This condition is not expected to be satisfied under conditions of aeronomic interest for which electron attachment is an important process.

(d) Dissociative Attachment

The dissociative attachment reaction is

$$e + XY \rightarrow X^- + Y \qquad [3]$$

and occurs at a rate of $k_3[XY][e]$, where [XY] is the concentration of the molecule with which the electron interacts. Laboratory studies of the dissociative attachment of electrons to gases of aeronomic interest have been carried out for many years (1, 8–10). In the case of O_2 at room temperature, dissociative attachment occurs only for electron energies above about 4.5 eV (85, 86). As the temperature, i.e. the degree of vibrational excitation, of the O_2 is increased, the threshold for attachment decreases until at 2000 °K the effective threshold is at about 2 eV (47). Although this threshold is still too large for dissociative attachment rate coefficients to be of significance in the earth's atmosphere, the studies of this process in O_2 (47, 49), H_2 (87), and other gases (88), have provided the theoretical background necessary for understanding the associative detachment process discussed in the next section.

Dissociative attachment appears to be the dominant attachment process in O_3 (46, 52) and as such may be a significant aeronomic process (5). Extrapolation of data obtained using swarm techniques (52) to thermal energies (300 °K) yields a rate coefficient for dissociative attachment to O_3 of 10^{-12} to 10^{-11} cm^3/s (see Table I). This value is about an order of magnitude smaller than that obtained from measurements in a flowing afterglow experiment (3) where the electrons may have been non-thermal (4). At present it is not known whether the value of k_3 for O_3 varies significantly with gas temperature at temperatures of aeronomic interest.

Dissociative attachment is an important process in N_2O although there has been considerable disagreement as to the effective threshold for this process (89, 90). It now appears that the early results include effects due to vibrationally excited N_2O (48) and that the rate coefficient for dissociative attachment to N_2O at 300 °K is less than 3×10^{-15} cm^3/s (68). Dissociative attachment in other minor constituents of the earth's atmosphere, e.g., NO, CO_2, and H_2O, occurs with sufficiently high electron energy thresholds and with sufficiently low rate coefficients at aeronomic temperatures so that the reactions can be neglected.

(e) Associative Detachment

Recent laboratory measurements of the rate coefficients for associative detachment reactions of ionospheric negative ions with atomic oxygen (2–4), have shown that these reactions must be included in any accurate ionospheric model (1, 3–5). The associative detachment reaction may be written as

$$X^- + Y \rightarrow XY + e \qquad [4]$$

Can. J. Chem. Downloaded from www.nrcresearchpress.com by 210.87.254.40 on 09/05/12
For personal use only.

and occurs at a rate of $k_4[X^-][Y]$. Values of the rate coefficient k_4 measured using the flowing afterglow technique (2, 4) and the swarm technique (17, 19) are listed in Table I. The flowing afterglow technique makes use of measurements of the rate of disappearance of ions while the swarm technique can be used to measure ion destruction (17) or the production of detached electrons (19).

Temperature dependences of the associative detachment rate coefficients have not been measured. Values of k_4 for O^- and H_2 have been found to be independent of ion energy for ion energies below about 0.16 eV, while the values of k_4 for O^- and NO appear to decrease with increasing ion energy (19).

Several theoretical studies have been made of associative detachment (80, 91) but only in the case of $H^- + H$ has theory led to quantitative predictions of rate coefficients (92) for comparison with experiment (93). As suggested by Dalgarno (94), associative detachment rate coefficients may be an appreciable fraction of the rate coefficient k_p for orbiting collisions in the polarization potential of the neutral molecule (10), i.e.

$$[5] \qquad k_p = 2\pi(e^2\alpha/M_r)^{1/2}$$

Here e is the electronic charge, α is the polarizability of the molecule, and M_r is the reduced mass of the colliding particles. In cases where the lifetime of a state of the XY^- complex formed initially in reaction [4] has a short lifetime against autodetachment, e.g. less than 10^{-14} s, a fixed fraction of the collisions will result in the formation of this state and in detachment. The contribution of this state to k_4 will then be a fixed fraction of k_p and, to the accuracy of this model, will be independent of temperature. The reaction of O^- with H_2 appears to be an example of this class (19). When the lifetime of the state is comparable with the duration of a collision ($\sim 10^{-13}$ s), one expects a contribution to k_4 which is smaller than in the case of a short lifetime and which is dependent on the gas temperature. The reaction of O^- with NO appears to be of this class (19). In the case of $O^- + N_2$ (2, 17, 19), associative detachment is not observed even though the reaction is exothermic. It has been pointed out (95) that the low value of k_4 may be due to unfavorable potential energy surfaces due to differences in the stable ground state configurations of the negative ion and the neutral molecule.

(f) Radiative Attachment

The results of determinations of radiative attachment cross sections from laboratory measurements of photodetachment have been reviewed by Branscomb (54). The radiative attachment process can be written as

$$[6] \qquad e + X \rightarrow X^- + h\nu$$

where $h\nu$ is the photon produced by the reaction. The rate of the reaction is $k_6[e][X]$, and the known values of k_6 are given in Table I.

The radiative attachment spectrum for atomic oxygen has been observed (96) and the spectroscopic features of the results are consistent with photodetachment results (54, 97). Direct laboratory measurements of radiative attachment cross sections for low energy electrons in molecular gases are desirable, because of the large uncertainties which result when these cross sections are derived from photodetachment data. These uncertainties may arise because of lack of data near threshold, as in the case of O_2^- (98); because of rotational structure in the photodetachment cross section, as in OH^- (55); or because of differences in equilibrium separation and vibrational level spacing between the neutral and the negative ion, as in O_2^- (44, 75).

(g) Electron Affinities

A knowledge of the electron affinity of a negative ion helps one to predict the behavior of the ion in aeronomic situations by setting limits on the threshold energy for dissociative attachment, collisional detachment, and photodetachment, and on allowed associative detachment and ion–molecule reactions. Table II lists the recommended values or limits on values of the electron

TABLE II

Electron affinity of atmospheric negative ions

Negative ion	Electron affinity* (eV)	Reference
NO^-	<0.43	(2)
O_2^-	0.43 ± 0.02†	(18)
CO_4^-	1.22 ± 0.07	(70)
O^-	1.47 ± 0.01	(49, 96, 97)
OH^-	1.83 ± 0.04	(55)
O_3^-	1.9 ± 0.4	(99)
CO_3^-	Unknown	
NO_3^-	Unknown	
NO_2^-	>3.8	(103)
	<3.8	(2)

*Here the energy quoted is that required to separate the electron from the most stable neutral species, e.g., $e + O_3$ and $e + O_2 + CO_2$.
†The effect of O_4^- formation (102) on the electron – O_2^- equilibrium is less than 20% at 375 °K so that the derived (18) electron affinity of O_2 remains within the error limits quoted.

affinities of negative ions of aeronomic interest. It is to be noted that only for O_2^-, CO_4^-, O^-, and OH^- are laboratory measurements available which give definite values for the electron affinities.

Discussion

The results of laboratory studies discussed in the preceding section show that while considerable progress has been made in determining the important attachment and detachment rate coefficients since the last of the Symposia in 1963, there is still much to be done. For example, while there is good agreement as to the rate coefficient for the attachment of thermal electrons to oxygen in air-like mixtures at room temperature and pressures below about 30 Torr, there is considerable disagreement as to the measured rate coefficient at temperatures near 200 °K and as to the predicted rate coefficients for pressures above 150 Torr. Similarly, while there is good agreement between various experiments as to the rate coefficients for associative detachment of O^- with gases like H_2 and NO, there is only one set of measurements for the important reaction of O^- and O_2^- with O. As yet there is no data regarding the temperature dependence of the associative detachment reactions involving O. At present, the attachment coefficient for thermal electrons to ozone has been obtained only by extrapolation from data obtained at electron energies of 0.1 eV and above, and the temperature dependence of the attachment coefficient has not been investigated.

Laboratory measurements of the rate coefficients for electron detachment as the result of collisions between various negative ions and excited species are necessary in order to allow proper evaluation of such processes in the earth's atmosphere (76) and in laboratory experiments (43, 44). The recent measurements (77) of collisional and associative detachment by $O_2(^1\Delta_g)$ are examples of such a process.

Future laboratory studies of reactions of aeronomic significance should include measurements of the role of water vapor in associative detachment, photodetachment, and negative ion – molecule reactions. Experiments thus far have shown that negative ions readily form complexes or clusters with water vapor (17, 100) and that the clusters are relatively stable (101). Quantitative measurements of the rate coefficients for cluster formation and destruction are required in order to make possible estimates of the importance of the clusters under aeronomic conditions.

Accurate laboratory determinations of the electron affinity of negative ions of aeronomic interest would be very helpful in setting limits on rate coefficients and checking the consistency of laboratory measurements.

1. L. M. Branscomb. Ann. Geophys. **20**, 88 (1964).
2. F. C. Fehsenfeld, E. E. Ferguson, and A. L. Schmeltekopf. J. Chem. Phys. **45**, 1844 (1966).
3. F. C. Fehsenfeld, A. L. Schmeltekopf, H. I. Schiff, and E. E. Ferguson. Planetary Space Sci. **15**, 373 (1967).
4. E. E. Ferguson. Rev. Geophys. **5**, 305 (1967).
5. R. E. Lelevier and L. M. Branscomb. J. Geophys. Res. **73**, 27 (1968).
6. R. I. Schoen. Can. J. Chem. This issue.
7. E. E. Ferguson. Can. J. Chem. This issue.
8. L. B. Loeb. Basic processes in gaseous electronics. University of California Press, Berkeley, California. 1955. Chap. 5.
9. A. N. Prasad and J. D. Craggs. Atomic and molecular processes. *Edited by* D. R. Bates. Academic Press, Inc., New York. 1962. Chap. 6.
10. E. W. McDaniel. Collision phenomena in ionized gases. John Wiley and Sons, Inc., New York. 1964. Chap. 8.
11. A. Doehring. Z. Naturforsch. **7a**, 253 (1952).
12. L. M. Chanin, A. V. Phelps, and M. A. Biondi. Phys. Rev. **128**, 219 (1962).
13. G. S. Hurst and T. E. Bortner. Phys. Rev. **114**, 116 (1959).
14. L. G. H. Huxley, R. W. Crompton, and C. H. Bagot. Australian J. Phys. **12**, 303 (1959).
15. J. A. Rees. Australian J. Phys. **18**, 41 (1965).
16. H. Eiber. Z. Angew. Phys. **15**, 103, 461 (1963).
17. J. L. Moruzzi and A. V. Phelps. J. Chem. Phys. **45**, 4617 (1966).
18. J. L. Pack and A. V. Phelps. J. Chem. Phys. **44**, 1870 (1966).
19. J. L. Moruzzi, J. W. Ekin, and A. V. Phelps. J. Chem. Phys. **48**, 3070 (1968).
20. V. A. J. van Lint, E. G. Wikner, and D. Trueblood. Bull. Am. Phys. Soc. **5**, 122 (1960). V. A. J. van Lint, J. Parez, D. Trueblood, and M. E. Wyatt. Rev. Sci. Instr. **36**, 521 (1965).
21. J. P. Doering and B. H. Mahan. J. Chem. Phys. **36**, 669 (1962).
22. P. N. Eisner, M. N. Hirsh, and J. A. Slevin. Bull. Am. Phys. Soc. **10**, 189 (1965). M. N. Hirsh, P. N. Eisner, and J. A. Slevin. Phys. Rev. In press.
23. R. C. Gunton and T. M. Shaw. Phys. Rev. **140**, A748 (1965).
24. C. S. Weller and M. A. Biondi. Bull. Am. Phys. Soc. **11**, 495 (1966); Phys. Rev. **172**, 198 (1968).
25. V. B. Brodskii and S. E. Zagik. Zh. Tekhn. Fiz. **36**, 672 (1966); English transl. Soviet Phys.-Tech. Phys. **11**, 498 (1966).
26. R. W. Fessenden and J. M. Warman. Advan. Chem. Ser. No. 81–82, **2**, 222 (1968).
27. B. H. Mahan and I. C. Walker. J. Chem. Phys. **47**, 3780 (1967).
28. J. A. Carruthers. Can. J. Phys. **40**, 1528 (1962).
29. B. G. Young, A. W. Johnson, and J. A. Carruthers. Can. J. Phys. **41**, 625 (1963).
30. M. A. Biondi. Phys. Rev. **84**, 1072A (1951).
31. E. H. Holt. Bull. Am. Phys. Soc. **4**, 112 (1959).
32. M. C. Sexton, M. J. Mulcahy, and J. J. Lennon. Proc. 4th Intern. Conf. Ionization Phenomena in

Can. J. Chem. Downloaded from www.nrcresearchpress.com by 210.87.254.40 on 09/05/12
For personal use only.

Gases. Vol. I. Uppsala, Sweden. North-Holland Publishing Co., Amsterdam. 1960. p. 94.
33. J. J. LENNON and M. J. MULCAHY. *In* Proc. Phys. Soc. **78**, 1543 (1961).
34. P. J. CHANTRY, J. S. WHARMBY, and J. B. HASTED. *In* Proc. 5th Intern. Conf. Ionization Phenomena in Gases. Munich. *Edited by* H. Meaker. North-Holland Publishing Co., Amsterdam. 1962. p. 630.
35. A. I. ANISINOV, N. I. VINOGRADOV, and V. E. GOLANT. Zh. Tekhn. Fiz. **33**, 1141 (1963); English transl. Soviet Phys.-Tech. Phys. **8**, 850 (1964).
36. R. HACKAM and J. J. LENNON. Proc. Phys. Soc. **86**, 123 (1965).
37. R. L. TAYLOR and K. V. NARASINGA RAO. *In* Proc. 7th Intern. Conf. Phenomena in Ionized Gases. Vol. I. Gradevinska Knjiga Publishing House, Beograd. 1966. p. 74.
38. M. H. MENTZONI. J. Appl. Phys. **36**, 57 (1965).
39. M. HIRSH, P. EISNER, J. SLEVIN, and G. HALPERN. Bull. Am. Phys. Soc. **11**, 495 (1966).
40. M. H. MENTZONI and R. V. ROW. Phys. Rev. **130**, 2312 (1963).
41. M. H. MENTZONI and K. V. NARASINGA RAO. Phys. Rev. Letters, **14**, 779 (1965).
42. R. D. HAKE, JR. and A. V. PHELPS. Phys. Rev. **158**, 70 (1967).
43. J. D. CRAGGS. *In* Proc. 3rd Intern. Conf. Ionization Phenomena in Gases. Italian Physical Society, Milan. 1957. p. 203.
44. M. A. BIONDI. Advances in electronics. Vol. 18. *Edited by* L. Marton. Academic Press, Inc., New York. 1963. p. 67.
45. G. J. SCHULZ. Bull. Am. Phys. Soc. **6**, 387 (1961).
46. R. K. CURRAN. J. Chem. Phys. **35**, 1849 (1961).
47. W. L. FITE, R. T. BRACKMAN, and W. R. HENDERSON. *In* Proc. 4th Intern. Conf. Electronic and Ionic Impact Phenomena. Science Bookcrafters, Inc., New York. 1965. p. 100. T. F. O'MALLEY. Phys. Rev. **155**, 59 (1967).
48. P. J. CHANTRY. Bull. Am. Phys. Soc. **14**, 258 (1969).
49. P. J. CHANTRY and G. J. SCHULZ. Phys. Rev. **156**, 134 (1967).
50. C. B. COLLINS and W. W. ROBERTSON. J. Chem. Phys. **40**, 2202, 2208 (1961).
51. R. A. YOUNG and G. ST. JOHN. Phys. Rev. **152**, 25 (1966).
52. J. L. MORUZZI and A. V. PHELPS. Bull. Am. Phys. Soc. **13**, 209 (1968).
53. A. K. GOSH, A. I. CARSWELL, and C. RICHARD. Phys. Fluids, **10**, 1100 (1967). A. C. MALLIARIS. Phys. Fluids, **11**, 698 (1968); J. Appl. Phys. **39**, 3675 (1968). T. W. JOHNSTON and A. K. GOSH. Phys. Fluids, **11**, 699 (1968).
54. L. M. BRANSCOMB. Atomic and molecular processes. *Edited by* D. R. Bates. Academic Press, Inc., New York. 1962. Chap. 4.
55. L. M. BRANSCOMB. Phys. Rev. **148**, 11 (1966).
56. G. TISONE and L. M. BRANSCOMB. Phys. Rev. Letters, **17**, 236 (1966); Phys. Rev. **170**, 169 (1968).
57. D. F. DANCE, M. F. A. HARRISON, and R. D. RUNDEL. Proc. Roy. Soc. London, Ser. A, **299**, 525 (1967).
58. J. B. HASTED. Physics of atomic collisions. Butterworths, Inc., Washington. 1964. Chap. 8.
59. T. L. BAILEY. *In* Proc. 2nd Intern. Conf. Physics of Electronic and Atomic Collisions. University of Colorado. W. A. Benjamin, Inc., New York. 1961. p. 54.
60. J. A. RUTHERFORD and B. R. TURNER. *In* Symp. Phys. and Chem. of Lower Atmosphere. Boulder, Colorado. 1966.
61. F. BLOCH and N. E. BRADBURY. Phys. Rev. **48**, 689 (1935).
62. D. C. CONWAY. J. Chem. Phys. **36**, 2549 (1962).
63. J. A. STOCKDALE, L. G. CHRISTOPHOROU, and G. S. HURST. J. Chem. Phys. **47**, 3267 (1967).
64. D. A. PARKES. Ph.D. Thesis. University of Cambridge, England. 1965.
65. M. A. BIONDI. Proc. 7th Intern. Conf. Phenomena in Ionized Gases. Vol. I. Graderinska Knjiga Publishing House, Beograd. 1966. p. 19.
66. M. H. MENTZONI and J. DONOHOE. Can. J. Phys. **45**, 1565 (1967).
67. J. M. WARMAN and R. W. FESSENDEN. J. Chem. Phys. **49**, 4718 (1968).
68. A. V. PHELPS and R. E. VOSHALL. J. Chem. Phys. **49**, 3246 (1968).
69. J. B. HASTED and S. BEG. Brit. J. Appl. Phys. **16**, 1779 (1965).
70. J. L. PACK and A. V. PHELPS. J. Chem. Phys. **45**, 4316 (1966).
71. S. TAKEDA and A. A. DOUGAL. J. Appl. Phys. **31**, 412 (1960).
72. G. S. HURST, G. A. STOCKDALE, and L. B. O'KELLY. J. Chem. Phys. **38**, 3572 (1963).
73. M. I. CHIBISOV. Zh. Eksp. Teor. Fiz. **49**, 852 (1965); English transl. Sov. Phys.-JETP **22**, 593 (1966). R. S. VITLINA and A. V. CHAPLIK. Zh. Eksperim. Teor. Fiz. **52**, 959 (1967); English transl. Sov. Phys.-JETP **25**, 634 (1967).
74. R. N. COMPTON, L. G. CHRISTOPHOROU, G. S. HURST, and P. W. REINHARDT. J. Chem. Phys. **45**, 4634 (1966).
75. P. E. CADE. Bull. Am. Phys. Soc. **11**, 42 (1966). R. F. W. BADER, W. H. HENNEKER, and R. E. CADE. J. Chem. Phys. **46**, 3341 (1967).
76. L. R. MEGILL and J. B. HASTED. Planetary Space Sci. **13**, 339 (1965).
77. F. C. FEHSENFELD, D. L. ALBRITTON, J. A. BURT, and H. I. SCHIFF. Can. J. Chem. This issue.
78. L. FROMMHOLD. Fortschr. Physik, **12**, 597 (1964).
79. B. M. SMIRNOW and O. B. FIRSOV. Zh. Eksperim. Teor. Fiz. **47**, 232 (1964); English transl. Sov. Phys.-JETP **20**, 156 (1965).
80. YU. N. DEMKOV. Zh. Eksperim. Teor. Fiz. **46**, 1126 (1964); **49**, 885 (1965); English transl. Sov. Phys.-JETP **19**, 762 (1964); **22**, 615 (1966).
81. D. R. BATES and J. C. G. WALKER. Proc. Phys. Soc. London, **90**, 333 (1967).
82. M. R. C. MCDOWELL and J. H. WILLIAMSON. Phys. Letters, **4**, 159 (1963).
83. B. M. SMIRNOV and M. I. CHIBISOV. Zh. Eksperim. Teor. Fiz. **49**, 841 (1965); English transl. Sov. Phys.-JETP **22**, 585 (1966).
84. S. GELTMAN. Proc. Phys. Soc. London, **75**, 67 (1960).
85. G. J. SCHULZ. Phys. Rev. **128**, 178 (1962).
86. L. G. CHRISTOPHOROU, R. N. COMPTON, G. S. HURST, and P. W. REINHARDT. J. Chem. Phys. **43**, 4273 (1965).
87. J. N. BARDSLEY, A. HERZENBERG, and F. MANDL. Proc. Phys. Soc. London, **89**, 321 (1966). G. J. SCHULZ and R. K. ASUNDI. Phys. Rev. **158**, 25 (1967). J. C. Y. CHEN and J. L. PEACHER. Phys. Rev. **163**, 103 (1967).
88. J. C. Y. CHEN. Phys. Rev. **148**, 66 (1966). T. F. O'MALLEY. Phys. Rev. **150**, 14 (1966).
89. R. K. CURRAN and R. E. FOX. J. Chem. Phys. **34**, 1590 (1961). G. J. SCHULZ. J. Chem. Phys. **34**, 1778 (1961).
90. F. KAUFMAN. J. Chem. Phys. **46**, 2449 (1967). E. E. FERGUSON, F. C. FEHSENFELD, and A. L. SCHMELTEKOPF. J. Chem. Phys. **47**, 3085 (1967).
91. J. C. Y. CHEN. Phys. Rev. **156**, 12 (1967). A. HERZENBERG. Phys. Rev. **160**, 80 (1967).

Can. J. Chem. Downloaded from www.nrcresearchpress.com by 210.87.254.40 on 09/05/12
For personal use only.

92. A. DALGARNO and J. C. BROWNE. Astrophys. J. **149**, 231 (1967).
93. A. L. SCHMELTEKOPF, F. C. FEHSENFELD, and E. E. FERGUSON. Astrophys. J. **148**, L155 (1967).
94. A. DALGARNO. Ann. Geophys. **17**, 16 (1961).
95. E. E. FERGUSON, F. C. FEHSENFELD, and A. L. SCHMELTEKOPF. J. Chem. Phys. **47**, 3085 (1967).
96. R. S. BERRY, J. C. MACKIE, R. L. TAYLOR, and R. LYNCH. J. Chem. Phys. **43**, 3067 (1965).
97. L. M. BRANSCOMB, D. S. BURCH, S. J. SMITH, and S. GELTMAN. Phys. Rev. **111**, 504 (1958).
98. D. S. BURCH, S. J. SMITH, and L. M. BRANSCOMB. Phys. Rev. **112**, 171 (1958); **114**, 1652 (1959).
99. R. H. WOOD and L. A. D'ORAZIO. J. Phys. Chem. **69**, 2562 (1965).
100. W. L. FITE and J. A. RUTHERFORD. Discussions Faraday Soc. **37**, 192 (1964).
101. P. KABARLE, M. ARSHADI, and J. SCARBOROUGH. J. Chem. Phys. In press.
102. D. CONWAY and L. E. NESBITT. J. Chem. Phys. **48**, 509 (1968).
103. R. K. CURRAN. Phys. Rev. **125**, 910 (1962).

Associative-detachment reactions of O^- and O_2^- by $O_2(^1\Delta_g)$

F. C. FEHSENFELD AND D. L. ALBRITTON
Environmental Science Services Administration Research Laboratories, Boulder, Colorado

AND

J. A. BURT AND H. I. SCHIFF
Center for Research and Experimental Space Science, York University, Toronto, Ontario

Received December 18, 1968

The flowing afterglow technique has been used to study the electron detachment reactions

$$O_2(^1\Delta_g) + O_2^- \rightarrow 2O_2 + e \quad \text{and} \quad O_2(^1\Delta_g) + O^- \rightarrow O_3 + e$$

The rates of these reactions are sufficiently fast to make them important processes in D region ionospheric chemistry.

Canadian Journal of Chemistry, **47**, 1793 (1969)

The dominant negative ion formed in the D region of the earth's ionosphere is O_2^-. The process for this formation is three-body electron attachment (1). Laboratory measurements have already indicated that the associative-detachment reaction between O_2^- and atomic oxygen is important in the determination of the electron density below 100 km (2). Recent rocket-borne photometric measurements have indicated appreciable concentrations of $O_2(^1\Delta_g)$ molecules in the D region (3). It has been suggested that electrons are detached from O_2^- by $O_2(^1\Delta_g)$ (4). Thus, this reaction might play an important role in determining electron densities at altitudes where the $O_2(^1\Delta_g)$ concentration becomes comparable with the atomic oxygen concentration.

The flowing afterglow technique (5) has recently been applied to the measurement of the reaction of O^- and O_2^- with $O_2(^1\Delta_g)$. A simplified schematic diagram of this apparatus is shown in Fig. 1. Both O_2^- and O^- were produced by flowing helium carrier gas containing O_2 past an electron gun. $O_2(^1\Delta_g)$ was added to the gas stream through a downstream port. It was produced by the passage of O_2 through a microwave discharge in a quartz side arm. The rate of production of $O_2(^1\Delta_g)$ was varied by changing the O_2 flow and the discharge power. The discharge products were passed over a glass wool plug containing mercuric oxide in order to remove atomic oxygen (6). This removal was essential since the O atoms associatively detach electrons from both O_2^- and O^- (2). The gas containing molecular oxygen was then passed through a cell 6 cm in diameter and 20 cm in length, located just before the inlet port of the flow tube, where the $O_2(^1\Delta_g)$ content of the gas was determined by measuring

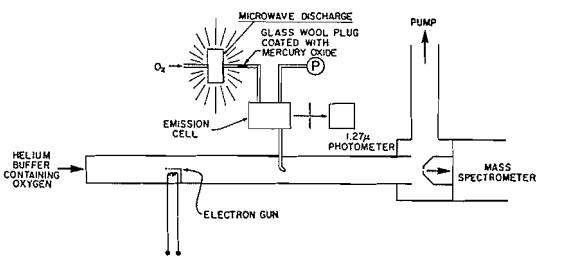

FIG. 1. A simplified schematic representation of the system.

Can. J. Chem. Downloaded from www.nrcresearchpress.com by 210.87.254.40 on 09/05/12
For personal use only.

92. A. DALGARNO and J. C. BROWNE. Astrophys. J. **149**, 231 (1967).
93. A. L. SCHMELTEKOPF, F. C. FEHSENFELD, and E. E. FERGUSON. Astrophys. J. **148**, L155 (1967).
94. A. DALGARNO. Ann. Geophys. **17**, 16 (1961).
95. E. E. FERGUSON, F. C. FEHSENFELD, and A. L. SCHMELTEKOPF. J. Chem. Phys. **47**, 3085 (1967).
96. R. S. BERRY, J. C. MACKIE, R. L. TAYLOR, and R. LYNCH. J. Chem. Phys. **43**, 3067 (1965).
97. L. M. BRANSCOMB, D. S. BURCH, S. J. SMITH, and S. GELTMAN. Phys. Rev. **111**, 504 (1958).
98. D. S. BURCH, S. J. SMITH, and L. M. BRANSCOMB. Phys. Rev. **112**, 171 (1958); **114**, 1652 (1959).
99. R. H. WOOD and L. A. D'ORAZIO. J. Phys. Chem. **69**, 2562 (1965).
100. W. L. FITE and J. A. RUTHERFORD. Discussions Faraday Soc. **37**, 192 (1964).
101. P. KABARLE, M. ARSHADI, and J. SCARBOROUGH. J. Chem. Phys. In press.
102. D. CONWAY and L. E. NESBITT. J. Chem. Phys. **48**, 509 (1968).
103. R. K. CURRAN. Phys. Rev. **125**, 910 (1962).

Associative-detachment reactions of O^- and O_2^- by $O_2(^1\Delta_g)$

F. C. FEHSENFELD AND D. L. ALBRITTON
Environmental Science Services Administration Research Laboratories, Boulder, Colorado

AND

J. A. BURT AND H. I. SCHIFF
Center for Research and Experimental Space Science, York University, Toronto, Ontario

Received December 18, 1968

The flowing afterglow technique has been used to study the electron detachment reactions

$$O_2(^1\Delta_g) + O_2^- \rightarrow 2O_2 + e \quad \text{and} \quad O_2(^1\Delta_g) + O^- \rightarrow O_3 + e$$

The rates of these reactions are sufficiently fast to make them important processes in D region ionospheric chemistry.

Canadian Journal of Chemistry, **47**, 1793 (1969)

The dominant negative ion formed in the D region of the earth's ionosphere is O_2^-. The process for this formation is three-body electron attachment (1). Laboratory measurements have already indicated that the associative-detachment reaction between O_2^- and atomic oxygen is important in the determination of the electron density below 100 km (2). Recent rocket-borne photometric measurements have indicated appreciable concentrations of $O_2(^1\Delta_g)$ molecules in the D region (3). It has been suggested that electrons are detached from O_2^- by $O_2(^1\Delta_g)$ (4). Thus, this reaction might play an important role in determining electron densities at altitudes where the $O_2(^1\Delta_g)$ concentration becomes comparable with the atomic oxygen concentration.

The flowing afterglow technique (5) has recently been applied to the measurement of the reaction of O^- and O_2^- with $O_2(^1\Delta_g)$. A simplified schematic diagram of this apparatus is shown in Fig. 1. Both O_2^- and O^- were produced by flowing helium carrier gas containing O_2 past an electron gun. $O_2(^1\Delta_g)$ was added to the gas stream through a downstream port. It was produced by the passage of O_2 through a microwave discharge in a quartz side arm. The rate of production of $O_2(^1\Delta_g)$ was varied by changing the O_2 flow and the discharge power. The discharge products were passed over a glass wool plug containing mercuric oxide in order to remove atomic oxygen (6). This removal was essential since the O atoms associatively detach electrons from both O_2^- and O^- (2). The gas containing molecular oxygen was then passed through a cell 6 cm in diameter and 20 cm in length, located just before the inlet port of the flow tube, where the $O_2(^1\Delta_g)$ content of the gas was determined by measuring

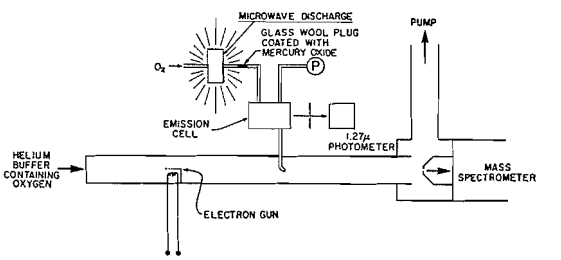

FIG. 1. A simplified schematic representation of the system.

Can. J. Chem. Downloaded from www.nrcresearchpress.com by 210.87.254.6 on 09/05/12
For personal use only.

TABLE I

Reaction rate constants* at 300 °K

Reaction	ΔE (eV)	k (cm^3 s^{-1})
$O^-(^2P) + O(^3P) \rightarrow O_2(^3\Sigma_g) + e$	3.6	2×10^{-10}
$O_2^-(^2\Pi_g) + O(^3P) \rightarrow O_3(^1A_1) + e$	0.6	3×10^{-10}
$O^-(^2P) + O_2(^1\Delta_g) \rightarrow O_3(^1A_1) + e$	0.6	$\sim3\times10^{-10}$
$O_2^-(^2\Pi_g) + O_2(^1\Delta_g) \rightarrow 2O_2(^3\Sigma_g) + e$	0.6	$\sim2\times10^{-10}$

*This table shows the measured reaction rates for the reaction of O^- and O_2^- with atomic oxygen and $O_2(^1\Delta_g)$. The approximate exothermicity of each reaction is listed under ΔE.

the intensity of the 1.27 μ emission from $O_2(^1\Delta_g)$. This emission was detected by a PbS photometer. From the measured emission intensity, the geometry of the cell, and the radiative lifetime (7), it was possible to calculate the concentration of $O_2(^1\Delta_g)$ molecules in the cell. This concentration, when combined with the mass flow rate of O_2 and the cell pressure, permits calculation of the flow rate of $O_2(^1\Delta_g)$. Reaction occurs between O^- and O_2^- ions and $O_2(^1\Delta_g)$ neutrals between the flow tube inlet port and the sampling orifice of the quadrupole mass spectrometer. The decrease in negative ion signal as a function of the rate of addition of $O_2(^1\Delta_g)$ provides the raw data from which the rate constants for reactions were determined.

Sample data for reaction of O^- with $O_2(^1\Delta_g)$ are shown in Fig. 2. This is a semilogarithmic plot of detected ion counts per second vs. the addition rate of $O_2(^1\Delta_g)$. This plot is made directly from the computer output of the raw data taken by an on-line data acquisition system; the scale factor for the $O_2(^1\Delta_g)$ flow is listed on the first line below the plot, while the initial O^- signal in counts per second is listed below this. The D's along the ordinate of the plot indicate decades of change in the O^- signal. The experimental points are given by pluses while the computer data fit is indicated by the asterisks.

The measured rate constants for the reactions of O^- and O_2^- with $O_2(^1\Delta_g)$ are shown in Table I. Also shown in this table are the previously measured values (8) for the detachment reactions of O^- and O_2^- with atomic oxygen. The approximate exothermicity of the reactions is also listed. Although the relative values of the $O_2(^1\Delta_g)$ reactions are probably accurate to better than 25%, no greater claim is made than an order of magnitude for the absolute accuracy of the individual values. The chief source of error lies in the uncertainty of the photometer calibration.

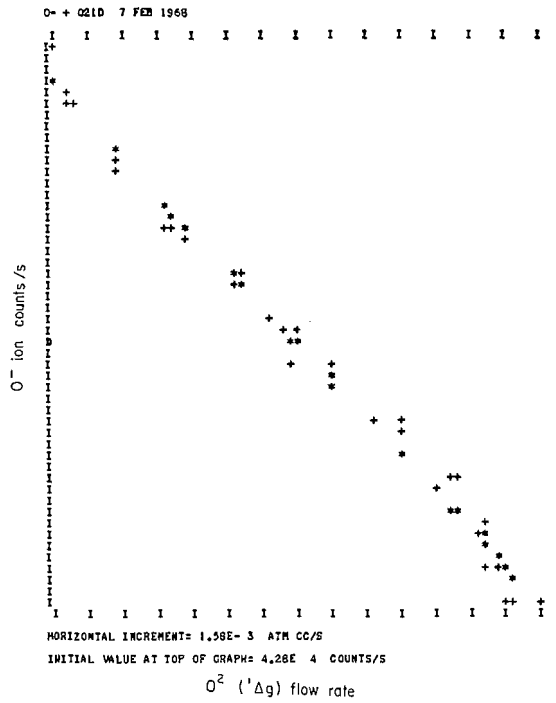

FIG. 2. A reproduction of the reduced data output from the on-line data acquisition system for the reaction of O^- with $O_2(^1\Delta_g)$. This is a semilogarithmic plot with the flow of $O_2(^1\Delta_g)$ in atm cm^3/s plotted along the abscissa and the O^- signal in counts/s plotted along the ordinate (the D's along the ordinate represent decade changes in the O^- signal). The pluses are the experimental points while the asterisks are the computer best fit to this data.

Nevertheless, the work to date has been sufficient to confirm the suspicion that the $O_2(^1\Delta_g)$ reactions play an important role in lower D region ionospheric chemistry.

1. L. M. CHANIN, A. V. PHELPS, and M. A. BIONDI. Phys. Rev. **128**, 219 (1962).
2. F. C. FEHSENFELD, A. L. SCHMELTEKOPF, and E. E. FERGUSON. Planetary Space Sci. **15**, 373 (1967).

Can. J. Chem. Downloaded from www.nrcresearchpress.com by 210.87.254.6 on 09/05/12
For personal use only.

3. W. F. J. EVANS, D. M. HUNTEN, E. J. LLEWELLYN, and A. VALLANCE JONES. J. Geophys. Res. **73**, 2885 (1968).
4. L. R. MEGILL and J. B. HASTED. Planetary Space Sci. **13**, 339 (1965).
5. F. C. FEHSENFELD, A. L. SCHMELTEKOPF, P. D. GOLDAN, H. I. SCHIFF, and E. E. FERGUSON. J. Chem. Phys. **44**, 4087 (1966); **44**, 4095 (1966). F. C. FEHSENFELD, E. E. FERGUSON, and A. L. SCHMELTEKOPF. J. Chem. Phys. **44**, 3022 (1966); **45**, 1844 (1966); **46**, 2802 (1967).
6. L. ELIAS, E. A. OGRYZLO, and H. I. SCHIFF. Can. J. Chem. **37**, 1680 (1959).
7. R. M. BADGER, A. C. WRIGHT, and R. F. WHITLOCK. J. Chem. Phys. **43**, 4345 (1965).
8. F. C. FEHSENFELD, A. L. SCHMELTEKOPF, H. I. SCHIFF, and E. E. FERGUSON. Planetary Space Sci. **15**, 373 (1967).

Comments

COMMENTS BY V. A. J. VAN LINT

Our measurements on NO_2 establish a very high rate of electron disappearance. The apparent three-body coefficient near 10^{-27} cm^6/s at 300 °K may be associated with N_2O_4 rather than NO_2. The only escape from this large cross section for NO_2 or N_2O_4 is to assume an even larger cross section for an impurity. The reaction appears to be three-body. There is some evidence that in pure NO_2 the electrons are not completely thermalized before attachment. Therefore, it is possible that the three-body pressure dependence actually reflects a dependence of electron energy on pressure.

Can. J. Chem. Downloaded from www.nrcresearchpress.com by 210.87.254.6 on 09/05/12
For personal use only.

3. W. F. J. EVANS, D. M. HUNTEN, E. J. LLEWELLYN, and A. VALLANCE JONES. J. Geophys. Res. **73**, 2885 (1968).
4. L. R. MEGILL and J. B. HASTED. Planetary Space Sci. **13**, 339 (1965).
5. F. C. FEHSENFELD, A. L. SCHMELTEKOPF, P. D. GOLDAN, H. I. SCHIFF, and E. E. FERGUSON. J. Chem. Phys. **44**, 4087 (1966); **44**, 4095 (1966). F. C. FEHSENFELD, E. E. FERGUSON, and A. L. SCHMELTEKOPF. J. Chem. Phys. **44**, 3022 (1966); **45**, 1844 (1966); **46**, 2802 (1967).
6. L. ELIAS, E. A. OGRYZLO, and H. I. SCHIFF. Can. J. Chem. **37**, 1680 (1959).
7. R. M. BADGER, A. C. WRIGHT, and R. F. WHITLOCK. J. Chem. Phys. **43**, 4345 (1965).
8. F. C. FEHSENFELD, A. L. SCHMELTEKOPF, H. I. SCHIFF, and E. E. FERGUSON. Planetary Space Sci. **15**, 373 (1967).

Comments

COMMENTS BY V. A. J. VAN LINT

Our measurements on NO_2 establish a very high rate of electron disappearance. The apparent three-body coefficient near 10^{-27} cm^6/s at 300 °K may be associated with N_2O_4 rather than NO_2. The only escape from this large cross section for NO_2 or N_2O_4 is to assume an even larger cross section for an impurity. The reaction appears to be three-body. There is some evidence that in pure NO_2 the electrons are not completely thermalized before attachment. Therefore, it is possible that the three-body pressure dependence actually reflects a dependence of electron energy on pressure.

Can. J. Chem. Downloaded from www.nrcresearchpress.com by 210.87.254.6 on 09/05/12
For personal use only.

Positive ion reactions

WADE L. FITE
Department of Physics, University of Pittsburgh, Pittsburgh, Pennsylvania 15213
Received November 21, 1968

Progress over the past five years in the measurement of rate coefficients and cross sections for interactions between positive ions and neutral molecules of particular interest to aeronomy is reviewed. Emphasis is placed on the methods of experimentation developed for studies in the range of thermal energies and slightly above. Along with discussion of the range of applicability of each of the techniques, illustrated by examples of measurements on processes of aeronomic interest, some evaluation of limitations of applicability and reliability of the measurements is made. A table summarizing results obtained to date on processes pertaining to the atmospheres of the earth and neighboring planets is presented.

Canadian Journal of Chemistry, 47, 1797 (1969)

Can. J. Chem. Downloaded from www.nrcresearchpress.com by 210.87.254.105 on 09/05/12
For personal use only.

Introduction

Five years ago at the symposium preceding the present one, two reports summarized experimental work on collisions between ions and neutral atomic systems of interest to aeronomy. Paulson (1) reviewed the situation with regard to experiments at thermal and low energies and the present author summarized experiments where the relative energy was sufficiently high that ion beam methods were employed (2). At that time the higher energy techniques were well established and a number of results had been obtained; however, to apply the results to problems of low energies, extrapolation by rather unreliable means had to be employed. In only a few cases were thermal and low energy data available since the techniques of experimenting at these low energies were in a very early stage of development.

The five years intervening between these symposia has seen the situation reverse itself. The development of low energy experimental methods has been rapid and the amount of low energy data on the principal atmospheric species is now quite large. To an ever-increasing extent, the role of the higher energy experiments is to examine details of reactions in order to better interpret the lower energy results as they apply to the atmosphere and to discover processes deserving of attention in thermal energy experiments.

Accordingly, it is appropriate here to review the principal laboratory methods now in use to obtain thermal energy data on total cross sections and reaction rate coefficients for ion–neutral reactions, to examine briefly the modifications of these methods and alternative methods by which the effects of increased kinetic energy and reactants being in excited states are assessed, and to discuss the ways in which higher energy experiments contribute additional knowledge.

In the interests of brevity the entire field of very high energy (i.e. 1 keV and up) processes will be omitted in this review despite their importance to certain atmospheric phenomena. Only reactions involving positive ions will be considered here, since negative ion reactions are being treated in a separate review by Ferguson (3). Only casual treatment of methods which were described in the reviews (1, 2) of the 1963 symposium will be made here, the reader being referred to these earlier papers; emphasis here will be placed instead on some of the more important newer developments. Lastly, no attempt will be made to present a complete compendium of reaction rate coefficient results; instead a summary of only those reaction rate coefficients most commonly used in chemical aeronomy at low energies is given.

Information Needs and Capabilities

The large bulk of information of present interest to aeronomy is limited to very low kinetic energies, i.e., in the energy range from about 0.015 eV to about 0.15 eV, for this is the range of temperatures in the ambient natural atmospheres of the earth and neighboring planets. While attention has been focussed initially on those atmospheric species which are the major constituents in the atmospheres, i.e., N_2, O_2, and O, it has become increasingly evident that major aeronomic effects involving ions arise through minor atmospheric components such as O_3, NO, OH, CO_2, He, and H. Additionally, mass spectrometric sampling of the D region by

TABLE I
Rate coefficients at 300 °K

Reaction	k (cm³/s)	Footnotes and comments
$He^+ + O_2 \rightarrow He + O + O^+$	$10 \pm 5\ (-10)$	1–7
$He^+ + N_2 \rightarrow He + N + N^+$	$12 \pm 5\ (-10)$ total	2–10
$He^+ + N_2 \rightarrow He + N_2^+$	Branching: $N^+ \sim 65\%$, $N_2^+ \sim 35\%$	
$O^+ + N_2 \rightarrow NO^+ + N$	$2 \pm 1\ (-12)$	5, 7, 9–12, 18, 19 Importance of vibrational temperature in N_2 established by Schmeltekopf *et al.* (13)
$O^+ + O_2 \rightarrow O + O_2^+$	$2 \pm 1\ (-11)$	7, 9–12, 14
$N_2^+ + O_2 \rightarrow N_2 + O_2^+$	$1 \pm .5\ (-10)$	1, 3, 5, 7, 9, 15
$N_2^+ + O \rightarrow NO^+ + N$	$2.5\ (-10)$	16
$N_2^+ + O \rightarrow N_2 + O^+$	$<1\ (-11)$	16
$O_2^+ + NO \rightarrow NO^+ + O_2$	$8\ (-10)$	7, 17
$O_2^+ + N_2 \rightarrow NO^+ + NO$	$<1\ (-15)$	7, 17
$O_2^+ + N \rightarrow NO^+ + O$	$18.\ (-10)$	17
$N_2^+ + NO \rightarrow NO^+ + N_2$	$5\ (-10)$	7, 17
$N^+ + O_2 \rightarrow NO^+ + O$	$3.5 \pm 1.5\ (-10)$	1, 5, 7, 9, 17
$N^+ + O_2 \rightarrow N + O_2^+$	$4.5 \pm 1.5\ (-10)$	5, 7, 9, 17
$N_2^+ + Na \rightarrow N_2 + Na^+$	$5.8 \pm 3.8\ (-10)$	20
$O_2^+ + Na \rightarrow O_2 + Na^+$	$6.7 \pm 2.1\ (-10)$	20
$O_2^+ + Na \rightarrow NaO^+ + O$	$7.7 \pm 2.4\ (-11)$	21 (Merging beam result)
$NO^+ + Na \rightarrow NO + Na^+$	$7 \pm 2\ (-11)$	20
$Mg^+ + O_3 \rightarrow MgO^+ + O_2$	$2.3\ (-10)$	22
$MgO^+ + O \rightarrow Mg^+ + O_2$	$\sim 1\ (-10)$	24
$Ca^+ + O_3 \rightarrow CaO^+ + O_2$	$1.6\ (-10)$	22
$Fe^+ + O_3 \rightarrow FeO^+ + O_2$	$1.5\ (-10)$	22
$Na^+ + O_3 \rightarrow NaO^+ + O_2$	$<1\ (-11)$	22 Very slow, unobservable in flowing afterglow
$NO^+ + O_3 \rightarrow NO_2^+ + O_2$		
$H_2O^+ + H_2O \rightarrow H_3O^+ + OH$	$8.5\ (-10)$	25
$H_2O^+ + O_2 \rightarrow O_2^+ + H_2O$	$\sim 2\ (-10)$	26
$O^+ + CO_2 \rightarrow O_2^+ + CO$	$1.2\ (-9)$	27
$N^+ + CO_2 \rightarrow CO_2^+ + N$	$1.3\ (-9)$	28
$N_2^+ + CO_2 \rightarrow CO_2^+ + N_2$	$9\ (-10)$	28
$N^+ + CO \rightarrow CO^+ + N$	$5\ (-10)$	28
$N_2^+ + CO \rightarrow CO^+ + N_2$	$7\ (-11)$	28
$C^+ + O_2 \rightarrow CO^+ + O$	$1.0 \pm .1\ (-9)$	29, 30
$C^+ + CO_2 \rightarrow CO^+ + CO$	$1.9\ (-9)$	29
$CO^+ + O_2 \rightarrow O_2^+ + CO$	$2.0\ (-10)$	29
$CO^+ + CO_2 \rightarrow CO_2^+ + CO$	$1.1\ (-9)$	29
$CO_2^+ + O_2 \rightarrow O_2^+ + CO_2$	$1.0\ (-10)$	31

Where several measurements exist ± indicates approximate range of measured values; where single measurements exist ± indicates estimated experimental uncertainty. Notation "$A(-B)$" implies $A \times 10^{-B}$. Extrapolated values from high energy data are not included in this table.

[1] W. L. Fite *et al.* Discussions Faraday Soc. 33, 264 (1962).
[2] J. Sayers and D. Smith. Discussions Faraday Soc. 37, 167 (1964).
[3] E. E. Ferguson *et al.* Planetary Space Sci. 12, 1169 (1964).
[4] F. C. Fehsenfeld *et al.* J. Chem. Phys. 44, 4087 (1966).
[5] V. Aquilanti and G. G. Volpi. Ric. Sci. 36, 359 (1966).
[6] J. Heimerl *et al.* Bull. Am. Phys. Soc. 13, 205 (1968).
[7] P. Warneck. Planetary Space Sci. 15, 1349 (1967); J. Geophys. Res. 72, 1651 (1967).
[8] T. F. Moran and L. Friedman. J. Chem. Phys. 45, 3837 (1966).
[9] D. B. Dunkin *et al.* J. Chem. Phys. 49, 1365 (1968).
[10] G. F. O. Langstroth and J. B. Hasted. Discussions Faraday Soc. 33, (1962).
[11] F. C. Fehsenfeld *et al.* Planetary Space Sci. 13, 219 (1965).
[12] M. F. Copsey *et al.* Planetary Space Sci. 14, 1047 (1966).
[13] A. L. Schmeltekopf *et al.* Planetary Space Sci. 15, 401 (1967).
[14] D. Smith *et al.* Planetary Space Sci. 16, 243 (1968).
[15] D. E. Golden *et al.* Phys. Rev. Letters, 20, 239 (1968).
[16] E. E. Ferguson *et al.* Planetary Space Sci. 13, 823 (1965).
[17] E. E. Ferguson *et al.* J. Geophys. Res. 70, 4323 (1965).
[18] M. M. Nakshbandi and J. B. Hasted. Planetary Space Sci. 15, 1781 (1967).
[19] D. K. Bohme *et al.* Planetary Space Sci. 15, 1777 (1967).
[20] A. L. Farragher *et al.* To be published.
[21] E. A. Entemann and P. K. Rol. To be published.
[22] F. C. Fehsenfeld *et al.* Bull. Am. Phys. Soc. 13, 212 (1968).
[23] A. L. Schmeltekopf *et al.* Bull. Am. Phys. Soc. 12, 235 (1967).
[24] E. E. Ferguson *et al.* To be published.
[25] V. L. Tal'rose and E. L. Frankevich. Zh. Fiz. Chem. 34, 2709 (1960).
[26] F. C. Fehsenfeld *et al.* J. Chem. Phys. 46, 2802 (1967).
[27] F. C. Fehsenfeld *et al.* J. Chem. Phys. 44, 3022 (1966).
[28] F. C. Fehsenfeld *et al.* J. Chem. Phys. 44, 4537 (1966) and 46, 2019 (1967).
[29] F. C. Fehsenfeld *et al.* J. Chem. Phys. 45, 23 (1966).
[30] J. L. Franklin and M. S. B. Munson. 10th Combustion Symposium, Combustion Institute Pittsburgh. 1965. p. 561.
[31] E. E. Ferguson *et al.* Space research. Vol. VII. North Holland Publ. Co., Amsterdam. 1967. p. 135.

Can. J. Chem. Downloaded from www.nrcresearchpress.com by 210.87.254.105 on 09/05/12
For personal use only.

Can. J. Chem. Downloaded from www.nrcresearchpress.com by 210.87.254.105 on 09/05/12
For personal use only.

Narcisi and his collaborators (4) has dramatically introduced an interest in reactions involving metals and other materials presumably of meteoritic origin.

While the catalogue of chemical species of interest has increased, the need for detailed information about the role of excited states of reactants has also become apparent. In several instances it has been found in the laboratory that cross sections and rate coefficients depend very strongly on the internal energy of one or both reactants. The importance of excited states in the normal atmosphere has not been well assessed as yet, but in rather special circumstances of a disturbed atmosphere, the effects of internal energy of reactants appear exceedingly important.

In general the information sought for low energy aeronomy is total cross section or reaction rate coefficient data and most experiments are directed at obtaining this type of information. The processes of interest that involve positive ions are (*a*) charge transfer, e.g., $A^+ + BC \rightarrow A + BC^+$, and (*b*) ion–molecule reactions (or ion–atom interchange), e.g., $A^+ + BC \rightarrow AB^+ + C$, the distinction between the two being whether the chemical identity of the reactants is preserved or altered in the collision. While these names are good on laboratory experimental grounds, since the ionic products can be unequivocally determined by using mass spectrometry, the distinction physically is less clear. While charge transfer, for example, can proceed by simple electron transfer as in the case at high energies, low energy charge transfer products can also be formed in one of the decay channels of a transitory complex ion, $(ABC^+)^*$. Since ion–molecule reactions are normally envisaged as proceeding through such a complex ion, some and probably most thermal energy charge transfer reactions are more nearly similar to ion–molecule reactions than to simple electron transfer processes.

In simple electron transfer between systems of the same ionization potential (resonant charge transfer) the energy dependence of the total cross section is given by

$$[1] \qquad Q = (A - B \log E)^2$$

where A and B are constants. When the process is endothermic this dependence is found at high energies, but as the energy is reduced the cross section reaches a maximum at a relative velocity $v_m \cong a|\Delta E|/h$, where ΔE is the energy defect and a is a length of atomic dimensions. At lower energies the cross section diminishes to zero at threshold energy in the center of mass coordinates (see, for example, ref. 5).

For exothermic processes the simple electron transfer cross section is expected to behave similarly to the endothermic case, where ΔE is now the excess energy in the process. However, in cases involving molecules or molecular ions the products can be left in excited states thus leaving ΔE effectively zero. In such cases of "accidental resonance" charge transfer, eq. [1] again describes the dependence of the cross section on energy.

The usual model taken for ion–molecule reaction collisions is that a collision complex is first formed, and redistribution of the atoms within this complex then occurs. In the case of ion–molecule reactions, the mechanism of complex formation is that an incoming ion induces an electric dipole moment in a neutral, and the charge-induced-dipole force attracts the two together. If the initial impact parameter is above a critical amount depending on the relative velocity, the ion will be deflected slightly but probably no reaction will occur; if smaller than this critical amount, the two particles orbit around each other and come closer to where reaction can occur. The cross section for forming an orbiting complex was given by Langevin as

$$[2] \qquad Q(v) = 2e\left(\frac{\alpha}{\mu}\right)^{\frac{1}{2}} \cdot \frac{1}{v}$$

where α is the polarizability of the neutral and μ the reduced mass. Gioumousis and Stevenson (6) and Field, Franklin, and Lampe (7) have established experimentally that for many ion–molecule reactions, eq. [2] does describe the cross sections at energies of a few eV and less. In some cases the inverse velocity dependence is observed but the absolute magnitude of a cross section is less than that predicted. In these cases, one recognizes that a collision complex can decay through various channels leading to new ionic products, to charge transfer and also to no change in products (i.e., scattering), and that the probability of decaying by any one channel will determine the cross section for that one process.

It is of interest to note that for processes described by eq. [2], the rate coefficient,

$$[3] \qquad k = \int Q(v) v f(v) \mathrm{d}v$$

where $f(v)$, the normalized velocity distribution

Can. J. Chem. Downloaded from www.nrcresearchpress.com by 210.87.254.105 on 09/05/12
For personal use only.

function, is independent of any other parameters that might appear in $f(v)$; most notably it is independent of the temperature in the case of a Maxwell–Boltzmann distribution.

The two energy dependences given in eqs. [1] and [2] are often used in extrapolation of high energy data to thermal energies, when it can be established that one or the other is valid at higher energies, and this procedure has usually given fairly good estimates of rate coefficients which have later been determined at very low energies.

In some cases it appears that charge transfer can proceed by both simple electron transfer and by complex formation, as evidenced by velocity dependences given by eq. [1] at higher energies and by eq. [2] at moderate energies. In some cases, most notably the important reaction $O^+ + N_2 \rightarrow NO^+ + N$, neither eq. [1] nor eq. [2] even crudely describes the experimental results.

It has already been pointed out that where a charge transfer process is exothermic, it can still display an energy dependence corresponding to one of resonance charge transfer, i.e., eq. [1]. This is usually taken to imply that the excess energy has been left as internal excitation in the products. Of course the possibility that a product of an ion–molecule reaction is left in an internally excited state is also present. Such products can radiate or dissociate, or, if metastable, remain to participate in future reactions. The last possibility is one of the reasons for studying the role of internal energy in aeronomic reactions even in the ambient atmosphere and the first two possibilities provide additional laboratory methods of studying reactions.

At higher energies, other two-body collisions processes occur. These include direct excitation and/or dissociation of either of the reactants, ionization of the target neutral, and removal of additional electrons from the incident ion, in addition to charge transfer. In general the formation of collision complexes is a low energy phenomenon and eq. [2] fails at ion energies of the order of tens of eV, with the cross section for ion–molecule reactions falling off much more rapidly as the energy is increased.

The principal three-body thermal energy process of interest to aeronomy is clustering, i.e., the addition of neutral molecules to existing ions. The case of clustering of one or more water molecules to ions is particularly noteworthy in the D region.

Laboratory Methods

The laboratory methods in use for the measurement of total cross sections and reaction rates for processes involving positive ions and neutrals can be grouped on the basis of the energy range in which they work. The principal general methods are

1. Thermal energy methods (0.008–0.05 eV):
   (*a*) mass spectrometry of stationary afterglows,
   (*b*) mass spectrometry of flowing afterglows, and
   (*c*) ion cyclotron resonance methods.
2. Thermal to medium energies (0.025–10 eV):
   (*a*) secondary ions in mass spectrometer sources,
   (*b*) pulsed sources on mass spectrometers,
   (*c*) drift tube methods, and
   (*d*) merging beam methods.
3. Medium to high energies:
   (*a*) beams into static gases, double mass spectrometer methods, and
   (*b*) crossed beam methods.

Most of these methods were described in the reviews given at this symposium five years ago (1, 2), and these will not be discussed to any extent in the present summary except to note certain innovations to these older techniques and new results of unusual interest. Three of the methods are new, however, and these will be discussed in some detail. The three new methods are flowing afterglows (1*b*), ion cyclotron resonance (1*c*), and merging beams (2*d*).

1. Thermal Energy Methods

(a) Mass spectrometry of stationary afterglows. Mass spectrometry of stationary afterglows was used several years ago to provide the earliest information on charge transfer and ion–molecule reactions of major importance to aeronomy. In this method a mixture of gases in widely disparate amounts are subjected to a pulse of excitation that produces primary ions from the original gases in amounts roughly proportional to their respective number densities. After cessation of the pulse, these primary ions react with the neutrals and the relative populations of the ions change in time. An aperture is placed in the afterglow chamber and ions emerging from the aperture are analyzed by a mass spectrometer. The assumption is made that the ion currents are proportional to the number densities of the ions in the vicinity of the aperture and the time history of each ion

Can. J. Chem. Downloaded from www.nrcresearchpress.com by 210.87.254.105 on 09/05/12
For personal use only.

is taken to represent the time history of the number density of each ion, from which a rate coefficient may be deduced if one also knows the partial pressures of the neutrals in the afterglow chamber. Such experiments were performed by Sayers and his associates (8, 11), Hasted and his collaborators (9), and by Fite *et al.* (10), and are described in ref. 1.

In the past five years, the principal work done with stationary afterglows has been to take advantage of the small volumes involved which makes rather easy the variation of temperature and the study of temperature dependences of ion–neutral reaction processes. Sayers and Smith (11) studied the temperature dependence of $O^+ + O_2 \rightarrow O + O_2^+$, finding a rate that diminished with temperature which has subsequently been determined by Smith and Fouracre (12) to vary as $T^{-0.48(\pm.05)}$ up to about 600 °K, in opposition to temperature independence expected on the basis of Langevin collisions. This result is in good agreement with a stationary afterglow experiment result of Nakshbandi and Hasted (13) and a flowing afterglow experiment of Dunkin *et al.* (14). At temperatures higher than 600 °K, the rate coefficients as determined in a drift tube experiment of Bohme *et al.* (15) and a secondary ion mass spectrometer experiment of Warneck (16) appear to be effectively temperature-independent up to several thousand degrees, i.e., in accord with the orbiting collision model (eqs. [2] and [3]) and then appear to increase with energy (15).

The fact that more has not been done with stationary afterglow mass spectrometry is due to two basic limitations of the general method. First, the gases admitted to the afterglow chamber must be chemically stable and second, all gases are subjected to the excitation pulse. Since the excitation pulse can partially dissociate and excite a neutral gas, one is rarely completely certain that an observed reaction process is occurring with a groundstate molecule of the neutral gas put into the chamber nor certain of the state of the ion. One must work very hard to ensure an unambiguous interpretation of an experimental result.

These two basic problems have been largely alleviated in the flowing afterglow approach.

(b) Mass spectrometry of flowing afterglows. In the flowing afterglow technique which was developed and very successfully used by Ferguson, Fehsenfeld, and Schmeltekopf and their collaborators (17) at the Environmental Sciences Services Administration laboratories in Boulder, Colorado, the variation of ion concentrations with time of the stationary afterglow approach is replaced by variation of ion concentrations with space as an afterglow flows rapidly down a tube. While this in itself offers no advantages, the method does represent a major step forward in that it permits injection of gases into the flow stream without their being subjected to the excitation mechanism making the primary ions and all that this implies.

In a typical experiment a buffer gas (usually helium) is admitted to the entrance end of the flow tube and subjected to electron impact bombardment or microwave power or some other means of producing ions. Slightly downstream, a primary gas is injected into the stream and charge transfer and Penning ionization operate to replace the helium ions by primary ions from the injected gas. Yet further downstream, a secondary gas is injected whose reactions with the primary ions are to be studied. Finally at the end of the flow tube the ions present are sampled by being taken into a differentially pumped mass spectrometer through an aperture normally on the axis of the flow tube. Typical flow speeds are 10^4 cm/s, tube lengths are normally about 1 m, and the gas pressure (being made up almost entirely of buffer gas partial pressure) range is generally between 0.1 and 1 Torr. The quantity of buffer gas handled is quite large and fast Roots pumps are used to maintain the flow and to exhaust the gas after the flow has passed the mass spectrometric sampling device.

As noted above, the advantage of this approach is that secondary gases are injected into the stream below the point where buffer gas ions and primary ions are made, thereby obviating questions of the uncontrolled production of excited states of the neutral reactants, questions which plague stationary afterglow experiments. Additional major advantages are that (*a*) the neutral gases need not be chemically stable but can be either partially dissociated, or put into some excited state, in some specific and separately controlled manner; (*b*) the spatial separations admit optical absorption spectroscopic monitoring of species and states at any point in the flow; (*c*) additional gases can be injected which quench out states and species of primary ions whose presence would confuse interpretation of an experiment, and (*d*) different methods of injection and points of injection can be used to maximize or minimize

Can. J. Chem. Downloaded from www.nrcresearchpress.com by 210.87.254.105 on 09/05/12
For personal use only.

either wanted or unwanted effects. The excitation means is usually run continuously, but the pulsed mode of excitation can also be employed to advantage. The flexibility afforded by being able separately to control so many of the parameters in flowing afterglow experiments is enormously greater than that available in stationary afterglow experiments, and the flowing afterglow method has now become the standard way of studying thermal ion–neutral reactions.

It would be misleading to suggest that the interpretation of flowing afterglow experiments is not without its problems. Some of these problems originate from the use of a flow system, and it is appropriate to consider the model of what takes place in the flowing afterglow. The flux of primary ions, $\boldsymbol{S}_1$, is presumed to be given by

$$[4] \qquad \boldsymbol{S}_1 = -D_1 N \boldsymbol{\Delta}_1 + N_1 \boldsymbol{v}$$

where N_1 is the primary ion number density, D_1 is the ambipolar diffusion coefficient of the primary ions through the buffer gas, and $\boldsymbol{v}$ is the vector velocity of the stream which is determined by the hydrodynamics of the flow. Applying continuity in the steady state one can write down

$$[5] \quad \nabla \cdot \boldsymbol{S}_1 = -kN_1 n_2 - \sum_{i \neq 2} \beta_i n_i N_1 - \alpha_1 n_e N_1 + \gamma_1 n_1$$

where the first term represents the loss of primary ions due to the reaction of interest with a neutral gas whose number density is n_2, the second term represents loss of primary ions due to other competing processes, the third term is the loss due to electron–ion recombination (and a similar term could be written down for ion–ion mutual neutralization), and the fourth term represents the production of primary ions by Penning ionization by He* and other processes.

Combining these equations

$$[6] \quad (\boldsymbol{v} \cdot \nabla) N_1 = -kn_2 N_1 - \sum \beta_i n_i N_1 - \alpha_1 n_e N_1 + \gamma n_1 + D_1 \nabla^2 N_1$$

The corresponding equation for a secondary ion formed as a product of the reaction between N_1 and n_2 is

$$[7] \quad (\boldsymbol{v} \cdot \nabla) N_2 = +kn_2 N_1 - \sum \delta_j n_j N_2 - \alpha_2 n_e N_2 + \sum \varepsilon_j n_2 N_j + D_2 \nabla^2 N_2 + \gamma_2 n_2$$

where the first term represents the process of interest, the second term losses of secondary ions in tertiary processes, the third term again recombination, the fourth term production of secondary ions in reactions with ions other than the desired primary, the fifth term the ambipolar diffusion losses, and the sixth term production of ions by Penning ionization, etc.

The number densities of the secondary gas(es) are themselves solutions of diffusion equations of the type

$$[8] \qquad (\boldsymbol{v} \cdot \nabla) n_2 = D_n \nabla^2 n_2$$

subject to the boundary conditions and whatever initial conditions are appropriate to the chosen manner of injection.

The complexity of using these three equations and treating them properly is staggering. However, one can manipulate the experimental conditions to simplify the problem somewhat by minimizing the contributions of separate terms. For example, by using sufficiently low plasma densities the recombination terms can be neglected; Penning ionization by He* as an unwanted source of primary or secondary ions can be excluded by admixing a small amount of argon to the helium buffer gas to quench the He*; using clean gases and controlling the means of production of chemically unstable neutral reactant species can minimize competing processes terms, etc. Indeed, much of the success of the ESSA group in using these experiments is due to their ingenuity in finding ways to manipulate gases and experimental parameters in order to display the process of interest.

There are additional problems, however. Questions of mixing of an injected reactant gas with the flow stream enter and are important especially at the high flow velocities used; the form of $\boldsymbol{v}$ is important and although indications are that laminar viscous (Poiseuille) flow is operative over most of the length of most flow tubes, one does not know $\boldsymbol{v}$ in the vicinity of obstructions such as nozzles where the reactant gases are injected. The fact that a pressure gradient along the tube is necessary to maintain the flow further complicates matters.

However, even under "ideal circumstances", i.e., no competing processes and Poiseuille flow, the situation is still not easy. In the cylindrically symmetric case, the equations become

$$[6'] \quad D_1 \frac{1}{r} \frac{\partial}{\partial r}\left(r \frac{\partial N_1}{\partial r}\right) + D_1 \frac{\partial^2 N_1}{\partial z^2} = v_0 \left(1 - \frac{r^2}{a^2}\right) \frac{\partial N_1}{\partial z} + kn_2 N_1$$

$$[7'] \quad D_2 \frac{1}{r}\frac{\partial}{\partial r}\left(r\frac{\partial N_2}{\partial r}\right) + D_2\frac{\partial^2 N_2}{\partial z^2} = v_0\left(1 - \frac{r^2}{a^2}\right)\frac{\partial N_2}{\partial z} - kn_2N_1$$

$$[8'] \quad D_n \frac{1}{r}\frac{\partial}{\partial r}\left(r\frac{\partial n_2}{\partial r}\right) + D_n\frac{\partial^2 n_2}{\partial z^2} = v_0\left(1 - \frac{r^2}{a^2}\right)\frac{\partial n_2}{\partial z}$$

where each D is a function of position due to the pressure gradient down the tube.

It is apparent that these three equations cannot be solved by separation of the variables due to the parabolic flow profile, and further approximations must be introduced. One of the simplest approximations assumes that n_2 is constant (i.e., the neutral reactant is distributed uniformly), that N_1 is initially a function of z only and independent of the radius r, and that the flow is "slug flow", i.e., that $v = v_0$ and is independent of r. Under these extreme simplifying assumptions, $N_1(z)$ is given by

$$[9] \quad N_1(z, n_2) = N_1(0)f(r) \times \exp\left[-\left(\frac{D_1}{\Lambda^2} + kn_2\right)\frac{z}{v_0}\right]$$

after sufficient time (distance) has elapsed for the flow to settle into the lowest radial diffusion mode, for which the diffusion length is Λ, and f is a Bessel function. Clearly, by varying n_2 and plotting N_1 on a semi-log plot, the slope gives an indication of the rate coefficient, k. This method of observing primary ion decay, after approximate corrections for parabolic flow, is that normally employed by the ESSA group and has the advantage that by holding the geometry constant, the spatial parameters in eq. [9] are unchanged. This also has the experimental advantage of making unnecessary the moving of sources of either the primary ions or the secondary gases.

It is to be pointed out, however, that if the ambipolar diffusion coefficient is dependent on n_2 this procedure can lead to erroneous results. Since ambipolar diffusion coefficients do change with relative concentrations in an ion mixture and since the ion concentrations are dependent on n_2 through the reaction, it would be expected that the ambipolar diffusion coefficient would be dependent on n_2.

An alternative procedure in data treatment can be used to minimize macroscopic effects of this kind (and also competing process effects). If one defines a ratio, $R = N_2/N_1$, eqs. [6'] and [7'] can be combined to give

$$[10] \quad (\mathbf{v}\cdot\nabla)R = kn_2(1 + R) + R\left\{D_2\frac{\nabla^2 N_2}{N_2} - D_1\frac{\nabla^2 N_1}{N_1}\right\}$$

which in the limit of small R gives

$$[11] \quad v\frac{\partial R}{\partial z} = kn_2(1 + R)$$

and which can be solved along the z-axis to give

$$[12] \quad \log(1 + R) = \frac{k}{v_0}\int n_2(0, E)\mathrm{d}z$$

In this approach, even if n_2 is not uniform, solution of eq. [8] is all that is needed in order to perform the integral.

This "ratio method" which was used by Farragher *et al.* (18) in studying charge transfer between atmospheric ions and sodium atoms, has the disadvantage that one must know the detection efficiency for the primary and secondary ions. If there is mass discrimination in the mass spectrometer or differences in secondary emission coefficient at the electron multiplier detector, these must be corrected for before correct answers can be hoped for.

A third method for analyzing data is to treat the appearance of the secondary ions. Like the decay of the primary ion method, it observes a single ion and therefore is not susceptible to mass discrimination effects. This method handles eq. [7'] in a manner analogous to that used for eq. [6'] in deriving eq. [9]. In an analogous manner, problems of changing diffusion coefficients and other macroscopic effects that depend on n_2 can again lead to erroneous results.

The complexity of properly treating the physics in flowing afterglows is evident from the above discussion. There are, of course, other problems which are shared with stationary afterglow methods which have not received detailed consideration as yet. In particular the processes by which ions emerge through apertures is not at all well understood. The practice of biassing an ion extraction aperture which is often done to improve signal strengths suggests that the ion extraction process is mobility limited. There is some evidence suggesting that the existence of

Can. J. Chem. Downloaded from www.nrcresearchpress.com by 210.87.254.105 on 09/05/12
For personal use only.

Can. J. Chem. Downloaded from www.nrcresearchpress.com by 210.87.254.105 on 09/05/12
For personal use only.

negative ions in the plasma affects positive ion extraction (19) and varying an added electronegative reactant gas may lead to spurious results using the primary ion decay method. There is a free jet expansion as the gas leaves the flow tube and enters the mass spectrometer's high vacuum; the extent to which altering gases affects this expansion and in turn the ion extraction has not been investigated.

In general, it seems appropriate to caution any user of rate coefficients obtained from flowing afterglow experiments that errors of a factor of two or three may still be in even the best measurements. The physics of afterglows is quite complex and of flowing afterglows even more so. Factors of two discrepancies are not uncommon with ostensibly identical flow tubes and data handling procedures, even for the simplest processes having the largest rate coefficients. Time and further work on this very fruitful approach will unquestionably clear up some of these remaining problems.

To turn to the positive aspects of flowing afterglow experiments, perhaps the best testament to the fruitfulness of the approach is the list of reactions at the end of this paper whose rate coefficients have been obtained by no other method. Two experiments are appropriate to recount here in the text as well. The first studied reactions of $N_2^+ + O$ (20). In this study nitrogen gas that had been partially dissociated in a separate discharge flowed through a side tube toward the flowing afterglow containing N_2^+ ions. Before admission to the flow, NO was added in the side tube and the titration reaction $NO + N \rightarrow N_2 + O$ produced oxygen atoms at the rate of one O for each NO added. Since the flow rate of NO could be measured, the flow of O into the afterglow was known and the experiment could proceed in a fairly conventional way.

The second particularly interesting experiment involved the reaction $O^+ + N_2 \rightarrow NO^+ + N$, thermal energy values of which had been particularly elusive and irreproducible from one investigator to another using stationary and flowing afterglows. The problem was traced down in the experiment of Schmeltekopf *et al.* (21) who excited the nitrogen in a separate gas discharge before admission to the flow tube. The excited neutral gas was then electron-impact excited to radiating states and from the vibrational temperature of the emitted radiation the vibrational temperature of the original excited N_2 gas was deduced. The remarkable finding was that as the vibrational temperature was increased the rate coefficient was increased enormously. Evidently the scatter in data from other experiments on this reaction arose from different experiments having nitrogen whose vibrational states were populated differently and the lowest value was the best. This $O^+ + N_2$ reaction has the strongest dependence on the internal energy state of the neutral reactant known so far. The fact that the process is also of unusual importance to aeronomy emphasizes the importance of excited states in understanding the upper atmosphere.

(c) Ion cyclotron resonance methods. Many of the uncertainties in the afterglow methods discussed above arise from lack of understanding of how ions emerge through apertures. Clearly these problems could be avoided if the rates of change of ion population could be determined while the ions were in the flow tube. A very attractive method by which this can be done is the use of ion cyclotron resonance.

In this method a magnetic field is put on the afterglow so that each ion follows a circular motion at the ion cyclotron resonance frequency

$$[13] \qquad f_c = \frac{1}{2\pi}\frac{eB}{mc}$$

where B is the magnetic induction, e is the charge, c is the velocity of light, and m is the ion mass. Obviously ions of different e/m will have different cyclotron energies. If a weak radio frequency electric field at the cyclotron frequency is also applied, an ion will pick up energy from the field and this energy absorption can be detected as a load on the rf oscillator. By sweeping either the magnetic field or the oscillator frequency, the appearance of loading on a marginal oscillator evidences the presence of each ion and the strength of the loading gives an indication of the number of ions present. By following the rise and decay rate of various ions one has the information from which reaction rate coefficients can be deduced.

This very attractive approach was first employed to study mobilities and total collision cross sections of ions by Wobschall, Graham, and Malone (22), where the cross section information could be deduced from line widths of the resonance absorption lines. More recently it has been applied to charge transfer and ion–molecule

Can. J. Chem. Downloaded from www.nrcresearchpress.com by 210.87.254.105 on 09/05/12
For personal use only.

reactions by Baldeschweiler and his associates (23) in nitrogen–hydrocarbon systems, which, unfortunately, are not of very great interest to aeronomy. It will be important to receive data on atmospheric reactions using ion cyclotron resonance in the future, both for what it can add in the way of new information and for what it will contribute to understanding of present afterglow data.

2. Thermal to Medium Energies

(a) Secondary ions in mass spectrometer sources. This method needs little discussion here, having been treated in ref. 1. However, an important new advance has been applied to this approach by the use of photoionization sources for the primary ions. By using light of a given wavelength, the primary ions can be much more selectively produced than on electron impact and production of ions in specific initial states is possible. Warneck (16) has been foremost in applying this important modification of an older method to problems of aeronomical interest.

(b) Pulsed sources on mass spectrometers. See ref. 1.

(c) Drift tube methods. In drift tube methods, primary ions are created at one end of a tube along the length of which a d.c. electric field exists. A primary ion assumes a velocity appropriate to its mobility at the gas pressure in the tube and for the applied electric field. One effectively increases the kinetic temperature of the interactants without appreciably altering the internal energy states populations. A mass spectrometer usually samples the ions emerging from the drift tube which contains a buffer gas and the reactant gas of interest.

Three recent drift tube experiments are noteworthy. In the first, Hasted and his associates (15, 24) changed the primary ion source to one which is mass analyzed and could be made state selective as well. Although the ion enters at relatively high energy (tens to hundreds of eV) it is rapidly moderated down in energy to the steady drift value. By inserting a selected ion into the drift tube, many of the ambiguities of interpretation of results are reduced.

Using groundstate O^+ ions reacting with N_2 to produce NO^+, an energy dependence of the rate coefficient which increased with energy was found, the increase being compatible with the increase in cross section for this reaction as obtained from crossed beam (25) and beam-in-static-gas (26) experiments. The apparent increase in rate coefficient for $O^+ + O_2 \rightarrow O + O_2^+$ at energies greater than 0.5 eV has already been noted earlier in this paper.

A second drift tube experiment of interest was the careful study of Heimerl, Johnsen, and Biondi (27) on reactions between He^+ and both N_2 and O_2, who showed that over the temperature range 300 to 1200 °K the reaction rate coefficients appear to be temperature-independent.

Yet a third drift tube experiment of interest is that of Golden, Sinnott, and Varney (28) who studied the reaction $N_2^+ + O_2 \rightarrow N_2 + O_2^+$ and found that it also appeared to have a temperature-independent rate coefficient in accordance with the Langevin orbiting complex model.

(d) Merging beam techniques. The newest experimental method to arrive on the experimental scene is also one of the most elegant and promises to be extremely useful. This is the technique of merging parallel beams. In this method a fast beam of selected ions of mass m_1 at laboratory energy E_1 is charge transfer neutralized and into this fast beam is merged a beam of ions of mass m_2 travelling at laboratory energy E_2. After the two merged beams have run along together a prescribed distance (i.e., time) the ions are separated out and from the relative signals of the primary and secondary ions the cross section as a function of relative energy, or energy in the center of mass system, may be deduced.

The relative energy is given by

$$[14] \quad E_r = \frac{1}{m_1 + m_2} [\sqrt{(m_2 E_1)} - \sqrt{(m_1 E_2)}]^2$$

It is clear that even though the laboratory energies of the beams are quite high (high enough to produce and handle high current beams), by adjusting E_1 and E_2 the relative energy can be made arbitrarily small. Furthermore the energy spread in the center of mass is scaled down from the laboratory energy spread by a factor comparable to the relative energy divided by the laboratory energy. In this approach it is not necessary to be content to measure only rate coefficients, but instead cross sections as a function of energy as measured on a very fine energy spread scale can be obtained.

This method which was first described by Trujillo, Neynaber, Marino, and Rothe (29)

Can. J. Chem. Downloaded from www.nrcresearchpress.com by 210.87.254.105 on 09/05/12
For personal use only.

has subsequently been applied by those authors to the charge transfer between $Ar^+ + Ar$. Of more interest for aeronomy, and also as an illustration of the unique potentialities of the merging beams technique, we can cite the very recent experiments of Entemann and Rol working in Dr. Neynaber's laboratory (33) who examined collisions between O_2^+ and Na. Analysis of the secondary ions revealed the appearance of NaO^+ which was unequivocally identified, and the cross section for its formation corresponded to a thermal energy rate coefficient of approximately 8×10^{-11} cm^3/s. This product was also sought in the flowing afterglow experiments of Farragher *et al.* (18) but without success due to general noise in the experiment.

While merging beam experiments are difficult to execute because of extremely low signal levels, they are extremely clean experiments and have very few interpretational pitfalls. The beams can be produced cleanly and impurity and competing process effects are automatically excluded; the product ions are unequivocally identified and there is no possibility of confusing different ions of the same e/m (e.g., $H_5O_2^+$ vs. NaN^+, K^+ vs. NaO^+, CO^+ vs. N_2^+, etc.) which can occur in afterglow and drift tube experiments.

The merging beam technique appears to this author to be uniquely able to investigate reactions having small rate coefficients. While flowing afterglows appear suitable for determining large rate coefficients, when small rate coefficients are of interest, one must be extremely cautious in the flowing afterglow because of competing processes, perhaps with unknown impurities, to produce the desired secondary ion, attack of the secondary ion through tertiary processes, etc. Concerns of this kind probably need be worried about only for processes with apparent rate coefficients of 10^{-11} cm^3/s and less.

The one present problem with merging beams for ion–neutral studies of total cross sections is that the neutrals are produced by charge transfer and one is not certain of the internal energy state population of the neutral beam. Unquestionably, techniques will be developed to select states, perhaps such as that described in the following section, and correct this present deficiency.

3. *Medium to High Energies*

At energies of a few eV and higher it is possible to produce ion beams of sufficiently high current to perform either beam-in-static-gas experiments or crossed beam experiments where the ion beam intersects a thermal energy molecular to atomic beam. Such experiments have been discussed in refs. 1 and 2.

Recent work along these lines has continued with a wide variety of processes being examined. The rocket observations of Narcisi (4) have prompted crossed beam experiments on reactions producing and destroying metal ions. Henderson, Mentall, and Fite (30) examined charge transfer between atmospheric ions and sodium, and Turner and Rutherford (34) have made measurements on production of Mg^+, Ca^+, as well as Na^+ in charge transfer reactions between the parent metal atoms and N_2^+, O_2^+, N^+, O^+, NO^+, H_2O^+, and H_3O^+ to supplement a wide variety of measurements on atmospheric reactions between normally gaseous components (31).

Potentially the most important of the recent studies at the higher energies are those of Turner, Rutherford, and Compton (32) on selective absorption of ions in beams passing through gases, for these point the way toward production of high currents of ions in specific states. A problem that has always plagued high energy experiments (and probably low energy experiments as well) is that it is difficult to produce ions in a single state and to know the state population in any ion beam. While one can produce the ions by electron bombardment immediately above threshold and gain reasonable assurance for most ions that only the groundstate ion is being produced, the ion currents so produced are often impossibly low. Turner and his associates took the approach to produce ions in an electron bombardment source at high electron energies where the beam current was high, and then passed the current through an absorbing gas. Those ions in states with high cross sections for charge transfer or ion–molecule reactions will interact with the absorbing gas and be greatly attenuated, while those with low cross sections will be largely transmitted. Experimenting with O^+ and O_2^+ passing through N_2, Ar, and H_2 and looking at the transmitted current as a function of absorbing gas pressure, it was found that two clearly defined straight line sections on a semi-log plot appeared, demonstrating the existence of at least two separate cross sections for reaction for the ions in the beam. By reducing the electron energy to just above threshold, a single straight line appeared

Can. J. Chem. Downloaded from www.nrcresearchpress.com by 210.87.254.105 on 09/05/12
For personal use only.

on the semi-log plot which was associated with the groundstate ion cross section. Comparing the semi-log plots, one can deduce (*a*) the fraction of ions in the beam which are excited when using the high electron energies, (*b*) the cross section for the excited states reacting with the absorbing gas, and (*c*) the cross section for the ground state reaction with the absorber. Among other things, it was learned that electron bombardment at energies typically used in ion sources produce 22 to 33% of the O_2^+ ions in the metastable $^4\Pi_u$ state and 27 to 30% of the O^+ appears to be in the ^2D metastable state.

The cross sections are sufficiently different in these cases that with an absorber gas, the excited states can be virtually completely removed while attenuating the groundstate ion component by a factor of only about 3 to 5. This can give an appreciable improvement in ion currents over sources operating immediately above threshold in order to produce the groundstate ion.

The potentialities of using selective attenuation to produce beams of ions in a given excited state are obvious and further experiments with different absorbing gases along these lines are clearly called for.

Of direct interest to aeronomy is the fact that the cross sections for reaction of the various states of O_2^+ colliding with N_2 at ion energies of about 100 eV differ by factors of 150! Whether many thermal reaction rates also have such spectacular variation with the state of the ionic reactant will be something very important to learn, especially for application to aeronomic situations where ions in excited states can be produced.

It is this author's expectation that a review paper on the subject of reactions between positive ions and neutral molecules given five years hence will have as its central theme the role of excited states.

1. J. F. Paulson. Ann. Geophys. **20**, 18 (1964).
2. W. L. Fite. Ann. Geophys. **20**, 31 (1964).
3. E. E. Ferguson. Can. J. Phys. (1968).
4. R. S. Narcisi. *In* Space research. Vol. 7. North-Holland Publishing Co., Amsterdam. 1967.
5. D. Rapp and W. E. Francis. J. Chem. Phys. **37**, 2631 (1962).
6. G. Gioumousis and D. P. Stevenson. J. Chem. Phys. **29**, 294 (1958).
7. F. H. Field, J. L. Franklin, and F. W. Lampe. J. Am. Chem. Soc. **79**, 2419 (1957).
8. P. G. Dickinson and J. Sayers. Proc. Phys. Soc. London, **76**, 137 (1960).
9. G. F. O. Langstroth and J. B. Hasted. Discussions Faraday Soc. **33**, 298 (1962).
10. W. L. Fite, J. A. Rutherford, W. R. Snow, and V. A. J. van Lint. Discussions Faraday Soc. **33**, 264 (1962).
11. J. Sayers and D. Smith. Discussions Faraday Soc. **37**, 167 (1964).
12. D. Smith and R. A. Fouracre. Planetary Space Sci. **16**, 243 (1968).
13. M. M. Nakshbandi and J. B. Hasted. Planetary Space Sci. **15**, 1781 (1967).
14. D. B. Dunkin, F. C. Fehsenfeld, A. L. Schmeltekopf, and E. E. Ferguson. J. Chem. Phys. In press.
15. D. K. Bohme, P. P. Ong, J. B. Hasted, and L. R. Megill. Planetary Space Sci. **15**, 1777 (1967).
16. P. Warneck. Planetary Space Sci. **15**, 1349 (1967).
17. F. C. Fehsenfeld, A. L. Schmeltekopf, P. D. Goldan, H. I. Schiff, and E. E. Ferguson. J. Chem. Phys. **44**, 4087 (1966); Goldan *et al.* J. Chem. Phys. **44**, 4095 (1966); F. C. Fehsenfeld *et al.* J. Chem. Phys. **45**, 1844 (1966).
18. A. L. Farragher, W. L. Fite, and J. A. Peden. J. Chem. Phys. In press.
19. W. L. Fite and J. A. Rutherford. Discussions Faraday Soc. **37**, 192 (1964).
20. E. E. Ferguson, F. C. Fehsenfeld, P. D. Goldan, A. L. Schmeltekopf, and H. I. Schiff. Planetary Space Sci. **13**, 823 (1965).
21. A. L. Schmeltekopf, F. C. Fehsenfeld, G. I. Gilman, and E. E. Ferguson. Planetary Space Sci. **15**, 401 (1967).
22. D. Wobschall, J. R. Graham, and D. P. Malone. Phys. Rev. **131**, 1565 (1963).
23. L. R. Anders, J. L. Beauchamp, R. C. Dunbar, and J. D. Baldeschweiler. J. Chem. Phys. **45**, 1062 (1966); J. L. Beauchamp. J. Chem. Phys. **46**, 1231 (1967).
24. Y. Kaneko, L. R. Megill, and J. B. Hasted. J. Chem. Phys. **45**, 3741 (1966).
25. R. F. Stebbings, J. A. Rutherford, and B. R. Turner. J. Geophys. Res. **71**, 771 (1966).
26. C. F. Giese. Advan. Chem. Ser. 25, Am. Chem. Soc., Washington, D.C. 1966. pp. 20–27.
27. J. Heimerl, R. Johnsen, and M. A. Biondi. Bull. Am. Phys. Soc. **13**, 205 (1968).
28. D. E. Golden, G. Sinnott, and R. N. Varney. Phys. Rev. Letters, **20**, 239 (1968).
29. S. M. Trujillo, R. H. Neynaber, L. Mariono, and E. W. Rothe. IVth International Conference on the Physics of Electronic and Atomic Collisions, Quebec, Canada, 1965. Science Bookcrafters, New York. 1965. p. 260.
30. W. R. Henderson, J. E. Mentall, and W. L. Fite. J. Chem. Phys. **46**, 3447 (1967).
31. B. R. Turner, J. A. Rutherford, and R. F. Stebbings. J. Geophys. Res. **71**, 4521 (1966).
32. B. R. Turner, J. A. Rutherford, and D. M. J. Compton. J. Chem. Phys. **48**, 1602 (1968).
33. P. K. Rol. Private communication. 1968.
34. B. R. Turner and J. A. Rutherford. Private communication. 1968.

Si^+ and SiO^+ reactions of atmospheric importance

F. C. FEHSENFELD
Environmental Science Services Administration Research Laboratories, Boulder, Colorado 80302

Received November 21, 1968

Flow system measurements are reported of the approximate rate constants for the gas phase reactions $Si^+ + O_2 \rightarrow SiO^+ + O$, $SiO^+ + N \rightarrow Si^+ + NO$ or $NO^+ + Si$, and $SiO^+ + O \rightarrow Si^+ + O_2$. The constants are, respectively, $< 10^{-11}$, $\sim 1.5 \times 10^{-10}$, $\sim 1.5 \times 10^{-10}$, and 2×10^{-10}, all in $cm^3\ s^{-1}$.

Canadian Journal of Chemistry, 47, 1808 (1969)

Can. J. Chem. Downloaded from www.nrcresearchpress.com by 210.87.254.42 on 09/05/12
For personal use only.

Recently rocket borne mass spectrometers have measured the positive ions present in the earth's lower ionosphere. These measurements indicate that ions of mass 28 and 44 are present in the ionosphere above 85 km. These ions have been tentatively identified as Si^+ and SiO^+. In this presentation I will report some recent laboratory measurements of the reactions of Si^+ with O_2 and SiO^+ with O_2 and atomic oxygen which are relevant to the ionospheric chemistry of Si^+ and SiO^+.

Figure 1 is a simplified schematic drawing of the apparatus used to make these measurements. The system is basically the same flowing afterglow described in the literature. There are, however, two features particular to the present system which will be briefly described. The first of these features is the method used to generate the silicon ions. To do this a few grams of the silicon monoxide is placed in a furnace. The furnace is mounted in a forward section of the flow tube. As the silicon monoxide vapor is evolved it is carried downstream by the buffer gas. In the studies involving SiO^+, argon is used as a buffer. Argon ions and metastables are produced by electron impact and produce SiO^+ from SiO by secondary processes. To produce Si^+ a helium buffer is used. The helium ion and metastables are energetically capable of dissociatively ionizing silicon monoxide. The actual resulting ion composition is roughly 50% Si^+ and 50% SiO^+.

The ions produced in the excitation region are carried down the tube by the flowing gas past a downstream port through which the reactant gas (in this case either O_2 or atomic oxygen) is added. In order to generate atomic oxygen the standard technique is used whereby atomic nitrogen is produced and then reacted with NO. To obtain the atomic nitrogen, N_2 is passed through a microwave discharge where a few tenths of 1% of the N_2 is dissociated. The N_2 containing atomic nitrogen then flows past an inlet where NO is

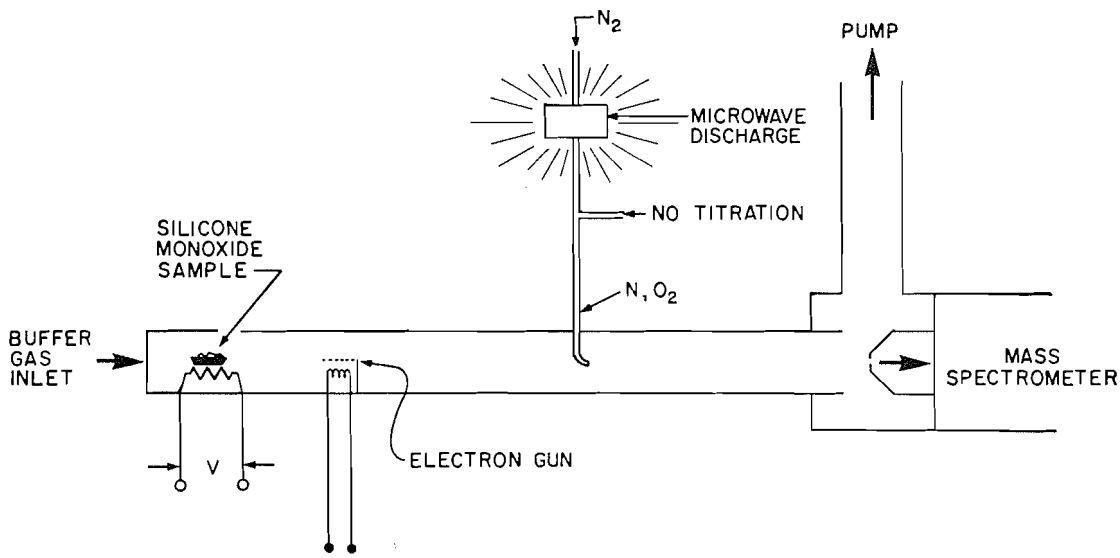

FIG. 1. A simplified schematic representation of the apparatus.

added. The NO rapidly reacts with the atomic nitrogen producing atomic oxygen. The end point of this titration may be detected optically or by the behavior of various ion signals. The measured NO flow at the end point is equal to the total flow of the atomic species. The mixture of N_2 and O then passes into the system. In the region between this inlet and the sampling orifice of the mass spectrometer the reactions between the reactant neutral and the ions take place.

$$Si^+ + O_2 \xrightarrow{k_1} SiO^+ + O$$
$$k_1 < 10^{-11}$$

$$SiO^+ + N \xrightarrow{k_{2a}} Si^+ + NO$$
$$\xrightarrow{k_{2b}} NO^+ + Si$$
$$k_{2a} + k_{2b} \cong 3 \times 10^{-10}\ cm^3/s,\ k_{2a} \cong 2k_{2b}$$

$$SiO^+ + O \xrightarrow{k_3} Si^+ + O_2$$
$$k_3 \cong 2 \times 10^{-10}\ cm^3/s$$

FIG. 2. The measured reaction rates for Si^+ with O_2 and SiO^+ with atomic nitrogen and atomic oxygen.

Figure 2 lists the measured rate constant for the reaction between Si^+ and O_2 and SiO^+ with the atoms of nitrogen and oxygen. The reaction of SiO^+ with atomic nitrogen is fast. The products of this reaction are $Si^+ + NO$ and $NO^+ + Si$. The relative intensity of the product ion signals indicates that about two-thirds of the reaction goes to Si^+ while one-third leads to NO^+. This result is not surprising because these reactions are strongly exothermic. The interesting result concerns the fast reaction of SiO^+ with atomic oxygen. Using the published results for the dissociation energy for SiO^+, this reaction should be about 0.5 eV endothermic. The observation of this reaction either indicates that the published dissociation energy of SiO^+ is high, or the SiO^+ that is present in our experiment is in an excited state. However, the fact that the reaction $Si^+ + O_2$ is slow also argues for the exothermicity of the reverse reaction.

In the atmosphere, SiO^+ is probably produced from SiO or SiO_2. These species probably are deposited in this region by meteor ablation. The reactions which have been reported would suggest that SiO^+ would be rapidly converted to Si^+ by atomic oxygen. The ionospheric measurements indicate that there is a significant concentration of SiO^+ relative to Si^+ in the atmosphere. To maintain such a ratio there is probably a rapid reconversion of Si^+ back to SiO^+.

Aeronomic importance of ion–molecule clustering reactions

D. K. BOHME[1]

Aeronomy Laboratory, Environmental Science Services Administration, Boulder, Colorado 80302

Received November 21, 1968

A literature survey of observations of ion clusters in mass spectrometers indicates that the association rate constant depends on the number of atoms in the cluster. An altitude profile of estimated apparent bimolecular rates of clustering in the atmosphere is made from this empirical correlation. Experimental measurements of the termolecular rate constant for clusters in formation are reported; the temperature dependence of some of these has been measured.

Canadian Journal of Chemistry, 47, 1809 (1969)

The recent mass spectrometric measurements of Narcisi (1) in the D region of the ionosphere have indicated appreciable concentrations of heavy positive ions with masses greater than 45 a.m.u. Some of these heavy ions have been attributed to hydrated cluster ions. The mass 37 ion, presumably the hydrated ion $H_3O^+.H_2O$, was found to be the dominant low-mass positive ion between 60 and 80 km.

Heavy cluster ions have now been identified in many laboratory experiments (2, 3). Recent D region simulation experiments performed in the E.S.S.A. flowing afterglow with air at a temperature of 162 °K and a pressure of 0.1 Torr have yielded evidence for hydrated H_3O^+ ions as

[1]National Research Council of United States Postdoctoral Resident Research Associate.

Can. J. Chem. Downloaded from www.nrcresearchpress.com by 210.87.254.42 on 09/05/12
For personal use only.

added. The NO rapidly reacts with the atomic nitrogen producing atomic oxygen. The end point of this titration may be detected optically or by the behavior of various ion signals. The measured NO flow at the end point is equal to the total flow of the atomic species. The mixture of N_2 and O then passes into the system. In the region between this inlet and the sampling orifice of the mass spectrometer the reactions between the reactant neutral and the ions take place.

$$Si^+ + O_2 \xrightarrow{k_1} SiO^+ + O$$
$$k_1 < 10^{-11}$$

$$SiO^+ + N \xrightarrow{k_{2a}} Si^+ + NO$$
$$\xrightarrow{k_{2b}} NO^+ + Si$$
$$k_{2a} + k_{2b} \cong 3 \times 10^{-10}\ cm^3/s,\ k_{2a} \cong 2k_{2b}$$

$$SiO^+ + O \xrightarrow{k_3} Si^+ + O_2$$
$$k_3 \cong 2 \times 10^{-10}\ cm^3/s$$

FIG. 2. The measured reaction rates for Si^+ with O_2 and SiO^+ with atomic nitrogen and atomic oxygen.

Figure 2 lists the measured rate constant for the reaction between Si^+ and O_2 and SiO^+ with the atoms of nitrogen and oxygen. The reaction of SiO^+ with atomic nitrogen is fast. The products of this reaction are $Si^+ + NO$ and $NO^+ + Si$. The relative intensity of the product ion signals indicates that about two-thirds of the reaction goes to Si^+ while one-third leads to NO^+. This result is not surprising because these reactions are strongly exothermic. The interesting result concerns the fast reaction of SiO^+ with atomic oxygen. Using the published results for the dissociation energy for SiO^+, this reaction should be about 0.5 eV endothermic. The observation of this reaction either indicates that the published dissociation energy of SiO^+ is high, or the SiO^+ that is present in our experiment is in an excited state. However, the fact that the reaction $Si^+ + O_2$ is slow also argues for the exothermicity of the reverse reaction.

In the atmosphere, SiO^+ is probably produced from SiO or SiO_2. These species probably are deposited in this region by meteor ablation. The reactions which have been reported would suggest that SiO^+ would be rapidly converted to Si^+ by atomic oxygen. The ionospheric measurements indicate that there is a significant concentration of SiO^+ relative to Si^+ in the atmosphere. To maintain such a ratio there is probably a rapid reconversion of Si^+ back to SiO^+.

Aeronomic importance of ion–molecule clustering reactions

D. K. BOHME[1]

Aeronomy Laboratory, Environmental Science Services Administration, Boulder, Colorado 80302

Received November 21, 1968

A literature survey of observations of ion clusters in mass spectrometers indicates that the association rate constant depends on the number of atoms in the cluster. An altitude profile of estimated apparent bimolecular rates of clustering in the atmosphere is made from this empirical correlation. Experimental measurements of the termolecular rate constant for clusters in formation are reported; the temperature dependence of some of these has been measured.

Canadian Journal of Chemistry, 47, 1809 (1969)

The recent mass spectrometric measurements of Narcisi (1) in the D region of the ionosphere have indicated appreciable concentrations of heavy positive ions with masses greater than 45 a.m.u. Some of these heavy ions have been attributed to hydrated cluster ions. The mass 37 ion, presumably the hydrated ion $H_3O^+.H_2O$, was found to be the dominant low-mass positive ion between 60 and 80 km.

Heavy cluster ions have now been identified in many laboratory experiments (2, 3). Recent D region simulation experiments performed in the E.S.S.A. flowing afterglow with air at a temperature of 162 °K and a pressure of 0.1 Torr have yielded evidence for hydrated H_3O^+ ions as

[1]National Research Council of United States Postdoctoral Resident Research Associate.

Can. J. Chem. Downloaded from www.nrcresearchpress.com by 210.87.254.42 on 09/05/12
For personal use only.

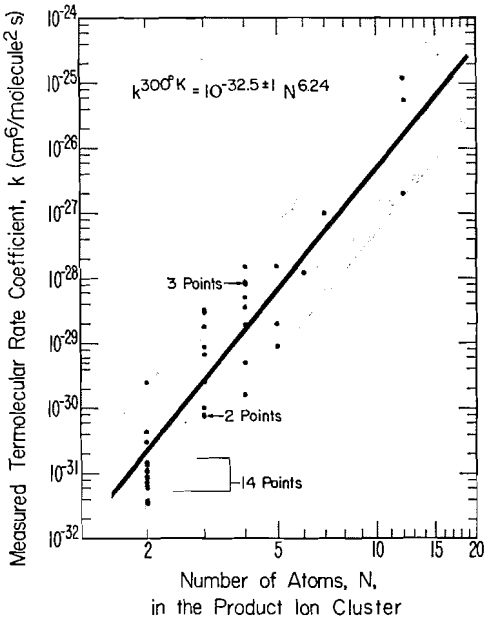

FIG. 1. The measured termolecular rate coefficient plotted as a function of the number of atoms in the product ion cluster.

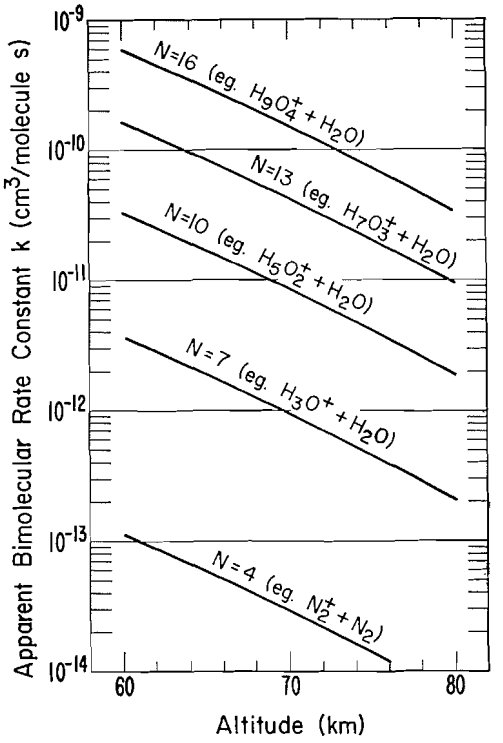

FIG. 2. The estimated apparent rate constant of ion cluster formation at 300 °K plotted as a function of altitude.

large as $H_3O^+.6H_2O$, as well as hydrated O_2^+ and NO^+ ions. The cluster ions N_6^+, N_7^+, N_8^+, N_9^+, as well as He_3^+ and Ar_3^+, were identified mass spectrometrically at 82 °K, apparently for the first time (4). Although observations of heavy cluster ions have been numerous, little is known about the magnitude of specific rates of cluster formation and the dependency of these rates on cluster size, temperature, and pressure.

A consideration of all available laboratory data found in the literature on ion–neutral termolecular association in which a stable cluster is formed indicates a surprisingly systematic variation of the termolecular rate coefficient with the number of atoms N in the product ion cluster. This is illustrated in Fig. 1 for 44 measurements of 27 ion–molecule association reactions. The spread in the data may be attributed, in part, to variations in the stabilization efficiency of the third body and the potential energy configuration of the ion cluster. Nevertheless, the following empirical relation, which allows an order-of-magnitude estimation of the specific termolecular rate k of cluster formation at about 300 °K, may be derived from the plot shown in Fig. 1:

$$[1] \qquad k^{300\,°K} = 10^{-32.5\pm1} N^{6.24}$$

An altitude profile of some estimated apparent bimolecular rates of clustering at 300 °K which can be constructed using eq. [1] is given in Fig. 2. A standard reference atmosphere was used to obtain neutral densities (5). The role of ion cluster formation can be seen to be more important at lower altitudes where the apparent bimolecular specific rates are larger. It is evident from Fig. 2 that the three-body formation of heavy ion clusters involving a large number of atoms ($N \gtrsim 10$) may readily compete with the fairly rapid two-body reactions occurring in the D region of the ionosphere. Atomic and molecular ions with very low specific rates of two-body conversion are likely to be bound to polyatomic molecules such as H_2O by the more rapid three-body formation of ion clusters. This would be the case for the terminal ions in the D region such as NO^+ and NO_3^- as well as atomic ions of low ionization potential such as Na^+, Ca^+, Mg^+, Fe^+, and Si^+.

Recent experiments conducted in the E.S.S.A. flowing afterglow system have indicated several additional empirical relationships. Table I is a list of some positive and negative three-body

Can. J. Chem. Downloaded from www.nrcresearchpress.com by 210.87.254.42 on 09/05/12
For personal use only.

Can. J. Chem. Downloaded from www.nrcresearchpress.com by 210.87.254.42 on 09/05/12
For personal use only.

TABLE I

Termolecular rate constants measured in the E.S.S.A. flowing afterglow system

Reaction	Temperature (°K)	Rate constant (cm^6/s)
$O_2^+ + O_2 + He$	82	3.1×10^{-29}
$N_2^+ + N_2 + He$	82	1.2×10^{-28}
	280	1.9×10^{-29}
$O^- + CO_2 + He$	280	1.5×10^{-28}
$O^+ + N_2 + He$	82	5.4×10^{-29}
$N^+ + N_2 + He$	82	7.2×10^{-29}
	280	8.6×10^{-30}
$Ar^+ + Ar + He$	82	1.6×10^{-30}
	290	$\sim1.3\times10^{-30}$
$O^- + N_2 + He$	82	1.3×10^{-30}
$Mg^+ + O_2 + Ar$	300	$\sim2.5\times10^{-30}$
$Fe^+ + O_2 + Ar$	300	$\sim1.0\times10^{-30}$
$Ca^+ + O_2 + Ar$	300	$\sim6.6\times10^{-30}$

ion–molecule reactions, the specific rates of which have recently been measured in the E.S.S.A. flowing afterglow at 82 and 280 °K with helium and argon as a third-body over a pressure range 0.1 to 3.0 Torr. At low pressures the kinetics of cluster formation was termolecular at both temperatures, as expected for the ground state ions investigated. The termolecular rate coefficients were found to increase significantly with decreasing temperature. Furthermore, the results indicate that termolecular cluster formation is less strongly dependent upon temperature as the number of atoms N in the product ion cluster increases according to the empirical relation

$$[2] \qquad k_1 = k_0 \left(\frac{T_0}{T_1}\right)^{\frac{N+2}{N}}$$

k_1 and k_0 are the termolecular specific rates at temperatures T_1 and T_0, where $T_0 > T_1$. Equation [2] was derived from the experimental results at the two temperatures 82 and 280 °K for the association of N_2^+ with N_2, N^+ with N_2, and Ar^+ with Ar in helium gas assuming that the termolecular rate coefficient varies as T^{-n}. Therefore, caution must be exercised when invoking eq. [2] to extrapolate the results shown in Figs. 1 and 2 to more realistic D region temperatures.

Finally, the E.S.S.A. flowing afterglow experiments have indicated (6) that the kinetics of the formation of O_4^+ and N_4^+ ion clusters at 82 °K becomes bimolecular above helium pressures of about 1.6 and 0.2 Torr, respectively, as demonstrated in Fig. 3. This result is qualitatively consistent with a clustering process involving a collision sequence of two steps, i.e. initial formation of the intermediate complex followed by stabilization upon collision with a third body. According to such a mechanism, the apparent bimolecular specific rate of ion cluster formation will never exceed the Langevin orbiting rate constant of the initial complex formation, i.e. of two-body ion–molecule reactions. In fact, for the case of O_4^+ and N_4^+ ion cluster formation, the flowing afterglow results at 82 °K indicate an apparent bimolecular specific rate at saturation of only about 7×10^{-12} cm^3/s. It is not yet known whether the apparent bimolecular specific rate of ion cluster formation at saturation is dependent on the gas temperature and on the complexity of the ion cluster.

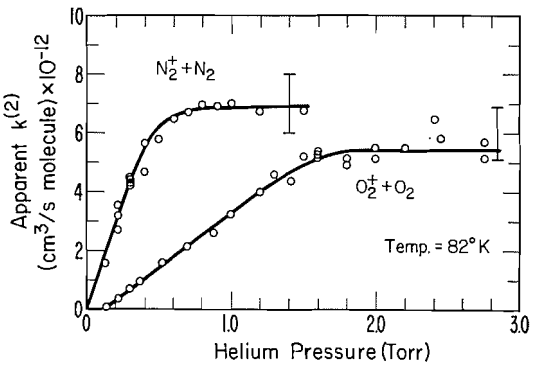

FIG. 3. The experimentally determined bimolecular rate coefficient, $k^{(2)}$, plotted as a function of helium pressure.

A full evaluation of the importance of three-body clustering reactions in the D region of the ionosphere will have to await more laboratory measurements of specific rates at various temperatures and pressures, the complete identification of the large concentrations of heavy positive ions observed in rocket flights, and measurements of neutral concentrations such as principally H_2O and possibly neutral clusters.

1. R. S. NARCISI. Ann. Geophys. **22**, 224 (1966).
2. P. KEBARLE, R. M. HAYNES, and S. SEARLES. Advan. Chem. Ser. **58**, 210 (1966).
3. M. M. SHAHIN. Advan. Chem. Ser. **58**, 315 (1966).
4. E. E. FERGUSON, D. B. DUNKIN, F. C. FEHSENFELD, and A. L. SCHMELTEKOPF. Bull. Am. Phys. Soc. **13**, 212 (1968).
5. Cospar International Reference Atmosphere 1965. North-Holland Publishing Co., Amsterdam. 1965.
6. D. K. BOHME, D. B. DUNKIN, F. C. FEHSENFELD, and E. E. FERGUSON. J. Chem. Phys. In press.

Comments, Replies, and Summary

COMMENTS BY M. A. BIONDI

As noted in Dr. Fite's review, drift tube/mass spectrometer measurements of the reaction rate for $N_2^+ + O_2 \rightarrow N_2 + O_2^+$ by Golden, Sinnott, and Varney (1) indicate no dependence on the ion's energy over the range from thermal energy to ~ 1 eV. Dr. Ferguson cited E.S.S.A. flowing afterglow measurements (2) over the temperature range 80–550 °K which revealed a substantial decrease in the reaction rate over this range. Using a drift tube/mass spectrometer to study the same reaction (3), we also find a substantial decrease in the reaction rate with increasing ion energy (see Fig. 1), in disagreement with the result of Golden *et al.* (1) and in agreement with the E.S.S.A. result (2). Also shown in the figure is the reaction $O^+ + CO_2 \rightarrow O_2^+ + CO$, which shows a slight decrease in rate with increasing ion energy, in agreement with the corresponding E.S.S.A. result (2), thus giving us additional confidence in the validity of our energy dependence determinations.

Finally, we include in the figure our results for the energy dependence of the ionospherically interesting charge transfer reaction $O_2^+ + NO \rightarrow O_2 + NO^+$, which has not previously been studied in this energy region.

1. D. E. GOLDEN, G. SINNOTT, and R. N. VARNEY. Phys. Rev. Letters, **20**, 239 (1968).
2. D. B. DUNKIN, F. C. FEHSENFELD, A. L. SCHMELTEKOPF, and E. E. FERGUSON. J. Chem. Phys. **49**, 1365 (1968).
3. R. JOHNSEN, L. BROWN, and M. A. BIONDI. Paper H-6, Gaseous Electronics Conference, Boulder, Colo., Oct. 16–18, 1968; Bull. Am. Phys. Soc. To be published.

COMMENTS BY E. E. FERGUSON[1]

Recently rate constants of some of the important ionospheric positive ion reactions have been measured over the temperature range 80 to

[1]Address: Aeronomy Laboratory, Environmental Science Services Administration Laboratories, Boulder, Colorado.

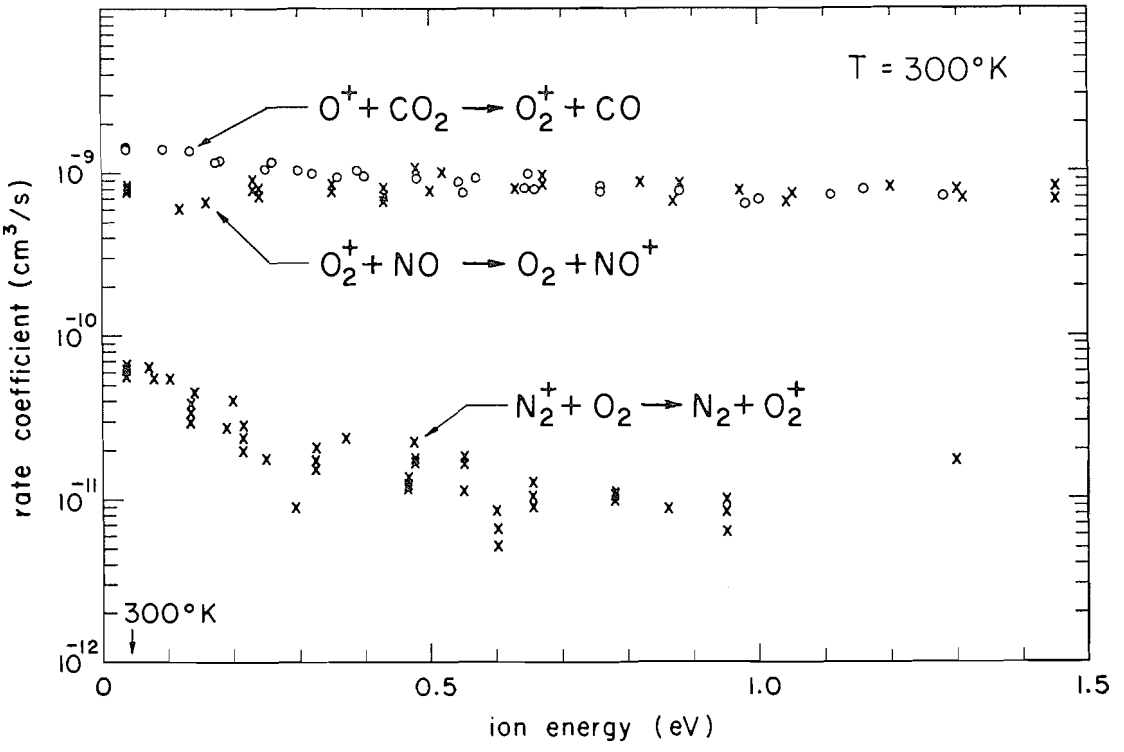

FIG. 1. Drift mobility tube/mass spectrometer determinations by Johnsen, Brown, and Biondi of the energy dependence of three ion–molecule reactions of aeronomic interest.

Can. J. Chem. Downloaded from www.nrcresearchpress.com by 210.87.254.40 on 09/05/12
For personal use only.

Can. J. Chem. Downloaded from www.nrcresearchpress.com by 210.87.254.40 on 09/05/12
For personal use only.

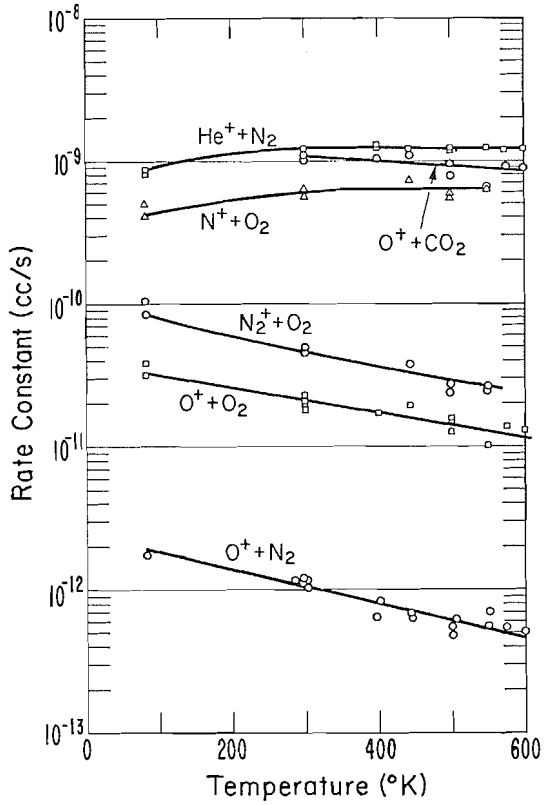

FIG. 2. Rate constants of some positive ion reactions over 80 to 600 °K.

600 °K, in the E.S.S.A. flowing afterglow system (4, 5). These results are shown in Fig. 2. The magnitude and constancy of the rate constant for $He^+ + N_2$ from 300 to 600 °K agrees with results of Heimerl *et al.* (6). The magnitude and temperature dependence of the $O^+ + O_2$ reaction is in excellent agreement with measurements of Smith and Fouracre (7) between 185 and 576 °K. There is a substantial disagreement among various experimenters concerning the $O^+ + N_2$ reaction. The current literature on all these reactions is discussed in ref. 1.

We have proposed a qualitative theory for the decrease in rate constant with increasing temperature for slow reactions in the near-thermal range (5). In brief, it is known from unimolecular decomposition theory and from the temperature dependence of three-body association reaction rate constants (8) that the lifetimes of the intermediate reaction complexes increase with decreasing temperature. It is also known from phase space theory that equilibration of vibrational modes in the complex, prior to breakup, favors the most exothermic breakup channel. The longer the complex lifetime, the nearer the approach to equilibration should be. Therefore, it follows that the reactions of Fig. 1, which are the most exothermic breakup channels, should be favored at low temperatures over thermoneutral elastic breakup (no reaction), as compared to higher temperatures.

4. D. B. DUNKIN, F. C. FEHSENFELD, A. L. SCHMELTEKOPF, and E. E. FERGUSON. J. Chem. Phys. **49**, 1365 (1968).
5. E. E. FERGUSON, D. K. BOHME, F. C. FEHSENFELD, and D. B. DUNKIN. J. Chem. Phys. To be published.
6. J. HEIMERL, R. JOHNSEN, and M. A. BIONDI. Bull. Am. Phys. Soc. **13**, 205 (1968).
7. D. SMITH and R. A. FOURACRE. Planetary Space Sci. **16**, 243 (1968).
8. D. K. BOHME, D. B. DUNKIN, F. C. FEHSENFELD, and E. E. FERGUSON. J. Chem. Phys. To be published.

COMMENTS BY MARK CHER[2]

I wish to report that we have solved eq. [6′], the continuity equation for Poiseuille flow, by neglecting the term $D_1\partial^2 N_1/\partial z^2$. This approximation is justified because in general, transport along the axial direction by diffusion is small everywhere in the tube (except perhaps very near the walls) compared with transport by convection. The other approximations are the usual ones, namely that D_1, v_0, k, and n_2 (in Fite's notation) are constants independent of position. The solution is

$$N_1(z, r) = N_1(0) \exp\left\{-\left[\frac{D_1\lambda_0^2}{a^2} + (1 + \varepsilon_1)kn_2 - \frac{\varepsilon_2 k^2 a^2 n_2^2}{D_1^2}\right]\frac{z}{v_0}\right\} f(r)$$

where $f(r)$ is the product of an exponential and a confluent hypergeometric function and λ_0, ε_1, and ε_2 are constants equal to 2.710, 0.237, and 0.00115, respectively. These constants were obtained numerically from the boundary condition requiring that N_1 vanish at the walls by setting $f(a) = 0$. Usually the concentration of the added gas n_2 is small, and the third term can be ignored. Note that v_0 in the above equation and in eq. [6′] refers to the *maximum* velocity in a parabolic flow profile, and its value is exactly twice the value of v_0 in eq. [9] for equivalent volumetric flows. Thus, the correction for parabolic flow which has to be applied to the rate

[2]Address: Science Center, North American Rockwell Corp.

constant obtained in the usual way from eq. [9] is the factor 2/1.237 = 1.617. Full details concerning the solution of the above differential equation will appear shortly[3].

REPLY TO MARK CHER

If one is willing to ignore the axial diffusion term in eq. [6′] the equation becomes immediately separable in its variables and can be readily solved as Dr. Cher has done. Other approximate solutions in series form can be obtained even while retaining the axial diffusion term, although the convergence of such series is unfortunately slow and particularly troublesome near walls and in the vicinity of point sources, i.e., exactly where neglect of the axial diffusion term in Cher's approach raises the most concern.

While one can hope that approximate solutions using either approach will not seriously affect the values of rate coefficients obtained in flowing afterglow experiments, I am not aware of any quantitative evaluations of the errors introduced by such approximations.

SUMMARY BY CHAIRMAN, T. M. DONAHUE[4]

As was the case with recombination coefficients, the general state of accord between laboratory measurements and ionospheric requirements is good for ion–molecule reactions. It is gratifying to find that the rate coefficients for removal of O^+ by N_2 and O_2 decrease with temperature as this chairman requested a couple of years ago. It remains to be seen whether the rate constant for $N_2^+ + O \rightarrow NO^+ + N$ will conform also.

On the other hand, it is alarming that the rate constant for $N^+ + O_2$ did not drop. This creates quite a problem because N^+ densities in the F region are much higher than can be reconciled with removal rate constants of order 10^{-9} cm^3 s^{-1} and conventional sources of N^+. Similar difficulties exist in explaining He^+ densities (and H^+ densities also). Except for O^+, in fact, atomic ion densities all seem to present aeronomic problems. Recent measurements in auroras by Narcisi and the Pittsburgh group show that even below 150 km there are three orders of magnitude greater He^+ densities than can be reconciled with a 10^{-9} cm^3 s^{-1} rate constant with N_2. The ratio of H^+ to O^+ at low altitudes suggests that $H^+ + O$ and $O^+ + H$ have different, temperature dependent, cross sections at low energy. The problems of getting rid of Mg^+, Ca^+, Na^+, etc. in "metal" ion layers is now acute in view of Fehsenfeld's report that the oxides of these ions are rapidly reduced by atomic oxygen.

Another problem to be solved is that of forming hydrates of hydronium ions in the D region. The B.R.L. group (9) (Lineberger and Puckett, 1968) has shown that NO^+ can be converted to $NO^+ \cdot H_2O$. Fehsenfeld and Ferguson (10) may have found a chain which converts this ion to $H_3O^+ \cdot (H_2O)_n$. This possibility richly deserves to be followed up.

It also would be interesting to know how the rate constant for $O^+ + N_2(V^*)$ varies with the kinetic energy of the collision partners for various vibrational levels. There is some good indication in auroras that removal of O^+ by N_2 may be slow in spite of high vibrational temperatures.

Problems obviously remain, and the general dependence of rate constants on excitation of ions and neutrals is an outstanding one. However, the situation is gratifyingly better than it was at the Berkeley symposium.

---

[3]M. Cher and C. S. Hollingsworth. *In* Advan. Chem. Ser. In press.

[4]Address: Physics Department, University of Pittsburgh, Pittsburgh, Pennsylvania 15213.

9. W. C. LINEBERGER and L. J. PUCKETT. DASA Symposium, Waltham, Mass. June 1968.
10. F. C. FEHSENFELD and E. E. FERGUSON. Private communication.

Can. J. Chem. Downloaded from www.nrcresearchpress.com by 210.87.254.40 on 09/05/12
For personal use only.

Can. J. Chem. Downloaded from www.nrcresearchpress.com by 210.87.254.40 on 09/05/12
For personal use only.

Negative ion – molecule reactions

E. E. FERGUSON
Aeronomy Laboratory, Environmental Sciences Services Administration Research Laboratories, Boulder, Colorado

Laboratory reaction rate constant measurements for negative ion – atom interchange reactions, negative ion charge transfer reactions, and negative ion three-body association reactions of aeronomic interest are reviewed and the available data tabulated. The present experimental techniques in use are briefly summarized. Most of the rate constants have been measured only at 300 °K; in a few cases data is available at energies $\gtrsim$ 1 eV, as well as at 300 °K, so that an indication of the energy dependence of the rate constants is available.

Canadian Journal of Chemistry, 47, 1815 (1969)

Introduction

Almost the entire available knowledge concerning negative ion – molecule reactions of atmospheric interest has been acquired since the I.A.G.A. Aeronomy Symposium held in Berkeley in 1963. The subject of positive and negative ion low energy charge exchange and ion – molecule reactions was reviewed then by Paulson (1), and at the time the only negative ion reaction rate of atmospheric interest known was the reaction

[1] $$O^- + NO_2 \rightarrow NO_2^- + O$$

which had been measured by Henglein and Muccini (2) and found to have a rate constant $\sim 3 \times 10^{-9}$ cm^3/s. (This rate constant has been subsequently measured by three groups and found to be 1.2×10^{-9} cm^3/s at 300 °K.) By way of contrast, a recent review (3) tabulated 15 negative ion neutral reactions of atmospheric interest and fairly detailed negative ion reaction schemes for the atmosphere have now been proposed (4, 5). At least 4 different laboratory groups, utilizing 4 different experimental techniques, have now obtained rate constant data on negative ion – neutral molecule reaction processes.

The negative ion composition of the ionosphere has as yet not been determined experimentally so that even the qualitative predictions based on laboratory measurements have not been subjected to critical test. This is in contrast to the situation for the positive ion chemistry in which direct rocket borne mass spectrometer ion measurements have allowed detailed, quantitative checks of the most important positive ion reaction rate constants, for at least the E and F1 ionospheric layers.

The present review is concerned only with negative ion reactions with neutral molecules, and specifically reactions in which a different heavy negative ion is a product of the reaction. This excludes processes of electron attachment and detachment from neutrals. One of the more important negative ion – neutral molecule reaction processes occurring in the D region is the associative-detachment process in which an electron is released from a negative ion. This process has long been expected theoretically, but was discovered experimentally only in 1966. This class of reactions is included in the electron attachment and detachment processes reviewed by Phelps (6) in the current symposium.

The binary negative ion reactions known which appear likely to be important in the earth's atmosphere are listed in Table I. Brief discussions of some aspects of the role of these reactions in the quiet D region have been given by Fehsenfeld *et al.* (4), Fehsenfeld and Ferguson (7), and Ferguson (3). Recently, LeLevier and Branscomb (5) have presented a discussion of the role of negative ion chemistry in certain disturbed atmospheric conditions. In many respects, more useful observations exist for comparison of the broad atmospheric negative ion behavior with theoretical prediction for disturbed atmospheric conditions. The limited available data for negative ion three-body association reactions are given in Table II.

Discussion of Measurements

Different measuring techniques are often complementary in their capabilities and the energy ranges over which they can be operated. It is very desirable (and of course generally recognized) that the important reactions should be

TABLE I

Binary ionospheric negative ion reactions

Reaction	Rate constant (cm^3/s)	Method†	Energy	Reference
$O^- + O_3 \rightarrow O_3^- + O$	7.0(−10)*	f.a.	300 °K	4
	5.3(−10)	f.a	300 °K	13
$O_2^- + O_3 \rightarrow O_3^- + O_2$	3.0(−10)	f.a.	300 °K	4
	4.0(−10)	f.a.	300 °K	13
$O^- + NO_2 \rightarrow NO_2^- + O$	1.2(−09)	f.a.	300 °K	13
	1.1(−09)	beam	extrap.‡	10
	~3.0(−09)	m.s.		2
	1.0(−09)	m.s.	~1 eV	8
$O^- + NO_2 \rightarrow O_2^- + NO$	1.8(−11)	m.s.	~1 eV	8
$O_2^- + NO_2 \rightarrow NO_2^- + O_2$	8.0(−10)	f.a.	300 °K	13
	1.5(−09)	beam	extrap.	10
$O_3^- + NO_2 \rightarrow NO_2^- + O_3$	7.0(−10)	beam	extrap.	10
$O_3^- + NO_2 \rightarrow$?§	1.9(−10)	f.a.	300 °K	16
$H^- + NO_2 \rightarrow NO_2^- + H$	2.9(−09)	f.a.	300 °K	13
	5.0(−10)	beam	extrap.	10
$OH^- + NO_2 \rightarrow NO_2^- + OH$	1.0(−09)	f.a.	300 °K	13
	1.4(−09)	beam	extrap.	10
$NH_2^- + NO_2 \rightarrow NO_2^- + NH_2$	1.0(−09)	f.a.	300 °K	13
$CO_3^- + NO \rightarrow NO_2^- + CO_2$	9.0(−12)	f.a.	300 °K	4
$F^- + NO_2 \rightarrow NO_2^- + F$	<2.5(−11)	f.a.	300 °K	13
	~1.5(−11)	beam	3 eV	14
$Cl^- + NO_2 \rightarrow NO_2^- + Cl$	<6.0(−12)	f.a.	300 °K	13
	slow	beam	5 eV	14
	4.0(−11) to 4.0(−10)	m.s.		9
$O_3^- + CO_2 \rightarrow CO_3^- + O_2$	4.0(−11)	f.a.	300 °K	4
$CO_3^- + O \rightarrow O_2^- + CO_2$	8.0(−11)	f.a.	300 °K	4
$O_3^- + NO \rightarrow NO_3^- + O$	1.0(−11)	f.a.	300 °K	4
$NO_2^- + O_3 \rightarrow NO_3^- + O_2$	1.8(−11)	f.a.	300 °K	7
$NO^- + O_2 \rightarrow O_2^- + NO$	9.0(−10)	f.a.	300 °K	15
$CO_3^- + NO_2 \rightarrow NO_3^- + CO_2$	8.0(−11)	f.a.	300 °K	16
$N_2O^- + O_2 \rightarrow O_3^- + N_2$	fast	f.a.	80 °K	16
$O_3^- + N_2 \rightarrow$ products	<1.0(−15)	f.a.	300 °K	16
$O_3^- + SiO \rightarrow SiO_3^- + O$	fast	f.a.	300 °K	16
$O_3^- + CO \rightarrow$ products	slow	f.a.	300 °K	16
$O_2^- + SO_2 \rightarrow SO_2^- + O_2$	5.4(−10)	f.a.	300 °K	16
$O_3^- + SO_2 \rightarrow SO_3^- + O_2$	5.1(−10)	f.a.	300 °K	16
$O_3^- + SO_2 \rightarrow SO_4^- + O$				

*(−10) ≡ 10^{-10}.
†m.s. refers to mass spectrometer ion source measurements, f.a. refers to flowing afterglow experiments, and beam refers to crossed beam studies.
‡Extrap. means that beam studies above 2 eV ion energy were extrapolated to thermal energy assuming a "smooth" energy dependence of the cross section.
§Product ion uncertain, either NO_3^- or NO_2^- or both.

measured in several different ways when this is possible. A comparison of measurements made by different techniques greatly aids in the evaluation of the precision and reliability of the different methods. It also acts as a safeguard against errors which may arise in experiments due to such factors as lack of knowledge of reactant states, and various subtle experimental problems which may be somewhat hidden in any particular experiment.

A. Mass Spectrometer Experiments

Historically, most positive ion reaction measurements have been carried out in mass spectrometer ion sources. This has not been true, however, of *ionospheric* positive ion reactions and is not true for negative ion reactions in general. The role of mass spectrometer ion source measurements in the elucidation of ionospheric negative ion chemistry is expected to continue to be limited because so many of the most critical re-

Can. J. Chem. Downloaded from www.nrcresearchpress.com by 210.87.254.40 on 09/05/12
For personal use only.

TABLE II

Three-body negative ion reactions

Reaction	Rate constant (cm^6/s)	Method*	Reference
$O^- + 2CO_2 \rightarrow CO_3^- + CO_2$	9.0(−29)	d.t.	17
$O^- + CO_2 + He \rightarrow CO_3^- + He$	1.5(−28)	f.a. (300 °K)	16
$O_2^- + 2CO_2 \rightarrow CO_4^- + CO_2$	9.0(−30)	d.t.	17
$O_2^- + CO_2 + O_2 \rightarrow CO_4^- + O_2$	2.0(−29)	d.t.	17
$O^- + 2O_2 \rightarrow O_3^- + O_2$	9.0(−31)	d.t.	18
	7.5(−31)	d.t.	19
$O^- + N_2 + He \rightarrow N_2O^- + He$	~1.0(−30)	f.a. (80 °K)	16
$O_3^- + 2N_2 \rightarrow$ products	<1.5(−31)	f.a. (300 °K)	16

*d.t. refers to drift tube, and f.a. refers to flowing afterglow experiments.

actions involve relatively unstable neutral reactants, such as atomic oxygen and ozone, which have not been successfully used in positive or negative ion studies in mass spectrometer ion sources. Also, the most important atmospheric negative ions (e.g. O_2^-, O_3^-, CO_3^-, etc.) are not produced by direct electron impact on a stable gas and accordingly are not suitable for the typical low pressure mass spectrometer ion source studies.

Several mass spectrometer ion source measurements are tabulated in Table I. The early observation by Henglein and Muccini (2) that O^- charge transfers rapidly with NO_2 has subsequently been borne out by more precise measurements. The recent measurement by Paulson (8) of the same reaction has been well supported by the flowing afterglow measurement.

The report by Curran (9) that Cl^- charge transfers rapidly with NO_2 has not been supported, however, by either the thermal energy flowing afterglow results (4) or by a reasonable extrapolation to low energies of the higher energy crossed beam measurements (10).

B. Crossed Beam Measurements

The crossed beam studies carried out by Rutherford and Turner (10) at General Atomic have been valuable in the study of charge transfers of various negative ions to NO_2. The measurements were actually carried out at energies above 2 eV, up to several hundred eV in most cases, and Rutherford and Turner extrapolated their values to thermal (ionospheric) energies. A comparison of their results with thermal energy measurements shows that the charge transfer rate constants do not have a marked energy dependence in the cases studied. The same conclusion was obtained for many positive ion charge transfer reactions studied as a function of energy using the crossed beam technique.

Negative ion – atom interchange reactions have not been studied in crossed beam experiments. Probably these reactions will often not be fast at the several volts and greater energies at which the beam reactions are studied. One complication in the extrapolation of charge transfer rate constants from beam energies to the ionospheric energy range arises if a fast ion – atom interchange process becomes significant at energies below the lowest beam energy studied. One example of such a situation may occur for the reaction

$$[2] \qquad O_3^- + NO_2 \rightarrow NO_2^- + O_3$$

which Rutherford and Turner (10) measured for kinetic energies from 25–400 eV. They extrapolated their data to obtain a 300 °K rate constant of 7×10^{-10} cm^3/s. However, it is not unlikely that at thermal energies, the reaction goes as

$$[3] \qquad O_3^- + NO_2 \rightarrow NO_3^- + O_2$$

rather than by charge transfer! The flowing afterglow results suggested that this might be the case, but were inconclusive and must be repeated with additional measurements (the O_3 concentration) simultaneously carried out in order to resolve this point.

C. Afterglow Measurements

Fite and Rutherford (11) made some interesting qualitative observations on negative ions in air and oxygen afterglows using a stationary afterglow method in which ions were sampled as a

Can. J. Chem. Downloaded from www.nrcresearchpress.com by 210.87.254.40 on 09/05/12
For personal use only.

Can. J. Chem. Downloaded from www.nrcresearchpress.com by 210.87.254.40 on 09/05/12
For personal use only.

function of time following cessation of a discharge in the gas. They found the ion sampling efficiency to vary with time in the afterglow and this effect precluded any quantitative rate measurements in the stationary afterglows.

The flowing afterglow system developed in the Environmental Sciences Services Administration Laboratory has proved to be very useful for negative ion reaction studies. Most of the reactions tabulated in Table I have been measured by this method. For the ion – atom interchange reactions, few other measurements exist. The flowing afterglow measurements of negative ions have so far been carried out at 300° K. Recently, a new temperature controlled flowing afterglow system has been constructed which operates in the temperature range 82–600 °K. The rate constants of Table I will in time be measured over this temperature range, which includes the temperature range of most concern for atmospheric negative ion reactions.

D. Drift Tube Measurements

So far the application of drift tubes to negative ion studies of atmospheric interest has been concentrated on three-body rate constant measurements. Most of the three-body rate constants of Table II have been measured in drift tubes. The recent upsurge in binary positive ion reaction measurements in drift tubes will perhaps be followed by similar negative ion measurements.

A particular advantage of the drift tube technique is in the capability of varying the reactant ion kinetic energy over a range of values. Variations in ion kinetic energy cannot be assumed in all cases to be equivalent to similar variations in gas temperature in which rotational and vibrational degrees of freedom are equilibrated as well as translational, but will in any case provide very useful data. The temperature or energy variation feature is not so important for ionospheric negative ion charge-transfer and ion – atom interchange reactions as it is in the case of ionospheric positive ion reactions, because the range of temperatures in the D region where negative ions can be important is so much more limited. However, three-body reaction rate constants appear to be much more dependent on temperature than binary reaction rate constants. One difficulty with drift tube measurements, as well as mass spectrometer ion source and crossed beam experiments, will be to achieve ion energies in the sub-300 °K temperature range characteristic of the D region. The afterglow technique, which has been successfully operated at 82 °K with all degrees of freedom equilibrated, has a distinct advantage in this respect.

On the other hand, the drift tube can be used to measure reactions which are endothermic at thermal energy. Slightly endothermic collisional dissociation of negative ion clusters may prove to be important in controlling their concentration in the D region, as one possible application where the drift tube could provide perhaps unique data. Moruzzi and Phelps have successfully determined the stability of the negative ion CO_4^- in drift tube studies, for example (17). The drift tube technique is, of course, quite restricted in the variety of reactants which can be studied.

General Discussion

The Cl^- charge transfer with NO_2 has been included in this review, not because that particular reaction is expected to be of direct ionospheric interest, but because Curran's report that this process was fast has led to the widely accepted conclusion that the process was exothermic, and consequently that the NO_2 electron affinity exceeded that of Cl. Since the recent studies do not find this charge transfer to occur at thermal energies, this conclusion should be reexamined. The value of the NO_2 electron affinity is of some importance in the physics and chemistry of the D region. The observation that F^- does not charge transfer rapidly with NO_2 is also reported in Table I for the same reason, F having about the same electron affinity as Cl. Observation of charge transfer reactions at thermal energy is often a useful way to obtain limits on electron affinities. For example, the observation of fast NO^- charge transfer with O_2 establishes an upper limit of 0.46 eV on the NO electron affinity.

Since there are no serious discrepancies between negative ion rate constants measured by different experimental techniques and since no quantitative atmospheric negative ion chemistry models or direct ionospheric negative ion measurements exist, the question of the precision of measurement is not at this time one of compelling urgency so far as aeronomy is concerned.

In favorable cases, the flowing afterglow and the mass spectrometer ion source techniques are probably reliable to within 30%. This is supported by the intercomparison of the techniques

Can. J. Chem. Downloaded from www.nrcresearchpress.com by 210.87.254.40 on 09/05/12
For personal use only.

on the $O^- + NO_2$ charge transfer (Table I) and by very much more extensive comparisons for positive ion reactions where the measurement precision considerations are presumably not essentially different. In addition, the flowing afterglow measurements on several negative ion associative-detachment reactions have been compared with drift tube measurements and the agreement has been consistent with such estimated error limits. The uncertainties in reactions involving unstable neutrals such as O, O_3, and even NO_2 are greater than for reactions involving stable neutral reactants such as NO and CO_2, however, due to the greater difficulty of reactant concentration measurements in these cases.

The unknown distribution of vibrational states in the *molecular* negative ion reaction experiments so far carried out adds an element of uncertainty to their measured reaction rate constants. In principle it seems possible to resolve this uncertainty to some extent in flowing afterglow experiments since the lifetime of the negative ion prior to reaction can be varied. Experience would suggest that exothermic charge transfer reactions will not be sensitive to the vibrational state of the molecular ion, since indeed they seem relatively insensitive even to the choice of ion.

Recent refinements in data analysis along with certain improvements in experimental apparatus suggest that flowing afterglow measurements can probably be refined to $\pm 10\%$ type errors in future experiments for favorable cases such as reactions involving stable neutral reactants.

For the near future, aeronomical D region calculations are more likely to be limited by uncertainties in the critical neutral constituent concentrations (e.g. NO, O_3, O, NO_2, and CO_2) than by the uncertainties in reaction rate constants.

Need for Future Work

Of most concern are the possibilities of important reactions not yet considered. To date, no negative ion reactions of the kind considered in this review have been measured involving excited states of the neutral reactants as one example of interest.

A possibility which has been pointed out by Pack and Phelps (12) is that the primary negative ions may rapidly cluster in the lower ionosphere. Ions such as CO_4^-, $O_2^-(H_2O)_n$, $NO_2^-(H_2O)_n$, etc., may be very important. Therefore a number of three-body association reactions of the type

$$X^- + A + M \rightarrow AX^- + M$$

may be of considerable importance. The very limited available data of this type is compiled in Table II, without regard for whether the specific processes tabulated there are likely to occur in the earth's atmosphere or not, since a knowledge of the magnitudes of the few observed rate constants may be helpful in attempting to estimate probable ranges of such three-body coefficients, prior to measurements of the appropriate processes in the laboratory.

A considerable amount of effort will be required in three-body measurements in order to furnish the data which can be expected to be important in the ionosphere. Each cluster ion forming reaction has the new degree of variability associated with different possible third bodies. One would like to know the efficiencies of both O_2 and N_2 in most D region negative ion association reactions. Additionally, the effect of temperature variations on three-body rate constants is generally very much greater than it is for the binary charge transfer and ion – atom interchange reactions.

Finally, one of the more important clustering agents in the D region is likely to be the polar H_2O molecule, which is very difficult to work with quantitatively in the laboratory. Recent developments in the technology of laboratory ion – molecule reaction rate constant measurements certainly will assure a steady increase in the quantitative data required for aeronomical applications.

1. J. F. PAULSON. Ann. Geophys. **20**, 18 (1964).
2. A. HENGLEIN and G. A. MUCCINI. J. Chem. Phys. **31**, 1426 (1959).
3. E. E. FERGUSON. Rev. Geophys. **5**, 305 (1967).
4. F. C. FEHSENFELD, A. L. SCHMELTEKOPF, H. I. SCHIFF, and E. E. FERGUSON. Planetary Space Sci. **15**, 373 (1967).
5. R. E. LELEVIER and L. M. BRANSCOMB. J. Geophys. Res. **73**, 27 (1968).
6. A. V. PHELPS. Can. J. Chem. This issue.
7. F. C. FEHSENFELD and E. E. FERGUSON. Planetary Space Sci. **16**, 701 (1968).
8. J. F. PAULSON. Advan. Chem. Ser. **58**, 28 (1966).
9. R. K. CURRAN. Phys. Rev. **125**, 910 (1962).
10. J. A. RUTHERFORD and B. R. Turner. J. Geophys. Res. **72**, 3795 (1967).
11. W. L. FITE and J. A. RUTHERFORD. Discussions Faraday Soc. **37**, 192 (1964).
12. J. L. PACK and A. V. PHELPS. J. Chem. Phys. **45**, 4316 (1966).
13. E. E. FERGUSON, F. C. FEHSENFELD, and A. L. SCHMELTEKOPF. Advan. Chem. Ser. In press.

14. B. R. TURNER, D. M. J. COMPTON, and J. W. McGOWAN. General Atomic Report 7419, Nov. 14, 1966.
15. F. C. FEHSENFELD, E. E. FERGUSON, and A. L. SCHMELTEKOPF. J. Chem. Phys. **45**, 1844 (1966).
16. F. C. FEHSENFELD. Unpublished results.
17. J. L. MORUZZI and A. V. PHELPS. J. Chem. Phys. **45**, 4617 (1966).
18. D. S. BURCH and R. GEBALLE. Phys. Rev. **106**, 183, 188 (1957).
19. E. C. BEATY, L. M. BRANSCOMB, and P. L. PATTERSON. Bull. Am. Phys. Soc. **9**, 535 (1964).

Comments

COMMENTS BY F. E. NILES

Your statement about the possible importance of clustering agents, particularly H_2O, in the D region for the negative ions is supported by recent laboratory measurements at BRL. Photoionization of a small admixture of NO in a few hundred mTorr of laboratory air resulted in $HN_2O_4^-$ (mass 93) being the dominant negative ion. Other negative ions in decreasing order of the mass spectrometric abundance were $NO_2^- \cdot H_2O$ (mass 64), $NO_2^- \cdot 2H_2O$ (mass 82), NO_2^- (mass 46), and $NO_2^- \cdot 3H_2O$ (mass 100). Other negative ions were also observed.

Can. J. Chem. Downloaded from www.nrcresearchpress.com by 210.87.254.40 on 09/05/12
For personal use only.

Can. J. Chem. Downloaded from www.nrcresearchpress.com by 210.87.254.40 on 09/05/12
For personal use only.

Absorption cross-sections of atmospheric gases for use in aeronomy

ROBERT E. HUFFMAN[1]
United States Air Force Cambridge Research Laboratory, Bedford, Massachusetts

Received November 21, 1968

The current status of absorption cross-section measurements for aeronomic use is reviewed. Recommended values for the gases O_2, N_2, O, and O_3 are given at wavelengths where there is strong atmospheric absorption in the 3500–10 Å region. A table of absorption and ionization cross-sections at important solar emission lines is given. The problem of insufficient resolution at some wavelengths is discussed, and information on photolysis products is given where available.

Canadian Journal of Chemistry, 47, 1823 (1969)

Introduction

The absorption of solar radiation in the ultraviolet to soft X-ray region is well established as one of the most important mechanisms for creating and maintaining the unique characteristics of the upper atmosphere. As the radiation is absorbed, new constituents such as ions, electrons, and atoms are formed, and the intensity at the absorbed wavelengths is reduced, until at ground level only wavelengths greater than about 2900 Å are observed. The pattern of the absorption is complicated, depending on the variation of absorption with wavelength for each constituent, the atmospheric composition as a function of altitude, and the detailed intensity distribution of the solar spectrum. To understand this absorption profile, it is necessary to have laboratory measurements of the absorption cross-section, or absorption coefficient, which is a measure of the total attenuation of radiation at a given wavelength. This information is useful in aeronomy both to find the altitudes at which solar energy is deposited and to evaluate the flux remaining for further absorption at lower altitudes.

This article reviews the present status of laboratory absorption cross-section measurements and provides recommended values for aeronomical problems. Only wavelength regions and gases particularly important for atmospheric absorption are discussed in detail. The wavelength region considered is from roughly 3500 to 10 Å. The gases discussed at length are molecular oxygen, molecular nitrogen, atomic oxygen, and ozone. These four gases account for most of the solar absorption. There are several older reviews of this general subject (1–3).

[1]1967–68 address: Department of Physics, Imperial College, London, England.

The Absorption Cross-section

The absorption cross-section is defined by the usual absorption law (Beer–Lambert Law)

$$[1] \qquad I(\nu) = I_0(\nu) \exp [-\sigma(\nu)N]$$

In this expression $I(\nu)$ is the transmitted intensity, $I_0(\nu)$ is the intensity incident on the absorbing gas column, $\sigma(\nu)$ is the cross-section, and N is the number of absorbers (molecules or atoms) per cm^2 column in the light path. The cross-section σ is generally given in units of Megabarn (Mb), which is equal to 10^{-18} cm^2. The data may also be presented as the absorption coefficient k, with units of cm^{-1}. It is equal to $\sigma n_0 \cdot 10^{-18}$, where σ is in Mb, and Loschmidt's number n_0, is 2.69×10^{19} cm^{-3}.

The measurement procedure for the absorption cross-section involves finding $I(\nu)$ and $I_0(\nu)$ at known values of ν and N. It is only necessary to measure the ratio $I_0(\nu)/I(\nu)$ and thus the simpler relative calibration of the detector is adequate. For many cases, $\sigma(\nu)$ as calculated from eq. [1] is constant over a range of N values, and this cross-section can then be used to calculate the absorption or the number of absorbing molecules in atmospheric problems. There are, however, important cases discussed in a separate section where the typical laboratory resolution is inadequate and various approximate $\sigma(\nu)$ values must be given.

No review of the experimental details of the light sources, monochromators and spectrographs, and detectors used will be given here. These are covered fully in the references and in reviews (4) and (5).

The absorption cross-section curve itself provides little information about products or excited states formed as a result of the absorption. At most wavelengths considered here, there are a

Can. J. Chem. Downloaded from www.nrcresearchpress.com by 210.87.254.40 on 09/05/12
For personal use only.

number of possibilities including excitation, dissociation, ionization, dissociative ionization, and various other combinations of these processes. The products of dissociation or ionization processes may be left in excited states, and in some cases these states may become deactivated by emission of radiation.

In the observed spectrum or cross-section curve, excitation produces the normal molecular bands and atomic lines generally measured and classified in absorption spectroscopy. Dissociation and ionization processes are indicated by absorption continua. Diffuse bands or lines are an intermediate case and indicate predissociation or autoionization processes. In the wavelength range discussed here, a number of different processes usually occur at the same wavelength.

The absorption cross-section can be considered to represent the sum of partial cross-sections of the various detailed processes. The partial cross-sections give the fractional amounts of the different products resulting from the absorption. For example, the cross-sections for ionized and non-ionized products can be given. For partial cross-sections, a quantitative measurement of the products is required, which generally presents experimental difficulties. Some processes can usually be ruled out by energy considerations. The cross-sections involving photoionization will be dealt with in a separate paper at this symposium.

The photodissociation cross-section and products are of considerable interest, for both the major and minor atmospheric gases, but little detailed information is available. Photochemical investigations may give information on products at some wavelengths. A review is available (6) for many atmospheric gases.

The absorption cross-section is also related to the oscillator strength of the transition (7), and the oscillator strength can be obtained directly from an integration of the observed cross-section curve at sufficiently high resolution. This aspect of the subject is not discussed since oscillator strengths are covered by another paper in this symposium.

Resolution Problems

The resolution of the spectrometer is generally not adequate for atomic lines or sharp molecular bands encountered in the spectrum. Using the normal procedure given above, the cross-section calculated from [1] is not constant but usually decreases with increase in N, and thus more detailed consideration must be given before applying the laboratory measurements to atmospheric problems. The actual cross-section is very large at the line center and rapidly becomes weak away from the center. When a measureable change in transmission is detectable, the narrow, strongly absorbing center of the line is already completely absorbed. The change in absorption with the change in number of absorbers is thus controlled by the weaker absorption in the wings of the line. The cross-section thus appears to become smaller as the amount of gas in the light-path increases.

The problem may be approached by examining the typical spectrometer experiment using continuum background radiation in more detail. The instrument provided a narrow range of frequencies around the nominal value, and an absorption measurement is actually made over this frequency range. If the intensity–frequency relation of the radiation provided at the exit slit at a given nominal spectrometer position ν_0 is $F(\nu)$, then the result of an absorption measurement will be

$$[2] \qquad \frac{I(\nu_0)}{I_0(\nu_0)} = \frac{\int F(\nu) \exp\left[-\sigma(\nu)N\right] d\nu}{\int F(\nu)\, d\nu}$$

The integrations are over the range where $F(\nu)$ has an appreciable value. For a continuum background source, $F(\nu)$ frequently has an almost triangular shape and in this case the integration is effectively between $\pm a$, where a is the half-width. For a light source emitting sharp atomic lines, the frequency range transmitted is generally less than the half-width of $F(\nu)$ and depends on the excitation conditions in the light source. If $\sigma(\nu)$ is constant over the range of frequencies provided by the spectrometer, the exponential may be taken outside the integral in eq. [2], and the usual absorption law eq. [1] results.

For an isolated non-autoionized atomic line, and ignoring pressure-broadening as usually unimportant under atmospheric conditions, the shape of the line is due to a combination of Doppler and natural broadening, which is sometimes called the Voigt profile (7). For oxygen atom at 300 °K and an imaginary line at 1000 Å, the Doppler half-width is 3.1×10^{-3} Å. The natural width for an allowed transition ($\tau = 10^{-8}$ s) at

Can. J. Chem. Downloaded from www.nrcresearchpress.com by 210.87.254.40 on 09/05/12
For personal use only.

1000 Å is 5.3×10^{-6} Å. The typical bandwidth available is from about 0.5 to 0.05 Å. Thus, the absorption line is much narrower than the bandwidth. The values of $I(\nu_0)/I_0(\nu_0)$ obtained depend on the line shape $\sigma(\nu)$ and $F(\nu)$ as shown in eq. [2], and in general $\sigma(\nu)$ cannot be evaluated without some knowledge of the line shape to be expected.

This problem of obtaining useful information under conditions of inadequate resolution is a well-known difficulty in astrophysical and infrared investigations, and several procedures have been developed (7, 8). One technique is to obtain the integral of the absorption curve over a range of N. This is called the equivalent width, or sometimes the total absorption. The equivalent width W is equal to the following

$$[3] \qquad W = \int_0^\infty [1 - \exp(-\sigma(\nu)N)]\, d\nu$$

One can then obtain the "curve of growth" by plotting W against N. This curve would allow an estimate of N to be made if W values were obtained under similar conditions of absorbing gas environment, since W is independent of resolution over fairly wide limits (7, 8). The complete curve of growth for an atomic line is rather complicated even for an isolated line with only natural and Doppler broadening. However, under many conditions the center is completely absorbed and the strong line approximation is applicable, which means that W is proportional to $\sqrt{N}$. This behavior is found when the line has a Lorentz shape, which occurs when the absorption is controlled by the wings of the line. A demonstration of this effect for sharp O_2 bands has been given (9). Although little absorption data on atmospheric gases is now presented in this way, it is suggested that curves of W against N would be of use in some cases. It will be most useful when the solar radiation background is a continuum or when an artificially introduced continuum light source is used. Difficulties include partly overlapped lines, unusual autoionization profiles, and molecular bands.

Continuum background light sources are considered more useful than line sources in general because they give the absorption curve at all wavelengths and lead to a more complete understanding of the absorption processes. However, they give difficulty when a solar line of interest falls at an absorption band or line of the atmospheric gas, since the bandwidth of the continuum usually employed is much larger than the solar line half-width. For these cases, one approach has been to use a light source emitting lines at the solar wavelengths rather than a continuum (10). These lines may be much narrower than the continuum background bandwidths generally available, and thus they more nearly approximate the solar lines in half-width. They are also more intense than usual continuum sources. This is a useful interim procedure, but it is open to criticism for several reasons. First, the lines emitted may be quite different from the solar lines in shape, self-absorption, or relative multiplet intensities, due to differences in excitation conditions in the sun and in laboratory discharges. In fact, the laboratory lines may be as much as 0.1 Å wide (10), which is within the capability of continuum measurements. Furthermore, solar lines from highly ionized atoms are not usually produced in the typical laboratory source, so the continuum background must be used for these cases. Even when using lines, in some cases where $\sigma(\nu)$ varies with N using continuum radiation, a similar variation occurs using line sources. For further progress, more information about the solar line-shapes coupled with high resolution continuum data is needed. Continuum sources offer the advantage of improving the resolution in a straightforward way and of eventually interpreting the data more completely. These improvements in resolution and in knowledge of the solar line shape are not likely to become available soon. Thus, both continuum and line data are valuable to have at the present time, where a large number of measurements have not been made at some wavelengths, and data from both sources is included here.

In conclusion, it is apparent that considerably more attention must be given to cases where resolution is insufficient in order to extract the most information of aeronomic interest from laboratory measurements. In addition, some difficulties in comparing photon absorption and various electron impact experiments might have been avoided by earlier recognition and discussion of these resolution problems (11). Where resolution is not adequate, information about the number of absorbing species must be given. This is now usually given only as a range of values. A plot of transmission or measured apparent absorption cross-section for atmosphere values of N

Can. J. Chem. Downloaded from www.nrcresearchpress.com by 210.87.254.40 on 09/05/12
For personal use only.

TABLE I

Absorption and ionization cross-section of O_2, N_2, and O at solar lines

Solar line λ (Å)	Classification	O_2		N_2		O
		σ	σ_i	σ	σ_i	$\sigma = \sigma_i$
1215.7	H Ly α	0.010	0	$<6\times10^{-5}$	0	0
1206.5	Si(III)	15	0	~0	0	0
1175.7[a]	C(III)	1.3	0	—	0	0
1085.7[a]	N(II)	2[b]	0	—	0	0
1037.6[a]	O(VI)	0.78	0	$<7\times10^{-4}$	0	0
1031.9	O(VI)	1.04	0	$<7\times10^{-4}$	0	0
1025.7	H Ly β	1.58	0.98	$<10^{-3}$	0	[e]
991.6[a]	N(III)	1.75	1.21	1.9	0[b,c]	0
989.8[a]	N(III)	1.4	0.95[b,c]	1.1	0[c]	[e]
977.0	C(III)	4.0	2.5	0.7	0[c]	0
972.5	H Ly	32	25[b]	370	0[b,c]	0
949.7	H Ly	6.3	—[b]	5.2	—[b]	0
937.8	H Ly	5.0	—	10	—[b]	[e]
930.7	H Ly	26	17[b]	4.8	—[b]	[e]
904	C(II)	11	6.3[b]	6.3	—	3.5
835.3	O(III)	10	3.7	15	—[b]	[f]
835.1	O(III)	10	3.7	26	—[b]	3.2
834.5	O(II)	11	4.0	3.3	—[b]	[f]
833.7	O(III)	13	5.1	—	—[b]	3.2
832.9, 832.7	O(III)[d]	26	10	—	—[b]	[f]
790.2	O(IV)	28	10[b]	24[c]	11[b,c]	3.2
790.1	O(IV)	28	10[b]	26[c]	12[b,c]	3.2
787.7	O(IV)	24	13[b]	9[c]	8[c]	[f]
780.3	Ne(VIII)	28	11[b]	19	—	3.3
770.4	Ne(VIII)	18	11	15	—	[e]
765.1	N(IV)	23	12[b]	85[c]	66[b,c]	3.3
761.1	O(V)	20	10	40	22	[f]
703.8	O(III)	26	23	26	—	7
702.3	O(III)	24	—	26	—	7
686.3	N(III)	22	22	25[c]	24[c]	[e]
685.8	N(III)	18	18	26[c]	25[c]	7
685.5	N(III)	18	18	25[c]	24[c]	[e]
685.0	N(III)	26	26	25[c]	24[c]	7
629.7	O(V)	30	29	24[c]	24[c]	12
625	MgX	25	24	24	23	12
610	MgX	27	25	24	24	12
599.6	O(III)	28	27	23	22	12
584.3	He(I)	23	23	23	23	13
555.3	O(IV)	26	25	25	24	13
554.5	O(IV)	26	26	25	23	13
554.1	O(IV)	26	25	25	24	13
553.3	O(IV)	26	24	25	24	13
537.0	He(I)	21	21	25	24	12
525.8	O(III)	25	24	26	26	12
522.2	He(I)	21	21	24	23	12
508.2	O(III)	24	23	22	22	12
507.7[d], 507.4	O(III)	23	22	24	24	12
435.0	O(III)	21	21	24	24	12
430.2[d], 430.0, 429.9	O(II)	18	18	21	21	12
303.8	He(I)	17	17	12	12	9

NOTE: cross-sections in Mb (10^{-18} cm^2). Values based on data in refs. 1, 10, 17, 23, 24, 25, 28, 29, 31, and 36. Table prepared in collaboration with R. I. Schoen.

[a]Blend of several lines observed in solar spectrum.

[b]The absorbing gas has discrete structure at this wavelength and thus the cross-section presently measurable given in the table may not be applicable. See text and references.

[c]Considerable variation among measurements.

[d]These lines not resolved in laboratory cross-section measurement.

[e]Possible overlap with atomic oxygen ground state (^{3}P) absorption line. See Table III.

[f]Possible overlap with atomic oxygen metastable state (^{1}D) absorption line. See Table III.

Can. J. Chem. Downloaded from www.nrcresearchpress.com by 210.87.254.40 on 09/05/12
For personal use only.

would be of considerably more value. Throughout this review, regions where the structure has not been adequately resolved will be mentioned.

Cross-section Measurements

General

The following cross-section curves and tables are considered to be the best values available at the present time. In this review, consideration was given to all published values known to the author. The wavelength range covers the upper wavelength where appreciable absorption begins to about 10 Å. These values should be useful at atmospheric densities, except in wavelength regions mentioned where resolution is a problem. The atmospheric temperature may be considerably above or below room temperature, but most cross-sections are measured at room temperature. Where data at other temperatures are available, they are mentioned. The % uncertainties have not been estimated, but they are in the range $\pm 10\%$ except at lines or bands.

In addition to the gases treated in detail, there are a number of minor constituents whose absorption cross-sections are of less importance in aeronomy. The atomic gases in this category include H, N, Ar, He, Na etc., and recent reviews are available (12, 13). Molecular gases include NO, NO_2, N_2O, H_2O, CO_2, CO, H_2, CH_4, etc. Data on these gases have been reviewed (1, 13).

The cross-section in regions where the solar radiation largely consists of strong emission lines is difficult to obtain from published curves. Table I lists the total absorption and total ionization cross-section at these lines from 1215.7 Å (H Ly α) to 304 Å (He Ly α). In order to provide a consistent review within this symposium, Table I was prepared jointly with R. I. Schoen, who discusses ionization cross-sections in detail in another paper.

One problem in the application of laboratory data to atmospheric problems is the unavailability of large-scale cross-section curves. These are frequently not published even when prepared because of space limitations in journals. Such curves are available to aeronomists, by request, from the author. These curves were prepared in connection with previous work from this laboratory. At present, N_2 and O_2 in the 600–1000 Å region at a bandwidth of 0.5 Å are available. It is planned to improve these data in wavelength range and resolution in the near future.

TABLE II

Absorption cross-sections[a] at wavelengths less than 304 Å.

Wavelength[b] (Å)	O_2	N_2	O
247.2	12.3	9.8	6
209.3	9.0	6.5	4
100	1.9	0.84	0.8
68.0	0.9	0.50	0.2
44.6	0.31	0.18	0.1
13.4	0.29	0.089	0.14[c]
9.9	0.14	0.042	0.071[c]

NOTE: Data primarily from refs. 12, 36, and 47. Cross-section in Mb (10^{-18} cm^2).

[a]These cross-sections are assumed to be equal to the ionization cross-section at least to 100 Å, although there are no yield measurements. See also paper by R. I. Schoen in this symposium.

[b]There are a number of solar lines in this region, but there have been few measurements, and also the cross-section curve appears to be relatively smooth. The wavelengths used should allow a reasonable estimate to be made.

[c]This value is one-half the O_2 cross-section.

Molecular Oxygen

Molecular oxygen has important absorption from 2600 Å to lower wavelengths. Cross-section data are given in Figs. 1 to 6. Lower wavelengths are included in the atomic oxygen cross-section curves presented later. Absorption cross-section values at the more intense solar lines are given in Table I, and Table II gives shorter wavelengths. In most cases, at least two measurements are available, and the data are in reasonably good agreement. There are many investigations of the absorption spectrum given in the references.

The weak Herzberg continuum in the 2600–1850 Å region shown in Fig. 1 is usually considered as the primary source of oxygen atoms below 80 km. In this dissociation process, two

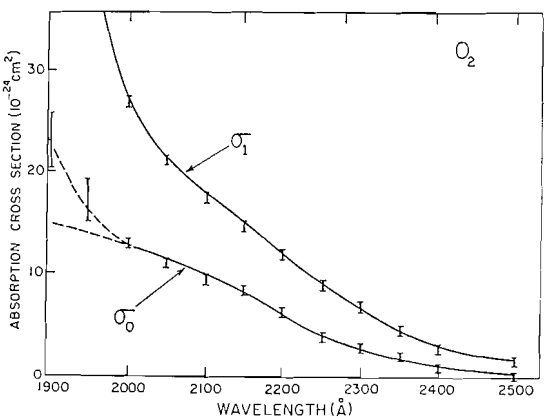

FIG. 1. Molecular oxygen absorption cross-sections; σ_0, value extrapolated to zero pressure; σ_1, 1 atm data, ref. (14).

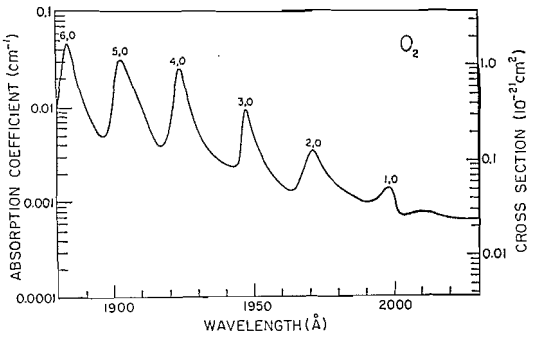

FIG. 2. Molecular oxygen absorption cross-sections, Schumann–Runge bands, ref. (9).

ground state (^3P) oxygen atoms are formed, since there is not sufficient energy to excite the metastable ^1D and ^1S atoms at these wavelengths. There are two measurements in fairly good agreement (14, 9). The cross-sections are very small, and the high pressures necessary result in formation of some O_4 dimer in the cell, so extrapolation to zero pressure is necessary.

The Schumann–Runge bands ($^3\Sigma_u^- \leftarrow {}^3\Sigma_g^+$) between 1750 and 2010 Å require high resolution to obtain accurate cross-sections (1, 9, 15). It is also difficult to separate the Herzberg continuum and the Schumann–Runge bands in the 1900–2030 Å region. Absorption data (9) are given in Figs. 2 and 3, but these are averaged values because of insufficient resolution. It is likely that much experimental work will be done on these bands in the future with high resolution.

The strong Schumann–Runge continuum (1250–1750 Å) is very important, since it is the primary source of oxygen atoms at altitudes greater than 80 km. The cross-section has been

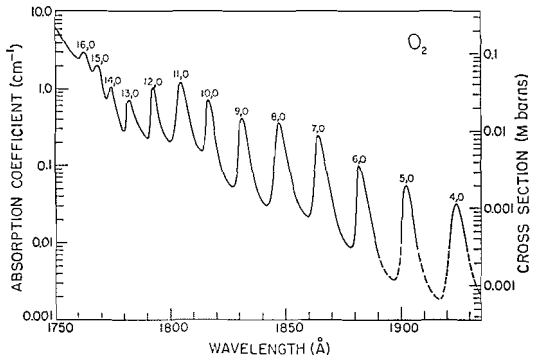

FIG. 3. Molecular oxygen absorption cross-sections, Schumann–Runge bands, ref. (9).

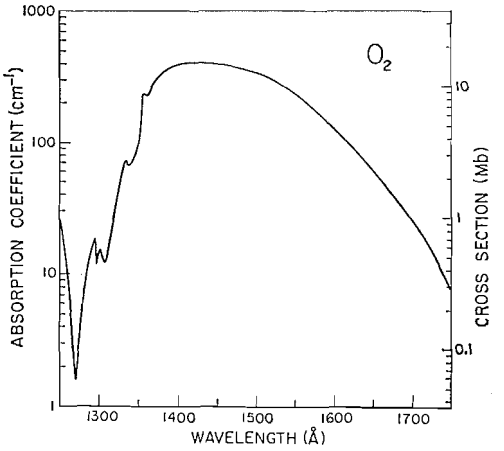

FIG. 4. Molecular oxygen absorption cross-sections, Schumann–Runge continuum, ref. (9).

measured repeatedly with photoelectric techniques with generally good agreement (1, 9, 16–18), and a representative curve (9) is given in Fig. 4. Absorption in the principal continuum is believed to produce one ground state (^3P) and one metastable (^1D) oxygen atom. Evidence from photochemically induced secondary reactions and from emission has been given for $O(^1D)$ production (19, 20), but more direct observation and quantitative cross-sections are also needed. A temperature effect has been discussed (21), and an increase in cross-section with temperature has been found in the 1580–1950 Å region (22).

The spectrum from 1250 Å to the ionization potential at 1027.8 Å is very complex (1, 16). There are several "windows" of low cross-section, one of which corresponds almost exactly to the intense H Ly line. As is well known, this ionizing radiation can penetrate much deeper into the atmosphere than nearby wavelengths.

The region 1070 to 600 Å shown in Figs. 5 and 6 has been studied several times recently with continuum sources (23–25) and a line source (10). The measurements of refs. (25) and (10) are in best agreement and are given more weight in Table I. In this region, ionization and dissociation continua are overlapped by rather diffuse and generally autoionized bands. The dissociation continua in this region have recently been given (25).

Appreciable quantities of the metastable O_2 $a^1\Delta_g$ molecule appear to be present in the upper

Can. J. Chem. Downloaded from www.nrcresearchpress.com by 210.87.254.40 on 09/05/12
For personal use only.

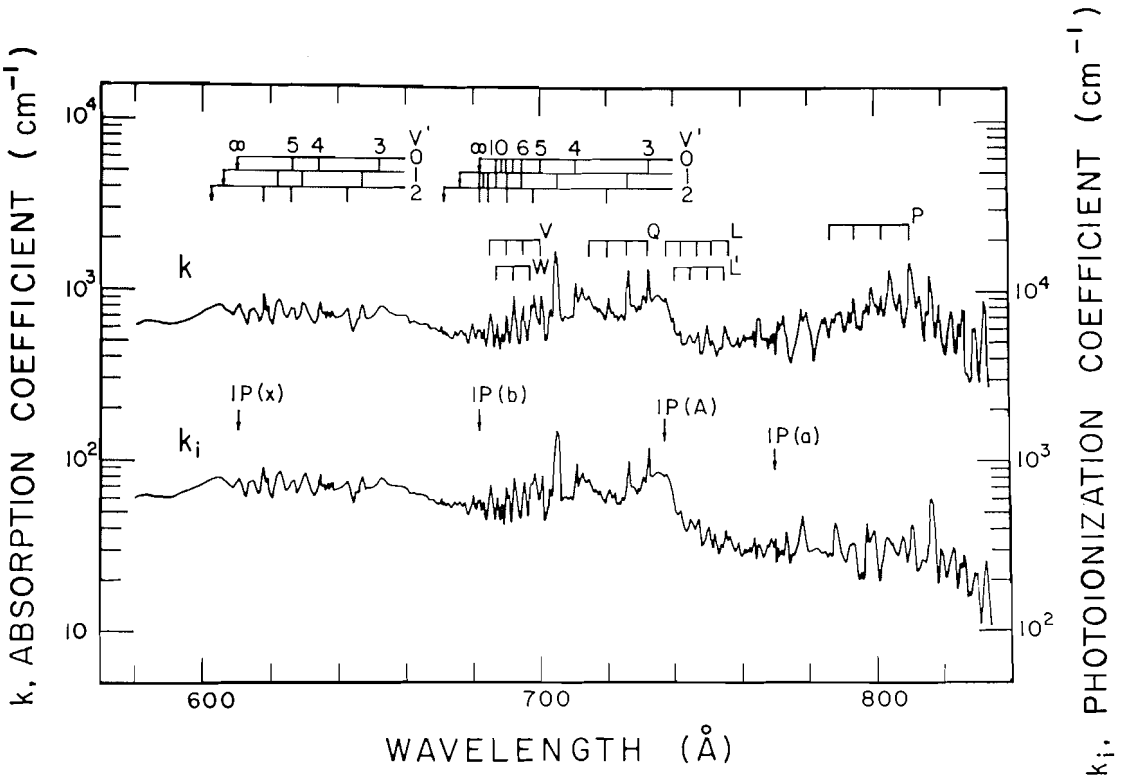

FIG. 5. Molecular oxygen absorption and ionization coefficients, ref. (25).

atmosphere (26, 27). It is conceivable that absorption by this molecule may be more significant than generally realized. Some intense bands attributed to absorption by the $a^1\Delta_g$, or less likely the $b^1\Sigma_g^+$, state have been observed recently in the 830–900 Å region, (28, 29), and recent work has found absorption bands of both the $a^1\Delta_g$ and the $b^1\Sigma_g^+$ states in the 1200–1600 Å region (30).

Molecular Nitrogen

The absorption cross-section of molecular nitrogen at important solar lines is given in Table I, which is based on several recent investigations (10, 31, 24). Table II gives shorter wavelength data. Cross-section curves obtained with continuum background sources in the region 600–1000 Å are given in Figs. 7 and 8. There is an extensive literature on the absorption spectrum which can be traced through the references given. There is one recent paper on absorption at wavelengths less than 600 Å (32).

Molecular nitrogen has a much smaller absorption cross-section than molecular oxygen at wavelengths longer than 1000 Å. The Lyman–Birge–Hopfield bands and several other forbidden transitions are present at wavelengths between 1450 and 1000 Å, but the maximum cross-sections measured are less than 10^{-3} Mb. The resolution is also generally inadequate for precise measurements. There are recent studies on high temperature absorption in this region (33).

There are no strong photodissociation continua for nitrogen, which is different from molecular oxygen. This fact helps to explain why atomic nitrogen is in very small concentration in the atmosphere, while atomic oxygen is a major constituent.

At wavelengths less than 1000 Å, there are a number of strong bands which cannot be measured accurately with the present resolution. The curve of Fig. 7 for the 800–1000 Å region must be regarded as approximate within regions of strong bands (11, 34), but it is useful for illustrating the general absorption in this region. One interesting situation is the coincidence of the strong H Ly γ solar line (972.5 Å) with one of the nitrogen

Can. J. Chem. Downloaded from www.nrcresearchpress.com by 210.87.254.40 on 09/05/12
For personal use only.

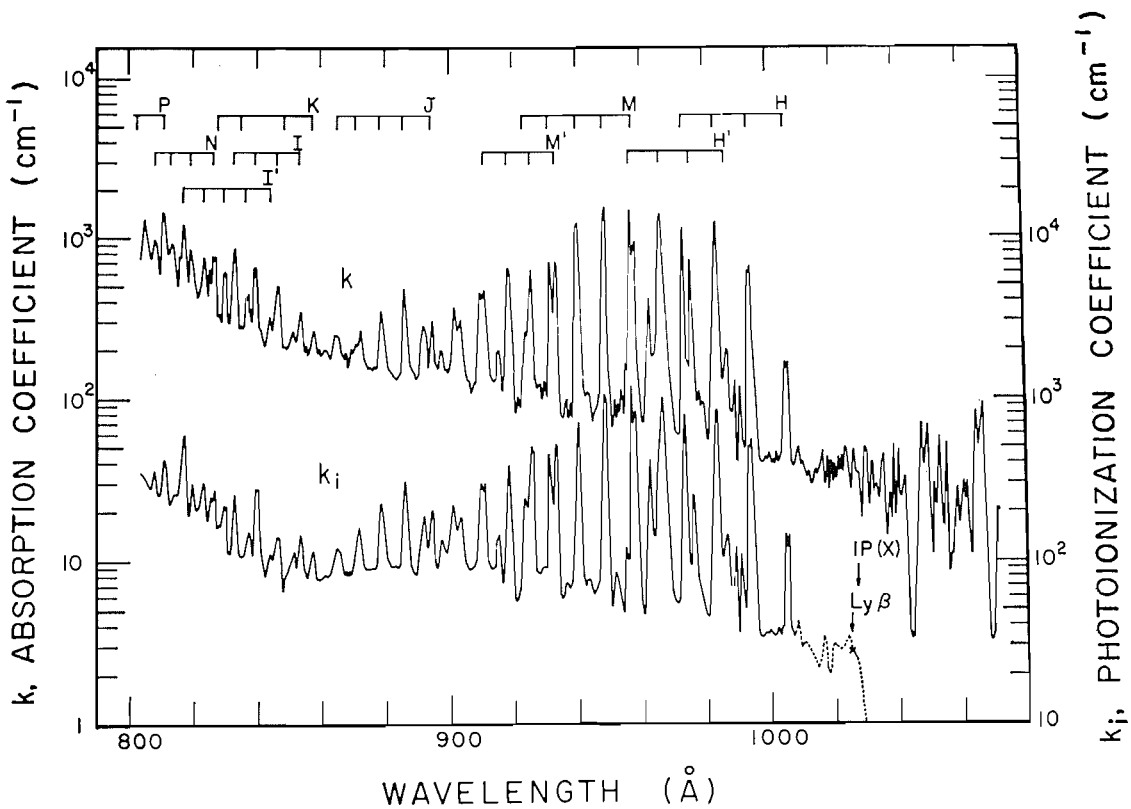

FIG. 6. Molecular oxygen absorption and ionization coefficients, ref. (25).

bands (35). At wavelengths less than the ionization threshold (795.8 Å), most bands become more diffuse because of autoionization, and they are superimposed on the ionization continuum. Thus, the curve of Fig. 8 should be more reliable. Recent unpublished results at Air Force Cambridge Research Laboratories indicate that the step at 661 Å is probably not real. The curve should be rescaled between 600 and 661 Å to form a smooth curve with the longer wavelength values.

Atomic Oxygen

The atomic oxygen spectrum consists of the ionization continuum at wavelengths less than the threshold at 910.4 Å and in addition, line series converging to limits corresponding to the electronic states of the ion. In the continuum region, there is good reason to believe that the absorption and ionization cross-sections are identical, in analogy with the ionization continua of the rare gases (12), except for a few non-autoionizing series lines. Most of the absorption lines at wavelengths less than the ionization threshold are autoionized.

Theoretical (36) and experimental (37, 38) cross-sections are given in Figs. 9 and 10. Table I gives cross-sections at important solar lines. Until quite recently there were no experimental values, but measurements using two independent techniques have now been published. One technique uses discharged oxygen, which requires correction for metastable molecules (37), and the other uses a beam technique requiring calibration against hydrogen atom (38). They are in only fair agreement with each other, but they generally bracket the theoretical curve. Despite these excellent experiments, the need for additional measurements is evident. Tables I and II rely primarily on the theoretical curves. Additional calculations have recently been published (39).

The large number of atomic oxygen absorption lines in the ionization continuum has only been realized recently with the measurement and classification of a number of these series (28). Some of the more intense series members are

Can. J. Chem. Downloaded from www.nrcresearchpress.com by 210.87.254.40 on 09/05/12
For personal use only.

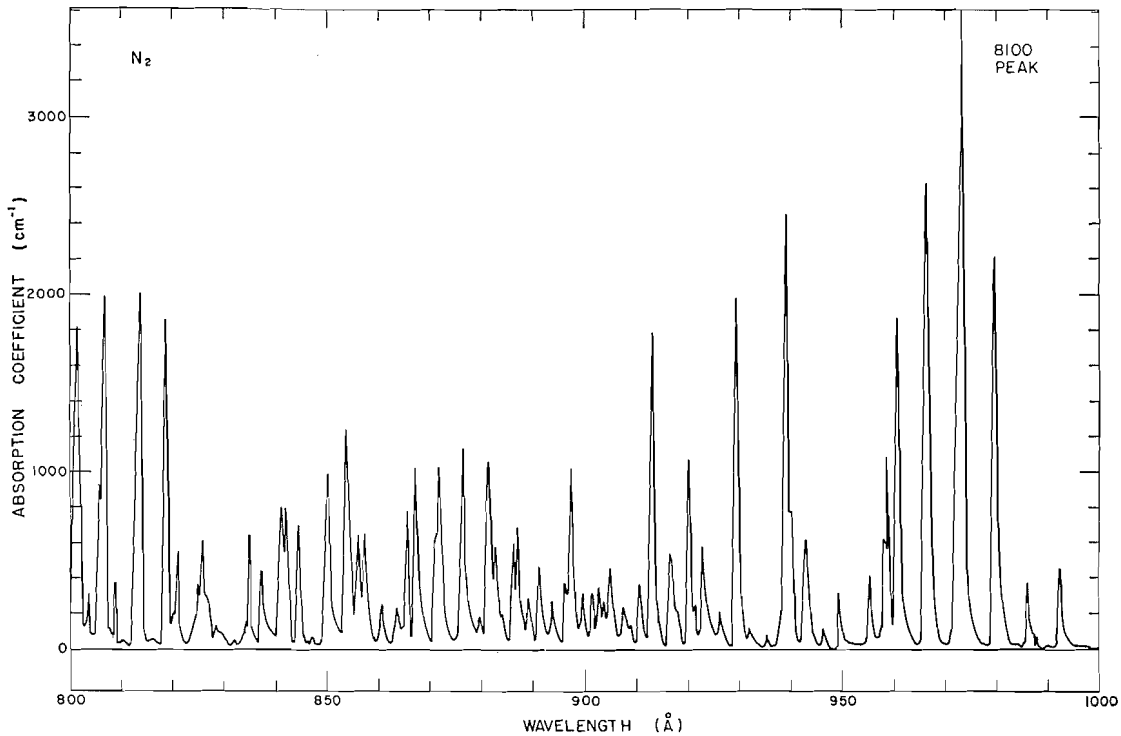

FIG. 7. Molecular nitrogen absorption cross-sections, refs. (31, 17).

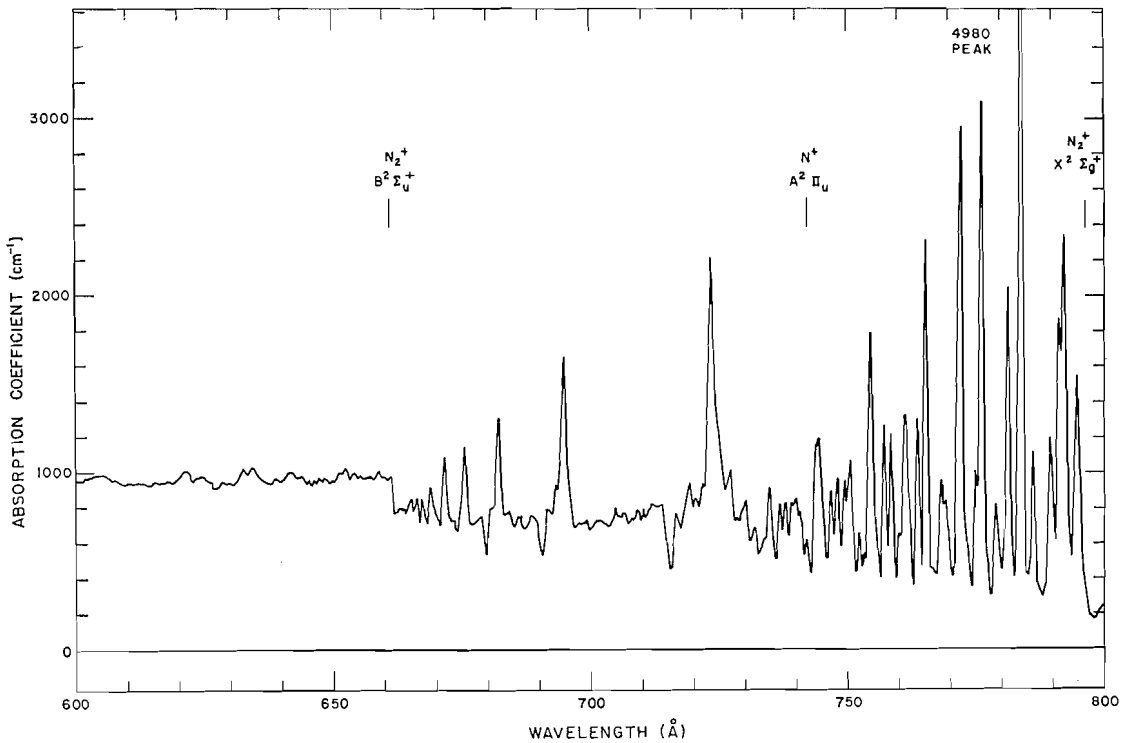

FIG. 8. Molecular nitrogen absorption cross-sections, refs. (31, 17).

Can. J. Chem. Downloaded from www.nrcresearchpress.com by 210.87.254.40 on 09/05/12
For personal use only.

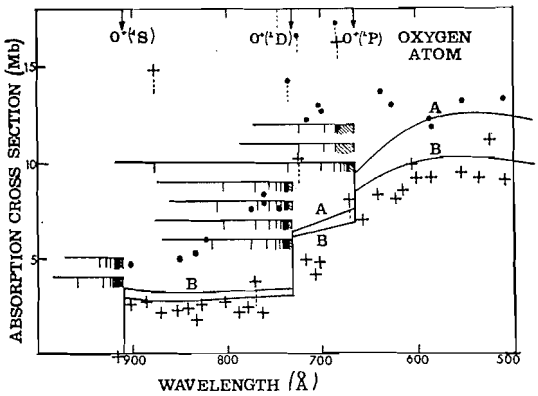

FIG. 9. Atomic oxygen cross-sections. Curve, ref. (36); A, dipole length; B, dipole velocity; filled circles, ref. (37); crosses, ref. (38); dashed line beneath point indicates absorption line; absorption series, ref. (28).

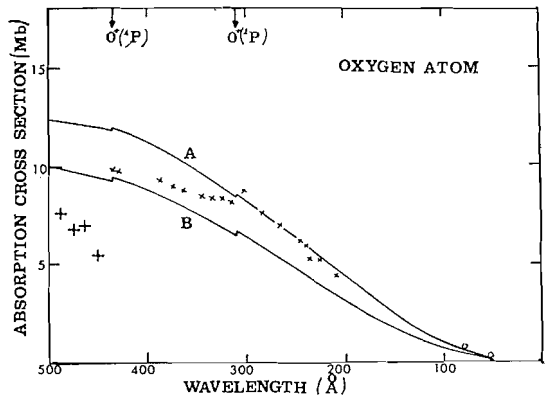

FIG. 10. Atomic oxygen cross-sections. See caption of Fig. 9. Symbol × represents one-half O_2 cross-section, based on ref. (37).

shown in Fig. 9, and it is clear that the lines used in some laboratory measurements were absorbed by oxygen atom lines, leading to high cross-section values (40), compared to nearby lines in the continuum region. If a solar line happens to overlap one of the atomic absorption lines, the absorption cross-section for this solar line will be much larger than the continuum value. The intensity profile with varying altitude will be dependent on the details of the two line shapes involved. Wavelengths where this effect is likely to be important for strong solar lines are given in Table I, and Table III gives the classification and additional wavelengths. The recent measurements also give absorption lines from the meta-stable $O(^1D)$ and $O(^1S)$ states (28), which may be important under special conditions.

TABLE III

Atomic oxygen lines which may absorb solar lines

Solar line (Å)	OI line (Å)	Classification	Remarks
1025.7	1025.76	$^3P_2$–$3d\,^3D^0$	*a*
989.8	990.13	$^3P_1$–$3s'\,^3D^0$	
937.8	937.84	$^3P_2$–$7s'\,^3S^0$	
930.7	930.89	$^3P_1$–$7d\,^3D^0$	
835.3	835.44	$^1D_2$–$10d'\,^1F^0$, $^1D^0$	
834.5	834.34	$^1D_2$–$12s'\,^1D^0$	
832.9	833.10	$^1D_2$–$12d'\,^1F^0$, $^1D^0$	
787.7	788.18	$^1D_2$–$5s''\,^1P^0$	*b*
770.4	770.35	$^3P_1$–$4d'\,^3P_2{}^0$	
761.1	761.26	$^1D_2$–$6d''\,^1F^0$, $^1D^0$	*b*
686.3	686.28	$^3P_1$–$5d''\,^3P^0$, $^3D^0$	*b,c*
685.5	685.54	$^3P_2$–$5d''\,^3P^0$, $^3D^0$	*b,c*

NOTE: atomic oxygen resonance lines (1302, 1305, 1306 Å) not included. References 28, 29, and 48 give details.
[a]Solar line known to be broad.
[b]Atomic oxygen line broadened by autoionization.
[c]These lines known to overlap. See refs. 40 and 37.

Ozone

Ozone (O_3) has important atmospheric absorption at wavelengths less than 3500 Å. The cross-section curves are given in Figs. 11 and 12. There have been several measurements in substantial agreement (41, 42). There is less atmospheric absorption at wavelengths less than 2000 Å, because solar radiation of these wavelengths does not penetrate to the altitudes where ozone is present, so this region is not reviewed.

Although the Hartley continuum in the 2000–3000 Å region (Fig. 11) has the larger cross-section, the greater solar intensity at wavelengths greater than 3000 Å makes absorption in the weaker Huggins bands also very important (43). The cross-section data in the region above 3000 Å should be improved in resolution to more

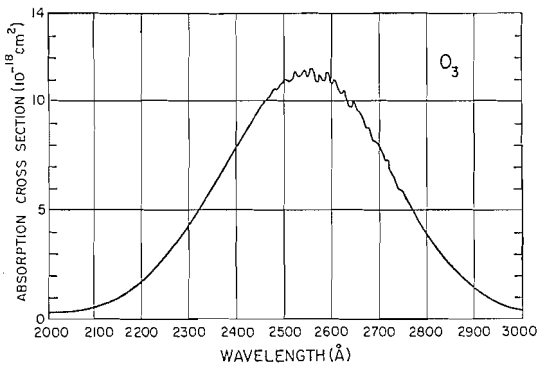

FIG. 11. Ozone absorption cross-sections, ref. (41).

Can. J. Chem. Downloaded from www.nrcresearchpress.com by 210.87.254.40 on 09/05/12
For personal use only.

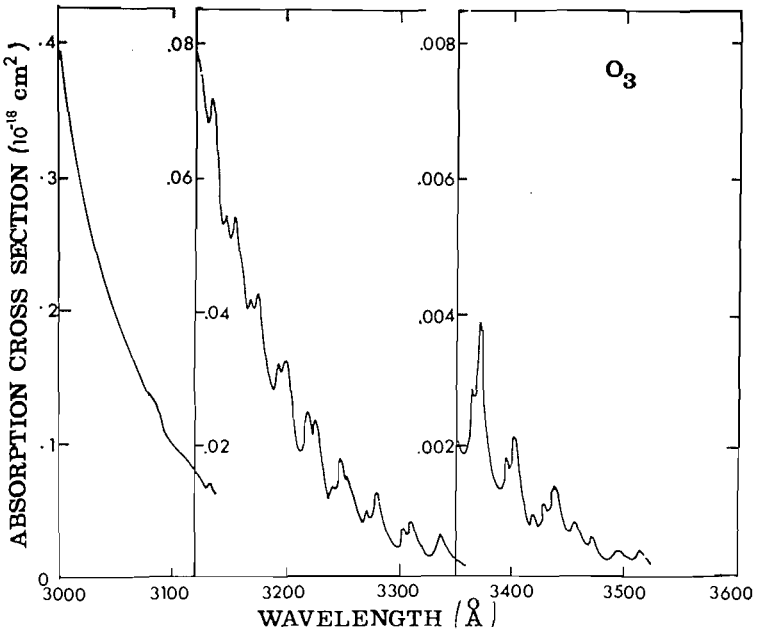

FIG. 12. Ozone absorption cross-sections, ref. (41).

accurately assess its importance. New data in this region have recently been published (44).

The photodissociation products of ozone are of considerable interest, since they appear to be one of the most likely sources of excited oxygen atoms and molecules. At wavelengths less than 3100 Å, it is energetically possible to have O_2 $^1\Delta_g$ and O ^{1}D as products of the ozone photolysis. The threshold for O ^{1}D formation is 4100 Å, but the process would also yield a ground state $X^3\Sigma_g^-$ molecule, which would be a forbidden transition (6). Discussions of the evidence for these products from flash and steady state photolysis have been given (27, 45), and a general conclusion is that O ^{1}D is much better established as a primary product than O_2 $a^1\Delta_g$. However, recent photolysis experiments at 2537 Å have succeeded in observing the O_2 $a^1\Delta_g \rightarrow X^3\Sigma_g^-$ infrared atmospheric bands in emission (49). The intense metastable O_2 absorption bands between 830 and 900 Å previously mentioned (28) have also been observed in the products of ozone photolysis at 2537 Å (50), which supports the presence of metastable O_2 in the products. It can therefore be considered as established that the absorption in this region does yield O_2 $a^1\Delta_g$, but the efficiency is not known.

Conclusions

There is a substantial body of information available on absorption cross-sections which may be used with considerable confidence for aeronomic calculations. Continued work is resulting in a convergence of values from different groups and techniques although this review notes many areas where work is needed. Agreement with the findings of rocket spectrophotometry (46) is also substantial; however, close interaction between laboratory and field studies is necessary to further reduce uncertainties.

Acknowledgments

The author would like to thank Professor W. R. S. Garton, for making facilities available in his group during preparation of this review. Illustrations and/or additional comment were provided by R. B. Cairns, W. Swider, K. Watanabe, and F. Matsunaga. Special thanks are due to Y. Tanaka and J. C. Larrabee for discussions over a period of many years.

1. K. WATANABE. Advances in geophysics. Vol. 5. *Edited by* H. E. Landsberg. Academic Press, Inc., New York. 1958. p. 153.
2. G. V. MARR. Proc. Roy. Soc. London, Ser. A, **228**, 531 (1965).

Can. J. Chem. Downloaded from www.nrcresearchpress.com by 210.87.254.40 on 09/05/12
For personal use only.

3. R. E. HUFFMAN. Handbook of geophysics and space environments. *Edited by* S. Valle. McGraw-Hill Book Co., Inc., New York. 1965. DASA reaction rate handbook, DASA 1948. Defense Atomic Support Agency, Washington. 1967.
4. G. L. WEISSLER. Handbuch der Physik. Vol. XXI. *Edited by* S. Flugge. Springer-Verlag, Berlin. 1956.
5. J. A. R. SAMSON. Techniques of vacuum ultraviolet spectroscopy. John Wiley and Sons, Inc., New York. 1967.
6. J. R. MCNESBY and H. OKABE. Advan. Photochem. **3**, 147 (1964).
7. A. C. G. MITCHELL and M. W. ZEMANSKY. Resonance radiation and excited atoms. Cambridge University Press, London. 1934.
8. R. M. GOODY. Atmospheric radiation. I. Theoretical basis. The Clarendon Press, Oxford. 1964.
9. A. J. BLAKE, J. H. CARVER, and G. N. HADDAD. J. Quant. Spectry. Radiative Transfer, **6**, 451 (1966).
10. J. A. R. SAMSON and R. B. CAIRNS. J. Geophys. Res. **69**, 4583 (1964).
11. V. D. MEYER, A. SKERBELE, and E. N. LASSETTRE. J. Chem. Phys. **43**, 3769 (1965).
12. J. A. R. SAMSON. Advan. At. Mol. Phys. **2**, 177 (1966).
13. G. V. MARR. Photoionization processes in gases. Academic Press, Inc., New York. 1967.
14. R. W. DITCHBURN and P. A. YOUNG. J. Atmospheric Terrest. Phys. **24**, 127 (1962).
15. B. A. THOMPSON, P. HARTECK, and R. R. REEVES. J. Geophys. Res. **68**, 6431 (1963).
16. P. H. METZGER and G. R. COOK. J. Quant. Spectry. Radiative Transfer, **4**, 107 (1964).
17. R. E. HUFFMAN, Y. TANAKA, and J. C. LARRABEE. Discussions Faraday Soc. **37**, 154 (1964).
18. R. GOLDSTEIN and F. N. MASTRUP. J. Opt. Soc. Am. **56**, 765 (1966).
19. J. O. SULLIVAN and P. WARNECK. J. Chem. Phys. **46**, 953 (1967).
20. R. A. YOUNG and G. BLACK. J. Chem. Phys. **47**, 2311 (1967).
21. J. S. EVANS and C. J. SCHEXNAYDER. NASA Technical Report R-92 (1961).
22. R. D. HUDSON, V. L. CARTER, and J. A. STEIN. J. Geophys. Res. **71**, 2295 (1966).
23. R. E. HUFFMAN, J. C. LARRABEE, and Y. TANAKA. J. Chem. Phys. **40**, 356 (1964).
24. G. R. COOK and P. H. METZGER. J. Chem. Phys. **41**, 321 (1964).
25. F. M. MATSUNAGA and K. WATANABE. Sci. Light, Tokyo, **16**, 31 (1967).
26. W. F. J. EVANS, D. M. HUNTEN, E. J. LLEWELLYN, and A. VALLANCE JONES. J. Geophys. Res. **73**, 2885 (1968).
27. R. P. WAYNE. Quart. J. Roy. Meteorol. Soc. **93**, 69 (1967).
28. R. E. HUFFMAN, J. C. LARRABEE, and Y. TANAKA. J. Chem. Phys. **46**, 2213 (1967).
29. R. E. HUFFMAN, J. C. LARRABEE, and Y. TANAKA. J. Chem. Phys. **47**, 4462 (1967).
30. F. ALBERTI, R. A. ASHBY, and A. E. DOUGLAS. Can. J. Phys. **46**, 337 (1968).
31. R. E. HUFFMAN, Y. TANAKA, and J. C. LARRABEE. J. Chem. Phys. **39**, 910 (1963).
32. K. CODLING. Astrophys. J. **143**, 552 (1966).
33. J. P. APPLETON and M. STEINBERG. J. Chem. Phys. **46**, 1521 (1967).
34. G. M. LAWRENCE, D. L. MICKEY, and K. DRESSLER. J. Chem. Phys. **48**, 1989 (1968).
35. M. OGAWA and R. B. CAIRNS. Planetary Space Sci. **12**, 656 (1964).
36. A. DALGARNO, R. J. W. HENRY, and A. L. STEWART. Planetary Space Sci. **12**, 235 (1964), and references therein.
37. R. B. CAIRNS and J. A. R. SAMSON. Phys. Rev. **139**, A1403 (1965).
38. F. J. COMES, F. SPEIER, and A. ELZER. Z. Naturforsch. **23a**, 114 (1968).
39. R. J. W. HENRY. Planetary Space Sci. **15**, 1747 (1967).
40. R. E. HUFFMAN, J. C. LARRABEE, and Y. TANAKA. Phys. Rev. Letters, **16**, 1033 (1966).
41. E. C. Y. INN and Y. TANAKA. J. Opt. Soc. Am. **43**, 870 (1953).
42. E. VIGROUX. Ann. Phys. **8**, 709 (1953).
43. P. A. LEIGHTON. Photochemistry of air pollution. Academic Press, Inc., New York. 1961. p. 48.
44. E. VIGROUX. Ann. Phys. **2**, 209 (1967).
45. W. B. DEMORE and O. RAPER. J. Chem. Phys. **44**, 1780 (1966).
46. L. A. HALL, W. SCHWEIZER, and H. E. HINTEREGGER. J. Geophys. Res. **70**, 105 (1965).
47. J. A. R. SAMSON and R. B. CAIRNS. J. Opt. Soc. Am. **55**, 1035 (1965).
48. R. E. HUFFMAN and J. C. LARRABEE. J. Geophys. Res. **73**, 7419 (1968).
49. R. P. WAYNE. Private communication.
50. J. C. LARRABEE and R. E. HUFFMAN. Unpublished results.

Absorption in the spectral range of the Schumann–Runge bands

M. ACKERMAN, F. BIAUME, AND M. NICOLET
Institut D'Aéronomie Spatiale de Belgique 3, Avenue Circulaire, Bruxelles 18, Belgique

Received November 21, 1968

Absorption of silicon lines by O_2 in the Schumann–Runge bands has been measured. The results lead to some conclusions about the nature of the absorption and about the general behavior of the spectrum.

Canadian Journal of Chemistry, 47, 1834 (1969)

Introduction

Early measurements, presented in Fig. 1, of the absorption coefficient of oxygen in the Schumann–Runge bands (1750–2000 Å) and in the Herzberg continuum ($\lambda < 2424$ Å) were mainly performed with light sources providing spectral emission

Can. J. Chem. Downloaded from www.nrcresearchpress.com by 210.87.254.40 on 09/05/12
For personal use only.

3. R. E. HUFFMAN. Handbook of geophysics and space environments. *Edited by* S. Valle. McGraw-Hill Book Co., Inc., New York. 1965. DASA reaction rate handbook, DASA 1948. Defense Atomic Support Agency, Washington. 1967.
4. G. L. WEISSLER. Handbuch der Physik. Vol. XXI. *Edited by* S. Flugge. Springer-Verlag, Berlin. 1956.
5. J. A. R. SAMSON. Techniques of vacuum ultraviolet spectroscopy. John Wiley and Sons, Inc., New York. 1967.
6. J. R. MCNESBY and H. OKABE. Advan. Photochem. **3**, 147 (1964).
7. A. C. G. MITCHELL and M. W. ZEMANSKY. Resonance radiation and excited atoms. Cambridge University Press, London. 1934.
8. R. M. GOODY. Atmospheric radiation. I. Theoretical basis. The Clarendon Press, Oxford. 1964.
9. A. J. BLAKE, J. H. CARVER, and G. N. HADDAD. J. Quant. Spectry. Radiative Transfer, **6**, 451 (1966).
10. J. A. R. SAMSON and R. B. CAIRNS. J. Geophys. Res. **69**, 4583 (1964).
11. V. D. MEYER, A. SKERBELE, and E. N. LASSETTRE. J. Chem. Phys. **43**, 3769 (1965).
12. J. A. R. SAMSON. Advan. At. Mol. Phys. **2**, 177 (1966).
13. G. V. MARR. Photoionization processes in gases. Academic Press, Inc., New York. 1967.
14. R. W. DITCHBURN and P. A. YOUNG. J. Atmospheric Terrest. Phys. **24**, 127 (1962).
15. B. A. THOMPSON, P. HARTECK, and R. R. REEVES. J. Geophys. Res. **68**, 6431 (1963).
16. P. H. METZGER and G. R. COOK. J. Quant. Spectry. Radiative Transfer, **4**, 107 (1964).
17. R. E. HUFFMAN, Y. TANAKA, and J. C. LARRABEE. Discussions Faraday Soc. **37**, 154 (1964).
18. R. GOLDSTEIN and F. N. MASTRUP. J. Opt. Soc. Am. **56**, 765 (1966).
19. J. O. SULLIVAN and P. WARNECK. J. Chem. Phys. **46**, 953 (1967).
20. R. A. YOUNG and G. BLACK. J. Chem. Phys. **47**, 2311 (1967).
21. J. S. EVANS and C. J. SCHEXNAYDER. NASA Technical Report R-92 (1961).
22. R. D. HUDSON, V. L. CARTER, and J. A. STEIN. J. Geophys. Res. **71**, 2295 (1966).
23. R. E. HUFFMAN, J. C. LARRABEE, and Y. TANAKA. J. Chem. Phys. **40**, 356 (1964).
24. G. R. COOK and P. H. METZGER. J. Chem. Phys. **41**, 321 (1964).
25. F. M. MATSUNAGA and K. WATANABE. Sci. Light, Tokyo, **16**, 31 (1967).
26. W. F. J. EVANS, D. M. HUNTEN, E. J. LLEWELLYN, and A. VALLANCE JONES. J. Geophys. Res. **73**, 2885 (1968).
27. R. P. WAYNE. Quart. J. Roy. Meteorol. Soc. **93**, 69 (1967).
28. R. E. HUFFMAN, J. C. LARRABEE, and Y. TANAKA. J. Chem. Phys. **46**, 2213 (1967).
29. R. E. HUFFMAN, J. C. LARRABEE, and Y. TANAKA. J. Chem. Phys. **47**, 4462 (1967).
30. F. ALBERTI, R. A. ASHBY, and A. E. DOUGLAS. Can. J. Phys. **46**, 337 (1968).
31. R. E. HUFFMAN, Y. TANAKA, and J. C. LARRABEE. J. Chem. Phys. **39**, 910 (1963).
32. K. CODLING. Astrophys. J. **143**, 552 (1966).
33. J. P. APPLETON and M. STEINBERG. J. Chem. Phys. **46**, 1521 (1967).
34. G. M. LAWRENCE, D. L. MICKEY, and K. DRESSLER. J. Chem. Phys. **48**, 1989 (1968).
35. M. OGAWA and R. B. CAIRNS. Planetary Space Sci. **12**, 656 (1964).
36. A. DALGARNO, R. J. W. HENRY, and A. L. STEWART. Planetary Space Sci. **12**, 235 (1964), and references therein.
37. R. B. CAIRNS and J. A. R. SAMSON. Phys. Rev. **139**, A1403 (1965).
38. F. J. COMES, F. SPEIER, and A. ELZER. Z. Naturforsch. **23a**, 114 (1968).
39. R. J. W. HENRY. Planetary Space Sci. **15**, 1747 (1967).
40. R. E. HUFFMAN, J. C. LARRABEE, and Y. TANAKA. Phys. Rev. Letters, **16**, 1033 (1966).
41. E. C. Y. INN and Y. TANAKA. J. Opt. Soc. Am. **43**, 870 (1953).
42. E. VIGROUX. Ann. Phys. **8**, 709 (1953).
43. P. A. LEIGHTON. Photochemistry of air pollution. Academic Press, Inc., New York. 1961. p. 48.
44. E. VIGROUX. Ann. Phys. **2**, 209 (1967).
45. W. B. DEMORE and O. RAPER. J. Chem. Phys. **44**, 1780 (1966).
46. L. A. HALL, W. SCHWEIZER, and H. E. HINTEREGGER. J. Geophys. Res. **70**, 105 (1965).
47. J. A. R. SAMSON and R. B. CAIRNS. J. Opt. Soc. Am. **55**, 1035 (1965).
48. R. E. HUFFMAN and J. C. LARRABEE. J. Geophys. Res. **73**, 7419 (1968).
49. R. P. WAYNE. Private communication.
50. J. C. LARRABEE and R. E. HUFFMAN. Unpublished results.

Absorption in the spectral range of the Schumann–Runge bands

M. ACKERMAN, F. BIAUME, AND M. NICOLET
Institut D'Aéronomie Spatiale de Belgique 3, Avenue Circulaire, Bruxelles 18, Belgique

Received November 21, 1968

Absorption of silicon lines by O_2 in the Schumann–Runge bands has been measured. The results lead to some conclusions about the nature of the absorption and about the general behavior of the spectrum.

Canadian Journal of Chemistry, 47, 1834 (1969)

Introduction

Early measurements, presented in Fig. 1, of the absorption coefficient of oxygen in the Schumann–Runge bands (1750–2000 Å) and in the Herzberg continuum ($\lambda < 2424$ Å) were mainly performed with light sources providing spectral emission

Can. J. Chem. Downloaded from www.nrcresearchpress.com by 210.87.254.6 on 09/05/12
For personal use only.

Can. J. Chem. Downloaded from www.nrcresearchpress.com by 210.87.254.6 on 09/05/12
For personal use only.

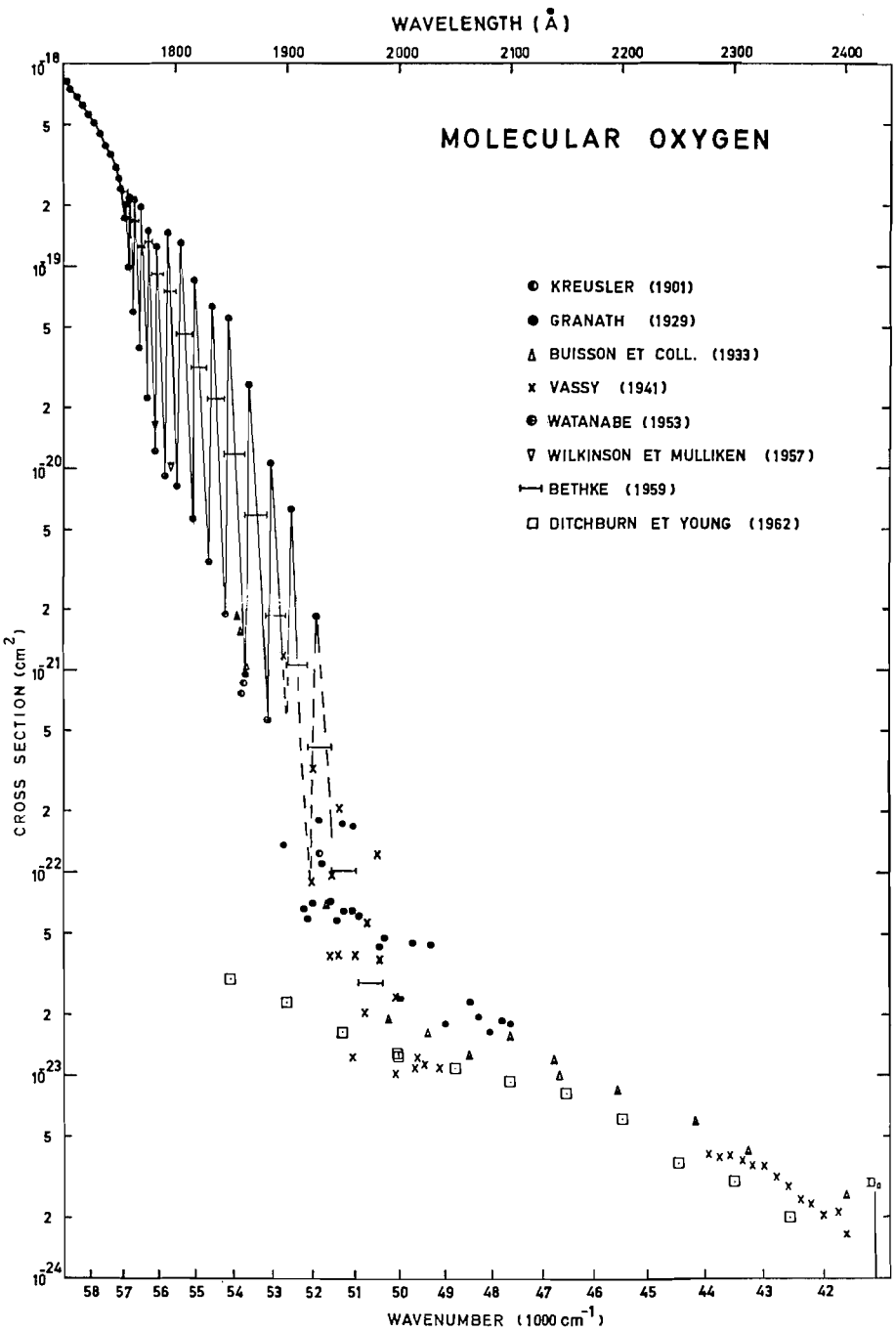

FIG. 1. Absorption cross section of molecular oxygen σ_{O_2} between 1700 and 2430 Å. The uncertainty remaining in the Schumann–Runge bands after measurements extending over a period of more than 60 years appears clearly.

Can. J. Chem. Downloaded from www.nrcresearchpress.com by 210.87.254.6 on 09/05/12
For personal use only.

TABLE I
Data

Band	Line	$\nu_{O_2}(cm^{-1})$	$\nu_{Si}(cm^{-1})$	$\Delta\nu(cm^{-1})$	$\overline{\Delta\nu}(cm^{-1})$	S Bethke (cm)	r_J	$\sigma_{\nu_0}(O_2)$ (cm^2)	$\sigma_\nu(Si)$ (cm^2)	$\frac{\sigma_\nu(Si)}{\Sigma\sigma_{\nu_0}(O_2)}$
5–0	7P	52 513.2		10.5			0.06589	4.24×10^{-20}		
	9R	52 511.9	52 502.7	9.2	13.2	6.44×10^{-19}	0.07434	4.79×10^{-20}	5.26×10^{-22}	2.99×10^{-3}
	9P	52 486.5		16.2			0.06690	4.31×10^{-20}		
	11R	52 485.5		17.2			0.06664	4.29×10^{-20}		
6–0	19P	52 823.3	52 819.2	4.1	3.8	1.53×10^{-18}	0.01186	2.89×10^{-20}	(1.31×10^{-21})	2.57×10^{-2}
	21R	52 822.6		3.4			0.01236	1.89×10^{-20}	1.23×10^{-21}	
6–0	13P	52 973.4	52 974.7	1.3	1.3	1.53×10^{-18}	0.05102	7.81×10^{-20}	(1.79×10^{-20})	1.20×10^{-1}
	15R						0.04198	6.42×10^{-20}	1.71×10^{-20}	
7–0	25P	53 141.1	53 139.1	2.0	2.5	3.15×10^{-18}	0.00380	1.20×10^{-20}	8.28×10^{-22}	4.49×10^{-2}
	27R	53 135.6		3.5			0.00204	6.43×10^{-21}		
7–0	19P	53 349.1		38.9			0.01886	5.94×10^{-20}		
	21R	53 345.4	53 310.2	35.2	33.2	3.15×10^{-18}	0.01236	3.89×10^{-20}	1.50×10^{-22}	1.05×10^{-3}
	21P	53 285.6		24.6			0.01180	3.72×10^{-20}		
	23R	53 281.4		28.8			0.00722	2.27×10^{-20}		
7–0	19P	53 349.1	53 337.8	11.3	9.8	3.15×10^{-18}	0.01886	5.94×10^{-20}	(4.06×10^{-22})	4.35×10^{-3}
	21R	53 345.4		7.6			0.01236	3.89×10^{-20}	4.28×10^{-22}	
7–0	17P	53 406.7		19.4			0.02821	8.89×10^{-20}		
	19R	53 403.6	53 387.3	16.3	26.6	3.15×10^{-18}	0.01986	6.26×10^{-20}	3.14×10^{-22}	1.26×10^{-3}
	19P	53 349.1		38.2			0.01886	5.94×10^{-20}		
	21R	53 345.4		41.9			0.01236	3.89×10^{-20}		
8–0	13P	54 000.4		18.5			0.05102	3.05×10^{-19}		
	15R	53 995.3	53 981.9	13.4	22.5	5.98×10^{-18}	0.04198	2.51×10^{-19}	(1.19×10^{-21})	1.14×10^{-3}
	15P	53 953.5		28.4			0.03936	2.35×10^{-19}	1.11×10^{-21}	
	17R	53 947.8		34.1			0.02987	1.79×10^{-19}		
8–0	13R	54 036.8	54 034.4	2.4	2.4	5.98×10^{-18}	0.05494	3.29×10^{-19}	(1.40×10^{-20}) 1.31×10^{-20}	3.98×10^{-2}
8–0	7P	54 104.1		13.4			0.06589	3.94×10^{-19}		
	9R	54 101.5	54 090.7	10.8	14.4	5.98×10^{-18}	0.07434	4.45×10^{-19}	(2.96×10^{-21})	2.07×10^{-3}
	9P	54 075.6		15.1			0.06690	4.00×10^{-19}	3.39×10^{-21}	
	11R	54 072.2		18.5			0.06664	3.99×10^{-19}		
8–0	7P	54 104.1	54 108.2	4.1	5.5	5.98×10^{-18}	0.06589	3.94×10^{-19}	(6.95×10^{-21})	9.19×10^{-3}
	9R	54 101.5		6.7			0.07434	4.45×10^{-19}	7.71×10^{-21}	
8–0	5P	54 126.7	54 128.0	1.3	2.4	5.98×10^{-18}	0.05637	3.37×10^{-19}	(3.20×10^{-20})	4.87×10^{-2}
	7R	54 124.7		3.3			0.07530	4.50×10^{-19}	3.83×10^{-20}	
8–0	1R	54 157.3		10.6			0.02726	1.63×10^{-19}		
	1P }	54 152.7	54 167.9	15.2	13.4	5.98×10^{-18}	0.01363	8.15×10^{-20}	(1.71×10^{-21})	3.01×10^{-3}
	3R }						0.05110	3.05×10^{-19}	1.85×10^{-21}	
9–0	23P	54 158.0		9.9		9.49×10^{-18}	0.00692	6.57×10^{-20}		

Can. J. Chem. Downloaded from www.nrcresearchpress.com by 210.87.254.6 on 09/05/12
For personal use only.

TABLE I (*Concluded*)

Band	Line	$\nu_{O_2}(cm^{-1})$	$\nu_{Si}(cm^{-1})$	$\Delta\nu(cm^{-1})$	$\overline{\Delta\nu}(cm^{-1})$	*S* Bethke (cm)	r_j	$\sigma_{\nu_0}(O_2)$ (cm^2)	$\sigma_\nu(Si)$ (cm^2)	$\frac{\sigma_\nu(Si)}{\Sigma\sigma_{\nu_0}(O_2)}$
8–0	1R	54 157.3		28.0			0.02726	1.63×10^{-19}		
	1P	54 152.7	54 185.3	32.6	33.2	5.98×10^{-18}	0.01363	8.15×10^{-20}		
	3R						0.05110	3.05×10^{-19}	(5.50×10^{-22})	6.43×10^{-4}
9–0	23R	54 218.6		33.3			0.00722	6.86×10^{-20}	5.12×10^{-22}	
	23P	54 158.0		27.3		9.49×10^{-18}	0.00692	6.57×10^{-20}		
	21P	54 231.8		46.5			0.01180	1.12×10^{-19}		
9–0	21P	54 231.8	54 236.7	4.9	4.9	9.49×10^{-18}	0.01180	1.12×10^{-19}	(2.06×10^{-21}) 2.11×10^{-21}	1.88×10^{-2}
10–0	29P	54 306.3	54 305.1	1.2	1.2	1.38×10^{-17}	0.00096	1.32×10^{-20}	(6.57×10^{-21}) 7.54×10^{-21}	5.71×10^{-1}
9–0	19P	54 298.1	54 313.8	15.7	15.2	9.49×10^{-18}	0.01886	1.79×10^{-19}	(2.95×10^{-22})	1.49×10^{-3}
10–0	29P	54 306.3		7.5		1.38×10^{-17}	0.00096	1.32×10^{-20}	2.87×10^{-22}	
9–0	13P	54 462.6	54 451.1	11.5	7.9	9.49×10^{-18}	0.05102	4.85×10^{-19}	(5.27×10^{-21})	4.80×10^{-3}
	15R	54 454.6		3.5			0.04198	3.99×10^{-19}	4.24×10^{-21}	
10–0	3P	55 037.4	55 038.0	0.6	0.6	1.38×10^{-17}	0.03883	5.29×10^{-19}	1.60×10^{-19}	3.02×10^{-1}
11–0	17P	55 160.2		35.8			0.02821	5.39×10^{-19}		
	19R	55 142.0	55 124.4	17.6	32.8	1.91×10^{-17}	0.01986	3.79×10^{-19}	(1.51×10^{-21})	1.25×10^{-3}
	19P	55 096.1		28.3			0.01886	3.60×10^{-19}	1.90×10^{-21}	
	21R	55 073.6		50.8			0.01236	2.36×10^{-19}		
11–0	13P	55 270.9	55 276.0	5.1	5.1	1.91×10^{-17}	0.05102	9.74×10^{-19}	1.15×10^{-20}	1.18×10^{-2}
11–0	11P	55 314.8	55 309.4	5.4	6.2	1.91×10^{-17}	0.06109	1.17×10^{-18}	1.21×10^{-20}	5.45×10^{-3}
	13R	55 302.3		7.1			0.05494	1.05×10^{-18}		
14–0	$7P_{2,3}$	55 280.37	56 280.19	0.18	0.18	2.87×10^{-17}	0.04392	1.26×10^{-18}	1.58×10^{-18}	1.25
15–0	$9R_1$	56 465.75		2.01			0.02478	7.14×10^{-19}		
	R_2	56 469.41	56 467.75	1.66	1.97	2.89×10^{-17}	0.02478	7.14×10^{-19}	4.24×10^{-20}	1.98×10^{-2}
	R_3	56 470.00		2.25			0.02478	7.14×10^{-19}		
15–0	$7P_1$	56 485.54		8.45			0.02196	6.35×10^{-19}		
	P_2	56 488.60		11.51			0.02196	6.35×10^{-19}		
	P_3	56 488.60		11.51		2.89×10^{-17}	0.02196	6.35×10^{-19}		
	$9R_1$	56 465.75		11.34			0.02478	7.14×10^{-19}		
	R_2	56 469.41	56 477.09	7.68	8.29		0.02478	7.14×10^{-19}	1.23×10^{-20}	2.35×10^{-3}
	R_3	56 470.00		7.09			0.02478	7.14×10^{-19}		
16–0	$15R_1$	56 472.60		4.49			0.01399	3.90×10^{-19}		
	R_2	56 479.69		2.60		2.80×10^{-17}	0.01399	3.90×10^{-19}		
	R_3	56 481.92		4.83			0.01399	3.90×10^{-19}		
16–0	$9P_1$	56 613.38	56 613.79	0.41	0.41	2.80×10^{-17}	0.02230	6.24×10^{-19}	3.46×10^{-19}	5.54×10^{-1}
16–0	$9P_2$	56 617.93		5.20			0.02230	6.24×10^{-19}		
	P_3	56 618.84	56 623.13	4.29	4.69	2.80×10^{-17}	0.02230	6.24×10^{-19}	2.65×10^{-20}	1.36×10^{-2}
	R_1	56 627.72		4.59			0.02480	6.94×10^{-19}		
16–0	$9R_2$	56 633.90		3.38		2.80×10^{-17}	0.02478	6.94×10^{-19}		
	R_3	56 633.32	56 637.28	3.96	3.19		0.02478	6.94×10^{-19}	1.42×10^{-19}	7.76×10^{-2}
17–0	$13P_1$	56 635.58		1.70		2.60×10^{-17}	0.01701	4.42×10^{-19}		
16–0	$7P_2$	56 655.68	56 656.27	0.59	0.59	2.80×10^{-17}	0.02196	6.15×10^{-19}	1.00×10^{-18}	8.13×10^{-1}
	P_3	56 655.68					0.02196	6.15×10^{-19}		
16–0	$3P_1$	56 700 37	56 700.25	0.12	0.12	2.80×10^{-17}	0.01278	3.58×10^{-19}	9.25×10^{-19}	1.04
17–0	$11P_2$	56 700.37				2.60×10^{-17}	0.02036	5.29×10^{-19}		

NOTE: Values obtained with the 2.17 m length cell are shown in parentheses; others were obtained with the 4.01 m length cell.

Can. J. Chem. Downloaded from www.nrcresearchpress.com by 210.87.254.6 on 09/05/12
For personal use only.

lines (1–4). Differences between measured values were not clearly understood before analysis of the rotational structure by Curry and Herzberg (5), Knauss and Ballard (6), and Brix and Herzberg (7), all of whom used continuous light sources and high resolution spectrographs.

Absorption measurements by Watanabe, Inn, and Zelikoff (8) using a hydrogen light source showed an apparent pressure effect due to insufficient resolution. They lead to an order of magnitude of absorption intensity useful for semiquantitative applications. Using a slightly higher resolution and assuming the spectral line width, Ditchburn and Heddle (9) have deduced values of the oscillator strengths of the bands. Such results do not agree with those of Bethke (10), deduced from integrated absorption coefficients measured at high pressure, or with those of Hudson (11), obtained recently at different temperatures. This discrepancy has lead to the conclusion that the line half-widths assumed by Ditchburn and Heddle were too small.

The present article reports measurements of the absorption coefficients of O_2 on more than 30 lines of atomic silicon excited in a microwave discharge tube. Such a light source, already described (12), presents various advantages; the spectral lines are narrow and their wavelengths are known with a high accuracy, the uncertainty being less than 0.0015 Å. In addition, such a source produces practically no continuous radiation.

Experimental

The spectral lines have been isolated in our experiments using a 50 cm focal length vacuum monochromator before entering the absorption cell which was a Pyrex tube closed at each end with a quartz lens. Two cell lengths have been used, 217 and 401 cm. The light intensity was monitored by an E.M.I. 6255 Cd photomultiplier. The output was recorded for various O_2 pressures measured by using mercury manometers and MacLeod gauges.

For the data obtained in the region between the 5–0 and the 17–0 band, Beer's law is obeyed and the values range from 1.5×10^{-22} to 1.6×10^{-18} cm^2 and are presented in Table I. In a few cases where the wavenumber of an O_2 rotational line differs only by a fraction of a cm^{-1} from the wavenumber of a silicon line at which the measurement takes place, the absorption cross-section has a negative pressure coefficient. In such cases an inferior limit for the absorption cross-section was obtained by extrapolating to zero pressure. For lower v' values a positive pressure coefficient appears which has already been reported by others (13, 14). We shall not deal here with this part of our data.

Interpretation

The absorption at 56 700.25 cm^{-1} of one of the Si lines corresponds to the maximum of the $3P_1$ line of the 16.0 band and the $11P_2$ line of the 17.0 band of O_2 which are blended at 56 700.37 cm^{-1}. We infer, from the integrated absorption coefficients given by Bethke and from the relative rotational population, that these lines have an equivalent rectangular width of 1 cm^{-1}.

This value is not in disagreement with those given by Wilkinson and Mulliken (15), Heddle (16), and Hudson (11). Assuming that this value is valid for the bands that we consider here, we have calculated the maxima of absorption cross-section at the center of the lines which are close to the silicon lines. We have then plotted the ratios of the measured values σ to the sum of the maximum values σ_i versus the distance $\Delta\nu$ in cm^{-1}, weighted according to the relation

$$\Delta\nu\,(\mathrm{cm}^{-1}) = \frac{\sum \Delta\nu_i \sigma_i}{\sum \sigma_i}$$

The graph of Fig. 2 shows the absorption dependence of the distance from the line even at 30 cm^{-1} from the line center. The error bars indicate only the uncertainty on the measured cross-sections. The scattering of the points can be attributed to the uncertainty of the wavenumbers for the bands having v' values lower than 12, to the assumption of a constant half-width and to the overlapping of the bands which affects Bethke's values.

The solid line represents Rice's formula (17) for the shape of a line broadened by predissociation. To obtain the best fit of this curve with our data the half-width has to be fixed at 1.4 cm^{-1}.

Conclusion

A line half-width of 1.4 cm^{-1}, which must be chosen to obtain the best fit to the data mainly at large values of $\Delta\nu$ where it has the largest influence on the ratio σ/σ_i, indicates that the band oscillator strengths given by Bethke may be too low by as much as a factor of two or three at least for the v' values smaller than 12.

No continuous absorption underlying the bands on which we report in this article can be deduced from our measurements. The data reported here enforce the old idea of Flory (18)

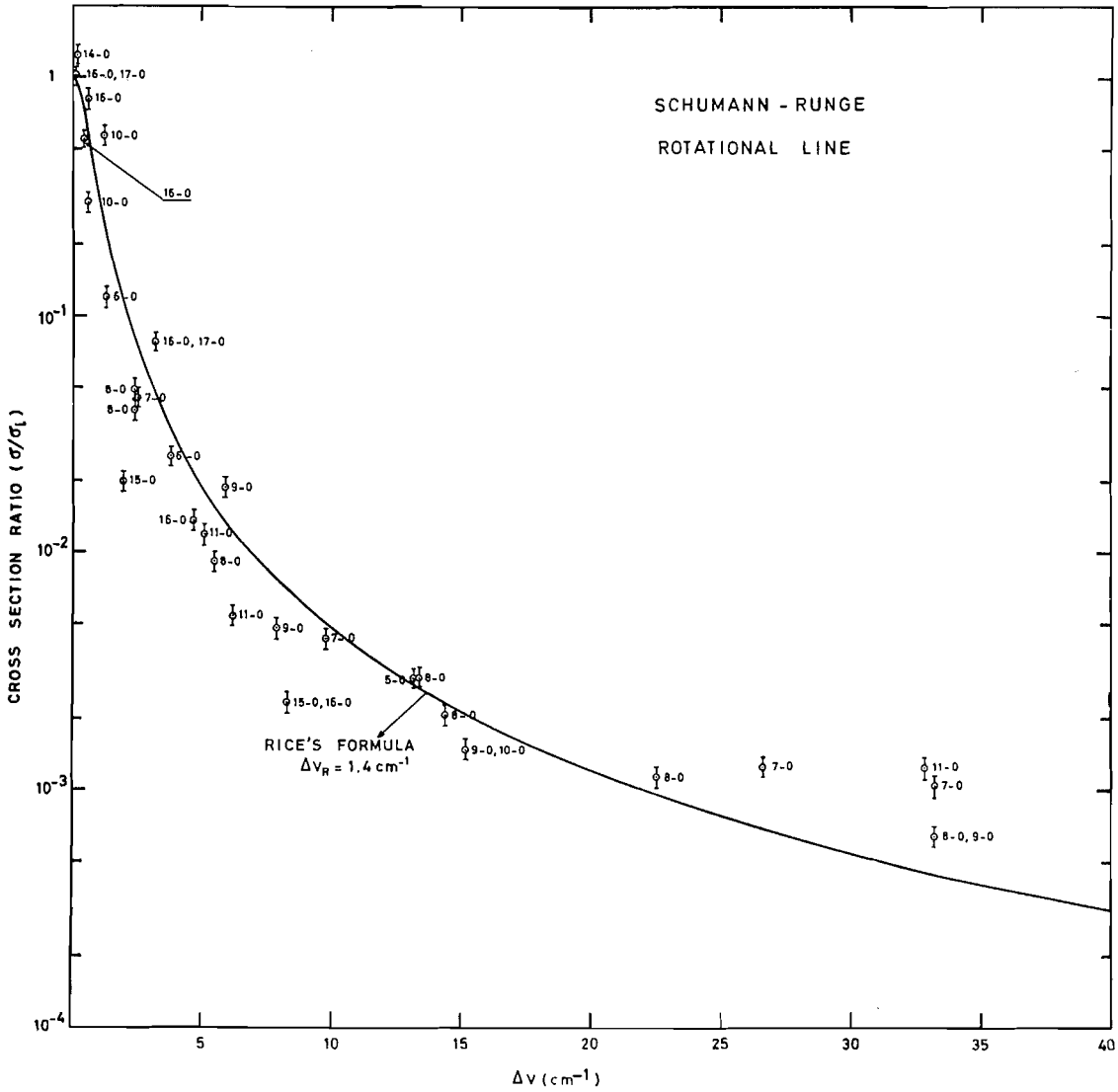

FIG. 2. Ratios σ/σ_l of the measured cross section σ and calculated cross section at the line center σ_l vs. the distance $\Delta\nu$ from the line center.

relating to the predissociation of the oxygen molecule in the Schumann–Runge bands.

A synthetic absorption spectrum can be computed using a line half-width of 1.4 cm^{-1} and Bethke's values for the band oscillator strengths. It exhibits minima and maxima of absorption cross-section which lead to unit optical depth in the atmosphere between altitudes at 25 and 120 km. The deduction of precise values will only become possible when the position of the lines and the strength of the bands has been accurately determined.

1. H. KREUSLER. Ann. Phys. **6**, 412 (1901).
2. L. P. GRANATH. Phys. Rev. **34**, 1045 (1929).
3. H. BUISSON, C. JAUSSERAN, and P. ROUARD. Rev. Optique, **12**, 70 (1933).
4. A. VASSY. Ann. Phys. Paris, **16**, 145 (1941).
5. J. CURRY and G. HERZBERG. Ann. Physik, 5 Folge, **19**, 800 (1934).
6. H. P. KNAUSS and S. S. BALLARD. Phys. Rev. **48**, 796 (1935).

Can. J. Chem. Downloaded from www.nrcresearchpress.com by 210.87.254.6 on 09/05/12
For personal use only.

7. P. BRIX and G. HERZBERG. Can. J. Phys. **32**, 110 (1954).
8. K. WATANABE, E. C. Y. INN, and M. ZELIKOFF. J. Chem. Phys. **21**, 1026 (1953).
9. R. W. DITCHBURN and D. W. O. HEDDLE. Proc. Roy. Soc. London, Ser. A, **226**, 509 (1954).
10. G. W. BETHKE. J. Chem. Phys. **31**, 669 (1959).
11. R. D. HUDSON and V. L. CARTER. Private communication.
12. V. KAUFMAN, L. J. RADZIEMSKI, and K. L. ANDREW. J. Opt. Soc. Am. **56**, 911 (1966).
13. W. HEILPERN. Helv. Phys. Acta, **14**, 329 (1941).
14. R. W. DITCHBURN and P. A. YOUNG. J. Atmospheric Terrest. Phys. **24**, 127 (1962).
15. P. G. WILKINSON and R. S. MULLIKEN. Astrophys. J. **125**, 594 (1957).
16. D. W. O. HEDDLE. J. Chem. Phys. **32**, 1889 (1960).
17. O. K. RICE. Phys. Rev. **35**, 1551 (1930).
18. P. J. FLORY. J. Chem. Phys. **4**, 23 (1936).

Can. J. Chem. Downloaded from www.nrcresearchpress.com by 210.87.254.6 on 09/05/12
For personal use only.

Predissociation in N_2 and O_2[1]

ROBERT D. HUDSON[2] AND VIRGINIA L. CARTER
Space Physics Laboratory, Aerospace Corporation, El Segundo, California

Received November 21, 1968

An outline discussion is given of some of the complications in the measurement of absorption cross sections which arise from finite instrumental bandwidths. Application is made to data on O_2 and N_2 from the literature.

Canadian Journal of Chemistry, 47, 1840 (1969)

Introduction

In a recent paper (1) we have shown that published absorption cross sections obtained at maxima or minima could be in error by as much as a factor of two, and that published line and band profiles are probably erroneous because of a failure to take into account the effects of finite instrumental bandwidths. In this paper we should like to present some measurements that we have performed on N_2 (2), and O_2 (3) at high resolution, and to show that another consequence of poor resolution is a loss of information regarding the physical processes that accompany the absorption.

Results

Molecular Oxygen

We would like to discuss the molecular oxygen results first. Our initial aim was to study the effect of temperature on the absorption of oxygen in the Schumann–Runge system, at an instrumental bandwidth of 0.075 Å. The results of our study of the dependence of the continuum on temperature were published some time ago (4). The dependence of the band structure is more complicated as is indicated in Fig. 1, which covers the spectral range from 1878 to 1894 Å. All three absorption traces were obtained with the same concentration of oxygen in the absorption cell, thus the effects that one sees are due entirely to the redistribution in the ground vibrational and rotational levels. The curve at 600 °K is of special interest as the fraction of molecules in the $v'' = 1$ state at that temperature is 0.0234, and yet the 9–1 band obviously gives rise to more absorption than the 6–0 band. This fact reflects the large increase in Franck–Condon factors from the $v'' = 0$ to the $v'' = 1$ levels due in part to the relatively large (0.4 Å) difference between the internuclear separations of the ground $X^3\Sigma_g^-$ and the excited $B^3\Sigma_u^-$ electronic states. One of the most important findings of the analysis was that all of the upper vibrational levels from $v' = 3$ to 17 were subject to predissociation, the individual rotational lines having half-widths varying from 0.5 to 2.3 cm^{-1}. Predissociation in these bands explains the failure, thus far, to observe fluorescence in the Schumann–Runge bands in the upper atmosphere, and provides an additional source of atomic oxygen between 65 and 95 km, both atoms of which will be left in the ^3P state with kinetic energies of up to 1 eV. We have recently measured this photodissociation rate in the laboratory, as a function of column height, at both 200 and 300° K and the resulting atomic oxygen production rate for the CIRA 1965 standard atmosphere (12) is shown in Fig. 2. The curve shown with the Schu-

[1]This work was supported by the United States Air Force under contract number FO4695-67-C-0158.

[2]Present address: The Joint Institute for Laboratory Astrophysics, The University of Colorado, Boulder, Colorado 80302.

7. P. BRIX and G. HERZBERG. Can. J. Phys. **32**, 110 (1954).
8. K. WATANABE, E. C. Y. INN, and M. ZELIKOFF. J. Chem. Phys. **21**, 1026 (1953).
9. R. W. DITCHBURN and D. W. O. HEDDLE. Proc. Roy. Soc. London, Ser. A, **226**, 509 (1954).
10. G. W. BETHKE. J. Chem. Phys. **31**, 669 (1959).
11. R. D. HUDSON and V. L. CARTER. Private communication.
12. V. KAUFMAN, L. J. RADZIEMSKI, and K. L. ANDREW. J. Opt. Soc. Am. **56**, 911 (1966).
13. W. HEILPERN. Helv. Phys. Acta, **14**, 329 (1941).
14. R. W. DITCHBURN and P. A. YOUNG. J. Atmospheric Terrest. Phys. **24**, 127 (1962).
15. P. G. WILKINSON and R. S. MULLIKEN. Astrophys. J. **125**, 594 (1957).
16. D. W. O. HEDDLE. J. Chem. Phys. **32**, 1889 (1960).
17. O. K. RICE. Phys. Rev. **35**, 1551 (1930).
18. P. J. FLORY. J. Chem. Phys. **4**, 23 (1936).

Can. J. Chem. Downloaded from www.nrcresearchpress.com by 210.87.254.6 on 09/05/12
For personal use only.

Predissociation in N_2 and O_2[1]

ROBERT D. HUDSON[2] AND VIRGINIA L. CARTER
Space Physics Laboratory, Aerospace Corporation, El Segundo, California

Received November 21, 1968

An outline discussion is given of some of the complications in the measurement of absorption cross sections which arise from finite instrumental bandwidths. Application is made to data on O_2 and N_2 from the literature.

Canadian Journal of Chemistry, 47, 1840 (1969)

Introduction

In a recent paper (1) we have shown that published absorption cross sections obtained at maxima or minima could be in error by as much as a factor of two, and that published line and band profiles are probably erroneous because of a failure to take into account the effects of finite instrumental bandwidths. In this paper we should like to present some measurements that we have performed on N_2 (2), and O_2 (3) at high resolution, and to show that another consequence of poor resolution is a loss of information regarding the physical processes that accompany the absorption.

Results

Molecular Oxygen

We would like to discuss the molecular oxygen results first. Our initial aim was to study the effect of temperature on the absorption of oxygen in the Schumann–Runge system, at an instrumental bandwidth of 0.075 Å. The results of our study of the dependence of the continuum on temperature were published some time ago (4). The dependence of the band structure is more complicated as is indicated in Fig. 1, which covers the spectral range from 1878 to 1894 Å. All three absorption traces were obtained with the same concentration of oxygen in the absorption cell, thus the effects that one sees are due entirely to the redistribution in the ground vibrational and rotational levels. The curve at 600 °K is of special interest as the fraction of molecules in the $v'' = 1$ state at that temperature is 0.0234, and yet the 9–1 band obviously gives rise to more absorption than the 6–0 band. This fact reflects the large increase in Franck–Condon factors from the $v'' = 0$ to the $v'' = 1$ levels due in part to the relatively large (0.4 Å) difference between the internuclear separations of the ground $X^3\Sigma_g^-$ and the excited $B^3\Sigma_u^-$ electronic states. One of the most important findings of the analysis was that all of the upper vibrational levels from $v' = 3$ to 17 were subject to predissociation, the individual rotational lines having half-widths varying from 0.5 to 2.3 cm^{-1}. Predissociation in these bands explains the failure, thus far, to observe fluorescence in the Schumann–Runge bands in the upper atmosphere, and provides an additional source of atomic oxygen between 65 and 95 km, both atoms of which will be left in the ^3P state with kinetic energies of up to 1 eV. We have recently measured this photodissociation rate in the laboratory, as a function of column height, at both 200 and 300° K and the resulting atomic oxygen production rate for the CIRA 1965 standard atmosphere (12) is shown in Fig. 2. The curve shown with the Schu-

[1]This work was supported by the United States Air Force under contract number FO4695-67-C-0158.

[2]Present address: The Joint Institute for Laboratory Astrophysics, The University of Colorado, Boulder, Colorado 80302.

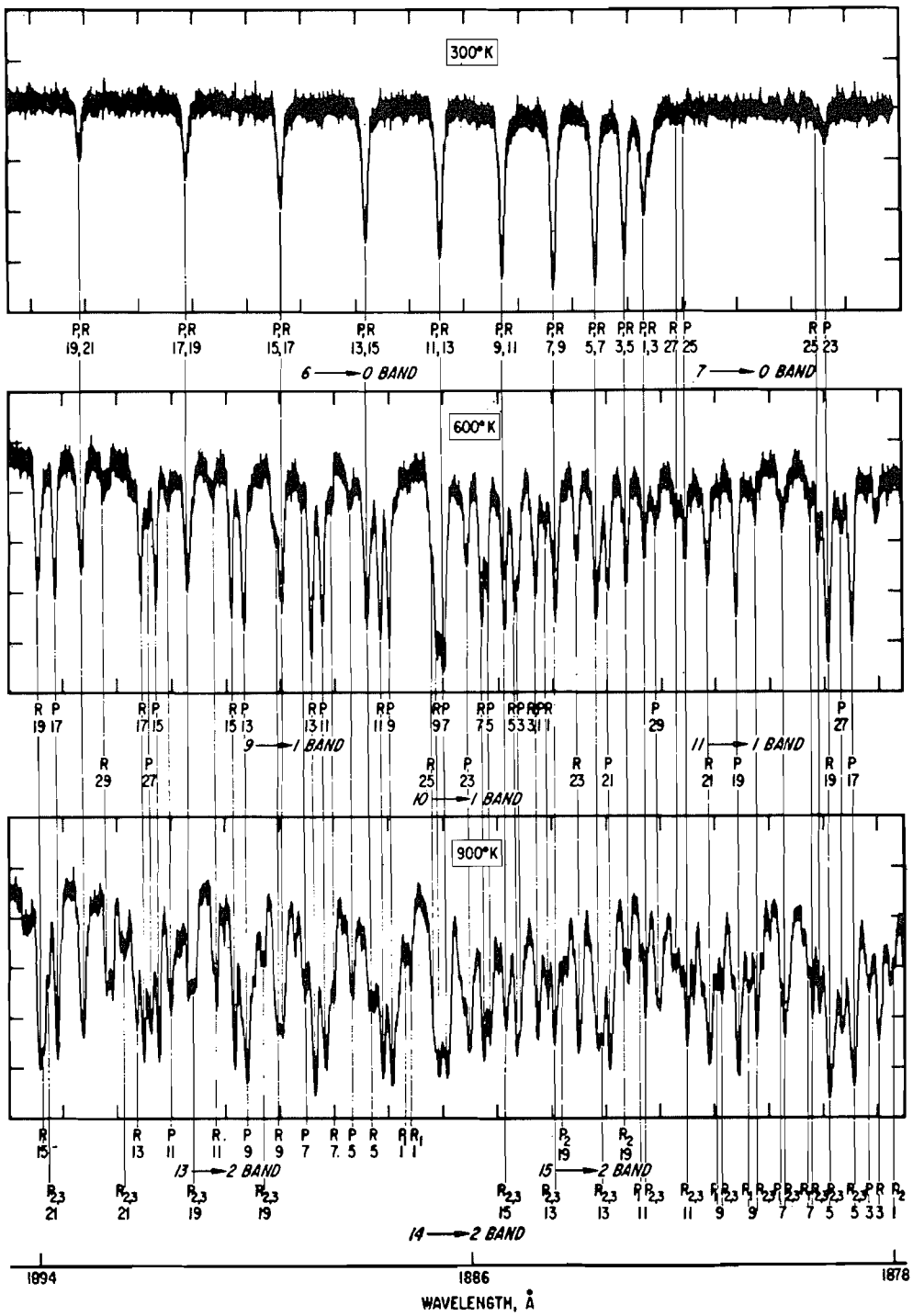

FIG. 1. Absorption by molecular oxygen between 1878 and 1894 Å at 300, 600, and 900 °K.

Can. J. Chem. Downloaded from www.nrcresearchpress.com by 210.87.254.6 on 09/05/12
For personal use only.

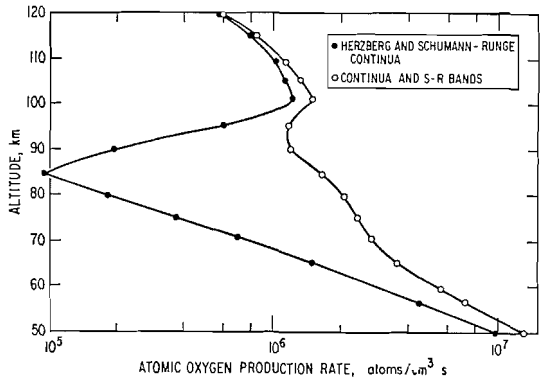

FIG. 2. Comparison of atomic oxygen production rate, between 50 and 120 km, with and without the assumption of predissociation in the Schumann–Runge system.

mann–Runge bands included, is the average of the 200 and 300 °K curves, as, within our experimental error, the results are the same for both temperatures. The additional atoms from predissociation can be seen to fill in the region from 65 to 95 km, giving an overall curve for atomic oxygen production that increases with a decrease in altitude.

Molecular Nitrogen

Figure 3 shows a small portion of the nitrogen absorption spectrum that we have obtained at 0.04 Å bandwidth using photoelectric techniques. We should like to stress that the plot here is of the average cross section over our bandwidth and not the true cross section. For comparison we show some previous experimental results (5, 6). Attempts to fit this curve to theoretical band profiles indicate that the widths of the individual rotational lines are greater than 2 cm^{-1} (compared to Doppler widths of 0.27 cm^{-1}). Line broadening of this magnitude has been reported by Lawrence *et al.* (7) for an absorption band in N_2 at 972 Å. Tilford and Wilkinson (8) have observed intensity anomalies in the emission spectrum of N_2 between 900 and 1130 Å which they ascribe to predissociation, and it seems reasonable to ascribe the broadening seen in absorption to the same phenomenon. We have made a preliminary survey, with 0.038 Å bandwidth, of the absorption bands of N_2 between 800 and 1000 Å, and it appears that most of the bands show widths significantly greater than the corresponding Doppler widths.

We have calculated the production rate of atomic nitrogen in the atmosphere above 150 km assuming (*a*) that all the absorption bands in N_2 between 800 and 1000 Å are indeed predissociated, (*b*) that the room temperature absorption cross sections given by Cook and Metzger (6), Huffman *et al.* (5), Samson and Cairns (9), and Watanabe and Marmo (10) are applicable, (*c*) the solar emission fluxes as given by Hinteregger and Hall (11), and (*d*) the CIRA 1965 standard atmosphere (12) is applicable. The results of this calculation versus altitude are shown in Fig. 4 along with calculated production rates resulting from ion–molecular reactions taken from a recent paper by Ghosh (13). These results indicate that the photoproduction of atomic nitrogen in the upper atmosphere could be a factor of 10^4 greater than has been assumed previously and could contribute significantly to the total production rate of atomic nitrogen in the atmosphere.

The actual photoproduction rate of atomic nitrogen in the upper atmosphere is likely to be different from that shown in Fig. 4, as the use of room temperature absorption cross sections may not be valid at altitudes where the temperature can range from 300 to 1500 °K. The band absorption profiles applicable to the conditions of temperature and pressure in the atmosphere above 120 km, can be calculated from room temperature data, but only when more definitive measurements of the absorption cross sections, band oscillator strengths, and line widths have been made. Account must also be taken of the variation of the Franck–Condon factors with v'' in view of the high probability that, in the upper atmosphere, non-thermal distributions prevail in the ground-state vibrational levels of molecular nitrogen (14).

Conclusion

In conclusion we should like to suggest (*a*) that predissociation in O_2 and N_2 could be of consequence in the chemistry of the upper atmosphere, (*b*) that the calculation of the dissociation rate of N_2 depends on an accurate knowledge of room temperature absorption profiles and Franck–Condon factors, and that the presently published data are insufficient, and (*c*) that physical information of great importance to aeronomic calculations can be lost when insufficient resolution is used in absorption spectroscopy.

Can. J. Chem. Downloaded from www.nrcresearchpress.com by 210.87.254.6 on 09/05/12
For personal use only.

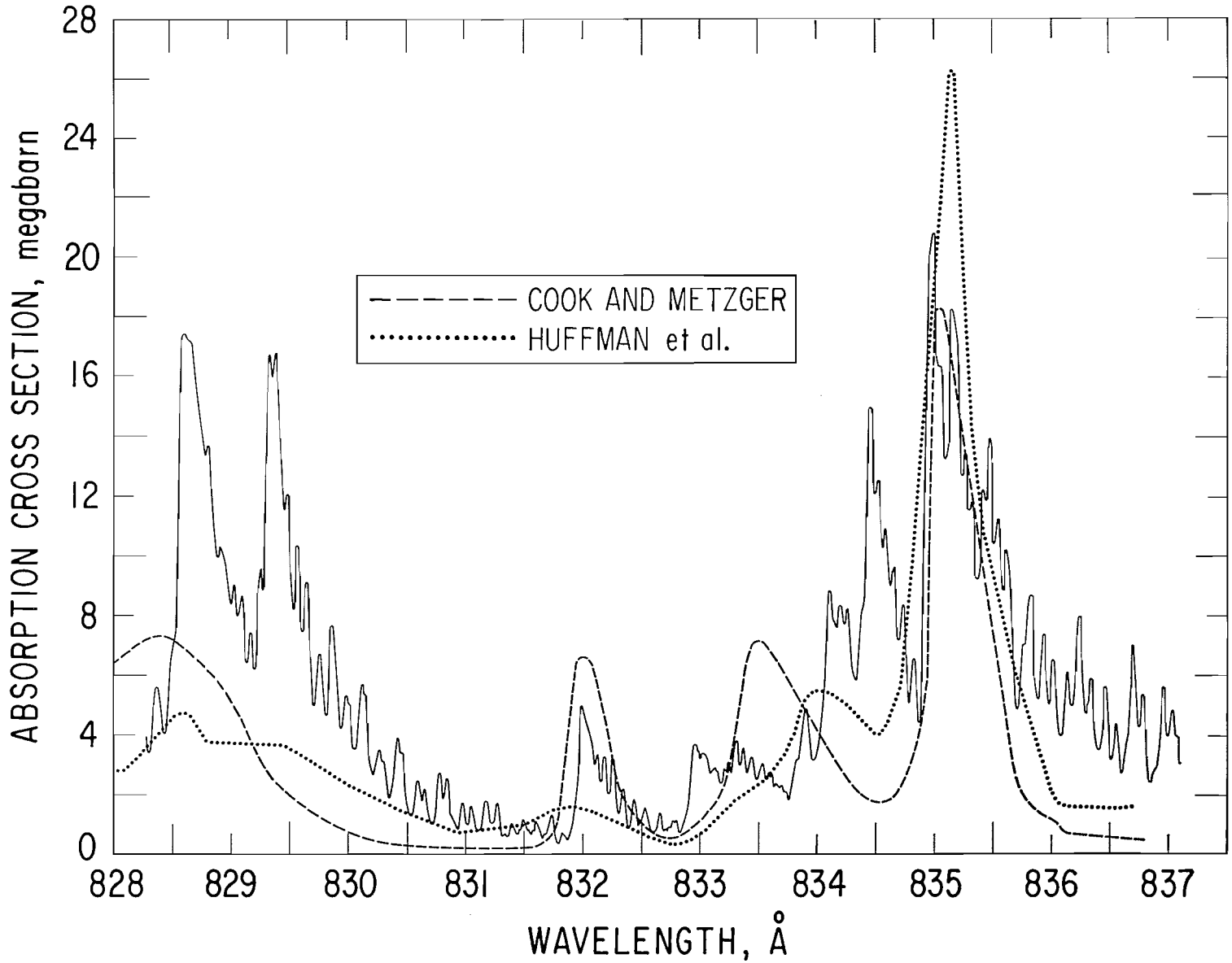

FIG. 3. The absorption cross section of molecular nitrogen between 828 and 838 Å. The solid curve is the result of this experiment at 0.04 Å bandwidth, the dotted curves were obtained at 0.5 Å bandwidth.

Can. J. Chem. Downloaded from www.nrcresearchpress.com by 210.87.254.6 on 09/05/12
For personal use only.

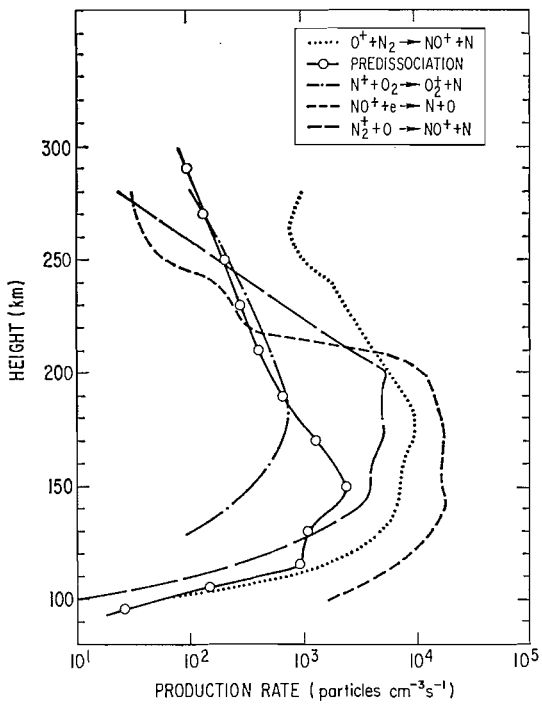

FIG. 4. Comparison of calculated atomic nitrogen production rates from ion–molecular reactions (13) and from predissociation (2).

Acknowledgments

Our thanks are due to Dr. R. A. Becker for his help and encouragement in this work and to R. Marcoe and M. E. Brennan for technical assistance.

1. R. D. HUDSON and V. L. CARTER. J. Opt. Soc. Am. **58**, 227, 1968.
2. R. D. HUDSON and V. L. CARTER. J. Geophys. Res. To be published. 1969.
3. R. D. HUDSON and V. L. CARTER. J. Opt. Soc. Am. To be published. 1969.
4. R. D. HUDSON, V. L. CARTER, and J. A. STEIN. J. Geophys. Res. **71**, 2295 (1966).
5. R. E. HUFFMAN, Y. TANAKA, and J. C. LARRABEE. J. Chem. Phys. **39**, 910 (1963).
6. G. R. COOK and P. H. METZGER. J. Chem. Phys. **41**, 321 (1964).
7. G. M. LAWRENCE, D. L. MICKEY, and K. DRESSLER. J. Chem. Phys. **48**, 1989 (1968).
8. S. G. TILFORD and P. G. WILKINSON. J. Mol. Spectry. **12**, 347 (1964).
9. J. A. R. SAMSON and R. B. CAIRNS. J. Geophys. Res. **69**, 4583 (1964).
10. K. WATANABE and F. F. MARMO. J. Chem. Phys. **25**, 965 (1956).
11. H. E. HINTEREGGER and L. A. HALL. Space Research V. Proc. Vth Intern. Space Sci. Sym. North Holland Publishing Co., Amsterdam. 1965.
12. CIRA 1965, COSPAR International Reference Atmosphere 1965. North Holland Publishing Co., Amsterdam. 1965.
13. S. N. GHOSH. J. Geophys. Res. **73**, 309 (1968).
14. J. C. G. WALKER. Planetary Space Sci. **16**, 321 (1968).

Comments, Replies, and Summary

COMMENTS BY G. M. LAWRENCE[1]

The high-resolution absorption measurements of Lawrence, Mickey, and Dressler were made to investigate the relation between electron impact cross-sections and ultraviolet absorption results. They concluded that agreement could be produced by going to low enough pressures and high enough resolution. Thus if one is interested in true absorption coefficients averaged over wavelength one might well consider using electron impact oscillator strengths.

COMMENTS BY J. W. McGOWAN[2]

Preliminary experiments have been carried out in our laboratory on the excitation of N_2 in the vacuum ultraviolet under electron impact. In particular, we have found evidence for the strong dissociative excitation of the first resonance line of atomic nitrogen

$$N_2 + e \rightarrow N(^4P) + N(^4S) + e$$
$$\searrow \rightarrow N(^4S) + h\nu\,(10.3\text{ eV})$$

Measurements were made on N_2 at a pressure near 10^{-6} Torr, using a source of monoenergetic electrons and a photo-multiplier with a LiF window and a KBr photocathode. The spectral sensitivity of our detector is from 1050 to $\sim$ 1450 Å, and therefore responds to radiation from the Lyman–Birge–Hopfield band system and the second negative system as well as the resonance radiation from the lowest ^4P states of the nitrogen atom.

Our preliminary results are shown in the Fig. 1. The approximate value of the cross-section for dissociative excitation is 4×10^{-17} cm^2 for 80 eV

[1]Address: Douglas Advanced Research Laboratories, Huntinton Beach, California.
[2]Address: Gulf General Atomic, P.O. Box 608, San Diego, California 92112.

Can. J. Chem. Downloaded from www.nrcresearchpress.com by 210.87.254.6 on 09/05/12
For personal use only.

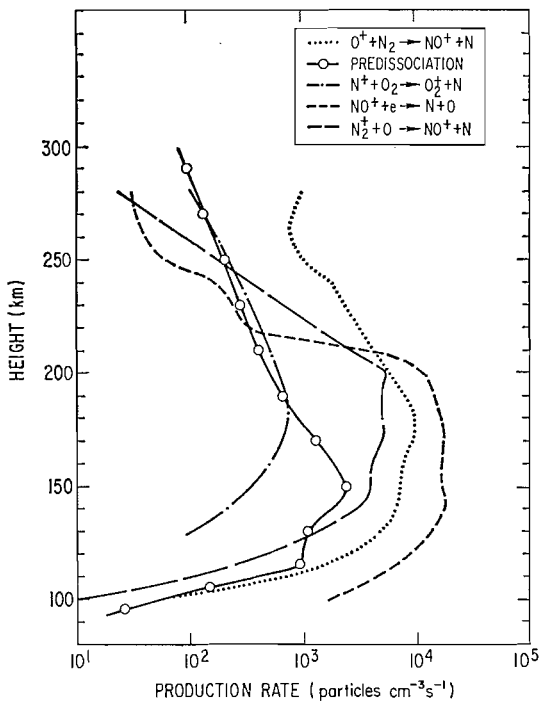

FIG. 4. Comparison of calculated atomic nitrogen production rates from ion–molecular reactions (13) and from predissociation (2).

Acknowledgments

Our thanks are due to Dr. R. A. Becker for his help and encouragement in this work and to R. Marcoe and M. E. Brennan for technical assistance.

1. R. D. HUDSON and V. L. CARTER. J. Opt. Soc. Am. **58**, 227, 1968.
2. R. D. HUDSON and V. L. CARTER. J. Geophys. Res. To be published. 1969.
3. R. D. HUDSON and V. L. CARTER. J. Opt. Soc. Am. To be published. 1969.
4. R. D. HUDSON, V. L. CARTER, and J. A. STEIN. J. Geophys. Res. **71**, 2295 (1966).
5. R. E. HUFFMAN, Y. TANAKA, and J. C. LARRABEE. J. Chem. Phys. **39**, 910 (1963).
6. G. R. COOK and P. H. METZGER. J. Chem. Phys. **41**, 321 (1964).
7. G. M. LAWRENCE, D. L. MICKEY, and K. DRESSLER. J. Chem. Phys. **48**, 1989 (1968).
8. S. G. TILFORD and P. G. WILKINSON. J. Mol. Spectry. **12**, 347 (1964).
9. J. A. R. SAMSON and R. B. CAIRNS. J. Geophys. Res. **69**, 4583 (1964).
10. K. WATANABE and F. F. MARMO. J. Chem. Phys. **25**, 965 (1956).
11. H. E. HINTEREGGER and L. A. HALL. Space Research V. Proc. Vth Intern. Space Sci. Sym. North Holland Publishing Co., Amsterdam. 1965.
12. CIRA 1965, COSPAR International Reference Atmosphere 1965. North Holland Publishing Co., Amsterdam. 1965.
13. S. N. GHOSH. J. Geophys. Res. **73**, 309 (1968).
14. J. C. G. WALKER. Planetary Space Sci. **16**, 321 (1968).

Comments, Replies, and Summary

COMMENTS BY G. M. LAWRENCE[1]

The high-resolution absorption measurements of Lawrence, Mickey, and Dressler were made to investigate the relation between electron impact cross-sections and ultraviolet absorption results. They concluded that agreement could be produced by going to low enough pressures and high enough resolution. Thus if one is interested in true absorption coefficients averaged over wavelength one might well consider using electron impact oscillator strengths.

COMMENTS BY J. W. McGOWAN[2]

Preliminary experiments have been carried out in our laboratory on the excitation of N_2 in the vacuum ultraviolet under electron impact. In particular, we have found evidence for the strong dissociative excitation of the first resonance line of atomic nitrogen

$$N_2 + e \rightarrow N(^4P) + N(^4S) + e$$
$$\searrow \rightarrow N(^4S) + h\nu\,(10.3\text{ eV})$$

Measurements were made on N_2 at a pressure near 10^{-6} Torr, using a source of monoenergetic electrons and a photo-multiplier with a LiF window and a KBr photocathode. The spectral sensitivity of our detector is from 1050 to $\sim$ 1450 Å, and therefore responds to radiation from the Lyman–Birge–Hopfield band system and the second negative system as well as the resonance radiation from the lowest ^4P states of the nitrogen atom.

Our preliminary results are shown in the Fig. 1. The approximate value of the cross-section for dissociative excitation is 4×10^{-17} cm^2 for 80 eV

[1]Address: Douglas Advanced Research Laboratories, Huntinton Beach, California.
[2]Address: Gulf General Atomic, P.O. Box 608, San Diego, California 92112.

Can. J. Chem. Downloaded from www.nrcresearchpress.com by 210.87.254.6 on 09/05/12
For personal use only.

electrons. This has been determined relative to the 2p excitation cross-section of atomic hydrogen.

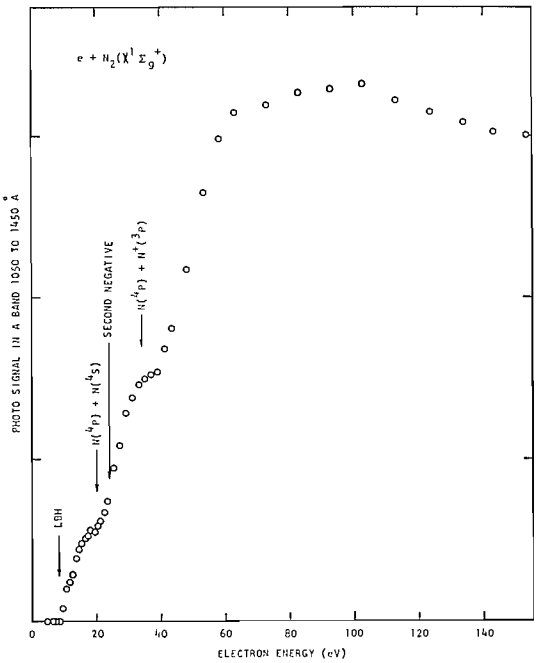

FIG. 1. Plot of photo signal vs. electron energy.

REPLY BY R. E. HUFFMAN

The interesting dissociative excitation process discussed in this comment has not been reported using photon absorption excitation, to the author's knowledge.

SUMMARY BY CHAIRMAN, F. R. GILMORE[3]

Measurements of absorption coefficients for atmospheric gases have been carried out for many years, yet important additions and improvements have just been made recently, and much still remains to be done. These conclusions are evident from R. E. Huffman's authoritative review which began this session. He pointed out that one of the most important problems is getting sufficient spectral resolution for precise measurements in regions where molecular bands or atomic lines are important. This point was reemphasized by the contributed papers of Ackerman, Biaume, and Nicolet, and of Hudson and Carter, which followed. Ackerman presented data on the O_2 Schumann–Runge bands with sufficient resolution to reveal, in considerable detail, the variation of absorption across individual rotational lines. Hudson presented data on N_2 and O_2 with a lesser resolution, but still sufficient to show that many of the line widths are much greater than Doppler widths, due to predissociation. Such predissociated bands may make important contributions to the production rates of atomic nitrogen and oxygen in the upper atmosphere.

As pointed out by both Huffman and Hudson, for atmospheric applications it is often necessary both to obtain good absorption cross sections and to determine the species and excitational states of the photo-absorption products. Much more work is needed in this field. High-resolution spectroscopy frequently provides good clues to the products, but in some cases direct detection schemes seem necessary.

Another area needing more work is the absorption spectroscopy of unstable or excited species, such as atomic oxygen and O_2 $a^1\Delta_g$.

The session concluded with a paper, "The N_2 Vegard–Kaplan System in Absorption", by D. E. Shemansky. This paper has been submitted to the Journal of Chemical Physics, and is not reproduced here. Its results are mentioned briefly in the Summary of the Session on Transition Probabilities and Lifetimes (see below).

[3]Address: The Rand Corporation, Santa Monica, California 90 406.

Can. J. Chem. Downloaded from www.nrcresearchpress.com by 210.87.254.6 on 09/05/12
For personal use only.

Can. J. Chem. Downloaded from www.nrcresearchpress.com by 210.87.254.5 on 09/05/12
For personal use only.

Aeronomically important transition probability data

R. W. NICHOLLS
Centre for Research in Experimental Space Science, York University, Toronto, Ontario

Received November 27, 1968

Since the 1963 I.A.G.A. conference at Berkeley our knowledge of radiative transitions which are aeronomically important has been extended particularly into the vacuum ultraviolet region of the spectrum. A brief review is made of the newly established important radiative transitions. Recent experimental and theoretical work on radiative transitions which have aeronomical applications is discussed.

Canadian Journal of Chemistry, 47, 1847 (1969)

Introduction

A review was made (1) at the I.A.G.A. Aeronomy Symposium at the 1963 I.U.G.G. Congress at Berkeley on the state of knowledge of transition probability parameters for radiative transitions in species of aeronomical importance. A wide range of aeronomical phenomena (cold air absorption, hot air absorption, aurora, dayglow, nightglow, twilight glow) were considered there. In this paper, which is not intended to be so extensive, the previous review is supplemented with an account of some of the developments which have occurred in the past few years. The emphasis is more molecular than atomic, and in view of the very large volume of new data treated, reference is made here to papers only.

In the past five years the direction of aeronomical spectroscopy has been by the increased use of rocket, balloon, and satellite techniques to extend the wavelength region of active study into the vacuum ultraviolet region of the spectrum. New firm data in the wavelength region (1000–3500 Å) have been established both in the aurora and in the airglow. Some extensions have also been made in the infrared.

Thus the wavelength region considered in this paper is 1 000 – 10 000 Å. Within this wavelength region height profiles of important species have also been studied, and a continuing debate proceeds on the kinetics of reactions necessary to maintaining the species concentrations. Such work also requires firm knowledge of radiative lifetimes of excited species so that radiative depopulation processes can be accurately compared with collision processes.

For collision processes and reactions, a few hundreds of processes at the most have to be considered and are reviewed in other papers of the symposium. For radiative processes a much greater volume of basic data has to be assessed for all of the thousands of radiative transitions involved. Thus no attempt is made there to present tabular data. There has been a great deal of laboratory and associated theoretical work in the past five years stimulated by the needs of observational aeronomy and astrophysics. Some of this is also reviewed below. Chamberlain's monograph (2) remains an essential reference work to the whole field.

General Concepts

Much of aeronomy consists of diagnostic studies of the upper atmosphere by using the methods of quantitative spectroscopy on auroral and airglow emissions. Clear quantitative discussion of radiative transitions has often been obscured by ambiguous use of the many transition probability parameters which are commonly employed. Tatum (3) has made a very clear exposition of the transition probability aspects of molecular spectra.

The controlling parameters of the $U, v', J' \leftrightarrow L', v'', J''$ radiative molecular transition (symbols conventional (4)) is the transition strength matrix element.

$$[1] \qquad S^{U,v',J'}_{L,v'',J''} = |\int \Psi_{Uv'J'} M \Psi_{Lv''J''} d\tau|^2$$

In most aeronomical situations it is possible to average over the rotational structure of (v',v'') bands. The dominating parameter for such a band is then the band strength

$$[2a] \qquad S_{v'v''} = |\int \psi_{v'} R_e(r) \psi_{v''} dr|^2$$

where the electronic transition moment $R_e(r)$ is defined in eq. [2*b*], and ψ_v are the vibrational wavefunctions.

$$[2b] \qquad R_e(r) = \int \psi_{eu} M \psi_{eL} \, d\tau_e$$

Can. J. Chem. Downloaded from www.nrcresearchpress.com by 210.87.254.5 on 09/05/12
For personal use only.

For many band systems it is possible to write eq. [2*a*] in the factored form

$$[2c] \qquad S_{v'v''} = R_e^2(\bar{r}_{v'v''})q_{v'v''}$$

where the *r*-centroid is given by

$$[2d] \qquad \bar{r}_{v'v''} = \int\psi_{v'}\psi_{v''}r\,dr/\int\psi_{v'}\psi_{v''}\,dr$$

and the Franck–Condon factor by

$$[2e] \qquad q_{v'v''} = |\int\psi_{v'}\psi_{v''}\,dr|^2$$

Commonly used transition probability parameters defined in terms of $S_{v'v''}$ are
Einstein *A* coefficient,

$$[3a] \qquad A_{v'v''} \propto \nu^3_{v'v''}S_{v'v''}$$

Einstein *B* coefficient,

$$[3b] \qquad B_{v'v''} \propto S_{v'v''}$$

linear absorption coefficient,

$$[3c] \qquad k_{v'v''} \propto \nu_{v'v''}S_{v'v''}$$

atomic or molecular absorption coefficient or cross section,

$$[3d] \qquad \alpha_{v'v''} \propto \nu_{v'v''}S_{v'v''}$$

intensity or flux,

$$[3e] \qquad I_{v'v''} \propto N_{v'}\nu^4_{v'v''}S_{v'v''}$$

photon mean free path,

$$[3f] \qquad \Lambda_{v'v''} = (k_{v'v''})^{-1} \propto (\nu_{v'v''}S_{v'v''})^{-1}$$

optical depth,

$$[3g] \qquad \tau_{v'v''} = \int k_{v'v''}\,dz \propto \nu_{v'v''}S_{v'v''}$$

oscillator strength,

$$[3h] \qquad f_{v'v''} \propto \nu_{v'v''}S_{v'v''}$$

and radiative lifetime of upper state,

$$[3i] \qquad \tau_{v'} = 1/\sum_{v''}A_{v'v''} = 1/\sum_{v''}\nu^3_{v'v''}S_{v'v''}$$

The band strength dominates all of these, and in that many of them are used diagnostically to determine aeronomic conditions, it is of the greatest importance that firm information be available on band strengths. Thus experimental programs of great variety have been in progress to determine band strengths, and associated theoretical programs have been in progress to study molecular potentials, calculate Franck–Condon factors (which dominate band strengths), and more recently a start has been made to calculate electronic transition moments for simple molecules from an ab initio basis. Until quite recently resort had to be made to experiment for this, as our knowledge of electronic wavefunctions was almost as primitive as the computation power necessary to calculate them to a sufficient degree of accuracy that derived functions of them could be calculated with some confidence. In later sections of this paper we shall very briefly review recent experimental and theoretical work on most aspects of the band strengths for aeronomically important transitions.

The above discussion relates to radiative transitions. Electron collision induced transitions (excitation and/or ionization) may be similarly treated. Cross-sections for excitation and ionization of molecules are controlled by a similar strength factor

$$[4a] \qquad P^{V,v',J'}_{L,v'',J''} = |\int\Psi' V\Psi''\,dr|^2$$

where Ψ's are the respective total wave functions of the system (molecule + electron) before and after collision and V is the potential field in which the electron moves (1, 5, 6). Appeal to the Born–Oppenheimer approximation and to the Born approximation allows eq. [4*a*] to be factored into

$$[4b] \qquad P_{v'v''} = G_e^2(\bar{r}_{v'v''})q_{v'v''}$$

where the perturbation integral $G_e(r)$ involves electronic wave functions of electrons (Ψ_{elec}) and molecule (Ψ_u or Ψ_L)

$$[4c] \qquad G_e(r) = \int\psi'_{elec}\psi_u V\psi''_{elec}\psi_L\,d\tau_e$$

The Franck–Condon factors thus control to a large extent the vibration levels which are excited in electron collisions of molecule, and thus the spectral character of the resulting radiation, provided that the exciting (and/or ionizing) electrons may be represented by plane waves. A classic series of researches by Lassettre and colleagues (see on) in electron energy loss spectroscopy has confirmed how closely the Franck–Condon principle is followed in electron excitation of molecules by relatively energetic electrons, where the Born approximation is applicable.

Aeronomically Important Species and Transitions

With the exception of NO, no great change has occurred during the past five years in the important species and transitions recognized in aero-

Can. J. Chem. Downloaded from www.nrcresearchpress.com by 210.87.254.5 on 09/05/12
For personal use only.

nomical spectra. In contrast, it is apparent from other papers of this symposium that a number of new active species have been proposed to play possible active roles in rate processes. Two atlases of cold air absorption have recently been published (7, 8). Two atlases of airglow spectra have also recently appeared (9, 10). These atlases together with those in Chamberlain's monograph (2) are valuable aids to identification. Krassovsky and Sefov (11) have published a useful review paper on the airglow which lists important emitters. Barth (12, 13) made a most important contribution to the field by firmly establishing NO as an airglow emitter (of the gamma bands). The spectra of N_2, N_2^+, O_2, O_2^+, NO, OH, NI, NII, OI, OII, Na, H, Li, He, and Ca in the airglow and aurora have, in a number of cases reviewed below, been extended into the vacuum ultraviolet and less frequently into the near infrared. A number of the predictions of Swings, Bosman-Crespin, and Arpingny (14) on the nature of the auroral spectrum in the ultraviolet have been borne out. A very useful quantitative review has been made by Marr (15) of the processes which attenuate solar radiation in the atmosphere, particularly in the ultraviolet region of the spectrum. There have been further studies on the emissivity of high temperature air which will not be reviewed here.

The following short list reviews features of atomic and molecular spectra particularly in the vacuum ultraviolet which have been established as important since the last symposium.

Atomic Features

Hydrogen

Lyman alpha at 1216 Å has been recognized as an important feature of the airglow spectrum for some years (16, 17). There is a continuing debate as to whether it is also part of the auroral spectrum (18). Miller, Fastie, and Isler (19) showed that while Lyman alpha, N, O, and N_2 features were detected in the 1050–1550 Å region using rocket techniques, the strength of the Lyman alpha feature seemed to be independent of the orientation of the rocket.

Helium

Krassovsky and Shefov (11) review Soviet interferometric work on the near infrared line at 10 830 Å in the airglow which arises from transition from the metastable 2^3P state at about 21 V to the 2^3S level at about 20 V. The upper state is thought to be excited by energetic photoelectrons produced in photoionizations from solar ultraviolet photons. Tinsley (20) has made similar measurements. Brandt, Broadfoot, and McElroy (21) report observation of the 3889 line of orthohelium in the twilight airglow. This arises from the 3^3P to 2^3S transition.

Oxygen

Vacuum ultraviolet transitions of O and N have been observed in both the aurora and the airglow spectra. For example Fastie, Crosswhite, and Heath (22) reported the strong transition between $^3S_1$ and ^3P ground state of OI. Components of this line lie at 1302, 1304, and 1306 Å. Also observed were the forbidden transition between $^5S_2$ and the ground state at 1355 and 1358 Å. The 1304 feature is one of the strongest in the vacuum ultraviolet spectrum of the aurora.

Nitrogen

Fastie, Crosswhite, and Heath (22) tentatively identified the NI 1200 Å ($2p^3$ 4S–$2p^2$ ^3S) line in the wing of Lyman alpha. The associated 1134 Å NI line was not observed because of decreasing instrumental sensitivity.

Molecular Features

There have been significant extensions to our knowledge of important molecular transitions in the aurora and airglow in recent years, particularly in the ultraviolet. The most important of these is the observation of NO gamma bands by Barth in the airglow and the observation of the Lyman–Birge–Hopfield bands of N_2 in the aurora by Fastie and colleagues. In addition to observational work there has been much activity in developing phenomenological theories of excitation of atmospheric luminosities by electron and photon streams by Barth, Green, and colleagues, in many of which account is taken of numerous molecular band systems.

Nitrogen

The band-system which has received the greatest attention is the $a^1\Pi$–$X^1\Sigma$ Lyman–Birge–Hopfield system of N_2. This has been studied in auroral spectra by Fastie, Crosswhite, and Markham (23), Isler and Fastie (24), Murcray (25), and Fastie, Miller, and Isler (26). There has been speculation that the Birge–Hopfield ($b^1\Pi$–$X^1\Sigma^+$) and the Watson–Koontz ($h^1\Sigma_u^+$–$X^1\Sigma_g^+$) band systems also occur in the auroral spectra. The Lyman–Birge–Hopfield system is the major emitter. Definitive identification or refutation of

Can. J. Chem. Downloaded from www.nrcresearchpress.com by 210.87.254.5 on 09/05/12
For personal use only.

other nitrogen systems may be possible through a photographic study of the vacuum ultraviolet spectrum of the aurora using rocket techniques such as is in progress in the author's laboratory. Recent work suggests that the Lyman–Birge–Hopfield system may well be the only strong emitter. It is surprising, however, that in view of the strength of the N_2^+ ($B^2\Sigma$–$X^2\Sigma$) First Negative spectra in the aurora that the Second Negative bands ($C^2\Sigma$–$X^2\Sigma$) which lie in the same wavelength region as the Lyman–Birge–Hopfield, have not yet been observed. About 23 V is required to excite them directly from the ground state.

In the phenomenological theoretical study of excitation of the ultraviolet spectrum of the aurora by the "stopping" of electron beams, Green and Barth (27) include contributions from the First Negative and Meinel bands of N_2^+, the Vegard–Kaplan, First Positive, Second Positive, Lyman–Birge–Hopfield, Birge–Hopfield, Janin–Watson–Koontz, Herman–Baydon band systems of N_2. This work is part of an extensive program of similar calculations by Green and colleagues. See, for example, Stolarski and Green (28), Green (29), Green and Stolarski (30), and Green and Barth (31). Recent rocket studies by Fastie, Miller, and Isler (26) suggest that some of the estimated contributions from band systems other than the Lyman–Birge–Hopfield may be too large. The Second Negative system of N_2^+ does not seem to have been considered.

Nitric Oxide

One of the most important observations of the past few years is that of Barth (12, 13) of the NO ($A^2\Sigma$–$X^2\Pi$) gamma bands in the spectrum of the airglow. He reports that no beta ($B^2\Pi$–$X^2\Pi$) bands were observed.

Oxygen

Many observations have been made of the O_2 atmospheric ($b^1\Sigma_g^+$–$X^3\Sigma_g^-$) and O_2 infrared atmospheric ($a^1\Delta_g$–$X^3\Sigma_g^-$) emissions from the airglow. No new band systems of O_2 have been observed. Hennes (142) reports extended observations on the O_2($A^3\Sigma$–$X^3\Sigma$) Herzberg I system into the 2300–3800 Å region in a rocket airglow observation. It had previously been observed, for many years, over a small wavelength region from ground-based observations. Barth (32) and Tohmatsu (33) have suggested that there may be a contribution to the dayglow from fluorescently excited O_2 Schumann–Runge ($B^3\Sigma$–$X^3\Sigma$). Although most photon–$O_2(X)$ collisions would dissociate the O_2, some transitions to bound B-levels could re-radiate and redistribute the radiation to longer wavelengths, according to the Franck–Condon principle. The predicted spectrum has been calculated by Barth and Tohmatsu between 1800 and 3000 Å but has not yet been observed.

Continua

The air afterglow continuum from NO + O $\rightarrow$ NO_2^* $\rightarrow$ NO_2 + $h\nu$ (2) which has been one possible contributor to the airglow continuum may be reinforced by the continuum from inverse photodissociation of ozone in the Chapuis region (Gadsen (34)). The process involved is $O_2(a^1\Delta)$ + $O(^3P)$ $\rightarrow$ O_3 + $h\nu$. This additional process may account for the peak in the airglow continuum at 6000 Å.

Experimental and Theoretical Work

Much experimental and theoretical work has been done during the past 5 years to provide reliable and firm data on the transition probability (and related) parameters reviewed in Section II for species of aeronomical importance.

Major trends in experimental work have been

Wavelength Measurements on New Band Systems

See, for example, the work of McFarlane (35) on new infrared band systems of N_2 and of Degen (145) on ultraviolet systems of O_2.

Intensity Measurements in Emission and Absorption

See, for example, the work of Chandriah and Shepherd (36) on band strengths of the N_2 Vegard–Kaplan system, the work of McEwen and Nicholls (37) on band strengths of the Lyman–Birge–Hopfield system of N_2, and the work of Cook and Ogawa (38) on the absorption photoionization spectrum of N_2.

Lifetime Measurements of Excited States

See, for example, the work of Jeunehomme (39, 40) on the radiative lifetimes of the $C^3\Pi$ and $B^3\Pi$ states of N_2 and the $B^2\Sigma$ state of N_2^+ from the decay time of discharges, the work of Fink and Welge (41) and of Hesser and Dressler and colleagues (42, 70) on the radiative life of many molecular states by the phase shift method. Transition oscillator strengths are often calculated from such measurements.

Electron Energy Loss Spectroscopy

Lassettre and colleagues in a distinguished and extensive series of papers in J. Chem. Phys. since

Can. J. Chem. Downloaded from www.nrcresearchpress.com by 210.87.254.5 on 09/05/12
For personal use only.

1964, have studied the electron energy loss spectra in many gases, including atmospheric gases. They have compared and correlated their cross section measurements with the equivalent optical transition probabilities by appeal to a property of the Bethe generalized oscillator strengths (43). The inelastic cross section is a function of the generalized oscillator strength which, in the limit of zero electron momentum change, becomes the optical transition probability. See ref. (44) for discussion of the relevant theory, and ref. (45) for an application of work to the Lyman–Birge–Hopfield system of N_2. See also Lassettre's review in this symposium.

Similar major trends in theoretical work have been

Ab Initio Quantal Calculations of Molecular Properties

Within the past few years it has become possible, using the capabilities of large electronic computers, to make a start to study from first principles the detailed properties of complex multi-particle systems such as light diatomic molecules, to a sufficient degree of accuracy that comparison with experiment may fairly confidently be made. In early work of this nature the sheer volume of calculation of wave functions precluded the study of them at more than one internuclear separation. The situation is rapidly changing and realistic ab initio calculations of molecular properties are being made in a number of laboratories, notably at the University of Chicago. The topic will not be pursued further here except to mention a recent review of Ohno (46) on calculations on O_2 and N_2.

Molecular Potentials, Molecular Wavefunctions, and Derived Quantities

It is clear from the equations of the section "General Concepts" that the Franck–Condon factors and *r*-centroids are important desiderata for the diagnostic interpretation of aeronomical spectral intensities. These quantities are derived from molecular vibrational (and vibration–rotation) wavefunctions which are themselves solutions of the Schrödinger equation for the one dimensional molecular vibrating rotator appropriate to a specific molecular potential. Thus much effort has been expended in compiling accurate and realistic numerical molecular potentials, using a variety of methods and using experimental measurements of molecular properties as basic data. Gilmore (47, 48) has calculated a definitive set of potentials of N_2, O_2, NO and their ions. Similar work of this nature has been done by Vanderslice (49) and Benesch, Vanderslice, Tilford, and Wilkinson (50). See also the review of Spindler (51) and of Steele, Lippincott, and Vanderslice (144).

There has also been much effort in a number of laboratories to develop efficient and comprehensive computer programs to solve the wave equation numerically appropriate to the numerical potentials and to compute derived quantities of these wavefunctions such as Franck–Condon factors and *r*-centroids. Such work has been done by Jarmain (52–54), Cooley (55, 56), Cashion (57), Zare, Larson, and Berg (58), and by Spindler (51). Work of a similar nature is in progress in the E.S.S.A. laboratories at Boulder (59), at the Air Force Special Weapons Laboratory, Kirtland, New Mexico (60), and in the author's laboratory (61) where a very comprehensive program has been prepared to produce automatically Franck–Condon factor and *r*-centroid arrays (including rotation–vibration interaction) for the variety of realistic potentials. Aeronomic and astrophysical transitions have been emphasized in this work and the results will shortly appear in a number of monographs.

There has also been some activity in the calculation of Franck–Condon factor arrays for a number of transitions appropriate to analytic potentials. A review has been made (62) of nearly 100 transitions studied by the author using the Morse model of potential, and ways by which interpolation among such arrays may be carried out. Not only have radiative transitions between bound states been considered but also excitation and ionization transitions of aeronomical interest with applications to eq. [4*b*] have been published (6, 63). Studies have also been made of Franck–Condon densities of photodissociation continua of O_2 (64, 65). The matrix multiplication property (66) of vibrational overlap integrals of transitions between three cyclically ordered states i, j, k

$$[5] \qquad (i,k) = \sum_j (i,j)(j,k)$$

may provide another rapid way of roughly estimating Franck–Condon factors.

The *r*-centroid concept has been under debate, particularly the circumstances under which it breaks down. A recent detailed study by Drake (67, 68) has shown explicitly the circumstances under which the concept is rigorously valid.

Can. J. Chem. Downloaded from www.nrcresearchpress.com by 210.87.254.5 on 09/05/12
For personal use only.

These include the large majority of aeronomic band systems.

Phenomenological Studies of Aeronomical Luminosities

Reference has already been made to the work of Green, Barth, and colleagues (see ref. 69) and relevant references under nitrogen in section above) on the use of phenomenological models for electron stopping power and fluorescence efficiencies to predict spectral energy distributions of aurorae and airglows in planetary atmospheres. This work is briefly discussed in the communication of Peterson at the symposium.

We now make a brief review of specific experimental and theoretical studies of aeronomic species and transitions.

Transitions: A, Molecular Transitions

Nitrogen (N_2)

Lifetime Measurements

Some of the most important experimental work on N_2 during the past five years has been lifetime measurements on electronic states. The triplet states have been the most studied. Jeunehomme (40) has measured the lifetimes of levels of the $B^3\Pi$ state as between 4 and 8 μs, which is equivalent to an oscillator strength f_{00} of the (0,0) band of the First Positive system of 2×10^{-3}. A number of measurements have been made on the lifetimes of levels of the $C^3\Pi$ state which is the upper state of the Second Positive system. Fink and Welge (41) measuring decay of the (0,0) and (0,1) Second Positive bands established a lifetime of 2.7×10^{-8} s for the $v = 0$ level from which an oscillator strength of the (0,0) band of 6.3×10^{-3} was inferred. Jeunehomme (39) measured the lifetime as 47×10^{-9} s, in agreement with the early work of Bennett and Dalby (71). The equivalent oscillator strength of the (0,0) band is 1.89×10^{-2}. He explains the discrepancy with the work of Fink and Welge in terms of recombination–cascade process. The metastable $A^3\Sigma$ state has received attention from a number of workers. Brower and Spieweck (72) measured the decay of the Vegard–Kaplan bands and find the lifetime of the $v = 0$ level to be about 10 s, in contrast with the previous work of Zipf (73), Noxon (74), and Phillips (75) leading to about 1 s and in rough agreement with an early suggestion of Hunten (76) of about 30 s. On the basis of measurements on the absorption coefficients of Vegard–Kaplan bands, Shemansky (77) reports a lifetime of the $A^3\Sigma$ state of 1.27 s (see his communication to the symposium). Brennen (78), on the basis of pressure dependence of N_2 band intensities, has suggested lower limits for the $B(v = 11)$ and $A(v = 0)$ state lifetimes as 2.4 μs and 12 s, respectively. It appears that Dunford's (79) indirect estimate of the A lifetime of 0.08 s is now unacceptable. Peterson (80) reported at the symposium lifetime measurements of the $A^2\Pi$ state of N_2^+ of 12.7 μs from decay of Meinel Band intensities in an N_2^+ molecular beam. Lawrence (81) reported on vacuum ultraviolet intensity measurements on N_2, C, N, O, using the phase shift method.

Intensity Measurements

Intensity measurements have been made in emission and absorption on a number of aeronomically important band systems of N_2.

(i) Vegard–Kaplan System ($A^3\Sigma_u^+$–$X^1\Sigma_g^+$): Chandriah and Shepherd (36) have measured the intensities in emission of 18 bands of the Vegard–Kaplan system, interpreted the results in terms of electronic transition moment variation, and reported an array of relative band strengths. Their measurements are in good accord with those of Carleton and Papaliolios (82) which were used by Nicholls (1) at the last symposium to place band strengths for the system on an absolute basis.

In view of the balance of experimental evidence cited above that the lifetime of $A^3\Sigma_u^+$ levels is about 1 s, it does not appear necessary to radically modify the absolute transition probabilities for Vegard–Kaplan bands presented in ref. 1.

(ii) Lyman–Birge–Hopfield System ($a^1\Pi_g$–$X^1\Sigma_g$): Intensity measurements have been made in emission on this system by McEwen (37, 83) who showed, as had been previously suggested (84), that the electronic transition moment was relatively insensitive to internuclear separation, and thus the band strengths followed Franck–Condon factors. These data may be placed on an absolute basis by use of the oscillator strengths of 10 bands of the $v'' = 0$ progression measured in absorption by Ching, Cook, and Becker (85). The results agree with those of McEwen, and the oscillator strengths of bands lie in the $1–5 \times 10^{-6}$ region. Vanderslice, Wilkinson, and Tilford (86) have confirmed the 1/3 ratio of electric quadrupole to magnetic dipole nature of the transition.

(iii) Other Vacuum Ultraviolet Band Systems: Appleton and Steinberg (87) using absorption through shock-heated N_2 have placed upper

Can. J. Chem. Downloaded from www.nrcresearchpress.com by 210.87.254.5 on 09/05/12
For personal use only.

limits on the oscillator strengths of the Birge–Hopfield $b^1\Pi$–$X^1\Sigma$ and $b'^1\Sigma$–$X^1\Sigma$ band systems which may have a place in the vacuum ultraviolet auroral spectrum. The absorption coefficient of N_2 between 1000 and 580 Å, which includes a number of potentially important band systems for the auroral spectra, has been measured by Huffman, Tanaka, and Larrabee (88, 89). The absorption and photoionization cross sections of N_2 and O_2 in the wavelength region 303–1037 Å have been measured at strong solar emission line wavelengths by Sampson and Cairns (90). Photoionization and absorption cross sections of N_2 and O_2 in the 600–1000 Å were measured by Cook and Metzger (91) and Cook, Ching, and Becker (92). Photoionization cross section of N_2 in the 734–805 Å region were studied by Cook and Ogawa (38). This work is discussed by Huffman at the symposium (93).

Theoretical Work

Insofar as theoretical work on N_2 is concerned, reference has been made earlier to the work of Gilmore (48) on potential curves. Benesch, Vanderslice, Tilford, and Wilkinson (50) have provided another authoritative set of potential curves for N_2 states below 11 eV derived from a critical assessment of molecular data. They point out inconsistencies in some of the similar curves computed by Zare, Larsen, and Berg (58) which in part invalidate some of the most useful Franck–Condon factor tables published by them for many N_2 transitions appropriate to realistic potentials. In two further papers (94, 95), Vanderslice, Tilford, and Wilkinson present Franck–Condon factor tables for a large number of N_2 transitions computed using realistic potentials. They point out that in a number of cases, earlier calculations using Morse potential are still quite acceptable. Halmann and Laulicht (96–100) published arrays for some N_2 and other band systems using the Morse and realistic potentials for isotopically substituted molecules. Nicholls (63) published Morse arrays for a number of excitation and ionization transitions of N_2.

Ionized Nitrogen (N_2^+)

Lifetime Measurements

Most of the work has been on $v' = 0$ level of the First Negative system for which the following data applies. Hesser and Dressler (42) quote a value of 59×10^{-9} s, Jeunehomme (39) quotes a value of 71.5×10^{-9} s, and Fink and Welge (41) quote a value of 45×10^{-9} s.

Intensity Measurements

Apart from the photoionization absorption work cited above few laboratory intensity measurements have been made recently. Some work on the Meinel and Second Negative systems is in progress in the author's laboratory.

Theoretical Work

A number of the papers cited above contain new data for N_2^+ band systems.

Oxygen (O_2)

Lifetime Measurements

Badger, White and Whitlock (101) in an absorption and curve of growth study of the $a^1\Delta$–$X^3\Sigma$ band at 1.26 μ have found that the lifetime of the isolated $a^1\Delta$ molecule is 45 min, and that this is reduced to 9 min at 1 atm.

Intensity Measurements

Ogryzlo and co-workers (102–104) have studied the intensity of the 6340 Å band of oxygen and shown kinetically that it most likely arises from the radiating collisions complex $(O_2(a^1\Delta))_2$. Intensity measurements have also been made on this feature in atmospheric absorption by Dianov-Klovov (105, 106) who in the last of these papers determines the oscillator strengths of the atmospheric bands ($b^1\Sigma$–$X^3\Sigma$) and the infrared atmospheric bands ($a^1\Delta$–$X^3\Sigma$) as 2.7×10^{-10}, respectively. He measured the lifetime of the $(O_2(^1\Delta))_2$ complex as greater than 0.3×10^{-13} s. Wark and Mercer (107) have measured the Einstein A coefficient of the atmospheric band as 0.145 s^{-1}.

Herzberg I ($A^3\Sigma_u^+$–$X^3\Sigma_g^-$) System: Degen and Nicholls (108) using a newly developed laboratory source of the bands (109) have measured the intensities of 36 bands of the system in the 2590–4880 Å region of the spectrum (110). It was found that the electronic transition moment was relatively independent of internuclear separation and that the relative band strengths follow the Franck–Condon factors quite closely. Some absorption measurements on the same system and its associated photodissociation continuum are in progress in the author's laboratory. Blake, Carver, and Haddad (111) have made some measurements on the continuum.

Schumann–Runge ($B^3\Sigma_g^-$–$X^3\Sigma_g^-$) System: The Schumann–Runge photodissociation continuum transition is one of the strongest sources of free atomic oxygen in the upper atmosphere (15). It has been studied by Metzger and Cook (112), Huffman, Tanaka, and Larabee (89), Goldstein and Mastrup (113), and Evans and

Can. J. Chem. Downloaded from www.nrcresearchpress.com by 210.87.254.5 on 09/05/12
For personal use only.

Schexnayder (114). Absorption measurements were made on isotopic bands by Halmann (96).

Vacuum-Ultraviolet Absorptions of O_2: The absorption coefficient of oxygen in the vacuum ultraviolet has been studied by Huffman, Larrabee, and Tanaka (115, 116) and Matsungaga and Watanabe (117).

Theoretical Work: Franck–Condon factors for O_2 transitions have been provided by Nicholls (118) for Morse models of potentials. Hubisz and Nicholls (61) have comparable unpublished data for Klein–Dunham potentials. Isotopic Franck–Condon factors were provided for the Schumann–Runge bands by Hallmann and Laulicht (97–100). Jarmain and Nicholls (64, 65) have made theoretical studies on the Franck–Condon densities of the Herzberg photodissociation continuum.

Ionized Oxygen (O_2^+)

Wavelength Measurements

Linton (119) has reported new bands and new vibrational assignments for bands of the O_2^+ Second Negative ($A^2\Pi_u$–$X^2\Pi_g$) system.

Lifetime Measurements

Jeunehomme (120) reports lifetime measurements and oscillator strengths for the First and Second Negative systems.

Theoretical Work

Nicholls (121) has published Franck–Condon factors for the O_2 First Negative and Second Negative systems.

Hydroxyl (OH)

Few recent laboratory measurements have been made on the vibration rotation spectrum of OH which makes such an important contribution to the airglow. Ferguson and Parkinson (122) present some new calculations on band strengths for this system. The violet electronic system ($A^2\Sigma$–$X^2\Pi$) has been more fully studied; Anketell and Pery-Thorne (123) and Anketell and Learner (124) have measured oscillator strengths of individual lines by the hook method. Bennett and Dalby (125) and Nicholls (141) have published Franck–Condon factors and band strengths.

Nitric Oxide (NO) (Gamma Bands)

The gamma band system of NO has been recently reported in the airglow by Barth. Recent laboratory and theoretical work on this band system is as follows. Jeunehomme (126) reports lifetime measurements and band strengths, as do Callear, Pilling, and Smith (127) and Marr (128). Nicholls (129) reports Franck–Condon factors.

Attention is drawn to the useful and recent privately circulated report by Main (130) on molecular transition probabilities of molecules.

Transitions: B, Atomic Transitions

Oscillator strengths of aeronomically important hydrogen lines (e.g. Lyman alpha) are available from exact theory (131). There have also been a number of recent extensive theoretical studies on atomic oxygen and nitrogen lines (132, 133) particularly those in the ultraviolet. See also the work of Kelly and Armstrong (134). Measurements have been made on OI line oscillator strengths by Parkes, Keyser, and Kaufman (135), McConkey, Burns, Moran, and Emeleus (136), Savage and Lawrence (137), LeBlanc, Oldenberg, and Carleton (138), and Morse and Kaufman (139). The measurements on OI and NI transition oscillator strengths of Prag, Fairchild, and Clark (140) are in good agreement with theory.

Acknowledgments

This work was supported in part by research grants from the National Research Council of Canada and contracts from the Department of Defence Production of Canada. The preparation of this paper would have been impossible without the skillful and effective bibliographic assistance of Mrs. Sandra Innanen.

1. R. W. NICHOLLS. Ann. Geophys. **20**, 144, 1964.
2. J. W. CHAMBERLAIN. Physics of the aurora and the airglow. Academic Press, Inc., New York. 1961.
3. J. B. TATUM. Ap. J. Supp. **14**, 21, 1967.
4. R. W. NICHOLLS and A. T. STEWART. Allowed transitions. *Edited by* D. R. Bates. Academic Press, Inc., New York. 1962. Chap. 2.
5. J. D. CRAGGS and H. S. W. MASSEY. Handbuch der Physik. Vol. **37**. *Edited by* S. Flugge. Springer-Verlag, Berlin. 1959. p. 314.
6. R. W. NICHOLLS. J. Phys. B. In press. 1968.
7. R. GERHARZ. J. Atmospheric Terrest. Phys. **27**, 1191 (1965).
8. J. A. CURCIO, L. F. CRUMMETER, and G. L. KESTRICH. Appl. Opt. **3**, 1401 (1964).
9. V. I. KRASSOVSKY, N. N. SHEFOV, and V. I. YARIN. Planetary Space Sci. **9**, 883 (1962).
10. A. L. BROADFOOT and K. R. KENDALL. J. Geophys. Res. **73**, 426 (1968).
11. V. I. KRASSOVSKY and N. N. SHEFOV. Space Science Rev. **4**, 176 (1965).
12. C. A. BARTH. J. Geophys. Res. **69**, 3301 (1964).
13. C. A. BARTH. Ann. Geophys. **22**, 198 (1966).
14. P. SWINGS, D. BOSMAN-CRESPIN, and C. ARPIGNY. Mem. Roy. Soc. Leige, **4**, 583 (1961).
15. G. V. MARR. Proc. Roy. Soc. London, Ser. A, **288**, 531 (1965).
16. E. J. BYRAM, T. A. CHUBB, H. FRIEDMAN, and J. E. KUPPERIAN. The threshold of space. *Edited by* M

Can. J. Chem. Downloaded from www.nrcresearchpress.com by 210.87.254.5 on 09/05/12
For personal use only.

Zelikoff. The Pergamon Press, Ltd., New York. 1965. p. 203.
17. T. M. DONAHUE. Ann. Geophys. **22**, 175 (1966).
18. V. I. KRASSOVSKY, N. N. SHEFOV, and O. L. VAISBERG. Ann. Geophys. **22**, 208 (1966).
19. R. E. MILLER, W. G. FASTIE, and R. C. ISLER. Rocket studies of far UV radiation in an aurora. Johns Hopkins, Technical Report 13, NASA Research Grant NsG 193–62. 1967.
20. B. A. TINSLEY. Planetary Space Sci. **16**, 91 (1968).
21. J. C. BRANDT, A. L. BROADFOOT, and M. B. MCELROY. Ap. J. **141**, 1584 (1965).
22. W. G. FASTIE, H. M. CROSSWHITE, and D. F. HEATH. J. Geophys. Res. **69**, 4129 (1964).
23. W. G. FASTIE, H. M. CROSSWHITE, and T. P. MARKHAM. Ann. Geophys. **17**, 1 (1961).
24. R. C. ISLER and W. G. FASTIE. J. Geophys. Res. **70**, 2613 (1965).
25. W. G. MURCRAY. J. Geophys. Res. **71**, 2739 (1966).
26. W. G. FASTIE, R. E. MILLER, and R. C. ISLER. Space Research VII. 1967.
27. A. E. S. GREEN and C. A. BARTH. J. Geophys. Res. **70**, 1083 (1965).
28. R. S. STOLARSKI and A. E. S. GREEN. J. Geophys. Res. **72**, 3967 (1967).
29. A. E. S. GREEN. J. Geophys. Res. **72**, 4950 (1967).
30. A. E. S. GREEN and R. S. STOLARSKI. *In* The middle ultraviolet; its science and technology. *Edited by* A. E. S. Green. John Wiley and Sons. Inc., New York. 1966. pp. 165–176.
31. A. E. S. GREEN and C. A. BARTH. J. Geophys. Res. **72**, 3975 (1967).
32. C. A. BARTH. *In* Dynamics of manned lifting planetary entry. *Edited by* S. M. Scala, A. C. Harrison, and M. Rodgers. John Wiley and Sons, Inc., New York. 1963. pp. 82–94.
33. T. TOHMATSU. Rep. Ionosph. Space Res. Japan, **17**, 187 (1963).
34. M. GADSEN. J. Atmospheric Terrest. Phys. **29**, 603 (1967).
35. R. A. MCFARLANE. Phys. Rev. **146**, 37 (1966).
36. G. CHANDRIAH and G. C. SHEPHERD. Can. J. Phys. **46**, 221 (1968).
37. D. J. MCEWAN and R. W. NICHOLLS. Nature, **209**, 902 (1966).
38. G. R. COOK and M. OGAWA. Can. J. Phys. **43**, 256 (1965).
39. M. JEUNEHOMME. J. Chem. Phys. **44**, 2672 (1966).
40. M. JEUNEHOMME. J. Chem. Phys. **45**, 1805 (1966).
41. VON E. FINK and K. H. WELGE. Z. Naturforsch. **19a**, 1193 (1964).
42. J. E. HESSER and K. DRESSLER. J. Chem. Phys. **45**, 3149 (1966).
43. N. F. MOTT and H. S. W. MASSEY. Theory of Atomic Collisions. 3rd ed. Oxford University Press, London, New York. 1965.
44. E. N. LASSETTRE. J. Chem. Phys. **43**, 4479 (1965).
45. E. N. LASSETTRE, V. D. MEYER, and M. S. LONGMIRE. J. Chem. Phys. **42**, 807 (1965).
46. K. OHNO. *In* Present status of calculation of properties of N_2 and O_2. *Edited by* A. E. S. Green. John Wiley and Sons, Inc., New York. 1966. pp. 73–82.
47. F. R. GILMORE. Potential energy curves for N_2, NO, O_2 and corresponding ions. Rand Memorandum RM 4034-PR. 1964.
48. F. R. GILMORE. J. Quant. Spectry. Radiative Transfer, **5**, 369, 1965.
49. J. T. VANDERSLICE. J. Chem. Phys. **37**, 384 (1962).
50. W. BENESCH, J. T. VANDERSLICE, S. G. TILFORD, and P. G. WILKINSON. Astrophys. J. **142**, 1227 (1965).
51. R. J. SPINDLER. J. Quant. Spectry. Radiative Transfer, **5**, 165 (1965).
52. W. R. JARMAIN. Numerical solution of the Schrödinger equation. Scientific Report 6, Contract AF 19(604) 4560. 1961.
53. W. R. JARMAIN. Can. J. Phys. **41**, 414 (1963).
54. W. R. JARMAIN. Can. J. Phys. **41**, 1926 (1963).
55. J. W. COOLEY. Math. of Comp. **15**, 363 (1961).
56. J. W. COOLEY. A. E. C. Report No. NYO-9490, 1961.
57. J. K. CASHION. J. Chem. Phys. **39**, 1872 (1963).
58. R. N. ZARE, E. O. LARSON, and R. A. BERG. J. Mol. Spectry. **15**, 117 (1965).
59. D. ALBRITTON. Private communication. 1967.
60. J. GENEROSA. Private communication. 1968.
61. J. HUBISZ and R. W. NICHOLLS. To be published.
62. R. W. NICHOLLS. J. Quant. Spectry. Radiative Transfer. **5**, 647 (1965).
63. R. W. NICHOLLS. J. Quant. Spectry. Radiative Transfer, **2**, 433 (1962).
64. W. R. JARMAIN and R. W. NICHOLLS. Proc. Phys. Soc. **84**, 417 (1964).
65. W. R. JARMAIN and R. W. NICHOLLS. Proc. Phys. Soc. **90**, 545 (1967).
66. R. W. NICHOLLS. Nature, **219**, 151 (1968).
67. J. DRAKE. M.Sc. Thesis. York University, Toronto, Ontario. 1967.
68. J. DRAKE and R. W. NICHOLLS. In press.
69. A. E. S. GREEN. The middle ultraviolet; its science and technology. John Wiley and Sons, Inc., New York. 1966.
70. J. E. HESSER. J. Chem. Phys. **48**, 2518 (1968).
71. W. BENNETT and F. W. DALBY. J. Chem. Phys. **31**, 434 (1959).
72. H. H. BROWER and F. SPEIVICK. Planetary Space Sci. **15**, 689 (1967).
73. E. C. ZIPF. J. Chem. Phys. **38**, 2034 (1963).
74. J. F. NOXON. J. Chem. Phys. **36**, 926 (1962).
75. L. F. PHILLIPS. Can. J. Chem. **43**, 369 (1965).
76. D. M. HUNTEN. Atmospheric Terrest. Phys. **7**, 141 (1955).
77. D. E. SHEMANSKY. Can. J. Chem. This issue.
78. W. BRENNEN. J. Chem. Phys. **44**, 1793 (1966).
79. H. B. DUNFORD. J. Phys. Chem. **67**, 258 (1963).
80. J. R. PETERSON. Can. J. Chem. This issue.
81. G. M. LAWRENCE. Can. J. Chem. This issue.
82. N. P. CARLETON and C. PAPALIOLIOS. J. Quant. Spectry. Radiative Transfer **2**, 241 (1962).
83. D. J. MCEWEN. Ph.D. Thesis. University of Western Ontario, London, Ontario. 1965.
84. R. W. NICHOLLS. Nature, **186**, 958 (1960).
85. B. K. CHING, G. R. COOK, and R. A. BECKER. J. Quant. Spectry. Radiative Transfer, **7**, 323 (1967).
86. J. T. VANDERSLICE, P. G. WILKINSON, and S. G. TILFORD. J. Chem. Phys. **42**, 2681 (1965).
87. J. P. APPLETON and M. STEINBERG. J. Chem. Phys. **46**, 1521 (1967).
88. R. E. HUFFMAN, Y. TANAKA, and J. C. LARRABEE. J. Chem. Phys. **39**, 910 (1963).
89. R. E. HUFFMAN, Y. TANAKA, and J. C. LARRABEE. Discussions Faraday Soc. **37**, 159 (1964).
90. J. SAMPSON and R. CAIRNS. J. Geophys. Res. **69**, 4583 (1964).
91. G. R. COOK and P. H. METZGER. J. Chem. Phys. **41**, 321 (1964).
92. G. R. COOK, B. K. CHING, and R. A. BECKER. Discussions Faraday Soc. **37**, 149 (1965).
93. R. E. HUFFMAN. Can. J. Chem. This issue.
94. W. BENESCH, J. T. VANDERSLICE, S. G. TILFORD, and P. G. WILKINSON. Astrophys. J. **143**, 236 (1966).
95. W. BENESCH, J. T. VANDERSLICE, S. G. TILFORD, and P. G. WILKINSON. Astrophys. J. **144**, 408 (1966).

96. M. HALMANN. J. Chem. Phys. **44**, 2406 (1966).
97. M. HALMANN and I. LAULICHT. J. Chem. Phys. **42**, 137 (1965).
98. M. HALMANN and I. LAULICHT. J. Chem. Phys. **43**, 438 (1965).
99. M. HALMANN and I. LAULICHT. J. Chem. Phys. **44**, 2398 (1966).
100. M. HALMANN and I. LAULICHT. J. Chem. Phys. **46**, 2684 (1967).
101. R. M. BADGER, A. C. WRIGHT, and R. F. WHITLOCK. J. Chem. Phys. **43**, 4345 (1965).
102. S. J. ARNOLD, E. A. OGRYZLO, and H. WITZKE. J. Chem. Phys. **40**, 1769 (1964).
103. S. J. ARNOLD, R. J. BROWNE, and E. A. OGRYZLO. Photochem. Photobiol. **4**, 963 (1965).
104. L. W. BADER and E. A. OGRYZLO. Discussions Faraday Soc. **37**, 46 (1964).
105. V. I. DIANOV-KLOKOV. Opt. Spectry. **16**, 224 (1964).
106. V. I. DIANOV-KLOKOV. Opt. Spectry. **17**, 76 (1964).
107. D. Q. WARK and D. M. MERCER. Appl. Opt. **4**, 839, 1965.
108. V. DEGEN and R. W. NICHOLLS. J. Geophys. Res. **71**, 3781 (1966).
109. V. DEGEN and R. W. NICHOLLS. J. Phys. B. **1**, 983 (1968).
110. V. DEGEN and R. W. NICHOLLS. To be published.
111. A. J. BLAKE, J. H. CARVER, and G. N. HADDAD. J. Quant. Spectry. Radiative Transfer, **6**, 451 (1966).
112. P. H. METZGER and G. R. COOK. J. Quant. Spectry. Radiative Transfer, **4**, 107 (1964).
113. R. GOLDSTEIN and F. N. MASTRUP. J. Opt. Soc. Am. **56**, 765 (1966).
114. J. S. EVANS and C. J. SCHEXNAYDER. An investigation of the effect of high temperature on the Schumann–Runge ultraviolet absorption continuum of O_2. NASA Tech. Rept. R-92. 1961.
115. R. E. HUFFMAN, J. C. LARRABEE, and Y. TANAKA. J. Chem. Phys. **40**, 356 (1964).
116. R. E. HUFFMAN, J. C. LARRABEE, and Y. TANAKA. J. Chem. Phys. **46**, 2213 (1967).
117. F. M. MATSUNGAGA and K. WATANABE. Sci. Light, **16**, 31 (1967).
118. R. W. NICHOLLS. J. Res. Natl. Bur. Std. A, **69**, 369, 1965.
119. C. LINTON. Nature, **212**, 1358 (1966).
120. M. JEUNEHOMME. J. Chem. Phys. **45**, 4433 (1966).
121. R. W. NICHOLLS. Can. J. Phys. **43**, 1390 (1964).
122. A. E. FERGUSON and D. PARKINSON. Planetary Space Sci. **11**, 149 (1963).
123. J. ANKETELL and A. PERY-THORNE. Proc. Roy. Soc. London, Ser. A, **301**, 343 (1967).
124. J. ANKETELL and R. C. M. LEARNER. Proc. Roy. Soc. London, Ser. A, **301**, 355 (1967).
125. W. BENNETT and R. W. DALBY. J. Chem. Phys. **40**, 1414 (1964).
126. M. JEUNEHOMME. J. Chem. Phys. **44**, 4253 (1966).
127. A. B. CALLEAR. M. J. PILLING, and I. I. SMITH. Trans. Faraday Soc. **62**, 2997 (1966).
128. G. V. MARR. Proc. Phys. Soc. **83**, 293 (1964).
129. R. W. NICHOLLS. J. Res. Natl. Bur. Std. A, 535 1964c.
130. R. P. MAIN. Annotated bibliography of transition probabilities in the electronic spectra of small free molecules. Heliodyne Corporation, Los Angeles. 1967.
131. H. A. BETHE and E. E. SALPETER. Quantum mechanics of one of two electron atoms. Academic Press, Inc., New York. 1957.
132. P. S. KELLY. Astrophys. J. **140**, 1247 (1964).
133. P. S. KELLY. J. Quant. Spectry. Radiative Transfer, **4**, 117 (1964).
134. P. S. KELLY and B. H. ARMSTRONG. Phys. Rev. Letters, **12**, 35 (1964).
135. D. A. PARKES, L. F. KEYSER, and F. KAUFMAN. Astrophys. J. **14**, 9217 (1967).
136. J. W. MCCONKEY, D. J. BURNS, K. A. MORAN, and K. G. EMELEUS. Phys. Letters, **22**, 416 (1966).
137. R. D. SAVAGE and G. M. LAWRENCE. Astrophys. J. **146**, 940 (1966).
138. F. J. LEBLANC, O. OLDENBERG, and N. P. CARLETON. J. Chem. Phys. **45**, 2200 (1966).
139. F. A. MORSE and F. KAUFMAN. J. Chem. Phys. **42**, 1785 (1965).
140. A. B. PRAG, C. E. FAIRCHILD, and K. C. CLARK. Phys. Rev. **137A**, 1358 (1965).
141. R. W. NICHOLLS. *In* Laboratory astrophysics and combustion spectroscopy. *Edited by* Olfe and Zackkay. The Pergamon Press, Ltd., New York. 1964. pp. 413–430.
142. J. P. HENNES. J. Geophys. Res. **71**, 763 (1966).
143. C. A. BARTH. *In* The middle ultraviolet; its science and technology. *Edited by* A. E. S. Green. John Wiley and Sons, Inc., New York. 1966. pp. 177–218.
144. D. STEELE, E. R. LIPPINCOTT, and J. T. VANDERSLICE. Rev. Mod. Phys. **34**, 239 (1962).
145. V. DEGEN. Can. J. Phys. **46**, 783 (1968).

Vacuum ultraviolet transition probabilities in C, N, O, and N_2

GEORGE M. LAWRENCE
Douglas Advanced Research Laboratories, Huntington Beach, California 92647

Received November 27, 1968

A review is made of the recent works on the transition probabilities for C, N, O, and N_2 in the vacuum ultraviolet.

Canadian Journal of Chemistry, 47, 1856 (1969)

Radiative lifetime measurements can provide accurate transition probabilities by bypassing the difficult task of determining absolute densities. With pulsed excitation, one determines a radiative lifetime by analysis of the observed decay curve. Another method, using radio frequency techniques, is the phase shift method, in which the phase delay between sine wave modulation of

Can. J. Chem. Downloaded from www.nrcresearchpress.com by 210.87.254.5 on 09/05/12
For personal use only.

96. M. HALMANN. J. Chem. Phys. **44**, 2406 (1966).
97. M. HALMANN and I. LAULICHT. J. Chem. Phys. **42**, 137 (1965).
98. M. HALMANN and I. LAULICHT. J. Chem. Phys. **43**, 438 (1965).
99. M. HALMANN and I. LAULICHT. J. Chem. Phys. **44**, 2398 (1966).
100. M. HALMANN and I. LAULICHT. J. Chem. Phys. **46**, 2684 (1967).
101. R. M. BADGER, A. C. WRIGHT, and R. F. WHITLOCK. J. Chem. Phys. **43**, 4345 (1965).
102. S. J. ARNOLD, E. A. OGRYZLO, and H. WITZKE. J. Chem. Phys. **40**, 1769 (1964).
103. S. J. ARNOLD, R. J. BROWNE, and E. A. OGRYZLO. Photochem. Photobiol. **4**, 963 (1965).
104. L. W. BADER and E. A. OGRYZLO. Discussions Faraday Soc. **37**, 46 (1964).
105. V. I. DIANOV-KLOKOV. Opt. Spectry. **16**, 224 (1964).
106. V. I. DIANOV-KLOKOV. Opt. Spectry. **17**, 76 (1964).
107. D. Q. WARK and D. M. MERCER. Appl. Opt. **4**, 839, 1965.
108. V. DEGEN and R. W. NICHOLLS. J. Geophys. Res. **71**, 3781 (1966).
109. V. DEGEN and R. W. NICHOLLS. J. Phys. B. **1**, 983 (1968).
110. V. DEGEN and R. W. NICHOLLS. To be published.
111. A. J. BLAKE, J. H. CARVER, and G. N. HADDAD. J. Quant. Spectry. Radiative Transfer, **6**, 451 (1966).
112. P. H. METZGER and G. R. COOK. J. Quant. Spectry. Radiative Transfer, **4**, 107 (1964).
113. R. GOLDSTEIN and F. N. MASTRUP. J. Opt. Soc. Am. **56**, 765 (1966).
114. J. S. EVANS and C. J. SCHEXNAYDER. An investigation of the effect of high temperature on the Schumann–Runge ultraviolet absorption continuum of O_2. NASA Tech. Rept. R-92. 1961.
115. R. E. HUFFMAN, J. C. LARRABEE, and Y. TANAKA. J. Chem. Phys. **40**, 356 (1964).
116. R. E. HUFFMAN, J. C. LARRABEE, and Y. TANAKA. J. Chem. Phys. **46**, 2213 (1967).
117. F. M. MATSUNGAGA and K. WATANABE. Sci. Light, **16**, 31 (1967).
118. R. W. NICHOLLS. J. Res. Natl. Bur. Std. A, **69**, 369, 1965.
119. C. LINTON. Nature, **212**, 1358 (1966).
120. M. JEUNEHOMME. J. Chem. Phys. **45**, 4433 (1966).
121. R. W. NICHOLLS. Can. J. Phys. **43**, 1390 (1964).
122. A. E. FERGUSON and D. PARKINSON. Planetary Space Sci. **11**, 149 (1963).
123. J. ANKETELL and A. PERY-THORNE. Proc. Roy. Soc. London, Ser. A, **301**, 343 (1967).
124. J. ANKETELL and R. C. M. LEARNER. Proc. Roy. Soc. London, Ser. A, **301**, 355 (1967).
125. W. BENNETT and R. W. DALBY. J. Chem. Phys. **40**, 1414 (1964).
126. M. JEUNEHOMME. J. Chem. Phys. **44**, 4253 (1966).
127. A. B. CALLEAR. M. J. PILLING, and I. I. SMITH. Trans. Faraday Soc. **62**, 2997 (1966).
128. G. V. MARR. Proc. Phys. Soc. **83**, 293 (1964).
129. R. W. NICHOLLS. J. Res. Natl. Bur. Std. A, 535 1964c.
130. R. P. MAIN. Annotated bibliography of transition probabilities in the electronic spectra of small free molecules. Heliodyne Corporation, Los Angeles. 1967.
131. H. A. BETHE and E. E. SALPETER. Quantum mechanics of one of two electron atoms. Academic Press, Inc., New York. 1957.
132. P. S. KELLY. Astrophys. J. **140**, 1247 (1964).
133. P. S. KELLY. J. Quant. Spectry. Radiative Transfer, **4**, 117 (1964).
134. P. S. KELLY and B. H. ARMSTRONG. Phys. Rev. Letters, **12**, 35 (1964).
135. D. A. PARKES, L. F. KEYSER, and F. KAUFMAN. Astrophys. J. **14**, 9217 (1967).
136. J. W. MCCONKEY, D. J. BURNS, K. A. MORAN, and K. G. EMELEUS. Phys. Letters, **22**, 416 (1966).
137. R. D. SAVAGE and G. M. LAWRENCE. Astrophys. J. **146**, 940 (1966).
138. F. J. LEBLANC, O. OLDENBERG, and N. P. CARLETON. J. Chem. Phys. **45**, 2200 (1966).
139. F. A. MORSE and F. KAUFMAN. J. Chem. Phys. **42**, 1785 (1965).
140. A. B. PRAG, C. E. FAIRCHILD, and K. C. CLARK. Phys. Rev. **137A**, 1358 (1965).
141. R. W. NICHOLLS. *In* Laboratory astrophysics and combustion spectroscopy. *Edited by* Olfe and Zackkay. The Pergamon Press, Ltd., New York. 1964. pp. 413–430.
142. J. P. HENNES. J. Geophys. Res. **71**, 763 (1966).
143. C. A. BARTH. *In* The middle ultraviolet; its science and technology. *Edited by* A. E. S. Green. John Wiley and Sons, Inc., New York. 1966. pp. 177–218.
144. D. STEELE, E. R. LIPPINCOTT, and J. T. VANDERSLICE. Rev. Mod. Phys. **34**, 239 (1962).
145. V. DEGEN. Can. J. Phys. **46**, 783 (1968).

Vacuum ultraviolet transition probabilities in C, N, O, and N_2

GEORGE M. LAWRENCE
Douglas Advanced Research Laboratories, Huntington Beach, California 92647

Received November 27, 1968

A review is made of the recent works on the transition probabilities for C, N, O, and N_2 in the vacuum ultraviolet.

Canadian Journal of Chemistry, 47, 1856 (1969)

Radiative lifetime measurements can provide accurate transition probabilities by bypassing the difficult task of determining absolute densities. With pulsed excitation, one determines a radiative lifetime by analysis of the observed decay curve. Another method, using radio frequency techniques, is the phase shift method, in which the phase delay between sine wave modulation of

Can. J. Chem. Downloaded from www.nrcresearchpress.com by 210.87.254.5 on 09/05/12
For personal use only.

TABLE I

f values, O(I), 1302 Å

Authors	Method, source of absolute scale	*f* value (× 1000)	Time (ns)	Reference	Year of work
Morse and Kaufman	Absorption, gas titration	33 ± 11	2.6	11	1965
Parkes, Keyser, and Kaufman	Absorption, gas titration	21 ± 3	4.0	12	1967
Savage and Lawrence	Phase shift lifetime	35 ± 4	2.4	8	1966
Boldt and Labuhn	Seeded arc, Saha equilibrium	180 ± 45	0.5	4	1967
Hesser and Gaillard	Phase shift lifetime	50 ± 9	1.7	10	1968
Lawrence	Pulse lifetime	46.3 ± 1.2	1.82	6, 7	1968

the excitation and the modulation of the emitted light is measured as a function of frequency. Results using the phase shift method are reported by Lawrence and Savage (1) for "resonance" lines of B, C, N, and their ions. The measurements have estimated error limits on the order of $\pm 15\%$ and can be used to make 20% corrections in some of the arc measurements compiled in the NBS tabulation (2). One important conclusion from the measurements is that central field calculations yield transition probabilities for partially filled p shells which are incorrect by factors of 3 or so. Calculations by Weiss (3) using extensive configuration mixing for C(I) and C(II) yield results within 25% of experiment. The resonance transition probabilities for O(I) at 1302 Å are not as well understood as there is a spread of an order of magnitude in the literature values. Measurements subsequent to those referenced by Professor Nicholls have been made by Boldt and Labuhn (4), Hesser and Gaillard (5), and by Lawrence (6, 7). Table I lists the *f* values. A major source of ambiguity in the lifetime measurements is the cascade correction. For O(I) 1302 Å measured with CO as a sample gas, this correction turned out to be larger than expected (8). The maximum cascading fraction from O(I) 1302 Å is 3.0 for CO, 1.6 for O_2, and 0.95 for H_2O. Such measurements of cascade amounts were made by numerical analysis of pulse-decay curves (9) and can be used to provide vacuum ultraviolet excitation functions by normalization against visible spectra.

Phase shift lifetimes for spectra of H_2, N_2, N_2^+, CO, CO^+, NO, NO^+, BF, CO, BCl, and CO_2^+ are reported by Hesser (10).

1. G. M. Lawrence and B. D. Savage. Phys. Rev. **141**, 67 (1966).
2. W. L. Wiese, M. W. Smith, and B. M. Glennon. NSRDS-NBS 4 Atomic transition probabilities, hydrogen through neon. 1966.
3. A. W. Weiss. Phys. Rev. **162**, 71 (1966).
4. G. Boldt and F. Labuhn. Z. Naturforsch. **22a**, 1613 (1967).
5. J. E. Hesser and M. Gaillard. Astrophys. J. **152**, 695 (1968).
6. G. M. Lawrence. Bull. Am. Phys. Soc. **13**, 424 (1968).
7. G. M. Lawrence and M. George. Phys. Rev. **175**, 40 (1968).
8. B. D. Savage and G. M. Lawrence. Astrophys. J. **146**, 940 (1966).
9. G. M. Lawrence. Bull. Am. Phys. Soc. **13**, 907 (1968).
10. J. E. Hesser. J. Chem. Phys. **48**, 2518 (1968).
11. F. A. Morse and F. Kaufman. J. Chem. Phys. **42**, 1785 (1965).
12. D. A. Parkes, L. F. Keyser, and F. Kaufman. Astrophys. J. **149**, 217 (1967).

Can. J. Chem. Downloaded from www.nrcresearchpress.com by 210.87.254.5 on 09/05/12
For personal use only.

Time of flight measurement of N_2 and N_2^+ lifetimes[1]

M. HOLLSTEIN[2], D. C. LORENTS[3], J. R. PETERSON, and J. R. SHERIDAN[4]
Stanford Research Institute, Menlo Park, California 94025

Received November 27, 1968

Lifetime measurements have been carried out on the N_2 first positive and N_2^+ Meinel systems by observing the spatial decay of radiation from fast beams. The neutral beam is excited by near-resonant charge transfer, and the N_2^+ excitation originates in the ion source. The (2,0), (3,0), (3,1), (5,2), (9,5), and (12,8) first positive bands have been measured and the results compare favorably with Jeunehomme's values. The Meinel studies are apparently the first to yield well-defined values for that system. We obtained 12.2 ± 0.2, 11.4 ± 0.2, and 12.2 ± 0.9 μs for the $v' = 3$, 4, and 5 levels, respectively.

Canadian Journal of Chemistry, 47, 1858 (1969)

Introduction

Oscillator strengths and transition probabilities for molecular bands have been determined experimentally by measuring the absorption or emission of radiation by a gas in a state of equilibrium at a known temperature, or by measuring radiative lifetimes. Radiative lifetimes have generally been measured by exciting a gas by a shock wave, discharge, or electron beam and observing the time decay of light in a specified wavelength interval emitted from the excited gas.

We have made direct measurements of lifetimes by using a time of flight method in which the desired species is excited in a monoenergetic beam and the variation in intensity of emitted light with distance along the beam is measured. In the case of neutral species, beam particles are excited in near-resonant charge transfer collisions. The desired species is isolated by mass analysis and ion–neutral separation. The time of flight technique avoids problems of collisional excitation and deactivation, and radiation trapping. The problem of interference from overlapping bands of other emitting systems is eliminated by isolation of the emitting species of interest. Since we excite neutral states of interest in near-resonant electron capture collisions, which preferentially populate the states of interest, problems resulting from cascade contributions to the observed emissions are greatly reduced.

[1]Work sponsored by Air Force Weapons Laboratory, Kirtland Air Force Base, New Mexico.
[2]Present address: Dornier G.M.B.H. Friederickshafen (Bodensee), Germany.
[3]On leave at Physics Department, University of Aarhus, Aarhus, Denmark.
[4]On leave from University of Alaska, College, Alaska.

Apparatus and Technique

Ions produced in an electron bombardment ion source (50 eV electrons) are focused, accelerated to energies from 400 to 2500 eV, and mass analyzed before entering an oven where near-resonant electron capture collisions with gases or alkali vapors can take place. After traversing the oven, the remaining ions are deflected from the beam. For lifetime measurements of ion states, the oven is evacuated and the ion beam is allowed to pass directly to the observation region. Figure 1 shows a schematic diagram of the apparatus. Typical operating pressures are 5×10^{-5} Torr in the ion source, about 5×10^{-2} Torr in the oven, 5×10^{-6} Torr in the center chamber, and 4×10^{-7} Torr in the observation chamber.

In the observation chamber, light is alternately sampled from two segments of the beam 2 cm long and 15 cm apart. This is accomplished by using three mirrors, two fixed and one rotatable, as shown in Fig. 2, to direct light alternately from each of the two beam segments through a lens and an interference filter onto the photocathode of a refrigerated EMI type 9558 photomultiplier. The relative intensity for each segment of the beam is determined by counting photoelectron pulses with pulse analyzing and counting circuits having a pulse-pair resolution of 100 mμs. Typical counting rates range from 100 to 10^4/s.

When the lifetimes of neutral species are measured, the background signal, obtained when the ion beam is deflected just before entering the oven, is subtracted from the signal. This background includes dark counts from the photomultiplier and any signal resulting from neutrals present in the beam before it enters the oven. The remaining signal, therefore, consists only of emissions from neutrals produced in the oven. When lifetimes for excited states of ions are measured, the background signal resulting when the ions are deflected from the beam after traversing the oven (which is then empty of vapor) is subtracted from the signal. The latter background includes dark counts and any signal resulting from neutrals present in the beam. For both ion and neutral species, the total measured background signal is, at most, a few % above that resulting from dark counts alone. In the case of neutral species, this reveals the relatively high efficiency of the near-resonant, electron capture collisions in producing the desired excited states.

The total flux of ions and/or neutrals in the beam is monitored with a secondary emission detector with

Can. J. Chem. Downloaded from www.nrcresearchpress.com by 210.87.254.5 on 09/05/12
For personal use only.

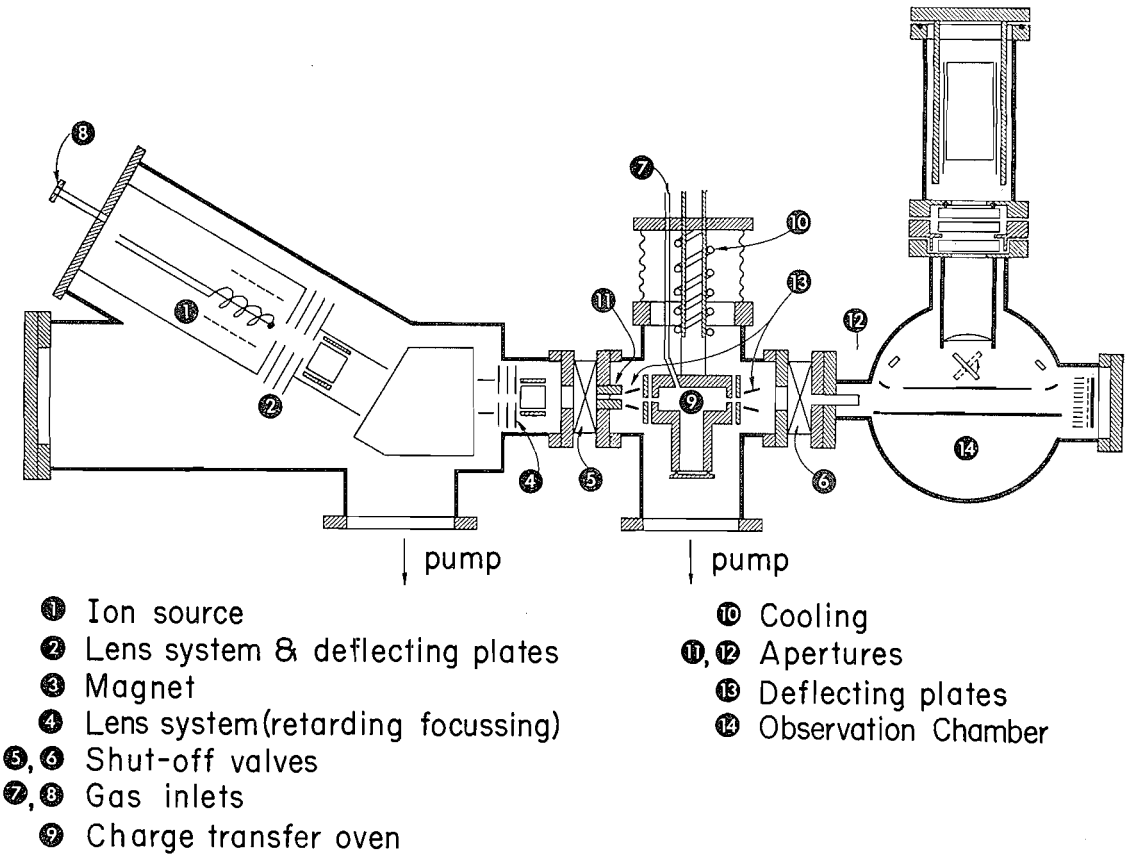

FIG. 1. Schematic diagram of the apparatus.

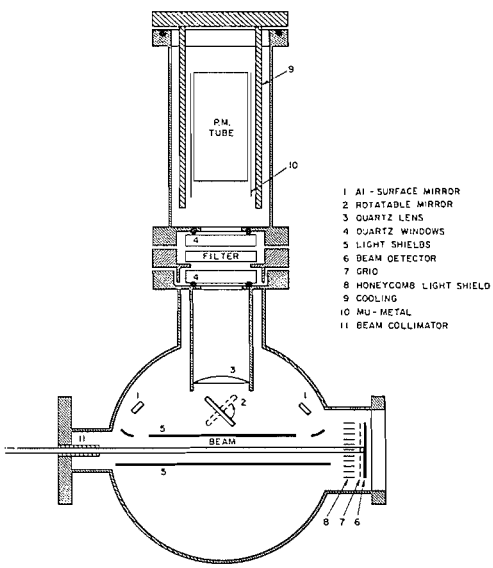

FIG. 2. Observation chamber.

appropriate light baffles to prevent fluorescence at the beam collector surfaces from producing an optical signal.

The optical system is adjusted so that the efficiency is very nearly (within 5%) the same for the detection of light from the two segments of the beam. This relative efficiency is periodically measured by observing light produced under conditions such that the light emitted from the two segments of the beam has the same intensity. As an example, we have used for this purpose the light emitted in the region of 3914 Å, produced in $He^+ + N_2$ collisions at low target gas pressures.

The relative detection efficiencies, $f_1(x)$ and $f_2(x)$, functions of position x along the first and second beam segments, are calculated from the geometry and also experimentally determined by measuring the optical signal from a uniform source as a function of the position along the beam axis. Both methods of determining $f_1(x)$ and $f_2(x)$ agree well.

Lifetimes are measured for a range of velocities from 0.5×10^7 to 1.3×10^7 cm/s. A lack of velocity dependence in the measurements is evidence that the overall relative detection efficiencies for the two beam segments have been properly corrected for, and that no significant

Can. J. Chem. Downloaded from www.nrcresearchpress.com by 210.87.254.5 on 09/05/12
For personal use only.

Can. J. Chem. Downloaded from www.nrcresearchpress.com by 210.87.254.5 on 09/05/12
For personal use only.

contribution to the signal comes from multiple exponential decays.

Reduction of Data

The variation in the intensity of light from excited beam particles as a function of the distance, x, along the beam is given by

$$[1] \qquad I = I_0 \exp(-x/\tau v)$$

where τ is the lifetime of the excited state and v is the particle velocity.

The optical signals, I_1 and I_2, observed from two beam segments of length a and separated by a distance b are then given by

$$[2] \qquad I_1 = \alpha K \int_0^a f_1(x) \exp(-x/\tau v)\, dx$$

and

$$[3] \qquad I_2 = K \exp(-b/\tau v) \int_0^a f_2(x) \exp(-x/\tau v)\, dx$$

where K is a constant for a given initial flux of excited beam particles and target gas density, α is the ratio of the total detection efficiency for the first beam segment to that for the second beam segment, and $f_1(x)$ and $f_2(x)$ represent the variation in detection efficiency as a function of position along the first and second beam segments, respectively.

The ratio of the measured signals is then

$$[4] \qquad I_1/I_2 = \alpha R(\tau v) \exp(b/\tau v)$$

where

$$R(\tau v) = \int_0^a f_1(x) \exp(-x/\tau v/dx) \int_0^a f_2(x) \exp(-x/\tau v)\, dx$$

The lifetime is then given by

$$[5] \qquad \tau = \left[\frac{v}{b}(\ln I_1/I_2 - \ln \alpha R)\right]^{-1}$$

For the conditions of our experiment, $R(\tau v)$ is always very close to 1 and the lifetime is obtained directly from eq. [5] by letting $R = 1$. However, a computer program has also been used to calculate τ from eq. [5] more exactly by using the known values of $f_1(x)$ and $f_2(x)$ and an iterative procedure.

Results

The first positive system of N_2 was used to determine the lifetime of the $B^3\Pi_g$ state of N_2. This state follows the rapid (0.047 μs) decay of the $C^3\Pi_u$ state which is produced by the electron capture of N_2^+ ions on Rb. The lifetime measurements were made at least 2 μs after the initial excitation, and all cascading from the C state had taken place.

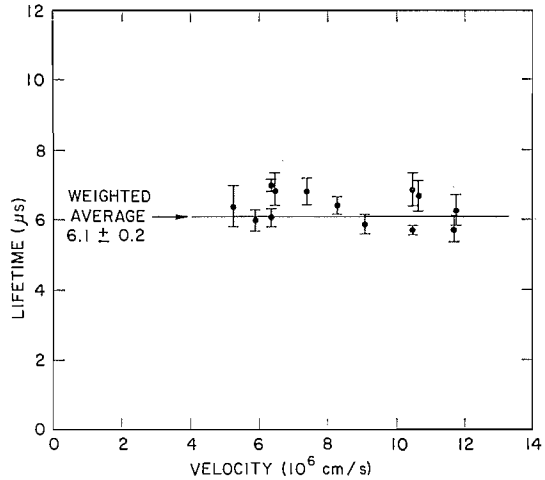

FIG. 3. Lifetime measurements for the $v' = 5$ level of the $B^3\Pi_g$ state of N_2 at various beam particle velocities.

A typical set of data is shown in Fig. 3 for the $v' = 5$ vibrational level of the $B^3\Pi_g$ state of N_2. The lifetime of this level was determined from the spatial decay of the 6705 Å (5,2) band of the first positive system. The errors shown represent the root mean square deviation of the data used for the corresponding points in the figure and arise primarily from the statistics of photon counting and from small beam fluctuations.

Lifetimes for the $v' = 2$, 9, and 11 and 12 (combined) levels of the $B^3\Pi_g$ state of N_2 were determined from the spatial decay of the 7753 (2,0), 5906 (9,5), 5804 (11,7) and 5755 Å (12,8) bands, respectively, of the first positive system of N_2. The lifetime for the $v' = 3$ level was measured by observing the spatial decay of both the 6875 Å (3,0) band and the 7626 Å (3,1) band. Both of the two latter measurements yielded the same lifetime, thus giving further evidence for the validity of the measurements. The results for the first positive system are shown in Table I along with the results of Jeunehomme (1) who measured the temporal decay of light from states excited in a discharge, used a computer program to separate multiple exponential decays, and extrapolated to zero pressure to obtain collision-free values. There is

TABLE I

N_2 first positive lifetimes

	N_2^+ lifetimes (μs)		
		Jeunehomme	
v'	This work	Interrupted discharge	Pulsed electrodeless discharge
0		8.0	
1		7.5	
2	7.5 ±0.20	7.0	7.0±0.4
3	6.6 ±0.30	6.8	6.8±0.3
4		6.5	6.7±0.7
5	6.1 ±0.20	6.2	6.7±1.0
6		6.0	7.0±0.7
7		5.3	5.4±0.8
8		5.1	5.4±0.8
9	4.87±0.25	4.8	5.4±0.5
10		4.4	
11			
12	4.14±0.15		
v'	N_2^+ Meinel lifetimes (μs)		
3	12.23±0.19		
4	11.42±0.16		
5	12.2 ±0.9		

good agreement between our results and those of Jeunehomme, with a possible discrepancy for $v' = 2$ which is, however, within the combined experimental errors.

We have also determined the lifetimes for the $v' = 3$, 4, and 5 levels of the $A^2\Pi_u$ state of N_2^+ from the spatial decay of the (3,0), (4,1), and (5,1) bands of the Meinel system of N_2^+, respectively. The $N_2^+(A^2\Pi_u)$ state is produced in the ion source, and sufficient quantities to permit measurement are left in the beam when it reaches the observation chamber about one meter from the source. Pressures in the observation chamber are about 4×10^{-7} Torr under these conditions. Increasing this pressure fivefold had no effect on the data.

The results of the Meinel measurements are also given in Table I. The lifetimes are about four times longer than the rough estimate made by Sheridan, Oldenberg, and Carleton (2).

1. M. JEUNEHOMME. J. Chem. Phys. **45**, 1805 (1966).
2. W. F. SHERIDAN, O. OLDENBERG, and N. P. CARLETON. *In* Atomic collision processes. *Edited by* M. R. C. McDowell. North-Holland Publishing. Co., Amsterdam. 1964. p. 440.

Summary

SUMMARY BY CHAIRMAN,
F. R. GILMORE[1]

Professor R. W. Nicholls opened the session with an able review of the new information on radiative transition probabilities which has been obtained since the last I.A.G.A. Symposium in 1963. Activity in this field has greatly increased, and Nicholls was able to reference nearly a hundred measurements of radiation intensities or lifetimes of atmospheric species, as well as several theoretical calculations. The considerable amount of new information on spectroscopic constants, potential curves, and Franck–Condon factors was also itemized. Reasonably good information on a majority of the transitions that are important to aeronomy is now available, although there are still a number of gaps and a few discrepancies.

After the review paper, G. M. Lawrence discussed the experimental advantages of determining transition probabilities by measuring lifetimes, and listed a number of very recent lifetime measurements on atmospheric species by himself and others. These new data fill in important gaps, especially for atomic oxygen and nitrogen.

The following paper, by Hollstein, Lorents, Peterson, and Sheridan, presented results obtained by a relatively unexploited method: measuring the decay of radiation along a molecular beam. Lifetimes for the N_2 First Positive bands were obtained which agreed with previous work, and the lifetimes of three N_2^+ Meinel bands were found to be about 12 μs.

The session concluded with a paper by D. E. Shemansky and N. P. Carleton, "Lifetime of the N_2 Vegard–Kaplan System" which has been submitted to the J. of Chem. Phys. and is not reproduced here. In this paper they reinterpreted some earlier measurements of Carleton and Oldenberg, and obtained lifetimes for N_2 $A^3\Sigma_u^+$ ($v = 0$) of 1.36 s for the $\Sigma = 0$ substate and 2.7 s for the $\Sigma = \pm 1$ substates. These results are in good agreement with results obtained in absorption by Shemansky, and reported in the session on absorption coefficients.

[1]Address: The Rand Corporation, Santa Monica, California 90406.

Can. J. Chem. Downloaded from www.nrcresearchpress.com by 210.87.254.5 on 09/05/12
For personal use only.

Can. J. Chem. Downloaded from www.nrcresearchpress.com by 210.87.254.5 on 09/05/12
For personal use only.

The collisional deactivation of metastable atoms and molecules in the upper atmosphere

E. C. ZIPF
Department of Physics, University of Pittsburgh, Pittsburgh, Pennsylvania 15213

Received December 13, 1968

It is now possible to produce comparatively large concentrations of highly reactive metastable species in laboratory sources and to study metastable atoms and molecules with very long radiative lifetimes by photoionization mass spectroscopy, by vacuum ultraviolet absorption techniques, or by direct observation of the feeble radiation emitted by these excited species. These methods are being used widely to study the collisional deactivation of aeronomically important metastable species by quenching or by reaction. New information on radiative lifetimes, diffusion coefficients, and reaction rate coefficients is now available. These results are tabulated and reviewed in the light of atmospheric measurements and current theories of the terrestrial airglow and aurora.

Canadian Journal of Chemistry, 47, 1863 (1969)

In recent years ground-based, satellite, and sounding rocket experiments have given us a much clearer picture of the remarkable chemical and physical properties possessed by the metastable species found in our upper atmosphere. During the same period a number of important technical advances in photomultiplier tube design, in digital data processing, in the techniques for further purifying reagent grade gas samples, and in the complementary use of ultra-high vacuum gas-handling systems under stationary or flowing gas conditions, have brought laboratory studies on the excitation and collisional deactivation of metastable species of aeronomic interest to a state of comparable maturity. It is now possible to produce comparatively large concentrations of highly reactive metastable species in laboratory sources and to study metastable atoms and molecules with very long radiative lifetimes (Table I) by photoionization mass spectroscopy, by vacuum ultraviolet absorption techniques, or by direct observation of the feeble radiation emitted by these excited species.

In this paper we are concerned primarily with those collision processes that depopulate a metastable atom or molecule, either by quenching or by reaction. Much of the experimental work in this field is still preliminary and unpublished. In Tables I–IX, presented in the following section, a representative sample of these results has been included. In a number of cases data obtained in sounding rocket studies of the airglow and aurora have guided and corrected the laboratory work and where it seemed appropriate, the atmospheric values have also been included. There is a notable unevenness in the laboratory results reported so far. It is commonplace to find experimenters agreeing on the magnitude of one specific quenching coefficient only to differ by an order of magnitude or more on another, in spite of using the same apparatus and techniques for both measurements. We are fortunate to this extent, however, that for most metastable species there is a consensus of opinion on the identity of the dominant quenching agent in the upper atmosphere and on the magnitude of the quenching coefficient required to account for the observational data. This information is summarized in Table X.

Tables and Notes

Notes on $O_2(a^1\Delta_g)$ Quenching, Table II

Oxygen molecules in the $a^1\Delta_g$ state are remarkably immune to quenching by the major atmospheric gases. Wall collisions are equally ineffective in deactivating this long-lived state. In the typical laboratory source the catalytic efficiency of the walls is generally in the range 10^{-2} to 2×10^{-3} (5, 57) and it is not uncommon to find as much as 10% of the total O_2 concentration in the

TABLE I
Radiative lifetimes

Metastable species	Lifetime	Reference
$O(I)(^1S)$	0.74 s	68–70
$O(I)(^1D)$	110 s	68–70
$O^+(^2P)$	5 s	68–70
$O^+(^2D)$	3.6 h	68–70
$N(I)(^2P)$	12 s	68–70
$N(I)(^2D)$	26 h	68–70
$N^+(^1S)$	0.90 s	68–70
$N^+(^1D)$	4.13 min	68–70
$N_2(A^3\Sigma_u^+)$	1.3 s (F_2); 2.5 s (F_1, F_3)	67
$O_2(a^1\Delta_g)$	45 min	64
$O_2(b^1\Sigma_g^+)$	12 s	65, 66, 95, 96

TABLE II

Quenching coefficients*

Quenching particle	Rate coefficient (cm^3/s)	Reference
$O_2(a^1\Delta_g)$	2.2×10^{-18}†	5
	$<10^{-17}$	6
	10^{-14}	7
	$\sim4\times10^{-17}$‡	60
	$(5\pm1)\times10^{-23}$§	63
$O_2(X^3\Sigma_g^-)$	$<2.6\times10^{-19}$	5
	$(1\pm0.5)\times10^{-17}$	61
$O_2^-(^2\Pi_g)$	10^{-9}	13
	2×10^{-10}	62
N_2	4×10^{-19}	8
O	$<10^{-15}$	8, 11
N	3×10^{-13}	12
O_3	2×10^{-15}	10
	2×10^{-14}	9

*Metastable species: $O_2(a^1\Delta_g)$, infrared atmospheric bands $[a^1\Delta_g \rightarrow X^3\Sigma_g^-]$.
†For the process $2[O_2(a^1\Delta_g)] \rightarrow O_2(^1\Sigma_g^+) + O_2(^3\Sigma_g^-)$.
‡For the process $2[O_2(a^1\Delta_g)] \rightarrow O_2(^3\Sigma_g^-) + O_2(^3\Sigma_g^-)$.
§For the process $2[O_2(a^1\Delta_g)] \rightarrow O_2(^3\Sigma_g^-) + O_2(^3\Sigma_g^-) + h\nu(6340\ Å)$.

$a^1\Delta_g$ state. In view of this overall inertness, it may come as something of a surprise to find $O_2(a^1\Delta_g)$ playing a very active role in the physics and chemistry of the D region.

Metastable $O_2(a^1\Delta_g)$ molecules are produced in the upper atmosphere principally by the photolysis of ozone (8),

$$O_3(^1A) + h\nu \rightarrow O_2(a^1\Delta_g) + O(^1D)$$

through the absorption of solar radiation in the Hartley continuum. Other processes that contribute in a minor way include the following

(*i*) Resonance–phosphorescence, (including cascading)

$$O_2(^3\Sigma^-) + h\nu(1.27 \text{ or } 0.76\ \mu) \rightarrow O_2(a^1\Delta_g)(+h\nu\ (1.9\ \mu))$$

(*ii*) Atomic oxygen – ozone reactions,

$$O_3 + O \rightarrow O_2 + O_2(a^1\Delta_g)$$

(*iii*) Chapman 3-body recombination,

$$O + O + M \rightarrow O_2(a^1\Delta_g) + M$$

The slow collisional deactivation of $O_2(a^1\Delta_g)$ coupled with a very long radiative lifetime allow these sources to create an abundant supply of $^1\Delta_g$ molecules above 40 km. Evans *et al.* (8), who measured the altitude profile of the infrared atmospheric system of oxygen $(a^1\Delta_g \rightarrow X^3\Sigma_g^-)$, found that the maximum $O_2(a^1\Delta_g)$ density occurred near 50 km where the concentration of this metastable species was about $3.7\times10^{10}\ cm^{-3}$. The integrated intensity of the infrared atmospheric bands above 30 km was approximately 21 MR, making these bands the brightest feature in the dayglow spectrum.

By analyzing the altitude distribution of $O_2(a^1\Delta_g)$ in the dayglow, Evans *et al.* (8) determined k_d, an overall quenching coefficient that was referred to the total particle concentration $n(M)$

$$O_2(a^1\Delta_g) + M \rightarrow O_2(^3\Sigma_g^-) + M$$

They found that $k_d = 3\times10^{-19}\ cm^3/s$. Although their experiment did not distinguish between O_2 or N_2 as the quenching agent, they concluded, in view of the laboratory work of Arnold and Ogryzlo (5), that N_2 was favored with a quenching coefficient $1.25k_d$. If, however, the quenching is attributed entirely to O_2, the corresponding rate coefficient would have a value of $1.5\times10^{-18}\ cm^3/s$. This is still an order of magnitude smaller than the preliminary value for $^1\Delta_g$ quenching by O_2 ($1\times10^{-17}\ cm^3/s$) obtained recently by Clark and Wayne (61) who detected the metastables by photoionization. If the larger quenching coefficient is accepted, then a much more efficient source of $O_2(a^1\Delta_g)$ molecules will have to be found to explain the comparatively large concentrations observed in the upper atmosphere.

Metastable $O_2(a^1\Delta_g)$ molecules appear to be a major source of O_2^+ ions in the D region. Hunten and McElroy (12) have shown that $O_2(a^1\Delta_g)$ can be ionized by the solar radiation in the wavelength band $\lambda = 1027$–1118 Å which penetrates deeply into the D region

$$O_2(a^1\Delta_g) + h\nu\ [1027\text{–}1118\ Å] \rightarrow O_2^+ + e$$

This mechanism may account for the unusual amount of O_2^+ observed in the D region by Narcisi and Bailey (90, 91).

Equally intriguing is the proposal by Hunten and McElroy (12) that metastable $O_2(a^1\Delta_g)$ may also produce most of the NO found in the D region through the following quenching reaction

$$[1] \qquad N + O_2(a^1\Delta_g) \rightarrow NO + O$$

This process would help account for the large quantities of NO implied by the dayglow observations of Barth (92, 93) provided the reaction coefficient for reaction [1] was about $3\times10^{-13}\ cm^3/s$.

Finally we should note that $O_2(a^1\Delta_g)$ molecules may influence the negative ion equilibrium in the D region through the fast detachment reaction,

$$O_2^- + O_2(a^1\Delta_g) \rightarrow 2[O_2(^3\Sigma_g^-)] + e$$

which proceeds at room temperature with a rate coefficient of $2\times10^{-10}\ cm^3/s$ (62).

Notes on $O_2(b^1\Sigma_g^+)$ Quenching, Table III

There is general agreement that molecular nitrogen is the dominant $O_2(b^1\Sigma_g^+)$ quenching agent in the upper atmosphere,

$$[2] \qquad O_2(b^1\Sigma_g^+) + N_2 \rightarrow O_2 + N_2$$

Laboratory measurements indicate a quenching coefficient $k_2 = (1.5\text{–}2.5)\times10^{-15}\ cm^3/s$ at room temperature. This is in good agreement with the results obtained by Wallace and Hunten (2) who found from sounding rocket studies of the O_2 atmospheric bands $[b^1\Sigma_g^+ \rightarrow X^3\Sigma_g^-]$ that $k_2 = 1.5\times10^{-15}\ cm^3/s$. Molecular oxygen is not an effective $^1\Sigma_g$ quenching agent,

$$[3] \qquad O_2(b^1\Sigma_g^+) + O_2 \rightarrow O_2 + O_2$$

with $k_3 \leqslant 10^{-16}\ cm^3/s$.

The much larger quenching coefficients (e.g., $k_2 = 5\times10^{-13}\ cm^3/s$) reported by Black *et al.* (1) are simply incompatible with the upper atmosphere data. Whether the presence or absence of vibrationally excited O_2

Can. J. Chem. Downloaded from www.nrcresearchpress.com by 210.87.254.5 on 09/05/12
For personal use only.

Can. J. Chem. Downloaded from www.nrcresearchpress.com by 210.87.254.5 on 09/05/12
For personal use only.

TABLE III

Quenching coefficients*

Quenching particle	Rate coefficient (cm^3/s)	Reference
O_2	3×10^{-13}	1
	$\leqslant 9\times10^{-16}$	2
	1×10^{-16}	3
	$\leqslant 1\times10^{-16}$	57
	10^{-18}	4
N_2	5×10^{-13}	1
	1.5×10^{-15}	2
	1.5×10^{-15}	3
	2.3×10^{-15}	57
	2.5×10^{-15}	60
CO	1.1×10^{-12}	1
	3×10^{-15}	3
	2.5×10^{-15}	60
CO_2	1.5×10^{-11}	1
	5×10^{-13}	3
	5×10^{-14}	60
O_3	6×10^{-13}	9
	7.1×10^{-12}	57
NO	6×10^{-12}	1

*Metastable species: $O_2(b^1\Sigma_g^+)$, atmospheric bands $[b^1\Sigma_g^+ \rightarrow X^3\Sigma_g^-]$.

molecules in the different laboratory experiments, as proposed by Black *et al.* (94), will explain the discrepancy remains to be seen. The explanation depends in part on the fact that the smaller values for k_2 and k_3 (3, 57, 60) were derived from measurements in which the O_2 pressure was much greater than 1 Torr, whereas in the work of Black and his collaborators, $p(O_2) \ll 1$ Torr. While this may have some bearing on the problem, it should be pointed out that the O_2 pressures in the experiments of Black *et al.* are duplicated in the upper atmosphere at altitudes above 50 km; it is precisely from observational data obtained in this region of the atmosphere that Wallace and Hunten (2) deduced the smaller quenching coefficient $k_2 = 1.5 \times 10^{-15}$ cm^3/s.

The presence of $O_2(b^1\Sigma_g^+)$ molecules in the upper atmosphere is an interesting example of how the collisional deactivation of one metastable species figures prominently in the excitation of still another. Metastable $O_2(b^1\Sigma_g^+)$ molecules are produced efficiently at the expense of metastable $O(^1D)$ atoms

$$[4] \quad O(^1D) + O_2(^3\Sigma_g^-) \rightarrow O_2(b^1\Sigma_g^+) + O(^3P)$$

In the region above 85 km $O(^1D)$ atoms are produced in the daytime by photodissociation of O_2 in the Schumann–Runge continuum [S.R.c.],

$$[5] \quad O_2(^3\Sigma_g^-) + h\nu\ [\text{S.R.c.}] \rightarrow O(^1D) + O$$

and by photodissociation of ozone at lower altitudes

$$[6] \quad O_3(^1A) + h\nu \rightarrow O_2(a^1\Delta_g) + O(^1D)$$

in the Hartley continuum. Although most of the ^1D atoms formed by processes [5] and [6] are quenched by N_2, making reaction [4] a minor ^1D loss process, O_2 quenching of $O(^1D)$ is the dominant source of $O_2(b^1\Sigma_g^+)$ above 100 km and it is still an important source at altitudes as low as 40 km (2).

Based on an analysis of the excitation of the atmospheric bands in auroras, Wallace and Chamberlain (32) concluded that the rate coefficient for reaction [4] was approximately 1×10^{-11} cm^3/s. This conclusion has been supported by the laboratory work of Young and his collaborators (23) and by Noxon (3) who find that an $O_2(b^1\Sigma_g^+)$ molecule is formed nearly every time an $O(^1D)$ atom is quenched by O_2. This is in disagreement with the recent work of Izod and Wayne (57) who report that an $O_2(b^1\Sigma_g^+)$ molecule is formed only once in 500 quenching collisions.

TABLE IV

Quenching coefficients*

Quenching particle	Rate coefficient (cm^3/s)	Reference
N_2	$\leqslant 1.2\times10^{-18}$	14
	10^{-19}	15
O_2	$\leqslant 4\times10^{-10}$	16
	$\sim10^{-13}$	17
NO	7×10^{-11}	18
N	5×10^{-11}	19
	5×10^{-12}	54
	5.4×10^{-11}	20
O	$\sim5\times10^{-11}$	17
	$\leqslant 3\times10^{-11}$	16
$N_2(A^3\Sigma_u^+;\ v'=0)$	$\sim2\times10^{-11}$†	55

*Metastable species: $N_2(A^3\Sigma_u^+)$, Vegard–Kaplan bands $[A^3\Sigma_u^+ \rightarrow X^1\Sigma_g^+]$.
†For the process: $2N_2(A^3\Sigma_u^+) \rightarrow N_2(C^3\Pi_u) + N_2$.

Notes on $N_2(A^3\Sigma_u^+)$ Quenching, Table IV

The Vegard–Kaplan bands $[A^3\Sigma_u^+ \rightarrow X^1\Sigma_g^+]$ appear prominently in the ultraviolet spectrum of an aurora; they have not been observed in the normal day or night airglow. In auroras, the Vegard–Kaplan system is excited principally by cascade radiation from two other closely related triplet states of nitrogen (40, 76)

$$N_2(X^1\Sigma_g^+) + e \rightarrow N_2(C^3\Pi_u) + e$$
$$N_2(C^3\Pi_u) \rightarrow N_2(B^3\Pi_g) + h\nu \text{ (second positive bands)}$$

$$N_2(X^1\Sigma_g^+) + e \rightarrow N_2(B^3\Pi_u) + e$$
$$N_2(B^3\Pi_g) \rightarrow N_2(A^3\Sigma_u^+) + h\nu \text{ (first positive bands)}$$

Atomic oxygen appears to be the dominant A state quenching agent in the upper atmosphere

$$[7] \quad N_2(A^3\Sigma_u^+) + O(^3P) \rightarrow N_2(X^1\Sigma_g^+) + O^*$$

where the product atom O* may be in the ^1S, ^1D, or ^3P state.

The quenching results based on atmospheric observations were derived by Hunten and McElroy (16) from a consideration of the high rotational temperature (800 °K or more; refs. 38–41) exhibited by the Vegard–Kaplan bands in auroras. When this analysis was undertaken, the accepted value for the radiative lifetime of the $A^3\Sigma_u^+$ ($v' = 0$) state was approximately 10–12 s (77, 78). It was then supposed that there would be sufficient time for $N_2(A)$ molecules formed in an aurora to come into thermal equilibrium with the ambient atmosphere prior

Can. J. Chem. Downloaded from www.nrcresearchpress.com by 210.87.254.5 on 09/05/12
For personal use only.

to radiating. The consistently high rotational temperatures would, therefore, indicate that the height of the emission is around 200 to 220 km and that below 200 km the Vegard–Kaplan system is effectively quenched. In this view the Vegard–Kaplan bands, like the O(I) red line [λ = 6300 Å], are emitted in a diffuse, high altitude glow that pervades the entire sky. If reaction [7] is the dominant quenching process, a quenching coefficient $k = 3 \times 10^{-11}$ cm^3/s would be required to account for the observations.

The agreement between the laboratory value for the quenching coefficient (5×10^{-11} cm^3/s; ref. 17) and the atmospheric estimate is remarkably good. The chief difficulty, however, with this otherwise self-consistent picture is the growing evidence from several recent auroral rocket experiments (ref. 28) that the bulk of the Vegard–Kaplan emission occurs in the vicinity of 120 km and that only very weak emission is observed above 170 km. These results would indicate that the apparent rotational temperature of the Vegard–Kaplan bands is not an accurate measure of the ambient temperature at the altitude of peak emission. The sounding rocket data indicate further that the product of the quenching coefficient and the radiative lifetime must be nearly one order of magnitude smaller than the value adopted by Hunten and McElroy (16). If we accept the laboratory value for the quenching coefficient as being essentially correct, then the radiative lifetime of the $A^3\Sigma_u^+$ state would have to be in the range of 1–2 s in order to be compatible with the observational data. This conclusion agrees well with the new experimental lifetime measurements of Shemansky (67) who finds that $\tau_r = 1.3$ s for the F_2 levels and 2.5 s for the F_1 and F_3 levels.

Notes on O(^{1}S) Quenching, Table V

The processes that create oxygen atoms in the metastable ^{1}S state in the upper atmosphere have been the subject of constant study and speculation since the green line ($^1S \rightarrow {}^1D$; λ = 5577 Å) was first detected in the nightglow by Campbell (79) in 1895. The excitation mechanisms most frequently discussed include the following

(*1*) In auroras (80, 81),

(*i*) Dissociative recombination of O_2^+

$$O_2^+ + e \rightarrow O(^1S, {}^1D, {}^3P) + O$$

(*ii*) Electron impact excitation

$$O(^3P) + e \rightarrow O(^1S) + e$$

(*2*) In the dayglow (37, 82),

(*iii*) Photodissociation of O_2 by solar vacuum ultraviolet (v.u.v.) photons (83)

$$O_2(X^3\Sigma_g^-) + h\nu\,(\text{v.u.v.}) \rightarrow O(^1S) + O$$

in addition to processes (*i*) and (*ii*).

(*3*) In the nightglow (84–86),

(*iv*) The Chapman mechanism

$$O + O + O \rightarrow O(^1S) + O_2$$

which may be an important source of ^{1}S atoms in the low altitude nightglow layer (87, 88), in addition to the dissociative recombination of O_2^+ ions (process (*i*)) which is a significant ^{1}S source in the night-time F region.

TABLE V

Quenching coefficients*

Quenching particle	Rate coefficient (cm^3/s)	Reference
O_2	$(2.1 \pm 0.4) \times 10^{-13}$	21
	1×10^{-13}	4
	3.2×10^{-13}	52
	5×10^{-13}	53
	4×10^{-15}	16
N_2	$< 10^{-15}$	15
	$< 10^{-17}$	4
	$< 2 \times 10^{-16}$	52
	1.3×10^{-15}	53
CO_2	2.5×10^{-14}	4
	$(3.18 \pm 0.30) \times 10^{-13}$	103
	4.6×10^{-13}	52
CO	9.4×10^{-14}	52
O	1.8×10^{-13}	4
	$< 4 \times 10^{-13}$	16
N_2O	1.5×10^{-11}	52
	1.6×10^{-11}	53
H_2O	$\sim 3 \times 10^{-10}$	52
H_2	1.5×10^{-15}	52
	2×10^{-13}	53
NO	4×10^{-10}	53

*Metastable species: O(^{1}S), auroral green line [$^1S \rightarrow {}^1D$; λ = 5577 Å].

Ground-based studies of the temporal behavior of the λ = 5577 Å emission in auroras (42–45) and in meteoric wakes (46) show that the ^{1}S state is collisionally deactivated in the upper atmosphere. The early work of Kvifte and Vegard (47) appeared to rule out O_2 as an important ^{1}S quenching agent. More recent laboratory work (21, 4, 52, 53), however, shows that this is not the case. It is now apparent that O_2 quenching competes effectively with radiation in depopulating O(^{1}S) atoms in the nightglow layer at 95 km; it is the dominant loss mechanism in the lower portion of that layer. Molecular nitrogen and atomic oxygen are not effective ^{1}S quenching agents in the upper atmosphere.

Among the minor atmospheric constituents in the D region only water vapor may deactivate O(^{1}S) atoms sufficiently fast to compete with radiation and O_2 quenching

[8] $$H_2O + O(^1S) \rightarrow OH + OH$$

Hesstvedt (89) finds, on the basis of numerical calculations, taking into account the effects of eddy and molecular diffusion fluxes as well as the standard photochemical reactions, that there could be a considerable H_2O density at the altitude of the λ = 5577 Å nightglow. In view of the large rate coefficient (3×10^{-10} cm^3/s) found by Stuhl (52) for process [8], water vapor quenching of O(^{1}S) is a distinct possibility.

Notes on O(^{1}D) Quenching, Tables VI and VII

There is little doubt that molecular nitrogen is the most important O(^{1}D) quenching agent in the upper atmosphere

[9] $$O(^1D) + N_2 \rightarrow O(^3P) + N_2^*$$

Can. J. Chem. Downloaded from www.nrcresearchpress.com by 210.87.254.5 on 09/05/12
For personal use only.

TABLE VI

Quenching coefficients*

Quenching particle	Rate coefficient (cm^3/s) $\times 10^{11}$	Reference
N_2	(2.2 ± 1)	22
	5	16
	5	23
	10	3
	5–10	27
	3	58, 59
O_2	(4×10^{-4})	16
	4	23
	6	3
	3	58, 59
NO	15	23
N_2O	18	23
H_2	19	23
	10	94
CO	<3	3
	1	99, 101
	5	23
CO_2	0.3	3
	23	23
	0.02	100

*Metastable species: $O(^1D)$, airglow red line [$^1D \rightarrow {}^3P$; $\lambda = 6300$ Å].

In fact, this process competes effectively against radiation up to altitudes of at least 250 km (37). At room temperature reaction [9] has a rate coefficient of approximately $5\text{–}10 \times 10^{-11}$ cm^3/s.

To what extent reaction [9] leads to the production of vibrationally excited nitrogen molecules, N_2^*, has not been determined. In view of the very efficient production of $O(^1D)$ in the daytime by photodissociation of O_2,

$$O_2(^3\Sigma_g^-) + h\nu \text{ [S.R.c.]} \rightarrow O(^1D) + O$$

and by electron impact,

$$O(^3P) + e \rightarrow O(^1D) + e$$

and dissociative recombination in auroras,

$$O_2^+ + e \rightarrow O(^1D) + O$$

this mechanism may indeed be very important in the thermal economy of the daytime E region and at auroral altitudes where it selectively heats the ambient electron gas via super-elastic collisions

[10] $N_2^*(v'' > 0) + e \rightarrow N_2^*(v' < v'') + e + \text{kinetic energy}$

The anomalously high electron temperatures observed in the daytime E region have been attributed by Walker (29) to reactions [9] and [10]. There is certainly ample energy available, but new data on the quenching of N_2^* by CO_2 (Table VIII) suggest that most of this energy is transferred to atmospheric CO_2 molecules where it is ultimately lost by radiation. This process may still be important at somewhat higher altitudes in auroras where very high electron temperatures (2000 °K or more) have been observed in sounding rocket experiments.

Vibrationally excited nitrogen formed by reaction [9] and electron impact may also figure prominently in auroras by enhancing the geophysically important ion–molecule reaction (30)

[11] $$O^+ + N_2^* \rightarrow NO^+ + N$$

At vibrational temperatures less than 1000 °K this reaction proceeds with a rate coefficient of 1×10^{-12} cm^3/s (31). Above 1000 °K the rate coefficient increases rapidly with the vibrational temperature reaching a value of 10^{-11} cm^3/s when $T_v = 2800$ °K. Direct evidence of the importance of this process was obtained by Zipf *et al.* (97) in a pulsating aurora in which the transient response of the ionosphere to incoming pulses of energetic electrons was studied in situ by simultaneous positive ion mass spectroscopy, optical photometry, and measurements of the primary and secondary electron energy spectrum with hemispherical analyzers.

Molecular oxygen also efficiently quenches the ^1D state

[12] $$O(^1D) + O_2(^3\Sigma_g^-) \rightarrow O(^3P) + O_2$$

Recent laboratory measurements (3, 23) indicate a quenching coefficient $k_{11} = 4\text{–}6 \times 10^{-11}$ cm^3/s. The early work of Kvifte and Vegard (47), as re-analyzed by Hunten and McElroy (16), yielded quenching coefficients that are much smaller than the recent laboratory results; presumably this discrepancy is due to the known complexity of an electrical discharge. Although O_2 quenching is not the dominant ^1D loss mechanism in the upper atmosphere, it is, as we have already noted, an important source of excited $O_2(b^1\Sigma_g^+)$ molecules via reaction [4].

TABLE VII

Relative $O(^1D)$ quenching coefficients

Relative quenching coefficients for quenching particle					
N_2	O_2	CO_2	N_2O	Argon	References
1.0	0.82	4.7	3.6	$<3.6 \times 10^{-2}$	23
1.0	—	4.1	4.2	4.1×10^{-2}	36
1.0	—	—	—	3.8×10^{-3}	22
1.0	0.6	3×10^{-2}	—	—	3
1.0	0.25	—	—	0.11	57
1.0	~1.0	—	—	—	58, 59
1.0	2.1	15	28	—	74, 75

Can. J. Chem. Downloaded from www.nrcresearchpress.com by 210.87.254.5 on 09/05/12
For personal use only.

TABLE VIII

Quenching coefficients

Metastable species	Quenching particle	Rate coefficient (cm^3/s)	Reference
$N(^2D)$	O_2	10^{-12}	16
$N(^2P)$	N_2	3×10^{-19}	15
O(II) [red multiplet]	N_2	10^{-10}	24
$O^+(^2D)$	N_2	$1 \rightarrow 0.3\times10^{-9}$	25, 26, 56
N_2^*, O_2^* [$v' = 1$]	—	3×10^{-18}	35
$N_2^*[v' = 1]$	CO_2	6×10^{-13}	57
$N_2^*[v' = 4-10]$	N_2	$10^{-14} \rightarrow 10^{-15}$	16, 34
$N_2^*[v' \geqslant 8]$	Na	10^{-10}	49, 50
N_2^*[vib]	O_3	6×10^{-13}	33
O_2^*[vib]*	Na	?	48

*Proposed as a possible energy source for the sodium nightglow.

The apparent disagreement between the dayglow measurements of the ^1D quenching rate above 100 km and Seaton's conclusions (51) based on an analysis of ground-based measurements of the λ5577/λ6300 intensity ratio in auroras has been resolved. Parkinson *et al.* (27) have found in a recent rocket experiment that the O(I) red and green emission lines are emitted from quite different altitude regions in an auroral display. As predicted by Hunten and McElroy (16), the O(I) red line was emitted from a high altitude, diffuse glow that pervaded the entire sky. The rocket experiment showed very clearly the strong deactivation of the ^1D state by N_2 and pointed out the hazards involved in ground-based auroral studies. The rocket data are compatible with an N_2 quenching coefficient of about $5\text{–}10 \times 10^{-11}$ cm^3/s.

The effectiveness of CO_2 as a ^1D quenching agent is the subject of some controversy as Table VII shows. Two groups (Young *et al.* (23), and Preston and Cvetanović (36)) find CO_2 four to five times more efficient than N_2 in depopulating $O(^1D)$ atoms. In neither experiment, however, are $O(^1D)$ atoms directly observed. Noxon (3) disagrees with this result. In an experiment in which he follows the behavior of $O(^1D)$ atoms in a photolysis cell by directly observing the λ = 6300 Å radiation emitted by this species, he concludes that CO_2 is 30 times *less* efficient than N_2. A somewhat similar result has been reported by Clerc and Reiffsteck (100). There is also a difference of opinion concerning the question of quenching versus reaction. Clerc and Reiffsteck have obtained some evidence that the reaction,

$$O(^1D) + CO_2 \rightarrow CO_3$$

is more important than simple quenching,

$$O(^1D) + CO_2 \rightarrow O(^3P) + CO_2$$

This finding disagrees, however, with the photolysis experiments of Slanger (102) which indicate that $O(^3P)$ is definitely one of the products of the ^1D loss mechanism.

Finally, Black *et al.* (98) suggest that the existence of an intermediate CO_3^* complex in equilibrium with the reactants

$$CO_2 + O(^1D) \underset{k_2}{\overset{k_1}{\rightleftarrows}} CO_3^* \xrightarrow{k_3} CO_2 + O(^3P) \text{ or } CO_3$$

may be the key to resolving the CO_2 efficiency problem. They postulate that in their experiment the equilibrium is upset by the presence of the NO used to detect ground-state oxygen atoms, in which case they obtain k_1. Noxon, on the other hand, obtains $k_1 \cdot [k_3/k_2]$ when he observes the $O(^1D)$ decay.

TABLE IX

Metastable diffusion coefficients

Metastable species	Gas	Diffusion coefficient*	Reference
$N_2(A^3\Sigma_u^+)$	N_2	153 ± 2	71, 72
$O(I)(^1S)$	O_2	260 ± 10	73
	Argon	257 ± 6	73
	Neon	405 ± 10	73

*At 1 Torr and 298 °K.

TABLE X

Summary

Metastable species	Collision partner*	Probable quenching coefficient (cm^3/s)
$O(^1D)$	N_2	8×10^{-11}
	O_2	5×10^{-11}
	CO_2	3×10^{-12}†
$O(^1S)$	O_2	2.1×10^{-13}
$O^+(^2D)$	N_2	3×10^{-10}
$N_2(A^3\Sigma_u^+)$	O	3×10^{-11}
$O_2(b^1\Sigma_g^+)$	N_2	1.5×10^{-15}
$O_2(a^1\Delta_g)$	N	3×10^{-13}
	$O_2(^2\Pi_g)$	2×10^{-10}
$N(^2D)$	O_2	10^{-12}

*Important quenching agents in our upper atmosphere.
†Controversial.

1. R. A. Young and G. Black. J. Chem. Phys. **47**, 2311 (1967).
2. L. Wallace and D. M. Hunten. J. Geophys. Res. **73**, 4813 (1968).
3. J. Noxon. Private communication.
4. R. A. Young and G. Black. J. Chem. Phys. **44**, 3741 (1966).
5. S. J. Arnold and E. A. Ogryzlo. Can. J. Phys. **45**, 2053 (1967).

Can. J. Chem. Downloaded from www.nrcresearchpress.com by 210.87.254.5 on 09/05/12
For personal use only.

6. A. M. WINER and K. D. BAYES. J. Chem. Phys. **70**, 302 (1966).
7. R. A. YOUNG and G. BLACK. J. Chem. Phys. **42**, 3740 (1965).
8. W. F. J. EVANS, D. M. HUNTEN, E. J. LLEWELLYN, and A. VALLANCE JONES. J. Geophys. Res. **73**, 2885 (1968).
9. R. E. MARCH, S. G. FURNIVAL, and H. I. SCHIFF. Photochem. Photobiol. **4**, 971 (1965).
10. R. J. MCNEAL and G. R. COOK. Trans. Am. Geophys. Union, **48**, 73 (1967).
11. D. M. HUNTEN. Space Sci. Rev. **6**, 493, (1967).
12. D. M. HUNTEN and M. B. MCELROY. J. Geophys. Res. **73**, 2421 (1968).
13. L. R. MEGILL and J. B. HASTED. Planetary Space Sci. **13**, 339 (1965).
14. E. C. ZIPF. Bull. Am. Phys. Soc. **9**, 185 (1964).
15. J. NOXON. J. Chem. Phys. **36**, 926 (1962).
16. D. M. HUNTEN and M. B. MCELROY. Rev. Geophys. **4**, 303 (1966).
17. R. A. YOUNG. Private communication.
18. R. A. YOUNG and G. A. ST. JOHN. J. Chem. Phys. **48**, 898 (1968).
19. R. A. YOUNG and G. A. ST. JOHN. J. Chem. Phys. **48**, 895 (1968).
20. K. L. WRAY. J. Chem. Phys. **44**, 623 (1966).
21. E. C. ZIPF. Bull. Am. Phys. Soc. **12**, 225 (1967).
22. D. R. SNELLING and E. J. BAIR. J. Chem. Phys. **47**, 228 (1967).
23. R. A. YOUNG, G. BLACK, and T. G. SLANGER. To be published.
24. A. DALGARNO and M. B. MCELROY. Planetary Space Sci. **13**, 947 (1965).
25. A. DALGARNO and M. B. MCELROY. Planetary Space Sci. **14**, 1321 (1966).
26. R. F. STEBBINGS, B. R. TURNER, and J. A. RUTHERFORD. J. Geophys. Res. **71**, 771 (1966).
27. T. M. PARKINSON, E. C. ZIPF, T. M. DONAHUE, J. P. DOERING, R. A. MILLER, and W. G. FASTIE. To be published.
28. W. G. FASTIE. Private communication.
29. J. C. G. WALKER. Planetary Space Sci. **16**, 321 (1968).
30. L. THOMAS and R. B. NORTON. J. Geophys. Res. **71**, 227 (1966).
31. A. L. SCHMELTEKOPF, F. C. FEHSENFELD, G. I. GILMAN, and E. E. FERGUSON. Planetary Space Sci. **15**, 401 (1967).
32. L. WALLACE and J. W. CHAMBERLAIN. Planetary Space Sci. **2**, 60 (1959).
33. J. E. MORGAN and H. I. SCHIFF. Can. J. Chem. **42**, 2300 (1964).
34. L. F. PHILLIPS and H. I. SCHIFF. J. Chem. Phys. **36**, 3283 (1962).
35. A. DALGARNO. Planetary Space Sci. **10**, 19 (1963).
36. K. F. PRESTON and R. J. CVETANOVIĆ. J. Chem. Phys. **45**, 2888 (1966).
37. L. WALLACE and M. B. MCELROY. Planetary Space Sci. **14**, 677 (1966).
38. W. PETRIE. Phys. Rev. **86**, 790 (1952).
39. L. V. WALLACE. J. Atmospheric Terrest. Phys. **17**, 46 (1959).
40. A. L. BROADFOOT and D. M. HUNTEN. Can. J. Phys. **42**, 1212 (1964).
41. A. VALLANCE JONES. *In* Aurora and airglow. Reinhold Publishing Co., New York. 1967.
42. A. OMHOLT and L. HARANG. J. Atmospheric Terrest. Phys. **7**, 247 (1955).
43. W. F. J. EVANS and A. VALLANCE JONES. Can. J. Phys. **43**, 697 (1965).
44. K. V. PAULSON and G. G. SHEPHERD. J. Atmospheric Terrest. Phys. **27**, 831 (1965).
45. T. PARKINSON, E. C. ZIPF, and T. M. DONAHUE. To be published.
46. I. HALLIDAY. Astrophys. J. **131**, 25 (1960).
47. G. KVIFTE and L. VEGARD. Geofys. Publikasjoner, Norske Videnskaps-Akad. Oslo, 17, No. 3, 1947.
48. A. E. POTTER and B. S. DEL DUCA. J. Geophys. Res. 65, 3915 (1960).
49. J. MENTALL, H. KRAUSE, and W. L. FITE. *In* The Fifth International Conference on the Physics of Electronic and Atomic Collisions. *Edited by* I. P. Flaks. Publishing House Nauka, Leningrad. 1967.
50. D. M. HUNTEN. J. Atmospheric Terrest. Phys. **27**, 583 (1965).
51. M. J. SEATON. Astrophys. J. **127**, 67 (1958).
52. F. STUHL and K. H. WELGE. Can. J. Chem. This issue.
53. G. BLACK, T. G. SLANGER, G. A. ST. JOHN, and R. A. YOUNG. Can. J. Chem. This issue.
54. B. A. THRUSH. J. Chem. Phys. **47**, 3691 (1967).
55. E. C. ZIPF. Bull. Am. Phys. Soc. **10**, 179 (1965).
56. P. BANKS. To be published.
57. T. P. J. IZOD and R. P. WAYNE. To be published.
58. W. B. DEMORE and O. F. RAPER. Astrophys. J. **139**, 1381 (1964).
59. W. B. DEMORE and O. F. RAPER. J. Chem. Phys. **44**, 1780 (1964).
60. E. A. OGRYZLO. Can. J. Chem. This issue.
61. R. P. WAYNE and I. D. CLARK. Private communication.
62. J. BURT, H. I. SCHIFF, and F. FEHSENFELD. Can. J. Chem. This issue.
63. A. M. FALIK and B. H. MAHAN. J. Chem. Phys. 47, 4778 (1967).
64. R. M. BADGER, A. C. WRIGHT, and R. F. WHITLOCK. J. Chem. Phys. **43**, 4345 (1965).
65. W. H. J. CHILDS and R. MECKE. Z. Physik, **68**, 344 (1931).
66. D. Q. WARK and D. M. MERCER. Appl. Opt. 4, 839 (1965).
67. D. SHEMANSKY. J. Chem. Phys. In press.
68. R. H. GARSTANG. Monthly Notices Roy. Astron. Soc. **111**, 115 (1951).
69. R. H. GARSTANG. Astrophys. J. **115**, 506 (1952).
70. R. H. GARSTANG. *In* The airglow and the aurora. *Edited by* E. B. Armstrong and A. Dalgarno. The Pergamon Press, Ltd., London. 1956. pp. 324–327.
71. E. C. ZIPF. J. Chem. Phys. **38**, 2034 (1963).
72. H. H. BROMER and F. SPIEWECK. Planetary Space Sci. **15**, 689 (1967).
73. E. C. ZIPF. Bull. Am. Phys. Soc. **14**, 264, (1969).
74. J. O. SULLIVAN and P. WARNECK. J. Chem. Phys. **46**, 953 (1967).
75. P. WARNECK and J. O. SULLIVAN. Proceedings of the International Conference on Photochemistry, Munich, 1967.
76. W. BENESCH, J. T. VANDERSLICE, and S. G. TILFORD. J. Atmospheric Terrest. Phys. **28**, 431 (1966).
77. N. P. CARLETON and O. OLDENBERG. J. Chem. Phys. **36**, 3460 (1962).
78. M. JEUNEHOMME and A. B. F. DUNCAN. J. Chem. Phys. **41**, 1962 (1964).
79. W. W. CAMPBELL. Astrophys. J. **2**, 162 (1895).
80. T. M. DONAHUE, T. PARKINSON, E. C. ZIPF, J. P. DOERING, W. G. FASTIE, and R. E. MILLER. Planetary Space Sci. **16**, 737 (1968).
81. M. H. REES, J. C. G. WALKER, and A. DALGARNO. Planetary Space Sci. **15**, 1097 (1967).
82. E. C. ZIPF. J. Geomag. Geoelec. Kyoto, **18**, 301 (1966).
83. J. C. G. WALKER. J. Atmospheric Sci. **22**, 361 (1965).
84. I. S. GULLEDGE, D. M. PACKER, S. G. TILFORD, and

J. T. VANDERSLICE. J. Geophys. Res. **73**, 5535 (1968).
85. V. L. PETERSON, T. E. VANZANDT, and R. B. NORTON. J. Geophys. Res. **71**, 2255 (1966).
86. W. E. BROWN and W. R. STEIGER. Nature, **216**, 47 (1967).
87. S. CHAPMAN. Proc. Roy. Soc. London, Ser. A, **132**, 353 (1931).
88. R. A. YOUNG. Can. J. Chem. This issue.
89. E. HESSTVEDT. Geophysica Norvegica, **27**, 4 (1968).
90. R. S. NARCISI and A. D. BAILEY. J. Geophys. Res. **70**, 3687 (1965).
91. R. S. NARCISI. Ann. Geophys. **22**, 224 (1966).
92. C. A. BARTH. Planetary Space Sci. **14**, 623 (1966).
93. C. A. BARTH. Ann. Geophys. **22**, 198 (1966).
94. G. BLACK, T. G. SLANGER, and R. A. YOUNG. Can. J. Chem. This issue.
95. D. E. BURCH and D. A. GRYVNAK. Strengths, widths, and shapes of the oxygen lines near 7600 Angstroms, Pub. no. U-4076, Philco–Ford Corp., Aeronutronic Div. 1967.
96. C. W. CHO, E. R. ALLIN, and H. L. WELSH. Can. J. Phys. **41**, 1991 (1963).
97. E. C. ZIPF, T. PARKINSON, T. M. DONAHUE, J. P. DOERING, K. DICK, and W. G. FASTIE. To be published.
98. G. BLACK, T. G. SLANGER, and R. A. YOUNG. Can. J. Chem. This issue.
99. M. CLERC and F. BARAT. J. Chim. Phys. **63**, 1525 (1966).
100. M. CLERC and A. REIFFSTECK. J. Chem. Phys. **48**, 2799 (1968).
101. M. CLERC and F. BARAT. J. Chem. Phys. **46**, 107 (1967).
102. T. SLANGER. Can. J. Chem. This issue.
103. E. C. Zipf. To be published.

Deactivation of $O(^1S)$ and $O_2(b^1\Sigma_g^+)$[1]

F. STUHL AND K. H. WELGE
Centre for Research in Experimental Space Science, York University, Toronto

Received December 13, 1968

Rate constants for the collisional deactivation of $O(^1S)$ and $O_2(b^1\Sigma_g^+)$ are reported. They are obtained by measuring the intensity decay of the $O(^1S \rightarrow {}^1D)$ and $O_2(b^1\Sigma_g^+ \rightarrow X^2\Sigma_g^+)$ emissions after a pulsed production of the excited species.

Canadian Journal of Chemistry, **47**, 1870 (1969)

We wish to report some rate constants for the deactivation of $O(^1S)$ and $O_2(b^1\Sigma_g^+)$ obtained by direct lifetime measurements. $O(^1S)$ and $O_2(b^1\Sigma_g^+)$ were produced in a pulsed mode, and the emissions of $O(^1S \rightarrow {}^1D)$ and $O_2(b^1\Sigma_g^+ \rightarrow X^3\Sigma_g^-)$ were detected photoelectrically. The rate constants were derived from the time-dependence of the excited state density.

The experimental arrangement, which will be described elsewhere in detail, consists in its main part of a repetitively pulsed vacuum-ultraviolet flash light source, a reaction cell, and a detector system at right angles to the exciting light beam. The characteristics of the light source are: flash duration < 2 μs, energy per discharge up to 10 J, repetition frequency up to 20 c.p.s. The low wavelength cut-off was provided by the use of LiF, MgF_2, CaF_2, and BaF_2 windows. The emissions were isolated by tilting narrow band interference filters with peak wavelengths at 5577.5 and 7622.5 Å. The signals were accumulated by signal averaging with a channel width of 10 μs.

[1]This research was supported by grants received from the National Research Council of Canada and the Defence Research Board of Canada.

$O(^1S)$

A suitable source for the formation of $O(^1S)$ was found to be the photodissociation

$$CO_2 + h\nu \rightarrow CO + O(^1S) \quad (\lambda < 1220\ \text{Å})$$

Flashing of CO_2 produced the $O(^1S \rightarrow {}^1D)$ emission when LiF and MgF_2 windows were used. The emission reached its maximum intensity synchronously with the flash. The decay rate was measured first using CO_2 and then later adding other gases. Pressures ranging from about 10^{-2} to a few 100 Torr were used. From the exponential decay, rate constants were obtained in a straightforward manner. The results are given in Table I.

$O_2(b^1\Sigma_g^+)$

For the production of $O_2(b^1\Sigma_g^+)$ the mechanism, as established recently by Noxon (1)

$$[1] \qquad O_2 + h\nu \rightarrow O(^1D) + O(^3P)$$

$$[2] \qquad O(^1D) + O_2 \rightarrow O_2(b^1\Sigma_g^+) + O(^3P)$$

Can. J. Chem. Downloaded from www.nrcresearchpress.com by 210.87.254.5 on 09/05/12
For personal use only.

J. T. VANDERSLICE. J. Geophys. Res. **73**, 5535 (1968).
85. V. L. PETERSON, T. E. VANZANDT, and R. B. NORTON. J. Geophys. Res. **71**, 2255 (1966).
86. W. E. BROWN and W. R. STEIGER. Nature, **216**, 47 (1967).
87. S. CHAPMAN. Proc. Roy. Soc. London, Ser. A, **132**, 353 (1931).
88. R. A. YOUNG. Can. J. Chem. This issue.
89. E. HESSTVEDT. Geophysica Norvegica, **27**, 4 (1968).
90. R. S. NARCISI and A. D. BAILEY. J. Geophys. Res. **70**, 3687 (1965).
91. R. S. NARCISI. Ann. Geophys. **22**, 224 (1966).
92. C. A. BARTH. Planetary Space Sci. **14**, 623 (1966).
93. C. A. BARTH. Ann. Geophys. **22**, 198 (1966).
94. G. BLACK, T. G. SLANGER, and R. A. YOUNG. Can. J. Chem. This issue.
95. D. E. BURCH and D. A. GRYVNAK. Strengths, widths, and shapes of the oxygen lines near 7600 Angstroms, Pub. no. U-4076, Philco–Ford Corp., Aeronutronic Div. 1967.
96. C. W. CHO, E. R. ALLIN, and H. L. WELSH. Can. J. Phys. **41**, 1991 (1963).
97. E. C. ZIPF, T. PARKINSON, T. M. DONAHUE, J. P. DOERING, K. DICK, and W. G. FASTIE. To be published.
98. G. BLACK, T. G. SLANGER, and R. A. YOUNG. Can. J. Chem. This issue.
99. M. CLERC and F. BARAT. J. Chim. Phys. **63**, 1525 (1966).
100. M. CLERC and A. REIFFSTECK. J. Chem. Phys. **48**, 2799 (1968).
101. M. CLERC and F. BARAT. J. Chem. Phys. **46**, 107 (1967).
102. T. SLANGER. Can. J. Chem. This issue.
103. E. C. Zipf. To be published.

Deactivation of $O(^1S)$ and $O_2(b^1\Sigma_g^+)$[1]

F. STUHL AND K. H. WELGE
Centre for Research in Experimental Space Science, York University, Toronto

Received December 13, 1968

Rate constants for the collisional deactivation of $O(^1S)$ and $O_2(b^1\Sigma_g^+)$ are reported. They are obtained by measuring the intensity decay of the $O(^1S \rightarrow {}^1D)$ and $O_2(b^1\Sigma_g^+ \rightarrow X^2\Sigma_g^+)$ emissions after a pulsed production of the excited species.

Canadian Journal of Chemistry, **47**, 1870 (1969)

We wish to report some rate constants for the deactivation of $O(^1S)$ and $O_2(b^1\Sigma_g^+)$ obtained by direct lifetime measurements. $O(^1S)$ and $O_2(b^1\Sigma_g^+)$ were produced in a pulsed mode, and the emissions of $O(^1S \rightarrow {}^1D)$ and $O_2(b^1\Sigma_g^+ \rightarrow X^3\Sigma_g^-)$ were detected photoelectrically. The rate constants were derived from the time-dependence of the excited state density.

The experimental arrangement, which will be described elsewhere in detail, consists in its main part of a repetitively pulsed vacuum-ultraviolet flash light source, a reaction cell, and a detector system at right angles to the exciting light beam. The characteristics of the light source are: flash duration < 2 μs, energy per discharge up to 10 J, repetition frequency up to 20 c.p.s. The low wavelength cut-off was provided by the use of LiF, MgF_2, CaF_2, and BaF_2 windows. The emissions were isolated by tilting narrow band interference filters with peak wavelengths at 5577.5 and 7622.5 Å. The signals were accumulated by signal averaging with a channel width of 10 μs.

[1]This research was supported by grants received from the National Research Council of Canada and the Defence Research Board of Canada.

$O(^1S)$

A suitable source for the formation of $O(^1S)$ was found to be the photodissociation

$$CO_2 + h\nu \rightarrow CO + O(^1S) \quad (\lambda < 1220\ \text{Å})$$

Flashing of CO_2 produced the $O(^1S \rightarrow {}^1D)$ emission when LiF and MgF_2 windows were used. The emission reached its maximum intensity synchronously with the flash. The decay rate was measured first using CO_2 and then later adding other gases. Pressures ranging from about 10^{-2} to a few 100 Torr were used. From the exponential decay, rate constants were obtained in a straightforward manner. The results are given in Table I.

$O_2(b^1\Sigma_g^+)$

For the production of $O_2(b^1\Sigma_g^+)$ the mechanism, as established recently by Noxon (1)

$$[1] \qquad O_2 + h\nu \rightarrow O(^1D) + O(^3P)$$

$$[2] \qquad O(^1D) + O_2 \rightarrow O_2(b^1\Sigma_g^+) + O(^3P)$$

Can. J. Chem. Downloaded from www.nrcresearchpress.com by 210.87.254.5 on 09/05/12
For personal use only.

TABLE I

Quenching rate coefficients

Quenching particle	Coefficients (cm^3 $molecule^{-1}$ s^{-1})	
	$O(^1S)$	$O_2(b^1\Sigma_g^+)$
CO_2	4.6×10^{-13}	2.0×10^{-13}
O_2	3.2×10^{-13}	1.1×10^{-16}
CO	9.4×10^{-14}	3.3×10^{-15}
H_2	1.1×10^{-15}	6.4×10^{-13}
N_2	$<5\times10^{-17}$	2.2×0^{-15}
Ar		3.2×10^{-16}
N_2O	1.5×10^{-11}	
H_2O	$\sim4\times10^{-10}$	$\sim2\times10^{-11}$

was used. The rate constant (1) for the energy transfer process is 6×10^{-11} cm^3 s^{-1}. When O_2 was flashed,the emission of $O_2(b^1\Sigma_g^+)$ was found to reach the maximum within less than 10 μs at pressures above a few 10^{-1} Torr. Under the above conditions the rapid rise of the emission intensity may be expected. Pressures of O_2 up to 40 Torr were used. From the decay rates with and without added gases the rate constants given in Table I were derived.

1. J. NOXON. Symposium on laboratory measurements of aeronomic interest. Toronto, 1968.

Comments, Replies, and Summary

COMMENTS BY E. A. OGRYZLO[1]

I would like to comment on the collection of quenching constants for $O_2(^1\Sigma_g^+)$ and $O_2(^1\Delta_g)$ which Dr. Zipf presents in Tables I and II. In a paper presented at the Symposium on "The physics and chemistry of the upper atmosphere", Saskatoon, Canada, June 1966, which unfortunately has not yet appeared in the literature, it was pointed out that the results of March *et al.* (9) yield a rate constant for the reaction

$$O_3 + O_2(^1\Sigma_g^+) \rightarrow 2O_2 + O$$

about a factor of 2 larger than the one reported by them, when a correction is made for the continuous formation of $O_2(^1\Sigma_g^+)$ in their system by the process

$$O_2(^1\Delta_g) + O_2(^1\Delta_g) \rightarrow O_2(^1\Sigma_g^+) + O_2(^3\Sigma_g^-)$$

It is probably worth emphasizing that we have not revised our estimation of the rate constant for this latter reaction. We have obtained evidence for a reaction which is second order in $O_2(^1\Delta_g)$ and about 20 times faster. However, we believe this to be the following process which is "spin allowed"

$$O_2(^1\Delta_g) + O_2(^1\Delta_g) \rightarrow O_2(^3\Sigma_g^-) + O_2(^3\Sigma_g^-)$$

The following rate constants (obtained by Arnold, Kubo, and Ogryzlo) for quenching of $O_2(^1\Sigma_g^+)$ which will appear shortly in "Advances in chemistry" may be added to those listed in Table I.

Quenching particles	Rate constants
N_2, Ar, and CO	2.5×10^{-15}
CO_2	5×10^{-14}
H_2O	1×10^{-13}

[1]Address: University of British Columbia, Vancouver, British Columbia.

COMMENTS BY G. BLACK, T. G. SLANGER, AND R. A. YOUNG[2]

We would like to make some comments on the large disparity between the several quenching rates for $O_2(b^1\Sigma_g^+)$ shown in Table I of Dr. Zipf's paper. Our value of 3×10^{-13} cm^3 $molecule^{-1}$ s^{-1} differs by a factor of almost 10^3 from the laboratory measurements of 1×10^{-16} cm^3 $molecule^{-1}$ s^{-1} by Noxon and $\leqslant 1 \times 10^{-16}$ cm^3 $molecule^{-1}$ s^{-1} by Izod and Wayne (not mentioned in the table but to be published in Proc. Roy. Soc.).

It has been suggested that our results pertain to $O(^1D)$ quenching and not $O_2(b^1\Sigma_g^+)$ quenching. Whereas this could be true for some of the N_2 data where a ratio of rate coefficients (nitrogen relative to oxygen) very close to that observed for $O(^1D)$ (Table V) is found, much greater quenching efficiencies were found for CO, N_2O, NO, and CO_2 relative to O_2 than the ratios observed for $O(^1D)$. This rules out the quenching of $O(^1D)$ as the main quenching reaction for these gases.

An explanation of the discrepancy lies, we think, in the different pressure regions of the

[2]Address: Stanford Research Institute, Palo Alto, California.

Can. J. Chem. Downloaded from www.nrcresearchpress.com by 210.87.254.5 on 09/05/12
For personal use only.

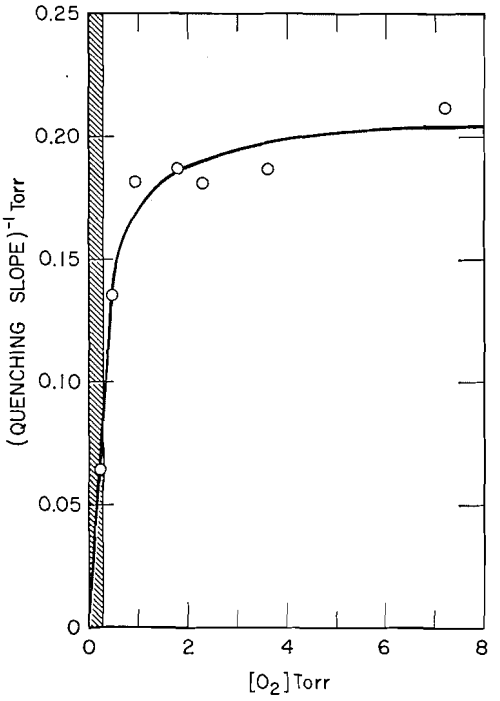

FIG. 1. N_2 quenching data. The reciprocal of the slope of Stern–Volmer graphs vs $[O_2]$; [He] = 10 Torr.

experiments. Our published measurements pertain to an O_2 pressure $\ll 1$ Torr, whereas the other measurements were made at O_2 pressures $\gg 1$ Torr. We took measurements up to O_2 pressures ~ 10 Torr at the same time as our low pressure results but found incompatibility between the low and high pressure data. This is illustrated for our N_2 quenching data in Fig. 1 where the shaded portion indicates the region covered in our previous publication. Similar shaped curves were obtained for CO, N_2O, NO, and CO_2. The ordinate of this graph is $(\tau_0 k_{N_2})^{-1}$ where τ_0 is the lifetime of the quenched species before quenching addition. We interpreted the low O_2 pressure data as pertaining to $O_2(b^1\Sigma_g^+)$ and deduced the value of k_{O_2} shown in Table I from the very strong dependence of τ_0 on O_2 in this pressure region. The high pressure "plateau" region, if interpreted in terms of $O_2(b^1\Sigma_g^+)$ quenching, would give much lower quenching efficiencies, particularly for oxygen, than those deduced in our paper. These are the findings of Noxon and Izod and Wayne. In fact, relative rate coefficients deduced from our "plateau" values for N_2:CO:CO_2 are 1:2:150 in satisfactory agreement with the ratio of 1:2:330 from the absolute values of Noxon using his unpublished value of 5×10^{-13} cm^3 molecule^{-1} s^{-1} for CO_2 quenching of $O_2(b^1\Sigma_g^+)$. Stuhl (unpublished) has recently determined $k_{CO_2} = 2 \times 10^{-13}$ cm^3 molecule^{-1} s^{-1} for this quenching rate. This would bring the ratios into very good agreement.

It is our feeling that the different quenching behavior in the two regions may well reflect quenching of vibrationally excited $O_2(b^1\Sigma_g^+)$ molecules. In unpublished work, $O_2(b^1\Sigma_g^+)$ in the $v' = 2$ has been seen by Noxon and we have seen the $v' = 1$ level (in the (1,1) transition at 7708 Å) with approximately one-tenth the emission intensity of the (0,0) band. The presence of these vibrationally excited molecules should not be surprising in view of the energy resonance with $O_2(b^1\Sigma_g^+)_{v'=2}$ when $O(^1D)$ transfers to O_2.

Definitive experiments to resolve this controversy are presently underway in our laboratory where the decay with time of $O_2(b^1\Sigma_g^+)$ in both ground and excited vibrational states is being determined in a pulsed system.

COMMENTS BY G. BLACK, T. G. SLANGER, G. A. ST. JOHN, AND R. A. YOUNG[2]

We would like to confirm the measurements of Stuhl and Welge on $O(^1S)$ deactivation. We have used a similar technique for obtaining the rate coefficients, that is, measurement of the decay time of the 5577 Å emission as a function of added gas pressure. Our light source was a pulsed 1470 Å Xe lamp, powered by an RF oscillator, while the $O(^1S)$ source was N_2O. The lamp was pulsed at up to 20 c.p.s., with an instrumental decay time of ~ 100 μs. The resulting 5577 Å emission pulse was registered in a signal accumulator and, after a few thousand cycles, an averaged $O(^1S)$ decay curve was displayed on an oscilloscope. The slope of a plot of reciprocal decay time vs. pressure is equal to the quenching rate coefficient of the added gas.

We have so far obtained the following values.

Quenching particle	Rate coefficient, cm molecule^{-1} s^{-1}
C_2H_4	6×10^{-10}
NO	5.5×10^{-10}
N_2O	1.6×10^{-11}
O_2	5×10^{-13}
CO_2	3×10^{-13}
H_2	1×10^{-15}
N_2, Ar, He	$< 3 \times 10^{-15}$

Can. J. Chem. Downloaded from www.nrcresearchpress.com by 210.87.254.5 on 09/05/12
For personal use only.

Can. J. Chem. Downloaded from www.nrcresearchpress.com by 210.87.254.5 on 09/05/12
For personal use only.

Because of the very rapid rates for the fastest reactants, it must still be confirmed that the values for the slowest reactants are not influenced by contamination.

Previous measurements of $O(^1S)$ deactivation rates (J. Chem. Phys. **44**, 3741 (1966)) gave values considerably lower than those now reported. In these earlier measurements, it was the product of the quenching coefficient and the zero pressure $O(^1S)$ decay time, $k\tau$, that was being measured. It was assumed that τ was the radiative lifetime, 1 s, and thus the quenching coefficients were obtained. The fact that they are too low means that either τ referred to a loss process other than radiation or that the 1 s value, a theoretically calculated number, is too high.

In the present system, the residual $O(^1S)$ lifetime, a value obtained by extrapolating N_2O and buffer gas pressures to zero, is 3 ms. This is certainly too short to be the radiative lifetime, but experiments are continuing to see whether a true value may be obtained.

By comparison of the emission intensity of $O(^1S)$ in N_2O photolysis with the intensity of emission from a reaction with a known quantum yield (for instance, the NO_2* chemiluminescence using O_2 photolysis as an $O(^3P)$ source), one may obtain a value for the $O(^1S)$ quantum yield. Using the new N_2O quenching coefficient of 1.6×10^{-11} cm^3 s^{-1} and a radiative lifetime of 1 s, the quantum yield is 0.5 ± 0.05. The value is proportional to the radiative lifetime, so any decrease in the lifetime will decrease the quantum yield. If the 1 s value is correct, then N_2O photolysis at 1470 Å is an excellent $O(^1S)$ source, and is the obvious system to use for product formation studies.

COMMENTS BY K. WELGE

By using various windows on our photolysis lamps, we find that $O(^1S)$ is not produced from CO_2 at wavelengths longer than about 1220 Å.

COMMENTS BY T. SLANGER

Our experiments confirm Dr. Welge's findings. We have used an absorption cell between a krypton resonance lamp and a photolysis cell. CO_2 was photolyzed, and the resulting 5577 Å emission was monitored. By observation of the change in emission intensity as CO_2 was added to the absorption cell, a value for the CO_2 absorption coefficient at the wavelength that was producing $O(^1S)$ could be measured. This value was found to agree well with the 1165 Å lamp component, and not at all with the one at 1236 Å, even though the 1236 Å intensity is ~ 5 times the 1165 Å intensity. Thus, the continuum in the CO_2 absorption curve that begins at 1190 Å presumably corresponds to the photodissociation

$$CO_2 \xrightarrow{h\nu} CO(X^1\Sigma^+) + O(^1S)$$

This is 0.7 eV more energy than is required on purely thermodynamical grounds.

COMMENTS BY J. NOXON

In connection with the quenching of $O(^1D)$ by CO_2 we have made the following observations.
(*1*) Emission of 6300 Å radiation following CO_2 photolysis indicates production of $O(^1D)$ which appears to be quenched with a rate constant of $k \simeq 3 \times 10^{-12}$.
(*2*) When 1–2% N_2 is added to the system the 6300 Å radiation is quenched.
(*3*) For O_2 photolysis a plot of the intensity of 7600 Å radiation from $O_2(b^1\Sigma_g^+)$ against added CO_2 shows a linear decrease up to ratios of $CO_2/O_3 \geqslant 10$ which indicates that, for the quenching of $O(^1D)$, $k_{CO_2} < 10\, k_{O_2}$ or $k_{CO_2} \simeq 6 \times 10^{-12}$.

COMMENTS BY G. BLACK, T. G. SLANGER, AND R. A. YOUNG

We were very pleased to hear Dr. Ferguson's theory yesterday, explaining the negative temperature coefficient for the reaction

$$N_2 + O^+ \rightarrow NO^+ + N$$

His explanation involved an intermediate, N_2O^{+}*, in equilibrium with the reactants

$$N_2 + O^+ \underset{k_2}{\overset{k_1}{\rightleftarrows}} N_2O^{+*} \xrightarrow{k_3} NO^+ + N$$

where $k_2 = 10^3 k_3$.

This is quite analogous to our scheme explaining the two orders of magnitude difference between our value for the rate coefficient for $O(^1D)$ deactivation by CO_2 and Noxon's. In this case, the intermediate is CO_3* and the proposed reaction is

$$CO_2 + O(^1D) \underset{k_2}{\overset{k_1}{\rightleftarrows}} CO_3^* \xrightarrow{k_3} \begin{matrix} CO_2 + O(^3P) \\ \text{or } CO_3 \end{matrix}$$

where $k_2 = 10^2 k_3$. In our experiments, which are always done in the presence of NO, we

Can. J. Chem. Downloaded from www.nrcresearchpress.com by 210.87.254.5 on 09/05/12
For personal use only.

suggest that a new loss process for CO_3* becomes available

$$CO_3^* + NO \xrightarrow{k_4} CO_3 + NO$$

where $k_4[NO] \gg k_2$. Thus, the equilibrium is upset, and our method of detection leads to a value for k_1. On the other hand, when $[O(^1D)]$ is measured, as in Noxon's experiments, it is not k_1, but $k_1 \cdot k_3/k_2 = 10^{-2}k_1$, that is obtained.

The obvious way to determine if this idea is tenable is to measure $O(^3P)$ in the absence of NO. If this results in a sharply decreased value for k_1, then the idea would appear to have merit. Such measurements are underway.

Some observations that support the equilibrium concept are available in a comparison of some of our data with Dr. Schiff's. In an article published (Can. J. Chem. **44**, 1981 (1966)), Schiff and Ung showed that the production of O_2 could be completely suppressed in the 1470 Å photolysis of 35 Torr CO_2 by the addition of 0.3 Torr CH_4. Once $O(^3P)$ is produced in the system, it may probably be assumed that it will lead to O_2 formation. Therefore, the data suggest that CH_4 removes $O(^1D)$ more than two orders of magnitude faster than does CO_2.

On the other hand, we find that when photolyzing 3 Torr CO_2 and 0.3 Torr NO, the $O(^3P)$ concentration is halved by the addition of 2 Torr CH_4, indicating that CO_2 and CH_4 remove $O(^1D)$ at comparable rates (the CH_4 needed to halve the $O(^3P)$ concentration is a function of CO_2, so it cannot be argued that NO is the principal deactivator). This observation tends to support the idea that when k_2 is the principal CO_3* loss, then CO_2 will appear to be an inefficient deactivator of $O(^1D)$, but when k_2 is small relative to another CO_3* loss mechanism, CO_2 will appear to be efficient.

COMMENTS BY H. I. SCHIFF

The discrepancy of a factor of 100 in the quenching rates of $O(^1D)$ by CO_2 among investigators is very puzzling. It has been suggested that this discrepancy is due to the difference in detection, whether one follows the disappearance of $O(^1D)$ or the formation of $O(^3P)$. And yet Noxon, who measures ^1D, and Clerc, who essentially measures ^3P, both find low values, while Cvetanović, who follows ^1D, and Black *et al.*, who follow ^3P, both find high values.

The explanation offered by Black *et al.*, referred to in Zipf's review, that it is due to the CO_3* equilibrium, may resolve the difference between them and Noxon, although it is difficult to understand why NO should be so unique in promoting dissociation of the complex to $O(^3P)$. (The stabilization of the CO_3 by NO would not be measured by their method.) It is even more difficult to see how this would help to resolve the difference in the results of Clerc and Cvetanović.

COMMENTS BY M. CLERC

From the measurement of the amount of O_3 produced by the vacuum ultraviolet flash photolysis of O_2–Ar mixtures (1), (O_2 = 1 Torr, Ar = 760 Torr), to which either CO_2 or CO is added, a value of the ratio $k_5/k_3 = 55 \pm 5$ has been determined for the reactions

[3] $$O(^1D) + CO_2 \rightarrow CO_3$$

[5] $$O(^1D) + CO \rightarrow CO_2$$

The results provide indirect evidence for the occurrence of reaction [3] instead of reaction [4]

[4] $$O(^1D) + CO_2 \rightarrow O(^3P) + CO_2$$

Consider the following mechanisms

[1] $$O_2(^3\Sigma_g^-) + h\nu \rightarrow O(^1D) + O(^3P)$$

[2] $$O(^3P) + O_2 + M \rightarrow O_3 + M$$

[6] $$O(^1D) + M \rightarrow O(^3P) + M$$

[7] $$O(^1D) + O_3 \rightarrow 2O_2$$

if the reaction between $O(^1D)$ and CO_2 was a simple collisional deactivation by reaction [4], no variation should be observed in the amount of O_3 formed at the equilibrium after the flash. However, if the $O(^1D)$ reacts with an efficient scavenger, before it can be de-excited by M, the ozone formation should have diminished by one-half. By addition of CO_2 (2 Torr) or CO (0.1 Torr), to the initial (O_2, 1 Torr + Ar, 760 Torr) mixture, the amount of O_3 formed at the equilibrium after the photolytic flash is divided by two. This result shows that by addition of CO_2, the principal reaction is [3], and that by addition of CO, reaction [5] is brought into play.

From the relationship between $[O_3]$ and the added $[CO_2]$ or [CO], the ratio of the rate constants $k_5/k_3 = 55 \pm 5$ is obtained.

Our previous results, (2, 3) have shown that $k_5 = 10^{-11}$ cm^3 molecule^{-1} s^{-1}, from which

one may calculate $k_3 = 2 \times 10^{-13}$ cm^3 molecule^{-1} s^{-1}.

1. M. CLERC and A. REIFFSTECK. J. Chem. Phys. **48**, 2799 (1968).
2. M. CLERC and F. BARAT. J. Chem. Phys. **46**, 107 (1967).
3. M. CLERC and F. BARAT. J. Chim. Phys. **63**, 1525 (1966).

QUESTION BY J. W. McGOWAN

Why don't you consider CO + O_2 as one of the possible competing product channels for the $O(^1D)$ + CO_2 quenching reaction. If these reaction products were formed along with $O(^3P)$ + CO_2, might this not give you a low production rate of $O(^3P)$ and therefore an apparently lower reaction rate?

REPLY BY M. CLERC

We have no direct evidence that CO + O_2 are products of the reaction $O(^1D)$ + CO_2. In any case, if a reaction such as

[1] $$O(^1D) + CO_2 \rightarrow CO + O_2$$

occurred to an important extent, it would lead to a CO quantum yield $1 < \phi_{CO} < 2$ in the photochemistry of CO_2, via the reaction

[2] $$CO_2 + h\nu \rightarrow CO + O(^1D)$$

[2] followed by [1]. A CO quantum yield close to 1 is generally obtained.

Evidently an analysis of the final products would give a definite reply to this question; this we intend to do.

REPLY BY T. SLANGER

At Stanford Research we have measured the $O(^3P)$ quantum yield for CO_2 photolysis at 1470 Å. By making measurements relative to O_2 photolysis, where the $O(^3P)$ quantum yield after $O(^1D)$ deactivation is 2, it is observed that the $O(^3P)$ quantum yield from CO_2 is 1.0. This implies that all of $O(^1D)$ initially produced is ultimately converted to $O(^3P)$. The $O(^3P)$ production rate was measured by chemiluminescence following the addition of NO. It may be argued that NO is then the $O(^1D)$ deactivator and not CO_2, but examination of the results in detail clearly shows that CO_2 is the deactivating species. Thus, the reaction

$$O(^1D) + CO_2 \rightarrow CO + O_2$$

cannot be important.

SUMMARY AND REMARKS BY CHAIRMAN D. M. HUNTEN[3]

This paper shows clearly that the study of metastables is coming of age, in both the laboratory and the upper atmosphere. In the laboratory, there are a variety of detection techniques, those mentioned by Zipf, and also the less direct methods based on differences in chemical reactivity. In the upper atmosphere the subject has been revolutionized by rocket probes of dayglow emissions. In nearly every case an unambiguous identification of the production process and its rate has been possible, and the quenching rate, therefore, follows immediately from the measurements; large systematic errors are nearly impossible. Identification of the quenching partner requires other evidence. Nevertheless, the results from the upper atmosphere can give a valuable check on the laboratory. Zipf has recognized this, but many other laboratory workers seem to ignore it, and some completely unacceptable results have been published.

Several years ago McElroy and I published (4) a predecessor of Zipf's paper; a good indication of the activity of the subject is the degree to which our evaluations must be changed. Among other things, we undertook an analysis of the classical data of Kvifte and Vegard (5) on the red and green lines of oxygen from an electrical discharge. The measurements were made under a wide range of conditions, pressure, tube diameter, and buffer gas, and seemed to give clear indications of the quenching rates for $O(^1S)$ by O_2. The interferences for $O(^1D)$ were less direct, and also were referred to the ^1S result. As Zipf points out (Tables V and VI), the results were low by two and four orders of magnitude. It now seems clear that the discharges were much more complicated than they seemed to be. We did point out that quenching by electrons should be considered, but there may well have been still other factors. In a similar high-power discharge, LeBlanc *et al.* (6) could find no evidence for collisionally-stimulated emission. But a further analysis of the results by Carleton (as yet unpublished) gave much larger quenching coefficients, in the same range as the other values quoted by Zipf. And in this case, laboratory and atmosphere are in excellent agreement.

[3]Address: Kitt Peak National Laboratory, Tucson, Arizona.

Can. J. Chem. Downloaded from www.nrcresearchpress.com by 210.87.254.5 on 09/05/12
For personal use only.

Can. J. Chem. Downloaded from www.nrcresearchpress.com by 210.87.254.5 on 09/05/12
For personal use only.

An unscheduled discussion session was held at the Symposium on the problems connected with the composition of the upper atmospheres of Mars and Venus following the paper by Zipf. This report, written after the meeting, attempts to state the problem and outline some of the current thinking. The atmospheres of these planets are mainly composed of CO_2; the problem is essentially that of understanding the photodissociation of this gas and the subsequent association of the products, CO and O. Superficially, the situation resembles that of O_2 on Earth, which decomposes into O above 90 to 100 km. CO_2, like O_2, has a strong dissociation continuum below about 1800 Å, and the daytime dissociation rate should be about 5×10^{12} cm^{-2} s^{-1} by the reaction

[1] $$CO_2(^1\Sigma) + h\nu \rightarrow CO(^1\Sigma) + O(^1D)$$

The upper atmospheres of Mars and Venus should thus be composed largely of CO and O, with some O_2 from the association of O atoms. A photochemical model of this sort is given by Chamberlain and McElroy (7).

The ionospheric heights and densities measured by Mariner IV on Mars and Mariner V on Venus show with considerable confidence that CO_2 is largely undissociated throughout the upper atmospheres of both planets. Relatively small admixtures of lighter gases would increase the scale heights so much as to make it impossible to fit the observed profiles of electron density. This conclusion is rather general, and independent of detailed ionic reaction mechanisms and rates. With pure CO_2, the Venus ionosphere can be fitted remarkably well; there is still a considerable discrepancy on Mars, but CO_2 is strongly suggested (8–11). A second line of evidence for Venus is the low intensity of the resonance triplet of O at 1304 Å; neither Venera 4 nor Mariner V detected it. Though there are problems of interpretation, these results at least suggest a very small abundance of O at great heights.

Planetary studies thus seem to require that CO and O react much faster than O and O. But the reaction is spin-forbidden (with ground-state O) and thus very slow

[2] $$CO(^1\Sigma) + O(^3P) + M \rightarrow CO_2(^1\Sigma) + M$$

Note that the allowed photodissociation, reaction [1], yields an excited O atom. The inverse of this reaction should be much faster than [2], but presumably a third body is still required. The maximum 3-body coefficient for a simple reaction (10^{-32} cm^6 s^{-1}) is still inadequate by far to maintain an undissociated upper atmosphere.

In the laboratory, it is usual to find that traces of water vapor efficiently catalyze the association by reactions such as

[3] $$CO + OH \rightarrow CO_2 + H$$

[4] $$CO + HO_2 \rightarrow CO_2 + OH$$

but in an upper atmosphere, at total concentrations of 10^{12} cm^{-3} or less, the re-oxidation of the H atoms is very inefficient, and these reactions can readily be ruled out as soon as actual quantities are considered (cf. McElroy (9)).

Laboratory photolysis experiments on CO_2 produce equally mysterious results. Reaction [1], followed by association of O, should produce CO with a quantum efficiency of 1, and O_2 with a quantum efficiency of $\frac{1}{2}$. Mahan (12) found a serious deficiency of O_2; Warneck (13) confirming this result, showed that the missing oxygen was not present as ozone. Taking up a suggestion of Katakis and Taube (14), he postulated a CO_3 molecule, and found indeed that most of the missing oxygen reappeared after a wait of 1 h. Ung and Schiff (15), and Slanger (16) showed that these results depend greatly on the condition of the walls; with certain treatments there is no deficiency of O_2. Young and Ung (17) searched without success for the forbidden 6300 Å emission from $O(^1D)$ and concluded that this metastable atom either reacts with or is quenched by CO_2 with a rate coefficient greater than 10^{-13} cm^2 s^{-1}.

Following the suggestion of Young and Ung, McElroy (8, 9) postulated the following reaction scheme for a planetary atmosphere. The CO_3* molecule is not the same as the CO_3 inferred from the work of Warneck; it is an excited state, best considered as a complex of CO_2 and $O(^1D)$, which can decay or be quenched into the more stable CO_3, or spontaneously dissociate.

[5] $$O(^1D) + CO_2 \rightleftarrows CO_3^*$$

[6] $$CO_3^* + CO \rightarrow 2CO_2$$

Taken together, [5] and [6] constitute a 3-body reaction. But the effective rate coefficient can be much greater than 10^{-32} cm^6 s^{-1}, in the same proportion as the lifetime of CO_3* exceeds

10^{-14} s. (At the Symposium, Phillips independently proposed the same scheme.)

It appears that CO_3 and CO_3* can explain most of the laboratory observations as well. In addition to those mentioned above, from which the suggestions arose, there is the flash photolysis study by Clerc and Barat (18), which showed a decrease of CO in the first 60 μs. Their explanation in terms of reaction with $O(^1D)$ could also be satisfied by CO_3*, which would form on about the same time scale. The latest work finds $k_5 = 2 \times 10^{-13}$ cm^3 s^{-1}. Noxon (19) finds that emission of the 6300 Å line is not strongly quenched by CO_2; the CO_3* would continuously regenerate $O(^1D)$ by the reverse of [5], and the same thing may be happening in the work of Clerc *et al.* But Young and associates (20) find strong quenching in the presence of NO, which presumably swallows up the CO_3* so fast that it cannot regenerate $O(^1D)$ (see their comments).

The explanation is not so clear-cut for the reaction

$$[7] \qquad N_2O + O(^1D) \rightarrow N_2 + O_2$$

Yamazaki and Cvetanović (21), and later Cvetanović (22), studied this reaction in the case where the $O(^1D)$ is produced by photolysis of the N_2O; the reaction is strongly quenched by added CO_2. Warneck (23) observed the reaction [7] to dominate in CO_2 with less than 1% added N_2O. Here, most of the excitation would reside in the form of CO_3*, but a small concentration of $O(^1D)$ would be maintained in equilibrium with it, to react in [7]. We must then postulate that a large excess of N_2O quenches CO_3* to CO_3, or to $CO_2 + O(^3P)$. Under these conditions, CO_2 acts as a quenching agent, or more properly a quenching catalyst.

Direct observations of CO_3 have been made by Moll, Clutter, and Thompson (24), by infrared absorption in a matrix of solid CO_2. The compound was formed in a stream of CO_2 by photolysis or electric discharge. Metastable CO_3* has considerably less status, and for the present its existence must be considered an ad hoc hypothesis. Perhaps its most unlikely property is its postulated formation in the 2-body process (8), though in the laboratory experiments stabilization by a third body is possible. Stabilization for periods as long as us in a planetary atmosphere would seem to require the improbable emission of an infrared photon. Moll *et al.* found that their CO_3 was readily dissociated by visible and near-ultraviolet radiation; its lifetime in sunlight would thus be very short, and that of CO_3* presumably even shorter.

4. D. M. Hunten and M. B. McElroy. Rev. Geophys. **4**, 303 (1966).
5. G. Kvifte and L. Vegard. Geofys. Publikasjoner, Norske Videnskaps. Akad. Oslo, **17**, no. 3 (1947).
6. F. J. LeBlanc, O. Oldenberg, and N. P. Carleton. J. Chem. Phys. **45**, 2200 (1966).
7. J. W. Chamberlain and M. B. McElroy. Science, **152**, 21 (1966).
8. M. B. McElroy. Astrophys. J. **150**, 1125 (1967).
9. M. B. McElroy. J. Geophys. Res. **73**, 1513 (1968); J. Atmospheric Sci. **25**, 574 (1968); J. Geophys. Res. *In* press.
10. D. M. Hunten. *In* The atmospheres of Venus and Mars. *Edited by* J. C. Brandt and M. B. McElroy. Gordon and Breach, New York. 1968. p. 147.
11. R. W. Stewart. J. Atmospheric Sci. **25**, 578 (1968).
12. B. H. Mahan. J. Chem. Phys. **33**, 959 (1960).
13. P. Warneck. J. Chem. Phys. **41**, 3435 (1964).
14. D. Katakis and H. Taube. J. Chem. Phys. **36**, 416 (1962).
15. A-Y. Ung and H. I. Schiff. Can. J. Chem. **44**, 1981 (1966).
16. T. G. Slanger. J. Chem. Phys. **45**, 4127 (1966).
17. R. A. Young and A. Y.-M. Ung. J. Chem. Phys. **44**, 3038 (1966); **47**, 1566 (1967).
18. M. Clerc and F. Barat. J. Chem. Phys. **46**, 107 (1967).
19. J. F. Noxon. Can. J. Chem. This issue.
20. R. A. Young, G. Black, and T. G. Slanger. To be published.
21. H. Yamazaki and R. J. Cvetanović. J. Chem. Phys. **39**, 1902 (1963).
22. R. J. Cvetanović. J. Chem. Phys. **43**, 1850 (1965).
23. P. Warneck. J. Chem. Phys. **43**, 1849 (1965).
24. N. G. Moll, D. R. Clutter, and W. E. Thompson. J. Chem. Phys. **45**, 4469 (1966).

Can. J. Chem. Downloaded from www.nrcresearchpress.com by 210.87.254.5 on 09/05/12
For personal use only.

Can. J. Chem. Downloaded from www.nrcresearchpress.com by 210.87.254.42 on 09/05/12
For personal use only.

Laboratory measurements of photoionization, photoexcitation, and photodetachment

RICHARD I. SCHOEN
Boeing Scientific Research Laboratories, Seattle, Washington 98124

Received December 18, 1968

This review is devoted to a discussion of laboratory measurements of ionization, fluorescence, and photodetachment. The review is limited to molecules of aeronomic interest but excludes atoms. The section on photodetachment includes only work which has appeared since 1964. Current data are presented on photoionization cross sections, dissociative ionization cross sections, cross sections for the excitation of particular states of ions, relative vibrational excitation probabilities, photodetachment cross sections, angular distributions of electrons from photoionization, and dissociative excitation of neutral molecules. Some suggestions are made for further work.

Canadian Journal of Chemistry, 47, 1879 (1969)

I Introduction

This review deals with those photoabsorption processes which cause the release of charged particles or photons. Laboratory measurements of photoionization cross sections are discussed, and cross sections of excitation into particular ionic states are considered. Some recent work on photodetachment is presented. Experiments in which fluorescence of molecular and atomic species is produced by photoabsorption are examined. The intent is to present values of cross sections and determinations of excitation to particular states which will be of use in aeronomic calculations, to indicate the accuracy of existing data where possible, and to point out areas where more work is needed.

In a preceding review Huffman (1) has discussed photoabsorption cross sections. Within the ionization continuum of any atom, its absorption and ionization cross sections will differ only at rare, non-autoionizing lines. Therefore photoionization cross sections of atoms are not considered here, nor are photoexcitation processes which reveal themselves in the photoabsorption spectrum. Information about states of excitation which is gathered by purely chemical means is also excluded.

Since the aim of this review is to present a critical discussion of current data, some detailed descriptions of experimental pitfalls have been included, and consideration of the pioneering work of purely historical interest has been curtailed. For discussions of the older literature on photoionization, the reader is referred to reviews by Weissler (2) and Watanabe (3). Ditchburn and Öpik (4) give a short discussion of theoretical and experimental aspects of photoionization. Branscomb has presented a comprehensive review of photodetachment (5). More recently Marr (6) has devoted a complete volume to photoionization, and Samson (7) a complete volume to vacuum ultraviolet (u.v.) techniques. The field of vacuum u.v. photochemistry has been reviewed by McNesby and Okabe (8), and the reader should consult their article for information on chemical techniques.

The rest of the paper is divided into topical sections. Section II is devoted to photoionization cross section measurements, section III to dissociative ionization cross sections, and section IV to cross sections for excitation to particular ionic states. In section V fluorescence of excited ions and neutrals is examined, and some recent work on photodetachment is discussed in section VI. Conclusions are presented in section VII.

II Photoionization Cross-section Measurements

The photoionization cross section, $\sigma_i(\lambda)$, is that part of the absorption cross section which represents ionization by absorption of photons of wavelength λ. It is usually assumed that only singly charged ions are produced by photoionization. This assumption is almost certainly correct for the wavelength region $\lambda > 300$ Å and the molecules discussed here. In a typical experiment an ion current, $i(\lambda)$, is produced by monochromatic radiation shining into a chamber like that of Fig. 1. The magnitude of this current is given in eq. [1]

$$[1] \quad i(\lambda) = I_0(\lambda)\{1 - \exp[-nl\sigma_T(\lambda)]\} \times e\sigma_i(\lambda)/\sigma_T(\lambda)$$

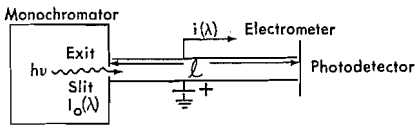

FIG. 1. A schematic diagram of a simple ion chamber. The entrance slit of the chamber is the exit slit of the monochromator.

$I_0(\lambda)$ is the photon flux in photons per second incident on the ion chamber; n is the number of molecules per unit volume; l is the chamber length; e is the electronic charge; and $\sigma_T(\lambda)$ is the cross section for all processes which remove photons from the beam. The ion current, the photon flux, and the cross sections are all functions of the wavelength of incident radiation, λ. The quantity $\sigma_i(\lambda)/\sigma_T(\lambda)$ is called the photoionization efficiency or yield and represents the fraction of absorption which leads to ionization. For our purposes, we assume $\sigma_T(\lambda)$ to be known from other experiments (1).

The "monochromatic" photon flux used in the measurements of photoionization cross sections discussed here comes from a vacuum grating monochromator with an appropriate light source. Neither light sources nor monochromators are discussed here. It should be noted that window materials absorb strongly in the spectral region between 1050 Å and a few hundred angstroms; thus while differential pumping is used to evacuate the monochromators, both light sources and experimental chambers may be gas-filled. If one demands that less than 1% of the light be absorbed in the monochromator, it is necessary that the pressure of absorbing gases in the monochromator be no more than a few times 10^{-5} Torr.

Several options are available to the experimenter who wishes to measure photoionization cross sections. He may choose a comparative method to measure yields, in which case he obtains the ratio of the ion current from the gas of interest to the ion current from a gas of known yield under conditions of incident flux and absorption in the chamber which can be compared quantitatively. He may choose an absolute method, in which case he must make absolute measurements of the incident photon flux, $I_0(\lambda)$, and the ion current, $i(\lambda)$, together with the absorption, $1 - \exp[-nl\sigma_T(\lambda)]$, to obtain the yield, or he must make further absolute measurements of the particle density, n, and the chamber length, l, to obtain the photoionization cross section directly in the small pressure limit. The comparative method is discussed in the next few paragraphs, the absolute method later.

When the comparative method is employed, comparison is usually made with a noble gas (9–12) in which the photoionization efficiency, $\sigma_i(\lambda)/\sigma_T(\lambda)$, is 1 (9, 11, 13). This comparison with a noble gas is limited to wavelengths shorter than 1023 Å (12.127 eV), the ionization threshold of Xe. If measurements in the gas of interest are labeled with subscript M and those in the noble gas with subscript N, we have in the case of identical absorption in the two gases

$$[2] \qquad i_M(\lambda)/i_N(\lambda) = [I_{0M}(\lambda)/I_{0N}(\lambda)][\sigma_{iM}(\lambda)/\sigma_{TM}(\lambda)]$$

or

$$\sigma_{iM}(\lambda) = \sigma_{TM}(\lambda)[i_M(\lambda)/i_N(\lambda)]\,[I_{0N}(\lambda)/I_{0M}(\lambda)]$$

At each wavelength, for each gas, it must be ascertained that a known fraction (generally equal to 1.00) of all the ions is collected, that no electrons are collected on the ion collector, that the photoelectron current from the ion collector is negligible, and that the electrons produced in the photoionization process or from metal surfaces do not produce ions in the gas. The fact that the noble gases all appear to have the same photoionization efficiencies (11, 13, 14) indicates that it is proper to neglect secondary electron emission from the ion collector, as all observers have done. The chief advantage of the comparative method is that absolute measurements of currents and number densities are not required, although number densities must ultimately be measured to obtain $\sigma_{TM}(\lambda)$, the absorption cross section (1).

Relative photon flux measurements are generally made through photoelectric conversion. The measurements may be made directly from the photoelectric emission of a metal plate or indirectly from measurements with a photomultiplier of the visible light output from a material, such as sodium salicylate, which fluoresces under vacuum u.v. radiation. Typically,

Can. J. Chem. Downloaded from www.nrcresearchpress.com by 210.87.254.42 on 09/05/12
For personal use only.

Can. J. Chem. Downloaded from www.nrcresearchpress.com by 210.87.254.42 on 09/05/12
For personal use only.

measurements of the incoming photon flux are made without an absorbing gas, to establish a relative value of $I_0(\lambda)$; measurements are then made with the absorbing gas and then measurements without absorbing gas are repeated. The light source is assumed to have an output constant in time, if no significant changes occur between the first and the last measurements (i.e. those measurements without absorbing gas). Cook and Metzger (12) indicate that their helium continuum source is constant to about 2%. Ditchburn (15) has suggested a double beam method to eliminate concern about variations of light source intensity, but his suggestion does not appear to have been used in photoionization measurements. The double ion chamber method (2, 10, 11) is almost equivalent to a double beam technique. Use of this method requires that the familiar single ion chamber be divided into two parts, typically two identical ion chambers. The distance between the front of the first and the front of the second chamber is measured, as is the distance from the photodetector to the chamber entrance slit. The ratio of the currents from the two ion chambers then gives the logarithmic decrement of light intensity in the chamber, and, from this decrement and the measured photodetector current, $I(\lambda)$, the current which the photodetector would give if it were placed at the chamber entrance is calculated. This latter current is the current which would be measured if no gas were in the chamber; thus a measure of $I_0(\lambda)$ can be obtained from $I(\lambda)$. The difficulty is that I_0/I may be a large number. It is doubtful that the accuracy of determining I_0 by this method is better than the 2% claimed above as the accuracy of the assumption that I_0 is a constant. The double ion chamber method does provide a useful check against larger variations in light source intensity.

Changes in the efficiency of a sodium salicylate converter may be misinterpreted as light source intensity changes. Efficiency changes have been noted many times (7), but they can, in most cases, be avoided by making measurements within a few hours of calibration. The cause for changes in the efficiency of the sodium salicylate is unknown. It is known, however, that some reactive gases such as NO_2 decrease the efficiency within minutes. In general, care must be taken that the gas does not affect the photodetector and that the photodetector does not affect the ion current measurements. The latter is especially important when photoemission from a metallic surface is used as a detector (12).

Problems of light scattered from the grating, light reflected from metal surfaces in the ionization chamber, and fluorescent light have been dealt with in some detail by various experimenters (12, 16, 17). These problems are not expected to be important in the work discussed here, nor are problems of wavelength identification.

The problem of resolution, however, is more difficult. When a continuum is used, the instrumental bandpass must be small compared to the width of an absorption feature, in order that measurements of ionization cross sections be reliable. In general, bandpasses which are not small compared with the widths of features produce cross sections which are too low at peaks and too high in valleys. Line sources in which lines are separated at the instrumental bandpass used give cross-section values which may depend upon line profiles in the source. In most cases the source-line widths are 0.1 Å or less (18) and probably are narrow enough. If several lines lie within the bandpass of the instrument used, the cross-section measurement will be accurate only if the cross section is the same for all lines.

The absorption cross section $\sigma_T(\lambda)$ is used directly to calculate the ionization cross section $\sigma_i(\lambda)$ from measured quantities (eq. [2]). Thus the error of measurement of the absorption cross section directly affects the photoionization cross sections measured by the comparative method. Absorption cross sections are discussed by Huffman in a preceding article (1), and a table of absorption and photoionization cross sections of O_2 and N_2 at solar lines is included. In all cases some variation of the comparative method was used in their measurement. Measurements in particular gases are discussed below.

O_2

Preferred values of the photoionization cross section of O_2 at particular solar lines are tabulated in a preceding article by Huffman. In all but a few cases these values are taken from Samson and Cairns (18) but have been rounded off. They are expected to be accurate to 10% except at those wavelengths at which several lines lie within the monochromator bandpass, and sharp variation of the cross section with wavelength is also found in the bandpass. Matsunaga and

Can. J. Chem. Downloaded from www.nrcresearchpress.com by 210.87.254.42 on 09/05/12
For personal use only.

Watanabe (19) have used both the helium continuum and the hydrogen many-lined source to obtain data in the 600–1020 Å region with resolution of 0.3 Å with the helium source and 0.2 Å with the hydrogen source. Agreement with the work of Samson and Cairns is within experimental error. The values of Matsunaga and Watanabe are recommended at wavelengths between 600–1020 Å other than those shown in the table. Except where there are strong bands, the values are probably within ±15% between 700–900 Å and somewhat less accurate at longer and shorter wavelengths.

The photoionization efficiencies of Cook and Metzger (12) and of Cook, Ching, and Becker (20), obtained with a continuum source, are lower than those of Samson and Cairns or Matsunaga and Watanabe over much of the spectral range. We think that the results of Cook and associates are less likely to be correct than those of Samson and Cairns or Matsunaga and Watanabe because: *(1)* the latter two groups are in agreement with each other but not with Cook and associates; *(2)* structure which has been found photographically (21, 22) in the absorption spectrum of O_2 in the spectral region 600–650 Å is found in the absorption and ionization cross section curves of Matsunaga and Watanabe but not those of Cook and associates; *(3)* it seems likely that at short wavelengths in regions in which the structure is not strong the photoionization yield should approach 1—Samson and Cairns, and Matsunaga and Watanabe find that it does; Cook and associates find that it does not; and *(4)* the double ion chamber methods used by Samson and Cairns are likely to be the most reliable for measuring the absorption cross section and for eliminating light source variation problems from the yield measurements.

N_2

The photoionization cross sections of Samson and Cairns (18) are preferred for the solar lines shown in the table in Huffman's article (1). The accuracy is again about 10% except in regions of strong band structure. In the spectral region 600–700 Å the results of Samson and Cairns are in good agreement with those of Cook and Metzger (12), who obtained cross sections with the aid of a continuum source and 0.5 Å resolution. The excellence of the agreement, however, is somewhat fortuitous because the absorption cross sections of Cook and Metzger are larger and the photoionization yields smaller than those of Samson and Cairns. In the range 750–800 Å the cross sections of Cook and Metzger and the cross sections of Cook and Ogawa (23), obtained with 0.2 Å resolution, do not agree well with those of Samson and Cairns. The differences are probably in part ascribable to the lack of resolution in a region of band structure. Cook and Ogawa used a technique which required pressure measurements at pressures of a few microns. Pressure measurement errors may have contributed substantially to their total error. The photoionization cross sections of Cook and Ogawa are recommended for those wavelengths between the 700–800 Å not tabulated, and the cross sections of Cook and Metzger are recommended from 600–700 Å. These cross sections are expected to be accurate to ±25%, except where strong band structure is found.

NO

Watanabe *et al.* (24) have worked in the range from 580–1350 Å with the helium continuum (580–950 Å) and the hydrogen many-lined source (860–1350 Å). Their resolution was 0.3 Å in the range 580–950 Å, 0.4 Å in the range 950–1100 Å, and 0.2 Å in the range 1060–1350 Å. These results supersede those of a previous paper (25) and are the preferred measurements. At wavelengths longer than 1020 Å, Watanabe *et al.* used calibration techniques to be described below; otherwise their techniques were the same as those used by Matsunaga and Watanabe (19). We judge that the cross section values given are probably accurate within ±10%, between 700–950 Å, and within ±20% at longer and shorter wavelengths, except in strong bands where the resolution may not be adequate. The photoionization cross section at Lyman-α (1215.7 Å) is 2.0 Mb, and the photoionization efficiency is 0.81.

Photoionization cross sections obtained by Metzger, Cook, and Ogawa (26) with the helium continuum and about 0.5 Å resolution in the spectral range 600–950 Å appear to be uniformly lower than those discussed above. The difference lies largely in the photoionization yields. For instance, Metzger *et al.* found yields to be 78% at 600 Å and less at longer wavelengths, while Watanabe *et al.* found the yields to exceed 90% for wavelengths less than 685 Å.

Can. J. Chem. Downloaded from www.nrcresearchpress.com by 210.87.254.42 on 09/05/12
For personal use only.

CO_2

The situation with respect to CO_2 is disturbing. Cairns and Samson (27) have made measurements with a line source and the double ionization chamber technique, while Nakata *et al.* (28) and Cook *et al.* (29) have used the helium continuum and single ion chamber with photomultiplier. In the almost structureless spectral region 600–686 Å, the ionization cross sections of Cairns and Samson are nowhere less than 48% larger than those of Nakata *et al.* and Cook *et al.* The latter two authors agree in this spectral range on the ionization cross sections to within 15%, but the agreement is partly fortuitous since Cook *et al.* find higher absorption cross sections and lower ionization efficiencies than do Nakata *et al.* Most of the difference between the results of Cairns and Samson and the other authors in this spectral region is ascribable to differences in absorption cross section, which are nowhere less than 30% of the values of Cook *et al.* Cook *et al.* and Nakata *et al.* differ by somewhat more than their stated probable errors toward the long wavelength end of the interval.

The helium continuum is weak at wavelengths shorter than 700 Å, and the measurement errors are consequently greater; but it is strong near 800 Å, and the accuracy should be better. At 840 Å the absorption cross section measured by Nakata *et al.* is 25% larger than that measured by Cook *et al.*, and at 880 Å the difference exceeds 40%.

On the basis of the number of electrons available, we would think that the absorption and ionization cross sections of CO_2 would be considerably greater than those of O_2 or CO in the spectral region near 600 Å. They appear to be from the work of Cairns and Samson, not from the work of Nakata *et al.* or Cook *et al.* The question of which values are best remains open, but we suggest those of Cairns and Samson when a choice must be made. It should be noted that the disparity between the results of these experienced and able groups of experimenters casts a shadow over all the cross sections of aeronomic interest mentioned previously.

Other Gases

Watanabe and co-workers (30) have examined the photoionization of NO_2, and Metzger and Cook (31) have measured photoionization cross sections of H_2O.

Absolute Methods and the Extension of the Comparative Method

If the experimenter requires photoionization yields at wavelengths longer than 1022 Å, the long wavelength limit of noble gas photoionization, he has several choices. He may extend the comparative method with transfer standards. To do this, he requires a detector the relative spectral response of which is known, such as a thermopile used with due caution (7). Typically the detector output at a wavelength λ_0 shorter than 1022 Å is measured with no gas in the ion chamber; the ion current from a rare gas is then measured under conditions of total radiation absorption. Measurements of the same quantities are obtained at the wavelength of interest λ_1 with the gas, M, and the yield obtained from the expression

$$\frac{\sigma_{iM}(\lambda_1)}{\sigma_{TM}(\lambda_1)} = \frac{k(\lambda_0)\, i_M(\lambda_1)\, I(\lambda_0)}{k(\lambda_1) i_M(\lambda_0)\, I(\lambda_1)}$$

in which the i_M is the ion chamber current, I is the detector current, and k is the relative sensitivity of the detector as a function of wavelength. For a thermopile, k may be taken as 1. For sodium salicylate, one might used published curves for k (7), which are no more accurate than the thermopile measurements on which they are based, or one might calibrate the sodium salicylate against the thermopile in the above relative sense at a few wavelengths at which large light fluxes are available. Due regard should be paid to the possible ageing of sodium salicylate if it is used (7), as it frequently is because of the much greater sensitivity available from it than from thermopiles.

Another choice is the measurement of absolute photon flux with a thermopile. This involves calibrating the thermopile in air, then recalibrating in vacuum if one wishes to work in a windowless system. After calibration, photon fluxes can be measured absolutely with no gas in the ion chamber, and then the ion chamber can be filled so that ion current can be measured with total absorption of the radiation. The yield is then the ratio of the number of ions detected per second to the number of photons absorbed per second. The absolute method is subject to additional error above that found in the comparative method in each of the extra steps of thermopile calibration and in the measurement of absolute

Can. J. Chem. Downloaded from www.nrcresearchpress.com by 210.87.254.42 on 09/05/12
For personal use only.

rather than relative ion chamber currents. Hinteregger (32) estimates that absolute calibration of thermoelectric detectors is usually not better than 20%. Watanabe *et al.* (24) have used the absolute method in their work on NO in calibrating their sodium salicylate detector, but they did have an ion chamber comparison with a noble gas to check their calibration at short wavelength.

It should be noted that at no point in measurements of photoionization efficiencies is it necessary to measure the absolute pressure, although it is necessary to measure it when the absorption cross section is measured, and it is necessary that the pressure should be uniform in ion chambers. The uniformity of the pressure has been carefully investigated by those experimenters who have used simple ion chambers (11, 12, 16). The data which have been presented here are thought to be free of errors caused by pressure non-uniformity. As one can see from eq. [1], the absorption cross section can be eliminated from consideration by working under optically thin conditions, i.e., at low pressures. However, one trades measurements of $\sigma_T(\lambda)$ made at relatively high pressures (tens or hundreds of microns) for measurements of $\sigma_i(\lambda)$ made at relatively low pressures (a few microns), with a consequent loss in accuracy in the pressure determination, thus in $\sigma_i(\lambda)$.

The foregoing remarks apply also to absolute measurements of photoionization cross sections in mass spectrometers in which measurements are made under optically thin conditions. In these instruments the ion chamber pressure is likely to be less than a micron, and the flow rates are likely to be high; thus pressure determinations are difficult. Furthermore, the definition of the effective path length of ionization and the collection and detection efficiencies are also difficult. Therefore measurements with mass spectrometers of absolute photoionization cross sections are likely to have much larger systematic errors than do ion chamber measurements.

Comes and Lessman (33) have made absolute photoionization cross section measurements in N_2 with a mass spectrometer. The measurements are in agreement with those of Samson and Cairns (18) below 500 Å but are consistently higher (by more than 50% in places) from 500–700 Å, where band structure should play no important role. Difficulties of absolute measurements of pressure and photon flux can be decreased by the introduction of a noble gas as an internal standard (at least for $\lambda < 1020$ Å).

In a photoionization cross section measurement, instead of allowing the photon beam to traverse an ionization chamber, one may allow it to intersect a molecular beam. In such beam-interaction experiments, which are generally done with mass spectrometers, absolute measurements are afflicted with all of the problems indicated immediately above, plus the problems involved in determining the effective beam–beam interaction region and the molecular density therein.

Very recently Comes and colleagues (34, 35) have measured the photoionization cross sections of atomic oxygen and nitrogen by this technique. The method is a comparative one. First a photodetector is calibrated by comparing its output current to the current from photoionization of a hydrogen atomic beam (36). The photoionization cross section for hydrogen is exactly calculable. Then the current from the photoionization of the atomic species in the atomic beam is measured and compared to the photodetector current to produce a relative atomic photoionization cross section as a function of wavelength. Next, the absolute photoionization cross section of the molecular species (O_2 or N_2, in this case) is measured at one wavelength in a separate ion chamber experiment. Finally, the absolute cross section is obtained by comparison of the photoionization currents from the atomic and molecular constituents of the beam at the wavelength for which the ion chamber experiment was done. It is assumed that the relative concentration of atoms to molecules in the beam can be obtained from the change in the molecular photoionization current produced by the discharge which dissociates some of the molecules to form atoms and a temperature measurement. It is too early for a definitive evaluation of the work; however, the beam method is a very important one for dealing with unstable species and will probably give the best cross sections for their photoionization.

III Dissociative Ionization

We have discussed ion chamber measurements of photoionization cross sections in which no distinction was made between one ion species and another. We now turn to a discussion of measurements of cross sections for the production of specific ion species from dissociative ionization. Such measurements are made by coupling mass spectrometers to monochromators (25, 37–40). Absolute cross sections for dissociative ionization

Can. J. Chem. Downloaded from www.nrcresearchpress.com by 210.87.254.42 on 09/05/12
For personal use only.

processes can be obtained in two ways. Absolute measurements may be made of the photon flux, neutral number density, the length of photon beam over which ions are collected, the ion current, and detector efficiency as discussed previously. On the other hand, measurements may be made of the relative probability for the production of various ion species, then cross sections for the production of particular species may be calculated by multiplying the relative probability of producing a particular ion type at one wavelength by the total photoionization cross section, which has been obtained at that wavelength in experiments of the kind previously discussed.

Two prominent sources of systematic error exist (38). First, ion fragments with kinetic energy of dissociation tend to be lost from the ion beam in the mass spectrometer because of their motion transverse to the beam direction (41, 42). This effect will always make fragment ions appear to be less numerous than they are. Second, when electron multipliers are used for ion detection (a common practice since photon-produced ion currents are small), ions of different masses and different chemical makeup may be detected with different efficiencies at the electron multiplier. This effect may cause errors in either direction, may depend upon the species being studied, the material of the first dynode of the multiplier, and possibly its surface contamination.

Because of the difficulties outlined above, together with the difficulties of measuring photoionization cross sections, there is relatively little accurate data on dissociative ionization of molecules of aeronomic interest. Selected data are presented below.

N_2

The cross sections for the production of N^+ from N_2, which have been measured by Comes and Lessman (33) with a vacuum monochromator and quadrupole mass spectrometer, are shown in Fig. 2. These recent measurements of Comes and Lessman are preferred to the earlier measurements of Weissler *et al.* (38) who used a vacuum monochromator coupled to a magnetic mass spectrometer. One can compare the "ions-per-photon" curves of Weissler *et al.* obtained by mass spectrometry with ionization cross sections measured with ion chambers. If we use the work of Cairns and Samson (27) for A, Samson and Cairns (18), and Matsunaga and Watanabe (19) for O_2, and Cook and Metzger for N_2 (12), one concludes that the work of Weissler *et al.* deviated by as much as a factor of 3 from accurate ion-chamber measurements.

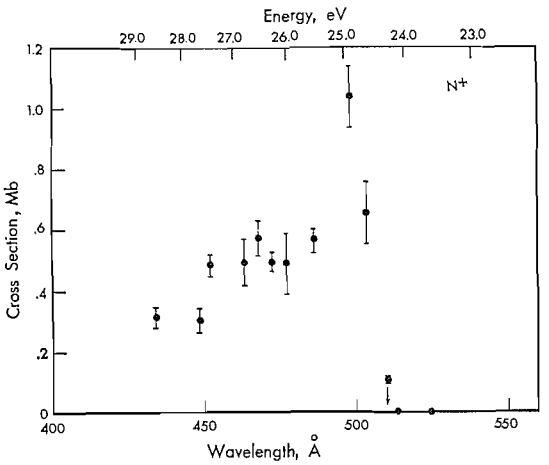

FIG. 2. The dissociative ionization cross section of N_2 as measured by Comes and Lessman (33).

Comparison of the N_2^+ cross sections of Comes and Lessman with photoionization cross sections of Samson and Cairns (18) reveals no systematic error in the wavelength range in which N^+ ions were produced, although there is a systematic error in the N_2^+ cross sections of Comes and Lessman at longer wavelength. It is difficult to estimate the magnitudes of systematic errors in these experiments. Doolittle and Schoen (unpublished) find no energetic ions from N_2 photoionization in this spectral range. Therefore there is probably no discrimination in the collection system between N^+ and N_2^+, but there may be discrimination in the detector, and the relative detection efficiencies for the two ions in this apparatus are not known.

O_2

The dissociative photoionization cross section for the production of O^+ from O_2, shown in Fig. 3, has been measured by Comes *et al.* (34). These measurements were made with a molecular beam. The cross sections were made absolute by comparison with the photoionization cross section leading to O_2^+. During these measurements Comes *et al.* determined the relative detection efficiency of their electron multiplier for O^+ and O_2^+ ions by comparing the pulse height distributions, thereby eliminating one serious measurement problem. It is shown below that dissociative

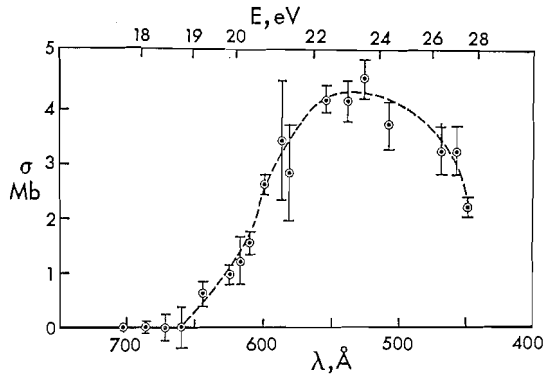

FIG. 3. The dissociative ionization cross section of O_2 as measured by Comes *et al.* (34).

ionization of O_2 produces energetic O^+ ions at wavelengths shorter than 584 Å. How much such energetic ions change the transmission of the time-of-flight mass spectrometer used by Comes and Lessman is not clear, but it is clear that the effect of energetic ions is to make the cross sections appear to be lower than they actually are. Thus the accuracy of the results shown is not known, but they are more likely to be low than high and likely to be more in error at shorter wavelengths than at longer.

Dibeler and Walker (43), without making any claim to measure cross sections, report an O^+ signal 0.03 of their O_2^+ signal at 584 Å. This signal represents a cross section of about 0.7 megabarn (Mb), but the relative transmission and counting efficiencies are unknown. Dibeler and Walker report the formation of O^+ and O^- in the spectral region 718.5–700 Å with a peak intensity of about 0.03 that of the O_2^+ ion at 718.5 Å. Because the correct normalization was very much in doubt, their cross-section curve was not included in Fig. 3. Somewhat earlier, Elder *et al.* (44) had obtained information similar to that of Dibeler and Walker, but at lower resolution.

Other Gases

Although they make no claim to measure photoionization cross sections, Dibeler and coworkers have obtained photoionization mass spectra of CO_2 (43), N_2O and NO_2 (45), and H_2O (46).

IV Excitation of Ions during Photoionization

Electron and Ion Energies

The study of the states of excitation of ions produced by photoionization is generally accomplished by measuring the kinetic energies of the charged particles released or by studying the fluorescence, if any, of the ions. Some of the processes which can take place during photoionization are illustrated in Fig. 4.

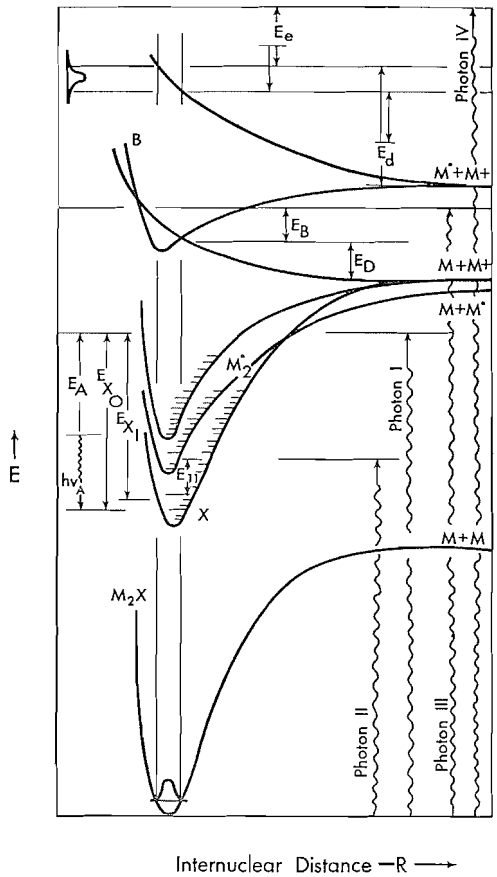

FIG. 4. Ionization processes in a mythical molecule, M_2.

Absorption of photon I may cause a transition to the ground electronic and vibrational state of the molecular ion with the release of an electron of energy E_{X0}, or a transition to the vibrationally excited ground electronic state with the release of an electron of energy E_{X1}, or a transition to the A excited state of the molecular ion with the release of an electron of energy E_A. If selection rules allow, excitation of state A may be followed by the emission of a photon of energy $h\nu_A$. Photon II may be absorbed to produce an excited state of the neutral M_2 which may decay by autoionization to a particular vibrational level of the X state of the molecular ion. The energy of

Can. J. Chem. Downloaded from www.nrcresearchpress.com by 210.87.254.42 on 09/05/12
For personal use only.

Can. J. Chem. Downloaded from www.nrcresearchpress.com by 210.87.254.42 on 09/05/12
For personal use only.

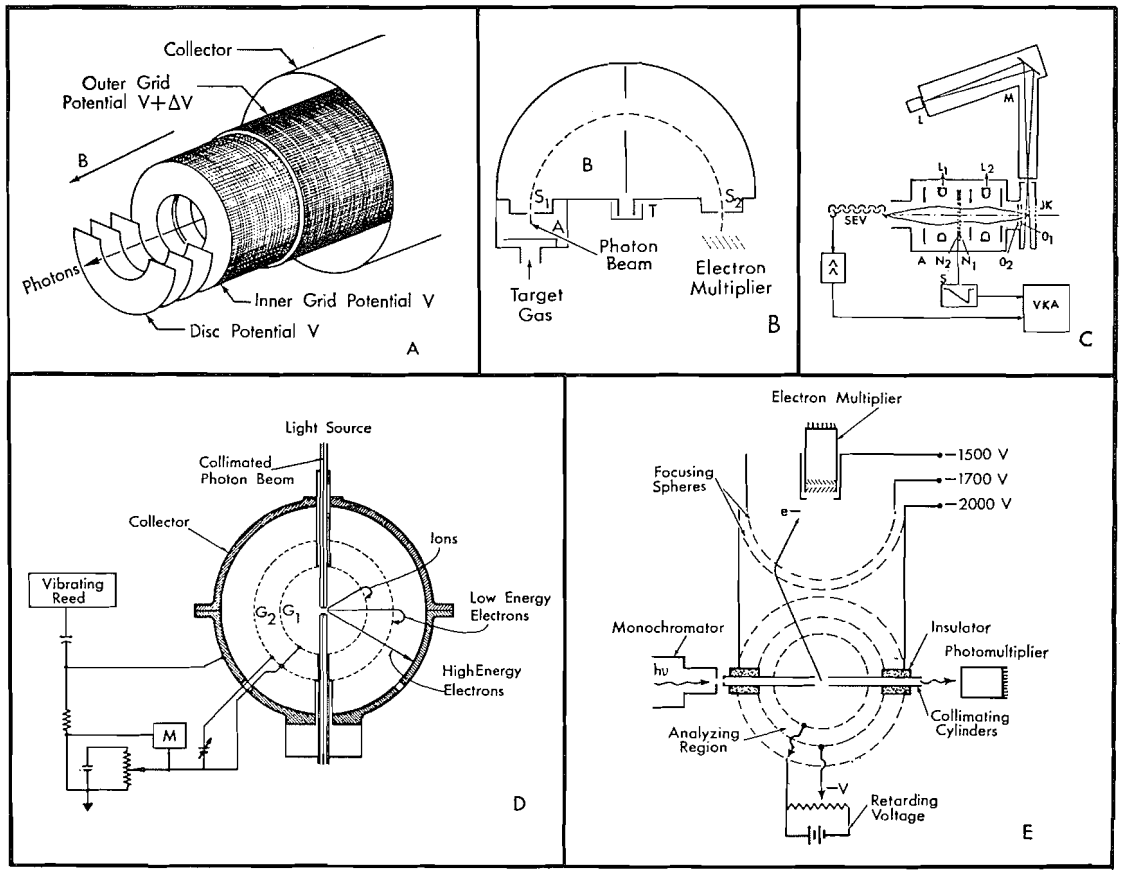

FIG. 5. Electron and ion energy measuring systems. A. Cylindrical retarding potential system, $B = 0$ for electron measurements, Doolittle and Schoen (unpublished). B. Magnetic analyzer, Turner and May (51). C. Lens system: L_1 and L_2, electron lenses; N_1 and N_2, retarding field grids; SEV, electron multiplier; M, monochromator; L, light source, Spohr and Puttkamer (54). D. Spherical analyzer, Frost *et al.* (52). E. Quasi-spherical system with electron multiplier, Samson (53).

the released electron in that case is E_{II}. Absorption of photon III may cause excitation of the B state of the molecular ion, the release of an electron of energy E_B, followed by the predissociation of the molecular ion to release fragments whose total energy is E_D. Photon IV may lead to ionization through a repulsive potential curve with release of an electron which lies in the continuous energy band E_e, and to release of heavy particles the sum of whose energies lies in the corresponding band E_d.

Energies of charged particles have been studied in cylindrical geometries (47–51), spherical (52) and quasi-spherical geometries (53), and with electron focusing systems and plane retarding fields (54–55). Simple retarding potential systems (47–50) and magnetic (51) and electrostatic (56) deflection analyzers have been used in cylindrical geometries as illustrated in Fig. 5A and B, while a lens system is shown in Fig. 5C. The common danger in the use of all cylindrical and focusing systems is that the ion currents measured depend on the angular distributions of the particles which in turn depend on the final states of the ions.

Even if one considers only one ionic final state, it is possible that the angular distribution of the charged particles released upon ionization will depend on the energies of the particles because of centrifugal pseudopotential terms in the Hamiltonian (57) and phases which are a function of energy. All distributions are expected to be in the form $A + B\cos^2\theta$ about the electric vector of polarized light (58–60) in the dipole approximation. A suitable average of this quantity must be

Can. J. Chem. Downloaded from www.nrcresearchpress.com by 210.87.254.42 on 09/05/12
For personal use only.

taken when partially polarized light from a grating, or unpolarized light from a lamp, is used.

True spherical symmetry has not been devised, but approximations thereto have been used by several groups (52, 53), as illustrated in Fig. 5D and E.

If a truly spherical collection system is not available, one might ask what can be used to obviate problems of angular distribution. When one examines the terms in the angular distribution, $A + B\cos^2\theta$, one notices that the average of the second term over a sphere is one-third. Thus, collection at an angle at which $\cos^2\theta$ is one-third will permit one to measure currents which are independent of the angular distribution. Thus, if one makes measurements at an angle of 54° 44′ with respect to the electric vector of polarized light, the measurements will be independent of the angular distribution of the emitted charged particles. Furthermore, one can show that if the light is unpolarized, a measurement at an angle of 54° 44′ with respect to the direction of propagation will be independent of the angular distribution. If one considers three cones of half angle 54° 44′ about three orthogonal axes, one of which is the direction of propagation, one finds that these cones intersect in a line (the 1, 1, 1 direction). Observations made along this line will be independent of angular distribution if the radiation is unpolarized, or if it is polarized, along one of the two axes perpendicular to the direction of propagation. Because of the symmetry of the problem with respect to planes containing any two axes, there are 6 cones and 8 directions of intersection which satisfy the requirement.

Suppose now that the radiation is partially polarized. Consider a plane perpendicular to the direction of propagation and within that plane define an axis parallel to the exit slit of a monochromator. Measure an angle, η, from that axis. Let $f(\eta)$ be the probability that the polarization of a photon lies in the interval $\eta \rightarrow \eta + d\eta$ and expand $f(\eta)$ in a Fourier series. Only terms involving sines and cosines of even multiples of η will occur, because $f(\eta) = f(\eta + \pi)$. By expanding $\cos^2\theta$ one can show that only constant terms and those involving 2η remain. If the distribution is symmetric about the axis chosen and if no term in sin 2η arises, the choice of a direction of observation described above is proper.

Furthermore, it can easily be shown that if no terms in sin 2η arise, the conclusions reached above hold true no matter what solid angle the detector subtends, provided that the detector is circularly symmetric about the line chosen to lie at 54° 44′ with respect to the appropriate axes.

In the systems discussed above, the gas to be ionized is distributed uniformly in vacuum tanks of one kind or another. By using an electrical lens system and the high local densities available from molecular beams, Berkowitz *et al.* (55) were able to make both retarding potential and angular distribution measurements. Vilesov *et al.* (61) have made angular distribution measurements without energy discrimination in a cylindrical tank system.

Two types of experiments may be distinguished: that with a monochromatic radiation source (He 584 Å resonance line) and no monochromator, and that with a monochromator and one of a number of kinds of light sources. In the former case it is expected that the light will be unpolarized; in the latter, partially polarized.

By attributing to each state a fraction of the photoionization cross section proportional to the electron current associated with it, cross sections for various states of excitation can be obtained. Problems which have been discussed previously, such as scattered light, photoelectrons from walls, light-source constancy, etc. are present in electron and ion-energy experiments also. Furthermore, in retarding potential experiments, the efficiency of collection of electrons or ions may depend upon the energy with which they impinge on the collector. Some improvement of collection efficiency can be achieved by coating the collector with carbon black (52), but one runs the risk of introducing inhomogeneities in the potential. Low energy electrons scattered from grids and plates have constituted a significant hindrance to electron energy measurements at low energies. When electron multipliers are used (53–55), care must be taken that the gases introduced do not cause changes in the efficiency or pulse height distribution during the course of the experiment. If electron energies are of interest, the local magnetic field must be reduced to a small fraction of the earth's field in the region of measurement. In all cases gas pressures must be low enough so that gas scattering is not important.

N_2

Berkowitz *et al.* (55) have measured the angular distribution of electrons for the cases in

Can. J. Chem. Downloaded from www.nrcresearchpress.com by 210.87.254.42 on 09/05/12
For personal use only.

TABLE I

Relative probabilities of exciting various electronic states with 584 Å radiation

Electronic state	Blake and Carver*	Berkowitz *et al.*†	Frost *et al.*‡	Samson§	Doolittle and Schoen‖	Spohr and Puttkamer¶
			N_2^+			
$X^2\Sigma$	0.34	0.78**	0.33	0.32	0.35	0.26
$A^2\Pi$	0.51	1.00**	0.60	0.55	0.45	0.58
$B^2\Sigma$	0.15		0.08	0.13	0.21	0.16
			O_2^+			
$X^2\Pi_g$	0.24		0.18	0.15		0.14
$a^4\Pi + A^2\Pi$	0.35		0.37	0.38		0.42
$b^4\Sigma_g$	0.26		0.24	0.27		0.44
$B^2\Sigma_g$	0.15		0.21	0.20		
			NO^+			
$X^1\Sigma$			0.36**			
$a^3\Sigma$			0.06**			
$^3\Delta$			1.00**			
$A^1\Pi$			0.51**			
			CO_2^+			
$^2\Pi_g$						0.16
$^2\Pi_u$						0.38
$^2\Sigma_u^+$						0.46

*Reference 50. These values are estimated from published curves. Blake and Carver used cylindrical retarding potential systems.

†Reference 55. Berkowitz *et al.* used electron lenses and plane retarding potential.

‡Reference 52 for N_2, but ref. 62 for O_2 and NO. Frost *et al.* used a spherical retarding potential system.

§Unpublished. See ref. 53 for method. The author thanks Dr. Samson for these data. Samson used a quasi-spherical system with focusing and an electron multiplier.

‖Unpublished. Doolittle and Schoen used cylindrical retarding potential systems.

¶Reference 54 and private communication. The author thanks Dr. Puttkamer for supplementary data. Puttkamer and Spohr used electron lenses and plane retarding potential.

**Relative values for several but not all states.

which the ions are left in either the $X^2\Sigma_g^+$ or the $A^2\Pi_u$ state by 584 Å radiation and found them both to be spherically symmetric as illustrated in Fig. 6. If in the ionization to the $B^2\Sigma_u$ state the electron angular distribution is also spherically symmetric, as might be expected from the removal of a σ_u electron to a σ_g (but not a Π_g state) state in the continuum, then all methods of electron energy measurement should give the same results. Table I contains relative excitation cross sections for the three electronic states of N_2^+ which can be excited with 584 Å radiation. It appears that while the relative cross sections for the X and the A states are known to perhaps 20%, that of the B state is known only within about a factor of two. Vibrational distributions have also been investigated at 584 Å and are presented in Table II with some calculated values. Rather large errors are quite possible for small transition probabilities to upper vibrational states in retarding potential measurements. These errors come from two sources: noise proportional to the total current collected and noise from scattered

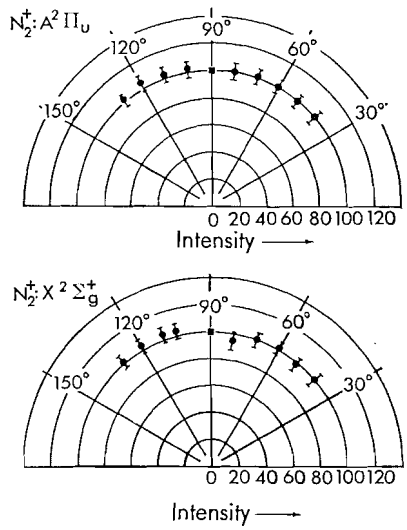

FIG. 6. Electron angular distributions resulting from photoionization which leaves the molecular ion in either the $A^2\Pi_u$ (top) or the $X^2\Sigma_g^+$ (bottom) states, from Berkowitz *et al.* (55).

TABLE II

Relative vibrational transition probabilities at 584 Å

Electronic state		Experimental					Theoretical	
		Spohr and Puttkamer*	Berkowitz *et al.*†	Frost *et al.*‡	Turner and May§	Watanabe‖	Nicholls¶	Wacks**
					N_2^+			
$X^2\Sigma_g$	0	1.00	1.00	1.00			1.00	
	1	0.09	>0.2	0.054			0.10	
$A^2\Pi_u$	0	0.86	0.84	0.85			0.78	
	1	1.00	1.00	1.00			1.00	
	2	0.78	0.73	0.71			0.72	
	3	0.38	0.39	0.46			0.40	
	4	0.16		0.21			0.18	
	5	0.07		0.14			0.08	
	6			0.08				
$B^2\Sigma_u$	0	1.00			1.00		1.00	
	1	0.18			0.11		0.11	
					NO^+			
$X^1\Sigma^1$	0	0.41	0.50	0.59		0.79	0.48	
	1	1.00	0.94	1.00		1.00	1.00	
	2	0.88	1.00	0.81		1.00	0.92	
	3	0.46	0.71	0.40		0.67	0.48	
	4	0.28		0.16			0.16	
					O_2^+			
$X^2\Pi_g$	0	0.50	0.53	0.43				0.60
	1	1.00	1.00	1.00				1.00
	2	0.97	0.98	0.98				0.67
	3	0.57	0.57	0.43				0.24
	4	0.09		0.14				0.05
$^4\Sigma_g$	0		0.53					1.00
	1		1.00					0.83
	2		0.98					0.40
	3		0.72					0.15
$^2\Sigma_g$	0				0.75			
	1				1.00			
	2				0.92			
	3				0.67			
	4				0.50			
	5				0.17			
	6				0.13			

*Reference 54.
†Reference 55.
‡Reference 52 for N_2, but ref. 62 for O_2 and NO.
§Reference 51.
‖Reference 65.
¶Reference 63.
**Reference 64.

low energy electrons, both of which are large at low electron energies in electron retarding potential experiments. In Table II agreement is reasonably good, both among experiments and between theory and experiments.

The spectral region around 584 Å does not have strong autoionization bands, but such bands are present at longer wavelengths and may have a large effect on the energy distribution of the outgoing electrons. Figure 7 illustrates the difference in the vibrational distribution in nitrogen in two autoionization bands within a few angstroms of each other. In such regions averages of cross sections for excitation to particular states of the ion over 5 or 10 Å are as likely to be as misleading as the ionization or absorption cross sections so averaged. Therefore investigation with high spectral resolution is required in each autoionization region of interest.

Nonetheless, the only direct information from electron energy experiments concerning the wavelength dependence of the cross sections for excit-

Can. J. Chem. Downloaded from www.nrcresearchpress.com by 210.87.254.42 on 09/05/12
For personal use only.

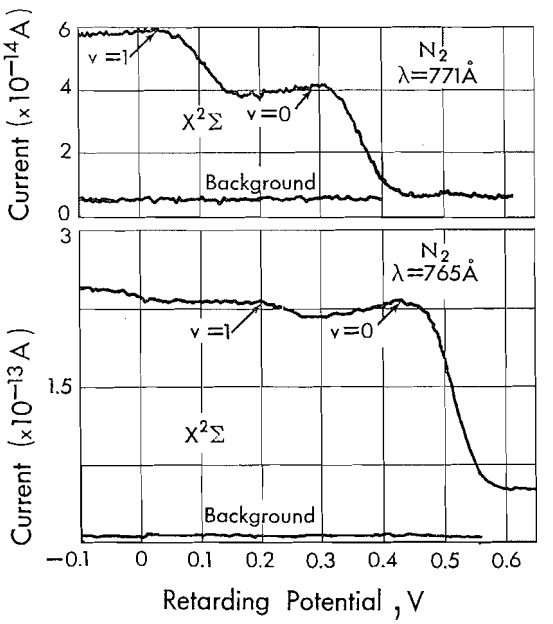

FIG. 7. Electron retarding potential measurements of vibrational excitation in an autoionization region, Schoen and Doolittle (unpublished). Step heights are proportional to excitation probabilities at each wavelength. Step heights at one wavelength should not be compared to step heights at another wavelength.

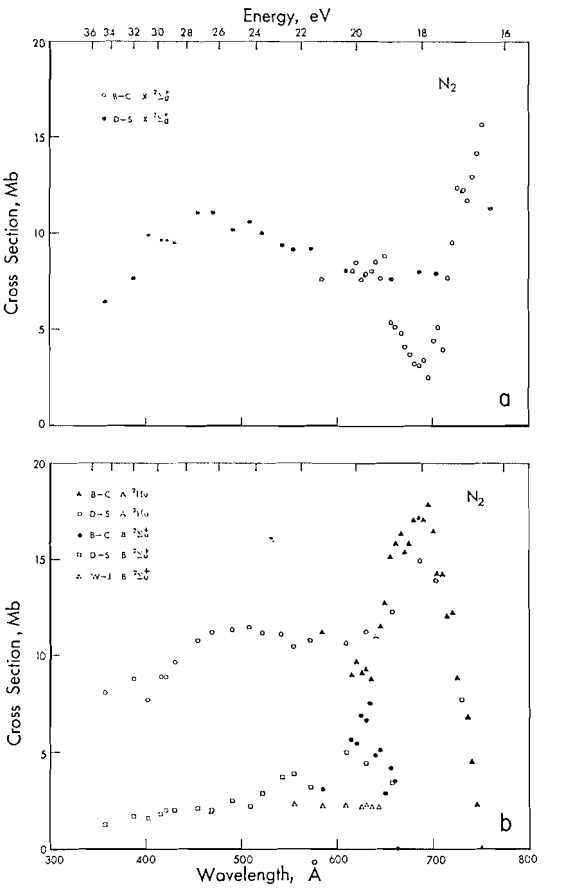

FIG. 8. Photoionization cross sections for the excitation of various states of N_2^+. B–C, Blake and Carver (50). Their results are normalized to the cross sections of Cook and Metzger (12). D–S, Doolittle and Schoen (unpublished). Their results are normalized to the cross sections of Samson and Cairns (18). W–J, Judge and Weissler (66) from fluorescence. Their results are normalized to Frost *et al.* (52) at 584 Å.

ing particular states of the N_2^+ ion has been obtained with relatively large bandwidths and cylindrical analyzers. Blake and Carver (50) have used a continuum source for these measurements (bandwidth $\approx$ 10 Å), and Doolittle and Schoen (unpublished) have used a line source (bandwidth $\approx$ 3 Å). Partial ionization cross sections from these two groups are shown in Fig. 8. There is no information about the angular distribution of the electrons at wavelengths other than 584 Å. To test for discrimination effects which change as the wavelength changes, it is advisable to sum quantities proportional to the cross sections for excitation of the individual states and compare the sum with the total ionization cross section. In a retarding potential experiment, this can be done by dividing the collector current associated with each ionic state by the photon detector current properly normalized to remove any wavelength dependence of photodetector efficiency. The ratio of the measured photoionization cross section to the sum of the quantities calculated above should be a constant independent of wavelength. Doolittle and Schoen (unpublished) have applied such a test to their raw data for N_2 and find that the sum of the partial cross sections appears to be as much as 40% high at long wavelengths and as much as 40% low at short wavelengths. Whether the cause lies in the sodium salicylate converter or in an energy dependence of collection efficiency is not clear. Their data shown in Fig. 8 have been corrected by normalization to the total cross section at each wavelength. Blake and Carver have tested the collection efficiency of their apparatus as a function of electron energy; they find no energy discrimination effects.

Can. J. Chem. Downloaded from www.nrcresearchpress.com by 210.87.254.42 on 09/05/12
For personal use only.

Can. J. Chem. Downloaded from www.nrcresearchpress.com by 210.87.254.42 on 09/05/12
For personal use only.

O_2

Berkowitz *et al.* (55) have found at 584 Å that the electrons released from O_2 in removal of a π_g electron to produce the $X^2\Pi_g$ state of the O_2^+ ion have a tendency to come out parallel or antiparallel to the direction of the photon beam, as shown in Fig. 9. Removal of other electrons appears to produce only spherically symmetric distributions. Therefore, the apparent cross section for the production of the ground state O_2^+ ion will appear to be too small when measured in cylindrical systems. Some measurements of the relative probabilities of transition to various electronic states with 584 Å radiation incident are given in Table I. No corrections have been made for angular discrimination.

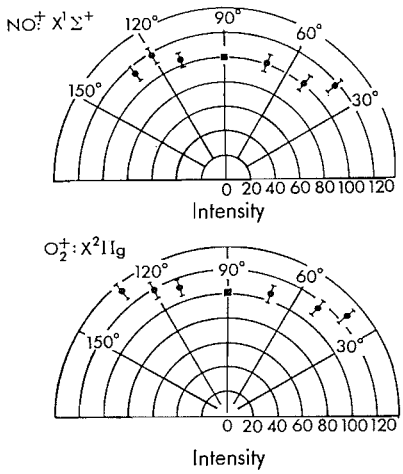

FIG. 9. Angular distribution measurements of electrons released in photoionization. Bottom—excitation of the $X^2\Pi_g$ state of O_2^+. Top—excitation of the $X^2\Pi_g^+$ state of NO^+ from Berkowitz *et al.* (55).

It is interesting that Blake and Carver (50), with a cylindrical apparatus, obtained a larger probability for transition to the $X^2\Pi$ state of O_2^+ than did Vroom (62), who used a spherical retarding potential system. Samson's results (private communication) are from a quasi-spherical geometry (Fig. 5E) and may be affected by polarization of the radiation, but relative transition probabilities certainly agree with Vroom's values to within experimental error. It should be noted that, even with resolution of the order of 20 mV (56), no one has been able to resolve the $A^2\Pi_u$ state from the $a^4\Pi_u$ state. Some relative excitation probabilities of vibrational states in several states, again with 584 Å radiation, are shown in Table II. Deviations from calculated values are significant.

At longer wavelengths, large deviations from the Franck–Condon principle occur in the autoionization region. Blake and Carver (50) ascribe some of the effects seen in this region to the series of events: transition to a super-excited neutral, radiation of a photon in the red or infrared, and finally autoionization. They used a helium continuum with about 10 Å resolution. Doolittle and Schoen (unpublished) have investigated the same spectral region with a line source and somewhat better energy resolution. At some wavelengths they observed strong deviations from the Franck–Condon principle, but no transitions which required the emission of a photon were noted. The difference in results may be ascribable to the differences in wavelengths actually studied and in resolution differences. Figure 10 shows the measured relative transition probabilities to various electronic states as a function of wavelength. In the region between 650 and 800 Å, Doolittle and Schoen made measurements on autoionization lines in a number of cases. Since they worked with a line spectrum and resolution of about 3 Å, it is not likely that in this spectral region their results will be comparable to those of Blake and Carver, who worked with a helium continuum and about 10 Å resolution.

NO

Angular distribution measurements at 584 Å by Berkowitz *et al.* (55) have shown that the removal of the π_g electron, as in the case of O_2, produces an angular distribution peaked along the photon beam (Fig. 9). The most surprising fact to arise from electron energy measurements in NO is that an NO^+ state, $a^3\Sigma$, previously thought to lie 14.22 eV above the ground state of the neutral (67), does not exist there but that there is a state at about 15.5 eV (49, 57) which had not been observed previously. Vroom (62) finds a state at 14.84 eV which he labels $a^3\Sigma$, but this finding is not confirmed by others. Table II gives the relative excitation probabilities of various vibrational states of the ground state of NO^+ with 584 Å incident. Data on the relative transition probabilities to a few, but not all, electronic states are given in Table I. No published data are available for other wavelengths.

CO_2

Measurements by Spohr and Puttkamer (54) on the relative excitation probabilities of various

Can. J. Chem. Downloaded from www.nrcresearchpress.com by 210.87.254.42 on 09/05/12
For personal use only.

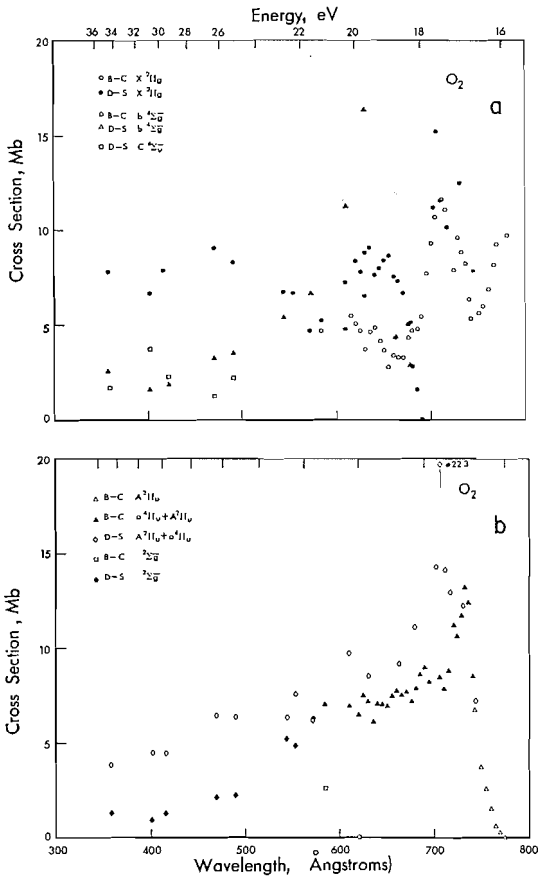

FIG. 10. Photoionization cross sections for the excitation of various states of O_2^+. B–C, Blake and Carver (50); their results normalized to the cross sections of Cook and Metzger (12). D–S, Doolittle and Schoen (unpublished); their results normalized to the cross sections of Samson and Cairns (18) 630 Å $\leqslant \lambda$ and Matsunaga and Watanabe (19) $\lambda \geqslant$ 630 Å.

electronic states excited with 584 Å radiation were obtained with an electron lens and retarding potential system. The results of these measurements are shown in Table I. Vibrational excitation probabilities were also investigated by these authors and by Turner and May (51) who used magnetic analysis.

Other Molecules

Of other molecules of some aeronomic interest, N_2O has been investigated by Turner and May (51), Spohr and Puttkamer (54), and Vroom (62), and NO_2 has been investigated by Spohr and Puttkamer (54) and Vroom (62). Blake and Carver (50) have measured the electron energy spectrum from H_2O with a cylindrical retarding potential analyzer from threshold to 584 Å.

Positive Ions

Positive ions may be studied by any of the various techniques outlined. The energy resolution is not nearly as good as it is for electron experiments because the motion of the neutral parent contributes significantly to the velocity of the ion fragment (68). Vroom (62) has measured the energy distribution of O^+ fragments from the photoionization of O_2 at 584 Å. He used a spherical retarding potential system. Doolittle *et al.* (69) have measured the energy distributions from dissociative photoionization of O_2 and N_2 in a cylindrical system at a number of wavelengths between 584 and 358 Å. No angular distribution measurements have been made.

Ion energy distribution measurements taken at 4 wavelengths in O_2 are shown in Fig. 11. Analysis of these and similar curves taken at other wavelengths and consideration of electron energy data and fluorescence data leads to a number of conclusions. First, the energies of these ions are great enough to cause significant loss from ion beams in some types of mass spectrometers, with consequent underestimation of the probability of formation of O^+ from O_2. Second, the $^2\Sigma^-$ state of O_2 predissociates, and other states of the molecular ion may predissociate. Third, some of the energetic neutrals accompanying the energetic ions are in metastable states.

Doolittle *et al.* (69) have made measurements of the dissociative ionization of O_2 in a mass spectrometer very sensitive to ion energies. They found that perhaps all, but not less than half, of the O^+ ions produced by 584 Å radiation had significantly more than thermal energy. At the same wavelength this group also used a cylindrical retarding potential analyzer to determine that 0.15 of all ions ($O_2^+ + O^+$) collected were energetic. Vroom (62), with a spherical retarding potential analyzer, found 0.075 were energetic. The difference in results might be ascribable to angular distribution effects or discrimination effects in one of the analyzers.

V Excitation of Ions and Neutrals

Fluorescence

While electron and ion energy distribution measurements are very useful in locating ionic

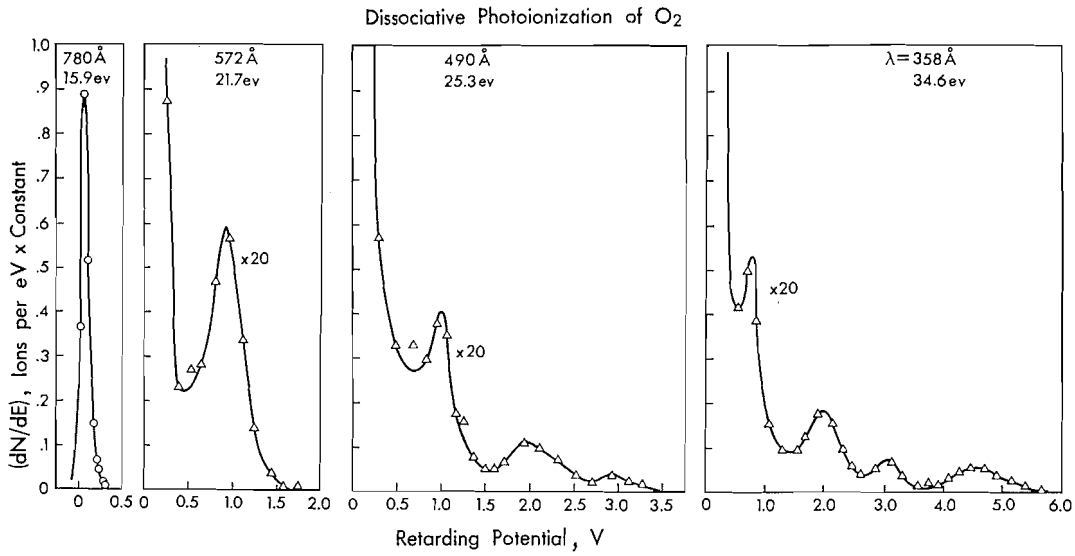

FIG. 11. Ion energy distributions measured at 4 wavelengths, Doolittle *et al.* (69). These curves are derivations of retarding potential curves. The ordinate is multiplied by 20 in the cases of the three shorter wavelengths.

states on energy level diagrams and in determining the relative probabilities of excitation of these states, such measurements give no information about neutrals, no information directly about the classification of electronic states, and occasionally fail to give information about the existence of electronic states, because of overlap of two or more vibrational progressions. Studies of fluorescence may give the missing information and may also give more precise results than electron and ion energy measurements do about the relative probabilities of exciting various electronic or vibrational states. Even failure to detect fluorescence when excitation is known to exist may be useful in determining classification when metastable states are possible.

In a typical fluorescence experiment, radiation of intensity $I_0(\lambda)$ from a monochromator is incident on gas in a cell such as that shown in Fig. 1, and the fluorescent radiation is viewed from the side with a photomultiplier or with a second monochromator and photomultiplier. Fluorescence is detected with an efficiency $F(x, \lambda,\lambda_f, n)$, which is a function of the position, x, of the fluorescing molecules in the chamber, of the incident wavelength, λ, of the fluorescent wavelength, λ_f, and of the molecular number density, n (if gas quenching, diffusion, or absorption of fluorescent radiation are important). If it is supposed that the detection efficiency is non-zero only between the distances L and $L + l$ measured from the chamber entrance, then the observed intensity of the fluorescence is given by

$$[3] \qquad I_f(\lambda,\lambda_f) = I_0(\lambda) \exp[-n\sigma_T(\lambda)L] \int_0^l n\sigma_f(\lambda,\lambda_f) \exp[-n\sigma_T(\lambda)x] F(x,\lambda,\lambda_f,n)\, dx$$

in which σ_f is the cross section for production of the fluorescing state and σ_T is the cross section for all processes which remove photons from the beam. This equation is generally simplified by making, implicitly or explicitly, the assumptions that $n\sigma_T L \ll 1$, $n\sigma_T l \ll 1$, and that the detection efficiency does not depend upon λ, x (between l and $L + l$), or upon n. Under these assumptions, eq. [3] can be simplified to the form

$$[4] \qquad I_f(\lambda,\lambda_f) = I_0(\lambda) nl\sigma_f(\lambda,\lambda_f) F(\lambda_f)$$

or

$$\sigma_f(\lambda,\lambda_f) = I_f(\lambda,\lambda_f)/I_0(\lambda) nlF(\lambda_f)$$

Under the conditions which allow the use of eq. [4], I_f/I_0 is proportional to the cross section for excitation of the fluorescing state. In no experi-

Can. J. Chem. Downloaded from www.nrcresearchpress.com by 210.87.254.42 on 09/05/12
For personal use only.

Can. J. Chem. Downloaded from www.nrcresearchpress.com by 210.87.254.42 on 09/05/12
For personal use only.

ments in which dispersed vacuum ultraviolet radiation stimulated fluorescence has there been a measurement of $F(\lambda_f)$ which allowed a direct determination of $\sigma_f(\lambda,\lambda_f)$; however, the dependence upon incident wavelength of the cross section has been determined in a number of cases. If the value of the cross section is taken from electron energy data at an incident wavelength at which measurement is particularly accurate (584 Å, for instance), then the value is determined at all incident wavelengths from the measured wavelength dependence.

In fluorescence experiments, particular care must be taken not to confuse radiation caused by electrons released from the gas or walls with radiation caused by photon absorption processes. Confusion can also be caused by a change in the polarization of the fluorescent radiation as a function of incident wavelength. Such a change might change the detection efficiency, F, and be confused with a change in the cross section, σ_f. No experimental information about polarization is at hand.

Fluorescence information has been obtained with dispersed, incident radiation only during the past eight years. Some results for specific molecules are given below.

N_2

Cook and Metzger (12) and Huffman *et al.* (17) have determined the threshold for the production of strong visible fluorescence in N_2 to be 661 Å. This is the energy required to excite the $B^2\Sigma_u$ state of N_2^+. Judge and Weissler (66) have dispersed the radiation, identified the expected first negative bands of N_2^+, and determined the variation of the cross section with wavelength. Judge and Weissler chose their cross section value at 584 Å equal to that measured by Frost *et al.* (52) and calculated the cross section at other wavelengths from their measurements of wavelength dependence. Their results are shown in Fig. 8. This wavelength dependence of the cross section for excitation to the $B^2\Sigma_u$ state of N_2^+ is probably more accurate than that obtained from electron energy measurements.

O_2

Beyer and Welge (70) have used magnetic strip multipliers with LiF and CaF_2 windows to detect fluorescence from excited O atoms produced in the dissociation of O_2, Fig. 12. They have observed the direct radiation at 1302, 1304, and

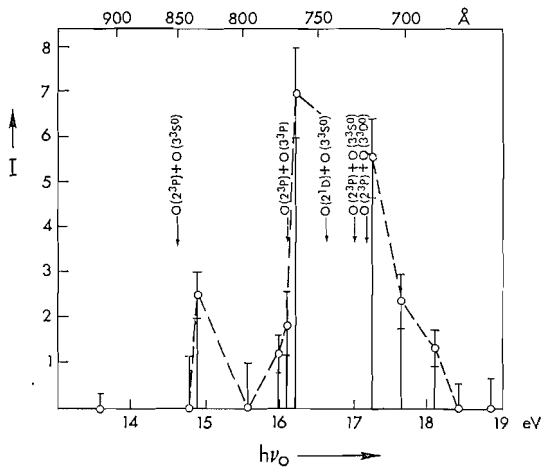

FIG. 12. Fluorescence of O_2 in the spectral range of fluorescent radiation 1250–1500 Å, Beyer and Welge (70). The ordinate is proportional to I_f/I_0. Incident photon energy is marked on the abscissa. These data were taken with a CaF_2 detector window. A LiF window did not change the intensity distribution.

1306 Å from the O(3s ^{3}S) state and the same radiation in cascade from the O(3p ^{3}P) state.

Cook and Metzger (12) and Huffman *et al.* (17) have observed a weak fluorescence in O_2 at thresholds which are identified as 736.5 and 722 ± 5 Å, respectively. The onset of this weak fluorescence is gradual; thus the threshold is difficult to determine. Cook and Metzger, with a photomultiplier which viewed from the side probably had more sensitivity than did Huffman *et al.* who view from the end with a sodium salicylate-coated multiplier. The fluorescence is probably from the $A^2\Pi_u$ state of O_2^+ and represents detection in a case in which electron energy measurements have not indicated a state. Confirmation with dispersed fluorescent radiation is awaited.

Judge and Weissler (unpublished) have detected radiation from the $b^4\Sigma_g^-$ state of O_2^+ and have observed several peculiar shifts of vibrational intensity at wavelengths above 600 Å. These shifts are probably related to autoionization.

NO

In Fig. 13 are shown relative fluorescence yields from NO measured by Beyer and Welge (70). The atomic oxygen lines at 1302, 1304, and 1306 Å that appeared from O_2 in these authors' measurements seem to appear here, also, both by

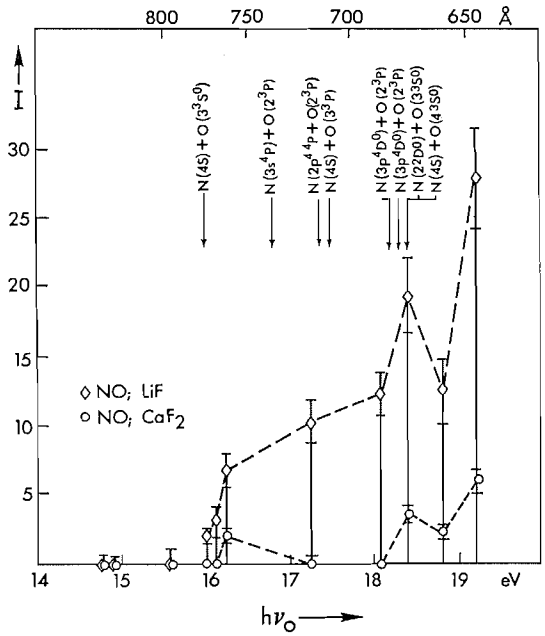

FIG. 13. Fluorescence of NO from Beyer and Welge (70). The ordinate is proportional to I_f/I_0. The incident photon energies are given on the abscissa. The spectral range of the detector was 1100–1500 Å with the LiF detector window and 1250–1500 Å with the CaF_2 window. Two figures in the original are combined here.

direct transition and by cascade. In addition, one or more radiations appear which are not transmitted by CaF_2 but are transmitted by LiF. These are attributed to the atomic nitrogen lines at 1200 and perhaps 1134 Å. In addition, Metzger *et al.* have observed radiation in the vacuum ultraviolet, which they attribute to the $A^1\Pi \rightarrow X^1\Sigma$ transition in NO^+, and have determined the threshold for excitation of this radiation to be 677.4 Å. Metzger *et al.* did not observe the transitions from the neutral atoms. It is not clear why.

VI Photodetachment

Since the whole field of photodetachment has been well reviewed during the last few years (5, 71), only recent work will be discussed here. Of particular interest are several new threshold determinations, cross section measurements, and angular distribution measurements.

The new data of Branscomb *et al.* (72) have been added to that of Smith (73) in Fig. 14 to show the photodetachment thresholds of O^- to form $O(^3P)$ and the $O(^1D)$. The authors point

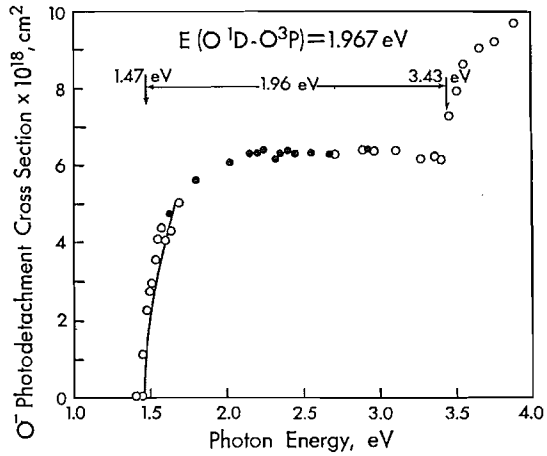

FIG. 14. The photodetachment cross section of O^- as a function of photon energy. The open circles are from Branscomb *et al.* (72); the filled circles are from Smith (73). The data of Branscomb *et al.* were normalized to that of Smith at 1.65 and 2.7 eV.

out that the rate of increase of the cross section above the second threshold is less than calculated, but calibration is very difficult when photon energies exceed 3.7 eV.

Branscomb (74) has measured cross sections for photodetachment of OH^- and OD^-, as shown in Fig. 15. The measurements themselves

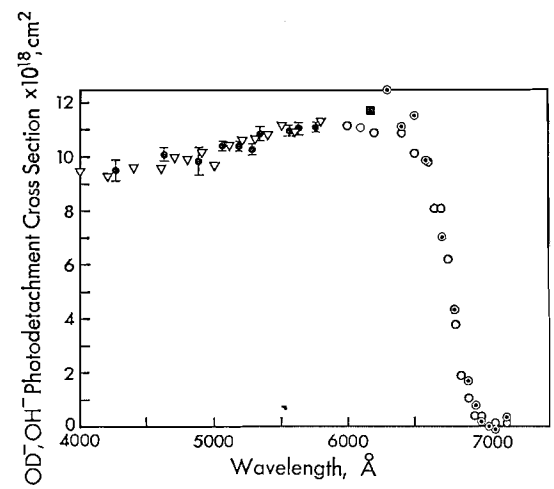

FIG. 15. The cross sections for photodetachment of OH^- and OD^- as a function of wavelength from Branscomb (74). The solid points refer to OH^-; the crosses and circles to OD. The error bars refer to unpublished data of Branscomb and Smith using bandpass filters at about 500 Å resolution. All other data were obtained at a resolution of 100 Å and were placed on an absolute scale by comparison with H^-.

Can. J. Chem. Downloaded from www.nrcresearchpress.com by 210.87.254.42 on 09/05/12
For personal use only.

Can. J. Chem. Downloaded from www.nrcresearchpress.com by 210.87.254.42 on 09/05/12
For personal use only.

are on a relative basis and were made absolute by comparison to the known H^- cross section photodetachment. We estimate that the cross section of OH^- should be accurate to 20%. Very recent measurements of photodetachment have been made in a drift tube by Woo *et al.* (75). They find the photodetachment rate of O_3^- to be 4.2% that of O^- or $6.0 \times 10^{-2}\ s^{-1}$.

The experimental work of Siegel and Hall (76) on the angular distribution of photodetached electrons from H^- and O^- is compared with the theoretical work of Cooper and Zare (77) in Fig. 16. Several striking facts emerge from the O^- study. First, the agreement of the theory with the measurements is very good. To obtain this agreement the authors had to calculate the mixing ratio of s to d wavefunctions in the outgoing electron wave. Second, the authors found a case in which a cylindrical analyzer might have missed a group of electrons entirely. Third, Cooper and Zare showed that the angular distribution varies with the energy of the incident photons. At threshold the distribution is isotropic. It becomes almost $\sin^2\theta$ (where θ is measured from the electric vector of the incident light) at photon energies roughly 0.8 eV above threshold and then becomes more isotropic with increasing photon energy. Such a change of angular distribution with energy would be interpreted as a change of cross section with energy in many electron energy measurements.

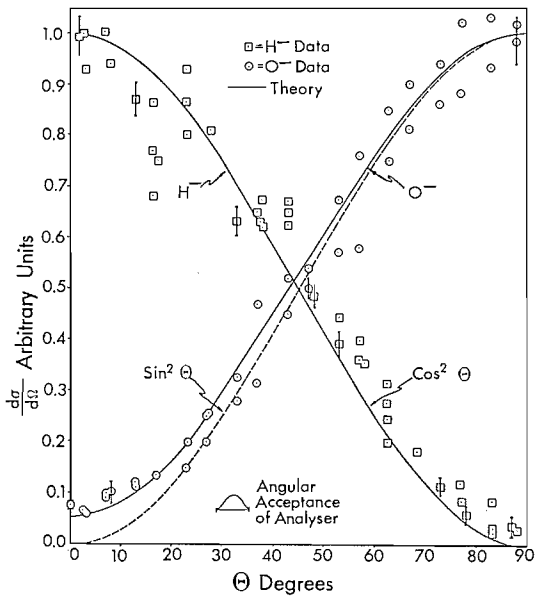

FIG. 16. A comparison of experimental, Siegel and Hall (76), with theoretical, Cooper and Zare (77), values for the angular distributions of electrons from photodetachment of H^- and O^-. The experimental points were obtained at the argon laser wavelength, 4880 Å. The solid curves are the calculated angular distributions.

VII Conclusions

For present purposes of aeronomy, the measurements of photoionization cross sections of O_2 and N_2 have been made with sufficient accuracy at wavelengths longer than 300 Å, except where strong band structure is present. At a few wavelengths where important solar lines lie within strong band structure, measurements with higher resolution may be required. A similar statement may be made about the photoionization cross section of NO at wavelengths longer than 600 Å. There is conflicting data on the photoionization cross section of CO_2 which casts a shadow over other measurements. Further investigation of the photoionization and photoabsorption cross sections of CO_2 are required.

At wavelengths shorter than 300 Å, it is likely that each photon absorbed produces an ion, but this assumption should be tested. There are no measured cross sections of excited species of stable molecules or of free molecular radicals such as OH. Cross sections of such species may be needed, and the beam methods for making the measurements are now being developed.

Much more work is required on the details of ionization processes. The dissociative ionization cross section of O_2 and N_2 should be checked with particular care devoted to the effects of energetic ions and of detector efficiency variation from species to species. The range of measurement should also be extended to wavelengths shorter than 400 Å, the present limit.

Electron and ion energy measurements are in their infancy. There is a need for a set of accurate measurements at wavelengths of solar lines from threshold to 100 Å. These measurements must be made in a system unaffected by the angular distribution of the charged particles. When used to make electron energy measurements, the system must have enough resolution to show vibrational states clearly. More information is needed about angular distributions. The work of Berkowitz *et al.* should be extended to cover other molecules and a wider range in angle and wavelength.

Can. J. Chem. Downloaded from www.nrcresearchpress.com by 210.87.254.42 on 09/05/12
For personal use only.

The combination of electron energy measurements, ion energy measurements, and fluorescence measurements presents a powerful array for the analysis of photoionization phenomena. At the present time, it appears that the most accurate cross sections for the excitation of those states which decay by fluorescence can be obtained by combining the best cross sections measured in electron energy experiments at 584 Å with relative fluorescence efficiencies measured over a range of wavelengths of the exciting vacuum u.v. radiation. Dispersion of the fluorescent radiation is highly desirable, but care must be taken to check for polarization effects, which may be a function of the wavelength of the exciting radiation. In many cases fluorescence represents the best method for detecting the existence of excited states. It would seem that much more work is required in the examination of fluorescence caused by vacuum u.v. radiation at all wavelengths of incidence and for most molecules of aeronomic interest.

The picture in photodetachment studies has been changed in the last few years by the increased appreciation of the role of ion–molecule reactions. Fehsenfeld *et al.* (78) have pointed out the importance of NO_2^-, NO_3^-, CO_3^-, and perhaps hydrates of these ions. Photodetachment of these ions will require measurements in the near u.v.

Acknowledgments

During the course of preparation of this paper, the author engaged in discussions and correspondence with a substantial fraction of those whose works are listed in reference and with a number of people working in related fields. To those who generously gave supplementary data, comments, and corrections, the author would like to express his thanks. The author is entirely responsible for the value judgments contained in this paper and for any errors of commission or omission.

1. R. E. HUFFMAN. See preceding article.
2. G. L. WEISSLER. *In* Handbuch der Physik. Vol. XXI. *Edited by* S. F. Flügge. Springer-Verlag, Berlin. 1956. p. 304.
3. K. WATANABE. Advan. Geophys. **5**, 153 (1958).
4. R. W. DITCHBURN and U. ÖPIK. *In* Atomic and molecular processes. *Edited by* D. R. Bates. Academic Press, Inc., New York. Chap. 3. 1962.
5. L. W. BRANSCOMB. *In* Atomic and molecular processes. *Edited by* D. R. Bates. Academic Press, Inc., New York. Chap. 4. 1962.
6. G. V. MARR. *In* Photoionization processes in gases. Academic Press, Inc., New York. 1967.
7. J. A. R. SAMSON. *In* Techniques of vacuum ultraviolet spectroscopy. John Wiley and Sons, Inc., New York. 1967.
8. J. R. MCNESBY and H. OKABE. Advan. Photochem. **3**, 157 (1964).
9. K. WATANABE and F. F. MARMO. J. Chem. Phys. **25**, 965 (1956); K. WATANABE and S. P. SOOD. Sci. Light, **14**, 36 (1965).
10. R. I. SCHOEN. J. Chem. Phys. **37**, 2032 (1962).
11. J. A. R. SAMSON. J. Opt. Soc. Am. **54**, 6 (1964).
12. G. R. COOK and P. H. METZGER. J. Chem. Phys. **41**, 321 (1964).
13. F. M. MATSUNAGA, R. S. JACKSON, and K. WATANABE. J. Quant. Spectry. Radiative Transfer, **5**, 329 (1965).
14. P. H. METZGER and G. R. COOK. J. Opt. Soc. Am. **55**, 516 (1965).
15. R. W. DITCHBURN. J. Quant. Spectry. Radiative Transfer, **2**, 361 (1962).
16. K. WATANABE and S. P. SOOD. Sci. Light, **14**, 36 (1965).
17. R. E. HUFFMAN, Y. TANAKA, and J. C. LARRABEE. J. Chem. Phys. **38**, 1920 (1963).
18. J. A. R. SAMSON and R. B. CAIRNS. J. Geophys. Res. **69**, 4583 (1964).
19. F. M. MATSUNAGA and K. WATANABE. Sci. Light, **16**, 31 (1967).
20. G. R. COOK, B. H. CHING, and R. A. BECKER. Discussions Faraday Soc. **37**, 149 (1964).
21. Y. TANAKA and T. TAKAMINE. Sci. Papers Inst. Phys. Chem. Res. Tokyo, **39**, 437 (1942).
22. K. CODLING and R. P. MADDEN. J. Chem. Phys. **42**, 3935 (1967).
23. G. R. COOK and M. OGAWA. Can. J. Phys. **43**, 256 (1965).
24. K. WATANABE, F. M. MATSUNAGA, and H. SAKAI. Appl. Opt. **6**, 391 (1967).
25. K. WATANABE. J. Chem. Phys. **22**, 1564 (1954).
26. P. H. METZGER, G. R. COOK, and M. OGAWA. Can. J. Phys. **45**, 203 (1967).
27. R. B. CAIRNS and J. A. R. SAMSON. J. Geophys. Res. **70**, 99 (1965).
28. R. S. NAKATA, K. WATANABE, and F. M. MATSUNAGA. Sci. Light, **14**, 54 (1965).
29. G. R. COOK, P. H. METZGER, and M. OGAWA. J. Chem. Phys. **44**, 2935 (1966).
30. TOSHIO NAKAYAMA, MORRIS Y. KITAMURA, and K. WATANABE. J. Chem. Phys. **30**, 1180 (1959).
31. P. H. METZGER and G. R. COOK. J. Chem. Phys. **41**, 642 (1964).
32. A. E. HINTEREGGER. Space Sci. Review, **4**, 461 (1965).
33. F. J. COMES and W. LESSMAN. Z. Naturforsch. **19a**, 65 (1964).
34. F. J. COMES, F. SPEIER, and A. ELZER. Z. Naturforsch. **23a**, 125 (1968).
35. F. J. COMES and A. ELZER. Z. Naturforsch. **23a**, 133 (1968).
36. F. J. COMES, A. ELZER, and F. SPEIER. Z. Naturforsch. **23a**, 114 (1968).
37. H. HURZELER, M. G. INGHRAM, and J. C. MORRISON. J. Chem. Phys. **28**, 76 (1958).
38. G. L. WEISSLER, J. A. R. SAMSON, M. OGAWA, and G. R. COOK. J. Opt. Soc. Am. **49**, 338 (1959).
39. C. A. MCDOWELL. *In* Mass spectrometry. McGraw-Hill Book Co., Inc., New York. 1963.

40. F. I. VILESOV. Usp. Fiz. Nauk. **81**, 669 (1963).
41. C. E. BERRY. Phys. Rev. **78**, 597 (1958). A. W. WASHBURN and C. E. BERRY. Phys. Rev. **70**, 559 (1946).
42. N. D. COGGESHALL. J. Chem. Phys. **12**, 19 (1947).
43. V. H. DIBELER and J. A. WALKER. J. Opt. Soc. Am. **57**, 1007 (1967).
44. F. A. ELDER, D. VILLARIO, and M. O. INGHRAM. J. Chem. Phys. **43**, 758 (1965).
45. V. H. DIBELER, J. A. WALKER, and SUSAN K. LISTON. J. Res. Natl. Bur. Std. (U.S.) **71A**, 371 (1967).
46. V. H. DIBELER, J. A. WALKER, and H. M. ROSENSTOCK. J. Res. Natl. Bur. Std. (U.S.) **70A**, 459 (1966).
47. B. L. KARBATOV, F. I. VILESOV, and A. N. TERENIN. Soviet Phys.-Doklady, **6**, 490 (1961); Soviet Phys.-Doklady, **6**, 883 (1962). See also ref. 37.
48. D. W. TURNER and M. I. AL-JOBOURY. J. Chem. Phys. **37**, 3007 (1962); J. Chem. Soc. 5141 (1963).
49. R. I. SCHOEN. J. Chem. Phys. **40**, 1830 (1964).
50. A. J. BLAKE and J. W. CARVER. J. Chem. Phys. **47**, 1038 (1967).
51. D. W. TURNER and D. P. MAY. J. Chem. Phys. **45**, 471 (1966); J. Chem. Phys. **46**, 1156 (1967).
52. D. C. FROST, C. A. MCDOWELL, and D. A. S. VROOM. Proc. Roy. Soc. London, **196**, 566 (1967).
53. J. A. R. SAMSON. J. Opt. Soc. Am. **56**, 552 (1966).
54. R. SPOHR and E. VON PUTTKAMER. Z. Naturforsch. **22a**, 705 (1967).
55. J. BERKOWITZ, H. EHRHARDT, and T. TEKAAT. Z. Physik, **200**, 69 (1967).
56. D. W. TURNER. 15th Ann. Conf. Mass Spectrometry and Allied Topics. Denver, Colorado. May, 1967. p. 121.
57. H. D. COHEN and U. FANO. Phys. Rev. **150**, 30 (1966).
58. R. N. ZARE. Lectures at summer school of theoretical physics, University of Colorado. 1968.
59. H. A. BETHE and E. E. SALPETER. *In* Handbuch der Physik. Vol. XXXV. *Edited by* S. F. Flügge. Springer-Verlag, Berlin. 1957. p. 88. See also Lester Lipsky. To be published.
60. S. T. MASON and J. W. COOPER. Phys. Rev. To be published.
61. F. I. VILESOV, M. E. AKOPYAN, S. N. LOPATIN, and V. I. KLEYMENOV. 5th Intern. Conf. Phys. Electronic and Atomic Collisions. Leningrad. July, 1967.
62. D. A. S. VROOM. Thesis (unpublished). University of British Columbia. 1966.
63. R. W. NICHOLLS. J. Quant. Spectry. Radiative Transfer, **2**, 433 (1962).
64. M. E. WACKS. J. Chem. Phys. **41**, 930 (1964).
65. K. WATANABE. J. Chem. Phys. **22**, 1564 (1954).
66. D. L. JUDGE and G. L. WEISSLER. J. Chem. Phys. To be published.
67. F. R. GILMORE. J. Quant. Spectry. Radiative Transfer **5**, 369 (1965).
68. P. J. CHANTRY and G. J. SCHULZ. Phys. Rev. Letters, **12**, 449 (1964).
69. P. H. DOOLITTLE, R. I. SCHOEN, and K. E. SCHUBERT. J. Chem. Phys. To be published.
70. K. D. BEYER and K. H. WELGE. Z. Naturforsch. **19a**, 19 (1964).
71. L. M. BRANSCOMB. Ann. Geophys. **20**, 88 (1964).
72. L. M. BRANSCOMB, S. J. SMITH, and G. TISONE. J. Chem. Phys. **43**, 2906 (1965).
73. S. J. SMITH. 4th Intern. Conf. Ionization Phenomena Gases. Uppsala. 1959. p. 219.
74. L. M. BRANSCOMB. Phys. Rev. **148**, 11 (1966).
75. S. B. WOO, E. C. BEATY, and L. M. BRANSCOMB. Bull. Am. Phys. Soc. **12**, 237 (1967).
76. M. W. SIEGEL and J. L. HALL. J. Chem. Phys. **48**, 943 (1968).
77. J. COOPER and R. N. ZARE. J. Chem. Phys. **48**, 942 (1968).
78. F. C. FEHSENFELD, A. L. SCHMELTEKOPF, H. I. SCHIFF, and E. E. FERGUSON. Planetary Space Sci. **15**, 373 (1967).

Comments and Summary

COMMENTS BY J. R. PETERSON[1]

McElroy asked for evidence to support his use of the ratio $N^+/N_2^+ \sim 0.28$ given by Rapp and Englander-Golden (unpublished?) from their electron-impact ionization work. I made measurements (1) on e + N_2 using a crossed beam arrangement and could measure directly the ratio $[N^+(+2N_2^{2+})]/N_2^+$. The absolute values of the cross sections had 20% uncertainties, but the relative values are better. The ratio is about 0.26 at 50 eV, reaches 0.30 at 100 eV, and gradually decreases to 0.25 at 500 eV, substantiating McElroy's choice. The ratio at high energy probably is the same as for photoionization.

1. J. R. PETERSON. *In* Atomic collision processes. *Edited by* M. R. C. McDowell. North Holland Publ. Co., Amsterdam, 1964. p. 465.

[1]Address: Stanford Research Institute, Menlo Park, California.

SUMMARY AND REMARKS BY CHAIRMAN, MICHAEL B. MCELROY

Despite Schoen's disclaimer, it would appear that, for N_2 and O_2 at least, the laboratory data on total photoabsorption and total photoionization cross-sections are adequate for aeronomical applications. The state of the art in aeronomy has not yet reached the point where inaccuracies of about 30% can be considered as bothersome. The situation with regard to dissociative photoionization is less satisfactory.

It is thought that the reaction

$$h\nu + N_2 \rightarrow N^+ + N + e$$

is the major source of atmospheric N^+. The ion has been observed mass-spectrometrically and is an important component of the ionosphere in the vicinity of the *F* peak where it accounts for

Can. J. Chem. Downloaded from www.nrcresearchpress.com by 210.87.254.42 on 09/05/12
For personal use only.

40. F. I. VILESOV. Usp. Fiz. Nauk. **81**, 669 (1963).
41. C. E. BERRY. Phys. Rev. **78**, 597 (1958). A. W. WASHBURN and C. E. BERRY. Phys. Rev. **70**, 559 (1946).
42. N. D. COGGESHALL. J. Chem. Phys. **12**, 19 (1947).
43. V. H. DIBELER and J. A. WALKER. J. Opt. Soc. Am. **57**, 1007 (1967).
44. F. A. ELDER, D. VILLARIO, and M. O. INGHRAM. J. Chem. Phys. **43**, 758 (1965).
45. V. H. DIBELER, J. A. WALKER, and SUSAN K. LISTON. J. Res. Natl. Bur. Std. (U.S.) **71A**, 371 (1967).
46. V. H. DIBELER, J. A. WALKER, and H. M. ROSENSTOCK. J. Res. Natl. Bur. Std. (U.S.) **70A**, 459 (1966).
47. B. L. KARBATOV, F. I. VILESOV, and A. N. TERENIN. Soviet Phys.-Doklady, **6**, 490 (1961); Soviet Phys.-Doklady, **6**, 883 (1962). See also ref. 37.
48. D. W. TURNER and M. I. AL-JOBOURY. J. Chem. Phys. **37**, 3007 (1962); J. Chem. Soc. 5141 (1963).
49. R. I. SCHOEN. J. Chem. Phys. **40**, 1830 (1964).
50. A. J. BLAKE and J. W. CARVER. J. Chem. Phys. **47**, 1038 (1967).
51. D. W. TURNER and D. P. MAY. J. Chem. Phys. **45**, 471 (1966); J. Chem. Phys. **46**, 1156 (1967).
52. D. C. FROST, C. A. MCDOWELL, and D. A. S. VROOM. Proc. Roy. Soc. London, **196**, 566 (1967).
53. J. A. R. SAMSON. J. Opt. Soc. Am. **56**, 552 (1966).
54. R. SPOHR and E. VON PUTTKAMER. Z. Naturforsch. **22a**, 705 (1967).
55. J. BERKOWITZ, H. EHRHARDT, and T. TEKAAT. Z. Physik, **200**, 69 (1967).
56. D. W. TURNER. 15th Ann. Conf. Mass Spectrometry and Allied Topics. Denver, Colorado. May, 1967. p. 121.
57. H. D. COHEN and U. FANO. Phys. Rev. **150**, 30 (1966).
58. R. N. ZARE. Lectures at summer school of theoretical physics, University of Colorado. 1968.
59. H. A. BETHE and E. E. SALPETER. *In* Handbuch der Physik. Vol. XXXV. *Edited by* S. F. Flügge. Springer-Verlag, Berlin. 1957. p. 88. See also Lester Lipsky. To be published.
60. S. T. MASON and J. W. COOPER. Phys. Rev. To be published.
61. F. I. VILESOV, M. E. AKOPYAN, S. N. LOPATIN, and V. I. KLEYMENOV. 5th Intern. Conf. Phys. Electronic and Atomic Collisions. Leningrad. July, 1967.
62. D. A. S. VROOM. Thesis (unpublished). University of British Columbia. 1966.
63. R. W. NICHOLLS. J. Quant. Spectry. Radiative Transfer, **2**, 433 (1962).
64. M. E. WACKS. J. Chem. Phys. **41**, 930 (1964).
65. K. WATANABE. J. Chem. Phys. **22**, 1564 (1954).
66. D. L. JUDGE and G. L. WEISSLER. J. Chem. Phys. To be published.
67. F. R. GILMORE. J. Quant. Spectry. Radiative Transfer **5**, 369 (1965).
68. P. J. CHANTRY and G. J. SCHULZ. Phys. Rev. Letters, **12**, 449 (1964).
69. P. H. DOOLITTLE, R. I. SCHOEN, and K. E. SCHUBERT. J. Chem. Phys. To be published.
70. K. D. BEYER and K. H. WELGE. Z. Naturforsch. **19a**, 19 (1964).
71. L. M. BRANSCOMB. Ann. Geophys. **20**, 88 (1964).
72. L. M. BRANSCOMB, S. J. SMITH, and G. TISONE. J. Chem. Phys. **43**, 2906 (1965).
73. S. J. SMITH. 4th Intern. Conf. Ionization Phenomena Gases. Uppsala. 1959. p. 219.
74. L. M. BRANSCOMB. Phys. Rev. **148**, 11 (1966).
75. S. B. WOO, E. C. BEATY, and L. M. BRANSCOMB. Bull. Am. Phys. Soc. **12**, 237 (1967).
76. M. W. SIEGEL and J. L. HALL. J. Chem. Phys. **48**, 943 (1968).
77. J. COOPER and R. N. ZARE. J. Chem. Phys. **48**, 942 (1968).
78. F. C. FEHSENFELD, A. L. SCHMELTEKOPF, H. I. SCHIFF, and E. E. FERGUSON. Planetary Space Sci. **15**, 373 (1967).

Comments and Summary

COMMENTS BY J. R. PETERSON[1]

McElroy asked for evidence to support his use of the ratio $N^+/N_2^+ \sim 0.28$ given by Rapp and Englander-Golden (unpublished?) from their electron-impact ionization work. I made measurements (1) on e + N_2 using a crossed beam arrangement and could measure directly the ratio $[N^+(+2N_2^{2+})]/N_2^+$. The absolute values of the cross sections had 20% uncertainties, but the relative values are better. The ratio is about 0.26 at 50 eV, reaches 0.30 at 100 eV, and gradually decreases to 0.25 at 500 eV, substantiating McElroy's choice. The ratio at high energy probably is the same as for photoionization.

1. J. R. PETERSON. *In* Atomic collision processes. *Edited by* M. R. C. McDowell. North Holland Publ. Co., Amsterdam, 1964. p. 465.

[1]Address: Stanford Research Institute, Menlo Park, California.

SUMMARY AND REMARKS BY CHAIRMAN, MICHAEL B. MCELROY

Despite Schoen's disclaimer, it would appear that, for N_2 and O_2 at least, the laboratory data on total photoabsorption and total photoionization cross-sections are adequate for aeronomical applications. The state of the art in aeronomy has not yet reached the point where inaccuracies of about 30% can be considered as bothersome. The situation with regard to dissociative photoionization is less satisfactory.

It is thought that the reaction

$$h\nu + N_2 \rightarrow N^+ + N + e$$

is the major source of atmospheric N^+. The ion has been observed mass-spectrometrically and is an important component of the ionosphere in the vicinity of the *F* peak where it accounts for

Can. J. Chem. Downloaded from www.nrcresearchpress.com by 210.87.254.40 on 09/05/12
For personal use only.

perhaps as much as 10% of the total ion density. In order to account for the observations I argued some time ago (2) that below 400 Å approximately 30% of all photoionization events in N_2 should be dissociative. This number seemed reasonable at the time. It was suggested by laboratory studies of electron impact ionization (3). It is not, however, compatible with the data discussed by Schoen. As he points out, serious experimental difficulties must be overcome before we can attach any confidence to the laboratory data. Until the position improves the aeronomer must grit his teeth and wait. Maybe the present theory of atmospheric N^+ is adequate. On the other hand there may be an important unidentified source of N^+. One possible such source not included in present theories is the reaction

$$O_2^+ + N(^2D) \rightarrow O_2 + N^+$$

Unpublished calculations by the writer suggest that this reaction may be competitive with dissociative ionization at higher altitudes.

The ability to study individual paths for photoionization processes represents an important advance in recent years. The data are invaluable not only for interpretation of dayglow emissions such as the first negative and Meinel bands of N_2^+, but are useful also for in-depth studies of the atmospheric heat budget. These studies are feasible with current data on electron collision processes. The energy of the photoelectron, which carries a major fraction of the incident photon energy, depends of course on the degree of internal excitation of the photoion.

Finally, I should draw attention to the need for data on photoabsorption by metastable species, especially long lived metastables such as $O_2(^1\Delta)$ and $N(^2D)$. Hunten and McElroy (4) have suggested that photoionization of the former molecule is an important source of O_2^+ in the D region. It can be ionized by relatively long wavelength radiation which penetrates deep into the atmosphere at selected frequencies where the O_2 absorption cross-section is small (in the so-called windows).

2. M. B. McElroy. Planetary Space Sci. **15**, 457 (1967).
3. P. Gordon and D. Rapp. Lockheed Missiles and Space Company Report No. LMSC 6-74-64-12. 1965.
4. D. M. Hunten and M. B. McElroy. J. Geophys. Res. **73**, 2421 (1968).

Can. J. Chem. Downloaded from www.nrcresearchpress.com by 210.87.254.40 on 09/05/12
For personal use only.

Can. J. Chem. Downloaded from www.nrcresearchpress.com by 210.87.254.40 on 09/05/12
For personal use only.

Neutral reactions involving oxygen and nitrogen

H. I. SCHIFF
Centre for Research in Experimental Space Science, York University, Downsview, Ontario

Received December 24, 1968

Methods of production and detection of reactive species of oxygen and nitrogen are discussed briefly. Kinetic data for reactions of these species which have aeronomic interest are reviewed. New data, obtained during the past 4 years are critically compared, and recommendations made for "best" values where possible. An attempt is also made to delineate important areas where additional work is needed to meet the demands of atmospheric modelling.

Canadian Journal of Chemistry, 47, 1903 (1969)

At the Berkeley I.A.G.A. symposium the author was privileged to review (1) the status of the laboratory work on oxygen and nitrogen as of August 1963. It appeared then, that with a few notable exceptions, rate constants for ground state atoms and molecules were known with sufficient accuracy for most aeronomic calculations at 300 °K. Temperature coefficients (or activation energies) were, however, largely lacking. Fortunately, many of the reactions of aeronomic interest have rate constants sufficiently close to collision frequencies that their activation energies could not exceed one kcal mole^{-1}. Two important exceptions were the reactions $O + O_3 \rightarrow 2O_2$ and $N + O_2 \rightarrow NO + O$. Also very little was known at that time about the reaction of metastable atoms, or of molecules which possess appreciable quantities of internal energy. But ground based (2) and rocket borne (2, 3) measurements have shown that considerable concentrations of these excited species are present in the chemosphere. A great deal of laboratory work on both these aspects, temperature dependence, and excited state reactions, has ensued. It is the intention of this paper to review some of the more significant recent developments.

A wide variety of methods has been used, both in the production and in the measurement of reactive species. Electrical discharge sources have enjoyed the widest popularity. Oxygen atoms have been produced directly by discharges through O_2 and indirectly by the now familiar titration reaction

$$N + NO \rightarrow N_2 + O$$

Such discharges also produce an embarassing richness of electronically and vibrationally excited molecules, and it is often difficult to account for their influence on the reaction under study. Discharges through Ar containing only a small amount of O_2 have been used in the hope that virtually complete dissociation will be achieved with no opportunity, therefore, for the formation of excited molecules. This assumption has yet to be unequivocally justified, and the absence of metastable Ar and O atoms demonstrated. Small concentrations of O atoms have been obtained by the total thermal decomposition of O_3 in a furnace (4, 5). Since the temperature used was just sufficient to break the bond, there should be no energy available to excite the products. However, verification should be sought that excited O_2 is not formed by surface-catalyzed recombination on the hot furnace walls. A recent modification of this method (6) consists of the partial decomposition of N_2O on a "Nernst glower" filament. N_2O is relatively inert to O atoms attack, as is the other pyrolysis product, N_2. In addition, any vibrational excitation of either N_2O or N_2 on the filament is known to be rapidly deactivated by the excess N_2O which acts as a carrier.

Photolysis provides a very clean source of excited atoms and molecules, and in many cases the choice of wavelength permits an exact knowledge of their excitation. This method is being exploited successfully to study radiative lifetimes and quenching cross sections. Unfortunately, the concentrations achievable are too low to provide much chemical kinetic data on the reactions. For example, quenching rates of $O(^1D)$ and $O(^1S)$ by N_2, NO, CO_2 etc. can be studied accurately (7, 8) but the nature of the products is not as yet known. Photolysis can be continued for times which are long compared with the half-lives of the reactions concerned in order that sufficient products can be accumulated to permit analysis. Kinetic data must then be inferred from an assumed mechanism which reduces its reliability. One need only

Can. J. Chem. Downloaded from www.nrcresearchpress.com by 210.87.254.40 on 09/05/12
For personal use only.

quote the example of the controversy which still exists over the photolysis of CO_2 (9).

Shock tube techniques can, in principle, provide kinetic data which, in combination with other methods at lower temperatures, provide more than a sufficient temperature range to span all planetary atmospheric conditions. Unfortunately, the method is largely restricted to studies of the rates of decomposition of diatomic and triatomic molecules which are of no direct interest in aeronomy. What are of interest, of course, are the rates of the reverse processes, viz. the recombination reactions. These are commonly calculated by combination of the dissociation rates with the equilibrium constant for the process. However, it is not clearly established that the use of equilibrium thermodynamics is justified in the time scales involved behind a shock front, particularly whether vibrational equilibrium is established. Recent theoretical work (10) indicated that the rate constant for dissociation could increase by as much as a factor of 3 between 1 and 100% dissociation. Activation energies for dissociation of diatomic molecules are consistently below the bond strengths. Also, temperature dependences of the dissociation are usually expressed in the form

$$k_d = AT^{-n} \exp(-D_0/RT)$$

where D_0 is the dissociation energy, and the equilibrium constant in the form

$$k_d/k_r = B \exp(-D_0/RT)$$

which ignores the change in entropy of the reaction with temperature. Combination of these two expressions gives, of course, an $A'T^{-n}$ dependence for k_r which is, therefore, open to question.

Flames and explosion limits also provide information about atom reactions at relatively high temperatures. Their drawback is that so many coupled reactions occur simultaneously that it is difficult to extract reliable rate constants for individual steps.

Methods for detecting and measuring atom concentrations have become even more diverse than methods of producing them. Titration techniques — NO for N atoms, and NO_2 for H and O atoms — have been widely used. Their validity, formerly challenged, now appears to be verified, the most direct comparison (11) being made with the very simple, but difficult, technique of isolating a known volume of the gas and measuring the pressure drop due to atom recombination. Care must be taken in using titration reactions for low atom concentrations since their rates will then be small even if the rate constant is large. This condition of low atom concentration will, of course, always obtain near the end point. One way to circumvent this difficulty is to add a large excess of the titrant (e.g. NO_2), thereby increasing the rate, and determining the amount consumed, rather than using the chemiluminescent end-point.

The chemiluminescent reactions, NO + O, N + N, N + O, H + NO have been used to follow atom reactions. Although the intensities of the glows resulting from these reactions have been shown to be proportional to atom concentrations, the proportionality factors may depend on the pressure and the nature of the other gases present.

Calorimetric probes covered with catalytic surfaces for atom recombination have been used successfully for following atom reactions when consideration is given to possible perturbations of the gas stream resulting from the removal of the atoms and the heat released. Their main drawback is their low level of specificity, since they may also respond to other energetic species. In fact, if the atom concentration is measured by another method (12), or is known to be zero (13), such probes can be used to study the kinetics of vibrationally (12) or electronically (13) excited molecules.

Absorption spectroscopy has been used in flash photolysis and in flow systems for vibrationally excited molecules (14) and free radicals (15). Resonance absorption by atoms occurs at energies close to the vacuum ultraviolet (u.v.) region and to date has only been used for ground state atoms (16). Emission spectroscopy has been used to study electronically excited molecules, but most of the work has been concerned with the physical processes of quenching and energy exchange rather than with the chemical reactions they undergo. Photoionization has also been used (17) to detect $O_2(^1\Delta_g)$ molecules.

Electron spin resonance (e.s.r.) has been finding increasing use in the study of atom reactions. The main difficulty with this technique appears to be that of calibration. In the most recent work this difficulty appears to be circumvented (18).

Mass spectrometry has the great advantage that reactants and products can, in principle, all

Can. J. Chem. Downloaded from www.nrcresearchpress.com by 210.87.254.40 on 09/05/12
For personal use only.

be identified. Difficulties are encountered with low sensitivities for free radicals and atoms resulting from deactivation by collisions with the walls of the ion chamber, and specially designed inlet systems and ion sources are required. Another difficulty is the overlapping of fragment ions with the same mass number. This difficulty can be overcome by using doubly charged ions (19) or by combining the mass spectrometer with titration (20) or chemiluminescent (21) techniques. Although in principle it is possible to identify excited molecules by their ionization potentials, in practice this is a difficult procedure.

Following this brief summary of methods of production and detection of reactive species, an attempt will be made to summarize some of the results obtained during the past 4 years. Heats of reaction are shown after each equation in kcal $mole^{-1}$, with the value in eV in brackets. These are calculated from JANAF tables and are at 1 atm and 298.15 °K, since this is the temperature at which the thermochemical data is most reliable, and the one at which many of the reactions discussed have been measured. Rate constants are given in particles cm^{-3} concentration units. Temperature coefficients are given in the Arrhenius form for second order reactions, $k = A \exp(-E/RT)$ where E is in kcal $mole^{-1}$, and either in this form or in the form $k = AT^{-n}$ for third order reactions. Some attempt will be made to suggest a "best" value. This task is often difficult because the rate constants obtained by various authors may differ by several hundred % even though the errors claimed by each are usually much less than 25%. This is largely the result of the time-honored confusion between precision and accuracy. It is relatively easy to evaluate the reproducibility of a set of experiments but much more difficult to assess the absolute errors in atom concentration measurements, flow rates, mixing coefficients, diffusion corrections, wall recombination, etc.

This review of aeronomically interesting reactions is probably not comprehensive. Readers are referred to the tabulation of rate data by Schofield (22), to the monographs by Wright and Winkler (24) for nitrogen reactions, and by Johnson (23) on oxygen reactions.

Reactions

[1] $O + O + M \rightarrow O_2 + M + 119.118(5.1653)$

Recent measurements by Campbell and Thrush (25) agree with earlier ones by Morgan and Schiff (26) at 300 °K for M = N_2 and He but not for M = Ar where they found $k_1(\mathrm{Ar}) = 1.7 \times 10^{-33}$ while the earlier work gave $k_1(\mathrm{Ar}) = 0.9 \times 10^{-33}$. Reeves *et al.* reported (27) a value of 2.8×10^{-33} for this third body but neglected to correct for wall recombination. Morgan and Schiff (26) showed that this would have lowered their value to somewhere between 0.8 and 1.1×10^{-33}. This discrepancy in the case of Ar is unfortunate since it is the only third body used in common in both the low temperature and the shock tube studies.

The most careful and comprehensive shock tube study appears to be that of Wray (28). The rate of O_2 dissociation was investigated from 5 000–18 000 °K and the recombination was studied separately from 1500–3000 °K following complete dissociation of O_3 by the shock. Comparison of these two sets of experiments led to the conclusion that the use of the thermodynamic equilibrium constant was justified in this case. A pre-exponential temperature dependence, T^{-1} was used for the equilibrium constant from 300–3500 °K and a $T^{\frac{1}{2}}$ dependence above 3500 °K. This then gave a $T^{-\frac{3}{2}}$ dependence for the recombination rate at the low temperature range of his measurements which extrapolates to $k = 0.48 \times 10^{-33}$ for M = Ar at 300 °K in satisfactory agreement with Morgan and Schiff (26). However, similar treatment of other shock tube data gives for the exponent, n in the T^{-n} form, 2.5 for O_2 (29) and 3.0 for M = O (30). There is also wide disagreement among shock tube workers regarding relative efficiencies of various third bodies. The temperature dependence should not, however, depend on the nature of the third body if recombination occurs via the very probable mechanism

$$O + O \rightleftarrows O_2^*$$

$$O_2^* + M \rightarrow + M$$

In fact Benson and Fueno (31), in a theoretical treatment of this reaction based on the assumption that M removes vibrational quanta from O_2^* stepwise in amounts $\approx kT$, conclude that the temperature dependence for all M's should be T^{-1}, and claim that all experimental work can be reconciled with this value, although it is difficult to see how Byron's results (29) can be fitted to this conclusion. The most recent shock tube work (32) with M = O_2 shows such a large temperature dependence for the recombination between 3000–3800 °K that it cannot be taken seriously.

Can. J. Chem. Downloaded from www.nrcresearchpress.com by 210.87.254.40 on 09/05/12
For personal use only.

From studies at 190–350 °K, Campbell and Thrush (25) find a T^{-3} dependence for M = N_2, He, and Ar. They conclude that the exponential form $k = 1.5 \times 10^{-34} \exp(1.4 \pm 0.35/RT)$ for M = Ar permits a better fit with shock tube results. Wray (28) also suggested that "n" in the power representation may change with temperature.

Johnson (23) has made a very careful statistical analysis of all available data on the recombination. He concludes that the shock tube data, and the low temperature data can be represented, within the very large scatter of the shock tube results by the expression

$$k_1(\mathrm{Ar}) = 3.6 \times 10^{-31} T^{-1} \exp(-0.34/RT)$$

for M = Ar over the temperature range, 300–15 000 °K. However, for M = O_2, the results of shock tube and low temperature studies cannot be reconciled, so that the corresponding expression

$$k_1(\mathrm{O_2}) = 3.8 \times 10^{-30} T^{-1} \exp(-0.34/RT)$$

was recommended only over the temperature range 1000–1800 °K. It is obvious that more work is required on the effect of temperature on this reaction.

Also in need of clarification is the relative efficiency of O atoms. There is agreement among shock tube workers that it is very high, as much as 50:18:1 for O:O_2:Ar. But Wray points out that this ratio decreases with decreasing temperature, which is also indicated by the failure of room temperature measurements to detect any unusually high efficiencies for O atoms as third bodies. This has some importance at high altitudes where this reaction constitutes a major O atom loss process and where O becomes a major atmospheric constituent.

[2] $O + O_2 + M \rightarrow O_3 + M + 25.45\ (1.103)$

This is the principal reaction responsible for recombination of O atoms below 100 km. When followed by

[3] $$O + O_3 \rightarrow 2O_2$$

the net effect is identical to reaction [1].

Studies of this reaction using discharged O_2 as the atom source have led to rate constants which differ from one another by amounts which are much greater than the uncertainties in the individual measurements. The values were also smaller than those determined indirectly from studies of ozone decomposition. During the past 4 years it has become apparent that these discrepancies were mainly due to two causes:

(*i*) The presence of hydrogenous impurities in the discharged gas which can give rise to H and OH, both of which can catalyze the recombination by the fast reactions

$$H + O_3 \rightarrow OH + O_2$$
$$O + OH \rightarrow O_2 + H$$

The net result of these reactions is kinetically indistinguishable from reaction [3] but occurs with a rate constant some 1000 times larger (33). Moreover the three body reaction (34)

$$H + O_2 + M \rightarrow HO_2 + M$$

is considerably faster than [2] and can feed the chain reactions via the production of OH from

$$HO_2 + O \rightarrow OH + O_2$$

(*ii*) There is now abundant evidence that electrically discharged O_2 contains appreciable quantities of electronically excited O_2 in the $^1\Delta_g$ and $^1\Sigma_g^+$ states which are capable of decomposing O_3.

[5] $$O_2^* + O_3 \rightarrow 2O_2 + O$$

Essentially, reaction [5] reverses the recombination sequence [2] and [3] and results in too low a value for the rate constant of [2]. Mathias and Schiff (35) found that more O_3 could be decomposed than there were O atoms in the discharged O_2, while Kaufman and Kelso (36) found an increase in O atoms when O_3 was added to discharged O_2. These findings not only explain the low values of k_2 found from the earlier discharge studies, but also explain the diversity of results obtained from these studies, since the concentration of electronically excited O_2^* molecules is known to be a sensitive function of gas pressure and purity.

Clyne *et al.* (37) attempted to overcome these problems by discharging argon containing less than 10^{-3} mole % of O_2 although there is some possibility that this method may also produce metastable atoms. They found that the addition of water vapor did not affect the recombination rate which they took as evidence that $O(^1D)$ was not present in their system. This conclusion does not seem to be warranted, however, since it has not been proved that the NO–O glow used to

TABLE I

Relative efficiencies based on Ar = 1

He	N_2	O_2	CO_2	N_2O	CF_4	SF_6	O_3	H_2O	Reference
1.4	1.6	1.7	4.2				4.2		41
1.0	1.4	1.6	3.7	3.7	4.0	8.5	—	15	36
0.68			4.1	3.5					39
		1.1	3.4						5
1.3	1.5	1.7	4.2				4.0		42
1.4	1.6	1.8	3.8				4.0		23

monitor the recombination is applicable to $O(^1D)$ atoms and no account was taken of the possible influence of water vapor on the wall recombination efficiency. They followed [O] by the NO–O glow which was put on an absolute basis by NO_2 titration. The difficulties in the use of this titration for low atom concentrations have been mentioned previously. The value they report for M = Ar is 7.8×10^{-34}.

Kaufman and Kelso (38) decomposed O_3 in a furnace to yield about 0.01% oxygen atoms, which should be free of electronically excited O_2. They followed the recombination by the NO–O glow and obtained at 300 °K, $k_2 = 6.5 \times 10^{-34}$ for M = O_2. Their value for M = Ar of 4×10^{-34} is about half that of the previous workers (37).

Mulcahy and Williams (5) also used thermal decomposition of O_3 as a source of O atoms and the NO–O glow to follow the recombination. Their value of $k_2 = (8.9 \pm 0.9) \times 10^{-34}$ for M = Ar, O_2 is in fair agreement with Kaufman and Kelso and their value of $(7.9 \pm 0.8) \times 10^{-34}$ agrees well with Clyne *et al.* Unfortunately their relative efficiencies for these two third bodies do not agree so well with other workers, as seen in Table I.

Sauer (39, 40) obtained rates for this reaction for pulsed radiolysis studies of CO_2 and N_2O in Ar. They obtained $k_2 = 2.8 \times 10^{-34}$ for M = Ar.

Benson and Axworthy (41) have reviewed the existing data on the thermal decomposition of O_3 and combined it with a new evaluation of the equilibrium constant. Their value for M = O_2 is 3.6×10^{-34}, about half that of Kaufman and Kelso (38). The relative efficiencies shown in Table I are, however, in excellent agreement.

Isotope exchange studies (43, 44) give a rate constant of 1×10^{-12} for exchange and an activation energy (45) of 1.1 ± 0.4.

Klein and Herron (43) ascribe rate constants to the individual steps in the mechanism

$$O + O_2 \underset{B}{\overset{A}{\rightleftarrows}} O_3^* \xrightarrow[(M)]{C} O_3 + M$$

to be $k_A = 1.5 \times 10^{-12}$, $k_B = 1.8 \times 10^{-9}$, $k_C = 7 \times 10^{-13}$. This interpretation has been criticized (41) on the basis that the expected lifetime of O_3^* would more likely correspond to k_B being an order of magnitude larger.

Temperature coefficients obtained by direct studies of this reaction are in good agreement. Clyne *et al.* (37) give an "activation energy" $E_2 = -(1.8 \pm 0.4)$ for M = Ar and $n = (3.4 \pm 0.8)$ in the T^{-n} representation in the range 190–350 °K. Mulcahy and Williams (5) give $E_2 = -(1.7 \pm 0.1)$ and $n = (3.0 \pm 0.2)$ for M = Ar, and $E_2 = -(1.45 \pm 0.14)$ and $n = (2.4 \pm 0.3)$ for M = CO_2 from 213–386 °K. On the other hand, Benson and Axworthy (41) in their review of the indirect value obtained from O_3 decomposition give $E_2 = -0.89$ for M = O_2 near 360 °K. Although the shock tube decomposition study of Jones and Davidson (46) gives $E_2 = -(1.7 \pm 0.3)$, their results are not readily reconciled with the low temperature measurements (37). Johnson has reviewed all existing data on this reaction and recommends

$$k_2 = 1.16 \times 10^{-35} \exp(2.10/RT)$$

for M = Ar with an uncertainty of about 50%.

In summary, it appears that the rate constant at 300 °K is known to within a factor of 2. However, there is a much greater uncertainty in the temperature dependence, or even whether a single analytical form for this dependence can be used over a wide temperature range. Certainly more work should be done between 350 and 1600 °K.

Can. J. Chem. Downloaded from www.nrcresearchpress.com by 210.87.254.40 on 09/05/12
For personal use only.

Can. J. Chem. Downloaded from www.nrcresearchpress.com by 210.87.254.40 on 09/05/12
For personal use only.

[3] $O + O_3 \rightarrow 2O_2 + 93.7$ (4.06)

There is increasing interest in the height distribution of O_3 in our atmosphere. Meteorologists have long used O_3 as an atmospheric tracer to study circulation patterns and have been concerned with its important contribution to the energy balance in the stratosphere. Aeronomists now realize that it is a major source of OH and O_2-($^1\Delta_g$) airglow emissions. Recently it has been shown (47) to be important in the negative ion chemistry of the D region ionosphere.

It is therefore unfortunate that reaction [3], which plays a dominant role in determining atmospheric O_3 composition, has proved to be so elusive to experimental measurement, particularly measurement of its temperature coefficient. Both direct and indirect methods have been used. The indirect method involves thermal decomposition of O_3, which is now conceded to occur via the mechanism

$$[d, 2] \qquad O_3 + M \rightleftarrows O_2 + O + M$$

$$[3] \qquad O + O_3 \rightarrow 2O_2$$

Only k_d and the ratio of $k_d \cdot k_3/k_2$ can be obtained from such measurements. The activation energy of [*d*] completely dominates the temperature dependence of the rate constant ratios, and has not been determined with sufficient accuracy to provide values for $E_3 - E_2$ which are accurate to better than about 2 kcal mole^{-1}. The uncertainty of E_2, noted in the previous section, makes the indirect method of doubtful value in providing reliable values of E_3. The decomposition of O_3 by visible light gives k_2/k_3 ratios directly (42), but unfortunately has been studied only over a small temperature range.

Direct methods in which O atoms are produced from electrical discharge sources are subject to the difficulties of O_3 decomposition by electronically excited O_2, or by H and OH from hydrogenous impurities, discussed above. Even the N–NO titration method cannot be used reliably since the titration reaction produces vibrationally excited $N_2^{\ddagger}$ which has been shown (48) to decompose O_3.

Mathias and Schiff (35) investigated these effects mass spectrometrically and were able to obtain a value of $k_3/k_2 = 1.2 \times 10^{-19}$ at 300 °K. Combination with Mulcahy and Williams' value (5) for k_2 gives $k_3 = 1.06 \times 10^{-14}$ while combination with Kaufman and Kelso's value (36) gives $k_3 = 0.66 \times 10^{-14}$.

Lundell *et al.* (6) have recently measured k_3 directly in a flow system in which O atoms were generated in the absence of energetic molecules by thermal decomposition of N_2O on a hot filament. They obtained a value of $(1.5 \pm 0.1) \times 10^{-14}$ at 300 °K.

Benson and Axworthy in a recent re-review of thermal O_3 decomposition data suggest

$$k_3 = 5.6 \times 10^{-11} \exp(-5.7/RT)$$

This is based on $E_2 = -0.89$. If, however, a value of $E_2 = -1.7$ is used, E_3 is reduced to 4.9. The shock tube data by Davidson and Jones have been interpreted (46) to give $k_3 = 5.7$ but more recent shock tube work suggests this value is too high (49).

Intezarova and Kondratjev (50) have recently reported a study of the thermal decomposition of O_3 in a flow system at atmospheric pressure from 410–500 °K. The authors claim that their data give them k_3/k_2 ratios directly. They combine this ratio with the value of k_2 derived from the O_3 equilibrium constant, $K = k_d/k_2$ and an average value of k_d from previous thermal decomposition studies. It is not obvious to this author, however, just how this average is obtained, or why they did not derive k_d from their own experiments directly. At any rate, their procedure gave $k_3 = (4.8 \pm 1.5) \times 10^{-12} \exp(3.7 \pm 0.3/RT)$. If their k_3/k_2 ratio is combined with the directly determined value of k_2 from Mulcahy and Williams (5) or Clyne *et al.* (37) the activation energy $E_3 = 3.0 \pm 0.4$ while at 300 °K, combination with Kaufman and Kelso's (38) value of k_2 gives $k_3 = 1.5 \times 10^{-14}$, and with Mulcahy and Williams' k_2, gives $k_3 = 2.1 \times 10^{-14}$.

Castellano and Schumachers' value for k_2/k_3, when combined with the expression by Clyne *et al.* (37) for k_2, gives $k_3 = (1.4 \pm 0.3) \times 10^{-12} \exp(-3.0 \pm 0.4/RT)$.

Lundell *et al.* (51) have recently made a direct measurement of this reaction using decomposition of N_2O on a "Nernst" glower to produce ground state atoms in the absence of O_2. For the temperature range 0–70 °C they obtained $k_3 = 3.2 \times 10^{-11} \exp(-4.5/RT)$.

Johnson (23), reviewed all the existing data on this reaction and recommends $k_3 = 2.00 \times 10^{-11} \exp(-4.79/RT)$.

[4] $O(^1D) + O_3 \rightarrow 2O_2 + 138.8$ (6.02)

The first evidence for this reaction comes from O_3 photolysis. At wavelengths greater than that required to produce $O(^1D)$, the O_3 quantum yield

Can. J. Chem. Downloaded from www.nrcresearchpress.com by 210.87.254.40 on 09/05/12
For personal use only.

is strictly 2 but at shorter wavelengths quantum yields as high as 16 have been reported. In flash photolysis McGrath and Norrish (52) observed vibrationally excited ground state $O_2^{\ddagger}$ molecules and postulated these and $O(^1D)$ to be the chain carriers

[4a] $O(^1D) + O_3 \rightarrow O_2 + O_2^{\ddagger}\ (v \geqslant 17)$

[4b] $O_2^{\ddagger} + O_3 \rightarrow O_2 + O_2 + O(^1D)$

To make reaction [4b] exoergic requires $O_2^{\ddagger}$ to have $v \geqslant 17$, and the sharp cut-off above the 17th level was taken as evidence for this mechanism. A similar chain could of course, be written for $O(^3P)$ and $O_2^{\ddagger}$ ($v \geqslant 5$) but this apparently does not happen since it is well established that one ^3P atom leads to the consumption of only one O_3 molecule (40, 53).

Bair and his co-workers (54–56), however, found a continuous vibrational distribution of the $O_2^{\ddagger}$ product and observed levels up to $v = 23$ with no sharp discontinuity at $v = 17$. They also found the relaxation of the vibrational distribution to be consistent with a single quantum ladder process and further argued that the population at $v \geqslant 17$ was always too small to account for any appreciable chain decomposition of O_3.

Norrish and Wayne (57) photolyzed O_3 at 2537 Å in the presence of other gases. They found the O_3 quantum yield to increase linearly to 16.7 with O_3 pressure, to decrease to 2 with increased partial pressures of N_2 or CO_2, and to approach zero with increasing O_2 partial pressure. To explain these results they proposed the mechanism

$$O_3 + h\nu \rightarrow O_2^* + O^*$$

$$O_2^* + O_3 \rightarrow 2O_2 + O$$

[4a] $$O^* + O_3 \rightarrow O_2^{**} + O_2$$

[4b] $$O_2^{**} + O_3 \rightarrow 2O_2 + O^*$$

$$O + O_2 + M \rightarrow O_3 + M$$

$$O_2^{**} + \text{wall} \rightarrow O_2$$

where O^* represents $O(^1D)$, O_2^* an excited molecule which can dissociate O_3 but cannot produce an O^*, and O_2^{**} one that can, and is therefore a chain carrier. They still believe, however, that O_2^{**} is a ground state $^3\Sigma_g^-$ molecule with $v \geqslant 17$.

McGrath and McGarvey (58) criticize this conclusion on the basis that it would require an unreasonable amount of energy to be imparted to the O_3^{**} molecule in reaction [4a] while [4b] would require a complex means of spin conversion. They feel it more likely that O_3^{**} is an electronically excited molecule, either in the $^3\Sigma_u^-$ or $^3\Sigma_u^+$ states, and favor the latter because of its greater lifetime.

McKenney and Laidler (59), from theoretical considerations of the potential energy surfaces, prefer the $^3\Sigma_u^-$ state even though reaction [4a] is then endoergic by about 2 kcal mole^{-1}. Molecules in this state should then rapidly radiate in the allowed Schumann–Runge system but the Franck–Condon factors are such that the lower state would be vibrationally excited and could then partake in the Norrish chain. Volman *et al.* (60) originally favored the transition of $^3\Sigma_u^-$ to $^1\Delta_g$ or $^1\Sigma_g^+$ states but chains would then not be possible on energetic grounds. Volman (61) points out that the $^3\Sigma_u^-$ state should also predissociate via the repulsive $^3\Pi$ state to form two $O(^3P)$ atoms. Benson (62) points out that if $^3\Sigma_u^-$ molecules were involved, fluorescence should be observed at about 3400 Å. Since it is not, he favors the $^3\Sigma_u^+$ state.

De More and Raper (63) studied the photolysis in the condensed phase and found that $O(^1D)$ atoms are produced at wavelengths shorter than 3100 Å but in the 3100–3400 Å region both $O(^1D)$ and $O(^3P)$ are formed. They confirm the increased quantum yields at these wavelengths and conclude that $^3\Sigma_u^-$ molecules are the chain carriers since no temperature dependence was observed and the reaction involving $^3\Sigma_u^-$ would require 2 kcal mole^{-1} activation energy.

McNesby and Okabe (64) showed that, at $\lambda \leqslant 2340$ Å, $O(^1S)$ can also be formed and give rise to $^3\Sigma_u^-$ with vibrational excitation.

One might also ask whether $O(^3P)$ atoms could react with O_3 to form $O_2(^1\Sigma_g^+)$ or $O_2(^1\Delta_g)$ which could then be a significant source of airglow emission from these species. However, both these species are known to decompose O_3 and no evidence for chain reactions has been obtained for $O(^3P)$ atoms.

Warneck (65), in a quantum yield study, concluded that $O(^1D)$ reacts with O_3 8 times faster than does $O(^3P)$. However, this conclusion does not appear to be warranted since it is based on the unlikely assumption that the rate of formation of O_3 from $O + O_2 + M$ is the same for both types of atoms. In fact DeMore and Raper (63) showed that O_2 quenched $O(^1D)$ rather than reacted with it.

Snelling and Bair (56) studied the effect of

Can. J. Chem. Downloaded from www.nrcresearchpress.com by 210.87.254.40 on 09/05/12
For personal use only.

added inert gases to the flash photolysis of O_3 and conclude that $k_4 = (3 \pm 1.5) \times 10^{-10}$, i.e. the reaction occurs at virtually every collision. This would be consistent with the finding of DeMore and Raper that the temperature coefficient is low but not with those of Sullivan and Warneck (66) who give $E_4 = 2.4 \pm 1$. However, the latter result must be viewed with suspicion since the ratios of k_4 to k_q, the quenching rate constant of $O(^1D)$ by O_2, obtained in this work, combined with currently acceptable (4) values of k_2 gives $k_4 \geqslant 10^{-8}$!

This discussion has probably emphasized the need for more definitive experiments on the rates and products of this reaction.

[5] $O_2^* + O_3 \rightarrow O_2 + O_2 + O$

In the foregoing sections we have seen that both photolysis and electrical discharge studies indicated the occurrence of this reaction. Wayne (67) pointed out that the occurrence of these reactions would lead to a quantum yield of 4 for O_3 decomposition at zero pressure in agreement with observations. Schiff and Megill (68) pointed out some possible aeronomic implications of these reactions. Although they might affect the rate of energy release and time for attainment of O_3 equilibrium, Hunt (69) has shown that they do not influence the O_3 height profile. Bader and Ogryzlo (13) found that the addition of O_3 decreased the intensity of the $^3\Sigma_g^- \leftarrow {}^3\Sigma_g^+$ emission but had a much smaller effect on the $^3\Sigma_g^- \leftarrow {}^1\Delta$ emission.

March *et al.* (70) studied the rate of the reaction with $O_2(^1\Sigma_g^+)$ and obtained $k_5(^1\Sigma_g^+) = 6 \times 10^{-13}$. They also made a rough estimate of the rate constant with $O_2(^1\Delta_g)$ of about 4×10^{-14}.

McNeal and Cook (17) followed the decrease in $O_2(^1\Delta_g)$ by photoionization as a function of added O_3 and obtained $k_5(^1\Delta_g) = (2.5 \pm 0.5) \times 10^{-15}$. They did not specifically rule out the possibility of photoionization of vibrationally excited O_2 with an equivalent amount of energy, although photolysis studies indicate that either vibrationally excited O_2 does not decompose O_3 or else it is very rapidly relaxed.

[6a] $O_2(^1\Delta_g) + O_2(^1\Delta_g) \rightarrow (O_4)^* \rightarrow 2O_2(^3\Sigma_g^-) + h\nu$ *(6340 and 7640 Å)*

[6b] $O_2(^1\Delta_g) + O_2(^1\Delta_g) \rightarrow O_2(^1\Sigma_g^+) + O_2(^3\Sigma_g^-)$

These very interesting reactions were first reported in the gas phase by Bader and Ogryzlo (13) and have received considerable attention subsequently. The first of these represent a pooling of the energies of the two $(^1\Delta_g)$ molecules to give out a single light quantum. The 6340 Å radiation corresponds to both $O_2(^3\Sigma_g^-)$ molecules being formed in their ground vibrational levels, while the 7640 Å radiation leaves one of the $^3\Sigma_g^-$ molecules in the first vibrational level. The O_4 intermediate has no binding energy and probably has a very transient existence although its radiative lifetime has been estimated (71) to be 3 s. These authors (72) measured the $(^1\Delta_g)$ concentration by means of an isothermal calorimetric probe and found (7) $k_{6a} = 2.5 \times 10^{-22}$. Falik and Mahan (73) measured the $(^1\Delta_g)$ concentration by e.s.r. and obtained $k_{6a} = 5 \pm 1 \times 10^{-23}$ which agrees reasonably well in view of the analytical techniques used.

The second reaction *[6b]* represents an alternative energy pooling process in which one of the O_2 molecules is promoted to the next higher electronic state while the other is deactivated to the ground state. The reaction represents a violation of the spin conservation rule. Young and Black (71) give as the rate constant $k_{6b} = 3 \times 10^{-14 \pm 0.5}$. If it were indeed as high as this it would have considerable aeronomic importance in explaining the persistance of the emission from O_2 $(^1\Sigma_g^+)$ in the airglow, since the radiative lifetime of $^1\Delta_g$ is some 10^3 times longer than that of $^1\Sigma_g^+$. However, Arnold and Ogryzlo (74) have shown fairly convincingly that their rate constant of $k_{6b} = 2.2 \times 10^{-18}$ is more likely to be correct which then renders this reaction too slow to provide a significant source of $O_2(^1\Sigma_g^+)$ molecules in the atmosphere.

[7] $O + N + M \rightarrow NO + M + 151.0$ *(6.55)*

Kretschmer and Petersen (75) followed this reaction in a flow system. They discharged a mixture of 5% O_2 in N_2, determined [O] quantitatively with a Wrede gauge, and followed the reaction by the accompanying NO* emission intensity. Their rate constant $k_7 = 9 \times 10^{-33}$ for $M = N_2$ at 350 °K is considerably higher than previous measurements (76). An interesting sidelight of this work was the evidence presented that at short times after the N_2 discharge, when the N_2 vibrational temperature was high, the dissociation reaction $N_2^{\ddagger} + O_2 \rightarrow N_2 + O + O$ occurred. The same work, however, gave a value

Can. J. Chem. Downloaded from www.nrcresearchpress.com by 210.87.254.40 on 09/05/12
For personal use only.

of $k = 8 \times 10^{-17}$ for the reaction $O + N_2 \rightarrow NO$ which is about 2 orders of magnitude lower than the values reported by other workers.

Campbell and Thrush (77) followed the reaction by simultaneously monitoring the intensities of the Lewis–Raleigh and O–NO afterglows in a system in which N atoms were partially titrated with NO. They obtained $k_7 = 1.1 \times 10^{-32}$, for $M = N_2$ at 300 °K in excellent agreement with the value above. They find only a small temperature dependence corresponding to $E_7 = -(0.3 \pm 0.1)$ or $n = 0.5 \pm 0.2$, the smallest coefficient observed for any three body recombination reaction. The efficiencies for Ar and He relative to N_2 were found to be 0.76 and 0.35 respectively.

[8] $O + NO + M \rightarrow NO_2 + M + 73.23$ (3.175)

Recent measurements using quite different techniques to follow the reaction agree remarkably well. Westenberg and de Haas (18) used e.s.r. to follow [O] and obtained 8.1×10^{-32} for $M = O_2$. Klein and Herron (78) followed the reaction mass spectrometrically and obtained $k_8 = 1.1 \times 10^{-31}$ for $M = N_2$ at 300 °K. They find a temperature dependence over the range 307–505 °K corresponding to $E_8 = -(1.9 \pm 0.1)$ while Clyne and Thrush (79) report $E_8 = -(1.8 \pm 0.4)$ from 212–315 °K. They report relative efficiencies of $N_2:O_2:Ar:He = 1.0:0.87:0.87:0.58$, in agreement with previous measurements. On the basis of these results Kaufman (80) recommended the use of a $T^{-(2.5 \pm 0.3)}$ dependence but the power representation does not fit the different temperature ranges used by these workers as well as does the exponential form.

Klein and Herron (78) also studied the isotopic exchange reaction from which they obtained an exchange rate of 1.8×10^{-12} and deduced the individual rate constants for the elementary processes

$$O + NO \underset{B}{\overset{A}{\rightleftarrows}} NO_2 \xrightarrow[(M)]{C} + M$$

to be $k_A = 3.7 \times 10^{-12}$, $k_B = 7.1 \times 10^{7}$, $k_C = 2 \times 10^{-12}$.

[9] $O + NO_2 \rightarrow NO + O_2 + 45.89$ (1.990)

The only new measurements of this reaction were made by Klein and Herron (78) using a mass spectrometric technique. Some difficulties were encountered with wall contamination of the ion chamber of the mass spectrometer, but studies over the temperature range 278–374 °K yielded the expression

$$k = (3.2 \pm 0.1) \times 10^{-11} \exp(-0.6 \pm 0.2/RT)$$

which gives 5.4×10^{-12} at 300 °K, about twice as large as the value reported earlier (20).

Klein and Herron also used isotopic labelling and report an exchange rate of 7×10^{-12} and rate constants of $k_A = 1.6 \times 10^{-11}$, $k_B = 5 \times 10^{7}$, $k_C = 1.3 \times 10^{-12}$, and $k_D = 2.6 \times 10^{7}$, for the individual steps in the mechanism

$$O + NO_2 \underset{B}{\overset{A}{\rightleftarrows}} NO_3^* \xrightarrow[(M)]{C} NO_3$$
$$\xrightarrow{D} NO + O_2$$

Benson and DeMore (81), however, criticized these values since they are based on the assumption that the same NO_3^* intermediate is involved in reactions C and D. They argue that D must result from an O—N—O—O intermediate while C comes from the symmetric

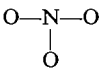

complex. Klein and Herron (82) reassessed their data accordingly and altered k_A to 1.0×10^{-11} while k_D can no longer be estimated from their data.

[10] $O + H_2 \rightarrow OH + H - 1.87$ (−0.081)

Recent measurements of this reaction are in excellent agreement. Westenberg and de Haas (83) added H_2 to discharged Ar–O_2 in a flow system and followed [O] by e.s.r. For the temperature range 400–950 °K they find $k_{10} = (8 \pm 3) \times 10^{-11} \exp(-10.2 \pm 0.5/RT)$ with a claimed accuracy of 10%. The same authors (84) also investigated the isotope effect when D_2 was substituted for H_2.

Hoyermann *et al.* (85) generated O atoms by N–NO titration and used e.s.r. to follow both O and H atoms over the temperature range 373–478 °K. They find

$$-\frac{d[O]}{dt} = \frac{d[H]}{dt} = 2k_{10}$$
$$= 2.2 \times 10^{-11} \exp(-9.4 \pm 0.15/RT)$$

Wong and Potter (19) used a stirred reactor and a time-of-flight mass spectrometer to follow [O]. They assumed that the secondary reactions were

Can. J. Chem. Downloaded from www.nrcresearchpress.com by 210.87.254.40 on 09/05/12
For personal use only.

$O + OH \rightarrow O_2 + H$ and $OH + H_2 \rightarrow H_2O + H$ and used Kaufman's value (15) for their rate constants. For the temperature range 396–597 °K they report

$$k_{10} = 7 \times 10^{-11} \exp(-10.2/RT)$$

The activation energy reported by these three groups is 0.8 kcal mole^{-1} higher than the value of an earlier investigation by Clyne and Thrush (86) using discharge techniques but 1.5 kcal mole^{-1} lower than that of Azatyan *et al.* (87) from flame measurements.

[10a] $O(^1D) + H_2 \rightarrow OH + H + 43.35$ *(1.88)*

De More (88), in a recent study of the photolysis of O_3–H_2 solutions at 87 °K found evidence for this reaction. He concluded that it occurs much more frequently than does straight quenching of the $O(^1D)$ atoms by H_2 and estimated that its rate constant is about $\frac{1}{4}$ that of the $O(^1D)$–O_3 reaction, i.e. about 10^{-11}, and that its activation energy is approximately zero.

[11] $O + CH_4 \rightarrow CH_3 + OH + 0.394$ *(0.0171)*

Avramenko and Kolesnikova (89) report that the reaction proceeds by two parallel primary steps

$$O + CH_4 \rightarrow CH_2O + H_2$$
$$\rightarrow CH_2 + H_2O$$

with an overall rate constant $k_{11} = 3.4 \times 10^{-11} \exp(-7.8/RT)$. Wong and Potter (90), however, did not observe any CH_2O formation mass spectrometrically while Brown and Thrush (91) detected the production of H atoms which can only be reconciled with the primary reaction

$$O + CH_4 \rightarrow CH_3 + OH$$

followed by the subsequent attack of O on OH to form H atoms. They produced O atoms by the N–NO titration technique and follow the reaction by e.s.r. They report, for the temperature range 450–600 °K

$$k_{11} = (1.1 \pm 0.3) \times 10^{-11} \exp(-7.7 \pm 0.3/RT)$$

Cadle and Allan (92) produced O atoms the same way and followed the kinetics by monitoring the O atoms with an isothermal calorimetric probe. Difficulty was encountered because of the complexity of secondary reactions when O_2 was present. On the other hand when O atoms were generated by N–NO titration the rates were so slow that large excesses of CH_4 had to be added. They report, for the range 295–533 °K

$$k_{11} = (1.2 \pm 0.6) \times 10^{-11} \exp(-7.3 \pm 1.5/RT)$$

Azatyan *et al.* (93) obtained a rate constant for this reaction by studying the effect of CH_4 addition to the explosion limit of H_2–O_2 mixtures. They give

$$k_{11} = 0.95 \times 10^{-10} \exp(-8.7/RT)$$

Wong and Potter (90) produced O atoms by the electrical discharge of 1.4% O_2 in Ar and detected them by time-of-flight mass spectrometry. This study gave, from 400–560 °K

$$k_{11} = 1.7 \times 10^{-11} \exp(-10.0/RT)$$

with an estimated accuracy of about ±50%, compared to their earlier study (19) which gave $1.6 \times 10^{-11} \exp(-8.2/RT)$. They attribute the difference in activation energies to the secondary reaction of the excess O_2 which was present in their earlier experiments. However, these earlier results are in better agreement with those of Brown and Thrush (91) who also used an O_2-free system.

Westenberg and de Hass (83) used discharge Ar–O_2 mixtures and e.s.r. detection and obtained, over the range 299–895 °K, with Ar, N_2, and He carriers

$$k_{11} = (2.8 \pm 0.2) \times 10^{-11} \exp(-8.7 \pm 0.7/RT)$$

Since this appears to be the most comprehensive study of this reaction and this rate constant represents a compromise of the other results it is the one recommended.

[11a] $O(^1D) + CH_4 \rightarrow OH + CH_3 + 45.66$ *(1.98)*

De More and Raper (94) photolyzed mixtures of CH_4 and O_3 dissolved in liquid argon. From quantum yield measurements of O_3 consumption they conclude that $O(^1D)$ reacts with CH_4 at a rate 4 times slower than it does with O_3 (i.e. $k_{11a} \approx 10^{-11}$), that about 30% of the collisions result in non-reactive quenching of the (^1D) atoms to $O(^3P)$, and that both processes occur with no activation energy.

[12] $O_2 + 2NO \rightarrow 2NO_2 + 27.34$ *(1.186)*

This reaction is the major oxidation process of NO in the lower atmosphere. Although it has been studied intensively for many years the exact order is still under debate. Tipper and Williams (95) claim that the order depends on pressure and

Can. J. Chem. Downloaded from www.nrcresearchpress.com by 210.87.254.40 on 09/05/12
For personal use only.

amount of inert gas present. Ashmore *et al.* (96) disagree and find that first and second order dependence on O_2 and NO respectively is strictly followed over a wide range of added N_2 pressure. Šolc (97), on the other hand, finds that the respective orders depend on the O_2/NO ratio, and claims that changes in this ratio can affect the rate constant by as much as a factor of 2.

The most recent study of this reaction was reported by Morecroft and Thomas (98) who agree with Ashmore *et al.* (96). The best value for the rate constant for this reaction appears to be $k_{15} = 1 \times 10^{-33}$ at 300° with a small negative activation energy of about 0.5 kcal mole^{-1}.

[13] $O_3 + NO \rightarrow NO_2 + O_2 + 47.8\ (2.07)$

The rate of this reaction was studied by Clyne *et al.* (99) over the temperature range 216–322 °K. The rate expression is given as

$$k_{13} = 0.95 \times 10^{-12} \exp(-2.46 \pm 0.15/RT)$$

which corresponds to 1.5×10^{-14} at 300 °K in satisfactory agreement with earlier determinations (20).

[14] $N + N + M \rightarrow N_2 + M + 226.0\ (9.80)$

Earlier measurements provided a rather wide range of values for the rate constant from 2×10^{-33} to 2×10^{-32} at 300 °K with M = N_2. Several recent measurements indicate that at least part of this spread may have been due to incorrect allowances being made for wall recombinations which seem to be particularly complex in the case of N atoms. Thus it now appears (100–103) that most of the heterogeneous recombination occurs via a process which is second order in [N], in contrast to the usual first order behavior exhibited by other atom wall recombinations. Very dramatic dependence of the wall recombination efficiencies on gas purity, has also been observed, with O_2 showing the greatest effects.

Kretschmer and Petersen (75) give the lowest value of 2.1×10^{-33} which they obtained by following the decay of the Lewis–Raleigh afterglow, both in flowing afterglow and in pulsed afterglow systems, using NO titration and the Wrede gauge for determining absolute concentrations. They attributed higher values obtained by other workers to H_2O impurities which they find can increase the N decay rate, presumably via the fast reaction $N + HO_2 \rightarrow NH + O_2$.

Evanson and Burch (100), however, took even greater precautions to remove water vapor from their flow system and obtained the highest reported value of $2.25 \pm 0.20 \times 10^{-32}$. They find an increase in recombination rate with time after the discharge. Their high value of the rate constant was obtained at times greater than 3 s in a static system using e.s.r. detection. At lower times they postulate the presence of excited N_2* molecules which decompose to N atoms, resulting in a slower apparent recombination rate. They ascribe the lower rate constants reported by other workers to measurements in this short time regime.

Campbell and Thrush (101) followed the "active nitrogen" glow in a flow system over the temperature range 196–327 °K. They report a value of $(3.8 \pm 0.3) \times 10^{-33}$ at 300 °K and a negative "activation energy" of 0.98 ± 0.14. The wall recombination was found to have the opposite temperature coefficient which, they say, explains why Herron *et al.* (102) found only a small temperature dependence. They find Ar to have a similar third body efficiency to N_2 but He, H_2O, and CO_2 to be more efficient by factors of 1.4, 1.6, and 1.9 respectively. They also claim that approximately 50% of the recombination produces N_2 in the $A^3\Sigma_u^+$ state.

Clyne and Stedman (103) report a value of $k_{14} = 7.4 \times 10^{-33}$ at 300 °K for M = N_2. They find they can fit their results over the wide temperature range 90–611 °K to high temperature shock tube values by the expression

$$k_{14} = 1.4 \times 10^{-33} \exp(1.0 \pm 0.3/RT)$$

but not by an AT^{-n} temperature dependence.

There is not, however, a high degree of consistency among shock tube data. Three of the most recent investigations (104–106) give rate constants which agree within the large combined estimated errors in the overlapping temperature range from 8 000–10 000 °K. They differ widely in the relative efficiencies of third bodies especially in the case where M = N. They differ also in the exponent in the temperature dependence T^{-n} Thus Cary (105) finds $n = 1.7$ for N_2 and 1.0 for N, He, and Ar, while Byron (104) finds $n = 0.5$ for N_2 and Ar, and 1.5 for N. Appleton *et al.* (106) find the same coefficient, $n = 1.6$ for Ar, N_2, and N. The very large spread of the rate constants at both high and low temperatures can be fitted equally well to values of n between 1.0 and 1.7. There are a number of theoretical treatments (31, 83, 107) which predict values of n from 0.5 to 1.5.

Can. J. Chem. Downloaded from www.nrcresearchpress.com by 210.87.254.40 on 09/05/12
For personal use only.

It is safe to say that the rate constant for this reaction and its temperature dependence still awaits unequivocal determinations. Fortunately this reaction is not a major loss process for atomic nitrogen in the earth's atmosphere.

[15] $O_2 + N \rightarrow NO + O + 31.9$ *(1.38)*

This reaction is believed to provide the major source of NO in the chemosphere. Kaufman (80) has recently reviewed the work on this reaction prior to 1964 and recommended for the rate constant

$$k_{15} = (1.4 \pm 0.2) \times 10^{-11} \exp(-7.1 \pm 0.4/RT)$$

The only recent measurement of this reaction was reported by Vlastaras and Winkler (108) for the temperature range 180–330 °K

$$k_{15} = 6.5 \times 10^{-12} \exp(-7.0/RT)$$

in reasonable agreement with the earlier measurements in spite of the neglect by the authors of atom recombination.

Reactions of N atoms with $O_2(^1\Delta_g)$ have not yet been reported but may be important in atmospheric NO production.

[16] $N + NO \rightarrow N_2 + O + 75.0$ *(3.25)*

This is one of the fastest known bimolecular reactions between neutral species. Its importance in the laboratory for the "titration" of N atoms and for the production of O atoms in the absence of O_2 is well known. Its importance in the atmosphere stems from its ability to convert N and O_2 into O and N_2 by the sequence of reactions [15] followed by [16]. The N_2 formed in this reaction has been shown (48) to be vibrationally excited with enough energy to dissociate O_3. No new measurements of the rate constant for this reaction have been reported so the value (20) of $k_{16} = (2.2 \pm 0.6) \times 10^{-11}$ at 300 °K still stands. Since this value is within a factor of 5 of the gas collision rate, the activation energy cannot exceed 0.5 kcal mole^{-1}.

[17]
$$N + NO_2 \xrightarrow{a} N_2O$$
$$\xrightarrow{b} 2NO$$
$$\xrightarrow{c} N_2 + O_2$$
$$\xrightarrow{d} N_2 + 2O$$

Although this reaction has little aeronomic importance it is interesting because of the variety of reaction channels available, all of which appear to occur. Phillips and Schiff (109) studied this reaction in a flow system using a combination of photometric and mass spectrometric detection. The overall rate constant was found to be $k_{17} = (1.8 \pm 0.2) \times 10^{-11}$ at 300 °K. The percentage reaction into the four channels were (*a*) 4.3 ± 4, (*b*) 33 ± 7, (*c*) 10 ± 12, and (*d*) 13 ± 11. The reaction rate is also so close to gas collision frequency that the activation energy cannot exceed 0.5 kcal mole^{-1}.

Summary

This brief review will at least have shown that neutral reactions involving nitrogen and oxygen have been actively studied during the past 4 years. Progress has been made on the temperature coefficients of a number of aeronomically important rate constants. But, as atmospheric measurements and model calculations improve, so the need for more accurate rate data will increase.

The field of excited atom and molecule reactions has just begun to be cultivated. To date, most of the work on excited species has dealt with quenching rather than with reactive collisions. It is probably safe to predict that two tools which will play major roles in breaking this new ground will be integrating spectroscopic techniques for studying excited reactants and molecular beam techniques for studying excitation of the products.

1. H. I. Schiff. Ann. Geophys. **20**, 86 (1964).
2. J. F. Noxon. Space Sci. Rev. **8**, 92 (1968).
3. W. F. Evans, D. M. Hunten, E. J. Llewelyn, and A. Vallance-Jones. J. Geoph. Res. **73**, 2885 (1968).
4. F. Kaufman and J. R. Kelso. Discussions Faraday Soc. **37**, 26 (1964); J. Chem. Phys. **40**, 1162 (1964).
5. M. F. R. Mulcahy and D. J. Williams. Trans. Faraday Soc. **64**, 59 (1968).
6. O. R. Lundell, R. D. Ketcheson, and H. I. Schiff. *In* 12th Intern. Symp. Comb. Poitiers, 1968.
7. J. F. Noxon. Private communication.
8. R. A. Young and G. Black. J. Chem. Phys. **44**, 3741 (1966).
9. A. Y. Ung and H. I. Schiff. Can. J. Chem. **44**, 1981 (1966).
10. V. LoDato and H. O. Pritchard. J. Phys. Chem. To be published.
11. L. Elias. J. Chem. Phys. **44**, 3810 (1966); **42**, 4311 (1965).
12. J. E. Morgan and H. I. Schiff. Can. J. Chem. **41**, 903 (1963).
13. L. Bader and E. A. Ogryzlo. Discussions Faraday Soc. **37**, 46 (1964).
14. N. Basco and R. G. W. Norrish. Can. J. Chem. **38**, 1769 (1960).

Can. J. Chem. Downloaded from www.nrcresearchpress.com by 210.87.254.40 on 09/05/12
For personal use only.

15. F. KAUFMAN and F. P. DEL GRECO. Discussions Faraday Soc. **33**, 128 (1962).
16. F. A. MORSE and F. KAUFMAN. J. Chem. Phys. **42**, 1785 (1965).
17. R. J. MCNEAL and G. R. COOK. J. Chem. Phys. **47**, 5385 (1967).
18. A. A. WESTENBERG and N. DE HAAS. J. Chem. Phys. **40**, 3087 (1964).
19. E. L. WONG and A. E. POTTER. J. Chem. Phys. **43**, 3371 (1965).
20. L. F. PHILLIPS and H. I. SCHIFF. J. Chem. Phys. **36**, 1509 (1962).
21. L. F. PHILLIPS and H. I. SCHIFF. J. Chem. Phys. **42**, 3171 (1965).
22. K. SCHOFIELD. Planetary Space Sci. **15**, 643 (1967).
23. H. S. JOHNSON. Natl. Std. Ref. Data Series, NSRDS-NBS20 (1968).
24. A. N. WRIGHT and C. A. WINKLER. Active nitrogen. Academic Press, Inc., New York. 1968.
25. I. M. CAMPBELL and B. A. THRUSH. Proc. Roy. Soc. London, Ser. A, **296**, 222 (1967).
26. J. E. MORGAN and H. I. SCHIFF. J. Chem. Phys. **38**, 1495 (1963).
27. R. R. REEVES, G. MANELLA, and P. HARTECK. J. Chem. Phys. **32**, 632 (1960).
28. K. L. WRAY. J. Chem. Phys. **38**, 1518 (1963). 10th Intern. Symp. Comb. 1965. p. 523.
29. S. R. BYRON. J. Chem. Phys. **30**, 1380 (1959).
30. M. CAMAC and A. VAUGHAN. J. Chem. Phys. **34**, 460 (1961).
31. S. W. BENSON and T. FUENO. J. Chem. Phys. **36**, 1597 (1962).
32. R. I. SALOUKHIN. Combust. Flames, II, 489 (1967).
33. L. F. PHILLIPS and H. I. SCHIFF. J. Chem. Phys. **37**, 1233 (1962).
34. F. S. LARKIN and B. A. THRUSH. Discussions Faraday Soc. **37**, 112 (1964).
35. A. MATHIAS and H. I. SCHIFF. Discussions Faraday Soc. **37**, 38 (1964).
36. F. KAUFMAN and J. R. KELSO. Discussions Faraday Soc. **37**, 26 (1964).
37. M. A. A. CLYNE, D. J. MCKENNEY, and B. A. THRUSH. Trans. Faraday Soc. **61**, 2701 (1965).
38. F. KAUFMAN and J. R. KELSO. J. Chem. Phys. **46**, 4541 (1967).
39. M. C. SAUER. J. Phys. Chem. **71**, 3311 (1967).
40. M. C. SAUER and L. M. DORFMAN. J. Am. Chem. Soc. **87**, 3801 (1965).
41. S. W. BENSON and A. E. AXWORTHY. J. Chem. Phys. **42**, 2614 (1965).
42. E. CASTELLANO and H. J. SCHUMACHER. Z. Physik. Chem. **34**, 198 (1962).
43. F. S. KLEIN and J. T. HERRON. J. Chem. Phys. **40**, 2731 (1964).
44. N. BRENNEN and H. NIKKI. J. Chem. Phys. **42**, 3725 (1965).
45. S. JAFFE and F. S. KLEIN. Trans. Faraday Soc. **62**, 3135 (1966).
46. W. M. JONES and N. DAVIDSON. J. Am. Chem. Soc. **84**, 2868 (1962).
47. F. C. FEHSENFELD, A. L. SCHMELTEKOPF, H. I. SCHIFF, and E. E. FERGUSON. Planetary Space Sci. **15**, 373 (1967).
48. J. E. MORGAN, L. F. PHILLIPS, and H. I. SCHIFF. Discussions Faraday Soc. **33**, 118 (1962).
49. J. H. KIEFER and R. W. LUTZ. 11th Intern. Symp. Comb. Academic Press, Inc., New York. 1966.
50. E. I. INTEZAROVA and V. N. KONDRATJEV. Izv. Akad. Nauk Leningrad, **11**, 2440 (1967).
51. O. R. LUNDELL, R. D. KETCHESON, and H. I. SCHIFF. Unpublished work.
52. W. C. MCGRATH and R. G. W. NORRISH. Proc. Roy Soc. London, Ser. A, **254**, 317 (1960).
53. L. F. PHILLIPS and H. I. SCHIFF. J. Chem. Phys. **37**, 924 (1962).
54. R. V. FITZSIMMONS and E. J. BAIR. J. Chem. Phys. **40**, 451 (1964).
55. D. R. SNELLING, V. D. BAIAMONTE, and E. J. BAIR. J. Chem. Phys. **44**, 4137 (1966).
56. D. R. SNELLING and E. J. BAIR. J. Chem. Phys. **47**, 228 (1967).
57. R. G. W. NORRISH and R. P. WAYNE. Proc. Roy. Soc. London, Ser. A, **288**, 200 (1965).
58. W. D. MCGRATH and J. J. MCGARVEY. Planetary Space Sci. **15**, 427 (1967).
59. D. J. MCKENNY and K. J. LAIDLER. Can. J. Chem. **40**, 539 (1962).
60. D. H. VOLMAN, K. GILL, and K. J. LAIDLER. J. Chem. Phys. **30**, 589 (1959).
61. D. H. VOLMAN. Advan. Photochem. **1**, 43 (1963).
62. S. W. BENSON. J. Chem. Phys. **33**, 939 (1960).
63. W. B. DE MORE and O. F. RAPER. J. Chem. Phys. **44**, 1780 (1966).
64. J. R. MCNESBY and H. OKABE. Advan. Photochem. **3**, 157 (1964).
65. P. WARNECK. Discussions Faraday Soc. **37**, 57 (1964).
66. J. O. SULLIVAN and P. WARNECK. J. Chem. Phys. **46**, 953 (1967).
67. R. P. WAYNE. J. Roy. Met. Soc. **93**, 69 (1967).
68. H. I. SCHIFF and L. R. MEGILL. J. Geophys. Res. **69**, 5120 (1964).
69. B. G. HUNT. J. Geophys. Res. **71**, 1385 (1966).
70. R. E. MARCH, S. G. FURNIVAL, and H. I. SCHIFF. Photochem. Photobiol. **4**, 971 (1966).
71. R. A. YOUNG and G. BLACK. J. Chem. Phys. **42**, 3740 (1965).
72. S. J. ARNOLD, R. J. BROWNE, and E. A. OGRYZLO. Photochem. Photobiol. **4**, 963 (1965).
73. A. FALIK and B. H. MAHAN. J. Chem. Phys. **47**, 4778 (1967).
74. S. J. ARNOLD and E. A. OGRYZLO. Can. J. Phys. **45**, 2053 (1967).
75. C. B. KRETSCHMER and H. L. PETERSEN. J. Chem. Phys. **39**, 1772 (1964).
76. C. A. BARTH. Ann. Geophys. **20**, 137 (1964).
77. I. M. CAMPBELL and B. A THRUSH. Proc. Roy. Soc. London, Ser. A, **296**, 222 (1967).
78. F. S. KLEIN and J. T. HERRON. J. Chem. Phys. **41**, 1285 (1964).
79. M. A. A. CLYNE and B. A. THRUSH. Proc. Roy. Soc. London, Ser. A, **269**, 404 (1962).
80. F. KAUFMAN. DASA Reaction Rate Handbook 14-1 (1967).
81. S. W. BENSON and W. B. DE MORE. Ann. Rev. Phys. Chem. **16**, 405 (1965).
82. F. S. KLEIN and J. T. HERRON. J. Chem. Phys. **44**, 3645 (1966).
83. A. A. WESTENBERG and N. DE HAAS. J. Chem. Phys. **46**, 490 (1967).
84. A. A. WESTENBERG and N. DE HAAS. J. Chem. Phys. **47**, 4241 (1967).
85. H. HOYERMANN, H. GG. WAGNER, and J. WOLFRUM. Bunsenges. Physik. Chem. **71**, 599 (1967).
86. M. A. A. CLYNE and B. A. THRUSH. Proc. Roy. Soc. London, Ser. A, **275**, 544 (1965).
87. V. V. AZATYAN, V. V. VOEVODSKY, and A. B. NALBANDYAN. Kinetika i Kataliz, **2**, 340 (1961).
88. W. B. DE MORE. J. Chem. Phys. **47**, 2777 (1967).
89. L. I. AVRAMENKO and R. V. KOLESNIKOVA. Advan. Photochem. **2**, 25 (1964).
90. E. L. WONG and A. E. POTTER. Can. J. Chem. **45**, 367 (1967).

91. J. M. BROWN and B. A. THRUSH. Trans. Faraday Soc. **63**, 630 (1967).
92. R. D. CADLE and E. R. ALLAN. J. Phys. Chem. **69**, 1611 (1965).
93. V. V. AZATYAN, A. B. NALBANDYAN, and T-M. YUAN. Kinetika i Kataliz, **5**, 201 (1964).
94. W. B. DE MORE and O. F. RAPER. J. Chem. Phys. **46**, 2500 (1967).
95. C. F. H. TIPPER and R. K. WILLIAMS. Trans. Faraday Soc. **57**, 79 (1962).
96. P. G. ASHMORE, M. G. BURNETT, and B. J. TYLER. Trans. Faraday Soc. **58**, 685 (1962).
97. M. ŠOLC. Nature, **209**, 706 (1966).
98. J. MORECROFT and J. H. THOMAS. J. Phys. Chem. **71**, 1543 (1967).
99. M. A. A. CLYNE, B. A. THRUSH, and R. P. WAYNE. Trans. Faraday Soc. **60**, 359 (1964).
100. K. M. EVANSON and D. S. BURCH. J. Chem. Phys. **45**, 2450 (1966).
101. I. M. CAMPBELL and B. A. THRUSH. Proc. Roy. Soc. London, Ser. A, **296**, 201 (1965).
102. J. T. HERRON, J. L. FRANKLIN, P. BRADT, and V. H. DIBELER. J. Chem. Phys. **30**, 879 (1959).
103. M. A. A. CLYNE and D. H. STEDMAN. J. Phys. Chem. **71**, 3071 (1967).
104. S. BYRON. J. Chem. Phys. **44**, 1378 (1966).
105. B. CARY. Phys. Fluids, **8**, 26 (1965).
106. J. P. APPLETON, M. STEINBERG, and D. J. LIQUORNIK. J. Chem. Phys. **48**, 599 (1968).
107. J. C. KECK and G. CARRIER. J. Chem. Phys. **43**, 2284 (1965).
108. A. S. VLASTARAS and C. A. WINKLER. Can. J. Chem. **54**, 2837 (1967).
109. L. F. PHILLIPS and H. I. SCHIFF. J. Chem. Phys. **42**, 3171 (1965).

Comments and Summary

COMMENTS AND SUMMARY BY CHAIRMAN, MICHAEL B. McELROY[1]

The most important problem in this area where laboratory data are inadequate concerns the chemistry of NO. To account for the atmospheric measurements of NO concentrations, (1, 2) one requires an efficient source of this gas in the sub 100 km region of the atmosphere. The temperature is low, less than 200 °K at about 90 km, and previously one could speculate that the reaction

[1] $$N + O_2 \rightarrow NO + O$$

was faster than might be expected from the Arrhenius equation, which employed an activation energy deduced from laboratory studies at relatively high temperatures (> 400 °K). The recent measurements by Vlastaras and Winkler (3), which extend down to 180 °K, would appear to eliminate this particular solution.

The most plausible alternative sources of NO involve metastable species. In particular either

[2] $$N(^2D) + O_2 \rightarrow NO + O$$

or

[3] $$N + O_2(^1\Delta) \rightarrow NO + O$$

could account for the observed NO concentrations if certain conditions are satisfied. It is well known (4) that $N(^2D)$ is quenched in the atmosphere. If reaction [2] is to be important source of NO then the quenching must proceed almost exclusively by this path. The rate coefficient should be of order 10^{-12} cm^3 s^{-1}. Reaction [3] will be important if the relevant rate coefficient is larger than 10^{-13} cm^3 s^{-1}. Laboratory studies of both reactions are urgently required. Until reliable data become available the problem of NO chemistry, a central one for D region ionospheric studies, must remain vexing but unsolved.

The laboratory data for other reactions discussed by Schiff appear adequate for aeronomical applications.

[1]Address: Kitt Peak National Observatory, Tucson, Arizona.

1. C. A. BARTH. J. Geophys. Res. **69**, 3301 (1964).
2. J. F. PEARCE. Ph.D. Thesis, University of Colorado, 1968.
3. A. S. VLASTARAS and C. A. WINKLER. Can. J. Chem. **45**, 2837 (1967).
4. D. M. HUNTEN and M. B. MCELROY. Rev. Geophys. **4**, 303 (1966).

Can. J. Chem. Downloaded from www.nrcresearchpress.com by 210.87.254.40 on 09/05/12
For personal use only.

Neutral reactions involving hydrogen and other minor constituents[1]

FREDERICK KAUFMAN
Department of Chemistry, University of Pittsburgh, Pittsburgh, Pennsylvania 15213
Received December 18, 1968

Experimental laboratory work is reviewed for the kinetics of 21 neutral, elementary reactions involving H, OH, HO_2, H_2, CO, N_2O, CH_4, and Na.

Canadian Journal of Chemistry, 47, 1917 (1969)

Introduction

Five years ago, at the Berkeley Symposium, this author presented a review of laboratory studies of relevant neutral reactions involving hydrogen (1). The present paper will attempt to bring that review up to date, and to discuss briefly the reactions of certain other minor constituents, not previously covered, at the suggestion of the organizers of this Symposium. It will not present, specifically, work done at the author's laboratory, and so is likely to be a drab recitation of experimentally measured rate parameters. The seemingly chaotic diversity and corresponding lack of clear trends among such rate parameters is, of course, a consequence of the greater inherent complexity of neutral reactions, whose cross sections are generally smaller, energy barriers larger, interactions weaker, and intermediate states less predictable than those involving electrons or ions. The lively progress of fundamental rate theory (2) during the last few years will, in general, not be reflected in this review. The day when the detailed course of most elementary reactions will be open to investigation by single-collision methods (e.g. crossed molecular beam) in addition to the varied arsenal of bulk methods (with increasing sophistication of specific quantum state analysis) is unfortunately not yet at hand (except for alkali atom reactions), but, hopefully, it is not far off. Until then, we must rely on chemical kinetic information obtained by various methods such as discharge-flow, flash photolysis, steady photolysis, high temperature kinetics and mechanism, flame sampling, shock-tube, and others. For the purpose of this Symposium where the interest centers on reactions of simple atomic species at temperatures from about 200 to 1000 °K, the discharge-flow method has become the most widely used. Its many variants include formation of reactive species in glow discharges, in thermal sources, or by chemical reaction of energetic precursors; reaction with added molecules along a cylindrical flow tube or in stirred-flow reactor; and detection by measurement of a simply related chemiluminescent emission, by wire calorimetry, optical absorption, election spin resonance (e.s.r.) absorption, mass spectrometry, gas titration of the reactive species, or by other methods. As one reviews the published results of such experiments critically, one should keep in mind all inherent limitations or assumptions which will tend to reduce the accuracy of their results. For example, the experimental errors introduced in the measurements of pressure in the 0.1 to 10 Torr range, of all flow rates (properly reduced to $cm^3\ s^{-1}$ at N.T.P. or particles s^{-1}), and of the geometry of the flow tube or reactor, and thereby the elapsed time, are likely to result in a minimum probable error of about 10% in the resultant rate constant. Next, major uncertainties arise from the oversimplification of the gas flow and from uncontrolled side reaction. Thus, for relatively slow reactions, concurrent surface recombination is always a serious problem, and for very fast reactions whose rate often can not be reduced by lowering reactant concentrations because of detector sensitivity, the flow velocity is likely to be high (0.2 to 1×10^4 cm s^{-1}) which complicates the reactant mixing problem, impedes the establishment of Poiseuille flow, and introduces axial pressure gradients. Probable errors of 10% due to these causes would seem to be conservative estimates in most cases. Finally, there are the errors associated with the method of detection. These are particularly serious when the absolute concentration of a reactive species must be

[1]This work was supported by the National Science Foundation under Grant GP-5369 and by the Defense Atomic Support Agency under Grant DA-ARO-D-31-124-G881.

known as in the calculation of bimolecular rate constants for the reaction involving two such molecules. In such cases, uncertainties in the optical or e.s.r. absorption coefficient, discrimination effects in mass spectrometric analysis, unknown detection efficiency and diffusion effects in probe calorimeters, and titration errors (especially overtitration) in chemiluminescent titrations, will add further errors which will usually amount to at least 10 to 20%. It is clear, of course, that in any one series of measurements most of these errors will tend to remain fairly constant, and that, therefore, the average deviation from the mean in such a series is likely to be much smaller than the true probable error. This rather obvious reminder of the difference between precision and accuracy would seem to be out of place in such a review, were it not for the alarming rise in the claimed accuracy of many reported kinetic parameters. Thus, claims of a probable error (single standard deviation) in a rate constant of less than about $\pm 15\%$ should in most cases be disregarded. As an example, one may cite one of the most easily measured rate constants by discharge-flow techniques, the recombination rate constant for

$$O + NO + O_2 \rightarrow NO_2 + O_2$$

which is not a subject of this review, for which six separate investigations have reported values of 5.1, 5.1, 6.0, 6.0, 7.6, and 8.0×10^{-32} cm^6 $molecule^{-2}$ s^{-1}, even though this is a pseudo first order process in which the concentrations of NO and O_2 are easily measured and remain constant and that of O, therefore, need not be known in absolute magnitude.

Review of Recent Rate Data

The writing of this review was much aided by other recent summaries, especially by the excellent evaluation of kinetic rate data of Schofield (3) and by other review articles (4–6). Reactions will be discussed in the approximate order of this author's earlier review (1), beginning with reactions of H, followed by OH, HO_2, H_2, and H_2O, and ending with a few reactions of CO_2, N_2O, CH_4, and of Na. Molecular units (cm^3 $molecule^{-1}$ s^{-1} or cm^6 $molecule^{-2}$ s^{-1}) will be used throughout, and should be assumed to apply when not specified. Specific rate constants are reported, i.e. for the reaction

$$2A \rightarrow B + C$$

$$k \equiv -1/2 \frac{d[A]}{dt} \Big/ [A]^2 = \frac{d[B]}{dt} \Big/ [A]^2$$

or for

$$2A + M \rightarrow A_2 + M$$

$$k \equiv -1/2 \frac{d[A]}{dt} \Big/ [A]^2[M] = \frac{d[A_2]}{dt} \Big/ [A]^2[M]$$

For each reaction, the energy change at absolute zero temperature, ΔE_0^0, will be given in units of kcal $mole^{-1}$, based on the thermochemical data from the JANAF tables (7). Where this author is unaware of new work since his earlier review, that recommended value will be repeated without discussion for increased usefulness. Lastly, apologies are again in order for possible crimes of omission or commission.

A. Reactions of H Atoms

[1] $$H + H + M \rightarrow H_2 + M$$
$$\Delta E_0^0 = -103.26$$

This reaction is of aeronomic interest only for the major planets. It continues to be studied over a wide temperature range, because it is the most important test case of theory and experiment of atom recombination. Larkin and Thrush (8) studied the T dependence (213 to 349 °K) for M = Ar and found $k = 1.2 \times 10^{-32} (273/T)^{0.7}$, in fairly good agreement with the theory of Benson and Fueno (9), although the latter predicts a weaker T dependence ($\sim T^{-0.3}$ for a Lennard–Jones potential for H + H collision complexes).

The extensive work at high T by shock tube techniques can not be reviewed here. Sutton (10) finds a T^{-1} dependence between 2800 and 4500 °K for M = H_2, and his k extrapolates well to discharge-flow data near 300 °K. His k for M = H is about 10 times larger. Hurle (11) is in good agreement with Sutton for M = H_2, but reports a very much larger k for M = H, with a very large negative T dependence, T^{-7}, between 4000 and 6000 °K. Such a value is clearly not extrapolatable to 300 °K, and Hurle is reported to have seen k come to maximum value near 3000 °K and to appear to decrease again at lower T (12). Rosenfeld (12) has suggested an explanation for this interesting observation. More experimental work is needed, especially in an intermediate T range. Although there is qualitative agreement on the relative efficiency of different M, i.e. Ar < N_2 < H_2O < H_2 < H, there remain wide discrepancies in their exact magnitude.

[2] $H + O_2 + M \rightarrow HO_2 + M$
$\Delta E_0^0 = -45.9$

Two studies near 300 °K, one using chemiluminescent (13) and the other probe (14) detection, have shown this to be a "normal" three-body atom–molecule recombination with a k of $(3 \pm 1) \times 10^{-32}$ (M = Ar) and a ratio of about 20 for $k_{H_2O}:k_{Ar}$. From the M-effect on the second explosion limit of H_2–O_2 explosions near 800 °K, similar relative M-efficiencies are obtained which place He and O_2 near Ar, N_2 1.5 to 2 times larger, H_2 3 times larger. Schofield (3) combined most available rate data to obtain $k = 3 \times 10^{-32} (273/T)^{1.3}$ which is likely to be approximately correct although the $T^{-1.3}$ dependence is weaker than that of several similar recombinations.

[3] $H + O_2 \rightarrow OH + O$
$\Delta E_0^0 = 16.63$

The reaction is sufficiently endothermic to be of no direct importance. There is no experimental information on the interesting possibility of a forward reaction with O_2, $X^3\Sigma_g^-$, $v'' \geqslant 4$ or with O_2, $a^1\Delta_g^+$ or $b^1\Sigma_g^+$. From the very large k of the reverse reaction, $(5 \pm 2) \times 10^{-11}$, (1), and the equilibrium constant, 21 exp $(16.8/RT)$, a value of 1×10^{-9} exp $(-16.8/RT)$ is obtained if the reverse reaction k is assumed to be T independent. If the reverse reaction produces substantial vibrational excitation in O_2, the above "thermal" k would be too large. The very large pre-exponential factor indirectly supports such a possibility.

[4] $H + NO + M \rightarrow HNO + M$
$\Delta E_0^0 = -48.6$

Further work on this reaction since the last review included measurement of k at 293 °K for six M as well as measurement of the relative M effect in the concurrent chemiluminescent reaction to form HNO* (15). For M = H_2, k is now found to be 5.7×10^{-32}, compared to 3.8×10^{-32} in the earlier work of the same laboratory (16). The relative efficiencies of M in the recombination, normalized to M = H_2 are: He, 0.47; Ar, 0.54; CO_2, 1.1; N_2O, 1.2; SF_6, 1.9; H_2O, 3.3. The formation of HNO* was found to depend on M in a similar manner. The further bimolecular reaction, $2HNO \rightarrow N_2O + H_2O$, was investigated by Clyne (17) who placed a lower limit of 0.5×10^{-16} on its rate constant, and by Kohout and Lampe (18) who find $k = 6.7 \pm 10^{-16}$ in a photolysis mass spectrometer study.

[5] $H + NO_2 \rightarrow OH + NO$
$\Delta E_0^0 = -29.5$

No new work is available. The direct measurement of Phillips and Schiff (19) at 300 °K gave $(4.8 \pm 0.5) \times 10^{-11}$. Rosser and Wise (20) reported a similar value based on the competition of reaction [5] with the reaction $H + Cl_2 \rightarrow HCl + Cl$. Schofield (3) recalculated k_5 from the data of ref. 20 using more recent kinetic data on $H + Cl_2$, and obtained an excessively large value. This indicates that the temperature dependence of the rate constant ratio is much smaller than reported in (20). Further unpublished work at the author's former laboratory has confirmed the earlier conclusion that there is very little, if any, vibrationally excited OH formed in this reaction.

[6] $H + O_3 \rightarrow OH + O_2$
$\Delta E_0^0 = -77.1$

This reaction was extensively discussed in the earlier review (1). No new data are available on its rate constant, $(2.6 \pm 0.5) \times 10^{-11}$ at 300 °K as reported by Phillips and Schiff (19). Further work in the author's former laboratory has confirmed the formation of highly vibrationally excited OH as a major reaction product and has provided information on its collisional deactivation by various added gases. Anlauf, Macdonald, and Polanyi (21) have recently studied the infrared chemiluminescence of this reaction at pressures down to 10^{-4} Torr under conditions where $OH^\ddagger$ would either react or be deactivated to $v'' = 0$ at the wall of the reactor. The infrared emission indicated a highly non-Boltzmann distribution of $OH^\ddagger$ with increasing populations up to $v'' = 9$, the highest available level, and about 80 to 85% of all molecules in $v'' \geqslant 4$ if the populations in $v'' = 0$ to 2 are estimated by extrapolation. This result is in good agreement with the earlier ultraviolet absorption work (1) in which only molecules with $v'' = 0$ and 1 were observed. The various fates of $OH^\ddagger$ as a result of radiation, physical quenching, or chemical reactions were presented in the earlier review. The detailed course of its reaction with O_3 has been further clarified by DeMore (22) who showed

that the reaction between $OH^{\ddagger}$ and O_3 may produce $H + 2O_2$ via highly excited HO_2 after a single collision rather than only by two successive collisional processes, i.e. $OH^{\ddagger} + O_3 \rightarrow OH + + O_2 + O$, followed by $OH + O \rightarrow O_2 + H$ (1). This helps to explain why the yield of OH, $v'' = 0$, does not increase strongly when very small concentrations of H are reacted with excess O_3.

[7] $$H + OH \rightarrow H_2 + O$$
$$\Delta E_0^0 = -1.9$$

This rate constant is best obtained from its much studied reverse reaction for which three new values have been reported since the last review: $7 \times 10^{-11} \exp(-10.2/RT)$ (23), $2 \times 10^{-11} \exp(-9.2/RT)$ (24), and $8 \times 10^{-11} \exp(-10.2/RT)$ (25). Combined with the equilibrium constant, $k = 0.44 \exp(-1.87/RT)$, and using the larger activation energy, one obtains $3 \times 10^{-11} \exp(8.3/RT)$ which, although differing fairly substantially from the earlier recommended expression (1), does not yield very different rate constants near 300 °K.

[8] $$H + HO_2 \rightarrow 2OH$$
$$\Delta E_0^0 = -38.8$$

[8′] $$H + HO_2 \rightarrow H_2 + O_2$$
$$\Delta E_0^0 = -57.3$$

No new work is available. The earlier rough estimates of $k_8 \geqslant 3 \times 10^{-12}$ stand (1).

B. Reactions of OH

[9] $$2OH \rightarrow H_2O + O$$
$$\Delta E_0^0 = -16.7$$

Since the earlier work (1) which reported $(1.4 \pm 0.3) \times 10^{-12}$ at 300 °K (the quoted 2.8×10^{-12} referred to $-d[OH]/dt = k[OH]^2$, i.e. twice the specific rate constant) several other values have been published. Westenberg and deHaas (26) found $(2 \pm 0.6) \times 10^{-12}$ by a similar method except for e.s.r. detection, and later work in the same laboratory (27) led to $(2.6 \pm 0.25) \times 10^{-12}$ (The stated errors are single standard deviations calculated from the published data.) Wilson and O'Donovan (28) recently re-analyzed Herron's (29) data on the CO + OH reaction and calculated $(1.1 \pm 0.1) \times 10^{-12}$ for the OH + OH reaction. They then performed similar experiments which yielded $(2.1 \pm 0.1) \times 10^{-12}$, but rejected both in favor of their earlier $(2.6 \pm 0.25) \times 10^{-12}$ (28). Several of these authors err in claiming excessive accuracy as discussed in the Introduction, i.e. they simply report the average deviation from the mean of their calculated values, which is sometimes as low as $\pm 3\%$. It is difficult to assess which of the two principal measurements, $(1.4 \pm 0.3) \times 10^{-12}$ by ultraviolet (u.v.) or $(2.6 \pm 0.25) \times 10^{-12}$ by e.s.r. absorption, is more reliable. Experimentally, the u.v. value has a slight edge, because it averages OH over a shorter distance along the flow tube, permits its measurement closer to the mixing point where OH is produced, and uses a better mixing device for the parent $H + NO_2$ reaction. The u.v. method was also used to measure the oscillator strength of the pertinent electronic transition, $^2\Sigma^+ - {}^2\pi$, and a result $f_{0,0} = (7.1 \pm 1.0) \times 10^{-4}$ was obtained (30) in good agreement with the best direct measurement of the radiative lifetime (31) which yields $(8.0 \pm 0.8) \times 10^{-4}$. The effect of adopting the slightly higher f would be a proportional decrease in all OH concentrations and an increase of k from 1.4 to $(1.6 \pm 0.3) \times 10^{-12}$. The higher e.s.r. value, on the other hand, is supported by measurement of the ratio $[O_2]_\infty/[CO_2]_\infty$ at large reaction times when the OH + CO reaction occurs concurrently, even though this support is predicated on the correctness of the OH + CO rate constant. Very likely, the correct k will lie somewhere between 1.4 and 2.6×10^{-11}, but exaggerated claims of high accuracy should be disregarded.

[10] $$OH + O \rightarrow O_2 + H$$
$$\Delta E_0^0 = -16.6$$

No further work is available. The earlier value of $(5 \pm 2) \times 10^{-11}$ at 300 °K stands.

[11] $$OH + O_3 \rightarrow HO_2 + O_2$$
$$\Delta E_0^0 = -38.3$$

DeMore's recent photolysis work (22, 32) supports the earlier conclusion (1) that ground-state OH does not react rapidly with O_3 ($k \leqslant 5 \times 10^{-13}$) whereas excited OH from the $H + O_3$ reaction does so. No direct proof is available for the often invoked chain decomposition of O_3 by this reaction followed by $HO_2 + O_3 \rightarrow OH + 2O_2$, and such a scheme should not be postulated without proof. With highly excited $OH^{\ddagger}$, the reaction proceeds to give $H + 2O_2$ as previously discussed.

[12] $OH + HO_2 \rightarrow H_2O + O_2$
$\Delta E_0^0 = -72.1$

The earlier recommendation of a fast reaction, $k \geqslant 10^{-11}$, on the basis of indirect information on HO_2 production, still stands.

[13] $OH + H_2 \rightarrow H_2O + H$
$\Delta E_0^0 = -14.7$

Two new measurements of this rate constant at 300 °K have been reported, both in good agreement with the earlier value of $(7 \pm 2) \times 10^{-15}$ (1). Dixon-Lewis, Wilson, and Westenberg (27) find $(6.5 \pm 0.5) \times 10^{-15}$ by e.s.r. and Greiner (33), $(6.7 \pm 0.4) \times 10^{-15}$ by flash photolysis and kinetic spectroscopy. Combined with flame and shock tube data, this value has led to several Arrhenius expressions for k such as $6.3 \times 10^{-11} \exp(-5.49/RT)$ (3), $1 \times 10^{-10} \exp(-5.9/RT)$ (1), and $3.8 \times 10^{-11} \exp(-5.2/RT)$ (27) which are also in close agreement over the relevant T range.

C. Reactions of HO_2

No new information is available for the reactions

$$O + HO_2 \rightarrow OH + O_2$$
$$k \geqslant 10^{-11}$$

and

$$2HO_2 \rightarrow H_2O_2 + O_2$$
$$k = 1.5 \times 10^{-12}$$

where k is the specific rate constant.

D. Reactions of H_2

[14] $O + H_2 \rightarrow OH + H$
$\Delta E_0^0 = +1.9$

Several new studies of this important reaction of ground-state oxygen, ^3P, have been reported, as noted above in the discussion of the reverse reaction. The rate expressions are: $7 \times 10^{-11} \exp(-10.2/RT)$ (23), $2 \times 10^{-11} \exp(-9.2RT)$ (24), and $8 \times 10^{-11} \exp(-10.2/RT)$ (25). Combining the first two of these with the earlier 2×10^{-11} $(-9.4/RT)$ (34), Schofield suggested $2.1 \times 10^{-11} \exp(-9.4/RT)$ (3). The most recent of these investigations, by Westenberg and de-Haas (25) who use the discharge-flow method and e.s.r. detection, also indicates deviations from an Arrhenius expression at the low T end of their range (350 °K) which may be due to tunnelling. The higher activation energy of 10.2 kcal seems to be slightly preferable, and an expression $7 \times 10^{-11} \exp(-10.2/RT)$ is recommended.

E. Reactions of CO and CO_2

As additional species are brought in for consideration and review, the number of possible reactions increases exponentially. Only very few of these reactions will be discussed, however, partly because of their low aeronomic interest and partly because of the paucity of laboratory data. Moreover, all reactions of excited states are discussed elsewhere.

[15] $OH + CO \rightarrow H + CO_2$
$\Delta E_0^0 = -24.4$

Three recent measurements near 300 °K have shown that this reaction has a much smaller activation energy than heretofore believed. Thus, Westenberg and Fristrom (35) combined available kinetic data in 1964 to give the rate expression $1.2 \times 10^{-11} \exp(-7.7/RT)$, based in part on incorrect early discharge work (36). Yet since then, all measurements have indicated that $E < 2$ kcal. Herron (30) reported $(8.5 \pm 3) \times 10^{-14}$ at 300 °K and derived $1.5 \times 10^{-12} \exp(-1.7/RT)$ by combination with explosion and flame data; Dixon-Lewis, Wilson, and Westenberg (28) obtained 1.9×10^{-13} at 300 °K and derived $5.0 \times 10^{-13} \exp(-0.6/RT)$; Greiner (34) obtained 1.5×10^{-13} at 300 °K; and Wilson and O'Donavan (29) also obtained 1.5×10^{-13} although they prefer the somewhat higher 1.7×10^{-13} based on the earlier measurement of reaction [9]. A three parameter expression for this rate constant has also been proposed (28) but is surely not warranted in view of the large spread of nearly an order of magnitude in the high T data. A compromise of $9 \times 10^{-13} \exp(-1.0/RT)$ is suggested, albeit without special evidence.

The reverse reaction is endothermic and therefore quite slow. Using the expression $2.3 \times 10^{-3} \exp(+24.7/RT)$ for the equilibrium constant over the range 300 to 1000 °K, the reverse k is $4.0 \times 10^{-10} \exp(-25.7/RT)$. At 1000 °K, the equilibrium constant is 620 which shows that the reverse reaction is not altogether negligible.

[16] $O + CO + M \rightarrow CO_2 + M$
$\Delta E_0^0 = -125.75$

Our understanding of this simple recombination reaction is still in a most unsatisfactory state. There is general agreement that the reaction is at

least two to three orders of magnitude slower than "normal" recombinations such as O + NO + M or H + O_2 + M, and therefore difficult to study in low pressure flow system. But there has been lack of agreement whether the process is of second or third order in the Torr pressure range, and whether it has a positive or negative T dependence. Clyne and Thrush (37) found no measurable reaction at 293 °K at a total pressure of 2 Torr and CO partial pressure up to 0.5 Torr, and placed an upper limit of 8×10^{-35} on the third order k. They also reported a second order chemiluminescent rate constant of $1 \times 10^{-17} \exp(-3.7/RT)$ for M = O_2, indicating a small energy barrier. Mahan and Solo (38) claim the recombination to be second order to pressures as low as 0.2 Torr and report $k = 1.6 \times 10^{-14} \exp(-4.0/RT)$ for the overall reaction and $2 \times 10^{-13} \exp(-9.5/RT)$ for the chemiluminescent reaction. The former value is almost four times as large as the above upper limit at 2 Torr and therefore inconsistent with it. Hartunian, Thompson, and Hewitt (39) studied only the chemiluminescent reaction in a glow-discharge shock tube and reported $1.6 \times 10^{-18} \exp(-2.5/RT)$, in fair agreement with ref. 37 and in good agreement with a value $0.5 \times 10^{-18} \exp(-2.5/RT)$ obtained by Myers and Bartle (40) from shock tube work near 3000 °K. Avramenko and Kolesnikova (41) also reported the overall reaction to be second order with $k = 1.6 \times 10^{-13} \exp(-3.8/RT)$, but this value gives much too high a k at 300 °K and is in strong disagreement with a recent measurement by Mulcahy and Williams (42), whose measured O + CO rate is 100 times slower than the above at 456 °K. In all, it seems likely that the reaction has a small energy barrier and is third order in the few Torr pressure range, but a definitive experimental study has yet to be undertaken.

[17] $$H + N_2O \rightarrow OH + N_2$$
$$\Delta E_0^0 = -62.8$$

The neutral chemistry of N_2O is unlikely to be of much importance in aeronomy because all its reactions involve fairly large energy barriers. This is true of the reaction O + $N_2O \rightarrow$ 2NO whose energy of activation is near 25 kcal and it also applies to this reaction although to a lesser extent. The H + N_2O reaction was investigated indirectly by Fenimore and Jones (43) at 1260 to 1780 °K by flame probe methods. These authors reported $7 \times 10^{-10} \exp(-16.3/RT)$, but this result was based on the high value of the activation energy for reaction [13], and the rate expression should, therefore, now be changed to $1.3 \times 10^{-10} \exp(-11.3/RT)$. This is in fair agreement with more recent measurements by Dixon-Lewis, Sutton, and Williams (44) whose k's indicate a similar activation energy of 10.1 kcal but are smaller in magnitude. Schofield (3) suggests the rate expression $5 \times 10^{-11} \exp(-10.8/RT)$ as a mean of the available data. Because of slowness of this and other N_2O reactions and because of the low concentrations of reactants, it seems clear that its photochemistry will be of much greater importance than the above collisional processes.

[18] $$H + CH_4 \rightarrow CH_3 + H_2$$
$$\Delta E_0^0 = -2.8$$

The above remarks are applicable here. With the exception of the reaction with $O(^1D)$, which is not covered in this review, all other neutral reactions of CH_4 of aeronomic applicability involve energy barriers and are likely to be slow compared with photoexcitation or dissociation. For the present reaction, the ΔE_0^0 of 2.8 kcal calculated from the JANAF tables should probably be replaced by a value of −0.6 kcal based on Golden, Walsh, and Benson's (45) value for the energy of formation of CH_3. Twelve investigations of this reaction are cited in a recent review (4). Reported activation energies range from 4.5 to 15.1 kcal and pre-exponential values from 10^{-14} to 5×10^{-10}, but there is much better agreement on the absolute value of k than is indicated by this large spread. Schofield (3) has combined the data of seven of these studies in an Arrhenius plot and reports $6.7 \times 10^{-11} \exp(-11.6/RT)$ which indicates that the reaction is negligibly slow near 300 °K.

[19] $$OH + CH_4 \rightarrow H_2O + CH_3$$
$$\Delta E_0^0 = -17.6$$

Similar considerations apply here regarding ΔE_0^0 which is more probably −15.4 in view of the recent work on CH_3 (45). This reaction has been studied repeatedly by a variety of experimental methods, with reported activation energies ranging from 5.0 to 9.0 kcal. Schofield's (3) analysis of most available data yields $1.2 \times 10^{-10} \exp(-5.9/RT)$. In view of the very rapid reaction

of OH with O, the steady-state OH concentration is probably very small, and the present reaction is of no importance.

[20] $$CH_4 + O \rightarrow CH_3 + OH$$
$$\Delta E_0^0 = -0.9$$

ΔE_0^0 is more probably +1.3 kcal (45). Several recent studies of this reaction over the T range 300 to 1000 °K are in surprisingly good agreement. Thus, Schofield (3) summarized the available data by the rate expression 5.3×10^{-11} exp $(-7.95/RT)$, where the specific investigations ranged only from 6.9 to 8.7 kcal in their activation energies. Since the time of that summary, two more studies have been published, both using discharge-flow e.s.r. methods: Brown and Thrush (46) obtain 1.2×10^{-11} exp $(-7.7/RT)$ and Westenberg and deHaas (25) report 2.8×10^{-11} exp $(-8.7/RT)$. The latter expression probably represents the most accurate work, and since it also covers a much larger T range than the former, it is to be preferred. It should be remembered that in this rate constant the subsequent reaction of CH_3 with excess O have been taken into account, i.e. the total O-atom decay rate constant is given by $4k$.

[21] $$Na + O_2 + M \rightarrow NaO_2 + M$$

No value of ΔE_0^0 is given for this reaction, because NaO_2 (g) is not listed in the JANAF tables. There exists a recent, indirect measurement of ΔE_0^0 by McEwan and Phillips (47) of -65 ± 3 kcal, based on the approach to equilibrium of the present reaction in O_2-rich H_2–O_2–N_2 flames. Compared with the corresponding values of -45.9 for HO_2, this seems unexpectedly high. These authors also report a value of 2.0×10^{-35} for the rate constant, surprisingly independent of T over the range 1380 to 2030 °K. This is in fairly good agreement with an earlier measurement by Kaskan (48) of 0.8×10^{-33} obtained from flame work at 1 atm pressure in which the reaction order could not be established. Recently, the pressure dependence of this process was investigated by Carabetta and Kaskan (49) over the pressure range from 100 to 1520 Torr, and the third order dependence was verified. A rate constant of 0.83×10^{-33} was reported near 1500 °K. With an assumed T^{-1} to T^{-2} dependence this will lead to a range of 0.5 to 2.5×10^{-32} near 300 °K, 200 to 1000 times smaller than similarly extrapolated results of Bawn and Evans (50) which are probably too large because of the neglect of quenching of $Na(^2P)$, by N_2 as discussed by Blamont and Donahue (51). However, this discrepancy appears too wide to be bridged by correction of the diffusion flame data (50). The flame k's are smaller than one would expect for a fully allowed three-body process involving a large atom and a moderately electronegative molecule, they show no T dependence over a fairly large range, and they lead to an unreasonably large bond energy. Additional work at low T is needed.

To this author's knowledge, no experimental data are available on the kinetics of the reactions $NaO_2 + O \rightarrow NaO + O_2$ and $NaO + O \rightarrow Na + O_2$. If the recent Na—$O_2$ bond strength of 65 kcal is correct and the JANAF value of 71.2 for the Na—O bond strength is accepted, the former process is only about 6 kcal exothermic and the latter 46.8 kcal, only 1.7 kcal less than the excitation energy of $Na(^2P_{1/2})$. The many other exothermic reactions of Na-oxides with H or OH can not be discussed for lack of any laboratory information.

1. F. KAUFMAN. Ann. Geophys. **20**, 106 (1964).
2. Discussions Faraday Soc. **44**, (1967).
3. K. SCHOFIELD. Planetary Space Sci. **15**, 643 (1967).
4. A. F. TROTMAN-DICKENSON and G. S. MILNE. Tables of Bimolecular Gas Reactions. U.S. Dept. of Commerce NSRDS-NBS 9, 1967.
5. B. H. MAHAN. Ann. Rev. Phys. Chem. **17**, 173 (1966).
6. S. W. BENSON and W. B. DEMORE. Ann. Rev. Phys. Chem. **16**, 397 (1965).
7. JANAF Thermochemical Tables. U.S. Dept. Commerce, Natl. Bur. Std. PB 168370, -1, -2, 1965, 1966, 1967.
8. F. S. LARKIN and B. A. THRUSH. *In* 10th Intern. Symp. Combustion. The Combustion Institute, Pittsburgh, Pa. 1965. p. 397.
9. S. W. BENSON and T. FUENO. J. Chem. Phys. **36**, 1697 (1962).
10. E. A. SUTTON. J. Chem. Phys. **36**, 2923 (1962).
11. I. R. HURLE. *In* 11th Intern. Symp. Combustion. The Combustion Institute, Pittsburgh, Pa. 1967. p. 827.
12. J. L. J. ROSENFELD. Discussions Faraday Soc. **44**, 89 (1967).
13. M. A. A. CLYNE and B. A. THRUSH. Proc. Roy. Soc. London, Ser. A, **275**, 559 (1963).
14. F. S. LARKIN and B. A. THRUSH. Discussions Faraday Soc. **37**, 112 (1964).
15. D. B. HARTLEY and B. A. THRUSH. Proc. Roy. Soc. London, Ser. A, **297**, 520 (1967).
16. M. A. A. CLYNE and B. A. THRUSH. Discussions Faraday Soc. **33**, 139 (1962).
17. M. A. A. CLYNE. *In* 10th Intern. Symp. Combustion. The Combustion Institute, Pittsburgh, Pa. 1965. p. 311.
18. F. C. KOHOUT and F. W. LAMPE. J. Chem. Phys. **46**, 4075 (1967).
19. L. F. PHILLIPS and H. I. SCHIFF. J. Chem. Phys. **37**, 1233 (1962).

20. W. A. ROSSER, JR. and H. WISE. J. Phys. Chem. **65**, 532 (1961).
21. K. G. ANLAUF, R. G. MACDONALD, and J. C. POLANYI. Chem. Phys. Letters, **1**, 619 (1968).
22. W. B. DEMORE. J. Chem. Phys. **46**, 813; **47**, 2777 (1967).
23. E. L. WONG and A. E. POTTER. J. Chem. Phys. **43**, 3371 (1965).
24. D. L. RIPLEY and W. C. GARDINER, JR. J. Chem. Phys. **44**, 2285 (1966).
25. A. A. WESTENBERG and N. DEHAAS. J. Chem. Phys. **46**, 490 (1967); **47**, 4241 (1967).
26. A. A. WESTENBERG and N. DEHAAS. J. Chem. Phys. **43**, 1550 (1965).
27. G. DIXON-LEWIS, W. E. WILSON, and A. A. WESTENBERG. J. Chem. Phys. **44**, 2877 (1966).
28. W. E. WILSON, JR. and J. T. O'DONOVAN. J. Chem. Phys. **47**, 5455 (1967).
29. J. T. HERRON. J. Chem. Phys. **45**, 1854 (1966).
30. D. M. GOLDEN, F. P. DELGRECO, and F. KAUFMAN. J. Chem. Phys. **39**, 3034 (1963).
31. R. G. BENNETT and F. W. DALBY. J. Chem. Phys. **40**, 1414 (1964).
32. W. B. DEMORE and O. F. RAPER. J. Chem. Phys. **46**, 2500 (1967).
33. N. R. GREINER. J. Chem. Phys. **46**, 2795 (1967).
34. M. A. A. CLYNE and B. A. THRUSH. Proc. Roy. Soc. London, Ser. A, **275**, 544 (1963); *In* 9th Intern. Symp. Combustion. The Academic Press, Inc., New York. 1963. p. 211.
35. A. A. WESTENBERG and R. M. FRISTROM *In* 10th Intern. Symp. Combustion. The Combustion Institute, Pittsburgh, Pa. 1965. p. 473.
36. L. I. AVRAMENKO and R. V. LORENTSO. Zh. Fiz. Khim. **24**, 207 (1950).
37. M. A. A. CLYNE and B. A. THRUSH. Proc. Roy. Soc. London, Ser. A, **269**, 404 (1962); *In* 9th Intern. Symp. Combustion. Academic Press, Inc., New York. 1963. p. 177.
38. B. H. MAHAN and R. B. SOLO. J. Chem. Phys. **37**, 2669 (1962).
39. R. A. HARTUNIAN, W. P. THOMPSON, and E. W. HEWITT. J. Chem. Phys. **44**, 1765 (1966).
40. B. F. MYERS and E. R. BARTLE. J. Chem. Phys. **47**, 1783 (1967).
41. L. I. AVRAMENKO and R. V. KOLESNIKOVA. Izv. Akad. Nauk SSSR, 1562 (1959); 561 (1960).
42. M. F. R. MULCAHY and D. J. WILLIAMS. Trans. Faraday Soc. **64**, 59 (1968).
43. C. P. FENIMORE and G. W. JONES. J. Phys. Chem. **63**, 1154 (1959).
44. G. DIXON-LEWIS, M. M. SUTTON, and A. WILLIAMS. *In* 10th Intern. Symp. Combustion. The Combustion Institute, Pittsburgh, Pa. 1965. p. 495; J. Chem. Soc. 5724 (1965).
45. D. M. GOLDEN, R. WALSH, and S. W. BENSON. J. Am. Chem. Soc. **87**, 4053 (1965).
46. J. M. BROWN and B. A. THRUSH. Trans. Faraday Soc. **63**, 630 (1967).
47. M. J. MCEWAN and L. F. PHILLIPS. Trans. Faraday Soc. **62**, 1717 (1966).
48. W. E. KASKAN. *In* 10th Intern. Symp. Combustion. The Combustion Institute, Pittsburgh, Pa. 1965. p. 41.
49. R. CABARETTA and W. E. KASKAN. J. Phys. Chem. **72**, 2483 (1968).
50. C. E. H. BAWN and A. G. EVANS. Trans. Faraday Soc. **33**, 1580 (1937).
51. J. E. BLAMONT and T. M. DONAHUE. J. Geophys. Res. **69**, 4093 (1964).

Comments, Replies, and Summary

COMMENTS BY A. FONTIJN[1]

The discrepancy between the determinations of the rate constant of the reaction $Na + O_2 + M \rightarrow NaO_2 + M$, noted in Professor Kaufman's article, may be readily explainable. In the atomic diffusion flame work of ref. 1, a "fog" of sodium oxide particles is present, thus creating a large surface area on which reactions can occur. The rates measured, therefore, may pertain to undefined combinations of homogeneous and heterogeneous reactions and the obtained rate constant may well be orders of magnitude too high, as the comparison to the "hot" flame work seems to suggest.

Steacie (2) has pointed out that reaction products, present in the form of solid particles, may participate in atomic alkali halide reactions. The present observation thus appears to confirm this possibility.

[1]Address: Aerochemistry Research Laboratories, Princeton, New Jersey.

1. C. E. H. BAWN and A. C. EVANS. Trans. Faraday Soc. **33**, 1580 (1937).
2. E. W. R. STEACIE. Atomic and free radical reactions. Vol. 1. 2nd ed. Reinhold Publishing Corp., New York. 1954. p. 22.

COMMENTS BY L. F. PHILLIPS[2]

Regarding NaO_2, I wish to make the following points:

1. The temperature coefficient (negative) of the reaction $Na + O_2 + M \rightarrow NaO_2 + M$ is obscured in flames by the fact that the nature of M changes with temperature, increasing T being accompanied by increasing partial pressure of H_2O.

2. Carabetta and Kaskan (1) believe that 65 kcal is too low a value for $D^0(Na—O_2)$ because, on the basis of the JANAF value of 90 kcal for D^0(Na—OH), the equilibrium $NaO_2 + H \rightleftharpoons NaOH + O$ would favor NaOH over NaO_2 in flames, contrary to observation. However, in this case

[2]Address: Lawrence Radiation Laboratory, Berkeley, California.

20. W. A. ROSSER, JR. and H. WISE. J. Phys. Chem. **65**, 532 (1961).
21. K. G. ANLAUF, R. G. MACDONALD, and J. C. POLANYI. Chem. Phys. Letters, **1**, 619 (1968).
22. W. B. DEMORE. J. Chem. Phys. **46**, 813; **47**, 2777 (1967).
23. E. L. WONG and A. E. POTTER. J. Chem. Phys. **43**, 3371 (1965).
24. D. L. RIPLEY and W. C. GARDINER, JR. J. Chem. Phys. **44**, 2285 (1966).
25. A. A. WESTENBERG and N. DEHAAS. J. Chem. Phys. **46**, 490 (1967); **47**, 4241 (1967).
26. A. A. WESTENBERG and N. DEHAAS. J. Chem. Phys. **43**, 1550 (1965).
27. G. DIXON-LEWIS, W. E. WILSON, and A. A. WESTENBERG. J. Chem. Phys. **44**, 2877 (1966).
28. W. E. WILSON, JR. and J. T. O'DONOVAN. J. Chem. Phys. **47**, 5455 (1967).
29. J. T. HERRON. J. Chem. Phys. **45**, 1854 (1966).
30. D. M. GOLDEN, F. P. DELGRECO, and F. KAUFMAN. J. Chem. Phys. **39**, 3034 (1963).
31. R. G. BENNETT and F. W. DALBY. J. Chem. Phys. **40**, 1414 (1964).
32. W. B. DEMORE and O. F. RAPER. J. Chem. Phys. **46**, 2500 (1967).
33. N. R. GREINER. J. Chem. Phys. **46**, 2795 (1967).
34. M. A. A. CLYNE and B. A. THRUSH. Proc. Roy. Soc. London, Ser. A, **275**, 544 (1963); *In* 9th Intern. Symp. Combustion. The Academic Press, Inc., New York. 1963. p. 211.
35. A. A. WESTENBERG and R. M. FRISTROM *In* 10th Intern. Symp. Combustion. The Combustion Institute, Pittsburgh, Pa. 1965. p. 473.
36. L. I. AVRAMENKO and R. V. LORENTSO. Zh. Fiz. Khim. **24**, 207 (1950).
37. M. A. A. CLYNE and B. A. THRUSH. Proc. Roy. Soc. London, Ser. A, **269**, 404 (1962); *In* 9th Intern. Symp. Combustion. Academic Press, Inc., New York. 1963. p. 177.
38. B. H. MAHAN and R. B. SOLO. J. Chem. Phys. **37**, 2669 (1962).
39. R. A. HARTUNIAN, W. P. THOMPSON, and E. W. HEWITT. J. Chem. Phys. **44**, 1765 (1966).
40. B. F. MYERS and E. R. BARTLE. J. Chem. Phys. **47**, 1783 (1967).
41. L. I. AVRAMENKO and R. V. KOLESNIKOVA. Izv. Akad. Nauk SSSR, 1562 (1959); 561 (1960).
42. M. F. R. MULCAHY and D. J. WILLIAMS. Trans. Faraday Soc. **64**, 59 (1968).
43. C. P. FENIMORE and G. W. JONES. J. Phys. Chem. **63**, 1154 (1959).
44. G. DIXON-LEWIS, M. M. SUTTON, and A. WILLIAMS. *In* 10th Intern. Symp. Combustion. The Combustion Institute, Pittsburgh, Pa. 1965. p. 495; J. Chem. Soc. 5724 (1965).
45. D. M. GOLDEN, R. WALSH, and S. W. BENSON. J. Am. Chem. Soc. **87**, 4053 (1965).
46. J. M. BROWN and B. A. THRUSH. Trans. Faraday Soc. **63**, 630 (1967).
47. M. J. MCEWAN and L. F. PHILLIPS. Trans. Faraday Soc. **62**, 1717 (1966).
48. W. E. KASKAN. *In* 10th Intern. Symp. Combustion. The Combustion Institute, Pittsburgh, Pa. 1965. p. 41.
49. R. CABARETTA and W. E. KASKAN. J. Phys. Chem. **72**, 2483 (1968).
50. C. E. H. BAWN and A. G. EVANS. Trans. Faraday Soc. **33**, 1580 (1937).
51. J. E. BLAMONT and T. M. DONAHUE. J. Geophys. Res. **69**, 4093 (1964).

Comments, Replies, and Summary

COMMENTS BY A. FONTIJN[1]

The discrepancy between the determinations of the rate constant of the reaction $Na + O_2 + M \rightarrow NaO_2 + M$, noted in Professor Kaufman's article, may be readily explainable. In the atomic diffusion flame work of ref. 1, a "fog" of sodium oxide particles is present, thus creating a large surface area on which reactions can occur. The rates measured, therefore, may pertain to undefined combinations of homogeneous and heterogeneous reactions and the obtained rate constant may well be orders of magnitude too high, as the comparison to the "hot" flame work seems to suggest.

Steacie (2) has pointed out that reaction products, present in the form of solid particles, may participate in atomic alkali halide reactions. The present observation thus appears to confirm this possibility.

[1]Address: Aerochemistry Research Laboratories, Princeton, New Jersey.

1. C. E. H. BAWN and A. C. EVANS. Trans. Faraday Soc. **33**, 1580 (1937).
2. E. W. R. STEACIE. Atomic and free radical reactions. Vol. 1. 2nd ed. Reinhold Publishing Corp., New York. 1954. p. 22.

COMMENTS BY L. F. PHILLIPS[2]

Regarding NaO_2, I wish to make the following points:

1. The temperature coefficient (negative) of the reaction $Na + O_2 + M \rightarrow NaO_2 + M$ is obscured in flames by the fact that the nature of M changes with temperature, increasing T being accompanied by increasing partial pressure of H_2O.

2. Carabetta and Kaskan (1) believe that 65 kcal is too low a value for $D^0(Na—O_2)$ because, on the basis of the JANAF value of 90 kcal for D^0(Na—OH), the equilibrium $NaO_2 + H \rightleftharpoons NaOH + O$ would favor NaOH over NaO_2 in flames, contrary to observation. However, in this case

[2]Address: Lawrence Radiation Laboratory, Berkeley, California.

Can. J. Chem. Downloaded from www.nrcresearchpress.com by 210.87.254.6 on 09/05/12
For personal use only.

Can. J. Chem. Downloaded from www.nrcresearchpress.com by 210.87.254.6 on 09/05/12
For personal use only.

JANAF is wrong, and the value of 77 kcal for D^0(Na—OH) given by Jensen and Padley (2) changes the picture so that the above equilibrium actually favors NaO_2, as observed.

3. Using the listed heat of formation (Gilles and Magrave) of 62 kcal for NaO_2(s) at 298 °K it is possible to deduce a heat of vaporization near 22 kcal for NaO_2(s) at 298 °K. This seems rather low (values for Na metal 26 kcal, NaI 48 kcal, NaOH 47 kcal) but may be reasonable in view of the instability of solid NaO_2 at room temperature. A higher D^0(Na—O_2) value would give a still lower heat of vaporization.

3. R. CABARETTA and W. E. KASKAN. J. Phys. Chem. **72**, 2483 (1968).
4. D. E. JENSEN and P. J. PADLEY. Trans. Faraday Soc. **62**, 2132 (1966).

REPLY BY F. KAUFMAN

I can not accept Dr. Phillips' second and third points. Regarding *2*, although the reaction $NaO_2 + H \rightarrow NaOH + O$ becomes slightly endothermic if the value of 77 kcal for D^0(Na − OH) is accepted, the more important process $NaO_2 + OH \rightarrow NaOH + O_2$ is still fairly exothermic. For either reaction (or for $NaO_2 + O \rightarrow NaO + O_2$) one should carry out equilibrium calculations rather than rely on qualitative arguments.

In *3*, it seems strange to rationalize an unusually low heat of vaporization as due to the instability of the solid (presumably with respect to other species in the solid phase). The melting point of NaO_2(c) has been reported to be 825 °K. There seems to be no reason why NaO_2(c) should not readily vaporize to NaO_2(g) if its ΔH_V is only 22 kcal and if the Na—O_2 bond energy is as large as 65 kcal, which makes NaO_2 the most stable gaseous Na-oxide by far, at moderate temperatures. I consider it more likely that the ΔH_V is near 40 kcal, the bond energy also near 40 to 45 kcal, and that the oxide is, therefore, extensively dissociated at elevated temperatures but is formed as an intermediate species which reacts further to produce NaO or NaOH.

SUMMARY AND REMARKS BY CHAIRMAN, D. M. HUNTEN[3]

In the Earth's atmosphere, the reactions of hydrogen and its compounds are of interest in three principal ways:

(*1*) as a possibly significant loss mechanism for ozone, whose concentrations are otherwise predicted to be greater than observed;

(*2*) in connection with the excitation of the Meinel (i.e. vibration–rotation) bands of OH, closely related to (*1*), because the important reaction is $H + O_3 \rightarrow OH + O_2$;

(*3*) as a source of atomic hydrogen, whose behavior is of great interest in the thermosphere and which dominates the exosphere.

An important obstacle to quantitative study has been the lack of certainty about the mixing ratio of H_2O at balloon altitudes. The best aircraft measurements in the lower stratosphere have given low values, but much higher results have frequently been obtained by balloon-borne instruments. There now seems little doubt that most of the difference has been H_2O released from the balloon; the effect is much less important for an aircraft, which does not float along in its own vapor cloud. The most careful work (1) shows consistently a mixing ratio of 3×10^{-6} by volume; the payload must be suspended far below the balloon, and the best measurements are made during descent, initiated by ejection of part of the lifting gas. Optical absorption is also subject to error; Zander (2) has published some direct observations of the vapor cloud, made as the line of observation to the Sun passed near the balloon.

A further uncertainty is the possible role of methane as a source of H atoms. Bates and Nicolet (3) point out that the mixing ratio is 1.5×10^{-6} in the tropopause, and if upward transport is fast enough, an additional 3×10^{-6} of H_2O would be produced. But it may be that the H_2O observations include this contribution.

Calculations of the O–O_3 equilibrium have been made by Hunt (4) with a water–vapor mixing ratio of 5×10^{-6}, close to what is suggested above, and using essentially the rate coefficients recommended by Kaufman. He finds that the inclusion of the hydrogen compounds produces a much better agreement with the observed ozone amounts. The important reactions at high altitudes are Kaufman's reactions [6] and [10], also responsible for the OH nightglow. At lower altitudes reaction [11] is invoked, followed by the reaction of HO_2 with O_3. Kaufman's warnings about this cycle should be kept in mind.

[3]Address: Kitt Peak National Observatory, Tucson, Arizona.

Near 90 km the dominant form of hydrogen becomes H (5), but the details are not well understood, especially the transport processes that must be included. At great enough heights, the H becomes the dominant constituent by gravitational separation, but the treatment is complicated by the upward flux that is required to replace the atoms that escape the Earth's gravitational field altogether.

Other planets show strikingly different problems, which have received less discussion. The atmospheres of the major planets are nearly all H_2, and the temperatures are low. The equilibrium between H_2 and H becomes the analogue of the familiar one between O_2 and O; a preliminary study has been made by Gross and Rasool (6). The minor constituents, CH_4 and NH_3, are subject to photolysis, but no obvious way exists of reforming them, except far down in the dense lower atmosphere (7).

On Mars and Venus there is much CO_2 but little free oxygen. McElroy has suggested that under these conditions much of the upper-atmospheric hydrogen will appear as H_2. Any effect of hydrogen compounds of the CO_2–CO equilibrium is likely to be small, because of the very small concentrations of both hydrogen and oxygen. Atomic hydrogen in the exosphere of Venus has been observed from two planetary probes by the scattered Lyman-α radiation. The radial distribution is anomalous, and one suggestion invoked H_2 in addition to H. The H_2 mechanism has been shown to be self-contradictory (8, 9), and the only remaining possibility seems to be deuterium. If this is so, many interesting problems of atmospheric chemistry and evolution will have to be considered.

5. H. J. MASTENBROOK. J. Atmospheric Sci. **25**, 299 (1968).
6. R. ZANDER. J. Geophys. Res. **71**, 3775 (1966).
7. D. R. BATES and M. NICOLET. Planetary Space Sci. **13**, 905 (1965).
8. B. G. HUNT. J. Geophys. Res. **71**, 1385 (1966).
9. E. HESSTVEDT. Geophysica Norvegica, **27**, no. 4 (1968).
10. S. H. GROSS and S. I. RASOOL. Icarus, **3**, 311 (1964).
11. R. D. CADLE. J. Atmospheric Sci. **19**, 281 (1962).
12. T. M. DONAHUE. J. Atmospheric Sci. **25**, 568 (1968).
13. M. B. MCELROY and D. M. HUNTEN. J. Geophys. Res. In press.

Can. J. Chem. Downloaded from www.nrcresearchpress.com by 210.87.254.6 on 09/05/12
For personal use only.

Can. J. Chem. Downloaded from www.nrcresearchpress.com by 210.87.254.105 on 09/05/12
For personal use only.

Chemiluminescent reactions in the airglow

ROBERT A. YOUNG
Center for Research in Experimental Space Science, York University, Toronto, Ontario

Received December 31, 1968

Laboratory experiments on chemiluminescent reactions involving atomic oxygen of pertinence to the earth's nightglow are reviewed. From simple consideration it is shown that the atomic oxygen concentration in the earth's upper atmosphere must be larger than the presently accepted value of 2×10^{11} atoms/cm^3 at the peak in the atomic oxygen altitude profile. Rocket measurements of the volume emission intensity of 5577 Å radiation and laboratory measurements of the rate of its excitation by three-body atomic oxygen association indicate a peak upper atmospheric atomic oxygen concentration near 10^{12} atoms/cm^3. The excitation of molecular oxygen emission in atomic association is a multistep process involving at least one quenchable precursor. Laboratory results are inadequate to define the excitation mechanism but a strongly temperature-dependent precursor deactivation process is required for laboratory observation to be consistent with the hypothesis that atomic association is the cause of nightglow O_2 emission. Other processes are briefly discussed.

Canadian Journal of Chemistry, 47, 1927 (1969)

Introduction

Planetary atmospheres are inhomogeneous, having a density which decreases approximately exponentially upward from the surface. Photodissociation of this atmosphere by solar radiation produces the reactants which later undergo exothermic reaction. Generally, the effective solar radiation is in the far ultraviolet and is strongly absorbed. Hence photodissociation occurs high in the atmosphere where the atmosphere is tenuous. Since re-association usually requires a three-body process, the fragments diffuse downward where recombination is possible and the resulting molecules diffuse upward. The reactive constituents have a maximum concentration below the height at which maximum photodecomposition occurs and above the height where recombination is more important than diffusion.

This combination of circumstances is usually not suitable for direct laboratory simulation and study, because the total pressure is so low that very large volumes must be employed if surface phenomena are to be sufficiently minimized, and the total rate of product formation is consequently too slow to be detectable. Hence laboratory measurements of possible chemiluminescent processes pertinent to the upper atmosphere are done at considerably higher densities of both the reactive and nonreactive constituents of planetary atmospheres. This increases both the rate of product formation and the rate of secondary collisional phenomena.

Since radiative deactivation of excited species is unimolecular, but collisional deactivation is bimolecular, the overall efficiency of chemiluminescent reactions decreases and emission from other components of the system may increase — because of energy transfer — as the pressure is raised to that necessarily employed in laboratory experiments. Hence collisional deactivation processes must be measured if laboratory results are to be applied in planetary atmospheres.

Since photodecomposition is the result of absorption of ultraviolet solar energy and this energy must drive all atmospheric exothermic processes, it is logical that associative reactions are the major chemical processes occurring in planetary atmospheres. Were this not the case, planetary atmospheres must decompose into simpler constituents. Presumably, this has already occurred if it is possible.

The night airglow is due almost exclusively to chemiluminescent processes utilizing energy stored in photodissociation products created during the day by solar radiation. Since the major effect of the sun on the upper atmosphere of the earth is to dissociate O_2, most nightglow emissions are expected to be produced by processes involving atomic oxygen. Hence it is not surprising to observe emission from O_2 and O. However, it may be surprising that the largest total photon flux is due to OH vibration–rotation bands from the ground electronic state. Table I contains a list of observed nightglow emissions and an estimate of their total intensity.

Overall Consideration of Nightglow Excitation

Before entering into a discussion of specific processes which produce the emissions tabulated

TABLE I*

Intensity of nightglow emissions

Emission	Species	Emission rate in a column of atmosphere (photons/cm² s)	Emission rate (Rayleighs)
5893 Å	Na	1×10^8	100
6300 Å	$O(^1D)$	1×10^8	100
5577 Å	$O(^1S)$	2.5×10^8	250
Continuum (400–10 000 Å)	$NO_2(?)$	1×10^9	10^3
Herzberg bands (3000–4000 Å)	$O_2(A^3\Sigma_u^+)$	1×10^9	10^3
Atmospheric bands (7000–9000 Å)	$O_2(b^1\Sigma_u^+)$	3×10^{10}	3×10^4
Infrared atmospheric (1 μ)	$O_2(a^1\Delta)$	5×10^{10}	5×10^4
Meinel bands (5000 Å – 5 μ)	OH	4.5×10^{12}	4.5×10^6

*This table is derived from Table II.1 in Appendix II of ref. 5 and modified as discussed in Sections 12.3, 13.4, and 13.5.

in Table I, a comparison of the total energy flux released by atomic oxygen association with the energy radiated in the nightglow is instructive. Figure 1 shows the theoretical computation of the altitude profiles of [O], [O_2], and [O_2] + [N_2] = [M] normalized to rocket data for [O] at 120 km. This profile is considered to be the best present knowledge of these constituents. Also shown are the rate of O_2 formation by

[*a*] $$O + O + M \rightarrow O_2 + M$$

and

[*b*] $$O + O_2 + M \rightarrow O_3 + M$$

[*c*] $$O + O_3 \rightarrow 2O_2$$

These production rates were computed using rate coefficients of 3×10^{-33}, 8×10^{-34} cm⁶/s for k_a and k_b (1)[1], and assuming that O_3 is in a steady state. Then the rate of O_2 formed by the series of reactions [*b*] and [*c*] is the rate of O_3 formation by reaction [*b*]. An upper limit to the energy released above 80 km by reaction [*a*] in a cm² column of the atmosphere is 5×10^{10} eV/cm² s and the upper limit by reactions [*b*] and [*c*] is 4×10^{12} eV/cm² s. The energy radiated from O_2 is 1×10^{11} eV/cm² s and that from OH is 5×10^{12} eV/cm² s. It is certain that all the energy which atomic oxygen can liberate by forming O_2, roughly 5 eV/molecule, is not radiated, especially in the atmospheric, infrared atmospheric, and OH Meinel bands.

[1]This reference contains an up-to-date compilation of rate coefficients pertinent to atmospheric phenomena.

These comparisons indicate that unless the atomic oxygen concentration profile (2), as currently accepted, is modified to indicate considerably larger concentration of atomic oxygen, atomic oxygen association by reactions [*a*], [*b*], and [*c*] cannot power the airglow. There is no doubt, in fact, that it does. It will not be surprising, then, if individual processes subsequently discussed are similarly found inadequate to account for specific emission features in the nightglow, if the presently accepted atomic oxygen profile is used.

Chemiluminescent Reactions

All exothermic chemical reactions are potentially chemiluminescent. Unless all the energy released in the chemical reaction is initially converted into kinetic energy, the products must contain excess rotational, vibrational, or electronic energy. In the absence of collision phenomena this energy can only be dissipated by radiation and the chemical reaction would be termed chemiluminescent.

Since the initial reaction involved a collision between reactants, the products must also suffer collisions. Luminescence will then result only when the rate of radiation is larger than the rate of collisional removal of energy. Hence the term "chemiluminescent reactions" is a relative one; an exothermic reaction will generally be luminescent provided radiation rather than collisional processes remove the excess internal energy.

Can. J. Chem. Downloaded from www.nrcresearchpress.com by 210.87.254.105 on 09/05/12
For personal use only.

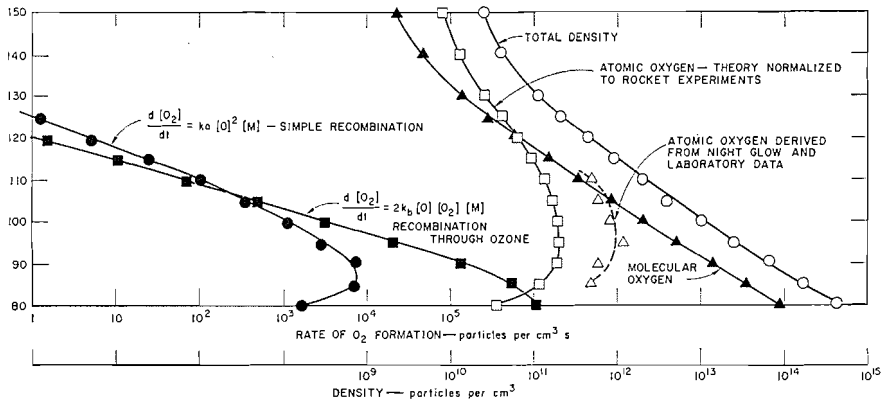

FIG. 1. This figure is a composite of (*a*) the densities of [O], [O_2] and [O_2] + [N_2] derived from calculations in ref. 2, normalized to rocket measurements of atomic oxygen at 120 km, and also adjusted so that [O]/[O_2] = 1 at this altitude in conformance to rocket measurement, (*b*) the rate of O_2 formation using the depicted densities and rate coefficients listed in the text, and (*c*) the atomic oxygen profile deduced from rocket measurement of 5577 Å emission in the nightglow as reported in ref. 8.

Because most exothermic chemical reactions lead to excited products, a study of chemiluminescent reactions is largely a study of the competition between radiation and collisional deactivation of excited atoms and molecules. For a given collision environment, the shorter the radiative lifetime of the excited species the more likely it is to dissipate its excess energy as radiation. Hence emission is more likely from electronically excited species than from vibrationally or rotationally excited species.

Although the energy released in reactions may not be significantly radiated from the initial products because of collisional effects, a large part of this energy may ultimately appear as radiation if deactivation of the products occurs by energy transfer to radiative states. This depends on the radiative lifetime of the acceptor relative to its collisional deactivation lifetime. In short, the appearance of emission during an exothermic chemical reaction depends upon the radiative and collisional characteristics of the entire system in which energy is being released. Because of this, different exothermic reactions may lead to similar emission phenomena provided other constituents are common elements of the two systems. The observed emission may not be unique to a single exothermic reaction.

Since energy radiated out of a reacting system is unavailable for further chemical use, excited products with short radiative lifetimes generally do not play a significant role in the evolution of the reacting system. However, metastable electronically excited species and vibrationally or rotationally excited species may have significant consequences for the evolution of a reaction system. Since the reactive character of a species is determined largely by its outer electronic structure, and electronic excitation changes this structure as significantly as changing its chemical identity, electronically excited species may have an entirely different chemical character from the same species in its unexcited state. Electronic excitation then adds entirely new reactants to a chemical system.

Vibrational and rotational excitation primarily affect the state of motion of the nuclei forming a molecule and have a less direct effect on its chemical behavior. Since the rate coefficients of many reactions depend strongly on temperature over an interval where significant change in the vibrational excitation of the gas does not occur, this dependence must be due either to effects of relative energy of collision or the rotational state of the reactant, or both. Of the two possibilities, the relative energy of the collision is considered more important in determining the rates of chemical processes. Vibrational energy is known to be effective in causing increases in reaction rates, but detailed studies are as yet incomplete.

Laboratory Experiments

Theory

Laboratory experiments generally consist of

Can. J. Chem. Downloaded from www.nrcresearchpress.com by 210.87.254.105 on 09/05/12
For personal use only.

Can. J. Chem. Downloaded from www.nrcresearchpress.com by 210.87.254.105 on 09/05/12
For personal use only.

measuring the intensity of emission from a particular excited state of a particular chemical species which might be called X_n^*. Then

$$[1] \qquad I(X_n^*) = \frac{[X_n^*]}{\tau(X_n^*)}$$

where $I(X_n^*)$ is the emission in photons/cm^3 s from X_n^* which has a density of $[X_n^*]$ molecules/cm^3 and $\tau(X_n^*)$ is the spontaneous radiative lifetime of X_n^*. If X_n^* is deactivated by species i in a process having coefficient k_i then in a steady state

$$[2] \qquad P(X_n^*) = (1/\tau(X_n^*) + \sum k_i[i])[X_n^*]$$

or

$$[3] \qquad P(X_n^*) = (1 + \tau(X_n^*)\sum k_i[i])I(X_n^*)$$

where $P(X_n^*)$ is the rate of production of X_n^* per cm^3. Since $P(X_n^*)$ is here due to chemical processes, it depends upon the constituents of the system, their densities, and the temperature. The dependence of $P(X_n^*)$ on [i] is the primary data desired from the experiment. From such data the mechanism of excitation and its rate coefficient may be deducible.

It is apparent, however, that steady-state experiments do not give $P(X_n^*)$ unless $\sum k_i[i]$ is known or negligible. Furthermore, unless the processes producing X_n^* are elementary, the functional dependence of $P(X_n^*)$ on [i] will not uniquely determine either the group of processes leading to excitation of X_n^* or the appropriate rate coefficients. This latter difficulty is important, fundamental, and often encountered. It can only be removed by measurement or manipulation of the intermediate compounds involved in the processes forming X_n^*.

Associative reactions are generally three-body processes, since both momentum and energy are unlikely to be conserved in two-body associative processes except through radiation. This is particularly true for atomic association as occurs in the earth's atmosphere. Hence $P(X_n^*)$ in its simplest form is

$$[4] \qquad P(X_n^*) = \sum \bar{k}_i[X][X_{n-1}][i]$$

implying (perhaps)

$$[d] \qquad X + X_{n-1} + i \rightarrow X_n^* + i$$

and then

$$[5] \qquad \sum \bar{k}_i[X][X_{n-1}][i] = (1 - \tau(X_n^*)\sum k_i[i])I(X_n^*)$$

This formulation singles out X and X_{n-1} on the left but not on the right side.

A somewhat more involved process is

$$[e] \qquad X + X_{n-1} + i \rightarrow X_n^* + i$$

$$[f] \qquad X_n^* + i \rightarrow X_n + i$$

$$[g] \qquad X_n^* \rightarrow X_n + h\nu$$

giving

$$[6] \qquad I(X_n^*) = \frac{\sum \bar{k}_i(e)[X][X_{n-1}][i]k_g}{\sum(k_g + \sum k_i(f))[i]}$$

This can be further complicated if an intermediate or precursor excited species is involved.

$$[h] \qquad X + X_{n-1} + i \rightarrow X_n^{**} + i$$

$$[j] \qquad X_n^{**} + i \rightarrow X_n^* + i$$

$$[l] \qquad X_n^{**} + i \rightarrow X_n + i$$

$$[m] \qquad X_n^{**} \rightarrow X_n + h\nu$$

$$[n] \qquad X_n^* + i \rightarrow X_n + i$$

$$[p] \qquad X_n^* \rightarrow X_n + h\nu$$

which leads to the complicated expression

$$[7] \qquad I(X_n^*) = \frac{(\sum \bar{k}_i(h)[X][X_{n-1}][i])(\sum k_i(j)[i])}{\{k_m + \sum(k_i(j) + k_i(l)[i])\}(k_p + \sum k_i(n)[i])}$$

From these formations it can be seen that interpretation of laboratory observation of $I(X_n^*)$ vs. [i] may be difficult.

How Atomic Oxygen Is Made and Measured in the Laboratory

Laboratory experiments on atomic oxygen airglow reactions consists of making, controlling, and measuring atomic oxygen in a largely N_2 atmosphere and measuring the intensity of emission from the appropriate emitting species.

Figure 2 schematically shows a suitable experimental system (3). Nitrogen flows through a microwave discharge at a few Torr pressure where it is partially dissociated, past an inlet for NO which reacts rapidly with N

$$[q] \qquad N + NO \rightarrow N_2 + O$$

to produce O from N, into a large observation bulb, and finally out to a fast mechanical pump.

Can. J. Chem. Downloaded from www.nrcresearchpress.com by 210.87.254.105 on 09/05/12
For personal use only.

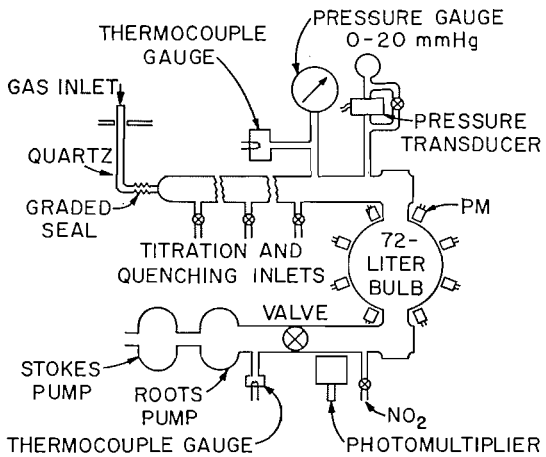

FIG. 2. A schematic diagram of a low pressure flow system suitable for investigating atmospheric chemiluminescent reactions.

The flow velocity in the 4 in. i.d. tubing is 8 m/s and the residence time of the gas in the 72 l bulb is approximately 1 s.

This indirect method of producing atomic oxygen is used to prevent the formation of excited O_2 molecules, except by atom association, and to permit [O] to be controlled by the rate of NO addition to the gas stream. The rate coefficient of reaction [*q*] was first measured using mass spectroscopic techniques (4) and the result has been repeatedly verified (1).

To measure [O], several subsidiary chemiluminescent reactions are utilized (3). The emission of the N_2 first positive bands occurs in the recombination of atomic nitrogen, the NO δ, γ, and β bands are excited in the association of N and O, and NO_2 "continuum" is excited in the association of O and NO. In each instance the intensity of emission is proportional to the simple product of reactant densities

$$[8] \qquad I_{N_2} = K_\alpha[N]^2$$

$$[9] \qquad I_{NO} = K_\beta[N][O]$$

$$[10] \qquad I_{NO_2} = K_\gamma[O][NO]$$

The constants of proportionality may depend upon both gas composition and pressure, but can be empirically obtained by using reaction [*q*]. As NO is added, [N] decreases and [O] increases. When I_{NO} is a maximum, [N] = [O], and [O] can be computed from the rate of [NO] addition and the rate of flow of the gas in the flow system. Knowing [N] and [O] permits K_α and K_β to be computed. As the flow rate of NO into the system is further increased I_{N_2} and I_{NO} decrease to zero when [N] = 0. Further addition of NO causes I_{NO_2} to increase from its previous near zero value. The point of minimum emission is called the null point and corresponds to [N] $\approx$ 0, [NO] $\approx$ 0 and [O] equals the concentration of [NO] that would be present if it did not react. Emission at the null point is, of course, not zero because emission from atomic oxygen association, which is to be studied, is occurring at a maximum rate. However, atomic oxygen association produces much less emission than the other processes.

As [NO] increases beyond the null point I_{NO_2} increases linearly so long as [O] is not appreciably decreased by reations with NO. This is because the series of reactions

$$[r] \qquad O + NO + M \rightarrow NO_2 + M$$

$$[s] \qquad NO_2 + O \rightarrow NO + O_2$$

catalytically recombine O but do not decrease NO. As [NO] increases reactions [*r*] and [*s*] become the dominant ones removing O, and I_{NO_2} decreases. If NO_2 were added to the stream containing only O, I_{NO_2} would increase as reaction [*s*] causes NO to increase, reach a maximum, and then decrease to zero when all O had been consumed. Since a null is more reliably measured, the NO_2 technique is less accurate and more difficult to use in measuring [O] than the NO titration technique.

Emission intensities are generally measured using photomultipliers with interference filters, to restrict their sensitivity to wavelength intervals which isolate the emission feature under study. The intervals to be used are determined from spectroscopic examination of the emission. The filtered photomultipliers are absolutely calibrated using the NO_2 continuum whose spectral distribution and proportionality constant K_γ have been carefully measured.

Excitation of $O(^1S)$

The most conspicuous features on nightglow spectrograms (5) are the 5577 and 6300, 6364 Å lines in the cascade from $O(^1S)$ to $O(^1D)$ to $O^3(P)$. (The third line in the ^1D–^3S transition is so weak as to be unobservable.) These have been studied much more than the other airglow features and their explanation has been sought for over half a century.

Can. J. Chem. Downloaded from www.nrcresearchpress.com by 210.87.254.105 on 09/05/12
For personal use only.

Over 30 years ago it was suggested (6) that $O(^1S)$ was excited by

[t] $$O + O + O \rightarrow O_2 + O(^1S)$$

If reaction [t] produces $O(^1S)$ then eq. [3] becomes

[11] $$k_t[O]^3 = (1 + \tau k_i[i])I(^1S)$$

and a plot of

[12] $$[O]^3/I(^1S) \text{ vs. } [O]$$

can be made. Figure 3 shows that this is a single straight line regardless of the other constituents in the system (3). The slope, $\tau k_0/k_t$ and intercept, k_t^{-1} (k_0 equal to the quenching rate coefficient of atomic oxygen) can be used to obtain τk_0 and k_t provided all other k_i are negligible. Since the data in Fig. 3 were taken at several pressures and compositions but fit the same line, this assumption appears to be true.

If other gases are added which do not change [O], then eq. [11] can be divided by a similar equation which now contains two terms in the right-hand side, $k_0[O] + k_Q[Q]$, where Q is the added gas. Rearrangement then gives

[13] $$\frac{I_0(^1S)}{I(^1S)} = 1 + \frac{\tau k_Q[Q]}{1 + \tau k_0[O]}$$

where I_0 referred to the intensity of 5577 Å emission when [Q] = 0. The slope of such a plot

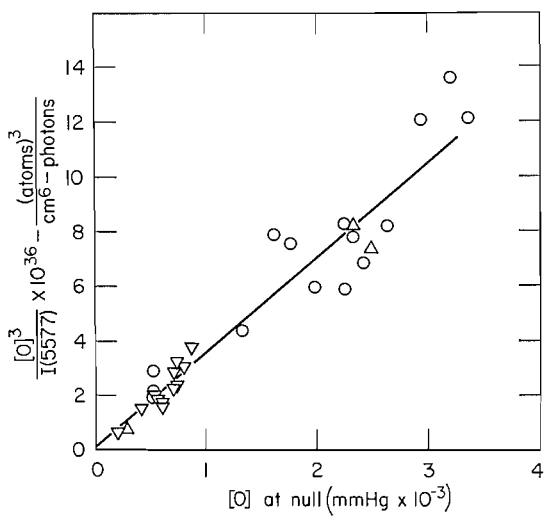

FIG. 3. The dependence of $[O]^3/I_c(5577)$ on [O]. Data are presented for N_2 (○), 1% N_2 in Ar (△), and 1% N_2 in He (▽).

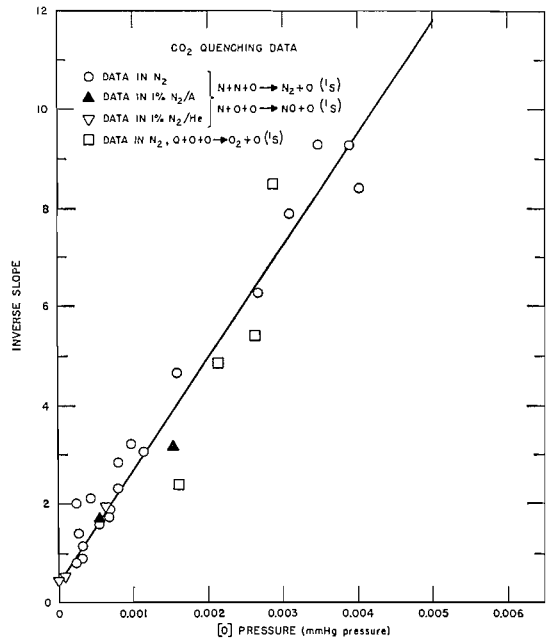

FIG. 4. CO_2 quenching data. The reciprocal of the slope of Stern–Volmer graphs vs. [O]. Data points were taken at total pressures from 0.2 to 11 mm Hg in N_2, 1% N_2 in He, and 1% N_2 in Ar. The $O(^1S)$ was produced by reactions [12], [13], and [14].

is $\tau k_Q/(1 + \tau k_0[O])$ and its inverse should be another straight line if plotted against [O], as Fig. 4 verifies. The intercept of this line is $(\tau k_Q)^{-1}$, its slope is k_0/k_Q, and the ratio is τk_0. Because the intercept in Fig. 3 is so small, it is preferable to use τk_0 obtained from Fig. 4 and the slope of Fig. 3 ($\tau k_0/k_t$) to compute k_t as 1.8×10^{-34} cm^6 molecule. Diffusion has been neglected in this analysis, but since the data of Figs. 3 and 4 are independent of pressure, this approximation is substantiated.

Using the value of τk_0 just obtained in eq. [13], less extensive measurements of I_0/I will give the k_Q/k_0 listed in Table II.

TABLE II*

Rate coefficients for the loss of $O(^1S)$

Rate coefficients	Value
$k_Q(N_2O)$	5.9×10^{-13}
$k_Q(O)$	1.8×10^{-13}
$k_Q(O_2)$	1.0×10^{-13}
$k_Q(CO_2)$	2.5×10^{-14}
$k_Q(H_2)$	3.0×10^{-15}
$k_Q(He,Ar,N_2)$	$< 10^{-17}$

*From ref. 3.

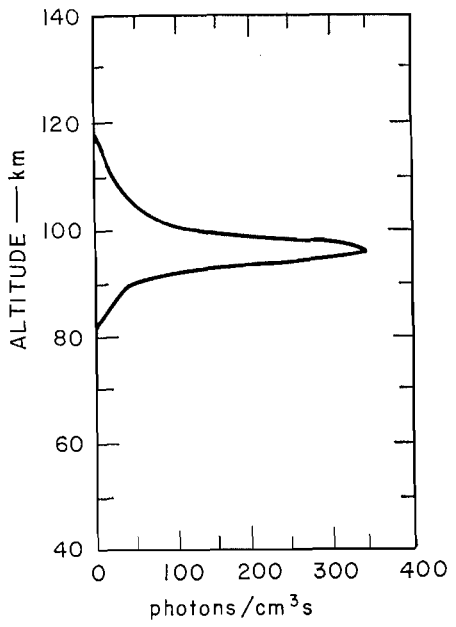

FIG. 5. The emission rate of 5577 Å per cm^3 as a function of altitude as measured by rocket instrumentation (ref. 8).

Using various models (7) of the earth's upper atmosphere, the rate of collisional deactivation of $O(^1S)$ can be computed using the rates listed in Table II — above about 90 km radiation predominates over collisional energy removal. The 5577 Å emission peaks near 100 km are shown (Fig. 5) by rocket probes (8) which penetrate the luminous layer.

From the rocket measurement of $I(^1S)$ as a function of altitude and the assumption that reaction [t] is the excitation process, [O] can be derived. The results of this reduction of rocket nightglow data are shown in Fig. 1, along with mass spectrometer measurement of [O] and theoretical extrapolation into the 100 km region. A very significant discrepancy exists since the atomic oxygen concentration derived from the nightglow observation is approximately 5 times larger than that implied by the theoretical extrapolation of rocket born mass spectrometer measurements. To bring the nightglow results into agreement with the atomic oxygen, it would require k_t to be $\approx 10^{-32}$ cm^6/s.

It has been suggested (9) that $O(^1S)$ is excited in a two step process

[u] $\quad O + O + M \rightarrow O_2^* + M$

[v] $\quad O_2^* + O(^3P) \rightarrow O_2 + O(^1S)$

[w] $\quad O_2^* + M \rightarrow O_2 + M$

[x] $\quad O_2^* \rightarrow O_2 + h\nu$

If reaction [w] dominates over reactions [v] and [x], then

$$[14] \qquad I(^1S) = \frac{k_v k_u}{k_w}[O]^3$$

This requires that $k_w[M] \gg k_v[O]$ or $[O]/[M] \ll k_w/k_v$. Since $k_u \leqslant 3 \times 10^{-33}$ cm^3/s (the measured total rate coefficient for atomic oxygen association), $k_v/k_w > 10^{-2}$ if $k_v k_u/k_w$ is as measured and $[O]/[M] < 10$. In the upper atmosphere near 100 km, $[O]/[M] \approx 10^{-2}$ (for the currently accepted atmosphere) as is also true in the laboratory experiments. Hence in the upper atmosphere eq. [14] is valid and hence the two-step process is also unable to account for the 5577 Å emission.

Only if the conditions under which laboratory experiments are carried out completely supress an excitation mechanism for $O(^1S)$ (which becomes dominant under the true conditions prevalent at 100 km), would it be possible for the presently accepted value of the oxygen concentration at 100 km in the earth's atmosphere to be compatible with the existing laboratory results. Further, if we retain the assumption that the energy eventually appearing as emission at 5577 Å is released in atomic oxygen association, then reaction [w] must so dominate reaction in the laboratory that $k_v k_u/k_w \ll 10^{-34}$ cm^3/s and hence the laboratory observation pertains only to reaction [t] while in the upper atmosphere k_w must decrease by several orders of magnitude. If $k_w = 0$ in the upper atmosphere and all O_2 formed in reaction [u] eventually excites O, $k_u > 10^{-34}$ cm^6/s to account for the observed green line intensity with a peak oxygen concentration $\approx 2 \times 10^{11}$ atoms/cm^3. Hence in the laboratory $k_v/k_w \ll 1$, perhaps 10^{-2}, if the multistep process is to be undetectable in laboratory measurements. Furthermore, this ratio must remain small even when M is Ar or He, since the laboratory results are independent of the gas composition.

The ratio of [O]/[M] in the upper atmosphere and in the laboratory is similar, so the only significant difference apparent between the laboratory environment and the environment near 100 km is the temperature. The temperature

Can. J. Chem. Downloaded from www.nrcresearchpress.com by 210.87.254.105 on 09/05/12
For personal use only.

Can. J. Chem. Downloaded from www.nrcresearchpress.com by 210.87.254.105 on 09/05/12
For personal use only.

dependence of k_u can be neglected. If k_v is constant with temperature, then k_w must have an activation energy of ≈ 0.2 eV. The assumption that $O_2{}^*$ has a radiative lifetime of less than 100 s implies that $k_v > 10^{-14}$ (probably near 10^{-13}) in the upper atmosphere if $O_2{}^*$ is to excite O rather than to radiate. Then k_w at 300 °K must be approximately 10^{-11} or larger. This is a very fast process, particularly for reactants such as He and Ar.

The situation concerning the excitation of the 5577 Å $O(^1S)$ emission in the nightglow is reduced to this: (1) the atomic oxygen concentration near 100 km is about 3 to 5 times larger than current theoretical extrapolations of rocket measurements imply, or (2) errors of a factor of 3 to 5 in atomic oxygen concentration have consistently been made in the laboratory over a period of years using different apparatus, or (3) the deactivation rate coefficient for $O(^1S)$ derived from laboratory experiments is in error, or (4) a two-step process excites $O(^1S)$ in the atmosphere but is subdued in the laboratory by strongly temperature-dependent deactivation processes which have rate coefficients near 10^{-11} cm^3/s even for He and Ar as reactants.

Without new rocket measurements of atomic oxygen by a technique different from mass spectroscopy (resonance absorption is the most promising) it is unlikely that systematic errors, if they exist, will be uncovered. Measurements near 100 km are most desirable because this region is where [O] is largest and where the airglow is strongest. Such measurements would also make comparison with the 5577 Å green line relatively independent of theoretical models of the earth's atmosphere and eddy diffusion coefficients.

It is very unlikely that laboratory measurements of [O] are too low by a factor of 3 to 5 as is required to bring the nightglow-derived atomic oxygen concentration into agreement with the mass-spectrometer-derived atomic oxygen concentrations. Although it is conceivable that more than one N atom is removed per NO molecule injected into the stream, there certainly cannot be more than one oxygen atom liberated per NO molecule added. Hence it is clearly impossible for the NO titration technique to give an underestimate. A laboratory underestimate of atomic oxygen concentration would mean that other rate constants (such as those for excitation of the first positive bands and the NO (β, γ, δ bands) would also be underestimated by a factor of 9 to 25. However, independent measurements do not show this much divergence. In fact, intercomparison of rate coefficients of chemiluminescent reactions made over a period of 5 years in two very different flow systems indicates that any errors in atomic oxygen concentration measurements using the NO-null technique are independent of almost all experimental parameters such as the geometry of the flow tube, the flow speed, the pressure, the residence time, the source of NO, the dissociative discharge conditions, etc.

The deactivation rate of $O(^1S)$ by atomic oxygen was deduced by comparing the rate of its removal by collisions with $O(^3P)$ to its apparent unimolecular rate of decay by radiation. The rate coefficients for $O(^1S)$ removal by several compounds relative to that of $O(^3P)$ were deduced from eq. [13]. There is recent evidence that some of the rates listed in Table II are much too low, perhaps by as much as a factor of 27, while others are approximately correct. Quenching by atomic oxygen has not been independently measured. Since k_t was derived from a measurement of $k_t/\tau k_0$, increasing k_0 by 27 would require that k_t be increased by 27 also, so that this combination of factors remains equal to the experimental results. Such an increase in k_t would decrease the computed atomic oxygen concentration at 100 km by a factor of 3 and reasonable agreement between optical and mass spectrometric measurements would result. This same factor must also be used in computing the rate of

$$[y] \qquad N + N + O \rightarrow N_2 + O(^1S)$$

$$[z] \qquad N + O + O \rightarrow NO + O(^1S)$$

The result of such a correction is that atomic oxygen is then a more efficient third-body for atomic association than are other, less reactive, species.

If the original measurements of $O(^1S)$ deactivation rate coefficients are in error then either the apparent unimolecular decay rate of $O(^1S)$ is faster than 1/s, or the measurements of atomic oxygen are too small. The latter is unlikely.

The same transient studies of $O(^1S)$ emission which implied much larger quenching rate coefficients than those listed in Table II, also implied an apparent unimolecular decay rate greater than 1/s which is associated with radiation. There is circumstantial evidence that this rapid

Can. J. Chem. Downloaded from www.nrcresearchpress.com by 210.87.254.105 on 09/05/12
For personal use only.

decay is due to collision of $O(^1S)$ with H_2O. To simulate, as previously observed the apparent independence of the rate of $O(^1S)$ removal on pressure, gas composition, flow rate, etc. H_2O must be in equilibrium with water sorbed on the walls of the experimental apparatus. If the rate coefficient for deactivation of $O(^1S)$ by H_2O is $\approx 10^{-10}$ cm^3/s then a partial pressure of 10^{-5} Torr would account for the necessary shortened lifetime of $O(^1S)$ during the measurements of k_t and k_0 discussed in this article.

The two-step mechanism is not excluded since it is not inconceivable that He, Ar, and N_2 all deactivate the precursor exciting $O(^3P)$ to $O(^1S)$ in the two-step process with rate coefficients of the order of 10^{-11} cm^3/s, although it seems unlikely. For the rare gases little energy is likely to be removed and the process must be vibration and rotation deactivation or non-radiative collision-induced transition within the precursor molecule. Helium is noted for not inducing electronic transitions, but is an efficient vibration and rotation relaxer. Since rotation relaxation involves too small an energy increment to lead to the large activation energy required to harmonize laboratory results with upper atmosphere observations, the effects of He must be due to vibrational relaxation. This, in turn, means that transfer of energy to $O(^3P)$ occurs only from vibrationally excited states of O_2* which need not be electronically excited. The final evaluation of the significance of vibrational relaxation of O_2*, formed in atomic association, for excitation of $O(^3P)$ to $O(^1S)$ is yet to be made.

In passing, it should be noted that the addition of O_2 to a mixture of O and N_2 indicated simple deactivation of $O(^1S)$ and no change in the excitation mechanism. Hence the presence of O_2 in the real atmosphere cannot account for the difference found between laboratory results and airglow observations.

Excitation of $O(^1D)$

The 6300 and 6364 Å lines from $O(^1D)$ originate mostly from above 200 km (8). This implies that $O(^1D)$ is collisionally deactivated in the 100 km region, since otherwise the 6300 and 6364 Å lines should be as intense as the 5577 Å line. Recent laboratory results (11) indeed verify that both O_2 and N_2 rapidly deactivate $O(^1D)$.

At the great altitudes from which $O(^1D)$ emission occurs, only dissociative recombination of O_2* can produce $O(^1D)$ sufficiently rapidly as has recently been verified by Zipf (10).

Excitation of the O_2 Herzberg Bands

The emission systems of O_2 observed in the O, N_2 afterglow (3) (the Herzberg and atmospheric bands) are also present in the nightglow. There is no doubt that the composite processes occurring in the laboratory cannot account for the airglow emissions. Unfortunately, these processes are not well known for two reasons: (1) the collisional deactivation processes removing the radiative states have not been separately measured, and (2) the excitation processes are complicated.

Figure 5 shows measurements of the intensity of the Herzberg bands of O_2 which occur between 3000 and 4000 Å. A straightforward interpretation of these data is

$$[aa] \qquad O + O + M \rightarrow O_2^* + M$$

$$[bb] \qquad O_2^* + M \rightarrow O_2 + M$$

$$[cc] \qquad O_2^* \rightarrow O_2 + h\nu$$

implying that

$$[15] \qquad I(\text{Herzberg}) = \frac{k_{cc}k_{aa}[O]^2[M]}{k_{cc} + k_{bb}[M]}$$

At low pressure I increases linearly with M giving $k_{aa} = 2.1 \times 10^{-37}$ cm^6/s and at high pressures where $k_{bb}[M] > k_{cc}$, I is constant giving $k_{cc}(k_{aa}/k_{bb}) = 2.3 \times 10^{-21}$ cm^3/s. It can be seen from Fig. 2 that the intensity of this emission would be insignificant. Again, in the nightglow, the conclusion is reached that if atomic association is the source of nightglow energy, there must exist yet unknown dissipative processes operating in the laboratory which do not operate in the upper atmosphere. The simplest reason for this is the difference in temperature between the laboratory and the atmosphere at 100 km. For this to be the case, excitation of $O_2(A^3\Sigma_u^+)$ must be by a multistep process which would replace reaction [*aa*]. Again, the most likely multistep process is vibrational relaxation or non-radiative collision-induced electronic transition.

Excitation of the Atmospheric O_2 Bands

The results of measurements (3) of atomic association to produce $O_2(b^1\Sigma)$ which emit the atmosphere bands are shown in Fig. 6 and again, taken at face value, they indicate that this mechanism is incapable of producing the observed nightglow emission intensities. Because

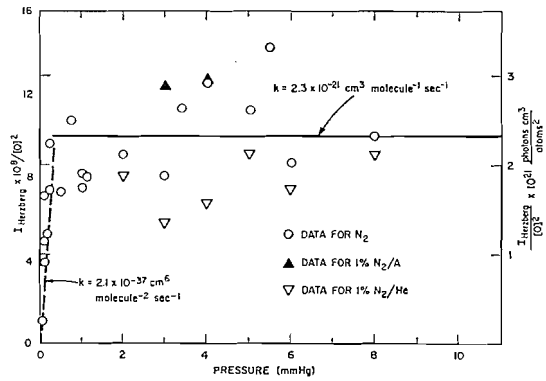

FIG. 6. The intensity of the ultraviolet Herzberg bands of O_2 divided by $[O]^2$ vs. pressure in N_2 (○), 1% N_2 in Ar (△), and 1% N_2 in He (▽).

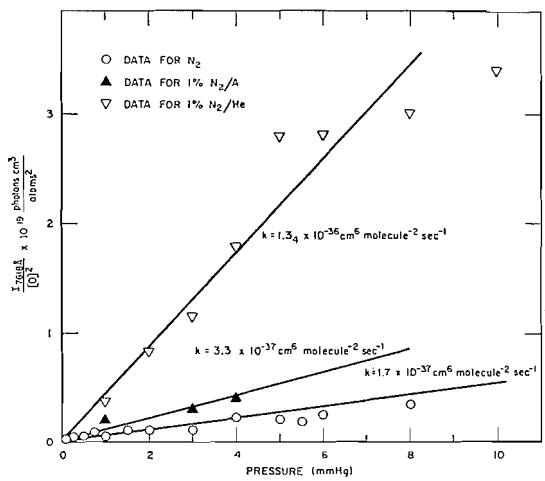

FIG. 7. The intensity of the (0,0) atmospheric band of O_2 at 7618 Å divided by $[O]^2$ vs. pressure in N_2 (○), 1% N_2 in Ar (△), and 1% N_2 in He (▽).

other measurements indicate that some precursor to the emission of both the Herzberg and atmospheric bands is deactivated by N_2, the single-step interpretation is unjustified. It is evident that the processes exciting O_2 are sufficiently complicated that present data in the 1 to 10 Torr range and at 300 °K are insufficient for extrapolating to the condition of 10^{-3} Torr and 200 °K existing in the nightglow region of our atmosphere.

Excitation of the OH Bands

The strong OH emission observed in the nightglow is presumed to arise from

[*dd*] $$H + O_3 \rightarrow OH^* + O_2$$

Such a process has been observed in the laboratory (12) but its rate coefficient has not yet been measured.

Excitation of the NO Bands

Very few nitrogen atoms are expected in the upper atmosphere where emission due to

[*ee*] $$N + O \rightarrow NO^*$$

[*ff*] $$NO^* \rightarrow NO + h\nu$$

will be weak. Reaction [u^{ee}] is a pre-association having a rate coefficient (13) of 1.5×10^{-17} cm^3/s. Emission in these bands occurs near 2000 Å and so would be observable only from above the ozone layer. To date, this emission has not been detected in rocket experiments (14) implying that $[N] < 10^7$ cm^3, using very rough approximations.

Conclusions

It is concluded on general grounds that the peak atomic oxygen concentration is considerably larger than the presently accepted value of 2×10^{11} atoms/cm^3 at 100 km. If the 5577 Å nightglow emission intensity obtained from rocket measurements is excited by reaction [*t*] (i.e., O + O + O → O_2 + $O(^1S)$) with the rate coefficient originally found from laboratory experiments, (1.5×10^{-34} cm^6/molecule s) the peak atomic oxygen concentration is approximately $10^{12}/cm^3$ near 100 km. If the implications of more recent measurements of the deactivation of $O(^1S)$ can be extended to deactivation by $O(^3P)$ then only 3×10^{11} atoms would be necessary to account for the observed nightglow emission of 5577 Å radiation. Although the excitation of molecular oxygen is probably due to three-body atomic oxygen association, this is a multistep process which, so far, has not been completely characterized in laboratory experiments. The excitation of OH has not been quantitatively studied in the laboratory but there is no evidence that reactions of H and O_3 cannot adequately account for nightglow observation.

1. K. SCHOFIELD. Planetary Space Sci. **15**, 643 (1967).
2. F. D. COLEGROVE, F. S. JOHNSON, and N. B. HANSON. J. Geophys. Res. **71**, 2227 (1966).
3. R. A. YOUNG and G. BLACK. J. Chem. Phys. **44**, 3741 (1966).
4. J. BERKOWITZ, W. A. CHUPKA, and G. B. KISTIAKOWSKY. J. Chem. Phys. **25**, 457 (1956).
5. J. W. CHAMBERLAIN. Physics of the aurora and airglow. Academic Press, Inc., New York. 1961.
6. S. CHAPMAN. Proc. Roy. Soc. London, Ser. A, **132**, 353 (1931).

Can. J. Chem. Downloaded from www.nrcresearchpress.com by 210.87.254.105 on 09/05/12
For personal use only.

7. Cospar International Reference Atmosphere, 1965. North Holland Publishing Company, Amsterdam. 1965; U.S. Standard Atmospheres. U.S. Govt. Printing Office, Washington, DC. 1962; U.S. Standard Atmospheres Supplement. U.S. Govt. Printing Office, Washington, DC. 1960; Handbook of Geophysics. Geophysics Research Directorate, Air Force Research Division, ARDC, MacMillan & Company Ltd., New York. 1960.
8. I. S. GULLEDGE, D. M. PACKER, S. G. TILFORD, and J. T. VANDERSLICE. J. Geophys. Res. In press.
9. C. A. BARTH. Sci. **134**, 1426 (1961); J. Geophys. Res. **67**, 1628 (1962).
11. R. A. YOUNG, T. SLANGER, and G. BLACK. J. Chem. Phys. In press. J. F. NOXON. Private communication.
12. D. GARVIN. J. Am. Chem. Soc. **81**, 3173 (1959).
13. R. A. YOUNG and R. L. SHARPLESS. J. Chem. Phys. **39**, 1071 (1963).
14. J. P. HENNES. J. Geophys. Res. **71**, 763 (1966).

Chemiluminescent reactions of He(2³S) atoms

MARK CHER AND C. S. HOLLINGSWORTH
Science Center, North American Rockwell Corporation, Thousand Oaks, California 91360

Received December 31, 1968

Rate coefficients for the reactions of He(2³S) atoms with N_2, O_2, CO, and CO_2 were determined by measuring the fractional absorption of 3889 Å light from a helium lamp as a function of the concentration of the neutral gas in a flowing afterglow apparatus. The rate coefficients are in reasonable agreement with those obtained previously from measurements of the emission intensity. It is concluded that the observed chemiluminescence arises from Penning ionization reactions involving the He(2³S) atom.

Canadian Journal of Chemistry, 47, 1937 (1969)

Can. J. Chem. Downloaded from www.nrcresearchpress.com by 210.87.254.105 on 09/05/12
For personal use only.

In previous publications (1, 2) we reported the results of the measurements of the rate coefficients for the chemiluminescent reactions of excited helium with various neutral gases. The technique used was based on the measurement of the spatial variation of the emission intensity in a flowing afterglow apparatus. The emitting species are well-known electronically excited ionic states of the added neutral gases. Although some evidence was presented which strongly suggested that the He(2³S) metastable is the dominant reactive helium species, a more direct identification of the reactant seemed desirable. In this paper we report the results of the measurements of the decay in the concentration of He(2³S) as a function of the concentration of the added gases using a light absorption technique. The purpose of the experiments was to determine rate coefficients for the disappearance of He(2³S) and to compare these with rate coefficients obtained previously from the rate of formation of excited ionized products.

Experimental

Relative concentrations of He(2³S) were obtained as a function of the concentration of the added gas by measuring the fractional absorption of incident 3889 Å light from a low pressure helium discharge lamp. The apparatus and procedure have been described previously (1, 2). Absorption at 3889 Å corresponds to the atomic helium transition $2^3S \rightarrow 3^3P$. The absorption intensity, which was always less than 1%, is consequently proportional to the concentration of He(2³S).

Theory

The two major processes for the disappearance of He(2³S) are diffusion to the walls and chemical reaction with the added neutral gas. The concentration of He(2³S) as a function of position was obtained by solving the continuity equation assuming Poiseuille flow (1) and is shown in eq. [1].

$$[1] \quad \ln [He^*] = \ln [He^*]_0 - \frac{(D_0 p_0)\pi x}{760 \sum FRT} \times \left(\frac{\lambda_0^2}{2}\right) - kx\pi \left(\frac{pr_0}{\sum FRT}\right)^2 \left(\frac{1+\varepsilon}{2}\right) F_N$$

Here [He*] represents the He(2³S) concentration, x is the axial distance from the inlet nozzle of the added gas, $D_0 p_0$ is the diffusion coefficient of He(2³S) at 1 Torr, $\sum F$ is total flow rate in moles/s, R is the gas constant, T is the temperature, p is the pressure, r_0 is the radius of the tube, F_N is the flow rate of the impurity gas, k is the rate coefficient, and λ_0, ε, and π are constants equal to 2.710, 0.237, and 3.14. Since the absorption intensity is proportional to the concentration of He(2³S), a plot of $\ln I_{abs}$ vs. F_N at constant x should produce a straight line with slope S given by

$$[2] \quad S = 1.237 \frac{k\pi x}{2} \left(\frac{pr_0}{\sum FRT}\right)^2$$

7. Cospar International Reference Atmosphere, 1965. North Holland Publishing Company, Amsterdam. 1965; U.S. Standard Atmospheres. U.S. Govt. Printing Office, Washington, DC. 1962; U.S. Standard Atmospheres Supplement. U.S. Govt. Printing Office, Washington, DC. 1960; Handbook of Geophysics. Geophysics Research Directorate, Air Force Research Division, ARDC, MacMillan & Company Ltd., New York. 1960.
8. I. S. GULLEDGE, D. M. PACKER, S. G. TILFORD, and J. T. VANDERSLICE. J. Geophys. Res. In press.
9. C. A. BARTH. Sci. **134**, 1426 (1961); J. Geophys. Res. **67**, 1628 (1962).
11. R. A. YOUNG, T. SLANGER, and G. BLACK. J. Chem. Phys. In press. J. F. NOXON. Private communication.
12. D. GARVIN. J. Am. Chem. Soc. **81**, 3173 (1959).
13. R. A. YOUNG and R. L. SHARPLESS. J. Chem. Phys. **39**, 1071 (1963).
14. J. P. HENNES. J. Geophys. Res. **71**, 763 (1966).

Chemiluminescent reactions of He(2³S) atoms

MARK CHER AND C. S. HOLLINGSWORTH
Science Center, North American Rockwell Corporation, Thousand Oaks, California 91360

Received December 31, 1968

Rate coefficients for the reactions of He(2³S) atoms with N_2, O_2, CO, and CO_2 were determined by measuring the fractional absorption of 3889 Å light from a helium lamp as a function of the concentration of the neutral gas in a flowing afterglow apparatus. The rate coefficients are in reasonable agreement with those obtained previously from measurements of the emission intensity. It is concluded that the observed chemiluminescence arises from Penning ionization reactions involving the He(2³S) atom.

Canadian Journal of Chemistry, 47, 1937 (1969)

Can. J. Chem. Downloaded from www.nrcresearchpress.com by 210.87.254.6 on 09/05/12
For personal use only.

In previous publications (1, 2) we reported the results of the measurements of the rate coefficients for the chemiluminescent reactions of excited helium with various neutral gases. The technique used was based on the measurement of the spatial variation of the emission intensity in a flowing afterglow apparatus. The emitting species are well-known electronically excited ionic states of the added neutral gases. Although some evidence was presented which strongly suggested that the He(2³S) metastable is the dominant reactive helium species, a more direct identification of the reactant seemed desirable. In this paper we report the results of the measurements of the decay in the concentration of He(2³S) as a function of the concentration of the added gases using a light absorption technique. The purpose of the experiments was to determine rate coefficients for the disappearance of He(2³S) and to compare these with rate coefficients obtained previously from the rate of formation of excited ionized products.

Experimental

Relative concentrations of He(2³S) were obtained as a function of the concentration of the added gas by measuring the fractional absorption of incident 3889 Å light from a low pressure helium discharge lamp. The apparatus and procedure have been described previously (1, 2). Absorption at 3889 Å corresponds to the atomic helium transition $2^3S \rightarrow 3^3P$. The absorption intensity, which was always less than 1%, is consequently proportional to the concentration of He(2³S).

Theory

The two major processes for the disappearance of He(2³S) are diffusion to the walls and chemical reaction with the added neutral gas. The concentration of He(2³S) as a function of position was obtained by solving the continuity equation assuming Poiseuille flow (1) and is shown in eq. [1].

$$[1] \quad \ln [He^*] = \ln [He^*]_0 - \frac{(D_0 p_0)\pi x}{760 \sum FRT} \times \left(\frac{\lambda_0^2}{2}\right) - kx\pi \left(\frac{pr_0}{\sum FRT}\right)^2 \left(\frac{1+\varepsilon}{2}\right) F_N$$

Here [He*] represents the He(2³S) concentration, x is the axial distance from the inlet nozzle of the added gas, $D_0 p_0$ is the diffusion coefficient of He(2³S) at 1 Torr, $\sum F$ is total flow rate in moles/s, R is the gas constant, T is the temperature, p is the pressure, r_0 is the radius of the tube, F_N is the flow rate of the impurity gas, k is the rate coefficient, and λ_0, ε, and π are constants equal to 2.710, 0.237, and 3.14. Since the absorption intensity is proportional to the concentration of He(2³S), a plot of $\ln I_{abs}$ vs. F_N at constant x should produce a straight line with slope S given by

$$[2] \quad S = 1.237 \frac{k\pi x}{2} \left(\frac{pr_0}{\sum FRT}\right)^2$$

Can. J. Chem. Downloaded from www.nrcresearchpress.com by 210.87.254.6 on 09/05/12
For personal use only.

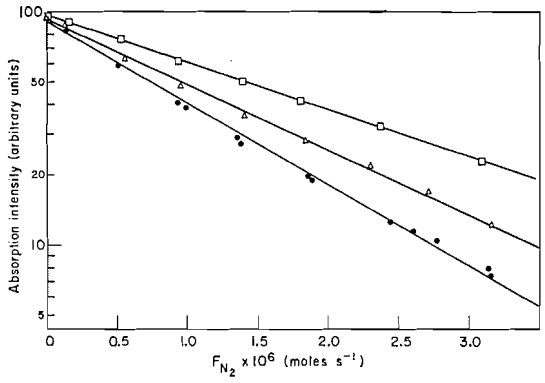

FIG. 1. Absorption at 3889 Å vs. nitrogen flow rate. Flow rate of helium in moles s^{-1}: ●, 2.98×10^{-3}; △, 4.44×10^{-3}; □, 6.51×10^{-3}.

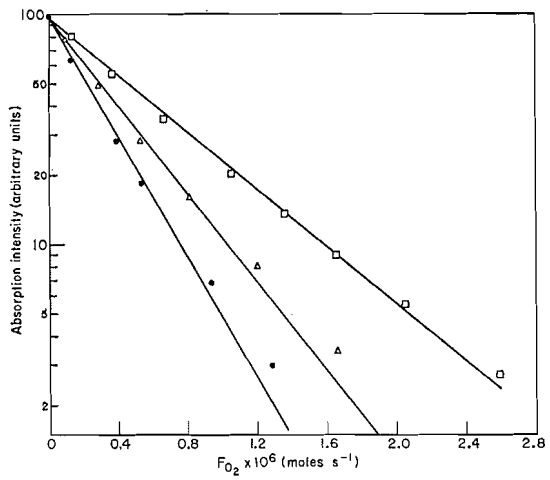

FIG. 2. Absorption at 3889 Å vs. oxygen flow rate. Flow rate of helium in moles s^{-1}: ●, 2.98×10^{-3}; △, 4.44×10^{-3}; □, 6.53×10^{-3}.

Results and Discussion

Measurements of absorption intensity were carried out at several different flow rates of helium in the presence of N_2, O_2, CO, and CO_2. Results are shown in Figs. 1–4. Rate coefficients were determined from the slopes of the graphs according to eq. [2] and are shown in Table I in the column labeled absorption. Because of the small absorption intensities and substantial signal-to-noise problems, these rate coefficients are less precise than those obtained from the emission experiments, and the probable error is estimated at about ±30%. The uncertainty is greater in the measurements with O_2 and CO_2 because of the

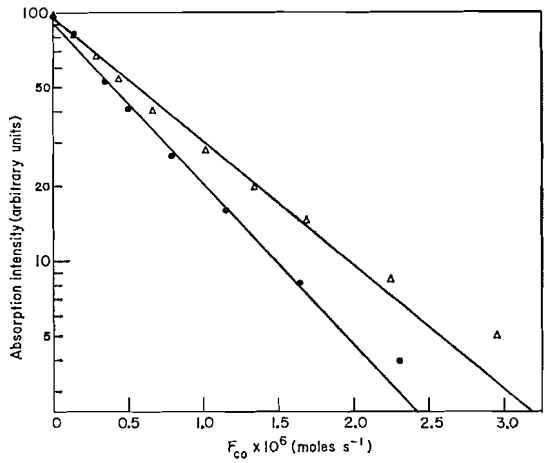

FIG. 3. Absorption at 3889 Å vs. carbon monoxide flow rate. Flow rate of helium in moles s^{-1}: ●, 2.98×10^{-3}; △, 4.45×10^{-3}.

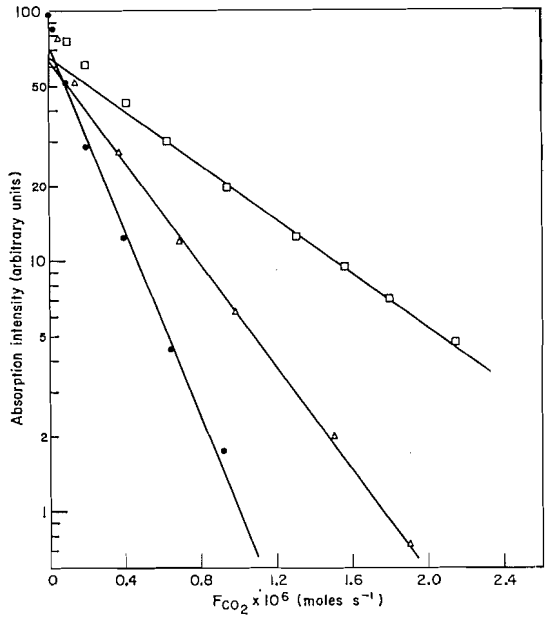

FIG. 4. Absorption at 3889 Å vs. carbon dioxide flow rate. Flow rate of helium in moles s^{-1}: ●, 2.98×10^{-3}; △, 4.45×10^{-3}; □, 6.53×10^{-3}.

shorter flames caused by larger rate coefficients. The value of k is within experimental error independent of pressure or flow rate of helium, as is to be expected.

Table I also shows rate coefficients[1] calculated

[1]It may be recalled that rate coefficients were shown to vary with temperature approximately as $k \sim T$.

TABLE I

Rate coefficients for reactions of 2^3S

Reactant	$F_{He} \times 10^3$ (moles s^{-1})	p (mm Hg)	T (°K)	$k \times 10^{10}$ (cc molecule^{-1}s^{-1}) Absorption	Emission	Emission spectrum
N_2	2.98	1.08	313	1.3		
	4.44	1.41	326	1.5		
	6.51	1.72	331	1.6		
			320	Ave. 1.4±0.3	1.0±0.3	N_2^+ (1st negative)
O_2	2.98	1.08	314	5.2		
	4.44	1.39	329	5.4		
	6.53	1.80	335	4.5		
			320	Ave. 5.0±1.5	3.8±0.9	O_2^+ (1st negative)
					3.4±0.9	O_2^+ (2nd negative)
CO	2.98	1.11	313	2.3		
	4.45	1.42	327	2.6		
			320	Ave. 2.5±0.7	1.8±0.5	CO^+ (Comet-tail)
					1.8+0.5	CO^+ (Baldet–Johnson)
CO_2	2.98	1.01	322	13		
	4.45	1.39	341	10		
	6.53	1.78	350	8.3		
			320	Ave. 10±3	8.3±2.5	CO_2^+

at 320 °K from the data based on the emission measurements. In the reactions of O_2 and CO rate coefficients were obtained by monitoring two different emission systems and they are listed separately. Although the rate coefficients from the absorption measurements appear to be consistently higher than the rate coefficients from the emission experiments, the discrepancy is within the rather large expected error, and consequently we consider the two sets of measurements to be in reasonable agreement. We conclude, therefore, that the observed chemiluminescence for all these processes is the result of the Penning ionization reaction

$$He(2^3S) + X \rightarrow He + X^{+*} + e^-$$

where X^{+*} is the upper electronic state of the emitting ion.

1. M. CHER and C. S. HOLLINGSWORTH. Chemical reactions in electrical discharges. Advan. Chem. Ser. **80**. In press.
2. M. CHER and C. S. HOLLINGSWORTH. J. Chem. Phys. In press.

Comments and Summary

COMMENTS BY A. O. C. NIER[1]

Dr. Young has suggested that the atomic oxygen concentration on the lower thermosphere may be many times larger than is generally supposed. It is perhaps worth commenting on the situation insofar as direct measurements are concerned. Atomic oxygen determinations have been by optical absorption techniques and by mass spectrometry. In general, but not always, the results lie below the model atmosphere values. These are based mainly on satellite drag measurements.

Von Zahn has suggested that the mass spectrometric atomic oxygen determinations may be too low because of the reaction of atomic oxygen with mass spectrometer ion source surfaces and the formation of compounds such as CO_2 or N_2O (mass 44). While undoubtedly effects such as these exist, it is hard to believe that the atomic oxygen readings could be low by a factor of 5 or more as required by Dr. Young's suggestion. In some of the experiments, such as those of Schaefer of Michigan, the ion sources are relatively open, and in some positions of the rocket there are almost no opportunities for oxygen atoms to collide with surfaces. Yet his values agree well with those of other mass spectrometer

[1]Address: University of Minnesota, Minneapolis, Minnesota.

Can. J. Chem. Downloaded from www.nrcresearchpress.com by 210.87.254.6 on 09/05/12
For personal use only.

TABLE I

Rate coefficients for reactions of 2^3S

Reactant	$F_{He} \times 10^3$ (moles s^{-1})	p (mm Hg)	T (°K)	$k \times 10^{10}$ (cc molecule^{-1}s^{-1}) Absorption	Emission	Emission spectrum
N_2	2.98	1.08	313	1.3		
	4.44	1.41	326	1.5		
	6.51	1.72	331	1.6		
			320	Ave. 1.4±0.3	1.0±0.3	N_2^+ (1st negative)
O_2	2.98	1.08	314	5.2		
	4.44	1.39	329	5.4		
	6.53	1.80	335	4.5		
			320	Ave. 5.0±1.5	3.8±0.9	O_2^+ (1st negative)
					3.4±0.9	O_2^+ (2nd negative)
CO	2.98	1.11	313	2.3		
	4.45	1.42	327	2.6		
			320	Ave. 2.5±0.7	1.8±0.5	CO^+ (Comet-tail)
					1.8+0.5	CO^+ (Baldet–Johnson)
CO_2	2.98	1.01	322	13		
	4.45	1.39	341	10		
	6.53	1.78	350	8.3		
			320	Ave. 10±3	8.3±2.5	CO_2^+

at 320 °K from the data based on the emission measurements. In the reactions of O_2 and CO rate coefficients were obtained by monitoring two different emission systems and they are listed separately. Although the rate coefficients from the absorption measurements appear to be consistently higher than the rate coefficients from the emission experiments, the discrepancy is within the rather large expected error, and consequently we consider the two sets of measurements to be in reasonable agreement. We conclude, therefore, that the observed chemiluminescence for all these processes is the result of the Penning ionization reaction

$$He(2^3S) + X \rightarrow He + X^{+*} + e^-$$

where X^{+*} is the upper electronic state of the emitting ion.

1. M. CHER and C. S. HOLLINGSWORTH. Chemical reactions in electrical discharges. Advan. Chem. Ser. **80**. In press.
2. M. CHER and C. S. HOLLINGSWORTH. J. Chem. Phys. In press.

Comments and Summary

COMMENTS BY A. O. C. NIER[1]

Dr. Young has suggested that the atomic oxygen concentration on the lower thermosphere may be many times larger than is generally supposed. It is perhaps worth commenting on the situation insofar as direct measurements are concerned. Atomic oxygen determinations have been by optical absorption techniques and by mass spectrometry. In general, but not always, the results lie below the model atmosphere values. These are based mainly on satellite drag measurements.

Von Zahn has suggested that the mass spectrometric atomic oxygen determinations may be too low because of the reaction of atomic oxygen with mass spectrometer ion source surfaces and the formation of compounds such as CO_2 or N_2O (mass 44). While undoubtedly effects such as these exist, it is hard to believe that the atomic oxygen readings could be low by a factor of 5 or more as required by Dr. Young's suggestion. In some of the experiments, such as those of Schaefer of Michigan, the ion sources are relatively open, and in some positions of the rocket there are almost no opportunities for oxygen atoms to collide with surfaces. Yet his values agree well with those of other mass spectrometer

[1]Address: University of Minnesota, Minneapolis, Minnesota.

Can. J. Chem. Downloaded from www.nrcresearchpress.com by 210.87.254.40 on 09/05/12
For personal use only.

Can. J. Chem. Downloaded from www.nrcresearchpress.com by 210.87.254.40 on 09/05/12
For personal use only.

experiments where the surface conditions are not so favorable. Nevertheless the absolute determination of atomic oxygen remains a serious problem, and the questions raised by Dr. Young should remind us of this fact.

COMMENTS BY K. H. BECKER[2]

1. Recently we have investigated (1) the NO + O air afterglow reaction in the pressure region of 2×10^{-3} to 3×10^{-2} Torr. A pressure dependence of the NO_2* chemiluminescence intensity due to a three-body recombination has been observed in a 200 l glass sphere. The derived quenching constants are in agreement with those of previous fluorescence measurements (2). Similar work on the NO_2* chemiluminescence in a flow-tube experiment (3) agrees with our results. Very recently we found that in a pressure region of about 10^{-4} Torr in a reaction volume as large as 2×10^5 l, no pressure dependence of I_{NO_2*} could be observed. This might indicate that at these low pressures NO_2* is formed by a two-body recombination. A rough comparison of these results with those in the higher pressure region would give an upper limit of 10^{-19} cm^3 (molecule s)$^{-1}$ for the two-body process, but the chemiluminescence spectrum at low pressures has not yet been compared with that at higher pressures.

2. Recently we have found (4) that reaction C_2O + O forms electronically excited CO* in the $A^1\Pi$, $d^3\Delta$, and $e^3\Sigma^-$ states, with an excitation energy up to almost 9 eV. It is known that by the photolysis of CO in the vacuum-ultraviolet C_2O is formed. It might be interesting to analyze the emission from the Martian and Venus atmospheres in search of CO* emission which could give some information about the CO photolysis in these atmospheres.

3. Very little is known about the chemiluminescent reaction O + H. Recently Ticktin, Spindler, and Schiff (5) have studied the OH* chemiluminescence in this system. The formation of OH*($A^2\Sigma^+$) was explained by a two-body recombination, especially indicated by an enhancement at $K' = 13$ ($13Q_2$) for $v' = 0$. A rate constant of 3×10^{-21} cm^3(molecule s)$^{-1}$ for the two-body reaction was derived. Dr. Kley and I have also been working on the O + H reaction recently.

Our findings that (*a*), no perturbation at $K' = 13$ for $v' = 0$ has been seen; (*b*), the OH* emission intensity was found to be linear in (O) but not in (H); (*c*), the rotational population of OH*($A^2\Sigma^+$, $v = 0$) was observed up to $K' = 27$, probably up to $K' = 30$; and (*d*), the reaction C_2H_4 + O showed (6) the same rotational distribution for the (0,0) band as the reaction O + H, both at a total pressure of 2 Torr, led us to the conclusion that the electronically excited OH* is formed neither by a two-body nor by a three-body reaction between O(^{3}P) and H(1^2S). A complex radical mechanism seems to be involved in the formation of the OH* chemiluminescence.

1. K. H. BECKER, W. GROTH, and F. JOO. Ber. Bunsenges. **72**, 157 (1968).
2. G. H. MYERS, D. M. SILVER, and F. KAUFMAN. J. Chem. Phys. **44**, 718 (1966).
3. N. JONATHAN and R. PETTY. Trans. Faraday Soc. **64**, 1240 (1968).
4. K. H. BECKER and K. D. BAYES. J. Chem. Phys. **48**, 653 (1968).
5. S. TICKTIN, G. SPINDLER, and H. I. SCHIFF. Discussions Faraday Soc. **44**, 218 (1967).
6. K. H. BECKER, D. KLEY, and R. J. NORSTROM. Intern. Symp. Comb. Poitiers. 1968.

COMMENTS BY H. I. SCHIFF

In connection with Dr. Becker's recent observations, it is difficult to see the connection between the OH emissions arising from the reaction of O atoms with C_2H_4 and with H atoms. Our most recent results indicate that the intensity of the (1,0) emission from the O + H reaction is first order in each of the reactants while the (0,0) intensity is first order in [O] but not in [H]. These results are consistent with the population of the $v' = 0$ level being third order but with H being a particularly effective third body.

REMARKS AND SUMMARY BY CHAIRMAN, MICHAEL B. McELROY[3]

Young's paper is concerned primarily with the mechanism for production of O(^{1}S) in the night-sky. He contends that the abundance of O must be larger than current models of the atmosphere suggest if laboratory and atmosphere are to be

[2]Address: Institut f. Physikalische Chemie, Universität Bonn, Germany.

[3]Address: Kitt Peak National Observatory, Tucson, Arizona.

compatible. Nier's comment suggests that the uncertainties in our present knowledge of the atmosphere are not large enough to bridge the gap from this direction alone. The vacillations of the laboratory chemists on the detailed laboratory mechanism for green line production inspires little confidence on the part of the aeronomer. It is this particular aeronomer's prejudiced view that further laboratory endeavors should justify Chapman's original mechanism

$$O + O + O \rightarrow O_2 + O(^1S)$$

and prove anew that not all that is recent is right and not all that is ancient is wrong.

Can. J. Chem. Downloaded from www.nrcresearchpress.com by 210.87.254.40 on 09/05/12
For personal use only.

Can. J. Chem. Downloaded from www.nrcresearchpress.com by 210.87.254.42 on 09/05/12
For personal use only.

Canadian Journal of Chemistry

Published by THE NATIONAL RESEARCH COUNCIL OF CANADA

VOLUME 47 JUNE 1, 1969 NUMBER 11

Polychloro-alicyclic ketones. I. Polychloro-2-methylcyclohexenones, polychloro-3-methylcyclohexenones, and related polychlorocyclohexadienones

EIICHI MORITA

Monsanto Company, Organic Chemicals Division, Rubber Chemicals Research Laboratories, Akron, Ohio

AND

MARTIN W. DIETRICH

Monsanto Company, Organic Chemicals Division, Research Department, St. Louis, Missouri

Received November 5, 1968

The structures of eighteen polychloro-alicyclic ketones prepared by the chlorination of chlorinated phenols, ortho and meta cresols, or the corresponding toluidines were determined by nuclear magnetic resonance, infrared, and ultraviolet spectroscopy. Stereochemistry and the sequence of the formation of these polychloro-alicyclic ketones are described.

Canadian Journal of Chemistry, 47, 1943 (1969)

Introduction

The chlorination of phenols and anilines in acetic acid is an exothermic reaction yielding polychlorocyclohexenones and polychlorocyclohexadienones. Zincke and co-workers (1–3) studied the chlorination products of *p*-cresol and monochloro-*o*-toluidines. von Walther and Zipper (4) prepared polychloro-3-methyl cyclohexenones by the chlorination of *m*-cresol. Muller and Linde (5) reported the preparation of polychlorocyclohexenones from 2,5-dimethylphenol. Denivelle and Fort (6) described the preparations of alkylated polychlorohexadienones. However, the application of current spectroscopic techniques to substantiate the assigned structures of polychloro-alicyclic ketones has been limited to the infrared and ultraviolet spectra of hexachlorocyclohexadienones and octachlorocyclohexenones obtained by Denivelle and Fort (7), and the infrared spectra of tetrachloro-3,5-dimethylcyclohexadien-1-one and hexachloro-3,5-dimethylcyclohexen-1-one reported by Kumamoto and Kato (8). Our recent investigation of these compounds indicates that several of the structures assigned earlier do not satisfy the spectral data. This report discusses the structures of known as well as numerous novel polychloro-alicyclic ketones prepared from chlorinated phenols, *o*- and *m*-cresols or the corresponding toluidines. The sequences of the formation of these compounds are also proposed.

Results and Discussion

Polychloro-acyclic Ketones from Chlorinated Phenols

The work of Denivelle and Fort on cyclohexadienones and cyclohexenones derived from pentachlorophenol has been invaluable as a reference for the structural determination in the present study. The significant infrared (i.r.) and ultraviolet (u.v.) absorptions of these compounds are given in Table I. We have observed that the same u.v. absorption maxima are obtained from these compounds using methanol solutions.

Table I illustrates the dependence of the i.r. absorption band of the carbonyl group on the number of chlorine atoms attached to the adjacent carbons. The effect of the types of conjugation is also evident and only 2,4-cyclohexadien-1-one type conjugation gives two olefinic absorption bands.

To obtain further spectral references for

TABLE I

Ultraviolet and infrared absorptions of perchloro-cyclohexadienones and cyclohexenones (7)

	Ultraviolet*		Infrared† (cm^{-1})	
	λ_{max} (mμ)	ε_{max}	C=O	C=C
Octachloro-3-cyclohexen-1-one	236	9 000	1780	1592
Octachloro-2-cyclohexen-1-one	267	10 500	1749	1581
Hexachloro-2,5-cyclohexadien-1-one	262	16 000	1691	1580
Hexachloro-2,4-cyclohexadien-1-one	365	4 000	1718	1590 s 1538 m

*Cyclohexane solution.
†Carbon disulfide and carbon tetrachloride solutions.

TABLE II

Preparations of polychloro-alicyclic ketones

Polychloro-alicyclic ketones	Melting point (°C)	Empirical formula	%Cl		Starting material	Chlorination media
			Calcd.	Found		
1	Liquid	$C_6H_2Cl_6O$	70.25	69.75	2,4,6-Trichlorophenol	AcOH/HCl
2	96–97*	C_6HCl_7O	73.59	73.84	2,3,4,6-Tetrachlorophenol	AcOH/HCl
3	117–118	$C_7H_4Cl_6O$	67.16	67.41	2,4,6-Trichloro-*m*-cresol	95% AcOH
4	89–90†	$C_7H_4Cl_4O$	57.69	58.38	2,4,6-Trichloro-*m*-cresol	95% AcOH
5	101–102†	$C_7H_3Cl_7O$§	70.65	70.57	Tetrachloro-*m*-cresol	AcOH/HCl
6	89–90*	$C_7H_3Cl_5O$	63.21	62.80	Tetrachloro-*m*-cresol	AcOH/HCl
7	Liquid	$C_7H_4Cl_4O$	57.67	58.02	2,4,6-Trichloro-*m*-cresol	CCl_4/pyridine (I)
8	58–59*	$C_7H_3Cl_5O$	63.24	63.44	Tetrachloro-*m*-cresol	CCl_4/pyridine (I)
A(9 + 10)	98–99	$C_7H_4Cl_6O$	67.16	68.19	3-Chloro-6-methylaniline	AcOH/HCl
B(11 + 12)	96–97	$C_7H_4Cl_6O$	67.16	67.60	3-Chloro-2-methylaniline	AcOH/HCl
C(9 + 11)	106–107*	$C_7H_4Cl_6O$	67.16	67.08	*o*-Cresol	95% AcOH
13	60–61*	$C_7H_3Cl_5O$	63.24	63.50	Tetrachloro-*o*-cresol	AcOH/HCl
14	88–89‡	$C_7H_3Cl_7O$‖	70.65	70.45	**13**	AcOH/HCl
15 (major)	Liquid	$C_7H_5Cl_5O$	62.60	60.78	4,6-Dichloro-*o*-cresol	AcOH/HCl
15 (major)	Liquid	$C_7H_5Cl_5O$	62.60	61.94	2-Chloro-6-methylaniline	AcOH/HCl
16	Liquid	$C_7H_5Cl_3O$	50.30	50.10	4,6-Dichloro-*o*-cresol	CCl_4/pyridine (I)
D(17 major)	Liquid	$C_7H_4Cl_4O$	57.69	59.29	Reduction product of **A**	CCl_4/pyridine (II)
E(18 major)	Liquid	$C_7H_4Cl_4O$	57.69	58.05	Reduction product of **B**	CCl_4/pyridine (II)

*Recrystallization from petroleum ether.
†Recrystallization from MeOH.
‡Recrystallization from EtOH.
§Anal. Calcd. C, 23.93; H, 0.86. Found: C, 23.93; H, 0.84.
‖Anal. Calcd. C, 23.93; H, 0.86. Found: C, 24.06; H, 0.94.

structural determinations by nuclear magnetic resonance (n.m.r.), hexachlorocyclohexenone (**1**) and heptachlorocyclohexenone (**2**) were prepared from 2,4,6-trichlorophenol and 2,3,4,6-tetrachlorophenol (9), respectively (Tables II and III). The u.v. and i.r. spectra indicate that the double bond present in both ketones is not conjugated to the carbonyl group, namely **1** and **2** are 3-cyclohexenones. Since the n.m.r. spectrum of **1** indicates two non-equivalent protons, the protons originally present at the meta positions are not substituted by the chlorination. Thus, the only structure for **1** that satisfies these conditions is 2,2,4,5,6,6-hexachloro-3-cyclohexen-1-one. The lower field chemical shift of δ 6.51 p.p.m. would then be the olefinic proton and δ 4.99 p.p.m. the other methine proton. The lower i.r. absorption frequency of C=C in **2** compared to **1** suggests that the proton in **2** is not attached to the double bond and the chemical shift of δ 5.18 p.p.m. favors the presence of a non-olefinic proton. Ketone **2** is, therefore, 2,2,3,4,5,6,6-heptachloro-3-cyclohexen-1-one.

Polychloro-3-methylcyclohexenones and Cyclohexadienones

A hexachloro-3-methylcyclohexenone (**3**), m.p. 117–118°, precipitates out of solution, when

Can. J. Chem. Downloaded from www.nrcresearchpress.com by 210.87.254.42 on 09/05/12
For personal use only.

TABLE III

Spectral data of polychloro-alicyclic ketones

Polychloro-alicyclic ketones	Nuclear magnetic resonance				Infrared (cm^{-1})		Ultraviolet	
	δ CH_3 (p.p.m.)	δ CH (p.p.m.)	δ C=CH (p.p.m.)	J(Hz)	C=O	C=O	λ_{max} mμ	ε_{max}
1	—	4.99 (d)	6.51 (d)	$J_{H-H}=1.5$	1775	1645	215	8 050
2	—	5.18 (s)	—	—	1770	1612	215	8 400
							230	7 280
3	2.30 (d)	5.06 (m)	—	$J_{H-CH_3}=0.6$	1770	1640	220	8 210
4	2.48 (s)	—	7.38 (s)	—	1688	1602	253	13 780
5	2.26 (s)	—	—	—	1770	1598	231	7 380
6	2.58 (s)	—	—	—	1685	1590	258	14 860
7*a*	2.41 (d)	—	6.79 (m)	$J_{H-CH_3}=0.4$	1703	1620	355	—
7*b*	2.33 (d)	—	7.25 (m)	$J_{H-CH_3}=0.4$		1560		
8*a*	2.52 (s)	—	—	—	1718	1590	363	2 980
8*b*	2.45 (s)	—	—	—		1538		
13	2.00 (s)	—	—	—	1695	1580	354	3 480
						1530		
14	2.11 (s)	—	—	—	1769	1600	232	7 450
15*a*	2.07 (s)	4.98 (d)	6.23 (d)	$J_{H-H}=1.5$	1760	1650	220	—
15*b*	1.89 (s)	4.97 (d)	6.24 (d)	$J_{H-H}=1.5$				
16	1.83 (s)	—	6.46 (d)	$J_{H-H}=2.3$	1698	1627	339	—
			7.16 (d)			1564		
17	1.86 (s)	—	6.72 (s)	—	1693	1610	345	—
						1535		
18	2.00 (s)	—	7.37 (s)	—	1695	1622	353	—
						1560		

either *m*-cresol, *m*-toluidine, or 2,4,6-trichloro-*m*-cresol is chlorinated in acetic acid. Previously, the structure of 2,4,4,5,6-pentachloro-3-chloromethyl-2,5-cyclohexadien-1-one (4) was assigned to **3**, which was also reported as 2,4,4,5,6,6-hexachloro-3-methyl-2-cyclohexen-1-one (5). However, the i.r. and u.v. spectra of **3** (Table III) are characteristic of a 3-cyclohexenone. Its n.m.r. spectrum indicates the presence of a methyl group (δ CH_3 = 2.30 p.p.m.), a single methine proton (δ CH = 5.06 p.p.m.) but no methylene group. Since the methine proton is originally meta to the methyl group, the small coupling between the methine and methyl protons (J_{H-CH_3} = 0.5 Hz) favors the structure with the methyl group attached to the double bond, which would give the HC—C=C—CH type coupling (10). Moreover, the chemical shift of the methine proton is in the region of the non-olefinic protons of **1** and **2**. The structure 2,2,4,5,6,6-hexachloro-3-methyl-3-cyclohexen-1-one satisfies all these spectral features of **3**.

The spectral data of the ketone (**4**), obtained from the filtrate of the chlorination product of 2,4,6-trichloro-*m*-cresol, indicate it is 2,4,4,6-tetrachloro-3-methyl-2,5-cyclohexadien-1-one as reported previously (6).

Chlorination of tetrachloro-*m*-cresol in acetic acid gives a heptachloro-3-methylcyclohexenone (**5**) and a pentachloro-3-methylcyclohexadienone (**6**). It is evident from the u.v. and i.r. spectra, which are very similar to those of octachloro-3-cyclohexen-1-one in Table I, that **5** is a 3-cyclohexenone. The methyl group is not attached to the double bond, since (*a*) the i.r. absorption frequency for C=C is lower than that of **3** and close to octachloro-3-cyclohexen-1-one, and (*b*) the chemical shift of the methyl protons is up-field relative to that in **3**, which would not be expected if the methine proton of **3** is replaced by a chlorine. The most probable structure of **5** is, therefore, heptachloro-5-methyl-3-cyclohexen-1-one. The spectral data of **6** are in agreement with the structure of 2,4,4,5,6-pentachloro-3-methyl-2,5-cyclohexadien-1-one reported previously (4).

The chlorination of 2,4,6-trichloro-*m*-cresol in carbon tetrachloride in the presence of an equimolar amount of pyridine yielded a mixture (ketone **7**) containing two major components. Both major components contain one methyl group and one olefinic proton. Elemental analysis indicates both are tetrachlorocyclohexadienones. Ultraviolet and i.r. absorption

Can. J. Chem. Downloaded from www.nrcresearchpress.com by 210.87.254.42 on 09/05/12
For personal use only.

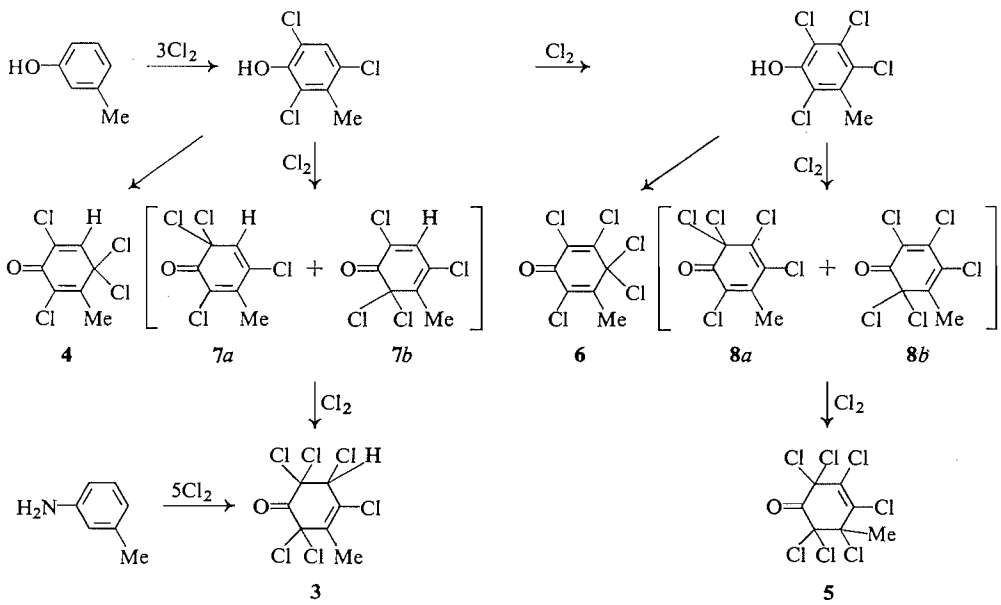

SCHEME I. Chlorination of *m*-cresols and *m*-toluidine.

peaks observed for the mixture are characteristic of 2,4-cyclohexadienones and show that neither contains the 2,5-dienone structure. The major components must therefore be the two isomeric 2,4-dienones. The chemical shift of the olefinic proton in the n.m.r. spectrum, by comparison to **17**, suggests one component, δ C=CH = 6.79 and δ CH_3 = 2.41 p.p.m. is probably 2,4,6,6-tetrachloro-3-methyl-2,4-cyclohexadien-1-one (*7a*). The other component, δ C=CH = 7.25 and δ CH_3 = 2.33 p.p.m. is then 2,4,6,6-tetrachloro-5-methyl-2,4-cyclohexadiene-1-one (*7b*). The chemical shift of the olefinic proton of the latter component is consistent with that observed for **18**. These compounds are unstable and further chlorination of **7** in acetic acid gives **3** as the major product. The ketone (**8**) obtained from tetrachloro-*m*-cresol by similar chlorination was also a mixture of two isomers in about equal proportions. The structure of these isomers are pentachloro-3-methyl-2,4-cyclohexadien-1-one (*8a*) (δ CH_3 = 2.52 p.p.m.) and pentachloro-5-methyl-2,4-cyclohexadien-1-one (*8b*) (δ CH_3 = 2.45 p.p.m.). It was shown by i.r. data that **8** is formed during the early stage of the chlorination of tetrachloro-*m*-cresol in glacial acetic acid.

Ketones **3**, **4**, **5**, and **6** were identified, by vapor-phase chromatography (v.p.c.) and i.r. spectra in the liquid fraction obtained by chlorination of *m*-cresol in acetic acid. It appears that exhaustive chlorination of *m*-cresol in acetic acid proceeds as shown in Scheme I.

Polychloro-2-methylcyclohexenones and Cyclohexadienones

Four distinct isomers, each with a methyl group and a methine proton with no observable coupling, were identified in the hexachlorocyclohexenones **A**, **B**, and **C** derived from 3-chloro-6-methylaniline, 3-chloro-2-methylaniline, and *o*-cresol, respectively. **A** is a mixture of ketones **9** and **10**; **B** a mixture of **11** and **12**; and **C** a mixture of **9** and **11**. The major component **9** of **C** was isolated by heating **C** with sodium acetate in ethyl alcohol, which decomposed **11**. Ketone **10**, the major component of **A**, was isolated by repeated fractional recrystallization from petroleum ether as the less soluble fraction. Ketones **11** and **12** were separated and isolated by repeated recrystallization of **B** from petroleum ether in which the major component **11** is less soluble. The physical data obtained for these isomers are given in Table IV.

The u.v. and i.r. spectra suggest that the isomers are all 3-cyclohexenones. Based on the n.m.r. spectra and on the position of the chlorine atom in the starting materials used for the preparation

Can. J. Chem. Downloaded from www.nrcresearchpress.com by 210.87.254.42 on 09/05/12
For personal use only.

TABLE IV

Hexachloro-3-cyclohexenones derived from *o*-cresol and *o*-toluidines

Compound	Melting point (°C)	Analyses*			Nuclear magnetic resonance (p.p.m.)		Infrared (cm^{-1})		Ultraviolet	
		C	H	Cl	δ CH_3	δ CH	C=O	C=C	λ_{max} (mμ)	ε_{max}
9	109–110	26.35	1.30	66.82	1.99 (e)	4.88	1760	1620	226	8300
10	123–124	26.51	1.30	66.71	2.12 (a)	4.87	1772 s 1745 w	1611	220	8000
11	112	26.60	1.37	66.81	2.17 (e′)	5.17	1758	1613	228	8300
12	61–62	26.42	1.26	66.87	2.01 (a′)	5.15	1768	1620	226	7800

*Anal. Calcd. for $C_7H_4Cl_6O$: C, 26.53; H, 1.27; Cl, 67.14.

of ketones **A** and **B**, **9** and **10** are 2,2,3,4,5,6-hexachloro-6-methyl-3-cyclohexen-1-ones, while **11** and **12** are 2,3,4,5,6,6-hexachloro-2-methyl-3-cyclohexen-1-ones. The identities of these structures are substantiated by the fact that the reduction of **A** and **B** by zinc in methyl alcohol gives 4,5,6-trichloro-*o*-cresol and 3,4,6-trichloro-*o*-cresol, respectively, besides tetrachloro-*o*-cresol. The similarity of the i.r. spectra shown in Fig. 1 suggests that **9** and **10** are stereoisomers as are **11** and **12**.

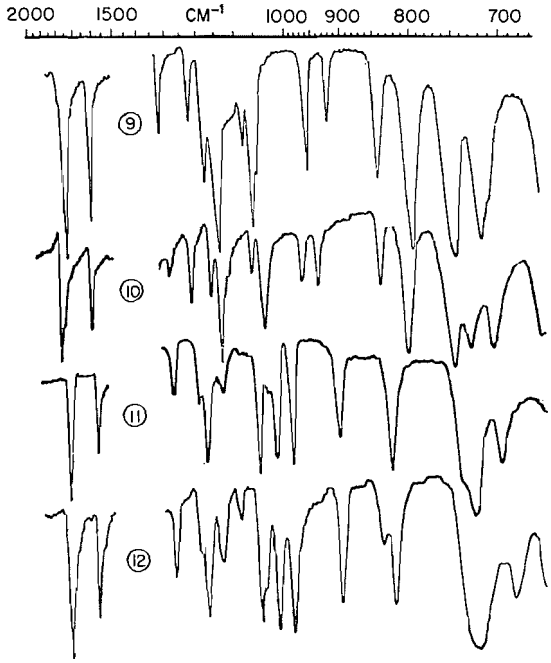

FIG. 1. Infrared spectra of hexachloro-3-cyclohexenones derived from *o*-cresol and *o*-toluidines. These spectra were obtained as Nujol mulls by P and E Model 137B Infracord.

The differences in the chemical shifts of the methyl protons of **9** and **10** (or **11** and **12**) may reflect the differences in the steric configuration of the methyl groups. The chemical shifts of the methine protons of these components are by contrast about equal, suggesting similar steric configurations. It has been shown that for cyclohexanones halogenated on the carbon adjacent to the carbonyl, a chlorine in an equatorial position shifts the i.r. absorption of the carbonyl to a higher frequency than a chlorine in an axial position (11). Also the u.v. absorption maximum of cyclohexanone is shifted to a longer wavelength when substituted by an axial chlorine and to a lower wavelength by an equatorial chlorine (12). Hence, the higher i.r. absorption frequency of the carbonyl in **10** than in **9** signifies that the chlorine in the 6-position is equatorial (e) and the methyl group axial (a) in **10**. Conversely, the methyl group in **9** would be equatorial (e). By analogous interpretation, the methyl group is quasiaxial (a′) in **12** and quasiequatorial (e′) in **11**, since the i.r. absorption frequency of the carbonyl is higher in **12** than **11**. The difference in the u.v. absorption maxima of these ketones is

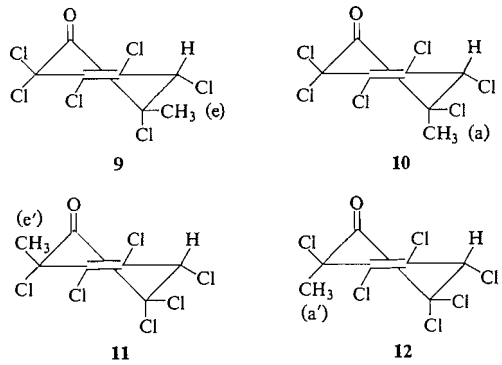

Can. J. Chem. Downloaded from www.nrcresearchpress.com by 210.87.254.42 on 09/05/12
For personal use only.

Can. J. Chem. Downloaded from www.nrcresearchpress.com by 210.87.254.42 on 09/05/12
For personal use only.

in agreement with the assigned configurations. The H-5 of the 3-cyclohexenones are probably quasiaxial, since the chemical shifts are up-field relative to H-4 (a′) (δ 5.29 p.p.m.) of 2-methyl naphthalene tetrachloride and the chemical shifts of quasiequatorial H-4 of other naphthalene tetrachlorides are further downfield (13).

Ketone **13** was previously considered to be either pentachloro-2-methyl-2,4-cyclohexadien-1-one or pentachloro-2-methyl-2,5-cyclohexadien-1-one (2). Its u.v. and i.r. spectra indicate that it is a 2,4-dienone. However, the single high field chemical shift of 2.00 p.p.m. observed for the methyl group means the methyl group is not attached to the conjugated double bond. Hence, **13** is 2,3,4,5,6-pentachloro-6-methyl-2,4-cyclohexadien-1-one.

A heptachloro-2-methylcyclohexenone (**14**) is obtained by further chlorination of **13** in concentrated hydrochloric acid/glacial acetic acid mixture. Compound **14** is also formed, together with **13**, as the major products by direct chlorination of tetrachloro-*o*-cresol in acetic acid. The u.v. and i.r. spectra indicate **14** is also a 3-cyclohexenone. The high i.r. absorption frequency of the carbonyl suggests that there are at least three chlorine atoms on the carbons adjacent to the carbonyl and that the methyl group is in the axial position as in **10** or **12**. Only **12** can give a down-field chemical shift of 2.11 p.p.m. for the methyl protons by a chlorine substitution of the methine proton. The most probable structure of **14**, therefore, appears to be 2,3,4,5,5,6,6-heptachloro-2-methyl-3-cyclohexen-1-one with the methyl group in the quasiaxial position. Similarity of the i.r. absorption bands of **12** and **14** between 850 and 1400 cm^{-1} supports this assigned structure.

Another ketone (**15**) was isolated from the liquid fraction of chlorinated *o*-cresol by v.p.c. This ketone, identified by i.r. spectra, eluted before the hexachloro-2-methylcyclohexenones. It was subsequently identified as the major component of the orange liquid obtained by chlorination of 4,6-dichloro-*o*-cresol or 2-chloro-6-methylaniline in concentrated hydrochloric acid/glacial acetic acid mixture. The chlorine contents of these liquids are close to those of a pentachloro-2-methylcyclohexenone. The common strong i.r. absorption bands at 1760 (C=O) and 1650 cm^{-1} (C=C) and u.v. absorption maximum at 220 mμ shown by these products indicate that **15** is a 3-cyclohexenone. It was found by n.m.r. data that they contain two principal components in common with mixtures of minor components. Each principal component has a methyl group and two non-equivalent methine protons. The two methine protons are coupled (J_{H-H} = 1.50 Hz) and neither is coupled to the methyl protons. The chemical shifts of the major component (**15***a*) are δ CH_3 = 2.07, δ CH = 4.98, δ C=CH = 6.23 p.p.m. and of the minor component (**15***b*) δ CH_3 = 1.89, δ CH = 4.97, δ C=CH = 6.24 p.p.m. Since one of the starting materials 4,6-dichloro-*o*-cresol has protons at only the 3- and 5-positions, it would be expected that the structure of **15** would be similar to **1** except for the presence of a methyl group. Comparison of the methine protons of **1** and **15***a* or **15***b* indicates that the chemical shifts of the non-olefinic protons are essentially equal and that of the olefinic proton of **15***a* or **15***b* is up-field relative to that of **1**. This signifies that the methyl group in both components is on the carbon adjacent to the double bond and that **15***a* and **15***b* are stereoisomers of 2,4,5,6,6-pentachloro-2-methyl-3-cyclohexen-1-one. This structure is supported by the possibility of **11** or **12**, but not **9** or **10**, to give **15** with a methine proton chemical shift of δ CH = 4.97 p.p.m., when the chlorine at the double bond is substituted by a proton. By analogy to **11** and **12**, δ CH_3 = 2.07 p.p.m. of **15***a* being down-field relative to δ CH_3 = 1.89 p.p.m. of **15***b*, the methyl group would be quasiequatorial in **15***a* and quasiaxial in **15***b*. The similar chemical shift differences of the methyl groups of **15***a* and **15***b* and of **11** and **12** support the proposed steric configuration.

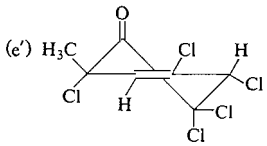

15*a*

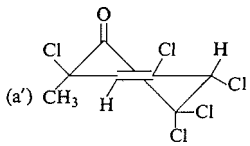

15*b*

Infrared and u.v. spectra indicate that chlorination of 4,6-dichloro-, 4,5,6-trichloro-, or 3,4,6-trichloro-*o*-cresol in carbon tetrachloride in the presence of pyridine gives yellow liquids with 2,4-hexadien-1-ones as the major component. The product from 4,6-dichloro-*o*-cresol contains a single 2,4-hexadienone (**16**) and mixtures of minor components. The two non-equivalent protons present in **16** are coupled

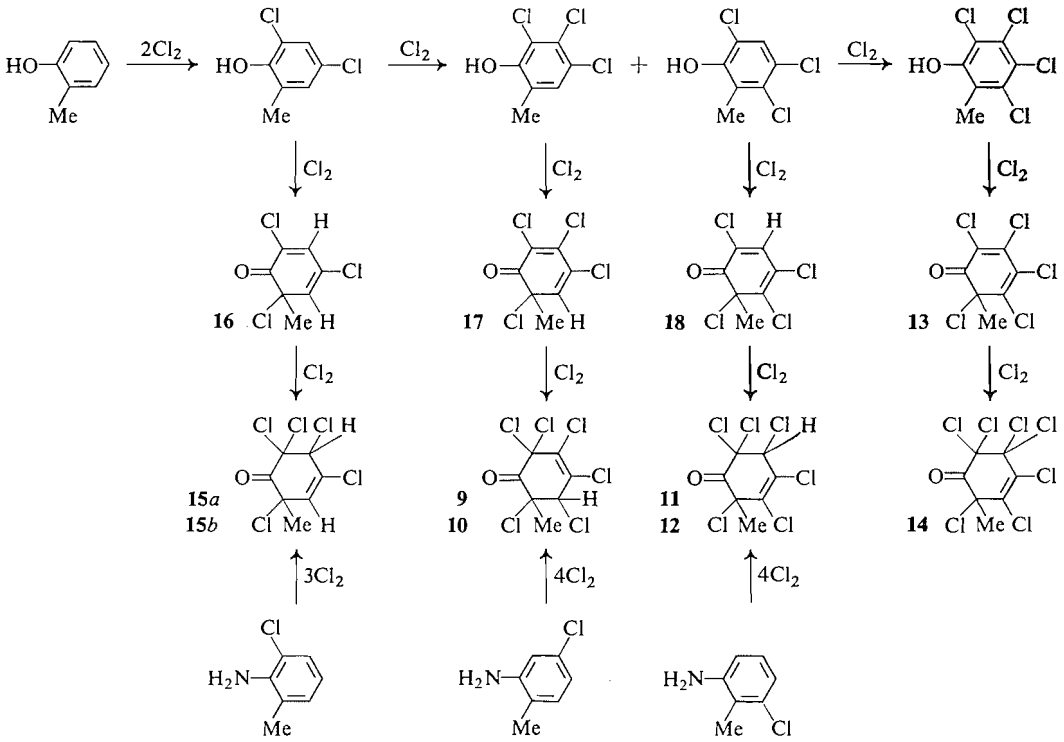

SCHEME II. Chlorination of *o*-cresol and *o*-toluidines.

(J_{H-H} = 2.3 Hz) but neither is coupled to the methyl protons. The high-field chemical shift and the lack of coupling of the methyl group indicate that **16** is 2,4,6-trichloro-6-methyl-2,4-cyclohexadien-1-one.

Ketone **D** obtained from a mixture of 4,5,6-trichloro- and tetrachloro-*o*-cresol consists of two principal components. The major component (**17**) (ca. 75%) contains a methyl group and an olefinic proton with no detectable coupling. For the same reason as for **16**, the structure of **17** is 2,3,4,6-tetrachloro-6-methyl-2,4-cyclohexadien-1-one. The other principal component (ca. 25%) is **13**. Ketone **E**, obtained from 3,4,6-trichloro-*o*-cresol, contains one principal component (ca. 85%) and a mixture of minor components. The principal component is probably 2,4,5,6-tetrachloro-6-methyl-2,4-hexadien-1-one (**18**) because of the high-field chemical shift of the methyl group.

The absence of 2-methyl-2,5- and 2-methyl-2,4-cyclohexadien-1-ones may be attributed to the greater ease of chlorination of a methylated carbon than a chlorinated carbon. The n.m.r. spectra indicated several minor compounds in the liquid fractions, but the compounds have not been isolated. In Scheme II is given the probable sequence leading to the major products by the chlorination of *o*-cresols and *o*-toluidines in acetic acid. The relative amounts of these products formed depend on the conditions during chlorination.

Experimental

Analyses

The ultraviolet (u.v.) spectra were obtained as MeOH solutions with a Cary model-11 spectrophotometer. The i.r. spectra of all solid compounds were obtained as Nujol mulls, and those of liquids as films between two NaCl plates using a Perkin–Elmer model-21 spectrophotometer unless specified otherwise. Nuclear magnetic resonance (n.m.r.) spectra were obtained from chloroform-*d* solutions using a Varian Associates A-60 spectrometer. Chemical shifts are reported in p.p.m. with respect to TMS ≡ 0.

Chlorine was determined using an Ag/AgCl half cell, by potentiometric titration of the chloride ion, formed by oxidation of the compounds with sodium peroxide in Parr Bomb.

Preparation of Cyclohexenones and 2,5-Cyclohexenones

The cyclohexenones and the 2,5-cyclohexadienones

Can. J. Chem. Downloaded from www.nrcresearchpress.com by 210.87.254.42 on 09/05/12
For personal use only.

Can. J. Chem. Downloaded from www.nrcresearchpress.com by 210.87.254.42 on 09/05/12
For personal use only.

were prepared by the chlorination of the appropriate phenols or toluidines in 95% AcOH or in a mixture of glacial AcOH and concentrated HCl (2, 3, 6). Initially, chlorine was passed very rapidly and the temperature was allowed to rise freely but not above 70°. Chlorination was generally continued at a range of 50–60°. The rate of chlorine feed was reduced and slight heating was required as the rate of chlorine uptake decreased. After an excessive amount of chlorine was used, the reaction mixture was allowed to cool to room temperature and solids formed were separated by filtration. The acetic acid solution obtained was concentrated in a rotary evaporator under reduced pressure and poured into a large volume of water. The non-aqueous layer was then dissolved in ethyl ether. The ethereal solution was washed with water, dried (Na_2SO_4), filtered, and the solvent removed *in vacuo*. Liquid products thus obtained were further bubbled with N_2 to remove residual solvents. Solid products were purified by recrystallization. These chlorination products and their analyses are given in Tables II, III, and IV. All 3-cyclohexenones are colorless and 2,5-cyclohexenones are yellowish crystals.

Preparation of 2,4-Cyclohexadienones

Method I (6)

To a stirred solution of cresols in CCl_4 a slight excess of chlorine was passed rapidly and an equimolar amount of pyridine as CCl_4 solution was added, while the temperature was maintained below 45° with cooling. After continued stirring for 45 min the reaction mixture was poured into a large volume of water. The CCl_4 layer was treated similarly to the aforementioned ethereal solution, to obtain the final products.

Method II

A very slight excess of chlorine was passed into a stirred solution of equimolar amounts of cresols and pyridine in CCl_4 with cooling at 20–25°. The subsequent treatment of the CCl_4 solution was the same as above. The data on the 2,4-cyclohexadienones obtained are given in Tables II and III.

Method III

Ketone **13**, m.p. 60–61°, was also prepared by heating ketone **B** in ethanol in the presence of sodium acetate (2). The i.r. spectra of ketone **13** prepared by Method II and III were superimposable.

Reduction of Ketones A and B

To a stirred slurry of **A** (40 g) in MeOH (200 ml) was added zinc powder (28 g) in small portions with stirring and slight heating initially. Vigorous exothermic reaction occurred after a slow start. After refluxing for 4 h, the solution was allowed to cool to room temperature and filtered. The filtrate was poured into 1 l of water slightly acidified with HCl. The solids formed were collected by filtration, washed with water, and air-dried at room temperature; crude yield: 29.1 g. The reduction product, recrystallized from petroleum ether and used to prepare ketone **D**, was a mixture of 3,4,6-trichloro-*o*-cresol [n.m.r.: δ 2.23 (s, CH_3) and 7.18 p.p.m. (s, C=CH)] (ca. 75%) and tetrachloro-*o*-cresol (ca. 25%).

By analogous procedure reduction products (25.6 g) were obtained from **B** (40 g). A mixture of 4,5,6-trichloro-*o*-cresol [n.m.r.: δ 2.33 (s, CH_3) and 7.30 p.p.m. (s, C=CH)] (ca. 95%) and tetrachloro-*o*-cresol (ca. 5%) was used to prepare ketone **E**.

Acknowledgments

We wish to express our thanks to Dr. R. H. Campbell and Mr. C. K. Harmon for the u.v. spectra determinations and to Mr. D. B. Graves for his assistance in the preparation of the compounds.

1. TH. ZINCKE, W. SCHNEIDER, and W. EMMERICH. Ann. Chem. **328**, 268 (1903).
2. TH. ZINCKE and W. PFAFFENDORFF. Ann. Chem. **394**, 11 (1912).
3. TH. ZINCKE and O. PREISS. Ann. Chem. **417**, 205 (1918).
4. R. FRH. VON WALTHER and W. ZIPPER. J. Prak. Chem. (2), **199**, 364 (1915).
5. H. MULLER and H. LINDE. J. Prak. Chem. **4**, 69 (1956).
6. L. DENIVELLE and R. FORT. Compt. Rend. **235**, 1514 (1952); R. FORT. Ann. Chim. (Paris) (13), **4**, 203 (1959).
7. L. DENIVELLE and R. FORT. Bull. Soc. Chim. France, 1834 (1956); L. DENIVELLE and R. FORT. Bull. Soc. Chim. France, 724 (1957); L. DENIVELLE and R. FORT. Bull. Soc. Chim. France, 459 (1958); L. DENIVELLE and R. FORT. Bull. Soc. Chim. France, 392 (1959).
8. J. KUMAMOTO and T. KATO. J. Ind. Chem. (Japan), **60**, 1325 (1957).
9. H. BILTZ and W. GIESE. Ber. Deut. Chem. Ges. **37**, 4017 (1904).
10. R. H. BIBLE, JR. Interpretation of n.m.r. spectra: an empirical approach. Plenum Press, New York. 1965. p. 38.
11. (*a*) K. KOZIMA and Y. YAMANOUCHI. J. Am. Chem. Soc. **81**, 4159 (1959); (*b*) N. I. ALLINGER, J. ALLINGER, L. A. FREIBERG, R. T. CZAJA, and N. A. LEBEL. J. Am. Chem. Soc. **82**, 5876 (1960): (*c*) K. KOZIMA and E. HIRANO. J. Am. Chem. Soc. **83**, 4300 (1961).
12. R. C. COOKSON. J. Chem. Soc. 282 (1954).
13. G. CUM, P. B. D. DE LA MARC, and J. S. LOMAS. J. Chem. Soc. B, 244 (1967).

Can. J. Chem. Downloaded from www.nrcresearchpress.com by 210.87.254.105 on 09/05/12
For personal use only.

Some benzophenanthridine alkaloids from *Bocconia arborea*

D. B. MacLean, D. E. F. Gracey, and J. K. Saunders
Department of Chemistry, McMaster University, Hamilton, Ontario

AND

R. Rodrigo and R. H. F. Manske
Department of Chemistry, University of Waterloo, Waterloo, Ontario

Received December 10, 1968

The minor alkaloids of *B. arborea* have been identified. Three of them have been shown to be dihydrosanguinarine, oxysanguinarine, and 11-*O*-methyldihydrochelerythrine respectively. The structure of the fourth has been established by physical methods and by synthesis as the hitherto unknown 1,3-bis(11-hydrochelerythrinyl)acetone. It does not appear to be an artefact. The high resolution mass spectra of some dihydrochelerythrine derivatives are discussed.

Canadian Journal of Chemistry, 47, 1951 (1969)

One of us had previously reported (1) the isolation of seven alkaloids from this source. We wish now to present evidence for the structures of the four alkaloids then unassigned and designated **A**, **B**, **C**, and **P61** respectively.

Alkaloid **A** (m.p. 304°) and dihydrochelerythrine, **2**, had ultraviolet (u.v.) spectra (in 1,4-dioxan) virtually superimposable on each other and infrared (i.r.) spectra (in $CHCl_3$) that were extremely similar but for the presence of carbonyl stretching absorption in the former at 1710 cm^{-1}. When the mass spectrum of alkaloid **A** was first recorded, the peak of highest mass was found at *m/e* 405 and corresponded in composition to $C_{24}H_{23}NO_5$ (calcd.: 405.1576; observed: 405.1583). The spectrum was similar to that reported (2) for 11-acetonyldihydrochelerythrine, **1** (m.p. 194°) with the base peak appearing at *m/e* 348 corresponding in composition to $C_{21}H_{18}NO_4$ (calcd.: 348.1236; observed: 348.1265). Unfortunately, a good quality proton magnetic resonance (p.m.r.) spectrum of **A** could not be obtained because of its very poor solubility in the common solvents.

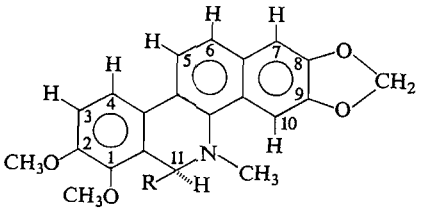

1 R = CH_2COCH_3
2 R = H
3 R = OCH_3
4 R = CH_2COCH_2—(2—H)

TABLE I

Nuclear magnetic resonance signals of dihydrochelerythrine and its derivatives

	1	2	3
2-CH_3O	3.89	3.89	3.92
1-CH_3O	3.93	3.93	3.96
O—CH_2—O	6.00	6.04	6.04
>N—CH_3	2.65	2.62	2.77
H_3	6.94	6.94	7.05
H_4	7.52	7.52	7.65
H_5	7.70	7.71	7.80
H_6	7.47	7.49	7.49
H_7	7.09	7.11	7.14
H_{10}	7.50	7.69	7.72
H_{11}	5.03	4.30	5.55
11-OCH_3	—	—	3.46

However, the close similarity of **A** to 11-acetonyldihydrochelerythrine led us to prepare the latter and carefully examine its spectroscopic properties.

The results of our p.m.r. examination are qualitatively similar to those reported by Desai *et al.* (2) but we have been able, with the use of a 100 MHz instrument and with the application of the nuclear Overhauser effect (n.O.e.) (3), to assign all the signals in the spectrum.

The 100 MHz spectrum (Table I, compound **1**) shows singlets of three protons each at δ 2.04 (CH_3—C(=O)—), δ 2.65 (>N—CH_3), δ 3.89 and 3.93 (2×—OCH_3), a two proton singlet at δ 6.00 assigned to the methylenedioxy group, and an ABX system associated with the proton at C_{11}

Can. J. Chem. Downloaded from www.nrcresearchpress.com by 210.87.254.105 on 09/05/12
For personal use only.

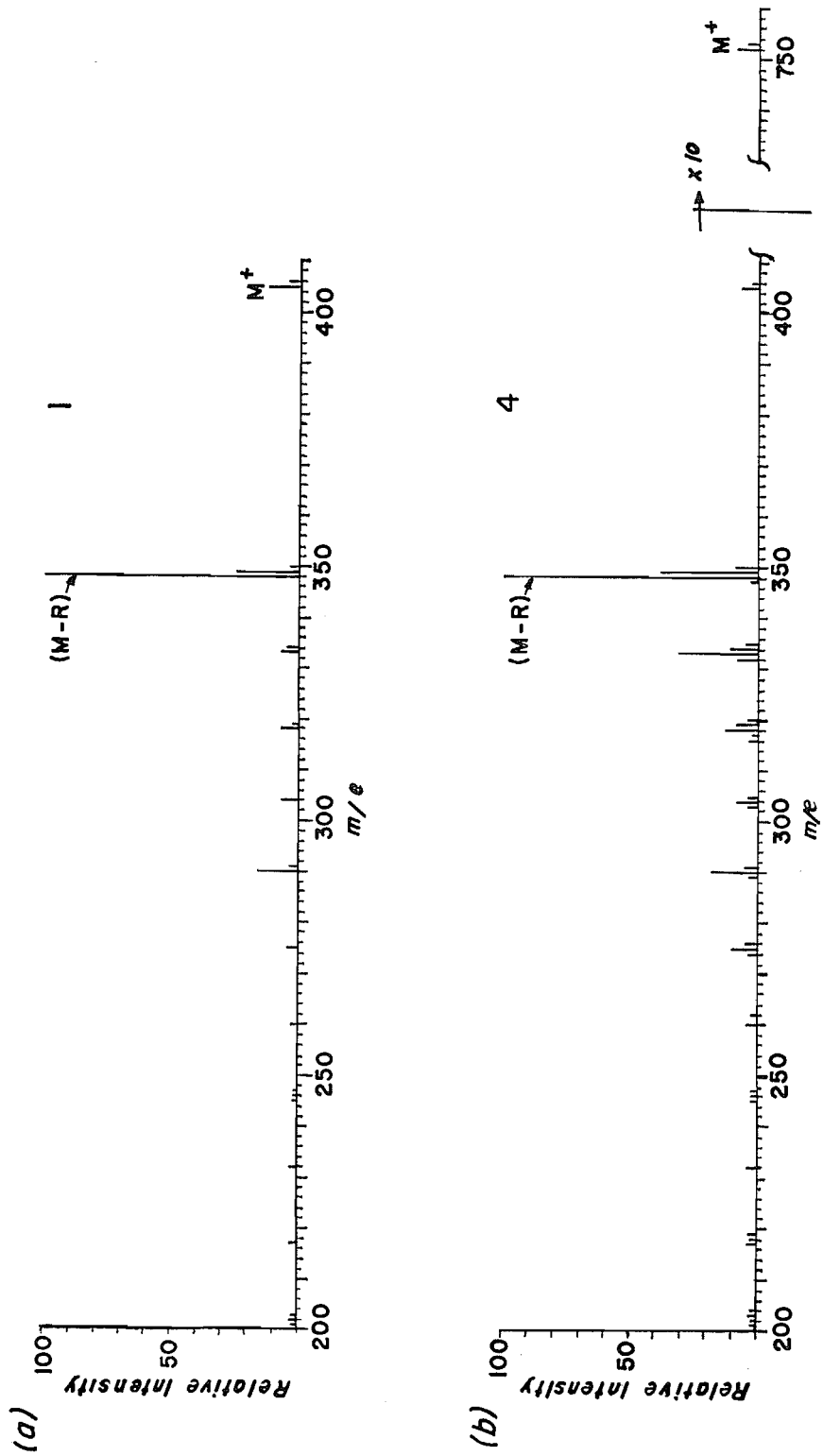

FIG. 1. The mass spectra of (*a*) 11-acetonyldihydrochelerythrine (**1**) and (*b*) 1,3-bis(11-hydrochelerythrinyl)acetone (**4**).

Can. J. Chem. Downloaded from www.nrcresearchpress.com by 210.87.254.105 on 09/05/12
For personal use only.

and the two protons at C_{12}. The signals associated with the ABX system are centered at δ 2.23, 2.57, and 5.03, respectively, with coupling constants, $J_{AX} = 4.0$, $J_{BX} = 9.0$, and $J_{AB} = 15.0$ Hz. The aromatic region integrates for six protons comprising two singlets at δ 7.09 (H_7) and 7.50 (H_{10}) and two AB quartets (δ H_3, 6.94; δ H_4, 7.52; $J_{H_3H_4} = 8.3$ Hz and δ H_5, 7.70; δ H_6, 7.47; $J_{H_5H_6} = 8.6$ Hz). The assignment of the signal at δ 7.50 to H_{10} is based on the existence of an n.O.e. between the $\overset{\diagdown}{\underset{\diagup}{N}}—CH_3$ and the signal centered at δ 7.50. Thus, when the sample was irradiated at δ 2.65 (the signal attributed to the $\overset{\diagdown}{\underset{\diagup}{N}}—CH_3$ group) an increase in area of 30% was observed for the signal at δ 7.50. It follows that the signal at δ 7.50 must be assigned to H_{10} while that at δ 7.09 is associated with H_7. Irradiation at δ 2.65 did not affect any other aromatic proton but caused an increase in area of the multiplet centered at δ 5.03 (assigned to H_{11}) by 23%. Similarly an n.O.e. of 24% was observed at the signal δ 6.94 when the methoxyl signals were irradiated. The signal at δ 6.94 must, therefore, be assigned to H_3 from which it follows that the signal at δ 7.52 must be attributed to H_4 since the two are coupled. The remaining AB quartet is assigned to the protons at H_5 and H_6. The lower field proton (δ 7.47) is assigned to H_6 on the basis of n.O.e. measurements. Irradiation at δ 7.09, the signal corresponding to H_7, caused an increase in area of 27% for the signal at δ 7.47. Thus the signal at δ 7.47 must be assigned to H_6 while that at δ 7.70 must be assigned to H_5. These assignments are in agreement with, and confirm, those of Slavik *et al.* (4) who examined other benzophenanthridine alkaloids.

Upon comparison of the spectrum of **1** with the poor quality spectra of alkaloid **A** obtained in DMSO-d_6 and pyridine-d_5, it was apparent that **A** was the bis adduct of chelerythrine and acetone, viz. 1,3-bis(11-hydrochelerythrinyl)-acetone, **4**.

The two compounds had the same ratios of methoxyl to $\overset{\diagdown}{\underset{\diagup}{N}}—CH_3$, to methylenedioxy and to aromatic protons. Moreover, compound **A** also had an ABX system, although not as well resolved as that in the acetone adduct. Compound **A**, however, lacked the singlet (three protons) at δ 2.04 found in the former.

Re-examination of the mass spectrum of **A** revealed an ion of low intensity at *m/e* 752 which had been missed earlier. Accurate mass measurement indicated that this ion had the composition $C_{45}H_{40}N_2O_9$ (calcd.: 752.2734; observed: 752.2759). This is compatible with **4**. Evidently, upon electron impact, hydrogen transfer accompanies the fragmentation process yielding a neutral species of mass 347 and an ion of *m/e* 405. The latter ion fragments as expected with loss of 57 mass units yielded the most intense ion of the spectrum at *m/e* 348. (The mass spectra of compounds **1** and **4** are shown in Fig. 1.) The loss of a substituent at C_{11} is characteristic of benzophenanthridine systems substituted at C_{11} as reported by Slavik *et al.* in their study (4) of the mass spectra of benzophenanthridine alkaloids including various 11-substituted dihydrochelerythrine derivatives. In the case of the latter compounds it was noted that the loss of the R group (Scheme 1) is characteristic of all these compounds and the ion $[M—R]^+$ which they designate '*a*' then undergoes a series of fragmentations via *a*-15, *a*-30, *a*-58, *a*-58-15, *a*-58-30, and *a*-(2 × 58). Slavik *et al.* have not, however, determined the composition of these ions but have drawn some conclusions with respect to their formation. Desai *et al.* (2) have reported that the mass spectrum of 11-acetonyldihydrochelerythrine, **1**, shows a molecular ion peak and an intense peak at *m/e* 348 but they have not commented further on the spectrum. The four compounds (**1**–**4**) which we have examined all show a peak at *m/e* 348 and the other fragment peaks described by Slavik *et al.*

The mass spectra of compounds **1** and **4** are shown in Fig. 1 and a general scheme for the fragmentation of 11-substituted dihydrochelerythrine derivatives in Scheme 1. The compositions given were deduced from the masses measured on a high resolution instrument. In all cases the measured masses agreed with the calculated values within ±3 milli mass units. All measurements were made on compound **1**. There appear to be three independent pathways by which the ion *m/e* 348 fragments further. Pathways *2* and *3* converge at *m/e* 303 or *m/e* 275. Pathway *1* also yields an ion of *m/e* 275 but of different composition. Pathway *1* appears to be dominant

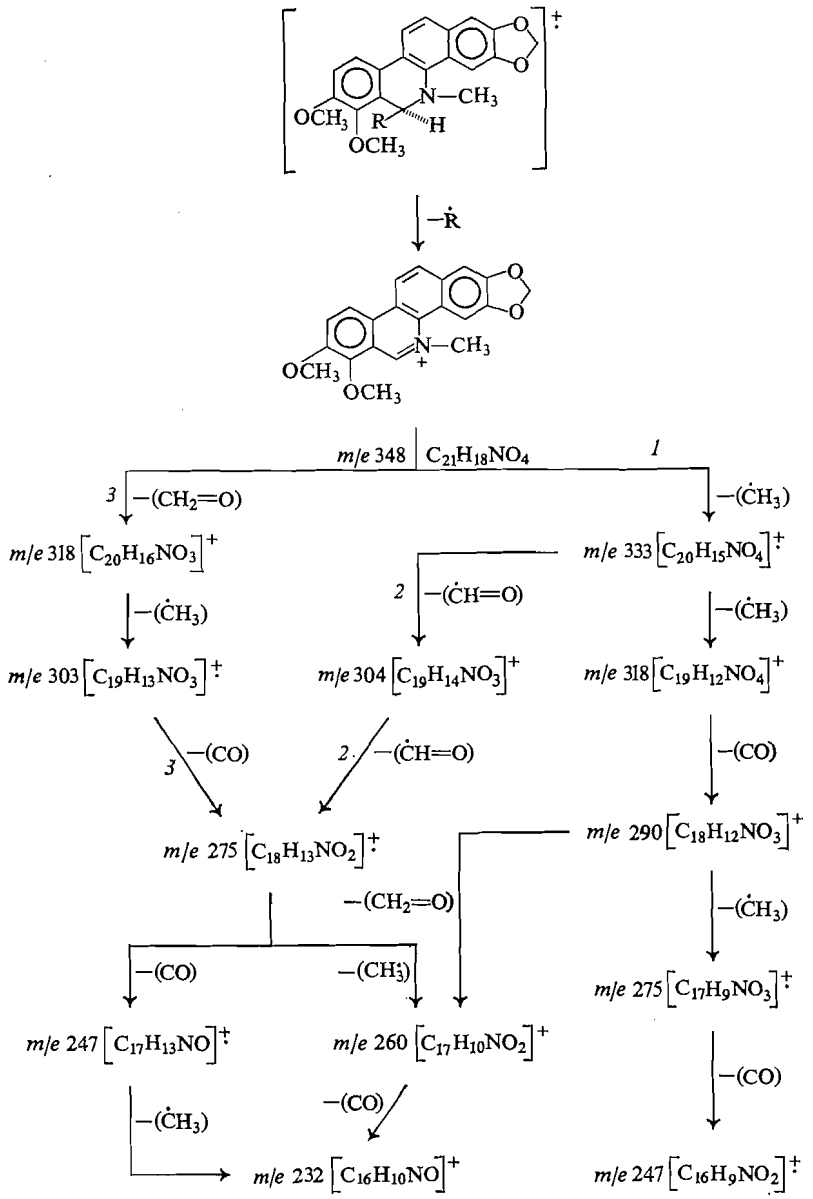

Scheme 1

since the doublets at *m/e* 318, 275, and 247 are enriched in the ions from pathway *1* by factors of 8, 6, and 2 respectively.

None of the pathways demand that CH_3 be lost consecutively from the two methoxyl groups as implied by Slavik *et al.* Instead, a loss of methoxyl methyl may be followed by loss of an N—CH_3 group and this in turn by loss of CO. It is impossible, without labelling studies, to decide the order of sequence of loss of OCH_3 vs. N—CH_3, or to decide whether the loss of CH_2=O and CH=O species arises from the methoxyl or methylenedioxy group. The same pattern of fragmentations is found in the spectra of compounds **2**–**4** and since all spectra contain the common ion of *m/e* 348 one can

Can. J. Chem. Downloaded from www.nrcresearchpress.com by 210.87.254.105 on 09/05/12
For personal use only.

Can. J. Chem. Downloaded from www.nrcresearchpress.com by 210.87.254.105 on 09/05/12
For personal use only.

assume that the composition of the fragment ions is the same in the spectra of all four compounds.

The structure of alkaloid **A**, inferred from the spectral data was confirmed by its synthesis by the base-catalyzed condensation of chelerythrine and acetone dicarboxylic acid. It is noteworthy that attempts to synthesize **A** by mild base-catalyzed condensation of chelerythrine with 11-acetonyldihydrochelerythrine were unsuccessful. It is therefore probable that **A** is indeed a naturally occurring alkaloid and not an artefact produced in the isolation process.

Alkaloid **P61** which had been earlier believed (5) to be a pure sample of chelerythrine by reason of its conversion to the pseudocyanide of the latter, is now recognized as 11-*O*-methyldihydrochelerythrine, **3**, on the basis of its p.m.r. spectrum in which every signal could be assigned by analogy with the spectrum of 11-acetonyldihydrochelerythrine (Table I). Furthermore, the mass spectrum of **P61** was in complete accord with the proposed structure and fitted perfectly into the general Scheme 1. **P61** is quite probably an artefact produced in the isolation of the alkaloids from the plant material and it is noteworthy that a similar artefact, the 11-*O*-ethyl derivative, has been isolated (6) from *F. xanthoxyloides.*

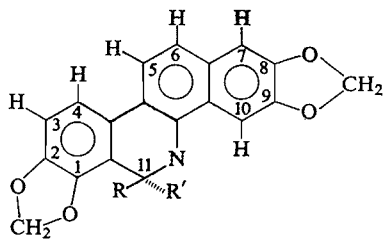

5 R = R′ = H
6 R + R′ = O

Alkaloid **B** (m.p. 191°) was recognized as dihydrosanguinarine, **5**, from its 100 MHz p.m.r. spectrum which had singlets at δ 2.58, 4.16, 6.03, and 6.04, corresponding in position and intensity to *N*-methyl, benzylic methylene, and two methylenedioxy groups respectively. The aromatic region of the spectrum integrated for six protons consisting of two singlets at δ 7.06 and δ 7.66 which could be assigned to the C_7 and C_{10} protons, respectively, and two AB quartets (δ H_3, 6.79; δ H_4, 7.24; $J_{H_3H_4}$ = 8.2 Hz and δ H_5, 7.63; δ H_6, 7.43; $J_{H_5H_6}$ = 8.0 Hz). These assignments could be made by comparison with the spectrum of dihydrochelerythrine, **2** (Table I). This structure of alkaloid B was confirmed by oxidation of B in chloroform solution with mercuric acetate to sanguinarine (m.p. 244°).

Alkaloid **C**, after a preliminary purification, crystallized from chloroform–methanol as white leaflets melting at 361° in an evacuated tube. It had a u.v. absorption spectrum typical of a benzophenanthridine alkaloid, and carbonyl stretching absorption at 1655 cm^{-1} in the i.r. spectrum characteristic of a six-membered aromatic lactam. The mass spectrum of **C** showed the molecular ion at *m/e* 347 corresponding to the expected composition $C_{20}H_{13}NO_5$ (calcd.: 347.0794; observed: 347.0796). The p.m.r. spectrum of **C** could not be determined because of its very poor solubility in the common solvents. However, on the basis of the foregoing properties it is clear that **C** is in fact oxysanguarine **6**.

Experimental

Melting points were determined using a Fisher Meltemp apparatus. Mass spectra were recorded on a CEC 21-110B double-focusing mass spectrometer. Samples were introduced through the direct inlet system. Accurate mass measurements (7) were carried out by reference to appropriate peaks in the spectrum of perfluorokerosene (8). Proton magnetic resonance spectra were recorded using the frequency sweep mode of a Varian HA-100 spectrometer. Samples were dissolved in $CDCl_3$, unless otherwise specified, using added TMS as the internal locking signal. Chemical shifts were measured relative to TMS using a V4315 frequency counter incorporated in the instrument. Double irradiation was achieved by employing a Hewlett–Packard 201C audiogenerator at the desired frequency. For n.O.e. measurements degassed solutions were used and a procedure similar to that of Anet and Bourn (3) was employed. A Beckmann I.R. 10 spectrometer was used to record i.r. spectra, and a Cary 14 spectrophotometer was used for the u.v. spectra.

11-Acetonyldihydrochelerythrine **1**

Chelerythrine chloride (1 g) was refluxed with acetone (50 ml) and aqueous sodium carbonate (10 ml, 2 g) for 6 h. The excess acetone was removed under reduced pressure and the residue washed thoroughly with water and chromatographed on a short column of silica gel in benzene–acetone (9:1). The product (u.v. blue fluorescent) was collected, the solvent removed, and the residue recrystallized from acetone from which it deposited large colorless plates (0.64 g) melting sharply at 199°, $\nu_{C=O}$(KBr) 1715 cm^{-1}.

1,3-bis(11-Hydrochelerythrinyl)acetone **4**

Chelerythrine (300 mg) was dissolved in pyridine (5 ml), freshly prepared acetone dicarboxylic acid (60 mg) was added, and the solution allowed to stand overnight. The pyridine was removed under reduced

pressure, the residue chromatographed on a column of silica gel in benzene–acetone (9:1), and the u.v. blue fluorescent band collected. This fraction was taken to dryness under reduced pressure and the residue further purified by thin-layer chromatography (t.l.c.) on several plates of silica gel G(20 × 20 × 0.1 cm) in benzene–acetone (9:1). The slower u.v. blue fluorescent major component was eluted and crystallized from chloroform–acetone as colorless plates, m.p. 304° (45 mg).

Alkaloid **A** was similarly freed of a minor impurity by preparative t.l.c. which raised its melting point to 304°.

*Oxidation of Alkaloid **B**, **5**, to Sanguinarine*

Alkaloid **B** (1 g) was refluxed with mercuric acetate (2 g) in chloroform (50 ml) for 12 h. Most of the chloroform was removed under reduced pressure, the solution allowed to cool, and filtered. The filtrate was evaporated to dryness and chromatographed on a short column of silica gel. The column was first eluted with chloroform (100 ml) and the eluate discarded. This was followed by elution with chloroform–acetone (9:1) (100 ml) and the eluate, upon evaporation to dryness and crystallization from chloroform–methanol, yielded colorless needles of sanguinarine, m.p. 244° (740 mg).

*Purification of Alkaloid **C***

Alkaloid C (150 mg) was chromatographed on a column of silica gel (13 × 1.8 cm) and the column was eluted first with hexane–acetone (9:1) (400 ml). The eluate upon crystallization from chloroform–methanol gave colorless crystals, m.p. 275° (62 mg). This compound did not contain nitrogen and was not investigated further. Upon subsequent elution with chloroform–acetone (9:1) (300 ml) the column gave an eluate which could be induced to crystallize from chloroform–methanol as white leaflets (75 mg) melting at 361° in an evacuated tube; u.v.: λ_{max}(dioxan) 284, 293, 334 (shoulder), 344 and 363 (shoulder), and 382 mμ; log ε 4.56, 4.62, 4.15, 4.17, 4.06, and 4.00; i.r.: $\nu_{C=O}$ (KBr) 1655 cm^{-1}.

Acknowledgments

Research support from the National Research Council of Canada is gratefully acknowledged. Thanks are due to Professor E. Bullock of Memorial University, Newfoundland for the 100 MHz spectrum of dihydrosanguinarine.

1. R. H. F. MANSKE. Can. J. Res. B, **21**, 140 (1943).
2. P. D. DESAI, T. R. GOVINDACHARI, K. NAGARAJAN, and N. VISWANATHAN. Ind. J. Chem. **5**, 41 (1967).
3. F. A. L. ANET and A. J. R. BOURN. J. Am. Chem. Soc. **87**, 5250 (1965).
4. J. SLAVIK, L. DOLEJŠ, V. HANUŠ, and A. D. CROSS. Coll. Czech. Chem. Commun. **33**, 1619 (1968).
5. R. H. F. MANSKE. The alkaloids. Vol. IV. Academic Press. New York. 1954. p. 255.
6. F. G. TORTO, P. SEKOVIC, and B. A. DADSON. Tetrahedron Letters, 181 (1966).
7. K. S. QUISENBERRY, T. T. SCOLMAN, and A. O. NIER. Phys. Rev. **102**, 1071 (1956).
8. F. W. MCLAFFERTY. Anal. Chem. **28**, 306 (1956).

Can. J. Chem. Downloaded from www.nrcresearchpress.com by 210.87.254.105 on 09/05/12
For personal use only.

Can. J. Chem. Downloaded from www.nrcresearchpress.com by 210.87.254.42 on 09/05/12
For personal use only.

Optical rotatory dispersion and circular dichroism of diastereoisomers. I. The ephedrines and chloramphenicols

L. A. MITSCHER, F. KAUTZ, AND J. LAPIDUS

Divisions of Medicinal and Natural Products Chemistry, College of Pharmacy, The Ohio State University, Columbus, Ohio 43210

Received July 11, 1968

Optical rotatory dispersion (o.r.d.) and circular dichroism measurements are reported for all four diastereoisomers in both the ephedrine and chloramphenicol series. The Cotton effect associated with the ^1L_b absorption band is a reliable guide to absolute configuration in both series whereas the ^1L_a band is not. Circular dichroism measurements are preferred as the ^1L_a band dominates the o.r.d. curves to such an extent that erroneous assignment is quite possible. An attempt to relate the sign and intensity of the ^1L_b Cotton effect with rotamer population failed due to lack of apparent correlation.

Canadian Journal of Chemistry, 47, 1957 (1969)

The absolute configurations of ephedrine (**1–4**) and chloramphenicol (**5–8**) isomers have been firmly established (1–6). As these two series are closely related to one another in a stereochemical sense and are related to a multitude of biologically important arylamines, we were interested in establishing a rapid, convenient, micromethod for configurational assignment based on optical rotatory dispersion (o.r.d.) and circular dichroism (c.d.) measurements. Insufficient information is presently available in the literature on compounds of this type upon which to make reliable assignments based upon empirical rules much less upon theoretical grounds (7, 8). Therefore, we decided to begin our studies in this area by measuring all of the diastereoisomers of ephedrine and chloramphenicol using modern instrumentation.

Some years ago a pioneering study on the optical rotatory dispersion of a variety of simple aromatic substances included, as one of the examples, (−)-(1R,2S)-ephedrine (9). The best instrumentation available at that time had limited penetrating power and, as will be seen below, the majority of the curve in the most interesting spectral region was unavoidably inaccessible. The results obtained seemed to demonstrate the first extremum of a *negative* Cotton effect. As will be seen from Fig. 1, in fact, when seen *in toto*, a series of low amplitude peaks and troughs are present in the 240–280 mμ region where one would expect the symmetry "forbidden" ^1L_b π–π^* transition to occur (10). These small peaks are superimposed upon large slopes which do not reach maxima above 200 mμ. This is attributed to the very large π–π^* transitions which occur at lower wavelengths in many simple monosubstituted benzenoids. As will be

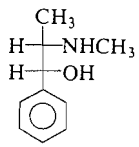

1

(−)-(1R,2S)-ephedrine

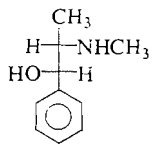

4

(+)-(1S,2S)-pseudoephedrine

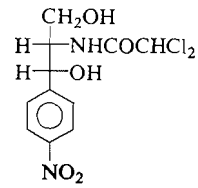

5

(+)-(1R,2S)-chloramphenicol

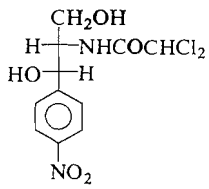

8

(+)-(1S,2S)-chloramphenicol

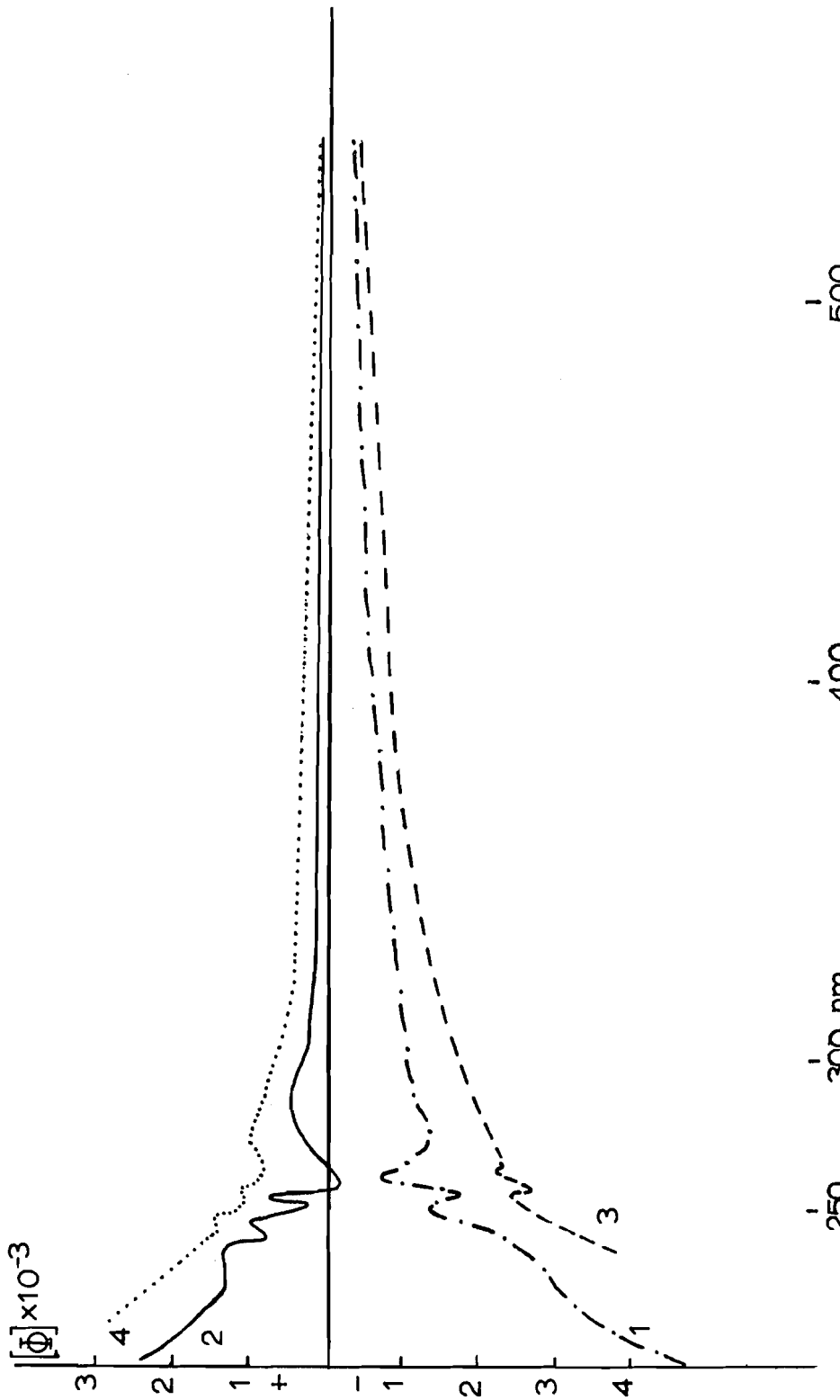

FIG. 1. Optical rotatory dispersion curves of the four isomeric ephedrine alkaloids **1**–**4** in methanol.

Can. J. Chem. Downloaded from www.nrcresearchpress.com by 210.87.254.42 on 09/05/12
For personal use only.

Can. J. Chem. Downloaded from www.nrcresearchpress.com by 210.87.254.42 on 09/05/12
For personal use only.

seen below most clearly in the case of the chloramphenicol isomers, for reasons that are presently obscure, not all of the factors that affect the shape of the spectra are sensitive to stereochemistry so the curves are not exactly enantiomeric. The slope of the curve is such that it is difficult to decide whether the first extremum of the group of peaks at 240–280 mμ is negative as previously assigned in the ephedrine case, or positive. This is a potentially serious problem for the sign of the first extremum at highest wavelength determines the optical family to which a substance is assigned (11).

A clear solution to this problem was found by using circular dichroism (c.d.) measurements. It is well known that whereas short wavelength absorbing functions ordinarily do not seriously interfere with c.d. measurements above 220 mμ, their influence is felt more or less strongly in o.r.d. measurements. This extensive "tailing effect" is not only a function of peak intensity but also of peak separation so that the effect is often minimal at wavelengths far removed from the absorption peak. In the cases at hand, the tailing effect of the short wavelength maxima is so pronounced that it virtually overwhelms the ^1L_b maxima and even dominates the o.r.d. spectrum all the way out to the sodium-D line (589.3 mμ)! The appropriate c.d. spectra of the ephedrines are recorded in Fig. 2 where it will be seen that (−)-(1R,2S)-ephedrine (**1**) and (−)-(1R,2R)-pseudoephedrine (**3**) hydrochlorides actually give a series of *positive* Cotton effects near 260 mμ. It is apparent, then, that the earlier incorrect attribution of a negative sign to this transition is a consequence of the slope of the curve in regions inaccessible at the time. Unfortunately, sensitivity was lost precisely at the wavelength where the low amplitude positive Cotton effects were beginning to appear. An exactly analogous case arising from a similar effect has recently been reported by Craig and his co-workers (12). The absolute configurations of the ephedrines have been firmly established by purely chemical means (1, 2) and so the reversal in designation of sign required by these data does not necessitate a corresponding change in configurational assignment.

So far as data is available to this point (but *vide infra*), the sign of the c.d. maxima of simple aryl chromophores in the 250–270 mμ range has proved to be a reliable guide to absolute con-

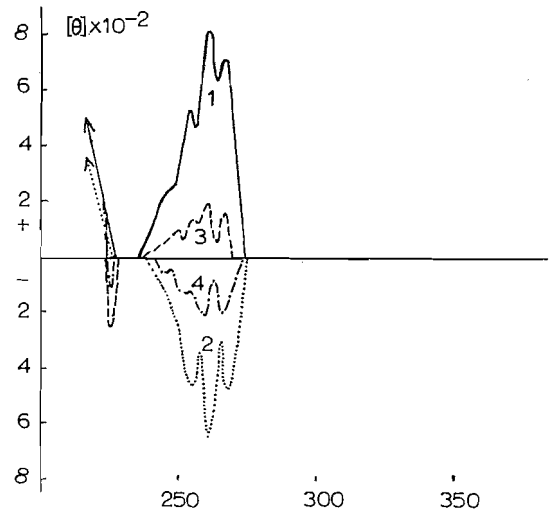

FIG. 2. Circular dichroism curves of the four isomeric ephedrine alkaloids **1–4** in methanol.

figuration, whereas the approach slopes of peaks below 200 mμ have not been directly correlatable with absolute configuration (7, 8, 12–19). Craig has even recorded an example wherein the sign of the latter transition and the corresponding sodium-D line rotation *inverted* when measuring successively the rotations of the free base and then the amine salt (12). The peaks at 250–270 mμ retained their sign although there were intensity differences. We have observed similar changes in intensity in this study but none so strong as to change the sign. In the absence of structural features containing n or p electrons capable of interacting with the benzenoid π cloud (for example, phenylalanine and 1-methylindane) the ^1L_b Cotton effects may be very difficult to detect at all (13, 20). From these findings, it is now clear that o.r.d. measurements of simple aryl chromophores are treacherous guides to absolute configuration whereas c.d. measurements of the ^1L_b band appear to lead to unambiguous answers.

The optical rotations of aryl chromophores of this type reflect the weighted average of the population of the various rotamers through their incremental optical rotatory contributions even though the intimate mechanisms are presently obscure. It seems likely that an explanation of the strong dependence of o.r.d. spectra on experimental conditions could be simply that the peaks below 200 mμ are more sensitive to small changes in

Can. J. Chem. Downloaded from www.nrcresearchpress.com by 210.87.254.42 on 09/05/12
For personal use only.

rotamer ratios than those at 260 mμ because of their much greater magnitude. It is obvious that differentiations between pairs of substances which differ configurationally at centers more distantly removed from the chromophore, such as (−)-ephedrine and (−)-pseudoephedrine, often must be made on the basis of peak amplitude rather than sign. With experimental parameters having a strong influence on amplitude, comparisons must be made between very close models and at as nearly identical conditions as are possible with respect to concentration, solvent and pH. The c.d. peaks at 260 mμ are apparently much less sensitive to the changes at lower wavelength with the exception of modifications in amplitude.

Turning once again to Fig. 2, it is apparent that, using the cautions enumerated above, the ^1L_b c.d. bands are a reliable indicator of the configurations of both asymmetric carbons of the ephedrines when the sign and amplitude are both considered. As expected, the configuration of C-1, which is closest to the aromatic ring, dominates the spectrum and determines the overall sign of the Cotton effect. The configuration of C-2 has an effect on the amplitude. Both (−)-(1R,2S)-ephedrine (**1**) and (−)-(1R,2R)-pseudoephedrine (**3**) hydrochlorides, which have the same configuration at C-1, give positive ^1L_b bands. On the other hand (+)-(1S,2R)-ephedrine (**2**) and (+)-(1S,2S)-pseudoephedrine (**4**) salts give closely enantiomeric c.d. spectra to those of their negative analogues. The *erythro* compounds (ephedrines) give curves with higher amplitudes than the *threo* compounds (pseudoephedrines). Analogous findings have been made with c.d. measurements on the related diastereoisomeric cinchona alkaloids (21). Thus, the diminution of amplitude observed in the *threo* compounds can serve as an indication of the configuration of C-2. The corresponding free bases of **1** and **3** were measured. With natural ephedrine (**1**), this change in conditions results in a considerable diminution of the ^1L_b band and a slight shift in peak positions. With pseudoephedrine (**2**), a slight intensification of the ^1L_b band was noted. Use of dioxane as a solvent in place of methanol (for pseudoephedrine free base) simply reduced the amplitude and brought out some added fine structure.

In cases where steric effects are large, or where overriding effects are present due to strong intramolecular hydrogen bonds, definite preferences will be found for a single rotamer even at ambient temperature. Strong intramolecular hydrogen bonding is indeed found with the ephedrines and has been the subject of a number of investigations (22–25). Most pertinent is a recent study by Portoghese utilizing nuclear magnetic resonance (n.m.r.) techniques whereby he was able to assess the rotameric situation in this series (22). Ephedrine, as the free base, can exist in three different staggered rotational conformations of which a definite preference for conformer **A** is apparent from the various coupling constants. Conformer **B** makes a small contribution whereas **C**, which is not capable of stabilization by intramolecular hydrogen bonding, is not present in significant amounts. In acidic solution, the conformational preference

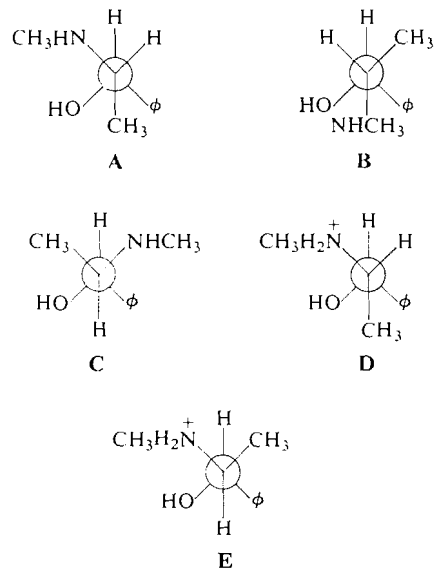

for **A** is reinforced at the expense of conformer **B** even though the hydrogen bonding is probably contributed by a different donor (**D**). Except for greater dilution, the conditions utilized in this study are similar, so these factors suggest that the o.r.d.–c.d. effects reported here are largely attributable to conformer **D**. Lesser amplitude observed with the free base may be due to an increased, and competing, contribution by conformer **B** and perhaps **C**. With pseudoephedrine, the corresponding most populous configuration is that of **E** which is closely analogous to rotamer **D** for ephedrine. This

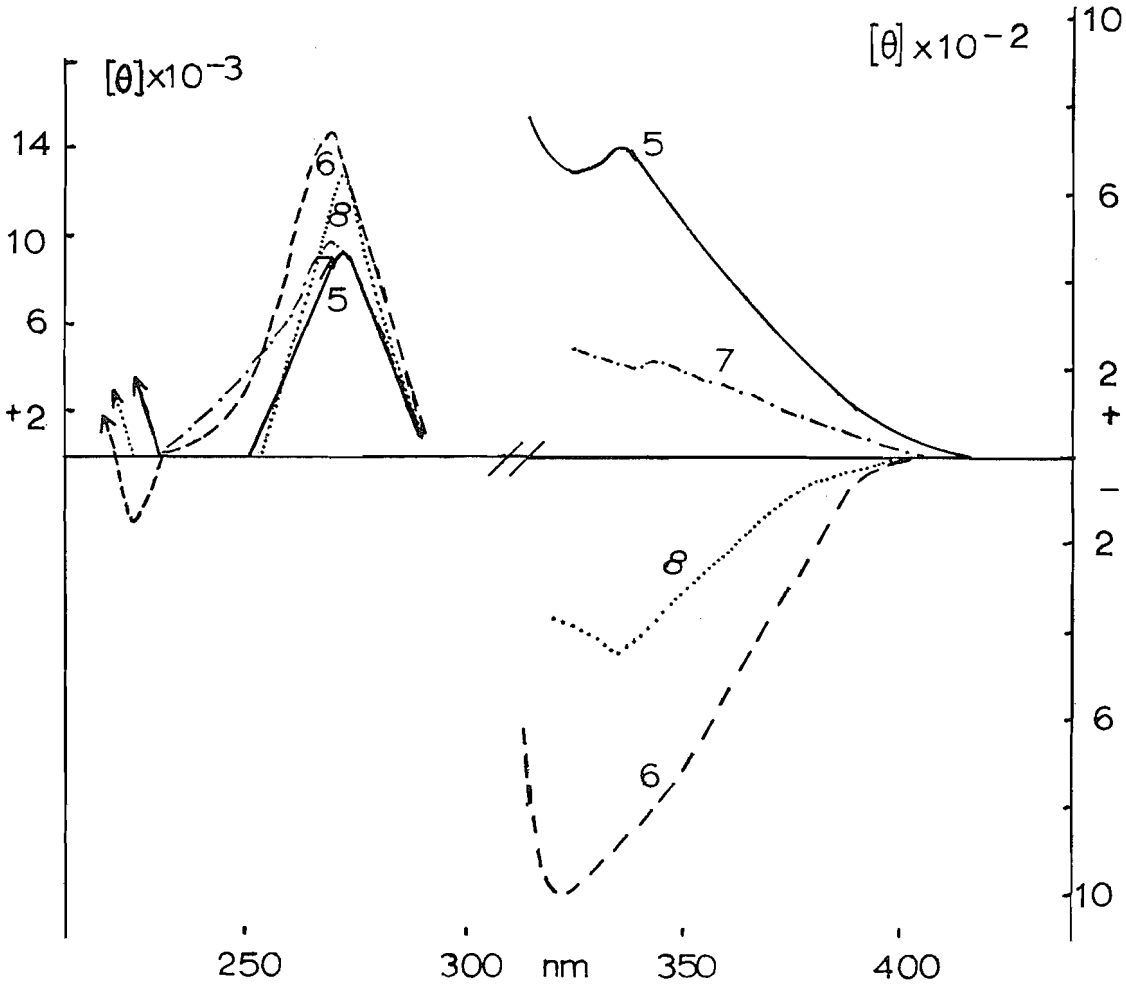

FIG. 3. Circular dichroism curves of the four isomeric chloramphenicol antibiotics **5–8**.

rotamer is strongly preferred for both the free base and the salt and in fact amplitude differences between the two forms are not sizable. The most notable difference between **D** and **E**, of course, is that the methyl group is on opposite sides of the chromophoric phenyl ring and may well distort the perpendicular magnetic moment (26) giving rise to the amplitude differences observed through its steric bulk effect.

These considerations make it extremely tempting to attribute the c.d. effects to the preference for a particular rotamer which has a dominant influence on the sign and intensity of the ^1L_b Cotton effect. In order to test this hypothesis we turned our attention to the chloramphenicols (**5–8**) where a series of apparently closely related isomers is available. The chloramphenicols have also been studied by n.m.r. techniques with regard to preferred conformation in solution (27). The appropriate c.d. curves are reproduced in Fig. 3. It will immediately be perceived that all 4 isomers have a Cotton effect of *the same sign* in the 260 mμ region! However, this is *not* the same transition which occurs in this region with the ephedrines but rather is the hitherto unavailable ^1L_a band which has now been shifted to higher wavelength due to the auxochromic effect of the *p*-nitro group. Now that this band is present in a relatively accessible spectral region and can be examined, it is clearly evident that

Can. J. Chem. Downloaded from www.nrcresearchpress.com by 210.87.254.42 on 09/05/12
For personal use only.

Can. J. Chem. Downloaded from www.nrcresearchpress.com by 210.87.254.42 on 09/05/12
For personal use only.

the sign and intensity of this transition does *not* reflect the absolute configuration of the side-chain in any clearly discernible manner any more than it seemed to in the ephedrine series. This finding can serve to rationalize difficulties others have experienced trying to correlate o.r.d. disappearance slopes and absolute configuration (12). The ^1L_b transition is now to be found at about 320–340 mμ and, as usual, is much less intense than the ^1L_b band and could be easily overlooked. Obviously in measuring c.d. spectra of compounds carrying auxochromic functions, then, appropriate wavelengths must be selected for comparison purposes.

The sign of the ^1L_b transition of the chloramphenicols is a reliable indicator of absolute configuration. The signs of the respective Cotton effects are the same and the relative intensities are parallel to the corresponding ephedrines.

It should be pointed out that the possibilities for hydrogen bonding are quite different in the chloramphenicol series as opposed to the ephedrines because of the addition of the primary hydroxyl group on C-3. Indeed, according to Jardetzky (27), it is the interaction between this function and the secondary hydroxyl on C-1 which exerts a dominant influence on the rotamer population.

Jardetzky's preferred rotamer for natural chloramphenicol (**7**; 1R,2R) (**F**) looks rather more like that of (−)-(1R,2S)-ephedrine (**D**) than that of (−)-(1R,2R)-pseudoephedrine (**E**) to which it correlates directly by virtue of its absolute configuration and c.d. spectrum. This apparent noncorrelation between preferred rotamer and sign of Cotton effect is disappointing. The present state of knowledge, then, does not seem sufficient to allow generalizations based on

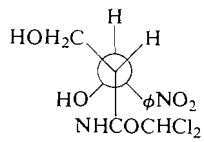

F

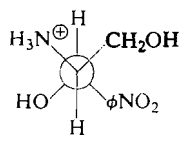

G

comparison of c.d. spectra and presumed rotamer population densities.

A great many more measurements will be needed on compounds of known absolute configuration and reasonably clear rotameric preference before generally useful empirical rules can be established in complicated cases of this type. These considerations are guiding extensions of this work currently under way in this laboratory.

Experimental

The o.r.d. and c.d. measurements were carried out using a Durrum–Jasco model ORD/UV-5 instrument equipped with a c.d. attachment and operating at ambient temperature (cell compartment temperature 29 °C). The solvent used was spectra grade methanol unless otherwise specified and concentrations were chosen so that peak absorption, as reflected by the photomultiplier voltage readings, did not exceed 0.8.

(−)-(1R,2S)-Ephedrine Hydrochloride (1)

Optical rotatory dispersion measurements at 2.43×10^{-3} *M*: $[\Phi]_{500}$ −370, $[\Phi]_{400}$ −575, $[\Phi]_{350}$ −780, $[\Phi]_{300}$ −1110, $[\Phi]_{280}$ −1320, $[\Phi]_{269}$ −780, $[\Phi]_{265}$ −1770, $[\Phi]_{262}$ −1360, $[\Phi]_{240}$ −3090, $[\Phi]_{230}$ −3700, $[\Phi]_{220}$ −4730.

Circular dichroism measurements at 1.48×10^{-3} *M*: $[\Theta]_{274}$ 0, $[\Theta]_{268}$ +700, $[\Theta]_{264}$ +635, $[\Theta]_{261}$ +800, $[\Theta]_{256}$ +470, $[\Theta]_{254}$ +535, $[\Theta]_{250}$ +270, $[\Theta]_{246}$ +200, $[\Theta]_{236}$ 0, $[\Theta]_{228}$ 0, $[\Theta]_{220}$ +400.

(−)-(1R,2S)-Ephedrine Free Base (1)

Circular dichroism measurements at 1.93×10^{-3} *M*: $[\Theta]_{276}$ 0, $[\Theta]_{268}$ +140, $[\Theta]_{266}$ +45, $[\Theta]_{262}$ +155, $[\Theta]_{258}$ +75, $[\Theta]_{256}$ +100, $[\Theta]_{250}$ +50, $[\Theta]_{246}$ +70, $[\Theta]_{234}$ 0 $[\Theta]_{230}$ −69.

(+)-(1S,2R)-Ephedrine Hydrochloride (2)

Optical rotatory dispersion measurements at 1.44×10^{-3} *M*: $[\Phi]_{589}$ +155, $[\Phi]_{500}$ +155, $[\Phi]_{400}$ +155, $[\Phi]_{300}$ +362, $[\Phi]_{286}$ +415, $[\Phi]_{274}$ +260, $[\Phi]_{268}$ −207, $[\Phi]_{264}$ +670, $[\Phi]_{262}$ +210, $[\Phi]_{257}$ +980, $[\Phi]_{254}$ +775, $[\Phi]_{250}$ +1240, $[\Phi]_{236}$ +1450, $[\Phi]_{224}$ +2170.

Circular dichroism measurements at 1.44×10^{-3} *M*: $[\Theta]_{274}$ 0, $[\Theta]_{268}$ −475, $[\Theta]_{266}$ −305, $[\Theta]_{261}$ −645, $[\Theta]_{258}$ −340, $[\Theta]_{255}$ −475, $[\Theta]_{250}$ −240, $[\Theta]_{245}$ −100, $[\Theta]_{240}$ 0, $[\Theta]_{226}$ 0, $[\Theta]_{220}$ +270.

(−)-(1R,2R)-Pseudoephedrine Hydrochloride (3)

Optical rotatory dispersion measurements at 2.13×10^{-3} *M*: $[\Phi]_{589}$ −320, $[\Phi]_{500}$ −500, $[\Phi]_{400}$ −825, $[\Phi]_{350}$ −1150, $[\Phi]_{300}$ −1740, $[\Phi]_{270}$ −2245, $[\Phi]_{266}$ −2660, $[\Phi]_{264}$ −2475, $[\Phi]_{256}$ −3160.

Circular dichroism measurements at 4.8×10^{-3} *M*: $[\Theta]_{270}$ 0, $[\Theta]_{267}$ +150, $[\Theta]_{264}$ +55, $[\Theta]_{261}$ +195, $[\Theta]_{258}$ +125, $[\Theta]_{255}$ +140, $[\Theta]_{252}$ +55, $[\Theta]_{250}$ +100, $[\Theta]_{237}$ 0, $[\Theta]_{228}$ 0, $[\Theta]_{225}$ −360, $[\Theta]_{223}$ 0.

(−)-(1R,2R)-Pseudoephedrine Free Base (3)

Circular dichroism measurements at 5.47×10^{-3} *M*: $[\Theta]_{271}$ 0, $[\Theta]_{267}$ +265, $[\Theta]_{265}$ +180, $[\Theta]_{262}$ +330, $[\Theta]_{258}$ +230 $[\Theta]_{245}$ +100, $[\Theta]_{236}$ 0, $[\Theta]_{228}$ 0, $[\Theta]_{225}$ +145.

Circular dichroism measurements in dioxane at 3.27×10^{-3} *M*: $[\Theta]_{280}$ 0, $[\Theta]_{275}$ +40, $[\Theta]_{270}$ 0, $[\Theta]_{268}$ +200, $[\Theta]_{264}$ +40, $[\Theta]_{260}$ +220, $[\Theta]_{258}$ +60, $[\Theta]_{254}$ +180, $[\Theta]_{252}$ +110, $[\Theta]_{250}$ +160, $[\Theta]_{242}$ +40, $[\Theta]_{236}$ 0, $[\Theta]_{220}$ +60.

(+)-(1S,2S)-Pseudoephedrine Hydrochloride (4)

Optical rotatory dispersion measurements at 1.32×10^{-3} *M*: $[\Phi]_{589}$ +110, $[\Phi]_{500}$ +160, $[\Phi]_{400}$ +270,

$[\Phi]_{350}$ +430, $[\Phi]_{300}$ +640, $[\Phi]_{272}$ +910, $[\Phi]_{269}$ +800, $[\Phi]_{264}$ +1070, $[\Phi]_{262}$ +1015, $[\Phi]_{257}$ +1495, $[\Phi]_{255}$ +1390, $[\Phi]_{250}$ +1710, $[\Phi]_{230}$ +2775.

Circular dichroism measurements at 7.2×10^{-3} *M*: $[\Theta]_{273}$ 0, $[\Theta]_{266}$ −200, $[\Theta]_{263}$ −85, $[\Theta]_{260}$ −220, $[\Theta]_{255}$ −140, $[\Theta]_{252}$ −130, $[\Theta]_{248}$ −45, $[\Theta]_{245}$ −65, $[\Theta]_{242}$ 0, $[\Theta]_{227}$ 0, $[\Theta]_{225}$ −100, $[\Theta]_{224}$ 0, $[\Theta]_{223}$ +220.

(+)-(1R,2S)-Chloramphenicol (5)

Circular dichroism measurements at 2.56×10^{-3} *M*: $[\Theta]_{400}$ +65, $[\Theta]_{380}$ +195, $[\Theta]_{360}$ +450, $[\Theta]_{340}$ +645, $[\Theta]_{335}$ +710, $[\Theta]_{330}$ +645, $[\Theta]_{325}$ +645, $[\Theta]_{315}$ +770.

Circular dichroism measurements at 2.41×10^{-4} *M*: $[\Theta]_{290}$ +1090, $[\Theta]_{280}$ +6280, $[\Theta]_{274}$ +9280, $[\Theta]_{270}$ +8730, $[\Theta]_{260}$ +4090, $[\Theta]_{250}$ 0, $[\Theta]_{230}$, then strongly positive.

(−)-(1S,2R)-Chloramphenicol (6)

Circular dichroism measurements at 3.15×10^{-3} *M*: $[\Theta]_{400}$ 0, $[\Theta]_{390}$ −50, $[\Theta]_{370}$ −365, $[\Theta]_{350}$ −730, $[\Theta]_{330}$ −940, $[\Theta]_{325}$ −990, $[\Theta]_{320}$ −990, $[\Theta]_{315}$ −630.

Circular dichroism measurements at 3.15×10^{-4} *M*: $[\Theta]_{290}$ +1670, $[\Theta]_{280}$ +8790, $[\Theta]_{269}$ +14 600, $[\Theta]_{260}$ +7320, $[\Theta]_{250}$ +2720, $[\Theta]_{230}$ 0, $[\Theta]_{223}$ −3560, $[\Theta]_{220}$ 0, then positive.

(−)-(1R,2R)-Chloramphenicol (7)

Circular dichroism measurements at 5.72×10^{-3} *M*: $[\Theta]_{410}$ 0, $[\Theta]_{390}$ +60, $[\Theta]_{370}$ +130, $[\Theta]_{350}$ +195 $[\Theta]_{345}$ +220, $[\Theta]_{340}$ +210, $[\Theta]_{330}$ +230, $[\Theta]_{325}$ +240.

Circular dichroism measurements at 2.17×10^{-4} *M*: $[\Theta]_{280}$ +7600, $[\Theta]_{270}$ +9440, $[\Theta]_{260}$ +6090, $[\Theta]_{250}$ +3950, $[\Theta]_{230}$ 0, then increasingly positive.

Circular dichroism measurements in ethyl acetate at 6.14×10^{-3} *M*: $[\Theta]_{410}$ 0, $[\Theta]_{390}$ +55, $[\Theta]_{370}$ +150, $[\Theta]_{350}$ +237, $[\Theta]_{340}$ +269, $[\Theta]_{330}$ +260.

Desdichloroacetyl-(1R,2R)-chloramphenicol Hydrochloride

Circular dichroism measurements at 7.18×10^{-3} *M*: $[\Theta]_{420}$ 0, $[\Theta]_{400}$ −45, $[\Theta]_{380}$ −140, $[\Theta]_{360}$ −275, $[\Theta]_{340}$ −370, $[\Theta]_{330}$ −415.

Circular dichroism measurements at 2.39×10^{-4} *M*: $[\Theta]_{320}$ −415, $[\Theta]_{315}$ −230, $[\Theta]_{275}$ +1930, $[\Theta]_{270}$ +2760, $[\Theta]_{265}$ +3040, $[\Theta]_{260}$ +2485, $[\Theta]_{255}$ +830, $[\Theta]_{253}$ 0, $[\Theta]_{250}$ +1105, then positive.

Desdichloroacetyl-(1R,2R)-chloramphenicol

Circular dichroism measurements at 5.73×10^{-3} *M*: $[\Theta]_{420}$ 0, $[\Theta]_{400}$ −90, $[\Theta]_{380}$ −200, $[\Theta]_{360}$ −400, $[\Theta]_{345}$ −575, $[\Theta]_{335}$ −548.

Circular dichroism measurements at 1.32×10^{-4} *M*: $[\Theta]_{330}$ −490, $[\Theta]_{325}$ −90, $[\Theta]_{300}$ +1460, $[\Theta]_{290}$ +2560, $[\Theta]_{270}$ +10 960, $[\Theta]_{260}$ +4020, $[\Theta]_{250}$ +1460, $[\Theta]_{240}$ +2190, $[\Theta]_{230}$ +3650.

(+)-(1S,2S)-Chloramphenicol (8)

Circular dichroism measurements at 3.62×10^{-3} *M*: $[\Theta]_{400}$ 0, $[\Theta]_{380}$ −45, $[\Theta]_{360}$ −230, $[\Theta]_{350}$ −320, $[\Theta]_{340}$ −410, $[\Theta]_{335}$ −455, $[\Theta]_{330}$ −410, $[\Theta]_{320}$ −365.

Circular dichroism measurements at 2.16×10^{-4} *M*: $[\Theta]_{290}$ +1460, $[\Theta]_{280}$ +7670, $[\Theta]_{274}$ +12 950, $[\Theta]_{270}$ +11 700, $[\Theta]_{260}$ +4020, $[\Theta]_{254}$ 0, strongly positive after 222 mμ.

Acknowledgment

The chloramphenicol isomers were a gift of Parke–Davis Company through the kindness of Dr. H. M. Crooks, Jr.

1. K. Freudenberg, E. Schoffel, and E. Braun. J. Am. Chem. Soc. **54**, 234 (1932).
2. K. Freudenberg and F. Nikolai. Ann. **510**, 223 (1934).
3. M. C. Rebstock, H. M. Crooks, Jr., J. Controulis, and Q. R. Bartz. J. Am. Chem. Soc. **71**, 2458 (1949).
4. G. Fodor, J. Kiss, and I. Sallay. J. Chem. Soc. 1858 (1951).
5. M. Honjo. J. Pharm. Soc. Japan, **73**, 368 (1953).
6. D. Fles and B. Balenovic. J. Am. Chem. Soc. **78**, 3072 (1956).
7. P. Crabbé. *In* Topics in stereochemistry. Vol. 1. *Edited by* N. L. Allinger and E. L. Eliel. Interscience Publishers, Inc., New York. 1967. p. 170.
8. P. Crabbé and W. Klyne. Tetrahedron, **23**, 3449 (1967).
9. G. G. Lyle and W. Lacroix. J. Org. Chem. **28**, 900 (1963). G. G. Lyle. J. Org. Chem. **25**, 1779 (1960).
10. J. R. Platt. J. Chem. Phys. **17**, 484 (1949).
11. P. Crabbé. Optical rotatory dispersion and circular dichroism in organic chemistry. Holden-Day, San Francisco. 1965. p. 16, 20.
12. J. C. Craig, R. P. K. Chan, and S. K. Roy. Tetrahedron, **23**, 3573 (1967).
13. J. H. Brewster and J. G. Buta. J. Am. Chem. Soc. **88**, 2233 (1966).
14. L. Verbit and P. J. Heffron. Tetrahedron, **23**, 3865 (1967).
15. H. E. Smith, M. E. Warren, Jr., and L. I. Katzin. Tetrahedron, **24**, 1327 (1968).
16. L. Verbit and P. J. Heffron. Tetrahedron, **24**, 1231 (1968).
17. L. Verbit and Y. Inouye. J. Am. Chem. Soc. **89**, 5717 (1967).
18. J. C. Craig and S. K. Roy. Tetrahedron, **21**, 391 (1965).
19. L. Verbit, E. Pfeil, and W. Becker. Tetrahedron Letters, 2169 (1967).
20. I. P. Dirkx and T. J. deBoer. Rec. Trav. Chim. **83**, 535 (1964).
21. H. Auterhoff and H. J. Pankow. Arch. Pharm. **299**, 789 (1966).
22. P. S. Portoghese. J. Med. Chem. **10**, 1057 (1967).
23. J. B. Hyne. Can. J. Chem. **39**, 2536 (1961).
24. J. B. Hyne. Can. J. Chem. **38**, 125 (1960).
25. T. Kanzawa. Bull. Chem. Soc. Japan, **29**, 398, 479 (1956).
26. A. Moscowitz, A. Rosenberg, and A. E. Hansen. J. Am. Chem. Soc. **87**, 1814 (1965).
27. O. Jardetzky. J. Biol. Chem. **238**, 2498 (1963).

Can. J. Chem. Downloaded from www.nrcresearchpress.com by 210.87.254.42 on 09/05/12
For personal use only.

Can. J. Chem. Downloaded from www.nrcresearchpress.com by 210.87.254.6 on 09/05/12
For personal use only.

Quantitative aspects of base-catalyzed Michael addition: Mechanistic study of structural and medium effects on rate[1]

JOHN A. MARKISZ AND JOSEPH D. GETTLER
Department of Chemistry, Nichols Laboratory, New York University, Bronx, New York 10453

Received September 10, 1968

The quantitative kinetics of the reactions of acrylonitrile and methyl vinyl ketone with ethyl acetoacetate and 2,4-pentanedione, and those of acrylonitrile with ethanol and methanol in basic solution were studied as functions of base concentration, temperature, ionic strength, and solvent composition. An expression is obtained which relates the observed rates to the basicity of the solution for the 2,4-pentanedione reactions by the amount of anion in solution. For the other systems, reasonable values of ionization constants obtained empirically, similarly correlate observed rates with the concentration of base in the system. A quantitative correlation with activity coefficients as expressed by the expanded form of the Debye–Hückel equation gave good agreement for most of the experimental data with ionic strength. A derivation for the particular type of system employed indicated that the activity coefficient for the double-bonded compounds appears to have to be treated as an ion with partial ionic charge. On the basis of experimental data reported, the mechanism proposed involves, (*i*) anion attack on a polarized double bond, (*ii*) formation of a cyclic intermediate, severely restricted because of π orbital overlap, and (*iii*) protonation of this intermediate to form product.

Canadian Journal of Chemistry, 47, 1965 (1969)

Introduction

The Michael condensation denotes nucleophilic addition to a carbon–carbon double bond and is important synthetically for its versatility and characteristic high product yields (1). Although a large number of specific reactions of this type occur in basic solution, quantitative mechanistic studies in basic media or, for that matter, in any medium are quite rare.

In the almost complete absence of mechanistic studies (2), it has been presumed that an α-hydrogen is abstracted from a donor species generating a carbanion.

[1] 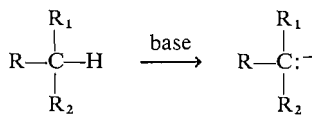

The carbanion, with the importance of resonance stabilization depending upon the substituents, attacks the β-carbon of a multiple bond system.

[2] 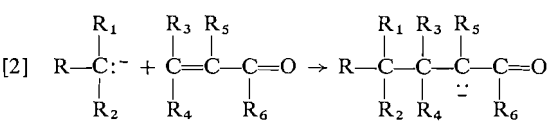

[1]Abstract of a dissertation submitted by John A. Markisz to the faculty of the Graduate School of Arts and Science, New York University, in partial fulfillment of the requirements for the degree of Doctor of Philosophy, June, 1966.

The resulting adduct can then be represented by the resonance structure, [3].

[3] 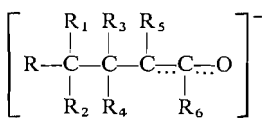

This species can accept a proton from a protonated base, a solvent molecule, or another donor molecule, and the resulting protonated enol then rearranges to give the more stable keto form, a 1,4 addition becoming essentially a 1,2 addition. The varieties of donor compounds which react in this way are numerous and include amines, amides, alcohols, mercaptans, aldehydes, ketones, esters, inorganic acids, and salts (3, 4).

Few quantitative kinetic or mechanistic studies have been reported on the Michael condensation, even though a large number of reactions of this type have been studied synthetically. Some very early work by Jones (5) on the rate of addition of hydrogen cyanide across a conjugated double bond was found to be dependent upon the concentration of cyanide ion. Kamlet and Glover (6*a*, *b*), studied the reaction of barbituric acid with β-nitro styrene in non-alkaline media, while Hine and Kaplan (7*a*) studied the addition of nitroform to β-nitro styrene in acidic methanol. Both of these investigations proposed mutually consonant mechanisms which involved carbanion attack on the β-nitro styrene, but they presented no

Can. J. Chem. Downloaded from www.nrcresearchpress.com by 210.87.254.6 on 09/05/12
For personal use only.

additional mechanistic information on base-catalyzed reactions. Kinetics of the reverse Michael reaction have been studied (*7b*), and Oda and Shono (*7c*) have attempted, with moderate success, to relate reactivity of Michael adducts to configuration and K_a with localized molecular orbital calculations for π electrons.

The present investigation was undertaken to elucidate the quantitative kinetics and mechanism of a number of base-catalyzed Michael condensations. All reaction systems investigated during the course of the current research were characterized by a double-bonded compound reacting with an α-hydrogen donor molecule. The kinetics of the following Michael additions were investigated:

reaction [4], methyl vinyl ketone (1 mole) with ethyl acetoacetate (1 mole) to yield ethyl 2-acetyl-5-keto hexanoate;

reaction [5], methyl vinyl ketone (2 moles) with ethyl acetoacetate (1 mole) to yield ethyl 2-acetyl-2-(4′-butanone)-5-keto hexanoate;

reaction [6], methyl vinyl ketone (1 mole) with 2,4-pentanedione (1 mole) to yield 3-acetyl-2,6-heptanedione;

reaction [7], methyl vinyl ketone (2 moles) with 2,4-pentanedione (1 mole) to yield 5,5-diacetyl-2,8-nonanedione;

reaction [8], acrylonitrile (1 mole) with ethyl acetoacetate (1 mole) to yield ethyl 2-(2′-cyanoethyl)-3-keto butanoate;

reaction [9], acrylonitrile (2 moles) with ethyl acetoacetate (1 mole) to yield ethyl 2,2-di(2′-cyanoethyl)-3-keto butanoate;

reaction [10], acrylonitrile (1 mole) with 2,4-pentanedione (1 mole) to yield 3-(2′-cyanoethyl)-2,4-pentanedione;

reaction [11], acrylonitrile (2 moles) with 2,4-pentanedione (1 mole) to yield 3,3-di(2′-cyanoethyl)-2,4-pentanedione;

reaction [12], acrylonitrile (1 mole) with methanol (1 mole) to yield methyl-2-cyanoethyl ether;

reaction [13], acrylonitrile (1 mole) with ethanol (1 mole) to yield ethyl-2-cyanoethyl ether.

Experimental

Materials

All chemicals employed in this research were commercially available. All organic reagents were liquids and were distilled before use, under nitrogen when necessary. All other compounds were reagent grade and used without further purification.

Preparation of Solutions

Buffer solutions were prepared in the conventional manner according to the formulations of Clark and Lubs (cited in ref. 8). The nominal values of buffer solutions were confirmed with a Sargent pH meter which had been previously standardized against commercially available buffer powders and buffer solutions of known pH. The pH meter was standardized with reference buffers at each of the temperatures at which rate constants were determined and the pH of each reaction mixture was measured before, during, and after the kinetic experiment at the relevant temperature. No variation was observed.

Standard solutions of base were prepared and standardized against standard hydrochloric acid solutions in the conventional manner. Salt solutions for ionic strength experiments were prepared by weighing portions of the desired salts into a tared volumetric flask, dissolving in distilled water, and diluting to the appropriate volume. Potassium chloride, sodium chloride, and lithium chloride were used in ionic strength experiments and no specific salt effects were observed.

Apparatus

The timing of kinetic experiments was done with an A.R. and J.E. Meylan one-fifth split second timer. Calibration of volumetric glassware and analytical weights met customary standards for precision experimentation. Reaction vessels were 250 ml Pyrex flasks fitted with 50 ml side-bulbs and standard tapered ground glass stoppers. The thermostats were of conventional design, and the temperature could be maintained to within ± 0.01 °C at 25 and 35°, and to within ± 0.05 °C at 50°. The composition of various reaction mixtures from kinetic experiments was studied, after suitable treatment, by gas–liquid chromatography (g.l.c.) on a Carbowax column.

Analytical Method

The analytical procedure employed during this research was based on the cyanoethylation of dodecyl mercaptan. This method is generally suited for the quantitative determination of acrylonitrile in dilute solutions (9), is unaffected by the presence of other species in the kinetic systems investigated, and is useful to determine as little as 2 mg (10). It was found here to be equally well suited for the determination of methyl vinyl ketone. Necessary reagents were prepared as follows:

(a) Basic Catalyst

Twenty-eight grams of potassium hydroxide were dissolved in 1 l of 95% ethanol, to prepare an approximately 0.5 *N* solution.

(b) Mercaptan Reagent

Twenty-five grams (31 ml) of crude *n*-dodecyl mercaptan were dissolved in 1 l of isopropyl alcohol (99%), and the resulting solution allowed to stand for at least two days before using.

(c) Standard Iodine Solution

An iodine–iodide (triiodide) solution was prepared in water and standardized against a solution of sodium thiosulfate, which had been standardized with potassium iodate.

(d) Acid Stop-Solution

Sixteen ml of concentrated hydrochloric acid were added to enough isopropyl alcohol to make 1 l.

Can. J. Chem. Downloaded from www.nrcresearchpress.com by 210.87.254.6 on 09/05/12
For personal use only.

In all analyses the following procedure was used. Twenty-five ml of mercaptan reagent were accurately transferred to a 250 ml iodine flask from a fast-flowing pipette. Similar mercaptan-containing flasks were prepared for each sample and one for a blank. A measured volume of an unknown sample was transferred into one of these flasks, which was then stoppered and the contents swirled. Two ml of the basic catalyst were added and the flask again stoppered and swirled to intermix the solutions. Two min after the catalyst addition, the reaction was suppressed by adding 125 ml of the acid stop-solution. The blank sample was afforded the same treatment, but in this case immediate titration was mandatory. Samples were titrated to a faint yellow color, permanent for at least 30 s of swirling, by the addition of standard triiodide solution.

Kinetic Procedure

Into the 50 ml side-bulb of a glass stoppered 250 ml reaction flask was pipetted an aliquot of acrylonitrile of known concentration in appropriate buffer and salt solution, and into the main section was pipetted the other reactant in a similar medium. The flask was then placed in a thermostat for a sufficient time to permit temperature equilibration. Reaction vessels for experiments with methyl vinyl ketone were prepared in a similar manner except that no base solution or basic buffer solution was mixed with the olefin while temperature equilibration was being affected. This procedural departure was necessary because methyl vinyl ketone reacts with the base itself. This complication is discussed more fully below. During this period, a series of iodine flasks containing mercaptan reagent was prepared, and the value of the blank determined. The reaction was initiated by removing the solution-containing reaction flask from the thermostat, inverting it, shaking vigorously to insure proper mixing, and returning it to the thermostat. This first inversion of the flask and mixing of the reactants was taken as zero time, the start of the reaction. Aliquots which were rapidly withdrawn using a fast-flowing pipette that had been sheathed in asbestos and kept in a glass well in the thermostat, were then delivered into the iodine flask containing mercaptan reagent. Resulting solutions were then analyzed for acrylonitrile or methyl vinyl ketone. The time was noted when the pipette started delivering solution, and to this was added the previously determined time of half-delivery for the pipette. This total time was used as the time t in kinetic calculations. Reaction mixtures were of sufficient volume so that 12–15 samples could be withdrawn for analysis during the course of a kinetic experiment.

Synthetic Experiments

The products of reactions [4] to [13] were synthesized by refluxing appropriate reaction mixtures over a steam bath for 3–4 h in the presence of approximately 1 g of sodium ethylate. Reaction mixtures of about 3:1 molar ratio of acrylonitrile or methyl vinyl ketone to α-hydrogen donor compound were used in reactions [5], [7], [9], and [11], while 1:3 molar ratios were used for the remaining reactions. Volatile components of reaction mixtures, essentially always the reactants, were expelled by gently heating, and the desired products were distilled under reduced pressure. Table I lists the boiling or melting points (experimental and reported) of the compounds prepared.

TABLE I

Boiling points of reaction products

Product of reaction no.	Experimental b.p. (°C)	Reported b.p. (°C)
[4]	131–132 at 5 mm	127–129 at 4.5 mm*
[5]	169–171 at 5 mm	160 at 3 mm†
[6]	113–116 at 6 mm‡	
[7]	155–159 at 6 mm‡	
[8]	137–139 at 5 mm	121 at 2 mm§
		126–127 at 3 mm‖
[9]	81.5 (m.p.)	82 (m.p.)¶
[10]	150–151 at 8 mm‡	
[11]	177–178 (m.p.)	180 (m.p.)¶
[12]	77–80 at 25 mm	77–78 at 25 mm**
[13]	88–90 at 50 mm	86 at 49 mm**

*Reference 15*b*.
†Reference 15*a*.
‡Not previously reported.
§Reference 22.
‖Reference 23.
¶Reference 24.
**Reference 25.

These compounds were used as standards to establish the identity of products formed in aqueous kinetic mixtures, extracted from such reaction mixtures, dried, and then subjected to g.l.c. analyses. The physical constants of products from reactions [6], [7], and [10] were not previously reported. Products from reactions [6] and [10], when treated with excess base and olefin, gave products from reactions [7] and [11], respectively. Elemental analysis confirmed their identity.

Calculations and Results

Although the Michael condensation is generally reversible (11), equilibrium constants under experimental conditions were so small that the reverse reaction could easily be neglected by selecting and imposing the proper conditions. The usual second-order irreversible rate expression was therefore used in rate calculations.

Thermodynamic activation quantities were calculated using the following equations (12):

$$[14] \qquad \Delta F^{\ddagger} = -RT \ln [kh/k_b T]$$

$$[15] \qquad \Delta H^{\ddagger} = RT^2 (\delta \ln k/\delta T) - RT$$

$$[16] \qquad \Delta S^{\ddagger} = [\Delta H^{\ddagger} - \Delta F^{\ddagger}]/T$$

where $F^{\ddagger}$, $H^{\ddagger}$, and $S^{\ddagger}$ are the activation free energy, enthalpy, and entropy, respectively, k is the rate constant, k_b is Boltzmann's constant, h is Planck's constant, R is the gas constant, T is the absolute temperature and $k_b T/h$ is the frequency factor of transition state theory.

Table II lists the experimentally observed rates of reaction for reactions [4]–[11] in aqueous solution. Table III lists the observed rates for reactions [4]–[12] which were run in methanol,

TABLE II

Specific rate constants in aqueous solution

Reaction	Temperature (°C)	pH	$k \times 10^2$, (l/mole/s) at ionic strength of: 0.104	0.201	0.599	1.05	1.30	1.65
[4]	25.00±0.01	7.40	0.540	0.525	0.511	0.487	0.298	0.210
		8.42	2.43	—	2.30	2.19	1.34	0.944
		8.86	3.19	—	3.02	2.87	1.75	—
		9.24	3.56	—	3.37	3.21	1.96	1.38
		9.80	3.79	—	3.59	3.42	2.09	—
	34.84±0.01	7.20	0.333	—	0.316	0.302	0.184	—
		7.40	0.427	—	0.404	0.385	0.235	—
		8.42	3.24	—	3.07	2.92	1.79	—
		8.86	5.05	4.91	4.77	4.55	2.74	1.95
		9.24	6.16	5.98	5.83	5.54	3.41	2.39
	50.46±0.05	7.20	0.329	—	0.311	0.297	—	—
		7.40	0.525	—	0.496	0.473	0.288	—
		8.01	1.97	—	—	1.78	—	0.765
		8.42	4.29	—	4.05	3.87	2.35	—
[5]	25.00±0.01	8.42	0.243	—	0.230	0.218	0.136	—
		8.86	0.583	—	0.542	0.522	0.359	—
		9.24	1.05	—	0.975	0.942	0.647	—
		9.80	1.83	—	—	1.64	—	—
	34.84±0.01	8.42	0.203	—	0.191	—	0.135	—
		8.86	0.520	—	—	—	0.349	—
		9.24	—	—	0.990	0.966	0.703	—
		9.80	2.30	—	—	2.12	1.54	—
[6]	25.00±0.01	7.20	0.731	0.711	0.692	0.658	0.465	0.323
		7.40	—	0.997	0.972	0.924	—	—
		8.01	2.11	—	—	1.89	1.32	—
		8.86	2.97	—	—	2.67	—	—
		9.80	3.15	—	2.99	2.83	1.99	—
	34.84±0.01	7.20	0.808	0.786	0.765	0.729	0.512	0.358
		8.01	3.14	—	2.97	—	—	—
		8.42	4.58	—	—	4.13	—	—
		8.86	5.67	—	5.36	5.11	—	—
		9.80	6.42	6.23	6.07	5.78	—	—
	50.46±0.05	7.20	0.956	0.930	0.905	0.864	—	—
		7.40	4.87	—	—	4.40	—	—
		8.01	8.85	—	—	7.95	—	—
[7]	25.00±0.01	8.01	0.456	—	0.431	0.410	—	—
		8.42	0.668	—	0.632	0.602	0.544	—
		8.86	0.830	0.805	0.785	0.747	0.676	—
	34.84±0.01	7.40	0.160	—	0.151	—	0.132	0.108
		8.01	—	0.491	—	0.455	—	—
		8.42	0.877	0.851	0.825	0.781	0.716	—
[8]	25.00±0.01	8.01	0.298	—	—	0.272	—	—
		8.42	0.476	—	0.448	0.429	—	—
		8.86	0.619	—	0.589	0.564	—	—
		9.24	0.689	—	0.657	0.628	—	—
		9.80	0.736	0.714	0.698	0.668	0.523	—
	34.84±0.01	8.01	0.370	—	0.351	0.337	0.265	—
		8.42	0.687	0.669	0.651	0.625	0.492	—
		8.86	—	1.04	—	0.973	0.766	—
		9.24	1.30	—	—	1.19	0.934	—
		9.80	1.47	—	—	1.34	1.06	—
	50.46±0.05	8.01	0.479	—	0.457	0.438	0.342	—
		8.86	2.09	—	1.96	1.86	—	—
		9.24	—	2.92	—	2.73	2.14	—

Can. J. Chem. Downloaded from www.nrcresearchpress.com by 210.87.254.6 on 09/05/12
For personal use only.

TABLE II (*Continued*)

Reaction	Temperature (°C)	pH	$k \times 10^2$, (1/mole/s) at ionic strength of: 0.104	0.201	0.599	1.05	1.30	1.65
[9]	25.00±0.01	8.42	0.0339	—	0.0322	0.0309	0.0218	—
		8.86	0.0844	—	0.0768	0.0702	0.0543	—
		9.24	0.161	—	—	0.144	—	—
		9.80	0.313	—	—	0.285	0.200	—
	34.84±0.01	8.86	0.0301	—	0.0286	0.0275	0.0196	—
		9.24	0.0679	0.0661	0.0645	0.0619	—	—
[10]	25.00±0.01	7.40	0.208	—	—	0.189	0.157	—
		8.01	0.426	—	—	0.388	0.322	—
		8.42	0.535	—	0.508	0.488	0.406	—
		8.86	0.600	—	0.570	0.547	0.454	—
		9.24	0.623	—	0.593	0.568	0.472	—
		9.80	0.638	—	0.607	0.582	0.483	—
	34.84±0.01	7.40	0.296	—	0.277	0.268	0.216	—
		8.01	0.766	0.743	0.718	0.694	—	—
		8.42	1.12	—	—	1.01	0.815	—
		8.86	—	1.34	—	1.25	—	—
		9.24	1.49	—	—	1.35	1.10	—
	50.46±0.05	7.20	0.276	—	—	0.252	0.210	—
		8.01	1.41	—	—	1.29	1.07	—
		8.42	2.55	—	—	2.33	1.93	—
		8.86	3.84	—	3.67	3.52	2.92	—
[11]	25.00±0.01	8.01	0.155	—	—	0.144	0.0857	—
		8.42	0.235	—	—	0.214	0.131	—
		8.86	0.301	—	—	0.274	0.167	—
	34.84±0.01	7.40	0.0501	—	0.0477	0.0457	0.0278	—
		8.01	0.163	—	—	0.149	0.0907	—
		8.42	0.294	—	—	0.268	0.163	—
		8.86	0.442	—	0.421	0.403	0.246	—

and Table IV lists the observed rates for reactions [4]–[11] and [13] which were run in ethanol. Table V lists the rates of reaction for the first-order basic decomposition of methyl vinyl ketone.

Discussion

Rate data accumulated during the present research indicate that all but reactions [12] and [13] are experimentally reversible. The rates of the reverse steps, however, are so slow that the extent of reversibility is easily controlled by the selection of proper experimental conditions. Consequently, forward specific rate constants can be readily determined. The production of the cyanoalkyl ethers, reactions [12] and [13], on the other hand, appear to be irreversibly second order under all conditions employed, since no measurable concentrations of reactants could be detected in basic solutions of these ethers over extended periods of time at any of the temperatures used. In any single kinetic experiment values of specific rate constants exhibit no noticeable trend with time. Practically all kinetic experiments were carried to approximately 75% completion, and a minimum of 10, and usually 12–15, experimental points were employed in the calculation of any particular rate constant.

An inspection of Tables II, III, and IV reveals that specific reaction rates of all reactions studied increase at higher base concentrations in all solvents, or at higher pH values in water, decrease with increasing ionic strength, increase with decreasing dielectric constant, and do not uniformly show linear Arrhenius plots, i.e., the logarithm of the rate constant versus the reciprocal of the absolute temperature. Some of the reactions investigated actually show inverted Arrhenius plots. Since this requires impossible negative activation energies, the reaction between uncharged reactant molecules, which is implied by using stoichiometric concentrations of reactants in the rate equations, cannot be considered valid.

Can. J. Chem. Downloaded from www.nrcresearchpress.com by 210.87.254.6 on 09/05/12
For personal use only.

Can. J. Chem. Downloaded from www.nrcresearchpress.com by 210.87.254.6 on 09/05/12
For personal use only.

TABLE III

Specific rate constants in methanol

Reaction	Temperature (°C)	Methanol (wt.%)	[Base]	Ionic strength	k (l/mole/s)
[8]	25.00±0.01	100	10^{-6}	0.104	0.00444
				0.355	0.00400
				0.700	0.00346
				1.03	0.00302
			5×10^{-6}	0.104	0.00567
				0.201	0.00535
				0.355	0.00511
				0.599	0.00492
				0.700	0.00441
				1.03	0.00384
			10^{-4}	0.104	0.00638
				0.355	0.00573
				0.700	0.00496
			5×10^{-4}	0.104	0.00644
				0.201	0.00608
				0.355	0.00579
				0.599	0.00559
				0.700	0.00500
				1.30	0.00465
	34.84±0.01	100	10^{-4}	0.104	0.0130
				0.355	0.0119
				0.599	0.0108
				0.700	0.00952
				1.02	0.00886
			5×10^{-4}	0.104	0.0132
				0.355	0.0118
				0.599	0.0112
				0.700	0.00952
				1.02	0.00893
[10]	25.00±0.01	100	10^{-4}	0.104	0.00550
				0.201	0.00520
				0.355	0.00495
				0.599	0.00474
				0.700	0.00421
	34.84±0.01	100	10^{-4}	0.104	0.0131
				0.201	0.0126
				0.355	0.0118
				0.599	0.0112
[12]	25.00±0.01.	100		0.104	0.00912
				0.201	0.00877
				0.355	0.00814
				0.599	0.00780
		80		0.201	0.00828
				0.355	0.00769
		60		0.201	0.00773
				0.355	0.00718
		40		0.201	0.00686
				0.355	0.00637
		20		0.201	0.00639
				0.355	0.00595
	34.84±0.01	100		0.104	0.0145
				0.355	0.0130
				0.599	0.0124
	50.46±0.05	100		0.104	0.0290
				0.201	0.0278
				0.599	0.0248

TABLE IV
Specific rate constants in ethanol

Reaction	Temperature (°C)	Ethanol (wt.%)	[Base]	Ionic strength	k (l/mole/s)
[8]	25.00±0.01	100	10^{-6}	0.104	0.00355
				0.201	0.00330
				0.599	0.00294
				0.700	0.00244
				1.03	0.00194
			10^{-4}	0.104	0.00573
				0.201	0.00533
				0.355	0.00500
				0.599	0.00475
				0.700	0.00394
				1.03	0.00316
			5×10^{-4}	0.104	0.00582
				0.201	0.00541
				0.355	0.00508
				0.599	0.00482
				0.700	0.00400
				1.03	0.00321
	34.84±0.01	100	6×10^{-5}	0.104	0.0116
				0.355	0.00998
				0.599	0.00901
				0.700	0.00980
				1.02	0.00817
			5×10^{-4}	0.104	0.0119
				0.355	0.0103
				0.599	0.00983
				0.700	0.00910
				1.02	0.00826
[10]	25.00±0.01	100	10^{-4}	0.104	0.00501
				0.201	0.00466
				0.355	0.00438
				0.599	0.00416
				0.700	0.00352
	34.84±0.01	100	10^{-4}	0.104	0.0118
				0.201	0.0109
				0.355	0.0102
				0.599	0.00972
[13]	25.00±0.01	100		0.104	0.00563
				0.201	0.00520
				0.355	0.00487
				0.599	0.00464
		80		0.201	0.00502
				0.355	0.00470
		60		0.201	0.00479
				0.355	0.00449
		40		0.201	0.00463
				0.355	0.00433
		20		0.201	0.00441
				0.355	0.00413
	34.84±0.01	100		0.104	0.00921
				0.201	0.00852
				0.355	0.00796
				0.599	0.00759
	50.46±0.05	100		0.104	0.0192
				0.201	0.0177
				0.355	0.0166
				0.599	0.0158

Can. J. Chem. Downloaded from www.nrcresearchpress.com by 210.87.254.6 on 09/05/12
For personal use only.

Can. J. Chem. Downloaded from www.nrcresearchpress.com by 210.87.254.6 on 09/05/12
For personal use only.

TABLE V

Specific rate constants for the basic decomposition of methyl vinyl ketone

Temperature (°C)	pH	Ionic strength	k (s^{-1})
25.00±0.01	8.42	0.104	0.000345
		0.599	0.000326
		1.05	0.000311
		1.30	0.000269
		1.65	0.000251
	8.86	0.104	0.000964
		0.201	0.000933
		0.599	0.000914
		1.05	0.000869
		1.30	0.000752
	9.24	0.104	0.00228
		1.05	0.00206
		1.30	0.00178
		1.65	0.00166
	9.80	0.104	0.00841
		0.201	0.00815
		0.599	0.00796
		1.05	0.00758
		1.30	0.00656
34.84±0.01	8.42	0.104	0.000466
		1.05	0.000418
		1.30	0.000363
		1.65	0.000334
	8.86	0.104	0.00130
		1.05	0.00117
		1.30	0.000934
	9.24	0.104	0.00308
		1.05	0.00277
		1.30	0.00240
		1.65	0.00221
	9.80	0.104	0.0113
		1.05	0.0102
		1.30	0.00885
50.46±0.05	8.42	0.201	0.000702
		0.599	0.000684
		1.05	0.000654
		1.30	0.000564
	8.86	0.104	0.00202
		1.05	0.00183
		1.30	0.00158
	9.24	0.104	0.00479
		1.05	0.00433
		1.30	0.00374
		1.65	0.00349
	9.80	0.104	0.0176
		1.05	0.0159
		1.30	0.0138

Since all but two of the reactions investigated are reversible, forward reactions were studied under carefully controlled experimental conditions in an effort to suppress kinetic complications generally concomitant with reverse reactions. For this reason, either experimental conditions were selected so that a large excess of the α-hydrogen donor compound was present to suppress reversal tendency, or kinetic measurement was stopped at about 75% completion, up to which point the reverse reaction, because of its slower rate, imposed no measurable effect on the kinetic results. Gas–liquid chromatographic analyses of kinetic reaction mixtures showed the investigated reactions to be the expected ones, since no unexplained product peaks were observed. No change in concentration of acrylonitrile or methyl vinyl ketone, in the absence of other reactants, but with all other reaction conditions prevailing, except as noted below, was detected in a period greater than seven half-lives of the slowest reaction, which suggested the impossibility of hydrolysis or polymerization of these compounds during a kinetic experiment. The possibility of radical reaction was discounted since no insoluble polymers were found in the reaction mixtures and these dilute solutions became only slightly colored after having reached equilibrium.

The reactions of methyl vinyl ketone at low pH values, 7 to 8, and low base concentrations were uncomplicated by side reactions, and the study of pertinent kinetics was essentially straightforward, being of the mixed second-order type, first-order in each of the reactants. At increased base concentrations, however, in addition to the condensation reactions [4]–[7] listed above, there was a first-order disappearance of methyl vinyl ketone to some undetermined product or products, which interfered quite significantly with the determination of rate constants for the principal reactions. This situation was handled with the aid of computer techniques which have been previously described (13). Briefly, the differential equation

$$[17] \qquad -\delta[a]/\delta t = k_1[a] + k_2[a][b]$$

was solved for k_2 by a series of six steps: (*1*) obtaining a polynomial which expressed the concentration of a, $[a]$, as a function of the time, t; (*2*) differentiation of the function found in (*1*) to obtain $\delta[a]/\delta t$; (*3*) determination of k_1 experimentally under reaction conditions where the second-order reaction was quenched and then calculation of the amount of a decomposed in this reaction in the first second; (*4*) calculation from the function obtained in (*1*) of the total amount of a reacted after one second (for both reactions); (*5*) calculation of the difference between the quantities of a obtained in sections (*4*) and (*3*), which is equal to the amount of a and the amount of b disappearing by the second-

Can. J. Chem. Downloaded from www.nrcresearchpress.com by 210.87.254.6 on 09/05/12
For personal use only.

order process; and (*6*) calculation of k_2 from eq. [17].

An inspection of the data in Tables II–V shows that for the reactions studied, at constant ionic strength, the specific rate constant increases with increasing concentration of base. A quantitative interpretation can be made if it is assumed that the anion, A^-, of the α-hydrogen donor molecule, HA, is the reactive species. This molecule, HA, would be in equilibrium with its conjugate base, A^-, as follows,

$$[18] \qquad HA \rightleftharpoons H^+ + A^-$$

for which there would be an equilibrium constant, K_a. The total concentration of HA, $[HA]_t$, would be equal to the sum of the un-ionized and anionic species,

$$[19] \qquad [HA]_t = [HA] + [A^-]$$

then,

$$[20] \qquad [A^-] = [HA]_t/(1 + [H^+]/K_a)$$

or,

$$[21] \qquad [A^-] = K_a[HA]_t[OH^-]/(K_w + K_a[OH^-])$$

where K_w is the ion product of water. If the rate determining step is represented by eq. [2], then the rate expression is,

$$[22] \qquad \delta[x]/\delta t = k[B][A^-]$$

where [B] is the concentration of olefin, and $[x]$ is the concentration of product. The values obtained in Tables II through IV were calculated using the total concentration of HA, $[HA]_t$,

$$[23] \qquad \delta[x]/\delta t = k'[B][HA]_t$$

where the observed rate constant, k', if eq. [2] correctly represents the rate determining step, would be equal to

$$[24] \qquad k' = k\,K_a[OH^-]/(K_w + K_a[OH^-])$$

K_w values used in this equation were those reported for the temperatures of kinetic experiments. The hydroxyl ion concentrations used were determined by measurement before, during and after a kinetic experiment. Salts were added initially to stock solutions of hydroxyl ion to prevent changes in ionic strength. K_a was assumed to be temperature independent over the temperature range investigated. This would introduce no error at 25° and a possible maximum error of about 4% at 50°. This latter error in k' would cause an error of about 0.3 cal/deg in activation entropy calculations, which is well within experimental limits.

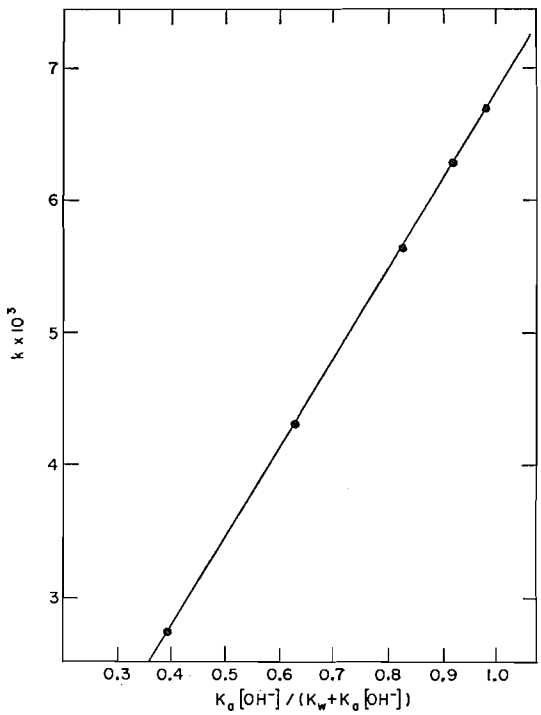

FIG. 1. k' vs. $K_a[OH^-]/(K_w + K_a[OH^-])$ for reaction [8], 25.00 °C; ionic strength = 1.05. Typical for the several reactions.

Equation [24] has been successfully employed for reactions [6] and [10], where K_a for 2,4-pentanedione (14) is 1.9×10^{-9}. A plot of k' against $K_a[OH^-]/(K_w + K_a[OH^-])$ is shown in Fig. 1 for these reactions at 25.00 °C. The assumption that K_a varies very little with temperature yielded satisfactory linear plots for data at all pertinent temperatures. The resultant specific rate constants, k, were found to be independent of base concentration. In the cases of reactions [5], [7], [9], and [11], occurring in water, K_a values are unavailable, so an alternate procedure was employed, which gave values of K_a for ethyl acetoacetate (reactions [4] and [8]) in very good agreement with reported values (7.1×10^{-11}) (14). Observed rates were plotted against $[OH^-]/(K_w + \beta[OH^-])$, where β is an empirically determined constant. This value is assumed equal to the ionization constant,

Can. J. Chem. Downloaded from www.nrcresearchpress.com by 210.87.254.6 on 09/05/12
For personal use only.

K_a, and the slope, from eq. [24], thus becomes equal to k/K_a or k/β. Specific rate constants obtained in this way are independent of base concentration. Values of k corrected for the influence of base are listed in Table VI, along with calculated values of β. An analysis of the data in Table VI indicates that the β parameter is always essentially the same for a given nucleophile, independent of both the temperature and the particular olefinic compound involved in the reaction. These k values also yielded a normal, linear Arrhenius plot, which will be discussed below.

Although all of the reactions studied were base-catalyzed, no attempt was made to account quantitatively for this phenomenon in alcoholic solvents, since values of K_a and K_w were unavailable for all of the reactants under these conditions, and attempting to fit the data to a line determined by two empirical constants would have been completely meaningless. It was found in these solvents, as well as in pure ethanol and pure methanol, that equimolar solutions of different bases (sodium ethoxide, sodium methoxide, triethyl amine) had no specific effect on the rate of the reactions. In these rather dilute solutions, the basic ionization was probably complete.

It was established that methyl vinyl ketone is unstable in basic solution in a first-order manner, with the rate constant increasing linearly with the concentration of hydroxyl ion, Table V. This presumably indicates a second-order reaction in which the hydroxyl ion, itself a superior nucleophilic agent, competes with the other anion for addition to the double bond. A product analysis was not possible, since amounts of products recovered by extractive procedures, as described above, were obtained only in trace quantities, and the addition of base to concentrated solutions induced polymerization which was probably anionic. This competitive reaction was slow, but significantly large so as to interfere with the rate calculations of the Michael condensation at high pH values. No comparable reactions or complications were detected for acrylonitrile. Previously, data of a synthetic study (15*a*) of a Michael reaction involving methyl vinyl ketone indicated an increase in product yield followed by a decrease, as the concentration of base was steadily increased. It now appears that it is the increase in the rate of this incompletely described decomposition of methyl vinyl ketone with an increasing amount of base which is responsible for this phenomenon.

The mechanism of nucleophilic addition, then, as indicated by the results of the present investigation, appears to be consistent with that

TABLE VI

Specific rate constants corrected for base concentration

Ionic strength	k (l/mole/s) at temperature (°C): 25.00	34.84	50.46	$K_a \times 10^{10}$
	Reaction [4]			
0.104	.0388	.0732	.184	.64
0.201	.0378	.0711	—	
0.599	.0368	.0692	.174	
1.05	.0350	.0660	.166	
1.30	.0214	.0403	.101	
1.65	.0151	.0284	—	
	Reaction [5]			
0.104	.0253	.0416	—	.041
0.599	.0235	.0393	—	
1.05	.0227	.0383	—	
1.30	.0156	.0279	—	
	Reaction [6]			
0.104	.0318	.0652	.186	19.
0.201	.0309	.0634	.181	
0.599	.0301	.0617	.176	
1.05	.0286	.0588	.168	
1.30	.0201	.0413	—	
	Reaction [7]			
0.104	.00959	.0168	—	.88
0.201	.00931	.0163	—	
0.599	.00907	.0158	—	
1.05	.00864	.0151	—	
1.30	.00780	.0137	—	
	Reaction [8]			
0.104	.00751	.0155	.0448	.64
0.201	.00732	.0151	—	
0.599	.00715	.0147	.0427	
1.05	.00685	.0141	.0409	
1.30	.00536	.0111	.0320	
1.65	.00420	—	—	
	Reaction [9]			
0.104	.00482	.00812	—	.029
0.599	.00458	.00772	—	
1.05	.00439	.00740	—	
1.30	.00310	.00522	—	
	Reaction [10]			
0.104	.00643	.0159	.0537	19.
0.201	—	.0154	—	
0.599	.00611	.0149	.0513	
1.05	.00586	.0144	.0491	
1.30	.00487	.0116	.0408	
	Reaction [11]			
0.104	.00357	.00614	—	.74
0.599	—	.00584	—	
1.05	.00325	.00560	—	
1.30	.00298	.00341	—	

Can. J. Chem. Downloaded from www.nrcresearchpress.com by 210.87.254.6 on 09/05/12
For personal use only.

presented in eqs. [1], [2], and [3], at least so far as the rate-determining step seems to be the addition of a nucleophile to the carbon–carbon double bond, eq. [2]. For the reaction of a donor substance bearing two α-hydrogens, there appears to be two separate and distinct nucleophilic additions, each with the mechanism proposed. The rate expression for these equations is

$$[25] \qquad \delta[x]/\delta t = k_1[a][b] + k_2[c][b]$$

where k_1 refers to the addition of the first mole of olefin to form the product c, and k_2 is the addition of a second mole of olefin to c. Since k_1 had been determined from weakly basic, dilute systems, the same procedure used to solve eq. [17] was employed here. Values of k_2 obtained agreed extremely well with second-order specific rate values obtained by reacting the products of reactions [4], [6], [8], and [10] with the appropriate olefin.

If the proposed mechanism is correct, a change of ionic strength would have little or no influence on the specific rate. Scatchard (16) has derived an expression, eq. [26], for the influence of ionic strength on the rate of reaction, where reactant molecules A and B, each with a charge z_a and z_b, respectively, form a complex X*, with a charge of $(z_a + z_b)$, which eventually yields products. The equation

$$[26] \qquad \ln k = \ln k_0 + 2z_a z_b A(I)^{1/2}$$

was derived assuming the natural logarithm of the activity coefficient to be the usual Debye–Hückel expression,

$$[27] \qquad \ln \gamma_a = -z_a^2 A(I)^{1/2}$$

where k is the rate constant at ionic strength I, k_0 is the rate constant at zero ionic strength, and A is a complex constant. Equation [26] would indicate no influence of ionic strength, since $z_b = 0$, a neutral molecule according to the mechanism of reaction [2]. However, an inspection of the data in Tables II–V shows a very pronounced decrease in rate with increasing ionic strength. Qualitatively, at least, this infers reaction between oppositely charged ions. For the systems of the present investigation it would mean that the rate-determining step could not be the one proposed, but should be rather the protonation of resonance structure [3]. This situation does not appear too reasonable, since protonation would be expected to occur very rapidly in the polar solvents employed (water, methanol, and ethanol), all of which are quite efficient proton donors as neutral molecules. The only other plausible alternate mechanism for these systems would be the rapid protonation of the double bond to form a carbonium ion, followed by the rate-determining step, reaction of the carbonium ion with the nucleophile. This possibility must also be rejected, firstly, because the rate would be expected to increase with decreasing base concentration and secondly, because from analyses of reaction products a primary carbonium ion must be generated, rather than the more stable secondary allylic carbonium ion.

A plot of log k against the square root of the ionic strength did not give a linear relationship in the case of any reaction studied, although this is not particularly surprising since the ionic strengths used in this investigation generally were outside the range of applicability of the Debye–Hückel equation used, [27]. Using a more precise equation (17):

$$[28] \qquad \log_{10} \gamma_a = -z_a^2 A(I)^{1/2}/(1 + \sigma B(I)^{1/2})$$

where $A = 1.8123 \times 10^6/(DT)^{3/2}$ and $B = 5.0288 \times 10^9/(DT)^{1/2}$. σ is a constant once considered to be the distance of closest approach of an oppositely charged field to the ion in question, but now considered to be purely an empirical parameter. D is the macroscopic dielectric constant and T is the absolute temperature. This would give the following expression for the influence of ionic strength on a specific rate constant.

$$[29] \qquad \log_{10} k = \log_{10} k_0 + 2z_a z_b A(I)^{1/2}/(1 + \sigma B(I)^{1/2})$$

It was found empirically that a value of $\sigma = 5$ gave a satisfactory linear plot of log k against the complex function on the right side of eq. [29], Fig. 2, for a sizeable fraction of the data at the low ionic strength portion of the curve, but the slope was much too small for an ionic reaction, being about 0.5 compared to a minimum of 2.0 for ionic reactions. Empirical equations of the type suggested by Debye and McAulay (18), such as

$$[30] \qquad \ln \gamma_a = \lambda_a I$$

for the influence of ionic strength on the activity coefficient of a neutral molecule, were applied to

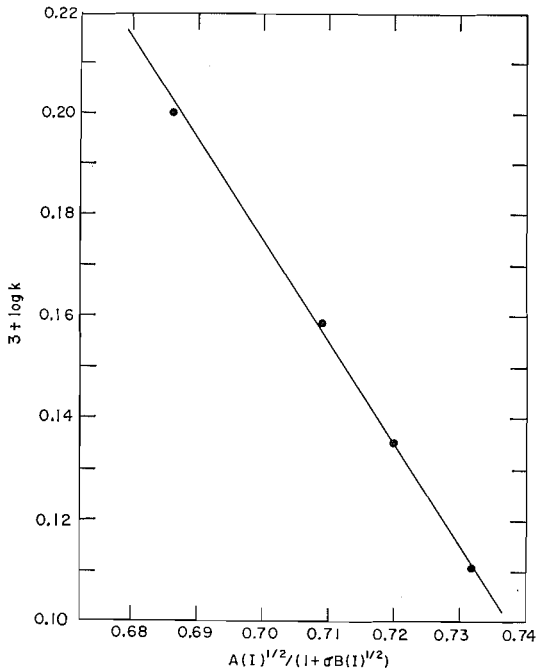

FIG. 2. Typical plot of log k against ionic strength function (eq. [29]), for reaction [8]; 25.00 °C; pH = 9.80.

the kinetic data without any success. The failure of these equations to correlate satisfactorily the data indicated the necessity for a new approach to the problem. With previous results pointing the way it was assumed that the olefin in eq. [2] was polarized prior to nucleophilic attack, and an attempt was made to treat theoretically this proposed mechanism to determine what effect, if any, ionic strength would have on rate.

The nucleophile, A^-, reacts with the positive end of the polarized double bonded compound, B, to form an activated complex, X*, in an equilibrium reaction. Ionic charges of the pertinent species are designated by z_a, z_b, and z_x, respectively, but now z_x is assumed equal only to z_a rather than the sum of z_a and z_b, since z_b is the charge at one end of a polarized molecule with no net charge on B, and the charge on the resulting complex, X*, will be that of the nucleophile A^-. Therefore,

$$[31] \qquad \text{rate} = k_0[X^*]$$

From the proposed equilibrium,

$$[32] \qquad K_x = \frac{[X^*]}{[A^-][B]} \cdot \frac{\gamma_x}{\gamma_a\gamma_b}$$

or,

$$[33] \qquad \text{rate} = (k_0K_x\gamma_a\gamma_b/\gamma_x)[A^-][B]$$

The observed rate constant, k, would then be given by,

$$[34] \qquad k = k_0K_x\gamma_a\gamma_b/\gamma_x$$

and since both A and X* are each singly negatively charged ions, it is to be expected that their activity coefficients, given by eq. [28], would be very similar and that the ratio of their activity coefficients, i.e., γ_a/γ_x, should be very close to unity. Then,

$$[35] \qquad k = k_0K_x\gamma_b$$

or,

$$[36] \qquad \log_{10} k = \log_{10} k' + \log_{10} \gamma_b$$

where k' is equal to k_0K_x, yielding

$$[37] \qquad \log_{10} k = \log_{10} k' - z_b^2A(I)^{1/2}/(1 + \sigma B(I)^{1/2})$$

if the polarized molecule behaves like an ion of partial electronic charge z_b, or,

$$[38] \qquad \log_{10} k = \log_{10} k' + \lambda_b I$$

if the polarized molecule behaves like a neutral molecule. Qualitatively, for the data in Tables II–V, eq. [38] predicts an increase in rate with increasing ionic strength (unless λ_b is negative) which was not found, and since no linear correlation of log k with ionic strength was found for any set of conditions, the possibility of eq. [30] accurately describing the behavior of the polarized molecule was discarded. Equation [37], however, not only correctly represents the influence of ionic strength on the rate, but also accurately describes the linearity predicted over most of the experimental range. That the upper ionic strength range does not fit to the desired curve, is probably due to non-ideal interactions in solution which limit the applicability of eq. [28] in this range. Although this function, eq. [37], may have no obvious theoretical validity for the systems under consideration, it is, nevertheless, useful for extrapolation back to zero ionic strength, yielding specific rate constants independent of the specific medium employed. The slopes of the lines for a given reaction are constant at different pH values or base concentrations within a given solvent. Table VII lists the slopes of the lines ($-z_b^2$)

Can. J. Chem. Downloaded from www.nrcresearchpress.com by 210.87.254.6 on 09/05/12
For personal use only.

Can. J. Chem. Downloaded from www.nrcresearchpress.com by 210.87.254.6 on 09/05/12
For personal use only.

for the various systems studied, which give values of z_b between 0.6–0.7 e.s.u. From these values it appears that the double bond is highly polarized by the groups conjugated to it, and must be treated as a positive ion with a fractional electronic charge, since its activity coefficient, in these reactions is unusually influenced, for a neutral molecule, by an ionic atmosphere.

There is a possibility that resonance might appreciably influence this treatment since the resonance structures of the nucleophile would not concentrate, strictly, a full negative charge on the carbon atom in question, but rather would tend to disperse it. If the charge dispersal effects were dissimilar for both the nucleophile and the transition state, the ratio of activity coefficients in eq. [34] would have a value other than unity, negating the validity of eq. [35] for the reactions treated here. The operation of such an effect is denied by an analysis of the data. Since 2,4-pentanedione has more important contributing resonance structures than does ethyl acetoacetate, the ratio of activity coefficients in eq. [34] would not be equal, and this would be evident from the differences in the slopes of the lines for their reactions with the same olefin (acrylonitrile or methyl vinyl ketone). Table VII shows that there is no such difference in slope, so that the effect of resonance in the nucleophile which would effectively reduce its charge and change its activity coefficient must also be operative in the resonance hybrid of eq. [3], thus maintaining the ratio at a value of unity. The values of the slopes for reactions [8] and [10] are almost identical to those for reactions [12] and [13] (all involving reactions with acrylonitrile), where the non-resonant methoxide and ethoxide ions are the nucleophilic reagents. Consequently the ratio of activity coefficients in these cases should also be unity.

It is not surprising that the absolute value of the slope should decrease with decreasing dielectric constant, if one considers z_b to be the partial positive charge on the primary carbon atom due to polarization by the conjugated electronegative groups. Water would be able to stabilize a positive charge much better than either ethanol or methanol, because it is much more polar, and would encounter much less steric hindrance. The carbon atom in question would therefore be able to accommodate a greater charge. The interpretation of the slopes of the lines for the ethanol and methanol systems is highly debatable, since in these much lower dielectric media there is a very great probability of ion-pair formation which would invalidate any quantitative treatment of the data. This possibility is further supported by the fact that only at very low ionic strengths does the data linearly fit eq. [37]. Table VIII lists the rate constants from Tables II–V, corrected for the influence of both base concentration and ionic strength.

TABLE VII

Average slopes for the several reactions calculated from eq. [35]

Reaction	Solvent	Temperature (°C)	−Slope
[4]	H_2O	25.00	.50
"	"	34.84	.51
"	"	50.46	.50
[5]	"	25.00	.50
"	"	34.84	.49
[6]	"	25.00	.50
"	"	34.84	.50
"	"	50.46	.49
[7]	"	25.00	.51
"	"	34.84	.50
[8]	"	25.00	.45
"	"	34.84	.45
"	"	50.46	.45
[9]	"	25.00	.45
"	"	34.84	.46
[10]	"	25.00	.45
"	"	34.84	.45
"	"	50.46	.44
[11]	"	25.00	.45
"	"	34.84	.45
[8]	CH_3OH	25.00	.41
"	"	34.84	.40
[10]	"	25.00	.41
"	"	34.84	.40
[12]	"	25.00	.40
"	"	34.84	.41
"	"	50.46	.40
[8]	CH_3CH_2OH	25.00	.39
"	"	34.84	.39
[10]	"	25.00	.39
"	"	34.84	.39
[13]	"	25.00	.38
"	"	34.84	.39
"	"	50.46	.39

Reactions [8], [10], [12], and [13] were investigated in methanol and in ethanol, as well as in aqueous solution, and it was found that a plot of log k against the reciprocal of the dielectric constant, $(1/D)$, was linear. The logarithm of the activity coefficient of an ion of radius ρ in a medium of dielectric constant D, relative to that of a vacuum, is given by (19):

$$[39] \quad \ln \gamma_a = -e^2 z_a^2 (1 - 1/D)/(2\rho k_b T)$$

where e is the electronic charge, z_a is the ionic charge, k_b is Boltzmann's constant, and T is the

Can. J. Chem. Downloaded from www.nrcresearchpress.com by 210.87.254.6 on 09/05/12
For personal use only.

TABLE VIII

Specific rate constants corrected for the influence of base concentration and ionic strength

Reaction	Solvent	k (l/mole/s) at temperature (°C): 25.00	34.84	50.46
[4]	H_2O	.0442	.0832	.209
[5]	"	.0287	.0473	—
[6]	"	.0361	.0741	.212
[7]	"	.0109	.0191	—
[8]	"	.00843	.0174	.0503
[8]	CH_3OH	.00883	.0183	—
[8]	CH_3CH_2OH	.00907	.0189	—
[9]	H_2O	.00541	.00911	—
[10]	"	.00721	.0171	.0604
[10]	CH_3OH	.00755	.0181	—
[10]	CH_3CH_2OH	.00776	.0188	—
[11]	H_2O	.00401	.00690	—
[12]	CH_3OH	.0126	.0201	.0400
[13]	CH_3CH_2OH	.00892	.0146	.0304
*	H_2O	151.	202.	315.

*Base-catalyzed decomposition of methyl vinyl ketone units for this reaction are s^{-1}.

absolute temperature. Assuming the proposed mechanism to be correct, and again using the method employed to obtain eq. [36],

$$[40] \quad \log_{10} k = \log_{10} k' - 2.303\, e^2 z_a^2 (1 - 1/D)/(2\rho k_b T)$$

or,

$$[41] \quad \log_{10} k = \text{const.} + 2.303\, e^2 z_a^2/(2\rho k_b T D)$$

Equation [41] predicts that the rate should increase with decreasing dielectric constant for the reactions studied, and this can be observed in Tables III and IV. The apparent linearity obtained is interesting in that it supports ionic strength measurements, indicating that the activity coefficients for the double bonded compounds can be treated as though they were those of ions of partial electronic charge. The limited scope of the present work, however, prohibits any conclusions beyond an interesting, although limited parallel. A more intensive study was attempted, without very much success, as shown below.

Reactions [12] and [13] were studied over a range of water–alcohol mixed solvents. Log k values were plotted against $1/D$, but no linear relationship was obtained. This result is probably due to a combination of contributing factors, such as non-uniform dielectric constant on a molecular level, increased importance of ion-pair formation as D decreases, variations in ionization constants over a range of mixed solvents, and appreciable changes in activity coefficient ratios as the dielectric constant is varied. For these reasons no detailed analysis of the slopes for any of these data was made.

The rates listed in Table VIII uniformly show a linear Arrhenius plot for log k vs. $1/T$. The activation entropy values reported in Table IX are apparently unusual in that they are abnormally large in a negative sense. Although highly negative entropy values have been assumed to be due to increased electrorestriction of solvent in the transition state, this would appear to be quite unlikely in this situation. These values should correspond to an intensely restricted transition state, which would most likely reflect a cyclic mechanism. Although these values are too negative to be consonant with earlier reported values for other cyclization processes (20), recent studies appear to agree with the present data in that Wulfman and co-workers (21) have reported an activation entropy of −55.6 e.u. for the reaction of diethyl malonate with methyl crotonate, leading them to a similar mechanistic interpretation.

Even though the entropies are highly unusual, they are quite plausible if the reaction course is considered in molecular detail. The anion, A^-, formed from HA, is a stable and readily formed species because of the formation of a resonance hybrid in which there is an overlap of π orbitals which restricts the 5 atoms (O—C—C—C—O) to a plane. The minimum energy path for anion attack and subsequent reaction requires that the

TABLE IX

Thermodynamic activation quantities at 25.00 °C

Reaction		$\Delta F^{\ddagger}$ (kcal/mole)	$\Delta H^{\ddagger}$ (kcal/mole)	$\Delta S^{\ddagger}$ (e.u.)
[4]		19.53	11.43	−27.18
[5]		19.78	9.03	−36.08
[6]		19.65	12.98	−22.38
[7]		20.36	10.15	−34.26
[8]		20.51	13.10	−24.87
[8]	CH_3OH	20.48	13.15	−24.59
[8]	CH_3CH_2OH	20.46	13.27	−24.13
[9]		20.77	9.40	−38.15
[10]		20.60	15.60	−16.78
[10]	CH_3OH	20.58	15.81	−16.01
[10]	CH_3CH_2OH	20.56	15.97	−15.40
[11]		20.95	9.86	−37.21
[12]		20.28	8.44	−39.73
[13]		20.48	8.80	−39.19
*		14.72	5.23	−31.85

*Base-catalyzed decomposition of methyl vinyl ketone.

four π orbitals of the conjugated olefinic molecule be similarly parallel, for maximum overlap and delocalization enabling reaction. Thus, there is not only restricted rotation for the 9 atoms, but a condition for reaction arises whereby rotation for the 9 atoms involved is almost totally forbidden, due to the necessity for total π orbital overlap. Sufficient degrees of freedom of the entire system are therefore lost, with nine π orbitals parallel and overlapping, to account qualitatively for the apparently extremely negative entropy values.

Structural effects are also quite significant. As far as the polarization of the double bond is concerned, the acetyl group is seen to be more powerfully electron withdrawing than the cyano group on the double bond, as evidenced by the data in Tables II to IV and VIII. An examination of the data for the reactions of 2,4-pentanedione and ethyl acetoacetate with either methyl vinyl ketone or acrylonitrile reveals that although the anion of the former is more easily formed, the specific reaction rate constant is smaller for the reaction than for that of the latter compound. The 2,4-pentanedione is less reactive as a nucleophile than is the ethyl acetoacetate, since anionic charges would be dispersed to a greater extent. For this same reason, the dione is more acidic as reflected by its larger K_a value as listed in Table VI.

On the basis of experimental evidence reported here, the following mechanistic statements appear to apply without exception to all examples of the Michael condensation investigated during the course of this research:

(*i*) The reaction involves an anion attack on a double bond, which has been polarized, to form an activated complex.

(*ii*) The activated complex forms an intermediate through cyclization in which there are intensely hindered rotations because of π orbital overlap.

(*iii*) The cyclic intermediate reacts, most probably with the solvent, to accept a proton and form terminal products.

(*iv*) The polarized double bond, insofar as rate measurements are concerned, can be treated as a partial ion (i.e., an ion of partial positive electronic charge).

The observed variations of rate in various media and under different experimental conditions can then be explained, at least on a semi-quantitative basis, in terms of the above four statements.

1. R. ADAMS. Organic reactions. Vol. X. John Wiley and Sons, Inc., New York. 1959. pp. 270–541.
2. R. ADAMS. Organic reactions. Vol. X. John Wiley and Sons, Inc., New York. 1959. p. 203.
3. G. WHELAND. Theory of resonance. John Wiley and Sons, Inc., New York. 1944. pp. 85, 135, 136.
4. CYANAMID. Nitrogen chemicals digest. The chemistry of acrylonitrile. American Cyanamid Co., Inc., New York. 1951. p. 26.
5. W. J. JONES. J. Chem. Soc. **105**, 1547 (1914).
6. (*a*) M. KAMLET. J. Am. Chem. Soc. **77**, 4896 (1955). (*b*) M. KAMLET and D. J. GLOVER. J. Am. Chem. Soc. **78**, 4556 (1956).
7. (*a*) J. HINE and L. KAPLAN. J. Am. Chem. Soc. **82**, 2915 (1960). (*b*) S. PATAI, S. WEINSTEIN, and Z. RAPPOPORT. J. Chem. Soc. 1741 (1962). (*c*) R. ODA and T. SHONO. J. Chem. Soc. Japan, **78**, 1680, 1683 (1957).
8. H. H. WILLARD, N. H. FURMAN, and C. E. BRICKER. Elements of quantitative analysis. D. Van Nostrand Co., Inc., Princeton, New Jersey. 1956. p. 195.
9. CYANAMID. Nitrogen chemicals digest. The chemistry of acrylonitrile. American Cyanamide Co., Inc., New York. 1951. p. 69.
10. D. W. BEESING, W. P. TAYLOR, D. M. KURTZ, and S. A. HARRISON. Anal. Chem. **21**, 1073 (1949).
11. R. ADAMS. Organic reactions. Vol. X. John Wiley and Sons, Inc., New York. 1959. p. 187.
12. S. W. BENSON. The foundations of chemical kinetics. McGraw-Hill Book Co., Inc., New York. 1960. p. 278.
13. J. A. MARKISZ and J. D. GETTLER. J. Phys. Chem. **71**, 3053 (1967).
14. D. J. CRAM and G. S. HAMMOND. Organic chemistry. McGraw-Hill Book Co., Inc., New York. 1964. p. 214.
15. (*a*) H. HENECKA. Chem. Ber. **81**, 197 (1948). (*b*) H. HENECKA. Chem. Ber. **81**, 179 (1948).
16. G. SCATCHARD. Chem. Rev. **10**, 229 (1932).
17. J. N. BUTLER. Ionic equilibria. A mathematical approach. Addison-Wesley Publishing Co., Inc., Reading, Mass. 1964. pp. 432–433.
18. P. DEBYE and J. MCAULAY. Z. Physik. **26**, 22 (1925).
19. S. W. BENSON. The foundations of chemical kinetics. McGraw–Hill Book Co. Inc., New York. 1960. p. 532.
20. J. HINE. Physical organic chemistry. McGraw–Hill Book Co., Inc., New York. 1962. pp. 506, 509, 515.
21. D. S. WULFMAN, K. R. MEHTA, R. P. SHETH, and P. R. SHAFER. Abstract of paper presented at 151st. Am. Chem. Soc. meeting. Pittsburgh, Pa., March 28–31, 1966.
22. N. F. ALBERTSON. J. Am. Chem. Soc. **72**, 2594 (1950)
23. C. W. YOHO and R. LEVINE. J. Am. Chem. Soc. **74**, 5597 (1952).
24. G. R. ZELLARS and R. LEVINE. J. Org. Chem. **13**, 911 (1948).
25. W. P. UTERMOHLEN. J. Am. Chem. Soc. **67**, 1505 (1945).

Can. J. Chem. Downloaded from www.nrcresearchpress.com by 210.87.254.6 on 09/05/12
For personal use only.

Can. J. Chem. Downloaded from www.nrcresearchpress.com by 210.87.254.5 on 09/05/12
For personal use only.

Etude de la décomposition des diazo-2 dicétones-1,3. I. Cas du diazo-2 diméthyl-5,5 cyclohexanedione-1,3

HENRI VESCHAMBRE[1] ET DANIEL VOCELLE[2]
Département de Chimie, Université de Montréal, Montréal, Québec

Reçu le 16 octobre 1968

La décomposition thermique dans le xylène et les décompositions photochimiques dans le tétrachlorure de carbone, les alcools méthylique et éthylique, et le cyclohexène, du diazo-2 diméthyl-5,5 cyclohexanedione-1,3 (**2**) ont été étudiées. La thermolyse donne le composé **4**. La photolyse dans le CCl_4 fournit **4** et **5** tandis que dans le méthanol **6** et **7** sont obtenus. L'éthanol conduit aux composés **8**, **9**, **10** et **11**. Enfin la photolyse dans le cyclohexène donne les produits **5** et **12**. Un mécanisme, expliquant la formation de ces différents composés, sera proposé.

Canadian Journal of Chemistry, 47, 1981 (1969)

La décomposition de diazo-dicétones du type **1** est fort mal connue.

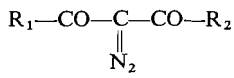

1

Quelques cas seulement ont été étudiés jusqu'à présent et souvent de façon incomplète (1, 2). Devant ces résultats fragmentaires, nous avons voulu faire une étude complète et approfondie de la décomposition des diazo du type **1** dans différents solvants. Pour ce faire, l'étude de la décomposition du diazo-2 diméthyl-5,5 cyclohexanedione-1,3 (**2**) a été entreprise.

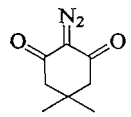

2

Le composé **2** a déjà été synthétisé. Pour notre étude nous avons utilisé la méthode mise au point par Yates *et al.* (3) en y apportant de très légères modifications (voir Partie expérimentale). Il existe deux modes principaux de décomposition de dérivés diazoïques (4): la thermolyse et la photolyse. Pour notre part, nous avons utilisé ces deux procédés; soit la thermolyse dans le benzène en présence de poudre de cuivre ou mieux encore dans le xylène, et la photolyse dans le tétrachlorure de carbone, dans les alcools méthylique et éthylique et dans le cyclohexène.

Résultats

Thermolyse

Le diazo **2**, porté à reflux dans le benzène en présence de poudre de cuivre pendant 30 h, n'a subi aucune décomposition. Toutefois à 140 °C et dans le xylène, sans poudre de cuivre, **2** a conduit au tétraméthyl-6,6,4′,4′ trioxo-2,4,2′ hexahydro-2,3,4,5,6,7 spiro[cyclopenta(*b*)pyran-3,1′ cyclopentane] (**4**) avec un rendement de 76%.

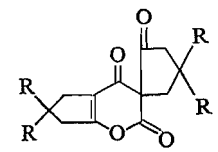

3, R = H **4**, R = CH_3

Ce composé présente les caractéristiques suivantes: spectre infrarouge (i.r.): bandes à 1647, 1678, 1752 et 1788 cm^{-1}. Stetter et Kiehs (1) attribuent au composé non méthylé **3** des bandes à 1647, 1672, 1744 et 1786 cm^{-1}. Le spectre u.v. de **4** dans le chloroforme possède un maximum à 278 mμ (ε_{max} = 7940) alors que pour **3** Stetter et Kiehs (1) ont obtenu λ_{max} = 277 mμ (ε_{max} = 7900).

Le spectre de résonance magnétique nucléaire (r.m.n.) est constitué par deux systèmes de bandes ayant les caractéristiques suivantes: un système localisé à 8.81, 8.78 et 8.72 τ répondant pour 12 protons (soit 4 CH_3) et un système comportant deux séries de bandes, l'une sous forme de deux pics mals séparés à 7.7 et 7.65 τ et l'autre sous

[1]En congé du CNRS (1967–1968). Etudiant post-doctoral du Conseil National de Recherches du Canada. Adresse actuelle: Laboratoire de Chimie Organique 3, Faculté des Sciences, 17 ter rue Paul-Collomp, 63 Clermont-Ferrand, France.

[2]Attaché de Recherche (1966–1968). Adresse actuelle: Collège Sainte-Marie, 1180 rue Bleury, Montréal, Québec et à qui toute demande d'information devra être adressée.

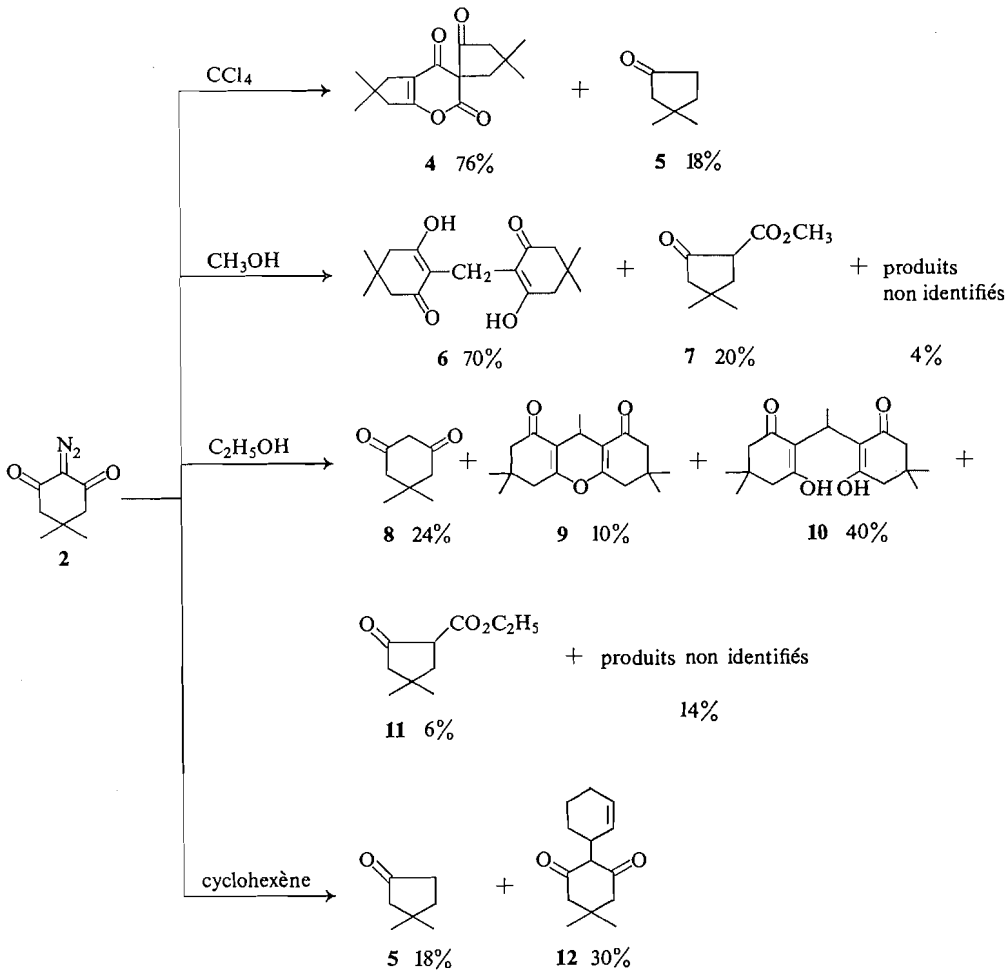

Schéma 1

forme de quatre pics mals résolus à 7.45, 7.37, 7.34 et 7.30 τ. L'ensemble de ce dernier système répond pour 8 protons (soit 4 CH_2). En outre l'analyse est en accord avec la formule brute de **4** soit $C_{16}H_{20}O_4$. L'ensemble de ces données vérifie bien la structure attribuée au composé **4** obtenu au cours de la thermolyse de **2** dans le xylène.

Photolyse

Les résultats de toutes les réactions photochimiques faites à partir de **2** paraissent au Schéma 1. Le même mode opératoire a été suivi dans presque tous les cas, soit une photolyse d'une heure sous atmosphère d'azote, avec une lampe Hanovia 450 W, sans filtre. Dans chaque cas, à la fin de la réaction, le solvant a été soigneusement éliminé par distillation. Le résidu obtenu consistait en un mélange de solides et de liquides qui furent séparés par filtration. Des analyses par chromatographie sur couches minces, suivies par des chromatographies sur colonne permirent d'isoler les produits réactionnels. Les pourcentages paraissant au Schéma 1 sont des pourcentages de récupération qui furent dans la presque totalité des cas supérieurs à 90%.

(a) Photolyse dans le tétrachlorure de carbone

Le solide obtenu de la photolyse (76%) a présenté un point de fusion et des spectres i.r., u.v. et de r.m.n. rigoureusement identiques à ceux obtenus pour le composé **4**; ce qui l'identifia.

Le liquide présentait après distillation une

Can. J. Chem. Downloaded from www.nrcresearchpress.com by 210.87.254.5 on 09/05/12
For personal use only.

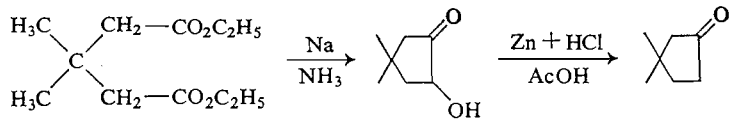

Schéma 2

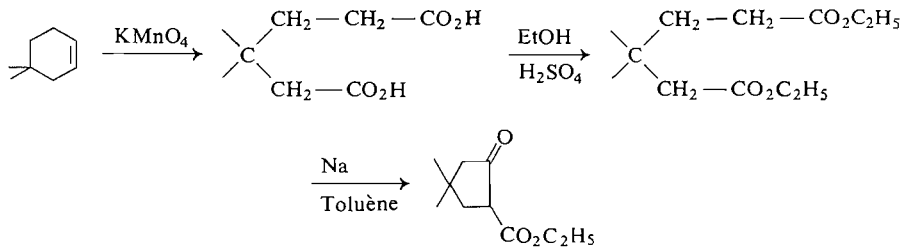

Schéma 3

bande i.r. à 1745 cm^{-1}, un dérivé dinitro-2,4 phénylhydrazone fondant à 145–146 °C et une semicarbazone fondant à 180–181 °C. Ces dérivés se sont révélés identiques à ceux obtenus d'un échantillon authentique de diméthyl-3,3 cyclopentanone synthétisé selon le mode réactionnel décrit au Schéma 2. De la photolyse il a été tiré 18% de diméthyl-3,3 cyclopentanone (**5**).

(b) Photolyse dans les alcools

Les photolyses dans le méthanol et l'éthanol donnèrent essentiellement les mêmes types de composés.

Dans le méthanol purifié, la photolyse de **2** donne 70% de dérivé dimédonique du méthanal (**6**) et 20% de diméthyl-4,4 oxo-2 cyclopentanecarboxylate de méthyle (**7**). De plus la chromatographie sur colonne de silicagel permet d'isoler un mélange de liquides (4%) qui présente en i.r. des bandes hydroxyle et carbonyle. En outre le spectre de r.m.n. de ce mélange indique l'incorporation de groupements méthoxy. Ce mélange ne fut pas étudié plus à fond. Le composé **6** a été identifié à l'aide d'un échantillon authentique obtenu par réaction de la dimédone sur le formaldéhyde selon la méthode de Horning et Horning (5). Le céto-ester a été identifié comme étant le diméthyl-4,4 oxo-2 cyclopentanecarboxylate de méthyle (**7**), par ses bandes i.r. à 1750 et 1730 cm^{-1} et par son spectre de r.m.n. dont les valeurs sont données ci-dessous. De plus l'hydrolyse acide de **7** conduit à la diméthyl-3,3 cyclopentanone (**5**).

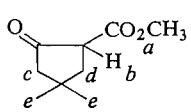

a: 6.24 τ (singulet)
b: 6.57 τ (triplet)
c: 7.78 τ (singulet)
d: 7.84 τ (doublet)
e: 8.77 et 8.93 τ (singulet)

Dans l'éthanol, les mêmes types de produits ont été observés. Ainsi 40% de dérivé dimédonique de l'acétaldéhyde (**10**) et 10% de dioxo-4,5 pentaméthyl-2,2,7,7,9 octahydroxanthène (**9**) ont été obtenus. Ils ont été identifiés à l'aide d'échantillons authentiques obtenus par réaction de la dimédone sur l'acétaldéhyde (5). De plus, 24% de dimédone (**8**) étaient présents de même que 6% de diméthyl-4,4 oxo-2 cyclopentanecarboxylate d'éthyle (**11**). Ce dernier composé a été identifié de deux façons: d'une part à l'aide d'un échantillon authentique obtenu selon le mode opérationnel décrit au Schéma 3, et d'autre part au moyen d'une hydrolyse acide de **11** qui donna **5**. Il a également été trouvé un mélange de plusieurs produits liquides (14%) qui n'ont pas été identifiés.

(c) Photolyse dans le cyclohexène

Lorsque nous avons utilisé du cyclohexène parfaitement pur, la photolyse a conduit aux composés **5** et **12** dans des proportions respectives de 18 et 30%. Un important résidu gommeux s'est également formé (1 g). Le composé **12** a été identifié par son spectre i.r.: bandes à 3020, 1755 et 1720 cm^{-1}, par une détermination de masse moléculaire: 222 ± 2 (théorique 220.3),

Can. J. Chem. Downloaded from www.nrcresearchpress.com by 210.87.254.5 on 09/05/12
For personal use only.

par analyse et par son spectre de r.m.n. dont les valeurs sont données ci-après:

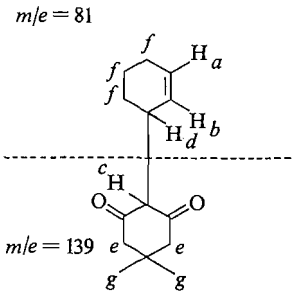

12

a et *b*: 4.0 à 4.5 τ (multiplet)
c: 4.75 τ (singulet très large)
d: 6.63 τ (triplet)
e: 7.8 et 8.0 τ (singulet)
f: 8.1 à 8.7 τ (multiplet)
g: 8.78 et 8.94 τ (singulet)

De plus le spectre de masse montre des fragments importants à m/e = 81 et 139. Le pic parent n'est pas présent.

Discussion

Le décomposition thermique et photolytique des diazocétones est fort bien connue (4). Elle conduit généralement à un cétène selon le mécanisme ci-dessous (Schéma 4)

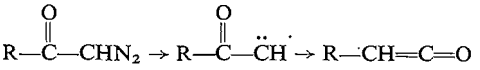

Schéma 4

Ce dernier n'est qu'un intermédiaire, car il réagit habituellement avec le solvant ou se réarrange pour donner des composés plus stables.

Dans le cas du diazo-2 diméthyl-5,5 cyclohexanedione-1,3 un tel mécanisme semble intervenir à la fois dans la thermolyse dans le xylène et dans la photolyse dans le tétrachlorure de carbone.

Ainsi Stetter et Kiehs (1), dans la décomposition thermique du diazo-2 cyclohexanedione-1,3, ont obtenu le composé **3** et préconisé un intermédiaire cétène pour expliquer leur résultat (Schéma 5, R = H).

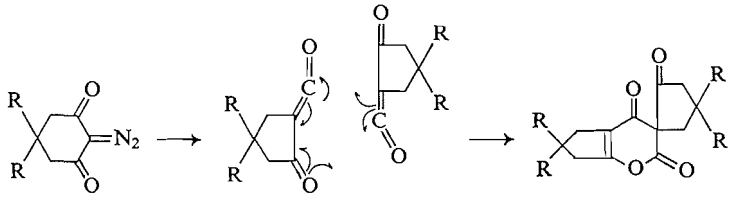

Schéma 5

La thermolyse de **2** donnant **4** (R = CH_3) a donc lieu selon le même mécanisme.

La photolyse du diazo **2** dans le tétrachlorure de carbone, conduisant à **4** et à la diméthyl-3,3 cyclopentanone (**5**), peut également s'expliquer par un mécanisme admettant le même cétène comme intermédiaire (Schéma 6).

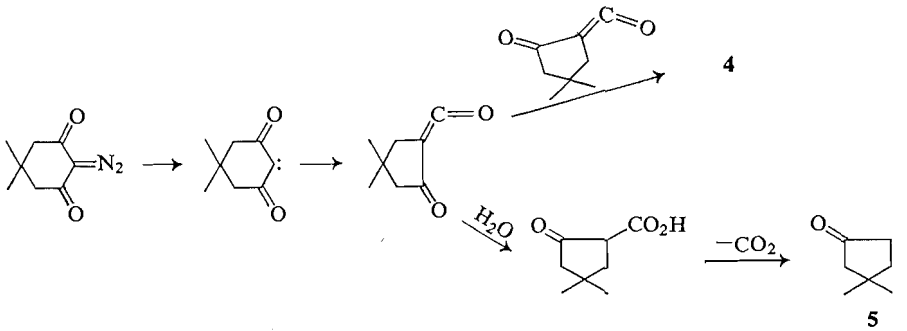

Schéma 6

Can. J. Chem. Downloaded from www.nrcresearchpress.com by 210.87.254.5 on 09/05/12
For personal use only.

La formation de la cétone **5** par réaction du cétène avec l'eau, suivie d'une décarboxylation, semble être confirmée par le fait que, plusieurs photolyses de **2** dans le tétrachlorure de carbone contenant une proportion variable d'eau, donnèrent un pourcentage plus élevé de **5** à mesure que la proportion d'eau dans le solvant augmentait. En effet, selon que l'on utilise un tétrachlorure de carbone séché, non séché ou saturé d'eau, les pourcentages en composé **5** passent respectivement de 18 à 40% et à 57%. (Il faudrait moins de 0.003% d'eau dans le tétrachlorure de carbone pour éviter toute formation de **5**.)

Les résultats des photolyses du diazo **2** dans les alcools méthylique et éthylique montrent que le mécanisme décrit au Schéma 6 n'est pas le seul à intervenir. En effet, la formation des composés **6**, **9** et **10**, ne peut que provenir d'une réaction de la dimédone sur le formaldéhyde et l'acétaldéhyde. Ceci implique d'une part l'oxydation du méthanol en formaldéhyde et de l'éthanol en acétaldéhyde et d'autre part la réduction du carbène en dimédone. Le mécanisme proposé pour le système d'oxydo–réduction est le suivant (Schéma 7).

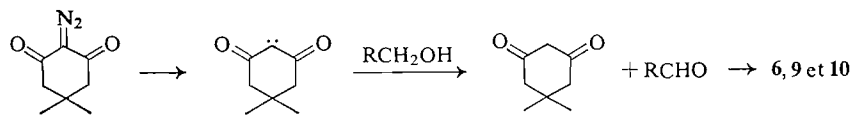

8

Schéma 7

Ce mécanisme est déjà confirmé par la présence de **8** dans les produits finaux de la réaction dans l'éthanol, et par la mise en évidence de la formation d'acétaldéhyde au cours de la réaction. Ainsi, lorsqu'on fait barbotter l'azote à la sortie de l'appareil de photolyse dans une solution de dinitro-2,4 phénylhydrazine, un précipité de dinitro-2,4 phénylhydrazone de l'acétaldéhyde est obtenu. Un système d'oxydo–réduction du même type a déjà été mentionné par Weygand, Schwenke et Bestmann (6).

Les céto-esters **7** et **11** sont obtenus par un réarrangement de Wolff classique (4) (Schéma 8).

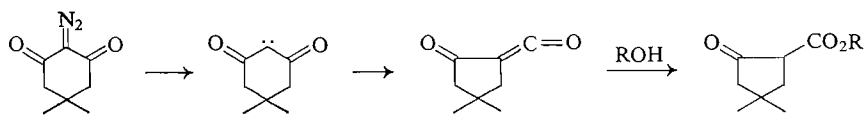

7, R = H
11, R = CH_3

Schéma 8

La formation de carbène, normale dans ces réactions (4), a cependant été confirmée par la photolyse du diazo **2** dans le cyclohexène. Elle donne le composé **12** typique d'une réaction d'un carbène sur une oléfine (2, 4).

Conclusion

L'ensemble des mécanismes, proposé pour expliquer la formation des composés obtenus au cours des décompositions du diazo-2 diméthyl-5,5 cyclohexanedione-1,3, montrent que ces produits se forment: soit par une contraction de cycle provenant de la transposition du carbène en cétène, soit par un système d'oxydo-réduction faisant intervenir le solvant et le carbène lui-même.

Partie expérimentale

Les points de fusion ont été déterminés dans l'appareil Büchi Modèle Dr. Tottoli et sont donnés sans correction. Les spectres i.r. ont été enregistrés sur un spectrophotomètre Beckman IR 8 et les spectres u.v. sur "spectronic 505" de Bausch and Lomb. Les spectres de r.m.n. ont été réalisés sur un appareil Jéol type C 60 H dans le chloroforme deutérié comme solvant. Les spectres de masse ont été pris sur un appareil Hitachi Perkin–Elmer RMU-6D. Les microanalyses on été effectuées par "Schwarzkoff Microanalytical Laboratory," Woodside, New York, U.S.A. Les poids moléculaires ont été déterminés sur un appareil Hewlett–Packard type Mechrolab 301 A. Les chromatographies en phase gazeuse ont été

Can. J. Chem. Downloaded from www.nrcresearchpress.com by 210.87.254.5 on 09/05/12
For personal use only.

Can. J. Chem. Downloaded from www.nrcresearchpress.com by 210.87.254.5 on 09/05/12
For personal use only.

réalisées sur un appareil F et M modèle 810; et les chromatographies sur couches minces ont été faites sur des "chromagram" Eastman-Kodak No. 6060. Dans ce dernier cas l'éluant utilisé a toujours été le mélange cyclohexane – acétate d'éthyle 75:25 en volume.

Synthèse du diazo-2 diméthyl-5,5 cyclohexanedione-1,3 (2)

Selon la méthode décrite par Rosenberg, Yates, Hendrickson et Wolf (3) un mélange de diméthyl-5,5 cyclohexanedione-1,3 et d'azoture de tosyle a été mis en suspension dans l'éther anhydre sous agitation. Lorsque la température est inférieure à 10 °C on ajoute rapidement de la triéthylamine et on abandonne 15 min à froid. Après 1 h à température ambiante, un abondant précipité s'est formé, il est filtré et lavé à l'éther. La solution éthérée est lavée à la soude 10% et à l'eau. Après séchage et élimination du solvant, le solide restant est recristallisé dans l'alcool à 95°; rendement 75%; p.f. 106–108° (litt. p.f. 106–108° (3)).

Infrarouge ($CHCl_3$): 2180, 2130 et 1640 cm^{-1}; r.m.n.: 7.8 τ (singulet 4 H) et 8.88 τ (singulet 6 H).

Décomposition thermique du diazo-2 diméthyl-5,5 cyclohexanedione-1,3 (2)

En solution dans le benzène, et en présence de poudre de cuivre, le diazo **2** ne subit aucune décomposition apparente même après 30 h de reflux.

Dans le xylène la décomposition s'effectue facilement: dans un ballon de 100 ml à 2 tubulures, muni d'un réfrigérant et d'une ampoule à brome, 30 ml de xylène ont été placés. Lorsque la température du bain d'huile, dans lequel est placé le ballon, atteint 140°, on ajoute goutte à goutte une solution de 1.5 g de **2** dans 20 ml de xylène. Le dégagement gazeux cesse 15 min après la fin de l'addition de la solution de diazo. La solution encore chaude est traitée par du charbon actif et filtrée. On élimine le xylène sous vide partiel, il reste une huile jaune claire qui cristallise au refroidissement. Après recristallisation dans l'éther un solide blanc est obtenu, p.f. 110–120°. Les propriétés spectrales sont rapportées dans le texte.

Anal. Calc. pour $C_{16}H_{20}O_4$ (276.3): C, 62.59; H, 7.25. Trouvé: C, 62.29; H, 7.23.

Décomposition photochimique du diazo-2 diméthyl-5,5 cyclohexanedione-1,3 (2)

Toutes les photolyses ont été faites avec une lampe Hanovia 450 W et sous courant d'azote.

(a) Photolyse dans le tétrachlorure de carbone

Une solution de 5 g de diazo **2**, dans 1 000 ml de tétrachlorure de carbone (Anachemia Reagent) séchés sur des tamis moléculaires, a été photolysée pendant 1 h. Après quoi, le solvant est éliminé par distillation. On obtient 3.8 g de résidu qui cristallise partiellement au refroidissement et dont les spectres i.r. indique l'absence complète de **2**. Par filtration, il fut séparé 3.2 g d'un solide qui après recristallisation dans l'éther fut identifié comme étant **4** et 0.6 g d'un liquide qui s'avéra être la diméthyl-3,3 cyclopentanone (5).

Le solide blanc homogène en chromatographie sur couches minces, présentait les mêmes spectres i.r., u.v. et de r.m.n. qu'un échantillon authentique de **4**. En outre, le point de fusion mixte ne donna aucune dépression.

Le liquide également homogène en chromatographie en phase gazeuse (colonne de 8 pieds de polyester de Craig 20% sur chromosorb P; T °C: 160; temps de rétention: 11 min) présente en i.r. une bande à 1745 cm^{-1}. En outre il forme très facilement une dinitro-2,4 phénylhydrazone (p.f. 145–146 °C) et une semicarbazone (p.f. 180–181 °C). Ces deux dérivés possèdent les mêmes points de fusion et les mêmes caractéristiques spectrales que ceux obtenus de la diméthyl-3,3 cyclopentanone (**5**) synthétisée, via une condensation acyloïne du diméthyl-3,3 glutarate d'éthyle (voir plus loin).

Une photolyse de **2** dans un tétrachlorure commercial non séché nous permet d'isoler de la même manière 1.8 g de **4** et 1.7 g de **5**. Une photolyse de **2**, dans du tétrachlorure de carbone ayant séjourné 48 h sur de l'eau, fournit 1.5 g de **4** et 2.4 g de **5**.

(b) Photolyse dans l'alcool méthylique

Une solution de 5 g de diazo-2 diméthyl-5,5 cyclohexanedione-1,3, dans 1000 ml de méthanol purifié selon la méthode de Lund et Bjerrum (7), a été photolysée pendant 1 h. Le méthanol est par la suite soigneusement distillé et le résidu obtenu cristallise en partie. Une filtration permet de recueillir 3.1 g de solide et 1 g de liquide.

Le produit solide est homogène (chromatographie sur couches minces) après une recristallisation dans le méthanol. Il fut identifié comme étant le dérivé dimédonique du formaldéhyde (6). Il présente en effet les caractéristiques suivantes: p.f. 191–192 °C (litt. p.f. 191–192 °C (5)); i.r. ($CHCl_3$): bande large entre 3400 et 2400 cm^{-1}, 1611 et 1592 cm^{-1}; u.v. (ethanol 95%): λ_{max} = 258 mμ ε_{max} = 20 300; r.m.n.: 8.96 τ (12 H singulet); 7.75 τ (4 H, singulet), 6.83 τ (2 H, singulet), −1.23 τ (2 H singulet).

Ces caractéristiques sont rigoureusement identiques à celles obtenues pour le dérivé dimédonique du formaldéhyde synthétisé à partir de dimédone et de formaldéhyde selon la méthode de Horning et Horning (5).

Le produit liquide est en fait un mélange assez complexe de plusieurs composés (chromatographie en phase gazeuse: colonne 8 pieds de Polyester de Craig 20% sur chromosorb P; T °C = 190; temps de rétention de 6 à 40 min). Toutefois un produit est nettement majoritaire. Une chromatographie sur colonne de silicagel (Baker Analyzed 150 g), en utilisant le mélange cyclohexane – acétate d'éthyle 75:25 en volume comme éluant, permet d'isoler le diméthyl-4,4 oxo-2 cyclopentane-carboxylate de méthyle ((**7**), 0.540 g, 20%). Les caractéristiques spectrales sont rapportées dans le texte.

La structure de ce composé a été confirmée par une hydrolyse acide qui donna la diméthyl-3,3 cyclopentanone (**5**). Celle-ci fut identifié par le point de fusion mixte de sa semicarbazone et de son dérivé dinitro-2,4 phénylhydrazone.

La chromatographie sur colonne ne put séparer les autres constituants du mélange (0.160 mg) qui ne furent pas identifiés.

(c) Phololyse dans l'alcool éthylique

De la même façon que pour le méthanol, 5 g de diazo **2** dans 1 000 ml d'éthanol purifié selon la méthode de Lund et Bjerum (7) ont été photolysés pendant 1 h. Le solvant a été soigneusement distillé, le résidu obtenu cristallise en partie et fournit après filtration une phase solide (3.3 g) et une phase liquide (1.2 g).

Can. J. Chem. Downloaded from www.nrcresearchpress.com by 210.87.254.5 on 09/05/12
For personal use only.

Une chromatographie sur couches minces du solide montra que celui-ci contenait au moins 3 produits. Une chromatographie sur colonne de silicagel (Baker Analyzed 300 g) fournit deux fractions. En éluant avec un mélange de cyclohexane – acétate d'éthyle (75:25 en volume) les composés **9** et **10** furent obtenus en mélange (2.3 g) et dans les proportions respectives de 20 et 80. Une cristallisation fractionnée dans le méthanol aqueux permet d'isoler d'abord le pentaméthyl-2,2,7,7,9 dioxo-4,5 octahydroxanthène (**9**) p.f. 178–179 °C (litt. p.f. 176–177 °C (5)) dont es caractéristiques sont les suivantes: i.r.: 1660 et 1620 cm^{-1}; u.v. (ethanol 95%): λ_{max} = 232 mμ ε_{max} = 15 000; r.m.n.: 6.34 τ (1 H quadruplet); 7.62 et 7.80 τ (8 H singulet); 8.86 (12 H singulet); 8.88 (3 H doublet).

L'addition supplémentaire d'eau permet d'obtenir le dérivé dimédonique de l'acétaldéhyde (**10**) pur, p.f. 142–143 °C (litt. p.f. 141–142 °C (5)). Dont les caractéristiques sont les suivantes:

Infrarouge: bande large entre 3400 et 2400 cm^{-1} et 1595 cm^{-1}; r.m.n.: 5.84 τ (1 H quadruplet); 7.7 (8 H singulet); 8.22 τ (3 H doublet); 8.95 (12 H singulet); −3.5 τ (2 H singulet).

Ces deux composés se sont révélés identiques au dérivé dimédonique de l'acétaldéhyde et à l'octahydroxanthène synthétisés à partir de la dimédone et d'acétaldéhyde selon le mode opératoire de Horning et Horning (5).

Le composé **10** obtenu par photolyse se transforme complètement en **11** par action de l'acide chlorhydrique en milieu éthanolique. Il a pu être montré que **9** est obtenu non pas au cours de la photolyse mais essentiellement pendant la distillation du solvant. En effet si le solvant est éliminé à froid, l'étude des composés obtenus ne montrent plus que la présence de traces de **9**.

La deuxième fraction de la chromatographie sur colonne est obtenue en éluant avec de l'acétate d'éthyle pur. Elle fournit 1 g de diméthyl-5,5 cyclohexanedione-1,3 (**8**) identifiée par comparaison avec un échantillon authentique.

La fraction liquide (1.2 g) était constituée de plusieurs composés comme le montra la chromatographie en couches minces. Elle fut traitée par la soude 10%. La solution sodique, acidifiée par HCl 10% et extraite à l'éther, fournit 0.500 g de diméthyl-4,4 oxo-2 cyclopentanecarboxylate d'éthyle (**11**). Ce composé présente les caractéristiques suivantes:

Infrarouge: 1745 et 1730 cm^{-1}; r.m.n.: 5.80 τ (2 H quadruplet); 6.60 τ (1 H triplet); 7.80 τ (2 H singulet); 7.85 τ (2 H doublet); 8.72 τ (3 H triplet); 8.75 τ (3 H singulet); 8.92 τ (3 H singulet).

Ces caractéristiques sont rigoureusement identiques à celles obtenues pour le diméthyl-4,4 oxo-2 cyclopentanecarboxylate d'éthyle provenant d'une condensation de Dieckman sur le diméthyl-3,3 adipate d'éthyle (voir synthèse plus loin). En outre la structure de **11** a été confirmée de la façon suivante: 0.250 g de **11** a été chauffé en suspension dans une solution d'acide chlorhydrique 10%; après 3 h de reflux et extraction à l'éther, on isole la diméthyl-3,3 cyclopentanone (**5**) qui fut identifiée par le point de fusion mixte de son dérivé dinitro-2,4 phénylhydrazone. La fraction non soluble dans la soude 10% (0.7 g) est un mélange de plusieurs composés. La chromatographie en phase gazeuse (colonne 8 pieds Polyester de Craig 20% sur chromosorb P; T °C = 190) a montré la présence d'au moins 4 produits qui n'ont pas été identifiés. Le spectre de r.m.n. de ce mélange indique l'incorporation de groupements éthyles.

(d) Photolyse dans le cyclohexène

Cas du cyclohexène purifié—Diazo-2 diméthyl-5,5 cyclohexanedione-1,3 (5 g) a été photolysé en solution dans 1 000 ml de cyclohexène purifiés selon la méthode de Waterman et Van Wester (8). La pureté du solvant a été vérifiée par chromatographie en phase gazeuse. Pour que tout le diazo disparaisse il a été nécessaire d'effectuer la photolyse pendant 4 h. Le cyclohexène fut ensuite distillé et le résidu liquide, par distillation fractionnée fournit 2 fractions:

Fraction 1 ($p.e._7$ = 48–50 °C (0.600 g))—Ce composé s'avèra être la diméthyl-3,3 cyclopentanone (**5**). Elle fut identifiée par comparaison des spectres i.r. et de r.m.n. et par le point de fusion mixte de son dérivé dinitro-2,4 phénylhydrazone.

Fraction 2 ($p.e._7$ = 145–155 °C (2.6 g))—Le liquide légèrement souillé par deux autres composés (chromatographie sur couches minces) fut purifié par une chromatographie sur colonne de silicagel (200 g Baker Analyzed). En éluant avec un mélange cyclohexane – acétate d'éthyle 75:25 en volume on obtient en tête 2.0 g de liquide pur. Ce liquide répond à la structure du (cyclohexen-2)yl-2 diméthyl-5,5 cyclohexanedione-1,3 (**12**) dont les caractéristiques spectrales sont rapportées dans le texte.

Anal. Calc. pour $C_{14}H_{20}O_2$ (220.3): C, 76.33; H, 9.15. Trouvé: C, 76.14; H, 9.39.

Spectre de masse: pic important à 81 (100%) et 139 (30%). On a également obtenu un abondant résidu gommeux (1 g) non distillable.

Synthèse de la diméthyl-3,3 cyclopentanone (5)

La diméthyl-3,3 hydroxy-5 cyclopentanone est d'abord préparée par une synthèse acyloïne à partir de diméthyl-3,3 glutarate d'éthyle en présence de sodium dans l'ammoniac. La méthode utilisée est celle décrite par Kwart et Ford (9).

L'acyloïne obtenue a été réduite en diméthyl-3,3 cyclopentanone par la poudre de zinc et l'acide chlorhydrique en milieu acétique selon le procédé de Prelog, Frenkiel, Kolbe et Barman (10).

La distillation finale conduit à un liquide $p.e._{12}$ = 55–60 °C (litt. $p.e._{760}$ = 154–155 °C (11)); semicarbazone: p.f. 180–181 °C (litt. p.f. 178–179 °C (11)); dinitro-2,4 phénylhydrazone: p.f. 145–146.5°.

Synthèse du diméthyl-4,4 oxo-2 cyclopentanecarboxylate d'éthyle

L'acide diméthyl-3,3 adipique a été obtenu par oxydation du diméthyl-4,4 cyclohexène par le permanganate de potassium tel que décrit par Hibbitt et Linstead (12).

Le diméthyl-3,3 adipate d'éthyle a été ensuite transformé en diméthyl-4,4 oxo-2 cyclopentanecarboxylate d'éthyle par une réaction de Dieckman utilisant le sodium dans le toluène selon la méthode de Pinkney (13).

Par distillation, on obtient un liquide $p.e._7$ = 100–105 °C et dont les caractéristiques spectrales sont les suivantes:

Infrarouge (pur): bandes à 1745 et 1730 cm^{-1}; r.m.n.: bandes à 5.80 τ (2 H quadruplet); 6.60 τ (1 H triplet); 7.80 τ (2 H singulet); 7.85 τ (2 H doublet), 8.72 τ (3 H triplet); 8.76 τ (3 H singulet); 8.92 τ (3 H singulet).

Mise en évidence de la formation d'acétaldéhyde au cours de la photolyse de **2** *dans l'éthanol*

La formation d'acétaldéhyde au cours de la photolyse de **2** dans 'éthanol a été mise en évidence en faisant barbotter l'azote, à la sortie de l'appareil de photolyse, dans une solution de dinitro-2,4 phénylhydrazine. Après 1 h de photolyse, un abondant précipité jaune orangé, s'est formé dans la solution-piège. Ce précipité était le dérivé dinitro-2,4 phénylhydrazone de l'acétaldéhyde, p.f. 159–161 °C. Le point de fusion mixte n'a donné lieu à aucune dépression.

Remerciements

Nous remercions Monsieur le Professeur H. Favre qui a gracieusement mis son laboratoire à notre disposition et sans qui ce travail n'aurait pu avoir lieu. Nos remerciements vont également à Monsieur R. Mayer pour les spectres de résonance magnétique nucléaire, à Monsieur J. C. Regenass pour les spectres de masse et à Monsieur R. Favier pour les déterminations de masse moléculaire. Finalement nous tenons à remercier le Conseil National de Recherches du Canada pour l'aide financière accordée et pour une bourse de recherches post-doctorale (subvention A-14).

1. H. Stetter et K. Kiehs. Chem. Ber. **98**, 1181 (1965).
2 F. Weygand, H. Dworschak, K. Koch et S. T. Konstas. Angew. Chem. **73**, 409 (1961).
3. M. Rosenberg, P. Yates, J. B. Hendrickson et W. Wolf. Tetrahedron Letters, **33**, 2285 (1964).
4. W. Kirmse. Carbene chemistry. Academic Press, Inc., New York. 1964. p. 119.
5. E. C. Horning et M. G. Horning. J. Org. Chem. **11**, 95 (1946).
6. F. Weygand, W. Schwenke et H. J. Bestmann. Angew. Chem. **70**, 506 (1958).
7. A. I. Vogel. A text-book of practical organic chemistry. John Wiley and Sons, Inc., New York. 1966. p. 167.
8. H. I. Waterman et H. A. Van Westen. Rec. Trav. Chim. **48**. 637 (1929).
9. H. Kwart et J. A. Ford, Jr. J. Org. Chem. **24**, 2060 (1959).
10. V. Prelog, L. Frenkiel, M. Kolbe et P. Barman. Helv. Chim. Acta, **30**, 1741 (1947).
11. G. Blanc. Bull. Soc. Chim. France, 783 (1908).
12. D. C. Hibbitt et R. P. Linstead. J. Chem. Soc. 470 (1936).
13. P. S. Pinkney. Org. Syn. Coll. Vol. II. 116 (1943).

Can. J. Chem. Downloaded from www.nrcresearchpress.com by 210.87.254.5 on 09/05/12
For personal use only.

Can. J. Chem. Downloaded from www.nrcresearchpress.com by 210.87.254.5 on 09/05/12
For personal use only.

Approaches to the synthesis of triterpenoids. I. Methyl group migration to the 9β-position in steroids as a route to the cucurbitacins. A possible structural feature directing epoxide cleavage rearrangements[1,2]

J. W. ApSimon, R. R. King, and J. J. Rosenfeld
Department of Chemistry, Carleton University, Ottawa, Canada

Received November 21, 1968

The BF_3 catalyzed cleavage of some steroidal 9α,11α-epoxides has been studied in an attempt to induce migration of the C-10 methyl group to C-9. In the case of 9α,11α-epoxyandrost-4-ene-3,17-dione, cleavage with BF_3 gas in benzene led to two major products. One of these was the required 3,11α-dihydroxy-9β-methylestra-1,3,5(10)-triene-17-one, thus leading to a novel class of steroids and possibly opening a route to the synthesis of compounds of the cucurbitacin class. The other main product was shown to be 11α-hydroxy-9β-androst-4,8(14)-diene-3,17-dione. A possible structural feature directing the rearrangement pathway to these materials is proposed from the study of other epoxide rearrangements and some reported in the literature.

Canadian Journal of Chemistry, 47, 1989 (1969)

The cucurbitacins (e.g. bryogenin **1** (1)) represent an interesting variation in the biogenetic pathways leading to the tetracyclic triterpenes, a migration of one methyl group from C-10 to C-9 in a lanostane precursor **2** (arrows) appearing to account for these compounds (2, 3). This series of compounds interested us from a synthetic point of view since there did not appear to be any direct correlation with other materials, and we felt that it was feasible to carry out such a methyl group migration chemically on a suitable triterpene precursor. This paper describes our initial studies in this direction.

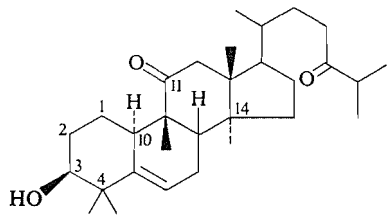

1

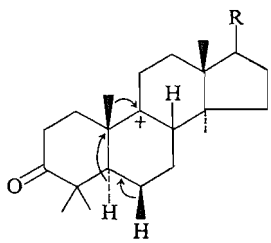

2

There are many reports of methyl group migrations in terpenoids usually initiated by protonation of a suitably situated double bond (4) such as the euphenol **3** to isoeuphenol **4** conversion (5).

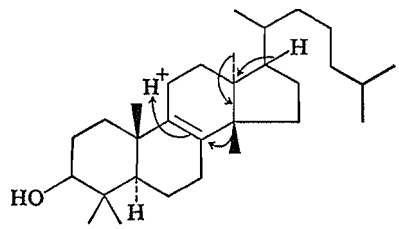

3

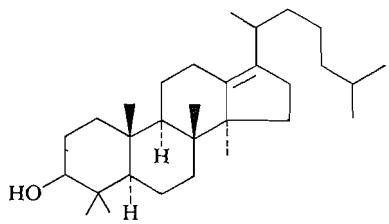

4

At the outset we rejected this type of rearrangement for our studies since it involved the saturation of a double bond at one terminus of the pathway and hence loss of some functionality required for further elaboration of the molecule at a later stage. We therefore decided to study the creation of a cationic center next to the methyl

[1]Presented in part at the 50th and 51st Canadian Chemical Conferences, Toronto, June 1967 and Vancouver, June 1968 respectively. Preliminary communication of part of this work has appeared in ref. 36.

[2]This work describes part of the M.Sc. Thesis of R. R. King, Carleton University, October 1967.

Can. J. Chem. Downloaded from www.nrcresearchpress.com by 210.87.254.5 on 09/05/12
For personal use only.

group of interest *via* the Lewis acid catalyzed cleavage of an epoxide. Thus, we reasoned that the methyl group could best be induced to migrate if it were *anti*-periplanar with respect to the opening end of an epoxide.[3] Since the systems required also have oxygenation at C-11, steroidal or tetracyclic triterpene 9α,11α-epoxides would appear to be the starting materials of choice. At first sight, the work of Henbest and Wrigley (7) appeared to militate against our ideas, since they had observed that the major product of BF_3-catalyzed opening of steroidal and some triterpene 9α,11α-epoxides was the corresponding 11-ketone. However, two factors induced us to continue. Firstly we felt that the particular model compound we wished to use, 9α,11α-epoxyandrost-4-ene 3,17-dione **5***a*, was ideally constructed for methyl migration, the expected concomitant aromatization of ring A acting as an extra driving force (arrows in **5**) to give the phenolic steroid **6***a*. Secondly, we were encouraged by reports on methyl group migrations, both single (8, 22) and multiple (9) induced by the acid-catalyzed cleavage of epoxides in steroids and triterpenes.

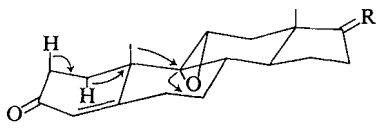

5

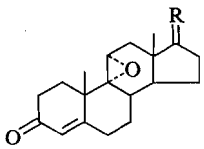

5*a* R = =O

b R = COCH$_3$ / H

The possibility that epoxides are involved in the biogenetic cyclization of squalene (10) suggested to us that perhaps this functional group could also play a role in further transformations of terpenoids in the plant. It is interesting to note that, at least in two cases where a triterpene series appears to have originated from a further methyl

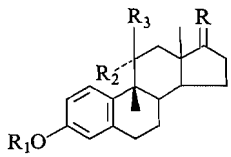

6*a* R = =O; R_1 = H; R_2 = OH; R_3 = H

b R = =O; R_1 = CH_3; R_2 = OH; R_3 = H

c R = =O; R_1 = CH_3; $R_2 + R_3$ = =O

d R = COCH$_3$ / H ; R_1 = H; R_2 = OH; R_3 = H

migration, there is an oxygen function at a position corresponding to the vestige of an epoxide. These are the cucurbitacins, e.g. **1**, and the meliacin series (11), e.g. **7**, this latter example being of particular note since there is a C-7α hydroxyl group having therefore the correct orientation for epoxide origin. In fact, since submission of our preliminary communication on this work,[2] two reports have appeared (12) describing the synthesis of this latter series by Lewis acid-catalyzed cleavage of a 7α,8α-epoxide, (**8** to **9**). Recent reports also suggest germacrane sesquiterpene epoxides as precursors of cyclized species (13).

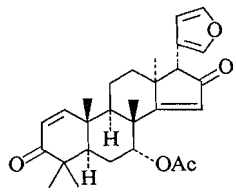

7

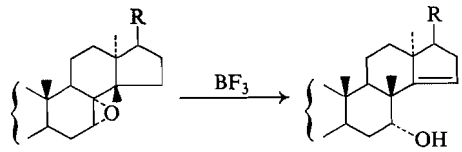

8 **9**

The epoxide **5***a* (14) was prepared from commercially available androst-4-ene-3,11,17-trione (adrenosterone)[4] *via* epoxidation of androst-4,9(11)-diene-3,17-dione (15) assuming the stereochemistry of this last step to be controlled by the

[3]For an excellent review of epoxide chemistry, see ref. 6.

[4]We thank the Upjohn Company for a generous gift of this material.

Can. J. Chem. Downloaded from www.nrcresearchpress.com by 210.87.254.5 on 09/05/12
For personal use only.

ease of approach of *m*-chloroperoxybenzoic acid to the 9(11)-double bond (16). Treatment of a dry benzene solution of this epoxide at room temperature with an excess of freshly distilled BF_3 etherate[5] for extended periods, or with $AlCl_3$ or $SnCl_4$ gave no indication of any reaction. Heating of these mixtures gave some cleavage products which could not be adequately characterized and appeared to be polymeric. However, when BF_3 gas was bubbled into a dry benzene solution of **5***a* at room temperature, a gel formed around the sides of the reaction flask characteristic of an epoxide–BF_3 complex (17). Immediate work-up of this solution gave only unchanged epoxide, but if the reaction mixture was left for 12 h at room temperature, the gel slowly turned purple and work-up gave phenolic and neutral products.

Phenolic Products

Extraction of the above reaction mixture followed by washing with 0.5 *N* sodium hydroxide yielded 30% phenolic material, m.p. 255–256°, analyzing for $C_{19}H_{24}O_3$. That this material can be assigned structure **6***a* follows from its spectral properties[6] and the predicted course of methyl migration in a *trans* and diaxial manner to the opening end of the epoxide. The phenol readily formed a monomethyl ether **6***b* with diazomethane which was not phenolic and which on oxidation yielded the diketone **6***c*. All of these compounds exhibited the required analytical and spectral properties. The stereochemistry assigned is supported by nuclear magnetic resonance (n.m.r.) since in **6***a* and **6***b* the C-1 proton is unusually deshielded, appearing at 8.1 δ. However, in the diketone **6***c* this signal appears at the more normal aromatic proton position of 6.5 δ. Considering the stereochemistry shown in **10** and viewing the molecule from end-on as in **11**, then it is apparent that there is a very strong nonbonded interaction between the C-1 proton and the hydroxyl group which can result in a strong compression effect evidenced as a large deshielding of that proton (19). On removal of this interaction by conversion to **6***c*, the C-1 proton is no longer subject to this Van der Waal's deshielding.[7] Through the kind cooperation of Professor R. A. Bell we have examined the nuclear Overhauser effects (n.O.e.) (20) of **6***b* in order to detect closely-spaced protons. Examination of **11** indicates that the 11α-hydroxyl proton is very close to H-1, at least some of the time and an Overhauser effect should be observable. When the signal for H-1 (8.12 δ) was integrated during irradiation of the 11α-hydroxyl proton signal (1.67 δ) a 10% increase in intensity was noted, supporting the stereochemistry assigned. It is also interesting to note that irradiation of the C-9 methyl group (1.43 δ) gives a 9% n.O.e. on H-1. No other possible structure for **6** appears consistent with these data.[8] A further indication of the proximity of the C-1 aromatic proton of **10** and the C-11α-hydroxy group is obtained from the n.m.r. spectrum of the phenol methyl ether of **10** (i.e. **6***b*) in pyridine-d_5. In this solvent, the H-1 doublet is deshielded by 0.85 p.p.m. appearing at 8.97 δ whereas the H-2 and H-4 signals were only deshielded by 0.2 p.p.m. This large deshielding effect is rationalized if an alcohol–pyridine association (probably by H bonding) is postulated, which leaves H-1 in the most highly deshielding region of the complex (21).

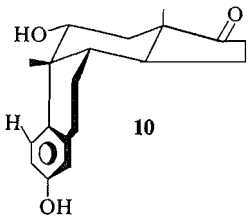

10

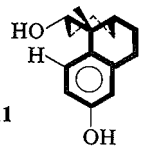

11

Neutral Products

Column chromatography on alumina (grade III neutral) yielded, besides unchanged epoxide, two products which could be fully characterized. The major product from this fraction we assign as **12***a*[6] arising from the alternative mode of rearrangement of epoxide **5***a* as shown. The structure of **12***a* follows from its analysis and spectroscopic properties and is supported by its oxidation to **13***a* with Jones' reagent. We had hoped to

[5]In order for BF_3 to exert its full effect as a Lewis acid it must be freed of nucleophilic fluorine-containing species (18). In none of the cases reported here did we observe the formation of fluorohydrins.

[6]If the spectroscopic and other properties of new compounds are unexceptional we will not elaborate on them further, apart from full information in the experimental section.

[7]It is also possible to use magnetic anisotropy arguments in this case, and though we prefer the compression deshielding argument at this time we are not in a position to decide unequivocally between the two.

[8]We are at present attempting a synthesis of this material and hope to report on this at a later date.

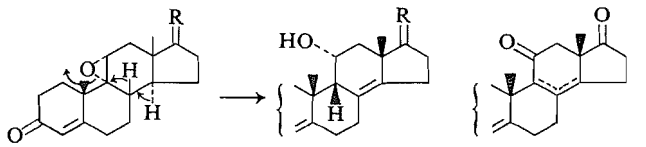

5*a*(or *b*) **12***a* R = =O, COCH$_3$ **13***a* $\Delta^{8,14}$, 9αH

b R = H *b* $\Delta^{8,9}$

isolate the 9β isomer of **13***a* thus confirming our assumption as to the stereochemistry of **12***a* at that position, but even on rapid treatment with Jones' reagent we were unsuccessful (22). On warming **13***a* with alcoholic hydrochloric acid, a di-α,β-unsaturated ketone **13***b* was obtained as evidenced by spectroscopy. Throughout this sequence, the only ethylenic proton observable in the n.m.r. spectra of the compounds prepared was that attributable to the C-4 proton. Thus, there is present in **12**, **13***a*, and **13***b*, a tetrasubstituted double bond, and hence the location of this unsaturation is as shown. There still exists some doubt as to the stereochemistry of **12***a* at C-9, although the C-8β hydrogen in **5***a* which would be expected to migrate in an *anti*-periplanar manner on epoxide cleavage would dictate this stereochemistry (23).

An alternative pathway leading to the 9α-isomer of **12***a* can also be formulated

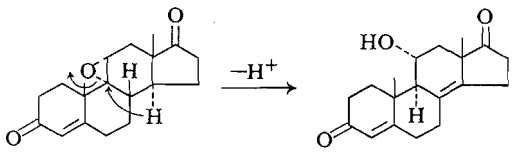

5 **12***a* (9αH)

However, we prefer the pathway proceeding *via anti*-periplanar movements of the migrating atoms with loss of the C-14 proton, rather than the alternative shown which involves *cis*-attack at the reaction site as well as a 1,3 hydrogen transfer.[9] Whilst there are reported examples of openings of epoxides with retention of configuration at the cleaved bond, these have been observed only when some neighboring group participation is involved (25). Thus, we favor the first route to **12***a* and hence its stereochemistry as shown.

The structure of **12***a* is further supported by an n.m.r. study (100 MHz of the 11β-hydrogen signal ($CDCl_3/D_2O$) which appears as a 5-line multiplet centered at 4.4 δ. The ratio of these lines, all equally spaced at 5 Hz intervals, is 1:2:2:2:1. This signal is best accommodated by coupling constants of $J_{9\beta,11\beta} = 5$ Hz; $J_{11\beta,12\alpha} = 10$ Hz; $J_{11\beta,12\beta} = 5$ Hz, being assigned by inspection of Dreiding models of **12***a* where the observed approximate dihedral angles are Θ, 11βH–12αH, 120°; Θ, 11β–12βH, 0°; Θ, 9βH–11βH, 45°.[10] On the other hand the 9α-H isomer of **12***a* would appear, from Dreiding models, to exist in only one conformation with dihedral angles of Θ, 9β–11βH, 150°; Θ, 11βH–12αH, 180°; Θ, 11βH–12βH, 60°, leading to a substantially different signal pattern for 11βH in the n.m.r. spectrum of this isomer. The same observation was made for compound **12***b*.

When the rearrangement of **5** was performed on a large scale we were able to isolate about 4% of the ketone **14**, whose structure follows by base-catalyzed inversion at C-9 to adrenosterone (**14** with C-9α). It therefore appears that in the rearrangement of **5** there are two main pathways induced by epoxide cleavage, whilst the more common ketone formation (7) is suppressed.[11]

Assuming that our structural assignments are correct, we must now consider the factors dictating the two pathways observed. The first point of note is that the aromatization of ring A is not the dominant effect. This was emphasized by a

[9]There is a report of 1,3 hydrogen transfer (24) during epoxide cleavage. However, here again, the migrating group is *trans* disposed to the opening end of the epoxide.

[10]The models show this to be a very flexible molecule and it is also possible to make other likely conformations which would be expected to show similar coupling constants. However, the one used is that most closely giving correct coupling constants according to Karplus' equation (26).

[11]It is interesting to note that in Henbests' report (7), hydroxyl-containing materials up to about 50% yield were noted but not further characterized. We hope to repeat this work to see if these materials fit into our framework of observations.

Can. J. Chem. Downloaded from www.nrcresearchpress.com by 210.87.254.5 on 09/05/12
For personal use only.

Can. J. Chem. Downloaded from www.nrcresearchpress.com by 210.87.254.5 on 09/05/12
For personal use only.

similar rearrangement of 9α,11α-epoxypregn-4-ene-3,20-dione, **5***b*, which might be expected to react in an analogous manner to **5***a* at least in that portion of the reaction leading to aromatization and methyl migration. In this case only 3% of rearrangement in this direction was noted yielding **6***d*, whilst the only other product present in detectable amount, **12***b*, was arising from formation of the 8,14 double bond. The structure was assigned in a similar manner to that used for **12***a*. Even in this latter case we were a little surprised since we had anticipated some concomitant migration of the C-13 methyl group to C-14 to give **15**, the formation of an α,β-unsaturated ketone driving this pathway.

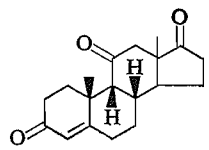

14

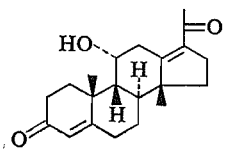

15

Thus, while the aromatization is probably responsible for directing the C-9 methyl migration, there must exist some other intrinsic structural feature acting in competition. We therefore believed that the alternate pathway (to **12***a* and **12***b*) represented a comparable energy barrier, the possibility of a concerted intramolecular process being favored.

At this stage of our work, we studied two more examples of epoxide cleavage. The first was 9α,11α-epoxy-5α-androstan-3,17-dione (**5***a* with 4,5 double bond removed) (27). In this case we hoped to observe some C-10 methyl migration with the formation of a 9β-methylandrost-1-ene-3-one system (28), but again the major product was that resulting from formation of the 8,14 double bond (**12***a* with 4,5 double bond saturated), whose structure follows from oxidation and conjugation to an αβ unsaturated ketone (see Experimental). The second example was the cleavage of 3α,4α-epoxyfriedelane **16** (29). We anticipated that Lewis acid cleavage of this epoxide might lead to extensive backbone rearrangement to β-amyrin derivative **17** (29) (see arrows in **16**) although the possibility of rearrangement to an intermediate compound must not be ignored (30). In fact this latter course was observed, the only isolable product from the reaction of **16** with stannic chloride in dry benzene[12] was alnus-5(10)-ene-3α-ol, **18**, characterized by conversion to alnus-1,5(10)-diene-3-one, **19** (31) as shown in Scheme I.

On considering the above 4 cases of formation of homoallylic alcohols and examining the structures of the parent epoxides, one common structural feature is recognizable which could account for this mode of rearrangement. There is always a hydrogen atom in a 1,3-diaxial relationship to the departing end of the epoxide, and we find an intramolecular proton abstraction pathway an attractive explanation for the formation of such products as shown in Scheme II, assuming

[12] BF_3 also gave the same product but in lower yield and with more polymerization. This is in contrast to the steroidal examples where BF_3 was best.

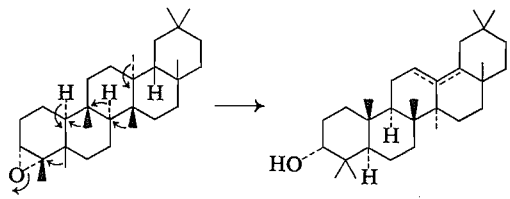

16 **17**

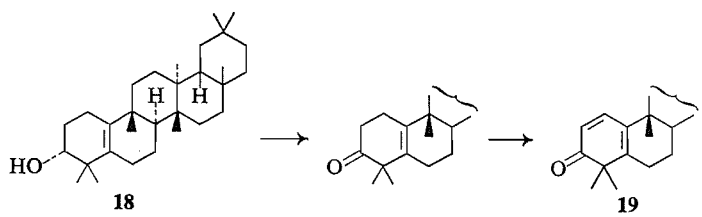

18 **19**

SCHEME I

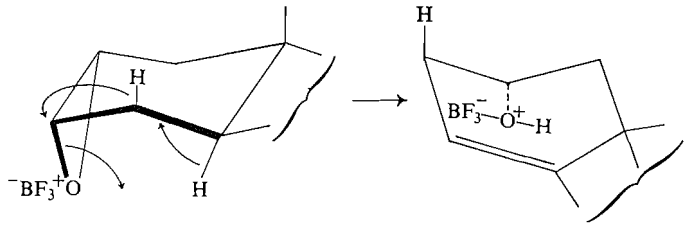

SCHEME II

of course that no major conformational factors lead to destabilization of this pathway.[13]

If it is borne in mind that in our cases only gaseous BF_3 or pure $SnCl_4$ in dry benzene was used as the Lewis acid, then the pathway shown could be favored since the only base available to aid in proton removal is the epoxide oxygen atom. By contrast, the more usual BF_3–etherate reagent used for epoxide rearrangements provides a proton acceptor in the ether and thus more varied reaction products may be anticipated. On considering our two initial cases, **5***a* and **5***b*, the only structural difference is in ring D at C-17. Examination of models shows that conversion of C-17 to a tetrahedral state introduces a new 1,3-diaxial interaction between the 17α- and the 12α- and 14α-hydrogens, as well as the introduction of further eclipsed cyclopentane vicinal interactions. If this effect is relieved by a slight flexing of the C and D rings then it becomes apparent from models that the C-14α hydrogen atom is pushed closer to the epoxide oxygen atom and is thus more available for abstraction on the basis of our hypothesis. This could then account for the large change in this direction of rearrangement, about 30% for **5***a* to **12***a* and about 75% for **5***b* to **12***b* and thus a corresponding reduction in the aromatization–methyl migration products.[14] Similar arguments account for some of the products observed in a number of published cases (12, 33), even where BF_3–etherate or mineral acid had at times been used for the cleavage. Such a pathway could even have biogenetic significance (11, 34).

We are at present exploring this concept of intramolecular proton abstraction in a number of other cases, especially with respect to earlier work (7). It is possible that this type of reaction could lead to some unique control in organic synthesis with suitably constructed epoxides.[15]

[13]This process may also be stepwise with the discrete formation of a carbonium ion. However, the example shown of a Wagner–Meerwein rearrangement on epoxide cleavage where the breaking bond is α to a carbonyl group (32) leads us to favor a generalized process in which there is little C—O bond cleavage before rearrangement, the BF_3 serving to increase bond polarization by complex formation. If a discrete carbonium ion was formed, this would necessitate the formation of a cationic center α to a carbonyl group whereas a cyclic process such as we envisage would not necessitate formation of such energetic species.

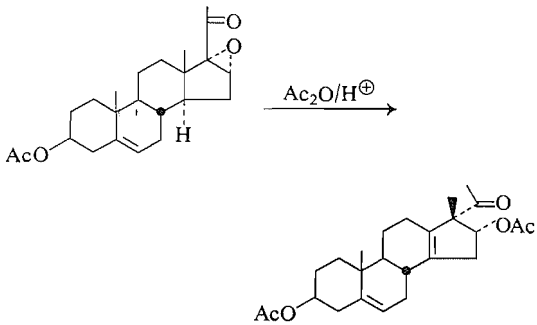

[14]In fact, the aromatization pathway can also be accounted for by this type of mechanism, the 1α hydrogen atom being in the correct orientation according to our proposal. This would then give **20** as the intermediate which by simple tautomerism would give **6**. The difference in the amounts of phenolic products from **5***a* and **5***b* is again a reflection of the ease of this 6-membered cyclic process in the two cases.

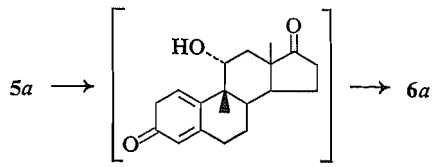

20

[15]For the present we have ignored the further effects of BF_3, such as complexation with keto groups present in some of the examples considered. Some of our examples quoted have no carbonyl groups, thus, if our hypothesis is correct, the complexation of BF_3 with keto groups distant from the epoxide grouping has little or no effect on the reaction pathway. We are, however, studying the effects of nearby carbonyl groupings.

Can. J. Chem. Downloaded from www.nrcresearchpress.com by 210.87.254.5 on 09/05/12
For personal use only.

Can. J. Chem. Downloaded from www.nrcresearchpress.com by 210.87.254.5 on 09/05/12
For personal use only.

Experimental

Infrared (i.r.) spectra were determined on Perkin–Elmer Infracord 137 and 237 spectrophotometers in Nujol mulls. Nuclear magnetic resonance spectra were determined at 60 MHz on a JEOLCO C-60, or at 100 MHz on a Varian HA 100 spectrometer. Chemical shifts are given in delta (δ) units relative to tetramethylsilane as internal standard. The following abbreviations were used to describe the signals—s, singlet; d, doublet; t, triplet; q, quartet; m, multiplet. Only signals deemed to be of interest in assigning structures have been quoted. Sample concentrations were approximately 10% (wt./vol.) in deuteriochloroform as a solvent. All optical rotations were taken at room temperature with absolute ethanol as solvent. Melting points are uncorrected and were determined on a Kofler hot stage. Thin-layer chromatography (t.l.c.) was carried out on silica gel plates. Mass spectra were obtained on the Perkin–Elmer–Hitachi instrument of McMaster University through the courtesy of Professors R. A. Bell and D. B. McLean. Microanalyses were determined by A. Spang, Ann Arbor, Michigan.

General Procedure for Epoxidation: Preparation of 9α,11α-Epoxyandrost-4-ene-3,17-dione (5)

Treatment of androst-4,9(11)diene-3,17 dione (6.1 g) with a slight excess of *m*-chloroperoxybenzoic acid (4.0 g) in spectra grade chloroform (200 cc) at 0 °C for 48 h gave complete reaction as indicated by t.l.c. (benzene – ethyl acetate 7:3). The chloroform solution was washed successively with sodium iodide in dilute sulfuric acid, dilute sodium sulfite, and saturated aqueous sodium bicarbonate, then dried and evaporated. Recrystallization of the product from acetone gave 5.3 g (87%) of pure (t.l.c.) epoxide **5***a*. Two more recrystallizations from acetone gave small colorless cubes, m.p. 273–275 °C; $[\alpha]_D$ +190°; ν_{max} 1740 (17 ketone), 1660 (3 ketone), 1620 cm^{-1} (Δ^4); λ_{max} 244 mμ, ε 15 800; n.m.r. signals at 6.85 (1H, s, 4-H), 3.27 (1H, t, 11βH).

Anal. Calcd. for $C_{19}H_{24}O_3$: C, 75.97; H, 8.05. Found: C, 75.80; H, 8.07.

General Procedure for BF_3 Rearrangements: Rearrangement of 9α,11α-Epoxyandrost-4-ene-3,17-dione (5a)

Epoxide **5***a* (1.0 g) was dissolved in freshly dried and distilled benzene (175 ml). BF_3 gas was bubbled through the solution until epoxide–BF_3 complexation commenced as manifested by the formation of a slight reddish-brown gel around the sides of the flask. The mixture was allowed to stand for 12 h after which time t.l.c. analysis of the gel (benzene – ethyl acetate 7:3) showed the formation of two major products and the disappearance of most of the starting material. The reaction was taken up in ether (125 cm^3) to give an orange solution. The ether–benzene layer was washed three times with saturated aqueous sodium bicarbonate and twice with water. Extraction with 0.5 *N* aqueous sodium hydroxide, acidification of the aqueous layer with 2 *N* HCl, and back extraction with ether gave the phenolic material; the ether–benzene layer of the alkaline extractions contained the neutral fraction.

Phenolic Fractions

The phenolic fraction gave a yellow oil (300 mg) which was taken up in a small amount of chloroform. Upon standing, the chloroform solution deposited 140 mg fine colorless prisms **6***a*, m.p. 254.5–255 °C; $[\alpha]_D$ +32°; ν_{max} 3550 (hydroxyl), 3300 (phenol), 1730 (17 ketone), 1610 and 1575 cm^{-1} (aromatic); λ_{max} 281 mμ, ε 1950 changing to λ_{max} 298 mμ, ε 3160 in base; n.m.r. signals 8.1 (1H, d, 1-H), 6.56 (2H, d + s, 2-H + 4H), 4.05 (1H, q, 11βH, $J_{11\beta,12\alpha}$ = 12 c.p.s., $J_{11\beta,12\beta}$ = 4 c.p.s.), 1.4 and 1.0 (3H, s, C-9 and C-18 methyls).

Anal. Calcd. for $C_{19}H_{24}O_3$: C, 75.97; H, 8.05. Found: C, 76.00; H, 8.02.

Methyl Ether of 6a

Treatment of **6***a* with dimethyl sulfate in methanolic potassium hydroxide gave **6***b* (65%). An analytical sample was prepared by crystallization from aqueous methanol followed by sublimation at 130 °C/10 mm to give colorless plates, m.p. 187–189 °C; ν_{max} 3550 (hydroxyl), 1730 (C-17 ketone), 1610 and 1575 cm^{-1} (aromatic); λ_{max} 278 mμ, ε 2140, no change in base; n.m.r. signals 8.12 (d, 1-H)4.00 (q, 11βH), 3.75 (3H, s, OMe), 1.43 (3H, s, C-9 CH_3), and 0.98 (3H, s, C-18 CH_3); *M* (mass spectral), 314.

Anal. Calcd. for $C_{20}H_{26}O_3$: C, 76.40; H, 8.33; Found: C, 76.13; H, 8.07.

9β-Methyl-3-hydroxy-1,3,5(10)-estratriene-11-one

Jones' oxidation of **6***a* followed by recrystallization from aqueous ethanol and sublimation at 200 °C/10 mm gave colorless plates, m.p. 278–280 °C; $[\alpha]_D$ +253°; ν_{max} 3400 (phenol), 1730 (17 ketone), 1695 (11 ketone), 1610 and 1595 cm^{-1} (aromatic); λ_{max} 282 mμ, ε 1980 changing to λ_{max} 300 mμ, ε 3010 in base; n.m.r. signals at 6.5 δ (3H, s, aromatic protons), 1.3 (3H, s, C-9 CH_3), 0.8 (3H, s, C-18 CH_3); *M* (mass spectral) 298. This compound was fairly unstable and it did not prove possible to obtain a sample pure enough for elemental analysis.

Neutral Fractions

The neutral fraction was chromatographed on neutral alumina. Elution with benzene gave **12***a* (260 mg, 26%) which was recrystallized from ethyl acetate. An analytical sample was obtained by further recrystallization from acetone to give colorless needles, m.p. 228–230 °C; $[\alpha]_D$ +350°; ν_{max} 3320 (hydroxyl), 1730 (17 ketone), 1650 (3 ketone); λ_{max} 245 mμ, ε 15 700; n.m.r. signals 5.58 (1H, s, 4H), 4.35 (1H, m, 11βH).

Anal. Calcd. for $C_{19}H_{24}O_3$: C, 75.96; H, 8.05. Found: C, 76.18; H, 8.05.

Repetition of the BF_3 catalyzed epoxide rearrangement on a 15 g scale gave 11.1 g of neutral material. Chromatography showed the presence of alcohol **12***a*, epoxide **5***a*, and triketone **14**. Chromatography on neutral alumina (Woelm) and elution with methylene chloride gave light-tan cubes (440 mg, 4%). Recrystallization from acetone gave colorless cubes (117 mg), m.p. 213–216 °C; ν_{max} 1749 (17 ketone), 1720 (11 ketone), 1660 (3 ketone), 1625 cm^{-1} (Δ^4); λ_{max} 245 mμ, ε 15 200; n.m.r. signals 5.78 (1H, s, 4H), 2.85 (1H, broad signal), 1.375 (3H, s), 1.28 δ (3H, s) (C_{18} + C_{19} methyl groups). Infrared, t.l.c., and n.m.r. indicated that this was not androst-4-ene-3,11,17-trione. Triketone **14** (40 mg) was treated with K_2CO_3 (30 mg) in methanol (3 cc). The solution was stirred overnight, poured into saturated salt solution (30 cm^3), extracted with ether, dried, and evaporated, to

Can. J. Chem. Downloaded from www.nrcresearchpress.com by 210.87.254.5 on 09/05/12
For personal use only.

give androst-4-ene-3,11,17-trione (15 mg) identical in all respects (m.p. and mixed m.p.; i.r., t.l.c., and n.m.r.) with an authentic sample.

Oxidation of ***12a***

Oxidation of alcohol **12***a* with Jones' reagent gave a near quantitative yield of triketone **13***a*. With some difficulty a small portion of this triketone was eventually crystallized from aqueous ethanol giving large colorless needles, m.p. 211.5–213 °C; $[\alpha]_D$ +165°; ν_{max} 1735 (17 ketone), 1700 (11 ketone), 1660 cm^{-1} (3 ketone); λ_{max} 244 mμ, ε 16 100; n.m.r. signals 5.83 (1H, s, 4H), 3.1 (1H, s, 9βH), 1.45 (3H, s), 1.05 (3H, s, C-18 + C-19 methyl groups).

Conjugation of ***13a*** *to* ***13b***

Compound **13***a* (10 mg) was treated with a drop of HCl in absolute ethanol (10 cc) and was warmed on a steam bath for 2 h. Work-up and recrystallization from ethyl acetate gave 3 mg of slightly yellow-colored needles, m.p. 186–188 °C; ν_{max} 1735 (17 ketone), 1660 cm^{-1} (11 and 3 ketones); λ_{max} 246 mμ, ε 19 700. This was too unstable to obtain an analytical sample.

*9α,11α-Epoxypregn-4-ene-3,20-dione (****5b****)*

Treatment of pregn-4,9(11)-diene-3,20-dione (1.2 g) (35) with *m*-chloroperoxybenzoic acid (0.8 g) in spectral grade chloroform (45 cc) at 0 °C for 30 h followed by a work-up as described above gave **5***b* (925 mg, 78%), upon recrystallization from ethyl acetate. An analytical sample was recrystallized from ethyl acetate to give large colorless needles, m.p. 183–185 °C; $[\alpha]_D$ +126°; ν_{max} 1710 (20 ketone), 1665 (3 ketone), 1620 cm^{-1} (Δ^4); λ_{max} 240 mμ, ε 15 800; n.m.r. signals at 5.8 (1H, s, 4H), 3.18 (1H, t, 11βH).

Anal. Calcd. for $C_{21}H_{28}O_3$: C, 76.79; H, 8.59. Found: C, 76.68; H, 8.54.

Rearrangement of 9α,11α-Epoxypregn-4-ene-3,20-dione

Rearrangement of **5***b* (450 mg) in freshly dried and distilled benzene was carried out as described above.

Phenolic Fraction

Recrystallization from benzene gave **6***d* (4 mg, 2%) as colorless flakes, m.p. 227–229 °C; $[\alpha]_D$ +77°; ν_{max} 3550 (hydroxyl), 3340 (phenol), 1690 (20 ketone), 1625 and 1590 cm^{-1} (aromatic); λ_{max} 282 mμ, ε 2020; n.m.r. signals at 8.2 (1H, d, 1H); 6.58 (1H, d, 2H), 6.47 δ (1H, s, 4H). This was too unstable to obtain an analytical sample.

Neutral Fraction

The neutral fraction was obtained in 89% yield (425 mg). Chromatography on neutral alumina and crystallization from acetone – petroleum ether gave **12***b* (290 mg, 61%) as fine white needles, m.p. 190–192 °C; $[\alpha]_D$ +376°; ν_{max} 3410 (hydroxyl), 1705 (20 ketone), 1650 (3 ketone), 1620 cm^{-1} (Δ^4); λ_{max} 242 mμ, ε 16 000; n.m.r. signals at 5.65 (1H, s, 4H), 4.45 (1H, m, 11βH).

Anal. Calcd. for $C_{21}H_{28}O_3$: C, 76.79; H, 8.59. Found: C, 76.95; H, 8.65.

Oxidation of **12***b* (100 mg) with Jones' reagent (5 drops) in acetone (15 ml) was complete in 2 min. Work-up as described for the oxidation of **12***a* and crystallization from ether gave the triketone (**13***a*, acetyl for C-17 ketone) as fine rosettes, m.p. 166–168 °C; $[\alpha]_D$ +518°; ν_{max} 1695–1705 (11 and 20 ketone), 1665 (3 ketone), 1620 cm^{-1} (Δ^4); λ_{max} 241 mμ, ε 16 200.

Anal. Calcd. for $C_{21}H_{26}O_3$: C, 77.27; H, 8.03. Found: C, 77.14; H, 7.96.

This ketone was readily conjugated by warming in alcoholic HCl to give an unstable di-α,β-unsaturated ketone (**13***b*, acetyl for C-17 ketone); ν_{max} 1710 (20 ketone), 1665 (3 + 11 ketone), 1625 cm^{-1} (Δ^4 and Δ^8); λ_{max} 245 mμ, ε 19 100.

9α,11α-Epoxy-5α-androstan-3,17-dione

5α-Androst-9(11)-ene-3,17-dione (530 mg) (27) was treated with a slight molar excess of *m*-chloroperoxybenzoic acid (400 mg) in spectral grade chloroform at 0 °C. Work-up has been previously described. Crystallization from acetone gave pure epoxide (390 mg, 73%). A further recrystallization from acetone gave colorless prisms, m.p. 212–214 °C; $[\alpha]_D$ +108° (27), ν_{max} 1735 (17 ketone), 1705 cm^{-1} (3 ketone); n.m.r. signals at 2.28 (1H, t, 11βH).

Anal. Calcd. for $C_{19}H_{24}O_3$: C, 75.96; H, 8.67. Found: C, 75.66; H, 8.61.

Rearrangement of 9α,11α-Epoxy-5α-androstan-3,17-dione

9α,11α-Epoxy-5α-androstan-3,17 dione (350 mg) (**5***a*, $\Delta^{4,5}$ saturated) in freshly dried and distilled benzene (20 ml) was saturated with BF_3 gas. The reaction went to completion in 35 min (t.l.c.): Quenching with saturated aqueous sodium bicarbonate, ether extraction, and crystallization of the oily residue from acetone – petroleum ether gave 11α-hydroxy-5α,9β-androst-8(14)-ene-3,17-dione (260 mg, 74%) as fine colorless prisms, m.p. 196–198.5 °C; $[\alpha]_D$ −87°; ν_{max} 3410 (hydroxyl), 1735 (17 ketone), 1700 cm^{-1} (3 ketone); n.m.r. signals at 3.75 (1H, m, 11βH).

Anal. Calcd. for $C_{19}H_{26}O_3$: C, 75.46; H, 8.67. Found: C, 75.41; H, 8.55.

Oxidation of this product (70 mg) (**12***a*, Δ^4 reduced, 5αH) with Jones' reagent (3 drops) in acetone (10 ml) was complete in 3 min. Work-up as described above and crystallization from acetone – petroleum ether (60–80°) gave coarse prisms of the triketone (**13***a*, Δ^4 reduced, 5αH), m.p. 202–204 °C; $[\alpha]_D$ +206°; ν_{max} 1740 (17 ketone), 1715 (11 ketone), 1705 cm^{-1} (3 ketone). Conjugation was achieved by hot alcoholic HCl to give a low yield of the unstable α,β-unsaturated ketone (**13***b*, Δ^4 reduced, 5αH), m.p. 148–152°; ν_{max} 1740 (17 ketone), 1710 (3 ketone), 1665 (11 ketone), 1610 cm^{-1} (Δ^8); λ_{max} 246 mμ, ε 12 100.

*3α,4α-Epoxyfriedelane (****16****)*

Friedel-3-ene (24) (1.2 g) was treated with *m*-chloroperoxybenzoic acid (550 mg) in spectral grade chloroform (80 ml) at 0 °C for 12 h. Work-up of the chloroform solution as described above and crystallization from 95% ethanol gave **16** (910 mg, 76%), m.p. 234–236 °C; $[\alpha]_D$ +540°; n.m.r. signals at 2.85 (1H, t, 3βH).

Anal. Calcd. for $C_{30}H_{50}O$: C, 84.44; H, 11.81. Found: C, 84.47; H, 11.69.

Rearrangement of 3α,4α-Epoxyfriedelane

A solution of 3α,4α-epoxyfriedelane (400 mg) in dry benzene (20 cc) was treated with $SnCl_4$ (0.2 cc). Work-up and recrystallization from methanol, then from hexane gave fine powdery flakes, m.p. 225–227 °C (300 mg); $[\alpha]_D$ −36°; ν_{max} 3510 cm^{-1} (hydroxyl) (BF_3 gave similar results but with lower yield).

Can. J. Chem. Downloaded from www.nrcresearchpress.com by 210.87.254.5 on 09/05/12
For personal use only.

The alcohol (200 mg) was treated with Jones' reagent (0.2 ml) until oxidation was complete. Quenching with water, filtration, and recrystallization gave a near quantitative yield of a ketone. Further recrystallization from hexane gave fine colorless plates, m.p. 248–250.5 °C; $[\alpha]_D$ −84°; ν_{max} 1710 cm^{-1} (3 ketone).

Anal. Calcd. for $C_{30}H_{48}O$: C, 84.84; H, 11.39. Found: C, 85.06; H, 11.30.

Spring (27) gives m.p. 250–252°; $[\alpha]_D$ −90°, and Chapon (36) gives m.p. 248°; $[\alpha]_D$ −84°.

The ketone was converted into alnusa-1,5-(10)-diene-3-one using the method of Spring and co-workers (27), m.p. 212.5–215°; ν_{max} 1690 cm^{-1} (3 ketone); λ_{max} 320, ε 5000. Spring (27) gives melting points between 211–215° and 216–217°; λ_{max} 322 mμ, ε 5500. A comparison sample was not available.

Acknowledgments

We thank the National Research Council of Canada for continued generous support and for a scholarship to J. J. Rosenfeld. One of us (R. R. King) is thankful to the Government of Ontario for a Graduate Fellowship. We are grateful to the Upjohn Company which provided generous samples of adrenosterone and 11-ketoprogesterone, and to the Armstrong Cork Company which supplied the cork wax for the extraction of friedelin. We express our gratitude to Mr. R. Sampson (n.m.r. spectra), Dr. R. R. Fraser (100 MHz n.m.r.), Dr. R. A. Bell, Dr. D. B. Maclean (mass spectra and n.O.e.), and finally to Professor Guy Ourisson (Institut de Chimie, Strasbourg, France) for his hospitality during the preparation of this manuscript.

1. G. Biglino, J. M. Lehn, and G. Ourisson. Tetrahedron Letters, 1651 (1963).
2. G. Ourisson, P. Crabbé, and O. Rodig. Tetracyclic triterpenes. Holden-Day, San Francisco. 1964. p. 123.
3. W. T. de Kock, P. R. Enslin, K. B. Norton, D. H. R. Barton, B. Sklarz, and A. A. Bothner-By. J. Chem. Soc. 3828 (1963).
4. J. F. King and P. de Mayo. Molecular rearrangements. *Edited by* P. de Mayo. Interscience Publishers, Inc., New York. 1964. p. 813; C. H. Heathcock and T. R. Kelly. Tetrahedron, **24**, 3753 (1968); M. M. Janot, C. Monneret, Q. Khuong-Huu, and R. Goutarel. Compt. Rend. C, **265**, 1468 (1967).
5. D. H. R. Barton, J. F. McGhie, M. K. Pradhan, and S. A. Knight. J. Chem. Soc. 876 (1955); D. Arigoni, R. Viterbo, M. Dunnenberger, O. Jeger, and L. Ruzicka. Helv. Chim. Acta, **37**, 2306 (1954).
6. A. Rosowsky. Heterocyclic compounds. Vol. 19. Part I. *Edited by* A. Weissberger. Interscience Publishers, Inc., New York. 1964. p. 1.
7. H. B. Henbest and T. I. Wrigley. J. Chem. Soc. 4596, 4765 (1957).
8. N. L. Wendler. Molecular rearrangements. *Edited by* P. de Mayo. Interscience Publishers, Inc., New York. 1964. p. 1022, and references cited therein; A. K. Ganguly, T. R. Govindachari, and A. Manmade. Tetrahedron, **23**, 3847 (1967).
9. J. W. Blunt, J. M. Coxon, M. P. Hartshorn, and D. N. Kirk. Tetrahedron, **23**, 1811 (1967); J. C. Jacquesy, J. Levisalles, and J. Wagnon. Chem. Commun. 25 (1967); M. Fetizon and P. Foy. Chem. Commun. 1005 (1967).
10. J. D. Willett, K. B. Sharples, K. E. Lord, E. E. van Tamelen, and R. B. Clayton. J. Biol. Chem. **242**, 4182 (1967), and references cited therein.
11. D. Lavie and M. K. Jain. Chem. Commun. 278 (1967).
12. G. P. Cotterrell, T. G. Halsall, and M. J. Wriglesworth. Chem. Commun. 1121 (1967); D. Lavie and E. C. Levy. Tetrahedron Letters, 2097 (1968).
13. E. D. Brown and J. K. Sutherland. Chem. Commun. 1060 (1968); H. Hikino, K. Agatsuna, and T. Takemoto. Tetrahedron Letters, 931 (1968). K. Wada and K. Murakata. Tetrahedron Letters, 4677 (1968).
14. C. J. Sih. J. Org. Chem. **26**, 4716 (1961).
15. S. Bernstein, R. Littell, and J. H. Williams. J. Am. Chem. Soc. **75**, 1482 (1953); S. Bernstein, R. H. Lenhard, and J. H. Williams. J. Org. Chem. **18**, 1166 (1953); **19**, 41 (1954).
16. E. Eliel. Stereochemistry of carbon compounds. McGraw-Hill Book Co., Inc., New York. 1962. p. 292.
17. J. M. Coxon, M. P. Hartshorn, and D. N. Kirk. Tetrahedron, **20**, 2531 (1964).
18. J. W. Blunt, M. P. Hartshorn, and D. N. Kirk. Tetrahedron, **22**, 3195 (1966).
19. R. W. Franck and K. Yanagi. J. Org. Chem. **33**, 811 (1968); W. Nagata, T. Terasawa, and K. Tori. J. Am. Chem. Soc. **86**, 3746 (1964); K. Tori and T. Komeno. Tetrahedron, **21**, 309 (1965); T. Schaefer, W. F. Reynolds, and T. Yonemoto. Can. J. Chem. **41**, 2969 (1963); S. Winstein, P. Carter, F. A. L. Anet, and A. J. R. Bourn. J. Am. Chem. Soc. **87**, 5247 (1965); W. H. Baarschers, R. R. Arndt, K. Pachler, J. A. Weisbach, and B. Douglas. J. Chem. Soc. 4778 (1964); B. V. Cheney. J. Am. Chem. Soc. **90**, 5386 (1968).
20. F. A. L. Anet and A. J. R. Bourn. J. Am. Chem. Soc. **87**, 5250 (1965). R. H. Martin and J. C. Nouls. Tetrahedron Letters, 2727 (1968), and references cited therein.
21. P. V. Demarco, E. Farkas, D. Doddrell, B. L. Mylari, and E. Wenkert. J. Am. Chem. Soc. **90**, 5480 (1968).
22. J. A. Marshall, N. Cohen, and K. R. Arenson. J. Org. Chem. **30**, 762 (1965); R. E. Ireland and P. W. Schiess. J. Org. Chem. **28**, 6 (1963); J. W. ApSimon, P. V. Demarco, and J. Lemke. Can. J. Chem. **43**, 2793 (1965).
23. E. L. Eliel, N. L. Allinger, S. J. Angyal, and G. A. Morrison. Conformational analysis. Interscience Publishers, Inc., New York. 1965. p. 296; E. L. Eliel. *In* Steric effects in organic chemistry. *Edited by* M. S. Newman. John Wiley and Sons, Inc., New York. 1956. p. 130.
24. N. L. Wendler, R. P. Graber, C. S. Snoddy, Jr., and F. W. Bollinger. J. Am. Chem. Soc. **79**, 4476 (1957).
25. S. O. Chan and E. J. Wells. Can. J. Chem. **45**, 2123 (1967), and references cited therein.
26. M. Karplus. J. Am. Chem. Soc. **85**, 2870 (1963); K. L. Williamson and W. S. Johnson. J. Am. Chem. Soc. **83**, 4623 (1961).

27. S. LIEBERMAN, L. B. HARITON, P. HUMPHRIES, C. P. RHOADS, and K. DOBRINER. J. Biol. Chem. **196**, 793 (1952); C. W. SHOPPEE. Helv. Chim. Acta, **30**, 766 (1947).
28. R. HODGES, S. G. MCGEACHIN, and R. A. RAPHAEL. J. Chem. Soc. 2515 (1963).
29. E. J. COREY and J. J. URSPRUNG. J. Am. Chem. Soc. **78**, 5041 (1956).
30. J. L. COURTNEY, R. M. GASCOIGNE, and A. Z. SZUMER. J. Chem. Soc. 881 (1958); R. M. COATES. Tetrahedron Letters, 4143 (1967); H. W. WHITLOCK, JR. and M. C. SMITH. Tetrahedron Letters, 821 (1968).
31. J. M. BEATON, F. S. SPRING, R. STEVENSON, and J. L STEWART. Tetrahedron, **2**, 246 (1958).
32. K. HEUSLER and A. WETTSTEIN. Chem. Ber. **87**, 1301 (1954); H. L. HERZOG, M. J. GENTLES, A. MITCHELL, E. B. HERSHBERG, and L. MANDELL. J. Am. Chem. Soc. **81**, 6478 (1954).
33. W. G. DAUBEN, G. A. BOSWELL, JR., W. TEMPLETON, J. W. MCFAFLAND, and G. H. BEREZIN. J. Am. Chem. Soc. **85**, 1672 (1963); J. BASCOUL and A. CRASTES DE PAULET. Chem. Commun. 256 (1968); J. W. BLUNT, M. P. HARTSHORN, and D. N. KIRK. J. Chem. Soc. C, 635 (1968); W. HERZ and H. J. WAHLBORG. J. Org. Chem. **30**, 1881 (1965); D. GOLDSMITH. Abstract F 27, 5th IUPAC Intern. Conf. Nat. Prod. London, July 1968; D. A. OKORIE and D. A. H. TAYLOR. Chem. Commun. 737 (1968); F. C. CHANG and C. K. CHIANG. Chem. Commun. 1156 (1968).
34. G. ADAM, K. SCHREIBER, J. TOMKA, Z. VOTICKY, and A. VASSOVA. Tetrahedron Letters, 2815 (1968).
35. G. ROSENKRANZ, O. MANCERA, and F. SONDHEIMER. J. Am. Chem. Soc. **76**, 2227 (1954).
36. J. W. APSIMON and R. R. KING. Chem. Commun. 1214 (1967).

Can. J. Chem. Downloaded from www.nrcresearchpress.com by 210.87.254.5 on 09/05/12
For personal use only.

Can. J. Chem. Downloaded from www.nrcresearchpress.com by 210.87.254.5 on 09/05/12
For personal use only.

Pyridazino[4,5-*b*]indole derivatives

THOMAS NOGRADY AND LEESON MORRIS
Chemistry Department, Loyola College, Montreal 262, Quebec

Received March 13, 1968

A series of pyridazino[4,5-*b*]indole lactams and their reduction products was prepared in an attempt to uncover monoamine oxidase inhibitory activity. The reduction and nuclear magnetic resonance spectra of these compounds are dealt with. Some are weak analgesics but no other pharmacological activity was found.

Canadian Journal of Chemistry, 47, 1999 (1969)

In our attempts to uncover novel monoamine oxidase inhibitory compounds we synthesized some 2-indolylcarbohydrazide derivatives (1). It seemed interesting to close ring C by insertion of one more carbon atom and this way obtain the pyridazino[4,5-*b*]indole ring system which can be considered as an azacarboline. Since many carboline alkaloids related to harmine are strong reversible MAO inhibitors (2), the combination of the carboline system with hydrazine seemed to be attractive also from a pharmacological point of view.

Only basic information is available on pyridazinoindoles and very few derivatives known. The [3,4-*b*] isomer was described by Kobayashi and Furukava (3). The [4,5-*b*] isomer was first reported by King and Stiller (4) who obtained it by heating 2-carbethoxy-3-formylindole *p*-nitrophenylhydrazone to 300° and obtained the cyclic hydrazide. Other authors (5–7) used basically the same method of ring closure, while some (8, 9) started from 2- or 3-indolylmethylhydrazines and condensed them with aldehydes to obtain the cyclized product.

In our series the 4-oxopyridazino[4,5-*b*]-indoles and their 1,2,3,4-tetrahydro derivatives were prepared according to the scheme shown below.

It is quite remarkable that the sequence of basically identical reactions, i.e. formylation and condensation with hydrazine derivatives, used in preparing the compounds, is responsible for the formation or absence of the Δ^1 double bond. This is due to the unusual formation of the

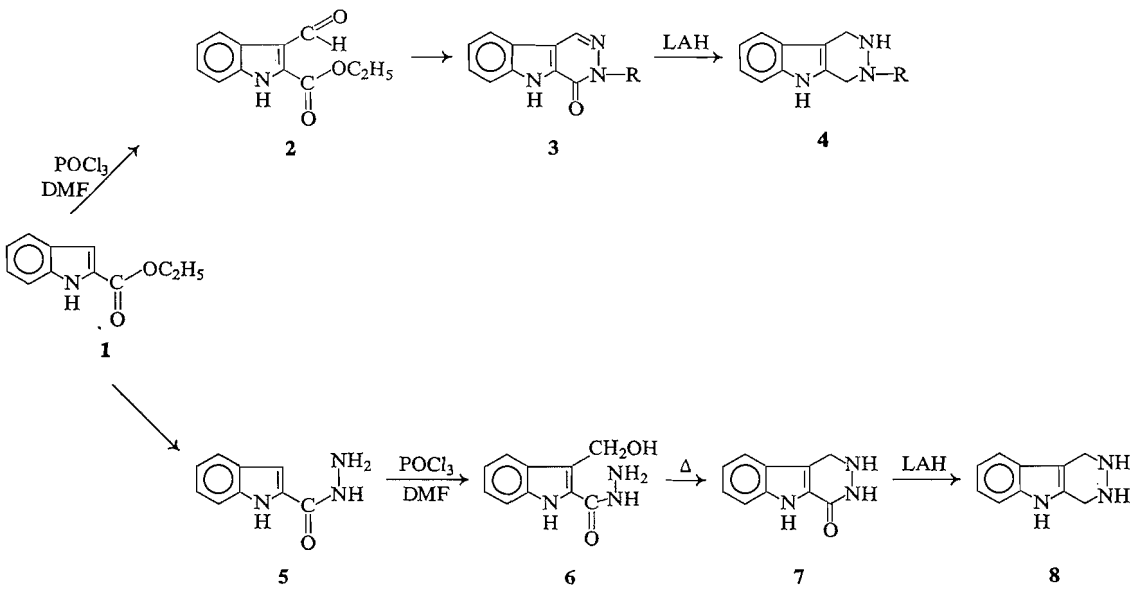

FIG. 1. Synthesis of pyridazoindoles.

TABLE I

3-Substituted 3,4-dihydro-4-oxo-pyridazino[4,5-*b*]indoles

Compound	R	Melting point (°C)	Solvent of crystallization	Nitrogen analysis Found	Nitrogen analysis Calcd.	Yield (%)	Method
9	—H	333–336	Dioxane	22.55	22.70	70	*
10	—CH(CH$_3$)$_2$	219–220	Ethanol	18.64	18.49	61	A
11	—CH$_3$	298–299	Butanol	20.87	21.09	95	A
12		229–230	DMF–water	15.71	16.08	85	B
13	—CH$_2$—CH$_2$—N(CH$_3$)$_2$	183–184	Ethanol	17.26 (2·HCl)	17.02	76	A
14	—CH$_2$—CH$_2$—CH$_2$—N(CH$_3$)$_2$	164–165	Methanol–water	21.01	20.72	77	C
15	—CH$_2$—CH$_2$—	224–225	Ethanol	23.42	23.55	70	C

*Method taken from ref. (7*a*).

3-hydroxymethylindole-2-carbohydrazine (**6**) during the DMF–$POCl_3$ formylation of indole-2-carbohydrazide (**5**) as described by Harradance and Lions (5), who obtained this compound in another way. The presence of the hydroxymethyl group (and the absence of any aldehyde proton) in **6** was proved by spectroscopy. The nuclear magnetic resonance (n.m.r.) spectrum of **6** (in DMSO-d_6) showed a CH_2 singlet at 2.80 p.p.m. (δ) integrating for two protons, an aromatic multiplet centered at 7.4 p.p.m., and two broad NH bands at 10.56 and 11.38 p.p.m., both exchangeable by D_2O. No aldehyde proton could be seen in the 9–10 p.p.m. region of the spectrum. The CH_2 singlet at 2.80 p.p.m. might appear more upfield than usual, since the corresponding resonance in benzyl alcohol is at 4.58. On inspecting the n.m.r. spectrum of 3-indolylmethanol however, one finds the CH_2 singlet at 3.83 p.p.m. (δ), also higher than expected.

In the ultraviolet (u.v.) spectrum, three maxima are visible: 306 (3.87), 251 (3.43), and 220 (3.69) mμ. In an alkaline medium practically no bathochromic shift could be seen, the maxima being at 310, 250, and 220 mμ. By comparison the ester-aldehyde **2** shows maxima at 322 (4.19), 253 (4.10), 245.5 (4.16), and 279.5 (4.22) mμ, which shift in an alkaline medium to 360 (4.79) and 273.5 (4.86), with strong tailing around 220–230 mμ. This bathochromic shift is due to the formation of the indolenine alcohol (cf. ref. 10).

The infrared (i.r.) spectrum (in KBr disk) shows a broad associated band in the OH/NH stretching region at 3.05–3.25 μ, the amide carbonyl at 6.40 μ, a fairly sharp, strong peak at 7.70 μ which could be O—H deformation, C—O stretching at 9.10 μ, and the disubstituted phenyl at 13.5 μ, as the principal peaks.

The condensation of 2-carbethoxy-3-formylindole (**2**) with hydrazine derivatives is more capable of variations in introducing a substituent in N-3, so our efforts were concentrated on preparing a series of 3,4-dihydro-4-oxopyridazines (Table I) rather than the tetrahydro derivatives and reduce them afterwards.

The reduction of the cyclic hydrazide (**3**) proved to be surprisingly facile considering reports on the failure to reduce aliphatic hydrazides (11) and 1-oxocarbolines (12) with $LiAlH_4$. The 4-oxopyridazino[4,5-*b*]indoles were refluxed overnight with a great excess of LAH in dioxane and excellent yields were obtained (Table II). After completion of our experiments the LAH reduction of 1-methyl-3-arylpyridaz-6-

Can. J. Chem. Downloaded from www.nrcresearchpress.com by 210.87.254.5 on 09/05/12
For personal use only.

TABLE II

3-Substituted 1,2,3,4-tetrahydro-pyridazino[4,5-*b*]indoles

Compound	R	Melting point (°C)	Solvent of crystallization	Nitrogen analysis Found	Nitrogen analysis Calcd.	Yield (%)
16	—H	235–237	Methanol	19.86	20.04	90
17	$-CH_3$	245–246	Methanol	18.29 (.HCl)	18.02	96
18	$-CH(CH_3)_2$	163–164	Methanol–water	19.65	19.52	95
19	—C$_6$H$_5$	222–223 (decomp.)	Acetone	16.55	16.99	95
20	$-CH_2-CH_2-N(CH_3)_2$	159–160	*i*-Propanol–hexane	22.66	22.93	90
21	$-CH_2-CH_2-CH_2-N(CH_3)_2$	146–147	Acetone	21.59	21.68	95
22	$-CH_2-CH_2-N$ piperazine NH	183–184	Benzene	24.66	24.54	86

one and related compounds was reported (13) but a 96 h reflux period yielded only 20% of pure reduced product.

In this reaction however the C=N double bond remains intact. In our reductions the C=N double bond is also reduced, as proved by n.m.r. spectra. In a representative example, the 1,2,3,4-tetrahydro-5*H*-pyridazino[4,5-*b*]indole (compound **17**), an N—CH_3 singlet is found at 2.88 p.p.m. (δ), and an aromatic multiplet centered at 7 p.p.m. The fairly well separated singlets at 4.16 and 4.23 p.p.m. (δ) are of equal intensity and integrate for 4 protons. They represent the 1- and 4-CH_2 groups; no olefinic protons are discernible. In the *N*-phenyl analogue, the corresponding protons are at 4.68 and 4.70 p.p.m. respectively.

In attempts to obtain the 4-methylpyridazino-[4,5-*b*]indole, the aza analogue of harmane, we tried the Bischler–Napieralski ring closure with phosphorus pentoxide, polyphosphoric acid, polyphosphate ester, and ethanolic HCl on 3-formylindole acetylhydrazone, without success.

Pharmacological Results

The only pharmacological effect shown by compounds **9**, **12**, **15**, and **16** was a weak analgetic activity (Median effective dose 50–150 mg/kg). No anti-histamine or central nervous system activity was noticed.

Experimental

All melting points were determined on a Gallenkamp block and are corrected; boiling points are uncorrected. The i.r. spectra were taken in KBr disks on a Beckman IR-8 instrument, and n.m.r. spectra were taken on a Varian A-60 spectrometer in trifluoracetic acid if not stated otherwise. Analyses were performed by Dr. C. Daesslé, Montreal.

3-Dimethylaminopropylhydrazine

Dimethylaminopropyl chloride·HCl (14.8 g) was dissolved in 75 ml ethanol, added slowly to 13.5 g refluxing hydrazine (anhydrous), and the solution refluxed for 4 h. After cooling, the precipitated hydrazine salt was filtered off, the solvent removed, and the residue distilled. The yield was 5.8 g (53.0%) b.p.$_{10}$ 75–80°; n_D^{20} 1.4611. The hydrochloride was prepared in ethanol–ether, and melted at 197–198°.

Anal. Calcd. for $C_5H_{15}N_3 \cdot 2HCl$: N, 22.05. Found: N, 21.78.

N-(β-Hydrazinoethyl)piperazine

N-(β-chloroethyl)piperazine (5 g) was dissolved in 10 ml water, 20 ml of anhydrous hydrazine added, and the solution refluxed for 4 h. After cooling, the solution was saturated with solid NaOH and the separated oil extracted with tetrahydrofuran. The organic phase was dried over K_2CO_3 and distilled; yield 3.2 g (95%), b.p.$_{12}$ 140–145°. The HCl salt, prepared in ethanol, melted at 107–109° (decomp.).

Can. J. Chem. Downloaded from www.nrcresearchpress.com by 210.87.254.5 on 09/05/12
For personal use only.

Can. J. Chem. Downloaded from www.nrcresearchpress.com by 210.87.254.5 on 09/05/12
For personal use only.

Anal. Calcd. for $C_6H_{16}N_4 \cdot 3HCl$: N, 22.09. Found: N, 21.70.

1,2,3,4-Tetrahydro-4-oxo-5H-pyridazino[4,5-b]indole (7) (5)

Indole-2-carbohydrazide **5** (ì) (0.5 g) was dissolved in 4 ml dimethyl formamide and added slowly to a solution of 0.5 ml $POCl_3$ in 4 ml dimethyl formamide. After 1 h at room temperature the solution was diluted with water and 0.41 g (77%) yellow crystals isolated by filtration, m.p. 195°. The melt resolidified and melted again at 285–288°. Recrystallized from *n*-butanol or dioxane they melted directly at 294–295°.

Anal. Calcd. for $C_{10}H_9N_3O$: C, 64.16; H, 4.85; N, 22.45. Found: C, 64.19; H, 4.63; N, 22.56.

The low melting compound is supposedly the 3-hydroxymethyl derivative **6** which cyclizes on heating in any way to **7**. Spectra of this compound were discussed in the theoretical part. The cyclized product shows a single carbonyl peak at 6.15 μ and broad indistinct bands in the 3–4 μ region.

*Method A. 3,4-Dihydro-3-methyl-4-oxo-5H-pyridazino[4,5-b]indole (**11**)*

A solution of 4.32 g 2-carbethoxy-3-formylindole and 7.5 ml methylhydrazine was refluxed gently in 50 ml glycerol for 15 min. The solution first became yellow, then colorless crystals separated. These were filtered off after cooling and dilution with water; yield 3.79 g (95%), m.p. 298–300°, unchanged after recrystallization from *n*-butanol.

Nuclear magnetic resonance spectrum: 4.30 (—CH_3) (3H), 7.2–8.2 (aromatic and C—H) (5H), 9.1 (N—H) (1H).

*Method B. 3,4-Dihydro-3-phenyl-4-oxo-5H-pyridazino[4,5-b]indole (**12**)*

2-Carbethoxy-3-formylindole (1.08 g) was dissolved in 20 ml glacial acetic acid and 2.5 ml freshly distilled phenylhydrazine were added. The solution became warm and yellow crystals of the phenylhydrazone separated, but dissolved upon heating. After refluxing for 1 h the crystals were filtered from the cooled reaction mixture and washed with water; yield 1.1 g (85%) m.p. 329–330° (from DMF–water).

Nuclear magnetic resonance spectrum: 7.6–8.6 (aromatic and C—H) (10H), 9.2 (N—H) (1H).

*Method C. 3,4-Dihydro-3-(γ-dimethylaminopropyl)-4-oxo-5H-pyridazino[4,5-b]indole (**14**)*

2-Carbethoxy-3-formylindole (1.08 g), 3.45 g 3-dimethylaminopropyl hydrazine, and 3 drops of glacial acetic acid were heated on the steam bath for 30 min until a gentle gas evolution ceased. The homogeneous mixture was now kept at 135–140° for 2 h more. On cooling, white needles separated which were filtered off, washed with water, and recrystallized from 50% methanol–water, yield 1.05 g (77%), m.p. 164–165°.

Reduction with $LiAlH_4$

The cyclic hydrazides were dissolved in 25–50 volumes of dry dioxane, an equal weight (5–8 moles) of $LiAlH_4$ was added cautiously, and the reaction mixture refluxed for 16 h. After cooling, 3 ml water were added for each gram of $LiAlH_4$ and worked up in the usual way. The pyridazines separated as solids in very good yields (see Table II).

Acknowledgments

This investigation was supported by Bristol Laboratories, Syracuse, New York. Pharmacological screening was performed by Dr. M. H. Pindell and his staff of Bristol Laboratories, to whom thanks are due.

1. T. Nogrady and L. Morris. J. Med. Chem. **9**, 438 (1966).
2. A. Pletscher, K. F. Gey, and P. Zeller. *In* Progress in drug research. Vol. 2. *Edited by* E. Jucker. Interscience Publishers, Inc., New York. 1960. p. 455.
3. G. Kobayashi and S. Furukawa. Chem. Pharm. Bull. **12**, 1129 (1964).
4. H. King and E. T. Stiller. J. Chem. Soc. 468 (1937).
5. R. H. Harradance and F. Lions. J. Proc. Roy. Soc. New South Wales, **72**, 221 (1939); Chem. Abstr. **33**, 6838 (1939).
6. R. S. Staunton and A. Topham. J. Chem. Soc. 1889 (1953).
7. (*a*) N. N. Suvorov, Zh. D. Ovchinnikova, and Yu. N. Sheinker. Zh. Obshch. Kim. **31**, 2333 (1961); Chem. Abstr. **56**, 3478 (1962). (*b*) N. N. Suvorov, Zh. D. Ovchinnikova, E. M. Peresleni, and Yu. N. Sheinker. Khim. Geterocikl. Soed. 926 (1965); Chem. Abstr. **64**, 17588 (1966).
8. J. Thesing and C. H. Willersinn. Chem. Ber. **89**, 1195 (1956).
9. H. Keberle and K. Hoffman. Gazz. Chim. Ital. **93**, 238 (1963).
10. M. F. Bartlett, D. F. Dickel, and W. I. Taylor. J. Am. Chem. Soc. **80**, 126 (1958).
11. R. L. Hinman. J. Am. Chem. Soc. **78**, 2463 (1956).
12. R. A. Abramovitch and D. Shapiro. J. Chem. Soc. 4589 (1956).
13. G. Leclerc and C. G. Wermuth. Bull. Soc. Chim. France, 1307 (1967).

Can. J. Chem. Downloaded from www.nrcresearchpress.com by 210.87.254.42 on 09/05/12
For personal use only.

Chemistry of the aminochromes. Part XI. Studies on 2-methylaminochromes[1,2,3]

O. HUTZINGER AND R. A. HEACOCK
Atlantic Regional Laboratory, National Research Council of Canada, Halifax, Nova Scotia

Received July 10, 1968

2-Methyladrenochrome and 1-ethyl-2-methylnoradrenochrome have been prepared by oxidation of 3,4-dihydroxyephedrine and 3,4-dihydroxyhomoephedrine with silver oxide. The corresponding 7-iodoaminochromes were obtained when the oxidations were carried out with potassium iodate. The expected 3,5,6-triacetoxyindoles were formed by treatment of these aminochromes with acetic anhydride and pyridine and the corresponding 5,6-dihydroxyindoles (isolated as their diacetyl derivatives) were obtained by reduction of the aminochromes with sodium borohydride or sodium hydrosulfite. An improved procedure for the synthesis of 3,4-dihydroxyephedrine (α-methyladrenaline) is also described.

Canadian Journal of Chemistry, 47, 2003 (1969

Only one 2-alkyl-substituted aminochrome had been isolated as a crystalline solid at the time that this investigation was begun. Bu'Lock and Harley-Mason obtained a deep-red crystalline product, described as 2-iodo-2-methylnoradrenochrome on oxidation of α-methylnoradrenaline (3,4-dihydroxynorephedrine) with potassium iodate (1). It has subsequently been shown that, like all other iodoaminochromes, this product is a 7-iodo derivative (i.e. 7-iodo-2-methylnoradrenochrome (**1**)) (2). 2-Methylnoradrenochrome (**2**) (1), 2-ethylnoradrenochrome (**3**) (3), and 2-methylnorepinochrome (**4**) (4) have been prepared in solution and a monosemicarbazone of **2** has been isolated as a crystalline solid (1).

The synthesis and some properties of 4-methyladrenochrome (**5**) and 7-methyladrenochrome (**6**) have recently been reported by the authors (5). This paper reports some of the results of a general extension of this research to aminochromes alkylated in the 2-position; in particular to 2-methyladrenochrome (**7**) and 2-methyl-1-ethylnoradrenochrome (**8**) and their 7-iodo derivatives **9** and **10**.

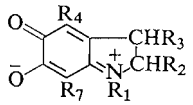

1, $R_1 = R_4 = H$; $R_2 = CH_3$; $R_3 = OH$; $R_7 = I$.
2, $R_1 = R_4 = R_7 = H$; $R_2 = CH_3$; $R_3 = OH$.
3, $R_1 = R_4 = R_7 = H$; $R_2 = C_2H_5$; $R_3 = OH$.
4, $R_1 = R_3 = R_4 = R_7 = H$; $R_2 = CH_3$.
5, $R_1 = R_4 = CH_3$; $R_2 = R_7 = H$; $R_3 = OH$.
6, $R_1 = R_7 = CH_3$; $R_2 = R_4 = H$; $R_3 = OH$.
7, $R_1 = R_2 = CH_3$; $R_3 = OH$; $R_4 = R_7 = H$.
8, $R_1 = C_2H_5$; $R_2 = CH_3$; $R_3 = OH$; $R_4 = R_7 = H$.
9, $R_1 = R_2 = CH_3$; $R_3 = OH$; $R_4 = H$; $R_7 = I$.
10, $R_1 = C_2H_5$; $R_2 = CH_3$; $R_3 = OH$; $R_4 = H$; $R_7 = I$.

Neither of the catecholamines required for the preparation of these aminochromes was available commercially. 3,4-Dihydroxyhomoephedrine (i.e. *N*-ethyl-α-methylnoradrenaline (**16**)) the precursor of **8** and **10** was prepared from veratrole (**11**) using essentially the method previously described by Lespagnol and Cuingnet (6) (i.e. **11** → **12** → **13** → **14** → **15** → **16**). An analogous route, used for the preparation of 3,4-dihydroxyephedrine (i.e. α-methyladrenaline (**19**)) is similar to a synthesis of this compound described in the patent literature (7). In the present case, however, the bromination reaction (i.e. **12** → **13**) was carried out in ether solution (cf. 6); the demethylation (**17** → **18**) by refluxing with concentrated hydrobromic acid, and a palladium–carbon, rather than a platinum catalyst was employed for the hydrogenation (**18** → **19**).

2-Methyladrenochrome (**7**) and 1-ethyl-2-methylnoradrenochrome (**8**) were both obtained, similarly to adrenochrome, as deep-red needles on oxidation of **19** and **16** with silver oxide in methanol (cf. 8). The monosemicarbazones **20** and **21** were obtained from aqueous solutions of the aminochromes **7** and **8**, prepared by oxidation of **19** and **16** with potassium ferricyanide in an aqueous sodium bicarbonate buffer (cf. 1). 7-Iodo-2-methyladrenochrome (**9**) and 1-ethyl-7-iodo-2-methylnoradrenochrome (**10**) were obtained as dark violet-brown crystalline solids

---

[1]NRCC No. 10375.
[2]Part X. W. Powell, R. A. Heacock, G. L. Mattok, and D. L. Wilson. Can. J. Chem. 47, 467 (1969).
[3]The preliminary phases of the work described in this paper were carried out by the authors in the laboratories of the Psychiatric Research Unit, University Hospital, Saskatoon, Saskatchewan.

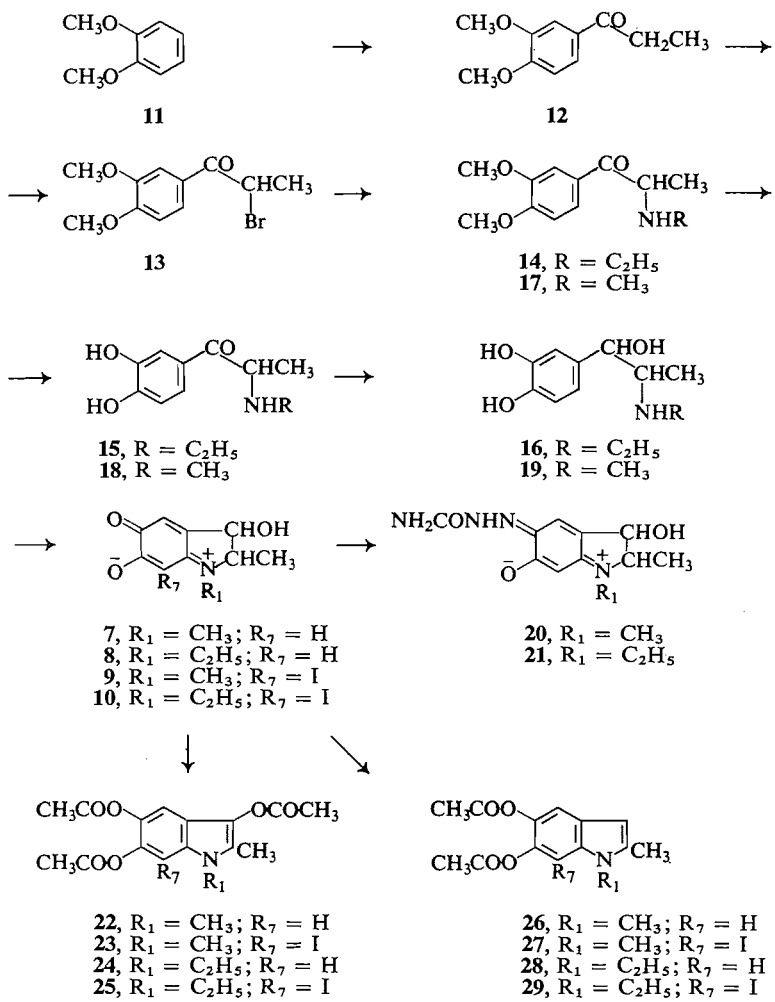

when **19** and **16** were oxidized with potassium iodate in aqueous solution.

The deep-red colors of aqueous solutions of the aminochromes **7** and **8** were rapidly discharged by alkali or aqueous zinc acetate; the resulting pale-yellow solutions probably contained the corresponding 5,6-dihydroxyindoxyls since, in ultraviolet light, they exhibited an intense yellow-green fluorescence, characteristic of this class of compounds (cf. ref. 9, p. 239). 3,5,6-Triacetoxyindoles are readily obtained from aminochromes with an OH group in the 3-position by treatment with a mixture of acetic anhydride and pyridine (cf. ref. 9, p. 242). 3,5,6-Triacetoxy-1,2-dimethylindole (**22**), 3,5,6-triacetoxy-7-iodo-1,2-dimethylindole (**23**), 3,5,6-triacetoxy-1-ethyl-2-methylindole (**24**), and 3,5,6-triacetoxy-1-ethyl-7-iodo-2-methylindole (**25**) were prepared in this manner from **7**, **8**, **9**, and **10** respectively.

5,6-Dihydroxyindoles are usually obtained on reduction of 3-hydroxy-substituted aminochromes (cf. ref. 9, p. 249). Because dihydroxyindoles of this type undergo oxidative polymerization in air to melanins, they are often more conveniently isolated as their diacetyl derivatives. 5,6-Diacetoxy-1,2-dimethylindole (**26**) and 5,6-diacetoxy-1-ethyl-2-methylindole (**28**) were obtained by acetylation of the corresponding 5,6-dihydroxyindoles, which, in turn, were prepared by reduction of the aminochromes **7** and **8** with sodium borohydride. The 5,6-diacetoxyindoles were prepared without the isolation of either the intermediate amino-

Can. J. Chem. Downloaded from www.nrcresearchpress.com by 210.87.254.42 on 09/05/12
For personal use only.

Can. J. Chem. Downloaded from www.nrcresearchpress.com by 210.87.254.42 on 09/05/12
For personal use only.

chromes or 5,6-dihydroxyindoles. 5,6-Diacetoxy-7-iodo-1,2-dimethylindole (**27**) and 5,6-diacetoxy-1-ethyl-7-iodo-2-methylindole (**29**) were prepared in an analogous manner from the 7-iodoaminochromes **9** and **10**. Here the oxidations were carried out in dilute aqueous solution with potassium iodate, and the reductions carried out with sodium hydrosulfite.

As would have been expected the presence of a 2-alkyl substituent in the aminochrome nucleus has little effect on the physical and chemical properties of the aminochromes. Further studies will be required to ascertain if the 2-alkyl group has any effect on the physiological activity of either the parent aminochromes (cf. ref. 9, p. 279) or the derived 5,6-dihydroxyindoles.

Experimental

*α-Methylamino-3,4-dimethoxypropiophenone Hydrochloride (**17**)*

A suspension of α-bromo-3,4-dimethoxypropiophenone (**13**) (119 g), prepared by the method of Lespagnol and Cuingnet (6), in a mixture of methanol (229 ml) and 30% w/v aqueous methylamine (150 ml), contained in a tightly stoppered flask, was stirred (magnetically) at room temperature until the solid had completely dissolved (ca. 45 min). The reaction mixture was then maintained at 37° overnight, after which time it was cooled and a mixture of 30% aqueous sodium hydroxide (200 ml) and ether[4] (200 ml) was added, with vigorous stirring. The system was allowed to separate into two phases and the ether layer was removed. The aqueous mother liquors were further extracted with ether (2 × 150 ml). The ether solutions were dried (K_2CO_3) and evaporated *in vacuo*. The oily residue was repeatedly evaporated with benzene to remove traces of water and was then dissolved in acetone (300 ml) and the solution saturated with dry hydrogen chloride gas. The hydrochloride (41.5 g; m.p. 207–209.5°) which separated as a colorless solid was removed by filtration and washed with a little cold acetone. The crude product was sufficiently pure to be used in the next stage of the synthesis.

An analytical sample of α-methylamino-3,4-dimethoxypropiophenone hydrochloride was obtained as colorless needles (m.p. 208–208.5° decomp.)[5] after repeated recrystallization from ethanol – ethyl acetate.

Anal. Calcd. for $C_{12}H_{18}ClNO_3$: C, 55.50; H, 6.98; N, 5.39; Cl, 13.65. Found: C, 55.25; H, 6.85; N, 5.49; Cl, 13.79.

*α-Methylamino-3,4-dihydroxypropiophenone (**18**)*

A solution of α-methylamino-3,4-dimethoxypropiophenone hydrochloride (40 g) in concentrated hydrobromic acid (124 ml) was boiled under reflux for 3 h. The dark solution was allowed to cool in a carbon dioxide atmosphere and then evaporated *in vacuo*. The dark residue was dissolved in methanol and decolorized with charcoal in a carbon dioxide atmosphere; after removal of the charcoal by filtration, dry ether was added to the yellowish-brown filtrate until a slight turbidity persisted. The solution was then saturated with dry ammonia gas. The impure base (mixed with ammonium bromide) which separated was filtered off, washed with a little cold acetone, and dried in a current of air. The crude material (17 g) was triturated with water (16 ml); the sludge so obtained was filtered and the remaining solid washed with water (5 × 10 ml) and acetone (2 × 25 ml). The α-methylamino-3,4-dihydroxypropiophenone (11.5 g), m.p. 191.5° (decomp.) obtained in this manner was sufficiently pure for the next stage in the synthesis and was not further purified.

*α-Methyladrenaline Hydrochloride (3,4-Dihydroxyphedrine Hydrochloride) (**19**)*

A suspension of α-methylamino-3,4-dihydroxypropiophenone (1.95 g) and 5% palladium–charcoal (1 g) in water (90 ml) and *N* hydrochloric acid (10 ml) was shaken in an atmosphere of hydrogen at atmospheric pressure and room temperature for 20 h. The reaction mixture was filtered and the filtrate evaporated *in vacuo* (T < 30°). The pale-violet residue (m.p. 182–182.5° decomp.) was repeatedly recrystallized from methanol – methyl acetate mixtures and gave α-methyladrenaline hydrochloride (1.5 g) in very small colorless plates, m.p. 190–191°; lit. m.p., 190–191° (10); 191–191.5° (11).

Anal. Calcd. for $C_{10}H_{16}ClNO_3$: C, 51.39; H, 6.90; N, 5.99; Cl, 15.17. Found: C, 51.50; H, 7.17; N, 5.71; Cl, 15.30.

*N-Ethyl-α-methylnoradrenaline Hydrochloride (3,4-Dihydroxyhomoephedrine Hydrochloride) (**16**)*

A suspension of α-ethylamino-3,4-dihydroxypropiophenone (2.09 g), prepared by the method of Lespagnol and Cuingnet (6), and 5% palladium–charcoal (1.0 g) in water (90 ml) containing *N* hydrochloric acid (10 ml) was shaken overnight in an atmosphere of hydrogen at atmospheric pressure and room temperature. After removal of the catalyst by filtration the solution was evaporated *in vacuo* (T < 50°). The white crystalline residue was repeatedly recrystallized from methanol–ether and gave *N*-ethyl-α-methylnoradrenaline hydrochloride as colorless prisms (1.15 g; m.p. 211–212°). Lespagnol and Cuingnet (6), who carried out the reduction in a slightly different manner reported m.p. 212–214°.

Anal. Calcd. for $C_{11}H_{18}ClNO_3$: C, 53.34; H, 7.32; N, 5.66; Cl, 14.32. Found: C, 53.36; H, 7.40; N, 5.52; Cl, 14.37.

*2-Methyladrenochrome (**7**)*[6]

Freshly prepared silver oxide (3.6 g) was added to a vigorously stirred solution of α-methyladrenaline hydrochloride (1.0 g) in methanol (20 ml). The stirring was continued for 3 min, after which time the reaction mixture

[4]Peroxide-free ether was used throughout this investigation.

[5]All melting points quoted in this paper are uncorrected.

[6]See preparation of adrenochrome by Heacock *et al.* (8).

Can. J. Chem. Downloaded from www.nrcresearchpress.com by 210.87.254.42 on 09/05/12
For personal use only.

was filtered through a Dowex-1 (Cl^-) resin bed[7] (diameter, 2.5 cm; height, 1.8 cm). Dry ether (30 ml) was added to the filtrate and 2-methyladrenochrome (0.22 g; totally decomposed without melting by 128°)[8] was obtained as dark-red needles after the solution had stood overnight at −20°.

Anal. Calcd. for $C_{10}H_{11}NO_3$: C, 62.16; H, 5.74; N, 7.25. Found: C, 62.11; H, 5.94; N, 7.10.

*1-Ethyl-2-methylnoradrenochrome (**8**)*

Oxidation of α-methyl-*N*-ethylnoradrenaline hydrochloride (1.0 g) with silver oxide (3.6 g) gave deep-red needles of 1-ethyl-2-methylnoradrenochrome (0.29 g; totally decomposed by 110°) when the product was isolated in the manner described above.

Anal. Calcd. for $C_{11}H_{13}NO_3$: C, 63.75; H, 6.32; N, 6.76. Found: C, 63.75; H, 6.34; N, 6.75.

*2-Methyladrenochrome Monosemicarbazone (**20**)*

A solution of α-methyladrenaline hydrochloride (0.5 g) in water (2.5 ml) was treated with potassium ferricyanide (2.35 g) and sodium bicarbonate (0.75 g) in water (6.25 ml). A solution containing semicarbazide hydrochloride (0.25 g) and sodium acetate (0.25 g) in water (2 ml) was added to the resulting deep-red 2-methyladrenochrome solution; after stirring at room temperature for 5 min the crude semicarbazone separated as an orange-brown solid (0.43 g). A pure sample of 2-methyladrenochrome monosemicarbazone was obtained as bright orange needles (totally decomposed by 222°) after repeated recrystallization of the crude product from aqueous pyridine.

Anal. Calcd. for $C_{11}H_{14}N_4O_3$: C, 52.79; H, 5.64; N, 22.39. Found: C, 52.80; H, 5.68; N, 22.19.

*1-Ethyl-2-methylnoradrenochrome Monosemicarbazone (**21**)*

1-Ethyl-2-methylnoradrenochrome monosemicarbazone (0.42 g) (orange-red prisms; m.p. 234° decomp.) was prepared from a solution of *N*-ethyl-α-methyladrenaline hydrochloride (0.5 g) (in 5 ml of water) in an analogous manner to that described above for the corresponding *N*-methyl derivative.

Anal. Calcd. for $C_{12}H_{16}N_4O_3$: C, 54.55; H, 6.10; N, 21.20. Found: C, 54.59; H, 6.26; N, 21.21.

*7-Iodo-2-methyladrenochrome (**9**)*

Potassium iodate (0.8 g) was added to a solution of α-methyladrenaline hydrochloride (0.5 g) in water (150 ml) and the reaction mixture stirred at room temperature for 1 h. 7-Iodo-2-methyladrenochrome (0.38 g) was obtained as a dark violet-brown crystalline solid (totally decomposed without melting by 96°) after the solution had stood at 4° for 2 h.

Anal. Calcd. for $C_{10}H_{10}INO_3$: C, 37.64; H, 3.16; N, 4.39; I, 39.78. Found: C, 37.57; H, 3.19; N, 4.22; I, 39.60

*1-Ethyl-7-iodo-2-methylnoradrenochrome (**10**)*

Potassium iodate (0.8 g) was added to a stirred solution of α-methyl-*N*-ethylnoradrenaline hydrochloride (0.5 g) in water (150 ml); the reaction mixture was stirred at room temperature for 1.5 h, and was then cooled in the refrigerator for a further 4.5 h. 1-Ethyl-7-iodo-2-methylnoradrenochrome (0.4 g) was obtained as a deep violet (almost black) crystalline solid (totally decomposed without melting by 97°).

Anal. Calcd. for $C_{11}H_{12}INO_3$: C, 39.66; H, 3.63; N, 4.20; I, 38.12. Found: C, 39.60; H, 3.74; N, 4.16; I, 38.26.

*3,5,6-Triacetoxy-7-iodo-1,2-dimethylindole (**23**)*

7-Iodo-2-methyladrenochrome (0.3 g) was dissolved in a mixture of acetic anhydride (5 ml) and dry pyridine (5 ml). The solution was allowed to stand overnight at room temperature and then added dropwise, with stirring, to an ice–water mixture. The aqueous product was extracted with ether (4 × 100 ml). The combined ether extracts were washed with 5% sodium bicarbonate solution (3 × 100 ml) and water (200 ml); benzene (100 ml) was added to the dried (Na_2SO_4) ethereal solution, and the ether removed *in vacuo*. The crude product, obtained in benzene solution, was purified chromatographically on a silica gel[9] column (3 in. × ¾ in.). Elution with benzene (600 ml) gave no identifiable products. Elution with ethyl acetate – benzene (5:95) (500 ml) gave a pale-pink solid which on recrystallization (charcoal) from benzene – light petroleum (b.p. 80–100°) gave colorless elongated prisms of 3,5,6-triacetoxy-7-iodo-1,2-dimethylindole (0.02 g; m.p. 186°).

Anal. Calcd. for $C_{16}H_{16}INO_6$: C, 43.15; H, 3.62; N, 3.15; I, 28.51. Found: C, 43.08; H, 3.65; N, 3.03; I, 28.75.

By analogous procedures the following compounds were prepared:

*3,5,6-Triacetoxy-1-ethyl-7-iodo-2-methylindole (**25**)*

Prepared from 1-ethyl-7-iodo-2-methylnoradrenochrome, as colorless prisms, m.p. 213°.

Anal. Calcd. for $C_{17}H_{18}INO_6$: C, 44.45; H, 3.95; N, 3.05. Found: C, 44.49; H, 4.04; N, 3.35.

*3,5,6-Triacetoxy-1,2-dimethylindole (**22**)*

Prepared from 2-methyladrenochrome, as colorless elongated prisms, m.p. 171°.

Anal. Calcd. for $C_{16}H_{17}NO_6$: C, 60.18; H, 5.37; N, 4.39. Found: C, 60.22; H, 5.30; N, 4.32.

*3,5,6-Triacetoxy-1-ethyl-2-methylindole (**24**)*

Prepared from 1-ethyl-2-methylnoradrenochrome, as colorless prisms, m.p. 152°.

Anal. Calcd. for $C_{17}H_{19}NO_6$: C, 61.25; H, 5.75; N, 4.20. Found: C, 61.05; H, 5.59; N, 4.14.

*5,6-Diacetoxy-1,2-dimethylindole (**26**)*

A solution of α-methyladrenaline hydrochloride (0.5 g) in water (10 ml) was oxidized by adding potassium ferricyanide (2.5 g) and sodium bicarbonate (0.8 g) in water (10 ml). Ether (50 ml) was added to the deep red aminochrome solution and solid sodium borohydride was then added portionwise until the red color of the aqueous phase had been totally discharged. The reaction mixture

[7]The resin (200/400 mesh size) was prepared by extensive washing with: (*1*) 3 *N* hydrochloric acid, (*2*) with water until neutral to litmus, and finally (*3*) with dry methanol.

[8]The decomposition points of all the aminochromes and aminochrome monosemicarbazones described in this paper were measured on a Leitz hot-stage instrument.

[9]In this and subsequent experiments the chromatographic silica gel used was obtained from the Koch-Light Laboratories Ltd. (200/300 mesh size).

Can. J. Chem. Downloaded from www.nrcresearchpress.com by 210.87.254.42 on 09/05/12
For personal use only.

was cautiously acidified with 2 *N* sulfuric acid; the ether layer was removed, and the mother liquors were extracted with a further quantity of ether (3 × 50 ml). A mixture of acetic anhydride (5 ml) and dry pyridine (5 ml) was added to the dried (Na_2SO_4) ethereal solutions. The ether was removed *in vacuo* (T < 30°) and, after standing at room temperature overnight, the acetylation mixture was added dropwise, with stirring, to an ice–water mixture. The product was extracted with ether (5 × 50 ml); the combined extracts were washed free of acetic acid with 5% aqueous sodium bicarbonate and water, and dried (Na_2SO_4). Evaporation *in vacuo* (T < 30°) gave a pale-yellow oil which slowly crystallized on standing. Recrystallization of the crude product from benzene – light petroleum (b.p. 80–100°) and finally from light petroleum alone gave very pale-yellow prisms of 5,6-diacetoxy-1,2-dimethylindole (0.01 g), m.p. 134–135°.

Anal. Calcd. for $C_{14}H_{15}NO_4$: C, 64.36; H, 5.79; N, 5.36. Found: C, 64.28; H, 5.76; N, 5.26.

5,6-Diacetoxy-1-ethyl-2-methylindole (28)

5,6-Diacetoxy-1-ethyl-2-methylindole (0.08 g) was obtained from *N*-ethyl-α-methylnoradrenaline hydrochloride (0.5 g) by an analogous procedure to that described above for the corresponding 1-methylindole (very pale-yellow needles from light petroleum (b.p. 100–120°), m.p. 137–138°.)

Anal. Calcd. for $C_{15}H_{17}NO_4$: C, 65.44; H, 6.22; N, 5.09. Found: C, 65.45; H, 6.22; N, 5.14.

5,6-Diacetoxy-7-iodo-1,2-dimethylindole (27)

Potassium iodate (0.9 g) was added to a solution of α-methyladrenaline hydrochloride (0.5 g) in water (400 ml) and the reaction mixture was stirred at room temperature for 2.5 h. Solid sodium hydrosulfite was added until the deep-violet color of the solution was completely discharged and the reaction mixture was extracted with ether (5 × 100 ml). A mixture of acetic anhydride (30 ml) and dry pyridine (30 ml) was added to the dried (Na_2SO_4) extract and the ether was removed *in vacuo* below 30°. After 16 h at room temperature, the reaction mixture was poured into an ice–water mixture; a white solid separated (0.25 g). On recrystallization from light petroleum (b.p. 80–100°) containing a little benzene this solid afforded 5,6-diacetoxy-7-iodo-1,2-dimethylindole (0.1 g) as colorless needles, m.p. 170–172°.

Anal. Calcd. for $C_{14}H_{14}INO_4$: C, 43.43; H, 3.65; N, 3.63; I, 32.79. Found: C, 43.48; H, 3.62; N, 3.58; I, 32.50.

5,6-Diacetoxy-1-ethyl-7-iodo-2-methylindole (29)

5,6-Diacetoxy-1-ethyl-7-iodo-2-methylindole was prepared from α-methyl-*N*-ethylnoradrenaline hydrochloride (0.5 g) in a similar manner to that described above for the corresponding 1-methyl compound. The product, (crude yield, 0.24 g) was obtained as colorless plates from benzene, m.p. 158–160°.

Anal. Calcd. for $C_{15}H_{16}INO_4$: C, 44.91; H, 4.02; N, 3.50; I, 31.64. Found: C, 44.97; H, 4.04; N, 3.53; I, 31.78.

Acknowledgment

The technical assistance of Mrs. B. D. Scott, of the Psychiatric Research Unit, University Hospital, Saskatoon, Saskatchewan is gratefully acknowledged.

1. J. Bu'Lock and J. Harley-Mason. J. Chem. Soc. 712 (1951).
2. R. A. Heacock, O. Hutzinger, B. D. Scott, J. W. Daly, and B. Witkop. J. Am. Chem. Soc. **85**, 1825 (1963).
3. C. Beaudet. Experientia, **7**, 291 (1951).
4. J. Bu'Lock and J. Harley-Mason. J. Chem. Soc. 2248 (1951).
5. R. A. Heacock and O. Hutzinger. Can. J. Chem. **43**, 2535 (1965).
6. A. Lespagnol and E. Cuingnet. Ann. Pharm. Franc. **18**, 445 (1960).
7. Les Laboratoires Dausse, French Patent No. 939,722, Nov. 23, 1948; Chem. Abstr. **45**, 5186 (1951).
8. R. A. Heacock, C. Nerenberg, and A. N. Payza. Can. J. Chem. **36**, 853 (1958).
9. R. A. Heacock. Advan. Heterocyclic Chem. **5**, 205 (1965).
10. M. Brockmühl, G. Ehrart, and L. Stein. U.S. Patent No. 1,877,756, Sept. 20, 1932; Chem. Abstr. **27**, 1095 (1933).
11. Ravensberg, G.m.b.H. Chemische Fabrik. German Patent No. 1,048,592, Jan. 15, 1959; Chem. Abstr. **55**, 4435 (1961).

Can. J. Chem. Downloaded from www.nrcresearchpress.com by 210.87.254.105 on 09/05/12
For personal use only.

Chemistry of the aminochromes. Part XII. Some new aminochromes and their derivatives[1-3]

R. A. HEACOCK AND O. HUTZINGER
Atlantic Regional Laboratory, National Research Council of Canada, Halifax, Nova Scotia

Received August 9, 1968

The synthesis of a number of new aminochromes (and their monosemicarbazones) derived from catecholamines containing: (*a*) a primary amino group and (*b*) an alkoxy group in the β-position of the ethylamine side chain is reported. Improved procedures for the preparation of some previously described aminochromes of these types including 7-iodonorepinochrome and adrenochrome methyl and ethyl ethers are also given.

Canadian Journal of Chemistry, 47, 2009 (1969)

In previous publications in this series the preparation, physical properties, and chemical reactivity of several new aminochromes have been described (1–3). This paper describes attempts to isolate a number of other new aminochromes as crystalline solids from catecholamines with: (*a*) a primary amino group and (*b*) an alkoxy group in the β-position of the ethylamine side chain.

Whilst the preparation of aminochromes from catecholamines containing a secondary amino group presents no particular problems (cf. review by Heacock, (4)) no simple non-halogenated aminochromes have, as yet, been obtained, as fully characterized crystalline solids, from primary catecholamines. Marquardt and Carl (5) reported that noradrenochrome (**1**) could be obtained as an ill-defined red-brown powder or as "red rings on the side of the flask" when noradrenaline (**2**) was oxidized with silver oxide in acetonitrile. The ultraviolet–visible absorption spectrum of **1** was described, but no other physical or analytical data were reported (5).

In view of the interest that has developed in recent years in the physiological activity of adrenochrome (cf. ref. 4, p. 279) it was considered desirable to investigate also the physiological activity of pure samples of noradrenochrome (**1**). However, attempts in the hands of the authors, to repeat and improve on the procedure of Marquardt and Carl for the preparation of **1** have met with little success. It was also not possible to obtain crystalline **1** by the oxidation of noradrenaline (**2**) with silver oxide in methanol, using the method commonly employed for the preparation of adrenochrome from adrenaline (6) or by oxidation of the base with the calculated quantity of iodic acid in aqueous methanol (cf. 7), a method that has been successfully used for the preparation of adrenochrome. Whilst red solutions were obtained using both of these procedures, only unidentified black amorphous solids could be isolated in either case. Similarly all attempts to prepare crystalline 2-methylnoradrenochrome (**3**) by the oxidation of 3,4-dihydroxynorephedrine (**4**) were unsuccessful.

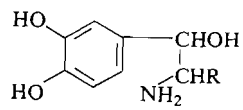

2, R = H
4, R = CH_3

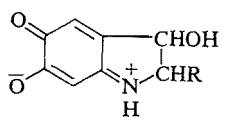

1, R = H
3, R = CH_3

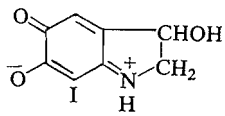

5

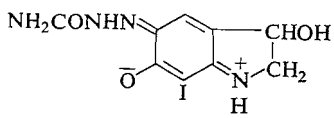

6

7-Iodonoradrenochrome (**5**) was first prepared by Bu'Lock and Harley-Mason in 1951 (8) by the oxidation of noradrenaline (**2**) with potassium iodate in aqueous solution. It was later shown that the copious formation of tarry by-products, that invariably occurred in this reaction, could be avoided if the reaction was carried out in more dilute solution under fairly strong acid conditions (9). A number of 7-halogenated aminochrome

[1]NRCC No. 10420.
[2]Part XI. Can. J. Chem. This issue.
[3]The preliminary phases of the work described in this paper were carried out by the authors in the laboratories of the Psychiatric Research Unit, University Hospital, Saskatoon, Saskatchewan.

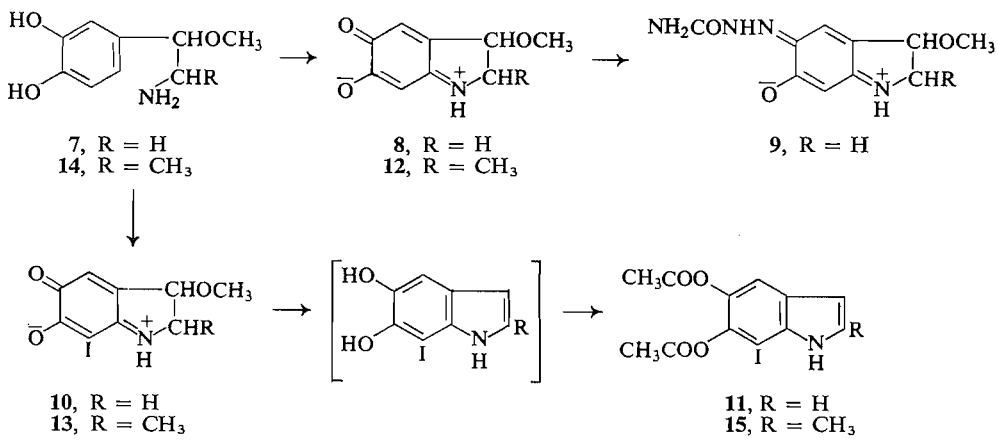

monosemicarbazones have recently been prepared by direct halogenation of the corresponding aminochrome monosemicarbazones and shown to exhibit potent hypotensive activity (10). A potentially very interesting member of this series, from the physiological standpoint, which was not reported in the original patent (10), is 7-iodonoradrenochrome monosemicarbazone (**6**). This compound has now been prepared by direct condensation of 7-iodonoradrenochrome (**5**) with semicarbazide.

Whilst red products were definitely obtained on the oxidation of noradrenaline methyl ether (**7**) with silver oxide either in methanol or acetonitrile it was not possible to isolate noradrenochrome methyl ether (**8**) as a crystalline solid from such solutions. However, noradrenochrome methyl ether monosemicarbazone (**9**) was obtained as a red microcrystalline solid from aqueous solutions of noradrenaline methyl ether (**7**) which had been oxidized with potassium ferricyanide. All attempts to prepare crystalline 7-iodonoradrenochrome methyl ether (**10**) by the oxidation of **7** with potassium iodate in aqueous solution were unsuccessful. There appears to be little doubt however that the iodoaminochrome **10** had formed, since the violet color of the solution was rapidly discharged by ascorbic acid, a reagent known to reduce aminochromes (cf. ref. 4, p. 253). 5,6-Diacetoxy-7-iodoindole (**11**) could be obtained by the acetylation of the ether-soluble reduction products. This product would have been expected since it is known that aminochromes with a 3-alkoxy group, like those with a 3-hydroxy group, give 5,6-dihydroxyindoles on reduction (11).

Similarly, all attempts to isolate crystalline 2-methylnoradrenochrome methyl ether (**12**) or 7-iodo-2-methylnoradrenochrome methyl ether (**13**) from solutions of oxidized α-methylnoradrenaline methyl ether (**14**) were not successful. As in the case of the oxidation products of noradrenaline methyl ether (**7**) however, it appeared that 7-iodo-2-methylnoradrenochrome methyl ether (**13**) was formed during the aqueous iodate oxidation since 5,6-diacetoxy-7-iodo-2-methylindole (**15**) was obtained on acetylation of the ether-soluble reduction products of **13**.

The formation of a crystalline iodo derivative of norepinochrome was first reported in 1951 (12). At that time neither the details of the preparative procedure nor the position of the iodine atom in the molecule was defined. This compound has now been obtained as a well-characterized violet-brown crystalline solid by the oxidation of dopamine (**16**) with potassium iodate under the conditions used to prepare 7-iodonoradrenochrome (**5**) (cf. 9). In common with all other iodoaminochromes the iodo derivative of norepinochrome is a 7-iodo derivative (i.e. **17**) since it gave 5,6-diacetoxy-7-iodoindole (**11**) on treatment with acetic anhydride and pyridine (cf. ref. 4, p. 242).

The iodoaminochrome **17** is probably the primary product obtained on oxidation of dopamine (**16**) with iodine, the reaction employed as the first stage of the commonly used estimation of dopamine in clinical chemistry. The chemistry of this method does not appear to be clearly understood (cf. ref. 4, p. 282).

The methyl and ethyl ethers of adrenochrome (**18** and **19**) were first isolated as their mono-

Can. J. Chem. Downloaded from www.nrcresearchpress.com by 210.87.254.105 on 09/05/12
For personal use only.

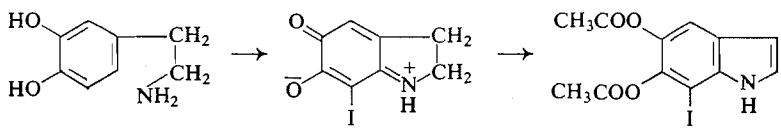

16 17 11

semicarbazones (13); the preparation of the crystalline aminochromes **18** and **19** in relatively poor yield was later reported by Heacock and Scott (1) who carried out the oxidation of adrenaline methyl and ethyl ether in acetonitrile with silver oxide. It has now been shown that **18** and **19** can be readily prepared by carrying out the oxidation in a methanol–ether medium.

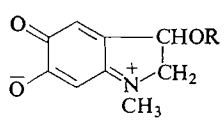

18, R = CH_3
19, R = C_2H_5

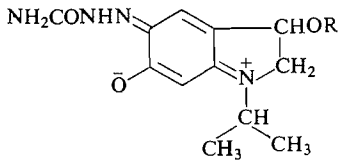

22, R = CH_3
23, R = C_2H_5

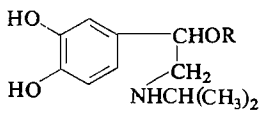

20, R = CH_3
21, R = C_2H_5

The preparation of the methyl and ethyl ethers of *N*-isopropylnoradrenaline (i.e. **20** and **21**) has recently been described (14). In view of the relatively small amount of research that has been carried out into the chemistry of the aminochrome ethers, attempts were made to prepare aminochromes (and their 7-iodo derivatives) from **20** and **21**. Whilst it was not possible to obtain these aminochromes in crystalline form it was possible to isolate crystalline monosemicarbazones of 1-isopropylnoradrenochrome methyl ether and 1-isopropylnoradrenochrome ethyl ether (i.e. **22** and **23**).

The results reported in this paper indicate some of the difficulties that are encountered in the synthesis of aminochromes derived from catecholamines containing a primary amino group or a β-alkoxy group in the ethylamine side chain.

Experimental

7-Iodonorepinochrome (17)

Potassium iodate (0.8 g) was added to a solution of dopamine hydrochloride (0.5 g) in water (150 ml). The reaction mixture was stirred at room temperature for 1 h, after which time the pH of the solution was adjusted to 2 by the dropwise addition of concentrated hydrochloric acid; 7-iodonorepinochrome (0.28 g; totally decomposed without melting by 106°[4]) was obtained as a violet-brown crystalline solid after the deep red-violet solution had been allowed to stand in the refrigerator overnight.

Anal. Calcd. for $C_8H_6INO_2$: C, 34.94; H, 2.20; N, 5.09; I, 46.15. Found: C, 34.85; H, 2.11; N, 5.16; I, 45.97.

Acetylation of 7-Iodonorepinochrome (17); Preparation of 5,6-Diacetoxy-7-iodoindole (11)

7-Iodonorepinochrome (1.2 g) was dissolved in a mixture of acetic anhydride (35 ml) and dry pyridine (35 ml) and the solution was allowed to stand at room temperature overnight. The reaction mixture was then added dropwise to a stirred ice–water mixture (1500 ml) and the aqueous reaction product was extracted with ether[5] (6 × 150 ml). The combined ether extracts were washed with saturated aqueous sodium bicarbonate (until free of acetic acid) and with water (2 × 100 ml). The yellow oily residue, which remained on concentration of the dried (Na_2SO_4) solution, *in vacuo*, gave after recrystallization from benzene – light petroleum (b.p. 80–100°), pale-fawn colored crystals (0.41 g; m.p. 123–126°) of crude 5,6-diacetoxy-7-iodoindole. This product was purified first by chromatography on a short silica gel[6] column with benzene – light petroleum (b.p. 60–80°) (2:1) as eluant and finally by further recrystallization from benzene – light petroleum (b.p. 80–100°). In this manner a pure sample of 5,6-diacetoxy-7-iodoindole (0.25 g; m.p. 127–128°) was obtained as a colorless crystalline solid. The melting point of a sample of 5,6-diacetoxy-7-iodoindole prepared by acetylation of the reduction product of 7-iodoadrenochrome (cf. 15) was undepressed on admixture with a sample of the same compound, prepared by the method described above.

7-Iodonoradrenochrome Monosemicarbazone (6)

A suspension of 7-iodonoradrenochrome (0.3 g), prepared by the method of Heacock and Scott (9), sodium acetate (0.5 g; anhydrous), and semicarbazide hydrochloride (0.5 g) in water (2.5 ml) was stirred at room temperature for 2 h. The crude product, an orange-brown solid (0.23 g), was filtered off, washed with a little cold water, and air dried. The residue was repeatedly extracted with boiling ethanol. The combined extracts were concentrated to small volume and an equal quantity of dry

[4]The decomposition points were measured on a Leitz hot-stage instrument.

[5]Peroxide-free ether was used throughout this investigation.

[6]In this and subsequent experiments the chromatographic silica gel used was obtained from the Koch-Light Laboratories Ltd. (200/300 mesh size).

Can. J. Chem. Downloaded from www.nrcresearchpress.com by 210.87.254.105 on 09/05/12
For personal use only.

Can. J. Chem. Downloaded from www.nrcresearchpress.com by 210.87.254.105 on 09/05/12
For personal use only.

benzene added. 7-Iodonoradrenochrome monosemicarbazone (0.04 g) was obtained as a deep cherry red crystalline solid (totally decomposed by 158°).

Anal. Calcd. for $C_9H_9IN_4O_3$: C, 31.05; H, 2.61; N, 16.10; I, 36.40. Found: C, 31.30; H, 2.73; N, 16.41; I, 36.49.

Oxidation of Noradrenaline Methyl Ether (7)

(i) Oxidation with Silver Oxide

No crystalline products could be isolated from solutions of noradrenaline methyl ether hydrochloride, in either methanol or acetonitrile, which had been oxidized with silver oxide.

(ii) Oxidation with Potassium Ferricyanide; Preparation of Noradrenochrome Methyl Ether Monosemicarbazone (9)

A solution of noradrenaline methyl ether hydrochloride (0.5 g, (14)) in water (2.5 ml) was oxidized with a solution of potassium ferricyanide (2.35 g) and sodium bicarbonate (0.75 g) in water (6.2 ml). After the oxidation had been allowed to proceed for 5 min a solution of semicarbazide hydrochloride (0.25 g) and sodium acetate (0.25 g) in water (1.5 ml) was added to the deep-red solution containing noradrenochrome methyl ether. A brown precipitate (0.25 g) separated after the reaction mixture had been allowed to stand at 4° overnight. Eventually a small quantity of noradrenochrome methyl ether monosemicarbazone was obtained as a deep-red microcrystalline powder (totally decomposed by 208°) by repeated recrystallization of the crude product from aqueous alcohol.

Anal. Calcd. for $C_{10}H_{12}N_4O_3$: C, 50.84; H, 5.12; N, 23.72. Found: C, 50.52; H, 5.29; N, 23.55.

(iii) Oxidation with Potassium Iodate

(*a*) Potassium iodate (0.8 g) was added to a solution of noradrenaline methyl ether hydrochloride (0.5 g; (14)) in water (150 ml). The reaction mixture was stirred at room temperature for 3½ h, after which time the deep-purple solution was filtered from a little dark-colored amorphous insoluble material. No significant precipitation occurred after the reaction mixture had been allowed to stand in the refrigerator overnight. The pH of the solution was then adjusted to 2 and it was allowed to stand at 4° for several hours; however, no crystalline iodoaminochrome was obtained.

The solution, presumed to contain 7-iodonoradrenochrome methyl ether (**10**), was treated with an excess of ascorbic acid and rapidly extracted with ether (4 × 60 ml). A mixture of acetic anhydride (10 ml) and dry pyridine (10 ml) was added to the dried (Na_2SO_4) ethereal extracts. After removal of the ether *in vacuo* the acetylation mixture was allowed to stand at room temperature overnight and was then poured dropwise with stirring into an ice–water mixture. The aqueous reaction mixture was ether extracted (4 × 60 ml) and the combined ether extracts washed free of acetic acid with 5% aqueous sodium bicarbonate and water. Benzene (50 ml) was added to the dried (Na_2SO_4) ether solution and the ether removed *in vacuo*. The crude product (in benzene solution) was purified chromatographically on a short silica gel column by adsorption from benzene – light petroleum (b.p. 60–80°) (1:1) and elution with a mixture (5:1) of these solvents. 5,6-Diacetoxy-7-iodoindole (0.13 g; m.p. 126–127°) was obtained when the partially purified product, obtained on concentration of the combined eluates, was recrystallized from benzene – light petroleum (b.p. 80–100°). This material did not depress the melting points of samples of 5,6-diacetoxy-7-iodoindole obtained from dopamine (see above) or noradrenaline (15).

(*b*) No crystalline products were obtained when more concentrated aqueous solutions of noradrenaline methyl ether hydrochloride were oxidized with potassium iodate in water at 0°. Repeated filtration from initially formed tarry by-products and adjustment of the pH of the solution to 2 were of no avail.

Oxidation of α-Methylnoradrenaline Methyl Ether (14)

An attempt to prepare 7-iodo-2-methylnoradrenochrome methyl ether (**13**) from α-methylnoradrenaline methyl ether hydrochloride (0.5 g), by a method analogous to that described above for the corresponding noradrenaline derivative was also unsuccessful. The deep-purple solution of the crude iodoaminochrome was reduced and the products acetylated as described previously. On pouring the acetylation mixture into ice–water a pale-brown solid was obtained. The product was dissolved in a mixture of benzene and light petroleum (b.p. 80–100°) (1:1) and adsorbed on a short silica gel column (2.5 × 2.2 cm). Elution of the column with benzene – light petroleum (b.p. 80–100°) (5:1) gave a solid product, which, on recrystallization from benzene – light petroleum (b.p. 100–120°), gave 5,6-diacetoxy-7-iodo-2-methylindole (0.055 g), m.p. 161–162°, undepressed on admixture with a sample prepared from α-methylnoradrenaline hydrochloride (16).

Adrenochrome Methyl Ether (18)

Freshly prepared silver oxide (5 g) was added to a solution of adrenaline methyl ether hydrochloride (1 g; (13)) in dry methanol (10 ml). The reaction mixture was shaken vigorously for 3–4 min and then filtered with suction through a Dowex-1 (Cl^-) resin bed.[7] Dry ether (30 ml) was added to the deep-red filtrate, which was cooled to −80°. After standing for several hours at this temperature adrenochrome methyl ether was obtained as a deep-red microcrystalline solid (m.p. softens at 81°; totally decomposed by 86°; undepressed on admixture with a sample of this compound prepared by the method previously described (1)). A second crop was obtained from the mother liquors after they had been allowed to stand at −80° overnight (total yield, 0.19 g).

Anal. Calcd. for $C_{10}H_{11}NO_3$: C, 62.16; H, 5.74. Found: C, 62.04; H, 5.71.

Adrenochrome Ethyl Ether (19)

Adrenochrome ethyl ether (0.25 g) was prepared as a deep-red microcrystalline solid (m.p. 79.5–81.5° with decomposition, undepressed on admixture with a sample of this compound prepared by the method previously described (1)) from adrenaline ethyl ether hydrochloride (1 g) by a method analogous to that described above for the preparation of adrenochrome methyl ether.

Anal. Calcd. for $C_{11}H_{13}NO_3$: C, 63.75; H, 6.32; N, 6.76. Found: C, 63.60; H, 6.32; N, 6.77.

---

[7]The resin (200/400 mesh size) was prepared by extensive washing with: (*1*) 3 *N* hydrochloric acid; (*2*) with water until neutral to litmus; and (*3*) finally with dry methanol. Column diameter, 2.5 cm; height, 1 cm.

1-Isopropylnoradrenochrome Methyl Ether Monosemicarbazone (22)

A solution of *N*-isopropylnoradrenaline methyl ether hydrochloride (0.25 g; (14)) in water (1.3 ml) was oxidized with a solution of potassium ferricyanide (1.17 g) and sodium bicarbonate (0.37 g) in water (3.1 ml). A solution containing semicarbazide hydrochloride (0.13 g) and sodium acetate (0.13 g) in water (0.7 ml) was added to the deep-red aminochrome solution; the resulting orange-colored solution deposited an orange-brown crystalline solid, m.p. 184–185° (decomp.) after being allowed to stand at 4° overnight. Recrystallization from water afforded 1-isopropylnoradrenochrome methyl ether semicarbazone (0.2 g) in reddish-orange elongated prisms, m.p. 190.5–191° (decomp.).

Anal. Calcd. for $C_{13}H_{18}N_4O_3$: C, 56.10; H, 6.52; N, 20.13. Found: C, 55.95; H, 6.56; N, 19.96.

1-Isopropylnoradrenochrome Ethyl Ether Monosemicarbazone (23)

1-Isopropylnoradrenochrome ethyl ether monosemicarbazone (0.21 g) (very small orange prisms; m.p. 187.5–188.5° (decomp.) was prepared from *N*-isopropylnoradrenaline ethyl ether hydrochloride (0.25 g; (14)) in a manner analogous to that described above for the corresponding methyl ether.

Anal. Calcd. for $C_{14}H_{20}N_4O_3$: C, 57.52; H, 6.90; N, 19.17. Found: C, 57.32; H, 6.84; N, 19.07.

Acknowledgment

The technical assistance of Mrs. B. D. Scott of the Psychiatric Research Unit, University Hospital, Saskatoon, Saskatchewan is gratefully acknowledged.

1. R. A. Heacock and B. D. Scott. Can. J. Chem. **38**, 516 (1960).
2. R. A. Heacock and O. Hutzinger. Can. J. Chem. **43**, 2535 (1965).
3. O. Hutzinger and R. A. Heacock. Can. J. Chem. This issue.
4. R. A. Heacock. Advan. Heterocyclic Chem. **5**, 205 (1965).
5. P. Marquardt and E. Carl. Naturwiss. **39**, 210 (1952).
6. R. A. Heacock, C. Nerenberg, and A. N. Payza. Can. J. Chem. **36**, 853 (1958).
7. E. Mácciotta. Gazz. Chim. Ital. **81**, 485 (1951).
8. J. D. Bu'Lock and J. Harley-Mason. J. Chem. Soc. 712 (1951).
9. R. A. Heacock and B. D. Scott. Experientia, **17**, 347 (1961).
10. N. Barsel. U. S. Patent No. 3,098,858. July 23, 1963. Chem Abstr. **60**, 506 (1964).
11. R. A. Heacock. Chem. Ind. London, 752 (1959).
12. R. Barer, H. Blaschko, and H. Langeman. J. Physiol. London, **112**, 21P (1951).
13. J. Hukki and N. Seppäläinen. Acta Chem. Scand. **12**, 1231 (1958).
14. R. A. Heacock, O. Hutzinger, and B. D. Scott. Can. J. Chem. **43**, 2437 (1965).
15. R. A. Heacock, M. E. Mahon, and B. D. Scott. Can. J. Chem. **39**, 231 (1961).
16. R. A. Heacock, O. Hutzinger, B. D. Scott, J. W. Daly, and B. Witkop. J. Am. Chem. Soc. **85**, 1825 (1963).

Can. J. Chem. Downloaded from www.nrcresearchpress.com by 210.87.254.105 on 09/05/12
For personal use only.

Can. J. Chem. Downloaded from www.nrcresearchpress.com by 210.87.254.42 on 09/05/12
For personal use only.

Dimethyl sulfoxide as a solvent in the Williamson ether synthesis[1]

RUSSEL G. SMITH, ALAN VANTERPOOL, AND H. JEAN KULAK[2]
Research Department, Canadian Chemical Company, P.O. Box 99, Edmonton, Alberta

Received September 9, 1968

Using the conventional Williamson ether synthesis, *n*-butyl ether was prepared from sodium hydroxide, *n*-butyl alcohol, and *n*-butyl chloride using excess of the alcohol as solvent in 61% yield after 14 h reaction time. However, when the excess alcohol was replaced by dimethyl sulfoxide, the yield of ether rose to 95% with 9.5 h reaction time. Other primary alkyl chlorides exhibited similar behavior to *n*-butyl chloride, but secondary alkyl chlorides and primary alkyl bromides gave little etherification, elimination being the major reaction. Unreactive halides, such as vinyl chloride, phenyl bromide, and 2,4-dinitrobromobenzene, were not etherified in dimethyl sulfoxide. The reaction products obtained from aliphatic dichlorides depended upon the relative positions of the chlorine atoms. Secondary alcohols reacted to give ethers, but tertiary alcohols were very unreactive. Polyols generally gave high yields of ethers, the major product being that in which all but one of the hydroxyl groups became etherified. Under forcing conditions, however, completely etherified polyols could be obtained.

Canadian Journal of Chemistry, 47, 2015 (1969)

Introduction

It has been shown by Cram and co-workers (1) that dimethyl sulfoxide (DMSO) is a useful solvent for the Williamson reaction (2). Working with phenyl bromide and potassium *t*-butoxide these authors obtained a greatly enhanced rate and a better overall yield of *t*-butyl phenyl ether in DMSO as compared to the conventional synthesis in *t*-butyl alcohol.

Later, workers studied the mechanism of the rate enhancement in greater detail and extended the application of the reaction in DMSO. Thus, ethers have been prepared from alkoxides and alkyl sulfonate esters (3, 4), from carbohydrates and dimethyl sulfate or methyl iodide (5, 6), from phenoxides and butyl halides (7), from methoxide and benzyl chlorides (8), from diphenoxides and dihaloaromatic compounds (9), and from methoxide and phenolates with poly[3,3-bis(chloromethyl)oxacyclobutane] (10). Zimmerman and Dathe (11) have shown polyol ethers can be obtained by reaction of the sodium alkoxide formed from the polyol and sodium hydroxide with alkyl chlorides.

The rate enhancement which occurs on transfer of a nucleophilic reaction from a protic solvent such as *t*-butanol to a dipolar aprotic solvent such as DMSO has been discussed in a review article by Parker (12). The rate enhancement is explained on the basis of the much greater solvation of anions in protic solvents along with the much greater solvation of polarized charged transition states in dipolar aprotic solvents. Consequently, for nucleophilic reactions the activation energy is less in dipolar aprotic solvents than in protic solvents. Rate enhancements by factors as large as 1×10^{10} have been observed for some nucleophilic reactions on transfer from protic solvents to dipolar aprotic solvents.

The use of sodium hydroxide to form alkoxides and subsequent reaction with alkyl chlorides as reported by Zimmerman and Dathe (11) is of interest since it is considerably less expensive than the conventional use of sodium metal and alkyl bromides. The purpose of the work reported here was to determine the limitations and advantages of this method of ether synthesis.

Experimental

In a typical preparation the hydroxyl containing compound, a stoichiometric excess of sodium hydroxide and DMSO (ca. 300 ml per mole of hydroxylic compound) was mixed and heated, with stirring. The temperature chosen was 5–10 °C below that at which discoloration occurred (usually 90–110 °C). When the precipitate had changed in physical appearance from a slimy to a granular form, the halide (in stoichiometric equivalence with caustic) was slowly added at such a rate that the temperature could be maintained at ca. 100 °C. Stirring and heating were maintained for 2–3 h after the addition was complete. The mixture was then cooled, and sufficient water added to dissolve the precipitated solids. The liquid layers were extracted with ethyl ether, the extracts combined, dried (sodium sulfate), and the ether removed by distillation. The residue was vacuum flashed, and the distillate analyzed by hydroxyl value and gas chromatography. Peak assignment, where possible, was made

[1]Presented in part to the 49th Annual Conference, Chemical Institute of Canada, Saskatoon, June 1966.
[2]Present address: 656 Thurber Drive, Columbus, Ohio 43215, U.S.A.

TABLE I

Effect of solvent on the yield of *n*-butyl ether prepared from *n*-butyl alcohol and *n*-butyl chloride

Solvent	Reaction time (h)		Products obtained	
	For alkoxide formation	For ether formation	% Alcohol converted to ether	% Halide converted to olefin
n-Butyl alcohol	4.0	10.0	61*	0
DMSO	2.5	3.5	62†	19
DMSO	7.0	2.5	95	‡

*Percent n-C_4H_9Cl converted to ether.
†Thirty-seven percent of the alcohol was recovered unchanged.
‡Not determined.

using known compounds. When these were not available, the assignment was chosen so as to agree with the determined hydroxyl value.

Volatile by-products were trapped in a dry ice – acetone bath and analyzed by mass spectrometry.

Results and Discussion

In general, it proved difficult to prepare alkoxides at practical synthetic levels in DMSO since both sodium hydroxide and the alkoxides studied had very limited solubility in DMSO. Consequently, long reaction times and high temperatures were necessary for the alkoxide production stage of the synthesis. Once the alkoxide had been formed, reaction with alkyl chlorides was rapid and ethers could be obtained in good yields. When *n*-butyl ether was prepared (Table I), it was obtained in 95% yield after a total of 9.5 h reaction time of which 7.0 h were required for alkoxide formation. This result compares favorably with a 61% yield obtained after 14 h reaction time, when *n*-butyl alcohol was used as the solvent instead of DMSO. When a reaction time of only 2.5 h for alkoxide formation in DMSO was allowed, the yield of the ether was only 62%.

In the synthesis of *n*-butyl ether in DMSO, a portion of the excess *n*-butyl chloride employed was converted to 1-butene. This elimination reaction did not occur in *n*-butyl alcohol solvent or when aqueous DMSO was employed. If stoichiometrically equivalent quantities of *n*-butyl alcohol, sodium hydroxide, and *n*-butyl chloride were used in the synthesis, a low yield of *n*-butyl ether was obtained due to this competing elimination. However, good yields of *n*-butyl ether could be obtained if a 1.5 fold excess of sodium hydroxide and *n*-butyl chloride was used over the *n*-butyl alcohol.

The synthesis gives good results when other primary alcohols and other primary chlorides are used. Thus, *n*-dodecyl ether was prepared (Table II) in 54% yield from *n*-dodecyl alcohol and *n*-dodecyl chloride.

A series of halides was reacted with *n*-butyl alcohol to determine the limitations to the type of halide which could be used in the synthesis. With isopropyl chloride (Table II), *t*-butyl chloride, and *n*-butyl bromide, the elimination reaction was sufficiently pronounced that little, if any, etherification occurred. On the other hand, vinyl chloride, 2,4-dinitrobromobenzene, and phenyl bromide failed to react at all (unreported experiments). This result is in contrast to the work of Cram *et al.* (1) where however, rigorously anhydrous conditions were employed.

Secondary alcohols, e.g., isopropyl alcohol, cyclohexyl alcohol, were found to be less reactive than *n*-butyl alcohol, while *t*-butyl alcohol was very unreactive (cf. Cram *et al.* (1)) (Table II). This lack of reactivity probably relates more to a difficulty in forming the alkoxide than to a difficulty in reacting the alkoxide with the halide. With phenol the reaction was particularly satisfactory since sodium phenoxide formed easily and was soluble in DMSO.

The reaction products obtained from aliphatic dichlorides depended on their structure. Thus, the *vicinal* dihalides studied (Table III) gave no ethers. Instead, appreciable amounts of acetylenes were formed, together with minor amounts of vinyl chlorides. With 1,3-dichloropropane

Can. J. Chem. Downloaded from www.nrcresearchpress.com by 210.87.254.42 on 09/05/12
For personal use only.

Can. J. Chem. Downloaded from www.nrcresearchpress.com by 210.87.254.42 on 09/05/12
For personal use only.

TABLE II

Ethers from monohydric compounds

Hydroxylic compound*	Halide	Moles halide per mole alcohol	Reaction time (h)		Products obtained			
			For alkoxide formation	For ether formation	% alcohol converted to ether	% unreacted alcohol recovered	% halide converted to olefin	% unreacted halide detected
n-C_4H_9OH	n-C_4H_9Cl	1.5	3.0	3.5	62	37	19	23
n-C_4H_9OH	i-C_3H_7Cl	1.5	2.5	3.5	0	†	79	†
n-C_4H_9OH	C_6H_5Br	1.2	3.0	10.0	11	61	0	53
n-$C_{12}H_{25}OH$	n-$C_{12}H_{25}Cl$	2.0	2.5	5.0	54	†	†	†
i-C_3H_7OH	n-C_4H_9Cl	1.5	5.0	3.0	55	†	32	3
$C_6H_{11}OH$	n-C_4H_9Cl	1.5	4.0	3.0	49	†	†	0
t-C_4H_9OH	n-C_4H_9Cl	1.5	6.0	4.0	13	†	43	6
t-C_4H_9OH	C_6H_5Br	1.0	6.0	8.0	0	†	0	†
C_6H_5OH	n-C_4H_9Cl	1.5	1.0	3.5	100	0	†	†

*One to five moles NaOH employed per mole of alcohol.
†Not determined.

TABLE III

Products obtained from the reaction of aliphatic dihalides with n-butyl alcohol

Dihalide	Reaction time (h)		% unreacted alcohol detected	% unreacted dihalide detected	Other products identified (% based on dihalide)	
	For butoxide formation	For ether formation				
1,2-Dichloroethane*	3.5	3.5	80	0	Acetylene	30
					Vinyl chloride	2
1,2-Dichloropropane†	3.5	5.0	74	24	Methylacetylene	36
					2-Chloropropene	4
1,3-Dichloropropane†	4.0	5.0	54	35	Allyl chloride	7
					Allyl ether	4
					Butyl allyl ether	35
					γ-Hydroxypropyl Butyl ether	7
1,4-Dichlorobutane*	5.5	6.5	63	8	1,3-Butadiene	42
					δ-Chlorobutyl Butyl ether	6
					1,4-Dibutoxybutane	16

*Used 1.0 mole NaOH and 0.5 mole of halide per mole of alcohol.
†Used 1.1 moles NaOH and 1.1 moles of halide per mole of alcohol.

Can. J. Chem. Downloaded from www.nrcresearchpress.com by 210.87.254.42 on 09/05/12
For personal use only.

TABLE IV

n-Butyl ethers of selected polyhydric alcohols made from *n*-butyl chloride

Polyol	Reaction temperature for salt formation (°C)	Reaction time (h)		Monoether (%)	Conversion of polyol to		
		For alkoxide formation	For ether formation		Diether (%)	Trie her (%)	Tetraether (%)
1,2-Dihydroxyethane*	100	3.0	4.5	22	66	—	—
1,2-Dihydroxypropane†	110	1.0	2.0	55‡	27	—	—
1,2,3-Trihydroxypropane*	140	4.5	4.5	0	41‡	24	—
2,2-bis(Hydroxymethyl)-propane†	100	1.0	2.0	41	36	—	—
2,2-bis(Hydroxymethyl)-butanol-1*	95	3.0	5.0	0	74	16	—
2,2-bis(Hydroxymethyl)-propanediol-1,3*	95	3.0	8.0	0	4	71	20

*Used 1.1 moles NaOH and 1.1 moles *n*-butyl chloride per mole of hydroxyl group.
†Used 1.5 moles NaOH and 1.5 moles *n*-butyl chloride per mole of hydroxyl group.
‡Combines total of the two possible isomers.

TABLE V

Selectivity in the preparation of ethers of pentaerythritol*

Ether desired	Moles NaOH used per mole pentaerythritol	Moles alkyl chloride used per mole pentaerythritol	Reaction time (h)		% Pentaerythritol converted to			
			For alkoxide formation	For ether formation	Monoether	Diether	Triether	Tetraether
di-*n*-Butyl	3.0	3.0	0.5	10.0	10	32	23	0
tri-*n*-Butyl†	8.0	8.0	0.5	5.0	0	4	88	6
tetra-*n*-Butyl‡	8.0	8.0	3.0	8.0	0	0	20	68
di-Allyl	3.0	3.0	0.5	3.5	0	42	31	2
tri-Allyl	3.6	3.6	0.5	4.5	0	26	56	5
tetra-Allyl	8.0	8.0	1.5	4.0	0	0	11	79

*Of the various reaction conditions examined, those shown gave the highest selectivity to the desired ether.
†Solvent was 66% aq. DMSO.
‡The mixed pentaerythritol alkoxides were isolated and dried before proceeding to ether formation.

Can. J. Chem. Downloaded from www.nrcresearchpress.com by 210.87.254.42 on 09/05/12
For personal use only.

there was a substantial amount of elimination to give allyl chloride, much of which reacted to form a mixture of ethers. However, there was also an appreciable degree of hydrolysis of the halides resulting, after subsequent reaction, in allyl ether and γ-hydroxypropyl butyl ether. 1,4-Dichlorobutane on the other hand, gave 1,3-butadiene as the major product with minor amounts of 1,4-dibutoxybutane and δ-chlorobutyl butyl ether. All these aliphatic dichlorides, however, were considerably less reactive than *n*-butyl chloride, as shown by the amount of unreacted *n*-butyl alcohol detected in the reaction product.

The reaction of several polyols with *n*-butyl chloride demonstrated (Table IV) that they were more reactive than the monohydric alcohols examined. This was to be expected on the basis of their higher acidity (13). However, mixtures of products were invariably obtained. Thus, ethylene glycol gave 22% monoether and 66% diether. With 1,2-propylene glycol, 27% of the fully etherified material was obtained along with 55% of the monoether. There were two monoethers formed, however; one, presumably 1-butoxy-2-hydroxypropane, to a much greater extent than the other (49% vs. 6%). With glycerol, no monoether was formed, only a mixture of diethers (34% of one isomer and 7% of the other) and the triether (24%). Trimethylolpropane and pentaerythritol also formed ethers in high conversion. The major product was that in which all but one of the hydroxyl groups had been etherified. *n*-Octyl chloride reacted with pentaerythritol in a similar manner to *n*-butyl chloride, while benzyl and methallyl chlorides gave results more similar to allyl chloride.

An appreciation of the selectivity of the reaction system, using pentaerythritol as an example can be gained from Table V. With either butyl or allyl chloride, no conditions were found which gave any appreciable amount of monoether. Diethers were obtained in modest conversions by using short reaction times for alkoxide formation and by reducing the moles of base and halide per mole of pentaerythritol. High conversion to tri-ether resulted when additional water was added to the solvent or by control of the stoichiometry. Tetra-ethers resulted when a large excess of alkyl chloride was employed with or without concomitant removal of water from the system. Previously it had not been found possible to make pentaerythritol tetraether in one step (14). The reaction using *n*-butyl chloride in DMSO resulted in production of 1-butene, *n*-butyl alcohol, and *n*-butyl ether by-products, but these were absent when the solvent was aqueous DMSO.

Polyallyl ethers of several other polyols were prepared. The mixed products were analyzed by determining hydroxyl number and iodine number. For materials, such as, sucrose, sorbitol, and inositol, which contain both primary and secondary hydroxyl groups, there was a low conversion (i.e., 10 to 30%) to highly etherified products. In each case, there was on an average, less than one free hydroxyl group remaining. Glucose was resinified by the highly alkaline reaction medium.

Acknowledgments

All analyses were performed by the Analytical Section of the Research Department of this Company.

The authors are indebted to the National Research Council of Canada for support of this work under an Industrial Research Assistant Grant.

1. D. J. Cram, B. Rickborn, and G. R. Knox. J. Am. Chem. Soc. **82**, 6412 (1960).
2. A. W. Williamson. J. Chem. Soc. **4**, 229 (1852).
3. C. H. Snyder. Chem. Ind. London, 121 (1963).
4. C. H. Snyder and A. R. Soto. J. Org. Chem. **29**, 742 (1964).
5. R. Kuhn and H. Trischmann. Ber. **96**, 284 (1963).
6. K. Wallenfels, G. Bechtler, R. Kuhn, H. Trischmann, and H. Egge. Angew. Chem. Intern. Ed. **2**, 515 (1963).
7. A. Berge and J. Ugelstad. Acta Chem. Scand. **19**, 742 (1965).
8. E. Tommila and M. Savolainen. Acta Chem. Scand. **20**, 946 (1966).
9. R. N. Johnson, A. G. Farnham, R. A. Clendinning, W. F. Hale, and C. N. Merriam. J. Polymer Sci. Pt. A-1, **5**, 2375 (1967).
10. Y. Minoura, K. Shiina, and K. Yoshikawa. J. Poly. Sci. Pt. A-1, **5**, 2843 (1967).
11. R. Zimmerman and W. Dathe. German Patent No. 1,178,840 (to Chemische Werke Albert). June 3, 1965.
12. A. J. Parker. Quart. Rev. **16**, 163 (1962).
13. J. Hine and M. Hine. J. Am. Chem. Soc. **74**, 5266 (1952).
14. W. Krey and K. Raichle. U.S. Patent No. 2,924,621 (to Farbenfabriken Bayer A.-G.). Feb. 9, 1960.

Can. J. Chem. Downloaded from www.nrcresearchpress.com by 210.87.254.105 on 09/05/12
For personal use only.

Reactions of cysteine with *N*-methyl-*N*-nitroso-*p*-toluenesulfonamide and *N*-methyl-*N'*-nitro-*N*-nitrosoguanidine

UWE SCHULZ AND D. R. MCCALLA
Department of Biochemistry, McMaster University, Hamilton, Ontario

Received December 10, 1968

The reaction between cysteine and *N*-methyl-*N*-nitroso-*p*-toluenesulfonamide affords almost quantitative yields of cystine and *N*-methyl-*p*-toluenesulfonamide. A mechanism based on the intermediacy of the *S*-nitroso derivative of cysteine and the intermediate formation of nitric oxide is proposed. Nitrous oxide is shown to be a final product. In the reaction of cysteine with *N*-methyl-*N'*-nitro-*N*-nitrosoguanidine a substantial yield of 2-nitramino-4-carboxyl-thiazoline is obtained. Cystine, *N*-methyl-*N'*-nitroguanidine and *S*-methylcysteine are formed in lesser amounts. The major product arises from nucleophilic attack on the imino carbon of *N*-methyl-*N'*-nitro-*N*-nitrosoguanidine. Concomitant elimination of the methylnitrosamino group accounts for the methylating ability of the system.

Canadian Journal of Chemistry, 47, 2021 (1969)

Previous work in this laboratory has shown that deoxyribonucleic acid (DNA) becomes methylated when it is allowed to react *in vitro* with either *N*-methyl-*N'*-nitro-*N*-nitrosoguanidine (NG) or with *N*-methyl-*N*-nitroso-*p*-toluenesulfonamide (MNTS) (1). Addition of cysteine to the reaction mixture was found to increase methylation by NG but to decrease dramatically methylation by MNTS, results which are of considerable interest in view of biological studies showing that cysteine has a protective action against certain types of alkylating agents (2).

Both NG and MNTS are well-established sources of diazomethane in their reactions with aqueous base (3, 4). For the reactions of NG and MNTS with nucleophilic reagents other than oxygen nucleophiles, a variety of products are reported. McKay and Wright (5) demonstrated that primary alkyl or aryl amines react with NG with the elimination of the methylnitrosamino group and the formation of *N*-substituted nitroguanidines. The only secondary amine to react with NG to give a *N*-disubstituted-*N'*-nitroguanidine is dimethylamine. Reaction of NG with other secondary amines resulted in denitrosation (6). In the reaction of NG with azide ion the methylnitrosamino group is eliminated and 5-nitroaminotetrazole is formed by cyclization of the intermediate nitroguanylazide (7). The reaction between MNTS and piperidine results in transfer of the nitroso group to form *N*-nitrosopiperidine without the formation of any diazomethane (4). Low yields of diphenylnitrosamine are reported to result from reaction of MNTS with diphenylamine (8).

Thus, while the existing literature pointed to the fact that the *N*-methyl-*N*-nitroso compounds under consideration exhibit two centers susceptible to nucleophilic attack, resulting in loss of the methylnitrosamino group and the nitroso function respectively, no information was available on their reactions with mercaptans. We report here data that provide a reasonable explanation for the difference in the behavior of NG and MNTS in the presence of cysteine.

Results and Discussion

Reactions of Cysteine with MNTS

The reactions of cysteine with MNTS were carried out at room temperature in aqueous 25% ethanol at pH 7 in an atmosphere of nitrogen. An ethanolic solution of MNTS was added to a magnetically stirred aqueous solution of cysteine at such a rate that the solution remained homogeneous. Upon addition of MNTS, the reaction mixture turned light-red and evolved gas. After most of the MNTS was added, a white solid precipitated. Preliminary experiments using a 1:1 ratio of reagents resulted in partial recovery of MNTS after an extended reaction period. Subsequently all experiments were carried out using a 1:2 ratio of MNTS and cysteine. Filtration after a reaction period of 20 h afforded an 85% yield of cystine. On ether extraction of the filtrate, *N*-methyl-*p*-toluenesulfonamide was isolated in 93% yield. The products were identified by their infrared spectra and their chromatographic behavior in comparison with that of

Can. J. Chem. Downloaded from www.nrcresearchpress.com by 210.87.254.105 on 09/05/12
For personal use only.

authentic samples. The amount of gas collected in a measuring cylinder during the reaction corresponded to 53 mole % based on the amount of MNTS. On exposure of the collected gas to air, brown fumes developed accompanied by a characteristic smell of nitrogen dioxide. This behavior pointed to the presence of nitric oxide. When the reaction was carried out in a closed system flushed with nitrogen and evacuated by means of an aspirator prior to addition of MNTS, the yield of cystine increased to 91%. The gaseous products at the end of the reaction were analyzed by mass spectrometry. The predominant peak was found at *m/e* 44 and was assigned to nitrous oxide. No peak was observed at *m/e* 30 corresponding to nitric oxide.

The observations described can be accounted for by the following mechanism:

[1] 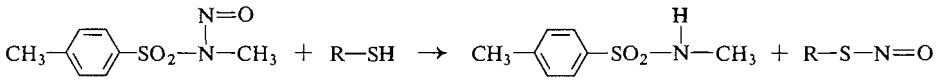

[2] $R{-}S{-}N{=}O \rightarrow R{-}S\cdot + \cdot N{=}O$

[3a] $R{-}S\cdot + R{-}S\cdot \rightarrow R{-}S{-}S{-}R$

[3b] $R{-}S\cdot + R{-}S{-}N{=}O \rightarrow R{-}S{-}S{-}R + \cdot N{=}O$

[4] $RSH + \cdot N{=}O \rightarrow R{-}S\cdot + HNO$

[5] $2HNO \rightarrow N_2O + H_2O$

$$R = H_2N{-}\underset{\displaystyle COOH}{\underset{|}{CH}}{-}CH_2$$

Initial nucleophilic attack by the sulfhydryl function on the nitroso group of MNTS results in the formation of *N*-methyl-*p*-toluenesulfonamide and of the *S*-nitroso derivative of cysteine. Subsequent reactions leading to the observed products involve radical intermediates formed by homolytic decomposition of the thionitrite.

Although in its entirety this mechanism is without precedent, the individual steps are supported by literature data and by additional experimental results described below. Isolation of *N*-methyl-*p*-toluenesulfonamide and appearance of a red color are considered sufficient evidence for eq. [1]. Solutions of thionitrites are known to be red (9, 10), though there is one report of green solutions of this class of compounds (11). Furthermore, the electronic spectrum of the reaction mixture shortly after mixing agreed closely with those reported for other thionitrites (12, 13). Thionitrites are relatively unstable compounds and are generally prepared in solution by action of nitrous acid (10) or nitrosyl chloride (9, 14) on the mercaptan. Thus, the reaction of a mercaptan with MNTS represents an alternative route to this class of compound and might have some practical value where strongly acidic (10) and anhydrous conditions (9, 14) are not expedient. Formation of a thiyl radical and nitric oxide has been reported in photolysis of thionitrites (12, 13). The thermal instability of the *S*-nitroso derivative of cysteine was indicated by our observation that exclusion of light had no noticeable effect on the rate of the reaction.

A somewhat disturbing fact was the report of a half-life of approximately 50 h for the *S*-nitroso derivative of cysteine when prepared from sodium nitrite in sulfuric acid in the presence of ammonium sulfamate (10). We therefore prepared the thionitrite in question by this latter method, but without addition of ammonium sulfamate. A deep red color resulted and persisted over a period of several hours. However, when the reaction mixture was adjusted to pH 7 immediately after mixing of the reagents, a vigorous evolution of gas set in within minutes, accompanied by precipitation of cystine and fading of the color. After 40 min a 78% yield of cystine was obtained. Thus, eq. [2] in the proposed reaction scheme is consistent with the behavior of the *S*-nitroso derivative of cysteine produced by an independent route.

The efficiency of eq. [2] does not have to be exceedingly high in view of a possible subsequent step [3*b*], a reaction that has precedence in the literature (12). Hydrogen atom abstraction from the sulfhydryl function of cysteine by nitric oxide should be an energetically favorable process considering the energy contents of the chemical bonds involved (15), and indeed reaction between an aqueous solution of cysteine and nitric oxide produced an almost quantitative yield of cystine. Preparation of disulfides in excellent yields has been reported for reactions of mercaptans with nitric oxide in the presence of hydroxide (16) and methoxide (17) ion. The

Can. J. Chem. Downloaded from www.nrcresearchpress.com by 210.87.254.105 on 09/05/12
For personal use only.

dimerization reaction of nitroxyl and subsequent decomposition follow from the work of Harteck (18) and seem to explain the formation of nitrous oxide. In this connection mention should be made of an investigation of the gas formation by cysteine during nitrite azotometry (19). Nitrous oxide was identified as product and the reaction mechanism was assumed to be as follows:

$$RSH + HNO_2 \rightarrow RSNO + H_2O$$

$$2RSNO \rightarrow RSSR + 2NO$$

$$2NO \rightarrow N_2O + O$$

Regarding the last step of this scheme we prefer our mechanistic proposal as it avoids the intermediacy of atomic oxygen which certainly would enter into further reactions.

Strong supporting evidence for the mechanism presented in this paper derives from variations in the stoichiometry under different reaction conditions. The fact that considerable amounts of unchanged MNTS could be recovered from reactions using a 1:1 ratio of MNTS and cysteine seems to indicate that the reaction steps [3–5] in our scheme involving radicals are fast compared to the initial nucleophilic attack on MNTS. The observed intermediacy of nitric oxide and the failure to detect any nitric oxide at the end of the reaction also support this notion. Finally, the decreased yield of cystine when the evolving gas is taken out of the reaction system during the reaction is in good agreement with the proposed mechanism.

Reactions of Cysteine with NG

The reactions of cysteine with NG were carried out in a manner analogous to that described for the reactions of cysteine with MNTS. Again a red color developed, gas evolved and precipitation of cystine took place. However, the yield of cystine (36%) was considerably lower and the amount of gas collected considerably higher than observed for the reaction of cysteine and MNTS. When the reaction was carried out in a closed system, the yield of cystine increased to 41%. Continuous extraction of the aqueous phase with ethyl acetate afforded a 22% yield of *N*-methyl-*N'*-nitroguanidine. When the aqueous phase was acidified and again extracted with ethyl acetate, a material was obtained which was shown to be homogeneous by thin-layer chromatography. After recrystallization from water the compound melted at 190–191°. Infrared spectroscopy indicated the presence of a nitro group and of a carbonyl function. The mass spectrum showed a molecular ion at *m/e* 191 and peaks at *m/e* 145 due to loss of the nitro group and at *m/e* 100 due to additional loss of the carboxyl group.

These findings suggested structure [**1**] for the material and the following pathway can account for its formation.

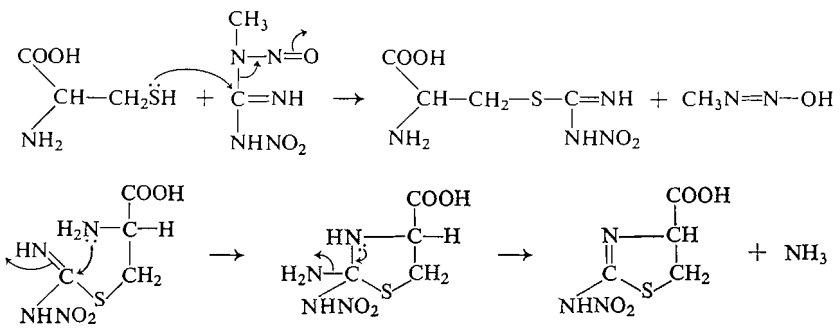

1

Elemental analysis and the nuclear magnetic resonance spectrum were in agreement with structure **1**. Another possible route for the formation of **1** is indicated in the sequence below:

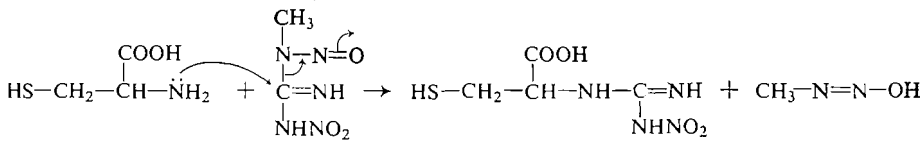

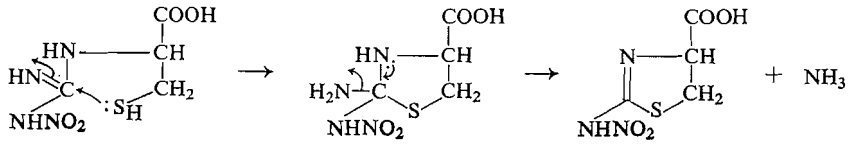

1

A comparison of the nucleophilic reactivities of the thiol and amino functions of cysteine should cast some light on the relative merits of these two alternatives. Ross has reported that the effective competition factor for the sulfhydryl group in cysteine is approximately 1000 times larger than that of α-amino groups (20). We therefore conclude that the thiazoline derivative is formed by almost exclusive operation of the first of the two sequences above.

Formation of the thiazoline derivative is reminiscent of the preparation of cyclic nitroguanidine derivatives from diamines and nitroguanidine with liberation of ammonia (21, 22). The possibility that 2-nitramino-4-carboxylthiazoline might arise from reaction of cysteine with *N*-methyl-*N'*-nitroguanidine can be eliminated, since no reaction took place on mixing cysteine and *N*-methyl-*N'*-nitroguanidine for 20 h at room temperature in aqueous ethanol.

The experiments indicate that the sulfhydryl function of cysteine can react with NG by nucleophilic attack at two reactive centers. Attack on the imino carbon of NG gives rise to the thiazoline derivative while attack on the nitroso group accounts for the formation of *N*-methyl-*N'*-nitroguanidine and cystine. The relative proportion of these two modes of attack can be assessed by the yields of the respective reaction products, if the products are stable under reaction conditions and if they do not arise from other reactions.

Based on the results from the reaction of cysteine with MNTS the two products from attack of the sulfhydryl function on the nitroso group were expected to be formed in equimolar amounts. However, *N*-methyl-*N'*-nitroguanidine was obtained in 22% yield while cystine was obtained in 41% yield. The reported decomposition of *N*-methyl-*N'*-nitroguanidine in aqueous solution at reflux (23), prompted us to check whether continuous extraction over 80 h in ethyl acetate saturated with water could cause decomposition of *N*-methyl-*N'*-nitroguanidine. A blank run resulted in recovery of 91% of *N*-methyl-*N'*-nitroguanidine and showed that decomposition if taking place at all could not be substantial enough to account for the observed imbalance of products in the reaction under investigation.

Chromatographic analysis of the aqueous solution after two continuous extractions with ethyl acetate revealed the presence of three compounds, one of which was identified as *S*-methylcysteine. Formation of this product serves as further evidence for the elimination of the methyl nitrosamino group from NG. The other two spots were shown to absorb ultraviolet light, but were not further identified.

Since the amount of nucleophilic attack by the sulfhydryl function on the nitroso group was not established with certainty, the respective yields of 22 and 41% can only be taken as lower and upper limits of the amount of this mode of attack. However, the 57% yield of the thiazoline derivative is believed to represent the percentage of attack on the imino carbon.

The results of our studies indicate a marked difference in mode of attack of cysteine on the two *N*-methyl-*N*-nitroso compounds under investigation. The reasons for this behavior are not obvious and are not discussed here. The interaction of *N*-methyl-*N*-nitrosourethane with cysteine in aqueous ethanol at room temperature is reported to afford a variety of compounds arising from nucleophilic attack of the thiol on the carbonyl group. Denitrosation reactions were not considered (24). We have conducted preliminary experiments in which *N*-methyl-*N*-nitrosourethane and *N*-methyl-*N*-nitrosourea in their reactions with cysteine in aqueous ethanol failed to yield any of the red color characteristic of *S*-nitroso compounds. Thus, it seems likely that at least under the conditions used, attack takes place exclusively on the carbonyl group of these compounds. Factors governing the relative proportion of nucleophilic attack on the nitroso group and the carbonyl carbon have been discussed recently for reactions of nitrosoalkylamine derivatives with alkoxide ions (25).

Can. J. Chem. Downloaded from www.nrcresearchpress.com by 210.87.254.105 on 09/05/12
For personal use only.

Can. J. Chem. Downloaded from www.nrcresearchpress.com by 210.87.254.105 on 09/05/12
For personal use only.

Our findings provide a possible explanation for the effects of added cysteine in the reactions of DNA with MNTS and NG. The reaction of cysteine with MNTS proceeds exclusively via attack on the nitroso group, a process that results in denitrosation and prevents MNTS from functioning as a methylating agent. This can explain the large decrease in methylation of DNA by MNTS when cysteine is added (1). In the reaction of cysteine with NG attack on both the nitroso group and the imino carbon are observed with the latter predominating. Nucleophilic attack on the imino carbon produces a fragment capable of methylation and thus allows qualitative rationalization of the increase in methyl incorporation into DNA in the presence of cysteine.

Experimental

Melting points were taken on a Gallenkamp apparatus and are uncorrected. Infrared spectra were recorded with a Beckman model IR5A spectrophotometer; nuclear magnetic resonance (n.m.r.) spectra with a Varian Associates model A-60 spectrometer; electronic spectra with a Beckman model DB spectrophotometer; mass spectra with a Hitachi model RMU-6A mass spectrometer. Microanalyses were by Galbraith Laboratories, Knoxville, Tennessee.

Thin-layer chromatograms were carried out on glass plates coated with silica gel H (E. Merck, Darmstadt) and were developed with iodine vapor. Paper chromatograms were run by the ascending method using the following solvent system (v/v/v): isopropanol – aqueous ammonia – water, 25:2:12. Spots were located in ultraviolet light or after spraying with a ninhydrin solution.

Nitrogen (Canadian Liquid Air) and nitric oxide (Matheson) were used as received. The following compounds were obtained from commercial sources: *N*-methyl-*N*-nitroso-*p*-toluenesulfonamide (Aldrich), *N*-methyl-*N'*-nitro-*N*-nitrosoguanidine (Aldrich) and cysteine hydrochloride (Baker).

Reaction of Cysteine with N-Methyl-N-nitroso-p-toluenesulfonamide (MNTS)

A 500 ml three-necked flask was equipped with an inlet tube for nitrogen, a dropping funnel, a magnetic stirring bar and a connecting tube leading to a measuring cylinder for the collection of evolved gas. The system was thoroughly flushed with nitrogen and 1.404 g (8.0 mmole) of cysteine hydrochloride monohydrate dissolved in 300 ml of water was placed into the flask. The pH of the solution was adjusted to 7 by addition of sodium hydroxide solution. The nitrogen inlet tube was quickly disconnected, the connecting tube opened and a solution of 0.860 g (4.0 mmole) of MNTS in 100 ml of 95% ethanol was added dropwise with magnetic stirring over a period of 40 min. Towards the end of the addition the slightly red solution turned cloudy due to precipitation. Evolution of gas (47 ml at STP) had ceased completely after an additional 2 h of stirring. When the collected gas was exposed to air, dark brown fumes with the characteristic smell of nitrogen dioxide formed immediately. Stirring of the aqueous reaction mixture was continued and after a total of 20 h the white precipitate was collected on a Buchner funnel (814 mg, corresponding to a yield of 85%). The material was identified as cystine by the R_f value of 0.3 on a paper chromatogram (ninhydrin) and by the infrared spectrum in comparison with an authentic sample (Sigma).

The filtrate was extracted with ether and the dried ether phase (sodium sulfate) was evaporated to dryness under vacuum. When the white residue was chromatographed on a neutral alumina column with petroleum ether – chloroform (1:1) as eluent, 692 mg, 93% yield of *N*-methyl-*p*-toluenesulfonamide was obtained. The infrared spectrum was identical to that of an authentic (26) sample. The melting point of 77–78° (lit. (27) 77.5–78.5) and a thin-layer chromatogram in chloroform, R_f 0.55, were confirmatory.

In another experiment, a similar apparatus was used except that the connecting tube was replaced by a gas trap that could be attached to the mass spectrometer. The system was evacuated by means of an aspirator prior to the reaction. Identical quantities were employed and the reaction was carried out as mentioned above. After 20 h the gaseous materials in the system were collected in the gas trap with the aid of liquid nitrogen. The mass spectrum of the gas sample showed a predominant peak at *m/e* 44 and did not show a peak at *m/e* 30. The described work-up yielded cystine in 91% yield (876 mg) and *N*-methyl-*p*-toluenesulfonamide in 93% yield (690 mg).

In an experiment on a smaller scale the colored solution of an early stage of the reaction was monitored spectrophotometrically in the visible region. Absorption maxima were observed at 340 and 550 mμ which agreed well with maxima of 340 and 550–560 mμ reported for other thionitrites (12, 13).

In a preliminary experiment employing a 1:1 ratio of cysteine and MNTS the reagents were allowed to react in 25% ethanol at room temperature for 20 h under a nitrogen atmosphere. The reaction mixture was extracted with ether and thin-layer chromatography showed the concentrate to contain considerable amounts of MNTS, R_f 0.55 in toluene

Reaction of Cysteine with Nitrous Acid

A 1 l three-necked flask was equipped with a connecting tube with parallel side arm, three dropping funnels and a gas inlet tube. The system was thoroughly flushed with nitrogen and 1.756 g (10 mmole) of cysteine hydrochloride hydrate dissolved in 180 ml of water was placed into the flask. To this solution was added 1 ml of concentrated sulfuric acid. The nitrogen stream was turned off and a solution of 0.69 g (10 mmole) of sodium nitrite in 30 ml of water was added within 2 min, followed by the rapid addition of 70 ml of 95% ethanol. The pH of the solution was then adjusted to 7 by addition of sodium hydroxide solution with moderate cooling. After a further 3 min a vigorous evolution of gas set in and the deep red solution turned cloudy due to precipitation accompanied by fading of the color. After 40 min the reaction mixture was filtered and 938 mg of cystine was collected corresponding to a 78% yield.

TABLE I

Paper chromatographic behavior of products in aqueous filtrate from reaction of cysteine with NG

R_f	Method of detection	Identity of spot
0.19	Ultraviolet light	Unknown
0.24	Ultraviolet light, ninhydrin	Unknown
0.29	Ninhydrin	Cystine
0.50	Ultraviolet light	2-Nitramino-4-carboxyl-thiazoline
0.62	Ninhydrin	S-Methylcysteine
0.75	Ultraviolet light	*N*-Methyl-*N'*-nitroguanidine

Reaction of Cysteine with Nitric Oxide

Into a 1 l three-necked flask equipped with three gas inlet tubes and a magnetic stirring bar was placed 1.756 g of (10 mmole) cysteine hydrochloride hydrate dissolved in 200 ml of water–ethanol (3:1). The system was thoroughly flushed with nitrogen and the solution was adjusted to pH 7 with sodium hydroxide. After repeated alternate flushing with nitrogen and evacuating by means of an aspirator the system was evacuated and a measured amount (10 mmole at STP) of nitric oxide was transferred in the reaction vessel. The solution was vigorously stirred for 20 h and the resulting precipitate was filtered off, 1.13 g, corresponding to a 94% yield of cystine. The material was identified by the infrared spectrum and by its paper chromatographic behavior.

Reaction of Cysteine with N-Methyl-N'-nitro-N-nitrosoguanidine (NG)

The reaction between 3.51 g (20 mmole) of cysteine hydrochloride monohydrate dissolved in 225 ml of water and 1.47 g (10 mmole) of NG dissolved in 75 ml of 95% ethanol was carried out as described for the reaction of cysteine with MNTS. Gas evolution amounted to 9 mmole at STP and the yield of cystine to 36% (0.869 g).

When the reaction was carried out in a closed system, cystine was obtained in 41% yield (0.989 g). A paper chromatogram of the aqueous filtrate indicated the presence of at least six compounds as shown in Table I. The major components of this reaction mixture could be identified as described below.

The filtrate was subjected to a continuous extraction with ethyl acetate over a period of 80 h. Evaporation of the organic phase to dryness gave 257 mg of a white solid, which was identical (infrared spectrum, thin-layer chromatogram in methanol, R_f 0.62) with authentic *N*-methyl-*N'*-nitroguanidine (5). After recrystallization from 95% ethanol the compound melted at 158–159°. Reported (5) m.p. 160–161°. The yield corresponded to 22%.

The aqueous layer was acidified to pH 1 by addition of concentrated hydrochloric acid and extracted with ethyl acetate over a period of 20 h. Concentration of the organic phase by rotary evaporation afforded 1.1 g of solid material which was shown to be homogeneous by thin-layer chromatography in 70% ethanol, R_f 0.78. After recrystallization from water the material melted at 190–191°. The infrared spectrum (Nujol) showed significant absorption at 1720 cm^{-1} (C=O) and at 1540 and 1260 cm^{-1} (nitro). The mass spectrum exhibited predominant peaks at *m/e* 191, 145 and 100. The n.m.r. spectrum (deuterium oxide) showed a quartet at τ 5.15 (J = 8.5 c.p.s., J = 6.5 c.p.s.) and doublets at τ 6.35 (J = 8.5 c.p.s.) and τ 6.42 (J = 6.5 c.p.s.). The ratio of the quartet at τ 5.15 and the sum of the doublets at τ 6.35 and 6.42 was 1.02:2. The yield corresponded to 57% of 2-nitramino-4-carboxyl-thiazoline.

Anal. Calcd. for $C_4H_5N_3O_4S$: C, 25.14; H, 2.64; N, 21.98; S, 16.77. Found: C, 25.20; H, 2.66; N, 21.88; S, 16.78.

A paper chromatogram of the aqueous phase indicated the presence of *S*-methylcysteine identified by comparison with authentic material (Sigma) and of unknown materials of R_f 0.19 and 0.24.

A sample of 100 mg of *N*-methyl-*N'*-nitroguanidine in 100 ml of ethyl acetate saturated with water was refluxed for 80 h. On concentration by rotary evaporation 91 mg of material was obtained which was found identical (infrared spectrum, thin-layer chromatogram in methanol, R_f 0.62) with authentic *N*-methyl-*N'*-nitroguanidine.

To a solution of 351 mg (2 mmole) of cysteine hydrochloride in 150 ml of water adjusted to pH 7 with sodium hydroxide was added 236 mg (2 mmole) of *N*-methyl-*N'*-nitroguanidine dissolved in 50 ml of 95% ethanol. The clear solution was stirred in a nitrogen atmosphere for 20 h and then concentrated to a volume of 30 ml by rotary evaporation. Paper chromatography showed only two spots which were identified as *N*-methyl-*N'*-nitroguanidine and cystine by comparison with authentic samples.

Acknowledgments

It is a pleasure to thank Messrs. Waldo Baerg and Antoon Reuvers for their assistance in the early stages of this work. Financial support from the National Cancer Institute of Canada and from the National Research Council of Canada is gratefully acknowledged.

1. D. R. McCalla. Biochim. Biophys. Acta, **155**, 114 (1968).
2. L. A. Elson. Radiation and radiomimetic chemicals. Butterworths, London. 1963. pp. 101–105.
3. A. F. McKay. J. Am. Chem. Soc. **70**, 1974 (1948).
4. H. J. Backer and T. J. de Boer. Proc. Koninkl. Ned. Akad. Wetenschap. **54B**, 191 (1951).
5. A. F. McKay and G. F. Wright. J. Am. Chem. Soc. **69**, 3028 (1947).

Can. J. Chem. Downloaded from www.nrcresearchpress.com by 210.87.254.105 on 09/05/12
For personal use only.

6. A. F. McKAY. J. Am. Chem. Soc. **71**, 1968 (1949).
7. R. A. HENRY and R. H. BOSCHAN. J. Am. Chem. Soc. **76**, 1949 (1954).
8. T. TAKIZAWA. J. Pharm. Soc. Japan, **70**, 490 (1950).
9. H. S. TASKER and H. O. JONES. J. Chem. Soc. **95**, 1910 (1909).
10. B. SAVILLE. Analyst, **83**, 670 (1958).
11. G. KRESZE and J. WINKLER. Ber. **96**, 1203 (1963).
12. J. BARRETT, D. F. DEBENHAM, and J. GLAUSER. Chem. Commun. 248 (1965).
13. J. BARRETT, L. J. FITZGIBBONS, J. GLAUSER, R. H. STILL, and P. N. W. YOUNG. Nature, **211**, 848 (1966).
14. H. RHEINBOLDT. Ber. **59**, 1311 (1926).
15. J. HINE. Physical organic chemistry. McGraw-Hill Book Co., Inc., New York. 1962. p. 32.
16. H. REIHLEN, A. v. FRIEDOLSHEIM, and W. OSWALD. Ann. **465**, 72 (1928).
17. R. LONGHI, R. O. RAGSDALE, and R. S. DRAGO. Inorg. Chem. **1**, 768 (1962).
18. P. HARTECK. Ber. **66**, 423 (1933).
19. M. HORI, H. KASHIWAGI, I. AOKI, and S. KUSUMOTO. Takeda Kenkyusho Nempo, **22**, 64 (1963); seen only as Chem. Abstr. **63**, 10688*c* (1965).
20. W. C. J. ROSS. Ann. N.Y. Acad. Sci. **68**, 669 (1957–1958).
21. A. F. McKAY and G. F. WRIGHT. J. Am. Chem. Soc. **70**, 430 (1948).
22. A. F. McKAY. Chem. Rev. **51**, 301 (1952).
23. T. L. DAVIS and R. C. ELDERFIELD. J. Am. Chem. Soc. **55**, 731 (1933).
24. R. SCHOENTAL and D. J. RIVE. Biochem. J. **97**, 466 (1965).
25. W. M. JONES and D. L. MUCK. J. Am. Chem. Soc. **88**, 3798 (1966).
26. D. R. McCALLA, A. REUVERS, and R. KITAI. Can. J. Biochem. **46**, 807 (1968).
27. T. J. DE BOER and H. J. BACKER. Rec. trav. chim. **73**, 229 (1954).

Can. J. Chem. Downloaded from www.nrcresearchpress.com by 210.87.254.105 on 09/05/12
For personal use only.

Chloral–ketone condensations in acetic anhydride. Reaction of chloral with butanone, 3-pentanone, cyclohexanone, and 4-methyl-2-pentanone

EBERHARD KIEHLMANN AND PUI-WAH LOO
Department of Chemistry, Simon Fraser University, Burnaby 2, British Columbia
Received November 5, 1968

In the presence of sodium acetate as catalyst, chloral hydrate undergoes a mixed aldol condensation with aliphatic and alicyclic ketones in acetic anhydride as solvent. Contrary to previous literature reports, reaction occurs at both the methyl and the methylene group in α-position to the carbonyl group of butanone, to give a mixture of 1,1,1-trichloro-2-hydroxy-4-hexanone (**1**) and 1,1,1-trichloro-2-hydroxy-3-methyl-4-pentanone (**2***a* and **2***b*, diastereomers). 3-Pentanone, cyclohexanone, and 4-methyl-2-pentanone yield 1,1,1-trichloro-2-hydroxy-3-methyl-4-hexanone (**3***a* and **3***b*, diastereomers), 2-(1-hydroxy-2,2,2-trichloroethyl-)cyclohexanone (**4***a* and **4***b*, diastereomers), and 1,1,1-trichloro-2-hydroxy-6-methyl-4-heptanone (**5**), respectively. Compound **5** is the exclusive product formed from chloral hydrate and 4-methyl-2-pentanone since attack at the methylene group is sterically hindered. The low-melting diastereomers **2***a*, **3***a*, and **4***a* which have not been characterized before, exhibit strong intramolecular hydrogen bonding and have been assigned the *threo* configuration on the basis of nuclear magnetic resonance and molecular model studies.

Canadian Journal of Chemistry, 47, 2029 (1969)

Can. J. Chem. Downloaded from www.nrcresearchpress.com by 210.87.254.42 on 09/05/12
For personal use only.

The condensation of chloral hydrate with aliphatic and alicyclic ketones is known to give aldol addition products which do not readily undergo dehydration when the reaction is carried out in acetic anhydride in the presence of sodium acetate as catalyst. According to Caujolle and co-workers (1), acetone, butanone, 3-pentanone, cyclohexanone, benzalacetone, and camphor yield only one addition product, respectively, under these experimental conditions although two asymmetric centers are generated, i.e., two diastereomeric products are possible when reaction occurs at the α-methylene group of butanone, 3-pentanone, or cyclohexanone. It has been postulated but not experimentally verified by the same authors (1), that chloral adds preferentially at the methylene group if a ketone e.g., butanone, contains both a methyl and a methylene group in α-position to the carbonyl function. The opposite view is held by Breusch and Keskin (2), who prepared a series of fourteen 1,1,1-trichloro-2-hydroxy-4-alkanones by refluxing the appropriate ketone, $R—CH_2—CO—CH_3$, with anhydrous chloral in glacial acetic acid. They determined the structure of the condensation product of 4-methyl-2-pentanone and chloral by synthesis and mixture melting point determination of 6-methyl-4-oxoheptanoic acid by two different routes, one of which involved 1,1,1-trichloro-2-hydroxy-6-methyl-4-heptanone (**5**) as an intermediate. On the basis of this experiment, the general structure $R—CH_2—CO—CH_2—CHOH—CCl_3$ resulting from addition of chloral at the ketone methyl group was assigned to all 14 reaction products.

Although the structure of **5** was subsequently verified by spectroscopic means (3), it appeared strange to us that the site of aldol addition changes from the α-methylene to the α-methyl group of a 2-alkanone when anhydrous chloral and glacial acetic acid are used instead of chloral hydrate and acetic anhydride. Therefore, we decided to reinvestigate the reaction of chloral hydrate with ketones in acetic anhydride in the presence of sodium acetate placing particular emphasis on the number and structure of the reaction products formed. This product study which made extensive use of modern techniques (vapor phase chromatography (v.p.c.) and nuclear magnetic resonance (n.m.r.)) not available to the authors of the original papers (1, 2) was also desirable as a first step toward future kinetic investigations of the addition step in mixed aldol condensations.

Results and Discussion

Chloral (trichloroacetaldehyde) appears to be a particularly suitable aldehyde component for studying the mechanism of mixed aldol condensations since due to the absence of α-hydrogens no self-condensation products are possible; thus, the desired mixed condensation product with the ketone component is expected to be formed exclusively. However, due to the inductive effect of the three chlorine atoms, the carbonyl group of chloral surpasses that of other aldehydes

TABLE I

Reaction products from chloral hydrate and various ketones*

Ketone	Reaction time (h)	Product yield (mole %)†‡ A	B	C	6	Literature‡§ yield (%)
Butanone	58	10.1	13.6	13.6	6.6	55 (B)
3-Pentanone	102	12.2	14.5	—	6.3	70 (B)
Cyclohexanone	45	5.2	18.3	—	23.5	70 (B)
4-Methyl-2-pentanone	52	—	—	17.7	5.3	—
Acetone	50	—	—	33.9	5.1	50 (C)
Benzalacetone	21	—	—	Trace	43‖	65 (C)

*Equation [1]: $RCOCH_2R' + CCl_3CH(OH)_2 \rightarrow RCOCHR'—CHOH—CCl_3$.
Experimental conditions: 1.25 moles ketone, 1 mole $CCl_3CH(OH)_2$, 1 mole Ac_2O, 10% (by weight) NaOAc, 70°.
†Determined by v.p.c. of crude product mixture on a 5 ft × ¼ in. SE-30 column (120–140°).
‡A = low-melting diastereomer, B = high-melting diastereomer, C = $RCOCH_2CHOHCCl_3$, 6 = $CCl_3CH(OAc)_2$.
§Reference (1).
‖Determined by n.m.r. of crude product mixture after removal of solvent, NaOAc, and unreacted chloral hydrate.

in additive ability and is readily attacked even by weak nucleophiles. It adds water to form a stable gem-diol (chloral hydrate), and acetic anhydride (4) to form 1,1-diacetoxy-2,2,2-trichloroethane (**6**) (trichloroethylidene diacetate). The latter is a stable compound which was obtained as the exclusive product in an attempt to prepare **5** from 4-methyl-2-pentanone and anhydrous chloral in acetic anhydride as solvent.

$$(CH_3)_2CHCH_2COCH_3 + CCl_3CHO + Ac_2O + NaOAc \rightarrow CCl_3CH(OAc)_2\ (71\%)$$
6

$$(CH_3)_2CHCH_2COCH_2CHOHCCl_3 \quad \text{(not observed)}$$
5

Chloral hydrate, on the other hand, is less reactive than anhydrous chloral as expected from its structure. It forms **6** in 5% yield when treated with acetic anhydride and sodium acetate for 52 h at 100°.

$$CCl_3CH(OH)_2 + Ac_2O \xrightarrow{NaOAc} HOAc + CCl_3CH(OAc)_2$$
6

Thus under the experimental conditions reported in the literature (1), i.e., treatment of a ketone with chloral hydrate, acetic anhydride and sodium acetate at 70° for several hours, we expected to obtain substantial quantities of **6** in addition to the desired chloral–ketone condensation products. The experimental results reported below were essentially in agreement with these expectations.

In contrast to the results reported by Caujolle and co-workers (1), we obtained three isomeric condensation products from butanone, two diastereomeric products each from 3-pentanone and cyclohexanone, respectively, and one product each from 4-methyl-2-pentanone, acetone and benzalacetone; considerable amounts of 1,1-diacetoxy-2,2,2-trichloroethane were found in all product mixtures, but no dehydration products of the type R—CO—CR′=CH—CCl_3 or acetylation products of the type R—CO—CHR′—CHOAc—CCl_3 were detected. This demonstrates that in general the aldol reaction between ketones of the type R—CO—CH_2—R′ (except when R′ is bulky, *vide infra*) and chloral hydrate leads to the formation of all possible isomeric condensation products resulting from attack at both the α-methyl (R = CH_3) and the α-methylene group of the ketone. Yields and product composition data for the condensation reaction [1] are summarized in Table I.

[1] $$RCOCH_2R' + CCl_3CH(OH)_2 \xrightarrow[70°]{Ac_2O,\ NaOAc} RCOCHR'—CHOH—CCl_3$$

1, R = Et, R′ = H
2, R = R′ = Me
3, R = Et, R′ = Me
4, R—R′ = —$(CH_2)_4$—
5, R = *i*-Bu, R′ = H
7, R = Me, R′ = H
8, R = *Ph*-CH=CH, R′ = H

Data for acetone and benzalacetone are included for comparison.

The same products and essentially the same product ratios were obtained under reflux conditions at atmospheric pressure and under the experimental conditions described in the literature (3) for the preparation of **5**. In the latter case, i.e., when anhydrous chloral and glacial acetic acid were used instead of chloral hydrate

Can. J. Chem. Downloaded from www.nrcresearchpress.com by 210.87.254.42 on 09/05/12
For personal use only.

Can. J. Chem. Downloaded from www.nrcresearchpress.com by 210.87.254.42 on 09/05/12
For personal use only.

and acetic anhydride, the desired condensation products were formed in higher yields.

The tabulated results (Table I) show that cyclohexanone and benzalacetone are less reactive than the other ketones studied, and that the α-methyl groups of acetone and 4-methyl-2-pentanone are approximately of equal reactivity toward chloral hydrate (taking into account a statistical factor of two for acetone). When two diastereomeric condensation products are possible, the high-melting isomer (**2***b*, **3***b*, **4***b*) is generally formed in higher yield than the low-melting compound (**2***a*, **3***a*, **4***a*).

The reaction between chloral hydrate and the 6 ketones listed in Table I is not accompanied by dehydration or acetylation of the condensation products. Only traces of unexpected by-products were detected by v.p.c. analysis of the slightly yellow, crude reaction mixtures; the ketone peak areas were found to correspond to 98–99% of the amount of unreacted ketone as calculated from the yield of condensation product. Thus, unreacted starting material, acetic acid, and the products listed in Table I account for more than 98% of the weight of the final reaction mixtures.

Butanone and Chloral Hydrate

Butanone reacts with chloral hydrate to form three isomeric condensation products and 1,1-diacetoxy-2,2,2-trichloroethane (**6**):

$$CH_3CH_2COCH_3 + CCl_3CH(OH)_2 \xrightarrow{Ac_2O} CH_3CH_2COCH_2CHOHCCl_3$$

1

$$+ CH_3COCH(CH_3)—CHOHCCl_3$$

2*a* and **2***b* (diastereomers)

$$+ CCl_3CH(OAc)_2$$

6

This demonstrates that contrary to a report in the literature (1), butanone undergoes condensation at both the methylene and the methyl group in α-position to the carbonyl function. Melting point and ease of crystallization indicate that the only product isolated by Caujolle and co-workers was ketol **1** and not the postulated isomeric ketol **2**. All three ketols are stable compounds which neither isomerize nor cleave to yield butanone and chloral when treated with acetic anhydride and sodium acetate under the preparative experimental conditions. The crude product mixture contains the straight-chain isomer (**1**) and the branched-chain isomers (**2***a* and **2***b*) in the approximate molar ratio 4:7 indicating that reaction occurs preferentially but not exclusively at the methylene group. However, the greater reactivity of the methylene group relative to the methyl group toward chloral hydrate appears to be specific for butanone (*vide infra*).

The n.m.r. and infrared (i.r.) spectra of the three isomeric condensation products exhibit a number of special features which permit conclusions to be drawn with respect to hydrogen-bonding and conformational interactions in these compounds. At a mole fraction of 0.08 in deuteriochloroform, the hydroxylic proton of **1**, **2***a*, and **2***b* appears as a sharp doublet at τ 5.83, 4.30, and 6.23, respectively. The coupling of this proton with the geminal proton (4.9–8.5 c.p.s.) suggests hydrogen-bonding association in $CDCl_3$ solution and a slow rate of proton exchange. Middleton and Lindsey (6) have reported similar retention of OH—H coupling for certain hydrogen-bonded solute–solvent complexes of 2*H*-hexafluoro-2-propanol.

The n.m.r. dilution shift data and i.r. absorption bands summarized in Table II provide evidence for different types of hydrogen bonds in the isomeric condensation products of butanone and chloral. Decreasing the mole fraction of the product in $CDCl_3$ from 0.25 to 0.04 results in an upfield shift of 36, 0, and 54 c.p.s. for the hydroxylic proton of **1**, **2***a*, and **2***b*, respectively. All three isomers exhibit an i.r. absorption band at 3600 cm^{-1} ("free" OH).[1] The "bonded" OH peak for **1** and **2***b* appears at 3470 to 3480 cm^{-1} (Δ_ν between "free" and "bonded" OH 120–130 wavenumbers) while the corresponding band for **2***a* is found at 3380 cm^{-1} ($\Delta_\nu = 220$ wavenumbers). The effect of concentration changes on the relative intensities of these i.r. absorption peaks is markedly different for **2***a* on one hand and **1** and **2***b* on the other hand. The "free" OH band of **2***a* is much less intense than the bonded OH band, and the ratio of peak intensities of the two bands remains essentially constant over the concentration range 0.5 *M* to 0.04 *M* in CCl_4. In contrast, dilute solutions (0.04 *M* in CCl_4) of **1** and **2***b* show a sharp, intense "free" OH band at 3600 cm^{-1} and a weak "bonded" OH band at 3475

[1]This band may be due to weakly hydrogen-bonded OH involving Cl as acceptor site, see ref. 9.

TABLE II

Nuclear magnetic resonance chemical shift and infrared absorption bands of OH group in R—CO—CHR′—CHOH—CCl_3*

Compound	Chemical shift mole fraction:†				Infrared absorption (cm^{-1})‡	
	0.25	0.15	0.08	0.04	"free" OH	"bonded" OH
1	273	260	250	237	3600	3470
2*a*	342	342	342	342	3600	3380
2*b*	265	243	226	211	3600	3480
3*a*	345	345	345	345	3600	3395
3*b*	268	250	230	215	3605	3490
4*a*		381	381		3600	3380
4*b*	248	232	218	206	3605	3500
5		252	238		3600	3450

*See eq. [1] for definition of R and R′.
†In c.p.s. downfield from TMS in $CDCl_3$ at 60 Mc.p.s.
‡0.5 *M* in CCl_4 (Beckman IR-12 or Perkin-Elmer 457) using NaCl window.

cm^{-1}. As the concentration is increased, the intensity of the bonded OH band increases at the expense of the "free" OH band. The absorption peak at 3600 cm^{-1} is entirely absent from the i.r. spectrum of a pure liquid (melt) film of **1** and **2***b* on sodium chloride plates.

It is apparent from these data that **2***a* is intramolecularly hydrogen-bonded involving the hydroxyl group as donor and the carbonyl oxygen as acceptor site (7, 8), while the isomeric ketols **1** and **2***b* form intermolecular hydrogen bonds at high concentrations. The possibility of weak Cl . . . . HO hydrogen bond interactions (9, 10) cannot be entirely excluded.

Molecular models show that only a limited number of conformations will satisfy the hydrogen-bonding requirements of the three isomeric condensation products **1**, **2***a*, and **2***b* if these assumptions are correct. These considerations prompted a conformational analysis of the two diastereomeric products **2***a* and **2***b*.

It is well known (11) that the coupling constant J_{ab} for the H_a—C—C—H_b fragment of ethane derivatives depends on the dihedral angle ϕ between the H_a—C—C and C—C—H_b planes. Although indiscriminate application of the theoretically derived correlation curve between J_{ab} and ϕ may lead to incorrect structural assignments (12), it may be used to estimate bond angles and conformations of organic molecules. Stiles and co-workers (13) investigated hydrogen bonding and conformational interactions in the diastereomeric condensation products of butanone with aromatic aldehydes by i.r. spectroscopy and measurement of the coupling constant J_{ab} between the tertiary hydrogens of CH_3—CO—$CH_a(CH_3)$—CH_bOH—Ar. They found intramolecular hydrogen bonding for both diastereomers and coupling constants of 8.0 and 3.0 c.p.s. for the *threo* (tertiary hydrogens *trans*) and *erythro* structure (tertiary hydrogens *gauche*), respectively.

After deuterium exchange, the n.m.r. spectrum of CH_3—CO—$CH_b(CH_3)$—CH_aOD—CCl_3 (**2***a* or **2***b*) exhibits a simple doublet due to the tertiary proton (H_a) of the —CH_aOD— group and a multiplet due to the tertiary proton (H_b) of the methyl-substituted carbon. Measurement of the H_b-methyl coupling in the methyl doublet and the H_a—H_b coupling in the H_a doublet allowed a satisfactory interpretation of the H_b signal, based upon simple splitting rules. The chemical shifts of the tertiary hydrogens and the coupling constants are summarized in Table III.

It is concluded from the magnitude of the splitting and from the inspection of molecular models that the H_a—C—C—H_b dihedral angle ϕ in the preferred conformation of **2***a* is close to 60 or 120° (Fig. 1, structures T-1 and T-2) while

TABLE III

Nuclear magnetic resonance chemical shifts and coupling constants J_{ab} of RCOCH_bR'—CH_aOD—CCl_3

Compound	Chemical shift (c.p.s.)*		J_{ab} (c.p.s.)
	H_a	H_b	
2*a*	246	207	1.9
2*b*	282	193	5.5
3*a*	247	208	2.0
3*b*	282	193	5.5
4*a*	238	183	2.0
4*b*	301	184	2.5

*Downfield from TMS in $CDCl_3$.

Can. J. Chem. Downloaded from www.nrcresearchpress.com by 210.87.254.42 on 09/05/12
For personal use only.

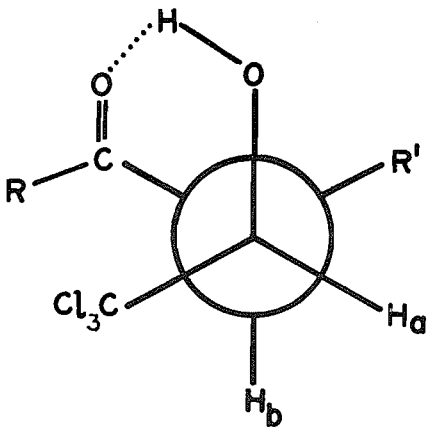

T-1 (threo)

2a, R = R' = Me
3a, R = Et, R' = Me

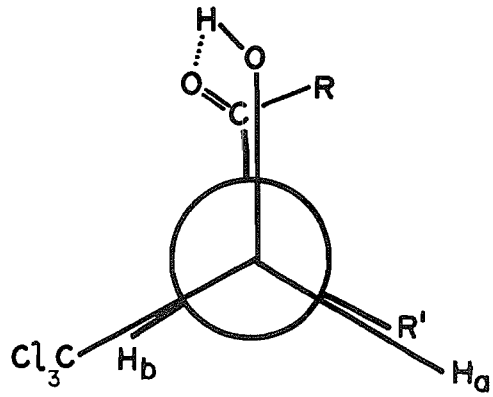

T-2 (threo)

2a, R = R' = Me
3a, R = Et, R' = Me
4a, R – R' = –$(CH_2)_4$–

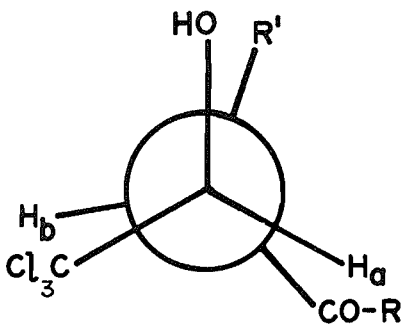

E-1 (erythro)

2b, R = R' = Me
3b, R = Et, R' = Me

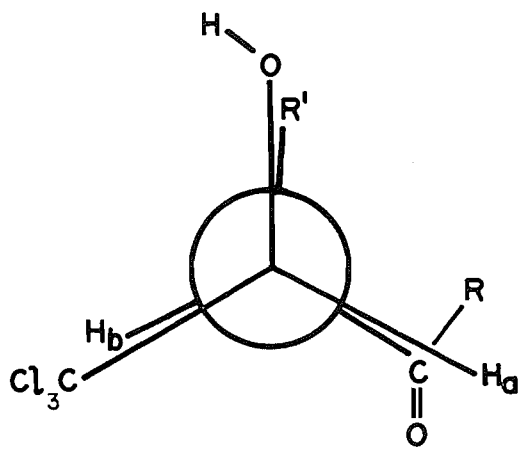

E-2 (erythro)

4b, R – R' = –$(CH_2)_4$–

FIG. 1. Conformational assignments for R—CO—CHR'—CHOH—CCl_3.

Can. J. Chem. Downloaded from www.nrcresearchpress.com by 210.87.254.42 on 09/05/12
For personal use only.

Can. J. Chem. Downloaded from www.nrcresearchpress.com by 210.87.254.42 on 09/05/12
For personal use only.

2*b* (and **1**) prefers a conformation with ϕ close to 140° (Fig. 1, structure E-1). Based on these results and the hydrogen-bond studies, the *threo* configuration has been assigned to **2***a* and the *erythro* configuration to **2***b*.[2]

The *erythro* configuration has been ruled out for the hydrogen-bonded structure **2***a* because molecular models of the two conformers obtained by 80° counterclockwise or 160° clockwise rotation of the rear carbon of structure E-1 (Fig. 1) indicate serious steric hindrance due to the eclipsing effect of the methyl and the trichloromethyl group, and all other conformers with an H_a—C—C—H_b dihedral angle of 60 or 120° (corresponding to the observed coupling constant J_{ab} = 1.9 c.p.s.) do not permit intramolecular hydrogen bonding. To minimize steric interaction between the R—CO— and the bulky trichloromethyl group of **2***b* (structure E-1, Fig. 1), a dihedral angle of 140° between the tertiary hydrogens is preferred to a 180° angle corresponding to a completely staggered conformation. For the same reason, the alternative *erythro* conformation with ϕ 140° (obtained by 80° clockwise rotation of the rear carbon of the structure E-1, Fig. 1) and all conformers with the alternative dihedral angle of 35° (corresponding to the observed coupling constant J_{ab} = 5.5 c.p.s.) are unfavorable for ketol **2***b*. It is therefore concluded that in contrast to the flat aryl groups of the compounds studied by Stiles and coworkers (13), the bulkiness of the trichloromethyl group prevents intramolecular hydrogen bonding in the *erythro* structure **2***b*, and in the straight-chain isomer **1** (see Table II).

It is hoped that high-resolution i.r. and n.m.r. spectral studies of very dilute solutions of **1**, **2***a*, and **2***b* in nonpolar solvents (presently in progress) will permit a quantitative estimate of the relative contribution of Cl . . . . H—O hydrogen-bonded structures and of conformational energy differences.

3-Pentanone and Chloral Hydrate

3-Pentanone reacts with chloral hydrate in acetic anhydride to form 1,1-diacetoxy-2,2,2-trichloroethane (**6**) and 1,1,1-trichloro-2-hydroxy-3-methyl-4-hexanone (**3***a*, m.p. 37–38°, and **3***b*, m.p. 57.5–58.5°). Pure samples of the two diastereomeric condensation products were obtained by partition chromatography of selected fractions of the high vacuum distillate on silicic acid using benzene as eluent.

Apparently Caujolle *et al.* (1) isolated only the high-melting isomer of this diastereomeric pair (m.p. 58.5°). We found that **3***a* and **3***b* are formed in the approximate molar ratio 5:6. The composition data of Table I show that the two methylene groups of 3-pentanone and cyclohexanone (*vide infra*) are less reactive toward chloral hydrate than the two methyl groups of acetone which is attributed to decreased nucleophilicity of the alkyl-substituted α-carbons.

The n.m.r. and i.r. spectra of the two diastereomers (Tables II and III) exhibit the same general features as the spectra of **2***a* and **2***b*, i.e. coupling of the hydroxylic proton with the geminal proton of the CHOH group, downfield position of the OH chemical shift of **3***a* relative to **3***b*, upfield shift of the OH proton signal of **3***b* (but not **3***a*) on dilution, concentration dependence of the i.r. absorption intensity ratio "free" OH: "bonded" OH for **3***b* only, and largely different coupling constants J_{ab} for the tertiary protons of **3***a* (2.0 c.p.s.) and **3***b* (5.5 c.p.s.), respectively. Applying arguments analogous to those advanced for the structural analysis of 1,1,1-trichloro-2-hydroxy-3-methyl-4-pentanone (**2***a* and **2***b*), it is concluded from these spectral data that **3***a* is an intramolecularly hydrogen-bonded *threo* structure (Fig. 1, conformer T-1 or T-2), and **3***b* is the *erythro* isomer existing predominantly in a conformation with ϕ close to 140° (Fig. 1, conformer E-1).

Cyclohexanone and Chloral Hydrate

The reaction between cyclohexanone and chloral hydrate in acetic anhydride has been reported (1) to give a 70% yield of a condensation product melting at 105°. Under the same reaction conditions we obtained a product mixture (47% yield) containing 1,1-diacetoxy-2,2,2-trichloroethane (**6**) as major component, and the two diastereomers of 2-(1-hydroxy-2,2,2-trichloroethyl-)cyclohexanone (**4***a* and **4***b*) in the approximate molar ratio 2:7. Ketol **4***b* (m.p. 101–102°) crystallized readily from the high-vacuum distillate of the crude product mixture but the isolation and purification of **4***a* (m.p. 43–44.5°) was found to be extremely difficult.

In close similarity to the structural features

[2]The *erythro*/*threo* nomenclature is used in this paper with reference to the two adjacent tertiary hydrogen atoms considering CCl_3—CH_a—CH_b—R′ as the main chain of the molecule and —OH and —CO—R as substituents.

Can. J. Chem. Downloaded from www.nrcresearchpress.com by 210.87.254.42 on 09/05/12
For personal use only.

observed for 1,1,1-trichloro-2-hydroxy-3-methyl-4-pentanone (**2***a* and **2***b*) and 1,1,1-trichloro-2-hydroxy-3-methyl-4-hexanone (**3***a* and **3***b*), i.r. and n.m.r. spectral data (Tables II and III) indicate strong intramolecular hydrogen bonding in **4***a* with the OH proton signal (381 c.p.s.) appearing considerably downfield from the position of the corresponding proton in **2***a* and **3***a* (342 and 345 c.p.s., respectively), and intermolecular hydrogen bonding in concentrated solutions of the more stable *erythro* structure **4***b*. The coupling constant J_{ab} between the two tertiary hydrogens was found to be 2.0 c.p.s. for **4***a* and 2.5 c.p.s. for **4***b* suggesting dihedral angles close to 60 or 120°. In order to satisfy these conformational requirements and to permit intramolecular C=O . . . H—O hydrogen bonding in **4***a*, the two diastereomers are believed to exist predominantly in the eclipsed conformations T-2 and E-2 (Fig. 1), respectively.

The rigidity of the cyclohexane ring prevents free rotation about the CHR′—CO single bond thus forcing the molecule into an eclipsed conformation in order to minimize steric interaction of the bulky CCl_3CHOH group with axial ring hydrogens or with the carbonyl group.

4-Methyl-2-pentanone and Chloral Hydrate

4-Methyl-2-pentanone yields only one condensation product, 1,1,1-trichloro-2-hydroxy-6-methyl-4-heptanone (**5**), when treated with chloral hydrate and acetic anhydride at 70°. In addition, 1,1-diacetoxy-2,2,2-trichloroethane is formed in low yield. It was not possible to detect any isomeric product by v.p.c. analysis using three different analytical columns. This finding, in conjunction with the experimental observation that 4,4-dimethyl-2-pentanone also undergoes condensation with chloral at the methyl group only, is indicative of steric factors being predominant in determining the product structure in crossed aldol condensations of unsymmetrical aliphatic ketones with chloral. Assuming that the reaction proceeds through an enol-like transition state rather than through an enolate intermediate, these results are in qualitative agreement with recent literature reports on the rate and orientation of the acid- and base-catalyzed deuteration of methyl ketones (5, 14, 15). The unusually high reactivity of the methylene group of butanone (see Table I) as compared to other methyl ketones of the general structure $CH_3—CO—CH_2—R$ has been attributed by Warkentin and Barnett (15) to a rate-accelerating polar effect of the alkyl group which "opposes the steric effect and is swamped by it in all the ketones except butanone". The same authors have shown that in the base-catalyzed deuteration of 4-methyl-2-pentanone in aqueous dioxane, enolization toward the methyl group is favored over enolization toward the methylene group by a factor of 2.38. The exclusive formation of **5** from chloral hydrate and 4-methyl-2-pentanone therefore indicates that this reaction cannot be simply interpreted in terms of two competitive rate-determining enolization steps, and that indiscriminate quantitative comparison of results obtained in different reaction media leads to incorrect predictions.

Further work will be needed to establish whether the transition state resembles ketone, enol or enolate, and to assess the importance of solvent effects and catalyst structure in determining the orientation of enolization of unsymmetrical aliphatic ketones and the rate of chloral addition. We are presently investigating the rate of acetate-catalyzed deuteration of ketones in acetic acid-d_4 and the kinetics of the reaction of anhydrous chloral with various methyl ketones in glacial acetic acid in order to gain further insight into the mechanism of this crossed aldol condensation.

On the basis of closely similar i.r. and n.m.r. spectra of **5** and **1**, intramolecular hydrogen bonding is believed to be weak or absent in straight-chain compounds of the type $R—CO—CH_2—CHOH—CCl_3$. In contrast to the spectral properties of the condensation products of butanone, 3-pentanone, and cyclohexanone with chloral hydrate, the OH proton signal of **5** appears as a broad singlet in the n.m.r. spectrum.

Experimental

Melting points are uncorrected. Analyses were performed by A. Bernhardt, Microanalytical Laboratory, Mülheim, Germany.

Infrared spectra were recorded on a Beckman IR-12 or a Perkin–Elmer 457 spectrometer using a CCl_4 solution or a thin film of neat liquid (melt) between sodium chloride plates. Ultraviolet (u.v.) spectra were run in 95% ethanol using a Unicam SP-200 spectrometer. Nuclear magnetic resonance spectra were recorded on a Varian A56/60 spectrometer using TMS as internal standard and $CDCl_3$ as solvent (unless specified otherwise). Chemical shifts are reported in c.p.s. downfield from TMS or in τ units. All spectral measurements were performed at room temperature.

Vapor-phase chromatographic analyses were carried out on a Varian Aerograph Model 1200-1 HY-FI III gas

Can. J. Chem. Downloaded from www.nrcresearchpress.com by 210.87.254.42 on 09/05/12
For personal use only.

chromatograph using a 5 ft × ⅛ in. column packed with 5% SE-30 on Aeropak 30 (column temperature 120–140°) and nitrogen as carrier gas (35 ml/min). All quantitative estimates of the composition of product mixtures by gas–liquid chromatographic (g.l.c.) analysis (Table I) are based on comparison of integrated peak areas obtained for the various components of a crude product mixture with those obtained for standard mixtures prepared from the pure components. The v.p.c. peak areas were measured planimetrically. For the purpose of analysis and identification, pure samples of all components of a product mixture were isolated by fractional distillation, crystallization and/or liquid partition chromatography on silica (Mallinckrodt, Silicic Acid A.R. 100 Mesh, Chromatographic Grade).

Butanone, 3-pentanone, cyclohexanone, and 4-methyl-2-pentanone (Matheson, Coleman, and Bell) were purified by fractional distillation; chloral hydrate (Matheson, Coleman, and Bell) and acetic anhydride (Baker and Adamson, Reagent grade) were used without further purification.

Reaction of Chloral Hydrate with Butanone

A mixture of 22.5 g (0.31 moles) of butanone, 41.1 g (0.25 moles) of chloral hydrate, 25.5 g (0.25 moles) of acetic anhydride, and 9.9 g (0.12 moles) of anhydrous sodium acetate was heated in a 200-ml pressure bottle at 70° for 58 h. Solvent, unreacted starting materials, and acetic acid were removed by distillation under reduced pressure. The yellow distillation residue was dissolved in 100 ml of ether, washed with water and sodium bicarbonate solution, and dried ($MgSO_4$). Evaporation of the ether gave 24.7 g of crude product (yellow) containing 30% (by weight) of ketol **1**, 23% of ketol **2***a*, 30% of ketol **2***b*, and 17% of 1,1-diacetoxy-2,2,2-trichloroethane (**6**) (analysis by v.p.c.). No dehydration or acetylation products and only trace amounts of other by-products were detected in the gas chromatogram. To separate **6** from the condensation products, the crude product mixture was distilled in high vacuum; ketols **1**, **2***a*, and **2***b* (total weight 15.4 g) were collected at 75–90°/0.02 mm (lit. (16), 135–138°/17 mm). Small samples of the pure components were isolated by liquid partition chromatography on silica using 20% (by volume) petroleum ether (30–60°) in benzene as eluent. Larger quantities of pure **2***a* and **2***b* were obtained by redistillation of the product mixture through a Vigreux column at high vacuum, v.p.c. analysis of each of the 15 fractions collected, seeding of selected fractions with **2***a* and **2***b*, respectively, filtration, and recrystallization from cyclohexane. Crystallization of **2***a* was extremely slow and inhibited by small amounts of impurities.

Characterization of **1**: m.p. 56–56.5° (lit. (1) 57°), b.p. 88–89°/0.02 mm.

Anal. Calcd. for $C_6H_9O_2Cl_3$: C, 32.83; H, 4.13; Cl, 48.46. Found: C, 32.78; H, 4.10; Cl, 48.38.

Ultraviolet: ν_{max}(EtOH) 212 mμ (ε 49), 276 mμ (ε 24); n.m.r. ($CDCl_3$): τ 8.91, triplet (3 protons, CH_3CH_2); 7.47, quartet (2, CH_3CH_2); 7.01, multiplet (2, CH_2-CHOH); 5.85, doublet (1, OH); 5.35, multiplet (1, CHOH).

Characterization of **2***a*: m.p. 33.5–34.5°, b.p. 69–71°/0.02 mm (estimated).

Anal. Calcd. for $C_6H_9O_2Cl_3$: C, 32.83; H, 4.13; Cl 48.46. Found: C, 32.72; H, 4.05; Cl, 48.33.

Ultraviolet: ν_{max}(EtOH) 210 mμ (ε 98), 278 mμ (ε 33); n.m.r.: τ 8.61, doublet (3, CH_3CH); 7.71, singlet (3, CH_3CO); 6.55, multiplet (1, CH_3CH); 5.90, multiplet (1, CHOH); 4.27, doublet (1, OH).

Characterization of **2***b*: m.p. 59.5–60.5°, b.p. 80–82°/0.02 mm.

Anal. Calcd. for $C_6H_9O_2Cl_3$: C, 32.83; H, 4.13; Cl, 48.46. Found: C, 32.95; H, 3.99; Cl, 48.36.

Ultraviolet: ν_{max}(EtOH) 214 mμ (ε 50), 276 mμ (ε 26); n.m.r.: τ 8.65, doublet (3, CH_3CH); 7.71, singlet (3, CH_3CO); 6.79, multiplet (1, CH_3CH); 6.25, doublet (1, OH); 5.31, multiplet (1, CHOH).

Reaction of Chloral Hydrate with 3-Pentanone

Following the procedure described in the preceding experiment (reaction time 102 h), 19.3 g of crude product (yellow) was obtained from 26.9 g (0.31 moles) of 3-pentanone, 41.1 g (0.25 moles) of chloral hydrate, 25.5 g (0.25 moles) of acetic anhydride, and 9.81 g (0.12 moles) of anhydrous sodium acetate. The crude product was found by v.p.c. analysis to contain 37% (by weight) of ketol **3***a*, 43% of ketol **3***b*, and 20% of **6**. High-vacuum distillation gave 13.4 g of a mixture of **3***a* and **3***b*, b.p. 79–89°/0.07 mm. Pure samples of the two diastereomers were obtained by fractional high-vacuum distillation and liquid partition chromatography with benzene as eluent (see preceding experiment for procedural details).

Characterization of **3***a*: m.p. 37–38°, b.p. 79–83°/0.07 mm.

Anal. Calcd. for $C_7H_{11}O_2Cl_3$: C, 36.00; H, 4.75; Cl, 45.55. Found: C, 36.05; H, 4.57; Cl, 45.45.

Ultraviolet: ν_{max}(EtOH) 213 mμ (ε 59), 279 mμ (ε 34); n.m.r. ($CDCl_3$): τ 8.95, triplet (3, CH_3CH_2); 8.61, doublet (3, CH_3CH); 7.33, quartet (2, CH_3CH_2); 6.53, multiplet (1, CH_3CH); 5.89, multiplet (1, CHOH); 4.17, doublet (1, OH).

Characterization of **3***b*: m.p. 57.5–58.5° (lit. (1) 58.5°), b.p. 85–89°/0.07 mm.

Anal. Calcd. for $C_7H_{11}O_2Cl_3$: C, 36.00; H, 4.75; Cl, 45.55. Found: C, 36.09; H, 4.70; Cl, 45.43.

Ultraviolet: ν_{max}(EtOH) 213 mμ (ε 51), 280 mμ (ε 31); n.m.r.: τ 8.93, triplet (3, CH_3CH_2); 8.71, doublet (3, CH_3CH); 7.37, quartet (2, CH_3CH_2); 6.78, multiplet (1, CH_3CH); 5.55, doublet (1, OH); 5.33, multiplet (1, CHOH).

Reaction of Chloral Hydrate with Cyclohexanone

Following the procedure described before, 28.9 g of crude product (yellow) was obtained by heating a mixture of 30.7 g (0.31 moles) of cyclohexanone, 41.1 g (0.25 moles) of chloral hydrate, 25.5 g (0.25 moles) of acetic anhydride, and 10.8 g (0.132 moles) of anhydrous sodium acetate at 70° for 45 h. The crude product mixture was found by v.p.c. analysis to contain 11% (by weight) of ketol **4***a*, 39% of ketol **4***b*, and 50% of **6**. High-vacuum distillation gave 10.4 g of a mixture of the two diasteromeric condensation products **4***a* and **4***b*. A pure sample of **4***b* was isolated by recrystallization of the solidified portion of the distillate from carbon tetrachloride. Purification of **4***a* was accomplished by liquid partition chromatography on silica using 20% (by volume) petroleum ether in benzene as eluent.

Can. J. Chem. Downloaded from www.nrcresearchpress.com by 210.87.254.42 on 09/05/12
For personal use only.

Characterization of **4***a*: m.p. 43–44.5°, b.p. 110–111°/0.04 mm.

Anal. Calcd. for $C_8H_{11}O_2Cl_3$: C, 39.13; H, 4.52; Cl, 43.32. Found: C, 39.22; H, 4.37; Cl, 43.28.

Nuclear magnetic resonance ($CDCl_3$): τ 6.03, multiplet (1, C*H*OH); 3.62, doublet (1, OH).

Characterization of **4***b*: m.p. 101–102° (lit. (1) 105°), b.p. 119–120°/0.04 mm.

Anal. Calcd. for $C_8H_{11}O_2Cl_3$: C, 39.13; H, 4.52; Cl, 43.32. Found: C, 39.22; H, 4.68; Cl, 43.23.

Ultraviolet: ν_{max}(EtOH) 214 mμ (ε 49), 283 mμ (ε 21); n.m.r.: τ 6.93, multiplet (1, C*H*—CHOH); 6.40, doublet (1, OH); 4.99, multiplet (1, C*H*OH).

1,1,1-Trichloro-2-hydroxy-6-methyl-4-heptanone (5)

Following the procedure outlined before (reaction time 52 h), 14.23 g of crude product (light yellow, partially solidified) was obtained from 31.25 g (0.31 moles) of 4-methyl-2-pentanone, 41.1 g (0.25 moles) of chloral hydrate, 25.5 g (0.25 moles) of acetic anhydride, and 10.9 g (0.133 moles) of anhydrous sodium acetate. The crude product mixture was found by v.p.c. analysis to contain 77% (by weight) of **5** and 23% of **6**. The residue left after removal of **6** by high vacuum distillation was recrystallized from carbon tetrachloride and cyclohexane to give 8.0 g of pure 1,1,1-trichloro-2-hydroxy-6-methyl-4-heptanone (**5**), m.p. 86–87° (lit. (3) 86–87°). Ketol **5** was shown by mixed melting point determination to be identical with a sample of the same compound prepared by the procedure described in the literature (3).

Characterization of **5**: u.v.: ν_{max}(EtOH) 213 mμ (ε 47), 239 mμ (ε 33), 280 mμ (ε 27); n.m.r. ($CDCl_3$): τ 9.07, doublet (6, $(CH_3)_2C$); 7.60, multiplet (3, $CHCH_2CO$); 7.05, multiplet (2, CH_2CHOH); 5.97, broad singlet (1, OH); 5.37, multiplet (1, C*H*OH).

1,1,1-Trichloro-2-hydroxy-4-pentanone (7)

Following the procedure outlined before (reaction time 50 h), 20.5 g of crude product (yellow, partially solidified) was obtained from 18.1 g (0.31 moles) of acetone, 41.1 g (0.25 moles) of chloral hydrate, 25.5 g (0.25 moles) of acetic anhydride, and 9.4 g (0.114 moles) of anhydrous sodium acetate. The crude product mixture containing 85% (by weight) of the desired ketol (7) and 15% of **6** was distilled at high vacuum to give 14.4 g of **7**, b.p. 100–105°/0.4 mm (lit (3) 100–105°/1 mm), m.p. 73.5–75° (lit. (1, 3, 17) 75–76°) after recrystallization from cyclohexane.

Characterization of **7**: u.v.: ν_{max}(EtOH) 219 mμ (ε 41), 275 mμ (ε 17); n.m.r. ($CDCl_3$): τ 7.75, singlet (3, CH_3CO); 7.00, multiplet (2, $COCH_2$); 5.90, doublet (1, OH); 5.35, multiplet (1, C*H*OH).

Reaction of Benzalacetone with Chloral Hydrate

Only trace amounts of 1,1,1-trichloro-2-hydroxy-6-phenyl-5-hexen-4-one (**8**) were obtained when a mixture of 45.6 g (0.31 moles) of benzalacetone, 41.1 g (0.25 moles) of chloral hydrate, 25.5 g (0.25 moles) of acetic anhydride, and 12.5 g (0.152 moles) of anhydrous sodium acetate was heated at 70° for 21 h. The usual work-up procedure (see before) gave a crude product mixture which was found by n.m.r. analysis (methyl peaks) to contain approximately 75 mole-% of benzalacetone and 25 mole-% of 1,1-diacetoxy-2,2,2-trichloroethane (**6**).

1,1-Diacetoxy-2,2,2-trichloroethane (**6**)

Compound **6** was obtained as the exclusive reaction product (71% yield) when a mixture of 31.25 g (0.31 moles) of 4-methyl-2-pentanone, 36.8 g (0.25 moles) of anhydrous chloral,[3] 25.5 g (0.25 moles) of acetic anhydride, and 5.2 g (0.063 moles) of anhydrous sodium acetate was heated at 100° for 52 h and worked up as described before. None of the desired 1,1,1-trichloro-2-hydroxy-6-methyl-4-heptanone (**5**) was detected by n.m.r. and v.p.c. analysis of the crude product mixture (44.4 g).

Characterization of **6**: b.p. 217–218°/750 mm, (lit. (18) 225°/750 mm); n.m.r. ($CDCl_3$): τ 7.81, singlet (6, CH_3); 2.28, singlet (1, CH); n_D^{23} 1.4570 (lit. (14), n_D^{20} 1.4567).

Acknowledgment

The support of this work by a grant from the National Research Council of Canada is gratefully acknowledged.

1. F. Caujolle, P. Couturier, and C. Dulaurans. Bull. Soc. Chim. France, **17**, 19 (1950).
2. F. L. Breusch and H. Keskin. Arch. Biochem. Biophys. **18**, 305 (1948).
3. W. Reeve and E. Kiehlmann. J. Org. Chem. **31**, 2164 (1966).
4. S. Mamedov and F. Gadshisade. Zh. Obshch. Khim. **32**, 799 (1962).
5. J. Warkentin and O. S. Tee. J. Am. Chem. Soc. **88**, 5540 (1966).
6. W. J. Middleton and R. V. Lindsey, Jr. J. Am. Chem. Soc. **86**, 4948 (1964).
7. M. Oki, H. Iwamura, J. Aihara, and H. Lida. Bull. Chem. Soc. Japan, **41**, 176 (1968).
8. L. Joris and P. von R. Schleyer. J. Am. Chem. Soc. **90**, 4599 (1968).
9. P. J. Krueger and H. D. Mettee. Can. J. Chem. **42**, 340 (1964).
10. T. M. Connor and C. Reid. J. Mol. Spectry. **7**, 32 (1961).
11. M. Karplus. J. Chem. Phys. **30**, 11 (1959).
12. M. Karplus. J. Am. Chem. Soc. **85**, 2870 (1963).
13. M. Stiles, R. Winkler, Y. Chang, and L. Traynor. J. Am. Chem. Soc. **86**, 3337 (1964).
14. C. Rappe and W. H. Sachs. J. Org. Chem. **32**, 3700, 4127 (1967).
15. J. Warkentin and C. Barnett. J. Am. Chem. Soc. **90**, 4629 (1968).
16. G. M. Baluja, A. M. Municio, and S. Vega. Anales. Real Soc. Espan. Fis. Quim. Madrid, Ser. B, **60**, 639 (1964).
17. W. Koenigs. Chem. Ber. **25**, 729 (1892).
18. N. A. D. Parlee, J. R. Dacey, and C. C. Coffin. Can. J. Res. B, **15**, 254 (1937).

[3]Anhydrous chloral was prepared from the commercially available material (chloral, practical, stabilized; Matheson Coleman and Bell) by distillation from phosphorus pentoxide.

Can. J. Chem. Downloaded from www.nrcresearchpress.com by 210.87.254.105 on 09/05/12
For personal use only.

Reactions of some 1,3-dipolarophiles with 1,2-dithioles and 1,2,4-dithiazoles

J. M. BUCHSHRIBER, D. M. MCKINNON, AND M. AHMED
Chemistry Department, University of Manitoba, Winnipeg, Manitoba

Received November 27, 1968

The reactions of 1,2-dithiole-3-thiones and 1,2,4-dithiazole-3-thiones with acetylenic esters provide initial 1,3-dithiole products by 1,3-dipolar additions. 3-Imino-1,2-dithioles react similarly to form thiazoles. Both these initial adducts react further with more acetylenic ester to form spiran type structures. The stereochemistry of these is discussed briefly and applied to their reactivity and spectroscopic properties.

Canadian Journal of Chemistry, 47, 2039 (1969)

1,2-Dithiole-3-thiones (**1**) have been shown to undergo 1,3-dipolar reactions with activated acetylenes (1–3). The reaction provides 1:1 adducts, formulated as 2-(2-thioacylmethylene)-1,3-dithioles (**2**). Further reaction may provide spirans (**3**) by further 1,4-addition of the activated acetylene with the initially formed adduct. Similarly, 1,2,4-dithiazole-3-thiones (**4**) react with activated acetylenes to give 2-thioacylimino -1,3-dithiole (**5**) initial products (3–5) which may react further with more acetylene to give spiran structures (6) (**6**).

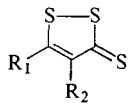

1

a $R_1 = R_2 = Ph$

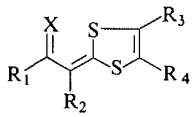

2

a $R_1 = R_2 = Ph, R_3 = R_4 = CO_2Me, X = S$
b $R_1 = R_2 = Ph, R_3 = H, R_4 = CO_2Et, X = S$
c $R_1 = Me, R_2 = H, R_3 = Ph, R_4 = H, X = O$
d $R_1 = R_2 = R_3 = Ph, R_4 = CO_2Et, X = S$

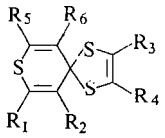

3

a $R_1 = R_2 = Ph, R_3 = R_4 = R_5 = R_6 = CO_2Me$
b $R_1 = R_2 = Ph, R_3 = CO_2Et, R_4 = R_5 = H, R_6 = CO_2Et$
c $R_1 = R_2 = Ph, R_3 = R_4 = CO_2Me, R_5 = H, R_6 = CO_2Et$

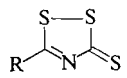

4

a R = Ph

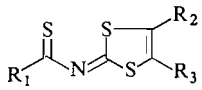

5

a $R_1 = Ph, R_2 = R_3 = CO_2Me$
b $R_1 = Ph, R_2 = R_3 = CF_3$
c $R_1 = Ph, R_2 = H, R_3 = CO_2Et$

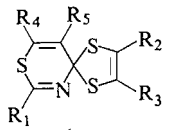

6

We were interested in the reactions of some dipolarophilic acetylenes with other such thiones and also with 3-imino-1,2-dithioles (**7***a*,*b*) which might be expected to undergo reactions similarly to the thiones, since partial ionic structures may be also written for these. Behringer reports (7) obtaining adducts by reaction of 5-iminoisothiazoles with dimethyl acetylenedicarboxylate. Probably the reaction of a 3-imino-1,2,4-dithiazole with dimethyl acetylenedicarboxylate (3) proceeds similarly.

4,5-Diphenyl-1,2-dithiole-3-thione (**1***a*) reacted with the three acetylenic esters studied; dimethyl acetylenedicarboxylate, ethyl propiolate, and ethyl phenylpropiolate. The first of these gave first a mono-adduct (**2***a*). The nuclear magnetic resonance (n.m.r.) spectrum of this showed two

Can. J. Chem. Downloaded from www.nrcresearchpress.com by 210.87.254.105 on 09/05/12
For personal use only.

singlets assigned to the methyls of the carbomethoxy groups which are not equivalent in this molecule. It is reported (4) however, that in the related thioacylimino-1,3-dithiole (**5***a*) the two carbomethoxy groups are equivalent. It is also found in 4,5-bistrifluoromethyl-2-thiobenziminо-1,3-dithiole (**5***b*) prepared by reaction of hexafluoro-2-butyne with 5-phenyl-1,2,4-dithiazole-3-thione (**4**) that the two trifluoromethyl groups are equivalent as indicated by n.m.r. It was initially suggested that the equivalence of the methyls was fortuitous, but it now appears more likely that they are in fact equivalent due to ready rotation of the side chain by a means which is not yet clear. Similarly, the n.m.r. spectrum of the ethyl ester (**5***c*) (4) showed the presence of only one carbethoxy group, instead of the two expected if two geometrical isomers had been obtained. Probably the greater electronegativity of the side chain nitrogen in these compounds (**5***a,b,c*) compared to the side chain carbon in compound **2***a* makes the exocyclic double bond acquire more single bond character, permitting free rotation. Such free rotation should be temperature dependent, but even at $-60°$, the n.m.r. spectrum of compound **5***c* indicated that only one compound was present. Further treatment of the mono-adduct (**2***a*) with dimethyl acetylenedicarboxylate provided a di-adduct (**3***a*). The two carbomethoxy groups in the five-membered ring are equivalent in the di-adduct, and this is confirmed by the n.m.r. A small amount of unidentified violet material was also isolated from this reaction.

With ethyl propiolate the thione (**1***a*) gave both mono- and di-adducts. The n.m.r. spectrum of the former (**2***b*) indicated that it was a mixture of two geometrical isomers. This has been previously suggested (8) for a related 1,3-dithiole ketone (**2***c*) and for some other thioacylmethylene-1,3-dithioles (3). These isomers could not be separated. The n.m.r. showed two different singlets at 2.26 τ and 2.13 τ due to the different protons on the five-membered rings of the mono-adducts. A possible mechanism for the 1,3-addition would involve initial β-addition of the thione group to the ethyl propiolate. This is inconsistent with the production of two isomers. Possibly these could interconvert under the conditions of the reaction, but Campaigne (8) has shown that for two such acylmethylene-1,3-dithiole isomers there was no interconversion at 140°.

The n.m.r. spectrum of the di-adduct (**3***b*) obtained was consistent with the presence of two enantiomers, both derived from the geometrical isomers of the mono-adduct. The two protons on the 1,3-dithiole rings absorbed at τ 3.5 and are equivalent in the enantiomers. The carbethoxy group of the thiopyran ring may be α or β to the sulfur atom, depending on the mode of addition of the acetylenic ester to the α,β-unsaturated thioketonic side chain of the initial adduct (**2***b*). Only one singlet for the proton on the thiopyran ring is apparent, hence only one isomer has been formed. Probably the mechanism again involves β-addition of the thione sulfur (from a vinylogous 1,3-dithiole-2-thione) to the acetylenic ester. Even the meribicyclic **6***a*, thiathiophthene system exhibits vinylogous 1,2-dithiole-3-thione properties in its reaction with methyl iodide (9). A 1,4-dipolar mechanism has been proposed (10) for this second addition of acetylenic ester.

A mixed di-adduct (**3***c*) was prepared by reaction of the mono-adduct (**2***a*) with ethyl propiolate to allow proper assignment of the protons in the different rings of the di-adduct (**3***b*). It demonstrated that the protons on the thiopyran ring of the di-adducts absorb at lower fields than those on the 1,3-dithiole ring.

The reaction of the thione (**1***a*) with ethyl phenylpropiolate provided a mono-adduct (**2***d*) only. Possibly steric hindrance or reduced reactivity of the acetylene made formation of a di-adduct more difficult. Examination of the n.m.r. spectrum again indicated that two geometrical isomers were present.

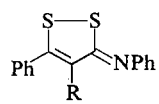

7

a R = H
b R = Ph

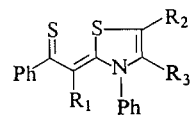

8

a R_1 = H,R_2 = R_3 = CO_2Me
b R_1 = Ph,R_2 = R_3 = CO_2Me
c R_1 = H,R_2 = CO_2Et,R_3 = H
d R_1 = H,R_2 = CO_2Et,R_3 = Ph

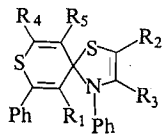

9

a $R_1 = H, R_2 = R_3 = R_4 = R_5 = CO_2Me$.
b $R_1 = Ph, R_2 = R_3 = R_4 = R_5 = CO_2Me$

Reaction of two 3-phenylimino-1,2-dithioles (**7***a,b*), prepared (11) by reaction of 3-methylthio-1,2-dithiolium salts with aniline, with dimethyl acetylenedicarboxylate gave no mono-adducts (**8**). Instead di-adducts were obtained. These may be formulated as spiran structures (**9***a,b*) respectively which have a thiazole nucleus joined to a thiopyran nucleus. Even when equivalent quantities of reagents were used, no mono-adducts (**8***a, b*) were isolated. Presumably these reacted more rapidly than the starting material with the acetylenic ester. However, Behringer (7) reports obtaining mono-adducts by reaction of isothiazole-3-imines with dimethyl acetylenedicarboxylate. In this case steric interference by phenyl groups on the nitrogen atoms of the side chain of the mono-adduct may hinder reaction with more acetylenic ester.

With the less reactive propiolic and phenylpropiolic esters, only 5-phenyl-3-phenylimino-1,2-dithiole (**7***a*) reacted. Mono-adducts (**8***c,d*) respectively were obtained. The n.m.r. spectrum was inconclusive in deciding whether the products were single compounds or mixtures of two geometrical isomers. Apparently, the ester groups are equivalent in the pairs of geometrical isomers in each case. 4,5-Diphenyl-3-phenylimino-1,2-dithiole (**7***b*) failed to react, probably due to steric hindrance. In these imines (**7***a,b*) the *N*-phenyl group may be "*cis*" or "*trans*" to the sulfur atoms. In the compound (**7***b*) however, steric hindrance by the 4-phenyl group makes the "*cis*" form more likely, and this form would in turn be less susceptible to approach by the acetylenic ester.

Also, the mono-adducts (**8***c,d*) formed may be either thiazole-4- or -5-carboxylic esters. They are formulated as the former since these would be the expected products of initial β-addition to the acetylenic ester.

Experimental

Thin-layer chromatography was performed on "Camag" silica gel type D.S.F. 5, supplied by Mondray Ltd. Development of plates was carried out using benzene with increasing proportions of chloroform and nuclear magnetic resonance spectra were obtained on a Varian model 56/60A spectrometer, in deuteriochloroform solution using tetramethylsilane as an internal standard.

Reaction of 4,5-Diphenyl-1,2-dithiole-3-thione with Dimethyl Acetylenedicarboxylate to form the Mono-adduct (2a)

4,5-Diphenyl-1,2-dithiole-3-thione (12) (381 mg) and dimethyl acetylenedicarboxylate (185 mg) in benzene (60 ml) were stirred together at room temperature for 18 h. The solution was evaporated to give a dark-green solid which was further purified by thin-layer chromatography. Dark-green needles m.p. 158.5–160.5° from chloroform (70%).

Anal. Calcd. for $C_{21}H_{16}O_4S_3$: C, 58.88; H, 3.74; S, 22.43. Found: C, 58.84; H, 3.72; S, 22.24.

Nuclear magnetic resonance 6.19 τ (3H singlet); 6.07 τ (3H singlet); 2.95 τ (5H singlet); 2.79 τ (5H singlet).

Reaction of 4,5-Diphenyl-1,2-dithiole-3-thione with Dimethyl Acetylenedicarboxylate to form the Di-adduct (3a)

4,5-Diphenyl-1,2-dithiole-3-thione (12) (285 mg) and dimethyl acetylenedicarboxylate (282 mg) in benzene (30 ml) were refluxed together for 15 h. The reddish-brown product obtained on evaporation was further purified by thin-layer chromatography. Two bands were obtained. The main product was the di-adduct. Yellow prisms m.p. 111–113° from ethanol (66%).

Anal. Calcd. for $C_{27}H_{22}O_8S_3$: C, 56.84; H, 3.86; S, 16.86. Found: C, 56.96; H, 3.75; S, 16.80.

Nuclear magnetic resonance 6.32 τ (6H singlet); 6.19 τ (3H singlet); 6.13 τ (3H singlet); 3.03–2.70 τ (5H multiplet); 2.77 τ (5H singlet).

A minor product was separated and crystallized from ethanol. Violet powder m.p. 161–163° (10 mg).

Reaction of 4,5-Diphenyl-1,2-dithiole-3-thione with Ethyl Propiolate (2b) and (3b)

The thione (213 mg) and the ester (74 mg) in benzene (50 ml) were refluxed 24 h. After evaporation the crude mixture was treated by thin-layer chromatography to separate the mono- and di-adducts.

Mono-adduct

Brownish-green powder from chloroform (29%) m.p. 175–178°.

Anal. Calcd. for $C_{20}H_{10}O_2S_3$: C, 62.50; H, 4.17; S, 25.00. Found: C, 61.00; H, 4.02; S, 23.89.

Nuclear magnetic resonance 8.72 τ (3H triplet, J = 7.2 c.p.s.); 8.62 τ (3H triplet, J = 7.2 c.p.s.); 5.67 τ (2H quartet, J = 7.2 c.p.s.); 5.57 τ (2H quartet, J = 7.2 c.p.s.); 2.98 τ (5H singlet); 2.80 τ (5H singlet); 2.26 τ (1H singlet); 2.13 τ (1H singlet).

Di-adduct

Yellow prisms from ethanol (70%) m.p. 149–151°.

Anal. Calcd. for $C_{25}H_{22}O_4S_3$: C, 62.24; H, 4.56; S, 19.92. Found: C, 61.98; H, 4.61; S, 19.83.

Nuclear magnetic resonance 8.79 τ (3H triplet, J = 7.0 c.p.s.); 8.69 τ (3H triplet, J = 7.0 c.p.s.); 5.9 τ (2H quartet, J = 7.0 c.p.s.); 5.67 τ (2H quartet, J = 7.0 c.p.s.); 3.50 τ (1H singlet); 2.93 τ (10H singlet); 2.49 τ (1H singlet).

Can. J. Chem. Downloaded from www.nrcresearchpress.com by 210.87.254.105 on 09/05/12
For personal use only.

Can. J. Chem. Downloaded from www.nrcresearchpress.com by 210.87.254.105 on 09/05/12
For personal use only.

Reaction of Dimethyl 2-(α-phenylthiophenacylidene)-1,3-dithiole-4,5-dicarboxylate with Ethyl Propiolate (3c)

The 1,3-dithiole dicarboxylic ester (151 mg) and ethyl propiolate (51 mg) in benzene (40 ml) were refluxed together for 4 days. The crude product was purified by thin-layer chromatography. Yellow needles from ethanol (62%) m.p. 148–150°.

Anal. Calcd. for $C_{26}H_{22}O_6S_3$: C, 59.32; H, 4.18; S, 18.25. Found: C, 59.12; H, 4.04; S, 18.17.

Nuclear magnetic resonance 8.77 τ (3H triplet, J = 7.0 c.p.s.); 6.38 τ (6H singlet); 5.63 τ (2H quartet, J = 7.0 c.p.s.); 3.02–2.50 τ (10H multiplet); 2.45 τ (1H singlet).

Reaction of 4,5-Diphenyl-1,2-dithiole-3-thione with Ethyl Phenylpropiolate (2d)

The thione (325 mg) and the ester (195 mg) in xylene (25 ml) were refluxed for 24 h. The solvent was removed under reduced pressure, and the crude product recrystallized from ethanol (56%) m.p. 183–185°.

Anal. Calcd. for $C_{26}H_{20}O_2S_3$: C, 67.82; H, 4.35; S, 20.87. Found: C, 67.62; H, 4.30; S, 20.85.

Nuclear magnetic resonance 8.92 τ (3H triplet, J = 7.2 c.p.s.); 8.80 τ (3H triplet, J = 7.2 c.p.s.); 5.90 τ (2H quartet, J = 7.2 c.p.s.); 5.78 τ (2H quartet, J = 7.2 c.p.s.); 3.05–2.53 τ (15H multiplet).

Reaction of 5-Phenyl-3-phenylimino-1,2-dithiole with Dimethyl Acetylenedicarboxylate (9a)

5-Phenyl-3-phenylimino-1,2-dithiole (**11**) (120 mg) and excess dimethyl acetylenedicarboxylate in benzene (50 ml) were refluxed for 18 h. The crude product obtained on evaporation was purified by thin-layer chromatography and crystallized from ethanol, orange prisms m.p. 173–175° (63%).

Anal. Calcd. for $C_{27}H_{23}NO_8S_2$: C, 58.59; H, 4.16; N, 2.53; S, 11.58. Found: C, 58.46; H, 4.10; N, 2.68; S, 11.68.

Nuclear magnetic resonance 6.42 τ (3H singlet); 6.32 τ (3H singlet); 6.20 τ (3H singlet); 6.12 τ (3H singlet); 3.75 τ (1H singlet); 2.83–2.62 τ (5H multiplet); 2.73 τ (5H singlet).

When the reaction was performed with equimolar quantities of reagents, the product was a mixture of di-adduct and unreacted imine.

Reaction of 5-Phenyl-3-phenylimino-1,2-dithiole with Ethyl Propiolate (8c)

The imine (400 mg) and the ethyl propiolate (150 mg) in benzene (20 ml) were refluxed for 18 h. The product obtained on evaporation was purified by thin-layer chromatography and crystallized from ethanol, dark orange needles, m.p. 221–223° (75%).

Anal. Calcd. for $C_{20}H_{17}NO_2S_2$: C, 65.39; H, 4.63; N, 3.82; S, 17.44. Found: C, 65.23; H, 4.66; N, 3.95; S, 17.47.

Nuclear magnetic resonance 8.70 τ (3H triplet, J = 7.2 c.p.s.); 5.83 τ (2H quartet, J = 7.2 c.p.s.); 3.12–2.59 τ (11H multiplet, due to 10 protons on the two benzene rings and one single proton on the thiazole ring); 2.47 τ (1H singlet; proton on side chain).

Reaction of 5-Phenyl-3-phenylimino-1,2-dithiole with Ethyl Phenylpropiolate (8d)

5-Phenyl-3-phenylimino-1,2-dithiole (11) (329 mg) and the ester (200 mg) in xylene (20 ml) were refluxed for 14 h. The solvent was removed under reduced pressure and the yellowish-orange residue was extracted with boiling ethanol (80 ml) to remove unreacted thione, and recrystallized from chloroform. Dark orange needles m.p. 261–263° (64%).

Anal. Calcd. for $C_{26}H_{21}NO_2S_2$: C, 70.43; H, 4.74; N, 3.16; S, 14.45. Found: C, 70.24; H, 4.86; N, 3.26; S, 14.26.

Nuclear magnetic resonance 8.80 τ (3H triplet, J = 7.0 c.p.s.); 5.77 τ (2H quartet, J = 7.0 c.p.s.); 2.97–2.28 τ (16H multiplet, due to 15 protons on the benzene rings and one proton on the thiazole ring).

Reaction of 4,5-Diphenyl-3-phenylimino-1,2-dithiole with Dimethyl Acetylenedicarboxylate (9b)

4,5-Diphenyl-3-phenylimino-1,2-dithiole (11) (330 mg) and the ester (132 mg) in xylene (30 ml) were refluxed for 72 h. The orange residue remaining after removal of the solvent under reduced pressure was recrystallized from ethanol. Yellow prisms m.p. 230–232° (75%).

Anal. Calcd. for $C_{33}H_{27}NO_8S_2$: C, 62.97; H, 4.29; N, 2.33; S, 10.17. Found: C, 62.73; H, 4.47; N, 2.17; S, 10.21.

Nuclear magnetic resonance 6.57–6.37 τ (12H, two main peaks but not properly resolved). 3.05–2.67 τ (15H multiplet, not properly resolved).

Reaction of 4,5-Diphenyl-3-Phenylimino-1,2-dithiole with Ethyl Propiolate

The imine was treated with excess ester in boiling xylene for 1 week. A thin-layer chromatography separation of the mixture indicated only unreacted starting materials.

Reaction of 4,5-Diphenyl-3-phenylimino-1,2-dithiole with Ethyl Phenylpropiolate

The imine was treated with excess ester in boiling xylene for 1 week. A thin-layer chromatography separation of the mixture indicated only unreacted starting materials.

Reaction of 5-Phenyl-1,2,4-dithiazole-3-thione with Hexafluoro-2-butyne (5b)

The thione (500 mg) was heated with excess hexafluoro-2-butyne in benzene (20 ml) in a sealed glass tube at 70° for 7 h. The benzene was evaporated and the product recrystallized from ethanol. Greenish needles m.p. 128–129° (89%).

Anal. Calcd. for $C_{12}H_5F_6NS_3$: C, 38.70; H, 1.30; F, 30.31; N, 13.69; S, 25.52. Found: C, 38.70; H, 1.53; F, 30.47; N, 3.81; S, 25.72.

Nuclear magnetic resonance gave a singlet at +3133 τ.

Low Temperature Nuclear Magnetic Resonance Study of Ethyl 2-Thiobenzimino-1,3-dithiole-4-carboxylate

The ester (4) was examined in saturated deuteriochloroform solution at temperatures to −60°. The absorption of the proton on the 1,3-dithiole ring at 1.98 τ remained a singlet over the temperature range studied.

Acknowledgments

This work was supported by the National Research Council of Canada. The authors wish to thank Mr. R. Fitch and Mr. R. Dickinson for

the preparation of nuclear magnetic resonance spectra.

1. D. B. J. EASTON and D. LEAVER. Chem. Commun. 585 (1965).
2. H. BEHRINGER and R. WIEDENMANN. Tetrahedron Letters, 3705 (1965).
3. H. BEHRINGER, D. BENDER, J. FALKENBERG, and R. WIEDENMANN. Ber. **101**, 1428 (1968).
4. J. W. MACDONALD and D. M. MCKINNON. Can. J. Chem. **45**, 1225 (1967).
5. H. BEHRINGER and D. DEICHMANN. Tetrahedron Letters, 1013 (1967).
6. G. LANG and J. VIAILLE. Bull. Soc. Chim. France, 2865 (1967).
7. H. BEHRINGER, J. KILGER, and R. WIEDENMANN. Tetrahedron Letters, 1185 (1968).
8. E. CAMPAIGNE and F. HAAF. J. Org. Chem. **30**, 732 (1965).
9. E. KLINGSBERG. J. Org. Chem. **33**, 2915 (1968).
10. H. DAVY, M. DEMUYNCK, D. PAQUER, A. ROUESSAC, and J. VIAILLE. Bull. Soc. Chim. France, 2057 (1968).
11. G. PAULMIER, Y. MOLLIER, and N. LOSAC'H. Bull. Soc. Chim. France, 2463 (1965).
12. M. G. VORONKOV, A. S. BROWN, and G. B. KARPENKO. J. Gen. Chem. USSR Eng. Transl., **19**, 395 (1949); Dokl. Akad. Nauk SSSR **59**, 1437 (1948).

Can. J. Chem. Downloaded from www.nrcresearchpress.com by 210.87.254.105 on 09/05/12
For personal use only.

Can. J. Chem. Downloaded from www.nrcresearchpress.com by 210.87.254.105 on 09/05/12
For personal use only.

Photolysis of benzil in 2-propanol and in cumene

DAVID L. BUNBURY AND TZE TANG CHUANG[1]
Chemistry Department, St. Francis Xavier University, Antigonish, Nova Scotia

Received October 9, 1968

Benzil has been irradiated in 2-propanol and in cumene with a mercury lamp filtered through Pyrex. The principal products are benzoin, 1,2,3,4-tetraphenyl-2,3-dihydroxybutane-1,4-dione (**3**), benzoin benzoate, benzaldehyde, benzoic acid, 1,2,3,4-tetraphenyl-2,3-dihydroxybutane-1,4-dione dibenzoate (**5**), and some unidentified high molecular weight compounds. The yield of **3** is strongly dependent on initial benzil concentration and temperature and on the solvent used. The quantum yield of benzil disappearance depends on initial benzil concentration to a lower limit which varies with solvent. At an initial benzil concentration of 0.083 moles/l, the quantum yield of benzil disappearance is 0.11 in 2-propanol and 0.018 in cyclohexane. Compound **3** does not appear to be formed by a coupling of the appropriate ketyl radicals, as in the benzophenone case but instead, a complex is formed between a benzil molecule and the ketyl radical. Compound **3** decomposes at temperatures as low as 25°. The principal path for the formation of benzaldehyde and benzoyl radicals is the dissociation of the ketyl radical. Excited benzil abstracts a hydrogen from 2-propanol at least ten times faster than it dissociates into two benzoyl radicals.

Canadian Journal of Chemistry, 47, 2045 (1969)

Introduction

The photo-reaction of benzil in cyclohexane has already been reported (1). This study has been extended using 2-propanol and cumene as solvents. Differences in kinds of products formed, in product distribution, and in concentration dependence, result when different solvents are used, particularly in the appearance of benzil pinacol (1,2,3,4-tetraphenyl-2,3-dihydroxy-1,4-butanedione). These differences seem to be related to the ease with which a hydrogen atom may be abstracted from the solvent. Benzoic acid appears as a product in all solvents used despite exclusion of oxygen during irradiation. Although similar to the photo-reduction of benzophenone (**2**) in the initial chemical step, subsequent reactions are more complicated.

Experimental

Materials

Benzil was from Eastman Organic Chemicals, and benzoin was Matheson, Coleman, and Bell, reagent grade. These were twice recrystallized from methanol. 2-Propanol and benzene, Fisher certified reagents, were freshly distilled. Cumene, Eastman Organic Chemicals, was distilled each time immediately before use. The silica gel used in column chromatography was 100–200 mesh Fisher certified grade, heated to 150 °C for 1 h and cooled to room temperature in a desiccator. Eastman Chromagram Sheet 6060 (silica gel with fluorescent indicator) was used in thin-layer chromatography (t.l.c.) and was heated to 100° for 20 min before use. Naphthalene, anthracene, and pyrene were chromatographed through activated alumina (3). Tri-*n*-butyltin hydride was prepared from tri-*n*-butyltin chloride (Aldrich Chemical Co. Inc.) by reduction with lithium aluminium hydride and vacuum distilled prior to use (4). Benzoin benzoate had been prepared previously. All other solvents used were freshly distilled.

Apparatus

All melting points were taken on a Fisher–Johns melting point apparatus and/or checked with a Mel-Temp melting point apparatus. Infrared (i.r.) spectra were determined on a Beckman IR 8 double beam spectrophotometer. Elemental analyses were done by Schwarzkopf Microanalytical Laboratory, 56–19 37th Avenue, Woodside, New York 11377, except for the dibenzoate analysis which was done by Dr. C. Daessle, Montreal, Quebec. Molecular weights were determined on a Hitachi Perkin–Elmer Model 115 molecular weight apparatus which uses an isopiestic method. Gas–liquid chromatography (g.l.c.) was performed on a Burrell model K-1 with a thermal conductivity detector. A 250 cm × ¼ in. internal diameter column filled with 20% Dow Corning high vacuum silicone grease on 80–100 mesh Chromosorb W was used for all compounds except acetone, for which 15% Apiezon L on the same supporting material was used. Standard solutions were run alternately with the irradiated solution for each peak of interest. Nuclear magnetic resonance (n.m.r.) spectra were obtained on a Varian A-60-A spectrometer, by courtesy of Dr. B. M. Lynch.

Three Raymaster Uviarc high pressure mercury lamps 420-UI (George W. Gates and Co., Inc., Franklin Square, Long Island, New York 11 010) were used in all irradiations except the actinometry runs. For these an Osram HBO 100 W/2 mercury super (high) pressure lamp (George W. Gates) with an arc size of 0.3 mm × 0.3 mm was used. Quantitative measurements were made on thin-layer chromatograms by a Photovolt Densicord, model 542 densitometer with a light source of 254 mμ.

[1]Taken from the M.Sc. Thesis of Tze Tang Chuang. Present Address: University of Alberta, Edmonton, Alberta.

Can. J. Chem. Downloaded from www.nrcresearchpress.com by 210.87.254.105 on 09/05/12
For personal use only.

Irradiation

Three types of irradiation were carried out. In the first type, 0.6 g of benzil were weighed into a 50 ml tube and made up to 35 ml with 2-propanol. This was attached to a vacuum line and, after degassing by at least three freeze pump thaw cycles, was sealed off the line and allowed to warm to room temperature. After solution of the benzil, it was irradiated for 7 min with external water cooling.

In the second type, 34.2 g of benzil were dissolved in 2 l of 2-propanol. The resulting solution was poured into a 3 l three-necked round bottom Pyrex flask fitted with reflux condenser and nitrogen sparger connections. The flask was surrounded by the 3 Uviarc mercury lamps and, after thorough flushing with nitrogen, it was irradiated. The temperature during irradiation was the boiling point of 2-propanol (82–85 °C).

Most of the irradiations were carried out using the third arrangement. In this, varying amounts of benzil and sometimes other reagents were dissolved in 500 ml of 2-propanol or other solvent and placed in a Vycor cylinder with a 600 ml capacity. This cylinder was placed inside a larger Pyrex cylinder and distilled water (25 °C) circulated through the Pyrex cylinder by means of a vibrostatic pump. Nitrogen was flushed through the solution for 30 min before irradiation and during the course of the irradiation. The few runs where nitrogen was not used are indicated.

Thin–Layer Chromatography

Standards were run at the same time as the irradiated solution. The developing solvent was hexane:ethyl ether (2:1). Quantitative analysis was carried out by measuring the area recorded on the densitometer and comparing it to the area produced by a standard solution. Using standard solutions, it was seen that there was a linear relationship between the area and amount of substance.

Column Chromatography

A check by t.l.c. showed no difference in the kinds of products between the sealed tube photolyses and the nitrogen flushed ones, so no further work was done on the sealed tube runs. In those runs in which a precipitate appeared, it was first filtered off and the filtrate treated the same as in those runs where there was no precipitate.

The 2-propanol was removed from the clear solution under reduced pressure. About 5 g of the residue were redissolved in 50 ml of ethyl ether and were added to 15 ml of saturated sodium bisulfite solution with continuous shaking. After separation, the ether layer was washed with 30 ml of saturated sodium bicarbonate twice, followed by two 50 ml portions of distilled water, and then dried over anhydrous sodium sulfate. The ether solution was then added to 30 g of silica gel, and the ether removed in a rotary evaporator. The dried residue was ground in a mortar with *n*-hexane and the mixture placed on top of 300 g of silica gel in a packed column. The column was eluted with 6 l of ethyl ether – hexane which varied in concentration from 0 to 60% ether (v/v), then 2.5 l of acetone. Each fraction was examined by either t.l.c. or g.l.c. Ether (5%) eluted the unreacted benzil and ether (15%) eluted the benzoin benzoate. The fractions eluted by 25–35% ether were combined for further column chromatography and yielded benzoin and dibenzoin dibenzoate.

The material eluted from the first column by 50% ether and by acetone could not be separated any further and was brownish in color; presumably this material was a high molecular weight product. There was also a very little material which could not be removed from the column. Runs made after identification of all the products had been completed were analyzed by t.l.c. after removal of the benzaldehyde and benzoic acid.

Determination of Quantum Yield

The actinometer used was that of Hatchard and Parker (5) and was stirred by a current of nitrogen during irradiation. The light from the lamp was passed through a collimating hole and then a No. 7-83 filter from Corning glass works. This filter has a peak at 368 mμ and a half band width of 22 mμ. The percentage transmission at the maximum is 16%. The same cell with plane glass windows was used both for the benzil solutions and for the actinometer. Complete absorption of light, as measured by a photocell, took place in the benzil solutions.

Isolation, Identification, and Estimation of Products

Benzil Pinacol

This compound appeared as a white precipitate after some irradiations. As there was sometimes supersaturation, the solution was always allowed to stand for several hours after irradiation before filtration. After filtering, the precipitate was purified by immersion in acetone for 24 h, filtered again, and dried in a vacuum desiccator. The i.r. spectrum showed a strong hydroxy peak at 3400 cm^{-1} and a carbonyl absorption at 1650 cm^{-1}. The melting point was 204° measured on a Koffler hot bench but decomposed at 130° when heated slowly in a capillary tube. If air was present, the decomposition product was benzil. When heated in a sealed degassed tube the decomposition products were benzoin and benzil. Quantitative analysis (weighing the total decomposition product and measuring the benzil by ultraviolet (u.v.) spectrometry) showed that the two were present in a 1:1 mole ratio.

Anal. Calcd. for $C_{28}H_{22}O_4$: C, 79.60; H, 5.25. Found: C, 79.14, 79.19; H, 5.20, 5.18.

The formula weight is 422. An outside laboratory reported a molecular weight of 278. Using tetrahydrofuran as solvent, we found the molecular weight to be 403 when measured as soon as the solution was made up. After standing for 4 h in tetrahydrofuran (0.9 g/100 ml at room temperature) the compound changed completely to benzil. The compound also dissolved in dioxane (0.7 g/100 ml at room temperature), and slightly in dimethyl sulfoxide. It was insoluble in all other solvents tried, changing in some of them to benzil (DMF 5 min, diphenylmethane 24 h). Alcohols and acetone at room temperature had absolutely no effect on either, neither did 1 *N* alcoholic NaOH. The fact that it changes to benzil over a period of hours would explain the molecular weight results. The insolubility in NaOH and the white color exclude the enol structure which might be expected in analogy with the dimerization of triphenylmethyl radicals to produce 1-diphenylmethylene-4-trityl-2,5-cyclohexadiene (6).

The n.m.r. spectrum in DMSO was run 6 times over a period of 135 min. The ratio of the area of the aromatic hydrogen and hydroxy hydrogen was plotted against

Can. J. Chem. Downloaded from www.nrcresearchpress.com by 210.87.254.105 on 09/05/12
For personal use only.

time and extrapolated to zero time. The intercept ArH/OH was 12. A ratio of 10 would be expected on the basis of the structure **3**. An excess of the compound was shaken with tetrahydrofuran, centrifuged, and the n.m.r. spectrum taken immediately. A value of 9.6 was obtained for the same ratio. When refluxed in 2-propanol or even just heated to 50 °C in 2-propanol, the compound changed to benzil. When added to styrene at room temperature the rate of polymerization increased. When added to a benzene solution of iodine which was then degassed and sealed, the color disappeared on warming to 50 °C. Apparently, the benzil pinacol dissociates very easily into two ketyl radicals. In the absence of oxygen, they disproportionate to benzil and benzoin. When O_2 is present, benzil is the sole product. Neckers and Schaap have recently reported that benzpinacol dissociates into free radicals at a temperature as low as 130 °C (7).

Benzaldehyde

This compound was measured by g.l.c. and its identity was checked by comparing its retention time with that of an authentic sample, and also by precipitating the 2,4-dinitrophenylhydrazone.

Unreacted Benzil

This compound was identified by its i.r. spectrum. It was measured by g.l.c.; one half of the benzoin had been subtracted. Benzoin disproportionates to benzil and deoxybenzoin on the g.l.c. column (8).

Benzoic Acid

This was recovered by acidification of the bicarbonate extract to pH 2 followed by two extractions with ether. The ether was washed, dried, and evaporated; the residue was identified by its m.p. and i.r. spectrum, and was weighed.

Benzoin Benzoate

The fraction eluted with 15% ethyl ether gave a substance which after recrystallization had m.p. 126 °C, lit. (17) 125 °C. The mixed m.p. with benzoin benzoate showed no depression and the i.r. and n.m.r. spectra were identical with authentic benzoin benzoate. The singlet at δ 7.19 in the n.m.r. spectrum is assigned to the aliphatic proton. It was measured either by weighing or by t.l.c.

Benzoin

This was obtained from column chromatography. It was identified by its m.p. and i.r. spectrum. It was measured either by weighing after column chromatography or by densitometry after t.l.c.

1,2,3,4-Tetraphenyl-2,3-dihydroxy-1,4-butanedione Dibenzoate (5) (di-(Benzoin Benzoate))

The second fraction after rechromatography yielded a compound which after recrystallization from *n*-hexane had m.p. 112–113 °C. It was first measured quantitatively by weighing and later by densitometry after t.l.c.

Anal. Calcd. for $C_{42}H_{30}O_6$ (mol. wt., 630.7): C, 79.98; H, 4.80. Found (mol. wt., 640): C, 78.82; H, 4.88.

The i.r. spectrum showed no aliphatic hydrogens or hydroxy groups and had the characteristic bands of the benzoyl group. The n.m.r. spectrum in dimethyl sulfoxide consisted only of unresolved aromatic absorption.

Further identification was made in two ways. The radicals produced by the abstraction of the aliphatic hydrogen of benzoin benzoate should couple to produce **5**. A mixture of benzoin benzoate with benzophenone was irradiated in a benzene–cyclohexane solvent (1:1, v/v). The solution was evaporated to dryness and the residue separated by column chromatography. One of the compounds obtained had an i.r. spectrum identical with that of **5** and m.p. 112 °C. A mixed m.p. with **5** showed no depression.

Rust *et al.* (9) found that heating benzaldehyde with *tert*-butyl peroxide leads to the formation of dihydrobenzoin dibenzoate by a mechanism involving the attack of benzoyl radicals on the oxygen of another benzaldehyde molecule, followed by a coupling of the resulting radicals. It was earlier reported by Bunbury and Wang (1) that adding benzil to the mixture of benzaldehyde and *tert*-butyl peroxide did not lead to the production of the dibenzoate. However, a careful check of the products from heating benzil, benzaldehyde, and *tert*-butyl peroxide leads to the isolation of several compounds. One of these compounds had m.p. 110–112 °C on recrystallization from *n*-hexane. The elementary analysis was C, 78.94; H, 4.80 and the measured molecular weight 648. A mixed m.p. with the product from the benzil in 2-propanol irradiation showed no depression. The n.m.r. spectrum showed only unresolved aromatic absorption.

Acetone

This was measured by g.l.c. and identified by its 2,4-dinitrophenylhydrazone.

Bicumyl

After irradiation of a cumene solution of benzil, the solvent was removed under reduced pressure, and the residue separated by column chromatography. The first fraction eluted with *n*-hexane was proved to be bicumyl by its m.p. and by comparison of its i.r. spectrum with that of an authentic sample. It was weighed.

Results and Discussion

The percentage of high molecular weight compounds appearing in Table I was obtained by difference. All runs in this table were carried to about 50% decomposition of the benzil.

Reducing the benzil concentration at constant light intensity has three effects: (1) the rate of benzil disappearance becomes steadily less until a constant value is reached, see runs 4–9, Table I and Fig. 1 curve A; (2) the percentage of benzil pinacol falls off to zero, see runs 4–9, Table I and Fig. 1 curve C; and (3) there is an increase in the amount of benzoin benzoate formed and even more in the amount of dibenzoin dibenzoate formed, see runs 4–9, Table I. Further, the initial concentration at which the benzil pinacol production becomes zero is the same as that at which the rate of benzil disappearance becomes constant.

Reducing the 2-propanol concentration with benzene leads to a marked reduction in rate and an elimination of benzil pinacol as a product, see run 13 Table I.

Can. J. Chem. Downloaded from www.nrcresearchpress.com by 210.87.254.105 on 09/05/12
For personal use only.

TABLE I

Reaction conditions and products of benzil photolysis in 2-propanol

Run number*	Reaction conditions	Solvent	Sample concentration (mmoles/l)	Time (min)	Benzil destroyed	Products (% of benzil lost)						
						Benzil pinacol	Benzaldehyde	Benzoic acid	Benzoin	Benzoin benzoate	Dibenzoin dibenzoate	High mol. wt. compound§
1	N_2-flushed	2-Propanol	83.1	185	84.2	‡	13.2	10.6	28.6	24.7	8.3	14.6
2	O_2-flushed	2-Propanol	83.0	81	22.3	‡	‡	91.2	‡	‡	‡	8.8
3	Stoppered	2-Propanol	83.5	70	20.3	28.6	4.5	14.7	14.5	10.2	5.4	22.1
4	N_2-flushed	2-Propanol	84.0	57	21.6	34.5	4.4	10.9	17.5	14.2	5.7	12.8
5	N_2-flushed	2-Propanol	51.9	51	11.4	20.3	5.7	11.1	18.0	16.1	11.2	17.6
6	N_2-flushed	2-Propanol	30.5	62	8.4	7.6	6.2	13.2	17.4	19.8	16.5	19.3
7	N_2-flushed	2-Propanol	16.6	55	4.4	0.4	5.9	12.0	20.5	19.3	17.3	24.6
8	N_2-flushed	2-Propanol	15.2	54	4.3	‡	†	†	†	†	†	†
9	N_2-flushed	2-Propanol	9.5	35	3	‡	7	11	20	17	18	27
10	N_2-flushed	Cumene	84.5	120	14.2	‡	†	†	†	†	†	†
11	N_2-flushed	Cumene	335.8	765	54.0	30.8	7.4	11.4	10.7	4.6	‡	35.1
12	N_2-flushed	Benzene	80.5	325	‡	‡	†	†	†	†	†	†
13	N_2-flushed	10% 2-propanol in benzene (v/v)	83.5	552	23.2	‡	15.3	18.8	17.1	18.4	10.2	20.2
19	N_2-flushed	2-Propanol	83.2	600	6.9	32.5	†	†	†	†	†	†

*Bath temperature was 25–30° in all runs except run 1; here it was 82–85°. The sample volume was 0.5 l except in run 1; here it was 2 l. Acetone (17 mmoles) was found in run 4, and 7 mmoles of bicumyl was found in run 11. There was weak light intensity in run 19. Runs were carried to 50% decomposition.

†Not measured.

‡None were found.

§High molecular weight compounds were obtained by difference.

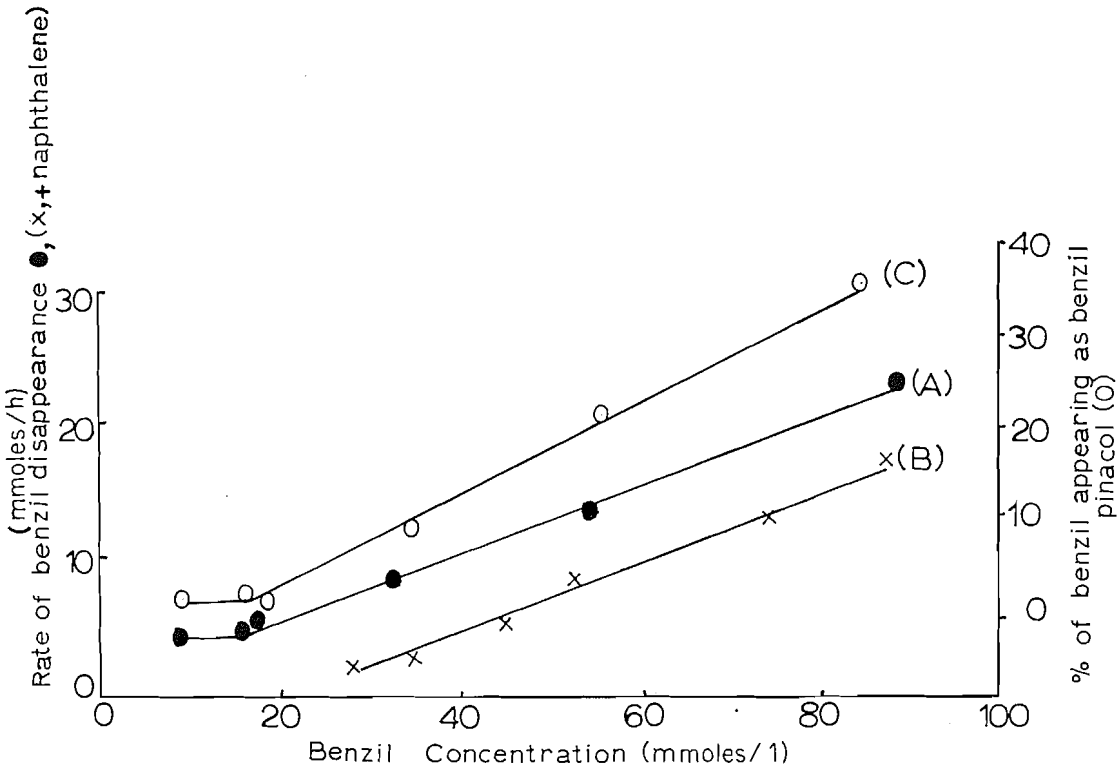

FIG. 1. Rate of benzil disappearance and pinacol formation as a function of benzil concentration in 2-propanol. Each curve was a separate series: curves A and B, 10% destruction of benzil; curve C, 40% destruction of benzil.

TABLE II

Reaction conditions and products of benzil photolysis in cumene

Run number*	Initial concentration of benzil (mole/l)	Rate of decomposition (mmole/h)	% benzil pinacol formed (% of decomposed benzil)	Benzoin	Benzoin benzoate	Benzaldehyde
1	0.405	3.54	23.0	7	3	†
2	0.362	3.15	15.7	7	5	†
3	0.272	2.50	9.4	10	5	†
4	0.248	2.38	0	14	10	†
5	0.226	2.33	0	13	13	†
6	0.092	2.60	0	†	†	†

*Total volume for irradiation is 50 ml of cumene solution. About 15% benzil was destroyed in each run. All runs were degassed.
†Not measured.

The behavior in cumene differs from that in 2-propanol in the following ways. The benzil concentration below which no benzil pinacol is formed is 250 mmoles/l in cumene as compared to 18 mmoles/l in 2-propanol. At a given concentration the rate is slower. The rate of change of the rate with concentration is 0.009 mmoles/h//mmoles/l while in 2-propanol it is 0.25 mmoles/h//mmoles/l. This is shown by runs 4, 10, and 11 in Table I, by Table II, and by Figs. 1 and 2.

The following series of steps seems best for rationalizing the results.

$$[1] \quad C_6H_5COCOC_6H_5 \xrightarrow{h\nu} {}^1C_6H_5COCOC_6H_5^*$$

$$[2] \quad {}^1C_6H_5COCOC_6H_5^* \rightarrow C_6H_5COCOC_6H_5$$

Can. J. Chem. Downloaded from www.nrcresearchpress.com by 210.87.254.105 on 09/05/12
For personal use only.

Can. J. Chem. Downloaded from www.nrcresearchpress.com by 210.87.254.105 on 09/05/12
For personal use only.

TABLE III

Effect of various adducts on the photolysis of benzil in 2-propanol*

Run number	Quencher	Concentration of quencher (mmoles/l)	Solvent	Benzil concentration (mmoles/l)	Time (min)	% benzil destroyed	Products (% benzil lost)			
							Benzil pinacol	Benzoin	Benzoin benzoate	Benzoic acid
4	‡	‡	2-Propanol	84.0	57	51.5	34.5	17.5	14.2	10.9
14	Naphthalene	3.75	2-Propanol	80.0	90	56.4	30.8	‡	‡	‡
15	Pyrene	4.05	2-Propanol	82.1	120	21.5	31.4	14.5	16.0	‡
16	Anthracene	3.1	Benzene (16.7%) in 2-propanol	81.7	120	24.5	32.2	13.6	17.4	‡
17†	Tri-*n*-butyltin hydride	40.3	2-Propanol	83.1	115	17.3	§	22.4	25.2	13.5
18	Iodine	1.0	2-Propanol	80.7	120	§	§	‡	‡	‡

*Reaction conditions: temperature 25–30 °C; volume 500 ml; nitrogen was flushed in all runs.
†Benzoin (0.41 mmoles) and 0.28 mmoles of benzoin benzoate were found in the dark and subtracted from the total to give the figures in the table.
‡Not measured.
§None were found.

TABLE IV

Rates of benzil disappearance and product appearance at constant light intensity for selected runs

Run number	Benzil concentration	mmoles benzil destroyed/h	Rates in mmoles/h							
			Pinacol	Benzaldehyde	Benzoin	Benzoin benzoate	Dimer	BB+2D*	Benzoin C_6H_5CHO	BB+2D* *o*-CHO
1	83.1	27.3	0.0	3.68	7.81	4.50	0.753	5.306	2.2	1.45
4	84.0	22.73	3.92	2.0	3.975	2.183	0.432	3.047	4.0	1.524
5	51.9	13.41	1.362	1.53	2.413	1.43	0.502	2.434	3.2	1.589
6	30.5	8.13	0.309	1.01	1.414	1.072	0.447	1.966	2.8	1.946
7	16.6	4.8	0.01	0.566	0.984	0.619	0.277	1.173	3.5	2.075
9	9.5	5.14	0.0	0.72	1.027	0.582	0.308	1.198	2.9	1.666

*Benzoin benzoate ≡ BB, dimer ≡ D.

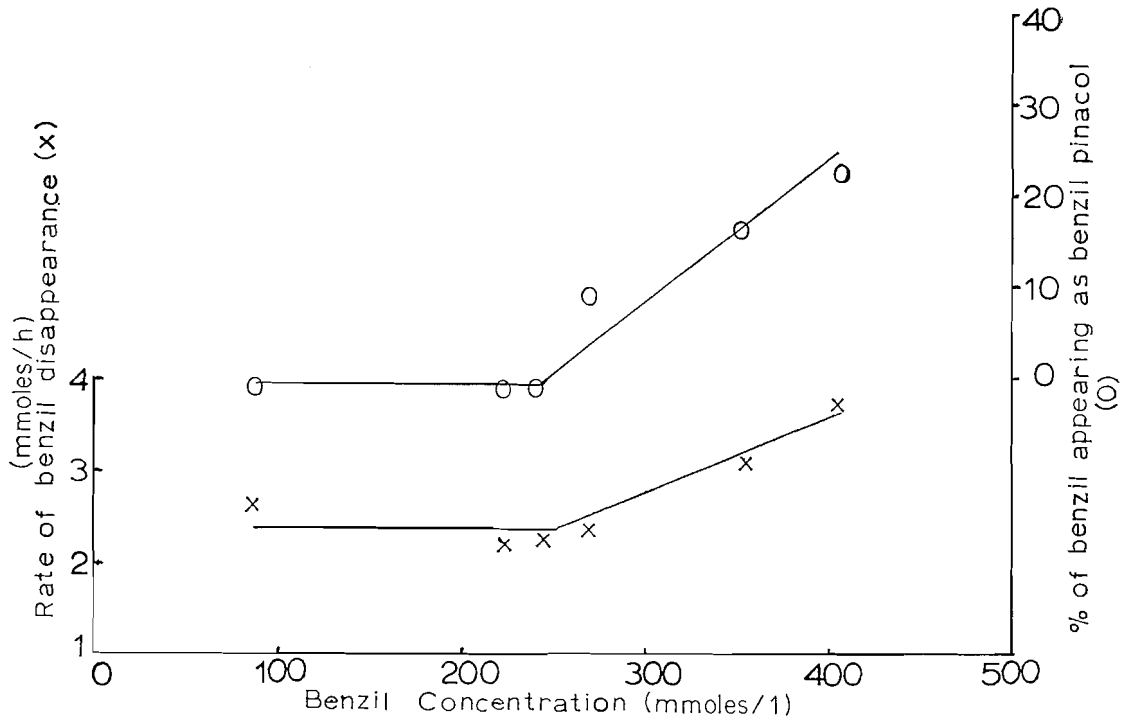

FIG. 2. Rate of benzil disappearance and pinacol formation as a function of benzil concentration in cumene.

[3] $C_6H_5COCOC_6H_5^* \rightarrow 2C_6H_5CO\cdot$

[4] $C_6H_5COCOC_6H_5^* + CH_3CHOHCH_3 \rightarrow C_6H_5\dot{C}OHCOC_6H_5 + CH_3\dot{C}OHCH_3$
2

[5] **1** + $CH_3\dot{C}OHCH_3 \rightarrow$ **2** + CH_3COCH_3

After reaction [1] the excited benzil molecule can do three things; lose its energy and revert to the ground state [2], split into two benzoyl radicals [3], or abstract a hydrogen atom from the solvent to form the ketyl radical [4]. That reaction [2] does occur is shown by the fact that the quantum yield of benzil decomposed depends strongly on the ease with which hydrogen is lost by the solvent. At an initial concentration of 83.4 mmoles/l the quantum yield of benzil disappearance in 2-propanol is 0.11 and in cyclohexane, 0.018. Anthracene and pyrene which have triplet energies below that of benzil are much more effective in slowing down the reaction than is naphthalene, the triplet energy of which is greater (10*a*), see Table III.

Reaction [3] is a minor reaction. Assume for the sake of argument that the benzoyl radicals so produced either abstract hydrogen from the solvent or react with benzil as proposed by Bunbury and Wang (1). Then the proportion of benzaldehyde should increase with the ease of hydrogen abstraction from the solvent but no such correlation is found; cyclohexane 6.2%, cumene 7.4%, 2-propanol 6%. Further, at lower benzil concentrations there should be an increase in the amount of benzaldehyde as there is less benzil to compete with the solvent for the benzoyl radicals. No such increase is found (Table I). The rate of decomposition in pure benzene, where reactions [4] and [5] cannot occur was found to be 0.323 mmoles/h at a concentration of 8 mmoles/l, and 0.526 mmoles/h at a concentration of 82.8 mmoles/l, under the same conditions as the runs in Table IV.

With the exception of the formation of benzoic acid, reactions [4] and [5] are the principal ones leading to products.

Reactions [6]–[9] show the different possible fates of the ketyl radical (**2**).

Reaction [6] shows the formation of benzil in a manner analogous to the formation of benzpinacol in the photolysis of benzophenone, **2.**

Can. J. Chem. Downloaded from www.nrcresearchpress.com by 210.87.254.105 on 09/05/12
For personal use only.

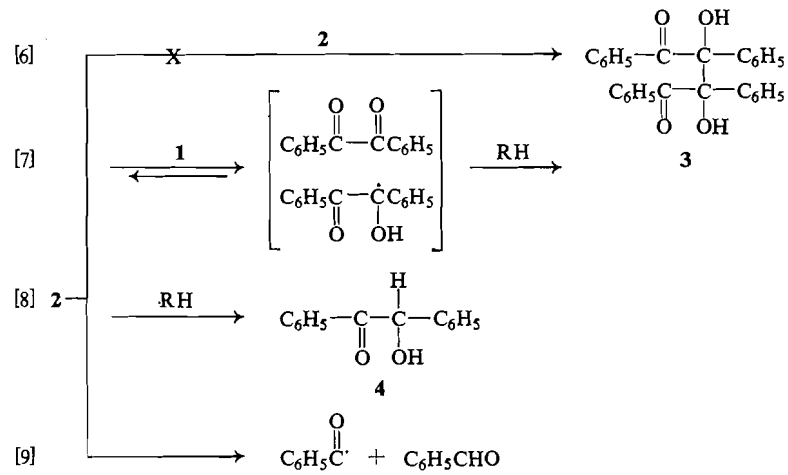

Dimerization of two ketyl radicals does not occur to any extent in the benzil system. If the benzil pinacol was produced by the combination of two ketyl radicals, its rate of production compared to that of benzoin should drastically decrease with a reduction in light intensity as the steady state concentration of ketyl radicals was reduced. No such decrease was found (run 19, Table I). Added quenchers which also reduce the steady state concentration of excited benzil, reduced the rate but had no effect on the proportion of benzil pinacol produced (Table III).

Since reduction of the benzil concentration causes a marked decrease in the production of benzil pinacol, we postulate a reversible complex formed between the ketyl radical and an unexcited benzil molecule and that this complex can abstract a hydrogen atom to form the benzil pinacol, reaction [7]. Also, since formation of the pinacol by this route uses a benzil molecule that would not otherwise be used, part of the fall in the quantum yield of benzil disappearance with fall in initial benzil concentration is explained. If the complex between the ketyl radical and a benzil molecule is a poor hydrogen abstractor, there should be an effect of solvent on pinacol formation. If we compare the reaction in cyclohexane, cumene, and 2-propanol, it is seen that there is no pinacol production in cyclohexane, and that the pinacol production becomes zero in cumene at an initial benzil concentration of 0.25 moles/l, and zero in 2-propanol at an initial benzil concentration of about 0.018 moles/l.

Metzger (11), in a study of the thermal decomposition of 1,1,2,2-tetraphenylethanol and of α-benzhydrylbenzoin says ". . . the experimental evidence leads to the conclusion that benzil is forming π-complexes with the radical intermediates . . .". One of the radicals for which complexes are postulated is the same ketyl radical as we have here.

In a recent paper, Filipescu and Minn (12) have shown that there is a long-lived intermediate formed between the PhĊOH radicals and the Me_2ĊOH radical during the photolysis of benzophenone in 2-propanol. This intermediate undergoes a slow dark reaction with benzophenone in the absence of oxygen to produce two PhĊOH radicals. Since the benzil pinacol usually took some time to precipitate after irradiation, we thought that perhaps an intermediate was intervening in a similar way. Shaking the irradiated mixture with air immediately after turning out the lights had no effect on the amount of benzil pinacol produced.

As mentioned above, the hydrogen-donating properties of the solvent have no effect on benzaldehyde production, therefore, benzaldehyde does not appear to be produced by hydrogen abstraction of benzoyl radicals. Further, the rate of benzoyl radical production by reaction [3] (as measured in pure benzene) is not nearly great enough to account for the rate of production of benzoin benzoate and its dimer (Table IV). Therefore, another source of benzoyl radicals, as well as a route for the production of benzal-

Can. J. Chem. Downloaded from www.nrcresearchpress.com by 210.87.254.105 on 09/05/12
For personal use only.

Can. J. Chem. Downloaded from www.nrcresearchpress.com by 210.87.254.105 on 09/05/12
For personal use only.

dehyde, is needed. Reaction [9] is suggested as a source of both benzaldehyde and benzoyl radicals. This reaction is similar to reaction [10]

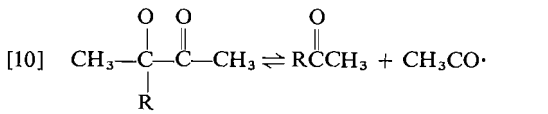

[10] $CH_3—\underset{\underset{R}{|}}{\overset{O}{\overset{||}{C}}}—\overset{O}{\overset{||}{C}}—CH_3 \rightleftharpoons R\overset{O}{\overset{||}{C}}CH_3 + CH_3CO\cdot$

proposed by Bentrude and Darnall (13) in both biacetyl photochemistry and the reaction of biacetyl with thermally generated radicals, and

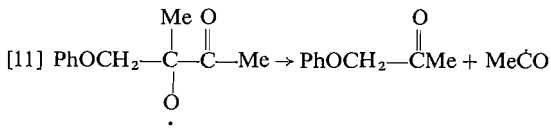

[11] $PhOCH_2—\underset{\underset{O\cdot}{|}}{\overset{Me\ O}{\overset{|\ \ ||}{C}}}—\overset{O}{\overset{||}{C}}—Me \rightarrow PhOCH_2—\overset{O}{\overset{||}{C}}Me + MeCO$

also to reaction [11] suggested by Baum and Norman (14) in a study of the photochemical reactions of biacetyl with some benzenoid compounds. In the photolysis of acetaldehyde, Zeldes and Livingston (15) propose reaction [12] which is the reverse of reaction [9] with methyls instead of phenyls

[12] $CH_3CO\cdot + CH_3CHO \rightarrow CH_3COCOHCH_3$

Reaction [9] is also supported by the finding that both benzoin and *benzoin benzoate* are produced by tri-*n*-butyl tin hydride acting on benzil in 2-propanol in the dark (Table III). Presumably, the tin hydride transfers a hydrogen atom to benzil forming the same ketyl radical, some of which then dissociates according to reaction [9]. In a given solvent the benzoin/benzaldehyde ratio would be expected to be independent of the benzil concentration as a certain fraction of the ketyl radicals would split and a certain fraction abstract hydrogen to form benzoin. On examining runs 4–7 in Table IV this is seen to be so. An increase in temperature would increase the rate of both reaction [8] and reaction [9] so the change in the ratio is not predictable. The ratio in fact shows slight if any change from 82–85 °C to 25–30 °C, 2.2 to 3.3. The more difficult it is to abstract a hydrogen atom from the solvent, the greater the amount of dissociation to benzoin formation would become. The benzoin/benzaldehyde ratio is 1.4 for cumene at 25°, and 1.1 for 10% 2-propanol in benzene at 25°.

If it is assumed that the rate of dissociation is the same in 2-propanol as in cumene, a comparison of the benzoin/benzaldehyde ratio in the two solvents gives the relative ease of hydrogen abstraction by the ketyl radical. The additional assumption that reaction [13]

[13] $\mathbf{2} + CH_3\dot{C}OHCH_3 \rightarrow \mathbf{4} + CH_3COCH_3$

does not take place to any appreciable extent must also be made. This appears to be so in the case of benzophenone; i.e. benzhydrol is not produced (10*b*).

With unsubstituted benzil, reaction [14] only results in a reduction of the quantum yield but it cannot be ruled out. Reaction [15] leads to benzoin benzoate, and di-(benzoin benzoate). Presumably, the high molecular weight compounds may be formed by other reactions involving benzoyl radicals. If reaction [9] was the only one forming benzoyl radicals, the moles of benzaldehyde should not be less than the moles of benzoin benzoate, plus twice the moles of benzoin benzoate dimer; further, the ratio of the two should remain constant. As can be seen from Table IV, the relative amount of benzoin benzoate and dimer increase with decreasing benzil concentration. Reaction [3] must be providing the additional benzoyl radicals. The thin-layer chromatogram of the pure benzene runs

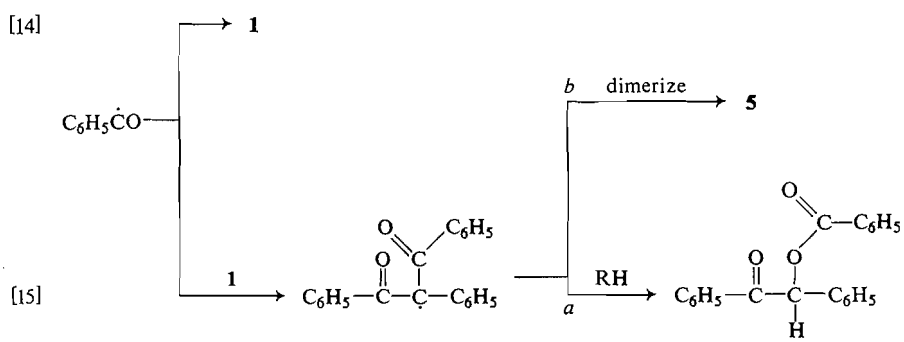

showed only two product spots, one that did not move and one that had an R_f corresponding to the dimer of benzoin benzoate. Apparently the sequence [1], [3], [15*b*] is followed in benzene. If twice the rate of decomposition in pure benzene (about 0.4 mmoles/h) is subtracted from the sum of the rate of benzoin benzoate formation and twice that of its dimer, the difference is approximately the rate of benzaldehyde production: i.e. benzaldehyde to benzoin benzoate plus twice the dimer ratio becomes more or less constant.

Apparently then, at constant light intensity, benzil dissociates into benzoyl radicals at a certain slow rate that is concentration independent, and also abstracts hydrogen from the solvent at a much faster rate that is solvent and, in some cases, concentration dependent. Thus, the proportion of benzil dissociating into two benzoyl radicals would become progressively larger at lower benzil concentrations (until the steady value is reached) thus explaining the relative increase in products involving the benzoyl radical as starting concentrations of benzil are reduced.

The decrease in the quantum yield of benzil destruction with decreasing benzil concentration is more than can be accounted for by the decrease in pinacol production. If each mole of pinacol is formed from an excited benzil molecule and one in the ground state, the rate of benzil disappearance when pinacol production reaches zero should be 22.7 – 3.9 = 18.8 mmoles/h. Instead, it falls to about 5 mmoles/h (Table IV). If at high benzil concentrations, reaction [5] is important and at low benzil concentrations becomes much less so, the 2-hydroxy-2-propyl radicals disappearing by disproportionation, this could account for an additional fall in the rate to about 9 mmoles/h. In cumene, the concentration effect disappears at a much higher initial benzil concentration and is much less marked than in 2-propanol; 0.009 mmoles/h//mmoles/l compared to 0.25 mmoles/h//mmoles/l.

It was originally thought that the tri-*n*-butyl tin hydride would suppress benzil pinacol formation by giving a hydrogen to the benzoin radicals before they had a chance to dimerize. Since that is apparently not the path of benzil pinacol formation we have no explanation for the suppression of benzil pinacol formation or for the fact that the tin hydride also slows down the rate of photochemical reaction.

That such a small amount of iodine should suppress the photochemical reaction is surprising (Table III). The iodine must either be a very efficient quencher or reacting in such a way that it is constantly being regenerated. For example, the following steps, [16] and [17], would provide such a path

[16] $$\underset{(I)}{\mathbf{2}} + I_2 \rightarrow \mathbf{1} + \underset{(HI)}{HI} + I$$

[17] $$CH_3\dot{C}(OH)CH_3 + HI \rightarrow CH_3CHOHCH_3 + I$$

This sequence is the same as the one proposed by Cohen *et al.* (16) for inhibition by disulfides and thiols in low concentration, of the photo-reduction of benzophenone, reactions [18] and [19].

[18] $$Ph_2\dot{C}OH + RS\cdot \rightarrow Ph_2CO + \underset{(R_2S_2)}{} \underset{(RSH + RS\cdot)}{RSH}$$

[19] $$Me_2\dot{C}OH + RSH \rightarrow Me_2CHOH + RS\cdot$$

The path to benzoic acid remains obscure. It is produced in all solvents used so far, cyclohexane (1), 2-propanol, cumene, and in later work here[2], triethylamine. The poorer hydrogen donors produce a larger percentage of benzoic acid. On the other hand, the presence of the very strong hydrogen donor, tri-*n*-butyl tin hydride does not affect the percentage of benzoic acid formed in 2-propanol. The reaction leading to the benzoic acid precursor must be a rapid one. The fact that it can exist in the presence of the tin hydride argues against it being a radical. It is not produced by oxygen during the reaction. When carried out in sealed degassed tubes, the same products were found comparable to run 4, Table I, benzil pinacol (not measured), benzoin 20%, benzoin benzoate 15%, benzoic acid 10% (analysis by t.l.c. only), and dibenzoin dibenzoate. Varying the flushing period before irradiation to a minimum of 15 min had no effect on the products. The u.v. spectrum (360–480 mμ) of a degassed sample was taken before irradiation, after irradiation, and after being opened to the air. The changes were not pronounced. Deliberately adding oxygen to the reaction mixture during irradiation leads to benzoic acid as the sole identifiable product with a reduction in rate

[2]Runs by Miss Han Ping Mak.

Can. J. Chem. Downloaded from www.nrcresearchpress.com by 210.87.254.105 on 09/05/12
For personal use only.

from 22.7 mmoles/h to 16.5 mmoles/h.[3] In oxygen-free solutions, the compound leading to benzoic acid might be an intermediate of the type proposed by Filipescu and Minn (12). In the case of benzophenone, it regenerates benzophenone on exposure to oxygen. In the case of benzil, it could lead to benzoic acid.

Acknowledgments

The authors thank the National Research Council of Canada for generous support and St. Francis Xavier University for help in the purchase of the densitometer.

[3]A referee has suggested that in this case the following chain leads to benzoic acid when oxygen is present.

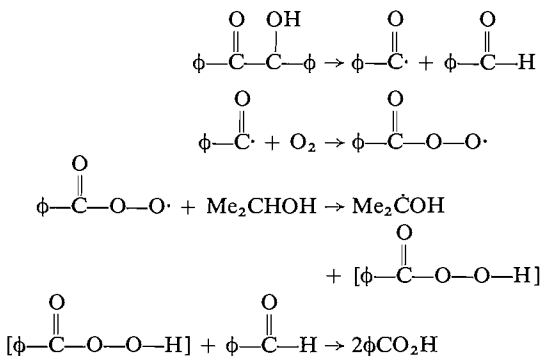

1. D. L. BUNBURY and C. T. WANG. Can. J. Chem. **46**, 1473 (1968).
2. J. N. PITTS, JR., R. L. LETSINGER, R. P. TAYLOR, J. M. PATTERSON, G. RECKTENWALD, and R. B. MARTIN. J. Am. Chem. Soc. **81**, 1068 (1959).
3. A. J. VOGEL. A textbook of practical organic chemistry. Longmans, Green and Co., Ltd. 1956. p. 944.
4. H. G. KUIVILA and O. F. BEUMEL, JR. J. Am. Chem. Soc. **83**, 1246 (1961).
5. C. G. HATCHARD and C. A. PARKER. Proc. Roy. Soc. London, Ser. A, **235**, 518 (1956).
6. H. LANKAMP, W. TH. NANTA, and C. MACLEAN. Tetrahedron Letters, 249 (1968).
7. D. C. NECKERS and A. P. SHAAP. J. Org. Chem. **32**, 22 (1967).
8. D. L. BUNBURY and M. S. OSYANY. J. Chromatog. **19**, 12 (1965).
9. F. F. RUST, F. H. SEUBOLD, and W. E. VAUGHN. J. Am. Chem. Soc. **70**, 3258 (1948).
10. N. J. TURRO. Molecular photochemistry. W. A. Benjamin, Inc., New York. 1965. (*a*) p. 132, (*b*) p. 143.
11. S. H. METZGER. Ph.D. Thesis. University of Illinois, Urbana, Illinois. 1962. p. 40 and pp. 69–74.
12. N. FILIPESCU and F. L. MINN. J. Am. Chem. Soc. **90**, 1544 (1968).
13. (*a*) W. G. BENTRUDE and K. R. DARNALL. J. Am. Chem. Soc. **90**, 3588 (1968); (*b*) W. G. BENTRUDE and K. R. DARNALL. Chem. Commun. 810 (1968).
14. E. J. BAUM and R. O. C. NORMAN. J. Chem. Soc. B, 227 (1968).
15. H. ZELDES and R. LIVINGSTON. J. Chem. Phys. **47**, 1465 (1967).
16. S. G. COHEN, S. ORMAN, and D. LAUFER. Proc. Chem. Soc. 301 (1961).
17. I. HEILBRON and H. M. BUNBERRY. Dictionary of Organic Compounds. 1ST ed. Vol. 1. Eyrie and Spottiswoode. 1953. p. 256.

Can. J. Chem. Downloaded from www.nrcresearchpress.com by 210.87.254.105 on 09/05/12
For personal use only.

Can. J. Chem. Downloaded from www.nrcresearchpress.com by 210.87.254.42 on 09/05/12
For personal use only.

Polymerization behavior of 2,6-dimethoxystyrene

W. Y. Lau and C. M. Burns
Department of Chemical Engineering, University of Waterloo, Waterloo, Ontario
Received November 18, 1968

Free radical, cationic, and anionic initiators were investigated as possible agents for the polymerization of 2,6-dimethoxystyrene. Polymerization was observed in all three cases, with rapid cross-linking apparently occurring with the cationic catalyst. Attempts at copolymerization with styrene and with methyl methacrylate resulted in the formation of homopolymers of 2,6-dimethoxystyrene, in the cationic cases, and of methyl methacrylate in the anionic cases. Random copolymers were obtained in the anionic case with styrene and in the free radical case with both comonomers. Monomer reactivity ratios were calculated, and the polymerization behavior was interpreted in terms of the molecular structure of 2,6-dimethoxystyrene.

Canadian Journal of Chemistry, 47, 2057 (1969)

In an investigation into graft copolymerization using cationic catalysts, we recently reported (1) an improved synthesis of 2,6-dimethoxystyrene. Using organometallic reagents it was possible to prepare this styrene derivative in high purity under relatively mild conditions in two steps, rather than in seven steps using the synthesis of Shamshurin (2) which was difficult to reproduce (3).

The methoxy groups in 2,6-dimethoxystyrene are electron-donating substituents which have been shown to increase greatly the susceptibility of the phenyl ring of styrene to electrophilic attack, while the solubility characteristics of the poly(2,6-dimethoxystyrene) surprisingly remain almost identical to those of the unsubstituted polystyrene (1). In this paper we report on the polymerization and copolymerization of this practically new monomer, and on the effects of these methoxy substituents upon the reactivity of this monomer in the presence of free radical, cationic, and anionic catalysts.

Experimental

2,6-Dimethoxystyrene

The synthesis followed our previous method (1) in which commercial 2,6-dimethoxyphenyllithium (Alfa Inorganics) was allowed to react with *N*-methylformanilide to form 2,6-dimethoxybenzaldehyde. The aldehyde was converted to 2,6-dimethoxystyrene by a Wittig reaction (4). An improved yield (97%) of the aldehyde was attributed to greater purity of 2,6-dimethoxyphenyllithium when received. The purity of the monomer was checked by infrared spectroscopy and gas–liquid chromatography.

The comonomers, styrene and methyl methacrylate, were purified by caustic extraction and distillation at reduced pressure.

Free Radical Polymerization

Measured quantities of bulk monomer (or comonomers) and 2,2′-azobis(2-methylpropionitrile) were added to a polymerization tube of about 8 ml capacity. The monomer was degassed by freezing and thawing and then sealed under vacuum. The tube was heated to 60 ± 1° for a pre-estimated period of time to give a desired conversion (below 10% in copolymerization experiments). The polymer was then precipitated in methanol, filtered, and dried. Three times the polymer was redissolved in 2-butanone, precipitated in methanol, filtered, and dried under vacuum at 50°.

Cationic Polymerization

Under dry nitrogen a solvent mixture was made up from freshly distilled nitrobenzene and carbon tetrachloride in a 1:1 mole ratio. The freshly distilled monomers were kept over silica gel. The polymerization vessel was a 15 ml glass bottle which had been heated and flushed with dry nitrogen and fitted with a self-sealing serum cap. Calculated quantities of materials were transferred to the polymerization vessel with syringes. The reaction was initiated when a calculated quantity of anhydrous stannic chloride in the solvent mixture was injected into the vessel at 0°. Of the remaining mixture stannic chloride was 0.5 wt. % and the solvent mixture was 85 wt. %. The polymers formed were purified as mentioned before.

Anionic Polymerization

Tetrahydrofuran was refluxed overnight with lithium aluminium hydride and distilled before use as solvent at a concentration of 60 wt. % of the polymerization mixture. *n*-Butyllithium in hexane was the anionic initiator so that the resulting initiator concentration was 1.6% by wt. The temperature was 30°. Techniques similar to those mentioned for cationic polymerization were used.

In order to determine whether polymers of reasonably high molecular weights were being produced, intrinsic viscosities of the polymers were measured in toluene at 30° in a Cannon-Ubbelohde viscometer with a flow-time for pure solvent of 153.0 s. The values of the intrinsic viscosities ranged between 0.1 and 1.1 dl/g, with the lower values about 0.1 being obtained in the ionic cases, and the higher values in the free radical cases.

Can. J. Chem. Downloaded from www.nrcresearchpress.com by 210.87.254.42 on 09/05/12
For personal use only.

Ultraviolet absorption spectroscopy was used to analyze quantitatively the compositions of the copolymers formed. Spectra were determined in methylene chloride at room temperature using a Cary 14 recording spectrophotometer.

Results

Ultraviolet Absorption Spectroscopy

Profiles of the absorption spectra in the ultraviolet region for the monomers and polymers studied show that at 278 mμ poly(2,6-dimethoxystyrene) absorbs strongly while polystyrene and poly(methyl methacrylate) absorb negligibly. Therefore the absorbances at 278 mμ of the copolymers were concluded to be entirely due to the presence of 2,6-dimethoxystyrene units in the copolymers. The absorbance at 278 mμ for poly(2,6-dimethoxystyrene) was found to increase linearly with concentration up to 0.16 g/l, with a specific extinction coefficient of 3.88 l g^{-1} cm^{-1}. Thus the amount of 2,6-dimethoxystyrene present in the copolymer was determined readily. The amount of comonomer (styrene or methyl methacrylate) present in the copolymer could then be obtained by difference.

Homopolymerization

It was found that the 2,6-dimethoxystyrene could be homopolymerized by free radical, cationic, and anionic catalysts. Very rapid polymerization was observed with the cationic system. The cross-linked material which was obtained may have been a result of a considerable amount of cationic grafting (1) or of cationic reaction with the polymeric main chain (5). Cross-linking had also resulted when 2,5-dimethoxystyrene had been polymerized cationically (6).

Copolymerization

For the cases of free radical copolymerization of 2,6-dimethoxystyrene with styrene and methyl methacrylate and of anionic copolymerization with styrene, the mole fraction of the 2,6-dimethoxystyrene taken up into the copolymer was found to be a monotonically increasing function of the mole fraction of the 2,6-dimethoxystyrene in the mixture of comonomers (Fig. 1).

This behavior was not observed in the other cases of copolymerization attempted. In the case of anionic polymerization of 2,6-dimethoxystyrene with methyl methacrylate, only pure poly(methyl methacrylate) was produced. In the case of cationic copolymerization of 2,6-dimethoxystyrene with unsubstituted styrene, only pure poly(2,6-dimethoxystyrene) was produced.

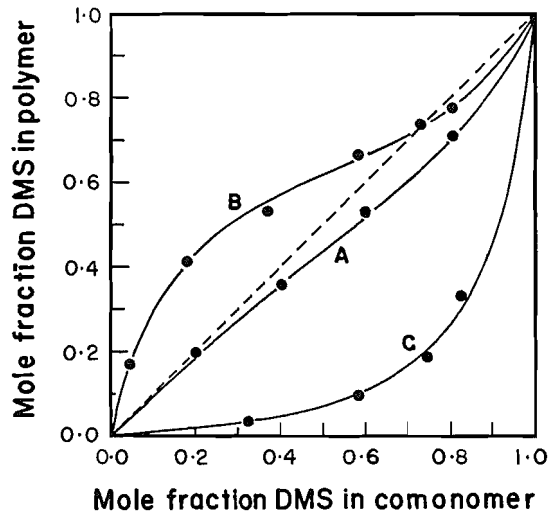

FIG. 1. Variation of copolymer composition with composition of comonomers: **A**, free radical copolymerization of 2,6-dimethoxystyrene (DMS) with styrene: **B**, free radical copolymerization of DMS with methyl methacrylate; **C**, anionic copolymerization of DMS with styrene.

Discussion

The presence of the two methoxy groups would be expected to increase the electron density of the vinyl group in styrene, so that it is noteworthy that 2,6-dimethoxystyrene can be homopolymerized by the anionic catalyst. The rapid polymerization and cross-linking in the cationic homopolymerization can be attributed to the increased electron density also, since it has been shown for *p*-methoxystyrene that the single methoxy substituent increases the reactivity of the phenyl ring to electrophilic attack one hundred times and the reactivity of the vinyl group four hundred times (7). The methoxy substituents in the 2- and 6-positions apparently do not sterically hinder the polymerization reaction although methyl substituents in the same positions had been observed to impede the polymerization (3).

In the cationic copolymerization of 2,6-dimethoxystyrene with styrene, the fact that only homopolymers of 2,6-dimethoxystyrene were formed indicates that the presence of the methoxy groups has made the vinyl group so electronegative that in the presence of cations it reacts preferentially to the exclusion of the styrene molecules. If cationic copolymerization had been attempted with 2,6-dimethoxystyrene and methyl methacrylate, homopolymers of 2,6-dimethoxystyrene would also be expected since methyl

TABLE I

Reactivity ratios and Q–e values of 2,6-dimethoxystyrene and copolymerization at 60°

Comonomers 1;2	r_1	r_2	Q	e
2,6-Dimethoxystyrene; styrene	0.55 ± 0.001	0.98 ± 0.004	1.9 ± 0.01	-1.6 ± 0.003
2,6-Dimethoxystyrene; methyl methacrylate	0.74 ± 0.04	0.14 ± 0.05	2.6 ± 0.7	-1.1 ± 0.1

methacrylate has an even more electropositive vinyl group than styrene.

The electropositive nature of the vinyl group of methyl methacrylate causes strong electrostatic attraction between it and anions, so that under anionic conditions methyl methacrylate is polymerized preferentially in mixtures with 2,6-dimethoxystyrene, in fact, to the complete exclusion of any 2,6-dimethoxystyrene. Copolymers of 2,6-dimethoxystyrene were formed anionically when styrene was used as the comonomer, but the electronegativity of the 2,6-dimethoxystyrene is so much greater that it is incorporated into the copolymer rather reluctantly and, at all relative concentrations of comonomers, the relative amount of 2,6-dimethoxystyrene in the copolymer is less than its relative amount in the comonomer (Fig. 1).

Copolymers of 2,6-dimethoxystyrene were obtained with both styrene and methyl methacrylate when a free radical catalyst was used. Computer techniques were used to show that the copolymerization data obtained in both the free radical and anionic cases were best described by the mechanism proposed by Mayo and Lewis (8), rather than the mechanisms of Wall (9) or Fontana and Kidder (10). At low conversions, the molar ratio of monomers being assimilated into the copolymer, m_1/m_2, is a function of the molar ratio of the monomers present, M_1/M_2, according to the following equation

$$\frac{m_1}{m_2} = \frac{r_1 \frac{M_1}{M_2} + 1}{1 + \frac{r_2 M_2}{M_1}}$$

r_1 ($= k_{11}/k_{12}$) and r_2 ($= k_{22}/k_{21}$) are called the monomer reactivity ratios.

The values of r_1 and r_2 were obtained after the equation was rearranged according to Fineman and Ross (11) and are given in Table I.

Since the reactivity ratios were all found to be less than one, all the radicals show a tendency to alternate, i.e. to add the other monomer. This tendency is strongest with the methyl methacrylate radical, apparently due to the large difference in its electronegativity with that of 2,6-dimethoxystyrene. The alternation tendency is much less pronounced in the styrene system.

Several schemes have been developed to assign to monomers characteristic parameters from which monomer reactivity ratios can be predicted (12). The Q–e scheme proposed by Alfrey and Price (13) is widely used. For the reaction of monomer j with radical i, the rate constant, k_{ij}, is considered in this scheme to be given by

$$k_{ij} = P_i Q_j \exp(- e_i e_j)$$

where P and Q refer to the resonance stabilization of radical and monomer, respectively, and e refers to the polar nature of the radical and monomer. The Q and e values for 2,6-dimethoxystyrene have been determined from the present copolymerization studies (Table I).

The standard deviations in the reactivity ratios determined in the styrene system (Table I) were much less than in the methyl methacrylate system so that the Q and e values determined from the styrene system are considered more reliable, and more likely to represent the monomer. Better agreement is obtained in the case of the Q values than in the case of the e values. A comparison of those Q and e values with those of other monomers (Table II) shows that the Q value for 2,6-dimethoxystyrene is remarkably large, indicating that the vinyl group of this monomer is considerably stabilized by resonance, while the e value for 2,6-dimethoxystyrene is quite negative, indicating that the vinyl group of this monomer has been made strongly electronegative by the electron-donating methoxy substituents in the 2- and 6-positions.

The small Q value of pentachlorostyrene has been attributed to the bulky substituents forcing the vinyl group out of coplanarity with the phenyl ring (15). A similar effect is believed to occur also with 2,6-dichlorostyrene as indicated by indirect evidence (16). The large Q value of 2,6-dimethoxystyrene indicates that the vinyl

Can. J. Chem. Downloaded from www.nrcresearchpress.com by 210.87.254.42 on 09/05/12
For personal use only.

TABLE II

Comparison of Q and e values of several monomers

Monomer	Q	e	Reference
2,6-Dimethoxystyrene	1.9	−1.6	Present study
2,5-Dimethoxystyrene	1.7	−1.0	(6)
p-Methoxystyrene	1.36	−1.1	(17)
Styrene	1.0	−0.8	(14)
Methyl methacrylate	0.74	0.4	(14)
Pentachlorostyrene	0.2	0.25	(15)

group is able to remain coplanar with the phenyl ring.

Acknowledgment

This work was supported in part by a grant from the National Research Council of Canada.

1. C. G. Overberger and C. M. Burns. J. Polymer Sci. To be published. C. M. Burns. Dissertation Abstracts. 1894B (1967).
2. A. A. Shamshurin. J. Gen. Chem. USSR, **16**, 99 (1946).
3. V. V. Korshak and N. G. Matveeva. Bull. Acad. Sci. USSR, Div. Chem. Sci. English Transl. 547 (1953).
4. A. Maercker. *In* Organic reactions. Vol. 14. *Edited by* A. C. Cope. John Wiley and Sons, Inc., New York. 1965. p. 270.
5. Ph. Teyssie and G. Smets. J. Polymer Sci. **20**, 351 (1956); Ph. Teyssie and G. Smets. J. Polymer Sci. **27**, 441 (1958).
6. H. Kamogawa and H. G. Cassidy. J. Polymer Sci. **A2**, 2409 (1964).
7. P. M. Kamath and H. C. Haas. J. Polymer Sci. **24**, 143 (1957).
8. F. R. Mayo and F. M. Lewis. J. Am. Chem. Soc. **66**, 1594 (1944).
9. F. T. Wall. J. Am. Chem. Soc. **63**, 1862 (1941).
10. R. B. Cundall. *In* The chemistry of cationic polymerization. *Edited by* P. H. Plesch. Pergamon Press, New York. 1963. p. 553.
11. M. Fineman and S. D. Ross. J. Polymer Sci. **5**, 259 (1950).
12. A. D. Jenkins. Advances in free-radical chemistry. Vol. 2. Lagos Press, London. 1967.
13. T. Alfrey, Jr. and C. C. Price. J. Polymer Sci. **2**, 101 (1947).
14. C. C. Price. J. Polymer Sci. **3**, 772 (1948).
15. T. Alfrey, Jr. and W. H. Ebelke. J. Am. Chem. Soc. **71**, 3235 (1949).
16. C. S. Marvel, G. E. Inskeep, R. Deanin, A. E. Juve, C. H. Schroeder, and M. M. Goff. Ind. Eng. Chem. **39**, 1486 (1947).
17. L. J. Young. J. Polymer Sci. **54**, 411 (1961).

Can. J. Chem. Downloaded from www.nrcresearchpress.com by 210.87.254.42 on 09/05/12
For personal use only.

Can. J. Chem. Downloaded from www.nrcresearchpress.com by 210.87.254.105 on 09/05/12
For personal use only.

Azaindoles. Part I. The syntheses of 5-aza- and 5,7-diazaindoles by the non-catalytic thermal indolization of 4-pyridyl- and 4-pyrimidylhydrazones respectively[1]

P. A. Crooks and B. Robinson
Department of Pharmacy, The University, Manchester 13, England

Received October 22, 1968

The thermal indolization of a series of 4-pyridyl- and 4-pyrimidylhydrazones has been investigated. Under these conditions, isobutyraldehyde and 2-methylbutyraldehyde 4-pyridylhydrazones afford only 5-aza-2,3-dimethylindole and 5-aza-2-ethyl-3-methylindole respectively, and both ethyl methyl ketone and isobutyraldehyde 4-pyrimidylhydrazones afford only 5,7-diaza-2,3-dimethylindole. Several attempts to effect a Chichibabin amination on 5-aza-2,3-dimethyl- and 5-aza-1,2,3-trimethylindole led only to the recovery of starting material.

Canadian Journal of Chemistry, 47, 2061 (1969)

Several synthetic approaches to the 5-azaindole system have been developed (1), but that involving the acid-catalyzed Fischer indolization (2) of 4-pyridylhydrazones has either failed or only succeeded under much more drastic conditions than employed for the indolization of the corresponding phenylhydrazones (1, 2). These limitations with 4-pyridylhydrazones are caused by deactivation of the pyridine nucleus towards intramolecular electrophilic attack, one of the stages in the mechanism of the Fischer indole synthesis, both by the inductive effect of the hetero-nitrogen atom and by protonation of this atom in the acidic reaction media (2). Recently (3, 4) protonation of this nitrogen atom during such indolizations has been prevented by employing the non-catalytic thermal indolization technique (5), several 2-pyridylhydrazones (3, 4) and cyclohexanone 4-pyridylhydrazone (3) having been converted into the corresponding 7-azaindoles and 6-aza-1,2,3,4-tetrahydrocarbazole respectively by boiling in di- or triethylene glycol. We have now investigated the application of this technique to the indolization of further 4-pyridylhydrazones.

The introduction of another nitrogen atom into the aromatic ring of a pyridylhydrazone affords, amongst other possible compounds, 4-pyrimidylhydrazones, in which the second hetero-nitrogen atom further reduces the nucleophilicity of the aromatic ring. This, however, does not prevent their non-catalytic thermal indolization to 5,7-diazaindoles in the examples which have been investigated in the present studies. Although syntheses of the 5,7-diazaindole ring system (6–8) and of 5,7-diazaindole itself (7,8) have been published, these are the first reports of such syntheses using Fischer indolizations, an approach which offers a versatile preparation of 5,7-diazaindoles having alkyl or aryl substituents in the 2- and/or 3-position(s), since 4-hydrazinopyrimidine is readily available (9, see also the Experimental).

The 4-pyridylhydrazones (Table I) were prepared by addition of the appropriate carbonyl compound to an aqueous or aqueous ethanolic solution of 4-hydrazinopyridine hydrochloride (10). Attempted preparation of ethyl pyruvate 4-pyridylhydrazone by condensation of ethyl pyruvate and 4-hydrazinopyridine hydrochloride under these conditions afforded only pyruvic acid 4-pyridylhydrazone. The 4-pyrimidylhydrazones (Table II) were prepared by condensation of the appropriate carbonyl compound with 4-hydrazinopyrimidine (9) in methanolic solution.

Attempted indolization of pyruvic acid 4-pyridylhydrazone by boiling a solution of it in mono-, di-, or triethylene glycol was unsuccessful, as were the similar attempts to prepare 5-aza-2-methylindole (**1**, R = R″ = H, R′ = CH_3, X = N, Y = CH) from acetone 4-pyridylhydrazone.

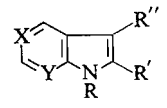

1

These results are analogous to those obtained from the previous unsuccessful attempts (4) to thermally indolize pyruvic acid and acetone 2-pyridylhydrazones: however, 5-aza-3-methylindole (**1**, R = R′ = H, R″ = CH_3, X = N, Y = CH) is produced by boiling a solution of

[1]Preliminary communication, P. A. Crooks and B. Robinson. Chem. Ind. London, 547 (1967).

TABLE I

Percentage yields, melting points, and analytical data of the 4-pyridylhydrazones

4-Pyridylhydrazone of:	Yield (%)	Melting point (°C)	Molecular formula	Analysis Calculated (%) C	Calculated (%) H	Found (%) C	Found (%) H
Pyruvic acid	91*	234–236 (decomp.)	$C_8H_9N_3O_2 \cdot \frac{1}{2}H_2O$	50.5	5.25 (N:22.1)	49.8	4.6 (N:22.1)
Acetone	98†	170–171 (lit. 23)					
		170–171	$C_8H_{11}N_3$	—	—	—	—
Propionaldehyde	98‡	79–85	$C_9H_{11}N_3$	Not analyzed			
Ethyl methyl ketone	89†	125–127	$C_9H_{13}N_3$	66.25	8.0	66.25	7.8
Isobutyraldehyde	92†	108–110	$C_9H_{13}N_3$	66.25	8.0	66.05	8.1
Methyl isopropyl ketone	86†	132–134	$C_{10}H_{15}N_3$	67.8	8.45	67.65	8.55
2-Methylbutyraldehyde	93‡	81–84	$C_{10}H_{15}N_3$	Not analyzed			

*Recrystallized from aqueous ethanol.
†Recrystallized from ether.
‡Could not be recrystallized.

TABLE II

Percentage yields, melting points, and analytical data of the 4-pyrimidylhydrazones

4-Pyrimidylhydrazone of:	Yield (%)	Melting point (°C)	Molecular formula	Analysis Calculated (%) C	Calculated (%) H	Found (%) C	Found (%) H
Cyclohexanone	80*	143–144	$C_{10}H_{14}N_4$	63.15	7.4	62.75	7.3
Ethyl methyl ketone	70†	109–112	$C_8H_{12}N_4$	58.85	7.3	58.35	7.2
Isobutyraldehyde	69†	120–121	$C_8H_{12}N_4$	58.85	7.3	58.75	7.2

*Recrystallized from aqueous methanol.
†Recrystallized from methanol.

propionaldehyde 4-pyridylhydrazone in diethylene glycol.

Since both cyclohexanone phenylhydrazone and 4-pyridylhydrazone have been indolized (3) in high yields using non-catalytic thermal conditions, the first attempted thermal indolization of a 4-pyrimidylhydrazone was effected on that of cyclohexanone in boiling diethylene glycol, a reaction which afforded a 32% yield of 6,8-diaza-1,2,3,4-tetrahydrocarbazole (**1**, R = H, R′ + R″ = $(CH_2)_4$, X = N, Y = CH). Boiling solutions of ethyl methyl ketone 4-pyridyl- and 4-pyrimidylhydrazones in diethylene glycol afforded only 5-aza- and 5,7-diaza-2,3-dimethylindoles (**1**, R = H, R′ = R″ = CH_3, X = N, Y = CH, and X = Y = N) respectively. These indolizations occurred as expected (2) exclusively on the methylene group of the ethyl group and not on the methyl group of the ketonic moiety.

In an attempt to extend this synthesis to the preparation of 5-aza- and 5,7-diaza-3*H*-indoles, solutions of isobutyraldehyde 4-pyridyl- and 4-pyrimidylhydrazones in monoethylene glycol were boiled, but no indolization of these compounds under these conditions could be detected, whereas in boiling diethylene glycol the hydrazones afforded only 5-aza- and 5,7-diaza-2,3-dimethylindoles (**1**, R = H, R′ = R″ = CH_3, X = N, Y = CH, and X = Y = N) respectively. Presumably, both these indoles are formed by a thermally-induced (11) Plancher rearrangement (12) of the initially-formed 5-aza- and 5,7-diaza-3,3-dimethyl-3*H*-indoles (**2**, R = H, R′ = CH_3, X = N, Y = CH, and X = Y = N) respectively. To eliminate the possibility that

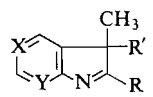

2

methyl group migration had occurred in the isobutyraldehyde 4-pyridyl- and 4-pyrimidylhydrazones (**3**, X = CH and N respectively) during their synthesis, the proton magnetic resonance (p.m.r.) spectra of these compounds were ex-

Can. J. Chem. Downloaded from www.nrcresearchpress.com by 210.87.254.105 on 09/05/12
For personal use only.

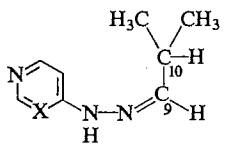

3

amined. Both spectra showed 6-proton doublets (J = 7 and 8 c.p.s. respectively) centered at τ 8.80 and 8.87 respectively (the two equivalent methyl groups on C_{10}), a 1-proton multiplet between τ 6.90–7.90 and τ 6.97–7.82 respectively [C_{10}—H], and a 1-proton doublet (J = 6 and 5 c.p.s. respectively) centered at τ 2.84 and τ 2.77 respectively [C_9—H]. In each case signals attributable to the N—H and aromatic protons were also obtained. In both spectra, after irradiation of the C_{10}—H one-proton multiplet, the 1- and 6-proton doublets collapsed to singlets. Boiling a solution of methyl isopropyl ketone 4-pyridylhydrazone in monoethylene glycol did, however, afford 5-aza-2,3,3-trimethyl-3*H*-indole (**2**, R = R′ = CH_3, X = N, Y = CH) in which a Plancher rearrangement to an indole is impossible.

It has been claimed (4), without the evidence of physical data, that the product obtained by thermal indolization of isobutyraldehyde 2-pyridylhydrazone in boiling diethylene glycol is 7-aza-3,3-dimethyl-3*H*-indole (**2**, R = H, R′ = CH_3, X = CH, Y = N); however, this product has an almost identical melting point to that of 7-aza-2,3-dimethylindole (**1**, R = H, R′ = R″ = CH_3, X = CH, Y = N), prepared by thermal indolization of ethyl methyl ketone 2-pyridylhydrazone in boiling diethylene glycol (4). In view of this and the above mentioned rearrangements it seems probable that the compound thought (4) to be 7-aza-3,3-dimethyl-3*H*-indole is, in fact, 7-aza-2,3-dimethylindole, a possibility which has now (13) been verified as correct.

2-Methylbutyraldehyde 4-pyridylhydrazone upon indolization in boiling diethylene glycol affords only 5-aza-2-ethyl-3-methylindole (**1**, R = H, R′ = C_2H_5, R″ = CH_3, X = N, Y = CH). In this case the intermediate 5-aza-3-ethyl-3-methyl-3*H*-indole (**2**, R = H, R′ = C_2H_5, X = N, Y = CH) has also undergone thermally-induced Plancher rearrangement under the indolization conditions. The exclusive formation of **1** (R = H, R′ = C_2H_5, R″ = CH_3, X = N, Y = CH) is in accord with the observation (14) that an ethyl group has a higher migratory aptitude than a methyl group and migrates preferentially to it in a Plancher rearrangement.

It has been suggested (15) that the "essential" molecular features of a purine antimetabolite are contained in a 1-unsubstituted 5-azaindole having a 4-substituent which is capable of forming a hydrogen bond, by hydrogen donation, with a nitrogen p-electron pair of a pyrimidine nucleus. Attempts have been made to synthesize a compound having these requirements by effecting a Chichibabin reaction (16) on **1** (R = H, R′ = R″ = CH_3, X = N, Y = CH), which, by analogy with this reaction on isoquinoline which affords (17) exclusively 1-amino-isoquinoline, would be expected to afford 4-amino-5-aza-2,3-dimethylindole. However, attempted amination of 5-aza-2,3-dimethylindole with sodamide in xylene and in *N*,*N*-dimethylaniline under various conditions failed, only starting material being recoverable from such reactions [cf. the failure to aminate 7-azaindole (18)]. It appeared likely that the failure of this reaction could be caused by the heterogeneous nature of these reaction mixtures owing to the insolubility of the sodium salt of the indole which is formed and precipitated out and/or by the presence of the negative charge on the indolic nucleus of this salt which would prevent attack on the nucleus by amide anion. This salt formation was overcome by 1-methylation of **1** (R = H, R′ + R″ = CH_3, X = N, Y = CH), with sodamide and methyl iodide (19) to afford **1** (R = R′ = R″ = CH_3, X = N, Y = CH), but attempted amination of this *N*-methylated derivative with sodamide in boiling decalin or xylene or with barium amide in liquid ammonia (20) again failed and led only to the recovery of starting material.

Experimental

Melting points were determined on a Köfler hot-stage apparatus and are uncorrected. Infrared (i.r.) spectra were recorded on a Perkin–Elmer 237 spectrophotometer, ultraviolet (u.v.) spectra were measured on a Perkin–Elmer 137 spectrophotometer, and p.m.r. spectra were recorded on a Varian A 60 spectrometer in deuteriochloroform solution (unless otherwise stated) using tetramethylsilane as internal standard. Solutions were dried over anhydrous magnesium sulfate and, unless otherwise stated, solvents were removed on a steam-bath under reduced pressure (water pump).

4-Pyridylhydrazones

4-Hydrazinopyridine hydrochloride (4.0 g) (10) was dissolved in water (10 ml) and the appropriate aldehyde or ketone (4 ml) was added. Ninety-five percent ethanol

Can. J. Chem. Downloaded from www.nrcresearchpress.com by 210.87.254.105 on 09/05/12
For personal use only.

Can. J. Chem. Downloaded from www.nrcresearchpress.com by 210.87.254.105 on 09/05/12
For personal use only.

(8 ml) was added, if required, to effect a homogeneous reaction mixture. After standing at room temperature for 4 h, the solution was basified with sodium hydroxide solution and the liberated oil extracted with ether (2 × 20 ml). The combined ethereal extracts were washed with water (2 × 20 ml), dried, and the solvent removed to afford the 4-pyridylhydrazones as oils which completely crystallized and which were recrystallized (except propionaldehyde and 2-methylbutyraldehyde 4-pyridylhydrazones) (Table I).

In the case of acetone 4-pyridylhydrazone a precipitate, and not an oil, was formed upon basification. This was collected, washed with water until the washings were neutral, dried over P_2O_5 *in vacuo*, and recrystallized (Table I).

4-Hydrazinopyridine hydrochloride was reacted with pyruvic acid and ethyl pyruvate as above, but after standing the reaction mixture at room temperature for 4 h, the ethanol was removed and the solid which separated was collected, washed with water, dried over P_2O_5 *in vacuo*, and recrystallized (Table I).

4-Hydrazinopyrimidine

The previously published (9, 21) method for the preparation of 4-hydrazinopyrimidine from 4-hydroxypyrimidine (22) was modified as follows to afford an increase in the yield of product.

A mixture of phosphoryl chloride (50 ml) and 4-hydroxypyrimidine (22) (14 g) was boiled under reflux on an oil-bath for 40 min. The cooled reaction mixture was then shaken with sodium-dried petroleum (6 × 40 ml, b.p. 40–60°) and to the resulting brown gum was carefully added dry methanol (120 ml) dropwise. After the vigorous reaction had ceased the resulting yellow-brown solution was poured into a methanolic solution of sodium methoxide (20 g of sodium in 250 ml of dry methanol) and the resulting suspension was boiled under reflux for 30 min. After cooling, carbon dioxide was passed through the suspension until it was saturated (3 h), the mixture was filtered, the precipitate was washed with dry methanol (2 × 20 ml), and the total methanolic filtrate was evaporated to dryness on a rotating evaporator at 25°. To the residue was added dry methanol (15 ml) and the methanol was again completely evaporated at 70°, this procedure being repeated one further time. The total methanolic distillate was then evaporated at room temperature on a rotating evaporator to a volume of approximately 30 ml, hydrazine hydrate (5 ml) was added, the mixture boiled under reflux for 2 h, a further quantity of hydrazine hydrate (5 ml) was added and the boiling under reflux continued a further 2 h. The solution was left standing at room temperature overnight and the solvent evaporated to afford 4-hydrazinopyrimidine as a pale-yellow crystalline solid (6.90 g, 41%) [lit. yield 15% (9, 21)] which was used to prepare the 4-pyrimidylhydrazones below without recrystallization. A small sample was recrystallized from methanol–benzene to afford pale-yellow prisms, m.p. 133–134° (decomp.) [lit. m.p. 132–134° (9)].

4-Pyrimidylhydrazones

4-Hydrazinopyrimidine (1.6 g) was dissolved in dry methanol (10 ml) and the ketone or aldehyde (3 ml) was added. An exothermic reaction occurred, after which the solutions were left standing overnight at room temperature.

Evaporation of the solvent then left the 4-pyrimidylhydrazones (Table II) as crystalline solids which were purified by recrystallization.

5-Aza-3-methylindole

A solution of propionaldehyde 4-pyridylhydrazone (3.0 g) in diethylene glycol (30 ml) was boiled under reflux for 10 h, then cooled to room temperature, and poured into cold water (250 ml). The liberated oil was extracted with chloroform (2 × 200 ml) and the combined chloroform extracts were washed with water (2 × 300 ml), dried, and the solvent removed to afford a tan-colored solid which after recrystallization from ethanol–ether afforded light-tan prisms (1.14 g, 34.5%), m.p. 144–145°.

Anal. Calcd. for $C_8H_8N_2$: C, 72.7; H, 6.1. Found: C, 72.5; H, 6.2.

λ_{max}(EtOH) 222 mμ, log ε 4.53; 275 mμ, log ε 3.39. λ_{Infl}(EtOH) 283 mμ, log ε 3.28. λ_{min}(EtOH) 245 mμ, log ε 3.04. λ_{max}(EtOH–HCl) 227.5 mμ, log ε 4.57; 284 mμ, log ε 3.34. λ_{Infl}(EtOH–HCl) 312 mμ, log ε 3.04. λ_{min} (EtOH–HCl) 246 mμ, log ε 2.92. These u.v. spectral data are similar to those reported (1) for 5-azaindole, the dissimilarities probably being caused by the bathochromic effect of the 3-methyl substituent. The p.m.r spectrum showed a 3-proton singlet at τ 7.83 [C_3—CH_3], a 1-proton singlet at τ 2.96 [C_2—H] (24), a 1-proton doublet (J = 5 c.p.s.) (ortho coupling) centered at τ 2.80 with each peak split into another doublet (J = 1.5 c.p.s.) (para coupling) [C_7—H], a 1-proton doublet (J = 5 c.p.s.) (ortho coupling) centered at τ 1.90 [C_6—H], a 1-proton doublet (J = 1.5 c.p.s.) (para coupling) centered at τ 1.25 [C_4 —H], and a broad 1-proton singlet at τ −1.36 which disappeared upon addition of D_2O (N—H).

5-Aza-2,3-dimethylindole

Ethyl methyl ketone 4-pyridylhydrazone (3.0 g) was boiled in diethylene glycol solution (30 ml) for 15 h, the reaction mixture cooled, and then poured into cold water. The resulting light-brown precipitate was collected, washed well with water followed by a little ether, and recrystallized from ethanol to afford light-tan prisms (1.41 g, 52.5%), m.p. 214–215°.

Anal. Calcd. for $C_9H_{10}N_2$: C, 73.5; H, 6.9. Found: C, 74.15; H, 6.85.

λ_{max}(EtOH) 226 mμ, log ε 4.54; 278 mμ, log ε 3.67. λ_{Infl}(EtOH) 286 mμ, log ε 3.54. λ_{min}(EtOH) 250 mμ, log ε 3.17. λ_{max}(EtOH–HCl) 231.5 mμ, log ε 4.62; 290 mμ, log ε 3.53. λ_{Infl}(EtOH–HCl) 314 mμ, log ε 3.17. λ_{min} (EtOH–HCl) 250 mμ, log ε 3.02. The p.m.r. spectrum included two 3-proton singlets at τ 7.80 and τ 7.68 [C_3—CH_3 and C_2—CH_3 respectively] (the high-field singlet is attributed to the C_3—CH_3 protons by comparison with the τ value of the singlet caused by the protons of this group in the spectrum of 5-aza-3-methylindole quoted above), a 1-proton doublet (J = 5.5 c.p.s.) (ortho coupling) centered at τ 2.76 with each peak split into further doublets (J = 1.5 c.p.s.) (para coupling) [C_7—H], a 1-proton doublet (J = 5.5 c.p.s.) (ortho coupling) centered at τ 1.89 [C_6 —H], a 1-proton doublet (J = 1.5 c.p.s.) (para coupling) centered at τ 1.32 [C_4 —H], and a 1-proton broad singlet between τ −1.33 and τ −0.93 which disappeared upon addition of D_2O (N—H).

Can. J. Chem. Downloaded from www.nrcresearchpress.com by 210.87.254.105 on 09/05/12
For personal use only.

When this reaction was repeated using isobutyraldehyde 4-pyridylhydrazone in place of ethyl methyl ketone 4-pyridylhydrazone, 5-aza-2,3-dimethylindole (identical m.p., mixture m.p., u.v., i.r., and p.m.r. spectra with that prepared above) was produced in 14.5% yield.

5-Aza-2,3,3-trimethyl-3H-indole

A solution of methyl isopropyl ketone 4-pyridylhydrazone (3.0 g) in diethylene glycol (30 ml) was boiled under reflux under an atmosphere of nitrogen for 6 h, and the reaction mixture worked up as described above for the preparation of 5-aza-3-methylindole. Evaporation of the chloroform extract afforded a dark-brown gum from which no recognizable product could be isolated.

The reaction was repeated in monoethylene glycol and after boiling for 6 h, the reaction mixture was cooled, poured into cold water (250 ml), and the aqueous suspension extracted with ether (3 × 150 ml). The combined ether extracts were washed with water (2 × 250 ml), dried, and the solvent removed to afford a brown oil (1.21 g) which could not be induced to crystallize and which had an u.v. spectrum (in EtOH) almost identical to that of the starting material. The aqueous phase remaining from the above ether extraction was extracted with chloroform (2 × 100 ml), the combined chloroform extracts washed with water (2 × 100 ml), dried, and the chloroform removed to afford a crystalline residue which upon sublimation [60–80° (bath temperature) at 74 mm] gave 5-aza-2,3,3-trimethyl-3*H*-indole as colorless needles (0.29 g, 10.5%), m.p. 86–87° [reported m.p. 81–81.5° (25)].

λ_{max}(EtOH) 243.5 mμ, log ε 3.56. λ_{infl}(EtOH) 299 mμ, log ε 2.78. λ_{min}(EtOH) 224 mμ, log ε 3.48. λ_{max}(EtOH–HCl) 277.5 mμ, log ε 3.85. λ_{infl}(EtOH–HCl) 308 mμ, log ε 2.94. λ_{min}(EtOH–HCl) 240 mμ, log ε 3.05. λ_{max} (conc. HCl) 256 mμ, log ε 3.84. λ_{infl}(conc. HCl) 313 mμ, log ε 2.43. λ_{min}(conc. HCl) 227 mμ, log ε 3.64. The p.m.r. spectrum showed a 6-proton singlet at τ 8.68 [C_3 $(CH_3)_2$], a 3-proton singlet at τ 7.75 [C_2 CH_3], a 1-proton doublet (J = 5 c.p.s.) (ortho coupling) centered at τ 2.75 with each peak split into further doublets (J = 1.5 c.p.s.) (para coupling) [C_7 —H], a 1-proton doublet (J = 1.5 c.p.s.) (para coupling) centered at τ 1.73 [C_4 —H], and a 1-proton doublet (J = 5 c.p.s.) (ortho coupling) centered at τ 1.70 [C_6 —H].

5-Aza-2-ethyl-3-methylindole

2-Methylbutyraldehyde 4-pyridylhydrazone (3.0 g) was indolized as described above for propionaldehyde 4-pyridylhydrazone, the boiling in diethylene glycol being continued for 16 h. The brown oil obtained by evaporation of the chloroform extract was subjected to column chromatography on alumina (grade 'H'). A light-brown band was eluted with ether, evaporation of the eluate yielding a light-brown oil which could not be crystallized and which showed no significant u.v. absorption. Elution with chloroform/ether (1:5 vol:vol) and then with chloroform, followed by evaporation of the eluates, afforded in each case a crystalline residue which after recrystallization from ethanol–ether gave light-tan prisms (0.54 g, 20%), m.p. 155–156°.

Anal. Calcd. for $C_{10}H_{12}N_2$: C, 75.0; H, 7.55. Found: C, 75.0; H, 7.25.

λ_{max}(EtOH) 227.5 mμ, log ε 4.57; 278 mμ, log ε 3.70. λ_{infl}(EtOH) 286 mμ, log ε 3.65. λ_{min}(EtOH) 250 mμ, log ε 3.51. λ_{max}(EtOH–HCl) 232 mμ, log ε 4.65; 289 mμ, log ε 3.65. λ_{infl}(EtOH–HCl) 316 mμ, log ε 3.28. λ_{min} (EtOH–HCl) 250 mμ, log ε 3.29 (these u.v. spectral data are almost identical with those recorded for 5-aza-2,3-dimethylindole recorded above). The p.m.r. spectrum (recorded in hexadeuteriodimethylsulfoxide) showed a 3-proton triplet (J = 7 c.p.s.) and a 2-proton quartet (J = 7 c.p.s.) centered at τ 8.75 and τ 7.26 respectively [C_2 C_2H_5], a 3-proton singlet at τ 7.78 [C_3 CH_3] [cf. the value of τ 7.83 and τ 7.80 for the protons of the C_3 CH_3 groups in 5-aza-3-methylindole and 5-aza-2,3-dimethylindole respectively], a 1-proton doublet (J = 5.1 c.p.s.) (ortho coupling) centered at τ 2.75 with each peak split into a further doublet (J = 1.5 c.p.s.) (para coupling) [C_7 —H], a 1-proton doublet (J = 5.1 c.p.s.) (ortho coupling) centered at τ 1.90 [C_6 —H], a 1-proton doublet (J = 1.5 c.p.s.) (para coupling) centered at τ 1.30 [C_4 —H], and a broad singlet between τ −1.40 and τ −0.92 which disappeared upon addition of D_2O (N—H).

The mother liquors remaining from the recrystallization of the 5-aza-2-ethyl-3-methylindole were evaporated and the p.m.r. spectrum of the residue was recorded (in hexadeuteriodimethylsulfoxide) and showed no trace of a singlet signal at ≏ τ 7.7, indicating the absence of a 2-methyl substituted 5-azaindole nucleus, since the C_2 CH_3 protons in 5-aza-2,3-dimethylindole give rise to a singlet at τ 7.68.

6,8-Diaza-1,2,3,4-tetrahydrocarbazole

Cyclohexanone 4-pyrimidylhydrazone (3.0 g) was dissolved in diethylene glycol (30 ml), the solution boiled under reflux for 5 h, and then worked up as described above for the preparation of 5-aza-3-methylindole. Evaporation of the chloroform extract afforded a light-brown oil which crystallized. Recrystallization from chloroform–ether afforded light-tan prisms (0.87 g, 32%), m.p. 233–235°.

Anal. Calcd. for $C_{10}H_{11}N_3$: C, 69.4; H, 6.4. Found: C, 69.2; H, 6.45.

λ_{max}(EtOH) 232.5 mμ, log ε 4.50; 274–275 mμ, log ε 3.38; 305 mμ, log ε 3.35. λ_{min}(EtOH) 251 mμ, log ε 3.24; 290 mμ, log ε 3.33. λ_{max}(EtOH–HCl) 236–237 mμ, log ε 4.47; 292–293 mμ, log ε 3.44. λ_{infl}(EtOH–HCl) 325 mμ, log ε 3.03. λ_{min}(EtOH–HCl) 258 mμ, log ε 3.23. λ_{max}(conc. HCl) 241.5 mμ, log ε 4.50; 299.5 mμ, log ε 3.73. λ_{infl}(conc. HCl) 320–330 mμ, log ε 3.50. λ_{min}(conc. HCl) 275 mμ, log ε 3.55. The p.m.r. spectrum (recorded in hexadeuteriodimethylsulfoxide) showed two 4-proton multiplets between τ 7.93 and τ 8.46 [C_2 H_2 and C_3 H_2] and τ 7.13 and τ 7.58 [C_1 H_2 and C_4 H_2], 1-proton singlets at τ 1.37 and τ 1.25 [C_5 H and C_7 H], and a 1-proton broad singlet at τ −1.66 which disappeared upon addition of D_2O (N—H).

5,7-Diaza-2,3-dimethylindole

Ethyl methyl ketone 4-pyrimidylhydrazone (1.60 g) was dissolved in monoethylene glycol (25 ml) and the solution was boiled under reflux for 12 h. After working up as described above for the preparation of 6,8-diaza-1,2,3,4-tetrahydrocarbazole, a brown oil was obtained but all attempts to obtain a crystalline or recognizable product from this failed.

The above procedure was repeated using diethylene glycol instead of monoethylene glycol and the brown oil obtained was subjected to column chromatography on

Can. J. Chem. Downloaded from www.nrcresearchpress.com by 210.87.254.105 on 09/05/12
For personal use only.

alumina (grade 'H') using chloroform as eluant. A brown band was initially eluted which upon removal of the solvent afforded a brown gum which could not be induced to crystallize and which had no significant u.v. absorption. A deep-yellow band was then eluted, removal of the solvent from which affording a pale-yellow crystalline solid (0.15 g, 10.5%) which after recrystallization from chloroform–ether and sublimation [140–160° (bath temperature) at 0.4 mm] yielded colorless prisms, m.p. 172–173°.

Anal. Calcd. for $C_8H_9N_3$: C, 65.3; H, 6.15. Found: C, 64.55; H, 6.0.

λ_{max}(EtOH) 231.5 mμ, log ε 4.39; 274–276 mμ, log ε 3.28; 307–308 mμ, log ε 3.26. λ_{min}(EtOH) 249 mμ, log ε 3.16; 290 mμ, log ε 3.24. λ_{max}(EtOH–HCl) 235 mμ, log ε 4.38; 293 mμ, log ε 3.30. λ_{infl}(EtOH–HCl) 323 mμ, log ε 3.15. λ_{infl}(EtOH–HCl) 323 mμ, log ε 3.15. λ_{min}(EtOH–HCl) 259 mμ, log ε 3.16. λ_{max}(conc. HCl) 241 mμ, log ε 4.38; 296 mμ, log ε 3.50. λ_{infl}(conc. HCl) 320–331 mμ, log ε 3.22. λ_{min}(conc. HCl) 275 mμ, log ε 3.28. The p.m.r. spectrum showed two 3-proton singlets at τ 7.73 [C_3CH_3] and τ 7.53 [C_2CH_3], a 2-proton singlet at τ 1.23 [C_4H and C_6H] and a 1-proton broad singlet at τ −1.93 which disappeared upon addition of D_2O (N—H).

The u.v. spectra reported above for 6,8-diaza-1,2,3,4-tetrahydrocarbazole and 5,7-diaza-2,3-dimethylindole are, as would be expected, closely similar to each other but bear no resemblance to the spectrum previously reported (8) for 5,7-diazaindole (i.e. λ_{max}(pH 6.8) 271 mμ, log ε 3.60. λ_{max}(HCl) 225 mμ, log ε 4.44; 265 mμ, log ε 3.49; 299 mμ, log ε 3.18. λ_{max}(NaOH) 273 mμ, log ε 3.59), although the spectrum of 5,7-diazaindole in hydrochloric acid solution as previously reported (8) and quoted above is closely similar to those of the two 5,7-diazaindoles presently reported in ethanolic solution. Since the structures of these two 5,7-diazaindoles are definitely established by their mode of synthesis and from their p.m.r. spectra, it appears that the solvents quoted in the published (8) u.v. spectrum of 5,7-diazaindole are erroneous.

Isobutyraldehyde 4-pyrimidylhydrazone (1.6 g) was indolized in boiling diethylene glycol by a procedure analogous to that described above for the indolization of ethyl methyl ketone 4-pyrimidylhydrazone. The column was initially eluted with ether–chloroform (1:1 vol:vol) until the eluate was colorless and a brown band was subsequently eluted with chloroform. Both these eluates upon evaporation of the solvents afforded crystalline residues (total 0.23 g, 16%) which after recrystallization from chloroform–ether and sublimation [140–160° (bath temperature) at 0.4 mm] gave colorless prisms which were identical (m.p., mixture m.p., and i.r., u.v., and p.m.r. spectra) to 5,7-diaza-2,3-dimethylindole described above.

Attempted Aminations of 5-Aza-2,3-dimethylindole

After boiling mixtures of 5-aza-2,3-dimethylindole (0.50, 0.30, and 0.30 g respectively) and sodamide (0.28, 0.20, and 0.80 g respectively) in dry xylene (6 ml) for 5 h, and *N,N*-dimethylaniline (6 ml) for 1 h and 5 h respectively, the only product which could be isolated from the reaction mixtures was unchanged 5-aza-2,3-dimethylindole (0.41, 0.12, and 0.17 g respectively).

5-Aza-1,2,3-trimethylindole

To a solution of sodamide in liquid ammonia (prepared from 8.0 g of sodium in 150 ml of liquid ammonia) was added 5-aza-2,3-dimethylindole (10 g). After stirring for 1.5 h, methyl iodide (20 ml) was added dropwise with stirring over 30 min, the stirring continued for 2.5 h, the ammonia and unreacted methyl iodide removed (steam-bath), and the residue shaken with water (150 ml).

The aqueous solution was basified with sodium hydroxide solution, the precipitate extracted with chloroform (3 × 200 ml), the combined extracts washed with water (2 × 200 ml), dried, and the solvent evaporated to afford a brown oil which was distilled (b.p. 160–164° at 1.5 mm) to give a pale-yellow oil which soon completely crystallized. Recrystallization afforded 5-aza-1,2,3-trimethylindole (7.20 g, 68%) as cream-colored prisms, m.p. 69–71°.

Anal. Calcd. for $C_{10}H_{12}N_2$: C, 75.0; H, 7.5. Found: C, 75.0; H, 7.85.

Attempted Aminations of 5-Aza-1,2,3-trimethylindole

Mixtures of 5-aza-1,2,3-trimethylindole (0.75 g) with sodamide (0.5 and 1.0 g respectively) were boiled in dry decalin (15 ml) for 1.5 h and dry xylene for 4 h respectively, and a mixture of 5-aza-1,2,3-trimethylindole (1.9 g) and barium nitrate (0.90 g) in a solution of barium amide in ammonia [prepared from barium (2.1 g), liquid ammonia (50 ml), and a trace of ignited barium oxide] was stirred for 24 h. The only product which could be isolated from all three reactions was 5-aza-1,2,3-trimethylindole (0.50, 0.46, and 1.62 g respectively).

Acknowledgment

One of us (P. A. C.) acknowledges the award of a Research Scholarship by the Science Research Council, London, England.

1. R. E. Willette. Advan. Heterocyclic Chem. **9**, 27 (1968).
2. B. Robinson. Chem. Rev. **63**, 373 (1963).
3. A. H. Kelly, D. H. McLeod, and J. Parrick. Can. J. Chem. **43**, 296 (1965).
4. A. H. Kelly and J. Parrick. Can. J. Chem. **44**, 2455 (1966).
5. J. T. Fitzpatrick and R. D. Hiser. J. Org. Chem. **22**, 1703 (1957).
6. T. B. Johnson. J. Am. Chem. Soc. **33**, 758 (1911); T. B. Johnson and E. F. Kohmann. Am. Chem. J. **49**, 186 (1913); Z. Foldi, G. Fodor, I. Demjen, H. Szekeres, and I. Halmos. Ber. **75**, 755 (1942); P. Nesbitt and P. Sykes. J. Chem. Soc. 3057 (1954); C. W. Noell and R. K. Robins. J. Heterocyclic Chem. **1**, 34 (1964); C. E. Taylor and R. W. Hendess. J. Am. Chem. Soc. **86**, 951 (1964); **87**, 1996 (1965); R. L. Tolman, R. K. Robins, and L. B. Townsend. J. Heterocyclic Chem. **4**, 230 (1967).
7. British Patent No. 812, 366 to Wellcome Foundation Ltd.; Chem. Abstr. **54**, 592 (1960).
8. J. Davoll. J. Chem. Soc. 131 (1960).
9. J. Chesterfield, J. F. W. McOmie, and E. R. Sayer. J. Chem. Soc. 3478 (1955).
10. F. G. Mann, A. F. Prior, and T. J. Willcox. J. Chem. Soc. 3830 (1959).
11. W. E. Noland and F. J. Baude. J. Org. Chem. **31**, 3321 (1966).
12. R. Robinson and H. Suginome. J. Chem. Soc. 298 (1932); F. J. Evans, G. G. Lyle, J. Watkins, and

R. E. LYLE. J. Org. Chem. **27**, 1553 (1962); F. J. EVANS and R. E. LYLE. Chem. Ind. London, 986 (1963); M. NAKAZAKI, K. YAMAMOTO, and K. YAMAGAMI. Bull. Chem. Soc. Japan, **33**, 466 (1960); M. NAKAZAKI. Bull. Chem. Soc. Japan, **33**, 472 (1960); P. L. JULIAN, E. W. MEYER, and H. C. PRINTY. Heterocyclic compounds. Vol. III. *Edited by* R. C. Elderfield. John Wiley and Sons, Inc., New York. 1952. pp. 79, 88, and 102; W. C. SUMPTER and F. M. MILLER. Heterocyclic compounds with indole and carbazole systems. *Edited by* A. Weissberger. Interscience Publishers, Inc., New York. 1954. p. 33.

13. J. PARRICK. Personal communication.
14. A. H. JACKSON and P. SMITH. Tetrahedron, **24**, 2227 (1968).
15. G. M. BADGER and R. P. RAO. Australian J. Chem. **17**, 1399 (1964).
16. A. E. CHICHIBABIN and O. SEIDE. J. Russ. Phys. Chem. Soc. **46**, 1216 (1914); M. T. LEFFLER. Organic reactions. Vol. I. John Wiley and Sons, Inc., New York. 1942. p. 91.
17. W. J. GENSLER. Heterocyclic compounds. Vol. IV. *Edited by* R. C. Elderfield. John Wiley and Sons, Inc., New York. 1952. p. 424.
18. M. M. ROBISON, B. L. ROBISON, and F. P. BUTLER. J. Am. Chem. Soc. **81**, 743 (1959).
19. K. T. POTTS and J. E. SAXTON. J. Chem. Soc. 2641 (1954).
20. F. W. BERGSTROM. J. Org. Chem. **2**, 411 (1938).
21. D. J. BROWN and L. N. SHORT. J. Chem. Soc. 331 (1953).
22. D. J. BROWN. J. Soc. Chem. Ind. **69**, 353 (1950).
23. E. KOENIGS, W. WEISS, and A. ZSCHAM. Ber. **59**, 316 (1926).
24. R. V. JARDINE and R. K. BROWN. Can. J. Chem. **41**, 2067 (1963).
25. G. E. FICKEN. Renwick Laboratory, Ilford Ltd., Ilford, Essex, England, personal communication. 1962.

Can. J. Chem. Downloaded from www.nrcresearchpress.com by 210.87.254.105 on 09/05/12
For personal use only.

Can. J. Chem. Downloaded from www.nrcresearchpress.com by 210.87.254.5 on 09/05/12
For personal use only.

Configuration of echinulin. II.[1] Optical rotatory dispersion of echinulin, hydroechinulin, and the stereoisomeric 3-methyl-6(indolyl-3-methyl)-piperazine-2,5-diones[2,3]

R. NAKASHIMA[4] AND G. P. SLATER

Prairie Regional Laboratory, National Research Council of Canada, Saskatoon, Saskatchewan

Received November 29, 1968

The optical rotatory dispersion spectra of echinulin and hydroechinulin have been compared with the spectra of the 4 stereoisomers of *cyclo*-alanyltryptophan. The results indicate appreciable differences in the spectra of the *cis*- and *trans*-piperazinediones and that echinulin has the *cyclo*-L-alanyl-L-tryptophan configuration.

Canadian Journal of Chemistry, 47, 2069 (1969)

Echinulin (**1***a*) is a white crystalline compound which was first isolated from a culture of *Aspergillus echinulatus* (Delacr) Thom & Church (1). The structure (**1***a*) was established by a series of degradations and partial synthesis (2) and is supported by nuclear magnetic resonance (n.m.r.) (3) and biochemical (4) studies.

Acid hydrolysis (5) of hexahydroechinulin (hydroechinulin) (**1***b*) gave L-alanine and the amino acid hexahydroechinin (hydroechinin) (**2***b*). Echinulin (**1***a*) may be regarded then as a piperazinedione formed by the condensation of L-alanine and the amino acid echinin (2′-(1,1-dimethylprop-2-enyl)-5′,7′-di-(3-methylbut-2-enyl)-tryptophan) (**2***a*) of unknown configuration.

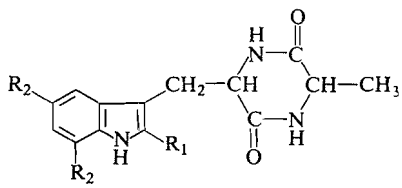

1

(*a*) $R_1 = -C(CH_3)_2-CH=CH_2$;
$R_2 = -CH_2-CH=C(CH_3)_2$

It has been found (6) that the absolute configuration of amino acids is indicated by their optical rotatory dispersion (o.r.d.) between 200 and 225 mμ. The configuration of echinin (**2***a*) could presumably be determined in this way also.

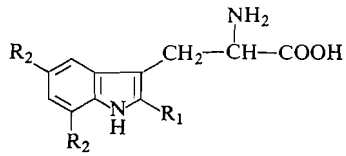

2

(*b*) $R_1 = -C(CH_3)_2-CH_2CH_3$;
$R_2 = -CH_2-CH_2-CH(CH_3)_2$

However, echinin (**2***a*) could not be obtained (5) by acid hydrolysis of echinulin (**1***a*) although hydroechinulin (**1***b*) gave hydroechinin (**2***b*) under the same conditions. The acid hydrolysis of hydroechinulin was previously used in this laboratory in connection with biosynthetic studies (7) but did not give a pure product. In view of this, and the observation (8) that the configuration of a piperazinedione can be determined by o.r.d., it was decided to compare the o.r.d. spectra of echinulin and the model *cyclo*-alanyltryptophans (**1**, $R_1 = R_2 = H$).

The piperazinediones were prepared by the cyclization (9) of alanyltryptophan or tryptophylalanine as shown in Fig. 1. In practice it was found more convenient to use the latter compound, as the synthesis of benzyloxycarbonyltryptophan presented less difficulty than the synthesis of tryptophan benzyl ester. Our investigations showed that the intermediate protected dipeptides obtained by the carbodiimide method (10) were identical in m.p. and specific rotation with the corresponding compounds prepared by the azide method (11). The various intermediates were obtained in good yield but since the carbodiimide method requires fewer steps than the azide method, the preferred synthesis of *cyclo*-alanyltryptophan is that shown in Fig. 1, route A.

---

[1]For Part I, see ref. 14.

[2]Presented in part to the 50th Annual Conference of the Chemical Institute of Canada, Toronto, June, 1967.

[3]NRCC No. 10637.

[4]NRCC Postdoctorate Fellow, 1966–1968. Present address: Department of Synthetic Chemistry, University of Kyoto, Kyoto, Japan.

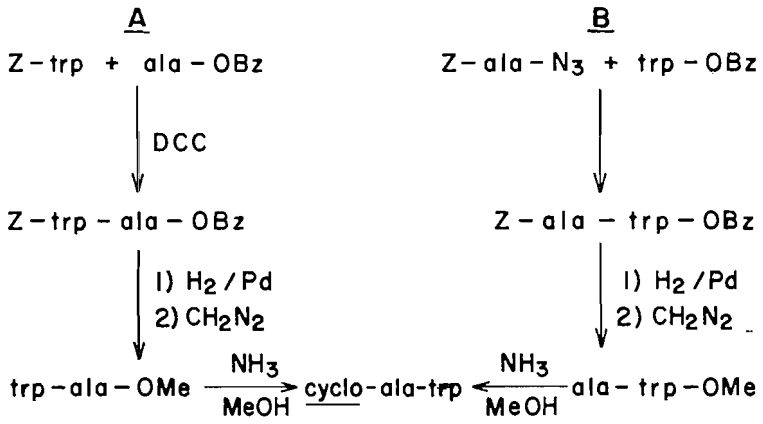

FIG. 1. Synthesis of *cyclo*-alanyltryptophan. Z = benzyloxycarbonyl, DCC = *N,N'*-dicyclohexylcarbodiimide.

Since this work was completed, two methods of preparing sterically pure piperazinediones have been reported (12, 13). A number of piperazinediones synthesized by Fischer's method (9) were found (13) to contain varying amounts of racemic material. However, thin-layer chromatography (t.l.c.) (13) of the piperazinediones used in the present work did not indicate racemization. The racemization may have been avoided by using shorter reaction times (5 h) than those (1–5 days) used by Nitecki *et al.* (13).

In a preliminary communication (14) the o.r.d. spectra of echinulin in chloroform and hydroechinulin in ethanol were compared with the o.r.d. spectra of *cyclo*-L-alanyl-L-tryptophan and *cyclo*-L-alanyl-D-tryptophan in diglyme–water (4:1) from 700–300 mμ. The similarity of the curves for *cyclo*-L-alanyl-D-tryptophan, echinulin, and hydroechinulin prompted the suggestion that the tryptophan moiety in echinulin has the D-configuration. The spectra of these compounds and the other stereoisomeric piperazinediones, *cyclo*-D-alanyl-D-tryptophan, and *cyclo*-D-alanyl-L-tryptophan, in ethanol are presented in Figs. 2–5. In the 650–350 mμ region these compounds possess plain dispersion curves as previously described (14). Below 350 mμ the spectra are more complex and more valuable in determining configuration, and only spectra covering this region have been reproduced. The spectra of the piperazinediones (Figs. 2–5) are divided into two parts (200–250 mμ and 230–320 mμ) with the ordinates in the ratio of 10:1. This method of presentation has been used because of the large differences in the molecular rotations and

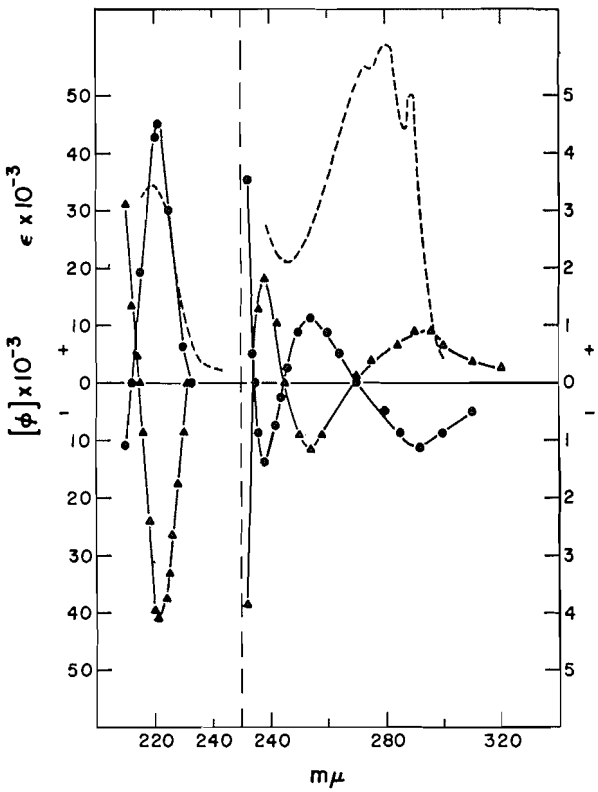

FIG. 2. Optical rotatory dispersion spectra of *cyclo*-L-alanyl-L-tryptophan (▲) and *cyclo*-D-alanyl-D-tryptophan (●) in ethanol. Ultraviolet spectrum in ethanol (– – –).

ultraviolet (u.v.) absorptions in these two regions. The spectra of echinulin (Fig. 4) and hydroechinulin (Fig. 5) have likewise been presented in two parts (200–280 mμ and 230–320 mμ)

Can. J. Chem. Downloaded from www.nrcresearchpress.com by 210.87.254.5 on 09/05/12
For personal use only.

Can. J. Chem. Downloaded from www.nrcresearchpress.com by 210.87.254.5 on 09/05/12
For personal use only.

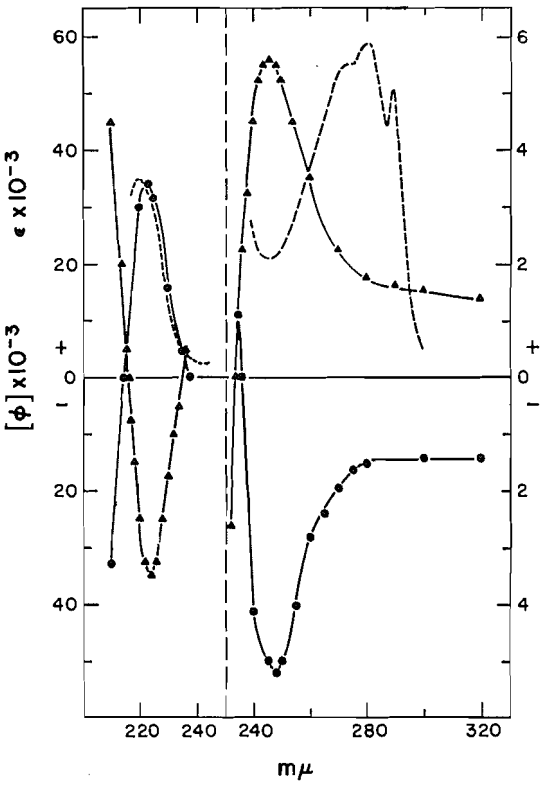

FIG. 3. Optical rotatory dispersion spectra of *cyclo*-D-alanyl-L-tryptophan (▲) and *cyclo*-L-alanyl-D-tryptophan (●) in ethanol. Ultraviolet spectrum in ethanol (– – –).

which allow for comparison with the spectra of the piperazinediones.

The o.r.d. spectra of the piperazinediones, echinulin, and hydroechinulin, show a number of differences in the 350–230 mμ region (cf. Figs. 2–5). The absence of a complex Cotton effect at 230–320 mμ in the spectra of the *trans*-piperazinediones may be due to the extrema near 246 mμ (Fig. 3) which mask the weak Cotton effects shown by the *cis*-piperazinediones (Fig. 2) in this region (the rotations of the *trans* compounds are almost three times the rotations of the *cis* compounds at these wavelengths). Echinulin (Fig. 4) and hydroechinulin (Fig. 5) also do not possess complex Cotton effects at 300–230 mμ but have instead a rather broad Cotton effect. The rotations of echinulin, hydroechinulin, and the *cis*-alanyltryptophans are of similar magnitude and the difference in the complexity of the spectra may be related to the steric effects of the alkyl substituents of echinulin and hydroechinulin.

Proton magnetic resonance (p.m.r.) studies (15) indicate that the preferred conformation of *cyclo*-alanylphenylalanine is such that the benzene and piperazinedione rings face each other. A similar folding would be expected of the *cyclo*-alanyltryptophans. Construction of models (Corey–Pauling–Koltun) (16) indicates that in the *cis* compounds, the indole nucleus can lie over the piperazinedione ring so that a hydrogen atom of the alanine methyl group is close to the mid-point of the bond common to the five- and six-membered rings (a model of *cis*-alanylphenylalanine shows that the corresponding hydrogen atom is near the center of the benzene ring). A model of echinulin in the folded form is very difficult to construct because of interference from the alkyl substituent in the α-position of the indole nucleus. The strain is not affected by placing the alanine methyl group in the *trans* position but is relieved by swinging the indole nucleus away from the

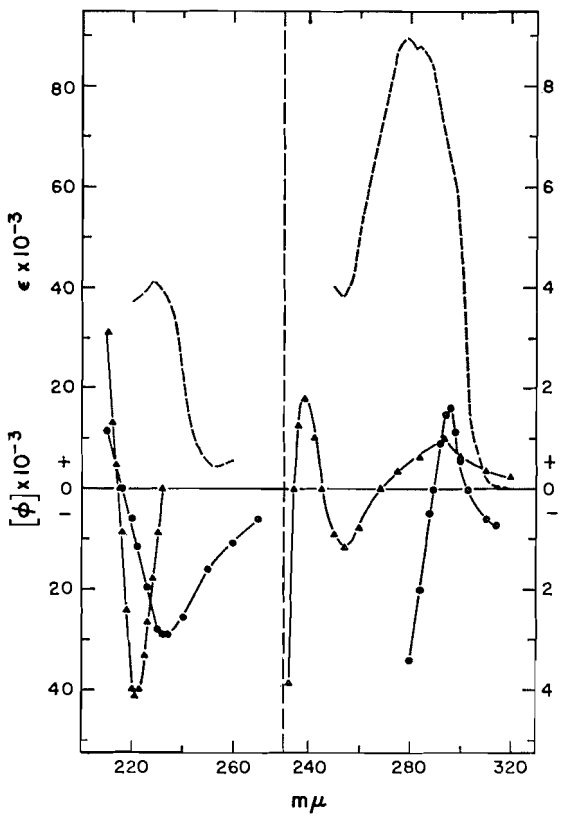

FIG. 4. Optical rotatory dispersion spectra of echinulin (●) and *cyclo*-L-alanyl-L-tryptophan (▲) in ethanol. Ultraviolet spectrum of echinulin in ethanol (– – –).

Can. J. Chem. Downloaded from www.nrcresearchpress.com by 210.87.254.5 on 09/05/12
For personal use only.

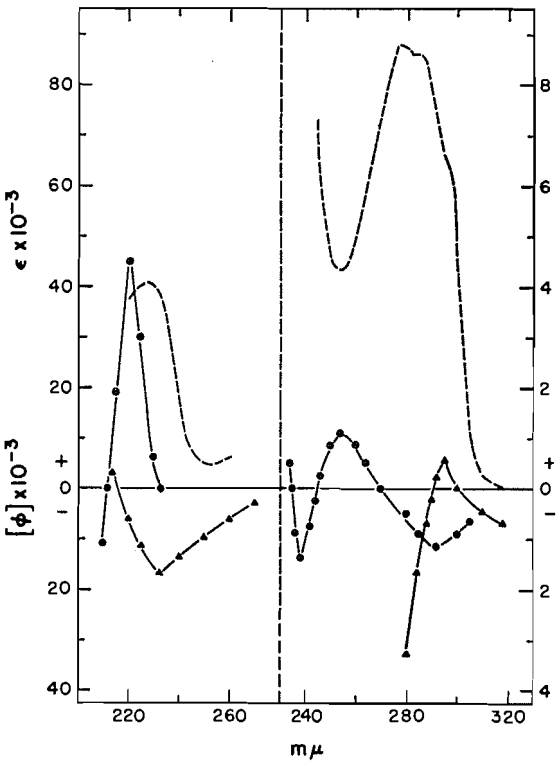

FIG. 5. Optical rotatory dispersion spectra of hydroechinulin (▲) and *cyclo*-D-alanyl-D-tryptophan (●) in ethanol. Ultraviolet spectrum of hydroechinulin in ethanol (– – –).

piperazinedione ring. Thus the molecular models indicate that interaction between the π-electrons of the indole and carbonyl groups would be expected to decrease in the order *trans-cyclo*-alanyltryptophan > *cis-cyclo*-alanyltryptophan > echinulin. Klyne *et al.* (17) have shown that the Cotton effects at 250–230 mμ of the heteroyohimbine alkaloids are influenced by the relative positions of the indole and carbomethoxy groups. Other examples of Cotton effects being related to the interaction of two π-electron systems are also known (18), and the results of the present study may be another instance of this type of relationship.

The o.r.d. spectra of echinulin (Fig. 4) and hydroechinulin (Fig. 5) possess the same broad positive Cotton effect in the 300–220 mμ region. These spectra are compared with the spectra of *cyclo*-L-alanyl-L-tryptophan (Fig. 4) and *cyclo*-D-alanyl-D-tryptophan (Fig. 5), respectively. The trough of the Cotton effects of echinulin and hydroechinulin are at longer wavelength (232 mμ) than the trough of the Cotton effect of *cyclo*-L-alanyl-L-tryptophan (221 mμ) (Fig. 4), or the corresponding trough of *cyclo*-D-alanyl-L-tryptophan (224 mμ) (Fig. 3). However, the troughs of these Cotton effects coincide with the relevant u.v. absorption maxima (cf. Figs. 2–5) and would thus appear to be related to the same chromophores. Comparison of the o.r.d. spectra of hydroechinulin and *cyclo*-D-alanyl-D-tryptophan (Fig. 5) shows that the latter has Cotton effects of opposite sign to the former. The o.r.d. spectra below 300 mμ therefore indicate that echinulin has the *cyclo*-L-alanyl-L-tryptophan configuration, and not the *cyclo*-L-alanyl-D-tryptophan configuration as previously suggested (14). This conclusion is supported by a recent o.r.d. study (19) of two *cyclo*-alanyltryptophans carrying a 1,1-dimethylprop-2-enyl substituent in the α-position of the indole nucleus (**1**, R_1 = —C$(CH_3)_2CH{=}CH_2$, R_2 = H).

The configuration of echinulin has also been investigated (20) by the t.l.c. method used to determine the steric purity of piperazinediones (13). Nitecki *et al.* (13) found that *cis*-piperazinediones have a lower R_f value than the corresponding *trans* compounds. Echinulin and *cyclo*-L-alanyl-L-tryptophan were racemized separately in boiling ethanol–triethylamine and the products, starting materials, and *cyclo*-L-alanyl-D-tryptophan were examined by t.l.c. The results (20) indicated that echinulin behaves like a *cis*-piperazinedione, and since the alanine portion has the L-configuration it follows that the tryptophan moiety must also have the L-configuration. Racemization experiments using the above-mentioned compounds and hydroechinulin gave results identical to those of Westley *et al.* (20).

Experimental

The optical rotatory dispersion (o.r.d.) measurements were made on a Jasco ORD/UV-5 spectropolarimeter. Optical rotations at the sodium-D line were measured at 25° on a Perkin–Elmer141 polarimeter. Ultraviolet absorption spectra were obtained with a Beckman DK-2 spectrometer. Melting points were determined on a Leitz hotstage and are uncorrected. Echinulin and hydroechinulin were obtained as previously described (7). The amino acids were obtained from the Sigma Chemical Company and had specific rotations in agreement with literature values and were used as supplied. The protected amino acids were synthesized by known methods and those previously described had melting points and specific rotations corresponding to the published values. The following derivatives do not appear to have been described previously: D-alanine benzyl ester benzene sulfonate (21), m.p.

Can. J. Chem. Downloaded from www.nrcresearchpress.com by 210.87.254.5 on 09/05/12
For personal use only.

120–121° (EtOH–Et_2O), $[\alpha]_D$ −8.1° (*c*, 3.1 pyridine); benzyloxycarbonyl-L-tryptophan hydrazide (24), m.p. 210–212° (EtOH–EtOAc), $[\alpha]_D$ −9.7° (*c*, 1.27 HOAc); D-isomer, m.p. 209–211°, $[\alpha]_D$ +9.2° (*c*, 1.31 HOAc); D-alanine ethyl ester hydrochloride (25*b*), m.p. 75–76° (EtOH–Et_2O), $[\alpha]_D$ +11.1° (*c*, 2.1 in 5 *N* HCl); D-tryptophan benzyl ester hydrochloride (23), m.p. 213–215° (EtOH–Et_2O), $[\alpha]_D$ −4.1° (*c*, 2.1 MeOH).

Benzyloxycarbonyltryptophylalanine Benzyl Ester

N,N'-dicyclohexylcarbodiimide (1.36 g, 0.006 mole) (23) was added to a mixture of benzyloxycarbonyltryptophan (22) (2.0 g, 0.0059 mole), alanine benzyl ester benzenesulfonate (21) (2.0 g, 0.0059 mole), and triethylamine (0.85 ml, 0.006 mole) in dichloromethane (25 ml). After stirring at room temperature for 4 h, acetic acid (0.2 ml) was added and the mixture filtered to remove dicyclohexylurea. The filtrate was washed with 0.5 *N* HCl, 0.5% $NaHCO_3$, and water. Evaporation of the dried ($MgSO_4$) solution left a mixture of dicyclohexylurea and an oil which was taken up in acetone and filtered. Addition of petroleum ether to the filtrate, and cooling, gave the product in 70–75% yield.

Benzyloxycarbonyl-L-tryptophyl-L-alanine benzyl ester, m.p. 150–152°, $[\alpha]_D$ −28.4° (*c*, 0.54 MeOH) (lit. (23) m.p. 153°, $[\alpha]_D^{25}$ −27° (*c*, 1 MeOH)).

Benzyloxycarbonyl-D-tryptophyl-D-alanine benzyl ester, m.p. 146–149°, $[\alpha]_D$ +27.4° (*c*, 0.58 MeOH).

Benzyloxycarbonyl-L-tryptophyl-D-alanine benzyl ester, m.p. 163–164°, $[\alpha]_D$ +9.8° (*c*, 0.59 MeOH).

Benzyloxycarbonyl-D-tryptophyl-L-alanine benzyl ester, m.p. 161–163°, $[\alpha]_D$ −9.2° (*c*, 0.72 MeOH).

Anal. Calcd. for $C_{29}H_{29}N_3O_5$: C, 69.7; H, 5.9; N, 8.4. Found: C, 69.5; H, 5.9; N, 8.7.

Coupling of benzyloxycarbonyltryptophan hydrazide (24) and alanylbenzyl ester (21) by the azide method (24) gave products identical to those from the carbodiimide method, although in lower yield (50–55%).

Cyclo-alanyltryptophan

A stream of hydrogen was passed through a stirred solution of benzyloxycarbonyltryptophylalanine benzyl ester (0.56 g, 0.0011 mole) in methanol (50 ml) containing palladium black (approximately 0.1 g) until carbon dioxide was no longer evolved (25*a*). If free peptide precipitated during hydrogenolysis it was dissolved by addition of water. The reaction mixture was filtered and the filtrate evaporated to dryness under reduced pressure at 50° to give tryptophylalanine as a white solid (90–95%) which was chromatographically pure (23). The tryptophylalanine tended to decompose (judged by the development of a yellow-brown color) when subjected to recrystallization procedures and the product obtained from hydrogenolysis was used directly in the following step.

The alanyltryptophan in methanol (50 ml) at room temperature was treated with an ether solution of diazomethane over 1 h. After stirring for a further 1 h the solvent was removed under reduced pressure and the residue dissolved in methanol (100 ml). The solution was cooled to 0° and saturated with dry ammonia gas (9). After stirring for 5 h the solvent was removed under reduced pressure at 40° and the product crystallized from ethanol – ethyl acetate in yields of 60–65%.

Cyclo-L-alanyl-L-tryptophan, m.p. 282–284° (decomp.) $[\alpha]_D$ +10.4°, (*c*, 0.48 EtOH).

Cyclo-D-alanyl-D-tryptophan, m.p. 281–283° (decomp.) $[\alpha]_D$ −10.2° (*c*, 0.048 EtOH).

Cyclo-D-alanyl-L-tryptophan, m.p. 265–267° (decomp.) $[\alpha]_D$ +75.6° (*c*, 0.049 EtOH).

Cyclo-L-alanyl-D-tryptophan, m.p. 264–267° (decomp.) $[\alpha]_D$ −74.2° (*c*, 0.051 EtOH).

λ_{max} (EtOH) 220 (35 700), 274 (5 790), 280 (5 870), 290 (5 080), mμ.

Anal. Calcd. for $C_{14}H_{14}N_3O_2$: C, 65.4; H, 5.9; N, 16.3. Found: C, 65.2; H, 5.8; N, 16.1.

Benzyloxycarbonylalanyltryptophan Benzyl Ester

Benzyloxycarbonylalanine hydrazide (24) (2.43 g, 0.0103 mole) in a mixture of acetic acid (12 ml), water (50 ml) and 5 *N* hydrochloric acid (5 ml) was treated with a solution of sodium nitrite (0.8 g, 0.0116 mole) in water (2.5 ml) as previously described (24). The dry ether solution of the azide was added to a solution of tryptophan benzyl ester (prepared by treating the hydrochloride (3.4 g, 0.0103 mole) in chloroform (20 ml) with triethylamine (5 ml, 0.0358 mole) at room temperature for 20 min, filtering, and evaporating to dryness). After standing at room temperature overnight, the reaction mixture was worked up in the usual way (24) and the solid product recrystallized from acetone – petroleum ether in yields of 75–80%.

Benzyloxycarbonyl-L-alanyl-L-tryptophan benzyl ester, m.p. 105–106°, $[\alpha]_D$ −23.2° (*c*, 1.1 MeOH) (lit. (23) m.p. 105°, $[\alpha]_D^{25}$ −22° (*c*, 1 MeOH)).

Benzyloxycarbonyl-D-alanyl-D-tryptophan benzyl ester, m.p. 104–105°, $[\alpha]_D$ +20.2° (*c*, 1.2 MeOH).

Benzyloxycarbonyl-D-alanyl-L-tryptophan benzyl ester, m.p. 158–160°, $[\alpha]_D$ +12.8° (*c*, 0.57 MeOH).

Benzyloxycarbonyl-L-alanyl-D-tryptophan benzyl ester, m.p. 158–160°, $[\alpha]_D$ −12.4° (*c*, 0.46 MeOH).

Anal. Calcd. for $C_{29}H_{29}N_3O_5$: C, 69.7; H, 5.9; N, 8.4. Found: C, 69.5; H, 5.8; N, 8.5.

Products identical to the above were obtained in 75–80% yield by treating benzyloxycarbonylalanine (26) and tryptophan benzyl ester with dicyclohexylcarbodiimide (23).

Cyclo-alanyltryptophan

Benzyloxycarbonylalanyltryptophan benzyl ester (2 g, 0.004 mole) in methanol (50 ml) containing palladium black (0.5 g) was hydrogenolyzed (25*a*) as for the benzyloxycarbonyltryptophylalanine benzyl ester to give alanyltryptophan in 90% yield. The peptide was methylated as before and the oily product treated with dry ammonia gas (9) as for the tryptophylalanine, to give *cyclo*-alanyltryptophan in yields of 65–70%. The piperazinediones prepared by this method were identical to the corresponding compounds synthesized from tryptophylalanine.

Racemization and Thin-Layer Chromatography

Samples (25 mg) of echinulin, hydroechinulin, and *cyclo*-L-alanyl-L-tryptophan in ethanol–triethylamine (1:1, 10 ml) were boiled under reflux for 3 days (20). The solvent was removed under reduced pressure and the residues, starting materials, and *cyclo*-L-alanyl-D-tryptophan examined by t.l.c. on silica gel G using diisopropyl ether – chloroform – acetic acid (6:3:2) (Nitecki *et al.* (13) used the ratio 6:3:1 but this was not sufficiently polar for our purpose). The spots were detected by exposing the air-dried plates to iodine vapor, which was

superior to the method of Nitecki *et al.* (13) for the compounds in this study.

Acknowledgments

The authors thank Mr. L. R. Hogge for producing echinulin and Mr. W. C. Haid for elemental analyses.

1. A. Quilico and L. Panizzi. Ber. **76**, 348 (1943).
2. A. Quilico. Res. Progr. Org. Biol. Med. Chem. **1**, 225 (1964), and references therein.
3. R. Romanet, A. Chemizart, S. Duhoux, and S. David. Bull. Soc. Chim. France, 1048 (1963).
4. A. J. Birch, G. E. Blance, S. David, and H. Smith. J. Chem. Soc. 3128 (1961).
5. A. Quilico, C. Cardani, and F. Piozzi. Gazz. Chim. Ital. **86**, 211 (1956).
6. I. P. Dirkx and F. L. J. Sixma. Rec. Trav. Chim. **83**, 522 (1964); W. Gaffield. Chem. Ind. London, 1460 (1964); J. P. Jennings, W. Klyne, and P. M. Scopes. J. Chem. Soc. 294 (1965); J. C. Craig and S. K. Roy. Tetrahedron, **21**, 391 (1965).
7. J. C. MacDonald and G. P. Slater. Can. J. Microbiol. **12**, 455 (1966).
8. D. Balasubramanian and D. B. Wetlaufer. J. Am. Chem. Soc. **88**, 3449 (1966).
9. E. Fischer. Ber. **39**, 2893 (1906).
10. J. C. Sheehan and G. P. Hess. J. Am. Chem. Soc. **77**, 1067 (1955).
11. T. Curtius. Ber. **35**, 3226 (1902).
12. K. D. Kopple and H. G. Ghazarian. J. Org. Chem. **33**, 862 (1968).
13. D. E. Nitecki, B. Halpern, and J. W. Westley. J. Org. Chem. **33**, 864 (1968).
14. R. Nakashima and G. P. Slater. Tetrahedron Letters, No. **45**, 4433 (1967).
15. K. D. Kopple and D. H. Marr. J. Am. Chem. Soc. **89**, 6193 (1967).
16. W. L. Koltun. Biopolymers, **3**, 665 (1965).
17. N. Finch, W. I. Taylor, T. R. Emerson, W. Klyne, and R. J. Swan. Tetrahedron, **22**, 1327 (1966).
18. P. Crabbe and W. Klyne. Tetrahedron, **23**, 3449 (1967).
19. E. Houghton and J. E. Saxton. Tetrahedron Letters, No. **52**, 5475 (1968).
20. J. W. Westley, V. A. Close, D. N. Nitecki, and B. Halpern. Anal. Chem. **40**, 1888 (1968).
21. J. E. Shields, W. H. McGregor, and F. H. Carpenter. J. Org. Chem. **26**, 1491 (1961).
22. E. L. Smith. J. Biol. Chem. **175**, 39 (1948).
23. M. Wilchek and A. Patchornik. J. Biol. Chem. **28**, 1874 (1963).
24. B. F. Erlanger and E. Brand. J. Am. Chem. Soc. **73**, 3508 (1951).
25. J. P. Greenstein and M. Winitz. *In* Chemistry of the amino acids. Vol. II. John Wiley and Sons, Inc., New York. 1961. (*a*) p. 1234, (*b*) p. 926.
26. M. Bergmann and L. Zervas. Ber. **65**, 1192 (1932).

Can. J. Chem. Downloaded from www.nrcresearchpress.com by 210.87.254.5 on 09/05/12
For personal use only.

Can. J. Chem. Downloaded from www.nrcresearchpress.com by 210.87.254.5 on 09/05/12
For personal use only.

Lignans and related phenols. Part IX.[1] Observations on the spectroscopic characterization and conformational analysis of apo-compounds of the arylnaphthalene class

D. C. AYRES

Department of Chemistry, Westfield College, University of London, Hampstead, London, N.W.3, England

Received December 2, 1968

The need for further spectroscopic characterization of apo-compounds of type **1** is discussed and details of proton magnetic resonance (p.m.r.) and optical rotatory dispersion (o.r.d.) spectra are given. Analysis of these spectra is relevant to the assignment of structure to the recently isolated thomasic acid and also reveals unusual conformational features in compounds of this group.

Canadian Journal of Chemistry, 47, 2075 (1969)

The presence of a carbon–carbon double bond in the B ring of these compounds (see Scheme 1[2]) may be indicated by weak infrared (i.r.) absorption. In apo-lactones (**1**, X → Y, CH_2—O—C=O) derived from picropodophyllin, (from **2** by elimination of —OH) this lies (7) at 1648(γ) or 1698 cm^{-1}(β). The intensity is not sensibly affected by conjugation and the absorption in methyl α-apopicropodophyllate (**1**, X = CH_2-OH, Y = CO_2Me) and its reduction product (α-apopicropodophyllol, X = Y = CH_2OH) lies at 1700 cm^{-1}. The peak due to the B ring unsaturation is obscured in the α-apo-lactone (1) and in acetyl α-apopicropodophyllol (2) and, when resolved, may not be readily correlated with structure. Thus the retro-system of thomasic acid (**3**) leads to absorption at 1695 cm^{-1} (3) close to that of α-apopicropodophyllate and of β-apopicropodophyllin, which in turn differ little from the γ-methyl ester (**1**, X = CH_2OH, Y = CO_2Me) absorbing at 1700 cm^{-1}.

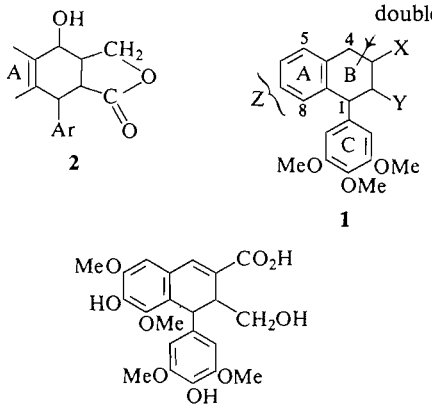

2 **1** **3**

SCHEME 1

In the ultraviolet (u.v.) spectra the effect of twisting the olefinic chromophore in the strained B ring of isomeric α- and γ-lactones has been referred to (4). Opening of the lactone ring causes only a slight blue shift (3 mμ) at longer wavelength when the α-lactone is converted into the corresponding methyl ester (**1**, X = CH_2OH, Y = CO_2Me; λ_{max} 310 mμ, log ε 3.80), but the carbonyl group is evidently much less effectively conjugated in methyl γ-apopicropodophyllate (λ_{max} 332.5 mμ, log ε 4.04) than in the corresponding lactone (λ_{max} 350, log ε 4.10); this must result from steric interaction between the methoxycarbonyl group and the adjacent aryl substituent. Provided regard is paid to this shift γ-apo-compounds can be characterized by their u.v. spectra. However, a distinction between α and β apo-derivatives by comparison of these spectra may not be possible; for example α-apopicrosikkimotoxin [**1**, Z = 6,7-dimethoxy, (5)] absorbs at shorter wavelength (λ_{max} 285 mμ) than either β-apopicropodophyllin (**1**, Z = 6,7-methylenedioxy) or its desmethylene derivative (λ_{max} 292 and 287.5 mμ respectively).

Opposition between factors favoring conjugation and those favoring strain relief leads to other uncertainties in the interpretation of u.v. spectra. Thus artifacts may arise in the presence of weak bases which readily isomerize α- to β-lactones

[1]For Part VIII see ref. 10.

[2]In the general structure **1**, α-apo implies unsaturation between C-3 and C-4, β-apo between C-2 and C-3, and γ-apo between C-1 and C-2; Z substituents on ring A are specified where relevant.

Can. J. Chem. Downloaded from www.nrcresearchpress.com by 210.87.254.5 on 09/05/12
For personal use only.

TABLE I

Table of chemical shifts of apo-compounds (τ values, 100 MHz)

Compound	Solvent	C-5 H*	C-8 H	C-2′ H C-6′ H	C-4 H	CH_2—O—CO or CH_2OH	C-2 H	C-1 H	—O—CH_2—O	—CO_2Me	MeO
Methyl γ-apopicropodophyllate	$CDCl_3$	3.27	3.64	3.64		—	—	—	4.08	6.53	6.09 (3H) 6.17 (6H)
β-Apopicropodophyllin	$CDCl_3$	3.33	3.42	3.68	ca. 6.3	5.19 Broad	—	ca. 5.2	4.10	—	6.26 (9H)
	CF_3CO_2H	3.24	3.36	3.42	ca. 6.2	4.95 Broad	—	5.14m	4.02 4.06 *J*1Hz	—	6.08 (3H) 6.15 (6 H)
Methyl α-apopicropodophyllate	$CDCl_3$	3.36	3.46	3.69	3.51m	5.81m	6.53d *J*4Hz	5.54d *J*4Hz	4.10	6.35	6.21 (3H) 6.24 (6H)
α-Apopicropodophyllin	CF_3CO_2H	3.41 or	3.87	3.33	3.63m	4.99 Broad	Obscured	5.96	4.23†	—	6.08 (3H) 6.16 (6H)
	$PhNO_2$‡	3.42 or	3.73	3.04	3.56m	4.88 Broad	—	5.90	4.12	—	6.04 (6H) 6.10 (3H)

*Location of the resonating proton.
†Peak width at half-height 3Hz.
‡60 MHz spectrum.

Can. J. Chem. Downloaded from www.nrcresearchpress.com by 210.87.254.5 on 09/05/12
For personal use only.

with reversion to the α-hydroxyacid on hydrolysis (1), whilst stronger bases may cause dehydrogenation to fluorescent arylnaphthalenes in non-hydrolytic media (6).

In their fundamental paper Schrecker and Hartwell (7) assigned configurations to the diastereoisomers of the desoxypicropodophyllin group (**2**, C-4 desoxy); their method depended on the hydrogenation of apo-precursors which were characterized in the u.v. It is apparent from the above remarks that additional evidence of the structures of these precursors is desirable. The following evidence of proton magnetic resonance (p.m.r.) spectroscopy confirms Schrecker and Hartwell's assignment and complements data given recently (3) for thomasic acid (**3**), the first fully characterized α-apo-compound of natural occurrence.

The p.m.r. spectrum of a model for γ-apopicropodophyllin (**1**,X,Y = CH_2—O—CO, rings A and C unsubstituted) has been recorded (8).[3] Points of interest in the spectrum of methyl γ-apopicropodophyllate (see Table I) are the shielding of the C-8 proton by the pendant aromatic ring, which also shields the ester protons, whose resonance lies about 18 Hz above the normal for an acrylic methyl ester (cf. Fig. 1). The shielded ester group must be forced above the plane of the aromatic ring and this is consistent with the blue shift in the u.v. spectrum noted above.

In the p.m.r. spectrum of β-apopicropodophyllin the C-4 protons and the C-1 proton form an ABX system, but the AB part is largely obscured beneath the ether peak (τ 6.25) in deuteriochloroform and although the high field portion is detectable in dimethyl sulfoxide-d_6 the resolution was not further improved on solution in trifluoroacetic acid. The X part of the spectrum appears at τ 5.20 in the less polar solvents, resonating at lower field than normal for a diphenylmethyl proton owing to deshielding by the C-2, C-3 unsaturation; in these solvents the resonance of the lactone protons is coincident with that at C-1. In trifluoroacetic acid the C-1 proton is resolved from the broad lactone peak at τ 4.95 as a multiplet (τ 5.14). The splitting of the methylenedioxy resonance must result from shielding of one of them by the pendant ring (9) when it occupies an axial conformation on the same face of the molecule; models show that these conformers are easily interconverted.[4]

Figure 1 shows the 100 MHz spectrum of methyl α-apopicropodophyllate (4). The broad peak at τ 5.80 was allocated to the hydroxymethylene protons as it was split on irradiation at τ 3.50 and the vinyl proton located here sharpened on irradiation at 5.80. Irradiation of the water peak in deuteriochloroform (τ 8.25) also sharpened the hydroxymethylene resonance because of exchange of the saturated water protons with those of the alcohol (11). The pair of doublets centered at τ 5.54 and 6.47 are allocated to C-1 H and C-2 H respectively. The former corresponds to the resonance C-1 H (τ 5.92) reported by Wallis (12) in a related structure (**1**, X = Y = Me, Z = 6,7,8-trimethoxy) and the latter to the resonance of C-2 H in thomasic acid dimethyl ether (τ 6.65 in $CDCl_3$) allowing for deshielding by the C-2 CO_2Me group of α-apopicropodophyllate (**4**). The coupling of 4 Hz between these protons was confirmed by irradiation at τ 5.54 and 6.47 and is small for a diaxial pair (**5**, Scheme 2). Chemical evidence for the *trans* configuration at C-1 and C-2 has been presented by a number of independent workers (e.g. 1, 5, 13, 14) and we must conclude that the conformation (**6**), having an axial aromatic substituent, contributes significantly to the equilibrium. Seikel[5] has

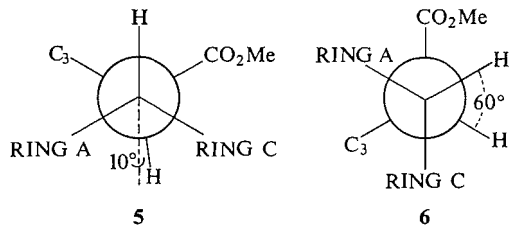

5 6

SCHEME 2

revised the structure of thomasic acid on chemical grounds and finds that its *trans*-1:2 configuration leads to a smaller coupling than that reported here for the α-apopicropodophyllate-ester, since the resonance of C-1 H (τ 5.16 in acetone) is broadened but not split. Wallis found a similar C-1 H resonance in the spectrum of his analogue [**1**, X = Y = Me, Z = $(MeO)_3$] which also had

[3]Some proton magnetic resonance data are also available for the γ-lactone, collinusin (**1**, X → Y CH_2—O—CO, Z = 6,7-dimethoxy, ring C 3,4-dimethoxyphenyl), see ref. 18.

[4]The conformational analysis of a related model is detailed in Part VIII of the series (10).

[5]Dr. M. K. Seikel, personal communication.

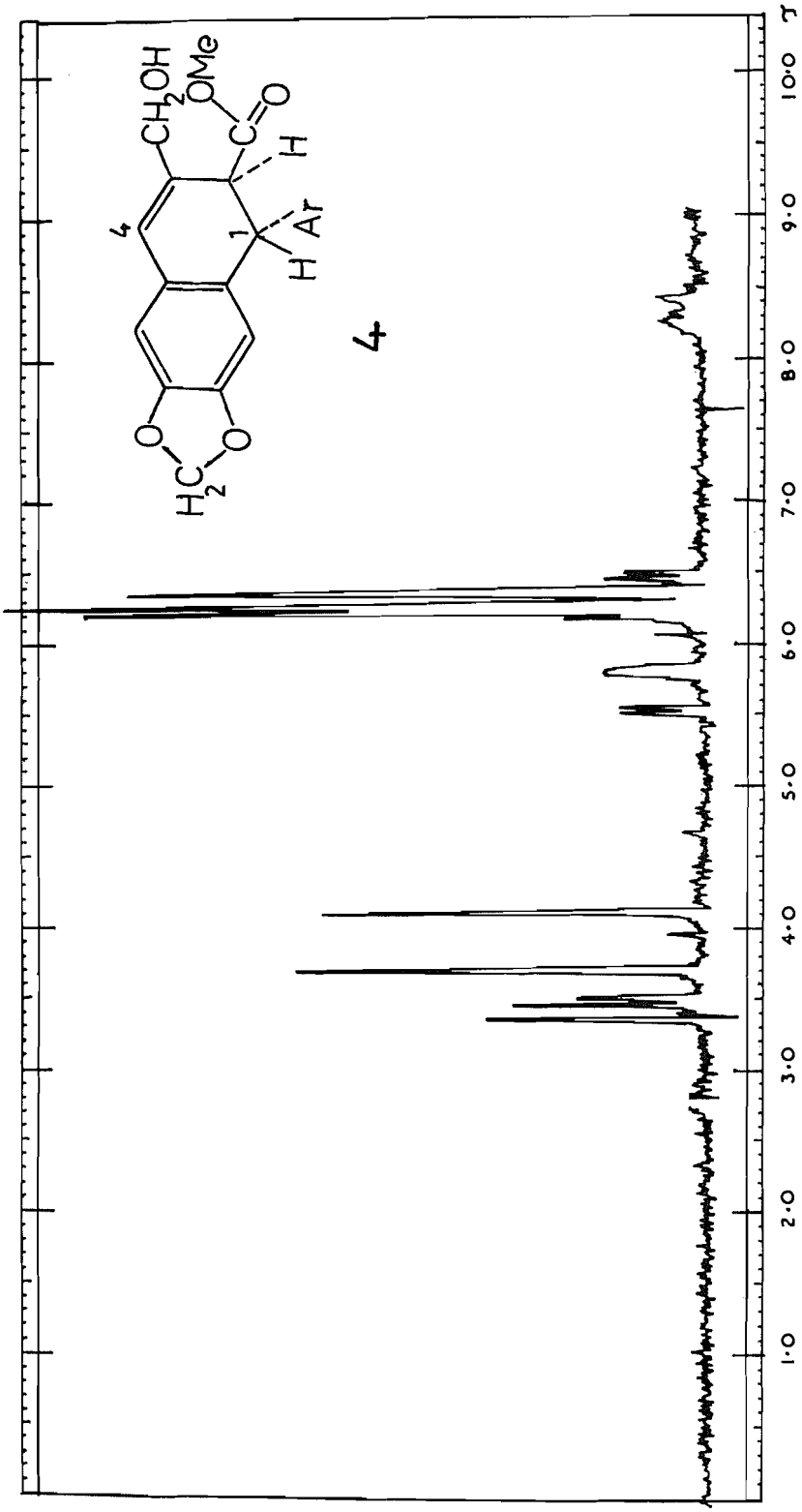

FIG. 1. The 100 MHz proton magnetic resonance spectrum of methyl α-apopicropodophyllate taken in $CDCl_3$.

Can. J. Chem. Downloaded from www.nrcresearchpress.com by 210.87.254.5 on 09/05/12
For personal use only.

Can. J. Chem. Downloaded from www.nrcresearchpress.com by 210.87.254.5 on 09/05/12
For personal use only.

the *trans*-1,2 configuration. It may be noted that when the aryl substituent adopts a quasi-axial conformation its interactions with an equatorial substituent at C-2 and with a hydrogen atom, or other group, at C-8 are diminished; further, no 1–3 interactions are established. The compounds described by Seikel *et al.* (3) and by Wallis (12) with a C-8 OMe substituent are expected to have an increased, even preponderant, proportion of axial substitution at C-1; this is in keeping with the smaller coupling constant $J_{H_1H_2}$ relative to that of methyl α-apopicropodophyllate.

In an attempt to evaluate the diaxial coupling constant $J_{H_1H_2}$ we examined the spectrum of α-apopicropodophyllin (**1**; X,Y = CH_2—O—CO, Z = 6,7-methylenedioxy) because the fused lactone ring prevents equilibration of conformers. Unfortunately the low solubility of this compound prevented its examination in chloroform. In deuteriodimethyl sulfoxide-d_6 the C-1 H resonance occurred at τ 5.96 as a broadened singlet whose intensity diminished during 15 min at 90° owing to isomerization to the β-apo-isomer; the C-2 H peak was obscured by the methoxyl proton resonances. The α-apo-lactone was unaffected (i.r. spectrum) after several hours in trifluoroacetic acid although it does react to give colored products on long-standing; in this solvent both the C-1 and C-2 H peaks were largely obscured by the methoxyl proton resonances.

Nitrobenzene gave a cold concentrated solution which did not deteriorate on keeping; here the C-1 H peak was identified (Fig. 2), and the protons of the lactone and the vinyl carbon were located at τ 4.88 and 3.56 respectively. The resonances of the aromatic ring protons are recorded in Table I, but their position is affected by the solvent so as to confuse the shielding correlation between C-8 H and the ring C conformation. The small coupling between C-1 H and C-2 H in the *trans* lactone must result from reduction in the dihedral angle (compare **5**) by rotation about the bond linking these carbon atoms, thus imparting axial character to the aryl substituent and bringing the C-3—C-4 double bond into more effective conjugation with ring A. This torsional effect also imparts axial character to the C-2 substituent so further straining the lactone ring, which in fact absorbs in KBr at a higher frequency (1770 cm^{-1}) in the i.r. than the strained lactone ring of podophyllotoxin (**2**, 1750 cm^{-1}); the conjugated lactones absorb at appreciably lower wavelengths (β-lactone 1750, γ-lactone 1745 cm^{-1}).

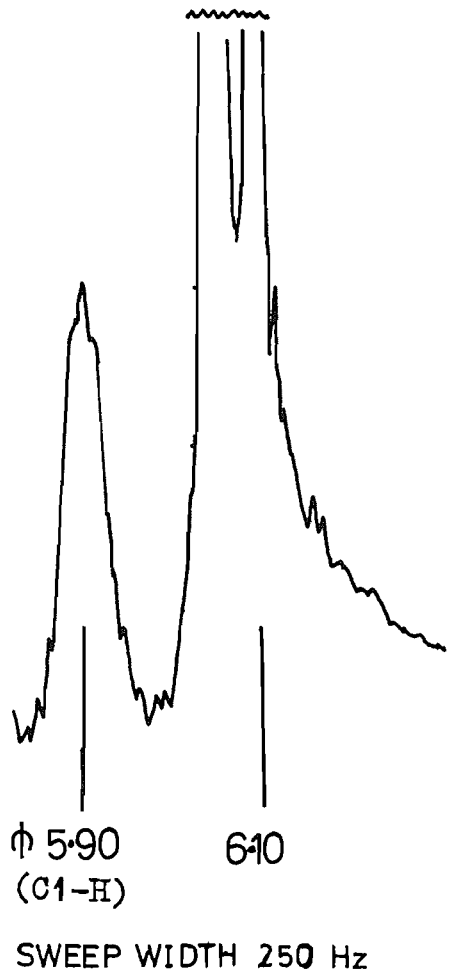

FIG. 2. The 60 MHz proton magnetic resonance spectrum of α-apopicropodophyllin (C-1 H peak).

The form of the optical rotatory dispersion (o.r.d.) curves (Fig. 3) of α-apopicropodophyllin (**7**) and of α-apopicropodophyllic acid (**8**) indicates that there are overlapping Cotton effects and that for fuller assignments circular dichroism measurements are required. However the considerable differences in the two curves cannot arise from minor differences in substituents at C-2 and C-3 (15), and must be due to differences in the conformation of the B ring: this is consistent with the interpretation of the p.m.r. spectra. The amplitude of the apparent Cotton effect near 285 mμ is much greater in the α-apo-acid and this can be attributed to the greater skewing between the aromatic chromophores (cf. 16) when the C ring adopts the quasi-axial conformation in this compound.

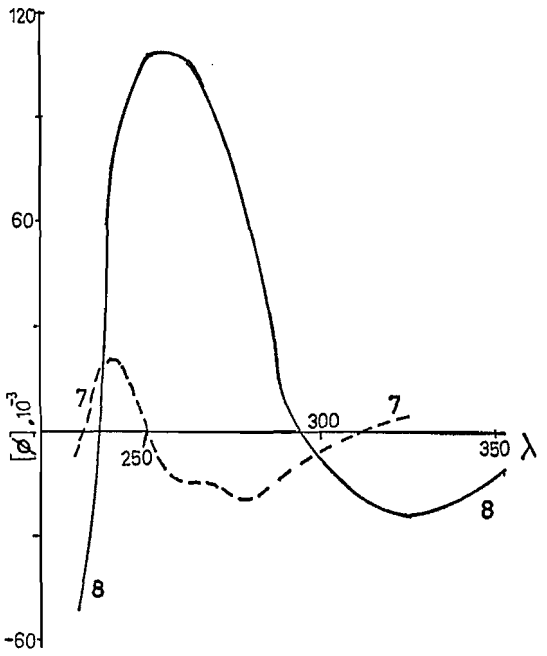

FIG. 3. Optical rotatory dispersion curves.

Experimental

With two exceptions the nuclear magnetic resonance (n.m.r.) spectra were measured on a Varian HA-100 spectrometer by the S.R.C. Spectroscopy Unit at Imperial College. Infrared (i.r.) spectra were measured with a Perkin–Elmer 127 spectrometer and ultraviolet (u.v.) spectra with a Unicam SP800 instrument. The optical rotatory dispersion measurements were made in methanol–dioxan 1:1 with the Bellingham and Stanley/Bendix Ericsson spectropolarimeter, Polarmatic 62, at a similar temperature (25–30°) to the proton magnetic resonance (p.m.r.) determination.

α-Apo-compounds

These were prepared and characterized as previously described. The method of Schrecker and Hartwell (1) was used for α- and β-apopicropodophyllin, α-apopicropodophyllic acid, and its methyl ester, while that of Haworth and Richardson (17) was used for γ-apopicropodophyllin, and the method of Ayres and Mundy (10) was used for methyl γ-apopicropodophyllate.

α-Apopicropodophyllin was obtained in almost quantitative yield without any discoloration by reducing the reaction time (1) of picropodophyllin in acetic anhydride/sulfuric acid to 2 min at 80–100°. The i.r., u.v., and p.m.r. spectra establish the structure of the product but the recorded (1) melting point was not observed on a heated microscope stage. Here the product was seen to melt at 161–163° and to crystallize at 165° on further slow heating; the material re-melted at 220–222° (cf. β-apopicropodophyllin). A sample of α-apopicropodophyllin kindly supplied by Dr. A. W. Schrecker behaved similarly.

Acknowledgments

We thank Dr. J. Feeney, Varian Associates Ltd., for the 100 MHz spectrum of **4** in $CDCl_3$ and Mr. P. B. Hulbert, Westfield College for the o.r.d. results. Dr. J. W. Mundy is thanked for the u.v. spectra.

1. A. W. SCHRECKER and J. L. HARTWELL. J. Am. Chem. Soc. **74**, 5676 (1952).
2. D. C. AYRES and P. J. S. PAUWELS. J. Chem. Soc. 5025 (1962).
3. M. K. SEIKEL, F. D. HOSTETTLER, and D. B. JOHNSON. Tetrahedron, 1475 (1968).
4. A. I. SCOTT. Interpretation of the ultraviolet spectra of natural products. The Pergamon Press Ltd., Oxford. 1964. p. 322.
5. E SCHREIER. Helv. Chim. Acta, **46**, 75 (1963).
6. D. C. AYRES and J. W. MUNDY. Chem. Commun. 1134 (1968).
7. A. W. SCHRECKER and J. L. HARTWELL. J. Am. Chem. Soc. **75**, 5916 (1953).
8. L. H. KLEMM, D. S. H. LEE, and C. E. KLOPFENSTEIN. J. Org. Chem. **31**, 2376 (1966).
9. C. E. JOHNSON and F. A. BOVEY. J. Chem. Phys. **29**, 1012 (1958).
10. D. C. AYRES and J. W. MUNDY. J. Chem. Soc. C. 637 (1969).
11. J. FEENEY and A. HEINRICH. Chem. Commun. 295 (1966).
12. A. F. A. WALLIS. Tetrahedron Letters, 5287 (1968).
13. W. J. GENSLER and C. D. GATSONIS. J. Org. Chem. **31**, 4005 (1966).
14. D. C. AYRES and S. E. MHASALKAR. J. Chem. Soc. 3586 (1965).
15. R. J. SWAN and W. KLYNE. Chem. Ind. London, 1218 (1965).
16. N. FINCH, W. I. TAYLOR, T. R. EMERSON, W. KLYNE, and R. J. SWAN. Tetrahedron, **22**, 1327 (1966).
17. R. D. HAWARTH and T. RICHARDSON. J. Chem. Soc. 348 (1936).
18. T. R. GOVINDACHARI, S. S. SATHE, and N. VISWANATHAN. Tetrahedron Letters, 4183 (1967).

Can. J. Chem. Downloaded from www.nrcresearchpress.com by 210.87.254.5 on 09/05/12
For personal use only.

Can. J. Chem. Downloaded from www.nrcresearchpress.com by 210.87.254.5 on 09/05/12
For personal use only.

Gas–liquid chromatography of terpenes. Part XVIII. The volatile oil of the leaves of *Juniperus communis* L.[1]

E. VON RUDLOFF AND V. K. SOOD[2]

Prairie Regional Laboratory, National Research Council of Canada, Saskatoon, Saskatchewan

Received January 2, 1969

The volatile leaf oil of the local common juniper was found to consist mainly of α-pinene (73 to 83%) and smaller amounts (0.5 to 5%) of β-pinene, 3-carene, myrcene, limonene, methyl citronellate, bornyl acetate, myrtenal, myrtenol, myrtenyl acetate, α-terpineol, citronellol, citronellyl acetate, nerolidol, farnesol, and an unusual hydroxy ketone. Of the many trace constituents, β-phellandrene, citronellal, "iso-" citronellal, linalool, geraniol, isopulegol, 4-terpinenol, and ε-cadinene were isolated, whereas camphene, sabinene, α-phellandrene, γ-terpinene, terpinolene, *p*-cymene, fenchone, thujone, isothujone and δ-cadinene could only be tentatively identified.

There was little variation in the quantitative composition of the leaf oil from one plant to another. Since the composition of this oil differs significantly from that of other juniper leaf oils, chemotaxonomic studies by means of leaf oil analysis are feasible.

Canadian Journal of Chemistry, 47, 2081 (1969)

Introduction

The common juniper, *Juniperus communis* L., is one of the most widely distributed conifers, occurring throughout the temperate zone of the northern hemisphere. On the North American continent it is found from the Maritimes through the Great Plains as well as the boreal region of Canada to the Rocky Mountains and the Pacific Coast. On this continent it seldom grows to more than 2 ft in height and it is generally referred to as the variety *depressa*. Sargent (1) lists the common juniper occurring at higher altitudes (Appalachians, Rocky Mountains, as well as the coast of Greenland to New England) as the variety *montana*. Fraser and Russell (2) refer to the common juniper found in the Prairie Provinces as *J. sibirica* Burgsd., *syn. J. communis* L. var. *saxatilis* Pall. The correct varietal names of two low-growing forms found in Europe were discussed by Hunt and Welch (3) recently.

Whereas the volatile oil of the berries of the common juniper has been investigated in considerable detail (4–6), the leaf oil has received scant attention, Hegnauer (5) listing only α-pinene, camphene, and cadinene as constituents. The components of the wood were investigated in detail by Bredenberg (7).

In the previous papers of this series the analyses by gas–liquid chromatography (g.l.c.) of the leaf oils of the Savin juniper (8), Rocky Mountain juniper (9), creeping juniper (10), Ashe juniper (11), and red juniper (12) were described. This communication deals with a similar analysis of the leaf oil of the local common juniper. As in the previous work, both quantitative and qualitative aspects were studied and the variation from one plant to another was determined to permit conclusions on chemotaxonomic aspects.

Experimental

The gas–liquid chromatography (g.l.c.) analyses were carried out with an F & M model 500 gas chromatograph (linear temperature programming, thermal conductivity dectector; F & M Scientific Instrument Inc.) and a unit of conventional design (isothermal operation). An Aerograph model A-700 (Autoprep, Varian-Aerograph) instrument was employed for preparative g.l.c. Helium was used as carrier gas in all instruments. The peak area and percentage composition were determined with an Aerograph model 471 digital integrator, the instrumental error being less than 0.1% on full scale recorder (1 mV) deflection with no baseline drift. Retention times were measured from the time of injection to the initial emergence of the peaks and tentative identity was established by comparison of relative retention data or by co-injection of reference terpenes. The liquid phases employed in the g.l.c. columns were polyethylene glycol (PEG) (Carbowax 20 M, 5% on Aeropak 30, 70–80 mesh and 15% on Gaschrom P, 60–80 mesh), silicone gum polymer (SE–30) (5% on Gaschrom Q, 60–80 mesh), fluorinated silicone polymer (QF-1) (15% and 20% on Gaschrom P, 60–80 mesh), β,β-oxydipropionitrile (ODPN) (ethylene glycol *bis*-propionitrile; 15% on Gaschrom P, 60–80 mesh), C-modified polyphenyl ether (PPE) (Monosanto MCS 652; 15% on Gaschrom P, 60–80 mesh). The 5% columns were used for analytical experiments (90–120 ml He/min) whereas the more heavily loaded ones were employed for preparative work (40–70 ml He/min). A typical gas chromatogram of the leaf oil of the common

[1]NRCC No. 10604 (Part XVII see ref. 12).

[2]Colombo Plan Fellow, 1968; present address: C.F.P. Branch, Forest Research Institute and Colleges, Dehra Dun (U.P.) India.

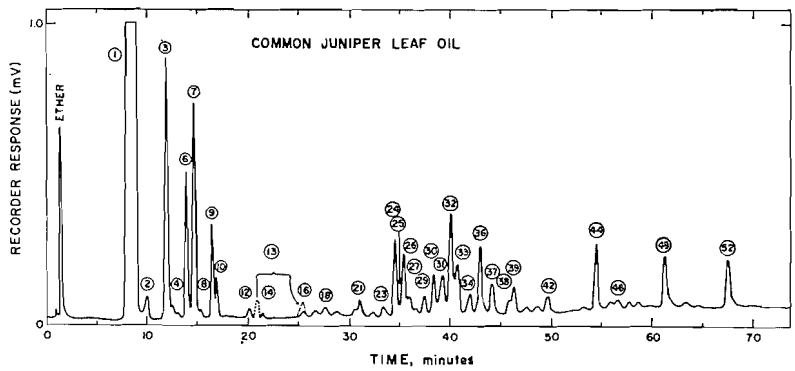

FIG. 1. Gas-liquid chromatogram of the leaf oil of *Juniperus communis* L. collected near Saskatoon, Saskatchewan; 5% PEG column (350 × 0.4 cm O.D.), 50° to 220° at 2.9°/min.

juniper as obtained on the 5% PEG column is shown in Fig. 1 and the individual components are numbered according to the sequence of elution on this column (50° to 220° at 2.9° per min). The isolated compounds were identified by comparison of the infrared (i.r.), proton magnetic resonance (p.m.r.), and ultraviolet (u.v.) spectra with those of authentic specimens. Infrared spectra were recorded as films between sodium chloride plates, using a Perkin–Elmer model 21 i.r. spectrophotometer. The p.m.r. spectra were obtained in carbon tetrachloride solution with tetramethyl silane as internal standard, using a Varian HA-100 (100 Hz) spectrometer. The u.v. spectra were determined in isooctane solution. Optical rotations were recorded in chloroform solution (2 to 5%) at 25° when a component was obtained in high purity and in sufficient amount (20 to 50 mg).

Plant Material and Recovery of the Volatile Oil

The foliage of the common juniper was collected along the eastern bank of the South Saskatchewan River 8 to 10 miles south of Saskatoon (Cranberry Flats to Beaver Creek area) during October and November, 1967, as well as April and May 1968. All woody branches were removed and the foliage was steam-distilled in 800 g batches in an all-glass apparatus (13) for 5 to 6 h. The oil was trapped in a small volume of ether and removed from time to time, a fresh aliquot of ether being added to the side-arm assembly after each withdrawal. After the distillation was completed, the residual water in the side-arm was extracted with ether. The ethereal extracts were combined and dried over anhydrous sodium sulfate and the ether was distilled off as described previously (12, 13). Small scale distillations (50 to 150 g foliage) were carried out in the same manner, but with a smaller apparatus (15). In later work it was discovered that the yield of the last component (farnesol, peak 53) could be increased by continuing the steam-distillation for a further 3 to 4 h. The yield of oil varied from 1.0 to 1.1% in the large scale distillation (same batch of plant material) and from 0.7 to 1.3% in the small scale work (individual plants); $[\alpha]_D$ −18 to −22°.

Prefractionation of the Volatile Oil

Aliquots (10.0 g) of the oil were chromatographed on modified silicic acid (120 g) as described previously (9–12). Elution of the column with petrol (Skellysolve F, b.p. 40–50°; 500 ml) gave a hydrocarbon fraction A (6.2 g), elution with methylene chloride (400 ml) a mid-fraction B (0.75 g), and elution with methanol (400 ml) a polar fraction C (2.0 g). Since the latter fraction was rather complex in composition attempts were made to separate this into distinct groups of compounds, but neither column chromatography nor preparative g.l.c. on QF-1 or SE-30 gave clear-cut separations.

Identification of Individual Compounds

a) Hydrocarbons

Analysis of the hydrocarbon fraction A on the analytical PEG, SE-30, PPE, and ODPN columns indicated that peaks 1 to 13 were monoterpene hydrocarbons with retentions corresponding to α-pinene, camphene, β-pinene, sabinene, an unknown, 3-carene, myrcene, α-phellandrene, limonene, β-phellandrene, γ-terpinene, *p*-cymene and terpinolene respectively. In some runs the camphene peak was partially resolved into two components, but the large amounts of α-pinene made separation and identification impossible. α-Pinene ($[\alpha]_D$ −20.2°), β-pinene ($[\alpha]_D$ −18.7°), 3-carene, myrcene, limonene and β-phellandrene were positively identified by their i.r. and nuclear magnetic resonance (n.m.r.) spectra, and *p*-cymene by its u.v. spectrum.

The relative amounts of component 13 (terpinolene) in the hydrocarbon fraction A were considerably lower than those recorded for the oil as a whole. On checking all analytical runs of the total oil and prefractionated material it could be found that a large portion of component 13 decomposed or rearranged during prefractionation. Also in most runs on the PEG columns a partial loss of component 13 with concomitant increase in the size of the double peak 15/16 was noticed. An attempt was made to isolate component 13 directly without prefractionation. The amount which could be collected barely sufficed for recording the i.r. spectrum in a micro cell (0.01 mm) path length. The weak spectrum was characterized by a broad CH peak (3000–2860 cm^{-1}), and relatively strong absorptions near 1730, 1645, 1455, 1380–1360 (doublet), 1260 (broad) and 870 cm^{-1} as well as a weak band near 3080 cm^{-1} ($\rangle C{=}CH_2$). Peak 13 must therefore consist mainly of a low boiling

Can. J. Chem. Downloaded from www.nrcresearchpress.com by 210.87.254.5 on 09/05/12
For personal use only.

Can. J. Chem. Downloaded from www.nrcresearchpress.com by 210.87.254.5 on 09/05/12
For personal use only.

labile ester containing a terminal methylene group and a trace of a hydrocarbon with the retention time of terpinolene.

The hydrocarbon fraction A also contained three trace peaks in the sesquiterpene range, retentions of which corresponded to those of ε-cadinene, δ-cadinene, and an unknown (peaks 34*b*, 36*b*, and 38*b* respectively). Only the first could be isolated in sufficient amount to give a weak i.r. spectrum and this was similar to that of the ε-cadinene isolated previously (15).

b) Midfraction

This fraction contained mainly peaks 21, 24, 26, 30, 31, 32, 34, and 35. Preparative g.l.c. on a QF-1 column (200 × 0.9 cm O.D.) gave these components as impure fractions and each was purified further on a PEG column (200 × 0.6 cm O.D.). In this manner components 24, 26, 30, 31, and 32 could be obtained practically pure and these were found to be methyl citronellate, bornyl acetate ($[\alpha]_D$ −30.5°), myrtenal ($[\alpha]_D$ +12.3°), citronellyl acetate, and myrtenyl acetate respectively. Refractionation of the methyl citronellate peak on a QF-1 column (180 × 0.9 cm O.D.) showed the presence of a small amount of an unknown alcohol (peak 25).

Component 21 was found to be an unknown aldehyde with a trisubstituted double bond; i.r. 1720 and 795 cm^{-1}, p.m.r. δ 9.73 Hz (1 H, partially split singlet, —CHO), 5.19 Hz (1 H, partially split singlet, $\rangle C=CH-$), 2.34 Hz (2 H complex multiplet, $-CH_2-C=C-$), 1.60 Hz (3 H, partially split singlet $CH_3-C=C$), 1.00 and 0.80 Hz (6 H, doublet, $(CH_3)_2CH-$).

Component 34 was found to be an unknown conjugated ketone with spectral properties differing from those of pulegone, piperitone, piperitenone, and carvone; i.r. bands near 2940 (s), 1760 (m), 1670 (s), 1615 (m), 1467 (m), 1432 (m), 1372 (m), 1335 (m), 1280 (m), 1240 (m), 1200 (m), 1030 (m), and 860 (m) cm^{-1}. The amount isolated was too small for recording a satisfactory p.m.r. spectrum.

Component 35 was isolated in very small amounts only and retention as well as the weak i.r. spectrum were in agreement with those of geranyl acetate. However, the isolated fraction was impure and since the i.r. spectrum of geranyl acetate does not contain a characteristic fingerprint region (it is very similar to that of neryl acetate) this identification is not entirely satisfactory. Subsequent refractionation of a concentrate of peaks 33 to 35 confirmed the presence of geranyl acetate. In addition a new ester was found in admixture with the conjugated ketone (peak 34).

c) Polar Fraction

This fraction consisted mainly of peaks 27, 33, 36, 37, 38, 44, 49 and 53. Preparative g.l.c. on a PEG column (200 × 0.6 cm O.D.) gave almost pure terpinen-4-ol (peak 27), α-terpineol (peak 33), citronellol (peak 36), myrtenol (peak 37), geraniol (peak 38), nerolidol (peak 44), and farnesol (peak 53).

Component 49 was obtained in what appeared to be a homogeneous main fraction (single peaks on QF-1, PEG and SE-30). The i.r. spectrum, 3430 (m), 2930 (s), 1705 (m), 1445 (m), 1375 (m); 820 and 795 (w) cm^{-1} suggested the main component to be a hydroxy ketone with at least one trisubstituted double bond. The p.m.r. spectrum differed from that of the known terpenoid hydroxy ketones (e.g. hydroxy camphor); δ 5.32 Hz (1 H, broad singlet, $\rangle C=CH-$), 5.05 Hz (1 H, triplet, J = 6, $\rangle C=CH-$), 4.22 Hz (1 H, broad, —OH), 1.95 Hz (4 to 6 H, unresolved multiplet), 1.66 Hz (3 H, singlet) and 1.62 Hz (3 H, singlet) (2 $CH_3-C=C$), and 1.08 Hz (3 H, singlet, $CH_3-C\langle$). The p.m.r. spectrum in deuterated dimethyl sulfoxide showed a sharp singlet near δ 3.80 Hz, which was removed on shaking with deuterium oxide (*tert* OH). The hydroxy ketone was hydrogenated in a Brown microhydrogenation apparatus. A slow uptake of approximately 2 mole equivalents of hydrogen was measured. The p.m.r. spectrum of the product showed singlets near δ 0.85, 0.90, 0.92, and 0.98 Hz, as well as a doublet near 1.02 Hz (J = 2) and a complex multiplet between δ 1.06 and 1.40 Hz. The amount available did not permit accurate integration.

Component 39 was isolated only in an impure state, the contaminant being geraniol (i.r., p.m.r.). The i.r. spectrum, 3460 (s), 3080 (w), 3000–2800 (s), 1635 (w), 1440 (s), 1375 (s), 1050 and 1025 (s), 950 (m), 880 (m), 810 (m), was indicative of an unsaturated alcohol containing a terminal methylene group. The p.m.r. spectrum showed resonance bands near δ 7.2 Hz (2 H, quartet as in estragol, or two doublets near 7.00 and 8.24, J = 16), 4.66 (1 H, singlet), 2.30 (2 H, doublet), 1.72 (4 H, multiplet), 1.58 and 1.55 (2 H and 1 H partially split doublet) and 1.48 Hz (3 H, singlet). The spectrum in deuterated dimethyl sulfoxide shifted the signals between 1.48 and 1.72 slightly upfield (by 0.03 to 0.09 Hz) and showed an unsymmetrical doublet at 4.80 Hz which was removed by shaking with deuterium oxide.

A small amount of component 50 was isolated and the i.r. (1720, 1705 cm^{-1}) and p.m.r. (δ 9.92 Hz (d)) spectra indicated this to be a conjugated keto aldehyde.

Results and Discussion

A typical gas–liquid chromatogram of the leaf oil of the common juniper as obtained on the standard 5% PEG column (12) is shown in Fig. 1. The individual components, identified by isolation and comparison of spectral properties as well as by retention data, and the percent composition are shown in Table I. This Table also lists the percent composition of five other leaf samples of common juniper collected in the same area along the South Saskatchewan River near Saskatoon. The results obtained show that there is little variation in the quantitative and qualitative composition of the leaf oil from one plant to another. The leaf oils of the local plants contain from 73 to 83% (−)-α-pinene. Since α-pinene has found extensive use in the synthesis of terpenes which are of value in the perfumery industry, this leaf oil may serve as a good source of this

Can. J. Chem. Downloaded from www.nrcresearchpress.com by 210.87.254.5 on 09/05/12
For personal use only.

TABLE I

Percentage composition of the leaf oil of *Juniperus communis* L.

Peak no.	Compound*	Sample†					
		A	B1	B2	B3	B4	B5
1	(−)-α-Pinene	73.5	81.0	80.5	83.0	75.5	81.2
2	(Camphene)	0.4	0.6	0.6	0.7	0.5	0.7
3	(−)-β-Pinene	4.9	5.2	4.9	4.6	4.2	4.9
4	(Sabinene)	0.1	0.3	0.2	0.3	0.3	0.1
5	Unidentified	Trace	Trace	Trace	Trace	Trace	Trace
6	3-Carene	2.8	1.4	2.9	0.3	5.3	0.2
7	Myrcene	4.0	3.4	4.1	3.8	4.2	4.3
8	(α-Phellandrene)	0.1	Trace	Trace	0.1	0.1	Trace
9	Limonene	1.2	1.0	1.1	0.9	1.2	1.2
10	β-Phellandrene	0.5	0.7	0.8	0.8	0.8	0.9
11	(γ-Terpinene)	Trace	Trace	Trace	Trace	Trace	Trace
12	(*p*-Cymene)	0.1	Trace	Trace	Trace	Trace	Trace
13*a*	(Terpinolene)	0.1–0.5	0.2	0.3	0.3	0.7	0.3
13*b*	Labile ester‡						
14	Unidentified	Trace	Trace	Trace	Trace	Trace	Trace
15	Rearrangement product‡	Trace	Trace	Trace	Trace	Trace	Trace
16	(Fenchone)	Trace	Trace	Trace	Trace	Trace	Trace
17	(Thujone)	Trace	Trace	Trace	Trace	Trace	Trace
18	(Isothujone)	Trace	Trace	Trace	0.1	Trace	0.1
19	Unidentified	Trace	Trace	Trace	Trace	Trace	Trace
20	Citronellal	Trace	Trace	Trace	Trace	Trace	Trace
21	"iso"-Citronellal	0.1	0.2	0.1	0.1	0.1	0.1
22	Unidentified	Trace	Trace	0.2	Trace	Trace	Trace
23	Linalool	0.1	0.3	0.1	Trace	0.1	Trace
24	Methyl citronellate	1.2	0.5	0.7	0.5	0.6	0.3
25	Isopulegol	0.2					
26	(−)-Bornyl acetate	1.1	0.6	0.5	0.7	0.6	0.6
27	Terpinen-4-ol	0.1	0.1	0.2	0.1	0.2	0.2
28	Unidentified	Trace	Trace	Trace	Trace	Trace	Trace
29	Unidentified	Trace	Trace	Trace	Trace	Trace	Trace
30	(+)-Myrtenal	0.5	0.3	0.1	0.1	0.2	0.2
31	Citronellyl acetate	0.6	0.2	Trace	0.1	0.2	0.1
32	Myrtenyl acetate	1.6	1.2	0.9	1.2	1.6	1.3
33	α-Terpineol	0.5	0.3	0.1	0.1	0.2	0.1
34*a*	Conjugated ketone	0.2	0.3	0.1	0.1	0.1	Trace
34*b*	ε-Cadinene	Trace					
35*a*	Geranyl acetate	0.1	Trace	Trace	0.1	0.2	0.1
35*b*	Unidentified ester	Trace					
36*a*	Citronellol	1.3	0.5	0.3	0.4	0.4	0.7
36*b*	(δ-Cadinene)	Trace					
37	Myrtenol	0.4	0.2	0.1	0.1	0.2	0.2
38*a*	Geraniol	0.1	Trace	Trace	Trace	Trace	Trace
38*b*	C_{15}-hydrocarbon	Trace					
39	Unidentified alcohol	0.3	0.1	Trace	0.1	0.1	0.6
40	Unidentified	Trace	Trace	Trace	Trace	Trace	Trace
41	Unidentified	Trace	Trace	Trace	Trace	Trace	Trace
42	Unidentified	0.1	Trace	Trace	Trace	Trace	Trace
43	Unidentified	Trace	Trace	Trace	Trace	Trace	Trace
44	(+)-Nerolidol	1.2	0.2	0.2	0.9	Trace	0.1
45	(Elemol)	Trace	Trace	Trace	Trace	Trace	Trace
46	Unsaturated alcohol	Trace	Trace	Trace	Trace	0.1	0.1
47	Unidentified	Trace	Trace	Trace	Trace	Trace	Trace
48	Unidentified	Trace	Trace	Trace	Trace	Trace	Trace
49	Hydroxy ketone§	1.0	0.3	0.1	0.5	2.1	1.0
50	Keto aldehyde	Trace	Trace	Trace	Trace	0.1	Trace
51	Unidentified	Trace	Trace	Trace	Trace	Trace	Trace
52	Unidentified	Trace	Trace	Trace	Trace	Trace	Trace
53	Farnesol	0.9	0.1	Trace	0.3	0.4	0.2

*Names in parentheses are tentatively identified compounds.
†A = large batch: B = small-scale distillation of leaf samples from individual plants.
‡Mainly a labile ester which decomposes or rearranges partially to a product with the retention of the double peak 15/16.
§ADDED IN PROOF: Component 49 has the retention of bisabolol.

Can. J. Chem. Downloaded from www.nrcresearchpress.com by 210.87.254.5 on 09/05/12
For personal use only.

monoterpene, especially where the yield of oil (0.7 to 1.3%) is relatively high. It is noteworthy that as with other conifer leaf oils (13) the composition was found to be rather constant during the fall and winter months.

Most of the minor and several of the trace constituents could be identified positively (see Table I). Of considerable interest from a phylogenetic point of view is the finding of myrtenal, myrtenol, and myrtenyl acetate. These terpenes are rarely found in essential oils and myrtenyl acetate does not appear to have been isolated previously from a natural source. These pinane derivatives may be readily identified by the characteristic chemical shifts of the *gem*-dimethyl groups in the p.m.r. spectra (14). It is possible that they may be detected in other oils containing smaller amounts of the pinanes by employing g.l.c. separation and p.m.r. spectroscopy.

From a chemical point of view the isolation of an isomer of citronellal (peak 21), and hydroxy ketone (peak 49) and what appears to be a ketoaldehyde (peak 50), are of interest. Retention and spectral characteristics showed component 21 to be an aliphatic aldehyde with a non-conjugated trisubstituted double bond. Since the p.m.r. spectrum indicates that one methyl group is situated next to the double bond whereas two more have the normal chemical shift (doublet at δ 1.00 and 0.80 Hz), of an isopropyl group the only acyclic terpenoid structure possible is 3,7-dimethyl-oct-3-en-1-al. However, the splitting constant of the two methyl groups ($J = 20$ c.p.s.) is very large for an isopropyl group (that in tetrahydro geraniol is only 7 c.p.s.). This aspect requires further study.

The retention time of the hydroxy ketone (peak 49) is typical for a monosubstituted sesquiterpene. Its i.r. spectrum shows the presence of a tertiary hydroxyl and a ketone group with strong indications that hydrogen bonding takes place. Internal hydrogen bonding between the hydroxyl and carbonyl functions would reduce the polarity sufficiently to account for the retention characteristics. The p.m.r. spectra confirmed the presence of a tertiary hydroxyl group and indicated the presence of an isopropylidene and at least one additional methyl group next to a double bond. Since all proton signals of the hydrogenated product were in the δ 0.85 to 1.0 Hz range none of the methyl groups can be adjacent to the oxygen functions. Although the spectra are fairly typical for terpenoid compounds (the single proton signals at low field as well as the methyl signals resembled those of farnesol) the above functions cannot be correlated with the basic farnesane, bisabolane, cadinane or eudesmane type of sesquiterpenes. The amounts of this hydroxy ketone, as well as the other partially characterized minor constituents which can be isolated in a fairly pure state by the present techniques are too small to permit structural investigations other than by spectral means. Large scale recovery of the oil and prefractionation by distillation may be an approach to obtain more of these compounds. Since several minor constituents of novel structure were also found in the leaf oils of the red, Ashe, Rocky Mountain and creeping junipers (9–12), new approaches to the isolation of larger amounts of such minor constituents are currently being studied.

Another minor constituent deserves attention in that it appears to rearrange during prefractionation. Component 13 has the retention time of terpinolene, but is almost completely lost in the prefractionation on silicic acid. Collection in a g.l.c. separation of the total oil gave only enough material for a weak i.r. spectrum. This indicated the compound to be an unsaturated acetate (bands at 1730, 1260, 1645, and 870 cm^{-1}) with a terminal methylene group. On reinjection to determine the purity two peaks with the retention time of peaks 13 and 15/16 were recorded, indicating that the ester was partially rearranged. The retention characteristics make it unlikely that it is a terpene acetate, but rather that a compound with six to eight carbon atoms is involved. Volatile aliphatic esters have been isolated from the leaf oil of the Douglas fir (16) and Sitka spruce (17), but component 13 differed from those reported.

The relatively small quantitative variation in the composition of the oil from one juniper plant to another (Table I, samples B1 to B5) make analysis of the leaf oil a suitable tool for chemotaxonomic studies. The common juniper is placed in the *Sectio oxycedrus*, whereas the junipers investigated previously by us (8–13) are all members of the *Sectio sabina*. This botanical difference is reflected in the chemical composition of the leaf oils. Whereas that of the common juniper is characterized by a large content of α-pinene and the presence of several terpenes belonging to the pinane (β-pinene, myrtenal,

myrtenol, and its acetate) and the acyclic (myrcene, linalool, citronellal, "iso"-citronellal, citronellol, geraniol, and possibly their acetates) groups, the oils of the other group of junipers contain mainly sabinene and its derivatives, elemol, the eudesmol isomers as well as safrole and other aromatic ethers. Hence, it appears relatively easy to distinguish between the two different groups on the basis of the types of terpenes found in their leaf oils. Noteworthy is, however, the finding of methyl citronellate in both groups. Since this ester is not widely found in conifer leaf oils, it may indicate the common ancestry of the two subsections of the genus *juniperus*. The fact that terpinen-4-ol and α-terpinenol, as well as several of the minor monoterpene hydrocarbons (and possibly the cadinenes) are also common to both sections, might at first sight also be listed in favor of common ancestry. However, since these terpenes are of widespread occurrence their phylogenetic value appears to be much more limited.

Finally, the occurrence of bornyl acetate in the oil of the common juniper deserves comment. Bornyl acetate is a typical constituent of the oils of the family Pinaceae, and with one noteworthy exception is absent from the members of the junipers (family Cupressaceae). The leaf oil of the Ashe juniper, *J. ashei* Buchh., was found to contain over 20% of bornyl acetate, as well as camphor, borneol and other terpenes which may be considered as typical of the family Pinaceae (11, 13). Hence, a biogenetic link between the conifers of the family Pinaceae, the Ashe juniper and the common juniper may be traced by the presence of bornyl acetate and related terpenes of the camphor group. Chemotaxonomic studies on this, as well as other North American junipers are in progress.

Acknowledgments

The grant of a Colombo Plan Fellowship by the Canadian International Development Agency to one of us (V. K. Sood) is gratefully acknowledged, as is the excellent technical assistance by Mr. M. Granat. The proton magnetic resonance and infrared spectra were recorded by Mr. M. Mazurek and Mr. W. C. Haid.

1. C. S. SARGENT. *In* Manual of the trees of North America. Vol. I and II. Dover Publications Inc., New York. 1965. p. 80.
2. W. P. FRASER and R. C. RUSSELL. An annotated list of the plants of Saskatchewan. University of Saskatchewan, Saskatoon, Saskatchewan. 1954. p. 3.
3. D. R. HUNT and H. J. WELCH. Taxon. **17**, 545 (1968).
4. E. GUENTHER. *In* The essential oils. Vol. VI. D. van Nostrand, Co., Inc., New York. p. 370.
5. R. HEGNAUER. *In* Chemotaxonomie der pflanzen. Vol. 1, Birkhauser, Verlag, Basel and Stuttgart. 1962. p. 367.
6. Y. HIROSE, N. NISHIMURA, and T. SAKAI. Nippon Kagaku Zasshi **81**, 1766 (1960), cf. Chem. Abstr. **56**, 6103*f* (1962).
7. J. B-SON BREDENBERG. Acta Chem. Scand. **15**, 961 (1961), and previous publications.
8. E. VON RUDLOFF. Can. J. Chem. **41**, 2876 (1963).
9. E. VON RUDLOFF and F. M. COUCHMAN. Can. J. Chem. **42**, 1890 (1964).
10. F. M. COUCHMAN and E. VON RUDLOFF. Can. J. Chem. **43**, 1017 (1965).
11. E. VON RUDLOFF. Can. J. Chem. **46**, 679 (1968).
12. A. R. VINUTHA and E. VON RUDLOFF. Can. J. Chem. **46**, 3743 (1968).
13. E. VON RUDLOFF. Can. J. Bot. **45**, 891 (1967).
14. R. B. BATES and V. P. THALACKER. J. Org. Chem. **33**, 1728 (1968).
15. E. VON RUDLOFF and F. W. HEFENDEHL. Can. J. Chem. **44**, 2015 (1966).
16. T. SAKAI, H. MAARSE, R. E. KEPNER, W. G. JENNINGS, and W. M. LONGHURST. J. Agr. Food Chem. **15**, 1070 (1967).
17. E. VON RUDLOFF. Can. J. Chem. **42**, 1057 (1964).

Can. J. Chem. Downloaded from www.nrcresearchpress.com by 210.87.254.5 on 09/05/12
For personal use only.

Can. J. Chem. Downloaded from www.nrcresearchpress.com by 210.87.254.42 on 09/05/12
For personal use only.

Structure of cryptosporiopsin: a new antibiotic substance produced by a species of *Cryptosporiopsis*[1]

G. M. STRUNZ, A. S. COURT, J. KOMLOSSY, AND M. A. STILLWELL
Canada Department of Forestry and Rural Development, Forest Research Laboratory, Fredericton, New Brunswick

Received November 13, 1968

The structure of cryptosporiopsin, a novel chlorine-containing antifungal agent produced by a species of *Cryptosporiopsis*, has been elucidated on the basis of spectral and chemical studies.

Canadian Journal of Chemistry, 47, 2087 (1969)

It was observed by Stillwell (1) that antifungal properties were associated with *Cryptosporiopsis* sp., an imperfect fungus isolated from yellow birch, *Betula alleghaniensis* Britt. Isolation from culture filtrates of the organism of a pure crystalline metabolite has recently been reported by Stillwell *et al.* (2). This compound, which was named cryptosporiopsin, was found to inhibit *in vitro* the growth of a wide variety of microorganisms (2).

In this paper, evidence is presented which allows the assignment of the structure **1** to cryptosporiopsin.

The metabolite was obtained as colorless crystals from *n*-hexane – methylene chloride, m.p. 133–137°, $[\alpha]_D^{25}$ +129°, (*c*, 1.35, chloroform). The molecular formula was established as $C_{10}H_{10}O_4Cl_2$ by elemental analysis and high resolution mass spectrometry. The infrared

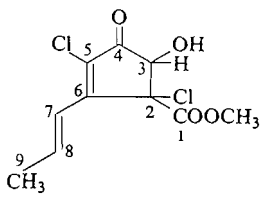

1

spectrum (KBr disk) of cryptosporiopsin exhibits bands at 1755 and 1730 cm^{-1}, attributed respectively to ester and conjugated five-membered ketone absorption. The relatively high frequency of both peaks is a consequence of chlorine substitution in the α-positions (3). A shoulder at 1737 cm^{-1} may be due to a rotational isomer of the chloroester in which the carbonyl group and the chlorine are staggered. The spectrum, measured at several concentrations in carbon tetrachloride, shows a strong sharp peak at 3500 cm^{-1} attributed to an intramolecularly hydrogen-bonded hydroxyl function. The carbonyl absorptions coalesce in the solution spectrum to a single sharp band at 1746 cm^{-1}.

The high resolution mass spectrum (see Experimental) shows, besides the molecular ion, peaks corresponding to loss from the latter of H_2O, Cl, $COOCH_3$ (base peak), and $COOCH_3$ plus CO.

The nuclear magnetic resonance (n.m.r.) spectrum of cryptosporiopsin (Fig. 1) shows a three-proton singlet at 6.12 τ attributable to the methyl ester hydrogens. A one-proton singlet at 5.31 τ slowly diminishes on addition of deuterium oxide and thus is assigned to the bonded hydroxyl hydrogen. A similar signal at 5.43 τ is shifted downfield to 4.91 τ on acetylation of the antibiotic, and clearly corresponds to the α-proton of a *secondary* alcohol. A three-proton doublet, centered at 7.99 τ (J = 6.2 c.p.s.) and a two-proton multiplet between 2.75 and 3.66 τ constitute an ABX_3-type pattern (4), in accord with the partial structure **2** (J_{AB} = 16.9 c.p.s.; no 1:3 coupling is evident). This assignment was corroborated by spin decoupling.

The metabolite exhibits an ultraviolet chromophore λ_{max}(95% EtOH) at 292 mμ (ε 22 800) indicating a system possessing extended conjugation, such as **3** (*vide infra*). The addition of alkali causes a negligible shift of the chromophore but gives rise to a time-dependent irreversible diminution of the extinction coefficient, demonstrating the lack of stability of the antibiotic in this medium. Since only two vinyl hydrogens appear in the n.m.r. spectrum, R_1 and R_2 must be alkyl substituents or chlorine atoms.

The molecular formula shows that the compound possesses five sites of unsaturation, four

[1]Presented at the Joint Meeting on the Chemistry of Natural Products, Fredericton, New Brunswick, August 1968.

Can. J. Chem. Downloaded from www.nrcresearchpress.com by 210.87.254.42 on 09/05/12
For personal use only.

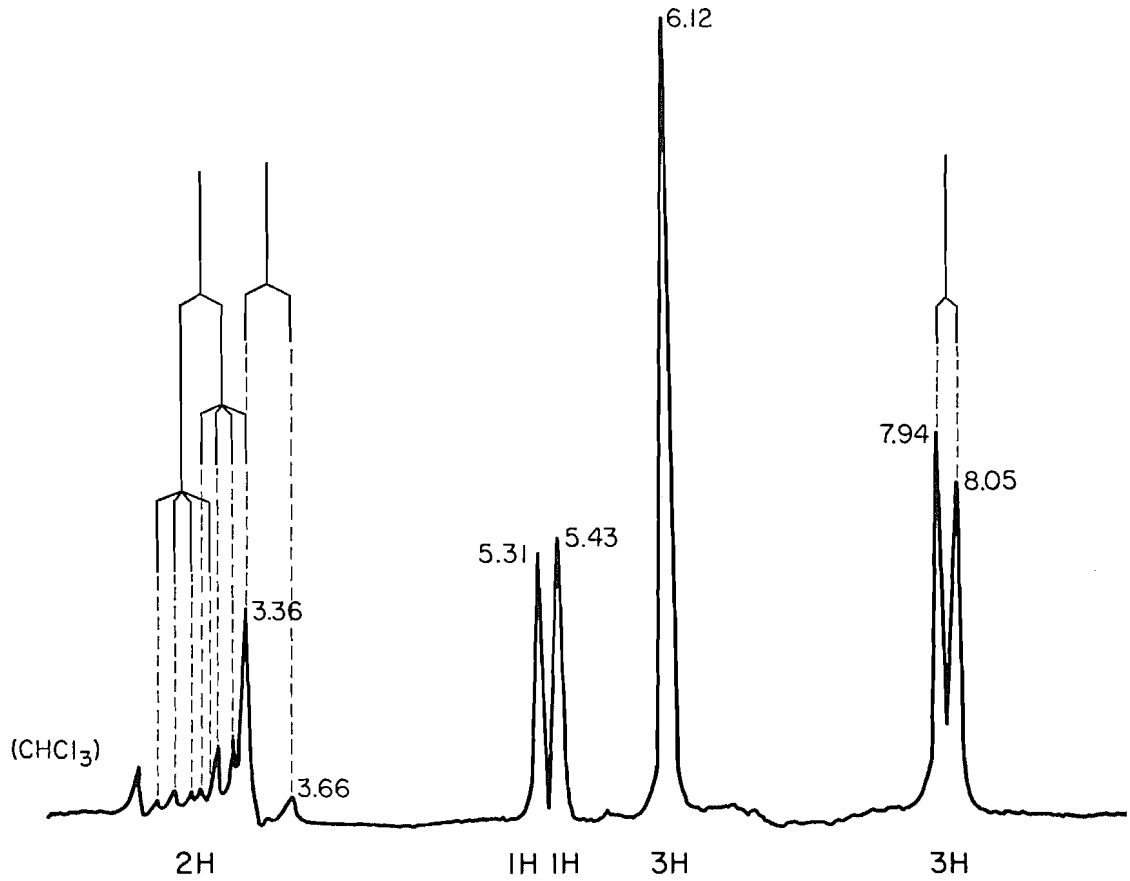

FIG. 1. The 56.4 Mc.p.s. nuclear magnetic resonance spectrum of cryptosporiopsin.

of these being accommodated in the ketone, ester, and double bonds; a ring accounts for the remaining unsaturation. The spectral data and degradative evidence (*vide infra*) eliminate structures possessing a conjugated ester group, and the remaining possiblities consistent with the cited information are represented in the partial formulae **4** and **5**.

Some structural features of the mould metabolite terrein **6** (5) suggested that the latter might be a useful model for spectroscopic comparison with cryptosporiopsin. Terrein shows ultraviolet absorption λ_{max}(EtOH) at 276 mμ (ε 25 000). The presence of a chlorine atom at the α-position would be expected to shift the maximum to 291 mμ (6), which coincides with the observed chromophore of cryptosporiopsin. Furthermore, infrared absorption (KBr disk) at 1635 and 1570 cm^{-1}, associated with the double bond system of cryptosporiopsin is also present in the terrein spectrum, as well as a peak at 965 cm^{-1} for the *trans* double bond (3).

Reduction of cryptosporiopsin with zinc in refluxing ethanol yielded an amorphous product, *m/e* 244, assigned the structure **7**. The relative abundance of the $M^+ + 2$ isotope peak demonstrates that **7** contains a single chlorine atom. The ultraviolet absorption λ_{max}(95% EtOH) at 285 mμ (ε 22 000) shows that the original chromophore is essentially unchanged. The presence of an *ethyl* ester is manifested in the n.m.r. spectrum, and in the mass spectral peak at *m/e* 171 (base peak) corresponding to the loss of the $COOC_2H_5$ fragment. The infrared spectrum (CCl_4) of **7** reveals again the presence of an internally-bonded hydroxyl group, and the carbonyl absorptions, in the absence of the chlorine α to the ester, now appear as a single band at 1730 cm^{-1}.

Can. J. Chem. Downloaded from www.nrcresearchpress.com by 210.87.254.42 on 09/05/12
For personal use only.

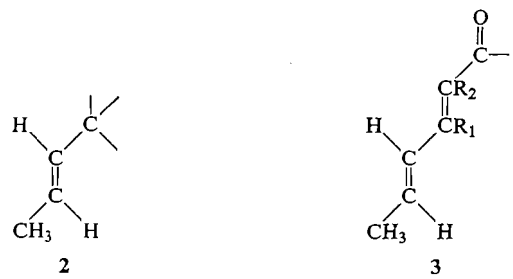

2 3

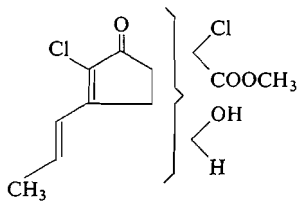

4

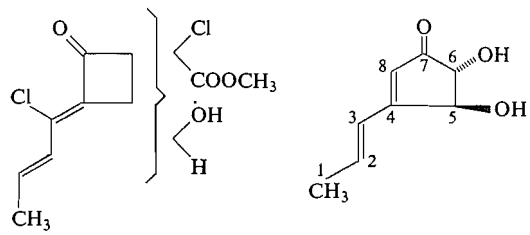

5 6

A dihydro product **8**, $C_{10}H_{12}O_4Cl_2$, *m/e* 266, was isolated from hydrogenation of cryptosporiopsin in ethyl acetate with a palladium-on-charcoal catalyst. Infrared absorption (KBr disk) at 1752 and 1738 cm^{-1} accounts for the chloroester and ketone respectively, while the double bond gives rise to a band at 1618 cm^{-1}. The hydroxyl shows again as a sharp peak at 3500 cm^{-1} in the spectrum measured in carbon tetrachloride solution. Ultraviolet absorption λ_{max} (absolute EtOH) at 244 mμ (ε 8300) agrees well with the predicted chromophore (6). The n.m.r. spectrum displays, *inter alia*, a two-proton multiplet at 7.35–7.61 τ, attributed to the allylic hydrogens of **8**. The methyl group appears as a poorly resolved triplet at 9.03 τ and no vinyl hydrogens are in evidence.

When hydrogenation with palladium-on-charcoal was conducted in ethanol, absorption ceased abruptly after uptake of 4 moles of hydrogen, and an oily product, *m/e* 182, corresponding to $C_{10}H_{14}O_3$ was obtained. Hydroxylic absorption is absent in the infrared spectrum

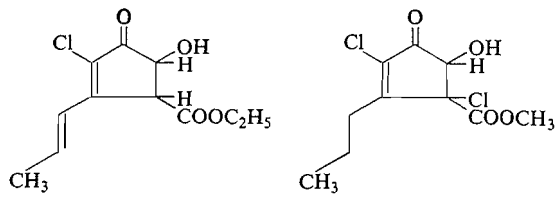

7 8

(CCl_4), and in addition to the carbonyl band at 1725 cm^{-1}, the spectrum surprisingly shows double bond absorption at 1610 cm^{-1}. Furthermore, the substance exhibits an ultraviolet maximum at 237 mμ (ε 10 000). This spectroscopic behavior can be readily interpreted in terms of the structure **9**. The primary reduction product is evidently the saturated hydroxy keto ester, which undergoes spontaneous dehydration on work-up.

Further support for structure **9** is found in the n.m.r. spectrum (4), in which the single vinyl hydrogen appears as a narrow doublet at 3.37 τ (J = 1.1 c.p.s.). A broad multiplet at 6.81 τ is attributed to the allylic proton; the low position of this resonance may be due to the anisotropy of the ester carbonyl. The two hydrogens on the saturated carbon α to the ketone constitute the AB part of an ABX system, and the appropriate pattern is discernible centered at 7.54 τ ($|J_{AB}|$ = 18.6 c.p.s.).

The mass spectrum exhibits, in addition to the molecular ion at *m/e* 182, peaks corresponding to the loss of methyl, ethyl, and propyl fragments, as well as $(M—OCH_3)^+$ and $(M—COOCH_3)^+$.

Reduction of **9** with zinc in acetic acid afforded a mixture of epimeric *cis* and *trans* keto esters **10**, not readily separable by thin-layer chromatography (t.l.c.). The mass spectrum of **10** shows

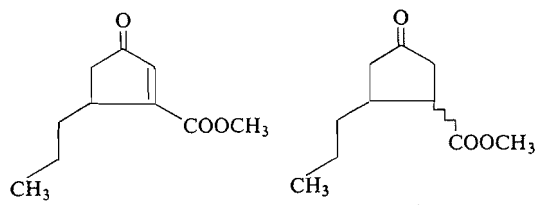

9 10

a molecular ion at *m/e* 184. A strong peak at *m/e* 114, and ions at *m/e* 97 and 87 can be rationalized in terms of the fragmentations shown in Fig. 2.

Separation of the *cis* and *trans* isomers could be effected by preparative vapor phase chromatography (v.p.c.), and the retention times of the

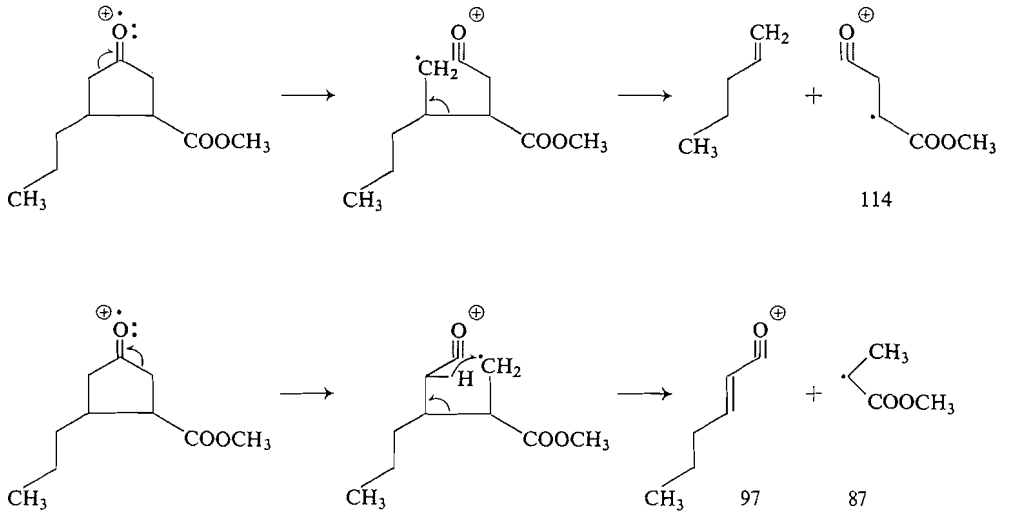

FIG. 2. The fragmentations of **10**

two fractions were identical with the major (*trans*) and minor (*cis*) constituents of a synthetic sample (*vide infra*). Comparison of the n.m.r., infrared, and mass spectra of the natural and synthetic *trans* keto esters confirmed their identities, and these compounds were further characterized as their 2,4-dinitrophenylhydrazones, $C_{16}H_{20}N_4O_6$.

Thus the skeletal structure of cryptosporiopsin is clearly defined, establishing the formulation **1** for the new antibiotic. Inspection of this structure suggests that, like terrein (7), it may arise from a polyketide chain precursor. In any scheme involving a purely polyketide route, the loss of one carbon atom must be accounted for. Birch *et al.* (7) has shown that terrein incorporates polyketide precursors with the unusual feature of two linked "carboxyl" carbons at the 6,7-positions (**6**), and attributes this distribution to a contraction of a six-membered precursor. It is reasonable to speculate that a common pathway is involved in the biosynthesis of cryptosporiopsin and terrein. Cyclization of a five-acetate unit chain with extrusion and the loss of one of the ring carbon atoms is seen to lead readily to the cryptosporiopsin system. Whereas the C-1 carboxyl is retained in cryptosporiopsin, this moiety is lost in the course of the terrein biosynthesis. Studies on further aspects of the chemistry, including stereochemistry, of cryptosporiopsin are in progress.

*Synthesis of 3-carbomethoxy-4-n-propyl Cyclopentanone **10**, cf. (8)*

2-Hexenoic acid, prepared from butyraldehyde and malonic acid by the Knoevenagel–Doebner reaction (9), was heated in a sealed vessel with butadiene to give the Diels–Alder adduct **11**, *m/e* 168. The product, after esterification, was cleaved by ozonolysis affording the ester diacid **13**, $C_{11}H_{18}O_6$. Esterification, followed by Dieckmann cyclization yielded the expected keto esters **15** (*a* and/or *b*). Hydrolysis and decarboxylation, followed by reesterification afforded *trans* and *cis* **10**, *m/e* 184, in the approximate ratio 25:4 (determined by v.p.c.).[2]

[2]This stereochemical assignment is based on the assumption that starting with predominantly *trans* 2-hexenoic acid (see Experimental), the preferred stereochemistry of the centers in question is *trans* throughout the synthetic sequence.

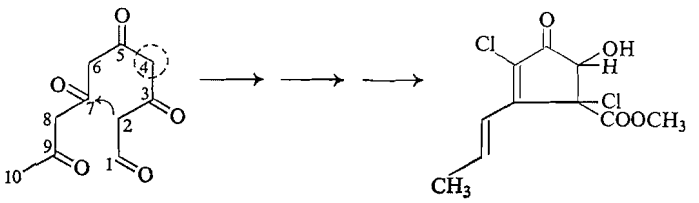

Can. J. Chem. Downloaded from www.nrcresearchpress.com by 210.87.254.42 on 09/05/12
For personal use only.

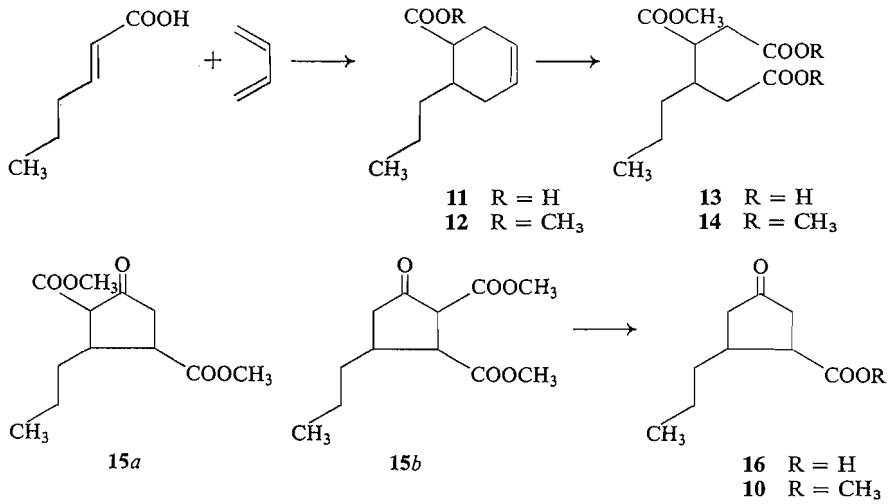

Experimental

Melting points were determined on a hot stage apparatus and are uncorrected. Infrared spectra were determined on a Beckmann IR-10 infrared spectrophotometer. Ultraviolet spectra were obtained on a Beckmann DK-2A spectrophotometer using 95% ethanol as solvent, except where otherwise indicated. Nuclear magnetic resonance spectra were measured in $CDCl_3$ solution with a Varian Associates 56.4 Mc.p.s. spectrometer.

The high resolution mass spectrum was obtained on a CEC 21-110B mass spectrometer, the other mass spectra were determined on a Hitachi Perkin–Elmer RMU-6D mass spectrometer. Microanalyses were performed by Spang Microanalytical Laboratory, Ann Arbor, Michigan, and by Dr. F. Pascher, Mikroanalytiches Laboratorium, Bonn, West Germany.

Cryptosporiopsin (1)

Isolation and purification of cryptosporiopsin have been described elsewhere (2). The metabolite is obtained as colorless crystals from methylene chloride – *n* – hexane, m.p. 133–137°, $[\alpha]_D^{25}$ +129° (*c*, 1.35, chloroform).

Anal. Calcd. for $C_{10}H_{10}O_4Cl_2$: C, 45.30; H, 3.80. Found: C, 45.45; H, 3.90.

Anal. Calcd. for $C_{10}H_{10}O_4Cl_2$ (high resolution mass spectrum): *m/e* 263.9956. Found: *m/e* 263.9943. Isotope peaks as percentages of M^+: $M^+ + 2$, 66%; $M^+ + 4$, 12%.

Acetylation of Cryptosporiopsin

Cryptosporiopsin (100 mg) was dissolved in acetic anhydride (6.0 ml). The solution was cooled to 0° and dry pyridine (0.6 ml) was added by syringe under nitrogen. The initially clear colorless solution was allowed to attain 25°, and was set aside with stirring in a nitrogen atmosphere for 22 h. The resulting brown reaction mixture was then evaporated to dryness and the residue was dissolved in an ether–water mixture. The organic phase was washed with 2% aqueous hydrochloric acid followed by water. The organic solution was subsequently dried over magnesium sulfate and the removal of the solvent under reduced pressure afforded 103 mg of brown gum. After chromatography on silica gel plates, 73 mg of pale-brown amorphous product was isolated. Infrared $\nu_{max}(CCl_4)$: 1741, 1759 cm^{-1} (no OH); n.m.r.: 2.78–3.77 τ (m, 2H), 4.83, 4.91 τ (s, ratio ca 0.4:1 for conformational or stereoisomers, 1H), 6.25 τ (s, 3H), 7.76, 7.83 τ (s, ratio ca 1:0.4 for conformational or stereoisomers, 3H) 7.97 τ (d, 3H); mass spectrum: M^+, 306; $M^+ + 2$, 66%; $M^+ + 4$ 12%.

Zinc–ethanol Reduction of Cryptosporiopsin

To cryptosporiopsin (100 mg, 0.377 mmole) in absolute ethanol (8 ml) was added zinc dust (131 mg, 0.002 g atom). The mixture was set aside with stirring at 25° for 20 h and was then refluxed for 7 h. Filtration removed the solid material, which was washed thoroughly with methylene chloride. The combined filtrates were washed with 2% sulfuric acid followed by water, and after drying over magnesium sulfate, removal of solvent yielded 85 mg of colorless gum. The product, 7, was chromatographed twice on preparative silica gel plates, but failed to crystallize. Infrared $\nu_{max}(CCl_4)$: 3515, 1730, 1642 cm^{-1}; ultraviolet λ_{max}(95% EtOH) 285 mμ (ε 22 000); n.m.r. 3.03–4.05 τ (m, 2H), 5.76 τ (q, J = 6.8 c.p.s., 2H), 6.01 τ (1H), 7.16, 7.22 τ (2H), 8.04 τ (d, 3H), 8.77 τ (t, J = 6.8 c.p.s., 3H); mass spectrum: M^+, 244; $M^+ + 2$, 34%.

Hydrogenation of Cryptosporiopsin, Palladium-on-charcoal – Ethyl Acetate

Cryptosporiopsin (70 mg) in ethyl acetate (30 ml) was stirred under hydrogen at atmospheric pressure and room temperature with a prehydrogenated 10% palladium-on-charcoal catalyst (30 mg) for 35 min. The catalyst was removed by filtration, and was washed thoroughly with ethyl acetate. The combined filtrates were evaporated to dryness furnishing 57 mg of colorless gum, which crystallized on standing. After recrystallization from ether–hexane the product, **8**, melted at 75–91° Spectral details are described in the text. Mass spectrum: M^+, 266; $M^+ + 2$, 66%; $M^+ + 4$, 12%.

Anal. Calcd. for $C_{10}H_{12}O_4Cl_2$: C, 44.96; H, 4.53; Cl, 26.55. Found: C, 45.00; H, 4.69; Cl, 26.49.

Can. J. Chem. Downloaded from www.nrcresearchpress.com by 210.87.254.42 on 09/05/12
For personal use only.

TABLE I

Cryptosporiopsin: accurate mass measurements of major peaks in the higher mass region of the spectrum

Peak*	Relative abundance	Observed mass	Composition	Calcd. mass (10)	Error (obs.–calcd.)	Fragment
264	36	263.9943	$C_{10}H_{10}O_4Cl_2$	263.9956	−0.0013	M^+
246	6	245.9865	$C_{10}H_8O_3Cl_2$	245.9850	+0.0015	$(M—H_2O)^+$
229	8	229.0268	$C_{10}H_{10}O_4Cl$	229.0268	0.0000	$(M—Cl)^+$
205	100	204.9828	$C_8H_7O_2Cl_2$	204.9823	+0.0005	$(M—COOCH_3)^+$
185	22	185.0375	$C_9H_{10}O_2Cl$†	185.0369	+0.0006	$(M—Cl \text{ and } CO_2)^+$
177	38	176.9871	$C_7H_7OCl_2$‡	176.9874	−0.0003	$(M—COOCH_3 \text{ and } CO)^+$

*Isotope peaks with appropriate relative intensities are present in each case.
†One of several plausible mechanistic rationales for a fragment with this composition involves migration of the ester methyl group to the carbon vacated by chlorine, through a four-center mechanism, with concomitant extrusion of CO_2. An alternative fragmentation pathway however appears also to be available for the $(M—Cl)^+$ ion. The spectrum shows a metastable peak at *m/e* 126.5 which corresponds to the decomposition 229 → 170, i.e. loss from $(M—Cl)^+$ of the $COOCH_3$ (mass, 59) fragment.
‡Metastable peak at *m/e* 153.5 (205 → 177).

Hydrogenation of Cryptosporiopsin, Palladium-on-charcoal – 95% Ethanol

Cryptosporiopsin (200 mg, 0.755 mmoles) in 95% ethanol (40 ml) was stirred under hydrogen at atmospheric pressure and 25° with a 10% prehydrogenated palladium-on-charcoal catalyst (90 mg). Absorption ceased abruptly after uptake of 4 moles of hydrogen. The catalyst was removed by filtration, and was washed thoroughly with ethanol. The combined filtrates upon the removal of solvent afforded 144 mg of pale-brown oil. Chromatography of 56 mg of this product on a silica gel preparative layer plate yielded 32 mg of colorless oily unsaturated keto ester **9**.

Spectral details are described in the text.

Due to asymmetric induction the hydrogenation product **9** was optically active, $[\alpha]_D^{30}$ −26.5° (*c*, 1.29, chloroform).

Zinc – Acetic Acid Reduction of 9

To a refluxing solution of the keto ester **9** (200 mg) in glacial acetic acid (30 ml) was added zinc dust (2.0 g) in three portions during 20 min. The resulting suspension was heated under reflux with stirring for 5 h. The solid material was removed by filtration, and was washed thoroughly with ether. The combined filtrates were evaporated to dryness, and the residue was redissolved in ether–water. The ether solution was washed with water and dried over magnesium sulfate. Removal of solvent *in vacuo* furnished 197 mg of pale-yellow gum. Chromatography on a preparative silica gel plate yielded 170 mg of colorless oil, consisting of a mixture of epimeric keto esters **10**. Although it was subsequently shown that t.l.c. did effect a partial separation of the isomers, their presence was not readily discernible on inspection of t.l.c. plates, but was however clearly manifested in the n.m.r. spectrum, in particular by the presence of two methoxyl peaks (6.24, 6.27 τ) together integrating for three protons. Separation of the epimers was effected by means of a Varian Aerograph Autoprep Model A-700; 20 ft by 3/8 in. column (30% SE 30 on Chromosorb W) at 205°, with helium as the carrier gas at 133 ml/min. Under these conditions the retention times of the two stereoisomers were (**10***a*) 21 min 15 s and (**10***b*) 22 min 55 s, identical with those of the major and minor epimeric constituents of an authentic synthetic product (considered to be *trans* and *cis* respectively—see text).

The infrared spectrum of **10***a* shows a broad carbonyl band at 1745 cm^{-1}. In the n.m.r. spectrum the methyl ester protons give rise to a sharp singlet at 6.28 τ, five deshielded hydrogens are included in a multiplet whose principal peaks are at 7.44 and 7.55 τ and the methyl protons of the propyl side chain appear as a poorly resolved triplet at 9.07 τ. The mass spectrum is similar to that of the epimer mixture **10**, and exhibits ions at *m/e* 184 (molecular ion, 5%), 114 (66%), 97 (7%), and 87 (32%) as described in the text. The base peak at *m/e* 55 corresponds to the ion $C_3H_3O^+$. In addition, peaks at *m/e* 155 (4%), 153 (5%), 141 (17%), and 125 (18%) correspond to the loss from the molecular ion of C_2H_5, OCH_3, C_3H_7, and $COOCH_3$ fragments respectively.

The infrared spectrum of the 2,4-dinitrophenylhydrazone of "natural" (dextrorotatory) **10***a*, was identical in all details with that of the derivative of racemic synthetic **10***a*.

An analytical sample, after four crystallizations from methanol, melted at 107–115°. Mass spectrum: *m/e* 364.

Anal. Calcd. for $C_{16}H_{20}N_4O_6$: C, 52.74; H, 5.53; N, 15.38. Found: C, 53.23; H, 5.61; N, 15.03.

2-Hexenoic Acid

2-Hexenoic acid was prepared according to the procedure of Niemann and Redemann (9). The crude reaction product crystallized on standing and was used in the subsequent Diels–Alder reaction without further purification. The n.m.r. spectrum indicates clearly that it consists principally of the *trans* isomer. A pair of partially superimposed triplets in the region 2.72–3.23 τ and a doublet at 4.25 τ (peaks slightly broadened due to 1,3-splitting) constitute the AB part of an ABX_2 spectrum. The coupling constant J_{AB} is 15.8 c.p.s., the correct magnitude for *trans* olefinic protons.

Preparation of 11 and 12

2-Hexenoic acid (14.3 g, 0.125 moles) was heated with butadiene (ca 7 g, 0.13 moles) and hydroquinone (100 mg) in a Parr bomb at 170–190° for 5 h.

Distillation of the brown reaction product afforded 11.7 g of colorless oily **11**, b.p. 140–150° /9 mm. In the

Can. J. Chem. Downloaded from www.nrcresearchpress.com by 210.87.254.42 on 09/05/12
For personal use only.

Can. J. Chem. Downloaded from www.nrcresearchpress.com by 210.87.254.42 on 09/05/12
For personal use only.

n.m.r. spectrum the two vinyl protons appear as a somewhat broadened singlet at 4.39 τ; the mass spectrum shows a molecular ion peak at *m/e* 168.

Conversion to the methyl ester **12** was effected by refluxing **11** (7.1 g) with anhydrous methanol (40 ml) in the presence of concentrated sulfuric acid (3 ml), monitoring the progress of the reaction by t.l.c. After work-up in the usual manner, the product was distilled, and the pure ester **12** was collected at 99–102° /11 mm. Infrared $\nu_{max}(CCl_4)$ 1737, 1658 cm^{-1}; n.m.r.: 4.39 τ (broad s, 2H), 6.33 τ (s, 3H); mass spectrum: molecular ion *m/e* 182.

*Preparation of **13** and **14***

An ozone–oxygen mixture was passed by means of a sintered glass bubbler into a solution of **12** (3.75 g, 20.6 mmoles) in ethyl acetate (100 ml) cooled in a dry ice – acetone bath. (Welsbach Model T-23 ozonator, operating at 90 V, 8 lb pressure, flow rate 0.02 ft^3/min). The end point was indicated by the development of a blue color in the solution, whereupon the system was flushed with nitrogen to remove excess ozone. The solution was then stirred vigorously under hydrogen at atmospheric pressure with a prehydrogenated 10% palladium-on-charcoal catalyst (304 mg), until the calculated volume of hydrogen had been taken up. The catalyst was removed by filtration, and the solvent was stripped off *in vacuo* below 30°.

The resulting dialdehyde ($\nu_{max}(CCl_4)$ 2720 cm^{-1}, broad carbonyl 1738–1715 cm^{-1}) was dissolved in acetone (200 ml), and the solution was cooled in an ice-bath. A solution of potassium permanganate (4.88 g, 30.9 mmoles) in distilled water (200 ml) was added slowly with stirring during 40 min, and the reaction mixture was set aside with stirring at 0–10° for a further 30 min. After addition of 20% sulfuric acid (2 ml), sulfur dioxide gas was passed in until a clear solution resulted; this was extracted exhaustively with ether. After drying over magnesium sulfate, removal of solvent under reduced pressure furnished 3.767 g of colorless oil, which partially crystallized on standing. Recrystallization from ether – *n*-hexane afforded colorless crystals of **13**, m.p. 128–132°.

Anal. Calcd. for $C_{11}H_{18}O_6$: C, 53.65; H, 7.37. Found: C, 53.83; H, 7.38.

Esterification was effected by sulfuric acid-catalyzed reaction with anhydrous methanol in the usual manner.

The pure triester **14** was eluted from a silica gel column with benzene–ether (95:5).

A somewhat broadened singlet at 6.32 τ in the n.m.r. spectrum accounts for the nine methoxyl protons; $\nu_{max}(CCl_4)$ 1740 cm^{-1}.

The same product was obtained by direct oxidation of the potassium salt of **11** with aqueous permanganate, followed by esterification.

*Dieckmann Condensation of **14***

To sodium hydride (306 mg, 12.75 mmoles, washed free of mineral oil with light petroleum) was added anhydrous tetrahydrofuran (30 ml) containing 5 drops of absolute methanol. The suspension was cooled in an ice-bath, and a solution of triester **14** (1.75 g, 6.37 mmoles) in dry tetrahydrofuran (70 ml) was added during 20 min with stirring. Moderate evolution of hydrogen occurred. When the addition was complete, and effervescence ceased, a nitrogen atmosphere was introduced, and the mixture was stirred at 25° for 15 h; it was then heated under reflux for 7 h. After cooling, methanol was added cautiously to decompose any unreacted hydride, and the solution was poured on to ice. The pH was adjusted to 2–3 by addition of 5% hydrochloric acid, and the mixture was extracted thoroughly with ether. The extracts were washed with sodium bicarbonate solution, dried over magnesium sulfate, and evaporated, yielding 1.214 g of crude oily product **15** (*a* and/or *b*). The cyclized material, which was not purified further exhibits ultraviolet absorption at λ_{max}(95% EtOH) 250 mμ (ε 2000). The addition of 1 drop 5% sodium hydroxide solution shifts and enhances the chromophore to 279 mμ (ε 15 000).

*Preparation of **10***

The crude Dieckmann product **15** (*a* and/or *b*) (3.4 g) was hydrolyzed and decarboxylated by refluxing with 4 *N* hydrochloric acid (25.2 ml) for 18 h. When cool, the mixture was extracted with ether, and the combined extracts were shaken with saturated sodium bicarbonate solution. Acidification of the aqueous phase, and extraction afforded 1.97 g of acidic product **16**.

Esterification was effected by refluxing **16** (1.97 g) with methanol (75 ml) and concentrated sulfuric acid (4 ml) for 3 h. After removal of the methanol under reduced pressure, work-up in the usual manner yielded 1.5 g of pale-yellow oil, which appeared homogeneous on t.l.c.

Vapor phase chromatographic analysis of synthetic **10** thus obtained revealed the presence of two components in the approximate ratio 25:4, corresponding to the *trans* and *cis* epimers **10***a* and **10***b* respectively (*vide supra*).

The infrared, n.m.r., and mass spectra of synthetic **10***a* were completely identical with the purified "natural" dextrorotatory *trans* epimer **10***a*.

Similarly the infrared spectrum of the 2,4-dinitrophenylhydrazone of racemic synthetic **10***a* was identical with that of the corresponding derivative of the "natural" keto ester.

An analytical sample, after four crystallizations from methanol melted at 103–109°.

Anal. Calcd. for $C_{16}H_{20}N_4O_6$: C, 52.74; H, 5.53; N, 15.38. Found: C, 52.83; H, 5.55; N, 15.31.

Acknowledgments

The authors thank Dr. P. Levins, Arthur D. Little Inc., Cambridge, Massachusetts for the high resolution mass spectrum, and Mr. J. E. Anderson, Harvard University for the spin decoupling study. Gratitude is expressed to Mrs. H. Moore, Mr. H. J. Liu, and Mr. K. T. Kan, all of the University of New Brunswick, for their contributions to this work in the form of nuclear magnetic resonance, mass spectra, and optical rotation measurements respectively.

1. M. A. STILLWELL. Can. J. Bot. **44**, 259 (1966).
2. M. A. STILLWELL, F. A. WOOD, and G. M. STRUNZ. Can. J. Microbiol. **15**, 501 (1969).
3. L. J. BELLAMY. The infrared spectra of complex molecules. 2nd ed. John Wiley and Sons, Inc., New York. 1958; K. NAKANISHI. Infrared absorption

spectroscopy, practical. Holden-Day, Inc., San Francisco. 1962.
4. L. M. JACKMAN. Applications of nuclear magnetic resonance spectroscopy in organic chemistry. The Pergamon Press, Ltd., New York. 1959; N. S. BHACCA and D. H. WILLIAMS. Applications of n.m.r. spectroscopy in organic chemistry. Holden-Day, Inc., San Francisco. 1964.
5. D. H. R. BARTON and E. MILLER. J. Chem. Soc. 1028 (1955); J. F. GROVE. J. Chem. Soc. 4693 (1954).
6. A. I. SCOTT. Interpretation of the ultraviolet spectra of natural products. The Pergamon Press, Ltd., New York. 1964.
7. A. J. BIRCH, A. CASSERA, and A. R. JONES. Chem. Commun. 167 (1965).
8. K. TOKI. Bull. Chem. Soc. Japan, **32**, 233 (1959).
9. C. NIEMANN and C. T. REDEMANN. J. Am. Chem. Soc. **68**, 1933 (1946).
10. J. H. BEYNON and A. E. WILLIAMS. Mass and abundance tables for use in mass spectrometry. American Elsevier Publishing Co. Inc., New York. 1963.

Can. J. Chem. Downloaded from www.nrcresearchpress.com by 210.87.254.42 on 09/05/12
For personal use only.

Can. J. Chem. Downloaded from www.nrcresearchpress.com by 210.87.254.42 on 09/05/12
For personal use only.

Pyrazolines VIII. Migration of a carbomethoxy group in a bromopyrazoline to pyrazole conversion[1]

D. E. McGreer and Y. Y. Wigfield
Department of Chemistry, University of British Columbia, Vancouver, British Columbia

Received December 9, 1968

The stereoisomers of 4-bromo-3-methyl-3-carbomethoxy-1-pyrazoline (**1** and **2**) have been prepared and are both transformed readily into 3-methyl-4-carbomethoxypyrazole (**6**). This transformation requires preferential migration of a carbomethoxy group over a methyl group.

Canadian Journal of Chemistry, 47, 2095 (1969)

Pyrazolines substituted with halo, nitrile, hydroxyl, amino, or nitro groups readily undergo elimination reactions to yield pyrazoles (1). Evidence has been presented that indicates that this reaction is both acid- and base-catalyzed (2). Aromatization occurs in preference to the elimination of nitrogen and formation of cyclopropane and olefin products (3). We have prepared the stereoisomers of 4-bromo-3-methyl-3-carbomethoxy-1-pyrazoline (**1** and **2**) in the hope that double substitution at C-3 would favor the reaction leading to loss of nitrogen. This would then provide a means for evaluating the migrational aptitudes of bromine and hydrogen in the olefin-forming reaction. The only reaction which could be induced, however, was pyrazole formation. As described below pyrazoles were formed by migration of a carbomethoxy group in preference to a methyl group.

Addition of diazomethane to methyl β-bromo-α-methacrylate, (E)-[2] (**3**) and (Z)- (**4**) gave the pyrazolines **1** and **2**. Compounds **1** and **2** could not be isolated pure due to their instability; however, conclusive evidence for their structures is found in the nuclear magnetic resonance (n.m.r.) spectra of solutions in tetrachloroethylene and chloroform-*d* (see Table I and the Experimental).

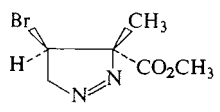

1

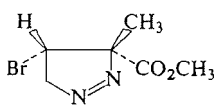

2

The magnitude of the coupling constant for the triplet and doublet multiplets is evidence that the carbon of the diazomethane has bonded to the β-carbons of **3** and **4**.

Warming of **1** or **2** neat or in solution led to an exothermic reaction which fumed apparently due to the hydrogen bromide formed. The reaction showed evidence of being autocatalytic due to a variable induction time with different samples and a sensitivity to the addition of traces of acid. The product from **1** and **2** was identical and was isolated as the hydrobromide and then converted to a pyrazole (m.p. 93–94 °C). Possibilities considered for the structure of this pyrazole were 3-carbomethoxy-4-methylpyrazole (**5**) and 3-methyl-4-carbomethoxypyrazole (**6**). An authentic sample of **5** (m.p. 171–171.5 °C, lit. (4) m.p. 172 °C) was prepared by the bromine oxidation of 3-carbomethoxy-4-methyl-2-pyrazoline (5) and proved different in many ways from our product. The pyrazole from **1** and **2** was converted to its ethyl ester (m.p. 46–48 °C, lit. (6) for the ethyl ester of **6**, m.p. 46 °C) confirming structure **6** for it.

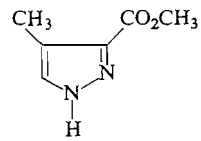

5

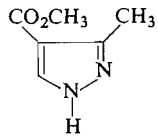

6

Treatment of **1** or **2** with base might permit isolation of a 3-methyl-3-carbomethoxy-(3*H*)-pyrazole. Attempts towards this end with pyridine or quinoline, however, yielded only intractable tars.

[1]Presented at the 51st meeting of the Chemical Institute of Canada Vancouver, British Columbia, June 1968.
[2]See ref. 12 for the use of this nomenclature.

TABLE I

The nuclear magnetic resonance spectra of **1** and **2** in C_2Cl_4 in τ units with external tetramethylsilane reference

Compound	C-5 (doublet)	C-4 (triplet)	CH_3-ester	CH_3 at C-3
1	5.12(J = 4.7 Hz)	5.28(J = 4.7 Hz)	6.21	8.09
2	4.96(J = 5.4 Hz)	5.80(J = 5.4 Hz)	6.15	8.48

The preferential migration of a carbomethoxy group over a methyl during acid-catalyzed aromatization is not without precedent. A number of dienones substituted on the 4 position by an alkyl group and a carboalkoxyl group undergo similar acid-catalyzed (7) and photochemical reactions (8). In the present case acid catalysis is presumably required to activate one molecule (by formation of its salt) towards elimination by another molecule of pyrazoline. We feel that elimination occurs as a distinct step prior to migration due to the fact that the same product is isolated from **1** and **2**. Concerted migration with elimination would be expected to lead to the migration of different groups from these different stereoisomers.

Experimental

Methyl β-Bromo-α-methacrylate, (E)- (3)

Methyl β-bromo-α-methacrylate, (E)- (b.p. 162–163 °C) was prepared by the procedure of Bieber (9) from methyl α,β-dibromoisobutyrate (10).

Methyl β-Bromo-α-methacrylate, (Z)- (4)

Methyl β-bromo-α-methacrylic acid, (Z)- was prepared from 50 g of *dl-erythro*-2,3-dibromo-2-methylsuccinic acid by the procedure of Rappe and Anderson (11). The acid obtained as an oil (2.8 g) contained 20% of the E form as determined by nuclear magnetic resonance (n.m.r.) spectroscopy. Treatment with 1 mole of diazomethane gave **4** and **3** in the ratio of 72:28 respectively. The equilibrium for these forms which can be achieved by heating to 120° or by acid catalysis is about 1:400 respectively as determined by vapor-phase chromatography.

Pyrazolines

All glassware for these preparations was conditioned by treatment with 10% aqueous sodium hydroxide followed by three washes with distilled water.

An excess of diazomethane in ether was added to **3** in ether and the solution let stand overnight. Evaporation of the ether at 0 °C gave an oily product. A solution in deuteriochloroform of the 3-carbomethoxy-3-methyl-4-bromo-1-pyrazoline (**1**), having the same *trans* orientation for the bromine and carbomethoxy groups as the starting material, showed n.m.r. signals at τ 5.00 (doublet, J = 4.7 Hz), τ 5.42 (triplet, J = 4.7 Hz), τ 6.27 and τ 9.02 against an internal TMS standard. No other physical properties could be determined as the pyrazoline even at room temperature readily reacted as described below.

Treatment in a similar manner of 1.9 g of **4** (containing 28% of **3**) yielded an oily pyrazoline mixture. The n.m.r. spectrum, given in Table I, indicated the presence of 55% of **2**, 20% of **1**, and 25% of unreacted **4**.

Pyrazoline Decomposition

On warming pyrazoline **1** a vigorous reaction took place with fuming due to hydrogen bromide gas which evolved and the hydrobromide of a pyrazole, m.p. 175–177.5 °C (white needles from ethanol) was formed. The n.m.r. spectrum taken in deuterium oxide showed peaks at τ 2.04 (1H), τ 6.30 (3H), and τ 7.68 (3H). Treatment of the hydrobromide with dilute sodium bicarbonate yielded a pyrazole (70%) which was extracted with chloroform. Evaporation of the chloroform gave a solid which when crystallized from methanol melted at 93–94 °C. The n.m.r. spectrum taken in deuteriochloroform gave peaks at τ 2.05 (1H), τ 6.17 (3H), and τ 7.46 (3H).

Anal. Calcd. for $C_6H_8N_2O_2$: C, 51.42; H, 5.75; N, 20.00. Found: C, 51.49; H, 5.85; N, 19.89.

In a similar way pyrazoline **2** (mixed with 28% of **1**) decomposed to the pyrazole hydrobromide, m.p. 175–177.5 °C. Treatment of this salt with dilute sodium bicarbonate yielded the pyrazole (76%), m.p. 93–94 °C, with n.m.r. peaks in deuteriochloroform at τ 2.00 (1H), τ 6.15 (3H), and τ 7.45 (3H).

3-Methyl-4-carboethoxypyrazole

A solution of 0.5 g of the pyrazole from **1** in 10 ml of 10% sodium hydroxide was heated under reflux for 3 h. After cooling and neutralization with concentrated hydrochloric acid, 0.3 g of the free acid was collected. A solution of the acid in 20 ml of absolute ethanol saturated with dry hydrogen chloride at 0 °C was refluxed for 3 h. After cooling the solution was made basic with sodium bicarbonate and the product was taken up into chloroform. Evaporation of the solvent gave 0.37 g of an oily material which crystallized, m.p. 46–48 °C, on standing. The melting point of 3-methyl-4-carboethoxypyrazole is 46 °C (4) thus identifying our pyrazole products from **1** and **2** as 3-methyl-4-carbomethoxypyrazole (6). The n.m.r. spectrum in deuteriochloroform showed peaks at τ 2.01 (1H), τ 5.67 (quartet, J = 7 Hz), τ 7.44, and τ 8.66 (triplet, J = 7 Hz).

Acknowledgments

The authors gratefully appreciate the support received for this work from the National Research Council of Canada and from the Committee on Research of the University of British Columbia. An NRCC scholarship to Y.Y.W. is hereby acknowledged.

Can. J. Chem. Downloaded from www.nrcresearchpress.com by 210.87.254.42 on 09/05/12
For personal use only.

1. A. N. KOST and I. J. GRANDBERG. *In* Advances in heterocyclic chemistry. Vol. 6. *Edited by* A. R. Katritzky and A. J. Boulton. Academic Press, Inc., New York. 1966. p. 381.
2. W. E. PARHAM and J. L. BLEASDALE. J. Am. Chem. Soc. **73**, 4664 (1951).
3. D. E. MCGREER and W.-S. WU. Can. J. Chem. **45**, 461 (1967), and earlier papers.
4. K. D. GUNDERMANN and R. THOMAS. Chem. Ber. **93**, 883 (1960).
5. D. E. MCGREER, W. WAI, and G. CARMICHAEL. Can. J. Chem. **38**, 2410 (1960).
6. H. BEYER and G. WOLTER. Chem. Ber. **89**, 1652 (1956).
7. S. INAYAMA and M. YANAGITA. J. Org. Chem. **27**, 1465 (1962).
8. P. J. KROPP. Tetrahedron Letters, 3647 (1964).
9. P. BIEBER. Ann. Chem. **9**, 674 (1954).
10. M. C. FORD and W. A. WATERS. J. Chem. Soc. 1851 (1951).
11. C. RAPPE and K. ANDERSON. Acta Chem. Scand. **21**, 1741 (1967).
12. J. E. BLACKWOOD, C. L. GLADYS, K. L. LOENING, A. E. PETRARCA, and J. E. RUSH. J. Am. Chem. Soc. **90**, 509 (1968).

Convenient new synthesis of 1,3-diaroylureas[1]

JAMES F. WOLFE AND GEORGE B. TRIMITSIS
Department of Chemistry, Virginia Polytechnic Institute, Blacksburg, Virginia 24061

Received January 14, 1969

It has been found that symmetrical 1,3-diaroylureas can be prepared in good yields by allowing urea to react with aromatic esters and excess sodium hydride in refluxing 1,2-dimethoxyethane. Applications of this method to the synthesis of unsymmetrical 1,3-diaroylureas and substituted monoaroylureas are also described.

Canadian Journal of Chemistry, 47, 2097 (1969)

In connection with a continuing study of base-catalyzed condensations involving nitrogen-containing carbonyl compounds (1, 2), we had occasion to investigate the reactions of urea and certain urea derivatives with aromatic esters, employing sodium hydride as the condensing agent. During the course of this investigation it became evident that these reactions provide a facile new method for the synthesis of 1,3-diaroylureas. Unlike several previously reported methods (3–6), which are either inconvenient or of untested generality, the present procedure utilizes readily available starting materials and appears to be quite general in scope.

Results

Treatment of urea with slightly more than two molecular equivalents of the appropriate aromatic ester and excess sodium hydride in refluxing 1,2-dimethoxyethane (DME) until hydrogen evolution was complete, produced symmetrical 1,3-diaroylureas **1***a–c*, eq. [1]. Similarly, dibenzoylurea (**1***a*) and unsymmetrical diaroylureas **2***a–b* were obtained from the reaction of benzoylurea

$$NH_2CONH_2 \xrightarrow[2.\ \text{Acid}]{1.\ ArCOOCH_3,\ NaH} ArCONHCONHCOAr \quad [1]$$

1*a*, Ar = C_6H_5
b, Ar = C_6H_4Cl-*p*
c, Ar = $C_6H_4OCH_3$-*p*

with methyl benzoate, methyl *p*-chlorobenzoate, and methyl anisate, respectively. In addition, this procedure was extended to the synthesis of monoaroylureas **3***a–b*, which were produced on treatment of methylurea and phenylurea with methyl

$C_6H_5CONHCONHCOAr$
2*a*, Ar = C_6H_4Cl-*p*
b, Ar = $C_6H_4OCH_3$-*p*

$RNHCONHCOC_6H_5$
3*a*, R = CH_3
b, R = C_6H_5

benzoate and sodium hydride in refluxing DME. The results of these experiments are presented in Table I where it may be seen that yields were generally good to excellent. Incidentally, in an attempt to effect dibenzoylation of biuret by the above method, cleavage of one of the amide groups occurred and dibenzoylurea, instead of the expected dibenzoylation product of biuret, was isolated from the reaction.

Structural assignments for new diaroylureas **1***b–c* and **2***a–b* were based on analyses (Table I)

[1]Supported by the United States Public Health Service, Research Grant No. GM-14340 from the National Institute of General Medical Sciences.

Can. J. Chem. Downloaded from www.nrcresearchpress.com by 210.87.254.42 on 09/05/12
For personal use only.

1. A. N. KOST and I. J. GRANDBERG. *In* Advances in heterocyclic chemistry. Vol. 6. *Edited by* A. R. Katritzky and A. J. Boulton. Academic Press, Inc., New York. 1966. p. 381.
2. W. E. PARHAM and J. L. BLEASDALE. J. Am. Chem. Soc. **73**, 4664 (1951).
3. D. E. MCGREER and W.-S. WU. Can. J. Chem. **45**, 461 (1967), and earlier papers.
4. K. D. GUNDERMANN and R. THOMAS. Chem. Ber. **93**, 883 (1960).
5. D. E. MCGREER, W. WAI, and G. CARMICHAEL. Can. J. Chem. **38**, 2410 (1960).
6. H. BEYER and G. WOLTER. Chem. Ber. **89**, 1652 (1956).
7. S. INAYAMA and M. YANAGITA. J. Org. Chem. **27**, 1465 (1962).
8. P. J. KROPP. Tetrahedron Letters, 3647 (1964).
9. P. BIEBER. Ann. Chem. **9**, 674 (1954).
10. M. C. FORD and W. A. WATERS. J. Chem. Soc. 1851 (1951).
11. C. RAPPE and K. ANDERSON. Acta Chem. Scand. **21**, 1741 (1967).
12. J. E. BLACKWOOD, C. L. GLADYS, K. L. LOENING, A. E. PETRARCA, and J. E. RUSH. J. Am. Chem. Soc. **90**, 509 (1968).

Convenient new synthesis of 1,3-diaroylureas[1]

JAMES F. WOLFE AND GEORGE B. TRIMITSIS
Department of Chemistry, Virginia Polytechnic Institute, Blacksburg, Virginia 24061

Received January 14, 1969

It has been found that symmetrical 1,3-diaroylureas can be prepared in good yields by allowing urea to react with aromatic esters and excess sodium hydride in refluxing 1,2-dimethoxyethane. Applications of this method to the synthesis of unsymmetrical 1,3-diaroylureas and substituted monoaroylureas are also described.

Canadian Journal of Chemistry, 47, 2097 (1969)

In connection with a continuing study of base-catalyzed condensations involving nitrogen-containing carbonyl compounds (1, 2), we had occasion to investigate the reactions of urea and certain urea derivatives with aromatic esters, employing sodium hydride as the condensing agent. During the course of this investigation it became evident that these reactions provide a facile new method for the synthesis of 1,3-diaroylureas. Unlike several previously reported methods (3–6), which are either inconvenient or of untested generality, the present procedure utilizes readily available starting materials and appears to be quite general in scope.

Results

Treatment of urea with slightly more than two molecular equivalents of the appropriate aromatic ester and excess sodium hydride in refluxing 1,2-dimethoxyethane (DME) until hydrogen evolution was complete, produced symmetrical 1,3-diaroylureas **1***a–c*, eq. [1]. Similarly, dibenzoylurea (**1***a*) and unsymmetrical diaroylureas **2***a–b* were obtained from the reaction of benzoylurea

$$NH_2CONH_2 \xrightarrow[2.\ \text{Acid}]{1.\ ArCOOCH_3,\ NaH} ArCONHCONHCOAr \quad [1]$$

1*a*, Ar = C_6H_5
b, Ar = C_6H_4Cl-*p*
c, Ar = $C_6H_4OCH_3$-*p*

with methyl benzoate, methyl *p*-chlorobenzoate, and methyl anisate, respectively. In addition, this procedure was extended to the synthesis of monoaroylureas **3***a–b*, which were produced on treatment of methylurea and phenylurea with methyl

$C_6H_5CONHCONHCOAr$
2*a*, Ar = C_6H_4Cl-*p*
b, Ar = $C_6H_4OCH_3$-*p*

$RNHCONHCOC_6H_5$
3*a*, R = CH_3
b, R = C_6H_5

benzoate and sodium hydride in refluxing DME. The results of these experiments are presented in Table I where it may be seen that yields were generally good to excellent. Incidentally, in an attempt to effect dibenzoylation of biuret by the above method, cleavage of one of the amide groups occurred and dibenzoylurea, instead of the expected dibenzoylation product of biuret, was isolated from the reaction.

Structural assignments for new diaroylureas **1***b–c* and **2***a–b* were based on analyses (Table I)

[1]Supported by the United States Public Health Service, Research Grant No. GM-14340 from the National Institute of General Medical Sciences.

Can. J. Chem. Downloaded from www.nrcresearchpress.com by 210.87.254.40 on 09/05/12
For personal use only.

TABLE I

Synthesis and properties of diaroylureas and substituted monoaroylureas

Starting material	Methyl ester	Product	Reaction period, h	Yield, %	Melting point, °C
Urea	Benzoate	1,3-Dibenzoylurea (**1***a*)	4	98	212–213[a,b]
Urea	*p*-Chlorobenzoate	1,3-Di(*p*-chlorobenzoyl)urea (**1***b*)[c]	2.5	80	241–243[d]
Urea	Anisate	1,3-Dianisylurea (**1***c*)[e]	6.5	66	212.5–213.5[a]
Benzoylurea	Benzoate	1,3-Dibenzoylurea (**1***a*)	3	88	212–213[a,b]
Benzoylurea	*p*-Chlorobenzoate	1-Benzoyl-3-(*p*-chlorobenzoyl) urea (**2***a*)[f]	6	76	207–209[a]
Benzoylurea	Anisate	1-Benzoyl-3-anisylurea (**2***b*)[g]	4	37	202–204[a]
Methylurea	Benzoate	1-Benzoyl-3-methylurea (**3***a*)	4	67	170–171[h,i]
Phenylurea	Benzoate	1-Benzoyl-3-phenylurea (**3***b*)	1	90	209–210[a,j]

[a]Recrystallized from absolute ethanol.
[b]Lit. (5) m.p. 208–209°.
[c]Anal. Calcd. for $C_{15}H_{10}N_2O_3Cl_2$: C, 53.43; H, 2.99; N, 8.31; Cl, 21.03. Found: C, 53.23; H, 2.96; N, 8.29; Cl, 20.94.
[d]Recrystallized from acetic acid.
[e]Anal. Calcd. for $C_{17}H_{16}N_2O_5$: C, 62.19; H, 4.91; N, 8.53. Found: C, 62.15; H, 4.86; N, 8.37.
[f]Anal. Calcd. for $C_{15}H_{11}N_2O_3Cl$: C, 59.51; H, 3.66; N, 9.26; Cl, 11.71. Found: C, 59.51; H, 3.92; N, 9.48; Cl, 11.90.
[g]Anal. Calcd. for $C_{16}H_{14}N_2O_4$: C, 64.42; H, 4.73; N, 9.39. Found: C, 64.34; H, 4.81; N, 9.42.
[h]Recrystallized from 95% ethanol.
[i]Dixon (7) reports m.p. 170–171°.
[j]Lit. (5) m.p. 210°.

and spectral data. The i.r. spectra of these compounds, which were similar to that of dibenzoylurea, had strong NH absorption at 3360–3400 and two intense carbonyl bands at 1670 and 1750 cm^{-1}. The nuclear magnetic resonance (n.m.r.) spectra had absorption for two NH protons at 12.1–13.2 and resonance for the appropriate number of aromatic protons at 7.8–8.5 p.p.m.; the methoxy protons of **1***c* (6H) and **2***b* (3H) appeared as singlets at 4.0 and 4.3 p.p.m., respectively.

Experimental[2]

Synthesis of Symmetrical Diaroylureas ***1****a–c*

These reactions were carried out in a 1 l two-necked flask equipped with a heating mantle, a magnetic stirring bar, and a reflux condenser, connected at its upper end through a cold trap (dry ice – acetone) to a Precision Scientific wet-test meter filled with water. The other neck of the flask was connected, through rubber tubing, to a 150 ml round-bottomed flask. The reaction flask was charged with 250 ml of DME[3] and 0.50 mole of sodium hydride,[4] and a slurry of 0.05 mole of urea and 0.125 mole of the appropriate ester in 60 ml of DME was placed in the addition flask. The system was then flushed with dry nitrogen and closed to the atmosphere. The sodium hydride – DME slurry was brought to reflux, and when thermal equilibrium had been established (15–20 min) an initial reading was taken on the test meter. The slurry of urea and ester in DME was then added during 5–7 min. Readings were taken periodically on the gas meter until hydrogen evolution had ceased.[5] Most of the solvent was then removed to give a pasty residue, which was cooled to 0° in an ice-water bath. Ether (150 ml) was added, and the resulting suspension was allowed to stir for 5–10 min. Cold water (100 ml) was added cautiously, and the solid which separated between the layers was collected by filtration and acidified with cold 6 *N* HCl. The resulting solid was collected, washed with 5% sodium bicarbonate solution, and recrystallized from the appropriate solvent (see Table I). Yields and analytical data for **1***a–c* are presented in Table I.

Synthesis of Unsymmetrical Diaroylureas ***2****a–b and Substituted Monoaroylureas* ***3****a–b*

These reactions were effected essentially as described above, employing 0.05 mole of the appropriate substituted urea, 0.08 mole of the appropriate aromatic ester, and 0.25 mole of sodium hydride. The reaction mixture was refluxed until hydrogen evolution ceased,[6] and the reaction mixture was processed in the usual manner. Recrystallization solvents, yields, and analytical data for the products obtained from these reactions are presented in Table I.

[2]Melting points were taken on a Thomas–Hoover "Uni-Melt" apparatus in open capillary tubes, and are corrected. Analyses were performed by Galbraith Laboratories, Knoxville, Tenn., and by Miss Q. H. Tan using an F & M model 185 C, H, and N analyzer. Infrared (i.r.) spectra were taken on a Beckman IR-5A infrared spectrophotometer using the potassium bromide pellet method. Nuclear magnetic resonance (n.m.r.) spectra were obtained on a Varian Associates A-60 spectrometer. Chemical shifts, relative to internal tetramethylsilane, were measured to the center of a singlet or multiplet. Dimethyl sulfoxide-d_6 was used as the n.m.r. solvent. Unless specified otherwise, chemicals were commercial reagent grade and were used without further purification.

[3]The DME was distilled from sodium ribbon immediately before use.

[4]This reagent was used as a 55% dispersion in mineral oil as obtained from Metal Hydrides, Inc., Beverly, Massachusetts.

[5]In all of these experiments four molecular equivalents of hydrogen were evolved.

[6]Three molecular equivalents of hydrogen were liberated in these experiments.

Can. J. Chem. Downloaded from www.nrcresearchpress.com by 210.87.254.40 on 09/05/12
For personal use only.

Attempted Dibenzoylation of Biuret

To a suspension of 0.50 mole of sodium hydride in 250 ml of refluxing DME was added a solution of 5.16 g (0.05 mole) of biuret and 17.02 g (0.125 mole) of methyl benzoate in 150 ml of DME. The reaction mixture was refluxed for 19.5 h and then processed in the usual manner to afford, after one recrystallization from absolute ethanol, 5.10 g (38%) of 1,3-dibenzoylurea (**1***a*), m.p. 215–217°; mixture m.p. 215–217°. The i.r. spectrum of this material was identical with that of a sample of **1***a* prepared from the dibenzoylation of urea.

1. J. F. Wolfe and G. B. Trimitsis. J. Org. Chem. **33**, 894 (1968).
2. J. F. Wolfe, G. B. Trimitsis, and C. R. Hauser. Can. J. Chem. **46**, 2561 (1968).
3. E. Schmidt. J. prakt. Chem. [2], **5**, 58 (1872).
4. A. F. Holleman. Chem. Ber. **23**, 3000 (1890).
5. O. C. Billeter. Chem. Ber. **36**, 3218 (1903).
6. R. A. Jacobsen. U.S. Patent 2,090,593 (1937); Chem. Abst. **31**, 7068 (1937).
7. A. E. Dixon. J. Chem. Soc. **75**, 383 (1899).

Selective reduction of esters with sodium trimethoxyborohydride

R. A. Bell and M. B. Gravestock

McMaster University, Hamilton, Ontario

Received December 27, 1968

The rate of reduction of representative methyl esters with sodium trimethoxyborohydride decreases in the order primary > secondary > tertiary. Sodium trimethoxyborohydride reduces with 100% selectivity the secondary ester group in the alicyclic diester–acid **2***c*.

Canadian Journal of Chemistry, 47, 2099 (1969)

Can. J. Chem. Downloaded from www.nrcresearchpress.com by 210.87.254.40 on 09/05/12
For personal use only.

Since its first preparation and brief examination of its properties in 1953 by Brown and Mead (1), sodium trimethoxyborohydride appears to have received little attention by organic chemists (2). We now report the 100% selective reduction of the alicyclic diester–acid **2***c* with sodium trimethoxyborohydride in refluxing dimethoxyethane. In order to gauge the synthetic utility of this reagent in selective ester reductions, we have measured the rates of reduction of the primary, secondary, and tertiary methyl esters, methyl 3-phenylpropionate, methyl cyclohexylcarboxylate, and methyl abietate **4**.

The diester–acid **2***c* was prepared from the known compound (3) methyl 12-oxopodocarp-13-en-16-oate **1**. Ozonolysis of **1** in ethyl acetate at 0°, followed by treatment with hydrogen peroxide in acetic acid yielded a dicarboxylic acid **2***a*, which on methylation with diazomethane afforded the triester **2***b*. Selective hydrolysis with one mole-equivalent of sodium hydroxide in methanol (4) yielded the diester–acid **2***c* in 75% overall yield from **1**.

The selective reduction of the secondary ester function in **2***c* was accomplished by treatment with a three mole-equivalent excess of sodium trimethoxyborohydride in refluxing dimethoxyethane. The ester – acid – alcohol **3** was obtained in greater than 95% yield, either as the free alcohol or in the form of its δ-lactone. Careful examination of the crude reaction product by proton magnetic resonance (p.m.r.) spectroscopy showed that the C-15 carbomethoxy group at 3.64 p.p.m. had suffered no observable reduction. The

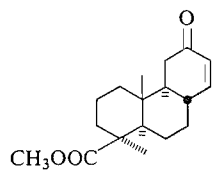

1

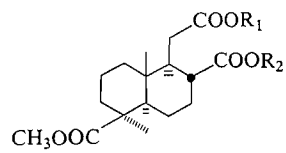

2 *a*, $R_1 = R_2 = H$
b, $R_1 = R_2 = CH_3$
c, $R_1 = H$; $R_2 = CH_3$

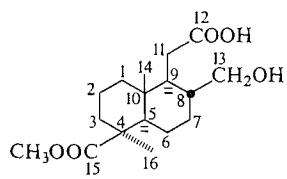

3

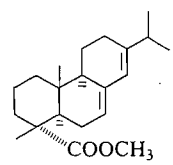

4

Attempted Dibenzoylation of Biuret

To a suspension of 0.50 mole of sodium hydride in 250 ml of refluxing DME was added a solution of 5.16 g (0.05 mole) of biuret and 17.02 g (0.125 mole) of methyl benzoate in 150 ml of DME. The reaction mixture was refluxed for 19.5 h and then processed in the usual manner to afford, after one recrystallization from absolute ethanol, 5.10 g (38%) of 1,3-dibenzoylurea (**1***a*), m.p. 215–217°; mixture m.p. 215–217°. The i.r. spectrum of this material was identical with that of a sample of **1***a* prepared from the dibenzoylation of urea.

1. J. F. Wolfe and G. B. Trimitsis. J. Org. Chem. **33**, 894 (1968).
2. J. F. Wolfe, G. B. Trimitsis, and C. R. Hauser. Can. J. Chem. **46**, 2561 (1968).
3. E. Schmidt. J. prakt. Chem. [2], **5**, 58 (1872).
4. A. F. Holleman. Chem. Ber. **23**, 3000 (1890).
5. O. C. Billeter. Chem. Ber. **36**, 3218 (1903).
6. R. A. Jacobsen. U.S. Patent 2,090,593 (1937); Chem. Abst. **31**, 7068 (1937).
7. A. E. Dixon. J. Chem. Soc. **75**, 383 (1899).

Can. J. Chem. Downloaded from www.nrcresearchpress.com by 210.87.254.5 on 09/05/12
For personal use only.

Selective reduction of esters with sodium trimethoxyborohydride

R. A. Bell and M. B. Gravestock
McMaster University, Hamilton, Ontario

Received December 27, 1968

The rate of reduction of representative methyl esters with sodium trimethoxyborohydride decreases in the order primary > secondary > tertiary. Sodium trimethoxyborohydride reduces with 100% selectivity the secondary ester group in the alicyclic diester–acid **2***c*.

Canadian Journal of Chemistry, 47, 2099 (1969)

Since its first preparation and brief examination of its properties in 1953 by Brown and Mead (1), sodium trimethoxyborohydride appears to have received little attention by organic chemists (2). We now report the 100% selective reduction of the alicyclic diester–acid **2***c* with sodium trimethoxyborohydride in refluxing dimethoxyethane. In order to gauge the synthetic utility of this reagent in selective ester reductions, we have measured the rates of reduction of the primary, secondary, and tertiary methyl esters, methyl 3-phenylpropionate, methyl cyclohexylcarboxylate, and methyl abietate **4**.

The diester–acid **2***c* was prepared from the known compound (3) methyl 12-oxopodocarp-13-en-16-oate **1**. Ozonolysis of **1** in ethyl acetate at 0°, followed by treatment with hydrogen peroxide in acetic acid yielded a dicarboxylic acid **2***a*, which on methylation with diazomethane afforded the triester **2***b*. Selective hydrolysis with one mole-equivalent of sodium hydroxide in methanol (4) yielded the diester–acid **2***c* in 75% overall yield from **1**.

The selective reduction of the secondary ester function in **2***c* was accomplished by treatment with a three mole-equivalent excess of sodium trimethoxyborohydride in refluxing dimethoxyethane. The ester – acid – alcohol **3** was obtained in greater than 95% yield, either as the free alcohol or in the form of its δ-lactone. Careful examination of the crude reaction product by proton magnetic resonance (p.m.r.) spectroscopy showed that the C-15 carbomethoxy group at 3.64 p.p.m. had suffered no observable reduction. The

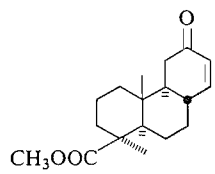

1

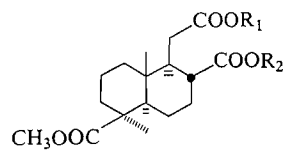

2 *a*, $R_1 = R_2 = H$
b, $R_1 = R_2 = CH_3$
c, $R_1 = H$; $R_2 = CH_3$

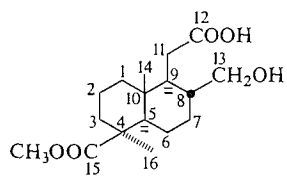

3

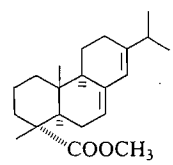

4

TABLE I

Reduction of esters by sodium trimethoxyborohydride*

Ester	Time for 50% reduction (min)	Time for 100% reduction (min)	Product
Methyl 3-phenylpropionate	17	40	3-Phenylpropanol
Methyl cyclohexylcarboxylate	27	60	Cyclohexylcarbinol
Diester–acid **2***c*	32	75	**3**
Methyl abietate **4**	255	600	Abietenol

*3 mole-equivalents excess in refluxing dimethoxyethane at 83°.

carboxyl function at C-12 was likewise completely unaffected as demonstrated by quantitative lactone formation.

To examine the general utility of sodium trimethoxyborohydride in dimethoxyethane in ester reductions, the rates of reaction of the esters, methyl 3-phenylpropionate, methyl cyclohexylcarboxylate, and methyl abietate were measured using the same procedure as above with three mole-equivalents excess of the reagent. Reduction times and products are summarized in Table I. The expected alcohols were all produced in essentially quantitative yield and were characterized by their p.m.r. spectra and as their 3,5-dinitrobenzoate derivatives.

Since sodium trimethoxyborohydride does not react with the carboxyl group (1, 2) (except to form the carboxylate anion) it would seem that the selective reduction of ester groups in the presence of carboxylic acids is readily achieved with this reagent. The relative rates of reduction of the primary and secondary esters methyl 3-phenylpropionate and methyl cyclohexanecarboxylate (1.6:1 respectively for 50% reduction) show that some selectivity (ca. 60%) may be achieved between them (5). This selectivity could probably be improved considerably by operating at lower temperatures, for example 0°. The very slow rate of reduction of the tertiary ester, methyl abietate, indicates that excellent selectivity can be achieved between primary and secondary esters in the presence of tertiary esters and that the reagent should be of synthetic use in these areas. The total non-reaction of the axial C-15 methyl ester in the diester–acid **2***c* arises because of the severe 1,3 diaxial interaction with the C-14 methyl group. This behavior may be compared with the more normal behavior of the tertiary, equatorial C-18 methyl ester in methyl abietate which, although slow, does undergo reduction.

Sodium borohydride in large excess in methanol (6) reduces aromatic carboxylic esters to alcohols in good yields, but results with aliphatic and alicyclic esters were less satisfactory. Lithium borohydride on the other hand reduces esters well, but also attacks carboxylic acids to varying extents (2, 7) so that selective reduction of esters in the presence of acids is rarely possible. It is likely that sodium trimethoxyborohydride, despite its reactivity, is more sensitive to the steric environment of the substrate than the tetrahydro reagents. Thus, like lithium tritertiarybutoxyaluminium hydride (8) it exhibits a wide range of relative reduction rates in its reaction with esters. A variety of selective reductions amongst different functional groups can be readily carried out with alkoxyaluminohydrides (8, 9). Lithium diethoxyaluminohydride has been reported to show some selectivity in the reduction of simple esters (10). However, on currently available evidence it would appear that sodium trimethoxyborohydride is the preferred reagent for achieving reasonable selectivity in ester reductions.

In view of Brown's report (1) that sodium trimethoxyborohydride reacted only slowly with esters in ethyl ether at reflux or in *n*-butyl ether at 110–140°, we are at present investigating the possibility of a specific solvent effect by dimethoxyethane. In addition, we are examining the effects of different alcohol moieties in the ester group with a view to further improving the selectivity between primary and secondary esters.

Experimental

Melting points are uncorrected and were determined on a Köfler hot-stage apparatus. Infrared spectra were recorded in chloroform. Proton magnetic resonance (p.m.r.) spectra were determined on Varian Associates HA-100 and A-60 spectrometers in deuteriochloroform with TMS as internal standard. Mass spectra were obtained on a Hitachi Perkin–Elmer RMU-6A spectrom-

Can. J. Chem. Downloaded from www.nrcresearchpress.com by 210.87.254.5 on 09/05/12
For personal use only.

Can. J. Chem. Downloaded from www.nrcresearchpress.com by 210.87.254.5 on 09/05/12
For personal use only.

eter. Carbon and hydrogen analyses were determined by Spang Microanalytical Laboratories, Ann Arbor, Michigan.

The sodium trimethoxyborohydride used in these experiments was obtained from Alfa Inorganics Inc., Beverly, Massachusetts.

4α,10-Dimethyl-4β-carbomethoxy-8α-carboxy-decahydro-9-naphthaleneacetic Acid 2a

The α,β-unsaturated ketone **1** (3) (1.00 g (3.45 mmoles)) m.p. 124–126°, was dissolved in 25 ml of dry ethyl acetate and oxygen containing ca. 2% ozone (Welsbach T-408 ozonizer) was passed through the solution at 0° for 30 min. After removal of excess ozone with a stream of nitrogen the solvent was removed *in vacuo* at 40°. To the residue were added 30 ml of acetic acid, 20 ml of 30% hydrogen peroxide, and 10 drops of concentrated hydrochloric acid and the mixture stirred at room temperature overnight and then heated for 1.5 h on the steam bath. The product was taken up in benzene, washed thoroughly with water, then with three 50 ml portions of saturated sodium carbonate solution, and finally once with 50 ml of water. The combined alkaline washings were acidified to pH 1 with 2 *N* sulfuric acid and extracted with benzene. The washed and dried (anhydrous sodium sulfate) benzene extract was evaporated *in vacuo* to give 0.90 g (80%) of **2a** as an oil which crystallized slowly on standing. Recrystallization from hexane – ethyl acetate (4:1) gave the diacid as colorless needles m.p. 182–184°; i.r. ν_{max}, 3500–2500 (COOH), 1730–1700 cm^{-1} (>CO, $COOCH_3$ and COOH); p.m.r. δ, 0.66 (s, 3H, C-14 CH_3); 1.20 (s, 3H, C-16 CH_3); 3.66 (s, 3H, $COOCH_3$); 10.5–11.5 p.p.m. (broad, 2H, COOH).

Anal. Calcd. for $C_{17}H_{26}O_6$: C, 62.56; H, 8.03. Found: C, 62.64; H, 8.11.

Methyl 4α,10-Dimethyl-14β,8α-dicarbomethoxy-decahydro-9-naphthalene-acetate 2b

Methylation of the diacid **2a** was carried out by the addition of a freshly prepared solution of diazomethane in ether to a stirred solution of 0.650 g (2 mmoles) of **2a** in ether–methanol at room temperature. Evaporation of the solvent *in vacuo* afforded 0.705 g (99–100%) of the crystalline triester **2b**. Recrystallization from hexane – ethyl acetate (9:1) yielded **2b** as colorless prisms m.p. 91.5–92.5°; i.r. ν_{max} 1740 (C-12 $COOCH_3$), 1735 (C-13 $COOCH_3$), 1725 (C-15 $COOCH_3$), 1220, and 1165 cm^{-1} (O—CH_3); p.m.r. δ, 0.59 (s, 3H, C-14 CH_3); 1.13 (s, 3H, C-16 CH_3), 3.53 (s, 3H, C-15 $COOCH_3$), 3.50 (s, 3H, C-13 $COOCH_3$), and 3.48 p.p.m. (s, 3H, C-12 $COOCH_3$); mol. wt. 354 (mass spectrum).

Anal. Calcd. for $C_{19}H_{30}O_6$: C, 64.38; H, 8.53. Found: C, 64.44; H, 8.11.

4α,10-Dimethyl-4β,8α-dicarbomethoxy-decahydro-9-naphthaleneacetic Acid 2c

To a sample of 1.00 g (2.83 mmoles) of triester **2b** (m.p. 89–91°) dissolved in 32 ml of methanol were added 2.85 ml of 1 *N* sodium hydroxide and 57.0 ml water (making the total solution 0.05 *N* in sodium hydroxide). The mixture was refluxed with stirring under nitrogen for 3.5 h. After removal of the majority of methanol *in vacuo*, the aqueous residue was washed with ether (3 × 50 ml) and the ethereal washings counterwashed with 50 ml of water. The aqueous phases were then combined and acidified to pH 1 with 2 *N* sulfuric acid and extracted with benzene. The benzene layer was washed with water, dried with anhydrous sodium sulfate, and after evaporation *in vacuo* yielded 875 mg (91%) of **2c** as an oil which crystallized on standing. Recrystallization from hexane – ethyl acetate (9:1) gave **2c** as colorless plates m.p. 138–139°; i.r. ν_{max} 3600–2600 (COOH), 1735 ($COOCH_3$), 1715 (COOH), 1220 and 1165 cm^{-1} (O—CH_3, CH_2—O); p.m.r. δ, 0.63 (s, 3H, C-14 CH_3), 1.16 (s, 3H, C-16 CH_3), 3.57 (s, 3H, C-15 $COOCH_3$), 3.54 (s, 3H, C-13 $COOCH_3$), 11.32 p.p.m. (broad, 1H, COOH).

Anal. Calcd. for $C_{18}H_{28}O_6$: C, 63.51; H, 8.29. Found: C, 63.54; H, 8.21.

Work-up of the neutral ether washings yielded 90 mg of crystalline unchanged starting material **2b**.

4α,10-Dimethyl-4β-carbomethoxy-8α-hydroxymethylene-decahydro-9-naphthaleneacetic Acid 3

A solution of 0.500 g (1.47 mmoles) of diester-acid **2c** in 50 ml dimethoxyethane (freshly distilled from calcium hydride) was added dropwise to 2.25 g (5.85 mmoles) of sodium trimethoxyborohydride in a 200 ml flask under a nitrogen atmosphere. After a short period of frothing and hydrogen evolution, the mixture was stirred and brought to reflux for 75 min. After cooling, the reaction mixture was poured into cold water, acidified with 2 *N* sulfuric acid and the liberated product extracted with benzene. The benzene extracts after washing with water, brine and drying (anhydrous sodium sulfate) afforded on evaporation *in vacuo* 0.45 g (98%) of crystalline hydroxy-acid **3**. However, recrystallization from hexane – ethyl acetate yielded colorless plates m.p. 136–137° which were found to be the δ-lactone of **3**. The impure crystalline **3** showed: i.r. ν_{max} 3600–2550 (COOH), 1730 ($COOCH_3$), 1720 cm^{-1} (COOH); p.m.r. δ, 0.68 (s, 3H, C-14 CH_3), 1.18 (s, 3H, C-16 CH_3), 3.64 (s, 3H, $COOCH_3$), 3.75 and 4.28 (m, 2H, AB part of an ABX, J_{AB} = 11 Hz, J_{BX} = 10 Hz, and J_{AX} = 5 Hz; C-13 CH_2), 8.70 p.p.m. (broad, 2H, COOH and OH). It was not possible to recrystallize **3** even from cold, nonpolar solvents without the loss of water and quantitative formation of the δ-lactone. The lactone showed: m.p. 136–137°; i.r. ν_{max} 1730 ($COOCH_3$), and 1725 cm^{-1} (δ-lactone); p.m.r. δ, 0.675 (s, 3H, C-14 CH_3), 1.16 (s, 3H, C-16 CH_3), 3.72 (s, 3H, $COOCH_3$), 3.66 and 4.20 (m, 2H, AB part of an ABX, J_{AB} = 11 Hz, J_{AX} = 5 Hz, and J_{BX} = 11 Hz; C-13 CH_2); mol. wt. 294 (mass spectrum).

Anal. Calcd. for $C_{17}H_{26}O_4$: C, 69.36, H, 8.90. Found: C, 69.38; H, 8.83.

The similarity in coupling constants for the ABX system formed by the C-13 protons (H_A and H_B) and the C-8 proton (H_X) for the δ-lactone and hydroxy-acid **3** suggests, not unexpectedly, that the hydroxyl group of **3** hydrogen bonds with the carboxyl and that **3** adopts a conformation very similar to that of the δ-lactone.

Reduction of Methyl Esters

The same procedure was followed for the three esters, methyl 3-phenylpropionate, methyl cyclohexylcarboxylate, and methyl abietate **4**.

To a solution of 5.0 mmoles of an ester in 50 ml of dimethoxyethane were added 20 mmoles of sodium trimethoxyborohydride and the mixture stirred under reflux under a nitrogen atmosphere. Five millilitre aliquots of the reaction mixture were withdrawn at appropriate times, quenched in dilute acid and examined by p.m.r. spectroscopy for the extent of reduction. In all three cases it was possible to observe the rate of disappearance of the ester group by integrating the area under the ester methyl absorption and comparing it with the area under absorptions arising from protons common to both the starting ester and the alcohol products. The results are shown in Table I. The 3,5-dinitrobenzoate derivatives of the products were prepared in the usual way and gave satisfactory melting points. The p.m.r. spectra of the products were consistent with expected alcohols.

Acknowledgments

We wish to thank the National Research Council of Canada and the Ontario Department of University Affairs for financial support of this work and the award of a Fellowship to M. B. Gravestock by the National Research Council of Canada.

1. H. C. Brown and E. J. Mead. J. Am. Chem. Soc. **75**, 6263 (1953).
2. E. Schenker. Angew. Chem. **73**, 81 (1961), and references therein.
3. R. H. Bible and R. R. Burtner. J. Org. Chem. **26**, 1174 (1961).
4. L. A. Paquette and N. A. Nelson. J. Org. Chem. **27**, 2272 (1962).
5. C. K. Ingold and F. R. Shaw. J. Chem. Soc. 2918 (1927).
6. M. S. Brown and H. Rapoport. J. Org. Chem. **28**, 3261 (1963).
7. R. Paul and N. Joseph. Bull. Soc. Chim. France. 758 (1953); R. F. Nystrom, S. W. Chaikin, and W. G. Brown. J. Am. Chem. Soc. **71**, 3245 (1949); H. C. Brown, E. J. Mead, and B. C. Subba Rao. J. Am. Chem. Soc. 77, 6209 (1955).
8. H. C. Brown and R. F. McFarlin. J. Am. Chem. Soc. **80**, 5372 (1958).
9. H. C. Brown and C. J. Shoaf. J. Am. Chem. Soc. **86**, 1079 (1964); H. C. Brown and P. M. Weissman. J. Am. Chem. Soc. **87**, 5614 (1965).
10. G. Hesse and R. Schrödel. Ann. **607**, 24 (1957).

Chemistry of the aminochromes. Part XIII. Some further observations on the reactions of the aminochromes with thioglycollic acid[1,2]

W. Powell[3,4] and R. A. Heacock[5]

Department of Chemistry, Dalhousie University, Halifax, Nova Scotia and Atlantic Regional Laboratory, National Research Council of Canada, Halifax, Nova Scotia

Received September 16, 1968

Thioglycollic acid reacts with adrenochrome in aqueous solution to give 5,6-dihydroxy-1-methylindole and 4-*S*-carboxymethylthio-5,6-dihydroxy-1-methylindole, together with smaller amounts of the lactone obtained by intramolecular cyclization of the latter compound. When the reaction is carried out in the absence of water the relative amount of 5,6-dihydroxy-1-methylindole formed is markedly reduced. At lower temperatures 4-*S*-carboxymethylthio-5,6-dihydroxy-1-methylindole is the main product obtained, whilst at higher temperatures the corresponding lactone predominates.

The major products obtained by the action of thioglycollic acid on 4- and 7-methyladrenochrome in aqueous solution were 5,6-dihydroxy-1,4-dimethylindole and 4-*S*-carboxymethylthio-5,6-dihydroxy-1,7-dimethylindole respectively.

Canadian Journal of Chemistry, 47, 2102 (1969)

The reduction of adrenochrome (**1**) by thioglycollic acid was first reported in 1945 (1). Some years later an examination by paper chromatography of the products formed when this reaction was carried out in aqueous solution at room temperature, indicated that two major products were consistently obtained and that they were accompanied by lesser amounts of two other products (2). The two major products have subsequently been identified as 5,6-dihydroxy-1-methylindole (**2**) and 4-*S*-carboxymethylthio-5,6-dihydroxy-1-methylindole (**3**) (3). Analogous products also appear to be formed by the action of thioglycollic acid on related simple aminochromes (3).

In the past the preliminary examination of

[1]NRCC No. 10533.
[2]Part XII. Can. J. Chem. This issue.
[3]Graduate student, Department of Chemistry, Dalhousie University, Halifax, Nova Scotia.
[4]Holder of an NRCC Bursary.
[5]Reprint requests and general correspondence concerning this paper should be addressed to this author (R.A.H.) at the Atlantic Regional Laboratory, National Research Council of Canada, Halifax, Nova Scotia.

Can. J. Chem. Downloaded from www.nrcresearchpress.com by 210.87.254.5 on 09/05/12
For personal use only.

To a solution of 5.0 mmoles of an ester in 50 ml of dimethoxyethane were added 20 mmoles of sodium trimethoxyborohydride and the mixture stirred under reflux under a nitrogen atmosphere. Five millilitre aliquots of the reaction mixture were withdrawn at appropriate times, quenched in dilute acid and examined by p.m.r. spectroscopy for the extent of reduction. In all three cases it was possible to observe the rate of disappearance of the ester group by integrating the area under the ester methyl absorption and comparing it with the area under absorptions arising from protons common to both the starting ester and the alcohol products. The results are shown in Table I. The 3,5-dinitrobenzoate derivatives of the products were prepared in the usual way and gave satisfactory melting points. The p.m.r. spectra of the products were consistent with expected alcohols.

Acknowledgments

We wish to thank the National Research Council of Canada and the Ontario Department of University Affairs for financial support of this work and the award of a Fellowship to M. B. Gravestock by the National Research Council of Canada.

1. H. C. Brown and E. J. Mead. J. Am. Chem. Soc. **75**, 6263 (1953).
2. E. Schenker. Angew. Chem. **73**, 81 (1961), and references therein.
3. R. H. Bible and R. R. Burtner. J. Org. Chem. **26**, 1174 (1961).
4. L. A. Paquette and N. A. Nelson. J. Org. Chem. **27**, 2272 (1962).
5. C. K. Ingold and F. R. Shaw. J. Chem. Soc. 2918 (1927).
6. M. S. Brown and H. Rapoport. J. Org. Chem. **28**, 3261 (1963).
7. R. Paul and N. Joseph. Bull. Soc. Chim. France. 758 (1953); R. F. Nystrom, S. W. Chaikin, and W. G. Brown. J. Am. Chem. Soc. **71**, 3245 (1949); H. C. Brown, E. J. Mead, and B. C. Subba Rao. J. Am. Chem. Soc. 77, 6209 (1955).
8. H. C. Brown and R. F. McFarlin. J. Am. Chem. Soc. **80**, 5372 (1958).
9. H. C. Brown and C. J. Shoaf. J. Am. Chem. Soc. **86**, 1079 (1964); H. C. Brown and P. M. Weissman. J. Am. Chem. Soc. **87**, 5614 (1965).
10. G. Hesse and R. Schrödel. Ann. **607**, 24 (1957).

Chemistry of the aminochromes. Part XIII. Some further observations on the reactions of the aminochromes with thioglycollic acid[1,2]

W. Powell[3,4] and R. A. Heacock[5]

Department of Chemistry, Dalhousie University, Halifax, Nova Scotia and Atlantic Regional Laboratory, National Research Council of Canada, Halifax, Nova Scotia

Received September 16, 1968

Thioglycollic acid reacts with adrenochrome in aqueous solution to give 5,6-dihydroxy-1-methylindole and 4-*S*-carboxymethylthio-5,6-dihydroxy-1-methylindole, together with smaller amounts of the lactone obtained by intramolecular cyclization of the latter compound. When the reaction is carried out in the absence of water the relative amount of 5,6-dihydroxy-1-methylindole formed is markedly reduced. At lower temperatures 4-*S*-carboxymethylthio-5,6-dihydroxy-1-methylindole is the main product obtained, whilst at higher temperatures the corresponding lactone predominates.

The major products obtained by the action of thioglycollic acid on 4- and 7-methyladrenochrome in aqueous solution were 5,6-dihydroxy-1,4-dimethylindole and 4-*S*-carboxymethylthio-5,6-dihydroxy-1,7-dimethylindole respectively.

Canadian Journal of Chemistry, 47, 2102 (1969)

The reduction of adrenochrome (**1**) by thioglycollic acid was first reported in 1945 (1). Some years later an examination by paper chromatography of the products formed when this reaction was carried out in aqueous solution at room temperature, indicated that two major products were consistently obtained and that they were accompanied by lesser amounts of two other products (2). The two major products have subsequently been identified as 5,6-dihydroxy-1-methylindole (**2**) and 4-*S*-carboxymethylthio-5,6-dihydroxy-1-methylindole (**3**) (3). Analogous products also appear to be formed by the action of thioglycollic acid on related simple aminochromes (3).

In the past the preliminary examination of

[1]NRCC No. 10533.
[2]Part XII. Can. J. Chem. This issue.
[3]Graduate student, Department of Chemistry, Dalhousie University, Halifax, Nova Scotia.
[4]Holder of an NRCC Bursary.
[5]Reprint requests and general correspondence concerning this paper should be addressed to this author (R.A.H.) at the Atlantic Regional Laboratory, National Research Council of Canada, Halifax, Nova Scotia.

Can. J. Chem. Downloaded from www.nrcresearchpress.com by 210.87.254.40 on 09/05/12
For personal use only.

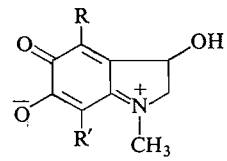

1 R = R′ = H
7 R = H; R′ = CH_3
12 R = CH_3; R′ = H

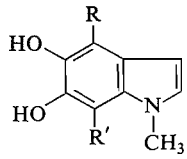

2 R = R′ = H
9 R = H; R′ = CH_3
11 R = CH_3; R′ = H

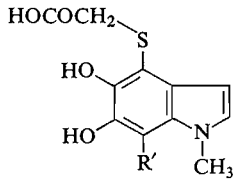

3 R′ = H
6 R′ = CH_3

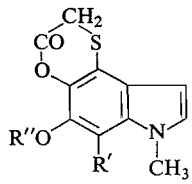

4 R′ = R″ = H
5 R′ = H; R″ = CH_3CO
8 R′ = CH_3; R″ = H
10 R′ = CH_3; R″ = CH_3CO

reaction mixtures, obtained by the action of thiols on aminochromes, has usually been carried out either spectroscopically or chromatographically on paper, with 2% acetic acid in water as running solvent and with descending or radial development. Using the descending technique the products **2** and **3** had R_f values of ca. 0.45 and ca. 0.50 respectively (2, 3). Whilst the chromatographic separation of **2** and **3** was not very good the products could easily be separated on the basis of the solubility of **3** in aqueous sodium bicarbonate. The more important minor product observed in the aqueous adrenochrome – thioglycollic acid reaction mixtures had an R_f value of ca. 0.18 under these conditions (2, 3). On the basis of the previously reported (2,3) color reactions of this product and the fact that it is not soluble in aqueous sodium bicarbonate, it appeared likely that the substance does not contain a carboxylic acid group but contains divalent sulfur, an indole nucleus, and phenolic groups.

It was observed in the course of preliminary chromatographic studies of this and other reactions of adrenochrome (**1**) that thin-layer chromatography (t.l.c.) of these reaction mixtures on cellulose layers was in many ways superior to paper chromatography, giving faster and in many cases better separations of the products. Consequently t.l.c. on cellulose layers using 2% acetic acid in water was used exclusively in this investigation.

The reaction between adrenochrome and thioglycollic acid has been studied under a variety of conditions including (*a*) reaction in aqueous solution at room temperature, (*b*) reaction under anhydrous conditions (i.e. in the absence of solvent) at room temperature, and (*c*) reaction under anhydrous conditions at 120°. The products were separated on cellulose layers using 2% acetic acid in water as running solvent.

In the first case the chromatographic picture was, as would have been expected, essentially the same as that previously observed (2, 3). The two main products detected were **2** and **3** with R_f values of 0.45 and 0.49 respectively. In order to observe the products clearly it was necessary to effect a preliminary separation of the reaction mixture on the basis of the solubility of **3** in aqueous sodium bicarbonate. The minor product, which was insoluble in aqueous sodium bicarbonate, and which had an R_f value of ca. 0.13 in this system was also observed as a fairly intense spot.

When the reaction was carried out under anhydrous conditions, however, the relative amounts of the products formed were quite different; the amount of 5,6-dihydroxy-1-methylindole (**2**) formed was considerably less and the relative amounts of 4-*S*-carboxymethylthio-5,6-dihydroxy-1-methylindole (**3**) and the unknown (R_f, 0.13) considerably increased. At room temperature significant amounts of **3** were present but when the reaction was carried out at elevated temperatures and for longer periods (i.e. at 120° for 3 h) the product R_f, 0.13 was the only major product observed. A more extensive survey of the color reactions of this compound suggested that, together with an indole nucleus (positive reactions with Ehrlich's reagent, cinnamaldehyde, and *p*-*N*,*N*-bis(2-chloroethyl)-aminobenzaldehyde) and divalent sulfur (positive reaction with the alkaline sodium nitroprusside reagent (cf. 4)), it contained a monophenolic hydroxyl group rather than the catechol system. Positive reactions for a phenolic hydroxyl group were obtained with ferric chloride, the Folin–Ciocalteu reagent, and Gibb's phenol reagent. A strongly positive reaction was obtained with the 4-aminoantipyrene reagent only after overspraying with potassium ferricyanide, suggesting that a monophenolic hydroxyl rather than an *o*-diphenol group was present in the molecule (cf. 5). All the evidence available at this point

Can. J. Chem. Downloaded from www.nrcresearchpress.com by 210.87.254.40 on 09/05/12
For personal use only.

TABLE I

Thin-layer chromatography* of the ether soluble products obtained in the reaction of adrenochrome with thioglycollic acid

Extract	R_f values and intensities of main spots†	Colors with chromogenic reagents‡								
		F_1	Ehr.	Cinn.	NaNP	F–C	$FeCl_3$	4AA	4AA[o]	Gib.
A	0.13 (s)§	B→V	B	R→V	G→GyG	Gy	Gy	Gy	Br	Br
	0.45 (w)	V	BV	OrBr→VBr	—	Gy	GyV	RBr	RBr	VBr
B	0.48 (s)	V	BV	OrR→GyV	BG→Bg	Gy	GyG	OrBr	OrBr	OrBr
C	0.13 (s)	B→V	B	R→V	G→GyG	Gy	Gy	Gy	Br	Br
D	0.48 (w)	V	BV	OrR→GyV	BG→Bg	Gy	GyG	OrBr	OrBr	OrBr
E	0.13 (m)	B→V	B	R→V	G→GyG	Gy	Gy	Gy	Br	Br
	0.45 (s)	V	BV	OrBr→VBr	—	Gy	GyV	RBr	RBr	VBr
F	0.48 (s)	V	BV	OrR→GyV	BG→Bg	Gy	GyG	OrBr	OrBr	OrBr

*Ascending development with 2% acetic acid in water on Eastman "Chromagram" cellulose sheets (20 × 20 cm).
†A spot R_f, 0.85 due to excess thioglycollic acid was also invariably observed in the acid extracts.
‡*Reagents*: F_1 = *p*-*N*,*N*-bis(2-chloroethyl)aminobenzaldehyde (Frinton Laboratories); Ehr. = Ehrlich's reagent; Cinn. = cinnamaldehyde; NaNP = sodium nitroprusside (6); F–C = Folin and Ciocalteu's reagent; $FeCl_3$ = 1% aqueous ferric chloride; 4AA = 4-aminoantipyrene (7); 4AA[o] = 4-aminoantipyrene followed by overspray with 1% aqueous potassium ferricyanide; Gib. = Gibb's reagent. *Colors*: B = Blue; BV = Blue-violet; V = Violet; GyV = Grey-violet; VBr = Violet-brown; OrBr = Orange-brown; OrR = Orange-red; R = Red; G = Green; GyG = Grey-green; BG = Blue-green; Bg = Biege; Gy = Grey.
§s, strong; m, medium; w, weak.

suggested that this product was the lactone **4** derived from 4-*S*-carboxymethylthio-5,6-dihydroxy-1-methylindole (**3**). This was confirmed by the isolation of the crystalline monoacetyl derivative of **4**, i.e. 6-acetoxy-4-*S*-carboxymethylthio-5-hydroxy-1-methylindole lactone (**5**). This product was identical in all respects to samples of **5** previously prepared by the treatment of **3** directly with acetic anhydride and pyridine (3).

An analogous lactone described as hydroquinone α-thioacetic acid lactone was obtained several years previously by Snell and Weissberger (6) when the crude products obtained by the action of thioglycollic acid on *p*-benzoquinone were either allowed to stand in a vacuum desiccator over phosphorous pentoxide or were heated to 150°.

The present investigation has confirmed previously reported preliminary results (3) which suggested that in general, thiols react with 4-alkyl substituted aminochromes to give only one significant product, namely the corresponding 4-alkyl-5,6-dihydroxyindole, whereas 7-alkyl substituted aminochromes give mainly the 7-alkyl-4-*S*-carboxymethylthio-5,6-dihydroxyindole derivative. 4-*S*-Carboxymethylthio-5,6-dihydroxy-1,7-dimethylindole (**6**) was the main product obtained by the action of thioglycollic acid on 7-methyladrenochrome (**7**) in aqueous solution. A smaller, but significant quantity of the corresponding lactone (i.e. **8**) was also formed at the same time; however, only minute amounts of a third product, which was probably 5,6-dihydroxy-1,7-dimethylindole (**9**), were detected in the reaction mixtures. The *O*-acetyl derivative (i.e. **10**) of the lactone **8** was isolated as a crystalline solid after treatment of the major product, i.e. 4-*S*-carboxymethylthio-5,6-dihydroxy-1,7-dimethylindole (**6**) with acetic anhydride and pyridine. 5,6-Dihydroxy-1,4-dimethylindole (**11**) was the only significant product formed by reduction of 4-methyladrenochrome (**12**) with thioglycollic acid.

Experimental

A. The Reaction of Adrenochrome with Thioglycollic Acid

Adrenochrome was prepared by the method of Heacock *et al.* (7).

I. Preliminary Reactions

(i) Non-aqueous reactions—Adrenochrome (3 mg) was dissolved in anhydrous thioglycollic acid (ca. 0.5 ml) and the resulting dark yellow-brown solution was divided into two approximately equal parts. After being allowed to stand at room temperature for ca. 1 h, one part of the reaction mixture was poured into water (3 ml) and excess solid sodium bicarbonate added; the reaction mixture was extracted with ether (4 × 2 ml) to remove phenolic but not acidic products (*extract A*). The mother liquors were acidified with 2 *N* hydrochloric acid and extracted with ether (4 × 2 ml) to remove acidic products (*extract B*). The second half of the original reaction mixture was heated on an oil-bath at 120° for 3 h, after which time it was cooled and poured into water (3 ml) and the products worked up in the manner described above, giving ether extracts containing phenolic (*extract C*) and acidic (*extract D*) products.

(ii) Aqueous reaction (cf. 2, 3)—Thioglycollic acid was added dropwise to a solution of adrenochrome (3 mg) in water (1 ml) until the red color of the solution was

Can. J. Chem. Downloaded from www.nrcresearchpress.com by 210.87.254.40 on 09/05/12
For personal use only.

TABLE II

Thin-layer chromatography* of the products obtained by the action of thioglycollic acid on 4- and 7-methyladrenochrome

Aminochrome	R_f values and colors† with the F_1‡ reagent			
4-Methyladrenochrome				
Total reaction mixture		0.39 (s)§		0.85‖
Phenolic products		0.39 (V)		
Acidic products				0.85 (Y)
7-Methyladrenochrome				
Total reaction mixture	0.06 (m)	0.33 (w)	0.40 (s)	0.85
Phenolic products	0.06 (B)	0.33 (B)		
Acidic products			0.40 (V)	0.85 (Y)

*Ascending development with 2% acetic acid in water on Eastman "Chromagram" cellulose sheets (20 × 20 cm).
†V = Violet; B = Blue; Y = Yellow.
‡F_1 = *p*-*N*,*N*-bis(2-chloroethyl)aminobenzaldehyde (Frinton Laboratories).
§s, strong; m, medium; w, weak.
‖The spot (R_f, 0.85), which was of variable intensity, was due to excess thioglycollic acid.

totally discharged. The aqueous reaction mixture was then treated with an excess of sodium bicarbonate and the products worked up in the manner described above to give ether extracts containing phenolic (*extract E*) and acidic (*extract F*) products.

(iii) Chromatography—The extracts *A*–*F* were examined by t.l.c. on cellulose layers (Eastman "Chromagram" sheet, 20 × 20 cm) using 2% acetic acid in water as running solvent. The developed chromatograms were dried and sprayed with several different chromogenic reagents. The results of the chromatographic examination of these extracts are shown in Table I.

*II. Isolation of 6-Acetoxy-4-S-carboxymethylthio-5-hydroxy-1-methylindole Lactone (**5**)*

A solution of adrenochrome (0.5 g) in thioglycollic acid (15 ml) was heated on an oil bath at 120° for 3 h. After cooling, the reaction mixture was poured into saturated aqueous sodium bicarbonate solution (200 ml) and the resulting suspension was extracted with ether (3 × 250 ml). A mixture of acetic anhydride (2.5 ml) and dry pyridine (2.5 ml) was added to the combined, dried (Na_2SO_4), ether extracts and the reaction mixture allowed to stand at room temperature overnight. After removal of the ether *in vacuo* the concentrated acetylation mixture was poured slowly, with stirring, into ice–water (250 ml). The pale-yellow gummy solid which was obtained was dissolved in benzene and purified chromatographically on a short silica gel[6] column (1.8 × 10 cm) with adsorption from and elution with benzene. The crude solid obtained on concentration of the benzene eluant gave 6-acetoxy-4-*S*-carboxymethylthio-5-hydroxy-1-methylindole lactone as colorless needles (125 mg; m.p. 156–159°). The identity of this product with samples of **5**, previously prepared, was established by the non-depression of m.p. and by the identity of their infrared and nuclear magnetic resonance spectra (cf. ref. 3).

Anal. Calcd. for $C_{13}H_{11}NO_4S$: C, 56.30; H, 4.00; N, 5.05; S, 11.57. Found: C, 56.69; H, 3.98; N, 5.07; S, 11.69.

[6]Malinckrodt "SilicaR" (100–200 mesh size) silica gel was used throughout this investigation.

B. The Reactions of 4- and 7-Methyladrenochrome with Thioglycollic Acid

4-Methyladrenochrome (**12**) and 7-methyladrenochrome (7) were prepared by the method of Heacock and Hutzinger (8).

I. Preliminary Reactions (cf. 2,3)

Thioglycollic acid was added dropwise to the aqueous aminochrome solution (2 mg/ml) until no further color changes occurred. The aqueous reaction mixtures were then treated with an excess of solid sodium bicarbonate and the products worked up in the manner described above for the reactions involving adrenochrome to give phenolic and acidic extracts.

The various extracts were examined by t.l.c. using the procedure described above. The results of the chromatographic investigations are given in Table II.

*II. Isolation of 6-Acetoxy-4-S-carboxymethylthio-5-hydroxy-1,7-dimethylindole Lactone (**10**)*

Thioglycollic acid (0.5 ml) was added, dropwise with stirring, to a solution of 7-methyladrenochrome (300 mg, prepared by the method of Heacock and Hutzinger (8)). The reaction mixture was stirred at room temperature for a further few minutes, after which time excess solid sodium bicarbonate was added. The neutralized reaction mixture was immediately extracted with peroxide-free ether (5 × 100 ml), cautiously acidified with 2 *N* hydrochloric acid, and further extracted with ether (5 × 100 ml). A mixture of acetic anhydride (1.5 ml) and pyridine (1.5 ml) was added to the combined, dried (Na_2SO_4) ether extracts of the acidified reaction mixture. The ethereal acetylation mixture was allowed to stand overnight at room temperature after which time the ether was removed *in vacuo* and the concentrated reaction mixture poured dropwise with stirring into ice–water (150 ml). The crude product, a light green tarry precipitate, was dissolved in benzene and purified chromatographically on a silica gel column (6 × 1.8 cm). The column was eluted with benzene and a series of 25 ml fractions collected. The fractions were monitored by t.l.c. using the F_1[7] reagent. The first three fractions did not react with

[7]See footnote ‡ in Table I.

Can. J. Chem. Downloaded from www.nrcresearchpress.com by 210.87.254.40 on 09/05/12
For personal use only.

this reagent and were discarded; fractions 4–11, which reacted positively with the F_1 reagent were combined and the benzene removed *in vacuo*. Recrystallization of the crude white crystalline solid, so obtained, from light petroleum (b.p. 80–100°) gave 6-acetoxy-4-*S*-carboxymethylthio-5-hydroxy-1,7-dimethylindole lactone (**10**) as white needles (53 mg, m.p. 202–204°). The proton magnetic resonance spectrum of this product in $CDCl_3$ indicated the presence of two C—CH_3 groups at τ 7.62 and 7.45; an S—CH_2— group at τ 6.54; an N—CH_3 group at τ 5.98; the indole β-proton at τ 3.64 ($J_{2,3}$ = 3 Hz); and the indole α-proton at τ 3.03 ($J_{2,3}$ = 3 Hz).

Anal. Calcd. for $C_{14}H_{13}NO_4S$: C, 57.80; H, 4.50; N, 4.81; S, 11.02. Found: C, 57.61; H, 4.36; N, 4.85; S, 10.69.

1. G. N. COHEN. Compt. Rend. **220**, 796 (1945).
2. R. A. HEACOCK and B. D. SCOTT. Can. J. Biochem. Physiol. **37**, 1087 (1959).
3. W. POWELL, R. A. HEACOCK, G. L. MATTOK, and D. L. WILSON. Can. J. Chem. **47**, 467 (1969).
4. D. K. BLACK. J. Chem. Soc. 1123 (1966).
5. T. A. LARUE and E. R. BLAKLEY. Anal. Chem. Acta, **31**, 400 (1964).
6. J. M. SNELL and A. WEISSBERGER. J. Am. Chem. Soc. **61**, 450 (1939).
7. R. A. HEACOCK, C. NERENBERG, and A. N. PAYZA. Can. J. Chem. **36**, 853 (1958).
8. R. A. HEACOCK and O. HUTZINGER. Can. J. Chem. **43**, 2535 (1965).

Coupling reaction between 4-*t*-butyl-*o*-benzoquinone and methyl linoleate

TAKASHI KATO, MAKOTO TANIAI, KAZUYUKI YOKOO, AND JU KUMANOTANI

The Engineering Research Institute, Faculty of Engineering, The University of Tokyo, Bunkyo-ku, Tokyo, Japan

Received January 2, 1969

This is the first report on the dehydrogenation-coupling reaction of an *o*-quinoid compound with a 1,4-diolefinic compound. The reaction of 4-*t*-butyl-*o*-quinone and methyl linoleate has been studied, and the product which has a 1-(2′-hydroxy-4′(or 5′)-*t*-butylphenoxy)-2,4-pentadienyl structure has been separated and identified.

Canadian Journal of Chemistry, 47, 2106 (1969)

Previously we reported that urushiol quinone reacts with the side chain of a triolefinic component of urushiol (3-(8′,11′,13′-pentadecatrienyl)-catechol) during the laccase-catalyzed oxidation process of Japanese lacquer, giving a coupling product with a phenyl ether linkage and a conjugated triene structure (1). As a further example of this type of reaction, we now describe the formation of a coupling product (**1**) in the reaction of 4-*t*-butyl-*o*-quinone with methyl linoleate at room temperature.

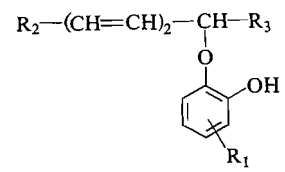

1

R_1 = *t*-butyl attached to 4 or 5 position

$\begin{cases} R_2 = (CH_2)_7—COOCH_3 \\ R_3 = (CH_2)_4—CH_3 \end{cases}$

and/or

$\begin{cases} R_2 = (CH_2)_4—CH_3 \\ R_3 = (CH_2)_7—COOCH_3 \end{cases}$

Concerning the reactions of *o*-quinones with unsaturated hydrocarbons, it is known that a high potential *o*-quinone, e.g., tetrachloro-*o*-quinone, abstracts hydrogen from the latter (2,3). It has been also reported that hydroquinone α-tetralyl ether derivatives were obtained by the reaction between the high potential *p*-quinone derivatives and tetralin (4,5). In those cases, however, an elevated temperature (4) or a radical initiator (5) was required. Therefore, this is the first report on the dehydrogenation-coupling reaction of an *o*-quinone with a 1,4-diene system.

The reaction product (**1**) was separated by thin-layer chromatography (t.l.c.) and identified. The results of the elemental analysis and the molecular weight measurement indicate that the compound is a coupling product between methyl linoleate and 4-*t*-butyl-*o*-quinone. The presence of a hydroxyl group and a benzene nucleus is obvious in view of the finding of the infrared (i.r.) absorptions at 3600–3200 cm^{-1}, and at 1599 and 1510 cm^{-1}, respectively. The conjugated diene structure was identified by the ultraviolet (u.v.) and i.r. absorptions at 234 mμ (ε 27 900) and 991

Can. J. Chem. Downloaded from www.nrcresearchpress.com by 210.87.254.40 on 09/05/12
For personal use only.

this reagent and were discarded; fractions 4–11, which reacted positively with the F_1 reagent were combined and the benzene removed *in vacuo*. Recrystallization of the crude white crystalline solid, so obtained, from light petroleum (b.p. 80–100°) gave 6-acetoxy-4-*S*-carboxymethylthio-5-hydroxy-1,7-dimethylindole lactone (**10**) as white needles (53 mg, m.p. 202–204°). The proton magnetic resonance spectrum of this product in $CDCl_3$ indicated the presence of two C—CH_3 groups at τ 7.62 and 7.45; an S—CH_2— group at τ 6.54; an N—CH_3 group at τ 5.98; the indole β-proton at τ 3.64 ($J_{2,3}$ = 3 Hz); and the indole α-proton at τ 3.03 ($J_{2,3}$ = 3 Hz).

Anal. Calcd. for $C_{14}H_{13}NO_4S$: C, 57.80; H, 4.50; N, 4.81; S, 11.02. Found: C, 57.61; H, 4.36; N, 4.85; S, 10.69.

1. G. N. COHEN. Compt. Rend. **220**, 796 (1945).
2. R. A. HEACOCK and B. D. SCOTT. Can. J. Biochem. Physiol. **37**, 1087 (1959).
3. W. POWELL, R. A. HEACOCK, G. L. MATTOK, and D. L. WILSON. Can. J. Chem. **47**, 467 (1969).
4. D. K. BLACK. J. Chem. Soc. 1123 (1966).
5. T. A. LARUE and E. R. BLAKLEY. Anal. Chem. Acta, **31**, 400 (1964).
6. J. M. SNELL and A. WEISSBERGER. J. Am. Chem. Soc. **61**, 450 (1939).
7. R. A. HEACOCK, C. NERENBERG, and A. N. PAYZA. Can. J. Chem. **36**, 853 (1958).
8. R. A. HEACOCK and O. HUTZINGER. Can. J. Chem. **43**, 2535 (1965).

Coupling reaction between 4-*t*-butyl-*o*-benzoquinone and methyl linoleate

TAKASHI KATO, MAKOTO TANIAI, KAZUYUKI YOKOO, AND JU KUMANOTANI

The Engineering Research Institute, Faculty of Engineering, The University of Tokyo, Bunkyo-ku, Tokyo, Japan

Received January 2, 1969

This is the first report on the dehydrogenation-coupling reaction of an *o*-quinoid compound with a 1,4-diolefinic compound. The reaction of 4-*t*-butyl-*o*-quinone and methyl linoleate has been studied, and the product which has a 1-(2′-hydroxy-4′(or 5′)-*t*-butylphenoxy)-2,4-pentadienyl structure has been separated and identified.

Canadian Journal of Chemistry, 47, 2106 (1969)

Previously we reported that urushiol quinone reacts with the side chain of a triolefinic component of urushiol (3-(8′,11′,13′-pentadecatrienyl)-catechol) during the laccase-catalyzed oxidation process of Japanese lacquer, giving a coupling product with a phenyl ether linkage and a conjugated triene structure (1). As a further example of this type of reaction, we now describe the formation of a coupling product (**1**) in the reaction of 4-*t*-butyl-*o*-quinone with methyl linoleate at room temperature.

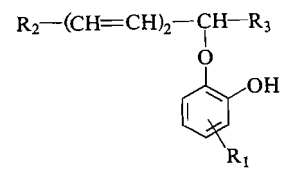

1

R_1 = *t*-butyl attached to 4 or 5 position

$\begin{cases} R_2 = (CH_2)_7—COOCH_3 \\ R_3 = (CH_2)_4—CH_3 \end{cases}$

and/or

$\begin{cases} R_2 = (CH_2)_4—CH_3 \\ R_3 = (CH_2)_7—COOCH_3 \end{cases}$

Concerning the reactions of *o*-quinones with unsaturated hydrocarbons, it is known that a high potential *o*-quinone, e.g., tetrachloro-*o*-quinone, abstracts hydrogen from the latter (2,3). It has been also reported that hydroquinone α-tetralyl ether derivatives were obtained by the reaction between the high potential *p*-quinone derivatives and tetralin (4,5). In those cases, however, an elevated temperature (4) or a radical initiator (5) was required. Therefore, this is the first report on the dehydrogenation-coupling reaction of an *o*-quinone with a 1,4-diene system.

The reaction product (**1**) was separated by thin-layer chromatography (t.l.c.) and identified. The results of the elemental analysis and the molecular weight measurement indicate that the compound is a coupling product between methyl linoleate and 4-*t*-butyl-*o*-quinone. The presence of a hydroxyl group and a benzene nucleus is obvious in view of the finding of the infrared (i.r.) absorptions at 3600–3200 cm^{-1}, and at 1599 and 1510 cm^{-1}, respectively. The conjugated diene structure was identified by the ultraviolet (u.v.) and i.r. absorptions at 234 mμ (ε 27 900) and 991

Can. J. Chem. Downloaded from www.nrcresearchpress.com by 210.87.254.105 on 09/05/12
For personal use only.

Can. J. Chem. Downloaded from www.nrcresearchpress.com by 210.87.254.105 on 09/05/12
For personal use only.

cm^{-1}, respectively. The nuclear magnetic resonance (n.m.r.) signal at τ 5.38 undoubtedly revealed the presence of the phenyl ether linkage by which two reactants were combined in this product (1, 6). Upon hydrogenation over 5% Pd-on-charcoal, this signal was observed to shift to an appreciably higher field at τ 5.73. This indicates that the phenyl ether bond is adjacent to the conjugated diene. Three different signals due to hydroxyl protons at τ 4.2–4.4 observed with the hydrogenated product may be attributed to the isomeric structures of the coupling product. However, the bonding position of the phenyl ether linkage in the olefinic chain and that of *t*-butyl in the benzene ring were not determined in this study.

Experimental

The infrared (i.r.) spectra were obtained with a Nihon-Bunko IR-spectrophotometer, model IR-S. The ultraviolet (u.v.) spectra were taken in ethanol with a Hitachi spectrophotometer, EPS-2. The nuclear magnetic resonance (n.m.r.) spectra were determined in deuteriochloroform at 60 Mc.p.s. with a Nihon-Denshi n.m.r. spectrometer, JMN C-60. The chemical shifts are described in τ values relative to tetramethylsilane as an internal standard. The molecular weights were measured in methyl ethyl ketone with a vapor pressure osmometer, model 301-A, Mechrolab., Inc. The silica gel layers used for thin-layer chromatography (t.l.c.) were made from Silica Rider (silica gel with 12–14% calcium sulfate, purchased from the Daiichi Pure Chemicals), and were activated at 105° for 1.5 h.

Materials

Methyl linoleate (93.8% with 6.2% of methyl oleate by gas–liquid chromatography (g.l.c.) was obtained from safflower oil. 4-*t*-Butyl-*o*-quinone was prepared from 4-*t*-butylcatechol (b.p. 129–131°/3 mm) by the method described in the literature (7).

Isolation of the Coupling Reaction Product between 4-t-Butyl-o-quinone and Methyl Linoleate

Methyl linoleate (7.19 g, 0.0245 mole) and 4-*t*-butyl-*o*-quinone (1.32 g, 0.0081 mole) were reacted at room temperature for 50 h. The reaction mixture was dissolved in *n*-hexane and applied as a spot on the silica gel layer (thickness, 0.25 mm). It was then chromatographed in an *n*-hexane–ether (4:1 v/v) solvent tank using the ascending technique. The developing distance was 12–14 cm. A filter paper (20 × 20 cm) impregnated with the developing solvent was inserted into the tank in order to saturate the atmosphere with the solvent vapor. The chromatogram gave, when sprayed with methanol – 1% $FeCl_3$ solution, the spots with R_f 0.43 (green, main) and 0.14 (dark brown), and the starting spot, and when further sprayed with an aqueous sulfuric acid solution (1:1) and heated at 150° for 30 min, it gave a new spot with R_f 0.60 (methyl linoleate). The compound with R_f 0.43 was collected by t.l.c. in the manner similar to that described previously (1), and a faintly yellow oil (**1**) was obtained (20% based upon the quinone).

Anal. Calcd. for $C_{29}H_{46}O_4$ (mol. wt. 458.7): C, 76.00; H, 10.12. Found (mol. wt. 514): C, 76.09; H, 10.06.

Infrared: ν_{max}(liquid film) 3600–3200 (m), 2930 (vs), 2870 (vs), 1745 (vs), 1657 (w), 1599 (w), 1510 (m), 1461 (m), 1435 (m), 1367 (m), 1279 (s), 1210 (vs), 1174 (s), 1125 (m), 991 (vs), 852 (w), 814 (w), and 727 cm^{-1} (w); u.v.: λ_{max} 234 (ε 27 900) and 283 mμ (3660); n.m.r.: τ 2.8–3.3 (3H, aromatic protons, multiplet), τ 3.3–5.0 (5H, olefinic and hydroxyl protons (1), multiplet), τ 5.38 (1H, phenoxymethine proton (6), broad), τ 6.33 (3H, protons of methyl ester, singlet), and τ 7.5–9.5 (34H, among broad signals were observed sharp signals at τ 8.69 due to methylene protons, τ 8.74 due to *t*-butyl protons and τ 9.13 due to methyl protons).

Hydrogenation of the Coupling Product

The coupling product (309 mg) was hydrogenated in ethyl acetate (10 ml) under an atmospheric pressure of hydrogen over 5% Pd-on-charcoal (51 mg) for 5 h; it absorbed 2.0 moles of hydrogen per mole. By removing the catalyst and the solvent from the reaction mixture the hydrogenated product resulted. It was further purified similarly by t.l.c. and a faintly yellow oil which gave one spot with R_f 0.52 was obtained.

Infrared: ν_{max}(liquid film, 1000–900 cm^{-1}) ca. 1005 cm^{-1} (m); u.v.: λ_{max} 231 (ε 5280, shoulder), and 283 mμ (2150); n.m.r.: τ 2.9–3.4 (3H, aromatic protons, quasi-triplet), τ 4.2–4.4 (1H, hydroxyl proton, quasi-triplet), τ 5.73 (1H, phenoxymethine proton, broad), τ 6.33 (3H, protons of methyl ester, singlet), τ 7.70 (2H, protons of the methylene adjacent to carbonyl, triplet, $J = 7$ c.p.s.), τ 8.0–9.0 (37H, methylene protons, signals were centered at τ 8.73), and τ 9.13 (3H, methyl protons, triplet, $J = 5$ c.p.s.).

Acknowledgment

The authors wish to express their gratitude to Dr. K. Yoshitomi (the Nisshin Oil Mills Ltd.) for the supply of methyl linoleate used in this study.

1. T. Kato and J. Kumanotani. J. Polymer Sci. Part A-1. To be published.
2. L. M. Jackman and D. T. Thompson. J. Chem. Soc. 4794 (1961).
3. N. N. Stefanovskaya, I. F. Gavrilenko, I. N. Markevich, V. L. Shmonina, E. I. Tinyakova, and B. A. Dolgoplosk. Izv. Akad. Nauk SSSR, Ser. Khim. 2355 (1967).
4. R. Criegee. Ber. **69**, 2758 (1936).
5. D. Koike. Nippon Kagaku Zasshi, **77**, 1051 (1956).
6. R. M. Silverstein and G. C. Bassler. Spectrometric identification of organic compounds. John Wiley and Sons, Inc., New York. 1967. p. 136.
7. S. Goldschmidt and F. Graef. Ber. **61**, 1858 (1928).

Mass spectral fragmentation of some bicyclic diketals. Evidence for ethylenedioxycarbene

GORDON WOOD AND E. P. WOO[1]
Department of Chemistry, University of Windsor, Windsor, Ontario
Received September 24, 1968

Some evidence is presented for a novel mass spectral fragmentation of certain bicyclic diketals.
Canadian Journal of Chemistry, 47, 2108 (1969)

Can. J. Chem. Downloaded from www.nrcresearchpress.com by 210.87.254.105 on 09/05/12
For personal use only.

In connection with the preparation and study of some bicyclic analogues of cyclohexane-1,4-dione (1) we had mass spectra of several intermediates determined.[2] We wish to report here some evidence for the loss of ethylenedioxycarbene (or its equivalent) as an important mode of fragmentation for diketals **1**, **2**, and **3**.

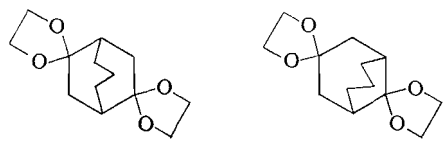

1 **2**

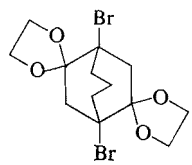

3

Table I lists the most abundant peaks of **1** and **2**, and selected peaks from **3**. It can be seen that both **1** and **2** show characteristic ketal peaks (2) at *m/e* 99 (base), 112, 125 etc. In addition, both show a significant peak at *m/e* 168. This peak corresponds to *P*-72 and if this peak arises directly from fragmentation of the parent, a metastable peak at *m/e* 117.6 would be anticipated. In both cases a metastable ion near *m/e* 118 is found.

Although considerable study has been done of mass spectral fragmentation of ketals (2–6), and the usefulness of these derivatives has been pointed out (3, 5, 6), to our knowledge mass spectral fragmentation involving the loss of a neutral species equivalent to ethylenedioxycarbene has not previously been observed.[3] We tentatively conclude that expulsion of the carbene may require a second ketal group or other functionality suitably located.[4]

TABLE I
Mass spectra of some bicyclic diketals

	Relative abundance*		
m/e	**1**	**2**	**3**
28	8.3	38.7	
41	19.9	17.0	
43	9.3	10.7	
45	5.5	10.1	
55	29.4	32.2	
86	33.1	17.0	
99	100 (base)	100 (base)	11.8
100	11.0	17.0	
112	8.3	18.0	8.0
113	12.4	37.4	61.5
125	35.9	24.1	17.3
139	4.1	22.2	
153	2.4	18.0	
168	13.4	15.8	
195	3.3	10.6	
240	13.4	10.0	
241	2.4	1.7	
245			100 (base)
247			98.0
317			88.5
319			86.0

*For **1** and **2** all ions of relative abundance 10% or greater in one of them are tabulated. For **3**, only selected ions are shown.

One rationale for the process does place positive charge on oxygen in the remaining ketal moiety.

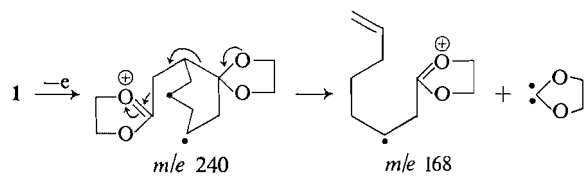

[1]Holder of a Province of Ontario Fellowship 1965–1968. Present address: Department of Chemistry, University College, London, England.
[2]Mass spectra were determined by Morgan Schaffer Corporation, Montreal.
[3]Some evidence for formation of this carbene and related species from thermal decomposition has been presented (7).
[4]The mass spectra of diketals in ref. 4 show no evidence of this process.

A mechanism may be drawn for **2** with the same structure for the *m/e* 168 ion. However, the substantial difference in the relative abundances of the ions between *m/e* 99 and *m/e* 168 suggests that a different *m/e* 168 ion may be involved.

Compound **3** yields an extremely rich spectrum in which the characteristic ketal peaks (*m/e* 99, etc.) are relatively weak. The strong peaks at *m/e* 317, 319 represent a monobromo species which differs from the parent (*P* = 396, 398, 400) only in the loss of one bromine atom. The

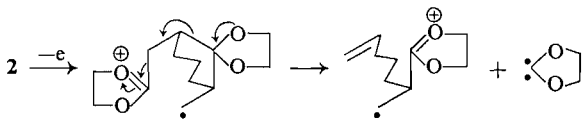

m/e 240 *m/e* 168

presence of a similar doublet at *m/e* 245, 247 and the broad metastable ion centered at *m/e* 190.5 (calcd. *m/e* 189.3 and 191.3) provides some evidence that loss of the ethylenedioxycarbene is involved here as well. Note that here the *m/e* 245 peak is the base peak.

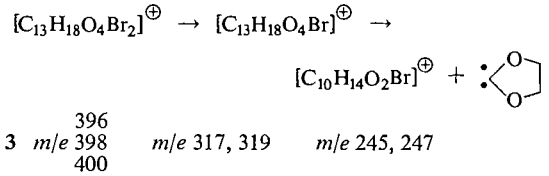

3 *m/e* 396, 398, 400 *m/e* 317, 319 *m/e* 245, 247

Acknowledgment

Financial support of this work by the National Research Council of Canada is gratefully acknowledged.

1. Gordon Wood and E. P. Woo. Can. J. Chem. **46**, 3713 (1968).
2. H. Audier, A. Diara, M. de J. Durazo, M. Fétizon, P. Foy, and W. Vetter. Bull. Soc. Chim. France, 2827 (1963).
3. Z. Pelah, D. H. Williams, H. Budzikiewicz, and C. Djerassi. J. Am. Chem. Soc. **86**, 3722 (1964).
4. H. Audier, J. Bottin, A. Diara, M. Fétizon, P. Foy, M Golfier, and W. Vetter. Bull. Soc. Chim. France, 2292 (1964).
5. H. Audier, M. Fétizon, J-C. Gramain, J. Schalbar, and B. Waegel. Bull. Soc. Chim. France, 1880 (1964).
6. H. Audier, M. Fétizon, and J-C. Gramain. Bull. Soc. Chim. France, 3088 (1965).
7. D. M. Lemal, E. P. Gosselink, and S. D. McGregor. J. Am. Chem. Soc. **88**, 582 (1966).

Structure and reactivity of the mono-oxime of 2,6-dimethoxy-1,4-benzoquinone

H. I. Bolker and F. L. Kung[1]

Department of Chemistry, McGill University, Montreal, Quebec and Organic Chemistry Division, Pulp and Paper Research Institute of Canada, Montreal, Quebec

Received August 9, 1968

Reaction of 2,6-dimethoxy-1,4-benzoquinone with hydroxylamine yielded 2,6-dimethoxy-4-oximino-2,5-cyclohexadienone-1 (**3**), as confirmed by spectroscopic analysis, and by independent synthesis from 5-nitro-1,2,3-trimethoxybenzene. Infrared and proton magnetic resonance spectra in solution showed no significant proportion of the tautomeric nitrosophenolic form of **3**. When **3** was heated for 3 min at 90–95° in 1.0 *N* HCl in $H_2{}^{18}O$, the N—OH group was stable, but the keto oxygen underwent complete exchange. Mass spectra of **3**, its ^{18}O- and deuterium-substituted derivatives indicated that a major process leading to fragmentation upon electron impact was loss of oxygen from N—OH to form the corresponding quinone imine.

Canadian Journal of Chemistry, 47, 2109 (1969)

In research aimed at elucidating the mechanism whereby 2,6-dimethoxy-1,4-benzoquinone (**1**) is formed by the action of nitrous acid on 1,2,3-trimethoxybenzene, we have found (1) that 2,6-dimethoxy-4-oximino-2,5-cyclohexadienone-1 (2,6-dimethoxy-1,4-benzoquinone-4-oxime) (**3**), a compound unknown until now, is an intermediate. Its relevance to current studies on the keto–enol equilibrium of nitrosophenols (2), and our findings concerning the exchangeability of its oxygen, have prompted separate publication of this part of the work.

Unsubstituted *p*-nitrosophenol is known to exchange 82% of one oxygen after only 5 min at

[1]From the Doctoral Thesis of F.L.K.; present address: College of Forestry, Syracuse University, Syracuse, New York.

Can. J. Chem. Downloaded from www.nrcresearchpress.com by 210.87.254.105 on 09/05/12
For personal use only.

A mechanism may be drawn for **2** with the same structure for the *m/e* 168 ion. However, the substantial difference in the relative abundances of the ions between *m/e* 99 and *m/e* 168 suggests that a different *m/e* 168 ion may be involved.

Compound **3** yields an extremely rich spectrum in which the characteristic ketal peaks (*m/e* 99, etc.) are relatively weak. The strong peaks at *m/e* 317, 319 represent a monobromo species which differs from the parent (*P* = 396, 398, 400) only in the loss of one bromine atom. The

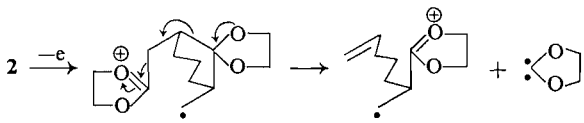

m/e 240 *m/e* 168

presence of a similar doublet at *m/e* 245, 247 and the broad metastable ion centered at *m/e* 190.5 (calcd. *m/e* 189.3 and 191.3) provides some evidence that loss of the ethylenedioxycarbene is involved here as well. Note that here the *m/e* 245 peak is the base peak.

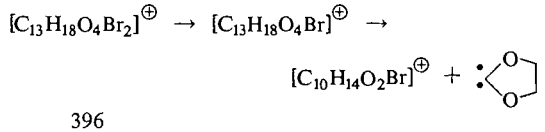

3 *m/e* 396, 398, 400 *m/e* 317, 319 *m/e* 245, 247

Acknowledgment

Financial support of this work by the National Research Council of Canada is gratefully acknowledged.

1. Gordon Wood and E. P. Woo. Can. J. Chem. **46**, 3713 (1968).
2. H. Audier, A. Diara, M. de J. Durazo, M. Fétizon, P. Foy, and W. Vetter. Bull. Soc. Chim. France, 2827 (1963).
3. Z. Pelah, D. H. Williams, H. Budzikiewicz, and C. Djerassi. J. Am. Chem. Soc. **86**, 3722 (1964).
4. H. Audier, J. Bottin, A. Diara, M. Fétizon, P. Foy, M Golfier, and W. Vetter. Bull. Soc. Chim. France, 2292 (1964).
5. H. Audier, M. Fétizon, J-C. Gramain, J. Schalbar, and B. Waegel. Bull. Soc. Chim. France, 1880 (1964).
6. H. Audier, M. Fétizon, and J-C. Gramain. Bull. Soc. Chim. France, 3088 (1965).
7. D. M. Lemal, E. P. Gosselink, and S. D. McGregor. J. Am. Chem. Soc. **88**, 582 (1966).

Structure and reactivity of the mono-oxime of 2,6-dimethoxy-1,4-benzoquinone

H. I. Bolker and F. L. Kung[1]

Department of Chemistry, McGill University, Montreal, Quebec and Organic Chemistry Division, Pulp and Paper Research Institute of Canada, Montreal, Quebec

Received August 9, 1968

Reaction of 2,6-dimethoxy-1,4-benzoquinone with hydroxylamine yielded 2,6-dimethoxy-4-oximino-2,5-cyclohexadienone-1 (**3**), as confirmed by spectroscopic analysis, and by independent synthesis from 5-nitro-1,2,3-trimethoxybenzene. Infrared and proton magnetic resonance spectra in solution showed no significant proportion of the tautomeric nitrosophenolic form of **3**. When **3** was heated for 3 min at 90–95° in 1.0 *N* HCl in $H_2{}^{18}O$, the N—OH group was stable, but the keto oxygen underwent complete exchange. Mass spectra of **3**, its ^{18}O- and deuterium-substituted derivatives indicated that a major process leading to fragmentation upon electron impact was loss of oxygen from N—OH to form the corresponding quinone imine.

Canadian Journal of Chemistry, 47, 2109 (1969)

In research aimed at elucidating the mechanism whereby 2,6-dimethoxy-1,4-benzoquinone (**1**) is formed by the action of nitrous acid on 1,2,3-trimethoxybenzene, we have found (1) that 2,6-dimethoxy-4-oximino-2,5-cyclohexadienone-1 (2,6-dimethoxy-1,4-benzoquinone-4-oxime) (**3**), a compound unknown until now, is an intermediate. Its relevance to current studies on the keto–enol equilibrium of nitrosophenols (2), and our findings concerning the exchangeability of its oxygen, have prompted separate publication of this part of the work.

Unsubstituted *p*-nitrosophenol is known to exchange 82% of one oxygen after only 5 min at

[1]From the Doctoral Thesis of F.L.K.; present address: College of Forestry, Syracuse University, Syracuse, New York.

Can. J. Chem. Downloaded from www.nrcresearchpress.com by 210.87.254.5 on 09/05/12
For personal use only.

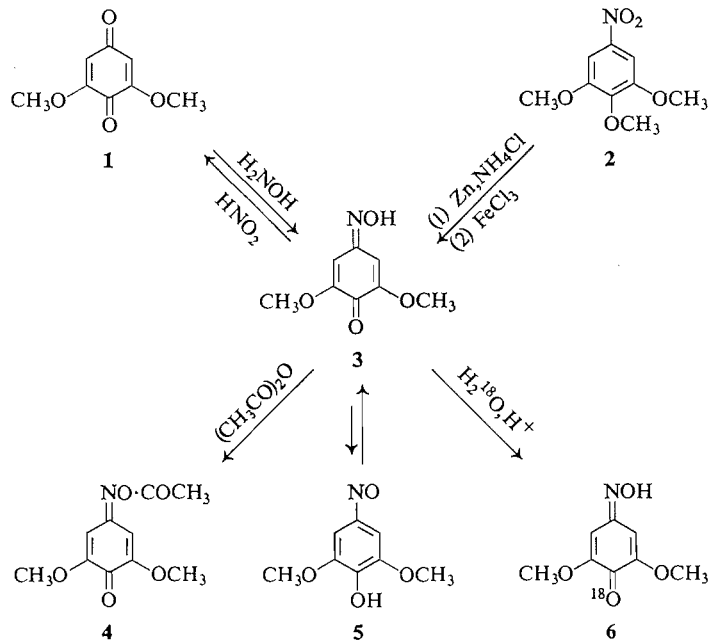

100° in 0.2 *N* alcoholic hydrogen chloride, and 1-nitroso-2-naphthol exchanges 84% in 5 min at 80° in the same solvent (3). However, the existence of the tautomeric keto-oximes has complicated interpretation of these reactions by suggesting that two exchangeable oxygens could be present. Nevertheless, it is proposed that only the carbonyl group of the keto-oxime is exchanged (3,4). In the present work, application of mass spectroscopy to compound **3** and its derivatives has produced evidence to support the original proposal.

The Structure of the Oxime (3)

Although the product **3** obtained by treating **1** with hydroxylamine in pyridine (5) was clearly a monoxime, an alternative synthesis (6) from 5-nitro-1,2,3-trimethoxybenzene (**2**) proved that the oximino group had been introduced in position-4, and not position-1. The products of the two reactions were identical in all respects, and, on acetylation, yielded the same acetate (**4**).

The proton magnetic resonance (p.m.r.) spectrum of **3** in deuteriodimethylsulfoxide showed the expected singlet at δ 3.58 corresponding to the 6 hydrogens of the methoxyl groups, and another singlet at δ 12.62 (eliminated on deuteration) due to a single hydroxyl proton. However, neither the spectrum of **3** in pure deuteriodimethylsulfoxide nor that in deuteriodimethylsulfoxide containing 50% D_2O exhibited any trace of the single peak which might have been expected to arise from the two identical phenyl ring protons of the tautomeric nitrosophenol (**5**). Rather, spectra of the compound in both solvents had a doublet at δ 6.30 and δ 6.64, corresponding to two phenyl ring protons with $J_{3,5} = 1.5$ c.p.s. This AB pattern suggests that the protons at positions-3 and -5 are not equivalent, undoubtedly because of the rigidity and non-linearity of the C=N—O group on position-4. Hence, even in aqueous solution, the oxime form of **3** is overwhelmingly predominant, as would be predicted from the literature already cited (2).

The oxime **3**, treated with nitrous acid, produced no 2,6-dimethoxy-4-nitrophenol but only 2,6-dimethoxy-1,4-benzoquinone (**1**) in 98% yield. In contrast, treatment of 2-methoxy-4-nitrosophenol with nitrous acid gave rise to the corresponding nitro compound (although it forms an oxime acetate upon acetylation (7)). In general, most other quinone monoximes (or *p*-nitrosophenols) are reported to exhibit reactions of both tautomers (2*c*, 8). In this respect the behavior of **3** is unusual.

Interpretation of Mass Spectra

From the mass spectra of **3** (Fig. 1) and

Can. J. Chem. Downloaded from www.nrcresearchpress.com by 210.87.254.5 on 09/05/12
For personal use only.

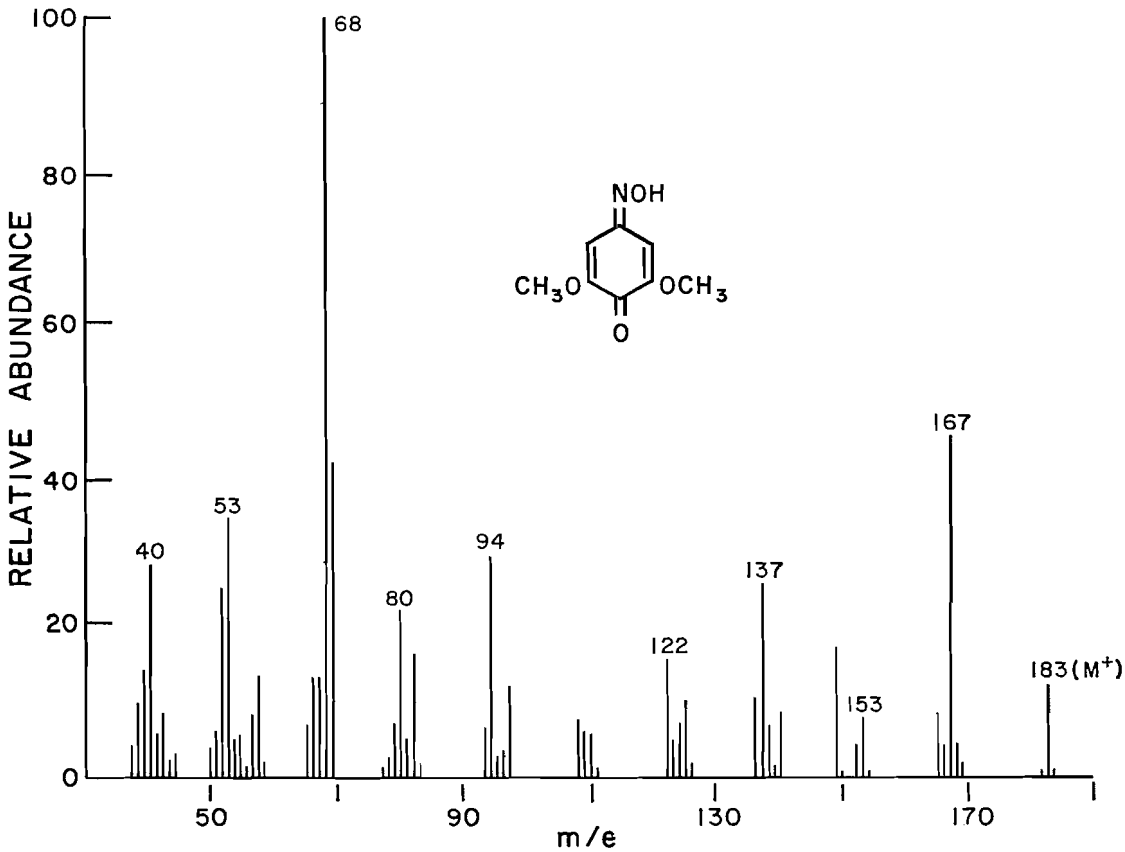

FIG. 1. Mass spectrum of 2,6-dimethoxy-4-oximino-2,5-cyclohexadienone-1 (**3**).

deuterated **3** (i.e. as =N—OD), we have deduced many of the details of the pattern of fragmentation (Scheme 1) arising from electron-impact, and have related this interpretation to the spectrum of the acetate (**4**), and hence deduced, in turn, the position of ^{18}O on compound **6** after exchange in acidified $H_2{}^{18}O$.

In the spectrum of deuterated **3**, all the peaks representing species listed in Scheme 1, except Path 3, exhibit intensification of the next higher mass unit ($m/e + 1$) over the corresponding peaks in the spectrum of the undeuterated **3** (Fig. 1). Therefore, these species have retained the deuterium introduced by exchange.

Thus, Path 1 demands tautomerization of species *a* to permit the expulsion of NO and formation of *e* ($m/e = 153$) without loss of label. In the light of the known tendency of **3** to retain its oxime form, Path 2 (by analogy with the fragmentation of benzophenone oxime (9)) requires transfer of the hydroxyl hydrogen to the ring, but may be a better interpretation for this compound. Paths 4, 5, and 6 have a common starting point, fragment *f*, which appears to have arisen in a one-step process (metastable ion is present) involving transfer of hydrogen to nitrogen simultaneously with the loss of oxygen. We have also observed the formation of a quinone imine corresponding to *f* in the fragmentation of the 4-monoxime of 2-methoxy-1,4-benzoquinone. We are therefore led to suggest that the quinone imine mechanism may prove to be common to the fragmentation processes of all quinone monoximes.

In the first step in each of the three pathways, 4, 5, and 6, whereby *f* undergoes further fragmentation, the products *h*, *i*, and *j* all retain their deuterium labels. The cleavage giving rise to *h* is similar to that of methoxybenzoquinones (10). In Path 5, the first two steps from *f* are the same

Can. J. Chem. Downloaded from www.nrcresearchpress.com by 210.87.254.5 on 09/05/12
For personal use only.

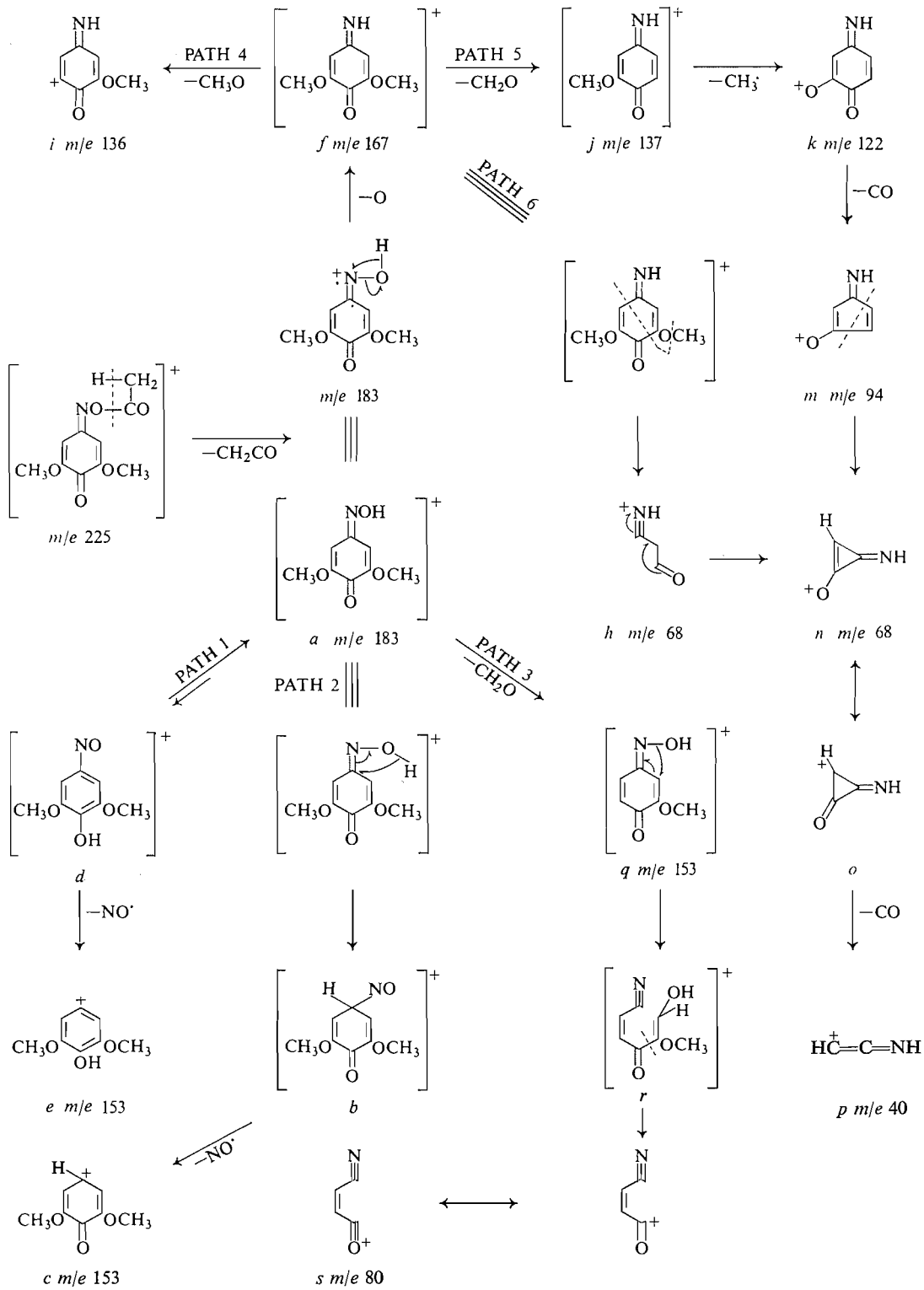

SCHEME 1. Fragmentation of 2,6-dimethoxy-4-oximino-2,5-cyclohexadienone-1 (**3**) and its acetate (**4**).

Can. J. Chem. Downloaded from www.nrcresearchpress.com by 210.87.254.5 on 09/05/12
For personal use only.

Can. J. Chem. Downloaded from www.nrcresearchpress.com by 210.87.254.5 on 09/05/12
For personal use only.

as those known for phenolic methyl ethers (11): loss of formaldehyde, then methyl. Two more steps are required to form *n* (*m/e* = 68), an isomer of *h*. The formation of *n* through two different paths, and the fact that it is resonance-stabilized, may account for *m/e* = 68 being the base peak of the spectrum.

In contrast with the other mechanisms, Path 3 alone leads to a product, *s*, which has lost its deuterium label.

With the exception of the transitions $183^+ \rightarrow 153^+ + 30$, $167^+ \rightarrow 68^+ + 99$, $153^+ \rightarrow 80^+ + 73$, all the fragmentation processes deduced from the spectra of **3** are further supported by the presence of appropriate metastable ions.

Exchange of Oxygen

For the experiment on the exchange of oxygen, **3** was dissolved in 1.0 *N* hydrochloric acid containing 10% of $H_2{}^{18}O$; the solution was rapidly heated to 90–95° and kept at that temperature for 3 min. Accurate measurement of the isotope content of the product by mass spectroscopic analysis (12) presented some difficulties, and it proved necessary to acetylate the compound to facilitate purification.

In the ^{18}O-containing acetate, the ratios of the peaks at *m/e* 225/227, 183/185, and 153/155 were all 100/12, while the same peaks in the unexchanged compound were in the ratio of 100/2. Thus 10% of ^{18}O had been incorporated in each of these species. (Natural relative isotopic abundance (13) of P_m/P_{m+2} for $C_{10}H_{11}NO_5$ (*m/e* 225) is 100/1.6, for $C_9H_9NO_4$ (*m/e* 183) is 100/1.2, and for $C_8H_9O_3$ (*m/e* 153) is 100/1.0.) The complete absence of spectral bands above *m/e* 225 + 2 clearly ruled out the possibility that ^{18}O might have been incorporated into more than one oxygen atom of **4**.

The main features of the spectra of the acetate are the same as those of the unacetylated oxime (Fig. 1), with the necessary exception that the first step in fragmentation is the loss of ketene (M-42), as has been observed in the spectra of *N*-acetyl alkylamines (14), and of sugar acetates (15). This loss occurred with retention of ^{18}O. Subsequent fragmentation through Paths 1, 2, 3, and 4 also led to retention of ^{18}O, as measured from the peaks for *c*, *e*, *i*, *s* (Scheme 1). However, in Paths 5 and 6, once the keto oxygen is lost (*h* in Path 6, *m* and subsequent fragments in Path 5) the ratios of *m/e*:*m/e* + 2 are the same for each *m/e* whether or not the compound originally contained ^{18}O.

The mass spectra of the oxime acetate (**4**), both with and without ^{18}O, thus serve on the one hand to confirm the previous interpretations of the spectrum of the free oxime, and, on the other, to demonstrate that, in accordance with earlier conjecture, the keto oxygen is the one which is exchangeable, in this instance, completely so.

Nucleophilic displacement of ring oxygen has also been reported to occur (16) as a minor pathway in the mechanism of direct alkylation of benzoquinone oxime by acidified alcohols (17). The major mechanism involves attack by protonated alcohol on carbonyl oxygen.

Experimental

All melting points were determined on a calibrated Fisher–Johns apparatus unless otherwise specified. Infrared (i.r.) spectra were recorded on a Perkin–Elmer spectrometer, model 337. The proton magnetic resonance (p.m.r.) spectra were recorded on a Varian A-60 spectrometer, with tetramethylsilane as an internal standard. Mass spectra were determined by the Morgan Schaffer Corp., Montreal, on a Hitachi Perkin–Elmer RMU60 mass spectrometer operating at 70 eV. Elemental analyses were done by Schwarzkopf Microanalytical Laboratory of Woodside, N.Y. Magnesium sulfate was used to dry all solvent extracts before concentration. Deuterium oxide and hydrogen oxide-^{18}O were products of Merck-Sharpe and Dohme. Known methods (1) were used to prepare 2,6-dimethoxy-1,4-benzoquinone (**1**) and 5-nitro-1,2,3-trimethoxybenzene (**2**). Solutions of nitrous acid were prepared according to the published procedure (18).

Preparation of 2,6-Dimethoxy-4-oximino-2,5-cyclohexadienone-1 (3) from 2,6-Dimethoxy-1,4-benzoquinone (1)

A solution of 20 g (0.12 mole) of **1** and 20 g (0.30 mole) of $NH_2OH \cdot HCl$ in 100 ml of anhydrous pyridine and 150 ml of anhydrous ethanol was boiled under reflux for 1 h with exclusion of moisture. The solution was then made alkaline with aqueous sodium hydroxide and concentrated by complete removal of the remaining pyridine under reduced pressure. Water (200 ml) was added and then the pyridine-free aqueous solution was extracted with methylene chloride (5 × 300 ml). Drying and evaporation of the combined extracts yielded 6.8 g (31%) of brown powder with m.p. 212–216°. Two recrystallizations from water containing 5% methanol gave 4.1 g, m.p. 218.8° (decomp.), of yellow plates. This compound was insoluble in ether and carbon tetrachloride, moderately soluble in cold water and chloroform, soluble in hot water, ethanol and methanol.

Anal. Calcd. for $C_8H_9NO_4$: C, 52.46; H, 4.92; N, 7.65. Found: C, 52.57; H, 5.01; N, 7.83.

The i.r. spectrum (KBr), 3270 cm^{-1} broad (OH), 1635 cm^{-1} (C=O), 1570 cm^{-1} (C=N), 1010 cm^{-1} (N—OH str.) and the absence of —N=O str. band at 1500 cm^{-1}, accorded with an oxime structure (19,20).

Preparation of 2,6-Dimethoxy-4-oximino-2,5-cyclohexadienone-1 (3) from 5-Nitro-1,2,3-trimethoxybenzene (2)

In a solution of 1.0 g of NH_4Cl in 50 ml of water

Can. J. Chem. Downloaded from www.nrcresearchpress.com by 210.87.254.5 on 09/05/12
For personal use only.

containing 20% methanol, 1.5 g of **2** were dissolved. The solution was heated to 60–65°, and zinc powder (2.5 g) was added over a period of 10 min with stirring. After rapid filtration by suction, the filter cake was washed with hot ethanol, the filtrate was cooled, and then was poured with stirring into 200 ml of water containing 10% ferric chloride. Steam distillation led to the recovery of 80 mg of starting material, **2**, in the distillate. The residue in the still (pH 2) was cooled and extracted with chloroform (3 × 100 ml). Drying and evaporation of the extract gave 1.1 g (85%) of light brown solid material with m.p. 210–215° (decomp.). One recrystallization from water containing 5% methanol gave 0.85 g of yellow plates with m.p. 218.0–218.5° (decomp.). This material exhibited an i.r. spectrum identical to that of a sample of **3**, prepared according to the method described in the preceding section, and showed no depression of melting point upon admixture.

Reaction of 2,6-Dimethoxy-4-oximino-2,5-cyclohexadienone-1 (3) with Nitrous Acid

This reaction was conducted in a flask fitted with a reflux condenser, with the top of the condenser connected, by means of rubber tubing, to two wash bottles in series. The first wash bottle was empty, and acted as a safety bottle. The second contained water, and its purpose was twofold: (*a*) to inhibit the escape of gases so that decomposition of nitrous acid would be retarded, and (*b*) to trap whatever oxides of nitrogen might otherwise tend to escape. A suspension of 10 mg of **3** in 20 ml of nitrous acid (pH 1) was placed in the flask and boiled under reflux for 1 h. The reaction mixture was then extracted with chloroform (3 × 10 ml). After drying and evaporation of the solvent, the yellow solid residue, 9 mg (98%), m.p. 250–252° was identified as **1** (by mixture m.p. and i.r. spectrum).

Reaction of 2-Methoxy-4-nitrosophenol with Nitrous Acid

A suspension of 10 mg of 2-methoxy-4-nitrosophenol (18) in 20 ml of nitrous acid (pH 1) was boiled under reflux for 1 h in the apparatus described in the previous section. The product solution was then extracted with chloroform (3 × 10 ml). Drying and evaporation of the extract yielded 10 mg (91%) of yellow solid, m.p. 90–96°. Two recrystallizations from ether with a few drops of petroleum ether added each time gave 7.3 mg of yellow needles, m.p. 100.3–100.4°, which proved to be identical (i.r. spectrum and mixture m.p.) with a sample of 4-nitroguaiacol prepared according to Pollecoff and Robinson (21). Thin-layer chromatography (on silica gel with methanol:benzene:acetic acid:petroleum ether (8:45:3.5:20) showed that the crude yellow solid contained a trace of 4,6-dinitroguaiacol (18).

Preparation of 2,6-Dimethoxy-4-oximino-2,5-cyclohexadienone-1 Acetate (4)

A solution of 1.0 g of **3** in 25 ml of acetic anhydride was boiled under reflux for 2 h. The hot solution was poured into 200 ml of ice water and extracted with chloroform (4 × 50 ml). Drying and evaporation of the extract, yielded a residue, which, after thorough washing with methanol and subsequent drying, was a yellowish material weighing 0.85 g (69%) with m.p. 179–181°. After two recrystallizations from ethanol, the product (0.61 g) appeared as yellow prisms, m.p. 181.8–182.0°.

Anal. Calcd. for $C_{10}H_{11}NO_5$: C, 53.33; H, 4.89; N, 6.22. Found: C, 52.84; H, 4.83; N, 6.31.

The i.r. spectrum (KBr) exhibited a band at 1795 cm^{-1} corresponding to C=O stretching vibration of acetoxyl (22).

Oxygen-18 Exchange Reaction of 2,6-Dimethoxy-4-oximino-2,5-cyclohexadienone-1 (3) Followed by Acetylation

To a solution of 1 ml of 6 *N* aqueous hydrochloric acid in 8 ml of water containing 10.6% ^{18}O, **3** (400 mg) was added. The resulting mixture was heated to 90–95° with constant stirring for 3 min. Extraction with chloroform, drying of the extract, and evaporation gave a yellowish product which was then acetylated by the same procedure as described in the preceding section. The purified labeled oxime acetate weighed 150 mg, m.p. 178.5–181.8°. The i.r. spectrum of the ^{18}O-containing compound showed no detectable difference from its unlabeled precursor (**3**). However, its mass spectrum indicated that 10% ^{18}O had been incorporated into the molecule.

Deuterium Exchange Reaction of 2,6-Dimethoxy-4-oximino-2,5-cyclohexadienone-1 (3)

A suspension of 100 mg of **3** in 3 ml of deuterium oxide was heated to boiling and filtered. The filtrate was allowed to stand at room temperature and the partially deuterated oxime gradually separated as yellow plates, m.p. 216.0–218.5° (turns brown at 210°), yield 75%. The i.r. spectrum exhibited an O—D stretching band at 2400 cm^{-1} (23).

Acknowledgment

This paper is based on results of research supported in part by a grant from the Department of Forestry of Canada.

1. H. I. Bolker and F. L. Kung. To be published.
2. (*a*) H. Uffmann. Tetrahedron Letters, **38**, 4631 (1966). (*b*) H. Uffmann. Z. Naturforsch. **22b**, 491 (1967). (*c*) R. K. Norris and S. Sternhell. Australian J. Chem. **19**, 841 (1966). (*d*) R. K. Norris and S. Sternhell. Tetrahedron Letters, **2**, 97 (1967).
3. (*a*) I. P. Gragerov and A. F. Levit. Zh. Obshch. Khim. **30**, 3726 (1960). (*b*) D. Samuel and B. L. Silver. Oxygen isotope exchange reactions of organic compounds. *In* Advances in physical organic chemistry. Vol. 3. *Edited by* V. Gold. Academic Press, Inc., New York. 1965. p. 176.
4. (*a*) S. Oae, T. Fukumoto, and R. Kiritani. Bull. Chem. Soc. Japan, **36**, 346 (1963). (*b*) S. Oae and R. Kiritani. Bull. Chem. Soc. Japan, **37**, 770 (1964).
5. S. J. Metro. J. Am. Chem. Soc. **77**, 2901 (1955).
6. E. Havinga and A. Schors. Rec. Trav. Chim. Pays-Bas, **69**, 466 (1950).
7. A. Pfob. Monatsh. Chem. **18**, 467 (1897).
8. E. H. Rodd. (Editor.) Chemistry of carbon compounds. Vol. III. Part A. Elsevier Publishing Co., Inc., New York. 1954. p. 446.
9. D. Goldsmith, D. Becher, S. Sample, and C. Djerassi. Tetrahedron, Supplement No. **7**, 145 (1966).
10. G. M. Clarke, R. Grigg, and D. H. Williams. J. Chem. Soc. 338 (1966).
11. H. Budzikiewicz, C. Djerassi, and D. H. Williams. Interpretation of mass spectra of organic compounds. Holden-Day, San Francisco. 1964. p. 179.

12. C. G. SWAIN, G. TSUCHIHASHI, and L. T. TAYLOR. Anal. Chem. **35**, 1415 (1963).
13. J. H. BEYNON and A. E. WILLIAMS. Mass and abundance tables for use in mass spectrometry. Elsevier Publishing Co., Inc., New York. 1963.
14. H. BUDZIKIEWICZ, C. DJERASSI, and D. H. WILLIAMS. Interpretation of mass spectra of organic compounds. Holden-Day, San Francisco. 1964. p. 67.
15. H. BUDZIKIEWICZ, C. DJERASSI, and D. H. WILLIAMS. Structure elucidation of natural products by mass spectrometry. Vol. 2. Holden-Day, San Francisco. 1964. p. 208.
16. Y. FURUYA, D. MORIKAWA, and K. ITOHO. Bull. Chem. Soc. Japan, **40**, 1425 (1967).
17. A. SCHORS, A. KRAAIJEVELD, and E. HAVINGA. Rec. Trav. Chim. **74**, 1243 (1955).
18. H. I. BOLKER, F. L. KUNG, and M. L. KEE. Tappi, **50**, 199 (1967).
19. D. HADZI. J. Chem. Soc. 2725 (1956).
20. H. STERK and E. ZIEGLER. Monatsh. Chem. **97**, 1131 (1966).
21. F. POLLECOFF and R. ROBINSON. J. Chem. Soc. 645 (1918).
22. L. J. BELLAMY. The infrared spectra of complex molecules. John Wiley and Sons, Inc., New York. 1958. p. 178.
23. D. M. W. ANDERSON, L. J. BELLAMY, and R. L. WILLIAM. Spectrochim. Acta, **12**, 233 (1958).

Can. J. Chem. Downloaded from www.nrcresearchpress.com by 210.87.254.5 on 09/05/12
For personal use only.

Can. J. Chem. Downloaded from www.nrcresearchpress.com by 210.87.254.40 on 09/05/12
For personal use only.

Electrochemical methoxylation of vinyl ethers: a novel anodic dimerization reaction

B. BELLEAU AND Y. K. AU-YOUNG
Department of Chemistry, University of Ottawa, Ottawa 2, Canada

Received March 24, 1969

Electrolysis of vinyl ethers in methanol using a platinum anode and nickel cathode was found to yield the corresponding 1,2-dimethoxylation products (60–66%) and products resulting from a tail-to-tail dimerization to succindialdehyde acetals (20–22%). A mechanism involving radical cation intermediates is proposed.

Canadian Journal of Chemistry, 47, 2117 (1969)

We have previously reported the electrochemical methoxylation of the isomeric dimethoxybenzene to *o*- and *p*-benzoquinone ketals (1), a class of substances inaccessible by other methods. Since benzene, simple ethers, and olefins react sluggishly or not at all under conditions which readily produce benzoquinone ketals from dimethoxybenzenes, it occurred to us that the only structural requirement in the latter for smooth anodic methoxylation could consist in the presence of vinyl ether units. Accordingly, a variety of aliphatic vinyl ethers were submitted to the conditions of electrochemical methoxylation described previously (1) using the same type of electrolysis cell (two concentric platinum gauze anodes and a nickel cathode; 1–0.5% KOH in methanol as the solvent). This work led to the discovery of two novel reactions of considerable practical and theoretical interest: (*a*) the dimethoxylation of the olefinic bond of vinyl ethers; and (*b*) the *dimerization* of vinyl ethers to succindialdehyde acetals.

A typical procedure was as follows. A one-litre electrolytic cell (160 cm^2 platinum gauze as anode and 240 cm^2 nickel as cathode) was charged with a solution of 42 g ethyl vinyl ether and 800 ml of methanol containing 5 g KOH. While stirring at $-5°$, a current of 4 A and 7 V was applied ($\sim$0.025 A/cm^2) for 24 h. The methanol was removed by distillation and the residue fractionated *in vacuo* (Todd column 30 cm) to give 1-ethoxy-1,2-dimethoxyethane, b.p. 58°/27 mm, n_D^{25}1.3954 (68% yield), 1,4-diethoxy-1,4-dimethoxylbutane, b.p. 110°/10 mm, n_D^{25}1.4148 (22% yield), and 2,4-dinitrophenylhydrazone m.p. 259–262° (decomp.). Other examples are assembled in Table I where it can be seen that the reaction is of general applicability.

The mechanism of this reaction is of considerable interest. The studies of Zweig *et al.* (2), revealed that the methoxybenzenes have remarkably low half-wave oxidation potentials. Their election spin resonance (e.s.r.) data show that anodic discharge readily produces absorbed radical cations, which they suggest could yield dimerization products. We have been unable to demonstrate this in our previous studies (1), presumably because of the very low discharge potential of the

TABLE I

Products of electrochemical methoxylation of vinyl ethers

Starting vinyl ether*	Dimethoxylation product (as in **4**)			2,2-Dimerization product (as in **2**)		
	Boiling point	n_D^{25}	% yield	Boiling point	n_D^{25}	% yield
Ethyl	58°/27 mm	1.3954	68	110°/10 mm	1.4148	22
Methyl	129–130°	1.3918	60	96°/12 mm	1.4136	20
Butyl	79–81°/12 mm	1.4063	75	92°/0.3 mm	1.4242	15
Δ^2-tetrahydropyran	85°/28 mm	1.4351	66	118°/1.5 mm	1.4684	24
1-ethoxycyclohexene	59°/1 mm	1.4408	66		Not isolated	
Methyl 1-decenyl	97°/1 mm	1.4288	40		Not isolated	

*All new products reported in this table had the correct empirical composition as determined by microanalysis.

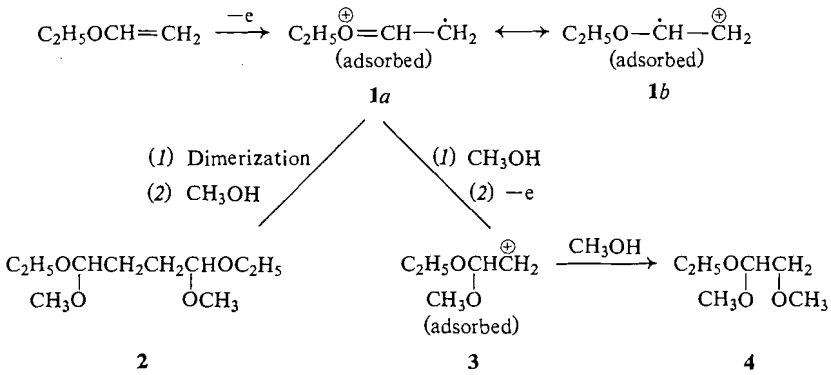

methoxybenzene radical cations. It is logical to suggest similarly that vinyl ethers readily discharge at the anode to give the adsorbed radical cation **1***a* ↔ **1***b*. Subsequently, **1***a* would dimerize to yield **2** after reaction with the solvent, but for reasons unknown as yet, the resonance form **1***b* does not give dimerization products. Alternatively, **1***a* would react rapidly with the solvent but would simultaneously discharge to give cation **3** which would finally yield **4** after reaction with the solvent. We feel that this mechanism accounts adequately for the substrate specificity of the anode in this reaction and for the observed products. Only one other anodic dimerization reaction in the non-aromatic series has general utility: the Kolbe synthesis (3). The anodic dimerization of vinyl ethers (**1***a* ↔ **2**) constitutes a second example which, because of the nature of the products, may have broader synthetic utility.

Acknowledgments

The financial support of the National Research Council of Canada is gratefully acknowledged.

1. B. Belleau and N. L. Weinberg. J. Am. Chem. Soc **85**, 2525 (1963).
2. A. Zweig, W. G. Hodgson, and W. H. Jura. J. Am. Chem. Soc. **86**, 4124 (1964).
3. B. C. L. Weedon. Advan. Org. Chem. **1**, 1 (1960).

A revised structure for the so-called "diadrenaline ether"[1]

Janet E. Forrest, S. Kašpárek[2], and R. A. Heacock
Atlantic Regional Laboratory, National Research Council of Canada, Halifax, Nova Scotia

AND

T. P. Forrest
Department of Chemistry, Dalhousie University, Halifax, Nova Scotia

Received March 27, 1969

The correct structure for the product, obtained by the action of 20% HCl on adrenaline (**1**) and previously described as diadrenaline ether (**2**), has been shown to be 6-(3′,4′-dihydroxy-α-methylaminomethylbenzyl)adrenaline (**3**). The trivial name adrepine is suggested for the base (**3**).

Canadian Journal of Chemistry, 47, 2118 (1969)

In 1923 Funk and Freedman obtained a crystalline product (m.p. 180–183°) from adrenaline (**1**) by the action of ethanolic hydrogen chloride at reflux temperatures (1). These authors proposed the "diadrenaline ether" (**2**) structure for this compound (isolated as the dihydrochloride) essentially on the basis of microanalytical data and its color reactions. Several years later Öppinger and Vetter obtained the

[1]NRCC No. 10738.
[2]NRCC Postdoctorate Fellow 1965–1967.

Can. J. Chem. Downloaded from www.nrcresearchpress.com by 210.87.254.40 on 09/05/12
For personal use only.

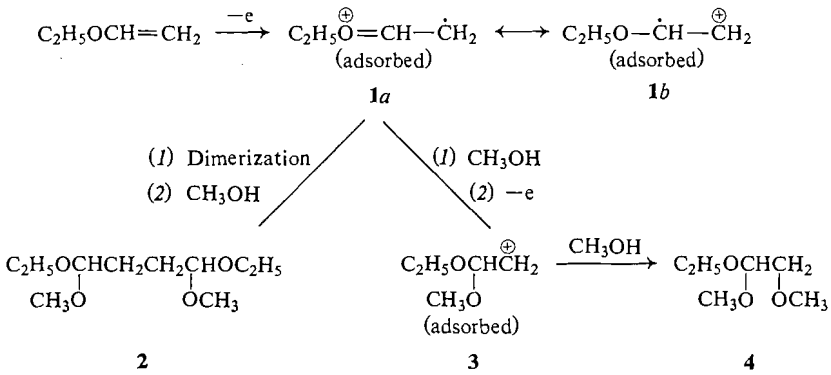

methoxybenzene radical cations. It is logical to suggest similarly that vinyl ethers readily discharge at the anode to give the adsorbed radical cation **1***a* ↔ **1***b*. Subsequently, **1***a* would dimerize to yield **2** after reaction with the solvent, but for reasons unknown as yet, the resonance form **1***b* does not give dimerization products. Alternatively, **1***a* would react rapidly with the solvent but would simultaneously discharge to give cation **3** which would finally yield **4** after reaction with the solvent. We feel that this mechanism accounts adequately for the substrate specificity of the anode in this reaction and for the observed products. Only one other anodic dimerization reaction in the non-aromatic series has general utility: the Kolbe synthesis (3). The anodic dimerization of vinyl ethers (**1***a* ↔ **2**) constitutes a second example which, because of the nature of the products, may have broader synthetic utility.

Acknowledgments

The financial support of the National Research Council of Canada is gratefully acknowledged.

1. B. Belleau and N. L. Weinberg. J. Am. Chem. Soc **85**, 2525 (1963).
2. A. Zweig, W. G. Hodgson, and W. H. Jura. J. Am. Chem. Soc. **86**, 4124 (1964).
3. B. C. L. Weedon. Advan. Org. Chem. **1**, 1 (1960).

A revised structure for the so-called "diadrenaline ether"[1]

Janet E. Forrest, S. Kašpárek[2], and R. A. Heacock
Atlantic Regional Laboratory, National Research Council of Canada, Halifax, Nova Scotia

and

T. P. Forrest
Department of Chemistry, Dalhousie University, Halifax, Nova Scotia

Received March 27, 1969

The correct structure for the product, obtained by the action of 20% HCl on adrenaline (**1**) and previously described as diadrenaline ether (**2**), has been shown to be 6-(3′,4′-dihydroxy-α-methylaminomethylbenzyl)adrenaline (**3**). The trivial name adrepine is suggested for the base (**3**).

Canadian Journal of Chemistry, 47, 2118 (1969)

In 1923 Funk and Freedman obtained a crystalline product (m.p. 180–183°) from adrenaline (**1**) by the action of ethanolic hydrogen chloride at reflux temperatures (1). These authors proposed the "diadrenaline ether" (**2**) structure for this compound (isolated as the dihydrochloride) essentially on the basis of microanalytical data and its color reactions. Several years later Öppinger and Vetter obtained the

[1]NRCC No. 10738.
[2]NRCC Postdoctorate Fellow 1965–1967.

Can. J. Chem. Downloaded from www.nrcresearchpress.com by 210.87.254.42 on 09/05/12
For personal use only.

Can. J. Chem. Downloaded from www.nrcresearchpress.com by 210.87.254.42 on 09/05/12
For personal use only.

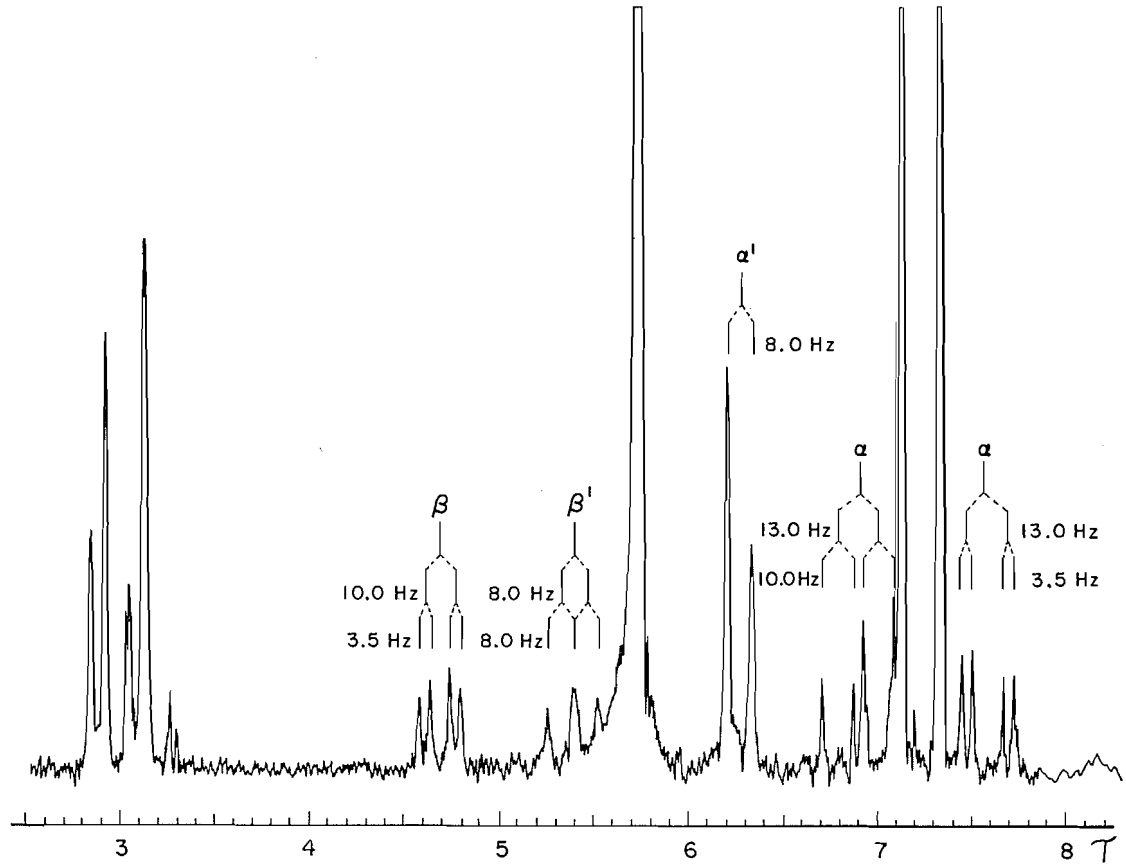

FIG. 1.

NOTE: The nuclear magnetic resonance spectrum of adrepine (**3**) dihydrochloride in D_2O with TMS as an external reference [τ 2.85 to τ 3.30, 5 aromatic protons; A_2X: τ 6.28 (d) and τ 5.40 (t); ABX: τ 7.75 (dd), τ 6.91 (dd), and 4.70 (dd); *N*—CH_3: τ 7.12 (s); *N*—CH_3: τ 7.32 (s)].

same product by the action of 20% aqueous hydrochloric acid on adrenaline (**1**) at 40° (2). The same product has also been detected chromatographically in solutions of adrenaline (**1**) in 10 *N* hydrochloric acid which have been allowed to stand for several days at room temperature (3).

In the course of a systematic study of the nuclear magnetic resonance (n.m.r.) spectra of a number of catecholamine derivatives, the spectrum of the compound described as diadrenaline ether (**2**) was recorded (see Fig. 1). It was immediately apparent that this compound could not have the symmetrical ether structure **2**. The spectrum showed the presence of five aromatic protons per molecule instead of the six required by structure **2**, indicating that substitution had occurred on one of the aromatic rings. The presence of two *N*-methyl peaks in the spectrum confirmed that the structure **2** was incorrect.

We now propose the structure **3** [i.e. 6-(3′,4′-dihydroxy-α-methylaminomethylbenzyl)adrenaline] for this product, which is usually isolated as the dihydrochloride and suggest the trivial name adrepine for the base. The observed n.m.r. spectrum of this product is fully compatible with a structure such as **3**.

Acetylation of adrenaline (**1**) with acetic anhydride in aqueous sodium bicarbonate gives the triacetyl derivative **4**, in which the alcoholic OH group is not acetylated (4); acetylation of adrenaline under more vigorous conditions (acetic anhydride and pyridine) gives the tetra-acetyl derivative **5** (5). Similarly **3** gives the

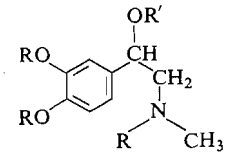

1 R = R′ = H
4 R = $COCH_3$; R′ = H
5 R = R′ = $COCH_3$

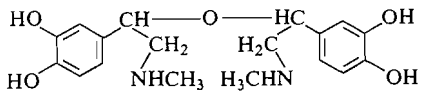

2

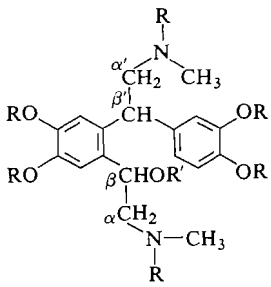

3 R = R′ = H
6 R = $COCH_3$; R′ = H
7 R = R′ = $COCH_3$

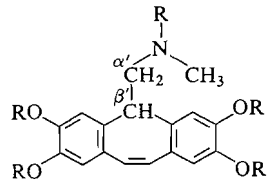

8 R = H

hexaacetate **6** ($C_{30}H_{36}N_2O_{11}$:[3] m.p. 91–92°; $\lambda_{max(EtOH)}$: 263; 272 mμ; $\nu_{max(Nujol)}$: 3300 (broad); 1770; 1630 cm^{-1}) under the former conditions of acetylation (cf. 4) and a heptaacetate **7** ($C_{32}H_{38}N_2O_{12}$: m.p. 167–170°; $\lambda_{max(EtOH)}$: 268; 274 mμ; $\nu_{max(Nujol)}$: 1775; 1755; 1735; 1640 cm^{-1}) under the latter, indicating that **3** contains an adrenaline type ethanolamine side chain. This fact can be verified by consideration of the n.m.r. spectra of **4**, **5**, **6**, and **7**. The signal due to the hydrogen atom on the β-carbon atom of the ethanolamine side chain in **6** is observed at τ 4.75 (the corresponding signal in **4** occurs at τ 5.10), whereas in **7** (in which the OH group on the β-carbon atom is acetylated) the corresponding peak is observed at τ 3.85, i.e. nearly 1 p.p.m. downfield. In tetraacetyladrenaline (**5**) the signal due to the β-proton is seen at τ 4.05, also ca. 1 p.p.m. downfield from its position in **4**. The heptaacetate **7** can also be obtained by acetylation of **6** with acetic anhydride and pyridine.

When **3** is heated above its melting point it decomposes and is converted to the dibenzocycloheptatriene derivative adnamine (**8**). This presumably accounts for the fact that all attempts to obtain a molecular ion in the mass spectrum of **3** have been unsuccessful; the highest mass fragment ion (*m/e* 299) observed appears to have been derived from **8**, formed by the thermal decomposition of **3** prior to ionization.

Kawazu had previously postulated the formation of **3** as a non-isolated intermediate in the formation of adnamine (**8**) from adrenaline (**1**) (6). The formation of **3** from **1** in acid solution can be readily explained mechanistically. It is well known that, in acid solution, the β-hydroxyl group in **1** is readily eliminated with the formation of the corresponding carbonium ion. The product **3** could then be formed by an electrophilic attack by this carbonium ion on the aromatic ring of a second adrenaline unit at a position *ortho* to the ethanolamine side chain.

The observed chemical shifts and coupling constants for the protons in the $-CH_2-CH<$ systems in **3**, **8** and a number of related β-arylepinines are very similar providing further evidence in support of structure **3**. The β′-proton is seen as a triplet in **3** (D_2O: τ 5.40; J = 8 Hz) and in **8** (D_2O: τ 5.90; J = 8 Hz). The α′-protons in **3** and **8** occur as doublets at τ 6.30 and τ 6.88 respectively.

This investigation is continuing and further details of the preparation and properties of a

[3]Satisfactory microanalytical data have been obtained for the new compounds described in this communication.

Can. J. Chem. Downloaded from www.nrcresearchpress.com by 210.87.254.42 on 09/05/12
For personal use only.

number of related β-phenylethylamine derivatives will be published in due course.

Acknowledgment

The authors wish to express their thanks to Mr. J. van Ingen of the Atlantic Regional Laboratory for recording some of the nuclear magnetic resonance spectra.

1. C. FUNK and L. FREEDMAN. J. Am. Chem. Soc. **45**, 1792 (1923).
2. H. ÖPPINGER and H. VETTER. Med. Chem. **4**, 343 (1942).
3. K. J. BROADLEY and D. J. ROBERTS. J. Chromatog. **27**, 407 (1967).
4. L. WELSH. J. Am. Chem. Soc. **74**, 4967 (1952).
5. H. BRETSCHNEIDER. Monatsh. **76**, 355 (1947).
6. M. KAWAZU. J. Pharm. Soc. Japan, **78**, 407 (1958); Chem. Abstr. **53**, 318 (1959).

Can. J. Chem. Downloaded from www.nrcresearchpress.com by 210.87.254.42 on 09/05/12
For personal use only.

On the mechanism of the Doebner–Miller reaction

T. P. FORREST, G. A. DAUPHINEE, AND W. F. MILES
Dalhousie University, Halifax, Nova Scotia

Received April 9, 1969

The reaction of acetaldehyde and aniline in deuterated media has led to substituted tetrahydroquinaldines. Analysis of the deuteration pattern indicates that the previously accepted mechanism of the reaction is incorrect. An alternative mechanism is proposed.

Canadian Journal of Chemistry, 47, 2121 (1969)

The mechanism of the Doebner–Miller synthesis of quinaldines has been the subject of many investigations, leading to the currently accepted mechanism which involves an aldol condensation forming an α,β-unsaturated aldehyde followed by Michael addition of the aromatic amine (1–3). We have carried out the reaction with acetaldehyde and aniline and present evidence that the reaction does not occur via the α,β-unsaturated aldehyde.

When acetaldehyde and aniline were reacted at low temperature in neutral or acidic medium a mixture of the *cis*- and *trans*-4-anilino-1,2,3,4-tetrahydroquinaldine (**1**) (4) could be isolated. The *cis* isomer is readily distinguished from the *trans* isomer by the coupling constants of the heterocyclic ring protons. In the *cis* isomer (m.p. 126°) the C-3 axial proton has coupling constants of 11.0 Hz with both vicinal protons indicating that the protons on C-2 and C-4 are both axial. In the *trans* isomer (m.p. 85°) the C-3 axial proton is coupled by 11.5 Hz to one of the vicinal protons and 4.0 Hz to the other indicating that one is axial and the other equatorial.

If the reaction is carried out in deuterated ethanol (C_2H_5OD) without acid, no deuterium is incorporated into either the *cis* or *trans* isomer of **1**. If the α,β-unsaturated aldehyde is an intermediate at least one deuterium atom would have to be incorporated at the C-3 position of the heterocyclic ring (eq. [1]).

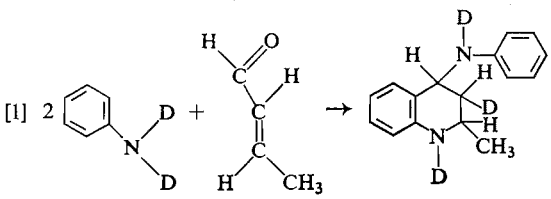

The reaction in non-acidic medium therefore does not proceed via the aldol condensation, but probably involves the condensation of the enamine with the Schiff's base (eq. [2]).

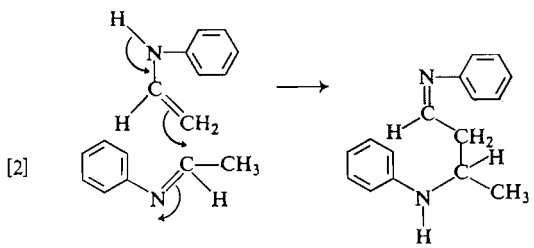

2

When the reaction was carried out in D_2O, DCl at room temperature the *cis*-4-anilino-1,2,3,4-tetrahydroquinaldine (**1** *cis*) was isolated. Nuclear magnetic resonance analysis showed some deuterium in the 3-position and in the

number of related β-phenylethylamine derivatives will be published in due course.

Acknowledgment

The authors wish to express their thanks to Mr. J. van Ingen of the Atlantic Regional Laboratory for recording some of the nuclear magnetic resonance spectra.

1. C. FUNK and L. FREEDMAN. J. Am. Chem. Soc. **45**, 1792 (1923).
2. H. ÖPPINGER and H. VETTER. Med. Chem. **4**, 343 (1942).
3. K. J. BROADLEY and D. J. ROBERTS. J. Chromatog. **27**, 407 (1967).
4. L. WELSH. J. Am. Chem. Soc. **74**, 4967 (1952).
5. H. BRETSCHNEIDER. Monatsh. **76**, 355 (1947).
6. M. KAWAZU. J. Pharm. Soc. Japan, **78**, 407 (1958); Chem. Abstr. **53**, 318 (1959).

Can. J. Chem. Downloaded from www.nrcresearchpress.com by 210.87.254.42 on 09/05/12
For personal use only.

On the mechanism of the Doebner–Miller reaction

T. P. FORREST, G. A. DAUPHINEE, AND W. F. MILES
Dalhousie University, Halifax, Nova Scotia

Received April 9, 1969

The reaction of acetaldehyde and aniline in deuterated media has led to substituted tetrahydroquinaldines. Analysis of the deuteration pattern indicates that the previously accepted mechanism of the reaction is incorrect. An alternative mechanism is proposed.

Canadian Journal of Chemistry, 47, 2121 (1969)

The mechanism of the Doebner–Miller synthesis of quinaldines has been the subject of many investigations, leading to the currently accepted mechanism which involves an aldol condensation forming an α,β-unsaturated aldehyde followed by Michael addition of the aromatic amine (1–3). We have carried out the reaction with acetaldehyde and aniline and present evidence that the reaction does not occur via the α,β-unsaturated aldehyde.

When acetaldehyde and aniline were reacted at low temperature in neutral or acidic medium a mixture of the *cis*- and *trans*-4-anilino-1,2,3,4-tetrahydroquinaldine (**1**) (4) could be isolated. The *cis* isomer is readily distinguished from the *trans* isomer by the coupling constants of the heterocyclic ring protons. In the *cis* isomer (m.p. 126°) the C-3 axial proton has coupling constants of 11.0 Hz with both vicinal protons indicating that the protons on C-2 and C-4 are both axial. In the *trans* isomer (m.p. 85°) the C-3 axial proton is coupled by 11.5 Hz to one of the vicinal protons and 4.0 Hz to the other indicating that one is axial and the other equatorial.

If the reaction is carried out in deuterated ethanol (C_2H_5OD) without acid, no deuterium is incorporated into either the *cis* or *trans* isomer of **1**. If the α,β-unsaturated aldehyde is an intermediate at least one deuterium atom would have to be incorporated at the C-3 position of the heterocyclic ring (eq. [1]).

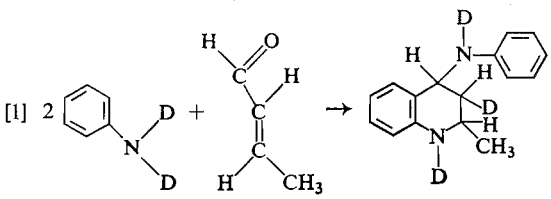

The reaction in non-acidic medium therefore does not proceed via the aldol condensation, but probably involves the condensation of the enamine with the Schiff's base (eq. [2]).

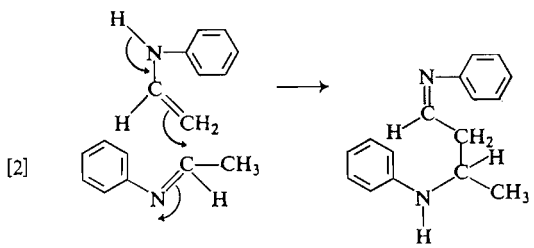

2

When the reaction was carried out in D_2O, DCl at room temperature the *cis*-4-anilino-1,2,3,4-tetrahydroquinaldine (**1** *cis*) was isolated. Nuclear magnetic resonance analysis showed some deuterium in the 3-position and in the

methyl group. Twenty-five percent of the compound contained no deuterium in the 3-position, thus showing that the α,β-unsaturated aldehyde is not required as an intermediate under acidic conditions.

The incorporation of deuterium in both the equatorial (65% D) and axial (30% D) positions of C-3 was greater than that in the methyl groups (15% D). The exchange in the methyl group could take place in the free acetaldehyde or its Schiff's base. No incorporation of deuterium takes place when **1** is treated with acid under the conditions used in the reaction. This indicates that exchange takes place in an intermediate and in a manner which differentiates the protons of the methylene group.

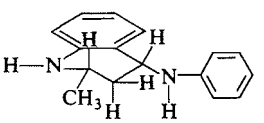

1 (*cis*)

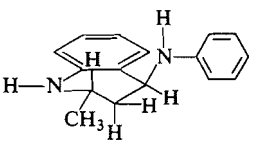

1 (*trans*)

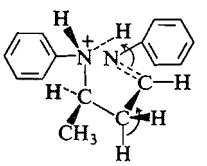

3

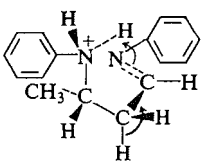

4

The differential exchange of the C-3 protons may be due to anchimeric assistance of the exchange through conformers **3** or **4**. The reactive *trans* proton of conformer **3** becomes the equatorial C-3 hydrogen in the final product (**1** *cis*). Conformer **3** should be more stable than **4** because of the greater non-bonded interaction of the methyl group in **4**. The predominance of conformer **3** therefore dictates that more deuterium appears in the C-3 equatorial position than in the C-3 axial position of **1** (*cis*).

Although it is true that crotonaldehyde can be used directly in this reaction our evidence indicates that it is not necessarily formed as an intermediate when acetaldehyde is used.

Acknowledgment

The authors wish to acknowledge the financial assistance of the National Research Council of Canada.

1. M. H. PALMER. The structure and reactions of heterocyclic compounds. Edward Arnold and Co., London. 1967. p. 110.
2. A. R. KATRITZKY and J. M. LAGOWSKI. The principles of heterocyclic chemistry. Methuen and Co. Ltd., London. 1967. p. 24.
3. G. M. BADGER, H. P. CROCKER, B. C. ENNIS, J. A. GAYLER, W. E. MATTHEWS, W. G. C. RAPER, E. L. SAMUEL, and T. M. SPOTSWOOD. Australian J. Chem. **16**, 814 (1963).
4. L. RAZUVAEV, and L. ZALUKAJEVS. Latvijas PSR Zinatnu Akad. Vestis 131, 747 (1951); Chem. Abstr. **48**, 10024 (1954).

Can. J. Chem. Downloaded from www.nrcresearchpress.com by 210.87.254.42 on 09/05/12
For personal use only.

Canadian Journal of Chemistry

Published by THE NATIONAL RESEARCH COUNCIL OF CANADA

VOLUME 47 JUNE 15, 1969 NUMBER 12

Polarography and coulometry of Rh(III) in a pyridine – pyridinium chloride electrolyte

LESLIE E. JOHNSTON[1] AND JOHN A. PAGE[1]

Lash Miller Chemical Laboratories, University of Toronto, Toronto 5, Ontario

Received October 17, 1968

The polarography and coulometry of Rh(III) has been studied in an aqueous pyridine – pyridinium chloride – sodium chloride electrolyte at pH 5.30 and ionic strength 0.30 *M* at 25.0 °C. Two distinct types of polarographic behavior were noted as the total Py concentration was varied between 0.05 and 0.45 *M*, a "normal" wave with $E_{1/2}$ of −0.43 V vs. a standard calomel electrode, and a second catalytic wave which under some conditions masked the normal wave.

For both types of behavior, controlled potential electrolysis gave a well-defined two electron reduction but there was a definite H^+ consumption in the electrolyses. It is postulated that hydride species are involved in the reduction according to the scheme

$\longrightarrow$ $Rh(III) + 2e \rightarrow Rh(I)$
"normal", diffusion controlled wave at dropping mercury electrode

"enhanced" wave
$Rh(I) + PyH^+ \rightarrow Rh(III) + H^- + Py$

surface reaction at dropping mercury electrode
$xRh(I) + yH^+ \rightarrow$ Products where $y > x$
slow, bulk solution in controlled potential electrolysis

Canadian Journal of Chemistry, 47, 2123 (1969)

Introduction

Nearly all of the analytical polarography of rhodium has been carried out employing a pyridine supporting electrolyte. The first investigations by Willis (1) and Repin (2) employed a Rh(III)–Py–KX(X = Cl^- or Br^-) system, and their work defined the position of the cathodic step on the potential axis. Pantani (3) examined their postulates on the number of electrons involved in the step and provided dubious evidence for a two electron reduction of the Rh(III). The nature of the solution species (oxidized or reduced) was not characterized. In another connection, Gillard *et al.* (4) have investigated the polarographic reduction of a number of Rh(III) complexes, among them $RhPy_4Cl_2{}^+Cl^-$. They postulated a two electron reduction step, but this was based on an estimate for the diffusion coefficient of the reducible species. The nature of the products of the reduction was not definitely established, but other work by these authors (5–7) indicated a Rh(III)-hydride as a possible product along with the more obvious Rh(I).

This study delineates the polarographic behavior, emphasizing the effect of solution composition on the wave. The nature of the reduction is characterized by analytical coulometry, half-wave potential measurements, and identification experiments on the oxidized and reduced solutions.

Experimental

All potentials reported are in volts relative to a mercury calomel electrode (m.c.e.) filled with saturated NaCl solution. The reference used throughout was a Metrohm EA-402 calomel electrode, or equivalent, containing saturated NaCl solution.

The polarograms were normally recorded on a Sargent Model XV polarograph with the damping set in the number one position. A conventional jacketed H-cell, thermostated at 25.0 °C, and employing a frit/NaCl agar

[1]Present Address: Department of Chemistry, Queen's University, Kingston, Ontario.

TABLE I

Determination of Py groups in the Rh(III) complex

Rh taken (moles × 10^5)	Py taken (moles × 10^5)	Py found (moles × 10^5)	Py groups per Rh(III)
1.134	126.1	121.3	4.2
2.831	126.1	115.3	3.8
2.831	126.1	115.1	3.9
2.831	126.1	114.6	4.0

gel to separate the working and counter (reference) compartments, was used. The dropping mercury electrode (d.m.e.) used for quantitative work had a flow rate of 1.597 mg s^{-1} with a drop time of 3.97 s at −0.60 V in a solution that was 0.453 m*M* in Rh(III) and 0.45 *M* in total Py at the chosen ionic strength and pH.

For the determination of the $E_{1/2}$ and wave form parameters, a three electrode system was used. This employed a Wenking Model 61 RS potentiostat, accurately calibrated for potential, to control the potential of the d.m.e. relative to a reference electrode in the working electrode compartment of the H-cell. The current was measured as the potential drop across a 10 KΩ load resistor; a Hewlett–Packard Model 7100B recorder with a response time of 0.5 s was used to record the current as a function of time over a series of mercury drops at a fixed potential.

Controlled potential coulometry was carried out in the H-cell with the three electrode system, but a Hg pool of 17.3 cm^2 area was used in place of the d.m.e. The pool was stirred mechanically in a reproducible fashion. The electrolysis current was integrated using an operational amplifier circuit with capacitance feedback (8). Background corrections, equal to the product of the final residual current and electrolysis time, were deducted from the total quantity of electricity.

For the measurement of pH, a Beckman Model G, or in the case of the precise electrolysis experiments involving H^+ consumption, a Beckman Research pH meter, was used. The glass electrode was a Beckman 40498 or equivalent and the meter was standardized against a KH phthalate solution prepared according to the directions of the National Bureau of Standards from their sample 185c (pH = 4.008 at 25.0 °C).

All solutions for polarography and coulometry were deaerated with nitrogen gas. Before use, the N_2 (Linde, less than 10 p.p.m. O_2) was passed through an acid vanadium(II) solution (9), scrubbed with water, then equilibrated with pyridine vapor by passage through three successive towers filled with supporting electrolyte at 25.0 °C.

Spectra in the ultraviolet (u.v.) and visible regions were obtained on either a Bausch and Lomb 505 Spectrophotometer using 10 cm quartz cells or on a Beckman DU Spectrophotometer using 1 cm quartz cells. The infrared (i.r.) spectra were obtained on a Perkin–Elmer Model 521 Grating i.r. spectrophotometer using Nujol mulls. Nuclear magnetic resonance (n.m.r.) information was obtained from the Varian Associates Model HR-100 n.m.r. spectrophotometer.

All chemicals used were reagent grade, and the pyridine was redistilled before use. The stock Rh(III) solutions were prepared by dissolution of $Na_3RhCl_6 \cdot 12H_2O$ (Alpha Inorganics Rh-103) in a 6 *M* HCl solution. Standardization of the resultant well characterized red $RhCl_6^{3-}$ species (10) was effected by controlled potential coulometry according to the method of Van Loon and Page (11). Typical analyses gave rhodium concentrations of 22.72 ± 0.04 m*M*.

The solutions for polarography and coulometry were prepared by refluxing aliquots of the stock Rh(III) solution with varying amounts of a 2.5 *M* aqueous Py solution for 15–20 min. The resulting pale yellow solution was diluted, and then neutralized to the appropriate pH by the addition of a 3 *M* HCl solution. The ionic strength was adjusted by the addition of the appropriate amount of a 2 *M* NaCl solution to give a final total ionic strength of 0.30 *M* on dilution to a volume of 100 ml. Spectrally, the complex prepared in this way was identical to $RhPy_4Cl_2^+$. Although the excess Py of the supporting electrolyte masked the u.v. region, the visible peak concurred with that reported. When the excess Py was removed by cryogenic distillation in the presence of NaOH in a closed evacuated system, and the residue taken up in water and acidified to pH 5, the absorbances found in the u.v. corresponded to those found in the literature for this complex (12, 13). Previous workers (14, 15) have indicated that a hydridic catalyst is necessary for the formation of this complex from Rh(III) chloro species.

Further confirmation of the number of Py groups coordinated to the Rh(III) was obtained by analysis; the total Py added in the preparation was compared to the free Py after reaction with the Rh(III). In each case the Py was separated from an aliquot of solution by a cryogenic distillation in a closed evacuated system after the addition of excess NaOH. The Py and water that distilled over were reacted with acetic anhydride, and then neutralized by excess standard $HClO_4$ in an HOAc solvent under non-aqueous conditions. Special care was required in the hydrolysis of the acetic anhydride. It was found that the reaction should be allowed to proceed overnight in the cold before completion through catalysis by addition of the excess standard $HClO_4$. The acid in excess was determined by a back titration with standard NaOAc solution to a potentiometric end point according to Kucharsky and Safarik (16). The results appear in Table I and clearly indicate four Py groups per Rh(III).

Results

Polarographic Reduction of $RhPy_4Cl_2^+$

The outlined method was used to prepare a series of Rh(III)–Py solutions, all with a final pH

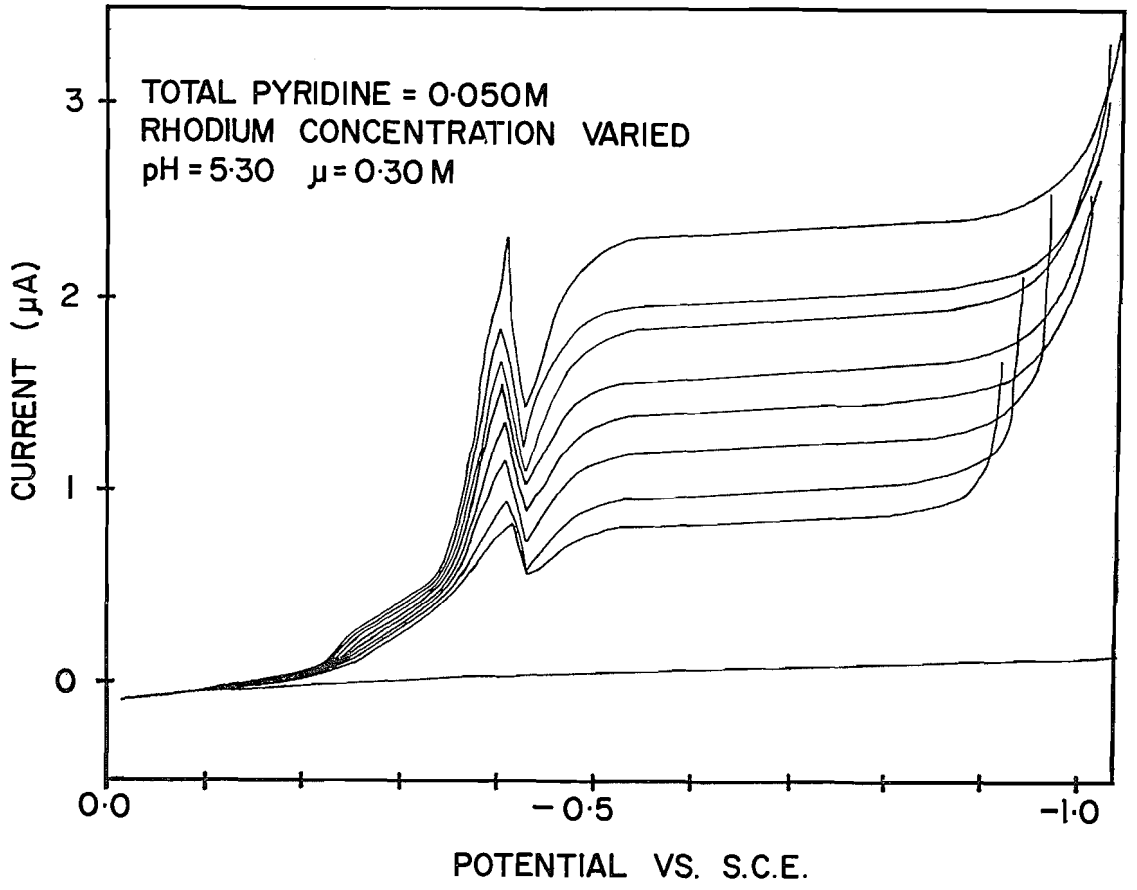

FIG. 1. Polarography at low total Py concentration. Curves from bottom to top are for 0.150, 0.180, 0.226, 0.270, 0.359, 0.385, and 0.453 m*M* Rh(III).

of 5.30. Two types of polarographic behavior were noted: a wave with normal parameters except for a spike on the rising part of the wave (Fig. 1) and a wave with abnormal parameters, the most apparent being the current enhancement over the normal wave (Fig. 2). The transformation from "normal" to "enhanced" behavior was noted as the Py concentration increased; both the spike width and a hump on the limiting current plateau grew until they merged to form the abnormal wave (Fig. 3). The decrease in current just prior to the discharge of the supporting electrolyte was also characteristic. The merging process was also a function of Rh(III) concentration in that at lower concentrations the abnormal wave formed more readily (Fig. 4).

The limiting current (i_l) of the "normal" wave exhibited a linear concentration dependence (Fig. 5*a*) and a temperature coefficient of +1.6% per °C over the range 15–30 °C. Diffusion control was indicated by the constancy of $i_l/h_{corr}{}^{1/2}$ (9) and also by the fact that the current–time curves for individual drops on the limiting plateau showed a $t^{1/6}$ behavior. The square root of the diffusion coefficient, calculated from the Ilkovic equation and an assumed 2 electron reduction, was 2.4×10^{-3} cm $s^{-1/2}$ compared with the value of 2.1×10^{-3} given by Gillard *et al.* (4) for $RhPy_4Cl_2{}^+$.

A solution 0.15 *M* in total Py and 0.38 m*M* in Rh(III) gave a "normal" wave with $E_{1/2} = -0.43$V. For this solution, the irreversibility of the assumed 2 electron reduction was noted from the slope of 57.7 mV for the plot of $E_{d.m.e.}$ vs. log $i/(i_d - i)$ and from the temperature coefficient of +1.6 mV per °C for $E_{1/2}$. In these, and in other cases, the log plot analysis was applied

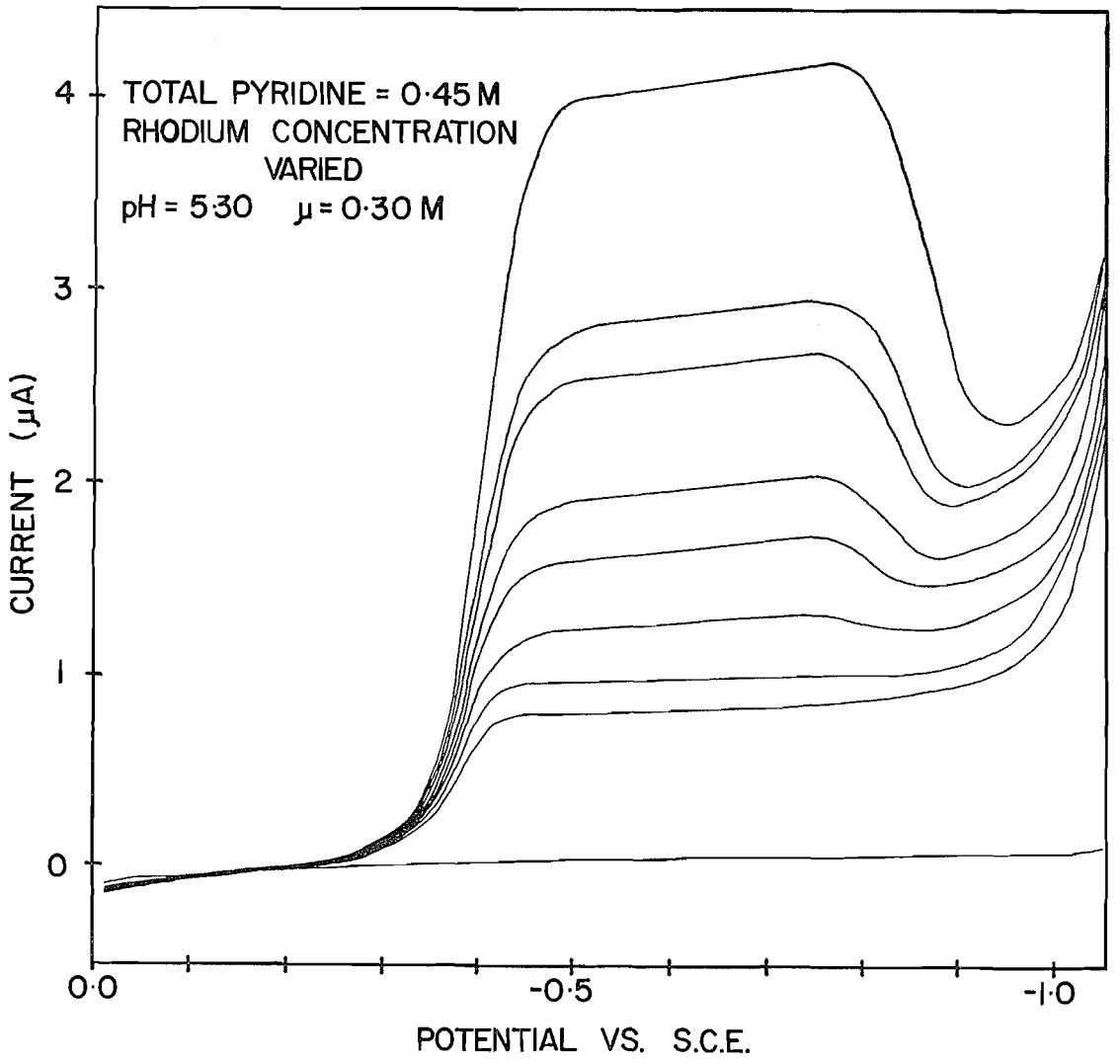

FIG. 2. Polarography at high total Py concentration. Rh(III) concentrations as in Fig. 1.

only on the part of the wave where the spike did not interfere.

The current on the plateau of the "enhanced" wave did not exhibit a linear concentration dependence (Fig. 5*a*), although the current at the minimum just prior to the discharge of the supporting electrolyte did show a linear dependence (Fig. 5*b*). Measurements on the limiting current plateau showed that i_l was invariant with h_{corr}. The temperature coefficient of i_l was +2.8% per °C. The current–time curves for individual drops on the plateau showed exponents of time increasing during drop life and tending to a $t^{2/3}$ behavior.

Lowering the temperature was found to result in a transformation from "enhanced" to "normal" behavior in a manner that was the reverse of that achieved with increasing Py concentration; the exact temperature range for the transformation was a function of both the Py and Rh(III) concentrations.

A solution 0.45 *M* in total Py and 0.45 m*M* in

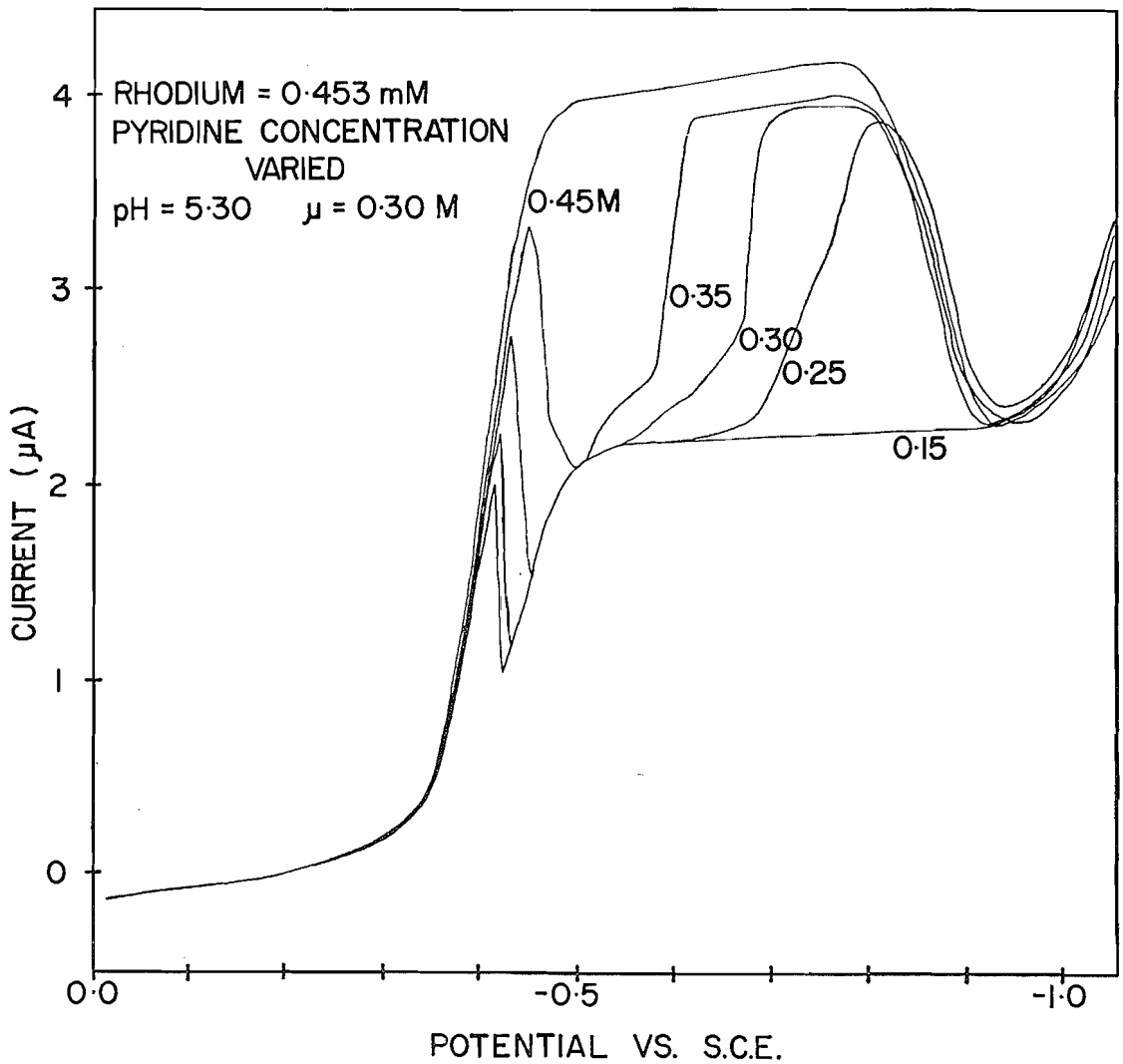

FIG. 3. Formation of "enhanced" polarographic wave.

Rh(III) gave an enhanced wave with $E_{1/2} = -0.40$ V. The plot of $E_{d.m.e.}$ vs. $\log i/(i_l - i)$ had a slope of 55.6 mV.

The effect of pH was investigated using solutions of fixed total Py and Rh(III) concentrations. The "normal" wave was found to break into two steps at pH > 5.8 (Fig. 6), although the total i_l measured just prior to the discharge of the supporting electrolyte remained constant with diffusion control demonstrated through the invariance of $i_l/h_{corr}^{1/2}$. For the first step at high pH, i_l showed neither diffusion or kinetic control when tested at various values of h_{corr}.

At pH > 10, the spike character of the first step disappeared. The wave height of this step was found to be insensitive to the Rh(III) concentration above a certain low value, and the current time curves for individual drops on the limiting current plateau exhibited a $t^{-1/3}$ behavior. This indicates an adsorption of the reduction product formed in the first step.

For the "normal" wave, the parameter $E_{1/2}{}^0$ was evaluated over a selected range of pH according to Meites (9) (Table II and Fig. 7). The linear variation from pH 4.1 to 5.8 shows a slope of 3.5 mV per pH unit; the experimental value of

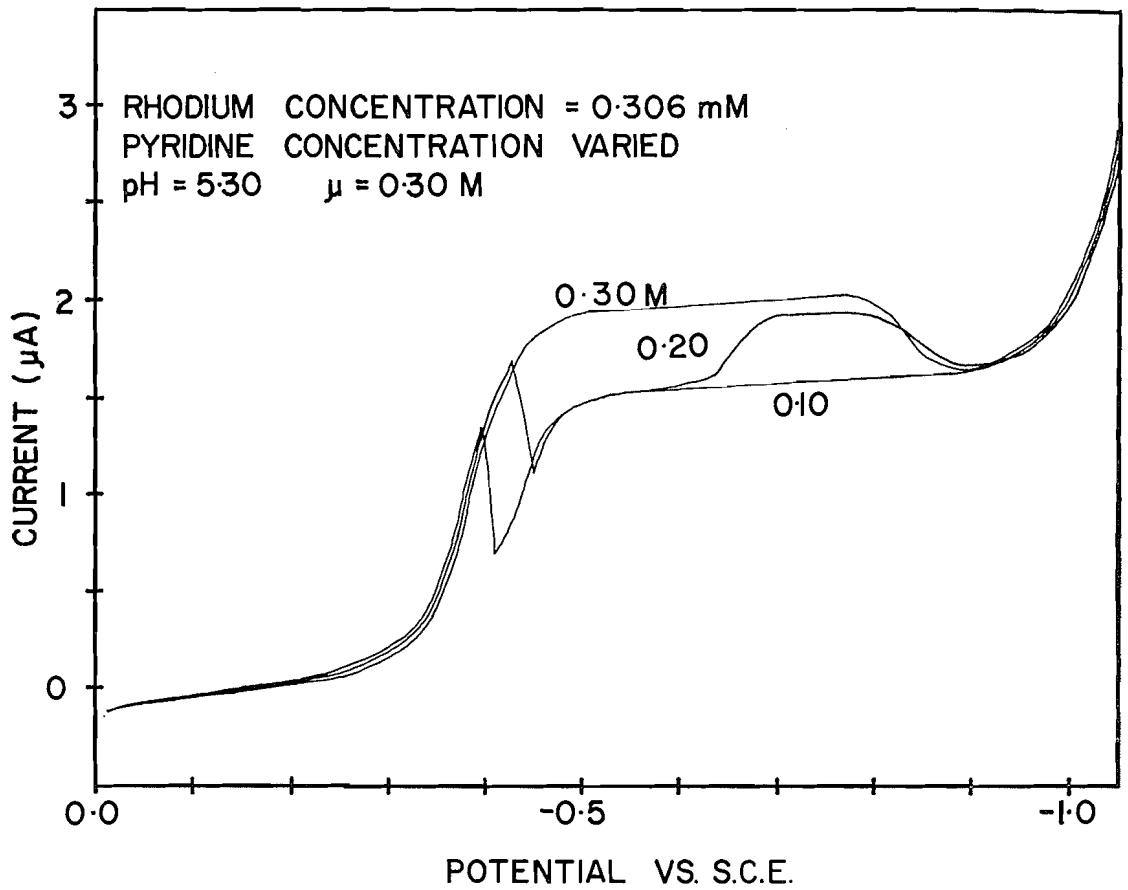

FIG. 4. Formation of "enhanced" polarographic wave at low Rh(III) concentration.
The wave at total Py > 0.30 *M* coincides with that at 0.30 *M*; for total Py < 0.10 *M* the wave coincides with that at 0.10 *M*.

TABLE II
Variation of $E_{1/2}{}^0$ with pH*

pH	Slope of log plot (−mV)	α	$E_{1/2}{}^0$ (V)
4.10	55	0.493	-0.428_5
4.43	51.5	0.525	-0.431_1
4.80	52.2	0.519	-0.430_4
5.36	51.2	0.528	-0.432_2
5.76	51.2	0.528	-0.435_9
6.19	52.6	0.515	-0.442_0
6.53	54.4	0.499	-0.452_7
6.77	53.6	0.505	-0.459_0
7.14	56.9	0.476	-0.473_6
7.84	68.2	0.398	-0.488_6

*$Rh(Py)_4Cl_2{}^+$ = 0.868 m*M*, total Py = 0.108 *M*, μ = 0.122 *M*.

TABLE III
Variation of $E_{1/2}{}^0$ with pH*

pH	Slope of log plot (−mV)	$E_{1/2}{}^0$ (V)
9.86	86.4	−0.835
10.13	83.8	−0.836
10.99	83.8	−0.843
11.48	83.8	−0.842
11.97	80.0	−0.854

*$RhPy_4Cl_2{}^+$ = 0.908 m*M*, total Py = 0.108 *M*, μ = 0.30 *M*.

αn over this pH range was 1.05. This independence on hydrogen ion concentration indicates that if the electron transfer step involves two electrons, the product of the reduction is a Rh(I) species rather than a Rh(III)-hydride species as suggested by Gillard *et al.* (4). While the variation of $E_{1/2}{}^0$ at pH > 5.8 seems to indicate hydrogen ion involvement, interpretation is difficult as the "normal" wave has begun to split.

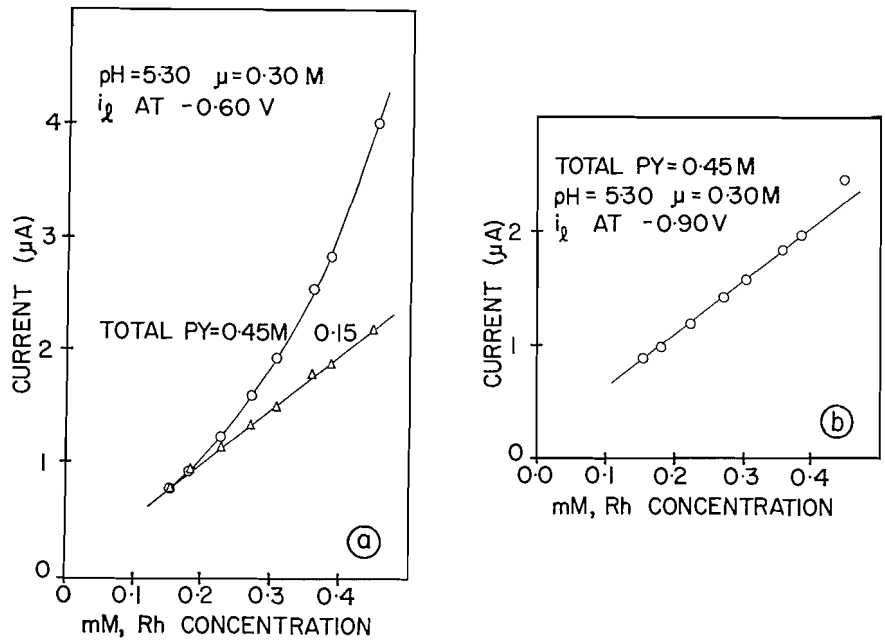

FIG. 5. Concentration dependence of limiting current. (*a*) "Normal" and "enhanced" polarographic waves. (*b*) Minimum of "enhanced" wave.

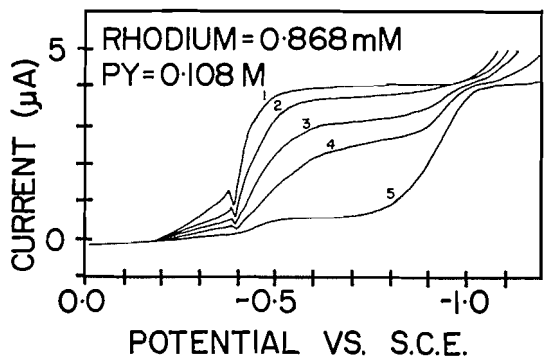

FIG. 6. Effect of pH on polarographic behavior. pH: 1, 5.76; 2, 6.53; 3, 7.14; 4, 7.84; 5, 10.67.

TABLE IV

Variation of $E_{1/2}$ with Cl^- concentration*

Cl^- (moles l^{-1})	Slope of log plot (−mV)	$E_{1/2}{}^0$ (V)
0.300	49.8	-0.441_3
0.250	50.0	-0.436_5
0.200	49.9	-0.430_3
0.150	50.2	-0.423_2
0.100	50.4	-0.413_2
0.0682	53.1	-0.405_1

*$RhPy_4Cl_2{}^+$ = 0.681 m*M*, total Py = 0.108 *M*, pH 5.0, μ = 0.30 *M* ($NaNO_3$).

The parameter $E_{1/2}{}^0$ was also evaluated for the second wave at high pH (Table III) and found to be relatively constant.

The effect of Cl^- concentration on the "normal" wave was also investigated at pH 5.0 and fixed total Py and Rh(III) concentrations (Table IV and Fig. 8). The data were analyzed according to the relation of Matsuda and Ayabe quoted in ref. 17

$$\frac{-dE_{1/2}{}^0}{d \ln [Cl^-]} = (m - i)\frac{RT}{\alpha n F}$$

where m is the number of Cl^- species on the Rh(III) species in bulk solution and i the number of Cl^- species on the electroactive species. The linear plot had a slope of −25.2 mV with αn = 1.08 yielding i = 0.94 for m = 2. This indicates that a fast reaction of the type

$$RhPy_4Cl_2{}^+ + X \rightleftharpoons RhPy_4ClX^{2+} + Cl^-$$

occurs prior to the assumed two electron reduction

$$RhPy_4ClX^{2+} + 2e \rightarrow RhPy_4ClX^0$$

The nature of X is not indicated by the experiment.

Controlled Potential Reduction of $RhPy_4Cl_2{}^+$

Large scale electrolyses were carried out at a

TABLE V

Coulometric reductions of Rh(III)*

Initial Rh(III) (mM)	Total Py (M)	Electrolysis (eq. × 10^5)	n	Comments
0.2260	0.124	3.37	1.99	†
		3.36	1.98	
0.3598	0.350	5.33	1.98	‡ §
		5.32	1.97	Electrolysis at 10 °C
0.1527	0.124	2.31	2.02	Electrolysis at 10 °C†
0.4500	0.450	6.77	2.00	§
		6.77	2.00	
		6.78	2.00	
		6.79	2.00	
0.2797	0.350	4.26	2.03	‡ §
		4.27	2.04	Electrolysis at 10 °C
0.4545	0.100	6.82	2.00	†
		6.85	2.01	

*74.93 ml of solution; electrolysis at 25 °C unless otherwise noted.
†Initial solution behavior: "normal" polarographic wave at 25.0 °C.
‡Initial solution behavior: "normal" polarographic wave at 10.0 °C.
§Initial solution behavior: "enhanced" polarographic wave at 25.0 °C.

TABLE VI

Determination of Rh in reduced solution

Rh taken (eq. × 10^5)	Vanadium catalyst (mg)	Net electrolysis (eq. × 10^5)	Vanadium correction (eq. × 10^5)	Rh found (eq. × 10^5)
4.20	0.51	4.34	0.192	4.15
4.20	0.51	4.36	0.192	4.17
6.79	0.051	6.75	0.019	6.73
6.79	0.051	6.70	0.019	6.68

Hg cathode controlled at -0.55 V and using conditions that produced either the "normal" or "enhanced" polarographic wave. In each case, the reduction proceeded to a negligible residual current (10–40 μA) and the quantity of electricity, when corrected for background effects, corresponded closely to 2 F per mole of Rh(III). The results, of analytical accuracy, are shown in Table V. Preelectrolysis to purify the electrolyte was not feasible because of the method of preparation of the complex, but blank electrolyses showed a negligible consumption of electricity.

When dealing with conditions that produced a "normal" polarographic wave, plots of ln i vs. time were always linear, indicating diffusion control. Slopes of the plot ran typically from 5×10^{-4} s^{-1} at 10 °C ($t_{1/2}$ = 1400 s) to 8×10^{-4} s^{-1} at 25 °C ($t_{1/2}$ = 850 s). In contrast, at high total Py concentration, a condition that showed an "enhanced" polarographic wave, the behavior was significantly different. The electrolysis current would decay to about 70% of the initial value, then jump back to about the initial value before decaying to the final background value. The effect was reproducible, but could be made to disappear by increasing the stirring to a much more rapid rate. Under this condition the plot of ln i vs. time was linear with slope typically 9×10^{-4} s^{-1} at 25 °C.

Hydrogen ion involvement in the Hg cathode electrolyses was studied in two series of runs. In the first, electrolyses were carried out at pH 4.5, a value somewhat less than that of the optimum buffer capacity of the Py system. Standard 0.01 M HCl solution was added to the system as necessary through the electrolysis to maintain the pH within ±0.001 unit of the initial value. Titrations of about 10 ml with a discrimination of 0.2 ml were typical. The moles of acid added were plotted against the quantity of electricity (Fig. 9), and the slope found for three such runs was $+0.68 \pm 0.03$ moles H^+ per F. This indi-

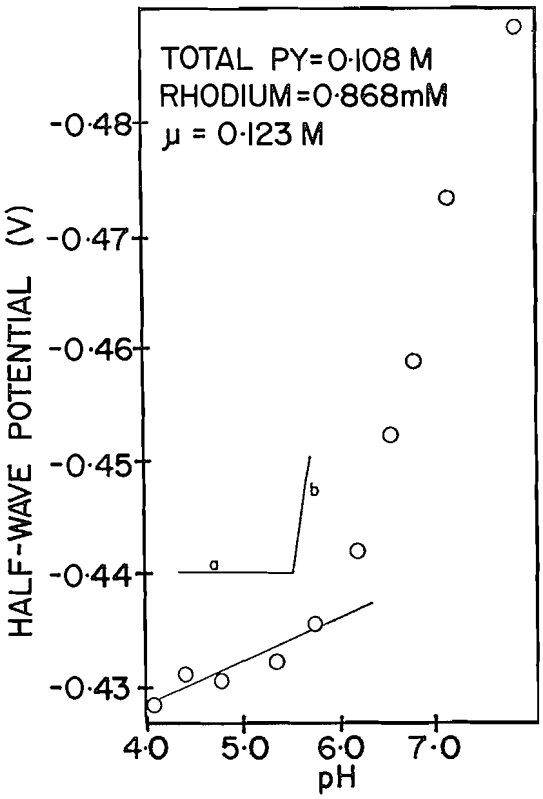

FIG. 7. Variation of $E_{1/2}$ with pH. Slope *a* corresponds to non-involvement of H^+; slope *b* corresponds to involvement of one H^+ in electrode reaction.

cates that 1.4 moles of H^+ are consumed during the reduction of each mole of Rh(III).

A second series of runs was carried out at pH 7.0, a value considerably above that of optimum buffer capacity. In these electrolyses, the meter was used to monitor the pH throughout the reduction. The total concentration of Py was determined by analysis of an aliquot of the solution before the run and checked by analysis of the reduced solution at the end of the run.

The concentration of H^+, calculated from the pH meter reading was plotted against the quantity of electricity (Fig. 10) and the slope found for 6 such runs was $-7.7 \pm 0.2 \times 10^{-4}$ moles l^{-1} H^+ per F. The rate of change of concentration of PyH^+ was then calculated

$$\frac{[Py][H^+]}{[PyH^+]} = K_a = 5.7 \times 10^{-6}$$

$$[Py] + [PyH^+] = C; [H^+] \approx 10^{-7}$$

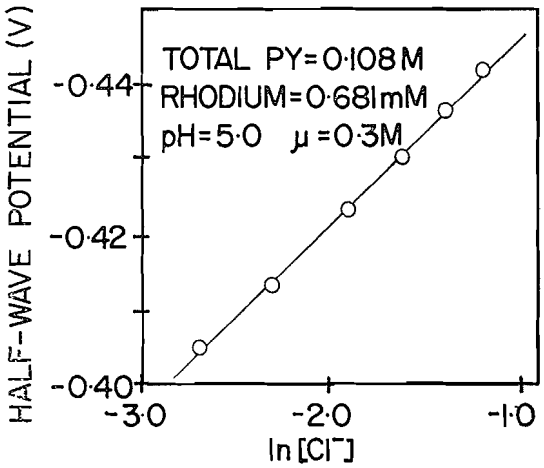

FIG. 8. Variation of $E_{1/2}$ with Cl^- concentration.

$$\frac{d[PyH^+]}{dQ} = \left\{\frac{C}{K_a + [H^+]} - \frac{[H^+]C}{(K_a + [H^+])^2}\right\}\frac{d[H^+]}{dQ}$$

and found to be -7.9 ± 0.2 moles l^{-1} per F. For the 90 ml electrolysis volume, this again indicated that 1.4 moles of protonic strength is consumed during the reduction of each mole of Rh(III).

Characterization of the Reduced Species

The reduced solution prepared by electrolysis was colorless. No adsorption peaks were found in the u.v.–visible spectrum other than the strong adsorption of the excess Py ($\lambda < 330$ mμ).

Since Gillard *et al.* (4) in their studies on rhodium hydrides found evidence that some metallic Rh was formed in the chemical reduction of Rh(III), the actual rhodium content of the reduced solutions was determined. The complex was destroyed by fuming the solution with a 1:1 mixture of nitric and perchloric acids in the presence of a metavanadate catalyst according to Smith (18). The resultant Rh(III) species was anated in hot 6 *M* HCl solution and determined coulometrically (11). A vanadium correction was determined by blank electrolyses. The results as shown in Table VI confirm the presence of all the rhodium in solution after reduction.

The reduced solutions on polarography yielded an oxidation wave with $E_{1/2} = -0.32$ V, but the limiting current of this wave was only about

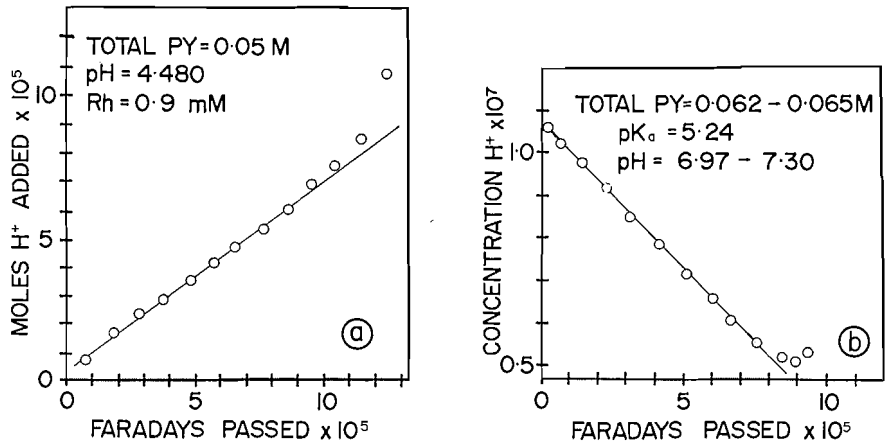

FIG. 9. Consumption of H^+ on electrolysis. (*a*) Electrolysis at fixed pH, (*b*) pH monitored through electrolysis.

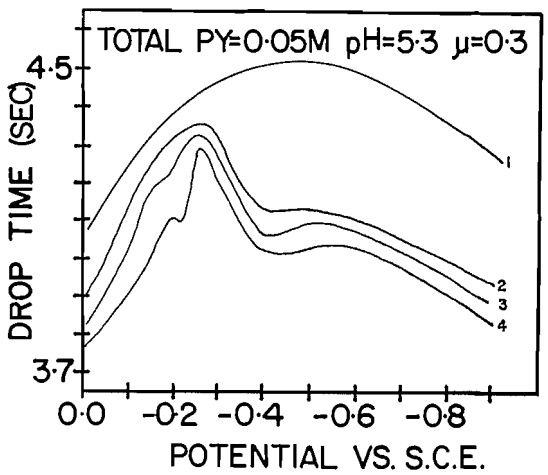

FIG. 10. Droptime vs. potential in 0.05 *M* total Py electrolyte. 1, 0; 2, 0.18; 3, 0.27; 4, 0.45 m*M* Rh(III).

15% of the reduction wave in the original unreduced solution. Investigations with a rotating Pt microelectrode showed no other reduction steps up to +0.9 V, indicating that this unexpectedly small wave at −0.32 V was not an absorption prewave.

Controlled potential electrolyses of the reduced solutions at a Hg anode at −0.1 V proceeded smoothly but required only about 15% of the quantity of electricity used in the original reduction. Subsequent re-reduction at −0.55 V after this oxidation required only the 15% quantity of electricity; if the solution was then electrolyzed again at −0.1 V there was a negligible consumption of electricity. This would indicate that each

TABLE VII

Reoxidation of reduced Rh solutions by reflux

Initial reduction (eq. × 10^5)	Second reduction (eq. × 10^5)
6.35	6.18
6.78	6.61
6.82	6.77
6.82	6.69

reduction produces a small proportion of an electroactive rhodium species, and a large proportion of an electroinactive species.

On the other hand, when the reduced solutions were refluxed under air, there was a complete reconversion to $RhPy_4Cl_2^+$. The refluxed solutions had the correct u.v.–visible spectrum and exhibited the proper coulometric behavior as summarized in Table VII.

The reduced solutions were also tested for catalytic activity as regards substitution of Py in a $RhCl_6^{3-}$ species. This experiment was suggested by the work of Rund *et al.* (19, 20) who distinguished between Rh(I) and Rh(III)-hydrides on the basis of such activity. The reaction was followed amperometrically using a Hg drop J-tube indicator electrode polarized at −0.20 V in a well stirred solution; the current at this potential was found to be proportional to the $RhCl_6^{3-}$ concentration. The catalyst was freshly prepared by electrolysis and added to the reaction mixture by pipette at zero time. The pyridination was found to be pseudo first order in $RhCl_6^{3-}$, but the catalytic activity of the electrolytically

TABLE VIII

Pyridination of $RhCl_6^{3-}$*

Reduced Rh added (moles $l^{-1} \times 10^6$)	Observed k_1† (s^{-1})	Catalytic activity‡ (l moles^{-1} s^{-1})
0.74	12.7×10^{-3}	3.6×10^3
0.87	16.6×10^{-3}	1.9×10^4
0.58	4.0×10^{-3}	2.4×10^4
0.99	4.6×10^{-3}	4.6×10^3
1.30	44.3×10^{-3}	3.4×10^4

*Initial $RhCl_6^{3-} = 1.0$ mM, Py = 0.1 M, NaCl = 0.1 M, pH 7–8, reaction at 25.0 °C.
†$d[RhCl_6^{3-}]/dt = -k_1[RhCl_6^{3-}]$.
‡Activity = k_1/[catalyst].

reduced rhodium solution was consistently much greater than that found by Rund for his active Rh(I) species (Table VIII).

It was hoped that further information could be obtained from i.r. and n.m.r. spectroscopy on the reduced solutions. A rhodium containing material was precipitated from the reduced dilute solution with tetraphenylborate but no peak was observed in the range 2000–2100 cm^{-1} where Rh—H stretches have previously been reported (5–7). Similarly, the high field line reported for Rh—H in the same papers could not be detected in the n.m.r. spectrum of a reduced saturated (ca. 0.01 M) $RhPy_4Cl_2^+$ solution, although the concentration range approached the detection limit for the n.m.r. configuration.

Discussion

The polarographic reaction of the $RhPy_4Cl_2^+$ species at the d.m.e. is complex but a possible scheme is given by

[1] $\longrightarrow$ Rh(III) + 2e → Rh(I)
"normal" diffusion controlled wave

[2] Rh(I) + PyH^+ → Rh(III) + Py + H^-

surface reaction at d.m.e.

The "normal" polarographic wave produces a Rh(I) species according to reaction [1]; this is consistent with the apparent 2 F per mole reduction. Since H^+ concentration appears to have little effect on $E_{1/2}{}^0$, the product of this electron transfer step is presumably not a hydride. However, the reaction is not completely "normal" in that there appears to be a strong adsorption of both the Rh(III) species and also of the product of the reduction. This can be concluded from Fig. 10 where the drop time of the d.m.e. in the presence of the Rh(III) species is plotted as a function of applied potential; it can also be inferred from the effect of temperature on the "enhanced" polarographic wave.

Under certain conditions, another reaction [2] may follow to produce an "enhanced" wave. The process envisioned would take place on the surface of the d.m.e.; it would involve a hydride intermediate which would decompose to regenerate Rh(III) and produce an enhanced polarographic current as the result of a cyclic or catalytic process.

The fact that a detectable enhancement is observed only over a restricted range of polarographic potentials can be explained if it is assumed that reaction [2] can only take place between adsorbed Rh(I) and adsorbed PyH^+ species. Three conditions could then result in a "normal" wave:

(*1*) No specific adsorption of either Rh(I) or PyH^+.

(*2*) A relatively strong adsorption of the Rh(I) produced by reaction [1]. If this was the case, the surface of the growing mercury drop would be saturated with Rh(I) to the exclusion of PyH^+ from almost the very beginning of the life of each drop.

(*3*) A relatively strong adsorption of the PyH^+. If this was the case, the Rh(I) formed by reaction [1] could not successfully compete for adsorption sites on a drop over its finite lifetime.

Intermediate situations could arise depending on the relative tendency of the Rh(I) and PyH^+ to be adsorbed. Thus it would be possible to have a catalytic process early in the life of a drop, but an increasing surface concentration of Rh(I) would finally result in an adsorption of this species to the exclusion of PyH^+. Thus only reaction [1] could proceed towards the end of the drop life.

The spike behavior of the "normal" wave would result from reaction [2] with the cyclic process inhibited by an increasingly strong adsorption of the Rh(I) as the potential of the d.m.e. becomes more negative. With electrolytes of low total Py concentration, the spike is followed by an enhancement at still more negative electrode potentials; this would follow from a change in relative adsorption characteristics with potential such that both species are again adsorbed. With electrolytes of high total Py concentration the spike and the enhancement are merged; this would follow if the higher concentration of PyH^+ in the electrolyte resulted in its adsorption, together with the Rh(I), over the given range of potential.

The final decrease to a "normal" current that is observed just prior to the discharge of the supporting electrolyte would again represent a change in relative adsorption or even a complete desorption of the two species.

In the large scale electrolysis, the coulometry shows a precise reduction of 2 F per mole of Rh(III). Thus there cannot be any appreciable net amount of the catalytic process represented by reaction [2], even under the same electrolyte conditions that produced an "enhanced" wave in polarography. It has been argued that this wave is associated with adsorption phenomena at the renewable surface of the d.m.e.; reaction [2] can proceed only when both Rh(I) and PyH^+ are present in the adsorbed state. It is possible that some of reaction [2] may indeed occur at the very beginning of a large scale electrolysis, but after passage of a small quantity of electricity, sufficient Rh(I) is produced to passivate the electrode by an adsorption of this species with an accompanying complete desorption of PyH^+. The quantity of electricity consumed in any accompanying cyclic process up to this point would be negligibly small relative to the total consumed in the quantitative reduction.

A possible scheme for the large scale reduction would require an electron transfer process followed by a protonation of part of the products of the electrode reaction

$$[3] \qquad \text{Rh(III)} + 2e \rightarrow \text{Rh(I)}$$

$$[4] \qquad x\text{Rh(I)} + y\text{H}^+ \rightarrow \text{Products} \quad \text{where } y > x$$

the nature of the protonated products being unknown. This scheme is supported by the precise 2 F per mole of Rh(III) reduced, the consumption of H^+ in the electrolysis, and evidence of a pair of products in that part of the reduced rhodium was present in an easily oxidized form (15%), the remainder in an electroinactive form (85%). The presence of some Rh(I) as a product follows from the proposal of Rund while a Rh(III)-hydride similar to the monohydride isolated by Wilkinson is an obvious possibility for a protonated product.

However, the observed consumption of 1.4 moles of H^+ per mole of Rh(III) reduced is not consistent with a single Rh(III)-hydride product, since even complete conversion to this species would require only one mole of H^+ per mole of Rh(III).

$$\text{Rh(III)} + \text{H}^+ + 2e \rightarrow \text{Rh(III)-H}$$

It is possible to explain the H^+ consumption at pH 4.5 if one proposes that one or more Py groups are displaced from the Rh(III) on reduction, the displaced Py being largely protonated at this pH. However, the same consumption of H^+ was noted at pH 7 where any displaced Py would be very largely unprotonated.

The difference between the consumption expected for the formation of Rh(III)-hydride and the value actually found appears to be significant and requires the formation of a more complex species as shown in reaction [4].

The failure to find a Rh—H stretch in the i.r. spectrum may or may not be significant in this regard. Some may have been formed but unobserved because of the relatively small quantities of this product; it may be that the proportion of stable Rh(III)-hydride is negligibly small.

Acknowledgments

This study was supported by operating grants from the National Research Council of Canada and the Province of Ontario. The award of a National Research Council of Canada Studentship to L. E. Johnston is also gratefully acknowledged.

1. J. Willis. J. Am. Chem. Soc. **66**, 1067 (1944).
2. S. A. Repin. J. Appl. Chem. USSR, English Transl. **20**, 46 (1947).
3. F. Pantani. J. Electroanal. Chem. **5**, 40 (1963).
4. R. D. Gillard, J. A. Osborn, and G. Wilkinson. J. Chem. Soc. 4107 (1965).
5. J. A. Osborn, R. D. Gillard, and G. Wilkinson. J. Chem. Soc. 3168 (1964).

6. B. N. FIGGIS, R. D. GILLARD, R. S. NYHOLM, and G. WILKINSON. J. Chem. Soc. 5189 (1964).
7. R. D. GILLARD and G. WILKINSON. J. Chem. Soc. 3594 (1963).
8. J. A. PAGE. Talanta, **9**, 365 (1962).
9. L. MEITES. Polarographic techniques 2nd ed. Interscience Publishers Inc., New York. 1965.
10. CHR. K. JORGENSEN. Acta Chem. Scand. **10**, 503 (1956).
11. G. VAN LOON and J. A. PAGE. Talanta, **12**, 227 (1965).
12. R. D. GILLARD and G. WILKINSON. J. Chem. Soc. 1226 (1964).
13. CHR. K. JORGENSEN. Acta Chem. Scand. **11**, 151 (1957).
14. R. D. GILLARD, J. A. OSBORN, and G. WILKINSON. J. Chem. Soc. 1951 (1965).
15. R. D. GILLARD, J. A. OSBORN, P. B. STOCKWELL, and G. WILKINSON. Proc. Chem. Soc. 284 (1964).
16. J. KUCHARSKY and L. SAFARIK. Titrations in non-aqueous solvents. Elsevier Publ. Co., Inc., Amsterdam. 1965.
17. J. HEYROVSKY and J. KUTA. Principles of polarography. Academic Press, Inc., New York. 1966. p. 222.
18. G. F. SMITH. Anal. Chim. Acta, **8**, 397 (1953).
19. J. V. RUND, F. BASOLO, and R. G. PEARSON. Inorg. Chem. **3**, 658 (1964).
20. J. V. RUND. Inorg. Chem. **7**, 24 (1968).

Can. J. Chem. Downloaded from www.nrcresearchpress.com by 210.87.254.6 on 09/05/12
For personal use only.

Kinetics and mechanism of the addition of dimethylarsine to hexafluorobutyne-2

W. R. CULLEN AND W. R. LEEDER
Chemistry Department, University of British Columbia, Vancouver 8, British Columbia

Received November 5, 1968

The addition of dimethylarsine to hexafluorobutyne-2 follows second order kinetics with activation energy, 6.09 ± 0.20 kcal/mole, and activation entropy, −48 ± 1 e.u. The product distribution of the competitive reaction of dimethylarsenic deuteride and diethylarsine with the acetylene shows that the addition mainly involves an intermolecular proton transfer. The mechanism of the addition is discussed.

Canadian Journal of Chemistry, 47, 2137 (1969)

Many investigations have been made of nucleophilic additions to acetylenes and a general rule of "*trans* addition" was postulated by Truce and Simms (1) and independently by Miller (2). This rule of stereospecific *trans* addition was based on product configuration. However, recently *cis* addition products have also been isolated (3, and references therein), mainly from reactions of primary and secondary amines, and with this discovery, the question of the mechanism of nucleophilic addition to alkynes has become of great interest. The mechanism suggested for these *cis* additions involves an intramolecular proton transfer (4). In general, the steric course of the reaction seems to depend on many variables such as the nature of the alkyne and amine (3), and the solvent (5, 6).

A predominantly *trans* addition product (90–98%) is obtained from the quantitative addition of dimethylarsine to hexafluorobutyne-2 (7) (reaction [1], R = R′ = CH_3). This reaction is clearly related to the amine additions and the present investigation was undertaken to establish if the mechanism of the arsine reaction involved a nucleophilic addition to form both products. It was also important to establish whether the hydrogen atom is transferred inter- or intra-molecularly.

Experimental

Volatile reagents and products were manipulated in a conventional vacuum system. Unless otherwise indicated, reactions were carried out in sealed Pyrex tubes. Nuclear magnetic resonance (n.m.r.) spectra were run on Varian A-60 and HA-100 instruments and are reported in p.p.m. downfield from external TMS. Ultraviolet (u.v.) spectra were recorded using a Cary Model 14 spectrophotometer; this was also used for the kinetic studies. Infrared (i.r.) spectra were run on a Perkin–Elmer Model 457 instrument.

Preparation of Dimethylarsine

The method used is a modification of that of Dehn and Wilcox (8). A 1-liter 3-necked flask was fitted with a dropping funnel, water-cooled condenser, stirrer, nitrogen purge, and cold traps (−196°) to condense any volatile products coming through the condenser. Mercuric chloride (30 g) and zinc dust (290 g) were placed in the flask and stirred vigorously with 100 ml of water. A solution of dimethylarsinic acid (50 g) in water (100 ml) was purged with nitrogen, transferred to the dropping funnel using a syringe, and combined with the slurry in the reaction flask. In a similar way 12 *N* hydrochloric acid (250 ml) was slowly added to the vigorously stirred flask. After 6 h, the contents of the traps were taken into the vacuum system and dried over P_2O_5. The yield of dimethylarsine was 34.1 g (89%). It had a very strong As—H stretching frequency at 2085 cm^{-1} and the n.m.r. spectrum showed a doublet at 0.82 p.p.m. (6H) and a septet at 2.82 p.p.m. (1H) (J_{CH_3H} = 7.0 Hz).

Preparation of Dimethylarsenic Deuteride

Dimethylarsine (10.8 g) was shaken with D_2O (30 g) and a trace of HCl (to speed exchange) for one week in a sealed tube. The arsine was separated and re-equilibrated with fresh D_2O. This yielded a product which is ~ 100% $(CH_3)_2AsD$ as detected by n.m.r.; (1:1:1 triplet at 0.82 p.p.m. (J_{CH_3D} = 1 Hz)). The i.r. spectrum showed a strong As—D stretching band at 1502 cm^{-1}.

Preparation of Diethylarsine

Chlorodiethylarsine was prepared from arsenic trichloride and tetraethyllead (9). The chloroarsine was then

[1] $$RR'AsH + CF_3C{\equiv}CCF_3 \longrightarrow \underset{90\text{–}98\%}{\overset{CF_3}{\underset{RR'As}{\diagdown C{=}C \diagup}}\overset{H}{\diagup\diagdown}\overset{}{CF_3}} + \underset{2\text{–}10\%}{\overset{CF_3}{\underset{RR'As}{\diagdown C{=}C \diagup}}\overset{CF_3}{\diagup\diagdown}\overset{}{H}}$$

Can. J. Chem. Downloaded from www.nrcresearchpress.com by 210.87.254.6 on 09/05/12
For personal use only.

reduced using lithium aluminium hydride (10). Diethylarsine had a very strong As—H stretching frequency at 2085 cm^{-1}. The n.m.r. spectrum showed a quintet at 2.43 p.p.m. (1H) (J = 6 Hz) and two multiplets (10H) at 1.42 and 1.15 p.p.m. respectively.

Reaction of Dimethylarsenic Deuteride with Hexafluorobutyne-2

Dimethylarsenic deuteride (0.95 g) and the acetylene (2.8 g) were left at 20° for 1 h. The product, 2-dimethylarsino-3-deutero-1,1,1,4,4,4-hexafluorobutene-2, condensed in a trap at −78°. The purity of the product was established by its n.m.r. spectrum which showed a quartet at 0.96 p.p.m. ($J \sim 1$ Hz). A small upfield quartet presumably corresponding with the *cis* adduct was also present. The amount of this was about 5% of the total product.

Reaction of Diethylarsine and Hexafluorobutyne-2

The arsine (2.43 g) and the acetylene (3.68 g) were left for 2 days at 20°. The product, 2-diethylarsino-1,1,1,4,4,4-hexafluorobutene-2, b.p. 146°, condensed in a trap cooled to −46°. The identity of the compound was established by its n.m.r. spectrum. This showed in the downfield region a quartet of quartets centered at 6.58 p.p.m. (J = 8 and 2 Hz) and another quartet at 5.85 p.p.m. (J = 8.3 Hz). The relative intensity of the two absorptions, 22:1, was the ratio of the *trans* to *cis* adducts (7). Upfield was a triplet (CH_3—CH_2—) at 0.94 p.p.m. (J = 7 Hz) and a complex multiplet at about 1.6 p.p.m. (CH_3—CH_2—). The relative areas of all multiplets were as expected.

Equilibrium Reaction of Diethylarsine and 2-Dimethylarsino-3-deutero-1,1,1,4,4,4-hexafluorobutene-2

Equal volumes of diethylarsine and the arsinobutene were sealed in an n.m.r. tube. The spectrum after 3 h at 20° showed no downfield absorption so that no exchange of D and H occurred.

Stability of the Products of the Dimethylarsine – Hexafluorobutyne-2 Reaction

The products from the reaction of reaction [1] (R = R′ = CH_3) can be separated by vapor-phase chromatography (v.p.c.) (silicone oil at 92°). The *trans* isomer was stable to air, diethyl ether, dimethylarsine, and mixtures of dimethylarsine and diethyl ether for extended periods of time (4 weeks). No isomerization to the *cis* isomer occurred. Similarly the *cis* isomer was stable and did not isomerize under the same conditions.

Kinetics of Secondary Arsine Additions to Hexafluorobutyne-2

The kinetics of the addition reactions were determined by following product formation using n.m.r. and u.v. spectroscopy.

In a typical n.m.r. monitored experiment, 0.1805 g of hexafluorobutyne-2, dimethylarsine (0.0554 g), and diethyl ether (total volume at 20° was 1.12 ml) were condensed into an n.m.r. tube. The tube was sealed. The sample was warmed to −35° and shaken just before placing it into the cooled probe (−30°) of the spectrometer. The rate of formation of the products was followed by integration. The results shown in Table I were found for the *trans* adduct.

The rate of formation of *cis* adduct was the same as the *trans* as the relative amounts of *trans* and *cis* products remained constant throughout the experiment.

TABLE I

Rate of *trans* product formation

t* (s)	Concentration of *trans* product (moles/l)
260	0.120
344	0.147
830	0.237
780	0.246
1587	0.337
1620	0.340
2420	0.388
2445	0.394
∞	0.493

*t = 0 is arbitrary.

Assuming that the reaction is bimolecular and first order in each of the starting materials, the following rate eq. [2] can be derived

$$[2] \qquad \log\left(\frac{A_0 - U}{B_0 - U}\right) = \frac{k_T(A_0 - B_0)}{2.303}\,t$$

where t = time, A_0 = initial concentration of acetylene, B_0 = initial concentration of dimethylarsine, U = concentration of one product formed, and k_T = rate constant at temperature T. Plotting t against $\log (A_0 - U/B_0 - U)$ for *trans* product formation gives a straight line (Fig. 1).

The experiments monitored by u.v. absorption were followed by measuring the increase in absorbance at 2610 Å (the products absorb there but not the reactants (11)). The reactants were condensed via a metal valve into a cold finger attached to a 1 or 0.1 mm path length silica cell. The arsine and ether (10 ml) were added first, mixed at room temperature, and then frozen. The hexafluorobutyne-2 was then condensed into the cold finger well above the arsine–ether mixture. The lower layer was quickly warmed and then vigorously shaken onto the still frozen acetylene. When the whole apparatus was at room temperature, it was placed in the adapted cavity of the spectrometer.

Second order kinetics were observed for all reactions until at least 50% completion. Allowance has been made for the solubility of hexafluorobutyne-2 determined below (Fig. 2). A summary of the experimental conditions used for the kinetic experiments is given in Table II. The rate constants obtained from each run are also listed.

Kinetics of the Addition of Diethylarsine to Hexafluorobutyne-2

This reaction was monitored by n.m.r. techniques as described above. Diethylarsine (0.052 g), the acetylene (0.1882 g), and diethyl ether were sealed in an n.m.r. tube. A plot for second order kinetics, first order in each of the starting materials, was linear. The rate was calculated to be 1.528×10^{-3} l $mole^{-1}s^{-1}$ at −10° in diethyl ether.

Competitive Reaction of Diethylarsine and Dimethylarsenic Deuteride with Hexafluorobutyne-2

Dimethylarsenic deuteride, diethylarsine, and hexafluorobutyne-2 were frozen into a Carius tube. The tube

TABLE II

Summary of results from dimethylarsine addition

Solvent	T (°C)	Concentration of $CF_3C{\equiv}CCF_3$ (mole/l)	Concentration of arsine (mole/l)	Means of monitoring	$k_T(\times 10^{-3}$ l mole^{-1} s$^{-1})$
Et_2O	$-30(\pm 3)$	0.998	0.469	n.m.r.	0.78 ± 0.01
Et_2O	-30	1.588	1.568	n.m.r.	0.778
Et_2O	-15	1.247	0.612	n.m.r.	1.69 ± 0.11
Et_2O	-15	1.205	0.5665	n.m.r.	2.15 ± 0.17
Et_2O	-15	1.184	0.549	n.m.r.	3.15 ± 0.5*
Et_2O	-5	1.016	0.492	n.m.r.	2.70 ± 0.4
Et_2O	$+22(\pm 5)$	0.376	0.0765	u.v.	5.26
Et_2O	$+22$	0.539	0.0671	u.v.	3.94
Et_2O	$+22$	0.2325	0.1031	u.v.	7.12
Et_2O	$+22$	0.101	0.185	u.v.	3.33
Et_2O	$+22$	0.115	0.4298	u.v.	3.03
Et_2O	$+22$	0.0892	0.2310†	u.v.	3.55
MeOH	$+22$	0.0093	0.0079	u.v.	560.00

*Inhibitor 2,2′-azobis(2-methylpropionitrile) 0.652 mole/l added.
†Dimethylarsenic deuteride used.

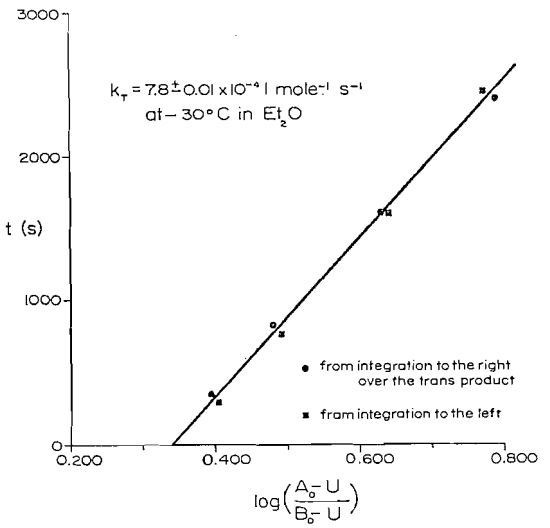

FIG. 1. Second order plot for the rate of formation of *trans*-$(CH_3)_2AsC(CF_3){=}C(CF_3)H$.

was warmed under water (15°) and vigorously shaken. After 5 min, the tube was frozen down, opened, and the contents taken into a vacuum system. The fraction which condensed at −78° was separated by v.p.c. (silicone, 128°). Four major fractions were found. These fractions were identified by n.m.r. to be *cis* and *trans* isomers of the arsine–butyne adducts. The weight of the separated isomers indicated that the reaction went 93% *trans*, 7% *cis* for adduct formations. The ratio of the products before and after separation was identical so no isomerization occurred while separating. From the integrals of the n.m.r. spectra, the percentage of hydrogen could be calculated for the separated fractions and from this the deuterium percentage could be found.

The results of two experiments are tabulated in Tables III and IV.

TABLE III

Initial concentration for competitive experiments

Experiment	Moles of Me_2AsD	Moles of Et_2AsH	Moles of $CF_3C{\equiv}CCF_3$
1	0.0113	0.0048	> 0.0225 (excess)
2	0.0059	0.0086	> 0.0586 (excess)

TABLE IV

Product distribution for competitive experiments

Fraction (v.p.c.)	Fraction identity	Exp. 1 %D	Exp. 1 %H	Exp. 2 %D	Exp. 2 %H
		70*	30*	40*	60*
1	*trans* Me_2As-	77	23	40	60
2	*cis* Me_2As-	70	30	49†	51†
3	*trans* Et_2As-	70	30	45	55
4	*cis* Et_2As-	‡	‡	40	60

*Initial percentages based on moles of reactants (Table III).
†Poor separation, two upfield proton peaks overlapped resulting in an inconclusive integral.
‡Insufficient product for an n.m.r. integral.

Reaction of Dimethylarsine and Hexafluorobutyne-2 in the Gas Phase

Gaseous hexafluorobutyne-2 and dimethylarsine were isolated separately in two evacuated bulbs separated by a valve. The valve was opened and the gas allowed to mix at room temperature. The extent of reaction could be followed by the pressure decrease in the system. In the absence of light, complete reaction required 3 days. Under identical initial conditions, but upon irradiation with u.v. light (100 W lamp, 20 cm from the air-stream cooled bulbs), the reaction required only 1 day to go to completion.

The analysis of the products from the two reactions showed 92% *trans* and 8% *cis* adducts from the u.v.

Can. J. Chem. Downloaded from www.nrcresearchpress.com by 210.87.254.6 on 09/05/12
For personal use only.

irradiated experiment, and 94% *trans* and 6% *cis* in absence of light. The small difference is not significant.

Solubility of Hexafluorobutyne-2 in Diethyl Ether

Hexafluorobutyne-2 (0.02615 g), trifluoroacetophenone (0.1295 g), and diethyl ether were sealed in an n.m.r. tube. The total volume was 1.0 ml and the concentration of gas corresponded closely with that of the n.m.r. kinetic studies. The trifluoroacetophenone was introduced as an internal standard. The ratio of the integrals in the ^{19}F n.m.r. spectrum of the sample was observed at various temperatures. At $-76°$ two phases appeared. The percentage of hexafluorobutyne-2 dissolved in the ether is plotted in Fig. 2.

In a separate experiment the vapor pressure increase found on adding the acetylene to ether solutions of the acetylene indicated that at 24°, 12% of the acetylene does not dissolve. This corresponds well with the n.m.r. results.

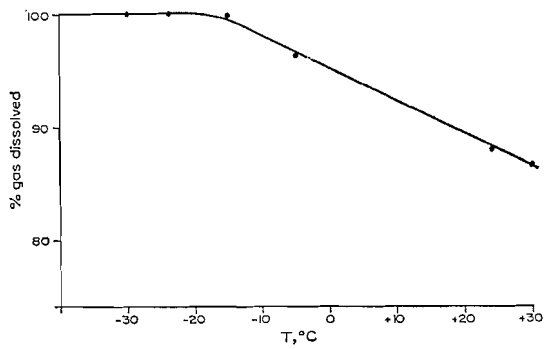

FIG. 2. Plot of % hexafluorobutyne-2 dissolved in diethylether as a function of temperature.

Discussion

Dimethylarsenic deuteride and diethylarsine have been found to add easily to hexafluorobutyne-2 in the same way as dimethylarsine (reaction [1], R = R′ = CH_3). The diethylarsine adduct is about 96% *trans* and the dimethylarsenic deuteride adduct is much the same. The n.m.r. spectrum of the deutero adduct shows that the peak due to the $(CH_3)_2As$ group is split into a quartet as has been observed previously for compounds with this type of structure (7, 12).

Kinetic Results

The addition of dimethylarsine to hexafluorobutyne-2 in ether solution is first order in both arsine and acetylene (Table II and Fig. 1). The rate constants determined from the n.m.r. monitored experiments are reproducible and an activation energy of 6.09 ± 0.20 kcal/mole for the reaction can be obtained from the variation of k_T with temperature. The activation entropy is -48 ± 1 e.u. at $-30°$ (13).

Although the u.v. monitored experiments gave good second order plots, the rate constants were inconsistent (Table II). This is probably due to the formation of variable amounts of polymeric $(CF_3C)_n$, visible in some cases. A small accelerating effect due to the u.v. radiation might also be expected since the slow gas phase addition rate is about three times faster when the reactants are irradiated with u.v. light. Good temperature control was not possible in the u.v. monitored experiment, so the rates would be expected to be nonreproducible on this account also. However, the greatly increased rate found when methanol was used as solvent is a real effect (*q.v*).

The product distribution of the liquid phase reaction is the same in a solvent as when the reactants are mixed neat, and is apparently unchanged when the reaction is done at lower temperatures. The rate of formation of the *cis* product always parallels that of the *trans*, suggesting that they are produced from the same intermediate.

In an attempt to determine if the As—H bond was involved in the rate determining step of the reaction, the rate of the addition of dimethylarsenic deuteride to the butyne was measured. However, this experiment, necessarily monitored by u.v. absorption, was inconclusive. The rate is similar to that found for the majority of the u.v. monitored experiments, (Table II).

The rate of addition of diethylarsine to the butyne is probably very little different from the rate of the addition of dimethylarsine. This can be deduced from the result that the diethylarsine rate at $-10°$ almost lies on the linear plot of log k_T against $1/T$ used to obtain the activation energy for the dimethylarsine addition.

Reaction Mechanism

Four general reaction paths can be considered for reaction [1]. The first, involving free radicals, can be eliminated mainly on the basis that the rate of addition of dimethylarsine to the acetylene is not significantly altered in the presence of an inhibitor and that the *cis* and *trans* isomers were again formed at the same rate. The increase in rate in methanol solution is against a free radical mechanism as is, to a lesser extent, the slight increase in the gas phase reaction found when the reactants are irradiated with u.v. light. The methanol experiment, monitored by u.v. spectroscopy, was checked against control unirradiated experiments. After a given time the reactions had proceeded to almost the same extent. The products from the gas phase reactions also have the same

Can. J. Chem. Downloaded from www.nrcresearchpress.com by 210.87.254.6 on 09/05/12
For personal use only.

Can. J. Chem. Downloaded from www.nrcresearchpress.com by 210.87.254.6 on 09/05/12
For personal use only.

isomer distribution as both the neat liquid reactions and the solution reactions, which indicates that the same sort of mechanism is operating in all cases.

A second possible mechanism involves pre-ionization of the arsine (reaction [3]). The rate law would be dependent on either the square root

[3] $(CH_3)_2AsH \rightleftarrows (CH_3)_2As^- + H^+$

of the arsine concentration or would be zero order in acetylene depending on the rate controlling step of the mechanism. The more likely pre-ionization step of reaction [4], could result in second

[4] $2(CH_3)_2AsH \rightleftarrows (CH_3)_2As^- + (CH_3)_2AsH_2^+$

order kinetics, first order in each of the starting materials, if addition of the arsine anion to the butyne is slower than the reverse step of reaction [4]. However, this pre-ionization step is not likely to contribute significantly to the overall mechanism of the addition reaction since the maximum rate of exchange of the label of diethylarsine with dimethylarsenic deuteride, regardless of mechanism, is 10^3 times slower than the rate of the addition reaction (11).

The third possible mechanism would involve electrophilic attack by the arsine which seems unlikely on chemical evidence. Haszeldine (14) has shown that electrophilic addition to hexafluorobutyne-2 is difficult and often needs a catalyst.

Considerable chemical evidence supports the fourth possible mechanism, nucleophilic attack by the arsine. Thus hexafluorobutyne-2 reacts easily with alkoxides and other nucleophiles (14, 15) and the ease of nucleophilic attack on hexafluorobutyne-2 is greater than on 3,3,3-trifluoropropyne, $CF_3C{\equiv}CH$ (14). It has already been shown that dimethylarsine reacts faster with the butyne than the propyne (7). Another piece of evidence pointing to nucleophilic attack is the result that as the groups R (reaction [1]) become more electronegative the reaction becomes more difficult. Thus the reaction rate decreases in the order (7)

$$(CH_3)_2AsH > (C_6H_5)(CH_3)AsH > (CF_3)_2AsH$$

an order which reflects the decreasing availability of the arsenic lone pair for nucleophilic attack because of the electron withdrawing effect of the groups attached to it (16).

In many amine additions to acetylenes the postulated mechanism involves an *intramolecular* proton transfer.

[5] $$R_2AsH + CF_3C{\equiv}CCF_3 \longrightarrow \begin{matrix} CF_3 & & CF_3 \\ & C{=}C & \\ R_2As\cdots\cdots & & H \end{matrix} \longrightarrow \begin{matrix} CF_3 & & CF_3 \\ & C{=}C & \\ R_2As & & H \end{matrix}$$

[6] $$\left.\begin{matrix}(C_2H_5)_2AsH \\ + \\ (CH_3)_2AsD\end{matrix}\right\} + CF_3C{\equiv}CCF_3 \longrightarrow \begin{matrix}(C_2H_5)_2AsC(CF_3){=}C(^{H}_{D})CF_3 \\ (CH_3)_2AsC(CF_3){=}C(^{H}_{D})CF_3\end{matrix}$$

This possibility (reaction [5]) must be considered for the arsine additions especially for the formation of the *cis* adduct. To check on this, the competitive experiment of reaction [6] was carried out on a preparative scale so that the *cis* and *trans* isomers of the products could be separated. The results are listed in Tables III and IV. The hydrogen–deuterium exchange reaction of reaction [7] when studied with neat liquids takes about 15 min for 50% equilibration at 35°, and in dilute solution is so slow compared with the rate of addition to the acetylene, that preequilibration of the arsines can be ignored (11).

[7] $(C_2H_5)_2AsH + (CH_3)_2AsD \rightleftarrows (CH_3)_2AsH + (C_2H_5)_2AsD$

Moreover, there is no exchange of the deuterium label on the products with another product or with a reactant, and there is no isomerization of the reaction products once they are formed even in the presence of unreacted arsine[1]. Thus the distribution of the deuterium label is significant and can be used as an aid to establish a mechanism for the reaction. Table V shows some of the mechanistic possibilities for the *trans* addition.

A similar table can be drawn up for the *cis* adducts. The results show that an *intramolecular* process is most unlikely for the formation of both isomers.

[1]Isomerization of tin hydride – acetylene adducts does occur in the presence of tin hydride (17).

TABLE V

Mechanistic possibilities for *trans* addition

trans Product	Exp. 1, %D		Exp. 2, %D		Mechanism
	Expt.	Calcd.	Expt.	Calcd.	
$(CH_3)_2As$	77	100	40	100	Intramolecular proton transfer
$(C_2H_5)_2As$	70	0	45	0	(*cis* addition is also intra)
$(CH_3)_2As$	77	95–100	40	95–100	Intramolecular proton transfer
$(C_2H_5)_2As$	70	≤5	45	≤5	(*cis* addition is inter)
$(CH_3)_2As$	77	70	40	40	Intermolecular proton transfer
$(C_2H_5)_2As$	70	70	45	40	(*cis* addition is inter)
$(CH_3)_2As$	77	65–70	40	35–40	Intermolecular proton transfer
$(C_2H_5)_2As$	70	65–70	45	35–40	(*cis* addition is intra)

[8] $$R_2AsH + CF_3C{\equiv}CCF_3 \xrightarrow{\text{slow}} \left[\begin{array}{c} CF_3 \quad\quad \bar{C} \\ \diagdown \quad / \\ C{=}C \\ / \quad \diagdown \\ R_2\overset{+}{A}sH \quad CF_3 \end{array} \rightleftarrows \begin{array}{c} CF_3 \quad\quad CF_3 \\ \diagdown \quad / \\ C{=}\underline{C} \\ / \quad \diagdown \\ R_2\overset{+}{A}sH \end{array} \right] \xrightarrow{R_2'AsH'} \begin{array}{c} CF_3 \quad\quad H' \\ \diagdown \quad / \\ C{=}C \\ / \quad \diagdown \\ R_2As \quad CF_3 \end{array} + \begin{array}{c} CF_3 \quad\quad CF_3 \\ \diagdown \quad / \\ C{=}C \\ / \quad \diagdown \\ R_2As \quad H' \end{array} + R_2'AsH$$

[9] $$R_2\overset{+}{A}sHC(CF_3){=}\bar{C}CF_3 + R_2'AsH' \rightarrow R_2\overset{+}{A}sHC(CF_3){=}CH'CF_3 + R_2'\bar{A}s$$

$$R_2'\bar{A}s + CF_3C{\equiv}CCF_3 \rightarrow R_2'AsC(CF_3){=}\bar{C}CF_3 \text{ etc.}$$

$$R_2\overset{+}{A}sHC(CF_3){=}CH'CF_3 \rightarrow R_2AsC(CF_3){=}CH'CF_3 + \overset{+}{H} \text{ (or } R_2\overset{+}{A}sH_2)$$

$$\overset{+}{H} \text{ (or } R_2\overset{+}{A}sH_2) + R_2'\bar{A}s \rightarrow R_2'AsH \text{ (+ } R_2AsH)$$

The following mechanism which most closely fits experimental results is proposed for the addition.

The *cis–trans* interconversion could proceed through a hyperconjugated intermediate as previously suggested (18). It is possible that at very low concentration the *cis* addition does go by an intramolecular process because of the lack of a second arsine molecule to donate its proton.

The low activation energy (6.09 kcal/mole) for the formation of the *trans* (and possibly *cis*) adduct fits in well with the idea of the arsenic atom easily donating its lone pair to the very electron defficient carbon–carbon triple bond. The activation entropy which is highly negative could be consistent with a charged transition state. The latter would account for the large increase in the rate of addition found when methanol is the solvent.

It should be noted that little can be said about the second part of the reaction, i.e. the formation of $R_2'AsH$. In fact it might not be formed at all since the anion $R_2'As^-$ might be stable enough to act as the nucleophile for further additions. This and some other possibilities are shown in reaction [9].

Acknowledgments

The authors are grateful to the National Research Council of Canada for financial support. They are indebted to Dr. D. E. McGreer for many helpful discussions. Thanks are also due to Dr. A. J. Leusink whose work on the mechanism of the hydrostannation reaction has helped to clarify our own problems.

1. W. E. Truce and J. A. Simms. J. Am. Chem. Soc. **78**, 2756 (1956).
2. S. I. Miller. J. Am. Chem. Soc. **78**, 6091 (1956).

Can. J. Chem. Downloaded from www.nrcresearchpress.com by 210.87.254.6 on 09/05/12
For personal use only.

3. E. WINTERFELDT. Angew. Chem. Intern. Ed. **6**, 423 (1967).
4. E. WINTERFELDT. Chem. Ber. **99**, 450 (1966).
5. J. E. DOLFINI. J. Org. Chem. **30**, 1298 (1965).
6. R. HUISGEN, B. GIESE, and H. HUBER. Tetrahedron Letters, **20**, 1883 (1967).
7. W. R. CULLEN, D. S. DAWSON, and G. E. STYAN. Can. J. Chem. **43**, 3392 (1965).
8. W. M. DEHN and B. B. WILCOX. Am. Chem. J. **35**, 1 (1906).
9. M. S. KARASCH, E. V. JENSEN, and S. WEINHOUSE. J. Org. Chem. **14**, 429 (1949).
10. A. TZSCHACH and W. LANGE. Z. Anorg. Allgem. Chem. **326**, 280 (1964).
11. W. R. CULLEN and W. R. LEEDER. To be published.
12. W. R. CULLEN, D. S. DAWSON, and G. E. STYAN. J. Organometal. Chem. Amsterdam, **3**, 406 (1965).
13. F. W. CAGLE and H. EYRING. J. Am. Chem. Soc. **73**, 5628 (1951).
14. R. N. HASZELDINE. J. Chem. Soc. 3490 (1952).
15. W. R. CULLEN and M. I. BRUCE. Fluorine chemistry reviews. *In* press.
16. W. R. CULLEN and D. C. FROST. Can. J. Chem. **40**, 390 (1962).
17. R. F. FULTON. Ph.D. Thesis, Purdue University. Lafayette, Indiana. 1960.
18. W. R. CULLEN and D. S. DAWSON. Can. J. Chem. **45**, 2887 (1967).

Can. J. Chem. Downloaded from www.nrcresearchpress.com by 210.87.254.6 on 09/05/12
For personal use only.

Solvolysis of alkyl chlorosulfates. Part III. Alcoholysis of *n*-propyl chlorosulfate

E. BUNCEL AND J. P. MILLINGTON
Department of Chemistry, Queen's University, Kingston, Ontario
Received November 25, 1968

The propanolysis reaction of *n*-propyl chlorosulfate has been examined quantitatively. Reaction at 25° yields the following products: di-*n*-propyl ether, *n*-propyl chloride, isopropyl chloride (trace), *n*-propyl hydrogen sulfate, di-*n*-propyl sulfate, and hydrogen chloride. It is found that the product distribution bears a direct relationship to the initial concentration of *n*-propyl chlorosulfate.

It is concluded that only di-*n*-propyl ether and di-*n*-propyl sulfate are formed in primary processes, that is solvolytic displacement at carbon and sulfur respectively, and that the other products arise through secondary reactions. Carbon displacement is the predominant primary process.

Canadian Journal of Chemistry, 47, 2145 (1969)

The alcoholysis of an alkyl chlorosulfate was first examined in 1879 by Claesson (1) who reported the formation of a variety of products. Thus ethyl chlorosulfate on treatment with ethanol gave rise to diethyl ether, ethyl chloride, diethyl sulfate, ethyl hydrogen sulfate, and hydrogen chloride (1). Subsequently the reaction of methyl chlorosulfate with methanol was reported to yield analogous products, but with the exception of dimethyl ether (2).

In our first systematic study of nucleophilic substitution in alkyl chlorosulfates (3, 4) the kinetics of hydrolysis in aqueous dioxan of a series of primary alkyl chlorosulfates was reported on (see also ref. 5). The relative rates of hydrolysis were in accord with a solvolytic displacement process at carbon (**1**) but the entropies of activation suggested the possibility of multiple bond fission (**2**) (cf. refs. 6, 7). The reaction of

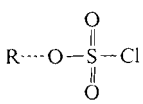

1

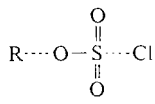

2

n-propyl chlorosulfate with some nucleophiles in aqueous dioxan was similarly interpreted as proceeding by displacement at carbon with $^-OSO_2Cl$ as the leaving group (8). In the alcoholysis of an alkyl chlorosulfate, the formation of dialkyl ether is indicative of carbon displacement, while the simultaneous formation of dialkyl sulfate would then suggest that nucleophilic displacement at sulfur has become an important competing process. The origin of the other products observed in the earlier studies (1, 2) is not so clear. The present study was initiated with the aim of elucidating these aspects and particularly to evaluate quantitatively the nucleophilicities towards carbon and towards sulfur in this system.

Results

The system chosen for study was that of *n*-propyl chlorosulfate with *n*-propanol, in which quantitative estimation of the various possible products should be readily feasible. As anticipated, gas–liquid chromatography (g.l.c.) allowed the quantitative analysis of di-*n*-propyl ether, *n*-propyl chloride, isopropyl chloride, and di-*n*-propyl sulfate, in *n*-propanol solvent. Hydrogen chloride was analyzed as chloride ion with silver nitrate, and *n*-propyl hydrogen sulfate was determined as the difference between the total acid, as titrated with sodium hydroxide, and the hydrogen chloride. Reaction was allowed to go to completion at 25° prior to product analysis. The effect of varying the initial chlorosulfate concentration on the proportion of the various products was evaluated.

The results of the product analyses are given in Tables I–III. For clarity the data are presented separately for the constituent portions of the substrate: the *n*-propyl residue (Table I), the chloride residue (Table II), and the sulfate moiety (Table III), in mole % throughout. The *n*-propyl hydrogen sulfate data are not included in Table I since, as is shown later, the alkyl moiety of this product originates not from the substrate but from the solvent through a secondary reaction. Isopropyl chloride constitutes only a very small proportion of the total alkyl halide and is formed

TABLE I

Propanolysis of *n*-propyl chlorosulfate at 25°*

[*n*-$PrOSO_2Cl$] (*M*/l)	*n*-PrCl (mole %)	iso-PrCl (mole %)	*n*-Pr_2O (mole %)	*n*-Pr_2SO_4 (mole %)	Total products (mole %)
0.00810	6.2†	—	96.0	—	—
0.00895	4.5†	—	95.5	—	—
0.0565	40.0	—	52.4	3.2	95.6
0.530	52.5	—	40.0	8.3	100.8
0.513	56.2	—	35.5	8.5	100.2
1.99	64.7	3.4	23.0	6.4	97.5

*Products derived from the alkyl residue.
†Obtained as the difference between 100% and the yield of HCl (see Table II).

TABLE II

Propanolysis of *n*-propyl chlorosulfate at 25°*

[$PrOSO_2Cl$] (*M*/l)	*n*-PrCl (mole %)	iso-PrCl (mole %)	HCl (mole %)	Total products (mole %)
0.00810	6.2†	—	93.8	—
0.00895	4.5†	—	95.5	—
0.0565	40.0	—	53.9	93.9
0.530	52.5	—	44.9	97.4
0.513	56.5	—	34.6	91.1
1.99	64.7	3.4	22.3	90.4

*Products derived from the chloride residue.
†Obtained as the difference between 100% and the yield of HCl.

TABLE III

Propanolysis of *n*-propylchlorosulfate at 25°*

[$PrOSO_2Cl$] (*M*/l)	*n*-Pr_2SO_4 (mole %)	*n*-$PrOSO_3H$ (mole %)	Total products (mole %)
0.00810	—	97.3	97.3
0.00895	—	96.0	96.0
0.0565	3.2	94.3	97.5
0.530	8.3	94.8	103.1
0.513	8.5	95.0	103.5
1.99	6.4	95.5	101.9

*Products derived from the sulfate moiety.

only with the highest *n*-propyl chlorosulfate concentration. Due to the very small yield of di-*n*-propyl sulfate and the consequent poor precision in analysis, it is not clear whether the apparent initial increase and subsequent decrease in the yield of this material is real, or whether its yield should be considered as invariant, within experimental error (i.e. a yield of 6 ± 2.5 mole%). The material balance in the various experiments is generally better than 90% of theoretical.

The effect of increasing the initial concentration of *n*-propyl chlorosulfate on the product distribution is seen more clearly with reference to the graphical representation in Figs. 1 and 2, for the volatile and the ionic products of reaction, respectively. Figure 1 shows that on increasing the initial substrate concentration from ca. 0.01 to 2 *M* the yield of di-*n*-propyl ether decreases, rapidly at first and then more gradually, while the yield of *n*-propyl chloride increases correspondingly. The di-*n*-propyl sulfate yield remains small throughout. Figure 2 shows that the decrease in the hydrogen chloride yield with increasing substrate concentration mirrors the trend with respect to di-*n*-propyl ether. The *n*-propyl hydrogen sulfate yield remains approximately constant.

Discussion

The results presented in Tables I–III and Figs. 1 and 2 show that there is a relationship between the spectrum of products and the initial substrate concentration. The proposed mechanistic rationale of the observations is as follows. The near quantitative formation of di-*n*-propyl ether in the most dilute reaction media indicates that the principal primary process, in the absence of complicating reactions which arise as the substrate concentration is increased, is solvolytic displacement by *n*-propanol nucleophile on carbon, with $^-OSO_2Cl$ as the leaving group. The near constancy in the di-*n*-propyl sulfate yield

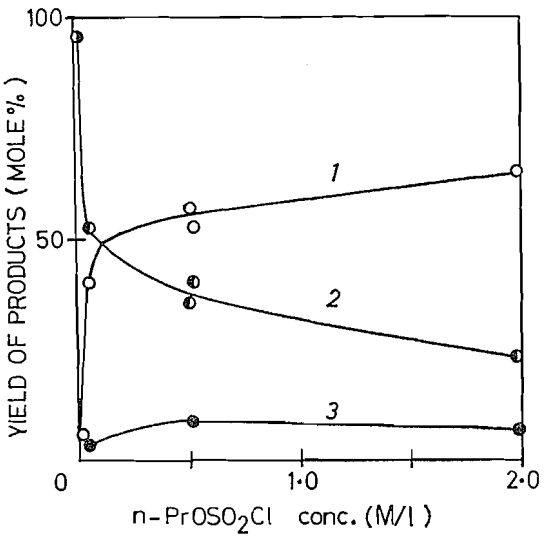

FIG. 1. Yield of gaseous products (mole %) in the propanolysis of *n*-propyl chlorosulfate at 25° as function of initial concentration. Curve 1, *n*-propyl chloride; curve 2, di-*n*-propyl ether; curve 3, di-*n*-propyl sulfate.

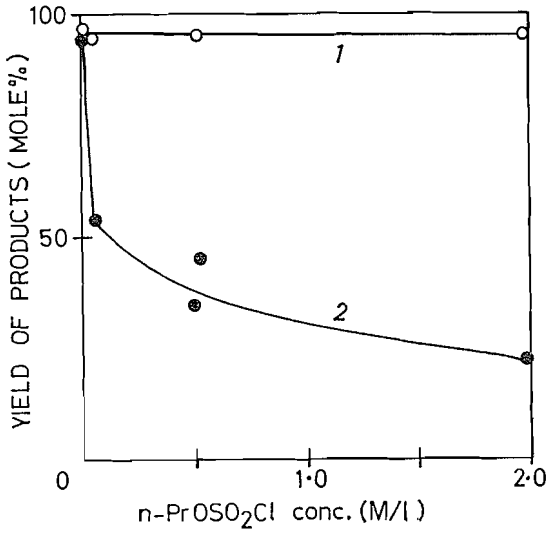

FIG. 2. Yield of ionic products (mole %) in the propanolysis of *n*-propyl chlorosulfate at 25° as function of initial concentration. Curve 1, *n*-propyl hydrogen sulfate; curve 2, hydrogen chloride.

over the range of substrate concentrations suggests that this compound is formed by a minor concurrent (parallel) process, that is, displacement by *n*-propanol nucleophile on sulfur, with chloride ion as the leaving group. The two primary processes, solvolytic displacement at carbon and at sulfur, are depicted in reactions [1] and [2]

[1] $PrOH + Pr\overset{\frown}{O}SO_2Cl \longrightarrow Pr_2O + HOSO_2Cl$

[2] $PrOH + PrOSO_2\overset{\frown}{Cl} \longrightarrow PrOSO_2OPr + HCl$

It is proposed that the other observed products arise as follows. The chlorosulfonic acid formed in the principal solvolytic process (reaction [1]) will be rapidly solvolyzed to form *n*-propyl hydrogen sulfate and hydrogen chloride (reaction [3]); this would account for the initial formation of hydrogen chloride in ca. 95% yield, as well as *n*-propyl hydrogen sulfate. Now as the concentration of hydrogen chloride increases, with increasing initial substrate concentration, chloride ion will effectively compete with *n*-propanol in nucleophilic displacement at the carbon center of *n*-propyl chlorosulfate (reaction [4]). (This reaction may be acid catalyzed, with protonation occurring on the ester oxygen, and may also account for the formation of isopropyl chloride through a minor ionization process.) Since

[3] $PrOH + HOSO_2\overset{\frown}{Cl} \longrightarrow PrOSO_2OH + HCl$

[4] $HCl + Pr\overset{\frown}{O}SO_2Cl \longrightarrow PrCl + HOSO_2Cl$

reaction [4] also consumes the substrate, the formation of propyl chloride must occur at the expense of the propyl ether (reaction [1]), as is in fact observed experimentally (Fig. 1). (Some *n*-propyl chloride may also be formed by reaction of hydrogen chloride with solvent but this should be a very minor process under the mild reaction conditions.) The chlorosulfonic acid formed in the latter reaction (reaction [4]) will react with solvent to give more *n*-propyl hydrogen sulfate, whose total yield will therefore equal the sum of the yields of propyl ether and propyl chloride. This also is borne out by the experimental findings.

The conclusion of the preceding discussion hence is that the primary processes in the propanolysis of *n*-propyl chlorosulfate are solvolytic displacements at carbon (reaction [1]) and at sulfur (reaction [2]), leading to propyl ether and propyl sulfate, respectively. Propyl chloride, propyl hydrogen sulfate, and hydrogen chloride are formed in secondary, consecutive, reactions (reactions [3] and [4]). Of the two primary processes, the predominance of solvolytic displacement at carbon requires comment. One factor

favoring attack at carbon is the great facility of $^-OSO_2Cl$ as a leaving group (cf. ref. 9). This is no doubt due in the main to the fact that $^-OSO_2Cl$ is the conjugate base of one of the strongest acids, but it may also result from the possibility of multiple bond fission (4). However, another pertinent factor may well be that the competing nucleophilic attack at sulfur will be discouraged, relatively, by the negative field effect of the sulfonyl oxygens (10, 11). A further electronic effect which will have the same influence is back-donation from an occupied p-orbital of chlorine to a vacant d-orbital of sulfur. The relevance of such p_π–d_π bonding to chlorosulfate reactivity will be further discussed at a later date (12).

Experimental

n-Propyl chlorosulfate was prepared according to the procedure of Binkley (13) and had physical properties as previously described (8). Di-*n*-propyl sulfate was prepared by the method of Nef (14) and had the following physical properties: b.p. 114–115°/15 mm, density 1.114 (22.5°), refractive index 1.4140 (25°), in close agreement with the literature values (14).

The reactions between *n*-propyl chlorosulfate and *n*-propanol were run in a thermostatted bath at 25° to completion. Product analysis was performed directly on aliquots of the reaction mixture. The ionic products (total acid, chloride ion, and propyl hydrogen sulfate by difference) were determined by volumetric procedures given previously (8). The volatile products were determined by quantitative g.l.c. using a Beckman G.C.2 chromatograph with a column of neopentylglycol sebacate, 10% on Embacel, and helium as carrier gas (40 p.s.i.). For analysis of di-*n*-propyl ether, *n*-propyl chloride, and isopropyl chloride, the column temperature was 70°, while for di-*n*-propyl sulfate the temperature was 190°. The yields of these products were determined by means of calibration curves (*n*-propanol solvent), constructed using the authentic compounds.

Acknowledgment

We thank the National Research Council of Canada for a grant in aid of research and for a scholarship (to J.P.M.).

1. P. Claesson. J. Pract. Chem. [2], **19**, 231 (1879).
2. R. Levaillant and L. J. Simon. Compt. Rend. **169**, 854 (1919).
3. E. Buncel and J. P. Millington. Proc. Chem. Soc. 406 (1964).
4. E. Buncel and J. P. Millington. Can. J. Chem. **43**, 556 (1965).
5. H. K. Hall, Jr. J. Am. Chem. Soc. **78**, 1450 (1956).
6. J. F. King and D. J. H. Smith. J. Am. Chem. Soc. **89**, 4803 (1967).
7. A. Queen. Can. J. Chem. **45**, 1619 (1967).
8. E. Buncel and J. P. Millington. Can. J. Chem. **43**, 547 (1965).
9. A. G. Cottrell, E. Buncel, and J. K. N. Jones. Chem. Ind. London, 552 (1966).
10. C. Y. Meyers. Tetrahedron Letters, **24**, 1125 (1962).
11. J. Strating. Organic sulfur compounds. Vol. 1. *Edited by* N. Kharasch. The Pergamon Press, Ltd., New York. 1961. p. 146.
12. E. Buncel and L.-I. Choong. To be published.
13. W. W. Binkley. J. Am. Chem. Soc. **60**, 2810 (1938).
14. J. U. Nef. Ann. **318**, 1 (1901).

Can. J. Chem. Downloaded from www.nrcresearchpress.com by 210.87.254.42 on 09/05/12
For personal use only.

Electron spin resonance studies of radicals condensed from irradiated water vapor: reactions of the radicals[1,2]

P. WARDMAN[3] AND W. A. SEDDON

Research Chemistry Branch, Atomic Energy of Canada Limited, Chalk River Nuclear Laboratories, Chalk River, Ontario

Received November 26, 1968

Electrons and hydroperoxyl radicals are trapped in polycrystalline ice after irradiation of water vapor and rapid condensation to 77 °K. Using higher sample flow rates than in the earlier work of Seddon, Smith, and Bindner, the electron spin resonance spectra of the trapped electrons (e_t^-) were obtained in both H_2O and D_2O ice with negligible interference from the underlying $HO_2\cdot$ ($DO_2\cdot$) radicals. Addition of $C(NO_2)_4$, H_2O_2, $(CH_3)_2SO$, and O_2 as radical scavengers confirmed the earlier prediction that reactions with the radicals do not occur in the vapor phase in this system. The results with $C(NO_2)_4$ and H_2O_2 also provided chemical evidence consistent with the spectroscopic assignment for $HO_2\cdot$ ($DO_2\cdot$) radicals. Experiments with added isobutylene suggested that hydrogen atoms are formed (possibly in a post-irradiation reaction during condensation) and are also produced on photobleaching e_t^- at 77 °K.

Canadian Journal of Chemistry, 47, 2149 (1969)

Introduction

Gamma irradiation of many glassy solids produces electrons which are trapped in the matrix with high efficiency. Typically, the yield (G) of trapped electrons (e_t^-) at 77 °K is in the range 0.5–3 per 100 eV energy absorbed (1, 2). In contrast, electrons produced by irradiation of the same materials in polycrystalline or single crystal forms are generally trapped with very low efficiency or not at all (e.g. in solute-free ice, $G(e_t^-) \simeq 2 \times 10^{-4}$ at 77 °K (3)). The observation by Marx, Leach, and Horani (4) and Seddon, Smith, and Bindner (5) that electrons could be efficiently trapped in polycrystalline ice when water vapor was irradiated and rapidly condensed to 77 °K, was therefore of considerable interest.

Further study of e_t^- in solute-free ice was made difficult by the presence of the underlying $HO_2\cdot$ electron spin resonance (e.s.r.) absorption, which entirely masked the e_t^- resonance in H_2O ice (4, 5). We have found that increasing the sample flow rate increased the ratio of e_t^- to $HO_2\cdot$ in the deposit and this permitted an extension of the earlier work (5). Hydrogen atoms and hydroxyl radicals are expected to be formed during irradiation in the vapor phase and reactive solutes have been added to the water vapor in an attempt to study the formation and reactivity of $HO_2\cdot$ and other radicals in this system.

Experimental

Materials

Dimethylsulfoxide-d_6 was supplied by Stohler Isotope Chemicals (99.5% D). Isobutylene was Phillips Research Grade, 99.84%. Nitric oxide (Matheson) was fractionally distilled several times in vacuo. Sodium deuteroxide was prepared by dissolving sodium in D_2O. Tetranitromethane (K and K Laboratories) was shaken with 0.1 *M* HCl ten times (6), degassed, and stored in vacuo at 77 °K. Water (H_2O and D_2O) was quadruply distilled and preirradiated as described previously (7). D_2O was 99.75% D, low tritium, high grade material supplied by A.E.C.L. All other chemicals were of reagent or spectroscopic grade.

Preparation of Samples

All samples were deaerated on a grease and mercury-free vacuum system by bulb-to-bulb distillation where appropriate. Samples of pure H_2O and D_2O (0.2 to 0.4 g) were distilled directly from the liquid into the target chamber but mixtures (0.1 g) were admitted from a 5 l bulb. After preliminary washing, glassware was cleaned by baking in an air oven for 12 h at 550 °C.

Irradiations

A 100 μA, 1 MeV He^+ ion beam was used for crossed-beam irradiations as described previously (5, 8). The sample introduction system was constructed entirely of stainless steel and the needle valve used in the previous work (5, 8) was omitted.

Preliminary experiments had shown that increasing the sample flow rate over that used in the earlier work (5, 8) increased the ratio of electrons to other radicals in the deposit and in all the experiments described below, the flow rates were up to five times greater than those used earlier. The pressure in the radiation zone was therefore slightly different from that measured previously (5). Pure water samples were introduced at a rate of about 0.1 g in 3 min and mixtures at about 0.1 g in 15 min. In the latter

[1]Issued as A.E.C.L. No. 3298.

[2]Presented in part at the 156th National Meeting of the American Chemical Society, Atlantic City, New Jersey. September 8–13, 1968.

[3]NRCC Postdoctorate Fellow 1967–1969.

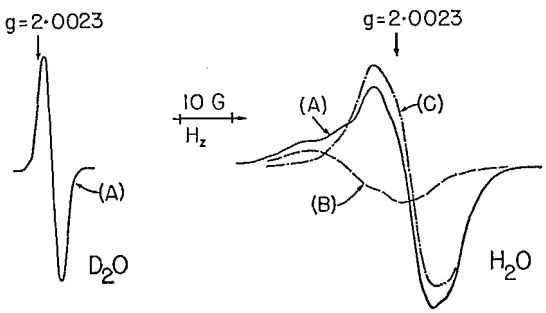

FIG. 1. Electron spin resonance absorption spectra of H_2O and D_2O at 77 °K after condensing irradiated water vapor. (A), before photobleaching (no saturation); (B), after photo bleaching; (C), calculated for e_t^-, i.e. (A) − (B).

case most of the sample was deposited in the first 5 min. Samples were then isolated under vacuum; light was excluded during irradiation and examination of samples.

Electron Spin Resonance Spectroscopy

A Varian V-4502 X-band spectrometer was used with the Fieldial and the TE_{104} cavity. Resonances exhibiting g-factor anisotropy were analyzed using Kneubühl's method (9). Frequency measurements were made with a Hewlett–Packard microwave frequency converter and electronic counter.

Deposits of ice on the cold finger were warmed by passing a stream of cold helium through the finger, displacing the liquid nitrogen. The temperature was measured with a thermocouple in the gas stream and was varied by controlling the helium flow rate.

Samples in the e.s.r. cavity were photobleached using a focussed 150 W tungsten filament lamp and Corning glass filters ($440 < \lambda < 740$ mμ).

Results and Discussion

(i) Pure Water Vapor

The e.s.r. absorption spectra of the deep blue colored deposit at 77 °K from irradiated D_2O and H_2O vapor are shown in Fig. 1. In D_2O at low microwave powers (3×10^{-8} to 10^{-6} W) only the singlet (A) of e_t^- was observed, but at higher powers, saturation of the e_t^- signal permitted the observation of an underlying radical, and the spectra were similar to those found earlier (5) for deposits containing fewer trapped electrons. In H_2O the singlet of e_t^- was four times broader than in D_2O and was slightly distorted by an underlying resonance even at low microwave powers (spectrum (A)). The absorption of e_t^- in H_2O was obtained (C) by photobleaching e_t^- completely and subtracting the underlying resonance (spectrum (B)) remaining after photobleaching. It was verified that the concentration of the underlying radicals (spectrum (B)) did not change during photobleaching e_t^-. The lines of e_t^- in D_2O and H_2O were closely Gaussian, with line widths between derivative maxima $\Delta H_{ms} = 2.7 \pm 0.3$ and 10.6 ± 1.5 G, respectively and both had $g = 2.0008 \pm 0.0003$.

Although ȮD was expected to be observed in the deposit (5), no evidence for the characteristic splitting of ȮD was observed in D_2O. The underlying resonance observed after removal of e_t^- by photobleaching was similar to that observed previously and assigned to the hydroperoxyl radical (5): cf. Fig. 2 (below). In H_2O, $g_{\parallel} = 2.034 \pm 0.001$ and $g_{\perp} = 2.0024 \pm 0.0008$; in D_2O, $g_{\parallel} = 2.034 \pm 0.001$ and $g_{\perp} = 2.004 \pm 0.001$, all at 77 °K. Splitting of the parallel feature was always observed in H_2O ($A_{\parallel} = 15 \pm 3$ G at 77 °K) but never in D_2O. An almost negligible splitting of the perpendicular feature was often seen in both H_2O and D_2O (similar to that observed in Fig. 2). In H_2O this may in part be attributable to proton hyperfine interaction, but there is a small difference between g_x and g_y for $HO_2\cdot$ or $DO_2\cdot$ in ice at 77 °K. These parameters are in good agreement with those well established for the hydroperoxyl radical (10, 11).

Warming the deposit without photobleaching resulted in the disappearance of both e_t^- and $HO_2\cdot$ ($DO_2\cdot$). The e_t^- signal began to decay at about 120 °K and the first half-life was 20 ± 2 min at 130 ± 5 °K in D_2O. The decay could not be followed to an extent sufficient to determine the kinetic order because of the underlying resonance. The $HO_2\cdot$ ($DO_2\cdot$) radicals were also decaying in this temperature region and decayed rapidly at 140 °K. The small splitting of the perpendicular feature of the $DO_2\cdot$ radical disappeared on warming to 110 °K.

The probable fate of e_t^- during thermal bleaching at about 130 °K is by reaction [1] rather than by the alternative reaction [2], because Bennett *et al.* (12) have shown that the electrons trapped in a similar ice matrix in the absence of solvated protons were observable at temperatures up to at least 170 °K. This

$$[1a] \qquad e_t^- + kT \rightarrow e_m^-$$

$$[1b] \qquad e_m^- + [(H_2O)_nH]^+ \rightarrow nH_2O + H\cdot$$

$$[2] \qquad 2\,e_m^- \rightarrow 2OH^- + H_2$$

Can. J. Chem. Downloaded from www.nrcresearchpress.com by 210.87.254.42 on 09/05/12
For personal use only.

Can. J. Chem. Downloaded from www.nrcresearchpress.com by 210.87.254.42 on 09/05/12
For personal use only.

comparison is justified because the ice matrix is produced in a very similar manner in both systems and the e.s.r. parameters for e_t^- in ice at 77 °K obtained in this work are closely similar to those obtained by Bennett *et al.* (12). It is very probable that the ice in these experiments is polycrystalline since vitreous ice is produced to a maximum thickness of 0.06 mm when wet nitrogen impinges slowly on a cold surface (13, 14).

(ii) The Line Shape of e_t^- in Ice

Our results confirm the suggestion of Bennett *et al.* (12) that the alkali metal ions do not broaden the e.s.r. line of e_t^- prepared by depositing sodium atoms and water vapor on a rotating drum at 77 °K. These authors observed 7 hyperfine lines ($A_H = 5.5 \pm 0.5$ G) in the e.s.r. spectrum of e_t^- in H_2O at 170 °K. If the spin density on the D atoms is the same for e_t^- in D_2O ice as it is on the H atoms in H_2O ice, then *F* center theory (15) predicts $\Delta H_{ms}(H_2O) = 4\,\Delta H_{ms}(D_2O)$; such a ratio was experimentally observed. However, computer simulation of the spectrum expected for e_t^- in D_2O at 77 °K assuming six equivalent D atoms and $A_D = 0.85 \pm 0.09$ G indicated that the minimum linewidth of the singlet would be $\Delta H_{ms} \simeq 4$ G. Thus either the 6 protons are not all equivalent or the spin density distribution is different in H_2O and D_2O.

(iii) The Effects of H_2O_2 and $C(NO_2)_4$

The e.s.r. spectrum of the deposit obtained from 7.5 mole % H_2O_2 in H_2O is shown in Fig. 2(A); no electrons were trapped in the deposit. The spectrum was closely similar to that obtained from pure H_2O after bleaching e_t^- and had $g_{\|} = 2.034 \pm 0.001$, $g_{\perp} = 2.0030 \pm 0.0006$, and $A_{\|} = 15 \pm 2$ G at 77 °K. A sample of D_2O containing 0.18% H_2O_2 gave the spectrum shown in Fig. 2(B) at 77 °K with $g_{\|} = 2.033 \pm 0.001$ and $g_{\perp} = 2.004 \pm 0.001$. (Since H_2O_2 exchanges in D_2O (16), a dilute solution of H_2O_2 in D_2O may be treated as D_2O_2 in D_2O.) On warming, the parallel feature became more prominent and at 130 °K (Fig. 2(C)), $g_{\|} = 2.032 \pm 0.001$ and $g_{\perp} = 2.0072 \pm 0.0005$. We conclude from the spectroscopic data that the addition of sufficient hydrogen peroxide prevents the trapping of electrons in the deposit and that the only remaining paramagnetic species is the hydroperoxyl radical.

It was found that the addition of hydrogen peroxide approximately doubled the concentration of $HO_2\cdot$ ($DO_2\cdot$) radicals in the deposit relative to that observed in the absence of this scavenger. This is expected if $\dot{O}H$ radicals produced during condensation by reaction [3] are converted to $HO_2\cdot$ in reaction [4] in preference to the dimerization reaction [5], which is important in the absence of H_2O_2.

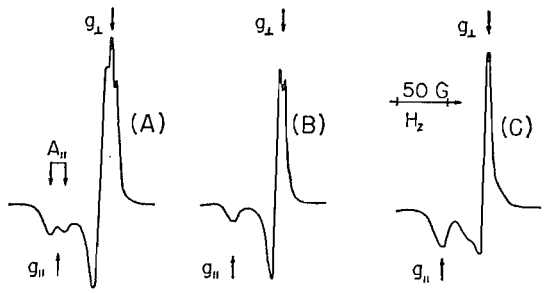

FIG. 2. Electron spin resonance absorption spectra of the deposit condensed from irradiated water vapor containing hydrogen peroxide. (A), 7.5 mole % H_2O_2 in H_2O at 77 °K; (B), 0.18 mole % D_2O_2 (see text) in D_2O at 77 °K; (C), sample (B) at 130 °K.

[3] $$e_m^- + H_2O_2 \rightarrow \dot{O}H + OH^-$$

[4] $$\dot{O}H + H_2O_2 \rightarrow H_2O + HO_2\cdot$$

[5] $$2\,\dot{O}H + M \rightarrow H_2O_2 + M$$

The ratio of $[e_t^-]/[DO_2\cdot]$ was measured in pure D_2O and found to be ~ 2.1, about 5 times higher than that measured in the earlier work (5). The increase in this ratio arose from about a doubling in the number of electrons trapped in the deposit and a halving of the concentration of $DO_2\cdot$ radicals with the increased sample flow rate. The reasons for this marked effect of deposition rate are not known.

Tetranitromethane reacts with both electrons and hydroperoxyl radicals to produce $C(NO_2)_3^-$ and NO_2 (6, 17). No trapped electrons were observed in the deposit condensed from an irradiated mixture of D_2O and 0.005 mole % $C(NO_2)_4$. The e.s.r. spectrum of the deposit is shown in Fig. 3(A) and is very similar to that ascribed by Symons *et al.* (18) to NO_2 in ice at 77 °K. The 3 hyperfine lines overlap to a negligible extent and were integrated to ascertain whether the $DO_2\cdot$ radical (which underlies only the central line of NO_2) was present. The integrated area under the central line was only about 10–15% higher than the outer lines (of the same

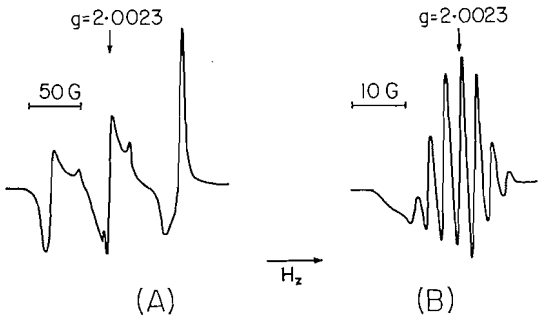

FIG. 3. Electron spin resonance absorption spectra of the deposit at 77 °K condensed from irradiated D_2O vapor containing: (A), 0.005 mole % $C(NO_2)_4$; (B), 0.5 mole % $(CD_3)_2SO$.

order of magnitude as the experimental error) even at $[C(NO_2)_4] = 0.1$ mole %.

The ratio of electrons to $DO_2\cdot$ radicals condensed in the deposit from pure D_2O is less than 2.1 under the conditions used for the samples containing solutes. If $C(NO_2)_4$ scavenged only the electrons and not the $DO_2\cdot$ radicals, the integrated area under the central line of the NO_2 triplet would be at least twice as great as the outer lines. No such difference was observed. This may indicate that $C(NO_2)_4$ was also reacting with $DO_2\cdot$ and is additional chemical evidence supporting our confirmation of the assignment (4, 5) of the underlying radical in pure water to the hydroperoxyl radical. An alternative explanation of the apparent absence of $DO_2\cdot$ upon the addition of $C(NO_2)_4$ is that the number of electrons reacting with $C(NO_2)_4$ is considerably greater than the number trapped in the absence of scavengers (see below).

(iv) Effects of $(CH_3)_2SO$, O_2, and NO

Earlier calculations (5) had predicted that only extremely rapid reactions with the major component of the vapor (such as ion–molecule reactions) could occur in the vapor phase in the time between irradiation and hitting the surface of the cold finger (ca. 10 μs). If this is correct then the efficiency of scavenging electrons and other radicals might depend on the efficiency with which the scavenger is condensed. Dimethylsulfoxide reacts with e_{aq}^- very slowly

$$k(e_{aq}^- + (CH_3)_2SO) = 1.7 \times 10^6\ M^{-1}\ s^{-1}$$

at ~ 20 °C in H_2O (19) but like $C(NO_2)_4$ has a melting point close to room temperature. Oxygen and nitric oxide have a reactivity towards e_{aq}^- similar to that of $C(NO_2)_4$ but the condensing efficiency will be much lower.

The e.s.r. spectrum of the deposit condensed from an irradiated mixture of 0.5% $(CD_3)_2SO$ in D_2O is shown in Fig. 3(B). The 7 lines of $CD_3\cdot$ ($A_D = 3.6 \pm 0.1$ G) are superimposed on a broad underlying resonance. No trapped electrons were observed, but at $[(CD_3)_2SO] = 0.01\%$, a small fraction of the electrons was not scavenged and e_t^- was observed in low yield. Hydroxyl radicals may also react with dimethylsulfoxide to produce methyl radicals (19, 20).

Even 0.7% O_2 had little or no effect on the radicals trapped in the deposit. When oxygen was admitted to the surface of the deposit whilst under e.s.r. examination, no change in the concentration of electrons was observed after several minutes exposure. A similar lack of effect of oxygen on $CD_3\cdot$ radicals trapped in the deposit suggested that oxygen could not diffuse through the ice at 77 °K, since the formation of alkyl peroxy radicals is known to be rapid even at low temperatures (11).

The deposit condensed from irradiated 0.2% NO in D_2O contained a very low concentration of NO_2 radicals in addition to $DO_2\cdot$ and a much lower concentration of electrons than normal. Blank experiments without irradiation produced an identical concentration of NO_2; admission of oxygen to the surface of the deposit at 77 °K had no effect on the e.s.r. spectrum.

The absence of an effect with O_2 may be contrasted with the effectiveness of $C(NO_2)_4$ and $(CD_3)_2SO$ at concentrations three orders of magnitude less. It seems likely that reaction of the electron with the solute must only occur either in the transient liquid phase during condensation or in the solid condensate at temperatures where the electrons are still mobile.

(v) Effect of $(CH_3)_2C{=}CH_2$: Photobleaching of e_t^-

Isobutylene (0.2%) in H_2O did not prevent the trapping of electrons in the deposit and the e.s.r. spectrum of the $(CH_3)_3C\cdot$ radical was observed ($A_H = 22.7 \pm 0.5$ G) superimposed on the e_t^- and $HO_2\cdot$ signals (Fig. 4(A)). The concentration of $(CH_3)_3C\cdot$ radicals was increased by 25% on photobleaching e_t^- at 77 °K (Fig. 4(B)). When 0.5% CO_2 (an electron scavenger) was added in

Can. J. Chem. Downloaded from www.nrcresearchpress.com by 210.87.254.42 on 09/05/12
For personal use only.

addition to 0.2% isobutylene, the contribution of $(CH_3)_3C\cdot$ to the total concentration of radicals was much less, the blue coloration of e_t^- was considerably diminished, and no increase in the $(CH_3)_3C\cdot$ radical concentration was observed on photobleaching the remaining e_t^- absorption.

The observation of *t*-butyl radicals upon the addition of isobutylene suggests that hydrogen atoms are produced. The effects of electron scavengers suggest that a major fraction of the alkyl radicals observed arise not from the hydrogen atoms produced in primary events during radiolysis (which would probably condense with low efficiency), but from hydrogen atoms produced during post-radiolysis events in the deposit. Electrons are mobile in ice at temperatures above about 130 °K and hydrogen atoms are expected to be produced in the deposit during cooling in the post-irradiation reaction [1*b*]. If reaction [1*b*] is indeed important during condensation, added scavengers would react with a much greater number of electrons than could be trapped in the absence of scavenger.

The increase in the $(CH_3)_3C\cdot$ radical signal observed on *photobleaching* e_t^- *in ice* condensed from H_2O containing $(CH_3)_2C{=}CH_2$ suggests that hydrogen atoms are produced during this process. It is experimentally difficult to determine whether a major fraction of spins is converted from e_t^- to $(CH_3)_3C\cdot$ during photobleaching, and it is impossible from this evidence alone to be sure that a reaction producing $H\cdot$ is the major photobleaching process. Ionic reactions such as [6] followed by [7] are also a possible explanation of the observations

$$[6] \quad H_3O^+ + (CH_3)_2C{=}CH_2 \rightarrow H_2O + (CH_3)_3C^+$$

$$[7] \quad (CH_3)_3C^+ + e_m^- \rightarrow (CH_3)_3C\cdot$$

and from the available thermochemical data (21) we cannot exclude this possibility.

Conclusions

The electrons trapped in polycrystalline ice after condensing irradiated water vapor have similar chemical properties to those trapped in glassy matrices. Chemical evidence to support the spectroscopic identification of the hydroperoxyl radical in the deposit has been obtained but only indirect evidence is available that the precursor

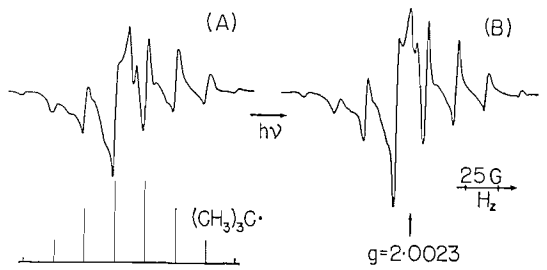

FIG. 4. Electron spin resonance absorption spectra of the deposit at 77 °K condensed from irradiated H_2O vapor containing 0.2 mole % $(CH_3)_2C{=}CH_2$; (A), before photobleaching e_t^- ($H_1 = 2 \times 10^{-2}$ G, e_t^- strongly saturated); (B), after photobleaching.

of $HO_2\cdot$ is[4] $\dot{O}H$. The $HO_2\cdot$ radical is also observed when water containing $\dot{O}H$ radicals, produced by a microwave discharge, is condensed and the problem is discussed in some detail elsewhere (22, 23). Recent work (24) indicates that reaction [4] has a surprisingly low activation energy (1.2 kcal mole^{-1}).

The disadvantages of this technique are that post-irradiation reactions may occur during condensation and the choice of scavengers is restricted. The absence of an effect of a scavenger (such as that with O_2) does not necessarily indicate that the species of interest are absent. Relative primary yields may not be deduced from an examination of the condensate.

Acknowledgments

Most of the apparatus and techniques used in this work were developed by Dr. D. R. Smith and co-workers (5, 25) and we thank Dr. Smith for helpful discussions. We thank Mr. G. A. Sims for his expert operation of the accelerator and Mr. P. E. Bindner for technical assistance.

1. W. H. HAMILL. *In* Radical ions. *Edited by* E. T. Kaiser and L. Kevan. Interscience Publishers, Inc., New York. 1968. p. 321.
2. *For a review see* L. KEVAN. Radiation chemistry of frozen aqueous solutions. 19th Farkas Memorial Symp., Jerusalem. 1967. U.S.A.E.C. report COO-1528.

[4]The addition of 0.2 mole% isopropanol did not prevent the trapping of electrons in the deposit and $(CH_3)_2\dot{C}OH$ radicals were observed together with $HO_2\cdot$ and e_t^-. It is possible that the $(CH_3)_2\dot{C}OH$ radicals arose from reaction with $H\cdot$ atoms rather than $\dot{O}H$, although no increase in the concentration of $(CH_3)_2\dot{C}OH$ was observed on photobleaching e_t^- (unpublished work by Wardman).

Can. J. Chem. Downloaded from www.nrcresearchpress.com by 210.87.254.42 on 09/05/12
For personal use only.

3. K. EIBEN and I. A. TAUB. Nature, **216**, 782 (1967).
4. R. MARX, S. LEACH, and M. HORANI. J. Chim. Phys. **60**, 726 (1963).
5. W. A. SEDDON, D. R. SMITH, and P. E. BINDNER. Can. J. Chem. **46**, 1747 (1968).
6. B. H. J. BIELSKI and A. O. ALLEN. J. Phys. Chem. **71**, 4544 (1967).
7. W. A. SEDDON and D. R. SMITH. Can. J. Chem. **45**, 3083 (1967).
8. W. A. SEDDON and D. R. SMITH. *In* Radiation chemistry. Vol. II. Advan. Chem. Ser. No. 82. *Edited by* R. F. Gould. Am. Chem. Soc. Washington, 1968. p. 163.
9. F. K. KNEUBÜHL. J. Chem. Phys. **33**, 1074 (1960).
10. S. J. WYARD, R. C. SMITH, and F. J. ADRIAN. J. Chem. Phys. **49**, 2780 (1968).
11. J. E. BENNETT, B. MILE, and A. THOMAS. 11th Intern. Symp. Combust. Aug. 14–20, 1966. University of California, Berkeley, California. 1967. p. 853.
12. J. E. BENNETT, B. MILE, and A. THOMAS. J. Chem. Soc. A, 1393, 1399 (1967).
13. J. A. PRYDE and G. O. JONES. Nature, **170**, 685 (1952).
14. L. G. DOWELL and A. P. RINFRET. Nature, **188**, 1144 (1960).
15. A. F. KIP, C. KITTEL, R. A. LEVY, and A. M. PORTIS. Phys. Rev. **91**, 1066 (1953).
16. H. ERLENMEYER and H. GÄRTNER. Helv. Chim. Acta, **17**, 970 (1934).
17. J. RABANI, W. A. MULAC, and M. S. MATHESON. J. Phys. Chem. **69**, 53 (1965).
18. P. W. ATKINS, N. KEEN, and M. C. R. SYMONS. J. Chem. Soc. 2873 (1962).
19. G. MEISSNER, A. HENGLEIN, and G. BECK. Z. Naturforsch. **22b**, 13 (1967).
20. W. T. DIXON, R. O. C. NORMAN, and A. L. BULEY. J. Chem. Soc. 3625 (1964).
21. G. R. FREEMAN. Rad. Res. Rev. **1**, 1 (1968).
22. M. VENUGOPALAN and R. A. JONES. Chemistry of dissociated water vapor and related systems. Interscience Publishers, Inc., New York. 1968.
23. M. VENUGOPALAN and R. A. JONES. Chem. Rev. **66**, 133 (1966).
24. N. R. GREINER. J. Phys. Chem. **72**, 406 (1968).
25. D. R. SMITH and J. C. TOLE. Can. J. Chem. **45**, 779 (1967).

Can. J. Chem. Downloaded from www.nrcresearchpress.com by 210.87.254.42 on 09/05/12
For personal use only.

Can. J. Chem. Downloaded from www.nrcresearchpress.com by 210.87.254.105 on 09/05/12
For personal use only.

Electron spin resonance studies of radicals condensed from irradiated water vapor: paramagnetic relaxation of trapped electrons in ice[1,2]

P. WARDMAN[3] AND W. A. SEDDON

Research Chemistry Branch, Atomic Energy of Canada Limited, Chalk River Nuclear Laboratories, Chalk River, Ontario

Received November 26, 1968

The spin–lattice relaxation time T_1 of electrons (e_t^-) trapped in several ice matrices at 77 °K has been estimated to be of the order of 10^{-2} s by observation of the electron spin resonance (e.s.r.) dispersion signal under fast passage conditions. These studies, together with measurements of the microwave power saturation of the e.s.r. absorption signal indicate that there is little difference in T_1 at 77 °K for e_t^- in solute-free polycrystalline H_2O or D_2O ice, γ-irradiated 8 *M* $NaOH/H_2O$ or $NaOD/D_2O$ glassy ices, and in 8 *M* $NaOD/D_2O$ glasses in which the electrons were produced by photoionization of ferrocyanide ion. This indicates that the predominant spin–lattice relaxation mechanism is not cross relaxation, and that correlations between T_1 and line width or trap depth are inappropriate.

Canadian Journal of Chemistry, 47, 2155 (1969)

Introduction

Electrons trapped in solute-free ice (e_t^-) by condensation of irradiated water vapor appear to have similar chemical properties to those trapped in ice containing high concentrations of electrolytes (1). It was of interest to compare some of the e.s.r. characteristics of e_t^- in solute-free, polycrystalline ice with those trapped in glassy ice containing high concentrations of solute. The close similarity of the small, negative *g*-shift for e_t^- in both types of system suggested similar interaction with the matrix via (weak) spin–orbit coupling, and by means of microwave power saturation characteristics we have investigated the interaction of e_t^- with the matrix to see whether any differences could be detected. A study has been published (2) of the saturation characteristics of e_t^- in γ-irradiated glassy ice containing ca. 8 *M* NaOH or NaOD, and we have, therefore, compared e_t^- in solute-free ice with those in γ-irradiated alkaline ice. In the latter case, enhanced spin–spin interaction due to the inhomogeneous spatial distribution of e_t^- could complicate the study, and hence we also compared the saturation behavior of e_t^- produced (presumably homogeneously) by photoionization of a dilute solution of ferrocyanide ion (3) in an identical glassy alkaline ice matrix.

[1]Issued as A.E.C.L. No. 3299.

[2]Presented in part at the 156th National Meeting of the American Chemical Society, Atlantic City, New Jersey. September 8–13, 1968.

[3]NRCC Postdoctorate Fellow 1967–1969.

Theory

During an e.s.r. experiment, the magnitude of the external magnetic field H_z is given by the expression

$$H_z = H_0(t) + H_m \cos(\omega_m t)$$

where $H_0(t)$ represents the direct current magnetic field, H_m is one half the peak-to-peak amplitude of the modulating field, ω_m the modulation frequency, and t the time. When $dH_0/dt \ll \omega_m H_m$ (as in this work), $dH_z/dt \simeq -\omega_m H_m \sin(\omega_m t)$ and the rate of passage through resonance is restricted by ω_m and H_m. The e.s.r. dispersion ($d\chi' H_1/dH_z$) and absorption ($d\chi'' H_1/dH_z$) signals depend both on the spin system (the spin–lattice and spin–spin relaxation times T_1 and T_2 and the width-at-half-height of the line envelope ΔH_{env}) and on the experimental parameters ω_m, H_m, and H_1 (the mean value at the sample of the circularly polarized magnetic component of the microwave field). The saturation behavior expected under several conditions of passage through resonance has been described at length (4–7). The important conditions are

(*a*) slow passage

$$(\gamma H_1)^{-1} \ll (T_1 T_2)^{1/2} \ll H_1 (dH_z/dt)^{-1}$$
$$H_m \ll \Delta H_{env}$$

(*b*) rapid passage: $H_1 (dH_z/dt)^{-1} \ll (T_1 T_2)^{1/2}$

(*c*) fast passage: $\omega_m T_1 \gg 1$, and

(*d*) adiabatic condition: $\gamma H_1^2 \gg dH_z/dt$

Can. J. Chem. Downloaded from www.nrcresearchpress.com by 210.87.254.105 on 09/05/12
For personal use only.

where γ is the gyromagnetic ratio of the electron. The validity of a particular restriction may vary throughout the modulation cycle, but since most of the signal arises near the extrema of the modulation cycle, for many purposes dH_z/dt may be replaced by $\omega_m H_m$. True slow passage, adiabatic conditions are a requirement for the treatment of progressive microwave power saturation data to obtain T_1 and T_2 using the Portis (8) and Castner (9) methods. Smith and Pieroni (10) developed these methods to demonstrate the spatial inhomogeneity of e_t^- and radicals in γ-irradiated 2-methyltetrahydrofuran glass, and Zimbrick and Kevan (2) later extended them to glassy alkaline ice. Progressive saturation under fast passage conditions is theoretically less satisfactory but may be used to compare relaxation characteristics under similar experimental conditions. By observation of the effects of fast passage on the dispersion signal, Bullock and Sutcliffe (7) estimated T_1 for a free radical in a solid matrix and we have also used this approach.

Experimental

Most of the experimental techniques have been described earlier (1).

Estimation of H_1 and H_m[4]

The microwave power P (W) incident at the cavity was measured using a Hewlett–Packard power meter, thermistor mount, and a 3 dB directional coupler. For powers less than 10^{-6} W the height of the diphenylpicrylhydrazyl (DPPH) standard was used to estimate H_1. For the V4531 TE_{102} cavity the maximum value of the microwave field H_1 at the sample is given by $H_1 = 1.41 \times 10^{-2} (Q_L P)^{1/2}$ G (12) where Q_L is the loaded Q (typically 4500), measured from the oscilloscope mode sweep pattern to $\pm 10\%$ as $f/\Delta f_{1/2}$ (9). For the TE_{104} cavity, $H_1 \simeq 1.0 \times 10^{-2} (Q_L P)^{1/2}$ G and this expression was taken to be the mean value of H_1 at the sample (variation of H_1 along a line sample may be neglected for our purposes using 100 kHz modulation (12)). The peak-to-peak modulation amplitude $2H_m$ was estimated (to $\pm 25\%$) from the effects of modulation broadening on signals from the $(SO_3)_2NO^{2-}$ and *p*-benzosemiquinone anion radicals (14).

Photoionization of Ferrocyanide Ion in Alkaline Ice

Samples contained ca. 1 m*M* $K_4Fe(CN)_6$ and were photolyzed at 77 °K with light from a low pressure mercury resonance lamp (Oriel Optics C-13-61) in conjunction with a Corning CS 7-54 glass filter, which together provide light of about 89% 254 mμ, 7% 313 mμ, and 4% 366 mμ.

Results

(i) Progressive Microwave Power Saturation of e_t^- in Ice

The effects of increasing microwave power on the e.s.r. absorption signal of e_t^- were investigated in two systems. System I was e_t^- in solute-free, polycrystalline D_2O ice at 77 °K (the deposit condensed from irradiated D_2O vapor) and system II was e_t^- in glassy 8 *M* NaOD in D_2O at 77 °K (after photoionization of ferrocyanide ion). In both systems, $[e_t^-] = 5 \times 10^{16}$ spins cm^{-3}, very approximately. The saturation factor Z was determined at several values of H_1 by measuring

$$Z_{H_1} = \chi''_{H_1}/\chi''_{\lim H_1 \to 0}$$

the ratio of the height of the first derivative absorption signal of e_t^- to that of a solid DPPH standard in the TE_{104} dual cavity (DPPH does not saturate under these conditions). Neither the shape nor the linewidth between derivative maxima ΔH_{ms} of the e_t^- resonance changed over the values of H_1 used. The underlying radical ($DO_2\cdot$) in system I did not interfere with the experiments; in system II there is no resonance underlying e_t^-.

The conditions used were $\omega_m = 2\pi \times 10^5$ rad s^{-1}, $H_m = 1.1 \pm 0.3$ G, $H_1 = 10^{-4}$ to 10^{-2} G, $dH_0/dt \simeq 0.5$ G s^{-1} (a value used throughout this work). Preliminary experiments (observation of passage effects on the dispersion signal, see below) had shown that $T_1 \gg 10^{-5}$ s in both systems and since $dH_0/dt \ll \omega_m H_m$, fast passage, strongly non-adiabatic conditions applied throughout most of the modulation cycle. The results are shown in Fig. 1; saturation of e_t^- ($Z < 1$) began at $H_1 \simeq 10^{-3}$ G and the dependence of Z on H_1 was

[4]Apparent discrepancies in published work often arise from the use of different equations for H_1. For example Smith and Pieroni (10) erroneously used Ingram's equation (11) for a TE_{102} cavity

$$H_1 = 5.7 \times 10^{-2} (Q_L P)^{1/2}$$

Using Hyde's equation (12) modified for a TE_{104} cavity

$$H_1 = 1.0 \times 10^{-2} (Q_L P)^{1/2}$$

lowers all of Smith's values of H_1 by a factor of 5.7. Since $T_1 T_2 = \gamma H_1^2$, Smith's T_1 is too short by a factor of $(5.7)^2 = 32.5$; the corrected value of T_1 is $7.5 \times 10^{-5} \times 32.5 = 2.4 \times 10^{-3}$ s. T_2 is unaffected by the error since it was obtained from the ratio of two H_1 values. The values of Williams *et al.* (13) may be compared to Smith's (10) by recalculation of Williams' data using Smith's measured $Q_L = 4440$ rather than Williams' assumed $Q_L = 6900$. This reduces the discrepancy with Smith's data still further. Williams' values of H_1 then become only a factor of 1.24 lower than Smith's. Such a small difference may arise in different laboratories from the use of quartz Dewars having different wall thicknesses. (Private communication from D. R. Smith.)

Can. J. Chem. Downloaded from www.nrcresearchpress.com by 210.87.254.105 on 09/05/12
For personal use only.

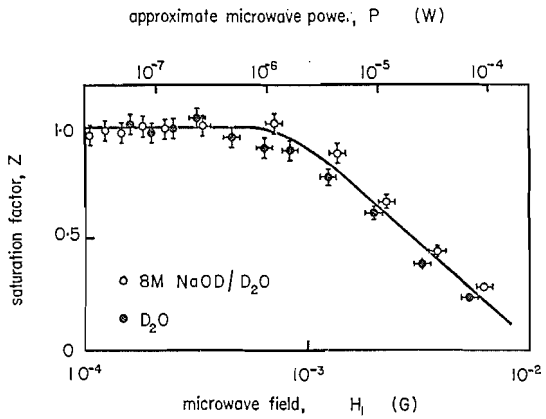

FIG. 1. Fast passage progressive microwave power saturation of the e.s.r. absorption of e_t^- at 77 °K. System I (●): solute-free, polycrystalline ice; system II (○): photolyzed glassy 8 *M* NaOD in D_2O containing $Fe(CN)_6^{4-}$.

similar for both systems. The difference in Z at a particular value of H_1 was only slightly outside the experimental precision in estimating Q_L and P as shown in Fig. 1 as error limits on H_1. Since different sample geometries were used in the two systems, the mean value of H_1 at the sample is expected to be slightly different for the same $Q_L P$.

(ii) Effects of Fast Passage on the Dispersion Signal

(a) Using 100 kHz Field Modulation

Figure 2 shows the effect on the dispersion signal of e_t^- of varying H_m under non-adiabatic fast passage conditions. The conditions used were $\omega_m = 2\pi \times 10^5$ rad s^{-1}, $H_1 = 2.0 \times 10^{-3}$ G and the signal was observed in phase with the modulating field. Figure 2 actually refers to e_t^- produced by photoionization of ferrocyanide ion in 8 *M* $NaOD/D_2O$ at 77 °K, but similar effects were observed with slightly different values of H_1 and H_m for e_t^- trapped in solute-free H_2O or D_2O ice and in γ-irradiated 8 *M* $NaOH/H_2O$ or $NaOD/D_2O$ glassy alkaline ice.

The first derivative dispersion signal was of the usual form (as observed for DPPH under these conditions) at $H_m > 4$ G but as H_m was reduced, the signal decreased and changed quite suddenly into a bell-shaped (approximately Gaussian) curve. This signal at first increased in size as H_m was reduced further, went through a maximum at $H_m \simeq 0.06$ G and then decreased approximately linearly with H_m. Below $H_m \simeq 0.2$ G the signal did not change in shape appreciably and

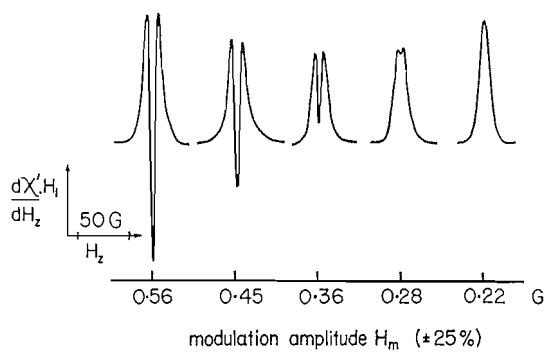

FIG. 2. Fast passage e.s.r. dispersion signal of e_t^- at 77 °K in the region of $2\gamma H_1^2 T_1/\pi H_m \sim 1$.

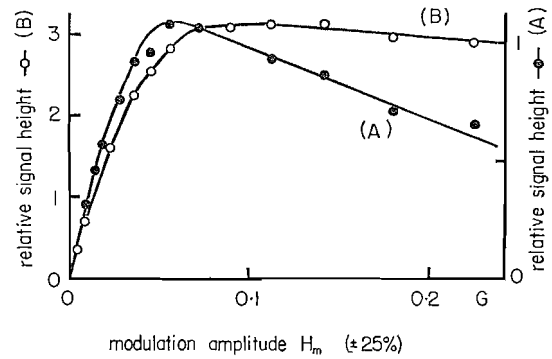

FIG. 3. Dependence of the height of the fast passage e.s.r. dispersion signal on H_m when $H_m < 2\gamma H_1^2 T_1/\pi$. Curve (A) (●): $H_1 = 2.0 \times 10^{-3}$ G; curve (B) (○): $H_1 = 6.6 \times 10^{-3}$ G.

the height of this "bell-shaped" signal is plotted as a function of H_m in Fig. 3, curve (A), for the same $NaOD/D_2O/Fe(CN)_6^{4-}$ sample. The form of the variation of the height of the "bell-shaped" signal with H_m depended on H_1 and in Fig. 3, curve (B), this variation is shown for the identical sample used for curve (A) but using a value of H_1 only three times as great. At the higher power, hardly any decrease in the height of the signal at high H_m was observable. At higher H_m than that shown in Fig. 3 the signal shape began to show the changes illustrated in Fig. 2.

The variations in the dispersion signal of e_t^- with H_m shown in Figs. 2 and 3 are qualitatively *identical* to the effects observed by Bugai (6) and Hyde (15) for *F* centers in potassium chloride crystals. Bullock and Sutcliffe (7) show that the overall change in signal form shown in Fig. 2 is expected to occur when

[1] $$2\gamma H_1^2 T_1/\pi H_m \sim 1$$

Can. J. Chem. Downloaded from www.nrcresearchpress.com by 210.87.254.105 on 09/05/12
For personal use only.

and one might therefore expect that for the same system (same T_1), identical "intermediate" shapes such as that observed at $H_m \simeq 0.4$ G in Fig. 2 would be observed at identical values of H_1^2/H_m. Fast passage dispersion effects were therefore investigated for the sample of photolyzed $Fe(CN)_6^{4-}$ in alkaline D_2O ice at several values of H_1 ($H_1^2 = 1.0$, 4.0, 14.5, 44, and 170×10^{-6} G^2). As expected, the values of H_m over which the change in form of the dispersion signal occurred did vary with H_1, but at no value of H_1^2/H_m could a constant intermediate shape be observed at the various values of H_1, contrary to what one expects from eq. [1]. This may be explained by the fact that at high H_1 the magnitude of the bell-shaped dispersion signal does not change rapidly with increasing H_m, whilst at lower values of H_1 the bell-shaped signal decreases very rapidly as H_m is increased. It is therefore not surprising that, as observed, the change in the form of the signal occurs rather more sharply at the lower values of H_1 and no "intermediate" shape of signal is found at a constant value of H_1^2/H_m.

These observations preclude reliable comparison between widely different systems unless the differences in T_1 are of orders of magnitude, but should not invalidate approximate comparison between the systems of interest in this work. We arbitrarily defined the signal shape corresponding to eq. [1] as that intermediate between those shown for $H_m = 0.45$ and 0.36 G in Fig. 2. We then compared the values of T_1 obtained from eq. [1] at similar values of H_1. Values of T_1 obtained were all in the range 7×10^{-3} to 4×10^{-2} s for e_t^- in solute-free, polycrystalline H_2O or D_2O ice, γ-irradiated 8 *M* NaOH/H_2O (NaOD/D_2O) glassy ice (dose ca. 1 Mrad), and photolyzed $Fe(CN)_6^{4-}$ in 8 *M* NaOD/D_2O glassy ice, all at 77 °K.

(b) Using Field Modulation at Audio Frequencies

Results using 100 kHz field modulation suggested that $T_1 \simeq 10^{-2}$ s and hence fast passage conditions should still be observable at modulation frequencies of about 10^2 Hz. (In fact one may obtain an estimate of T_1 simply by reducing ω_m until passage effects are not observed, although since the restrictions vary throughout the modulation cycle, this method is unsuitable for detecting small differences.) Working at $\omega_m = 2\pi \times 200$ rad s^{-1} also had the advantage that values of H_1 could be used such that approximately adiabatic conditions were obtained, and the results could be compared with those observed under strongly non-adiabatic conditions at $\omega_m = 2\pi \times 10^5$ rad s^{-1}.

The dispersion signal in phase with the modulating field for γ-irradiated NaOD/D_2O ice was investigated as a function of H_m at $H_1 = 10^{-2}$ G, $\omega_m = 2\pi \times 200$ rad s^{-1}, and $H_m = 0.2$–2 G ($\gamma H_1^2 \simeq dH_z/dt$). Results qualitatively similar to those shown in Fig. 2 were obtained and at the same value of H_1, the change in form of the signal with H_m was identical at $\omega_m = 2\pi \times 200$ and $2\pi \times 10^5$ rad s^{-1}, within the precision of comparing H_m ($\pm 15\%$).

(c) The Phase Lag of the Fast Passage Dispersion Signal

Hyde (5, 16) has shown that for *F* centers in LiF crystals, the phase of the rapid-passage (bell-shaped) dispersion signal lags the modulating field by 90° (i.e. the signal is in quadrature) when $\omega_m T_1 < 1$. It is expected that when $\omega_m T_1$ is of the order of unity, a rapid-passage dispersion signal will be observed of about equal intensity both in phase and in quadrature with the modulating field. The dispersion signals at these two settings of the reference phase in the phase sensitive detector were examined for e_t^- in polycrystalline D_2O using $H_1 = 1.9 \times 10^{-3}$ G and $\omega_m = 2\pi \times 200$ rad s^{-1}. The in phase signal (an approximately Gaussian, bell-shaped curve) was about one-sixth the intensity of the similarly shaped in quadrature signal. It is impossible to place quantitative significance on these ratios because of the variation of passage conditions during the modulation cycle but these results do confirm the prediction above that T_1 is of the order of 10^{-2} to 10^{-3} s.

Discussion

The theoretical treatment of the fast passage dispersion experiments used to derive eq. [1] applies to inhomogeneously broadened lines. Whilst an important source of broadening is in fact inhomogeneous (the presence of unresolved hyperfine lines), in γ-irradiated samples homogeneous contributions are also important (2, 10) because of the non-uniform distribution of the electrons. The e.s.r. absorption of electrons trapped with different local concentrations even in the same matrix will have different spin packet width and since the behavior observed is in part a

Can. J. Chem. Downloaded from www.nrcresearchpress.com by 210.87.254.105 on 09/05/12
For personal use only.

function of this quantity (6), meaningful interpretation of small apparent differences is impossible. We may draw no comparison, for example, between our estimate of $T_1 \simeq 10^{-2}$ s in ice at 77 °K and the value of 5×10^{-3} s estimated by Tsujikawa *et al.* (17) for e_t^- in triethylamine glass at 77 °K in a brief application of the same technique. Kevan's estimates (2) of $(T_1T_2)^{1/2}$ and T_2 for γ-irradiated alkaline ice gave a value of T_1 in agreement with our estimates.

For fast passage progressive saturation of an inhomogeneously broadened line under adiabatic conditions, T_1 may be estimated from eq. [2] (7)

$$[2] \qquad Z = [1 + (2\gamma H_1^2 T_1/\pi H_m)]^{-1}$$

In fact the line drawn through the points in Fig. 1 gives $Z = 0.5$ at $H_1 = 3.0 \times 10^{-3}$ G and using eq. [2], $T_1 = 1 \times 10^{-2}$ s. Such agreement with the dispersion data may be fortuitous because of the disturbance of adiabaticity (7). Variation of Z with H_1 may also be used under slow passage, adiabatic conditions to distinguish between homogeneous and inhomogeneous line broadening mechanisms (8, 9). Such a treatment of the data in Fig. 1 suggested that the line broadening mechanism was entirely inhomogeneous. Much less homogeneous broadening is expected in the two systems presented in Fig. 1 than in the γ-irradiated case, because of the lower value of the spin packet width compared to the line envelope width in the former systems (a higher local concentration of electrons increases the spin packet width (10)). However, it is apparent from earlier work (7) that the large disturbance from adiabaticity under these conditions may have entirely masked any homogeneous contribution. The absence of an increased e.s.r. absorption line width with increasing H_1 for electrons trapped in solute-free ice and glassy alkaline ice after photoionization of $Fe(CN)_6^{4-}$ is in accord with the expected major contribution of inhomogeneous broadening to the line width and supports our use of the fast passage effects to estimate T_1.

The fast passage saturation characteristics of the e.s.r. absorption signal of e_t^- in solute-free or glassy ice shown in Fig. 1 confirm our conclusion from the dispersion studies that T_1 is similar in both systems. It is important to realize that even if relaxation times are determined under the theoretically better understood slow passage, adiabati cconditions, the results obtained are probably quantitatively no more reliable than our estimates. Recent comparisons of relaxation data obtained by the Castner and Portis methods with more direct spin-echo or pulse measurements confirm this conclusion (18). The precise estimation of H_1 is very difficult because of the distortion of radio-frequency fields by the quartz. When T_1 is as long as in this case it is experimentally very difficult to obtain true slow passage adiabatic conditions over the whole range of H_1 required. The important conclusion from slow passage studies as applied by Smith and Pieroni (10) is the estimate of T_2 and hence the local concentration of electrons.

Conclusions

We have estimated the spin–lattice relaxation time for electrons trapped at 77 °K in solute-free, polycrystalline ice and glassy alkaline ice (for both H_2O and D_2O matrices) to be 10^{-2} s *within an order of magnitude*. The absence of significant variation in T_1 indicates that the interaction of the electron with the environment via spin–lattice relaxation is similar in the various ices. Cross relaxation processes (2) are probably excluded since in addition to e_t^-, hydroperoxyl radicals are present in the polycrystalline ice, O^- radical-ions in the γ-irradiated alkaline ice (with a different spatial distribution to $HO_2\cdot$ in the former case), and neither of these latter species are present after photolysis of alkaline ice containing ferrocyanide. Further discussion of the relaxation mechanism is unjustified. The results also indicate that correlations between T_1 and line width or trap depth (17) are inappropriate.

The value of T_1 obtained is of interest in: (*i*) the possible application of the slow passage saturation technique (10) to determine T_2 and the spatial distribution of e_t^- generated photolytically in alkaline ice and in the ice condensed from irradiated water vapor; (*ii*) the choice of H_1 to avoid saturation effects in the routine observation of e_t^- in ice under fast passage conditions; (*iii*) distinguishing between e_t^- and other species with similar e.s.r. absorptions but different T_1's; and (*iv*) in the application of electron nuclear double resonance to investigate the hyperfine interactions of e_t^- in ice (a knowledge of saturation and passage conditions is required).

Acknowledgments

We thank Dr. D. R. Smith and Professor M. Fujimoto (University of Guelph, Ontario) for helpful discussions.

1. P. WARDMAN and W. A. SEDDON. Can. J. Chem. This issue.
2. J. ZIMBRICK and L. KEVAN. J. Chem. Phys. **47**, 2364 (1967).
3. P. B. AYSCOUGH, R. G. COLLINS, and F. S. DAINTON. Nature, **205**, 965 (1965).
4. M. WEGER. Bell System Tech. J. **39**, 1013 (1960).
5. J. S. HYDE. Phys. Rev. **119**, 1483, 1492 (1960).
6. A. A. BUGAI. Soviet Phys.-Solid State, English transl. **4**, 2218 (1963).
7. A. T. BULLOCK and L. H. SUTCLIFFE. Trans. Faraday Soc. **60**, 2112 (1964).
8. A. M. PORTIS. Phys. Rev. **91**, 1071 (1953).
9. T. G. CASTNER, JR. Phys. Rev. **115**, 1506 (1959).
10. D. R. SMITH and J. J. PIERONI. Can. J. Chem. **43**, 876 (1965).
11. D. J. E. INGRAM. Free radicals as studied by electron spin resonance. Butterworth Scientific Publications, London. 1958. p. 133.
12. J. S. HYDE. Experimental techniques in E.P.R. Varian Associates' Sixth Annual N.M.R.–E.P.R. Workshop. November 5–9, 1962.
13. J. LIN, K. TSUJI, and F. WILLIAMS. J. Am. Chem. Soc. **90**, 2766 (1968).
14. Varian Associates' V-4502 E.P.R. systems instruction manual. Publication no. 87-100-074. p. 5-6.
15. J. S. HYDE. Varian Associates' E.P.R. at work. No. 20.
16. J. S. HYDE. *In* N.M.R. and E.P.R. spectroscopy (Varian Associates, Third Annual N.M.R.–E.P.R. Workshop). The Pergamon Press, Ltd., New York. 1960. pp. 252, 279.
17. H. TSUJIKAWA, K. FUEKI, and Z. KURI. J. Chem. Phys. **47**, 256 (1967).
18. V. V. VOEVODSKY. 8th Intern. Symp. Free Radicals. Plenary lecture. (*Read by* YU. D. TSVETKOV.) July 26–31, 1967.

Can. J. Chem. Downloaded from www.nrcresearchpress.com by 210.87.254.105 on 09/05/12
For personal use only.

Can. J. Chem. Downloaded from www.nrcresearchpress.com by 210.87.254.105 on 09/05/12
For personal use only.

Translational freezing in free jet expansions, with special reference to molecular beam formation[1]

RODNEY L. LEROY[2] AND JACQUES M. DECKERS
Lash Miller Chemical Laboratories, University of Toronto, Toronto 5, Ontario

Received November 15, 1968

A theoretical model is described which can be used to calculate the velocity distribution function in the transition region of a free jet expansion. It makes use of a simple mechanism to account for the way in which collisions "perturb" the distribution function which would apply in the absence of collisions. The results are compared with experimental studies of argon beams isolated from free jet sources. If the collision frequency is calculated using a hard sphere collision cross section of (25 ± 5) Å^2, good agreement with experimental beam intensity profiles is obtained. In the transition region computed values of the bulk mass velocity, and of the parallel and perpendicular temperatures, are intermediate between the values which would be found if the flow were collision-dominated or free molecular. In particular the perpendicular temperature varies slowly from a dependence on the $-4/3$ power of the distance from the source, approaching monotonically a -2 power dependence at large distances.

Canadian Journal of Chemistry, 47, 2161 (1969)

Introduction

Following the suggestion of Kantrowitz and Grey (1), free jets are now used in many laboratories as molecular beam sources. In this application the core of the jet must be "skimmed" at a point where the local mean free path is considerably greater than the diameter of the skimming orifice (2). This condition usually[3] requires that the skimmer sample the free jet in the transition region of the expansion, where the flow is no longer "collision-dominated".

Brook and Oman (4) attempted the first study of this transition region by solution of the Boltzmann equation, and their approach was extended and improved upon by Edwards and Cheng (5) and by Hamel and Willis (6). These latter two groups arrived at equivalent results. Their work constitutes an essentially complete theoretical description of source flow expansions. Hamel and Willis (6) examined their solution by fitting it to an ellipsoidal (two-temperature) function superimposed on the bulk mass velocity. Although the resulting predictions of the terminal value of the parallel temperature ($T_\parallel$) were in reasonable agreement with experimental measurements (7–10), those of the perpendicular temperature ($T_\perp$) were not. The theory predicts that at large distances from the source, $T_\perp$ approaches a direct dependence on the inverse of the nozzle–skimmer separation s. This may be compared with the $T \propto s^{-4/3}$ dependence which applies in the collision dominated region, or with the $T_\perp \propto s^{-2}$ dependence which applies in the limit of free molecular flow. Values of $T_\perp$ deduced from measurements of beam profiles downstream of the skimmer (9, 10), and of beam intensities as a function of skimmer area (11, 12), always show a dependence on s which is intermediate between the results expected in the collision dominated and free molecular limits.

The discrepancy between theory and experiment was clarified by Edwards and Cheng's analysis (13) of the asymptotic solution which they had obtained previously (5). They found that it can be represented by a bimodal function — the sum of an ellipsoidal function corresponding to a low value of $T_\perp \propto s^{-2}$, and a broad function (high $T_\perp$) which describes those molecules whose trajectories in the transition region are affected by collisions. Molecules contributing to this broader distribution likely make a negligible contribution to experimental beam intensities downstream of the skimmer on or near the centerline. In fact such molecules can be considered to have been self-scattered out of the beam for purposes of predicting centerline molecular beam intensities (14).

Thus the discrepancy is only apparent. Experimental determinations of $T_\perp$ which are carried out by fitting beam profiles to a Maxwellian distribution are quite insensitive to the "tails" of the profile. In fact the signal is generally

[1]Supported by grants from the National Research Council of Canada.

[2]Present address: Department of Chemistry, University of Colorado, Boulder, Colorado 80302.

[3]A notable exception being the experiments reported recently by Bossel, Hurlburt, and Sherman (3).

Can. J. Chem. Downloaded from www.nrcresearchpress.com by 210.87.254.105 on 09/05/12
For personal use only.

lost in noise when the beam intensities are measured more than a few degrees from the centerline. Hence it is likely that if the distribution functions obtained by solution of the Boltzmann equation were used directly to predict beam intensity profiles downstream of a skimmer, they could reasonably reproduce the experimental measurements

In the calculation outlined below we make use of a simple model to approximate the way in which collisions affect the distribution of molecular speeds in the transition region of a free jet expansion. Throughout the calculation distribution functions are truncated quite near the centerline, at angles which are scaled so that they adequately cover the experimental profiles at the skimmer. Several approximations are made: near its centerline the expansion is assumed to have spherical symmetry about the source; a hard sphere collision model is used to calculate collision probabilities in the transition region, although the formalism is not restricted to such a model; and collisions in the transition region are assumed to take place only on a series of well defined surfaces. By varying the separation between such surfaces, this latter approximation was shown to introduce a negligible error. The collision cross section in the transition region is used as a fitting parameter, and is derived by comparison with typical experimental beam profiles.

The description of the expansion which results is neither rigorous nor complete, but the distributions obtained are in good agreement with experimental measurements of molecular beam intensities.

Theory

The velocity distribution function in the collision dominated region of the expansion is well known, so we start the calculation in this region at a distance s_q from the nozzle throat. The distribution function downstream of s_q is evaluated on a series of spheres which are so spaced that the collision probability between any two is much less than unity (a typical value being 0.2). The velocity distribution function on a given sphere of radius $R + \Delta R, f'(v,\theta)$, is derived from the known function $f(v,\theta)$ on the sphere of radius R, using the relation

$$[1]\quad f'(v,\theta) = [1 - P(v,\theta)]f_{geom}(v,\theta) + P(v,\theta)f_{coll}(v,\theta)$$

Here $P(v,\theta)$ is the probability that a particle with a trajectory defined by v and θ suffers a collision between the two spheres, $f_{geom}(v,\theta)$ is a geometrically altered function describing those particles which do not suffer a collision, and $f_{coll}(v,\theta)$ is a function which describes those particles which do suffer a collision. All three functions are defined with respect to the space element $dvd\theta$. Because of the assumed spherical symmetry of the expansion, they are independent of the azimuthal angle ϕ.

The probability that a particle (1 say) collides between the two spheres of radius R and $(R + \Delta R)$ is

$$[2]\quad P(v_1,\theta_1) = 4\frac{n(R')d_1}{v_1}\int_0^{2\pi}\int_0^{\pi}\int_0^{\infty} g_r Q(g_r) \times f(v,\theta)\, dv\, d\theta\, d\phi$$

where

$$d_1 = -R\cos\theta_1 + [R^2\cos^2\theta_1 + \Delta R(2R + \Delta R)]^{1/2}$$

The number density n is taken as its value on an intermediate sphere of radius $R' = [R(R + \Delta R)]^{1/2}$, chosen such that $n(R)/n(R') = n(R')/n(R + \Delta R)$. g_r is the relative velocity of collision between particles with velocities $\boldsymbol{v}_1(v_1,\theta_1,\phi_1 = 0)$ and $\boldsymbol{v}(v,\theta,\phi)$, and it may be derived in analytical form if we consider collisions between R and $(R + \Delta R)$ to occur at R'. The result is

$$g_r = [v_1^2 + v^2 - 2v_1v(\cos\alpha\cos\beta + \sin\alpha\sin\beta\cos\phi)]^{1/2}$$

where $\alpha = \arcsin(R\sin\theta_1/R')$ and $\beta = \arcsin(R\sin\theta/R')$, $Q(g_r)$ is the collision cross section.

In the absence of collisions, a particle which crosses the sphere of radius R at an angle θ_1 with respect to the radial direction will cross the sphere of radius $(R + \Delta R)$ at an angle $\theta = \arcsin[R\sin\theta_1/(R + \Delta R)]$. Thus $f_{geom}(v,\theta)$ can be derived directly from the known function $f(v,\theta_1)$

$$[3]\quad f_{geom}(v,\theta) = \left[\left(\frac{R + \Delta R}{R}\right)^2 - \sin^2\theta_1\right]^{1/2} \times \frac{f(v,\theta_1)}{\cos\theta_1}$$

To construct an appropriate collisionally altered distribution function, we equipartition the available energy at R' among the three transla-

Can. J. Chem. Downloaded from www.nrcresearchpress.com by 210.87.254.105 on 09/05/12
For personal use only.

tional degrees of freedom. The appropriate conservation law (see, for example, ref. 10) is

$$[4] \quad mv_b^2/2 + 3kT_{\parallel}/2 + kT_{\perp} = 5kT_0/2$$

where m is the molecular mass, k is the Boltzmann constant, and T_0 is the source temperature. v_b is the bulk mass velocity, evaluated at R' from[4]

$$[5] \quad v_b = \langle v \cos\theta \rangle$$

The "collisional distribution function" at R' in (v,θ') space is thus

$$[6] \quad f_{coll}(v,\theta') = \left(\frac{m}{2\pi kT}\right)^{3/2} \exp\left[-\frac{m}{2kT} \times (v^2 + v_b^2 - 2vv_b\cos\theta')\right] 2\pi v^2 \sin\theta'$$

where[5]

$$T = T_0 - \frac{mv_b^2}{5k}$$

A geometric correction (cf. eq [3]) is applied to obtain $f_{coll}(v,\theta)$ at $(R + \Delta R)$.

The distribution function on a new sphere may thus be evaluated from eq. [1]. A computation is started with the known function in the collision dominated region on the sphere of radius s_q, and $f(v,\theta)$ is computed on successive spheres until the skimmer plane is reached.

Results and Comparison with Experiment

It is apparent that the terms on the right hand side of eq. [1] cannot be obtained in analytical form, and hence that $f(v,\theta)$ must be carried through the computation as a two-dimensional table of numbers. The numerical techniques which we use are detailed elsewhere (15).

The computed distribution function at the skimmer may be compared with experimental measurements of the beam intensity profile downstream of the skimmer. Suitable flux measurements were published by Anderson and Fenn[6] (7) and are reproduced in Fig. 1. These data

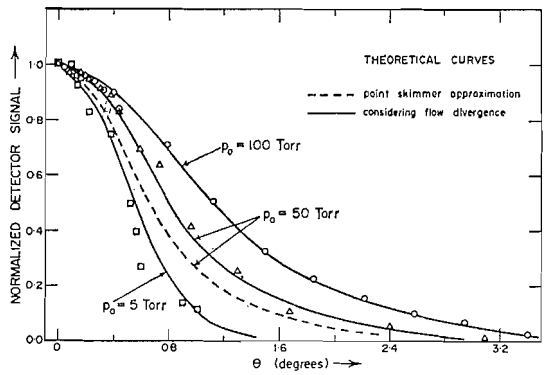

FIG. 1. Experimental and theoretical profiles of a nozzle beam downstream of an 0.35 mm skimmer. Source pressure, 50 Torr; nozzle exit diameter, 0.33 mm; nozzle–skimmer separation, 2.1 cm.

were obtained by moving an ionization gauge perpendicular to the beam axis, 63 cm downstream of an 0.35 mm skimmer. The nozzle diameter was 0.33 mm and the nozzle–skimmer separation was 2.1 cm. To make comparison with these data, the flux distribution $vf(v,\theta)$ was determined at the skimmer for each pressure. In each case the distance s_q from the nozzle was taken rather arbitrarily from Anderson and Fenn's empirical correlation for the value of the terminal mach number (7).

The solid curves in Fig. 1 were obtained by suitable integration of the flux distribution at the skimmer over velocity, and over the dimensions of the skimmer orifice (15). The broken curve illustrates the effect of ignoring the finite divergence of the flow at the skimmer. A hard sphere cross section of 25 Å^2 was used to compute collision frequencies in the calculations summarized in Fig. 1. Profiles were also computed using cross sections of 15 and 35 Å^2, and in both cases the agreement with experiment was poor. The larger cross section broadened the computed profiles, while the smaller cross section narrowed them. We conclude that the effective collision cross section for argon is (25 ± 5) Å^2. This is comparable to the values determined by Knuth and Fisher (10, 16) in their study of a similar free jet expansion, although we should emphasize that the cross section is a function of the local temperature, and thus of the source conditions (see ref. 16).

Finally we examine the variation of v_b, $T_{\perp}$, and $T_{\parallel}$ in the expansion downstream of the "quitting"

[4]The nomenclature

$$\langle \psi(v,\theta) \rangle = \int_0^{\infty} \int_0^{\pi} \psi(v,\theta)\, f(v,\theta)\, d\theta\, dv$$

is introduced here.

[5]Using this expression our considerations are restricted to gases for which the heat capacity ratio is 5/3.

[6]We are grateful to Professor Anderson for providing us with the original data which were used in the plotting of Fig. 11 of ref. 7.

Can. J. Chem. Downloaded from www.nrcresearchpress.com by 210.87.254.105 on 09/05/12
For personal use only.

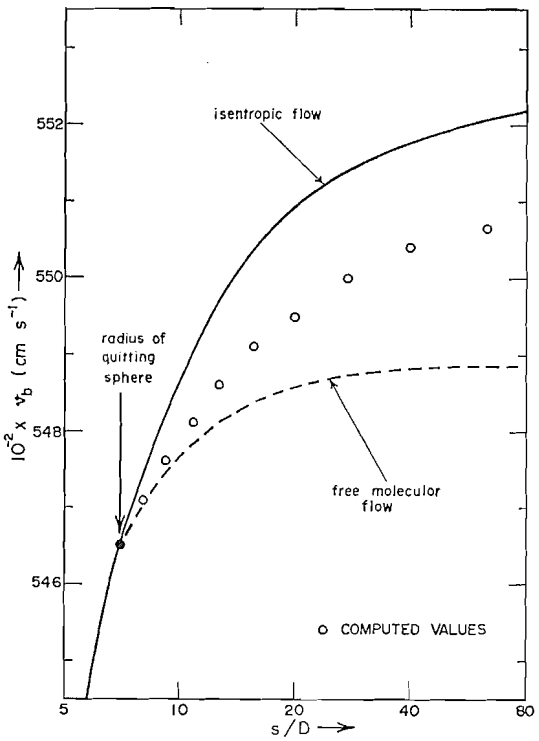

FIG. 2. Variation of the bulk mass velocity v_b with distance downstream of s_q. The computed results are compared with the variation which would be found in the limits of collision dominated and free molecular flow.

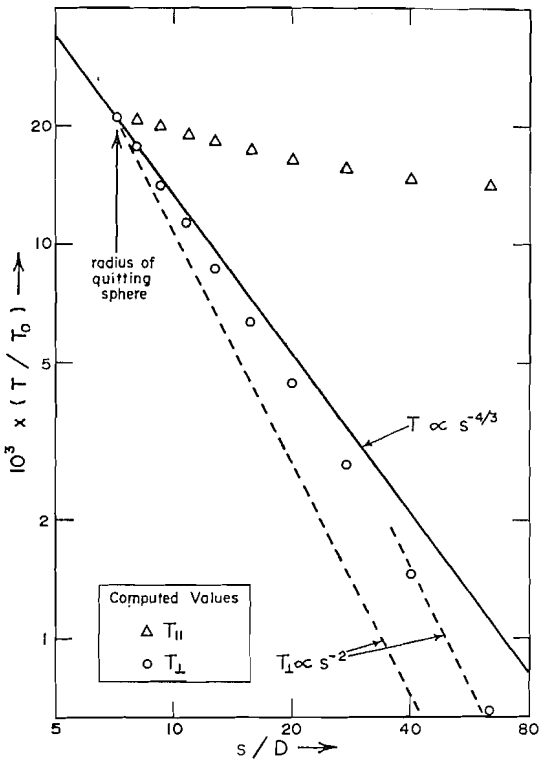

FIG. 3. Variation of the perpendicular temperature $T_\perp$ and the parallel temperature $T_{||}$ with distance downstream of s_q.

surface. These quantities are computed on each sphere from eq. [5] and the relations

$$[7] \qquad T_\perp = \frac{m}{2k}\langle(v \sin\theta)^2\rangle$$

and

$$[8] \qquad T_{||} = \frac{m}{2k}\langle(v \cos\theta - v_b)^2\rangle$$

The specific results presented correspond to a source pressure of 50 Torr and $Q = 25$ Å^2.

In Fig. 2, the solid curve illustrates the increase of bulk mass velocity with distance in an isentropic expansion, while the broken curve indicates the variation which would be observed if the flow became suddenly free molecular at s_q (15). The computed velocities (eq. [5]) are intermediate between these two limits. Increasing Q increases v_b, while decreasing it has the opposite effect. Values of $T_\perp$ and $T_{||}$ (eqs. [7] and [8]) are plotted as a function of the distance from the nozzle in Fig. 3. The solid line represents the local temperature in an isentropic expansion, and the broken line illustrates the variation of $T_\perp$ with distance which would be observed in the absence of collisions downstream of s_q. The computed variation is intermediate, and falls off slowly from $T_\perp \propto s^{-4/3}$ to approach $T_\perp \propto s^{-2}$, 50 diameters downstream of the source. This is not unlike the experimental dependence of $T_\perp$ on s which Abuaf *et al.* (9) report for similar source conditions. In fact our calculations seem to agree with the experiments of Scoles and his co-workers (11, 12) and of Abuaf *et al.* (9) in indicating that the $s^{-4/3}$ dependence persists far downstream of a "quitting" surface whose position is calculated from the terminal mach number. As we might expect, increasing Q causes the $s^{-4/3}$ dependence to persist to larger distances, and decreasing it has the opposite effect.

Conclusions

We have outlined above a simple method which is capable of predicting velocity distribution

functions in the transition region of a free jet expansion. The results are in good agreement with molecular beam measurements. A simple model is used to account for the way in which collisions redistribute translational energy. The approach is essentially equivalent to a solution of the Boltzmann equation, although its success may reflect the fact that our distribution functions are tabulated near the centerline, at angles which are scaled so that they adequately cover the experimental profiles at the skimmer. In this way the calculation exhibits the same prejudice as a molecular beam experiment; it is relatively insensitive to the broad tails of the distribution function.

Acknowledgments

The authors are deeply indebted to Professor J. P. Valleau for his assistance throughout this work. Also we are grateful for stimulating discussions with many people, especially Miss Wong Wan Yin, Dr. R. G. Albright, Professors G. Scoles, R. P. Andres and J. B. Anderson, and Mr. T. R. Govers. One of us (R.L.L.) thanks the National Research Council of Canada for the award of a Studentship.

1. A. KANTROWITZ and J. GREY. Rev. Sci. Instr. **22**, 328 (1951).
2. J. B. FENN and J. M. DECKERS. *In* Rarefied gas dynamics. *Edited by* J. A. Laurmann. Vol. 1. Academic Press, Inc., New York. 1963. p. 497.
3. U. BOSSEL, F. C. HURLBURT, and F. S. SHERMAN. Proc. 6th Intern. Symp. Rarefied Gas Dynamics. In press.
4. J. W. BROOK and R. A. OMAN. *In* Rarefied gas dynamics. *Edited by* J. H. DeLeeuw. Vol. 1. Academic Press, Inc., New York. 1965. p. 125.
5. R. H. EDWARDS and H. K. CHENG. A.I.A.A. Journal, **4**, 558 (1966).
6. B. B. HAMEL and D. R. WILLIS. Phys. Fluids, **9**, 829 (1966).
7. J. B. ANDERSON and J. B. FENN. Phys. Fluids, **8**, 780 (1965).
8. J. E. SCOTT, JR. and J. A. PHIPPS. *In* Rarefied gas dynamics. *Edited by* C. L. Brundin. Vol. 2. Academic Press, Inc., New York. 1967. p. 1337.
9. N. ABUAF, J. B. ANDERSON, R. P. ANDRES, J. B. FENN, and D. R. MILLER. *In* Rarefied gas dynamics. *Edited by* C. L. Brundin. Vol. 2. Academic Press, Inc., New York. 1967. p. 1317.
10. S. S. FISHER. University of California Department of Engineering Report No. 67–5. Los Angeles. March, 1967.
11. G. SCOLES and F. TORELLO. Meccanica, **3**, 20 (1968).
12. C. GAZZOLA, G. SCOLES, and F. TORELLO. Proc. 6th Intern. Symp. Rarefied Gas Dynamics. In press.
13. R. H. EDWARDS and H. K. CHENG. *In* Rarefied gas dynamics. *Edited by* C. L. Brundin. Vol. 2. Academic Press, Inc., New York. 1967. p. 819.
14. J. M. DECKERS, T. R. GOVERS, and R. L. LEROY. To be published.
15. R. L. LEROY. Ph.D. Thesis, University of Toronto, Toronto. 1968.
16. E. L. KNUTH and S. S. FISHER. J. Chem. Phys. **48**, 1674 (1968).

Can. J. Chem. Downloaded from www.nrcresearchpress.com by 210.87.254.105 on 09/05/12
For personal use only.

Can. J. Chem. Downloaded from www.nrcresearchpress.com by 210.87.254.42 on 09/05/12
For personal use only.

Nuclear magnetic relaxation of 1,2-dichloroethane in deuterated benzene and carbon disulfide solution at 20 °C

E. Bock
Parker Chemistry Laboratory, University of Manitoba, Winnipeg, Manitoba

AND

E. Tomchuk
Department of Physics, University of Winnipeg, Winnipeg, Manitoba

Received January 10, 1969

The molecular rotational relaxation time of the 1,2-dichloroethane molecule in deuterated benzene and carbon disulfide solution was determined by pulsed nuclear magnetic resonance techniques. It was found that the rotational relaxation time, τ_r, in infinitely dilute deuterated benzene solution and in infinitely dilute carbon disulfide solution was 1.3×10^{-12} and 0.6×10^{-12} s, respectively. Both values are in fair agreement with the dielectric molecular relaxation time for 1,2-dichloroethane in dilute benzene, *p*-xylene, and *n*-hexane solution reported by Chitoku and Higasi (1).

Canadian Journal of Chemistry, 47, 2167 (1969)

Introduction

Chitoku and Higasi (1) found that 1,2-dichloroethane exhibits an exceptionally high electric dipole moment and dielectric relaxation time in dilute benzene and *p*-xylene solution as compared to other non-polar, non-aromatic solvents, viz. 1.80 D and 3.69×10^{-12} s in benzene as compared to 1.35 D and 1.31×10^{-12} s in hexane. The above authors attributed the exceptional behavior of 1,2-dichloroethane in benzene solution to the existence of a particular conformer of the molecule in solution, the *gauche* form, and to the formation of a weak complex between the solute and solvent molecules. On the other hand, other workers who investigated the same problem have interpreted the anomalous behavior of 1,2-dichloroethane molecule in benzene solution in terms of different conformations of the molecule (2), formations of definite complexes (3), or different types of interaction between solvent and solute molecules (4). In order to shed some new light on this problem we have determined the nuclear magnetic spin–lattice relaxation of the protons of the 1,2-dichloroethane molecule in two different non-magnetic solvents, viz. perdeutero benzene and carbon disulfide. Although perdeutero benzene is not really an entirely non-magnetic solvent, we nevertheless chose this solvent because the efficiency of the deuteron nucleus in causing nuclear relaxation as compared to that of the proton is only 1/24 of the latter and because all the other properties of perdeutero benzene closely resemble those of ordinary benzene.

Experimental

Solvents

The benzene-d_6, 99.5 atom % D, was obtained from Merck, Sharp, and Dohme of Canada Ltd., and was used without further purification. The carbon disulfide, Fisher certified reagent, was deodorized by prolonged shaking, ~ 12 h, with mercury and saturated mercuric chloride and potassium permanganate solutions, in that order, and distilled from P_2O_5.

Solute

The 1,2-dichloroethane was obtained from Eastman Organic Chemicals and was used without further purification.

Apparatus and Procedure

The spin–lattice relaxation time of pure 1,2-dichloroethane and of 4 different solutions of progressively lower concentration of 1,2-dichloroethane in heavy benzene and carbon disulfide was determined at 20 °C on a PS-60A NMR Specialities pulsed nuclear magnetic resonance (n.m.r.) spectrometer using a 180–90° pulse sequence (5). The experimental solutions were carefully degassed by repeated freeze–pump–thaw cycles to remove dissolved oxygen and were sealed under vacuum. To minimize vaporization from the liquid phase the experimental glass sample tubes, 8 mm in diameter, were provided with a restriction leading to the vapor space as suggested by Green and Powles (6).

Results and Discussion

The experimental results are shown graphically in Fig. 1 in a form of a graph of T_1^{-1} vs. the mole fraction of 1,2-dichloroethane in solution. In

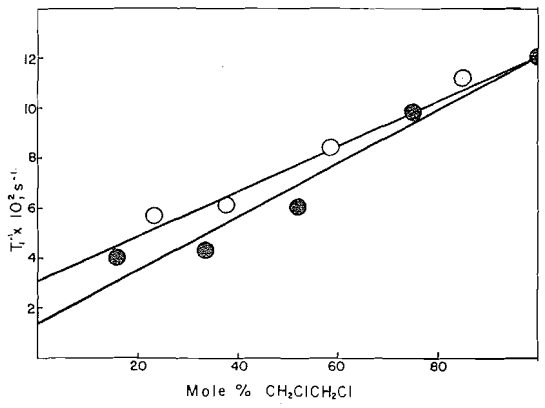

FIG. 1. Graph of T_1^{-1} vs. mole % 1,2-dichloroethane in solution. ○, heavy benzene; ●, carbon disulfide.

each case the experimental points were fitted to a straight-line plot by a least squares fitting procedure; the average deviation from the straight line was, in the case of heavy benzene, 0.34 T_1^{-1} units and in the case of carbon disulfide, 0.66 T_1^{-1} units. The rotational relaxation time, τ_r, was calculated using the extrapolated value of T_1^{-1} and the following relationship between the intramolecular relaxation time, i.e. the extrapolated value of T_1, and the rotational relaxation time, τ_r (7).

$$[1] \qquad T_1^{-1}\,(\text{intra}) = A\tau_r$$

$$[2] \qquad A = \frac{\hbar^2\gamma^4}{n}\sum_i\sum_j \beta_{ij} d_{ij}^{-6}$$

Here n is the number of protons in the molecule, β_{ij} is a constant factor equal to 3/2 for equivalent protons and 1 for nonequivalent protons, γ is the magnetogyric ratio of the proton, and d_{ij} is the distance between proton i and proton j. The necessary data for the calculation of the constant A in eq. [2] were taken from the literature (8). In the calculation it was assumed, following the suggestion of Chitoku and Higasi (1), that the solute molecules exist in two conformations only, viz. the *gauche* and *trans* conformation respectively. The resulting value for the molecular rotational relaxation time, τ_r was found to be 1.31×10^{-12} and 0.57×10^{-12} s for heavy benzene and carbon disulfide solvents, respectively. Both values are in reasonable agreement with the dielectric relaxation values reported by Chitoku and Higasi (1), viz. 3.69×10^{-12} s in benzene, 4.53×10^{-12} s in *p*-xylene, and 1.31×10^{-12} s in hexane solution, see Table I. In making the above comparison it should be remembered that on theoretical grounds (9) it is expected that the n.m.r. relaxation time, τ_r, is 1/3 of the dielectric relaxation time, τ_D, and that according to the Debye relationship, the rotational relaxation time for a sphere rotating in a viscous medium is proportional to the viscosity of that medium. This means that our value of 1.31×10^{-12} s for benzene should be compared with one third of the value obtained by Chitoku and Higasi (1) for benzene and *p*-xylene solutions, i.e. 1.23×10^{-12} s and 1.51×10^{-12} s respectively. Also our value for carbon disulfide should be compared with one third of their value obtained in hexane solution, but, corrected for the different viscosities of the two solvents. The viscosity of hexane and carbon disulfide at 20 °C is 0.308 cP (1) and 0.367 cP (10), respectively. If our value of 0.57×10^{-12} s is multiplied by the ratio of the viscosities for hexane and carbon disulfide and the result is multiplied by 3, there results a relaxation time of 1.44×10^{-12} s, which compares favorably with the dielectric value for hexane solution reported by Chitoku and Higasi (1), viz. 1.31×10^{-12} s. The reason we chose hexane for our comparison from the 5 different solvents studied by Chitoku and Higasi (1) was that the viscosity, and hence also the macro hydrodynamical properties of this solvent, most closely resemble the viscosity and the hydrodynamical properties of carbon disulfide.

Although there is fair agreement between our values and those found by Chitoku and Higasi (1), which argues in favor of their interpretation that the "situation may possibly be described in the first approximation by a picture of rotating *gauche* molecules in a viscous medium", it will be noticed that in each case our values are larger than the values found by Chitoku and Higasi. We

TABLE I

Comparison of dielectric, τ_D, and magnetic, τ_r, relaxation times, of 1,2-dichloroethane in different solvents

Solvent	τ_r (ps)	$\tau_D/3$ (ps)	η (cP)
Benzene	1.31	1.23	0.652
p-Xylene	—	1.51	0.638
CS_2	0.57 (0.48)*	—	0.367
Hexane	—	0.44	0.308

*Corrected for the different viscosities of carbon disulfide and hexane.

Can. J. Chem. Downloaded from www.nrcresearchpress.com by 210.87.254.42 on 09/05/12
For personal use only.

Can. J. Chem. Downloaded from www.nrcresearchpress.com by 210.87.254.42 on 09/05/12
For personal use only.

believe that this discrepancy is due to either spin–rotation and/or spin – internal rotation interaction. It is well known that if parts of a molecular structure are capable of rotating about some internal molecular axis, then, depending on the relative speeds of rotation of the over all, end-for-end tumbling motion of the molecule and the internal rotary motion, the measured value of τ_r will be decreased by a certain factor which in the limit, when the speed of the internal rotary motion far exceeds the speed of the tumbling motion, assumes a value of 1/4 (11). In our case we evaluated the rotational relaxation time, i.e. the relaxation time for the tumbling motion, on the assumption that the molecule was rigid; the internal rotation of the two chloromethyl groups was neglected. Now as a first approximation the total intra molecular spin–lattice relaxation rate, T_1^{-1} may be written as a sum of two parts, one corresponding to the tumbling motion and the other to the internal rotation, viz.

$$[3] \quad T_1^{-1}(\text{intra}) = T_1^{-1}(\text{tumb}) + T_1^{-1}(\text{int rot})$$

From eqs. [3] and [1] it is obvious that the neglect of the internal rotation contribution to T_1^{-1} (intra) will result in a larger calculated value for τ_r. Chitoku and Higasi (1) noted that the Cole–Cole parameter for benzene and *p*-xylene solution was 0.11–0.14 and 0.17–0.21, respectively, suggesting the existence of two or more polar molecular species. However, the above authors did not think that the accuracy of their data warranted an analysis of their measurements into two or more different absorption peaks. We, too, think that the precision of our data does not permit a more elaborate analysis of our data, but, the fact that our values in both cases are larger than those of Chikotu and Higasi, values which reflect the tumbling motion of the molecule only, does suggest that the tumbling motion of the molecule is accompanied to some, albeit small, degree by an internal rotation of the two chloromethyl groups.

Acknowledgments

We thank Mr. R. Long for some of the experimental measurements and Dr. T. Schaefer for helpful discussions. The financial assistance of the National Research Council of Canada is very much appreciated.

1. K. Chitoku and K. Higasi. Bull. Chem. Soc. Japan, **40**, 773 (1967).
2. H. Muller. Physik. Z. **34**, 689 (1933).
3. M. Kubo. Bull. Inst. Phys. Chem. Res. Tokyo, **13**, 1221 (1934).
4. A. Neckel and H. Volk. Z. Elektrochem. **62**, 1104 (1958).
5. A. Laukien. Handbuch der Physik. Vol. XXXVIII. Springer-Verlag, Berlin. 1958. p. 20.
6. D. K. Green and J. G. Powles. Proc. Phys. Soc. London, **85**, 87 (1965).
7. J. G. Powles. Ber. Bunsenges Physik. Chem. **67**, 328 (1963).
8. Tables of interatomic distances and configuration in molecules and ions. Chem. Soc. London. Spec. Publ. No. 11 (1958).
9. A. Abragam. Principles of nuclear magnetism. Oxford Univ. Press, London. 1961. p. 300.
10. Thorpe and Rodger. Phil. Trans. **185A**, 397–710 (1894).
11. D. E. Woessner. J. Chem. Phys. **36**, 1 (1962).

Can. J. Chem. Downloaded from www.nrcresearchpress.com by 210.87.254.105 on 09/05/12
For personal use only.

Electrochemical reactions at PbO_2 electrodes. Part IV. Electrochemical behavior of α-PbO_2 in acid perchlorate electrolytes

N. A. HAMPSON, P. C. JONES[1], AND R. F. PHILLIPS
Department of Chemistry, Loughborough University of Technology, Leicestershire, England

Received May 27, 1968

The cathodic passivation and the exchange reactions at α-PbO_2 electrodes in acid perchlorate electrolytes have been investigated using the galvanostatic technique. The results are generally closely similar to those previously reported for β-PbO_2 but some differences occur and these are explained in terms of an α–β-PbO_2 equilibration process.

Canadian Journal of Chemistry, 47, 2171 (1969)

Introduction

Lead dioxide exists in two polymorphic states, known as the α and the β forms. As usually produced, both forms exist together, but under controlled experimental conditions either may be prepared substantially free of the other. In general, the less reactive β-modification is obtained from acid solutions, and the α-modification from alkaline solutions, but precise control of temperature and, in anodic deposition, current density is necessary. The electrochemical behavior of β-PbO_2 electrodes in acid lead perchlorate electrolytes has been described in previous papers (1–3). The present paper describes similar studies at α-PbO_2 electrodes.

Experimental

The electrolytic cell, electrical circuit, electrolyte purification procedure, and electrode geometry and construction have been described (1).

Deposition of α-PbO_2 on Platinum

Counter, test, and reference electrodes were prepared by electrodeposition of α-PbO_2 from alkaline sodium plumbite (2 *M* NaOH, saturated with PbO) at a rate of 0.8 mA cm^{-2} at 30 °C on etched (1:1, HNO_3:H_2SO_4) platinum, (see ref. 4). Comparative X-ray diffraction measurements were made to establish the initial freedom of the preformed α-PbO_2 deposits from β-PbO_2.

Electrolytes

Two series of acidified $Pb(ClO_4)_2$ electrolytes were used, the first at constant $[H^+]$ and variable $[Pb^{2+}]$ and the second at constant $[Pb^{2+}]$ and variable $[H^+]$. The total perchlorate concentration was maintained (added $NaClO_4$) at 6.85 *M* throughout.

Electrometric Measurements

After allowing 10 min for stabilization of the electrode–electrolyte system, measurements were made of transition time and overpotential in the same manner as previously reported (1).

Results

The Galvanostatic (Cathodic) Passivation of α-PbO_2 in Acid Perchlorate Electrolytes

During the cathodic polarization of α-PbO_2 in acid perchlorate electrolytes, two abrupt changes in potential were recorded corresponding to transitions respectively between the following reactions

[1] $$\alpha\text{-}PbO_2 + 4H^+ + 2e \rightarrow Pb^{2+} + 2H_2O$$

[2] $$Pb^{2+} + 2e \rightarrow Pb$$

[3] $$2H^+ + 2e \rightarrow H_2$$

Subsequent ex situ examination of the electrode after stage [3], however, showed only a reddish-brown film containing Pb(II) with no evidence of metallic lead (no amalgamation when the film was treated with Hg). The non-appearance of elemental Pb contrasts with that observed when using β-PbO_2 electrodes (1).

For each electrolyte system the equation

[4] $$(i - i_l)t_p^{\frac{1}{2}} = k_p$$

was obeyed, where t_p (< 20 s) is the time taken to reach the first transition at the current density, i, and k_p and i_l are constants for a given solution. Both k_p and i_l vary with $[H^+]$. The dependence of k_p on $[H^+]$ calculated using the method of least squares is (at 23 °C)

[5] $$k_p = 0.197\ [H^+] + 0.015$$

From eq. [5], using the theory developed in Part I (1), values of δ, the thickness of the diffusion layer, have been calculated and these are shown in Table I.

[1]Present address: Energy Conversion Ltd., Basingstoke, Hampshire, England.

Can. J. Chem. Downloaded from www.nrcresearchpress.com by 210.87.254.105 on 09/05/12
For personal use only.

TABLE I

Calculated diffusion layer thickness (δ cm) for observed i_l at 23 °C*

$[H^+]$, M	k_p, A cm^{-2}s$^{\frac{1}{2}}$	i_l, A cm^{-2}	δ, cm
0.027	0.020	0.002	0.035
0.24	0.061	0.006	0.035
0.94	0.195	0.015	0.046
3.0	0.60	0.050	0.042

*α-PbO_2 electrodes in acid perchlorate electrolytes. Total concentration of ClO_4^-, 6.85 M with $NaClO_4$.

TABLE II

Mean double layer capacitances at 23 °C*

$[Pb^{2+}]$, M	$[H^+]$, M	C_L, μF cm^{-2}
0.001	3.0	137.3
0.0098	3.0	141.3
0.063	3.0	124.0
0.50	3.0	139.9
0.10	0.24	138.0
0.098	0.027	139.0

*α-PbO_2 electrodes in acid lead perchlorate electrolytes. Total concentration of ClO_4^-, 6.85 M with $NaClO_4$.

TABLE III

Exchange currents and charge transfer coefficients at 23 °C*

Concentration	i_0†, mA cm^{-2}	i_0‡, mA cm^{-2}	α‡
3.0 M H^+			
0.005 M Pb^{2+}	0.137	0.143	0.15
0.0098 M Pb^{2+}	0.156	0.163	0.17
0.063 M Pb^{2+}	0.194	0.197	0.20
0.50 M Pb^{2+}	0.266	0.276	0.20
0.1 M Pb^{2+}			
0.24 M H^+	0.207	0.212	0.22
0.027 M H^+	0.214	0.210	0.17

*α-PbO_2 electrodes in acid lead perchlorate electrolyte. Total concentration of ClO_4^-, 6.85 M with $NaClO_4$.
†Determined geometrically.
‡Determined iteratively.

Overpotential – Current Density Data

Double Layer Capacitances

Double layer capacitances calculated (2) from the rise of electrode potential during the very early stages of galvanostatic polarization are shown in Table II.

Lower Overpotential Region (η_D < 10 mV)

Linear plots were obtained of charge transfer overpotential, η_D, vs. current density. The exchange current, i_0, was calculated from the slope of these plots at the origin, using

$$[6] \qquad \left(\frac{\partial \eta_D}{\partial i}\right)_{\eta_D=0} = -\frac{RT}{2F}\cdot\frac{1}{i_0}$$

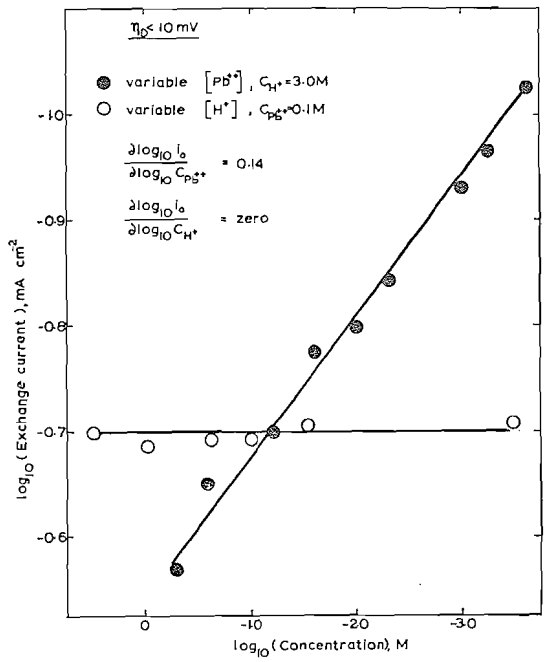

FIG. 1. Variation of exchange current with $[Pb^{2+}]$ and $[H^+]$ α-PbO_2 electrode; total $[ClO_4^-]$, 6.85 M (with $NaClO_4$) at 23 °C.

Satisfactory agreement was obtained (Table III) between these values of i_0 and those obtained using the iterative technique (5). The charge transfer coefficients derived by the iterative method also agree with the value calculated from the dependence of i_0 on $[Pb^{2+}]$ (Fig. 1). The dependence of i_0 on $[H^+]$, also shown in Fig. 1, suggests an abnormally high value for the charge transfer coefficient and possibly indicates some adsorption of H^+ (2).

The effect of temperature on current density – overpotential relationships is shown in Fig. 2*a*. $\log_{10} i$ vs. $1/T$ °K Arrhenius plots (Fig. 2*b*) suggest two approximately linear parts, corresponding to activation enthalpies of ~ 3 kcal mole^{-1} in the low temperature range and ~ 10 kcal mole^{-1} in the higher temperature range. Figure 2*b* was typical of all the electrolytes investigated.

Can. J. Chem. Downloaded from www.nrcresearchpress.com by 210.87.254.105 on 09/05/12
For personal use only.

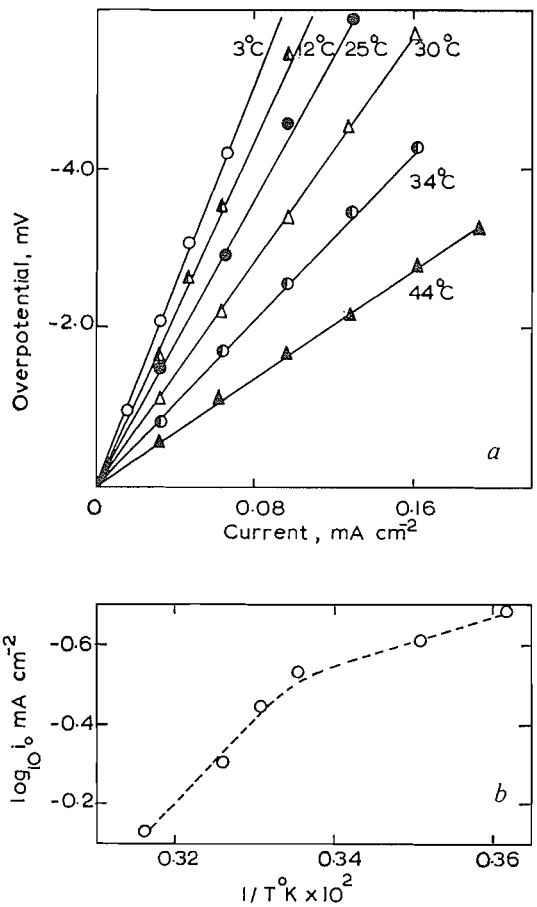

FIG. 2. Temperature dependence of current–overpotential curves for α-PbO_2. Electrolyte: 0.025 *M* Pb^{2+} plus 3.0 *M* H^+, total $[ClO_4^-]$, 6.85 *M*.

High Overpotential Region ($\eta_D > 10$ mV)

Figure 3 shows Tafel plots ($\log_{10} i$ vs. η_D) for different $[Pb^{2+}]$ at constant $[H^+]$. Potentials $E_{3M}{}^{\alpha}$ refer to the α-PbO_2/3.0 *M* H^+, 1.0 *M* Pb^{2+} system as the reference potential.

Figure 4 shows Tafel plots for electrolytes of constant $[Pb^{2+}]$ and variable $[H^+]$. The potentials $E_{M'}{}^{\alpha}$ refer to the α-PbO_2/0.1 *M* Pb^{2+}, 1.0 *M* H^+ system as a similar arbitrary standard. In both series of experiments the reference electrode was connected using saturated sodium perchlorate electrolyte through a tap and sintered frits of low porosity. Over the concentration ranges investigated experimental values of the equilibrium potential agreed with calculated values, confirming that the liquid junction potential had been eliminated.

TABLE IV

Potential limits of constant αZ. Potential region (about the equilibrium) in which the reaction conforms to a simultaneous two-electron transfer process

Concentration, *M*	Potential region, ± 5 mV
1. Pb^{2+} concentration at constant $[H^+] = 3.0$ *M*, $[ClO_4^-] = 6.85$ *M*	
0.025	−22 mV to +13 mV
0.0098	−32 mV to +12 mV
0.0050	−38 mV to +14 mV
2. H^+ concentration at constant $[Pb^{2+}] = 0.1$ *M*, $[ClO_4^-] = 6.85$ *M*	
0.94	−35 mV to + 9 mV
0.24	−39 mV to +13 mV
0.027	−25 mV to +10 mV

Following the procedure adopted in Part III (3) the effect of increases in $|\eta_{D_{max}}|$ (the maximum numerical value of the overpotential) on "αZ" was examined, where "αZ" is part of the exponent in the charge transfer equation

$$[7] \quad i = i_0\left[\exp -\frac{\alpha ZF}{RT}\eta_D - \exp\frac{(1-\alpha)ZF}{RT}\eta_D\right]$$

Table IV shows the limits within which "αZ" remained constant.

Discussion

Galvanostatic Passivation of α-PbO_2

For a given electrolyte the similarity of k_p, i_l, and δ for both α- and β-PbO_2 indicates that for the first transition point, which is controlled by mass transport in the electrolyte phase, the effective surface area of each modification involved in this diffusion controlled process is substantially the same.

The absence of detectable lead and the presence of Pb(II) on the electrode when the latter, polarized to the point of hydrogen evolution, is removed from the electrolyte and examined chemically, represents a notable difference from the behavior of the β-electrode. This difference might be attributed to a greater oxidizing power of α-PbO_2 promoting the reaction

$$[8] \quad \text{Pb(IV)} + \text{Pb} \rightarrow \text{Pb(II)}$$

and so chemically converting metallic lead to Pb(II) as it forms at the electrode. An alternative

Can. J. Chem. Downloaded from www.nrcresearchpress.com by 210.87.254.105 on 09/05/12
For personal use only.

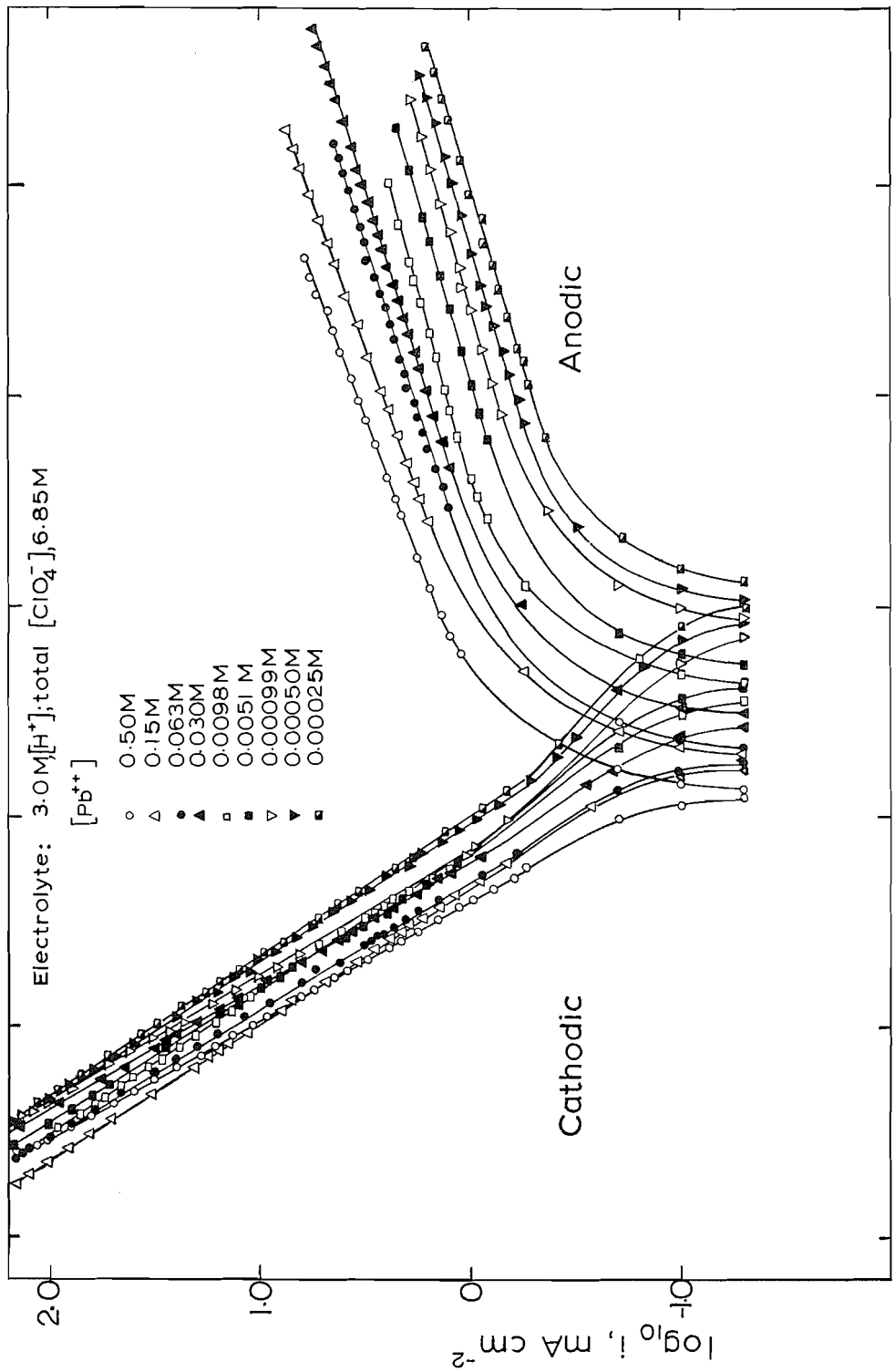

FIG. 3. Cathodic and anodic current density – potential curves for α-PbO_2 at variable Pb(II) concentration in 3.0 *M* H^+ at 23 °C; total $[ClO_4^-]$, 6.85 *M*.

Can. J. Chem. Downloaded from www.nrcresearchpress.com by 210.87.254.105 on 09/05/12
For personal use only.

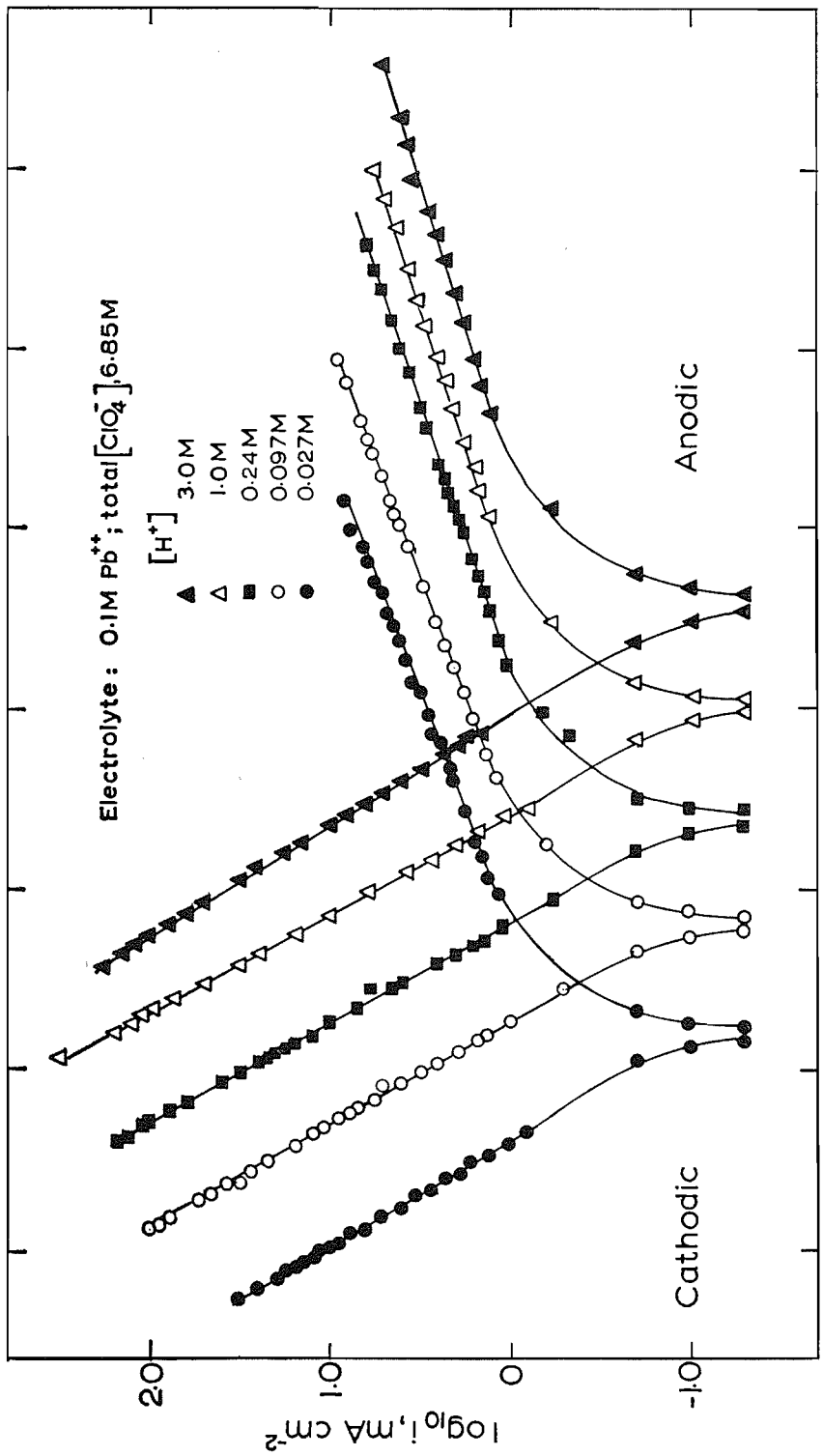

FIG. 4. Cathodic and anodic current density – potential curves for α-PbO_2 at variable H^+ concentration in 0.1 *M* Pb^{2+} at 23 °C; total [ClO_4^-], 6.85 *M*.

Can. J. Chem. Downloaded from www.nrcresearchpress.com by 210.87.254.105 on 09/05/12
For personal use only.

explanation may be obtained by analogy with the work of Mark (7) who found that, in the discharge of α- and β-PbO_2 in dilute H_2SO_4, the final $PbSO_4$ product in the case of α-PbO_2 remains as a tightly adherent film on the surface of the undischarged PbO_2, whereas in the case of β-PbO_2, the $PbSO_4$ film is much less adherent. This might suggest in our experiments the initial formation of an adherent Pb(II) film, which on further reduction produces Pb in close contact with the PbO_2 electrode with which it simultaneously reacts chemically to form PbO (8) or some corresponding salt of perchloric acid. The lead product film in the case of β-PbO_2, however, being in less perfect physical contact with the underlying electrode, would on this evidence be expected to react at a much slower or even negligibly slow rate.

Overpotential – Current Density Measurements

The mean value of the double layer capacitance (138 μF cm^{-2}) is substantially higher than that found for β-PbO_2 (78 μF cm^{-2}). This might suggest a greater degree of electrode surface roughness in the case of α-PbO_2.

Low Overpotential Region

The equality respectively of the anodic and cathodic exchange currents and of the charge transfer coefficients, in the low overpotential region, indicates that in this region the rate controlling reaction is the same for both the anodic and cathodic processes, and for reasons adduced in the closely similar case of β-PbO_2 (2, 3) is a simultaneous two-electron transfer process.

The observation that the activation enthalpy increases with temperature (Figs. 2*a* and 2*b*) was confirmed in a number of replicate experiments. Such changes were not observed with β-PbO_2 (3). It is interesting to report that Angstadt, Venuto, and Ruetschi (9) in their investigations of PbO_2 in H_2SO_4 in the same temperature range as reported here, found a pronounced change in slope of the electrode potential versus temperature curve in the case of α-PbO_2 but not in the case of β-PbO_2.

High Overpotential Region

Figure 3 shows a family of anodic and cathodic $\log_{10} i$ vs. η_D curves, corresponding to varying $[Pb^{2+}]$ at constant $[H^+]$. The *cathodic branch* of this family of curves is of particular interest.

For the exchange reaction

$$[9] \qquad PbO_2 + 4H^+ + 2e = Pb^{2+} + 2H_2O$$

we can write for constant potential conditions

$$[10] \qquad i_C = k_C a_{PbO_2} a_{H^+}{}^m$$

$$[11] \qquad i_A = k_A a_{Pb(II)} a_{H^+}{}^n$$

where i_C and i_A are cathodic and anodic current, respectively, k_C and k_A are potential dependent rate constants, m and n are the numbers of H^+ involved in the rate determining step in the cathodic and anodic directions respectively, and a is the activity[2].

The faradaic current ($i = i_C - i_A$) reduces to i_C at sufficiently high cathodic potentials since i_A becomes negligibly small. At these high cathodic potentials i would be expected to follow eq. [10] and to be dependent on a_{PbO_2} and $a_{H^+}{}^m$ but to be independent of $a_{Pb(II)}$. For β-PbO_2 only one cathodic Tafel line was observed, as expected under these conditions. For α-PbO_2, however, Fig. 3 shows a closely spaced set of cathodic Tafel lines indicating a reduction in reaction rate with increased [Pb(II)]. That is, at constant potential in the cathodic Tafel region, the current flowing decreases with increased [Pb(II)]. Reference to eq. [10] indicates that at constant pH and potential, the cathodic current is reduced only by a decrease in PbO_2 activity. This reduction must therefore be brought about by increased [Pb(II)].

To explain these results, one must either assume direct participation of Pb^{2+} in the cathodic reaction, or consider the possibility of a change in the activity of the PbO_2 electrode, in the direction of a decrease of PbO_2 activity with increase in $[Pb^{2+}]$. The appearance of a single cathodic Tafel line in the β-PbO_2 experiments must rule out the first of these hypotheses, and focus attention on PbO_2 as the only difference in the two series of experiments.

The key observation from Fig. 3 is the shift of the cathodic Tafel line towards the β-PbO_2 cathodic Tafel line with increase in $[Pb^{2+}]$. At

---

[2] a_{H^+} occurs in both eqs. [10] and [11] since eq. [9] may be balanced in other ways with respect to H^+ (or OH^-), e.g. in a reaction such as

$$PbO_2 + 3H^+ + 2e = Pb^{2+} + H_2O + OH^-$$

m would be 3 and n would be −1.

TABLE V

Characteristics of Tafel plots. α-PbO_2 electrode: total [ClO_4^-] 6.85 *M* (with added $NaClO_4$) at 23 °C

Concentration, *M*		Cathodic coefficient $-2.3\frac{RT}{F}\cdot\frac{\partial \log_{10} i_c}{\partial \eta_D}$	Anodic coefficient $2.3\frac{RT}{F}\cdot\frac{\partial \log_{10} i_A}{\partial \eta_D}$	Intercepts at $\eta_D = 0$ mA cm^{-2}	
Pb^{2+}	H^+			$2i_{0a}$	$2i_{0b}$
0.25	3.0	0.94	0.22	0.117	0.630
0.0098	3.0	0.90	0.20	0.0690	0.479
0.0050	3.0	0.94	0.18	0.0417	0.407
0.0010	3.0	0.92	0.18	0.0141	0.355
0.098	0.24	0.98	0.20	0.0955	0.531
0.10	0.027	1.00	0.18	0.100	0.569
0.10	0.0001	0.84	0.18	0.123	0.501

equilibrium the extent of the exchange reaction [9] is governed by the activities of the electroactive species H^+, Pb(II), and PbO_2. Increases in activities of the electroactive species increase the rate of exchange between Pb(II) in the solution and PbO_2 in the electrode surface. If this is linked with the known higher stability of β-PbO_2 in acid media, the effect of increasing the [Pb^{2+}] is to be seen to progressively alter the electrode surface from α- to β-PbO_2. The resultant equilibrium situation would be controlled by the [Pb^{2+}] and be established by the exchange current (i_0) during the interval (10 min) preceding the polarization measurements (< 80 ms duration). Schematically we have

$$\alpha\text{-}PbO_2 \overset{Pb^{2+}}{\rightleftharpoons} \binom{Pb^{2+}}{H^+} \overset{Pb^{2+}}{\rightleftharpoons} \beta\text{-}PbO_2$$

The results reported in Fig. 3 are the overpotential values extrapolated to time $t = 0$, and thus refer to the electrode in its initial (Pb^{2+} controlled) equilibrium state.

Coming next to the anodic polarization curves of Fig. 3, the results are virtually identical with the similar family of curves reported (3) for β-PbO_2. This is in agreement with the fact that the PbO_2 (whether α or β) is not involved as a reactant in this anodic process. The situation is precisely similar for the anodic family of curves shown for constant [Pb^{2+}] but varying [H^+] (Fig. 4).

When we come to consider the cathodic family of curves of Fig. 4, similar arguments for an equilibrated α/β-PbO_2 electrode surface would apply, following the scheme

$$\alpha\text{-}PbO_2 \overset{H^+}{\rightleftharpoons} \binom{Pb^{2+}}{H^+} \overset{H^+}{\rightleftharpoons} \beta\text{-}PbO_2$$

The equilibrium proportion of β-PbO_2 would thus be expected to increase in proportion to some power of the [H^+].

The corresponding rate eq. [10] now becomes

$$[12] \qquad i_C = k_C' \, a_{H^+}^{(m+x)}$$

x, reflecting the dependence of the α/β equilibrium process of [H^+]. From this we deduce

$$(\partial \log i_C/\partial \log[H^+]) = m + x$$

If our value of 2.0 is now compared to the value of 1.5 reported for $\partial \log i/\partial \log[H^+]$ for β-PbO_2, the increase represents the effect of [H^+] on the α/β-PbO_2 equilibration process.

Characteristics of Tafel Plots

The results in the present series of experiments (see Figs. 3 and 4) provide the same evidence as reported for β-PbO_2 (3), for a change of the charge transfer mechanism from a simultaneous two-electron transfer to two consecutive single-electron transfer steps with increase in overpotential. This follows from

(*a*) the sum of the cathodic and anodic coefficients

$$\left[-\left(\frac{RT}{F}\right)\cdot \partial \log_e i_C/\partial \eta_D \quad \text{and} \quad \left(\frac{RT}{F}\right)\cdot \partial \log_e i_A/\partial \eta_D\right]$$

is significantly less than two (Table V).

(*b*) The anodic and cathodic exchange currents, i_{0a} and i_{0b}, obtained by extrapolating Tafel plots to η_D equals zero, are both appreciably different from each other (Table V).

(*c*) The charge transfer resistances, R_D, observed in the low overpotential region differ

Can. J. Chem. Downloaded from www.nrcresearchpress.com by 210.87.254.105 on 09/05/12
For personal use only.

TABLE VI

Charge transfer resistances. Comparison of experimental charge transfer resistance (for $\eta_D <$ 10 mV) with those calculated for $\eta_D >$ 50 mV

Concentration, M		Charge transfer resistance, Ω cm^2	
Pb^{2+}	H^+	Experimental	Calculated
0.005	3.0	93.3	340.0
0.0098	3.0	80.0	212.8
0.063	3.0	65.8	158.8
0.50	3.0	48.0	121.0
0.098	0.24	61.8	157.0
0.100	0.027	61.0	150.1

from those calculated from high overpotential measurements (Table VI) using

$$[13] \qquad R_D = \frac{RT}{4F} \cdot \left(\frac{1}{i_{0a}} + \frac{1}{i_{0b}} \right)$$

(*d*) Two distinct rectilinear regions are identifiable in the cathodic branch of Fig. 3; Fig. 5, which gives the full range of results for the 0.005 M Pb^{2+} case, shows this in greater detail.

In these terms, the reaction sequence (written for the reduction process) at overpotentials greater than $\sim$ 80 mV is

$$[14] \qquad PbO_2 \xrightarrow{i_{0a},\ \alpha_a} Pb(III)$$

followed by

$$[15] \qquad Pb(III) \xrightarrow{i_{0b},\ \alpha_b} Pb(II)$$

Following the procedure outlined in Part III, the rate determining step in the cathodic reduction of PbO_2 and also in the anodic oxidation of Pb^{2+} is the step leading to the formation of the Pb(III) intermediate. The experimental parameters calculated from the slope of cathodic and anodic Tafel plots

$$-2.3 \frac{RT}{F} \cdot \left(\frac{\partial \log_{10} i_C}{\partial \eta_D} \right) = \alpha_a$$

$$2.3 \frac{RT}{F} \cdot \left(\frac{\partial \log_{10} i_A}{\partial \eta_D} \right) = (1 - \alpha_b)$$

and intercepts ($2i_{0a}$ and $2i_{0b}$) are shown in Table V and are of similar order to the corresponding parameters observed for β-PbO_2.

Comparison of α- *and* β-PbO_2

Passivation (discharge) data are very similar for electrodeposited α- and β-PbO_2, although

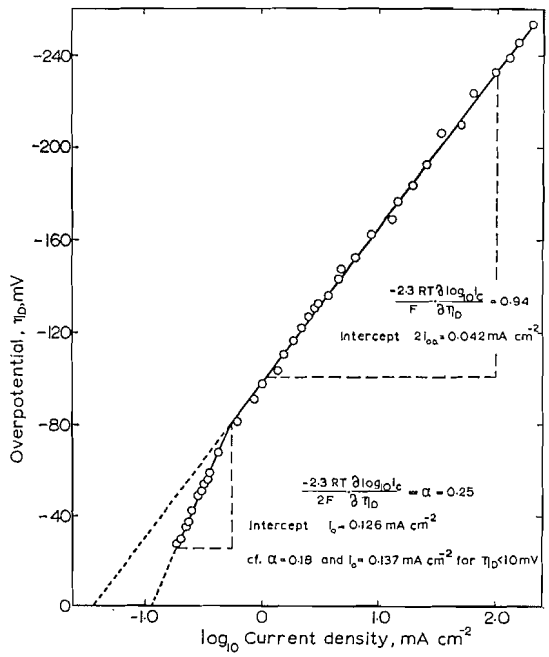

FIG. 5. Cathodic Tafel plot for α-PbO_2. Electrolyte: 0.005 M Pb^{2+} plus 3.0 M H^+; total [ClO_4^-], 6.85 M at 23 °C.

capacitance results indicate a greater true surface area in the case of the α-modification. This is to be expected since on the time scale of the passivation experiments, the diffusion layer is thick and reflects the apparent area of the electrodes, whereas electrode capacitances calculated in the first few milliseconds of electrode polarization when the diffusion layer is thin, reflect the true surface area.

The charge transfer process is similar for both α- and β-PbO_2. It is desirable to compare the numerical magnitude of characteristic thermodynamic and kinetic data for α- and β-PbO_2. Comparative data concerning oxidizing power, enthalpy of activation, exchange current density, and transfer coefficients would be particularly interesting. However, it is clear that experiments with α-PbO_2 in acid solutions have certain limitations which preclude a quantitative interpretation of the results. The isolation therefore of exact kinetic data for α-PbO_2 in acid perchlorate electrolytes has not proved possible. As suggested earlier in the paper, the reason for this is likely to be the formation of β-PbO_2 in addition to α-PbO_2 as products of the exchange reaction

Can. J. Chem. Downloaded from www.nrcresearchpress.com by 210.87.254.105 on 09/05/12
For personal use only.

which occurs from the instant the PbO_2 electrode comes into contact with the electrolyte.

Qualitatively it can nevertheless be concluded that the exchange current density for α-PbO_2 in perchlorate electrolytes is approximately twice as large as that for β-PbO_2, the charge transfer coefficients being approximately the same.

1. N. A. HAMPSON, P. C. JONES, and R. F. PHILLIPS. Can. J. Chem. **45**, 2039 (1967).
2. N. A. HAMPSON, P. C. JONES, and R. F. PHILLIPS. Can. J. Chem. **45**, 2045 (1967).
3. N. A. HAMPSON, P. C. JONES, and R. F. PHILLIPS. Can. J. Chem. **46**, 1325 (1968).
4. V. DODSON. J. Electrochem. Soc. **108**, 401 (1968).
5. J. P. G. FARR, N. A. HAMPSON, and M. E. WILLIAMSON. J. Electroanal. Chem. **13**, 462 (1967).
6. S. J. BONE, K. P. SINGH, and W. F. K. WYNNE-JONES. Electrochim. Acta, **4**, 288 (1961).
7. H. B. MARK, JR. J. Electrochem. Soc. **109**, 634 (1962).
8. J. J. LANDER. J. Am. Electrochem. Soc. **98**, 200 (1951).
9. R. T. ANGSTADT, C. J. VENUTO, and P. RUETSCHI. J. Electrochem. Soc. **109**, 177 (1962).

Can. J. Chem. Downloaded from www.nrcresearchpress.com by 210.87.254.105 on 09/05/12
For personal use only.

Can. J. Chem. Downloaded from www.nrcresearchpress.com by 210.87.254.105 on 09/05/12
For personal use only.

Studies on metal hydroxy compounds. VI. Kinetics of thermal decomposition of zinc and cadmium halide (Cl, F) derivatives

P. RAMAMURTHY AND E. A. SECCO
Chemistry Department, St. Francis Xavier University, Antigonish, Nova Scotia

Received October 31, 1968

Kinetics of thermal decomposition of zinc and cadmium hydroxides along with their halide (Cl, F) derivatives are reported. The kinetic results are discussed in terms of the appropriate reaction mechanism. The rates are also discussed using activated complex theory in a manner outlined by Cordes (9) where the effect of molecular rotation in both the reactants and the activated complex is considered. Furthermore, the abnormally high preexponential factors are speculated to have their origin in an active translational mode on the surface.

Canadian Journal of Chemistry, 47, 2181 (1969)

Introduction

The observed rates of solid-state decompositions are extremely difficult to interpret in terms of elementary steps, in contrast to gas-phase and liquid-phase reactions, because the rate is not controlled by the molecularity or chemistry alone, but is also controlled by the geometry of the solid, i.e. its topochemistry.

The purpose of this research is to study in detail a series of compounds within a certain restricted class in order to obtain a better understanding of the fundamental chemical aspect of solid-state decomposition reactions. The class of metal hydroxy compounds present, to our view, the requisite features which would allow a systematic investigation of the structural and substituent parameters on their reaction kinetics.

This communication, representing the first part of a systematic program of study on solid-state decomposition kinetics, reports on the kinetics of thermal decomposition of cadmium and zinc hydroxides and their halide (Cl, F) derivatives. Details of these decomposition reactions and analyses have already been reported (1–3).

Experimental

All compounds used in this study were prepared in this laboratory using procedures already described (1, 2).

The decomposition kinetics were determined gravimetrically, i.e. weight loss vs. time, using a duPont TGA-950 plug-in module for the duPont DTA-900 thermal analyzer console. To do kinetic studies with this unit the *x*-axis drive for the recorder must be accurately calibrated for time and temperature.

The time base calibration was done by switching the "Program Mode" selector to "Isothermal" and setting the appropriate controls on the 900 console and 950 module as recommended in the manufacturer's manual. The time intervals for a number of trial scans were checked against a stop watch; periodic checks were also made during the course of a reaction.

The temperature was calibrated by determining the relation between "Starting Temperature" dial setting and the "Isothermal" temperature. A plot of this relationship allowed us to choose the "Isothermal" experimental temperature from the "Starting Temperature" dial setting.

The recorded weight loss vs. time trace was converted to yield decomposition fraction, α, vs. time plot. The kinetic data were further processed to obtain the best straight line or linear fit with the known rate expressions.

All decomposition runs were done in nitrogen gas atmosphere. A current of nitrogen (Matheson Prepurified Grade with a stated impurity of 0.003% oxygen) was passed through the assembly at a constant flow rate of 2SCFH.

Results and Discussion

The kinetic data for the decomposition reactions occurring according to the following general reaction equations

$$[1]\quad Me(OH)_{2(s)} \rightarrow MeO_{(s)} + H_2O_{(g)}$$

$$[2]\quad 2MeOHX_{(s)} \rightarrow MeO_{(s)} + MeX_{2(s)} + H_2O_{(g)}$$

where Me represents the metal (Cd, Zn) and X the halogen (Cl, F), are presented in Table I.

The experimental α, t data were processed through a large number of kinetic equations. The best fit between the experimental data and the known rate expressions over the maximum reaction fraction $\alpha \geqslant 0.8$ and over the temperature ranges studied is given in Table I. In all cases, except CdOHF, the fitting of the data to a particular rate expression was straight-forward and clear-cut. On the other hand, the CdOHF data are fitted equally well to three known rate equations: (*i*) Avrami–Erofeyev (A–E) type with $n = 3/2$, (*ii*) the contracting formula or Roginskii–Todes–Mampel (R–T–M) equation, and (*iii*)

TABLE I

Kinetic data for decomposition reactions

Compound	Temperature range (°C)	Number of temperatures	Rate expression	Activation energy E_a (kcal)	log A	Heat of reaction ΔH (kcal)
ε-$Zn(OH)_2$	110–145	5	First order	10.2±1.5	4.4	11.6
β-ZnOHCl	250–290	6	First order	67.3±4.1	25.6	5.6
ZnOHF	370–400	4	First order	70.6±5.2	21.9	4.7
$Cd(OH)_2$	170–210	5	First order	26.3±2.1	10.9	12.1
CdOHCl	300–350	5	$1/(1-\alpha) = 1+kt$	54.3±3.4	9.2	9.8
CdOHF	290–330	5	$\ln(1-\alpha) = kt^{3/2}$	18.3±1.8		
			$1-(1-\alpha)^{1/3} = kt$	18.8±2.0	4.7	9.0
			$\log(\alpha/1-\alpha) = k \log t + c$	8.0±4.0		

modified Prout–Tompkins (P–T) in the order of listing in Table I.

The values of the preexponential factor A in the Arrhenius equation indicate a dependence on the E_a values. However, there is no dependence of E_a on ΔH indicated. The contents of Table I are grouped on the basis of their kinetic behavior and discussed under three categories: (*a*) zinc compounds and $Cd(OH)_2$, (*b*) CdOHCl, and (*c*) CdOHF.

(a) Zinc Compounds and $Cd(OH)_2$

The simple first-order kinetics obeyed by this group of compounds suggests the absence of a nucleation-controlled mechanism with the solid particle presenting a reaction zone or reactant/product interface where each molecule possesses an equal probability for decomposition. The low activation energies for the two hydroxides are in sharp contrast to the high E_a values for ZnOHCl and ZnOHF. In the latter reactions, one of the decomposition products, that is, $ZnCl_2$ or ZnF_2, is known to be hygroscopic. It thus presents the strong possibility of the decomposition water becoming chemisorbed at the reactant/product interface. The chemisorbed water could hinder the reaction by stabilizing the reaction interface. The above mode of action is in accord with the higher E_a values and lower rates observed, i.e. factor of 10^3, in ZnOHCl and ZnOHF relative to $Zn(OH)_2$. Zhabrova and his co-workers (4) have reported similar retardation effects with ambient gases (O_2, N_2, H_2O) on the dehydration kinetics of $Mg(OH)_2$ and $Al(OH)_3$.

(b) CdOHCl

The decomposition data for CdOHCl fit the second-order rate law represented in its integrated form by

$$1/(1 - \alpha) = 1 + kt$$

The integrated form of the second-order rate law is considered in solid state kinetics as a special case of the treatment given by Avrami (5), which was cast into a second-order rate expression by Honig *et al.* (6) at sufficiently large t to yield

$$[3a] \qquad 1/(1 - \alpha) = 1 + \sigma N_g G t$$

where σ is a shape factor, G is the lineal growth rate of the new phase, N_g is the initial density of germ nuclei, and t is the time. The composite quantity $\sigma G N_g$ is taken to be the formal rate constant k.

With σ and N_g effectively constant, the rate constant dependence on temperature originates with the term G in the composite rate constant, i.e. $\sigma N_g G$. The observed activation energy appears, therefore, to represent the rate of growth of the new phase or in this case, the advancement of the product/reactant interface.

In this reaction, as in the case of ZnOHCl and ZnOHF, one of the products $CdCl_2$ has a strong affinity for water. The action of chemisorbed water on a product retarding the progressive movement of the product/reactant interface is again in evidence resulting in a high activation energy for the reaction.

(c) CdOHF

The kinetics of CdOHF decomposition are quite well described by three rate expressions, which illustrates that the kinetics analysis, while a necessary one, is not sufficient alone to define the nature of the decomposition reaction. However, there is justification in disregarding the modified P–T equation on grounds of the low E_a value relative to the higher E_a value obtained for the other two equations. Furthermore, since no theoretical justification accompanies the A–E

Can. J. Chem. Downloaded from www.nrcresearchpress.com by 210.87.254.105 on 09/05/12
For personal use only.

Can. J. Chem. Downloaded from www.nrcresearchpress.com by 210.87.254.105 on 09/05/12
For personal use only.

type equation with $n = 3/2$, we are left with the contracting formula

$$1 - (1 - \alpha)^{1/3} = kt$$

The contracting formula is valid where the rate of advance in directions parallel to the surface is very fast compared with the rate perpendicular thereto, and—provided the surface is reasonably well nucleated—the surface then rapidly becomes covered with a layer of product which consumes the particle at a constant linear rate; the interface retains the shape of the original solid particle. The equation

$$1 - (1 - \alpha)^{1/3} = kt$$

applies specifically to spherical particles but in general to any isodimensional particles.

Attempts to analyze and interpret the pre-exponential factors of solid-state decomposition reactions in terms of fundamental molecular kinetic steps have been unsuccessful. The first such effort (7) made use of the Polanyi–Wigner equation, i.e. rate $= C.\nu.e^{-E_a/RT}$, and applied to decomposition of salt hydrates, where C is a constant computed from the number of water molecules per unit area of the interface and ν is the vibration frequency responsible for initiating decomposition with an expected order of magnitude of $5 \times 10^{12}\ s^{-1}$. The main hurdle encountered in this type of analysis was to reconcile experimental values of ν that differed by a factor as much as 10^{10}, e.g. $\nu \sim 10^5$–10^{22}.

Several applications have been made of the theory of the activated complex to solid decompositions with the most recent treatments embracing monomolecular and bimolecular cases given by Shannon (8) and Cordes (9) respectively. The treatment hinges on the critical parameter of the number of active degrees of freedom in the reactant and the complex contributing to their respective partition functions in the equation of absolute rate theory

$$k_r = A \exp\left(-E_a/kT\right) = \left[\frac{kT}{h}\cdot\frac{Q^*}{Q}\right] \exp\left(-E_a/kT\right)$$

where Q^* and Q represent the complete partition functions of the activated complex, excluding the reaction coordinate, and of the reactant, respectively, with the remaining terms following the conventional notation of rate theory.

The association is made between the experimental A term and the theoretical composite term

$$\left[\frac{kT}{h}\cdot\frac{Q^*}{Q}\right]$$

so that we have

$$\left[10^{13}\cdot\frac{Q^*}{Q}\right] = A$$

leading to three distinct limiting cases:

(i) $Q^* > Q$ yielding $A > 10^{13}$,
(ii) $Q^* < Q$ yielding $A < 10^{13}$, and
(iii) $Q^* = Q$ yielding $A = 10^{13}$.

Case (*i*) is visualized for a complex located on the surface exercising a larger number of active degrees of freedom relative to the reactant incorporated or locked in the crystal interior. Case (*ii*) is the converse, that is, the complex is more restricted in its freedom on the surface or in the bulk relative to the reactant. Case (*iii*) obviously refers to the situation where the complex and the reactant resemble each other within the limits of absolute rate theory.

Unfortunately, it is not possible now to make a rigorous test for the kinetics of the reactions reported here in terms of absolute rate theory, owing to the lack of the complete infrared spectrum for the reactant, that is, data on lattice vibrations, torsional oscillations, etc. We can, however, speculate on the nature of these reactions using Cordes' general analysis considering only rotational freedom for empirical first-order preexponential factors.

Following Cordes' treatment we envisage a reaction scheme for decomposition as follows

(a) Hydroxides

[1] HO—Me—OH → [HO--Me--OH]*
→ Me—OH + OH

[2] OH + Me—OH → [Me—OH---OH]*
→ MeO + H_2O

(b) Basic Halides

[1] X—Me—OH → Me—X + OH

[2] OH + X—Me—OH → [X—Me—OH---OH]*
→ X—Me—O + H_2O

[3] Me—X + X—Me—O → [X—Me---X---Me—O]*
→ MeX_2 + MeO

We further envisage the rate determining steps to be reaction [1] or [2]. Although an activated

complex is shown in reaction [3] to represent an intermediate species prior to the stable products, we cannot appreciate this reaction since this step is not accompanied by a weight loss and is therefore unobservable in our experiments.

In the case of hydroxides with reaction [1] as the slow step, the overall decomposition rate will be monomolecular first-order. If the limiting aspect of this reaction is a surface one, a surface regression rate which is pseudo-first-order is observed. The activated complex formed is highly restricted in rotation with a very low preexponential factor $\sim 10^5$ predicted. This predicted value agrees very well with the observed value for ε-$Zn(OH)_2$. On the other hand, if the complex enjoys a "freer" condition on the surface, then the predicted factor of 10^9 is again in fair agreement with the observed value for $Cd(OH)_2$. Alternatively for $Cd(OH)_2$, if reaction [2] is the limiting step, the reaction will be bimolecular first-order with a predicted preexponential factor range 10^9–10^{11}. This situation includes the case where the bond length between the two parts of the complex, i.e. —(OH---OH), is such to permit free rotation.

The preexponential factors observed for ZnOHCl and ZnOHF rates are more difficult to interpret from Cordes' analysis because these rates are complicated by the intervention of H_2O vapor giving rise to extremely high preexponential values. However, we can imagine the adsorbed H_2O to provide a mobile layer on the reactant/product surface to permit the complex to execute one or two translational modes of freedom where these modes are absent in the reactant. The contribution to the overall partition function by one additional translational mode in the complex is ca. 10^8, yielding a predicted A value of ca. 10^{21} which is within the order of magnitude observed experimentally.

Acknowledgment

The authors are indebted to the National Research Council of Canada for financial support of this research program.

1. O. K. Srivastava and E. A. Secco. Can. J. Chem. **45**, 579 (1967).
2. O. K. Srivastava and E. A. Secco. Can. J. Chem. **45**, 1375 (1967).
3. P. Ramamurthy and E. A. Secco. Can. J. Chem. In press.
4. G. M. Zhabrova, B. M. Kadenatzi, O. V. Krylov, A. V. Shkarin, and V. A. Gordeeva. 6th Intern. Symp. Reactivity Solids. *Edited by* J. W. Mitchell. Schenectady, New York. 1969.
5. M. Avrami. J. Chem. Phys. **8**, 212 (1940).
6. A. W. Czanderna, J. M. Honig, and C. N. R. Rao. Trans. Faraday Soc. **54**, 1069 (1958).
7. P. W. M. Jacobs and F. C. Tompkins. Chemistry of the solid state. *Edited by* W. E. Garner. Butterworths Scientific Publications, London. 1955. Chap. 7.
8. R. D. Shannon. Trans. Faraday Soc. **60**, 1902 (1964).
9. H. F. Cordes. J. Phys. Chem. **72**, 2185 (1968).

Can. J. Chem. Downloaded from www.nrcresearchpress.com by 210.87.254.105 on 09/05/12
For personal use only.

Can. J. Chem. Downloaded from www.nrcresearchpress.com by 210.87.254.6 on 09/05/12
For personal use only.

Studies on metal hydroxy compounds. VII. Thermal analyses of copper derivatives

P. RAMAMURTHY AND E. A. SECCO
Chemistry Department, St. Francis Xavier University, Antigonish, Nova Scotia

Received November 15, 1968

Copper basic halide compounds have been studied by thermogravimetric and differential thermal analyses. This study reveals the general pattern of thermal stability observed for cadmium and zinc basic halides.

The initial mode of decomposition varied within the copper group. The iodides, bromides, and chlorides all decomposed via dehydroxylation and in this way resembled the Cd and Zn basic halides. The copper basic fluorides, on the other hand, decomposed by simultaneous dehydroxylation and dehydrofluorination which is in distinct contrast to the Cd and Zn basic fluorides.

Canadian Journal of Chemistry, 47, 2185 (1969)

Introduction

A program of research on metal basic halides was initiated in our laboratory with studies on Zn and Cd compounds reported earlier (1, 2). Since other transition metals, such as Cu, Ni, Co, and Fe form two types of basic halides, i.e. MeOHX and $Me_2(OH)_3X$, it was considered worthwhile to extend our studies to include this group of compounds. In this communication we report on the differential thermal analysis (d.t.a.) and thermogravimetric analysis (t.g.a.) of copper basic halides.

Wheeler and Handler (3) studied the decomposition of $CuF_2 \cdot 2H_2O$ and CuOHF by d.t.a. and proposed the following reactions

$$[1a] \quad 2Cu_2F \cdot 2H_2O \xrightarrow{130\text{–}150\ ^\circ C} Cu_2(OH)F_3 + HF + 3H_2O$$

$$[1b] \quad Cu_2(OH)F_3 \xrightarrow{420\ ^\circ C} CuO + CuF_2 + HF$$

$$[2a] \quad 4CuOHF \xrightarrow{370\ ^\circ C} Cu_2(OH)F_3 + 2CuO + HF + H_2O$$

$$[2b] \quad Cu_2(OH)F_3 \xrightarrow{420\ ^\circ C} CuO + CuF_2 + HF$$

Recently, Le Van My and co-workers (4) reported $CuF_2 \cdot 2H_2O$ to decompose in vacuum as follows

$$[3a] \quad CuF_2 \cdot 2H_2O \xrightarrow{130\ ^\circ C} CuOHF + H_2O + HF$$

$$[3b] \quad 4CuOHF \xrightarrow{350\ ^\circ C} Cu_2(OH)F_3 + 2CuO + H_2O + HF$$

$$[3c] \quad Cu_2(OH)F_3 \xrightarrow{420\ ^\circ C} CuO + CuF_2 + HF$$

When our study was nearing completion a report by Ball and Coultard (5) appeared on the t.g.a. of a number of copper basic halides conducted in air. This latter report contained results which were in disagreement with the already published decomposition reactions and, therefore, added to the existing controversy.

The purpose of this communication is to clarify the growing controversy on the modes of decomposition of copper basic halides and to contrast these modes of decomposition with those of their zinc and cadmium analogues.

Experimental

All the compounds used in this study were prepared in this laboratory by following known methods with slight modification of the procedures. Brief descriptions of the procedures are given below; all chemicals used in these preparations were of reagent grade.

(i) CuOHCl

This was prepared by heating a mixture of $CuCl_2 \cdot 2H_2O$ and CuO at 110 °C for one week in a sealed Pyrex tube (6, 7).

(ii) α-$Cu_2(OH)_3Cl$

This was prepared by reacting $3Cu(OH)_2 \cdot CuSO_4$ with

TABLE I

Thermogravimetric analyses

Compound	Step number	Temperature range* (°C)	% of total weight lost: Observed	% of total weight lost: Calculated	Reaction
CuOHCl	1	230–350	7.52	7.76	[I*a*]
	2	410–550	16.49	23.04	[I*b*]
	3	550–720	79.72	65.70	Volatilization Cu_2Cl_2
	4	Above 800			Disproportionation CuO†
α-$Cu_2(OH)_3Cl$	1	220–350	12.68	12.64	Dehydroxylation
	2	400–465	17.19	20.95	Disproportionation $CuCl_2$
	3	470–720	55.29	44.12	Volatilization Cu_2Cl_2
β-$Cu_2(OH)_3Cl$	1	250–400	12.65	12.64	
	2	405–480	17.25	20.95	
	3	480–720	56.20	44.12	
γ-$Cu_2(OH)_3Cl$	1	280–390	12.62	12.64	
	2	430–490	18.10	20.95	Same as for α-$Cu_2(OH)_3Cl$
	3	490–720	56.35	44.12	
δ-$Cu_2(OH)_3Cl$	1	240–300	12.66	12.65	
	2	400–470	17.30	20.95	
	3	470–700	55.94	44.12	
$Cu_2(OH)_3Br$	1	250–340	25.12	25.96	Dehydroxylation, disproportionation of $CuBr_2$
	2	370–740	52.56	53.56	Volatilization Cu_2Br_2
$Cu_2(OH)_3I$	1	170–260	28.46	29.66	Dehydroxylation, disproportionation of CuI_2
	2	300–690	59.29	60.89	Volatilization Cu_2I_2
$CuF_2 \cdot 2H_2O$	1	135–220	27.04	26.90	[V*a*]
	2	250–500	34.96	34.16	[V*b*]
	3	Above 800			Volatilization CuF_2,‡ disproportionation CuO
$Cu_2(OH)F_3$	1	220–450	9.70	9.90	[V*b*]
CuOHF	1	300–430	14.49	14.57	[VII*a*], [VII*b*]
$Cu_2(OH)_3F$	1	285–450	18.81	19.28	[VIII*a*]
	2	Above 800			Disproportionation CuO

*Onset and terminal temperatures.
†Observed with all chlorides, bromide, and iodide compounds, but not cited to avoid unnecessary repetition.
‡Observed with all fluorides except $Cu_2(OH)_3F$.

saturated aqueous solution of NaCl at room temperature for 48 h (8).

(iii) β-*$Cu_2(OH)_3Cl$*

This was prepared by digesting CuO with medium concentrated aqueous solution of $CuCl_2$ at 110 °C for one week (7).

(iv) γ-*$Cu_2(OH)_3Cl$*

This was prepared by the oxidation of Cu_2Cl_2 in solution of $CuCl_2$ with oxygen (8).

(v) δ-*$Cu_2(OH)_3Cl$*

This was prepared by adding excess NH_3 to 1 *M* $CuCl_2$ solution with slow evaporation of NH_3 at 50 °C (8).

(vi) $Cu_2(OH)_3Br$

This was prepared by digesting CuO with medium concentrated aqueous solution of $CuBr_2$ at 110 °C for one week (9).

(vii) $Cu_2(OH)_3I$

This was prepared by heating aqueous solution of cupric acetate with KI at 60–70 °C overnight (10).

All preparations involving the basic fluorides were carried out in polyethylene or platinum containers.

(viii) $CuF_2 \cdot 2H_2O$

This was prepared by the action of aqueous HF on $CuCO_3$ (3). This compound was used immediately after preparation.

(ix) $Cu_2(OH)F_3$

This was prepared by heating $CuF_2 \cdot 2H_2O$ for 2 h in N_2 atmosphere (3) at 160 °C.

(x) CuOHF

This was prepared by the hydrolysis of $CuF_2 \cdot 2H_2O$ in air at 100 °C for 10 h (3).

(xi) $Cu_2(OH)_3F$

This was prepared by dissolving $CuCO_3$ in aqueous HF and then adding concentrated NH_3 until the blue color of the ammonium complex appeared. The resulting solution was diluted with distilled H_2O and hydrolyzed slowly (11).

The identity and purity of the compounds were confirmed by the available infrared (i.r.) spectra and X-ray diffraction patterns (9, 12).

Can. J. Chem. Downloaded from www.nrcresearchpress.com by 210.87.254.6 on 09/05/12
For personal use only.

Can. J. Chem. Downloaded from www.nrcresearchpress.com by 210.87.254.6 on 09/05/12
For personal use only.

The thermograms were recorded on a DuPont Thermal Analyzer, DTA-900 and TGA-950, and DuPont 1200 °C DTA cell, as previously described (1). In the case of the fluorides, only the 1200 °C d.t.a. cell equipped with platinum cups and liners was used; experiments with the fluorides in the 850 °C cell equipped with quartz sample holders were complicated by reaction of the quartz with the fluoride compound.

The heating rate used for most thermograms was 20 °C/min. In the case of overlapping processes, slow heating rates of 4 and 2 °C/min were used in an attempt to resolve the processes. An ambient atmosphere of dry N_2 (Matheson Prepurified Grade with a stated impurity of 0.003% oxygen) was maintained during both the d.t.a. and t.g.a. measurements unless otherwise specified.

Results and Discussion

Thermogravimetric Analysis

The results of t.g.a. are presented in Table I and each compound is discussed in sequence. The proposed reactions for each compound are those which best fit the observed weight loss; the intermediate and final products were further identified by X-ray diffraction and correlated with d.t.a. thermograms.

(I) CuOHCl

The first step is the dehydroxylation to the oxide and halide according to

[I*a*] $$2CuOHCl \rightarrow CuO + CuCl_2 + H_2O$$

which was followed by disproportionation of the halide, i.e.

[I*b*] $$2CuCl_2 \rightarrow Cu_2Cl_2 + Cl_2$$

The third step involves the volatilization of Cu_2Cl_2 leaving CuO which itself disproportionates above 800 °C to yield a residue of Cu_2O.

The observed weight loss values assigned to reaction [I*b*] in all cases of basic chlorides are lower than their calculated values. This discrepancy arises from the overlap of $CuCl_2$ disproportionation with Cu_2Cl_2 volatilization as shown graphically in Fig. 1.

In all cases of the basic chlorides, i.e. CuOHCl and $Cu_2(OH)_3Cl$, it was observed that the weight loss up to the CuO product stage was always greater than calculated. This discrepancy was interpreted in terms of chlorination of CuO to form the volatile Cu_2Cl_2, i.e.

[I*c*] $$2CuO + Cl_2 \rightarrow Cu_2Cl_2 + O_2$$

which contributes to the higher weight losses observed. This interpretation was confirmed with 2:1 mole ratio physical mixture of CuO:$CuCl_2$ which showed a loss of 56.33%, whereas the predicted value, in the absence of the chlorination step, is 45.80%.

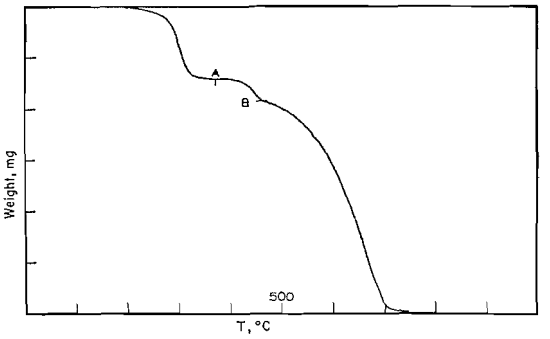

FIG. 1. Thermogravimetric analysis curve for α-$Cu_2(OH)_3Cl$ illustrating the initial dehydroxylation step followed by the disproportionation of $CuCl_2$ overlapping with Cu_2Cl_2 volatilization. A, represents weight value used to calculate weight loss for dehydroxylation; B, represents the weight value used to calculate weight loss for $CuCl_2$ disproportionation.

(II) α-, β-, γ-, and δ-$Cu_2(OH)_3Cl$

All four forms of this basic chloride undergo decomposition in the same manner, namely, dehydroxylation, similar to reaction [I*a*] accompanied by a slight variation in the temperature range. The subsequent processes of disproportionation of $CuCl_2$ and volatilization of Cu_2Cl_2, along with the partial chlorination and disproportionation of CuO, are observed as described above for CuOHCl.

Ball and Coultard in their experiments done in air observed Cu_2Cl_2 as an intermediate only in the decomposition of $CuCl_2 \cdot 2H_2O$. Their claim that the basic chlorides undergo only dehydroxylation with direct oxidation of $CuCl_2$ to CuO is in contrast to our observations. In view of the possibility that the course of the reaction is determined by the experimental conditions, particularly the nature of the atmosphere in contact with the compound, we carried out the decomposition in our instrument using air instead of N_2. The formation of Cu_2Cl_2 was confirmed consistently as identified by X-ray diffraction and supported by d.t.a. thermograms.

(III) $Cu_2(OH)_3Br$

The initial step corresponds to simultaneous dehydroxylation and disproportionation of $CuBr_2$, i.e.

[III*a*] $$2Cu_2(OH)_3Br \rightarrow 3CuO + \tfrac{1}{2}Cu_2Br_2 + \tfrac{1}{2}Br_2 + 3H_2O$$

Can. J. Chem. Downloaded from www.nrcresearchpress.com by 210.87.254.6 on 09/05/12
For personal use only.

On the premise that disproportionation should follow the formation of $CuBr_2$ from dehydroxylation, several unsuccessful attempts were made at low heating rates to resolve these two processes. From the d.t.a. measurements, it is obvious that $CuBr_2$ disproportionates at the same temperature as dehydroxylation occurs. The second step in the thermogram corresponds to volatilization of Cu_2Br_2 which is followed by disproportionation of CuO.

Ball and Coultard reported the mode of decomposition in air as follows

$$[IIIb]\quad 2Cu_2(OH)_3Br + \tfrac{1}{2}O_2 \rightarrow 3Cu(OH)_2,CuO + Br_2$$

and

$$[IIIc]\quad 3Cu(OH)_2, CuO \xrightarrow{370\text{–}435\ ^\circ C} 4CuO + 3H_2O$$

Since these reactions appeared unreasonable on the basis that it demands the copper hydroxide be stable up to 400 °C, compared to its experimentally determined value of 200 °C, the thermogravimetry of $Cu_2(OH)_3Br$ was repeated by us in air and at the same heating rate given by Ball and Coultard. The thermogram clearly displayed two steps, with slight overlap, corresponding to 24.96 and 38.00% weight loss, respectively. These observed weight losses are fitted to the following reactions

$$2Cu_2(OH)_3Br \rightarrow 3CuO + \tfrac{1}{2}Cu_2Br_2 + \tfrac{1}{2}Br_2 + 3H_2O$$

and

$$Cu_2Br_2 + O_2 \rightarrow 2CuO + Br_2$$

which predict weight losses of 25.96 and 38.33%, respectively.

The slight discrepancy between our observed and predicted values is attributed to the overlap. Furthermore, an X-ray diffractogram of the residue after heating $Cu_2(OH)_3Br$ in air up to 320 °C showed peaks characteristic of Cu_2Br_2 and CuO.

(IV) $Cu_2(OH)_3I$

In common with the basic bromide, the initial step corresponds to simultaneous dehydroxylation and disproportionation of CuI_2, i.e. reaction [III*a*]; the second step involves volatilization of Cu_2I_2 which is followed by disproportionation of CuO at high temperatures.

The decomposition of $Cu_2(OH)_3I$ in air for the first two steps leaving CuO as the product shows weight losses of 46.55 and 50.00%, respectively; the predicted weight loss after the second step is 50.49%. The high value of 46.55% in air relative to 28.46% in N_2 must include partial oxidation of Cu_2I_2; a thermogram of pure Cu_2I_2 carried out in air revealed almost complete oxidation between 280–350 °C.

(V) $CuF_2 \cdot 2H_2O$

The mode of decomposition involves dehydroxylation and dehydrofluorination forming a basic fluoride which in turn breaks down by further dehydrofluorination, yielding the oxide and fluoride in the residue, i.e.

$$[Va]\quad 2CuF_2 \cdot 2H_2O \rightarrow Cu_2(OH)F_3 + HF + 3H_2O$$

and

$$[Vb]\quad Cu_2(OH)F_3 \rightarrow CuO + CuF_2 + HF$$

These steps are followed by volatilization of CuF_2 and disproportionation of CuO at high temperatures. The mode of decomposition represented by reactions [V*a*] and [V*b*] is in agreement with Wheeler and Handler (3).

(VI) $Cu_2(OH)F_3$

The initial step is dehydrofluorination as described by reaction [V*b*].

(VII) CuOHF

Our results are best fitted to a dehydroxylation and dehydrofluorination and the formation of $Cu_2(OH)F_3$ with its subsequent decomposition overlapping, i.e.

$$[VIIa]\quad 4CuOHF \rightarrow Cu_2(OH)F_3 + 2CuO + HF + H_2O$$

and

$$[VIIb]\quad Cu_2(OH)F_3 \rightarrow CuO + CuF_2 + HF$$

Attempts to resolve these reaction processes at low heating rates, 1.4 °C/min, were unsuccessful.

(VIII) $Cu_2(OH)_3F$

Decomposition occurs via dehydroxylation and dehydrofluorination to yield only CuO in the residue, i.e.

$$[VIIIa]\quad Cu_2(OH)_3F \rightarrow 2CuO + H_2O + HF$$

Differential Thermal Analysis

The results of d.t.a. measurements are presented in Table II and each compound is discussed in sequence to accompany the t.g.a. results.

(I) CuOHCl

Four endotherms are observed on heating to 1200 °C; these endotherms are identified with (*a*) dehydroxylation, (*b*) disproportionation of $CuCl_2$, (*c*) volatilization of Cu_2Cl_2, and (*d*) dis-

TABLE II

Differential thermal analyses

Compound	Peak number*	Peak temperature (°C)	Reaction
CuOHCl	1	272	Dehydroxylation
	2	485	Disproportionation $CuCl_2$ †
	3	880	Volatilization Cu_2Cl_2 †
	4	995	Disproportionation CuO †
α-$Cu_2(OH)_3Cl$	1	275	Dehydroxylation
β-$Cu_2(OH)_3Cl$	1	301	Dehydroxylation
γ-$Cu_2(OH)_3Cl$	1	301	Dehydroxylation
δ-$Cu_2(OH)_3Cl$	1	265	Dehydroxylation
$Cu_2(OH)_3Br$	1	295	Dehydroxylation, disproportionation of $CuBr_2$
	2	395	(γ → β) Cu_2Br_2
	3	472	(β → α) Cu_2Br_2
	4	490	Fusion Cu_2Br_2
	5	995	Disproportionation of CuO, volatilization of Cu_2Br_2
$CuBr_2$	1	300	Disproportionation of $CuBr_2$
	2	395	(γ → β) Cu_2Br_2 ‡
	3	472	(β → α) Cu_2Br_2 ‡
	4	490	Fusion Cu_2Br_2 ‡
	5	995	Volatilization of Cu_2Br_2 ‡
$Cu_2(OH)_3I$	1	225	Dehydroxylation, disproportionation of CuI_2
	2	368	(γ → β) Cu_2I_2
	3	405	(β → α) Cu_2I_2
	4	605	Fusion Cu_2I_2
	5	1075	Disproportionation of CuO, volatilization of Cu_2I_2
$CuF_2 \cdot 2H_2O$	1	175	Decomposition
	2	420	Dehydroxylation of intermediate
	3	1000	Disproportionation of CuO§
$Cu_2(OH)F_3$	1	430	Dehydroxylation
CuOHF	1	385	[VII*a*]
	2	421	[VII*b*]
$Cu_2(OH)_3F$	1	375	[VIII*a*]

*All endotherms.
†Observed in all chlorides but not cited to avoid unnecessary repetition.
‡Confirmed with Cu_2Br_2.
§Observed in all fluorides except $Cu_2(OH)_3F$.

proportionation of CuO, respectively. Cooling the thermogram from 700 °C revealed two exotherms at 460 and 422 °C, identified with freezing of Cu_2Cl_2 and structural transition, respectively (13). The heating and cooling thermograms of pure Cu_2Cl_2 reveal the corresponding endo- and exotherms.

(II) α-, β-, γ-, δ-$Cu_2(OH)_3Cl$

All four forms of $Cu_2(OH)_3Cl$ show the same thermogram pattern with slight variation only in the peak temperatures of the first endotherm. The endotherms are identified with similar processes described above for CuOHCl.

(III) $Cu_2(OH)_3Br$

The thermogram revealed five endotherms associated with (*a*) dehydroxylation and disproportionation of $CuBr_2$, (*b*) (γ → β), (*c*) (β → α) structural transitions (14), (*d*) fusion of Cu_2Br_2, and (*e*) disproportionation of CuO accompanied by volatilization of Cu_2Br_2, respectively. The endotherms associated with reversible processes (*b*), (*c*), and (*d*) as expected appeared as exotherms on cooling from 700 °C.

The heating thermograms of pure $CuBr_2$ confirmed the endotherms identified above involving $CuBr_2$ and Cu_2Br_2.

(IV) $Cu_2(OH)_3I$

Five endotherms were observed on heating to 1200 °C identified with (*a*) dehydroxylation and disproportionation of CuI_2, (*b*) (γ → β), (*c*) (β → α) structural transformations of Cu_2I_2 (15), (*d*) fusion of Cu_2I_2, and (*e*) volatilization of Cu_2I_2 along with disproportionation of CuO, respectively. The endotherms associated with reversible processes (*b*), (*c*), and (*d*) as expected appeared as exotherms on cooling from 700 °C. The solidification exotherm, however, appeared as a doublet, 620 and 605 °C. The doublet only occurs when

Can. J. Chem. Downloaded from www.nrcresearchpress.com by 210.87.254.6 on 09/05/12
For personal use only.

Can. J. Chem. Downloaded from www.nrcresearchpress.com by 210.87.254.6 on 09/05/12
For personal use only.

CuO is present with Cu_2I_2 as confirmed with 3:1 mole ratio $CuO:Cu_2I_2$ mixture. The origin of the doublet, which will be a subject for further study, is speculated to arise from a compound or a solid solution of partial miscibility.

(V) $CuF_2 \cdot 2H_2O$

The thermogram showed three endotherms associated with (*a*) decomposition of dihydrate, (*b*) decomposition of the intermediate species $Cu_2(OH)F_3$, and (*c*) disproportionation of CuO. These observations agree with Wheeler and Handler (3) up to 500 °C. In a later study by Handler and co-workers (16) on d.t.a. of CuF_2 in CaF_2 and quartz matrix, they reported an endotherm at 770 °C, an exotherm at 780 °C, and a strong endothermic effect at 870–900 °C. In all our basic fluorides where CuF_2 was a product, corresponding peaks were not observed except for a very weak exotherm at 715 °C.

(VI) $Cu_2(OH)F_3$

Two endotherms were observed and identified with processes (*b*) and (*c*) stated above under (V).

(VII) CuOHF

The three endotherms in this thermogram are identified with decomposition and the subsequent two processes (*b*) and (*c*) characteristic of $Cu_2(OH)F_3$ which forms in the initial step.

(VIII) $Cu_2(OH)_3F$

The thermogram consisted of two endotherms which were associated with decomposition and subsequent disproportionation of CuO.

Conclusions

The thermal analyses of copper basic halides reveal the general pattern of thermal stability observed for Cd and Zn compounds, i.e. $Me(OH)_2 < Me(OH)I < Me(OH)Br < Me(OH)Cl < Me(OH)F$. The initial mode of decomposition varied within the copper group. The iodides, bromides, and chlorides all decomposed via dehydroxylation and in this way resembled the Cd and Zn halide derivatives. The copper basic fluorides, on the other hand, decomposed by simultaneous dehydroxylation and dehydrofluorination which is in distinct contrast to the Cd and Zn basic fluorides.

The work confirms the results by Wheeler and Handler (3) and therefore disagrees with Le Van My and co-workers (4) on the mode of decomposition of $CuF_2 \cdot 2H_2O$, namely the formation of CuOHF instead of $Cu_2(OH)F_3$, i.e. reactions [1*a*] and [3*a*]. Since CuOHF is formed by the action of H_2O vapor on $Cu_2(OH)F_3$, as reported earlier (3) and confirmed in this laboratory, we conclude that sufficient H_2O vapor is accumulated during the experiments of Le Van My to effect the formation of Cu(OH)F from the primary product $Cu_2(OH)F_3$.

The identification of Cu_2Cl_2 and Cu_2Br_2 as secondary products in the decomposition of $Cu_2(OH)_3Cl$ and $Cu_2(OH)_3Br$, respectively, in this work is at variance with the results of Ball and Coultard (5). There is a further inconsistency in the latters reporting of Cu_2Cl_2 as a secondary product in the dehydration of $CuCl_2 \cdot 2H_2O$ in air.

Acknowledgment

The authors acknowledge the financial support of this research program by the National Research Council of Canada.

1. O. K. Srivastava and E. A. Secco. Can. J. Chem. **45**, 579 (1967).
2. O. K. Srivastava and E. A. Secco. Can. J. Chem. **45**, 1375 (1967).
3. C. M. Wheeler and H. H. Handler. J. Am. Chem. Soc. **76**, 263 (1954).
4. Le Van My, G. Perinet, and P. Bianco. J. Chim. Phys. **63**, 719 (1966).
5. M. C. Ball and R. F. M. Coultard. J. Chem. Soc. A, **6**, 1417 (1968).
6. E. Hayek. Z. Anorg. Allgem. Chem. **210**, 241 (1933).
7. W. Feitknecht and K. Maget. Helv. Chim. Acta, **32**, 1639 (1949).
8. H. R. Oswald and W. Feitknecht. Helv. Chim. Acta, **47**, 272 (1964).
9. P. Tarte. Spectrochim. Acta, **13**, 107 (1958).
10. O. V. Dubsky, E. Terarik, and A. Okac. Collection Czech. Chem. Commun. **2**, 226 (1930).
11. U. Mannweiler. Licentiatsarbeit Universitat Bern. 1961.
12. A.S.T.M. Index to Powder Diffraction File (1963).
13. M. R. Lorenz and J. S. Prener. Acta Cryst. **9**, 538 (1956).
14. S. Hoshino. J. Phys. Soc. Japan, **7**, 560 (1952).
15. V. V. Pechkovskii and A. V. Sofronova. Russ. J. Inorg. Chem. English Transl. **10**, 825 (1965).
16. H. M. Handler, L. H. Towle, E. F. Bennett, and W. L. Patterson. J. Am. Chem. Soc. **76**, 2178 (1954).

Can. J. Chem. Downloaded from www.nrcresearchpress.com by 210.87.254.105 on 09/05/12
For personal use only.

Behavior of lead electrodes in sulfuric acid solutions. II[1]

E. TARTER AND K. EKLER[2]
Department of Chemistry, Loyola College, Montreal, Quebec

Received September 26, 1968

An attempt was made to clarify the question whether the variation in the length of the "first discharge plateau" with change in H_2SO_4 concentration was caused by a change in the efficiency of PbO_2 formation or by a variation in its discharge rate. The relationships between acid concentration, "passivation time", amount of $PbSO_4$ formed during passivation, and the quantity of PbO_2 derived therefrom during charging were investigated. The amount of $PbSO_4$ on the anode increased with a decrease in passivating acid concentration. More PbO_2 was formed at lower charging acid concentrations. The higher the discharge acid concentration, the greater was its stabilizing effect on PbO_2 discharge. The combination of two factors, i.e. a decrease of the amount of PbO_2 formed at higher acid concentrations together with an increase in the PbO_2 stability, gave rise to the maximum 10.5 *N* H_2SO_4.

Canadian Journal of Chemistry, 47, 2191 (1969)

Introduction

In a previous publication the conversion of $PbSO_4$ to PbO_2 in H_2SO_4 solutions and the reverse reaction were studied by the galvanostatic method and by making potential–time records during charging and self-discharge of the lead anode (1).

Since the behavior of the anode was sensitive to the "immersion time", i.e. the time during which the anode had been in contact with the H_2SO_4 before polarization, the results are here reported for anodes which were immersed in the electrolyte for the shortest possible time ("short immersion").

When the current was turned off and the electrode allowed to self-discharge on open-circuit, there was a drop of about 300 mV from the "charging-plateau" to a level that was termed the "first discharge plateau" (Fig. 1). The duration of the latter was dependent on acid concentration, with a particularly long first discharge plateau being observed in 10.5 *N* H_2SO_4.

An attempt was made to investigate the relationships between acid concentration and "passivation time" (Fig. 1, A to C), amount of $PbSO_4$ formed during passivation, and quantity of PbO_2 derived therefrom during charging, as well as the stability of PbO_2 in various acid concentrations.

Experimental

Procedure

The galvanostatic method was used for the polarization of the anode and has been described in an earlier paper (1). The cell was immersed in a constant temperature bath (Lauda Ultra Kryostat, UK 40 SD) in which temperatures between +30 and −50 °C could be controlled to ±0.02 °C. The coolant was methanol. The direct current was supplied by a Harrison power-supply (881-A, 1.0 A capacity). The preparation of the anodes was identical to that reported previously.

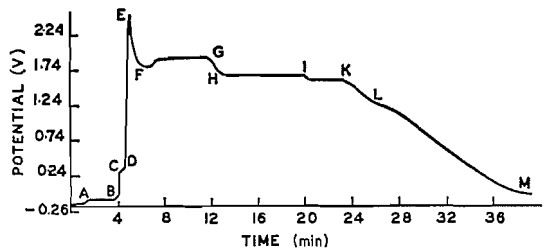

FIG. 1. Typical potential–time recording for short-immersion electrode. A to G, charging; G to N, discharging; A, $Pb/PbSO_4$ potential; F to G, "charging plateau" (PbO_2/O_2 potential); H to K, "first discharge plateau" ($PbSO_4/PbO_2$ potential); L, mixed potentials.

In experiments where an anode was transferred from one acid to another of a different concentration, the electrode was allowed to drain for 3 s before it was immersed in the second acid and was then drawn back and forth through the electrolyte for about 10 s to insure mixing.

When an anode was force-discharged by applying a current in the reverse direction, resistors ranging from 7 to 30 kΩ, depending on the discharge current used, were incorporated into the circuit to avoid short-circuiting the anode and cathode through the low-impedance power-supply while force-discharge was taking place. The method of Rüetchi and Cahan (2) was employed to obtain the maximum anodic charge by force-discharging at successively higher current densities (i) and extrapolating the product $i \times t$ to zero time, where t is the discharge time in s.

Analytical Methods

The quantity of $PbSO_4$ formed on the anode during

[1]To be presented at the C.I.C. Conference, Montreal, Quebec, May 1969.
[2]To whom all correspondence should be addressed.

Can. J. Chem. Downloaded from www.nrcresearchpress.com by 210.87.254.105 on 09/05/12
For personal use only.

the passivation time was determined polarographically (Radiometer, Polariter P O 4). The passivated electrode was thoroughly rinsed with distilled H_2O and immersed for 3 min with constant agitation in 18.0 ml 4.0 *N* CH_3COONa. When solution of the $PbSO_4$ had taken place the electrode was removed, drained, the liquid mixed with 18.0 ml 4.0 *N* CH_3COOH, and the polarogram taken. A calibration curve was established using 1.0 to 10.0 mg samples of $PbSO_4$. A blank in which a freshly etched electrode was agitated in H_2SO_4 for 3 min showed a negligible amount of Pb.

The PbO_2 formed on the anode on charging was determined by a semi-micro titration adapted from a standard method (3). To minimize self-discharge the charged anode was rinsed with distilled water as rapidly as possible and then submerged in an excess (40.0 ml) of 0.004 *N* As_2O_3. The unreacted As_2O_3 was back-titrated (in the presence of 1.5 *N* HCl and 0.5 g KBr) with 0.004 *N* $KBrO_3$, using one drop of 0.1% methyl orange as indicator. A blank had shown that 0.70 ml $KBrO_3$ was required to oxidize the indicator. Near the end-point the $KBrO_3$ was added at intervals of 20 s or more. The method was tested with 5.0–10.0 mg samples of PbO_2, in the presence and absence of finely divided Pb-powder, and was capable of detecting 96–98% of the PbO_2. Analyses were unaffected by digestion of the PbO_2 in H_2SO_4 and were reproducible to ± 0.05 mg PbO_2.

Materials

During the earlier part of the investigation the 2.5 cm × 10.0 cm electrodes were cut from $\frac{1}{4}$ in. rolled Pb-sheet (Canada Metal Co., Montreal) identical to that used in the previous paper. Later, 0.025 in. sheet was used (International Nickel Co., Sheridan Park, Ontario) of the following analysis: Sn, <0.0001%; Sb, 0.0001%; As, 0.0001%; Ag, 0.0003%; Cu, 0.0002%; Bi, 0.0008%; Fe, 0.0001%; Zn, 0.0001%. The following reagent grade chemicals were used: H_2SO_4 and CH_3COOH (Nicholls), As_2O_3, $KBrO_3$, and KBr (J. T. Baker), NH_2SO_3H and $CH_3COONa \cdot 3H_2O$ (Anachemia), and PbO_2 (Fisher). The H_2O was doubly distilled from KOH.

Results and Discussion

To obtain first discharge plateaux which were long enough to minimize self-discharge during force-discharging and to yield $PbSO_4$ and PbO_2 in sufficient quantity to allow a quantitative determination with the required precision, the influence of temperature on the length of the plateaux was investigated in the range −40 to +70 °C. The plateau for an electrode charged at 5.0 °C and 0.5 mA/cm² for 14 min showed a several-fold increase in length relative to that at 25.0 °C and 1 mA/cm², the latter having been reported previously (1), and therefore most of the experiments were made at the lower temperature and current density. The plateau lengths for various acid concentrations again showed the peculiar maximum in 10.5 *N* H_2SO_4 (Fig. 2).

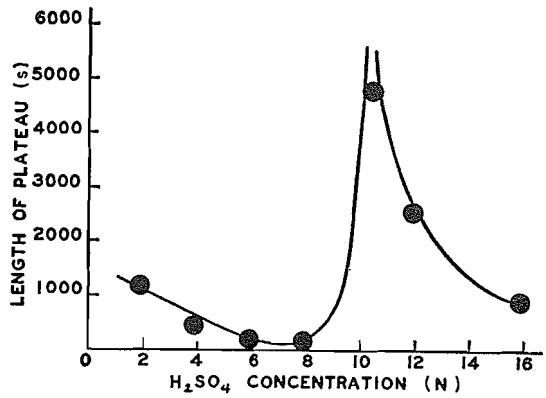

FIG. 2. Acid-dependence of "first discharge plateau" for electrodes charged at 5.0 °C and 0.5 mA/cm² for 14 min (self-discharge).

(a) $PbSO_4$ Formation

The passivation time was recorded for anodes in acids ranging from 1.0–14.0 *N* at 5.0 °C and 0.5 mA/cm² and found to increase with a decrease in H_2SO_4 concentration in a similar manner to that reported before for 25.0 °C and 1.0 mA/cm² (1).

A difference in the character of the $PbSO_4$ layer seems to be involved, since the coating formed in 2.0 *N* H_2SO_4 had a dull grey appearance, whereas at higher acid concentrations it was transparent. This is in agreement with the findings of Kabanov *et al.* (4) who found that $PbSO_4$ formed in concentrated acid crystallizes in a denser layer than in dilute solution. The cause for this is probably the decrease of the diffusion coefficient of $PbSO_4$ at higher H_2SO_4 concentrations.

The polarographic determination of the amounts of anodic $PbSO_4$ indicated that the longer passivation times in more dilute acids corresponded to progressively larger amounts of $PbSO_4$ (Fig. 3).

(b) PbO_2 Formation

(i) Passivating and Charging, Acid Concentration Constant

To correlate the amounts of $PbSO_4$ and PbO_2 formed during passivation and charging, respectively, anodes were passivated and charged in the same acid ranging in concentration from 1.0 to 16.0 *N* and, immediately after the charging current was turned off, the PbO_2 was determined by titration (Fig. 4*b*). The amount of PbO_2 formed,

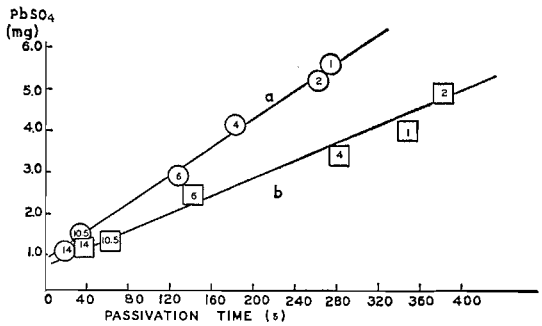

FIG. 3. Dependence of $PbSO_4$ formation on passivation time. (*a*) current density = 1.0 mA/cm², temperature = 25.0 °C; (*b*) current density = 0.5 mA/cm², temperature = 5.0 °C. The numbers inside circles and squares refer to acid concentrations.

similar to that of $PbSO_4$, increased with a decrease in acid concentration. This, however, could be anticipated, as it is well recognized that the amount of PbO_2 formed, for short charging periods in strongly acidic solutions, is approximately equivalent to the $PbSO_4$ deposited on the electrode during passivation (5, 6)

$$PbSO_4 + 2H_2O \rightarrow \beta\text{-}PbO_2 + 2H^+ + H_2SO_4 + 2e$$

(ii) Passivating, Acid Concentration Constant—Charging, Acid Concentration Variable

In a series of experiments in which anodes were passivated in one acid and transferred to be charged in a second acid of a different concentration, the results indicated that a given quantity of $PbSO_4$ on the anode is less completely oxidized to PbO_2 the higher the charging acid concentration. The amount of PbO_2 was determined by titration.

(iii) Passivating and Discharging, Acid Concentration Constant—Charging, Acid Concentration Variable

The observations were supported by another set of experiments in which the anodes were passivated in one acid, transferred and charged in a second acid, as before, but then were returned to the first acid to be force-discharged (Fig. 5). The shortening of the plateaux with an increase in charging acid concentration reflects the lesser amounts of PbO_2 formed on the anodes with an increase in the passivating and/or charging acid concentration.

Similar evidence was obtained with anodes which were passivated in one acid (2.0 *N*), transferred for charging to progressively more concentrated solutions (2.0–14.0 *N*), and then returned to the first acid (2.0 *N*) for self-discharging. The continuous decrease of plateau length (Table I) for charging acid concentrations between 2.0 and 14.0 *N* was attributed to incomplete oxidation of $PbSO_4$ to PbO_2 during charging.

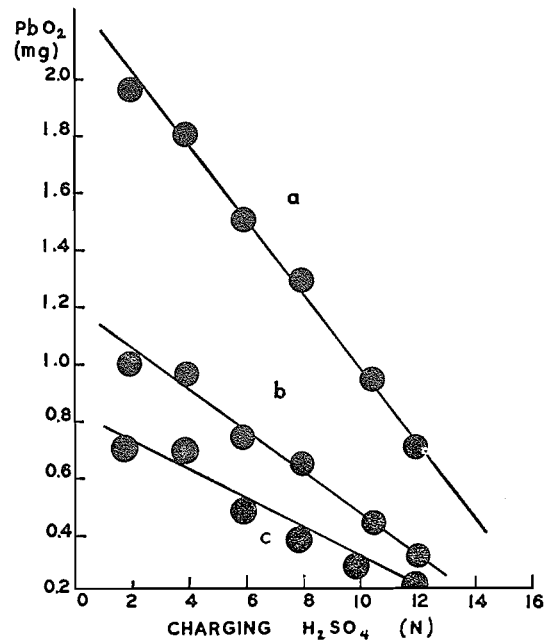

FIG. 4. PbO_2-determinations by (*a*) extrapolation; (*b*) titration; and (*c*) "inert PbO_2". Electrodes charged at 5.0 °C and 0.5 mA/cm² for 14 min.

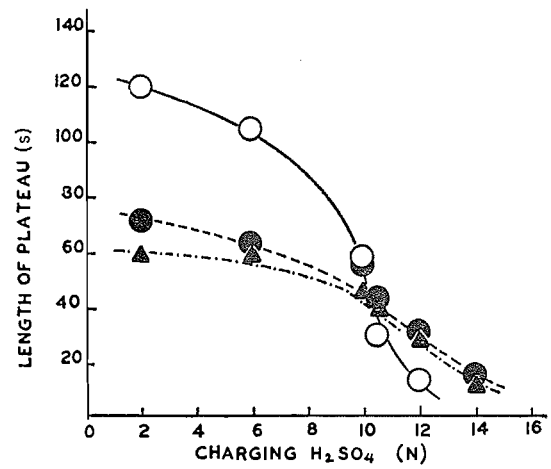

FIG. 5. Dependence of force-discharge plateau on charging acid concentration for electrodes charged at 5.0 °C and 0.5 mA/cm² for 14 min. Force-discharge current density = 0.7 mA/cm². Passivating and discharge acid concentration: ○, 2 *N*; ●, 6 *N*; ▲, 10.5 *N*.

It is known that two reactions can occur, among

Can. J. Chem. Downloaded from www.nrcresearchpress.com by 210.87.254.105 on 09/05/12
For personal use only.

Can. J. Chem. Downloaded from www.nrcresearchpress.com by 210.87.254.105 on 09/05/12
For personal use only.

TABLE I

Influence of charging acid concentration on self-discharging plateau

$H_2SO_4(N)$			
Passivating	Charging	Self-discharge	Plateau-length (s)
2.0	2.0	2.0	306
2.0	6.0	2.0	306
2.0	10.0	2.0	100
2.0	10.5	2.0	75
2.0	12.0	2.0	57
2.0	14.0	2.0	12

*Temperature = 25.0 °C; charging current density = 1 mA/cm²; charging time = 7 min.

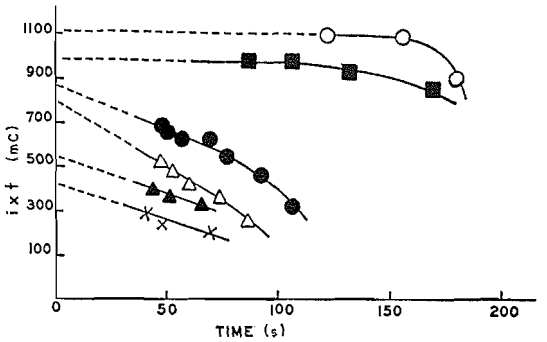

FIG. 6. Dependence of amount of PbO_2 (extrapolation) on force-discharge time for electrodes charged at 5.0 °C and 0.5 mA/cm² for 14 min. ○, 2 *N*; ■, 4 *N*; ●, 6 *N*; △, 8 *N*; ▲, 10.5 *N*; ×, 12 *N*.

others, at the PbO_2/O_2 potential during anodization, i.e. the conversion of $PbSO_4$ to β-PbO_2 at the $PbSO_4$–electrolyte interface and secondly the oxidation of the underlying Pb to α-PbO_2, due to the basic conditions possibly prevailing there. According to Burbank (7) "the rate of formation of α-PbO_2 is controlled by the rate of penetration of the oxygen species through the β-PbO_2 layer." Presumably, the rate of penetration would be increased in more dilute acids. This would give rise to an amount of α-PbO_2 at the metal boundary in addition to the β-PbO_2 obtained at the electrolyte interface, thus causing more PbO_2 (α + β) to be formed in more dilute solutions.

Electrochemical reduction (Fig. 6) was used as an alternative method for the determination of "initial PbO_2" (the quantity of PbO_2 formed during anodization), Rüetchi and Cahan (8) having reported that "the titration of the absolute amount of PbO_2 in a freshly formed oxide-layer was inconclusive because of self-discharge effects

TABLE II

Quantity of PbO_2 by extrapolation method

Passivating, charging, and force-discharge H_2SO_4 (*N*)	"Zero time" PbO_2 (mg)	"Inert" PbO_2 (mg)	Total PbO_2 (mg)
2	1.26	0.70	1.96
4	1.11	0.70	1.81
6	1.00	0.48	1.48
8	0.92	0.38	1.30
10.5	0.63	0.26	0.81
12	0.50	0.21	0.79

*Temperature = 5.0 °C; current density = 0.5 mA/cm²; charging time = 14 min.

... a much smaller error might be anticipated when discharged layers were titrated." The product $i \times t$ was extrapolated to zero time, converted to mg PbO_2 to which was added the value for "inert PbO_2" (electrochemically undischargeable PbO_2), determined by titration after force-discharging (Table II). Voss and Freundlich (9) have postulated several reasons for the existence of "inert PbO_2" with reference to battery plates, e.g. the electrical isolation of PbO_2 crystallites by $PbSO_4$. The amount of "inert PbO_2" in the present case was essentially independent of the force discharge current density.

A comparison of the results obtained by the extrapolation and titration methods together with the "inert PbO_2" is given in Fig. 4. Although self-discharge took place to a considerable degree when the titration-method was used, the trend was similar for both curves. Both methods indicated the fact that in higher charging acid concentrations, less PbO_2 was formed for a given quantity of charge passed.

(c) Stability of PbO_2

(i) Passivating and Charging, Acid Concentration Constant—Discharge, Acid Concentration Variable

To examine the question of whether different acid concentrations caused a variation in the discharge-rate of a given quantity of PbO_2, electrodes were both passivated and charged in one acid, transferred to a second acid of a different concentration, and allowed to self-discharge. The lengths of the plateaux were dependent on two factors, firstly the amount of "initial PbO_2" and secondly the self-discharge acid concentration (Table III). Anodes which were both passivated and charged in successively more concentrated acids and were then self-discharged in one particular acid, yielded pro-

TABLE III

Dependence of plateau on the amount of "initial PbO_2" and self-discharge acid concentration

Experiment	Passivating and charging H_2SO_4 (N)	Self-discharge H_2SO_4 (N)	Plateau length (min)	PbO_2 formed (mg)
1	2.0	2.0	16	1.12
2	2.0	6.0	5	
3	2.0	10.5	57	
4	2.0	16.0	550	
5	6.0	2.0	5	0.74
6	6.0	6.0	2.5	
7	6.0	10.5	60	
8	6.0	16.0	250	
9	10.5	2.0	1.25	0.43
10	10.5	6.0	3	
11	10.5	10.5	42	
12	10.5	16.0	57	
13	16.0	2.0	0	0.21
14	16.0	6.0	0.5	
15	16.0	10.5	1.25	
16	16.0	16.0	3.25	

*Temperature = 5.0 °C; current density = 0.5 mA/cm²; charging time = 14 min.

gressively shorter plateaux, reflecting the lesser amounts of "initial PbO_2". On the other hand, the lengths of the plateaux underwent a very large increase when anodes, passivated as well as charged in one particular acid, were transferred to be discharged in an acid varying from 2.0–16.0 N. Since the quantity of "initial PbO_2" was maintained constant, it can be concluded that the higher the discharge acid concentration, the greater is its stabilizing effect on the PbO_2 discharge.

The peculiar maximum observed for the self-discharge plateau in 10.5 N H_2SO_4 (Fig. 2) can be explained in terms of the above data. Experiment Nos. 1, 6, 11, and 16 (Table III) correspond to some of the key points of Fig. 2. A gradual decrease in the amount of PbO_2 formed, coupled with a simultaneous increase in discharge acid concentration are opposing factors, giving rise to the maximum in 10.5 N H_2SO_4. Thus for anodes which were both passivated and charged in the same acid, the lengths of the self-discharge plateaux depended on both "initial PbO_2" and the self-discharge acid concentration.

(ii) Passivating, Acid Concentration Constant—Charging and Discharging, Acid Concentration Variable

The plateau lengths again passed through a maximum when anodes were passivated in one

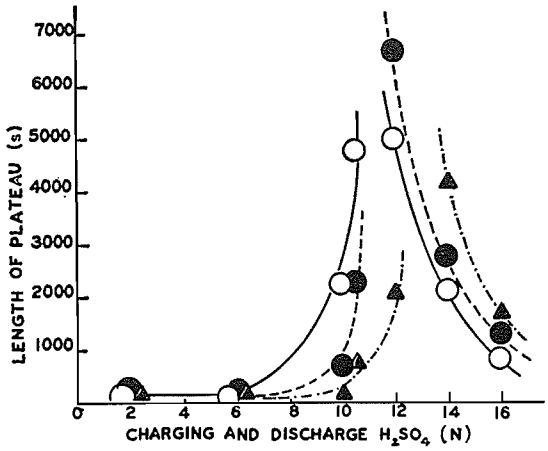

FIG. 7. Dependence of "first discharge plateau" on charging and/or discharge acid concentration for electrodes charged at 25.0 °C and 1 mA/cm² for 7 min (self-discharge). Passivating acid concentration: ○, 2 N; ●, 6 N; △, 10.5 N.

acid, and transferred to a second acid ranging from 2.0–16.0 N for charging as well as self-discharging (Fig. 7). This also was probably due to the fact that a given passivating acid concentration controlled the amount of $PbSO_4$ formed during passivation. The $PbSO_4$ was less completely oxidized when transferred to greater charging acid concentrations. Nevertheless, the lengths of the plateaux increased because of the stabilizing effect of the second acid.

The greater stability of PbO_2 in more concentrated H_2SO_4 solutions (Table III) is in accordance with the work of Rüetchi and Cahan (2) who reported a similar behavior with PbO_x electrodes (where x has a value from 1.4–1.6): "Potential measurements in H_2SO_4 more dilute than specific gravity 1.225 indicated that self-discharge strongly increased with decreasing acid concentration." Rüetchi and Angstadt (10) formulated a self-discharge mechanism as follows: "At the surface of the film nearest the electrolyte β-PbO_2 is electrochemically reduced in acid medium according to

$$[1]\quad 2e + \beta\text{-}PbO_2 + HSO_4^- + 3H^+ \rightarrow PbSO_4 + 2H_2O$$

and

$$[2]\quad 2e + \beta\text{-}PbO_2 + SO_4^{2-} + 4H^+ \rightarrow PbSO_4 + 2H_2O$$

As the surface becomes covered with $PbSO_4$, further reduction of β-PbO_2 and underlying α-PbO_2 to $PbSO_4$ is inhibited because of slow diffusion of H_2SO_4 into the film." They reported

Can. J. Chem. Downloaded from www.nrcresearchpress.com by 210.87.254.105 on 09/05/12
For personal use only.

Can. J. Chem. Downloaded from www.nrcresearchpress.com by 210.87.254.105 on 09/05/12
For personal use only.

further that electrons for these reactions are supplied during self-discharge by reactions such as

[3] $$H_2O \rightarrow \tfrac{1}{2}O_2 + 2H^+ + 2e$$

[4] $$Pb + SO_4^{2-} \rightarrow PbSO_4 + 2e$$

[5] $$Pb + 2OH^- \rightarrow PbO + H_2O + 2e$$

and that [4] would proceed faster and with less restrictions than the other reactions. Referring to Table III it seems that the greater self-discharge rate in lower acid concentrations is governed by increased solubility of $PbSO_4$ in the acid, allowing reaction [4] to proceed at a higher rate. The solubility of $PbSO_4$ in H_2SO_4 was determined by Kameyama and Fukumoto (11) from 0.5–10.5 *N* H_2SO_4 and by Craig and Vinal (12) to 14.2 *N* and shows a maximum in 2.0 *N* where PbO_2 is the least stable.

Conclusions

The present study showed that the longer passivation times in dilute acids correspond to increased yields of $PbSO_4$ on the electrodes, that the efficiency of oxidation to PbO_2 of the $PbSO_4$ thus formed is higher the more dilute the acid, and that the stability of the PbO_2 in turn is greater the more concentrated the acid. The maximum length of the self-discharge plateau in 10.5 *N* H_2SO_4 can be explained in terms of the influence of two opposing factors, i.e. a decrease of the amount of PbO_2 formed on the anode and a simultaneous increase in PbO_2 stability with an increase in acid concentration.

Acknowledgments

The present investigation was made with financial assistance from the Defence Research Board of Canada, Grant Number 5480-14, to whom grateful acknowledgment is made.

Thanks are due to Messrs. M. Lam, A. Lam, and J. Beck (student assistants) who helped with the experiments during the summer months.

The writer would like to express his appreciation to Dr. E. J. Casey and Dr. G. Nagy of the Defence Research Chemical Laboratories for several valuable discussions, Dr. C. A. Winkler, McGill University, for his continued encouragement and advice, and Dr. M. M. Wright (International Nickel Company, Sheridan Park, Ontario) for the generous gift of high-purity lead sheet.

1. K. Ekler. Can. J. Chem. **42**, 1355 (1964).
2. P. Rüetchi and B. D. Cahan. J. Electrochem. Soc. **105**, 369 (1958).
3. I. M. Kolthoff and E. B. Sandell. Textbook of quantitative inorganic analysis. Macmillan, New York. 3rd ed. 1952. p. 557.
4. B. N. Kabanov, D. I. Leikis, and E. I. Krepakova. Dokl. Akad. Nauk SSSR, **98**, 989 (1954).
5. P. Jones, R. Lind, and W. F. K. Wynne-Jones. Trans. Faraday Soc. **50**, 972 (1954).
6. W. FeitKnecht. Z. Elektrochem. **62**, 795 (1958).
7. J. Burbank. J. Electrochem. Soc. **104**, 693 (1957).
8. P. Rüetchi and B. D. Cahan. J. Electrochem. Soc. **104**, 406 (1957).
9. E. Voss and J. Freundlich. Proc. 3rd Intern. Symp. Batteries. Bournemouth, England. October 1962. Macmillan, New York. 1963.
10. P. Rüetchi and R. T. Angstadt. J. Electrochem Soc. **111**, 1323 (1964).
11. N. Kameyama and T. Fukomoto. J. Soc. Chem. Ind. Japan, **46**, 1022 (1943).
12. D. N. Craig and G. W. Vinal. J. Res. Natl. Bur. Stds. **22**, 55 (1939).

Diffusivity measurements of the argon–mercury vapor system

H. B. SPENCER, J. M. TOGURI, AND J. A. KURTIS
Department of Metallurgy and Materials Science, University of Toronto, Toronto 5, Ontario
Received November 18, 1968

An experimental method for the determination of the diffusivities of metal vapor – gas mixtures has been examined. An investigation of the mercury vapor – argon system in the temperature range 180–340 °C indicated that the experimental diffusivities agreed well with the diffusivities calculated from the kinetic theory of gases. The temperature dependence of the diffusivity was found to vary with the absolute temperature to the 1.7 power.

Canadian Journal of Chemistry, 47, 2197 (1969)

Can. J. Chem. Downloaded from www.nrcresearchpress.com by 210.87.254.105 on 09/05/12
For personal use only.

Introduction

In reactions involving condensed systems with gaseous components, molecular diffusion in the gas phase can often be a rate-controlling step. Consequently, a knowledge of diffusivities is essential to the analysis of such processes. For high temperature systems, however, data on the diffusivities of metal vapor – gas mixtures are scarce.

Predictions of vapor and gas diffusivities can be obtained from the Chapman and Cowling (1) approximation (eq. [1]) of the rigorous theory developed by Enskog and Chapman for monoatomic gases

$$[1] \qquad D_{12} = \frac{0.0018583 T^{1.5}(1/M_1 + 1/M_2)^{1/2}}{P C r_{12}^{\,2}}$$

where D_{12} is the binary diffusivity in cm^2/s, T the absolute temperature in °K, M_1 and M_2 the molecular weights of the species 1 and 2 respectively, P the pressure in atm, C the collision integral, and r_{12} the arithmetic mean of the diameters of the colliding molecules in Å.

The derivation of eq. [1] is based on nonreacting systems of monatomic gases which are nonpolar and spherically symmetric. Furthermore, the gas densities must be low enough to allow collisions involving only two molecules to dominate.

The Lennard–Jones (12-6) model of intermolecular forces can be used as the basis for a numerical evaluation of the collision integral and collision diameter. The collision integral accounts for the dynamics of molecular interaction including the speeds, the masses, and the angles involved in the collisions. The values of this complex function based on the Lennard–Jones (12-6) model have been tabulated by Hirschfelder *et al.* (2) in terms of a reduced temperature, T_R, where $T_R = (k/\varepsilon)T$, and ε/k is the force constant.

For many gases and vapors, the force constants for the individual species are available from viscosity data or from calculations involving the second virial coefficient. However, for most metal vapors these sources of information are not available and, hence, empirical relationships based on the law of corresponding states are useful to determine the force constants. Hirschfelder *et al.* (2) showed that force constants for the Lennard–Jones (12-6) model, the reduced temperature T_R, and other reduced properties approximate to universal constants at critical points.

Based on these empirical relations, force constants and collision diameters may be estimated from the following expressions

$$[2] \qquad \varepsilon/k = 0.77\, T_c \quad \text{in °K}$$

$$[3] \qquad \varepsilon/k = 1.15\, T_b \quad \text{in °K}$$

$$[4] \qquad r = 0.841\, (V_c)^{1/3} \quad \text{in Å}$$

$$[5] \qquad r = 1.166\, (V_b)^{1/3} \quad \text{in Å}$$

The subscripts b and c refer to the boiling and critical temperatures respectively. V_b and V_c are the respective molar volumes of the liquid at the boiling and critical temperatures in $cm^3\ mole^{-1}$.

For mercury, the necessary parameters have been determined experimentally from viscosity measurements of mercury vapors. For the calculations in this paper, the data for mercury and argon cited by Hirschfelder are used. As shown in Table I, the mercury–argon system showed good correlation between the force constants obtained from the empirical equations and those calculated from viscosity data. The calculations also demonstrate that the calculated diffusivities

TABLE I

Comparison of force constants and diffusivities based on viscosity data and on empirical relationships for the argon–mercury vapor system

	Viscosity			Empirical	
	Ar	Hg	Ar–Hg	Hg	Ar–Hg
r (Å)	3.46	2.90	3.18	2.92*	3.19‡
ε/k (°K)	116	851	314	724†	287§
D_{12} at 550 °K (cm²/s)			0.364		0.372

*Calculated from V_b.
†Calculated from T_b.
‡Calculated from $\left(\frac{r_{Hg} + r_{Ar}}{2}\right)$.
§Calculated from $(\varepsilon_{Hg} \cdot \varepsilon_{Ar})^{1/2}$.

for the mercury–argon system were relatively insensitive to changes in the force constants. Hence, eqs. [2]–[5] appear to be satisfactory approximations in the determination of diffusivities of systems involving metal vapors for which no viscosity data are available. This view is also supported by Turkdogen (3).

The cumbersome nature of eq. [1] and the apparent deviation of experimental diffusivities from the theoretical values have led to many attempts to develop relationships with improved predictive powers. Generally these relationships have tended to be empirical. Two notable examples are the relationships developed by Chen and Othmer (4) and by Wilke and Lee (5).

The expression of Wilke and Lee is a modification of eq. [1] and is expressed as follows

$$[6] \qquad D_{12} = \frac{2BT^{3/2}\left(\frac{1}{M_1} + \frac{1}{M_2}\right)^{1/2}}{PCr_{12}^{\,2}}$$

where

$$B = 10.7 - 2.46\left(\frac{1}{M_1} + \frac{1}{M_2}\right)^{1/2}$$

The diffusivity becomes more dependent upon the molecular weights. The expression for B is determined empirically.

The Chen–Othmer approach is more rigorous. The lengthy collision integral table is eliminated by relating the collision integral to an expression containing the force constant, ε/k, and the absolute temperature. The force constants are then replaced by expressions involving critical temperatures and critical volumes. These relationships are then incorporated into the equation derived from the kinetic theory of gases. The various parameters required in the development of the relationship are determined by fitting the expression to the experimental data. The resulting equation is presented below

$$[7] \qquad D_{12} = \frac{0.43\left(\frac{T}{100}\right)^{1.81}\left(\frac{1}{M_1} + \frac{1}{M_2}\right)^{1/2}}{P\left(\frac{T_{C1}\,T_{C2}}{10\,000}\right)^{0.1405}\left[\left(\frac{V_{C1}}{100}\right)^{0.4} + \left(\frac{V_{C2}}{100}\right)^{0.4}\right]^2}$$

where C refers to the critical points.

The expression proves to be effective in predicting diffusivities of many systems. However, some difficulty can be expected in metal vapor systems where reliable critical data are scarce. This lack of data for metal vapor systems has prevented the estimation of reliable diffusivities for metal vapor – gas mixtures.

The present study was therefore carried out to examine a method of determining experimental values for the diffusivities of metal vapors in non-reacting atmospheres. The experimental technique is a modified version of the Stefan method (6). This method has been used by many investigators (7, 8) for measuring rates of evaporation of organic liquids near room temperature. In this investigation the technique was modified to examine the mercury–argon system in the temperature range 180–340 °C. The mercury–argon system was selected since the experimental

Can. J. Chem. Downloaded from www.nrcresearchpress.com by 210.87.254.105 on 09/05/12
For personal use only.

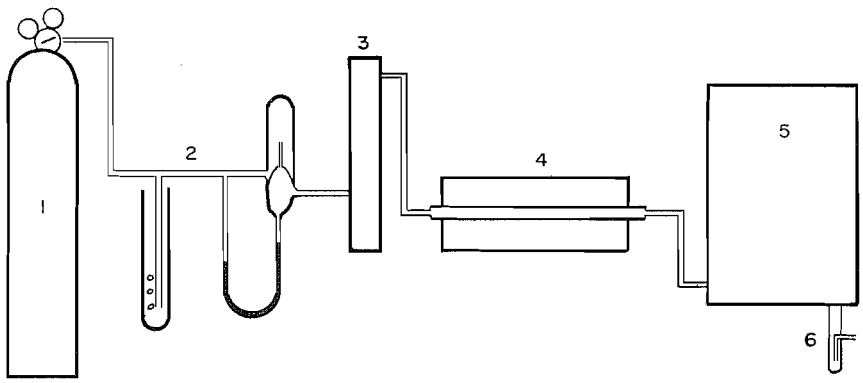

FIG. 1. Diagram of apparatus.

diffusivities could be compared with those calculated from the kinetic theory and from certain empirical relationships.

Experimental

(1) Theoretical Basis

Based on the Stefan method, a gas stream was passed over a vertical open mouth tube which was partially filled with the condensed phase of one of the components. A measure of the mass flux or the change in height of the column of the condensed phase allowed the determination of the diffusivity of the system.

The diffusion of the mercury vapor through the argon is accompanied by a bulk flow in the same direction, i.e. away from the surface of the condensed phase. At the same time, the corresponding upward bulk flow of argon is much smaller and is balanced by the downward molecular diffusion of the argon. Therefore, the argon gas above the mercury in the diffusion tube is considered to be a stagnant layer. The general expression for the molecular flux in a binary gas mixture is as follows

$$[8] \qquad N_1 = \frac{-D_{12}}{RT}\frac{dP_1}{dx} + \frac{P_1}{P_T}(N_1 + N_2)$$

where N_1 is the molar flux in g mole/cm² s, R the gas constant in mm Hg cc/g-mole °K, P_T the total pressure of system in mm Hg, and P_1 the partial pressure of species 1.

For the system under investigation, i.e. steady state diffusion of mercury vapor through stagnant argon, integration of eq. [8] and application of the condition $N_{Ar} = 0$ results in the following expression.

$$[9] \qquad N_{Hg} = \frac{D_{12} \cdot P_T \cdot (p_0 - p_s)}{R \cdot T \cdot L \cdot p_{lm}}$$

where L is the diffusion length in cm and p_0, p_s, and p_{lm} are partial pressures at the mouth of the diffusion tube, at the surface of the condensed phase, and the logarithmic mean of argon pressures, respectively.

Further reduction of the terms and conversion to c.g.s. units of mass flux produces the expression which was used in the present calculations

$$[10] \qquad D_{12} = 0.1757 \frac{T}{\alpha} \cdot \frac{w}{t} \cdot L$$

where w is the weight of condensed vapor in grams, t is the duration of the run in hours, and

$$\alpha = P_T \cdot \ln\left(\frac{P_T - p_0}{P_T - p_s}\right)$$

In this development, the diffusion length, L, is assumed to remain constant. This condition is approximated by keeping the change in length during a run to a small percentage of the overall diffusion length.

(2) Apparatus and Procedure

A schematic diagram of the apparatus is presented in Fig. 1. The copper gettering furnace, operated at 600 °C, reduced the oxygen pressure of the argon carrier gas to less than 10^{-10} mm Hg. The low oxygen pressure prevented the formation of an oxide film on the liquid mercury and also eliminated any chance of enhanced vaporization due to the formation of an oxide fog above the liquid (9). Calcium sulfate was used as the drying agent.

Figure 2 shows the arrangement of the diffusion and condensation cell with the furnace. In order to minimize temperature gradients along the vertical length of the diffusion cell, a graphite block was placed around the cell. The cell temperature was controlled to within ±1 °C. The gas entering the furnace was pre-heated in the vertical column filled with glass beads before passing over the diffusion cell.

Can. J. Chem. Downloaded from www.nrcresearchpress.com by 210.87.254.105 on 09/05/12
For personal use only.

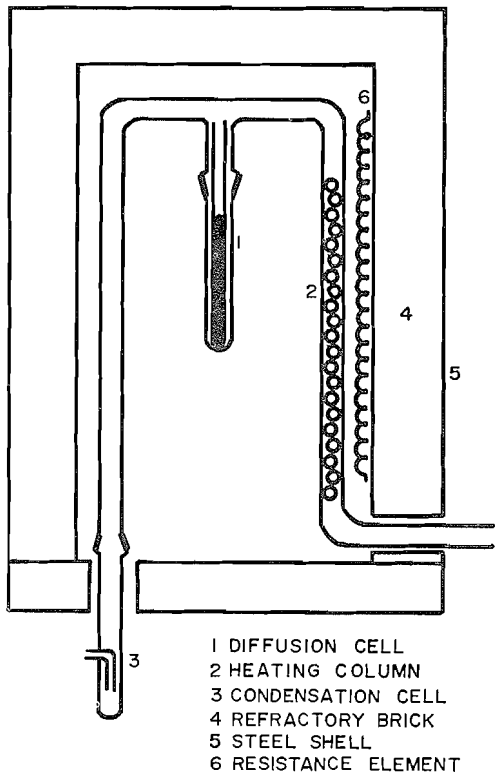

FIG. 2. Arrangement of diffusion and condensation cell.

The diffusion cell contained the Pyrex diffusion tube which was 15 cm in height and 0.792 ± 0.001 cm in internal diameter (i.d.). After passing over the diffusion cell and sweeping the mercury vapor away, the carrier gas entered the condensation cell. As the gas left the furnace and cooled, the mercury vapor condensed. The condensation cell extended into the furnace to insure that all condensation occurred within the cell. The lower 3 in. of the cell were immersed in an ice – water mixture to maintain a constant temperature for the effluent gas and to minimize vapor losses. The temperature of the effluent gas was 22 °C.

Before each run, the system was completely evacuated and then flushed with argon gas. This procedure eliminated an "incubation period" during the initial stages of the experiment. If air was left in the system, in particular in the stagnant gas layer above the condensed phase, molecular diffusion of oxygen and nitrogen was found to interfere with the diffusion of the mercury vapor for periods of 20–24 h.

The flow rate of the argon gas was 2.4 cc/s, a rate suggested by the earlier work of Kurtis (10). When the furnace had been at thermal equilibrium for 1 h, the condensation cell was inserted into the gas train. At the end of the run, the cell was removed. To prevent vapor losses from the cell as it cooled, the hot end of the condensation cell was stoppered. When the furnace had cooled to room temperature, the mercury level in the diffusion tube was measured. The final diffusion path length and the weight of condensed material collected provided the data necessary for the determination of the interdiffusivity of the system.

Runs lasted from 10–24 h depending on the initial height of mercury in the diffusion tube and on the temperature. Doubly distilled mercury was used throughout this study.

(3) Treatment of Data

At the end of each run, the distance from the top of the diffusion tube to the point of contact between the liquid mercury and the glass was measured. The change in height during the experiment was determined in the following manner

$$\text{Volume} = \frac{\text{weight}}{\text{density}}$$

$$\frac{\pi}{4} d^2 \Delta h = \frac{w}{\rho_{RT}}$$

$$[11] \qquad \Delta h = 0.150\, w$$

where d = i.d. of the diffusion tube in cm, Δh = the change in height in cm of the mercury column during the run, and ρ_{RT} = the density of mercury at room temperature in g/cc.

Two other corrections were necessary. Some factor was required to account for the meniscus, the top of which in the present case was 0.14 cm above the measured point at room temperature. In addition, when the furnace was cooled after the run, some diffusion still occurred. The resulting change in height combined with the effect of the meniscus was determined as 0.10 cm.

To estimate the effective diffusion length at operating conditions, the thermal expansion of the mercury column was considered. Neglecting the relatively small thermal expansion of the Pyrex tube, the correction took the following form

$$[12] \qquad L_T = (\rho_{RT}/\rho_T - 1) L_{Hg}$$

where L_T = change due to thermal expansion in cm, ρ_T = the density of mercury in g/cc at operating temperature, and L_{Hg} = the length of the mercury column at room temperature in cm.

The expression for the average diffusion length, L, is

$$[13] \qquad L = \frac{(2L_f - \Delta h)}{2} - 0.10 - L_T$$

where L_f = the measured length at the end of the run in cm.

The mercury vapor pressure at the mouth of the diffusion tube (p_0) can be assumed to be zero only if a high flow rate of carrier gas is used. The magnitude of p_0 was determined by assuming ideal behavior of the mercury vapor and by considering the flow rate and mass flux of the vapor. Thus

$$[14] \qquad p_0 = 0.0352 T \frac{w}{t}$$

Can. J. Chem. Downloaded from www.nrcresearchpress.com by 210.87.254.105 on 09/05/12
For personal use only.

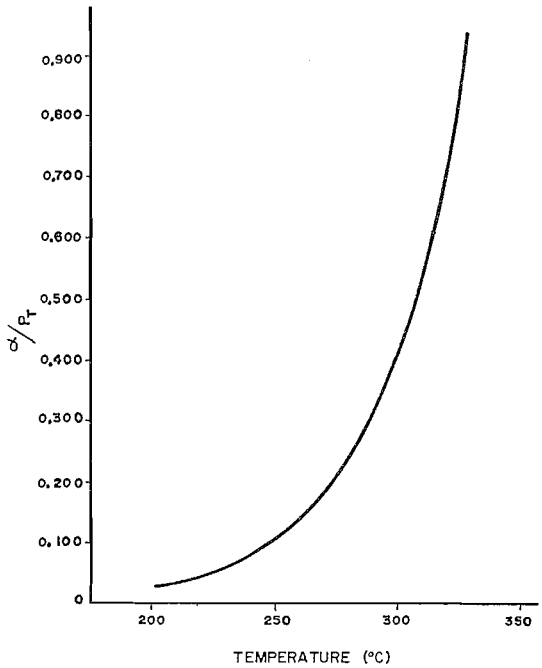

FIG. 3. Temperature dependence of α.

This correction was incorporated in the present calculations.

With the two quantities, p_0 and L, determined, the calculation of the diffusivity from eq. [10] is straightforward.

Results and Discussion

The temperature dependence of the diffusivity in eq. [10] centers on the absolute temperature, T, and the inverse of the function α. As shown in Fig. 3, the latter dependence was critical in the experimental analysis. Because of the strong dependence of this function on temperature, particularly above 280 °C, isothermal conditions were essential. A temperature profile study of the diffusion tube revealed that the temperature at the mouth of the tube was slightly higher (about 1 °C) than the temperature at a point 12 cm lower in the tube. This temperature gradient combined with the small diameter of the tube effectively eliminated any convection effects.

Wilke and Lee (8) have investigated the inherent errors in the Stefan tube technique. The turbulence effect at the mouth of the tube is of primary importance since it shortens the effective diffusion length. If turbulence occurs, the measured or apparent diffusion length is greater than the true length. The error introduced by this condition is calculated by plotting the inverse of the apparent diffusivities, all at the same temperature, against the inverse of the corresponding apparent diffusion lengths. A similar study was undertaken to determine the effect of turbulence in this experiment. At 278 °C, experimental values of 0.386 ± 0.024 and 0.389 ± 0.024 cm^2/s had diffusion lengths of 5.87 and 12.30 cm, respectively. Since the experimental uncertainty was greater than the difference between the two values and since the diffusivity with a shorter diffusion length was the smaller of the two, this quantitative study indicated that the turbulence effect was negligible. Accordingly, the effect was neglected in the calculations.

The experimental results are presented in Table II. A comparison of experimental and theoretical values found from eq. [1], using force constants and collision diameters estimated from viscosity data, is shown in Fig. 4. Data from other metal vapor – inert gas systems (3) are also included.

In Fig. 5, a comparison of the experimental diffusivities and the diffusivities calculated from eqs. [1], [6], and [7] are shown. At the higher

TABLE II

Experimental data

Temperature (°C)	Weight collected (g)	Time (h).	Atmospheric pressure (mm Hg)	Length (cm)	Diffusivity* (cm^2/s)
186	0.1241	20.134	754.5	6.48	0.291
224	0.3031	23.800	751.6	10.80	0.316
265	0.6921	15.134	755.6	10.15	0.372
278	1.7986	15.967	752.6	5.87	0.386
278	1.1714	21.500	753.1	12.30	0.389
303	1.6045	13.350	751.6	10.73	0.401
326	3.8492	16.117	751.6	10.98	0.440
334	2.9474	9.816	750.4	11.11	0.434

*All diffusivities presented in this work have been reduced to 760 mm Hg pressure.

Can. J. Chem. Downloaded from www.nrcresearchpress.com by 210.87.254.105 on 09/05/12
For personal use only.

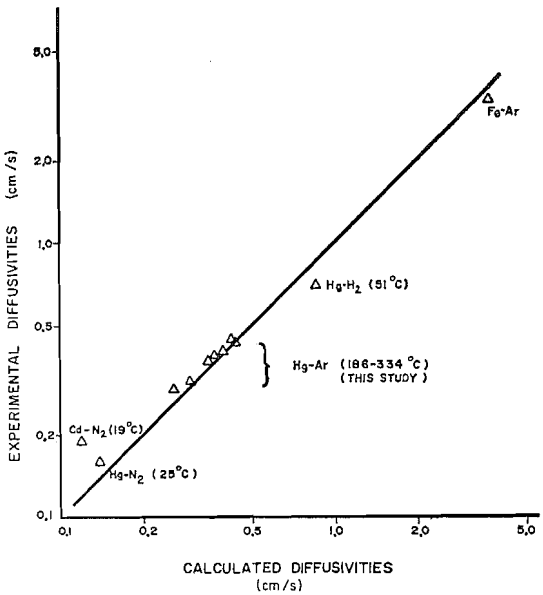

FIG. 4. Comparison of experimental and calculated diffusivities for various metal vapor – vapor systems.

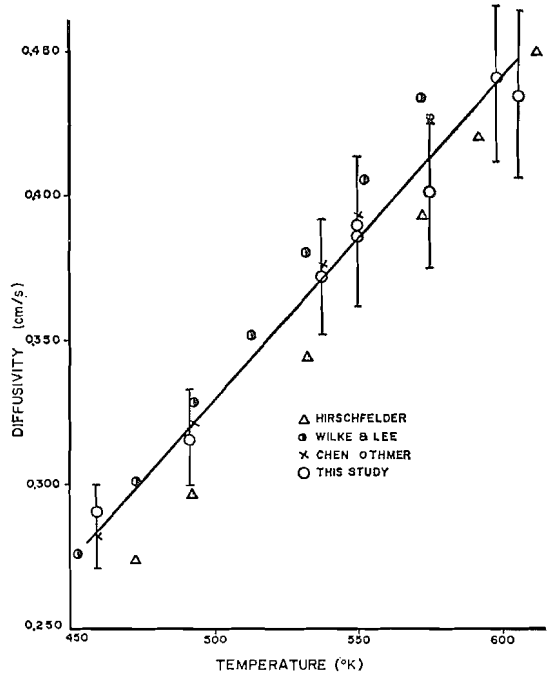

FIG. 5. Diffusivities for the Hg–Ar system as a function of temperature.

temperatures, the results tend to deviate from the trend established at the lower temperatures. The sensitivity of the function α accounts for a good part of the discrepancy, and for the large error limits in this range. The error limits of the value at 186 °C represent effects of a temperature decrease of 3 °C during part of the run.

Examination of Fig. 5 reveals good correlation of the data with the empirical relationships of eqs. [6] and [7], particularly with the Chen–Othmer relationship. Considering that the empirical expressions for diffusivities are based on studies of systems involving gases and organic vapors, the correlation obtained for this metal vapor system is excellent.

The experimental values of the diffusivities were consistently higher than the theoretical values found from eq. [1]. This may be due to the inadequacy of the Lennard–Jones (12-6) model and to the empirical rules for combining collision diameters and force constants to describe the binary mixtures. A further possible explanation for the high results depends on the existence of a more pronounced turbulence effect than that determined in the investigation of this condition. Turbulence to a depth of 1 cm in the diffusion tube would bring the experimental data into very good agreement with the theoretical values. However, a study of the turbulence effect did not justify a correction of this magnitude to the effective diffusion length.

As shown in eq. [1], the kinetic theory predicts that the temperature dependence of the diffusivity is the absolute temperature to the 3/2 power. A least mean squares analysis of the data from the runs between 180 and 326 °C inclusive produced a value of 1.70. This value is in good agreement with the results of similar analyses of other monatomic systems (11).

Conclusions

The results of this study demonstrated that the proposed technique can be useful in the investigation of the diffusivities of metal vapors. The experimental results for the mercury vapor – argon system were found to be in reasonably good agreement with values predicted by both the kinetic theory and other empirical relationships.

The effect of temperature on the diffusivity of mercury vapor – argon has been found to vary as $T^{1.7}$.

The temperature range over which the Stefan

Can. J. Chem. Downloaded from www.nrcresearchpress.com by 210.87.254.105 on 09/05/12
For personal use only.

tube technique can be usefully employed is somewhat restricted. At low temperatures, the small vapor pressures make it increasingly difficult to obtain suitably large samples in a reasonable period of time. At high temperatures, the increased sensitivity of the function α to temperature becomes important. Furthermore, this technique can not be used above the boiling point of the metal under consideration.

Acknowledgment

The research for this paper was supported by the National Research Council of Canada Grant A 3676 for which the authors are grateful.

1. S. CHAPMAN and T. G. COWLING. The mathematical theory of nonuniform gases. Cambridge University Press, London. 1939.
2. J. O. HIRSCHFELDER, C. F. CURTISS, and R. B. BIRD. Molecular theory of gases and liquids. John Wiley and Sons, Inc., New York. 1954.
3. E. T. TURKDOGAN. Steelmaking. Chipman Conference. M.I.T. Press. 1962.
4. N. H. CHEN and D. F. OTHMER. J. Chem. Eng. Data, **7**, No. 1, 37 (1962).
5. C. R. WILKE and C. Y. LEE. Ind. Eng. Chem. **47**, 1253 (1955).
6. J. STEFAN. Wien. Ber. II, **68**, 385 (1873).
7. J. F. RICHARDSON. Chem. Eng. Sci. **10**, 234 (1959).
8. C. R. WILKE and C. Y. LEE. Ind. Eng. Chem. **46**, 2381 (1954).
9. E. T. TURKDOGAN, P. GRIEVESON, and L. S. DARKEN. Trans. AIME, **67**, 1647 (1963).
10. J. A. KURTIS. B.A.Sc. Thesis. University of Toronto, Toronto, Ontario, 1967.
11. E. H. FULLER, P. D. SCHETTLER, and J. C. GIDDINGS. Ind. Eng. Chem. **58**, No. 5, 19 (1966).

Can. J. Chem. Downloaded from www.nrcresearchpress.com by 210.87.254.105 on 09/05/12
For personal use only.

Can. J. Chem. Downloaded from www.nrcresearchpress.com by 210.87.254.40 on 09/05/12
For personal use only.

Oxidative addition of silicon hydrides to hydridocarbonyltris(triphenylphosphine)iridium(I)

J. F. HARROD, D. F. R. GILSON, AND R. CHARLES
Chemistry Department, McGill University, Montreal, Quebec

Received November 12, 1968

Complexes have been prepared by oxidation of hydridocarbonyltris(triphenylphosphine)iridium(I) with a variety of silicon hydrides. The complexes were very stable with respect to thermal loss of either silicon hydride or molecular hydrogen.

An unequivocal assignment of stereochemistry of the complexes was obtained from a combination of infrared and proton nuclear magnetic resonance (n.m.r.) techniques. Addition of the silicon hydride to the iridium complex was found to be stereospecifically *cis*.

Canadian Journal of Chemistry, 47, 2205 (1969)

Introduction

The oxidative addition of silicon hydrides to chlorocarbonylbis(triphenylphosphine)iridium(I) was previously studied as part of an investigation of the mechanism of metal ion catalyzed olefin hydrosilation (1). The complexes formed in this reaction were not suitable for an intensive investigation of structure and physical properties, because of their instability in solution and because the reaction was limited to silicon hydrides bearing electronegative substituents.

The present study was undertaken after it was established that hydridocarbonyltris(triphenylphosphine)iridium(I), **1**, reacted readily with silicon hydrides, and that even triaryl and trialkylsilanes yielded relatively stable adducts. These reactions were of particular interest because, on the one hand, there existed the possibility of an unequivocal assignment of stereochemistry using proton n.m.r. and infrared spectroscopies, and on the other hand, it was expected that reductive elimination of hydrogen from the adducts would provide a synthetic route to the hitherto unknown silylcarbonylbis(triphenylphosphine)iridium(I) complexes.

In the course of the present investigation the addition of some chloro-substituted silicon hydrides to tris(triphenylphosphine)chlororhodium(I) was reported by de Charentenay *et al.* (2). The presence of Rh—H in the adducts was detected by n.m.r., but a complete assignment of stereochemistry was not possible.

Results and Discussion

A variety of silicon hydrides was found to react rapidly with **1** to yield adducts according to [1]

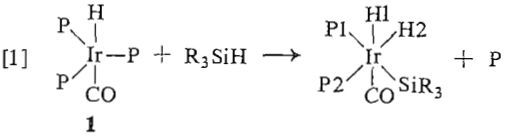

1

where P = $(C_6H_5)_3P$.

Chemical analyses were obtained for the crystalline products resulting from additions of $(C_6H_5)_3SiH$, $(C_2H_5O)_3SiH$, and Cl_3SiH. Although difficulties were experienced in obtaining adducts with other silicon hydrides that were sufficiently pure for chemical analysis, the similarity of the infrared or n.m.r. spectra of all of the adducts leaves little doubt that they were isostructural.

All of the adducts exhibited a strong and weak band in the region of 2100 cm^{-1} in the infrared. These bands are assigned to the symmetric and antisymmetric Ir—H vibrations. In addition all complexes exhibited a band at ca. 1950 cm^{-1} due to the carbonyl group. Infrared data on all of the complexes prepared are summarized in Table I.

Proton n.m.r. spectra in the high field region, characteristic of protons directly bonded to transition metals, were obtained with the adducts derived from $(C_2H_5O)_3SiH$, $(C_6H_5)_3SiH$, and $(C_6H_5)(CH_3)_2SiH$. Each of these complexes gave a complicated splitting pattern interpreted as a 16 line spectrum, according to the correlation diagram illustrated in Fig. 1 for the triethoxysilyl derivative. The chemical shifts and coupling constants for all 3 complexes are listed in Table II. The 16 line spectrum is in accord with the stereochemistry depicted for the product in reaction [1], with regard to the relative positions of the protons and the phosphines, but does not

TABLE I

Infrared absorption data for silyliridium(III) complexes*

Addend	ν_{Si-H} of parent silane	ν_{C-O}	ν_{Ir-H}
Cl_3SiH	2275 vs (*b*)	2010 vs (*a*)	2117 vs (*a*)
CH_3Cl_2SiH	2210 vs (*b*)	1995 vs (*a*) 1990 vs (*b*, *c*)	2108 vs 2142 m (*a*) 2108 vs (*b*, *c*)
$(C_2H_5O)_3SiH$	2210 vs (*b*)	1963 vs (*a*, *d*) 1966 vs (*c*)	2075 vs 2120 m(*a*, *d*) 2090 vs (*b*) 2090 s (*c*)
$(C_6H_5)_3SiH$	2120 vs (*a*)	1963 vs (*a*, *c*)	2075 vs 2134 m (*a*, *b*, *c*)
$(C_6H_5)(CH_3)_2SiH$	2125 vs (*b*)	1963 vs (*a*, *c*, *d*)	2080 vs (*a*, *b*, *c*, *d*)
$(CH_3)_3SiH$	2125 vs (*b*)	1960 vs (*c*)	Obscured by ν_{SiH}

*The notation *a*, *b*, *c*, and *d* refers to state of sample: *a*, KBr pellet; *b*, benzene solution; *c*, dichloromethane solution; *d*, film on NaCl plate produced by solvent evaporation.

TABLE II

Proton n.m.r. data for silyliridium(III) complexes

	Coupling constants* (Hz)					Chemical shifts (τ)	
Addend	*J*(P2–H1)	*J*(P1–H1)	*J*(H2–H1)	*J*(P2–H2)	*J*(P1–H2)	H1	H2
$(C_2H_5O)_3SiH$	22	17	4	110.5	18.5	20.2	21.5
$C_6H_5(CH_3)_2SiH$	23.5	16	4.5	113.5	19.5	20.0	21.0
$(C_6H_5)_3SiH$	20	15.5	4.5	110.5	17	19.5	20.7

*All atoms labelled as in reaction [1].

give any unequivocal indication of the relative position of the silicon and carbonyl groups. The insensitivity of the chemical shift values to variation of the substituents on the silicon suggested that the structure as in reaction [1] was in fact the correct one.

In order to prove the latter conclusion, a reaction was carried out between triethoxysilane and deuteridocarbonyltris(triphenylphosphine)-iridium(I) in equimolar amounts. The product of this reaction exhibited two carbonyl bands at 1965 and 2000 cm^{-1} and gave an n.m.r. spectrum identical to that shown in Fig. 1 except that the H–H coupling was no longer evident. These results find a ready interpretation in terms of the structure shown in Fig. 1, if it is assumed that the deuterium is equally distributed between the hydride positions. The carbonyl band at 2000 cm^{-1} may be assigned to CO *trans* to deuterium (3).

Some Properties of the Dihydridosilyliridium(III) Complexes

The adducts synthesized in the present work are of considerably greater stability than those formed from chlorocarbonylbis(triphenylphosphine)iridium(I), as evidenced by the ready formation of complexes with trialkyl and triarylsilanes. The order of stability, however, seems to be similar, since the trimethyl- and phenyl-dimethylsilyl derivatives were only completely formed in the presence of excess silane, whilst silanes containing a chloro- or ethoxy substituent gave an essentially complete reaction with equimolar quantities of reactants. This enhanced stability is in accord with the currently held belief that oxidative addition is promoted by the presence of electron releasing ligands on the reactant complex (4), hydride being more electron releasing than chloride.

The remarkable stability of the adducts with respect to loss of molecular hydrogen, may also be understood in terms of the above hypothesis. Pure samples of the triethoxy- and triphenylsilyl derivatives could be heated up to temperatures where charring occurred without loss of hydrogen or silicon hydride. Since silyl ligands seem to be very strong σ-donors (5), it would be expected (at least with the benefit of hindsight) that the hydrogen adduct of a silylcarbonylbis(triphenylphosphine)iridium complex would be extremely

Can. J. Chem. Downloaded from www.nrcresearchpress.com by 210.87.254.40 on 09/05/12
For personal use only.

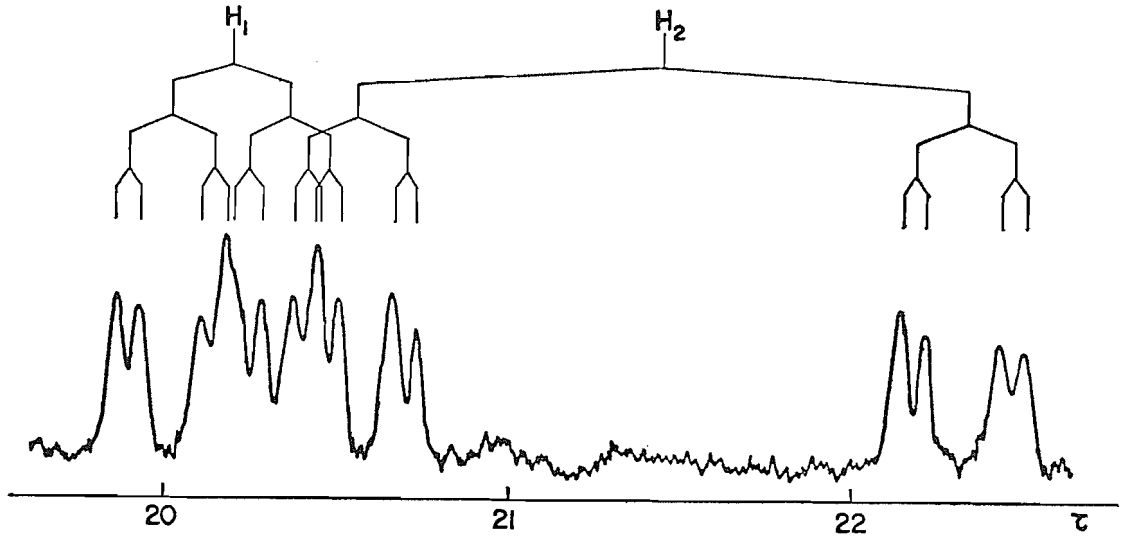

FIG. 1. Proton n.m.r. spectrum of dihydridotriethoxysilylcarbonylbis(triphenylphosphine)iridium(III) in the high field region (the coupling constants for this complex are given in Table II).

stable, and that our objective of preparing the latter by dehydrogenation of the former would not be realized.

At the time we obtained our results, we were surprised to find that the structure of our adducts was one in which the phosphine ligands were *cis* to each other, since all other analogous bisphosphine complexes for which structures had been reported contained the phosphines in the *trans* position. We could find no evidence for isomerization occurring, even though spectra could be run within a very short time of mixing the reactants.

Since we obtained these results, the addition of allyl halides to chlorocarbonylbis(phenyldimethylphosphine)iridium(I) to yield products with mutually *cis* phosphines has been reported by Deeming and Shaw (6). The similarity of the above reaction to the silicon hydride additions studied by us (at least from the point of view of stereochemistry) suggests a possible similarity in mechanism. Such an analogy would require a predissociation of the 5-coordinate complex **1** to a square planar intermediate as depicted in reaction [2]. Approach of the addend along the axis perpendicular to the plane of the molecule, accompanied by a simultaneous migration of the phosphine ligands in a direction away from the approaching addend, would give the required stereochemistry as in reaction [3].

A serious objection to such a simple scheme is

[2] 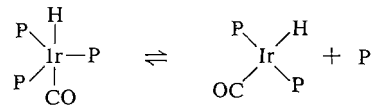

1 **2**

[3] 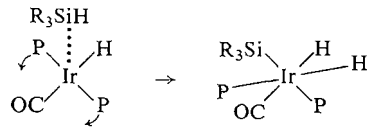

that the results of the experiment, where triethyoxysilane was added to the deuterido analogue of **1**, indicated that either of the hydrogen ligands in the product may originate from the silicon hydride. The fact that Deeming and Shaw obtained a mixture of isomers from the addition of allyl chloride to *trans* bromocarbonylbis(phenyldimethylphosphine)iridium (I), indicates that a similar lack of stereospecificity may also arise in that reaction.

The catalysis of SiH–SiD exchange by chlorocarbonylbis(triphenylphosphine)iridium(I) has been reported by Sommer and Lyons (7). We have found that hydridodeuteridotriethoxysilylcarbonylbis(triphenylphosphine)iridium(III) undergoes exchange with triethoxysilane. In principle such an exchange could occur, if reaction [1] was a rapid equilibrium, by repetitive oxidative addition and reductive elimination. Such a possibility does not, however, exist for the

Can. J. Chem. Downloaded from www.nrcresearchpress.com by 210.87.254.40 on 09/05/12
For personal use only.

chloro complex. In view of the extreme stability of the triethoxy derivative with respect to loss of silicon hydride, it seems more probable that these exchange reactions occur by a concerted bimolecular process. A kinetic investigation of such exchange reactions is in progress to test the validity of this hypothesis.

Experimental

Iridium trichloride trihydrate was obtained from Engelhard Industries Ltd. Chlorocarbonylbis(triphenylphosphine)iridium(I) was prepared by the method of Collman and Kang (8). Hydridocarbonyltris(triphenylphosphine)iridium(I) was prepared by the method of Vaska and Bath (9) in the initial stages of this work, but subsequently we obtained much better yields by the dehydrochlorination of chlorodihydrocarbonylbis(triphenylphosphine)iridium(III) with KOH in ethanol (10). Deuteridocarbonyltris(triphenylphosphine)iridium(I) was prepared according to Vaska (11).

Triphenyl-, trimethyl-, triethoxy-, and trichloro-silanes were obtained from Penninsular Chemresearch Ltd. Methyldichlorosilane and phenyldimethylsilane were gifts from the General Electric Co.

Preparation of Dihydrido(triethoxysilyl)bis(triphenylphosphine)iridium(III)

A sample of **1** (0.3 g) was dissolved in dry benzene (5 ml) and placed on a vacuum transfer line. After the solution had been thoroughly degassed, triethoxysilane (1.0 g) was distilled onto it and the reactants were then left at room temperature for 1 h. During this time the initially yellow solution became almost colorless. All volatile material was pumped off by prolonged evacuation at room temperature to yield a yellow oil. Trituration of this oil with a small amount of hexane yielded pale yellow crystals, which on recrystallization from hexane became white. Yield (after recrystallization): 0.24 g (78%), melting point 152–154 °C.

Anal. Calcd. for $IrC_{45}H_{47}O_4P_2Si$: C, 56.72; H, 5.17; Si, 3.08; P, 6.80. Found: C, 56.68; H, 5.35; Si, 2.84; P, 6.63.

The phenyldimethylsilane adduct was prepared by the same procedure, but the complex underwent dissociation during attempts to recrystallize. An impure sample of the phenyldimethyl adduct was found to undergo loss of silane on heating to ca. 120 °C.

Preparation of the Trichlorosilane and Methyldichlorosilane Adducts

A sample of **1** was dissolved in dry dichloromethane (0.3 g in 10 ml) and attached to a vacuum transfer line. Trichlorosilane (0.6 g) was distilled onto the solution and the mixture was allowed to warm to room temperature. On reducing the volume of the solution, white crystals of the product were obtained. The product was filtered in nitrogen, washed with a little dry dichloromethane, and dried *in vacuo*. The product neither melted nor decomposed below 300 °C. Yield: 0.24 g (88%).

Anal. Calcd. for $C_{37}H_{32}OP_2Cl_3SiIr$: C, 50.4; H, 3.64; Si, 3.2; P, 7.04. Found: C, 51.0; H, 3.83; Si, 3.76; P, 6.90.

The methyldichlorosilane adduct was prepared by the same procedure and had physical properties virtually identical to the trichlorosilane adduct.

Anal. Calcd. for $C_{38}H_{35}OP_2Cl_2SiIr$: C, 53.0; H, 4.1; Si, 3.3; P, 7.2. Found: C, 57.0; H, 4.9; Si, 3.3; P, 7.5.

The very high values for C, H, and P in this analysis indicate incomplete separation of the product from uncomplexed triphenylphosphine.

Preparation of the Triphenylsilane Adduct

A mixture of **1** (0.22 g) and triphenylsilane (0.06 g) was dissolved in dry benzene (10 ml). The solution was evaporated to dryness on a vacuum transfer line and the residue was redissolved in benzene. Careful addition of hexane to this solution caused the product to precipitate free of triphenylphosphine. The precipitate was filtered and washed with hexane. Yield: 0.20 g (90%), decomposing at 160 °C.

Anal. Calcd. for $C_{55}H_{47}OP_2SiIr$: C, 65.68; H, 4.71; Si, 2.79; P, 6.17. Found: C, 65.87; H, 4.9; Si, 3.08; P, 6.09.

The Trimethylsilane Adduct

Excess trimethylsilane was distilled directly from the cylinder onto a solution of **1** in benzene at 0 °C. On warming the solution to room temperature the intense yellow color characteristic of **1** faded considerably, indicating rapid formation of the adduct. All attempts to isolate the adduct, either by solvent removal, or by precipitation, resulted in the decomposition of the adduct by loss of silane.

Spectroscopic Measurements

Infrared spectra were measured on a Perkin–Elmer model 257 spectrometer.

Proton n.m.r spectra were measured with a Varian A60 spectrometer coupled to a Varian C1024 averaging computer. Generally about 50 scans at 250 s were required for spectra such as those illustrated in Fig. 1. Samples were saturated solutions in dichloromethane.

Acknowledgment

The authors would like to acknowledge financial support for this work by grants from the National Research Council of Canada.

1. A. J. Chalk and J. F. Harrod. J. Am. Chem. Soc. **87**, 16 (1965).
2. F. de Charentenay, J. A. Osborne, and G. Wilkinson. J. Chem. Soc. 787 (1968).
3. L. Vaska. J. Am. Chem. Soc. **88**, 4100 (1966).
4. J. P. Collman. Accounts of Chemical Research, **1**, 136 (1968).
5. W. A. G. Graham. Inorg. Chem. 7, 315 (1968).
6. A. J. Deeming and B. L. Shaw. Chem. Commun. 751 (1968).
7. L. H. Sommer and J. E. Lyons. J. Am. Chem. Soc. **90**, 4199 (1968).
8. J. P. Collman and J. W. Kang. J. Am. Chem. Soc. **89**, 844 (1967).
9. L. Vaska and S. S. Bath. J. Am. Chem. Soc. **85**, 3500 (1963).
10. J. F. Harrod, D. F. R. Gilson, and R. Charles. Can. J. Chem. In press.
11. L. Vaska. Proc. 8th. Intern. Conf. on Co-ord. Chem. 1964. *Edited by* V. Gutman. p. 99.

Can. J. Chem. Downloaded from www.nrcresearchpress.com by 210.87.254.40 on 09/05/12
For personal use only.

Can. J. Chem. Downloaded from www.nrcresearchpress.com by 210.87.254.6 on 09/05/12
For personal use only.

Complexes of Group IV halides with mercuric thiocyanate and mercuric cyanide as ligands

S. C. JAIN AND R. RIVEST
Department of Chemistry, University of Montreal, Montreal 3, Quebec

Received October 21, 1968

Coordination compounds between mercuric thiocyanate and mercuric cyanide as ligands and the Group IV halides as Lewis acids have been prepared and their infrared (i.r.) spectra (4000–200 cm^{-1}) examined. Two types of compounds, $MX_4 \cdot L$ and $MX_4 \cdot 2L$ where M = Ti, Sn; X = Cl, Br; and L = $Hg(SCN)_2$ or $Hg(CN)_2$ were characterized. On the basis of i.r. spectral results, possible coordination through the thiocyanato and cyano groups has been discussed.

Les composés de coordination entre le thiocyanate mercurique et le cyanure mercurique comme ligands et les halogénures des éléments du Groupe IV comme acides de Lewis ont été préparés et leurs spectres infrarouges mesurés de 4000 à 200 cm^{-1}. Deux genres de composés ont été obtenus soit: $MX_4 \cdot L$ et $MX_4 \cdot 2L$ où M = Ti, Sn; X = Cl, Br; et L = $Hg(SCN)_2$ ou $Hg(CN)_2$. D'après les résultats obtenus dans l'infrarouge on discute de la coordination possible par l'intermédiaire du groupe thiocyanato et cyano.

Canadian Journal of Chemistry, 47, 2209 (1969)

Introduction

We have previously reported the formation of coordination complexes between organic cyanides (nitriles) (1) or organic thiocyanates (2) and Group IV halides. Since Jones (3) and Lewis *et al.* (4) have concluded that the Hg—C bond in $Hg(CN)_2$ and Hg—S bond in $Hg(SCN)_2$ are strong covalent bonds, it was considered interesting to use $Hg(CN)_2$ and $Hg(SCN)_2$ as ligands towards Group IV halides and compare their donor behavior with those of organic cyanides and thiocyanates.

Experimental

Since the Group IV halides are highly hygroscopic, all the experimental manipulations were carried out in a dry box continuously flushed with dry nitrogen. The experimental set up and the method of preparation of the complexes were similar to the ones discussed previously (1, 5). Lewis acids used were purified by suitable methods (1) and the solvent methylene chloride was dried over phosphorus pentoxide and fractionally distilled before use. Mercury thiocyanate and cyanide (purified) were obtained from the City Chemical Corporation, New York, and used as such after drying in vacuo.

Since the mercury compounds were found insoluble in common organic inert solvents, the reactions were performed in large excesses of Lewis acids by taking the ligands in suspension (6). The reactants were normally allowed to react for 4–6 days with magnetic stirring at room temperature. In each case solid powdery compounds were obtained which were filtered, washed with the solvent, and dried in vacuo at room temperature.

The analyses for titanium and mercury were made gravimetrically by weighing as TiO_2 and $[Cuen_2][HgI_4]$ (7) respectively. Sulfur, nitrogen, and halogens were determined by Organic Micro-analyses, 5757 Decelles Ave., Montreal. The analytical results are included in Table I.

The i.r. spectra were recorded on a Perkin–Elmer spectrophotometer model 621 in Nujol mull. In the case of mercuric cyanide compounds, cesium iodide disks were used over the range 4000–200 cm^{-1}. In the case of mercuric thiocyanate coumpounds, however, where cesium iodide seems to interact, sodium chloride disks were used over the range of 4000-600 cm^{-1} and polyethylene disks were used for the range 600–200 cm^{-1}. The i.r. spectral results are reported in Table II.

Results and Discussion

The analytical results (Table I) indicate that Group IV halides form two types of adducts with $Hg(SCN)_2$ and $Hg(CN)_2$ i.e. 1:1 and 1:2. It is well known (1, 8, 9) that as a result of coordination through the electron pair on nitrogen of the cyano group, the cyano stretching frequency, ν(CN) shows a hypsochromic effect. A coordination through the π electrons of the triple bond, on the other hand, would result in the appearance of a bathochromic effect on the CN stretching frequency (10–12).

The i.r. spectral results in the cyano stretching region (Table II) for the 1:1 adducts show the ν(CN) shifted to higher positions, whereas for the 1:2 adducts both shifted and unshifted bands are observed (Fig. 1). The increase in ν(CN) for the compounds may be attributed to a change in CN force constant, or may be due to bridging between two metal atoms. Since the 1:2 adducts display both shifted and unshifted ν(CN) bands and the 1:1 adducts display only shifted ν(CN) bands, it seems more likely that the increase in

Can. J. Chem. Downloaded from www.nrcresearchpress.com by 210.87.254.6 on 09/05/12
For personal use only.

TABLE I

Analytical results

Compound	Color	Melting point* (°C)	Composition (%) Metal† Calcd.	Metal† Found	Halogen Calcd.	Halogen Found	Nitrogen Calcd.	Nitrogen Found	Sulfur Calcd.	Sulfur Found	Mercury Calcd.	Mercury Found	Nature of adduct
$TiCl_4 \cdot Hg(SCN)_2$	Orange	170–172 (d)	9.45	9.2	27.93	27.7	5.53	5.8	12.63	11.2	39.59	39.6	1:1
$TiBr_4 \cdot Hg(SCN)_2$	Dark brown	168–170 (d)	7.01	7.1	46.72	46.8	4.09	4.3	9.35	8.9	29.3	28.9	1:1
$SnCl_4 \cdot Hg(SCN)_2$	Cream	> 400	20.56	20.2	24.55	25.1	4.85	4.9	11.09	11.2			1:1
$SnBr_4 \cdot 2Hg(SCN)_2$	Cream	> 400	11.08	10.7	29.83	30.0	5.22	5.6	11.94	12.7			1:2
$TiCl_4 \cdot Hg(CN)_2$	Yellow	~ 300 (d)	10.83	10.4	32.05	32.0	6.33	5.6			45.34	45.2	1:1
$TiBr_4 \cdot 2Hg(CN)_2$	Orange	~ 250 (d)	5.49	5.7	36.63	36.2					45.95	45.2	1:2
$SnCl_4 \cdot 2Hg(CN)_2$	White	~ 250 (d)	15.50	15.3	18.51	17.5	7.31	7.3					1:2
$SnBr_4 \cdot 2Hg(CN)_2$	White	~ 280 (d)	12.58	12.8	33.90	33.4	5.93	5.6					1:2

*d = decomposed by turning black.
†Group IV metal.

TABLE II

Infrared spectra results* in Nujol mull (cm^{-1})

(*a*) $MX_4 \cdot nHg(SCN)_2$ compounds (n = 1 or 2)

Compounds	ν(C≡N)	ν(C—S)	δ(S—C≡N)	ν(Hg—S)	ν(M—X)
Hg(SCN) (L$_A$)	2116 s	722 m	459 m 427 s	306	—
$TiCl_4 \cdot L_A$	2171 s	738 s	550 m, 497 m 469 w, 449 m	301 m	396 vsb, 375 sh
$TiBr_4 \cdot L_A$	2121 s	725 s	552 m, 476 m 450 w, 422 sh	305 sh	370 vsb, 330 ssh 240 m
$SnCl_4 \cdot L_A$	2167 s	730 sh	551 m, 473 w 424 m	305 w	333 vs, 320 ssh
$SnBr_4 \cdot 2L_A$	2124 s 2108 sh	730 sh 720 w	553 m, 468 m 447 m	300 sh	320 sh, 280 s 256 sb

(*b*) $MX_4 \cdot nHg(CN)_2$ compounds (n = 1 or 2)

Compounds	ν(C≡N)	ν(Hg—C)	δ(Hg—C≡N)	ν(M—X)
$Hg(CN)_2$ (L$_B$)	2195 s	442 vs 411 w	338 w	—
$TiCl_4 \cdot L_B$	2241 s	502 m 495 m	336 w	394 vs, 370 s
$TiBr_4 \cdot 2L_B$	2227 s 2196 m	500 m, 477 m 443 s, 410 sh	336?	350 sh, 336 s, 300 sh
$SnCl_4 \cdot 2L_B$	2249 s 2197 s	498 s, 478 m 443 s, 410 w	336?	353 s, 336 vs
$SnBr_4 \cdot 2L_B$	2238 s 2197 m	479 s, 445 s 410 w	330 w	252 s, 245 sh 225 sb

*s: strong, m: medium, w: weak, sh: shoulder, v: very, b: broad, ?: band probably hidden under strong (M—X) band.

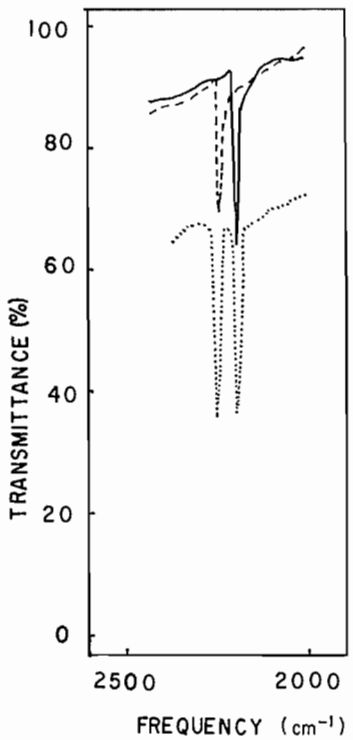

FIG. 1. Infrared spectra in ν(CN) region; —, $Hg(CN)_2$; - - -, $TiCl_4 \cdot Hg(CN)_2$; · · ·, $SnCl_4 \cdot 2Hg(CN)_2$.

ν(CN) is mainly due to bridging between two metal atoms. ν(CN) is known (13) to appear at a higher position for a bridging cyano group than for a non-bridging one. Mitchell and Williams (14) reached a similar conclusion with regard to the cyanide stretching frequency for a bridging thiocyanate group. Such a group has two possibilities for bridging, i.e. either through the sulfur atom or through the nitrogen atom as shown below.

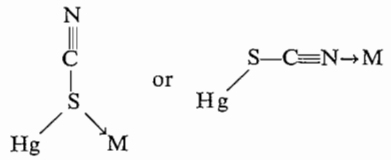

On the basis of X-ray crystallography Chatt and Hart (15) have concluded that in the great majority of bridged complex thiocyanates, bridging takes place through both the sulfur and the nitrogen atoms. In fact, AgSCN in the pure state consists of infinite chains of structure (16) ··Ag—S—C—N→Ag··· in which the thiocyanato bridge is also formed through both the sulfur and the nitrogen atoms. In the pure state mercuric thiocyanate is also likely to consist of bridging thiocyanate groups similar to AgSCN.

Can. J. Chem. Downloaded from www.nrcresearchpress.com by 210.87.254.6 on 09/05/12
For personal use only.

Can. J. Chem. Downloaded from www.nrcresearchpress.com by 210.87.254.6 on 09/05/12
For personal use only.

In our 1:1 adducts, it seems that both the cyano groups of $Hg(CN)_2$ or $Hg(SCN)_2$ coordinate to the Group IV metal atoms but in the 1:2 adducts only one of the functional group coordinates, while the other one remains unaffected. The i.r. spectrum shows two ν(CN) peaks corresponding to the two types of thiocyanato or cyano groups (14). The fact that these compounds are not soluble in commonly used organic inert solvents makes it rather difficult to study further their physico-chemical nature in support of their structure. Since the cyano (17) and the thiocyanato groups are almost linear in nature, it is reasonable to believe that in the 1:1 adducts both the functional groups coordinate to different metal atoms forming compounds polymeric in nature. On the other hand, in the 1:2 adducts, the unshifted ν(CN) bands may be due to terminal CN or SCN groups or to bridging functional groups between two mercury atoms. Since the position of these bands is almost the same in the complexes and in pure $Hg(CN)_2$, where the CN groups are known to be bridging between two mercury atoms (13), it is quite sure that the same type of bridging still exists in the complexes with Group IV halides. As a result of this, these compounds also are probably polymeric in nature.

Another important feature of the i.r. results is that in the compounds formed, the cyano or thiocyano groups are not completely ionic, because a free ionic CN^- group displays a ν(CN) band at a much lower region (18) than the ones observed in the present case. Moreover, $Hg(CN)_2$, being a covalent molecule (3), is less likely to ionize in a nonpolar solvent like CH_2Cl_2 to give CN^- ions.

A comparison of $Hg(CN)_2$ or $Hg(SCN)_2$ with organic cyanides or thiocyanates (1, 2) as ligands towards Group IV halides, is difficult to make. $Hg(SCN)_2$ or $Hg(CN)_2$ as solids are said to contain SCN or CN bridging between neighboring Hg atoms (13). So the shift or increase in ν(CN) on coordination with Group IV metals is not necessarily the difference between the ν(CN) of the terminal cyano group and the bridging cyano group.

To obtain the position of terminal ν(CN) and ν(SCN) bands we recorded i.r. spectra of $Hg(CN)_2$ and $Hg(SCN)_2$ in Nujol mulls and compared them with those taken in tetrahydrofuran solution. In the case of $Hg(CN)_2$ the i.r. spectrum recorded in solution showed the ν(CN) band 8 cm^{-1} lower than the one observed in the spectrum taken in Nujol, while in the case of $Hg(SCN)_2$, the ν(SCN) band position remained unchanged. This would suggest that there is only very weak bridging interaction between two $Hg(SCN)_2$ or two $Hg(CN)_2$ molecules. The fact that the N—Hg distance in solid $Hg(CN)_2$ is 2.70 Å as compared to 1.99 Å for Hg—C (19) strongly indicates that the bridging effect in the ligands in the pure state is very weak. Actually a fairly strong N—Hg bond would be needed to effect the ν(CN) vibration. If one considers the magnitude of the positive shift, Δν(CN) as the measure of basicity of the CN or S—CN groups in an organic or inorganic ligand and takes 2195 and 2116 cm^{-1} as the terminal ν(CN) bands for $Hg(CN)_2$ and $Hg(SCN)_2$, respectively, then it is interesting to note that in organic cyanides and thiocyanates (1, 2), cyanide seems to be a better donor than the corresponding thio compound as shown below

Compound	Δν(CN) (cm^{-1})	Reference
$TiCl_4(—CH_2CN)_2$	53	1
$TiCl_4(—CH_2SCN)_2$	30	2
$2TiCl_4(—CH_2CN)_2$	56	1
$2TiCl_4(—CH_2SCN)_2$	40	2
$TiCl_4 \cdot Hg(CN)_2$	46	This work
$TiCl_4 \cdot Hg(SCN)_2$	55	This work

but in the case of $Hg(CN)_2$ and $Hg(SCN)_2$, the thiocyanate molecule shows a larger Δν(CN) on coordination with titanium.

Far Infrared Spectral Studies

(a) MX_4 and $Hg(CN)_2$ Compounds

In addition to the metal–halogen and the metal–ligand stretching bands, these compounds would exhibit Hg—C stretching, and Hg—CN and C—Hg—C bending bands in the low frequency region. Since the C—Hg—C bending band appears below the 200 cm^{-1} range (20) we will discuss only the ν(M—X), ν(Hg—C), and δ(Hg—CN) bands.

ν(M—X) bands

The ν(M—X) bands are usually strong bands and their identification can be made easily by comparing the positions of ν(M—Cl) and ν(M—Br) bands in identical compounds. ν(M—Br) bands normally appear in a much lower region than the ν(M—Cl) bands. Our assignments of the ν(M—X) bands are given in Table II and the results are in good agreement with the

values reported previously (6, 21, 22), and correspond to the value for which the central metal atom exhibits a coordination number six (23).

ν(Hg—C) bands

The bands at 411 and 422 cm^{-1} for $Hg(CN)_2$ are assigned to ν(Hg—C) (3). In the 1:1 adduct $TiCl_4 \cdot Hg(CN)_2$ these bands disappear and new medium bands appear at 502 and 495 cm^{-1} which probably are shifted ν(Hg—C) bands. Shifting of the ν(Hg—C) bands to a higher frequency region may be due to coupling of the ν(Hg—C) with the ν(CN) in the Hg—CN part of the molecule. Since the ν(CN) shifts to a higher position on coordination, the ν(Hg—C) should show a similar effect. It is interesting to note that in the $MX_4 \cdot 2Hg(CN)_2$ compounds the i.r. spectra show both the shifted ν(Hg—C) bands due to coordinated (bridged) cyano group and the unshifted bands due to the CN groups which remain unaffected. In fact a similar effect in the ν(CN) region further supports our interpretation that in the 1:2 adducts we have two types of cyano groups, one bridging between mercury and titanium, and another probably bridging between mercury and mercury.

δ(Hg—CN) bands

In the spectrum of $Hg(CN)_2$ we observed δ(Hg—CN) at 338 cm^{-1} as a weak band. In the literature (3) the value reported for this band is 341 cm^{-1}. In the complexes of Group IV halides this band seems to remain almost unchanged. Since strong ν(Ti—Br) and ν(Sn—Cl) bands also appear in the same region, in the spectra of the complexes $TiBr_4 \cdot 2Hg(CN)_2$ and $SnCl_4 \cdot 2Hg(CN)_2$ most probably the δ(Hg—CN) bands are hidden under the strong ν(M—X) bands.

(b) MX_4 and $Hg(SCN)_2$ Compounds

ν(M—X) bands

Assignment of the ν(M—X) bands in these compounds is in good agreement to the corresponding bands already discussed in the previous section. In these compounds also the Group IV metals seem to exhibit a coordination number of six.

ν(C—S) bands (4, 24, 25)

For a thiocyanato group the ν(C—S) occurs between 690 and 720 cm^{-1} (24, 25). In the i.r. spectrum of $Hg(SCN)_2$ we assign a band at 722 cm^{-1} to the ν(C—S) vibration. As a result of coordination, the ν(C—S) shifts to a higher position. Clark and Williams (24) also observed that both the ν(C—N) and ν(C—S) stretching frequencies increase on coordination of the thiocyanate ion to the metal.

The Thiocyanato Bending Mode δ(S—C≡N) (4, 25)

The behavior of N—C≡S bending vibration has been discussed by Sabatini and Bertini (25) on the basis of its bonding to the metal atom through the sulfur or nitrogen. The S-bonded thiocyanato compounds absorb at a lower frequency region than the N-bonded ones. The S-bonded groups also show more than one δ(SCN) band. In the case of S-bonded $Hg(SCN)_2$ we observe two bands in the δ(SCN) range, Table II. The spectra of complexes with Group IV halides show 3–4 bands in this region which appear at higher positions than the bands for pure $Hg(SCN)_2$. In a system where S—C≡N is bridging between two different metals Hg—S—C≡T—Ti, there are both S-bonded and N-bonded groups at the same time; thus an increase in the number and the positions of δ(SCN) is not surprising.

Mercury–Sulfur Stretching Band: ν(Hg—S)

Sabatini *et al.* (25) report the ν(Hg—S) band at 285 cm^{-1} for $K_2[Hg(SCN)]_4$ compound. The spectrum of $Hg(SCN)_2$ shows a strong band at 306 cm^{-1} which could be associated with the ν(Hg—S) vibration. Since a number of ν(M—X) bands also appear in this region (Table II), it is not safe to comment on the effect of coordination of $Hg(SCN)_2$ to MX_4 on the ν(Hg—S) vibration. However, a band at 301 cm^{-1} for $TiCl_4 \cdot Hg(SCN)_2$ where the ν(Ti—Cl) are expected to appear at a higher position than 300 cm^{-1} shows that the ν(Hg—S) is not much affected when the SCN groups of $Hg(SCN)_2$ coordinate to titanium through the nitrogen atom. Clark (24) also noticed the very small effect that bridging of the NCS group has on the (M—NCS) stretching mode.

Acknowledgment

The authors gratefully acknowledge the continued financial assistance from The National Research Council of Canada.

1. S. C. Jain and R. Rivest. Can. J. Chem. **41**, 2130 (1963).
2. S. C. Jain and R. Rivest. Can. J. Chem. **43**, 787 (1965).
3. L. H. Jones. J. Chem. Phys. **27**, 665 (1957).

Can. J. Chem. Downloaded from www.nrcresearchpress.com by 210.87.254.6 on 09/05/12
For personal use only.

4. J. LEWIS, R. S. NYHOLM, and P. W. SMITH. J. Chem. Soc. 4590 (1961).
5. S. C. JAIN and R. RIVEST. Can. J. Chem. **40**, 2243 (1962).
6. S. C. JAIN and R. RIVEST. J. Inorg. Nucl. Chem. **29**, 2787 (1967).
7. A. I. VOGEL. A textbook of quantitative inorganic analysis. 3rd ed. 1961. p. 488.
8. R. A. WALTON. Quart. Rev. London, **19**, 126 (1965).
9. M. KUBOTA and D. L. JOHNSTON. J. Inorg. Nucl. Chem. **29**, 769 (1967).
10. S. C. JAIN and R. RIVEST. Inorg. Chem. **6**, 467 (1967).
11. M. F. FARONA and N. J. BREMER. J. Am. Chem. Soc. **88**, 3735 (1966).
12. H. BOCK and H. DIEK. Ber. **99**, 213 (1966).
13. D. A. DOWS, A. HAIM, and W. K. WILMARTH. J. Inorg. Nucl. Chem. **21**, 33 (1961).
14. P. C. H. MITCHELL and R. J. P. WILLIAMS. J. Chem. Soc. 1912 (1960).
15. J. CHATT and F. A. HART. J. Chem. Soc. 1416 (1961).
16. I. LINDQVIST. Acta Cryst. **10**, 20 (1957).
17. J. HVOSLEF. Acta Chem. Scand. **12**, 1568 (1958).
18. K. NAKAMOTO. Infrared spectra of inorganic and coordination compounds. John Wiley and Sons, Inc., New York. 1963. p. 169.
19. R. W. G. WYCKOFF. Crystal structures. Vol. I. 2nd ed. Interscience Publishers, Inc., New York. 1963.
20. K. NAKAMOTO. Infrared spectra of inorganic and coordination compounds. John Wiley and Sons, Inc., New York. 1963. p. 171.
21. S. C. JAIN and R. RIVEST. Can. J. Chem. **45**, 139 (1967).
22. S. C. JAIN and R. RIVEST. J. Inorg. Nucl. Chem. **31**, 399 (1969).
23. R. J. H. CLARK. Spectrochim. Acta, **21**, 955 (1965).
24. R. J. H. CLARK and C. S. WILLIAMS. Spectrochim. Acta, **22**, 1081 (1966).
25. A. SABATINI and I. BERTINI. Inorg. Chem. **4**, 959 (1965).

Can. J. Chem. Downloaded from www.nrcresearchpress.com by 210.87.254.6 on 09/05/12
For personal use only.

Crystal structure of $\beta'Mn_3(PO_4)_2$

J. S. STEPHENS[1] AND C. CALVO

Department of Physics and Institute for Materials Research, McMaster University, Hamilton, Ontario

Received March 19, 1968

$\beta'Mn_3(PO_4)_2$ crystallizes as a monoclinic crystal with lattice parameters $a = 8.94(3)$ Å, $b = 10.04(2)$ Å, $c = 24.12(12)$ Å, $\beta = 120.8(1)°$, and $Z = 12$. The diffraction pattern shows a pronounced superlattice phenomenon with reflections generally weak if their l index $\neq 0$ mod 3. The conventional R value for a total of 3516 reflections, of which 1637 were strong enough to be measured,was reduced to 0.09 by full matrix least squares procedures. This structure is related to that of $\beta Zn_3(PO_4)_2$ whose unit cell dimensions are comparable save for a tripled c axis in $\beta'Mn_3(PO_4)_2$. In addition, the latter compound is isostructural with the low temperature form of $Cd_3(PO_4)_2$. The PO_4^{3-} groups are slightly irregular tetrahedra with a mean P—O bond distance of 1.54 ± 0.01 Å. The coordination numbers of the cations have increased on the average in comparison to $\beta Zn_3(PO_4)_2$ where they are 4, 5, and 5 for the three unique cations. In $\beta'Mn_3(PO_4)_2$ each cation shows 5 strong Mn—O bonds and most cations have one additional bond of intermediate strength. The metal–oxygen atom bond distances in $\beta'Mn_3(PO_4)_2$ range from 2.03 to 2.31 Å although there are some additional long ones ranging from 2.4 to 3.0 Å which can be correlated with normal bond lengths in $\beta Zn_3(PO_4)_2$.

Canadian Journal of Chemistry, 47, 2215 (1969)

Can. J. Chem. Downloaded from www.nrcresearchpress.com by 210.87.254.105 on 09/05/12
For personal use only.

Introduction

Two crystalline modifications of $Mn_3(PO_4)$ are known (1). One has a structure similar to that of the mineral graftonite, a solid solution represented as $(Fe,Mn,Ca)_3(PO_4)_2$ (2). The second has a Debye–Scherrer pattern very similar to that of $\beta Zn_3(PO_4)_2$. Further, the pattern of $Cd_3(PO_4)_2$ (3) also appeared closely related to that of $\beta Zn_3(PO_4)_2$ and therefore a structural similarity was anticipated. The close structural relationship between $Cd_3(PO_4)_2$ and $\beta Zn_3(PO_4)_2$ was confirmed in that single crystal data from the former phase were used in elucidating the crystal structure of $\beta Zn_3(PO_4)_2$ (4). The structure of this phase of $Mn_3(PO_4)_2$ was examined in detail in order to consider further the question of direct cation substitution of Mn^{2+} in $\beta Zn_3(PO_4)_2$.

This and related crystallographic studies on the $M_3(XO_4)_2$ systems, where the XO_4^{3-} group has a tetrahedral configuration and M is a divalent ion of moderately small radius ($\leqslant 1$ Å), show a surprising number of crystallographically distinct phases. Even among those phases of a common structural type, the cations coordination numbers vary as the composition of a given cation site is changed (5). A comparison of the structures of $\beta Zn_3(PO_4)_2$ and $\beta'Mn_3(PO_4)_2$ indicates that similar changes occur here, resulting in slightly different structures for these phases.

Katnack and Hummel (6) have studied the phase diagram of the $ZnO - MnO - P_2O_5$ system. Above 900 °C the β form of $Zn_3(PO_4)_2$ appears to be stable up to a composition of about 30 mole % of Mn^{2+}. Beyond this composition $\beta Zn_3(PO_4)_2$ is no longer the stable phase although this instability might be due to the oxidation of Mn (6). Below 900 °C and above 5% $Mn_3(PO_4)_2$ a solid solution, commonly called "γ" $Zn_3(PO_4)_2$, is stable. The structure of this phase has been reported previously (7).

The structural similarity between $\beta Zn_3(PO_4)_2$ and $Cd_3(PO_4)_2$ and this phase of $Mn_3(PO_4)_2$ can be implied by labelling these phases as $\beta'Cd_3(PO_4)_2$ and $\beta'Mn_3(PO_4)_2$. $\beta'Cd_3(PO_4)_2$ has a high temperature phase transition necessarily involving small atomic displacements (8) and therefore may transform to a phase like that of $\beta Zn_3(PO_4)_2$ but not identical with it.

Experimental

$Mn_3(PO)_2 \cdot 7H_2O$, obtained from Fisher Scientific Co., was dried to remove the water and then fused in a sealed evacuated Vycor tube with an oxygen-gas flame. Crystals were grown upon slowly removing the flame and allowing the sample to cool across its melting temperature, reported to be 1119 °C (9). The crystals, whose color varied from dirty brown to nearly colorless, had plate-like morphologies. Preliminary X-ray photographs showed that they were monoclinic with the space group $P2_1/c$, since the systematic extinctions were the l odd reflections of $h0l$ set and k odd reflections of $0k0$ set. Also it was

[1]Present address: Chemistry Department, University of Manchester Institute of Science and Technology, Manchester 1, England.

Can. J. Chem. Downloaded from www.nrcresearchpress.com by 210.87.254.105 on 09/05/12
For personal use only.

apparent, particularly at low angles, that the structure showed a pronounced superstructure. This indicated that the c axis was tripled, because of small displacements of the atoms from an average structure, since all strong reflections had their l Miller index equal to 0 mod 3.

A small fragment, broken from one of the less colored single crystals, was mounted on a glass fiber and aligned so as to rotate around the b axis. The crystal had dimensions $0.07 \times 0.15 \times 0.10$ mm^3 with the long axis parallel to the axis of rotation. Intensity data of the $h0l$ and the $h1l$ planes were recorded with a Weissenberg camera using MoKα radiation while the [100] and [001] zones were photographed on a precession camera with the same radiation. The intensities of these reflections were estimated visually and corrected for Lorentz and polarization effects but not for absorption.

The lattice parameters were determined with the same crystal. The b axis length was determined from a rotation photograph calibrated by a superimposed TiO_2 pattern. The lattice parameters of the rutile crystals, which had been grown by the Verneuil technique, were taken to be $a = 4.5929(5)$ Å and $c = 2.9591(3)$ Å, after Cromer and Herrington (10).

The lengths of the reciprocal axes, a^* and c^*, were determined from the films of the [100] and [001] zones calibrated by the previously determined b axis. The β angle was determined from the spindle readings on the precession camera when the [100] and [001] zones were photographed. The density was measured with a pycnometer. The crystal data are recorded in Table I.

In addition to forming the β′ structure, $Mn_3(PO_4)_2$ can be crystallized with the graftonite structure. The conditions which determine the formation of each of these phases are uncertain. Although the graftonite-like phase appears with greater frequency than the β′ phase and can be produced at will, both phases have been obtained a number of times. An effort was made to determine the systematics for the formation of the β′ phase. An analysis of Fisher's "$Mn_3(PO_4)_2 \cdot 7H_2O$" showed it contained a substantial amount of $MnHPO_4$. Thus, it was postulated that the β′ structure formed in the presence of $Mn_2P_2O_7$, which is the decomposition product of $MnHPO_4$. This can be understood if graftonite is regarded as the stable phase at the melting temperature, the β′ phase is stable at lower temperatures, and if the transformation between the phases is irreversible and sluggish. The β′ phase would then result if the melting temperature of $Mn_3(PO_4)_2$ could be reduced by adding a compound like $Mn_2P_2O_7$ to the liquid phase. Attempts to prove this hypothesis by obtaining the β′ phase from $Mn_3(PO_4)_2$ – $Mn_2P_2O_7$ mixtures proved unsuccessful since only the graftonite form could be detected.

TABLE I
Crystal data of β′$Mn_3(PO_4)_2$

Lattice parameters	Unit	Value*
a	Å	8.94 (3)
b	Å	10.04 (2)
c	Å	24.14 (12)
β	degrees	120.8 (1)
Z		12
Extinctions	$h0l$, l odd $0k0$, k odd	
Densities	$\rho_{exp} = 4.1$ g cc^{-1} $\rho_{calcd} = 3.92$ g cc^{-1}	
Linear absorption coefficient for MoKα = 118 cm^{-1}		

*Estimated standard deviations in parentheses.

Structure Solution

The structure was solved by taking advantage of the fact that both $\beta Zn_3(PO_4)_2$ and $\beta' Cd_3(PO_4)_2$ have structures similar to that of $\beta' Mn_3(PO_4)$. The average cation positions in $Cd_3(PO_4)_2$ were determined from Patterson projections prepared with the $l = 0$ mod 3 reflections. These were used to elucidate the cation positions in $\beta Zn_3(PO_4)_2$ and eventually the entire structure of this compound (4). The final atomic coordinates of $\beta Zn_3(PO_4)_2$ were used to find the "average" positions of the atoms in $Cd_3(PO_4)_2$ and $Mn_3(PO_4)_2$ using the $l = 0$ mod 3 data only. By "average" or "average structure" is meant the positions r_j where the position of the jth atom in the nth sub-cell along the c axis is given by $R_{jn} = r_j + \varepsilon_{jn} + nc/3$ and $n (= 0, 1, 2)$ is the index defining the sub-cell. The average positions are chosen so that the displacements from these positions, ε_{jn}, average to zero, i.e. $\sum_{n=0} \varepsilon_{jn} = 0$. The structure factor for these $l = 0$ mod 3 reflections is

$$[1] \quad F(H) = \sum_n \sum_j f_j(H)\, e^{2\pi i H\cdot(r_j+\varepsilon_{jn}+nc/3)} = \sum_n \sum_j f_j(H)\, e^{2\pi i H\cdot(r_j+\varepsilon_{jn})} = \sum_j f_j(H)\, e^{2\pi i H\cdot r_j} \sum_n (1 + 2\pi i H\cdot\varepsilon_{jn} + \ldots)$$

If the ε_{jn}'s are small and/or if only low order reflections are used, the structure factor

$$[2] \quad F(H) = \sum_j f_j(H)\, e^{2\pi i H\cdot r_j}$$

is that corresponding to the average structure only. The "average" β′ structure was refined by difference synthesis and least squares refinement until the value of

$$R_2 = \left[\frac{(\sum\omega||F_o| - |F_c||)^2}{\sum\omega|F_o|^2}\right]^{\frac{1}{2}}$$

had reached a minimum for $Cd_3(PO_4)_2$ first. These coordinates were then used as those of the average structure of $\beta' Mn_3(PO_4)_2$. Refinement was continued until no further improvement in the agreement was noted. At this point R_2 was

Can. J. Chem. Downloaded from www.nrcresearchpress.com by 210.87.254.105 on 09/05/12
For personal use only.

0.2 but the PO_4^{3-} groups were unrealistically distorted and the isotropic temperature factors for the oxygen atoms ranged from moderate negative values to large positive values.

The values for the ε_{jn} were now determined. Since the average intensity of the $l \neq 0$ mod 3 reflections relative to that of the $l = 0$ mod 3 reflections was larger in β′$Mn_3(PO_4)_2$ than in β′$Cd_3(PO_4)_2$, the data of the former were used to obtain the trial structure for the proper unit cell.

The signs of 15 reflections of the type $h0l$ with $l \neq 0$ mod 3 were determined using inequality relationships amongst the unitary structure factors (11). Of these 15 signs, 13 were related to a parameter p, which could be + or −; the remaining two signs were predicted to be +, independent of the choice of sign for p.

Subsequent electron density sections were calculated in the region of the average cation positions using these 15 reflections for both $p = -$ and +. These sections were treated as though they were difference density maps, and the displacements, ε_{jn}, for the cations estimated from the density gradients at their average positions. Subsequent structure factor calculations using all the $h0l$ data yielded slightly better agreement for the choice $p = +$. The refinement was continued with the set of displacements resulting from this choice, but the $h1l$ data were excluded, so that it could be used as an independent check on the validity of the displacements at a later stage. Scattering factors were obtained from the International tables for X-ray crystallography (12).

The phosphorus and oxygen atoms were placed close to their average positions such that the PO_4^{3-} groups became regular tetrahedra and their coordinates refined by least squares. A full matrix least squares program, written by one of the authors (J.S.S.) for the I.B.M. 7040, was employed. The temperature factors were not varied during the initial stages, and approximate tetrahedral geometry was enforced on the phosphate groups by shifting the oxygen atoms radially to give P—O bond lengths of 1.54 Å whenever these distances departed by more than 0.05 Å from this value.

After several cycles of refinement, the $|F_c|$ (calculated structure factors), seemed to be too small for the $l \neq 0$ mod 3 reflections. The weighing scheme was changed from unit weights on all reflections to one where the weights of $l \neq 0$ mod 3 reflections were gradually reduced to 0.75 over several least squares cycles. The least squares residues, which had previously been 0.10 and 0.23 for the $l = 0$ mod 3 and $l \neq 0$ mod 3 data respectively, fell to 0.09 and 0.13.

The choice of $p = +$ was then confirmed by calculating structure factors for the unused $h1l$ data, first with the ε_{jn} just determined, and then with the inverse of these displacements. By eq. [2], this reversal is equivalent to changing the signs of the $l \neq 0$ mod 3 reflections while leaving the average structure unchanged. This latter calculation yielded very poor agreement between $|F_o|$ and $|F_c|$ while the original set of displacements gave a value for R_2 with $h1l$ data of 0.13 after a cycle of least squares. The choice of $p = +$ was then considered to be correct.

An additional three cycles of least squares refinement were carried out using all the data measured to this point, isotropic temperature factors for all the atoms, and with weights chosen, as suggested by Cruickshank *et al.* (13). The oxygen atoms were no longer shifted between cycles. Unobserved reflections were given zero weight if $|F_c| < |F_{min}|$, and $|F_o|$ the observed structure factor was taken as 0.85 $|F_{min}|$ when the calculated structure factor, $|F_c|$, exceeded the minimum observable structure factor $|F_{min}|$. Although the R value was 0.089 at this point, only 821 reflections out of 1289 recorded reflections were intense enough to be measured. Since there were 160 variables, including 4 scale constants, in the least squares refinement an honest skepticism concerning the validity of the structure could persist.

The intensity of the hnl ($n = 2, 3, 4, 5$) reflections were then measured by visual comparison from Weissenberg photographs taken with MoKα radiation. In addition, the intensities of the [10$\bar{3}$] zone again taken with MoKα radiation, were measured with a Joyce–Loebl densitometer from integrated precession photographs. This yielded an additional 2500 reflections of which 816 has measurable intensity. The amount of data now exceeded the mount conveniently handled by our IBM 7040 computer. Therefore, only those unobserved reflections whose $|F_c| > 0.85\ |F_{min}|$ on a previous refinement cycle were included in subsequent cycles. The final cycles used 1679 reflections with 177 positional parameters, 39 isotropic temperature factors, and 9 independent scale constants. Of this total about one-third were observed $l \neq 0$ mod 3 reflections.

TABLE II
Atomic parameters for $\beta'Mn_3(PO_4)_2$*

Atom	Coordinates			B(Å^2)
	x	y	z	
Mn(1A)	−0.0046(4)	0.0943(5)	0.05984(15)	0.68(6)
(1B)	0.0098(4)	0.0847(5)	0.71662(15)	0.71(6)
(1C)	−0.0068(4)	0.1061(5)	0.39303(15)	0.63(6)
Mn(2A)	0.2982(5)	0.3872(5)	0.07566(16)	0.82(6)
(2B)	0.2877(4)	0.3886(5)	0.74362(16)	0.78(6)
(2C)	0.3107(4)	0.3882(5)	0.41667(15)	0.65(6)
Mn(3A)	0.4036(4)	−0.2193(4)	0.14067(16)	0.66(6)
(3B)	0.3975(5)	−0.2038(5)	0.79645(16)	0.65(6)
(3C)	0.4127(5)	−0.2168(5)	0.45732(15)	0.67(6)
P(1A)	0.3610(8)	0.0557(8)	0.06056(25)	0.68(9)
(1B)	0.3696(7)	0.0688(8)	0.71873(24)	0.51(9)
(1C)	0.3609(8)	0.0753(8)	0.39423(26)	0.80(9)
P(2A)	0.1269(8)	−0.3523(8)	−0.00080(27)	0.73(9)
(2B)	0.1220(7)	−0.3672(7)	0.67189(25)	0.63(9)
(2C)	0.1398(8)	−0.3559(8)	0.33141(26)	0.78(9)
O(1A)	0.1675(21)	0.0205(20)	0.02095(71)	1.01(27)
(1B)	0.1727(20)	0.0336(20)	0.67531(67)	0.79(25)
(1C)	0.1694(20)	0.0294(19)	0.36052(47)	0.76(25)
O(2A)	0.1871(24)	−0.3521(22)	0.07176(82)	1.73(32)
(2B)	0.1377(22)	−0.4243(22)	0.73481(75)	1.49(31)
(2C)	0.1620(21)	−0.4312(21)	0.38906(71)	0.18(28)
O(3A)	0.4735(21)	−0.0677(20)	0.09654(68)	0.85(25)
(3B)	0.4780(19)	−0.0538(18)	0.75588(60)	0.34(22)
(3C)	0.4849(20)	−0.0397(19)	0.42906(66)	0.81(26)
O(4A)	0.2373(20)	−0.2617(20)	−0.01395(68)	0.83(26)
(4B)	0.2632(21)	−0.2566(20)	0.69071(72)	1.07(26)
(4C)	0.2718(21)	−0.2441(21)	0.35373(71)	0.98(28)
O(5A)	0.4268(21)	0.1083(20)	0.01677(70)	1.03(27)
(5B)	0.4419(22)	0.1185(21)	0.67696(73)	1.11(27)
(5C)	0.4006(23)	0.1363(21)	0.34536(77)	1.36(29)
O(6A)	0.1382(20)	−0.5019(20)	−0.01833(68)	0.88(25)
(6B)	0.1646(21)	−0.4832(20)	0.64126(72)	1.16(27)
(6C)	0.1730(23)	−0.4421(22)	0.28557(78)	0.63(31)
O(7A)	0.3876(21)	0.1720(20)	0.10796(71)	0.87(27)
(7B)	0.3837(23)	0.1829(20)	0.76378(73)	1.13(28)
(7C)	0.3862(20)	0.1841(19)	0.44181(68)	0.64(25)
O(8A)	−0.0562(20)	−0.2966(24)	−0.04244(78)	1.54(32)
(8B)	−0.0514(20)	−0.3047(20)	0.62517(69)	0.83(26)
(8C)	−0.0457(30)	−0.2927(27)	0.29481(99)	2.73(41)

*Estimated standard deviations in parentheses.

The weights were chosen as indicated above with ω given by $[30 + 0.25F_o + 0.0075F_o^2]^{-1}$. The measured structure factors of common reflections were averaged and randomly assigned to the possible scale constant groups. The final atomic parameters are listed in Table II, where the atoms are labelled with letters A, B, or C denoting the particular sub-cell to which they belong (n = 0, 1, or 2 respectively.) The final least square residues are $R = 0.096$ and $R_2 = 0.123$. The observed and calculated structure factors are found in Table III[2].

[2]Table III has been placed in the Depository of Unpublished Data. Photocopies may be obtained free of charge, upon request, from: Depository of Unpublished Data, National Science Library, National Research Council of Canada, Ottawa, Canada.

Description of the Structure

A strong similarity between the structures of $\beta'Mn_3(PO_4)_2$ and that of $\beta Zn_3(PO_4)_2$ has been noted. Therefore, the rather complex structure of $\beta'Mn_3(PO_4)_2$ will be described in terms of similarities and differences between these structures. Each phosphorus atom is surrounded, roughly tetrahedrally, by 4 oxygen atoms. The average value of the P—O bond distances is 1.54 Å with the value for any individual tetrahedra deviating by no more than 0.01 Å. These distances have not been corrected for the effects of thermal motion. The range of the phosphorus–oxygen bond distances about any phosphorus atom does not exceed 0.08 Å. Since the extremes lie within two standards of the mean values, the deviations of the tetrahedra from regularity do not appear

Can. J. Chem. Downloaded from www.nrcresearchpress.com by 210.87.254.105 on 09/05/12
For personal use only.

TABLE IV

(*a*) Bond distances in PO_4 tetrahedra in β′$Mn_3(PO_4)_2$*

Bonded atoms	Distance (Å)	Bonded atoms	Distance (Å)
P(1A)—O(1A)	1.53(2)	P(2A)—O(2A)	1.55(2)
P(1A)—O(3A)	1.55(2)	P(2A)—O(4A)	1.49(2)
P(1A)—O(5A)	1.54(2)	P(2A)—O(6A)	1.58(2)
P(1A)—O(7A)	1.56(2)	P(2A)—O(8A)	1.52(2)
P(1B)—O(1B)	1.56(2)	P(2B)—O(2B)	1.56(2)
P(1B)—O(3B)	1.55(2)	P(2B)—O(4B)	1.56(2)
P(1B)—O(5B)	1.53(2)	P(2B)—O(6B)	1.53(2)
P(1B)—O(7B)	1.54(2)	P(2B)—O(8B)	1.51(2)
P(1C)—O(1C)	1.54(2)	P(2C)—O(2C)	1.51(2)
P(1C)—O(3C)	1.52(2)	P(2C)—O(4C)	1.51(2)
P(1C)—O(5C)	1.52(2)	P(2C)—O(6C)	1.55(2)
P(1C)—O(7C)	1.52(2)	P(2C)—O(8C)	1.56(2)

(*b*) Bond angles in PO_4 tetrahedra in β′$Mn_3(PO_4)_2$

Bonded atoms	Angle (°)	Bonded atoms	Angle (°)
O(1A)—P(1A)—O(3A)	112	O(2A)—P(2A)—O(4A)	111
O(1A)—P(1A)—O(5A)	111	O(2A)—P(2A)—O(6A)	106
O(1A)—P(1A)—O(7A)	109	O(2A)—P(2A)—O(8A)	112
O(3A)—P(1A)—O(5A)	107	O(4A)—P(2A)—O(6A)	113
O(3A)—P(1A)—O(7A)	112	O(4A)—P(2A)—O(8A)	104
O(5A)—P(1A)—O(7A)	106	O(6A)—P(2A)—O(8A)	112
O(1B)—P(1B)—O(3B)	111	O(2B)—P(2B)—O(4B)	109
O(1B)—P(1B)—O(5B)	110	O(2B)—P(2B)—O(6B)	106
O(1B)—P(1B)—O(7B)	107	O(2B)—P(2B)—O(8B)	115
O(3B)—P(1B)—O(5B)	107	O(4B)—P(2B)—O(6B)	109
O(3B)—P(1B)—O(7B)	113	O(4B)—P(2B)—O(8B)	107
O(5B)—P(1B)—O(7B)	108	O(6B)—P(2B)—O(8B)	112
O(1C)—P(1C)—O(3C)	111	O(2C)—P(2C)—O(4C)	110
O(1C)—P(1C)—O(5C)	110	O(2C)—P(2C)—O(6C)	113
O(1C)—P(1C)—O(7C)	108	O(2C)—P(2C)—O(8C)	109
O(3C)—P(1C)—O(5C)	110	O(4C)—P(2C)—O(6B)	106
O(3C)—P(1C)—O(7C)	110	O(4C)—P(2C)—O(8B)	108
O(5C)—P(1C)—O(7C)	107	O(6C)—P(2C)—O(8B)	111

*Estimated standard deviations in parentheses.

significant by this criterion. On the other hand, the O—P—O bond angles, also found in Table IV, suggests that the tetrahedron about P(2) may be irregular.

These tetrahedra connect sheets of cation polyhedra extended parallel to the ($\bar{1}$13) plane with those related by the 2_1 axes extended parallel to the ($\bar{1}\bar{1}$3) plane. Although the major bonding between the oxygen atom polyhedra surrounding the cations lies in the sheet, there are some bonds involving shared oxygen atom between sheets often involving long cation–oxygen atom bond lengths. In β′$Mn_3(PO_4)_2$ these sheets, shown in Fig. 1, are composed of three sub-units each similar to the ($\bar{1}$11) planes in β$Zn_3(PO_4)_2$, seen in Fig. 2. In the latter case, this unit has a center of symmetry in the sheets while in β′$Mn_3(PO_4)_2$, two of the sub-units are related by the center of symmetry lying at the center of the third.

In the structure of β$Zn_3(PO_4)_2$ a pair of cations of type 1, related by a center of symmetry, share a common edge. These cations show four-fold coordination with oxygen atoms. A fifth oxygen atom, O(4), lies 2.55 Å from this cation. This group shares an oxygen atom, O(8), on each side with an edge-shared pair of five-fold coordinated Zn ions involving cations 2 and 3. These latter cations then share an oxygen atom with the centro-symmetrically related cation pair. Bonding between sheets is propagated through long cation–oxygen bonds, involving O(6) between Zn(2) and Zn(1), and O(4) between Zn(3) and Zn(1). In addition, there are strong bonds between sheets involving O(7), Zn(2), and Zn(3).

Can. J. Chem. Downloaded from www.nrcresearchpress.com by 210.87.254.105 on 09/05/12
For personal use only.

Can. J. Chem. Downloaded from www.nrcresearchpress.com by 210.87.254.105 on 09/05/12
For personal use only.

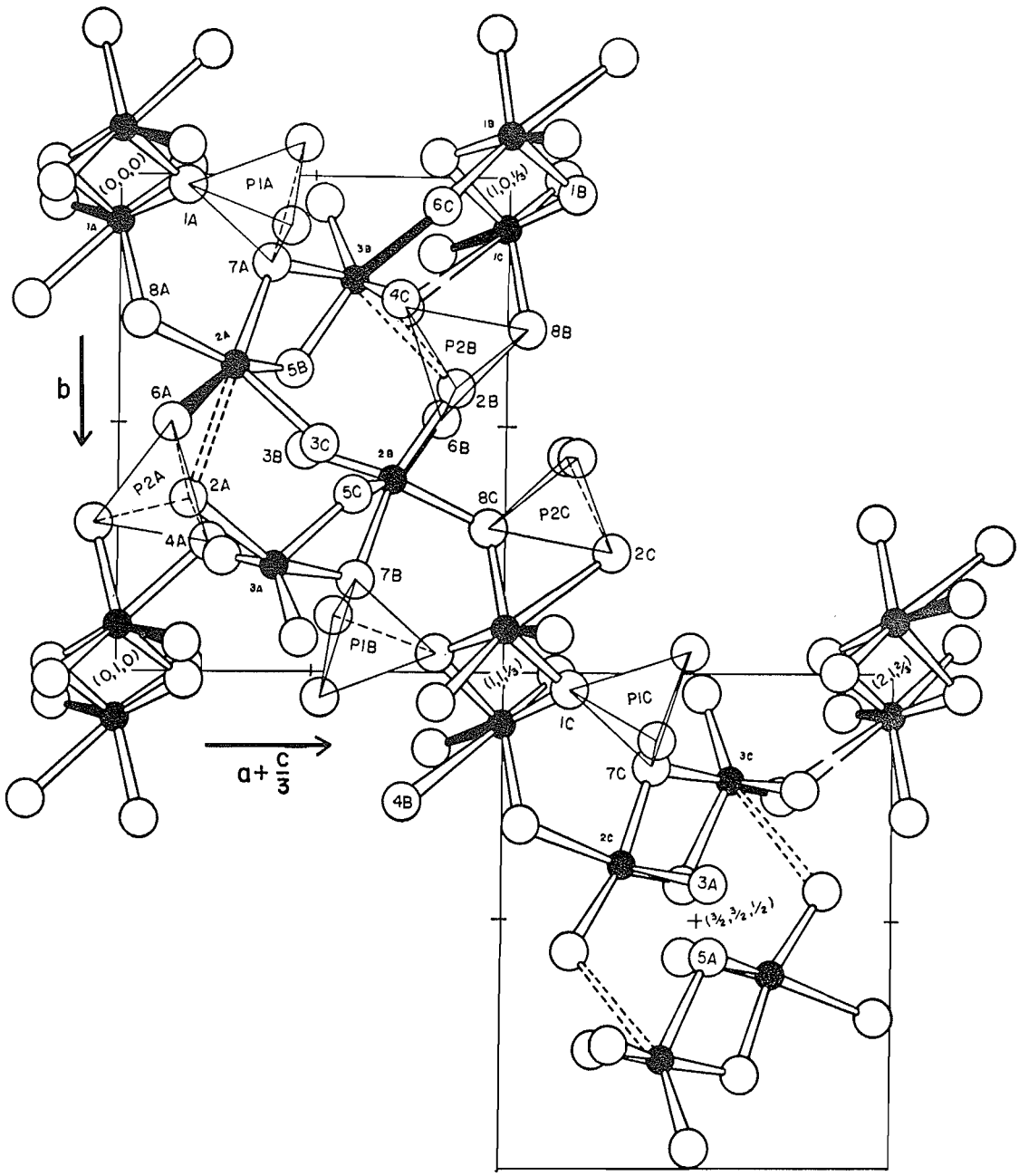

FIG. 1. The structure of $\beta'Mn_3(PO_4)_2$ near the $(\bar{1}13)$ plane is shown. The large open circles represent oxygen atoms while the filled ones depict the cations. The 4 oxygen atoms comprising the PO_4^{3-} tetrahedra are connected outlining this group. The filled bonds represent new bonds with respect to the $\beta Zn_3(PO_4)_2$ structure while the dotted bonds have been broken in comparison to that structure.

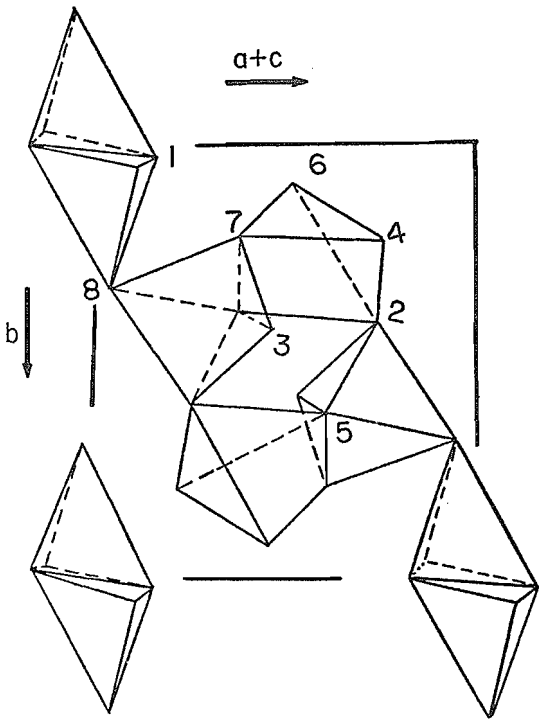

FIG. 2. The cation polyhedra in plane in $\beta Zn_3(PO_4)_2$ analogous to that of β′$Mn_3(PO_4)_2$ seen in Fig. 1 are shown. The oxygen atoms are labelled by analogy to that of β′$Mn_3(PO_4)_2$.

In β′$Mn_3(PO_4)_2$ each sub-unit consists of a pair of a polyhedra of oxygen atoms, each containing a cation of type 1, sharing an edge and lying at the corner of each of the reduced cells. This group then shares an oxygen atom, O(8), with the edge-shared polyhedral group containing cations 2 and 3. Cations 2 and 3 "share" a pair of oxygen atoms with a similar cation pair (3 and 2) but in this structure, in contrast to $\beta Zn_3(PO_4)_2$, these bonds are long. These bonds are shown dotted in Fig. 1.

We now turn to a detailed examination of the difference between the three sub-cells in β′$Mn_3(PO_4)_2$. All the cations show at least 5 acceptable Mn—O bonds. Mn(1A) has a sixth near neighbor oxygen atom, O(4A), at 2.45 Å; Mn(3B) has its sixth oxygen atom, O(6C) which lies 2.39 Å away; and Mn(2B) has its sixth neighbor, O(6B), at 2.49 Å from the cation. Each of the remaining cations, except Mn(2C), has a sixth oxygen atom within 3.0 Å of the cation but at distances greater than 2.6 Å. The detailed cation–oxygen atom bond lengths are compared with the analogous bonds in $\beta Zn_3(PO_4)_2$ in Table V. The average length of the 5 nearest Mn—O bonds, also included in Table V, shows values ranging from 2.13 to 2.19 Å.

Mn(1A) shares the O(1A) – O(1Ā′) edge across the center of symmetry at the origin. The cation–oxygen atom bond lengths about Mn(1A) range from 2.08 to 2.45 Å, with an average of 2.19 Å for the 5 shortest. The 4 shortest bond lengths involve the same oxygen atoms as in $\beta Zn_3(PO_4)_2$ while in each structure there is a long bond involving O(4). There are 5 short bonds about Mn(1B), with an average cation–oxygen atom bond length of 2.14 Å, while the sixth oxygen atom, O(4C), lies at 2.72 Å from the cation. Oxygen atoms O(1B) and O(1C) are shared between cation Mn(1B) and Mn(1C). The environment of Mn(1C) is similar to Mn(1B) with O(4B), the long sixth oxygen atom bond, lying at 2.62 Å. The five shorter cation–oxygen lengths range from 2.09 to 2.23Å with an average of 2.16 Å. All the individual cation–oxygen atom bond lengths about cation site 1 in the three sub-cells are insignificantly different except those to O(4). O(2), which lies more than 3.0 Å away from cation site 1 in $\beta Zn_3(PO_4)_2$, shows a modest deviation of ±0.08 Å from the average value of 2.23 Å in this structure.

In $\beta Zn_3(PO_4)_2$ cation site 2 shows five-fold coordination with an average Zn—O bond length of 2.09 Å and an additional oxygen atom, O(6), displaced by 2.51 Å from this cation. In β′$Mn_3(PO_4)_2$, Mn(2A) shows five-fold coordination with an average Mn—O bond length of 2.18 Å but the sixth oxygen atom, O(2A), is removed by 2.79 Å. Mn(2B) again has 5 strong bonds with an average value of 2.17 Å and a sixth, involving O(6), subtending a length of 2.49 Å. Oxygen atom, O(6C), lies more than 3.0 Å away from Mn(2C) and, therefore, this cation has only 5 cation–oxygen atom bonds. In both sub-cell B and C, O(2) forms a normal bond to the cation in contrast to the long bond in sub-cell A.

Of the three cation types, cation 3 shows the greatest variation in bonding amongst the sub-cells. Two of these cations, Mn(3A) and Mn(3C) clearly show five-fold coordination involving, however, oxygen atoms of different types. Mn(3B) has 5 bonds in the range 2.10 to 2.26 Å with the sixth, O(6C), at 2.39 Å. O(2B) lies more than 3 Å from this cation. O(6) lies about 2.96 Å from Mn(3A) while O(2A) is bonded normally

Can. J. Chem. Downloaded from www.nrcresearchpress.com by 210.87.254.105 on 09/05/12
For personal use only.

Can. J. Chem. Downloaded from www.nrcresearchpress.com by 210.87.254.105 on 09/05/12
For personal use only.

TABLE V

Cation–oxygen bond lengths in $\beta'Mn_3(PO_4)_2$ compared to $\beta Zn_3(PO_4)_2$*

Bonded atoms	Distance (Å)	Bonded atoms	Distance (Å)	Bonded atoms	Distance (Å)	Bonded atoms	Distance (Å)
Mn(1A)—O($\bar{1}$A)	2.08(2)	Mn(1B)—O($\bar{1}$C)	2.07(2)	Mn(1C)—O($\bar{1}$B)	2.09(2)	Zn(1)—O(1)	1.95
Mn(1A)—O(1A)	2.30(2)	Mn(1B)—O(1B)	2.21(2)	Mn(1C)—O(1C)	2.23(2)	Zn(1)—O(1)	2.11
Mn(1A)—O(6B′)	2.08(2)	Mn(1B)—O(6C′)	2.11(2)	Mn(1C)—O(6A′)	2.12(2)	Zn(1)—O(6)	1.89
Mn(1A)—O($\bar{8}$A)	2.20(2)	Mn(1B)—O($\bar{8}$C)	2.15(2)	Mn(1C)—O($\bar{8}$B)	2.16(2)	Zn(1)—O(8)	1.96
Mn(1A)—O($\bar{4}$A)†	2.45(2)	Mn(1B)—O($\bar{4}$C)†	2.72(2)	Mn(1C)—O($\bar{4}$B)†	2.62(2)	Zn(1)—O(4)	2.55
Mn(1A)—O($\bar{2}$C)	2.31(2)	Mn(1B)—O($\bar{2}$B′)	2.17(3)	Mn(1C)—O($\bar{2}$A′)	2.21(3)	Zn(1)—O(2)	—
<Mn(1A)—O>	2.19	<Mn(1B)—O>	2.14	<Mn(1C)—O>	2.16	<Zn(1)—O>	1.98
Mn(2A)—O(2A)†	2.78(2)	Mn(2B)—O(2B)	2.25(2)	Mn(2C)—O(2C)	2.14(2)	Zn(2)—O(2)	1.99
Mn(2A)—O(7A)	2.30(2)	Mn(2B)—O(7B)	2.19(2)	Mn(2C)—O(7C)	2.15(2)	Zn(2)—O(7)	2.02
Mn(2A)—O($\bar{8}$A)	2.09(2)	Mn(2B)—O($\bar{8}$C)	2.10(2)	Mn(2C)—O($\bar{8}$B)	2.17(2)	Zn(2)—O(8)	2.05
Mn(2A)—O(5B′)	2.10(2)	Mn(2B)—O(5C′)	2.14(2)	Mn(2C)—O(5A′)	2.08(2)	Zn(2)—O(5)	2.09
Mn(2A)—O($\bar{3}$C′)	2.13(2)	Mn(2B)—O($\bar{3}$B′)	2.16(2)	Mn(2C)—O($\bar{3}$A′)	2.16(2)	Zn(2)—O(3)	2.28
Mn(2A)—O(6A)	2.26(2)	Mn(2B)—O(6B)†	2.49(2)	Mn(2C)—O(6C)	—	Zn(2)—O(6)	2.51
<Mn(2A)—O>	2.18	<Mn(2B)—O>	2.17	<Mn(2C)—O>	2.13	<Zn(2)—O>	2.09
Mn(3A)—O(4B′)	2.16(2)	Mn(3B)—O(4C′)	2.24(2)	Mn(3C)—O(4A′)	2.03(2)	Zn(3)—O(4)	1.92
Mn(3A)—O(3A)	2.13(2)	Mn(3B)—O(3B)	2.10(2)	Mn(3C)—O(3C)	2.12(2)	Zn(3)—O(3)	2.00
Mn(3A)—O($\bar{5}$C′)	2.16(2)	Mn(3B)—O($\bar{5}$B′)	2.17(2)	Mn(3C)—O($\bar{5}$A′)	2.15(2)	Zn(3)—O(5)	2.01
Mn(3A)—O($\bar{2}$A)	2.23(2)	Mn(3B)—O(2B)	3.00(2)	Mn(3C)—O(2C)†	2.93(2)	Zn(3)—O(2)	2.17
Mn(3A)—O($\bar{7}$B)	2.14(2)	Mn(3B)—O($\bar{7}$A)	2.14(2)	Mn(3C)—O($\bar{7}$C)	2.19(1)	Zn(3)—O(7)	2.26
Mn(3A)—O(6B′)†	2.96(2)	Mn(3B)—O(6C′)†	2.39(2)	Mn(3C)—O(6A)	—	Zn(3)—O(6)	—
Mn(3A)—O(4A)	—	Mn(3B)—O(4B)	2.26(2)	Mn(3C)—O(4C)	2.16(2)	Zn(3)—O(4)	—
<Mn(3A)—O>	2.16	<Mn(3B)—O>	2.18	<Mn(3C)—O>	2.13	<Zn(3)—O>	2.08

*Estimated standard deviations in parentheses.
†Not included in average. Atoms X($\bar{n}$) and X(n') are derived from X(n) by the inversion and glide plane operations respectively.

TABLE VI

Atomic parameters of β′$Mn_3(PO_4)_2$ (For the $l = 0$ mod 3 data)*

Atom	Coordinates			$B(T)$
	x	y	z	
Mn(1)	−0.0013(5) [−0.0005]	0.0951(6) [0.0950]	0.1710(6) [0.1694]	1.05
Mn(2)	0.2989(5) [0.2989]	0.3877(5) [0.3880]	0.2359(6) [0.2359]	0.78
Mn(3)	0.4040(6) [0.4046]	−0.2121(5) [−0.2133]	0.3945(6) [0.3943]	1.14
P(1)	0.3642(9) [0.3638]	0.0673(9) [0.0671]	0.1720(10) [0.1736]	0.81
P(2)	0.1298(9) [0.1298]	−0.3579(9) [−0.3585]	0.0032(11) [0.0030]	0.95
O(1)	0.1696(26) [0.1701]	0.0329(24) [0.0292]	0.0550(29) [0.0564]	1.50
O(3)	0.4791(22) [0.4780]	−0.0537(21) [−0.0531]	0.2765(26) [0.2716]	0.77
O(5)	0.4220(25) [0.4239]	0.1207(25) [0.1215]	0.0366(29) [0.0389]	1.46
O(7)	0.3862(26) [0.3861]	0.1770(24) [0.1814]	0.3153(30) [0.3135]	1.02
O(2)	0.1645(35) [0.1609]	−0.4046(32) [−0.4033]	0.1946(39) [0.1956]	2.89
O(4)	0.2666(28) [0.2573]	−0.2518(27) [−0.2534]	0.0632(31) [0.0297]	1.63
O(6)	0.1577(35) [0.1591]	−0.4851(32) [−0.4756]	−0.0762(39) [−0.0703]	2.87
O(8)	−0.0529(25) [−0.0510]	−0.2936(24) [−0.2968]	−0.1220(28) [−0.1222]	1.39

*The average atomic coordinates of the final structure are enclosed in square brackets and the estimated standard deviations obtained the $l = 0$ mod 3 data.

at 2.25 Å and O(4A) is unbonded. In the case of Mn(3C), it is O(6A) which lies more than 3 Å from the cation while O(2C) lies 2.93 Å away. The average Mn(3)—O bonds are 2.16, 2.18, and 2.13 Å for sub-cells A, B, and C, respectively. In β$Zn_3(PO_4)_2$, O(6) and O(4) lie beyond the primary coordination sphere around cation 3.

In summary, Mn(1), in comparison with β$Zn_3(PO_4)_2$, takes O(2) as its fifth strong oxygen atom bond. Cation 2 retains O(7), O(8), O(5), and O(3) as strong bonds in all sub-cells. There are strong bonds to O(2) in two of the sub-cells. In the remaining sub-cell the fifth strong bond is formed with O(6). Cation 3 shows strong bonds to O(4), O(3), O(5), and O(7). In one sub-cell cation 3 retains the strong bond to O(2), analogous to β$Zn_3(PO_4)_2$. The remaining sub-cells adopt O(4), as the fifth strong bond.

The values of the ε_{jn}'s, the deviations from the average structure, are of some interest. Therefore, the final values of the atomic coordinates using only the $l = 0$ mod 3 reflections are tabulated in Table VI. From these the values of ε_{jn} can easily be obtained. The average parameters obtained from the final β′$Mn_3(PO_4)_2$ atomic parameters are also shown. These indicate that the two average values almost always differ insignificantly. They differ most for the y coordinates of O(7) and O(6), and the z coordinates of O(4).

Discussion

The mean P—O bond length at 1537 ± 0.005 Å agrees well with the accepted value for this bond in PO_4^{3-} groups. The temperature factors of the cations and the phosphorus atoms show modest variation. The mean value (1.03 $Å^2$) and the variation in these values for the oxygen atoms exceeds that of the cations, but there does not appear to be any correlation among those expected

Can. J. Chem. Downloaded from www.nrcresearchpress.com by 210.87.254.105 on 09/05/12
For personal use only.

Can. J. Chem. Downloaded from www.nrcresearchpress.com by 210.87.254.105 on 09/05/12
For personal use only.

to be sensitive to positional disorder. The standard deviations of these thermal parameters seem to be about 25% too small since 4 lie more than 2 standard deviations from the mean. This likely results from the lack of adsorption corrections.

The mean displacement of the cations, and P(1) from the positions determined from the $l = 0$ mod 3 reflections is about 0.1 Å while that of oxygen atoms about this phosphorus atom is about 0.2 Å. The displacements about P(2) are about twice as great. Although the major component of this displacement is along the c axis for the cations, this is not necessarily the case for the phosphorus and oxygen atoms. The largest displacement found, that of O(2A), is about 0.6 Å. An examination of Table V shows that it is exclusively the oxygen atoms about P(2) that are involved in the difference in bonding between the β and β′ structure and the sub units of the latter phase.

The studies of Pearson, Turkdogan, and Fenn (9) suggest, in agreement with the present studies, that the stable phase of $Mn_3(PO_4)_2$ at the melting temperature is the graftonite form since the density they report agrees with that of the mineral. The value for the density of $\beta'Mn_3(PO_4)_2$ is substantially larger, 3.92 g/cm^3 compared to graftonite 3.756 g/cm^3. Further, the value of specific volume versus composition in the range between $Mn_3(PO_4)_2$ and MnO is linear with MnO composition, suggesting that the graftonite phase remains stable down to the eutectic temperature of 1044 °C. The field stability of $\beta'Mn_3(PO_4)_2$ is unknown and the variables leading to the stability cannot be ascertained without a more careful study. Finally, $\beta'Cd_3(PO_4)_2$ shows a phase transformation at high temperatures apparently removing the superstructure, but $\beta Zn_3(PO_4)_2$ down to at least −100 °C does not manifest a superstructure. Whether $\beta'Mn_3(PO_4)_2$ shows a transformation analagous to $\beta'Cd_3(PO_4)_2$ is unknown.

It is difficult to avoid some remarks concerning the driving force which generates the superstructure of the β′ structure. Divalent Mn can be regarded as unstable if coordinated to less than 5 oxygen atoms and will seek higher coordination numbers if possible. Thus, $Mn_3(PO_4)_2$, in the hypothetical β structure, would distort in such a manner as to increase the coordination number of site 1 to at least 5. The most obvious mode, shortening of the cation 1 – O(4) bond length, is not favored since as a result this Mn would share an edge involving two strong oxygen atom bonds with the PO_4^{3-} about P(1). In fact, in both the $\beta Zn_3(PO_4)_2$ and $\beta'Mn_3(PO_4)_2$ structures when an edge is shared with a PO_4^{3-} group, one of the cation–oxygen atom bonds is significantly longer than normal. An apparently more favorable change involves the acquisition of O(2) by Mn(1) from the adjacent sheet. In order to tolerate this change, one of the strong bonds between this oxygen atom and a cation, either 2 or 3, is broken. Mn(2A) exchanges the weak bond to O(6A) and strong bond to (2A) of the β structure for a strong bond to O(6A) and a weak one to O(2A). Mn(2B) maintains the status quo while Mn(2C) ignores O(6C) entirely. The bond to O(2) in the latter two cases is broken at cation 3 i.e. Mn(3B) and Mn(3C). These latter cations complete their coordination requirements by bonding both O(4B) and O(6C) to Mn(3B) and only O(4C) to Mn(3C).

Although the assumption of the desire of Mn for coordination numbers of 5 or greater while not sharing an edge strongly with the PO_4^{3-} group yields a plausible explanation for the difference between the β and β′ structures, other structures can not easily be excluded. In particular, that of $Cu_3(AsO_4)_2$ (14) shows all 5 cation ligand bonds in sheets paralleling (100) planes. Further, one would hope to derive a justification for the superstructure rather than just a structure having the β phase unit cell dimensions but with a higher coordination number for Mn(1). In fact, an examination of the sub-cell about the center of symmetry at 3/2 3/2 1/2 in Fig. 1 shows that the requirements assumed to be desirable can be fulfilled with a structure with this sub-cell as the unit cell, provided that the Mn(1)—O(8) bond is made long while the Mn(1)—O(4) bond is assumed normal. Each cation would then show 5 strong bonds and avoid sharing a strongly bound edge with any phosphorus tetrahedra. Under these circumstances O(4) would be tightly bonded to three cations while O(6) would be bonded to only one. This can be regarded as unfavorable. Since there is no convenient way, under our assumptions, to bond O(6) to cation 3 it does not appear that one can easily find a β-like analogue of $Mn_3(PO_4)_2$.

In considering the role of the structure on the energy levels of Mn^{2+} in doped compounds such

as $\beta Zn_3(PO_4)_2$, one has to know the detailed environment of the impurity. The levels involved in transition near the visible range of the spectrum seem to be particularly sensitive to the "cubic" components of the electric field and these would be dominated by the near neighbors. Mn^{2+} in $\beta Zn_3(PO_4)_2$ will adopt an environment which will be a compromise between that found for the cation in the β′ structure and that in the β structure. It is not at all certain that this compromise will be dominated by the host lattice. Therefore, it cannot be concluded what will be the detailed environment of the Mn^{2+} in $\beta Zn_3(PO_4)_2$.

Acknowledgments

This work has been supported by a grant from the National Research Council of Canada and a Fellowship from the Ontario Government (to J.S.S.).

1. J. S. Stephens. Ph.D. Thesis, McMaster University, Hamilton, Ontario. 1967.
2. C. Calvo. Am. Mineralogist, **53**, 742 (1968).
3. R. C. Ropp, R. W. Mooney, and C. W. W. Hoffman. Anal. Chem. **33**, 1687 (1961).
4. J. S. Stephens and C. Calvo. Can. J. Chem. **45**, 2303 (1967).
5. C. Calvo and J. S. Stephens. Can. J. Chem. **46**, 903 (1968).
6. F. L. Katnack and F. A. Hummel. J. Electrochem. Soc. **105**, 125 (1958).
7. C. Calvo. Phys. Chem. Solids, **24**, 141 (1963).
8. J. J. Brown and F. A. Hummel. J. Electrochem. Soc. **110**, 1218 (1963).
9. J. Pearson, E. T. Turkdogan, and E. M. Fenn. J. Iron Steel Inst. **176**, 441 (1954).
10. D. J. Cromer and K. Herrington. J. Am. Chem. Soc. **77**, 4708 (1955).
11. M. M. Woolfson. Direct methods in crystallography. Oxford at the Clarendon Press, London. 1961.
12. International tables for X-ray crystallography. Vol. II. Kynoch Press, Birmingham, England. 1959.
13. D. W. J. Cruickshank, D. E. Pilling, A. Bujosa, F. M. Louell, and M. R. Truter. *In* Computing methods and the phase problem in X-ray crystal analysis. *Edited by* R. Pepinsky, J. B. Robertson, and J. C. Speakman. The Pergamon Press, Ltd., New York. 1961.
14. S. J. Poulsen and C. Calvo. Can. J. Chem. **46**, 917 (1968).

Can. J. Chem. Downloaded from www.nrcresearchpress.com by 210.87.254.105 on 09/05/12
For personal use only.

Can. J. Chem. Downloaded from www.nrcresearchpress.com by 210.87.254.105 on 09/05/12
For personal use only.

Electron paramagnetic resonance spectroscopic study of nitroxide radicals formed from oximes[1]

P. SMITH AND W. M. FOX
Department of Chemistry, Duke University, Durham, North Carolina 27706

Received September 13, 1968

The addition of hydroxyl radicals to each of the oximes, acetaldoxime, acetoxime, and 2,3-butanedione monoxime, has been studied by mixing titanous chloride, hydrogen peroxide, and the oxime in an aqueous continuous-flow system. In each case a β-hydroxy nitroxide (functional structure $\rangle C(OH)—NH—O\cdot$) is formed. In confirmation of these results, amino and hydroxymethyl radicals were added to the oximes using similar procedures to give in each case the radicals of functional structure $\rangle C(NH_2)—NH—O\cdot$ and $\rangle C(CH_2OH)—NH—O\cdot$, respectively. Attempts to add methyl radicals, prepared by the reaction between titanous chloride and *t*-butyl hydroperoxide, to these oximes gave no observable products save the methyl radicals. However, use of titanous chloride and peracetic acid gave results consistent with the addition of hydroxyl radicals. The addition of hydroxyl radicals to the oxime-*O*-methyl ethers of acetaldehyde and acetone gave radicals of functional structure $\rangle C(OH)—\dot{N}—O—CH_3$ ($|a_N|$, ca. 14 G; $|a_H^{OCH_3}|$, ca. 3 G) which have not previously been identified unambiguously. On the assumption that $|Q_N| = |Q_H^{NH}| = 23$ G in all these radicals, ρ_N^π has been calculated and used to obtain a value for $|Q_H^{OCH_3}|$ of ca. 11 G which is within the range of other estimates in the literature.

Canadian Journal of Chemistry, 47, 2227 (1969)

Introduction

The reaction between titanous chloride and hydrogen peroxide in the presence of an organic substrate within an aqueous flow system has been shown (1) to be an effective method for the generation of transient free radicals for the purpose of electron paramagnetic resonance (e.p.r.) observations. A number of investigations using this generative method have been reported already from this laboratory (2–6). The present investigation concerns an extension of this method to a range of simple oximes. All aliphatic oximes proved to be highly reactive and underwent hydroxyl-radical addition to the carbon of the C=N bond. The few aromatic oximes studied were unreactive. In addition, some of these substrates were successfully investigated with the use of other radical-generating methods similar to that involving titanous chloride and hydrogen peroxide.

The results obtained from this present investigation confirm and considerably extend those of a recent study of Adams (7) which came to our attention after this work was complete.

[1]This work was supported by National Science Foundation Grant GP 7534.

Experimental

The experimental arrangement and procedures were essentially as described before (5).

The acetaldoxime, acetoxime, and 2,3-butanedione monoxime were all Eastman White Label. The other substrates were prepared with the use of reagent-grade materials. Of these other substrates, the simple oximes examined were prepared by the reaction between hydroxylamine and the carbonyl compound in alkaline solution, following which they were recrystallized from methanol until satisfactory melting points were obtained. In addition, acetaldoxime-*O*-methyl ether and acetoxime-*O*-methyl ether were prepared by mixing the carbonyl compound with an equivalent amount of methoxyamine hydrochloride in alkaline solution, and were used without further purification.

The following reaction conditions were employed: total flow rate, 2–9 ml s^{-1}, divided equally between the two streams; the reaction temperature, 25 ± 2 °C; the titanous chloride concentration in the reducing stream, 0.01–0.005 *M*; the hydrogen peroxide concentration in the oxidizing stream, 0.05 *M*; unless otherwise stated, the only acid present was that originating in the Fischer (2–6) titanous chloride solution[2] used in making up the reducing stream; similarly, except where specified to the contrary, the oxime was included only in the oxidizing stream, its concentration being about 0.02 *M*. When it was hoped to add methyl radicals to the oxime, the above

[2]A typical analysis of this solution (20% titanium trichloride) provided by the supplier gives: titanous chloride, titanic chloride, zinc chloride, hydrochloric acid, and phosphoric acid, 20.0, 0–5.0, 15.6, 7–9, and 3 wt./wt. %, respectively.

Can. J. Chem. Downloaded from www.nrcresearchpress.com by 210.87.254.105 on 09/05/12
For personal use only.

conditions were modified so as to use as the oxidizing stream 0.1 *M* peracetic acid (1) (Pflatz and Bauer, Inc., 40% wt./wt. solution) or saturated *t*-butyl hydroperoxide (1, 6, 8–10) (Borden Chemical Co.) instead of 0.05 *M* hydrogen peroxide. When the addition of amino radicals was to be studied, the hydrogen peroxide in the oxidizing stream was replaced by hydroxylamine hydrochloride (11, 12) (Eastman White Label) at a concentration of 0.1 *M*. The reaction between titanous chloride and hydrogen peroxide was conducted with both reactant streams 25 v/v % with respect to methanol (Baker and Adamson reagent grade) when the addition of hydroxymethyl radicals, $\cdot CH_2OH$, was to be investigated (11). It was found that both sulfuric acid and titanous chloride broadened the lines of the radical spectra, and consequently the best results were obtained when their concentrations were kept as low as possible.

When Fenton's reagent (1, 13, 14) was used, the titanous chloride normally present in the reducing stream was omitted and, instead, this stream was made 0.01 *M* in ferrous sulfate (Fischer Certified Reagent) and 0.05 *M* in ethylenediamine tetra-acetic acid, EDTA (G. Frederick Smith Chemical Co.).

All *g* values were measured with the use of peroxylamine disulfonate, the maximum uncertainty of the results being ±0.0002. In most instances the method followed was that described before (5), where the peroxylamine disulfonate was dissolved in the oxidizing stream. However, when hydroxylamine hydrochloride and oxime were present in this stream, it was found that the peroxylamine disulfonate tended to be particularly unstable. Consequently, for those cases, it was preferable to omit the peroxylamine disulfonate from the oxidizing stream and to utilize instead a solution of the peroxylamine disulfonate within an external, thin-walled Pyrex capillary held to the side of the mix-and-flow cell (both methods give the same results).

Results

It was found that the reaction between titanous chloride, hydrogen peroxide, and acetoxime, $(CH_3)_2C{=}NOH$, with the use of the flow system, gave rise to a spectrum of four equally-spaced lines of relative intensity 1:2:2:1 separated by 13.3 G. This pattern of absorption is characteristic of equal coupling to a nitrogen nucleus and a proton, and the coupling constants are similar to those reported by Gutch and Waters (15) for hydroxylamine radicals (nitroxides) of functional structure

$$\rangle C{-}NH{-}O\cdot$$

produced by oxidation of the corresponding hydroxylamine. It is assumed that the basic reactions which took place may be represented (1) as follows

[1] $\quad Ti(III) + H_2O_2 \rightarrow Ti(IV) + OH^- + \cdot OH$

[2] $\cdot OH + (CH_3)_2C{=}N{-}OH \rightarrow (CH_3)_2C(OH){-}\dot{N}{-}OH$

[3] $(CH_3)_2C(OH){-}N{-}OH \rightarrow (CH_3)_2C(OH){-}NH{-}O\cdot$

1

although there is some question (16) about the mechanistic details of the titanous chloride – hydrogen peroxide radical-generating system. The titanous chloride and hydrogen peroxide react to give a hydroxyl radical which adds exclusively to the carbon of the C=N bond of the oxime. Addition of a hydroxyl radical to the nitrogen end of the double bond would have been expected to have given an iminoxy radical

[4] $(CH_3)_2C{=}N{-}OH + \cdot OH \rightarrow (CH_3)_2\dot{C}{-}N(OH)_2$

[5] $(CH_3)_2\dot{C}{-}N(OH)_2 \rightarrow (CH_3)_2\dot{C}{-}N{=}O + H_2O$

[6] $\quad (CH_3)_2\dot{C}{-}N{=}O \leftrightarrow (CH_3)_2C{=}N{-}O\cdot$

Iminoxy radicals have been well characterized by e.p.r. spectroscopy (17) but none was observed in this investigation.

The presence of the $(CH_3)_2C(OH)$— group in radical **1** is difficult to establish as none of the protons in this group interact appreciably with the unpaired electron. However, the addition of hydroxyl radicals to acetaldoxime, $CH_3CH{=}NOH$, should give rise to the radical $CH_3CH(OH)$-$NHO\cdot$ with an interacting β-CH proton[3]. Furthermore, amino radicals from the reaction between titanous chloride and hydroxylamine hydrochloride would be expected (11, 12) to give with acetoxime the radical $(CH_3)_2C(NH_2)NHO\cdot$. The nitrogen of the amino group in this radical would be expected to have an appreciable interaction (11) identifying the position of radical attack. Both of these species were readily detected and the expected splittings observed. It was felt that these results adequately confirmed the position of radical addition. A typical spectrum obtained by adding amino radicals to acetoxime is shown in Fig. 1.

The addition of hydroxyl radicals to 2,3-butanedione monoxime, $CH_3COC(=NOH)CH_3$, produced a spectrum consistent with the formation of the expected product $CH_3COC(CH_3)$-$(OH)NHO\cdot$. This spectrum was sufficiently intense for carbon-13 satellites ($a_{^{13}C}$ equal to 6.0 G) to be relatively easily observed. However, these satellite lines were not sufficiently well resolved

[3]The sites in radicals of this type are labelled with respect to the nitrogen atom, i.e.

$$\begin{matrix}\gamma & \beta & \alpha\end{matrix}$$
$$—C—C—NH—O\cdot$$

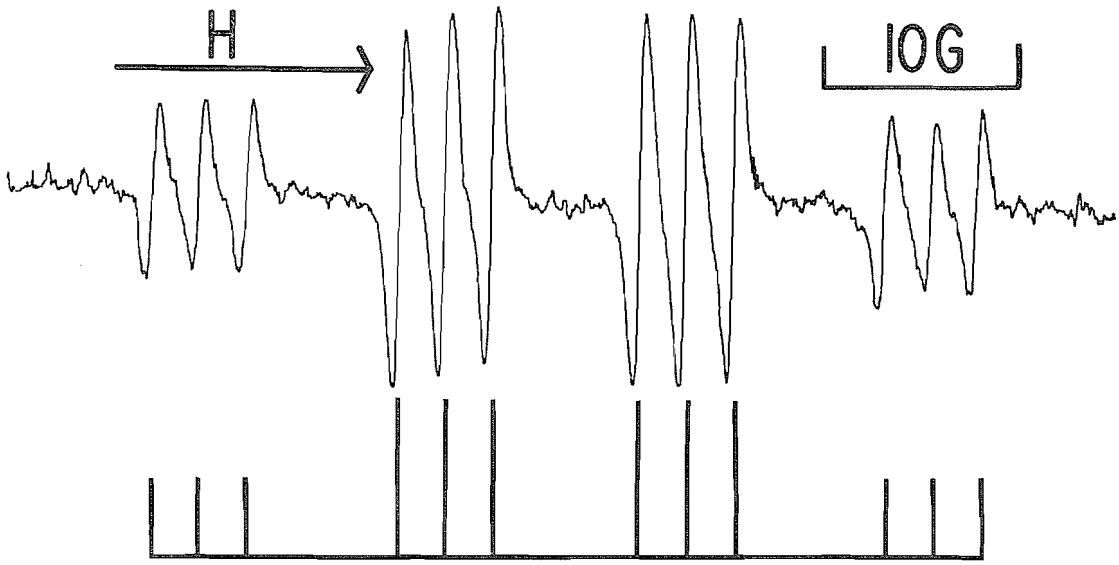

FIG. 1. First-derivative plot of the e.p.r. spectrum for the addition of amino radicals to acetoxime: temperature 25 °C; no sulfuric acid added to either stream; [$TiCl_3$] in the reducing stream, 0.005 *M*; [$NH_2OH{\cdot}HCl$] and [acetoxime] in the oxidizing stream, 0.1 and 0.02 *M*, respectively; total flow rate, 9.5 ml s^{-1} equally divided between both streams. The stick plot shows the positions and theoretical intensity distribution of the lines for the radical $(CH_3)_2C(NH_2)$—NH—O·, a quartet (1:2:2:1) of triplets (1:1:1).

for the number of interacting nuclei to be determined.

Hydroxyl radicals also added to the *O*-methyl ethers of acetoxime and acetaldoxime, $(CH_3)_2C{=}NOCH_3$ and $CH_3CH{=}NOCH_3$, respectively. In the former case, a rather broad-line spectrum (linewidth, between points of maximum slope, ca. 1.0–1.5 G) was observed, showing a 3.2 G interaction with a methyl group and a 13.7 G interaction with a nitrogen nucleus. No interaction was observed which could be due to a proton bonded directly to the nitrogen, hence the radical was thought to be $(CH_3)_2C(OH)$—$\dot{N}$—O—CH_3. A more clearly defined spectrum was obtained using acetaldoxime-*O*-methyl ether. It exhibited an interaction with the aldehyde CH-group proton in addition to the nitrogen and methyl-group proton hyperfine couplings, i.e., consistent with the expected structure, $CH_3CH(OH)$—$\dot{N}$—O—CH_3. Figure 2 shows a typical spectrum obtained by adding hydroxyl radicals to acetaldehyde-*O*-methyl ether.

The reaction between oximes, titanous chloride, and hydrogen peroxide in aqueous solutions 25 v/v % with respect to methanol did not produce the same radical as these reactants gave in the absence of methanol. The interacting nuclei were the same in the two cases but the magnitudes of the hyperfine couplings were different. The following reaction scheme is suggested by analogy with recent work (11) on vinyl compounds under comparable conditions

[1] $Ti(III) + H_2O_2 \rightarrow Ti(IV) + OH^- + {\cdot}OH$

[7] ${\cdot}OH + CH_3OH \rightarrow {\cdot}CH_2OH + H_2O$

[8] ${\cdot}CH_2OH + \rangle C{=}N{-}OH \rightarrow R_2C(CH_2OH){-}NH{-}O{\cdot}$

where $\rangle C{=}N{-}OH$ denotes the oxime.

Methyl-radical addition to oximes was investigated by mixing titanous chloride and either peracetic acid or *t*-butyl hydroperoxide in the presence of the three oximes, acetaldoxime, acetoxime, and 2,3-butanedione monoxime. Both these radical-generating systems produce two radicals by way of two-step reactions (1, 6, 8–10), viz.,

[9] $Ti(III) + CH_3CO(OOH) \rightarrow Ti(IV) + CH_3CO(O{\cdot}) + OH^-$

[10] $CH_3CO(O{\cdot}) \rightarrow {\cdot}CH_3 + CO_2$

or

[11] $Ti(III) + (CH_3)_3C{-}O{-}OH \rightarrow Ti(IV) + (CH_3)_3C{-}O{\cdot} + OH^-$

Can. J. Chem. Downloaded from www.nrcresearchpress.com by 210.87.254.105 on 09/05/12
For personal use only.

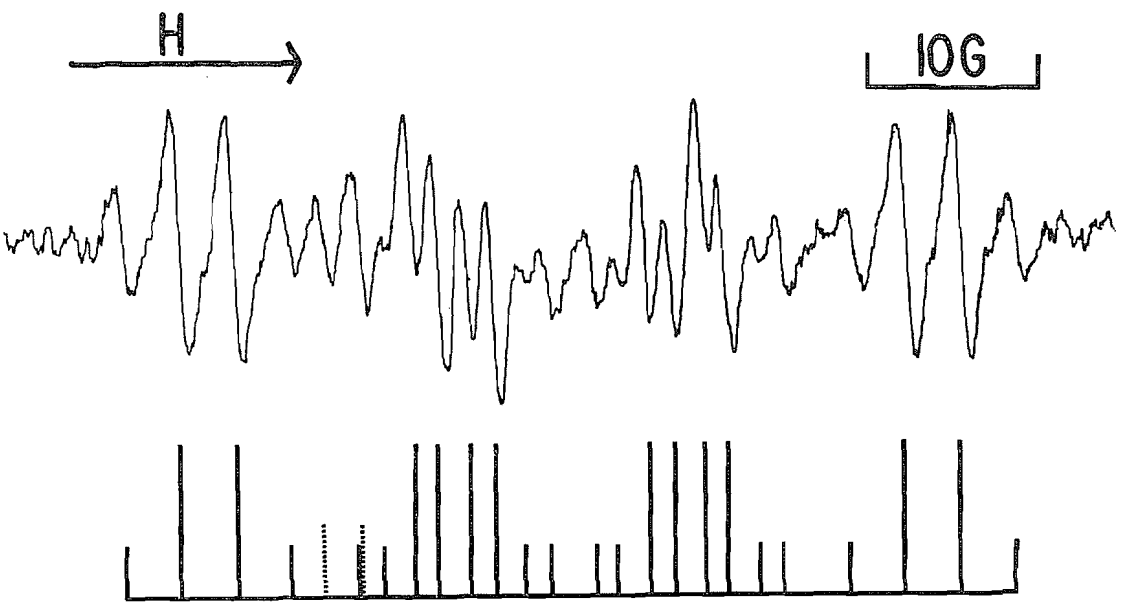

FIG. 2. First-derivative plot of the e.p.r. spectrum for the addition of hydroxyl radicals to acetaldoxime-*O*-methylether: temperature, 25 °C; no sulfuric acid added to either stream; [$TiCl_3$] in the reducing stream, 0.005 *M*; [H_2O_2] and [acetaldoxime-*O*-methylether] in the oxidizing stream, 0.05 and 0.02 *M*, respectively; total flow rate, 9.5 ml s^{-1} equally divided between both streams. The stick plot shows the positions and theoretical intensity distribution of the lines for the radical $CH_3CH(OH)—\dot{N}—O—CH_3$, a doublet (1:1) of triplets (1:1:1) of quartets (1:3:3:1); the two broken sticks indicate lines which arise from inorganic reaction products with *g* values estimated in this present work to equal about 2.0119 and 2.0132 (16).

[12] $(CH_3)_3C—O\cdot \rightarrow \cdot CH_3 + (CH_3)_2CO$

and, consequently, their use is attended by an element of ambiguity in that a suitably reactive substrate may perhaps react with the unstable radical precurser of the methyl radical, $(CH_3)_3CO(O\cdot)$ or $(CH_3)_3C—O\cdot$. No clear evidence for this sort of complication was found even in the case of the substrate acetaldoxime, for which such evidence might be the most easily discerned on account of the likely presence of an interacting β-CH group proton in the radicals expected from this substrate (see above). Another kind of complication was noticed, however. This appears to be the more relevant to the present work and hence it will be taken up in detail. In all instances where peracetic acid was used, the spectrum of the methyl radical was observed superimposed on a nitroxide spectrum of comparable intensity. It was found that the nitroxide radicals observed under these conditions had the same hyperfine interactions as the corresponding species formed by hydroxyl-radical addition with the use of the regular titanous chloride – hydrogen peroxide system. This may indicate that the radicals $\rangle C(OH)NHO\cdot$ and $\rangle C(CH_3)NHO\cdot$ formed by hydroxyl- and methyl-radical addition to oximes, happen to have the same magnetic properties. Alternatively, hydroxyl radicals may be formed from the hydrogen peroxide in equilibrium with the peracetic acid by way of the reaction

[13] $CH_3CO(OOH) + H_2O \leftrightharpoons CH_3CO(OH) + H_2O_2$

which has an equilibrium constant at 25 °C of ca. 4 (18), and the hydroxyl radicals so formed attack the oxime while the methyl radicals are relatively unreactive. In all cases where *t*-butyl hydroperoxide was used, the methyl-radical spectrum was observed but the nitroxide spectrum was absent. This suggests that methyl radicals are indeed relatively unreactive towards oximes, and that the radical formed in the presence of peracetic acid is the result of hydroxyl-radical addition.

The reaction between the ferrous–EDTA complex and hydrogen peroxide also gives rise to the $\rangle C(OH)NHO\cdot$ radical. No differences were observed between the splittings obtained with the use

Can. J. Chem. Downloaded from www.nrcresearchpress.com by 210.87.254.105 on 09/05/12
For personal use only.

TABLE I

Hyperfine coupling constants at 25 ± 2 °C for radicals formed from oximes

Radical	Coupling constants (G)*		
	$a_{N,H}^{NH}$†	$a_N^{NH_2}$	a_H^{CH}
$(CH_3)_2C(OH)NHO\cdot$	13.35‡	—	—
	13.28§	—	—
	(13.4)	—	—
$(CH_3)_2C(CH_2OH)NHO\cdot$	13.97	—	—
$(CH_3)_2C(NH_2)NHO\cdot$	12.40	2.3	—
$CH_3CH(OH)NHO\cdot$	13.13‡	—	8.95‡
	13.14§	—	8.92§
	(13.2)	—	(8.8)
$CH_3CH(CH_2OH)NHO\cdot$	13.69	—	10.33
$CH_3CH(NH_2)NHO\cdot$	12.27	2.9	9.20
$CH_2(OH)NHO\cdot$	(13.0)	—	(7.8) (CH_2)
$CH_3COC(CH_3)(OH)NHO\cdot$	12.65‡	—	†‖
	12.61§	—	—
$CH_3COC(CH_3)(CH_2OH)NHO\cdot$	13.14	—	—
$CH_3COC(CH_3)(NH_2)NHO\cdot$¶	11.90	2.6	—
$(CH_3)_2C(OH)\dot{N}OCH_3$	14.2‡**	—	3.1 (OCH_3)
$CH_3CH(OH)\dot{N}OCH_3$	13.7‡**	—	15.3 3.2 (OCH_3)

*Throughout this paper, signs of a and Q parameters are omitted. Of the a values from this present investigation and reported in this table, those cited to two decimal places have a maximum uncertainty of ca. 0.05 G and the rest have a maximum uncertainty of ca. 0.1 G. Numbers in parentheses are taken from ref. 7.

†$a_N^{NH} = a_H^{NH}$.

‡Obtained with the use of Ti(III) – H_2O_2; Fe(II) – EDTA – H_2O_2 gave the same result.

§Obtained with the use of Ti(III) – $CH_3CO(OOH)$.

‖$a_{^{13}C} = 6.0$ G.

¶This radical was prepared from $CH_3COC(CH_3)$=NOH in the presence of NH_2OH, and hence, may perhaps be derived from the corresponding dioxime, i.e., it may be $CH_3C(=NOH)$-$C(CH_3)(NH_2)NHO\cdot$.

**a_N only.

of this system and those found with the use of the titanous chloride – hydrogen peroxide system.

The reaction between titanous chloride and hydrogen peroxide was performed in the presence of two oximes having aromatic substituents (benzophenone oxime, $(C_6H_5)_2C$=NOH and benzaldoxime, C_6H_5CH=NOH) but no signals from free radicals derived from these oximes were observed. This suggests that conjugation with the aromatic ring reduces the reactivity of the oxime group towards hydroxyl-radical addition.

To summarize, hydroxyl, hydroxymethyl, and amino radicals were successfully added to all three oximes, acetaldoxime, acetoxime, and 2,3-butanedione monoxime, but attempts to add methyl radicals to these same oximes failed; hydroxyl radicals were successfully added to the oxime-*O*-methyl ethers of acetoxime and acetaldoxime, but attempts to add hydroxyl radicals to benzophenone oxime and benzaldoxime failed. Table I lists all the hyperfine coupling constants obtained.

The g values for the β-hydroxy and β-hydroxymethyl nitroxides were equal to 2.0059; those for the β-amino nitroxides were 2.0062. The g values for the radicals formed by hydroxyl-radical addition to the oxime-*O*-methyl ethers were found to be 2.0047. It can be seen that g values for disubstituted radicals of structure R—$\dot{N}$—O—CH_3, where R is a substituted alkyl group, are lower than those for monosubstituted radicals of structure R—NH—O·. The g values for the dialkyl nitroxides $(CH_3)_2$N—O· and $(C_2H_5)_2$N—O· have been recently reported (19) to be 2.0055 and 2.0054, respectively. These results also are less than those found in this present work for monosubstituted nitroxide radicals.

Discussion

Adams (7) has recently reported the results of an e.p.r. study of the radicals formed from formaldoxime, acetaldoxime, and acetoxime with the use of the chemical reaction of titanous chloride with hydrogen peroxide in dilute aqueous sulfuric acid solution within a continuous-flow system. These results show that hydroxyl radicals

Can. J. Chem. Downloaded from www.nrcresearchpress.com by 210.87.254.105 on 09/05/12
For personal use only.

add to the carbon end of the C=N bond in each case to give a β-hydroxy nitroxide radical and reveal the presence of hindered internal rotation about the C—N bond in these species

$$>C(OH)—NHO\cdot$$

The results in this present work partly overlap with, and considerably extend, those reported by Adams (7) and serve to confirm the identity of the radicals thought (7) to be formed by aliphatic oximes in this reaction system. In addition, in this present work the reactivity of aliphatic oximes has been investigated under other conditions and with other radicals (section I).

The addition of hydroxyl radicals to oxime-*O*-methyl ethers and the relevance of the products to the structure of other species are discussed in section II, while the estimation of spin densities from isotropic hyperfine splittings is considered in section III.

I. The Specificity of Radical Attack on Oximes

Shiga and co-workers (13, 14) have compared the reactivity of Fenton's reagent and the titanous chloride – hydrogen peroxide system to a variety of organic substrates. They conclude that in most cases the two systems give rise to a different distribution of products. In the present work these two systems are found to give the same products in the presence of an oxime; however, this possibly reflects only the favorability of producing a nitroxide from an oxime, but does not necessarily prove that it was formed by the same reaction in both cases.

Adams (7) has suggested that, in the case of the titanous chloride – hydrogen peroxide system, the specificity of hydroxyl-radical addition is due to the protonation of the nitrogen atom of the C=N bond of the oxime. In a similar fashion with this same radical-generating system, the protonation of the nitrogen atom of the amino group of a saturated aliphatic amine deactivates the amine with respect to hydrogen-atom abstraction (20). Attempts to confirm this were made with the use of the ferrous – EDTA – hydrogen peroxide system. In these attempts the oxime was included only in the reducing stream and this stream was made progressively less acidic and eventually alkaline by addition of reagent grade sodium hydroxide. Thus, the deprotonated oxime should be attacked when the oxidizing stream containing the hydrogen peroxide is mixed with the reducing stream. The only noticeable effect was to reduce the intensity of the β-hydroxy nitroxide spectrum until it finally disappeared when the mixed streams were of pH 8–9.

The radicals $\cdot OH$, $\cdot NH_2$, $\cdot CH_2OH$, and $\cdot CH_3$ were prepared in the presence of the aliphatic oximes (see Table I) and all except the methyl radical seemed to react[4]. The low reactivity of methyl radicals with respect to addition to a C=N bond under these conditions is paralleled by the work of Smith and Wood (6) on radical attack on allyl alcohol under reaction conditions similar to those of the present investigation. In this latter work (6), with the use of the titanous chloride – hydrogen peroxide system, the two species formed by addition of hydroxyl radicals to either end of the C=C bond of the allyl alcohol were more readily observed than that formed by hydrogen-atom abstraction from the 1 position, viz. the allylic radical CH_2-$=CH\dot{C}HOH$. But the reverse was true with the use of the titanous chloride – *t*-butyl hydroperoxide system, i.e. the allylic radical was the chief radical product observed. Further support for the idea that methyl-radical addition by way of the titanous chloride – *t*-butyl hydroperoxide system is less effective than hydroxyl-radical addition by way of the titanous chloride – hydrogen peroxide system is provided by recent studies with the use of these systems and the substrate acrylic acid (10). These show that methyl-radical addition is more selective than hydroxyl-radical addition. At present, it seems hardly worthwhile to speculate here on the reasons for the differences in the effectiveness of these two radical-generating systems until more is known about their reaction kinetics and mechanisms (8, 16)[5] and the factors which determine the orientation of free-radical addition to double bonds (23). Similar considerations apply to the other radical-generating systems where related questions arise.

[4]For the sake of simplicity of language, this statement and similar ones elsewhere in the text rest on the assumption that the operating mechanism of the Ti(III) – H_2O_2 system is as represented in eqs. [1]–[3]. A similar comment applies to the other radical-generating systems employed.

[5]A complication worth consideration in the case of the titanous chloride – *t*-butyl hydroperoxide system stems from formation of the *t*-butoxyl radical, $(CH_3)_3CO\cdot$, as a precursor of the methyl radical (see eqs. [11] and [12]). This radical is particularly effective in hydrogen-atom abstraction processes (21, 22).

Can. J. Chem. Downloaded from www.nrcresearchpress.com by 210.87.254.105 on 09/05/12
For personal use only.

Can. J. Chem. Downloaded from www.nrcresearchpress.com by 210.87.254.105 on 09/05/12
For personal use only.

II. Radicals Formulated as R—Ṅ—O—R′

The azobisisobutyronitrile-initiated oxidation of liquid aniline (24) has been shown to give a stable radical which was thought to be a time average of the structures C_6H_5—Ṅ—O—H and C_6H_5—NH—O·. Subsequently, this species has been prepared in aqueous solution by reduction of nitrosobenzene with sodium dithionite (25) and by the oxidation of *N*-phenyl hydroxylamine and triphenylhydrazine (26), and the radical was assigned the structure C_6H_5—Ṅ—O—H (25, 26). Russell and co-workers (27) have suggested that a more likely general structure is

[14] 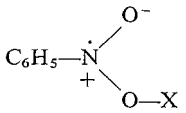

2

where X is an unspecified group.

Until now no radical of the type R—Ṅ—O—R′, where R and R′ are hydrocarbon or substituted hydrocarbon groups, has been prepared, and hence, it has been difficult to predict the magnetic properties of C_6H_5—Ṅ—O—H. However, assuming $(CH_3)_2C(OH)$—Ṅ—O—CH_3 has magnetic properties similar to those of $(CH_3)_2C(OH)$—Ṅ—O—H, we are able in this present work to assess the properties of R—Ṅ—O—H radicals.

The results of this present investigation show that

(*a*) radicals of the type R—Ṅ—O—R′ do exist even in acid solution and are not observed as the protonated species R—$\dot{N}\overset{+}{H}$—O—R′,

(*b*) the nitrogen hyperfine splittings of R—NH—O·, R—Ṅ—O—R′, and hence probably R—Ṅ—O—H, are very similar, and

(*c*) as R—Ṅ—O—CH_3 shows a methyl-group proton hyperfine interaction of 3.2 G, so R—Ṅ—O—H should also possess a hydroxyl-proton splitting of approximately the same value. None is observed in the spectrum attributed (25, 26) to C_6H_5—Ṅ—O—H, although the resolution is sufficient to reveal the 0.9 G interaction of the *meta*-protons in the phenyl group. Of these three observations, the first two suggest that it is possible for the radical observed (24–26) by earlier workers to be C_6H_5—Ṅ—O—H. The third observation suggests that it is not.

It should be possible to distinguish between C_6H_5—Ṅ—O—H and $C_6H_5\dot{N}O_2X$ (**2**) purely on the magnetic properties resulting from restricted rotation about the C—N bond. Both the nitrosobenzene radical anion, $C_6H_5NO^-$, and C_6H_5—NH—O· exhibit this restricted rotation (27, 28) which holds the —NO group and the benzene ring coplanar for a time longer than ca. 10^{-6} s for the former, or for a time comparable to 10^{-6} s for the latter. This results in unsymmetrical coupling to the protons of the benzene ring. Thus, the two *ortho* protons have hyperfine couplings which differ by 0.3 G or more depending on the solvent. Protonation of the oxygen should not obliterate either the restricted rotation or the assymetry of the hyperfine couplings of the protons in the benzene ring. This has been confirmed experimentally, for example, in the case of the benzaldehyde radical anion, $C_6H_5CHO^-$ (29), and $C_6H_5\dot{C}HOH$ (30). In contrast, $C_6H_5\dot{N}O_2X$ would be expected to show symmetrical couplings to the protons in the benzene ring by analogy with the recently reported results for similar radicals (31).

III. Q-Parameter Values for the Isotropic Interaction of Protons in N—H and N—CH_3 Groups

Attempts to relate the spin-density distribution in an organic radical to the observed hyperfine interactions using predictable constants have been made on several levels of sophistication. The Karplus and Fraenkel equation (32) assumes that the isotropic hyperfine coupling constant of a nucleus results from the polarization of electron pairs by spin density in an orbital on that nucleus and also in orbitals on adjacent nuclei. The equation was first proposed to account for the isotropic hyperfine interaction of an sp^2-hybridized carbon atom that is bonded to three other atoms and was used with some success (32, 33). However, attempts to extend its use to nitrogen-containing radicals have been less profitable, and no unique, universally acceptable set of ρ–π or Q parameters has emerged (34–36). The equation yields self-consistent parameters for a series of closely related radicals, but it has been suggested that the greater variations of charge and hybridization of nitrogen compared with carbon in organic radicals prevents simple correlation between different series. Thus, no attempt was made to use this equation to estimate the spin-density

TABLE II

Hyperfine coupling constants and Q parameters for nitrogen and hydrogen nuclei in N—H groups in a representative selection of radicals

Radical	a_N (G)	a_H^{NH} (G)	a_N/a_H^{NH}	Q_N (G)	Q_H^{NH} (G)	Reference
$CH(NH_2)COOH$	6.3	5.4	1.17	—	—	*
$H_2NO\cdot$	11.9	11.9	1.00	—	—	(34)
$[H_2NNH_2]^+\cdot$	11.5	11.0	1.05	23	22	(39)
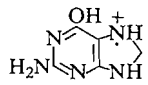	8.0	8	1	21	21	(40)†
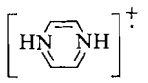	7.60 7.40	8.30 7.94	0.92 0.93	33 32	36 34	(41) (42)
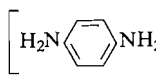	5.29	5.88	0.90	22	25	(43)
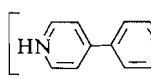	3.54 3.56	4.00 4.06	0.89 0.88	22 32	25 34	(44) (42)
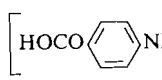	7.8	9.6	0.81	—	—	(45)
$C_6H_5NHO\cdot$	8.89	11.7	0.76	—	—	(27)
$[\cdot NH_3]^+$	19.5	25.9	0.75	20	26	(46)
$NH_2CONHO\cdot$	8.3	12.1	0.68	20	30	(47)†
$CH_3CH_2OCONHO\cdot$	7.0	11.1	0.63	—	—	(15)
$C_6H_5CONHO\cdot$	6.10	10.40	0.59	—	—	(48)
$2,4,6\text{-}(t\text{-}C_4H_9)_3C_6H_2\dot{N}H$	6.83	11.98	0.57	—	—	(49)
$CCl_3CONHO\cdot$	5.00	9.95	0.50	—	—	(48)

*W. M. Fox, D. J. McGinty, P. Smith, and P. B. Wood, unpublished results obtained with the use of glycine and Ti(III) – H_2O_2 at 25 °C.
†The data refer to the α-NH group.

distribution in the nitroxide radicals presented here.

A more simple approach postulates that the proton hyperfine interaction of a proton or of a methyl group bonded to an sp^2-hybridized carbon, a_H^{CH} or $a_H^{CCH_3}$, respectively, is an indication of the spin density in the $2p_z$ orbital on that carbon, ρ_C^π, using eq. [15] or [16]

$$[15] \qquad a_H^{CH} = Q_H^{CH}\rho_C^\pi$$

$$[16] \qquad a_H^{CCH_3} = Q_H^{CCH_3}\rho_C^\pi$$

However, even here there is uncertainty as to which of the two ρ–π parameters, Q_H^{CH} or $Q_H^{CCH_3}$, if either, has a generally applicable value. Fessenden and Schuler (37) have estimated a value of $Q_H^{CCH_3}$ equal to 29.3 G from a study of a series of alkyl radicals and suggested that this parameter is more likely than Q_H^{CH} to be a universal constant. Fischer (38) has shown that, if this is true, Q_H^{CH} is strongly dependent upon the substituents at the trigonal carbon atom in aliphatic radicals. His values of Q_H^{CH} varied between 18.3 and 26.2 G. Consequently, it may be possible to determine the spin density on a nitrogen atom in an organic radical in an analogous fashion from any of the following equations

$$[17] \qquad a_H^{NH} = Q_H^{NH}\rho_N^\pi$$

$$[18] \qquad a_H^{NCH_3} = Q_H^{NCH_3}\rho_N^\pi$$

$$[19] \qquad a_N = Q_N\rho_N^\pi$$

Tables II and III give representative data for radicals bearing N—H and N—CH_3 groups. These data show that the ratios a_N/a_H^{NH} and $a_N/a_H^{NCH_3}$ vary considerably between different types of radical or even within an apparently similar group of radicals, e.g., radicals containing functional groups —NHO· or —CONHO·. Thus, all three equations cannot be valid simultaneously. Furthermore, the few estimates for the three Q values in eqs. [17]–[19] given in Tables II and III suggest that these too, vary appreciably (Q_N, 20–35 G; Q_H^{NH}, 21–36 G; $Q_H^{NCH_3}$, 20–36 G).

Can. J. Chem. Downloaded from www.nrcresearchpress.com by 210.87.254.105 on 09/05/12
For personal use only.

TABLE III

Hyperfine coupling constants and Q parameters for nitrogen and hydrogen nuclei in N—CH_3 groups in a representative selection of radicals

Radical	a_N (G)	$a_H^{CH_3}$ (G)	$a_N/a_H^{CH_3}$	Q_N (G)	$Q_H^{NCH_3}$ (G)	Reference
$(CH_3)_2NO\cdot$	15.2	12.3	1.24	25*	20*	(34)
	17.1	14.6	1.17	—	—	(19)
$C_6H_5N(CH_3)O\cdot$	11.0	10.4	1.06	—	—	(51)
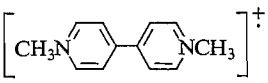	4.23	3.99	1.06	26	25	(44)
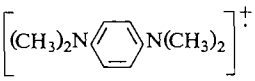	6.99	6.76	1.03	—	—	(52)
$[\cdot N(CH_3)_3]^+$	27.5	27.8	0.99	35†	36†	(53)
	18.0	26.7	0.67	24†	34†	(54)
$(^-OCO)N(CH_3)O\cdot$	10.8	11.3	0.96	—	—	(15)
$CH_3CH_2OCON(CH_3)O\cdot$	9.1	10.1	0.90	—	—	(15)
$C_6H_5CON(CH_3)O\cdot$	7.67	8.57	0.88	—	—	‡
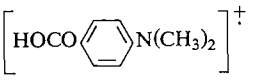	10.8	12.7	0.85	—	—	(45)

*For di-*t*-butyl nitroxide a_N has been reported (50*a*) to equal 15.4 G and sufficient anisotropic hyperfine coupling constant data are presented (50*a*) to enable ρ_N^π to be calculated. The value of ρ_N^π obtained is ca. 0.61 and is based on the assumption that unit spin density in a $2p_z$ orbital on nitrogen gives an interaction of ca. 17 G (50*b*). This information and the assumption that $a_N((CH_3)_2NO\cdot)$: $a_N((t\text{-}C_4H_9)_2NO\cdot)$ equals $\rho_N^\pi((CH_3)_2NO\cdot)$: $\rho_N^\pi((t\text{-}C_4H_9)_2NO\cdot)$ lead to an estimate for $\rho_N^\pi((CH_3)_2NO\cdot)$ of ca. 0.60 from which the Q values of this present work were deduced.

†Calculated in this present work on the assumption, analogous to that originally made in the case of alkyl radicals (37), that each α-methyl group removes 8.1% of the unpaired spin density from the $2p_z$ orbital of the adjacent unsaturated nucleus, i.e., ρ_N^π equals 0.776.

‡This radical was prepared at 25 °C from $C_6H_5CON(CH_3)OH$ with the use of aqueous ceric ammonium sulfate ca. 0.1 *M* with respect to sulfuric acid and the procedures are described in the main text. The $C_6H_5CON(CH_3)OH$ was prepared from $C_6H_5COOC_2H_5$ and CH_3NHOH (48).

Since there appears to be no simple generally applicable method of determining the spin density on nitrogen in the nitroxides discussed in this paper, it was thought that the most appropriate method was to choose values of Q_H^{NH} and Q_N and assume the validity of eqs. [17] and [19] for this limited range of radicals. The values $Q_N = Q_H^{NH} = 23$ G derived from the hydrazine radical cation, $[NH_2NH_2]^+$ (39), have been chosen because of the similarity between the hyperfine interactions of this radical and those of the simplest nitroxide radical $NH_2O\cdot$ (34). Both of the above radicals and the monoalkyl nitroxides, $RNHO\cdot$ (15, 32), are unusual in that their nitrogen and proton hyperfine interactions are about equal (see Tables I and II).

The values of ρ_N^π obtained in this way for the radicals listed in Table I vary between 0.62 for $(CH_3)_2C(OH)\dot{N}OCH_3$ and 0.52 for $CH_3COCCH_3(NH_2)\dot{N}HO\cdot$. The value of ρ_N^π equal to 0.62 for $(CH_3)_2C(OH)\dot{N}OCH_3$ would indicate ρ_O^π to be between 0.25 and 0.35, by analogy with work on alkyl radicals (37) which suggests that an α-alkyl group withdraws about 8% of the unpaired spin density from the $2p_z$ orbital of the adjacent unsaturated carbon atom. Hence, a value of $Q_H^{OCH_3}$ equal to 12.4–8.9 G can be estimated. If the highest value of Q_N given in Tables II and III, viz., 35 G, is used, the apparent spin density on oxygen increases and $Q_H^{OCH_3}$ decreases to between 5.5 and 6.7 G. The coupling constant data for $CH_3CH(OH)\dot{N}OCH_3$ are similar to those for $(CH_3)_2C(OH)\dot{N}OCH_4$ and yield estimates of $Q_H^{OCH_3}$ of about the same size. Values of $Q_H^{OCH_3}$ found by other workers vary between 5.6 and 19 G, while values of Q_H^{OH} are in the range 7 to 21 G (55–57).

Acknowledgment

The hydrogen peroxide used in this work was kindly provided by the Food Machinery and Chemical Corporation, Becco Chemical Division.

1. W. T. Dixon and R. O. C. Norman. J. Chem. Soc. 3119 (1963).
2. J. T. Pearson, P. Smith, and T. C. Smith. Can. J. Chem. **42**, 2022 (1964).
3. P. Smith, J. T. Pearson, P. B. Wood, and T. C. Smith. J. Chem. Phys. **43**, 1535 (1965).

Can. J. Chem. Downloaded from www.nrcresearchpress.com by 210.87.254.105 on 09/05/12
For personal use only.

4. P. SMITH, J. T. PEARSON, and R. V. TSINA. Can. J. Chem. **44**, 753 (1966).
5. P. SMITH and P. B. WOOD. Can. J. Chem. **44**, 3085 (1966).
6. P. SMITH and P. B. WOOD. Can. J. Chem. **45**, 649 (1967).
7. J. Q. ADAMS. J. Am. Chem. Soc. **89**, 6022 (1967).
8. M. F. R. MULCAHY, J. R. STEVEN, and J. C. WARD. Australian J. Chem. **18**, 1177 (1965).
9. H. FISCHER. Makromol. Chem. **98**, 179 (1966).
10. H. FISCHER and G. GIACOMETTI. J. Polymer Sci. Part C, **16**, 2763 (1967).
11. C. CORVAJA, H. FISCHER, and G. GIACOMETTI. Z. Phys. Chem. Frankfurt am Main, **45**, 1 (1965).
12. W. E. GRIFFITHS, G. F. LONGSTER, J. MYATT, and P. F. TODD. J. Chem. Soc. B, 3119 (1967).
13. T. SHIGA. J. Phys. Chem. **69**, 3805 (1965).
14. T. SHIGA, A. BOUKHORS, and P. DOUZOU. J. Phys. Chem. **71**, 3559 (1967); **71**, 4264 (1967).
15. C. J. W. GUTCH and W. A. WATERS. J. Chem. Soc. 751 (1965).
16. H. FISCHER. Ber. **71**, 685 (1967); K. TAKAKURA and B. RÅNBY. J. Phys. Chem. **72**, 164 (1968); R. O. C. NORMAN. Proc. Roy. Soc. London, Ser. A, **302**, 315 (1968).
17. R. O. C. NORMAN and B. C. GILBERT. J. Phys. Chem. **71**, 14 (1967).
18. J. A. JOHN and F. J. WEYMOUTH. Chem. Ind. London, 62 (1962).
19. R. E. FLORIN. J. Chem. Phys. **47**, 345 (1967).
20. W. T. DIXON, R. O. C. NORMAN, and A. L. BULEY. J. Chem. Soc. 3625 (1964).
21. C. WALLING. Pure Appl. Chem. **15**, 69 (1967).
22. P. GRAY, R. SHAW, and J. C. J. THYNNE. Progr. Reaction Kinetics, **4**, 63 (1967).
23. J. M. TEDDER and J. C. WALTON. Progr. Reaction Kinetics, **4**, 37 (1967).
24. J. C. BAIRD and J. R. THOMAS. J. Chem. Phys. **35**, 1507 (1961).
25. P. B. AYSCOUGH, F. P. SARGENT, and R. WILSON. J. Chem. Soc. B, 903 (1966).
26. K. MARUYAMA, T. OTSUKI, and T. IWAO. J. Org. Chem. **32**, 82 (1967).
27. G. A. RUSSELL, E. J. GEELS, F. J. SMENTOWSKI, K.-Y. CHANG, J. REYNOLDS, and G. KAUPP. J. Am. Chem. Soc. **89**, 3821 (1967).
28. TH. A. J. W. WAJER, A. MACKOR, TH. J. DE BOER, and J. D. W. VAN VOORST. Tetrahedron Letters, 1941 (1967).
29. N. STEINBERGER and G. K. FRAENKEL. J. Chem. Phys. **40**, 723 (1964).
30. H. FISCHER. Z. Naturforsch. **20A**, 488 (1965).
31. D. J. COWLEY and L. H. SUTCLIFFE. Chem. Commun. 201 (1968).
32. M. KARPLUS and G. K. FRAENKEL. J. Chem. Phys. **35**, 1312 (1961).
33. M. K. CARTER and G. VINCOW. J. Chem. Phys. **47** 308 (1967).
34. J. Q. ADAMS, S. W. NICKSIC, and J. R. THOMAS. J. Chem. Phys. **45**, 654 (1966).
35. J. M. GROSS and M. C. R. SYMONS. J. Chem. Soc. A, 451 (1966).
36. G. A. RUSSELL, J. MCDONNELL, and C. MYERS. J. Phys. Chem. **72**, 1386 (1968).
37. R. W. FESSENDEN and R. H. SCHULER. J. Chem. Phys. **39**, 2147 (1963).
38. H. FISCHER. Z. Naturforsch. **20A**, 428 (1965).
39. J. Q. ADAMS and J. R. THOMAS. J. Chem. Phys. **39** 1904 (1963).
40. C. ALEXANDER and W. GORDY. Proc. Natl. Acad. Sci. U.S. **58**, 1279 (1967).
41. J. R. BOLTON, A. CARRINGTON, and J. DOS SANTOS-VEIGA. Mol. Phys. **5**, 465 (1962).
42. B. L. BARTON and G. K. FRAENKEL. J. Chem. Phys. **41**, 1455 (1964).
43. M. T. MELCHIOR and A. H. MAKI. J. Chem. Phys. **34**, 471 (1961).
44. C. S. JOHNSON and H. S. GUTOWSKY. J. Chem. Phys. **39**, 58 (1963).
45. W. M. FOX and W. A. WATERS. J. Chem. Soc. Suppl. 2, 6010 (1964).
46. T. COLE. J. Chem. Phys. **35**, 1169 (1961).
47. W. M. FOX and P. SMITH. J. Chem. Phys. **48**, 1868 (1968).
48. J. V. RAMSBOTTOM and W. A. WATERS. J. Chem. Soc. B, 132 (1966).
49. N. M. ATHERTON, E. J. LAND, and G. PORTER. Trans. Faraday Soc. **59**, 818 (1963).
50. (*a*) N. EDELSTEIN, A. KWOK, and A. H. MAKI. J. Chem. Phys. **41**, 179 (1964); (*b*) P. B. AYSCOUGH. Electron spin resonance in chemistry. Methuen and Co. Ltd., London. 1967. Appendix 3.
51. G. CHAPELET-LETOURNEUX, H. LEMAIRE, and A. RASSAT. Bull. Soc. Chim. France, 3283 (1965).
52. J. R. BOLTON, A. CARRINGTON, and J. DOS SANTOS-VEIGA. Mol. Phys. **5**, 615 (1962).
53. G. SCHOFFA. J. Chem. Phys. **40**, 908 (1964).
54. A. J. TENCH. J. Chem. Phys. **38**, 593 (1963).
55. G. P. RABOLD, R. T. OGATA, M. OKAMURA, L. H. PIETTE, R. E. MOORE, and P. J. SCHEUER. J. Chem. Phys. **46**, 1161 (1967).
56. A. B. BARABAS, W. F. FORBES, and P. D. SULLIVAN. Can. J. Chem. **45**, 267 (1967).
57. P. D. SULLIVAN. J. Am. Chem. Soc. **89**, 4294 (1967).

Can. J. Chem. Downloaded from www.nrcresearchpress.com by 210.87.254.105 on 09/05/12
For personal use only.

Can. J. Chem. Downloaded from www.nrcresearchpress.com by 210.87.254.105 on 09/05/12
For personal use only.

Infrared spectroscopic studies of adsorption and catalysis. Part 3. Carboxylic acids and their derivatives adsorbed on silica

R. P. YOUNG[1]

School of Chemical Sciences, University of East Anglia, Norwich, England

Received February 20, 1969

Infrared spectra in the region 4000–1300 cm^{-1} have been obtained of acetic acid, acetyl chloride, acetic anhydride, propionic acid, and propionyl chloride adsorbed on discs of pressed silica powder. In all cases the spectra showed the presence of both the simple hydrogen-bonded species

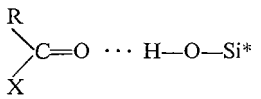

where X = OH, Cl, or O.CO.R and Si* represents a surface silicon atom, and also chemisorbed surface ester groups R.CO.O—Si*. The latter were characterized by a $\nu_{C=O}$ frequency in the 1760–1740 cm^{-1} region, whereas in the case of hydrogen-bonded physical adsorption, the $\nu_{C=O}$ frequency was about 20–30 cm^{-1} lower than that of the same molecule in the vapor phase. At high temperatures (150–200 °C) the water or hydrogen chloride eliminated in the surface esterification reaction was desorbed, and high conversions of surface OH to surface ester groups were observed. Under these conditions the carboxylic acid was formed from both the chloride and the anhydride; the latter was also produced at room temperature from the acid chloride. A scheme is suggested for the equilibration of these compounds on hydroxylated silica surfaces. The chemisorbed ester groups were susceptible to hydrolysis by water vapor, thus regenerating the original silanol OH groups.

Canadian Journal of Chemistry, 47, 2237 (1969)

Introduction

In continuation of recent spectroscopic studies of the adsorption of organic carbonyl compounds, the adsorption of a range of carboxylic acids and their derivatives at various temperatures on pressed discs prepared from pure silica powder has been examined. The adsorption of these compounds has not previously been investigated in very much detail by infrared (i.r.) spectroscopy, although formic acid was studied by Hirota (1) on silica and alumina, and by Clarke and Pullin (2) on silica-supported nickel. Noto *et al.* (3) have recently examined the decomposition of formic acid over alumina and silica and concluded that on the latter at 180 °C the adsorbate was stable, although deuterium exchange occurred with the hydrogen atom of the surface hydroxyl groups. Eischens (4) showed that acetic acid interacted with a silica – magnesium oxide surface to form chemisorbed surface acetyl groups. The adsorption of acetyl chloride and acetic anhydride on solid aluminium chloride was studied by Bertoluzza and co-workers (5, 6).

This paper describes the i.r. spectra obtained from acetic acid, acetic anhydride and acetyl chloride, and propionic acid and propionyl chloride adsorbed on Cab-O-Sil powder at temperatures between 25 and 200 °C. In each case the spectra show that several surface species are formed, indicating that an equilibrium is established on the surface between the acid, the chloride, and the anhydride, whereby they may be interconverted one with another. Chemisorbed surface ester groups R.CO.OSi* were observed as a predominant species, although in the presence of water vapor they were found to be easily hydrolyzed, thus regenerating the original surface hydroxyl groups.

Experimental

The adsorbates were distilled under dry nitrogen immediately before use, and thoroughly degassed by repeated freeze–thaw–pumping cycles just prior to admission of the pure vapor to the adsorption cell at 25 °C. Spectra were taken before and after sample admission, and again after various intervals of standing and/or heating. The adsorption cell and the spectrometer have been described before (7). The silica used was Cab-O-Sil HS powder (kindly donated by the Cabot Corporation, Boston, Mass.), which was ignited for 12 h at 600 °C, and then pressed for 2 min at 5 tons/sq in. into thin discs 1 in. diameter and weighing about 100 mg.

---

[1]Present address: Division of Pure Chemistry, National Research Council of Canada, Ottawa, Canada.

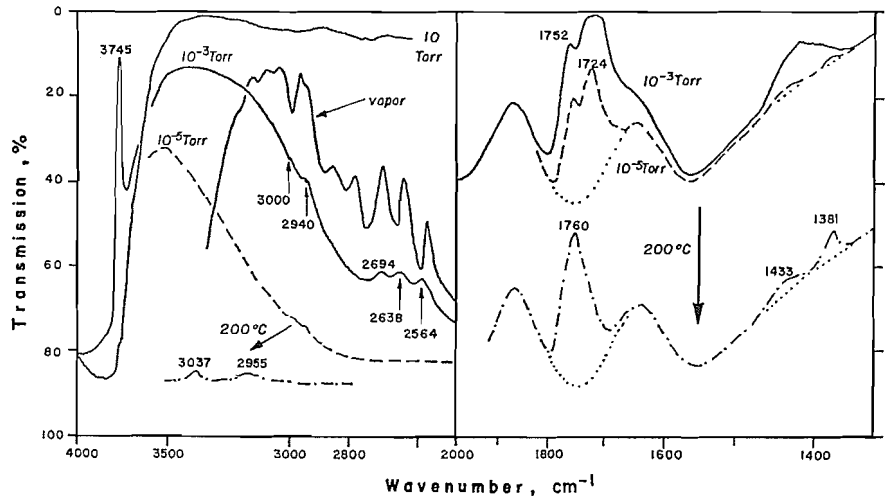

FIG. 1. Acetic acid adsorbed on Cab-O-Sil powder. 25 °C at 10, 10^{-3}, and 10^{-5} Torr (dashed); 200 °C at 10 Torr for 15 h and evacuated at 100 °C to 10^{-5} Torr (dot–dashed).

Results

A. *Acetic Acid, Acetyl Chloride, and Acetic Anhydride*

(i) Acetic Acid

Exposure of a Cab-O-Sil sample to acetic acid vapor (10 Torr) resulted in the very highly absorbing spectrum shown as the upper solid line in Fig. 1 (4000–2700 cm^{-1} region). The ν_{O-H} band of free surface hydroxyl groups at 3745 cm^{-1} had completely disappeared and was replaced by the very strong $\nu_{O-H\cdots O}$ band which extended well below 3000 cm^{-1}, and obscured all the detail of the ν_{C-H} bands. The vapor phase spectrum in this region showed the main ν_{O-H} absorption and also the overtone and combination satellite bands characteristic of the hydrogen-bonded cyclic dimer (8)

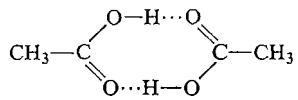

Similar bands were also seen in the adsorbed phase after evacuation to 10^{-3} Torr, indicating that this species was also present on the surface; the free OH groups of the silica surface were largely restored. At this pressure the $\nu_{C=O}$ region showed a very strong band at 1724 cm^{-1} and a weaker one at 1752 cm^{-1}. On further evacuation to 10^{-5} Torr (dashed line) there was a general loss of intensity in this region of the spectrum, the 1724 cm^{-1} band becoming weaker relative to that at 1752 cm^{-1}. The characteristic overtone and combination bands below 2700 cm^{-1} and the broad band at 1410 cm^{-1} of the dimer were no longer visible, suggesting that at this pressure monomeric acetic acid is the principal physically adsorbed species. When a further sample of acetic acid vapor was admitted and heated overnight at 200 °C, followed by evacuation to 10^{-5} Torr at 100 °C, the spectrum given by the dot–dashed line was obtained. This showed very weak ν_{C-H} bands at 3037 and 2955 cm^{-1}, a single $\nu_{C=O}$ band at 1760 cm^{-1}, and CH deformation bands at 1433 and 1381 cm^{-1} (see also Table I). These new bands were not diminished at all by prolonged evacuation and most probably arose from chemisorbed species formed by reaction between the acid vapor and the surface hydroxyl groups. This residual spectrum is characteristic of the acetyl group, and can reasonably be attributed to a surface acetyl species formed by the esterification reaction

$$CH_3.COOH + HOSi^* \rightarrow CH_3.CO.OSi^* + H_2O$$

As will be described below, the reactions of both acetyl chloride and acetic anhydride give rise to virtually identical residual spectra, suggesting that the chemisorbed product is the same in each case. We may therefore confidently assign the strong band at 1760 cm^{-1} to the $\nu_{C=O}$ mode of chemisorbed surface acetyl groups. The 1724 cm^{-1} band, which was strong initially but was

Can. J. Chem. Downloaded from www.nrcresearchpress.com by 210.87.254.105 on 09/05/12
For personal use only.

TABLE I

Infrared frequencies (cm^{-1}) and relative intensities of acetic acid adsorbed on Cab-O-Sil

Mode of vibration	Gas phase*	At 25 °C, 10^{-3} Torr		At 200 °C, 10^{-5} Torr	
		Frequency	Optical density	Frequency	Optical density
ν_{C-H}	3145				
	3092			3037	0.016
	3030	~3000	~0.02		
	2964	~2940	~0.05	2955	0.016
	2850				
Overtones and combinations‡	2783				
	2703	2694	0.080		
	2646	2638	0.046		
	2570	2564	0.056		
$\nu_{C=O}$	1790†	~1752	0.76	1760	0.70
	~1745‡	1724	~1.6		
δ_{C-H}	1432			1433	0.07
				1381	0.27
ν_{C-O}/δ_{O-H}		1410	0.38, broad		

*See ref. 8.
†Monomer.
‡Dimer.

entirely eliminated by evacuation at 100 °C, was attributed to physically adsorbed acetic acid.

The observation by Noto and co-workers (3) that D.CO.OD participated in deuterium exchange with surface OH groups suggests that the hydroxylic hydrogen atom of the acid molecule interacts directly with the surface. The $\nu_{C=O}$ frequency of $\sim 1720\ cm^{-1}$ which we observe for the physically adsorbed acetic acid, indicates that the carbonyl group also is hydrogen-bonded to surface OH groups. However, it is not clear from the i.r. spectra alone, whether the acetic acid molecule is held to the silica surface by one or by two silanol groups, e.g.

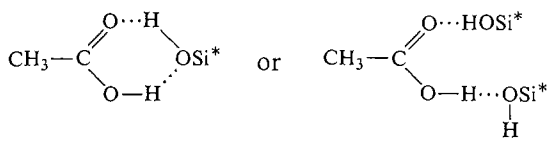

(ii) Acetyl Chloride

Figure 2(*a*) shows the spectra obtained immediately after the adsorption of acetyl chloride (10 Torr, solid line; 10^{-5} Torr, dashed line). Of particular note are the two $\nu_{C=O}$ bands; the one at 1795 cm^{-1} was completely removed after brief evacuation (dashed line), and was therefore assigned as the $\nu_{C=O}$ mode of acetyl chloride held to the surface by relatively weak hydrogen-bonds

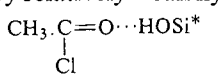

The 1742 cm^{-1} band, on the other hand, was retained even after evacuation for several hours at 25 °C, and was attributed to chemisorbed surface acetyl groups (the intensity ratio of the ν_{C-H} and $\nu_{C=O}$ bands was similar to that observed above in the case of acetic acid adsorption). The hydrogen chloride liberated in the surface esterification was not observed, presumably because it was removed from the adsorption cell by evacuation before the spectrum was recorded. When a further sample of acetyl chloride vapor (10 Torr) was allowed to stand over the silica surface for 15 h at 25 °C, not only did the ν_{C-H} and $\nu_{C=O}$ bands of the surface ester groups become stronger, but in addition a new weak $\nu_{C=O}$ band appeared at 1842 cm^{-1} (Fig. 2(*b*), solid line). As before, evacuation to 10^{-5} Torr at 25 °C removed all the physically adsorbed acetyl chloride (as shown by the disappearance of bands at 1795 and 1364 cm^{-1}, dashed line) but the new 1842 cm^{-1} band remained, and was only finally removed by evacuation for 30 min at 150 °C (at 10^{-5} Torr). That the adsorption of this new species was physical, and not chemical in nature, was established by the eventual disappearance of the 1842 cm^{-1} band, in contrast to the surface acetyl groups which were retained at 150 °C. The high frequency of the $\nu_{C=O}$ band (1842 cm^{-1}) suggests the possible formation of an acid anhydride; the strong retention on the silica surface is consistent with the relatively high boiling point

Can. J. Chem. Downloaded from www.nrcresearchpress.com by 210.87.254.105 on 09/05/12
For personal use only.

Can. J. Chem. Downloaded from www.nrcresearchpress.com by 210.87.254.105 on 09/05/12
For personal use only.

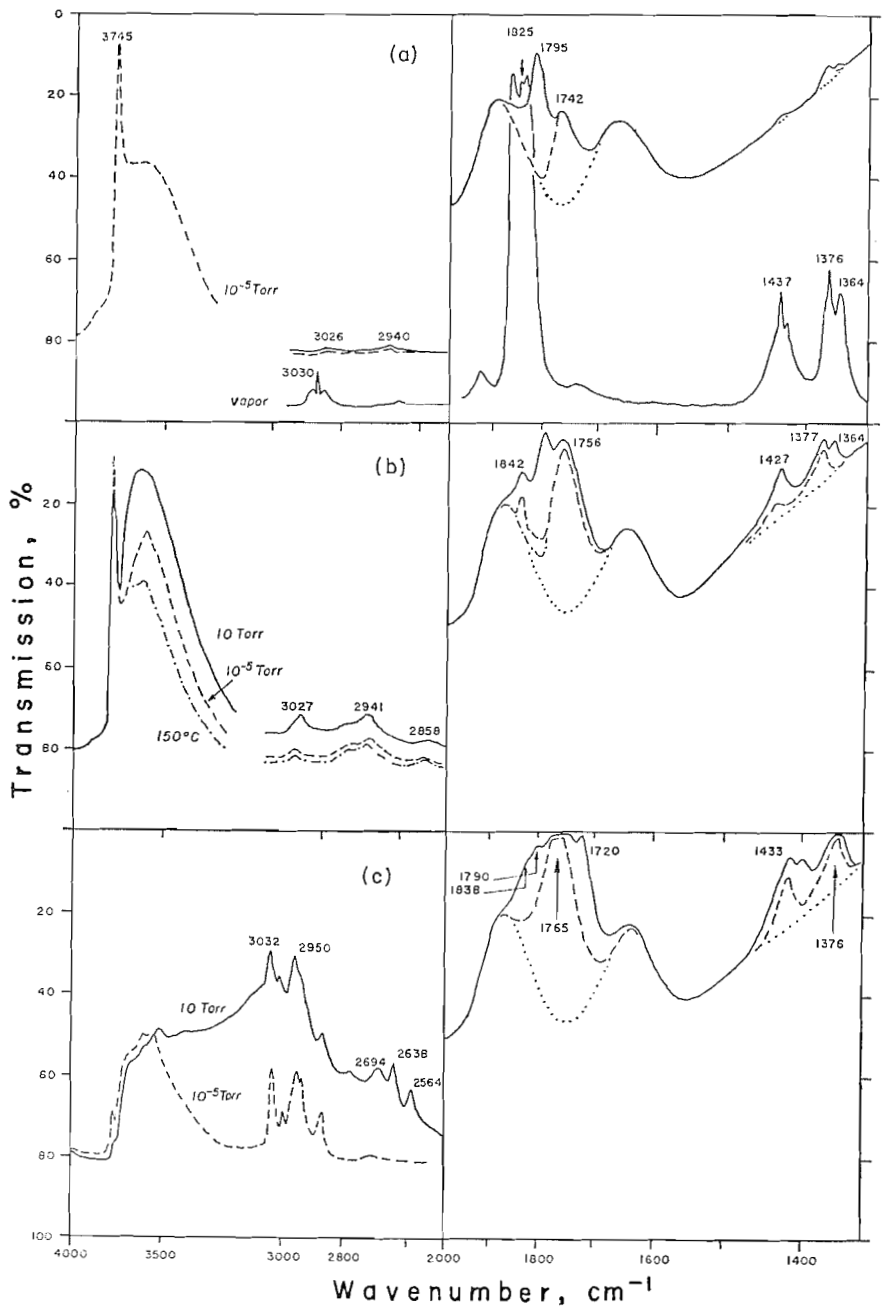

FIG. 2. Acetyl chloride adsorbed on Cab-O-Sil powder. (*a*) 10 Torr at 25 °C for 10 min, and after immediate evacuation to 10^{-5} Torr (dashed); (*b*) 10 Torr at 25 °C for 15 h, evacuated to 10^{-5} Torr (dashed), and after final evacuation at 150 °C (dot–dashed); (*c*) 10 Torr at 150 °C for 15 h, and evacuated to 10^{-5} Torr (dashed).

TABLE II

Infrared frequencies (cm^{-1}) and relative intensities of acetyl chloride adsorbed on Cab-O-Sil*

Mode of vibration	Frequency† (gas phase)	25 °C, 10 min at 10 Torr		25 °C, 15 h at 10 Torr		150 °C, 15 h at 10 Torr	
		Frequency	Optical density	Frequency	Optical density	Frequency	Optical density
ν_{C-H}	3030	3036	<0.01‡	3027	0.028	3032	0.200¶
						2995	0.134¶
				2965 (sh)		2950	0.220¶
	2930	2940	<0.01‡	2941	0.045	2940	~0.2¶
				2858	0.016	2860	0.050¶
Overtones and combinations						2694	0.060‖
						2638	0.074‖
						2564	0.050‖
ν_{C-O}	1825	1795	0.66‡	1842	0.32§	1838	0.53§
				1792	~1.3‡	1790	0.98‡
		1742	0.27¶	1756	~1.0¶	1765	>2
						1720	~1.5‖
δ_{C-H}	1437	~1430		1427	0.3	1433	0.55¶
ν_{C-O}/δ_{O-H}						1420 (sh)‖	
δ_{C-H}	1376	1381¶		1377	~0.5¶	1376	>2¶
	1364	1364‡		1364	~0.4‡		

*For adsorption on solid aluminium chloride, see ref. 5.
†For vapor and solution spectra, see ref. 11.
‡Physically adsorbed acetyl chloride.
§Physically adsorbed acetic anhydride.
‖Physically adsorbed acetic acid.
¶Chemisorbed surface acetyl groups.

(140 °C) of acetic anhydride. The lower frequency component (at ~ 1785 cm^{-1}) of the expected anhydride $\nu_{C=O}$ doublet was obscured by the broad strong band at 1756 cm^{-1} of the surface ester groups still retained at 10^{-5} Torr. This assignment of the 1842 cm^{-1} band was confirmed by experiments with acetic anhydride itself (see following section). A further sample of acetyl chloride (10 Torr) was admitted and heated overnight at 150 °C; subsequent cooling to 25 °C yielded the spectrum shown in Fig. 2(*c*), solid line. In addition to $\nu_{C=O}$ bands characteristic of physically adsorbed acetyl chloride (1790 cm^{-1}), acetic anhydride (1838 cm^{-1}, shoulder), and chemisorbed surface acetyl groups (~ 1765 cm^{-1}, very strong), bands characteristic of physically adsorbed acetic acid dimer were also observed (2800–2600 cm^{-1} region, 1720 and 1410 cm^{-1}). Evacuation at 100 °C removed all these physically adsorbed species, leaving only the surface ester groups which had almost completely replaced the original free hydroxyl groups (Fig. 2(*c*), dashed line). The residual $\nu_{O-H\cdots O}$ band at about 3600 cm^{-1} (dashed) possibly arises from hydrogen-bonding between a small number of surface acetyl groups and unreplaced OH groups

$$CH_3.CO.OSi^*$$
$$\vdots$$
$$HOSi^*$$

The variation of $\nu_{C=O}$ frequency within the 1760–1740 cm^{-1} range is discussed later in terms of hydrogen-bonding to OH groups, either on the silica surface or in vapor phase molecules. The frequencies and optical densities of all the observed bands are listed in Table II.

(iii) Acetic Anhydride

In order to confirm the assignment of the 1842 cm^{-1} band observed with acetyl chloride, spectra were recorded using acetic anhydride itself as adsorbate. In Table III are listed the frequencies of the bands shown in Fig. 3 for the adsorption of acetic anhydride at 3 Torr on Cab-O-Sil. The dashed line represents the spectrum obtained after evacuation to 10^{-5} Torr at 25 °C, and shows both physically adsorbed acetic anhydride (1839 cm^{-1}) and surface acetyl groups (1755 cm^{-1}). After reaction at 200 °C for 12 h the surface OH groups were replaced to a considerable extent by acetyl groups (dot–dashed line), as in the cases of acetic acid and acetyl chloride. The ν_{C-H} region is shown expanded. Because of the low volatility of acetic anhydride, the silica surface was exposed

Can. J. Chem. Downloaded from www.nrcresearchpress.com by 210.87.254.105 on 09/05/12
For personal use only.

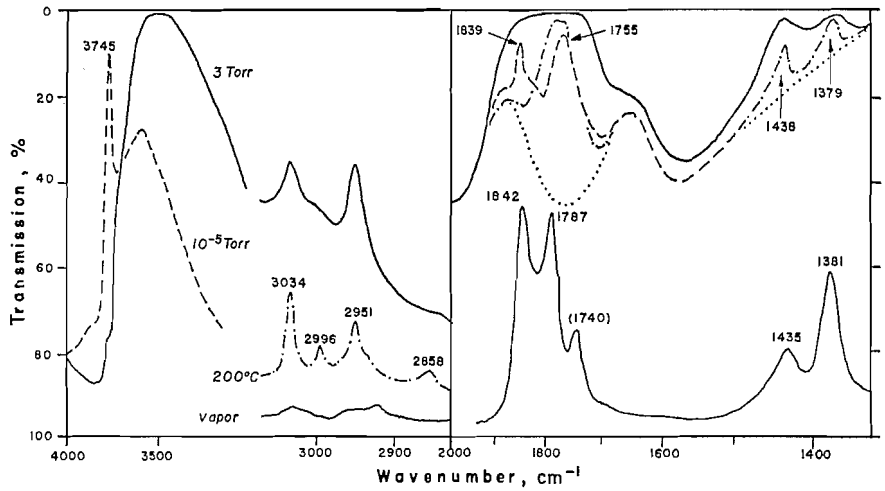

FIG. 3. Acetic anhydride adsorbed on Cab-O-Sil powder. 25 °C at 3 Torr and 10^{-5} Torr (dashed); 200 °C at 10 Torr for 15 h and evacuated to 10^{-5} Torr (dot–dashed).

TABLE III

Infrared frequencies (cm^{-1}) and relative intensities of acetic anhydride adsorbed on Cab-O-Sil*

Mode of vibration	Frequency (gas phase)	25 °C, 3 Torr		200 °C, 10^{-5} Torr	
		Frequency	Optical density	Frequency	Optical density
ν_{C-H}	3035	3031	0.162	3034	0.133
	~2962	2995 (sh)		2996	0.050
	~2925	2948	0.234	2951	0.090
				2858	0.025
$\nu_{C=O}$†	1842	1839	>2		
	1787	1755	>2	1765	>2
δ_{C-H}	1435	1438	~1.4	1439	0.41
	1381	1379	>2	1377	>1.5

*For adsorption on solid aluminium chloride, see ref. 6.
†For a study of $\nu_{C=O}$ spectra of anhydrides in solution, see ref. 12.

for several minutes to the saturated vapor pressure (~ 3 Torr at 25 °C). This may account for the breadth of the bands recorded at this pressure, since some condensation may have occurred on the sample. The vapor phase also appeared to contain a small amount of acid (1740 cm^{-1}) although none was observed in the spectrum of the adsorbed phase.

B. Propionic Acid and Propionyl Chloride

(i) Propionic Acid

At room temperature and a pressure of 1 Torr the spectrum shown in Fig. 4(*a*) was obtained; the ν_{C-H} bands were superimposed on the broad $\nu_{O-H\cdots O}$ absorption and the $\nu_{C=O}$ band was broad and unresolved, and centered at about 1720 cm^{-1}. On evacuation to 10^{-5} Torr the maximum shifted to 1745 cm^{-1}, after removal of the low frequency component responsible for the original breadth of the band (although this was still visible as a shoulder at 10^{-5} Torr). By analogy with the case of adsorbed acetic acid, the 1720 cm^{-1} band has been assigned to the $\nu_{C=O}$ mode of physically adsorbed propionic acid; at 1 Torr there was less evidence of the dimer than with acetic acid at 10^{-3} Torr, since the overtone and combination bands below 2700 cm^{-1} were scarcely visible, although a rather broad band was present at 1420 cm^{-1} corresponding to the 1410 cm^{-1} band of acetic acid dimer. The residual

Can. J. Chem. Downloaded from www.nrcresearchpress.com by 210.87.254.105 on 09/05/12
For personal use only.

TABLE IV

Infrared frequencies (cm^{-1}) and relative intensities of propionic acid* adsorbed on Cab-O-Sil

Mode of vibration	25 °C, 1 Torr		25 °C, 10^{-5} Torr	
	Frequency	Optical density	Frequency	Optical density
ν_{C-H}	2992	0.27	2995	0.118
	2953	0.21	2956	0.058
	2928	0.12	2934	0.030
	2896	0.13	2897	0.022
$\nu_{C=O}$	1750–1720	~2	1745	0.45
δ_{C-H}	1470	0.69	1470	0.10
ν_{C-O}/δ_{O-H}	1420	0.48 (broad)		
δ_{C-H}	1387	0.30		

*For solution spectra, see refs. 13 and 14.

spectrum ($\nu_{C=O}$ at 1745 cm^{-1}, and ν_{C-H} bands as shown) has been taken to represent chemisorbed surface propionyl groups $CH_3CH_2.CO.OSi$*. The frequencies of the bands are listed in Table IV. Virtually identical spectra were observed from the ester groups formed from propionyl chloride (see following section).

(ii) Propionyl Chloride

The spectrum of propionyl chloride adsorbed on silica, shown in Fig. 4(*b*), was analogous to that observed with acetyl chloride. Thus, physically adsorbed propionyl chloride

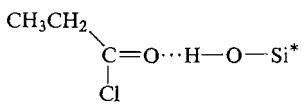

showed a $\nu_{C=O}$ band at 1786 cm^{-1} which was easily removed by evacuation, and a persistent band at 1828 cm^{-1} attributed to the anhydride. Room temperature evacuation to 10^{-5} Torr removed the acid chloride (dashed line), revealing the $\nu_{C=O}$ band of chemisorbed $CH_3CH_2.CO.OSi$* groups at 1742 cm^{-1}. In the ν_{C-H} region the intensity pattern was very similar to that observed with methyl ethyl ketone (7) and diethyl ketone (9), which also contain the propionyl group. The rather pronounced adsorbed anhydride $\nu_{C=O}$ band may have been slightly enhanced by the possible presence of traces of anhydride impurity in the sample (see the weak high frequency shoulder on the vapor phase $\nu_{C=O}$ band).

When heated overnight at 200 °C in the presence of 10 Torr propionyl chloride, the surface OH groups were replaced almost completely by $CH_3CH_2.CO.OSi$* groups. Considerable amounts of propionic acid were also formed, as shown by the characteristic dimer bands in the 2800–2600 cm^{-1} region, the broad 1427 cm^{-1} band, and the $\nu_{C=O}$ band at 1725 cm^{-1} (Fig. 4(*c*), solid line). All the physically adsorbed acid, acid chloride, and acid anhydride were removed by evacuation to 10^{-5} Torr at 100 °C, leaving on the surface almost exclusively the chemisorbed propionyl groups. The weak band at about 3500 cm^{-1} on the side of the residual $\nu_{O-H\cdots O}$ band (dashed) was assigned as the overtone of the $\nu_{C=O}$ fundamental at 1764 cm^{-1}. The frequencies of all the other observed bands are listed in Table V.

Discussion

It is concluded that the species responsible for the strong absorption band in the 1760–1740 cm^{-1} region is chemisorbed, since prolonged evacuation at elevated temperatures fails to remove it from the surface. Moreover, the similarity observed in these residual spectra, whether the initial adsorbate is the carboxylic acid, the acid chloride, or the acid anhydride, suggests that the same species is formed in each case. There is, in fact, little doubt that the surface silanol groups are esterified to form chemisorbed acetyl and propionyl groups, i.e. $CH_3.CO.OSi$* and $CH_3CH_2.CO.OSi$*. This assignment is fully confirmed, at least in the acetyl case, by a comparison with the vapor phase spectra of silyl acetate reported by Robiette and Thompson (10). There is surprisingly little difference between $CH_3.CO.OSi$*, $CH_3CO.OSiH_3$, and $CH_3.CO.OSiD_3$ in any of the vibrational frequencies, as is shown in Table VI.

The only frequency which is significantly affected by the presence of the silica surface is that

Can. J. Chem. Downloaded from www.nrcresearchpress.com by 210.87.254.105 on 09/05/12
For personal use only.

Can. J. Chem. Downloaded from www.nrcresearchpress.com by 210.87.254.105 on 09/05/12
For personal use only.

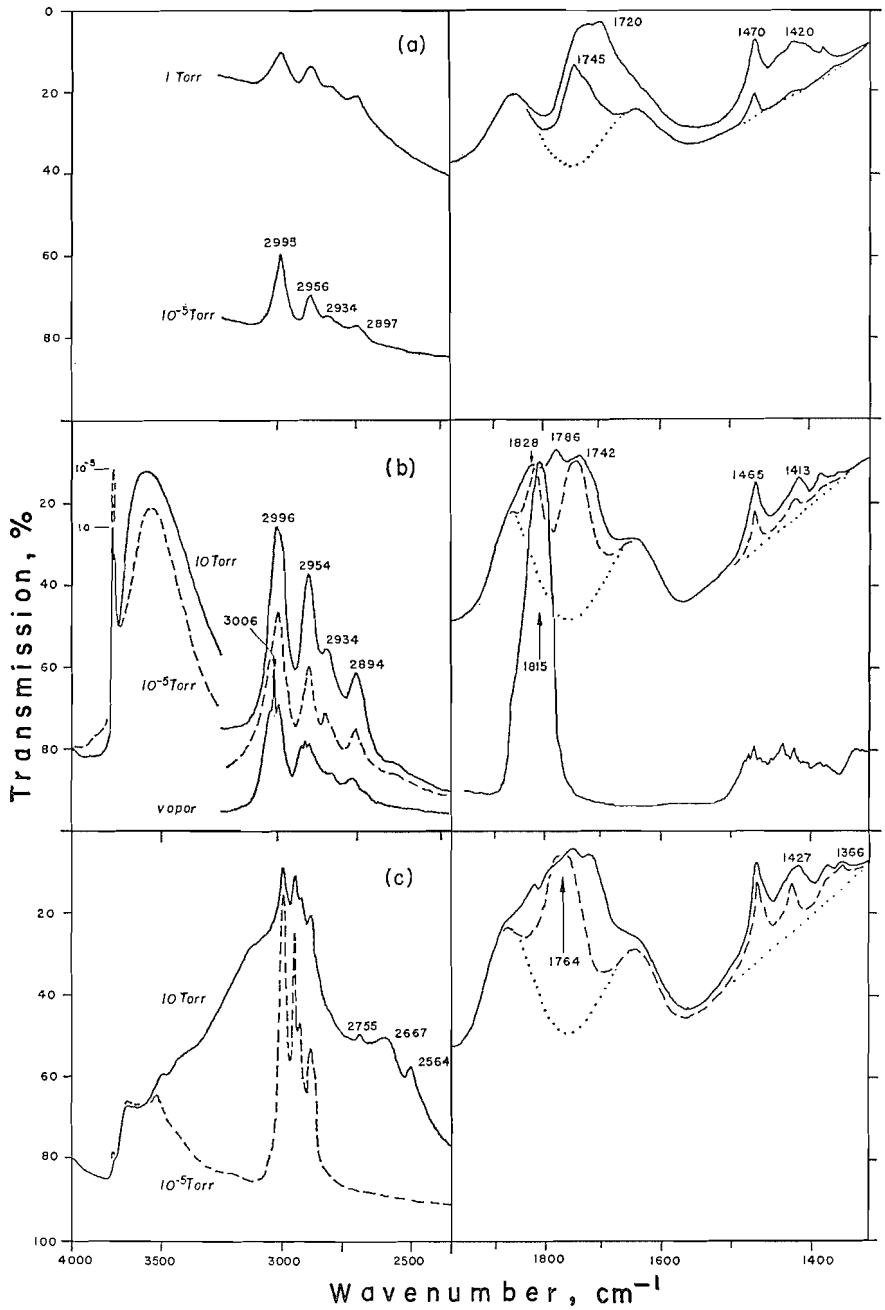

FIG. 4. (*a*) Propionic acid adsorbed on Cab-O-Sil powder at 25 °C at 1 and 10^{-5} Torr. (*b*) Propionyl chloride adsorbed on Cab-O-Sil powder at 25 °C at 10 and 10^{-5} Torr. (*c*) Proprionyl chloride adsorbed on Cab-O-Sil powder at 200 °C at 10 Torr for 15 h, and after evacuation to 10^{-5} Torr (dashed).

TABLE V

Infrared frequencies (cm^{-1}) and relative intensities of propionyl chloride* adsorbed on Cab-O-Sil

Mode of vibration	Frequency (gas phase)	25 °C, 10 Torr		200 °C, 10^{-5} Torr	
		Frequency	Optical density	Frequency	Optical density
ν_{C-H}	3006	2996	0.485	2996	0.80‖
	2961	2954	0.340	2958	0.56‖
	~2930	2934	0.170	2939	0.25‖
	2898	2894	0.140	2897	0.20‖
		2855		2855‖	
Overtones and combinations				2755§	
				2667§	
				2564§	
$\nu_{C=O}$	1860 (sh)	1828	0.49‡	1828	0.15‡
	1815	1786	0.78†		
		1742	0.73‖	1764	1.0‖
				1725 (sh)§	
δ_{C-H}	1464	1465	0.32	1471	0.50‖
ν_{C-O}/δ_{O-H}				1427	0.30§
δ_{C-H}	1416	1413	0.20‡		
	1381	1387	0.12	1366	0.41‖

*For liquid and solid spectra, see ref. 15; for solutions, see ref. 16.
†Physically adsorbed propionyl chloride.
‡Physically adsorbed propionic anhydride.
§Physically adsorbed propionic acid.
‖Chemisorbed surface propionyl groups.

TABLE VI

Observed infrared spectra of species containing acetyl groups

Mode of vibration	Description	Frequency (cm^{-1})†		
		$CH_3.CO.OSi$*‡	$CH_3CO.OSiH_3$§	$CH_3CO.OSiD_3$§
ν_1	Asymmetric	3034 (w)	3037 (w)	3037 (w)
ν_{18}	CH_3 stretch	2996 (w)	2990 (w)	2999 (w)
ν_2	Symmetric CH_3 stretch	2951 (w)	2951 (w)	2955 (w)
ν_5	C=O stretch	~1765 (s)	1750 (s)	1750 (s)
ν_{20}, ν_6	Asymmetric CH_3 bend	1439 (m)	1447 (s)	1446 (mw)
			1437 (m)	1444 (mw)
ν_7	Symmetric CH_3 bend	1377 (s)	1376 (s)	1376 (s)

†The intensity is indicated as strong (s), medium (m), or weak (w).
‡Taken from the data in Table III, representing acetylation of silica by acetic anhydride at 200 °C. The asterisk denotes surface Si atom.
§Taken from ref. 10.

of the carbonyl stretching mode, which is increased by about 15 cm^{-1} relative to silyl acetate. Inspection of Tables I–V and Figs. 1–4 reveals that the observed frequency of the $\nu_{C=O}$ band of the surface ester groups varies within the range 1765–1740 cm^{-1}. There is, however, a consistent trend in every case; the frequency after brief adsorption at 25 °C is always between 1755 and 1740 cm^{-1}, and rises to over 1760 cm^{-1} after long periods at high temperature (note that all the spectra were recorded with the sample at 25 °C). Closely parallelling the frequency rise in the $\nu_{C=O}$ vibration is the intensity decrease of the ν_{O-H} band of the surface OH groups. This strongly suggests that it is the surface OH concentration which influences the behavior of the ester groups replacing them on the surface. It seems not unlikely that at low ester group concentrations, hydrogen-bonding to adjacent, unreplaced, silanol groups may occur. As the

Can. J. Chem. Downloaded from www.nrcresearchpress.com by 210.87.254.105 on 09/05/12
For personal use only.

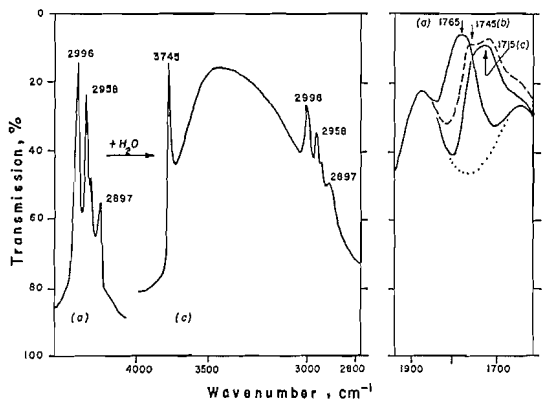

FIG. 5. Hydrolysis of surface propionyl groups by water vapor at 25 °C. (*a*) Surface as in Fig. 4 (*c*-dashed); (*b*) immediately after addition of water vapor (dashed line); (*c*) after standing in water vapor at 10 Torr for 14 h and evacuation to 10^{-4} Torr.

temperature is raised, the conversion of OH to ester groups increases and such neighboring group interactions become less numerous. Such interactions would be expected to cause a shift of about -20 cm^{-1} to the $\nu_{C=O}$ frequency (7, 9). To test the hypothesis that hydrogen-bonding to OH groups can cause a frequency shift from ~ 1760 to ~ 1740 cm^{-1} in the $\nu_{C=O}$ mode of surface carbonyl groups, a fully esterified surface was exposed to water vapor at 25 °C. The propionylated surface represented by the dashed line in Fig. 4(*c*) was used, and the results are shown in Fig. 5. The spectrum before the adsorption is shown in the $\nu_{C=O}$ region as curve (*a*), with a peak intensity at 1765 cm^{-1}. Immediately after the surface was exposed to water vapor the dashed curve (*b*) was observed, with maximum absorption at 1745 cm^{-1}, in support of the view that this lower frequency refers to hydrogen-bonded surface carbonyl groups

$$\mathrm{CH_3CH_2.CO.OSi^*} \quad \text{or} \quad \mathrm{CH_3CH_2.CO.OSi^*}$$
$$\vdots \qquad\qquad\qquad\qquad \vdots$$
$$\mathrm{H{-}O{-}H} \qquad\qquad\qquad \mathrm{H{-}OSi^*}$$

In addition to this change, a band at 1715 cm^{-1} also appeared on addition of water. This was attributed to physically adsorbed propionic acid, formed by the hydrolysis of the surface ester groups by the added water vapor

$$\mathrm{CH_3CH_2.CO.OSi^* + H_2O \rightarrow HOSi^* + CH_3CH_2.COOH}$$

Support for this view was found when, after standing overnight at 25 °C in water vapor (10 Torr), the spectrum of the surface again showed bands in the 2800–2600 cm^{-1} region characteristic of the dimeric acid. Moreover, on evacuation to 10^{-4} Torr, the "free" ν_{O-H} band at 3745 cm^{-1} was partially restored and the ν_{C-H} bands of the $CH_3CH_2.CO.OSi^*$ groups were considerably weaker (Fig. 5, curve (*c*)). These observations are similar to those of Eischens (4) who reported bands at 1747 and 1389 cm^{-1} which he attributed to chemisorbed acetyl groups formed by the interaction of acetic acid with a mixed silica/magnesium oxide surface; however, on pure silica he found these bands to be very weak, and concluded that the ester groups were formed mainly on the magnesium oxide. He also noticed that the addition of water led to a decrease in the concentration of these ester groups, and the appearance of a weak band at 1701 cm^{-1} indicated the regeneration of the free acid.

From the results presented here, it is clear that surface ester groups are readily formed on pure silica and, in addition, that the same chemisorbed ester groups are also formed from acid chlorides and anhydrides. In these cases, however, more than one surface species is usually formed, and these can generally be identified by the $\nu_{C=O}$ frequency. The highest conversions of surface hydroxyl to surface ester groups were achieved at high temperatures, when the water or hydrogen chloride released in the reaction was desorbed from the surface. Under these conditions the carboxylic acid was formed from both the chloride and the anhydride; the latter was also observed during the room temperature adsorption of the acid chloride. It is evident, therefore, that an equilibrium is established on the surface between the acid, the chloride, and the anhydride, whereby they may be interconverted with each other; the actual products obtained depend on the conditions employed. This may be represented schematically as shown below.

In this scheme, † denotes physical adsorption by hydrogen-bonding to surface OH groups; (A) ~ 1720 cm^{-1}; (B) ~ 1840 cm^{-1}; (C) ~ 1790 cm^{-1}; (D) 1760–1740 cm^{-1}, these limits represent "essentially free" and "essentially hydrogen-bonded" surface carbonyl groups respectively.

Finally, it is concluded that the esterification of surface silanol groups by carboxylic acids and their derivatives is reversible with respect to hydrolysis by water vapor, which is consistent with Eischens (4) observations of the behavior

Can. J. Chem. Downloaded from www.nrcresearchpress.com by 210.87.254.105 on 09/05/12
For personal use only.

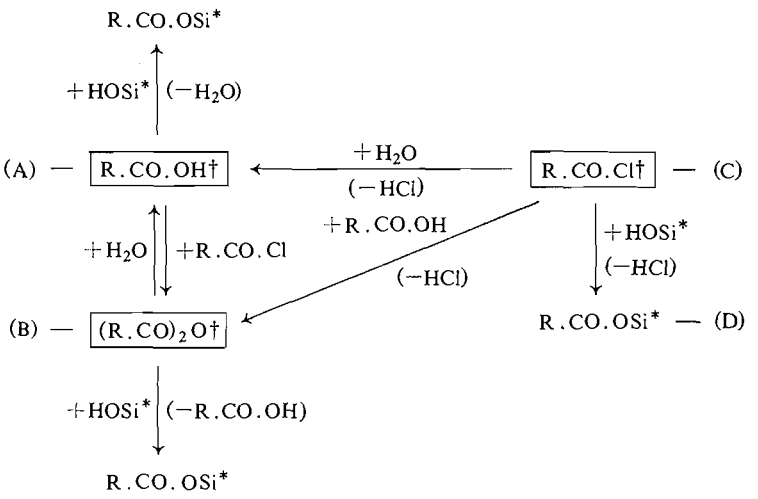

SCHEME 1

of ester groups on silica/magnesium oxide surfaces.

Acknowledgments

I am grateful to Professor N. Sheppard for many helpful discussions during the course of this work, and to the Science Research Council, London, England, for a Research Studentship.

1. K. HIROTA. Bull. Chem. Soc. Japan, **32**, 1261 (1959).
2. J. K. A. CLARKE and A. D. E. PULLIN. Trans. Faraday Soc. **56**, 534 (1960).
3. Y. NOTO, K. FUKUDA, T. ONISHI, and K. TAMARU. Trans. Faraday Soc. **63**, 2300 (1967).
4. R. P. EISCHENS. Science, **146**, 486 (1964).
5. A. BERTOLUZZA, G. FABBRI, and G. FARNE. Atti Accad. Nazl. Lincei, Rend., Classe Sci. Fiz., Mat. Nat. **36**, 481 (1964).
6. A. BERTOLUZZA, M. A. B. MORELLI, and C. CASTELLARI. Atti Accad. Nazl. Lincei, Rend., Classe Sci. Fiz., Mat. Nat. **38**, 686 (1965).
7. R. P. YOUNG and N. SHEPPARD. Trans. Faraday Soc. **63**, 2291 (1967).
8. J. K. WILMHURST. J. Chem. Phys. **25**, 1171 (1956).
9. R. P. YOUNG. Ph.D. Thesis, University of East Anglia, Norwich, England. 1967.
10. A. G. ROBIETTE and J. C. THOMPSON. Spectrochim. Acta, **21**, 2023 (1965).
11. J. OVEREND, R. A. NYQUIST, J. C. EVANS, and W. J. POTTS. Spectrochim. Acta, **17**, 1205 (1961).
12. L. J. BELLAMY, B. R. CONNELLY, A. R. PHILPOTTS, and R. L. WILLIAMS. Z. Elektrochem. **64**, 563 (1960).
13. J. WENOGRAD and R. A. SPURR. J. Am. Chem. Soc. **79**, 5844 (1957).
14. R. N. JONES. Can. J. Chem. **40**, 321 (1962).
15. K. K. DEB. Ind. J. Phys. **36**, 290 (1962).
16. J. E. KATON and W. R. FEAIRHELLER. J. Chem. Phys. **44**, 144 (1966).

Can. J. Chem. Downloaded from www.nrcresearchpress.com by 210.87.254.105 on 09/05/12
For personal use only.

Coefficient of thermal expansion of solid cyclohexane by means of dielectric constant measurements

R. K. CHAN AND H. A. CHEW
Department of Chemistry, University of Western Ontario, London, Ontario

Received February 6, 1969

A method has been devised to measure the coefficient of thermal expansion of solid cyclohexane from −80 to 0 °C by means of dielectric constant measurements in a spring-loaded apparatus. Assuming the Clausius–Mosotti equation to be valid, the coefficient of thermal expansion is given by

$$\alpha = -\frac{3}{(\varepsilon - 1)(\varepsilon + 2)}\left(\frac{\partial \varepsilon}{\partial T}\right)_p$$

$(\partial\varepsilon/\partial T)_p$ for solid cyclohexane is found to be -9.6×10^{-4} °C^{-1}. Therefore, $\alpha = 6.0 \times 10^{-4}$ °C^{-1} at −40 °C and $(\partial\alpha/\partial T)_p = 6.4 \times 10^{-7}$ °C^{-2}.

According to Crowe and Smyth $(\partial\varepsilon/\partial T)_p$ is $+7 \times 10^{-4}$ °C^{-1} because it has been measured with a fixed amount of solid cyclohexane between the electrodes. Using a model calculation based on the equivalent circuit consisting of 3 series capacitors filled alternately with air and sample, it is shown that the apparent value of $(\partial\varepsilon/\partial T)_p$ actually changes sign.

Canadian Journal of Chemistry, 47, 2249 (1969)

Can. J. Chem. Downloaded from www.nrcresearchpress.com by 210.87.254.40 on 09/05/12
For personal use only.

The coefficient of thermal expansion, α, of solids can be calculated simply from the dimensional changes as a function of temperature. For solids with well-defined dimensions such as metals, the measurement of α is straightforward. Various methods have been reviewed by Hidnert and Souder (1). However, these methods are not adaptable to polycrystalline organic or inorganic solids because of their volatility and tendency to fracture upon cooling. These complications have adverse effects on the dimensional stability of the specimen. Garner and Ryder (2) measured the densities of solid fatty acids using the dried air displacement method. Because of the high compressibility of air they had to take extraordinary precautions to maintain a constant temperature and to measure pressures very accurately. A convenient method has been devised to measure the coefficient of thermal expansion of non-polar polycrystalline solids over a considerable temperature range using dielectric constant measurements.

Experimental

The dielectric constant of solid cyclohexane was measured by a General Radio 1615-A transformer ratio arm capacitance bridge capable of 0.01% precision from 1–10 kHz. The signal was supplied by a Hewlett–Packard 200 CD oscillator and the unbalanced signal was amplified by a Rohde–Schwarz UBM tunable indicating amplifier. The temperature was measured to ±0.1 °C by means of a duplex copper–constantan thermocouple with a Leeds and Northrup K-3 universal potentiometer. The thermocouple was calibrated at the freezing point of mercury and the sublimation point of solid carbon dioxide at 1 atm. The spring-loaded 3-terminal dielectric cell is shown in Fig. 1. The tension of the spring equivalent to 10 atm kept the solid sample under an essentially constant pressure. The dielectric cell was made of stainless steel and insulated with teflon and mica. A system of 3-terminal coaxial electrodes similar to that employed by Davidson and Cole (3) was used. The nominal dimension of the inner electrode was 0.5 in. in diameter and the outer electrode was 0.75 in. in diameter by 1.25 in. in length. With the dielectric cell empty, the cell constant was 4.443 ± 0.002 pF independent of frequency from 1–10 kHz. The cyclohexane was Fisher certified spectranalyzed grade which was distilled fractionally from calcium hydride at atmospheric pressure before use. The cyclohexane was frozen by packing the outside of the dielectric cell with a small amount of dry ice. After the spring was loaded the dielectric cell was introduced into a copper tube wound with insulated heater wire, this assembly being placed in the center of a metal can containing polyurethane foam insulation. The entire assembly was placed in a stainless steel Dewar and was cooled by liquid nitrogen. The heater was controlled to ±0.1 °C by a Philips automatic compensator using a thermocouple as the sensing element. The temperature of the solid cyclohexane was cycled between −80 and 0 °C until the dielectric constant in the warming and cooling cycles agreed to within ±0.1% or better. About 4 cycles were required and each cycle took 2 days. The solid sample remained at constant temperature for at least 2 h before the final readings were taken.

Results

The dielectric constants of cyclohexane at 10 kHz are shown in Table I and Fig. 2. The conductance of the sample was approximately $10^{-10}\ \Omega^{-1}\ \text{cm}^{-1}$. According to the Clausius–Mosotti equation the dielectric constant of a

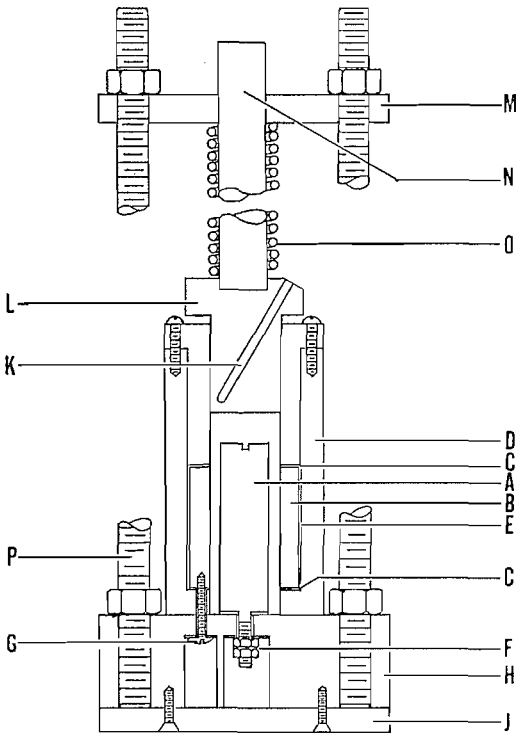

FIG. 1. Spring-loaded three-terminal dielectric cell. A, inner electrode; B, outer electrode; C, mica insulation; D, guard electrode; E, teflon insulation; F, lead for inner electrode; G, lead for outer electrode; H, base; J, base for shielding the electrodes; K, thermocouple well; L, piston; M, top plate for holding spring tension; N, rod; O, compression spring; P, supporting rods.

non-polar substance is related to the molar polarization by

$$[1] \qquad \frac{\varepsilon - 1}{\varepsilon + 2}\frac{M}{\rho} = P$$

where ε is the dielectric constant, M is the molecular weight, ρ is the density, and P the molar polarization. If the molar polarization is independent of temperature

$$[2] \quad \alpha = -\left(\frac{\partial \ln \rho}{\partial T}\right)_p = -\frac{3}{(\varepsilon - 1)(\varepsilon + 2)}\left(\frac{\partial \varepsilon}{\partial T}\right)_p$$

where α is the coefficient of thermal expansion. Since α is normally a positive quantity, ε should increase with a decrease of temperature. For liquid cyclohexane the temperature coefficient of dielectric constant is $-1.6 \times 10^{-3}\ °C^{-1}$ and the dielectric constant is 2.023 at 20 °C (4). According to eq. [2], $\alpha = 1.16 \times 10^{-3}\ °C^{-1}$. The densities

TABLE I

Dielectric constants of cyclohexane at 10 kHz

Cooling temperature (°C)	ε	Warming temperature (°C)	ε
−20.0	2.137	−104.2	2.167
−28.3	2.145	−97.0	2.166
−36.5	2.153	−88.0	2.165
−42.9	2.159	−85.9	2.184
−46.4	2.162	−85.4	2.188
−55.0	2.169	−85.2	2.189
−62.0	2.175	−85.1	2.190
−71.4	2.184	−85.0	2.195
−78.0	2.192	−84.8	2.196
−82.2	2.198	−84.5	2.200
−84.9	2.200	−72.4	2.185
−86.8	2.199	−63.5	2.179
−86.8	2.197	−53.2	2.169
−86.8	2.189	−46.0	2.163
−86.8	2.181	−36.2	2.152
−86.9	2.180	−35.0	2.153
−87.0	2.176	−22.2	2.139
−87.1	2.172	−6.2	2.125
−87.2	2.167	−0.3	2.117
−89.0	2.165	+2.3	2.111
−98.4	2.167	3.3	2.109
−111.1	2.170	4.2	2.107
		5.3	2.103
		5.8	2.096
		5.9	2.084
		6.0	2.071
		7.5	2.051
		8.5	2.042
		15.0	2.030
		20.0	2.022

of liquid cyclohexane are 0.77855 and 0.77389 g cm^{-3} at 20 and 25 °C respectively (5), $\alpha = 1.20 \times 10^{-3}\ °C^{-1}$. Therefore, the value of α obtained from dielectric constant compares favorably with that obtained from the density for liquid cyclohexane. It is assumed that similar calculations apply to solid cyclohexane. The temperature coefficient of dielectric constant for solid cyclohexane from −80 to 0 °C is $-9.6 \times 10^{-4}\ °C^{-1}$ which is independent of temperature within the experimental error. Values of α for various temperatures are given in Table II. The temperature coefficient of α is $6.4 \times 10^{-7}\ °C^{-2}$. Garner and Ryder (2) quoted the mean α for solid octoic, nonoic, decoic, undecoic, and lauric acids between 0 and 50 °C as $7.7 \times 10^{-4}\ °C^{-1}$ compared to $6.0 \times 10^{-4}\ °C^{-1}$ at −40 °C for solid cyclohexane.

Discussion

The dielectric behavior of cyclohexane has been investigated by Crowe and Smyth (6). They took the precaution of eliminating voids and cracks

Can. J. Chem. Downloaded from www.nrcresearchpress.com by 210.87.254.40 on 09/05/12
For personal use only.

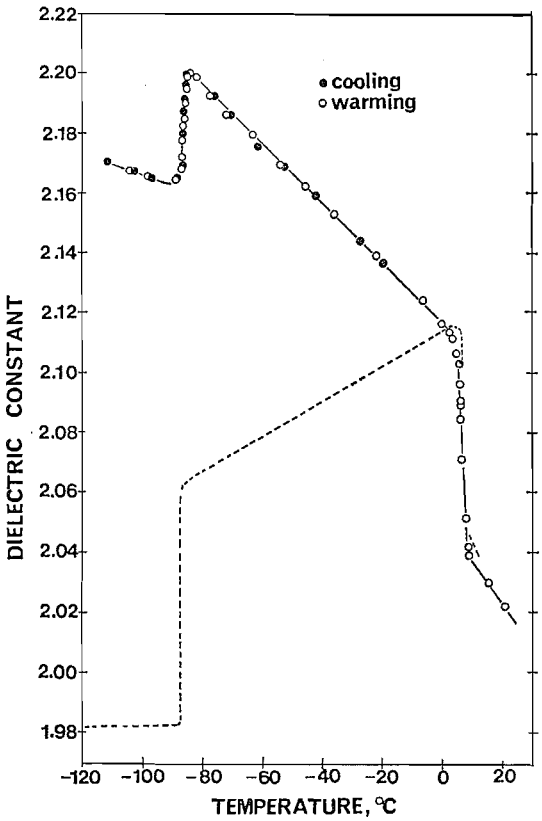

FIG. 2. Dielectric constant of cyclohexane at 10 kHz. The dashed line represents the data of Crowe and Smyth (6).

by freezing and thawing the sample repeatedly. Consequently, the value of the dielectric constant for solid cyclohexane slightly below the freezing point agreed well with the results of this investigation. Their results are represented by a dashed line in Fig. 2. With the use of a spring-loaded dielectric cell, the solid sample always filled the space between the electrodes. Increase in density as the temperature was decreased inevitably resulted in an increase of dielectric constant according to eq. [1], provided the molar polarization remained constant. The decrease of dielectric constant of solid cyclohexane observed by Crowe and Smyth can be explained if air gaps were present when the sample was cooled below the freezing point. Consequently, their measurements were most probably made on the solid–vapor equilibrium line. Since the amount of solid material between the electrodes was constant, shrinkage at low temperature could cause cracks

TABLE II

Variation of coefficient of thermal expansion of solid cyclohexane from −80 to 0 °C

Temperature (°C)	$\alpha(10^4\,°C^{-1})$
0	6.26
−20	6.12
−40	6.00
−60	5.86
−80	5.75

to appear. It was demonstrated conclusively by Auty and Cole (7) that air gaps parallel to the electrodes caused a decrease in dielectric constant of ice. Consider two parallel electrodes with area A and separation d. The capacitance in pF is given by

$$[3] \qquad C = \frac{\varepsilon A}{4\pi d}$$

where ε is the dielectric constant of the medium. If a parallel air gap of fractional width $\delta/2$ separates each electrode from the solid dielectric, the apparent capacitance of this compound capacitor, which is equivalent to 3 capacitors in series with the solid dielectric sandwiched between 2 air capacitors, is

$$[4] \qquad \frac{1}{C_{app}} = \frac{1}{C_{air}} + \frac{1}{C_{solid}} + \frac{1}{C_{air}}$$

Combining eqs. [3] and [4], one gets

$$[5] \qquad \frac{1}{\varepsilon_{app}} = \frac{\delta}{2} + \frac{1-\delta}{\varepsilon_{solid}} + \frac{\delta}{2}$$

or

$$\varepsilon_{app} = \frac{\varepsilon_{solid}}{1 + \delta(\varepsilon_{solid} - 1)}$$

In order to account for the result of Crowe and Smyth with ε_{app} being 2.07 at −80 °C, the fractional width of the air gaps, δ, must be 5.0%. In other words, the sample has to contract 5.0% in a direction perpendicular to the electrodes. The volume contraction of the sample from the freezing point to −80 °C is 5.2%. If the sample contracts uniformly, the fractional width of air gaps should be approximately one third of volume contraction, i.e. 1.7%, which is substantially below the predicted value of 5.0%. At least the prediction is in the right direction even though the quantitative agreement is poor. On the other hand, if the contraction is not uniform, the

Can. J. Chem. Downloaded from www.nrcresearchpress.com by 210.87.254.40 on 09/05/12
For personal use only.

extreme case would give rise to a value of 5.2% for the fractional width of air gaps. Granting such a case, the apparent dielectric constant of solid cyclohexane would be represented almost exactly by the dashed line in Fig. 2. It is worthwhile to point out that the apparent dielectric constant at −80 °C is only 0.13 less than the true value. For most dielectric constant measurements this is within the experimental error. Therefore, the slight error due to incomplete filling of the space between the electrodes will not show under normal circumstances.

Acknowledgment

It is a pleasure to acknowledge the financial support of the National Research Council of Canada for the undertaking of this project.

1. P. H. HIDNERT and W. SOUDER. Thermal expansion of solids; Natl. Bur. Stds. Circ. 486 (1950).
2. W. E. GARNER and E. L. RYDER. J. Chem. Soc. **127**, 720 (1925).
3. D. W. DAVIDSON and R. H. COLE. J. Chem. Phys. **19**, 1484 (1951).
4. A. A. MARYOTT and E. R. SMITH. Table of dielectric constants of pure liquids; Natl. Bur. Stds. Circ. 514 (1951).
5. A. F. FORZIATI, A. R. GLASGOW, JR., C. B. WILLIAMHAM, and F. D. ROSSINI. J. Res. Natl. Bur. Stds. **36**, 129 (1946).
6. R. W. CROWE and C. P. SMYTH. J. Am. Chem. Soc. **73**, 5406 (1951).
7. R. P. AUTY and R. H. COLE. J. Chem. Phys. **20**, 1309 (1952).

Can. J. Chem. Downloaded from www.nrcresearchpress.com by 210.87.254.40 on 09/05/12
For personal use only.

Dielectric properties of hexafluoroacetone and hexachloroacetone

R. K. CHAN
Department of Chemistry, University of Western Ontario, London, Ontario
Received February 7, 1969

The dielectric constants of hexafluoro- and hexachloro-acetone are measured in the solid and liquid state. They show negligible association in the liquid state. The dipole moments are 0.648 D measured in the gaseous state and 0.63 D in pure liquid for hexafluoroacetone, and 1.24 D in carbon tetrachloride solution and 1.34 D in pure liquid for hexachloroacetone. If the differences between inductive effects due to CX_3 and C=O groups can be ignored, the vector addition of bond moments gives values of dipole moment which are compatible with the experimental values.

Canadian Journal of Chemistry, 47, 2253 (1969)

Can. J. Chem. Downloaded from www.nrcresearchpress.com by 210.87.254.40 on 09/05/12
For personal use only.

Recently Plaush and Pace (1) studied the thermodynamic properties of hexafluoroacetone from 12 °K to its normal boiling point. A survey of the literature revealed that the dielectric properties of hexafluoroacetone and hexachloroacetone had never been investigated. The objectives of this work were to measure their dielectric constants in the gas, liquid, and solid state and in solution.

Experimental

The chemically pure grade of hexafluoroacetone was supplied by the Matheson Co. It was purified by fractional distillation in a standard vacuum apparatus. The melting point was 147.5 °K as determined by the dielectric constant measurements compared to the literature value of 147.70 °K (1). The reagent grade hexachloroacetone was supplied by Aldrich Chemical Co. It was purified by refluxing with calcium hydride and fractionally distilled at 1 atm. The constant boiling fraction of 476–477 °K was retained. The boiling point given in the literature was 475–477 °K (3).

The apparatus for measuring the dielectric constants in the gas phase was constructed according to Shoemaker and Garland (4). It consisted of a General Radio 1304-B beat frequency audio generator, an oscilloscope, and a GR 1422-ME precision variable capacitor. The frequency of the resonance circuits was 200 kHz. The dielectric cell was made of 3 concentric cylinders insulated by quartz separators. The cell constant measured in vacuum after the lead correction was 297 ± 0.5 pF, effectively independent of temperature. The gas dielectric cell was placed in a fiber glass insulated aluminium block which was heated by two embedded calrod elements. After thermal equilibrium was established, a constant voltage was enough to maintain the temperature drift to less than 0.1° per h. For measurements taken below the room temperature, ice water was circulated through a copper coil placed between the aluminium block and the fiber glass insulation. The temperature was measured by a calibrated chromel p-alumel thermocouple with a Leeds and Northrup K-3 universal potentiometer.

The dielectric constants of the sample in the solid and liquid state were measured in a 3-terminal dielectric cell similar to the one used by Gross and Taylor (5). A General Radio 1615-A transformer ratio arm capacitance bridge with a precision of better than 0.01% was used.

The dielectric constants of the solutions at 25 °C were measured by a Dipolmeter type DM01 manufactured by Wissenschaftlich-Technische Werstätten, Germany. It was calibrated with freshly dried and distilled cyclohexane, benzene, and carbon tetrachloride. The refractive indices (n_D) were measured by an Abbe refractometer thermostated at 25 °C.

Results

The dielectric constants of gaseous hexafluoroacetone were measured up to 1 atm from 276–528 °K (Table I). Using the Debye equation the total molar polarization in $cm^3\ mole^{-1}$ was given by

$$[1] \qquad [P] = 17.53 + \frac{2.556 \times 10^3}{T}$$

corresponding to a dipole moment value of 0.64_8 D. The values of the total molar polarization at various temperatures have been corrected for the non-ideal behavior of the gas by means of the Berthelot equation (6) with the critical temperature of 357.25 °K and the critical pressure of 27.97 atm (1). The calculated molar polarization at the sodium D line was 16.82 $cm^3\ mole^{-1}$ based on the bond refraction values of Smyth (7), and was considered to be in satisfactory agreement with the intercept of 17.53 $cm^3\ mole^{-1}$ in eq. [1] in view of the uncertain contribution due to the atomic polarization.

The gaseous hexafluoroacetone was condensed into the dielectric cell and it was cycled three times through the melting point before the measurements for the solid phase were taken. The dielectric constants of solid and liquid hexafluoroacetone at 10 kHz are shown in Fig. 1 and Table II. At 147.5 °K the solid sample melted sharply with only a slight premelting. The

Can. J. Chem. Downloaded from www.nrcresearchpress.com by 210.87.254.40 on 09/05/12
For personal use only.

TABLE I

Total molar polarization of gaseous hexafluoroacetone as a function of temperatures

T (°K)	P (cm^3 mole^{-1})
276.4	26.65
295.2	26.22
350.2	24.97
403.2	24.01
452.9	23.16
528.5	22.24

TABLE II

Dielectric constants of hexafluoroacetone at 10 kHz

T(°K)	ε	State
110.0	1.899	solid
123.7	1.902	solid
140.9	1.907	solid
145.5	1.910	solid
146.5	1.913	melting
146.9	1.924	melting
147.4	1.971	melting
147.5	2.304	melting
146.3	2.396	supercooled liquid
150.6	2.363	liquid
153.6	2.345	liquid
157.8	2.322	liquid
164.5	2.285	liquid
168.7	2.260	liquid
173.5	2.234	liquid
186.1	2.176	liquid
190.6	2.162	liquid
202.2	2.104	liquid
218.2	2.040	liquid
220.9	2.032	liquid
223.8	2.014	liquid
232.3	1.994	liquid
238.1	1.958	liquid

conductance of the liquid was estimated to be $\sim 10^{-10}\ \Omega^{-1}\ \text{cm}^{-1}$ at 200 °K. Using the Onsager equation (8)

$$[2] \qquad \mu^2 = \frac{9kT}{4\pi N}\,\frac{(\varepsilon - n^2)(2\varepsilon + n^2)}{\varepsilon(n^2 + 2)^2}$$

where N is the number of molecules in 1 cm^3 of liquid. The dipole moments were calculated to be 0.61, 0.63, and 0.64 D at 200, 220, and 240 °K, respectively, with an average of 0.63 ± 0.01 D. The density data were taken from Plaush and Pace (1). The refractive index was estimated by means of the Lorenz–Lorentz equation. The molar refraction was taken as the sum of the bond refractions at the sodium D line less 4% contribution due to atomic polarization (7).

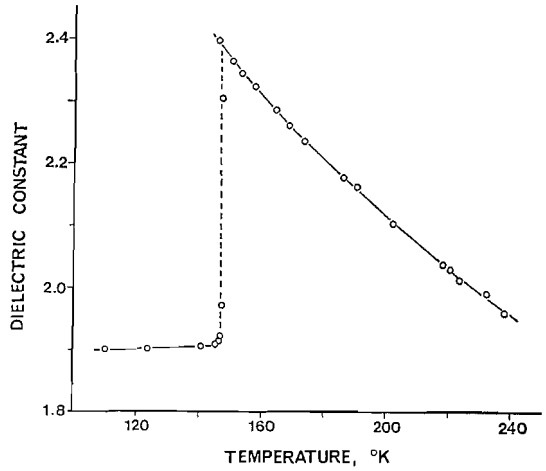

FIG. 1. The dielectric constants of hexafluoroacetone.

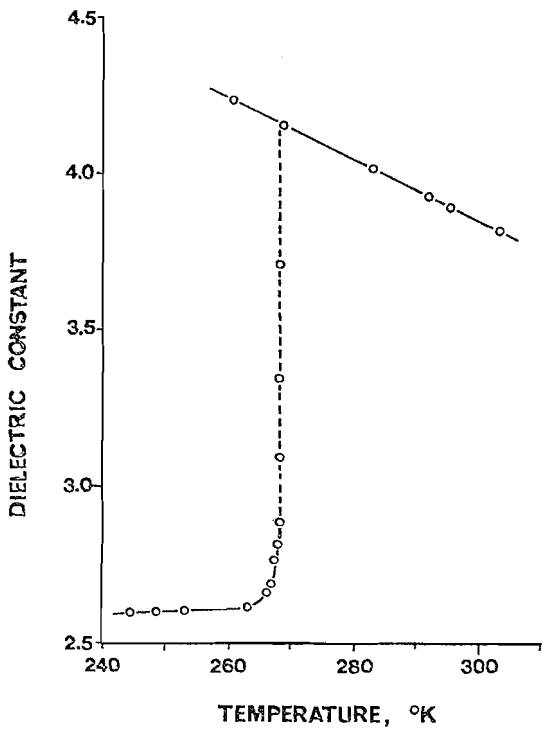

FIG. 2. The dielectric constants of hexachloroacetone.

The dielectric constants of solid and liquid hexachloroacetone at 10 kHz are shown in Fig. 2 and Table III. At 280 °K the conductance of the liquid was $\sim 3 \times 10^{-8}\ \Omega^{-1}\ \text{cm}^{-1}$. With a slight premelting, the solid sample melted sharply at 268.2 °K in fair agreement with the literature value of 269–270 °K (9).

Can. J. Chem. Downloaded from www.nrcresearchpress.com by 210.87.254.40 on 09/05/12
For personal use only.

TABLE III

Dielectric constants of hexachloroacetone at 10 kHz

T (°K)	ε	State
244.2	2.594	solid
248.5	2.600	solid
253.0	2.604	solid
263.2	2.612	solid
266.3	2.659	melting
266.8	2.684	melting
267.3	2.767	melting
267.6	2.814	melting
268.2	2.885	melting
268.2	3.090	melting
268.2	3.341	melting
268.2	3.710	melting
260.6	4.234	supercooled liquid
268.7	4.153	liquid
282.8	4.013	liquid
291.9	3.925	liquid
295.2	3.890	liquid
303.3	3.816	liquid

The densities of liquid hexachloroacetone were determined in a 10 cm^3 bicapillary pycnometer calibrated with freshly distilled water in the temperature range of 275 to 315 °K

[3] $d(\text{g cm}^{-3}) = 2.1673 - 0.00145\,T$

the uncertainty being 0.01%. At 285 °K the rather old literature value was 1.744 g cm^{-3} (3) compared to the calculated value of 1.7540 g cm^{-3}. The calculated Onsager dipole moments of liquid hexachloroacetone were 1.32, 1.34, and 1.34 D at 270, 285, and 300 °K, respectively, with an average of 1.33 ± 0.01 D.

The dipole moment of hexachloroacetone was also determined in the carbon tetrachloride solutions at 25 °C. The results were given in Table IV. The dipole moment was calculated according to the Guggenheim method (10). The limiting slopes of the dielectric constants and squares of the refractive index as a function of weight fractions of solute were 1.279 and 0.156, respectively, giving a dipole moment of 1.24 D for the solute.

Discussion

The dielectric constants of solid and liquid hexafluoro- and hexachloro-acetone are normal, both exhibiting a sharp rise at the melting point. The rise of the dielectric constant is three times larger for hexachloroacetone than hexafluoroacetone because the former is considerably more polar. The dipole moments of hexachloroacetone, 1.24 D (solution) and 1.34 D (liquid), are higher than those of hexafluoroacetone, 0.648 D (gas) and 0.63 D (liquid). Since the dipole moment in the liquid state is comparable to that obtained by other means, it implies that neither of the liquids associates to any appreciable extent. Acetone behaves similarly with dipole moments of 2.86 D (gas) and 3.0 D (liquid) (11).

TABLE IV

Weight fraction w, dielectric constant ε, and refractive index n_D of hexachloroacetone in carbon tetrachloride solutions at 25 °C

$w \times 10^2$	ε	n_D
0	2.2263	1.4570
1.269	2.2423	1.4575
1.797	2.2495	1.4579
2.885	2.2634	1.4584
3.237	2.2693	1.4588
4.200	2.2815	1.4591
4.902	2.2923	1.4597
5.353	2.2980	1.4598
6.366	2.3143	1.4605
6.614	2.3166	1.4606
7.960	2.3386	1.4616

TABLE V

Values of dipole moment from McClellan (11)

Substance	μ_{gas} (D)
CH_3F	1.83
CHF_3	1.64
CH_3Cl	1.94
$CHCl_3$	1.05
CH_2O	2.32

An attempt is made to calculate the dipole moments of hexafluoro- and hexachloro-acetone by the vector addition of bond moments. Since the C—C—C bond angle is normal (12)

[5] $\mu_{calculated} = \mu_{C=O} - 2\mu_{CX_3} \cos 60°$

Because all 3 halogen atoms are bonded to the same carbon atom, the inductive effect will be considerable (2). Consequently, an effective fractional positive charge is induced in the carbon atom resulting in a reduction of the CX_3 group moment. The difference of dipole moments between CHX_3 and CH_3X is explained usually in this manner since all the bond angles are essentially tetrahedral (see Table V). If it is assumed that the differences between inductive effects on the carbon atom are negligible for CHX_3 and CH_2O, then the vector addition of bond moments

as illustrated in configurations **1** and **2**, will yield dipole moment values of 0.68 D for hexafluoroacetone and 1.27 D for hexachloroacetone.

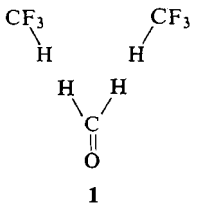

1

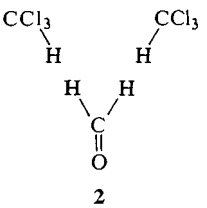

2

Admittedly, the values of dipole moments in Table V are uncertain to the extent of ~0.05 D and, therefore, the calculated dipole moments are probably accurate to ~0.1 D. Their agreement with the experimental values must be considered satisfactory.

Acknowledgment

The financial support of the National Research Council of Canada is greatly appreciated.

1. A. C. PLAUSH and E. L. PACE. J. Chem. Phys. **47**, 44 (1967).
2. J. W. SMITH. Electric dipole moments. Butterworths Scientific Publication, London. 1955. p. 172.
3. BEILSTEIN. Handbuch der Organischen Chemie. 4th ed. Vol. 1. 1918. p. 657.
4. D. P. SHOEMAKER and C. W. GARLAND. Experiments in physical chemistry. 2nd ed. McGraw-Hill Book Co., Inc., New York. 1967. p. 303.
5. P. M. GROSS, JR. and R. C. TAYLOR. J. Am. Chem. Soc. **72**, 2075 (1950).
6. S. GLASSTONE. Physical chemistry. 2nd ed. D. Van Nostrand Co., Inc., New York. 1946. p. 295.
7. C. P. SMYTH. Dielectric behavior and structure. McGraw-Hill Book Co., Inc., New York. 1955. pp. 409 and 419.
8. C. J. F. BÖTTCHER. Theory of electric polarization. Elsevier Publishing Co., Amsterdam. 1952. p. 192.
9. E. G. EDWARDS, D. P. EVANS, and H. B. WATSON. J. Chem. Soc. 1942 (1937).
10. E. A. GUGGENHEIM. Trans. Faraday Soc. **47**, 573 (1951)
11. A. L. MCCLELLAN. Tables of experimental dipole moments. W. H. Freeman and Co., San Francisco and London. 1963.
12. G. A. BOULET. Ph.D. Dissertation. University of Michigan, 1964. See also Dissert. Abstr. **25**, 3283 (1964–65).

Can. J. Chem. Downloaded from www.nrcresearchpress.com by 210.87.254.40 on 09/05/12
For personal use only.

Substitution reactions at octahedral centers. IV. Acid and base hydrolysis of chloropentakis(alkylamine)chromium(III) ions

M. PARRIS[1] AND W. J. WALLACE[2]

Department of Chemistry, University of Alberta, Edmonton, Alberta

Received November 28, 1968

The compounds $[Cr(RNH_2)_5Cl](ClO_4)_2$, where R = H, CH_3, C_2H_5, n-C_3H_7, and n-C_4H_9, have been prepared and the replacement of chloride by either water or hydroxide ion subjected to kinetic examination. Below about pH 7 the reaction was acid independent, and ΔH_A^* was 22.4 kcal mole^{-1} when ammonia was the inert ligand compared with about 26.4 kcal mole^{-1} when the inert ligand was a primary amine. The corresponding ΔS_A^* values increased continuously with R from H to n-C_4H_9. At higher pH the rate became inversely dependent upon the acidity of the solution, and ΔH_B^* decreased from 26.7 kcal mole^{-1} for ammonia as the inert ligand to 25.4 kcal mole^{-1} for an amine as the inert ligand. For the pH dependent reaction the values obtained for ΔS_B^* were much larger than for the pH independent reaction but the pattern of variation as the inert ligands were changed was quite similar in the two cases. The great similarity in the trends of ΔS^* values for the acid and base hydrolysis reactions has been interpreted in terms of a rate-determining step that is primarily dissociative in both cases.

Canadian Journal of Chemistry, 47, 2257 (1969)

Introduction

There have been a number of investigations of the kinetics of substitution reactions on octahedral chromium and the mechanism of removal of a simple anion and its replacement by water (eq. [1]) seems well understood (1–5). The mechanism of the companion reaction in more

[1] $Cr(NH_3)_5X^{2+} + H_2O \rightarrow Cr(NH_3)_5H_2O^{3+} + X^-$

basic solution where the replacing group is hydroxide (eq. [2]) remains a problem. The interpretation of the kinetics of alkaline hydrolysis of the halopentamminechromium(III) ions (eq. [2])

[2] $Cr(NH_3)_5X^{2+} + OH^- \rightarrow Cr(NH_3)_5OH^{2+} + X^-$

in mechanistic terms is complicated by the presence of labile hydrogen atoms, which give rise to the possibility of reaction through a conjugate base intermediate (6) kinetically indistinguishable from a bimolecular reaction between the complex and hydroxide ions.

The validity of a conjugate base mechanism hinges on the comparative kinetic behavior of otherwise similar complexes at high pH in both the presence and the absence of a moderately acidic proton. A number of aprotic cobalt complexes have been studied and found to hydrolyze at a rate which is independent of hydroxide ion even at high pH (7, 8). However, in each of these studies the change in the inert ligands may have introduced inductive and mesomeric terms that changed the mechanism. Examination of the activation parameters for these systems would reveal such effects, but these data have not been available.

It seemed, then, to be of interest to attempt to prepare a series of complex ions related to the pentammine by progressive substitution of inert groups for the hydrogens on nitrogen. It has been possible to prepare the series of complexes in which aliphatic straight chain primary amines replace ammonia as inert ligands. However, even this limited series of compounds introduces significant variation into the solvation and acidic properties of the complex ions, and these differences are shown to be mechanistically significant.

Experimental

Preparation of Compounds

The chloropentakis(alkylamine)chromium(III) chlorides were prepared by the slow addition of anhydrous chromic chloride to the refluxing amines as described by Rogers and Staples (5). A reaction similar to that occurring in liquid ammonia in the absence of basic catalysts (9) takes place and a suspension of the chloropentakis(alkylamine)chromium(III) chloride is formed. Too high a temperature, produced for example, by rapid addition of the chromic chloride, caused the formation of apparently polymeric products. Excess amine was removed by decanting, washing with ether, and vacuum pumping. Precipitation from aqueous acetone solution with perchloric acid was followed by recrystallization from the same solvent until the product gave no test for ionic chloride.

[1]Present address: Department of Chemistry, Carleton University, Ottawa, Canada.

[2]Present address: Department of Chemistry, University of Saskatchewan, Regina, Saskatchewan.

Can. J. Chem. Downloaded from www.nrcresearchpress.com by 210.87.254.5 on 09/05/12
For personal use only.

Can. J. Chem. Downloaded from www.nrcresearchpress.com by 210.87.254.5 on 09/05/12
For personal use only.

Chloropentamminechromium(III) Perchlorate

The preparation and properties have been described elsewhere (4).

Chloropenta(methylamine)chromium(III) Perchlorate

This was obtained as carmine red platelets, soluble in water, alcohol, and acetone.

Anal. Calcd. for $C_5H_{25}N_5O_8Cl_3Cr$: Cr, 11.8; N, 15.9; Cl, 24.0. Found: Cr, 12.0; N, 15.9; Cl, 23.5.

Chloropenta(ethylamine)chromium(III) Perchlorates

These were obtained as very dark red platelets very soluble in water, alcohol, and acetone.

Anal. Calcd. for $C_{10}H_{35}N_5O_8Cl_3Cr$: Cr, 10.2; N, 13.7; Cl, 20.8. Found: Cr, 10.1; N, 13.6; Cl, 20.7.

Chloropenta(n-propylamine)chromium(III) Perchlorate

This was obtained as a reddish-purple powder, soluble in water and very soluble in alcohol and acetone.

Anal. Calcd. for $C_{15}H_{45}N_5O_8Cl_3Cr$: Cr, 8.95; N, 12.0; Cl, 18.2. Found: Cr, 8.9; N, 11.9; Cl, 18.2.

Chloropenta(n-butylamine)chromium(III) Perchlorate

This was obtained as a reddish powder with a pronounced purple tinge, slightly soluble in water, but very readily precipitated by perchlorate and soluble in alcohol and acetone.

Anal. Calcd. for $C_{20}H_{55}N_5O_8Cl_3Cr$: Cr, 7.98; N, 10.7; Cl, 16.3. Found: Cr, 7.6; N, 10.3; Cl, 16.1.

Analyses

Analyses were performed by standard methods: nitrogen by the Kjeldahl method, chloride gravimetrically as silver chloride, and chromium by oxidation with alkaline peroxide and back titration with ferrous sulfate.

n-Amylamine and *n*-hexylamine gave tacky, apparently polymeric products, tenaciously retaining excess amine and difficultly soluble in acetone. Secondary and tertiary amines even in the presence of sodamide gave no reaction upon heating for prolonged periods in sealed tubes.

Upon heating and occasionally upon concussion, the dry perchlorates explode, but the reaction becomes less violent as the size of the alkyl group is increased.

Kinetic Studies

Solutions were made up to 10^{-3} *M* in complex ion at a selected pH, controlled by amine–perchlorate buffers and adjusted to ionic strength $\mu = 0.2$, as described previously (4). By adjustment of the buffering amine and/or the buffer ratio the pH could be controlled to any value over the range shown in Fig. 1. The solutions were then thermostated at the desired temperature and the reaction allowed to proceed. The extent of reaction was followed by removing an aliquot, quenching, either by cooling or lowering the pH or both, and determining the liberated chloride polarographically. Pseudo first order plots were obtained over the first two half lives of the reaction. No attempt was made to isolate the liberated aquo complex because loss of chloride was followed by rapid loss of amine.

Results

The data plotted in Fig. 1 show that, on the basis of its pH dependence, the process leading to the hydrolytic removal of chloride from all the chloropentamminechromium(III) complexes can be divided into the same two parts.

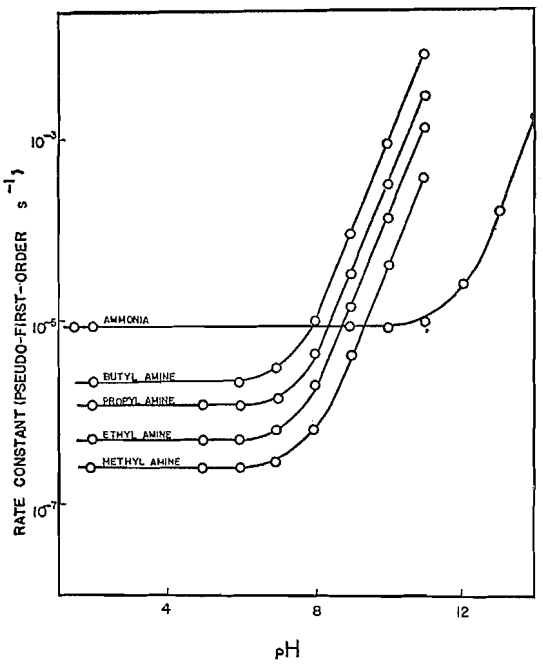

FIG. 1. pH profiles for the hydrolysis of some chloropentamminechromium(III) complex ions at 25 °C.

Over the entire pH range the rate law is given by

$$\text{Rate} = k_A[\text{complex}] + k_B[\text{complex}][OH^-]$$

However, when the pH of the reaction mixture is not controlled by buffering, the scatter of the data is much greater and a superimposed pH dependence of the type reported by Rogers and Staples (5) is observed (11).

The rate constants for acid hydrolysis are sensitive to the amount and kind of electrolyte present in the reaction system. Such electrolyte effects must be taken into account in making comparisons among published rate data for the pentamminechromium(III) complexes (4, 5, 10).

The data in Table I show the variation of the rate constants as a function of temperature for both the acid and base hydrolysis. These data have been used to calculate the activation parameters reported in Table II. Individual chloride determinations were within $\pm 3\%$ of the true value and 6 points obtained over two half lives of the reaction gave rate constants with an average deviation over 5 values at 25° of $\pm 1\%$. Some replicate values are given in Table I to illustrate the quality of the data but in general the values reported are averages obtained from three indi-

Can. J. Chem. Downloaded from www.nrcresearchpress.com by 210.87.254.5 on 09/05/12
For personal use only.

TABLE I

Temperature dependence of the rate constants for the hydrolytic removal of chloride from the complexes $Cr(Am)_5Cl^{2+}$

Temperature (°C)	Acid hydrolysis, $k_A \times 10^6$ (s^{-1})				
	NH_3	$MeNH_2$	$EtNH_2$	n-$PrNH_2$	n-$BuNH_2$
25.3	8.70	0.261	0.512	1.20	2.11
	8.78	0.264	0.508	1.24	2.10
	8.65	0.262	0.509	1.19	2.15
	8.72				
35.1	28.3	1.05	2.06	4.85	8.51
46.2	95.4	4.39	8.60	20.4	35.6
58.3	332	19.0	37.4	89.1	154
	328	19.0	37.0	89.0	155
	331	19.2	37.2	89.5	157
Temperature (°C)	Base hydrolysis, k_B ($mole^{-1}$ s^{-1})				
	NH_3	$MeNH_2$	$EtNH_2$	n-$PrNH_2$	n-$BuNH_2$
0.0			0.0287	0.0604	0.177
15.2		0.101	0.353	0.758	2.18
		0.103	0.352	0.756	2.19
		0.104	0.356	0.755	2.15
25.3	0.00192	0.432	1.61	3.53	9.81
35.1	0.00778	1.64	6.06	13.4	37.4
	0.00785	1.64	6.10	13.3	37.0
	0.00771	1.68	6.16	13.9	37.9
46.2	0.0332	6.56			
58.3	0.148				

TABLE II

Activation parameters for the hydrolytic removal of chloride from $Cr^{III}(RNH_2)_5Cl^{2+}$

R	Acid hydrolysis			Base hydrolysis		
	$k_A \times 10^6$ (s^{-1}) at 25.3°	H_A^* (kcal $mole^{-1}$)	S_A^* (e.u.)	k_B ($l\ mole^{-1}\ s^{-1}$) at 25.3°	H_B^* (kcal $mole^{-1}$)	S_B^* (e.u.)
H	8.70	22.3	−6.9	0.00192	26.7	+18.5
	7.3[a]	22.9[a]	−5.4			
Methyl	0.261	26.3	−0.5	0.432	25.4	+24.6
Ethyl	0.512	26.3	+0.8	1.61	25.2	+27.2
	0.42[a]	26.6[a]	+1.4			
n-Propyl	1.20	26.4	+2.5	3.53	25.4	+28.8
n-Butyl	2.11	26.3	+3.6	9.91	25.3	+30.8

[a]Reference 5. Rate constants at 25.3° obtained by extrapolation.

vidual runs at the appropriate temperature. The activation enthalpy values reported in Table II are uncertain by ±0.1 kcal and the activation entropies by ±0.3 e.u.

Discussion

The patterns exhibited by the pH profiles of the rate constants (Fig. 1) suggest that there are two distinct mechanistic processes operating in this series of complexes.

In acid hydrolysis ΔH^* increases from 22.3 to 26.3 kcal/mole when the inert ligand is changed from ammonia to methyl amine, but lengthening of the carbon chain produces no further increase. By contrast the same changes in the inert ligand produce, for the base hydrolysis, an initial ΔH^* decrease from 26.7 to 25.4 kcal/mole then no further change. For both the acid and base hydrolyses, the pattern of entropy changes is very nearly the same. The initial increase, $\delta\Delta S^*$, of about 7 e.u. when the inert ligand is changed from ammonia to methyl amine is followed by progressive increases of about 2 e.u. per carbon increase in the chain length. These observations are

Can. J. Chem. Downloaded from www.nrcresearchpress.com by 210.87.254.5 on 09/05/12
For personal use only.

most easily rationalized in terms of models which allow a progressive but similar loosening of the molecular constraints in the transition state for both acid and base hydrolyses but which require opposite enthalpy effects.

An explanation for the entropy variation which is compatible with the experimental observations can be drawn from the picture of ion–solvent interaction painted by Frank and Evans (12), and modified and expanded by Nemethy and Scheraga (13). In this view of aqueous solutions, a non-polar solute molecule induces solvent molecules in its near vicinity to interact with each other in such a way that, on the average, these molecules are more ordered than are those of the bulk solvent. By contrast, specific interaction between polar solutes and the solvent tends to destroy the "iceberg" structure by reorienting the water molecules so that they are no longer favorably disposed to fit such a configuration.

The complex ions studied in this work have large radii so that despite their charge they should orient but not polarize the solvent, and their effect upon the solvent should be analogous to alkali metal ions of the same charge density. Consequently, the data of Frank and Evans (12) for the alkali metal ions have been used to produce a charge density–structural entropy calibration curve. Then, using this calibration curve together with estimates of the sizes of the complex ions involved in this study, it is possible to estimate the entropy change produced in the solvent as a function of ion size and ion charge. The estimates obtained in this way are given in Table III.

The hydrolysis reaction illustrated in reaction [1] represents an actual case in which the ion charge is increased from 2+ to 3+ in proceeding from reactant to product. This should mean that as the reacting ion moves up to and through the transition state, its interaction with the solvent will tend to cause the structural entropy of the ion in solution to decrease progressively, as the breaking bond distorts. It might be expected that if a pair of ions reacts by the same mechanism, there will be a correlation between the change in the structural entropy produced by the increase in ionic charge in the transition state and the change in the activation entropy for the one ion compared with that for the other. If the charge separation in the transition state is the same for the two ions, then the correlation between the change in structural entropy and the change in activation entropy for the two ions may depend only on the relative sizes of the two ions. An attempt to make such a correlation is shown in the last two columns of Table III. Even though the estimates of the structural entropy differences for the various ions are very crude, it is quite clear that there is a real correlation between these two parameters. In fact, the correlation that is obtained would suggest that the change in structural entropy is the principal reason for the change in the activation entropy through the series of complexes.

The obvious, mechanistically distinct, processes involving the hydroxide ion are described as displacement, ion pair, and conjugate base mechanisms (14). The first two seem unlikely both in terms of the low concentration of hydroxide at the onset of the base catalyzed reaction, and of the difficulty in fitting them to the observed pattern of activation entropies. The conjugate base mechanism (reactions [3], [4], and [5]) seems better suited to the observations on both counts.

[3] $Cr(NH_3)_5Cl^{2+} \rightleftarrows [Cr(NH_3)_4NH_2Cl]^+ + H^+$

[4] $[Cr(NH_3)_4NH_2Cl]^+ + H_2O \rightarrow Cr(NH_3)_5OH$

[5] $H^+ + OH^- \rightarrow H_2O$

This mechanism is a composite of two acid–base equilibria (reactions [3] and [5]) and a rate determining dissociation (reaction [4]). The observed activation parameters are summations of the appropriate thermodynamic parameters for each of the steps. Within the series of compounds investigated here the hydronium ion – hydroxide ion recombination makes a constant contribution of +19.3 e.u. (15) to the measured entropy of activation. The entropy change in the acid dissociation of the bound amine (reaction [3]) is much more in doubt because there are no direct measurements reported in the literature. However, it may be possible to get some feel for the order of magnitude of this quantity by analogy with the corresponding systems involving water. The acid dissociation of the chromium(III) aquo ion (reaction [6]) involves an entropy change of

[6] $Cr(H_2O)_6^{3+} \rightarrow Cr(H_2O)_5OH^{2+} + H^+$

+24 e.u. (16). This means that there is a difference between the entropy of dissociation of water and that of coordinatively bound water of about +43 e.u. For other trivalent aquo ions the difference is comparable (17). If the assumption is made that this difference is transferable to the

TABLE III

Structural entropies estimated for various pentaminechromium(III) complex ions

Amine	Radius[c]	ΔS_{ST} 2+ Ion	ΔS_{ST} 3+ Ion	$\delta\Delta S_{ST}$[a]	$\delta\Delta S^*$[b]
NH_3	2.5	10.4	−2.0		
CH_3NH_2	5.4	23.6	17.8	+6.6	+ 6.6
$C_2H_5NH_2$	6.5	25.5	20.9	+7.8	+ 8.0
$C_3H_7NH_2$	7.7	27.1	23.1	+8.4	+10.2
$C_4H_9NH_2$	8.9	28.2	24.6	+8.8	+11.0

[a]Change in ΔS_{ST} as the ion charge is increased from +2 to +3 compared with the same change for the ammonia complex.
[b]Change in ΔS^* for the acid hydrolysis reaction compared with that for the ammonia complex (Table I).
[c]Based upon the distance of closest approach of a water molecule to a non-bonding hydrogen on the terminal carbon assuming the most compact configuration for the alkyl chain.

corresponding ammonia systems, it would be expected that the entropy of dissociation would increase from −39.1 e.u. for free ammonia (17) to about +4 e.u. for ammonia bound to chromium(III). Then, a rough order of magnitude value for the entropy change involved in reaction [3] might be 0–10 e.u. Combination of this value with that for step [5] easily accounts for the 25 e.u. which separate the entropies of activation for the acid and base hydrolyses. If it is then assumed that the dissociation of the amines follows the dissociation of the corresponding ammonium salts (18), only small variations in the entropy of dissociation would be expected as the amine is changed through the series. This would mean that the entropy change in reaction [3] is roughly the same for all the amine complexes and that the sum of entropy changes for steps [3] and [5] would remain the same through the series of complexes. Consequently the predissociation steps do not contribute to the differences in the activation entropies between complexes, and the pattern of activation entropies that are observed would be expected to arise in reaction [4].

It is suggested that the similarity in the pattern of activation entropy variation through the series of complexes for the acid and base hydrolyses indicates a mechanistic similarity as well. Thus, the argument presented about the role of solvation in determining the entropy differences as the inert ligands were varied could apply equally well to both acid and base hydrolysis reactions. So, if the acid hydrolysis is primarily dissociative in character, it is at least plausible to propose that the base hydrolysis is also. This is exactly what might be expected for the rate determining step (reaction [4]) in the conjugate base mechanism.

If the conjugate base model is correct, the transition state for the base hydrolysis should differ from that for the acid hydrolysis only in the absence of one proton from one of the nitrogens, and if a similar degree of charge separation is attendant upon the base hydrolysis (as was suggested by the entropy changes) then, by analogy with the acid hydrolysis, the enthalpy of activation might have been expected to increase by about 4 kcal in going from the ammonia complex to the methyl amine complex. The decrease that actually occurred must represent a complication in the system and may have its origin in the pre-equilibrium acid dissociation to produce the conjugate base intermediate. This would have the enthalpy change in the acid dissociation of a bound primary amine less than that of bound ammonia. On the basis of purely electronic effects this is unlikely (19). However, calorimetric measurements of the heats of protonation of alkyl amines in aqueous solution (20, 21) show that replacement of a single hydrogen on ammonia by an alkyl group produces the expected increase, but two alkyl groups produce a decrease of about 1 kcal $mole^{-1}$ and a third alkyl group reduces the binding of the new proton by a further 4 kcal $mole^{-1}$. These changes have been interpreted in terms of the inefficient solvation of the substituted ammonias, making an unbound fully solvated proton increasingly favored as the degree of substitution on ammonia increased (21, 22).

When the alkyl amines are bound in the chromium complex, they are much more restricted in their interaction with the solvent than they would be as free amines in solution. It would not then be surprising that the alkyl substituents would exhibit an unusually large effect in shielding the remaining amino protons from interaction with the solvent. In this case it might be expected

Can. J. Chem. Downloaded from www.nrcresearchpress.com by 210.87.254.5 on 09/05/12
For personal use only.

that acid dissociation would be energetically favored in an attempt to reduce the positive charge on the metal complex, and distribute it into the bulk solvent (via the proton) where it could be effectively solvated. If this is correct then a decrease of the enthalpy associated with a process involving hydrogen dissociation could be expected. If all other factors were to remain constant a decrease of the activation energy for reaction through the conjugate base path is reasonable.

The experimental results presented here and the arguments which have been drawn from them are consistent with a mechanism for both the acid and base hydrolysis of these complexes which has as its rate determining step a primarily dissociative process.

Acknowledgment

The authors wish to acknowledge financial support of the work from the National Research Council of Canada.

1. Y. P. NAZARENKO and Y. I. BRATUSHKO. Ukr. Khim. Zh. **28**, 17 (1962).
2. H. FREUNDLICH and R. BARTELS. Z. Physik. Chem. Leipzig, **101**, 177 (1922).
3. R. E. OGARD and H. TAUBE. J. Am. Chem. Soc. **80**, 1084 (1958).
4. M. A. LEVINE, T. P. JONES, W. E. HARRIS, and W. J. WALLACE. J. Am. Chem. Soc. **83**, 2453 (1961).
5. A. ROGERS and P. J. STAPLES. J. Chem. Soc. 6834 (1965).
6. R. G. PEARSON and F. BASOLO. J. Am. Chem. Soc. **78**, 4878 (1956).
7. F. BASOLO, J. G. BERGMANN, R. E. MEEKER, and R. G. PEARSON. J. Am. Chem. Soc. **78**, 2676 (1956).
8. A. W. ADAMSON and F. BASOLO. Acta Chem. Scand. **9**, 1261 (1955).
9. W. C. FERNELIUS (*Editor*). Inorganic syntheses. Vol. II. McGraw-Hill Book Co., Inc., New York. 1946. p. 196.
10. T. P. JONES, W. E. HARRIS, and W. J. WALLACE. Can. J. Chem. **39**, 2371 (1961).
11. M. A. LEVINE. M.Sc. Thesis, University of Alberta, Edmonton, Alberta. 1959.
12. H. FRANK and M. EVANS. J. Chem. Phys. **13**, 507 (1945).
13. G. NEMETHY and H. A. SCHERAGA. J. Chem. Phys. **36**, 3382 (1962).
14. F. BASOLO and R. G. PEARSON. Mechanisms of inorganic reactions. John Wiley and Sons, Inc., New York. 1968.
15. K. H. PITZER. J. Am. Chem. Soc. **59**, 2365 (1937).
16. R. J. P. WILLIAMS. J. Phys. Chem. **58**, 121 (1954).
17. L. G. SILLEN. Stability constants. The Chemical Society, London. 1958.
18. R. STEWART and J. P. O'DONNELL. Can. J. Chem. **45**, 925 (1967).
19. R. G. PEARSON and D. C. VOGELSONG. J. Am. Chem. Soc. **80**, 1038 (1958).
20. R. P. BELL. The proton in chemistry. Cornell Univ. Press, Ithaca, New York. 1959.
21. D. R. WEIR. Ph.D. Thesis, University of Alberta, Edmonton, Alberta. 1966.
22. R. STEWART and J. P. O'DONNELL. Can. J. Chem. **42**, 1681 (1964).

Can. J. Chem. Downloaded from www.nrcresearchpress.com by 210.87.254.5 on 09/05/12
For personal use only.

Can. J. Chem. Downloaded from www.nrcresearchpress.com by 210.87.254.6 on 09/05/12
For personal use only.

Protonation of conjugated carbonyl groups in sulfuric acid solutions. II. Protonation and basicity of α,β-unsaturated alicyclic ketones[1, 2]

R. I. ZALEWSKI[3] AND G. E. DUNN
Department of Chemistry, University of Manitoba, Winnipeg 19, Manitoba

Received December 16, 1968

The protonation of 14 α,β-unsaturated alicyclic ketones, B, by sulfuric acid leads to values of log [B]/[BH^+] which, when plotted against the amide acidity function, H_A, give straight lines of unit slope. The pK_{BH^+} values thus obtained show substituent effects which are additive and can be interpreted in terms of polar and resonance effects.

Canadian Journal of Chemistry, 47, 2263 (1969)

The first paper of this series described the use of the amide acidity function, H_A, to study the protonation of the carbonyl group in non-Hammett bases (1). These included some alicyclic α,β-unsaturated ketones. In this paper, data for more compounds of this class of bases are presented.

The protonation of α,β-unsaturated ketones has not been a point of great interest in the past. Deno reported that α,β-unsaturated ketones in concentrated sulfuric acid solutions exist as mesomeric carbonium ions (2), with an absorption maximum near 287 mμ (3). However, no systematic study of the protonation of simple α,β-unsaturated ketones has been undertaken.

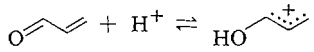

Not long ago, Zalewski studied the protonation of α,β-unsaturated ketosteroids and concluded that these compounds do not follow Hammett's H_0 acidity function (4). This investigation also clearly showed an influence of acid strength on the location and shape of the absorption curve in the ultraviolet region (4, 5). The present paper will present protonation data for a set of alicyclic α,β-unsaturated ketones having 5- and 6-membered rings, and show that these are better accommodated by the H_A acidity function than the H_0 function. A correlation between basicity and the electronic effects of substituents attached to the chromophore will be demonstrated.

[1]Presented in part at the 51st Conference of C.I.C. Vancouver 3–5, June 1968.
[2]For Part I, see ref. 1.
[3]University of Manitoba Postdoctorate Fellow, 1967–1968. Present address: Katedra Chemii Ogolnej W.S.E. Poznan (Poland) ul. Marchlewskiego 146.

Experimental

Materials

Compounds[4] used in this study were commercially available except **2** and **3**. Compounds **3**, **4**, **9–13** were used without purification. Compounds **1**, **2**, **5–8** and **14** were purified by the following procedure. About 1 g of ketone was mixed with 1 ml of *n*-heptane, filtered through Al_2O_3, and eluted by *n*-heptane. The eluent was removed by evaporation.

The sulfuric acid solutions were prepared by dilution of Allied Chemical C.P. Reagent sulfuric acid (min. 95.5%) and the concentrations were determined by density measurements for higher concentrations, by titration and density measurements for lower concentrations. The sulfuric acid concentrations were read from density data in the International Critical Tables. The corresponding H_0 or H_A values were read from graphs of acidity function vs. concentration, constructed from the data of Jorgenson and Hartter (6), and Yates *et al.* (7), respectively.

Method

The protonation of several classes of organic compounds has been intensively investigated in recent years, mostly by spectrophotometric methods in sulfuric acid solutions. An organic base may be considered to exist as free base, B, in water or dilute acid solutions, while in strongly acidic solutions it is protonated to its conjugate acid, BH^+. Since B and BH^+ usually have different absorption spectra, a wavelength can be found (often in the ultraviolet region) where the absorbance changes as the compound is protonated. From the absorbance change, it is in general possible to calculate K_{BH^+}, the equilibrium constant for the protonation reaction, in terms of an acidity function H (such as pH, H_0, H_A, etc.), in two ways (10).

(a) A plot of absorbance against H gives a titration curve, at the inflection point of which $H = pK_{BH^+}$.

(b) Absorbances can be used to calculate the quantity

$$[1] \qquad \frac{[B]}{[BH^+]} = \frac{\varepsilon_{BH^+} - \varepsilon}{\varepsilon - \varepsilon_B}$$

[4]The names corresponding to compound numbers are found in Table II.

from which pK_{BH^+} is obtained by the relationship

$$[2] \qquad pK_{BH^+} = H - \log \frac{[B]}{[BH^+]}$$

where B is the organic base, BH^+ is its conjugate acid, ε is the absorptivity of the solution at acidity H, and ε_B, ε_{BH^+} are the absorptivities of the base and conjugate acid, respectively, at the wavelength where ε is measured.

Sometimes it is very difficult to determine the coordinates of the inflection point in the first method, or the values of ε_B and ε_{BH^+} in the second method. We have attempted to overcome these difficulties by the use of a computer program based on the following considerations.

Generally, for the protonation of an organic base, B, under conditions where activities may be approximated by concentrations, the ionization constant is expressed by

$$K_{BH^+} = \frac{[B][H^+]}{[BH^+]}$$

where the quantities in square brackets represent molar concentrations. If the total concentration of base (free and ionized) is [C] then the absorbance, A, measured in a solution where the base is only partly ionized, can be shown (20) to be given by

$$[3] \qquad A = [C] \frac{\varepsilon_B K_{BH^+} + \varepsilon_{BH^+}[H^+]}{K_{BH^+} + [H^+]}$$

Equation [3] is an adequate representation of the titration curve at constant ionic strength in the region of acidity, where $[H^+]$ may be approximated from pH. For use in strong solutions of sulfuric acid, pH is replaced by an acidity function, such as H_0, which expresses the deviation of the system from ideality. Constancy of ε_B and ε_{BH^+} over the necessary range of sulfuric acid concentration is still assumed, of course.

Since A, $[H^+]$, and [C] are observable quantities, eq. [3] contains three unknowns: K_{BH^+}, ε_{BH^+}, and ε_B. In principle ε_B and ε_{BH^+} can be determined experimentally by measurements made in solutions with $[H^+] = pK_{BH^+} + 2$ and $[H^+] = pK_{BH^+} - 2$, respectively. However, in practice, they may not be so readily accessible, because the base is subject to further protolytic or non-protolytic reactions at high or low acidity, because the solvent absorbs at the necessary acidity, or for a variety of other reasons. In moderately concentrated sulfuric acid solutions, it is often observed that ε_B and ε_{BH^+} are not constant, even in the region of acid concentrations where the organic base should be present as a single species, either free base or conjugate acid (8–14). It is therefore probable that ε_B and ε_{BH^+} will vary across the range of acidities where both species contribute to the absorbance. Various methods have been proposed to take account of this variation (10–13), most of them based on extrapolation of ε_B and ε_{BH^+} from regions of acidity outside the titration range. The extrapolation requires that absorbance by the substrate outside the titration range be subject only to medium effects (no protolytic, hydrolytic, or other reactions), and that the medium effects be linear in the acidity function used. For many bases these conditions cannot be satisfied, so in the present work, a procedure was used which makes some allowance for medium effects, even when extrapolation is not possible. Absorbances were measured at 12 or more intervals in the titration range, and used in a least-squares computer program to solve eq. [3] for the 3 disposable parameters K_{BH^+}, ε_B, and ε_{BH^+}. This procedure is an extension of one suggested by Flexser *et al.* (10) and, in effect, gives the best average values of ε_B and ε_{BH^+} over the titration range.

Measurements were made at the wavelength, λ_B, characteristic of the base, and at the wavelength, λ_{BH^+}, characteristic of the conjugate acid, so that two largely independent estimates were obtained for each of the 3 unknowns. Measurements at the 2 wavelengths were also combined by the Stewart–Granger procedure (*8a*), to give a third set of estimates intermediate between the first two.

Absorption Spectra Measurements

Aqueous stock solutions (10^{-3} M) of the ketones were diluted with sulfuric acid solutions to concentrations of about 5×10^{-5} M for absorbance measurement on a Beckman DK-1 spectrophotometer. Three ketones which were not easily soluble were treated differently. Compounds **9** and **10** were dissolved in 10 ml of concentrated sulfuric acid, then diluted to 250 ml with water to give the 10^{-3} M stock solutions. Compounds **5**, **6**, and **7** gave the same spectral and pK data by this procedure and the standard one, so it appears that most α,β-unsaturated ketones are unaffected by concentrated sulfuric acid, except for protonation. For *d*-carvone, which does react with sulfuric acid of more than 70% concentration, 10 ml of methanol was used instead of 10 ml of sulfuric acid to prepare the stock solution.

Results and Discussion

In Fig. 1 are shown spectra from 210 to 265 mμ of 2-cyclopentenone in various concentrations of sulfuric acid, as well as in methanol and in water. These are typical of the spectra obtained from all the α,β-unsaturated ketones examined. It is observed that the $\pi \rightarrow \pi^*$ band shifts bathochromically with increasing solvent polarity, from 218.5 mμ in methanol, to 221.5 mμ in water. A further bathochromic shift occurs in sulfuric acid solution (Figs. 1 and 2).

Figure 2 shows a typical relation between the acidity of the solvent and the location of the $\pi \rightarrow \pi^*$ maximum. The lower part of the curve represents the absorption maximum for the α,β-unsaturated ketone as a base, where the concentration of the conjugate acid is small. The small bathochromic shift in this region can be explained by increasing interaction between the carbonyl group and solvent. The upper part of the curve represents the absorption maximum for the conjugate acid of the ketone, where the concentration of unprotonated ketone is small. Again there is a small bathochromic shift with increasing acid

Can. J. Chem. Downloaded from www.nrcresearchpress.com by 210.87.254.6 on 09/05/12
For personal use only.

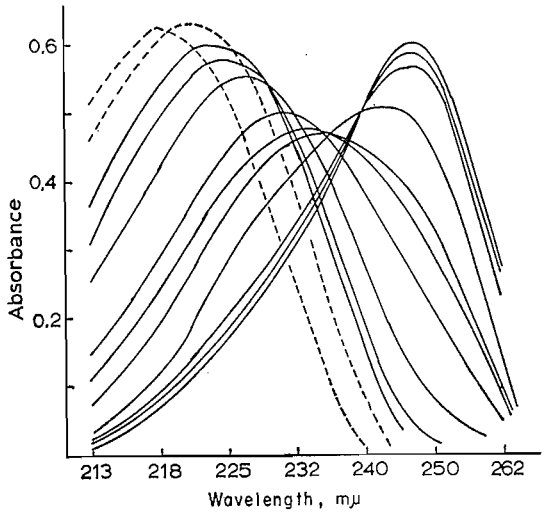

FIG. 1. Absorbance of 2-cyclopentenone as a function of sulfuric acid concentration. Solvent (top to bottom at left-hand margin); methanol, water, sulfuric acid 38.0, 51.0, 57.3, 66.0, 69.1, 71.5, 74.2, 83.9, 94.1, and 96%.

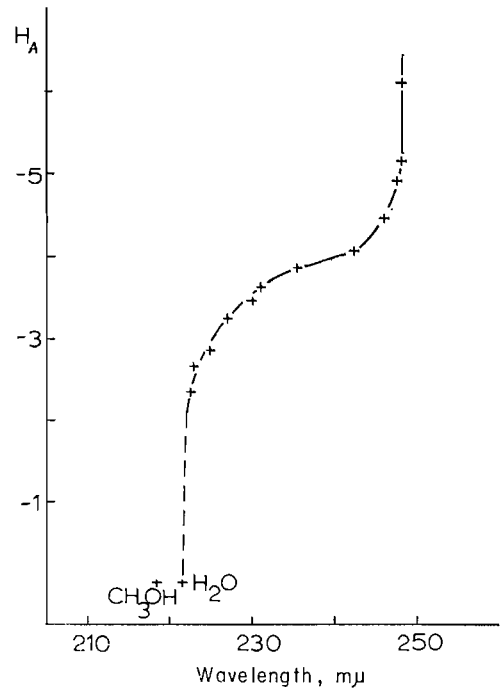

FIG. 2. Effect of sulfuric acid concentration on λ_{max} of 2-cyclopentenone.

concentration as the result of changing interaction between cation and solvent (15). The middle part of the curve represents the broad, irregular maxima, resulting from the overlapping absorptions of mixtures of the 2 species. Curves similar to those in Fig. 2 were observed for all the α,β-unsaturated ketones examined.

The solvent shifts in λ_{max} described above are such that there is no single isosbestic point in Fig. 1. In the region of acidities where the ketone should be present as unionized base (lower vertical part of Fig. 2), the gradual shift in λ_{max} results in the convergence of the absorbance curves into an apparent isosbestic point at 230 mμ. A similar convergence occurs at 240.5 mμ for the conjugate acid (acidities in the upper vertical part of Fig. 2). The true isosbestic point, where $\varepsilon_B = \varepsilon_{BH^+}$, lies at about 236 mμ. Here the approximate convergence of the absorption curves shows that, within the region of acidities corresponding to the non-vertical part of Fig. 2, the variation in ε_B and ε_{BH^+} is not large. It is in this region that pK_{BH^+} measurements were made.

The primary objective of the present investigation was to examine the effect of structural changes on the basicities of α,β-unsaturated ketones. In order to do this, of course, it is necessary to find an acidity function which adequately represents the ability of acid solutions to protonate ketones. Ideally, this requires that the activity coefficient ratio, f_B/f_{BH^+}, must exactly parallel that of the indicator bases used to establish the acidity function through the whole range of acidities from the neutralization point to dilute aqueous solution. Such information is rarely available, so that an organic base is usually considered to obey an acidity function satisfactorily, if the activity coefficient ratio parallels that of the indicators through the titration range of acidities. Tests for this minimum requirement are provided by eqs. [2] and [3]. The pK_{BH^+} values calculated from eq. [2] must be independent of acidity and the plot of log $[B]/[BH^+]$ vs. the acidity function must have a slope of unity. The acidity function which best satisfies eq. [3] is the one which most closely reproduces the experimental absorbances.

Table I presents the numerical data for acidity, H_0 and H_A, of sulfuric acid solutions, the wavelength λ_{max}, and the absorbance A_{max} of the $\pi \rightarrow \pi^*$ transitions of 2-cyclopentenone and its conjugate acid. Also presented, for the wavelength characteristic of the base, λ_B, and that characteristic of the conjugate acid, λ_{BH^+}, are the experimental absorbances ($A = \varepsilon[C]$), and those calculated from eq. [3]. It is seen that the values of A_B, A_{BH^+}, and pK_{BH^+} have a smaller standard

Can. J. Chem. Downloaded from www.nrcresearchpress.com by 210.87.254.6 on 09/05/12
For personal use only.

Can. J. Chem. Downloaded from www.nrcresearchpress.com by 210.87.254.6 on 09/05/12
For personal use only.

TABLE I

Absorbance and acidity data for 6.5×10^{-5} *M* 2-cyclopentenone in sulfuric acid

Concentration (%)	$-H_0$	$-H_A$	λ_{max} (mμ)	A_{max}	$A_{\lambda BH^+}$			$A_{\lambda u}$			$-pK_{BH^+}$	
					Observed	Calculated H_A	Calculated H_0	Observed	Calculated H_A	Calculated H_0	H_0	H_A
	—	—	—	—	A_{BH^+}*	0.584± ±0.005	0.552± ±0.013		0.185± ±0.010	0.213± ±0.010	—	—
94.0	9.68	6.00	248.0	0.590	—	—	—	—	—	—	—	—
86.1	8.29	5.12	248.0	0.570	0.570	0.571	0.552	0.200	0.198	0.214	6.85	3.68
83.3	7.97	4.90	247.8	0.560	0.560	0.563	0.551	0.210	0.206	0.215	6.77	3.70
79.4	7.18	4.45	246.0	0.530	0.530	0.527	0.545	0.230	0.240	0.221	6.26	3.53
79.2	6.41	4.03	242.5	0.510	0.490	0.454	0.509	0.290	0.303	0.259	5.99	3.61
71.5	5.95	3.85	235.5	0.470	0.400	0.407	0.453	0.350	0.341	0.311	5.76	3.66
69.1	5.65	3.67	231.0	0.480	0.340	0.351	0.374	0.395	0.383	0.377	5.65	3.67
66.0	5.20	3.45	230.0	0.500	0.260	0.278	0.246	0.445	0.436	0.466	5.42	3.67
62.0	4.70	3.20	227.0	0.520	0.170	0.197	0.133	0.490	0.489	0.531	5.13	3.63
57.3	4.05	2.87	225.0	0.555	0.115	0.112	0.070	0.545	0.541	0.562	4.85	3.67
51.0	3.32	2.57	223.0	0.575	0.065	0.061	0.052	0.570	0.569	0.571	4.40	3.63
46.3	3.08	2.33	222.5	0.580	0.040	0.036	0.049	0.580	0.583	0.572	4.34	3.59
38.0	2.30	1.90	222.0	0.595	0.010	0.013	0.047	0.595	0.595	0.573	4.07	3.67
—	—	—	—	—	A_B*	0.000± ±0.005	0.046± ±0.012	—	0.602± ±0.003	0.573± ±0.010	—	—
—	—	—	—	—	pK_{BH^+}*	−3.49± ±0.03	−5.39± ±0.13	—	−3.62± ±0.03	−5.57± ±0.11	—	—

*Calculated from eq. [3].

Can. J. Chem. Downloaded from www.nrcresearchpress.com by 210.87.254.6 on 09/05/12
For personal use only.

deviation when calculated from H_A than from H_0, and that the values from H_A give much better reproduction of the experimental absorbances than do those from H_0. The last 2 columns of Table I show pK_{BH^+} calculated from eq. [2] at λ_B using the values of A_B and A_{BH^+} from eq. [3]. The values calculated from H_A are approximately constant while those from H_0 show a pronounced drift. Figure 3 shows the plot of log $[B]/[BH^+]$ vs. H_A with slope 1.01 and vs. H_0 with slope 0.52. It is evident that the protonation of 2-cyclopentenone very closely parallels that of the amides used to establish the H_A acidity function. Similar behavior was observed for all the other α,β-unsaturated ketones tested.

Data for all the α,β-unsaturated ketones are presented in abbreviated form in Table II. Spectral data are given for the ketone as base, B, and as conjugate acid, BH^+, together with values for pK_{BH^+} obtained from eq. [3] using the Stewart–Granger procedure, and for the slopes of the lines log $[B]/[BH^+]$ vs. H_A and H_0. It is clear that for all the α,β-unsaturated ketones, the slopes are those to be expected from the H_A acidity function. In the absence of activity data over the whole acidity range, it is not known whether or not the pK_{BH^+} values derived from H_A are thermodynamic ones or not, but they should be satisfactory for interpreting structural effects upon acidity within a single series of bases[5].

The effect of structure on the basicities of α,β-unsaturated ketones may now be considered. In

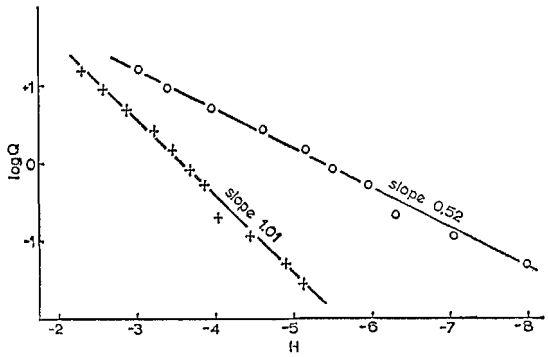

FIG. 3. Plot of log $[B]/[BH^+]$ (= log Q) vs. acidity for 2-cyclopentenone. Crosses represent H_A and circles represent H_0.

general, the ability of the base to accept a proton depends on factors affecting the electron density at the basic center, in our case the carbonyl group. These are customarily divided into polar, resonance, and steric factors. Polar and resonance effects on the basicities of α,β-unsaturated ketones are easily demonstrated from the pK_{BH^+} data of Table II, but effects specifically attributable to steric factors are not evident. It is noticeable in this connection that similarly substituted 2-cyclopentenones and 2-cyclohexenones (**1** and **5**, **2** and **6**) have almost identical pK_{BH^+} values. Apparently this much variation in ring size does not affect basicity.

Ketones substituted by methyl groups in the β-position (**2**, **6**) are stronger bases than the unsubstituted ones by 0.75 pK_{BH^+} unit. β-Methylene (**9**) has the same acid-strengthening effect as β-methyl. Further methyl substitution in the δ-position (**7**) does not effect the basicity. These facts are all explainable in terms of the +I inductive effect of the methyl group, which stabilizes the conjugate acid more than the ketone. Hyperconjugation will have a similar influence.

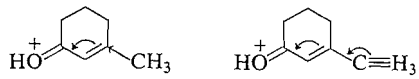

α-Methyl substitution (**8**) also makes the base stronger. Unfortunately *d*-carvone is not stable in more concentrated solutions of sulfuric acid so that it is impossible to find λ_{BH^+}. Consequently, pK_{BH^+} was calculated at only one wavelength (λ_B) and for only part of the titration curve. A more reliable demonstration of the base-strengthening effect of α-methyl substitution is obtained by

[5]Bunnett and Olsen (16) and Greig and Johnson (13) prefer to relate the protonation of all bases to the original Hammett acidity function, H_0, by use of the observation that all acidity functions are linearly related to H_0 (12). If

$$H = mH_0 + b$$

then eq. [2] becomes

$$pK_{BH^+} = mH_0 + b - \log([B]/[BH^+])$$

Since all acidity functions must converge in dilute acid, b should be zero. This is observed to be the case except for the amide acidity function (12), where a plot of H_A vs. H_0 deviates from linearity at low acidity, so that in the region of acidities used in most of this work, $H_A = 0.53H_0 + 0.68$. Hence, for a base which fits the H_A scale, a plot of log $[B]/[BH^+]$ vs. H_0 should have a slope of 0.53. Table II shows that this prediction is correct, except for compounds **13** and **14**, where pK_{BH^+} lies on the curved part of the H_A vs. H_0 plot. Except for these 2 compounds, the pK_{BH^+} preferred by the above authors will be obtained by adding 0.68 to the values given in Table II. Without activity data, it is not known whether either set is thermodynamic, and the latter set rests upon the as yet unproved assumption that the H_A scale is incorrectly based, so we have used the set based on H_A and eq. [3].

Can. J. Chem. Downloaded from www.nrcresearchpress.com by 210.87.254.6 on 09/05/12
For personal use only.

TABLE II

Absorbance and acidity data for α,β-unsaturated alicyclic ketones

	Compound	λ_B (mμ)	$\varepsilon_B \times 10^{-3}$	λ_{BH^+} (mμ)	$\varepsilon_{BH^+} \times 10^{-3}$	$-pK_{BH^+}$	Slope log Q vs. H_A	Slope log Q vs. H_0
1.	2-Cyclopenten-1-one	222	9.3	248	9.0	3.55±0.03	1.01	0.52
2.	3-Methyl-	232	14.3	254	16.0	2.82±0.03	1.00	0.54
3.	2,3-Dimethyl-	240	11.1	266	13.6	2.55±0.02	0.97	0.53
4.	3-Methyl-2-hydroxy-	258	10.6	292	12.0	3.27±0.04	1.03	0.54
5.	2-Cyclohexen-1-one	231	7.5	271	9.4	3.60±0.04	1.01	0.50
6.	3-Methyl-	241	13.1	277	13.8	2.83±0.03	1.03	0.51
7.	3,5-Dimethyl-	243	12.9	278	13.3	2.86±0.04	1.01	0.51
8.	*d*-Carvone	293	8.2	—	—	2.92±0.07	1.01	0.55
9.	3-Methyl-$\Delta^{1,9}$-octalone-2	249	11.0	287	11.1	2.82±0.03	0.98	0.50
10.	1-Methyl-$\Delta^{1,9}$-octalone-2	258	11.0	297	11.3	2.47±0.03	0.99	0.50
11.	9-Methyl-$\Delta^{5(10)}$-octalin-1,6-dione	250	11.7	279	11.2	3.54±0.04	0.97	0.51
12.	2,8*a*-Dimethyl-3,4,8,8*a*-tetrahydro-1,6(2*H*,7*H*)-naphthalene-dione	259	12.0	299	12.3	3.32±0.03	0.98	0.52
13.	3-Hydroxy-2-cyclohexen-1-one	256	16.1	273	20.5	0.84±0.02	1.00	—
14.	3-Ethoxy-2-cyclohexen-1-one	257	17.6	273	21.0	0.77±0.04	0.94	—

Can. J. Chem. Downloaded from www.nrcresearchpress.com by 210.87.254.6 on 09/05/12
For personal use only.

comparing the pK_{BH^+} values of 2,3-dimethylated ketones (**3**, **9**) with those of 3-methylated ones (**2**, **6**). The additional methyl group in the α-position strengthens the base by 0.3 pK_{BH^+} unit.

Resonance stabilization may produce much larger changes in basicity, as is illustrated by compounds **13** and **14** which are about 2.6 pK_{BH^+} units more basic than the unsubstituted α,β-unsaturated ketones. Compound **13** is 1,3-cyclohexanedione but this is reported by Schwarzenbach and Felder to be more than 90% enolized in aqueous solution (17). Its high basicity has previously been noted by Eistert *et al.* (18), whose pK value agrees satisfactorily with the one reported here. The very close agreement in basicity between this compound and 3-ethoxy-2-cyclohexenone (**14**) tends to confirm the enol structure. The inductive effect (−I) of hydroxy and alkoxy groups should be base-weakening, so the great basicity of the β-oxy compounds must be the result of resonance stabilization of their conjugate acids. This should be of special importance because of the equivalence of the two main con-

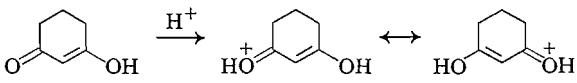

tributing structures. Such resonance stabilization is not possible when the hydroxy group is in the α-position, so the inductive effect should be revealed. Compound **4** illustrates these conclusions. It is 3-methyl-1,2-cyclopentanedione which is also completely enolized in aqueous solution (19). The α-hydroxy group makes the base weaker than the corresponding unsubstituted compound (**2**) by about 0.45 pK_{BH^+} unit. Evidently the inductive effect predominates here. The α-fluoro substituent behaves similarly in α,β-unsaturated ketosteroids (21).

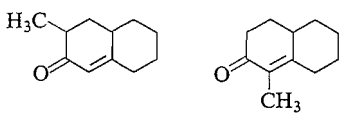

9 **10**

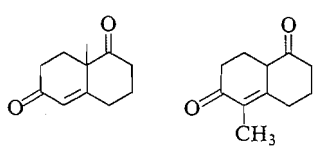

11 **12**

TABLE III

The effects of substituents on basicity of α,β-unsaturated ketones

Substituent	ΔpK_{BH^+}
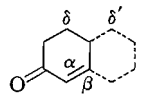	0.00
α-CH_3	+0.30
β-CH_3, —CH_2—	+0.75
α-OH	−0.50
β-OH	+2.60
δ′-C=O	−0.75
δ-CH_3	0.00

The basicities of molecules such as **11** and **12**, which contain a second (unenolized) carbonyl group in the δ-position, are smaller than those of the corresponding unsubstituted compounds (**9** and **10**, respectively) by about 0.75 pK_{BH^+} unit. No doubt this is the result of the inductive effect (−I) of the highly polar carbonyl group. A similar result is seen in α,β-unsaturated ketosteroids with a carbonyl group at C-11, which are weaker than the corresponding unsubstituted compounds by about 0.2 pK_{BH^+} unit (5). In these compounds, the substitution is more remote from the basic center, so the effect is smaller.

The effects of substituents on pK_{BH^+} of α,β-unsaturated ketones may be summarized in terms of differences ΔpK_{BH^+} between substituted and unsubstituted molecules, as shown in Table III. Also, ΔpK_{BH^+} values are additive, at least within the series of compounds examined, so that the basicity of an α,β-unsaturated ketone can be calculated by eq. [5], with a maximum error of 0.05 pK_{BH^+} unit.

$$[5] \qquad pK_{BH^+} = -3.57 + \sum \Delta pK_{BH^+}$$

Acknowledgments

The authors are grateful to the National Research Council of Canada for financial support and to Dr. T. Sorenson for valuable discussions as well as for the gift of compounds **2** and **3**.

1. R. I. Zalewski and G. E. Dunn. Can. J. Chem. **46**, 2469 (1968).
2. N. C. Deno, H. G. Richey, N. Friedman, J. D. Hodge, J. J. Houser, and Ch. U. Pittman, Jr. J. Am. Chem. Soc. **85**, 2991 (1963).
3. G. A. Olah, Ch. U. Pittman, Jr., R. Waack, and M. Donar. J. Am. Chem. Soc. **88**, 1488 (1966).
4. R. I. Zalewski. Ph.D. Thesis, University of Poznan, Poland. 1967.

5. A. M. SMOCZKIEWICZ and R. I. ZALEWSKI. Steroids, **12**, 391 (1968).
6. M. J. JORGENSON and D. R. HARTTER. J. Am. Chem. Soc. **85**, 878 (1963).
7. K. YATES, J. B. STEVENS, and A. R. KATRITZKY. Can. J. Chem. **42**, 1957 (1967).
8. (*a*) R. STEWART and M. GRANGER. Can. J. Chem. **39**, 2508 (1961). (*b*) CH. T. DAVIS and T. A. GEISSMAN. J. Am. Chem. Soc. **76**, 3507 (1959).
9. K. YATES and H. WAI. Can. J. Chem. **43**, 2131 (1965).
10. L. A. FLEXSER, L. P. HAMMETT, and A. DINGWALL. J. Am. Chem. Soc. **57**, 2103 (1935).
11. R. L. REEVES. J. Am. Chem. Soc. **88**, 2240 (1966).
12. K. YATES and R. A. MCCLELLAND. J. Am. Chem. Soc. **89**, 2686 (1967).
13. C. C. GREIG and C. D. JOHNSON. J. Am. Chem. Soc. **90**, 6453 (1968).
14. E. M. ARNETT. Progr. Phys. Org. Chem. **1**, 223 (1963).
15. N. S. BAYLIS and E. G. MCRAE. J. Phys. Chem. **58**, 1002 (1959).
16. J. F. BUNNETT and F. P. OLSEN. Can. J. Chem. **44**, 1899 (1966).
17. G. SCHWARZENBACH and E. FELDER. Helv. Chim. Acta, **27**, 1019 (1944).
18. B. EISTERT, E. MERKEL, and W. REISS. Chem. Ber. **87**, 1573 (1959).
19. G. SCHWARZENBACH and C. WITTWER. Helv. Chim. Acta, **30**, 663 (1947).
20. G. E. DUNN and FEI-LIN KUNG. Can. J. Chem. **44**, 1261 (1966).
21. R. I. ZALEWSKI. Unpublished data.

Can. J. Chem. Downloaded from www.nrcresearchpress.com by 210.87.254.6 on 09/05/12
For personal use only.

Can. J. Chem. Downloaded from www.nrcresearchpress.com by 210.87.254.40 on 09/05/12
For personal use only.

Osmotic and activity coefficients of some simple borates in aqueous solution at 25°

R. F. PLATFORD
Canada Centre for Inland Waters, Burlington, Ontario

Received December 19, 1968

Activity coefficients for sodium tetraborate, potassium tetraborate, sodium metaborate, sodium fluoroborate, and orthoboric acid were derived from isopiestic vapor pressure measurements. The osmotic behavior of sodium tetraborate, at concentrations up to its solubility limit, was the same as that of the more soluble potassium salt. The mean activity coefficients of both tetraborates were quite low: 0.355 at 0.1 *m*; the activity coefficients of sodium metaborate and fluoroborate were less than those of sodium chloride, indicating partial association in solution.

The boric acid results were not very reliable because boric acid apparently volatilized during the measurements, but the results obtained indicated that it behaves like a non-electrolyte at all concentrations up to saturation, with an activity coefficient never less than 0.92.

Canadian Journal of Chemistry, 47, 2271 (1969)

Introduction

Borax ($Na_2B_4O_7 \cdot 10H_2O$) is a common mineral and its osmotic properties in aqueous solution should be of interest to geochemists. It is not, however, very soluble in water and therefore is not very suitable for isopiestic studies, but its analogue, potassium tetraborate, is soluble enough to make such measurements worthwhile, and to provide insight into the behavior of the less soluble borax. The metaborates and fluoroborates are also soluble salts of interest, the latter particularly so because a fluoroborate ion electrode has recently been marketed[1].

Another soluble boron compound worth investigating is boric acid, which, with its pK_a of 9.2 (1), should behave like a non-electrolyte in solution.

The measurements described here are preliminary to a study of multicomponent borate systems of geochemical interest.

Experimental

The reference salt, sodium chloride, was recrystallized from water and dried at 120°.

Sodium tetraborate was recrystallized twice from water at 55° and dried over a saturated solution of sucrose and sodium chloride to give $Na_2B_4O_7 \cdot 10H_2O$ (2). The solubility (reported as molality of the salt at 25°) determined by titration with HCl was 0.158 *m*; the literature value is 0.157 *m* (3). The solubility measured by the isopiestic method described by Scatchard *et al.* (4) was 0.154_3 *m*. This last value refers to an air-free solution at a total pressure of ~ 23 Torr, and the difference in values may be due to the different conditions.

[1]Orion Research Incorporated, Cambridge, Mass., 02139.

Potassium tetraborate was recrystallized twice from water and dried at 60° to give $K_2B_4O_7 \cdot 4H_2O$ (5). The solubility at 25° determined by three different methods, was: by titration, 0.660 *m*; by evaporation at 60°, 0.65 *m*; and by the isopiestic method, 0.648_4 *m* (literature value, 0.65 *m* (5)).

Sodium metaborate was recrystallized from water and dried at 80° to give the dihydrate. Some runs were also done with reagent grade tetrahydrate. The solubility of sodium metaborate determined by titration was 4.29 *m* and by the isopiestic method was 4.423 *m* (literature value, 4.19 *m* (3)).

Sodium fluoroborate was recrystallized from water and dried at 120°. Its solubility, determined by evaporation to dryness at room temperature, was 9.4_6 *m*, and by the isopiestic method was 9.87 *m* (literature value, 9.8 *m* (6)).

Orthoboric acid was recrystallized twice from water and dried at 60°. This sample slowly lost weight, apparently by sublimation, as it always assayed 100 ± 0.5% pure. Volatilization also occurred at the low pressures under which the isopiestic measurements were made, but not to a great enough extent to be readily detectable by analysis of the small volumes (1–2 ml) of final solutions, resulting from the isopiestic measurements. Because of this volatilization, or for some unknown reason, the isopiestic results for boric acid were quite badly scattered, and the concentrations reported (which were usually determined by weighing as described below) may not be better than ±0.005 *m*, even though they are reported to 0.001 *m*. (This difficulty was also observed with the sodium fluoroborate solutions although to a lesser extent than with the boric acid.)

The solubility of boric acid at 25°, determined by titration with $Ba(OH)_2$ in the presence of mannitol (7), was 0.927 *m*. Evaporation of saturated solutions to dryness at room temperature gave a solubility of 0.929_5 *m* and the isopiestic method gave 0.92 *m* (literature value, 0.934 *m* (3)).

Isopiestic comparisons were made either in 7 silver dishes or in 4 platinum dishes (for $NaBF_4$) set in gold plated copper blocks (8). The pure dry salts were weighed into the dishes and a suitable amount of distilled water was added to each. The dishes and block were set in a

Can. J. Chem. Downloaded from www.nrcresearchpress.com by 210.87.254.40 on 09/05/12
For personal use only.

TABLE I

Isopiestic concentrations at 25 °C

Molality (m)		
NaCl	$K_2B_4O_7$	H_3BO_3
0.0948	0.0377	0.181
0.1297	0.0523*	0.245
0.1587	0.0668	—
0.1922	—	0.362
0.2706	0.1321*	—
0.3071	0.1543*†	—
0.3160	—	0.588
0.3177	0.1643	—
0.3858	—	0.725
0.4095	0.2333	0.773
0.4553	—	0.845
0.4915	—	0.92†
0.5416	0.3447	—
0.6123	0.4106	—
0.6990	0.4980	—
0.7847	0.5917	—
0.8379	0.6484†	—
1.0045	0.8473	—
1.2670	1.1940	—
±0.0003	±0.0004	±0.002

Molality (m)			
NaCl	$NaBO_2$	NaCl	$NaBF_4$
0.2543	0.2664	0.2352	0.2402
0.5170	0.5709	0.5527	0.5986
0.6485	0.7321	1.2275	1.4635
1.0661	1.2815	1.4384	1.7601
1.2281	1.5042	2.0760	2.7585
1.5263	1.9213	2.3458	3.2086
1.9543	2.5104	2.8099	4.0465
2.2121	2.8546	3.5743	5.5435
2.9112	3.7699	4.1148	6.7168
3.2341	4.1660	4.9274	8.6242
3.4408	4.4235†	5.42	9.87†
±0.0006	±0.0012	±0.0007	±0.0011

*$Na_2B_4O_7$.
†Saturated solution.

desiccator which was then evacuated, and the solutions were equilibrated for 3–5 days in a thermostat at 25.00° before the dishes were reweighed. Some solutions were frozen before evacuation in order to reduce bumping and volatilization. Each set contained 2 or 3 sodium chloride reference solutions. The isopiestic concentrations reported in Table I are averages of 2 or 3 replicates corrected to vacuum. The last figure in each column is the average precision of all the replicate measurements for that salt.

Potassium tetraborate solutions supersaturated so easily that measurements on this salt were extended to concentrations of nearly 1.2 m.

Results and Discussion

The osmotic coefficients were calculated from the equation

$$[1] \qquad \phi = 2m_R\phi_R/\nu m$$

where m_R and ϕ_R are respectively the molality and osmotic coefficient of sodium chloride (9), ν is the number of moles of ions formed per mole of borate, and m is the molality of the borate in equilibrium with the reference solution.

For boric acid, ν was put equal to 1 (H_3BO_3 is the predominant species in solution at all concentrations) and for the two tetraborates it was necessary to put $\nu = 6$, in order that $\phi \to 1$ as $m \to 0$. This value for ν is consistent with the dissociation

$$[2] \quad Na_2B_4O_7 + 7H_2O \rightarrow 2Na^+ + 2B(OH)_4^- + 2H_3BO_3$$

because borax in solution is equivalent to boric acid titrated halfway to the equivalence point with strong base. If the dissociations of sodium metaborate and sodium fluoroborate are given by reactions [3] and [4]

$$[3] \quad NaBO_2 + 2H_2O \rightarrow Na^+ + B(OH)_4^-$$

$$[4] \quad NaBF_4 \rightarrow Na^+ + BF_4^-$$

then $\nu = 2$ for these two salts. The fluoroborate ion hydrolyzes (10) slightly in solution to give H_3BO_3 and HF. This hydrolysis causes some uncertainty in the values of ϕ and $\gamma_\pm$ for $NaBF_4$, which will have to be determined by electrode measurements.

The osmotic coefficients interpolated at round molalities are given in Table II. The sodium and potassium tetraborates have such similar osmotic coefficients over their common concentration range, that any difference is indistinguishable on an ordinary plot. Therefore, the values in Table II refer to either of these salts up to 0.15 m.

The mean activity coefficients were calculated from the standard equation (9)

$$[5] \quad -\ln \gamma_\pm = 1 - \phi + 2\int_0^{m^{\frac{1}{2}}} \frac{(1-\phi)}{m^{\frac{1}{2}}} dm^{\frac{1}{2}}$$

and are reported in Table II. The integral in eq. [5] was evaluated graphically.

The uncertainties in ϕ are about 0.002 for the borates, and because of the uncertainties mentioned earlier, are about 10 times greater for the boric acid. The uncertainties in $\gamma_\pm$ are as much as 0.01 depending on how the integral in eq. [5] is evaluated at low concentrations.

Because borax in solution can be formed by mixing aqueous sodium metaborate and boric acid, it should be possible to calculate changes in

TABLE II

Osmotic and activity coefficients for borates

	$K_2B_4O_7$ ($Na_2B_4O_7$)		H_3BO_3			$NaBO_2$		$NaBF_4$	
m	ϕ	$\gamma_\pm$	ϕ	$\gamma_\pm$	m	ϕ	$\gamma_\pm$	ϕ	$\gamma_\pm$
0.01	0.89	0.74	—	0.99	0.1	0.925	0.797	0.934	0.818
0.05	0.76	0.48	—	0.98	0.5	0.843	0.613	0.864	0.652
0.1	0.671	0.355	0.99	0.97	1.0	0.795	0.515	0.820	0.560
0.2	0.562	0.246	—	0.96	1.5	0.771	0.461	0.791	0.502
0.3	0.501	0.192	—	0.95	2.0	0.760	0.426	0.768	0.461
0.4	0.462	0.159	—	—	2.5	0.763	0.405	0.751	0.428
0.5	0.433	0.137	0.98	0.94	3.0	0.774	0.393	0.737	0.404
0.6	0.410	0.120	—	—	3.5	0.791	0.386	0.727	0.384
0.7	0.392	0.107	—	0.93	4.0	0.814	0.385	0.718	0.367
0.8	0.376	0.097	—	—	5.0	—	—	0.705	0.339
0.9	0.363	0.089	0.98	0.92	6.0	—	—	0.695	0.318
1.0	0.351	0.082	—	—	7.0	—	—	0.686	0.300
1.1	0.341	0.077	—	—	8.0	—	—	0.680	0.286
1.2	0.333	0.072	—	—	9.0	—	—	0.676	0.275

ideality resulting from the reverse of the process in eq. [2]. This is done by comparing ϕ(borax) with the weighted sum of $\phi(NaBO_2)$ and $\phi(H_3BO_3)$. The ϕ values are measures of the colligative properties of solutions, and any difference is directly related to the excess free energy of mixing (11) or change in ideality on mixing.

For example, if 0.3 mole of $NaBO_2$ in 0.667 kg of water is added to 0.3 mole of H_3BO_3 in 0.333 kg of water to give 0.15 mole of $Na_2B_4O_7$ in 1.0081 kg of water, the process will have taken place at a nearly constant νm of 0.9. (The small amount of water required to hydrate the $NaBO_2$ has been ignored.) The change in ideality on mixing is given by

$$\Delta = \phi\,(0.15\,m\,Na_2B_4O_7) - 2/3\,\phi\,(0.45\,m\,NaBO_2) - 1/3\,\phi\,(0.9\,m\,H_3BO_3)$$

where $\Delta \to 0$ as $m \to 0$. For the process above

$$\Delta = 0.60 - 2/3 \times 0.85 - 1/3 \times 0.98 = -0.29$$

This dimensionless quantity is directly related to the excess free energy of mixing, and is fairly large in comparison with the Δ for other mixing processes (11). The actual free energy change cannot be calculated with any confidence from these data alone but if it is relatively large, as the large value of Δ indicates, it shows that borax in solution has behavior more complicated than that represented by eq. [2].

Acknowledgments

Dr. C. L. Christ of the U.S. Geological Survey first suggested to me that I study the tetraborates isopiestically, and he corrected my naïve ideas on what species exist in borate solutions. I am grateful to the Fisheries Research Board of Canada for the loan of the apparatus used in this work, and to Dr. M. E. Thompson for helpful suggestions during the writing of this paper.

1. B. B. Owen. J. Am. Chem. Soc. **57**, 1526 (1935).
2. D. D. Perrin, W. L. F. Armarego, and D. R. Perrin. Purification of laboratory chemicals. The Pergamon Press, Ltd., London. 1966. p. 327.
3. N. P. Nies and R. W. Hulbert. J. Chem. Eng. Data, **12**, 303 (1967).
4. G. Scatchard, W. J. Hamer, and S. E. Wood. J. Am. Chem. Soc. **60**, 3061 (1938).
5. J. Sauka and J. Putnins. Zh. Analit. Khim. **11**, 668 (1956).
6. I. G. Ryss and V. A. Plit. J. Gen. Chem. USSR, **25**, 17 (1955).
7. A. I. Vogel. A text-book of quantitative inorganic analysis. 2nd ed. Longmans, Green and Co., Ltd., London. 1951. p. 245.
8. R. F. Platford. Can. J. Chem. **45**, 821 (1967).
9. R. A. Robinson and R. H. Stokes. Electrolyte solutions. Revised 2nd ed. Butterworths, London. 1965. p. 476.
10. I. G. Ryss and D. B. Donskaya. Zh. Fiz. Khim. **33**, 107 (1959).
11. A. K. Covington, T. H. Lilley, and R. A. Robinson. J. Phys. Chem. **72**, 2759 (1968).

Can. J. Chem. Downloaded from www.nrcresearchpress.com by 210.87.254.40 on 09/05/12
For personal use only.

Can. J. Chem. Downloaded from www.nrcresearchpress.com by 210.87.254.105 on 09/05/12
For personal use only.

Some substituted urea and thiourea complexes of Co(II), Mn(II), and Cr(III)[1]

PAKINAM ASKALANI[2] AND R. A. BAILEY
Department of Chemistry, Rensselaer Polytechnic Institute, Troy, New York 12181

Received December 11, 1968

Complexes of Co(II), Mn(II), and Cr(III) with N-butylurea, N-methylthiourea, and N,N′-dimethylthiourea, and Cl^-, Br^-, NO_3^-, and ClO_4^- anions were prepared and characterized using infrared and visible spectroscopy, and magnetic susceptibility. The urea is bonded through oxygen, and the thioureas through sulfur in all cases. The Co–N-butylurea compounds are octahedral, mostly with CoL_6X_2 stoichiometries, but some compounds involving coordinated anions and possibly bridging butylurea ligands were found. The Co–thioureas are tetrahedral. Octahedral Cr(III) compounds of the type CrL_3X_3 and $CrL_6(ClO_4)_3$ were prepared, and the CrS_6 chromophore characterized. Mn(II)–butylureas are octahedral, while the thioureas show MnL_6X_2 and MnL_4X_2 stoichiometries. X-ray diffraction established some of the latter to be isostructural with the analogous tetrahedral Co(II) compounds. Ligand field parameters *Dq* and *B* have been evaluated for the Co(II) and Cr(III) compounds.

Canadian Journal of Chemistry, 47, 2275 (1969)

Introduction

Urea, thiourea, and their N-substituted forms have recently been subject to some investigations due to their ability to behave as oxygen (sulfur in the case of thioureas) or nitrogen coordinating ligands. Much of the attention has been given to the infrared (i.r.) spectra of their coordination compounds to determine the bonding atom of the ligand (which is usually but not always oxygen or sulfur for most of the first row transition elements which have been considered), although some studies on the different structural aspects of their transition metal complexes have been reported. Among these are the studies on Co(II) compounds with thiourea (1); ethylenethiourea and N,N′-diethylthiourea (2); N,N′-diethylthiourea, N,N′-dibutylthiourea, and N,N′-diphenylthiourea (3); and N-methylurea, N-ethylurea, N,N′-dimethylurea, N,N′-diethylurea, and ethyleneurea (4). In general, it has been found that thiourea and its N-substituted forms tend to surround Co(II) ions in a tetrahedral geometry, while urea and its substituted forms give octahedral Co(II) compounds, although exceptions to this generalization have been reported.

Cr(III) compounds with urea and N,N′-dimethylurea are evidently octahedral, (5–7), although only Stonestreet *et al.* (7) have considered properties other than i.r. spectra. Thiourea complexes of this ion have been still less studied; recently Cervone *et al.* (8) obtained octahedral compounds of the sort CrL_3Cl_3 where L = thiourea, N,N′-diethylthiourea, and N,N′-dibutylthiourea, but were unable to obtain species with a CrS_6 chromophore. The C—S bond is difficult to form, and spectral and magnetic properties for such compounds are of interest. While ligand field spectra of the above compounds imply sulfur bonding, no confirming i.r. data are available.

Infrared evidence for sulfur bonding of thiourea with Mn(II), (9, 10) and of oxygen bonding of dimethylurea (7) has been presented, but no structures are known for the thiourea compounds which are of the form $Mn(thiourea)_4X_2$. The hexakis-N-methylurea complex (11) has been shown to be oxygen bonded and octahedral.

The present study was undertaken to fill in some of the gaps in the knowledge of the behavior of Cr(III) and Mn(II) with this class of ligands. Work on Co(II) has been included as well, since this, along with previously published work, provides a series of well characterized complexes with the same ligands for a number of first row transition metal ions. Effects of different anions can be correlated, as can trends in ligand field parameters with changing substituent on the organic ligands.

Experimental

Chemicals

All chemicals used were reagent grade when possible,

[1]Taken from a thesis presented by Pakinam Askalani to the Graduate School of Rensselaer Polytechnic Institute in partial fulfillment of the requirements for the Ph.D. degree.

[2]Present address: Department of Physical Science, American University in Cairo, Cairo, United Arab Republic.

Can. J. Chem. Downloaded from www.nrcresearchpress.com by 210.87.254.105 on 09/05/12
For personal use only.

TABLE I

Preparative and analytical data

Compound (empirical formula)	Preparative solvent	Color	Yield (%)	Melting point (°C)	% Metal		% Total nitrogen		%(Cl^-, Br^-, NO_3^-, or ClO_4^-)	
					Calcd.	Found	Calcd.	Found	Calcd.	Found
$Co(BU)_2Cl_2$	Ethanol	Pink	42	—	16.27	16.21	15.47	15.54	19.58	19.62
$Co(BU)_6Br_2$	$CHCl_3$–ethanol	Pink	90	135	6.43	6.38	18.34	18.07	17.41	17.45
$Co(BU)_4(NO_3)_2$	$CHCl_3$–ethanol	Pink	41	d >60‡	9.10	9.16	21.63	21.70	19.15	19.04
$Co(BU)_6(NO_3)_2$	$CHCl_3$–ethanol	Pink	27	123	6.70	6.79	22.29	22.28	14.09	13.98
$Co(BU)_6(ClO_4)_2$	$CHCl_3$	Pink	58	150	6.17	6.36	17.60	17.60	20.83	21.04
$Co(MTU)_2Cl_2$	$CHCl_3$–ethanol	Blue	30	125	19.00	19.11	18.07	18.11	22.86	22.88
$Co(MTU)_2Br_2$	$CHCl_3$–ethanol	Blue	12	89	14.67	14.72	14.04	13.85	40.05	39.98
$Co(MTU)_3(NO_3)_2$*	Isopropanol	Blue	20	—	12.99	12.96	24.72	24.63	27.36	27.45
$Co(MTU)_4(ClO_4)_2$*	Isopropanol	Blue	30	—	9.53	9.35	18.12	18.20	32.17	31.97
$Co(DMTU)_2Cl_2$	Methanol	Blue	53	222	17.43	17.41	16.57	16.49	18.95†	18.95†
$Co(DMTU)_2Br_2$	Methanol	Blue	40	179	13.80	13.85	13.12	13.09	15.02†	15.15†
$Co(DMTU)_3(NO_3)_2$	Isopropanol	Blue	36	134	11.89	11.77	22.62	22.56	25.02	24.86
$Co(DMTU)_4(ClO_4)_2$	$CHCl_3$–ethanol	Blue-green	70	141	8.73	8.53	16.61	16.57	29.49	29.59
$Cr(BU)_6Cl_3$*	Acetone	Green	—	—	6.08	6.25	19.66	19.72	12.42	12.43
$Cr(BU)_6Br_3$*	Acetone	Green	—	—	5.26	5.20	17.00	17.22	24.25	24.19
$Cr(BU)_6(ClO_4)_3$*	Ethanol	Green	—	—	4.96	5.04	16.05	15.83	28.50	28.77
$Cr(MTU)_3Cl_3$	Acetone	Brown	45	d >35‡	12.13	12.04	19.60	19.46	24.80	24.69
$Cr(MTU)_6(ClO_4)_3$	Acetone	Brown	60	d >75‡	5.83	5.70	18.86	18.76	33.48	33.67
$Cr(DMTU)_3Cl_3$	Acetone	Brown	13	215	11.05	11.11	17.85	17.98	22.58	22.74
$Cr(DMTU)_3Br_3$	Acetone	Brown	20	d >105‡	8.62	8.71	13.91	13.70	39.67	39.51
$Cr(DMTU)_6(ClO_4)_3$	Ethanol	Yellow-brown	26	188	5.33	5.19	17.24	17.30	30.59	30.88
$Mn(BU)_6Cl_2$	Methanol	White	48	108	6.70	6.79	20.43	20.31	8.62	8.85
$Mn(BU)_6Br_2$	Methanol	White	77	135	6.02	5.86	18.44	18.20	17.54	17.49
$Mn(MTU)_2Cl_2$	Acetone	White	47	176	17.95	18.15	18.31	18.30	23.16	23.08
$Mn(MTU)_6(ClO_4)_2$	Isopropanol	White	60	159	6.91	6.80	21.15	21.30	25.03	24.87
$Mn(DMTU)_2Cl_2$	Methanol	White	50	205	16.44	16.38	16.77	16.49	21.22	21.41
$Mn(DMTU)_2Br_2$	Isopropanol	White	24	157	12.98	13.10	13.24	13.35	37.77	37.83
$Mn(DMTU)_4(ClO_4)_2$	Isopropanol	White	53	128	8.19	8.05	16.71	16.55	29.67	29.90

*Oil.
†Sulfur content rather than halogen content.
‡Decomposed.

Can. J. Chem. Downloaded from www.nrcresearchpress.com by 210.87.254.105 on 09/05/12
For personal use only.

and were used without further purification. N-butylurea was obtained from K and K Laboratories, Inc., and the two thioureas from Chemicals Procurement Laboratories. The metal halides were anhydrous, but hydrated perchlorates and nitrates were employed.

Preparations

The compounds were prepared by dissolving the metal salt and ligand in a hot organic solvent (shown for each case in Table I), heating for 30–60 min, and cooling in ice with vigorous stirring to help initiate crystallization. For chromium halide compounds, zinc was used as a catalyst to break the auto-complex. This, along with any unreacted halide, was filtered from the hot reaction mixture. In some cases, ether or benzene was added to induce crystallization. The solvent used was determined by trial, and depended on solubilities. All solid products were recrystallized, usually from the solvent used in the preparation. A number of products could not be obtained as solids, and were characterized as oils. They were thoroughly washed with solvents which would dissolve unreacted starting materials, and dried under vacuum until pure. All analytical data are given in Table I.

For the $Co(NO_3)_2$ – N-butylurea system, the product isolated depended on the ratio of ligand to metal salt, with $Co(BU)_4(NO_3)_2$ being formed if this ratio were much below 6.

Most of these compounds showed color changes in dilute solution, raising the possibility of dissociation or other reaction with the solvent. In these cases, solution data were not considered to be reliable indications of structures of the solid compounds.

Physical Measurements

Magnetic susceptibilities were taken by the Gouy technique, using $[Hg\,Co(NCS)_4]$ as calibrant and measurements were corrected for diamagnetism in the usual manner. Measurements were made at room temperature, and at lower temperatures by surrounding the specimen with a suitable coolant in a Dewar flask. Measurement results were independent of field strength.

Electronic spectra were taken by reflection from finely powdered samples, using a Beckman DU spectrophotometer and $MgCO_3$ as standard. Oils were pressed between quartz plates and measured by transmission on a Beckman DK-2A spectrophotometer. Neither technique can provide extinction coefficients.

Infrared spectra were taken on a Perkin–Elmer 621 spectrophotometer. Solids were pressed in KBr discs and checked in mulls, while oils were pressed between salt plates.

X-ray powder diffraction patterns were taken with a Philips X-ray unit, type 12045B/3 and a Philips high angle goniometer, type 42267/0. Nickel filtered copper radiation was used.

Conductance measurements, when it was felt that these would be significant, were taken at 25 °C on 0.001 *M* solutions using an Industrial Instruments, Inc., model RC 16B2 conductance bridge.

Analyses

Manganese and cobalt were determined by EDTA titration methods, while chromium was found spectrophotometrically as CrO_4^{2-}. Total nitrogen was estimated by the Kjeldahl technique with selenium or copper sulfate as catalyst, while nitrate was determined gravimetrically as nitron nitrate. Halides were analyzed potentiometrically with silver nitrate, and perchlorates were precipitated as tetraphenylarsonium perchlorate. Sulfur was determined as $BaSO_4$ after decomposition by Eschka's mixture.

Results and Discussion

Infrared Spectra

Shifts in the i.r. spectra of the coordinated ligands can be used to indicate the mode of bonding of the organic ligands in these compounds. For N-butylurea, comparison with other substituted ureas (12) suggests that the most distinctive change expected on coordination through oxygen is a decrease in the energy of the C=O stretching band at 1650 cm^{-1}. This is found here at 1625–1640 cm^{-1}. The N—H stretching region near 3400 cm^{-1} shows no shift to lower energy, and other bands behave similarly to those observed in other oxygen-bonded N-butylurea complexes (12).

The bonding criteria of N-methylthiourea have been suggested by Lane *et al.* (13) and Gosavi and Rao (14), and for N,N′-dimethylthiourea by Gosavi and Rao (14). The spectra of the complexes of N-methylthiourea were in good agreement with what is expected for sulfur bonding on the basis of the above, while those of N,N′-dimethylthiourea showed only slight discrepancies from the sulfur-bonding criteria. (The N—H out-of-plane bending mode at 718 cm^{-1} in the free ligand is expected to increase for S-bonding and to decrease for N-bonding. It was found in these complexes at 710–720 cm^{-1}.)

The above conclusions, that all N-butylurea compounds are bonded through oxygen, while all those of the thioureas are sulfur bonded, are in keeping with most of the previous observations on urea and thiourea complexes of the metals of the first transition series. The electronic spectra below provide some further evidence to this point.

Magnetism

The magnetic data for the compounds prepared here are reported in Table II. Measurements were made at three or more temperatures, but only the room temperature data are tabulated; the values given for θ permit the lower temperature data to be recovered. Moments are corrected for diamagnetism and temperature independent paramagnetism when the latter

TABLE II

Magnetic data of the Co(II), Mn(II), and Cr(III) compounds

Compound (empirical formula)	Diamagnetic correction × 10^6	$\chi_M \times 10^6$ uncorrected	μ_{eff} (B.M.)	θ (degrees)
$Co(BU)_2Cl_2$	−188	9 710	4.88	—
$Co(BU)_6Br_2$	−493	9 890	4.99	—
$Co(BU)_4(NO_3)_2$	−320	9 920	4.96	—
$Co(BU)_6(NO_3)_2$	−462	9 930	4.99	—
$Co(BU)_6(ClO_4)_2$	−487	10 820	5.19	—
$Co(MTU)_2Cl_2$	−142	8 310	4.49	−12
$Co(MTU)_2Br_2$	−164	8 240	4.46	−12
$Co(MTU)_3(NO_3)_2$	−181	7 830	4.24	− 4
$Co(MTU)_4(ClO_4)_2$	−250	7 570	4.29	−13
$Co(DMTU)_2Cl_2$	−191	8 720	4.49	−10
$Co(DMTU)_2Br_2$	−213	9 400	4.56	− 9
$Co(DMTU)_3(NO_3)_2$	−216	8 310	4.49	− 2
$Co(DMTU)_4(ClO_4)_2$	−353	9 450	4.61	−10
$Cr(BU)_6Cl_3$	−494	5 390	3.72	−10
$Cr(BU)_6Br_3$	−527	5 120	3.78	− 7
$Cr(BU)_6(ClO_4)_3$	−513	4 510	3.70	− 7
$Cr(MTU)_3Cl_3$	−213	4 730	3.68	−10
$Cr(MTU)_6(ClO_4)_3$	−376	6 530	3.85	−22
$Cr(DMTU)_3Cl_3$	−287	6 460	3.92	−19
$Cr(DMTU)_3Br_3$	−320	5 950	3.88	−28
$Cr(DMTU)_6(ClO_4)_3$	−523	6 900	4.16*†	
$Mn(BU)_6Cl_2$	−470	15 700	5.95	−22
$Mn(BU)_6Br_2$	−493	15 130	5.97	−19
$Mn(MTU)_2Cl_2$	−142	13 350	5.73	− 1
$Mn(MTU)_6(ClO_4)_2$	−346	14 350	5.76	− 4
$Mn(DMTU)_2Cl_2$	−191	13 930	5.74	− 1
$Mn(DMTU)_2Br_2$	−213	15 110	5.96†	—
$Mn(DMTU)_4(ClO_4)_2$	−353	13 570	5.73†	—

*Moment decreased with decreasing temperature. Believed to be a packing difficulty.
†μ_{eff} was calculated from the Curie law; θ was not determined.

is significant (Cr(III) and tetrahedral Co(II) compounds).

The Co–N-butylurea compounds all have moments suggesting octahedral geometry (15), 4.88–5.17 B.M. Moments decreased with decreasing temperature, as is characteristic of a $^4T_{1g}$ ground state; plots of $1/\chi_M$ vs. temperature were not linear. Moments of the substituted thiourea complexes with Co, on the other hand, are clearly in the range for tetrahedral symmetry. All obeyed the Curie–Weiss law with relatively small values of θ (Table II). Room temperature moments in the table were calculated from the relation $\mu = 2.84\ (T - \theta)^{\frac{1}{2}}$ B.M., although we make no claims as to the significance of θ.

Moments for all of the chromium compounds are also in the range characteristic of octahedral geometry (15), and behave in a straight-forward manner. Those for the manganese compounds are typical for Mn(II) in a weak ligand field; they are not characteristic of geometry for a d^5 ion. The Curie-Weiss law was obeyed in both cases.

Electronic Spectra

Three spin allowed transitions are predicted for Co(II) in an octahedral ligand field; these are, in order of energy

$$^4T_{1g}(F) \rightarrow {}^4T_{2g}(F)$$

$$^4T_{1g}(F) \rightarrow {}^4A_{2g}(F)$$

$$^4T_{1g}(F) \rightarrow {}^4T_{1g}(P)$$

Of these, the second corresponds to a 2-electron jump and is expected to be very weak (16); it is usually obscured by the tail of the more intense third band (4). The five pink Co–N-butylurea compounds which appear to be octahedral on the basis of magnetic data show two major bands; one around 8 000 cm^{-1} and the other at 19 000 – 20 000 cm^{-1} with a shoulder at higher energies (Table III, Fig. 1). It is reasonable to assign these bands to first and third transitions, respectively, with the shoulder on the latter probably due to spin–orbit splitting of the $^4T_{1g}(P)$ state (16). The band listed under the ν_2 transition in Table III is

Can. J. Chem. Downloaded from www.nrcresearchpress.com by 210.87.254.105 on 09/05/12
For personal use only.

Can. J. Chem. Downloaded from www.nrcresearchpress.com by 210.87.254.105 on 09/05/12
For personal use only.

TABLE III

Visible spectral data of the Co(II) and Cr(III) compounds

Compound (empirical formula)	Band positions (cm^{-1})*			Dq (cm^{-1})	B (cm^{-1})	β
	ν_1	ν_2	ν_3			
$Co(BU)_2Cl_2$	7 600	14 800	19 200, 21 500	950	900	0.93
$Co(BU)_6Br_2$	8 100	14 500	19 600, 21 000	1010	900	0.93
$Co(BU)_4(NO_3)_2$	8 100	15 000	19 400, 20 700	1010	888	0.91
$Co(BU)_6(NO_3)_2$	8 100	15 500	19 300, 20 500	1010	882	0.90
$Co(BU)_6(ClO_4)_2$	8 030		19 600, 20 800	1000	904	0.93
$Co(MTU)_2Cl_2$		8 000	15 500	470	627	0.65
$Co(MTU)_2Br_2$		7 900	14 900	460	600	0.62
$Co(MTU)_3(NO_3)_2$		8 200	15 500	490	607	0.63
$Co(MTU)_4(ClO_4)_2$		8 400	15 100	500	593	0.61
$Co(DMTU)_2Cl_2$		7 900	15 200	470	600	0.62
$Co(DMTU)_2Br_2$		7 800	14 600	460	573	0.59
$Co(DMTU)_3(NO_3)_2$		8 200	15 500	490	600	0.62
$Co(DMTU)_4(ClO_4)_2$		8 000	14 400	480	527	0.56
$Cr(BU)_6Cl_3$	16 400	22 700		1640	627	0.68
$Cr(BU)_6Br_3$	16 350	22 700		1640	627	0.68
$Cr(BU)_6(ClO_4)_3$	16 400	22 800		1640	627	0.68
$Cr(MTU)_3Cl_3$	14 300	19 300		1430	480	0.52
$Cr(MTU)_6(ClO_4)_3$	14 500	19 000		1450	420	0.46
$Cr(DMTU)_3Cl_3$	13 800	19 200		1380	547	0.59
$Cr(DMTU)_3Br_3$	13 700	18 400		1370	486	0.53
$Cr(DMTU)_6(ClO_4)_3$	14 000	18 200		1400	394	0.43

*For assignments, see text.

rather low in energy, and is almost certainly the spin-forbidden transition to the ^2E_g state which also lies in this region; it was not used in obtaining the ligand field parameters, and does not agree well with the parameters given if it is the $^4A_{2g}$ band. Values of both Dq and B (the Racah parameter, Table III) are comparable to those of other oxygen coordinated ligands with Co(II) (4).

Spectra of the deep blue cobalt – substituted thiourea compounds do not fit an octahedral case, and magnetic results above indicate a tetrahedral geometry. Three ligand field bands are expected in this case, with the lowest energy band (equal to 10 Dq) below the range of measurement. Two bands were observed, near 8 000 and 15 000 cm^{-1} with the latter showing much fine structure which is common for tetrahedral Co(II) (2). The transition energy (Table III) was taken as the center of gravity of this band; the individual peaks (usually three) have not been listed. These bands can be assigned to the transitions $^4A_2(F) \rightarrow {}^4T_1(F)$ and $^4A_2(F) \rightarrow {}^4T_1(P)$, and Dq and B evaluated from the relationships of Underhill and Billings (17). The data are given in Table III. Both parameters are reasonable when compared to other tetrahedral Co(II) systems. In particular, values of B of about 600 cm^{-1} were reported by Cotton *et al.* (1) for other Co(II)–thiourea compounds. Such small values are reasonable only if the ligand is bonded through sulfur, which lies high in the nephelauxetic series.

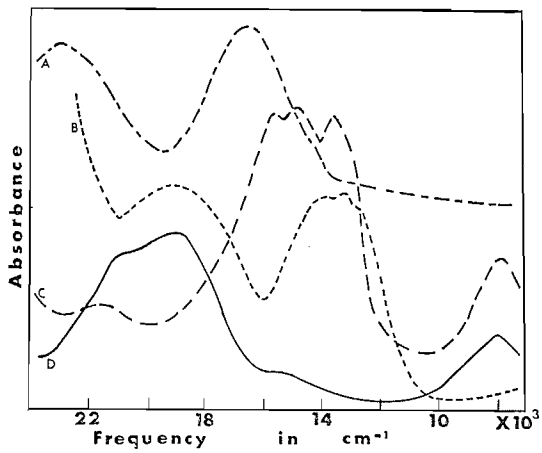

FIG. 1. Representative electronic spectra of Co(II) and Cr(III) complexes. (A), $[Cr(BU)_6](ClO_4)_3$; (B), $[Cr(DMTU)_3Cl_3]$; (C), $[Co(DMTU)_2Br_2]$; (D), $[Co(BU)_6](ClO_4)_2$.

Cr(III) should exhibit three bands in an octahedral field

ν_1: $^4A_{2g}(F) \rightarrow {}^4T_{2g}(F)$

ν_2: $^4A_{2g}(F) \rightarrow {}^4T_{1g}(F)$

ν_3: $^4A_{2g}(F) \rightarrow {}^4T_{1g}(P)$

Can. J. Chem. Downloaded from www.nrcresearchpress.com by 210.87.254.105 on 09/05/12
For personal use only.

In addition, spin-forbidden bands may appear.

The chromium–butylurea spectra exhibit two major bands, near 16 400 and 22 700 cm^{-1} (Table III). A small shoulder appears at 14 300 cm^{-1} in the spectra of all these compounds. These band positions are similar to those reported with other oxygen coordinating ligands (7, 18); the major bands can be assigned to the ν_1 and ν_2 transitions. The position of ν_3 can be predicted to be above 35 000 cm^{-1} where it is obscured by charge transfer bands. The weak shoulder, on the other hand, can be attributed to the $^4A_{2g}(F) \rightarrow {}^2E_g(G)$, $^2T_{1g}(G)$ doublet, which has been observed as a single band at this energy in other Cr(III) complexes. (These levels are independent of ligand field.) The methylthiourea and most dimethylthiourea compounds are similar to the above, but B is much smaller, again in keeping with S-bonded organic ligands (19). A value of 1400–1450 cm^{-1} for Dq of the Cr(III)–S_6 chromophore may be compared with that of 1510 cm^{-1} calculated by Cervone *et al.* (8) from average ligand field arguments; this is an average for the three thiourea ligands which they used. Dq for the N,N′-dibutylurea complexes, 1640 cm^{-1}, is slightly greater than the 1540 cm^{-1} of N,N′-dimethylurea given by Stonestreet *et al.* (7). Substitutents on the urea ligands have some effect on the coordination strengths toward Cr(III) as toward Ni(II) (12).

The spectra of the chloride and perchlorate of the chromium dimethylthioureas exhibit three peaks in the region assigned to ν_1. A similar observation on other Cr(III) compounds was explained by Bates (18) on the basis that, in the region where the three energy levels ^2E_g, $^2T_{1g}$, and $^4T_{2g}$ cross, mixing occurs which gives all three levels intermediate doublet–quartet character. Transitions to all should then have comparable probabilities. Since none of these bands can be assigned definitely to the ν_1 transition, the center of this triplet band was used in calculating Dq, and only this is tabulated.

No visible spectra were obtained for compounds of manganese. This is not unexpected, since all bands would be spin-forbidden.

In all of the above compounds, N,N′-dimethlythiourea has a slightly weaker ligand field strength than N-methylthiourea. Both are slightly stronger than Cl^- and considerably weaker than butylurea. Substituted ureas and thioureas are stronger than the unsubstituted ligands, since presumably substitution increases the electron density around the O (or S) atom. The greater tendency for butylurea compounds to be octahedral with cobalt may be related to the greater ligand field stabilization energy associated with the octahedral geometry which is more significant with this ligand than with the weaker thioureas. However, the same observations on structure seem to hold for some of the Mn(II) compounds (see below) where this stabilization energy is zero, so that other factors must be important.

The Co–N-butylurea compounds were shown above to be octahedral, indicating the existence of the $[Co(BU)_6]^{2+}$ cation in the bromide, nitrate, and perchlorate compounds. $Co(BU)_4(NO_3)_2$ may have two coordinated nitrate ions to complete the octahedral geometry. This could not be confirmed. Infrared evidence was inconclusive, as some of the nitrate regions are obscured by bands from the organic ligands; however, nitrate bands at 823 and 1300–1400 cm^{-1} (very broad) best fit ionic nitrate (20). In fact, these regions of the i.r. spectrum match almost exactly those of $[Co(BU)_6](NO_3)_2$ where the nitrates are without doubt ionic. Conductance data were not useful, as a color change in all suitable solvents investigated implied further changes. If the nitrates are ionic, bridging butylurea would be indicated (bridging through the oxygen, based on the i.r. spectrum and the similarity of the ligand field spectrum to that of $[Co(BU)_6](NO_3)_2$).

Octahedral $Co(BU)_2Cl_2$ must also be a bridged structure. Bridging of both butylureas, or both chlorides, or one of each, could lead to an octahedral geometry. Application of the average ligand field rule (21) to the various possibilities leads to the following calculated values for 10 Dq (assuming only O-bonding, as indicated by the i.r. evidence): 4 butylureas and 2 chlorides around each Co(II), 9060 cm^{-1}; 4 chlorides and 2 butylureas around each Co(II), 8130 cm^{-1}; 3 chlorides and 3 butylureas around each Co(II), 8600 cm^{-1}. The observed value is 9500 cm^{-1}. While the rule is only approximate, and will be influenced by bond lengths, it usually holds to within a few hundred wavenumbers in systems similar to this. It seems to rule out bridging chlorides. While bridging of 2 metal ions by the oxygen atom of a urea type ligand has not previously been established, it is known with the sulfur of thiourea systems (22). Clearly, addi-

TABLE IV

X-ray diffraction data of DMTU complexes of cobalt and manganese halides

$Co(DMTU)_2Cl_2$		$Mn(DMTU)_2Cl_2$		$Co(DMTU)_2Br_2$		$Mn(DMTU)_2Br_2$	
d (Å)	Intensity*	*d* (Å)	Intensity*	*d* (Å)	Intensity*	*d* (Å)	Intensity*
7.55	m	7.55	m	7.26	m	7.26	m
7.00	s	6.88	s	6.11	m	6.11	s
5.97	m	5.83	m	3.95	s	3.99	s
5.31	w	5.42	m	3.83	m	3.87	m
4.01	w	4.05	m	3.70	w	3.68	w
3.83	m	3.79	s	3.53	m	3.56	s
3.76	s	3.74	m	3.47	m	3.47	m
3.67	m	3.67	m	3.36	s	3.38	s
3.45	s	3.47	s	—	—	3.09	w
3.30	m	3.32	m	2.99	m	2.98	m
3.16	w	3.19	m	2.50	m	2.51	m
3.00	m	3.02	m				
2.94	m	2.93	m				
2.74	w	2.71	w				
2.51	w	2.52	w				
2.45	m	2.46	m				
2.19	m	2.19	m				

*s = strong, m = medium, w = weak.

tional structural data would be valuable in this case. This last compound is the first cobalt urea complex with coordinated anions.

This last compound is very unstable, rapidly but incompletely decomposing on standing to a gummy, deep blue material which exhibits a spectrum characteristic of tetrahedral cobalt, and a reduced magnetic moment (4.6 B.M.). The blue product was soluble in ether, so could be washed away as formed. However, different samples of it varied in composition, and no single product could be isolated. Interestingly, the other possibly bridged compound of this series, $Co(BU)_4(NO_3)_2$, also decomposes readily to a blue, tetrahedral species. A similar decomposition was observed by Costamagna and Levitus (4), who believed the reaction to be

$$ML_{6(oct)} \rightarrow ML_2X_{2(tet)} + 4L$$

in their case. The tetrahedral species could not be isolated and characterized.

The Co – substituted thiourea compounds are tetrahedral. Since $Co(MTU)_2Cl_2$ and $Co(DMTU)_2Cl_2$ are non-electrolytes in nitromethane, the anions are believed to be coordinated. The compounds $CoL_3(NO_3)_2$ may have one coordinated nitrate or a bridged structure; conductance data were again invalid due to changes in color in solution. For the methylthiourea compound, the i.r. spectrum showed bands at 822 and 1350 cm^{-1} attributable to ionic nitrate, but also gave a band at 1025 cm^{-1} which can be assigned to a coordinated nitrate (20). Other possible nitrate bands, and the 1025 cm^{-1} region in the dimethylthiourea compound, were obscured by ligand absorptions. We suggest very tentatively one coordinated NO_3^- group. Meneces *et al.* (23) describe analogous cobalt thiourea halides.

The Cr(III) compounds are all octahedral; this is the usual geometry for this ion. Compounds of the butylurea series contain the $[Cr(BU)_6]^{3+}$ cation, while those of formulas CrL_3X_3 contain coordinated anions, as shown by Cervone *et al.* (8).

No structural data can be obtained for the Mn(II) compounds from magnetic or spectral measurements. It is presumed that those of formula MnL_6X_2 are octahedral. In an attempt to relate structures of the remaining compounds to others of similar formulas and known structures, X-ray powder patterns were examined. Identical powder patterns for two such compounds (except for slight differences in d spacings) can be taken as evidence that the compounds are isostructural and therefore contain units with the same coordination geometry. This is the case, for example, with $[Mn(BU)_6]Br_2$ and $[Co(BU)_6]Br_2$. The compounds $Mn(DMTU)_2Cl_2$, $Mn(DMTU)_2Br_2$, and $Mn(DMTU)_4(ClO_4)_2$ have the same stoichiometries as the analogous cobalt compounds, and the

Can. J. Chem. Downloaded from www.nrcresearchpress.com by 210.87.254.105 on 09/05/12
For personal use only.

first two of these are isostructural with their cobalt analogues as shown in Table IV. Tetrahedral species are thus indicated for these Mn(II)–thiourea systems, while the ureas are octahedral, as for Co(II). The manganese chloride compound was a non-conductor in nitromethane as the proposed structure requires.

$Mn(DMTU)_4(ClO_4)_2$ is not isostructural with its cobalt analogue. Its conductance in nitromethane, ca. 125 Ω^{-1} cm^2, is in the range of a 1:2 electrolyte. $Mn(MTU)_2Cl_2$ is not isostructural with $Co(MTU)_2Cl_2$, $Fe(MTU)_2Cl_2$ (24), or $Ni(MTU)_2Cl_2$ (12). This does not preclude a similar coordination structure to any one of them, but a different crystal structure. It was dissociated in solution.

It is interesting that the stoichiometry of the Mn(II) perchlorate compounds varies with the substituents on the thiourea ligands. The methylthiourea species is evidently octahedral, unlike the thiourea–Co(II) systems. It is likely that compounds of both stoichiometries $MnL_4(ClO_4)_2$ and $MnL_6(ClO_4)_2$ could be formed under proper conditions with these ligands.

Acknowledgment

We wish to thank Mr. T. R. Peterson for experimental assistance and helpful discussion.

1. F. A. Cotton, C. D. Faut, and J. T. Mague. Inorg. Chem. **3**, 17 (1964).
2. R. C. Carlin and S. L. Holt. Inorg. Chem. **2**, 849 (1963).
3. O. Piovesana and C. Furlani. J. Inorg. Nucl. Chem. **30**, 1249 (1968).
4. J. A. Costamagna and R. Levitus. J. Inorg. Nucl. Chem. **28**, 2685 (1966).
5. G. A. Barbieri. Atti Acad. Lincei, **22**, 867 (1913).
6. R. B. Penland, S. Mizushima, C. Curran, and J. V. Quagliano. J. Am. Chem. Soc. **79**, 1575 (1957).
7. B. C. Stonestreet, W. E. Bull, and R. J. Williams. J. Inorg. Nucl. Chem. **28**, 1895 (1966).
8. E. Cervone, P. Cancellieri, and C. Furlani. J. Inorg. Nucl. Chem. **30**, 2431 (1968).
9. K. C. Dash, M. Ali, R. N. Patel, and D. V. R. Rao. J. Indian Chem. Soc. **44**, 246 (1967).
10. K. Swaminathan and H. M. N. H. Irving. J. Inorg. Nucl. Chem. **26**, 1291 (1964).
11. M. Nardelli and L. Coghi. Gazz. Chim. Ital. **88**, 355 (1958); Ric. Sci. Suppl. **29**, 134 (1959).
12. R. A. Bailey, I. R. Feins, and T. R. Peterson. Can. J. Chem. **47**, 171 (1969).
13. T. J. Lane, A. Yamaguchi, J. V. Quagliano, J. A. Ryan, and S. Mizushima. J. Am. Chem. Soc. **81**, 3824 (1959).
14. R. K. Gosavi and C. N. R. Rao. J. Inorg. Nucl. Chem. **29** 1937 (1967).
15. B. N. Figgis and J. Lewis. *In* Progress in inorganic chemistry. *Edited by* F. A. Cotton. Interscience Publishers, Inc., New York. 1964. Chap. 2.
16. C. J. Ballhausen. Introduction to ligand field theory. McGraw Hill Book Co., Inc., New York. 1962. pp. 256–257.
17. A. E. Underhill and D. E. Billings. Nature, **210**, 834 (1966).
18. T. Bates. *In* Modern aspects of the vitreous state. Vol. 2. *Edited by* J. D. Mackenzie. Butterworths, London. 1962. p. 195.
19. C. K. Jorgensen. Absorption spectra and chemical bonding in complexes. The Pergamon Press, Ltd., London. 1961. pp. 110–111.
20. K. Nakamoto. Infrared spectra of inorganic and coordination compounds. John Wiley and Sons, Inc., New York. 1963. p. 159.
21. B. N. Figgis. Introduction to ligand fields. Interscience Publishers, Inc., New York. 1966. Chap. 9.
22. M. Nardelli, A. Braibanti, and G. Fava. Gazz. Chim. Ital. **87**, 1209 (1957).
23. N. Meneces, C. Piriz-MacColl, and R. Levitus. Inorg. Nucl. Chem. Letters, **4**, 597 (1968).
24. R. A. Bailey and T. R. Peterson. Can. J. Chem. **45**, 1135 (1967).

Can. J. Chem. Downloaded from www.nrcresearchpress.com by 210.87.254.105 on 09/05/12
For personal use only.

An analytical method of calculating thermodynamic data in ternary systems

A. D. PELTON AND S. N. FLENGAS
Department of Metallurgy and Materials Science, University of Toronto, Toronto, Ontario

Received September 27, 1968

Relationships between the coefficients of series expansions in the composition variables for isothermal partial molar properties of all components, and for the corresponding integral property in a ternary system, have been developed. These relationships allow the calculation of the isothermal partial properties of mixing of all components, from experimental values of this property for one component, or from experimental measurements of the corresponding integral property of mixing. The form of the series expansions is such as to permit the easy fitting of the experimental data by standard least-squares techniques. Experimental data in a binary sub-system or experimentally determined phase boundary positions may easily be used to give end-points for the calculation. The method is faster and more accurate than the older graphical integration techniques. The simplicity of the method depends upon the proper choice of composition variables. Sample calculations have been done for the Cd–Bi–Sn system, using computer programs designed for the purpose.

Canadian Journal of Chemistry, 47, 2283 (1969)

Can. J. Chem. Downloaded from www.nrcresearchpress.com by 210.87.254.105 on 09/05/12
For personal use only.

Introduction

As is well-known, if values of the isothermal excess free energy of mixing of one component in a system are known over a composition range, then values of the excess free energy of mixing of all the other components, and values of the excess integral free energy of mixing, may be calculated by use of the Gibbs–Duhem relation. For binary systems, the calculations may be done by the well-known graphical techniques or by analytical techniques such as that proposed by Margules (1).

For ternary systems, such calculations have only been done by the graphical techniques of Darken (2), Wagner (3), Schuhmann (4), and Gokcen (5). These techniques are long and tedious. They involve several steps such as the graphical determination of slopes of tangent lines. Unless great care is taken, the results can be inaccurate. Quantities are calculated at one composition at a time. The experimental data must be available along simple composition paths (such as quasi-binary lines or constant mole fraction lines) so that interpolations may be made, and slopes and areas may be determined graphically. If the available data points are scattered at random over the composition range, interpolation can be very difficult.

In the present investigation, an analytical method has been developed which overcomes these difficulties. In this method, relationships between the coefficients of series expansions in the composition variables for the isothermal excess partial and integral free energies of mixing, are found. If the coefficients of the expansion for one component are found by a least-squares surface fitting technique to experimental data, then the coefficients of the expansions for the properties of all the other components, and for the integral property, are immediately and exactly determined. The method is readily adaptable for use with a digital computer.

The Analytical Method in Binary Systems

The following modification of the analytical method of Margules (1) for binary systems will serve as a basis for the later extension to ternary systems.

Let f_1 and f_2 be the partial molar excess free energies of mixing of components *1* and *2*, and let f be the excess integral molar free energy of mixing. If f_1, f_2, and f are expressed as power series in X_2, the mole fraction of component *2*, as follows

$$[1] \qquad f_1 = \sum_{j=2}^{j'} a_j X_2^{\,j}$$

$$[2] \qquad f_2 = \sum_{j=0}^{j'} b_j X_2^{\,j}$$

$$[3] \qquad = \sum_{j=1}^{j'} \phi_j X_2^{\,j}$$

then the relationships between the coefficients, as derived by Margules (1) from the Gibbs–Duhem relation, take the following form

$$[4] \qquad b_j = a_j - \left(\frac{j+1}{j}\right) \cdot a_{j+1} \qquad j \geqslant 1$$

$$[5] \qquad \phi_j = a_j/(1-j) \qquad j \geqslant 2$$

The expansion for f_1 must start with the

Can. J. Chem. Downloaded from www.nrcresearchpress.com by 210.87.254.105 on 09/05/12
For personal use only.

$j = 2$ term. The missing coefficient a_0 is zero because $f_1 = 0$ when $X_2 = 0$, and the fact that the missing coefficient a_1 is zero follows from eq. [5], since ϕ_1 must be finite. In the expansion [3] for f, the missing coefficient ϕ_0 is zero, since $f = 0$ when $X_2 = 0$. If the coefficients a_j have been determined by fitting a curve to the experimental values of f_1 over a composition range, then all the coefficients, b_j and ϕ_j, may be calculated from eqs. [4] and [5] except for b_0 and ϕ_1. The determination of these two coefficients requires the experimental knowledge of one end-point value of f_2 (or f) at the boundary of the composition range studied.

In the simple case when f_1 has been measured over the composition range down to $X_2 = 1$, the boundary conditions that $f_2 = 0$ and $f = 0$ when $X_2 = 1$ may be used, and no independent measurement of f_2 (or f) is required to give end-point values. In this case it may easily be shown that b_0 and ϕ_1 are given by the explicit forms

$$[6] \qquad b_0 = -\sum_{j=1}^{j'} b_j$$

$$[7] \qquad \phi_1 = -\sum_{j=2}^{j'} \phi_j$$

It is well-known that partial molar excess free energies of mixing are well-fitted by an expansion, such as that in eq. [1]. For most systems, a very good fit may be obtained with only three or four terms.

The Form of the Series Expansions for Ternary Systems

The composition variables chosen in this work for the series expansions were designated y and t where

$$[8] \qquad y = (1 - X_1)$$

$$[9] \qquad t = \frac{X_3}{X_2 + X_3}$$

where X_1, X_2, and X_3 are the mole fractions of the three components. The inverse transformations are

$$[10] \qquad \begin{aligned} X_1 &= (1 - y) \\ X_2 &= (1 - t)y \\ X_3 &= ty \end{aligned}$$

In the composition triangle of an isothermal ternary system, t is constant along quasi-binary lines of constant X_3/X_2 ratio. The variable can assume values from $t = 0$ in the *1–2* binary system to $t = 1$ in the *1–3* binary system. The variable y is constant along lines parallel to the *2–3* binary line, and can assume values from $y = 0$ for pure component *1* to $y = 1$ in the *2–3* binary system. This is shown on the ternary composition triangle in Fig. 1. These variables were first suggested by Wagner (3) for his graphical treatment, and have also been found particularly useful for the present analytical method.

The partial and integral excess molar free energies of mixing are expressed as power series in y and t as follows

$$[11] \qquad f_1 = \sum_{j=2}^{j'} \sum_{k=0}^{k'} a_{jk} y^j t^k$$

$$[12] \qquad f_2 = \sum_{j=0}^{j'} \sum_{k=0}^{k'} b_{jk} y^j t^k$$

$$[13] \qquad f_3 = \sum_{j=0}^{j'} \sum_{k=0}^{k'} c_{jk} y^j t^k$$

$$[14] \qquad f = \sum_{j=1}^{j'} \sum_{k=0}^{k'} \phi_{jk} y^j t^k$$

where f_1, f_2, and f_3 are the partial molar excess free energies of mixing of components *1*, *2*, and *3*, respectively, and f is the excess integral molar free energy of mixing.

The upper limits of the summations can be selected in accordance with the number of terms found necessary to fit the data for a particular system. In many cases, it may be expedient for the upper limit k' to be a function of j'. An example of this is given later.

Equation [11] may be written in expanded form as

$$[15] \qquad \begin{aligned} f_1 = {} & (a_{20} + a_{21}t + a_{22}t^2 + \cdots\cdot)y^2 \\ & + (a_{30} + a_{31}t + a_{32}t^2 + \cdots\cdot)y^3 \\ & + \cdots\cdots\cdots\cdots \end{aligned}$$

Along a line of constant t, each of the bracketed factors in eq. [15] becomes constant, and f_1 is simply a power series in $y = (1 - X_1)$ starting with the y^2 term, which is of the same form as eq. [1] for binary systems. In the *1–2* and *1–3* binary sub-systems, y becomes equal to X_2 or X_3, respectively, and eq. [15] reduces exactly to eq. [1]. It is in this sense that the lines of constant t are called quasi-binary lines.

The expansion [11] for f_1 starts with the $j = 2$ term. That the missing coefficients a_{0k} are zero for all values of k follows from the condition that $f_1 = 0$ when $y = 0$. That the missing coefficients a_{1k} are all zero follows from the Gibbs–Duhem relation as will be discussed shortly. In the

Can. J. Chem. Downloaded from www.nrcresearchpress.com by 210.87.254.105 on 09/05/12
For personal use only.

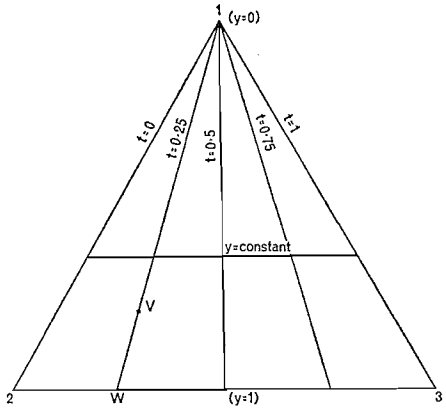

FIG. 1. Quasi-binary lines in a ternary system.

expansion [14] for f, the missing coefficients ϕ_{0k} for $j = 0$ must all be zero because of the condition that $f = 0$ when $y = 0$. The analogy with the binary case is clear.

Calculation of the Excess Integral Molar Free Energy of Mixing

By substituting the inverse transformations [10] into the well-known expression

$$[16] \qquad f = X_1 f_1 + X_2 f_2 + X_3 f_3$$

and into the Gibbs–Duhem equation

$$[17] \qquad X_1 df_1 + X_2 df_2 + X_3 df_3 = 0$$

it may be shown (see Appendix I) that

$$[18] \qquad f - f_1 = y\left(\frac{\partial f}{\partial y}\right)_t$$

Substitution of eqs. [11] and [14] into eq. [18] yields the equation

$$[19] \quad \sum_{j=1}\sum_{k=0}\phi_{jk}y^j t^k - \sum_{j=2}\sum_{k=0}a_{jk}y^j t^k = y\sum_{j=1}\sum_{k=0}\phi_{jk}(j)y^{j-1}t^k$$

By equating coefficients of $y^j t^k$ for each pair of values of j and k, the following relationship is obtained

$$[20] \qquad a_{jk} = (1 - j)\phi_{jk}$$

For $j = 1$, it is seen from eq. [20] that $a_{1k} = 0$ for all values of k, since the coefficients ϕ_{1k} must be finite. This proves the assertion made previously.

From eq. [20], the coefficients ϕ_{jk} in the expression for f, may be found from a knowledge of the coefficients a_{jk} for all values of j and k except for $j = 1$. These coefficients, ϕ_{1k}, must be found from boundary conditions as will be discussed shortly.

Calculation of the Partial Molar Excess Free Energies of Mixing

By taking the partial differentials of f in eq. [16] with respect to t and y, it may be shown (see Appendix II), that

$$[21] \qquad f_2 = f_1 + \left(\frac{\partial f}{\partial y}\right)_t - \frac{t}{y}\left(\frac{\partial f}{\partial t}\right)_y$$

Substituting the expressions for f_1, f_2, and f from eqs. [11], [12], and [14] into eq. [21] and simplifying (see Appendix II) yields the following relationship

$$[22] \quad \sum_{j=0}\sum_{k=0}b_{jk}y^j t^k = \sum_{j=2}\sum_{k=0}a_{jk}y^j t^k + \sum_{j=0}\sum_{k=0}\phi_{(j+1)k}(j + 1 - k)y^j t^k$$

By equating coefficients of $y^j t^k$ for each pair of values of j and k for $j \geqslant 1$, the following relationship is obtained

$$[23] \qquad b_{jk} = a_{jk} + (j + 1 - k)\phi_{(j+1)k} \qquad j \geqslant 1$$

By substitution from eq. [20], it is seen that

$$[24] \qquad b_{jk} = a_{jk} - \left(\frac{j + 1 - k}{j}\right)a_{(j+1)k} \qquad j \geqslant 1$$

The relationship between the coefficients c_{jk} and the coefficients a_{jk} may be derived in a similar manner (see Appendix III). The relationship is

$$[25] \quad c_{jk} = a_{jk} - \left(\frac{j + 1 - k}{j}\right)a_{(j+1)k} - \left(\frac{k + 1}{j}\right)a_{(j+1)(k+1)} \qquad j \geqslant 1$$

In applying eqs. [24] and [25], if j' is the upper summation index, then the coefficients $a_{(j'+1)k}$ must be taken to be zero.

From eqs. [24] and [25], the coefficients b_{jk} and c_{jk} of the expansions for f_2 and f_3 may be determined from a knowledge of the coefficients a_{jk}, except for the case when $j = 0$. These coefficients, b_{0k} and c_{0k}, must be determined from boundary values as discussed in the next section.

The Inclusion of Boundary Values

Equation [12] for f_2 may be expanded as follows

$$[26] \quad f_2 = (\sum_{k=0}b_{0k}t^k) + \sum_{j=1}\sum_{k=0}b_{jk}y^j t^k$$

Can. J. Chem. Downloaded from www.nrcresearchpress.com by 210.87.254.105 on 09/05/12
For personal use only.

As stated previously, the coefficients b_{0k} cannot be calculated from eq. [24] and must be found from boundary values of f_2.

The undetermined term, $(\sum_{k=0} b_{0k}t^k)$, in eq. [26], is constant along a quasi-binary line where t is constant. The knowledge of one end-point value of f_2 along a quasi-binary line is thus sufficient to give values of f_2 at any point on that line.

Let $f_{2(y^*,t)}$ be some known end-point value of f_2 at some point where $y = y^*$ along a quasi-binary line where t is constant. Then

$$[27]\quad f_{2(y^*,t)} = (\sum_{k=0} b_{0k}t^k) + \sum_{j=1}\sum_{k=0} b_{jk}y^{*j}t^k$$

Let $f_{2(y,t)}$ be the value of f_2 at any value of y along the same quasi-binary. Substitution of eq. [27] into eq. [26] then gives

$$[28]\quad f_{2(y,t)} = f_{2(y^*,t)} + \sum_{j=1}\sum_{k=0} b_{jk}(y^j - y^{*j})\,t^k$$

In Fig. 1, then, values of $f_{2(y,t)}$ at any point along the quasi-binary line *1*–W are given by a knowledge of $f_{2(y^*,t)}$ at any point on this line, say at point V, which could lie on a phase boundary such as a liquidus. It is thus seen that the use of end-point values permits f_2 to be found in the ternary system, without the explicit determination of the coefficients b_{0k}.

If values of f_1 were measured and fitted down to the *2–3* binary line where $y = 1$, then the experimental value of f_2 at point W, obtained from measurements in the *2–3* binary system, could be used as an end-point. In this case, $y^* = 1$, and eq. [28] takes the simple form

$$[29]\quad f_{2(y,t)} = f_{2(1,t)} + \sum_{j=1}\sum_{k=0} b_{jk}\,(y^j - 1)\,t^k$$

If f_2 has been measured in the *2–3* binary system as a function of concentration, then $f_{2(1,t)}$ may be written as a function of t (where $t = X_3$ in the *2–3* binary system from the definition [9]). The functional form of $f_{2(1,t)}$ would be as in eq. [1]. Equation [29] would then be a complete analytical equation for f_2 in the ternary system.

In the *1–2* binary system, the end-point condition that $f_2 = 0$ when $X_2 = 1$ can be used if values of f_1 are available down to $X_2 = 1$. This determines values of f_2 in this binary system, and in particular it fixes a value of f_2 at $X_1 = 1$ ($y = 0$). From Fig. 1, it may be seen that this value, $f_{2(0,t)}$, could then be used as an end point value in any quasi-binary. No independent measurements of f_2 anywhere would then be required to give values of f_2 at any point in the ternary composition triangle.

In fact, in this case, the boundary condition used, (that $f_2 = 0$ when $X_2 = 1$), could be employed to give explicit equations for the coefficients b_{0k} analogous to eq. [6] for binary systems.

However, this method requires that extremely accurate values of f_1 be known in the region near $X_1 = 1$, since f_2 is usually quite large in this region and, through the Gibbs–Duhem relation, is very sensitive to changes in the partial derivatives of f_1 with y and t. However, f_1 is very small in this region, and it is very difficult to determine the partial derivatives with any accuracy. Attempts to use this technique in the Cd–Bi–Sn system, discussed later, failed completely. Thus, in practice, end-point values obtained from independent measurements of f_2 are always required. All the graphical Gibbs–Duhem integration techniques (2–5) require the knowledge of end-point values for the same reason.

Equations completely analogous to eqs. [28] and [29] may be written for f_3

$$[30]\quad f_{3(y,t)} = f_{3(y^*,t)} + \sum_{j=1}\sum_{k=0} c_{jk}\,(y^j - y^{*j})\,t$$

Or, if values of f_3 in the *2–3* binary system may be used as end points

$$[31]\quad f_{3(y,t)} = f_{3(1,t)} + \sum_{j=1}\sum_{k=0} c_{jk}\,(y^j - 1)\,t^k$$

$f_{3(1,t)}$ could be expressed as a power series in t to give a complete analytical solution for f_3 in the ternary system.

For the excess integral free energy of mixing, f, eq. [14] may be expanded as

$$[32]\quad f = y\sum_{k=0}\phi_{1k}t^k + \sum_{j=2}\sum_{k=0}\phi_{jk}y^jt^k$$

If $f_{(y^*,t)}$ is some known value of f at a point where $y = y^*$ along a quasi-binary line, then

$$[33]\quad f_{(y^*,t)} = y^*\sum_{k=0}\phi_{1k}t^k + \sum_{j=2}\sum_{k=0}\phi_{jk}y^{*j}t^k$$

By substitution of eq. [33] into eq. [32], it may be seen that $f_{(y,t)}$ at any point on the quasi-binary

Can. J. Chem. Downloaded from www.nrcresearchpress.com by 210.87.254.105 on 09/05/12
For personal use only.

line may then be calculated from the equation

$$[34]\quad f_{(y,t)} = \left(\frac{y}{y^*}\right) f_{(y^*,t)} + \sum_{j=2}\sum_{k=0} \phi_{jk}(y^j - y y^{*(j-1)})t^k$$

And in the simple case where values of f in the *2–3* binary system may be used as end-points

$$[35]\quad f_{(y,t)} = y f_{(1,t)} + \sum_{j=2}\sum_{k=0} \phi_{jk}(y^j - y)\, t^k$$

$f_{(1,t)}$ may be expressed as a power series in t to give a complete analytical solution for f in the ternary system.

Although explicit equations for the coefficients c_{0k} and ϕ_{1k} could be found from the boundary conditions at the corners of the composition triangle, this method fails to give accurate results for the same reasons as discussed previously for the case of f_2, and so in practice, end-point values of f_3 and f from independent measurements are always required.

Summary of Method

Experimental values of f_1 over a composition range of a ternary system are fitted by a least-squares technique to an equation of the form of eq. [11]. The expansions for f_2, f_3, and f are then of the forms of eqs. [28], [30], and [34]. The coefficients b_{jk}, c_{jk}, and ϕ_{jk} are calculated from eqs. [24], [25], and [20]. The terms $f_{2(y^*,t)}$, $f_{3(y^*,t)}$, and $f_{(y^*,t)}$ are end-point values which must be determined at one point ($y = y^*$) on each quasi-binary line (t = constant), along which values of f_2, f_3, and f are to be calculated.

In the simple case in which values of f_1 have been measured and fitted over a composition range which has the *2–3* binary line as a boundary, experimental end-point values $f_{2(1,t)}$, $f_{3(1,t)}$, and $f_{(1,t)}$ obtained from measurements in this binary system, may be used. These could be expressed as power series in t (where $t = X_3$ in this binary system from the definition [9]). Suppose, for instance, that experimental values of $f_{2(1,t)}$ in the *2–3* binary system were available. These values could be fitted to an equation of the form of eq. [1]

$$[36]\quad f_{2(1,t)} = \sum_{j=2}^{j'} a_j t^j$$

Then, $f_{3(1,t)}$ and $f_{(1,t)}$ are given by equations of the form of eqs. [2] and [3]

$$[37]\quad f_{3(1,t)} = \sum_{j=0}^{j'} b_j t^j$$

$$[38]\quad f_{(1,t)} = \sum_{j=1}^{j'} \phi_j t^j$$

where the coefficients b_j and ϕ_j are given by eqs. [4]–[7].

Example of Application

The activities of Cd at several compositions in the Cd–Bi–Sn system have been determined with the aid of e.m.f. measurements at 500 °C by Mellgren (6). Also, the activities of Sn in the Bi–Sn binary system have been measured by Seltz and Dunkerley (7), and were corrected to 500 °C with the aid of the Gibbs–Helmholz equation by Mellgren (6). Using this data, Mellgren (6) applied the graphical Gibbs–Duhem integration techniques of Darken (2) and Wagner (3) to obtain activities of Bi and Sn at several compositions in the ternary system.

In the following discussion, the analytical method is applied to this system, and the results compared to those obtained graphically.

Cd, Bi, and Sn are taken as components *1*, *2*, and *3*, respectively.

A Fortran IV computer program was written to determine the coefficients a_{jk} for f_1 by a least-squares technique. The form of the expansion for f_1 used was as follows

$$[39]\quad \begin{aligned} f_1 = {} & (a_{20} + a_{21}t + a_{22}t^2 + a_{23}t^3 + a_{24}t^4)\, y^2 \\ & + (a_{30} + a_{31}t + a_{32}t^2 + a_{33}t^3)\, y^3 \\ & + (a_{40} + a_{41}t + a_{42}t^2) y^4 \\ & + (a_{50} + a_{51}t)\, y^5 \\ & + (a_{60})\, y^6 \end{aligned}$$

That is, 15 coefficients were used. Since y and t are never greater than unity, terms in $y^j t^k$ become progressively less significant as $(j + k)$ becomes larger. Thus, truncation in this manner with $(j + k) \leqslant 6$ was considered to be the most logical.

Another least-squares fit with $(j + k) \leqslant 5$ (10 coefficients), was done. Results for the 10 and 15 coefficient cases differed very little. The 15 coefficient fit seemed slightly better, however, and is reported here.

Values of the coefficients a_{jk} are listed in Table I. In Fig. 2 the fit between the calculated surface

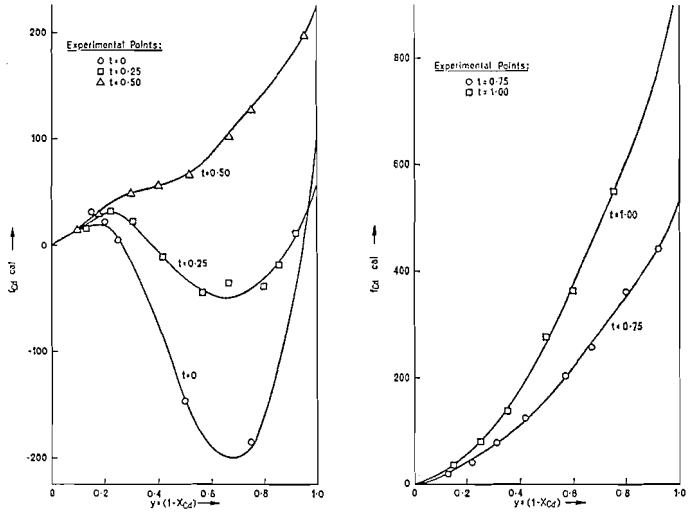

FIG. 2. Least-squares fit to experimental values (6) of the partial molar excess free energy of mixing of Cd along quasi-binary lines in the Cd–Bi–Sn system at 500 °C. Solid lines are the least-squares fit. $t = X_{Sn}/(X_{Bi} + X_{Sn})$.

and the experimental points is illustrated. The standard error of estimate was 6.58 cal.

Since the calculated values of f_2, f_3, and f depend upon the partial slopes of the tangents to the f_1 surface (through the Gibbs–Duhem relation), it is most important, when the analytical method is used, that the least-squares fit to the data be plotted as in Fig. 2 in order to make sure that a smooth fit without "hills and valleys" has been obtained.

The coefficients b_{jk}, c_{jk}, and ϕ_{jk} of the expansions for f_2, f_3, and f were determined, with the aid of a digital computer, from eqs. [24], [25], and [20] and are listed in Table I.

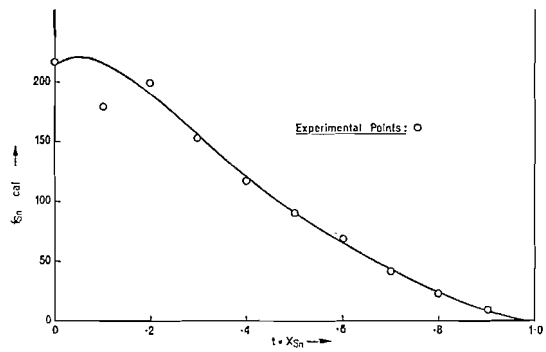

FIG. 3. Least-squares fit to experimental values (6, 7) of the partial molar excess free energy of mixing of Sn in the Bi–Sn system at 500 °C. Solid line is the least-squares fit. (Point at $t = 0.1$ was not included in least-squares fit.)

From the data in the *2–3* binary system, $f_{2(1,t)}$, $f_{3(1,t)}$, and $f_{(1,t)}$ as functions of t were determined by a least-squares fit, followed by an application of eqs. [4]–[7]. A good fit was obtained using 4 coefficients. The coefficients a_j, b_j, and ϕ_j of the expansions [36]–[38] are listed in Table I, and the fit between the calculated curve for $f_{3(1,t)}$ and the experimental points is illustrated in Fig. 3. (The actual method employed was to fit $f_{3(1,t)}$ as a series in X_2, to use eqs. [4]–[7] to obtain the coefficients for $f_{2(1,t)}$ and $f_{(1,t)}$ as series in X_2, and then to apply the relation, $X_2 = (1 - X_3)$, to obtain the coefficients of the expansions in $t = X_3$. Matters would have been facilitated if Sn rather than Bi had been defined as component *2*. However, this makes no difference to the final result.) The standard error of estimate was 3.5 cal.

Complete solutions for f_2, f_3, and f in the form of eqs. [29], [31], and [35] were thus obtained.

Values of f_2 and f_3 at the compositions at which Mellgren graphically determined values, were calculated, and are compared to his results in Table II. The two sets of results compare within the limits of experimental accuracy. Also, graphical plots of f_2 and f_3 over the entire composition range for the ternary system are in agreement with the curves given by Mellgren (6).

Although the two sets of calculations done by Mellgren (Table II) appear to agree more closely with each other than with the analytical calcula-

Can. J. Chem. Downloaded from www.nrcresearchpress.com by 210.87.254.105 on 09/05/12
For personal use only.

TABLE I

Coefficients of series expansions*

Coefficients a_{jk} of f_1 (cal) as in eq. [11] from least-squares fit to data. Standard error of estimate = 6.58 cal

a_{20} = 3 122.87	a_{21} = − 545.90	a_{22} = −1786.85	a_{23} = 1061.06	a_{24} = 384.51
a_{30} = −19 363.44	a_{31} = 13 980.85	a_{32} = 524.58	a_{33} = −2312.40	
a_{40} = 35 337.37	a_{41} = −21 816.32	a_{42} = 3707.95		
a_{50} = −26 567.48	a_{51} = 7 660.68			
a_{60} = 7 575.58				

Coefficients b_{jk} of f_2 (cal) obtained from eq. [24]

b_{10} = −6 245.74	b_{11} = 545.90	b_{12} = 0.00	b_{13} = 1061.06	b_{14} = 769.02
b_{20} = 32 168.03	b_{21} = −14 526.75	b_{22} = −2049.14	b_{23} = 1061.06	b_{24} = 384.51
b_{30} = −66 479.93	b_{31} = 35 797.17	b_{32} = −1947.39	b_{33} = −2312.40	
b_{40} = 68 546.72	b_{41} = −29 477.00	b_{42} = 3707.95		
b_{50} = −35 658.18	b_{51} = 7 660.68			
b_{60} = 7 575.58				

Coefficients c_{jk} of f_3 (cal) obtained from eq. [25]

c_{10} = −5 699.84	c_{11} = 4 119.60	c_{12} = −3183.18	c_{13} = −476.98	c_{14} = 769.02
c_{20} = 25 177.60	c_{21} = −15 051.33	c_{22} = 1419.46	c_{23} = 1061.06	c_{24} = 384.51
c_{30} = −59 207.83	c_{31} = 33 325.20	c_{32} = −1947.39	c_{33} = −2312.40	
c_{40} = 66 631.55	c_{41} = −29 477.00	c_{42} = 3707.95		
c_{50} = −35 658.18	c_{51} = 7 660.68			
c_{60} = 7 575.58				

Coefficients ϕ_{jk} of f (cal) obtained from eq. [20]

ϕ_{20} = −3 122.87	ϕ_{21} = 545.90	ϕ_{22} = 1786.85	ϕ_{23} = −1061.06	ϕ_{24} = −384.51
ϕ_{30} = 9 681.72	ϕ_{31} = −6990.42	ϕ_{32} = −262.29	ϕ_{33} = 1156.20	
ϕ_{40} = −11 779.12	ϕ_{41} = 7272.11	ϕ_{42} = −1235.98		
ϕ_{50} = 6 641.87	ϕ_{51} = −1915.17			
ϕ_{60} = −1 515.12				

Coefficients a_j of $f_{2(1,t)}$ (cal) as in eq. [36]

a_2 = −123.05	a_3 = 1770.07	a_4 = −2939.24	a_5 = 1730.59

Coefficients b_j of $f_{3(1,t)}$ (cal) as in eq. [37] calculated from eqs. [4] and [6]

b_0 = 214.89	b_1 = 246.10	b_2 = −2778.15	b_3 = 5689.06
b_4 = −5102.48	b_5 = 1730.59		

Coefficients ϕ_j of $f_{(1,t)}$ (cal) as in eq. [38] calculated from eqs. [5] and [7]

ϕ_1 = 214.89	ϕ_2 = 123.05	ϕ_3 = −885.04	ϕ_4 = 979.75	ϕ_5 = −432.65

*Cd = *1*, Bi = *2*, Sn = *3*; 500 °C.

tions, it should be noted that Mellgren's calculations are the result of two different graphical integrations, on the same set of smoothed plots of the experimental data. The analytical calculations are the result of treating a slightly different basic interpolation of the data.

Discussion

Although the analytical method should find most application with partial molar excess free energies of mixing as obtained from activity measurements, all the derived equations are valid for any partial molar property of mixing to which the Gibbs–Duhem relationship may be applied, provided that the partial property of every component and the corresponding integral property and their derivatives are continuous and finite functions, in and on the boundary of the entire composition range, so that series expansions as in eqs. [11]–[14] may be written.

Can. J. Chem. Downloaded from www.nrcresearchpress.com by 210.87.254.105 on 09/05/12
For personal use only.

TABLE II

Comparison of values of f_2 and f_3 as calculated by graphical and by analytical methods*

			f_2 (cal)		
t	X_1/X_3	y	Calculated graphically using Darken's method (6)	Calculated graphically using Wagner's method (6)	Calculated analytically
0.25	1/3	0.9231	− 3	+ 2	+ 4
0.50	1/3	0.8571	− 13	− 16	− 9
0.75	1/3	0.8000	− 30	− 20	− 38
0.25	1/1	0.8000	− 24	− 20	− 13
0.50	1/1	0.6667	−110	−116	−111
0.75	1/1	0.5714	−204	−216	−221
0.25	3/1	0.5714	− 90	−102	− 86
0.50	3/1	0.4000	−260	−292	−263
0.75	3/1	0.3077	−360	−372	−351

			f_3 (cal)		
t	X_1/X_2	y	Calculated graphically using Darken's method (6)	Calculated graphically using Wagner's method (6)	Calculated analytically
0	1/3	0.7500	360	330	274
0.25	1/3	0.8000	264	290	276
0.50	1/3	0.8571	168	175	168
0.75	1/3	0.9231	60	65	64
0	1/1	0.5000	750	650	608
0.25	1/1	0.5714	504	480	504
0.50	1/1	0.6667	310	310	306
0.75	1/1	0.8000	120	120	122
0	3/1	0.2500	820	880	847
0.25	3/1	0.3077	700	710	731
0.50	3/1	0.4000	520	520	539
0.75	3/1	0.5714	250	270	279

*Cd = *1*, Bi = *2*, Sn = *3*; 500 °C.

The enthalpy of mixing and the excess entropy of mixing are examples of properties to which the method may be applied. The method may not be applied to the total free energy of mixing or to the total entropy of mixing, since in these cases the partial property of mixing of a component becomes infinite as the mole fraction of that component approaches zero.

It is also evident that, with slight modification, the present method could be used to calculate partial molar properties of mixing, by fitting an equation of the form of eq. [14] to experimentally available values of the corresponding integral molar property of mixing, such as to calorimetrically measured values of the enthalpy of mixing.

Relationships between the coefficients of series expansions of partial and integral molar properties of mixing in ternary systems have been previously calculated by Wohl (8). Wohl used the mole fractions as composition variables. Nikol'skii (9) has recently generalized and simplified Wohl's equations. The drawback to using Wohl's or Nikol'skii's equations in a Gibbs–Duhem treatment of experimental data, however, is that it is not possible to utilize end-point values as is done in eqs. [28], [30], and [34]. The boundary conditions at the corners of the composition triangle are implicit in the equations. As discussed earlier, the use of these boundary conditions can lead to very serious inaccuracies. Also, the use of these boundary values renders the use of Wohl's and Nikol'skii's equations impossible if experimental data are available only over a restricted region of the composition triangle. Besides this, Wohl's and Nikol'skii's equations are in a form not easily fit by a least-squares technique.

Conclusions

An analytical technique based upon the Gibbs–

Can. J. Chem. Downloaded from www.nrcresearchpress.com by 210.87.254.105 on 09/05/12
For personal use only.

Duhem relation has been developed for calculating isothermal partial molar properties of mixing of the second and third components in a ternary system, when experimental measurements for one component or for the corresponding integral property are available. The method overcomes the problems inherent in graphical integration techniques. Data points may be scattered randomly over the composition range. The technique is not subject to human error. Equations are determined which allow the calculation of the quantities to be quickly made at any composition. The method is thus faster and more accurate than the graphical techniques.

The relationships developed are simple and readily adaptable to solution by a digital computer, and they reduce directly to the equations of Margules for binary systems. The use of quasi-binary lines along which one composition variable is constant makes the method simple, permits the easy utilization of end-point data, and aids in the visualization of the procedure.

Acknowledgments

The authors wish to thank Professor F. G. Smith of the Department of Geology, University of Toronto, for his valuable contribution in writing the computer programs used in this investigation. Financial support from the National Research Council of Canada and a maintenance fellowship for one of the authors (A.D.P.) from Shell Canada, are also gratefully acknowledged.

1. M. MARGULES. Sitz-Ber. Math.-Naturw. Kl. Bayer. Akad. Wiss. München. IIa, **104**, 1243 (1895).
2. L. S. DARKEN. J. Am. Chem. Soc. **72**, 2909 (1950).
3. C. WAGNER. Thermodynamics of alloys. Addison–Wesley Publishing Co., Inc., Reading, Mass. 1952. p. 15–21.
4. R. SCHUHMANN. Acta Met. **3**, 219 (1955).
5. N. A. GOKCEN. J. Phys. Chem. **64**, 401 (1960).
6. S. MELLGREN. J. Am. Chem. Soc. **74**, 5037 (1952).
7. H. SELTZ and F. J. DUNKERLEY. J. Am. Chem. Soc. **64**, 1392 (1942).
8. K. WOHL. Trans. Am. Inst. Chem. Engr. **42**, 215 (1946).
9. S. S. NIKOL'SKII. Russ. J. Phys. Chem. **39**, 1541 (1965).

Can. J. Chem. Downloaded from www.nrcresearchpress.com by 210.87.254.105 on 09/05/12
For personal use only.

Appendix I

Substitute eq. [10] into eq. [16] and collect terms

[A-1] $$f = (1 - y)f_1 + y(1 - t)f_2 + tyf_3$$

[A-2] $$f = f_1 + y(f_2 - f_1) + ty(f_3 - f_2)$$

Differentiate eq. [A-2] with respect to y at constant t

[A-3] $$\left(\frac{\partial f}{\partial y}\right)_t = \left[\left(\frac{\partial f_1}{\partial y}\right)_t + y\left(\frac{\partial(f_2 - f_1)}{\partial y}\right)_t + ty\left(\frac{\partial(f_3 - f_2)}{\partial y}\right)_t\right] + [(f_2 - f_1) + t(f_3 - f_2)]$$

Substitute eqs. [10] into eq. [17] and collect terms

[A-4] $$(1 - y)\,df_1 + y(1 - t)\,df_2 + ty\,df_3 = 0$$

[A-5] $$df_1 + y\,d(f_2 - f_1) + ty\,d(f_3 - f_2) = 0$$

Since eq. [A-5] holds everywhere, it also holds along a line where t is constant. Thus, by eq. [A-5], the first term on the right-hand-side of eq. [A-3] is zero. By substitution from eq. [A-2], the second term on the right-hand-side of eq. [A-3] is given, with the result that

[A-6] $$\left(\frac{\partial f}{\partial y}\right)_t = \frac{f - f_1}{y}$$

Can. J. Chem. Downloaded from www.nrcresearchpress.com by 210.87.254.105 on 09/05/12
For personal use only.

Appendix II

Differentiate eq. [A-2] with respect to t at constant y

$$[A\text{-}7] \qquad \left(\frac{\partial f}{\partial t}\right)_y = \left[\left(\frac{\partial f_1}{\partial t}\right)_y + y\left(\frac{\partial(f_2 - f_1)}{\partial t}\right)_y + ty\left(\frac{\partial(f_3 - f_2)}{\partial t}\right)_y\right] + y(f_3 - f_2)$$

From eq. [A-5], it is seen that the first term on the right-hand-side of eq. [A-7] is zero. Multiplying through in eq. [A-3] by y, multiplying through in eq. [A-7] by t, and subtracting the resulting equations, yields the following

$$[A\text{-}8] \qquad y\left(\frac{\partial f}{\partial y}\right)_t - t\left(\frac{\partial f}{\partial t}\right)_y = y(f_2 - f_1)$$

which may be written

$$[A\text{-}9] \qquad f_2 = f_1 + \left(\frac{\partial f}{\partial y}\right)_t - \frac{t}{y}\left(\frac{\partial f}{\partial t}\right)_y$$

Substitute eqs. [11], [12], and [14] into eq. [A-9] and simplify

$$[A\text{-}10] \qquad \sum_{j=0}\sum_{k=0} b_{jk}y^j t^k = \sum_{j=2}\sum_{k=0} a_{jk}y^j t^k + \sum_{j=1}\sum_{k=0} \phi_{jk}(j)y^{j-1}t^k - \frac{t}{y}\sum_{j=1}\sum_{k=0} \phi_{jk}(k)y^j t^{k-1}$$

Whence

$$[A\text{-}11] \qquad \sum_{j=0}\sum_{k=0} b_{jk}y^j t^k = \sum_{j=2}\sum_{k=0} a_{jk}y^j t^k + \sum_{j=1}\sum_{k=0} \phi_{jk}(j-k)\, y^{j-1}t^k$$

Alter the dummy variable j in the second term on the right-hand-side of eq. [A-11]

$$[A\text{-}12] \qquad \sum_{j=0}\sum_{k=0} b_{jk}y^j t^k = \sum_{j=2}\sum_{k=0} a_{jk}y^j t^k + \sum_{j=0}\sum_{k=0} \phi_{(j+1)k}(j+1-k)\, y^j t^k$$

Appendix III

Re-arrange eq. [A-7]

$$[A\text{-}13] \qquad f_3 = f_2 + \frac{1}{y}\left(\frac{\partial f}{\partial t}\right)_y$$

Substitute eqs. [12], [13], and [14] into eq. [A-13]

$$[A\text{-}14] \qquad \sum_{j=0}\sum_{k=0} c_{jk}y^j t^k = \sum_{j=0}\sum_{k=0} b_{jk}y^j t^k + \frac{1}{y}\sum_{j=1}\sum_{k=0} \phi_{jk}(k)y^j t^{k-1}$$

Alter both dummy variables, j and k, in the second term on the right-hand-side of eq. [A-14]

$$[A\text{-}15] \qquad \sum_{j=0}\sum_{k=0} c_{jk}y^j t^k = \sum_{j=0}\sum_{k=0} b_{jk}y^j t^k + \sum_{j=0}\sum_{k=-1} \phi_{(j+1)(k+1)}(k+1)\, y^j t^k$$

Equate coefficients of $y^j t^k$ for each pair of values of j and k for $j \geqslant 1$

$$[A\text{-}16] \qquad c_{jk} = b_{jk} + (k+1)\,\phi_{(j+1)(k+1)} \qquad j \geqslant 1$$

Substitute eqs. [20] and [24] into eq. [A-16]

$$[A\text{-}17] \qquad c_{jk} = a_{jk} - \left(\frac{j+1-k}{j}\right)a_{(j+1)k} - \left(\frac{k+1}{j}\right)a_{(j+1)(k+1)} \qquad j \geqslant 1$$

Reaction of chromyl chloride with donor molecules[1]

R. C. MAKHIJA[2] AND R. A. STAIRS
Chemistry Department, Trent University, Peterborough, Ontario

Received December 11, 1968

Reaction of chromyl chloride with various donor molecules led to solid products of compositions $CrO_2Cl_2.2D$ (D = acetone or dimethylsulfoxide), $2CrO_2Cl_2.3D$ (D = tetrahydrofuran, 1,4-dioxan, or 4-picoline), $CrO_2Cl_2.D$ (D = diethyl ether, triphenylphosphine, or triphenylarsine), and $2CrO_2Cl_2.(C_6H_5)_3N$. Acetonitrile failed to react. Infrared and ultraviolet spectra, X-ray diffraction and magnetic measurements, and the organic products obtained on hydrolysis were interpreted as showing that none of these complexes are Lewis adducts of chromyl chloride, but that all contain chromium(IV).

Canadian Journal of Chemistry, 47, 2293 (1969)

Can. J. Chem. Downloaded from www.nrcresearchpress.com by 210.87.254.5 on 09/05/12
For personal use only.

Introduction

Chromyl chloride, CrO_2Cl_2, has been used as an oxidant for hydrocarbons from time to time for many years, and its reactions with saturated and unsaturated molecules have been extensively studied (1–8). In the course of recent investigations of the structure of the main product of the Etard reaction of chromyl chloride with toluene (9), it was found that this product could react with two molecules of a Lewis base to form complexes containing the elements of the hydrocarbon, chromyl chloride, and the base, in the approximate molar proportions 1:2:2. (We will refer to this as a "ternary complex".) It was considered desirable to investigate the possibility of direct reaction of chromyl chloride as a Lewis acid with the base. Possible Lewis acid character also seemed relevant to the rapid cyclization of tetraphenylethylene by chromyl chloride which has been recently reported (10, 11).

The only past work on Lewis adducts of chromyl chloride is that of Bernard and Camelot (12), who have reported what appear to be 1:1 and 1:2 adducts with pyridine, which are formed only at temperatures below $-30\,^{\circ}C$, and decompose with reduction of the chromium on warming. Necsoiu and co-workers (4) have reported a 1:1 complex with ether which, however, clearly involves oxidation–reduction. Apsit, Sauka, and Blum (13) have reported a complex with hydrogen sulfide, which also probably contains reduced chromium.

Formation of an adduct by chromyl chloride requires that the coordination number of chromium be increased above 4. Unlike molybdenum and tungsten (14–16), chromium does not, on presently available evidence, appear to do this in its hexavalent state. Durrant and Durrant (17) describe the crystal structure of chromium trioxide as having the AlF_3 structure, with six-coordinate chromium, but Bystrom and Wilhelmi (18) describe the structure as made up of chains of CrO_4 tetrahedra.

In this work, chromyl chloride in dilute solution in an inert solvent (carbon tetrachloride or carbon disulfide) was reacted with a variety of molecules containing nitrogen, phosphorus, arsenic, oxygen, and sulfur as potential electron-pair donors. The complexes which were produced were then examined analytically, spectroscopically, by X-ray diffraction, and in one case each, by magnetic susceptibility and by electron spin resonance spectrometry (e.s.r.), for evidence that chromium was still hexavalent and that it was bonded directly to the donor atom.

Experimental

Reagents

Chromyl chloride (Alfa) was distilled, and the middle fraction, b.p. 114.5–115.5 °C used. Carbon tetrachloride, petroleum ether, diethyl ether, dioxan, tetrahydrofuran, 4-picoline, acetone, and acetonitrile were dried and purified as described earlier (9). Triphenylamine (Eastman), triphenylphosphine, and triphenylarsine (Alfa) were used as received.

Preparation and Analysis of Complexes

All operations were performed in a nitrogen atmosphere. Most of the preparations were carried out several times. The same procedure was used for all. Sufficient carbon tetrachloride and chromyl chloride were distilled into a three-necked flask to give an approximately 2% solution of the latter. A 2% solution of the donor substance was added slowly with continuous stirring,

[1]Presented at the 51st Annual Conference of the Chemical Institute of Canada, Vancouver, June, 1968.
[2]Teaching Postdoctoral Fellow.

TABLE I

Stoichiometry of the complexes

D	Ratio CrO_2Cl_2:D		Analysis*					Apparent oxidation number of Cr
	Taken	In product	C	H	N	Cr	Cl	
THF	1:8	2:3	27.4	4.6	—	19.8	27.0	3.12
			28.7	5.0	—	19.3	26.4	
Dioxan	1:8	2:3	25.1	4.2	—	18.1	24.7	3.66
			23.9	3.9	—	17.3	23.9	
4-Picoline	1:8	2:3	33.3	3.6	7.1	17.7	24.1	4.27
			33.2	3.4	6.6	16.6	24.6	
DMSO	1:6	1:2	15.4	3.9	—	16.7	—	3.92
			16.1	4.4	—	17.5	—	
Acetone	1:6	1:2	—	—	—	19.2	26.2	3.33
			—	—	—	19.3	26.4	
Ether	1:8	1:1	—	—	—	22.7	31.0	3.0
			—	—	—	23.0	33.1	
$(C_6H_5)_3N$	1:4	2:1	38.9	2.7	2.5	18.7	25.6	—
			37.8	2.9	2.5	17.7	25.3	
$(C_6H_5)_3P$	1:4	1:1	51.8	3.6	—	12.5	17.0	—
			48.2	3.7	—	13.3	15.5	
$(C_6H_5)_3As$†	1:4	1:1	46.9	3.3	—	11.3	15.4	—
			40.4	3.3	—	11.8	16.2	

*The upper figure is the calculated value and the lower figure is that found experimentally.
†Anal Calcd. for $3CrO_2Cl_2.2(C_6H_5)_3As$: C, 40.2; H, 2.80; Cr, 14.5; Cl, 19.8.

TABLE II

Infrared spectra of CrO_2Cl_2 complexes (type A) in 1250–200 cm^{-1} region

Complex or ligand	COC(asym) or C=O (cm^{-1})	Cr—Cl	Cr—O	Cr—O coordinated	Cr—N coordinated
C_4H_8O	1070s	—	—	—	—
$2CrO_2Cl_2.3C_4H_8O$	1030m	325s, 305sh	530–510mb, 435m	270w	—
$C_4H_8O_2$	1110s	—	—	—	—
$2CrO_2Cl_2.3C_4H_8O_2$	1080m, 1045m	360m	540–520mb, 450w	275w	—
$2CrO_2Cl_2.3$(4-picoline)	—	368m, 330s	550m, 515m, 428	—	285m
CH_3COCH_3	1710s	—	—	—	—
$CrO_2Cl_2.2CH_3COCH_3$	1665, 1635s	370, 330mb	570m, 445m, 430m	—	—

until it was in excess as noted in Table I. Stirring was continued until the color of chromyl chloride was discharged from the solution. This took place within a few minutes, except in the case of acetonitrile, which failed to react not only at room temperature, but also at the boiling point of carbon tetrachloride and at dry-ice temperature. (Prolonged refluxing of acetonitrile and chromyl chloride in carbon tetrachloride led to formation of a metal-free tar, which appeared to be a polymer of acetonitrile.) The precipitate that formed was removed by filtration, washed with several portions of solvent, and dried in vacuum at room temperature for 2–3 days.

Chromium and chlorine were estimated as Cr_2O_3 and as AgCl as described earlier (9). Some determinations of chromium as $BaCrO_4$ were also carried out as a check. Carbon, hydrogen, and nitrogen analyses were performed by a commercial analyst. The results are summarized in Table I, together with the compositions deduced therefrom, and the calculated analyses. Agreement between the analyses found and calculated is moderately good, with the notable exceptions of the results for carbon in the triphenylphosphine and triphenylarsine complexes. The latter figure would be in better accord with an assumed stoichiometry $3CrO_2Cl_2.2(C_6H_5)_3As$, but the analyses for H, Cr, and Cl are inconsistent with this, and are in agreement with the composition noted in the Table.

Physical Measurements

Infrared (i.r.) spectral measurements on the complexes were carried out in the frequency range 4000–200 cm^{-1} using a Perkin–Elmer 621 grating instrument purged with nitrogen. Samples were examined in Nujol or Fluorolube mulls between CsI plates. Ultraviolet (u.v.) spectra were obtained with a Unicam SP.800 spectrophotometer, using dioxan or tetrahydrofuran as solvent. Concentrations were not measured, but were estimated to be 10^{-5}–10^{-6} *M*. The path length of the cells used was 1 cm. Results of spectral measurements are summarized in Tables II, III, and IV.

The apparent oxidation state of chromium in the complexes was determined iodometrically. A weighed sample was added to an acidified aqueous solution of potassium iodide, allowed to stand in the dark in a stoppered flask

Can. J. Chem. Downloaded from www.nrcresearchpress.com by 210.87.254.5 on 09/05/12
For personal use only.

TABLE III

Infrared spectra of CrO_2Cl_2 complexes (type B) in 1250–200 cm^{-1} region

Complex or ligand	Cr=O (tentative)	Cr—Cl	Frequency (M=O)*	x-Sensitive† q r t	Unassigned
$(C_6H_5)_3PO$	—	—	1182s	1115 721 457,451	—
CrO_2Cl_2	1000s, 990s	—	—	— — — —	—
$CrO_2Cl_2.(C_6H_5)_3P$	955m, 935m	340m	1130, 1145	1103 720 450,433	768, 665
$(C_6H_5)_3AsO$	—	—	880s	1086 512 429,460	—
$CrO_2Cl_2.(C_6H_5)_3As$	970m, 950m	350s	885s	1082 — 470,455	—
$2CrO_2Cl_2.(C_6H_5)_3N$	965m, 945m	320–330mb	—	1085 510 440,400	—

*Where M = P, As.
†See footnote 1 and ref. 32.

for 2–3 min, and the liberated iodine titrated with sodium thiosulfate solution, using starch as indicator. The color change at the end point was sharp, from blue to green. The apparent oxidation numbers found are listed in Table I.

The organic products of hydrolysis were sought in the solutions resulting from addition of 2–3 g of the complexes in water saturated with sulfur dioxide. Chromium was removed by precipitation as hydroxide by ammonia, filtered off, and washed. The filtrate and washings were extracted with carbon tetrachloride, and both layers separately examined. Some products were identified by their i.r. or u.v. spectra only, but those that could be separated by evaporation of their solutions were crystallized where possible, and derivatives prepared. In Table V the results are summarized, including yields where determined (based on the assumed total amount of the organic reactant in the complex), frequencies of identifying u.v. or i.r. absorption bands, and m.p. of crystalline products and derivatives prepared.

X-ray powder diffraction patterns were taken using an 11.46 cm Debye-Scherrer camera with nickel-filtered copper Kα radiation. The magnetic susceptibility was measured by the Gouy method, at temperatures from 143 to 300 °K, on a powdered sample.

Discussion

The products of the reactions studied may be divided roughly into two classes, according to their stoichiometry and their i.r. and u.v. spectra. Class A, which is typified by the products of reaction of chromyl chloride with dioxan and tetrahydrofuran, is characterized by a combining ratio CrO_2Cl_2:D of 2:3 (D is the organic molecule) the presence in the i.r. absorption spectrum of the band assigned to OH, and the absence of the pair at 970–945 cm^{-1} tentatively assigned to O=Cr=O vibrations, as well as the presence of the series of bands in the u.v. from 37.9 to 41.9 kK. The product from 4-picoline lacks one qualification for this class, agreeing in stoichiometry and in the i.r. spectrum, and the product from diethyl ether agrees in the i.r. spectrum alone. The appearance of the OH band in the i.r. spectrum of all these suggests that an Etard-type oxidation has occurred, with transfer of a hydrogen to chromyl chloride at the same time reducing the Cr—O bond order, and therefore shifting the two Cr—O stretching bands to longer wavelengths. The i.r. spectra of the diethyl ether, tetrahydrofuran, and dioxan complexes also show features typical of the coordinated, but not oxidized molecules in the range 1250–200 cm^{-1}; in particular, the peak associated with the C—O—C antisymmetric stretch is split, and shows the expected frequency decrease, in each case (19, 20), i.e. the strong 1070 cm^{-1} band in tetrahydrofuran moves to 1030(m) and 1000(s) cm^{-1}, and the strong 1124 cm^{-1} band of dioxan appears at 1045(m) and 1015(m) cm^{-1}; also the tetrahydrofuran band at 908 cm^{-1} moves to 850 cm^{-1}, and the dioxan band at 878 cm^{-1} splits to give peaks at 868 and 820 cm^{-1}.

The u.v. bands observed in the complexes of dioxan and tetrahydrofuran (the spectra were taken using these same substances as solvents) may be characteristic of chromium(IV) complexed by a cyclic ether, for they also appeared weakly in the spectra of the complexes of triphenylamine and its analogues, which were taken in dioxan as solvent. That they appear only weakly suggests that dioxan is unable to displace extensively the other ligands.

The hydrolysis products from class A consist in each case, including the marginal ones, of some unchanged base and some that has been oxidized. Allowing for the possibility of some further reaction on working up, it appears probable that the reactions in this class can be viewed as a two-step process, viz. an Etard-type reaction of two molecules of chromyl chloride with one molecule of the base at a carbon adjacent to oxygen or the aromatic ring followed

Can. J. Chem. Downloaded from www.nrcresearchpress.com by 210.87.254.5 on 09/05/12
For personal use only.

TABLE IV

Ultraviolet spectra

Complex	Solvent	Peak positions (kK)
$2CrO_2Cl_2.N(C_6H_5)_3$	Dioxan	33.56 38.17 39.06 41.84
$CrO_2Cl_2.P(C_6H_5)_3$	Dioxan	36.56 37.45 38.31 39.21 42.01
$CrO_2Cl_2.As(C_6H_5)_3$	Dioxan	36.76 37.73 41.89
$2CrO_2Cl_2.3C_4H_8O$	THF	37.88 38.54 39.68–39.05 40.48–40.00 41.07 41.93
$2CrO_2Cl_2.3C_4H_8O_2$	Dioxan	37.88 38.61 39.53 40.33 41.15 41.93
$2CrO_2Cl_2.3C_5H_4(CH_3)N$	Dioxan	40.00
$CrO_2Cl_2.(C_2H_5)_2O$	Diethylether	44.05 43.86
$CrO_2Cl_2.2$ acetone	Dioxan	41.49 or 41.50
$CrCl_3.2NMe_3$*	Reflectance	37.50 45.60
$CrCl_3.3C_4H_8O$†	THF	36.60sh. 41.70
CrO_2Cl_2	CCl_4	33.33 35.71

*Reference 33.
†Reference 19.

TABLE V

Organic products of hydrolysis

From complexes of	Product (yield)	Identified by
THF	THF	i.r.: 1070 cm^{-1}
	γ-Butyrolactone (35%)	i.r.: 2850, 1175 cm^{-1}
Dioxan	Dioxan	i.r.: 1110 cm^{-1}
	Glyoxal	2,4-Dinitrophenylhydrazone, m.p. 331 °C
	Ethylene glycol	i.r.: 3350, 1640, 1670, 1040 cm^{-1}
	Oxalic acid	i.r.: 1680, 1740 cm^{-1}
4-Picoline	4-Picoline	i.r.: (C=N) 1600 cm^{-1}
	Isonicotinic acid (30%)	u.v.: 39.0kK, m.p. 305 °C
DMSO	DMSO	
	Dimethylsulfone	i.r.: 1380, 1145 cm^{-1}
Acetone	Acetone	i.r.: 1710 cm^{-1}
Diethyl ether	Ethyl acetate	i.r.: 1715 cm^{-1}
	Acetaldehyde	2,4-Dinitrophenylhydrazone, m.p. 147 °C
Triphenylamine	Tetraphenylbenzidine (60%)	m.p. 224 °C
Triphenylphosphine	Triphenylphosphine oxide (75%)	m.p. 158 °C i.r.: P=O 1182 cm^{-1}
Triphenylarsine	Triphenylarsine oxide monohydrate (75%)	m.p. 179–180 °C i.r.: As=O 880 cm^{-1}

by reaction of two further molecules of the base with the first product, giving rise in effect to a ternary complex like those mentioned above. On hydrolysis two moles of unchanged base and one of oxidized base should be obtained for each mole of the complex $2CrO_2Cl_2.3D$ reacting. We have not succeeded in making a quantitative recovery of the products of hydrolysis but the complexes from 4-picoline, dioxan, and tetrahydrofuran each yielded unchanged base as a major component.

The oxidized products are concordant with the known behavior of chromyl chloride. Attack by chromyl chloride appears to be facilitated by the presence of one single-bonded oxygen on a carbon atom, but hindered by more than one electronegative substituent, whether oxygen or another such as chlorine. There seems to be, also, a strong tendency for chromium(IV) to form binuclear complexes and a lesser tendency to further polymerization. It is probably for both these reasons that the Etard reaction proceeds two steps from toluene to aldehyde, but not further. In certain cases a single molecule of chromyl chloride only appears to be involved. An example that is somewhat uncertain, as different workers disagree about the composition of the complex, is triphenylmethane (5, 21). Here there is only one oxidizable C—H, and apparently the three bulky phenyl groups preclude dimerization to form a binuclear chromium(IV) complex. A consequence is the binding, in an

Can. J. Chem. Downloaded from www.nrcresearchpress.com by 210.87.254.5 on 09/05/12
For personal use only.

Can. J. Chem. Downloaded from www.nrcresearchpress.com by 210.87.254.5 on 09/05/12
For personal use only.

unknown manner, of additional chromyl chloride, so that various workers have reported ratios of chromyl chloride to hydrocarbon ranging from 1.2 to nearly 2.

With the cyclic ethers the organic products can be explained by assuming attack of two molecules of chromyl chloride, on the same carbon of tetrahydrofuran, and on adjacent carbons of dioxan. The tetrahydrofuran product appears to involve an unusual attack on a carbon bearing two oxygens, facilitated by the formation of the binuclear complex. The main oxidized product of hydrolysis should then be γ-butyrolactone, as observed. In the dioxan product, attack on the carbon already bearing two oxygens by the second chromyl chloride molecule is avoided, and the adjacent carbon is attacked instead. We postulate that the primary product of hydrolysis is the cyclic double hemiacetal **1**, and that this is partly hydrolyzed to glyoxal and glycol and partly oxidized to ethylene oxalate, **2**, in a similar manner to the ether complex, discussed below.

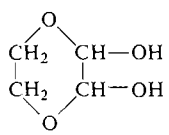

1

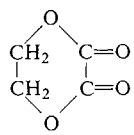

2

We have not yet been able to detect or isolate **1**, but believe that it may be more resistant to hydrolysis than are ordinary non-cyclic hemiacetals, as we could not detect glyoxal in the reaction mixture from hydrolysis of the complex, but found it in the steam distillate.

Hydrolysis of the complexes of the cyclic ethers in the presence of iodide, and titration of the liberated iodine, gave apparent oxidation numbers lower than 4 for chromium. The assumption that these complexes contain chromium(IV) was based in part on the results of e.s.r. spectrum measurements (22). The samples examined all gave identical spectra consisting of a broad, intense line with g close to 2 and a half-width of the order of 500 G, unaffected by cooling to 77 °K, and apparently identical to that observed by Necsoiu and co-workers (3) with the Etard product obtained from toluene. This is believed to contain chromium(IV) in a similar state of bonding to that in the present complexes. In the discussion of the diethyl ether complex, below, an explanation of the low apparent oxidation numbers found by titration is proposed, which is probably applicable here also.

Class B contains the products of reactions of 1:1 stoichiometry, which show no OH band in the i.r., but do show the bands assigned to Cr=O, and in the u.v. show a single intense absorption maximum at about 230 mμ. We were tempted to conclude that these were Lewis adducts, but the magnetic susceptibility of the triphenylphosphine product was incompatible with chromium(VI). In fact, it is in close agreement with the other measurements on complexes believed to contain chromium(IV) (9). (The value obtained for the magnetic moment of $CrO_2Cl_2.(C_6H_5)_3P$ was 3.00 ± 0.05 B.M.) The arsenic analogue was presumed to be similar. Since each yielded the oxide of the base (or its hydrate) on hydrolysis, it is clear that the interaction with chromyl chloride was through oxygen.

We were puzzled by the persistence in the i.r. of bands similar to the O=Cr=O bands of chromyl chloride, shifted only about 20–30 cm^{-1}. This may be due to interaction in the solid between Cr=O groups in neighboring molecules. Brisdon and Edwards (23) and Bagnall *et al.* (24) came to a similar conclusion with regard to the spectrum of $ReOCl_4$, taken in Nujol mull, which contained a pair of bands at 1033 and 1016 cm^{-1}. If our bands at 955 and 935 cm^{-1} in the triphenylphosphine product and 970 and 950 cm^{-1} in the triphenylarsine product are due to splitting of a single Cr=O band in the solid state, they should reduce to one sharp, strong absorption band in solution. We have not yet found a suitable solvent. There should be a band due to coordinated Cr—O, in the region 450–350 cm^{-1} (25), which may be obscured by the Cr—Cl stretching vibrations. As is well established, the ν(P=O) and ν(As=O) absorptions move to lower frequencies on coordination (26–31). In our complexes the medium broad absorption bands at 1130–1145 and 885 cm^{-1} are assigned to coordinated P=O and As=O respectively. All the Whiffen bands (32) *q*, *r*, and *t* show small shifts in frequency[3]. The frequencies and assignments are listed in Table III.

[3]Modes in which ring vibrations are coupled to C—P or (C—As) motion, and which are sensitive to coordination.

Can. J. Chem. Downloaded from www.nrcresearchpress.com by 210.87.254.5 on 09/05/12
For personal use only.

The products that fall neither into class A nor class B are those obtained from dimethylsulfoxide, triphenylamine, acetone, and diethyl ether. The first of these we have been unable to characterize, the complex being excessively unstable. The hydrolyzed products included dimethylsulfone, which suggests that one molecule of dimethylsulfoxide is attacked by chromyl chloride at the sulfur to give a complex of the sulfone which is further complexed by a second dimethylsulfoxide molecule. The last two present some unusual features, but can be considered as variants of class A. Triphenylamine behaved in a distinctly different manner in that oxidative coupling to tetraphenyl benzidene occurred. This is a common product of oxidation of triphenylamine, so we did not investigate it further at this time.

Necsoiu and co-workers (4) report that diethyl ether reacts with only one molecule of chromyl chloride, as we have confirmed. The hemiacetal, which would be the "normal" product of hydrolysis of the complex according to the above proposal for class A, presumably suffers further oxidation and hydrolysis leading to the reported products, ethyl acetate and acetaldehyde. (Ethanol would also be expected, but was not detected.) This complex, when hydrolyzed in water containing potassium iodide, liberated almost no iodine, so the chromium was apparently reduced very rapidly to chromium(III). A possible sequence of reactions on hydrolysis might be

[1] $C_2H_5—O—\underset{\displaystyle CH_3}{\underset{|}{CH}}—O—Cr(OH)Cl_2 + H_2O \rightarrow C_2H_5O—\underset{\displaystyle CH_3}{\underset{|}{CHOH}} + [Cr^{IV}(OH)_2Cl_2]$

[2] $2Cr^{IV} \rightarrow Cr^{V} + Cr^{III}$

[3] $C_2H_5O\underset{\displaystyle CH_3}{\underset{|}{CHOH}} + Cr^{V} \rightarrow C_2H_5O\underset{\displaystyle CH_3}{\underset{|}{C}}=O + Cr^{III}$

[4] $C_2H_5O\underset{\displaystyle CH_3}{\underset{|}{CHOH}} \rightarrow C_2H_5OH + CH_3CHO$

If this is to be accomplished without oxidation of iodide by the very reactive chromium(IV) and (V) species, steps [1] to [3] must take place within such a closed environment as that afforded by a binuclear complex. We suggest, therefore, that the structure of the ether complex is something resembling **3**, which is in accord with the facts noted above, and is analogous with the structure proposed earlier for the ternary complexes.

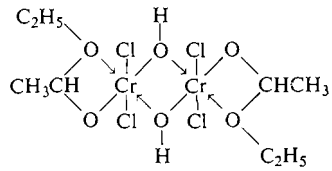

3

The product obtained with acetone showed both OH and Cr=O bands in the i.r., and conformed to class B in the u.v., but to neither class in stoichiometry. If the regularly spaced group of u.v. bands is characteristic of the complexes of the cyclic ethers with chromium-(IV), the probability is that the acetone product is in other respects similar to class A. The significance of the 1:2 stoichiometry is not clear but it can be accommodated by the structure **4**, which on hydrolysis should yield equal amounts of acetone and hydroxyacetone or its oxidation products.

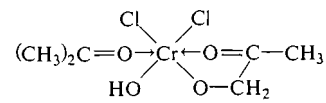

4

We have not succeded in identifying the oxidized products.

The X-ray powder diffraction photographs of the complexes $CrO_2Cl_2.2CH_3COCH_3$, $2CrO_2Cl_2.3C_4H_8O$, $2CrO_2Cl_2.3C_4H_8O_2$, $CrO_2Cl_2.(C_2H_5)O$, and $CrO_2Cl_2.P(C_6H_5)_3$ show no lines, and hence the complexes are amorphous. The complexes $CrO_2Cl_2.2DMSO$ and $2CrO_2Cl_2.3(CH_3)C_5H_4N$ show a few lines, but not enough for indexing. These lines are due neither to dimethylsulfone nor to 4-picolinium chloride. The three strongest lines are at approximately 4.1, 3.7, and 6.6 Å in $2CrO_2Cl_2.3(CH_3)C_5H_4N$ and 2.72, 1.93, and 1.58 Å in $CrO_2Cl_2.2DMSO$.

We conclude that, if chromyl chloride is a Lewis acid, it is a very weak one. None of the products examined were pure molecular addition compounds. In all of the cases studied, chromyl chloride is reduced and the ligand is oxidized. The two main different types of compounds

obtained are (*a*) Etard-type products with additional coordinated base and (*b*) the products of reaction of triphenyl-phosphine and -arsine, which we conclude should be considered as complexes of the base oxides with chromium(IV) oxydichloride.

Acknowledgments

The authors wish to acknowledge generous help from Professor A. D. Westland of Ottawa University with the magnetic measurements, and from Dr. Norman Bright, and Mr. J. F. Rowland of Mines Branch, Department of Energy, Mines and Resources, Ottawa, with X-rays. The work was made possible by grants from the National Research Council of Canada and Trent University.

1. W. H. HARTFORD and M. DARRIN. Chem. Rev. **58**, 1 (1958).
2. K. B. WIBERG and R. EISENTHAL. Tetrahedron, **20**, 1151 (1964).
3. I. NECSOIU, A. T. BALABAN, I. PASCARU, E. SLIAM, M. ELAIN, and C. D. NENITZESCU. Tetrahedron, **19**, 1133 (1963).
4. I. NECSOIU, V. PRZCMETCHI, A. GHENCIULESCU, C. N. RENTEA, and C. D. NENITZESCU. Tetrahedron, **22**, 3037 (1966).
5. C. N. RENTEA, I. NECSOIU, M. RENTEA, A. GHENCIULESCU, and C. D. NENITZESCU. Tetrahedron, **22**, 3501 (1966).
6. O. H. WHEELER. Can. J. Chem. **38**, 2137 (1960).
7. O. H. WHEELER. Can. J. Chem. **42**, 706 (1964).
8. R. A. STAIRS, D. G. M. DIAPER, and A. L. GATZKE. Can. J. Chem. **41**, 1059 (1963).
9. R. C. MAKHIJA and R. A. STAIRS. Can. J. Chem. **46**, 1255 (1968).
10. C. D. NENITZESCU. Bull. Soc. Chim. France, **4**, 1349 (1968).
11. A. L. GATZKE, D. G. M. DIAPER, and R. A. STAIRS. Can. J. Chem. **46**, 3695 (1968).
12. J. BERNARD and M. CAMELOT. Compt. Rend. **258**, 5881 (1964).
13. A. APSIT, J. SAUKA, and A. YA. BLUM. Uch. Zap. Rizhsk Politekhn. Ins. **6**, 63 (1962). Chem. Abstr. **59**, 7149*h* (1963).
14. C. G. HULL and M. H. B. STIDDARD. J. Chem. Soc. 1633 (1966).
15. MELVIN L. LARSON and FRED W. MOORE. Inorg. Chem. **5**, 801 (1966).
16. B. J. BRISDON. Inorg. Chem. **6**, 1791 (1967).
17. P. J. DURRANT and B. DURRANT. Advanced inorganic chemistry. 2nd ed. Longman's Green, London. 1962. pp. 989–990.
18. A. BYSTROM and K. A. WILHELMI. Acta Chem. Scand. **4**, 1131 (1950).
19. G. W. A. FOWLES, P. T. GREEN, and T. F. LESTER. J. Inorg. Nucl. Chem. **29**, 2365 (1967).
20. R. J. KERN. J. Inorg. Nucl. Chem. **24**, 1105 (1962).
21. R. C. MAKHIJA. Unpublished results.
22. M. C. R. SYMONS. Private communication.
23. B. J. BRISDON and D. A. EDWARDS. Inorg. Chem. **7**(9), 1898 (1968).
24. K. W. BAGNALL, D. BROWN, and R. COLTON. J. Chem. Soc. 3017 (1964).
25. J. P. CLARK, V. M. LANGFORD, and C. J. WILKINS. J. Chem. Soc. 792 (1967).
26. F. A. COTTON, R. D. BARNES, and E. BANNISTER. J. Chem. Soc. 2179 (1960).
27. D. M. L. GOODGAME and F. A. COTTON. J. Chem. Soc. 2298 (1961); 3735 (1961).
28. J. C. SHELDON and S. Y. TYREE. J. Am. Chem. Soc. **80**, 4775 (1958).
29. M. J. FRAZER, W. GERRARD, and R. TWAITS. J. Inorg. Nucl. Chem. **25**, 637 (1963).
30. G. B. DEACON and J. H. S. GREEN. Spectrochim. Acta, **24A**, 845 (1968).
31. G. B. DEACON and J. H. S. GREEN. Chem. Ind. London, 1031 (1965).
32. D. H. WHIFFEN. J. Chem. Soc. 1350 (1956).
33. M. W. DUCKWORTH, G. W. A. FOWLES, and P. T. GREENE. J. Chem. Soc. 1592 (1967).

Can. J. Chem. Downloaded from www.nrcresearchpress.com by 210.87.254.5 on 09/05/12
For personal use only.

Can. J. Chem. Downloaded from www.nrcresearchpress.com by 210.87.254.42 on 09/05/12
For personal use only.

Molecular rotational relaxation time of aniline in deuterated benzene solution at 20 °C

E. BOCK
Parker Chemistry Laboratory, University of Manitoba, Winnipeg, Manitoba

AND

E. TOMCHUK
Department of Physics, University of Winnipeg, Winnipeg, Manitoba

Received October 21, 1968

The molecular rotational relaxation time of the aniline molecule in deuterated benzene solution was determined at 20 °C by pulsed nuclear magnetic resonance (n.m.r.) techniques. It was found that the rotational relaxation time, τ_r, in infinitely dilute deuterated benzene solution was 3.2×10^{-12} s, a value which is in fair agreement with the dielectric molecular relaxation time reported by Grubb and Smyth for aniline in dilute benzene solution.

Canadian Journal of Chemistry, 47, 2301 (1969)

Introduction

The dielectric relaxation of NR_3 type molecules has been the subject of many investigations (1, 2). The reason for the great interest shown in the relaxation behavior of the above type molecules is that these molecules may possess a relaxation mechanism whereby the electric dipole moment may reverse direction by an inversion process in addition to a simple molecular rotation process. To the best of our knowledge there has been only one attempt made to determine the molecular rotational relaxation time of the aniline molecule by other means than by dielectric relaxation techniques, viz. by n.m.r. technique (3). However, the measurements reported in ref. 3 were made on pure aniline and, moreover, the experimental data were interpreted on the assumption that the intermolecular contribution to the spin–lattice relaxation time, T_1, is relatively unimportant and makes only a minor contribution to the measured value of T_1. We thought it, therefore, not inappropriate to redetermine the molecular rotational relaxation time of the aniline molecule using a pulsed n.m.r. method and an experimental technique which permitted the separation of the *inter-* and *intra-*molecular contributions to the overall measured spin–lattice relaxation time T_1.

Experimental

Solvent

The solvent used, benzene-d_6, 99.5 atom % D, was obtained from Merck, Sharp, and Dohme Co. of Canada Ltd., and was used without further purification.

Solute

The aniline, obtained from Eastman Organic Chemicals, was further purified by redistillation from anhydrous KOH.

Apparatus and Procedure

The spin–lattice relaxation time of pure aniline and four different solutions of progressively lower concentration of aniline in heavy benzene was determined at 20 °C on a PS-60A NMR specialties pulsed n.m.r. spectrometer using a 180–90° pulse sequence (4). The experimental solutions were carefully degassed by repeated freeze–pump–thaw cycles to remove dissolved oxygen and were sealed under vacuum. To minimize vaporization from the liquid phase the experimental glass sample tubes, 8 mm diameter, were provided with a restriction leading to the vapor space as suggested by Green and Powles (5).

Results and Discussion

The experimental results are shown graphically in Fig. 1 in a form of a graph of T_1^{-1} vs. the mole fraction of aniline in solution. The rotational relaxation time, τ_r, was calculated using the extrapolated value of T_1^{-1} and the following relationship between the intramolecular relaxation time, i.e. the extrapolated value of T_1, and the rotational relaxation time, τ_r (6).

$$[1] \qquad T_1^{-1}\,(\text{intra}) = A\tau_r$$

$$[2] \qquad A = \frac{\hbar^2\gamma^4}{n}\sum_i\sum_j \beta_{ij} d_{ij}^{-6}$$

Here n is the number of protons in the molecule,

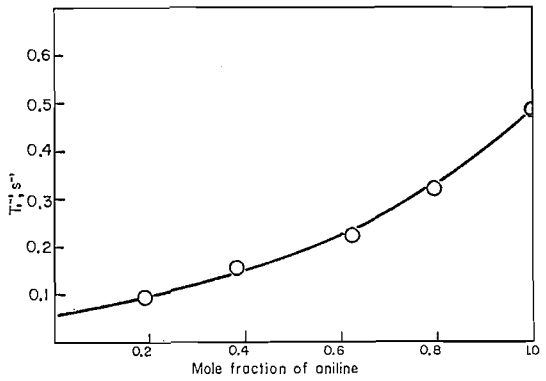

FIG. 1. Plot of T_1^{-1} vs. mole fraction of aniline in C_6D_6.

β_{ij} is a constant factor equal to 3/2 for equivalent protons and 1 for nonequivalent protons, γ is the magnetogyric ratio of the proton, and d_{ij} is the distance between proton i and proton j. The necessary data for the calculation of the constant A in eq. [2] was taken from the microwave data of Lister and Tyler (7). The resulting value for the molecular rotational relaxation time, τ_r, was found to be 3.2×10^{-12} s. This value may be compared with the dielectric molecular, i.e. rotational, relaxation time, τ_D, obtained by Fischer, 6.7×10^{-12} s (8), and by Grubb and Smyth, 8.0×10^{-12} s (1), in dilute benzene solution at 20 °C. In making this comparison it should be remembered that on theoretical grounds it is expected that $\tau_D = 3\tau_r$ (9). Considering that the probable error in τ_r is at least 10%, the agreement between $3\tau_r = 9.6 \times 10^{-12}$ s and τ_D of Grubb and Smyth, viz. 8.0×10^{-12} s, is quite satisfactory. The agreement is not quite as close when the value for τ_D determined by Fischer is used for comparison, but there is reason to believe that Fischer's value is less accurate than the value reported by Grubb and Smyth since the latter workers were able to measure the dielectric loss of their solutions at frequencies nearer to the maximum dielectric absorption than was Fischer. One tentative conclusion which may be drawn from the close agreement between τ_D and $3\tau_r$ is that either the inversion process contributes little to the rotational part of the spin–lattice relaxation time, or that the ring and amide group motions are essentially similar, as suggested by Powles and Neale (3). However, it should be pointed out that in our interpretation of the experimental results we assumed the existence of but one correlation time; also in our experimental measurements we were unable to distinguish between the relaxation times of the ring protons and $-NH_2$ protons.

In our opinion, no meaningful comparison can be made between our results and those obtained by Powles and Neale (3), except to note that our value of T_1 for pure aniline is in fair agreement with that reported by them, viz. ~2 s in both cases. The measurements of Powles and Neale were made on pure aniline only. It was impossible for them on the basis of their measurements to separate the translational and rotational contributions to T_1. In fact, they assumed that the translational or intermolecular contribution to T_1 was negligible. But they did point out that this assumption, viz. neglect of intermolecular contribution to T_1, could be checked by comparing "the pure liquid T_1's with those for dilute solution in the perdeutero compound". In part we have done just that, but only in part. For it may be fairly assumed that perdeutero benzene molecule closely simulates the motional properties of the ring fragment of the aniline molecule, but what is missing is the $-ND_2$, and it may be that the presence of this group severely alters the motional properties of the molecule by the formation of hydrogen bonds with the neighboring molecules. At any rate, our measurements show that T_1 does become significantly longer with increase in dilution, and that in perdeutero benzene solution at least the intermolecular contribution to T_1 is not negligible. However, it may very well be that in perdeutero aniline the intermolecular contribution to T_1 is negligible as assumed by Powles and Neale. The fact that their measured value of $3\tau_r$ does agree with the measured value of τ_D for pure aniline does suggest that their assumption is probably correct.

Acknowledgments

Firstly we would like to thank both referees for pointing out to us a glaring error in our calculation of the constant A of eq. [2]. We thank Dr. T. Schaefer for helpful suggestions. Finally the financial assistance of the National Research Council of Canada is deeply appreciated.

1. E. L. GRUBB and C. P. SMYTH. J. Am. Chem. Soc. **83**, 4879 (1961).
2. G. WILLIAMS. Trans. Faraday Soc. **64**, 1219 (1968).
3. J. G. POWLES and D. J. NEALE. Proc. Phys. Soc. **78**, 377 (1961).

Can. J. Chem. Downloaded from www.nrcresearchpress.com by 210.87.254.42 on 09/05/12
For personal use only.

4. A. LAUKIEN. Handbuch der Physik. Vol. XXXVIII. Springer-Verlag, Berlin. 1958. p. 120.
5. D. K. GREEN and J. G. POWLES. Proc. Phys. Soc. London, **85**, 87 (1965).
6. J. G. POWLES. Ber. Bunsenges. Physik. Chem. **67**, 328 (1963).
7. D. G. LISTER and J. K. TYLER. Chem. Commun. 152 (1966).
8. E. FISCHER. Z. Physik, **127**, 49 (1949).
9. A. ABRAGAM. Principles of nuclear magnetism. Oxford Univ. Press, London. 1961. p. 300.

Addendum: Studies on metal hydroxy compounds. VIII. Heats of decomposition of twelve copper halide derivatives

P. RAMAMURTHY AND E. A. SECCO
Chemistry Department, St. Francis Xavier University, Antigonish, Nova Scotia

Received January 27, 1969

(Ref. Can. J. Chem. This issue)

Canadian Journal of Chemistry, 47, 2303 (1969)

The calorimetric results (1) along with related enthalpic values for the decomposition of 12 copper hydroxy-halide compounds are presented in Table I according to the following equations showing the onset and terminal temperatures

[1] $Cu(OH)_{2(c)} \xrightarrow{140\text{–}205\ ^\circ C} CuO_{(c)} + H_2O_{(g)}$

[2] $2Cu(OH)Cl_{(c)} \xrightarrow{240\text{–}310\ ^\circ C} CuO_{(c)} + CuCl_{2(c)} + H_2O_{(g)}$

[3] $2\alpha\text{-}Cu_2(OH)_3Cl_{(c)} \xrightarrow{220\text{–}310\ ^\circ C} 3CuO_{(c)} + CuCl_{2(c)} + 3H_2O_{(g)}$

[4] $2\beta\text{-}Cu_2(OH)_3Cl_{(c)} \xrightarrow{250\text{–}350\ ^\circ C} 3CuO_{(c)} + CuCl_{2(c)} + 3H_2O_{(g)}$

[5] $2\gamma\text{-}Cu_2(OH)_3Cl_{(c)} \xrightarrow{250\text{–}350\ ^\circ C} 3CuO_{(c)} + CuCl_{2(c)} + 3H_2O_{(g)}$

[6] $2\delta\text{-}Cu_2(OH)_3Cl_{(c)} \xrightarrow{210\text{–}300\ ^\circ C} 3CuO_{(c)} + CuCl_{2(c)} + 3H_2O_{(g)}$

[7] $2Cu_2(OH)_3Br_{(c)} \xrightarrow{240\text{–}320\ ^\circ C} 3CuO_{(c)} + \tfrac{1}{2}Cu_2Br_{2(c)} + 3H_2O_{(g)} + \tfrac{1}{2}Br_{2(g)}$

[7*a*] $\longrightarrow 3CuO_{(c)} + CuBr_{2(c)} + 3H_2O_{(g)}$

[8] $2Cu_2(OH)_3I_{(c)} \xrightarrow{185\text{–}260\ ^\circ C} 3CuO_{(c)} + \tfrac{1}{2}Cu_2I_{2(c)} + 3H_2O_{(g)} + \tfrac{1}{2}I_{2(g)}$

[8*a*] $\longrightarrow 3CuO_{(c)} + CuI_{2(c)} + 3H_2O_{(g)}$

[9] $2CuF_2 \cdot 2H_2O_{(c)} \xrightarrow{130\text{–}220\ ^\circ C} Cu_2(OH)F_{3(c)} + HF_{(g)} + 3H_2O_{(g)}$

[10] $Cu_2(OH)F_{3(c)} \xrightarrow{250\text{–}430\ ^\circ C} CuO_{(c)} + CuF_{2(c)} + HF_{(g)}$

[11] $4Cu(OH)F_{(c)} \xrightarrow{260\text{–}430\ ^\circ C} 3CuO_{(c)} + CuF_{2(c)} + 2HF_{(g)} + H_2O_{(g)}$

[11*a*] $\longrightarrow Cu_2(OH)F_{3(c)} + 2CuO_{(c)} + HF_{(g)} + H_2O_{(g)}$

[12] $Cu_2(OH)_3F_{(c)} \xrightarrow{260\text{–}430\ ^\circ C} 2CuO_{(c)} + H_2O_{(g)} + HF_{(g)}$

Can. J. Chem. Downloaded from www.nrcresearchpress.com by 210.87.254.42 on 09/05/12
For personal use only.

4. A. LAUKIEN. Handbuch der Physik. Vol. XXXVIII. Springer-Verlag, Berlin. 1958. p. 120.
5. D. K. GREEN and J. G. POWLES. Proc. Phys. Soc. London, **85**, 87 (1965).
6. J. G. POWLES. Ber. Bunsenges. Physik. Chem. **67**, 328 (1963).
7. D. G. LISTER and J. K. TYLER. Chem. Commun. 152 (1966).
8. E. FISCHER. Z. Physik, **127**, 49 (1949).
9. A. ABRAGAM. Principles of nuclear magnetism. Oxford Univ. Press, London. 1961. p. 300.

Addendum: Studies on metal hydroxy compounds. VIII. Heats of decomposition of twelve copper halide derivatives

P. RAMAMURTHY AND E. A. SECCO
Chemistry Department, St. Francis Xavier University, Antigonish, Nova Scotia

Received January 27, 1969

(Ref. Can. J. Chem. This issue)

Canadian Journal of Chemistry, 47, 2303 (1969)

The calorimetric results (1) along with related enthalpic values for the decomposition of 12 copper hydroxy-halide compounds are presented in Table I according to the following equations showing the onset and terminal temperatures

[1] $Cu(OH)_{2(c)} \xrightarrow{140\text{–}205\ ^\circ C} CuO_{(c)} + H_2O_{(g)}$

[2] $2Cu(OH)Cl_{(c)} \xrightarrow{240\text{–}310\ ^\circ C} CuO_{(c)} + CuCl_{2(c)} + H_2O_{(g)}$

[3] $2\alpha\text{-}Cu_2(OH)_3Cl_{(c)} \xrightarrow{220\text{–}310\ ^\circ C} 3CuO_{(c)} + CuCl_{2(c)} + 3H_2O_{(g)}$

[4] $2\beta\text{-}Cu_2(OH)_3Cl_{(c)} \xrightarrow{250\text{–}350\ ^\circ C} 3CuO_{(c)} + CuCl_{2(c)} + 3H_2O_{(g)}$

[5] $2\gamma\text{-}Cu_2(OH)_3Cl_{(c)} \xrightarrow{250\text{–}350\ ^\circ C} 3CuO_{(c)} + CuCl_{2(c)} + 3H_2O_{(g)}$

[6] $2\delta\text{-}Cu_2(OH)_3Cl_{(c)} \xrightarrow{210\text{–}300\ ^\circ C} 3CuO_{(c)} + CuCl_{2(c)} + 3H_2O_{(g)}$

[7] $2Cu_2(OH)_3Br_{(c)} \xrightarrow{240\text{–}320\ ^\circ C} 3CuO_{(c)} + \tfrac{1}{2}Cu_2Br_{2(c)} + 3H_2O_{(g)} + \tfrac{1}{2}Br_{2(g)}$

[7*a*] $\longrightarrow 3CuO_{(c)} + CuBr_{2(c)} + 3H_2O_{(g)}$

[8] $2Cu_2(OH)_3I_{(c)} \xrightarrow{185\text{–}260\ ^\circ C} 3CuO_{(c)} + \tfrac{1}{2}Cu_2I_{2(c)} + 3H_2O_{(g)} + \tfrac{1}{2}I_{2(g)}$

[8*a*] $\longrightarrow 3CuO_{(c)} + CuI_{2(c)} + 3H_2O_{(g)}$

[9] $2CuF_2 \cdot 2H_2O_{(c)} \xrightarrow{130\text{–}220\ ^\circ C} Cu_2(OH)F_{3(c)} + HF_{(g)} + 3H_2O_{(g)}$

[10] $Cu_2(OH)F_{3(c)} \xrightarrow{250\text{–}430\ ^\circ C} CuO_{(c)} + CuF_{2(c)} + HF_{(g)}$

[11] $4Cu(OH)F_{(c)} \xrightarrow{260\text{–}430\ ^\circ C} 3CuO_{(c)} + CuF_{2(c)} + 2HF_{(g)} + H_2O_{(g)}$

[11*a*] $\longrightarrow Cu_2(OH)F_{3(c)} + 2CuO_{(c)} + HF_{(g)} + H_2O_{(g)}$

[12] $Cu_2(OH)_3F_{(c)} \xrightarrow{260\text{–}430\ ^\circ C} 2CuO_{(c)} + H_2O_{(g)} + HF_{(g)}$

Can. J. Chem. Downloaded from www.nrcresearchpress.com by 210.87.254.42 on 09/05/12
For personal use only.

TABLE I

Compound	Reaction	Heat of decomposition*		ΔH_f^0 (kcal/mole)	
		ΔH of H_2O formed (kcal/mole)	ΔH of compound decomposed (kcal/mole)	This work†	Literature
$Cu(OH)_2$	[1]	11.68±0.03	11.68±0.03	−106.6	−107.2†
CuOHCl	[2]	16.14±0.02	8.07±0.01	−79.6	—
α-$Cu_2(OH)_3Cl$	[3]	14.51±0.04	21.79±0.06	−188.8	—
β-$Cu_2(OH)_3Cl$	[4]	15.13±0.02	22.69±0.03	−189.6	—
γ-$Cu_2(OH)_3Cl$	[5]	15.15±0.03	22.72±0.05	−189.7	—
δ-$Cu_2(OH)_3Cl$	[6]	14.65±0.01	21.98±0.02	−188.9	—
$Cu_2(OH)_3Br$	[7]		23.61±0.01	−176.7	
	[7a]	11.62±0.02	17.43±0.03	−176.7	−186.8
$Cu_2(OH)_3I$	[8]		17.06±0.05	−171.2	
	[8a]	18.69±0.03	28.04±0.05	−171.2	—
$CuF_2\cdot 2H_2O$	[9]		28.06±0.12	−247.0	−274.5
$Cu_2(OH)_3F$	[10]		28.67±0.33	−256.9	—
CuOHF	[11]		16.54±0.22	−122.7	
	[11a]		9.36±0.22	−122.6	—
$Cu_2(OH)F_3$	[12]		21.86±0.06	−188.8	—

*All determinations were done in duplicate; ΔH values are given with their average deviations.
†ΔH_f^0 values of compounds used in our calculations are from N.B.S. Circular No. 500 (1951). The above ΔH_f^0 values were calculated using Kopp's Rule approximation with $\Delta C_p^0 \approx 0$ in the equation

$$\Delta H_T^0 = \Delta H_{298\,^\circ K}^0 + \int_{298\,^\circ K}^{T} \Delta C_p^0 dT$$

because ΔC_p^0 values for most compounds in the decomposition reactions are unavailable to us. Integral term was negligible for $Zn(OH)_2$ (1).

Our value of ΔH_f^0 for $Cu(OH)_2$ compares very well with the literature value, but the ΔH_f^0 values for $Cu(OH)_3Br$ and $CuF_2\cdot 2H_2O$ from this work and the literature (2, 3) differ considerably. Our ΔH_f^0 values for these latter two compounds are internally consistent with two or more reactions, namely, reactions [7] and [7*a*] for $Cu(OH)_3Br$ and reactions [9], [10], and [11*a*] for $CuF_2\cdot 2H_2O$.

$CuBr_2$ disproportionates concomitantly with dehydroxylation in the $Cu_2(OH)_3Br$ reaction. If one assigns the experimentally observed ΔH of decomposition for the two combined processes to reaction [7*a*], a value of −182.9 kcal/mole is obtained which approaches the literature value of −186.8 kcal/mole. In the case of $CuF_2\cdot 2H_2O$, the literature ΔH_f^0 value (3) was obtained on the basis of simple dehydration

$$[13] \qquad CuF_2\cdot 2H_2O_{(c)} \rightarrow CuF_{2(c)} + 2H_2O_{(v)}$$

The assignment of our observed ΔH of reaction to [13] yields a ΔH_f^0 value of −270.6 kcal/mole, approaching the literature value of −274.5 kcal/mole.

The slight variations in the ΔH values of the four structural forms, α-, β-, γ-, and δ-$Cu_2(OH)_3Cl$ are associated with their lattice arrangements.

The column of values for ΔH per mole of H_2O formed indicates higher values for the copper hydroxychlorides and hydroxyiodide relative to the parent $Cu(OH)_2$; the sole exception to this pattern is the bromide. The decomposition behavior of the basic fluorides involving dehydrofluorination along with dehydroxylation does not permit a similar comparison. The above pattern in basic chlorides and basic iodide of copper parallels the cadmium hydroxyhalide where it was interpreted that the Cd—OH bond increases in strength by substitution of the halogen in the parent hydroxide.

The decomposition temperatures for the derivative compounds are all higher relative to their parent hydroxides. This is attributed primarily to increased separation of neighboring OH groups by interposition of the halogen substituent. The halogen substituent in $Cu_2(OH)_3Br$ effects a higher decomposition temperature but weakens the bonding between the OH group and the copper cation; such effects parallel the halogen substituent in ZnOHCl and ZnOHF.

Acknowledgment

This research work has received generous support from the National Research Council of Canada.

1. P. Ramamurthy and E. A. Secco. Can. J. Chem. **46**, 3605 (1968).
2. P. Sabatier. Compt. Rend. **125**, 301 (1897).
3. W. Jahn-Held and K. Jellinek. Z. Elektrochem. **42**, 401 (1936).

Can. J. Chem. Downloaded from www.nrcresearchpress.com by 210.87.254.42 on 09/05/12
For personal use only.

Background scattering of a supersonic free jet: source temperature dependence[1,2]

RODNEY L. LEROY[3,4], THOMAS R. GOVERS[3], AND JACQUES M. DECKERS
Lash Miller Chemical Laboratories, University of Toronto, Toronto 5, Ontario

Received November 7, 1967

The attenuation of nozzle beams by scattering on background gas in the expansion chamber is examined experimentally. It is found that, due to the velocity dependence of the collision cross section, this attenuation is significantly reduced as the source temperature is increased.

Canadian Journal of Chemistry, 47, 2305 (1969)

Can. J. Chem. Downloaded from www.nrcresearchpress.com by 210.87.254.5 on 09/05/12
For personal use only.

The intensities of nozzle beams can be strongly affected by background scattering of the expanding jet in the nozzle exhaust chamber (1–4). The purpose of this note is to illustrate that the importance of this effect is reduced at elevated nozzle stagnation temperatures.

The apparatus has been described elsewhere (4). Center-line beam fluxes (I) were measured as a function of the background pressure in the nozzle exhaust chamber (p_b) for various combinations of the nozzle–skimmer separation s, the source pressure p_0, and the source temperature T_0. Argon was used throughout. Typical primary data are shown in Fig. 1.

Following a procedure similar to that proposed by Fenn and Anderson (2), we correlated the data obtained for different values of s and p_0 by plotting the quantity $-(\mathrm{d} \ln I/\mathrm{d}n_b)/p_0$ vs. s/p_0 (n_b is the number density corresponding to p_b). This is illustrated in Fig. 2. For each of the source temperatures shown, the data at larger values of s/p_0 can be represented by an equation of the form

$$\frac{1}{p_0}\frac{\mathrm{d} \ln I}{\mathrm{d}n_b} = -\frac{Q_{\mathrm{eff}}}{p_0}(s - s_p)$$

where Q_{eff} is the slope of the limiting straight lines in Fig. 2, and s/p_0 is the intercept with the abscissa. Q_{eff} can be regarded as an effective scattering cross section, and s_p as the distance from the source at which the background gas has completely penetrated the jet. The source temperature dependence of the scattering data is further illustrated in Fig. 3. These results were obtained at source pressures low enough ($15 \leqslant p_0 \leqslant 20$ Torr) to ensure effective background penetration of the expansion. For a given value of s/p_0, an increase in T_0 from 290 to 1200 °K reduced the attenuation coefficient $\mathrm{d} \ln I/\mathrm{d}n_b$ by about 40%. Since s_p/p_0 remained nearly constant

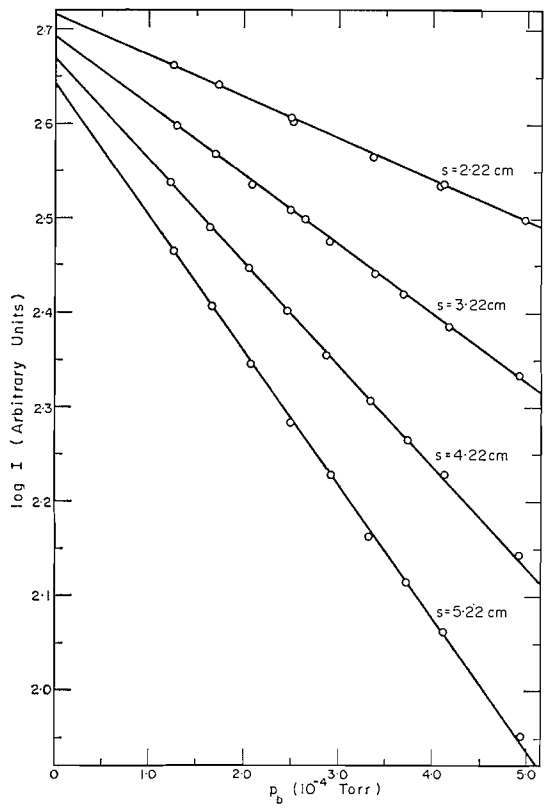

FIG. 1. Typical primary scattering data. The beam flux is plotted logarithmically against the pressure in the nozzle exhaust chamber. Source conditions are $p_0 = 19.6$ Torr and $T_0 = 476$ °K.

[1]Supported by grants from the National Research Council of Canada.
[2]Revision received March 3, 1969.
[3]Holder of a National Research Council of Canada Studentship.
[4]Present address: Department of Chemistry, University of Colorado, Boulder, Colorado 80302.

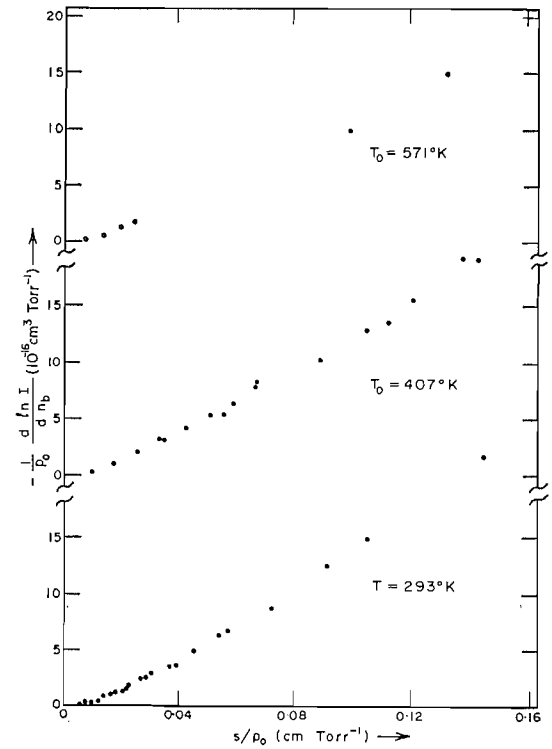

FIG. 2. Correlation of data obtained at different source pressures. Results at $T_0 = 293$ and 407 °K include data taken at $p_0 = 15$, 30, 60, and 120 Torr, while the results at $T_0 = 571$ °K were obtained at two source pressures ($p_0 = 15$ and 60 Torr).

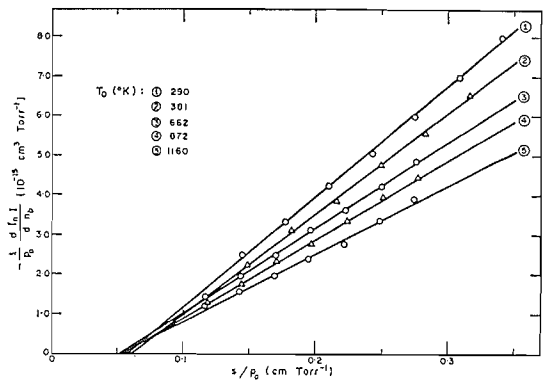

FIG. 3. Plots of $-(\mathrm{d} \ln I/\mathrm{d}n_b)/p_0$ vs. s/p_0 for different source temperatures. The source pressure p_0 was between 15 and 20 Torr for all the data indicated.

(constant "x intercept" in Fig. 3), this reduction can be attributed mainly to the velocity dependence of Q_{eff}. In fact the slopes of the straight lines in Fig. 3 ($=Q_{\mathrm{eff}}$) vary as the $-2/3$ power of the relative velocity of jet and background molecules (5), as expected on the basis of simple classical scattering theory (6).

The observations presented here may be of practical interest when limited pumping speeds in the nozzle exhaust chamber result in significant background scattering of the jet.

1. K. BIER and O. HAGENA. *In* Rarefied gas dynamics. Vol. 2. *Edited by* J. H. deLeeuw. Academic Press, Inc., New York. 1966. p. 260.
2. J. B. FENN and J. B. ANDERSON. *In* Rarefied gas dynamics. Vol. 2. *Edited by* J. H. deLeeuw. Academic Press, Inc., New York. 1966. p. 311.
3. R. F. BROWN and J. H. HEALD, JR. *In* Rarefied gas dynamics. Vol. 2. *Edited by* C. L. Brundin. Academic Press, Inc., New York. 1967. p. 1407.
4. T. R. GOVERS, R. L. LEROY, and J. M. DECKERS. Proc. 6th Intern. Symp. Rarefied Gas Dynamics. M.I.T. 1968. In press.
5. T. R. GOVERS. Ph.D. Thesis, University of Toronto, Toronto, Ontario. 1969.
6. F. VON BUSCH. Z. Physik, **193**, 412 (1966).

The stabilization of alkoxide anions

N. C. BAIRD
Department of Chemistry, University of Western Ontario, London, Ontario

Received January 22, 1969

Molecular orbital calculations by the MINDO method are reported for the valence electrons of HO^- and a number of small alkoxide anions. The acidity order isopropanol > ethanol > methanol ≫ water is predicted, in agreement with recent ion cyclotron resonance studies. The electron density distributions within the ions are discussed with reference to current models of the polarizability of alkyl groups.

Canadian Journal of Chemistry, 47, 2306 (1969)

Recently Brauman and Blair (1) have demonstrated by ion cyclotron resonance measurements that alkyl groups are effective in stabilizing negative charge in the gaseous alkoxide anions. This result is the reverse of that expected from classical inductive effect considerations, and is

Can. J. Chem. Downloaded from www.nrcresearchpress.com by 210.87.254.5 on 09/05/12
For personal use only.

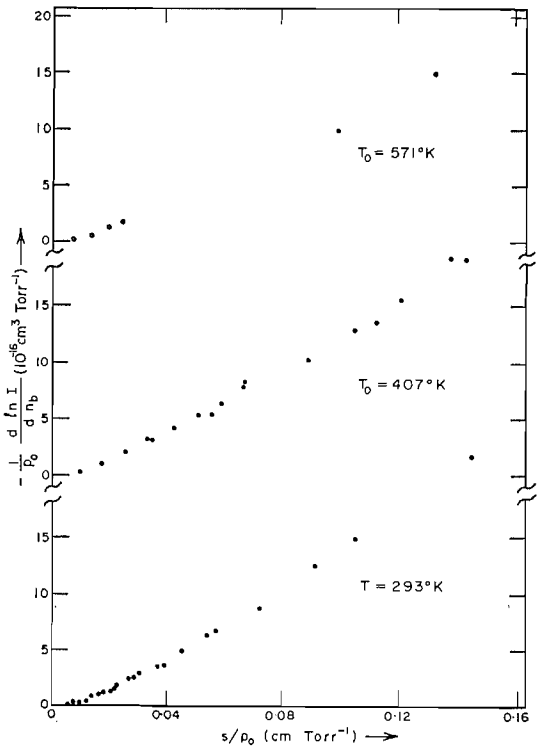

FIG. 2. Correlation of data obtained at different source pressures. Results at T_0 = 293 and 407 °K include data taken at p_0 = 15, 30, 60, and 120 Torr, while the results at T_0 = 571 °K were obtained at two source pressures (p_0 = 15 and 60 Torr).

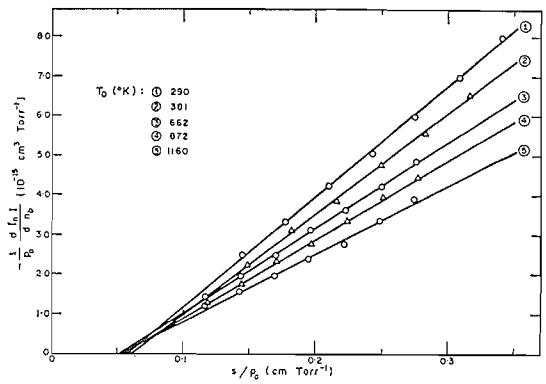

FIG. 3. Plots of $-(\mathrm{d} \ln I/\mathrm{d}n_b)/p_0$ vs. s/p_0 for different source temperatures. The source pressure p_0 was between 15 and 20 Torr for all the data indicated.

(constant "x intercept" in Fig. 3), this reduction can be attributed mainly to the velocity dependence of Q_{eff}. In fact the slopes of the straight lines in Fig. 3 ($=Q_{\mathrm{eff}}$) vary as the $-2/3$ power of the relative velocity of jet and background molecules (5), as expected on the basis of simple classical scattering theory (6).

The observations presented here may be of practical interest when limited pumping speeds in the nozzle exhaust chamber result in significant background scattering of the jet.

1. K. BIER and O. HAGENA. *In* Rarefied gas dynamics. Vol. 2. *Edited by* J. H. deLeeuw. Academic Press, Inc., New York. 1966. p. 260.
2. J. B. FENN and J. B. ANDERSON. *In* Rarefied gas dynamics. Vol. 2. *Edited by* J. H. deLeeuw. Academic Press, Inc., New York. 1966. p. 311.
3. R. F. BROWN and J. H. HEALD, JR. *In* Rarefied gas dynamics. Vol. 2. *Edited by* C. L. Brundin. Academic Press, Inc., New York. 1967. p. 1407.
4. T. R. GOVERS, R. L. LEROY, and J. M. DECKERS. Proc. 6th Intern. Symp. Rarefied Gas Dynamics. M.I.T. 1968. In press.
5. T. R. GOVERS. Ph.D. Thesis, University of Toronto, Toronto, Ontario. 1969.
6. F. VON BUSCH. Z. Physik, **193**, 412 (1966).

The stabilization of alkoxide anions

N. C. BAIRD
Department of Chemistry, University of Western Ontario, London, Ontario

Received January 22, 1969

Molecular orbital calculations by the MINDO method are reported for the valence electrons of HO^- and a number of small alkoxide anions. The acidity order isopropanol > ethanol > methanol ≫ water is predicted, in agreement with recent ion cyclotron resonance studies. The electron density distributions within the ions are discussed with reference to current models of the polarizability of alkyl groups.

Canadian Journal of Chemistry, 47, 2306 (1969)

Recently Brauman and Blair (1) have demonstrated by ion cyclotron resonance measurements that alkyl groups are effective in stabilizing negative charge in the gaseous alkoxide anions. This result is the reverse of that expected from classical inductive effect considerations, and is

Can. J. Chem. Downloaded from www.nrcresearchpress.com by 210.87.254.6 on 09/05/12
For personal use only.

Can. J. Chem. Downloaded from www.nrcresearchpress.com by 210.87.254.6 on 09/05/12
For personal use only.

attributed by Brauman and Blair to differences in the polarizabilities of alkyl groups and hydrogen atoms (1).

To investigate these effects further, we have performed self-consistent field molecular orbital calculations for the valence electrons of a number of small alkoxide anions RO^-, by the semi-empirical MINDO method (2). The MINDO procedure is a variant of the INDO method described recently by Pople *et al.* (3) and has been found to accurately predict the bonding energies and heats of formation of a wide variety of neutral organic molecules (2) and carbonium ions (4). For the anions considered, the bond lengths and idealized bond angles established for the neutral alcohols ROH (2) have been used. Both experimental (5) and theoretical (6) studies indicate that the O—H bond distance in HO^- is virtually identical to that in HO·. No structural information is as yet available for the other anions considered.

In Table I, the heats for the reactions

$$[1] \qquad ROH + R'O^- \rightarrow RO^- + R'OH$$

calculated from the heats of formation of the alcohols (2) and of the alkoxide anions, are listed for R, R′ = H, CH_3, CH_3CH_2, and $(CH_3)_2CH$. In agreement with the ion cyclotron results, the acidity order isopropanol > ethanol > methanol ≫ water is obtained.

TABLE I

Calculated ΔH for reaction [1] (kcal/mole)

R or R′	H	CH_3	CH_3CH_2	$(CH_3)_2CH$
H	0.0	+23.8	+28.9	+33.3
CH_3	−23.8	0.0	+5.1	+9.5
CH_3CH_2	−28.9	−5.1	0.0	+4.4
$(CH_3)_2CH$	−33.3	−9.5	−4.4	0.0

Following Streitwieser and Hammons (7) the energetics of the reaction

$$[2] \qquad ROH \rightarrow RO^- + H^+$$

can be analyzed as the sum of contributions from the processes: (*i*) bond dissociation to RO· and H·; (*ii*) ionization of H· to H^+; and (*iii*) formation of RO^- from RO·. The electron affinities of the radicals RO· (step *iii*), have been computed from the calculated heats of formation of the ROH and RO^- species, together with the known energy requirements for step *i* (104 kcal/mole for R = alkyl (1) and 119.2 kcal/mole for R = H (8) and for step *ii* (313.5 kcal/mole (2)), and are predicted to increase in the order HO· (+30 kcal/mole), CH_3O· (+38), CH_3CH_2O· (+43), and $(CH_3)_2CHO$· (+48)[1].

Hence alkyl groups are effective in stabilizing the net negative charge associated with the oxygen atom. The stabilization order isopropyl > ethyl > methyl ≫ hydrogen found for these anions is identical to that predicted for carbonium ions (4).

The electron density distributions calculated for the anions support the interpretation of Brauman and Blair (1), that polarization of alkyl groups is responsible for the order of stabilization observed for alkoxide anions. The calculations predict that all the carbon–hydrogen bonds in the hydrocarbon fragments of such species become strongly polarized in the direction $C^{\delta+}H^{\delta-}$. For example, the carbon atom in CH_3O^- carries a net positive charge of +0.77e, and a net charge of −0.29e is associated with each hydrogen atom. Each of these C—H dipoles is of the correct direction and magnitude to stabilize the net charge of ∼ −1e associated with the oxygen atom by a charge–dipole interaction

The calculations also predict that a portion of the total stabilization occurs via hyperconjugative release of electron density from oxygen, since the oxygen atom net charge decreases from −1.08e in HO^- to −0.91e in CH_3O^-, to −0.85e in $CH_3CH_2O^-$, and to −0.81e in $(CH_3)_2CHO^-$.

Acknowledgment

Support of this research by the National Research Council of Canada is gratefully acknowledged.

1. J. I. Brauman and L. K. Blair. J. Am. Chem. Soc. **90**, 6561 (1968).
2. N. C. Baird and M. J. S. Dewar. J. Chem. Phys. **50**, 1262 (1969). N. C. Baird, M. J. S. Dewar, and R. Sustmann. J. Chem. Phys. **50**, 1275 (1969).
3. J. A. Pople, D. L. Beveridge, and P. A. Dobosh. J. Chem. Phys. **47**, 2026 (1967).
4. N. C. Baird and M. J. S. Dewar. J. Am. Chem. Soc. In press.
5. L. M. Branscomb. Phys. Rev. **148**, 11 (1966).
6. P. E. Cade. J. Chem. Phys. **47**, 2390 (1967).
7. A. Streitwieser, Jr. and J. H. Hammons. Progr. Phys. Org. Chem. **3**, 41 (1965).
8. J. A. Kerr. Chem. Rev. **66**, 465 (1966).

[1]Recent experimental data for the simplest species of this series, HO·, yield an electron affinity of +42.2 ± 0.9 kcal/mole (5). The present calculation represents an improvement over the Hartree–Fock prediction of −2.3 kcal/mole (6), but is not as accurate as the Hartree–Fock result corrected for correlation energy (6).

Polarizations of atomic and molecular charge distributions

R. F. W. BADER, I. KEAVENY[1], AND G. RUNTZ
Department of Chemistry, McMaster University, Hamilton, Ontario

Received November 25, 1968

It is shown that the dominant polarization of a molecular charge distribution in the region of a nucleus of an atom which employs p orbitals in its bonding (Be → F, Mg → Cl) is quadrupolar in nature, and dipolar for an atom which employs s orbitals (H, He, Li, Na). That these polarizations are of a fundamental nature is demonstrated by showing that they represent the primary response of a charge distribution to an electric field, whether it be internal or external, static or dynamic.

Canadian Journal of Chemistry, 47, 2308 (1969)

The polarization of a molecular charge distribution measured relative to the charge densities of its constituent separated atoms is determined by a density difference distribution $\Delta\rho_{SA}(r)$. Such a distribution is constructed by subtracting from the molecular distribution, one obtained from the overlap of the undistorted atomic densities, the atomic densities being centered at the same nuclear positions as in the molecule. An extensive investigation of such $\Delta\rho_{SA}(r)$ distributions (1–4)[2] for diatomic molecules formed from atoms in the first two rows of the periodic table, has revealed that the component atomic densities exhibit one of two dominant polarizations on the formation of a chemical bond. The polarization of atoms which employ principally s orbitals in their bonding, e.g., H, He, Li, and Na, is *dipolar* in character. The $\Delta\rho_{SA}(r)$ distribution in the vicinity of such a nucleus shows that the change in the atomic charge density corresponds to a simple transfer of charge from one side of the nucleus to the other. This is exemplified by the $\Delta\rho_{SA}(r)$ map in the region of the proton for the OH molecule (Fig. 1(*a*)). The redistribution of charge found in the $\Delta\rho_{SA}(r)$ distributions for Be → F or Mg → Cl atoms is characterized by an increase in charge density along the bond axis on both the bonded *and* nonbonded sides of the nucleus, and in its removal from a torus-like region perpendicular to the bond axis at the position of the nucleus. Such a *quadrupolar* polarization, i.e., charge increase along one axis and its removal from another perpendicular to it, results in a gross accumulation of charge density in the antibinding as well as in the binding region and is illustrated by the charge redistribution in the region of the oxygen nucleus in the $\Delta\rho_{SA}(r)$ map for OH.

In this note we wish to point out that the dipolar, and in particular, the quadrupolar polarizations, are the dominant ones in the formation of polyatomic systems as well, and offer evidence that such polarizations represent the primary response of a charge distribution to an imposed field.

Figure 1(*b*) shows a $\Delta\rho_{SA}(r)$ map for the water molecule in the plane of the nuclei[3]. The pattern of the charge rearrangement in the vicinity of the oxygen nucleus is quadrupolar, and dipolar in the region of each proton. In fact, there is a striking similarity between this $\Delta\rho_{SA}(r)$ map and the map for the OH diatomic molecule. The *principal* increase in charge density again occurs along a single axis, the two-fold symmetry axis, and charge is again concentrated in both the binding and antibinding regions of the oxygen nucleus. As in the OH molecule, the charge decrease occurs in a belt perpendicular to the axis of charge increase at the position of the oxygen nucleus. These same features persist in the plane perpendicular to the nuclear plane.

[1]Present address: Department of Chemistry, University of California, San Diego, La Jolla, California 92037.

[2]In addition, density distributions over 300 diatomic molecular states have been obtained in preparation of a research monograph by Bader and Cade on molecular charge distributions.

[3]The density distribution for the water molecule was determined from a linear combination of atomic orbital molecular orbital wave function. The basis set consisted of the self consistent field atomic functions of Clementi (13), for the ^3P state oxygen and a 1s orbital ($\zeta = 1.32$) on each H atom. The wavefunction was determined by requiring the charge density to balance the forces on the nuclei and give the measured dipole moment. The resulting density gives expectation values for other one-electron properties in excellent agreement with experiment. Further details may be found in ref. 14. The configuration $1s^2 2s^2 2p_x^1 2p_y^1 2p_z^2$ (where the x and y axes lie in the molecular plane) was used in the construction of the $\Delta\rho_{SA}(r)$ map. This gives circular contours for the O atom density in the plane of the nuclei.

Can. J. Chem. Downloaded from www.nrcresearchpress.com by 188.143.235.115 on 09/06/12
For personal use only.

Can. J. Chem. Downloaded from www.nrcresearchpress.com by 188.143.235.115 on 09/06/12
For personal use only.

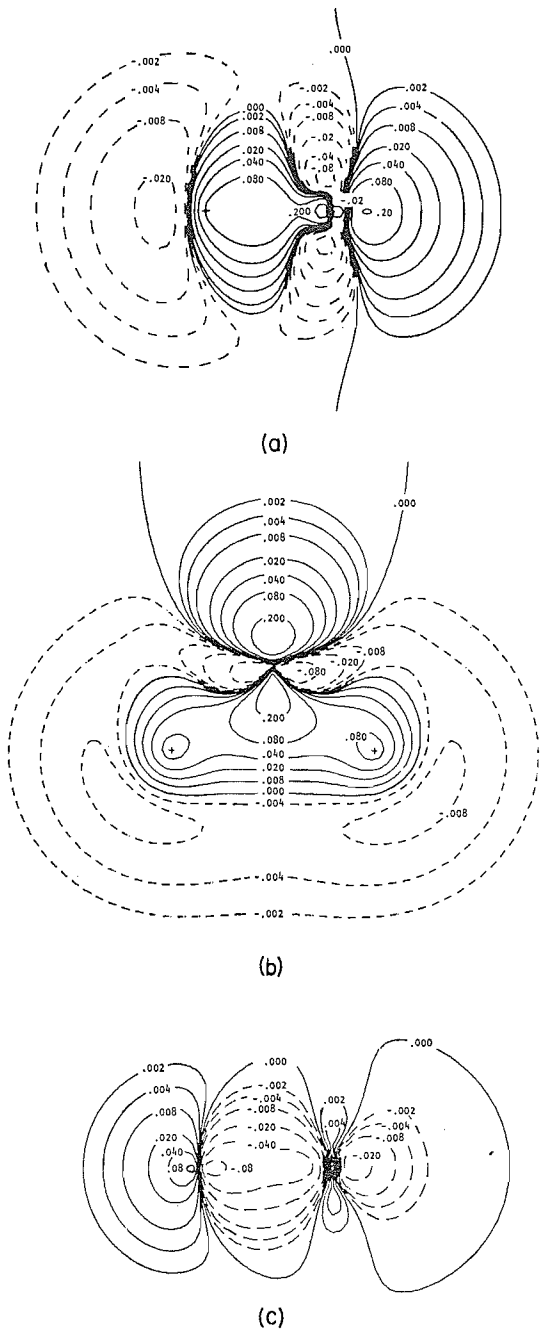

FIG. 1. (*a*) Density difference map $\Delta\rho_{SA}(r)$ for the OH molecule at the equilibrium separation of 1.8342 a.u. (*b*) Density difference map $\Delta\rho_{SA}(r)$ for the water molecule at the equilibrium geometry. Note the similarity in the values of the contours between the OH and H_2O molecules. (*c*) A density difference map showing the change in density for the OH molecule when the bond length is *increased* by 0.166 a.u. The O nucleus is held stationary. For a bond *contraction* the algebraic signs of the contours are reversed.

The polarization in the vicinity of each proton is a simple dipolar one; charge is removed from the antibinding region and concentrated in the binding region. The only major difference between the $\Delta\rho_{SA}(r)$ maps for the H_2O and OH molecules is the spreading of the charge increase in the binding region of the water molecule to encompass the protons which lie off the axis of the principal charge increase. The formation of the ammonia molecule exhibits the same type of reorganization with respect to the separated atoms as noted for the water molecule (or for NH or OH). A $\Delta\rho_{SA}(r)$ map for an approximate density for NH_3 has been previously given (5). The principal charge increase occurs along the three-fold symmetry axis both on the bonded and nonbonded side of the nitrogen nucleus. The charge removal again occurs in a torus-like region around the nitrogen nucleus, perpendicular to the symmetry axis.

In terms of the molecular charge distributions, the principal features of the binding in the diatomic hydrides NH, OH, HF, and the polyatomic hydrides NH_3 and H_2O are the same. The main increase in charge density occurs along one principal axis of polarization and the charge is removed from a region perpendicular to this axis at the heavy nucleus[4]. This preferred quadrupolar polarization in the region of the heavy nucleus overrides the "line of sight" field between the heavy nucleus and each proton, and density is not concentrated directly along each O—H or N—H internuclear axis.

We have previously pointed out that such a disposition of the charge increase on the bonded side of the O and N nuclei in H_2O and NH_3 molecules is the expected one, in terms of regions where charge must be accumulated to achieve electrostatic equilibrium (5). One can determine a spatial region in a polyatomic molecule, the binding region, in which the electron density binds all the nuclei simultaneously. It can also be shown that a $\Delta\rho_{SA}(r)$ map must exhibit a charge increase in the binding region if the system is to achieve electrostatic equilibrium (6). The binding region in the water molecule is triangular in shape, subtending an angle at the oxygen nucleus slightly less than the bond angle. In the ammonia molecule, the binding region is pyramidal in

[4]Such a quadrupole polarization is not possible for the C atom in CH_4 in which case an octupole moment is the lowest moment allowed by the tetrahedral symmetry.

Can. J. Chem. Downloaded from www.nrcresearchpress.com by 188.143.235.115 on 09/06/12
For personal use only.

shape, enclosed within the region of all 4 nuclei with its apex at the nitrogen nucleus. The $\Delta\rho_{SA}(r)$ maps for H_2O and NH_3 demonstrate that the charge increase arising from the quadrupolar type polarization on the N and O nuclei effectively concentrates charge density in the central portion of the binding for both molecules.

The polarization of the charge density along a single axis in H_2O is evident in the total molecular charge density in the form of ellipsoidal contours centered on the oxygen nucleus with their major axis coincident with the symmetry axis. The same ellipsoidal polarizations of the total charge density are evident in the regions of the apex nuclei in contour plots of the charge densities for NO_2^- and FO_2 (7). Quadrupole polarizations are also found in the regions of heavy nuclei in linear molecules (8).

When a system is placed in an external electric field, the polarizations of the charge distribution again exhibit the same dipolar and quadrupolar rearrangements. Stevens and Lipscomb (9, 10) have determined the first-order change in the charge distributions of the HF and F_2 molecules when they are perturbed by an external electric field. The density difference maps given by these authors

$$\Delta\rho(r) = \rho(\text{molecule in field}) - \rho(\text{unperturbed molecule})$$

are remarkably similar in appearance to the $\Delta\rho_{SA}(r)$ maps for the same molecules in the regions of the fluorine nuclei. The results of Stevens and Lipscomb for HF (9) show that when the direction of the positive field is from the proton to the fluorine, charge is removed from a torus-like region perpendicular to the axis at the position of the F nucleus, and transferred to both the binding and antibinding regions of the F nucleus along the internuclear axis. Thus the polarizations evident in the $\Delta\rho_{SA}(r)$ maps, which show the response of the atomic charge densities to a field resulting from the close approach of nuclei, are identical in form to the response of a system to an externally applied field.

The manner in which a molecular charge distribution relaxes during a vibrational motion of the nuclei may be illustrated in the form of a density difference map between the extended and equilibrium molecular charge distribution. Such charge relaxation diagrams exhibit a striking correlation with their corresponding $\Delta\rho_{SA}(r)$ maps (11). As an example, Fig. 1(*c*) shows such a relaxation map for an outward displacement of the oxygen nucleus in the OH molecule. Inasmuch as increasing the bond length is the reverse of bond formation, one might expect the relaxation map for bond extension to exhibit a reversal of the polarizations depicted in the $\Delta\rho_{SA}(r)$ map. Figure 1(*c*) shows this to be the case. The charge relaxation in the region of the oxygen nucleus is quadrupolar in character, corresponding to a removal of charge density from along the bond axis and to its accumulation in a belt around the axis at the oxygen nucleus. The relaxation in the neighborhood of the proton is a simple dipolar transfer of charge from the binding to the antibinding region. The vibrational relaxation maps involve the difference between two molecular charge densities and hence show directly the polarizations induced in a molecular charge distribution by a change in the nuclear potential field.

The same polarizations are also evident in the approach of two molecules in a chemical reaction. Using the wavefunctions of McLean and Yoshimine (12) we have investigated the change in the charge distributions of the HF molecule and the F^- ion as they approach one another to form the $(FHF)^-$ ion (8). The results indicate that the field of the fluoride ion causes a removal of charge from the region of the proton, enhancing the positive field directed at the fluorine nucleus in the HF molecule. This increased field, in complete analogy with the results of Stevens and Lipscomb (9), enhances the quadrupole polarization already present in the region of the fluorine nucleus in HF, with the result that still more charge is transferred from the perpendicular belt-like region to the binding and antibinding regions of the fluorine nucleus along the internuclear axis.

Granted the nonclassical concept of a charge distribution, the simple dipolar polarization as exemplified in the $\Delta\rho_{SA}(r)$ maps by the hydrogen atom is the expected one on classical grounds; a build-up of charge in the region of low potential between the nuclei and its depletion from the regions of relatively high potential energy on the nonbonded side of the nucleus. The quadrupolar-type polarization is, however, not anticipated by classical arguments. It is instead a direct conse-

quence of quantum mechanics and its effect of imposing a preferred spatial direction on the motions of electrons which possess angular momentum in the field of a nucleus. When the angular momentum arises from the occupation of p orbitals and the symmetry of the field is less than cubic[5], the result is an increase in the charge density along the principal axis of the field and a decrease in the charge density in a continuous ring about this axis. Within the framework of an orbital description, the quadrupolar polarization is the result of an increase in the population of the $p\sigma$ orbitals at the expense of the s orbitals, and of a polarization of the $p\pi$ orbitals away from the perpendicular plane. The examples given in this note demonstrate that the dipolar or quadrupolar polarizations are the dominant ones regardless of the exact symmetry of the field provided it is less than cubic, and regardless of whether it is static or dynamic, internal or external. The quadrupolar-type polarization in particular must play a dominant role in determining reaction mechanisms and molecular geometry.

[5]In a field of cubic symmetry all three p orbitals are equivalent and the lowest possible polarization is an octupolar one.

1. R. F. W. Bader, W. H. Henneker, and P. E. Cade. J. Chem. Phys. **46**, 3341 (1967).
2. R. F. W. Bader, I. Keaveny, and P. E. Cade. J. Chem. Phys. **47**, 3381 (1967).
3. R. F. W. Bader and A. D. Bandrauk. J. Chem. Phys. **49**, 1653 (1968).
4. P. E. Cade, R. F. W. Bader, W. H. Henneker, and I. Keaveny. J. Chem. Phys. In press.
5. R. F. W. Bader and H. J. T. Preston. Can. J. Chem. **44**, 1131 (1966).
6. R. F. W. Bader. J. Am. Chem. Soc. **86**, 5070 (1964).
7. R. Bonaccorsi, C. Petrongolo, E. Scrocco, and J. Tomasi. J. Chem. Phys. **48**, 1497 (1968).
8. R. F. W. Bader and G. Runtz. Unpublished results.
9. R. M. Stevens and W. N. Lipscomb. J. Chem. Phys. **41**, 184 (1964).
10. R. M. Stevens and W. N. Lipscomb. J. Chem. Phys. **41**, 3710 (1964).
11. R. F. W. Bader and A. D. Bandrauk. J. Chem. Phys. **49**, 1666 (1968).
12. A. D. McLean and M. Yoshimine. Tables of Linear Molecule Wave Functions. I.B.M. Journal of Research. 1967.
13. E. Clementi. Tables of Atomic Wave Functions. I.B.M. Journal of Research. 1965.
14. I. Keaveny. Ph.D. Thesis, McMaster University, Hamilton, Ontario. 1967.

Radiation induced bonding of hexamethyldisiloxane to silica

R. S. Chahal and L. E. St. Pierre

Department of Chemistry, McGill University, Montreal, Quebec

Received November 22, 1967[1]

An infrared technique was used to study the interfacial interaction between silica and hexamethyldisiloxane systems in the absence and presence of a radiation field. In the absence of the radiation, physisorbed hexamethyldisiloxane and higher molecular weight silicone compounds could be completely removed from the silica surface. In the irradiated samples, however, relatively large amounts of hexamethyldisiloxane were found to be chemisorbed on the surface. The evidence presented supports a radiation-induced chemical bonding of the products of the radiolysis of hexamethyldisiloxane to a silica surface at coverages of less than a monolayer.

Canadian Journal of Chemistry, 47, 2311 (1969)

The crosslinking of silica-filled polydimethylsiloxane by high-energy radiation has been investigated (1, 2), and a G value of 2.5 ± 0.4, equal to that found for the unfilled system, has been reported (3–9). Similar observations were made by Charlesby *et al.* for the same system (10) and for another involving squalene and silica (11).

[1]Revision received November 29, 1968.

The influence of the silica on the radiation-induced crosslinking efficiency was thus regarded to be negligible, and the possibility of covalent bonding of the irradiation products to the silica was discounted (10). This conclusion has been resisted by some workers (12, 13) who have had to invoke attachment of polymer molecules to filler particles in order to rationalize the results of swelling and modulus experiments. However, they have been reluctant to define their "firm

Can. J. Chem. Downloaded from www.nrcresearchpress.com by 188.143.235.115 on 09/06/12
For personal use only.

quence of quantum mechanics and its effect of imposing a preferred spatial direction on the motions of electrons which possess angular momentum in the field of a nucleus. When the angular momentum arises from the occupation of p orbitals and the symmetry of the field is less than cubic[5], the result is an increase in the charge density along the principal axis of the field and a decrease in the charge density in a continuous ring about this axis. Within the framework of an orbital description, the quadrupolar polarization is the result of an increase in the population of the $p\sigma$ orbitals at the expense of the s orbitals, and of a polarization of the $p\pi$ orbitals away from the perpendicular plane. The examples given in this note demonstrate that the dipolar or quadrupolar polarizations are the dominant ones regardless of the exact symmetry of the field provided it is less than cubic, and regardless of whether it is static or dynamic, internal or external. The quadrupolar-type polarization in particular must play a dominant role in determining reaction mechanisms and molecular geometry.

[5]In a field of cubic symmetry all three p orbitals are equivalent and the lowest possible polarization is an octupolar one.

1. R. F. W. Bader, W. H. Henneker, and P. E. Cade. J. Chem. Phys. **46**, 3341 (1967).
2. R. F. W. Bader, I. Keaveny, and P. E. Cade. J. Chem. Phys. **47**, 3381 (1967).
3. R. F. W. Bader and A. D. Bandrauk. J. Chem. Phys. **49**, 1653 (1968).
4. P. E. Cade, R. F. W. Bader, W. H. Henneker, and I. Keaveny. J. Chem. Phys. In press.
5. R. F. W. Bader and H. J. T. Preston. Can. J. Chem. **44**, 1131 (1966).
6. R. F. W. Bader. J. Am. Chem. Soc. **86**, 5070 (1964).
7. R. Bonaccorsi, C. Petrongolo, E. Scrocco, and J. Tomasi. J. Chem. Phys. **48**, 1497 (1968).
8. R. F. W. Bader and G. Runtz. Unpublished results.
9. R. M. Stevens and W. N. Lipscomb. J. Chem. Phys. **41**, 184 (1964).
10. R. M. Stevens and W. N. Lipscomb. J. Chem. Phys. **41**, 3710 (1964).
11. R. F. W. Bader and A. D. Bandrauk. J. Chem. Phys. **49**, 1666 (1968).
12. A. D. McLean and M. Yoshimine. Tables of Linear Molecule Wave Functions. I.B.M. Journal of Research. 1967.
13. E. Clementi. Tables of Atomic Wave Functions. I.B.M. Journal of Research. 1965.
14. I. Keaveny. Ph.D. Thesis, McMaster University, Hamilton, Ontario. 1967.

Radiation induced bonding of hexamethyldisiloxane to silica

R. S. Chahal and L. E. St. Pierre

Department of Chemistry, McGill University, Montreal, Quebec

Received November 22, 1967[1]

An infrared technique was used to study the interfacial interaction between silica and hexamethyldisiloxane systems in the absence and presence of a radiation field. In the absence of the radiation, physisorbed hexamethyldisiloxane and higher molecular weight silicone compounds could be completely removed from the silica surface. In the irradiated samples, however, relatively large amounts of hexamethyldisiloxane were found to be chemisorbed on the surface. The evidence presented supports a radiation-induced chemical bonding of the products of the radiolysis of hexamethyldisiloxane to a silica surface at coverages of less than a monolayer.

Canadian Journal of Chemistry, 47, 2311 (1969)

The crosslinking of silica-filled polydimethylsiloxane by high-energy radiation has been investigated (1, 2), and a G value of 2.5 ± 0.4, equal to that found for the unfilled system, has been reported (3–9). Similar observations were made by Charlesby *et al.* for the same system (10) and for another involving squalene and silica (11). The influence of the silica on the radiation-induced crosslinking efficiency was thus regarded to be negligible, and the possibility of covalent bonding of the irradiation products to the silica was discounted (10). This conclusion has been resisted by some workers (12, 13) who have had to invoke attachment of polymer molecules to filler particles in order to rationalize the results of swelling and modulus experiments. However, they have been reluctant to define their "firm

[1]Revision received November 29, 1968.

attachment" as covalent bonding and instead have proposed it to be strong multipoint physical adsorption.

During the course of investigations into systems similar to those described above, we have utilized infrared (i.r.) spectroscopy as an analytical tool and the results have caused us to come to a conclusion as to the nature of the bonding. Results of experiments involving radiolysis of hexamethyldisiloxane physisorbed on silica surfaces suggest that chemical bonding between one or several of the products of radiolysis and the surface of silica occurs.

Experimental

Samples of thermal silica, Cab-O-Sil M-5, with a surface area of 200 m^2/g (determined by nitrogen adsorption) were placed in a flask to which was attached a side arm. In the side arm were placed known amounts of carefully purified hexamethyldisiloxane, sealed in breakable ampoules, as in Fig. 1. The silica was then dried at 100 °C and 10^{-3} mm Hg pressure for 1 h and the flask sealed. The ampoule containing hexamethyldisiloxane was then broken and the system was allowed to equilibrate overnight at room temperature. By suitable choice of sample sizes of silica and hexamethyldisiloxane, different initial surface coverages could be obtained. Infrared absorption measurements at 2960 cm^{-1} (ν asymmetric CH_3) were performed on discs pressed out of 30 mg samples of silica at a pressure of 5000 p.s.i. Comparisons of absorption intensity were made between samples with physisorbed hexamethyldisiloxane, the same sample washed and devolatilized, and a duplicate sample irradiated and then washed and devolatilized, see Fig. 2.

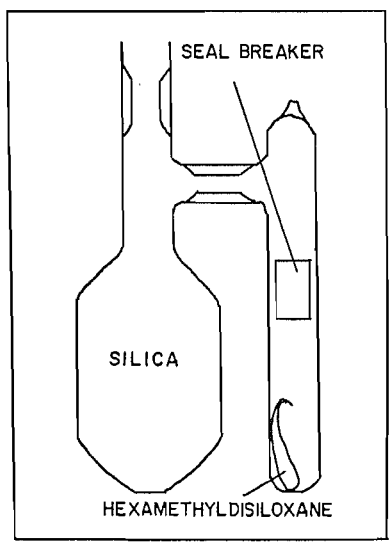

FIG. 1. Apparatus for adsorption of hexamethyldisiloxane on silica.

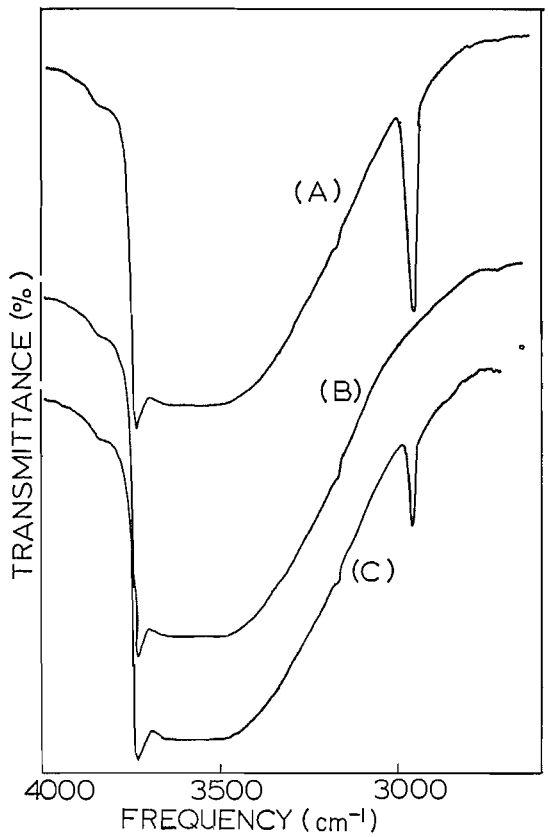

FIG. 2. Infrared absorption: (A) hexamethyldisiloxane adsorbed on silica, (B) after washing and devolatilization of adsorbed hexamethyldisiloxane, (C) after irradiation of adsorbed hexamethyldisiloxane, washing, and devolatilization.

The irradiations were performed in a ^{60}Co source at a dose rate of 2.73×10^4 rads/h.

The pre-irradiation coverage could not be calculated precisely since the adsorption isotherm was not obtained. However, the ratios of materials used were such that if all the hexamethyldisiloxane was adsorbed, coverages of less than 0.6 monolayer would have resulted.

Results and Discussion

In discussing the results, it must be kept in mind that, since the nature of the post-irradiation products is unknown, a quantitative definition of the amount of irradiation-induced chemisorption is impossible. Nevertheless, we can, through comparisons of the i.r. absorption (Fig. 2), establish whether chemisorption of irradiation products does occur, since the absorption at 2960 cm^{-1}, after irradiation and devolatilization, can

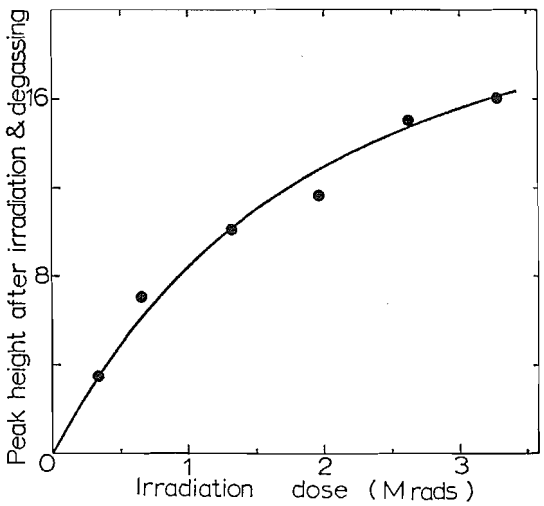

FIG. 3. Radiation products retained on the surface vs. dose at a given concentration of hexamethyldisiloxane (by i.r. absorption at 2960 cm^{-1}).

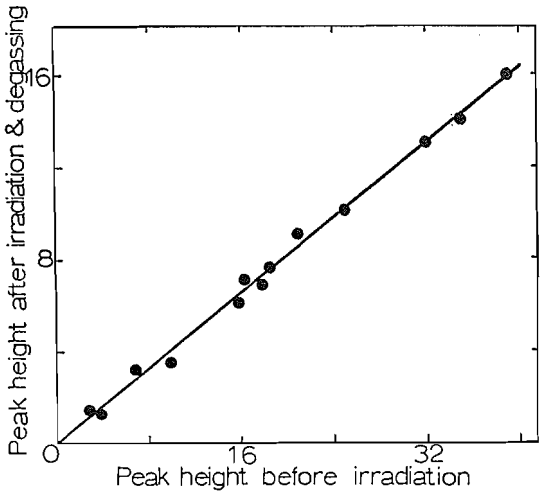

FIG. 4. Radiation products retained on the silica surface relative to initial concentration of hexamethyldisiloxane (by relative i.r. absorption at 2960 cm^{-1}) at constant radiation dose of 3.27 Mrads.

only be due to irradiation fragments from the hexamethyldisiloxane which have become chemically attached to the silica. The possibility that the retained absorption is due to the physisorption of silicone compounds is rejected on the grounds that molecules more than ten times as large as hexamethyldisiloxane are completely removed by the washing and devolatilization techniques used.

The relationship between the irradiation dose and the amount of C—H containing materials (those which absorb at 2960 cm^{-1}) remaining on the surface after washing and devolatilization can be seen from Fig. 3. The initial coverage of hexamethyldisiloxane was the same in all cases, approximately 0.6 monolayer, assuming total adsorption. The data are plotted in terms of relative i.r. absorption at 2960 cm^{-1}.

The non-linearity in the yield with dose is to be expected since the surface concentration of unreacted hexamethyldisiloxane is reduced with increasing dose.

The relationship between the amount of hexamethyldisiloxane on the silica prior to irradiation to the amount of material retained after, at constant dose, is shown in Fig. 4. The relationship is one of strict linearity.

Prior to the identification of the irradiation products, including those which remain chemically attached to the silica, it is not considered to be meaningful to calculate G values for the chemisorption or indeed to speculate too far on the nature of the adsorbed species. However, the results of Dewhurst and St. Pierre (14), who performed irradiation experiments on liquid and solid hexamethyldisiloxane, suggest numerous possibilities for the formation of species which could react with the surface SiOH groups on the silica. While they identified products which indicated that there was cleavage of all types of bonds present in the hexamethyldisiloxane, they found a considerable amount of product resulting from cleavage of the siloxane bond itself. Recombination of these fragments to form Me_3SiOH or Me_3SiH, both reactive with silanol groups, could result in reactions to form chemical bonds to the surface. Indeed, other studies involving heterogeneous systems (15, 16) and work presently under way in these laboratories suggest a considerable enhancement in total irradiation yields of physisorbed species, which would in turn result in increased chemisorption.

Work aimed at a more quantitative definition of the radiation chemistry of the physisorbed species is presently under way. However, the results disclosed in this note are considered proof of irradiation-induced chemical bonding of hexamethyldisiloxane irradiation fragments to silica. With the establishment of the quantitative aspects of this bonding, it will be possible to

expand present theories of network structure in filled polymers to allow a more complete understanding of the structure – physical property relationship.

Acknowledgments

The authors wish to acknowledge the generous assistance of the Defence Research Board of Canada, the National Research Council of Canada, and the Research Committee of McGill University, whose grants provided us with the equipment and materials necessary to execute this work. The support of R.S.C. by the Xerox Corporation through a fellowship is also gratefully acknowledged.

1. E. L. WARRICK. Ind. Eng. Chem. **47**, 2388 (1955).
2. R. K. TRAEGER and T. T. GASTONGUAY. J. Appl. Polymer Sci. **10**, 535 (1966).
3. A. CHARLESBY. Proc. Roy. Soc. London, Ser. A, **230**, 120 (1955).
4. M. G. ORMEROD and A. CHARLESBY. Polymer Sci. London, **4**, 459 (1963).
5. A. M. BUECHE. J. Polymer Sci. **19**, 292 (1958).
6. L. E. ST. PIERRE, H. A. DEWHURST, and A. M. BUECHE. J. Polymer Sci. **36**, 105 (1959).
7. W. BARNES, H. A. DEWHURST, R. W. KILB, and L. E. ST. PIERRE. J. Polymer Sci. **36**, 525 (1959).
8. F. BUECHE. J. Polymer Sci. **19**, 297 (1956).
9. A. A. MILLER. J. Am. Chem. Soc. **82**, 3519 (1960).
10. D. BAKER, A. CHARLESBY, and J. MORRIS. Polymer Sci. London, **9**, 437 (1968).
11. A. CHARLESBY. Irradiation of polymers. *Edited by* R. F. Gould. Advan. Chem. Ser. 66. Am. Chem. Soc. Washington, D.C. 1967.
12. A. M. BUECHE. J. Polymer Sci. **15**, 105 (1955); **25**, 139 (1959).
13. E. L. WARRICK and P. C. LAUTERBUR. Ind. Eng. Chem. **47**, 486 (1955).
14. H. A. DEWHURST and L. E. ST. PIERRE. J. Phys. Chem. **64**, 1063 (1960).
15. H. W. KOHN. J. Am. Chem. Soc. **87**, 3521 (1965).
16. J. G. RABE, R. RABE, and A. O. ALLEN. J. Am. Chem. Soc. **86**, 3887 (1964).

Excitation and ionization of Hg by metastable states of N_2 and CO[1]

C. H. DUGAN
Department of Physics, York University, Toronto 12, Ontario

Received November 13, 1968

When metastable states of N_2 and CO collide with mercury atoms, the excitation energy can be transferred to the mercury atom, yielding a fluorescence in the spectral lines of mercury. This note describes observations of this process using a thermal beam of metastable molecules excited by electron impact. Metastable CO excites only the 6^3P levels of Hg. Metastable N_2 excites predominantly 6^3P, but some 10% of collisions excite 6^1P, and higher states are also excited. In addition, ionization of Hg by excited N_2 (but not by CO) is reported. Other observations are reported briefly.

Canadian Journal of Chemistry, 47, 2314 (1969)

This note reports an experimental study of processes involving excitation and ionization of Hg using thermal velocity beams of metastable excited electronic states of N_2. The excitation curve for the ionization produced by N_2^* in collision with Hg is presented, and a rudimentary spectral analysis of the emitted light is given. Experiments with other gases are also reported.

Hg is of interest because of the possibility of using it as an "indicator" for the presence of various metastable species: it might be used in an experiment in which both the optical and ionic mass spectra of an afterglow are studied with the goal of investigating the time history of the several excited species of N_2. Čermák (1) has reported recently on Penning ionization by N_2^* of molecules whose ionization potentials are higher than that of Hg (10.38 eV) so that it might be expected that Penning ionization ($N_2^* + Hg \rightarrow N_2 + Hg^+ + e$) will occur.

Experimental Procedure

Several earlier publications have dealt with the instrumentation of the experiments here (2). Briefly, the arrangement is this: an electron beam of variable energy but constant current excites a thermal velocity beam that enters a collision chamber after travelling some 10 cm in a vacuum of 10^{-5} to 10^{-6} Torr. The collision chamber contains a higher pressure of some added gas (earlier: NO at about 1 mTorr, here Hg at some 10^{-4} Torr) with

[1]Work performed at the Smithsonian Astrophysical Observatory, Cambridge, Massachusetts.

expand present theories of network structure in filled polymers to allow a more complete understanding of the structure – physical property relationship.

Acknowledgments

The authors wish to acknowledge the generous assistance of the Defence Research Board of Canada, the National Research Council of Canada, and the Research Committee of McGill University, whose grants provided us with the equipment and materials necessary to execute this work. The support of R.S.C. by the Xerox Corporation through a fellowship is also gratefully acknowledged.

1. E. L. WARRICK. Ind. Eng. Chem. **47**, 2388 (1955).
2. R. K. TRAEGER and T. T. GASTONGUAY. J. Appl. Polymer Sci. **10**, 535 (1966).
3. A. CHARLESBY. Proc. Roy. Soc. London, Ser. A, **230**, 120 (1955).
4. M. G. ORMEROD and A. CHARLESBY. Polymer Sci. London, **4**, 459 (1963).
5. A. M. BUECHE. J. Polymer Sci. **19**, 292 (1958).
6. L. E. ST. PIERRE, H. A. DEWHURST, and A. M. BUECHE. J. Polymer Sci. **36**, 105 (1959).
7. W. BARNES, H. A. DEWHURST, R. W. KILB, and L. E. ST. PIERRE. J. Polymer Sci. **36**, 525 (1959).
8. F. BUECHE. J. Polymer Sci. **19**, 297 (1956).
9. A. A. MILLER. J. Am. Chem. Soc. **82**, 3519 (1960).
10. D. BAKER, A. CHARLESBY, and J. MORRIS. Polymer Sci. London, **9**, 437 (1968).
11. A. CHARLESBY. Irradiation of polymers. *Edited by* R. F. Gould. Advan. Chem. Ser. 66. Am. Chem. Soc. Washington, D.C. 1967.
12. A. M. BUECHE. J. Polymer Sci. **15**, 105 (1955); **25**, 139 (1959).
13. E. L. WARRICK and P. C. LAUTERBUR. Ind. Eng. Chem. **47**, 486 (1955).
14. H. A. DEWHURST and L. E. ST. PIERRE. J. Phys. Chem. **64**, 1063 (1960).
15. H. W. KOHN. J. Am. Chem. Soc. **87**, 3521 (1965).
16. J. G. RABE, R. RABE, and A. O. ALLEN. J. Am. Chem. Soc. **86**, 3887 (1964).

Excitation and ionization of Hg by metastable states of N_2 and CO[1]

C. H. DUGAN
Department of Physics, York University, Toronto 12, Ontario

Received November 13, 1968

When metastable states of N_2 and CO collide with mercury atoms, the excitation energy can be transferred to the mercury atom, yielding a fluorescence in the spectral lines of mercury. This note describes observations of this process using a thermal beam of metastable molecules excited by electron impact. Metastable CO excites only the 6^3P levels of Hg. Metastable N_2 excites predominantly 6^3P, but some 10% of collisions excite 6^1P, and higher states are also excited. In addition, ionization of Hg by excited N_2 (but not by CO) is reported. Other observations are reported briefly.

Canadian Journal of Chemistry, 47, 2314 (1969)

This note reports an experimental study of processes involving excitation and ionization of Hg using thermal velocity beams of metastable excited electronic states of N_2. The excitation curve for the ionization produced by N_2^* in collision with Hg is presented, and a rudimentary spectral analysis of the emitted light is given. Experiments with other gases are also reported.

Hg is of interest because of the possibility of using it as an "indicator" for the presence of various metastable species: it might be used in an experiment in which both the optical and ionic mass spectra of an afterglow are studied with the goal of investigating the time history of the several excited species of N_2. Čermák (1) has reported recently on Penning ionization by N_2^* of molecules whose ionization potentials are higher than that of Hg (10.38 eV) so that it might be expected that Penning ionization ($N_2^* + Hg \rightarrow N_2 + Hg^+ + e$) will occur.

Experimental Procedure

Several earlier publications have dealt with the instrumentation of the experiments here (2). Briefly, the arrangement is this: an electron beam of variable energy but constant current excites a thermal velocity beam that enters a collision chamber after travelling some 10 cm in a vacuum of 10^{-5} to 10^{-6} Torr. The collision chamber contains a higher pressure of some added gas (earlier: NO at about 1 mTorr, here Hg at some 10^{-4} Torr) with

[1]Work performed at the Smithsonian Astrophysical Observatory, Cambridge, Massachusetts.

Can. J. Chem. Downloaded from www.nrcresearchpress.com by 210.87.254.6 on 09/05/12
For personal use only.

Can. J. Chem. Downloaded from www.nrcresearchpress.com by 210.87.254.6 on 09/05/12
For personal use only.

which collisions occur. We compare different ways of detecting the metastable species. In striking a metal surface they release electrons if they have enough internal energy (Auger effect). We collected these electrons. Second, we detected the emission of light, either from the beam or (with a target gas added) due to collisions and transfer of excitation to the struck molecules. Light from the collision region was detected directly by a quartz envelope photomultiplier attached (inside the vacuum system) to the collision chamber, viewing the interior through a LiF window. To study the spectral distribution of the light, we inserted filters in front of the photomultiplier to isolate broad spectral regions. We used these filters: (*a*) a window of Vycor whose transmission at λ2537 Å is about 70%, which does not transmit λ1849 Å; (*b*) a Pyrex window that blocks both λ1849 and λ2537 Å but transmits light of wavelength $\lambda > 3000$ Å. This allowed us to "resolve" the light into three important spectral regions: $\lambda < 2000$ Å, 2000 Å $< \lambda <$ 3000 Å, and $\lambda > 3000$ Å, in order to detect separately the two resonance emissions and the emission in transitions among higher excited levels.

Finally, we detected positive ions formed by Penning collisions. Ions were observed by collecting the positive ions on a fine wire electrode biased negative with respect to the chamber walls; a detector of small area was used to avoid a signal due to Auger electron emission from the detector caused by elastically scattered metastable particles striking the detector.

The energy resolution possible with this electron gun is poor because the rather long filament was directly heated, giving a 0.5 V potential drop along the filament, approximately.

Summary of Experiments

Several exploratory experiments were conducted using different gases in the source and target. These are listed below, along with those to be described in more detail. Figure 1 is an energy level diagram of several relevant molecules.

(*a*) A beam of N_2 was excited by electron impact and collided with Hg. Both light and ions were detected. This is discussed below.

(*b*) A beam of CO was excited by electron impact and collided with Hg. Light was observed but no ionization was detected. Electrons were not ejected by CO* from the metal target owing to the high work functions of the metal used as a target. The light that was observed is discussed below.

(*c*) A beam of Ar was excited before collisions with Hg. No light was observed. Ar* in collision with CO and O_2 yielded no light emission. Ar* in collision with N_2 yielded a light signal that was strong by the standards of this experiment. These results agree with flow-tube observations of Robertson (3). Electrons ejected by Ar* from metallic targets were readily observed (2). Penning ionization was not studied.

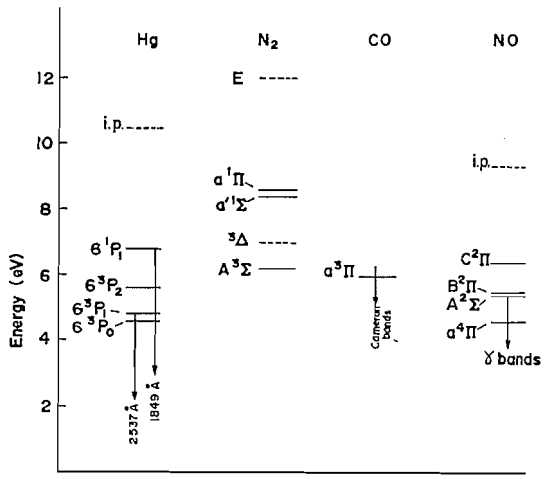

FIG. 1. Energy levels of molecules and atoms considered in the present experiment.

(*d*) A beam of NO was excited by electron impact; in collision with Hg the metastable states (if present) produced no light signal, and no Auger-ejected electrons were found using a NO beam. Vibrational levels $v \geq 2$ in NO ($a^4\Pi$) have sufficient energy to populate Hg (6^3P).

N_2 + Hg*

Brennen and Kistiakowsky (4) observed excitation of λ2537 Å and longer wavelengths in the afterglow of a nitrogen discharge when Hg was added; this was attributed to energy transfer from excited molecules. They reported no observation of λ1849 Å, and they found that radiation from higher excited states accounted for only 2% of their signal. The presence of only a very small emission from any singlet Hg atom was cited as evidence that spin-conservation was effective in the collision. They consider it unlikely that highly excited vibrational states of $N_2(X^1\Sigma)$ caused the emission, but as with the proposed $A^3\Sigma_u^+$ component, their experiment did not observe the active species directly.

The use of a beam that is detected independently offers some simplification in interpretation. Direct excitation of high vibrational levels of $X^1\Sigma$ is unlikely; the vibrationally excited ground-state molecules that are present come mostly from downward transition from excited electronic states. This means that they are not greatly more

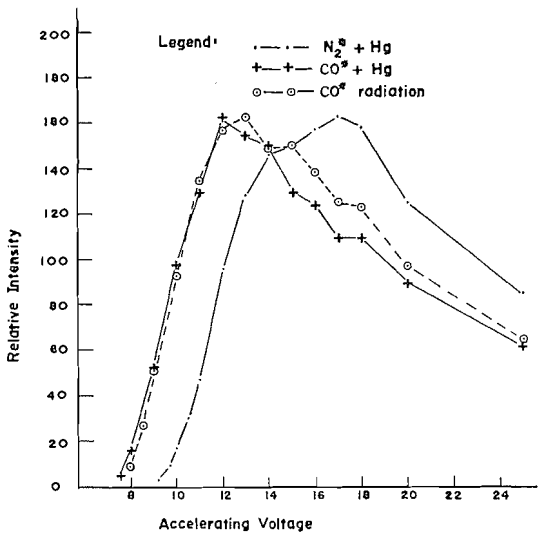

FIG. 2. Excitation function for production of light by collision of metastable molecules with Hg. Also shown is the excitation function of the emission directly from the excited CO beam.

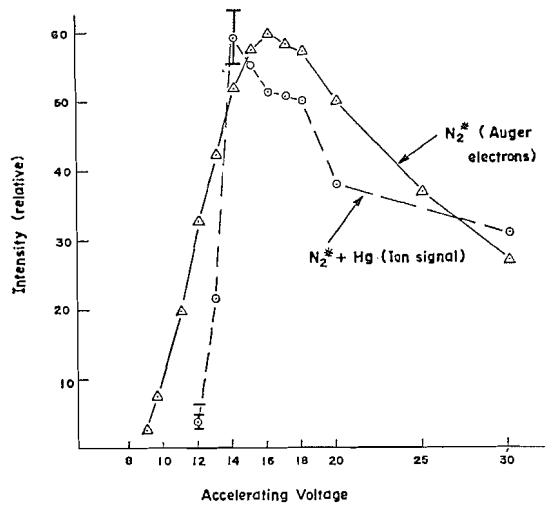

FIG. 3. Penning ionization of Hg by N_2^*. The excitation function for this process is compared with the signal due to electrons emitted from a metallic detector by N_2^*.

numerous than long-lived excited electronic states, as they might be in an afterglow. Earlier (2), we discussed whether atoms can play a part in causing these emissions and explained that it seems most unlikely. The presence of energetic photons in the beam may be expected and this has been studied previously (2). It is not a significant feature in this experiment. We can thus confidently assert that the predominant excited species in the beam is electronically excited molecules.

The distribution of excited states found in the beam will be somewhat different from that found in an afterglow and the excitation produced in Hg may be expected to be different. Based on the signals we detected we assign the light to mercury radiation at appropriate wavelengths. For electrons with an excitation energy of 15 eV, the N_2 beam produces a fluorescence that is 12% at λ1849 Å, 81% at λ2537 Å, and 7% for $\lambda > 3000$ Å. At an excitation energy of 30 eV, the fluorescence is 9% at λ1849 Å, 74% at λ2537 Å, and 17% at $\lambda > 3000$ Å. (Of course, every photon emitted at $\lambda > 3000$ Å gives rise to the emission of a photon at λ1849 or λ2537 Å.) These numbers were obtained in a way that makes the determination of the fraction above the Pyrex cut-off most reliable, although there are uncertainties of a few percent in these values. Less accurate is the determination of the fractions of the light in the two resonance lines, because uncertainty in the $\lambda > 3000$ Å component and in the measurement of window transmission propagates in determinations of the other two fractions. It was not possible to isolate the light signal at λ1849 Å with a narrow-band filter or monochromator, so that we had to rely on transmission of various materials to isolate the spectral region rather than the line. An additional qualification is the fact that this assignment of fractions of the light is simply an assignment of the current to the anode of an uncalibrated photo-multiplier. In assigning the fractions to the light we assumed that the photo-multiplier response is constant; this is not true, but calibrating the multiplier at λ1849 Å was not something we were equipped to do.

The possibility that different Hg states are excited preferentially by any of the possible N_2^* states could in principle be studied with the present experimental technique by recording excitation curves for different Hg emissions. Unfortunately we were unable to accomplish this goal satisfactorily. Figure 2 gives excitation functions for the total light emitted by Hg when excited by N_2^*. In an earlier study (2) of excitation of NO by N_2^* the excitation curve showed two distinct maxima; we see only one peak in this experiment.

The positive ion signal collected in the detection chamber as a function of exciting electron

Can. J. Chem. Downloaded from www.nrcresearchpress.com by 210.87.254.6 on 09/05/12
For personal use only.

energy is shown in Fig. 3, and for comparison purposes we show the Auger electron signal obtained with a Ni target. The threshold is higher for the Penning ion formation than for the appearance of ejected electrons at the metal surface. The decrease in the Penning signal for higher energies appears to be more rapid than for the total metastable signal, although the error flag shown for the Penning signal near the peak of the curve makes it uncertain that we can distinguish between the shapes of the two curves. (Signals near threshold do not have such a large error flag.)

No vibrational state of $N_2(A^3\Sigma)$ is sufficiently energetic to cause ionization in Hg. The state responsible must, therefore, be one of the other metastable states having a higher dissociation limit. Molecules in the state $a^1\Pi_g$ with vibrational quantum number 10 have sufficient energy to ionize Hg. Čermák reported the ionization of C_2H_2 (ionization potential = 11 eV) by N_2* in his experiment[2].

CO + Hg*

CO ($a^3\Pi$) is long-lived and readily excited by electron impact (2, 5), and it has sufficient energy to excite the 6^3P level of Hg. However, we found no evidence to suggest that a state whose energy is above the ionization potential of Hg is excited; we found no Penning ionization of Hg using CO. Based on an observation (6) of CO* using a detector unfavorable for the detection of $a^3\Pi$ it was conjectured earlier that the state $b^3\Sigma^+$ at 10.9 eV was detected. This state should ionize Hg unless selection rules prevent it; if it was present in the beam, it was below the detection threshold of this experiment. As reported earlier (5) the CO beam excited by electron impact yields an observable radiation even in the absence of any target gas; very likely we saw the Cameron bands. Figure 2 shows the total light signal excited by CO* in Hg; it is distinguishable from the corresponding curve for N_2* in its energies at threshold and at the maximum signal. Of this light, less than 1% had $\lambda > 3000$ Å; 6% of the light was at λ1849 Å.

[2]Since the completion of this note, Dr. R. S. Freund has informed me that he has observed the emission spectrum of this state, $N_2(E)$, in a beam experiment. I am grateful to him for sending me a pre-publication copy of his paper.

1. V. Čermák. J. Chem. Phys. **44**, 1318 (1966).
2. C. H. Dugan. J. Chem. Phys. **45**, 87 (1966); **46**, 1534 (1967). (The schematic sketch given in the 1966 paper is of an earlier equipment.)
3. W. W. Robertson. J. Chem. Phys. **44**, 2456 (1966).
4. W. Brennen and G. B. Kistiakowsky. J. Chem. Phys. **44**, 2695 (1966). Other relevant observations are summarized in A. N. Wright and C. A. Winkler. Active nitrogen. Academic Press Inc., New York. 1968.
5. (*a*) C. D. Papliolios. Ph.D. Thesis, Harvard University, Cambridge, Mass. 1965. (*b*) C. H. Dugan. Ph.D. Thesis, Harvard University, Cambridge, Mass. 1963.
6. J. Olmstead, III, A. S. Newton, and K. Street. J. Chem. Phys. **42**, 2321 (1965).

Characterization and photolysis of octacyanomolybdic(IV) acid: isolation of a red photoproduct

R. P. Mitra, B. K. Sharma, and Hari Mohan

Department of Chemistry, University of Delhi, Delhi -7, India

Received November 13, 1968

pH and conductometric titration of aqueous octacyanomolybdic acid shows that it has 4 strong H^+ ions per Mo(IV). Photolysis of an ice-cold solution of the acid gives a red anion, $[Mo(CN)_7H_2O]^{3-}$, which has been isolated as a silver salt. When the corresponding (red) acid is titrated, 3 strong H^+ ions are first neutralized and then one more equivalent of the base is consumed in a slow substitution reaction to give a yellow anion, $[Mo(CN)_7OH]^{4-}$.

Canadian Journal of Chemistry, 47, 2317 (1969)

Yellow needle-shaped crystals of octacyanomolybdic(IV) acid were obtained by bubbling hydrogen chloride gas into a concentrated cold (0 °C) solution of the acid prepared by the percolation of aqueous potassium octacyanomolybdate(IV) through beds of the cation exchanger, Amberlite I.R. 120 resin (H form). The infrared (i.r.) spectrum of the solid acid showed C≡N

Can. J. Chem. Downloaded from www.nrcresearchpress.com by 210.87.254.6 on 09/05/12
For personal use only.

energy is shown in Fig. 3, and for comparison purposes we show the Auger electron signal obtained with a Ni target. The threshold is higher for the Penning ion formation than for the appearance of ejected electrons at the metal surface. The decrease in the Penning signal for higher energies appears to be more rapid than for the total metastable signal, although the error flag shown for the Penning signal near the peak of the curve makes it uncertain that we can distinguish between the shapes of the two curves. (Signals near threshold do not have such a large error flag.)

No vibrational state of $N_2(A^3\Sigma)$ is sufficiently energetic to cause ionization in Hg. The state responsible must, therefore, be one of the other metastable states having a higher dissociation limit. Molecules in the state $a^1\Pi_g$ with vibrational quantum number 10 have sufficient energy to ionize Hg. Čermák reported the ionization of C_2H_2 (ionization potential = 11 eV) by N_2* in his experiment[2].

CO + Hg*

CO ($a^3\Pi$) is long-lived and readily excited by electron impact (2, 5), and it has sufficient energy to excite the 6^3P level of Hg. However, we found no evidence to suggest that a state whose energy is above the ionization potential of Hg is excited; we found no Penning ionization of Hg using CO. Based on an observation (6) of CO* using a detector unfavorable for the detection of $a^3\Pi$ it was conjectured earlier that the state $b^3\Sigma^+$ at 10.9 eV was detected. This state should ionize Hg unless selection rules prevent it; if it was present in the beam, it was below the detection threshold of this experiment. As reported earlier (5) the CO beam excited by electron impact yields an observable radiation even in the absence of any target gas; very likely we saw the Cameron bands. Figure 2 shows the total light signal excited by CO* in Hg; it is distinguishable from the corresponding curve for N_2* in its energies at threshold and at the maximum signal. Of this light, less than 1% had $\lambda > 3000$ Å; 6% of the light was at λ1849 Å.

[2]Since the completion of this note, Dr. R. S. Freund has informed me that he has observed the emission spectrum of this state, $N_2(E)$, in a beam experiment. I am grateful to him for sending me a pre-publication copy of his paper.

1. V. Čermák. J. Chem. Phys. **44**, 1318 (1966).
2. C. H. Dugan. J. Chem. Phys. **45**, 87 (1966); **46**, 1534 (1967). (The schematic sketch given in the 1966 paper is of an earlier equipment.)
3. W. W. Robertson. J. Chem. Phys. **44**, 2456 (1966).
4. W. Brennen and G. B. Kistiakowsky. J. Chem. Phys. **44**, 2695 (1966). Other relevant observations are summarized in A. N. Wright and C. A. Winkler. Active nitrogen. Academic Press Inc., New York. 1968.
5. (*a*) C. D. Papliolios. Ph.D. Thesis, Harvard University, Cambridge, Mass. 1965. (*b*) C. H. Dugan. Ph.D. Thesis, Harvard University, Cambridge, Mass. 1963.
6. J. Olmstead, III, A. S. Newton, and K. Street. J. Chem. Phys. **42**, 2321 (1965).

Characterization and photolysis of octacyanomolybdic(IV) acid: isolation of a red photoproduct

R. P. Mitra, B. K. Sharma, and Hari Mohan

Department of Chemistry, University of Delhi, Delhi -7, India

Received November 13, 1968

pH and conductometric titration of aqueous octacyanomolybdic acid shows that it has 4 strong H^+ ions per Mo(IV). Photolysis of an ice-cold solution of the acid gives a red anion, $[Mo(CN)_7H_2O]^{3-}$, which has been isolated as a silver salt. When the corresponding (red) acid is titrated, 3 strong H^+ ions are first neutralized and then one more equivalent of the base is consumed in a slow substitution reaction to give a yellow anion, $[Mo(CN)_7OH]^{4-}$.

Canadian Journal of Chemistry, 47, 2317 (1969)

Yellow needle-shaped crystals of octacyanomolybdic(IV) acid were obtained by bubbling hydrogen chloride gas into a concentrated cold (0 °C) solution of the acid prepared by the percolation of aqueous potassium octacyanomolybdate(IV) through beds of the cation exchanger, Amberlite I.R. 120 resin (H form). The infrared (i.r.) spectrum of the solid acid showed C≡N

Can. J. Chem. Downloaded from www.nrcresearchpress.com by 210.87.254.6 on 09/05/12
For personal use only.

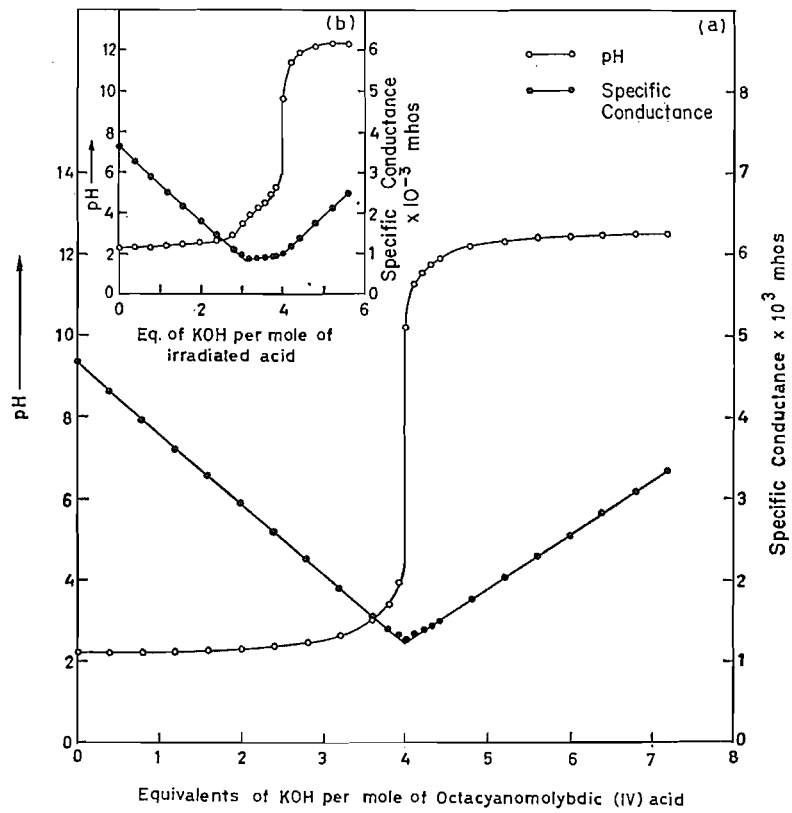

FIG. 1*a*. pH and conductometric titration curves of 5.0×10^{-3} f octacyanomolybdic(IV) acid with KOH.
1*b*. (Inset) pH and conductometric titration curves of photolyzed solution of 5×10^{-3} f octacyanomolybdic(IV) acid corresponding to the stage of maximum optical density at 512 mμ.

stretching frequencies 2160, 2130, and 2090 cm^{-1}. Aqueous solutions of the acid gave absorption peaks at 368 and 240 mμ characteristic of the $Mo(CN)_8^{4-}$ ion (1, 2). The conductometric titration curve of the aqueous acid showed a sharp minimum and its pH titration curve showed a corresponding pronounced inflexion (Fig. 1*a*), at which 4 equivalents of strong H^+ ions were neutralized for each equivalent of Mo(IV), as estimated by redox titration against potassium permanganate.

Anal. Calcd. for $H_4Mo(CN)_86H_2O$: Mo, 23.05; C, 23.08; N, 26.92; H_2O, 25.95. Found: Mo, 22.94; C, 23.07; N, 26.89; H_2O, 26.2.

On irradiation with ultraviolet (u.v.) light from a Philips mercury discharge lamp with a filter which transmitted radiation of wavelengths in the range 340–430 mμ, the yellow solution of octacyanomolybdic acid turned first red and then brown. Adamson and Perumareddi (1) reported a transient red species which was formed by the action of u.v. light on aqueous $K_4Mo(CN)_8$ and showed an absorption peak at 510 mμ. The red species could not be isolated by them. Its production was accompanied by a release of CN^- ions. Hydrolysis of these ions caused the pH to rise to 9.5. Since we used octacyanomolybdic acid which had a pH as low as 2.2, almost all the CN^-, which would be disengaged by the action of the u.v. light, would be present as HCN. When the irradiation of the acid was stopped and the solution kept in the dark, the red color disappeared to give back the original yellow solution. To prevent the back (thermal) reaction, the temperature of the solution was maintained at 0 °C and HCN was removed as fast as it was formed by bubbling N_2 gas through the solution as it was irradiated. During irradiation, the peak at 368 mμ decayed

Can. J. Chem. Downloaded from www.nrcresearchpress.com by 210.87.254.6 on 09/05/12
For personal use only.

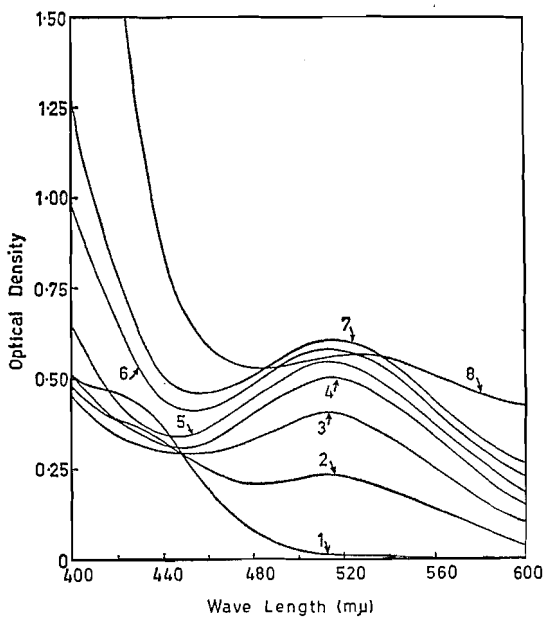

FIG. 2. Spectral variations of a 5×10^{-3} f solution of octacyanomolybdic(IV) acid during irradiation with u.v. light (1 cm light path). Curve numbers 1, 2, 3, 4, 5, 6, 7, and 8 refer to irradiation times of 0, 4, 9, 12, 14, 15, 17.5, and 30 min, respectively.

and a new peak at 512 mμ, synchronizing with the appearance of the red color, was observed. This peak grew in height as the red color deepened (Fig. 2) and, later on, it decayed. A titrimetric and spectral study of aliquots taken out at regular intervals showed that H^+ ions were lost (as HCN) as irradiation proceeded and, further, when the loss was one equivalent, the peak at 512 mμ, characterizing the red species, attained its maximum height (Fig. 2, curve 7).

To isolate the red species, an intense beam of u.v. light was next switched on to a fresh 100 cc of the (5×10^{-3} f) acid which had been cooled to 0 °C and through which N_2 gas was kept bubbling. When one equivalent of H^+ was lost as found by titration, an ice-cold solution of $AgNO_3$ was added. A red silver salt was precipitated.

Anal. Calcd. for $Ag_3Mo(CN)_7H_2O$: Ag, 52.21; C, 13.56; N, 15.81; Mo, 15.47; H_2O, 2.93. Found: Ag, 52.46; C, 13.6; N, 15.97; Mo, 15.73; H_2O, 3.4.

Redox titrations of aliquots of the irradiated solution against $KMnO_4$ indicated that up to the stage where the red species was precipitated as silver salt, the oxidation state of molybdenum did not change; 1.0 equivalent of $KMnO_4$ was taken up per Mo(IV). The standard redox [Mo(IV) $\rightleftharpoons$ Mo(V)] potential also remained constant (0.799 V at 0 °C).

The i.r. spectrum of the red silver salt gave a peak at 898 cm^{-1} consistent with the presence of coordinated water (3). This peak was not found in the spectrum of the solid acid. The formulation of Jakob *et al.* (4–5) of the red species as a super complex, $[Mo(CN)_8 2H_2O]^{4-}$, does not agree with the composition of our red silver salt and it does not fit with our observation that HCN is liberated when the red species is formed. We think that the red anion is $[Mo(CN)_7H_2O]^{3-}$. According to Carassiti and Claudi (6), it could be one of the photoproducts of the $Mo(CN)_8^{4-}$ ion. They, however, neither isolated it nor characterized it by its absorption spectrum. Adamson and Perumareddi (1), like us, thought that the red species would be an aquocomplex. According to them, it would function as a weak acid and would have the composition $[Mo(CN)_7OH]^{4-}$ at pH 9.5. When we titrated the red acid, $H_3[Mo(CN)_7H_2O]$, in the photolyzed solution at the stage where the silver salt was precipitated, we found that, first, three strong H^+ ions were neutralized and, then, a slow reaction set in, in which one equivalent of the base was consumed (Fig. 1*b*). This slow reaction could not be due to proton loss from coordinated water. We believe that it is one of ligand exchange in which the coordinated water in $[Mo(CN)_7H_2O]^{3-}$ is replaced by an OH^- ion. The change from red to yellow by the action of an alkali was not reversible. The solution remained yellow when kept in the dark at room temperature (30 °C). The red color did not return even on acidification.

1. A. W. ADAMSON and J. R. PERUMAREDDI. Inorg. Chem. **4**, 247 (1965).
2. J. R. PERUMAREDDI, A. D. LIEHR, and A. W. ADAMSON. J. Am. Chem. Soc. **85**, 249 (1963).
3. K. NAKAMOTO. Infrared spectra of inorganic and coordination compounds. John Wiley and Sons, Inc., New York. 1963. p. 156.
4. W. JAKOB and Z. JAKOB. Roczniki Chem. **36**, 601 (1962).
5. W. JAKOB, A. SAMOTUS, Z. STASICKA, and A. GOLEBIEWSKI. Z. Naturforsch. **21b**, 819 (1966).
6. V. CARASSITI and M. CLAUDI. Ann. Chim. Rome, **49**, 1697 (1959).

Can. J. Chem. Downloaded from www.nrcresearchpress.com by 210.87.254.6 on 09/05/12
For personal use only.

Studies on the solvent extraction of metal dithiocarbamates[1,2]

VEDULA S. SASTRI, KEIJO I. ASPILA, AND CHUNI L. CHAKRABARTI[3]
Department of Chemistry, Carleton University, Ottawa 1, Canada

Received July 8, 1968

Studies on the solvent extraction of morpholine dithiocarbamic acid complexes of divalent metal ions Mn, Fe, Co, Ni, Cu, Zn, Pb, Cd, Hg, and Sn were carried out, and the extraction constants and the overall stability constants were determined. The stability constants of complexes of Cu(II) formed with various substituted dithiocarbamic acids, showed a variation of the stability constants with the basicity of the nitrogen and sulfur atoms in the reagents.

Canadian Journal of Chemistry, 47, 2320 (1969)

Can. J. Chem. Downloaded from www.nrcresearchpress.com by 210.87.254.105 on 09/05/12
For personal use only.

Introduction

Complexation reactions of various substituted dithiocarbamates have been reviewed by Hulanicki (1). Most of the analytical methods for metals which use dithiocarbamic acids, involve extraction with organic solvents like chloroform or carbon tetrachloride, followed by the spectrophotometric determination. Thus, solvent extraction of the metal dithiocarbamate is an important step in analytical procedures. Solvent extraction has been extensively used in the determination of stability constants of metal complexes (2–6) and in the study of the equilibria of complex-ions (7–12). The present investigation was directed at (*i*) determination of the extraction constants for divalent metal ions with morpholine DTC (dithiocarbamate) as the complexing agent, and the overall stability constants of the complexes, and (*ii*) to determine the effect of various substituents at the nitrogen atom in disubstituted dithiocarbamic acids on the magnitude of the stability constants.

Theory

Dithizone Extraction

Studies on solvent extraction of metal dithizonates of copper, lead, cadmium, and nickel in the presence of bis(carboxymethyl)dithiocarbamate as a masking agent, were carried out by Hulanicki and Minczewska (13), and the stability constants of the metal dithiocarbamates were calculated (13).

In the solvent extraction of metal dithizonate (MDZ) in the absence of masking agent, morpholine DTC,

$$M^{2+} + 2(HDZ)_0 \rightleftarrows (MDZ_2)_0 + 2H^+$$

the distribution ratio, D, can be written as

$$[1] \qquad D = K\frac{[HDZ]_0^2}{[H^+]^2}$$

where K represents the extraction constant for the metal dithizonate. At $pH_{\frac{1}{2}}$ the distribution ratio is unity, and thus

$$[2] \qquad 2pH_{\frac{1}{2}} = -\log K - 2\log [HDZ]_0$$

In the case of the masked extraction with morpholine DTC as the masking agent, the contribution of the metal–dithiocarbamate complexes in masking the extraction of the metal–dithizonate complex depends on the values of the stability constants β_i for the various complexes, and also on the concentration of free dithiocarbamic acid, and is given by a complexation function F, defined by

$$[3] \qquad F = \sum_{i=0}^{N} \beta_i[\text{Morpholine DTC}]^i$$

where $\beta_0 = 1$

For the masked extraction the distribution ratio D^* is

$$[4] \qquad D^* = K\frac{[HDZ]_0^{*2}}{[H^+]^{*2}F}$$

where K has the same value as in eq. [1].

Equation [4] can be written in the form

$$[5] \qquad -\log K = 2\log [HDZ]_0^* + 2pH_{\frac{1}{2}}^* - \log F$$

where symbols with an asterisk refer to the masked extraction. From eqs. [2] and [5], one can write

$$[6] \qquad -\log F = 2(pH_{\frac{1}{2}}^* - pH_{\frac{1}{2}}) + 2\log\frac{[HDZ]_0^*}{[HDZ]_0}$$

[1]Presented at the 51st Canadian Chemical Conference and Exhibition, Vancouver, B. C., June 3–5, 1968.
[2]This paper was taken in part from the Ph.D. thesis of Keijo I. Aspila.
[3]All correspondence should be addressed to this author.

Can. J. Chem. Downloaded from www.nrcresearchpress.com by 210.87.254.105 on 09/05/12
For personal use only.

The stability constants of the complexes formed by divalent metal ions, Sn, Pb, Ni, and Cd, with morpholine DTC, were obtained by the use of eqs. [6] and [3].

At the pH values used for the extraction of the metal dithizonates in the presence of morpholine DTC, both the aqueous and the organic phase were analyzed, and it was found that the amount of metal morpholine DTC complex extracted into the organic phase was negligible.

Extraction of Metal–Morpholine DTC Complexes

Stary and Kratzer (14) have determined the extraction constants and the overall two-phase stability constants of several metal ions with diethyl–dithiocarbamic acid. The theory of the extraction has been outlined by Stary (4), and the basic equations applicable to the extraction of metal–morpholine DTC complexes are given below.

Solvent extraction of metal ions by a chloroform solution of morpholine DTC occurs thus

$$M^{n+} + n(HA)_{org} \rightleftharpoons MA_n + nH^+$$

and the extraction constant for the process is given by

$$[7] \qquad K = \frac{[MA_n]_{org}[H^+]^n}{[M^{n+}][(HA)_{org}]^n}$$

In the cases where the distribution ratio of the metal–dithiocarbamate complex was high, masking agents, e.g., EDTA, oxalate, and iodide, were used to form the non-extractable metal complex, MX_y, where X stands for the anion of the masking agent.

$$[8] \qquad K = q\{1 + \beta_y[X^{n-}]^y\}\frac{[H^+]^n}{[(HA)_{org}]^n}$$

where q is the distribution ratio of the metal in the presence of the masking agent, and where β_y is the stability constant of the metal complex MX_y. The stability constant of the metal–dithiocarbamate complex was calculated by the use of eqs. [9] and [10].

$$[9] \qquad \beta_{n_{org}} = \frac{[MA_n]_{org}}{[M^{n+}][A^-]^n} = K\left(\frac{p_{HA}}{K_{HA}}\right)^n$$

where p_{HA} is the partition coefficient of HA and is defined as

$$p_{HA} = \frac{[HA]_{org}}{[HA]}$$

and K_{HA} is the dissociation constant of HA and is defined as

$$K_{HA} = \frac{[H^+][A^-]}{[HA]}$$

$$[10] \qquad \log \beta_{n_{org}} = \log K + n \log\left(\frac{p_{HA}}{K_{HA}}\right)$$

The use of eqs. [7] or [8] in combination with eq. [9] enabled the determination of the stability constants of complexes of divalent metal ions, Mn, Fe, Co, Zn, Cu, and Hg, formed with morpholine DTC.

In the case of Cu^{2+}, the stability constant of the complex was also determined by the competition method of Janssen (15) using oxine as the competing ligand in 75% alcohol–water medium.

Experimental

Reagents

Analytical-reagent grade chemicals were used. (*a*) Stock solutions of 0.1 *M* of all the metals were prepared from the corresponding metal nitrates. (*b*) Dithizone solution in chloroform was prepared fresh just before use. (*c*) Morpholine DTC solutions were prepared fresh before use. (*d*) Spectral-grade chloroform was used for extraction.

Apparatus

A Bausch and Lomb spectronic 505 spectrophotometer was used for recording absorbance values.

Procedure

(a) Metal Dithizonates (13, 16)

For every metal ion, two series of experiments were done: (*i*) extraction in the absence of morpholine DTC; (*ii*) extraction in the presence of morpholine DTC. Extraction was done using 25 ml of aqueous solution which was 10^{-4}–10^{-5} *M* in metal ion and 10^{-3} *M* in morpholine DTC. This was extracted with 25 ml of dithizone reagent in chloroform. The time of equilibration was 10 min. All experiments were done at a temperature of 25 ± 1 °C.

The following points may also be noted. (*i*) In the pH range of non-masked extraction, Cd^{2+}, Pb^{2+}, Ni^{2+}, and Sn^{2+} do not form any hydroxocomplexes, (*ii*) pH of the solutions were maintained by using buffer solutions, (*iii*) the ionic strength was kept constant at 0.1 by the addition of potassium nitrate, (*iv*) the formation of mixed complexes was checked spectrophotometrically by comparison of the spectra with those of the corresponding complexes obtained in the absence of morpholinodithiocarbamic acid, and it was found that mixed complexes were absent, (*v*) the absorbance of the metal dithizonate in the organic phase was used for obtaining the % extraction as a function of pH, both in the absence and presence of morpholinedithiocarbamic acid from which the $pH_{\frac{1}{2}}$ values were evaluated.

(b) Metal Dithiocarbamates (14)

(*i*) 25 ml of a solution of morpholine DTC in chloroform was equilibrated with an equal volume of aqueous

Can. J. Chem. Downloaded from www.nrcresearchpress.com by 210.87.254.105 on 09/05/12
For personal use only.

solution of the metal salt of appropriate pH for about 10 min, and the equilibrium concentrations of the free ligand and metal ion were determined spectrophotometrically. This was used as the reference solution against which the extent of formation of the metal–morpholine complexes under the conditions given in (*ii*) below, was compared, (*ii*) 25 ml of an aqueous solution containing the metal ion of appropriate pH, and 0.1 *M* of EDTA or oxalate ion, was equilibrated with 25 ml of chloroform solution of morpholine DTC, and the equilibrium concentrations of the metal ion and the ligand were determined spectrophotometrically. Extraction was carried out also in the absence of masking agent. All extractions were carried out at a temperature of 25 ± 1 °C. The time of equilibration for Mn^{2+}, Fe^{2+}, Co^{2+}, Zn^{2+}, Cu^{2+}, and Hg^{2+} was 30 min. The masking agents were as follows

Metals	Masking agents
Mn^{2+}, Fe^{2+}, Co^{2+}, Zn^{2+}	Oxalate
Cu^{2+}	EDTA
Hg^{2+}	Iodide

The concentrations used in (*b*) metal–dithiocarbamates (*i*) and (*ii*) were as follows: metal 10^{-4}–10^{-5} *M*, morpholine DTC 10^{-3}–10^{-4} *M*, and masking agents 10^{-2} *M*.

In both cases of extraction of (*a*) metal dithizonates and (*b*) metal dithiocarbamates, the process was continued for a further period of time up to 2 h in order to test for completion of the equilibration, and it was found that the equilibration was complete in the time mentioned in (*a*) and (*b*) above.

Results and Discussion

In Table I, data for the stability constants of copper dithiocarbamate complexes for various substituted dithiocarbamic acids are presented together with p*K*'s for the nitrogen and sulfur sites of the reagents. In general, the stability constants increase with increasing basicity of the sulfur site of the reagent, with the exception of diphenyldithiocarbamate. A similar correlation of the stability constants is seen with the basicity of nitrogen centers (pK_N) of the reagents, with the exception of morpholine dithiocarbamic acid.

The data on the stability constants and extraction constants of complexes of Mn(II), Fe(II), Co(II), Ni(II), Cu(II), Zn(II), Pb(II), Cd(II), Sn(II), and Hg(II), are given in Table II. In discussing the order of stability constants for complexes of Mn(II), Fe(II), Co(II), Cu(II), and Zn(II) with sulfur, nitrogen, and oxygen substituted iminodiacetic acids, Burger (17) invoked the concept of the π bonding ability of sulfur atoms, and concluded that this was responsible for the deviation in the order of stability constants from the natural order of stability predicted by Irving and Williams (18). However, the experimental evidence shows that the stability constants of complexes of divalent metal ions with sulfur donors, such as S-ethylthioglycolic, 3-(S-ethyl)mercaptopropionic, and *o*-ethylmercaptobenzoic acids (19), and thiodiglycolic acid (20, 21), follow the natural order, i.e.,

$$Cu > Ni > Pb > Co > Zn > Cd$$

In the case of diethyl (14) and morpholine dithiocarbamate complexes, the order of stability constants has been found to be

$$Mn(II) < Fe(II) < Co(II) < Ni(II) < Cu(II) > Zn(II)$$

and

$$Mn(II) < Fe(II) > Co(II) < Ni(II) < Cu(II) > Zn(II)$$

respectively.

Data on the extraction constants of morpholine and diethyl dithiocarbamate complexes show the order of decreasing extraction

$$Hg > Cu > Zn > Fe > Co > Mn$$

which agrees well with the previous findings of Stary and Kratzer (14) and Eckert (22).

TABLE I

Stability constants of the complexes, and p*K*'s for the nitrogen and sulfur sites of the reagents

Solvent	Reagent	$pK_{Cu(DTC)_2}$	pK_S	pK_N
$CHCl_3$	Diethyl	27.10	6.2	4.0 (1)
	Morpholine	26.05	6.13	5.2 (1)
	Pyrrolidine	24.7	6.0	3.0
	Diphenyl	23.9	8.1	<0.8

TABLE II

Stability constants and extraction constants of the complexes

	Morpholine DTC	
Metal ion (M^{2+})	log K_{ML_n}	log *K* (extraction constant)
Mn	9.10	−3.18
Fe	15.48	3.22
Co	13.60	1.33
Ni	14.70	—
Cu	26.05	14.06
Zn	16.60	4.32
Pb	21.90	—
Cd	16.45	—
Sn	16.12	—
Hg	41.00	28.7

Acknowledgments

The authors are grateful to the National Research Council of Canada and the Ontario

Department of University Affairs for research grants.

1. A. HULANICKI. Talanta, **14**, 1371 (1967).
2. M. M. JONES. Elementary coordination chemistry. Prentice-Hall, Inc., New Jersey. 1964. p. 307.
3. G. H. MORRISON and H. FREISER. Solvent extraction in analytical chemistry. John Wiley and Sons, Inc., New York. 1957.
4. J. STARY. The solvent extraction of metal chelates. The Pergamon Press, Ltd., Oxford, England. 1964. Chap. 2.
5. J. RYDBERG. Acta Chem. Scand. **14**, 157 (1960).
6. T. SCHUBERT, E. L. LIND, W. M. WESTFALL, R. PFLEGER, and N. C. LI. J. Am. Chem. Soc. **80**, 4799 (1958).
7. R. E. CONNICK and W. H. MCVEY. J. Am. Chem. Soc. **71**, 3182 (1949).
8. R. A. DAY, JR. and R. M. POWERS. J. Am. Chem. Soc. **76**, 3895 (1954).
9. D. DRYSSEN and L. G. SILLEN. Acta Chem. Scand. **7**, 663 (1953).
10. H. IRVING, F. J. C. ROSSOTTI, and R. J. P. WILLIAMS. J. Chem. Soc. 1906 (1955).
11. J. RYDBERG. Acta Chem. Scand. **4**, 1503 (1950).
12. J. RYDBERG and J. C. SULLIVAN. Acta Chem. Scand. **13**, 2057 (1959).
13. A. HULANICKI and M. MINCZEWSKA. Talanta, **14**, 677 (1967).
14. J. STARY and K. KRATZER. Anal. Chim. Acta, **40**, 93 (1968).
15. M. J. JANSSEN. Rec. Trav. Chim. **75**, 1411 (1956).
16. E. B. SANDELL. Colorimetric determination of traces of metals. 3rd ed. Interscience Publishers, Inc., New York. 1959.
17. K. BURGER. Talanta, **8**, 769 (1961).
18. H. IRVING and R. J. P. WILLIAMS. Nature, **162**, 746 (1948).
19. F. P. DWYER and D. P. MELLOR. Chelating agents and metal chelates. Academic Press, Inc., New York. 1964. p. 125.
20. M. YASUDA, K. YAMASAKI, and H. OHTAKI. Bull. Chem. Soc. Japan, **33**, 1067 (1960).
21. K. SUZUKI and K. YAMASAKI. J. Inorg. Nucl. Chem. **28**, 473 (1960). K. SUZUKI, C. KARAKI, S. MORI, and K. YAMASAKI. J. Inorg. Nucl. Chem. **30**, 167 (1968).
22. E. ECKERT. Z. Anal. Chem. **155**, 23 (1957).

Effects of hydrogen bonding and homoconjugation on the titration curves of a synthetic polynuclear phenolic compound in non-aqueous solvents

S. K. CHATTERJEE
Department of Chemistry, Delhi University, Delhi-7, India

Received December 31, 1968

A straight chain polynuclear phenolic compound containing 9 phenolic nuclei has been synthesized and titrated in several non-aqueous solvents. In some of the solvents, a stepwise neutralization of OH groups in the compound has been observed. Some of the OH groups in the compound have a hyper-acid character, and a sharp increase in conductance was observed as these OH groups are neutralized by the base. Some of these features have been discussed in terms of intramolecular hydrogen bonding and homoconjugation between the acid and its anion.

Canadian Journal of Chemistry, **47**, 2323 (1969)

The presence of hydrogen bonds has often been postulated to explain the peculiar behavior of certain phenolic resin intermediates (1, 2). Coggeshall's (3) infrared spectroscopic results on ortho diphenyl methanes have shown the presence of intramolecular hydrogen bonds in these compounds. Sprengling (4) potentiometrically titrated some *o,o'*-dihydroxy diphenyl methane type of compounds in benzene – isopropyl alcohol mixture, and observed that one of the OH groups in the molecule had a strong acid character. He suggested that the cause of the strong acid character was to be found in an intramolecular hydrogen bond formation between neighboring OH groups in the molecule, as shown in **1–3**

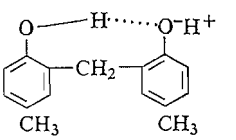

1

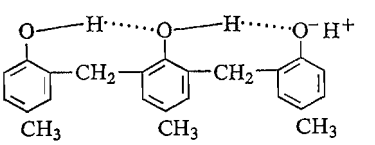

2

Can. J. Chem. Downloaded from www.nrcresearchpress.com by 210.87.254.105 on 09/05/12
For personal use only.

Department of University Affairs for research grants.

1. A. HULANICKI. Talanta, **14**, 1371 (1967).
2. M. M. JONES. Elementary coordination chemistry. Prentice-Hall, Inc., New Jersey. 1964. p. 307.
3. G. H. MORRISON and H. FREISER. Solvent extraction in analytical chemistry. John Wiley and Sons, Inc., New York. 1957.
4. J. STARY. The solvent extraction of metal chelates. The Pergamon Press, Ltd., Oxford, England. 1964. Chap. 2.
5. J. RYDBERG. Acta Chem. Scand. **14**, 157 (1960).
6. T. SCHUBERT, E. L. LIND, W. M. WESTFALL, R. PFLEGER, and N. C. LI. J. Am. Chem. Soc. **80**, 4799 (1958).
7. R. E. CONNICK and W. H. MCVEY. J. Am. Chem. Soc. **71**, 3182 (1949).
8. R. A. DAY, JR. and R. M. POWERS. J. Am. Chem. Soc. **76**, 3895 (1954).
9. D. DRYSSEN and L. G. SILLEN. Acta Chem. Scand. **7**, 663 (1953).
10. H. IRVING, F. J. C. ROSSOTTI, and R. J. P. WILLIAMS. J. Chem. Soc. 1906 (1955).
11. J. RYDBERG. Acta Chem. Scand. **4**, 1503 (1950).
12. J. RYDBERG and J. C. SULLIVAN. Acta Chem. Scand. **13**, 2057 (1959).
13. A. HULANICKI and M. MINCZEWSKA. Talanta, **14**, 677 (1967).
14. J. STARY and K. KRATZER. Anal. Chim. Acta, **40**, 93 (1968).
15. M. J. JANSSEN. Rec. Trav. Chim. **75**, 1411 (1956).
16. E. B. SANDELL. Colorimetric determination of traces of metals. 3rd ed. Interscience Publishers, Inc., New York. 1959.
17. K. BURGER. Talanta, **8**, 769 (1961).
18. H. IRVING and R. J. P. WILLIAMS. Nature, **162**, 746 (1948).
19. F. P. DWYER and D. P. MELLOR. Chelating agents and metal chelates. Academic Press, Inc., New York. 1964. p. 125.
20. M. YASUDA, K. YAMASAKI, and H. OHTAKI. Bull. Chem. Soc. Japan, **33**, 1067 (1960).
21. K. SUZUKI and K. YAMASAKI. J. Inorg. Nucl. Chem. **28**, 473 (1960). K. SUZUKI, C. KARAKI, S. MORI, and K. YAMASAKI. J. Inorg. Nucl. Chem. **30**, 167 (1968).
22. E. ECKERT. Z. Anal. Chem. **155**, 23 (1957).

Effects of hydrogen bonding and homoconjugation on the titration curves of a synthetic polynuclear phenolic compound in non-aqueous solvents

S. K. CHATTERJEE
Department of Chemistry, Delhi University, Delhi-7, India

Received December 31, 1968

A straight chain polynuclear phenolic compound containing 9 phenolic nuclei has been synthesized and titrated in several non-aqueous solvents. In some of the solvents, a stepwise neutralization of OH groups in the compound has been observed. Some of the OH groups in the compound have a hyper-acid character, and a sharp increase in conductance was observed as these OH groups are neutralized by the base. Some of these features have been discussed in terms of intramolecular hydrogen bonding and homoconjugation between the acid and its anion.

Canadian Journal of Chemistry, **47**, 2323 (1969)

The presence of hydrogen bonds has often been postulated to explain the peculiar behavior of certain phenolic resin intermediates (1, 2). Coggeshall's (3) infrared spectroscopic results on ortho diphenyl methanes have shown the presence of intramolecular hydrogen bonds in these compounds. Sprengling (4) potentiometrically titrated some *o,o'*-dihydroxy diphenyl methane type of compounds in benzene – isopropyl alcohol mixture, and observed that one of the OH groups in the molecule had a strong acid character. He suggested that the cause of the strong acid character was to be found in an intramolecular hydrogen bond formation between neighboring OH groups in the molecule, as shown in **1–3**

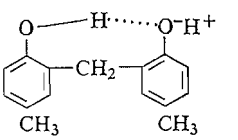

1

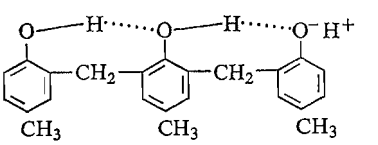

2

Can. J. Chem. Downloaded from www.nrcresearchpress.com by 210.87.254.6 on 09/05/12
For personal use only.

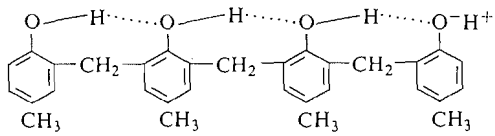

3

However, he failed to observe any stepwise neutralization of phenolic OH groups in these compounds. Mitra and Chatterjee (5–7) titrated a series of low molecular weight synthetic polynuclear phenolic compounds in various non-aqueous solvents, and showed that a stepwise neutralization of phenolic OH groups in these compounds could be obtained if solvents and titrant bases were properly chosen. This note is intended to present certain facts concerning intramolecular hydrogen bonding and homoconjugation, and their influence on the titration curves of a large synthetic polynuclear phenolic compound. The structure and the chain length of the synthetic compound (4) used in this investigation were known from its synthesis.

Experimental

For the preparation of the synthetic polynuclear phenolic compound (4), the methods of Kammerer and Rausch (8) were followed

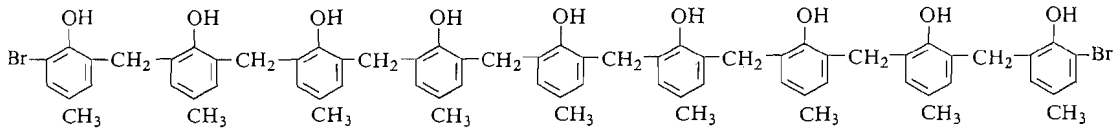

4

p-Cresol (0.01 mole) was condensed with slightly more than 0.02 mole of 3-bromo, 3′-hydroxy methyl, 2-2′-dihydroxy, 5-5′-dimethyl diphenyl methane (Br–2–CH_2–OH) in the presence of concentrated HCl as a catalyst. The resultant dibromo pentanuclear compound is then dehalogenated with Raney nickel. The dehalogenated pentanuclear compound was (0.01 mole) further condensed with slightly more than 0.02 mole of Br-2-CH_2OH in the presence of concentrated HCl as a catalyst. After the reaction, the fused mass was dissolved in dioxan and precipitated with methanol.

For potentiometric work, glass electrodes (Beckman), saturated calomel electrodes (as reference half cells), and a Beckman *pH* meter (H-2 model) were employed. For conductometric titrations, a Pt–Ir bridge was used in conjuction with a Muirhead audio frequency oscillator as the source of alternating electromotive force. Analytical grade solvents were used without further purification.

Results and Discussions

Figure 1 shows the titration curves of the nonanuclear compound (4) in various non-aqueous solvents. The conductometric titration of the compound in acetone with sodium methoxide as the titrant base is shown in curve 1. It shows 5 breaks in all, and the smallest interval between two successive breaks is found to be 80 meq. of base per 100 g of the compound. This amount of base incidently coincides with the calculated quantity of base required to neutralize one OH group in the compound. Therefore, from the quantities of base required at the various stages of neutralization of the conductometric titration curve, the number of OH groups neutralized at different steps can be ascertained. The corresponding potentiometric curve is shown by curve 2, which indicates only three inflexions. One OH group each is neutralized at the first two inflexions, and the third inflexion accounts for the neutralization of two more OH groups. The final break of the conductometric titration curve accounts for the neutralization of all the 9 OH groups of compound (4). However, the complete neutralization of the compound is not indicated by the potentiometric curve. Curves 3 and 4 in the same figure show the conductometric and potentiometric titration curves, respectively, of compound (4) in acetonitrile with sodium methoxide. The potentiometric curve shows two inflexions, where two OH groups are neutralized at each step. However, the corresponding conductometric curve (cf. curve 3) shows 6 breaks in all, and each of the first 4 breaks coincides with the neutralization of one OH group. On comparing the conductometric curves with the potentiometric curves, it can be seen that OH are neutralized mostly in a stepwise manner in the conductometric curve and more often they are lumped in the potentiometric curve. These extremely interesting observations can be interpreted in terms of homoconjugation as proposed by Kolthoff *et al* (9–11). Kolthoff defined homo-

Can. J. Chem. Downloaded from www.nrcresearchpress.com by 210.87.254.6 on 09/05/12
For personal use only.

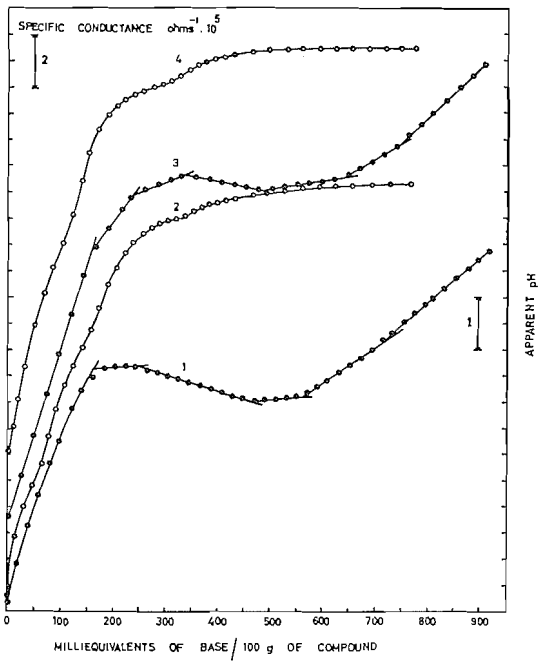

FIG. 1. Titration curves of compound (**4**) in acetone and acetonitrile with sodium methoxide. (*1*) Conductometric titration curve in acetone; (*2*) *pH* titration curve in acetone; (*3*) conductometric titration curve in acetonitrile; (*4*) *pH* titration curve in acetonitrile.

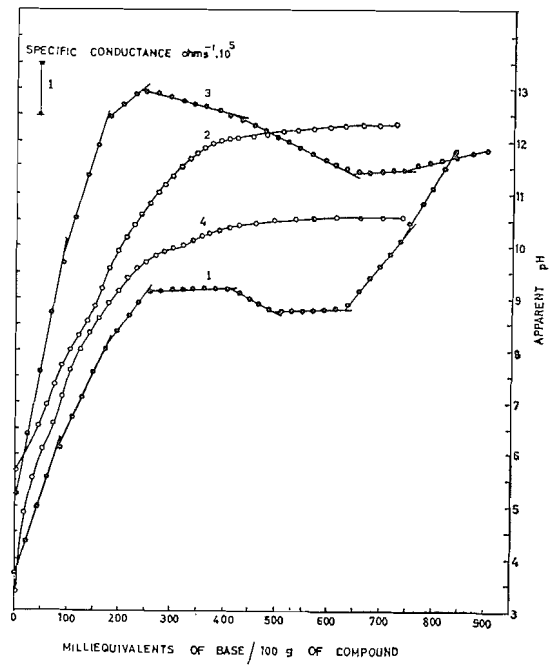

FIG. 2. Titration curves of compound (**4**) in some mixed solvents with sodium methoxide. (*1*) Conductometric titration curve in 1:1 DMF and B; (*2*) *pH* titration curve in 1:1 DMF and B; (*3*) conductometric titration curve in 1:1 AN and B; (*4*) *pH* titration curve in 1:1 AN and B.

conjugation as the association of an anion with its conjugate acid:

$$A^- + HA \rightleftarrows AHA^-$$

In solvents that are weak hydrogen bond doners, such as acetonitrile and acetone, homonuclear phenols form very stable homoconjugate complexes AHA^-. It seems likely that some of this tendency will persist with polynuclear phenols. In fact the observed maxima in the conductometric titration curves are exactly what would be expected if homoconjugation occurs. The formation of AHA^- and its effect on the characteristics of conductometric (12–14), and potentiometric (14, 15) titration curves have been considered in some recent publications. The large synthetic polynuclear molecule (**4**) in solution is likely to have intramolecular hydrogen bonds consisting of 2, 3, or 4 OH groups. In fact, the number of hydroxyl groups involved in the hydrogen bond formation should depend on the particular orientation of the molecule in solution. It may thus be considered that the polynuclear molecule (**4**) may dissociate in solution to give rise to a series of anions. The presence of various anions in solution may lead to the formation of a number of acid–anion complexes. Perhaps the difference of degree of dissociation of some of these homoconjugate complexes may be responsible for the stepwise neutralization of phenolic OH groups in the conductometric titration curves.

Van Meurs and Dahmen (16) showed that dielectric constant of the solvent and size of cation of titrant base play an important role in getting a particular shape of the titration curve. Therefore, it was considered of interest to vary the dielectric constant of the solvent by mixing with a solvent of low dielectric constant, such as benzene, and to study its influence on the nature of titration curves. In Fig. 2 are presented the titration curves of the polynuclear phenolic compound (**4**) in some mixed solvents. Curve 1 is the conductometric titration curve of the compound in a 1:1 mixture of dimethyl formamide (DMF) and benzene (B) with sodium methoxide as the titrant base. It shows 7 well defined breaks in all, and one OH group is neutralized at each of the first three

Can. J. Chem. Downloaded from www.nrcresearchpress.com by 210.87.254.6 on 09/05/12
For personal use only.

steps. The complete neutralization of all the OH groups in compound (**4**) is indicated by the final break of the conductometric titration curve. The neutralization of the first two OH groups of the compound is also indicated by the two inflexions of the potentiometric curve (cf. curve 2).The conductometric titration curve of the compound in a 1:1 mixture of acetonitrile (AN) and benzene (B) shows 6 breaks in all (cf. curve 3). The corresponding potentiometric titration curve indicates only two inflexions, where one OH group is neutralized at the first step and three in the subsequent step. Since the smallest interval between 2 successive breaks or inflexions in the titration curve coincides with the calculated amount of base required to neutralize one OH group of the compound, one can, therefore, make use of this fact to calculate average degree of polymerization (*DP*) of linear polymers having acidic or basic functional groups. The average *DP* would be obtained by dividing the total amount of base (740 meq.), expressed in meq./100 g of compound, added up to the final break in the titration curve, by the amount added during the smallest interval (80 meq.). Thus the average *DP* of the compound (**4**), would be equal to 740/80 = 9(approx.). This number, interestingly enough, coincides with the number of repeat units of the compound (**4**), which is known from its synthesis. It may thus be concluded that conductometric titration in suitable non-aqueous solvents provides an excellent method for quantitative estimation of phenolic OH groups in a polynuclear phenolic compound.

Acknowledgment

The author expresses his sincere thanks to Professor R. P. Mitra, Head of the Department of Chemistry, Delhi University, Delhi, for helpful discussions.

1. K. Hultzsch. Angew. Chem. **61**, 93 (1949).
2. H. S. Lillney. J. Soc. Chem. Ind. **67**, 196 (1948).
3. N. D. Coggeschall. J. Am. Chem. Soc. **72**, 2836 (1950).
4. G. R. Sprengling. J. Am. Chem. Soc. **76**, 1190 (1954).
5. R. P. Mitra and S. K. Chatterjee. J. Sci. Ind. Res. India, **20B**, 310 (1961).
6. R. P. Mitra and S. K. Chatterjee. Indian J. Chem. **1**, 62 (1963).
7. R. P. Mitra and S. K. Chatterjee. Indian J. Chem. **2**, 85 (1964).
8. H. Kammerer and W. Rausch. Makromol. Chem. **24**, 152 (1957).
9. I. M. Kolthoff, S. Bruckenstein, and M. K. Chantooni. J. Am. Chem. Soc. **83**, 3927 (1961).
10. I. M. Kolthoff and M. K. Chantooni. J. Am. Chem. Soc. **85**, 2195 (1963).
11. I. M. Kolthoff and M. K. Chantooni. J. Am. Chem. Soc. **87**, 1004 (1965).
12. N. Van Meurs and E. Dahmen. Anal. Chim. Acta, **19**, 64 (1958).
13. P. R. Bryant and A. H. Wardrup. J. Chem. Soc. 895 (1957).
14. D. B. Bruss and G. Harlow. Anal. Chem. **30**, 1833, 1836 (1958).
15. H. B. Van der Heijde. Anal. Chim. Acta, **16**, 392 (1957).
16. N. Van Meurs and E. Dahmen. Anal. Chim. Acta, **21**, 10 (1959).

Determination of the activity of water in highly concentrated perchloric acid solutions

Henry Wai[1] and Keith Yates

Department of Chemistry, University of Toronto, Toronto 5, Ontario

Received November 25, 1968

The water activities of concentrated aqueous perchloric acids in the range 40–75% have been determined at 25 °C using a modified isopiestic method.

Canadian Journal of Chemistry, 47, 2326 (1969)

In connection with our studies of equilibria (1) and rates (2) in concentrated mineral acids, we have found that the available data for the activity of water (3, 4) in perchloric acid solutions are rather inadequate for correlation purposes, because such data are only available up to about 60% acid (4). We have estimated the activity of water in perchloric acid ranging from 40–75%

[1]Present address: Department of Chemistry, Massachusetts Institute of Technology, Cambridge, Massachusetts 02139.

Can. J. Chem. Downloaded from www.nrcresearchpress.com by 210.87.254.6 on 09/05/12
For personal use only.

steps. The complete neutralization of all the OH groups in compound (**4**) is indicated by the final break of the conductometric titration curve. The neutralization of the first two OH groups of the compound is also indicated by the two inflexions of the potentiometric curve (cf. curve 2).The conductometric titration curve of the compound in a 1:1 mixture of acetonitrile (AN) and benzene (B) shows 6 breaks in all (cf. curve 3). The corresponding potentiometric titration curve indicates only two inflexions, where one OH group is neutralized at the first step and three in the subsequent step. Since the smallest interval between 2 successive breaks or inflexions in the titration curve coincides with the calculated amount of base required to neutralize one OH group of the compound, one can, therefore, make use of this fact to calculate average degree of polymerization (*DP*) of linear polymers having acidic or basic functional groups. The average *DP* would be obtained by dividing the total amount of base (740 meq.), expressed in meq./100 g of compound, added up to the final break in the titration curve, by the amount added during the smallest interval (80 meq.). Thus the average *DP* of the compound (**4**), would be equal to 740/80 = 9(approx.). This number, interestingly enough, coincides with the number of repeat units of the compound (**4**), which is known from its synthesis. It may thus be concluded that conductometric titration in suitable non-aqueous solvents provides an excellent method for quantitative estimation of phenolic OH groups in a polynuclear phenolic compound.

Acknowledgment

The author expresses his sincere thanks to Professor R. P. Mitra, Head of the Department of Chemistry, Delhi University, Delhi, for helpful discussions.

1. K. Hultzsch. Angew. Chem. **61**, 93 (1949).
2. H. S. Lillney. J. Soc. Chem. Ind. **67**, 196 (1948).
3. N. D. Coggeschall. J. Am. Chem. Soc. **72**, 2836 (1950).
4. G. R. Sprengling. J. Am. Chem. Soc. **76**, 1190 (1954).
5. R. P. Mitra and S. K. Chatterjee. J. Sci. Ind. Res. India, **20B**, 310 (1961).
6. R. P. Mitra and S. K. Chatterjee. Indian J. Chem. **1**, 62 (1963).
7. R. P. Mitra and S. K. Chatterjee. Indian J. Chem. **2**, 85 (1964).
8. H. Kammerer and W. Rausch. Makromol. Chem. **24**, 152 (1957).
9. I. M. Kolthoff, S. Bruckenstein, and M. K. Chantooni. J. Am. Chem. Soc. **83**, 3927 (1961).
10. I. M. Kolthoff and M. K. Chantooni. J. Am. Chem. Soc. **85**, 2195 (1963).
11. I. M. Kolthoff and M. K. Chantooni. J. Am. Chem. Soc. **87**, 1004 (1965).
12. N. Van Meurs and E. Dahmen. Anal. Chim. Acta, **19**, 64 (1958).
13. P. R. Bryant and A. H. Wardrup. J. Chem. Soc. 895 (1957).
14. D. B. Bruss and G. Harlow. Anal. Chem. **30**, 1833, 1836 (1958).
15. H. B. Van der Heijde. Anal. Chim. Acta, **16**, 392 (1957).
16. N. Van Meurs and E. Dahmen. Anal. Chim. Acta, **21**, 10 (1959).

Determination of the activity of water in highly concentrated perchloric acid solutions

Henry Wai[1] and Keith Yates
Department of Chemistry, University of Toronto, Toronto 5, Ontario
Received November 25, 1968

The water activities of concentrated aqueous perchloric acids in the range 40–75% have been determined at 25 °C using a modified isopiestic method.

Canadian Journal of Chemistry, 47, 2326 (1969)

In connection with our studies of equilibria (1) and rates (2) in concentrated mineral acids, we have found that the available data for the activity of water (3, 4) in perchloric acid solutions are rather inadequate for correlation purposes, because such data are only available up to about 60% acid (4). We have estimated the activity of water in perchloric acid ranging from 40–75%

[1]Present address: Department of Chemistry, Massachusetts Institute of Technology, Cambridge, Massachusetts 02139.

Can. J. Chem. Downloaded from www.nrcresearchpress.com by 210.87.254.105 on 09/05/12
For personal use only.

TABLE I

Isopiestic solutions of perchloric and sulfuric acids at 25 °C

$HClO_4$		H_2SO_4			
%	Molality	%	Molality	$-\log a_w$*	a_w*
40.03	6.645	38.97	6.509	0.231	0.587
48.90	9.526	49.77	10.10	0.447	0.357
51.29	10.48	52.88	11.44	0.535	0.292
55.87	12.60	59.05	14.70	0.752	0.177
57.53	13.48	61.42	16.23	0.854	0.140
60.18	15.04	65.05	18.98	1.022	0.095
62.11	16.32	67.53	21.21	1.178	0.0664
62.43	16.54	68.20	21.87	1.222	0.0600
63.62	17.57	69.69	22.55	1.321	0.0478
64.43	18.03	70.63	24.52	1.392	0.0406
65.77	19.12	72.43	26.79	1.526	0.0298
66.38	19.66	73.11	27.72	1.578	0.0264
67.24	20.43	74.22	29.36	1.680	0.0209
67.98	21.13	75.20	30.92	1.771	0.0169
69.09	22.25	76.50	33.18	1.896	0.0127
69.63	22.82	77.30	34.73	1.976	0.0106
71.15	24.55	79.01	38.37	2.165	0.00684
71.45	24.91	79.49	39.52	2.217	0.00607
72.45	26.18	80.76	42.79	2.368	0.00429
73.30	27.33	82.06	46.64	2.526	0.00298
74.78	29.52	83.22	50.56	2.679	0.00209

*Water activity values are interpolated graphically from data in ref. 7. Plots of a_w or $-\log a_w$ versus $\%H_2SO_4$ were used for the interpolations in less than and more than 66% (w/w) H_2SO_4 respectively.

acid at 20 °C by the isopiestic method (5) in a modified apparatus (see Experimental section) using sulfuric acid as the reference solution. This extends the useful range of water activity for acidity function work by more than three logarithmic units (on the H_0 scale). The results are listed in Table I, and are plotted as a function of acid concentration in Fig. 1.

The activity of water in perchloric acid up to 12 molal (ca. 55%) has been determined by Pearce and Nelson (3) by the dynamic method. It has also been determined by Robinson and Baker (4) up to 16 molal (ca. 62%) by the isopiestic method, using sodium chloride solution as the reference for perchloric acid below 4.5 molal and sulfuric acid above that[2]. These results agree closely with one another. It can be seen from Fig. 1 that the smoothed data from the literature (3, 4) and the raw data from the present work follow virtually the same curve in the regions where they overlap. This shows that the values in Table I, which are easily obtained by the

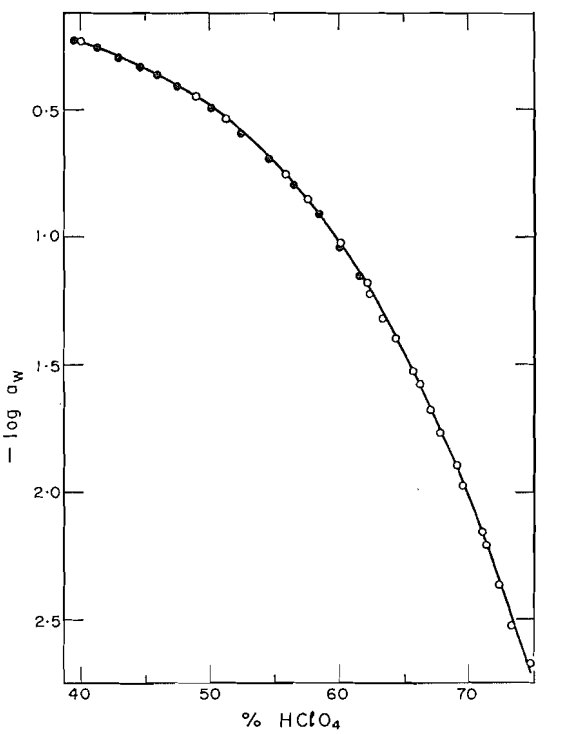

FIG. 1. Variation of water activity ($-\log a_w$) as a function of acid concentration in aqueous perchloric acid at 20 °C; ○, present work; ●, data taken from refs. 3 and 4.

[2]Some limited data at higher concentrations of perchloric acid have been reported by Haldna, Koppel, and Kuura (6). However, these are of questionable value since they were apparently based on isopiestic measurements at 20 °C using sulfuric acid reference data obtained at 25 °C (7).

Can. J. Chem. Downloaded from www.nrcresearchpress.com by 210.87.254.105 on 09/05/12
For personal use only.

present modified apparatus, may be used with confidence and that this simple method could be used to extend the somewhat sparse water activity data available for other concentrated acid systems. It can also been seen from Table I that for a pair of isopiestic solutions, sulfuric acid is generally much more concentrated than perchloric acid in the highly concentrated regions. This suggests that the amount of "free" water available in perchloric acids is much less than that in sulfuric acids of comparable concentration.

Experimental

A "Labconco" fiberglass glove box was converted to a constant temperature controlled box by fitting the built-in circulating duct with a "muffin fan" made by Rotron Manufacturing Co., Glendale, California. A 100-W wire heater was mounted in front of the fan which had a circulating capacity of 100 cu. ft/min. The box was thermostatically controlled at 25 ± 0.1 °C by means of a solid-state relay box connected to the heater.

The modified apparatus for the isopiestic determination of water activity is shown in Fig. 2. By using this all-glass apparatus, not only the necessity of very expensive platinum dishes (5) can be eliminated, but also the possibility of platinum catalyzed decomposition of perchloric acid (8) (especially in the highly concentrated region). Thermal communication between the two solutions in this glass apparatus is not a problem, since the whole apparatus is placed in the constant-temperature air-bath.

Perchloric acid solutions (Baker and Adamson reagent (70% minimum) and G. Frederick Smith Chemical Co. $HClO_4$ monohydrate) and sulfuric acid solutions (CIL C.P. reagent) were put separately into the pairs of flasks. Each flask had an indentation at the bottom to help provide turbulence. The common atmosphere above the acids was evacuated with a rotary vacuum pump to accelerate the attainment of equilibrium. The flasks were allowed to equilibrate (with gentle shaking) in the thermostatically controlled glove box at 25 ± 0.1 °C for 48 to 72 h, depending on the concentrations used. At the end of the equilibration, the concentrations of the acids were determined titrimetrically with standard sodium hydroxide solution, prepared from Fisher certified reagent concentrated solution. The times necessary to achieve isopiestic equilibrium were established by means of repeat determinations on duplicate samples, which had been equilibrated for different lengths of time, until constant titration values were obtained. The activity of water in each pair of the two isopiestic acids was interpolated graphically from data compiled by Robinson and Stokes for sulfuric acid (9).

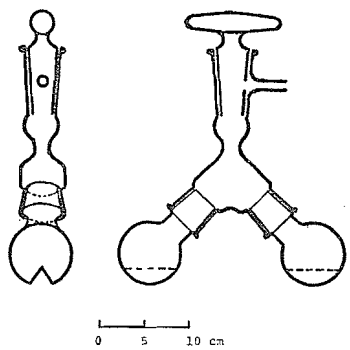

FIG. 2. Diagram of all glass apparatus used for equilibration of isopiestic acid solutions.

That the equilibration did not lead to any molecular transfer of the two mineral acids themselves was demonstrated in the following manner. A saturated barium hydroxide solution when added to the diluted perchloric acid after equilibration failed to detect the presence of any sulfate. To test for the presence of perchloric acid in the sulfuric acid after equilibration, the latter was carefully neutralized with analytical grade sodium hydroxide (British Drug Houses). The solution was evaporated to dryness and the sample was analyzed for chlorine content. In eight different samples analyzed by two independent microanalysis laboratories, chlorine was only found in one sample to the extent of 0.07%, the rest being reported as 0.00%. These results do not support the previously reported (6) suggestion that the isopiestic method is only valid up to about 72% $HClO_4$ because of volatilization of the acid.

Acknowledgments

This study was supported in part by a grant from the Defense Research Board of Canada. We are also grateful to the National Research Council of Canada for financial support and for a Studentship to one of us (H. W.)

1. (*a*) K. YATES and H. WAI. J. Am. Chem. Soc. **86**, 5408 (1964). (*b*) H. WAI and K. Yates. Unpublished results.
2. K. YATES and R. A. MCCLELLAND. J. Am. Chem. Soc. **89**, 2686 (1967).
3. J. N. PEARCE and A. F. NELSON. J. Am. Chem. Soc. **55**, 3075 (1933).
4. R. A. ROBINSON and O. J. BAKER. Trans. Roy. Soc. New Zealand, **76**, 250 (1946).
5. R. A. ROBINSON and R. H. STOKES. Electrolyte solutions. 2nd ed. Butterworths Publications, Ltd., London. 1961. Chap. 8.
6. Y. L. HALDNA, I. A. KOPPEL, and K. I. KUURA. Zh. Fiz. Khim. **40**, 1657 (1968).
7. W. G. GIAUQUE, E. W. HORNUNG, J. E. KUNZEL, and T. T. RUBIN. J. Am. Chem. Soc. **82**, 62 (1960).
8. G. S. PEARSON. Perchloric acid. *In* Advances in inorganic chemistry and radiochemistry. 1966. p. 8.
9. R. A. ROBINSON and R. H. STOKES. Electrolyte solutions. 2nd ed. Butterworths Publications, Ltd., London. 1961. p. 477.

Can. J. Chem. Downloaded from www.nrcresearchpress.com by 210.87.254.105 on 09/05/12
For personal use only.

Formation of 2,3-epoxyperfluoropropionylfluoride from the mercury photosensitized oxidation of 1,3-perfluorobutadiene

WAYNE STUCKEY, JULIAN HEICKLEN[1], AND VESTER KNIGHT
Aerospace Corporation, El Segundo, California 90045

Received October 30, 1968

The mercury photosensitized oxidation of 1,3-C_4F_6 gives nearly equal amounts of CF_2O and a new compound 2,3-epoxyperfluoropropionylfluoride and smaller amounts of *c*-C_3F_4. The infrared (i.r.) and mass spectra of 2,3-epoxyperfluoropropionylfluoride are presented.

Canadian Journal of Chemistry, 47, 2329 (1969)

Can. J. Chem. Downloaded from www.nrcresearchpress.com by 84.22.46.98 on 09/08/12
For personal use only.

We wish to report the synthesis and identification of 2,3-epoxyperfluoropropionylfluoride (1)

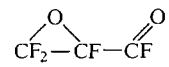

1

This molecule is prepared, along with CF_2O and *c*-C_3F_4, in the mercury-photosensitized oxidation of 1,3-C_4F_6 at room temperature. The experimental procedure was identical to that used in the study in the absence of O_2 (1). CF_2O and $OCF_2CFC(F)O$ were produced in nearly equal amounts under all operating conditions, though their absolute quantum yields varied markedly. Perfluorocyclopropene, which has been described previously (2), is produced in smaller quantities.

A possible reaction sequence[2] leading to products is

$$\begin{aligned}
&Hg + h\nu(2537\ \text{Å}) \rightarrow Hg^*\\
&Hg^* + 1,3\text{-}C_4F_6 \rightarrow 1,3\text{-}C_4F_6^*\\
&Hg^* + O_2 \rightarrow Hg + O_2^*\\
&O_2^* + 1,3\text{-}C_4F_6 \rightarrow O_2 + 1,3\text{-}C_4F_6^*\\
&1,3\text{-}C_4F_6^* + O_2 \rightarrow CF_2O_2 + C_3F_4 \rightarrow c\text{-}C_3F_4\\
&\qquad\qquad \rightarrow CF_2\ (\text{triplet}) + CF_2{=}CFC(F)OO\\
&CF_2\ (\text{triplet}) + O_2 \rightarrow CF_2O_2\\
&\qquad 2\ CF_2O_2 \rightarrow 2\ CF_2O + O_2
\end{aligned}$$

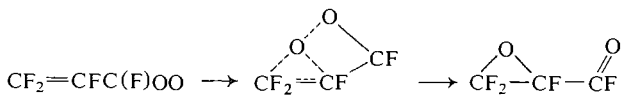

Other reactions which deactivate the excited states must also occur to account for the variation in quantum yields which varied from 0.1 to 0.8 for the major products under our experimental conditions, i.e. $[O_2] = 1.5$–100 Torr, $[1,3\text{-}C_4F_6] =$ 0.9–100 Torr, $I_a = 7.4 \times 10^{12} - 1.5 \times 10^{14}$ quanta/cc s. *It is clear that O_2 does not add across the double bonds in 1,3-C_4F_6*; if it did, no reasonable mechanism exists which leads to the observed products.

The molecular weight of $OCF_2CFC(F)O$ was obtained from vapor density measurements. Two determinations gave 145.7 and 143.0 which compare favorably to the theoretical value of 144. Further confirmation comes from the mass spectrum shown in Fig. 1. The peak of highest *m/e* is at 144 and all the cracking peaks are consistent with $C_3F_4O_2$. In fact no carbon–fluorine–oxygen molecule with a different empirical formula has a molecular weight of 144. The predominant cracking peaks corresponding to CFO^+, CF_2^+, and $C_2F_2O^+$ suggest the presence of these groups in the molecule. The peak corresponding to CF_3^+ must be a mass spectral rearrangement peak, since fluorine migration is not likely under the oxidation conditions employed. The presence of CF_3^+ is often found in mass spectra of compounds with no CF_3 groups (2).

[1]Present Address: Department of Chemistry, The Pennsylvania State University, University Park, Pennsylvania 16802.

[2]A referee has suggested that an alternative to intramolecular rearrangement in the biradical $CF_2{=}CFC(F)OO$ would be the addition of a second O_2, to give $O_2CF_2CF{=}CFO_2$ which could convert to $OCF_2CFC(F)O$ by reaction with other peroxide radicals, or by intramolecular elimination of O_2.

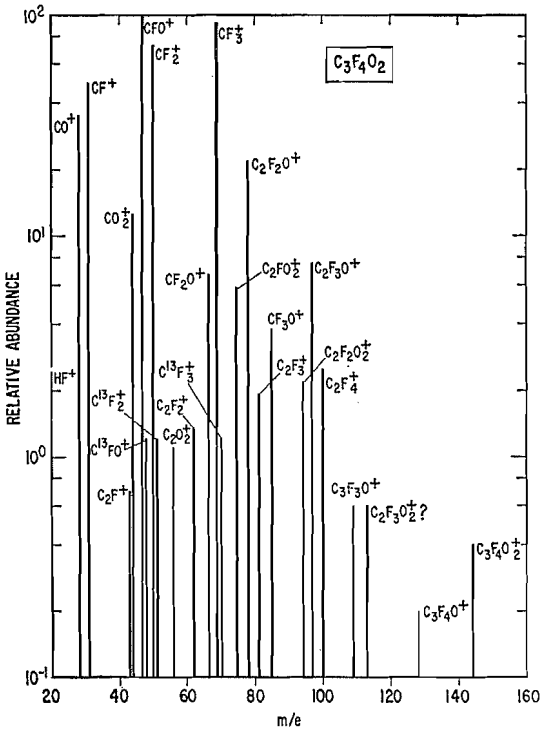

FIG. 1. Mass spectrum of $OCF_2CFC(F)O$ at 70 eV ionizing voltage.

Final confirmation of the structure comes from the i.r. spectrum, shown in Fig. 2. Bands appear at 5.35, 6.61, 7.72, 7.42, 8.65, 9.00, 9.84, 12.30, 13.00, and 13.82 μ. The strong band at 5.35 μ is characteristic of the —C(F)O group and the

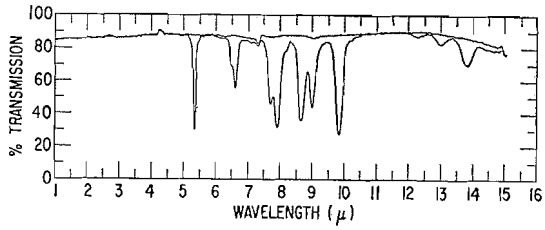

FIG. 2. Infrared spectrum of $OCF_2CFC(F)O$ taken at about 2 Torr pressure on a Beckman IR5A spectrometer.

weaker band at 6.61 μ can be identified with the perfluorinated epoxide group; e.g. the epoxide band in OCF_2CFCF_3 is at 6.45 μ (3).

The heat of vaporization of $OCF_2CFC(F)O$ was measured between −97 and −73 °C and found to be 6.9 kcal/mole with an extrapolated boiling point of 16 °C; the resulting Trouton's constant is 23.0.

Acknowledgment

This work was supported under U.S. Air Force contract No. 04(695)-1001 for which we are grateful.

1. W. STUCKEY and J. HEICKLEN. Can. J. Chem. **46**, 1361 (1968).
2. W. STUCKEY and J. HEICKLEN. J. Am. Chem. Soc. **90**, 3952 (1968).
3. J. HEICKLEN and T. JOHNSTON. J. Phys. Chem. **71**, 1391 (1967)

Can. J. Chem. Downloaded from www.nrcresearchpress.com by 84.22.46.98 on 09/08/12
For personal use only.

Can. J. Chem. Downloaded from www.nrcresearchpress.com by 210.87.254.5 on 09/05/12
For personal use only.

Canadian Journal of Chemistry

Published by THE NATIONAL RESEARCH COUNCIL OF CANADA

VOLUME 47 JULY 1, 1969 NUMBER 13

Nuclear magnetic resonance investigation of intermediates formed by the action of nucleophiles on substituted stilbenes

C. A. FYFE[1,2]

Department of Chemistry, University of British Columbia, Vancouver 8, British Columbia

Received September 18, 1968

A nuclear magnetic resonance investigation of the colored species formed by the action of bases on a series of α-cyano-4-nitro-4′-X-stilbenes characterizes these as the intermediate carbanions formed by the addition of base to the β-carbon atom of the double bond. The nuclear magnetic resonance spectra reveal that, whereas there is free rotation about the β-phenyl—Cβ and Cβ—Cα bonds in these adducts, there is restricted rotation around the α-phenyl—Cα bond due to very substantial delocalization of the negative charge into this ring. It has been verified that the same intermediates are formed by the action of bases on either the *cis* or *trans* isomers of α-cyano-4-nitrostilbene. The relation of these observations to the theory of alkene nucleophilic substitution reactions is discussed.

Canadian Journal of Chemistry, 47, 2331 (1969)

Introduction

Alkenes substituted by one more electronegative groups are susceptible to nucleophilic attack by a variety of bases (1). Almost all proposed mechanisms (1, 2) for alkene nucleophilic substitution reactions have the formation of the carbanion (**1**) as the first step [1], the particular products in a given reaction depending on the subsequent reaction of (**1**).

[1] 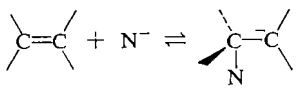

1

The color producing reactions between alkoxide ion and a large number of α-cyano-4,4′-disubstituted stilbenes have recently been investigated by Stewart and Kroeger using ultraviolet (u.v.) spectroscopy (5, 6). From the similarity between the u.v. spectra of the products formed from α-cyano-4-nitro-4′-X-stilbenes and those of the anion of 4-nitrophenylacetonitrile (5), and the general effect of substituents on the equilibrium (6), it was concluded that the colored species formed was the anion (**2**) formed by the addition of the alkoxide ion [2], and not (**3**) which would be formed by proton abstraction by the base [3]. It is known (1) that cleavage of α-cyanostilbenes can occur in basic media in the presence of labile hydrogens. Although the systems used were, as far as possible, anhydrous, in view of the general arguments used concerning the nuclear magnetic resonance (n.m.r.) data, consideration must be given to the possible occurrence of reaction [4] forming the anion of 4-nitrophenylacetonitrile.

Results and Discussion

The present investigation was of the intermediate formed by the attack of various nucleophiles on a series of α-cyano-4′-X-stilbenes. The substitution in the 4-position was purely for simplification of the n.m.r. spectra. For comparison, the anion of 4-nitrophenylacetonitrile was investigated under the same experimental conditions.

The n.m.r. spectra of the products of reactions corresponding to [2]–[4] would be expected to be quite different and diagnostic. Thus one would expect the product (**2**) to have an n.m.r.

[1]Killam Postdoctoral Fellow.
[2]Address as of August 1, 1969, Department of Chemistry, University of Guelph, Guelph, Ontario.

[2]

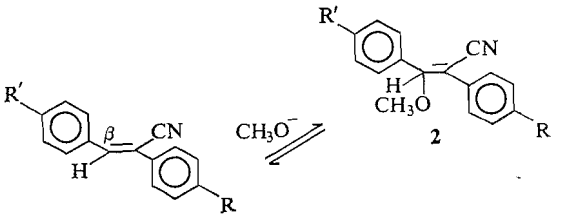

[3]

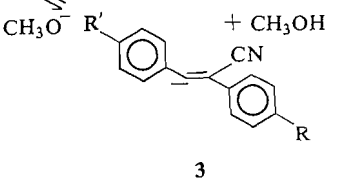

3

[4]

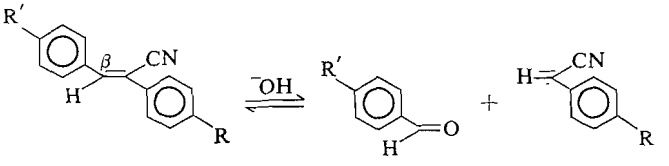

spectrum consisting of a 'normal' aromatic spectrum for the β-phenyl ring and a spectrum closely corresponding to the spectrum of the anion of 4-nitrophenylacetonitrile for the α-phenyl ring, but showing some variation with both nucleophile and substituents. There should be a large change in the chemical shift of Hβ from an alkene hydrogen at low field to an sp^3 hydrogen at higher field, whose chemical shift would be dependent on the nature of the nucleophile.

The spectra produced by reaction [4] would be similar to those from reaction [2], but in this case the complete spectrum should be *independent* of the nature of the nucleophile. Thus the α-phenyl ring should show exactly the spectrum of the anion of 4-nitrophenylacetonitrile with the methylene hydrogen at high field, and the β-phenyl ring the spectrum of 4-X-benyaldehyde, with the aldehydic proton at low fields and again independent of nucleophile.

The spectrum of compound (**3**) would be quite different, a critical feature being the complete lack of an absorption corresponding to the abstracted alkene proton Hβ.

The experimental results for the different systems are quite diagnostic and are discussed individually.

Section I: The Anion of 4-Nitrophenylacetonitrile

(a) By the Action of Anhydrous Sodium Methoxide in DMSO Solution

The addition of less than one equivalent of anhydrous sodium methoxide to a solution of 4-nitrophenylacetonitrile in DMSO causes the appearance of two new multiplets at higher fields, centered at $\delta = -7.39$ (relative intensity 2) and $\delta = -6.27$ (relative intensity 2), and a sharp singlet at $\delta = -3.95$ (relative intensity 1). These resonances can be assigned to the anion. The spectrum of the unreacted substrate is present simultaneously, indicating that under these conditions there is no significant anion–substrate exchange. However, in contrast to the spectrum of the ion which is quite sharp, that of the substrate is very broad and shows no fine structure whatsoever. This broadening is due to exchange with radicals produced in the system (the solutions show intense electron spin resonance absorptions[3]), but since there is no anion–substrate exchange, they do not affect the spectrum of the anion.

Addition of further quantities of methoxide

[3]The nature and reactions of these, and related radicals are at present under investigation.

Can. J. Chem. Downloaded from www.nrcresearchpress.com by 210.87.254.5 on 09/05/12
For personal use only.

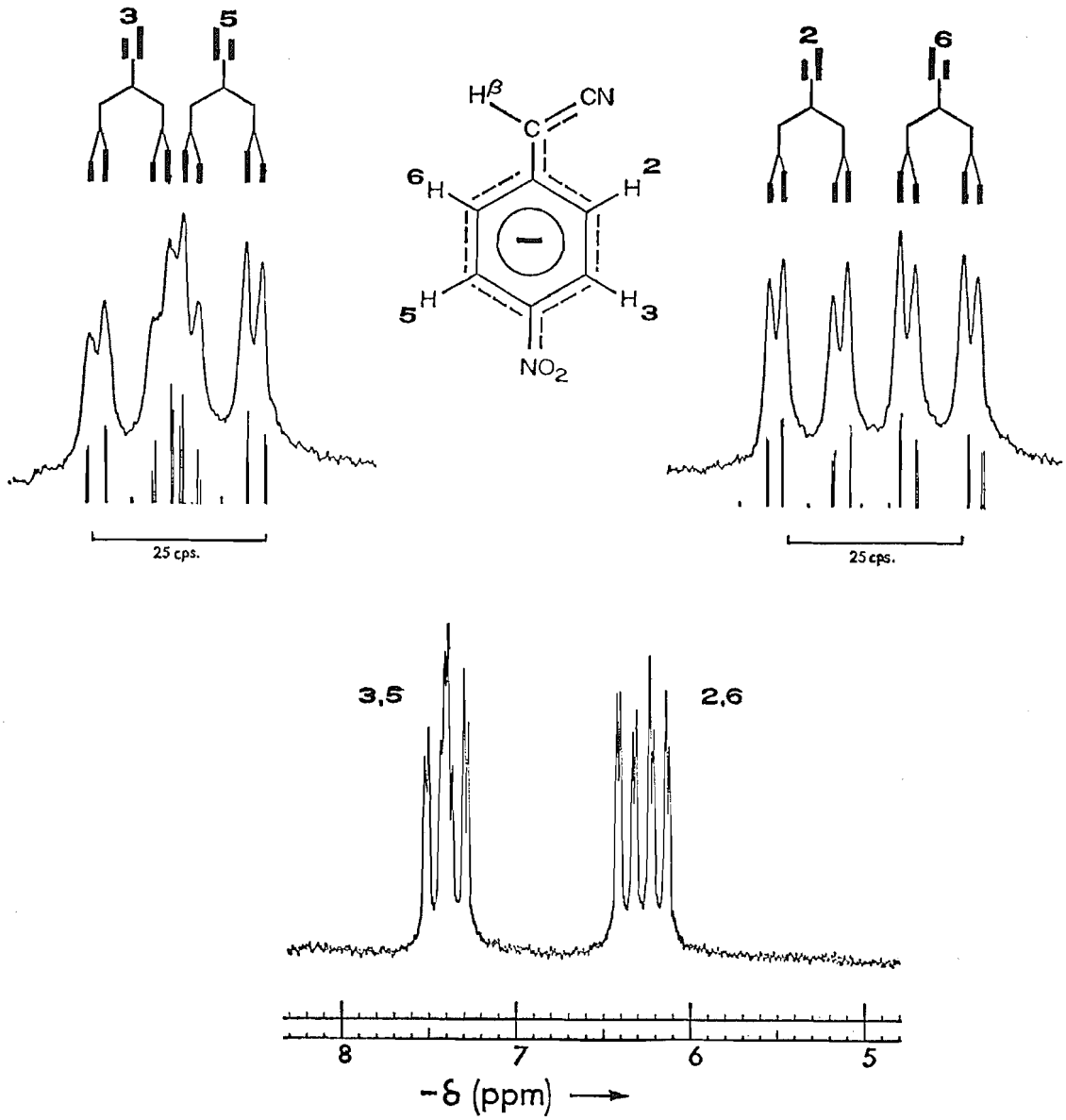

FIG. 1. The 100 MHz nuclear magnetic resonance spectrum of ring hydrogen resonances of 4-nitrophenylacetonitrile anion in DMSO solution with (inset) expended spectra of the multiplets and calculated spectra based on parameters given in the text.

increases the resonances of the ion and decreases those of the substrate until the spectrum shown in Fig. 1 is obtained. The major splittings in this spectrum are similar to those in the 100 MHz spectrum in 70% DMSO/30% MeOH solution recently observed by Crampton (7). The spectrum can be interpreted as an ABXY spectrum with $J_{2,3} = J_{5,6} = 9.0$ Hz, $J_{2,5} = J_{3,6} = 0.0$ Hz, $J_{2,6} = 2.3$ Hz, $J_{3,5} = 2.6$ Hz, $\nu_0\delta$ 3,5 = 13.0 Hz, and $\nu_0\delta$ 2,6 = 19.0 Hz, as shown in Fig. 1. The non-equivalence within the two pairs of ring protons is due (7) to restricted rotation about the (phenyl—carbon) bond. Similar conclusions have been drawn from the spectrum of the

Can. J. Chem. Downloaded from www.nrcresearchpress.com by 210.87.254.5 on 09/05/12
For personal use only.

Can. J. Chem. Downloaded from www.nrcresearchpress.com by 210.87.254.5 on 09/05/12
For personal use only.

anion of *N*-methylpicramide (8, 9). Although a reasonable assignment can be made on a first-order basis as shown in Fig. 1, the calculated spectrum shows that in fact that situation is more complex. Second-order effects will become more important in cases where the chemical shift differences within the AB and XY multiplets become smaller.

The non-observation by Crampton (7) of the smaller 2,6 and 3,5 couplings may be due to a small amount of anion–substrate exchange under the conditions of his experiment as this system contains 30% MeOH. There is no evidence for any exchange of this type under the conditions of the present experiments. There is, however, exchange between the substrate and anion radicals produced in the system, as evidenced by the extreme broadening of the spectrum of unreacted 4-nitrophenylacetonitrile. In general, this exchange reaction will greatly simplify spectra of ions produced under these conditions by effectively removing the spectrum of any unreacted aromatic material.

The observation of the n.m.r. spectra of ions in general will only be evidence for the absence of radicals where it can also be shown that ion substrate exchange exists.

(b) By the Action of Anhydrous Sodium Methoxide in Acetone Solutions

The addition of anhydrous sodium methoxide to an acetone solution of 4-nitrophenylacetonitrile did not give rise to an n.m.r. spectrum corresponding to that observed in the previous section, although some coloration was produced. The anion was, however, produced by the addition of anhydrous sodium methoxide to a solution of 4-nitrophenylacetonitrile in a solvent system of 80% acetone – 20% DMSO. The spectrum was similar to that in Fig. 1, but showed minor changes with the change in solvent. The two multiplets were centered at $\delta = -6.25$ p.p.m. and $\delta = -7.37$ p.p.m. with $J_{2,3} = J_{5,6} = 8.9$ Hz, $J_{2,5} = J_{3,6} = 0.0$ Hz, $J_{2,6} = 2.1$ Hz, $J_{3,5} = 2.5$ Hz, $V_{o\delta}$ 2,6 = 23.5 Hz, $V_{o\delta}$ 3,5 = 13.5 Hz. Again there was pronounced broadening of the spectrum of the substrate, due to the presence of radicals.

Section II: Intermediates Produced by the Action of Bases on α-Cyano-4-nitro-4′-methoxystilbene

(a) By Addition of Methoxide Ion

The addition of anhydrous sodium methoxide to a DMSO solution of the above stilbene gives an intense violet-pink coloration (λ_{max} 550 mμ) and causes the broadening and eventual disappearance of the spectrum of the stilbene and the appearance of a new spectrum at higher fields (Fig. 2). The new spectrum consists of an AA′XX′ pattern centered at $\delta = -6.95$ (relative intensity 4), two multiplets centered at $\delta = -7.34$ (doublet, relative intensity 2), and $\delta = -6.38$ (approximately a triplet with further splitting, relative intensity 2), and a sharp singlet at $\delta = -5.01$ (relative intensity 1). The spectrum is consistent with the formation of the intermediate (**4**), R = OCH_3, as shown in Fig. 2.

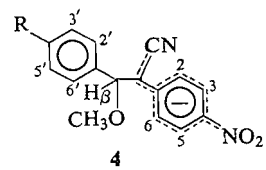

4

It is inconsistent with the occurrence of either reactions [3] or [4]. Thus the AA′XX′ pattern can be assigned to the four hydrogens on the β-phenyl ring and the singlet at $\delta = -5.01$ to the Hβ proton. The shifts of other two multiplets correspond very closely to those observed for the ring hydrogens of 4-nitrophenylacetonitrile anion, although the multiplet structures are different, and can be assigned to the four hydrogens of the α-phenyl ring. That these do not form a simple AA′XX′ system suggests that, as in the case of the 4-nitrophenylacetonitrile anion, there is restricted rotation around the α-phenyl—Cα bond, the complexity of the resonance at $\delta = -6.38$ arising because $J_{2,3} = V_{o\delta}$ 2,6. This, and the very large changes in the chemical shifts of the α-phenyl resonances suggest very substantial delocalization of the negative charge into the α-phenyl ring, so that the complex is probably more properly formulated as in (**4**), rather than with the negative charge localized on the α-carbon atom as is usually done. This is thought to be the case for all the compounds studied. Such a delocalization would be favored by a planar rather than a tetrahedral configuration at the α-carbon atom, and it is possible that this is the case for stilbenes with very electronegative groups in the 4-position.

The sharpness of the Hβ resonance would suggest that there is free rotation round the Cα—Cβ bond, as required for such intermediates

Can. J. Chem. Downloaded from www.nrcresearchpress.com by 210.87.254.5 on 09/05/12
For personal use only.

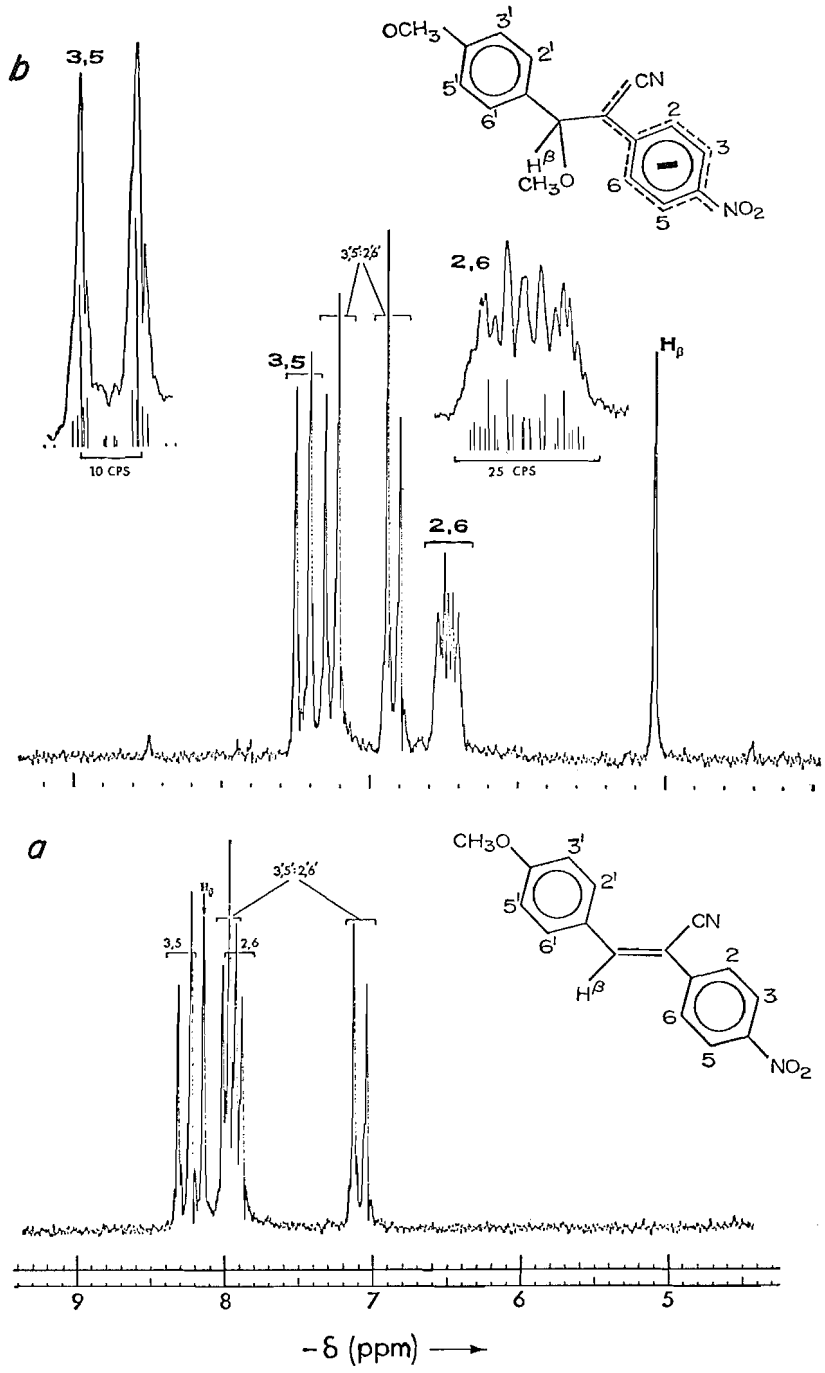

FIG. 2. The 100 MHz nuclear magnetic resonance spectra of (*a*) α-cyano-4-nitro-4′-methoxystilbene in DMSO solution and (*b*) this solution after the addition of anhydrous sodium methoxide

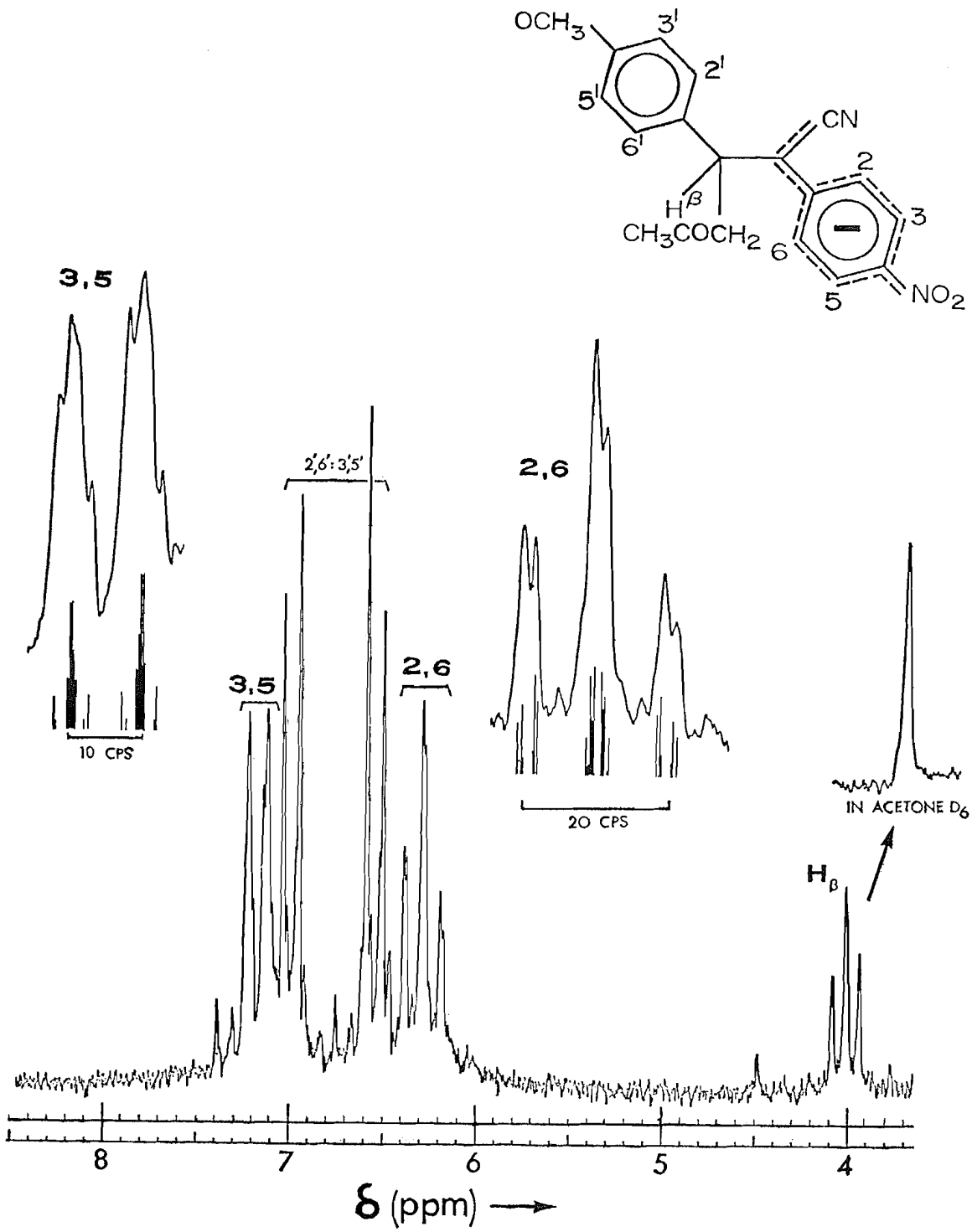

FIG. 3. The 100 MHz nuclear magnetic resonance spectrum of a solution of α-cyano-4-nitro-4′-methoxystilbene in acetone, after the addition of anhydrous sodium methoxide.

Can. J. Chem. Downloaded from www.nrcresearchpress.com by 210.87.254.5 on 09/05/12
For personal use only.

Can. J. Chem. Downloaded from www.nrcresearchpress.com by 210.87.254.5 on 09/05/12
For personal use only.

to take part in the *cis–trans* isomerization of alkenes (11).[4]

The solutions are quite stable for several days.

(b) By Addition of Acetone Anion

The addition of anhydrous sodium methoxide to a solution of α-cyano-4-nitro-4′-methoxystilbene in acetone gives rise to an intense coloration (λ_{max} 543 mμ, 576 mμ) and causes the broadening and disappearance of the stilbene spectrum and the appearance of a new spectrum at high fields (Fig. 3). This is similar in general appearance to that in Section II*a*, but different in several significant respects. The spectrum can be rationalized in terms of the intermediate (**5**) R = OCH_3 as shown in Fig. 3. The postulated addition of the acetone anion to the stilbene double bond may not be by direct attack, but by solvolysis of the methoxy adduct (**4**) R = OCH_3. An identical spectrum can be obtained by the addition of acetone to a DMSO solution of (**4**) R = OCH_3.

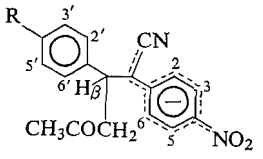

5

The spectrum is again inconsistent with the occurence of reactions [3] or [4]. The AA′XX′ spectrum of the β-phenyl ring is centered at δ = −6.87 and the multiplets corresponding to H_2, H_6 and H_3, H_5 occur at δ = −6.47 "triplet" (relative intensity 2) and δ = −7.35 "doublet" (relative intensity 2). The shift values of the α-phenyl ring hydrogens are very similar to those observed for the anion of 4-nitrophenylacetonitrile although the multiplet structures are again different. The complexity of the multiplets indicate restricted rotation about the α-phenyl—Cα bond, and a structure close to that of the methoxy adduct. That they are not exactly the same as those of the methoxy adduct is evidence against the occurrence of reaction [4].

The absorption at δ = −4.17 assigned to Hβ is now a triplet (relative intensity 1, J = 3.7 Hz), due to coupling with the two methylene hydrogens of the acetone moiety. Generation of the adduct in acetone-d_6 causes this resonance to collapse to a broad singlet (Fig. 3, inset), confirming the assignment of Hβ. In structures of type (**5**), Cβ is an asymmetric carbon atom and, in principle, Hβ could give a more complicated absorption than the simple triplet observed due to the effect of the asymmetric center on the methylene protons. The complete assignment of the spectrum is given in Table II.

The spectrum is unchanged over several days. In particular, there is no change in the triplet splitting of Hβ. It has been suggested (10) that adducts formed by nucleophiles with active methylene groups may undergo an isomerization involving hydrogen transfer, to form a carbanion with the nucleophile to give, in this case, compound (**6**) R = OCH_3. This would be expected to have quite a different n.m.r. spectrum from (**5**) R = OCH_3. The lack of change in the spectrum observed here suggests that there is no fast conversion of (**5**) into (**6**) to any appreciable extent.

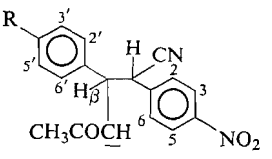

6

Section III: Intermediates Produced by the Action of the Bases on α-Cyano-4-nitro-4′-methylstilbene

(a) Addition of Methoxide Ion

Treatment of a DMSO solution of α-cyano-4-nitro-4-methylstilbene with methoxide causes similar changes in the u.v. and n.m.r. spectra to those described in the previous section. The n.m.r. spectrum is in accordance with the formation of (**4**), R = CH_3 as indicated in Fig. 4. Although this spectrum is similar in general appearance to that observed in Section II*a* (Fig. 2), there are significant differences, especially in the resonances ascribed to the α-phenyl ring hydrogens (inset). These differences argue strongly that an intermediate is being formed in each case, and eliminate further the possibility of breaking of the Cα—Cβ bond via reaction [4].

[4]This observation is also consistent with either the Hβ proton resonances having identical chemical shifts in the different conformers or the system being entirely in one fixed conformation, but these are considered less likely as they would have to be the case for all the compounds studied.

Can. J. Chem. Downloaded from www.nrcresearchpress.com by 210.87.254.5 on 09/05/12
For personal use only.

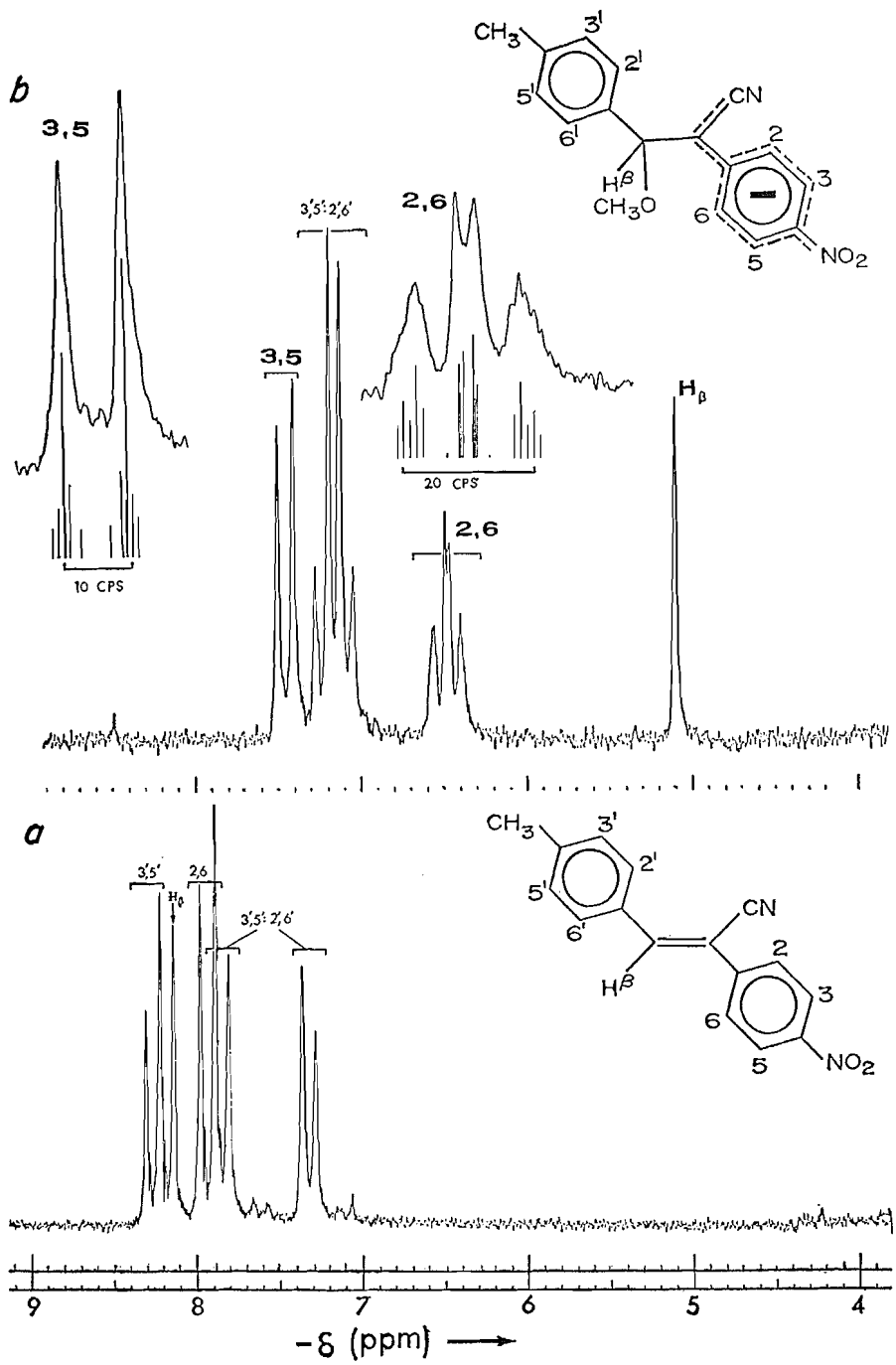

FIG. 4. The 100 MHz nuclear magnetic resonance spectra of (*a*) α-cyano-4-nitro-4′-methylstilbene in DMSO solution, and (*b*) this solution after the addition of anhydrous sodium methoxide.

Can. J. Chem. Downloaded from www.nrcresearchpress.com by 210.87.254.5 on 09/05/12
For personal use only.

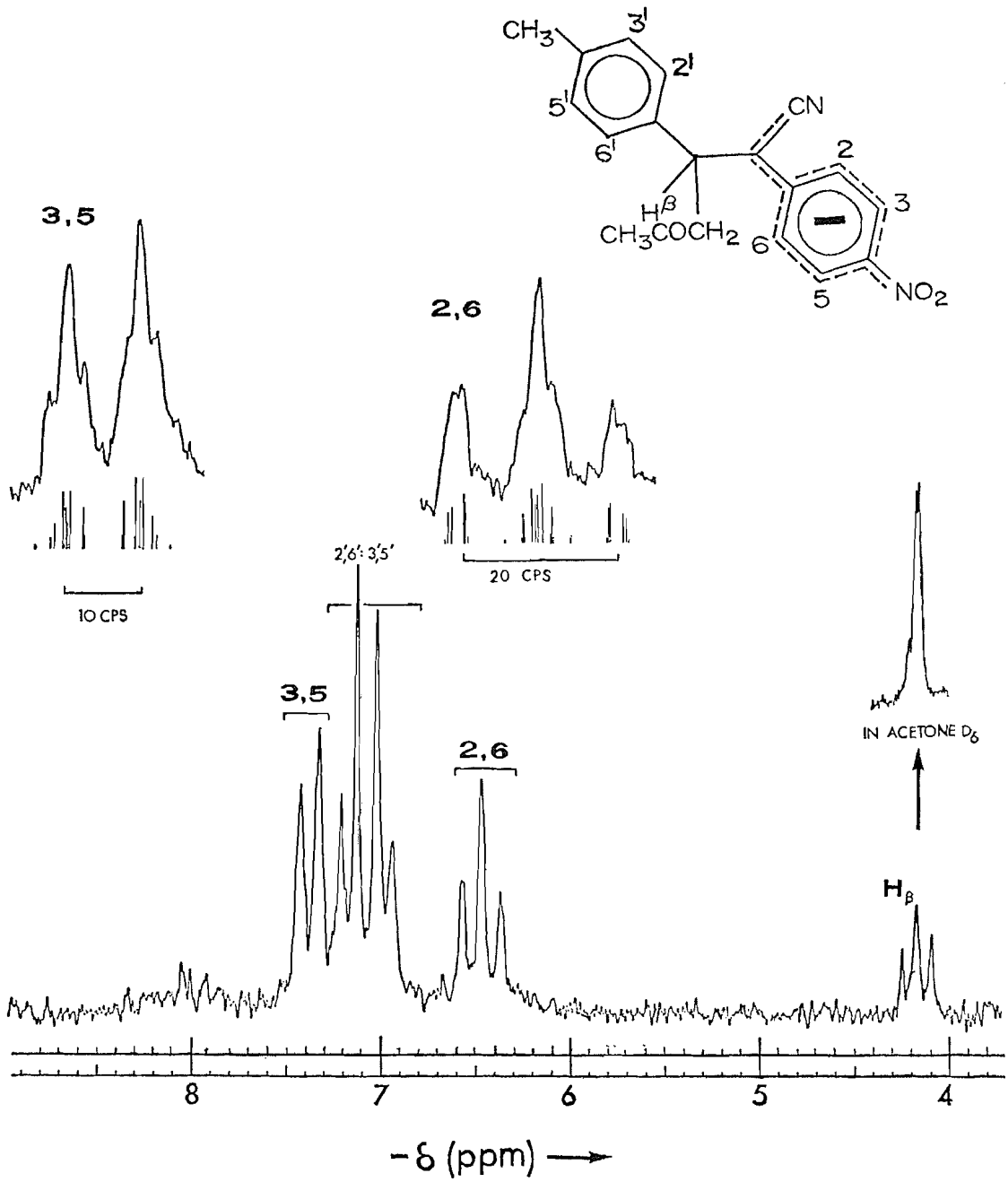

FIG. 5. The 100 MHz nuclear magnetic resonance spectrum of a solution of α-cyano-4-nitro-4′-methylstilbene in acetone after the addition of anhydrous sodium methoxide.

Can. J. Chem. Downloaded from www.nrcresearchpress.com by 210.87.254.5 on 09/05/12
For personal use only.

TABLE I*

Chemical shift data ($-\delta$, p.p.m.), coupling constants (Hz), and chemical shift differences (Hz) from the 100 MHz nuclear magnetic resonance spectra of compounds of general formula (**4**) in DMSO solution

R	Hβ	H 2,6†	$\nu_0\delta$ 2,6	$J_{2,6}$	$J_{2,3}$:$J_{5,6}$	$J_{3,5}$	$\nu_0\delta$ 3,5	H 3†,5	β Phenyl ring§
OCH_3	5.0_1	6.38	5.0±0.5	2.5±0.4	9.5±0.5	1.8±0.3	0.0±0.5	7.34	AA′ XX′ system
CH_3	5.09	6.44	8.5±0.5	2.1±0.3	9.5±0.5	1.8±0.3	0.0±0.5	7.45	AA′ BB′ system
NO_2‡	5.36	6.56	18 ±0.5	—	10.0±0.5	—	—	7.50	AA′ XX′ system
H	5.16	6.51	9.5±0.3	2.3±0.3	10 ±0.3	1.8±0.3	0.5±0.4	7.47	Unresolved multiplet

†Denotes multiplet center.
‡Owing to radical exchange broadening, only the major splittings were properly resolved.
§Assignment of lines indicated in figures.

TABLE II*

Chemical shift data ($-\delta$, p.p.m.), coupling constants (Hz), and chemical shift differences (Hz) from the 100 MHz nuclear magnetic resonance spectra of compounds of general formula (**5**) in acetone solution

R	Hβ	H 2,6†	$\nu_0\delta$ 2,6	$J_{2,6}$	$J_{2,3}$:$J_{5,6}$	$J_{3,5}$	$\nu_0\delta$ 3,5	H 3†,5	β Phenyl ring§
OCH_3	4.17	6.47	9.0±0.5	1.7±0.3	9.5±0.5	1.8±0.3	1.0±0.5	7.35	AA′ XX′ system
CH_3	4.15	6.48	11.5±0.6	1.7±0.3	9.5±0.5	1.8±0.3	2.0±0.5	7.36	AA′ BB′ system
NO_2‡	4.27	6.40	14 ±0.6	—	9.5±0.5	—	—	7.34	AA′ XX′ system
H	4.25	6.52	9.5±0.5	1.7±0.3	10.0±0.5	1.8±0.3	1.0±0.5	7.40	Unresolved multiplet

†Denotes multiplet center.
‡Owing to radical-exchange broadening, only the major splittings were properly resolved.
§Assignments of lines indicated in figures.

*NOTE: The data is presented in this way because it is felt that, in general, in a system of this complexity, no one assignment can be regarded as entirely unambiguous, and in these particular spectra, the ratio of observed peaks to possible transitions is so low that the presentation of absolute chemical shift values from the data would not be meaningful. However, calculated spectra from this data agree reasonably well with those observed experimentally both at 100 MHz (as shown inset in the figures) and also at 60 MHz, (although in these spectra the signal/noise ratio was much worse). None of the multiplets can be interpreted in terms of an AA′ XX′ spectrum. The errors given indicate the approximate variation in the parameters which still gives approximate agreement with the observed spectrum, all the other parameters being kept constant at the values in the Tables I and II.

Can. J. Chem. Downloaded from www.nrcresearchpress.com by 210.87.254.5 on 09/05/12
For personal use only.

(b) Addition of Acetone Anion

Base addition to an acetone solution of the stilbene as in Section II*b* causes intense coloration (λ_{max} 543 mμ, 576 mμ) and the appearance of a new n.m.r. spectrum, ascribed to (**5**), R = CH_3 as shown in Fig. 5. The complete assignment is given in Table II. Again it is thought that the differences in the multiplets assigned to the α-phenyl ring hydrogens in Figs. 3 and 5 are evidence that the spectral changes are not caused by reaction [4].

Section IV: Intermediates formed by the Action of Bases on α-Cyano-4-nitro-4′-nitrostilbene

The addition of anhydrous methoxide to solutions of this stilbene in DMSO or acetone gives rise to spectra which can be assigned to (**4**), R = NO_2 (λ_{max} 555 mμ) and (**5**), R = NO_2 (λ_{max} 550 mμ, 510 mμ) respectively. The complete assignments of the n.m.r. spectra are given in Tables I and II. In the case of this particular stilbene, the assignment of the resonances of the two rings is made unambiguous by the broadening and gradual disappearance of the resonances of the β-phenyl ring while the rest of the spectrum is only slightly broadened.

These changes are probably due to the formation of anion radicals on the β-phenyl ring, which in this particular complex is very electronegative. Electron transfer exchange of this radical with the complex will cause the disappearance of the β-phenyl resonances but would affect the α-phenyl resonances only slightly as an extremely small electron density would be expected in this ring in the radical due to repulsion by the negative charge already localized there.

Section V: Intermediates Produced by the Action of Bases on cis- and trans-α-Cyano-4-nitrostilbene

An important test of the conclusions drawn in the previous sections, and one directly connected to the theory of base-catalyzed *cis–trans* isomerizations (1, 3, 4) is that, if the species observed here do have the proposed structures, then the same species should be formed from both *cis* and *trans* isomers, giving consequently identical n.m.r. spectra.

(a) Addition of Methoxide Ion

Addition of anhydrous sodium methoxide to a solution of either *cis*- or *trans*-α-cyano-4-nitrostilbene in DMSO, produces an intense coloration (λ_{max} 547 mμ) and a new n.m.r. spectrum at higher fields than those of either of the stilbenes. The two spectra are absolutely identical, and can be rationalized in terms of (**4**), R = H as indicated in Fig. 6*a*. The number of peaks resolved in this spectrum makes it unlikely that the correspondence in the two spectra is a fortuitous one, and the spectrum is considered good evidence that the same compound is being formed in both instances. The resonances ascribed to Hβ and the α-phenyl ring hydrogens correlate well with the results of previous sections (Table I).

(b) Addition of Acetone Anion

The addition of anhydrous sodium methoxide to a solution of either *cis*- or *trans*-α-cyano-4-nitrostilbene in acetone gives a bright pink-violet coloration (λ_{max} 542 mμ, 578 mμ) and again gives rise to identical spectra from both isomers. This spectrum is in agreement with the formation of (**5**) (R = H), in both cases as indicated in Fig. 6*b*. Again, it is thought that the resolution of the spectrum is sufficient to make a fortuitous agreement extremely unlikely.

In this spectrum, Hβ does not appear as a simple triplet, but shows a splitting of the center peak due to slightly different couplings (J_1 = 3.4 Hz, J_2 = 4.1 Hz) from the methylene hydrogens caused by the asymmetry at Cβ. The multiplet collapses to a broad singlet in acetone-d_6.

Although the observation of identical spectra from both isomers in these two cases does not constitute proof as to the nature of the complexes formed, it is *required* by the suggestion that these have the structures (**4**) and (**5**) and, if this is the case, has direct relevance to the theory of *cis–trans* isomerizations referred to earlier.

In general, the various aspects of the n.m.r. spectra produced by the attack of bases on the substituted stilbenes can all be interpreted in terms of the general structure corresponding to (**1**). If this interpretation is correct, then the results would suggest that the intermediates are quite stable compounds (at least in solution). The n.m.r. spectra reveal restricted rotation around the α-phenyl—Cα bond in all the complexes and delocalization of the negative charge into the α-phenyl ring, suggesting perhaps the favoring of a planar configuration at this carbon atom.

The above effects will, in general, be very

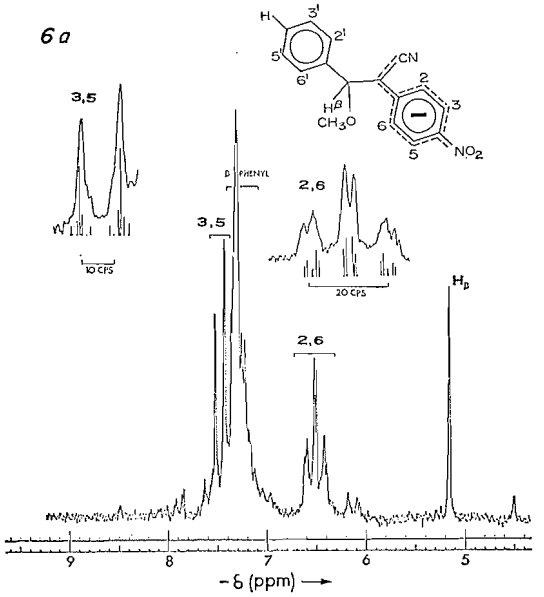

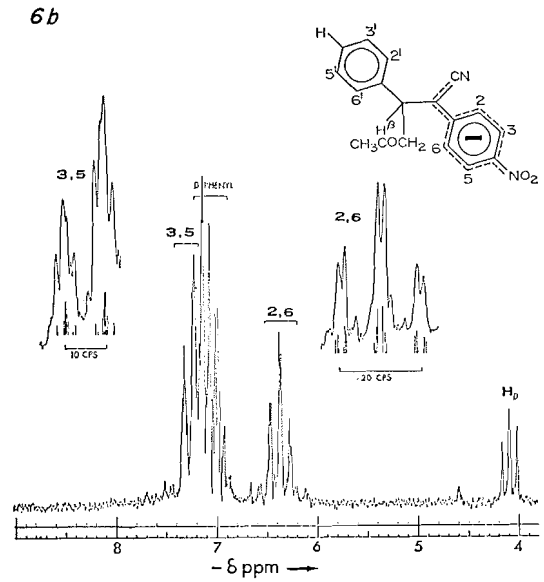

FIG. 6.(*a*) The 100 MHz nuclear magnetic resonance spectrum of a DMSO solution of *trans*-α-cyano-4-nitrostilbene after the addition of anhydrous sodium methoxide (the *cis* isomer gives an identical spectrum).

FIG. 6.(*b*) The 100 MHz nuclear magnetic resonance spectrum of an acetone solution of *cis*-α-cyano-4-nitrostilbene after the addition of anhydrous sodium methoxide (the *trans* isomer gives an identical spectrum).

dependent on the nature and position of substituents in the α-phenyl ring, but it is thought that the results obtained from these more activated substrates may be of general applicability.

Experimental

The n.m.r. spectra were recorded at 60 MHz on a Varian A60 spectrometer and at 100 MHz on a Varian HA100 spectrometer. Theoretical spectra were calculated using a copy of the n.m.r. program "TWOSUM" originally written by Dr. J. Martin which was available in this department. The program was used in its non-itterative mode. The u.v. spectra were measured on a Beckman S.P. 800 spectrophotometer.

The chemicals used were either from commercial sources or prepared by literature methods, and on purification gave melting points in agreement with published values: *p*-nitrophenylacetonitrile was a purified sample supplied by Eastman–Kodak, α-cyano-4-nitro-4′-methoxystilbene and α-cyano-4-nitro-4′-methylstilbene were generous gifts from Dr. R. Stewart (U.B.C.). The other stilbenes were prepared by the methods indicated: α-cyano-4-nitro-4′-nitrostilbene (11), *trans*-α-cyano-4-nitrostilbene (12), *cis*-α-cyano-4-nitrostilbene (13). Anhydrous grade DMSO supplied by Matheson, Coleman and Bell was distilled from calcium hydride and stored over Linde 5A molecular sieve.

Acknowledgments

The author would like to acknowledge the help given by Miss P. A. Watson in the measurement of the 60 MHz n.m.r. spectra; and Drs. R. Foster, L. D. Hall, and R. Stewart for helpful advice and discussion; also the help given by Professor C. A. McDowell during this work; the Department of Chemistry for the provision of facilities; and the University of British Columbia for the award of a Killam Postdoctoral Fellowship.

1. S. PATAI and A. RAPPOPORT. *In* The chemistry of the alkenes. *Edited by* S. Patai. Interscience Publishers, Inc., London. 1964. Chap. 8.
2. S. PATAI and Z. RAPPOPORT. J. Chem. Soc. 377 (1962).
3. Z. RAPPOPORT, C. DEGANI, and S. PATAI. J. Chem. Soc. 4513 (1963).
4. S. PATAI and Z. RAPPOPORT. J. Chem. Soc. 396 (1962).
5. D. J. KROEGER and R. STEWART. Can. J. Chem. **45**, 2163 (1967).
6. R. STEWART and D. J. KROEGER. Can. J. Chem. **45**, 2173 (1967).
7. M. R. CRAMPTON. J. Chem. Soc. B, 85 (1967).
8. K. L. SERVIS. J. Am. Chem. Soc. **87**, 5495 (1965).
9. M. R. CRAMPTON and V. GOLD. J. Chem. Soc. B, 893 (1966).
10. S. PATAI and A. RAPPOPORT. *In* The chemistry of the alkenes. *Edited by* S. PATAI. Interscience Publishers, Inc., London. 1964. p. 508.
11. R. MERCKX. Bull. Soc. Chim. Belges. **58**, 460 (1949).
12. A. SCHONNE, E. BRAYE, and A. BRUYLANTS. Bull. Soc. Chim. Belges. **62**, 155 (1953).
13. P. SCHMID. United States Atomic Energy Comm. VCRL 8883, 114, (1959).

Can. J. Chem. Downloaded from www.nrcresearchpress.com by 210.87.254.5 on 09/05/12
For personal use only.

Can. J. Chem. Downloaded from www.nrcresearchpress.com by 210.87.254.42 on 09/05/12
For personal use only.

Synthesis of acetylenic diols

SHOJI WATANABE, KYOICHI SUGA, AND TOSHIMITSU SUZUKI
Department of Applied Chemistry, Faculty of Engineering, Chiba University, Yayoicho, Chiba, Japan

Received February 6, 1969

Lithium naphthalene reacts with acetylenic carbinol, such as 3-methyl-1-butyn-3-ol or propargyl alcohol, to give the corresponding dilithio compounds. The reaction of these dilithio compounds with various ketones gives the corresponding acetylenic diols in good yield. By the new convenient one-step procedure for chain-lengthening, various acetylenic diols can be prepared from two kinds of ketones and acetylene using lithium naphthalene.

Canadian Journal of Chemistry, 47, 2343 (1969)

Synthesis of acetylenic diols is achieved by the interaction of acetylenic Grignard reagents or lithium derivatives of acetylenic compounds with carbonyl compounds: for example, 1-(1′-hydroxylcyclohexan-1′-yl)-3-methyl-1-pentyn-3-ol (**5**) can be prepared by the action of the dimagnesium bromide of ethynylcyclohexanol (**2**) with methyl ethyl ketone (**4**). When cyclohexanone (**1**) is used as the starting material, two reactions, namely the ethynylation of **1** and the Grignard reaction of **2** with **4**, are necessary for the preparation of **5**.

Recently, it was reported by us that lithium naphthalene in tetrahydrofuran solution is an excellent agent for the oligomerization of conjugated dienes (1–2). The previous paper indicated that α,β-unsaturated ketones react with various alkylacetylenes in the presence of lithium naphthalene in a tetrahydrofuran solution (3). This article concerns new convenient procedures for the preparation of acetylenic diols using lithium naphthalene under mild conditions. The authors have now found two such procedures for the preparation of long-chain acetylenic diols.

Thus, one mole of compound **2** was dropped very slowly into a solution of lithium naphthalene (two moles of lithium) and this underwent reaction for several hours to give the dilithio derivatives (**3**) of compound **2**. One mole of **4** was added to this solution and an acetylenic diol (**5**) was obtained in 60% yield. The composition ($C_{12}H_{20}O_2$) was confirmed by an elementary analysis. The infrared (i.r.) absorption spectrum showed characteristic bands of the tertiary alcohol group at 3440 and 1060 cm^{-1}. The absorptions of a terminal ethynyl group at 3320 and 2120 cm^{-1} disappeared. The nuclear magnetic resonance (n.m.r.) spectrum showed the signals of methyl protons ($-CH_2-CH_3$) at 1.02 p.p.m., methyl protons of $-\overset{\displaystyle CH_3}{\underset{\displaystyle OH}{\overset{|}{\underset{|}{C}}}}-$ at 1.45 p.p.m., methylene protons at 1.2–1.9 p.p.m., and hydroxyl protons at 2.18 p.p.m. These results indicated that this diol (**5**) was 1-(1′-hydroxylcyclohexane-1′-yl)-3-methyl-1-pentyn-3-ol. Similarly, various

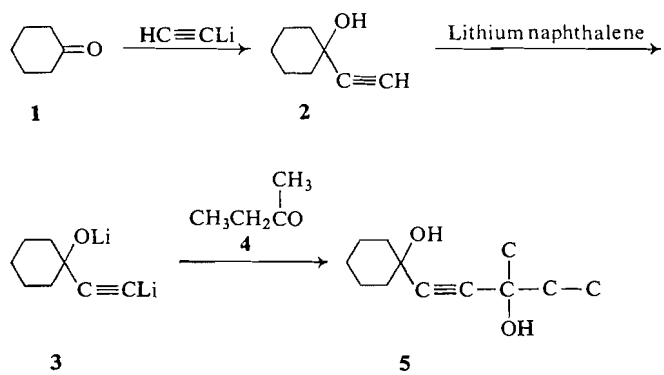

Can. J. Chem. Downloaded from www.nrcresearchpress.com by 210.87.254.42 on 09/05/12
For personal use only.

TABLE I

Reaction of ketones with acetylenic carbinols

Acetylenic carbinol	Ketone	Product*	Yield (%)	Boiling point (°C/10^{-3} Torr)	Infrared absorption spectra (cm^{-1})
Propargyl alcohol	Mesityloxide	4,6-Dimethyl-5-hepten-2-yn-1,4-diol	50	80–90	3420, 1060, 820
	Cyclohexanone	1-(1′-Hydroxylcyclohexan-1′-yl)-1-propyn-3-ol	50	130–140	3440, 1040
	Citral	6,10-Dimethyl-5,9-undecadien-2-yn-1,4-diol	37	80–110	3440, 1030, 830
	β-Ionone	1-(2′,6′,6′-Trimethyl-1′-cyclohexen-1′-yl)-3-methyl-1-hexen-4-yn-3,6-diol	50	130–150	3440, 1040, 970, 745
3-Methyl-1-butyn-3-ol	Methyl ethyl ketone	2,5-Dimethyl-3-heptyn-2,5-diol	80	80–90	3400, 1030
	Cyclohexanone	1-(1′-Hydroxylcyclohexan-1′-yl)-3-methyl-1-butyn-3-ol	60	100–110	3400, 1070
	Pulegone	1-(1′-Hydroxyl-2′-isopropyliden-5′-methyl-cyclohexan-1′-yl)-3-methyl-1-butyn-3-ol	32	110–120	3400, 1040
	Acetophenone	2-Phenyl-5-methyl-3-hexyn-2,5-diol	30	120–130	3440, 1040, 750, 690
	β-Ionone	1-(2′,6′,6′-Trimethyl-1′-cyclohexen-1′-yl)-3,6-dimethyl-1-hepten-4-yn-3,6-diol	50	130–150	3440, 1030, 970
	α-Ionone	1-(2′,6′,6′-Trimethyl-2′-cyclohexen-1′-yl)-3,6-dimethyl-1-hepten-4-yn-3,6-diol	44	130–150	3440, 1040, 970, 830
Ethynylcyclohexanol	Methyl ethyl ketone	1-(1′-Hydroxylcyclohexan-1′-yl)-3-methyl-1-pentyn-3-ol	50	100–120	3440, 1060
3,7,11-Trimethyl-1-dodecen-3-ol	Methyl ethyl ketone	3,6,10,14-Tetramethyl-4-pentadecyn-3,6-diol	70	110–130	3440, 1040, 740
Ethynyl-β-ionol	Methyl ethyl ketone	1-(2′,6′,6′-Trimethyl-1′-cyclohexen-1′-yl)-3,6-dimethyl-1-octen-4-yn-3,6-diol	55	130–150	3420, 1040, 970, 750

*Elementary analyses of carbon and hydrogen agreed with the calculated data.

Can. J. Chem. Downloaded from www.nrcresearchpress.com by 210.87.254.42 on 09/05/12
For personal use only.

TABLE II

Preparation of acetylenic diols from acetylene and two kinds of ketones

Ketone (1)*	Ketone (2)*	Product†	Yield (%)	Boiling point (°C/10^{-3} Torr)	Infrared absorption spectra (cm^{-1})
Acetone	Acetone	2,5-Dimethyl-3-hexyn-2,5-diol	20	75–90	3420, 1010
Acetone	Cyclohexanone	1-(1′-Hydroxyl-cyclohexan-1′-yl)-3-methyl-1-butyn-3-ol	30	110–115	3400, 1070
Cyclohexanone	Acetone	1-(1′-Hydroxyl-cyclohexan-1′-yl)-3-methyl-1-butyn-3-ol	50	110–115	3400, 1070
Cyclohexanone	Methyl ethyl ketone	1-(1′-Hydroxyl-cyclohexan-1′-yl)-3-methyl-1-pentyn-3-ol	52	100–120	3440, 1060
β-Ionone	Methyl ethyl ketone	1-(2′,6′,6′-Trimethyl-1′-cyclohexen-1′-yl)-3,6-dimethyl-1-octen-4-yn-3,6-diol	50	130–150	3420, 1040, 970, 750
Acetophenone	Acetone	2-Phenyl-5-methyl-3-hexyn-2,5-diol	50	100–110	3440, 1040, 750, 690
Citral	Acetone	2,7,11-Trimethyl-6,10-dodecadien-3-yn-2,5-diol	39	110–130	3440, 1040, 830
β-Ionone	Acetophenone	1-(2′,6′,6′-Trimethyl-1′-cyclohexen-1′-yl)-6-phenyl-1,6-dimethyl-1-hexen-4-yn-3,6-diol	30	150	3440, 1040, 970, 750, 690
β-Ionone	β-Ionone	1,8-*bis*-(2′,6′,6′-Trimethyl-2′-cyclohexen-1′-yl)-3,6-dimethyl-1,7-octadien-4-yn-3,6-diol	39	160–180	3440, 1040, 970
α-Ionone	Methyl ethyl ketone	1-(2′,6′,6′-Trimethyl-2′-cyclo-hexen-1′-yl)-3,6-dimethyl-1-octen-4-yn-3,6-diol	24	130–150	3440, 1040, 830

*At first, ketone 1 was reacted with acetylene and continually ketone 2 was reacted.
†Elementary analyses of carbon and hydrogen agreed with the calculated data.

TABLE III

Effect of various metallating agents* on the preparation of 1-(1′-hydroxylcyclohexyl-1′-yl)-3-methyl-1-pentyn-3-ol (**5**) from cyclohexanone, acetylene, and methyl ethyl ketone

Metallating agent (I)	Metallating agent (II)	Yield of compound **5** (%)
Lithium naphthalene	Lithium naphthalene	50
Lithium naphthalene	Sodium naphthalene	30
Lithium naphthalene	*n*-Butylmagnesium bromide	15
Sodium naphthalene	Lithium naphthalene	13
Sodium naphthalene	Sodium naphthalene	13
Sodium naphthalene	*n*-Butylmagnesium bromide	18
n-Butylmagnesium bromide	Lithium naphthalene	7
n-Butylmagnesium bromide	Sodium naphthalene	5
n-Butylmagnesium bromide	*n*-Butylmagnesium bromide	5

*Acetylene was passed into a solution of metallating agent (I). The resulting solution of ethynylcyclohexanol was metallated with metallating agent (II).

acetylenic diols were obtained from other acetylenic carbinols and various ketones. The addition products and their properties are given in Table I.

Various organic reactions for carbon chain-lengthening method are known. We have found that a new convenient one-step procedure for chain-lengthening can be carried out by the action of lithium naphthalene in tetrahydrofuran solution. For example, compound **5** can also be synthesized as follows: to lithium acetylide prepared from acetylene and lithium naphthalene (one mole of lithium), one mole of **1** was added to give the mono lithio salt of **2**. Without decomposition of this mixture, one mole of metallic lithium was added continuously, and interestingly, the metallic lithium cuts dissolved easily in this solution to give the dilithio compound (**3**). One mole of methyl ethyl ketone (**4**) was added to the resulting solution and the compound **5** was obtained in 50–60% yield. The identity of **5** was confirmed by comparison of the i.r. and n.m.r. spectra with those of an authentic sample. If the usual synthetic method is employed to prepare a long-chain diol such as **5**, at least two reactions are necessary. By our new one-step synthetic method, the preparation of long-chain diols can be performed easily and in high yield. Similarly, from the other ketones and acetylene, high conversions of acetylenic diols can be achieved by this new method. The addition products and their properties are given in Table II.

In our new one-step synthetic method, the effect of metallating agents has been examined, and typical results are presented in Table III. Sodium naphthalene and alkyl magnesium bromide both resulted in the formation of an acetylenic diol in low yield. Combination of lithium naphthalene and other metallating agents did not give a good result. The use of lithium naphthalene gave the optimum yield.

The foregoing observations indicate that long-chain acetylenic diols can be prepared easily by using lithium naphthalene in tetrahydrofuran solution.

Experimental

Materials

Commercial tetrahydrofuran was purified by drying it with metallic sodium and then distilling it over metallic sodium under nitrogen. Naphthalene and other reagents were purified. Nitrogen and acetylene were dried by passing them through columns of calcium chloride. All the experiments were carried out in a dry apparatus under nitrogen.

Reaction of Ethynylcyclohexanol with Methyl Ethyl Ketone

To a mixture of 5.2 g (0.04 mole) of naphthalene and 150 ml of tetrahydrofuran, 0.6 g (0.08 mole) of metallic lithium was added, and the mixture was agitated at room temperature in an atmosphere of dry nitrogen. After 1 h, a mixture of 5.0 g (0.04 mole) of ethynylcyclohexanol (**2**) and 10 ml of tetrahydrofuran was added very slowly to give the dilithio compound **3**. When the mixture was added rapidly, the lithium naphthalene complex tended to be destroyed. To the tetrahydrofuran solution, 2.9 g (0.04 mole) of methyl ethyl ketone (**4**) were gradually added, and the mixture was stirred for an additional 3 h at room temperature. The reaction mixture was decomposed with saturated ammonium chloride solution, and the organic layer was isolated with isopropyl ether. The isopropyl ether extracts were washed with water and dried over anhydrous sodium sulfate. After low boiling fractions were removed by vacuum distillation, the residue was distilled with a pot type molecular distillation still to give 4.5 g of a pale-yellow viscous oil (**5**). It had the following properties: b.p. 100–120° at 10^{-3} Torr; infrared (i.r.): 3440 and 1060 cm^{-1} (OH); nuclear magnetic

Can. J. Chem. Downloaded from www.nrcresearchpress.com by 210.87.254.42 on 09/05/12
For personal use only.

resonance (n.m.r.) (δ, p.p.m.): 1.02 (3 H, triplet, —CH_2—CH_3), 1.45 (3 H, singlet, HO—C(—CH_3)—), 1.9–1.2 (12 H multiplet, —CH_2—), 2.18 (2 H, singlet, —O*H*).

Anal. Calcd. for $C_{12}H_{20}O_2$: C, 73.5; H, 10.2. Found: C, 73.2; H, 10.1.

The identity of **5** was confirmed by comparison of the i.r. and n.m.r. spectra with those of an authentic sample. Authentic **5** was prepared from the dimagnesium bromide of compound **2** with compound **4** in the usual way.

Other acetylenic diols were prepared and identified similarly. Typical results are presented in Table I.

Synthesis of Acetylenic Diols by New One-step Method

Reaction of Acetylene with Cyclohexanone and Methyl Ethyl Ketone

Purified dry acetylene was slowly passed into a tetrahydrofuran solution (150 ml) of 0.1 mole of lithium and 0.1 mole of naphthalene to give lithium acetylide quantitatively. Cyclohexanone (0.1 mole) was gradually added to the tetrahydrofuran solution, and the mixture was stirred for an additional 2 h at room temperature. Without decomposition of this mixture, 0.1 mole of metallic lithium was added continuously. The metallic lithium dissolved slowly in the solution producing green lithium naphthalene. After 1 h, 0.1 mole of methyl ethyl ketone was added, and the tetrahydrofuran solution was stirred for an additional 2 h at room temperature. The reaction mixture was decomposed with saturated ammonium chloride solution, and the organic layer was extracted with isopropyl ether. The isopropyl ether solution was treated as usual. After low boiling fractions were removed by vacuum distillation, the residue (10 g) was distilled with a molecular distillation still to give 7.5 g of a pale-yellow oil (**5**), b.p. 100–120 °C at 10^{-3} Torr. The identity of **5** was confirmed by comparison of spectral data with those of an authentic sample.

Other acetylenic diols were prepared and identified similarly. Typical results are presented in Table II.

Reaction of Acetylene with Cyclohexanone and Methyl Ethyl Ketone Using Other Metallating Agents

Acetylene was passed slowly into a tetrahydrofuran solution of sodium naphthalene, which had been prepared from 0.1 mole of naphthalene and 0.1 mole of sodium cuts. Cyclohexanone (0.1 mole) was added to the solution. After 1 h, 0.1 mole metallic sodium was added as the second metallating agent. After 3 h, 0.1 mole of methyl ethyl ketone was added, and the reaction mixture was treated in the usual way to give compound **5**. As the second metallated agent, metallic lithium, *n*-butylmagnesium bromide or ethylmagnesium bromide were used as mentioned above. The identity of **5** was confirmed by comparison of the i.r. absorption spectra with those of an authentic sample. Typical results are given in Table III.

Infrared Absorption Spectra

Spectra were measured on a Koken IRS spectrophotometer.

Nuclear Magnetic Resonance Spectra

Spectra were determined on a Japan Electron Optics Lab. instrument (60 Mc.p.s.) with carbon tetrachloride solutions and with tetramethylsilane as an internal standard.

Acknowledgments

The authors thank Dr. Sanae Tanaka of Mitsubishi Petrochemical Co., Ltd., for his measurement of the nuclear magnetic resonance spectra, and Dr. Akira Komatsu of Takasago Perfumary Co., Ltd., for materials.

1. K. SUGA, S. WATANABE, H. KIKUCHI, and T. WATANABE. Can. J. Chem. **46**, 2619 (1968).
2. K. SUGA, S. WATANABE, and K. KAMMA. Can. J. Chem. **45**, 933 (1967).
3. K. SUGA, S. WATANABE, and T. SUZUKI. Can. J. Chem. **46**, 3041 (1968).

Can. J. Chem. Downloaded from www.nrcresearchpress.com by 210.87.254.42 on 09/05/12
For personal use only.

Sur les *tert*-butyl-4 triméthyl-1,2,2 cyclohexanols epimères

JEAN-CLAUDE RICHER ET CLAUDE LAMARRE
Département de Chimie, Université de Montréal, Boite Postale 6128, Montréal, Québec

Reçu le 1 octobre 1968

La stéréochimie des alcools tertiaires isomères formés par addition de l'iodure de méthylmagnésium sur la *tert*-butyl-4 diméthyl-2,2 cyclohexanone est déterminée. La transformation des acétates de ces alcools en *tert*-butyl-4 diméthyl-2,2 méthylènecyclohexane et en *tert*-butyl-4 triméthyl-1,6,6 cyclohexène a été effectuée. La stéréochimie de l'époxydation de ces alcènes a aussi été établie.

Canadian Journal of Chemistry, 47, 2349 (1969)

Introduction

Dans le cadre de nos travaux (1–4) sur la stéréochimie des produits dérivés de la *tert*-butyl-4 diméthyl-2,2 cyclohexanone (**1***b*), il nous apparaissait intéressant d'établir la stéréochimie de l'addition de l'iodure de méthylmagnésium sur cette cétone, et d'en comparer les résultats avec ceux obtenus (5–7) dans une réaction semblable sur la *tert*-butyl-4 cyclohexanone non substituée (**1***a*) afin d'évaluer l'influence des groupes méthyles en position-2 sur la stéréochimie de cette addition. Les résultats obtenus au cours de cette étude font l'objet de la présente communication.

Résultats et discussion

L'addition de l'iodure de méthylmagnésium sur la *tert*-butyl-4 diméthyl-2,2 cyclohexanone (**1***b*) effectuée d'après la procédure expérimentale décrite précédemment (5) conduit à un mélange d'alcools tertiaires **2***b* et **3***b* qui a été analysé par chromatographie en phase gazeuse (c.p.g.), et qui serait formé de 40% de *tert*-butyl-4 triméthyl-1,2,2 cyclohexanol *cis*[1] et 60% de l'isomère *trans*. Ce mélange d'alcools tertiaires a pu être transformé en acétates correspondants (**2***c* et **3***c*) selon la technique habituelle (8); l'analyse par c.p.g. effectuée sur ces dérivés confirme le résultat analytique précédent puisque les acétates seraient présents dans le mélange réactionnel dans la proportion de 39% de l'acétate du *tert*-butyl-4 triméthyl-1,2,2 cyclohexanol *cis* (**2***c*) et de 61% de l'isomère *trans* (**3***c*). Alors que la réaction de Grignard décrite dans le présent travail conduit à la formation prépondérante de l'alcool *trans* **3***b*, il est maintenant bien établi (6–9) que la même réaction effectuée sur la *tert*-butyl-4 cyclohexanone (**1***a*) conduit à la formation préférentielle de l'alcool *cis* **2***a*; cette différence serait dûe à l'influence du groupe méthyle axial en position-2 (3) qui provoque une attaque du réactif nucléophile par la face opposée de la molécule.

La stéréochimie de ces alcools qui peut être présumée d'après les quantités relatives formées au cours de cette réaction de Grignard (3) est attribuée en se basant sur les temps relatifs de rétention de ces alcools en c.p.g. (2, 9) et grâce à la position dans la résonance magnétique nucléaire (r.m.n.) des pics dus aux protons des groupes OH par comparaison avec les résultats rapportés récemment par Meakins *et al.* (9). Il est à noter aussi que, conformément aux observations de Laszlo et Welvart,[2] la largeur ($w_{1/2}$) de cette bande est plus grande pour l'isomère *cis* que pour l'isomère *trans*. D'autre part, Corey et Chaykovsky (10) ont démontré que le traitement de la *tert*-butyl-4 cyclohexanone (**1***a*) par l'ylide (**6**) conduit à l'époxyde *cis* (**4***a*); appliquée à la *tert*-butyl-4 diméthyl-2,2 cyclohexanone (**1***b*) cette méthode conduit à un mélange 84/16 d'époxydes (**4***b*/**5***b*) qui par réduction avec $LiAlH_4$ conduit à un mélange 88/12 des alcools tertiaires **2***b* et **3***b*. Par comparaison de ces résultats avec ceux obtenus par Corey et Chaykosvky, il est possible d'attribuer la configuration *cis* à l'époxyde formé d'une façon prépondérante, et cette conclusion basée sur une réaction chimique est en accord avec les configurations assignées précédemment en se basant sur des méthodes physiques.

Pour fins de comparaison, la stéréochimie de

[1]La notation *cis* ou *trans* pour les alcools tertiaires se rapporte à la position relative des groupes *tert*-butyles et hydroxyles.

[2]P. Laszlo and Z. Welvart. Communication personnelle.

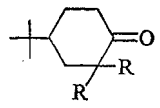

1

a) R = H
b) R = CH_3

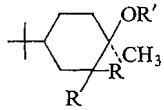

2

a) R = R′ = H
b) R = CH_3, R′ = H
c) R = CH_3, R′ = $-C(=O)-CH_3$
d) R = CH_3, R = $-C(=O)-C_6H_4NO_2(p)$

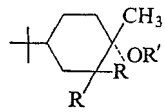

3

a) R = R′ = H
b) R = CH_3, R′ = H
c) R = CH_3, R′ = $C(=O)-CH_3$
d) R = CH_3, R′ = $C(=O)-C_6H_4NO_2\,(p)$

l'époxydation, par l'acide *p*-nitroperbenzoique, du *tert*-butyl-4 diméthyl-2,2 méthylène cyclohexane (**7***b*) obtenu d'après la réaction de Wittig (11), sur la *tert*-butyl-4 diméthyl-2,2 cyclohexanone, (**1***b*), et du *tert*-butyl-4 triméthyl-1,6,6 cyclohexène (**8***b*), obtenu par déshydratation du mélange des alcools tertiaires (**2***b* et **3***b*) par l'iode (12) a aussi été examinée; les résultats obtenus sont présentés dans le Tableau I en regard de ceux rapportés dans la littérature pour les réactions similaires effectuées sur les produits non méthylés **1***a*, **7***a*, et **8***a*. Il ressort d'un examen de ces données que le groupe méthyle axial en position-2, présent dans les molécules examinées au cours du présent travail, a comme effet de cacher une face de la molécule et de provoquer l'addition des réactifs par la face opposée conduisant ainsi à des produits contenant une proportion plus grande de la dernière fraction

TABLEAU I

	Pourcentage de produits *cis* (%)	
	Série R = CH_3	Série R = H
1 + CH_3MgI	40	50 (5, 6)
1 + **6**	84	100 (10)
7 + 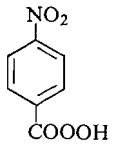	72	70 (14)
8 + 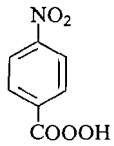	79	55 (13)

introduite en position axiale. Ces résultats sont en accord avec ceux rapportés précédemment (2) pour la réduction de la *tert*-butyl-4 diméthyl-2,2 cyclohexanone (**1***b*) et supportent la théorie complètement stérique proposée (3) pour expliquer la stéréochimie des additions (non réversibles) sur des carbones du type sp^2 contenus dans des cycles.

Au cours du présent travail, il a été observé que la chromatographie sur alumine, en présence de pentane, des acétates **2***c* et **3***c* des *tert*-butyl-4 triméthyl-1,2,2 cyclohexanols provoque une élimination d'acide acétique et la formation soit exclusive du *tert*-butyl-4 triméthyl-1,6,6 cyclohexène (**8***b*) à partir de l'acétate *cis* **2***c* soit d'un mélange 72/28 des alcènes **8***b*/**7***b* en partant de l'acétate **3***c*. Cette réaction inusitée pourrait être attribuée à l'encombrement stérique présent dans les acétates **2***c* et **3***c* qui serait provoqué par la présence de quatre substituants en positions-1 et -2 de ces cyclohexanes. Le fait qu'un des acétates conduise à une seule oléfine alors que l'autre conduit à un mélange suggère que les alcènes ne sont pas équilibrés dans les conditions de la réaction.

Partie expérimentale

Les techniques expérimentales générales ont été décrites dans les publications précédentes (1). Les propriétés physiques des produits obtenus au cours de cette étude sont résumées dans le Tableau II. Les époxydes tant endocycliques (**9***b*) qu'exocycliques (**4***b* et **5***b*) n'ont pu être obtenus stéréochimiquement purs; les propriétés

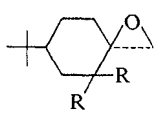

4

a) R = H
b) R = CH_3

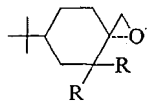

5

a) R = H
b) R = CH_3

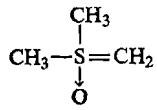

6

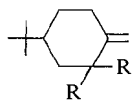

7

a) R = H
b) R = CH_3

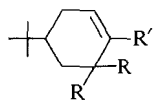

8

a) R = H, R′ = CH_3
b) R = R′ = CH_3

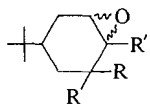

9

a) R = H, R′ = CH_3
b) R = R′ = CH_3

rapportées doivent donc être jugées pour les compositions mentionnées. Tous les pourcentages relatifs d'épimères qui sont rapportés ont été déterminés en faisant l'hypothèse (15) que dans le cas de composés épimères les surfaces relatives sous les pics peuvent être assimilées aux pourcentages relatifs de produits présents.

Synthèse de la tert-butyl-4 diméthyl-2,2 cyclohexanone (1b)

(Réf. 2)

Synthèse du tert-butyl-4 diméthyl-2,2 méthylène-1 cyclohexane (7b)

A 330 g de bromure de méthyl-triphénylphosphonium dans 1 l d'éther anhydre, on ajoute sous atmosphère d'azote, 64 g de butyl lithium en solution dans l'hexane. Après l'addition, l'agitation est maintenue pendant 2 h. La solution devient jaunâtre. A cette solution de méthylène triphénylphosphine, 55 g de cétone (**1***b*) en solution dans 200 ml d'éther anhydre sont ajoutés goutte à goutte. L'addition se fait sur une période de 2 h et l'agitation est maintenue pendant 1 h supplémentaire à la température de la pièce. La solution est portée à reflux 2 h. L'éther est déplacé par distillation et 1 l de tétrahydrofurane est ajouté pendant cette distillation. Le mélange réactionnel est ensuite porté à reflux 13 h. Après refroidissement et agitation supplémentaire de 3 h, 1 l d'eau y est ajouté. Le méthylène (**7***b*) est extrait par l'éther, la phase organique est lavée à l'eau saturée de chlorure de sodium, séchée sur sulfate de sodium anhydre, et évaporée sous vide. Le résidu est filtré sur alumine (activité I) en employant l'éther de pétrole 30–60 °C comme éluant. Le méthylène est obtenu avec un rendement de 81% (45.0 g).

tert-Butyl-4 triméthyl-1,2,2 cyclohexanols-1 cis et trans (2b et 3b)

Une solution de 25.3 g de cétone (**1***b*) dans 50 ml d'éther anhydre est traitée à 0 °C par de l'iodure de méthyl magnésium (préparé à partir de 5.0 g de magnésium et de 13 ml d'iodure de méthyle dans 160 ml d'éther anhydre), à la façon habituelle. Le mélange d'alcools est obtenu avec un rendement de 87% (24.0 g). Ce mélange d'alcools (9.3 g) est mis en solution dans 100 ml d'hexane et chromatographié sur 500 g d'alumine Merck. Le diamètre de la colonne est de 50 mm. L'élution de la colonne, en augmentant la polarité de l'hexane pur à de l'éther pur (variation de la concentration de 10% tous les 100 ml d'éluant) ne conduit à aucun produit. Avec de l'éther pur il est récupéré : 1°—1.6 g d'alcool *cis* **2***b* contaminé par des traces de cétone **1***b* de départ. 2°—3.2 g d'un mélange d'alcools *cis* et *trans* **2***b* et **3***b*; 3°—4.3 g d'alcool *trans* pur.

Synthèse de l'acétate du tert-butyl-4 triméthyl-1,2,2 cyclohexanol-1 cis (2c)

En suivant le mode opératoire de DePuy et King (8), 512 mg de *tert*-butyl-4 triméthyl-1,2,2 cyclohexanol-1 *cis* (**2***b*) conduisent à 520 mg d'acétate (**2***c*), soit un rendement de 84%.

Synthèse de l'acétate du tert-butyl-4 triméthyl-1,2,2 cyclohexanol-1 trans (3c)

Selon le mode opératoire de DePuy et King (8), 410 mg de *tert*-butyl-4 triméthyl-1,2,2 cyclohexanol-1 *trans* (**3***b*) conduisent à 428 mg d'acétate (**3***c*), soit un rendement de 86%.

p-Nitrobenzoates des tert-butyl-4 triméthyl-1,2,2 cyclohexanol-1 cis et trans (2d et 3d)

Ils sont préparés selon Hennion et Barrett (16); *cis* : p.f 153–154 °C (EtOH). *trans* : p.f. 178–179 °C (EtOH).

Elimination d'acide acétique lors de la chromatographie des acétates cis et trans (2c et 3c) sur alumine

Essai sur l'acétate cis (2c)

Une solution de 155 mg d'acétate *cis* (**2***c*) dans 10 ml pentane est chromatographiée sur une colonne de 12 mm de diamètre contenant 19 g d'alumine Merck. L'élution par 250 ml de pentane donne 102 mg (88%) de *tert*-butyl-4 triméthyl-1,6,6 cyclohexène (**8***b*) identifié par superposition en c.p.g., infrarouge (i.r.), et r.m.n.

Essai sur l'acétate trans (3c)

Dans les conditions identiques décrites précédemment, 154 mg d'acétate *trans* (**3***c*) conduisent à 100 mg (86%) d'un mélange de 72% de *tert*-butyl-4 triméthyl-1,6,6 cyclohexène (**8***b*) et 28% de *tert*-butyl-4 diméthyl-2,2 méthylènecyclohexane (**7***b*). Les deux alcènes (**7***b* et **8***b*) sont identifiés par c.p.g., i.r., et r.m.n.

Essai sur un mélange d'acétates cis et trans (2c, 3c)

Dans les mêmes conditions décrites précédemment, 115 mg d'acétates *cis* et *trans* (**2***c* et **3***c*) donne 75 mg (87%) d'alcènes (**7***b* et **8***b*). L'analyse en c.p.g. montre que l'alcène (**8***b*) est présent à 83%, tandis que l'alcène (**7***b*) est à 17%.

Synthèse du tert-butyl-4 triméthyl-1,6,6 cyclohexène (8b)

Selon le mode opératoire décrit par Hammond et

TABLEAU II

Propriétés physiques*

	p.e. (mm Hg)	n_D (°C)	p.f. (°C)	I.R. ν(cm^{-1})	C.P.G.	Résonance magnétique nucléaire: *t*-Bu p.p.m.	Résonance magnétique nucléaire: CH_3 p.p.m.	Particularités
2*b*	56–60 °C (0.25)	1.4659 (26)		3620 3500 (CCl_4)	Colonne A T_R.: 11.5 min	0.75	0.75 0.80 0.92	OH: 3.65 p.p.m. (DMSO) $w_{1/2}$: 0.45 c.p.s.
2*c*	72 °C (1.7)	1.4565 (25.5)		1730	Colonne B T_R.: 13.5 min	0.82	0.92 (2) 1.35	O—C—CH_3: 1.88 p.p.m. (CCl_4) ‖ O
2*d*			153–154 (EtOH)			0.80	1.00 1.10 1.56	Protons aromatiques 8.18 p.p.m. (CCl_4) *J*: 2.5 c.p.s.
3*b*	130 °C (22)		62–64	3615 3481 (CCl_4)	Colonne A T_R.: 15.5 min	0.80	0.80 0.88 1.03	OH: 3.81 p.p.m. (DMSO) $w_{1/2}$: 0.15 c.p.s.
3*c*	60–65 °C (0.25)	1.4588 (25.5)		1730	Colonne B T_R.: 15.5 min	0.82	1.00 1.20 1.45	O—C—CH_3: 1.85 p.p.m. (CCl_4) ‖ O
3*d*			178–179 (EtOH)			0.86	1.05 1.20 1.65	Protons aromatiques 8.16 p.p.m. (CCl_4) *J*: 3.0 c.p.s.
4*b* et **5***b*	120 °C (18)	1.4622 (25.5)		850 910 940	Colonne C T_R.: 4.5 min (84%) T_R.: 5.0 min (16%)	0.88	0.70 1.04	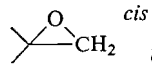 *cis* δ_A: 2.62 p.p.m. J_{AB}: 5 δ_B: 2.24 p.p.m. *trans* δ_A: 2.69 p.p.m. (CCl_4) δ_B: 2.21 p.p.m. J_{AB}: 5
7*b*	92–94 °C (20)	1.4590 (27.3)		3090 1640 900	Colonne D T_R.: 16.0 min	0.85	1.02 1.05	Double liaison exocyclique 4.62 p.p.m. (CCl_4)
8*b*	84–86 °C (1.5)	1.4603 (25.5)		3020 815	Colonne D T_R.: 17.0 min	0.83	0.96 (2) 1.56	Proton éthylénique 5.20 p.p.m. (CCl_4)
9*b*	115–118 °C (18)	1.4588 (26)		885 825	Colonne C T_R.: 5 min (79%) T_R.: 10.5 min (21%)	0.81	0.89 1.01 1.15	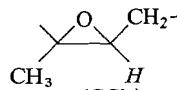 2.82 p.p.m. *J*: 5.3 c.p.s. (CCl_4)

*Les produits rapportés dans ce tableau sont à notre connaissance nouveaux; ils ont été caractérisés d'après leurs propriétés physiques. Les analyses par chromatographie en phase gaseuse (c.p.g.) ont été effectuées à l'aide des appareils Burrel (Kromatog K-2) colonne A : Carbowax 20 M 20%/Chromosorb P 30–60, 2.5 m, diamètre ¼ po., *T*: 176 °C, He : 50 ml/min. Colonne B : Micro Tek à conductivité thermique : SE-52/5% chromport. XXX, 15 pieds, diamètre ¼ po., *T*: 200 °C, He : 40 ml/min. Colonne C : Burrel (Kromatog K-2. D.E.G.S. 10%/Chromosorb G 80-100 DMCS, 2.5 m, diamètre ¼ po., *T*: 175 °C, He : 45 ml/min. Colonne D : F et M (modèle 810) Ucon Polar 20%/Chromosorb W30-60, 15 pds, diamètre ¼ po., *T*: 130 °C : He : 50 ml/min.

Navitt (12), 4.58 g d'alcools *cis* et *trans* (**2***b* et **3***b*) chauffés en présence de 60 mg d'iode à 148 °C pendant 1 h et demie, conduisent à 3.28 g d'alcène **8***b* (78%).

Synthèse des époxydes cis et trans (4b et 5b)

Epoxydation de la tert-butyl-4 diméthyl-2,2 cyclohexanone (1b)

A 1.3 g d'hydrure de sodium (suspension 50%), recouvert de 15 ml de diméthyl sulfoxyde anhydre (distillé sur hydrure de calcium), on ajoute d'un coup 5.25 g d'iodure de triméthyl-oxosulfonium et 5 ml de diméthyl sulfoxyde. Après quelques instants, la solution devient grise et très visqueuse, alors 6 ml de diméthyl sulfoxyde y sont ajoutés de façon à avoir une agitation. Après 2 h d'agitation 1.83 g de cétone (**1***b*) en solution dans 5 ml de diméthyl sulfoxyde sont ajoutés goutte à goutte. Le mélange est ensuite agité pendant 22½ h sous une atmosphère d'azote. Le mélange réactionnel est ensuite chauffé à 65 °C pour 3 h, et ensuite l'agitation est maintenue 21 h à la température ambiante. La solution est hydrolysée par 20 ml d'eau et reprise par de l'éther. La phase éthérée est lavée par de l'eau jusqu'à neutralité, séchée sur sulfate de sodium anhydre, et évaporée. On obtient 1.1 g (54%) d'époxydes *cis* et *trans* (**4***b* et **5***b*), dans un rapport 84/16.

Des essais de séparation de ces époxydes par chromatographie en phase gazeuse préparative n'ont conduit qu'a des produits de décomposition et ont du être abandonnés.

Les configurations *cis*/*trans* ont été établies par réduction du mélange des époxydes en *tert*-butyl-4 triméthyl-1, 2,2 cyclohexanol-1 *cis* (**2***b*) et *trans* (**3***b*).

A une suspension agitée de 300 mg d'hydrure de lithium et d'aluminium dans 10 ml de tétrahydrofurane, on ajoute une solution de 200 mg du mélange des époxydes *cis* (**4***b*) et *trans* (**5***b*) dans 7 ml de tétrahydrofurane. Le mélange est chauffé à reflux pendant 20 h, puis le complexe est décomposé par l'addition à 0 °C de 25 ml d'une solution d'acide chlorhydrique à 10%. Le mélange d'alcool (193 mg de **2***b* et **3***b*) est extrait de la façon habituelle. L'analyse du produit brut par c.p.g. a donné 88% de l'alcool *cis* **2***b* et 12% de l'alcool *trans* **3***b*.

Expoxydation du tert-butyl-4 diméthyl-2,2 méthylène-1 cyclohexane (7b)

A 2.0 g de tert-butyl-4 diméthyl-2,2 méthylène-1 cyclohexane, on ajoute 30 ml d'une solution chloroformique (10 ml) et dichlorométhane (20 ml), d'acide para-nitro perbenzoique (préparé selon la réf. 17) contenant 4.0 g de peracide. Le mélange est refluë 1 h sous atmosphère d'azote et ensuite agité 16 h à la température de la pièce, la solution est filtrée, et le précipité est lavé par du dichlorométhane. Le filtrat est lavé par de l'eau et la phase aqueuse est reprise par de l'éther. Les phases chloroformique/dichlorométhane et éthérée sont réunies et lavées successivement par 200 ml d'une solution de sulfite acide de sodium 10%, par 300 ml d'hydroxyde de sodium 5% et par de l'eau jusqu'à neutralité puis séchées et évaporées. On obtient 1.65 g d'époxydes *cis* **4***b* (72%) et *trans* **5***b* (28%) avec une rendement de 76%.

Les configuration *cis–trans* ont été établies par réduction du mélange des époxydes en *tert*-butyl-4 triméthyl-1,2,2 cyclohexanol-1 *cis* (**2***b*) et *trans* (**3***b*).

Selon le mode opératoire décrit précédemment, 200 mg d'époxydes *cis* **4***b* et *trans* **5***b* sont réduits avec un rendement brut de 95% par 300 mg d'hydrure de lithium et d'aluminium. L'analyse par c.p.g. montre que l'alcool *cis* (**2***b*) forme 72% du mélange tandis que l'alcool *trans* (**3***b*) en forme 28%.

Epoxydes cis et trans du tert-butyl-4 triméthyl-1,6,6 cyclohexène (9b)

En suivant fidèlement le mode opératoire décrit précédemment on obtient en partant de 2.0 g de *tert*-butyl-4 triméthyl-1,6,6 cyclohexène (**8***b*), 1.15 g (52%) du mélange d'époxydes *cis* et *trans* (**9***b*). Les deux époxydes sont dans un rapport *cis*/*trans* (79/21). Les configurations *cis–trans* ont été établies par réduction du mélange des époxydes en alcools *cis* (**2***b*) et *trans* (**3***b*)[3]. Selon le mode opératoire décrit précédemment, 200 mg d'époxydes (**9***b*) sont réduits avec un rendement brut de 98% par 300 mg d'hydrure de lithium et d'aluminium. L'analyse par c.p.g. indique que les alcools *cis* (**2***b*) et *trans* (**3***b*) sont dans un rapport 78/22.

Remerciements

Les auteurs remercient vivement le Conseil National de Recherches du Canada et le Ministère de l'Education de la Province de Québec pour l'aide financière apportée sous forme d'octrois et de bourses de recherches.

1. J.-C. RICHER et P. BELANGER. Can. J. Chem. **42**, 2398 (1964).
2. J.-C. RICHER et G. PERRAULT. Can. J. Chem. **43**, 18 (1965).
3. J.-C. RICHER. J. Org. Chem. **30**, 324 (1965).
4. J.-C. RICHER et C. GILARDEAU. Can. J. Chem. **43**, 538 (1965).
5. H. FAVRE et D. GRAVEL. Can. J. Chem. **39**, 1548 (1961).
6. WILLIAM J. HOULIHAN. J. Org. Chem. **27**, 3860 (1962).
7. B. CROSS et G. H. WHITHAM. J. Chem. Soc. 3892 (1960).
8. C. H. DEPUY et R. W. KING. J. Am. Chem. Soc. **83**, 2743 (1961).
9. G. D. MEAKINS, R. K. PERCY, E. E. RICHARDS, et R. W. YOUNG. J. Chem. Soc. C, 1106 (1968).
10. E. J. COREY et MICHAEL CHAYKOVSKY. J. Am. Chem. Soc. **87**, 1353 (1965).
11. G. WITTIG et U. SCHÖLLKOPF. Chem. Ber. **87**, 1318 (1954).
12. G. S. HAMMOND et T. D. NEVITT. J. Am. Chem. Soc. **76**, 4121 (1954).
13. N. A. LEBEL et G. G. ECKE. J. Org. Chem. **30**, 4316 (1965).
14. H. FAVRE et D. GRAVEL. Can. J. Chem. **41**, 1452 (1963).
15. E. L. ELIEL, S. H. SCHROETER, T. J. BRETT, F. J. BIROS, et J.-C. RICHER. J. Am. Chem. Soc. **88** 3327 (1966).
16. G. F. HENNION et S. OLIVIA BARRETT. J. Am. Chem. Soc. **79**, 2146 (1957).
17. M. VILKAS. Bull. Soc. Chim. France, 1401 (1959).
18. H. O. HOUSE. Modern synthetic reactions. W. A. Benjamin, Inc., New York. 1965. p. 38.

[3]Même s'il est possible d'envisager que la réduction par $LiAlH_4$ du mélange d'époxydes *cis* et *trans* (**9***b*) peut conduire à quatre alcools (dont deux secondaires et deux tertiaires), il est supposé (voir réf. 18) que ces réductions étant des processus S_N2 elles ne conduisent qu'aux alcools tertiaires provenant d'une attaque sur le carbone le moins substitué.

Can. J. Chem. Downloaded from www.nrcresearchpress.com by 210.87.254.40 on 09/05/12
For personal use only.

Base strengths of substituted 2- and 4-styrylpyridines in the ground and excited states

J. C. DOTY, J. L. R. WILLIAMS, AND P. J. GRISDALE
Research Laboratories, Eastman Kodak Company, Rochester, New York 14650

Received November 18, 1968

The base strengths of various 2- and 4-styrylpyridines in the ground state and first-excited-singlet state have been determined. The base strengths are found to conform to the Hammett equation if the proper σ values are chosen.

Canadian Journal of Chemistry, 47, 2355 (1969)

The base strengths (pK_a) of various 2- and 4-styrylpyridines (1) substituted in the 3′- or 4′-positions have been measured by the procedure described previously (2). The excited-state base strengths (pK_a^*) were calculated from the absorption spectra of the free bases and their conjugate acids (Table I) by the method employed by Jaffe, Jones, and Isaks (3) for the excited-state pK_a^* of azobenzene.

In the cases of mono-substituted azo and azoxybenzenes it was found that the best correlations were obtained when both the σ^+ and σ^- values for mesomerically electron donating and withdrawing groups respectively were used. This was attributed to the high polarity of the compounds. We have applied the same reasoning to the 2- and 4-styrylpyridine series.

In the present work it was impossible to use the measurements of fluorescent emission since the *cis* isomers do not fluoresce. Jaffe and Jones (4) have discussed the requirements and assumptions necessitated by the use of the absorption spectral data rather than fluorescent emission data in the Forster cycle. The results are listed in Tables II–IV.

The pK_a values obtained are in agreement with those found by Katritzky *et al.* (5) and Cauzzo *et al.* (6). A direct comparison cannot be made, however, since different solvent systems were used in each case.

The ground state (pK_a) and first-excited-singlet state (pK_a^*) values were first plotted versus the corresponding Hammett σ constants (7). It was found that the substituents which are able to participate in resonance with the large conjugated system did not fit on the line obtained. The pK_a values were then plotted by using the extreme σ values (Figs. 1–8) for the substituents capable of resonance participation. The substituents that

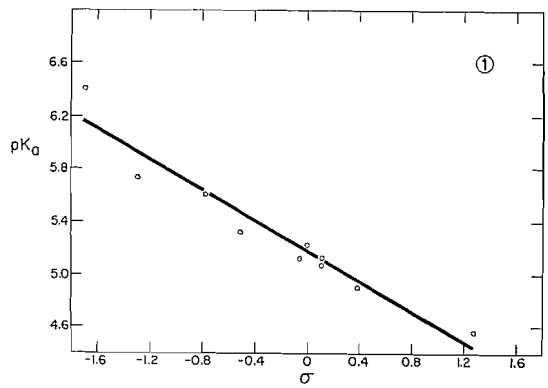

FIG. 1. pK_a Values of substituted *trans*-2-styrylpyridines vs. σ.

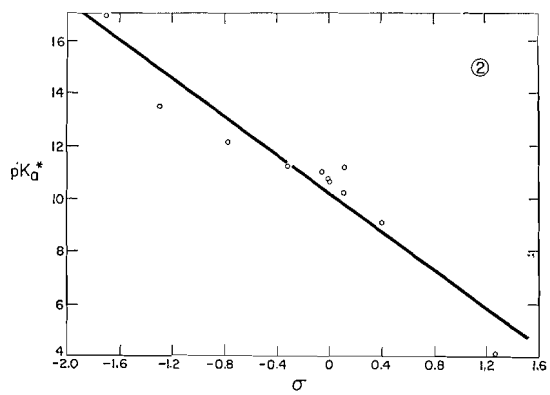

FIG. 2. pK_a^* Values of substituted *trans*-2-styrylpyridines vs. σ.

can donate electrons were represented by σ^+ (8) and those capable of withdrawing electrons were represented by σ^- (9). The equation of the straight line that best fit these points was calculated by the least-squares method. The ρ values

TABLE I

Absorption maxima and extinction coefficients of the styrylpyridines and their salts

Compound	Solvent	Free base		Hydrochloride	
		λ_{max}	ε	λ_{max}	ε
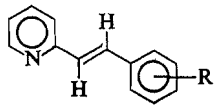					
where R =	H_2O				
p-$N(CH_3)_2$		348	26 200	425	17 900*
p-NH_2		337	30 100	385	32 100*
p-OCH_3		322	29 900	358	31 000
p-CH_3		313	29 500	343	31 000
m-CH_3		309	25 500	337	26 800
p-$NHCOCH_3$		323	36 300	353	34 300
H		309	26 300	334	27 900
p-Cl		312	31 100	339	32 500
m-OCH_3		308	23 800	333	24 100
m-Cl		308	26 400	329	28 400
p-NO_2		344	26 100	341	35 000
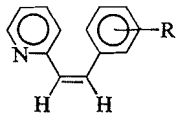					
where R =	H_2O				
p-$N(CH_3)_2$		323	10 900	410	8 000*
p-NH_2		313	12 800	378	10 320*
p-OCH_3		295	10 400	346	9 190
p-CH_3		292	10 100	329	9 000
H		288	9 500	317	9 680
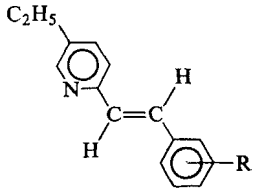					
where R =	H_2O				
p-OCH_3		324	31 900	358	33 300
p-CH_3		316	28 600	343	31 500
H		312	29 500	334	31 300
p-NO_2		350	24 200	344	37 500
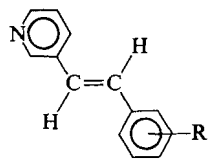					
where R =	50% aqueous MeOH				
p-$N(CH_3)_2$		369	27 500	462	34 100*
p-NH_2		344	27 300	414	27 700*
p-OCH_3		324	31 700	372	33 500
p-CH_3		313	33 000	353	34 000
m-CH_3		308	29 400	342	30 600
H		308	30 800	341	31 800
p-Cl		311	32 600	343	33 500
m-OCH_3		300	25 700	338	24 300
m-Cl		300	29 200	332	29 500
p-NO_2		341	36 600	333	27 200

*Calculated value, ref. 2.

Can. J. Chem. Downloaded from www.nrcresearchpress.com by 210.87.254.40 on 09/05/12
For personal use only.

Can. J. Chem. Downloaded from www.nrcresearchpress.com by 210.87.254.40 on 09/05/12
For personal use only.

TABLE II

Base strengths of 3′- and 4′-substituted-2-styrylpyridines†

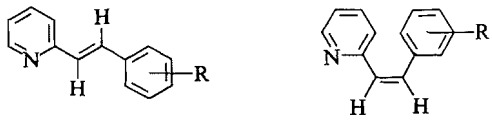

R	pK_a	pK_a*	pK_a	pK_a*
p-$N(CH_3)_2$	6.40	17.00	5.52	19.12
p-NH_2	5.72	13.44	5.78	17.25
p-OCH_3	5.60	12.15	5.44	15.14
p-CH_3	5.31	11.26	5.17	13.49
m-CH_3	5.13	11.01		
p-$NHCOCH_3$	5.19	10.78		
H	5.23	10.67	5.20	12.04
p-Cl	5.07	11.17		
m-OCH_3	5.13	10.35		
m-Cl	4.90	9.10		
p-NO_2	4.56	4.05		

†Measured in water at 25°.

TABLE III

Base strengths of substituted-5-ethyl-2-styrylpyridines†

R	pK_a	pK_a*
p-OCH_3	5.97	12.22
p-CH_3	5.65	10.79
H	5.62	10.18
p-NO_2	4.96	3.86

†Measured in water at 25°; general formula:

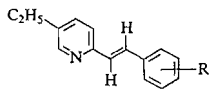

TABLE IV

Base strengths of 3′- and 4′-substituted-4-styrylpyridines†

R	pK_a	pK_a*
p-$N(CH_3)_2$	5.85	17.10
p-NH_2	5.62	15.44
p-OCH_3	5.17	13.55
p-CH_3	5.17	12.82
m-CH_3	4.99	11.98
H	5.02	11.76
p-Cl	4.88	11.20
m-OCH_3	4.93	13.02
m-Cl	4.68	11.66
p-NO_2	4.47	5.64

†Measured in 50% aqueous MeOH at 25°; general formula:

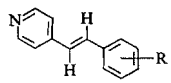

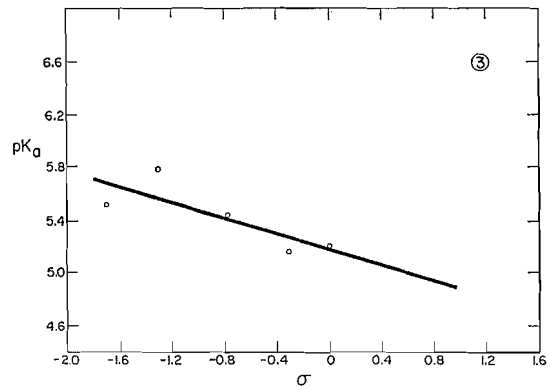

FIG. 3. pK_a Values of substituted *cis*-2-styrylpyridines vs. σ.

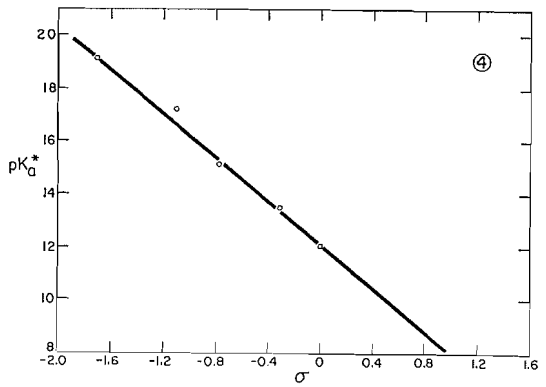

FIG. 4. pK_a* Values of substituted *cis*-2-styrylpyridines vs. σ.

were found to be similar to those found for the azobenzenes (3). The equations and correlation coefficients (r) are listed in Table V.

The correlation coefficients found for these lines indicate that the Hammett equation can predict the effects of the influence of 3′- and 4′-substituents on the base strengths of the styrylpyridines. The correlation coefficient is low for the *cis* form of the 2-styrylpyridine in the ground state. The *cis*-2-styrylpyridine molecule is very similar to *cis*-stilbene and is nonplanar in the ground state (10). The nonplanarity reduces the amount of resonance interaction between the rings.

Since we are trying to correlate the effect of substitution in one ring with the base strength of the nitrogen in the second ring, it is not surprising that the results for *cis*-2-styrylpyridine are not accurately predicted by the Hammett equation.

TABLE V

Equations of line obtained from least-squares calculations and correlation coefficients

Series	Equation of line	r
trans-2-Styrylpyridines	$pK_a = 5.175-0.573\sigma$	-0.971
	$pK_a^* = 10.249-3.626\sigma$	-0.952
cis-2-Styrylpyridines	$pK_a = 5.182-0.292\sigma$	-0.814
	$pK_a^* = 12.074-4.076\sigma$	-0.999
trans-5-Ethyl-2-styrylpyridines	$pK_a = 5.571-0.479\sigma$	-0.992
	$pK_a^* = 9.451-4.177\sigma$	-0.989
trans-4-Styrylpyridines	$pK_a = 4.972-0.468\sigma$	-0.979
	$pK_a^* = 11.667-3.322\sigma$	-0.943

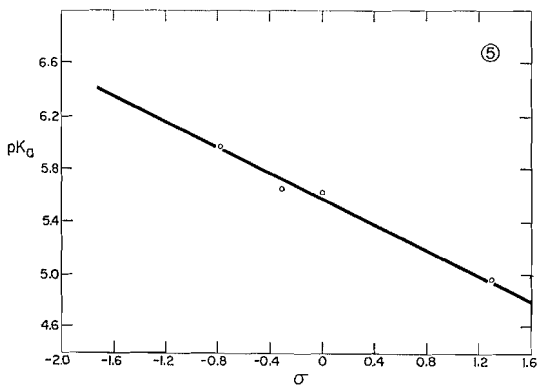

FIG. 5. pK_a Values of substituted *trans*-5-ethyl-2-styrylpyridines vs. σ.

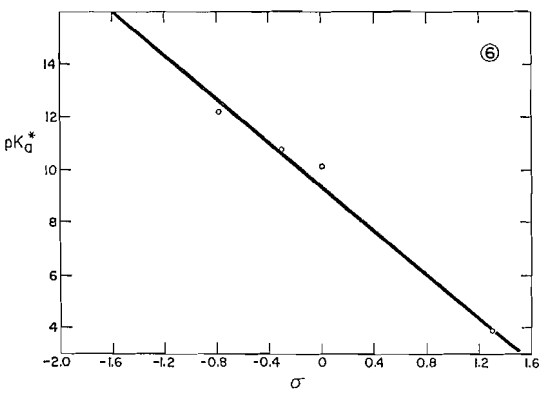

FIG. 6. pK_a^* Values of substituted *trans*-5-ethyl-2-styrylpyridines vs. σ.

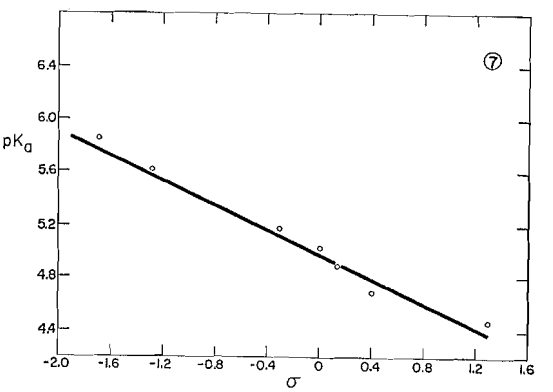

FIG. 7. pK_a Values of substituted *trans*-4-styrylpyridines vs. σ.

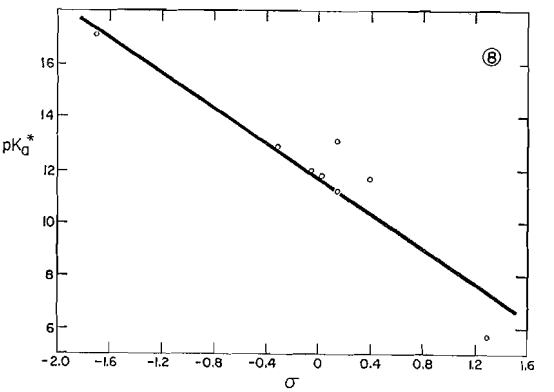

FIG. 8. pK_a^* Values of substituted *trans*-4-styrylpyridines vs. σ.

However, in the excited state, the correlation coefficient for *cis*-2-styrylpyridine is quite good. This would suggest that the planarity of the molecule is much greater in the excited state than in the ground state and that greater interaction between the rings takes place.

The ρ value of the Hammett equation represents a measure of the sensitivity of the molecular system to substitution. The excited-state ρ values of the styrylpyridine systems are 8–10 times greater than those of the ground-state molecules. The greater effect of substituents on the excited-

Can. J. Chem. Downloaded from www.nrcresearchpress.com by 210.87.254.40 on 09/05/12
For personal use only.

TABLE VI

Physical constants of 3′-substituted styrylpyridine derivatives

Compound	Melting or boiling point	% Yield*	Formula	Analysis calculated C	H	Cl	N	Analysis found C	H	Cl	N
2-(3-Methoxystyryl)-	152–155°/0.4mm	33	$C_{14}H_{13}NO$	79.5	6.2	—	6.6	79.3	6.4	—	6.8
4-(3-Methoxystyryl)-	160–164°/0.4mm	28	$C_{14}H_{13}NO$					79.3	5.9	—	6.4
2-(3-Methylstyryl)-	142–146°/0.8mm	30	$C_{14}H_{13}N$	86.1	6.7	—	7.2	85.7	7.1	—	6.9
4-(3-Methylstyryl)-	75–76°	5	$C_{14}H_{13}N$					85.9	6.9	—	7.2
2-(3-Chlorostyryl)-	52–54°	49	$C_{13}H_{10}ClN$	72.4	4.7	16.5	6.5	72.4	4.8	16.2	6.7
4-(3-Chlorostyryl)-	59–61°	35	$C_{13}H_{10}ClN$					72.1	4.7	16.7	6.3

*Analytical sample.

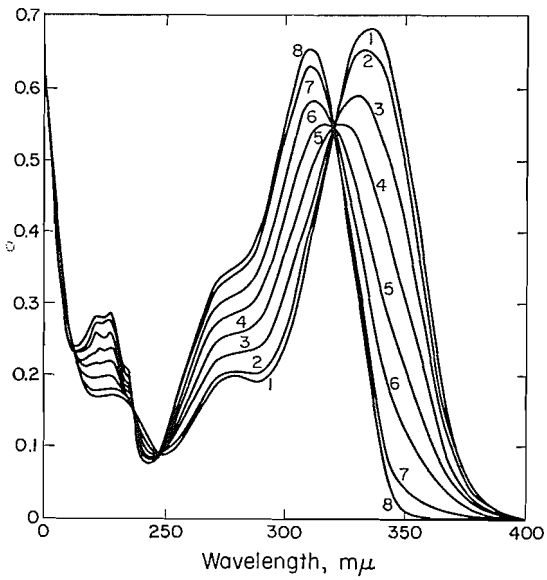

FIG. 9. Absorption spectra of *trans*-2-styrylpyridine at various pH values in water: curve 1 (pH 2.75), curve 2 (pH 4.05), curve 3 (pH 4.50), curve 4 (pH 5.03), curve 5 (pH 5.35), curve 6 (pH 5.62), curve 7 (pH 6.34), curve 8 (pH 9.17).

state pK_a* can be rationalized in terms of the electron distribution in the conjugated system, the electron distribution of which must be very different in the excited state from that in the ground state, since a drastic increase in base strength of unsubstituted compounds occurs in the excited state. In the ground state, the pK_a's of the styrylpyridines are not very different from that of pyridine. This would indicate that the styryl group does not contribute much to the basicity. Since the absorption spectrum of the pyridinium ion is shifted slightly bathochromically compared to the free base, the excited-state pK_a* should be slightly lower. Since the styrylpyridines become much stronger bases in the excited state, a very significant contribution is made by the styryl part of the molecule. Substitutions on the phenyl ring would then also be expected to affect the basicity of the pyridine nitrogen more in the excited state.

The results of the measurement of the base strength of the substituted styrylpyridines in the ground state and the corresponding calculated base strengths of the first-excited-singlet state show that the substituent effects are those predicted by the Hammett equation in both electronic states.

Experimental

The physical constants of various *trans*-3′-substituted styrylpyridines are listed in Table VI. The general synthesis was described previously (1).

The absorption spectra at various values of pH showed very sharp isosbestic points indicative of isomerically pure compounds. All of the compounds investigated were sufficiently soluble in water at all pH values as indicated by the sharp isosbestic points. A typical set of absorption spectra at various pH values is shown in Fig. 9.

1. J. L. R. WILLIAMS, R. E. ADEL, J. M. CARLSON, G. A. REYNOLDS, D. G. BORDEN, and J. A. FORD, JR. J. Org. Chem. **28**, 387 (1963).
2. J. L. R. WILLIAMS, R. E. ADEL, J. M. CARLSON, and G. A. REYNOLDS. Can. J. Chem. **43**, 1345 (1965).
3. H. H. JAFFE, H. JONES, and M. ISAKS. J. Am. Chem. Soc. **86**, 2934 (1964).
4. H. H. JAFFE and H. JONES. J. Org. Chem. **30**, 964 (1965).
5. A. R. KATRITZKY, D. J. SHORT, and A. J. BOULTON. J. Chem. Soc. 1511 (1960).
6. G. CAUZZO, G. GALIAZZO, U. MAZZUCATO, and N. MONGIAT. Tetrahedron, **22**, 589 (1966).
7. H. H. JAFFE. Chem. Rev. **53**, 191 (1953).
8. H. C. BROWN and T. OKAMOTO. J. Am. Chem. Soc. **80**, 4979 (1958).
9. J. HINE. Physical organic chemistry. 2nd ed. McGraw-Hill Book Co., Inc., New York. 1962. p. 90.
10. H. H. JAFFE and M. ORCHIN. Theory and applications of ultraviolet spectroscopy. John Wiley and Sons, Inc., New York. 1942. p. 429.

Can. J. Chem. Downloaded from www.nrcresearchpress.com by 210.87.254.40 on 09/05/12
For personal use only.

2,4,4-Trimethylpentenyl anions

D. H. HUNTER AND R. W. MAIR
Department of Chemistry, University of Western Ontario, London, Ontario
Received March 4, 1969

The allylic anions derived by proton abstraction from 2,4,4-trimethyl-1-pentene **1** and 2,4,4-trimethyl-2-pentene **2** have been studied as short-lived intermediates. The anions were generated in *t*-butyl alcohol-*O*-*d*-potassium *t*-butoxide at 215 °C and relative rates of hydrogen–deuterium exchange and isomerization were compared. The isomerization of the thermodynamically less stable **2** to **1** occurs through the *cis*-allylic anion with a low 10% intramolecular component. The intermediate anion preferentially collapses to give **2** (3 to 1). Treatment of **1** leads more frequently into the less substituted allylic anion.

Canadian Journal of Chemistry, **47**, 2361 (1969)

Can. J. Chem. Downloaded from www.nrcresearchpress.com by 210.87.254.6 on 09/05/12
For personal use only.

Introduction

Allylic anions have been implicated as intermediates in most base-catalyzed allylic isomerizations and their detailed behavior has been investigated for a number of systems (1). The features of the isomerizations that have received much attention are the intramolecularity of the 1,3-proton transfer (2), the collapse ratio in carbanion protonation (3), and the stability of the carbanions (4). For the phenyl substituted anions it has been possible to study the effect of medium, base, and substrate structure on all of these features. For the less stable anions derived from simple alkenes, the solvent–base pair widely employed has been dimethyl sulfoxide – potassium *t*-butoxide (5). While the effect of olefin structure in the alkenes has been extensively investigated, this solvent has limited the conclusions that could be drawn about intramolecularity and collapse ratios.

As a result we felt it would be interesting to change the solvent–base system to see what effect this would have, particularly upon the intramolecularity. Desiring a protic solvent and a strong base, we chose *t*-butyl alcohol-*O*-*d*-potassium *t*-butoxide which, however, required a high temperature (~215 °C) to effect reaction. The olefin pair selected for study was 2,4,4-trimethyl-1-pentene (**1**) and 2,4,4-trimethyl-2-pentene (**2**).

These olefins have been studied previously to obtain an estimate of their acidity (4) and to determine the gross amounts of hydrogen exchange (6) but no attempt had been made to discuss the details of their interconversion.

Results and Discussion

Equilibration

The relative stability of 2,4,4-trimethyl-1-pentene (**1**) and 2,4,4-trimethyl-2-pentene (**2**) were established under the present reaction conditions by reacting the olefins individually. The results of treatment of **1** and **2** with potassium *t*-butoxide in *t*-butyl alcohol at 215 °C for about 100 h are reported in Table I. The equilibrium composition corresponds to an equilibrium constant of 2.36 at 215 °C favoring the terminal olefin **1**. The thermodynamic relations between this pair of olefins has received considerable previous attention. Equilibrium has been observed with acid ($K = 5.3$ at 25 °C) (7), base ($K = 5.6$ at 55 °C) (4), and silica gel ($K = 5$ at 25 °C) (8). Heats of combustion, hydrogenation, and free energies have been obtained by several workers (9). These results are in substantial agreement and show that 2,4,4-trimethyl-1-pentene is thermodynamically more stable than 2,4,4-trimethyl-2-pentene under all the conditions employed. This observation has been rationalized in terms of the interactions between the *t*-butyl group and the *cis*-methyl in the **2**-isomer (10).

TABLE I

Equilibration of the 2,4,4-trimethyl-1 and 2-pentenes (0.23 *M*) in 0.42 *N* $KOC(CH_3)_3$ – $HOC(CH_3)_3$ at 215 °C

Run no.	Substrate	Time in h.	%**1***	%**2***
1	**1**	124	70.5	29.5
2	**2**	90	69.9	30.1

*±0.5%.

Relative Reactivities of the Olefins

Treatment of the 2,4,4-trimethylpentenes with the base was expected to lead into three distinct allylic anion systems. Anions *cis*-**A** and *trans*-**A** would provide routes for isomerization between the olefins **1** and **2** and concurrent exchange

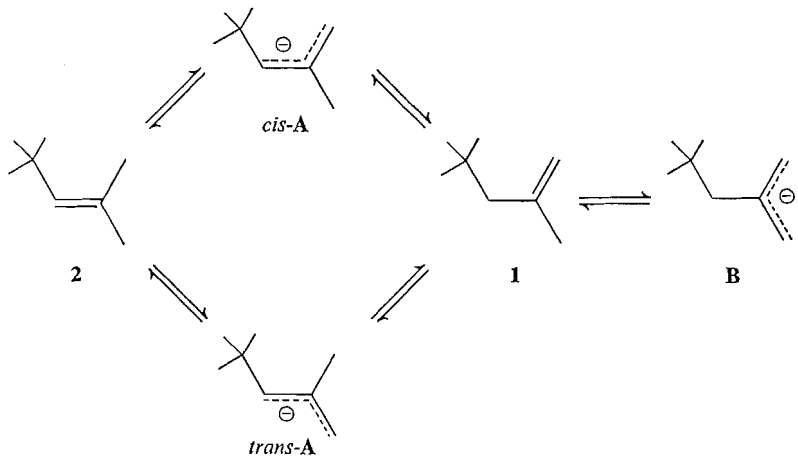

while anion **B** would only provide a mechanism for hydrogen–deuterium exchange of **1**.

Since nuclear magnetic resonance (n.m.r.) was used to determine the hydrogen–deuterium exchange behavior of **1** and **2**, the HA-100 n.m.r. spectra of 2,4,4-trimethyl-1-pentene **1** and 2,4,4-trimethyl-2-pentene **2** (5 wt. % in CCl_4) are shown in Figs. 1 and 2 along with the results of a first-order analysis of the spectrum of **2**.

As will be shown later, the relative ease of formation of *cis*-**A** and *trans*-**A** was determined from deuterium incorporation into the allylic methyls of olefin **2**. Therefore, nuclear Overhauser experiments were run to assign these methyl protons. Frequencies in the region of the allylic methyl groups were systematically irradiated and the peak corresponding to the olefinic proton was integrated. Results were obtained with varying irradiating powers, on two different Varian HA-100 spectrometers and on a Varian HA-60 spectrometer. At 100 MHz experiments were attempted, locking on TMS and on benzene. Irradiation of the upfield methyl group provided an average enhancement in the integral of 17 ± 4% while the downfield methyl showed 6 ± 4%. As a result the downfield peaks (1.68 p.p.m. from TMS) have been assigned to the methyl hydrogens *cis* to the *t*-butyl group as in Fig. 2. The opposite conclusion had been reached on the basis of chemical shifts (11) but our assignment agrees with more recent evidence, for example, ref. 12.

In the hydrogen–deuterium exchange reactions, samples of 2,4,4-trimethyl-1 and 2-pentene were treated separately with 0.16 *M* potassium *t*-butoxide in *t*-butyl alcohol-*O*-*d* in sealed degassed Carius tubes at 215 °C. After gas–liquid phase chromatography (g.l.p.c.) analysis, the mixture of olefins obtained from each reaction was separated by preparative g.l.p.c. and the individual olefins were analyzed for deuterium uptake by n.m.r. spectroscopy. Runs 3 and 4 of Table II contain the results obtained at two times with olefin **1** as the substrate. Runs 5–8 of Table II contain the results at varying times with olefin **2**.

As is evident from runs 7 and 8 the incorporation of deuterium as a function of the percentage of isomerization is quite reproducible. On the other hand for most runs time–isomerization results are reproduced only approximately, presumably due to the relatively large vertical temperature gradient (≃ 15 °C) across the sample tubes. Since conclusions were reached by comparing isomerization and exchange within a run, the time variations should not be very important. In all the exchange runs the percentage of protons in the solvent pool was kept below 5% throughout the run.

The results of Table II (in particular, run 3) can be used to obtain an estimate of the ease of formation of anion **B** relative to *cis*-**A** and *trans*-**A**. From the extensive exchange of the methyl and vinyl protons relative to the methylene protons of the recovered **1**, anion **B** is formed about 10 times more readily than the *cis*-**A** and *trans*-**A** anions. When the temperature effects are included, this difference in rate is approximately that calculated from the results of a study comparing the relative rates of base-catalyzed isomerization of several alkenes (4).

The relative rates of formation of such allylic

Can. J. Chem. Downloaded from www.nrcresearchpress.com by 210.87.254.6 on 09/05/12
For personal use only.

Can. J. Chem. Downloaded from www.nrcresearchpress.com by 210.87.254.6 on 09/05/12
For personal use only.

TABLE II

Exchange and isomerization of 2,4,4-trimethyl-1 and 2-pentene in 0.16 *N* $KOC(CH_3)_3$ – $DOC(CH_3)_3$ at 215 °C

Run no.	Substrate		Time (min)	1				2			
					Atoms D/molecule				Atoms D/molecule		
	Nature	Concentration		%	CH_3	CH_2	Vinyl-CH_2	%	*cis*-CH_3	*trans*-CH_3	Vinyl-H
3	**1**	0.21	1200	88.4	1.69	0.30	1.09	11.6	—	—	—
4	**1**	0.21	2640	74.3	2.36	0.25	1.57	25.7	3.0	0.88	1.0
5	**2**	0.74	380	8.5	0.40	0.56	0.30	91.2	0.09	0.08	0.07
6	**2**	0.20	408	16.0	—	—	—	83.7	0.43	0.12	0.08
7	**2**	0.19	670	26.3	1.44	0.82	0.88	74.4	0.71	0.12	0.19
8	**2**	0.20	760	27.0	1.40	0.83	0.62	72.7	0.70	0.10	0.10

Can. J. Chem. Downloaded from www.nrcresearchpress.com by 210.87.254.6 on 09/05/12
For personal use only.

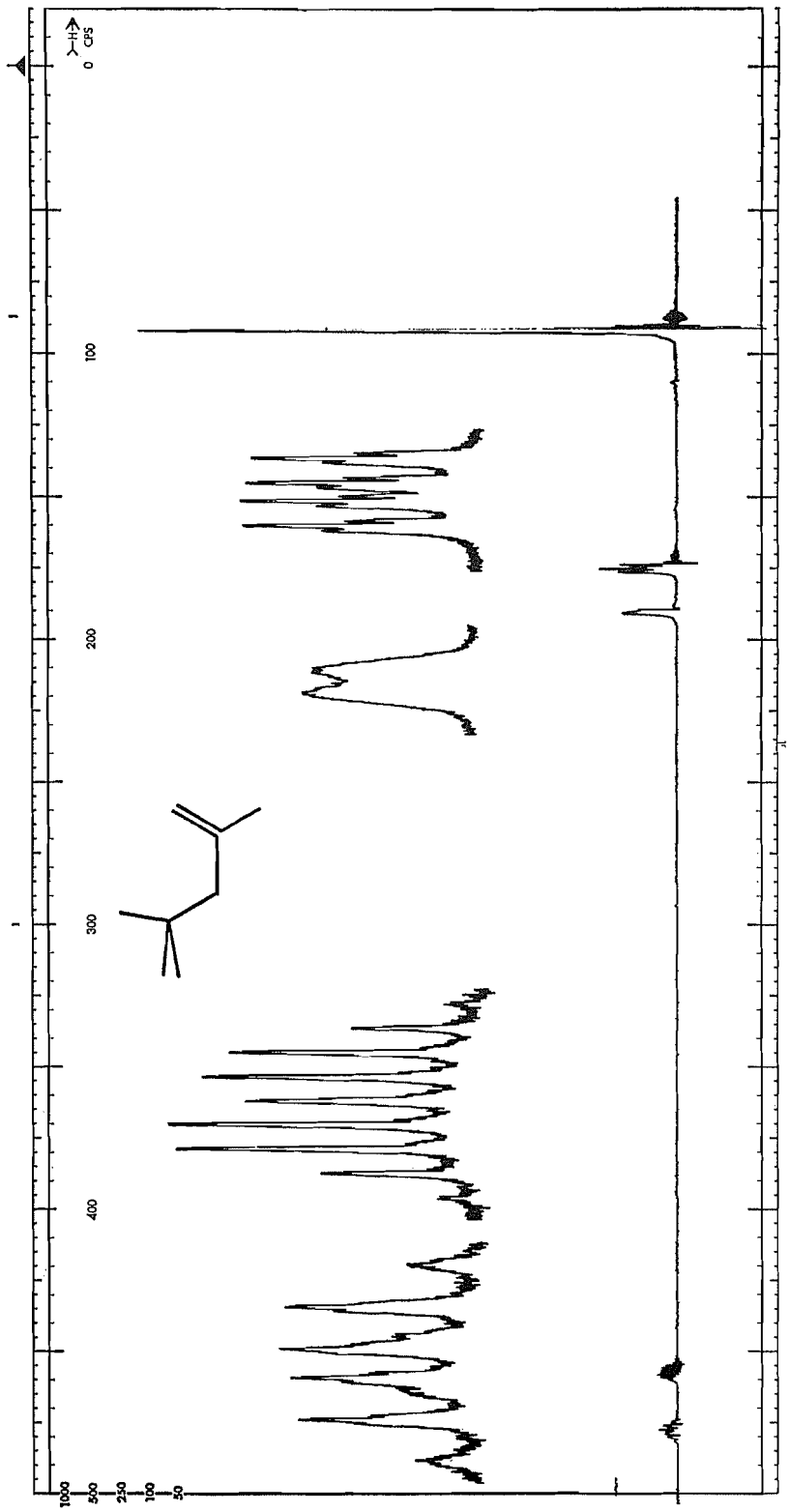

FIG. 1. The 100 MHz nuclear magnetic resonance spectrum of 2,4,4-trimethyl-1-pentene with sweep widths of 1000 and 50 Hz.

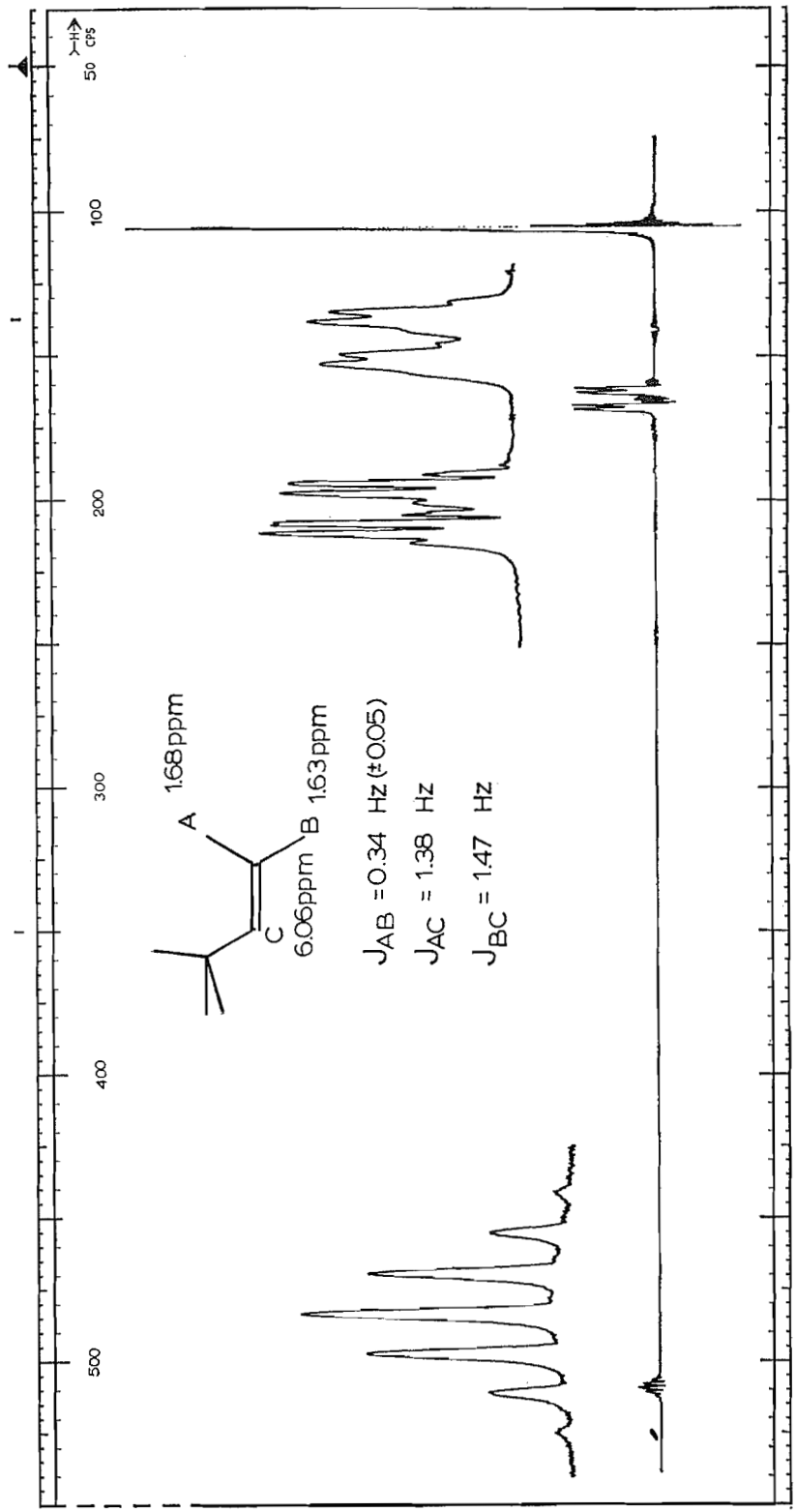

FIG. 2. The 100 MHz nuclear magnetic resonance spectrum of 2,4,4-trimethyl-2-pentene with sweep widths of 1000 and 50 Hz.

Can. J. Chem. Downloaded from www.nrcresearchpress.com by 210.87.254.6 on 09/05/12
For personal use only.

Can. J. Chem. Downloaded from www.nrcresearchpress.com by 210.87.254.6 on 09/05/12
For personal use only.

carbanions have been rationalized in terms of inductive and steric effects in the transition states for anion formation (4). While these factors are involved it is interesting to compare our extended Hückel calculations on the *cis*- and *trans*-butenyl systems with the isobutenyl system. For the allylic cations *trans*-butenyl is about 9 kcal/mole more stable than *cis*-butenyl or isobutenyl while for the anions, isobutenyl is about 9 kcal/mole more stable than the *cis*- or *trans*-butenyl anions. The π-molecular orbital being filled in passing from cation to anion in the butenyl systems involves considerable mixing of the orbitals on the methyl group. Thus hyperconjugation could be playing an important part in affecting anion stability and consequently a significant role in determining which anion is formed.

Reactivity of Geometric Isomers

Olefin **2** can lead to either of two anions (*cis*-**A** or *trans*-**A**). Collapse of these anions could regenerate **2** or produce **1** (both either exchanged or unexchanged). By comparing the relative amounts of exchange of the allylic methyl hydrogens in **2**, it is possible to determine which anion is preferentially formed. This assumes that *cis*-**A** and *trans*-**A** provide the major pathway for exchange and that exchanged **1** is not significantly involved. This assumption will be justified in a later section.

As the results of Table II show, the methyl *cis* to the *t*-butyl group in **2** exchanges faster than the *trans*-methyl and the relative amounts of exchange yield a factor of at least 11. On this basis the anion *cis*-**A** is the dominant intermediate and presumably the more stable anion. The preferential formation of *cis*-allylic anions appears to be a general phenomenon when stabilizing groups such as phenyl rings are absent (13). A variety of explanations have been offered to interpret these results. Among these are dipole moments of the anions (14), electronic stability of the anions as obtained by extended Hückel calculations (15), steric effects on solvation of the anions (1), ground state conformational preferences (16), and non-bonded interactions in the anions (17).

Intramolecularity

Before further consideration can be given to the exchange results reported in Table II, it is necessary to correct for the fact that 3.2% of **1** was present in **2**. The pertinent corrected results are contained in Table III. With these results and the equilibrium data of Table I, we have obtained information on the intramolecularity of the 1,3-proton shift in the allylic isomerization of **2** to **1** and on the energy profile for the interconversion.

Although we have assumed above that intermediates are involved in these isomerizations based upon analogy with similar systems (1), their involvement can be readily demonstrated with this olefin pair. Ignoring isotope effects, the equilibrium results show that the relative rates for interconversion of the olefins **1** and **2** are in the ratio of 2.4:1.

Assuming the kinetic scheme depicted in the heading of Table IV, the percentages of the two olefins that would have arisen were calculated to simulate the results collected in Table III. It is clear that even at the greatest extent of reaction, very little **2** has been regenerated (symbolized **2′**). If no intermediates were involved then the only source of deuterium in **2** would be from regenerated **2′**. The results of Table III show on the other hand that considerable incorporation of

TABLE III

Corrected and calculated exchange and isomerization results for 2,4,4-trimethyl-2-pentene

	1					**2**				
		Atoms D/molecule in CH_2					Atoms D/molecule in *cis*-CH_3			
			Calculated*					Calculated*		
Run no.	%	Corrected	2	3	4	%	Corrected	2	3	4
5	5.3	0.91	0.90	0.90	0.90	94.7	0.09	0.10	0.16	0.21
6	12.8	—	0.90	0.91	0.91	87.2	0.43	0.26	0.38	0.49
7	23.1	0.93	0.91	0.91	0.92	76.9	0.71	0.48	0.68	0.86
8	23.8	0.94	0.91	0.91	0.92	76.2	0.70	0.48	0.68	0.86

*The headings 2, 3, and 4 represent the ratio of k_a/k_d chosen for the calculation of that column.

deuterium has occurred while little **2′** has been produced and thus an intermediate must be invoked. The results of Table IV are of further significance since they justify ignoring further reactions of **1** for the periods of reaction studied since only 1.3% of **2′** has been formed, although 23% of **2** has reacted. Generation of anion **B** is a probable exception to this rule but it produces only exchange of the methyl and vinyl protons of **1** which need not be considered in the further discussion.

With these results in mind, the data of Table III were considered in terms of the partial mechanistic scheme depicted below. In this working

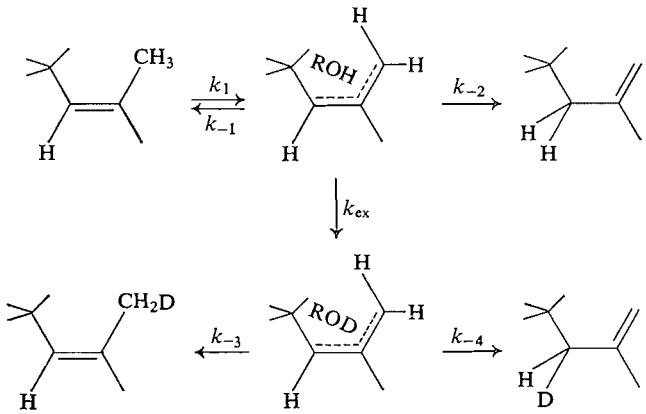

model the intermediate anions are represented in a grossly oversimplified manner in which the details of solvation and the mechanism for exchange are excluded. This is intentional since our evidence does not bear directly on these points. To facilitate kinetic analysis this mechanism was converted to the scheme shown below.

Rate constants were assigned to the kinetic scheme to obtain a best fit. The general scheme followed in assigning rate constants is as follows: (*1*) a ratio of k_a/k_d was chosen; (*2*) a ratio of k_d/k_c was chosen; (*3*) a kinetic isotope effect was then assumed.

Applying this isotope effect and with statistical weighting, the ratio of k_a/k_b is then fixed. Similarly the ratios $k_c:k_e:k_g$ and $k_d:k_f:k_h$ are fixed.

The calculated deuterium incorporation into the methylene group of olefin **1** depended only upon the ratio assumed for k_d/k_c in the range of k_a/k_d chosen. A good fit was obtained for k_d/k_c = 9. The ratio k_a/k_d determined the extent of deuterium incorporation into the methyl group of olefin **2** at a particular extent of isomerization. The sensitivity of the results to the assumed k_a/k_d ratio can be seen from the calculated results included in Table III. For these calculations the ratio $k_d/k_c = 9$ and the kinetic isotope effect

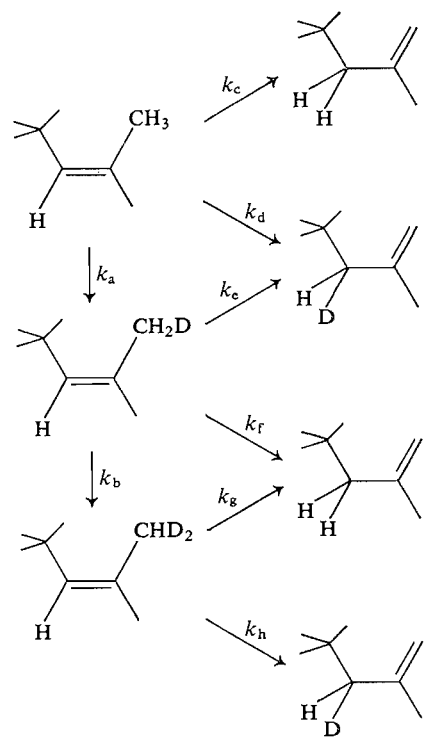

Can. J. Chem. Downloaded from www.nrcresearchpress.com by 210.87.254.6 on 09/05/12
For personal use only.

TABLE IV

Calculated percentages of interconversion between 2,4,4-trimethyl-1 and 2-pentene corresponding to the results of Table III

		Calculated*			
Run no.	Observed %(2+2′)	2.4† 2 ⟶	1 ⟶	2′ ⟶	2.3 1′
5	94.7	94.2	5.8	0.07	0.001
6	87.2	87.6	12.0	0.33	0.01
7	76.9	75.9	22.7	1.3	0.1

*The symbols **2** and **1** refer to unreacted 2,4,4-trimethyl-2 and 1-pentene respectively while **2′** and **1′** refer to the regenerated olefins.
†The relative rate constants are assigned from the equilibrium constant since $K = k_2/k_1 = 2.37$.

$k_H/k_D = 1$. The best fit is obtained for $k_a/k_d = 3$. This result was insensitive to the magnitude of the kinetic isotope effect presumably because of the small extent of deuterium incorporation. While definite values can be assigned to the ratios, the inaccuracies in the n.m.r. method of deuterium analysis suggest that $k_a/k_d = 3 \pm 0.5$ and $k_d/k_c > 8$.

The calculated ratios can be interpreted in terms of the mechanistic scheme by noting that with a steady state approximation for the anions

$$k_a = k_1k_{ex}k_{-3}/(k_{-1} + k_{-2} + k_{ex})(k_{-3} + k_{-4})$$

$$k_c = k_1k_{-2}/(k_{-1} + k_{-2} + k_{ex})$$

$$k_d = k_1k_{ex}k_{-4}/(k_{-1} + k_{-2} + k_{ex})(k_{-3} + k_{-4}).$$

One of the interesting results of this study was the lack of a significant intramolecular proton transfer component in the isomerization. The isolated olefin **1** contained 0.9 of an atom of deuterium or only 10% of the isomerization had occurred with an intramolecular 1,3-proton transfer. This is in direct contrast to results obtained for perdeuterio-1-pentene in 0.4 *M* *t*-butyl alcohol in dimethyl sulfoxide – potassium *t*-butoxide at 55 °C where isomerization led total exchange by a factor of 16 (18). The ratio of isomerization to total exchange $(k_c + k_d)/(k_a + k_d)$ for 2,4,4-trimethyl-2-pentene in *t*-butyl alcohol potassium *t*-butoxide at 215 °C is about 0.27. This corresponds to a factor of 60 difference in relative rates between the two studies. This 10% intramolecular proton transfer is one of the lowest that has been observed even for more delocalized anionic intermediates (1).

The large difference between the intramolecularity in 0.4 *M* *t*-butyl alcohol dimethyl sulfoxide and *t*-butyl alcohol probably has two major causes; temperature and proton (deuteron) availability. In terms of a mechanism like that shown on p. 2367, it is possible to estimate the change in $k_{ex}/(k_{-1} + k_{-2})$ that has occurred in these two contrasting experiments. Assuming that the intermediate in the perdeuterio-1-pentene isomerization collapses predominantly to 2-pentene, the change is a factor of 145. The *t*-butyl alcohol concentration has changed by a factor of about 25 and should account for a major portion of the rate ratio change.

Such a conclusion is supported by a calculation of the difference in $\Delta H^{\ddagger}$ between k_{ex} and $(k_{-1} + k_{-2})$ if the rate ratio changes were ascribed to temperature alone. The $\Delta\Delta H^{\ddagger}$ is calculated to be about 10 kcal/mole which is unreasonably high since both reactions are undoubtedly low energy processes.

On the basis of these arguments it seems sensible to expect that the absence of readily exchangeable hydrogens in the medium is an important factor in the high intramolecularity in dimethyl sulfoxide and that the high temperature is mainly responsible for the low intramolecularity in *t*-butyl alcohol.

Collapse Ratio

From the exchange and isomerization results it is possible to deduce the collapse ratio (k_{-1}/k_{-2} or k_{-3}/k_{-4}) for the proposed anionic intermediates. From the ratio $k_a/k_d = k_{-3}/k_{-4} = 3 \pm 0.5$, it is apparent that deuteron (and proton) capture by the allylic intermediate occurs more readily at the less substituted carbon to give the less stable isomer. This result can be interpreted as a steric interaction outweighing a thermodynamic effect. Extended Hückel results on the analogous *cis*-butenyl anion indicate a higher charge density on the 1-carbon than 3-carbon.

Can. J. Chem. Downloaded from www.nrcresearchpress.com by 210.87.254.6 on 09/05/12
For personal use only.

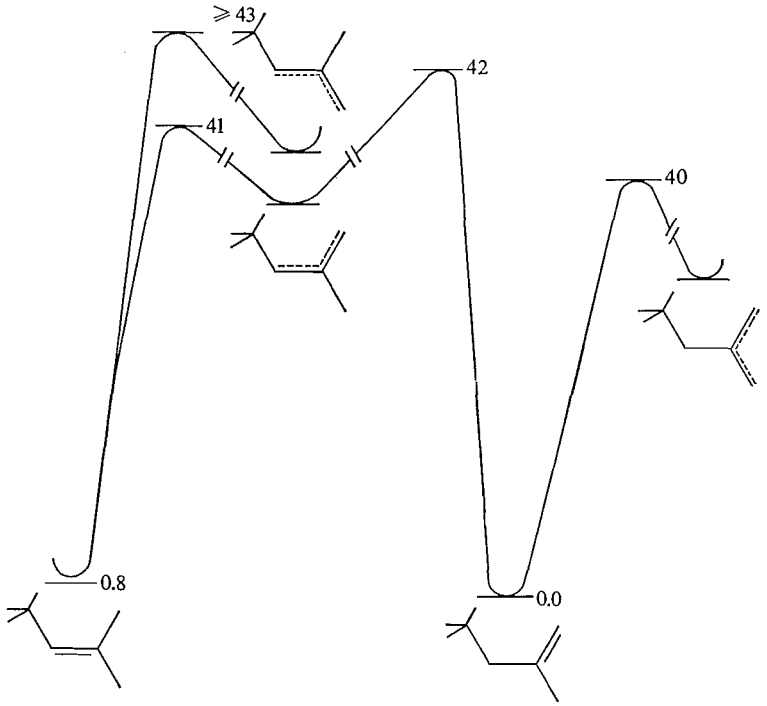

Although calculated values for absolute charges are not to be trusted (19), the relative charge distribution in the anion itself is consistent with favored attack at the less substituted carbon.

The kinetic results are summarized in the accompanying free energy diagram. Energies are in kcal/mole at 215 °C.

Experimental

Compounds

The 2,4,4-trimethyl-1-pentene and 2,4,4-trimethyl-2-pentene (Phillips Petroleum Co.) were distilled before use. The 2,4,4-trimethyl-1-pentene was judged to be 99.5% pure by gas–liquid partition chromatography analysis. The 2,4,4-trimethyl-2-pentene contained 3.2% of 2,4,4-trimethyl-1-pentene and 0.3% of an unidentified impurity as estimated by g.l.p.c. This impurity persisted through the isomerization and exchange reactions but was separated before deuterium analysis.

The *t*-butyl alcohol-*O-d* (0.98 atoms D/molecule as determined by nuclear magnetic resonance (n.m.r.)) was prepared as previously reported (20). The base solutions were obtained by dissolving freshly cut potassium metal in the alcohol under a nitrogen atmosphere.

Nuclear Magnetic Resonance Spectra

Proton spectra were run on the Varian HA-100 and A-60A spectrometers using a C-1024 time average computer for the more dilute samples. Deuterium analyses were obtained on carbon tetrachloride solutions of olefins obtained directly from preparative g.l.p.c. Integrations are the average of 10 scans with maximum expanded range and are relative to the 9 protons of the *t*-butyl group in each olefin.

Nuclear Overhauser experiments were run on degassed solutions of the olefins in carbon tetrachloride. Ten integrals were run at each irradiating frequency.

Exchange and Isomerization Reactions

Typically the substrate and base solution were sealed under vacuum after degassing in a Carius tube. The tube was then submerged in a thermoregulated Wood's metal bath for the reported time. The vertical temperature gradient in the bath was about 15 °C and the average temperature is reported.

After cooling the tube was opened and the solution was treated with pentane and three water extractions. After drying the excess pentane was carefully removed by distillation and the residual oil analyzed by g.l.p.c. A 1/4 in. × 18 ft column of 10% SE-30 on 40/60 mesh firebrick was employed for the analyses. Area percentages are reported.

Preparative separation of the olefin mixture was obtained with a 3/8 in. × 15 ft glass column of 10% SE-30 on 40/60 mesh firebrick. The eluted olefins were transferred with small amounts of carbon tetrachloride into n.m.r. tubes for deuterium analysis. Typical recoveries are estimated at 30% with the major loss occurring in transferring from the g.l.p.c. collector to the n.m.r. tubes.

Extended Hückel Calculations

Calculations were run on three basic allylic skeletons (isobutenyl, *cis*-butenyl, and *trans*-butenyl) looking at both the cations and the anions. In all these calculations

Can. J. Chem. Downloaded from www.nrcresearchpress.com by 210.87.254.6 on 09/05/12
For personal use only.

idealized bond angles were employed and the bond lengths were chosen on the basis of a preprint kindly supplied to us by one of the authors (21). In all three systems the methyl group was rotated and the lowest energy form chosen.

The program employed involved conventional extended Hückel calculations analogous to the program available from the Quantum Chemistry Program Exchange.

Kinetic Calculations

The mechanistic schemes analyzed in this article were obtained as limiting cases of a more general scheme developed for another study in progress. This general case is shown below

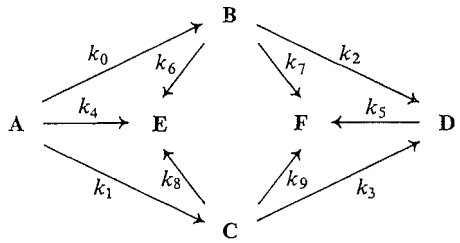

Setting $A + B + C + D + E + F = 1$, $A_o = 1$ and $B_o = C_o = D_o = E_o = F_o = 0$ the solution is

$$A = \exp -k_a t$$

$$B = k_0/(k_b - k_a)[(\exp -k_a t) - (\exp -k_b t)]$$

$$C = k_1/(k_c - k_a)[(\exp -k_a t) - (\exp -k_c t)]$$

$$D = (\alpha + \beta)/(k_5 - k_a)[(\exp - k_a t) - (\exp -k_5 t)] - \alpha/(k_5 - k_b)[(\exp -k_b t) - (\exp -k_5 t)] - \beta/(k_5 - k_c)[(\exp -k_c t) - (\exp -k_5 t)]$$

$$E = \delta/k_b[(\exp -k_b t) - 1] + \gamma/k_c[(\exp -k_c t) - 1] - \varepsilon/k_a[(\exp -k_a t) - 1]$$

$$F = 1 - A - B - C - D - E,$$

where $k_a = k_0 + k_1 + k_4$; $k_b = k_2 + k_6 + k_7$; $k_c = k_3 + k_8 + k_9$; $\alpha = k_0 k_2/(k_b - k_a)$; $\beta = k_1 k_3/(k_c - k_a)$; $\gamma = k_1 k_8/(k_c - k_a)$; $\delta = k_0 k_6/(k_b - k_a)$; and $\varepsilon = k_4 + \delta + \gamma$.

Acknowledgments

The authors wish to thank J.B. Stothers and N.C. Baird for their generous assistance and the Agricultural Research Institute for use of their n.m.r. facilities. We also wish to thank the National Research Council of Canada and the Department of University Affairs of the Province of Ontario for their financial assistance.

1. D. J. Cram. Fundamentals of carbanion chemistry. Academic Press, Inc., New York. 1965. Chapter 5.
2. J. Almy, R. T. Uyeda, and D. J. Cram. J. Am. Chem. Soc. **89**, 6768 (1967) and cited examples.
3. S. W. Ela and D. J. Cram. J. Am. Chem. Soc. **88**, 5791 (1966).
4. A. Schriesheim, C. A. Rowe, and L. Naslund. J. Am. Chem. Soc. **85**, 2111 (1963).
5. A. Schriesheim, J. E. Hofmann, and C. A. Rowe. J. Am. Chem. Soc. **83**, 3731 (1961) and subsequent publications.
6. (*a*) A. I. Shatenshtein, L. N. Vasil'eva, N. M. Dykhno, and E. A. Izrailevich. Dokl. Akad. Nauk SSSR, **85**, 381 (1952); (*b*) A. I. Shatenshtein and L. N. Vasil'eva. Dokl. Akad. Nauk SSSR, **95**, 115 (1955); (*c*) A. I. Shatenshtein, L. N. Vasil'eva, and N. M. Dykhno. Zh. Fiz. Khim. **28**, 193 (1954).
7. E. D. Hughes, C. K. Ingold, and V. J. Shiner. J. Chem. Soc. 3827 (1953).
8. W. S. Gallaway and M. J. Murray. J. Am. Chem. Soc. **70**, 2584 (1948).
9. J. D. Rockenfeller and F. D. Rossini. J. Phys. Chem. **65**, 267 (1961) and cited references.
10. R. B. Turner, D. E. Nettleton, and M. Perelman. J. Am. Chem. Soc. **80**, 1430 (1957).
11. L. M. Jackman and R. H. Wiley. J. Chem. Soc. 2881 (1960).
12. B. V. Cheney. J. Am. Chem. Soc. **90**, 5386 (1968).
13. (*a*) S. Bank, A. Schriesheim, and C. A. Rowe. J. Am. Chem. Soc. **87**, 3244 (1965); (*b*) S. W. Ela and D. J. Cram. J. Am. Chem. Soc. **88**, 5777 (1966).
14. S. Bank. J. Am. Chem. Soc. **87**, 3245 (1965).
15. R. Hoffmann and R. A. Olofson. J. Am. Chem. Soc. **88**, 943 (1966).
16. C. C. Price and W. H. Snyder. Tetrahedron Letters, 69 (1962).
17. W. O. Haag and H. Pines. J. Am. Chem. Soc. **82**, 387 (1960).
18. S. Bank, C. A. Rowe, and A. Schriesheim. J. Am. Chem. Soc. **85**, 2115 (1963).
19. R. Hoffmann. J. Chem. Phys. **39**, 1397 (1963).
20. D. J. Cram and B. Rickborn. J. Am. Chem. Soc. **83**, 2178 (1961).
21. N. C. Baird and M. J. S. Dewar. J. Chem. Phys. To be published.

Can. J. Chem. Downloaded from www.nrcresearchpress.com by 210.87.254.6 on 09/05/12
For personal use only.

Thermal decomposition of optically active unsymmetrical azoalkanes. (−)-(*S*)-1,1′-Diphenyl-1-methylazomethane[1]

KARL R. KOPECKY AND THOMAS GILLAN[2]
Department of Chemistry, University of Alberta, Edmonton, Alberta
Received December 24, 1968

The ratio, $(k_c/k_r)_{cage}$, of the rate of coupling of the 1-phenylethyl radical with the benzyl radical to the rate of its rotation with respect to the benzyl radical in the solvent cage has been determined for several solvents. The optically pure title compound, (−)-(*S*)-**4**, has been prepared and its absolute configuration determined. Thermal decomposition of (−)-(*S*)-**4** yields (−)-(*R*)-1,2-diphenylpropane, (−)-(*R*)-**9**, with partial retention of configuration. The maximum rotation of (−)-(*R*)-**9** has been determined. At 100° in benzene, cyclohexane, chlorobenzene, (all containing ca. 1 *M* butanethiol) and butanethiol, the cage effects for the decomposition of (±)-**4** were found to be 28.3, 31.7, 33.4, and 18.2%, respectively. Under these conditions (−)-(*R*)-**9** was formed from (−)-(*S*)-**4** with 10.3, 10.9, 13.0, and 17.3% net retention of configuration, respectively. A simple expression for $(k_c/k_r)_{cage}$ can be derived:

$$(k_c/k_r)_{cage} = F(1 - f)[(-)\text{-}(R)\text{-}\mathbf{9}/(+)\text{-}(S)\text{-}\mathbf{9} - 1]$$

F is the fraction of radicals consumed within the solvent cage and *f* is the fraction of radicals consumed within the solvent cage that disproportionate. Under the above conditions values for $(k_c/k_r)_{cage}$ were found to be 0.059, 0.069, 0.090, and 0.070, respectively. The values of the cage effect and $(k_c/k_r)_{cage}$ given were calculated assuming $f = 0.1$, but change little if *f* is assumed to be 0. The relevance of these results to the stereochemistry of the Wittig and Meisenheimer rearrangements and of the decomposition of diacyl peroxides is discussed.

Canadian Journal of Chemistry, 47, 2371 (1969)

The stereochemical fate of free radicals generated from optically active precursors has not yet received the systematic study accorded that of carbonium ions and carbanions derived from such sources. This appears to be due to a number of factors including the observations of essentially complete loss of either optical activity (1) or isomeric identity (2) in early systems studied, and ambiguity (3) concerning the mechanisms of decomposition of diacyl peroxides from which optically active products have been obtained (4).

In reactions which almost certainly proceed by radical pathways, stereoselectivity has been observed in the decomposition of substituted pyrazolines (5) and substituted tetrahydropyridazines (6) to substituted cyclopropanes and substituted cyclobutanes, respectively, photochemical decomposition of acyclic azoalkanes in frozen solution at low temperature (7), in a cage disproportionation reaction (8), in perester decompositions under very high pressures of oxygen (9), in addition of hydrogen bromide to olefins at low temperature and at high hydrogen bromide concentration (10), in certain photobromination reactions at low temperature (11), and in the cyclization of a propargylic ester to a γ-lactone (12). In the reactions involving open-chain systems stereoselectivity decreased with both increasing temperature (7, 9–11) and with decreasing concentration of radical trapping species (9–11). In all these cases radicals were generated with either another radical or a very efficient radical trapping species either within or as part of the solvent cage. Only in frozen solution was complete stereospecificity observed (7). It is clear that free radicals formed in the liquid or vapor phase by homolytic fission of a bond at an asymmetric carbon atom cannot maintain asymmetry for longer than ca. 10^{-9} s, if at all. One cannot tell if loss of asymmetry is due to a requirement that the radical assume a planar conformation or is due to rapid interconversion between two pyramidal conformations. Spectral studies of free radicals indicate that the planar conformation is the more stable (13), but radicals can be formed at the bridgehead carbon atom of small, bicyclic ring systems with energy requirements not much greater than in those systems in which radicals can assume a planar conformation (14, 3).

---

[1]Presented in part at the 51st Annual Conference of the Chemical Institute of Canada, Vancouver, British Columbia. June, 1968, abstracts, p. 57.

[2]Holder of an NRCC Studentship, 1966–1968; a Province of Alberta Fellowship, 1966–1967; a Province of Alberta Scholarship, 1967–1968; and a University of Alberta Dissertation Fellowship, 1968.

Can. J. Chem. Downloaded from www.nrcresearchpress.com by 210.87.254.105 on 09/05/12
For personal use only.

Can. J. Chem. Downloaded from www.nrcresearchpress.com by 210.87.254.105 on 09/05/12
For personal use only.

Vinyl radicals also lose geometrical identity quite rapidly (15) and these species can be trapped before isomerization only at low temperatures and with high concentrations of reactive hydrogen atom donors (16).

In order to be able to detect asymmetric products from radical reactions in solution involving asymmetric substrates it is necessary to use a reaction in which radicals are consumed at a rate which can compete with the rates of their diffusion and rotation.

The decomposition of a series of optically active unsymmetrical azoalkanes, eq. [1], appears well suited for a general and systematic investi-

[1] $$R{-}N{=}N{-}R' \rightarrow R{-}R' + R{-}R + R'{-}R' + N_2$$

gation of the stereochemical capabilities of free radicals and of the relative rates of the various processes which radicals formed in pairs in close proximity to each other can undergo. The radical nature of the decomposition of azoalkanes is well known and there is good evidence in both cyclic (*5b*, 17) and acyclic (18) systems that the decomposition is a concerted process which gives directly a molecule of nitrogen and a pair of radicals. These can combine at a rate which competes with the rate of their diffusion apart (19). The study of the decomposition of unsymmetrical azoalkanes offers several advantages over that of symmetrical azoalkanes. Separation of diastereomeric starting materials is unnecessary. Stereoselectivity would only be observed as a result of a cage recombination (19) reaction which can produce only the unsymmetrical coupling product R—R′. This product should be easily separable from the symmetrical products, R—R and R′—R′, which are only formed by combination of radicals which have diffused away from their original partners. The yield of symmetrical coupling products is dependent upon the proportion of radicals which diffuse away from their original partners. This could allow an estimate to be made of the proportion of cage recombination which occurs without recourse to the radical counting techniques usually required, and/or allow an estimate to be made of the relative rates of coupling between various radicals. Finally, the nature of the groups R and R′ can be varied independently and in a way that the stereochemistry of even bulky radicals can be studied. For example, if R is big, R′ can be made small so that a significant amount of cage recombination might still occur. Only a very small amount of cage recombination is observed in decomposition in solution of symmetrical azoalkanes with bulky alkyl groups (7).

The preparation and some studies of the decomposition of racemic and optically active 1,1′-diphenyl-1-methylazomethane are presented in this report. After the experimental work reported in this paper had been completed a report of the stereochemistry of decomposition of (−)-1,1′-diphenylazoethane was presented (20). The results described in that report are in excellent agreement with those of the present study.

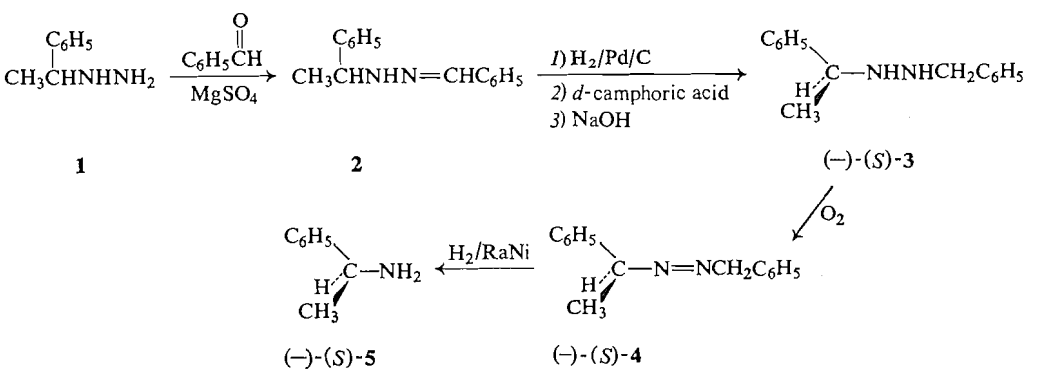

$[\alpha]_D^{25}$ −31.4°(*c*, 5.4, dioxane) $[\alpha]_D^{25}$ −125° (*c*, 1.06, benzene)

Rotations given are experimentally observed

CHART I

Can. J. Chem. Downloaded from www.nrcresearchpress.com by 210.87.254.105 on 09/05/12
For personal use only.

Absolute Configurations of Starting Material and Product

The preparation of (−)-(*S*)-1,1′-diphenyl-1-methylazomethane, (−)-(*S*)-**4**, and its degradation to (−)-(*S*)-1-phenylethylamine, (−)-(*S*)-**5**, are outlined in Chart I.

N-Benzyl-*N*′-(1-phenylethyl)-hydrazine, **3**, was prepared by condensation of 1-phenylethylhydrazine, **1** (18*c*), with benzaldehyde followed by reduction of the benzaldehyde 1-phenylethylhydrazone, **2**, formed. The compound, **3**, was quite sensitive to air oxidation and was readily oxidized to **4** by stirring solutions containing it under an atmosphere of oxygen. The azoalkane, **4**, was very sensitive to acid, base, and light. Rearrangement to the hydrazone, **2**, occurred readily under the influence of any one of these catalysts. This behavior contrasts with that of 1,1′-diphenylazoethane which in our hands is much less sensitive. Distillation of **4** was not attempted. It was purified by concentration of solutions containing it until the refractive index of the residual oil remained constant. When the preparation of **4** was carried out in the dark using carefully neutralized apparatus, the product was analytically pure, contained less than 1–2% hydrazone, **2**, as determined by ultraviolet (u.v.) spectroscopy, and no extraneous peaks could be detected in its nuclear magnetic resonance (n.m.r.) spectrum.

The resolution of **3** was accomplished by fractional crystallization of the *d*-camphorate salt until the rotation of the salt remained constant. Attempts to obtain the rotation of (−)-(*S*)-**3** gave variable results because of its ready oxidation to (−)-(*S*)-**4**. A sample of (−)-(*S*)-**4**, $[\alpha]_D^{25}$ −152° (*c*, 1.06, benzene), was hydrogenolyzed with Raney nickel in methanol at 25° to (−)-(*S*)-1-phenylethylamine, (−)-(*S*)-**5**, $[\alpha]_D^{25}$ −31.4° (*c*, 5.4, dioxane), whose absolute configuration is established (21) and whose maximum rotation (22) under these conditions was determined: $[\alpha]_D^{25}$ −39.6° (*c*, 5.4, dioxane). This result indicates that either this sample of (−)-(*S*)-**4** was 79% optically pure or racemization took place under the conditions of the hydrogenolysis. There was no racemization of (−)-(*S*)-**5** under the reaction conditions. Racemization could occur before hydrogenolysis, either by the process involved in the racemization which accompanies reduction in the catalytic hydrogenation of (−)-(*R*)-3-phenyl-1-butene to (−)-(*R*)-2-phenylbutane (23), or as a result of isomerization, by base adsorbed on the catalyst, of (−)-(*S*)-**4** to the benzylhydrazone of acetophenone, **10**, followed by reduction and hydrogenolysis.

In an alternate attempt to determine the maximum rotation of (−)-(*S*)-**4** a sample (−)-(*S*)-**5**, $[\alpha]_D^{25}$ −36.6° (neat, *l* 1 dm), was converted to

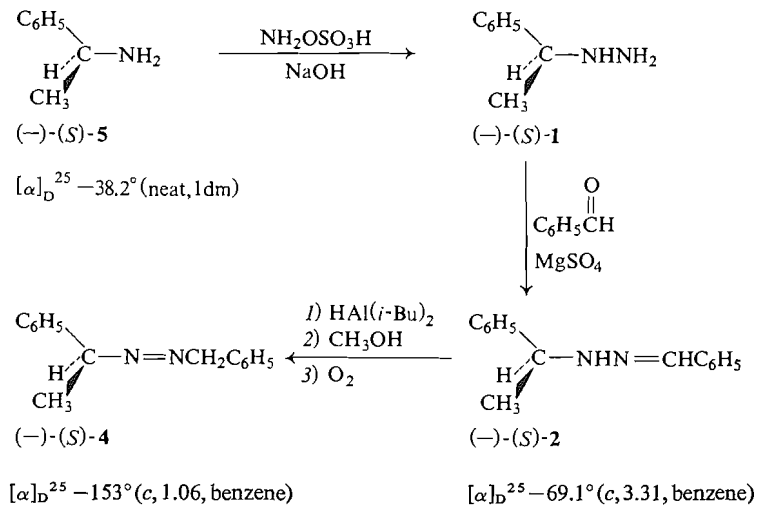

Rotations given are for optically pure compounds

CHART II

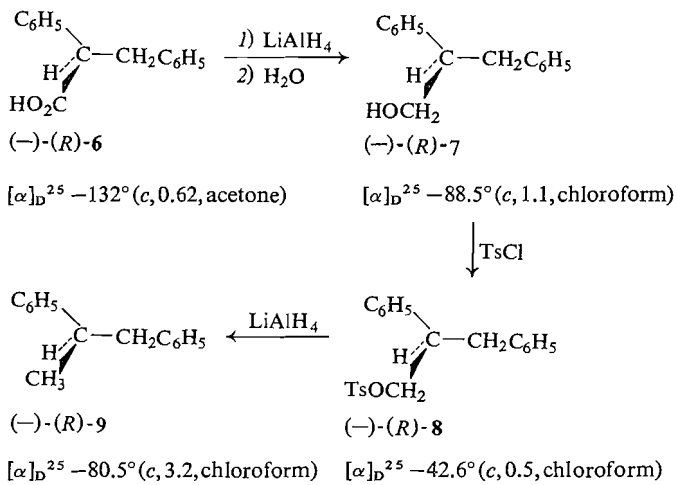

Rotations given are for optically pure compounds; Ts = *p*-toluenesulfonyl

CHART III

(−)-(*S*)-**4**, $[\alpha]_D^{25}$ −146° (*c*, 1.36, benzene),[3] by a route which quite certainly does not affect the asymmetric center (Chart II). On the basis that the maximum rotation of (−)-(*S*)-**5** is 38.2° (neat, *l* 1 dm) (22) the maximum rotation of (−)-(*S*)-**4** determined in this manner would then be −153°. This is essentially identical with the value obtained by resolution, and (−)-(*S*)-**4** of $[\alpha]_D^{25}$ −152° must be optically pure or very nearly so.

The absolute configurations of the 1,2-diphenylpropanes, (+)- and (−)-**9**, the unsymmetrical coupling products expected from decomposition of (+)-(*R*)- and (−)-(*S*)-**4**, have been determined (24), but there appeared to be some doubt about the maximum rotation of these compounds. Values of $[\alpha]_D^{19}$ −63.5° (24), $[\alpha]_D^{25}$ +76.7° (25), and $[\alpha]_D^{25}$ −76.3° (25) (all *c*, 2.2–2.3, chloroform) have been reported for these materials prepared by different routes. An independent determination of the maximum rotation of these materials seemed necessary[4] and was carried out by the route shown in Chart III. Optically pure (−)-(*R*)-2,3-diphenylpropanoic acid, (−)-(*R*)-**6** (28), was converted to (−)-(*R*)-**9**, $[\alpha]_D^{25}$ −80.5° (*c*, 3.2, chloroform), by reactions which did not involve the asymmetric center. This sequence establishes chemically the absolute configuration of (−)-(*R*)-**6**[5] as well as the maximum rotations of (−)-(*R*)-**9** and the intermediates shown in Chart III. The enantiomers of **9** prepared previously were clearly not optically pure (25).

Kinetic Studies

The rates of decomposition of **4** in cumene were determined by measuring the rates of nitrogen evolution. An insufficient amount of nitrogen was evolved in each of the kinetic runs and plots of log $(V_\infty - V_0)/(V_\infty - V_t)$ vs. time showed considerable curvature, especially at the lower temperature. The rate constants given in Table I were determined from the initial slopes of the plots using the theoretical values for V_∞. The initial rates are independent of concentration. An n.m.r. spectral analysis of a run at 106° indicated that considerable amounts of hydrazone, **2**, had been formed. There was no evidence for the presence of any of the isomeric hydrazone, acetophenone benzylhydrazone, **10**. It was

[3]After correction for the presence of 8 mole % of (−)-(*S*)-**1**.

[4]Raney nickel reduction of a sample of (−)-(1*S*,2*S*)-1,2-diphenyl-1-propanol (26) afforded the enantiomer with $[\alpha]_D^{25}$ − 76.3°, while the enantiomer with $[\alpha]_D^{25}$ +76.7° had been prepared by a sequence involving Raney nickel hydrogenolysis of a hydroxyl group at the asymmetric center. This hydrogenolysis would have to have proceeded with 100% retention of configuration if the (−)-enantiomer were optically pure and if no optical fractionation occurred during further reactions leading to the (+)-enantiomer. Such a high degree of stereospecificity does not appear to occur in Raney nickel hydrogenolyses of other systems (27).

[5]The absolute configuration of (+)-(*S*)-**6** has been assigned correctly on the basis of empirical methods (29). Also, (+)-methyl-1,2-methyl-1,2-diphenylpropionate, obtained by a degradation process, has been converted to (+)-(*S*)-**9** (25).

Can. J. Chem. Downloaded from www.nrcresearchpress.com by 210.87.254.105 on 09/05/12
For personal use only.

TABLE I

Rates of decomposition of **4** in cumene

Temperature (°C)	Concentration (M)	Moles N_2†	$k‡ \times 10^6$ (s^{-1})
106.0	0.084	0.59	8.44
	0.15	0.69	8.05
	0.13	0.67	8.29
127.9	0.12	0.90	124
	0.18	0.83	120
	0.15	0.86	111

†Moles N_2 per mole of **4**.
‡At 106° ΔH^* 35.6 ± 1.0 kcal/mole, ΔS^* 12.1 ± 2.6 e.u.

shown in separate experiments that **2** did not evolve nitrogen under these reaction conditions.

It can be predicted from the summary (30) of the activation parameters of a series of azoalkanes that ΔH^* for the decomposition of **4** should be about 33.5–34.5 kcal/mole and ΔS^* about 6 e.u. The value of ΔH^* obtained for the decomposition of **4**, Table I, is in good agreement with this prediction but the value for ΔS^* appears to be significantly different.

Products

Decomposition of **4** in benzene solution results in the formation of products according to eqs. [5]–[13]. The decomposition of **4** produces benzyl radicals and 1-phenylethyl radicals in a solvent cage (19). These radicals can react within the solvent cage to form the unsymmetrical coupling product, **9**, and the disproportionation products styrene and toluene, or in a competitive process, diffuse away from each other. The radicals which have diffused away from the solvent cage may now encounter and react with one of their own kind. An encounter between two 1-phenylethyl radicals will result in coupling to form *meso* and *dl*-2,3-diphenylbutane, *meso*- and *dl*-**11**, and in disproportionation to form styrene and ethylbenzene. The only reaction resulting from an encounter between two benzyl radicals will be coupling to form bibenzyl. An encounter between a 1-phenylethyl radical and a benzyl radical will result in the same products as are formed in the original solvent cage. The product distributions over a range of concentrations are given in Table II. No styrene could be found in the run at 0.5 M **4**. It was probably consumed by radical addition reactions. The amounts of the low molecular weight products, styrene, ethylbenzene, and toluene, formed in runs at the lower concentrations in benzene, could not be determined because the benzene peak in the gas–liquid chromatogram (g.l.c.) was so broad.

The ratio of the two kinds of symmetrical coupling products, *meso*- and *dl*-**11** to bibenzyl, decreases as the initial concentration of **4** decreases to a limiting value of about 0.90–0.94. The larger ratio at the higher initial concentrations of **4** reflects the greater reactivity of the benzyl radical as compared to the 1-phenylethyl radical in hydrogen abstraction from **4** and from reaction products, and in addition to any styrene formed. As the initial concentration of **4** is decreased such radical–molecule reactions become less important. The fact that the ratio, *meso*- and *dl*-**11** to bibenzyl, tends to a limit indicates that at an initial concentration of **4** of

Can. J. Chem. Downloaded from www.nrcresearchpress.com by 210.87.254.105 on 09/05/12
For personal use only.

TABLE II

Product distribution from thermal decomposition of **4** at 110° in benzene

[4]* (M)	Relative yield (%)					Ratio of *meso-* + *dl*-**11**: bibenzyl
	Toluene	Ethyl-benzene	Bibenzyl	**9**	*meso-* + *dl*-**11**†	
0.5	18	12	7.1	44	17.5	2.5
0.03	—	—	12.7, 12.0	65.3, 70.9	22.0, 17.1	1.7, 1.4
0.0063	—	—	16.9, 17.1	63.3, 64.0	19.8, 18.9	1.2, 1.1
0.0013	—	—	17.7, 19.7	65.6, 63.4	16.7, 17.3	0.94, 0.90

*Not corrected for volume expansion.
†Equal amounts of *meso-* and *dl*-**11** were formed.

ca. 1×10^{-3} M, all radicals produced are consumed by radical–radical reactions. The ratio would be expected to be 1.0 if there were no disproportionation between two 1-phenylethyl radicals, and if the rate constants for the coupling reactions that form bibenzyl, **9** and *meso-* and *dl*-**11** are all equal (see below). The actual ratio indicates that there is ca. 6–10% disproportionation. This appears to be a reasonable value. The amount of disproportionation observed during the decomposition of azocumene is 6% (30). No attempt was made in this study to determine accurately the amount of disproportionation which occurs during the decomposition of **4** and no study seems to have been made of the disproportionation occurring during decomposition of 1,1′-diphenylazoethane, but there is no reason to believe that disproportionation in these systems will be much different from 6–10%.

Cage Effect

If the radicals derived from **4** which have diffused from the original solvent cage couple randomly, an estimate of the cage effect in the decomposition of **4** may be made on the basis of the relative yields of the coupling products in decompositions at low initial concentrations of **4**. In the absence of disproportionation the amounts of bibenzyl, **9** and the sum of *meso-* and *dl*-**11** formed outside the original solvent cage would be in the ratio 1:2:1. The amount of **9** formed in excess of this ratio would represent the amount of **9** formed by cage recombination. In practice there is disproportionation which reduces the relative amounts of **9**, *meso-* and *dl*-**11** which would otherwise be formed. Noting that in the absence of disproportionation the amounts of *meso-* plus *dl*-**11** should equal the amount of bibenzyl formed, and correcting the amount of **9** found by the amount of disproportionation which occurs between benzyl and 1-phenylethyl radicals, the cage effect can be calculated from eq. [13]. The assumption

$$[13] \quad \% \text{ cage recombination} = 100\left(\frac{\mathbf{9} - 2 \times \text{bibenzyl}}{\mathbf{9} + 2 \times \text{bibenzyl}}\right)$$

is also made that the amount of disproportionation is the same within the original solvent cage as it is without.

The cage effect can also be calculated from the product distribution resulting from the decomposition of **4** in the presence of butanethiol. Butanethiol will scavenge all radicals which diffuse away from the original solvent cage, converting them to toluene and ethylbenzene. This assumption is shown to be correct for no trace of the symmetrical coupling products, bibenzyl and *meso-* and *dl*-**11** can be found when **4** is decomposed in the presence of butanethiol. The cage effect can then be calculated from the relative yields of **9** and ethylbenzene or toluene. Such a procedure has previously been used in the study of the decomposition of azocumene (31).

There are two values for the size of the cage effect for each entry in Table III. One value is calculated without correction for disproportionation between the benzyl and the 1-phenylethyl radicals. The other is calculated assuming 10% disproportionation. For the runs in the presence of butanethiol there is a difference of from 1.2 to 3% between these values depending on the magnitude of the cage effect and the method by which it is obtained. It is likely that 10% disproportionation is a maximum value so that the true values of the cage effects probably lie between the "corrected" and "uncorrected" values listed in Table III. The size of the cage

Can. J. Chem. Downloaded from www.nrcresearchpress.com by 210.87.254.105 on 09/05/12
For personal use only.

TABLE III

Cage effects in the decomposition of **4**

Solvent	[**4**] (M*)	[C_4H_9SH] (M)*	Temperature (°C)	% Cage reaction†	
				Uncorrected‡	Corrected§
Benzene	0.0013	0	110	30.2, 24, 4	34.4, 28.5
Benzene	0.13	0.97	110	26.3±0.5	28.3±0.5
Cyclohexane	0.09	1.3	115	29.7±0.4	31.7±0.4
Chlorobenzene	0.30	1.1	108	30.4±0.2	33.4±0.2
Butanethiol	0.22	9.3	110	16.9±0.8	18.2±0.8

*Concentrations refer to solutions as made up at 25° and are not corrected for solvent expansion.
†Values from runs in the presence of butanethiol are averages of at least 3 determinations, and are based on relative yields of ethylbenzene and 9 except in chlorobenzene. In chlorobenzene, values are based on relative yields of toluene and 9. Values in first entry are calculated using eq. [13]. Errors are average errors.
‡Calculated from experimentally observed product ratios.
§Calculated from experimentally observed product ratios corrected for an assumed 10% disproportionation between benzyl and 1-phenylethyl radicals.

effect in solvent butanethiol is considerably smaller than it is in the other three solvents. This is probably due to a solvent effect and not due to scavenging of radicals from within the solvent cage or of interception to secondary recombination processes. The rate constant for hydrogen atom abstraction from benzylmercaptan by the benzyl radical is $5.1 \times 10^4\ M^{-1}\ s^{-1}$ at 25° (32). The rate constants for hydrogen atom abstraction from butanethiol by the radicals derived from **4** should have a similar magnitude and are surely much too small for butanethiol to interfere with primary and secondary recombination processes (19) in the present system.

The presence of ca. 1 M butanethiol in the other solvents probably reduces the size of the cage effect by about 2% from what it would be in the pure solvents. The solvent order of increasing size of the cage effect, benzene, cyclohexane, chlorobenzene is also observed in the decomposition of azocumene (31), where the difficulties involved in interpreting such solvent effects have already been discussed. The "corrected" cage effect for the decomposition of **4** in benzene containing butanethiol agrees well with the value of 29% found for the cage effect found in the decomposition of 1,1′-diphenylazoethane at 105° in benzene (18*e*). This is a system for which a cage effect similar to that found in the decomposition of **4** is to be expected (7).

There is considerable error in calculating cage effects from product distributions in the absence of scavenger using eq. [13] in the present system (first entry in Table III). The products upon which this calculation is based are eluted quite closely together under the best g.l.c. conditions we were able to obtain. Small samples had to be injected to prevent overlap so that peak heights probably were not optimum. There is, however, fair agreement between these "corrected" values and the "corrected" value found in benzene in the presence of 0.97 M butanethiol. This indicates that radicals which have escaped from the original solvent cage do in fact react in a random manner. The difference in stability between benzyl and 1-phenylethyl radicals is not reflected in the rates of their various reactions among each other. Lack of sensitivity to radical stability in the rate of radical–radical coupling reactions (33) and the relative rates of coupling and diffusion of radicals formed in a solvent cage (7) have already been noted.

Attempts to determine the cage effect in the photochemical decomposition of **4** were unsuccessful. Photolysis of **4** resulted in the almost exclusive formation of the hydrazones, **2** and **10**. Similar results were obtained in the photolysis of *cis*-3,6-diphenyl-3,4,5,6-tetrahydropyridazine (*6b*), in which mainly the corresponding hydrazone was formed.

Stereochemistry of Cage Recombination

Optically pure (−)-(*S*)-**4** was decomposed thermally in several solvents with and without butanethiol as scavenger. In all cases the unsymmetrical coupling product, (−)-(*R*)-**9**, was formed. It was shown above that (−)-(*S*)-**4** and (−)-(*R*)-**9** have the same configuration so that (−)-(*R*)-**9** is formed with retention of configuration. The results in Table IV show that extensive racemization has occurred even in the presence of butanethiol where the unsymmetrical coupling

Can. J. Chem. Downloaded from www.nrcresearchpress.com by 210.87.254.105 on 09/05/12
For personal use only.

TABLE IV

Stereochemistry of (−)-(*R*)-**9** from the thermal decomposition of (−)-(*S*)-**4**, $[\alpha]_D^{25}$ −152°

Solvent	Temperature (°C)	[4]* (*M*)	[C_4H_9SH]* (*M*)	$[\alpha]_D^{25}$ (deg)†	Retention (%)	$(k_c/k_r)_{cage}$‡	
Benzene	132	0.13	0	−3.28	4.1		
	132	0.12	1.7	−9.29	11.5		
	110	0.082	0	−4.49	5.6		
	110	0.13	1.2	−8.27	10.3	0.059	0.061
	110	0.13	4.8	−13.5	16.7		
Butanethiol	110	0.19	9.3	−13.9	17.3	0.069	0.071
	132	0.14	9.3	−11.7	14.5		
Chlorobenzene	107	0.27	0	−6.60	8.2		
	107	0.33	1.1	−11.5	13.0	0.090	0.091
Cyclohexane	115	0.089	0	−5.10	6.3		
	115	0.089	1.3	−8.8	10.9	0.070	0.071
			0				

*Not corrected for volume expansion.
†Rotation of (−)-(*R*)-**9** taken in chloroform, *c* 1–2. Optically pure (−)-(*R*)-**9** has $[\alpha]_D^{25}$ −80.5° (*c*, 3.2, chloroform).
‡Values in first column calculated on basis of "corrected" cage effect, Table III; values in second column calculated on basis of "uncorrected" cage effect, Table III.

product is formed only by recombination within the original solvent cage. It is possible that the low optical yield obtained in the presence of butanethiol is due to racemization of starting material and product as a result of reversible hydrogen atom abstraction from these materials by butanethiyl radicals as shown in Chart IV. Hydrogen atom abstraction from hydrocarbons

$$C_6H_5\dot{C}HCH_3 \text{ or } C_6H_5\dot{C}H_2 + C_4H_9SH \rightarrow C_6H_5CH_2CH_3 \text{ or } C_6H_5CH_3 + C_9H_9S\cdot$$

$$(-)\text{-}(R)\text{-}\mathbf{9} + C_4H_9S\cdot \rightleftarrows \begin{matrix} C_6H_5 \\ \diagdown \\ \cdot\!C\!-\!CH_2C_6H_5 \\ \diagup \\ CH_3 \end{matrix} \rightleftarrows (+)\text{-}(S)\text{-}\mathbf{9} + C_4H_9S\cdot$$

Chart IV

by thiyl radicals is a well known reaction (34). Qualitative evidence that such a hydrogen atom abstraction occurs in the present system is furnished by the observation that small amounts of a light-yellow, low-melting solid were formed in all reactions carried out in the presence of butanethiol. Larger amounts were formed when butanethiol was used as solvent. This material had a g.l.c. retention time similar to that of (−)-(*R*)-**9**. It was not investigated further but is assumed to be the unsymmetrical azine, acetophenone benzaldehyde azine, **12**, formed by dehydrogenation of (−)-(*S*)-**4**. Such a dehydrogenation reaction is also observed in the decomposition of 1,1′-diphenylazoethane in the presence of octanethiol in which acetophenone azine is formed (35). These dehydrogenations may be initiated by hydrogen abstraction from the azo compounds by thiyl radicals.

$$\begin{matrix} & CH_3 & \\ & | & \\ C_6H_5\!-\!C\!=\!N\!-\!N\!=\!CHC_6H_5 & & \end{matrix}$$

12

Two control experiments were carried out in an attempt to determine the amounts of racemization of starting material and product which might occur during decomposition of (−)-(*S*)-**4** in the presence of butanethiol. In the first a solution of optically pure (−)-(*R*)-**9** and 1,1′-diphenylazoethane in butanethiol was heated at 110° for a time equivalent to ∼ 10 half lives of decomposition of the azo compound. Recovered (−)-(*R*)-**9** was 20% racemized. While 1,1′-diphenylazoethane and (−)-(*S*)-**4** decompose at somewhat different rates, the steady state concentration of butanethiyl radicals generated by the decomposing azo compounds should be closely similar in each case. The amount of racemization observed in the control experiment should represent an upper limit for the amount of racemization of (−)-(*R*)-**9** after its formation during the decomposition of (−)-(*S*)-**4** in butanethiol for two reasons. The concentration of (−)-(*R*)-**9** in the control experiment was already at its maximum value at the beginning of the reaction while during the decomposition of (−)-(*S*)-**4** it built up from 0. Since racemization is first order in both (−)-(*R*)-**9** and butanethiyl radicals, it proceeded at a faster rate in the control reaction during most of the run. Also, in butanethiol, (−)-(*S*)-**4** probably isomerizes to hydrazone much faster than does 1,1′-diphenylazoethane. Both azo compounds had probably

Can. J. Chem. Downloaded from www.nrcresearchpress.com by 210.87.254.105 on 09/05/12
For personal use only.

Can. J. Chem. Downloaded from www.nrcresearchpress.com by 210.87.254.105 on 09/05/12
For personal use only.

completely disappeared as a result of decomposition and isomerization well before the reactions were stopped, but (−)-(*S*)-**4** disappeared faster. The result is that radicals were generated for a longer period of time in the control run, again giving more racemization of (−)-(*R*)-**9**.

In the second control run a decomposition of (−)-(*S*)-**4** in butanethiol at 110° was interrupted after a time equivalent to ~ 20% decomposition. The coupling product, (−)-(*R*)-**9**, which was isolated was 17.3% optically pure. This optical yield is identical to that from a run under the conditions which had gone to completion and shows that little, if any, racemization of (−)-(*R*)-**9** occurs after its formation. This also indicates that there is little, if any, racemization of (−)-(*S*)-**4** during its decomposition. The greater amount of racemization which was observed in the control run probably occurs for the reasons cited above.

Recovery of starting material from the interrupted reaction gave a mixture, $[\alpha]_D^{25}$ −101°, consisting of 71.5% (−)-(*S*)-**4** and 28.5% of the hydrazone, (−)-(*S*)-**2**, as determined by n.m.r. spectroscopy. On the assumption that the (−)-(*S*)-**2** present was optically pure the recovered azo compound would have $[\alpha]_D^{25}$ −114°, indicating that it was 25% racemized. This, however, represents an upper limit for the amount of racemization for racemic azo compound may have been introduced during work-up. The unreacted azo compound was reduced with a 13-fold excess of diimide to the hydrazine which was then extracted into aqueous acid to free it from hydrazones, azine, and (−)-(*R*)-**9** which are also present in the reaction mixture. The hydrazine was liberated and oxidized back to the azo compound with oxygen. Diimide was used because it reduces azo compounds rapidly, it reduces polar double bonds such as are present in the hydrazones and azine more slowly (36), and because catalytic hydrogenation was precluded by the presence of sulfur compounds. It is possible that some reduction of acetophenone benzylhydrazone, if present, and azine, **12**, occurred. This would have resulted in the formation of racemic hydrazine, **3**, and, thus, racemic azo compound, **4**. The actual amount of racemization of (−)-(*S*)-**4**, may thus have been quite small, as was concluded above by comparing the optical yields of (−)-(*R*)-**9** isolated from the interrupted and completed runs.

Consideration of the stereochemistry of the decompositions in pure solvents in the absence of butanethiol also leads to the conclusion that there is little racemization of either starting material or product during decompositions in the presence of butanethiol. In chlorobenzene, for example, the cage effect in the decomposition of **4** is 33%. In the absence of hydrogen abstraction from starting material by the radicals which have escaped from the original solvent cage, the amounts of unsymmetrical coupling product formed from (−)-(*S*)-**4** inside and outside the original solvent cage would be equal.[6] That portion formed outside the original solvent cage will surely be racemic so that (−)-(*R*)-**9** formed by recombination within the original solvent cage would have twice the optical purity of the material actually isolated. The (−)-(*R*)-**9** isolated from a decomposition in pure chlorobenzene is 8.2% optically pure. That portion formed in the original solvent cage should then be 16.4% optically pure. This is greater than the 13% observed when the decomposition is carried out in the presence of 1.1 *M* butanethiol where only cage product is formed. It was shown from the dependence of product ratios upon initial concentration of **4** that a significant fraction of the radicals which escape from the original solvent cage do not give coupling products at the concentration used for decomposition of (−)-(*S*)-**4**. Less of the racemic coupling product would then be produced outside the original solvent cage. An accurate correction cannot be made for this effect, but any correction would be in a direction so as to make the stereochemistry of the cage recombination in pure chlorobenzene more similar to that in the presence of butanethiol.

Taken together, all the evidence indicates that any racemization of starting material or product during decomposition of (−)-(*S*)-**4** in the presence of butanethiol cannot be significant. The low optical yield of (−)-(*R*)-**9** from decomposition of (−)-(*S*)-**4** in the presence of butanethiol then must be almost entirely due to a racemization process taking place within the solvent cage after decomposition of (−)-(*S*)-**4** and before coupling of the radicals to (−)-(*R*)-**9**.

[6]Of the ca. 67% of the coupling products which are formed outside the original solvent cage ca. 1/4 is bibenzyl, 1/4 is *meso*- + *dl*-**11**, and 1/2 is **9**.

Can. J. Chem. Downloaded from www.nrcresearchpress.com by 210.87.254.105 on 09/05/12
For personal use only.

Although the 1-phenylethyl radical must be either planar or very nearly so and rapidly inverting, it is in an asymmetric environment after it is generated as long as it remains in the original solvent cage (Chart V). Coupling product of inverted configuration can result from cage recombination only if the 1-phenylethyl radical rotates with respect to the benzyl radical before coupling with it. The relative rates of rotation, k_r, of the 1-phenylethyl radical with respect to the benzyl radical and of coupling k_c, of the two radicals within the solvent cage can be calculated with the information at hand. Chart V illustrates all the possible reactions of the caged radical pair. The 1-phenylethyl radical is assumed to be planar and the nitrogen molecule is not shown although it is present in the original solvent cage and must be displaced from between the radicals before they can couple. Equation [14] is derived by using the steady

$$[14]\quad \frac{(-)\text{-}(R)\text{-}\mathbf{9}}{(+)\text{-}(S)\text{-}\mathbf{9}} = 1 + \left(\frac{k_c + k_{disp} + k_{diff}}{k_r}\right)_{cage}$$

state assumption for the concentrations of the enantiomeric radical pairs within the original solvent cage. An expression for $(k_c/k_r)_{cage}$, eq. [15], can now be obtained using the relationships

$$[15]\quad (k_c/k_r)_{cage} = F(1-f)\left(\frac{(-)\text{-}(R)\text{-}\mathbf{9}}{(+)\text{-}(S)\text{-}\mathbf{9}} - 1\right)$$

between k_c, k_{disp}, and k_{diff} which are given in eqs. [16] and [17]. F is the fraction of radicals which

$$[16]\quad \left(\frac{k_c + k_{disp}}{k_c + k_{disp} + k_{diff}}\right)_{cage} = F$$

$$[17]\quad \left(\frac{k_{disp}}{k_c + k_{disp}}\right)_{cage} = f$$

are consumed by coupling and disproportionation before diffusion from the original solvent cage and f is the fraction of radicals consumed in this way which undergo disproportionation. In general it will be assumed that the relative amount of disproportionation will be the same within and without the original solvent cage.

The two sets of values for $(k_c/k_r)_{cage}$ in Table IV, calculated assuming either 0 or 10% disproportionation, are very similar and show that the ratio, $(k_c/k_r)_{cage}$, is not very sensitive to reasonable errors ($\sim 10\%$) in the determination of the cage effect. Even within the original solvent cage the rate of rotation of the 1-phenylethyl radical with respect to the benzyl radical about any axis perpendicular to the line joining the two is much greater than its rate of coupling with the benzyl radical. The rate of such rotation of 1-phenylethyl radicals within the solvent cage is also found to be much greater than their rate of coupling during the decomposition of (−)-1,1′-diphenylazoethane in benzene at 110° (20). There

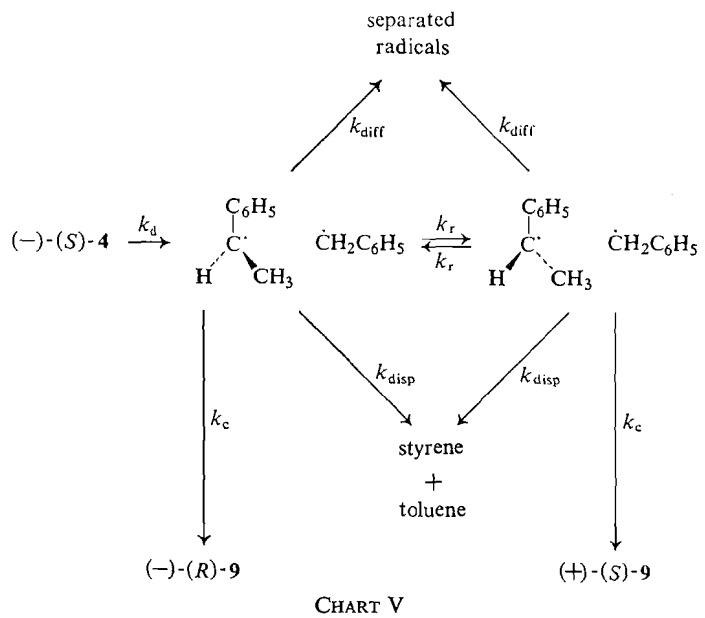

CHART V

Can. J. Chem. Downloaded from www.nrcresearchpress.com by 210.87.254.105 on 09/05/12
For personal use only.

is no significant solvent effect on the ratio, $(k_c/k_r)_{cage}$.

This very small ratio of coupling to rotation contrasts dramatically with ratios of coupling to rotation found in studies of diradicals generated from cyclic precursors (6, 33) in which k_c/k_r can be greater than 50 (6*a*). This must be due to the position of the nitrogen atom in the solvent cage in the acyclic systems. Decomposition of acyclic azo compounds most probably occurs with the groups in the *trans* arrangement about the N=N bond. When formed the two radicals have a nitrogen molecule situated between them on the line joining them, eq. [18]. Numerous collisions may take place before the nitrogen molecule is

[18] 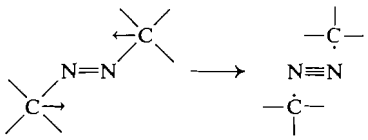

displaced from this position allowing ample time for rotation to take place. Diradicals generated from the cyclic systems studied do not have any such molecules situated between them even when these are derived from azo compounds, eq. [19], and there is no such hindrance to coupling.

[19] 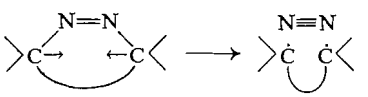

Even in acyclic systems there is a very large spread in the values of $(k_c/k_r)_{cage}$ among the only three systems already studied. In frozen solution $(k_c/k_r)_{cage}$ for the 3-methyl-2-phenyl-2-butyl radical pair, generated photochemically from either *meso*- or *dl*-3,3′-dimethyl-2,2′-diphenyl-azo-2-butane, appears to be as large as 50 (7), while for the 1-phenylethyl-benzyl radical pair in liquid solution at 110° it is as small as 0.060. This is a range of $\sim 10^3$ and leaves much room for further investigation.

The optically active esters obtained from decomposition of optically active diacyl peroxides are formed with very high (75–90%) retention of configuration in the alcohol part of the ester (4). On the basis of the results observed in the present study the very high degree of retention observed in the diacyl peroxide decompositions does not seem to be compatible with a process in which the ester is formed by the cage recombination of an acyloxy radical with an alkyl radical. The formation of the alkyl radical would have to be a two-step process proceeding via the acyloxy radical and the present results indicate that the orientation of the two acyloxy radicals with respect to one another must very rapidly become randomized. The original interpretation that ester does not arise by a free radical process (4*a*) thus gains added support, and it is likely that at least the majority of the ester is formed by an alternative route (3) which should give high retention.

Stereoselective cage recombinations of radicals are probably involved in other processes. The Wittig rearrangement of metallated benzyl ethers to benzyl carbinol salts proceeds with partial retention of configuration when optically active substrates are used (37) as does the Meisenheimer rearrangement (38). It now appears that stereoselective free radical cleavage – recombination processes are involved in both the Wittig (39, 40) and Meisenheimer (38, 41) rearrangements. The chromic acid oxidation of tertiary hydrocarbons to tertiary alcohols proceeds with a high degree of retention of configuration and it has been suggested that this reaction also proceeds by a free radical pathway involving stereoselective cage recombination (42). All three of these reactions proceed with a considerably higher degree of retention of configuration (~ 30 to $\sim 100\%$) than is observed in the cage recombination of the radicals derived from (−)-(*S*)-**4**. In each of these reactions there is no hindrance to the recombination of the fragments as is provided by the nitrogen molecule during the decomposition of (−)-(*S*)-**4** so that a higher degree of retention might be expected. The formulation of these reactions as proceeding via radical intermediates is therefore entirely consistent with the results of the studies of decomposition of optically active azo compounds.

Experimental

All melting points and boiling points are uncorrected. Elemental analyses were performed by Mrs. Darlene Mahlow and Mrs. Andrea Dunn. Nuclear magnetic resonance (n.m.r.) spectra were recorded on a Varian A-60 analytical spectrometer using tetramethylsilane as internal standard. Unless otherwise specified spectra were taken of 10–20% w/v solutions in carbon tetrachloride. Infrared (i.r.) spectra were recorded on a Perkin–Elmer recording infrared spectrophotometer, model 421. Ultraviolet

Can. J. Chem. Downloaded from www.nrcresearchpress.com by 210.87.254.105 on 09/05/12
For personal use only.

spectra were recorded on a Bausch and Lomb Spectronic 600 spectrophotometer. Optical rotations were measured with a Rudolph polarimeter, model 80, or with a Perkin–Elmer 141 polarimeter. Optical rotatory dispersion (o.r.d.) measurements were taken on a model ORD/uv-5 Japan Spectroscopic Company spectrophotometer. Gas–liquid chromatographic (g.l.c.) analyses were done with an Aerograph A90-P3 fractometer using helium as the carrier gas. Unless otherwise indicated a 6 ft × ¼ in. stainless steel column filled with 20% SF-96 on 60/80 Chromosorb P was used.

Solvents

Benzene, cumene, and cyclohexane were shaken with cold sulfuric acid until colorless, several times with water, and once with sodium carbonate solution. After drying over sodium carbonate the solvents were distilled from sodium through a short Vigreaux column and then redistilled through an annular Teflon spinning band distillation column. The middle fraction was taken and stored over sodium. Solvents were redistilled as required just before use. Chlorobenzene was purified in a similar manner except that the preliminary distillation was made over phosphorous pentoxide and it was stored over molecular sieves. Butanethiol was purified by distillation of commercial material, to which some sodium had been added, through a 6 in. Vigreaux column. This was stored for short periods in a brown bottle.

(−)-(S)-1-Phenylethylhydrazine, (−)-(S)-1

A mixture of 80 g (0.66 mole) of (−)-(*S*)-1-phenylethylamine (22) $[\alpha]_D^{25}$ −36.6° (neat, *l* 1 dm), 95% optically pure, and 500 ml water containing 25 g (0.45 mole) potassium hydroxide was stirred vigorously while a solution of 25 g (0.22 mole) freshly prepared (43) hydroxylamine-*O*-sulfonic acid dissolved in the minimum amount of water was added over a 30 min period (44). The temperature rose slowly to 50° during the addition. The reaction mixture was stirred for 2 h longer, cooled, and extracted twice with ether. The combined extracts were dried over sodium carbonate and then concentrated to an oil. The oil was distilled through a 6 in. Vigreaux column until most of the amine had distilled, b.p. 80–90° (25–35 mm), leaving a small amount of higher boiling material. The recovered amine was recycled through the reaction procedure twice more. Twenty-eight grams of starting material were recovered. The high boiling residues were combined and distilled twice through a 6 in. Vigreaux column. The fraction b.p. 70° (1 mm) was collected, 4.5 g (8%), n_D^{25} 1.5436, $[\alpha]_D^{25}$ −29.0° (*c*, 0.784, benzene). Reported (45) for (±)-**1**, b.p. 69° (0.8 mm), n_D^{25} 1.5436. A satisfactory rotation on the pure liquid could not be obtained as bubbles always formed in the polarimeter tube and variable readings were obtained.

Benzaldehyde 1-Phenylethylhydrazone, 2

To a stirred solution of 6.8 g (0.05 mole) 1-phenylethylhydrazine (45) in 80 ml ether were added 6 g anhydrous magnesium sulfate and, 5.5 g (0.052 mole) of freshly distilled benzaldehyde was then added over a period of 30 min. The resulting mixture was stirred overnight and filtered. The solvent was removed under reduced pressure to give a light-yellow oil. Pentane solutions of the oil deposited white crystals, m.p. 50–54°, whose melting point did not change upon recrystallization. Both the oil and the crystals had the same n.m.r. spectrum which showed absorption τ 2.5–3.1 (multiplet, 11.4 H), τ 4.6 (broad singlet, 0.93 H), τ 5.65 (quartet, J = 6.5 c.p.s., 0.93 H), and at τ 8.57 (doublet, J = 6.5 c.p.s., 3.0 H).

(+)-(R)-Benzaldehyde 1-Phenylethylhydrazone, (+)-(R)-2

(+)-(*R*)-1-Phenylethylamine (22), $[\alpha]_D^{25}$ +35.1° (neat, *l* 1 dm), 92% optically pure, was converted to (+)-(*R*)-**1** by the procedure used for the preparation of (−)-(*S*)-**1**. This was converted to (+)-(*R*)-**2**, using the procedure described for the preparation of **2**. After all traces of solvent were removed at reduced pressure (+)-(*R*)-**2** had $[\alpha]_D^{25}$ +63.5° (*c*, 3.31, benzene).

N-Benzyl-N′-(1-phenylethyl)-hydrazine, 3

A solution of hydrazone, **2**, prepared from 42 g of **1** was hydrogenated directly without removing the ether solvent with 5 g of 5% palladium-on-charcoal under an initial pressure of 50 lb hydrogen until uptake of hydrogen ceased. The mixture was filtered under an atmosphere of nitrogen and 39 g of oxalic acid dihydrate dissolved in the minimum amount of hot ethanol was added. An immediate precipitate formed. The mixture was filtered to give 72 g white crystals, m.p. 180–183° after 4 recrystallizations.

Anal. Calcd. for 1:1 base:acid, $C_{17}H_{20}N_2O_4$: C, 64.54; H, 6.40; N, 8.86.

Anal. Calcd. for 2:1 base:acid, $C_{32}H_{38}N_4O_4$: C, 70.82; H, 7.06; N, 10.32. Found: C, 66.30, 66.76; H, 6.58, 6.68; N, 9.63.

The results of the elemental analysis indicate that the salt has the approximate composition $(C_{15}H_{18}N_2)_{1.5}C_2O_4H_2$.

The free hydrazine, **3**, was obtained by addition of 60 g of the recrystallized oxalate salt to an excess of aqueous potassium hydroxide. The aqueous layer was extracted several times with methylene chloride and the combined organic layers were dried over sodium carbonate. After removal of the solvent under reduced pressure the residual oil was distilled to give 41.8 g of a colorless liquid, b.p. 135° (0.5 mm), n_D^{25} 1.5685. All operations were carried out under an atmosphere of nitrogen. The n.m.r. spectrum of **3** showed absorption at τ 2.83 (2 over-lapping singlets, 10 H), τ 6.16 (quartet, J = 7.0 c.p.s.) over-lapping with absorption at τ 6.28 (singlet) due to the hydrogens of the methylene group, (combined area 3.07 H), τ 6.95 (singlet, 2.0 H), and at τ 7.89 (doublet, J = 7.0 c.p.s., 2.94 H).

This material was very sensitive to air oxidation and a satisfactory elemental analysis was not obtained.

1,1′-Diphenyl-1-methylazomethane, 4

Solutions of **3** in ether were allowed to stand under an initial pressure of 10 lb oxygen until oxygen uptake stopped. The ether solution was shaken several times with water and dried over sodium carbonate. The ether was removed under reduced pressure using a rotary evaporator and evaporation continued until there was no further change in refractive index. Yields were quantitative, n_D^{25} 1.5598; λ_{max} (benzene) 358 mμ (ε 51). The n.m.r. spectrum showed absorption at τ 2.80 (multiplet, 10.6 H), τ 5.18 (singlet, ~ 2H) over-lapping with absorption at τ 5.42 (quartet, J = 7.0 c.p.s., ~ 1H) (combined

Can. J. Chem. Downloaded from www.nrcresearchpress.com by 210.87.254.105 on 09/05/12
For personal use only.

area 2.90 H), and at τ 8.50 (doublet, J = 7.0 c.p.s., 3.10 H).

Anal. Calcd. for $C_{15}H_{16}N_2$: C, 80.32; H, 7.19; N, 12.49. Found: C, 80.21; H, 6.99; N, 12.67.

(−)-(S)-1,1'-Diphenyl-1-methylazomethane, (−)-(S)-4

A Via Resolution of 3

A solution of 96 g (0.48 mole) of *d*-camphoric acid in 300 ml ethyl acetate was added to a solution of 108 g (0.51 mole) of **3** dissolved in 325 ml dioxane. The mixture was allowed to stand overnight at 25° and the precipitate which formed was filtered and washed with ether to give 115 g of white crystals, $[\alpha]_D^{25}$ +11.2° (*c*, 3.8, methanol). This material was recrystallized twice: first recrystallization, 55 g, $[\alpha]_D^{25}$ +2.73° (*c*, 3.3, methanol); second recrystallization, 30 g, m.p. 95–105° $[\alpha]_D^{25}$ −2.50° (*c*, 2.5, methanol). Further recrystallization did not alter the rotation or the melting point. The salt could be stored indefinitely at 0° but decomposed slowly at 25°.

The twice crystallized camphorate salt was added to excess aqueous sodium bicarbonate and the resulting oil extracted into ether. The hydrazine was usually not isolated but was converted to the corresponding azo compound by the oxidation procedure described above, $[\alpha]_D^{25}$ −152° (*c*, 1.06, benzene). Material obtained from a second resolution had $[\alpha]_D^{25}$ −150° (*c*, 1.1, benzene). Optical rotatory dispersion (*c*, 0.0179, cyclohexane): $[\Phi]_{600}$ −209°, $[\Phi]_{500}$ −377°, $[\Phi]_{450}$ −628°, $[\Phi]_{400}$ −1676°, $[\Phi]_{380}$ −2528°, $[\Phi]_{354}$ ±0°, $[\Phi]_{350}$ +726°, $[\Phi]_{330}$ +2095°, $[\Phi]_{320}$ +1732°.

Samples of (−)-(*S*)-**3** which were isolated by evaporation of solvent exhibited a negative rotation which varied widely from run to run.

B From (−)-(S)-1

In another experiment a mixture made up from 2.2 g (0.016 mole) of (−)-(*S*)-**1**, prepared from (−)-(*S*)-**5** of $[\alpha]_D^{25}$ −36.6° (neat, *l* 1 dm), 95% optically pure, 1 g magnesium sulfate, and 2.1 g (0.019 mole) benzaldehyde in 10 ml benzene was allowed to stand several hours. The reaction mixture was then filtered and 40 ml of a 25% solution of diisobutylaluminium hydride in benzene were added dropwise to the stirred filtrate under a nitrogen atmosphere. The addition required 30 min. The reaction mixture, which had become warm, was stirred at 25° for 2 days and then cooled in an ice bath. A solution of benzene–methanol (1:1) was added dropwise until there was no vigorous reaction on further addition. This was followed by the addition of 5 ml water, 10 ml 15% potassium hydroxide, and then 5 ml water. The aqueous layer was extracted with ether. The organic fractions were combined, dried over sodium carbonate, and poured into a solution of 2.6 g oxalic acid dihydrate in 10 ml of 98% ethanol. A white precipitate formed immediately. The mixture was allowed to stand at 0° for several hours and then filtered. The crystals, 1.9 g, were recrystallized from ethanol and the resulting solid, 1.5 g, was converted to the free hydrazine, (−)-(*S*)-**3**, as described previously. This material was not isolated but was oxidized directly to the azo compound as described above. The product after removal of the ether using a rotary evaporator contained 7.5% of (−)-(*S*)-**1**, by n.m.r. analysis, and had $[\alpha]_D^{25}$ −140° (*c*, 1.36, benzene). No other absorptions could be found. On the basis that the (−)-(*S*)-**1** present had $[\alpha]_D^{25}$ −28° and has the same density as (−)-(*S*)-**4**, (−)-(*S*)-**4** in the mixture has $[\alpha]_D^{25}$ −146°. Optically pure (−)-(*S*)-**4** would then have $[\alpha]_D^{25}$ −153°.

Hydrogenolysis of (−)-(S)-4

A mixture of 1.7 g (−)-(*S*)-**4**, $[\alpha]_D^{25}$ −152° (*c*, 1.06, benzene), 2 g Raney nickel, and 40 ml methanol was stirred at 25° in a microhydrogenation apparatus at atmospheric pressure. One equivalent of hydrogen was taken up within a few minutes and a second equivalent after two days. Analysis by g.l.c. showed that the main products were benzylamine and (−)-(*S*)-**5** together with small amounts of toluene and ethylbenzene. The mixture was filtered and the filtrate concentrated to a small volume. The residual oil was injected in 100 μl portions into the SF-96 g.l.c. column operating at 160° with a flow rate of 150 ml/min of helium. Partial separation of the amines was achieved in this way.

Material rich in (−)-(*S*)-**5** was collected from the effluent stream. Recycling of this material afforded 55 mg of pure (g.l.c.) (−)-(*S*)-**5**, $[\alpha]_D^{25}$ −31.4° (*c*, 5.4, dioxane). Optically pure (−)-(*S*)-**5** is calculated from literature data (46, 22) to have $[\alpha]_D^{25}$ −39.6° under these conditions.

In a control experiment 2 g of (−)-(*S*)-**5**, $[\alpha]_D^{25}$ −36.6° (neat, *l* 1 dm), in 40 ml methanol was stirred under the above hydrogenolysis conditions with 2 g Raney nickel for three days. The recovered amine had n_D^{25} 1.5245, $[\alpha]_D^{25}$ −36.5° (neat, *l* 1 dm).

2,3-Diphenyl-1-propanol, 7

A solution of 11 g (0.049 mole) of 2,3-diphenylpropionic acid, **6**, in 100 ml ether was added slowly to a slurry of 4.75 g (0.125 mole) of lithium aluminium hydride in 180 ml ether. The reaction mixture was stirred overnight and then hydrolyzed by the addition of water, followed by sulfuric acid. The ether layer was shaken twice with aqueous sodium carbonate, dried over sodium carbonate, and concentrated. Distillation of the residue gave 6.0 g (60%) of a light yellow oil, b.p. 140° (0.4 mm), n_D^{25} 1.5758; reported (47) b.p. 300–302°. The n.m.r. spectrum showed absorption at τ 2.95 (multiplet, 10.0 H), τ 6.3–7.4 (broad multiplet, 5.0 H), and at τ 8.05 (singlet, 1.1 H).

(−)-(R)-2,3-Diphenylpropanol, (−)-(R)-7

Using the above procedure, (−)-(*R*)-**6** (28), $[\alpha]_D^{25}$ −132° (*c*, 0.062, chloroform), 100% optically pure, was converted to (−)-(*R*)-**7**, n_D^{25} 1.5745, $[\alpha]_D^{25}$ −88.5° (*c*, 1.08, chloroform). Reported (25) for (+)-(*S*)-**7**, n_D^{25} 1.5742, $[\alpha]_D^{25}$ +76.3° (*c*, 5.3, chloroform).

2,3-Diphenyl-1-propyl p-Toluenesulfonate, 8

This material was prepared from **7** by the procedure of Schleyer (48), m.p. 79.5–89.5° after recrystallization from ligroin.

Anal. Calcd. for $C_{22}H_{22}O_3S$: C, 72.10; H, 6.05; S, 8.75. Found: C, 72.34; H, 5.88; S, 8.96.

(−)-(R)-2,3-Diphenyl-1-propyl p-Toluenesulfonate, (−)-(R)-8

This material was prepared from (−)-(*R*)-**7**, $[\alpha]_D^{25}$ −88.5°, 100% optically pure, by the above procedure, m.p. 91.0–93.5°, $[\alpha]_D^{25}$ −42.6° (*c*, 0.51, chloroform); reported (25) for (+)-(*S*)-**8**, m.p. 89–90°, $[\alpha]_D^{25}$ +40.2° (*c*, 2.4, acetone).

Can. J. Chem. Downloaded from www.nrcresearchpress.com by 210.87.254.105 on 09/05/12
For personal use only.

(−)-(R)-1,2-Diphenylpropane, (−)-(R)-9

A solution of 0.40 g of (−)-(*R*)-**8**, $[\alpha]_D^{25}$ −42.6°, 100% optically pure, in 15 ml ether was added dropwise to a slurry of 1.0 g lithium aluminium hydride in 40 ml ether. The reaction mixture was stirred for two days at 25°. It was hydrolyzed by adding ice water and then 6 *N* hydrochloric acid dropwise. The ether layer was dried over sodium carbonate and then concentrated to an oil. Analysis by g.l.c. showed only one product which was collected from the effluent stream, 0.074 g (30%), m.p. 22.0–23.0°, n_D^{25} 1.5572, $[\alpha]_D^{25}$ −80.5° (*c*, 3.2, chloroform). Optical rotatory dispersion (*c*, 1.54, cyclohexane): $[\Phi]_{600}$ −167°, $[\Phi]_{450}$ −333°, $[\Phi]_{350}$ −833°, $[\Phi]_{300}$ −1666°, $[\Phi]_{280}$ −2666°.

The g.l.c. retention time of this material was identical with a sample of **9** (49) prepared by the hydrogenation of α-methylstilbene; reported (25) for (−)-(*R*)-**9**, n_D^{25} 1.5553, $[\alpha]_D^{25}$ −76.3° (*c*, 2.2, chloroform), for (+)-(*S*)-**9**, n_D^{25} 1.5558, $[\alpha]_D^{25}$ +76.7° (*c*, 2.3, chloroform).

1,1′-Diphenylazoethane

This material was prepared by the published procedure (18*b*) except that the oxidation of the corresponding hydrazone was carried out with oxygen as described for the preparation of **4**, m.p. 68–71°; reported (18*b*), m.p. 72.3–72.9°.

Kinetic Studies

The rates of evolution of nitrogen from solutions of **4** (~ 0.1–0.2 *M*) in cumene were measured using an apparatus and a procedure similar to that described by Peterson(50). Rate constants were determined from the initial slopes of plots of log $(V_\infty - V_0/V_\infty - V_t)$ vs. time using the theoretical value of V_∞. V_0 was determined as described by Petersen *et al.* (50). The results are summarized in Table I.

Product Studies

For quantitative analyses solutions of **4** were placed in Pyrex tubes, degassed by several freeze-thaw cycles, and then heated at the appropriate temperature for at least 6 half-lives after the tubes were sealed. After cooling to −78° the tubes were opened and the solutions analyzed directly by temperature-programmed g.l.c. The temperature of the column was raised from 100 to 200° over a 35 min period beginning immediately after injection. The helium flow rate was 50 ml/min.

Hydrocarbon products were identified by comparison of g.l.c. retention times with those of authentic samples, and in the cases of bibenzyl, **9** and *meso*- and *dl*-**11** also by comparison of the n.m.r. spectra of isolated materials with those of authentic samples. The order of elution of the higher molecular weight products was bibenzyl, **9**, *dl*-**11**, and *meso*-**11**. Authentic samples of *meso*- and *dl*-**11** were prepared by the method of Barber *et al.* (51). Relative thermal response factors for the hydrocarbons were determined to be: toluene, 55; ethylbenzene, 60; bibenzyl, 85; **9**, 100; and *meso*- and *dl*-**11**, 95.

In preparative runs solutions of 1–2 g of (±)-**4** or optically pure (−)-(*S*)-**4** in 20–50 ml of solvent were placed in a 75 ml stainless steel bomb, flushed several minutes with nitrogen, and heated at the appropriate temperature for at least 7 half-lives. Most of the solvent was then removed through the spinning band column. When butanethiol was not present, the products were isolated from the residual oil by temperature-programmed preparative g.l.c. using the above conditions. When butanethiol was present in solution by-products formed which were eluted slowly from the g.l.c. column and repetitive injections of the residual oil could not be made. In these cases the by-products were removed by adsorbing the residual oil on a 5 cm × 40 cm column of activated basic alumina and eluting the hydrocarbon present with 200 ml hexane. After concentration of the hexane eluent through the spinning band column (±)-**9** or (−)-(*R*)-**9** were isolated from the residual oil by preparative g.l.c. using a steady column temperature of 205°. Amounts of (±)-**9** or (−)-(*R*)-**9** obtained, ranged from 10 to 100 mg. The smaller amounts were obtained when the sample had some impurities present after the first g.l.c. pass and had to be recycled.

From decompositions of (−)-(*S*)-**4** carried out in pure butanethiol as solvent, a yellow solid could be isolated which has a g.l.c. retention time very similar to that of (−)-(*R*)-**9**. It was not investigated further but is presumed to be the mixed azine of acetophenone and benzaldehyde. Smaller amounts of this yellow material were formed in decomposition in 1 *M* butanethiol.

Control Experiments

A Racemization of (−)-(R)-9 in Butanethiol

A solution made up of 1.2 g of 1,1′-diphenylazoethane, 36 ml butanethiol, and 80 mg of optically pure (−)-(*R*)-**9**, $[\alpha]_D^{25}$ −80.5° (*c*, 3.2, chloroform), was heated in the bomb at 110° for 12 h (~ 10 half-lives of decomposition of the azo compound); recovered (−)-(*R*)-**9** had $[\alpha]_D^{25}$ −64.1° (*c*, 1.42, chloroform).

B Interrupted Decomposition of (−)-(S)-4

A solution of 2.0 g optically pure (−)-(*S*)-**4** in 30 ml butanethiol was heated in the bomb at 110° for 5 h (~ 20% decomposition). Butanethiol was removed under reduced pressure and the residue was taken up in 50 ml methanol. Twenty grams of potassium azodicarboxylate were added, followed by the dropwise addition of acetic acid until the reaction mixture became colorless. Ether, 100 ml, was added and the resulting mixture was shaken with dilute sulfuric acid. The aqueous layer was shaken several times with ether, made alkaline with dilute potassium hydroxide solution, and shaken twice with ether. The latter ethereal extracts were combined, allowed to stand under an atmosphere of oxygen for several hours, shaken with water, and then dried over sodium carbonate. Removal of the ether gave a small amount of an oil $[\alpha]_D^{25}$ −101° (*c*, 1.3, benzene). The n.m.r. spectrum of this oil showed it to be a mixture of (−)-(*S*)-**4**, 71.5% and of (−)-(*S*)-**2**, 28.5%. No absorptions other than those due to these materials could be detected. On the basis that the (−)-(*S*)-**2** present is optically pure and has $[\alpha]_D^{25}$ −69°, the rotation of the recovered azo compound would be $[\alpha]_D^{25}$ −114°.

The ether layer remaining after the extraction with sulfuric acid was concentrated to an oil. The oil was chromatographed on alumina and the hydrocarbon, (−)-(*R*)-**9**, 0.012 g, isolated from the concentrated eluent by g.l.c. had $[\alpha]_D^{25}$ −13.9° (*c*, 1.2, chloroform).

Can. J. Chem. Downloaded from www.nrcresearchpress.com by 210.87.254.105 on 09/05/12
For personal use only.

Acknowledgment

This research was supported in part by a grant from the National Research Council of Canada.

1. (*a*) H. C. Brown, M. S. Kharasch, and T. H. Chao. J. Am. Chem. Soc. **62**, 3435 (1940); (*b*) E. L. Eliel, P. H. Wilken, F. T. Fang, and S. H. Wilen. J. Am. Chem. Soc. **80**, 3303 (1958); (*c*) H. J. Dauben, Jr. and L. L. McCoy. J. Am. Chem. Soc. **81**, 5404 (1959); (*d*) J. T. Gruver and J. G. Calvert. J. Am. Chem. Soc. **80**, 3524 (1958); (*e*) W. von E. Doering, M. Farber, M. Sprecher, and K. B. Wiberg. J. Am. Chem. Soc. **74**, 3000 (1952); (*f*) D. B. Denny and W. F. Beach. J. Org. Chem. **24**, 108 (1959); F. D. Greene. J. Am. Chem. Soc. **81**, 2688 (1959).
2. (*a*) F. D. Greene, C.-C. Chu, and J. Walia. J. Org. Chem. **29**, 2685 (1964); (*b*) S. J. Cristol, J. R. Douglas, W. C. Firth, Jr., and R. E. Krall. J. Org. Chem. **27**, 2711 (1962).
3. F. D. Greene, H. P. Stein, C.-C. Chu, and F. M. Vine. J. Am. Chem. Soc. **86**, 2080 (1964).
4. (*a*) M. S. Kharasch, J. Kuderna, and W. Nudenberg. J. Org. Chem. **19**, 1283 (1954); (*b*) F. D. Greene. J. Am. Chem. Soc. **77**, 4689 (1955); (*c*) D. F. De Tar and C. Weis. J. Am. Chem. Soc. **79**, 3045 (1957).
5. (*a*) R. Moore, A. Mishra, and R. J. Crawford. Can. J. Chem. **46**, 3305 (1968); (*b*) R. J. Crawford and A. Mishra. J. Am. Chem. Soc. **87**, 3768 (1965); (*c*) T. V. Von Auken and K. L. Rinehart. J. Am. Chem. Soc. **84**, 3736 (1964); (*d*) C. G. Overberger, N. Weinshenker, and J.-P. Anselme. J. Am. Chem. Soc. **86**, 5364 (1964); (*e*) C. G. Overberger, R. E. Zangaro, and J.-P. Anselme. J. Org. Chem. **31**, 2046 (1966).
6. (*a*) P. D. Bartlett and N. A. Porter. J. Am. Chem. Soc. **90**, 5317 (1968); (*b*) S. Evani. Ph.D. Thesis, University of Alberta, Edmonton, Alberta. 1967.
7. P. D. Bartlett and J. D. McBride. Pure Appl. Chem. **15**, 89 (1967).
8. H. M. Walborsky and C.-J. Chen. J. Am. Chem. Soc. **89**, 5499 (1967).
9. P. D. Bartlett, R. E. Pincock, J. H. Rolston, W. G. Schindel, and L. A. Singer. J. Am. Chem. Soc. **87**, 2590 (1965).
10. (*a*) H. L. Goering and D. W. Larsen. J. Am. Chem. Soc. **81**, 5937 (1959); (*b*) P. S. Skell and R. G. Allen. J. Am. Chem. Soc. **81**, 5383 (1959); (*c*) P. S. Skell and P. Freeman. J. Org. Chem. **29**, 2524 (1964).
11. (*a*) P. S. Skell, D. L. Tuleen, and P. D. Readio. J. Am. Chem. Soc. **85**, 2849 (1963); (*b*) W. O. Haag and E.-A. I. Heiba. Tetrahedron Letters, 3679 (1965).
12. E.-A. I. Heiba and R. M. Dessau. J. Am. Chem. Soc. **89**, 2238 (1967).
13. (*a*) M. Karplus. J. Chem. Phys. **30**, 15 (1959); (*b*) M. Karplus and G. K. Fraenkel. J. Chem. Phys. **35**, 1312 (1961); (*c*) R. W. Fessenden and R. H. Shuler. J. Chem. Phys. **39**, 2147 (1963); (*d*) S. Ogawa and R. W. Fessenden. J. Chem. Phys. **41**, 994 (1964); (*e*) G. Herzberg. Ann. Rev. Phys. Chem. **9**, 327 (1958); (*f*) G. Herzberg. Proc. Roy. Soc. London, Ser. A, **262**, 291 (1961).
14. (*a*) M. S. Kharasch, F. E. Engleman, and W. H. Urry. J. Am. Chem. Soc. **65**, 2428 (1943); (*b*) P. Wilder and A. Winston. J. Am. Chem. Soc. **75**, 5370 (1953); (*c*) P. D. Bartlett and F. D. Greene. J. Am. Chem. Soc. **76**, 1088 (1954); (*d*) F. D. Greene, M. L. Savitz, F. D. Osterholtz, H. H. Lau, W. N. Smith, and P. M. Zanet. J. Org. Chem. **28**, 55 (1963); (*e*) D. E. Applequist and L. Kaplan. J. Am. Chem. Soc. **87**, 2194 (1965); (*f*) L. B. Humphrey, B. Hodgson, and R. E. Pincock. Can. J. Chem. **46**, 3099 (1968); (*g*) R. C. Fort, Jr. and R. E. Franklin. J. Am. Chem. Soc. **90**, 5267 (1968); (*h*) J. P. Lorand, S. D. Chodroff, and R. W. Wallace. J. Am. Chem. Soc. **90**, 5266 (1968).
15. (*a*) J. A. Kampmeier and R. M. Fantazier. J. Am. Chem. Soc. **88**, 1959 (1966); (*b*) L. A. Singer and N. P. Kong. J. Am. Chem. Soc. **88**, 5213 (1966).
16. (*a*) P. S. Skell and R. G. Allen. J. Am. Chem. Soc. **80**, 5997 (1958); (*b*) S. Grover. M.Sc. Thesis, University of Alberta, Edmonton, Alberta. 1966.
17. (*a*) R. J. Crawford and D. M. Cameron. Can. J. Chem. **45**, 691 (1967); (*b*) B. H. Al-Sader and R. J. Crawford. Can. J. Chem. **46**, 3301 (1968).
18. (*a*) S. Seltzer and S. G. Mylonakis. J. Am. Chem. Soc. **89**, 6584 (1967); (*b*) S. Seltzer. J. Am. Chem. Soc. **83**, 2625 (1961); (*c*) S. Seltzer. J. Am. Chem. Soc. **85**, 15 (1963); (*d*) S. Seltzer and F. T. Dunne. J. Am. Chem. Soc. **87**, 2628 (1965); (*e*) S. Seltzer and E. J. H. Hamilton, Jr. J. Am. Chem. Soc. **88**, 3775 (1966).
19. (*a*) J. Franck and E. Rabinowitch. Trans. Faraday Soc. **30**, 120 (1934); (*b*) R. M. Noyes. J. Am. Chem. Soc. **77**, 2042 (1955); (*c*) H. P. Waits and G. S. Hammond. J. Am. Chem. Soc. **86**, 1911 (1964); (*d*) F. W. Lampe and R. M. Noyes. J. Am. Chem. Soc. **76**, 2140 (1954).
20. F. D. Greene and M. A. Berwick. 156th Natl. Meeting Am. Chem. Soc. Abstracts. Atlantic City, New Jersey. September, 1968.
21. W. Leithe. Chem. Ber. **64**, 2827 (1931).
22. W. Thielacker and H. G. Winkler. Chem. Ber. **87**, 690 (1954).
23. D. J. Cram. J. Am. Chem. Soc. **74**, 5518 (1952).
24. R. A. Barnes and B. R. Juliano. J. Am. Chem. Soc. **81**, 6462 (1959).
25. H. R. Sullivan, J. R. Beck, and A. Pohland. J. Org. Chem. **28**, 2381 (1963).
26. F. A. Abd Elhafez and D. J. Cram. J. Am. Chem. Soc. **74**, 5846 (1952).
27. (*a*) W. A. Bonner, J. A. Zderic, and G. A. Casaletto. J. Am. Chem. Soc. **74**, 5086 (1952); (*b*) D. J. Cram and J. Allinger. J. Am. Chem. Soc. **76**, 4516 (1954); (*c*) W. A. Bonner and J. A. Zderic. J. Am. Chem. Soc. **78**, 3218 (1956); (*d*) E. W. Garbisch. J. Org. Chem. **27**, 3363 (1962).
28. K. Pettersson. Arkiv Kemi, **7**, 339 (1954).
29. K. Pettersson. Arkiv Kemi, **10**, 297 (1957).
30. S. F. Nelson and P. D. Bartlett. J. Am. Chem. Soc. **88**, 137 (1966).
31. S. F. Nelson and P. D. Bartlett. J. Am. Chem. Soc. **88**, 143 (1966).
32. R. D. Burkhart. J. Am. Chem. Soc. **90**, 273 (1968).
33. J. A. Berson and E. J. Walsh, Jr. J. Am. Chem. Soc. **90**, 4731 (1968).
34. C. Walling and R. Rabinowitz. J. Am. Chem. Soc. **81**, 1137 (1959).
35. A. F. Bickel and E. C. Kooyman. Nature, **170**, 211 (1952).
36. E. E. van Tamelen, R. S. Dewey, and R. J. Timmons. J. Am. Chem. Soc. **83**, 3725 (1961).
37. (*a*) U. Schöllkopf and W. Fabian. Ann. **642**, 1 (1961); (*b*) U. Schöllkopf and A. Schäfer. Ann. **663**, 22 (1963).
38. (*a*) U. Schöllkopf, M. Patsch, and H. Schäfer.

Tetrahedron Letters, 2515 (1964); (*b*) U. SCHÖLLKOPF and H. SCHÄFER. Ann. **683**, 42 (1965).
39. P. T. LANSBURY, V. A. PATHSON, J. D. SEDLER, and J. BIEBER. J. Am. Chem. Soc. **88**, 78 (1966).
40. H. SCHÄFER, U. SCHÖLLKOPF, and D. WALTER. Tetrahedron Letters, 2809 (1968).
41. (*a*) U. SCHÖLLKOPF and U. LUDWIG. Chem. Ber. **101**, 2224 (1968); (*b*) U. SCHÖLLKOPF, U. LUDWIG, M. PATSCH, and W. FRANKEN. Ann. **703**, 77 (1967).
42. K. B. WIBERG and G. FOSTER. J. Am. Chem. Soc. **83**, 423 (1961).
43. H. J. MATSUMAGA and L. F. AUDRIETH. Inorg. Syn. **5**, 122 (1957).
44. A. MEUWSEN and R. GÖSL. Chem. Ber. **92**, 252 (1959).
45. C. G. OVERBERGER and A. V. DIGUILIO. J. Am. Chem. Soc. **80**, 6562 (1958).
46. D. J. CRAM and R. J. GUTHRIE. J. Am. Chem. Soc. **88**, 5760 (1966).
47. M. FREUND and P. REMSE. Chem. Ber. **23**, 2859 (1890).
48. P. VON R. SCHLEYER. *Reported in* L. F. Fieser and M. Fieser. Reagents for organic synthesis. John Wiley and Sons, Inc., New York. 1967. p. 1182.
49. M. TUOT and M. GURYARD. Bull. Soc. Chim. France, 1087 (1947).
50. R. C. PETERSEN, J. H. MARKGRAF, and S. D. ROSS. J. Am. Chem. Soc. **83**, 3819 (1961).
51. H. J. BARBER, R. STACK, and A. M. WOOLMAN. J. Chem. Soc. 99 (1943).

Can. J. Chem. Downloaded from www.nrcresearchpress.com by 210.87.254.105 on 09/05/12
For personal use only.

Can. J. Chem. Downloaded from www.nrcresearchpress.com by 210.87.254.6 on 09/05/12
For personal use only.

Stéréochimie de l'addition de réactifs de Grignard sur la *t*-butyl-2 cyclohexanone

JEAN-CLAUDE RICHER ET DENIS EUGÈNE
Département de Chimie, Université de Montréal, Boîte Postale 6128, Montréal, Québec

Reçu le 8 octobre 1968

Les configurations relatives des *t*-butyl-2 éthyl-1 cyclohexanols ont été déterminées. La stéréochimie de l'addition de réactifs de Grignard sur la *t*-butyl-2 cyclohexanone a été étudiée. Les résultats obtenus sont interprétés en fonction d'une théorie complètement stérique.

Canadian Journal of Chemistry, 47, 2387 (1969)

Introduction

La stéréochimie de l'addition de réactifs de Grignard sur la *t*-butyl-4 cyclohexanone (**1**) a été étudiée par plusieurs auteurs (1–4). Toutefois aucune étude parallèle dans le domaine de la *t*-butyl-2 cyclohexanone (**2**) où le carbonyle est soumis à l'encombrement stérique du groupe *t*-butyle de la position-2 n'a été rapportée. Considérant l'importance que pourrait avoir ce substituant volumineux sur la réactivité de la cétone adjacente il apparaissait opportun d'examiner les résultats stéréochimiques de l'addition des réactifs de Grignard sur cette cétone. Les résultats obtenus au cours de cette étude font l'objet de la présente communication.

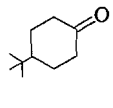

1

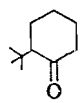

2

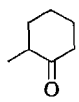

6

Résultats

Les résultats obtenus lors de l'addition des magnésiens (**3**) d'éthyle, de vinyle et d'éthynyle sur la *t*-butyl-2 cyclohexanone sont rapportés dans le tableau I. Les configurations relatives des alcools tertiaires qui en dérivent ont été établies.

La chromatographie sur alumine du produit obtenu par addition d'un grand excès de bromure d'éthylmagnésium (**3***a*) sur la *t*-butyl-2 cyclohexanone (**2**) permet d'obtenir le *t*-butyl-2 éthyl-1 cyclohexanol *trans*[1] (**5***a*) à l'état pur. Le même alcool est aussi obtenu d'une part par hydrogénation catalytique du *t*-butyl-2 vinyl-1 cyclohexanol *trans* (**5***b*) formé en prépondérance lors de l'addition du bromure de vinylmagnésium (**3***b*) sur la *t*-butyl-2 cyclohexanone (**2**) et d'autre part par hydrogénation catalytique du *t*-butyl-2 éthynyl-1 cyclohexanol *trans* (**5***c*) obtenu par l'action du bromure d'éthynylmagnésium (**3***c*) sur la *t*-butyl-2 cyclohexanone (**2**). Ces résultats indiquent que les alcools obtenus en prépondérance par action des magnésiens sur la *t*-butyl-2 cyclohexanone ont tous la même configuration relative.

TABLEAU I

Stéréochimie des additions des réactifs de Grignard **3** sur la cétone **2**

Grignard **3**	% alcools **5** formés
3*a*	97*
3*b*	95
3*c*	80

*Quantités équimoléculaires de cétone **2** et de magnésien **3***a*.

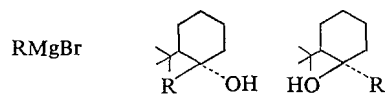

3 **4** **5**

a) R = $CH_3—CH_2—$
b) R = $CH_2=CH—$
c) R = $H—C\equiv C—$
d) R = H

Les alcools tertiaires de la série *cis* (**4**) ont tous été obtenus à partir du *t*-butyl-2 éthynyl-1 cyclohexanol *cis* (**4***c*) préparé par réaction de la *t*-butyl-2 cyclohexanone (**2**) avec l'acétylure de lithium complexé par l'éthylène diamine (**5**) utilisant le tétrahydrofuranne comme solvant. Il a été bien établi (6) à l'aide de la méthyl-2 cyclohexanone (**6**) que l'addition de sels métalliques d'acétylène conduit à des résultats où le rapport d'alcool tertiaires *cis*/*trans* varie considérablement en fonction des conditions de la réaction.

[1]Les configurations se rapportent à la relation existant entre les groupes alkyles portés par les noyaux cyclohexaniques.

TABLEAU II

Propriétés comparées des alcools **4***a* et **5***a*

Produit	i.r. (cm^{-1})*	r.m.n.† p.p.m.	r.m.n.† $\Delta w_H OH$(c.p.s.)
4*a*	1010–1040	3.45	0.78
5*a*	956	3.32	1.95

*Fréquence de la vibration C—O.
†Spectres déterminés à 84.8 mg/0.5 ml DMSO-d_6.

Les conditions choisies dans la présente étude correspondent à celles qui ont fourni un rapport d'alcool *cis*/*trans* maximum.

La configuration relative des alcools tertiaires obtenus est inférée à partir des résultats de l'analyse chromatographique en phase gazeuse qui indiquent que les alcools formés en prédominance (**5***a*) par l'action des Grignard sur la *t*-butyl-2 cyclohexanone ont les temps de rétention les plus courts; il est maintenant bien établi (4) que ces produits doivent contenir un groupe OH en position axiale. Les fréquences d'absorption dans l'infrarouge ont aussi été fréquemment utilisées (4, 7, 8) afin d'établir des configurations relatives de produits hydroxylés. Le tableau II montre les positions des bandes d'absorption dans la région de 1000 cm^{-1} pour les alcools tertiaires obtenus au cours de ce travail et ces données supportent les configurations proposées précédemment. La résonance magnétique nucléaire (voir tableau II) corrobore ces conclusions tant par la position (déplacement chimique) des protons hydroxyliques (4) que par la largeur de ces bandes (9, 10)[2] grâce à l'observation selon laquelle les largeurs à demi-hauteur des bandes dues à des protons de groupes hydroxyles axiaux sont plus faibles que celles des protons des groupes hydroxyles équatoriaux; cette différence a été attribuée au fait que le couplage à longue distance est plus facile dans un cas que dans l'autre.

L'ensemble des résultats rapportés ici présente une image consistante qui indique que les alcools tertiaires formés en prépondérance lors de l'addition d'un réactif de Grignard sur la *t*-butyl-2 cyclohexanone possèdent la configuration *trans* (**5***b*, et **5***c*). La stéréochimie observée pour ces réactions pourrait à notre avis être attribuée au fait qu'une attaque axiale en position-2 du

groupe *t*-butyle serait empêchée à cause de l'interaction 1,3 diaxale qui se développerait entre le réactif introduit et l'un des groupes méthyles du groupement *t*-butyle présent en position-2; cette proposition est en parfait accord avec les rapports récents soumis pour expliquer les vitesses relatives d'oxydation chromique d'alcools secondaires (11), la stéréochimie d'addition de boranes sur le *t*-butyl-3 cyclohexène (12), ou pour expliquer la stéréochimie des époxidations de cet hydrocarbure (13). L'ensemble de ces observations implique d'une part que la stéréochimie des réactions d'addition de réactifs de Grignard sur des cétones cycliques (14) peut être expliquée grâce à la théori complètement stérique (15) proposée pour expliquer la stéréochimie des additions nucléophiles sur ces cétones et d'autre part qu'un groupement *t*-butyle ne doit pas être considéré comme sphérique mais que les conformations privilégiées de ce groupement doivent toujours être envisagées.

Partie expérimentale

Les techniques expérimentales générales sont décrites dans des publications précédentes (14, 16). Les détails expérimentaux et les spectres de masse sous forme de graphiques sont rapportés dans le mémoire de Maîtrise de M. Denis Eugène dont une copie est déposée à la bibliothèque du Conseil National de Recherches du Canada. Les poids moléculaires sont déterminés au moyen d'un osmomètre à pression de vapeur de la compagnie Hewlett–Packard modèle 301 A. Les chromatographies en phase gazeuse ont été effectuées à l'aide d'un appareil de la compagnie F et M, modèle 810 à ionisation de flamme utilisée avec la colonne A de 8 pd. × 1/4 po. contenant 15% de diglycérol avec 2% d'eau sur du Chromosorb W "non acid wash", maintenue à 110 °C et le débit d'azote au cours de ces études est de 35 ml/min; un appareil Microtek à conductivité thermique a été utilisée avec la colonne B de 10 pd. × 1/4 po. contenant 15% d'hyprose sur du Chromosorb P est maintenue à 170 °C et dans ces conditions le gaz porteur, l'hélium, a un débit de 75 ml/min.

t-Butyl-2 éthynyl-1 cyclohexanols (4c et 5c)

t-Butyl-2 éthynyl-1 cyclohexanol trans (5c)

Par l'intermédiaire d'un tube barboteur, un léger courant d'acétylène purifiée et anhydre est envoyé dans 175 ml de THF anhydre pendant 2 h de façon à saturer le THF en d'acétylène. En maintenant toujours sous un courant acétylène, 60 ml d'une solution tétrahydrofuranique 3.1 *N* de bromure d'éthyl magnésium sont ajoutés goutte à goutte; après cette addition le milieu réactionnel est laissé à la température de la pièce pour 45 min. Le

[2]P. Laszlo et Z. Welvart. Communication personnelle.

Can. J. Chem. Downloaded from www.nrcresearchpress.com by 210.87.254.6 on 09/05/12
For personal use only.

Can. J. Chem. Downloaded from www.nrcresearchpress.com by 210.87.254.6 on 09/05/12
For personal use only.

magnésien formé est insoluble dans le THF à cette concentration. Le courant d'acétylène est arrêté et 24 g de *t*-butyl-2 cyclohexanone (0.156 mole) sont additionnés lentement. La réaction est laissée 48 h à température de la pièce et après hydrolyse avec une solution de NH_4Cl à 10% les produits sont extraits à l'éther à la façon habituelle pour fournir 25 g d'un produit qui par chromatographie en phase gazeuse contiendrait encore 59% de cétone qui n'a pas réagie; l'alcool désiré forme 80% de la fraction alcoolique. Après distillation de la cétone, l'alcool désiré est obtenu par chromatographie sur alumine de la fraction alcoolique en employant un mélange cyclohexane: acétate d'éthyle à 3% comme solvant. L'alcool (**5***c*) pur se présente sous forme d'un liquide incolore; p.e.: 60°/0.25 mm Hg; n_D^{26}: 1.4810; infrarouge (i.r.): bandes à 3520, 3325, 2100 et 968 cm^{-1}; spectre résonance magnétique nucléaire (r.m.n.): le groupe *t*-butyle à 1.04 p.p.m., proton acétylénique à 3.12 p.p.m. et proton hydroxylique à 3.36 p.p.m.; les temps de rétention en chromatographie en phase gazeuse sont sur la colonne A de 22 min et sur la colonne B de 11 min 30. Ce produit peut être caractérisé sous forme d'acétate: p.é.: 54°/0.05 mm Hg; n_D^{26}: 1.4720; poids moléculaire calculé: 222; trouvé: 221: spectre i.r.: bandes à 3300 cm^{-1} et 1730 cm^{-1}; r.m.n.: groupe *t*-butyle à 1.06 p.p.m., proton acétylénique à 2.62 p.p.m., CH_3 de l'acétate à 1.96 p.p.m.

t-Butyl-2 éthynyl-1 cyclohexanol cis (4c)

Une solution de 12.5 g d'acétylure de lithium complexé par l'éthylènediamine dans 110 ml de THF anhydre est maintenue à une température de 45° sous un léger courant d'acétylène purifié et séché sur H_2SO_4. Sous agitation, 15 g de *t*-butyl-2 cyclohexanone sont introduits goutte à goutte et une fois l'addition terminée le chauffage, l'agitation et le courant d'acétylène sont laissés pendant 22 h. Pour effectuer l'hydrolyse 50 ml d'eau sont introduits et un chauffage de 1 h au léger reflux permet de chasser l'excès d'acétylène dissous dans la solution. L'extraction à la manière habituelle conduit à 17.2 g de produit qui par chromatographie en phase gazeuse contiendrait 9% de cétone **2** qui n'a pas réagie: dans ce mélange l'alcool désiré *cis* (**4***c*) forme 88% du total. Cet alcool est un solide qui recristallisé deux fois dans un mélange d'éthanol–eau présente les caractéristiques suivantes: p.f.: 68°; i.r.: bandes à 3630, 3460, 1057 et 3330 cm^{-1}; spectre r.m.n.: groupe *t*-butyle à 1.01 p.p.m., proton acétylénique à 3.16 p.p.m., proton hydroxylique à 3.36 p.p.m.; chromatographie en phase gazeuse: temps de rétention sur la colonne A de 28.3 min et sur la colonne B de 12 min. Cet alcool peut être caractérisé par l'intermédiaire de son acétate: p.é.: 60°/0.08 mm Hg; n_D^{26}: 1.4762 poids moléculaire calculé: 222; trouvé: 220.8; i.r.: bandes à 3300 et 1735 cm^{-1}; r.m.n.: groupe *t*-butyle à 1.09 p.p.m., proton acétylénique 2.68 p.p.m. et CH_3 de l'acétate à 2.00 p.p.m.

t-Butyl-2 vinyl-1 cyclohexanols (4b et 5b)

t-Butyl-2 vinyl-1 cyclohexanol trans (5b)

A une solution de magnésien du bromure de vinyle préparée selon la méthode de Normant (17) à partir de 22.7 g de magnésium et de 100 g de bromure de vinyle, 15 g de cétone **2** sont ajoutés goutte à goutte à la température de la pièce; le mélange est maintenu sous agitation à cette température pendant 36 h. Après extraction à la manière habituelle, 15.6 g de produit sont obtenus; la chromatographie en phase gazeuse indique qu'il reste 44% de cétone **2** qui n'a pas réagie et que l'alcool désiré **5***b* forme 95% de la fraction alcoolique. Le produit ainsi obtenu est traité par 5 g de $LiAlH_4$ dans 200 ml d'éther et extrait à la manière habituelle. La chromatographie de ce mélange d'alcool utilisant 250 g d'alumine permet d'isoler 3.5 g du *t*-butyl-2 vinyl-1 cyclohexanol *trans* (**5***b*) pur: p.é.: 47°/0.07 mm Hg; n_D^{27}: 1.4779; i.r.: bandes à 3630, 3520, 3100, 1638, 1005, 910 cm^{-1}; r.m.n.: groupe *t*-butyle à 0.97 p.p.m., proton hydroxylique à 4.01 p.p.m., protons A, B, et C du groupe vinyle respectivement à 6.1, 4.88 et 5.15 p.p.m. (les constantes de couplages sont J_{AB} 10.25 c.p.s., J_{AC} 17.25 c.p.s. et J_{BC} 1.75 c.p.s.); chromatographie en phase gazeuse: temps de rétention sur la colonne A de 11 min et sur la colonne B de 7.20 min; spectre de masse: pic parent à 182. Cet alcool peut être caractérisé par l'intermédiaire de son acétate: p.é.: 54°/0.07 mm Hg; n_D^{26}: 1.4764; poids moléculaire calculé: 224; trouvé: 222.8; i.r.: bandes à 3080, 1738, 1640 cm^{-1}; r.m.n.: groupe *t*-butyle apparaît à 1.0 p.p.m., CH_3 de l'acétate à 2.05 p.p.m., protons A, B, et C du groupe vinyle respectivement à 6.36, 5.06 et 4.97 p.p.m. (J_{AB} = 12 c.p.s., J_{AC} = 18 c.p.s. et J_{BC} = 1 c.p.s.).

t-Butyl-2 vinyl-1 cyclohexanol cis (4b)

L'hydrogénation de 1.62 g de *t*-butyl-2 éthynyl-1 cyclohexanol *cis* (**4***c*) dissous dans 10 ml de méthanol en présence de 40 mg de palladium sur carbonate de calcium (5%) empoisonné par 40 mg de quinoléine préalablement distillée conduit après distillation à 1.3 g du produit attendu (**4***b*); p.é.: 94°/11 mm Hg; n_D^{26}: 1.4863; i.r.: bandes à 3650, 3490, 3095, 1631, 995, 912 cm^{-1}; r.m.n.: groupe *t*-butyle à 0.96 p.p.m., proton hydroxylique à 4.14, protons A, B et C du groupe vinyle respectivement à 6.42, et 5.04 et 5.32 (J_{AB} = 10.12, J_{AC} = 16.5, et J_{BC} = 2.5 c.p.s.); chromatographie en phase gazeuse: temps de rétention sur la colonne A de 13.3 min et sur la colonne B de 8.3 min; spectre de masse: pic parent à 182. Cet alcool peut être caractérisé par l'intermédiaire de son acétate: p.é.: 55°/0.8 mm Hg; n_D^{26}: 1.4955; poids moléculaire calculé: 224; trouvé: 222.1; i.r.: bandes à 3100, 1730, 1635, 995 et 905 cm^{-1}; r.m.n.: groupe *t*-butyle à 1.0 p.p.m., CH_3 de l'acétate à 1.75 p.p.m., protons A, B et C du groupe vinyle respectivement à 6.25, 4.89 et 4.82 p.p.m. (J_{AB} = 12, J_{AC} = 18 et J_{BC} = 1 c.p.s.).

t-Butyl-2 éthyl-1 cyclohexanol (4a et 5a)

t-Butyl-2 éthyl-1 cyclohexanol trans (5a)

A une solution de 4 moles de magnésien du bromure d'éthyle dans l'éther, 60 g (0.39 mole) de cétone (**2**) sont ajoutés goutte à goutte et une fois l'addition terminée, l'agitation est maintenue pendant 48 h. L'hydrolyse du milieu réactionnel est faite à l'aide d'une solution aqueuse de chlorure d'ammonium dans la glace et l'extraction des produits réactionnels à la manière habituelle conduit à 11 g de produit brut contenant d'après la c.p.g. 23% de cétone qui n'a pas réagi **2**, 22% d'alcools de réduction (**4***d* et **5***d*) et 55% d'alcools d'addition (**4***a* et **5***a*) parmi lesquels le produit désiré *trans*, **5***a* forme 91% du total. Cet alcool est purifié par chromatographie de 11 g de produit brut sur 800 g d'alumine; l'élution à l'éther de pétrole 30–60 permet de

Can. J. Chem. Downloaded from www.nrcresearchpress.com by 210.87.254.6 on 09/05/12
For personal use only.

récupérer la cétone qui n'a pas réagi alors que l'alcool **5***a* est élué grâce à un mélange contenant du benzène et 20% d'éther anhydre. Il se présente sous forme d'une huile incolore. p.é.: 54°/0.18 mm Hg; n_D^{27}: 1.4731; i.r.: bandes à 3630, 3520 et 956 cm^{-1}; r.m.n.: groupe *t*-butyle à 1.03 p.p.m., proton hydroxylique (DMSO-d_6) à 3.32 p.p.m., groupes méthyle et méthylène de l'éthyle à 0.89 et 1.67 p.p.m. respectivement avec $J = 7.5$ c.p.s.; chromatographie en phase gazeuse: temps de rétention sur la colonne A, 13 min, et sur la colonne B, 8 min; spectre de masse: pic parent à 184. Cet alcool peut être caractérisé par l'intermédiaire de son acétate: p.é.: 57°/0.08 mm Hg; n_D^{27}: 1.4672; poids moléculaire calculé: 226; trouvé: 223.9; i.r.: bandes à 1730, 1247, 1265 et 1277 cm^{-1}; r.m.n.: groupe *t*-butyle à 1.05 p.p.m., méthyle de l'acétate à 1.95 p.p.m. et méthyle du groupe éthyle à 0.93 p.p.m.

Cet alcool peut aussi être obtenu par hydrogénation totale en présence d'oxyde de platine dans le méthanol soit des *t*-butyl-2 éthynyl-1 (**5***c*) ou vinyl-1 (**5***b*) cyclohexanols décrits précédemment. La similitude des produits est démontrée grâce à la spectroscopie i.r. et la chromatographie en phase gazeuse.

t-Butyl-2 éthyl-1 cyclohexanol cis (4a)

L'hydrogénation de 3 g de l'alcool **4***b* dissous dans 50 ml de méthanol en présence de 50 mg de PtO_2 conduit après extraction des produits à la manière habituelle à 2.5 g (85% du rendement théorique) de l'alcool désiré (**4***a*): p.é.: 46°/0.07 mm Hg; n_D^{27}: 1.4747; i.r.: bandes à 3640, 3520, 1040 et 1010 cm^{-1}; r.m.n.: groupe *t*-butyle à 1.04 p.p.m., méthyle et méthylène du groupe éthyle respectivement à 0.89 et 1.63 p.p.m. avec $J = 7.5$ c.p.s., proton hydroxylique (DMSO-d_6) à 3.45 p.p.m.; chromatographie en phase gazeuse: temps de rétention sur la colonne A, 15 min et sur la colonne B, 8.6 min; spectre de masse: pic parent à 184. Cet alcool peut être caractérisé par l'intermédiaire de son acétate: p.é.: 58°/0.07 mm Hg; n_D^{27}: 1.4722; poids moléculaire: calculé 226; trouvé 224.2; i.r.: bandes à 1727, 1263, 1250 et 1240 cm^{-1}; r.m.n.: groupe *t*-butyle à 1.05 p.p.m., groupe méthyle de l'acétate à 2.00 p.p.m. et groupe méthyle de l'éthyle à 0.91 p.p.m. Le même alcool peut être obtenu par hydrogénation de l'alcool (**4***c*) en présence de PtO_2 dans le méthanol; l'identité des produits est démontrée grâce à l'i.r. et la chromatographie en phase gazeuse.

Remerciements

Les auteurs remercient vivement le Conseil National de Recherches du Canada et le service de la Coopération avec l'extérieur du Ministère de l'Education de la Province de Québec pour l'aide financière apportée sous forme d'octrois de recherches et de bourse d'étude.

1. B. Cross et G. H. Whitham. J. Chem. Soc. 3892 (1960).
2. W. J. Houlihan. J. Org. Chem. **27**, 3860 (1962).
3. H. O. House et W. L. Respess. J. Org. Chem. **30**, 301 (1965).
4. G. D. Meakins, R. K. Percy, E. E. Richards et R. N. Young. J. Chem. Soc. (London) (C) 1106 (1968).
5. O. F. Beumel Jr. et R. F. Harris. J. Org. Chem. **29**, 1872 (1964).
6. J. N. Nazarov et A. A. Akhrem. Izv. Akad. Nauk SSSR (Otd. Khim. Nauk) **3**, 631 (1958).
7. A. R. H. Cole, R. N. Jones et K. Dobriner. J. Am. Chem. Soc. **74**, 5571 (1952).
8. J.-C. Richer et P. Belanger. Can. J. Chem. **44**, 2057 (1966).
9. J. C. Jochins, G. Taigel, A. Seeliger, P. Lutz et H. E. Driesen. Tetrahedron Letters, 4363 (1967).
10. C. W. Shoppee, F. P. Johnson, R. E. Lack, J. S. Shannon et S. Sternhell. Tetrahedron Supplement **8**, Part II. 421 (1966).
11. J.-C. Richer, L. A. Pilato et E. L. Eliel. Chem. Ind. 2007 (1961).
12. D. J. Pasto et F. M. Klein. J. Org. Chem. **33**, 1468 (1968).
13. J.-C. Richer et C. Freppel. Can. J. Chem. **46**, 3709 (1968).
14. J.-C. Richer et P. Belanger. Can. J. Chem. **44**, 2067 (1966).
15. J.-C. Richer. J. Org. Chem. **30**, 324 (1965).
16. J.-C. Richer et C. Lamarre. Can. J. Chem. **45**, 1581 (1967).
17. H. Normant. Bull. Soc. Chim. France, 728 (1957).

Can. J. Chem. Downloaded from www.nrcresearchpress.com by 210.87.254.40 on 09/05/12
For personal use only.

Influence of Lewis acids on the Diels–Alder reaction. Part I. An improved synthesis of 7-azanorbornadiene, 3-azaquadricyclane, and azepine derivatives[1]

R. C. BANSAL,[2] A. W. MCCULLOCH, AND A. G. MCINNES
Atlantic Regional Laboratory, National Research Council of Canada, Halifax, Nova Scotia

Received November 28, 1968

Depending on the experimental conditions the $AlCl_3$-promoted reaction of 1-carbomethoxypyrrole and dimethyl acetylenedicarboxylate yields 2,3,7-tricarbomethoxy-7-azanorbornadiene, either in almost quantitative yield or together with dimethyl 1-carbomethoxy-2-pyrrolyl maleate and fumarate. The azanorbornadiene has been quantitatively converted to 1,4,5-tricarbomethoxyazepine via the corresponding 3-azaquadricyclane. The proton magnetic resonance spectra were analyzed with the aid of the Laocoon II program.

Canadian Journal of Chemistry, 47, 2391 (1969)

Prinzbach and co-workers (1, 2) have recently reported the preparation of a number of 7-azanorbornadiene derivatives (**2***a*–**2***e*). These adducts were prepared by heating the appropriate *N*-substituted pyrrole (**1***a*–**1***e*) with a large excess of dimethyl acetylenedicarboxylate (DMAD). Adducts **2***a*–**2***d*, however, were only isolated in yields of 30 to 45% because of the high reaction temperatures (105–142°), the reversible nature of the reactions (see reaction *b*), and in one case a retro Diels–Alder reaction which produced **7***a* and acetylene from **2***a* (see also ref. 16). Adducts **2***e* were prepared at lower temperatures (40–95°) but with one exception (**2***e*, Y = NO_2) their thermal instability limited yields to about 25%.

Up until 1968 the only 7-azanorbornadiene derivatives reported were those prepared from *N*-benzyl-, *N*-1-naphthyl-, and *N*-carbomethoxypyrrole with acetylenedicarboxylic acid (3, 4, 16), and recently Prinzbach and co-workers have isolated the corresponding adduct of *N*-methylpyrrole (2). These adducts exist as zwitterions and their isolation has been attributed to their insolubility in the reaction medium (4). Sauer in a recent review article (5) has incorrectly claimed that *N*-benzyl-, *N*-1-naphthyl-, and *N*-triphenylmethylpyrrole react with DMAD to yield adducts. The dienophile used in these reactions, however, was acetylenedicarboxylic acid and the latter diene was unreactive (4). Derivatives **2***a*–**2***e* (1, 2) were the first examples in which an acetylenedicarboxylic ester was used as dienophile. Previous attempts to isolate adducts of such a dienophile with 2-methyl- (6) or *N*-methylpyrrole (7), or with unsubstituted and substituted **1***a* (8), were unsuccessful, although these adducts have been postulated as reaction intermediates (7, 8).

As part of a comprehensive study of the influence of Lewis acids on the Diels–Alder reaction we have recently studied the reaction of substituted furans with acetylenedicarboxylic esters and were able to draw the following conclusions: (*a*) Lewis acids cause an enormous increase in the rate of adduct formation thereby permitting the use of lower temperatures and shorter reaction times (9, 10); (*b*) the addends and adduct all complex with Lewis acids (9); (*c*) conversion of addends to adduct was irreversible in contrast to the thermal reaction due to the formation of a strong adduct – Lewis acid complex.

During the above studies we were able to isolate the previously inaccessible adduct diethyl 1,4-diphenyl-7-oxabicyclo[2·2·1]2,5-heptadiene-2,3-dicarboxylate (9). This suggested that Lewis acids might promote the formation of similar adducts of other heterocyclic dienes. For one such study we chose the reaction of **1***a* with DMAD. When this work was started the adduct **2***a* had not been prepared.[3] Our approach to the synthesis of **2***a* differs significantly from that of Prinzbach (2). We felt that the combination of milder reaction conditions, the irreversible nature of the reaction and the formation of a **2***a* – Lewis acid complex [see (*a*)–(*c*) above] might enable

[1]NRCC No. 10602.
[2]NRCC Postdoctorate Fellow 1967–1968.

[3]This work was reported at the 51st Annual Conference of the Chemical Institute of Canada which was held in Vancouver, British Columbia, on June 3–6, 1968.

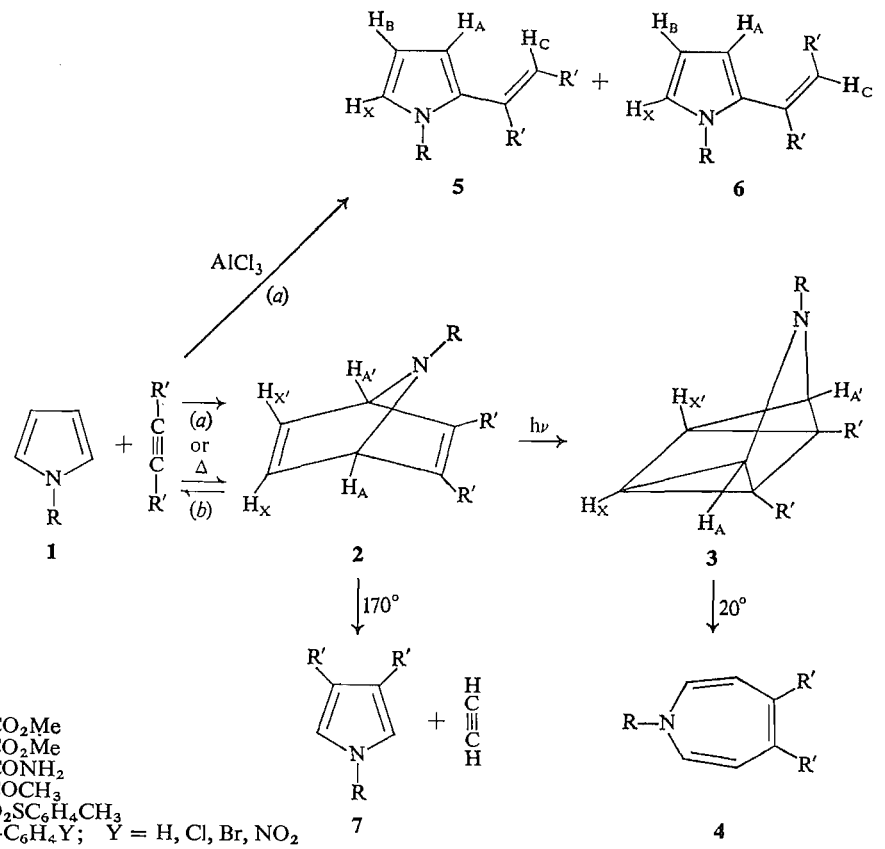

this adduct to be prepared in the presence of $AlCl_3$. By analogy with the synthesis of oxepine derivatives (11, 12) **2***a* could then be converted to the azepine **4***a* via the 3-azaquadricyclane derivative **3***a*. Prinzbach and co-workers have used this approach in the synthesis of the azepines **4***c* and **4***d* (1). This communication reports the synthesis of **2***a* in virtually quantitative yield and our independent investigations in developing a facile azepine synthesis. Our mechanistic studies on the formation of adducts like **2***a* in the presence of Lewis acids will be reported elsewhere.

The $AlCl_3$-promoted reaction of **1***a* and DMAD in CH_2Cl_2 yields variable amounts of **2***a*, **5***a*, and **6***a* (see reaction *a*) depending on the reaction conditions. Compounds similar to **5***a* and **6***a* have been obtained previously from thermal reactions of other substituted pyrroles with acetylenedicarboxylic acid or DMAD (3, 6, 16) and are believed to be formed by a Michael type addition (13).

Independent experiments established that **5***a* was isomerized to **6***a* but that neither compound was interconvertible with **2***a* in the presence of $AlCl_3$. Consequently, the formation of **2***a* and **5***a* must have occurred by independent routes with subsequent conversion of the latter to **6***a*. Our results in Table I clearly indicate that low temperatures (≪25°) favor the production of **5***a*

TABLE I

Yields of products obtained from the reaction of **1***a*, DMAD and $AlCl_3$ in CH_2Cl_2*

$AlCl_3$: addend ratio	Temperature	Time (h)	Mole % yield†		
			5*a*	**6***a*	**2***a*
1:1	−75°	2	No reaction		
1:1	−10°	4	36	36	18
1:1	25°	2	34	22	34
1:1	40°	0.5	30	4	54
3:1	40°	1	—	19	76
5:1	40°	1	—	—	93

*Reaction solutions were 0.1 molar in the three reagents, except in the last two experiments in which the $AlCl_3$ concentration was increased by a factor of 3 or 5.

†Reaction composition was determined by proton magnetic resonance.

Can. J. Chem. Downloaded from www.nrcresearchpress.com by 210.87.254.40 on 09/05/12
For personal use only.

Can. J. Chem. Downloaded from www.nrcresearchpress.com by 210.87.254.40 on 09/05/12
For personal use only.

and **6***a* when the reactants are present in equimolar amounts. Synthesis of **2***a* is favored and side reactions producing **5***a* and **6***a* are minimized at higher reaction temperatures (40°).

Increasing the $AlCl_3$ concentration had a dramatic effect on the product composition (see Table I). A three-fold increase in the $AlCl_3$ concentration at 40° not only raised the yield of **2***a* from 54 to 76% but caused total isomerization of **5***a* to **6***a*. This had important experimental implications since **2***a* could be separated from **6***a* by chromatography on silicic acid impregnated with silver nitrate while its separation from **5***a* was difficult and laborious. The isolable yields of **2***a* were therefore much lower than those estimated by proton magnetic resonance (p.m.r.) when the $AlCl_3$:addend ratio was 1:1 while at higher ratios the estimated and actual yields did not differ significantly. When the $AlCl_3$:addend ratio was increased to 5:1 **2***a* was obtained and could be isolated in almost quantitative yield (≈90%). Since **1***a* and DMAD do not react in CH_2Cl_2 at 40° in the absence of $AlCl_3$ it is clear that the latter must cause an enormous enhancement in the rates of formation of both **2***a* and **5***a*. It should be noted that the preferred formation of **5***a* rather than **6***a* in the initial stages of reaction implies the stereospecific *cis*-addition of the diene to the triple bond of DMAD. The mechanism of this addition is under investigation.

Photochemical conversion of **2***a* to **3***a* was quantitative and the latter rearranged to **4***a* at temperatures $> -20°$.

The molecular formulae of **2***a*, **4***a*, and **6***a* were determined by mass spectral analyses and the structures of these compounds together with those of **3***a* and **5***a* were established by p.m.r. Analyses of the characteristic AXX'A' systems in **2***a* and **3***a*, and the ABX systems in **5***a* and **6***a*, were carried out with the aid of the Laocoon II program (14). Observed and calculated spectra agreed within experimental error. Some spin–spin coupling constants were checked by spin-decoupling. The retro Diels–Alder conversion of **2***a* to **7***a* and acetylene at 170° was additional evidence for its structure. All spectral data are reported in the Experimental. Since Prinzbach and co-workers (2) did not analyze the p.m.r. spectrum of **2***a* the data for this compound have also been included.

The mild reaction conditions and high yields characteristic of the present study suggest that the use of Lewis acids to promote the formation of 7-azanorbornadiene derivatives from pyrroles, containing an electron acceptor substituent on nitrogen, and acetylene derivatives, may have certain advantages over the thermal reaction.

Experimental

The proton magnetic resononce (p.m.r.) spectra were recorded using a Varian HA-100 or A 60-A spectrometer equipped with a variable temperature probe and spin decoupler. Mass spectra were recorded using a Consolidated Electrodynamics Corporation 21-110B mass spectrometer and mass measurements employed electrical detection.

Preparation of 2a, 5a, and 6a

A 10 ml solution of **1***a* (1.26 g; 0.01 *M*) in CH_2Cl_2 was added to a 90 ml solution of DMAD (1.42 g; 0.01 *M*) and $AlCl_3$ (6.70 g; 0.05 *M*) in the same solvent, and the mixture stirred at 40° for 1 h. At the end of this period the dark-red reaction solution was washed with water to remove the Lewis acid and stop the reaction. After drying the organic layer and removing the solvent the dark-red oily residue (2.61 g) containing **2***a* and **6***a* was chromatographed on silicic acid (200 g) using a mixture of petroleum ether (60–80°) and ethyl acetate in the ratio of 7:3 as eluant.

2*a* was isolated in 90% yield as a yellow oil,[4] $n_D^{25} = 1.6560$ which gave a parent molecular ion at *m/e* 267. From its 60 MHz p.m.r. spectrum in $CDCl_3$ signals could be assigned to the bridgehead (2H, multiplet, average $\tau = 4.48$), olefinic (2H, multiplet, average $\tau = 2.83$), *N*-carbomethoxy (3H, singlet, τ 6.35) and carbomethoxy (6H, singlet, τ 6.18) protons. Analysis of the AXX'A' system[5] for the bridgehead and olefinic protons gave: $\Delta\nu_{AX} = 98.7$, $J_{AA'} = 2.2$, $J_{XX} = 5.1$, $J_{AX} = J_{A'X'} = 2.7$ and $J_{AX'} = J_{A'X} = 0.5$ Hz. Identical parameters (except ΔJ_{AX}) were obtained from the 100 MHz spectrum and $J_{XX'} = 5.0$ Hz was determined independently by irradiating the A protons and observing the ^{13}C—H satellite (doublet) of the X-protons.

When the $AlCl_3$:addend ratio was 1:1 **2***a*, **5***a*, and **6***a* were isolated by preparative thin-layer chromatography on silica gel G impregnated with 10% silver nitrate (15) using the solvent mixture described above as eluant. Samples of **5***a* were always contaminated with **2***a* although the amounts of the latter did not prevent the structure of **5***a* being deduced from its p.m.r. spectrum.

5*a* was obtained as a yellow oil and signals in its 60 MHz p.m.r. spectrum in $CDCl_3$ could be assigned to one olefinic proton (singlet, τ 3.64), an *N*-carbomethoxy (3H, singlet, τ 6.24) and two chemically non-equivalent carbomethoxy (6H, 2 singlets, τ 6.10 and 6.22) groups. Analysis of the ABX system for the three pyrrole ring protons (AB multiplet centered at τ 3.67 and X multiplet

[4]Prinzbach and co-workers reported that **2***a* crystallized from petroleum ether, m.p. 56–57° (2). Samples prepared in this laboratory by the thermal or Lewis acid-promoted reaction, although identical (p.m.r., infrared (i.r.)), could not be crystallized.

[5]Refer to figure for the labelling of protons in **2***a*–**6***a*.

at τ 2.62) gave $\Delta\nu_{AB} = 11.3$, $J_{AB} = 3.3$, $J_{AX} = 3.4$, and $J_{BX} = 1.9$ Hz. The chemical shift of the olefinic proton in **5***a* was similar to that for the corresponding protons in dimethyl maleate (τ 3.84).

6*a* was obtained as pale-yellow hexagonal prisms from CH_2Cl_2 – ether, m.p. 61–62° [lit. (16), m.p. 63°]. The 60 MHz p.m.r. spectrum of this compound in $CDCl_3$ gave signals for one olefinic proton (singlet, τ 3.04), one *N*-carbomethoxy (3H, singlet, τ 6.33) and two carbomethoxy (6H, 2 singlets, τ 6.10 and 6.23) groups. Analysis of the ABX system[5] for the three pyrrole ring protons (AB multiplet centered at τ 3.73 and X multiplet at τ 2.64) gave $\Delta\nu_{AB} = 3.2$, $J_{AB} = 3.3$, $J_{AX} = 3.4$ and $J_{BX} = 1.9$ Hz.

Preparation of 3a and 4a from 2a

2*a* (50 mg) was converted quantitatively to **3***a* when a solution in CD_2Cl_2 (2 ml) was irradiated at 3100 Å (Pyrex filter, Rayonet Photochemical Reactor) for 2 h at −25°. The reaction was monitored by p.m.r. and signals in the final 60 MHz spectrum could be assigned to one *N*-carbomethoxy (3H, singlet, τ 6.17) and two chemically equivalent carbomethoxy (6H, singlet, τ 6.32) groups. The remaining four protons formed an AXX′A′ system. The A type (2H, octet, average τ 5.42) and X type (2H, octet, average τ 7.11) protons appeared as deceptively simple doublets with a spacing of 4.8 Hz at a sweep width of 500 Hz. Analysis of this system[5] gave $\Delta\nu_{AX} = 100.0$, $J_{AA'} = 1.8$, $J_{XX'} = 3.1$, $J_{AX} = J_{A'X'} = 4.8$, and $J_{AX'} = J_{A'X} = 0$ Hz. Identical parameters (except $\Delta\nu_{AX}$) were obtained from the 100 MHz spectrum.

3*a* was not isolated because it gradually changes to **4***a* at temperatures above −20°. At room temperature this conversion is complete in 10 min.

4*a* was obtained as a yellow oil, $n_D^{25} = 1.5112$. Molecular ion mass: Anal. Calcd. for $C_{12}H_{13}NO_6$, 267.0743. Found: *m/e* 267.0742. Ultraviolet spectrum (EtOH) $\lambda\lambda_{max}$ 207 (ε 17 300) and 346 mμ (ε 1430). Its 60 MHz p.m.r. spectrum in CD_2Cl_2 contained signals for one *N*-carbomethoxy (3H, singlet, τ 6.21) and two chemically equivalent carbomethoxy (6H, singlet, τ 6.25) groups. The azepine ring protons gave a characteristic AB spectrum (centered at τ 4.16) with $\Delta\nu_{AB} = 27.3$ and $J_{AB} = 8.0$ Hz with an intensity corresponding to 4 protons. The value of J_{AB} was confirmed by decoupling. (It seems reasonable that the protons attached to the carbon atoms bearing nitrogen will appear at lowest field.)

Large amounts of **4***a* were obtained by scaling up the procedure described above.

Acknowledgments

We wish to thank Mr. D. G. Smith and Mr. J. van Ingen for recording the proton magnetic resonance spectra and Mr. D. J. Embree for the mass spectra.

1. H. PRINZBACH, R. FUCHS, and R. KITZING. Angew. Chem. Intern. Ed. Engl. **7**, 67 (1968).
2. R. KITZING, R. FUCHS, M. JOYEUX, and H. PRINZBACH. Helv. Chim. Acta. **51**, 888 (1968).
3. L. MANDELL and W. A. BLANCHARD. J. Am. Chem. Soc. **79**, 6198 (1957).
4. L. MANDELL, J. U. PIPER, and C. E. PESTERFIELD. J. Org. Chem. **28**, 574 (1963).
5. J. SAUER. Angew. Chem. Intern. Ed. Engl. **5**, 211 (1966).
6. O. DIELS, K. ALDER, H. WINCKLER, and E. PETERSON. Ann. **498**, 1 (1932).
7. R. M. ACHESON and J. M. VERNON. J. Chem. Soc. 1148 (1962).
8. N. W. GABEL. J. Org. Chem. **27**, 301 (1962).
9. A. W. MCCULLOCH, B. STANOVNIK, and A. G. MCINNES. Chemistry in Canada, Oct. 1966. p. 46.
10. A. W. MCCULLOCH and A. G. MCINNES. Chemistry in Canada, Sept. 1967. p. 51.
11. H. PRINZBACH, M. ARGUELLES, and E. DRUCKREY. Angew. Chem. Intern. Ed. Engl. **5**, 1039 (1966).
12. H. PRINZBACH, P. VOGEL, and W. AUGE. Chimia, (Aarau) **21**, 469 (1967).
13. R. M. ACHESON. Advan. Heterocyclic Chem. **1**, 125 (1963).
14. S. CASTELLANO and A. A. BOTHNER-BY. J. Chem. Phys. **41**, 3863 (1965).
15. C. B. BARRETT, M. S. J. DALLAS, and F. B. PADLEY. Chem. and Ind. London, 1050 (1962).
16. R. M. ACHESON and J. M. VERNON. J. Chem. Soc. 1008 (1963).

Can. J. Chem. Downloaded from www.nrcresearchpress.com by 210.87.254.40 on 09/05/12
For personal use only.

Conformations of some dianhydrohexitols

F. J. HOPTON AND G. H. S. THOMAS
Ontario Research Foundation, Sheridan Park, Ontario

Received October 23, 1968

Proton magnetic resonance spectra of three known diastereoisomers 1,4:3,6-dianhydro-D-glucitol, 1,4:3,6-dianhydro-D-mannitol, 1,4:3,6-dianhydro-L-iditol, and their diacetyl and dimesyl derivatives have been analyzed. The coupling constants obtained have been utilized to determine the conformation of the five-membered rings. Constancy of the couplings between ring protons throughout the series of compounds indicates the existence of one conformation common to all, and this appears to be a composite of the C_s and C_2 forms. It is significant that intramolecular hydrogen bonding, which occurs in two of the three diastereoisomers, has little or no effect on ring conformation.

Canadian Journal of Chemistry, 47, 2395 (1969)

Can. J. Chem. Downloaded from www.nrcresearchpress.com by 210.87.254.105 on 09/05/12
For personal use only.

It is well known that the hexitols L-iditol, D-glucitol, and D-mannitol readily form 1,4:3,6-dianhydrides under acidic conditions (1). These 1,4:3,6-dianhydrides each have two free hydroxyl groups located at the C-2 and C-5 positions.

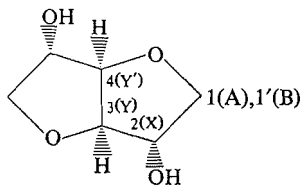

1

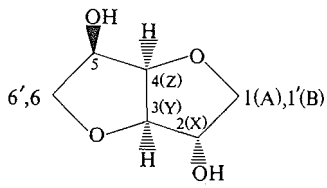

2

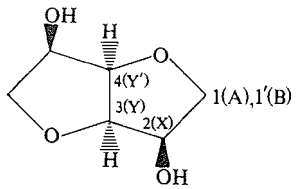

3

From inspection of molecular models the 1,4:3,6-dianhydrohexitols have two nearly planar *cis*-fused five-membered rings in the form of a "V" with the hydroxyl groups at the C-2 and C-5 positions either inside or outside the "V" shaped wedge. As in other ring systems the configuration of a group inside the wedge is designated as *endo* whereas one outside the wedge is *exo*. In the L-iditol derivative **1** both hydroxyl groups are *exo*, in the D-mannitol derivative **3** both are *endo*, and in the D-glucitol derivative **2** the hydroxyl at C-2 is *exo* and that at C-5 is *endo*.

The stereochemistry of these compounds has been discussed by Mills (2) and the order of stability of the three compounds as deduced from their ease of formation (3, 4), epimerization (5), and general chemical properties (6, 7) indicates that the presence of an *exo* substituent increases the stability of the ring to which it is attached, by virtue of the diminished opportunities for interaction between non-bonded substituents. Furthermore the faces of the rings inside the "V" are less accessible than the faces outside, so *exo* and *endo* isomers exhibit differences in reactivity in the direction determined by the steric requirements of the reaction in question (8, 9). The extent of intramolecular hydrogen bonding, as determined by infrared spectroscopy in this series of compounds (10) illustrates the influence of structure on such bonding. The C-2 and C-3, and C-4 and C-5 oxygen bonds in the iditol derivative are *trans* related as in L-threitan so that intramolecular bonding is precluded. A *cis* relation of the C-4 and C-5 oxygen bonds exists in the D-glucitol analogue permitting a single intramolecular hydrogen bond. In D-mannitol the C-2 and C-3, and C-4 and C-5 oxygen bonds are *cis* related; two intramolecular hydrogen bonds may occur and the absence of detectable absorption for free hydroxyl groups indicates the completeness of the hydrogen bonding.

Correlation of nuclear magnetic resonance

Can. J. Chem. Downloaded from www.nrcresearchpress.com by 210.87.254.105 on 09/05/12
For personal use only.

(n.m.r.) coupling constants (J) with dihedral angles (ϕ) is a major step in conformational and configurational analysis. Nuclear magnetic resonance has proved to be an effective means of determining possible conformations of carbohydrate ring systems in solution (11, 12). This paper is concerned with the n.m.r. study of three dianhydrohexitols and their diacetyl and dimesyl derivatives in an attempt to determine their conformations.

Experimental

Spectra (60 Mc.p.s. and 100 Mc.p.s.) were recorded on Varian A60 and HA-100 spectrometers respectively at 33 °C. The spectra were of 1–10 mole % solutions in both acetone-d_6 and deuteriochloroform with tetramethylsilane (TMS) as internal reference. Some spectra of the compounds in pyridine as solvent were also determined. Spin-decoupling and spin-tickling experiments were carried out with the HA-100 spectrometer.

L-Iditol was prepared from L-sorbose by reduction using sodium borohydride. The L-iditol was separated from accompanying D-glucitol by fractional crystallization of the hexaacetyl derivatives (13). The parent hexitol was obtained by deacetylation of the hexaacetyl-L-iditol using sodium methoxide.

The dianhydrohexitols were prepared by the method given by Shen for the preparation of 1,4:3,6-dianhydro-D-glucitol (14). The diacetyl and dimesyl derivatives of the dianhydrohexitols were prepared by standard methods. In all instances the compounds were either recrystallized or distilled until their physical constants corresponded closely with the reported values.

Analysis and Discussion

The ring protons in one ring of any one of the compounds studied constitute either an ABXYY′ or an ABXYZ system. Numbering of these protons is as indicated in formulas [**1**–**3**] and their 100 Mc.p.s. spectra are shown in Figs. 1, 2, and 3. For the symmetric molecules **1**, **3**, and their derivatives, the ring protons are classified as A(H-1, H-6) B(H-1′, H-6′) X(H-2, H-5) Y(H-3) Y′(H-4). In the parent compounds **1** and **3**, H-2 and H-5 are coupled to OH protons. This coupling was removed by addition of a few drops of acid to the sample causing rapid exchange of the OH protons.

The procedure used for simplification of the spectra obtained was to irradiate at the resonance position of H-3 and H-4 with a secondary radio frequency (r.f.) field to clarify the ABX

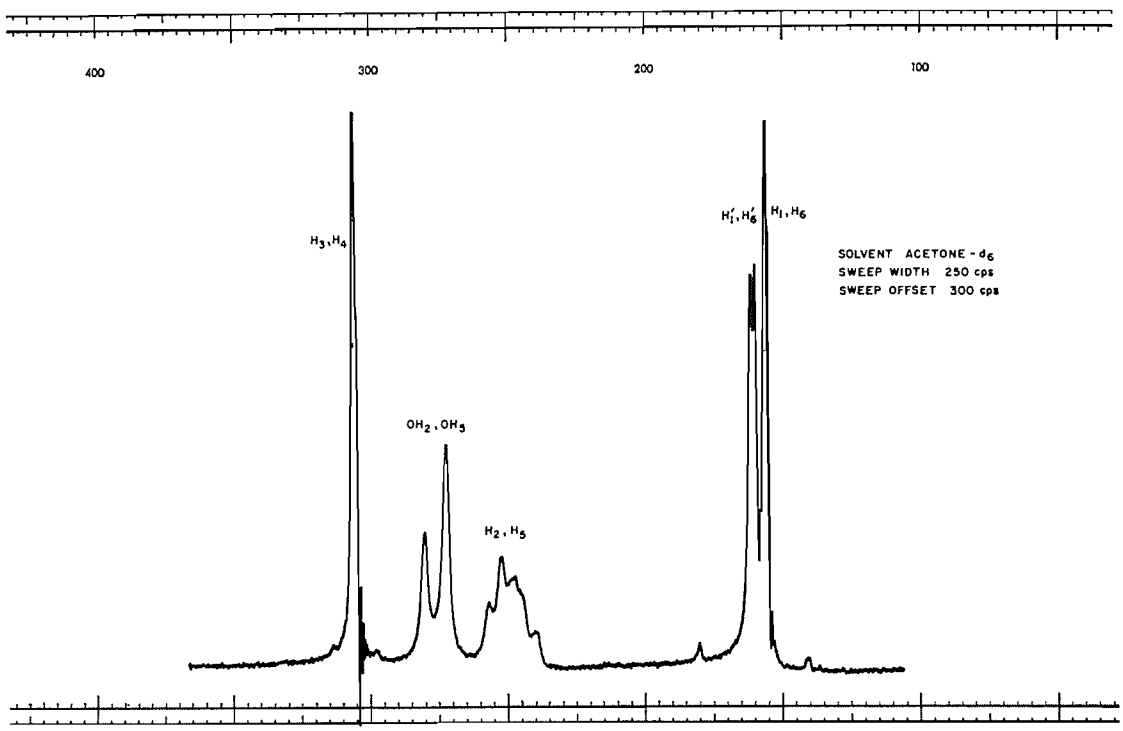

FIG. 1. The 100 Mc.p.s. nuclear magnetic resonance spectrum of 1,4:3,6-dianhydro-L-iditol.

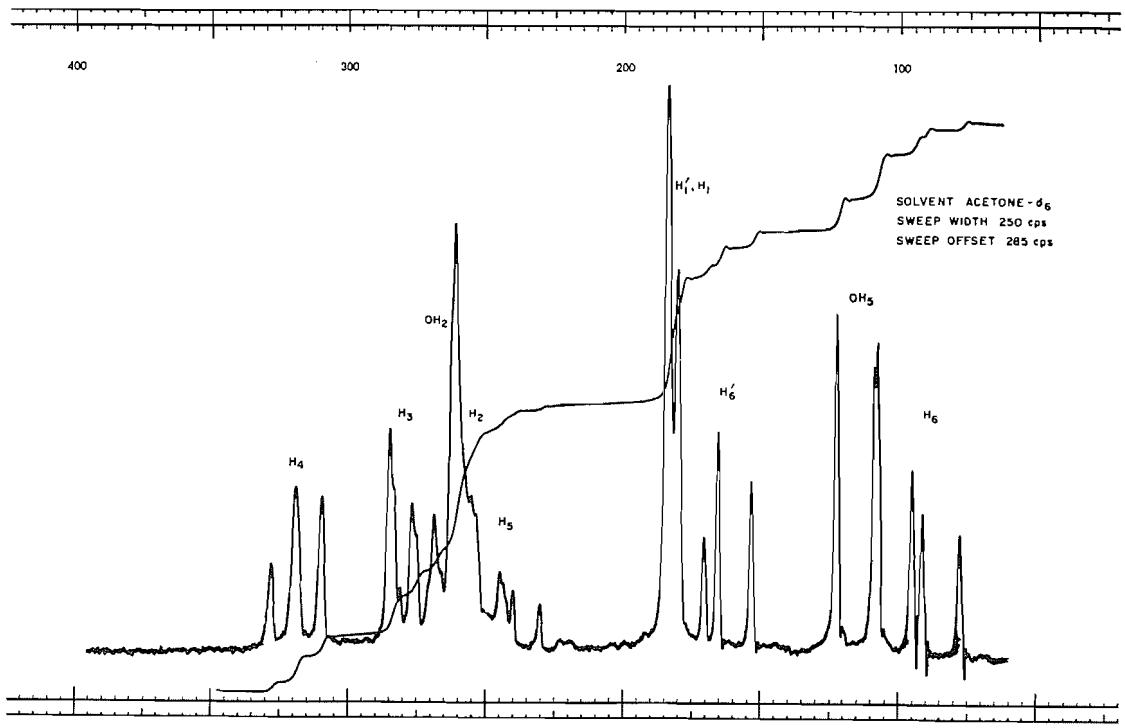

FIG. 2. The 100 Mc.p.s. nuclear magnetic resonance spectrum of 1,4:3,6-dianhydro-D-glucitol.

pattern of H-1, H-1′, and H-2 (H-6, H-6′, and H-5), followed by irradiation at a point midway between the resonance positions of H-1 (H-6) and H-1′ (H-6′) revealing an XX′YY′ pattern, very often approaching MM′YY′ for H-2, H-5, H-3, and H-4. Analysis of the ABX and XX′YY′ patterns was accomplished using established procedures (15). In cases where $\delta_{AB} \ll J_{AB}$ and fewer lines than expected were observed, analysis was made using methods published for other deceptively simple spectra (16). Additional decoupling and tickling experiments were performed to confirm the assignments made and to verify that the geminal coupling constant J_{AB} was of opposite sign to that of the vicinal coupling constants J_{AX} and J_{BX}.

The increased complexity of the spectra of compound **2** and its derivatives arises from a lack of symmetry in these compounds such that H-3 and H-4, H-1 and H-6, H-1′ and H-6′, H-2 and H-5 are no longer chemically equivalent. The procedures for analysis described above were, however, sufficient to evaluate all the chemical shifts and coupling constants from the spectra. Spectra of these compounds in pyridine as solvent were also used to facilitate some of the analyses.

Long range coupling between H-2 and H-4, and H-3 and H-5 is evident for most compounds, though it is extremely small. Irradiation at the H-2 or H-5 resonance with a secondary r.f. field sharpens the lines in the resonance patterns of H-3 and H-4, respectively. A long range coupling of significance is observed in the dimesyl derivative of **2** between H-3 and one of the geminal protons H-1 or H-1′. The spatial arrangement of these protons is most suited to a coupling between H-3 and H-1′ as labelled in **2** where the intervening bonds approach a planar W formation (17). However, this coupling is not observed in the corresponding derivative of **1** where the arrangement of protons must be very similar. The fact that long range coupling between H-3 and H-1′ is to be preferred over a similar coupling between H-3 and H-1 enables identification of the geminal protons to be made, with H-1′ being at lower field than H-1. This is also assumed to be the case in the spectra of the other compounds studied.

Coupling constants and chemical shifts are

Can. J. Chem. Downloaded from www.nrcresearchpress.com by 210.87.254.105 on 09/05/12
For personal use only.

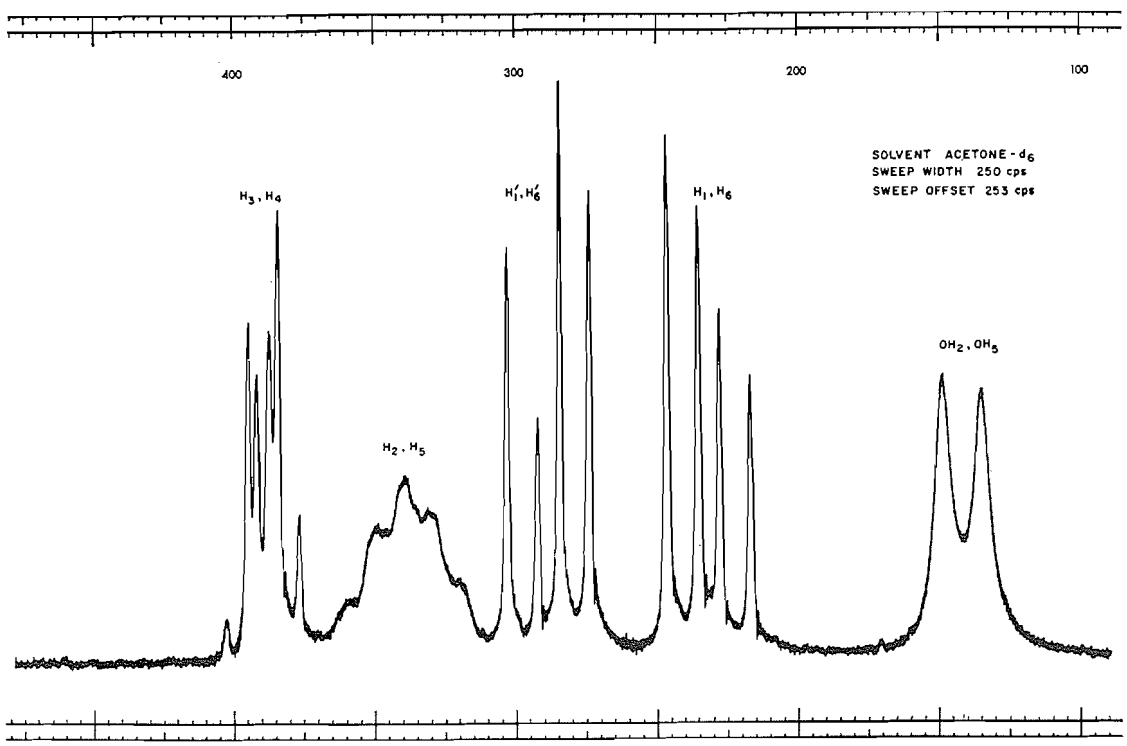

FIG. 3. The 100 Mc.p.s. nuclear magnetic resonance spectrum of 1,4:3,6-dianhydro-D-mannitol.

TABLE I
Coupling constants (J, c.p.s.)

Compound	$J_{11'}$	J_{12}	$J_{1'2}$	J_{23}	J_{34}	J_{45}	J_{56}	$J_{56'}$	$J_{66'}$	Other coupling	
1,4:3,6-Dianhydro-L-iditol-**1**	−9.5	3.8	0.7	0.5	3.8	0.5	0.7	3.8	−9.5	$J_{H_2(5)OH_2(5)}$	3.9
Diacetyl-**1**	−10.7	3.7	1.6	0.5	3.9	0.5	1.6	3.7	−10.7		
Dimesyl-**1**	−11.0	3.6	0.9	0.7	3.8	0.7	0.9	3.6	−11.0		
1,4:3,6-Dianhydro-D-glucitol-**2**	−8.5	3.4	0.5	0.8	4.4	4.7	5.8	5.9	−9.5	$J_{H_2OH_2}$	3.8
Diacetyl-**2**	−10.5	4.6	0.2	0.6	4.8	5.0	5.5	6.0	−9.7	$J_{H_5OH_5}$	7.5
Dimesyl-**2**	−11.4	3.4	0.5	1.0	4.6	5.1	5.0	5.6	−10.1	$J_{1'3}$	±1.1
1,4:3,6-Dianhydro-D-mannitol-**3**	−9.2	5.1	5.4	5.4	5.4	5.4	5.1	5.4	−9.2	$J_{H_2(5)OH_2(5)}$	6.9
Diacetyl-**3**	−9.0	7.0	6.5	5.5	5.0	5.5	7.0	6.5	−9.0		
Dimesyl-**3**	−9.5	6.1	6.8	5.5	4.8	5.5	6.1	6.8	−9.5		

TABLE II
Chemical shifts (p.p.m.)

Compound	H-1	H-1′	H-2	H-3	H-4	H-5	H-6	H-6′	OH_2	OH_5
1,4:3,6-Dianhydro-L-iditol-**1**	3.78	3.81	4.25	4.54	4.54	4.25	3.78	3.81	4.38	4.38
Diacetyl-**1**	3.80	3.92	5.12	4.56	4.56	5.12	3.80	3.92	CH_3	2.03
Dimesyl-**1**	3.90	3.99	5.02	4.76	4.76	5.02	3.90	3.99	CH_3	3.16
1,4:3,6-Dianhydro-D-glucitol-**2**	3.74	3.78	4.16	4.26	4.44	4.08	3.37	3.63	4.17	3.43
Diacetyl-**2**	3.90	3.94	5.12	4.42	4.76	5.09	3.75	3.87	CH_3	2.03, 2.08
Dimesyl-**2**	4.0	4.11	5.06	4.65	4.89	5.14	3.80	3.95	CH_3	3.13, 3.16
1,4:3,6-Dianhydro-D-mannitol-**3**	3.69	3.97	4.23	4.48	4.48	4.23	3.69	3.97	3.24	3.24
Diacetyl-**3**	3.60	3.86	4.91	4.54	4.54	4.91	3.60	3.86	CH_3	2.02
Dimesyl-**3**	3.88	3.96	5.02	4.65	4.65	5.02	3.88	3.96	CH_3	3.06

Can. J. Chem. Downloaded from www.nrcresearchpress.com by 210.87.254.105 on 09/05/12
For personal use only.

Can. J. Chem. Downloaded from www.nrcresearchpress.com by 210.87.254.105 on 09/05/12
For personal use only.

given in Tables I and II respectively. It is apparent that substitution has some effect on both vicinal and geminal coupling constants. A decrease in J_{gem} (increased negative value) occurs as the hydroxyl group is replaced by acetoxy and then by mesyloxy. This change in J_{gem} is greater when the substituent is *exo* rather than *endo*, providing further evidence that coupling is dependent both on the electronegativity of a group on an adjacent carbon atom and on the orientation of that group with respect to the geminal protons (18). Vicinal coupling constants vary with orientation of electronegative substituents (19). This stereochemical dependence is readily observed provided other factors, such as bond angles and bond lengths, remain unchanged. No attempt has been made in this study of dianhydrohexitols to correlate changes of particular vicinal coupling constants with electronegativity of substituent groups, because it is thought that the breaking of strong intra- and intermolecular hydrogen bonds, caused by substitution, effect changes in bond angles and possibly bond lengths.

Coupling of the hydroxyl proton to the proton on the same carbon atom when the hydroxyl group is *endo* is almost twice that observed when the hydroxyl group is *exo*. Intramolecular hydrogen bonding fixes the hydroxylic proton for the *endo* hydroxylic group such that the protons concerned are more or less *trans* oriented with respect to the C—O bond giving rise to a coupling of 7.5 c.p.s. When the hydroxylic group is *exo*, the hydroxylic proton has a random orientation with respect to the vicinal C—H proton, even though hydrogen bonding to a solvent may occur, and the coupling observed is much smaller (ca. 4 c.p.s.). It is thought that a conformational dependence exists for J_{HCOH} similar in qualitative form to that observed for J_{HCCH}. A value of 12–13 c.p.s. (20) has been found for J_{HCOH}^{trans} whereas the "free rotation" value of J_{HCOH} is 4 c.p.s.

The Karplus equation (21) and other modified versions (11, 22, 23) have been extensively used to calculate dihedral angles in five- and six-membered ring compounds from observed coupling constants. Variation of vicinal coupling constant J with the dihedral angle ϕ may be expressed by an equation of the following form

$$J = A\cos^2\phi + B$$

where A and B are constants and A is greater for $\phi > 90°$ than for $\phi < 90°$. The value of A in particular is found to vary for different systems in order to give consistent results. However, whatever values the parameters A and B have been given, J always decreases to approximately zero as ϕ increases from 0° to 90°, and increases again as ϕ further increases from 90° to 180°. Thus a small coupling of 1 c.p.s. or less corresponds to an angle of approximately 90°, and any other value of J will give two angles for ϕ, one between 0 and 90° and the other between 90 and 180°. Most of the constants obtained fall in the intermediate range of 3.5–6.0 c.p.s. and, using average values for the parameters A and B taken from the literature, correspond to dihedral angles of 50–30° or 125–145°.

Five-membered rings are generally accepted to be significantly non-planar; the rings may be described in terms of various planes through sets of four or three atoms, or in terms of various dihedral angles. Of the various puckered forms of cyclopentane (24) the so-called C_s or "envelope" form and the C_2 or "twist" (T) form have greater symmetry than all other possibilities, and substituted cyclopentanes exist preferentially with a geometry close to one or other of these forms.

Furthermore, calculations on cyclopentane derivatives containing sp^2 hybridized atoms, e.g. cyclopentanone or hetero-atoms, e.g. tetrahydrofuran, suggest (25) that such molecules exist in the twist form with the maximum puckering occurring at C-3 and C-4, i.e. away from the sp^2 hybridized or hetero-atom. An sp^2 hybridized atom in planar surroundings is not seriously troubled by bond eclipsing (unlike an sp^3 hybridized atom) and it is therefore reasonable that whatever puckering occurs should involve mainly other parts of the molecule. The fact that atoms with free pairs of electrons such as O, S, and N should behave similarly implies that the free pairs give rise to little or no eclipsing of their own. Qualitatively fused ring systems resemble single ring systems of analogous conformation, though a certain rigidity is associated with the bond common to the two fused rings.

For the purposes of comparison of the three diastereoisomers, reference is made to compound **2** in which C-1 – C-4 indicate an iditan-type moiety (*exo*-hydroxyl) and C-3 – C-6 indicate a mannitan-type moiety (*endo*-hydroxyl). The two fused rings in dianhydro-mannitol and dianhydro-iditol are identical in each case and

Can. J. Chem. Downloaded from www.nrcresearchpress.com by 210.87.254.105 on 09/05/12
For personal use only.

hence only the coupling in one ring need be discussed. From the data given in Table I, only two conformations are acceptable for either ring. The first of these is the C_S or envelope conformation in which C-3 is displaced out of the plane formed by atoms C-1, C-2, C-4, and the oxygen in that ring, and C-4 is displaced out of the plane formed by C-3, C-5, C-6, and the oxygen in that ring. This displacement is in such a way as to cause a decrease in angle between the ring planes thus described. The alternative conformation is the C_2 or half chair conformation in which C-2 and C-3 are displaced (symmetrically) below and above (respectively) the plane defined by C-1 and C-4 and the oxygen between them, and C-4 and C-5 are similarly disposed about a plane defined by C-3 and C-6 and the oxygen between them.

It has been shown that the molecular framework of *cis*-fused molecules is fairly rigid and conformational possibilities are restricted (25), and furthermore, that the energy difference between C_2 and C_S conformations for *cis*-fused five-membered rings, such as in the hydrindanes, is small. Unless, therefore, a distinct difference in dihedral angles occurs in the two conformations a preference of one form over the other on the basis of coupling constants is somewhat tenuous. Application of calculated angles obtained for both C_S and C_2 conformations to a mannitan-type ring in the systems under discussion would require the following dihedral angles

C_S conformation	C_2 conformation
$\phi_{45} = \phi_{34} = 46°$ (4.5)	$\phi_{45} = 48°$ (4.3)
$\phi_{56} = 29°$ (6.9)	$\phi_{56} = \phi_{34} = 39°$ (5.4)

The figures shown in parentheses above represent coupling constant values derived from a typically modified Karplus equation previously used for five-membered ring compounds (11).

Average values of the coupling constants J_{34}, J_{45}, and J_{56} taken from Table I for all rings of this type are 4.8, 5.2, and 5.7 c.p.s. respectively. It is readily seen that neither the C_S nor C_2 conformation is preferentially suited to such values. However, since J_{34} is always found to be less than or equal to J_{45}, and J_{56} varies quite considerably with differing substituents on C-5, the C_S conformation appears to be the more favored one. A slight displacement of C-5 from its position in a C_S conformation towards its position in a C_2 conformation would readily account for the coupling constants found. This displacement might well arise from a certain restriction to displacement of C-4 due to its involvement in the bond common to both rings. Similar arguments apply equally well to the iditan-type ring, so that in all the compounds studied, the rings are thought to have the same conformation.

Abraham *et al.* (11) have described in detail the conformation of the rings of 3,6-anhydro-1,2-*O*-isopropylidene-5-*O*-tosyl-α-D-glucofuranose evaluated from coupling constants obtained from a proton resonance study. Both the C_S and C_2 conformations are found to exist in this compound with the anhydro ring in the C_S conformation. These findings are based on an equality of particular coupling constants as a result of symmetric buckling in the ring. However, our results indicate that only a small deformation of either the C_S or C_2 arrangement of atoms can give rise to very similar coupling constant values.

From a paper by Cameron *et al.* (26) on the X-ray crystallographic study of 2-*O*-(*p*-bromobenzenesulfonyl)-1,4:3,6-dianhydro-D-glucitol-5-nitrate, calculations of the atomic positions, using data given in Table II of that publication, indicate the conformations of the two five-membered rings to be very similar. In this compound the most significant non-bonded intramolecular contact is between a nitro group oxygen and the oxygen atoms in the other ring, and the relatively short approach is probably the result of some attractive interaction between the two atoms. This interaction which exists in one ring only has little effect on the ring conformation. In the present study we find that intramolecular hydrogen bonding, which exists in both 1,4:3,6-dianhydro-D-glucitol and 1,4:3,6-dianhydro-D-mannitol, has very little effect on ring conformation.

Acknowledgments

This research was made possible by funds received by the Ontario Research Foundation from the Ontario Department of Trade and Development.

1. L. F. WIGGINS. Advan. Carbohydrate Chem. **5**, 191 (1950).
2. J. A. MILLS. Advan. Carbohydrate Chem. **10**, 1 (1955).

3. R. MONTGOMERY and L. F. WIGGINS. J. Chem. Soc. 390 (1946).
4. R. MONTGOMERY and L. F. WIGGINS. J. Chem. Soc. 433 (1947).
5. H. G. FLETCHER, JR. and R. M. GOEPP, JR. J. Am. Chem. Soc. **67**, 1042 (1945).
6. S. SOLTZBERG, R. M. GOEPP, JR., and W. FREUDENBERG. J. Am. Chem. Soc. **68**, 919 (1946).
7. R. MONTGOMERY and L. F. WIGGINS. J. Chem. Soc. 237 (1948).
8. N. K. MATHESON and S. J. ANGYAL. J. Chem. Soc. 1133 (1952).
9. A. C. COPE and T. Y. SHEN. J. Am. Chem. Soc. **78**, 3177 (1956).
10. J. S. BRIMACOMBE, A. B. FOSTER, M. STACEY, and D. H. WHIFFEN. Tetrahedron, **4**, 351 (1962).
11. R. J. ABRAHAM, L. D. HALL, L. HOUGH, and K. A. MCLAUCHLAN. J. Chem. Soc. 3699 (1962).
12. L. D. HALL. Chem. & Ind. (London), 950 (1963).
13. W. G. M. JONES and L. F. WIGGINS. J. Chem. Soc. 363 (1944).
14. T. Y. SHEN. Methods in Carbohydrate Chem. II, 191 (1963).
15. H. J. BERNSTEIN, J. A. POPLE, and W. G. SCHNEIDER. Can. J. Chem. **35**, 65 (1957).
16. R. J. ABRAHAM and H. J. BERNSTEIN. Can. J. Chem. **39**, 216 (1961).
17. N. S. BHACCA and D. H. WILLIAMS. Applications of n.m.r. spectroscopy in organic chemistry. Holden-Day Inc., San Francisco. (1964).
18. A. A. BOTHNER-BY. Advan. magnetic resonance. Vol. 1. *Edited by* J. S. Waugh. Academic Press, Inc., New York. 1965. p. 196.
19. H. BOOTH. Tetrahedron Letters, No. 7, 411 (1965).
20. N. L. BAULD and Y. S. RIM. J. Org. Chem. **33**, 1303 (1968).
21. M. KARPLUS. J. Chem. Phys. **30**, 11 (1959).
22. M. KARPLUS. J. Am. Chem. Soc. **85**, 2870 (1963).
23. R. U. LEMIEUX and J. W. LOWN. Can. J. Chem. **42**, 893 (1964).
24. J. E. KILPATRICK, K. S. PITZER, and R. SPITZER. J. Am. Chem. Soc. **69**, 2483 (1947).
25. K. S. PITZER and W. E. DONATH. J. Am. Chem. Soc. **81**, 3213 (1959).
26. A. CAMERON, N. CAMERON, and J. TROTTER. Acta Cryst. **19**, 449 (1965).

Can. J. Chem. Downloaded from www.nrcresearchpress.com by 210.87.254.105 on 09/05/12
For personal use only.

Can. J. Chem. Downloaded from www.nrcresearchpress.com by 210.87.254.42 on 09/05/12
For personal use only.

Sur l'acylation de l'éthyl-1 cyclohexène en présence de chlorure stannique

JEAN ALLARD[1] ET NORMAND DUFORT
Département de Chimie, Université de Montréal, Montréal, Québec

Recu le 18 décembre 1968

L'acylation de l'éthyl-1 cyclohexène par l'anhydride acétique et le chlorure d'acétyle est effectuée en présence de chlorure stannique. Le produit majeur de l'acylation par le chlorure d'acétyle est bicyclique. L'isomérisation et la réduction chimique et catalytique de ce composé bicyclique sont rapportées et les produits formés sont identifiés.

Canadian Journal of Chemistry, 47, 2403 (1969)

A la suite d'un travail publié (1) en particulier sur la condensation de l'éthyl-1 cyclohexène avec l'anhydride acétique en présence de $ZnCl_2$, nous rapportons les résultats de l'acylation de l'éthyl-1 cyclohexène par l'anhydride acétique et le chlorure d'acétyle en présence de $SnCl_4$.

L'acylation de l'éthyl-1 cyclohexène par l'anhydride acétique en présence de $SnCl_4$ indique à l'analyse par chromatographie en phase gazeuse (c.p.g.) la formation de 36% d'acétyl-1 éthylidène-2 cyclohexane (**1**), 43% d'acétyl-1 éthyl-2 cyclohexène-2 (**2**), 12% d'acétyl-1 éthyl-2 cyclohexène-1 (**3**), et deux autres composés formés à 4 et 5% qui n'ont pas été identifiés. L'isomérisation de ces produits en présence d'acide oxalique donne d'après l'analyse par c.p.g. 14% de composé **1**, 22% de composé **2**, et 64% de composé **3**.

L'acylation de l'éthyl-1 cyclohexène par le chlorure d'acétyle en présence de $SnCl_4$ suivie d'une déshydrochloruration par NaOH indique à l'analyse par c.p.g. la présence de 31% d'un mélange formé d'environ 25% de composé **1** et 6% d'un composé non identifié parce qu'il a été impossible de l'isoler à l'état pur (même en variant la longueur de la colonne, l'adsorbant et la température lors de la chromatographie, il fut impossible de bien séparer ces deux composés). Il y a également formation de 18% de composé **2**, 10% de composé **3**, et 41% d'un nouveau composé.

Ce dernier composé pur présente une bande à 1685 cm^{-1} dans l'infrarouge et une absorption maximum à 213 mμ (log ε: 3.65), dans l'ultraviolet indiquant que le groupe carbonyle est

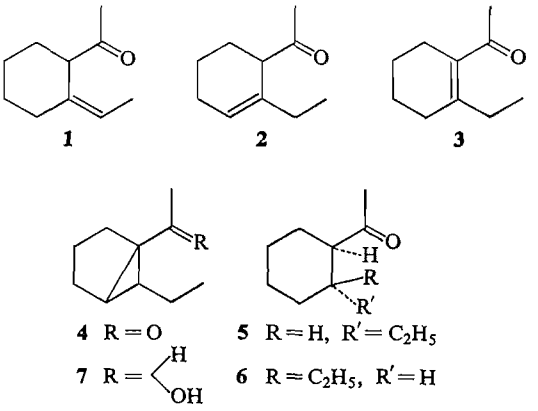

1 **2** **3**

4 R = O

5 R = H, R' = C_2H_5

7 R = H, OH

6 R = C_2H_5, R' = H

conjugué à un cyclopropane (2, 3). Ce composé résiste à l'ozone ce qui confirme la présence d'un cyclopropane dans sa structure. Son spectre de résonance magnétique nucléaire (r.m.n.) présente un multiplet à 1.01 p.p.m. (3H) pour le méthyle de la chaine éthyle et un singulet à 2.01 p.p.m. (3H) pour le méthyle adjacent au carbonyle. Vu qu'il n'y a que trois hydrogènes sous forme de multiplet dans la région de 0–1 p.p.m., la seule structure qui est conforme au spectre r.m.n. et qui a un cyclopropane conjugué avec le carbonyle est l'acétyl-1 éthyl-6 bicyclo[3.1.0]hexane (**4**). En se basant sur un travail fait sur le méthyl-1 cyclohexène (4), ce composé pourrait être l'isomère endo, mais aucune preuve absolue n'a été apportée pour déterminer la configuration de ce composé.

De plus, le composé **4** isomérisé en présence d'acide oxalique donne 14% de composé **1**, 37% de composé **2**, et 49% de composé **3**. La réduction catalytique du composé **4** donne 95% de *trans* acétyl-1 éthyl-2 cyclohexane (**5**) et 5% de *cis* acétyl-1 éthyl-2 cyclohexane (**6**). Ces cétones saturées sont préparées par réduction catalytique d'un mélange des composés **1**, **2**, et **3** et leur

[1]Extrait du mémoire présenté par J. Allard en vue de l'obtention du grade de Maître-ès-Sciences, Faculté des Sciences, Université de Montréal, Montréal, Québec, septembre 1966.

Can. J. Chem. Downloaded from www.nrcresearchpress.com by 210.87.254.42 on 09/05/12
For personal use only.

configuration est déterminée par leur mise en équilibre en présence d'acide oxalique.

La réduction du composé **4** par $LiAlH_4$ indique à l'analyse par c.p.g. la formation d'un seul composé: l'éthyl-6 (hydroxy-1 éthyl)-1 bicyclo[3.1.0]hexane (**7**). Cet alcool oxydé par le complexe anhydride chromique – pyridine (5) redonne la cétone de départ.

Partie expérimentale

Les températures n'ont pas été corrigées. Les analyses par c.p.g. ont été effectuées à l'aide d'un appareil F et M modèle 810 en utilisant une colonne de 2.5 m. contenant 10% d'hyprose supporté sur du chromosorb P. Les spectres de r.m.n. ont été déterminés avec un appareil modèle A60 de la Compagnie Varian pour des solutions dans le CCl_4 et utilisant le tétraméthylsilane comme référence interne.

Condensation de l'éthyl-1 cyclohexène avec l'anhydride acétique

L'éthyl-1 cyclohexène est condensé avec l'anhydride acétique en présence de $SnCl_4$ selon le procédé de Royals et Hendry (6); mais le tout est traité par une solution alcoolique de NaOH 12% pendant 20 h. Il y a formation de 36% de composé **1**, 43% de composé **2**, 12% de composé **3**, et deux autres produits formés à 4 et 5%. Les constantes physiques et spectrales des composés **1** et **2** correspondent à ceux de la littérature (1). Le composé **3** distille à 130°/75 mm; n_D^{25}: 1.4945; i.r.: bande carbonyle à 1675 cm^{-1}; λ_{max} (EtOH): 249 mμ, log ε: 3.75; r.m.n.: triplet à 1.00 p.p.m. (3H, J = 7.5 c.p.s.) et singulet à 2.17 p.p.m. (3H).

Anal. Calc. pour $C_{10}H_{16}O$: C, 78.90; H, 10.59. Trouvé: C, 78.74; H, 10.37.

La semicarbazone (méthanol) fond à 203–204°.

Anal. Calc. pour $C_{11}H_{19}N_3O$: C, 63.12; H, 9.15; N, 20.08. Trouvé: C, 63.19; H, 9.14; N, 19.62.

Condensation de l'éthyl-1 cyclohexène avec le chlorure d'acétyle

A 60 ml de $SnCl_4$ en solution dans 250 ml de CS_2 purifié, sont ajoutés lentement 50 g d'éthyl-1 cyclohexène et 36 g de chlorure d'acétyle à une température inférieure à 0°. Après une agitation de 2 h à la température de la pièce, le tout est refroidi à 0° et 350 g de glace sont ajoutés. Le reste est conforme au procédé de Turner et Voitle (7). L'analyse par c.p.g. indique la présence de 31% d'un mélange formé d'environ 25% de composé **1** et 6% d'un composé non identifié, 18% de composé **2**, 10% de composé **3**, et 41% de composé 4. Ce dernier composé distille à 97°/10 mm; n_D^{25}: 1.4777.

Anal. Calc. pour $C_{10}H_{16}O$: C, 78.90; H, 10.59. Trouvé: C, 78.66; H, 10.41.

La semicarbazone (méthanol) fond à 155.5–156.5°

Anal. Calc. pour $C_{11}H_{19}N_3O$: C, 63.12; H, 9.15; N, 20.08. Trouvé: C, 63.03; H, 9.18; N, 20.24.

Réduction catalytique du mélange de cétones insaturées

Dix grammes de cétones venant de l'acylation de l'éthyl-1 cyclohexène par l'anhydride acétique en solution dans 200 ml d'éthanol absolu sont hydrogénés en présence de 6 g de Pd/C 10%. Il se forme 67% de *trans* acétyl-1 éthyl-2 cyclohexane (**5**) et 33% de *cis* acétyl-1 éthyl-2 cyclohexane (**6**) qui sont séparés par c.p.g. préparative. Le composé **6** distille à 98°/25 mm; n_D^{25}: 1.4551; i.r.: bande carbonyle à 1705 cm^{-1}; r.m.n.: multiplet à 0.99 p.p.m. (3H) et singulet à 2.05 p.p.m. (3H).

Anal. Calc. pour $C_{10}H_{18}O$: C, 77.87; H, 11.76. Trouvé: C, 78.13; H, 11.52. Le composé **5** distille à 130°/110 mm; n_D^{25}: 1.4530; i.r.: bande carbonyle à 1705 cm^{-1}; r.m.n.: multiplet à 0.94 p.p.m. (3H) et singulet à 2.04 p.p.m. (3H).

Anal. Calc. pour $C_{10}H_{18}O$: C, 77.87; H, 11.76. Trouvé: C, 78.06; H, 11.55.

Mise en équilibre d'un mélange de trans et cis acétyl-1 éthyl-2 cyclohexane (5) et (6)

Dix grammes d'un mélange formé de 30% de composé **6** et de 70% de composé **5** sont traités par 25 g d'acide oxalique en solution dans 60 ml d'eau à 110° durant 24 h sous atmosphère d'azote. A l'équilibre, il y a formation de 24% de composé **6** et de 76% de composé **5**.

Réduction catalytique de l'acétyl-1 éthyl-6 bicyclo[3.1.0]-hexane (4)

Deux-cent cinquante milligrammes de composé **4** en solution dans 20 ml d'éthanol absolu sont hydrogénés en présence de 100 mg de Pd/C 10%. Il se forme 95% de composé **5** et 5% de composé **6**.

Réduction chimique de l'acétyl-1 éthyl-6 bicyclo[3.1.0]-hexane (4)

Sept grammes de composé **4** sont réduits par $LiAlH_4$ de la manière habituelle mais l'excès d'hydrure est détruit par l'addition de quelques ml d'eau et de 3 ml d'une solution saturée de Na_2SO_4. Après extraction et évaporation de l'éther, l'analyse par c.p.g. du résidu sur une colonne (2.5 m) de glycérol 20% indique la présence d'un seul composé. La distillation du résidu donne 6.1 g d'éthyl-6 (hydroxy-1 éthyl)-1 bicyclo[3.1.0]hexane (**7**): p.e.: 110°/32 mm; i.r.: bande alcool à 3300 cm^{-1}; r.m.n.: multiplet à 1.1 p.p.m. (6H) méthyle de la chaine éthyle et méthyle adjacent à l'hydroxyle, singulet à 2.93 p.p.m. (1H) hydrogène du OH; quadruplet à 3.62 p.p.m. (1H, J = 6.5 c.p.s.) hydrogène carbinolique.

Anal. Calc. pour $C_{10}H_{18}O$: C, 77.92; H, 11.78. Trouvé: C, 77.92; H, 11.94.

Oxydation de l'éthyl-6 (hydroxy-1 éthyl)-1 bicyclo[3.1.0]-hexane (7)

Cinq cent milligrammes de composé **7** sont oxydés par le complexe anhydride chromique – pyridine selon le procédé de Poos *et al.* (5). L'analyse par c.p.g. des produits d'oxydation indique la présence d'un seul composé qui est identifié comme étant la cétone de départ (**4**).

Remerciements

Les auteurs remercient le Conseil National de Recherches du Canada pour l'aide financière accordée sous forme d'octroi de recherches (A 2030); le service de l'aide aux étudiants de la Province de Québec pour l'aide financière

accordée sous forme de bourses d'études de perfectionnement des professeurs (J.A).

1. J. K. GROVES et N. JONES. J. Chem. Soc. 2215 (1968).
2. A. B. F. DUNCAN, W. GORDY, R. N. JONES, F. A. MATSEN, C. SANDORFY, et W. WEST. Chemical applications of spectroscopy. Vol. IX. Interscience Publishers Inc., New York. 1956. p. 445.
3. W. G. DAUBEN et G. H. BEREZIN. J. Am. Chem. Soc. **89**, 3449 (1967).
4. N. DUFORT et J. LAFONTAINE. Can. J. Chem. **46**, 1065 (1968).
5. G. I. POOS, G. E. ARTH, R. E. BEYLER, et L. H. SARETT. J. Am. Chem. Soc. **75**, 422 (1953).
6. E. E. ROYALS et C. M. HENDRY. J. Org. Chem., **15**, 1147 (1950).
7. R. B. TURNER et D. M. VOITLE. J. Am. Chem. Soc. **73**, 1403 (1951).

Can. J. Chem. Downloaded from www.nrcresearchpress.com by 210.87.254.42 on 09/05/12
For personal use only.

Can. J. Chem. Downloaded from www.nrcresearchpress.com by 210.87.254.105 on 09/05/12
For personal use only.

Proton magnetic resonance studies of hydrogen bonding of formamide with bromide ion in solution. The non-equivalence of the amide hydrogens

R. D. GREEN
Department of Chemistry, University of Alberta, Edmonton, Alberta
Received November 18, 1968

The proton magnetic resonance spectrum of a dilute solution of formamide—^{15}N in CH_3CN at 15 °C undergoes definite changes as bromide ion in the form of $(C_4H_9)_4NBr$ is added. The two amide resonances shift downfield, but at different rates. It is found that each amide hydrogen forms hydrogen bonds with bromide ions, apparently by way of independent equilibrium processes. The hydrogen bond at the *trans* position to the carbonyl oxygen is favored by about 0.7 kcal mole^{-1} over that at the *cis* position. It is postulated that electrostatic repulsion between any base and the carbonyl oxygen of an amide group, tends to favor formation of hydrogen bonds at the more remote, *trans*, hydrogen. This may account for the formation of hydrogen-bonded chains by *N*-monosubstituted amides preferentially with the amide hydrogen *trans* to oxygen.

Canadian Journal of Chemistry, 47, 2407 (1969)

Introduction

In the interactions of unsubstituted and monosubstituted amides with bases, both dipolar and monopolar, there has been some evidence that an amide hydrogen in the position *cis* to the carbonyl oxygen does not behave in exactly the same way as hydrogen in the *trans* position (1–4). For example, *N*-monosubstituted amides tend to have the amide hydrogen *trans* to oxygen, encouraging the formation of long hydrogen-bonded chains of molecules (1).

In the interesting case of the simplest of all amides, formamide, there are several pieces of evidence available which indicate that the *trans*

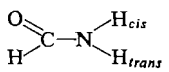

hydrogen is more electrophilic than the *cis*. Perhaps the most cogent argument is derived from the X-ray-determined crystal structure of formamide (2).

According to the evidence gathered by Pimentel and McClellan (5), there is every reason to believe that hydrogen bond strength correlates with the distances A—H and A—B in the hydrogen bond A—H . . . B; the shorter the bond length, the stronger is the bond. In the formamide crystal, both amide hydrogen atoms are involved in hydrogen bonds to carbonyl oxygens of other formamide molecules. However, the N—H_{cis} . . . O distance is 2.93$_5$ Å, whereas the N—H_{trans} . . . O distance is only 2.880 Å. The shorter hydrogen bond length is presumed to accompany the stronger interaction.

A note of caution should be sounded here. The C—N—O angle from the X-ray crystal data (2), is not the same in each case as is the C—N—H angle, determined by microwave spectroscopy (6), these angles taking the values 109 and 120.6° on the *trans* side, and 118.5 and 117.1° on the *cis* side. Hence, the shorter N—H_{trans} . . . O distance may be due to the fact that the hydrogen atom is not situated on the N—O axis; this would permit a shorter N—O distance without necessarily implying a stronger hydrogen bond. Hence, the crystal data are not conclusive concerning the relative bonding energies.

It has been found (3) that the enthalpy of solvation of ions by formamide is dependent on the orientation of the formamide molecules with respect to the ions. However, it is not possible from solvation enthalpies to establish the geometry of the formamide–anion solvates.

Nevertheless, it was determined (4) that the enthalpies of solvation of a series of salts with a common cation give a linear correlation with the inverse of the anion radius. This is taken as evidence that the anion–formamide interaction is essentially electrostatic in nature.

Results and Discussion

As a part of a continuing study of anion–molecule association in solution, the interaction of formamide—^{15}N with bromide ion in ethanenitrile solvent has been investigated by essentially the same technique as that developed earlier (7). The ^{15}N species was used to make

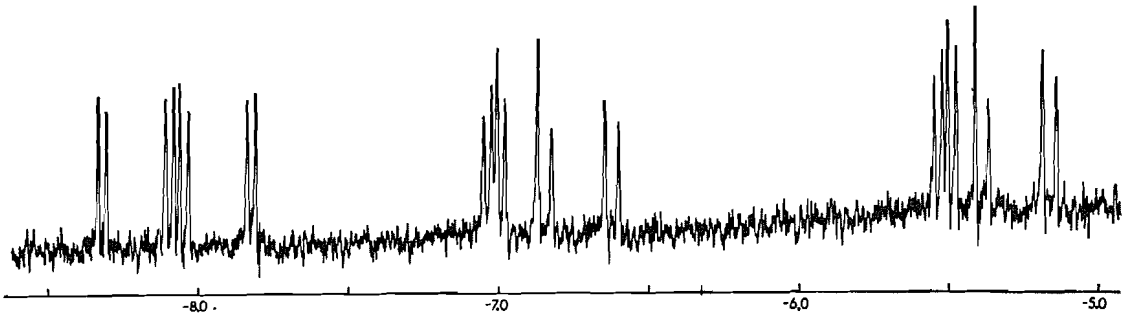

FIG. 1. The 60 MHz nuclear magnetic resonance spectrum of 0.25 *M* formamide—^{15}N in CH_3CN.

observation of the N—H signals a tractable matter. Successive amounts of tetrabutylammonium bromide were added to a 0.1 *M* solution of formamide—^{15}N in CH_3CN. The nuclear magnetic resonance (n.m.r.) signals due to the three protons were monitored as a function of salt concentration; the temperature was maintained at 15 °C, since at higher temperatures, rotation about the C—N bond begins to broaden the signals noticeably. The spectrum of dilute (0.25 *M*) formamide—^{15}N is shown in Fig. 1.

The chemical shift and coupling constant data for the various solutions are presented in Table I. Several trends are evident. First, all three proton signals show a monotonic downfield shift as the salt concentration increases. Second, the formyl proton signal shift is so small as to have no real significance. Third, the two amide proton signals shift significantly downfield, but not by equal amounts. Figure 2 demonstrates that the H_{trans} signal shifts farther than that of H_{cis}, and that its shift-concentration curve is levelling off more quickly.

A Benesi–Hildebrand–Scott analysis of the data (see p. 3660 of ref. 7) yields the complex shifts and equilibrium constants for the association of bromide ion with N—H_{cis} and N—H_{trans}; these are given in Table II. The indicated uncertainties are the standard errors derived as in the Appendix to ref. 7; these make allowance for uncertainties in the experimental measurements, as well as for deviations of the data points from a straight line.

The treatment of the data as representing essentially only hydrogen bonding processes involving bromide ion, appears to be justifiable. Formamide self-association is occurring, but only to a small extent: the shifts of H_{cis} and H_{trans} in neat formamide are −7.2 and −7.4 p.p.m. respectively (8); in a 0.25 *M* solution in CH_3CN, they are −6.0 and −6.3 p.p.m., while in a 0.10 *M* solution, they have changed to only −5.9 and −6.2 p.p.m. In addition, the effect of hydrogen bonding with the solvent is not likely to be very great, since acetonitrile is not a strong base: studies by n.m.r. (7) and infrared (9) spectroscopy confirm that $CHCl_3$ does not hydrogen bond with CH_3CN, although it does complex to an appreciable extent with bromide ions. Hence, the association equilibrium with bromide ion may be expected to predominate.

Equilibrium Constants

The difference in equilibrium constants is sufficiently large to require explanation. It would

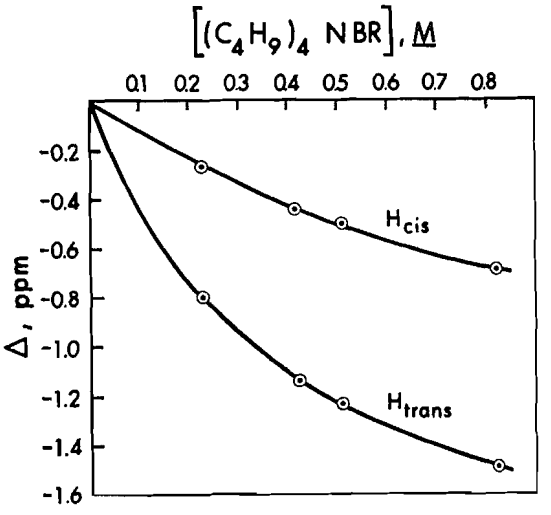

FIG. 2. The salt concentration dependence of the amide proton chemical shifts in 0.1 *M* formamide—^{15}N dissolved in CH_3CN.

Can. J. Chem. Downloaded from www.nrcresearchpress.com by 210.87.254.105 on 09/05/12
For personal use only.

TABLE I

Nuclear magnetic resonance data for 0.1 *M* formamide—^{15}N in CH_3CN upon addition of tetrabutylammonium bromide

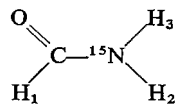

[Salt] *M*	δ_H, p.p.m. from TMS			$J_{p,q}$, Hz					
	H_1	H_2*	H_3*	1, 2	1, 3	2, 3	1, N	2, N	3, N
0	−8.060	−6.185	−5.888	1.5_5	13.5	2.7	16.3	90.1	87.5
0.228	−8.069	−6.981	−6.161	1.5_5	13.5_5	2.7	16.1	89.7	86.8
0.413	−8.073	−7.322	−6.330	1.6_5	13.5	2.9	16.1	89.6	86.7
0.510	−8.073	−7.418	−6.388	1.6_5	13.8	3.1	15.9	89.0	86.6
0.821	−8.075	−7.673	−6.573	1.7	13.7	2.9	15.9	89.5	87.0

**cis* and *trans* Protons assigned as in reference 8.

TABLE II

Complex formation data for formamide–bromide ion association in CH_3CN at 15 °C

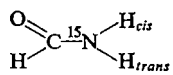

	Equilibrium constant K, M^{-1}	Complex shift Δ_c, p.p.m.
H_{cis}	1.02±0.10	−1.54±0.13
H_{trans}	3.21±0.23	−2.10±0.08

appear that formamide forms hydrogen-bonded complexes with bromide ion at the two N—H sites, by way of independent equilibrium processes. The complex involving H_{trans} is evidently considerably favored over that at H_{cis}, the $\Delta(\Delta G)$ being ca. 0.7 kcal mole^{-1}. Certainly, the data cannot be explained on the basis of one bromide ion interacting with both hydrogens simultaneously.

The explanation for the discrepancy in free energy of formation of the two complexes probably lies in electrostatic repulsion of the bromide ion by the carbonyl oxygen. When the ion is hydrogen bonded at the *cis* position, this repulsion should be considerably greater than when it is at the *trans* position, resulting in a less stable complex.

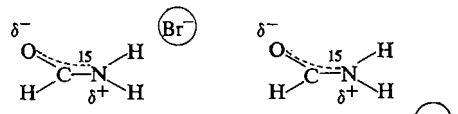

more electrostatic repulsion
less stable

The difference in free energy of hydrogen bonding between the two possible sites may account, at least in part, for the observation that polypeptide and protein molecules tend to adopt a *trans* configuration preferentially, although packing and structural factors undoubtedly play a major role also. Nonetheless, in the absence of other restraints, the present results indicate that the *trans* configuration should be favored by a little less than 1 kcal mole^{-1}.

The Complex Shifts

If the assumption is made that a particular molecular species is present in solution in two forms, the "free" molecule and the molecule complexed with a base, then the difference in shifts of any proton in the two forms is given by the Buckingham equation (10)

$$[1] \qquad \Delta_c = AE_z - BE^2$$

which expresses the complex shift as a function of the first and second powers of the electrostatic field of the base (bromide ion). This equation has been found to be applicable to hydrogen-bonded complexes of C—H compounds (7) and O—H compounds (11) with bromide ion. There is no reason to believe that it will not apply to N—H compounds also.

Now, the term in E_z is proportional to cos θ, where θ is the angle between the X—H and H. . . base vectors. Therefore, the magnitude of the shift decreases rapidly as the source of the field moves away from the X—H axis. This fact may be used as a further source of information.

Can. J. Chem. Downloaded from www.nrcresearchpress.com by 210.87.254.105 on 09/05/12
For personal use only.

Can. J. Chem. Downloaded from www.nrcresearchpress.com by 210.87.254.105 on 09/05/12
For personal use only.

Assuming that the *A* coefficient is characteristic of the N—H bond, and hence is the same for both bonds in the formamide molecule, it is evident that the two N—H...Br^- complexes are not of the same geometry. If the *trans* complex is collinear, then the N—H...Br^- angle in the *cis* complex is about 40°; this non-linearity would presumably be due to the electrostatic repulsion of the bromide ion at the *cis* position by the carbonyl oxygen.

Effect of the Cation

The present results are inconsistent with any considerable interaction between formamide and the tetrabutylammonium ion. Since the salt exists in acetonitrile solution primarily in the form of ion pairs (12), the question of the location of the cation arises.

If the counterion is separated from the molecule by the bromide ion, its effect is predicted by eq. [1] to be no more than about 10–20% of the magnitude of that of the bromide ion, and in the opposite sense. That is, it would have the effect of reducing the proton shift in the complex by 0.2–0.4 p.p.m. This difference would not be detectable in this experiment.

If the counterion were to interact with the formamide molecule, only one possible configuration seems reasonable: *viz.* the ion pair would be coplanar with the molecule. This

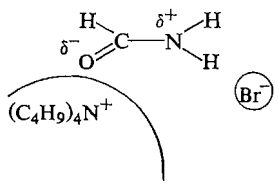

configuration would favor complex formation by H_{cis} over H_{trans}, since the complex with H_{cis} permits the cation to interact more strongly with the carbonyl oxygen atom. Since the opposite result is actually obtained, this mode of interaction appears unlikely.

Coupling Constants in Formamide—^{15}N

The variation of each coupling constant with increasing salt concentration (see Table I) is very small, and is not readily assigned any significance. This finding is in sharp contrast to the marked differences found by Sunners *et al.* (8) between formamide—^{15}N solutions in acetone (10 mole %), water (8 mole %), and the neat liquid. In all cases, the present values are within 2% of the ones they found in acetone solution; however, they found changes of up to 50% on going to an aqueous solution, or to the neat liquid, particularly in couplings to the nitrogen nucleus. It may be that there is some fundamental difference in the nature of the hydrogen-bonding interaction of the amide N—H group with a dipolar base. This conclusion would be consistent with an earlier finding (7) that hydrogen bonding of halide ions to C—H appears to differ qualitatively from the interaction of dipolar pyridine with the same molecules.

Experimental

Materials

Formamide—^{15}N (98% isotopic purity) was used as received from Isomet Corporation. The purification of the other materials is described elsewhere (7).

Procedures

All spectra were obtained on a Varian HA-60 spectrometer operating in internal lock mode. Each resonance line (24 per spectrum) was measured by setting the sweep oscillator at the resonance, and measuring the difference between its frequency and that of the lock-in oscillator which was locked onto the tetramethylsilane signal.

Line positions were measured with a precision of approximately ±0.1 Hz. Since the largest ratio of J/Δ encountered was 0.15, all the spectra were analyzed by a first-order analysis; errors caused by this approximation should not exceed 0.1 Hz. Because of the large number of spin–spin couplings in this small molecule, each chemical shift obtained was the average of four measurements, and each coupling constant was the average of four measurements in the case of couplings to ^{15}N, and eight measurements in the case of couplings to other protons. The uncertainties are estimated to be ±0.005 p.p.m. for the shifts, and ±0.1 Hz for the coupling constants.

Acknowledgments

The author is indebted to Dr. John S. Martin for many helpful discussions and for providing the formamide—^{15}N used in this work. The author also wishes to acknowledge gratefully the financial support of the National Research Council of Canada.

1. (*a*) A. E. Lutskii and S. A. Mikhailenko. J. Struct. Chem. USSR, **4**, 323 (1963); (*b*) R. E. Carter. Acta Chem. Scand. **21**, 75 (1967).
2. J. Ladell and B. Post. Acta Cryst. 7, 559 (1954).
3. G. Somsen. Rec. Trav. Chim. **85**, 526 (1966).
4. G. Somsen. Rec. Trav. Chim. **85**, 517 (1966).
5. G. C. Pimentel and A. L. McClellan. The hydrogen bond. W. H. Freeman and Co., San Francisco 1960. p. 83.
6. C. C. Costain and J. M. Dowling. J. Chem. Phys. **32**, 158 (1960).

7. R. D. GREEN and J. S. MARTIN. J. Am. Chem. Soc. **90**, 3659 (1968).
8. B. SUNNERS, L. H. PIETTE, and W. G. SCHNEIDER. Can. J. Chem. **38**, 681 (1960).
9. B. N. KHARE, S. S. MITRA, and G. LENGYEL. J. Chem. Phys. **47**, 5173 (1967).
10. A. D. BUCKINGHAM. Can. J. Chem. **38**, 300 (1960).
11. R. D. GREEN, J. S. MARTIN, W. B. MCG. CASSIE, and J. B. HYNE. Can. J. Chem. **47**, 1639 (1969).
12. D. F. EVANS, C. ZAWOYSKI, and R. L. KAY. J. Phys. Chem. **69**, 3878 (1965).

Can. J. Chem. Downloaded from www.nrcresearchpress.com by 210.87.254.105 on 09/05/12
For personal use only.

Can. J. Chem. Downloaded from www.nrcresearchpress.com by 210.87.254.105 on 09/05/12
For personal use only.

Some piperazino analogues of methadone and related ketones: a novel conversion of an *N*-carbethoxy to a triethylmethyl group

J. R. DIMMOCK,[1] N. J. HARPER, R. ISLAM, AND A. F. CASY

School of Pharmacy, Chelsea College of Science and Technology, University of London, London, S.W. 3, England

Received November 21, 1968

A number of derivatives of methadone and related compounds have been prepared, where the dimethylamino group has been replaced by a 4-substituted piperazino function. The preparation of these compounds involved the reaction of *N*-ω-cyanoalkyl-*N'*-carbethoxy piperazines with ethyl magnesium bromide, and various products were obtained. These included replacement of the *N'*-carbethoxy group by a triethylmethyl function and cleavage of the carbethoxy group. In some cases the ω-cyano group reacted to give the corresponding ketone. Reactions of 1-benzyl-4-carbethoxy piperazine with ethyl magnesium bromide and phenyl magnesium bromide gave no evidence for the formation of the triethylmethyl group. However, cleavage of the carbethoxy group occurred and there was evidence for the formation of the corresponding amide.

Canadian Journal of Chemistry, 47, 2413 (1969)

Introduction

Structural modifications of the narcotic analgesic methadone (**1***a*) involving replacement of the terminal dimethylamino group by an alicyclic *t*-basic function have led to several potent compounds, two of which, namely dipipanone (**1***b*) and phenadoxone (**1***c*), have been used clinically (1, 2). The *N'*-methylpiperazino analogue (**1***d*) has also been examined and is significantly active as an analgesic being half as potent as methadone in mice (3). In analgesics based upon 4-phenylpiperidine (e.g. pethidine) and those in which this structural unit forms part of a polycyclic molecule (e.g., dromoran), substitution of *N*-methyl by arylalkyl functions such as 2-phenethyl and 3-phenpropyl generally yields a more potent product (2), while oxygenated functions [e.g. $(CH_2)_4OH$ and $(CH_2)_2OEt$] effectively raise the activity of pethidine (4).

In the light of these findings, it was considered of interest to examine piperazino analogues of methadone and related compounds which carried aryl–alkyl and oxygenated-alkyl *N'*-substituents.

The general route used to prepare the desired methadone analogues is illustrated for one series in Scheme 1. *N'*-Carbethoxy intermediates (**2**) rather than those unsubstituted at this position were chosen on account of the need to avoid active hydrogen sites in certain of the reactions, and also because of the possibility of subsequent replacement of *N'*-CO_2Et in the ketone **3** by a variety of R substituents. It was recognized that the *N'*-CO_2Et group in the cyanide **2** might provide a further point of Grignard attack but this was not considered a disadvantageous complication since it could lead directly to the N'H analogue of **3**. Other piperazino cyanides subjected to the same reaction sequence were the trimethylene analogue **4** and the branched chain derivatives **5***a* and **5***b*. The latter pair both resulted when diphenylacetonitrile was alkylated with *N*-2-chloropropyl-*N'*-carbethoxy piperazine and their structures were established by converting one member to the corresponding *N'*-methyl derivative, previously prepared by an unambiguous route (5).

Reaction of the cyanides **2**, **4**, and **5** with ethyl magnesium bromide (excess of reagent in benzene at the reflux temperature) led in all cases to basic mixtures from which crystalline products could in some instances be isolated as hydrochloride salts. Further evidence of reaction pathways was provided by the nature of products obtained from the uncrystallizable residues after hydrolysis and *N'*-alkylation procedures. With the exception of the highly hindered cyanide **5***b*, all substrates suffered attack at the cyano function and were converted to corresponding ethyl ketones. These were isolated as the *N'*-alkylated products required for pharmacological evaluation. Direct evidence of the removal of the *N'*-CO_2Et group was only obtained in the case of cyanide **4**, through the isolation of the

[1]Correspondence should be addressed to this author. Present address: College of Pharmacy, University of Saskatchewan, Saskatoon, Saskatchewan.

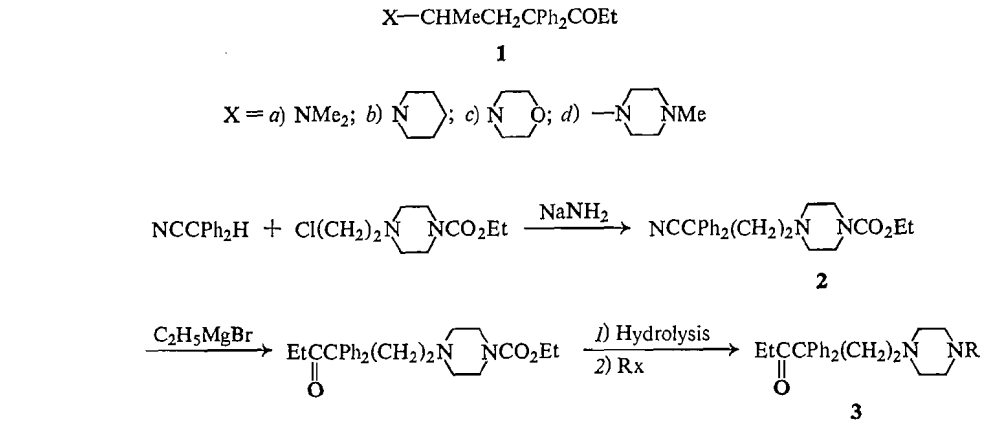

SCHEME 1

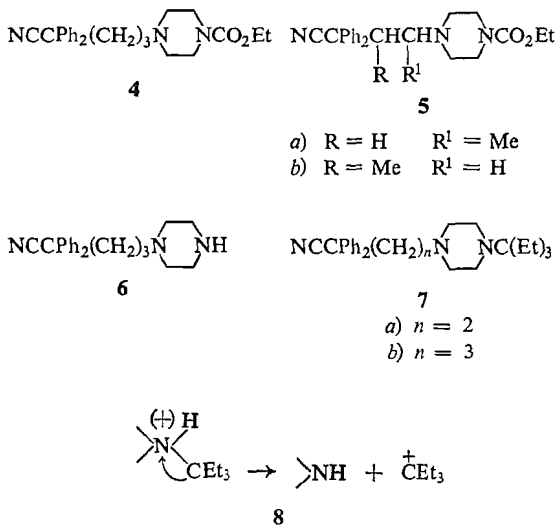

sec-amine **6** as a hydrochloride, while an unexpected reaction between the *N*-carbethoxy group and ethyl magnesium bromide, namely its conversion to a triethylmethyl function, was detected in two cases. Structural evidence for the cyanide 2-ethyl Grignard reaction product **7***a* is detailed below:

(*1*) The cyano group of this product is intact because the infrared spectrum of the free base shows a typical $\nu C{\equiv}N$ band at 2280 cm^{-1} (obscured in the salt by the broad $\nu N^{+}H$ band); the N'-CO_2Et group has been modified, however, since the pronounced $\nu C{=}O$ band near 1700 cm^{-1} of the precursor cyanide is absent, as are other bands in the carbonyl stretching region (1800–1620 cm^{-1}).

(*2*) The 60 MHz proton magnetic resonance (p.m.r.) spectrum of the salt demonstrates the presence of three identical *C*-ethyl groups (a 9 proton deformed triplet near 9 τ and a 6 proton multiplet near 8.25 τ). Their identity is supported by the fact that these signals were not further resolved when a spectrum was recorded at 100 MHz (Fig. 1).

(*3*) The mass spectrum of the hydrochloride showed a peak of highest *m/e* ratio at 403, corresponding with the dihydrochloride monohydrate of **7***a*. Prominent peaks consistent with likely fragments were found at 374 (loss of Et), 304 (loss of CEt_3), 192 (due to $NCCPh_2$), and 112 (due to CH_2CH_2N⟨ ⟩N), while a peak at 99 (CEt_3) was also recorded.

(*4*) Elemental analysis of the salt supported the dihydrochloride monohydrate structure **7***a*. Evidence for water of crystallization was provided by a loss on drying determination and infrared characteristics (broad band near 3500 cm^{-1}) of the salt.

A dihydrochloride monohydrate, isolated from the cyanide 4-ethyl Grignard reaction product, was similarly assigned the *N*-triethylmethyl structure **7***b* on the basis of analytical and infrared spectroscopic evidence. Its N'-substituent could be removed under acid conditions (18% HCl—H_2O at the reflux temperature) giving the *sec*-base **6**, and this unusual result (most *N*-alkyl derivatives are stable towards acids) may be attributed to resonance stabilization of the triethyl carbonium ion **8**, a likely reaction intermediate. *N*-Alkyl fission of certain benzhydryl-

Can. J. Chem. Downloaded from www.nrcresearchpress.com by 210.87.254.105 on 09/05/12
For personal use only.

Can. J. Chem. Downloaded from www.nrcresearchpress.com by 210.87.254.105 on 09/05/12
For personal use only.

amines with water or mineral acid represents an analogous example (6).

Literature data upon the fate of an *N*-carbethoxy group following attack by an organometallic reagent is sparse [chemically *N*-carbethoxy piperazines are substituted urethanes, a class to which no reference is made in standard works on the Grignard reaction (7, 8)], and a tentative reaction mechanism for (*a*) its conversion to a triethylmethyl function and (*b*) its removal is given below (Scheme 2).

Although the amide **10**, proposed as a common intermediate for both pathways, was not detected in reactions involving **3** and **4**, the analogous benzamide was isolated in 28% yield from the analogous reaction between phenyl magnesium bromide and *N*-benzyl-*N'*-carbethoxy piperazine. Treatment of this *N*-benzyl derivative with ethyl magnesium bromide gave *N*-benzyl piperazine (loss of the N'-CO_2Et group) together with the impure *N'*-propionyl amide (infrared evidence). No evidence for pathway (*a*) was obtained in either reaction of the simpler piperazine derivative. Although Scheme 2 depicts N'-CO_2Et loss via the amide **10**, the secondary amine **11***b* might also form upon initial Grignard attack through cleavage of the N—C rather than O—C bond within the complex **9**. However, amides have already been shown to react with Grignard reagents to yield *t*-alkyl amines (9) and secondary amines (10) analogous to **11***a* and **11***b* respectively.

A number of compounds described in this work were evaluated for analgesic activity after subcutaneous injection in mice by a pinch tail method and a modification of the hot plate method described by Janssen and Jageneau (11). Only three compounds showed activity at a dose range of 100 mg/kg, namely **12**, **20**, and **21** (Table I), with approximately 10–15% of the

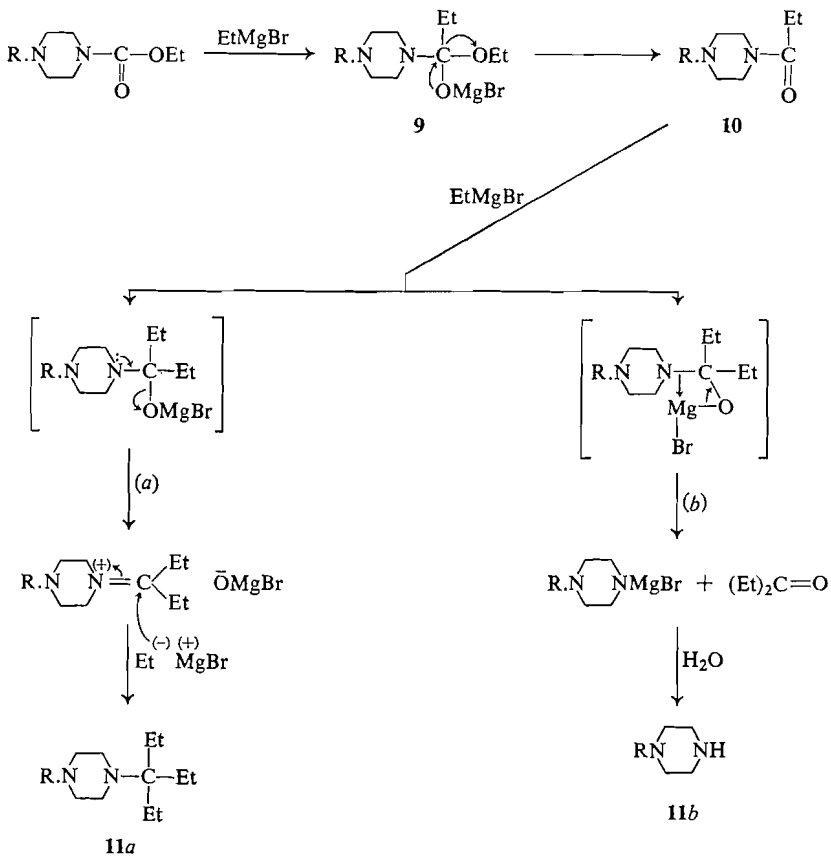

SCHEME 2

Can. J. Chem. Downloaded from www.nrcresearchpress.com by 210.87.254.105 on 09/05/12
For personal use only.

TABLE I

Compounds isolated* by alkylation of the product between ethyl magnesium bromide and the amino cyanides **2**, **4**, **5***a* and **5***b*

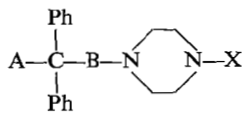

Compound	A	B	X	m.p. (°C)	Molecular formula	Analysis							
						Calculated				Found			
						C	H	N	Equiv.	C	H	N	Equiv.
12	COC_2H_5	$(CH_2)_2$	$(CH_2)_3C_6H_5$	215–217	$C_{31}H_{40}Cl_2N_2O$	70.6	7.6	5.3	263	69.9	7.8	5.1	260
13	CN	$(CH_2)_2$	$(CH_2)_3C_6H_5$	278–280	$C_{29}H_{35}Cl_2N_3$†			8.4	248			8.3	250
14	CN	$(CH_2)_2$	$CH_2CH{=}CHC_6H_5$	250–252	$C_{29}H_{33}Cl_2N_3$	70.5	6.7	8.5	247	70.0	6.4	8.7	250
15	COC_2H_5	$(CH_2)_2$	CH_2CH_2OH	210–211	$C_{24}H_{34}Cl_2N_2O\cdot H_2O$	61.3	7.7	6.0	235.5	61.7	7.8	6.2	237
16	CN	$(CH_2)_2$	CH_2CH_2OH	239–240	$C_{22}H_{29}Cl_2N_3O\cdot H_2O$	59.9	7.1	9.5	220	59.7	7.0	9.7	222
17	COC_2H_5	$(CH_2)_3$	$(CH_2)_2C_6H_5$	254	$C_{31}H_{40}Br_2N_2O$	60.4	6.5	4.5	308	60.9	6.8	4.8	311
18	COC_2H_5	$(CH_2)_3$	$(CH_2)_3C_6H_5$	274	$C_{32}H_{42}Br_2N_2O$	61.0	6.7	4.5	315	60.6	6.8	4.7	318
19	COC_2H_5	$(CH_2)_3$	$CH_2CH{=}CHC_6H_5$	249	$C_{32}H_{40}Cl_2N_2O$	70.2	7.5	5.2	270	70.4	7.4	5.8	267
20	COC_2H_5	$(CH_2)_3$	CH_2CH_2OH	244.5	$C_{25}H_{36}Cl_2N_2O_2$	64.2	7.8	6.0	235	64.1	7.8	6.3	230
21	COC_2H_5	$CH_2\cdot CH(CH_3)$	$(CH_2)_2C_6H_5$	232	$C_{31}H_{39}BrN_2O$	69.5	7.3	5.2	268	68.9	7.5	5.3	266
22	COC_2H_5	$CH_2\cdot CH(CH_3)$	$(CH_2)_3C_6H_5$	214	$C_{32}H_{41}BrN_2O$	69.9	7.5	5.1	275	69.5	8.0	5.2	273

*As the mono- or di-hydrohalide salts.
†Anal. Calcd.: Cl, 14.3. Found: Cl, 14.0.

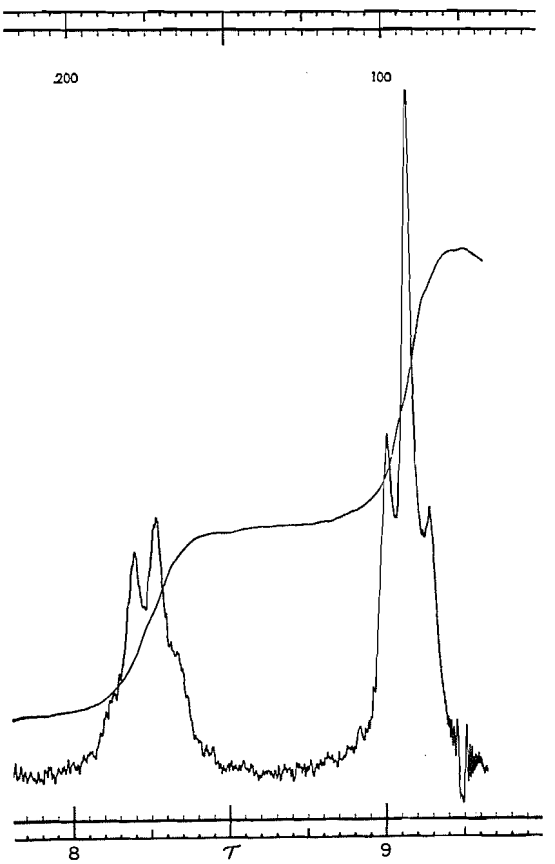

FIG. 1. The 100 MHz proton magnetic resonance spectrum of *7a* in DMSO-d_6.

activity of methadone. None of the cyanides possessed analgesic activity.

Experimental

All melting points and boiling points are uncorrected. The infrared spectra were determined on Unicam SP 100 and Unicam SP 200 spectrophotometers. The proton magnetic resonance (p.m.r.) spectra were recorded on Perkin–Elmer R 10 and Varian HA-100 instruments in dimethyl sulfoxide, operating at 60 and 100 MHz/s respectively with TMS as standard. Equivalent weights of bases and salts were determined by titration with 0.02 *N* perchloric acid in glacial acetic acid with Oracet Blue B as indicator. Microanalyses were performed by Mr. G. S. Crouch, School of Pharmacy, University of London, Dr. G. Weiler and Dr. F. B. Strauss, Microanalytical Laboratory, Oxford, and Mr. M. Ellison, Chesterford Park Research Station, Saffron Waldon, Essex. All organic extracts were washed several times with water and dried over anhydrous sodium sulfate prior to removal of the solvent. Unless otherwise stated, compounds were recrystallized from ethanol or 96% ethanol.

3-(4-Carbethoxypiperazino)-1,1-diphenylpropyl Cyanide (2)

Sodamide (8.6 g) was added to a solution of diphenylacetonitrile (37.6 g) in dry benzene (280 ml) under nitrogen. The mixture was stirred for 1 h and heated under reflux for 4.5 h during which time a further 230 ml of benzene were added. On cooling, a solution of 1-(2-chloroethyl)-4-carbethoxy piperazine (38.5 g) in dry benzene (100 ml) was added and the mixture heated under reflux for 5.5 h. After standing overnight, the excess of sodamide was decomposed with water and the organic extract separated; removal of benzene gave an oil which solidified on trituration with petroleum ether (b.p. 40–60 °C) to give the aminocyanide **2** as yellow crystals (70 g). An analytical sample, melted at 111.5–112.5 °C.

Anal. Calcd. for $C_{23}H_{27}N_3O_2$ (equiv., 377): C, 73.1; H, 7.3. Found (equiv., 372): C, 73.5; H, 7.3.

It gave a hydrochloride m.p. 176.5–178 °C.

Anal. Calcd. for $C_{23}H_{28}ClN_3O_2$ (equiv., 414): C, 66.7; H, 6.8; Cl, 8.6; N, 10.2. Found (equiv., 413): C, 66.6; H, 6.9; Cl, 8.5; N, 10.3.

4-(4-Carbethoxypiperazino)-1,1-diphenylbutyl Cyanide (4)

Reaction between diphenylacetonitrile and 1-(3-chloropropyl)-4-carbethoxy piperazine using the method described in the previous experiment gave the aminocyanide **4**, as pale-yellow crystals, m.p. 139 °C.

Anal. Calcd. for $C_{24}H_{29}N_3O_2$ (equiv., 391): C, 73.6; H, 7.5; N, 10.7. Found (equiv., 390): C, 73.6; H, 7.5; N, 10.9.

Preparation and Proof of Structure of the Isomeric Cyanides 5a and 5b

Diphenylacetonitrile (37.6 g) was condensed with 1-(2-chloropropyl)-4-carbethoxy piperazine (41.3 g) using the method described previously to give an oil (72.0 g), which yielded pale-yellow crystals (40.0 g) from ethanol, m.p. 119–122 °C. Recrystallization gave **5a**, m.p. 122 °C.

Anal. Calcd. for $C_{24}H_{29}N_3O_2$ (equiv., 391): C, 73.7; H, 7.4; N, 10.7. Found (equiv., 392): C, 74.4; H, 7.4; N, 10.8.

The hydrochloride melted at 177–178 °C.

Anal. Calcd. for $C_{24}H_{30}ClN_3O_2$ (equiv., 427.5): C, 67.4; H, 7.0; Cl, 8.3; N, 9.8. Found (equiv., 428): C, 67.1; H, 7.2; Cl, 8.2; N, 9.3.

Evaporation of the combined ethanolic mother liquors gave an oil (28.0 g) which could not be crystallized. A solution of the oil in a mixture of equal parts of benzene and petroleum ether (b.p. 40–60 °C) was chromatographed on alumina, followed by elution with petroleum ether containing increasing concentrations of benzene gave the isomeric cyanide **5b** (23.0 g), m.p. 113–114 °C from ethanol. It gave a hydrochloride, m.p. 124–125.5 °C.

Anal. Calcd. for $C_{24}H_{30}ClN_3O_2$ (equiv., 427.5): C, 67.4; H, 7.0; Cl, 8.3. Found (equiv., 430): C, 66.8; H, 7.1; Cl, 8.3.

5a (15.0 g) was heated under reflux for 6 h with 20% alcoholic potassium hydroxide solution (100 ml). After removal of the alcohol the reaction product was extracted with chloroform to give 3-piperazino-1,1-diphenylbutyl cyanide (11.0 g), the picrate crystallizing from acetone as solvated needles, m.p. 208–210 °C.

Anal. Calcd. for $C_{21}H_{25}N_3 \cdot 2C_6H_3N_3O_7 \cdot C_3H_6O$: C, 51.7; H, 4.5; N, 15.1. Found: C, 52.0; H, 4.6; N, 15.9.

Can. J. Chem. Downloaded from www.nrcresearchpress.com by 210.87.254.105 on 09/05/12
For personal use only.

Can. J. Chem. Downloaded from www.nrcresearchpress.com by 210.87.254.105 on 09/05/12
For personal use only.

This cyanide (3.2 g), 90% formic acid (1.2 g) and 36% formaldehyde solution (0.5 g), were heated under reflux for 6 h after which time hydrochloric acid was added and the formic acid and formaldehyde removed by distillation. Basification of the reaction mixture and extraction with chloroform gave an oil which solidified on titration with petroleum ether (b.p. 40–60 °C) to give a solid (3.3 g) which on recrystallization from petroleum ether (b.p. 80–100 °C) gave 3-(4-methylpiperazino)-1,1-diphenylbutyl cyanide, m.p. 107 °C, lit. m.p. 108–110 °C (5).

Calcd. for $C_{22}H_{27}N_3$: equiv., 166.5. Found: equiv., 168.

Reaction of Ethyl Magnesium Bromide with 3-(4-Carbethoxypiperazino)-1,1-diphenylpropyl Cyanide (2)

A solution of **2** (12.0 g) in dry benzene (100 ml) was added to a solution of ethyl magnesium bromide (prepared from 13.9 g of ethyl bromide and 3.05 g of magnesium) in ether (90 ml). After removal of the ether the mixture was stirred at room temperature for 4 h and then heated under reflux for 16 h. On cooling the product was decomposed with ice and dilute hydrochloric acid and the benzene layer was separated. Basification of the aqueous phase followed by extraction with ether and subsequent evaporation of the solvent gave an oil (12.2 g) which could not be crystallized. The oil (9.05 g) was dissolved in ethanol and treated with ethanolic hydrochloric acid and stored one month at 1 °C when **7***a* separated as the dihydrochloride monohydrate (2.8 g), m.p. 190 °C from ethanol.

Anal. Calcd. for $C_{27}H_{39}Cl_2N_3 \cdot H_2O$ (equiv., 247): C, 65.6; H, 8.4; Cl, 14.3; N, 8.5. Found (equiv., 245): C, 65.8; H, 8.3; Cl, 14.1; N, 8.7. Loss of H_2O at 120 °C. Anal. Calcd. for 1 H_2O: 3.6. Found: 3.85.

ν(Nujol): 3450 (OH), 670,710 (monosub., aromatic) cm^{-1}; ν(neat, free base), 2280 (CN) cm^{-1}: p.m.r. characteristics in DMSO-d_6: 9.03 (deformed triplet, 9H), 8.23 (multiplet, 6H), 6.90 (triplet, 2H), 2.56 (multiplet, 10H). Prominent *m/e* peaks: 403(**7***a*), 374[loss of C_2H_5], 304 [loss of $C(C_2H_5)_3$], 192[due to NC.C. $(C_6H_5)_2$], 112 [due to CH_2CH_2N⟨⟩N], 99[due to $C(C_2H_5)_3$].

The residue (30 g) from the mother liquors of several batches was heated under reflux with 18% hydrochloric acid (300 ml) for 5.5 h. The free base recovered from the aqueous phase was an oil **A** which could not be crystallized or converted to a solid salt. It was characterized by alkylation as follows.

2-Phenylethyl Bromide

A mixture of the oil **A** (5.3 g), 2-phenylethyl bromide (1.6 g), sodium bicarbonate (2.0 g), and ethanol (25 ml) was heated under reflux for 5.5 h. After removal of the inorganic matter by filtration, the ethanol was removed and the resultant oil basified with ammonia and extracted with ether. Evaporation of the solvent gave an oil which when treated with ethanolic hydrochloric acid gave 3-[4-(2-phenylethylpiperazino)]-1,1-diphenylpropyl cyanide dihydrochloride (2.5 g), m.p. 264–266 °C. An analytical sample melted at 266–267 °C.

Anal. Calcd. for $C_{28}H_{33}Cl_2N_3$ (equiv., 241): C, 69.7; H, 6.9; N, 8.7. Found (equiv., 244): C, 69.0; H, 7.0; N, 9.0.

Further alkylated derivatives together with compounds isolated from the aminocyanides **4**, **5***a*, and **5***b* were prepared by similar procedures. Relevant analytical and physical data are given in Table I.

Reaction of Ethyl Magnesium Bromide with 4-(4-Carbethoxypiperazino)-1,1-diphenylbutyl Cyanide (4)

Ethyl magnesium bromide (prepared from 65.4 g ethyl bromide and 14.6 g magnesium) was reacted with **4** (58.6 g) using the conditions described previously.

The product (55 g) was acidified with ethanolic hydrogen chloride and fractionally crystallized from ethanol to give

(i) 4-piperazino-1,1-diphenylbutyl cyanide dihydrochloride (6) (5.0 g), m.p. 260–261 °C from ethanol.

Anal. Calcd. for $C_{21}H_{27}Cl_2N_3$ (equiv., 196): C, 64.2; H, 6.9; Cl, 18.1; N, 10.7. Found (equiv., 198): C, 64.2; H, 6.8; Cl, 18.4; N, 10.9.

(ii) 4-(4-triethylmethylpiperazino)-1,1-diphenylbutyl cyanide dihydrochoride monohydrate (7b) m.p.. 180–182 °C.

Anal. Calcd. for $C_{28}H_{41}Cl_2N_3 \cdot H_2O$ (equiv., 254): C, 66.1; H, 8.6; N, 8.3. Found (equiv., 256): C, 66.3; H, 8.4; N, 8.5. Its infrared spectrum was similar to that of **7***a*.

A mixture of **7***b* (30.0 g) and 18% hydrochloric acid (300 ml) was heated under reflux for 6 h. The free base, recovered as usual, was acidified with ethanolic hydrochloric acid to give 4-piperazino-1,1-diphenylbutyl cyanide dihydrochloride, m.p. and mixture m.p. 260–261 °C.

Hydrolysis of residues from the mother liquors of the Grignard reaction product, carried out as before, gave an oil from which 7-piperazino-4,4-diphenylheptan-3-one dihydrochloride monohydrate m.p. 105–110 °C was obtained.

Anal. Calcd. for $C_{23}H_{32}Cl_2N_2O \cdot H_2O$ (equiv., 220): C, 62.6; H, 7.8; N, 6.3; Cl, 16.0. Found (equiv., 222): C, 62.5; H, 8.2; N, 6.3; Cl, 15.5.

ν(Nujol): 3350(H_2O), 1700(CO) cm^{-1}.

Reaction of Ethyl Magnesium Bromide with 3-(4-Carbethoxypiperazino)-1,1-diphenylbutyl Cyanide 5a

Reaction between the cyanide **5***a* (39 g) and ethyl magnesium bromide (prepared from 43.1 g of ethyl bromide and 8.8 g magnesium) gave an oil (35.0 g) from which an unidentified solid **A** (11 g) separated as a hydrochloride. This salt was hydrolyzed with 18% hydrochloric acid as usual and the product alkylated with 2-phenylethyl bromide to give 3-[4-(2-phenylethylpiperazino)]-1,1-diphenylbutyl cyanide dihydrobromide m.p. 282 °C, undepressed by an authentic sample of the salt prepared in the following manner. The carbethoxy group of **5***a* (15.0 g) was hydrolyzed with 20% alcoholic potassium hydroxide solution (100 ml) and the product alkylated.

Anal. Calcd. for $C_{29}H_{35}Br_2N_3$ (equiv., 292): C, 59.5; H, 6.0; Br, 27.3; N, 7.2. Found (equiv., 294): C, 59.6; H, 6.1; Br, 27.4; N, 7.1.

Hydrolysis of the residues from the mother liquors remaining after solid **A** had separated (18.0 g) with excess 18% hydrochloric acid gave 6-piperazino-4,4-diphenylheptan-3-one (14.0 g)' identified as the picrate, m.p. 259–260 °C (from acetone).

Anal. Calcd. for $C_{23}H_{30}N_2O \cdot 2C_6H_3N_3O_7$: C, 51.9; H, 4.5; N, 13.8. Found: C, 50.6; H, 4.6; N, 13.5.

Can. J. Chem. Downloaded from www.nrcresearchpress.com by 210.87.254.105 on 09/05/12
For personal use only.

Reaction of Ethyl Magnesium Bromide with 3-(4-Carbethoxypiperazino)-1,1-diphenyl-2-methylpropyl Cyanide 5b

Ethyl magnesium bromide (prepared from 4.4 g of ethyl bromide and 1.0 g of magnesium) was reacted with **5b** (3.9 g) using the method described previously to give an oil **B** (3.6 g) which failed to solidify or form a crystalline salt.

Hydrolysis of the Oil B

Hydrolysis of **B** (3.4 g) with 18% hydrochloric acid (30 ml) gave another oil **C** (2.7 g) which similarly failed to solidify or give a crystalline derivative.

Alkylation of the Oil C

Alkylation of **C** (2.0 g) with 2-phenylethyl bromide gave 3-[4-(2-phenylethyl)piperazino]-1,1-diphenyl-2-methylpropyl cyanide dihydrobromide (2.8 g) m.p. 297–299 °C.

Anal. Calcd. for $C_{29}H_{35}Br_2N_3$ (equiv., 293): C, 59.5; H, 6.0; Br, 27.3; N, 7.2. Found (equiv., 294): C, 59.7; H, 6.2; Br, 27.2; N, 7.1.

The compound was also prepared from **5b** by hydrolysis and subsequent alkylation with 2-phenylethyl bromide by the methods described previously.

Reaction of Phenyl Magnesium Bromide with 1-Benzyl-4-carbethoxy Piperazine

1-Benzyl-4-carbethoxy piperazine (12.5 g) and phenyl magnesium bromide (from 17.5 g phenyl bromide and 2.6 g of magnesium) were reacted under conditions described previously, except that the time of heating under reflux was 4 h. Treatment of the crude reaction product with ethanolic hydrobromic acid gave a solid, fractionally crystallizing from ethanol to give

(i) 1-benzyl-4-benzoyl piperazine hydrobromide (1.35 g) m.p. 250 °C. An analytical sample, melted at 257–259 °C, undepressed when mixed with an authentic sample prepared below.

Anal. Calcd. for $C_{18}H_{21}BrN_2O$ (equiv., 361): C, 59.8; H, 5.9; Br, 22.1; N, 7.8. Found (equiv., 370): C, 60.4; H, 6.2; Br, 21.7; N, 8.1. Benzoylation of 1-benzyl piperazine gave 1-benzyl-4-benzoyl piperazine hydrochloride m.p. 247.5–248.5 °C (lit. m.p. 245 °C (12)).

Calcd. for $C_{18}H_{21}ClN_2O$: equiv., 315.5. Found: equiv., 317.

Liberation of the free base followed by treatment with ethanolic hydrobromic acid yielded an authentic sample of 1-benzyl-4-benzoyl piperazine hydrobromide.

(ii) 1-benzyl-4-carbethoxy piperazine hydrobromide (0.94 g) m.p. 215.5–217 °C. Recrystallization raised the m.p. to 219.5–220.5 °C, undepressed when mixed with an authentic sample prepared below.

Calcd. for $C_{14}H_{21}BrN_2O_2$: equiv., 329. Found: equiv., 325.

1-Benzyl-4-carbethoxy piperazine, prepared from an authentic sample of the hydrochloride, on treatment with ethanolic hydrobromic acid gave an authentic sample of the salt, m.p. 227–227.5 °C. Found: equiv., 327.

Evaporation of the ethanolic mother liquors gave an oil (1.62 g) from which no further crystalline material could be isolated.

Reaction between Ethyl Magnesium Bromide and 1-Benzyl-4-carbethoxy Piperazine

1-Benzyl-4-carbethoxy piperazine (9.64 g) was reacted with ethyl magnesium bromide (from 9.36 g ethyl bromide and 2.07 g of magnesium) under the conditions of the previous experiment to give a golden oil (8.01 g). Treatment of the oil with ethanolic hydrochloric acid gave a solid which was fractionally crystallized from ethanol and ether–ethanol to give

(i) 1-benzyl piperazine dihydrochloride (1.79 g), 239 °C decomp.). An analytical sample melted at 256 °C (lit. m.p. 253° C (12)).

Anal. Calcd. for $C_{11}H_{18}Cl_2N_2$: C, 53.0; H, 7.3. Found: C, 53.0; H, 7.3.

(ii) 1-benzyl-4-carbethoxy piperazine hydrochloride (2.15 g) m.p. 210–212 °C. Recrystallization raised the m.p. to 215.5–217.5 °C, undepressed when mixed with an authentic sample.

(iii) a fawn solid (2.40 g). The infrared spectrum (Nujol) indicated the presence of 1-benzyl-4-carbethoxy piperazine hydrochloride (νCO, 1710 cm^{-1}) and a small peak at 1650 cm^{-1} (tertiary amide) indicated the presence of 1-benzyl-4-propionyl piperazine hydrochloride.

Acknowledgments

We should like to thank Mr. R. F. Branch of the School of Pharmacy, Chelsea College of Science and Technology, and Professor J. A. Elvidge of the Department of Chemistry, University of Surrey for profitable discussions. We are grateful to Smith, Kline & French Laboratories who undertook the pharmacological testing and provided samples of the cyanides **2**, **4**, and **5**. Dr. D. H. Williams of the University Chemical Laboratories, Cambridge, kindly determined the 100 MHz proton magnetic resonance spectrum.

1. O. J. Braenden, N. B. Eddy, and H. Halbach. Bull. World Hlth. Organ. **13**, 937 (1955).
2. A. H. Beckett and A. F. Casy. Progress in medicinal chemistry. *Editors.* G. P. Ellis and G. B. West. Vol. 2. Butterworth and Co. Ltd., London. 1962. p. 43.
3. J. Cymerman-Craig, R. J. Harrisson, M. E. Tate, R. H. Thorp, and R. Ladd. Australian J. Chem. **9**, 89 (1956).
4. D. G. Hardy, R. E. Lister, and E. S. Stern. J. Med. Chem. **8**, 847 (1965).
5. J. Redel and A. Bouteville. Bull. Soc. Chim. France, 1411 (1955).
6. R. Cantarel. Compt. Rend. **226**, 931 (1948).
7. M. S. Kharasch and O. Reinmuth. Grignard reactions of non-metallic substances. Constable and Co., Ltd., London. (1954).
8. F. Runge. Organo-metallverbindungen. 2nd ed. Wissenschaftliche, Verlagsgesellschaft M.G.H., Stuttgart. (1944).
9. M. Montagne. Compt. Rend. **183**, 216 (1926).
10. M. Busch and M. Fleischmann. Chem. Ber. **43**, 2553 (1910).
11. P. A. J. Janssen and A. Jageneau. J. Pharm. Pharmacol. **9**, 381 (1957).
12. R. Baltzly, J. S. Buck, E. Lorz, and W. Schön. J. Am. Chem. Soc. **66**, 263 (1944).

Can. J. Chem. Downloaded from www.nrcresearchpress.com by 210.87.254.5 on 09/05/12
For personal use only.

Total synthesis of anisomycin

C. M. Wong, J. Buccini, I. Chang, J. Te Raa, and R. Schwenk
Department of Chemistry, University of Manitoba, Winnipeg, Manitoba

Received January 7, 1969

Two synthetic approaches to anisomycin had been studied. One approach used 2R 3R tartaric acid as starting material and was successfully converted to the hydrochlorides of (+)-anisomycin (**22**) in an overall yield of about 5% and (−)-anisomycin (**1**) in about 1% yield. Liberation of the free bases gave (+)-anisomycin and (−)-anisomycin. The other approach started with α-anisyl pyrrole and was converted to (±)-deacetyl anisomycin **2**. The conversion of **2** to anisomycin was done by treating natural deacetyl anisomycin with benzyl bromide to give **9**. Conversion of **8** and **9** to (+)-anisomycin and (−)-anisomycin was done by selective acetylation with acetic anhydride and debenzylation under hydrogenation condition.

Canadian Journal of Chemistry, 47, 2421 (1969)

Introduction

Anisomycin (**1**) (1) was isolated from cultures of various streptomyces species. It was reported to be active against some pathogenic protozoa (2). The correct structure was elucidated by X-ray crystallography (3) which revealed only the relative stereochemistry.

We reported in our previous work the absolute configuration of anisomycin and a simple approach to deacetyl anisomycin (4, 5) and recently Oida (7) reported the total synthesis of (DL)-anisomycin.

Results and Discussion

N-Benzyl tartrimide prepared from 2R 3R tartaric acid reacting with anisylmagnesium chloride in tetrahydrofuran gave the keto-amide **3** (5). Heating **3** in absolute ethanol at 140 °C under nitrogen atmosphere gave the unsaturated lactam (**4**).[1] Hydrogenation of **4** using 5% Pd/C as catalyst in ethanol gave the lactam **5** and a minor compound (**6**). The separation of **5** from **6** was not successful and the presence of the small amount of **6** in the hydrogenation reaction was uncovered only after the lithium aluminium hydride reduction of **5** and **6** to **7** and **9**. Separation of **7** from **9** was easily done by thin-layer chromatography (t.l.c.) on silica. The overall yields of **7** and **9** from *N*-benzyl tartrimide were 37% and 1% respectively. The conversion of **7** to the epoxide (**11**) via the monoacetate (**10**) and the conversion of **10** to (+)-deacetyl anisomycin (**20**) was reported earlier (5).

The (±)-deacetyl anisomycin was also prepared starting with α-anisyl pyrrole (3). Clemmenson reduction of α-anisyl pyrrole gave 2-anisyl 3-pyrroline (**12**). Acetylation of **12** with acetic anhydride followed by peracetic acid oxidation gave the epoxide (**13**) as the major product together with a small amount of epoxide (**14**). Separation of **13** from **14** by t.l.c. or vapor-phase chromatography (v.p.c.) was unsuccessful. However, epoxide **14** gave the monoacetates **15** and **16** by refluxing in glacial acetic acid for 16 h while the epoxide **13** gave the monoacetate **17**. The opening of the epoxide ring of **13** was very slow compared with that of **14**. Thus careful column chromatography on alumina of the reaction mixture gave **13**, **15**, **16**, **17**, and the diol **18** which was formed by prolonged contact of the epoxide **13** with alumina. The acetate **15** was isolated only in negligible quantities and its structure was assigned only by comparing the infrared (i.r.) spectra with that of *N*-acetyl isoanisomycin (6), prepared from natural anisomycin. Acetates **16** and **17** were characterized by elemental analyses, mass spectra, and hydrolysis of both monoacetates to the diol **18**. Only the acetate **17** could be converted to the epoxide **14** by phosphorus pentachloride followed by alcoholic potassium hydroxide solution. The

[1]A by-product possibly (*i*) was isolated in about 1% yield. Hydrogenation of (*i*) and **4** gave the same product.

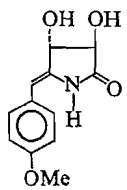

(*i*)

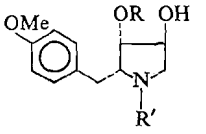

(1) R = Ac R′ = H
(2) R = R′ = H
(9) R = H R′ = CH_2–Ph

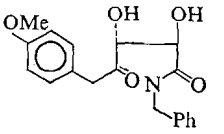

(3)

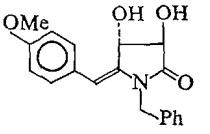

(4)

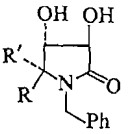

(5) R = CH_2– R′ = H
(6) R = H R′ CH_2–

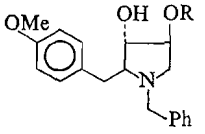

(7) R = H
(10) R = Ac

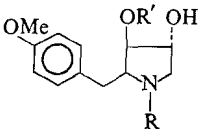

(8) R = CH_2Ph R′ = H
(21) R = CH_2Ph R′ = Ac
(22) R = H R′ = Ac
(20) R = R′ = H

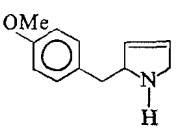

(12)

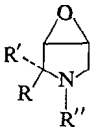

(11) R = CH_2– 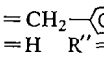 R′ = H R″ = CH_2Ph
(13) R = H R″ = Ac R′ = CH_2– 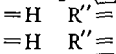
(14) R = CH_2– 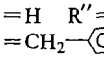 R′ = H R″ = Ac

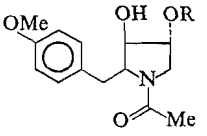

(15) R = Ac

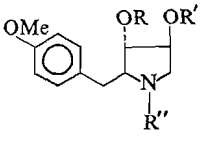

(16) R = R″ = Ac R′ = H
(17) R = H R′ = R″ = Ac
(18) R = R′ = H R″ = Ac
(19) R = R′ = R″ = H

epoxide **14** was also prepared from anisomycin (6)[2] for comparison. The i.r. spectra were superimposable. Refluxing **14** in glacial acetic acid followed by basic hydrolysis gave a mixture of racemic deacetyl anisomycin (**2**). Treating (−)-deacetyl anisomycin with benzyl bromide gave *N*-benzyl deacetyl anisomycin (**9**).

Conformation controlled selective acetylation[3] of (+)-*N*-benzyl deacetyl anisomycin (**8**) with acetic anhydride gave (+)-*N*-benzyl anisomycin (**21**). Debenzylation of **21** with 5% Pd/C in acidic ethanolic solution under hydrogenation condition gave the hydrochloride salt of (+)-anisomycin. Liberation of the free base by dilute sodium hydroxide solution gave (+)-anisomycin (**22**). The i.r., nuclear magnetic resonance (n.m.r.) spectra of **22** were superimposable to those of natural anisomycin.

[2]The stereochemistry of the epoxide prepared from anisomycin as described in (6) should be shown as (*i*).

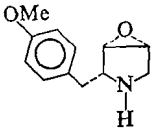

(*i*)

[3]

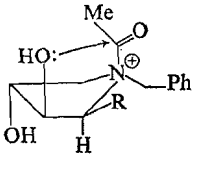

Experimental

All i.r. spectra were measured on a Perkin–Elmer 137 i.r. spectrophotometer using methylene chloride as solvent or as otherwise specified. Nuclear magnetic resonance (n.m.r.) spectra were measured on a Varian A 56/60 A spectrometer using tetramethylsilane as internal standard, and deuterated chloroform as solvent. Mass spectra were measured on a Hitachi Perkin–Elmer RMU-6D mass spectrometer. Melting points were measured by a Fisher–Johns melting point apparatus and are uncorrected. Microanalyses were performed by Dr. Daesslé of Montreal and optical rotations were measured on a Carl Zeiss polarimeter.

Can. J. Chem. Downloaded from www.nrcresearchpress.com by 210.87.254.5 on 09/05/12
For personal use only.

Can. J. Chem. Downloaded from www.nrcresearchpress.com by 210.87.254.5 on 09/05/12
For personal use only.

Preparation of the Unsaturated Lactam (4)

The keto-amide (**3**) (5) (6.4 g) and anhydrous magnesium sulfate (6.4 g) in anhydrous alcohol (100 ml) were heated at 135 °C under nitrogen atmosphere of 50 P/in^2 for 7 h in a high pressure hydrogenation apparatus. The magnesium sulfate was filtered off and the alcohol solution was evaporated to dryness under reduced pressure, giving an orange gummy residue. Crystallization of the residue from benzene gave the lactam **4** (3.5 g). The mother liquor was purified by t.l.c. on silica giving an additional amount of the lactam **4** (1.3 g). Yield, 80%; m.p. 148–149 °C; i.r. 3600, 3400, 1720, 1655, 1605 cm^{-1}; n.m.r. (τ) 2.80 (s, 5H's aromatic), 2.77–3.33 (A_2B_2, 4H's aromatic), 4.20 (d, 1H, J = 1.5 c.p.s., vinylic), 4.94 (q, 1H, J = 1.5 and 3.5 c.p.s., C_3—H), 5.27 (s, 2H's, N—CH_2—ph), 5.50 (d, 1H, J = 3.5 c.p.s., C_4—H), 6.30 (s, 3H's, —OCH_3).

Anal. Calcd. for $C_{19}H_{19}O_4N$: C, 70.14; H, 5.89; N, 4.13. Found: C, 70.28; H, 6.06; N, 4.32.

Preparation of the Diol 7 from the Lactam 4

To an alcoholic solution of **4** (50 ml, 2.2 g) was added 5% Pd/C (1.1 g) and the solution was hydrogenated for 18 h at room temperature under 450 P/in^2 of hydrogen. After filtering off the catalyst, the ethanol was removed under reduced pressure. The residue was recrystallized from benzene giving the crystalline lactam **5** (1.8 g). M.p. 111–112 °C; i.r: 3600, 3400, 1695, 1605 cm^{-1}.

Anal. Calcd. for $C_{19}H_{21}O_4N$: C, 69.71; H, 6.46; N, 4.27. Found: C, 69.93; H, 6.26; N, 4.49.

The saturated lactam (**5**) (1.9 g) dissolved in anhydrous tetrahydrofuran (20 ml) was added slowly to a suspension of lithium aluminium hydride (1.06 g) in anhydrous tetrahydrofuran (80 ml), and was refluxed for 7 h. The tetrahydrofuran (60 ml) was removed by distillation and wet ether (100 ml) was added slowly to the residue. Water (50 ml) was then added. The ether layer was separated from the aqueous layer which was extracted exhaustively with ether. The ether solution was evaporated to dryness and the residue was dissolved in benzene (20 ml) which was extracted with 5% hydrochloric acid (30 ml). The acidic solution was then made basic and the basic solution was then extracted with chloroform. Evaporation of the chloroform solution to dryness under reduced pressure gave a light yellow residue (1.85 g). Recrystallization of the residue from benzene heptane (1:1) solution gave the crystalline diol **7** (1.6 g), identical to the sample prepared earlier by another method (5). The mother liquor was purified by t.l.c. on silica to give more diols (**7**) (50 mg) and (**9**) (20 mg).

The Clemmenson reduction of α-Anisyl Pyrrole.

An amalgam was prepared by mixing zinc (100 g) and mercuric chloride (10 g) with hydrochloric acid (0.6 *N*, 130 ml). After stirring for 10 min, the aqueous solution was decanted and the amalgam was placed in a 2 l, 3-necked flask, equipped with an overhead stirrer, a reflux condenser, and a dropping funnel. Sea sand and hydrochloric acid (7 *N*, 175 ml) were added to the amalgam and the mixture was heated to a reflux. A solution of α-anisyl pyrrole (23 g) in ethanol (35 ml) was added very slowly over a period of 3 h. When one-third of the solution had been added, an additional amount of hydrochloric acid (7 *N*, 195 ml) was added to the reaction mixture. When the addition of α-anisyl pyrrole was completed, freshly prepared amalgam and hydrochloric acid were added (25 g amalgam, 40 ml acid) to the reaction mixture. Three further additions of the same amount of amalgam and hydrochloric acid were added at an interval of 1 h. After the last addition of amalgam, the solution was refluxed for 4 h. The reaction mixture was cooled and the residue was removed by filtration. The filtrate was extracted with ethyl acetate (7 × 500 ml) and the aqueous layer was discarded. The ethyl acetate was concentrated and the residue was dissolved in water (150 ml). Sodium hydroxide solution (40%) was added until the zinc hydroxide was redissolved. The strongly basic solution was then exhaustively extracted with ether and the ether solution, dried over magnesium sulfate, was removed under reduced pressure, giving an oily residue (23 g) which was purified by distillation. The fraction distilling out at 109–112 °C/0.5 mm Hg was collected (18.3 g). n_D^{25} = 1.5502; i.r: 3300, 1625, 1575, 1500 cm^{-1}; n.m.r: (τ) 3.17–3.60 (A_2B_2, 4 H's aromatic), 4.52 (m, 2 H's, olefinic), 6.15 (m, 1 H, —N—CH—), 6.50 (s, 3 H's, —OCH_3), 6.55 (t, 2 H's, —N—CH_2—), 7.50 (d, 2 H's, benzylic), 8.38 (s, 1 H, —NH—).

Anal. (as HCl salt) Calcd. for $C_{12}H_{16}ONCl$: C, 63.85; H, 7.14; N, 6.21; Cl, 15.71. Found: C, 64.08; H, 6.90; N, 6.25; Cl, 15.84.

Preparation of the Epoxide (13), Hydroxy Acetates (15), (16), and (17)

2-Anisyl 3-pyrroline (17.7 g) was added dropwise to ice-cooled acetic anhydride (47 g) with stirring. After stirring for 17 h, the acetic anhydride was evaporated under reduced pressure and the oily residue was distilled at 155 °C/0.5 mm Hg giving *N*-acetyl 2-anisyl 3-pyrroline (19.1 g).

A solution of *N*-acetyl 2-anisyl 3-pyrroline (10.7 g), concentrated H_2SO_4 (0.5 g), and glacial acetic acid (65 g) was warmed in an oil bath at 45 °C. To the solution was added H_2O_2 (90%, 7 g) in 3 equal portions at 1 h intervals. After 7 h, sodium bisulfite solution was added to the ice-cooled reaction mixture and the solution was then neutralized by sodium hydroxide solution. Exhaustive extraction of the solution with chloroform and evaporating the chloroform solution to dryness gave an oily residue (12.5 g). The residue was then refluxed in glacial acetic acid (100 ml) for 16 h to convert all epoxide **14** to the hydroxyacetates **15** and **16**. Evaporating the glacial acetic acid solution under reduced pressure gave a gummy residue. Careful chromatography of the residue on alumina gave the starting material *N*-acetyl 2-anisyl 3-pyrroline (1 g), the epoxide **13** (1.8 g), the hydroxyacetate **15** (negligible amount), the hydroxyacetate **16** (1 g), the hydroxyacetate **17** (3.3 g), and the diol **18** (2.3 g) which was shown to form by prolong contact of **13** with grade 1 alumina. The epoxide **13** showed i.r. absorption at 1645, 1620, 1505, 848 cm^{-1}; n.m.r. (τ) at 2.7–3.3 (A_2B_2, 4 H's aromatic), 6.25 (s, 3 H's —OCH_3), 8.06 and 8.13 (d, 3 H's, N—$COCH_3$).[4]

[4]All *N*-acetyl or *O*-acetyl groups in the intermediates showed hindered rotation. Temperature studies showed that the activation energies of free rotation calculated from the coalescence temperatures and the Eyring equation for the *N*-acetyl groups of all the intermediates are 18–22 kcal/mole (8).

The hydroxyacetate **16** m.p. 138–140 °C, showed i.r. absorption at 3580, 1735, 1640, and 1610 cm^{-1}; M^+/e; 307, 186, 144, 126, 121, and 84. The hydroxyacetate **17** m.p. 108–109 °C showed i.r. absorption at 3580, 1750, 1650, and 1615 cm^{-1}; M^+/e 307, 186, 144, 126, 121, and 84.

Anal. Calcd. for $C_{16}H_{21}O_5N$: C, 62.53; H, 6.89; N, 4.56. Found: C, 62.13; H, 6.85; N, 4.72.

The diol **18** m.p. 149–151 °C showed i.r. absorption at 3550, 3300, and 1630 cm^{-1}.

Anal. Calcd. for $C_{14}H_{19}O_4N$: C, 63.38; H, 7.22; N, 5.28. Found: C, 63.56; H, 7.11; N, 5.57.

Conversion of the Hydroxy Acetate (17) to the Epoxide (14)

To an ice-cooled chloroform solution (30 ml) containing the hydroxy acetate **17** (1.52 g) was added in portions (1.04 g) of phosphorus pentachloride. After stirring for 1 h at room temperature, the chloroform solution was evaporated to dryness under reduced pressure leaving an orange foam. Ethanol (8 ml) was added followed by alcoholic potassium hydroxide solution (15 ml, 20%). The solution was stirred for 1 h and then diluted with water (100 ml). The aqueous solution was extracted exhaustively with chloroform. Evaporating the chloroform solution to dryness, followed by purification of the residue by t.l.c. on silica gave the epoxide **14** (640 mg); i.r.: 1610, 1500, and 865 cm^{-1}, superimposable with that of the epoxide derived from natural anisomycin.

Preparation of Racemic Deacetyl Anisomycin (2)

The epoxide **14** (220 mg) was refluxed in glacial acetic acid for 12 h. Evaporating the acetic acid solution to dryness under reduced pressure gave an oily residue which was refluxed overnight under nitrogen in aqueous alcoholic sodium hydroxide solution (20 ml, 5 *N*). The solution was neutralized with hydrochloric acid and extracted continuously by chloroform. Evaporating the chloroform solution to dryness gave a foamy residue (100 mg). Separation of the residue by t.l.c. on silica gave the racemic diols **19** (20 mg) and **2** (25 mg). The diol **19** was identical in every respect with the hydrolysis product of **16**, **17**, and **18**. The racemic deacetyl anisomycin **2**, m.p. 170–172 °C showed a slight difference in the i.r. spectra (Nujol) compared with that of the natural deacetyl anisomycin. The racemic **2** was then converted into the corresponding hydrochloride by adding a few drops of concentrated hydrochloric acid into the methanolic solution containing the racemic base **2**. Evaporating the methanolic solution to dryness gave a solid residue which was recrystallized from methanolic ether solution, m.p. 220–222 °C. The i.r. spectrum was identical with that of deacetyl anisomycin hydrochloride.

Preparation of (+)-Anisomycin (22)

(+)-*N*-Benzyl deacetyl anisomycin was dissolved in acetic anhydride (10 ml) and the solution was stirred for 20 min. The acetic anhydride solution was evaporated to dryness under reduced pressure at 50 °C water bath. The residue was purified by t.l.c. on silica to give (+)-*N*-benzyl anisomycin (280 mg) (**21**)[5] which was then dissolved in ethanol (5 ml) containing concentrated hydrochloric acid (4 drops) and 5% Pd/C (50 mg). The solution was hydrogenated at atmospheric pressure and room temperature for 2 h. After filtering off the catalyst and evaporating the ethanol solution to dryness, the crystalline residue was recrystallized from methanol–ether to give the hydrochloride of (+)-anisomycin (**22**) (140 mg), m.p. 188–189 °C, $[\alpha]_D^{25} = -3.6°$ i.r. spectra (Nujol) was superimposable to that of natural anisomycin hydrochloride. From the mother liquor was isolated (+)-deacetyl anisomycin. Liberation of the free base by dilute sodium hydroxide solution gave (+)-anisomycin (70 mg) plus a small amount of deacetyl anisomycin. They were separated from each other by t.l.c. on silica. The (+)-anisomycin is identical in every respect to the natural anisomycin except an opposite sign of specific rotation and possibly no activity against protozoa (7).

Acknowledgments

The authors wish to express their gratitude to the National Research Council of Canada and Charles Pfizer & Co. Inc., for financial assistance and the supply of natural anisomycin.

1. B. A. Sobin and F. W. Tanner, Jr. J. Am. Chem. Soc. **76**, 4053 (1954).
2. J. E. Lynch, A. R. English, H. Bauck, and H. Deligianis. Antibiot. Chemotherapy, **4**, 844 (1954).
3. J. P. Schaefer and P. F. Wheatley. J. Org. Chem. **33**, 166 (1968).
4. C. M. Wong. Can. J. Chem. **46**, 1101 (1968).
5. C. M. Wong, J. Buccini, and J. Te Raa. Can. J. Chem. **46**, 3091 (1968).
6. J. J. Beereboom, K. Butler, F. C. Pennington, and I. A. Solomons. J. Org. Chem. **30**, 2334 (1965).
7. Sadao Oida. Chem. Pharm. Bull. (Tokyo), **16**, 2086 (1968).
8. Horst Kessler and Anton Rieker. Ann. Chem. **708**, 57 (1967).

[5]A very small amount of by-product possibly *N*-benzyl acetyl anisomycin was isolated which was converted back to *N*-benzyl deacetyl anisomycin (8) by basic hydrolysis.

Can. J. Chem. Downloaded from www.nrcresearchpress.com by 210.87.254.5 on 09/05/12
For personal use only.

Leaf coumarins of *Angelica archangelica*[1]

WARREN STECK AND B. K. BAILEY
Prairie Regional Laboratory, National Research Council of Canada, Saskatoon, Saskatchewan
Received February 4, 1969

Coumarin derivatives are abundant in leaves of *Angelica archangelica*, and differ in kind from those of the roots. Angelicin, bergapten, imperatorin, isopimpinellin, xanthotoxin, oxypeucedanin, and five unidentified coumarins were isolated from leaves. A time study of their development was carried out. Methods for the isolation of leaf neutral coumarins are described.

Canadian Journal of Chemistry, 47, 2425 (1969)

Can. J. Chem. Downloaded from www.nrcresearchpress.com by 210.87.254.40 on 09/05/12
For personal use only.

Introduction

Many plants of the family *Umbelliferae* are known to accumulate coumarin derivatives in their roots and seeds (1). The species *Angelica archangelica* L. has been particularly well studied in this respect. Späth and Pesta (2) found the main root coumarin to be osthol (**2** in Fig. 1), accounting for nearly 0.2% of the dry weight. Among the many other coumarins subsequently isolated from this source were osthenol and angelicin (**3**) (2); imperatorin (**8**), bergapten (**5**), umbelliprenin, xanthotoxol, and xanthotoxin (**6**) (3); oxypeucedanin (**9**), oreoselone, and archangelicin (4). The seeds contain a similarly complex array of coumarins (5).

The study of plant leaf coumarins has received less attention, and presents certain difficulties. The main problem is the separation of the ether-soluble neutral coumarins from the chlorophylls, waxes, and other constituents of similar solubility. Occasionally the appreciable solubility of neutral coumarins in hot water has been used to effect the separation directly (6), but more usually an alcohol extract has been made and treated with aqueous alkali for several hours to open the lactone ring and give coumarinate salts, other components then being removed by ether extraction. The coumarin derivatives can themselves be ether-extracted subsequent to their regeneration on acidification of the medium. Washing the final ether extract with carbonate leaves a lactone fraction. In the presence of chlorophyll, which is degraded to dark products by alkali, the isolation of such a lactone fraction is not usually clean-cut and may have to be done twice (7). A more serious objection to the use of alkali is the loss of ester linkages, which are not uncommon in *Angelica* coumarins. For example, ostruthol is transformed to oxypeucedanin.

We report in this paper a general method of leaf treatment which avoids entirely the use of alkali, yet affords a fraction from which neutral coumarins may be conveniently isolated and purified. We have used the technique with several umbellifers, but the case of *A. archangelica*, with its interesting biosynthetic implications, is alone described below.

Methods and Results

Fresh leaves were homogenized in boiling methanol and the hot filtrate adjusted to 60% aqueous methanol, then washed twice with Skelly B (*n*-hexane) to remove chlorophylls and other fatty materials. The Skelly B was back-extracted once with 60% methanol and this was added to the main alcoholic solution. This procedure was shown to retain more than 98% of the xanthotoxin and bergapten in the aqueous part while removing about 70–80% of the total weight of the original methanol extract. Concentration of the alcohol solution resulted in an aqueous suspension; this was extracted overnight with ether to remove the coumarins present.

The ether extract was chromatographed on silicic acid, eluting with 1:1 Skelly B:ether. This solvent mixture is slightly more polar than that used successfully for *Citrus* coumarins by Stanley and Vannier (8), and somewhat less solublizing than the system of Floss and Mothes (9), which was not entirely successful with *Pimpinella* coumarins. The fractions collected were allowed to evaporate overnight to allow deposition of crystalline material.

The first crystalline sample, long needles

[1]NRCC No. 10670.

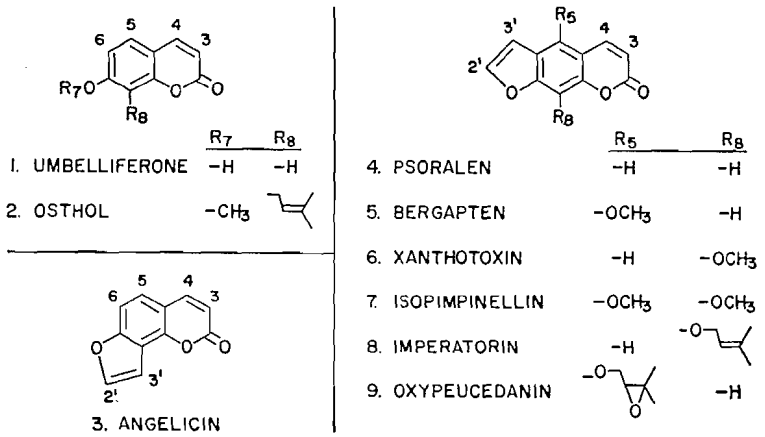

FIG. 1. Some coumarins mentioned in the text.

melting at 97.5–99.5°, was a lactone having an ultraviolet (u.v.) spectrum suggestive of a xanthotoxol derivative. The nuclear magnetic resonance (n.m.r.) spectrum indicated the presence of five aromatic protons: two were typical coumarin pyrone ring doublets ($J = 10$ c.p.s.); two others were typical furan ring doublets ($J = 2 \sim 2.5$ c.p.s.); the fifth was a singlet. All had very nearly the same chemical shifts as those of xanthotoxin. A dimethylallyl group was also evident. The material thus appeared to be imperatorin, lit. m.p. 102° (10). A mixed melting point with an authentic sample (m.p. 96–99°) was undepressed, and the u.v. and n.m.r. spectra of the standard were superimposable upon those of the isolated compounds. Chromatography on paper and examination of fluorescence properties confirmed the identity.

The second group of crystals, m.p. 188–190° with sublimation, also showed lactonic properties. A u.v. maximum near 306 mμ suggested a bergaptol or isobergaptol derivative. The n.m.r. spectrum showed the H_4 signal at $\delta > 8.0$, indicating substitution at the 5-position. The existence of 5 appropriate aromatic protons and a single aromatic methoxyl group suggested bergapten, lit. m.p. 188–189° with sublimation (11), as the identity of the material. A mixed melting point with authentic material was undepressed and direct comparison of u.v., n.m.r., fluorescence, and chromatographic data for isolated and authentic material showed no differences between the two.

The third crystalline deposit, a lactone melting at 144–145°, had the u.v. spectrum of a xanthotoxol derivative. The n.m.r. spectrum, indicating a monomethoxy furocoumarin, was identical with that of xanthotoxin (lit. m.p. 145–146° (12)), and an authentic sample of xanthotoxin had the same chromatographic and fluorescence properties. A mixed melting point was undepressed.

The fourth batch of crystals, melting at 147–149°, gave an absorption maximum at 311 mμ. A furocoumarin with two methoxy groups, one in the 5-position ($\delta > 8.0$ for H_4) was indicated by the n.m.r. spectrum. Since all the pyrone and furan ring protons appeared to be present in the spectrum, the only structures possible, assuming the usual 7-oxy-substitution, were pimpinellin (5,6-dimethoxyangelicin) and isopimpinellin (7), lit. m.p. 148–151° (13). A mixed melting point with an authentic sample of the latter was undepressed, and the u.v. and n.m.r. spectra of the isolated and authentic samples were identical. The fluorescence and chromatographic properties were also those of isopimpinellin. This coumarin, while known in other *Angelica* species, does not seem to have been reported previously in *A. archangelica.*

From the mother liquors of the bergapten fractions, another coumarin was isolated by gas–liquid chromatography (g.l.c.). Collection and recrystallization from alcohol gave crystals melting at 137–138°. Analysis by n.m.r. revealed six protons, all aromatic. The u.v. and n.m.r. spectra of angelicin (lit. m.p. 138–139.5° (2)) were identical with those of the isolated sample, and a mixed melting point showed no depression.

Can. J. Chem. Downloaded from www.nrcresearchpress.com by 210.87.254.40 on 09/05/12
For personal use only.

Can. J. Chem. Downloaded from www.nrcresearchpress.com by 210.87.254.40 on 09/05/12
For personal use only.

Co-chromatography confirmed the identification.

Leaves of plants from different seed sources gave differing amounts of the above coumarins. The plants examined in the work described here contained relatively large amounts of xanthotoxol derivatives, in contrast to another strain which afforded primarily bergaptol derivatives. Examination of this latter strain showed the presence of all the coumarins described above, and in addition demonstrated the presence of a lactone (m.p. 140–142°) eluting from silicic acid along with isopimpinellin. Its u.v. and n.m.r. spectra strongly suggested it to be racemic oxypeucedanin (lit. m.p. 142–143° (14)). The optically active (+)-isomer, which was available for comparison, gave identical u.v. and n.m.r. spectra.

Study of the non-crystalline fractions from silicic acid was carried out by g.l.c. In this way several other leaf coumarins were detected, but because of their scarcity, none was identified. These included three compounds U_1, U_2, and U_3 eluting with isopimpinellin and having identical xanthotoxol ether u.v. spectra; a compound U_4 eluting with bergapten and having a u.v. spectrum like osthol or herniarin but with chromatographic properties unlike those of any reference compound available; and a compound U_5 eluting just before bergapten in very small quantities, believed (on the basis of its chromatographic behavior) to be psoralen (**4**).

It might be noted here that g.l.c. analyses demonstrated the absence of other simple furocoumarins such as isobergapten (5-methoxyangelicin), sphondin (6-methoxyangelicin), pimpinellin (5,6-dimethoxyangelicin), and phellopterin (5-methoxy-8-dimethylallyloxypsoralen). Neither could osthol be detected, a point to be discussed further below.

Examination of the leaf water-solubles by acid hydrolysis and re-extraction with ether were carried out to test for the presence of furocoumarin glycosides, such as occur in some plants (e.g. ref. 15). No neutral coumarins were liberated by the hydrolysis, but umbelliferone (**1**) was found. It appeared to be present in unhydrolyzed extracts principally as the glucoside, skimmin.

Although osthol could be readily detected in root extracts, we were unable to find it in the leaves. This and the quantitative variation in coumarins from different seed strains prompted us to assay growing *A. archangelica* shoots and roots at various stages of development. This was done by direct g.l.c. of prepared coumarin-rich fractions, with estimation of the detected coumarins by comparison with standard area curves. The results for the seed strain whose component coumarins have just been described are shown in Figs. 2 and 3. The two outstanding features of these results are the selective accumulation of osthol in the roots and the early appearance of leaf coumarins. The data clearly show that the coumarins in the leaves undergo no great qualitative changes during the maturation of the

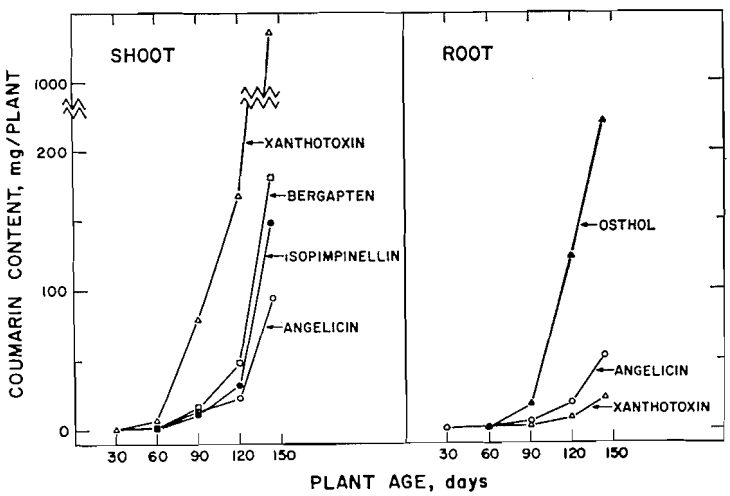

FIG. 2. Development of coumarins in *Angelica archangelica*; total content of some coumarins in shoots and roots.

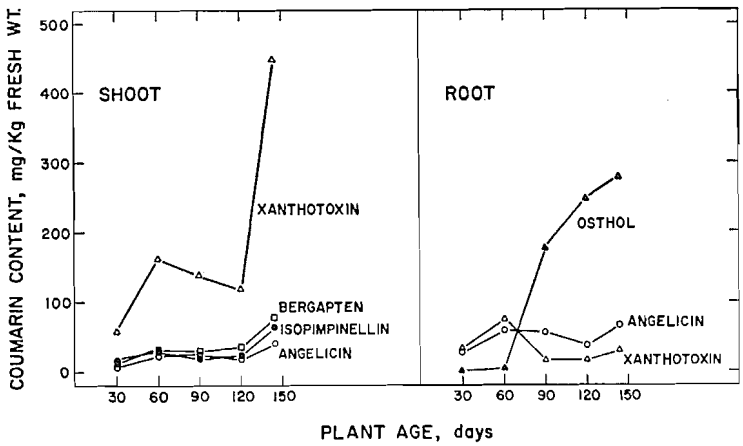

FIG. 3. Development of coumarins in *Angelica archangelica*; concentration of some coumarins in shoots and roots.

plant; they are apparently synthesized simultaneously and in more or less fixed ratios one to another. Moreover, their appearance ahead of, or coincident with the root coumarins suggests the leaves as an independent site of furocoumarin formation.

The situation in the roots is different. Here the main coumarins are angelicin and xanthotoxin in the first two months, but after this time the xanthotoxin concentration falls and osthol begins to accumulate, becoming, as reported in the literature, the main coumarin of the mature roots. How this accumulation comes about is impossible to say at this time, as the biosynthetic pathways leading to osthol and to the furocoumarins are not known with certainty. However, as osthol was not detected in the leaves, it seems probable that it is formed in the roots.

Experimental

A. archangelica was grown from seed in the greenhouse and the plants maintained hydroponically. A constant day length of 14 h was imposed.

Fresh leaves (1720 g, i.e. 300 g dry weight) of three month old plants, trimmed free of petioles and stems, were boiled and homogenized in 3 l methanol. The alcohol solution was adjusted to contain 60% methanol by concentration, then was washed with two 400 ml portions of Skelly B. This petroleum ether was backwashed with 60% methanol and the alcoholic solutions combined; methanol was removed from the orange solution and the aqueous residue continuously extracted overnight with ether. A small amount of white precipitate was filtered off before the extract was concentrated to the point of dryness.

A 4 × 35 cm column of silicic acid (Mallinckrodt, 100 mesh, used as received. Other brands gave less sharp separations.) was prepared by slurrying 200 g powder in about 1 l of 1:1 ether:Skelly B (60–80°), pouring this into the column, and allowing settling until the meniscus approached the top of the silicic acid. The ether extract, dissolved in about 50 ml of the same solvent mixture, was carefully poured upon the top of the column and washed in with a little extra solvent. Two hundred 15 ml fractions were collected and allowed to stand for a day or two to permit the ether to evaporate and thus bring about the slow crystallization of the chief coumarins. These were then filtered off, the appropriate fractions combined, and each crystalline substance recrystallized from ethanol.

Imperatorin

Fractions 41–47 deposited needles of imperatorin, m.p. 97.5–99.5°; λ_{max}(EtOH) 221, 248, 264 (shoulder), and 298 mμ. The n.m.r. spectrum (Varian HA-100, solvent deuterochloroform, internal standard tetramethylsilane) showed signals at δ = 6.32 (H_3) and 7.71 (H_4), both doublets having J = 10 c.p.s.; at 7.31 (H_5), 7.64 ($H_{2'}$), and 6.77 ($H_{3'}$), for a total of 5 aromatic protons. The assignments of aromatic signals here and below follow those of Sheinker *et al.* (16) and Batterham and Lamberton (17). The later work of Reisch *et al.* (18) has also been considered. Other signals, present at 4.97 (CH_2), 5.58 (unsaturated CH), and 1.74 (vinyl methyls), were typical for a 3,3-dimethylallyl substituent. Authentic imperatorin was identical in all respects. The yield was 170 mg; abundance = 0.57 mg/g dry leaves.

Bergapten

Fractions 54–62 gave bergapten, m.p. 188–190° with sublimation; λ_{max}(EtOH) 221, 247, 257, 266, and 306 mμ. The n.m.r. spectrum showed signals at δ = 6.25 (H_3) and 8.14 (H_4) (both doublets, J = 10 c.p.s.); at 7.12 (H_8), 7.59 ($H_{2'}$), and 7.02 ($H_{3'}$). A single aromatic methoxyl group was present at δ = 4.25. Authentic bergapten was identical in all respects. The yield was 46 mg; abundance = 0.15 mg/g.

Angelicin

The bergapten mother liquors were concentrated to

Can. J. Chem. Downloaded from www.nrcresearchpress.com by 210.87.254.40 on 09/05/12
For personal use only.

Can. J. Chem. Downloaded from www.nrcresearchpress.com by 210.87.254.40 on 09/05/12
For personal use only.

small volume and a little more bergapten was filtered off. Gas–liquid chromatography of the remaining solution showed several components, the major one emerging, after about 5 min. This was collected and recrystallized to colorless needles, m.p. 137–138°; λ_{max}(EtOH) 218, 242 (shoulder), 248, and 297 mμ. The n.m.r. showed only 6 protons, all in the aromatic region, at δ = 6.36 (H_3), 7.78 (H_4), both J = 10 c.p.s.; 7.40 (H_5), 7.38 (H_6), 7.67 ($H_{2'}$), and 7.12 ($H_{3'}$). Authentic angelicin was identical in all respects. Estimated leaf content = 42 mg; abundance = 0.14 mg/g.

Xanthotoxin

Fractions 67–81 gave crystals of xanthotoxin, m.p. 144–145°; λ_{max}(EtOH) 221, 242 (shoulder), 247, 260 (shoulder), and 297 mμ. The n.m.r. signals were located at δ = 6.32 (H_3) and 7.72 (H_4), both doublets of J = 10 c.p.s.; at 7.31 (H_5), 7.65 ($H_{2'}$), 6.78 ($H_{3'}$), and 3.25 (aromatic OCH_3). Authentic xanthotoxin was identical in all respects. The yield was 260 mg; abundance = 0.87 mg/g.

Isopimpinellin

Fractions 82–88 contained isopimpinellin, deposited as very pale yellow needles, m.p. 147–149°. (In some plants the amount of xanthotoxin present was so large relative to isopimpinellin that the latter was best purified in small quantities by g.l.c.) λ_{max}(EtOH) 221, 240, 247, 266–270 (broad), and 311 mμ. The n.m.r. signals, located at δ = 6.25 (H_3) and 8.08 (H_4), both doublets of J = 10 c.p.s., and at 7.59 ($H_{2'}$) and 6.96 ($H_{3'}$), doublets of J = 2 c.p.s., showed the presence of unsubstituted pyrone and furan rings. Two aromatic methoxyl groups were indicated by a six-proton signal at δ = 4.14. Authentic isopimpinellin was identical in all respects to the isolated material. Estimated leaf content = 34 mg; abundance = 0.11 mg/g.

Oxypeucedanin

Fractions 80–90 from one strain of plants deposited this racemic compound as prisms, m.p. 140–142°. The u.v. spectrum, with λ_{max}(EtOH) 221, 247, 257, 266, and 305 mμ, indicated a bergapten-type nucleus. The n.m.r. signals were seen at δ = 6.24 (H_3) and 8.15 (H_4), doublets of J = 10 c.p.s.; 7.11 (H_8), 7.57 ($H_{2'}$), and 6.92 ($H_{3'}$) for a total of 5 aromatic protons. In addition there were multiplets centered at δ = 4.49 (CH_2) and 3.20 (saturated CH) and sharp three-proton singlets at 1.40 and 1.32 (aliphatic CH_3). Although no authentic racemic sample was available for comparison, (+)-oxypeucedanin gave the same spectra. Abundance in the strain = 0.46 mg/g.

Unidentified Coumarins

U_1, U_2, and U_3 from fractions 82–88 emerged from the gas chromatograph at retention times of 6.2, 6.6, and 8.0 (relative to angelicin = 1.0). All had u.v. maxima at 221, 242 (shoulder), 248, 261 (shoulder), and 298 mμ, suggesting xanthotoxol derivatives.

U_4 from fractions 54–62, relative retention time 3.9, had λ_{max}(EtOH) 218, 247, 256, and 320 mμ, indicating a coumarin without a furan ring. No available coumarin derivative co-chromatographed (e.g. osthol, relative retention time (r.r.t.) 2.6 and herniarin, r.r.t. 1.08).

U_5 from fractions 48–56 was not always present. Its retention times relative to angelicin under several conditions of g.l.c. exactly matched those of psoralen, (r.r.t. = 1.15 under stated g.l.c. conditions).

Development of Coumarins in the Plant

Plants of the same strain were taken 30, 60, 90, 120, and 144 days after germination and separated into weighed root and shoot portions. Both portions were worked-up as above, but the ether-soluble fractions were analyzed directly by g.l.c. The same conditions were used for these analyses as for those above: a 0.25 in. × 10 ft copper column, packed with 5% silicone (SE-30) on acid-washed Chromosorb W-DMCS support (70–80 mesh), was operated at 205°. Injector and detector temperatures were 252 and 264° respectively. A helium flow of 60 ml/min was employed. Imperatorin, most phenolic coumarins, and many complex neutral coumarins do not pass through the g.l.c. column under these conditions, but other simple neutral coumarins could be separated and quantitated in this way. Details of this method and its further applications will appear elsewhere.

Osthol

This coumarin was found at a retention time of 2.6 relative to angelicin in the gas chromatograph. It was collected and crystallized to m.p. 82–84° (lit. m.p. 84° (2)); λ_{max}(EtOH) 219, 247, 256, and 320 mμ indicated the absence of a furan ring. The n.m.r. spectrum showed doublets at δ = 6.19 (H_3), 7.59 (H_4), 7.28 (H_5), and 6.82 (H_6), altogether 4 aromatic protons. Other signals were present at δ = 3.52 (CH_2), 5.23 (unsaturated CH), 3.90 (aromatic OCH_3), 1.83, and 1.67 (vinyl methyls). Authentic osthol gave identical spectra. Finally, a mixed melting point of the sample with authentic osthol showed no depression.

Acknowledgments

The authors wish to thank Dr. B. A. Bohm for his generous gift of authentic isopimpinellin and imperatorin; Dr. G. Caporale for bergapten; Dr. J. M. Baskin for psoralen; and Dr. T. O. Soine for osthol. Thanks are also extended to Mr. M. Mazurek, who recorded the nuclear magnetic resonance spectra.

1. W. Karrer. Konstitution and Vorkommen der Organischen Pflanzenstoffe. Birkhäuser Verlag, Basel. 1958.
2. E. Späth and O. Pesta. Chem. Ber. **67**, 853 (1934).
3. E. Späth and E. Vierhapper. Monatsh. Chem. **72**, 179 (1938).
4. A. Baerheim-Svendsen. Chemistry of Norwegian Umbellifers. Johan Grundt Tanum Forlag, Oslo. 1954. Chem. Abstr. **52**, 2173g (1958).
5. A. Chatterjee, A. Chakravarty, and R. Mukherjee. J. Ind. Chem. Soc. **44**, 110 (1967).
6. K. Okahara. Bull. Chem. Soc. Japan, **11**, 389 (1936).
7. E. Späth and O. Neufeld. Chem. Ber. **71**, 353 (1938).
8. W. L. Stanley and S. H. Vannier. J. Am. Chem. Soc. **79**, 3488 (1957).
9. H-G. Floss and U. Mothes. Phytochem. **5**, 161 (1966).

10. E. SPÄTH and H. HOLZEN. Chem. Ber. **66**, 1137 (1933).
11. W. N. HOWELL and A. ROBERTSON. J. Chem. Soc. 293 (1937).
12. H. THOMS. Chem. Ber. **44**, 3325 (1911).
13. F. WESSELY and F. KALLAB. Monatsh. Chem. **59**, 161 (1932).
14. E. SPÄTH and K. KLAGER. Chem. Ber. **66**, 914 (1933).
15. J. M. BASKIN, C. J. LUDLOW, T. M. HARRIS, and F. T. WOLF. Phytochem. **6**, 1209 (1967).
16. YU. N. SHEINKER, G. YU. PEK, and M. E. PEREL'SON. Dokl. Akad. Nauk SSSR, **158**, 1382 (1964).
17. T. J. BATTERHAM and J. A. LAMBERTON. Australian J. Chem. **17**, 1305 (1964).
18. J. REISCH, I. NOVAK, K. SZENDREI, and E. MINKER. Die Pharmazie, **22**, 205 (1967).

Can. J. Chem. Downloaded from www.nrcresearchpress.com by 210.87.254.40 on 09/05/12
For personal use only.

Can. J. Chem. Downloaded from www.nrcresearchpress.com by 210.87.254.40 on 09/05/12
For personal use only.

A synthesis in the series of aconitine and delphinine

K. WIESNER, WEN-LING KAO, AND J. ŠANTROCH
Natural Product Research Center, University of New Brunswick, Fredericton, New Brunswick

Received December 24, 1968

The synthesis of compound **3** is described. This synthesis represents the solution of most of the problems which will be encountered in the approach to the delphinine and aconitine aromatization products **1** and **2**. The synthetic compound **3** incorporates the complete skeleton and functionality of **1** and **2** except the substitution of ring A.

Canadian Journal of Chemistry, 47, 2431 (1969)

In 1959 we deduced the structures of the highly substituted and notorious aconite alkaloids delphinine (1*a*) and aconitine (1*b*).[1] In this structure determination aromatization products of the type **1** and **2** played a considerable role.[2] Our interest in these compounds is two-fold: (*a*) since they may be obtained in relatively good yields and only a few steps from delphinine and aconitine, the products **1** and **2** could serve as a relay in the total synthesis of complex poly-substituted aconite alkaloids; (*b*) the structure of the C/D ring system is one of the several features of aconitine and delphinine which follow with complete rigor from our chemical degradations (1*a*, 1*b*, 2, 3). Since the anisole ring of **1** and **2** has been generated from the C/D ring system of the parent alkaloids, while the remainder of the molecule remained completely intact, it is clear that a total synthesis of the aromatization products would represent a mathematically rigorous and simple structure proof for delphinine and aconitine, based on chemistry alone. This has not been accomplished in the past for too many natural products as complicated as the poly-substituted aconite alkaloids.

In view of our extensive and long standing interest in diterpene alkaloid chemistry we have decided to carry out the synthesis of **1** and **2** and thus to accomplish at least the second of the two objectives. The chief consideration in the total synthesis of the natural alkaloids themselves would then be the cost of such an undertaking. In the present communication we wish to describe the synthesis of compound **3** which represents the solution of most of the problems facing us in the synthesis of **1** and **2**. The synthesis of the fully

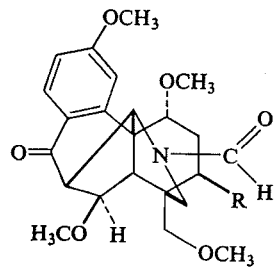

1 R = H
2 R = OH

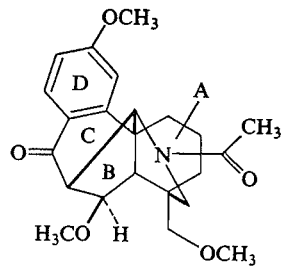

3

SCHEME 1

substituted aromatization products and the correlation of "natural" and synthetic materials will be reported separately.

The synthetic strategy, which we developed in model experiments (4) involved the alkylation of the tetralone **4** with a long-chain iodide destined to form ring A, followed by an alkylation with allyl bromide (see Scheme 2). In the present synthesis it was consequently our first task to prepare the methoxy benzyloxy iodopentane **12** needed for the first alkylation step.

A convenient starting material was the γ-lactone **7** described by Leuchs *et al.* in 1912 (5). This lactone was hydrolyzed by aqueous alkali to the salt of the corresponding hydroxy acid and the hydrolysis mixture was treated with benzyl

[1]The latter was deduced jointly with Professor Büchi's group at the Massachusetts Institute of Technology.
[2]For a full discussion of these compounds, see reference 2.

Can. J. Chem. Downloaded from www.nrcresearchpress.com by 210.87.254.40 on 09/05/12
For personal use only.

chloride in benzene. The resulting acid **8** was esterified with methanolic hydrochloric acid and the ester **9** obtained in an overall yield of 80% was purified by distillation and characterized by its nuclear magnetic resonance (n.m.r.) spectrum, which showed quantitatively the presence of all three of its functional groups.[3]

The ester **9** was now reduced with lithium aluminium hydride to the alcohol **10**, this material was tosylated to **11**, and finally the iodide **12** was obtained by exchanging the tosyloxy group in **11** for iodine with sodium iodide in acetone. Compound **12** was an oil which was purified by chromatography and characterized by thin-layer chromatography (t.l.c.) and a quantitative evaluation of the n.m.r. spectrum. The overall yield of the conversion **8** → **12** was 72%.

With the side-chain **12** available, it was now possible to proceed with the necessary alkylations of the tetralone **4** (6). After unsuccessful preliminary attempts to introduce the allyl chain first and the methoxy benzyloxy pentyl chain in the second alkylation stage, we have turned our attention to the preparation of the compound **5**. This caused considerable difficulties, since the most obvious method, the Stork reaction, did not yield the desired product. Finally, we have been able to prepare **5** in a 50% yield by treating the tetralone **4** with 2 moles of the iodide **12** and 1 mole of sodium methoxide in methanol.

At this stage it should be pointed out that the seven intermediates of the synthesis between compounds **5** and **18**, inclusive, were mixtures of diastereoisomers resulting from the uncontrolled asymmetric centers marked by the asterisks. They were all purified by careful chromatography until they were apparently homogeneous on a thin-layer plate. Characterization was performed by a quantitative evaluation of the n.m.r. spectrum. This was considered very reliable since n.m.r. spectrography showed clearly the presence of all the functional groups, which were derived from all three components of the molecule (see Experimental). However, in spite of the confidence in this method, we were very relieved when we obtained the highly crystalline intermediates **21** and **22** which allowed not only spectral, but also a full classical characterization.

The introduction of the allyl group into the mono-substituted tetralone **5** was performed with allyl bromide and sodium hydride in dry benzene. The yield of the disubstituted tetralone **6** obtained in this manner was 90%. The next two steps, i.e. the hydroxylation of **6** to the diol **13** and the oxidation of this compound to the aldehyde **14** were accomplished in almost quantitative yield, and the products were found (by spectroscopy and t.l.c.) to be pure enough for further work. The hydroxylation was performed with a catalytic amount of osmic acid in the presence of an excess of sodium chlorate in aqueous tetrahydrofuran. The subsequent glycol cleavage was accomplished by metaperiodate in the same solvent.

The ring closure of the keto-aldehyde **14** to the tricyclic bridged hydroxy ketone **15** is a simple aldol condensation and is portrayed by the arrow in formula **14**. The reaction took place readily at 50 °C in aqueous methanolic sodium hydroxide in an 87% yield. The product was purified by chromatography in the form of its tetrahydropyranyl derivative **16**. The infrared (i.r.) spectrum of **16** showed a single sharp carbonyl band at 1755 cm^{-1} for the ketone in the apex of the 1,2,3-bicyclooctane system and no hydroxyl peak.

The next task which had to be accomplished was the conversion of the ketone in **16** to a primary amino group. The required configuration of this group was *anti* to the anisole ring. This was the first asymmetric center which had to be controlled, since all the others would be abolished in the further course of the synthesis. We have established already in our first model study (4) that reductive amination of the ketone with alcoholic ammonia and Raney nickel under high pressure yielded the most favorable proportion of the *anti* and *syn* isomers. In the present case this ratio turned out to be approximately 4:1 in favor of the desired *anti* isomer and the synthesis was thus almost stereospecific. Nevertheless, the two nitrogen epimers were separated only at a later stage, when all the remaining asymmetric centers disappeared.

The mixture of diastereoisomeric amino alcohols **17** which was obtained by the amination of compound **16** (yield 80%) was converted into the acetates **18** and this material was subjected to mild alkaline hydrolysis, hydrogenolysis with palladium on charcoal (to liberate the acetylated and benzylated alcoholic functions), and Jones' oxidation. All these processes gave good yields and the oxidation has reduced the number of

[3]Spectral data are discussed in the Theoretical section only in specially relevant cases. For spectral data of all compounds see the Experimental.

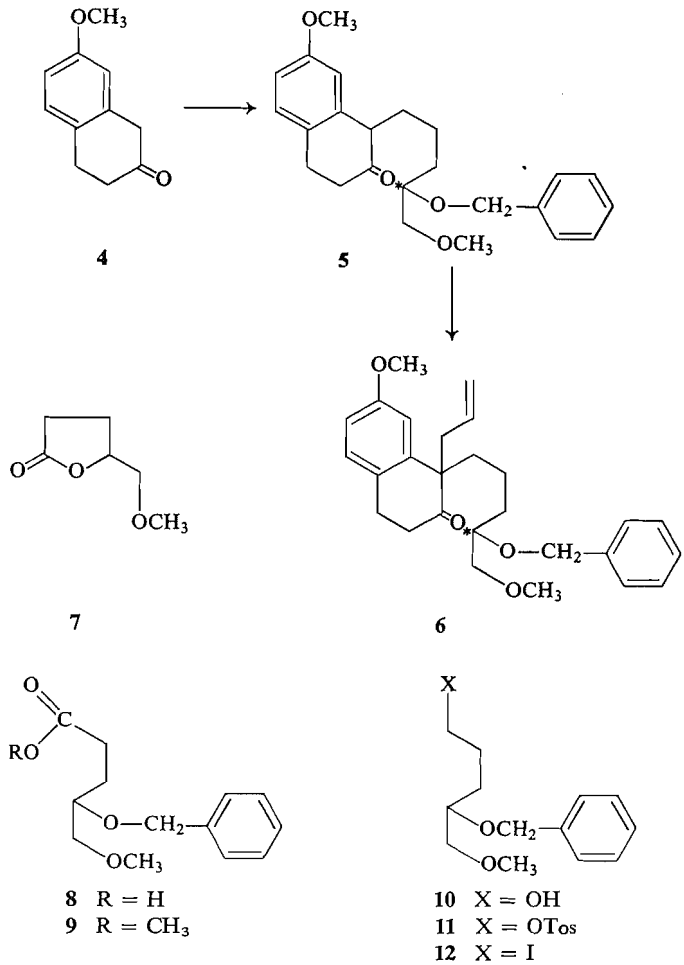

SCHEME 2

diastereoisomers to only two, i.e. the products **19** and **20**. These two epimeric acetylamino diketones were finally separated by careful chromatography on a column of silica gel. The ratio of **19** to **20** obtained in this manner was 4:1 and the required compound **19** crystallized as a waxy low-melting solid, which could not be recrystallized from a solvent.

The i.r. spectrum of **19** showed ketonic maxima at 1750 and 1725 cm^{-1} (five-membered and side-chain ketones), an amide carbonyl group at 1675 cm^{-1}, and the NH of the secondary amide group at 3500 cm^{-1}.

The n.m.r. spectrum of **19** displayed two methoxyl singlets (3H each) at τ = 6.54 and 6.12 p.p.m., the methylenic group unshielded by the primary methoxyl as a singlet (2H) at τ = 5.93 p.p.m., the acetyl methyl group as a singlet (3H) at τ = 7.93 p.p.m., and the hydrogen unshielded by the acetylamino group as a doublet (1H) at τ = 5.28 and 5.43 p.p.m.

The spectral data of compound **20** were similar except that the hydrogen unshielded by the acetylamino group appeared in the n.m.r. spectrum of **20** as a multiplet centered at τ = 5.25 p.p.m.

One can see readily that the n.m.r. peak of the hydrogen unshielded by the acetylamino group is a significant indicator of the configuration at this center. Nevertheless we have not attempted to assign the configurations by a fundamental analysis of the n.m.r. spectra.

Since we have prepared previously configurationally defined model compounds (4) we knew empirically that the doublet displayed by compound **19** corresponded to the desired *anti* configuration of the acetylamino group. A rigorous

Can. J. Chem. Downloaded from www.nrcresearchpress.com by 210.87.254.40 on 09/05/12
For personal use only.

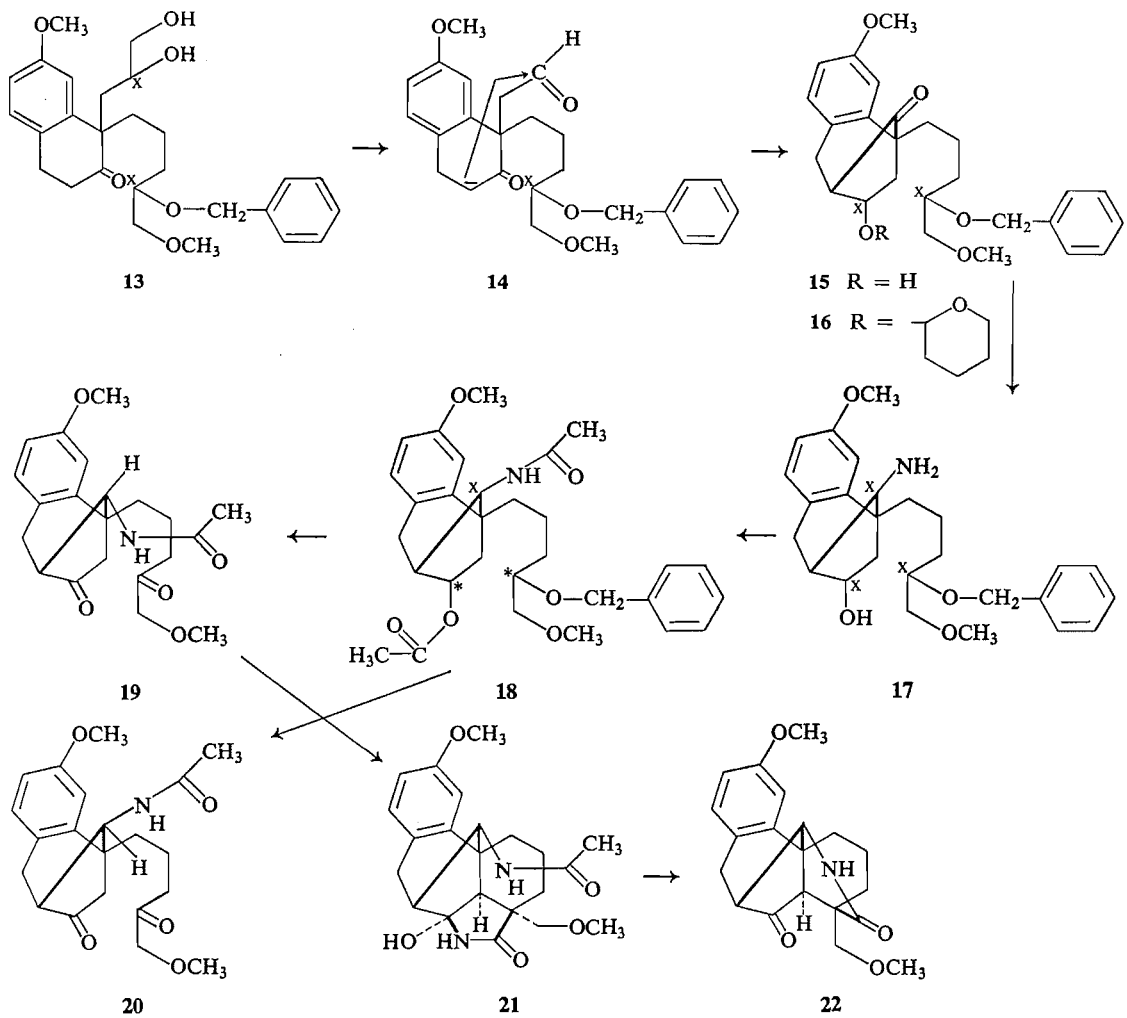

SCHEME 3

chemical corroboration of this preliminary configurational assignment followed subsequently from the conversion of compound **19** to the pentacyclic lactam **22**.

With the configurationally pure acetylamino diketone **19** in hand, the stage was set for the construction of ring A and the nitrogen ring. It was our intention to close ring A by an aldol condensation of diketone **19** and to complete the assembly of the entire carbon system by adding hydrogen cyanide across the double bond of the resulting α,β-unsaturated ketone.

We were not certain that this hydrocyanation reaction would yield a product possessing the required configuration with the nitrile and acetylamino groups *syn*. However, it would probably be simple to settle this point experimentally by ring formation between these two functional groups. As it turned out, the best method to perform the aldol condensation and hydrocyanation reactions was to combine them into one step. Prolonged reflux of the diketone **19** with a moderate excess of alcoholic potassium cyanide gave the highly crystalline sharply-melting lactamol **21** in an 80% yield. Clearly a hydrolysis of the nitrile group to a primary amide and interaction of this function with the five-membered ring B ketone followed the hydrocyanation. The analytical and spectral investigation of compound **21** (see Experimental) supported unambiguously

Can. J. Chem. Downloaded from www.nrcresearchpress.com by 210.87.254.40 on 09/05/12
For personal use only.

Can. J. Chem. Downloaded from www.nrcresearchpress.com by 210.87.254.40 on 09/05/12
For personal use only.

the structure assigned to it. On the other hand, the configuration of the lactamol which is portrayed in the formula **21** followed only from the success of the subsequent step, i.e. **21** → **22**.

This crucial process, which gave us the final proof for the configurations of the intermediates **19** and **21** and at the same time completed the construction of the desired skeleton, was brought about in a yield of 80% by refluxing the lactamol **21** with a mixture of methanol and concentrated hydrochloric acid.

The keto lactam **22** was a beautifully crystalline substance, which gave a correct elemental analysis and a strong molecular ion in mass spectroscopy. Its i.r. and n.m.r. spectra left no doubt about the correctness of the structural assignment. The i.r. spectrum in chloroform showed the five-membered ketonic carbonyl at 1750 cm^{-1}, the lactam carbonyl at 1665 cm^{-1}, and the lactam NH at 3400 cm^{-1}. The n.m.r. spectrum displayed two methoxyls as singlets (3H each) at τ = 6.67 and 6.22 p.p.m., the methylenic group unshielded by the primary methoxyl as a singlet (2H) at τ = 6.55 p.p.m. and aromatic hydrogen (3H) at τ = 3.08–3.21 p.p.m.

The synthesis of compound **22** was reported in a preliminary communication (7) by two of the present authors (K.W. and J.Š.). It was subsequently repeated on a larger scale (by W.K.) and the individual steps were not only corroborated, but the overall yield was increased by a factor of 3.

The stage was consequently set for the final adjustment of the functional groups. To this end it was necessary to change the ketone of compound **22** into an *exo*-methoxyl and to introduce a new keto group into conjugation with the anisole ring.

The reduction of the keto group in compound **22** caused considerable difficulties and about 500 mg of substance were consumed in attempts to find a stereospecific method. Finally the keto lactam **22** was reduced with lithium aluminium hydride, the product was acetylated, and the *O*-acetyl group saponified by mild reflux with methanolic alkali. All three steps proceeded in good yields (about 90%) and gave a mixture of the *N*-acetyl alcohols **23** and **24** (ratio about 5:4). These two epimers were readily separated by chromatography and subjected (separately) to methylation with dimethyl sulfate and sodium hydride in dry dioxane. The desired *exo*-methoxy compound **25** obtained by methylation of **23** crystallized nicely from ether and showed,

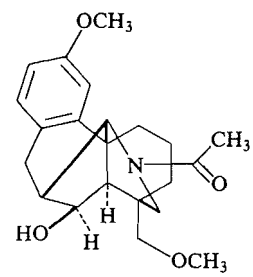

23

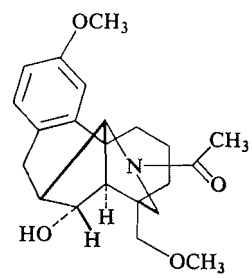

24

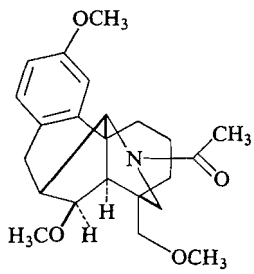

25

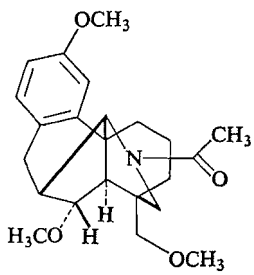

26

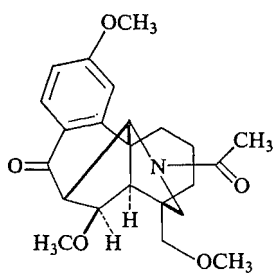

3

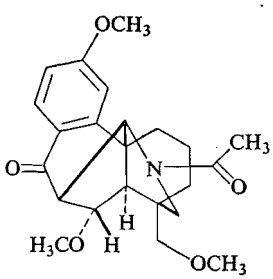

27

besides a correct molecular ion in mass spectroscopy, i.r. and n.m.r. spectral properties in agreement with expectations; n.m.r.: singlet (3H) τ = 6.27 p.p.m. (aromatic —OCH_3), singlet (6H) τ = 6.75 p.p.m. (two aliphatic —OCH_3), singlet (3H) τ = 7.98 p.p.m. (acetyl —CH_3), multiplet (3H) centered at τ = 3.20 p.p.m. (aromatic hydrogen); i.r.: no —OH or NH band, amide carbonyl at 1651 cm^{-1}.

The *endo*-methoxy compound **26** remained amorphous even when it was completely pure (t.l.c.). Its mass spectrum was identical with the mass spectrum of **25**, which is good evidence for the epimeric relationship of the two products. The i.r. spectra of **25** and **26** showed small but distinct differences only in the finger-print region. However, the n.m.r. spectrum of **26** displayed a major difference with respect to the spectrum of

Can. J. Chem. Downloaded from www.nrcresearchpress.com by 210.87.254.40 on 09/05/12
For personal use only.

25 and this enabled us to assign to the two products the configurations portrayed in the formulae. The secondary methoxyl singlet which in the n.m.r. spectrum of **25** coincides with the primary methoxyl at $\tau = 6.75$ p.p.m. is shifted in the n.m.r. spectrum of **26** strongly up-field to $\tau = 6.93$ p.p.m. The aromatic and primary methoxyl signals of **25** and **26** are at almost identical τ values and also the remaining peaks in both spectra are very similar. On inspection of the models of compounds **25** and **26** the reason for this n.m.r. behavior becomes clear. The secondary methoxyl of **26** is located in the shielding region of the anisole ring and thus its n.m.r. peak is shifted up-field.[4]

The last operation which faced us in the synthesis was the introduction of a new carbonyl group into conjugation with the anisole ring. No difficulties were encountered in this task, which was accomplished in a yield of 77% by Jones' oxidation. In this way the two compounds **25** and **26** were converted to the final products **3** and **27**, respectively.

This time the *endo*-methoxy product **27** was crystalline and the desired *exo*-methoxy derivative **3** remained amorphous, although it was completely homogeneous on t.l.c. in several systems. Both products gave not only correct molecular ion peaks in mass spectroscopy, but the entire mass spectra were practically identical. The i.r. spectrum of **3** showed no peak in the OH—NH region and three peaks in the carbonyl region at 1680, 1642, and 1600 cm^{-1}. The i.r. spectrum of **27** was practically the same and showed only small differences in the finger-print region. The ultraviolet (u.v.) spectra of **3** and **27** were identical and superimposable on the spectrum of the "natural" aromatization products **1** and **2** [$\lambda_{max} = 278$ mμ ($\log \varepsilon = 4.12$), $\lambda_{max} = 230$ mμ ($\log \varepsilon = 4.09$)].

Our final compound **3** contains the complete functionality of the aromatization products **1** and **2** except the substitution of ring A. In order to synthesize by the same method the "natural" compound **1** itself, it is clearly necessary to prepare an analogue of the intermediate **19** with an additional methoxyl suitably placed in the side-chain. This task is very laborious, but it has now been accomplished on a small scale by two routes.[5] It will be reported in due course.

[4]In this connection it might be mentioned that the "natural" aromatization products of aconitine (2) display methoxyl signals exactly like the epimer **25** and unlike **26**. However, we do not wish to use this as a corroboration of our assignment, which is quite unambiguous in its own right, since one of the purposes of the present work is a rigorous synthetic structure proof for aconitine.

Addendum

While this paper was being refereed and a high resolution mass spectrum of the final product obtained at the suggestion of the referee, we finally succeeded in securing a sufficient supply of pure aconitine to prepare the aromatization product **2** and convert it into the optically active forms of **25** and **3**. These "natural" compounds were shown to be identical with the corresponding synthetic racemates by t.l.c. (in six different systems using two adsorbents), i.r., n.m.r., and mass spectroscopy. This work completes a rigorous purely chemical structure proof for aconitine and delphinine, and also proves the configuration of the ring B methoxyl in these alkaloids. The entire structural argument will be reviewed in a future publication.

Experimental

Preparation of the Methoxy Benzyloxy Methyl Ester **9**

The lactone **7** (5) (13 g) was added to a mixture of dioxane (35 ml) and sodium hydroxide (20 g). The resulting suspension was stirred for 1 h at 80°. After this time the suspension was diluted with dry benzene (100 ml) and benzyl chloride (40 ml) was added dropwise over a period of 10 h. In the course of this addition the temperature was maintained at 80° and rapid stirring was continued. The acid **8** was isolated from the reaction mixture in the usual manner. The yield was 21 g (88%) and it was converted to the ester **9** without further purification. The acid **8** (23.8 g) was dissolved in absolute methanol (100 ml) and the solution was cooled to −15°. Gaseous hydrogen chloride was introduced for 30 min and the solution was allowed to stand overnight at room temperature. The solution was then neutralized with sodium bicarbonate, the methanol evaporated *in vacuo*, and the residue dissolved in ether. The ether solution was washed with water, dried, and the ether distilled off. The residue was fractionated *in vacuo*. The fraction boiling at 115–120° (0.2 mm Hg) was the pure ester **9** homogeneous in t.l.c. and g.l.c. The yield was 22.8 g (90%). Infrared spectrum: no OH band; 1740 cm^{-1} (ester carbonyl). Nuclear magnetic resonance spectrum: singlet (5H) $\tau = 2.75$ p.p.m. (aromatic hydrogen); singlet (2H) $\tau = 5.40$ p.p.m. (benzylic hydrogen); two singlets (3H each) $\tau = 6.35$ and 6.60 p.p.m. (2 —OCH_3). Mass spectrum: strong peaks at *m/e* 207 ($CH_3O_2C(CH_2)_2CHOCH_2C_6H_5$); 45 ($CH_2$-

[5]C. Demerson, E. Jay, and T. Kanno. Unpublished results.

Can. J. Chem. Downloaded from www.nrcresearchpress.com by 210.87.254.40 on 09/05/12
For personal use only.

OCH_3); 59 (CO_2CH_3); 91 ($CH_2C_6H_5$); 115 (CH_3CO_2-$(CH_2)_2CO$).

Preparation of the Methoxy Benzyloxy Iodopentane **12**

The ester **9** (25.2 g) was heated under reflux in dry ether (250 ml) with lithium aluminium hydride (3.7 g). Work-up in the usual manner gave the alcohol **10** (22.5 g) as a colorless oil in a quantitative yield. It was pure in t.l.c. and was immediately used for further work. Infrared spectrum: 3480 cm^{-1} (hydroxyl); no carbonyl peak. Nuclear magnetic resonance spectrum: singlet (5H) τ = 2.67 p.p.m. (aromatic hydrogen); singlet (2H) τ = 5.46 p.p.m. (benzylic hydrogen); singlet (3H) τ = 6.60 p.p.m. (—OCH_3).

The alcohol **10** (22.4 g) was dissolved in dry pyridine (40 ml) and cooled to −15°. Tosyl chloride (20 g) was gradually added under vigorous stirring and cooling. After the addition was completed the stirring was continued at 0° for 1 h. After this period, water (250 ml) and crushed ice were added and the oily suspension was extracted with ether. The ether solution was washed with dilute hydrochloric acid, aqueous bicarbonate and water, dried, and evaporated to dryness. The yield was 34 g (90%) of the crude tosylate **11**. This material (37.9 g) was dissolved in dry acetone, the solution was cooled to 0° and sodium iodide (75 g) was added to it. The mixture was stirred for 12 h after which time the acetone was distilled off *in vacuo* and water (300 ml) and crushed ice were added. The aqueous mixture was extracted with ether and the combined ether extracts were washed with a 10% thiosulfate solution and with water. After drying and evaporation to dryness the crude oily product was chromatographed on silica gel. Ether in benzene (5%) eluted the iodo compound **12**. It was homogeneous in t.l.c. and was obtained in a yield of 80% (26.8 g).

Mol. Wt. Calcd. for $C_{13}H_{19}O_2I$: 334. Found (mass spectrometry): 334.

Infrared spectrum: no OH and carbonyl band. Nuclear magnetic resonance spectrum: singlet (5H) τ = 2.61 p.p.m. (aromatic hydrogen); singlet (2H) τ = 5.37 p.p.m. (benzylic hydrogen); singlet (3H) τ = 6.52 p.p.m. (—OCH_3); multiplet (4H) centered at τ = 8.34 p.p.m. (C—CH_2—CH_2—C).

Preparation of the Monoalkylated Tetralone **5**

The methoxy tetralone **4** (6) (35.2 g) was added to a solution of sodium (4.6 g) in absolute methanol (1000 ml) under nitrogen. The solution was stirred for 1 h after which time the iodide **12** (120 g) was added and the stirring was continued at 25° for 48 h. The methanol was evaporated and water (500 ml) was added to the residue. The aqueous phase was extracted with ether (5 × 200 ml) and 2% aqueous sodium hydroxide (50 ml) was added to the combined ether extracts. Air was vigorously bubbled through both phases for a short time, after which the aqueous alkaline phase was separated and discarded. This operation destroyed the remaining starting material **4** while leaving the product **5** unaffected. The ether layer was now dried, evaporated to dryness, and the residue chromatographed on silica gel (3.2 kg). The product **5** was eluted with benzene–ether (10:1) as a colorless oil. The yield was 39 g (51%) and the product was apparently homogeneous in t.l.c. Infrared spectrum: no OH band; 1710 cm^{-1} (ketone). Nuclear magnetic resonance spectrum: singlet (5H) τ = 2.72 p.p.m. (aromatic hydrogen of the benzyl group); multiplet (3H) τ = 2.97–3.38 p.p.m. (aromatic hydrogen of the anisole ring); singlet (2H) τ = 5.48 p.p.m. (benzylic hydrogen); singlets (3H each) τ = 6.25 and 6.66 p.p.m. (2 —OCH_3).

Preparation of the Dialkylated Tetralone **6**

Compound **5** (38.2 g) was added to dry benzene (250 ml) containing a 50% emulsion (3.1 g) of sodium hydride in mineral oil. The mixture was stirred at room temperature for 1 h, after which time it was cooled in an ice bath and allyl bromide (24.2 g) was added over a period of 30 min. The temperature was then gradually raised to 45° and the stirring was continued for 24 h. After cooling, the reaction mixture was washed with water, dried, evaporated to dryness, and the residue was chromatographed on silica gel (2 kg). The product **6** was eluted with benzene–ether (20:1). It was a colorless oil homogeneous in t.l.c. and was obtained in a yield of 90%. Infrared spectrum: no OH band; 1720 cm^{-1} (ketone); 928 cm^{-1} (C=CH_2). Nuclear magnetic resonance spectrum: singlet (5H) τ = 2.77 p.p.m. (aromatic hydrogen of the benzyl group); multiplet (3H) τ = 3.02–3.22 p.p.m. (aromatic hydrogen of the anisole ring); multiplet (3H) centered around τ = 5.06 p.p.m. (vinylic hydrogen); singlet (2H) τ = 5.53 p.p.m. (benzylic hydrogen); two singlets (3H each) τ = 6.23 and 6.68 p.p.m. (2 —OCH_3).

Preparation of the Aldehyde **14**

The disubstituted tetralone **6** (21 g) was dissolved in tetrahydrofuran (100 ml) and a solution of osmium tetroxide (0.06 g) in tetrahydrofuran (6 ml) was added. The mixture was stirred for 10 min at room temperature, after which time sodium chlorate (6 g) in water (25 ml) was added. The stirring was continued at room temperature for 48 h. After this period most of the tetrahydrofuran was distilled off *in vacuo*, water was added, and the aqueous layer was exhaustively extracted with ether. After drying and evaporation to dryness the ether extract gave a quantitative yield (22.8 g) of a compound which was apparently homogeneous in t.l.c. and showed a strong hydroxyl band in the i.r. spectrum. It was converted to the aldehyde **14** without purification. To this end the above material (22.8 g) was dissolved in aqueous tetrahydrofuran (1:1, 400 ml) and sodium metaperiodate (81.1 g) was added to the solution. The mixture was vigorously stirred under nitrogen for 5 h at room temperature. During this time a heavy precipitate was formed. It was filtered off and washed thoroughly with ether. The ether was in turn washed with water, dried, and evaporated to dryness. The residue was the practically pure (t.l.c.) aldehyde **14** (21.2 g) obtained in quantitative yield. It was purified by chromatography on silica gel and stored under nitrogen. Infrared spectrum: no OH band, 2710 cm^{-1} (aldehyde); 1730 and 1725 cm^{-1} (aldehyde and ketone carbonyls); no vinyl group around 900 cm^{-1}. Nuclear magnetic resonance spectrum: narrow multiplet (1H) τ = 0.61 p.p.m. (aldehyde hydrogen); singlet (5H) τ = 2.73 p.p.m. (aromatic hydrogen of the benzyl group); multiplet (3H) τ = 3.26–3.38 p.p.m. (aromatic hydrogen of the anisole ring); singlet (2H) τ = 5.50 p.p.m. (benzylic hydrogen); two singlets (3H each) τ = 6.24 and 6.70 p.p.m. (2 —OCH_3).

Can. J. Chem. Downloaded from www.nrcresearchpress.com by 210.87.254.40 on 09/05/12
For personal use only.

Preparation of the Tetrahydropyranyl Ketone **16**

The keto aldehyde **14** (21.2 g) was dissolved in methanol (700 ml) and sodium hydroxide (2 g) in water (30 ml) was added under vigorous stirring. The stirring was continued under nitrogen at 50–55° for 24 h. After this time the methanol was partly evaporated *in vacuo*, ice water (150 ml) was added, and the solution was extracted with ether. After washing and drying the ether extract was evaporated to dryness. The yield was 18.15 g (86.5%) of the crude hydroxy ketone **15**. For purification it was converted into the tetrahydropyranyl derivative **16**. Infrared spectrum of crude **15**: 3500 cm^{-1} (OH); 1755 cm^{-1} (five-membered ketone). The crude hydroxy ketone **15** (21.2 g) was dissolved in dry chloroform (250 ml) and dihydropyran (22 g) was added to the solution. After the addition of two drops of concentrated hydrochloric acid the solution was allowed to stand for 24 h at room temperature. The chloroform was then washed with a dilute sodium bicarbonate solution and water, dried, and evaporated to dryness. The residue was chromatographed on neutral alumina (1.1 kg). Petroleum ether – dry chloroform (1:1) eluted 18.2 g (72%) of the t.l.c. homogeneous compound **16**. Infrared spectrum: no OH band; 1755 cm^{-1} (five-membered ketone). Nuclear magnetic resonance spectrum: singlet (5H) τ = 2.70 p.p.m. (aromatic hydrogen of the benzyl group); multiplet (3H) τ = 3.26–3.38 p.p.m. (aromatic hydrogen of the anisole ring); singlet (2H) τ = 5.34 p.p.m. (benzylic hydrogen); multiplet (13H) between singlets at τ = 6.24 and 6.58 p.p.m. (hydrogens unshielded by oxygen plus the two methoxyls).

Preparation of the N,O-Diacetyl Derivative **18**

The tetrahydropyranyl ketone **16** (18 g) was dissolved in methanol (60 ml) and the solution was saturated with ammonia. The solution was then hydrogenated at 2500 p.s.i. for 8 h in the presence of Raney nickel (4 g) at 165°. The catalyst was filtered off and the filtrate was evaporated to dryness. The basic fraction was separated in the usual manner and yielded 12 g of crude compound **17**. This material was dissolved in methylene dichloride (100 ml) and triethylamine (25 g) was added to the solution. The solution was then cooled in an ice bath and acetyl chloride (12.5 g) was added dropwise with vigorous stirring. The stirring was continued at room temperature for 24 h. After this time the mixture was diluted with chloroform, washed with dilute hydrochloric acid, aqueous sodium bicarbonate and water, dried, and evaporated to dryness. The residue was chromatographed on silica gel (600 g). The diacetyl compound **18** was eluted with ether–methanol (10:1) as an oil (11 g), apparently homogeneous in t.l.c. Infrared spectrum: 3450 cm^{-1} (NH); 1730 cm^{-1} (O—CO—CH_3); 1670 cm^{-1} (N—CO—CH_3). Nuclear magnetic resonance spectrum: singlet (5H) τ = 2.78 p.p.m. (aromatic hydrogen of the benzyl group); multiplet (3H) τ = 3.10–3.36 p.p.m. (aromatic hydrogen of the anisole ring); singlet (2H) τ = 5.48 p.p.m. (benzylic hydrogen); two singlets (3H each) τ = 6.30 and 6.66 p.p.m. (2 —OCH_3); two singlets (3H each) τ = 7.97 and 8.15 p.p.m. (2 —C(=O)—CH_3).

Preparation of the Acetylamino Diketone **19**

Compound **18** (10 g) was dissolved in methanol (200 ml) and 10% aqueous sodium hydroxide (40 ml) was added. The solution was refluxed for 1 h after which time the methanol was evaporated *in vacuo*, water (200 ml) was added, and the product extracted with chloroform. The chloroform extracts were washed with dilute hydrochloric acid, aqueous bicarbonate and water, dried, and evaporated to dryness. The residue (6.5 g) was practically homogeneous in t.l.c. and showed no acetoxy band in the i.r. spectrum. It was dissolved in ethanol (200 ml) and acetic acid (2 ml) was added. The solution was hydrogenated for 24 h at atmospheric pressure with 10% palladium on charcoal (2 g). The hydrogenation mixture was worked up as usual and gave after chromatography on silica gel (200 g, eluant chloroform–methanol 10:1) an oily product (4 g) which showed the absence of both the acetoxy and the benzyl group in the i.r. and the n.m.r. spectrum. This material was dissolved in acetone (250 ml) and the solution was cooled in an ice-bath to 5°. Jones' reagent was then added dropwise with stirring until the solution became orange. Stirring was continued for 20 min after which period the reaction mixture was neutralized with a saturated solution of sodium bicarbonate in water. The precipitate which had formed was filtered off and the filtrate was evaporated to dryness. The residue was suspended in water (50 ml) and extracted with chloroform (6 × 50 ml). The chloroform extract was dried, evaporated to dryness, and the residue was chromatographed on silica gel (400 g). Chloroform–methanol (25:1) eluted the pure epimer **19** as an oil which gradually crystallized to a low melting solid and was homogeneous in several t.l.c. systems. The yield was 2 g (50%).

Mol. Wt. Calcd. for $C_{21}H_{27}NO_5$: 373. Found (mass spectrometry): 373.

For the i.r. and n.m.r. spectra, see the Theoretical section.

Preparation of the Lactamol **21**

The diketone **19** (1.015 g) was dissolved in ethanol (50 ml) and a solution of potassium cyanide (0.54 g) in water (4 ml) was added. The mixture was heated under reflux for 18 h. The solvent was evaporated *in vacuo*, the residue was taken up in water (40 ml), and extracted with chloroform (6 × 50 ml). The chloroform extract was washed with dilute hydrochloric acid and water, dried, and evaporated to dryness. The crude product was chromatographed on silica gel (40 g). Chloroform–methanol (100:3) eluted the pure crystalline lactamol **21**. It was recrystallized from methanol to a melting point of 236–238°. The yield was 0.86 g (80%).

Anal. Calcd. for $C_{22}H_{28}N_2O_5$: C, 66.00; H, 7.00; N, 7.00. Found: C, 65.89; H, 6.69; N, 6.96.

Infrared spectrum (KBr pellet): 1670 and 1715 cm^{-1} (*N*-acetyl and five-membered lactam). Nuclear magnetic resonance spectrum: singlets (3H each) τ = 6.20 and 6.70 p.p.m. (2 —OCH_3); singlet (2H) τ = 6.54 p.p.m. (CH_2 unshielded by primary methoxyl); singlet (3H) τ = 8.10 p.p.m. (—C(=O)—CH_3). Mass spectrum: strong peak at *m/e* 382 (M—H_2O).

Preparation of the Keto Lactam **22**

The crystalline lactamol **21** (1.2 g) was heated under reflux with a mixture of methanol (30 ml) and concen-

Can. J. Chem. Downloaded from www.nrcresearchpress.com by 210.87.254.40 on 09/05/12
For personal use only.

trated hydrochloric acid (70 ml) for 24 h. After this time the solution was evaporated to dryness *in vacuo*. The residue was dissolved in chloroform and filtered through a column of neutral alumina (50 g). Evaporation of the filtrate yielded the pure crystalline keto lactam **22**. It was recrystallized from methanol and melted at 185–186°. The yield was 820 mg (80%).

Anal. Calcd. for $C_{20}H_{23}NO_4$ (mol. wt. 341): C, 70.50; H, 6.75; N, 4.12. Found (mol. wt. by mass spectrometry, 341): C, 70.49; H, 6.74; N, 4.36.

For i.r. and n.m.r. spectra, see the Theoretical section.

*Preparation of the Epimers **25** and **26***

The keto lactam **22** (400 mg) was dissolved in dry dioxane (20 ml) and heated under reflux for 24 h with an excess of lithium aluminium hydride (800 mg). After work-up in the usual manner 314 mg (85%) of reduced material were obtained. It was dissolved in dry pyridine (6 ml), acetic anhydride (5 ml) was added, and the mixture was allowed to stand overnight at room temperature. Work-up in the usual manner yielded 373 mg (92%) of the *N,O*-diacetate. This material was dissolved in methanol (6 ml) and a 10% aqueous potassium hydroxide solution (5 ml) was added to it. The reaction mixture was stirred overnight at room temperature. After this time the methanol was evaporated *in vacuo*, water (25 ml) was added, and the mixture was extracted with chloroform (7 × 50 ml). The chloroform solution was washed, dried, and evaporated to dryness. It yielded 311 mg of a colorless oil which showed two spots corresponding to the two epimeric alcohols **23** and **24** in a thin-layer chromatogram. The two epimers were separated by chromatography on silica gel (34 g). The epimer **23** (122 mg) was eluted with methanol–ether (3:100) and the epimer **24** (110 mg) with methanol–ether (5:100). Both compounds were oils homogeneous in t.l.c.

Compound **23** has an i.r. spectrum: 3395 cm^{-1} (—OH); 1621 cm^{-1} (N—C—CH_3; $\underset{\underset{O}{\|}}{}$); and an n.m.r. spectrum: multiplet (3H) τ = 2.99–3.15 p.p.m. (aromatic hydrogen); singlets (3H each) τ = 6.22, 6.69, and 7.88 p.p.m. (2 —OCH_3, N—C—CH_3; $\underset{\underset{O}{\|}}{}$).

Compound **24** has an i.r. spectrum: 3395 and 3595 cm^{-1} (—OH); 1625 cm^{-1} (N—C—CH_3; $\underset{\underset{O}{\|}}{}$); and an n.m.r. spectrum: multiplet (3H) τ = 2.95–3.15 p.p.m. (aromatic hydrogen); singlets (3H each) τ = 6.22, 6.71, and 7.93 p.p.m. (2 —OCH_3, N—C—CH_3; $\underset{\underset{O}{\|}}{}$).

The acetylamino alcohol **23** (130 mg) was dissolved in dry dioxane (7 ml) and a suspension of sodium hydride in mineral oil (30 mg) was added. The mixture was stirred overnight at room temperature. After this time dimethyl sulfate (0.25 ml) was added and the solution was heated under reflux for 12 h. The reaction mixture was cooled, water (20 ml) was added, and the solution was extracted with chloroform (7 × 50 ml). The chloroform extract was washed, dried, and evaporated to dryness. The crude product was chromatographed on silica gel (8.5 g). The compound **25** was eluted with benzene–chloroform (1:1) and recrystallized from ether to a constant melting point of 128–130°. The yield was 79 mg.

Mol. Wt. Calcd. for $C_{23}H_{31}NO_4$: 385. Found (mass spectrometry): 385.

For the i.r. and n.m.r. spectra, see the Theoretical section.

The methylation of the acetylamino alcohol **24** to compound **26** was performed in exactly the same manner. From 134 mg of **24** 87 mg of pure compound **26** were obtained. This material remained oily, but was completely homogeneous in t.l.c. and gave a mass spectrum identical with the mass spectrum of the crystalline epimer **25**.

Mol. Wt. Calcd. for $C_{23}H_{31}NO_4$: 385. Found (mass spectrometry): 385.

Infrared spectrum: no OH band; 1655 cm^{-1} (N—C—CH_3; $\underset{\underset{O}{\|}}{}$). Nuclear magnetic resonance spectrum: multiplet (3H) around τ = 3.20 p.p.m. (aromatic hydrogen), singlets (3H each) τ = 6.30, 6.73, 6.93, and 7.99 p.p.m. (3 —OCH_3, N—C—CH_3; $\underset{\underset{O}{\|}}{}$).

*Preparation of the Compounds **3** and **27***

The compound **25** (50 mg) was dissolved in pure acetone (20 ml) and the solution was cooled to 5°. Jones' reagent was added dropwise with stirring until the color of the reaction mixture changed from green to orange. Stirring was continued for 3 h 30 min after which time methanol (5 ml) was added and the mixture was neutralized with sodium bicarbonate. The precipitate was filtered off, the filtrate evaporated to dryness, dissolved in water (10 ml), and extracted with chloroform (6 × 25 ml). After washing and drying, the chloroform extract was evaporated to dryness and the residue was chromatographed on silica gel (15 g). Methanol–ether (8:92) eluted the pure compound **3**. It was an oil homogeneous in t.l.c. Its mass spectrum was identical with the mass spectrum of the crystalline epimer **27**. The yield was 40 mg.

Mol. Wt. Calcd. for $C_{23}H_{29}NO_5$: 399.2046. Found (mass spectrometry): 399.2042.

For the i.r. and u.v. spectra, see the Theoretical section.

The oxidation of compound **26** was performed in exactly the same manner. From 40 mg of **26** 30 mg of compound **27** were obtained. The material was purified by preparative t.l.c. on silica gel and crystallization from ether. It melted at 197–199°.

Mol. Wt. Calcd. for $C_{23}H_{29}NO_5$: 399. Found (mass spectrometry): 399.

Infrared spectrum (KBr pellet): 1678, 1645 and 1600 cm^{-1}. For the u.v. spectrum, see the Theoretical section.

Acknowledgments

We wish to thank the National Research Council of Canada for generous support of this work. We also thank Hoffmann-La Roche Inc.,

Nutley, New Jersey, and Schering Corporation, Bloomfield, New Jersey, for grants which helped to cover part of the costs.

1. *a*) K. WIESNER, F. BICKELHAUPT, D. R. BABIN, and M. GÖTZ. Tetrahedron Letters, No. 3, 11 (1959). *b*) K. WIESNER, M. GÖTZ, D. L. SIMMONS, L. R. FOWLER, F. W. BACHELOR, R. F. C. BROWN, and G. BÜCHI. Tetrahedron Letters, No. 2, 15 (1959).
2. K. WIESNER, M. GÖTZ, D. L. SIMMONS, and L. R. FOWLER. Collection Czech. Chem. Commun. **28**, 2462 (1963).
3. K. WIESNER, F. BICKELHAUPT, D. R. BABIN, and M. GÖTZ. Tetrahedron, **9**, 254 (1960).
4. K. WIESNER, K. K. CHAN, and C. DEMERSON. Tetrahedron Letters, 2893 (1965).
5. H. LEUCHS, M. GIUA, and J. F. BREWSTER. Chem. Ber. **45**, 1960 (1912).
6. J. W. CORNFORTH, R. H. CORNFORTH, and R. ROBINSON. J. Chem. Soc. 689 (1942).
7. K. WIESNER and J. ŠANTROCH. Tetrahedron Letters, 5939 (1966).

Can. J. Chem. Downloaded from www.nrcresearchpress.com by 210.87.254.40 on 09/05/12
For personal use only.

Can. J. Chem. Downloaded from www.nrcresearchpress.com by 210.87.254.6 on 09/05/12
For personal use only.

Photochemistry of nitroso compounds in solution.[1] X. The reaction pattern of photo-excited nitrosamides

Y. L. CHOW, N. S. TAM, AND A. C. H. LEE
Department of Chemistry, Simon Fraser University, Burnaby 2, British Columbia

Received October 10, 1968

The initial step in photolysis of alkyl *N*-nitrosamides **1** and **2** has been shown to be homolysis of the N—N bond, giving amidyl radicals and nitric oxide. Under the reaction conditions nitric oxide disproportionated, in part, to NO_2 and NO_3 radicals. The amidyl radicals abstracted hydrogen atoms intermolecularly from the solvent as well as intramolecularly from the δ-carbon of the alkyl chain, but not from that of the acyl chain. The combined pathways lead to the observed products as shown in Schemes 1 and 2. By this photolysis, the functionalization at the unactivated δ-carbon site of the alkyl chain could be achieved in 55% yield.

Canadian Journal of Chemistry, **47**, 2441 (1969)

Recent studies (1–6) have established that amidyl radicals can abstract a hydrogen atom from a saturated carbon center. We, as well as other groups,[2] have been studying the photolysis of nitrosamides aiming to unravel the reactions of transient amidyl radicals. We now amplify the preliminary report (7) to describe the detailed reaction pattern of nitrosamide photolysis. In particular we were concerned with intramolecular reaction of acyclic amidyl radicals. Since photolysis of nitrosamides in protic solvent gave complicated mixtures (8), the present work concentrated on reactions in hydrocarbon solvents.

Results

Owing to thermal lability of nitrosamides (9), all the preparations and photolyses of these compounds were carried out at a temperature near or below ambient. The crude nitrosamides **1** and **2** were not purified further and exhibited the expected physical properties as summarized in Table I. The apparatus and procedure of the irradiation were described in detail in Experimental. The photodecompositions of the nitrosamides were shown to follow zero-order kinetics up to 75% completion.

The photolysis of *N*-nitroso-*N*-(4-phenylbutyl)-acetamide (**1***a*) in petroleum ether gave *anti*-*N*-(4-phenyl-4-oximinobutyl)acetamide (**3***a*) and *N*-(4-phenylbutyl)acetamide. The structure of the former was determined by the conversion of the oxime to *N*-(4-phenyl-4-oxobutyl)acetamide (**4**) and further to 2-phenylpyrrolidine *p*-toluenesulfonamide (**5**) by standard methods. The *anti*-configuration of the oxime was decided by the nuclear magnetic resonance (n.m.r.) triplet signal τ 7.1 (N=C—CH_2—) by analogy with the chemical shift (τ 7.22) of the α-protons of β-methylbutyrophenone oxime (10). Careful chromatography revealed no other type of oxime (or corresponding *C*-nitroso compound) in the product.

The photolysis of *N*-nitroso-*N*-hexylacetamide (**1***c*) in benzene yielded the *trans*-dimer of *N*-(4-nitrosohexyl)acetamide (**6**) and the parent amide (**7**) in nearly equal amount. The structure of **6** was proven by conversion to *N*-(4-oxohexyl)-acetamide (**8**) through a depolymerization, tautomerization, and deoximation sequence. Decoupling experiments of **8** at 100 Mc.p.s. demonstrated the presence of the CH_3CH_2CO moiety with the chemical shifts at τ 8.99 (t) and 7.56 (q, J = 7 c.p.s.). The *trans* configuration of the dimer **6** was indicated by the strong infrared (i.r.) absorption at 1205 cm^{-1} (11, 12).[3] Careful chromatography did not reveal any γ- or ε-nitroso[4] derivatives isomeric to **6**, but instead afforded *N*-nitro-*N*-hexylacetamide (**9**) and a nitrato derivative of *N*-hexylacetamide. In agreement with an authentic sample prepared according to the known procedure (13), **9** exhibits the typical i.r. absorption at 1720, 1630, and 1570

[1]Part IX of this series; Y. L. Chow and C. J. Colon. Can. J. Chem. **45**, 2559 (1968).

[2]The authors are grateful to Dr. O. E. Edwards of the National Research Council of Canada, and Dr. L. P. Kuhn of Aberdeen Proving Ground, Maryland, who have informed us of their independent studies.

[3]The *trans*-dimers have been shown to isomerize upon low temperature irradiation (320–360 mμ region) to the *cis*-dimers which revert to the *trans*-dimers again on warming to −70° (see ref. 19).

[4]The Greek alphabets γ, δ, and ε refer to the positions of carbon chain with respect to the amide nitrogen atom, throughout this report.

TABLE I

Physical properties of nitrosamides

Nitrosamide	Infrared (cm^{-1})	Nuclear magnetic resonance (τ value)	Ultraviolet (mμ)
$C_6H_5(CH_2)_4$—N(NO)—C(=O)—CH_3	1730 1510	7.2 (s, 3H) 6.3 (m, 2H)	382, 397 415, 435
C_6H_{13}—N(NO)—C(=O)—H	1730 1520	6.3 (t, 2H) 0.63 (s, 1H)	388, 408 426
C_6H_{13}—N(NO)—C(=O)—CH_3	1725 1503	7.28 (s, 3H) 6.29 (t, 2H)	395, 406 425
C_5H_{11}—C(=O)—N(NO)—CH_3	1725 1500	9.09 (t, 3H) 7.00 (s, 3H) 6.92 (t, 2H)	376, 390 408, 427

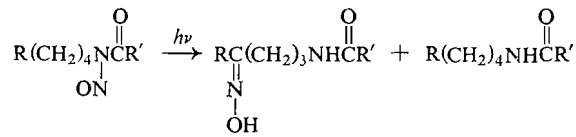

1 **3**

a: R = C_6H_5, R′ = CH_3 *b*: R = CH_2CH_3, R′ = H

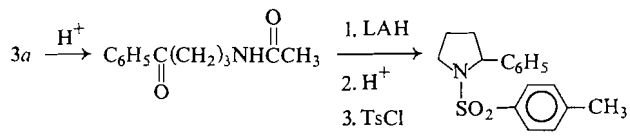

4 **5**

cm^{-1} and the methyl singlet (for the CH_3CO group) at very low field[5] of τ 6.43. The nitrato compound did not have the ester group on C-5 since the methyl signal in the n.m.r. spectrum was triplet. Since selective δ-hydrogen abstraction is the rule in the photolysis (2), it is almost certainly *N*-(4-nitratohexyl)acetamide (**10**).

The optimum condition for the formation of the *C*-nitroso dimer (**6**) was found to be the exposure of an *n*-pentane solution of **1***c* in sunlight for several days, from which **6** deposited in 40–45% yield. A similar irradiation of *N*-nitroso-*N*-hexylformamide (**1***b*) with sunlight, however, afforded *N*-(4-oximinohexyl)formamide (**3***b*) in 28% yield, in addition to the parent amide. That **3***b* was a mixture of *anti* and *syn* isomers was shown by the superimposed triplets at τ 7.3–7.9. The low yield was probably due to the thermal instability of **1***b* by which it decomposed to *n*-hexylformate (9).

The formation of **9** and **10** from **1***c* was reminiscent of the nitric oxide disproportionation reaction (14–16) and led us to examine similar

[5]The drastic shift to a downfield of this methyl proton must be due to the anisotropic effect of the nitro group.

Can. J. Chem. Downloaded from www.nrcresearchpress.com by 210.87.254.6 on 09/05/12
For personal use only.

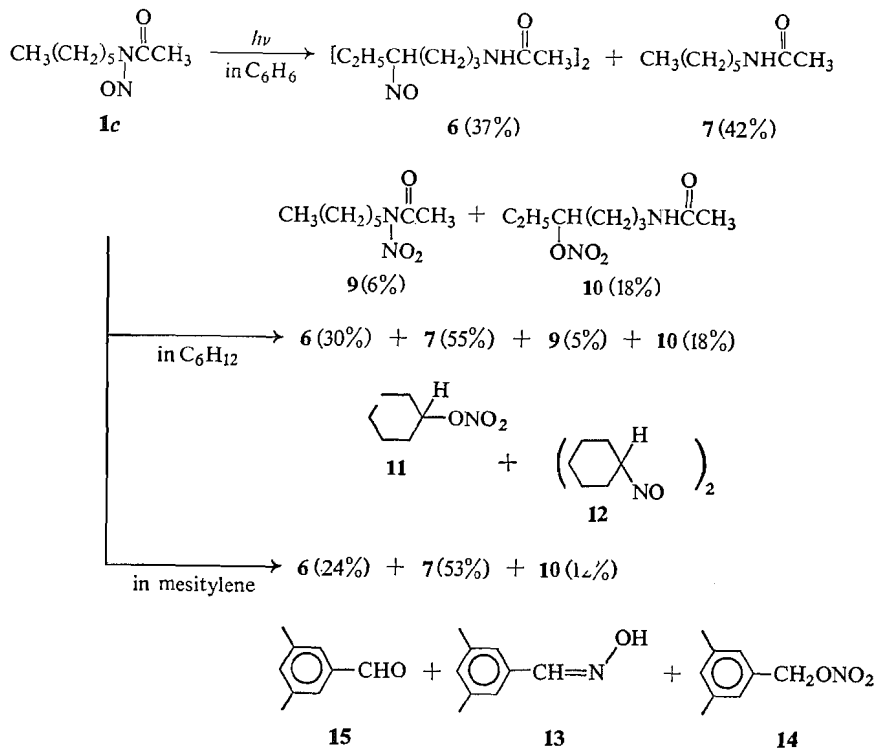

SCHEME I

photolysis in hydrogen donating solvents. The results are summarized in Scheme 1. While the yields of the parent amide **7** increased considerably at the cost of the intramolecular hydrogen exchange products (**6** and **10**), small amounts of the products derived from an intermolecular hydrogen exchange reaction were also obtained. When the photolysis was run in cyclohexane, the products were the *trans*-dimer of nitrosocyclohexane (**12**)[6] (17) and cyclohexylnitrate (**11**); when run in mesitylene, they were 3,5-dimethylbenzaldehyde (**15**) and its oxime (**13**), and 3,5-dimethylbenzylnitrate (**14**). The identity of these compounds was confirmed from their expected spectroscopic data (see Experimental).

The photolysis of *N*-nitroso-*N*-methylhexanamide (**2**, see Scheme 2) in benzene was shown to afford the parent amide (**16**), *N*-nitro-*N*-methylhexanamide (**17**) and the trimer of *N*-formylidenehexanamide (**18**). No intramolecular nitroso–hydrogen exchange product similar to **6** and **10** was obtained. The i.r. spectrum of **18** was consistent with *N*,*N*′,*N*″-trihexanoylhexahydro-*s*-triazine which gave *m*/*e* 281 as the highest mass peak equivalent to M^+-($C_5H_{11}COH$). The N—CH_2—N ring protons show an irregular multiplet due to restricted rotation about N—CO bonds (18, 19). When moisture was not rigorously excluded, hexanamide was isolated instead of **18**. The structure of the nitramide **17** was determined by spectroscopy, analogous to that used for the nitramide **9**. In cyclohexane, the photolysis yielded hexanoic acid, in addition to the nitrate **11** and the *C*-nitroso dimer **12**. Predictably, in a mesitylene solution the photolysis gave, in addition to **16**, good yields of **13**, **14**, and **15**. Variations of the photolysis conditions did not prove to be effective in producing the intramolecular nitroso–hydrogen exchange reaction. It should be added that dimeric compounds derived from solvents (such as dicyclohexyl and 1,2-diphenylethane) were not detected although the photolyzates were extensively analyzed by vapor-phase chromatography.

[6]It is interesting to point out that the *C*-nitroso dimer corresponding to crossed dimerization of nitrosocyclohexane and *N*-(4-nitrosohexyl)acetamide was not isolated from the photolyzate.

Can. J. Chem. Downloaded from www.nrcresearchpress.com by 210.87.254.6 on 09/05/12
For personal use only.

Can. J. Chem. Downloaded from www.nrcresearchpress.com by 210.87.254.6 on 09/05/12
For personal use only.

In order to prove the free radical chain process, the quantum yield of the disappearance of the nitrosamides was determined using potassium ferric oxalate actinometry (20). In benzene solutions, the nitrosamide **1***c* gave $\Phi = 2.5 - 3$ while **2** gave $\Phi = 2 - 2.5$.

Discussion

To facilitate the clarity of the discussion, hydrogen abstractions and the formation of *C*-nitroso compounds (and the derivatives thereof) will be described first, followed by the disproportionation of nitric oxide and the by-products therefrom.

Formation of C-Nitroso Compounds

The amidyl free radicals derived from the photolysis of nitrosamides **1** apparently undergo, in part, an intramolecular hydrogen abstraction from the δ-position via a favored transition state (**1** → **19** → **20**) in analogy with the abstraction mechanism proposed by Barton *et al.* (1) and Akhtar (2) and Walling and Padwa (21). The δ-nitroso amides (**21**) are then formed by a reaction of **20** with either another molecule of **1** (chain propagation) or nitric oxide in the bulk (chain termination).

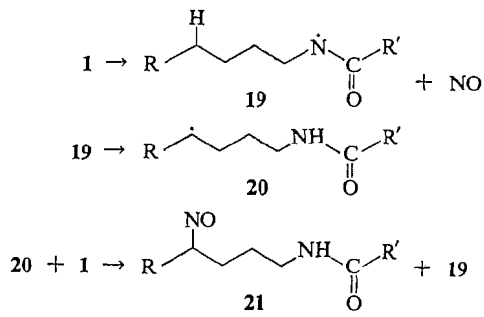

20 + NO → **21**

19 (or20) + SH → S· + **7**

Concurrently an intermolecular hydrogen abstraction by **19** or **20** from the solvent (SH) is expected to compete with the intramolecular hydrogen abstraction process, though not favorably in view of lack of hydrogen abstraction exhibited by amidyl radicals (22–25) and a low entropy factor involved in an intramolecular reaction. The formation of *C*-nitroso compounds (S—NO) derived from the solvent is thus analogous to the intramolecular hydrogen–nitroso group exchange mechanism; the increased yield of the parent amide **7** in cyclohexane and mesitylene is thus to be expected. A possibility of hydrogen abstraction by nitric oxide is considered to be unimportant in view of the reported inertness of this radical (26–28).

Spontaneous formation of *trans*-dimers from *C*-nitroso compounds (**21** and S—NO) leads to **6** and **12** (11). We have demonstrated as other groups have also done (12) that a *C*-nitroso dimer[7] upon irradiation in a Pyrex vessel dissociates to a *C*-nitroso monomer, which slowly tautomerizes to the corresponding oxime. The oxime **3***b* is formed from over-irradiation while **3***a* is favored over the corresponding *C*-nitroso dimer from a facile tautomerization (29). The complete absence of the γ-nitroso (or corresponding γ-oximino) derivative in the photolysis of **1** indicates such intramolecular hydrogen transfer must be highly selective.

It is surprising that the product due to intramolecular hydrogen–nitroso exchange does not form at all when the nitrosamide **2** is photolyzed under various conditions. This implies that intramolecular hydrogen abstraction similar to the process **19** → **20** does not take place with the *N*-methylhexanamidyl radical, which is certainly formed as indicated by the presence of the intermolecular hydrogen–nitroso group exchange products **12** and **13**. That an amidyl free radical does not intramolecularly abstract a δ-hydrogen atom of the acyl chain was also confirmed by other groups (5, 6). Interestingly, in the photolysis of *N*-haloamides (1, 3, 4), varied extents of δ-hydrogen abstraction from the acyl side chain took place depending on the type of halogen substitution and the type of *N*-alkyl group. Two plausible explanations, based on the stereochemistry of the transition state, have been postulated, one by us in our brief communication (7) and the other by Kuhn *et al.* (6). Since no new evidence is available for a refinement, no further comment is necessary at this stage.

In a benzene solution (Scheme 2) since both hydrogen abstraction pathways are blocked, the hexanamidyl radical undergoes a disproportionation reaction involving a β-scission of the C—H bond to give *N*-formylidenehexanamide which is isolated as the trimer **18** or as hexanamide

[7]A *C*-nitroso dimer usually has a strong ultraviolet absorption in the 280 mμ region which tails strongly above 300 mμ.

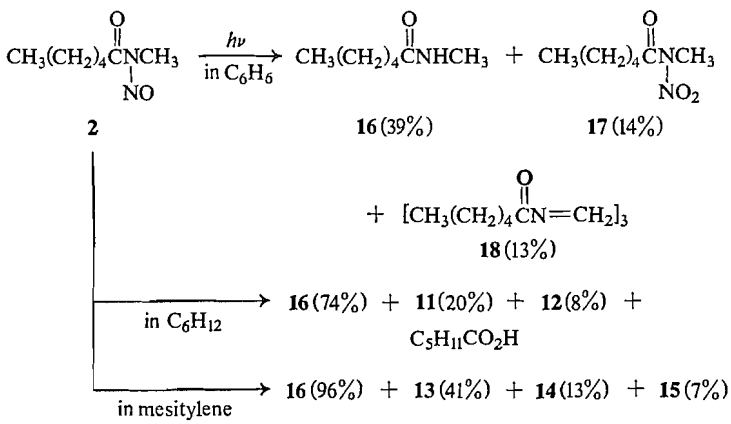

SCHEME 2

(see Experimental). The β-scission of the C—H bond in an alkoxy radical (30) is highly endothermic (31) and, therefore, a scarcely known process except as a part of a disproportionation reaction. Energetically the β-scission process of an amidyl radical is expected to be even more endothermic[8] than that of an alkoxyl radical (31). The overall results, therefore, demonstrate that the intramolecular hydrogen abstraction from the acyl chain is an extremely unfavorable process requiring even higher energy than the β-scission process.

Formation of By-products

The present nitrosamide photolysis differs from the nitrite photolysis (2) in that *N*-nitramides (**9** and **17**) and nitrates (**10**, **11**, and **14**) are formed as the by-products. These products are obviously derived from a combination of the hydrogen transfer reactions and a disproportionation of nitric oxide. Although by itself nitric oxide is unreactive (14), in the presence of a catalytic amount of nitrogen dioxide (and therefore of air), it displays a complex pattern of ill-defined redox reactions (14–16). Whatever the processes are, nitric oxide appears to be disproportionated to N_2, $\cdot NO_2$, and $\cdot NO_3$ (and probably N_2O also) (32) in the process of interacting with a free radical. Reaction of the respective carbon radicals (**20** and S·) with $\cdot NO_3$ would give **10**, **11**, and **14** and that of nitrogen radicals (**19**) with $\cdot NO_2$, **9**, and **17**. These reactions also serve as the chain termination steps. The observed by-products could not be due to an oxidation by traces of oxygen impurity in the nitrogen since the % yields were not significantly changed under various rates of nitrogen purging (down to nil). To form (6 + 18%) of **9** and **10** would have required 52 ml of oxygen if it was the source of these products. This seems impossible in view of the purity of the nitrogen.

3,5-Dimethylbenzaldehyde is probably not derived from the hydrolysis of **13** which is shown to be stable under these conditions. It can be visualized as formed by the elimination of nitrous acid from **14**, which was indeed found to decompose similarly during the working up.

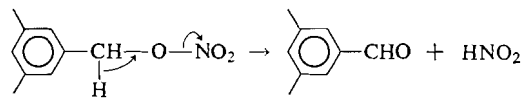

14 **15**

Other oxidation processes are also possible, particularly if the disproportionation of ·NO generates a singlet state O_2 (32), and cannot be excluded at this stage. The formation of hexanoic acid from the photolysis of **2** in cyclohexane was quite unexpected since the thermal decomposition was shown to be absent in the control. Any speculation on the pathway leading to hexanoic acid seems futile unless a far reaching assumption can be made. In any case, the original aim of functionalization at the δ-carbon atom could be achieved readily with a reasonably good yield (up to 55%) which compares favorably with nitrite photolyses.

[8]The heat of formation of an amidyl free radical is expected to be lower than that of an alkoxy free radical since the former is resonance stabilized.

Can. J. Chem. Downloaded from www.nrcresearchpress.com by 210.87.254.6 on 09/05/12
For personal use only.

Can. J. Chem. Downloaded from www.nrcresearchpress.com by 210.87.254.6 on 09/05/12
For personal use only.

Lastly, the evidence outlined above proves that photolyses of nitrosamides operate exclusively through cleavage of the N—NO bond in sharp contrast to the exclusive N—CO cleavage in the thermolysis of nitrosamides (9). It is indeed very extraordinary that such a clear-cut difference in the bond-breaking process is operating in nitrosamides. We have suggested previously that this difference may be ascribed to the different excited states (vibrational or electronic) from which the bond-breaking processes take place (8).

Experimental

Unless specified otherwise, the i.r. spectra were taken in liquid phase with a Unicam SP 200 spectrophotometer, the n.m.r. spectra in carbon tetrachloride solution with a Varian A56/60 instrument (using TMS as an internal standard), the u.v. spectra were obtained in cyclohexane solution with a Cary 14 spectrophotometer, and the mass spectra were taken at 80 eV with a heated inlet using a Hitachi–Perkin–Elmer RMU-6E instrument. The melting points were taken in a Fisher–Johns hot stage and were uncorrected. The actinometry followed the procedure of Hatchard and Parkers (20). The silicic acid chromatography was carried out with silicic acid by Mallinckrodt, (100 mesh) and chloroform (Shawinigan Chemicals). The pure grade nitrogen (99.995%) was scrubbed with Fieser's solution and dried with sulfuric acid before being introduced to the reaction vessel. The coupling pattern of the n.m.r. spectra was denoted by t (triplet), d (doublet), q (quartet), and m (multiplet), and the number of protons was expressed by *H*. The microanalyses were performed by Dr. A. Bernhardt, West Germany.

Preparation of N-Nitrosamides

The nitrosamides were prepared by nitrosation of the respective amides with excess sodium nitrite in a mixture of acetic acid and acetic anhydride as described in the previous paper (8). Their physical properties are summarized in Table I.

General Procedure of Photolysis

The photolysis was generally carried out in a flat Pyrex flask in order to spread the solution wide and thin and, thus, to increase the irradiation area. Into this flask, a solution (100 ml) about 0.1 *M* in nitrosamide was introduced. The solution was kept under a nitrogen atmosphere. The flask was submerged in a cooling water-bath. In all cases, the temperature of the photolysis was controlled by the running cold water (ca. 10–15°). The solution was irradiated with a G.E. Par 38 (black light) spot lamp unless specified otherwise. The photolysis was continued until the typical u.v. absorption of the nitrosamides (420–430 mμ region) disappeared completely. At intervals aliquots were withdrawn and were diluted (1/10) to record the u.v. absorbance. A plot of the optical density against time gave a straight line up to 75% completion. The plot curved upward slightly from this point. A small portion of the photolysis solution was placed in a flask covered with aluminium foil. This flask was placed in the same water bath as the photolysis apparatus. The u.v. absorption spectrum of this solution remained unchanged over the entire period of photolysis showing that no thermal reaction took place.

*Photolysis of N-Nitroso-N-(4-phenylbutyl)acetamide (**1a**)*

The nitrosamide **1***a* (5.03 g) in petroleum ether (100 ml) was irradiated for 31 h to give a supernatant solution and an oily precipitate. The solution was evaporated to give a liquid which was shown to be mainly 4-phenylbutylacetate by the i.r. (1705, 1630, 1604, and 1262 cm^{-1}) and the n.m.r. (τ 6.34, t, J = 7.5 c.p.s.) spectra.

A liquid (3.98 g) was obtained after the solvent was removed from the oil. The liquid (1 g) was chromatographed on a neutral alumina column. Elution with chloroform–benzene (1:9) gave 4-phenylbutylacetamide (317 mg), the i.r. and n.m.r. spectra of which were shown to be identical with those of an authentic sample. Elution with 2% ethanol in chloroform gave crystals (335 mg) which were recrystallized from ethanol–petroleum ether to yield **3***a*, m.p. 112–113°. **3***a* gave i.r. absorptions at 3360, 1618, 1572, 940, 758, and 690 cm^{-1}; n.m.r. signals at τ 8.25 (q, J = 6.5 c.p.s., 2H), 8.04 (s, 3H), 7.1 (t, J = 7 c.p.s., 2H), and 6.72 (q, J = 6.5 c.p.s., 2H) and λ_{EtOH} 243 mμ.

Anal. Calcd. for $C_{12}H_{16}N_2O_2$: C, 65.42; H, 7.32; N, 12.72. Found: C, 65.45; H, 7.36; N, 12.92.

The liquid (1.2 g) was hydrolyzed with 1 *N* methanolic hydrochloric acid (250 ml). The total extract (408 mg) from the hydrolysis was reduced with lithium aluminium hydride (5.2 g) by refluxing in tetrahydrofuran (80 ml). The basic extract of this reduction was treated with *p*-toluenesulfonyl chloride in 10% sodium hydroxide solution. The precipitate was chromatographed on a silicic acid column to yield pale-yellow crystals which were recrystallized from methanol–petroleum ether to yield **5**, m.p. 103–105 °C. **5** gave i.r. absorptions at 1600 (w), 1343(s), and 1154(s) cm^{-1}; n.m.r. signals at τ 5.2 (t, J = 5 c.p.s., 1H) 6.9 (m, 2H), 7.6 (s, 3H); mass peaks at 301 (9.6%), 224 (30.2%), 155 (19.8%), 146 (100%), and 91 (67%).

When the total extract of the acid hydrolyzate was chromatographed on a neutral alumina column, a white solid was obtained on elution with chloroform. The solid was recrystallized to afford 4-phenyl-4-ketobutylacetamide (**4**), m.p. 93–94.5°; n.m.r. signals at τ 8.02 (s, 3H), 6.92 (t, 2H), 6.64 (t, 2H), 2.5 (m, 3H), and 2.05 (m, 2H); i.r. peaks at 3350, 1680, 1630, and 1560 cm^{-1}.

*Photolysis of N-Nitroso-N-hexylformamide (**1b**)*

The nitrosamide **1***b*, (5.99 g) in *n*-pentane (100 ml) was photolyzed for 10 days in sunlight to give an oily precipitate and a supernatant solution. The solution gave, after removal of the solvent, a liquid (1.12 g) which possessed a strong i.r. peak at 1775 cm^{-1} (hexyl formate). The oil was stripped off the *n*-pentane to give a liquid (4.6 g). A part of the liquid (1.99 g) was chromatographed on an alumina column. Elution with chloroform–benzene (1:1) gave *N*-hexylformamide (405 mg) as was shown by the superimposable i.r. spectrum with that of an authentic sample. Elution with 5% ethanol in chloroform gave an oil (727 mg) which was distilled to afford a *syn* and *anti* mixture of *N*-4-oximinohexylformamide (**3***b*). **3***b* gave n.m.r. signals at τ 8.9 (t, J = 7.5 c.p.s., 3H), 7.3–7.9 (m, 4H), 6.7 (q, J = 6.2 c.p.s.), 1.85 (s, 1H); i.r. absorptions at

Can. J. Chem. Downloaded from www.nrcresearchpress.com by 210.87.254.6 on 09/05/12
For personal use only.

3400, 1670, 1550, and 940 cm^{-1}; mass peaks at *m/e* 158 (0.3%), 156 (2.0%), 141 (5.0%), 130 (1.8%), and 58 (100%).

Anal. Calcd. for $C_7H_{14}N_2O_2$: C, 53.15; H, 8.92. Found: C, 53.37; H, 8.82.

Photolysis of N-Nitroso-N-hexylacetamide (1c)

(*a*) The nitrosamide **1***c* (2.16 g) was photolyzed in benzene (100 ml) for 2 h. An oil (2.29 g) was obtained after evaporation of the solvent. The crude oil (1.67 g) was chromatographed on a silicic acid column to give the following compounds. The first fraction (109 mg) eluted with chloroform was distilled twice to give *N*-nitro-*N*-hexylacetamide (**9**). Infrared absorptions at 1720, 1630, 1570, 1300, 1220, and 1115 cm^{-1}; n.m.r. signals at τ 5.95 (t, J = 7 c.p.s., 2H), 6.43 (s, 3H), 9.1 (t, 3H); mass peak at *m/e* 141 ($M^+ - HNO_2$). The i.r. and n.m.r. spectra were superimposable with those of an authentic sample prepared according to the known method (13). The second fraction (550 mg) eluted with pure chloroform was *N*-hexylacetamide (**7**). The following fraction (350 mg) was vacuum distilled twice to give *N*-(4-nitratohexyl)acetamide (**10**); i.r. absorptions at 1630, 1550, 1275, 865, 755, and 700 cm^{-1}; n.m.r. signals at τ 9.1 (t, 3H), 8.20 (s, 3H), 6.78 (q, 2H), 5.0 (m, 1H); mass peaks at *m/e* 141 (14%), 100 (20%), 86 (30%), 82 (20%), 73 (70%), 72 (75%), 60 (50%), and 43 (68%). Under high vacuum distillation conditions (0.01 mm/80°), **10** decomposes slightly giving no satisfactory sample for analysis.

Elution with 2% methanol in chloroform gave a crystalline fraction (593 mg) which was recrystallized from acetone–pentane mixture to give *C*-nitroso dimer **6**, m.p. 125–127°. **6** has i.r. bands at 3280, 1646, 1555, 1205, and 1170 cm^{-1}; n.m.r. signals at τ 9.1 (t, J = 7 c.p.s., 3H), 8.0 (s, 3H), 6.75 (q, J = 6 c.p.s., 2H), and 4.60 (quintet, J = ca. 5 c.p.s., 2H). The cryoscopic molecular weight determination in water gave 336.

Anal. Calcd., for $C_{16}H_{32}N_4O_4$: C, 55.82; H, 9.36; N, 16.27. Found: C, 56.07; H, 9.35; N, 16.51.

These crystals **6** were warmed in levulinic acid over a water-bath for 2 h. After the usual working up, an oil was obtained which was distilled. The oil had i.r. bands at 3300, 1708, 1650, and 1555 cm^{-1}; n.m.r. signals at τ 8.99 (t, J = 7.2 c.p.s., 3H), 8.04 (s, 3H), 7.56 (q, J = 7.2, 2H), and 6.78 (q, J = 6.5 c.p.s., 2H). When the triplet at τ 8.99 was irradiated in a Varian HA-100 machine, the quartet at 7.56 collapsed to a singlet and vice versa.

The % yields[9,10] of the products are **6** (37%), **7** (42%), **9** (6%), and **10** (18%). The 2,4-dinitrophenylhydrazone of this oil was recrystallized from ethanol–water to give yellow needles, m.p. 119–121°.

Anal. Calcd. for $C_{14}H_{19}N_5O_5$: C, 49.82; H, 5.69; N, 20.76. Found: C, 49.89; H, 5.85; N, 20.81.

(*b*) The nitrosamide **1***c* (2.19 g) was similarly photolyzed in mesitylene (100 ml) for 1.5 h. Mesitylene was distilled off to give an oily residue (4.87 g). A similar chromatography gave, in order of elution, a hydrocarbon fraction (2.43 g), **14** (42 mg), **15** (42 mg), **13** (80 mg), **7** (960 mg), **10** (310 mg), and **6** (520 mg). The vapor-phase chromatographic analyses of the hydrocarbon fraction on an 8 ft SE-30 column at various temperatures showed only one corresponding peak to mesitylene. The % yields of the products were **6** (24%), **7** (53%), and **10** (12%).

(*c*) The nitrosamide **1***c* (1.01 g) in cyclohexane (100 ml) was irradiated for 2 h. Cyclohexane was evaporated to leave a yellow oil (1.11 g). The silicic acid chromatography of this oil (1.10 g) gave three fractions with chloroform. The first fraction (72 mg) was further distilled to an oily **11** which has i.r. absorptions at 1630, 1280, and 870 cm^{-1}; n.m.r. signals at τ 4.9 (broad, 1H) and 8.2 (10 H); mass peaks at *m/e* 145 and 98.

The second fraction (55 mg) was solid and was recrystallized from petroleum ether to give **12**, m.p. 112° (lit. (17) m.p. 116°); i.r. bands at 1390, 1260, and 1200 cm^{-1}; n.m.r. signals at τ 5.1 (broad, 1H) and 8.15 (broad, 10 H); mass peaks at *m/e* 113, 83, 55, and 41. The third fraction (58 mg) was distilled to give **9**. These fractions were followed by, in order of elution, **7** (453 mg), **10** (213 mg), and **6** (300 mg). The % yields of the products were **6** (30%), **7** (55%), **9** (5%), and **10** (18%).

(*d*) The nitrosamide **1***c* (3.12 g) in *n*-pentane (50 ml) was photolyzed in sunlight to give a crystalline deposit which could be recrystallized to give **6**. The oil obtained from pentane solution and the mother liquor were chromatographed on a silicic acid column to give **10** (795 mg) and more **6**. Total yield of **6** was 1.45 g.

Photolysis of N-Nitroso-N-methylhexanamide (2)

(*a*) The nitrosamide **2** (1.87 g) was photolyzed in benzene (100 ml) for 8 h. Benzene was removed by vacuum evaporation to leave an oil (1.78 g). The silicic acid chromatography of this oil (1.29 g) gave, with chloroform, an oil (212 mg) which was distilled twice to afford *N*-nitro-*N*-methylhexanamide (**27**); i.r. absorptions at 1720, 1620, 1570, 1300, and 1220 cm^{-1}; n.m.r. signals at τ 6.43 (s, 3H) and 7.10 (t, 2H). This was followed by **16** (435 mg) and then a solid fraction (136 mg) which was recrystallized from petroleum ether–benzene (1:1) mixture to give **18**, m.p. 172–176°; i.r. peak at 1655 cm^{-1}; n.m.r. signals at τ 5.32 (m, 2H), 7.8 (t, J = 6 c.p.s., 2H), and 9.1 (t, J = 6 c.p.s., 3H). The mass spectrum of **18** showed 281, 167, 127, and 71 peaks. Two more unidentified fractions were obtained. The % yields of the products were **16** (39%), **17** (14%), and **18** (13%).

(*b*) The nitrosamide **2** (1.78 g) was photolyzed in mesitylene (100 ml) for 3 h to afford a residue (4.39 g) after removal of the solvents. This oil was chromatographed on a silicic acid column to afford the following compounds in the order of elution. (*i*) 3,5-Dimethylbenzylnitrate (**14**, 262 mg); i.r. absorptions at 1630, 1270, 860, and 770 cm^{-1}; n.m.r. signals at τ 7.82 (s, 6H), 4.80 (s, 2H), 3.2 (m, 3H); mass peaks at *m/e* 181, 134, 133, 120, 105, and 91. (*ii*) 3,5-Dimethylbenzaldehyde (**15**, 115 mg), i.r. absorptions at 2870, 2730, 1700, 1650, 1570, and 860 cm^{-1}; n.m.r. signals at τ 7.6 (s, 6H), 2.6 (m, 3H), and 0.15 (s, 1H); M^+ of 134. (*iii*) 3,5-Dimethylbenzaldehyde oxime (**13**, 705 mg) which was recrystallized from petroleum ether, m.p. 125–127°; i.r. absorption at 1600, 1470, 1380, 995–960, and 860 cm^{-1}; n.m.r. signals at

[9]The % yields in this report were calculated based on one mole of the product being formed from one mole of the starting nitrosamide.

[10]The percentages were calculated from the results of a small scale column chromatography, a minor weighing error of which caused the total percentage to exceed 100. The percentages, however, accurately represent the ratio of the products.

τ 7.80 (s, 6H), 3.0 (m, 3H), and 2.08 (s, 1H); M^+ at 149. (*iv*) N-Methylhexanamide (**16**, 1.4 g). The % yields of the products were **16** (96%), **13** (41%), **14** (13%), and **15** (7%).

(*c*) A solution of the nitrosamide **2** (1.79 g) in cyclohexane (100 ml) was photolyzed for 3 h. Cyclohexane was evaporated to leave an oil (2.09 g). The oil (1.18 g) was chromatographed on a silicic acid column to give **11** (187 mg), **12** (59 mg), hexanoic acid (122 mg), and **14** (609 mg). Hexanoic acid was identified by comparing the i.r. spectrum with that of an authentic sample. The % yields of the products were **16** (74%), **11** (20%), and **12** (8%).

(*d*) The nitrosamide **2** (5.38 g) in petroleum ether (90 ml) was photolyzed in sunlight for 4 weeks. A brown liquid (5.65 g) was obtained when the solvent was removed. This oil (1.47 g) was chromatographed on a neutral alumina column. Elution with chloroform–benzene (1:9) gave **16** (224 mg). Elution with chloroform–benzene (1:1) gave a solid fraction (100 mg) which was sublimed to give white needles, m.p. 91–94° and mixture m.p. with an authentic hexanamide (m.p. 96–97°) 95–96°. The i.r. and the n.m.r. spectra of the needles were superimposable with those of hexanamide.

Acknowledgments

The authors are grateful for grants from the Defence Research Board in support of this research (DRB 9530-68) and for the capital equipment grants from the National Research Council of Canada for purchase of Hitachi–Perkin – Elmer RMU-6E mass spectrometer (E-1328).

1. D. H. R. Barton, A. L. J. Beckwith, and A. Goosen. J. Chem. Soc. 181 (1965).
2. M. Akhtar. *In* Advances in photochemistry. Vol. 2. Interscience Publishers, Inc., New York. 1964. pp. 263–303.
3. R. C. Petterson and A. Wambsgans. J. Am. Chem. Soc. **86**, 1648 (1964).
4. R. S. Neale, N. L. Marcus, and R. G. Schepers. J. Am. Chem. Soc. **88**, 3051 (1966).
5. O. E. Edwards and R. S. Rosich. Can. J. Chem. **45**, 1287 (1965).
6. L. P. Kuhn, G. G. Kleinspehn, and A. C. Duckworth. J. Am. Chem. Soc. **89**, 3858 (1967).
7. Y. L. Chow and A. C. H. Lee. Chem. Ind. 827 (1967).
8. Y. L. Chow and A. C. H. Lee. Can. J. Chem. **45**, 311 (1967).
9. E. H. White and G. A. Aufdermarsch, Jr. J. Am. Chem. Soc. **83**, 1174, 1179 (1961) and other references therein.
10. N. S. Bhacca, L. F. Johnson, and J. N. Shoolery. Nuclear magnetic resonance spectra catalog. Vol. 2, No. 585. Varian Associates. Palo Alto, California. 1962.
11. B. G. Gowenlock and W. Lüttke. Quart. Rev. 321 (1958).
12. A. Mackor, Th. A. J. W. Wajer, and Th. J. de Boer. Tetrahedron Letters, 2757 (1967).
13. E. H. White and D. W. Grisley, Jr. J. Am. Chem. Soc. **83**, 1191 (1961).
14. J. F. Brown, Jr. J. Am. Chem. Soc. **79**, 2480 (1957).
15. E. Weitz, L. Müller, and K. Dinges. Chem. Ber. **85**, 878 (1952).
16. F. H. Westheimer, E. Segel, and R. Schramm. J. Am. Chem. Soc. **69**, 776 (1947).
17. E. Müller and H. Metzger. Chem. Ber. **88**, 165 (1955); **90**, 1179 (1957).
18. W. D. Phillips. J. Chem. Phys. **23**, 1363 (1955).
19. H. S. Gutowsky and C. H. Holm. J. Chem. Phys. **25**, 1228 (1956).
20. C. G. Hatchard and C. A. Parkers. Proc. Roy. Soc. A, **235**, 518 (1956).
21. C. Walling and A. Padwa. J. Am. Chem. Soc. **83**, 2207 (1961).
22. R. E. Pearson and J. C. Martin. J. Am. Chem. Soc. **85**, 354, 3142 (1963).
23. G. A. Russell, C. DeBoer, and K. M. Desmond. J. Am. Chem. Soc. **85**, 365 (1963).
24. C. Walling, A. L. Rieger, and D. D. Tanner. J. Am. Chem. Soc. **85**, 3129 (1963).
25. C. Walling and A. L. Rieger. J. Am. Chem. Soc. **85**, 3134 (1963).
26. R. G. W. Norrish and G. L. Pratt. Nature, **197**, 143 (1965).
27. M. H. Back and K. J. Laidler. Can. J. Chem. **44**, 215 (1966).
28. B. G. Gowenlock. *In* Progress in reaction kinetics. Vol. 3. *Edited by* G. Porter. The Pergamon Press, Ltd., Oxford. 1965. p. 171.
29. Y. L. Chow, S. C. Chen, and C. J. Colon. J. Org. Chem. **32**, 2109 (1967).
30. E. R. Bell, J. H. Raley, F. F. Rust, F. H. Seubold, and W. E. Vaughan. Discussions Farad. Soc. **10**, 242 (1951).
31. P. Gray and A. Williams. Chem. Rev. **59**, 239 (1959).
32. O. P. Strausz and H. E. Gunning. Can. J. Chem. **39**, 2549 (1961).

Can. J. Chem. Downloaded from www.nrcresearchpress.com by 210.87.254.6 on 09/05/12
For personal use only.

Can. J. Chem. Downloaded from www.nrcresearchpress.com by 210.87.254.105 on 09/05/12
For personal use only.

Alkaloids of *Lycopodium alopecuroides*. Part 2. Alopecurine, a new type of Lycopodium alkaloid

W. A. AYER, B. ALTENKIRK, N. MASAKI, AND S. VALVERDE-LOPEZ
Department of Chemistry, University of Alberta, Edmonton, Alberta

Received February 17, 1969

Alopecurine, a pentacyclic Lycopodium alkaloid, has been shown to possess structure **1**. The structure, including the absolute stereochemistry, was established by X-ray analysis of debenzoylalopecurine hydrobromide, and further confirmed by X-ray analysis of alopecurine methobromide. Some chemical and spectroscopic properties of alopecurine are described. The isolation of four alkaloids in addition to those already reported from *L. alopecuroides* is described. These alkaloids include the known compound fawcettidine and three new bases, acetyldebenzoylalopecurine, alolycopine, and lycopecurine.

Canadian Journal of Chemistry, 47, 2449 (1969)

In Part 1 of this series (1) we reported on the isolation and characterization of alopecurine, $C_{23}H_{29}O_3N$, an alkaloid of *Lycopodium alopecuroides* L. It was shown that alopecurine contains a benzoyloxy group, a hydroxyl group, and a tertiary nitrogen and that the alkaloid is probably pentacyclic. We now wish to report that alopecurine possesses structure **1**, a new type of ring system for this group of alkaloids.

A study of the nuclear magnetic resonance (n.m.r.) spectrum of alopecurine (Fig. 1) indicates that the benzoyloxy group is located in the environment shown in part structure **2**. The signal for the proton geminal to the benzoyloxy group (H_a) appears as a complex multiplet ($w_{1/2} \simeq 15$ c.p.s., axial proton (2)) centered at τ 4.65. By spin decoupling of H_a it is possible to locate the signals due to the protons labelled

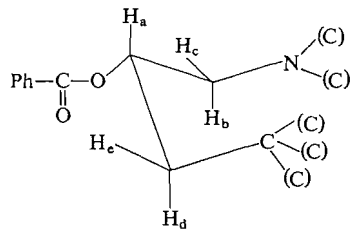

2

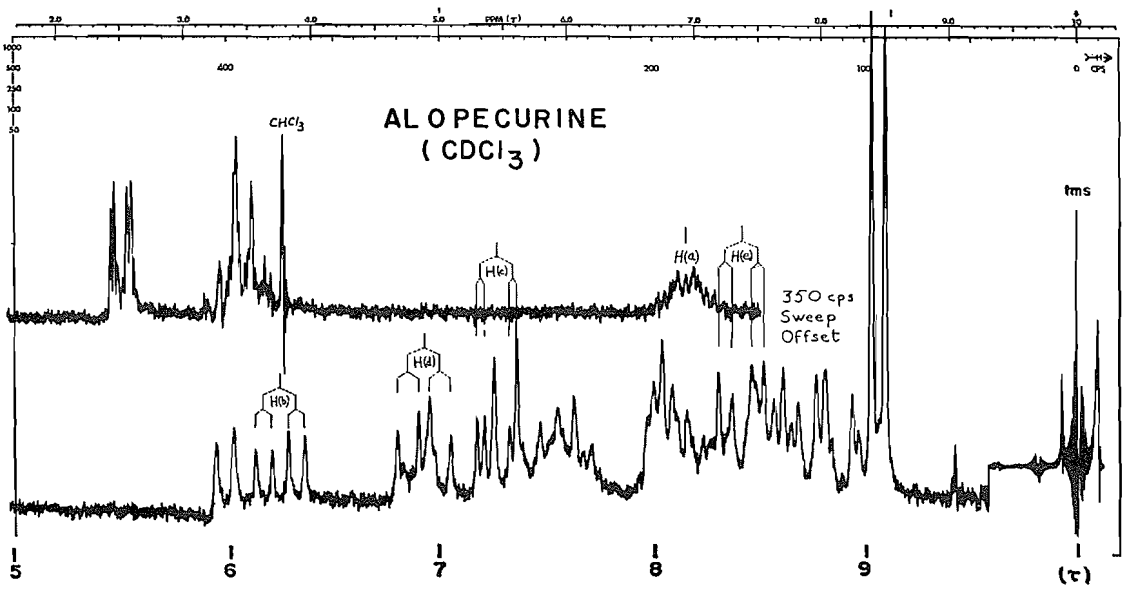

FIG. 1. Nuclear magnetic resonance spectrum (100 Mc.p.s.) of alopecurine in $CDCl_3$.

Can. J. Chem. Downloaded from www.nrcresearchpress.com by 210.87.254.105 on 09/05/12
For personal use only.

H_b, H_c, H_d, and H_e in **2**. Simultaneous irradiation of H_a causes the quartet (J = 7.5 and 15.5 c.p.s.) centered at τ 6.25 to collapse to a doublet (splitting 15.5 c.p.s.). Irradiation at τ 6.25 not only simplifies the multiplet at τ 4.65 but also causes the partially obscured quartet (J = 5 and 15.5 c.p.s.) centered at τ 7.28 to collapse to a doublet (splitting 5 c.p.s.). Triple irradiation (τ 4.65 and τ 7.28) causes the quartet at τ 6.25 to collapse to a singlet. In a similar manner the other two protons vicinal to H_a were located. The chemical shifts and coupling constants for these protons are given in Table I.

Of the four methylene protons, the one at lowest field (τ 6.25) was assumed to be on a carbon α to nitrogen to account for its chemical shift and was assigned the axial conformation because of its relatively large vicinal coupling. The signal at τ 6.93 is assigned to the axial proton (H_d), again on the basis of its vicinal coupling constant (10 c.p.s.). It is assumed that the 15 and 15.5 c.p.s. couplings are geminal couplings (3). Since neither H_d nor H_e is further coupled, it appeared that this methylene group is linked to a quaternary carbon.

The doublet (J = 8 c.p.s.) at τ 5.98 in the n.m.r. spectrum of alopecurine is due to the proton geminal to the hydroxyl group, since this signal is shifted to τ 4.80 in *O*-acetylalopecurine and is not present in the spectrum of dehydroalopecurine, prepared by Jones' oxidation of alopecurine. Dehydroalopecurine shows carbonyl absorption at 1715 and 1690 cm^{-1}, the former attributed to the benzoyloxy carbonyl and the latter to the newly formed keto group. Sodium borohydride reduction of dehydroalopecurine gave alopecurine. Hydrolysis of dehydroalopecurine gave debenzoyldehydroalopecurine which absorbs at 1690 cm^{-1} in the infrared (i.r.). Both of these compounds show an absorption band at 1410 cm^{-1}, not present in alopecurine itself, suggesting that the keto group is flanked, at least on one side, by a methylene group. Oxidation of either debenzoylalopecurine or debenzoyldehydroalopecurine gave the corresponding diketone which displays carbonyl absorption at 1720 and 1690 cm^{-1}.

TABLE I

Nuclear magnetic resonance data for ring C protons in alopecurine

Proton	Chemical shift (τ)	Coupling constants (c.p.s.)
H_a	4.65	J_{ab}7.5, J_{ac}5, J_{ad}10, J_{ae}6
H_b	6.25	J_{ab}7.5, J_{bc}15.5
H_c	7.28	J_{ac}5, J_{bc}15.5
H_d	6.93	J_{ad}10, J_{de}15
H_e	8.43	J_{ae}6, J_{de}15

Dehydration of alopecurine with thionyl chloride in benzene gave anhydroalopecurine which shows two olefinic protons in its n.m.r. spectrum, one appearing as a doublet (J = 9 c.p.s.) at τ 4.50 and the other as a quartet (J = 9 and 2 c.p.s.) at τ 4.65.

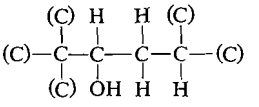

3a

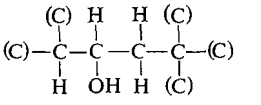

3b

The datum above indicates that the environment of the hydroxyl group is as shown in *3a* or *3b*, with *3a* preferred since the proton geminal to the hydroxyl group appears as a doublet in the n.m.r. spectrum (i.e., *3a* requires that only one coupling constant be zero).

Since at this stage it appeared that an unambiguous chemical solution to the structural problem was not close at hand, an X-ray crystallographic study was undertaken. Four heavy atom derivatives of alopecurine were prepared. Both the hydrobromide and the hydrochloride formed tetragonal crystals of large unit cell volume and were rejected. Alopecurine methobromide formed monoclinic crystals, space group $P2_1$, containing two molecules per unit cell of dimensions a = 10.96, b = 10.42, and c = 9.48 Å, β = 90.0°. Debenzoylalopecurine hydrobromide crystallized from methanol–acetone in the orthorhombic system space group $P2_12_12_1$, with four molecules in the unit cell of dimensions a = 7.52, b = 28.05, c = 7.05 Å. Since the $P2_12_12_1$ system is more suitable for application of the heavy atom method, debenzoylalopecurine hydrobromide was selected for the analysis. The X-ray reflections were recorded on equi-inclination Weissenberg photographs taken along the a and c axes with CuK_α radiation. The structure was solved by the heavy-atom method and refined by full-matrix least squares methods to an R-factor of 11.1%.[1] The molecular

[1]Full details of the X-ray analysis will be published separately.

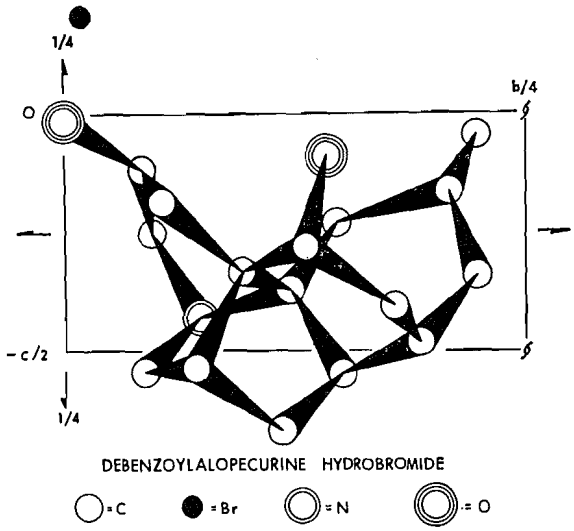

FIG. 2. Perspective drawing of a molecule of debenzoylalopecurine hydrobromide.

structure so derived is shown in Fig. 2, which also depicts the correct absolute configuration as determined by anomalous dispersion calculations. Structure **4** (**4***a* and **4***b* are other representations of the same molecule) thus represents debenzoylalopecurine. Since the n.m.r. evidence clearly indicates that the carbon bearing the benzoyloxy group is flanked on both sides by methylene groups, alopecurine itself is **1** (= **1***a* = **1***b*). As may be seen in **1** and as is emphasized by **1***a*, alopecurine contains the lycopodine-type skeleton with an extra bond connecting C-4 and C-10. As in most Lycopodium alkaloids, C-5 is oxygenated. However, this is the first example of an alkaloid of this group oxygenated at C-2, as well as being the first reported benzoylated Lycopodium alkaloid.

Another interesting feature revealed by the X-ray analysis is that ring C adopts a twist conformation in the crystal. The n.m.r. data quoted previously (Table I) indicates that this is also the preferred conformation of the free base in solution. The value J_{ad} = 10 c.p.s. is consistent only with a dihedral angle approaching 180°. The rather large values for J_{ae} and J_{ae} (5 and 6 c.p.s., respectively) and the relatively small value for J_{ab} (7.5 c.p.s.) may reflect some distortion in this ring, although our lack of knowledge of the effect of the nitrogen (4) on the couplings of H_b and H_c seems to make further speculation on the n.m.r. data unwarranted. In the crystal, the internuclear distance between C-2 and C-14 is 3.10 Å while in Dreiding models of the "undistorted" molecule, measurements indicate an internuclear distance of about 2.5 Å. Apparently the severe nonbonded interaction between the hydroxyl substituent at C-2 and the *exo*-hydrogen at C-9 (see **5**) makes the chair form **5** less stable than the twist form **4**.

The X-ray analysis also reveals a distortion of rings B and D. The internuclear distance between the C-5 oxygen and C-15 is 3.09 Å. In Dreiding models of the "undistorted" molecule, this distance is about 2.0 Å. As mentioned previously, the proton at C-5 gives rise to a doublet, $J \simeq 8$ c.p.s., in the n.m.r. spectrum. This can be accounted for if ring B is distorted toward the half-chair to such an extent that the dihedral angle between the hydrogen at C-5 and the axial hydrogen at C-6 approaches 0°. In this case the dihedral angle which the C-5 hydrogen makes with the equatorial hydrogen at C-6 is close to 90°, and explains the negligible coupling between these two protons. Dehydration of alopecurine, as mentioned, proceeds readily to give anhydro-

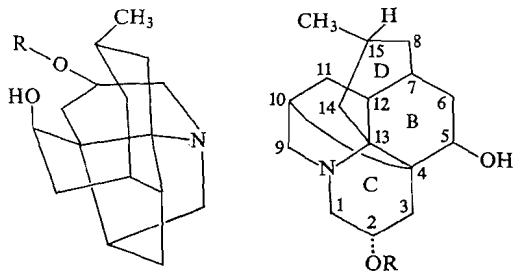

1 R = COPh
4 R = H
8 R = $COCH_3$

1*a* R = COPh
4*a* R = H

1*b* R = COPh
4*b* R = H

Can. J. Chem. Downloaded from www.nrcresearchpress.com by 210.87.254.105 on 09/05/12
For personal use only.

Can. J. Chem. Downloaded from www.nrcresearchpress.com by 210.87.254.105 on 09/05/12
For personal use only.

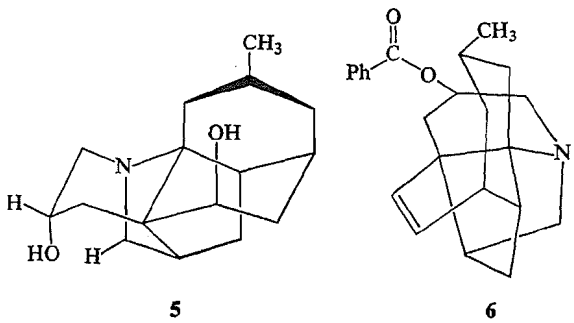

5

6

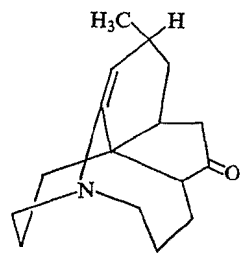

7

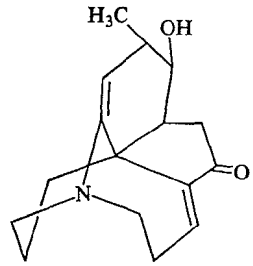

9

alopecurine (**6**), which from its spectroscopic properties appears to be unrearranged.

Because of the unusual nature of the ring system the X-ray analysis of alopecurine methobromide has also been completed[1] and the result (Fig. 3) fully confirms structure **1**, with ring C in a twist conformation.

Since our initial report on the isolation of the alkaloids of *L. alopecuroides* (1) we have succeeded in isolating 4 more alkaloids from this plant. One of these is fawcettidine (**7**) (5). The others are new alkaloids: (*i*) a compound $C_{18}H_{27}O_3N$, m.p. 238–240°. It was apparent from the i.r., n.m.r. (Fig. 4), and mass spectra of this alkaloid that it is acetyldebenzoylalopecurine (**8**), in which the benzoyl group of alopecurine is replaced by an acetyl group. Alkaline hydrolysis of **8** gave debenzoylalopecurine (**4**). Oxidation gave the corresponding ketone; (*ii*) a compound $C_{16}H_{21}O_2N$, m.p. 53–56°, which we have named alolycopine, and which has been shown to possess structure **9** (6); (*iii*) a compound $C_{16}H_{25}ON$, m.p. 239–241°, which we have called lycopecurine. The oxygen is present as a hydroxyl group and since there is no evidence for the presence of unsaturation, lycopecurine also appears to be pentacyclic.

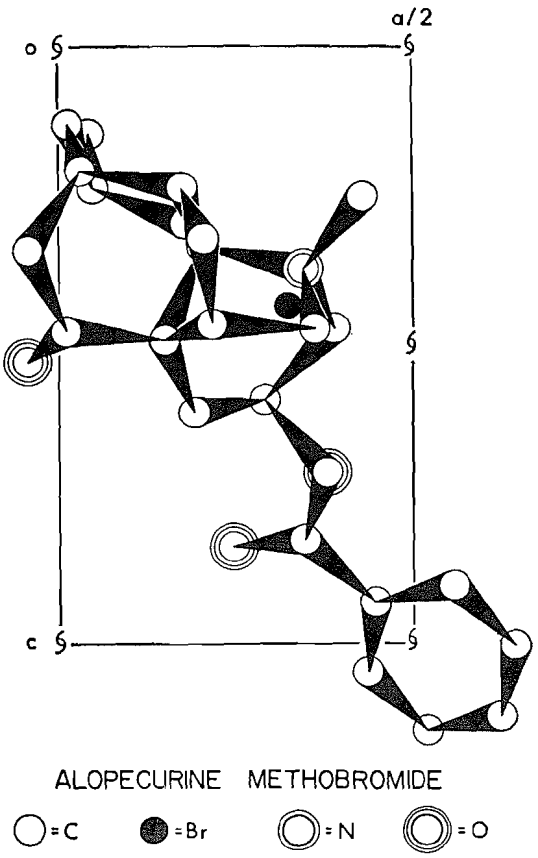

FIG. 3. Perspective drawing of a molecule of alopecurine methobromide.

Experimental

General

Infrared (i.r.) spectra were measured on a Perkin–Elmer model 441 or model 337 spectrophotometer, nuclear magnetic resonance spectra were measured on a Varian Associates model HA-100 spectrometer, and mass spectra were determined on an AEI MS-9 mass spectrometer. Alumina, unless otherwise specified refers to basic alumina of activity II–III (Brockmann scale). Thin-layer chromatograms (t.l.c.) were carried out on Alumina G (American Optical Corporation, Richmond, California) and developed with iodine and/or Dargendorff's reagent. Microanalyses were performed by A. B. Gygli, Toronto. Crystal densities were determined by the neutral buoyancy method using chlorobenzene and carbon tetrachloride.

Alopecurine

Alopecurine, m.p. 244–245°, $[\alpha]_D -105°$, $[\alpha]_{300} -420°$, (*c*, 0.5 MeOH) was isolated as previously described (1). The n.m.r. spectrum is shown in Fig. 1. Mass spectrum: *m/e* 367 (M^+, 26), 352(22), 262(55), 246(30), 245(59), 230(21), 219(38), 204(25), 178(26), 151(19), 122(19), 105(100), 77(50). The i.r. and ultraviolet spectra have been reported (1).

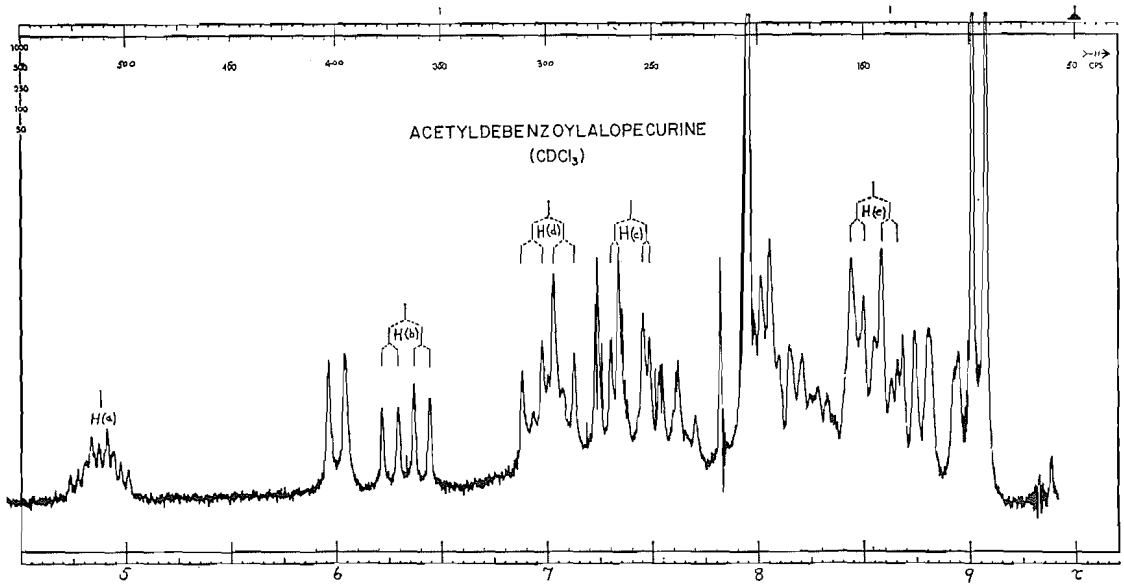

FIG. 4. Nuclear magnetic resonance spectrum (100 Mc.p.s.) of acetyldebenzoylalopecurine.

The *hydrobromide* was prepared in the usual fashion and recrystallized from methanol–acetone to give tetragonal crystals, m.p. > 300° (decomp.), $d^{25°} = 1.35$ g/cm³.

The *hydrochloride* was prepared in methanol and recrystallized from acetone, m.p. 290–300° (decomp.), $d^{25°} = 1.257$ g/cm³.

The *methobromide* was prepared as follows. Alopecurine (10 mg) was dissolved in acetone (6 ml) and a few drops of methyl iodide were added. The solution was heated on the steam bath for 2 h, then the solvents were evaporated, and the glassy residue was crystallized from acetone–ether. The methiodide, m.p. 250°, was dissolved in water and passed through a column of bromide loaded Dowex 2-X8 anion exchange resin (1 g). Evaporation of the water yielded alopecurine methobromide (11 mg), which after recrystallization from methanol–acetone melted at 247–249°, $d^{25°} = 1.397$ g/cm³. Infrared spectrum (Nujol mull): 3300, 1725, 1595, 1580, 1260 cm^{-1}.

Anal. Calcd. for $C_{24}H_{32}O_3NBr$: C, 62.33; H, 6.97. Found: C, 62.26, 62.44; H, 7.12, 7.04.

Debenzoylalopecurine Hydrobromide

The hydrobromide was prepared in the usual way and recrystallized from acetone–methanol, m.p. 249–251°, $d^{25°} = 1.481$ g/cm³.

Anal. Calcd. for $C_{16}H_{26}O_2NBr$: C, 55.81; H, 7.61. Found: C, 55.97, 56.02; H, 7.43, 7.53.

Dehydroalopecurine

Jones' reagent (8 drops) was added to a solution of alopecurine (46 mg) in acetone. After 5 min methanol (10 drops) was added and the solution concentrated almost to dryness. The residue was dissolved in chloroform and washed with dilute sodium bicarbonate. Evaporation left an oil which was homogeneous as determined by t.l.c. but which could not be induced to crystallize. The oil was purified by evaporative distillation (150°/0.1 mm); calculated mol. wt. for $C_{23}H_{27}O_3N$: 365. Found: 365 (mass spectrometry). Infrared spectrum ($CHCl_3$): 1715, 1690, 1410 cm^{-1}. Nuclear magnetic resonance spectrum ($CDCl_3$): τ 2.0–2.5 (5 H, aromatic protons), 4.75 (1 H, multiplet, $w_{1/2} \simeq 15$ c.p.s.), 6.25 (1 H, quartet, $J = 16$ and 7.5 c.p.s.), 7.1 (1 H, quartet, $J = 16$ and 8 c.p.s.), 7.2 (1 H, quartet, $J = 16$ and 2 c.p.s.), 8.1 (1 H, quartet, $J = 16$ and 2 c.p.s.) (the last 4 protons are all coupled to the τ 4.75 proton as shown by spin-decoupling), 9.03 (3 H, doublet, splitting 6 c.p.s.).

Debenzoyldehydroalopecurine

Dehydroalopecurine (36 mg) was dissolved in dioxane (2 ml) and 5% aqueous potassium hydroxide (0.3 ml) was added. After 12 h at room temperature, most of the solvent was evaporated, the residue taken up in water, and extracted with chloroform. Evaporation gave a solid (21 mg) which after recrystallization from acetone melted at 160–162°. Infrared spectrum (Nujol mull): 3100, 1690, 1412 cm^{-1}. Calculated mol. wt. for $C_{16}H_{23}O_2N$: 261.1728. Found: 261.1729 (high resolution mass spectrometry (h.r.m.s.)).

Oxidation of Debenzoylalopecurine

Debenzoylalopecurine (6 mg) was dissolved in acetone (2 ml) and Jones' reagent (2 drops) was added. Methanol (2 drops) was then added and the solution evaporated to dryness. The residue was dissolved in chloroform and washed with dilute sodium bicarbonate. Evaporation of the chloroform gave an oil which was purified by evaporative distillation (130°/0.1 mm). Infrared spectrum ($CHCl_3$): 1720, 1690, 1430, 1410 cm^{-1}. Calculated mol. wt. for $C_{16}H_{21}O_2N$: 259.1572. Found (h.r.m.s.): 259.1574.

The *hydrobromide* was prepared in the normal way and melted at 248–250° (decomp.).

Can. J. Chem. Downloaded from www.nrcresearchpress.com by 210.87.254.105 on 09/05/12
For personal use only.

Can. J. Chem. Downloaded from www.nrcresearchpress.com by 210.87.254.105 on 09/05/12
For personal use only.

Oxidation of Debenzoyldehydroalopecurine

The oxidation was carried out as described for debenzoylalopecurine and the product obtained was identical with the diketone described above.

Anhydroalopecurine

Alopecurine (25 mg) was dissolved in benzene (10 ml) and thionyl chloride (0.5 ml) was added. The solution was heated under reflux overnight, then water was added, followed by aqueous ammonia. The benzene layer was separated and the aqueous layer extracted twice more with benzene. Evaporation of the benzene left an oil (20 mg) which was chromatographed over alumina (Woelm neutral, activity II, 1 g). Elution with ether gave *anhydroalopecurine* (15 mg) which crystallized from ether, m.p. 105–107°. Infrared spectrum ($CHCl_3$): 1720, 1610, 1590, 1280 cm^{-1}. Nuclear magnetic resonance spectrum ($CDCl_3$): τ 2–2.5 (5 H, aromatic protons), 4.50 and 4.65 (2 H, AB portion of ABX system, J_{AB} = 9 c.p.s., J_{AX} = 0 c.p.s., J_{BX} = 2 c.p.s.), 4.70 (1 H, multiplet), 6.25 (1 H, quartet, J = 16 and 6.5 c.p.s.), 7.00 (1 H, quartet, J = 16 and 1 c.p.s.), 7.55 (1 H, quartet, J = 17 and 8.5 c.p.s.), 8.00 (1 H, quartet, J = 17 and 2.5 c.p.s.), 9.01 (3 H, doublet, splitting 6 c.p.s.). Calculated mol. wt. for $C_{23}H_{27}O_2N$: 349.2042. Found (h.r.m.s.): 349.2045.

Isolation of Fawcettidine

Fraction 3 from the initial chromatographic separation of the crude alkaloids (see ref. 1) was subjected to gas–liquid chromatography (190°, 5 ft × ¼ in. column, 10% QF-1 on Chromosorb W, flow rate (He) 60 ml/min, Aerograph A-90-P3). The middle fraction (of 3, retention time 5 min) was collected and treated with an ethereal solution of picric acid. The picrate thus obtained, m.p. 220–222°, was identical (m.p., m.m.p., i.r. spectrum) with fawcettidine picrate.

Isolation of Acetyldebenzoylalopecurine

Fraction 7 (1) and the mother liquors from fraction 8 were chromatographed over alumina. Elution with ether gave first alopecurine and then a fraction which on crystallization from acetone afforded *acetyldebenzoylalopecurine*, m.p. 238–240°. Infrared spectrum ($CHCl_3$): 3610, 1725, 1240 cm^{-1}. Nuclear magnetic resonance spectrum: see Fig. 4. Mass spectrum: *m/e* 305 (M^+, 41), 290(58), 262(50), 246(60), 245(100), 219(51), 204(46), 178(40). Calculated mol. wt. for $C_{18}H_{27}O_3N$: 305.1991. Found (h.r.m.s.): 305.1990.

Hydrolysis of Acetyldebenzoylalopecurine

Acetyldebenzoylalopecurine (19 mg) in methanol (5 ml) and 5% aqueous KOH (2 ml) were kept at room temperature for 24 h. Work-up in the usual manner gave debenzoylalopecurine (13 mg), m.p. 229–231°, identical with an authentic sample.

Oxidation of Acetyldebenzoylalopecurine

The oxidation of acetyldebenzoylalopecurine (10 mg) with Jones' reagent (10 drops) was carried out in the usual manner. The product (9 mg) was a solid, m.p. 241–243° after recrystallization from acetone. Infrared spectrum (Nujol mull): 1750, 1695, 1230 cm^{-1}. Calculated mol. wt. for $C_{18}H_{25}O_3N$: 303.1834. Found (h.r.m.s.): 303.1834.

Isolation of Alolycopine

The mother liquors from fraction 9 (1) and from several fractions from the chromatogram above showed a strong band at 1640 cm^{-1} in the i.r. These fractions (0.28 g) were combined and subjected to "dry-column" chromatography (7) over neutral alumina (125 g). The column was developed with chloroform–methanol (49:1, 100 ml). From this chromatography an apparently homogeneous (determined by t.l.c.) oil (0.12 g, $R_f \simeq 0.6$) was obtained which, however, could not be induced to crystallize. This oil, which showed hydroxyl absorption in the i.r., was treated at room temperature for 12 h with acetic anhydride – pyridine (4 ml of 1:1). Evaporation left an oil which was dissolved in ether and filtered through basic alumina. Crystallization of the residue from a small volume of ether provided *O*-acetylalolycopine (0.1 g), m.p. 180–182°. Calculated mol. wt. for $C_{18}H_{23}O_3N$: 301.1678. Found (h.r.m.s.): 301.1678.

Hydrolysis of *O*-acetylalolycopine at room temperature in aqueous methanolic potassium hydroxide gave crystalline alolycopine, which after recrystallization from ether melted at 53–56°. The i.r. spectrum of this material was virtually identical with that of the oil obtained from the "dry-column" chromatography. Calculated mol. wt. for $C_{16}H_{21}O_2N$: 259.1572. Found: 259.1571.

A full description of the properties of alolycopine is provided in the following paper (6).

Isolation of Lycopecurine

After standing for several months, the acetone mother liquors remaining from the isolation of alopecuridine (1) deposited crystals (24 mg) of a compound melting at 239–241°, which does not appear to have been described previously. The i.r. spectrum ($CHCl_3$) showed hydroxyl absorption at 3620 cm^{-1} but no absorption in the 1500–1800 cm^{-1} region. High resolution mass spectrometry suggests the molecular formula $C_{16}H_{25}ON$ (calculated mol. wt. 247.1936. Found: 247.1932). The base peak in the mass spectrum occurs at *m/e* 232. The n.m.r. spectrum determined on a small amount of the compound was poorly defined but did reveal the presence of a secondary *C*-methyl group (doublet at τ 9.08) and a lack of olefinic protons. An X-ray crystallographic analysis of the hydrobromide of lycopecurine is in progress.

Acknowledgments

We wish to thank the Smith, Kline, and French Laboratories, Philadelphia and especially Dr. J. A. Weisbach for the supply of crude alkaloids, and the National Research Council of Canada for financial support. We also wish to thank Mrs. Judith Westwood, Dr. A. N. Hogg, and Messrs. R. N. Swindlehurst and G. Bigam for their help in various phases of this work, and Professor David Hall for his help with the X-ray analysis.

1. W. A. Ayer, B. Altenkirk, S. Valverde-Lopez, B. Douglas, R. F. Raffauf, and J. A. Weisbach. Can. J. Chem. **46**, 15 (1968).

2. A. HASSNER and C. HEATHCOCK. J. Org. Chem. **29**, 1350 (1964).
3. R. C. COOKSON, T. A. CRABB, J. J. FRANKEL, and J. HUDEC. Tetrahedron Suppl. **7**, 355 (1966).
4. W. A. THOMAS. *In* Annual review of NMR spectroscopy. Vol. 1. *Edited by* E. F. Mooney. Academic Press, Inc., New York. 1968. pp. 72–74.
5. H. ISHII, B. YASUI, T. HARAYAMA, and Y. INUBUSHI. Tetrahedron Letters, 6215 (1966).
6. W. A. AYER and B. ALTENKIRK. Can. J. Chem. This issue.
7. B. LOEW and K. M. SNADER. Chem. Ind. London, 15 (1965).

Can. J. Chem. Downloaded from www.nrcresearchpress.com by 210.87.254.105 on 09/05/12
For personal use only.

Can. J. Chem. Downloaded from www.nrcresearchpress.com by 210.87.254.105 on 09/05/12
For personal use only.

Alkaloids of *Lycopodium alopecuroides*. Part 3. Structure of alolycopine

W. A. AYER AND B. ALTENKIRK

Department of Chemistry, University of Alberta, Edmonton, Alberta

Received February 17, 1969

The alkaloid alolycopine is shown to have structure **4***a*. The structural assignment is based on the interpretation of the infrared, ultraviolet, and nuclear magnetic resonance spectra of alolycopine and *O*-acetylalolycopine, and on a correlation of the latter with acetylanhydroaposerratinine (**6**).

Canadian Journal of Chemistry, 47, 2457 (1969)

In Part 2 (1) we reported the isolation of an alkaloid $C_{16}H_{21}O_2N$, m.p. 53–56°, from *Lycopodium alopecuroides* L. This paper describes the elucidation of the structure of this minor alkaloid, which has been named alolycopine.

An examination of the infrared (i.r.), ultraviolet (u.v.), and nuclear magnetic resonance (n.m.r.) spectra of alolycopine and *O*-acetylalolycopine suggested that part structures **1** and **2** are present in the alkaloid.

Part Structure 1

The presence of the hydroxyl group was indicated by i.r. absorption at 3625 cm^{-1}. Its secondary nature was suggested by the signal at τ 5.46 (quartet, J = 12 and 5 c.p.s.) in the n.m.r. spectrum (Fig. 1) of *O*-acetylalolycopine. Since the i.r. spectrum of *O*-acetylalolycopine shows no NH absorption, the nitrogen is tertiary. The presence of the vinyl amine grouping was suggested by the relatively intense carbon–carbon double bond absorption at 1665 cm^{-1} (Fig. 2), similar to that in fawcettidine (**3**) (2, 3), and by the fact that the n.m.r. signal (τ 4.54, Fig. 1) attributed to the proton on this double bond is shifted downfield by about 0.8 p.p.m. when trifluoroacetic acid is added to the solution, again similar to the case of fawcettidine (3). The fact that this proton, subsequently shown to be β to the nitrogen, gives rise to a signal at τ 4.54 rather than at the normal enamine position ($\simeq$ 5.5 (4)), indicates that there is no overlap possible between the nitrogen lone pair orbital and the π orbital of the double bond (i.e., the nitrogen is at a bridgehead). The signal for this olefinic proton, a doublet (J = 6 c.p.s.), was spin-decoupled by double irradiation at τ 7.3. Double irradiation at τ 7.3 also spin-decoupled the methyl doublet at τ 9.03 and removed the 5 c.p.s. coupling from the signal for the proton geminal to the acetoxyl group, *indicating that the carbon bearing the methyl group is situated between the carbon carrying the enamine proton and the carbon carrying the acetoxyl group*. Since the signal for the proton geminal to the acetoxyl is further split, part structure **1** is defined.

Part Structure 2

Both alolycopine and *O*-acetylalolycopine show intense absorption at 1715 and 1640 cm^{-1} in the i.r. (Fig. 2) and at 237 mμ in the u.v., consistent with the presence of an α,β-unsaturated cyclopentanone system. Both the position of the u.v. maximum (5) and the intensity of the carbon–carbon double bond absorption in the i.r. (6) indicate that the α,β-unsaturation is

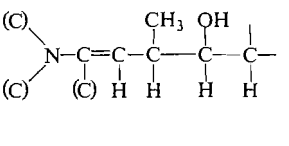

1

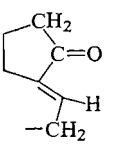

2

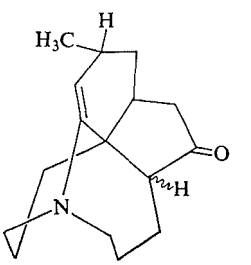

3

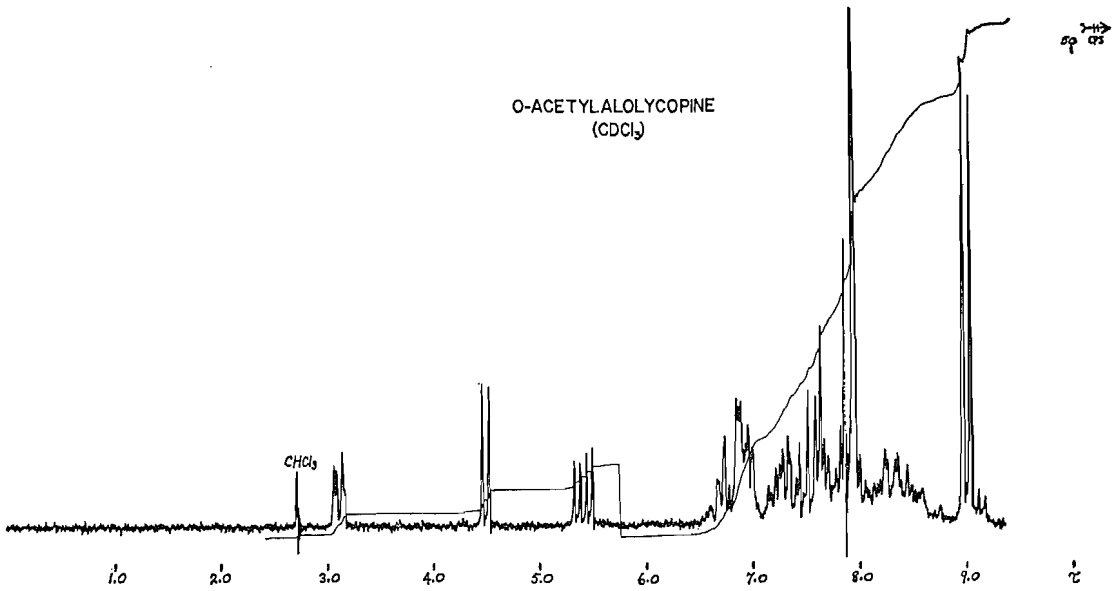

FIG. 1. Nuclear magnetic resonance spectrum (100 Mc.p.s.) of *O*-acetylalolycopine in $CDCl_3$.

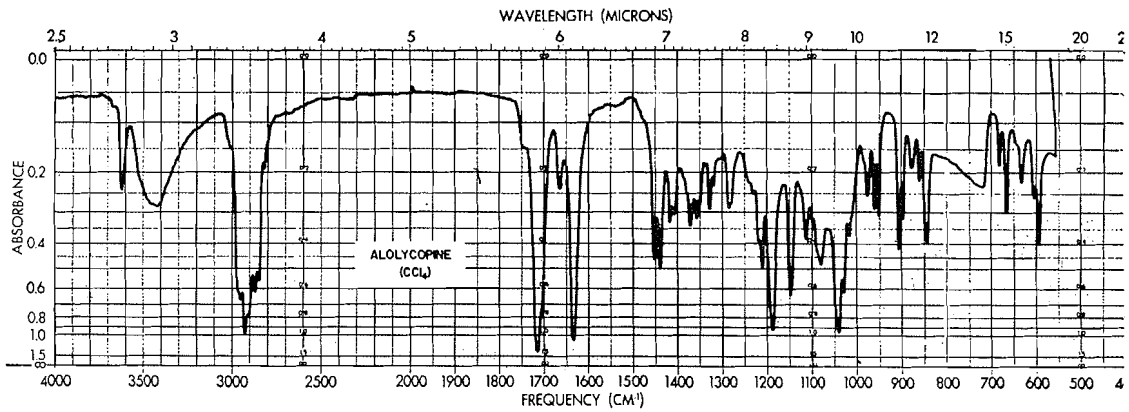

FIG. 2. Infrared spectrum (CCl_4) of alolycopine.

exocyclic to the cyclopentanone ring, and the appearance of a signal at τ 3.18 (quartet, $J = 6$ and 1.5 c.p.s.) in the n.m.r. shows the presence of a β-proton (7). The multiplicity of this signal suggests that the proton is coupled to two vicinal protons, although the possibility of a long range coupling cannot be excluded. The presence of an absorption band at 1410 cm^{-1} in the i.r. spectra of both alolycopine and its acetyl derivative indicates that the carbonyl group is flanked on one side by a methylene group (8).

The part structures **1** and **2** are readily accommodated by a fawcettidine (**3**)-type skeleton, **4**. During the study of the alkaloids serratinine and serratinidine (**5**) Inubushi and co-workers (9) prepared and established the structure of acetylanhydroaposerratinine (**6**). Catalytic hydrogenation of *O*-acetylalolycopine (**4***b*) at atmospheric pressure over palladium–charcoal in methanol gave acetylanhydroaposerratinine (**6**), establishing the structure and stereochemistry of alolycopine as that shown in **4***a*.

Can. J. Chem. Downloaded from www.nrcresearchpress.com by 210.87.254.105 on 09/05/12
For personal use only.

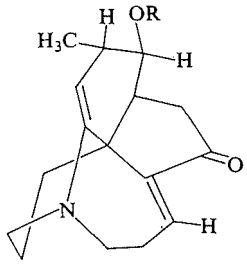

4*a* R = H
4*b* R = Ac

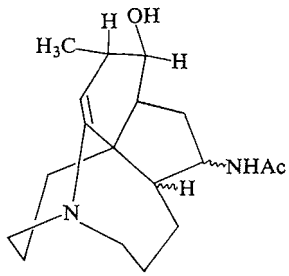

5

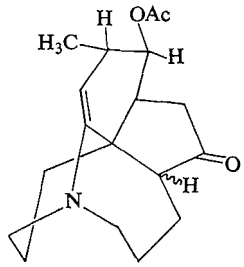

6

Experimental[1]

Alolycopine

Alolycopine, m.p. 53–56°, was isolated as previously described (1). Infrared spectrum: see Fig. 2. Ultraviolet spectrum: λ_{max}(MeOH) 237 mμ (ε 5000). Mass spectrum: *m/e* 259(M^+, 76), 244(15), 242(9), 216(11), 202(9), 188(12), 177(16), 176(100), 175(18), 174(16), 160(22).

O-Acetylalolycopine

O-Acetylalolycopine, m.p. 180–182°, was prepared as described previously (1). Infrared spectrum (Nujol mull): 1740, 1715, 1665, 1640, 1410, 1235 cm^{-1}. Ultraviolet spectrum: λ_{max}(MeOH) 237 mμ (ε 6000). Nuclear magnetic resonance spectrum: see Fig. 1. Mass spectrum: *m/e* 301(M^+, 100), 259(39), 258(26), 242(46), 218(59), 198(24), 176(43), 160(28).

Hydrogenation of O-Acetylalolycopine

O-Acetylalolycopine (25 mg) in methanol (30 ml) was stirred under hydrogen at atmospheric pressure in the presence of 5% palladium-on-charcoal (25 mg) for 2 h. The catalyst was removed by filtration and the solvent evaporated to leave a solid residue which on thin-layer chromatographic (t.l.c.) analysis showed one major component and three minor components. The solid was adsorbed on alumina (1 g) and eluted with ether 10 ml fractions). Fractions 2, 3, and 4 were combined (nd recrystallized from ether to give acetylanhydroaposerratinine (12 mg), m.p. 144–146°, identical (i.r. spectrum, t.l.c. behavior, mixture melting point undepressed) with an authentic sample (9) kindly provided by Professor Y. Inubushi.

[1]The general experimental details are the same as those given in Part 2 of this series (1).

Acknowledgments

We wish to thank Professor Y. Inubushi, Kyoto University, for the sample of acetylanhydroaposerratinine. We are grateful to the National Research Council of Canada and the University of Alberta for financial support of this work.

1. W. A. Ayer, B. Altenkirk, N. Masaki, and S. Valverde-Lopez. Can. J. Chem. This issue.
2. H. Ishii, B. Yasui, T. Harayama, and Y. Inubushi. Tetrahedron Letters, 6215 (1966).
3. B. Altenkirk. Ph.D. Thesis, University of Alberta, Edmonton, Alberta. 1969.
4. G. Stork, A. Brizzolara, H. Landesman, J. Szmuszkovicz, and R. Terrell. J. Am. Chem. Soc. **85**, 207 (1963).
5. A. I. Scott. Interpretation of the ultraviolet spectra of natural products. The Pergamon Press, Ltd., New York. 1964. p. 55.
6. R. L. Erskine and E. S. Waight. J. Chem. Soc. 3425 (1960).
7. N. S. Bhacca and D. H. Williams. Applications of NMR spectroscopy in organic chemistry. Holden-Day, Inc., San Francisco. 1964. p. 89.
8. R. N. Jones and C. Sandorfy. Technique of organic chemistry. Vol. IX. Interscience Publishers, Inc., New York. 1956. p. 498.
9. B. Yasui, H. Ishii, T. Harayama, R. Nishino, and Y. Inubushi. Tetrahedron Letters, 3967 (1966).

Can. J. Chem. Downloaded from www.nrcresearchpress.com by 210.87.254.105 on 09/05/12
For personal use only.

Can. J. Chem. Downloaded from www.nrcresearchpress.com by 210.87.254.40 on 09/05/12
For personal use only.

Tertiary phosphite – alkyl halide reactions in acetonitrile

LANE J. GOODELL AND JOHN T. YOKE
Department of Chemistry, Oregon State University, Corvallis, Oregon 97331

Received February 28, 1969

Olefin elimination does not occur during the interaction of ca. 0.2 *M* triisopropyl phosphite and isopropyl iodide (and of other simple tertiary phosphite – alkyl halide mixtures) in acetonitrile, contrary to a previous report. At and below 50°, the Arbuzov reaction does occur very slowly in these systems. The reaction of trimethyl phosphite and *n*-butyl iodide in acetonitrile gives a larger yield of dimethyl methylphosphonate than of dimethyl *n*-butylphosphonate.

Canadian Journal of Chemistry, 47, 2461 (1969)

There have been several recent kinetic investigations of the Arbuzov reaction

$$(RO)_3P: + R'X \rightarrow R'(RO)_3PX \rightarrow R'P(O)(OR)_2 + RX$$

using dilute solutions in acetonitrile (1, 2). In an infrared (i.r.) spectral study of the triisopropyl phosphite reaction with isopropyl iodide, Aksnes and Aksnes (3) observed that diisopropyl hydrogen phosphonate was formed instead of the Arbuzov product. Propene elimination was postulated to account for this. Olefin elimination from tri-*t*-butyl phosphite to give isobutylene and di-*t*-butyl hydrogen phosphonate has been reported (4) to occur readily either on warming the neat reagent, or (as the major reaction path) in its low temperature Arbuzov reaction with methyl iodide *in the absence of solvent*.

In the present work, several reactions in acetonitrile of tertiary phosphites with alkyl iodides were reinvestigated, with emphasis placed on isolation of products, and especially the detection of any olefins formed. Another aspect of the work dealt with the question of possible competition of the alkyl halide produced in the Arbuzov reaction with a different alkyl halide starting material; the system trimethyl phosphite – *n*-butyl iodide in acetonitrile was chosen for this study.

Experimental

Materials and Equipment

Transfers of reagents to reaction vessels and spectral cells were conducted in a nitrogen-filled dry box. Additions to and separations from reaction mixtures of solvent and volatile reagents, the final purification stages of such reagents, and the reactions themselves were conducted in an all glass high vacuum line in which the residual gas pressure had been reduced to $< 10^{-5}$ Torr.

Acetonitrile was repeatedly shaken with phosphorus(V) oxide, distilled from fresh phosphorus(V) oxide onto calcium hydride, and then redistilled from calcium hydride into the vacuum line. The alkyl iodides were doubly distilled. Trimethyl phosphite (Hooker Chemical Co. and Monsanto Chemical Co. samples) was redistilled in dry nitrogen; nuclear magnetic resonance (n.m.r.) (neat): δ 3.15 (d, J_{POCH} = 11 Hz, OCH_3). Triisopropyl phosphite (Mobil Chemical Co.) was purified as follows. Sodium wire was added to react with any dialkyl hydrogen phosphonate present. After evolution of hydrogen had ceased, the liquid phase was decanted and distilled under reduced pressure in nitrogen using a Nester–Faust Teflon spinning band column. A middle fraction was taken, and then similarly redistilled; n.m.r. (neat): δ 0.98 (d, J = 6 Hz, $CH(CH_3)_2$), 4.05 (m, $CH(CH_3)_2$). Tri-*n*-butyl phosphite (Eastman Kodak) was purified in an identical fashion; n.m.r. (neat): δ 3.59 (m, CH_2O—).

Authentic samples of dialkyl hydrogen phosphonates and dialkyl alkylphosphonates were needed for analytical standards. Commercial samples of the following were redistilled under reduced pressure, with a middle fraction taken: dimethyl hydrogen phosphonate (Mobil Chemical Co. and Monsanto Chemical Co.); n.m.r. (neat): δ 3.55 (J_{POCH} = 12 Hz, OHC_3), 6.55 (d, J_{PH} = 694 Hz, PH); di-*n*-butyl hydrogen phosphonate (Mobil); n.m.r. (neat): δ 3.85 (m, OCH_2), 12.30 (one component of PH doublet, other component obscured by CH_3); dimethyl methylphosphonate (Aldrich); n.m.r. (neat): δ 3.54 (d, J_{POCH} = 12 Hz, OCH_3), 1.32 (d, J_{PCH} = 18 Hz, PCH_3). Diisopropyl hydrogen phosphonate was prepared (3) by boiling triisopropyl phosphite with water in acetonitrile under nitrogen. The solvent and water were stripped off and the product (60%) distilled: b.p. 73–74° (9 mm); n.m.r. (neat): δ 1.07 (d, J = 7 Hz, $CH(CH_3)_2$), 4.50 (m, $CH(CH_3)_2$), 6.78 (d, J_{PH} = 704 Hz, PH). The previously unreported dimethyl *n*-butylphosphonate was prepared by the Arbuzov reaction from neat trimethyl phosphite and *n*-butyl bromide at ca. 110°, with methyl bromide evolved. The product (25%) was distilled: b.p. 76–78° (19 mm); n.m.r. (neat): δ 3.55 (d, J_{POCH} = 11 Hz, OCH_3). Di-*n*-butyl ethylphosphonate was synthesized by treating di-*n*-butyl hydrogen phosphonate in hexane first with sodium and then with ethyl bromide. The reaction mixture was washed with water to remove sodium bromide, the solvent was stripped off, and the product (60%) was distilled under reduced pressure using a spinning band column; n_D^{25} 1.4258 [lit. (5), n_D^{25} 1.4258]; n.m.r. (neat): δ 3.86 (m, OCH_2). An attempted synthesis of diisopropyl isopropylphosphonate by the Arbuzov reaction using neat triisopropyl phosphite and isopropyl bromide was unsuccessful. However, a sample was obtained in very low yield after heating a mixture of 50 ml of triisopropyl phosphite, 25 ml of isopropyl bromide,

TABLE I

Reaction conditions and results

Reaction conditions	% 3° Phosphite remaining	Products observed by g.l.c.	Comments
0.193 *M* $(n\text{BuO})_3\text{P}$ + 0.213 *M* EtI 7 days, 31°	83*	$(n\text{BuO})_2\text{P(O)Et}$, *n*BuI	Nuclear magnetic resonance accounted for by $(n\text{-BuO})_3\text{P}$ + $(n\text{-BuO})_2\text{P(O)Et}$
0.203 *M* $(\text{MeO})_3\text{P}$ + 0.215 *M* *n*BuI 7 days, 50°	87†	$(\text{MeO})_2\text{P(O)Me}$ (10%), $(\text{MeO})_2\text{P(O)}n\text{Bu}$ (2%), HP(O)(OMe)_2 (1%), MeI, MeOH	No P—H apparent in nuclear magnetic resonance or infrared spectroscopy
0.214 *M* $(\text{isoPrO})_3\text{P}$ + 0.229 *M* isoPrI 13.5 days, 50°	100‡	$(\text{isoPrO})_2\text{P(O)(isoPr)}$, X§	Essentially no reaction; gas–liquid chromatography shows products as traces only. Slight development of P=O (but no P—H) in infrared; only starting material apparent in nuclear magnetic resonance

*By quantitative infrared spectrophotometry at 870 cm^{-1}.
†By gas–liquid chromatography.
‡By quantitative infrared spectrophotometry at 862 cm^{-1}.
§Trace of unknown impurity.

and a trace of iodine in 200 ml of purified anhydrous acetonitrile at 78° for 10 days. The solvent and unreacted isopropyl bromide were stripped off and the residue was distilled. Most of the starting phosphite was recovered: b.p. 64–69° (11.5 mm), and then a small fraction (6%) of the desired product was collected: b.p. 92° (11.5 mm); infrared (i.r.): (CCl_4) 1202 and 1242 cm^{-1} (P=O); n.m.r. (neat): δ 4.46 (m, $\text{C}H(\text{CH}_3)_2$), 1.14 (d, J = 5 Hz, $\text{OCH}(\text{C}H_3)_2$), 0.82 (d, J = 6 Hz, $\text{PCH}(\text{C}H_3)_2$). The ratio of the (planimeter) integrated intensities of the latter two doublets was 1.8 ± 0.2, theory 2.0.

An F and M model 700 chromatograph was used for gas–liquid chromatography (g.l.c.) analyses, with dual 6 ft stainless steel columns and helium as the carrier gas. Two sets of columns were used: (*A*) 1/8 in., 10% silicone oil W98 on 80–100 mesh Chromosorb W; (*B*) 1/4 in., 20% Reoplex 400 on 30–60 mesh Chromosorb W. Spectra were obtained with a Varian A-60 proton n.m.r. spectrometer and a Beckman Microspec double beam recording i.r. spectrophotometer.

Reaction Studies

For each tertiary phosphite – alkyl iodide combination studied, the reaction flask was connected through the vacuum system to a manometer and gas storage bulb. The reaction conditions, degrees of conversion, and analytical observations are indicated in Table I. For each system, the vapor pressure of the reaction mixture remained constant during the entire period, and the equilibrium pressure dropped to < 1 mm when the reaction was terminated by quenching to −63.5°. The i.r. and g.l.c. analyses involved comparison of the acetonitrile reaction solutions with acetonitrile solutions of the reference standards. Where quantitative i.r. spectrophotometric analysis is indicated, the validity of Beer's Law and the lack of interference by other components had been established. Nuclear magnetic resonance spectra were obtained on the neat residues remaining after distillation of the volatile solvent and alkyl halides in the vacuum line.

Results and Discussion

The Arbuzov reactions of aliphatic tertiary phosphites and iodides in dilute solution in acetonitrile at and below 50° are very slow. In each of the systems studied, the major portions of the starting materials were recovered unchanged after a week or more. A previous report (1) of more rapid reaction in such systems has been attributed (2) to possible contamination of the solvent by traces of water. The present experimental results definitely prove that no olefin was formed in any of the systems studied, including the triisopropyl phosphite – isopropyl iodide system in which propene elimination had been postulated (3). The report of the formation of diisopropyl hydrogen phosphonate in that study (3) presumably may also be attributed to impurities in the solvent.[1]

That polar solvents may be of practical synthetic value as Arbuzov reaction media is suggested by the present work. Under typical synthetic conditions (neat reagents at reflux), triisopropyl phosphite and isopropyl bromide gave no reaction. When the reaction was conducted in acetonitrile at reflux, diisopropyl isopropylphosphonate slowly formed. The use of a higher boiling solvent should provide a more practical synthetic method for sterically hindered phosphonates. Alternatively, photolysis has been

[1]G. Aksnes. Personal communication.

Can. J. Chem. Downloaded from www.nrcresearchpress.com by 210.87.254.40 on 09/05/12
For personal use only.

used (6) to generate diisopropyl isopropylphosphonate from the tertiary phosphite.

An explanation for this effect of a polar solvent may be suggested. Aksnes and Aksnes have reported (2) that the first step of the reaction is rate-determining in acetonitrile. That the second step is normally rate-determining is indicated by the isolation of the intermediate in aliphatic (7) as well as aromatic systems. The presence of a polar solvent would markedly increase (7) the ionic dissociation of a phosphorane or ion-paired phosphonium halide intermediate. The change in kinetics and the reduction in steric hindrance may both be attributed to this change in the structure of the intermediate.

Additional evidence is the formation of five times as much dimethyl methylphosphonate as dimethyl *n*-butylphosphonate, in the reaction of trimethyl phosphite with *n*-butyl iodide in acetonitrile. In the absence of a solvent, such competition of an alkyl halide product with a different alkyl halide starting material is not a practical problem. To the extent that formation of the intermediate is the fast step (and irreversible), the tertiary phosphite would no longer be available. Even in acetonitrile, the effect is not seen unless the alkyl halide formed is significantly more reactive; thus no mixed products were observed in the tri-*n*-butyl phosphite–ethyl iodide system.

Acknowledgment

Acknowledgment is made to the donors of the Petroleum Research Fund, administered by the American Chemical Society, for the support of this work.

1. F. C. Buck and J. T. Yoke. J. Org. Chem. **27**, 3675 (1962).
2. G. Aksnes and D. Aksnes. Acta Chem. Scand. **17**, 2121 (1963); **18**, 38 (1964).
3. G. Aksnes and D. Aksnes. Acta Chem. Scand. **19**, 898 (1965).
4. V. Mark and J. R. Van Wazer. J. Org. Chem. **29**, 1006 (1964).
5. G. M. Kosolapoff. J. Am. Chem. Soc. **67**, 1180 (1945).
6. R. B. LaCount and C. E. Griffin. Tetrahedron Letters, 3071 (1965).
7. A. I. Razumov and N. N. Bankouskaya. Zh. Obshch. Khim. **34**, 1859, 3423 (1964).

Can. J. Chem. Downloaded from www.nrcresearchpress.com by 210.87.254.40 on 09/05/12
For personal use only.

Can. J. Chem. Downloaded from www.nrcresearchpress.com by 210.87.254.105 on 09/05/12
For personal use only.

Optical rotatory dispersion studies of 2*H*-naphtho(1,8-*bc*)- and naphtho(2,3-*b*)furan derivatives

P. Joseph-Nathan and Ma. P. González[1]

Departamento de Química del Centro de Investigación y de Estudios Avanzados, Instituto Politécnico Nacional, P.O. Box 14-740, Mexico City, Mexico

Received December 20, 1968

The study of the optical rotatory dispersion (o.r.d.) curves of some derivatives of the title systems, possessing various degrees of oxidation which contain asymmetrical centers near the chromophores, permits correlations between Cotton effects and stereochemistry. The configurations of those asymmetrical centers not known earlier, have been determined with the aid of the o.r.d. curves.

Canadian Journal of Chemistry, **47**, 2465 (1969)

The appearance of papers dealing with the use of optical rotatory dispersion (o.r.d.) and circular dichroism (c.d.) for studying the behavior of aromatic compounds with asymmetrical centers in the vicinity of their chromophores, has increased in the last years due to the advent of instruments capable of measuring optical activity to below 200 mμ (for a recent survey see ref. 2). However, the Cotton effects exhibited by many optically active aromatic substances, have not as yet been studied adequately (3–8). Therefore, we describe the o.r.d. spectra of some derivatives of the 2*H*-naphtho(1,8-*bc*)- and the naphtho(2,3-*b*)-furan systems, which were obtained during the elucidation of structures and chemical behavior of some Mexican natural products. Some of the substances studied here, should later be useful as o.r.d. models for other compounds, since they have small conformational flexibilities, and with few exceptions, their stereochemistry is known through independent chemical work.

According to the definitions of aromatic structures given by Crabbé and Klyne (2), the derivatives of the naphthofuran systems possess arylic heteroatoms and benzylic asymmetrical centers. Simultaneously such compounds as cacalone (**2***a*) and perezinone dibenzoate (**4**) can be classified as containing inherently dissymmetric chromophores. Some of the compounds contain quinonoid type rings which have not been considered adequately (2). We propose that the definitions of structures given recently (2) should be extended to quinones, which can be considered as aromatic compounds, since there is a measurable degree of cyclic delocalization of π-electrons (9).

[1]Taken in part from ref. 1.

Another important analogy between the compounds is that they possess a methyl group inserted in an asymmetrical center located α to the chromophore. Its configuration has been established in all compounds by degradative oxidation and chemical correlation (10–15). Application of the Sequence Rule (16) shows that in all cases, the methyl group is located in an asymmetrical center with absolute configuration (*R*). In addition, compounds **7** to **9** possess a second center of asymmetry, whose configuration was determined from the o.r.d. data.

It is well known that aromatic compounds show three major transitions in the ultraviolet (u.v.) region, two of which are strong absorptions near 180 and 200 mμ, and the third a weak one, generally with considerable fine structure, at about 260 mμ. We shall refer to the last one, known as the ^1L_b band in the Platt notation (17), since in dissymmetric aromatic compounds this π–π* transition is optically active.

Cacalol (**1***a*), cacalol acetate (**1***b*), and methyl cacalol (**1***c*) show very similar isotropic absorption spectra and similar o.r.d. curves (Fig. 1). They contain asymmetrical chromophores (the benzofuran system) which are dissymmetrically perturbed by the methyl group. The π–π* transition of their hexasubstituted benzene ring (near 260 mμ) is associated with strong positive Cotton effects with some fine structure, whose amplitude ranges between 169 in cacalol acetate (**1***b*) and 207 in methyl cacalol (**1***c*). The nearest analogy to this behavior appears to be shown by some 1-substituted indanes (18) with an absolute configuration (*R*), which give rise to weak positive Cotton effects with similar fine structures as compounds **1***a*, **1***b*, and **1***c* in the 260–270 mμ region. However, no Cotton effect was observed in the

Can. J. Chem. Downloaded from www.nrcresearchpress.com by 210.87.254.105 on 09/05/12
For personal use only.

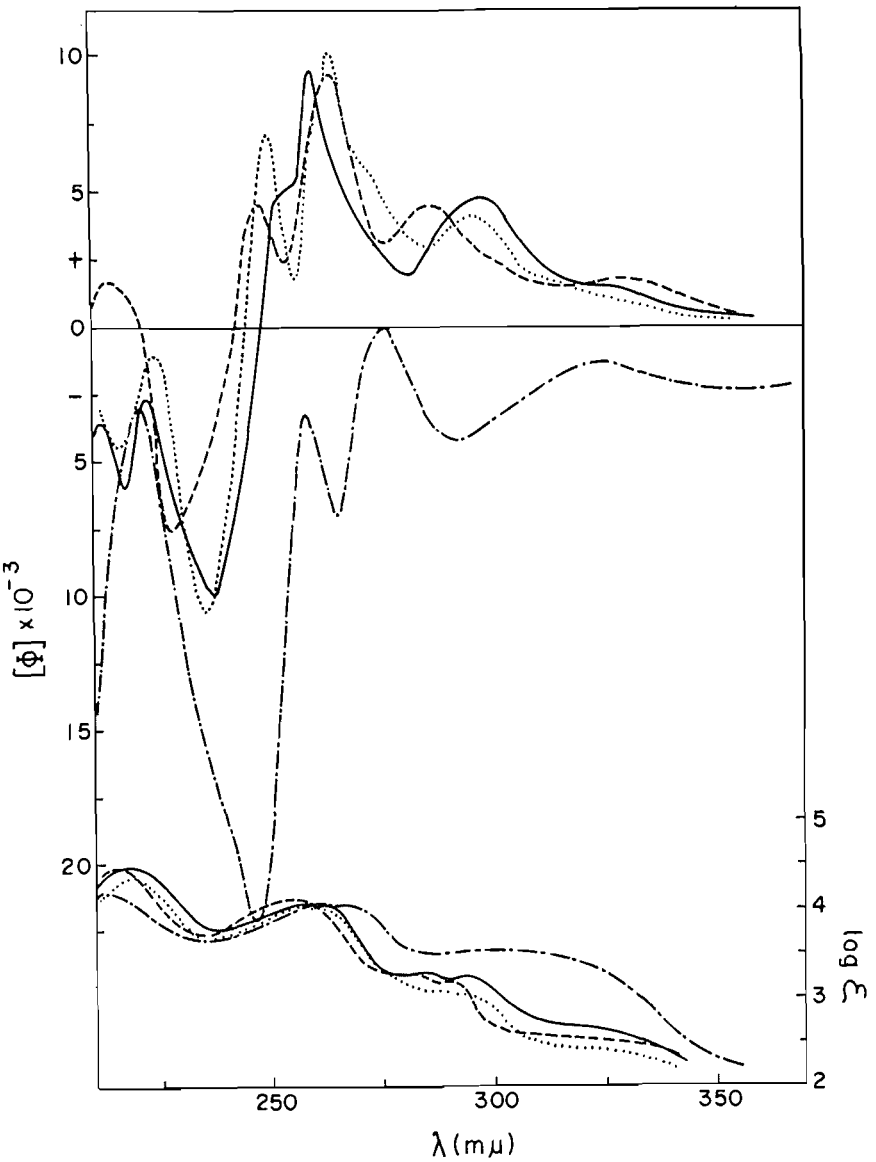

FIG. 1. The optical rotatory dispersion (in MeOH) and ultraviolet (in EtOH) curves of cacalol (**1***a*,———), cacalol acetate (**1***b*, - - - - -), methyl cacalol (**1***c*, ...), and the norquinone **3** (—.—.—.—.). (Ultraviolet spectra determined in MeOH are similar to those depicted. See Experimental.)

o.r.d. curve of (*R*)-1-methyl-indane (18). This fact, as well as the differences in the intensities of the Cotton effects, can be justified since cacalol (**1***a*) and its derivatives (**1***b* and **1***c*) possess two heterosubstituents on the aromatic ring itself, which appear to be necessary to provide an optically active transition of high intensity (19).

The o.r.d. curve (Fig. 1) of the norquinone (**3**) obtained by oxidation of cacalol (**1***a*) (10, 11) showed a negative Cotton effect in the 300 mμ region. The absolute configuration of its asymmetrical center must be the same (*R*) as that of its precursor (**1***a*), since this center is not affected during oxidation. This is demonstrated by the

Can. J. Chem. Downloaded from www.nrcresearchpress.com by 210.87.254.105 on 09/05/12
For personal use only.

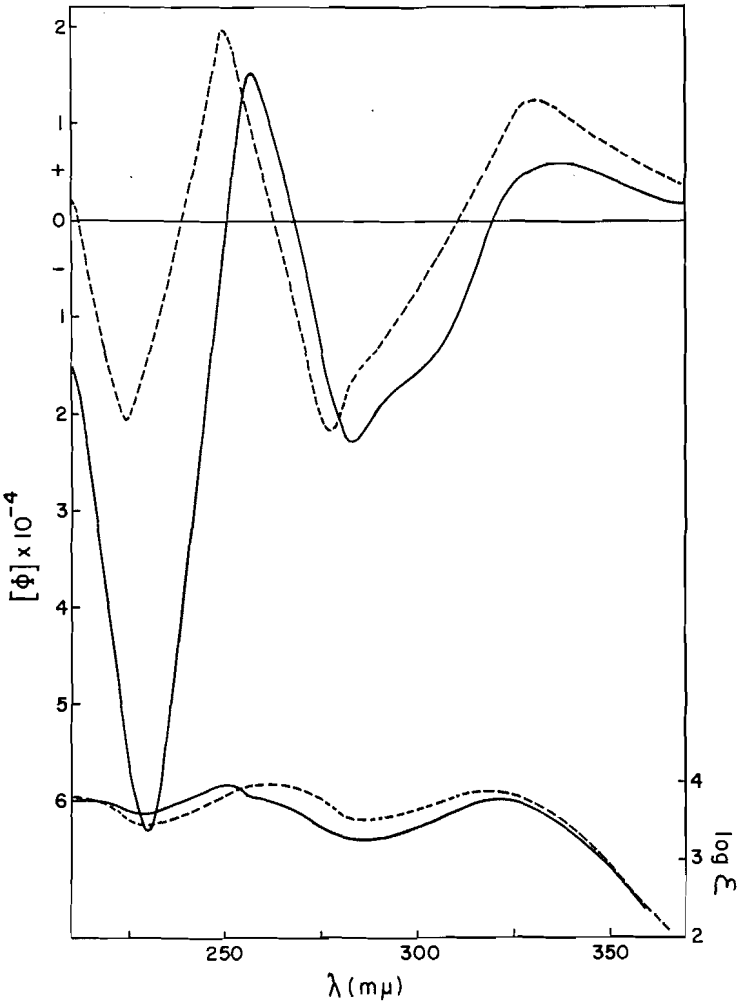

FIG. 2. The optical rotatory dispersion (in MeOH) and ultraviolet (in EtOH) curves of cacalone (**2***a*, ———) and cacalone acetate (**2***b*, - - - - -). (Ultraviolet spectra determined in MeOH are similar to those depicted. See Experimental.)

fact that some *p*-quinones possessing a center of asymmetry with absolute configuration (*R*) in the vicinity of their chromophores, give rise to negative Cotton effects in the 300 mμ region (20, 21), and the o.r.d. curve of the norquinone (**3**) resembles to some extent that of a *p*-quinone obtained by oxidation of latifolin (22).

Cacalone (**2***a*) and its acetate (**2***b*) belong to the class of compounds possessing inherently dissymmetric chromophores (2), since a carbonyl group is conjugated with the benzofuran system. They contain two optically active transitions in the u.v. region, each with positive Cotton effects, the first (near 320 mμ) being due to the carbonyl group (Fig. 2) and the second to the ^1L_b band of the aromatic moiety. Although some o.r.d. studies of substituted 1-tetralones have been described (23, 24), since their true aromatic Cotton effects have not been reached due to equipment limitations, and since they possess (23, 24) more than one asymmetric center near the chromophore, they are not suitable models for the natural product (**2***a*) and its acetate (**2***b*), which have only one center of asymmetry.

However, as in the case of compounds **1***a*, **1***b*, and **1***c*, the ^1L_b transition of cacalone (**2***a*) and its acetate (**2***b*) displayed positive Cotton effects.

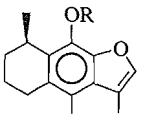

1 *a*: R = H
b: R = Ac
c: R = Me

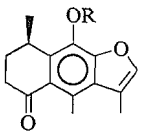

2 *a*: R = H
b: R = Ac

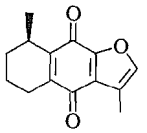

3

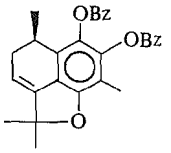

4

NOTE ADDED IN PROOF: Very recent evidence (28)[2] implies that the structure of compounds **1** to **3** are as shown:

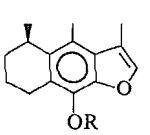

1

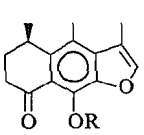

2

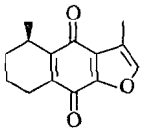

3

The change in position of the methyl group does not affect either the assignments or conclusions of the present work.

Another type of inherently dissymmetric chromophore having only one asymmetrical center is represented by perezinone dibenzoate (**4**). Its u.v. spectrum showed (12) three major transitions ca. 235, 270, and 325 mμ; the first and second bands contain isotropic absorption contributions from the benzoate aromatic rings (25) whereas the second and third bands are optically active. The positive Cotton effect associated with the 270 mμ band can be rationalized in terms of the ^1L_b band of the aromatic ring, since this transition is perturbed by the (*R*)-methyl group in a similar way as in the naphtho(2,3-*b*)furan derivatives **1***a*, **1***b*, and **1***c*.

Valuable information could be obtained from the o.r.d. curves of the hydroxyquinonemethide perezinone (**5**) and of the hydroxydihydro-*amphi*-quinone oxoperezinone (**6**). Their isotropic absorption and o.r.d. spectra are shown in Fig. 3. The o.r.d. curves reveal that their transitions are optically active, having negative Cotton effects with fine structure. This fact is in excellent accord with the o.r.d. curve of the norquinone (**3**) which also gave a negative Cotton effect (*vide supra*), since the three quinones (**3**, **5**, and **6**) possess a methyl group with absolute configuration (*R*) located *alpha* to the chromophore.

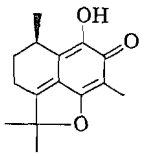

5

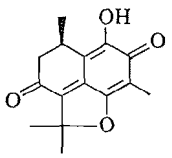

6

Hydrogenation of perezinone (**5**) (13) and oxoperezinone (**6**) (12) in the presence of Ac_2O afforded the diacetates **7** and **8** respectively, whereas *m*-chloroperbenzoic acid treatment of perezinone dibenzoate (**4**) gave compound **9** (12). The three reaction products contain in addition to the (*R*)-methyl group a second center of asymmetry which is also located *alpha* to the aromatic ring. Its configuration is deduced from the o.r.d. data as follows: the ^1L_b band of leuco-dihydroperezinone diacetate (**7**) shows a negative Cotton effect (26) in contrast to the positive ones displayed by the furotetralin derivatives **1***a*, **1***b*, and **1***c* which contain only the methyl group located at a center of asymmetry. After considering that in compound **7** the carbon having the *gem*-dimethyl group contributes more to the Cotton effect due to its size than the C-5 methyl group, the only way to explain the ^1L_b negative transition is to assume that the second asymmetrical center possesses an absolute configuration (*S*). During the transformation of **5** into **7**, hydrogen would be expected to attack the under, less hindered side of the molecule since the methyl group on the upper side hinders its approach. This was indeed observed, in good agreement with the Cotton effects. On the other hand, since compounds **7** and **8** were obtained from **5** and **6** under identical reaction conditions, and had similar geometry, the new asymmetric center in the products should have the same configuration. This can be proved easily by applying the octant rule (3, 6) to the keto group of leuco-dihydro-

[2]The authors are indebted to Dr. J. Romo (University of México) for this information prior to publication.

Can. J. Chem. Downloaded from www.nrcresearchpress.com by 210.87.254.105 on 09/05/12
For personal use only.

Can. J. Chem. Downloaded from www.nrcresearchpress.com by 210.87.254.105 on 09/05/12
For personal use only.

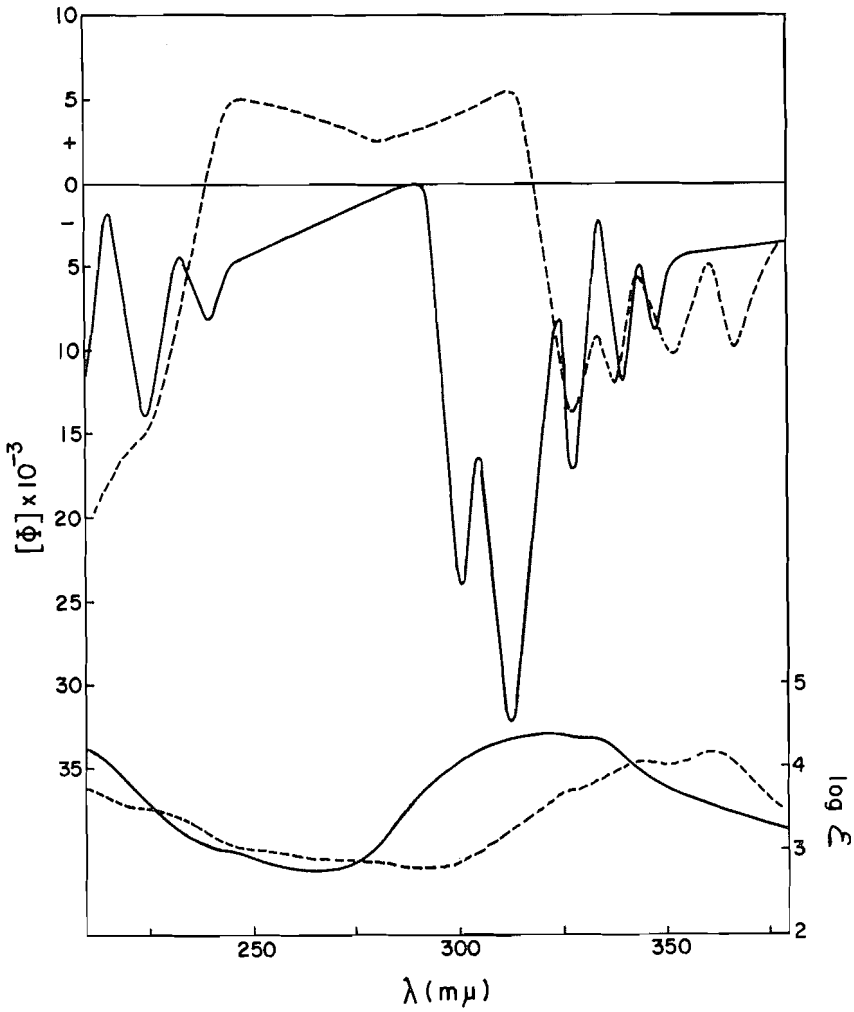

FIG. 3. The optical rotatory dispersion (in MeOH) and ultraviolet (in EtOH) curves of perezinone (**5**, ———) and oxoperezinone (**6**, ----). (Ultraviolet spectra determined in MeOH are similar to those depicted. See Experimental.)

öxoperezinone diacetate (**8**). Construction of Dreiding models reveals that when the hydrogen atom at the new asymmetric center is *beta* (absolute configuration (*R*)) the transition of the carbonyl group should give a negative Cotton effect, whereas an absolute configuration (*S*) would give a positive one. The o.r.d. curve of **8** displayed a weak positive Cotton effect with fine structure in the 320 mμ region. Furthermore the ^1L_b transition of the aromatic ring again showed a negative Cotton effect as in the case of the diacetate (**7**). It is also very reasonable that the Cotton effect in the 320 mμ region **8** is a weak one, since necessarily an equatorial or *quasi*-equatorial

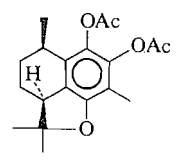

7

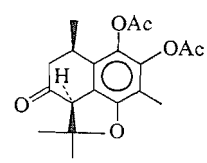

8

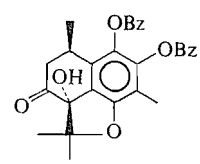

9

Can. J. Chem. Downloaded from www.nrcresearchpress.com by 210.87.254.105 on 09/05/12
For personal use only.

bond of the tetrahydrobenzene ring must be used for the junction to the furan ring.

The fact that compound **9** showed a strong positive Cotton effect with similar fine structure as **8** in the 320 mμ region is also congruent with the above observations. This can only be explained adequately in terms of formula **9** after proper application of the octant rule, since the reverse stereochemistry at the carbon having the hydroxyl group, leads to a negative Cotton effect. The higher intensity of the Cotton effect associated with the 320 mμ band of **9** compared to **8**, is due to the presence of the axial hydroxyl group since it is well known (3, 6) that axial substituents *alpha* to carbonyl contribute much more to Cotton effects than equatorial ones, and **9** has both axial and equatorial substituents, whereas **8** possesses only an equatorial one. In addition the ^1L_b band of compounds **8** and **9**, as expected from the observations described herein, give negative Cotton effects.

We can tentatively conclude that asymmetric centers located on the aliphatic ring *alpha* to the aromatic ring in tetralins, will show positive Cotton effects associated to the aromatic ^1L_b transitions, when the absolute configuration is (*R*); whereas if the absolute configuration is (*S*), these tetralins will show negative Cotton effects. It is also apparent that when the aromatic ring of a tetralin has quinonoid character, an asymmetric center located in the aliphatic ring *alpha* to the oxidized ring, gives rise to negative Cotton effects in the 300–320 mμ region when its absolute configuration is (*R*). However, these conclusions must be applied with care until more data are available. It would be helpful to study this type of compounds by c.d., but unfortunately we do not have access to such equipment.

The conformation of the aliphatic ring of all compounds, has recently been determined by 100 MHz double nuclear magnetic resonance spectroscopy (27).

Experimental

Materials

All derivatives of the naphtho(2,3-*b*)furan system were isolated or prepared as described (10, 11) for the structural elucidation of cacalol (**1***a*) and cacalone (**2***a*) and the 2*H*-naphtho(1,8-*bc*)furan derivatives were obtained as published recently (12, 13).

Measurements

The ultraviolet (u.v.) spectra of perezinone (**5**) and its derivatives were taken from the recent published data (12), whereas those of the naphtho(2,3-*b*)furan were repeated on Unicam SP800 in ethanolic solutions. They are plotted in Figs. 1 and 2 and are in good agreement with earlier reported values (10, 11).

For elegance in comparison between u.v. and optical rotatory dispersion (o.r.d.) spectra, the former were also determined in methanolic solutions and the pertinent data are given in this section.

A detailed comparison of the u.v. curves determined in MeOH, with those obtained in EtOH, reveals that solvent effects are negligible.

The o.r.d. curves were obtained with a JASCO ORD/UV-5 spectropolarimeter using JASCO 10 mm path dismountable Teflon cell in methanolic solutions between 22 and 26°.

*Cacalol (**1a**)*

Figure 1; o.r.d. (*c*, 0.0072): $(\Phi)_{700}$ ±0°, $(\Phi)_{400}$ ±0°, $(\Phi)_{348}$ +500°, $(\Phi)_{319}$ +1600°, $(\Phi)_{299}$ +4900°, $(\Phi)_{290}$ +3800°, $(\Phi)_{282}$ +1900°, $(\Phi)_{260}$ +9500°, $(\Phi)_{257}$ +5400°, $(\Phi)_{252}$ +4600°, $(\Phi)_{249}$ ±0°, $(\Phi)_{238}$ −10 000°, $(\Phi)_{223}$ −2700°, $(\Phi)_{218}$ −6000°, $(\Phi)_{212}$ −3500°, $(\Phi)_{210}$ −6500°; u.v. (MeOH) λ_{max}: 325, 296, 285, 262, 254, 218; log ε: 3.11, 3.20, 3.20, 3.84, 3.88, 4.28.

*Cacalol Acetate (**1b**)*

Figure 1; o.r.d. (*c*, 0.0067): $(\Phi)_{700}$ ±0°, $(\Phi)_{550}$ ±0°, $(\Phi)_{400}$ +500°, $(\Phi)_{350}$ +700°, $(\Phi)_{330}$ +1700°, $(\Phi)_{320}$ +1000°, $(\Phi)_{300}$ +2400°, $(\Phi)_{286}$ +4500°, $(\Phi)_{276}$ +3100°, $(\Phi)_{264}$ +9300°, $(\Phi)_{254}$ +2400°, $(\Phi)_{248}$ +4500°, $(\Phi)_{243}$ ±0°, $(\Phi)_{228}$ −7600°, $(\Phi)_{222}$ ±0°, $(\Phi)_{214}$ +1700°, $(\Phi)_{210}$ ±0°; u.v. (MeOH) λ_{max}: 291, 280, 255, 215; log ε: 3.20, 3.27, 4.13, 4.49.

*Methyl Cacalol (**1c**)*

Figure 1; o.r.d. (*c*, 0.0069): $(\Phi)_{700}$ ±0°, $(\Phi)_{400}$ ±0°, $(\Phi)_{338}$ +600°, $(\Phi)_{324}$ +1200°, $(\Phi)_{308}$ +2100°, $(\Phi)_{296}$ +4200°, $(\Phi)_{286}$ +3000°, $(\Phi)_{270}$ +6300°, $(\Phi)_{264}$ +10 200°, $(\Phi)_{256}$ +1800°, $(\Phi)_{250}$ +7200°, $(\Phi)_{245}$ ±0°, $(\Phi)_{235}$ −10 500°, $(\Phi)_{224}$ −1200°, $(\Phi)_{216}$ −4500°, $(\Phi)_{210}$ −2300°; u.v. (MeOH) λ_{max}: 292, 282, 261, 256, 218; log ε: 3.20, 3.32, 4.11, 4.13, 4.52.

*Cacalone (**2a**)*

Figure 2; o.r.d. (*c*, 0.0027): $(\Phi)_{700}$ ±0°, $(\Phi)_{450}$ ±0°, $(\Phi)_{370}$ +1500°, $(\Phi)_{335}$ +6100°, $(\Phi)_{319}$ ±0°, $(\Phi)_{300}$ −16 100°, $(\Phi)_{283}$ −23 000°, $(\Phi)_{268}$ ±0°, $(\Phi)_{257}$ +15 400°, $(\Phi)_{251}$ ±0°, $(\Phi)_{230}$ −63 000°, $(\Phi)_{210}$ −15 300°; u.v. (MeOH) λ_{max}: 321, 249, 207; log ε: 3.72, 3.89, 3.75.

*Cacalone Acetate (**2b**)*

Figure 2; o.r.d. (*c*, 0.0053): $(\Phi)_{700}$ ±0°, $(\Phi)_{550}$ ±0°, $(\Phi)_{420}$ +800°, $(\Phi)_{370}$ +3700°, $(\Phi)_{330}$ +12 000°, $(\Phi)_{312}$ ±0°, $(\Phi)_{285}$ −16 100°, $(\Phi)_{278}$ −22 500°, $(\Phi)_{263}$ ±0°, $(\Phi)_{250}$ +18 900°, $(\Phi)_{230}$ ±0°, $(\Phi)_{225}$ −21 200, $(\Phi)_{212}$ ±0°, $(\Phi)_{210}$ +2300°; u.v. (MeOH) λ_{max}: 317, 258, 206; log ε: 3.83, 3.95, 3.80.

*Norquinone (**3**)*

Figure 1; o.r.d. (*c*, 0.0058): $(\Phi)_{700}$ ±0°, $(\Phi)_{400}$ ±0°, $(\Phi)_{380}$ −1300°, $(\Phi)_{370}$ −2000°, $(\Phi)_{355}$ −2350°, $(\Phi)_{325}$ −1300°, $(\Phi)_{292}$ −4400°, $(\Phi)_{275}$ ±0°, $(\Phi)_{265}$ −7100° $(\Phi)_{258}$ −3400°, $(\Phi)_{246}$ −22 200°, $(\Phi)_{220}$ −3000°, $(\Phi)_{210}$ −15 300°; u.v. (MeOH) λ_{max}: 302, 266, 260, 216; log ε: 3.53, 4.06, 4.08, 4.12.

Can. J. Chem. Downloaded from www.nrcresearchpress.com by 210.87.254.105 on 09/05/12
For personal use only.

Perezinone Dibenzoate (4)

Optical rotatory dispersion (*c*, 0.009): $(\Phi)_{700}$ ±0°, $(\Phi)_{400}$ ±0°, $(\Phi)_{350}$ −3000°, $(\Phi)_{332}$ −6900°, $(\Phi)_{320}$ ±0°, $(\Phi)_{312}$ +900°, $(\Phi)_{306}$ +6000°, $(\Phi)_{300}$ +4700°, $(\Phi)_{280}$ +9900°, $(\Phi)_{272}$ ±0°, $(\Phi)_{267}$ +3000°, $(\Phi)_{264}$ ±0°, $(\Phi)_{252}$ −12 000°, $(\Phi)_{238}$ +850° ±0°, $(\Phi)_{231}$ −13 700°, $(\Phi)_{225}$ −4700°, $(\Phi)_{210}$ −34 300°; u.v. (MeOH) λ_{max}: 327, 315, 268, 234, 204; log ε: 3.93, 3.89, 4.06, 4.60, 4.34.

Perezinone (5)

Figure 3; o.r.d. (*c*, 0.0069): $(\Phi)_{700}$ ±0°, $(\Phi)_{400}$ ±0°, $(\Phi)_{370}$ −3500°, $(\Phi)_{353}$ −4400°, $(\Phi)_{348}$ −8900°, $(\Phi)_{344}$ −5100°, $(\Phi)_{340}$ −12 100°, $(\Phi)_{334}$ −2500°, $(\Phi)_{328}$ −17 100°, $(\Phi)_{325}$ −8250°, $(\Phi)_{313}$ −32 400°, $(\Phi)_{305}$ −16 500, $(\Phi)_{301}$ −24 100°, $(\Phi)_{291}$ ±0°, $(\Phi)_{245}$ −5100°, $(\Phi)_{240}$ −8250°, $(\Phi)_{233}$ −4400°, $(\Phi)_{225}$ −14 000°, $(\Phi)_{216}$ −1900°, $(\Phi)_{210}$ −15 200°; u.v. (MeOH) λ_{max}: 354, 330, 323, 208; log ε: 3.75, 4.38, 4.42, 4.23.

Oxoperezinone (6)

Figure 3; o.r.d. (*c*, 0.008): $(\Phi)_{700}$ ±0°, $(\Phi)_{420}$ ±0°, $(\Phi)_{385}$ −2800°, $(\Phi)_{367}$ −9900°, $(\Phi)_{361}$ −5000°, $(\Phi)_{352}$ −10 200°, $(\Phi)_{343}$ −6100°, $(\Phi)_{338}$ −12 200°, $(\Phi)_{334}$ −9400°, $(\Phi)_{328}$ −13 800°, $(\Phi)_{318}$ ±0°, $(\Phi)_{313}$ +5500°, $(\Phi)_{282}$ +2500°, $(\Phi)_{246}$ +5000°, $(\Phi)_{240}$ ±0°, $(\Phi)_{223}$ −15 500°, $(\Phi)_{210}$ −19 900°; u.v. (MeOH) λ_{max}: 361, 343, 325, 268, 225, 204; log ε: 4.14, 4.05, 3.69, 2.87, 3.48, 3.47.

Leuco-dihydroperezinone Diacetate (7)

Optical rotatory dispersion (*c*, 0.0041): $(\Phi)_{700}$ ±0°, $(\Phi)_{450}$ ±0°, $(\Phi)_{400}$ −1700°, $(\Phi)_{370}$ −3400°, $(\Phi)_{345}$ −4800°, $(\Phi)_{315}$ −4800°, $(\Phi)_{301}$ −6800°, $(\Phi)_{290}$ −10 250°, $(\Phi)_{268}$ −2050°, $(\Phi)_{250}$ −6800°, $(\Phi)_{230}$ −25 300°, $(\Phi)_{220}$ −10 900°, $(\Phi)_{210}$ −36 200°; u.v. (MeOH) λ_{max}: 286, 232, 209; log ε: 3.48, 3.74, 4.51.

Leuco-dihydroöxoperezinone Diacetate (8)

Optical rotatory dispersion (*c*, 0.0077): $(\Phi)_{700}$ ±0°, $(\Phi)_{380}$ ±0°, $(\Phi)_{360}$ +400°, $(\Phi)_{337}$ +1100°, $(\Phi)_{328}$ +2700°, $(\Phi)_{324}$ +1900°, $(\Phi)_{318}$ +2700°, $(\Phi)_{310}$ +800°, $(\Phi)_{306}$ +1100°, $(\Phi)_{300}$ ±0°, $(\Phi)_{286}$ +8400°, $(\Phi)_{274}$ ±0°, $(\Phi)_{268}$ −2400°, $(\Phi)_{254}$ −3800°, $(\Phi)_{232}$ −17 200°, $(\Phi)_{215}$ ±0°, $(\Phi)_{210}$ −7600°; u.v. (MeOH) λ_{max}: 325, 286, 207; log ε: 3.10, 3.40, 4.33.

Leuco-hydroxyoxoperezinone Dibenzoate (9)

Optical rotatory dispersion (*c*, 0.0085): $(\Phi)_{700}$ ±0°, $(\Phi)_{470}$ ±0°, $(\Phi)_{410}$ +1000°, $(\Phi)_{387}$ +2900°, $(\Phi)_{370}$ +3400°, $(\Phi)_{348}$ +7300°, $(\Phi)_{336}$ +16 000°, $(\Phi)_{331}$ +16 000°, $(\Phi)_{330}$ +17 000°, $(\Phi)_{325}$ +17 000°, $(\Phi)_{323}$ +17 500°, $(\Phi)_{318}$ +11 700°, $(\Phi)_{316}$ +10 700°, $(\Phi)_{310}$ +5300°, $(\Phi)_{308}$ ±0°, $(\Phi)_{291}$ −28 200°, $(\Phi)_{273}$ −15 100°, $(\Phi)_{262}$ −20 900°, $(\Phi)_{254}$ −16 000°, $(\Phi)_{238}$ −26 200°, $(\Phi)_{234}$ −17 500°, $(\Phi)_{212}$ −30 600°, $(\Phi)_{210}$ −26 200°; u.v. (MeOH) λ_{max}: 283, 230, 205; log ε: 3.68, 4.56, 4.52.

1. MA. P. GONZÁLEZ. Thesis for the degree of Maestro en Ciencias en Química. Departmento de Química del Centro de Investigacíon y de Estudios Avanzados, Instituto Politécnico Nacional, Mexico City, Mexico. (1969).
2. P. CRABBÉ and W. KLYNE. Tetrahedron, **23**, 3449 (1967).
3. C. DJERASSI. Optical rotatory dispersion; applications to organic chemistry. McGraw-Hill Book Co., Inc., New York. 1960.
4. W. KLYNE. *In* Advances in organic chemistry. Vol. 1. *Edited by* R. A. Raphael, E. C. Taylor, and H. Wynberg. Interscience Publishers, Inc., New York. 1960. p. 239.
5. G. G. LYLE and R. E. LYLE. *In* Determination of organic structures by physical methods. Vol. 2. *Edited by* F. C. Nachod and W. D. Phillips. Academic Press, Inc., New York. 1962. Chap. 1.
6. P. CRABBÉ. Optical rotatory dispersion and circular dichroism in organic chemistry. Holden Day, San Francisco. 1965. Applications de la dispersion rotatoire optique et du dichroisme circulaire optique en chimie organique. Gauthier-Villars, Paris. 1968.
7. L. VELLUZ, M. LEGRAND, and M. GROSJEAU. Optical circular dichroism. Principles, measurements, and applications. Verlag Chemie, Weinheim. 1965.
8. P. CRABBÉ. *In* Topics in stereochemistry. *Edited by* N. L. Allinger and E. L. Eliel. Interscience Publishers, Inc., New York. 1967. p. 93.
9. F. SONDHEIMER. Pure Appl. Chem. **7**, 363 (1963).
10. J. ROMO and P. JOSEPH-NATHAN. Tetrahedron, **20**, 2331 (1964).
11. P. JOSEPH-NATHAN, J. J. MORALES, and J. ROMO. Tetrahedron, **22**, 301 (1966).
12. P. JOSEPH-NATHAN, J. REYES, and MA. P. GONZÁLEZ. Tetrahedron, **24**, 4007 (1968).
13. F. WALLS, J. PADILLA, P. JOSEPH-NATHAN, F. GIRAL, M. ESCOBAR, and J. ROMO. Tetrahedron, **22**, 2387 (1966).
14. D. A. ARCHER and R. H. THOMSON. J. Chem. Soc. C, 1710 (1967).
15. D. ARIGONI and O. JEGER. Helv. Chim. Acta, **37**, 881 (1954).
16. R. S. CAHN, C. K. INGOLD, and V. PRELOG. Angew. Chem. Intern. Ed. **5**, 385 (1966), and previous papers.
17. J. R. PLATT. J. Chem. Phys. **17**, 484 (1949).
18. J. H. BREWSTER and J. G. BUTA. J. Am. Chem. Soc. **88**, 2233 (1966).
19. L. VERBIT. J. Am. Chem. Soc. **87**, 1617 (1965).
20. W. B. EYTON, W. D. OLLIS, I. O. SUTHERLAND, O. R. GOTTLIEB, M. TAVIERA MAGALHAES, and L. M. JACKMAN. Tetrahedron, **21**, 2683 (1966).
21. W. B. EYTON, W. D. OLLIS, I. O. SUTHERLAND, O. R. GOTTLIEB, M. TAVIERA MAGALHAES, and L. M. JACKMAN. Tetrahedron, **21**, 2697 (1966).
22. D. KUMASI, S. K. MUKERJEE, and T. R. SESHADRI. Tetrahedron Letters, 3767 (1966).
23. A. K. BOSE, M. S. MANHAS, and R. C. CAMBIE. J. Org. Chem. **30**, 501 (1965), and earlier papers.
24. C. DJERASSI, W. D. OLLIS, and R. C. RUSSELL. J. Chem. Soc. 1448 (1961).
25. H. E. UNGNADE and R. W. LAMB. J. Am. Chem. Soc. **74**, 3789 (1952).
26. J. PADILLA, J. ROMO, F. WALLS, and P. CRABBÉ. Rev. Soc. quím. Méx. **11**, 7 (1967).
27. P. JOSEPH-NATHAN, MA. P. GONZÁLEZ, and E. DIÁZ. Rev. Soc. quím. Méx. In press.
28. H. KAKISAWA, Y. INOUYE, and J. ROMA. Tetrahedron Letters. In press.

Can. J. Chem. Downloaded from www.nrcresearchpress.com by 210.87.254.40 on 09/05/12
For personal use only.

Nuclear magnetic resonance studies of hydrogen bonding in acetylenes containing oxygen functions[1]

W. E. BENTZ[2] AND L. D. COLEBROOK
Department of Chemistry, University of Rochester, Rochester, New York 14627

Received August 16, 1968

Dilution shifts in carbon tetrachloride and cyclohexane solution have been obtained for the terminal acetylenic proton signals in the nuclear magnetic resonance (n.m.r.) spectra of some acetylenes. The presence of an oxygen atom results in a significant increase in the magnitude of the dilution shift, suggesting that oxygen is an important proton acceptor site in these compounds. Steric influences on the dilution shift and differences between the infinite dilution chemical shifts in the two solvents used, have been observed.

Canadian Journal of Chemistry, 47, 2473 (1969)

It has been known for some time that compounds with terminal acetylene groups are capable of forming hydrogen bonds between the slightly acidic acetylenic hydrogen atom and electron donor groups. Weak hydrogen bonds of this type are amenable to study by nuclear magnetic resonance (n.m.r.) methods and several reports of work in this area have appeared (1).

Hatton and Richards (2) have examined the n.m.r. spectra of propargyl chloride, phenylacetylene (3), and benzoylacetylene in various solvents. They found that dilution with a poor electron donor solvent, such as cyclohexane, resulted in a small upfield shift of the acetylenic proton line position. It was assumed that, at infinite dilution in cyclohexane, acetylene–acetylene interactions were at a minimum. The lower field position of the acetylene proton resonance in the neat liquid was taken as evidence for deshielding produced by weak intermolecular hydrogen bonding between the acetylenic protons and the π-electron system. Whipple and co-workers (3) obtained comparable results when studying the spectrum of propargyl bromide in similar solvents.

Elsakov and Petrov (4, 5) have studied the dilution shifts in carbon tetrachloride of a number of acetylenes, including one containing an ether oxygen atom. Their results suggested that hydrogen bonding may be more extensive in acetylenes containing oxygen than in the corresponding hydrocarbons.

In order to obtain more information on the chemical shifts of acetylenic protons than has been available in the literature, we have undertaken a study to ascertain the extent to which the presence of an oxygen atom influences the magnitude of the dilution shift. Carbon tetrachloride was selected as the main solvent since it is a poor proton acceptor and it is a commonly used solvent for n.m.r. studies. However, in a study of the O—H stretching frequencies of a number of alcohols in several solvents, Allerhand and Schleyer (6) have found that $\Delta\nu = \nu_{\text{"free"}} - \nu_{H\text{-bonded}}$ is larger in carbon tetrachloride than in cyclohexane. Since $\nu_{\text{"free"}}$ and $\nu_{H\text{-bonded}}$ were found to be shifted to different extents in going from cyclohexane to carbon tetrachloride, these authors concluded that the latter solvent must interact in some specific way with solute molecules, and thus is not a totally "inert" solvent. Schaefer *et al.* (7) have also reported results which they interpret as evidence for a solvent effect on proton chemical shifts by carbon tetrachloride as compared to cyclohexane. For these reasons we have also determined the dilution shifts of some of the acetylenes in the apparently "more inert" solvent cyclohexane. The chemical shifts of the acetylenic protons of a number of compounds, some with oxygen atoms and some without, were measured as a function of concentration in carbon tetrachloride and cyclohexane. Concentrations in both solvents ranged from almost neat liquids to the lowest mole fraction which yielded spectra that could be measured with tolerable accuracy. The dilution curves obtained in this way were extrapolated to mole fractions of 1.00 and 0.00 (see Fig. 1 for carbon tetrachloride dilution curves). Extrapolation error was small because in no case was

[1]This work was supported by Grant No. GM-12 468 from the National Institutes of Health, United States Public Health Service.
[2]National Defense Education Act Predoctoral Fellow.

Can. J. Chem. Downloaded from www.nrcresearchpress.com by 210.87.254.40 on 09/05/12
For personal use only.

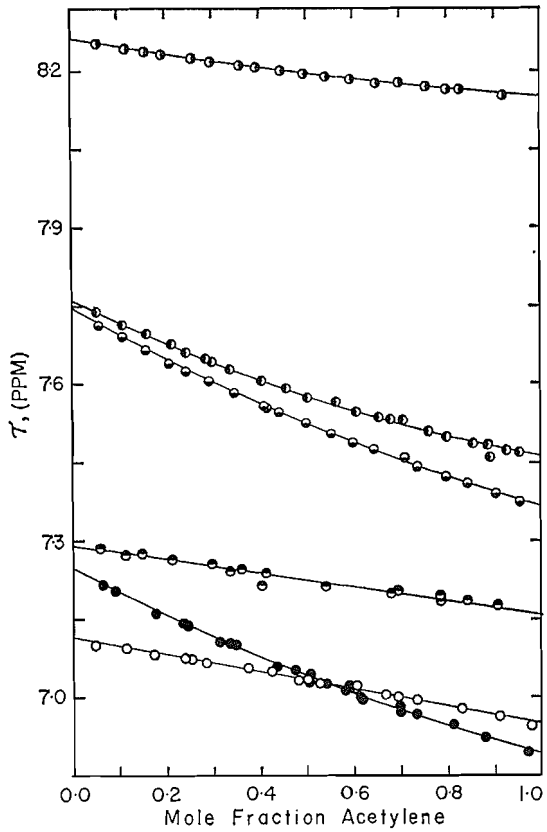

FIG. 1. Chemical shift vs. concentration in carbon tetrachloride solution of acetylenic protons: ◑, compound **1**; ◓, compound **2**; ○, compound **3**; ●, compound **4**; ◐, compound **5**; ◒, compound **6**. See Table I.

the curvature of the plot very great. The chemical shifts of the neat liquids and of the infinitely dilute solutions in carbon tetrachloride and cyclohexane are shown in Table I. Some data from ref. 2 are included for comparison purposes. Internal references were used in all cases.

Measurement of Spectra

All samples were prepared by weighing an appropriate amount of the acetylene directly into the sample tube. Carbon tetrachloride samples were prepared by weighing a solution of 5 or 15% of tetramethylsilane in the solvent into the tube. Cyclohexane solutions of **6** (see Table I) were prepared similarly, while samples of **2** and **3** were prepared without the addition of tetramethylsilane. The weight of tetramethylsilane was taken into account in calculating the mole fractions, which were accurate to ±0.003 or better. Analytical grade carbon tetrachloride and cyclohexane were dried by standing over Fisher type 4A molecular sieve before use.

The spectra of compounds **1**, **5**, and **6** in carbon tetrachloride and **2**, **3**, and **6** in cyclohexane were determined using a JEOLCO 4H-100 spectrometer operating at 100 MHz. Line positions, accurate to ±0.1 Hz, were measured directly from the recorded peak maxima using the internal frequency counter. The spectra of compound **2** in carbon tetrachloride were determined with a Varian HR-60 spectrometer and the spectra of compounds **3** and **4** in carbon tetrachloride with an A-60 spectrometer, both instruments operating at 60 MHz. Line positions were measured by the sideband method, using a Hewlett Packard 200 CD audio oscillator and a CMC 201 B frequency counter, to an accuracy of ±0.2 Hz.

Results and Discussion

Weak hydrogen bonds of the type studied in this project must be considered as transient on the n.m.r. time scale. At a given instant some molecules will be bonded and some will be "free". When several electron donor sites exist (as many as three in the current series), acetylenic protons will be present in a number of hydrogen-bonded complexes as well as in the "free" or unassociated state. The observed time-averaged chemical shift must be dependent on the chemical shift of protons in each of the environments, and on the relative numbers of protons in each state. If the chemical shift at infinite dilution is the true "free" chemical shift then the observed dilution shift (the difference between the chemical shift of the neat liquid and that of the infinitely dilute solution) will be a measure of the net effect of the factors which displace the chemical shift from its "free" value. If the solvent is not completely "inert", as may be the case with carbon tetrachloride, the chemical shift of acetylene molecules bonded to solvent molecules will also influence the resultant chemical shift. A change in molecular structure which alters the chemical shift of protons bound at a particular site, or which affects the relative numbers of molecules bound at that and other sites, may be expected to influence the resultant chemical shift.

Compounds **1**–**6** may be grouped into two distinct classes on the basis of their dilution

TABLE I

Acetylene proton dilution shifts

No.	Compound	Solvent	Infinite dilution (τ)	Neat liquid (τ)	Dilution shift (Δτ, p.p.m.)
1	$CH_3(CH_2)_5C{\equiv}CH$	CCl_4	8.262	8.150	0.112
2	$CH_2{=}C(CH_3)C{\equiv}CH$	CCl_4	7.290	7.162	0.128
		C_6H_{12}	7.388	7.150	0.238
3	$C_6H_5C{\equiv}CH$	CCl_4	7.115	6.950	0.165
		C_6H_{12}	7.203	6.935	0.268
		C_6H_{12}	7.26*	6.91*	0.35*
4	*cis*-$CH_3OCH{=}CHC{\equiv}CH$	CCl_4	7.247	6.894	0.353
5	$CH_3OC(CH_3)_2C{\equiv}CH$	CCl_4	7.764	7.458	0.306
6	$CH_3OCH_2C{\equiv}CH$	CCl_4	7.750	7.388	0.362
		C_6H_{12}	7.870	7.387	0.483

*See ref. 2.

shifts in carbon tetrachloride solution. The hydrocarbons show dilution shifts of less than 0.2 p.p.m. whereas the compounds containing oxygen show dilution shifts greater than 0.3 p.p.m. (Table I). The magnitude of the dilution shift is an unreliable indication of the strength of the hydrogen bonds since the chemical shift of a bonded hydrogen atom is determined by magnetic anisotropy as well as by the electron polarization produced by bond formation. However, the greater dilution shift (by a factor of 2 to 3 or more) when an oxygen atom is present in the molecule suggests that this atom can be an important proton acceptor site in these compounds. The presence of an oxygen atom may also influence the extent of hydrogen bonding at other electron donor sites.

Compounds **2**, **3**, and **6** were also examined in cyclohexane solution (Table I). Compounds **2** and **6** were selected for this study to determine whether or not the large difference in dilution shift between compounds with and without oxygen functions is also observable in this solvent. A logical choice for a non-oxygen containing acetylene would have been **1**, but the acetylenic proton of this compound absorbs too close to the cyclohexane solvent line position for accurate analysis. Compound **3** was reinvestigated in this solvent because its dilution shift in cyclohexane reported by Hatton and Richards (2) was more than double that found in this laboratory for carbon tetrachloride solutions.

The dilution shifts of both **2** and **6** were found to be increased by approximately 0.12 p.p.m. in cyclohexane as compared to carbon tetrachloride. Compound **6** still shows a shift larger by a factor of 2 than that of **2**, which supports the inference that the oxygen atom is a major electron donor in hydrogen bond formation in these compounds. In this respect, the results are the same in the two solvents. The dilution shift of **3** is also increased in cyclohexane compared to that in carbon tetrachloride. However, the shift was not found to be as large as that reported previously by Hatton and Richards.

In all cases the differences between the dilution shifts in the two solvents result from the infinite dilution chemical shifts in cyclohexane being at higher field than those seen in carbon tetrachloride. The small differences in the chemical shifts reported for the neat solutions in Table I reflect extrapolation errors. These results imply that carbon tetrachloride undergoes some type of specific association with the acetylene molecules, which causes a small downfield shift in the acetylenic proton signals.

Steric factors which hinder the approach of an acetylenic hydrogen atom to a donor site may be expected to reduce the magnitude of the dilution shift. This steric effect is likely to be particularly marked if a major bonding site which makes an important contribution to the total chemical shift is affected. This situation is well illustrated by a comparison of the dilution shifts in carbon tetrachloride of 3-methoxy-1-propyne (**6**), and 3-methyl-3-methoxy-1-butyne (**5**). These two compounds have the same carbon skeleton but differ in that **5** has two methyl substituents on C-3. Since the infinite dilution chemical shifts of these compounds are very similar, it is clear that the structural differences have little

Can. J. Chem. Downloaded from www.nrcresearchpress.com by 210.87.254.40 on 09/05/12
For personal use only.

Can. J. Chem. Downloaded from www.nrcresearchpress.com by 210.87.254.40 on 09/05/12
For personal use only.

direct effect on the shielding of the acetylenic proton. The two methyl groups on the carbon bearing the oxygen atom in **5** should be expected to hinder the approach of another molecule of the acetylene, particularly to the bonding site on oxygen. It is found that the dilution shift of the more hindered compound, **5**, is about 15% smaller than that of the less hindered compound **6**, in accord with this prediction. The dilution shift of **5** is also substantially smaller than that of compound **4**, which is relatively unhindered.

Introduction of a double bond has little effect on the dilution shift in carbon tetrachloride. Elsakov and Petrov have noted (4) that conjugation of a double bond with the acetylenic triple bond has only a small effect on the magnitude of the shift. The presence of the phenyl group conjugated with the triple bond in **3** results in a more marked increase in the magnitude of the dilution shift. Interpretation of the shift in this case is complicated by the effect of the anisotropy of the aromatic ring.

Elsakov and Petrov (4, 5) have reported dilution shifts in carbon tetrachloride for compound **2** ($\Delta\tau = 0.16$ p.p.m.) and compound **4** ($\Delta\tau = 0.28$ p.p.m.), plus the additional compounds vinylacetylene ($\Delta\tau = 0.09$ p.p.m.) and 3-methyl-1-butyne ($\Delta\tau = 0.07$ p.p.m.). The last compound would be expected to show a dilution shift similar to that observed for 1-octyne, (**1**), in this laboratory. The agreement is reasonable, but not excellent. While the reported dilution shifts for compounds **2** and **4** are in general agreement with our results, they differ somewhat in magnitude. Experimental data obtained at the lower concentrations contain the main source of the discrepancies. The dilution shift reported for compound **4** is smaller than we obtained and tends to de-emphasize the role of oxygen as a proton acceptor site. Data reported by these authors were obtained from a much smaller number of measurements than were made in the present study.

Jouve (8) has determined the chemical shifts at infinite dilution in carbon tetrachloride of a number of terminal acetylenes and has presented an explanation of these shifts in terms of the molecular environment of the acetylenic protons. The reported infinite dilution chemical shifts of several straight chain terminal acetylenes (C-3 to C-7) show close agreement with the value obtained in this laboratory for 1-octyne. From the information now available it may be concluded that the chemical shift at infinite dilution in carbon tetrachloride of the acetylenic proton in compounds of this type is likely to fall in the range τ 8.24–8.27. Jouve has also reported infinite dilution chemical shifts for compounds **2**, **3**, and **6** in carbon tetrachloride differing by no more than 0.04 p.p.m. from the values obtained in this laboratory. The experimental data now available are adequate to indicate the approximate range within which the acetylenic protons of a variety of compounds may be expected to absorb in carbon tetrachloride solution. By combining the infinite dilution chemical shifts given in ref. 8 with the dilution shifts of representative compounds given in Table I and in refs. 4 and 5, it should be possible to make a reasonably satisfactory prediction of the chemical shifts of the acetylenic protons of many compounds at typical concentrations in carbon tetrachloride solution.

Hatton and Richards (2) have observed that the methylene protons of propargyl chloride were shifted by 0.26 p.p.m. when this compound was diluted with cyclohexane. We have observed a similar effect when compound **4** is diluted with carbon tetrachloride, the lines arising from the protons on the double bond undergoing an upfield shift (Table II). The chemical shift of the protons of the methyl group in this compound is essentially independent of concentration.

Experimental

Boiling points are uncorrected.

1-Octyne (1)

1-Octyne was obtained from Chemical Procurement Laboratories. Before use it was distilled twice, yielding a colorless liquid, b.p. 125–127°, n_D^{26} 1.4165. Samples with mole fractions of 0.056–0.920 were prepared in carbon tetrachloride and the chemical shift of the acetylenic proton from an internal TMS lock was measured. The position of the center peak of the triplet arising from the acetylene proton was taken as the chemical shift.

TABLE II

Vinyl proton chemical shifts of *cis*-methoxy-1-butene-3-yne (**4**) (carbon tetrachloride solutions)

Proton	Infinite dilution (τ)	Neat liquid (τ)	Dilution shift ($\Delta\tau$, p.p.m.)
C_2-H	5.647	5.558	0.089
C_1-H	3.824	3.616	0.208

Can. J. Chem. Downloaded from www.nrcresearchpress.com by 210.87.254.40 on 09/05/12
For personal use only.

2-Methyl-1-butene-3-yne (2)

Compound **2**, obtained from the Aldrich Chemical Company, was distilled before use. The colorless distillate, b.p. 33–34°, n_D^{25} 1.4123, was used to prepare samples with mole fractions of 0.060–0.908 in carbon tetrachloride. The chemical shift from TMS of the broad acetylenic singlet was measured. Samples of mole fraction 0.084–0.897 were prepared using cyclohexane as solvent. The position of the broad acetylenic singlet relative to cyclohexane was determined. This shift was then added to the slightly concentration dependent cyclohexane–TMS separation for the concentration in question in order to obtain the chemical shift relative to TMS.

Phenylacetylene (3)

This compound was obtained from Eastman Organic Chemicals Company and was distilled before use, yielding a colorless distillate, b.p. 138.5–139.5°, n_D^{26} 1.5461. Samples with mole fractions of 0.048–0.980 were prepared with carbon tetrachloride as solvent. The position of the acetylenic proton singlet relative to TMS was measured. Samples with mole fractions of 0.086–0.964 were prepared in cyclohexane. In this case the acetylene–cyclohexane separation was measured. This was then added to the concentration dependent cyclohexane–TMS separation to obtain the acetylene–TMS separation.

cis-1-Methoxy-1-butene-3-yne (4)

This compound was obtained from the Aldrich Chemical Company as an 80% solution in methanol. Fractional distillation in small quantities immediately before use yielded a colorless liquid, b.p. 59–61° (60 mm), n_D^{24} 1.4789. Samples with mole fractions of 0.066–0.975 in carbon tetrachloride solution were analyzed. The position of the highest field member of each acetylenic and olefinic proton quartet was measured with respect to TMS. Chemical shifts for each proton were taken to be the centers of the respective quartets.

3-Methoxy-3-methyl-1-butyne (5)

This compound was prepared in a manner similar to that of Kreevoy *et al.* (9). The entire reaction was carried out at 0 °C. 48 ml (0.15 mole) of dimethyl sulfate (Eastman Organic Chemicals practical grade) were added with stirring to a mixture of 42 g (0.50 mole) of 2-methyl-3-butyne-2-ol (Eastman Organic Chemicals practical grade), 53 ml of water, and 5 g of 50% sodium hydroxide solution. To this an additional 50 g of 50% sodium hydroxide solution (a total of 0.69 mole) were added slowly over a period of several hours. The upper layer of the resulting two phase system was extracted with cold water and dried over $MgSO_4$. The dried material was fractionally distilled, the fraction boiling at 70–87° being collected. This fraction was then redistilled using an 18 in. spinning band column. The desired material (8.6 g, 8.8%) was collected at 77–78.5°, n_D^{22} 1.3988. Samples with mole fractions of 0.054–0.956 in carbon tetrachloride were prepared and the position of the acetylenic proton singlet measured. The singlet at 1.385 p.p.m. from TMS arising from the geminal dimethyls was used as the lock signal. It was found that the position of this signal was independent of concentration.

3-Methoxy-1-propyne (6)

This compound was prepared from 3-hydroxy-1-propyne, obtained from Eastman Organic Chemicals Company, by the method of Reppe (10) yielding 41% of the desired product, b.p. 57–61°, n_D^{25} 1.3931. Samples with mole fractions of 0.057–0.993 were prepared in carbon tetrachloride, while cyclohexane was used to prepare samples of mole fractions 0.115–0.993. In both solvents the slightly concentration dependent methoxyl singlet at approximately 3.3 p.p.m. from TMS was used as the lock signal. The methoxyl–acetylene and methoxyl–TMS separations were measured for each sample. Subtraction of the former from the latter yielded the acetylene–TMS separation.

Acknowledgments

We are indebted to Mr. David M. Morse for some of the preliminary measurements and to one of the referees for helpful suggestions.

1. J. W. Emsley, J. Feeney, and L. H. Sutcliffe. High resolution nuclear magnetic resonance spectroscopy. Vol. II. The Pergamon Press Ltd., Oxford. 1965. pp. 848–851.
2. J. V. Hatton and R. E. Richards. Trans. Faraday Soc. **57**, 28 (1961).
3. E. B. Whipple, J. H. Goldstein, L. Mandell, G. S. Reddy, and G. R. McClure. J. Am. Chem. Soc. **81**, 1321 (1959).
4. N. V. Elsakov and A. A. Petrov. Opt. Spectry. (USSR) English Transl. **16**, 77 (1964).
5. N. V. Elsakov and A. A. Petrov. Opt. Spectry. (USSR), English Transl. **16**, 434 (1964).
6. A. Allerhand and P. von R. Schleyer. J. Am. Chem. Soc. **85**, 371 (1963).
7. T. Schaefer, B. Richardson, and R. Schwenk. Can. J. Chem. **46**, 2775 (1968).
8. P. Jouve. Compt. Rend. **256**, 1497 (1963).
9. M. M. Kreevoy, H. B. Charman, and D. R. Vinard. J. Am. Chem. Soc. **83**, 1978 (1961).
10. W. Reppe. Ann. Chem. **596**, 74 (1955).

NOTES

Contribution à l'étude du mécanisme d'oxydation chromique de cycloalcanols secondaires

JEAN-CLAUDE RICHER ET NGUYEN THI THANH HOA[1]
Département de Chimie, Université de Montréal, Boîte Postale 6128, Montréal, Québec
Reçu le 9 mai 1968

Les vitesses d'oxydation chromique d'alcools secondaires cycliques ont été étudiées en fonction de la grandeur des cycles, ceux-ci ayant un nombre de carbones de 4 à 13 et 15. Les vitesses d'oxydation mesurées à quatre températures différentes ont permis de calculer les entropies, enthalpies et énergies libres d'activation. Les résultats sont discutés en fonction de la grandeur des cycles. L'effect isotopique cinétique a été déterminé pour les oxydations chromiques de certains cyclanols.

Canadian Journal of Chemistry, 47, 2479 (1969)

Introduction

Au cours d'un travail précédent (1) il a été suggéré, à la suite de Rocek (2) et de Venkatasubramian (3) que les états de transition dans des oxydations chromiques d'alcools épimères se rapprochent de beaucoup du produit final, à savoir de la cétone. Cette hypothèse a toutefois été prise à partie par Kwart (4, 5) en se basant entre autres sur le fait que les vitesses d'oxydation du cyclopentanol et du cyclohexanol ne diffèrent que très peu l'une de l'autre alors que les vitesses de solvolyse des tosylates correspondants sont très différentes. Les résultats rapportés dans la présente communication ont été obtenus au cours d'un travail entrepris afin d'établir des résultats expérimentaux pour les vitesses d'oxydation chromique de cyclanols couvrant la gamme des cycles classiques, moyens et des grands cycles; il était envisagé que les résultats obtenus pourraient être discutés en fonction des notions de la théorie des tensions internes développées par Brown (6–8).

Partie expérimentale

Les alcools examinés au cours du présent travail ont été obtenus de sources commerciales ou par réduction de la cétone correspondante avec de l'hydrure double de lithium et d'aluminium ou par le deutérure double de lithium et d'aluminium. L'homogénéité (pureté plus grande que 99%) des alcools étudiés a été établie grâce à la chromatographie en phase gazeuse; leurs propriétés physiques sont résumées dans le tableau I.

Les constantes de vitesses d'oxydation chromique ont été mesurées dans l'acide acétique aqueux à l'aide d'un spectrophotomètre Perkin–Elmer modèle 4000 A, d'après le protocole expérimental décrit précédemment (1). Les calculs de ces constantes et des facteurs d'activation qui en découlent ont été faits à l'aide de l'ordinateur électronique 3400 de la compagnie CDC au Centre de Calcul de l'Université de Montréal utilisant la méthode des moindres carrés et le programme "Fast Regress". Une description détaillée de la procédure expérimentale et des méthodes de calcul utilisées est présentée dans la thèse de doctorat de Mlle Nguyen dont copie est déposée à la Bibliothèque du Conseil National de Recherches du Canada.

Résultats et discussion

En se basant sur le fait qu'un effet isotopique primaire de 5.9 est observé au cours de l'oxydation chromique du cyclohexanol-d_1, il a été conclu (4) que l'étape déterminante de cette réaction implique la rupture du lien carbone–hydrogène carbinolique. Afin de s'assurer que dans le cas des composés à cycle moyen l'étape déterminante de la réaction d'oxydation chromique est toujours l'enlèvement de l'atome d'hydrogène carbinolique, l'effet isotopique primaire de cette réaction a été établi pour un nombre représentatif de ces cyclanols. Les résultats obtenus sont rapportés dans le tableau II; les effets isotopiques primaires observés permettent de conclure que dans les oxydations chromiques d'alcools secondaires de cycles moyens comme dans le cas général observé par Westheimer et

[1]Les résultats rapportés dans le présent travail sont tirés en partie de la thèse de doctorat soumise par Mlle Nguyen Thi Thanh Hoa en vue de l'obtention du grade de Doctorat es Sciences, Faculté des Sciences, Université de Montréal, août 1967.

TABLEAU I

Propriétés physiques des cyclanols

$(CH_2)_{n-1}CHOH$ $n=$	p.e.(°C/mmHg) ou p.f. Observé	Littérature	n_D^{20}* Observé	Litt.	Réf.
4	45/25	125/760	1.4345	1.4367	9
5		139/760	1.4517	1.4530	10
6	68/3.3	158–159/760	1.4641	1.4642	11
7	50–51/2.8	83–84/14	1.4748	1.4705	12
				1.4753	13
8	70–72/3.3	89–90/11	1.4851	1.4868	14
				1.4844	15
9	69–70/0.8	115–119/15	1.4900	1.4903	16
10	p.f. = 40–41	125/12 p.f. = 40–41		1.4926	17
11	96/4	128–131/20	1.4914		17
12	p.f. = 76–78	p.f. = 80			17
13	104/4 p.f. = 59–60	p.f. = 60–60.5			17
15	p.f. = 84–85	p.f. = 81			17

*Les n_D sont tous ramenés à 20 °C, s'il y a lieu. Le facteur de correction utilisé est de 0.0004/°C.

TABLEAU II

Constantes de vitesses et effets isotopiques cinétiques de quelques cyclanols

$(CH_2)_{n-1}C(OH)X$	$k_2 \times 10^3$ (1 mole s^{-1})* X = H	X = D	k_H/k_D
$n = 8$	25.89	3.74	6.9
$n = 9$	23.16	3.42	6.8
$n = 10$	22.11	2.98	7.4
$n = 12$	15.05	2.02	7.4

*Mesures effectuées à ~25 °C dans une solution aqueuse d'acide acétique à 79.63% P/V.

Nicolaides (18) l'étape déterminante de la réaction est vraiment la rupture du lien carbone–hydrogène carbinolique et non pas la formation de l'ester chromique (19).

Les constantes de vitesse d'oxydation chromique des cyclanols sont reportées dans le tableau III alors que les facteurs thermodynamiques de ces réactions qui peuvent être déduites de ces données sont résumés dans le tableau IV.

Dans le tableau V les vitesses d'oxydation chromique des cyclanols sont mises en regard et des vitesses d'acétolyse des tosylates correspondants et de la fréquence de la vibration C=O

TABLEAU III

Constantes de vitesse d'oxydation chromique à différentes températures

$(CH_2)_{n-1}CHOH$	$k_2 \times 10^3$(1 $mole^{-1}s^{-1}$)* 33.25 °C	28.38 °C	25.10 °C	19.92 °C
$n = 4$	12.5_9	9.5_7	8.2_2	5.7_7
$n = 5$	12.2_6	9.5_6	7.6_5	5.4_8
$n = 6$	6.8_3	5.0_5	3.6_8	2.8_4
$n = 7$	31.5_3	22.5_6	17.6_9	12.4_7
$n = 8$	35.3_2	24.9_1	19.1_2	12.3_0
$n = 9$	32.4_1	23.6_0	18.5_2	12.6_3
$n = 10$	28.7_7	22.7_2	18.1_6	12.7_6
$n = 11$	25.4_5	18.8_1	16.2_6	10.8_6
$n = 12$	19.8_8	14.67	12.3_4	8.3_9
$n = 13$	21.7_0	16.4_0	13.0_6	9.0_7
$n = 15$	20.6_7	14.7_8	12.0_6	9.5_7†

*Mesures effectuées aux températures indiquées dans des solutions aqueuses contenant 27.71 g d'acide acétique par 100 ml de solution. Les constantes de vitesse données sont les moyennes de trois valeurs. L'erreur relative moyenne est d'environ ± 1%.
†Dans ce cas la mesure a été effectuée à 21.35 °C.

TABLEAU IV

Facteurs d'activation dans les réactions d'oxydation chromique de cyclanols

$(CH_2)_{n-1}CHOH$	$\Delta H^{\neq}$ (Kcal/mole)	$\Delta S^{\neq}$ (cal/°K mole)	$\Delta G^{\neq}$ (Kcal/mole)
$n = 4$	9.7_4	-35.4_9	20.3_2
$n = 5$	10.2_7	-33.7_9	20.3_5
$n = 6$	11.4_4	-31.2_0	20.7_4
$n = 7$	11.8_7	-26.7_3	19.8_4
$n = 8$	13.5_6	-20.9_7	19.8_1
$n = 9$	12.0_7	-26.0_1	19.8_2
$n = 10$	10.3_9	-31.6_9	19.8_4
$n = 11$	10.8_4	-30.4_4	19.9_2
$n = 12$	11.0_7	-30.2_0	20.0_7
$n = 13$	11.3_6	-29.0_7	20.0_2
$n = 15$	11.3_1	-29.3_8	20.0_7

TABLEAU V

Constantes de vitesse d'oxydation chromique de cyclanols comparées aux constantes de vitesse d'acétolyse des tosylates correspondants

$(CH_2)_{n-1}C(X)H$	X = OH*		X = OTs†		νC=O de la cétone correspondante cm^{-1}
	$10^3 k_{ox}$	$\log k_{ox}/k_6$	$10^5 k_{sol}$	$\log k_{sol}/k_6$	
$n = 4$	8.2_2	0.35	26.7	1.05	1775‡
$n = 5$	2.6_5	0.32	33.2	1.15	1751‡ (1748‖)
$n = 6$	3.6_8	0	2.37	0	1714§ (1716‖)
$n = 7$	17.6_9	0.68	60.0	1.40	1702§ (1705‖)
$n = 8$	19.1_2	0.72	452	2.28	1701§ (1704‖)
$n = 9$	18.5_2	0.70	408	2.24	1702§
$n = 10$	18.1_6	0.70	800	2.58	1702§
$n = 11$	16.2_6	0.65	116	1.69	1709§
$n = 12$	12.3_4	0.53	7.7	0.51	1710§
$n = 13$	13.0_6	0.55	8.3	0.54	1713§
$n = 15$	12.0_6	0.52	5.18	0.40	1712§

*Vitesses d'oxydation chromique déterminées à ~25 °C et rapportées dans le présent travail.
†Vitesses de solvolyse déterminées à ~70 °C et rapportées dans la réf. 8.
‡Voir réf. 21.
§Voir réf. 22.
‖Voir réf. 23.

(20); utilisant la notation de Brown (8), les valeurs de log K_n/K_6 (constante de vitesse d'un produit cyclanique correspondant contenant n chainons/ la vitesse correspondante en série cyclohexanique) sont aussi rapportées. Si une comparaison des résultats log K_{nox}/K_6 est faite avec les valeurs log $K_{nsolv.}/K_6$ et les fréquences de vibration du groupement carbonyle de la cétone correspondante (en excluant comme l'a fait Foote (20) les résultats obtenus en séries cyclobutaniques et cyclopentaniques où des effets supplémentaires sont en causes) un parallélisme étroit entre toutes ces données est alors observé; il peut alors en être conclu que les vitesses d'oxydation chromique d'alcools secondaires, comme les vitesses de solvolyse des tosylates correspondants sont directement reliées à la stabilité de la cétone qui se forme. Cette conclusion implique, comme il a été proposé précédemment (1–3), que l'état de transition des réactions d'oxydation chromique d'alcools secondaires ressemble au produit final et comporte un caractère cétonique bien développé.

Remerciements

Les auteurs remercient vivement le Conseil

National de Recherches du Canada et le Bureau de l'Aide Extérieure du Canada (Plan Colombo) pour l'aide financière apportée sous forme d'octrois et de bourse de recherches.

Les auteurs remercient également M. G. Marchand du Centre de Calcul de l'Université de Montréal et Mme M. C. Baskevitch pour l'aide apportée dans les calculs des vitesses d'oxydation.

1. J.-C. RICHER et C. GILARDEAU. Can. J. Chem. **43**, 538 (1964).
2. J. ROCEK. Coll. Czech. Chem. Commun. **25**, 1052 (1960).
3. N. VENKATASUBRAMIAN. Indian J. Chem. **3**, (5) 225 (1965).
4. H. KWART. Suomen Kemistilehti, A, **34**, 173 (1961).
5. H. KWART. Chem. and Ind. London, 610 (1962).
6. H. C. BROWN, R. S. FLETCHER, et R. B. JOHANNESEN. J. Am. Chem. Soc. **73**, 212 (1951).
7. H. C. BROWN et M. BORKOWSKI. J. Am. Chem. Soc. **74**, 1894 (1952).
8. H. C. BROWN et G. HAM. J. Am. Chem. Soc. **78**, 2735 (1956).
9. J. D. ROBERTS et C. W. SAUER. J. Am. Chem. Soc. **71**, 3925 (1949).
10. C. R. NOLLER et R. ADAMS. J. Am. Chem. Soc. **48**, 1080 (1926).
11. H. E. UNGNADE et D. NIGHTINGALE. J. Am. Chem. Soc. **66**, 1218 (1944).
12. C. RUZICKA, P. A. PLATTNER et H. WILD. Helv. Chim. Acta, **28**, 395 (1945).
13. J. BÖESEKEN et C. J. A. HANEGRAAFF. Rec. Trav. Chim. **61**, 69 (1942).
14. H. H. ZEISS et M. TSUTSUI. J. Am. Chem. Soc. **75**, 897 (1953).
15. L. RUZICKA et H. H. BOEKENOOGEN. Helv. Chim. Acta, **14**, 1319 (1931).
16. A. T. BLOOMQUIST, L. H. LIV et J. C. BOHRER. J. Am. Chem. Soc. **74**, 3643 (1952).
17. M. KOBELT, P. BARMAN, V. PRELOG et L. RUZICKA. Helv. Chim. Acta, **32**, 256 (1949).
18. F. H. WESTHEIMER et N. J. NICOLAIDES. J. Am. Chem. Soc. **71**, 25 (1949).
19. J. ROCEK, F. H. WESTHEIMER, H. ESCHENMOSER, L. MOLDOVANYI et J. SCHREIBER. Helv. Chim. Acta, **45**, 2554 (1962).
20. C. S. FOOTE. J. Am. Chem. Soc. **86**, 1853 (1964).
21. T. BIIRER et H. H. GUNTHARD. Helv. Chim. Acta, **39**, 356 (1956).
22. N. J. LEONARD et F. H. OWENS. J. Am. Chem. Soc. **80**, 6039 (1958).
23. A. P. KRAPCHO et J. E. MCCOULLOUGH. J. Org. Chem. **32**, 2453 (1967).

Thermal decomposition of alkyl *N*-(*o*-nitrophenyl)carbamates: A novel synthesis of benzofurazan

J. M. PROKIPCAK, P. A. FORTE, AND D. D. LENNOX
Department of Chemistry, University of Guelph, Guelph, Ontario

Received January 30, 1969

Several alkyl *N*-(*o*-nitrophenyl)carbamates have been shown to undergo thermal breakdown to give benzofurazan with the methyl derivative giving the optimum results.

Canadian Journal of Chemistry, 47, 2482 (1969)

During an investigation into the mechanism of the breakdown of nitrourethanes, it was found that alkyl *N*-(*o*-nitrophenyl)carbamates could be converted into benzo-2,1,3-oxadiazole (benzofurazan) by heating the carbamates to 250–270°.

Gaughran *et al.* (1) have prepared benzofurazan by the reduction of benzofurazan *N*-oxide with alkaline hydroxylamine. The benzofurazan *N*-oxide can be obtained by the oxidation of *o*-nitroaniline (1, 2) or by the pyrolysis of *o*-nitrophenyl azide (3). The method used in our laboratory involved the pyrolysis of alkyl *N*-(*o*-nitrophenyl)carbamates and afforded a ready source of pure benzofurazan in yields up to 53% in the case of the methyl carbamate.

The alkyl *N*-(*o*-nitrophenyl)carbamates were made using the method outlined by Synerholm *et al.* (4). Table I indicates the carbamates synthesized and used in the preparation of benzofurazan.

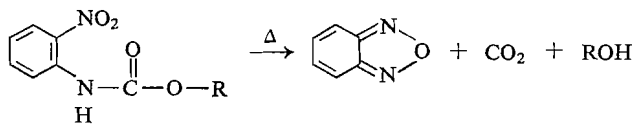

National de Recherches du Canada et le Bureau de l'Aide Extérieure du Canada (Plan Colombo) pour l'aide financière apportée sous forme d'octrois et de bourse de recherches.

Les auteurs remercient également M. G. Marchand du Centre de Calcul de l'Université de Montréal et Mme M. C. Baskevitch pour l'aide apportée dans les calculs des vitesses d'oxydation.

1. J.-C. RICHER et C. GILARDEAU. Can. J. Chem. **43**, 538 (1964).
2. J. ROCEK. Coll. Czech. Chem. Commun. **25**, 1052 (1960).
3. N. VENKATASUBRAMIAN. Indian J. Chem. **3**, (5) 225 (1965).
4. H. KWART. Suomen Kemistilehti, A, **34**, 173 (1961).
5. H. KWART. Chem. and Ind. London, 610 (1962).
6. H. C. BROWN, R. S. FLETCHER, et R. B. JOHANNESEN. J. Am. Chem. Soc. **73**, 212 (1951).
7. H. C. BROWN et M. BORKOWSKI. J. Am. Chem. Soc. **74**, 1894 (1952).
8. H. C. BROWN et G. HAM. J. Am. Chem. Soc. **78**, 2735 (1956).
9. J. D. ROBERTS et C. W. SAUER. J. Am. Chem. Soc. **71**, 3925 (1949).
10. C. R. NOLLER et R. ADAMS. J. Am. Chem. Soc. **48**, 1080 (1926).
11. H. E. UNGNADE et D. NIGHTINGALE. J. Am. Chem. Soc. **66**, 1218 (1944).
12. C. RUZICKA, P. A. PLATTNER et H. WILD. Helv. Chim. Acta, **28**, 395 (1945).
13. J. BÖESEKEN et C. J. A. HANEGRAAFF. Rec. Trav. Chim. **61**, 69 (1942).
14. H. H. ZEISS et M. TSUTSUI. J. Am. Chem. Soc. **75**, 897 (1953).
15. L. RUZICKA et H. H. BOEKENOOGEN. Helv. Chim. Acta, **14**, 1319 (1931).
16. A. T. BLOOMQUIST, L. H. LIV et J. C. BOHRER. J. Am. Chem. Soc. **74**, 3643 (1952).
17. M. KOBELT, P. BARMAN, V. PRELOG et L. RUZICKA. Helv. Chim. Acta, **32**, 256 (1949).
18. F. H. WESTHEIMER et N. J. NICOLAIDES. J. Am. Chem. Soc. **71**, 25 (1949).
19. J. ROCEK, F. H. WESTHEIMER, H. ESCHENMOSER, L. MOLDOVANYI et J. SCHREIBER. Helv. Chim. Acta, **45**, 2554 (1962).
20. C. S. FOOTE. J. Am. Chem. Soc. **86**, 1853 (1964).
21. T. BIIRER et H. H. GUNTHARD. Helv. Chim. Acta, **39**, 356 (1956).
22. N. J. LEONARD et F. H. OWENS. J. Am. Chem. Soc. **80**, 6039 (1958).
23. A. P. KRAPCHO et J. E. MCCOULLOUGH. J. Org. Chem. **32**, 2453 (1967).

Thermal decomposition of alkyl *N*-(*o*-nitrophenyl)carbamates: A novel synthesis of benzofurazan

J. M. PROKIPCAK, P. A. FORTE, AND D. D. LENNOX
Department of Chemistry, University of Guelph, Guelph, Ontario

Received January 30, 1969

Several alkyl *N*-(*o*-nitrophenyl)carbamates have been shown to undergo thermal breakdown to give benzofurazan with the methyl derivative giving the optimum results.

Canadian Journal of Chemistry, 47, 2482 (1969)

During an investigation into the mechanism of the breakdown of nitrourethanes, it was found that alkyl *N*-(*o*-nitrophenyl)carbamates could be converted into benzo-2,1,3-oxadiazole (benzofurazan) by heating the carbamates to 250–270°.

Gaughran *et al.* (1) have prepared benzofurazan by the reduction of benzofurazan *N*-oxide with alkaline hydroxylamine. The benzofurazan *N*-oxide can be obtained by the oxidation of *o*-nitroaniline (1, 2) or by the pyrolysis of *o*-nitrophenyl azide (3). The method used in our laboratory involved the pyrolysis of alkyl *N*-(*o*-nitrophenyl)carbamates and afforded a ready source of pure benzofurazan in yields up to 53% in the case of the methyl carbamate.

The alkyl *N*-(*o*-nitrophenyl)carbamates were made using the method outlined by Synerholm *et al.* (4). Table I indicates the carbamates synthesized and used in the preparation of benzofurazan.

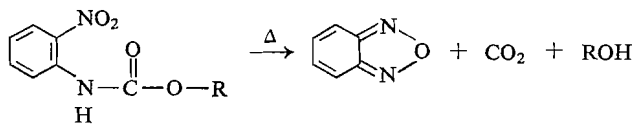

Can. J. Chem. Downloaded from www.nrcresearchpress.com by 210.87.254.6 on 09/05/12
For personal use only.

TABLE I

Preparation and decomposition of alkyl *N*-(*o*-nitrophenyl)carbamates*

R	Melting point (°C)	% Composition Calculated C	Calculated H	Calculated N	Found C	Found H	Found N	% Yield benzofurazan
CH_3—	51–52†	48.98	4.11	14.28	48.89	4.01	14.28	53
CH_3CH_2—	55–56‡	51.43	4.79	13.33	51.10	4.65	13.54	25
CH_2=CH—CH_2—	20–21	54.05	4.54	12.61	54.16	4.79	12.65	25
Me—O-C$_6$H$_4$-CH_2—	99.5–100.5	59.60	4.67	9.27	59.79	4.66	9.52	9
C$_6$H$_5$-CH_2—	64.5–66.0§	61.76	4.44	10.29	61.57	4.31	10.06	12
O_2N-C$_6$H$_4$-CH_2—	143–145	53.00	3.49	13.24	52.90	3.33	13.06	27

*General formula: 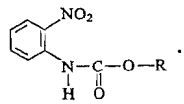 .

†Reported m.p. 53 °C (5).
‡Reported m.p. 57 °C (5).
§Reported m.p. 61–62 °C (6).

Undoubtedly an intermediate reaction that had to be considered was the formation of isocyanate (7, 8). The carbamates could be decomposing into the *o*-nitrophenyl isocyanate which then could lead to the formation of benzofurazan. However, when the *o*-nitrophenyl isocyanate was subjected to the same conditions as the carbamates, only a very small amount of benzofurazan (5%) was obtained, the major portion being a black tar. Thus the benzofurazan formation from the carbamate does not seem to include preliminary isocyanate formation.

The rate at which decomposition temperature was reached played an important part in the yield of benzofurazan. When the flask contents were brought to decomposition temperature slowly, the yield of benzofurazan was quite low (10%). However, if the flask contents were brought to the decomposition temperature rapidly, the yield of benzofurazan was greatly increased. This could be due to a decrease in the competing isocyanate reaction.

Thus thermal decomposition of methyl *N*-(*o*-nitrophenyl)carbamate has been shown to afford a quick method of preparing pure benzofurazan in good yields. Further investigation on this reaction is in progress.

Experimental

All melting points were determined on the Fisher–Johns melting point apparatus and are uncorrected. Analyses were performed by Organic Microanalyses, 5757 Decelles Avenue, Montreal, Quebec.

The preparation of the carbamates and their decomposition can be outlined by describing the general procedure used for the methyl *N*-(*o*-nitrophenyl)carbamate.

Preparation of Methyl N-(o-nitrophenyl)carbamate

o-Nitrophenyl isocyanate (16.4 g, 0.10 mole) was added over a period of 10 min to a solution of 3.5 g (0.11 mole) methanol in 150 ml of dry benzene. The reaction mixture was refluxed for a period of 2 h. The benzene was removed *in vacuo* and the resultant oil was taken up in hot hexane. After filtration, the solution was cooled and the resultant crystals were recovered by filtration, m.p. 51–52°. The yields for the different carbamates varied from 60–90%.

Thermal Decomposition of Methyl N-(o-nitrophenyl)-carbamate

Using a simple distillation set-up, 30 g (0.15 mole) of the carbamate were placed in a 50 ml distilling flask. The flask contents were heated quickly to 250–270 °C by means of a heating mantle. The gas evolved was allowed to escape into the atmosphere and the alcohol which distilled off was collected. The benzofurazan then began to distil over (distilling head temperature 190°) and solidified in the condenser. The crude product (11.40 g) was collected and purified by sublimation to give 9.70 g of pure benzofurazan, m.p. 51.5–53.0° in a 53% yield.

By comparison of physical properties and infrared spectra this compound was shown to be identical with

Can. J. Chem. Downloaded from www.nrcresearchpress.com by 210.87.254.6 on 09/05/12
For personal use only.

benzofurazan prepared by the method of Gaughran *et al.* (1). In all cases, the remainder of the flask contents was unidentified.

Acknowledgment

We acknowledge the National Research Council of Canada for financial support of this research.

1. R. J. Gaughran, J. P. Picard, and I. V. R. Kaufman. J. Am. Chem. Soc. **76**, 2233 (1954).
2. K. H. Pausacker and J. G. Scroggie. J. Chem. Soc. 4499 (1954).
3. P. A. F. Smith and J. H. Boyer. Org. Syn. **31**, 14 (1951).
4. M. E. Synerholm, N. W. Gilman, J. W. Morgan, and R. K. Hill. J. Org. Chem. **33**, 1111 (1968).
5. J. A. Attaway, R. W. Wolford, and G. E. Alberding. Anal. Chem. **34**, 671 (1962).
6. T. Mukaiyama and M. Iwanami. J. Am. Chem. Soc. **79**, 73 (1957).
7. M. Metayer. Bull. Soc. Chim. France, 802 (1951).
8. W. Siefken. Ann. **562**, 75 (1949).

Anodic addition of hydroxy and benzoyloxy groups to stilbenes[1]

Kikuhiko Koyama, Tatsuyoshi Ebara, Tadahiko Tani, and Shigeru Tsutsumi
Department of Chemical Technology, Faculty of Engineering, Osaka University, Yamadakami, Suita, Japan

Received May 28, 1968

The anodic reaction of benzoic acid in acetonitrile has been carried out in the presence of *trans*- and *cis*-stilbenes using platinum electrodes. The reaction with added *trans*-stilbene gave meso-hydrobenzoin dibenzoate together with *threo*-2-benzoyloxy-1,2-diphenylethanol. Under similar conditions, *cis*-stilbene also gave these products. No evidence for the isomerization of *cis*-stilbene to the *trans*-isomer during the electrolysis was found. Stereoisomeric *dl*-hydrobenzoin dibenzoate and erythro-2-benzoyloxy-1,2-diphenylethanol were not obtained from either stilbene. For comparison, the "wet" Prévost reaction of *cis*-stilbene with silver acetate and iodine was studied. These results are discussed on the basis of a stepwise oxidation mechanism which involves a cyclic 1,2-benzoxonium ion intermediate.

Canadian Journal of Chemistry, 47, 2484 (1969)

Over the last decade, considerable attention has been devoted to electrochemical addition reactions. An example of such reactions is the polymerization of vinyl monomers during the Kolbe electrolysis (1, 2). The free radicals produced by the Kolbe electrolysis are capable of attacking 1,3-dienes present, giving rise to the additive dimers (3–5). Smith *et al.* (6) have investigated the stereochemistry of the addition of free radicals to dienes in the anodic oxidation of carboxylic anions.

A previous communication (7) from this laboratory indicated that the electrolysis of sodium methoxide in methanol in the presence of *trans*- and *cis*-stilbenes afforded a mixture of meso- and *dl*-hydrobenzoin dimethyl ethers. More *cis*-adduct than *trans*-adduct was formed in each case. These results seem to be consistent with simultaneous addition of two methoxy radicals to a carbon–carbon double bond of an adsorbed stilbene from one side of the double bond, analogous to the catalytic hydrogenation of unsaturated compounds. An alternative mechanism involves a benzylic cation intermediate formed from stilbene during a stepwise two-electron transfer to the anode (8).

Recently, Mango and Bonner (9) found that electrolysis of sodium acetate in acetic acid in the presence of *trans*-stilbene yielded mainly meso-hydrobenzoin diacetate under anhydrous conditions, and *threo*-2-acetoxy-1,2-diphenylethanol together with a mixture of epimers of 1,2-diphenyl-1-propyl acetate under moist conditions. The stereoisomeric *erythro*-hydroxyacetate was not obtained from either experiment with added *trans*-stilbene. They concluded that the mechanism involved a cyclic acetoxonium ion intermediate **1** which was formed stereoselectively on the surface of an anode. Although the details of the formation of the cyclic intermediate ion, **1**, in this mechanism were not completely clear from their work, they suggested two possibilities; one-step and two-step oxidation mechanisms, as illustrated in Schemes 1 and 2, respectively.

The present study deals with the mechanism of

[1]Presented partly at the 18th Annual Meeting of the Chemical Society of Japan, Osaka, April, 1965, and the 17th Meeting of C.I.T.C.E., Tokyo, September, 1966.

Can. J. Chem. Downloaded from www.nrcresearchpress.com by 210.87.254.6 on 09/05/12
For personal use only.

benzofurazan prepared by the method of Gaughran *et al.* (1). In all cases, the remainder of the flask contents was unidentified.

Acknowledgment

We acknowledge the National Research Council of Canada for financial support of this research.

1. R. J. Gaughran, J. P. Picard, and I. V. R. Kaufman. J. Am. Chem. Soc. **76**, 2233 (1954).
2. K. H. Pausacker and J. G. Scroggie. J. Chem. Soc. 4499 (1954).
3. P. A. F. Smith and J. H. Boyer. Org. Syn. **31**, 14 (1951).
4. M. E. Synerholm, N. W. Gilman, J. W. Morgan, and R. K. Hill. J. Org. Chem. **33**, 1111 (1968).
5. J. A. Attaway, R. W. Wolford, and G. E. Alberding. Anal. Chem. **34**, 671 (1962).
6. T. Mukaiyama and M. Iwanami. J. Am. Chem. Soc. **79**, 73 (1957).
7. M. Metayer. Bull. Soc. Chim. France, 802 (1951).
8. W. Siefken. Ann. **562**, 75 (1949).

Anodic addition of hydroxy and benzoyloxy groups to stilbenes[1]

Kikuhiko Koyama, Tatsuyoshi Ebara, Tadahiko Tani, and Shigeru Tsutsumi
Department of Chemical Technology, Faculty of Engineering, Osaka University, Yamadakami, Suita, Japan

Received May 28, 1968

The anodic reaction of benzoic acid in acetonitrile has been carried out in the presence of *trans*- and *cis*-stilbenes using platinum electrodes. The reaction with added *trans*-stilbene gave meso-hydrobenzoin dibenzoate together with *threo*-2-benzoyloxy-1,2-diphenylethanol. Under similar conditions, *cis*-stilbene also gave these products. No evidence for the isomerization of *cis*-stilbene to the *trans*-isomer during the electrolysis was found. Stereoisomeric *dl*-hydrobenzoin dibenzoate and erythro-2-benzoyloxy-1,2-diphenylethanol were not obtained from either stilbene. For comparison, the "wet" Prévost reaction of *cis*-stilbene with silver acetate and iodine was studied. These results are discussed on the basis of a stepwise oxidation mechanism which involves a cyclic 1,2-benzoxonium ion intermediate.

Canadian Journal of Chemistry, 47, 2484 (1969)

Over the last decade, considerable attention has been devoted to electrochemical addition reactions. An example of such reactions is the polymerization of vinyl monomers during the Kolbe electrolysis (1, 2). The free radicals produced by the Kolbe electrolysis are capable of attacking 1,3-dienes present, giving rise to the additive dimers (3–5). Smith *et al.* (6) have investigated the stereochemistry of the addition of free radicals to dienes in the anodic oxidation of carboxylic anions.

A previous communication (7) from this laboratory indicated that the electrolysis of sodium methoxide in methanol in the presence of *trans*- and *cis*-stilbenes afforded a mixture of meso- and *dl*-hydrobenzoin dimethyl ethers. More *cis*-adduct than *trans*-adduct was formed in each case. These results seem to be consistent with simultaneous addition of two methoxy radicals to a carbon–carbon double bond of an adsorbed stilbene from one side of the double bond, analogous to the catalytic hydrogenation of unsaturated compounds. An alternative mechanism involves a benzylic cation intermediate formed from stilbene during a stepwise two-electron transfer to the anode (8).

Recently, Mango and Bonner (9) found that electrolysis of sodium acetate in acetic acid in the presence of *trans*-stilbene yielded mainly meso-hydrobenzoin diacetate under anhydrous conditions, and *threo*-2-acetoxy-1,2-diphenylethanol together with a mixture of epimers of 1,2-diphenyl-1-propyl acetate under moist conditions. The stereoisomeric *erythro*-hydroxyacetate was not obtained from either experiment with added *trans*-stilbene. They concluded that the mechanism involved a cyclic acetoxonium ion intermediate **1** which was formed stereoselectively on the surface of an anode. Although the details of the formation of the cyclic intermediate ion, **1**, in this mechanism were not completely clear from their work, they suggested two possibilities; one-step and two-step oxidation mechanisms, as illustrated in Schemes 1 and 2, respectively.

The present study deals with the mechanism of

[1]Presented partly at the 18th Annual Meeting of the Chemical Society of Japan, Osaka, April, 1965, and the 17th Meeting of C.I.T.C.E., Tokyo, September, 1966.

Can. J. Chem. Downloaded from www.nrcresearchpress.com by 210.87.254.6 on 09/05/12
For personal use only.

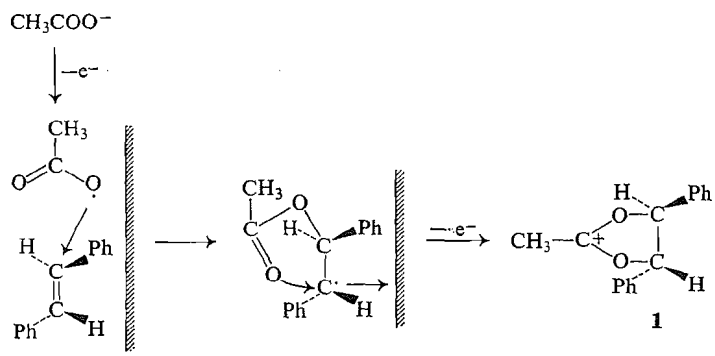

SCHEME 1

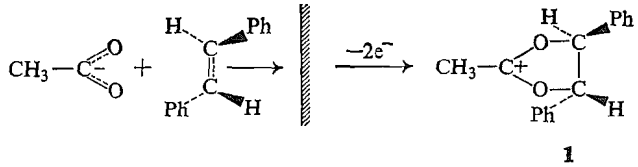

SCHEME 2

anodic addition of hydroxy and benzoyloxy groups to the stilbenes.

Results and Discussion

The electrolysis of benzoic acid in acetonitrile containing a small amount of triethylamine was conducted in the presence of *trans*-stilbene. After the usual work-up, the products which could be isolated were characterized by comparison with authentic samples, and found to consist of meso-hydrobenzoin dibenzoate **2** and *threo*-2-benzoyloxy-1,2-diphenylethanol, **3**. When benzoic acid was electrolyzed in the presence of *cis*-stilbene, it was also converted into a mixture of **2** and **3** in a fairly good yield. Each electrolysis was repeated several times, but no other compounds could be identified. In some cases, however, a small amount of a thick yellow oil, which gave an infrared (i.r.) spectrum displaying major absorption bands at 710, 760, 1110, 1270, 1670, and 1710 cm^{-1}, was produced. None of the stereoisomeric *erythro*-monobenzoate and *dl*-dibenzoate was obtained in either case. The relative yield of the diester, **2**, to the monoester, **3**, appeared to be affected by water present in the solvent; the ratio increased markedly when the solvent freshly distilled from phosphorus pentoxide, while it decreased when the solvent had been stored without any protection from moisture.

There was no evidence of isomerization of *cis*- to *trans*-stilbene under the electrolytic conditions employed; ultraviolet (u.v.) spectra of crude *cis*-stilbene recovered from the electrolyzed mixture showed no absorbance at 295 and 310 mμ characteristic for the *trans*-isomer.

As has been established in the stereochemistry of the "dry" and "wet" Prévost reactions, the stereoselective addition of hydroxy and benzoyloxy groups to the stilbenes, i.e., *cis*-hydroxylation and *trans*-benzoyloxylation, strongly suggests the formation of a common cyclic benzoxonium ion intermediate, **4**, from both stilbenes.

The inversion of configuration during anodic addition to *cis*-stilbene also suggests that the formation of **4** proceeds through a stepwise transfer of two electrons to the anode. If a cyclic ion intermediate were formed from an adsorbed *cis*-stilbene on the anode surface in one step as illustrated in Scheme 2, the *cis*-stilbene would be converted with retention of configuration into *dl*-hydrobenzoin dibenzoate and *erythro*-monobenzoate.

The u.v. analyses rule out the possibility of *cis–trans* inversion before the attack of a benzoate anion or radical on an anodically adsorbed stilbene.

The Prévost reaction on *cis*-stilbene, which so far as we know has not been reported, was

Can. J. Chem. Downloaded from www.nrcresearchpress.com by 210.87.254.6 on 09/05/12
For personal use only.

examined using silver acetate in wet acetic acid. It also afforded *threo*-2-acetoxy-1,2-diphenylethanol as the sole product, but the epimeric *erythro*-monoacetate was not produced.

Winstein and Seymour (10) have suggested that the diastereomeric stilbene dichlorides are first converted mainly into *erythro*-acetoxychloride when the dichlorides are treated with silver acetate in dry or moist acetic acid. The present investigation, however, affords evidence for the possible inversion of configuration during the formation of the cyclic ion intermediate **4**.

Our conclusion, based on the evidence above, is that the anodic addition of hydroxy and benzoyloxy groups to stilbenes proceeds via the formation of the cyclic benzoxonium ion intermediate **4** with the more stereochemically favorable configuration. It seems probable that two electrons are transferred stepwise from stilbene or from benzoate anion and stilbene to the anode.

Experimental

All melting points and boiling points are uncorrected. The i.r. spectra were obtained with a Shimadzu IR spectrophotometer IR-27C. The electrolyses were carried out in a cylindrical glass cell equipped with a reflux condenser, thermometer, and electrode unit. The electrode unit consisted of two platinum foil electrodes having an area of ca. 3 cm^2 each, spaced 1 cm apart. The cell was immersed in a water-bath, and the contents were stirred magnetically.

Electrolysis of Benzoic Acid in the Presence of trans-Stilbene

A solution of benzoic acid (6.1 g, 0.05 mole) and *trans*-stilbene (4.5 g, 0.025 mole) in acetonitrile (90 ml) containing triethylamine (2 g) was electrolyzed at 20–25 °C for 14 h (electric current; 0.1 A, applied potential; 31–35 V).

The bulk of the solvent was removed by evaporation at reduced pressure, and the residue was dissolved in chloroform. The chloroform solution was extracted twice with 5% aqueous sodium bicarbonate solution, then washed with water, dried over anhydrous magnesium sulfate, filtered, and evaporated to give a thick brown oil (7 g). A portion (3 g) of the crude product was chromatographed on silica gel (50 g), and eluted with chloroform–methanol mixtures. After removal of the solvent, the

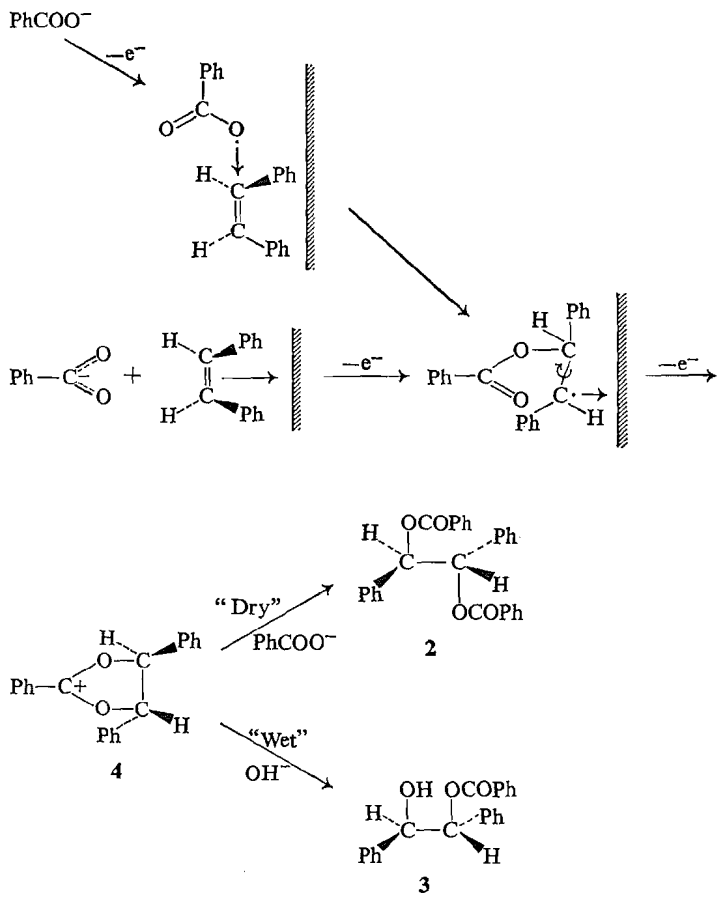

Can. J. Chem. Downloaded from www.nrcresearchpress.com by 210.87.254.6 on 09/05/12
For personal use only.

Can. J. Chem. Downloaded from www.nrcresearchpress.com by 210.87.254.6 on 09/05/12
For personal use only.

collected fractions were combined on the basis of the i.r. and thin-layer chromatography (t.l.c.) analyses.

The first combined residue (0.8 g) was shown by its i.r. spectrum to be unchanged stilbene. Recrystallization from *n*-hexane – benzene yielded white crystals, m.p. 122–124 °C, which showed no melting point depression when mixed with authentic *trans*-stilbene.

The second combined fraction (1.2 g) was recrystallized from *n*-hexane – benzene yielding 0.8 g of white crystals, m.p. 243–245 °C, which was identified as meso-hydrobenzoin dibenzoate, **2**, (m.p. 244–245 °C (11)). The product and an authentic sample of **2** had identical i.r. spectra and, on admixture, showed no melting point depression.

Anal. Calcd. for $C_{28}H_{22}O_4$: C, 79.60; H, 5.25. Found: C, 79.83; H, 5.61.

The third fraction, a yellow oil, gave an i.r. spectrum with major absorption bands at 710, 760, 1110, 1270, 1670, and 1710 cm^{-1}, and was examined by t.l.c. It consisted of several compounds, which were not further investigated.

The electrolysis was repeated in slightly wetted solvent. After working up the electrolyzed mixture in a manner similar to the experiment described above, the crude product (11.6 g) was subjected to chromatographic separation, and gave 4 combined fractions. The first combined fraction (0.2 g) consisted mainly of unchanged *trans*-stilbene, m.p. and mixed m.p. 121–123 °C. The second combined fraction (1.5 g) was filtered to separate a thick solid (0.03 g), m.p. 183–228 °C. The solid was washed with a *n*-hexane – benzene mixture, and recrystallized from boiling toluene to yield white crystals, m.p. 237–240 °C, which were identified as **2** (mixed m.p. 240–242 °C).

The third combined residue (3.9 g) was dissolved in benzene and, after addition of *n*-hexane to the solution, yielded a white solid (3.1 g), m.p. 149–152 °C. It was identified after recrystallization from benzene – *n*-hexane mixture as *threo*-2-benzoyloxy-1,2-diphenylethanol, **3**, m.p. 152.5–154.5 °C, undepressed on admixture with an authentic sample. The i.r. spectra of the product and authentic **3** were identical.

Anal. Calcd. for $C_{21}H_{18}O_3$: C, 79.22; H, 5.70. Found: C, 79.12; H, 5.74.

A dark-brownish residue (0.5 g) was not investigated.

Electrolysis of Benzoic Acid in the Presence of cis-Stilbene

A solution of benzoic acid (6.1 g, 0.05 mole) and *cis*-stilbene (4.5 g, 0.025 mole) in acetonitrile (90 ml) containing triethylamine (2 g) was electrolyzed in the manner described above for experiments with *trans*-stilbene. After the electrolysis, a portion (3.2 g) of the crude product (9.6 g) was subjected to chromatographic separation.

The first combined residue (0.61 g) was shown to be unchanged *cis*-stilbene by its i.r. spectra. The u.v. spectrum of this residue in ethanol solution showed the absorption band at 280 mμ, but no absorptions at 295 and 310 mμ which are characteristic for *trans*-stilbene.

The second combined residue (0.2 g), a white solid, was identified after recrystallization from toluene as **2**, m.p. 244–245 °C, not depressed by mixture with an authentic sample. The i.r. spectra of these two samples were identical.

Anal. Calcd. for $C_{28}H_{22}O_4$: C, 79.60; H, 5.25. Found: C, 80.56; H, 5.37.

The third combined residue (0.6 g) gave, after recrystallization from *n*-hexane – benzene, white crystals, m.p. 150–152 °C, not depressed by mixture with an authentic **3**.

Anal. Calcd. for $C_{21}H_{18}O_3$: C, 79.22; H, 5.70. Found: C, 79.83; H, 5.94.

A portion (0.1 g) of the third fraction was heated under reflux with 20% potassium hydroxide in aqueous ethanol for 2.5 h, and the solvent was then removed under reduced pressure. The residue was extracted three times with ether, and the combined ethereal solutions were washed twice with sodium bicarbonate solution, then with water, and were then dried over anhydrous magnesium sulfate. The evaporation of ether left a small amount of a white solid, which was characterized after two recrystallizations from *n*-hexane – benzene mixtures as *dl*-hydrobenzoin, m.p. 119–120 °C, undepressed on admixture with an authentic sample.

The last combined residue (0.34 g) was a dark-brownish semisolid, which was not characterized.

Authentic **2** (m.p. 244–245 °C, 78% yield) was prepared from meso-hydrobenzoin. Authentic **3** (m.p. 154.5 °C, 76.5% yield) was prepared from *erythro*-1-benzoyloxy-2-bromo-1,2-diphenylethane by a method similar to that described by Wiberg and Saegebarth (11), and was hydrolyzed to give authentic *dl*-hydrobenzoin, m.p. 118 °C.

The "Wet" Prévost Reaction on cis-Stilbene

The method used here was virtually identical with that of Mango and Bonner (9). To a solution of *cis*-stilbene (4.5 g, 0.025 mole) and silver acetate (10.5 g, 0.06 mole) in glacial acetic acid (75 ml) containing water (1 ml) was added powdered iodine (6.4 g, 0.05 mole) in small portions with vigorous stirring over a period of 1 h at room temperature. After all of the iodine was added to the solution, the mixture was heated at 90–95 °C for 3 h with vigorous stirring. The usual work-up of the reaction mixture gave a thick oil (5.3 g), which crystallized on standing. Recrystallization from a benzene – *n*-hexane mixture gave white crystals, m.p. 87–89 °C, undepressed on admixture with authentic *threo*-2-acetoxy-1,2-diphenylethanol.

1. S. Goldschmidt and E. Stockel. Chem. Ber. **85**, 630 (1952).
2. W. B. Smith and H.-G. Gilde. J. Am. Chem. Soc. **82**, 659 (1960).
3. R. V. Lindsey, Jr. and M. L. Peterson. J. Am. Chem. Soc. **78**, 2073 (1956).
4. W. B. Smith and H.-G. Gilde. J. Am. Chem. Soc. **81**, 5325 (1959).
5. M. Ya. Fioshin, A. I. Kamneva, L. A. Mirkind, and L. A. Salimia. Chem. Abstr. **55**, 18586 (1961).
6. W. B. Smith and H.-G. Gilde. J. Am. Chem. Soc. **83**, 1355 (1961).
7. T. Inoue, K. Koyama, T. Matsuoka, K. Matsuoka, and S. Tsutsumi. Tetrahedron Letters, 1409 (1963).
8. T. Inoue, K. Koyama, T. Matsuoka, and S. Tsutsumi. Bull. Chem. Soc. Japan, **40**, 162 (1967).
9. F. D. Mango and W. A. Bonner. J. Org. Chem. **29**, 1367 (1964).
10. S. Winstein and D. Seymour. J. Am. Chem. Soc. **68**, 119 (1946).
11. K. B. Wiberg and K. A. Saegebarth. J. Am. Chem. Soc. **79**, 6256 (1957).

Réactions de Ritter sur les *tert*-butyl-4 méthyl-1 cyclohexanols *cis* et *trans*

JEAN-CLAUDE RICHER ET ROBERT BISSON
Département de Chimie, Faculté des Sciences, Université de Montréal, Montréal, Québec

Reçu le 6 novembre 1968

La réaction de Ritter a été effectuée sur les *tert*-butyl-4 méthyl-1 cyclohexanols, et la stéréochimie de ces réactions a été déterminée. Les amines qui peuvent en découler ont été isolées et caractérisées.

Canadian Journal of Chemistry, 47, 2488 (1969)

Can. J. Chem. Downloaded from www.nrcresearchpress.com by 210.87.254.5 on 09/05/12
For personal use only.

Introduction

Il semble maintenant bien établi (1) que la réaction de Ritter procède par l'intermédiaire d'un carbocation. Formellement la réaction de l'acide cyanhydrique (ou d'un cyanure) sur ce carbocation serait une réaction d'addition nucléophile qui pourrait être rapprochée des additions nucléophiles sur le carbone des groupements carbonyles. Il s'avérait donc intéressant d'examiner la stéréochimie des produits issus de la réaction de Ritter sur les *tert*-butyl-4 méthyl-1 cyclohexanols (**1***a* et **2***a*) et de comparer les quantités relatives de produits formés à celles obtenues lors d'additions nucléophiles sur la *tert*-butyl-4 cyclohexanone (**A**) qui est formellement l'analogue carbonylé du carbocation **B** considéré comme intermédiaire dans la réaction de Ritter sur les alcools **1** et **2**.

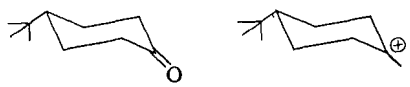

A **B**

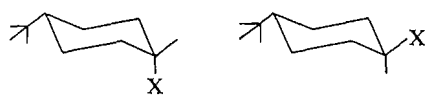

1 **2**

a) X = OH
b) X = NH_2
c) X = NH_3+
d) X = $NHSO_2C_6H_4CH_3$—*p*
e) X = $N(CH_3)_2$
f) X = N—C—H (‖ O)

Résultats et discussion

Les alcools tertiaires désirés **1***a* et **2***a* ont été préparés d'après la méthode décrite par Gravel (2). La réaction de Ritter a été effectuée sur chacun de ces alcools et sur un mélange approximativement 50/50 de chacun. Les produits obtenus ont été hydrolysés en milieu acide et les amines libres isolées ont été chromatographiées en phase gazeuse. Les pourcentages de *tert*-butyl-4 méthyl-1 cyclohexylamine *cis*[1] (**1***b*) obtenus dans chacune des réactions sont rapportés dans le tableau I.

TABLEAU I

Pourcentages* d'amine *cis* (**1***b*) formé au cours des réactions de Ritter

Alcool utilisé	1° essai	2° essai	Moyenne
1*a*	94	93	93,5
2*a*	88	90	89
45% **1***a*/55% **2***a*	91	94	92,5
			91,6

*Valeurs déterminées par chromatographie en phase gazeuse à 140 °C, utilisant une colonne de 10 pds. × 1/4 po. contenant du Chromosorb W 30–60 imprégné de 5% de KOH, 4% d'hyprose et 15% de Carbowax 20 M. Avec un débit d'hélium de 75 ml/min les temps de rétention sont de 19 min pour **1***b* et 25 min pour **2***b*.

Chacune des amines obtenue a été caractérisée et leur configuration relative a été attribuée en se basant d'une part sur leur temps de rétention relatif en chromatographie en phase gazeuse et grâce à leur pK_a, et d'autre part en notant comme l'ont fait Alleon-Aimi *et al.* (3) dans le cas des amines **1***e* et **2***e* que la transformation des amines **1***b* et **2***b* en leur chlorhydrate provoque dans les spectres de résonance magnétique nucleaire (r.m.n.) de **1***c* un déplacement chimique du groupe *tert*-butyle vers les champs faibles tandis qu'il n'y a aucun déplacement lorsqu'on passe de **2***b* à **2***c*. Les résultats stéréochimiques obtenus indiquent que l'addition du groupe NC sur le carbocation **B** s'effectue à 90% par le côté axial de la molécule. Ce résultat est en parfait accord avec ceux obtenus lors des additions nucléophiles par des

[1]La stéréochimie reflète la position relative des groupes fonctionnels et du groupe tertiobutyle.

Can. J. Chem. Downloaded from www.nrcresearchpress.com by 210.87.254.5 on 09/05/12
For personal use only.

petits réactifs sur la *tert*-butyl-4 cyclohexanone (4); ces résultats ont été expliqués grâce à une interprétation toute stérique qui serait aussi valable pour expliquer la stéréochimie des réactions de Ritter. La proposition récente de Cherest et Felkin (5) qui attribue ces résultats à des intéractions de torsion (plutôt qu'à des intéractions stériques) entre les réactifs et les substituants axiaux en position-2 et -6 permettrait aussi de rendre compte des résultats expérimentaux obtenus.

Partie expérimentale

Les spectres de résonance magnétique nucléaire ont été pris sur un spectromètre A-60 de la compagnie Varian; le $CDCl_3$ est utilisé comme solvant et les déplacements chimiques (δ), exprimés en p.p.m., se réfèrent au tétraméthylsilane utilisé comme standard interne. Les spectres infrarouges des produits ont été pris entre deux plaques de chlorure de sodium à l'état pur lorsque liquides et en suspension dans du Nujol lorsque solides; l'appareil utilisé est un spectromètre IR-8 à double faisceau de la compagnie "Beckman". Les analyses par chromatographie en phase gazeuse ont été effectuées sur un chromatographe F et M, modèle 810. Les indices de réfraction ont été mesurés à l'aide d'un réfractomètre, modèle 44 061 de la compagnie Zeiss. Les points de fusion ont été mesurés sur un appareil "Hot Stage" de la compagnie "Reichert".

tert-Butyl-4 méthyl-1 cyclohexanols **1***a et* **2***a*

Ils sont préparés selon les indications de Gravel (2). L'alcool **1***a* fond à 71–71.5° (litt. (2) 71°) alors que le p.f. de l'alcool **2***a* est de 99–99.5° (litt. (2) 98–99°).

tert-Butyl-4 méthyl-1 cyclohexylamines **1***b et* **2***b*

D'une manière générale, une solution contenant 0.1 mole d'alcool tertiaire (**1***a*, **2***a* ou mélange contenant 45% **1***a* et 55% **2***a*) dans 65 ml d'éther butylique anhydre et contenant 0.25 mole de cyanure de sodium finement pulvérisé est traitée, goutte à goutte tout en maintenant sous bonne agitation et à une température n'excédant pas 40–45 °C par 30 ml d'acide sulfurique concentrée. Lorsque l'addition est terminée l'agitation est maintenue durant 1 h, le mélange réactionnel ramené à la température de la pièce puis versé sur 300 ml d'eau glacée. L'extraction des produits réactionnels est effectuée à la manière habituelle par de l'éther après avoir alcalinisé le milieu par addition de soude 20%. Les dérivés formylés (**1***f* et **2***f*) ainsi obtenus sont hydrolysés par ébullition durant 5 h avec deux fois leur volume d'acide chlorhydrique concentré. L'extraction des amines libres (**1***b* et **2***b*) se fait par de l'éther à la manière habituelle; le rendement global est d'environ 80%.

Le mélange d'amine obtenu précédemment est mis en solution dans 150 ml d'éther anhydre; on y fait barboter du HCl gazeux jusqu'à ce que la précipitation soit complète. Les chlorhydrates d'amines **1***c* et **2***c* sont recueillis par filtration et se présentent sous forme de cristaux différents qui peuvent être séparés manuellement.

tert-Butyl-4 méthyl-1 cyclohexylamine cis **1***b*

Le chlorhydrate recueilli d'une façon prépondérante (**1***c*) a un p.f. de 256° (tube capillaire) et se sublime. Son spectre r.m.n. montre la présence de singulets à 0.88 p.p.m. (*tert*-butyle) et 1.43 p.p.m. (méthyle en position-1— voir. réf. 3). L'amine libre **1***b* régénérée serait pure par c.p.g. et se présente sous forme de liquide incolore, p.e.: 84°/11 mm Hg; n_D^{20}: 1.4562 montrant une bande de vibration N—H à 1610 cm^{-1} dans son spectre infrarouge, un pic *m/e* à 169 dans son spectre de masse et des singulets à 0.85 p.p.m. (*tert*-butyle) et 1.05 p.p.m. (méthyle) dans son spectre r.m.n. Cette amine peut être caractérisée sous forme de *p*-toluènesulfonamide **1***d* de p.f. 173° montrant dans son spectre r.m.n. des pics à 0.76 p.p.m. (*tert*-butyle) et 1.16 p.p.m. (méthyle). Le pK_a de cette amine déterminé[2] dans le méthylcellosolve est de 9.54.

tert-Butyl-4 méthyl-1 cyclohexylamine trans **2***b*

Le chlorhydrate recueilli d'une façon mineure (**2***c*) peut être recristallisé dans un mélange éther–éthanol. Son point de fusion est de 310–320 °C (déc.) et son spectre r.m.n. montre des singulets à 0.84 p.p.m. (*tert*-butyle) et 1.41 p.p.m. (méthyle). L'amine libre **2***b* régénérée est chromatographiquement pure; elle présente les caractéristiques suivantes: p.f. 41.5–43.5°; pK_a (méthylcellosolve)[2]:8.97; i.r.: bande à 1580 cm^{-1} (N—H); spectre de masse: pic parent à *m/e* de 169; r.m.n. singulets à 0.84 p.p.m. (*tert*-butyle) et 1.04 p.p.m. (méthyle). Cette amine donne une *p*-toluènesulfonamide de p.f. 129–130° qui montre dans son spectre r.m.n. des pics à 0.80 p.p.m. (*tert*-butyle) et 1.21 p.p.m. (méthyle).

Remerciements

Les auteurs remercient vivement le Conseil National de Recherches du Canada pour l'aide financière apportée sous forme d'octrois. Les auteurs remercient aussi la Compagnie Dow Chemicals pour un généreux échantillon de *tert*-butyl-4 cyclohexanone utilisée au cours de ce travail.

1. H. Christol et G. Solladie. Bull. Soc. Chim. France, 1299 (1966).
2. D. Gravel. Thèse de Doctorat, Faculté des Sciences, Université de Montréal (1962).
3. J. Alleon-aimi, D. Cabaret, J. P. Mazaleyrat et Z. Welvart. Bull. Soc. Chim. France, 4235 (1968).
4. J.-C. Richer. J. Org. Chem. **30**, 324 (1965).
5. M. Cherest et H. Felkin. Tetrahedron Letters, 2205 (1968).

[2]Les auteurs remercient vivement le Dr. Z. Welvart et ses collaborateurs, CNRS, Groupe de Vitry-Thias (94), France pour cette détermination.

Erratum: Thiazoloisoquinolines. III. Structure and methylation of 2-hydroxythiazolo[4,5-*c*]- and -[5,4-*c*]isoquinolines

CATHERINE E. HALL AND ALFRED TAURINS
Department of Chemistry, McGill University, Montreal, Quebec

Received January 27, 1969
(Ref.: Can. J. Chem. **46**, 691 (1968))

Canadian Journal of Chemistry 47, 2490 (1969)

On page 692, the structures **5** and **6** should be

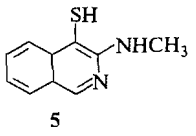

5

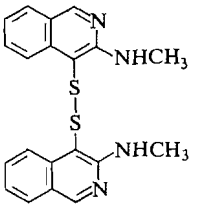

6

and not

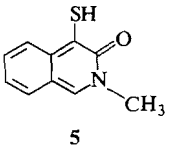

5

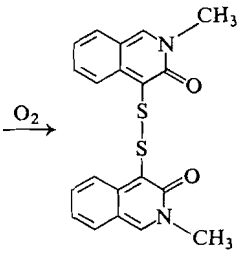

6

Erratum: Enzymic deacylation of esterified mono- and disaccharides. 3. The location of acetylated positions in partially acetylated sugars

A. L. FINK AND G. W. HAY
Department of Chemistry, Queen's University, Kingston, Ontario

Received March 17, 1969
(Ref. Can. J. Chem. **47**, 845 (1969))

Canadian Journal of Chemistry, 47, 2490 (1969)

In Scheme 1 p. 846, the second line is:

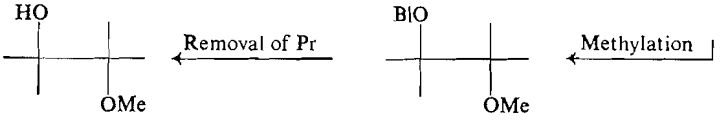

This should be changed to:

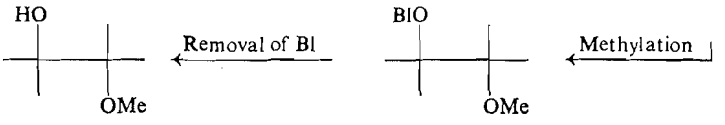

In Table I p. 847, "pentakis" should replace "pentabis" in the names of the top two compounds as well as in the compound of footnote†, Table I: in the same table, "tetrakis" should replace "tetrabis" in the names of the third and fourth compounds.

On p. 850, lines 40 and 41 should include the prefix "penta-kis" and not "penta-bis".

Can. J. Chem. Downloaded from www.nrcresearchpress.com by 210.87.254.105 on 09/05/12
For personal use only.

Epoxides of 1,1-dichloro-2,2-difluoroethylene and chlorotrifluoroethylene

D. CHOW, M. H. JONES, M. P. THORNE, AND E. C. WONG
Department of Physical Chemistry, Ontario Research Foundation, Sheridan Park, Ontario

Received February 6, 1969

The major products from the photochemically initiated oxidation of 1,1-dichloro-2,2-difluoroethylene and chlorotrifluoroethylene in the liquid phase are the corresponding epoxides and acyl halides. The epoxides have been isolated in pure form and characterized.

Canadian Journal of Chemistry, 47, 2491 (1969)

Can. J. Chem. Downloaded from www.nrcresearchpress.com by 210.87.254.42 on 09/05/12
For personal use only.

Halogenated derivatives of ethylene are susceptible to direct oxidation by molecular oxygen because of the electronegativity of the substituents and this represents a potential method for preparation of the corresponding epoxides. However, a variety of oxidation products may be obtained depending on the structure of the olefin and the reaction conditions. For example, dibromofluoroethylene reacts readily with oxygen to give the acyl bromide (1). Similarly, the major product in the photochemically initiated oxidation of chlorotrifluoroethylene is reported (2) to be the acyl fluoride, although the epoxide (3) has been isolated in substantial yield from direct oxidation of the olefin at its boiling point. More recently, it has been shown (4–6) that the photochemical and γ-ray initiated oxidation of tetrafluoroethylene yields primarily the epoxide and carbonyl fluoride.

The oxidation of 1,1-dichloro-2,2-difluoroethylene and chlorotrifluoroethylene by molecular oxygen at temperatures of −60 to +20 °C is slow, but the reaction can be accelerated appreciably by ultraviolet (u.v.) irradiation, particularly in the shorter wavelength region of 2000–3000 Å where significant absorption by the olefin occurs (7). The most convenient preparative method for the epoxides has been found to be irradiation of the olefin under reflux at atmospheric pressure, while bubbling dry oxygen through the liquid. The progress of the reaction may be followed by means of the infrared (i.r.) absorption bands of the mono and dichloro olefins at 1792 and 1740 cm^{-1} respectively.

With both olefins, at least 90% of the oxidation products are volatile and consist of the epoxide and acyl halides. Liquid peroxides occur in both cases but represent less than 5% of the total products. With chlorotrifluoroethylene, a small quantity of solid precipitates during the reaction and was shown to be polychlorotrifluoroethylene by i.r. analysis. In a typical photo-oxidation of 1,1-dichloro-2,2-difluoroethylene, approximately 40% of the volatile product is the epoxide, 50% is chlorodifluoroacetyl chloride, and 10% is dichlorofluoroacetyl fluoride. In the case of chlorotrifluoroethylene, the epoxide constitutes approximately 60% of the volatile product, the remainder being chlorodifluoroacetyl fluoride.

Isolation of the epoxides from the acyl halides proved to be difficult. Fractional distillation, gas–liquid chromatographic and adsorption methods were unsuccessful, resulting in either little or no separation of the components, or decomposition of the epoxides. Two procedures were employed. For the 1,1-dichloro-2,2-difluoroethylene oxide, the acyl halides were removed by successive extraction of a heptane solution with ice water and the epoxide recovered by nitrogen stripping of the heptane at ambient temperature. With the chlorotrifluoroethylene oxide, the acyl fluoride was separated by gas scrubbing with water and a dilute sodium hydroxide solution at 0 °C, using nitrogen as a carrier gas. In both cases the purity of the epoxide was at least 98% in terms of residual acyl halide and olefin as determined by i.r. analysis. However, aqueous treatments resulted in considerable decomposition of the epoxides, the yields of purified material being 10–30%.

As 1,1-dichloro-2,2-difluoroethylene oxide has not been described previously and information on chlorotrifluoroethylene oxide is limited, the epoxides were characterized and their physical properties determined. The data are given in Table I and the i.r. spectra of the two derivatives are shown in Fig. 1. The mass spectra did not show parent ions but the fragmentation patterns were consistent with the epoxide structures.

Both epoxides have limited thermal and hydrolytic stability. For example, a small sample of 1,1-dichloro-2,2-difluoroethylene oxide isom-

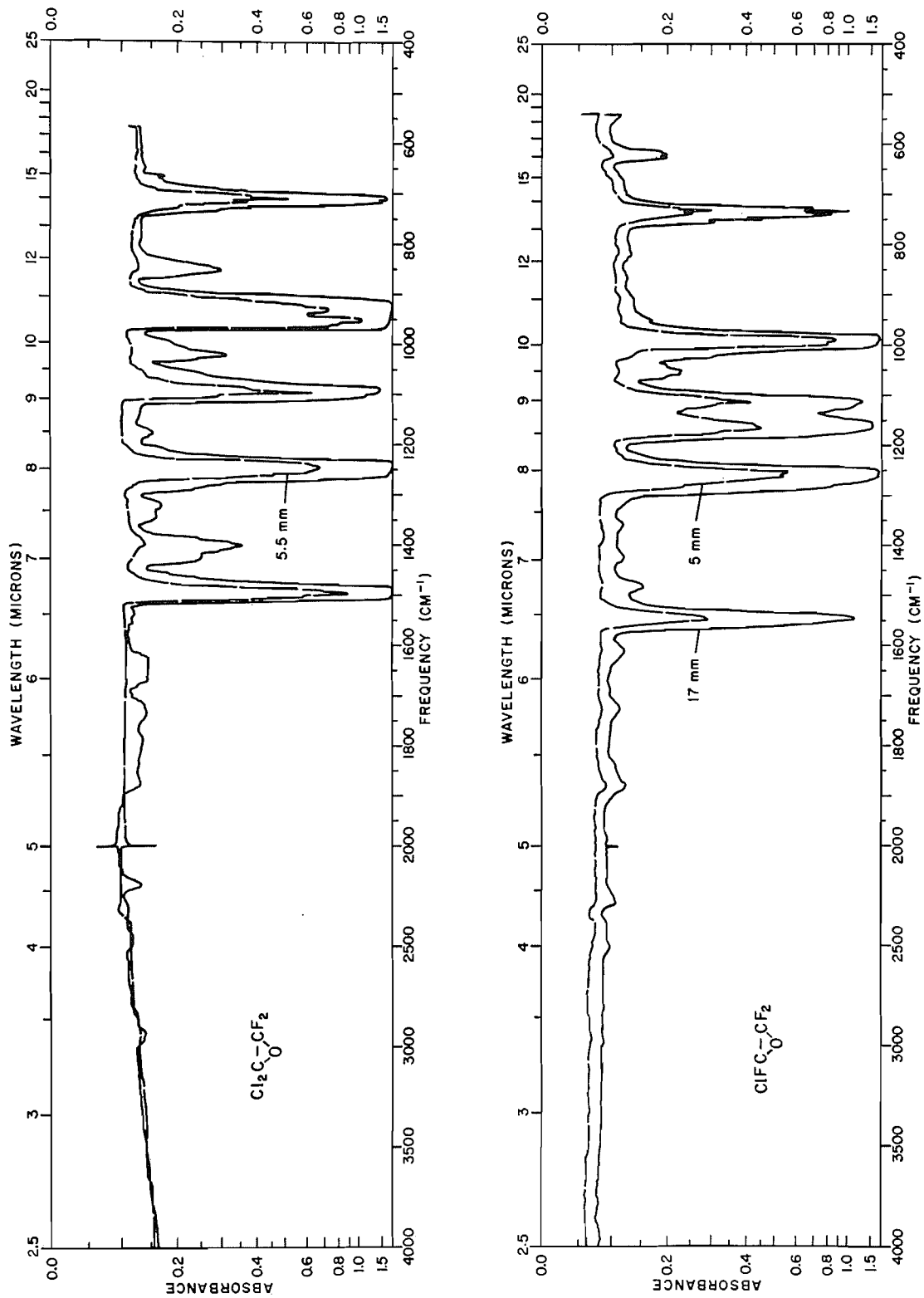

FIG. 1. Infrared absorption spectra of 1,1-dichloro-2,2-difluoroethylene oxide and chlorotrifluoroethylene oxide; 10 cm gas cell.

Can. J. Chem. Downloaded from www.nrcresearchpress.com by 210.87.254.42 on 09/05/12
For personal use only.

TABLE I
Characterization of epoxides

		Epoxide	
		$Cl_2C—CF_2$ (O)	ClFC—CF_2 (O)
Molecular weight*	Calcd.	149	132.5
	Found	147	132
Elemental analysis† C	Calcd.	16.11	18.11
C	Found	16.14	18.15
Cl	Calcd.	47.65	26.79
Cl	Found	45.71	26.73
F	Calcd.	25.50	43.02
F	Found	25.75	42.80
Mass spectrum		No parent ion	No parent ion
Characteristic i.r. absorption band		1500 cm^{-1}	1545 cm^{-1}(1550 cm^{-1})‡
Boiling point, micro, (°C)		$+20.2 \pm 0.5$	-22.0 ± 0.5 (−19)‡
Freezing point		-93.5 ± 0.6	-130.2 ± 0.8

*By vapor density.
†Performed by Swarzkopf Microanalytical Laboratory, New York.
‡From ref. 3.

erized almost entirely to dichlorofluoroacetyl fluoride on standing at 10 °C for 3 days. This rearrangement reaction, involving fluorine migration, is probably catalyzed by traces of moisture or acid and a similar process occurs with chlorotrifluoroethylene oxide. With the latter it has been shown, also, that contact with an excess of water results in complete hydrolysis to oxalic acid and hydrogen halides as indicated by Meyer (8).

Experimental

Materials

The 1,1-dichloro-2,2-difluoroethylene (99% pure) was obtained from Peninsula Chemresearch Inc., and chlorotrifluoroethylene (99% pure) was obtained from Matheson Company. In both cases, the materials were given a bulb to bulb distillation or distilled into the reaction flask to eliminate the inhibitor. Dry oxygen (99.65% purity) was obtained from Linde Company.

Photo-oxidation Reaction

A 3-necked quartz flask (250 ml) was equipped with a dry-ice reflux condenser and gas inlet and outlet tubes. Exit locations were protected from moisture ingress by tubes containing Drierite. Approximately 100 g of the required olefin were condensed in the flask and allowed to reflux. Oxygen, dried by passing through a bed of Linde 13X molecular sieve, was bubbled through the liquid olefin at a rate of 6–9 l/h. A Westinghouse H44-4AB medium pressure mercury lamp (100 W) was used as the ultraviolet (u.v). source and a roughly collimated beam covering the flask area was obtained with a quartz lens. Progress of the reaction was followed by vaporizing small samples of the liquid reaction mixture into an evacuated 10 cm gas cell with KBr windows and measuring the optical density of the olefin absorption band ($Cl_2C=CF_2$, 1740 cm^{-1}; $ClFC=CF_2$, 1792 cm^{-1}). On complete consumption of the olefin, the volatile products, consisting of the epoxide and acyl halide, were vacuum distilled into a second container. The peroxide content of the liquid residue could be determined by iodine titration.

Isolation of Epoxide

For 1,1-dichloro-2,2-difluoroethylene oxide, the volatile reaction product was dissolved in a 10–20 fold excess of cold heptane, extracted 4 times with ice water and once with dilute sodium hydroxide solution (0.1 *N*) at 0 °C. The heptane solution was dried over anhydrous magnesium sulfate and the epoxide recovered by stripping with dry nitrogen at room temperature. The product was given a final bulb-to-bulb distillation at low temperature to remove traces of heptane.

For chlorotrifluoroethylene oxide, a flask containing the volatile reaction product was connected to a gas scrubbing system consisting of two aqueous washes and a sodium hydroxide wash (0.1 *N*), the scrubbers being maintained at 0 °C. The reaction product was maintained 5–10° below its boiling point and the vapor carried through the train by a stream of nitrogen. It was found necessary to use small quantities of the reaction mixture (10–15 ml) to limit acid build-up in the scrubbers which accelerates decomposition of the epoxide. The vapor stream was dried with a bed of Drierite and the product condensed in a dry-ice – acetone trap, protected by a liquid nitrogen trap. This technique can also be applied to separation of the epoxide from the reaction product of 1,1-dichloro-2,2-difluoroethylene. The purified epoxides were stored at −80 °C.

Can. J. Chem. Downloaded from www.nrcresearchpress.com by 210.87.254.42 on 09/05/12
For personal use only.

Acknowledgment

This work was supported by funds received from the Province of Ontario through the Department of Trade and Development.

1. E. T. McBee, O. R. Pierce, and D. L. Christman. J. Am. Chem. Soc. 77, 1583 (1955).
2. R. N. Haszeldine and F. Nyman. J. Chem. Soc. 1084 (1959).
3. W. Müller and E. Walaschewsky. German Pat. No. 947 364. August 16, 1954.
4. H. H. Gibbs and J. L. Warnell. French Pat. No. 1 322 597. February 18, 1963.
5. V. Caglioti, M. Lenzi, and A. Mele. Nature, **201**, 610 (1964).
6. V. Caglioti, A. Delle Site, M. Lenzi, and A. Mele. J. Chem. Soc. 5430 (1964).
7. J. R. Lacker, L. E. Hummel, E. F. Bohmfalk, and J. D. Park. J. Am. Chem. Soc. **72**, 5486 (1950).
8. R. L. Meyer. Ind. Eng. Chem. **45**, 1783 (1953).

Synthesis of some methylated tetroses and pentoses

G. G. S. Dutton, K. B. Gibney, and P. E. Reid[1]

Department of Chemistry, University of British Columbia, Vancouver, British Columbia

Received March 27, 1968

Oxidation of 2,3-di-*O*-methyl-D-glucitol (≡ 4,5-di-*O*-methyl-L-gulitol) and 2,3-di-*O*-methyl-D-mannitol (≡ 4,5-di-*O*-methyl-D-mannitol) with an excess of periodate gave 2,3-di-*O*-methyl-L-threose and 2,3-di-*O*-methyl-D-erythrose, each characterized as the 2,4-dinitrophenylhydrazone. Borohydride reduction of the sugars gave 2,3-di-*O*-methyl-L-threitol and 2,3-di-*O*-methylerythritol characterized as their di-*p*-nitrobenzoates. Oxidation of the hexitols with 1 mole of periodate gave 3,4-di-*O*-methyl-L-xylose characterized as methyl 3,4-di-*O*-methyl-α-L-xylopyranoside and 3,4-di-*O*-methyl-D-arabinose identified as 3,4-di-*O*-methyl-D-arabonamide. 2-*O*-Methyl-D-erythritol (≡ 3-*O*-methyl-L-erythritol) and 1-*O*-methyl-D-threitol (≡ 4-*O*-methyl-D-threitol) were also prepared and characterized as the tri-*p*-nitrobenzoates.

Canadian Journal of Chemistry, 47, 2494 (1969)

Complex polysaccharides on methylation and hydrolysis may give isomeric methylated sugars, the separation and identification of which can be difficult. Sequential periodate oxidation and borohydride reduction of such mixtures may facilitate the process (1–3), particularly when partially methylated pentoses and tetroses are available as reference compounds. A previous paper (4) has described the 2,4-di-*O*-methyl-D- (and L-) tetroses and the present paper reports some mono- and di-*O*-methyltetroses and two di-*O*-methylpentoses (Table I).

Oxidation of 2,3-di-*O*-methyl-D-glucitol and 2,3-di-*O*-methyl-D-mannitol with an excess of periodate yielded respectively 2,3-di-*O*-methyl-L-threose and 2,3-di-*O*-methyl-D-erythrose, characterized as their 2,4-dinitrophenylhydrazones. Each tetrose was reduced to the glycitol and characterized as the *p*-nitrobenzoate. Oxidation of the two hexitols with one mole of periodate (5–8) gave high yields of 3,4-di-*O*-methyl-D-arabinose and 3,4-di-*O*-methyl-L-xylose, indicating a preferential attack of the C-5, C-6 bond.

4-*O*-Methyl-D-threose (9) was prepared by periodate oxidation of methyl 6-*O*-methyl-αβ-D-galactofuranosides. These furanosides form very readily and pure samples of the α-D- and β-D-furanosides were separated by cellulose-column chromatography and characterized. The periodate oxidation required about 50 h for completion in agreement with the findings of Jackson and Hudson (10) but longer than the time reported by Richards (9). The dialdehyde obtained was subjected to methanolysis in an attempt to reduce the extensive decomposition which has been reported on hydrolysis (9). In spite of some decomposition, the 4-*O*-methyl-D-threose was isolated as the dimethylacetal but could only be characterized through the threitol.

Similar difficulties were encountered in the attempted preparation of 2-*O*-methyl-D-erythrose from methyl 4-*O*-methyl-α-D-mannoside. The dialdehyde was resistant to hydrolysis or methanolysis and it was eventually reduced with borohydride before hydrolysis to give directly 2-*O*-methyl-D-erythritol.

[1]Present address: Department of Pathology, University of British Columbia, Vancouver, British Columbia.

Can. J. Chem. Downloaded from www.nrcresearchpress.com by 210.87.254.42 on 09/05/12
For personal use only.

Acknowledgment

This work was supported by funds received from the Province of Ontario through the Department of Trade and Development.

1. E. T. McBee, O. R. Pierce, and D. L. Christman. J. Am. Chem. Soc. 77, 1583 (1955).
2. R. N. Haszeldine and F. Nyman. J. Chem. Soc. 1084 (1959).
3. W. Müller and E. Walaschewsky. German Pat. No. 947 364. August 16, 1954.
4. H. H. Gibbs and J. L. Warnell. French Pat. No. 1 322 597. February 18, 1963.
5. V. Cagliotti, M. Lenzi, and A. Mele. Nature, **201**, 610 (1964).
6. V. Cagliotti, A. Delle Site, M. Lenzi, and A. Mele. J. Chem. Soc. 5430 (1964).
7. J. R. Lacker, L. E. Hummel, E. F. Bohmfalk, and J. D. Park. J. Am. Chem. Soc. **72**, 5486 (1950).
8. R. L. Meyer. Ind. Eng. Chem. **45**, 1783 (1953).

Synthesis of some methylated tetroses and pentoses

G. G. S. Dutton, K. B. Gibney, and P. E. Reid[1]

Department of Chemistry, University of British Columbia, Vancouver, British Columbia

Received March 27, 1968

Oxidation of 2,3-di-*O*-methyl-D-glucitol (≡ 4,5-di-*O*-methyl-L-gulitol) and 2,3-di-*O*-methyl-D-mannitol (≡ 4,5-di-*O*-methyl-D-mannitol) with an excess of periodate gave 2,3-di-*O*-methyl-L-threose and 2,3-di-*O*-methyl-D-erythrose, each characterized as the 2,4-dinitrophenylhydrazone. Borohydride reduction of the sugars gave 2,3-di-*O*-methyl-L-threitol and 2,3-di-*O*-methylerythritol characterized as their di-*p*-nitrobenzoates. Oxidation of the hexitols with 1 mole of periodate gave 3,4-di-*O*-methyl-L-xylose characterized as methyl 3,4-di-*O*-methyl-α-L-xylopyranoside and 3,4-di-*O*-methyl-D-arabinose identified as 3,4-di-*O*-methyl-D-arabonamide. 2-*O*-Methyl-D-erythritol (≡ 3-*O*-methyl-L-erythritol) and 1-*O*-methyl-D-threitol (≡ 4-*O*-methyl-D-threitol) were also prepared and characterized as the tri-*p*-nitrobenzoates.

Canadian Journal of Chemistry, 47, 2494 (1969)

Complex polysaccharides on methylation and hydrolysis may give isomeric methylated sugars, the separation and identification of which can be difficult. Sequential periodate oxidation and borohydride reduction of such mixtures may facilitate the process (1–3), particularly when partially methylated pentoses and tetroses are available as reference compounds. A previous paper (4) has described the 2,4-di-*O*-methyl-D- (and L-) tetroses and the present paper reports some mono- and di-*O*-methyltetroses and two di-*O*-methylpentoses (Table I).

Oxidation of 2,3-di-*O*-methyl-D-glucitol and 2,3-di-*O*-methyl-D-mannitol with an excess of periodate yielded respectively 2,3-di-*O*-methyl-L-threose and 2,3-di-*O*-methyl-D-erythrose, characterized as their 2,4-dinitrophenylhydrazones. Each tetrose was reduced to the glycitol and characterized as the *p*-nitrobenzoate. Oxidation of the two hexitols with one mole of periodate (5–8) gave high yields of 3,4-di-*O*-methyl-D-arabinose and 3,4-di-*O*-methyl-L-xylose, indicating a preferential attack of the C-5, C-6 bond.

4-*O*-Methyl-D-threose (9) was prepared by periodate oxidation of methyl 6-*O*-methyl-αβ-D-galactofuranosides. These furanosides form very readily and pure samples of the α-D- and β-D-furanosides were separated by cellulose-column chromatography and characterized. The periodate oxidation required about 50 h for completion in agreement with the findings of Jackson and Hudson (10) but longer than the time reported by Richards (9). The dialdehyde obtained was subjected to methanolysis in an attempt to reduce the extensive decomposition which has been reported on hydrolysis (9). In spite of some decomposition, the 4-*O*-methyl-D-threose was isolated as the dimethylacetal but could only be characterized through the threitol.

Similar difficulties were encountered in the attempted preparation of 2-*O*-methyl-D-erythrose from methyl 4-*O*-methyl-α-D-mannoside. The dialdehyde was resistant to hydrolysis or methanolysis and it was eventually reduced with borohydride before hydrolysis to give directly 2-*O*-methyl-D-erythritol.

[1]Present address: Department of Pathology, University of British Columbia, Vancouver, British Columbia.

Can. J. Chem. Downloaded from www.nrcresearchpress.com by 210.87.254.40 on 09/05/12
For personal use only.

Can. J. Chem. Downloaded from www.nrcresearchpress.com by 210.87.254.40 on 09/05/12
For personal use only.

The difficulty of isolating 2-*O*-methyl-D-erythrose as such, poses an interesting point in the general use of this degradative method for identifying higher sugars. Whereas 2- and 3-*O*-methyl-D-erythrose are structural isomers with distinct physical properties, the corresponding glycitols, 2-*O*-methyl-D-erythritol and 3-*O*-methyl-D-erythritol or 2-*O*-methyl-L-erythritol are enantiomorphs. These could be distinguished by reduction with sodium borodeuteride and mass spectrometry. A similar technique has recently been used with great success by Lindberg *et al.* (11) for labelling the terminal position in partially methylated alditols.

As it is most likely that the tetroses and tetritols described here will be encountered in various chromatographic procedures their mobilities are recorded in two common solvents (Table I). Only the essential points are given in the Experimental as further details may be found elsewhere (12).

Experimental

Evaporations were carried out *in vacuo* at a bath temperature of 35–45°. Borate was removed by distillation with 1% methanolic hydrogen chloride. Optical rotations were measured at 21 ± 2°. Gas–liquid chromatographic (g.l.c.) separations were made on an F and M model 720 instrument using an 8 ft × 0.5 in. column packed with 20% SF 96 on 80–100 mesh Diatoport S (F and M Division, Hewlett Packard, Avondale, Pennsylvania). Butanone–water azeotrope was used for all chromatographic separations unless otherwise specified and silica gel was used for thin-layer chromatography (t.l.c.). 2,4-Dinitrophenylhydrazones were prepared as previously described (4), purified by t.l.c. using ether–toluene (2:1), and recrystallized from aqueous ethanol. *p*-Nitrobenzoates were similarly purified. Melting points are uncorrected.

2,3-Di-O-methyl-L-threose

Methyl 2,3-di-*O*-methyl-α-D-glucopyranoside was synthesized by the method of Irvine and Scott (13) and hydrolyzed to the free glycose. 2,3-Di-*O*-methyl-D-glucose (3.0 g) was reduced with sodium borohydride (0.6 g) for 36 h and gave 2,3-di-*O*-methyl-D-glucitol (3.1 g), as a syrup $[\alpha]_D$ 15° (*c*, 3 in H_2O); lit. (14) $[\alpha]_D$ 13° (*c*, 2.54 in H_2O). 2,3-Di-*O*-methyl-1,4,5,6-tetra-*O*-*p*-nitrobenzoyl-D-glucitol crystallized from acetone–methanol had m.p. 88–91°.

Anal. Calcd. for $C_{36}H_{30}O_{18}N_4$: C, 52.0; H, 3.6. Found: C, 52.3; H, 3.8.

2,3-Di-*O*-methyl-D-glucitol (2.02 g) was dissolved in water (1 l) and oxidized with sodium metaperiodate (6.12 g, 3 moles) for 4 h. The product (1.35 g) was shown to contain two components (R_f 0.67 and 0.59) by t.l.c. and evaporation of an aqueous solution containing pyridine gave pure 2,3-di-*O*-methyl-L-threose $[\alpha]_D$ 12° (*c*, 1.6 in MeOH).

Anal. Calcd. for $C_6H_{12}O_4$: C, 48.6; H, 8.2. Found: C, 48.4; H, 8.3. The 2,4-dinitrophenylhydrazone had m.p. 125–126°.

Anal. Calcd. for $C_{12}H_{16}O_7N_4$: C, 43.9; H, 4.9; N, 17.1. Found: C, 44.0; H, 5.1; N, 16.9.

2,3-Di-*O*-methyl-L-threose (100 mg) was reacted for 16 h with sodium borohydride (200 mg) to give 2,3-di-*O*-methyl-L-threitol (65 mg) as a syrup, $[\alpha]_D$ 76° (*c*, 1.4 in MeOH).

Anal. Calcd. for $C_6H_{14}O_4$: C, 48.0; H, 9.3. Found: C, 48.2; H, 9.5.

The derivative 2,3-di-*O*-methyl-1,4-di-*O*-*p*-nitrobenzoyl-L-threitol had m.p. 143–144°.

Anal. Calcd. for $C_{20}H_{20}O_{10}N_2$: C, 53.6; H, 4.5; N, 6.3. Found: C, 53.3; H, 4.6; N, 6.2.

2,3-Di-O-methyl-D-erythrose

Methyl-α-D-mannopyranoside (15) was converted to methyl-4,6-*O*-benzylidene-α-D-mannoside (16) which was methylated to give methyl-4,6-*O*-benzylidene-2,3-di-*O*-methyl-α-D-mannoside as a syrup, $[\alpha]_D$ 60.7° (*c*, 2.4 in $CHCl_3$); lit. (17) $[\alpha]_D$ 62.7° (*c*, 1.18 in $CHCl_3$). Acid hydrolysis of this syrup (3.0 g) followed by borohydride reduction gave 2,3-di-*O*-methyl-D-mannitol (1.8 g) which was recrystallized from ethyl acetate, m.p. 101–102°; lit. (18), m.p. 101–103°.

Anal. Calcd. for $C_8H_{18}O_6$: C, 45.7; H, 8.6. Found: C, 45.6; H, 8.5.

2,3-Di-*O*-methyl-D-mannitol (1.0 g) was dissolved in water (500 ml) and oxidized for 4 h with sodium metaperiodate (3.06 g, 3 moles). The product (885 mg) contained two components on t.l.c. Pure 2,3-di-*O*-methyl-D-erythose was separated on a cellulose–hydrocellulose column (19) and had $[\alpha]_D$ −55.3° (*c*, 1.13 in MeOH).

Anal. Calcd. for $C_6H_{12}O_4$: C, 48.6; H, 8.2. Found: C, 48.4; H, 8.3.

2,4-Dinitrophenylhydrazone had m.p. 100–101°.

Anal. Calcd. for $C_{12}H_{16}O_7N_4$: C, 43.9; H, 4.9; N, 17.1. Found: C, 44.1; H, 5.1; N, 17.0.

Borohydride reduction of the glycose (50 mg) gave 2,3-di-*O*-methylerythritol (35 mg).

Anal. Calcd. for $C_6H_{14}O_4$: C, 48.0; H, 9.4. Found: C, 48.3; H, 9.3.

The derivative 2,3-di-*O*-methyl-1,4-di-*O*-*p*-nitrobenzoylerythritol had m.p. 178°.

Anal. Calcd. for $C_{20}H_{20}O_{10}N_2$: C, 53.5; H, 4.5; N, 6.3. Found: C, 53.5; H, 4.4; N, 6.4.

2-O-Methyl-D-erythritol

Methyl-α-D-mannopyranoside (25 g) was dissolved in 98–100% formic acid (100 ml) and acetone (750 ml) was added. Drierite (30 g) was added on the fourth day and the reaction was allowed to proceed for a total of 14 days. The Drierite was removed by filtration and the filtrate poured into a slight excess of 15% sodium hydroxide. The acetone was evaporated and the residue extracted with chloroform (3 × 500 ml) and with ether (3 × 500 ml). The extracts were combined, concentrated, and the residue was dissolved in water. This solution was extracted with 30–60° petroleum ether (3 × 300 ml) to remove all the methyl-2,3;4,6-di-*O*-isopropylidene-α-D-mannoside. The aqueous solution was concentrated to a syrup which was dissolved in hot ethyl acetate to yield

Can. J. Chem. Downloaded from www.nrcresearchpress.com by 210.87.254.40 on 09/05/12
For personal use only.

TABLE I

Properties of some methylated tetroses, pentoses, and tetritols

Compound	$[\alpha]_D^{21}$	R_F (solvent)*	Derivative (melting point, °C)
2,3-Di-*O*-methyl-D-erythrose	−55.3° (MeOH)	0.69 (*a*)	2,4-Dinitrophenylhydrazone, (100–101)
2,3-Di-*O*-methyl-L-threose	12° (MeOH)	0.83 (*a*) 0.80 (*b*)	2,4-Dinitrophenylhydrazone, (125–126)
3,4-Di-*O*-methyl-D-arabinose	−118° (H_2O)	0.19 (*a*) 0.49 (*b*)	3,4-Di-*O*-methyl-D-arabonamide, (132–133)
3,4-Di-*O*-methyl-L-xylose	−29° (H_2O)	0.55 (*a*) 0.65 (*b*)	Methyl-3,4-di-*O*-methyl-L-xyloside, (87–89)
2-*O*-Methyl-D-erythritol	12° (H_2O)	0.16 (*a*) 0.46 (*b*)	2-*O*-Methyl-1,3,4-tri-*O*-*p*-nitrobenzoyl-D-erythritol,‡ (151–152)
1-*O*-Methyl-D-threitol	4.7° (H_2O)	0.23 (*a*) 0.51 (*b*)	1-*O*-Methyl-2,3,4-tri-*O*-*p*-nitrobenzoyl-D-threitol,‡ (129)
2,3-Di-*O*-methylerythritol	—	0.37†	2,3-Di-*O*-methyl-1,4-di-*O*-*p*-nitrobenzoylerythritol,‡ (178)
2,3-Di-*O*-methyl-L-threitol	7.6° (MeOH)	0.37†	2,3-Di-*O*-methyl-1,4-di-*O*-*p*-nitrobenzoyl-L-threitol,‡ (143–144)

*Solvent: *a*, butanone–water azeotrope; *b*, butan-1-ol – ethanol – water (4:1:5 top layer).
†Thin-layer chromatography on silica gel in solvent *a*.
‡After purification by t.l.c. in ether–toluene (2:1).

Can. J. Chem. Downloaded from www.nrcresearchpress.com by 210.87.254.40 on 09/05/12
For personal use only.

methyl-2,3-*O*-isopropylidene-α-D-mannopyranoside (10.9 g), m.p. 107–108°; lit. (20), m.p. 105°.

Methyl-4-*O*-methyl-α-D-mannoside was prepared according to Smith (21) and a pure sample isolated from a cellulose–hydrocellulose column slowly crystallized from butanone, m.p. 101–102°; lit. (22), m.p. 101–103°. This glycoside (0.8 g) was oxidized with sodium metaperiodate (1.2 g, 1.5 moles) in water (200 ml) for 24 h. Treatment with barium acetate and reduction with sodium borohydride for 24 h followed by dilute acid hydrolysis gave 2-*O*-methyl-D-erythritol (0.39 g) $[\alpha]_D$ 12° (*c*, 0.8 in H_2O).

Anal. Calcd. for $C_5H_{12}O_4$: C, 44.1; H, 8.9. Found: C, 44.2; H, 8.8.

The derived 2-*O*-methyl-1,3,4-tri-*O*-*p*-nitrobenzoyl-D-erythritol had m.p. 151–152° after purification by t.l.c.

Anal. Calcd. for $C_{26}H_{21}O_{13}N_3$: C, 53.7; H, 3.7; N, 7.2. Found: C, 53.6; H, 3.5; N, 7.2.

Samples obtained by recrystallization only had melting points varying from 140 to 220°. This value of 151–152° corrects that previously reported (23).

4-O-Methyl-D-threose

6-*O*-Methyl-D-galactose was prepared from 1,2;3,4-di-*O*-isopropylidene-D-galactose and after recrystallization from ethanol had m.p. 128°, $[\alpha]_D$ 115° (*c*, 2.1 in H_2O); lit. (24), m.p. 128°, $[\alpha]_D$ 114° (*c*, 2.1 in H_2O).

A 2% methanolic solution of 6-*O*-methyl-D-galactose (5 g) containing 0.012% hydrogen chloride (25) was refluxed for 18 h by which time the solution was only faintly reducing (Fehling test). The syrup obtained on neutralization and concentration was separated into 3 fractions on a cellulose–hydrocellulose column. The flow rate was 30 ml/h and tubes were collected at 30 min intervals.

Fraction 1, tubes 23–38: 2.48 g, methyl 6-*O*-methyl-β-D-galactofuranoside $[\alpha]_D$ −117° (*c*, 4.7 in MeOH); methyl 6-*O*-methyl-2,3,5-tri-*O*-*p*-nitrobenzoyl-β-D-galactofuranoside, m.p. 82–85°.

Anal. Calcd. for $C_{29}H_{25}O_{15}N_3$: C, 53.2; H, 3.85. Found: C, 53.0; H, 3.75.

Fraction 2, tubes 42–60: 0.74 g, methyl 6-*O*-methyl-α-D-galactofuranoside $[\alpha]_D$ 95° (*c*, 1.96 in MeOH); methyl 2,3,5-tri-*O*-*p*-nitrobenzoyl-α-D-galactofuranoside, m.p. 107–110°. Found: C, 53.1; H, 3.80.

Fraction 3, tubes 100–160: 0.15 g, methyl 6-*O*-methyl-α-D-galactopyranoside, m.p. 132–134°.

The observed anomeric proton coupling constant for fraction 1 was 1.6 c.p.s. in agreement with the value of 2 c.p.s. or less for 1,2-*trans*-furanosides (26). The value for fraction 2 was 4.4 c.p.s. corresponding closely to the value for methyl α-D-galactofuranoside (26).

Methyl 6-*O*-methyl-αβ-D-galactofuranoside (3.0 g) was oxidized with sodium metaperiodate (1.5 moles) in water (1.2 l) for 3 days to give 2.87 g of product which was refluxed with 3% methanolic hydrogen chloride for 24 h. Column chromatography of the resulting syrup (1.67 g) gave a fraction (0.63 g) with properties consistent with the dimethylacetal of 4-*O*-methyl-D-threose having 3 methoxyl and 2 hydroxyl groups in its proton magnetic resonance (p.m.r.) spectrum and $[\alpha]_D$ 5° (*c*, 0.8 in MeOH). Hydrolysis with sulfuric acid (0.5 *N*) gave 4-*O*-methyl-D-threose $[\alpha]_D$ 5° (*c*, 1.3 in H_2O); lit. (9), $[\alpha]_D$ 3° (*c*, 2 in H_2O).

Sodium borohydride reduction of a portion of periodate oxidized furanosides (1.0 g), followed by hydrolysis gave 1-*O*-methyl-D-threitol $[\alpha]_D$ 4.7° (*c*, 1.2 in H_2O).

Anal. Calcd. for $C_5H_{12}O_4$: C, 44.1; H, 8.9. Found: C, 44.1; H, 8.7.

The derivative 1-*O*-methyl-2,3,4-tri-*O*-*p*-nitrobenzoyl-D-threitol had m.p. 129°.

Anal. Calcd. for $C_{26}H_{21}O_{13}N_3$: C, 53.5; H, 3.6; N, 7.2. Found: C, 53.3; H, 3.6; N, 7.2.

3,4-Di-O-methyl-L-xylose

Oxidation of 2,3-di-*O*-methyl-D-glucitol (1.11 g) with sodium metaperiodate (1.12 g, 1 mole) in water (175 ml) for 24 h showed 1 major and 3 minor products by t.l.c. The major component was isolated by column chromatography to give 3,4-di-*O*-methyl-L-xylose (0.74 g), $[\alpha]_D$ −14.6° (*c*, 2.1 in MeOH); lit. (27) for the D-isomer $[\alpha]_D$ 13° (*c*, 1.6 in MeOH). Methanolysis and separation by g.l.c. gave a pure sample of methyl-3,4-di-*O*-methyl-α-L-xyloside, m.p. 87–89°; lit. (28) for the D-isomer, m.p. 89–90°.

Anal. Calcd. for $C_8H_{16}O_5$: OMe, 48.3. Found: OMe, 48.2.

3,4-Di-O-methyl-D-arabinose

Similarly the oxidation of 2,3-di-*O*-methyl-D-mannitol (1.15 g) with 1 mole of periodate gave 1 major and 3 minor products. Column chromatography gave as the major product 3,4-di-*O*-methyl-D-arabinose (0.83 g) having $[\alpha]_D$ −118° (*c*, 1.3 in H_2O); lit. (27) for the L-isomer $[\alpha]_D$ 125° (*c*, 2.4 in H_2O). Oxidation with bromine water and conversion of the lactone to the amide gave 3,4-di-*O*-methyl-D-arabonamide which, crystallized from acetone, had m.p. 132–133°; lit. (27) for the L-isomer, m.p. 133°.

Anal. Calcd. for $C_7H_{15}NO_5$: C, 43.5; H, 7.8. Found: C, 43.5; H, 7.9.

Acknowledgments

The financial support of the National Research Council of Canada and of the University of British Columbia is gratefully acknowledged. We are indebted to Mr. P. Borda of this department for the analyses.

1. R. U. Lemieux and H. F. Bauer. Can. J. Chem. **31**, 814 (1953).
2. A. M. Stephen. J. Chem. Soc. 2030 (1962).
3. G. G. S. Dutton and A. M. Unrau. J. Chromatog. **20**, 78 (1965).
4. G. G. S. Dutton and K. N. Slessor Can. J. Chem. **42**, 614 (1964).
5. E. F. Garner, I. J. Goldstein, R. Montgomery, and F. Smith. J. Am. Chem. Soc. **80**, 1206 (1958).
6. J. C. P. Schwarz. J. Chem. Soc. 276 (1957).
7. J. E. Courtois and M. Guernet. Compt. Rend. **245**, 1273 (1957).
8. J. E. Courtois and M. Guernet. Bull. Soc. Chim. France, 1388 (1957).
9. G. N. Richards. J. Chem. Soc. 3222 (1957).
10. E. L. Jackson and C. S. Hudson. J. Am. Chem. Soc. **59**, 994 (1937).
11. C. G. Hellerquist, B. Lindberg, S. Svensson, T. Holme, and A. A. Lindberg. Carbohydrate Res. **8**, 43 (1968).

12. K. B. GIBNEY. M.Sc. Thesis. University of British Columbia, Vancouver, British Columbia. 1967.
13. J. C. IRVINE and J. P. SCOTT. J. Chem. Soc. **103**, 575 (1913).
14. R. A. BOISSONAS. Helv. Chim. Acta, **30**, 1689 (1947).
15. F. SMITH and J. W. VAN CLEVE. J. Am. Chem. Soc. **77**, 3159 (1955).
16. J. G. BUCHANAN and J. C. P. SCHWARZ. J. Chem. Soc. 4770 (1962).
17. G. J. ROBERTSON. J. Chem. Soc. 330 (1934).
18. K. PIERRE. M.Sc. Thesis. University of British Columbia, Vancouver, British Columbia. 1962.
19. J. D. GEERDES, B. A. LEWIS, R. MONTGOMERY, and F. SMITH. Anal. Chem. **26**, 264 (1954).
20. R. G. AULT, W. N. HAWORTH, and E. L. HIRST. J. Chem. Soc. 1012 (1935).
21. F. SMITH. J. Chem. Soc. 2652 (1951).
22. O. T. SCHMIDT and H. MÜLLER. Ber. **76**, 344 (1943).
23. G. G. S. DUTTON and A. M. UNRAU. Can. J. Chem. **41**, 1417 (1963).
24. K. FREUDENBERG and K. SMEYKAL. Ber. **59**, 100 (1926).
25. I. AUGESTAD and E. BERNER. Acta Chem. Scand. **8**, 251 (1954).
26. B. CAPON and D. THACKER. Proc. Chem. Soc. 369 (1964).
27. G. G. MAHER. Advan. Carbohydrate Chem. **10**, 257 (1955).
28. L. HOUGH and J. K. N. JONES. J. Chem. Soc. 4349 (1952).

Synthesis of 3-hexuloses

K. G. A. JACKSON AND J. K. N. JONES
Department of Chemistry, Queen's University, Kingston, Ontario

Received February 17, 1969

A general procedure for the syntheses of derivatives of 3-hexuloses from L-*threo*-hexeno-furano lactone is described[1].

Une méthode générale de synthèse de 3-hexuloses avec du L-*threo*-hexeno-furano lactone est décrite.

Canadian Journal of Chemistry, 47, 2498 (1969)

The recent isolation from an antibiotic, and identification of coriose (1), as D-*altro*-3-heptulose, previously isolated by Begbie and Richtmyer (2) prompts us to give details of a general synthesis of 3-hexuloses. In an earlier publication (3) the synthesis of 2-*O*-methyl-3-hexuloses and 2-*O*-methyl-3-heptuloses was described and a modification of this synthesis was later (4) suggested which might lead to the 3-hexuloses. It is now shown that this suggested procedure does in fact lead to the synthesis of sugars named in the title of this paper.

L-Ascorbic acid (**1**, $R^2 = R^3 = H$) is readily acetonated to yield 5,6-*O*-isopropylidene-L-ascorbic acid (**2**, $R^2 = R^3 = H$) (5). Treatment of this substance with one equivalent of diazomethane produces mainly the 3-*O*-methyl ether (**2**, $R^2 = H$; $R^3 = CH_3$) (4). The sodium salt of this compound reacts with benzyl chloride to give crystalline **2** ($R^2 = CH_2Ph$; $R^3 = CH_3$). Elimination of acetone by acid hydrolysis yields 2-*O*-benzyl-3-*O*-methyl-L-ascorbic acid (**1**, $R^2 = CH_2Ph$; $R^3 = CH_3$). 2,3-Di-*O*-substituted derivatives of L-ascorbic acid rearrange in the presence of base (6), to yield furanoside derivatives by addition at the vinylic carbon, in this case to yield **3** ($R^2 = CH_2Ph$; $R^3 = CH_3$) which reduces 0.97 equivalent of periodate. Reduction of the lactone by lithium aluminium hydride then results in the formation of a methyl glycoside of a 3-hexulose derivative. If now the benzyl residue is removed by hydrogenation and the resultant glycoside **4** ($R^2 = H$; $R^3 = CH_3$) treated with acid a 3-hexulose **4** ($R^2 = R^3 = H$) results, which consumes 1.7 equivalent of periodate and yields 0.81 equivalent of formaldehyde. However in the rearrangement described above two new asymmetric centers are produced at C-2 and C-3, but only two products are detected. Models indicate that the addition at C-3 yields the less strained component which contains two *cis*-fused five-membered rings. The two isomers produced are separable by thin-layer and gas–liquid chromatography (t.l.c. and g.l.c.). The absolute configuration of the

[1]Abstracted from the Ph.D. Thesis of K.G.A. Jackson (1966).

Can. J. Chem. Downloaded from www.nrcresearchpress.com by 210.87.254.40 on 09/05/12
For personal use only.

12. K. B. GIBNEY. M.Sc. Thesis. University of British Columbia, Vancouver, British Columbia. 1967.
13. J. C. IRVINE and J. P. SCOTT. J. Chem. Soc. **103**, 575 (1913).
14. R. A. BOISSONAS. Helv. Chim. Acta, **30**, 1689 (1947).
15. F. SMITH and J. W. VAN CLEVE. J. Am. Chem. Soc. **77**, 3159 (1955).
16. J. G. BUCHANAN and J. C. P. SCHWARZ. J. Chem. Soc. 4770 (1962).
17. G. J. ROBERTSON. J. Chem. Soc. 330 (1934).
18. K. PIERRE. M.Sc. Thesis. University of British Columbia, Vancouver, British Columbia. 1962.
19. J. D. GEERDES, B. A. LEWIS, R. MONTGOMERY, and F. SMITH. Anal. Chem. **26**, 264 (1954).
20. R. G. AULT, W. N. HAWORTH, and E. L. HIRST. J. Chem. Soc. 1012 (1935).
21. F. SMITH. J. Chem. Soc. 2652 (1951).
22. O. T. SCHMIDT and H. MÜLLER. Ber. **76**, 344 (1943).
23. G. G. S. DUTTON and A. M. UNRAU. Can. J. Chem. **41**, 1417 (1963).
24. K. FREUDENBERG and K. SMEYKAL. Ber. **59**, 100 (1926).
25. I. AUGESTAD and E. BERNER. Acta Chem. Scand. **8**, 251 (1954).
26. B. CAPON and D. THACKER. Proc. Chem. Soc. 369 (1964).
27. G. G. MAHER. Advan. Carbohydrate Chem. **10**, 257 (1955).
28. L. HOUGH and J. K. N. JONES. J. Chem. Soc. 4349 (1952).

Synthesis of 3-hexuloses

K. G. A. JACKSON AND J. K. N. JONES
Department of Chemistry, Queen's University, Kingston, Ontario

Received February 17, 1969

A general procedure for the syntheses of derivatives of 3-hexuloses from L-*threo*-hexeno-furano lactone is described[1].

Une méthode générale de synthèse de 3-hexuloses avec du L-*threo*-hexeno-furano lactone est décrite.

Canadian Journal of Chemistry, 47, 2498 (1969)

The recent isolation from an antibiotic, and identification of coriose (1), as D-*altro*-3-heptulose, previously isolated by Begbie and Richtmyer (2) prompts us to give details of a general synthesis of 3-hexuloses. In an earlier publication (3) the synthesis of 2-*O*-methyl-3-hexuloses and 2-*O*-methyl-3-heptuloses was described and a modification of this synthesis was later (4) suggested which might lead to the 3-hexuloses. It is now shown that this suggested procedure does in fact lead to the synthesis of sugars named in the title of this paper.

L-Ascorbic acid (**1**, $R^2 = R^3 = H$) is readily acetonated to yield 5,6-*O*-isopropylidene-L-ascorbic acid (**2**, $R^2 = R^3 = H$) (5). Treatment of this substance with one equivalent of diazomethane produces mainly the 3-*O*-methyl ether (**2**, $R^2 = H$; $R^3 = CH_3$) (4). The sodium salt of this compound reacts with benzyl chloride to give crystalline **2** ($R^2 = CH_2Ph$; $R^3 = CH_3$). Elimination of acetone by acid hydrolysis yields 2-*O*-benzyl-3-*O*-methyl-L-ascorbic acid (**1**, $R^2 = CH_2Ph$; $R^3 = CH_3$). 2,3-Di-*O*-substituted derivatives of L-ascorbic acid rearrange in the presence of base (6), to yield furanoside derivatives by addition at the vinylic carbon, in this case to yield **3** ($R^2 = CH_2Ph$; $R^3 = CH_3$) which reduces 0.97 equivalent of periodate. Reduction of the lactone by lithium aluminium hydride then results in the formation of a methyl glycoside of a 3-hexulose derivative. If now the benzyl residue is removed by hydrogenation and the resultant glycoside **4** ($R^2 = H$; $R^3 = CH_3$) treated with acid a 3-hexulose **4** ($R^2 = R^3 = H$) results, which consumes 1.7 equivalent of periodate and yields 0.81 equivalent of formaldehyde. However in the rearrangement described above two new asymmetric centers are produced at C-2 and C-3, but only two products are detected. Models indicate that the addition at C-3 yields the less strained component which contains two *cis*-fused five-membered rings. The two isomers produced are separable by thin-layer and gas–liquid chromatography (t.l.c. and g.l.c.). The absolute configuration of the

[1]Abstracted from the Ph.D. Thesis of K.G.A. Jackson (1966).

Can. J. Chem. Downloaded from www.nrcresearchpress.com by 210.87.254.6 on 09/05/12
For personal use only.

L-*xylo*-isomer was determined by reducing the 3-hexulose to a mixture of glucitol and galactitol, the acetates of which were identified by g.l.c. (7). A syrupy dinitrophenylhydrazone **5** of **4** ($R^2 = R^3 = H$) was prepared. Its oxidation produced formaldehyde (1.5 moles) and formic acid (0.78) with a consumption of 2.8 moles of periodate per mole. These figures obtained from a product isolated by chromatography, are in reasonable agreement with the theoretical values which are 2.0, 1.0, and 3.0 respectively (see below). The subsequent isolation of 2,4-dinitrophenylazomalondialdehyde is in agreement with the structure postulated, **5** (8).

Experimental

For details of separations of sugar derivatives by paper chromatography and t.l.c. see Jackson and Jones (4).

5,6-O-Isopropylidene-L-ascorbic acid (2, $R^2 = R^3 = H$)

A mixture of L-ascorbic acid (10 g) in acetone (40 ml) containing acetyl chloride (1.0 ml) was shaken mechanically. Crystalline 5,6-*O*-isopropylidene-L-ascorbic acid separated from the solution soon after the L-ascorbic acid had dissolved. After storage at 0° there was obtained on filtration, 10.1 g of needle-shaped crystals of m.p. 217–223° (5). This material was used in the next step without further purification.

2-O-Benzyl-5,6-O-isopropylidene-3-O-methyl-L-ascorbic acid (2, $R^2 = CH_2Ph$; $R^3 = CH_3$)

A methanolic solution of 5,6-*O*-isopropylidene-L-ascorbic acid (35 g) was treated at 0° with an ethereal solution of diazomethane to a yellow end point which persisted for about 1 min. Evaporation of the solvent yielded a mobile syrup which was dissolved in methanol and converted to the sodium salt by the addition of methanolic sodium methoxide (6.0 *N*, 21.0 ml).

After evaporation of the methanol the residual brown gum was dispersed in benzyl chloride (70 ml) and the mixture was heated at 80° (2.5 h) and then poured into water. After evaporation of excess benzyl chloride, the product crystallized and was recrystallized from methanol to yield the product (16.0 g) of m.p. 85–87°, identical with that described earlier (4) but in higher yield.

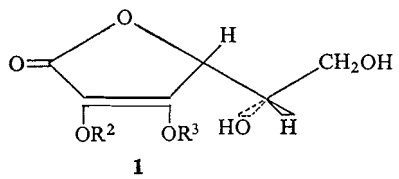

1

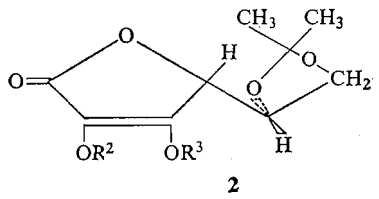

2

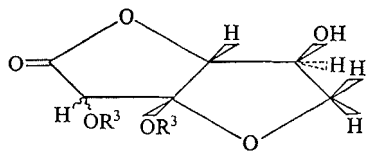

3

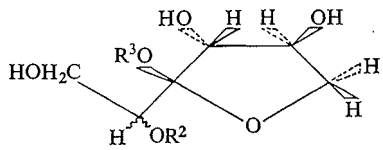

4

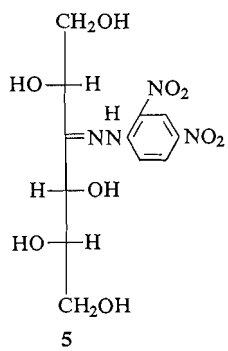

5

Can. J. Chem. Downloaded from www.nrcresearchpress.com by 210.87.254.6 on 09/05/12
For personal use only.

Can. J. Chem. Downloaded from www.nrcresearchpress.com by 210.87.254.6 on 09/05/12
For personal use only.

2-O-Benzyl-3-O-methyl-L-ascorbic acid (1, $R^2 = CH_2Ph$; $R^3 = CH_3$)

A solution of the above isopropylidene derivative (3.0 g) above in acetic acid (50%, 50 ml) was heated at 90–100° for 4 h. Water (200 ml) was then added and the solution was extracted with chloroform (2 × 200 ml). The chloroform extracts were dried ($MgSO_4$), filtered, and the filtrate was evaporated. The crystalline residue (1.3 g) was recrystallized from chloroform. The product had m.p. 124° and $[\alpha]_D = +48° \pm 1°$ (*c*, 1.0 in methanol).

Anal. Calcd. for $C_{14}H_{15}O_6$: C, 60.0; H, 5.7. Found: C, 59.6; H, 5.5.

The infrared (i.r.) spectrum (KBr disk) revealed strong absorptions at 1660, 1745, and 3300 cm^{-1}. The nuclear magnetic resonance (n.m.r.) spectrum (DMSO-d_6) revealed peaks at τ 2.61 (singlet, 5 aromatic protons), and 6.09 (singlet, 3 methyl protons) as well as other peaks.

Methyl 2-O-Benzyl-L-(lyxo + xylo)-3-hexulofuranosidonolactones (3, $R^2 = CH_2Ph$; $R^3 = CH_3$)

An aqueous solution of **1** ($R^2 = CH_2Ph$; $R^3 = CH_3$) (8.3 g) was saponified at 60° with sodium hydroxide (1.96 *N*, 11.2 ml). The solution was then passed down a column of ion exchange resin (H^+) and the acidic effluent collected. The column was washed with warm water until the effluent gave a negative Molisch test and the aqueous solutions were concentrated and extracted with chloroform (2 × 10 ml). The extracts were dried ($MgSO_4$), filtered, and the filtrate was evaporated to a syrup (6.6 g) which had $[\alpha]_D = -10° \pm 1°$ (*c*, 1.0 in methanol). Two components were detected by paper chromatograms (solvent *a*) and were visualized in iodine vapor. The i.r. absorption ($CHCl_3$) revealed absorptions at 1800 cm^{-1} (strong) and 3450 cm^{-1} (medium).

Methyl 2-O-Benzyl-L-(lyxo + xylo)-3-hexulosides (4, $R^2 = CH_2Ph$; $R^3 = CH_3$)

The syrupy product above (14.3 g from two preparations) was dissolved in ether (100 ml) and the solution added dropwise to a solution of $LiAlH_4$ (14.0 g) in ether (200 ml). An immediate precipitate resulted. Ten minutes after completion of the addition, excess of $LiAlH_4$ was destroyed with ethyl acetate (300 ml) followed by the cautious addition of water (200 ml). The ethyl acetate layer was separated and the residue was extracted with a further quantity of ethyl acetate (100 ml). The combined extracts were washed with water (100 ml), dried ($MgSO_4$), filtered, and the filtrate was evaporated to a pale yellow syrup (10.5 g) of $[\alpha]_D = -6° \pm 1°$ (*c*, 1.0 in methanol). Analysis by t.l.c. indicated the presence of two components of R_f 0.6 and 0.7 in the approximate ratio 2:3. The i.r. absorption of the mixture in chloroform indicated a peak at 3500 cm^{-1} (medium) but none at 1605–2000 cm^{-1}.

Periodate Oxidation of the Syrupy Mixture of Glycosides

Periodate uptake and formic acid yield on 116 mg of the mixture, dissolved in water (100 ml) were carried out in the usual way (4) using screened (methylene-blue)-methyl red indicator.

Found: Moles periodate consumed per mole of compound at the times indicated: 0.31, (0.5 h); 0.38 (1 h); 0.51 (2 h); 0.72 (4.5 h); 0.91 (20 h); 0.97 (94 h). The yield of formic acid rose from 0.02 to 0.08 in the same period.

Methyl L-(lyxo + xylo)-3-hexulosides (4, $R^2 = H$; $R^3 = CH_3$)

The syrupy mixture of glycosides (9.0 g) (above) was dissolved in ethanol (100 ml) and reduced with Raney nickel catalyst and hydrogen at 2 atmospheres pressure during 4 days. At the end of this time reaction was complete as judged by t.l.c. The solution was filtered and the filtrate evaporated to a syrup which was dissolved in water and extracted with chloroform (100 ml) to remove the last traces of toluene. Evaporation of the aqueous layer afforded a syrup (5.6 g) of $[\alpha]_D = +35° \pm 1°$ (*c*, 1.0 in methanol). Paper chromatography (solvent *a*) revealed one component with $R_f = 0.48$ and $R_{rhamnose} = 1.45$.

Periodate Oxidation of Methyl L-(lyxo + xylo)-3-hexulosides

Periodate uptake, formic acid production, and formaldehyde release were determined in the usual manner on 110 mg syrup in water (100 ml).

Found: Uptake of periodate at the times indicated: 0.91 (0.25 h); 1.05 (1 h); 1.26 (3.5 h); 1.45 (10 h); 1.64 (23 h); 1.70 (30 h). Formaldehyde yield: 0.02 (0.4 h); 0.81 (21 h). The formic acid yield changed from 0.01 (0.25 h) to 0.04 (23 h). All results are given in mole/mole of glycoside.

Methyl 1,2,4,5-Tetra-O-acetyl-L-(lyxo + xylo)-3-hexulosides

The mixed glycosides (1.0 g) were acetylated with pyridine (30 ml) and acetic anhydride (5 ml) at 0° for 12 h. The acetylated products were isolated in the usual manner as a clear colorless syrup. Thin-layer chromatography revealed components at $R_f = 0.60$ (medium) and 0.75 (major). Analysis by gas–liquid chromatography (g.l.c.) using 5% LAC-4-R-886 (Chromatographic Specialities, Brockville, Ontario) at 200° and at a flow rate of 100 cc/min (Pye Argon g.l.c.) showed two components, the L-*xylo* and L-*lyxo* derivatives respectively, 3.5 min and 5.8 min, in the ratio 55:45.

Separation of the Glycosides

A portion of the mixture was separated by preparative t.l.c. on plates 8 in. × 8 in. coated with silica gel G using chloroform, methanol (9:1 v/v) as eluant. The bands of material could be located visually or better with the aid of an ultraviolet lamp. The faster moving component (540 mg) isolated after extraction of the appropriate region of the silica gel G with acetone had a retention time of 3.5 min (see above) and had $[\alpha]_D = +14° \pm 1°$ (*c*, 1.0 in methanol) and was identified as methyl 1,2,4,5-tetra-*O*-acetyl-L-*xylo*-3-hexuloside (see below).

Anal. Calcd. for $C_{15}H_{22}O_{10}$: C, 49.7; H, 6.1. Found: C, 50.0; H, 6.4.

The slower moving component (200 mg) was therefore methyl 1,2,4,5-tetra-*O*-acetyl-L-*lyxo*-3-hexuloside with $[\alpha]_D = +5° \pm 1°$ (*c*, 1.0 in methanol). It was not further examined. The i.r. spectra of these two substances ($CHCl_3$) were indistinguishable and revealed absorption bands at 1730 cm^{-1} (strong) and at 1375 cm^{-1} (medium).

Purification of Methyl L-xylo-3-hexuloside

Methyl 1,2,4,5-tetra-*O*-acetyl-L-*xylo*-3-hexuloside (540 mg) was deacetylated by the method of Zemplén. After

12 h the product was isolated as a clear colorless syrup (250 mg) with $[\alpha]_D = -29° \pm 1°$ (*c*, 1.0 in methanol). On periodate oxidation of a sample (5.5 mg) formaldehyde (0.31 mole/mole, 21 h) was produced.

L-xylo-3-Hexulose (4, $R^2 = R^3 = H$)

The glycoside (100 mg) was dissolved in water (20 ml) and hydrolyzed at 80° with acid ion exchange resin (Amberlite IR-120) during 0.33 h. At the end of this time hydrolysis was complete as indicated by paper chromatography. The product in solvent *a* had $R_{rhamnose} = 0.69$; $R_{tagatose} = 1.25$ and $R_{sorbose} = 1.45$ and gave a bright-yellow color with the *p*-anisidine hydrochloride spray. The reducing sugar was isolated as a syrup after removal of the ion exchange resin and evaporation of the solution. It had $[\alpha]_D = +10° \pm 1°$ (*c*, 0.5 in water).

Sodium Borohydride Reduction of L-xylo-3-Hexulose (4, $R^3 = R^4 = H$) and Identification of the Resultant Hexitols

The ketose **4** ($R^3 = R^4 = H$) (20 mg) was reduced in water (50 ml) by addition of sodium borohydride (30 mg). When reduction was complete, as indicated by paper chromatography, the solution was passed through a column of ion exchange resin (Amberlite i.r. 120 H) and the effluent evaporated to dryness. Boric acid was removed as methyl borate by co-distillation with methanol and the residue acetylated (pyridine and acetic anhydride) in the usual way. The mixture of acetates was then examined by g.l.c. and was resolvable into two components which were indistinguishable, on an F and M model 500 g.l.c. machine, from sorbitol and dulcitol hexa-acetates under standardized conditions.

L-xylo-3-Hexulose 2,4-Dinitrophenylhydrazone (5)

The L-*xylo*-methyl glycoside (**4**, $R^2 = H$; $R^3 = CH_3$) (0.175 g) was dissolved in dimethyl sulfoxide (2 ml) containing 1 drop of conc. hydrochloric acid and 2,4-dinitrophenylhydrazine (0.165 g). After 2 h, paper chromatography (solvent *a*) indicated the presence of a yellow major component with $R_f = 0.66$, $R_{rhamnose} = 1.78$. This substance was isolated as a yellow gum after preparative chromatography on six 8 in. × 8 in. glass plates coated with silica gel G. The product (93 mg) had $[\alpha]_D = 20° \pm 4°$ (*c*, 0.9 in methanol) and was homogeneous by paper chromatography.

Periodate Oxidation of L-xylo-3-Hexulose 2,4-Dinitrophenylhydrazone

The hydrazone derivative (37.5 mg) was oxidized in duplicate in the usual manner.

Found: Mole of formic acid produced by moles of periodate consumed per mole of compound at the times indicated: 0.78, 2.8 (0.17 h); 0.7, 2.8 (0.67 h). Formaldehyde produced mole/mole 1.50 (0.5 h).

During the oxidation a yellow precipitate separated from solution. It had m.p. 160° and its i.r. spectrum (KBr disk) showed strong peaks at 1590, 1655, and 1685 cm^{-1} with no absorption in the region 1700–2300 cm^{-1}. The ultraviolet absorption was strong at $\varepsilon_{max} = 395$ mμ with $\varepsilon = 2.5 \times 10^4$. 2,4-Dinitrophenylazomalondialdehyde has m.p. 160–161°, $\varepsilon_{max} = 395$ mμ with $\varepsilon = 2.45 \times 10^4$ (8).

Acknowledgments

The authors thank the National Research Council of Canada for a Scholarship (to K.G.A.J.) and for a Grant (NRC A-19) and Queen's University for financial assistance. They also thank Dr. E. Buncel for his interest and advice.

1. T. Okuda and K. Konishi. Chem. Commun. 553, 671 (1968); Tetrahedron **24**, 6907 (1968).
2. R. Begbie and N. K. Richtmyer. Carbohyd. Res. **2**, 272 (1966).
3. J. K. N. Jones. J. Am. Chem. Soc. **78**, 2855 (1956).
4. K. G. A. Jackson and J. K. N. Jones. Can. J. Chem. **43**, 450 (1964).
5. K. Heyns. Ann. Chem. **558**, 177 (1947).
6. W. N. Haworth, E. L. Hirst, and F. Smith. J. Chem. Soc. 829 (1937); E. G. E. Hawkins, E. L. Hirst, and J. K. N. Jones. J. Chem. Soc. 246 (1939).
7. S. W. Gunner, J. K. N. Jones, and M. B. Perry. Can. J. Chem. **39**, 1892 (1961); H. G. Jones. Ph.D. Thesis, Queen's University, Kingston, Ontario. 1964.
8. F. Mashio and Y. Kimura. Nippon Kagaku Zasshi, **83**, 303 (1962); Chem. Abstr. **59**, 3841 (1963).

Total synthesis of (±)ochotensine

R. B. Kelly and B. A. Beckett
Department of Chemistry, University of New Brunswick, Saint John, New Brunswick

Received February 20, 1969

A total synthesis of (±)ochotensine is described.

Canadian Journal of Chemistry, 47, 2501 (1969)

A very recently published total synthesis of (±)ochotensine (**1**) (1) by Irie *et al.* (2) has just come to our attention, prompting us to report an independent, but similar, synthesis of this alkaloid. An account (3) of our total synthesis of analogues **5** and **6** of ochotensine and ochotensimine respectively, appeared some months ago. We anticipated (3) that the synthesis of

Can. J. Chem. Downloaded from www.nrcresearchpress.com by 210.87.254.6 on 09/05/12
For personal use only.

12 h the product was isolated as a clear colorless syrup (250 mg) with $[\alpha]_D = -29° \pm 1°$ (*c*, 1.0 in methanol). On periodate oxidation of a sample (5.5 mg) formaldehyde (0.31 mole/mole, 21 h) was produced.

L-xylo-3-Hexulose (4, $R^2 = R^3 = H$)

The glycoside (100 mg) was dissolved in water (20 ml) and hydrolyzed at 80° with acid ion exchange resin (Amberlite IR-120) during 0.33 h. At the end of this time hydrolysis was complete as indicated by paper chromatography. The product in solvent *a* had $R_{rhamnose} = 0.69$; $R_{tagatose} = 1.25$ and $R_{sorbose} = 1.45$ and gave a bright-yellow color with the *p*-anisidine hydrochloride spray. The reducing sugar was isolated as a syrup after removal of the ion exchange resin and evaporation of the solution. It had $[\alpha]_D = +10° \pm 1°$ (*c*, 0.5 in water).

Sodium Borohydride Reduction of L-xylo-3-Hexulose (4, $R^3 = R^4 = H$) and Identification of the Resultant Hexitols

The ketose **4** ($R^3 = R^4 = H$) (20 mg) was reduced in water (50 ml) by addition of sodium borohydride (30 mg). When reduction was complete, as indicated by paper chromatography, the solution was passed through a column of ion exchange resin (Amberlite i.r. 120 H) and the effluent evaporated to dryness. Boric acid was removed as methyl borate by co-distillation with methanol and the residue acetylated (pyridine and acetic anhydride) in the usual way. The mixture of acetates was then examined by g.l.c. and was resolvable into two components which were indistinguishable, on an F and M model 500 g.l.c. machine, from sorbitol and dulcitol hexa-acetates under standardized conditions.

L-xylo-3-Hexulose 2,4-Dinitrophenylhydrazone (5)

The L-*xylo*-methyl glycoside (**4**, $R^2 = H$; $R^3 = CH_3$) (0.175 g) was dissolved in dimethyl sulfoxide (2 ml) containing 1 drop of conc. hydrochloric acid and 2,4-dinitrophenylhydrazine (0.165 g). After 2 h, paper chromatography (solvent *a*) indicated the presence of a yellow major component with $R_f = 0.66$, $R_{rhamnose} = 1.78$. This substance was isolated as a yellow gum after preparative chromatography on six 8 in. × 8 in. glass plates coated with silica gel G. The product (93 mg) had $[\alpha]_D = 20° \pm 4°$ (*c*, 0.9 in methanol) and was homogeneous by paper chromatography.

Periodate Oxidation of L-xylo-3-Hexulose 2,4-Dinitrophenylhydrazone

The hydrazone derivative (37.5 mg) was oxidized in duplicate in the usual manner.

Found: Mole of formic acid produced by moles of periodate consumed per mole of compound at the times indicated: 0.78, 2.8 (0.17 h); 0.7, 2.8 (0.67 h). Formaldehyde produced mole/mole 1.50 (0.5 h).

During the oxidation a yellow precipitate separated from solution. It had m.p. 160° and its i.r. spectrum (KBr disk) showed strong peaks at 1590, 1655, and 1685 cm^{-1} with no absorption in the region 1700–2300 cm^{-1}. The ultraviolet absorption was strong at $\varepsilon_{max} = 395$ mμ with $\varepsilon = 2.5 \times 10^4$. 2,4-Dinitrophenylazomalondialdehyde has m.p. 160–161°, $\varepsilon_{max} = 395$ mμ with $\varepsilon = 2.45 \times 10^4$ (8).

Acknowledgments

The authors thank the National Research Council of Canada for a Scholarship (to K.G.A.J.) and for a Grant (NRC A-19) and Queen's University for financial assistance. They also thank Dr. E. Buncel for his interest and advice.

1. T. Okuda and K. Konishi. Chem. Commun. 553, 671 (1968); Tetrahedron **24**, 6907 (1968).
2. R. Begbie and N. K. Richtmyer. Carbohyd. Res. **2**, 272 (1966).
3. J. K. N. Jones. J. Am. Chem. Soc. **78**, 2855 (1956).
4. K. G. A. Jackson and J. K. N. Jones. Can. J. Chem. **43**, 450 (1964).
5. K. Heyns. Ann. Chem. **558**, 177 (1947).
6. W. N. Haworth, E. L. Hirst, and F. Smith. J. Chem. Soc. 829 (1937); E. G. E. Hawkins, E. L. Hirst, and J. K. N. Jones. J. Chem. Soc. 246 (1939).
7. S. W. Gunner, J. K. N. Jones, and M. B. Perry. Can. J. Chem. **39**, 1892 (1961); H. G. Jones. Ph.D. Thesis, Queen's University, Kingston, Ontario. 1964.
8. F. Mashio and Y. Kimura. Nippon Kagaku Zasshi, **83**, 303 (1962); Chem. Abstr. **59**, 3841 (1963).

Total synthesis of (±)ochotensine

R. B. Kelly and B. A. Beckett

Department of Chemistry, University of New Brunswick, Saint John, New Brunswick

Received February 20, 1969

A total synthesis of (±)ochotensine is described.

Canadian Journal of Chemistry, 47, 2501 (1969)

A very recently published total synthesis of (±)ochotensine (**1**) (1) by Irie *et al.* (2) has just come to our attention, prompting us to report an independent, but similar, synthesis of this alkaloid. An account (3) of our total synthesis of analogues **5** and **6** of ochotensine and ochotensimine respectively, appeared some months ago. We anticipated (3) that the synthesis of

Can. J. Chem. Downloaded from www.nrcresearchpress.com by 210.87.254.5 on 09/05/12
For personal use only.

Can. J. Chem. Downloaded from www.nrcresearchpress.com by 210.87.254.5 on 09/05/12
For personal use only.

these analogues would serve as a model for us for a total synthesis of ochotensine (**1**). Both the synthesis of Irie *et al.* (2) and that reported here parallel exactly our model synthesis (3) of **5** and **6**. However, they differ considerably in execution. We therefore feel that the experimental details of our synthesis would be of value, especially in view of the intense interest shown recently in the synthesis of ochotensine (**1**) and ochotensimine (**2**) (2, 3, 4). A total synthesis of the latter by McLean *et al.* (4) has appeared within the past year.

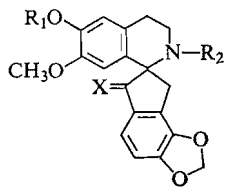

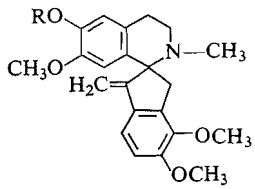

1 R_1 = H, R_2 = CH_3, X = CH_2
2 R_1 = R_2 = CH_3, X = CH_2
3 R_1 = R_2 = H, X = O
4 R_1 = H, R_2 = CH_3, X = O

5 R = H
6 R = CH_3

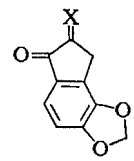

7 X = O
8 X = NOH

2,3-Dihydroxybenzoic acid, prepared from *o*-vanillin by a published route (5) was used as starting material for the synthesis of the indanedione **7**. Methyleneation of the ethyl ester of this acid by the method of Dallacker and Korb (6) gave 2,3-methylenedioxybenzoic acid (cf. ref. 7). The ethyl ester of the latter benzoic acid was reduced with lithium aluminium hydride and the resulting benzyl alcohol was oxidized to 2,3-methylenedioxybenzaldehyde with manganese dioxide under mild conditions. The aldehyde was converted to the known (7) 2,3-methylenedioxycinnamic acid by a Knoevenagel reaction and the cinnamic acid was reduced catalytically under mild conditions to 2,3-methylenedioxyhydrocinnamic acid. The acid chloride of the hydrocinnamic acid was cyclized, in 28% yield, in benzene with aluminium chloride as catalyst to 4,5-methylenedioxyindane-1-one which was converted via the oximinoketone (**8**) to the indanedione (**7**). Unless otherwise indicated, the yields of the individual steps of the above sequence were 80–90%.

A Pictet–Spengler condensation between the indanedione **7** and 3-hydroxy-4-methoxyphenethylamine (8) in ethanolic hydrochloric acid afforded the condensation product (**3**) in 46% yield. The condensation product was converted to the *N*-methylamine (**4**) by heating with an aqueous mixture of formic acid and formaldehyde. A Wittig reaction carried out on the tetrahydropyranyl derivative of **4**, chromatography of the crude product on silica gel and acid hydrolysis gave, in 35% yield, (±)ochotensine.

The ultraviolet (u.v.) and infrared (i.r.) spectra and the fragmentation pattern of the mass spectrum of the synthetic ochotensine were superimposable on the corresponding spectra of the natural alkaloid. Furthermore, the synthetic alkaloid exhibited the same behavior on thin-layer chromatography as the natural alkaloid.

Experimental

Ethyl 2,3-Dihydroxybenzoate

2,3-Dihydroxybenzoic acid (10.0 g) (5) was esterified in absolute ethanol saturated with dry hydrochloric acid gas in the usual manner. Crystallization of the product from ethanol–water afforded 10.1 g (86%) of the ester, m.p. 69°; ν_{max} (Nujol) 1705 cm^{-1} (ester).

Anal. Calcd. for $C_9H_{10}O_4$: C, 59.34; H, 5.53. Found: C, 59.16; H, 5.44.

2,3-Methylenedioxybenzoic Acid

A solution of 45.5 g of ester in 125 ml of ethylene glycol was saturated with hydrogen gas and the reaction was then carried out in a hydrogen atmosphere as follows. To the glycol solution were added 70 g of anhydrous potassium carbonate and 50 g of bromochloromethane. The temperature of the reaction mixture was gradually raised to 120° over a period of 4 h and thereafter maintained at 100–120° for 18 h. Solvent (65 ml) was removed by distillation *in vacuo* and water (1 l) was added to the concentrate. The resulting solution was cooled and acidified (Congo paper) with 6 *N* hydrochloric acid whereupon the desired product, 2,3-methylenedioxybenzoic acid crystallized. The crystalline acid (36.0 g, 87%) melted at 225° (lit. (7) m.p. 227°).

The *ethyl ester*, prepared by treatment of the acid with ethanol saturated with dry hydrogen chloride and distillation of the product, melted at 35° (lit. (7) m.p. 35.5°); ν_{max} (Nujol) 1710 (ester) and 915 cm^{-1} (—O—CH_2—O—).

Anal. Calcd. for $C_{10}H_{10}O_4$: C, 61.85; H, 5.19. Found: C, 62.01; H, 5.11.

2,3-Methylenedioxybenzaldehyde

Lithium aluminium hydride (6.2 g) was added from a

Can. J. Chem. Downloaded from www.nrcresearchpress.com by 210.87.254.5 on 09/05/12
For personal use only.

Soxhlet apparatus over a period of 1.5 h to a refluxing solution of 52.0 g of ethyl 2,3-methylenedioxybenzoate in 500 ml of ether. After stirring at room temperature for 1 h, 15 ml of concentrated brine were added to the reaction mixture and stirring was continued for 1 h. Anhydrous sodium sulfate was added, the mixture was filtered, and the solid material was washed well with ether. The combined filtrate and washings, on evaporation *in vacuo*, afforded 40.5 g of oil which was dissolved in 250 ml of chloroform and treated with 120 g of activated manganese dioxide (9). The mixture was stirred at room temperature for 5 h then filtered. The solid material was washed well with chloroform. The combined filtrate and washings were evaporated *in vacuo* and the residue was crystallized from petroleum ether (b.p. 40–60°) whereby 37.9 g (94%) of the desired product was obtained, m.p. 35° (lit. (7) m.p. 34°); ν_{max} (neat) 1685 (—CHO) and 925 cm^{-1} (—O—CH_2—O—).

Anal. Calcd. for $C_8H_6O_3$: C, 64.00; H, 4.03. Found: C, 63.84; H, 4.03.

2,3-Methylenedioxyhydrocinnamic Acid

2,3-Methylenedioxycinnamic acid prepared from 2,3-methylenedioxybenzaldehyde by the method of Perkin and Trikojus (7) was reduced catalytically as follows. A solution of 2.00 g of the acid in 250 ml of absolute alcohol was hydrogenated over 200 mg of Pd/C (10%) catalyst at 2 atm and room temperature for 2 h. Removal of the catalyst by filtration and evaporation of the filtrate gave 1.80 g (89%) of crystalline product, m.p. 72–75°. Recrystallization from ether – petroleum ether (b.p. 40–60°) afforded a sample melting at 76–78° (lit. (2) m.p. 78–79°); ν_{max} (Nujol) 1710 (COOH) and 925 cm^{-1} (—O—CH_2—O—).

Anal. Calcd. for $C_{10}H_{10}O_4$: C, 61.85; H, 5.19. Found: C, 61.73; H, 5.47.

4,5-Methylenedioxyindane-1-one

A solution of 10.0 g of 2,3-methylenedioxyhydrocinnamic acid in 125 ml of dry benzene was cooled on an ice bath and treated with 9.25 ml of freshly distilled oxalyl chloride. After stirring on an ice bath for 1 h, the solution was left at room temperature for 5 h. The solvent was removed by evaporation *in vacuo*. A solution of the acid chloride in 230 ml of dry benzene was cooled to −10° and treated, over a period of 5 min, with 13.3 g of freshly sublimed aluminium chloride. The mixture was then stirred on an ice bath for 30 min and finally at room temperature for 15 min. The reaction mixture was decanted onto ice and the resulting mixture was extracted with chloroform. The chloroform extracts were washed with 1 *N* sodium carbonate, brine, and finally water, dried over anhydrous sodium sulfate, and evaporated *in vacuo*. The residue, on crystallization from methylene chloride – ether yielded 1.98 g (28%) of desired product, m.p. 167–168° (lit. (2) m.p. 164–167°; (4) m.p. 165–168°); λ_{max}(EtOH) 285 mμ (ε 8950), 300 mμ (sh) (ε 7300); ν_{max} (Nujol) 1700 (ketone) and 925 cm^{-1} (—O—CH_2—O—).

Anal. Calcd. for $C_{10}H_8O_3$: C, 68.18; H, 4.58. Found: C, 68.29; H, 4.37.

4,5-Methylenedioxyindane-1,2-dione (7)

A stirred mixture of 500 mg of 4,5-methylenedioxyindane-1-one and 10 ml of methanol was cooled on an ice bath and treated with 0.75 ml of isoamyl nitrite and 0.25 ml of concentrated hydrochloric acid. After stirring at 50° for 15 min, the mixture was cooled to 0° and the product collected and washed with ethanol. Recrystallization from a large volume of ethanol gave 476 mg of the hydroxyimino derivative (**8**), m.p. 237–240° (decomposed) (lit. (2) m.p. 245–250°). This derivative (470 mg) was mixed with 5.5 ml of a solution of formaldehyde and concentrated hydrochloric acid (8:2). The resulting mixture was placed in a water bath at 50° and the temperature was raised, with vigorous stirring to 90° over a period of 10 min. After cooling, a yellow precipitate was collected and crystallized from benzene whereby 350 mg (64%) of **7** were obtained, m.p. 170–178° (lit. (4) m.p. 158–168°; (2) m.p. 171–178°); λ_{max}(EtOH) 293 mμ (ε 8500), 310 mμ (sh) (ε 7800); ν_{max}($CHCl_3$) 1715 and 1765 cm^{-1} (ketone).

Anal. Calcd. for $C_{10}H_6O_4$: C, 63.16; H, 3.18. Found: C, 63.35; H, 3.21.

Pictet–Spengler Condensation Product (3)

A mixture of 915 mg of the indanedione (**7**), 934 mg of 3-hydroxy-4-methoxyphenethylamine (**8**), 5 ml of concentrated hydrochloric acid and 95 ml of absolute ethanol were stirred at 55° for 60 h. The solvent was evaporated *in vacuo* and the residue was dissolved in the minimum volume of chloroform and ether was added until precipitation of solid material ceased. The precipitate was dissolved in 75 ml of 1 *N* ammonium hydroxide and the aqueous solution was extracted with chloroform. The chloroform extracts were washed with brine then with water and dried over anhydrous sodium sulfate. Crystallization of the residue obtained by evaporation of the chloroform extracts *in vacuo* from ethanol afforded 746 mg (46%) of **3**, m.p. 100–104° (lit. (2) m.p. 194–195°; (4) m.p. 104–107°);[1] λ_{max}(EtOH) 236 mμ (ε 28 500), 290 mμ (ε 12 100), 315 mμ (sh) (ε 7000); ν_{max}($CHCl_3$) 3525 (phenol) and 1710 cm^{-1} (ketone).

Anal. Calcd. for $C_{19}H_{17}NO_5$: C, 67.24; H, 5.05; N, 4.13. Found: C, 67.18; H, 5.25; N, 3.86.

N-Methylamine (4)

A solution of 750 mg of **3** in 4 ml each of 88% formic acid and 37% formaldehyde was stirred at 95° for 4 h. The cooled reaction solution was diluted with 20 ml of water, adjusted to pH 7 with concentrated ammonium hydroxide and extracted with chloroform. The chloroform extracts were washed with brine then with water, dried over anhydrous sodium sulfate, and evaporated *in vacuo*. The residue on crystallization from benzene, gave 578 mg (74%) of **4**, m.p. 100–103° (lit. (2) m.p. 101–103°); u.v. spectrum, similar to **3**, ν_{max}($CHCl_3$) 3525 (phenol) and 1708 cm^{-1} (ketone).

The *picrate*, crystallized from ethanol, melted at 213–217° (lit. (2) m.p. 213–217°).

Anal. Calcd. for $C_{26}H_{22}N_4O_{12}$: C, 53.61; H, 3.81; N, 9.62. Found: C, 53.37; H, 3.96; N, 9.78.

---

[1]It is suspected that the discrepancies between the reported melting points of this compound are due to dimorphism. Similar behavior has been observed, but not reported, by the authors in related compounds (3).

(±)Ochotensine (1)

A solution of 293 mg of **4** in 4.2 ml of dimethyl sulfoxide was treated, while cooled on an ice bath, with 4.2 ml of dihydropyran and 0.83 ml of trifluoroacetic acid. The resulting solution was left at room temperature for 4 h, cooled on an ice bath, and treated with 30 ml of 1 *N* sodium hydroxide. The alkaline solution was extracted with chloroform and the extracts were washed successively with 1 *N* sodium hydroxide and water, then dried over anhydrous sodium sulfate. The Wittig reaction was carried out on the oily tetrahydropyranyl derivative (362 mg), obtained by evaporation of the chloroform extracts, in an atmosphere of dry, oxygen-free nitrogen. Thus, a stirred mixture of 886 mg of methyltriphenylphosphonium bromide in 9 ml of ether was treated with 1.20 ml of a 2.3 *M* ethereal solution of *n*-butyllithium and the mixture was stirred for 2 h at room temperature. The resulting orange solution was treated with a solution of 362 mg of the tetrahydropyranyl derivative in 9 ml of tetrahydrofuran. After stirring at room temperature for 1 h, the ether was removed by distillation and replaced by 5 ml of tetrahydrofuran. The reaction solution was then heated under reflux for 3 h, cooled, treated with 1 ml of water, and the solvent was evaporated *in vacuo*. The residue was dissolved in chloroform and washed with water. The chloroform solution, after drying over potassium carbonate, was evaporated *in vacuo*. The residue was chromatographed on a column (diameter 2.5 cm) of 20 g of silica gel. The column was developed with 50% petroleum ether (b.p. 30–60°) in ether and the tetrahydropyranyl derivative was eluted with 25% petroleum ether in ether. Combination of the appropriate column fractions and evaporation of the solvent gave 126 mg of residue. This was stirred with 1.2 ml each of absolute ethanol and 4 *N* hydrochloric acid at room temperature for 5 h. Evaporation of the solvent and crystallization of the residue from ethanol afforded (113 mg, 35%) of the crystalline (±)ochotensine hydrochloride, m.p. 205–212°. The free alkaloid was obtained quantitatively from the hydrochloride by dissolving the salt in 0.1 *N* NaOH, adjusting the alkaline solution to pH 8.0, collecting the precipitate and crystallizing it from ethylene dichloride. The synthetic (±)ochotensine melted at 238–239° (lit. (2) m.p. 241–243.5°); λ_{max}(EtOH) 226 mμ (ε 25 800), 287 mμ (ε 15 800); ν_{max}(KBr) 1645 and 1605 cm^{-1} (C=C).

The u.v., i.r., and mass spectra of the synthetic ochotensine were superimposable on the corresponding spectra of the natural alkaloid. The synthetic alkaloid was not separated from the natural alkaloid on thin-layer chromatograms developed in benzene – methanol (95:5) and in ethylene dichloride – methanol (95:5).

Calcd. for $C_{21}H_{21}NO_4$: molecular weight 351. Found: molecular weight 351 (mass spectrum).

Acknowledgments

We are grateful to the National Research Council of Canada for a grant in aid of this work and to Professor Stewart McLean, University of Toronto, for a sample of natural ochotensine.

1. R. F. MANSKE. Can. J. Chem. **18**B, 75 (1940); S. MCLEAN, M. -S. LIN, and R. F. MANSKE. Can. J. Chem. **44**, 2449 (1966); S. MCLEAN, M. -S. LIN, A. C. MACDONALD, and J. TROTTER. Tetrahedron Letters, **2**, 185 (1966).
2. H. IRIE, T. KISHIMOTO, and S. UYEO. J. Chem. Soc. Ser. C, 3051 (1968).
3. B. A. BECKETT and R. B. KELLY. J. Heterocyclic Chem. **5**, 685 (1968).
4. S. MCLEAN, M. -S. LIN, and J. WHELAN. Tetrahedron Letters, **20**, 2425 (1968).
5. F. E. KING, J. H. GILKS, and M. W. PARTRIDGE. J. Chem. Soc. 4206 (1955).
6. F. DALLACKER and W. KORB. Ann. **694**, 98 (1966).
7. W. H. PERKIN and V. M. TRIKOJUS. J. Chem. Soc. 2925 (1926).
8. J. A. RAMIREZ and A. BURGER. J. Am. Chem. Soc. **72**, 2781 (1950).
9. J. ATTENBURROW, A. F. B. CAMERON, J. H. CHAPMAN, R. M. EVANS, B. A. HEMS, A. B. A. JANSEN, and T. WALKER. J. Chem. Soc. 1094 (1952).

2-Amino-4-methyl-5-hexenoic acid, a naturally occurring antimetabolite antibiotic

R. B. KELLY,[1] D. G. MARTIN, AND L. J. HANKA

Research Laboratories, The Upjohn Company, Kalamazoo, Michigan, 49001

Received March 17, 1969

A new antimetabolite antibiotic has been isolated from a *Streptomyces* culture. The antibiotic has been shown to be 2-amino-4-methyl-5-hexenoic acid, a hitherto unknown compound.

Canadian Journal of Chemistry, 47, 2504 (1969)

Previously we reported (1) the isolation and structure elucidation of an antimetabolite antibiotic, the antimicrobial activity of which was reversed by biotin. This was shown to be a new compound, α-dehydrobiotin (double bond in conjugation with the carboxyl group). We now wish to describe the isolation and structure

[1]Present address: Department of Chemistry, University of New Brunswick, Saint John, New Brunswick.

Can. J. Chem. Downloaded from www.nrcresearchpress.com by 210.87.254.5 on 09/05/12
For personal use only.

(±)Ochotensine (1)

A solution of 293 mg of **4** in 4.2 ml of dimethyl sulfoxide was treated, while cooled on an ice bath, with 4.2 ml of dihydropyran and 0.83 ml of trifluoroacetic acid. The resulting solution was left at room temperature for 4 h, cooled on an ice bath, and treated with 30 ml of 1 *N* sodium hydroxide. The alkaline solution was extracted with chloroform and the extracts were washed successively with 1 *N* sodium hydroxide and water, then dried over anhydrous sodium sulfate. The Wittig reaction was carried out on the oily tetrahydropyranyl derivative (362 mg), obtained by evaporation of the chloroform extracts, in an atmosphere of dry, oxygen-free nitrogen. Thus, a stirred mixture of 886 mg of methyltriphenylphosphonium bromide in 9 ml of ether was treated with 1.20 ml of a 2.3 *M* ethereal solution of *n*-butyllithium and the mixture was stirred for 2 h at room temperature. The resulting orange solution was treated with a solution of 362 mg of the tetrahydropyranyl derivative in 9 ml of tetrahydrofuran. After stirring at room temperature for 1 h, the ether was removed by distillation and replaced by 5 ml of tetrahydrofuran. The reaction solution was then heated under reflux for 3 h, cooled, treated with 1 ml of water, and the solvent was evaporated *in vacuo*. The residue was dissolved in chloroform and washed with water. The chloroform solution, after drying over potassium carbonate, was evaporated *in vacuo*. The residue was chromatographed on a column (diameter 2.5 cm) of 20 g of silica gel. The column was developed with 50% petroleum ether (b.p. 30–60°) in ether and the tetrahydropyranyl derivative was eluted with 25% petroleum ether in ether. Combination of the appropriate column fractions and evaporation of the solvent gave 126 mg of residue. This was stirred with 1.2 ml each of absolute ethanol and 4 *N* hydrochloric acid at room temperature for 5 h. Evaporation of the solvent and crystallization of the residue from ethanol afforded (113 mg, 35%) of the crystalline (±)ochotensine hydrochloride, m.p. 205–212°. The free alkaloid was obtained quantitatively from the hydrochloride by dissolving the salt in 0.1 *N* NaOH, adjusting the alkaline solution to pH 8.0, collecting the precipitate and crystallizing it from ethylene dichloride. The synthetic (±)ochotensine melted at 238–239° (lit. (2) m.p. 241–243.5°); λ_{max}(EtOH) 226 mμ (ε 25 800), 287 mμ (ε 15 800); ν_{max}(KBr) 1645 and 1605 cm^{-1} (C=C).

The u.v., i.r., and mass spectra of the synthetic ochotensine were superimposable on the corresponding spectra of the natural alkaloid. The synthetic alkaloid was not separated from the natural alkaloid on thin-layer chromatograms developed in benzene – methanol (95:5) and in ethylene dichloride – methanol (95:5).

Calcd. for $C_{21}H_{21}NO_4$: molecular weight 351. Found: molecular weight 351 (mass spectrum).

Acknowledgments

We are grateful to the National Research Council of Canada for a grant in aid of this work and to Professor Stewart McLean, University of Toronto, for a sample of natural ochotensine.

1. R. F. MANSKE. Can. J. Chem. **18**B, 75 (1940); S. MCLEAN, M. -S. LIN, and R. F. MANSKE. Can. J. Chem. **44**, 2449 (1966); S. MCLEAN, M. -S. LIN, A. C. MACDONALD, and J. TROTTER. Tetrahedron Letters, **2**, 185 (1966).
2. H. IRIE, T. KISHIMOTO, and S. UYEO. J. Chem. Soc. Ser. C, 3051 (1968).
3. B. A. BECKETT and R. B. KELLY. J. Heterocyclic Chem. **5**, 685 (1968).
4. S. MCLEAN, M. -S. LIN, and J. WHELAN. Tetrahedron Letters, **20**, 2425 (1968).
5. F. E. KING, J. H. GILKS, and M. W. PARTRIDGE. J. Chem. Soc. 4206 (1955).
6. F. DALLACKER and W. KORB. Ann. **694**, 98 (1966).
7. W. H. PERKIN and V. M. TRIKOJUS. J. Chem. Soc. 2925 (1926).
8. J. A. RAMIREZ and A. BURGER. J. Am. Chem. Soc. **72**, 2781 (1950).
9. J. ATTENBURROW, A. F. B. CAMERON, J. H. CHAPMAN, R. M. EVANS, B. A. HEMS, A. B. A. JANSEN, and T. WALKER. J. Chem. Soc. 1094 (1952).

2-Amino-4-methyl-5-hexenoic acid, a naturally occurring antimetabolite antibiotic

R. B. KELLY,[1] D. G. MARTIN, AND L. J. HANKA

Research Laboratories, The Upjohn Company, Kalamazoo, Michigan, 49001

Received March 17, 1969

A new antimetabolite antibiotic has been isolated from a *Streptomyces* culture. The antibiotic has been shown to be 2-amino-4-methyl-5-hexenoic acid, a hitherto unknown compound.

Canadian Journal of Chemistry, 47, 2504 (1969)

Previously we reported (1) the isolation and structure elucidation of an antimetabolite antibiotic, the antimicrobial activity of which was reversed by biotin. This was shown to be a new compound, α-dehydrobiotin (double bond in conjugation with the carboxyl group). We now wish to describe the isolation and structure

[1]Present address: Department of Chemistry, University of New Brunswick, Saint John, New Brunswick.

Can. J. Chem. Downloaded from www.nrcresearchpress.com by 210.87.254.5 on 09/05/12
For personal use only.

Can. J. Chem. Downloaded from www.nrcresearchpress.com by 210.87.254.5 on 09/05/12
For personal use only.

determination of another member of this class of antibiotics. The new antibiotic is produced by a *Streptomyces* (Sp. UC5159), is active against a variety of gram-positive organisms[2] and its antimicrobial activity is reversed by the presence of leucine. Valine or isoleucine were less effective reversing agents.

Details of fermentation and isolation procedures are given in the Experimental section. Elemental analyses (C, H, and N) of the crystalline antibiotic were in excellent agreement with the formula $C_7H_{13}NO_2$. A violet color developed on heating the antibiotic with ninhydrin reagent and the infrared (i.r.) spectrum displayed bands attributable to an α-amino acid. Bands at 1645, 995, and 920 cm^{-1}, consistent with the structural feature $CH_2 = CHR$, were also prominent in the i.r. spectrum. The nuclear magnetic resonance (n.m.r.) spectrum (Table I) in conjunction with the above data uniquely defined the structure of the antibiotic as 2-amino-4-methyl-5-hexenoic acid (**1**), a hitherto unknown compound. The structural relationship to the novel amino acid, hypoglycin A (**2**), (2), isolated from the fruits of *Blighia sapida* ("Ackee"), is noteworthy. A double bond isomer of **1**, 2-amino-4-methyl-4-hexenoic acid, has been synthesized and found to be a competitive antagonist of both phenylalanine and leucine (3).

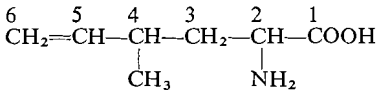

1

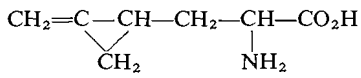

2

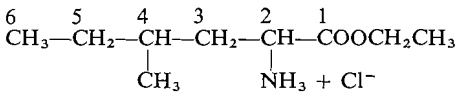

3

An optical rotatory dispersion (o.r.d.) curve with positive Cotton effect (peak 215 mμ) indicates that the antibiotic has the same configuration at C-2 as the naturally occurring α-amino acids (4).

The antibiotic was further characterized by catalytic reduction to the corresponding substituted hexanoic acid and conversion of the latter to the crystalline ethyl ester hydrochloride (**3**). In the n.m.r. spectrum of **3** taken in deuteriochloroform,[3] 14 protons were detected in the region δ 0.70–2.30 due to 3 methyl groups, 2 methylenes (at C-3 and C-5), and the methine at C-4. This region contained a triplet at δ 1.32 (J = 7 Hz) due to the methyl group in the ester; the overlapping signals of the other two methyl groups were at ca. δ 0.97. The methylene in the ester group appeared as a quartet at δ 4.28 (J = 7 Hz) superimposed on the signal for the methine at C-2. A broad singlet due to NH_{3+} was centered at δ 8.58 (3H, exchangable with D_2O). A prominent peak in the mass spectrum at *m/e* 173 established the molecular weight of the free ester of **3** as 173 ($C_9H_{19}NO_2$) and consequently that of the antibiotic **1** as 143 ($C_7H_{13}NO_2$). Elemental analyses of the ester hydrochloride (**3**) are in agreement with the formula $C_9H_{19}NO_2 \cdot HCl$.

The above data support the structure of the derived ester hydrochloride as **3** thus corroborating structure **1** for the antibiotic.

Experimental

Fermentation and Isolation

Fermentations were carried out at 32 °C in media consisting of 1% each of mannitol, starch, and Phytone,[4] 5% of calcium carbonate, and 0.2% of sodium chloride. Peak titres were reached after 4 or 5 days of incubation. The antimicrobial activity of fermentation liquors was determined by assay against *Escherichia coli* grown in a synthetic medium. This assay also served as a guide during isolation.

Two l of filtered fermentation liquor was percolated through a column of 400 ml of carbon. After washing the column with 2 l of water and 800 ml of 2% acetone in water, an active fraction was eluted with 4 l of 5% acetone in water. Evaporation of the active eluate *in vacuo* left 7.00 g of residue which was applied in 200 ml of water to a column of 400 ml of Dowex 50 (H+) resin. After washing the column with 2 l of water, an active fraction was eluted with 2.8 l of 1 *N* ammonium hydroxide. Evaporation of the active eluate left 1.26 g of crystalline residue. Five recrystallizations of this material from 95% ethanol afforded 191 mg of antibiotic having m.p. 260° (decomposing). The following data pertain to the o.r.d. curve in water (*c*, 0.993; 0.1 dm cell): $[\theta]_{300}$,

[2]For example, *Staphylococcus aureus*, *Sarcina lutea*, and *Bacillus subtilis*.

[3]Determined on a Varian A-60 instrument with tetramethylsilane as internal standard.

[4]A bacteriological peptone procured from Baltimore Biological Laboratory, Baltimore, Maryland.

TABLE I

Nuclear magnetic resonance data for antibiotic*

Shift (δ in p.p.m.)	Number of protons	Multiplicity	Assignment
1.05	3	Doublet (J = 7 Hz)	CH_3
1.80	2	Multiplet	Methylene at C-3
2.30	1	Broad multiplet	Methine at C-4
3.69	1	Doublet of doublets	Methine at C-2
5.10	2	Complex multiplet	Terminal methylene
5.83	1	Complex multiplet	Proton at C-5
4.72	3	Singlet	Protons exchanged with D_2O

*Determined in D_2O with a Varian A-60 instrument. Chemical shifts are relative to tetramethylsilane as internal standard.

+92; $[\theta]_{280}$, +138; $[\theta]_{260}$, +255; $[\theta]_{240}$, +590; $[\theta]_{220}$, +1840; $[\theta]_{216}$, +2130; $[\theta]_{214}$, +2130; $[\theta]_{212}$, +2080; $[\theta]_{210}$, +1815.

Anal. Calcd. for $C_7H_{13}NO_2$: C, 58.72; H, 9.15; N, 9.78. Found: C, 58.72; H, 9.43; N, 10.04.

Conversion of the Antibiotic to 3

The antibiotic (120 mg) was hydrogenated at room temperature and atmospheric pressure over 100 mg of palladium–charcoal (10%) catalyst in 95% ethanol. The theoretical quantity of hydrogen was absorbed within 30 min. The catalyst was removed by filtration and the residue obtained by evaporation of the filtrate *in vacuo* was treated with 30 ml of absolute ethanol saturated with dry HCl gas. The resulting solution was left for 2 h at room temperature then evaporated *in vacuo* to dryness. The residue was treated twice with ethanolic hydrochloric acid as above. Crystallization of the resulting solid from ethyl acetate afforded the ethyl ester hydrochloride **3** melting at 118–122 °C. The infrared (i.r.) spectrum (Nujol) had a series of bands between 3000 and 2500 cm^{-1} attributable to the ammonium ion. There was also a band at 1745 cm^{-1} due to the ester.

Anal. Calcd. for $C_9H_{20}ClNO_2$: C, 51.54; H, 9.61; Cl, 16.90; N, 6.68. Found: C, 51.26; H, 9.53; Cl, 16.89; N, 6.97.

Acknowledgment

This work was supported in part by Contract PH43-62-168, Cancer Chemotherapy National Service Center (CCNSC), National Cancer Institute, National Institutes of Health, Bethesda, Maryland.

1. L. J. HANKA, M. E. BERGY, and R. B. KELLY. Science, **145**, 1667 (1966).
2. S. WILKINSON. Chem. Ind. 17 (1958).
3. J. EDELSON, C. G. SKINNER, J. M. RAVEL, and W. SHIVE. J. Am. Chem. Soc. **81**, 5150 (1959).
4. P. CRABBE. Optical rotatory dispersion and circular dichroism in organic chemistry. Holden-Day, San Francisco. 1965. Chap. 11.

Carbon-13 kinetic isotope effects. V.[1] Substituent effects on k_{12}/k_{13} for alcoholysis of 1-phenyl-1-bromoethane

JAN BRON AND J. B. STOTHERS

Department of Chemistry, University of Western Ontario, London, Ontario

Received November 25, 1968

As a test of our earlier interpretations of the ^{13}C kinetic isotope effects found for alcoholysis of 1-phenyl-1-bromoethane, we have examined the effect of the *p*-methyl and *p*-bromo substituents on the ^{13}C fractionations in ethanol and methanol. Isotopic fractionation at the α-carbon is found to be substituent dependent, and the observed trend is consistent with the proposal that stabilization of the cationic center by the phenyl ring is a major factor governing the isotope effect in these systems. The first example of an inverse primary kinetic isotope effect for carbon ($k_{12}/k_{13} < 1$) is described.

Canadian Journal of Chemistry, 47, 2506 (1969)

Earlier it was found that k_{12}/k_{13} is 1.0065 for the methanolysis of 1-phenyl-1-bromoethane (**1**) at 25 °C (1). This relatively small isotope effect was attributed to resonance stabilization of the carbonium ion intermediate by the phenyl group, as well as to hyperconjugative interaction with the α-methyl group. The latter point has recently received support from measurements of the

[1]For Part IV, see ref. 4.

Can. J. Chem. Downloaded from www.nrcresearchpress.com by 210.87.254.5 on 09/05/12
For personal use only.

TABLE I

Nuclear magnetic resonance data for antibiotic*

Shift (δ in p.p.m.)	Number of protons	Multiplicity	Assignment
1.05	3	Doublet (J = 7 Hz)	CH_3
1.80	2	Multiplet	Methylene at C-3
2.30	1	Broad multiplet	Methine at C-4
3.69	1	Doublet of doublets	Methine at C-2
5.10	2	Complex multiplet	Terminal methylene
5.83	1	Complex multiplet	Proton at C-5
4.72	3	Singlet	Protons exchanged with D_2O

*Determined in D_2O with a Varian A-60 instrument. Chemical shifts are relative to tetramethylsilane as internal standard.

+92; $[\theta]_{280}$, +138; $[\theta]_{260}$, +255; $[\theta]_{240}$, +590; $[\theta]_{220}$, +1840; $[\theta]_{216}$, +2130; $[\theta]_{214}$, +2130; $[\theta]_{212}$, +2080; $[\theta]_{210}$, +1815.

Anal. Calcd. for $C_7H_{13}NO_2$: C, 58.72; H, 9.15; N, 9.78. Found: C, 58.72; H, 9.43; N, 10.04.

Conversion of the Antibiotic to 3

The antibiotic (120 mg) was hydrogenated at room temperature and atmospheric pressure over 100 mg of palladium–charcoal (10%) catalyst in 95% ethanol. The theoretical quantity of hydrogen was absorbed within 30 min. The catalyst was removed by filtration and the residue obtained by evaporation of the filtrate *in vacuo* was treated with 30 ml of absolute ethanol saturated with dry HCl gas. The resulting solution was left for 2 h at room temperature then evaporated *in vacuo* to dryness. The residue was treated twice with ethanolic hydrochloric acid as above. Crystallization of the resulting solid from ethyl acetate afforded the ethyl ester hydrochloride **3** melting at 118–122 °C. The infrared (i.r.) spectrum (Nujol) had a series of bands between 3000 and 2500 cm^{-1} attributable to the ammonium ion. There was also a band at 1745 cm^{-1} due to the ester.

Anal. Calcd. for $C_9H_{20}ClNO_2$: C, 51.54; H, 9.61; Cl, 16.90; N, 6.68. Found: C, 51.26; H, 9.53; Cl, 16.89; N, 6.97.

Acknowledgment

This work was supported in part by Contract PH43-62-168, Cancer Chemotherapy National Service Center (CCNSC), National Cancer Institute, National Institutes of Health, Bethesda, Maryland.

1. L. J. HANKA, M. E. BERGY, and R. B. KELLY. Science, **145**, 1667 (1966).
2. S. WILKINSON. Chem. Ind. 17 (1958).
3. J. EDELSON, C. G. SKINNER, J. M. RAVEL, and W. SHIVE. J. Am. Chem. Soc. **81**, 5150 (1959).
4. P. CRABBE. Optical rotatory dispersion and circular dichroism in organic chemistry. Holden-Day, San Francisco. 1965. Chap. 11.

Can. J. Chem. Downloaded from www.nrcresearchpress.com by 210.87.254.42 on 09/05/12
For personal use only.

Carbon-13 kinetic isotope effects. V.[1] Substituent effects on k_{12}/k_{13} for alcoholysis of 1-phenyl-1-bromoethane

JAN BRON AND J. B. STOTHERS

Department of Chemistry, University of Western Ontario, London, Ontario

Received November 25, 1968

As a test of our earlier interpretations of the ^{13}C kinetic isotope effects found for alcoholysis of 1-phenyl-1-bromoethane, we have examined the effect of the *p*-methyl and *p*-bromo substituents on the ^{13}C fractionations in ethanol and methanol. Isotopic fractionation at the α-carbon is found to be substituent dependent, and the observed trend is consistent with the proposal that stabilization of the cationic center by the phenyl ring is a major factor governing the isotope effect in these systems. The first example of an inverse primary kinetic isotope effect for carbon ($k_{12}/k_{13} < 1$) is described.

Canadian Journal of Chemistry, 47, 2506 (1969)

Earlier it was found that k_{12}/k_{13} is 1.0065 for the methanolysis of 1-phenyl-1-bromoethane (**1**) at 25 °C (1). This relatively small isotope effect was attributed to resonance stabilization of the carbonium ion intermediate by the phenyl group, as well as to hyperconjugative interaction with the α-methyl group. The latter point has recently received support from measurements of the

[1]For Part IV, see ref. 4.

Can. J. Chem. Downloaded from www.nrcresearchpress.com by 210.87.254.42 on 09/05/12
For personal use only.

β-deuterium isotope effects in solvolyses of **1**, the corresponding chloride, and several substituted derivatives (2). Indirect support for the proposal of an appreciable influence of the phenyl ring on k_{12}/k_{13} has been presented by Kresge, Lichtin, Rao, and Weston (3) from their study of the dissociation of trityl chloride in liquid SO_2. In addition, crude calculations show (4) that the loss of the C—Br stretching mode in the initial state can be offset, in the transition state, by a reasonable degree of Ar—C^+ bond strengthening by π-overlap via resonance. Intuitively, stabilization by the phenyl ring should be governed by the polarity of ring substituents, and the present study was undertaken to examine the effect of *p*-methyl and *p*-bromo groups on k_{12}/k_{13} for alcoholysis to test our original proposal (1).

The ^{13}C isotope effects for 1-(4′-methylphenyl)-1-bromoethane in methanol and ethanol at 0° and for 1-(4-bromophenyl)-1-bromoethane in methanol at 0 and 25 °C were determined. The results are listed in Table I together with some data obtained previously (5).

As noted previously (1), there is evidence that the major path for alcoholysis of 1-phenyl-1-bromoethane itself is through an intimate ion-pair, i.e. the process is a limiting S_N1 reaction proceeding via a carbonium ion intermediate. A plot of the present kinetic data (see Experimental) for methanolysis at 0° *vs.* the σ^+ parameter yields a ρ value of −5.4 which is consistent with the foregoing. Thus, it is to be expected that generation of positive charge at the benzylic carbon will be assisted by resonance interaction with the phenyl ring, the extent of which may be governed by *p*-substituents. The methyl group should increase the interaction while a *p*-bromo atom should reduce electron supply from the aryl ring, both relative to **1**. If the fractionation at the benzylic carbon is sensitive to conjugative interaction with the aryl ring, as we have proposed (1), the k_{12}/k_{13} values should reflect this.

Of the reaction conditions examined, one is common to the three reactants, methanolysis at 0°, and it is clear that the isotope effect is largest for the electron-withdrawing *p*-Br group and smallest for the electron-releasing methyl substituent. In fact the latter value represents an inverse effect, i.e. the ^{13}C isotope reacts faster, and we believe this to be the first example of a primary inverse *kinetic* effect for carbon isotopy, although inverse equilibrium isotope effects for carbon have been reported (3). The precision of the present measurements is sufficient to establish that the trend from *p*-Me → *p*-Br is real. Further evidence is given by the 25° results for **1** and its *p*-bromo derivative.

As noted above, semi-quantitative estimations of the ^{13}C isotope effect for **1** in solvolysis have shown that the α-phenylethyl carbonium ion model for the transition state can accommodate the observed results, on the basis of the Bigeleisen formulation (6), and that a strengthening of the Ar—C^+ bond in the transition state can offset the loss of the C—Br stretching mode in the initial state (5). Arguments to support the view that the carbonium ion is an appropriate model have been presented (1). Kresge *et al.* (3) have shown, for the closely related dissociation of trityl chloride in sulfur dioxide, that the carbon–phenyl bonds in the triphenyl-carbonium ions must be much stronger than those in trityl chloride. These authors have discussed an extension of their reasoning to provide an explanation for the relatively small kinetic isotope effects found for S_N1 processes. As discussed in an earlier part of this series (5), it is difficult to make quantitative estimates of the magnitudes of the vibrational frequency differences for the

TABLE I

^{13}C kinetic isotope effects* in the alcoholyses of 1-(*p*-substituted phenyl)-1-bromoethane

	MeOH†		EtOH†	
	0°	25°	0°	25°
p-Me	−0.05 ± 0.05 (7)	—	0.05 ± 0.12 (6)	—
p-H	0.50 ± 0.04 (9)	0.65‡	0.18‡	0.44‡
p-Br	1.27 ± 0.06 (7)	1.13 ± 0.09 (12)	—	—

*$(k_{12}/k_{13} - 1)100$.
†Standard deviation of the mean is given with the number of separate runs in brackets.
‡From refs. 1 and 5.

Can. J. Chem. Downloaded from www.nrcresearchpress.com by 210.87.254.42 on 09/05/12
For personal use only.

change, initial state → transition state. It is gratifying, however, to find that the experimental results agree qualitatively with the predictions based on the model which is intuitively reasonable.

Although the correspondence between the experimental results for the substituent effect and the predicted trend appears to be intuitively satisfactory, there is another explanation of the fact that the carbon isotope effect is larger for the *p*-bromo derivative. If the reaction of 1-(4′-bromophenyl)-1-bromoethane with methanol does not proceed exclusively through a limiting carbonium ion mechanism, but rather involves the incursion of some nucleophilic character, the isotopic fractionation at the α-carbon would be expected to be greater than that found for a pure S_N1 process, on the basis of the available isotope effect data for processes believed to be "pure" S_N2 reactions (4, 7). For example, the S_N2 reaction of 1-phenyl-1-bromoethane with a ethoxide ion exhibits a carbon isotope effect of 3.2–3.6% over the temperature range 0–25 °C (4). Clearly, the 1.1–1.3% effect found for the *p*-bromo derivative over the same range is much smaller and somewhat less sensitive to a change in temperature. For the bimolecular displacements, k_{12}/k_{13} decreases with increasing temperature while the opposite trend is found for alcoholyses of 1-phenyl-1-bromoethane itself (5). Because the reactivity of the *p*-methyl derivative in alcohol limits the conveniently accessible temperatures at which determinations may be done, its isotope effect was measured only at a single temperature, 0 °C, in both ethanol and methanol. Of the three compounds, however, the *p*-methyl derivative is the most likely to exhibit truly limiting behavior.

In any event, on the available evidence it is not possible to decide whether the influence of these substituents on the carbon isotope effect is signalling a mechanistic shift from the limiting case for the *p*-methyl derivative to one in which there is some nucleophilic character for the *p*-bromo compound, or whether the substituents govern the degree of resonance stabilization in the carbonium ion. It can be noted that the α- and β-deuterium secondary isotope effects for a series of substituted α-phenylethyl chlorides and bromides undergoing solvolysis in aqueous solution, suggest that the reaction is partly nucleophilic for those reactants having electron-withdrawing substituents (2). It is reasonable to assume that the secondary deuterium effects for alcoholysis would exhibit similar behavior and it would be interesting to measure these effects.

Experimental

The methods employed in this study were somewhat modified from those described previously (1, 4, and 5). After quenching a given isotope effect run, the remaining bromide was hydrolyzed completely to α-phenylethyl alcohol by heating, with vigorous stirring, at 50–60° for 12 h with aqueous sodium carbonate before isolation of the ether by fractional distillation.[2] Gas–liquid chromatography and refractive index determinations were used to assess the purity of the isolated product. To compare the results obtained by this modification with our previous data, the isotope effect for methanolysis of 1-bromo-1-phenyl-ethane was redetermined at 0 °C and found to agree precisely with our earlier data.

The oxidative degradations to the benzoic acids were also modified in this work. For the *p*-methyl derivatives, oxidation to *p*-toluic acid was accomplished in the following way. The methyl ether (1 g) was added to an ice-cold solution of potassium dichromate (9 g) in 300 ml of 45% (w/w) sulfuric acid. The mixture was shaken for 30 min while warming to room temperature. After extraction with low-boiling petroleum ether (3 times), the combined extracts were washed with saturated sodium bicarbonate solution and dried. To the residue, after removal of the solvent in vacuum, was added a solution containing sodium hydroxide (5 g), sodium hypochlorite solution (100 ml of Javex), and water (200 ml). The mixture was shaken for 1 h at room temperature before the addition of sodium metabisulfite (15 g). After the addition of ice, concentrated hydrochloric acid (40 ml) was added and the *p*-toluic acid extracted with ether. Removal of the solvent afforded *p*-toluic acid in 92% yield, m.p. 177–179°, completely free of terephthalic acid.

The *p*-bromo derivatives were oxidized in a manner similar to that described previously (1) except that the manganese dioxide was not removed by filtration after completion of the oxidation. Instead the MnO_2 was destroyed, after the addition of 30% sulfuric acid, by the addition of sodium metabisulfite. The *p*-bromobenzoic acid precipitated from solution and was isolated by filtration in 95% yield, m.p. 253–254°.

As in the earlier work (1, 4, and 5), the kinetics were measured by acid–base titration, at least in duplicate, and the data are:

1-(4′-bromophenyl)-1-bromoethane. Methanolysis; $k_1 = 4.17 \times 10^{-7}$ s^{-1} (0°), 1.27×10^{-5} s^{-1} (25°).

1-(*p*-tolyl)-1-bromoethane. Ethanolysis; $k_1 = 7.81 \times 10^{-6}$ s^{-1} (0°); methanolysis, $k_1 = 1.07 \times 10^{-4}$ s^{-1} (0°).

[2]Within the limits of the methods employed, there is no evidence of styrene formation under these reaction conditions. Thus we conclude that the amount formed is much less than 1%.

Acknowledgments

We are grateful to the National Research Council of Canada for generous support of this investigation and to Professor V. J. Shiner for making his results available to us prior to publication.

1. J. B. Stothers and A. N. Bourns. Can. J. Chem. **38**, 923 (1960).
2. V. J. Shiner, W. E. Buddenbaum, B. L. Murr, and G. Lamaty. J. Am. Chem. Soc. **90**, 418 (1968).
3. A. J. Kresge, N. N. Lichtin, K. N. Rao, and R. E. Weston. J. Am. Chem. Soc. **87**, 437 (1965).
4. J. Bron and J. B. Stothers. Can. J. Chem. **46**, 1825 (1968).
5. J. Bron and J. B. Stothers. Can. J. Chem. **46**, 1435 (1968).
6. J. Bigeleisen and M. Wolfsberg. Advan. Chem. Phys. **1**, 15 (1958).
7. K. R. Lynn and P. E. Yankwich. J. Am. Chem. Soc. **83**, 53, 790, 3220 (1961); M. L. Bender and D. F. Hoeg. J. Am. Chem. Soc. **79**, 5649 (1957); G. J. Buist and M. L. Bender. J. Am. Chem. Soc. **80**, 4308 (1958); A. J. McNamara and J. B. Stothers. Unpublished results.

Can. J. Chem. Downloaded from www.nrcresearchpress.com by 210.87.254.42 on 09/05/12
For personal use only.

Can. J. Chem. Downloaded from www.nrcresearchpress.com by 210.87.254.40 on 09/05/12
For personal use only.

COMMUNICATION

Synthesis of buf-20(21)-enolides and bufa-20,22-dienolides[1]

GEORGE R. PETTIT, DYRAL C. FESSLER, KENNETH D. PAULL,
PETER HOFER, AND JOHN C. KNIGHT
Department of Chemistry, Arizona State University, Tempe, Arizona 85281

Received February 7, 1969

A practical three-step procedure for converting an aldehyde to a 5-substituted dihydro-2-pyrone or by an additional step to the corresponding 2-pyrone has been summarized. Synthesis of 2-pyrone **5**, buf-20(21)-enolide **9** (and Δ^5-derivative) and bufadienolide **10** were used for illustration.

Canadian Journal of Chemistry, 47, 2511 (1969)

The intriguing biological properties[2] of bufalin (1) and related naturally occurring bufadienolides led us to investigate synthetic routes to 5-substituted 2-pyrones.[3] From a variety of approaches to 5-substituted 2-pyrones evaluated, we wish to report the following new route and application to synthesis of buf-20(21)-enolides and corresponding bufa-20,22-dienolides.

Heptaldehyde provides an illustration. Piperidine enamine **2** derived (7) from *n*-heptaldehyde was condensed in acetonitrile solution with methyl acrylate. Following mild (acetic acid – water) hydrolytic cleavage of the resulting enamine, aldehyde **3**, b.p. 114°[4] (4 mm) was isolated in 45% yield. The aldehyde proton appeared as a doublet (J = 4 c.p.s.) at 9.54 δ. Gentle saponification (sodium carbonate in water – methanol – tetrahydrofuran), acidification, and subsequent treatment (12 h) with *p*-toluenesulfonic acid in refluxing benzene provided (50%) enol lactone **4**: b.p. 102–103° (1.5 mm); vinyl proton as a broad signal centered at 6.4 δ. Dehydrogenating (8) enol lactone **4** (0.3 g) with 10% palladium on carbon (0.15 g) in refluxing *p*-cymene (50 ml, with nitrogen passing through the solution) afforded 2-pyrone **5** (0.14 g), boiling at 101–102° (0.8 mm) and exhibiting vinyl proton signals at 6.15 (H_a, doublet, J = 11 c.p.s.), 7.20 (H_b, set of doublets, J = 11 c.p.s. and J = 3 c.p.s.), 7.23 (H_c, doublet, J = 3 c.p.s.): M^+ 166.105060.

Application of the preceding four-step synthesis of 5-substituted 2-pyrones to obtaining representatives of the hitherto unknown bufa-20(21)-enolides proved satisfactory. First, nitrile **6** (m.p. 199–200°) was prepared in one step by condensing 3β-acetoxy-17-oxo-5α-androstane with the phosphorane (9) prepared from diethyl cyanomethylphosphonate and sodium hydride in tetrahydrofuran. Hydrogenation of olefin **6** with 5% palladium-on-calcium carbonate suspended in tetrahydrofuran yielded (100%) nitrile **7a**, m.p. 200–202°. Hydrolysis (potassium hydroxide in ethylene glycol) of the nitrile followed by acetylation (acetic acid – acetic anhydride) gave carboxylic acid **7b**, m.p. 190–195°. Rosenmund reduction (10% palladium on barium sulfate, refluxing toluene, 2 h) of the corresponding acid chloride (oxalyl chloride – benzene, 1.5 h at room temperature) provided (86–96%) aldehyde **7c** melting at 109–110.5°. Reacting aldehyde **7** (2.7 g) with piperidine in toluene solution and treating the resulting enamine as summarized above for enamine **2** gave aldehyde **8** (1.5 g, with 0.45 g of aldehyde **7c** recovered). The methyl ester protons appeared as a singlet at 3.65 δ and the aldehyde proton as a doublet with J = 4 c.p.s. at 9.5 δ. The remaining step to

[1]Steroids and Related Natural Products. LIX. For part LVIII, refer to (1).

[2]For example, local anesthetic (2), cardiac (2, 3), vasopressor (2*a*, 4), respiratory (2*a*, 4), and possibly of most potential importance, antitumor activity (5).

[3]When the present general study was initiated no bufadienolide (**1**) had been obtained by total synthesis and, in fact, no method (6*a*) was available which could be extended to this problem. Meanwhile, preliminary summaries of syntheses leading to two steroidal α-pyrones of the bufadienolide-type have been reported (6*b* and 6*c*).

[4]Each new substance gave satisfactory elemental analytical data and proton magnetic resonance spectra were obtained with a Varian A-60 spectrometer (deuteriochloroform as solvent with tetramethylsilane as internal standard).

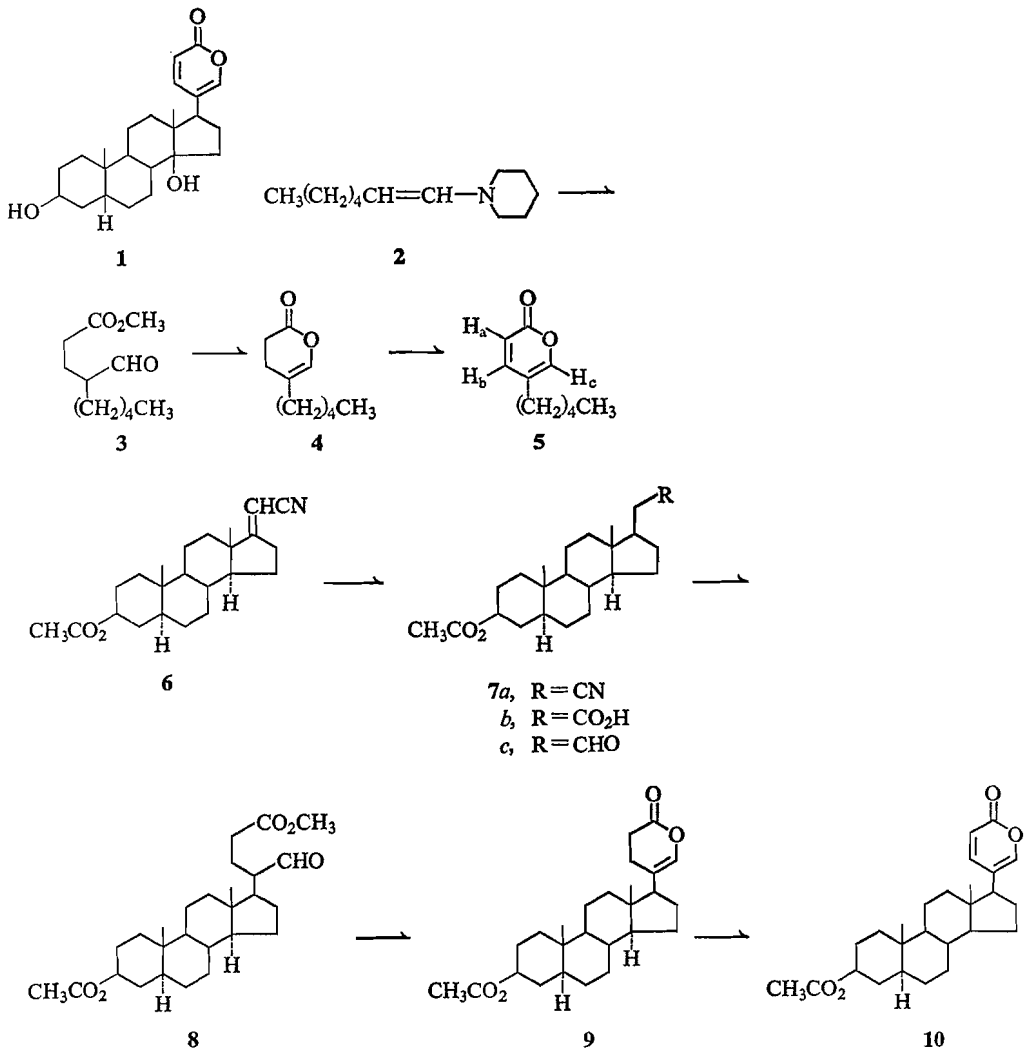

bufa-20(21)-enolide **9** (40% yield, m.p. 177–179°, 21-vinyl proton at 6.36 δ) was performed as noted above for enol lactone **4**. By an analogous series of reactions 3β-acetoxy-bufa-5,20(21)-dienolide (m.p. 184–186°) was also prepared.

The preceding approach to bufa-20(21)-enolides appears generally useful and is presently being utilized in one synthetic approach to bufa-20,22-dienolides. For example, heating (221–227°, 30 min) a mixture of sulfur (0.2 g) and buf-20(21)-enolide **9** (0.1 g) readily afforded (0.06 g, m.p. 194–195°) bufa-20,22-dienolide **10**. The sulfur reaction represents a new approach to 2-pyrones. A variety of more obvious dehydrogenation methods including those that performed well with enol lactone **4** were quite unsuccessful when applied to the superficially easy buf-20(21)-enolide → bufa-20,22-dienolide transformation.

Acknowledgments

This investigation was supported by Public Health Service Research Grant CA-10115-01 and CA-10115-02 from the National Cancer Institute. We also wish to thank Prof. P. Brown for the high resolution mass spectra (Atlas SM-1B) and P. A. Whitehouse for performing accessory experiments.

Can. J. Chem. Downloaded from www.nrcresearchpress.com by 210.87.254.40 on 09/05/12
For personal use only.

1. J. C. KNIGHT, G. R. PETTIT, and P. BROWN. J. Org. Chem. **34**. To be published.
2. *a*. M. OKADA, F. SAKAI, and T. SUGA. Itsuu Kenkyusho Nempo, **67**, 75 (1960); Chem. Abstr. **55**, 16798 (1961); *b*. K. K. CHEN, R. C. ANDERSON, and F. G. HENDERSON. Proc. Soc. Exptl. Biol. Med. **76**, 372 (1951); Chem. Abstr. **45**, 5812 (1951).
3. H. MURASE. Japan J. Pharmacol. **15**, 72 (1965); Chem. Abstr. **63**, 7517 (1965); W. FOERSTER. Acta Biol. Med. Ger. **9**, 341 (1962); Chem. Abstr. **58**, 11846 (1963).
4. M. KOMATSU and T. KAMANO. United States Patent 3,342,812 (1967); Chem. Abstr. **68**, 6179 (1968).
5. S. M. KUPCHAN, R. J. HEMINGWAY, and J. C. HEMINGWAY. Tetrahedron Letters, 149 (1968); S. M. KUPCHAN, R. W. DOSKOTCH, P. BOLLINGER, A. T. MCPHAIL, G. A. SIM, and J. A. SAENZ RENAULD. J. Am. Chem. Soc. **87**, 5805 (1965).
6. *a*. J. FRIED and R. C. ELDERFIELD. J. Org. Chem. **6**, 566 (1941); R. NICOLETTI. Ann. Chim. (Rome) **51**, 1260 (1961); *b*. D. BERTIN, L. NÉDÉLEC, and J. MATHIEU. Comp. Rend. **253**, 1219 (1961); *c*. Unpublished experiments by F. Sondheimer, Y. Mazur, and E. Levy summarized in a review by F. Sondheimer, Chem. Brit. **1**, 454 (1965); F. SONDHEIMER, W. MCCRAE, and W. G. SALMOND. J. Am. Chem. Soc. **91**, 1228 (1969).
7. R. DULONG, E. ELKIK, and A. VEILLARD. Bull. Soc. Chim. France, 967 (1960); G. STORK, A. BRIZZOLARA, H. LANDESMAN, J. SZMUSZKOVICZ, and R. TERRELL. J. Am. Chem. Soc. **85**, 207 (1963).
8. D. ROSENTHAL, P. GRABOWICH, E. F. SABO, and J. FRIED. J. Am. Chem. Soc. **85**, 3971 (1963).
9. A. K. BOSE and R. M. RAMER. Steroids, **11**, 27 (1968); A. K. BOSE and R. T. DAHIL, JR. J. Org. Chem. **30**, 505 (1965).

Can. J. Chem. Downloaded from www.nrcresearchpress.com by 210.87.254.40 on 09/05/12
For personal use only.

Can. J. Chem. Downloaded from www.nrcresearchpress.com by 210.87.254.40 on 09/05/12
For personal use only.

Canadian Journal of Chemistry

Published by THE NATIONAL RESEARCH COUNCIL OF CANADA

VOLUME 47 JULY 15, 1969 NUMBER 14

Raman and far infrared spectra of *s*-trinitrobenzene and *s*-trinitrobenzene-d_3

H. F. SHURVELL AND A. R. NORRIS
Department of Chemistry, Queen's University, Kingston, Ontario

AND

D. E. IRISH
Department of Chemistry, University of Waterloo, Waterloo, Ontario

Received January 30, 1969

Raman spectra have been recorded of *s*-trinitrobenzene and *s*-trinitrobenzene-d_3 both in solution and in the solid phase. Eighteen of the 22 Raman active fundamentals in D_{3h} have been observed for both molecules.

Two fundamentals have been observed in the far infrared spectrum of each molecule.

Nous avons enregistré les spectres Raman du *s*-trinitrobenzène et *s*-trinitrobenzène-d_3 en solution et aussi l'état solide. Dix-huit des 22 vibrations fondamentales ont été observées pour les deux molécules.

Deux vibrations fondamentales ont été observées dans les spectres infrarouge lointain pour chaque molécule.

Canadian Journal of Chemistry, 47, 2515 (1969)

Introduction

The infrared (i.r.) spectra of *s*-trinitrobenzene and *s*-trinitrobenzene-d_3 have been discussed previously (1). Although assignments were compatible with a molecule of D_{3h} symmetry, Raman spectra were desired to substantiate that conclusion and give a more complete vibrational assignment. The far i.r. spectrum was also needed, since two of the i.r. active fundamentals were not observed in the previous work (1).

Experimental

Materials were prepared in the same way as for the i.r. work (1). Raman spectra were recorded from chloroform and acetone solutions and from the polycrystalline solid. Raman spectra of solid *s*-trinitrobenzene and *s*-trinitrobenzene-d_3 are shown in Figs. 1 and 2.

Spectra were recorded on three different spectrometers; one a Cary model 81 instrument with mercury arc excitation, and two different experimental assemblies employing argon ion laser excitation and Spex 1400 double monochromators with photoelectric detection systems. One of these experimental assemblies is in the laboratory of Dr. H. J. Bernstein at the National Research Council of Canada, Ottawa; the other is in the Department of Physics at the University of Waterloo. In recording spectra of solid *s*-trinitrobenzene and *s*-trinitrobenzene-d_3, both the 4880 and the 5145 Å argon ion laser lines

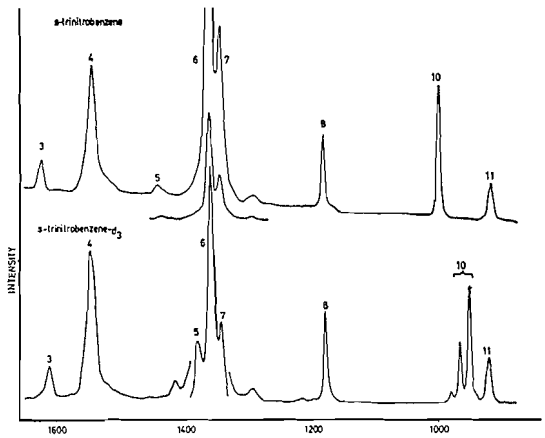

FIG. 1. Raman spectra of solid *s*-trinitrobenzene and *s*-trinitrobenzene-d_3 in the region 800–1600 cm^{-1}, excited by the 5145 Å line of an argon ion laser.

TABLE I

Raman and infrared frequencies (in cm^{-1}) for *s*-trinitrobenzene and *s*-trinitrobenzene-d_3

	s-Trinitrobenzene		*s*-Trinitrobenzene-d_3			
Identification	Raman*	Infrared†	Raman*	Infrared†	Assignment	
1	3100 w‡	3100	2310 vw‡	2305	νCH (νCD)	E'
2	3100 w‡	—	2310 vw‡	—	νCH (νCD)	A_1'
3	1623 m, dp	1625	1608 m, dp	1606	νCC	E'
4	1547 vs, dp	1545	1548 s, dp	1545	NO_2 asym. stretching	E'
—	1520 vw, sh	—	1420 vw	—	c	—
5	1440 w	1443	1384 w, dp	1385	νCC	E'
6	1365 vvs, p	—	1363 vs, p	—	NO_2 sym. stretching	A_1'
7	1345 s, dp	1345	1348 m	1345	NO_2 stretching	E'
—	1296 vw	—	1298 vw	—	c	—
8	1184 s, p	—	1185 s, p	—	νCN	A_1'
9	—	1075	—	806	βCH (βCD)	E'
—	—	—	989 vw	—	c	—
10	1002 s, p	—	976 m, p 960 s, p	Fermi resonance	Ring mode	A_1'
11	918 m, dp	918	930 m, dp	926	ν CN	E'
12	825 s, p	—	830 s, p	—	NO_2 sym. def.	A_1'
—	—	—	754 vw	—	c	—
13	754 w	—	704 w	—	γCH (γCD)	E''
14	726 vw	728	727 vw	725	NO_2 in-plane def.	E'
15	—	620	520 vw	518	αCCC	E'
16	370 m	360	368 w, dp	360	NO_2 rock	E'
17	355 m, p	—	334 m, p	—	Ring def.	A_1'
18	212 s	—	204 s	—	φCC	E''
19	200 sh	—	192 sh	—	NO_2 out-of-plane def.	E''
20	160 w	156	160 w	155	βCN	E'
21	133 sh	—	132 sh	—	NO_2 out-of-plane def.	E''

*v = very, s = strong, m = medium, w = weak, p = polarized, dp = depolarized, c = combination or overtone frequency, sh = shoulder.
†Infrared frequencies taken from ref. (1), except the lowest frequency for each molecule.
‡Frequency used twice.

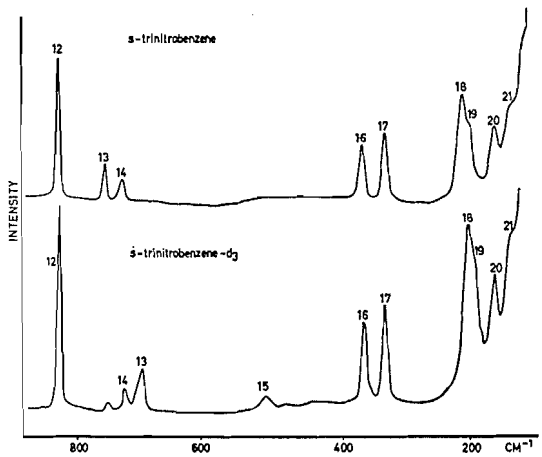

FIG. 2. Raman spectra of solid *s*-trinitrobenzene and *s*-trinitrobenzene-d_3 in the region 100–800 cm^{-1}, excited by the 4880 Å line of an argon ion laser.

were used to excite the Raman spectra. Most of the frequencies listed in Table I are the averages of several runs on solution and solid phase samples. The frequencies are believed to be correct to within ± 2 cm^{-1} in most cases. However, for the CH and CD stretching frequencies and for frequencies below 400 cm^{-1}, the errors are somewhat larger. The last 4 frequencies for each molecule in Table I were taken from spectra of the solids excited by the 4880 Å argon ion line.

The polarization data were obtained from acetone solutions, using the Cary 81 spectrometer.

Far i.r. spectra of Nujol mulls of *s*-trinitrobenzene and *s*-trinitrobenzene-d_3 supported between polyethylene discs were recorded on a Perkin–Elmer model 301 spectrophotometer in the laboratory of Dr. E. Whalley at the National Research Council of Canada, Ottawa, and are shown in Fig. 3.

Results and Discussion

Spectra obtained from chloroform and acetone solutions were essentially the same as the solid state spectra shown in Figs. 1 and 2. Some relative intensity differences were noted, but no evidence of splittings attributable to crystal effects was observed.

The normal vibrations of the *s*-trinitrobenzene molecule span the irreducible representations of the point group D_{3h} as follows

$$6\,A_1' + 5\,A_2' + 11\,E' + 1\,A_1'' + 4\,A_2'' + 5\,E''$$

Of these, only those vibrations belonging to the

Can. J. Chem. Downloaded from www.nrcresearchpress.com by 210.87.254.40 on 09/05/12
For personal use only.

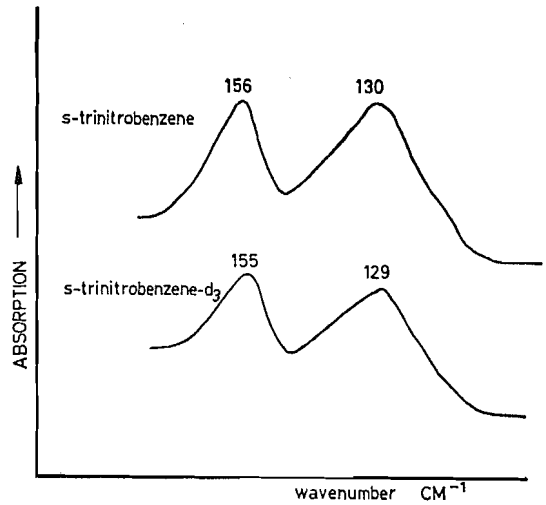

FIG. 3. Far infrared spectra of Nujol mulls of *s*-trinitrobenzene and *s*-trinitrobenzene-d_3 suspended between polyethylene plates.

species E' and A_2'' are i.r. active, while those belonging to the species A_1', E', and E'' are Raman active. Thus the Raman spectrum should contain 22 fundamentals of which 6 of species A_1' will be polarized, 11 will coincide with i.r. active fundamentals of species E', and the remaining 5 will be the E'' modes.

Discussion of the assignments will be facilitated by using descriptions of normal vibrations based on symmetry coordinates. In certain cases it is probable that the symmetry coordinate will provide a good description of the normal mode; for example the symmetrical CH stretching mode of species A_1'. In other cases, particularly for the modes of low frequency, considerable mixing may occur and the description will be at best approximate. By using the coordinates of the various groups of atoms as bases for reducible representations of the point group D_{3h} (2), we may predict qualitatively the numbers and types of group vibrations to be expected in the Raman spectrum.

Following this procedure, the Raman active vibrations may be described as follows. There are 6 vibrations involving the carbon atoms of the benzene ring, 4 CH vibrations, 4 CN vibrations, and 8 NO_2 group vibrations. This qualitative approach, coupled with previous evidence from various nitrobenzenes (3–7) and *s*-trichlorobenzene (8), has lead to the assignments given in Table I. The assignments to the various symmetry species are based on polarization studies and on coincidences with i.r. absorption frequencies. The notation used to describe the various vibrations of the substituted benzene ring is due to Whiffen (9).

A_1' Vibrations

There are 6 Raman active, totally symmetric fundamentals of the *s*-trinitrobenzene molecule, which should give rise to polarized lines in the spectra. One of the modes of species A_1' involves the hydrogen atoms. This can only be a symmetric stretching vibration and should be found near 3100 cm^{-1} in *s*-trinitrobenzene and 2300 cm^{-1} in the deuterated molecule. In the spectrum of the normal molecule, we have observed a weak line at about 3100 cm^{-1}, and a very weak line near 2310 cm^{-1} for the deuterated sample. These frequencies were only observed for solid samples, and no polarization data are available. There is therefore no way of distinguishing the symmetry species and we have assigned these frequencies to both A_1' and E' species of the CH and CD stretching modes.

The NO_2 symmetric stretching mode is assigned to a very strong polarized line at 1365 cm^{-1}, which is virtually unshifted on deuteration. This frequency is well within the usual range observed for symmetric NO_2 stretching vibrations in various nitrobenzenes (3–7). The frequency is 20 cm^{-1} higher than that of the doubly degenerate NO_2 stretching mode of species E' in the same molecule. A strong, polarized line at 1184 cm^{-1} is assigned to the symmetric CN stretching mode. The frequency of this mode is also unaffected by deuteration of *s*-trinitrobenzene. The frequencies of the corresponding mode in *s*-trichlorobenzene, (normal and deuterated) are 1149 and 1146 cm^{-1}, respectively (8).

A strong, polarized line at 1002 cm^{-1} in the spectrum of *s*-trinitrobenzene is assigned to the ring "breathing" mode. This vibration usually gives rise to frequencies near 1000 cm^{-1} in monosubstituted benzenes (9), and Scherer *et al.* have reported a frequency of 995 cm^{-1} in the Raman spectrum of *s*-trichlorobenzene (8). In the spectrum of deuterated *s*-trinitrobenzene, a doublet is observed at 976, 960 cm^{-1}. Both components are polarized and must therefore be assigned to vibrations of A_1' symmetry. Since only one fundamental is expected in this region, these two lines probably arise as a result of Fermi

Can. J. Chem. Downloaded from www.nrcresearchpress.com by 210.87.254.40 on 09/05/12
For personal use only.

Can. J. Chem. Downloaded from www.nrcresearchpress.com by 210.87.254.40 on 09/05/12
For personal use only.

resonance between the ring breathing fundamental of species A_1', and an overtone or combination line belonging to the same irreducible representation. None of the i.r. or Raman active fundamentals would have an overtone in the region of 970 cm^{-1}, and no combination of these fundamentals belonging to species A_1' lies in this region. The second component of the Fermi doublet must be either an overtone of an inactive fundamental or involve an inactive fundamental. The observed frequency of the ring breathing mode in *s*-trichlorobenzene-d_3 was 956 cm^{-1} (8).

A polarized line at 825 cm^{-1} is assigned to the NO_2 symmetric deformation mode. In the i.r. spectrum of nitrobenzene, Stephenson *et al.* (5) have assigned a peak at 850 cm^{-1} to this vibration. We have previously assigned i.r. bands near 725 cm^{-1} in the spectra of normal and deuterated *s*-trinitrobenzene to a symmetric NO_2 deformation mode of species E' (1). At that time we stated that this provided support for the assignment made by Green *et al.* (4) of a peak at 677 cm^{-1} in the i.r. spectrum of *s*-trinitrobenzene to the NO_2 symmetric deformation mode. In view of the present Raman spectra, it would appear that the assignment of Stephenson *et al.* (5) is the better one, and this conclusion is in agreement with the work of Pinchas *et al.* (6) on ^{18}O labelled nitrobenzene.

The last polarized line at 355 cm^{-1} is attributed to a symmetric ring deformation. In *s*-trichlorobenzene the corresponding mode gives rise to a Raman line at 379 cm^{-1}. This vibration involves motion of the carbon atoms to which the NO_2 groups are attached (or Cl atoms in the case of *s*-trichlorobenzene). Scherer (10) has given diagrams of the planar vibrations of *s*-trichlorobenzene and *s*-trichlorobenzene-d_3, and it is likely that the corresponding A_1' modes in *s*-trinitrobenzene have similar forms, with the chlorine atoms replaced by nitro groups.

E' Vibrations

The 11 E' type vibrations are active in both the i.r. and Raman spectra. However, definite coincidences have been observed in only 7 cases. The agreement between i.r. and Raman frequencies is good in these cases. The doubly degenerate CH and CD stretching modes should give rise to Raman lines near 3100 cm^{-1} for *s*-trinitrobenzene and 2300 cm^{-1} for the deuterated molecule. Only one line has been observed in each region. These lines have been assigned to the CH and CD stretching modes of species A_1', but it is possible that the E' modes could have similar frequencies. We have therefore attributed the observed lines to both A_1' and E' type fundamentals.

One of the far i.r. frequencies should be due to an E' type fundamental and a coincident Raman line is expected. We have assigned the line at 160 cm^{-1} in the spectrum of *s*-trinitrobenzene to the lowest frequency E' fundamental, an in-plane CN deformation mode (βCN). A line at the same frequency was observed for the deuterated molecule. The corresponding frequencies in the far i.r. region were 156 and 155 cm^{-1} for the normal and deuterated molecules respectively. The differences between i.r. and Raman frequencies are 5 cm^{-1}, which is probably within experimental error.

A second far i.r. band was observed at 130 cm^{-1} for *s*-trinitrobenzene, and at 129 cm^{-1} for the deuterated molecule. These appear to coincide with Raman features observed as shoulders on the exciting line at 133 and 132 cm^{-1} for the normal and deuterated molecules respectively, and offer an alternative assignment for the lowest frequency E' mode. However, we have assigned the i.r. bands to the A_2'' mode of lowest frequency, and the Raman lines to an E'' mode in each molecule.

The i.r. frequencies assigned to E' type modes but not observed in the present Raman spectra were at 1075 and 620 cm^{-1} for *s*-trinitrobenzene and 806 and 518 cm^{-1} for the deuterated molecule (1). These were assigned respectively to the in-plane CH deformation (βCH) and ring deformation (αCCC) vibrations. A very weak Raman line observed at 520 cm^{-1} in the spectrum of solid *s*-trinitrobenzene-d_3, probably corresponds to the 518 cm^{-1} i.r. absorption.

The assignments of the other E' type vibrations are the same as for the previous i.r. work (1).

E'' Vibrations

There should be 5 depolarized lines in the Raman spectra of both *s*-trinitrobenzene and *s*-trinitrobenzene-d_3, having no counterparts in the i.r. spectra. These are the out-of-plane E'' vibrations. Two lines and two shoulders have been located in the spectrum of each molecule. A weak line at 754 cm^{-1} that is displaced to 704 cm^{-1} on deuteration is attributed to the out-of-plane CH bending mode (γCH). The corresponding pair of lines in the Raman spectra of normal and deuterated *s*-trichlorobenzene were located

Can. J. Chem. Downloaded from www.nrcresearchpress.com by 210.87.254.40 on 09/05/12
For personal use only.

at 869 and 712 cm^{-1}. The smaller shift in the trinitro compounds is difficult to explain.

A fairly strong line at 212 cm^{-1} in the spectrum of *s*-trinitrobenzene shifts to 204 cm^{-1} in the spectrum of the deuterated molecule. These frequencies are assigned to an out-of-plane ring deformation (ϕCC). Coupling with other E'' type vibrations could account for the low frequency of this mode in *s*-trinitrobenzene as compared with other substituted benzenes (11). The other normal modes of species E'' are two out-of-plane NO_2 deformations and an out-of-plane CN bending mode (γCN). We have arbitrarily assigned the two shoulders to NO_2 deformations. The missing line may either be too weak to be observed in the Raman spectrum, or is obscured by another fundamental.

Far Infrared Spectra

The far i.r. spectra of *s*-trinitrobenzene and *s*-trinitrobenzene-d_3 are shown in Fig. 3. The observed frequencies were 156 and 130 cm^{-1} for the normal molecule and 155 and 129 cm^{-1} for the deuterated compound. The absorption at higher frequency coincides with a Raman line for both molecules, and this is assigned to the in-plane CN deformation mode of species E'. The lower frequency absorption is then assigned to the out-of-plane CN deformation of species A_2''.

Overtones and Combinations

Two very weak lines in the Raman spectrum of *s*-trinitrobenzene at 1520 and 1296 cm^{-1} have been assigned to overtone or combination frequencies. In the spectrum of *s*-trinitrobenzene-d_3, 4 very weak lines at 1420, 1298, 989, and 754 cm^{-1}, in addition to one component of the Fermi doublet at 976, 960 cm^{-1} have been assigned to combinations or overtones.

Conclusions

We have observed 18 of the 22 Raman active fundamentals in D_{3h} of *s*-trinitrobenzene and *s*-trinitrobenzene-d_3 in the present work and have made qualitative assignments to these frequencies in terms of symmetry coordinates based on group vibrations. Three of the remaining Raman active fundamentals belonging to the E' species have been observed in previous i.r. spectra. The two fundamentals observed in the far i.r. spectra complete the total of 15 i.r. active modes. There remain, however, 6 fundamentals inactive in both spectra, and the frequencies of these modes can only be estimated from normal coordinate calculations. We hope to make these calculations in the near future.

Acknowledgments

We are very grateful to Dr. H. J. Bernstein and Dr. E. Whalley of the National Research Council of Canada, Ottawa, and Dr. A. Anderson of the Department of Physics, University of Waterloo, for placing the facilities of their laboratories at our disposal. We thank Mr. E. A. Symons for help with the preparation and analysis of *s*-trinitrobenzene-d_3, and Mrs. J. Weerheim for technical assistance. The financial support of the National Research Council of Canada is gratefully acknowledged.

1. H. F. SHURVELL, J. A. FANIRAN, E. A. SYMONS, and E. BUNCEL. Can. J. Chem. **45**, 117 (1967).
2. F. A. COTTON. Chemical applications of group theory. John Wiley and Sons, Inc., New York. 1964.
3. R. R. RANDLE and D. H. WHIFFEN. J. Chem. Soc. 4153 (1952).
4. J. H. S. GREEN, W. KYNASTON, and A. S. LINDSEY. Spectrochim. Acta, **17**, 486 (1961).
5. C. V. STEPHENSON, W. C. COBURN, JR., and W. S. WILCOX. Spectrochim. Acta, **17**, 933 (1961).
6. S. PINCHAS, D. SAMUEL, and B. L. SILVER. Spectrochim. Acta, **20**, 179 (1964).
7. K. C. MEDHI. Spectrochim. Acta, **20**, 675 (1964).
8. J. R. SCHERER, J. C. EVANS, W. W. MUELDER, and J. OVEREND. Spectrochim. Acta, **18**, 57 (1962).
9. D. H. WHIFFEN. J. Chem. Soc. 1350 (1956).
10. J. R. SCHERER. Planar vibrations of chlorinated benzenes. The Dow Chemical Company, Midland, Michigan. 1963.
11. F. F. BENTLEY, L. D. SMITHSON, and A. L. ROZEK. Infrared spectra and characteristic frequencies. Interscience Publishers, Inc., New York. 1968.

Can. J. Chem. Downloaded from www.nrcresearchpress.com by 210.87.254.6 on 09/05/12
For personal use only.

Three forms of aluminium in aqueous systems determined by 8-quinolinolate extraction methods[1]

R. C. TURNER
Soil Research Institute, Canada Department of Agriculture, Ottawa, Canada

Received December 5, 1968

8-Quinolinolate extraction methods for the determination of Al^{3+} plus mononuclear hydroxyaluminium ions, polynuclear hydroxyaluminium ions, and the initial solid phase formed when a base is added to $AlCl_3$ solutions, are presented. The methods are based on the rates of reactions of 8-quinolinol with the 3 forms of aluminium substances. Results under a variety of experimental conditions are reported.

Canadian Journal of Chemistry, 47, 2521 (1969)

Introduction

Okura *et al.* (1) proposed an 8-quinolinolate method of analysis of Al in solution which is supposed to measure only the Al^{3+} and mononuclear (with respect to Al) hydroxyaluminium ions. The principle involved is that 8-quinolinol reacts instantaneously with the mononuclear ions but more slowly with polynuclear hydroxyaluminium substances. Consequently, their method requires that the length of time of contact between the test solution and the 8-quinolinol should be kept at a minimum. The method proposed by them is as follows. Pour 10 ml of H_2O and 2 ml portions of 8-quinolinol (dissolve 2.0 g of 8-quinolinol in 5 ml of glacial acetic acid and dilute to 200 ml with H_2O) and sodium acetate (1 *M*) into a separatory funnel. Add exactly 10 ml of chloroform. Add an appropriate volume of the test sample and shake immediately for 10 s. Allow the mixture to separate into two layers and draw off the chloroform layer. Determine the Al extracted in the chloroform colorimetrically.

This method was further investigated using dilute $AlCl_3$ solutions which had been neutralized or partially neutralized with NaOH, with the object of developing methods for differentiating between Al^{3+} plus mononuclear hydroxyaluminium ions, polynuclear hydroxyaluminium ions, and the initial solid phase formed when a base is added to an $AlCl_3$ solution.

Experimental

Mononuclear Ions

Preliminary experiments showed that, with dilute $AlCl_3$ solutions (10^{-3} to 2×10^{-1} *M*) which had been partially neutralized with NaOH, shaking the solutions in the separatory funnels for lengths of time greater than the 10 s prescribed by Okura *et al.* (1) increased the amount of Al in the chloroform extract. It was found, however, that if the 8-quinolinol plus test solution was shaken for a given length of time before adding the chloroform, followed by 10 s shaking with chloroform, the amount of Al in the chloroform was much greater than if the chloroform was present during the entire shaking period. Since the length of time that the test solution was in contact with the 8-quinolinol before shaking with chloroform commenced was very critical, the procedure outlined by Okura *et al.* (1) was modified to reduce this to a minimum. The modification was to mix the 8-quinolinol and sodium acetate solutions and H_2O together so that all the reagents could be added in one operation. In this way, the length of time between the first contact of the 8-quinolinol with the test solution and the beginning of shaking was reduced to a few seconds, regardless of how much of the test solution was required. Even with this modification, reproducible results could not always be obtained with the partially neutralized $AlCl_3$. This was apparently caused by the fact that there was some foreign substance in the solutions that slowed down the separation of the chloroform and aqueous phases, which defeated the effect of the short time of shaking. Centrifuging the test solution at 18 000 r.p.m. for 20 min did not eliminate the problem. Filtering through a 10 mμ pore size "Millipore" filter, however, removed a considerable portion of the total Al in the systems, and the separation of the 2 phases in the separatory funnels was normal when the filtrates were analyzed. (It should be pointed out that Goto and Yotsuyanagi (2) eliminated this problem of slow separation of the two phases by adding the surfactant sodium dodecyl sulfate after shaking.)

The procedure for determining the concentration of mononuclear ions in solution that resulted from these experiments is as follows. Filter an appropriate aliquot of the test solution through a 10 mμ pore size "Millipore" filter under suction. Discard the first aliquot that passes the filter, pass a second aliquot through the filter, and use the second filtrate for analysis. The loss in weight due to evaporation under suction must be determined by the difference between the weight of the aliquot poured on the filter and that of the resulting filtrate. Transfer an appropriate aliquot of the filtrate to a separatory funnel which

[1]Contribution No. 293.

Can. J. Chem. Downloaded from www.nrcresearchpress.com by 210.87.254.6 on 09/05/12
For personal use only.

contains 5 ml of H_2O and add exactly 10 ml of chloroform. Introduce 14 ml of the composite 8-quinolinol reagent by means of a plunger-type repipet and shake immediately for 10 s. Allow the chloroform phase to separate and drain it off. Place cotton wool in the end of the drainage tube of the funnel to remove moisture from the chloroform as it drains from the funnel. Determine the concentration of Al in the chloroform extract with a spectrophotometer at a wavelength of 395 mμ. Correct the result for the loss in weight during filtration. The composite 8-quinolinol reagent consists of 10 ml H_2O to 2 ml of the 8-quinolinol solution to 2 ml of molar sodium acetate.

Polynuclear Ions

The method for determining the concentration of Al in the form of polynuclear hydroxyaluminium ions was developed on the basis of the rate of reaction of these ions with 8-quinolinol. Both the polynuclear ions and the initial solid phase reacted with 8-quinolinol in the absence of chloroform, but more slowly than did the mononuclear ions. When the polynuclear ions and solid phase were present, the rate of the reaction or reactions did not seem to follow any particular order of reaction based on the Al present. The concentration of 8-quinolinol was suffciently large relative to that of the Al present that changes in its concentration from the reactions could be ignored and the reaction was irreversible. When the filtrates which passed through a 10 mμ pore size "Millipore" filter were used in the rate studies, the reactions followed a first order process with respect to the Al present. The specific rate constant was 0.18 per min at 26 °C, providing the partially neutralized systems were allowed to react for one day or more before filtering. When the reaction was studied immediately after adding the base to the $AlCl_3$ solution, the reaction started at a relatively fast rate and slowed down to a first order process after the first few minutes. In all cases, however, the reaction was essentially complete after 30 min. The procedure for determining the polynuclear ions which developed from these experiments is as follows. Transfer an appropriate aliquot of a filtrate obtained as described in the method for mononuclear ions, to a separatory funnel containing 5 ml of H_2O. Add 14 ml of composite 8-quinolinol reagent with a plunger-type repipet and shake for 30 min at room temperature (the temperature should be 25 °C or above). Add exactly 10 ml of chloroform and shake for 10 s. Drain off the chloroform and proceed as described in the method for mononuclear ions. The difference between the Al found after 30 min shaking and after zero time shaking (mononuclear ions) is the amount in the polynuclear form. The determination must be done immediately after filtering.

Initial Solid Phase

When the $AlCl_3$ solutions were 100% neutralized with NaOH, the rate of the reactions between 8-quinolinol and the Al material in the systems immediately after adding the base followed a two-third order reaction to a fairly good approximation. The length of time required for complete reaction was less than 3 h at 25 °C. The procedure for determining the Al in the initial solid phase is as follows. Transfer an appropriate aliquot of the unfiltered test suspension to a separatory funnel containing 5 ml of H_2O. Add 14 ml of the composite 8-quinolinol reagent by means of a plunger-type repipet and shake immediately for 3 h at room temperature (the temperature of the reaction mixture should not be less than 25 °C). Add exactly 10 ml of chloroform and shake 10 s. Drain off the chloroform and determine the Al in this chloroform extract. The Al thus determined, less that determined as mono plus polynuclear ions, is the Al in the initial solid phase.

Experimental Results

Method for Mononuclear Ions

The method for mononuclear ions was tested by comparing the results obtained with concentrations estimated from neutralization curves. When partially neutralized $AlCl_3$ solutions are titrated with a base, after various lengths of time of reaction, there are two buffer zones in the neutralization curves (3). The first occurs in the same pH range as for fast titrations of $AlCl_3$ solutions to which no base had been added prior to titration (3, 4), and the second in a pH range considerably above this.

Figure 1 shows neutralization curves for 5.8×10^{-2} *M* solutions of $AlCl_3$ which had been partially neutralized and then aged for various lengths of time. At the same time as the titrations were done, the Al concentration in the mononuclear form was determined by the 8-quinolinolate extraction method described above. The lower section of Fig. 1 shows the similarity between the first buffer zone of the neutralization curve of 5.8×10^{-2} *M* solution which had been 50% neutralized and aged for 1 day (curve *a*), and the neutralization curve of a 2.2×10^{-2} *M* solution to which no base had been added prior to titration (curve *b*). The volume of solutions titrated and the concentration of NaOH used were the same for the two titrations. Although it is impossible to determine the exact end point for the titration of the material that caused the first buffer zone with the partially neutralized sample, it is obvious that the amount was only slightly greater than that in the 2.2×10^{-2} *M* $AlCl_3$ solution, which is in excellent agreement with 2.3×10^{-2} *M* found by the 8-quinolinolate extraction method. The upper section of Fig. 1 shows the neutralization curves for a 5.8×10^{-2} *M* solution which had been 80% neutralized and aged for two different lengths of time before titration with NaOH. When the solution had been aged for only 1 h, there was not a clear distinction between the two buffer zones (curve *e*) so that it was impossible to make a very good estimate of the concentration of Al represented by the first buffer zone. Comparison with the

Can. J. Chem. Downloaded from www.nrcresearchpress.com by 210.87.254.6 on 09/05/12
For personal use only.

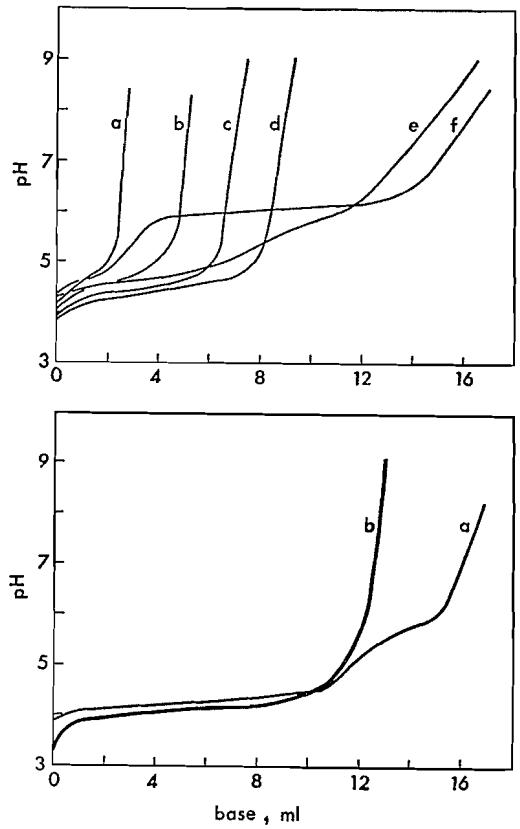

FIG. 1. Neutralization curves of $AlCl_3$ and partially neutralized $AlCl_3$ solutions. *Upper section*, 50 ml of solution titrated with 0.10 *N* NaOH. Curves *a*, 1.8×10^{-3}; *b*, 3.5×10^{-3}; *c*, 4.7×10^{-3}; *d*, 6.0×10^{-3} *M* $AlCl_3$ solutions. Curves *e*, 80% neutralized 5.8×10^{-2} *M* $AlCl_3$ aged 1 h; *f*, 80% neutralized $AlCl_3$ aged 23 days. *Lower section*, 20 ml of solution titrated with 0.10 *N* NaOH. Curve *a*, 60% neutralized 5.8×10^{-2} *M* $AlCl_3$ aged 1 day; Curve *b*, 2.2×10^{-2} *M* $AlCl_3$ solution.

neutralization curves for 4.7×10^{-3} and 6.0×10^{-3} *M* $AlCl_3$ solutions (curves *c* and *d*), however, shows that the concentration was between these two, and the mononuclear concentration determined by the 8-quinolinolate extraction method was 5.9×10^{-3} *M*. When the 80% neutralized solution was aged for 23 days, there was a distinct break between the two buffer zones (curve *f*) and there is no doubt that the Al concentration represented by the first buffer zone was considerably less than 3.5×10^{-3} *M* (curve *b*) and only somewhat greater than 1.8×10^{-3} *M* (curve *a*), which agrees with 2.0×10^{-3} *M* found by the 8-quinolinolate extraction method.

The results in Fig. 1 present rather convincing evidence that the method proposed measures only the mononuclear Al ions. Since the partially neutralized systems had pH values near 4 in all cases, however, Al^{3+} must have been essentially the only mononuclear ions present so that one can not conclude from these results that the method measures mononuclear hydroxyaluminium ions. The fact that $AlOH^{2+}$ is measured along with Al^{3+} was demonstrated with a 10^{-4} *M* solution of $AlCl_3$. This solution had a pH of 4.64 which means that $AlOH^{2+}$ represented roughly 30% of the total Al (Al^{3+} + $AlOH^{2+}$) present (5) and all the Al present was measured by the method. Furthermore, it was found that when a 10^{-3} *M* $AlCl_3$ solution was 100% neutralized the method showed essentially no mononuclear Al present, but when the base added exceeded the equivalent amount by 20%, the method showed a concentration of 2.3×10^{-4} *M* for mononuclear Al expressed as Al^{3+}. This shows that the method also measured the mononuclear hydroxyaluminium ions $Al(OH)_4^-$.

Methods for Polynuclear Ions and the Initial Solid Phase

The experimental evidence supporting the validity of these methods is based on the rate and nature of the reactions between polynuclear ions, initial solid phase, and 8-quinolinol, by which the hydroxyaluminium materials are destroyed. The test solutions or suspensions were shaken at constant temperature, for various lengths of time with the 8-quinolinol reagent as described in the previous section. Chloroform was then added and the mixture again shaken for 10 s after which the Al in the chloroform extract was determined colorimetrically. Since, as mentioned above, there was a great excess of 8-quinolinol in the reaction mixtures, any change in its concentration could be ignored and the reaction was irreversible. The rates of the reactions were thus dependent on the concentration of hydroxyaluminium material present. It was assumed that the reactions destroyed the hydroxyaluminium material and that Al^{3+} was the product so that the results could be expressed in moles per liter of Al.

The polynuclear ions, i.e., the material that passed through 10 mμ pore size "Millipore" filters but was not measured as mononuclears, reacted with 8-quinolinol much more slowly than did the mononuclear ions. When the filtrates from partially neutralized $AlCl_3$ solutions which had been aged for 1 day or more were used, the reaction followed a first order process with a rate

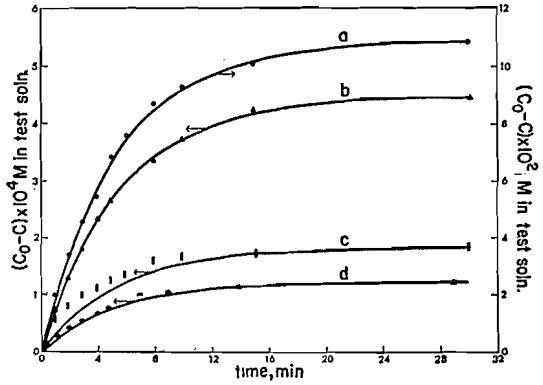

FIG. 2. Rate curves for the reaction with polynuclear ions at 26 °C. The smooth curves are first order curves with rate constants of 0.18 per min. The experimental points are for 80% neutralized 1.95×10^{-1} *M* $AlCl_3$ solutions aged 93 days (curve *a*); 80% neutralized 1.0×10^{-3} *M* $AlCl_3$ solutions aged 1 day (curve *b*); 80% neutralized 1.0×10^{-3} *M* $AlCl_3$ solutions not aged (curve *c*); 80% neutralized 1.0×10^{-3} *M* $AlCl_3$ solution not aged, with 1 min made zero time (curve *d*).

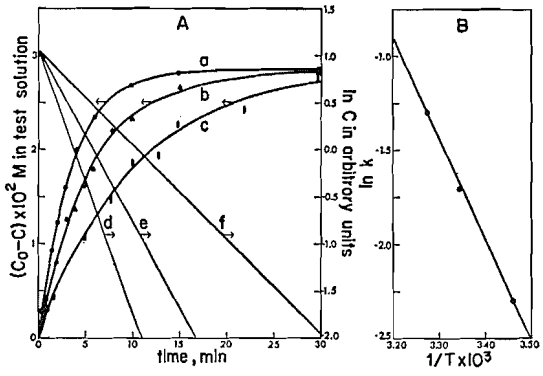

FIG. 3. Effect of temperature on the rate of the reaction with polynuclear ions. *Left section*, the smooth curves are first order curves with rate constants 0.28 at 34 °C (curve *a*); 0.18 at 26 °C (curve *b*); 0.10 at 16 °C (curve *c*) per min. Curves *d*, *e*, and *f* are the ln *C* vs. *t* plots from the smooth curves *a*, *b*, and *c*, respectively. The experimental points are for a 50% neutralized 5.8×10^{-2} *M* $AlCl_3$ solutions. *Right section*, the Arrhenius plots from which an activation energy of 11 kcal/mole was calculated.

constant of 0.18 per min at 26 °C (Fig. 2, curves *a* and *b*) regardless of the initial concentration of $AlCl_3$. When the filtrates were from unaged partially neutralized systems, the rate of reaction was much faster during the first few minutes than was predicted by a rate constant of 0.18 per min (Fig. 2, curve *c*) but if the reaction during the first minute was ignored, i.e., 1 min was made zero time, the reaction followed the first order process with the correct rate constant (Fig. 2, curve *d*). These results (curves *c* and *d*) probably mean that polynuclear material started as very low molecular weight ions and increased in size to a maximum. In any event the reaction with 8-quinolinol was complete in 30 min (curves *a*, *b*, *c*, and *d*). The effect of temperature on the rate of reaction with the polynuclear ions is shown in Fig. 3. The smooth curves *a*, *b*, and *c* in the left section of Fig. 3 were constructed with rate constants of 0.28, 0.18, and 0.10 for 34, 26, and 16 °C, respectively. Curves *d*, *e*, and *f* are the ln *C* vs. *t* plots from the smooth curves *a*, *b*, and *c*, respectively. The right section of Fig. 3 shows the Arrhenius plot from which an activation energy of the reaction of 11 kcal/mole was calculated.

The reaction with the initial solid phase was studied by using aliquots of the unfiltered suspensions immediately after adding the base to the $AlCl_3$ solutions. When the solutions of $AlCl_3$ were 100% neutralized no correction for polynuclear ions was necessary because they did not exist in the systems. It was necessary, however, to make corrections for the polynuclear ions when partially neutralized systems were used, and this was done by making parallel rate experiments on the filtrates from systems prepared in exactly the same way.

In all cases the reaction with the initial solid phase was a two-thirds order process. The simple model used as a guide for interpreting the experimental results was the one in which all the solid phase particles are identical and symmetrical in shape, e.g. spheres or cubes. It was assumed that the rate of the reaction was proportional to the surface area of the particles exposed to the 8-quinolinol reagent, that the 8-quinolinol was in sufficient excess that its concentration remained constant throughout the reaction, and that the reactions were irreversible. If there are *n* particles in a given volume, the rate of the reaction can be expressed by the equation

$$[1] \qquad (nM_0)^{1/3} - (nM)^{1/3} = n^{1/3} k't$$

where M_0 is the mass of a single particle at zero time, M is its mass at time t, and k' is a combination of constants including the specific rate constant. Furthermore, nM_0 and nM are proportional to C_0 and C, respectively, where C_0 and C are the number of moles of Al per liter which

Can. J. Chem. Downloaded from www.nrcresearchpress.com by 210.87.254.6 on 09/05/12
For personal use only.

exists in the solid phase at zero time and at time t, respectively. Therefore

$$[2] \qquad C_0^{1/3} - C^{1/3} = n^{1/3}kt = k_c t$$

where k is a constant and k_c is a constant at any given concentration. It follows that the time for a complete reaction is independent of the concentration of the solid phase and the slope of the $C^{1/3}$ vs. t plot, k_c, is proportional to $n^{1/3}$ and, therefore, to $C_0^{1/3}$.

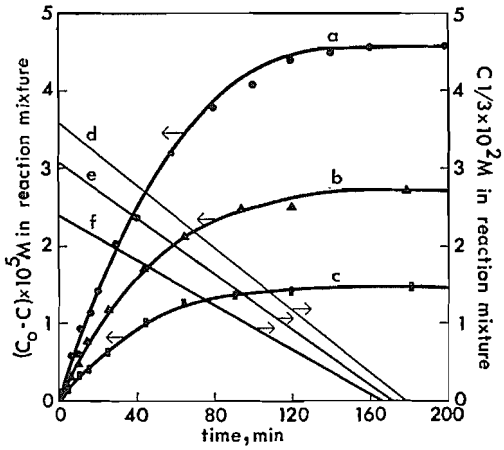

FIG. 4. Rate curves for the reaction with the initial solid phase at 25 °C. The experimental points are for 1.0×10^{-3} M solutions of $AlCl_3$ with 3 different degrees of neutralization. The smooth curves are two-thirds order rate curves with $k_c = 2.0 \times 10^{-4}$ for 100% neutralization (curve *a*); $k_c = 1.8 \times 10^{-4}$ for 80% neutralization (curve *b*); $k_c = 1.5 \times 10^{-4}$ $C^{1/3}$/min for 60% neutralization (curve *c*). Curves *d*, *e*, and *f* are the $C^{1/3}$ vs. t plot from the smooth curves *a*, *b*, and *c*, respectively.

Figure 4 shows the results obtained at 25 °C from a solution of 1.0×10^{-3} M $AlCl_3$ which had been 100, 80, and 60% neutralized. The smooth curves *a*, *b*, and *c* were constructed with k_c equal to 2.0×10^{-4}, 1.8×10^{-4}, and 1.5×10^{-4}, respectively, assuming a two-thirds order process. Equation [2] predicts that the k_c's should have been in the ratio 2.0:1.7:1.4 which shows that the experimental systems did not behave exactly according to the theoretical model to which the equation applies. This is shown in another way by the fact that curves *d*, *e*, and *f*, which are the $C^{1/3}$ vs. t plots for the smooth curves *a*, *b*, and *c*, respectively, did not intersect at zero concentration. The differences between experimental results and those predicted by the model are small, however, and it can be concluded that the experimental systems behaved like the model to a good approximation. From a practical point of view, curves *d*, *e*, and *f* show that the time required for complete reaction is very little affected by the concentration of solid phase present or the degree of neutralization. Since both the concentration of solid phase and the degree of neutralization varied in these experiments, other experiments were made in which only 100% neutralized systems were used.

The results obtained with 100% neutralized $AlCl_3$ solutions where the concentration in the reaction mixture was varied by using different amounts of the test suspension, are shown in Fig. 5. The ratio of the volumes used were 1:2.5:7.5 and the reactions were studied at 34 °C. The smooth curves *a*, *b*, and *c* in Fig. 5 were constructed with k_c equal to 8.2×10^{-4} for the highest, 5.8×10^{-4} for the intermediate, and 4.8×10^{-4} for the lowest Al concentration, respectively. The values of k_c according to eq. [2] should have been in the ratio of 8.2:5.3:4.1 and

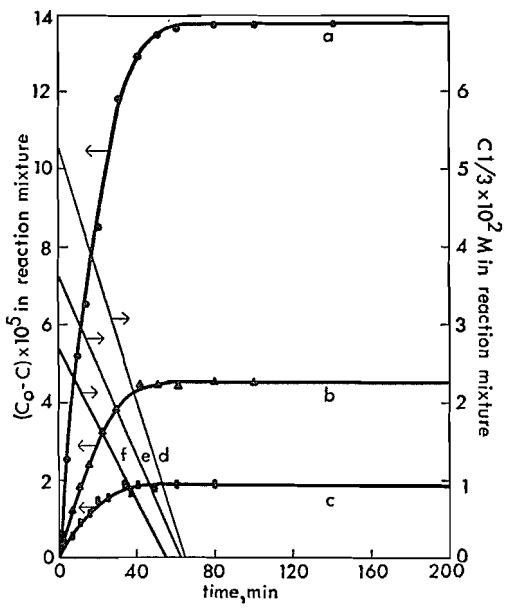

FIG. 5. Rate curves for the reaction with the initial solid phase at 34 °C. The experimental points are for a 100% neutralized 1.0×10^{-3} M $AlCl_3$ solution with 3 different concentrations of solid phase in the reaction mixture. The smooth curves are two-thirds order rate curves with $k_c = 8.2 \times 10^{-4}$ with 3 ml of test solution (curve *a*); $k_c = 5.8 \times 10^{-4}$ with 1 ml of test solution (curve *b*); $k_c = 4.8 \times 10^{-4}$ $C^{1/3}$ per min with 0.4 ml of test solution (curve *c*). Curves *d*, *e*, and *f* are the $C^{1/3}$ vs. t plots from the smooth curves *a*, *b*, and *c*.

Can. J. Chem. Downloaded from www.nrcresearchpress.com by 210.87.254.6 on 09/05/12
For personal use only.

the $C^{1/3}$ vs. t plots (curves d, e, and f) should have intersected at zero concentration, showing that even when all the initial solid phase was prepared under the same conditions, the experimental results did not agree exactly with eq. [2]. As with the systems in which the concentration of the solid phase was varied by changing the degree of neutralization (Fig. 4), however, the experimental systems behaved like the assumed model to a fairly good approximation.

The effect of temperature on the rate of the reaction with the initial solid phase is shown in Fig. 6. The smooth curves a, b, and c in the lower section were constructed with k_c equal to 5.8×10^{-4} at 34 °C, 2.0×10^{-4} at 25 °C, and 0.67×10^{-4} at 16 °C, respectively. The upper section of the Fig. 6 shows the Arrhenius plot from which an activation energy of 20 kcal/mole was calculated.

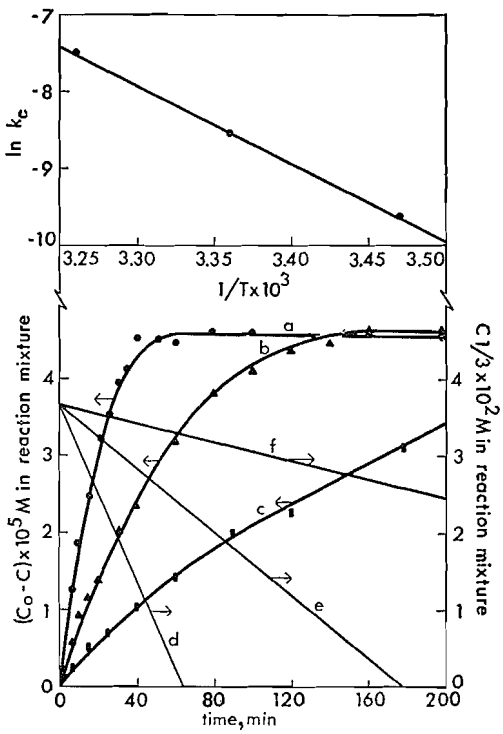

FIG. 6. Effect of temperature on the rate of reaction with the initial solid phase. *Lower section*, the smooth curves are two-thirds order rate curves with $k_c = 5.8 \times 10^{-4}$ at 34 °C (curve *a*); $k_c = 2.0 \times 10^{-4}$ at 25 °C (curve *b*); $k_c = 0.67 \times 10^{-4}$ $C^{1/3}$ per min at 16 °C (curve *c*). Curves *d*, *e*, and *f* are the $C^{1/3}$ vs. t plots from the smooth curves *a*, *b*, and *c*, respectively. The experimental points are for a 100% neutralized 1.0×10^{-3} M $AlCl_3$ solution. *Upper section*, the Arrhenius plot from which an activation energy of 20 kcal/mole was calculated.

Discussion

The object of the experiments discussed above was to show that the proposed methods measure quantitatively 3 distinct forms of Al, i.e., mononuclear ions, polynuclear ions, and the initial solid phase formed when a base is added to an $AlCl_3$ solution. The evidence that there are in fact these 3 distinct forms is very convincing: (*a*) the mononuclear ions react, for all practical purposes, instantaneously with 8-quinolinol whereas the other 2 forms react much more slowly; (*b*) the polynuclear ions are not separated from the liquid phase by filtration through a 10 mμ pore "Millipore" filter whereas the initial solid phase is; (*c*) the reaction between the polynuclear ions and an excess of 8-quinolinol is a first order process whereas the corresponding reaction with the initial solid phase is a two-thirds order process, and the activation energy of the reaction with the solid phase was almost double that for the reaction with the polynuclear ions. The evidence that the material, designated as polynuclear ions, is cations in moderately acid solutions and a component of the liquid phase is very strong: (*a*) they show exchange properties with clays (6) and exchange resins (7) as do simple cations such as Ca^{2+} and Na^+; (*b*) they are not separated from solution by filtration; (*c*) the reaction between them and an excess of the other reactant in solution is a first order process. (This conclusion should be compared with the results obtained by Goto and Yotsuyanagi (2) who found that the initial reaction without removing the solid phase was a first order process.) The evidence that the initial solid phase is a solid phase in fact as well as in name is also very strong: (*a*) it can be separated from solution by filtration; (*b*) the reaction between it and an excess of 8-quinolinol is a two-thirds order process which, to a good approximation, behaves as if it consisted of uniform solid particles with the rate of the reaction proportional to the surface exposed to the other reactant; (*c*) it is removed from the liquid phase by clays but not in an exchangeable form (6). Finally, there is the quantitative aspect of the analytic methods. The results in Fig. 1 show that if the partially neutralized systems are allowed to react for some time, the method for mononuclear ions does not measure anything but mononuclear ions. Furthermore, the experiment with 10^{-4} M $AlCl_3$ shows that the method

Can. J. Chem. Downloaded from www.nrcresearchpress.com by 210.87.254.6 on 09/05/12
For personal use only.

measures $AlOH^{2+}$ as well as Al^{3+}, and the experiment in which the neutralization was carried beyond 100% showed that it also measures $Al(OH)_4^-$. There is, however, a problem concerning the unaged partially neutralized systems. In this case, the rate of the reaction of the polynuclear ions with 8-quinolinol starts at a faster rate than usual and slows down after the first minute or so to the usual 1st order process (Fig. 2, curves *c* and *d*). Analogous to this behavior is the fact that the neutralization curves for the unaged partially neutralized systems did not show a distinct break between the two buffer zones (Fig. 1, curve *f*). It is probable as mentioned above, that some very low molecular weight polynuclear ions are present immediately after adding the base and gradually disappear with the formation of higher molecular weight ions. There is no convincing experimental evidence that these low molecular weight ions are excluded entirely from the mononuclear ions by the method proposed. Okura *et al.* (1), however, claimed that their experiments showed that ions with more than 2 Al atoms were excluded and there is no experimental evidence that those with 2 Al atoms are included with the mononuclear ions. Consequently, it must be kept in mind that there may be a small error in assuming that the method measures only mononuclear ions, but if the error does exist it must be very small. With respect to the methods for the polynuclear ions and the initial solid phase, the rates of their reactions with 8-quinolinol have been studied under such a variety of conditions. For example, Figs. 2–6 show that there is no doubt that the methods as outlined measure these 2 forms. It should be pointed out, however, that the initial solid phase changes fairly rapidly with length of time of aging and it is only the initial solid phase that is measured. After 24 h, for instance, only a fraction of the solid phase present is measured by the method. This will be the subject of a later communication.

1. T. OKURA, K. GOTO, and T. YOTSUYANAGI. Anal. Chem. **34**, 581 (1962).
2. K. GOTO and T. YOTSUYANAGI. Nippon Kagaku Zasshi, **89**, 49 (1968).
3. R. C. TURNER. Soil Sci. **106**, 338 (1968).
4. C. R. FRINK and B. L. SAWHNEY. Soil Sci. **103**, 144 (1967).
5. C. R. FRINK and M. PEECH. Inorg. Chem. **2**, 473 (1963).
6. R. C. TURNER. Can. J. Soil Sci. **47**, 217 (1967).
7. M. HONDA. Nippon Kagaku Zasshi, **72**, 555 (1951).

Can. J. Chem. Downloaded from www.nrcresearchpress.com by 210.87.254.6 on 09/05/12
For personal use only.

Can. J. Chem. Downloaded from www.nrcresearchpress.com by 210.87.254.105 on 09/05/12
For personal use only.

Photo-initiated reactions of thiols and olefins. III. Addition of methanethiol to acetylene and butadiene-1,3

D. M. GRAHAM AND J. F. SOLTYS
Department of Chemistry, University of Western Ontario, London, Ontario

Received November 27, 1968

The kinetics of addition of methanethiol to acetylene and butadiene-1,3 have been investigated. The butadiene reaction exhibits no chain character due to the low reactivity of the adduct radical formed, and no rate constants could be determined. Thiyl radical addition to acetylene was found to be reversible at 25 °C, and the results obtained are consistent with the mechanism previously postulated for olefins, except that in this case, the rate of dehydrogenation of thiol by the adduct radical is comparable to the rate of radical decomposition. This competition permitted determination of the ratio of rate constants for these two reactions, and the rate constant for thiyl radical attack on acetylene.

Canadian Journal of Chemistry, 47, 2529 (1969)

Introduction

In Part II (2) it was shown that the photo-initiated addition of methanethiol to an olefin (A) could be described by the following mechanism over the concentration range available to gas phase measurements.

$$CH_3SH + h\nu \rightarrow CH_3S + H \qquad (\text{rate} = r_i)$$

[1] $$CH_3S + A \rightarrow X$$

[2] $$X + CH_3SH \rightarrow XH + CH_3S$$

[3] $$X \rightarrow A + CH_3S$$

[4] $$2CH_3S \rightarrow CH_3SSCH_3$$

Because of the reversibility of the attack step [1], only the rate constant ratio k_1k_2/k_3 is obtainable from addition rate measurements. This results from the fact that, over all experimentally feasible ranges of concentration and temperature, the rate of reaction [3] is much greater than reaction [2]. The rate constant for reaction [1] may be obtained directly only if *cis* and *trans* forms of the olefin exist (or may be synthesized by deuteration); this seriously limits any investigation of double bond reactivity where reversible attack occurs. In order to gain further insight into this problem, a kinetic study has been made of the addition of methanethiol to two different molecules, acetylene and butadiene-1,3, for which the rates of reactions [2] and [3] might differ appreciably from those for the simple olefins.

Experimental

The techniques used were as previously outlined (1, 2), except for the following differences. In order to decrease the size of the correction for non-uniform absorption of light, a shorter cell, 2 cm in length and 5 cm in diameter, was used. Addition rates were measured using a more sensitive differential pressure transducer. This gauge consists of 2 stainless-steel bellows (one for temperature compensation) connected to a linear variable differential transformer, the output of which is rectified and applied to a recorder. The gauge was found to be completely linear over a range of about 50 Torr, and its maximum sensitivity was limited by temperature control of the reaction cell thermostat. A sensitivity of 3 Torr per mV was found to be sufficient for measurement of reaction rates at conversions of less than 1%. The internal volume of the gauge and connecting tubing was less than 1% of that of the reaction flask, and no correction was made for this volume. In all cases, the relation between concentration change and pressure change was checked, over the entire concentration range of the experiments, by gas chromatography and, in some cases, by running the reaction to completion.

Mean square-root initiation rates, $\overline{r_i^{\frac{1}{2}}}$, were obtained from rates of thiyl catalyzed isomerization of *cis*-butene-2, and are ultimately related to rates of hydrogen production of pure thiol, corrected for non-uniform light absorption (1). The rate constants given here therefore are essentially relative rate constants.

Acetylene (Matheson 99.6% min.) and butadiene-1,3 (Matheson 99.5% min.) were purified by trap-to-trap distillations using the appropriate slush baths. Rates measured using samples purified by gas chromatography were identical with those obtained from the distilled compounds.

Results

Acetylene

The addition of methanethiol and ethanethiol to monosubstituted acetylenes in solution has been shown to proceed through the mono- to the di-adduct in an anti-Markownikoff manner (3–5). Although no attempt at product analysis was made in this investigation, an addition rate study carried out to completion indicated that 2 moles of thiol add to 1 mole of acetylene, and that addition to the mono-adduct is a little faster than to acetylene itself.

TABLE I

Addition to acetylene*

Methanethiol (moles l^{-1}) × 10^3	$r_i^{\pm}$ (moles l^{-1} s^{-1})$^{\pm}$ × 10^4	R_a (moles l^{-1} s^{-1}) × 10^7			
		25 °C	40 °C	55 °C	70 °C
2.15	3.36	3.24	2.32	1.72	1.37
2.69	4.00	4.40	3.28	2.36	1.85
3.76	5.00	6.62	5.58	3.58	2.78
5.38	6.18	9.54	8.94	5.66	4.72
9.14	8.90	15.3	14.6	10.9	9.78

*[Acetylene] = 2.15 × 10^{-3} moles l^{-1}.

The effect of temperature on the initial rate of addition (R_a) is shown in Table I. It is apparent from these results that the attack step [1] must be reversible since the rates decrease with increasing temperature. The overall activation energy varies from −2.1 to −4.0 kcal at 9.14 × 10^{-3} and 2.15 × 10^{-3} moles l^{-1} methanethiol, respectively.

For reversible addition the rate is given by (2)

$$[5]\quad R_a = -\frac{d[A]}{dt} = \frac{r_i^{\pm}}{(2k_4)^{\pm}} \frac{k_1[A]k_2[RSH]}{k_3 + k_2[RSH]}$$

Using calibrated screens, it was demonstrated that R_a was proportional to the half power of the incident light intensity, and hence to $r_i^{\pm}$, over the full concentration range of the results presented here. The first order dependence on acetylene is illustrated in Fig. 1. If eq. [5] holds for this reaction, a plot of $r_i^{\pm}/R_a$ against the inverse of the thiol concentration should be linear, and since k_4 is known (2), k_1 may be obtained from the intercept, and k_2/k_3 from the intercept/slope ratio. Two sets of results obtained at different acetylene concentrations are shown in Fig. 2. These give k_1 = 8.00 × 10^4 and 7.86 × 10^4 l $mole^{-1}$ s^{-1}, and k_2/k_3 = 297 and 270 l $mole^{-1}$. Inverse plots at different temperatures using the data of Table I are shown in Fig. 3. Least-square fits to this data yield scattered intercepts, and a value for E_1

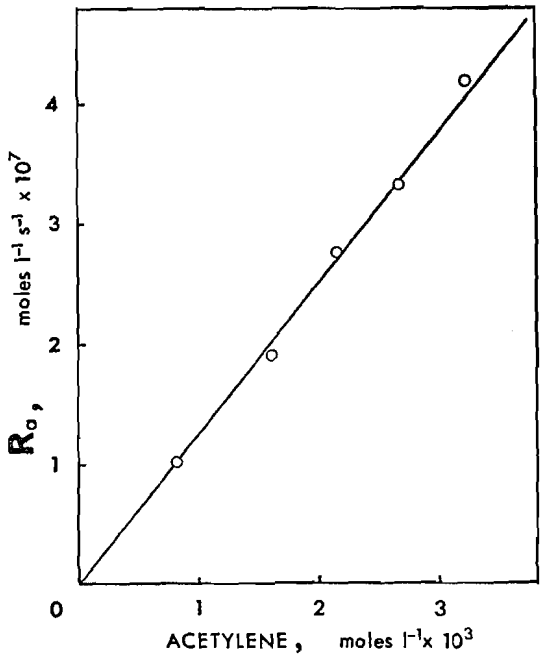

FIG. 1. Dependence of the addition rate on acetylene concentration; methanethiol = 2.69 × 10^{-3} mole l^{-1}; T = 25 °C.

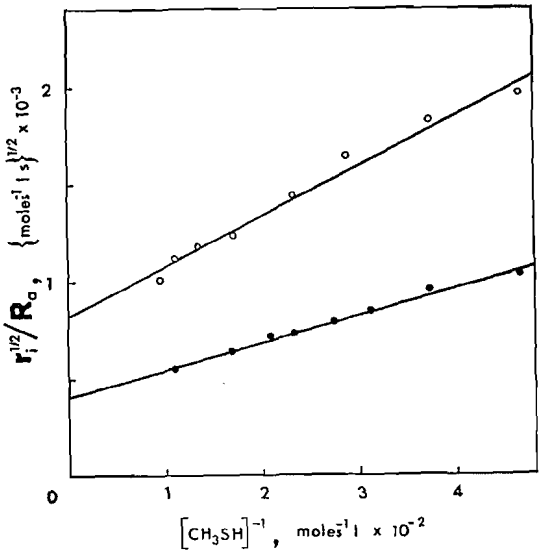

FIG. 2. Dependence of the rate of addition to acetylene on methanethiol concentration; ●, acetylene = 2.15 × 10^{-3}; ○, acetylene = 1.08 × 10^{-3} moles l^{-1}; T = 25 °C.

Can. J. Chem. Downloaded from www.nrcresearchpress.com by 210.87.254.105 on 09/05/12
For personal use only.

TABLE II

Addition to butadiene-1,3 at 25 °C

Butadiene (moles l^{-1}) × 10^3	Methanethiol (moles l^{-1}) × 10^3	R_a (moles l^{-1} s^{-1}) × 10^8	$(\overline{r_i^{\ddagger}})^2$ (moles l^{-1} s^{-1}) × 10^8	$R_a/(\overline{r_i^{\ddagger}})^2$	n*
0.161	10.8	3.32	6.64	0.50	0.99
0.538	10.8	3.36	6.64	0.50	1.00
1.08	10.8	3.24	6.64	0.49	1.00
1.61	10.8	3.32	6.64	0.50	0.98
1.61	30.7	7.00	10	0.70	0.86
1.61	8.60	2.92	6.04	0.49	1.00
1.61	6.45	2.24	5.12	0.49	—
1.61	4.30	1.72	3.49	0.49	—
1.61†	5.38	11.6	15.6	0.74	0.88
2.25†	9.02	17.8	22.0	0.81	0.84
1.35†	16.1	25.3	28	0.90	0.73
1.08	24.2	40.0	44	0.90	—
1.08	37.7	55.2	52	1.0	0.84

*n is the order dependence on light intensity.
†At 125 °C.

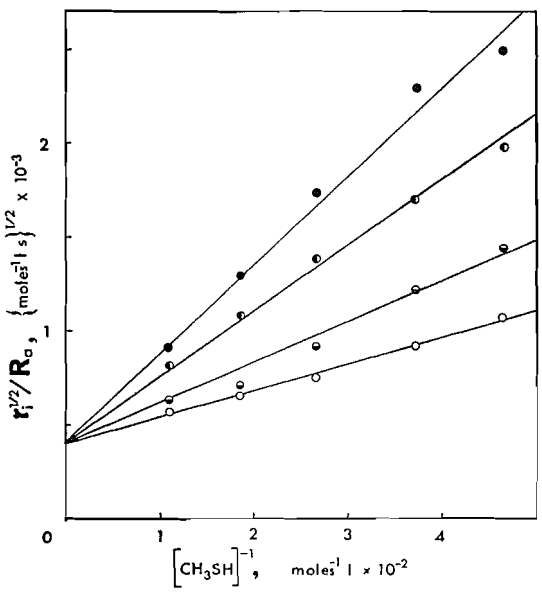

FIG. 3. Dependence of the rate of addition to acetylene on temperature; acetylene = 2.15×10^{-3} moles l^{-1}; ○, 25 °C; ◒, 40 °C; ◐, 55 °C; ●, 70 °C.

of -1.6 ± 1.3 kcal which is obviously meaningless. In order to obtain a better estimate for $E_2 - E_3$, therefore, it was assumed that $E_1 \simeq 0$, and that all intercepts were identical with that calculated using the average value of k_1 obtained at 25 °C from Fig. 2. The Arrhenius plot of the k_2/k_3 values obtained from these lines (shown in Fig. 3) is given in Fig. 4 which gives $E_2 - E_3 = -5.6$ kcal.

Butadiene-1,3

Free radical addition of simple aliphatic thiols to butadiene in solution has been found to yield predominantly the 1,4-mono-adduct with up to about 5% of the 1,2-addition product (6, 7). Gas chromatographic analysis, on a 300 ft Apiezon capillary column, of the products at low conversion of the gas phase reaction showed one broad peak and a smaller peak representing 94% and 5% of the total area, respectively. These peaks had retention times that would be expected for the adduct species. The mass spectrum of the reaction products is also consistent with the 1,4-mono-adduct being the primary product. The highest mass peaks observed were 102 and 101; the strongest peak occurred at 55, which

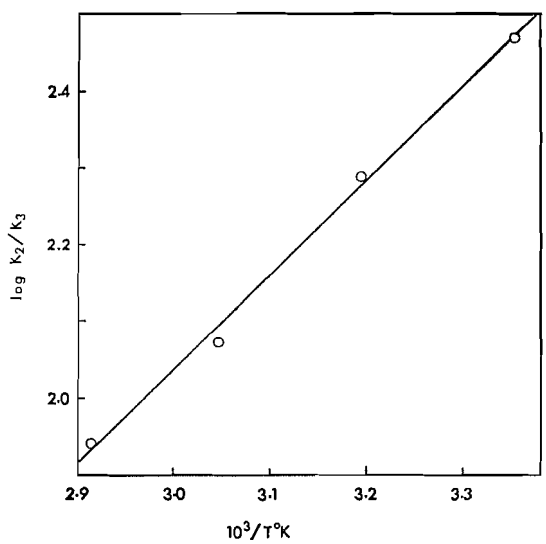

FIG. 4. Temperature variation of k_2/k_3 for acetylene.

Can. J. Chem. Downloaded from www.nrcresearchpress.com by 210.87.254.105 on 09/05/12
For personal use only.

Can. J. Chem. Downloaded from www.nrcresearchpress.com by 210.87.254.105 on 09/05/12
For personal use only.

could arise from allyl scission of the 1,4-adduct. In addition, fairly strong peaks due to 2,3-dithiabutane were seen.

The addition rate measurements are given in Table II. It is apparent that the reaction is zero order with respect to reactants, and approximately first order on the rate of thiol photolysis. This suggested the possibility that the reaction may have been occurring on the walls of the reaction vessel. In fact, during reaction, on the illuminated face of the cell, a mist was observed which disappeared immediately the light was blocked off. Heterogeneous effects probably may be eliminated however, since cleaning the cell with hydrofluoric acid, coating it with a baked film of dimethyldichlorosilane, or increasing the surface 13 times with glass-wool had no effect on the reaction rate.

The apparent chain lengths shown in the 5th column indicate that the reaction cannot properly be treated as a chain reaction. The chain length seems to increase with increasing thiol concentration and temperature, although these trends may only be apparent. Because of non-uniform initiation along the length of the cell, $(\overline{r_i^{\frac{1}{2}}})^2 \leq \overline{r_i}$, and the chain lengths may be overestimated at large thiol concentrations. Also, thermally induced reactions of butadiene may complicate the picture at the higher temperatures.

Discussion

Because of the very short chain lengths observed for butadiene, it is necessary to modify the kinetic treatment given previously to include a more detailed description of the primary initiation step. The rates of the following reactions must therefore be considered

$$CH_3SH + h\nu \rightarrow CH_3S + H \quad (\text{rate} = r_i/2)$$

[a] $$H + CH_3SH \rightarrow CH_3S + H_2$$

[b] $$H + A \rightarrow R$$

[c] $$R + CH_3SH \rightarrow RH + CH_3S$$

Addition of radicals other than thiyl to butadiene can probably be neglected since this is unlikely to be competitive with the attack on thiol. In solution, for example, the ratio of the rate constant for propagation of butadiene polymerization to that for dehydrogenation of straight chain thiols is 0.06 at 50 °C (8).

Assuming thiyl radical combination is the most important termination reaction, steady state analysis now gives the rate of addition as

$$[6] \quad R_a = \frac{(r_i/2)k_b[A]}{k_b[A] + k_a[RSH]} + \left(\frac{r_i}{2k_4}\right)^{\frac{1}{2}} \frac{k_1[A]k_2[RSH]}{k_3 + k_2[RSH]}$$

Thus, inclusion of these additional reactions introduces an extra term which is first order on light intensity. Since addition to butadiene produces an allyl-type radical, the activation energy for the reverse reaction should be about 20 kcal. The results indicate a small positive overall activation energy, and reaction [3] can probably be neglected. Hence, in the presence of butadiene, the thiyl radical population will be appreciably smaller than that for the adduct radical, X, and the main mode of termination should involve this latter species. The presence of appreciable disulfide in the reaction products, and the lower limit of 0.5 for the apparent chain length, suggest that the termination reaction should be $CH_3S + X$. Neglecting the chain propagation step [2] for the moment, and assuming the allyl radicals R and X to be kinetically indistinguishable, a steady state analysis with this termination yields $R_a = r_i/2$ which is consistent with the observed zero order kinetics. The detected addition products would appear to arise from radical combination reactions rather than from reaction [2].

As the thiol concentration or the temperature is increased, reaction [2] must become competitive with termination. This would produce an additional term in R_a proportional to $r_i^{\frac{1}{2}}$. The increase in chain length could also be due to a change in termination mechanism (X + X, for example, would yield $R_a = r_i$). However, since the increase occurs simultaneously with a decrease in the order dependence on light intensity, onset of chain propagation appears a more likely explanation.

In the case of acetylene also, low chain lengths were observed, particularly at lower thiol concentrations and higher temperatures. A more correct expression for the rate therefore would be eq. [6]. Since half-order dependence on light intensity was observed even at chain lengths less than unity, the first term of the equation must be negligible. The only way that this could occur,

Can. J. Chem. Downloaded from www.nrcresearchpress.com by 210.87.254.105 on 09/05/12
For personal use only.

which would be consistent with the kinetic measurements, would be for $k_a[\mathrm{RSH}] \gg k_b[\mathrm{A}]$. It may be crudely estimated that, over the concentration ranges used, as long as $k_a \gtrsim 3k_b$, contributions from the first term would be negligible within experimental error. The effect of the first term would be greater at higher temperatures, and could possibly produce the apparent deviation from linearity of the 70 °C results, in which case, $E_2 - E_3$ has been overestimated.

Thus butadiene and ethylene appear to be at opposite extremes. Addition to ethylene produces a very unstable radical which decomposes much more rapidly than it dehydrogenates thiol, and kinetic measurements can yield only the ratio k_1k_2/k_3, whereas addition to butadiene produces a very stable radical which reacts only very slowly with thiol, and no rate constants may be determined from rate studies. Acetylene represents an intermediate case, because the very reactive vinyl adduct radical attacks thiol at about the same rate that it decomposes. This competition allows k_1 and k_2/k_3 to be separately determined.

TABLE III

Kinetic data for reaction with methanethiol*

Reactant	$k_1k_2/k_3 \times 10^{-5}$	$k_1 \times 10^{-5}$	$E_1 + E_2 - E_3$
Acetylene	230	0.79	−5.6
Ethylene	20	4.8	−5.1
Propylene	51	—	−5.4
Butene-2	15	16†	−6.4

*Rate constants are in units of moles, l, and s; activation energies in kcal; temperature equals 25 °C.
†*cis–trans* equilibrium weighted rate constant (eq. [5], ref. 2).

For comparison, the kinetic data obtained so far are shown in Table III. In calculating the results given in Parts I and II (1, 2), a factor involving the length of the cell was inadvertently omitted in correcting for non-uniform light absorption. The corrected rate constant for thiyl radical recombination is now $2k_4 = 5.0 \times 10^9$ l mole^{-1} s^{-1} and the new values of the other rate constants are listed in Table III. In addition, the activation energy given in Part II (2) for butene-2 is in error (probably as a result of a leaky pressure gauge). The activation energies have all been redetermined using the more sensitive transducer gauge and are given in the table as well.

The lower reactivity of acetylene and the relatively small trend in k_1 values may be rationalized by postulating π-complex formation in the initial stages of attack. The zero activation energy observed for this step also is consistent with this idea. However, it is probably presumptuous to attempt to generalize at this time on the basis of only three results.

Acknowledgments

We are grateful to the National Research Council of Canada for the financial support bestowed, and to the Province of Ontario for a Fellowship awarded to J.F.S.

1. D. M. GRAHAM, R. L. MIEVILLE, and C. SIVERTZ. Can. J. Chem. **42**, 2239 (1964).
2. D. M. GRAHAM, R. L. MIEVILLE, R. H. PALLEN, and C. SIVERTZ. Can. J. Chem. **42**, 2250 (1964).
3. K. GRIESBAUM, A. A. OSWALD, E. R. QUIRAM, and W. NAEGELE. J. Org. Chem. **28**, 1952 (1963).
4. T. L. JACOBS and G. E. ILLINGWORTH, JR. J. Org. Chem. **28**, 2692 (1963).
5. A. T. BLOMQUIST and J. WOLINSKY. J. Org. Chem. **23**, 551 (1958).
6. J. LONGFIELD, R. JONES, and C. SIVERTZ. Can. J. Res. **B28**, 373 (1950).
7. A. A. OSWALD, K. GRIESBAUM, W. A. THALER, and B. E. HUDSON, JR. J. Am. Chem. Soc. **84**, 3897 (1962).
8. E. J. MEEHAN, I. M. KOLTHOFF, and P. R. SINHA. J. Polymer Sci. **16**, 471 (1955).

Can. J. Chem. Downloaded from www.nrcresearchpress.com by 210.87.254.6 on 09/05/12
For personal use only.

Kinetic study of the reduction of cobalt(II) by carbon monoxide in an aqueous system

H. N. HALVORSON
Technical Research Centre, Cominco Ltd., Trail, British Columbia

AND

E. PETERS
Department of Metallurgy, University of British Columbia, Vancouver, British Columbia

Received December 27, 1968

A study of the catalyzed reduction of cobalt(II) to metal by carbon monoxide from aqueous, ammoniacal solutions between 180 and 230 °C and from 0 to 50 atm CO is reported.

The reaction proceeds through the intermediate formation of a cobalt carbonyl anion. Under the conditions of this study this intermediate is produced homogeneously and also heterogeneously in the presence of cobalt sulfide. Metal formation occurs only in the presence of cobalt sulfide.

The stoichiometry of the production of cobalt carbonyl anion is consistent with the equation

$$2Co(NH_3)_n^{2+} + 11CO + (12 - 2n)NH_3 + 6H_2O \rightarrow 2Co(CO)_4^- + 3CO_3^{2-} + 12NH_4^+$$

Metal formation follows the stoichiometry of the equation

$$9Co(NH_3)_n^{2+} + 2Co(CO)_4^- + (32 - 9n)NH_3 + 16H_2O \xrightarrow[CoS_x]{} 11Co^0 + 8CO_3^{2-} + 32NH_4^+$$

A mechanism that is consistent with the kinetic observations is presented.

Canadian Journal of Chemistry, 47, 2535 (1969)

Introduction

Recovery of metals from aqueous leach solutions has been achieved traditionally by cementation, by electrowinning, and more recently, by displacement with reducing gases. Hydrogen has been the most commonly used gas but there has been a growing interest in the use of carbon monoxide for this application.

To assess the potential of carbon monoxide for use as a reductant in hydrometallurgy and also to gain fundamental knowledge of the mechanisms involved in such reactions, various metal ion – carbon monoxide systems have been studied. Most of this work has been done at the Department of Metallurgy at the University of British Columbia over the period 1956 to 1965.

Detailed kinetic studies of the reaction of carbon monoxide with Cu(II), Ni(II), Ag(I), Hg(II), MnO_4^-, $Cr_2O_7^{2-}$, and OH^- are reported (1–7). Briefly, these studies demonstrated that in most cases the formation of a carbon monoxide insertion complex of the type

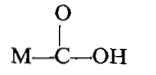

was suggested as an intermediate in the reactions. In addition, it was shown that only the most noble metals were finally obtained as metals. With nickel, only the carbonyl $Ni(CO)_4$ was obtained.

Cobalt, from thermodynamic considerations, is probably the least noble metal that can be reduced by carbon monoxide. No literature references were found for the reduction of Co(II) by carbon monoxide in aqueous systems. There are, however, many references to the formation of cobalt carbonyls in organic systems. These references demonstrate the ease of formation and the marked stability of these compounds. Therefore, if a reaction between Co(II) and carbon monoxide in aqueous medium were found to occur, it may be expected that (*1*) a cobalt carbonyl, rather than metallic cobalt might be the end product of the reaction, and (*2*) that a cobalt – carbon monoxide insertion complex might be a reaction intermediate from similarity with other CO reductions.

It was the purpose of this work to investigate the Co(II)–CO–H_2O system to determine if a reaction occurred and, if so, to establish its mechanism.

Experimental

(*a*) *Apparatus*

A 2 l Parr pressure reaction autoclave, series 4500, was used. It was of 316 stainless steel construction with a

titanium liner. Stirrer shafts were belt driven at speeds between 800 and 1000 r.p.m. Heating was provided by a ring-type burner acting as a pilot light with a bunsen burner controlled by a solenoid valve activated by a Thermistemp temperature controller, model 71. Using a thermister probe and this heating system, temperature control was maintained to within ± 0.3 °C. Reactor pressures were measured with a 1500 p.s.i. helicoid gauge.

(b) Procedure

The experimental procedure involved preparing the charge under an argon atmosphere to minimize Co(III) formation, transferring the charge to the autoclave while flushing with argon, and heating to the required temperature. Carbon monoxide partial pressure was applied and the reaction followed by taking slurry and gas samples. The total pressure in the vessel was maintained constant by admitting more carbon monoxide. At the end of the run the entire reaction vessel was quenched in cold water.

The kinetics of the reaction were determined primarily by analyzing the Co(II) content in solution of the periodic slurry samples using EDTA with murexide as indicator. Carbon monoxide, carbon dioxide, and hydrogen were determined in the gas samples using standard gas–liquid chromatography (g.l.c.) techniques. Other standard assays employed were the acid titration method for CO_3^{2-} and the acidification and distillation method for $HCOO^-$. A special technique reported by Hieber (8, 10) for $Co(CO)_4^-$ determination involving its gravimetric determination as $[Ni(1,10\text{-phenantholine})_3][Co(CO)_4]_2$ was used.

Results

1. Stoichiometry

Preliminary experiments established that Co(II) and CO did react under reasonably attainable laboratory conditions. Typical conditions established for convenient rate measurements were: 1 liter of solution (3 *M* Co(II), 1 *M* $(NH_4)_2SO_4$, and 3–5 *M* NH_3), 25 atm CO, 215 °C, and 0.06 *M* S^{2-}. Under these conditions, the reaction times were about 15 min. It was shown, however, that cobalt metal did not result from this reaction unless a catalyst was present. In the absence of this catalyst the cobalt reaction product was a cobalt carbonyl.

The catalyst found active in promoting metal formation was a cobalt sulfide formed by adding $(NH_4)_2S$ to the system. X-ray and electron diffraction patterns indicated the sulfide to be either γ-Co_6S_5 or Co_9S_8. Chemical analysis indicated that γ-Co_6S_5 was the more likely form. CoS_x and CuS were the only materials found active as catalysts for Co metal production in this system. The known homogeneous catalysts for CO – metal ion reactions, (Cu(II), Ag(I), Hg(II), and Hg_2(II)), were inactive as were Hg, Ag, Ti, Ni, and Cu metals, CdS, and the ions Fe(II), Cd(II), Ni(II), and Zn(II). Two materials, cyanide and tartrate ions, were found to catalyze the production of the cobalt carbonyl but their effect, if any, on metal formation was not established.

The presence of a cobalt carbonyl compound was established during the reaction of CO and Co(II). In the absence of CoS_x, it was the only cobalt end product of the reaction. In the presence of CoS_x, it was often observed along with cobalt metal. It was present as sparingly-soluble, white crystalline flakes, floating on the aqueous solution. If air were excluded from such mixtures, this compound was stable at room temperature and atmospheric pressure for several months. Chemical assay and infrared spectrophotometry suggested the material to be a Co(II) salt of cobalt hydrocarbonyl, i.e. $Co(NH_3)_6[Co(CO)_4]_2$. Hieber (10) describes such a compound and elsewhere (8) reports an analytical method specific for $Co(CO)_4^-$. This test confirmed that the unknown was the cobalt salt of $Co(CO)_4^-$.

To determine the role of $Co(CO)_4^-$ in the mechanism, the following two part experiment was done under conditions with which experience had shown both cobalt metal and substantial amounts of carbonyl were formed. At the end of the run the autoclave was quenched, CO gas released, and all residual CO was flushed from the vessel with N_2. The bomb was opened, fresh $CoSO_4 \cdot 7H_2O$ was added to replenish the initial $Co(NH_3)_n^{2+}$ concentration, the bomb was closed, and the charge taken to temperature where it was held without CO addition. Liquid samples were taken to see if reduction of Co(II) occurred. The result is shown in Fig. 1.

It is evident that Co(II) is reduced by $Co(CO)_4^-$. However, this experiment did not establish the role of CoS_x in this reduction. To answer this point, two additional experiments were conducted. The first of these (experiment 151) was identical to the one above except that no S^{2-} was added to either part A or B; the second (experiment 155) had CoS_x present only in part B. The rate of reduction of Co(II) is shown in Fig. 2.

Without the addition of S^{2-} to part A, only $Co(CO)_4^-$ is produced. Only when S^{2-} is added to part B does the reduction of Co(II) by $Co(CO)_4^-$ occur.

A material balance determination of both parts

Can. J. Chem. Downloaded from www.nrcresearchpress.com by 210.87.254.6 on 09/05/12
For personal use only.

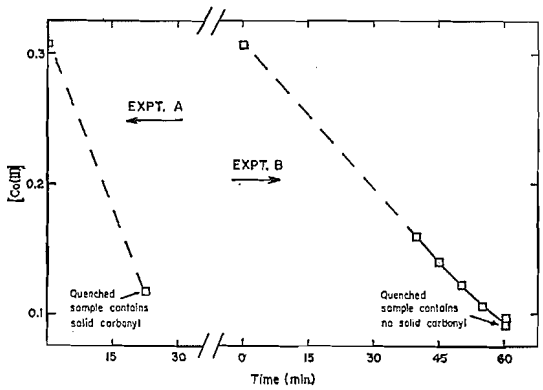

FIG. 1. Reduction of Co(II) by $Co(CO)_4^-$. *Experiment A*, production of $Co(CO)_4^-$ by reaction of CO and Co(II) in the presence of CoS_x; initial conditions: 0.046 M S^{2-}, 4.9 M NH_3, 1.1 M $(NH_4)_2SO_4$, 27.2 atm CO. *Experiment B*, reduction of Co(II) by the end products of experiment A in the absence of CO; initial conditions: 0.046 M S^{2-}, 4 M NH_3, 1.6 M $(NH_4)_2SO_4$, all reduction products from experiment A.

A and B of run 155 indicated the following stoichiometry

A. Reaction of CO with Co(II)

[1] $Co(NH_3)_n^{2+} + 5.5CO + 6NH_3 + 3H_2O \rightarrow Co(CO)_4^- + 1.5CO_3^{2-} + 6NH_4^+ + nNH_3$

B. Reaction of $Co(CO)_4^-$ with Co(II)

[2] $4.5Co(NH_3)_n^{2+} + Co(CO)_4^- + 16NH_3 + 8H_2O \xrightarrow{CoS_x} 5.5Co^0 + 4CO_3^{2-} + 16NH_4^+ + 4.5nNH_3$

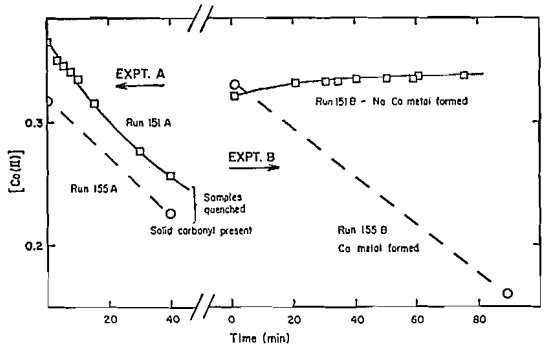

FIG. 2. Role of CoS_x in the reduction of Co(II) by $Co(CO)_4^-$. *Experiment A*, production of $Co(CO)_4$ in the absence of CoS_x; initial conditions: 1.1 M $(NH_4)_2SO_4$, 26 atm CO, 5 M NH_3, 190 °C. *Experiment B*, reactions of Co(II) with $Co(CO)_4^-$ produced in A in the absence of CoS_x (run 151 B) and in the presence of CoS_x (run 155 B); initial conditions: run 151 B: > 1.1 M $(NH_4)_2SO_4$, > 5 M NH_3, all products of experiment A, 190 °C, no S^{2-}; run 115 B: > 1.1 M $(NH_4)_2SO_4$, > 5M NH_3, all products of experiment A, 190 °C, 0.05 M S^{2-}.

The summation of eqs. [1] and [2] indicates that the overall reduction of Co(II) to metal by CO in the presence of the catalyst CoS_x should follow the stoichiometry

[3] $Co(NH_3)_n^{2+} + CO + 4NH_3 + 2H_2O \xrightarrow{CoS_x} Co^0 + CO_3^{2-} + 4NH_4^+ + nNH_3$

The comparison of the calculated stoichiometry of an overall reaction using eq. [3] and the experimental stoichiometry obtained with a typical run showed discrepancies of 9, 14, and 10% for the amount of CO consumed, NH_3 neutralized, and CO_3^{2-} produced. The agreement is sufficiently close to support the above hypothesis.

2. Kinetics

Stoichiometric studies indicated two major steps in the mechanism. Kinetic studies were used to elucidate more details of the reaction mechanism.

The rate of reduction of Co(II) was followed by determining the Co(II) content of periodically taken samples. Typical rate curves are shown in Fig. 3. Data so obtained fit no simple zero, first, or second order rate laws. It was observed, however, that maximum rates taken from zero order rate curves gave reproducible rates (maximum variation of $\pm 10\%$) and these rates were used throughout the study for evaluation of the kinetics. Using this technique, the effect on the rate of the experimental parameters was established.

Figure 4 shows the effect of the initial concentration of NH_3, $[NH_3]_i$, on the rate at three catalyst addition levels. The rate appears to be first order in initial NH_3 concentration up to about 3 M (or more correctly, for $[NH_3]_i/[Co(II)]_i < 10$) after which the reaction is independent of NH_3. By consideration of the simultaneous effect of the initial $(NH_4)_2SO_4$ and NH_3 concentration on the rate, it was established that the effect of NH_3 on the rate was due to changing the OH^- concentration and not to NH_3 complexing of Co(II). The rate determining step was, therefore, concluded to be first order in initial OH^- concentration below $[NH_3]_i/[Co(II)]_i = 10$ and to approach zero order in OH^- above this ratio.

The effect of the amount of CoS_x catalyst present was investigated at two levels of initial NH_3 concentration to determine the effect in

Can. J. Chem. Downloaded from www.nrcresearchpress.com by 210.87.254.6 on 09/05/12
For personal use only.

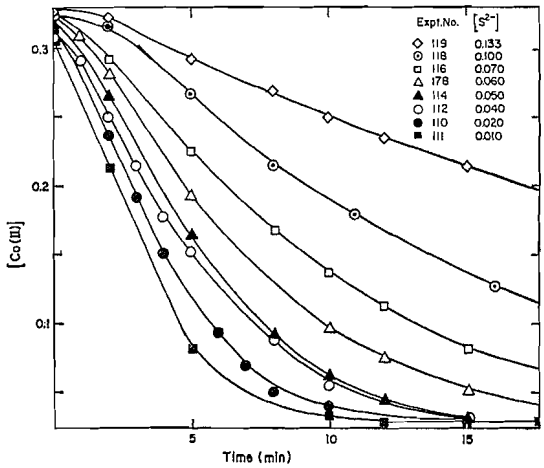

FIG. 3. Typical rate curves. Initial conditions: > 3.3 *M* NH_3, 1.1 *M* $(NH_4)_2SO_4$, 26 atm CO, 215 °C.

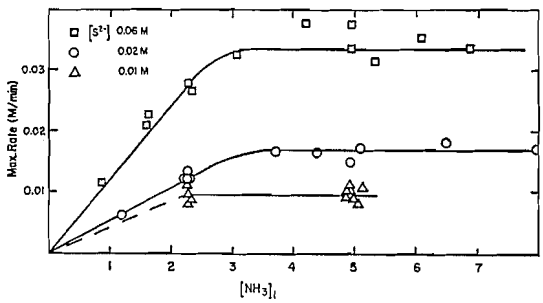

FIG. 4. Effect of initial NH_3 concentration on reduction rate at 215 °C. Initial conditions: 1.2 *M* $(NH_4)_2SO_4$, 0.31 *M* Co(II), and 26 atm CO.

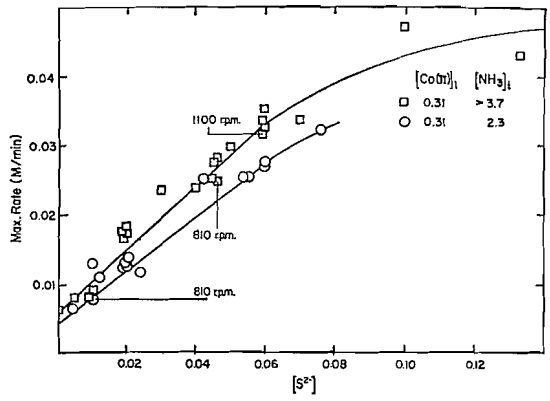

FIG. 5. Effect of S^{2-} addition on rate. Initial conditions: 1.1 *M* $(NH_4)_2SO_4$, 26 atm CO, 1005 r.p.m. stirring speed, 215 °C.

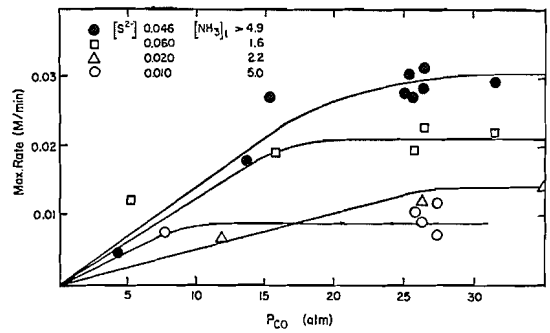

FIG. 6. Effect of initial CO pressure on rate. Initial conditions: 0.31 *M* Co(II), 1.2 *M* $(NH_4)_2SO_4$, 215 °C.

regions of zero and first order dependency on initial NH_3 concentration. The results are shown in Fig. 5. In both cases there is a measurable rate of Co(II) removal from solution in the absence of CoS_x. This is due to $Co(CO)_4^-$ formation and is sufficiently small, compared to total rates when CoS_x is present, to be ignored. With the addition of increasing amounts of S^{2-} the rate increases. A plot of log rate vs. log $[S^{2-}]$ indicated the order in S^{2-} addition to be about 0.6 to 0.7. This dependency is consistent with a linear dependency in surface area if the CoS_x particle numbers and shapes are unchanged with increasing S^{2-} concentration, but the sizes of the precipitate particles are larger.

The effect of CO pressure is shown in Fig. 6. Four series at various S^{2-} and initial NH_3 concentrations were done to check for possible interdependence of the variables. Initially the rate is apparently first order in P_{CO} but this dependency becomes zero order at high P_{CO}. The level at which the rate is independent of P_{CO} varies according to the NH_3 and S^{2-} concentrations but at the P_{CO} usually used in the study (26 atm), the rate is independent of P_{CO}.

Figure 7 demonstrates the effect of the initial Co(II) concentration. The rate determining step appears first order in initial Co(II) concentration at low levels decreasing to an apparent zero order at high levels.

The temperature dependence of the reaction was determined over the range 180–230 °C at high S^{2-} additions and at 3 different initial NH_3 levels. The corresponding Arrhenius plots are shown in Fig. 8. The calculated activation energies are within experimental error of the same value and indicate that the same mechanism is rate-

Can. J. Chem. Downloaded from www.nrcresearchpress.com by 210.87.254.6 on 09/05/12
For personal use only.

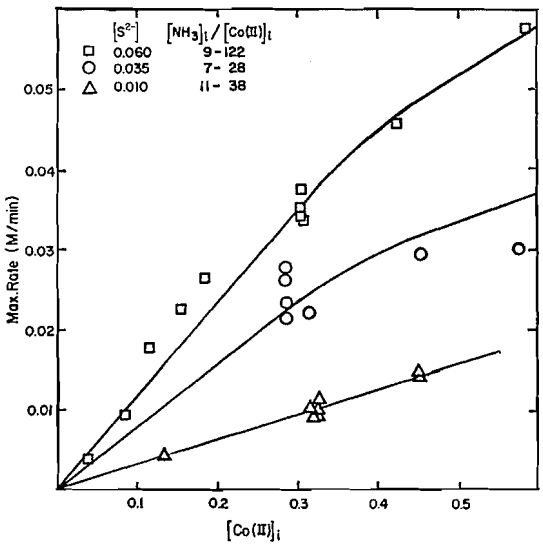

FIG. 7. Effect of initial Co(II) concentration on rate. Initial conditions: 1.1 M $(NH_4)_2SO_4$, 26 atm CO, 215 °C.

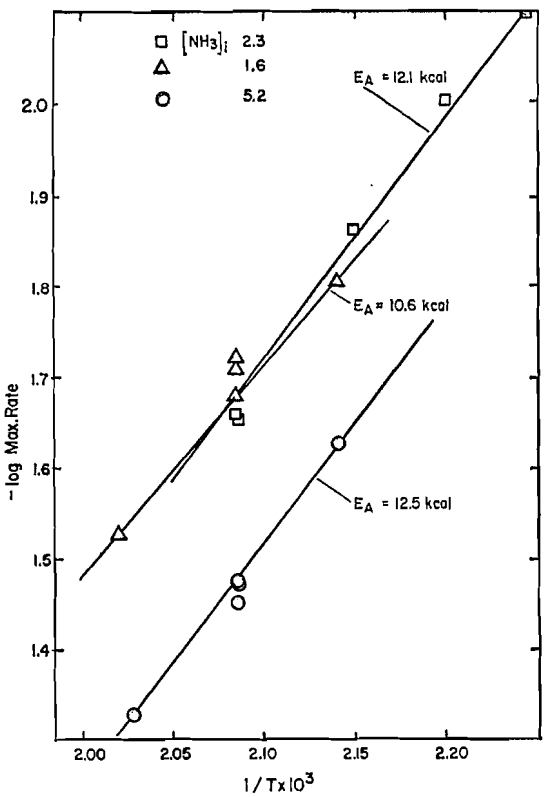

FIG. 8. Arrhenius plot. Initial conditions: 0.31 M Co(II), 0.06 M S^{2-}, 26 atm CO, 1.2 M $(NH_4)_2SO_4$.

controlling over the range of conditions used in this work, with an apparent activation energy of 11 ± 1 kcal/mole. This value is too high for diffusional mass transfer in aqueous solutions.

No dependency on the rate of stirring, or on Co(III) and CO_3^{2-} concentrations was observed. Adding Mg(II) and K(I) had no effect on the rates.

By-product formation of H_2 and $HCOO^-$ was observed in this study. Separate tests showed that $HCOO^-$ does not reduce Co(II) at an appreciable rate under the test conditions used in this study. H_2 reduction of Co(II) occurs under the conditions of this study but at a much lower rate, calculated to be equivalent to about 2% of the CO reduction rates at the H_2 pressures generated during these experiments.

To establish the effect on the rate of the presence of the Co metal produced, one recycling test was done. The procedure consisted of using the reduced solution and solids from a first run as partial feed to a second (in addition, $CoSO_4 \cdot 6H_2O$, NH_3, and H_2O were added to regain the original concentrations). The second run was, therefore, identical to the first except that CoS_x was not fresh and that Co metal was present from the start. The results of this recycling are shown in Fig. 9. The two runs have rates identical within experimental error, indicating the rate is independent of the amount of Co metal present and that

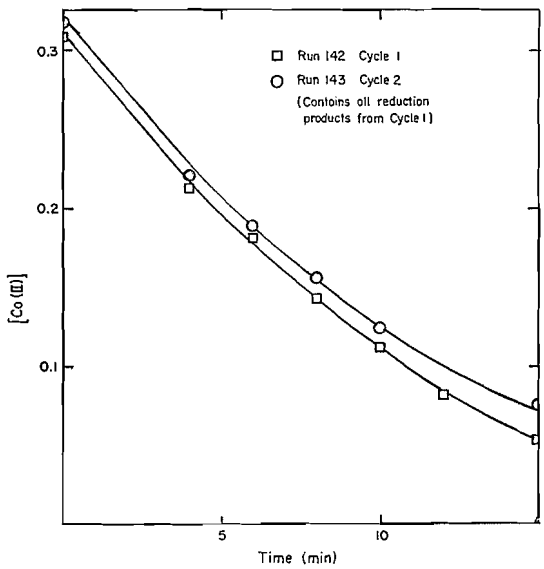

FIG. 9. Effect of recycling on rate. Initial conditions: 0.046 M S^{2-}, > 5 M NH_3, > 1.2 M $(NH_4)_2SO_4$, 26.5 atm CO, 215 °C.

Can. J. Chem. Downloaded from www.nrcresearchpress.com by 210.87.254.6 on 09/05/12
For personal use only.

Can. J. Chem. Downloaded from www.nrcresearchpress.com by 210.87.254.6 on 09/05/12
For personal use only.

the active sites on CoS_x are not destroyed by coating with Co metal. Electron microscopy partially confirmed this conclusion by indicating that the CoS_x was present as spherical particles while Co metal was present as platelets. A cobalt particle completely free of CoS_x was found.

3. Experimental Rate Law

The kinetic data produced the following experimental rate laws

Condition A

$$[4]\quad \frac{-d[Co(II)]}{dt} = k_1[OH^-][S^{2-}]^{0.6}[Co(II)]P_{CO}$$

valid for

$$0 < [NH_3]_i/[Co(II)]_i < 10$$
$$0 < [S^{2-}]$$
$$0 < P_{CO} < 26 \text{ atm}$$
$$0 < [Co(II)]_i < 0.6$$

Condition B

$$[5]\quad \frac{-d[Co(II)]}{dt} = k_2[S^{2-}]^{0.6}$$

valid for

$$[NH_3]_i/[Co(II)] > 10$$
$$0 < [S^{2-}]$$
$$P_{CO} > 26 \text{ atm}$$
$$[Co(II)]_i > 0.6$$

Conditions intermediate between *A* and *B* have not received enough experimental attention for complete resolution of a rate law.

In these rate law expressions the contribution of the homogeneous formation of $Co(CO_4)^-$ to the overall rate is omitted because it is small in comparison to the heterogeneous contribution at a finite S^{2-} addition.

Discussion

The mechanism has been shown to consist of two distinguishable stages: the formation of $Co(CO)_4^-$ and the formation of Co metal. Based on the literature, the kinetics in this present study would be expected to involve a rate-determining step consisting of the formation of a CO insertion complex. In the case of Cu(II), Ag(I), and Hg(II) similar insertion complexes react with another metallic ion resulting in reduced net valence states for the metals. In the case of Ni(II) the insertion complex reacts with further CO to form stable $Ni(CO)_4$ and no metal results. This present work indicates that Co(II) behavior is more comparable to the Ni(II) reaction than with those of the others, since a stable carbonyl also forms. This is the product of the reaction, unless a catalyst is present which permits this carbonyl to react with additional Co(II) ions forming metal, not unlike the reaction of the insertion complexes of Ag(I), Hg(II), and Cu(II). The formation of $Co(CO)_4^-$ is more complicated than that of $Ni(CO)_4$ in that the cobalt product has an awkward electronic change not obtainable through simple capture of CO molecules and normal decomposition of the Co(II) insertion complex. Rather, the cobalt – CO insertion complex must be further reduced. CoS_x is a likely vehicle for the reduction by reason of its content of metal in a variable valence.

The following assumed mechanism is consistent with both the experimental kinetics obtained and steps that would be expected in the literature

$$[6]\quad Co(NH_3)_n^{2+} + CO + NH_3 + H_2O \overset{K_1}{\rightleftharpoons} [(NH_3)_nCo{-}\overset{\overset{O}{\|}}{C}{-}OH]^+ + NH_4^+$$

$$[7]^1\quad [(NH_3)_nCo{-}\overset{\overset{O}{\|}}{C}{-}OH]^+ + C_S \xrightarrow{k_r} [(NH_3)_nCo{-}\overset{\overset{O}{\|}}{C}{-}OH]^+_{ads}$$

$$[8]^1\quad [(NH_3)_nCo{-}\overset{\overset{O}{\|}}{C}{-}OH]^+_{ads} + CoS_x \xrightarrow[\text{fast}]{} [(NH_3)_nCo{-}\overset{\overset{O}{\|}}{C}{-}OH]^0_{ads} + CoS_x^+$$

cathodic reaction

[1]Reactions [8] and [10] are coupled; i.e., as they occur stoichiometric with respect to each other, there is no net change in the electronic charge of CoS_x. Similarly eqs. [7] and [9] are coupled to maintain a constant concentration of vacant adsorption sites C_2 on the surface of CoS_x particles.

Can. J. Chem. Downloaded from www.nrcresearchpress.com by 210.87.254.6 on 09/05/12
For personal use only.

$$[9] \quad [(NH_3)_nCo{-}\overset{\overset{O}{\|}}{C}{-}OH]^0_{ads} \xrightarrow{k_{r_1}} [(NH_3)_nCo{-}\overset{\overset{O}{\|}}{C}{-}OH]^0 + C_S$$

$$[10]^1 \quad CoS_x^+ + \tfrac{1}{2}CO + 2NH_3 + H_2O \xrightarrow[\text{fast}]{} CoS_x + \tfrac{1}{2}CO_3^{2-} + 2NH_4^+$$

anodic reaction

$$[11] \quad [(NH_3)_nCo{-}\overset{\overset{O}{\|}}{C}{-}OH]^0 + 4CO + (3-n)NH_3 + H_2O \xrightarrow[\text{fast}]{} Co(CO)_4^- + CO_3^{2-} + 3NH_4^+$$

$$[12] \quad Co(CO)_4^- + 4.5Co(NH_3)_n^{2+} + (16 - 4.5n)NH_3 + 8H_2O \xrightarrow[\text{fast}]{CoS_x} 5.5Co^0 + 4CO_3^{2-} + 16NH_4^+$$

where CoS_x^+ denotes the removal of an electron from a CoS_x crystal. Adjustments in the charged double layer on the CoS_x crystal can neutralize the change in charge with a negligible change in potential for each electron.

Experimentally, the CoS_x surface can be considered as playing two independent roles. The first is to act as an electron source for adjusting the valence of Co during conversion from the insertion complex

$$[(NH_3)_n\,Co{-}\overset{\overset{O}{\|}}{C}{-}OH]^+$$

to the carbonyl anion $Co(CO)_4^-$. CoS_x is not necessary for this to occur but the rate is much faster in its presence. The second is to provide a path for metal crystal formation from $Co(CO)_4^-$ ions and unreduced Co(II) species.

Equation [12] is the overall stoichiometric statement for metal formation. It can be subdivided in several alternate ways, depending on whether the catalyst CoS_x can only exchange electrons or can also add or release cobalt atoms. Eventually, metal nucleation and growth is probably the result of homogeneous decomposition of the species $Co_4(CO)_{12}$, viz.

$$2Co_4(CO)_{12} \rightarrow 2Co^0 + 3Co_2(CO)_8$$

This would mean the above equation would generate $Co_4(CO)_{12}$ on the CoS_x surface utilizing a combination of $Co(CO)_4^-$ (ads), $Co_2(CO)_8$, and $Co(NH_3)_4^{2+}$ for this purpose.

Alternative metal deposition equations require the loss of carbon monoxide in homogeneous reaction. It has already been shown that all carbon monoxide initially in the form of $Co(CO)_4^-$ is oxidized. This could not happen if it was not returned to the surface as some cobalt carbonyl species such as $Co_2(CO)_8$.

The absence of cobalt metal on the catalyst surface precludes a mechanism as simple as eq. [12] seems to suggest, i.e. not involving additional carbonyl compounds of cobalt not shown in the stoichiometry.

In the mechanism as shown, if the assumption is made that $k_r > k_{r_1}$ for high values of P_{CO_i}, $[NH_3]_i/[Co(II)]_i$, and $[Co(II)]_i$ and $k_r < k_{r_1}$ for low values of P_{CO_i}, $[NH_3]_i/[Co(II)]_i$, and $[Co(II)]_i$, then adsorption of the cobalt insertion complex on the CoS_x surface (eq. [7]) becomes rate determining at low reactant concentrations, while the desorption of the reduced insertion complex (eq. [9]) is rate determining at high reactant concentrations.

If the reaction shown in eq. [7] is rate determining, the rate of reduction is given by

$$[13] \quad \frac{-d[Co(II)]}{dt} = \theta k_r \frac{K_1}{K_2}[Co(II)]P_{CO}[OH^-][S^{2-}]^{0.6}$$

where θ is the proportionality constant relating the amount of CoS_x present and the number of active adsorption sites and

$$K_2 = \frac{[NH_4^+][OH^-]}{NH_3}$$

Equation [13] is identical to eq. [4], the experimental rate law for low reactant concentrations, if

$$k_1 = \frac{\theta k_r K_1}{K_2}$$

If the rate determining step is that given by

eq. [9], then the rate of reduction is given simply by

$$[14] \qquad \frac{-d[Co(II)]}{dt} = \theta_1 k_{r_1}[S^{2-}]^{0.6}$$

where θ_1 is the proportionality constant relating the amount of CoS_x present with the number of sites available for adsorption. Equation [14] is identical to eq. [5], the experimental rate law at high reactant concentrations, if $k_2 = \theta k_{r_1}$.

From the experimental data, the values of k_1 and k_2 were determined. The value of k_1 was found to be about 3.3×10^4 l^2 mole^{-2} and k_2 to be about 0.39/min. From the literature K_2 is reported to be 2×10^{-6} moles/l at 215 °C. Using these values and the integrated forms of eqs. [13] and [14], it is possible to calculate reduction rate curves. Such calculated curves are compared with experimental rate curves in Figs. 10 and 11. The agreement between calculated and experimental curves is considered sufficiently good in both cases to support the mechanism.

Conclusions

In ammoniacal solutions in the temperature range 180 to 230 °C and CO pressures from 0 to 50 atm, the reduction of Co(II) to metal by CO in aqueous solution is found to proceed through the formation of $Co(CO)_4^-$ as an intermediate step. The production of metal results from the reduction of $Co(NH_3)_n^{2+}$ by $Co(CO)_4^-$. CoS_x catalyzes both steps of the overall reaction. $Co(CO)_4^-$ can be produced by a homogeneous step but at a much slower rate than when CoS_x is present. The rate determining step at low reactant concentrations is postulated to be the adsorption of a CO insertion complex of $Co(NH_3)_n^{2+}$ on a CoS_x surface. At high reactant concentrations the rate determining step is postulated to be the desorption of the reduced insertion complex. A mechanism consistent with the experimental rate measurements can be postulated involving these steps. A contribution to the overall rate by a homogeneous step for the production of $Co(CO)_4^-$ is neglected. The role of the cobalt sulfide catalyst is supposed to be electrochemical in that it acts as a source and sink for electrons so that otherwise awkward

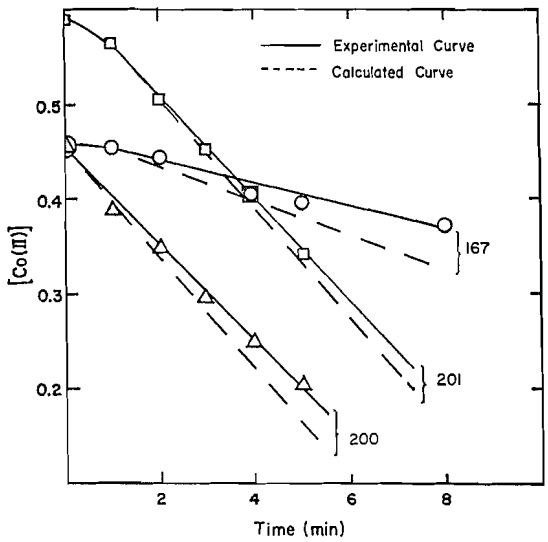

FIG. 10. Comparison of calculated and experimental rate curves in the region of high initial concentrations of NH_3, Co(II), and P_{CO}. ○, experiment number 167: $[NH_3]_i$, 7.25; $[S^{2-}]$, 0.01; P_{CO}, 27.9; error in rate, 35%; Δ, experiment number 200: $[NH_3]_i$, 5.20; $[S^{2-}]$, 0.06; P_{CO}, 27.2; error in rate, 20%; □, experiment number 201: $[NH_3]_i$, 5.20; $[S^{2-}]$, 0.06; P_{CO}, 27.2; error in rate, 5%. Rate should obey equation

$$[Co(NH_3)_n^{2+}] = -\theta_1 k_{r_1}[S^{2-}]^{0.6}t + [Co(NH_3)_n^{2+}]_i$$

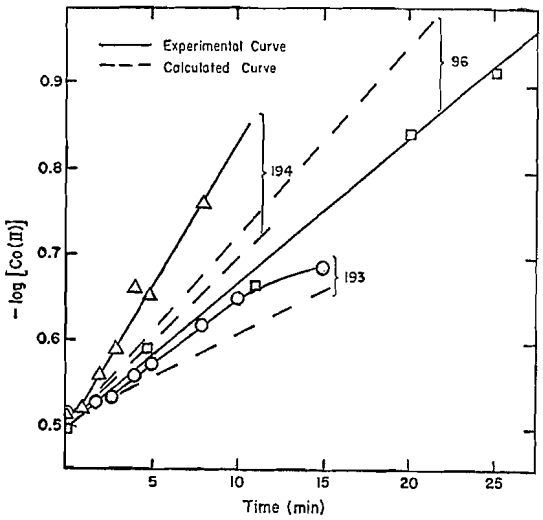

FIG. 11. Comparison of calculated and experimental rate curves in region of low initial reactant concentrations. □, experiment number 96: $[OH^-]$, 14.0×10^{-7}; $[S^{2-}]$, 0.03; P_{CO}, 11.9; error in rate, 35%; ○, experiment number 193: $[OH^-]$, 8.7×10^{-7}; $[S^{2-}]$, 0.06; P_{CO}, 5.3; error in rate, 44%; Δ, experiment number 194: $[OH^-]$, 8.7×10^{-7}; $[S^{2-}]$, 0.03; P_{CO}, 15.6; error in rate, 44%. Rate should obey equation

$$\log [Co(NH_3)_n^{2+}] = \frac{k_r \theta K_1}{2.3K_2}[OH^-][S^{2-}]^{0.6} P_{CO}\, t + \log [Co(NH_3)_n^{2+}]_i$$

Can. J. Chem. Downloaded from www.nrcresearchpress.com by 210.87.254.6 on 09/05/12
For personal use only.

charge changes in reacting species are accommodated.

CO reacts with OH^- to form $HCOO^-$ which in the presence of CoS_x reacts to form H_2. Under the conditions used in this work CO is a more effective reductant for Co(II) than is H_2.

1. A. C. HARKNESS. Kinetics of some oxidation-reduction reactions in aqueous solutions. Ph.D. Thesis, Department of Chemistry, University of British Columbia, Vancouver, British Columbia. 1963.
2. S. NAKAMURA. Reduction of silver ammine complexes by CO. M.Sc. Thesis, Department of Chemistry, University of British Columbia, Vancouver, British Columbia. 1962.
3. R. T. MCANDREW and E. PETERS. Can. Met. Quart. **3**, 153 (1964).
4. J. J. BYERLEY and E. PETERS. *In* Unit processes in hydrometallurgy. AIME, Met. Soc. Conf. Vol. 24. Gordon and Breach Science Publishers, New York. 1964. p. 183–203.
5. E. HIRSCH and E. PETERS. Can. Met. Quart. **3**, 137 (1964).
6. R. D. MCDONALD. The kinetics of CO adsorption in basic solutions at elevated temperatures. M.Sc. Thesis, Department of Metallurgy, University of British Columbia, Vancouver, British Columbia. 1963.
7. R. ROYEN. Erdol u. Kohle, **9**, 19 (1956).
8. W. HIEBER and H. FRAENKEL. Chem. Ber. **86**, 710 (1953).
9. I. WENDER. Anal. Chem. **24**, 174 (1952).
10. W. HIEBER. Z. Anorg. Allgem. Chem. **240**, 261 (1939); Chem. Abstr. **33**, 3285[5] (1939).

Can. J. Chem. Downloaded from www.nrcresearchpress.com by 210.87.254.6 on 09/05/12
For personal use only.

Can. J. Chem. Downloaded from www.nrcresearchpress.com by 210.87.254.42 on 09/05/12
For personal use only.

Infrared study of the interactions of acetone and siliceous surfaces

J. C. McManus, Yoshio Harano, and M. J. D. Low
Department of Chemistry, New York University, New York 10453

Received November 13, 1968

Adsorbed acetone is held to silica surfaces by hydrogen bonds between surface silanols and the acetone carbonyl groups. Acetone is adsorbed by this mechanism on porous glass surfaces but there is also some decomposition, as shown by the increase in surface B—OH groups and by formation of new C—H absorptions at 2984 and 2940 cm^{-1}. Experiments with boron-impregnated silica indicated that the presence of boron in the porous glass can account for this decomposition process. Bands at 1660–1670 and 1650 cm^{-1}, observed when acetone and acetone-d_6, respectively, were adsorbed on either porous glass or boron-impregnated silica, are attributed to ν(C=O) of the carbonyl group coordinated with a surface boron atom. The surface hydroxyls of both silica and porous glass could exchange with the deuterium of acetone-d_6 via a mechanism involving an enol intermediate.

Canadian Journal of Chemistry, 47, 2545 (1969)

Introduction

Recent work has shown that many of the differences in the surface properties of porous glass and pure silica can be attributed to the minority constituents on the glass (1, 2). Pure silica is relatively inert, but can be made "active," so that it resembles porous glass in behavior, by impregnating the silica with oxides such as alumina or boria. As much of the recent infrared (i.r.) work had been carried out with water (3) and nitrogenous compounds (4–6), it was thought desirable to extend the studies to oxygen-containing adsorbates such as methanol (7) and acetone, so that information would be available on the reactions of adsorbates having different "functional groups".

The present paper describes our attempts to characterize the interactions of acetone with porous glass and some silicas by i.r. techniques. The acetone – porous glass system has been examined previously (8, 9), but the studies were brief. Also, i.r. studies involving adsorbates such as acetone are fraught with difficulty because there is always the possibility that grease may be transported from joints onto the adsorbent surface. In the present experiments we approached this problem by using acetone and acetone-d_6 which were purified and stored in a grease-free system. Work with isotopic acetone not only gave more reliability to the results but also enabled the interactions to be more fully characterized.

Experimental

Acetone ("Baker Analysed"), acetone-d_6 (Stohler Isotope Chemicals, 99% D), and 1,1,3-trifluorotrichloroacetone (Aldrich Chemical Co.) were stored and purified in a section of the apparatus made entirely from glass and Teflon stopcocks. These adsorbates were dried *in vacuo* over either anhydrous copper or calcium sulfates and degassed by freeze–pump–thaw cycles until no pressure burst was evident on the Pirani gauge. Infrared spectra of acetone and acetone-d_6 in both the gas and liquid phase showed excellent agreement with the data of Dellepiane and Overend (10). Corning Grade 7930 porous glass was used in the form of 1 mm-thick plates. Thinner, ground samples (approx. 0.2 mm) were used in some experiments. Other samples were self-supporting discs of Cab-O-Sil (Cab-O-Sil M5 Silica, supplied by G. Cabot, Boston, Mass.), and of Cab-O-Sil impregnated with either 1% of boron or 1% of aluminium by the incipient-wetness method. All samples were outgassed *in vacuo* at 600° for 3 h, heated in 50 Torr oxygen for 6 h at 600°, and then degassed for 12 h at 800°.

Spectra were recorded with a Perkin–Elmer Model 621 spectrophotometer, using ordinate and abscissa scale expansion as required. A reference cell was always used to compensate for the absorptions of the atmosphere and the gaseous adsorbate.

Results and Discussion

A large number of experiments were carried out with various adsorbents. Each of these had its complexities and a number of reactions were observed. Thus, for the sake of simplicity, a summary of the bands of adsorbed acetone and their assignments is given in Table I, and each of the adsorbents is considered in turn.

Cab-O-Sil Silica

The reaction of acetone and also of acetone-d_6 with pressed Cab-O-Sil pellets was studied to evaluate the contribution of silica to the activity of porous glass. Figure 1 shows the results of the interaction of acetone with deuteroxylated Cab-O-Sil. Our results for acetone adsorption on

TABLE I

Summary of bands and assignments

Cab-O-Sil (cm^{-1})	B-impregnated Cab-O-Sil (cm^{-1})	Al-impregnated Cab-O-Sil (cm^{-1})	Porous glass (cm^{-1})	Assignment	
3745	3745	3745	3745	ν(O—H)	Si—OH
	3703		3703	ν(O—H)	B—OH
			3410	2ν(C═O)	Acetone
3400	3400	3400	3400	ν(OH···O═C)	H-bonding
			3390	2ν(C═O)	Acetone-d_6
3003	3001	3005–3000	3003	ν(C—H)	Acetone
2960	2970–2960	2975–2960			
2926	2925	2924–2917	2927		
3003	3001	2960	3003	ν(C—H)	Decomposition products
	2982		2984		
	2940		2940		
2761	2761		2761	ν(O—D)	Si—OD
	2727		2727	ν(O—D)	B—OD
2500	2540–2510		2520–2500	ν(OD···O═C)	H-bonding
2260	2254		2260	ν(C—D)	Acetone-d_6
2224	2225		2220		
	2236–2233		2236	ν(C—D)	Decomposition product
1711	1707	1692	1710	ν(C═O)	Acetone
1700	1700		1700	ν(C═O)	Acetone-d_6
	1661		1670–1665	ν(C···O → B)	Acetone, coordinated
	1650		1650	ν(C···O → B)	Acetone-d_6, coordinated
1415				$\delta_a(CH_3)$	Acetone
1360				$\delta_s(CH_3)$	Acetone

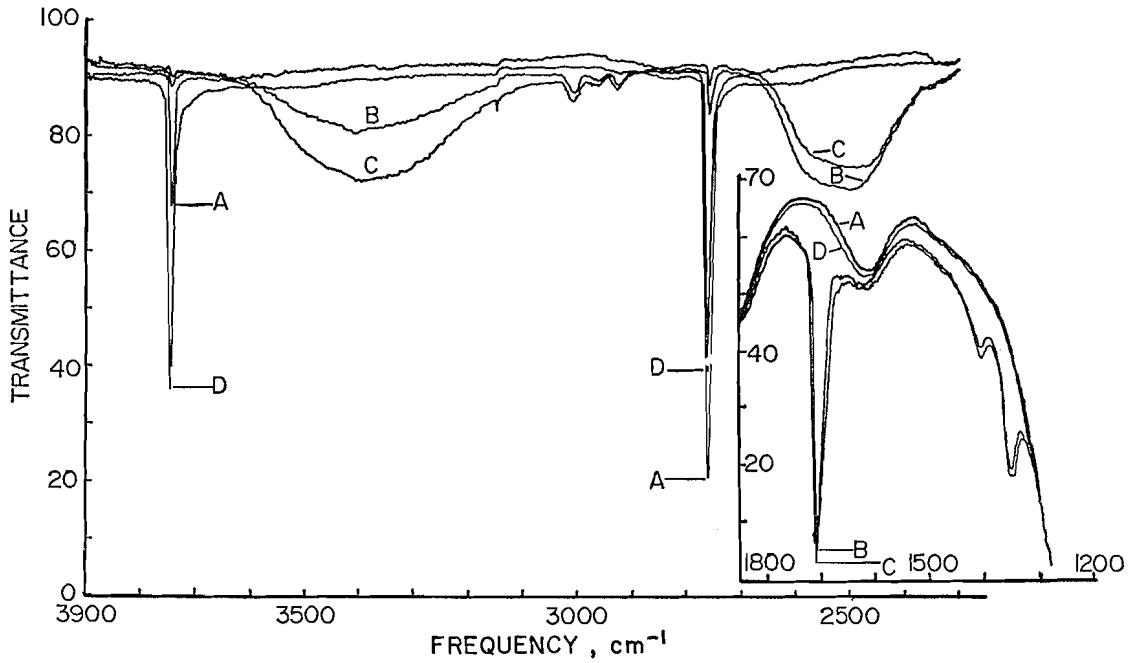

FIG. 1. Acetone sorption on deuterated silica. A: after deuteration and degassing at 800°; B: after exposure to 20 Torr acetone; C: after 3 h exposure to 20 Torr acetone; D: after leaving the cell isolated for 14 h and then evacuating for 50 min at 25°.

Can. J. Chem. Downloaded from www.nrcresearchpress.com by 210.87.254.42 on 09/05/12
For personal use only.

hydroxylated and deuteroxylated Cab-O-Sil surfaces showed that, in the main, acetone was held to the surface by a hydrogen-bonding mechanism involving surface silanol groups and the carbonyl grouping of acetone. This is in agreement with the work of Young and Sheppard (11). In addition to the bands due to "perturbed" hydroxyls at 3400 cm^{-1} and adsorbed acetone at 3003, 2960, 2926, and 1711 cm^{-1} observed by those workers, we obtained absorption bands at 1415 and 1360 cm^{-1}. These latter bands were in a similar position to those respectively observed for the asymmetric and symmetric CH_3 deformation vibrations of acetone (10) and, since they were not observed when acetone-d_6 was adsorbed, we believe that these vibrations are the cause of the absorptions. The position of ν(C=O) was insensitive to surface coverage and remained constant to ± 1 cm^{-1} over the absorbance range 0.1–0.9 during adsorption and desorption. The other bands of adsorbed acetone showed similar behavior. Like Young and Sheppard, we were unable to detect the splitting of ν(C=O) reported by Bertoluzza *et al.* (12).

After 30 min evacuation at room temperature, no bands due to adsorbed acetone could be observed and the concentration and type of silanol groups appeared to be unchanged from the initial state. This was found for samples outgassed in the range 450–800°. However, in many experiments, a small band (approx. 1% absorption) was detected at 3003 cm^{-1} when no absorption due to ν(C=O) could be observed. This band was not observed when the sample was treated with acetone-d_6 but no band was observed in the ν(C—D) region either. However, extinction coefficients of C—D absorptions are smaller

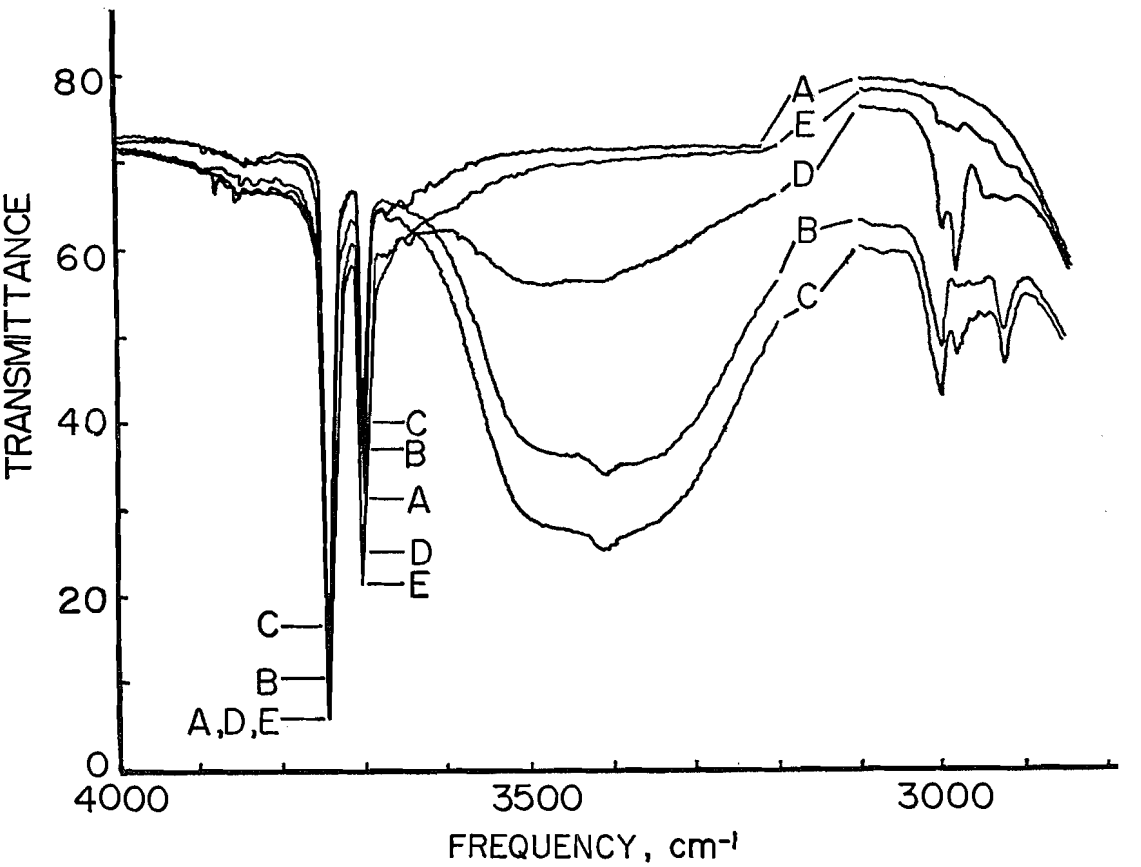

FIG. 2. Acetone sorption on porous glass. A: after outgassing at 840°; B: after exposure to 17 Torr acetone; C: after exposure for 1 h to 17 Torr acetone; D: after 14 h degassing at 25°; E: after 30 min degassing at 170°. The ordinates of spectra A, E, and D were displaced in the 3100–2800 cm^{-1} region to prevent overlapping.

Can. J. Chem. Downloaded from www.nrcresearchpress.com by 210.87.254.42 on 09/05/12
For personal use only.

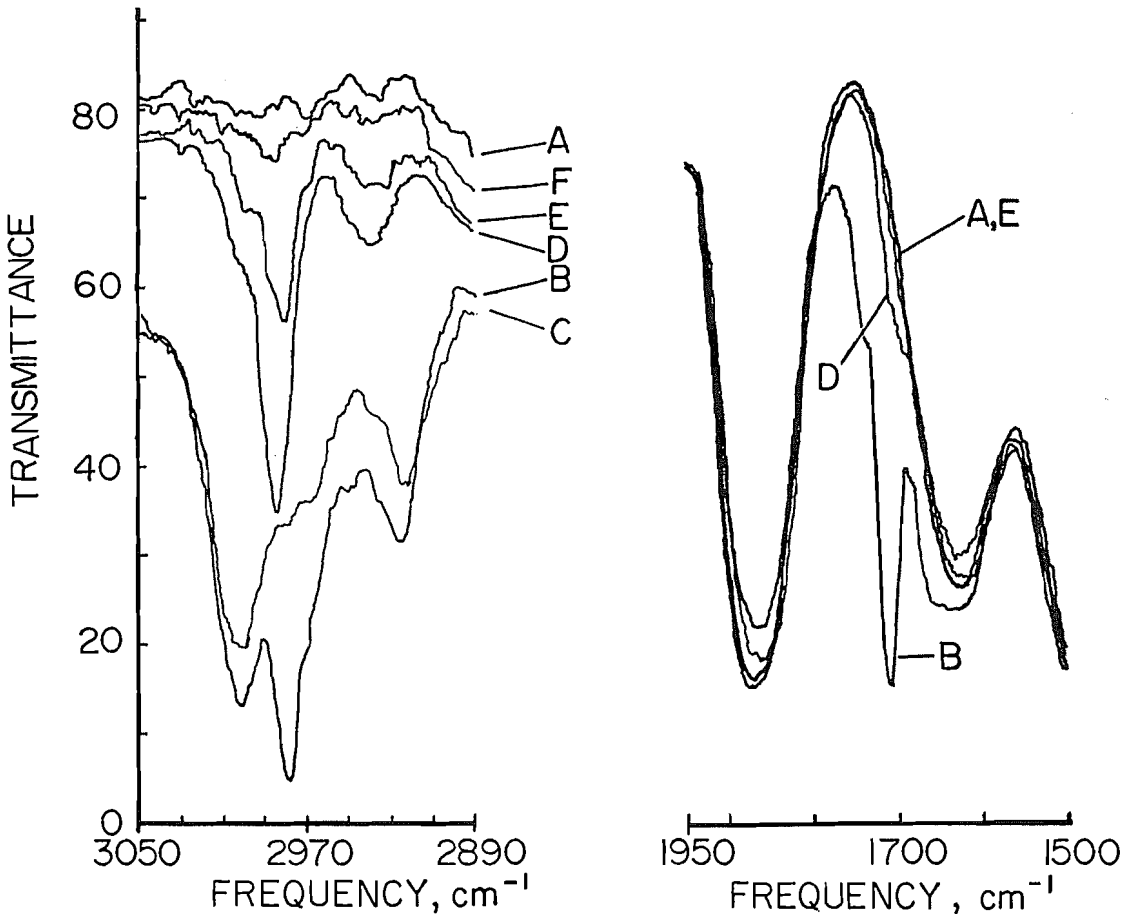

FIG. 3. Acetone sorption on thin porous glass. A: after outgassing at 800°; B: after exposure to 25 Torr acetone; C: 13 h after the addition of acetone; D: after 4 h degassing at 25°; E: after 30 min degassing at 70°; F: after 30 min degassing at 165°. For the 3050–2890 cm^{-1} region, 2.5-fold abscissa and 5-fold ordinate scale expansions were used. For the 1950–1500 cm^{-1} region, screen compensation with the 2× slit program (256 μ at 1800 cm^{-1}) was used.

than those of the corresponding C—H absorptions. The presence of this C—H band was briefly mentioned by Young and Sheppard. It seems unlikely that the 3003 cm^{-1} band was due to residual acetone because of the failure to observe ν(C═O). The species responsible for the absorption did not desorb until degassing temperatures of 90° were used and its exact nature remains uncertain. Figure 1 clearly shows that exchange between surface deuteroxyl groups and hydrogen in the acetone occurred, but discussion of this is left until later.

Porous Glass

As can be seen from Fig. 2, the main interaction of acetone with porous glass surfaces involved hydrogen-bonding between surface hydroxyls and the acetone carbonyl groups. The interaction was very similar in magnitude to that observed with Cab-O-Sil. The bands at 3745 and 3703 cm^{-1} are due to "free" Si—OH and B—OH groups (1, 2) respectively. When thick samples of high surface area were used, a band at 3410 cm^{-1}, superimposed on the broad absorption, was observed. The 3410 cm^{-1} band is attributed to the first overtone of ν(C═O). Both Figs. 2 and 3 show that, when porous glass was initially exposed to acetone, bands could be observed at 3003 and 2927 cm^{-1}. However, when the acetone remained in contact with the surface, a new band formed at 2984 cm^{-1}. Evacuation at room temperature for 30 min removed much of the hydro-

Can. J. Chem. Downloaded from www.nrcresearchpress.com by 210.87.254.42 on 09/05/12
For personal use only.

Can. J. Chem. Downloaded from www.nrcresearchpress.com by 210.87.254.42 on 09/05/12
For personal use only.

gen-bonded acetone, but the band at 2984 cm^{-1} was little affected. This treatment revealed a new band at 2940 cm^{-1} (which was probably obscured at higher coverage by the acetone C—H bands), and the intensity of the 3703 cm^{-1} B—OH band increased. These facts suggest that, apart from reversible adsorption, some chemisorption had also taken place. We were unable to observe a band at 2960 cm^{-1} to correspond with that observed when acetone was adsorbed on Cab-O-Sil. Figure 1 shows that that band was weak, and we therefore believe that it was probably obscured by other C—H absorptions (including possible small contributions at 2984 and 2940 cm^{-1}).

The spectra below 2000 cm^{-1} in Fig. 3 were obtained with a 0.2 mm-thick sample using a slit program wider (256 μ at 1800 cm^{-1}) than normally required, together with a scanning speed of 20 cm^{-1} per min and 2.5-fold abscissa expansion; the reference beam was attenuated with a wire screen. The absorption due to ν(C═O) is clearly revealed at 1710 cm^{-1}. However, making allowance for the background, a plot of absorbance vs. wavenumber for trace B in Fig. 3 indicates the presence of a band at 1665–1670 cm^{-1}. The experimental difficulties were quite large, but further evidence tends to substantiate this observation. Figure 3 shows that, in contrast to Cab-O-Sil, the ν(C═O) band did not entirely disappear until the sample had been degassed at 70°. Even so, it is evident that the absorptions at 2984 and 2940 cm^{-1} and at least some of the absorption at 3003 cm^{-1} were not related to ν(C═O), but show the presence of a new product or products. Degassing temperatures of 150° were required to remove these bands. Also, results for acetone-d_6 adsorption on porous glass could be satisfactorily compared with the acetone – porous glass system. Figure 4 shows that, initially, hydrogen-bonded acetone-d_6 was present on the surface, the C—D bands at 2260 and 2220 cm^{-1} being similar in position to those of liquid acetone-d_6, while the first overtone of ν(C═O) was shifted to 3390 cm^{-1}. However, some decomposition process is indicated; 18 h after the addition of the acetone-d_6 the lower-frequency C—D band shifted to 2230 cm^{-1} and, while degassing at 50° removed most of the hydrogen-bonded material, a pronounced band remained at 2236 cm^{-1}. We think that this band is due to a product similar in nature to that responsible for the absorption at 2984 cm^{-1} observed with the acetone – porous glass system. At no time were bands observed in the ν(C—H) region. Figure 4 also shows that exchange had occurred between the surface OH groups on porous glass surfaces and the deuterium in acetone-d_6, but discussion of this is deferred. Experiments with thin porous glass samples (Fig. 5) showed that ν (C═O) had its maximum absorption at 1700 cm^{-1}. The lowering in wavenumber (also observed for the acetone-d_6 – Cab-O-Sil system) of the band-head position compared to acetone may be caused by the heavier reduced mass of the acetone-d_6 molecule. Plots of absorbance vs. wavenumber again revealed the presence of a second, weaker band at 1650 cm^{-1}, which is 15 cm^{-1} lower than that found for acetone.

Impregnated Silicas

The effects of surface boron on adsorption properties were studied using a self-supporting disc of Cab-O-Sil containing 1% boron. The results given in Fig. 6 show that boron-impregnated silica behaved very much like porous glass. There was evidence for much acetone held by hydrogen-bonding forces to surface hydroxyls, but decomposition products which absorbed at 3001, 2982, and 2940 cm^{-1} were observed as with porous glass, and the concentration of B—OH groups increased. Similarly, as with the acetone-d_6 – porous glass system, a decomposition product which absorbed at 2236 cm^{-1} was observed. In addition to these findings, strong absorptions were observed at 1661 and 1650 cm^{-1} when pressures greater than 10 Torr acetone and acetone-d_6 respectively were in contact with boron-impregnated silica. Thus it seems that the presence of boron can account for all the observable differences between porous glass and silica. To see if aluminium acted in a similar way, some experiments were carried out with a Cab-O-Sil pellet containing 1% aluminium. These showed that some acetone was adsorbed by a hydrogen-bonding mechanism, but much of the acetone decomposed, as would be expected from the results of Hair and Chapman (13). The decomposition product gave a strong absorption at 2960 cm^{-1}. A similar product was not observed on porous glass, indicating that while a similar reaction involving aluminium is not ruled out, aluminium can play only a minor role compared to boron.

Can. J. Chem. Downloaded from www.nrcresearchpress.com by 210.87.254.42 on 09/05/12
For personal use only.

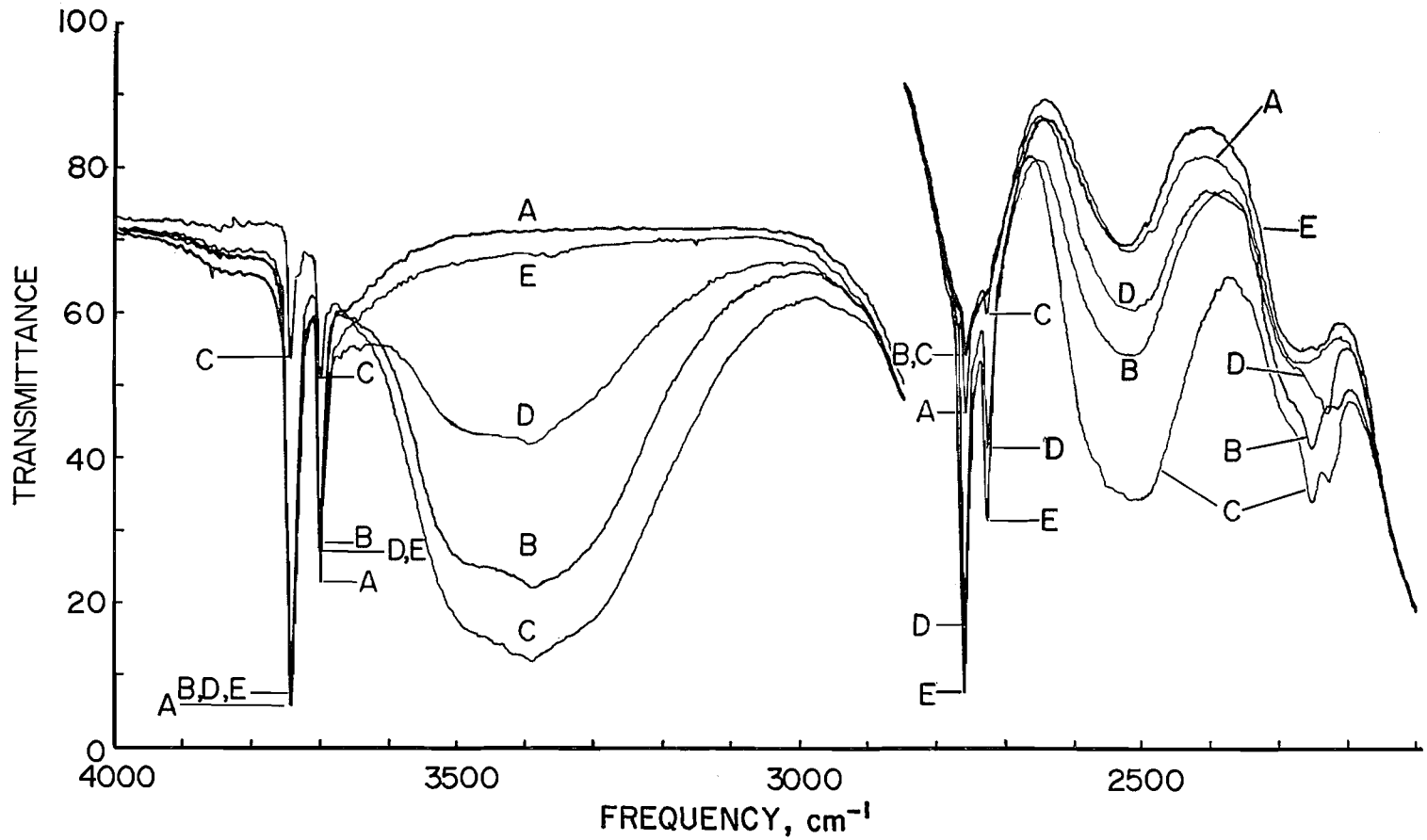

FIG. 4. Acetone-d_6 sorption on porous glass. A: after degassing at 800°; B: after exposure to 21 Torr acetone-d_6; C: 19 h after the acetone-d_6 addition; D: after 2 h degassing at 60°; E: after 70 min degassing at 110°. All spectra were screen-expanded below 2850 cm^{-1}.

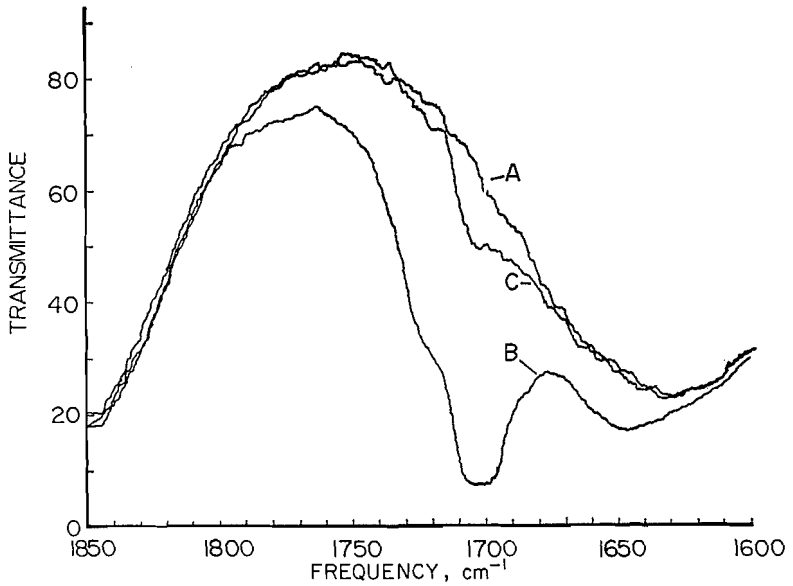

FIG. 5. Acetone-d_6 sorption on thin porous glass. A: after degassing at 800°; B: after exposure to 26 Torr acetone-d_6; C: after 30 min degassing at 25°. Ordinate expansion using screens, 5-fold abscissa scale expansion, and the 2× slit program (256 μ at 1800 cm^{-1}) were used.

The Absorptions at 1650–1660 cm^{-1}

It is likely that the bands in the region of 1650–1660 cm^{-1} were observed with greater ease on the boron-impregnated Cab-O-Sil samples because the surface area and radiation-transmitting properties of this material were greater than those of porous glass. There are two possible interpretations of the bands. (*a*) The bands at 1661 and 1650 cm^{-1} may be due to acetone and acetone-d_6 respectively coordinated to surface boron. Complexes of BF_3 and acetone have been prepared (14), and it was shown that the carbonyl absorption band frequency was lowered by 72 cm^{-1} whereas the C—H band positions were not affected. (*b*) The bands may be due to ν(C=C) of an enolic structure.

Attempts were made to differentiate between these two possibilities by observing the spectrum of adsorbed 1,1,3-trifluorotrichloroacetone. The 1,1,3-trifluorotrichloroacetone pressure was in the range 25–30 Torr. A single band at 1784 cm^{-1} was detected on Cab-O-Sil, but this band was accompanied by a second small band at 1747 cm^{-1} on boron-impregnated Cab-O-Sil. Porous glass spectra clearly showed the 1784 cm^{-1} band, but only a slight asymmetry could be observed on its low wavenumber side. In view of the similarities mentioned previously, the failure to observe a definite band in the 1740–1750 cm^{-1} region with porous glass was probably due to the lower surface area of this sample compared to that of boron-impregnated silica. We feel that a good interpretation of this lower-frequency band is that it was caused by the carbonyl grouping coordinated to a surface boron atom. This must be an uncertain assignment, but it has been shown that a ketone which could not enolize gave two bands in the carbonyl region when adsorbed on boron-containing silica surfaces. Moreover, there were no olefinic C—H or C—D bands which could be related to those at 1661 or 1650 cm^{-1}. These facts do not support assignment (*b*) but tend to give more credence to the assignment that the bands at 1661 and 1650 cm^{-1} were due to carbonyl bonds coordinated with surface boron atoms.

The Decomposition Reaction

The nature of the decomposition process is obscure because it is not possible to identify the products merely from their C—H stretching vibrations. However, the fact that new B—OH groups were formed suggests that surface B—O—B bridges were able to abstract hydrogen from adsorbed acetone. It is possible that part of this process resulted in the formation of a species

Can. J. Chem. Downloaded from www.nrcresearchpress.com by 210.87.254.42 on 09/05/12
For personal use only.

Can. J. Chem. Downloaded from www.nrcresearchpress.com by 210.87.254.42 on 09/05/12
For personal use only.

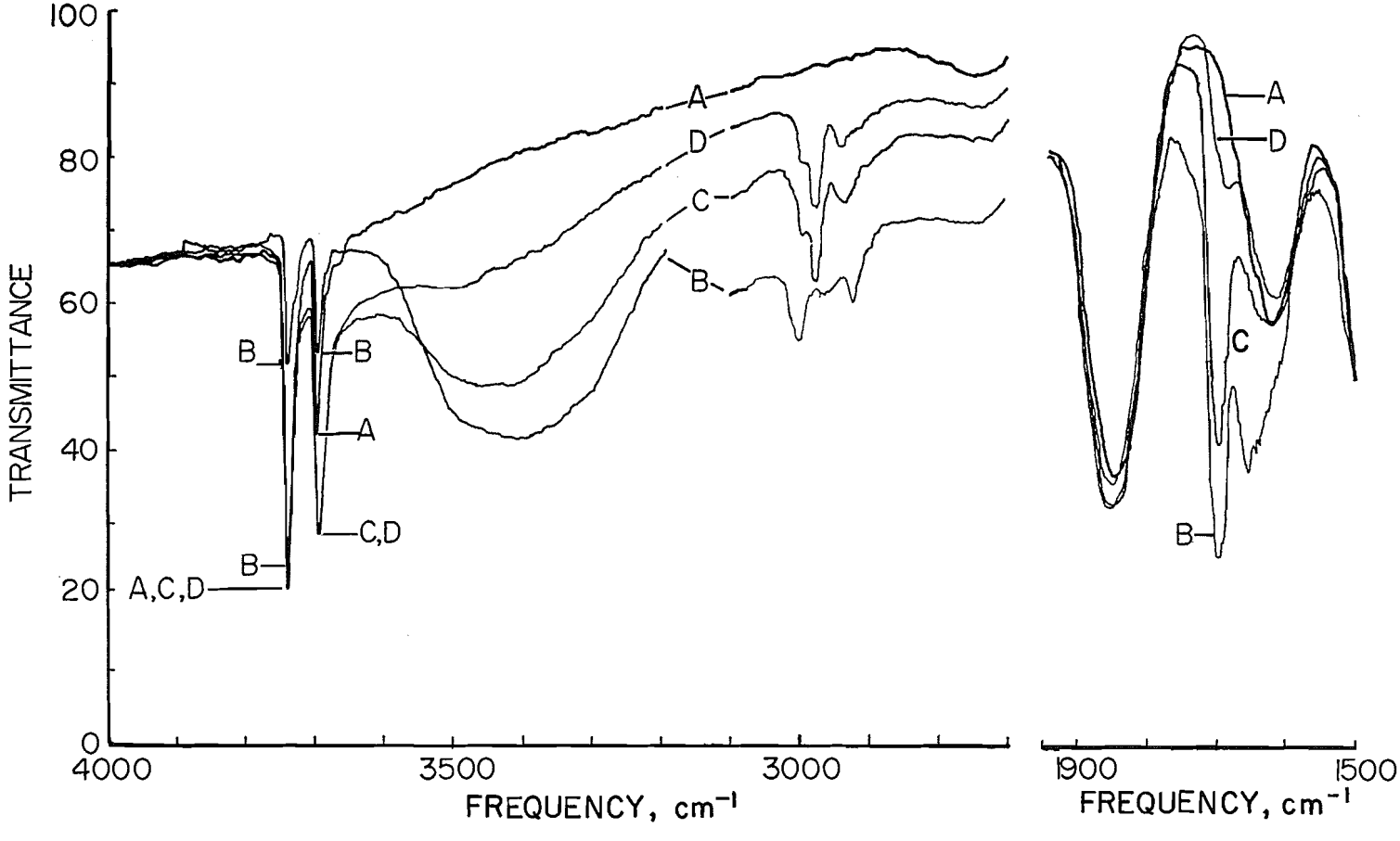

FIG. 6. Acetone sorption on boria-silica. A: after outgassing at 800°; B: after exposure to 20 Torr acetone; C: the cell was isolated for 17 h and then evacuated for 15 s at 25°; D: after 4.5 h degassing at 25°. The ordinates of spectra B and C were displaced in the 3100–1700 cm^{-1} region to avoid overlapping.

of the type $\equiv B—CH_2—CO—CH_3$. Such species would explain the added stability of ν(C═O) on porous glass and on boron-impregnated silica surfaces compared to Cab-O-Sil, because ν(C═O) and ν(C—H) should be very similar to those found in acetone. However, there must have been further reaction to give the species having absorption bands at 2984, 2940, and 3003 cm^{-1}. No mechanism is given because of the difficulty of identifying the species.

The Exchange Reaction

Figure 1 shows that, after exposing a silica surface containing mainly OD groups to 20 Torr acetone, there was, in addition to bands of acetone hydrogen-bonded to deuteroxyl groups, a broad absorption, centering at 3400 cm^{-1}, attributed to perturbed hydroxyl groups. After 15 h of isolation the concentration of adsorbed acetone increased to a slight extent but the concentration of perturbed OH groups increased quite markedly, while OD concentration decreased. Thus, some time-dependent exchange process occurred between surface OD groups and the hydrogen of the acetone. Qualitative experiments showed that the amount of exchange was also related to the gas phase pressure (and, thus, to surface concentration) of acetone. We tentatively propose the following mechanism for the exchange process

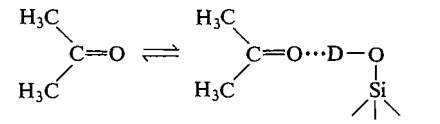

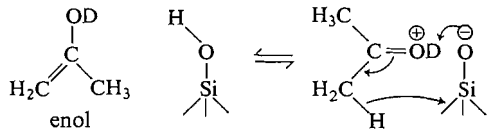

Enol must migrate and react with another OD group if the scheme is to account for exchange after acetone has been removed from the surface. Thus

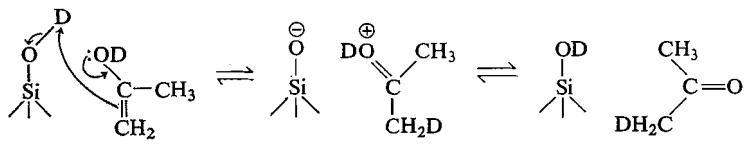

Justification for this mechanism comes mainly from the fact that exchange reactions involving ketones in solution are thought to involve an enol intermediate (15); a different intermediate is difficult to visualize. Absorbance vs. wavenumber plots in the region 1850–1550 cm^{-1} derived from data carefully obtained using scanning speeds of 30 cm^{-1}/min and 2.5-fold abscissa expansion revealed only a slight asymmetry on the low-frequency side of the 1711 cm^{-1} carbonyl band. This may contain a contribution from ν(C═C) of an enolic structure, but there is no definite proof of this (16). Figure 4 shows that exchange occurred on porous glass and that B—OH groups were active in the process, but there is nothing to suggest that they were much more active than Si—OH groups. Experiments with a thin, hydroxylated porous glass sample showed that when the sample was exposed to 3 Torr acetone-d_6, exchange took place and "free" OD groups formed. This indicates that there was no close interaction of the exchange products. As suggested by the mechanism, these are probably free to migrate on or desorb from the surface. This also seems to explain convincingly the failure to observe bands due to C—H absorption when acetone-d_6 interacted with hydroxylated porous glass.

Acknowledgment

Support by grants from the National Center for Air Pollution Control and the Communicable Disease Center is gratefully acknowledged.

1. M. J. D. Low and N. Ramasubramanian. J. Phys. Chem. **70**, 2740 (1966).
2. M. J. D. Low and N. Ramasubramanian. Preprints, Division of Petroleum Chemistry. 152nd Natl. Meeting Am. Chem. Soc. New York. Sept. 1966. p. 133.
3. M. J. D. Low and N. Ramasubramanian. J. Phys. Chem. **71**, 3077 (1967).
4. M. J. D. Low, N. Ramasubramanian, and V. V. Subba Rao. J. Phys. Chem. **71**, 1726 (1967).
5. M. J. D. Low, N. Ramasubramanian, P. Ramamur-

Can. J. Chem. Downloaded from www.nrcresearchpress.com by 210.87.254.42 on 09/05/12
For personal use only.

THY, and A. V. DEO. J. Phys. Chem. **72**, 2371 (1968).
6. M. J. D. LOW and V. V. SUBBA RAO. Can. J. Chem. **46**, 3255 (1968).
7. M. J. D. LOW and Y. HARANO. J. Res. Inst. Catalysis, Hokkaido Univ. **16**, 271 (1968).
8. M. FOLMAN and D. J. C. YATES. Proc. Roy. Soc. London, Ser. A, **246**, 32 (1958).
9. A. N. SIDOROV. Dokl. Akad. Nauk SSSR, **95**, 1235 (1954).
10. G. DELLEPIANE and J. OVEREND. Spectrochim. Acta, **22**, 593 (1966).
11. R. P. YOUNG and N. SHEPPARD. J. Catalysis, **7**, 223 (1967).
12. A. BERTOLUZZA, G. B. BONINO, G. FABRI, and V. LORENZELLI. J. Chim. Phys. **63**, 395 (1966).
13. M. L. HAIR and I. D. CHAPMAN. J. Phys. Chem. **69**, 3949 (1965).
14. D. CASSIMATIS and B. P. SUSZ. Helv. Chim. Acta, **43**, 852 (1960).
15. R. P. BELL. Acid-base catalysis. Oxford Univ. Press, Oxford, England. 1941.
16. R. P. YOUNG and N. SHEPPARD. Trans. Faraday Soc. **63**, 2291 (1967).

Can. J. Chem. Downloaded from www.nrcresearchpress.com by 210.87.254.42 on 09/05/12
For personal use only.

The germanium–selenium phase diagram[1]

L. Ross and M. Bourgon
Department of Chemistry, University of Montreal, Montreal, Quebec

Received January 31, 1969

The Ge–Se phase diagram was determined in the composition range 0–66.67 at. % Se by the method of differential thermal analysis. The diagram differs totally from the one reported by Liu *et al.* (1) but is in good agreement with the diagram recently reported by Karbanov *et al.* (13). In its broad features the Ge–Se phase diagram is quite similar to the diagrams of the Ge–S, Sn–S, and Sn–Se systems.

Canadian Journal of Chemistry, 47, 2555 (1969)

Can. J. Chem. Downloaded from www.nrcresearchpress.com by 210.87.254.105 on 09/05/12
For personal use only.

Introduction

Liu *et al.* (1) investigated the germanium–selenium system over the whole composition range. The main features of the reported phase diagram are

(*a*) The existence of two selenides of germanium, GeSe and $GeSe_2$; the diselenide melts congruently at 740 °C while the monoselenide melts incongruently at 670 °C according to the reaction

[1] $$GeSe(s) \rightarrow GeSe_2(s) + \text{liquid}$$

(*b*) The existence of a Ge–GeSe eutectic at 650 °C (40 at. % Se).

(*c*) The existence of a polymorphic transformation at 620 °C in GeSe. The thermal arrest corresponding to this transition was detectable readily on the cooling curves of the GeSe–Ge alloys. Resolution of this effect was considerably worse on the heating curves. In the GeSe–$GeSe_2$ region, the transformation of the monoselenide was recorded only on cooling curves, for compositions close to GeSe.

The three IV–VI compounds GeS, SnS, and SnSe are isostructural with GeSe (black-phosphorus-type structure) (2). Furthermore, the Ge–S (3, 4), Sn–S (5), and Sn–Se (6) phase diagrams show strong similarities; they are characterized by the presence of a monotectic reaction on the metal-rich side, by the presence of a eutectic in the MX–MX_2 region (X = chalcogen), and a degenerate eutectic in the MX_2–X region.

The Ge–Se phase diagram, as reported by the above investigators, is quite different from the phase diagrams of the Ge–S, Sn–S, and Sn–Se systems. Because of this discrepancy and because of the fact, also, that results obtained during the course of electrical conductivity measurements on liquid GeSe could not be reconciled entirely with the reported Ge–Se diagram, the latter was re-examined to the composition of $GeSe_2$ (66.67 at. % Se); the method of differential thermal analysis (d.t.a.) was used in the study of this diagram.

Experimental

Preparation of the Ge–Se Alloys

Alloys corresponding to the different compositions were prepared in 2 g quantities by fusing together weighed amounts of the elements in evacuated and sealed quartz vials. The germanium used (Sylvania Corporation) was of electronic grade with a minimum resistivity, at 27 °C, of 40 Ω cm. High purity selenium shot containing at least 99.99% selenium was obtained from Canadian Copper Refiners. To prevent the loss of selenium during sealing of the vials and to ensure a minimum vapor space, the following procedure was used.

Quartz tubes (12 cm long, 0.5 cm internal diameter) were constricted at two different levels. Germanium and selenium, ground to pass a 10 mesh sieve, were weighed directly in the tubes; the rough grinding prevented sticking of germanium or selenium powder to the tubes during weighing. The tubes were then evacuated (10^{-3} mm Hg) and sealed at the upper constriction. The samples were contracted to a point below the lower constriction by heating just above the melting point of selenium (220 °C); during this operation, a small quantity of selenium sublimed to the top of the tube. The sublimed selenium was returned below the constriction by placing the upper part of the tube in a small furnace heated at approximately 700 °C while the lower part of the tube was surrounded by a water-cooled brass block. After all the selenium had returned to the bottom of the tube, the latter was sealed at the lower constriction. It is believed that the percentage compositions were known to better than 0.03%. Each vial was then enclosed in a second quartz tube also sealed under vacuum; this last precaution was taken to avoid oxidation of the samples in case of inner vial breakage during cooling.

The germanium-rich samples (Ge > 50 at. %) were homogenized in the liquid state at a temperature of 960 °C i.e. just above the melting point of germanium; the selenium-rich samples were homogenized in the

[1]This paper was presented at the 36th Annual Conference of the Association Canadienne-Française pour l'Avancement des Sciences (ACFAS), Ottawa, November 1968.

Can. J. Chem. Downloaded from www.nrcresearchpress.com by 210.87.254.105 on 09/05/12
For personal use only.

liquid state at a temperature of 850 °C for a period of 1 h. All samples were baked at 765 °C for 2 days and at 690 °C for 5 h; they were then annealed at 650 °C for 17 h, at 600 °C for 8 h, and at 550 °C for 24 h, in a controlled furnace with a 13 cm constant temperature zone. Since preliminary work had indicated the possible existence of a monotectic reaction on the germanium-rich side, all samples containing between 2–50 at. % Se were mixed thoroughly, by rocking the furnace vigorously during the entire period that they were in the liquid state; this precaution was taken in order to prevent separation of two liquid phases which would increase the necessary equilibration time at the lower temperatures. After annealing, all the samples were cooled to room temperature, in the furnace, at the rate of approximately 10 °C/min. The samples were then ground to a fine powder as a preparation for d.t.a.

Some samples corresponding to the overall compositions GeSe and $GeSe_2$ were prepared as described above. The selenides were also obtained by subliming stoichiometric alloys; the GeSe was sublimed at 425 °C under vacuum while the $GeSe_2$ was sublimed at 550 °C under an atmospheric pressure of helium. Germanium diselenide disproportionates to some extent during sublimation. This is evidenced by the presence of three rather sharply defined sections in the sublimate which correspond to Se, GeSe, and $GeSe_2$. The monoselenide has a bright metallic appearance while the diselenide is orange-yellow.

Differential Thermal Analysis

The d.t.a. instrument and the technique used for preparing the samples have been described in a previous publication (4). All the thermograms were obtained from undiluted samples (2–3 mg), sealed in quartz under vacuum, at a heating rate of 4–5 °C/min and at a cooling rate of 4–6 °C/min. Platinel thermocouples were used. The calibration curves of the thermocouples provided by the manufacturer of the d.t.a. instrument were used as such. It is believed that the temperatures reported are precise to ±2 °C. The temperatures given are those of the maximum of the peaks since they proved to be the most reproducible. An empty quartz capsule was used as reference material. The measured melting points of pure germanium and pure selenium were 950 and 220 °C, respectively.

X-Ray Diagrams

The X-ray diagrams were taken with a Philips instrument (Cu Kα radiation, Ni filter) using a Guinier camera; exposure time varied between 4–14 h depending on the particular information required. Diffractograms also were obtained by means of a Norelco diffractometer.

Results

The germanium–selenium phase diagram as determined in this investigation is shown in Fig. 1. The diagram was traced from the data obtained during heating cycles; small Ge–Se samples are subject to severe supercooling and for this reason, not much information on equilibrium freezing temperatures can be obtained from cooling curves. The points obtained during cooling are shown on the diagram. All transformations observed during heating cycles were endothermic, and during cooling cycles all were exothermic. It should perhaps be emphasized that the pressure over the samples was not 1 atm but rather the equilibrium vapor pressure at a particular temperature–composition.

The Ge–GeSe Region

The addition of selenium depresses the melting point of germanium to a minimum of 900 °C, the temperature of the monotectic reaction; the thermal effect corresponding to this reaction was large and easily detectable during both heating and cooling cycles. Further evidence for this monotectic reaction was obtained by visual examination of samples held vertically in the furnace, at 960 °C, for a period of 2 h and quenched to room temperature. Two layers could be distinguished: one layer was hard and had the physical aspect of germanium; the d.t.a. trace of this layer showed two small peaks at 660 and 666 °C and a rather large one at 900 °C. The other layer was flakier and resembled GeSe; the thermogram showed two large peaks at 660 and 666 °C and a small one at 900 °C. The approximate compositions of the two liquid phases in equilibrium at the monotectic temperature are respectively 11–12 at. % Se on the germanium-rich side and 40–42 at. % Se on the selenium-rich side.

The temperature limits of immiscibility in the two-liquid region could not be determined by d.t.a. because of small heat effects. Between 900 and 666 °C the liquidus is quite steep. By successive heating and cooling of samples, approximate points on the liquidus curve could be obtained for some compositions. The point at 710 °C which corresponds to the GeSe composition was obtained during the course of electrical conductivity measurements on liquid GeSe (7); this point was obtained under equilibrium conditions and can be regarded with some degree of confidence.

The two thermal effects at 661 and 666 °C were detectable easily on heating curves of all samples of composition between 2–50 at. % Se; these arrests were also very sharp on cooling curves but they occurred at lower temperatures. No evidence was found that would indicate the existence of a Ge–GeSe eutectic.

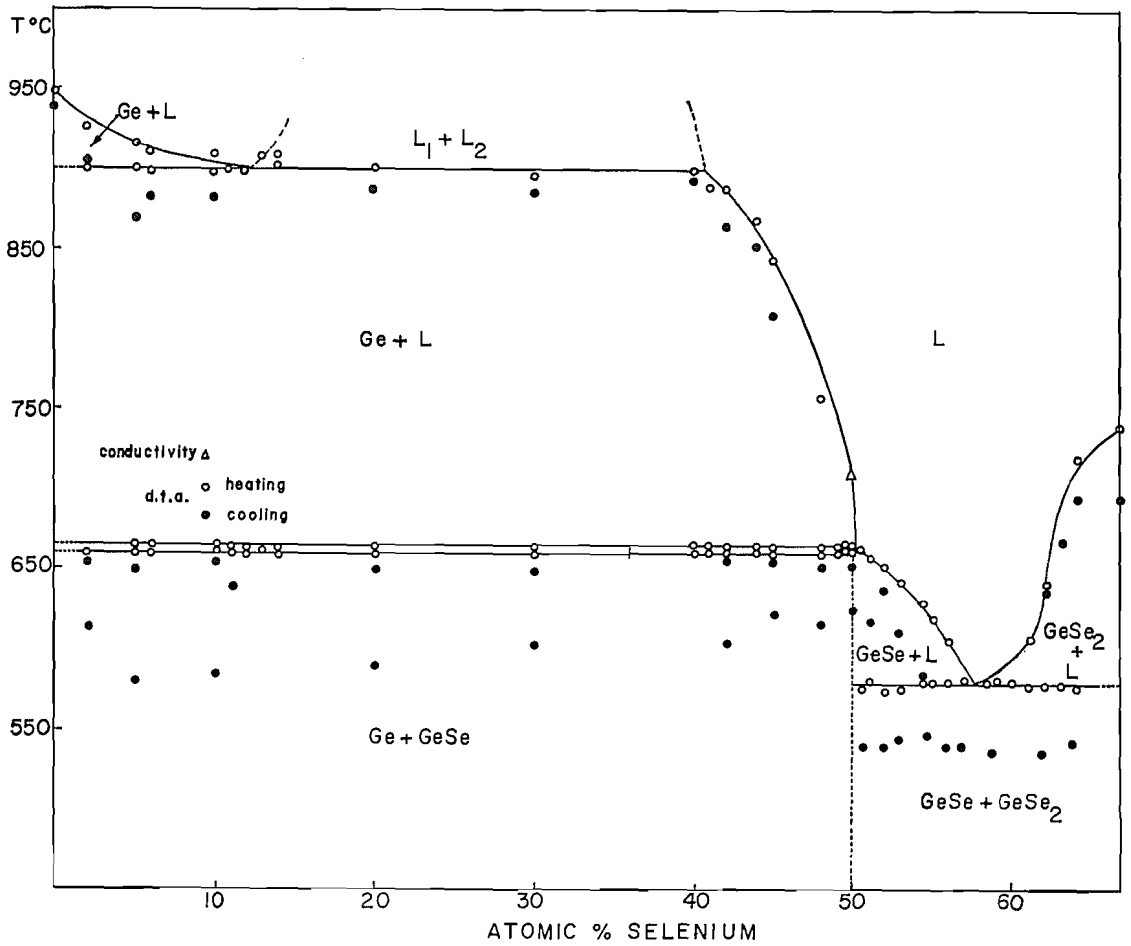

FIG. 1. The germanium–selenium phase diagram.

The Compounds $GeSe_2$ and GeSe

Congruent melting of $GeSe_2$ at 740 °C is confirmed in the present investigation; the same melting point was obtained from annealed samples prepared by weighing and from sublimed samples. X-Ray diagrams were obtained from sublimed $GeSe_2$ samples; the calculated spacings of the lattice planes were identical with those reported by Pashinkin *et al.* (8). According to these investigators, the structure of germanium diselenide is apparently a highly deformed version of an eight-layered cadmium iodide type.

All GeSe samples, sublimed or annealed and quenched, gave identical X-ray diagrams. The diagrams of the quenched samples showed a regular increase in the unit cell parameters as a function of temperature of annealing due, presumably, to dilation of the lattice or to the changing stoichiometry of GeSe on heating. The symmetry of the lattice and the parameters of the unit cell were determined from the X-ray diagrams of samples annealed at 350 °C and quenched; all the lines could be accounted for on the basis of a unit cell of orthorhombic symmetry, space group *Pcmn*, of parameters: $a = 4.38$ Å, $b = 3.83$ Å, $c = 10.78$ Å. These results are in substantial agreement with those of the literature (2, 9, 10).

The peak at 661 °C which appears on the thermograms of all samples on the germanium-rich side of the diagram is due presumably to a solid-state transition which occurs in GeSe; this transition could not be detected on the selenium-rich side of the diagram. The importance of the

Can. J. Chem. Downloaded from www.nrcresearchpress.com by 210.87.254.105 on 09/05/12
For personal use only.

peak is more indicative of a first-order transition. Transformations of the second order are known to exist in the compounds SnS (11) and SnSe (12) which are isostructural with GeSe: in both these cases, however, the thermal effects are very small and barely detectable on a d.t.a. trace. Attempts were made to fix the high temperature crystalline form of GeSe by quenching; this proved to be impossible.

No extensive study of the homogeneity region of GeSe was made; preliminary results seem to indicate, however, that this region is very narrow.

All the evidence accumulated during the course of this investigation leads to the conclusion that germanium monoselenide melts incongruently because of the peritectic disproportionation

$$[2] \qquad GeSe(s) \rightarrow Ge_{(1-x)}Se(l) + xGe(s)$$

where the phase $Ge_{(1-x)}Se$ can be considered as a solution of $GeSe_2$ in GeSe. Germanium lines could not be detected on the X-ray diagrams of GeSe samples annealed at 690 °C and quenched; this is an indication that the peritectic point lies quite close to the composition GeSe.

The GeSe–$GeSe_2$ Region

The GeSe–$GeSe_2$ region of the phase diagram is of the simple eutectic type; the eutectic has the composition 57–58 at. % Se and melts at 578 °C. The thermal effect corresponding to melting of the eutectic was detectable readily at all compositions between GeSe and $GeSe_2$. The liquidus temperatures were determined without difficulty at compositions lying to the left of the eutectic point; the phase reactions which correspond to crossing of the liquidus at compositions to the right of the eutectic point were, however, very sluggish and the temperatures were determined with more difficulty. It should be mentioned that samples prepared by different methods gave essentially the same results. Some alloys were prepared as described above, others were prepared by weighing the necessary quantities of sublimed GeSe and $GeSe_2$ with or without annealing.

X-Ray diffractograms obtained from samples in the selenium-rich region consistently showed the presence of both the $GeSe_2$ and the GeSe peaks; the $GeSe_2$ peaks were more intense to the right of the eutectic point while the GeSe peaks were more intense to the left of the eutectic point.

Discussion

The phase diagram as determined in this work is quite different from the one obtained by Liu *et al.* (1). These investigators did not detect the monotectic reaction on the germanium-rich side of the diagram. Furthermore, the thermal arrests which they observed on the thermograms of germanium-rich samples occurred at lower temperatures than the ones that were observed in this work; a possible explanation is that they determined these points from cooling curves. Their results on the selenium-rich side of the diagram are in direct contradiction with our results; no explanation for this discrepancy can be suggested; no single piece of evidence was found that would agree with reaction [1].

The very recent work of Karbanov *et al.* (13) on the Ge–Se phase diagram is in close agreement with the present work although the two diagrams differ in some details. Their diagram was plotted from d.t.a. data, using 2 g samples. The liquidus line was plotted from heating data (3 °C/min) and only the region between the GeSe–$GeSe_2$ eutectic and $GeSe_2$ was plotted from cooling data (3 °C/min). Karbanov *et al.* made the following observations.

(*a*) The melting points of Ge and Se were found to be 941 and 218 °C respectively. GeSe melts incongruently at 675 °C according to reaction [2]; the peritectic point was found to lie at 50.5 at. % Se. $GeSe_2$ melts congruently at 740 °C.

(*b*) A region of immiscibility was found to exist in the liquid at 17–40 at. % Se; the monotectic reaction occurs at 905 °C.

(*c*) Heating and cooling curves indicated an endothermic effect, corresponding to a polymorphic transformation of GeSe, at 664 °C. Effects, related to changes in the crystal structure of GeSe, were observed on cooling curves at 645 °C, in the region of 20–50 at. % Se. (In the present work, the transition was observed at 661 °C on heating curves only. The first arrest, on cooling curves, occurred in the vicinity of 650 °C while a second arrest was observed at temperatures between 580 and 620 °C, depending on composition.)

(*d*) In the GeSe–$GeSe_2$ region, the GeSe transformation was detected on heating and cooling curves at 579 °C while a eutectic, of composition 56.5 at. % Se, was found to melt at 587 °C. (In the present work, one peak only was

Can. J. Chem. Downloaded from www.nrcresearchpress.com by 210.87.254.105 on 09/05/12
For personal use only.

found on heating curves at 578 °C; during cooling this peak occurred in the vicinity of 540–550 °C and it was observed that this temperature decreased if the rate of cooling was increased.)

The Ge–Se phase diagram as determined in this work and in the work of Karbanov *et al.* is more consistent with the phase diagrams of the Ge–S (3, 4) and the Ge–Te (14) systems. Regular trends can be observed in these diagrams.

(*a*) The width of the two-liquid region decreases on going from the Ge–S system to the Ge–Te system; in fact, this two-liquid region has disappeared in the Ge–Te system; this is consistent with the increasing metallic character of the melt on going from the Ge–S to the Ge–Te system.

(*b*) The melting point of the dichalcogenide decreases from GeS_2 to $GeSe_2$ and in the Ge–Te system the ditelluride does not exist.

(*c*) A solid-state transition exists in GeTe at 430 °C; at this temperature the rhombohedral structure changes to the NaCl structure. As discussed above, a solid-state transition seems to exist in the Ge–Se system, but at a higher temperature. There is no evidence for the existence of a polymorphic transformation in GeS (4).

(*d*) The peritectic point approaches the composition 50 at. % chalcogen on going from GeS to GeTe; in fact, it is not definitely known whether melting of GeTe is congruent or incongruent. Also, the melting point of the monochalcogenide increases on passing from GeS to GeTe.

Acknowledgments

The financial support of the National Research Council of Canada is gratefully acknowledged. One of us (L.R.) wishes to thank the National Research Council of Canada for assistance in the form of a bursary. Thanks are due to Professor Guy Perreault of the Ecole Polytechnique for letting us use the X-ray diffraction instrument, and to Mr. L. Lebuis for technical assistance. Thanks are also due to Canadian Copper Refiners who, through the courtesy of Dr. C. Cooper of Noranda Research Center, provided us with high purity selenium.

1. Liu Ch'un-hua, A. S. Pashinkin, and A. V. Novoselova. Dokl. Akad. Nauk SSSR, **146**, 1092 (1962).
2. S. N. Dutta and G. A. Jeffrey. Inorg. Chem. **4**, 1363 (1965).
3. Liu Ch'un-hua, A. S. Pashinkin, and A. V. Novoselova. Dokl. Akad. Nauk SSSR, **151**, 1335 (1963).
4. L. Ross and M. Bourgon. Can. J. Chem. **46**, 2464 (1968).
5. M. I. Karakhanova, A. S. Pashinkin, and A. V. Novoselova. Izv. Akad. Nauk SSSR, Neorg. Mater. **2**, 991 (1966).
6. M. I. Karakhanova, A. S. Pashinkin, and A. V. Novoselova. Izv. Akad. Nauk SSSR, Neorg. Mater. **2**, 1186 (1966).
7. G. Handfield and M. Bourgon. Can. J. Chem. To be published.
8. Liu Ch'un-hua, A. S. Pashinkin, and A. V. Novoselova. Russ. J. Inorg. Chem. English Transl. **7**, 1117 (1962).
9. Liu Ch'un-hua, A. S. Pashinkin, and A. V. Novoselova. Russ. J. Inorg. Chem. English Transl. **7**, 496 (1962).
10. C. R. Kannewurf, A. Kelley, and R. T. Cashman. Acta Cryst. **13**, 449 (1960).
11. R. L. Orr and A. V. Christensen. J. Phys. Chem. **62**, 124 (1958).
12. S. A. Dembovskii, B. N. Egorov, A. S. Pashinkin, and Yu. A. Polyakov. Russ. J. Inorg. Chem. English Transl. **8**, 530 (1963).
13. S. G. Karbanov, V. P. Zlomanov, and A. V. Novoselova. Vestn. Mosk. Univ. Ser. II Khim. **23**, 96 (1968).
14. J. P. McHugh and W. A. Tiller. Trans. AIME, **218**, 187 (1960).

Can. J. Chem. Downloaded from www.nrcresearchpress.com by 210.87.254.105 on 09/05/12
For personal use only.

Can. J. Chem. Downloaded from www.nrcresearchpress.com by 210.87.254.5 on 09/05/12
For personal use only.

N-Chlorination of secondary amides. I. Kinetics of N-chlorination of N-methyl acetamide

M. WAYMAN AND E. W. C. W. THOMM

Department of Chemical Engineering and Applied Chemistry, University of Toronto, Toronto 5, Ontario

Received November 1, 1968

The rate of N-chlorination of N-methyl acetamide has been studied in acetate buffered hypochlorous acid solutions. The reaction rate is dependent upon pH, chloride ion concentration, and acetic acid concentration. The results fit the following rate expression

$$d[CH_3CO.NCl.CH_3]/dt = k_{obs}[CH_3CO.NH.CH_3][HOCl]$$

The observed rate constant, k_{obs}, has three components

$$k_{obs} = k_1 + k_2[H^+][Cl^-] + k_3[CH_3COOH]$$

The results suggest that the active chlorinating species in the pH range 3.0–6.0 are HOCl, Cl_2, and CH_3COOCl, in order of increasing reactivity. The values of the corresponding rate constants at 25 °C are $k_1 \simeq 0.1$, $k_{Cl} \simeq 5.0 \times 10^3$, and $k_{AcOCl} \simeq 5.8 \times 10^5$ l mole^{-1} min^{-1}, the last two rate constants being related to k_2 and k_3 through the respective equilibrium constants.

At temperatures near room temperature, the N-chlorination reaction has an apparent activation energy of 14 kcal/mole when Cl_2 is the active species, and 5 kcal/mole when CH_3COOCl is the chlorinating agent.

Canadian Journal of Chemistry, 47, 2561 (1969)

Introduction

The kinetics of N-chlorination of N-methyl acetamide in hypochlorous acid solutions has been previously studied over a narrow range of conditions. Soper and co-workers (1, 2) investigated the N-chlorination of the amide by hypochlorous acid in aqueous solutions, buffered with acetate solutions containing acetic acid up to 0.12 *M* at 25 °C, pH 5 and 6. Mauger and Soper (1) proposed that the active chlorinating agents under their conditions were hypochlorite ion and acetyl hypochlorite. The specific rate constant for acetyl hypochlorite, however, was not obtained. The role of chlorine in the chlorination of N-methyl acetamide was not determined.

Recently, Wayman *et al.* (3) have reported the development of chlorine exchange resins which contain amide functional groups, of which the nitrogen atoms take up positive chlorine reversibly. In order to shed more light on this N-chlorination process, it was decided to re-investigate the N-chlorination of N-methyl acetamide in the pH range 3–5, in which the resins are most useful. Accordingly, the results extended those of Soper and co-workers. N-Methyl acetamide was chlorinated in hypochlorous acid solutions buffered with acetic acid – sodium acetate solutions. The effects of pH, chloride ion concentration, acetic acid concentration, and temperature were investigated.

Experimental

(a) Reagents

N-Methyl acetamide was purchased from Eastman Kodak Co. It was distilled under reduced pressure in a nitrogen atmosphere before use. The undistilled amide showed no significant difference from the distilled product in the kinetic runs, and later experiments were carried out using the amide as purchased.

Sodium hypochlorite was purchased from Fisher Scientific Co., as a 5% solution. The chloride and hydroxide contents of the solutions made up from this concentrated solution were determined before use. Hypochlorous acid was prepared by acidifying the hypochlorite solutions.

Other reagents were British Drug Houses "AnalaR" grade chemicals.

(b) Experimental Procedure

Kinetic runs were carried out according to Mauger and Soper (1). A brief outline is presented below.

Hypochlorous acid and N-methyl acetamide solutions of twice the required concentration were prepared in acetic acid – sodium acetate buffers, to which sodium chloride had been added. The acetic acid concentration was corrected for the hydroxide content of the sodium hypochlorite stock solution. The chloride concentration was determined by a Mohr titration. When both solutions had attained the temperature of the thermostat, which was held to ±0.02 °C, 100 ml of the hypochlorous acid solution was added to an equal volume of the amide solution. The pH of the reacting solution was frequently measured during the course of the reaction.

The N-chloro-N-methyl acetamide content of the reaction mixture was determined at suitable intervals by pipetting 5 ml portions into 5 ml of saturated, freshly prepared phenol solutions and stirring for 30 s. This was followed by the addition of 5 ml of 3 *N* acetic acid, and then 1 g of potassium iodide. The liberated iodine was

titrated with standardized sodium thiosulfate solutions.

The combined hypochlorous acid plus chloroamide content was determined by the same procedure but omitting the addition of the phenol solution.

It was verified by determination that the chloroamide did not react with phenol to any noticeable extent in the duration of the analysis. The decomposition of the hypochlorous acid was found to be negligible during the time of the reaction.

Results of a typical run

Time (min)	Titre of N—Cl (ml)	Total titre (ml)	pH
0		13.89	5.01
5	3.50		
10	5.77	13.89	
15	7.47		5.01
20	8.65	13.87	
25	9.55		
30	10.40	13.80	5.01

NOTE: Reaction conditions: 25 °C, $[CH_3COOH] = 0.25\ M$, $[Cl^-] = 0.032\ M$, $[CH_3CO.NH.CH_3]_0 = 0.0060\ M$, $[Na_2S_2O_3] = 0.00206\ N$.

(c) Treatment of Data

All results fit the following rate expression

$$\frac{d[CH_3CO.NCl.CH_3]}{dt} = k_{obs}[CH_3CO.NH.CH_3][HOCl]$$

Thus, k_{obs} was calculated from the best straight line of the plot of log $[CH_3CO.NH.CH_3]/[HOCl]$ vs. time.

Results and Discussions

The observed rate constants, k_{obs}, at different pH, acetic acid concentration, and temperature, are presented in Figs. 1 – 5 as a function of chloride concentration. It was found that k_{obs} is a linear function of $[Cl^-]$. Furthermore by comparing the slopes $\Delta k_{obs}/\Delta[Cl^-]$ in Figs. 1, 2, and 3, it can be readily seen that k_{obs} is also a linear function of the hydrogen ion concentration, as shown in Table I.

By extrapolating the lines in Figs. 1–5 to zero chloride concentration, rate constants, k_0, are

TABLE I

Variation of "observed" rate constants, k_{obs}, with chloride concentration at 25 °C

pH	$\Delta k_{obs}/\Delta[Cl^-]$ ($l^2\ mole^{-2}\ min^{-1}$)
5	103
4	1 030
3	10 600

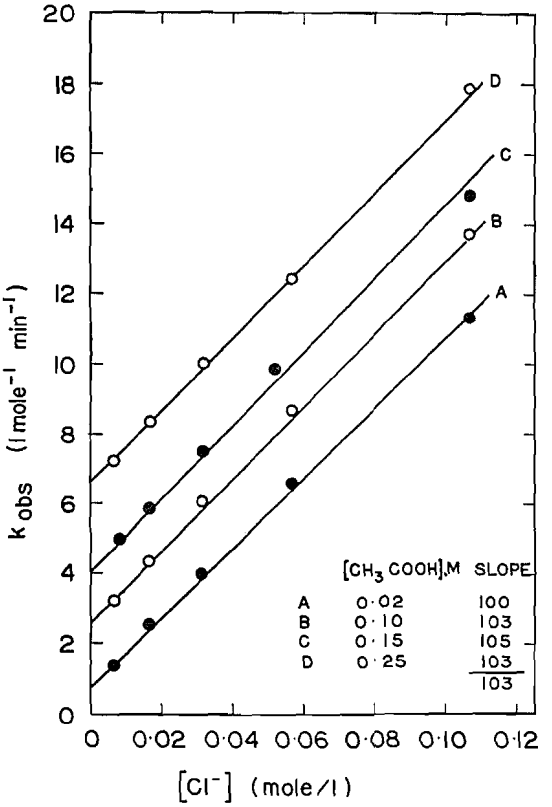

FIG. 1. k_{obs} at pH 5.00, 298 °K.

obtained, and have been presented in Fig. 6 as a function of the acetic acid concentration of the buffer. As can be seen, k_0 is a linear function of the acetic acid concentration, and is independent of hydrogen ion concentration. The extrapolated k_0 values at pH 3, 4, and 5 agree very well with the observations at pH 5 and 6 reported by Mauger and Soper (1).

The rate constant k_0 is primarily the contribution to the total rate constant, k_{obs}, by the active species formed by reaction between hypochlorous acid and acetic acid, and is independent of $[Cl^-]$ and pH, plus a small residual value k_1. As can be seen in Fig. 6, the k_0 vs. $[CH_3COOH]$ lines do not go through the origin, but result in this residual value. The agreement between the k_0 values at 25° and the data of Mauger and Soper obtained in the absence of chloride lends support to the validity of the extrapolation.

The total rate constant k_{obs} can be broken up into three components: (*i*) the residual part that is independent of hydrogen ion and chloride ion

Can. J. Chem. Downloaded from www.nrcresearchpress.com by 210.87.254.5 on 09/05/12
For personal use only.

Can. J. Chem. Downloaded from www.nrcresearchpress.com by 210.87.254.5 on 09/05/12
For personal use only.

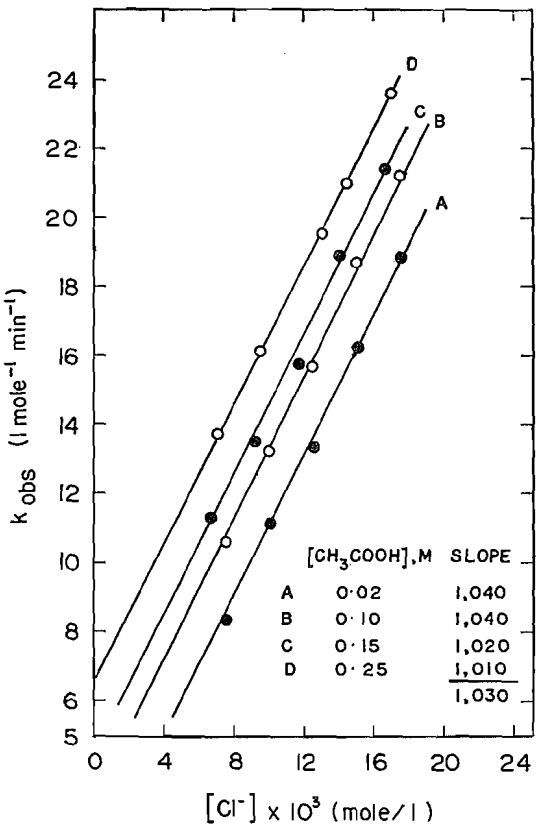

FIG. 2. k_{obs} at pH 4.00, 298 °K.

concentrations; (*ii*) the contribution from the involvement of hydrogen ions and chloride ions in the reaction; and (*iii*) the contribution due to acetic acid.
Thus

$$k_{obs} = k_1 + k_2[H^+][Cl^-] + k_3[CH_3COOH]$$

and

$$k_0 = k_1 + k_3[CH_3COOH]$$

In the absence of Cl^- and CH_3COOH, the rate of N-chlorination of the amide is slight. The chlorinating species may be hypochlorous acid itself or its dissociation products. At these pH values, the proportion of OCl^- is very small. It was proposed by de la Mare *et al.* (4) that the positive chloride ion, Cl^+, is a possible chlorinating species.

$$ClOH + H^+ \rightleftharpoons ClOH_2^+ \rightleftharpoons Cl^+ + H_2O$$

However, this is inconsistent with the present findings. If positive chloride ions were so formed, then k_1 would be a function of the hydrogen ion concentration. This has not been found over a 1000-fold variation of $[H^+]$ (pH 3–6). Similar argument can be presented against the following equilibrium

$$HOCl \rightleftharpoons Cl^+ + OH^-$$

Thus, under these conditions, we believe that molecular hypochlorous acid is the most likely chlorinating agent

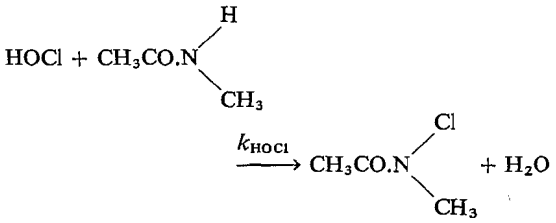

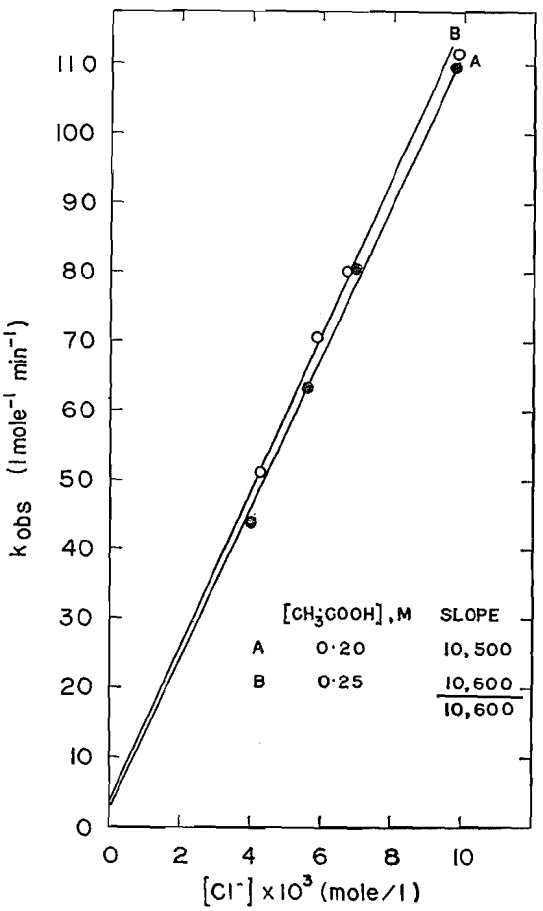

FIG. 3. k_{obs} at pH 3.00, 298 °K.

with the rate law expression

$$\frac{d[CH_3CO.NCl.CH_3]}{dt} = k_{HOCl}[HOCl][CH_3CO.NH.CH_3]$$

where $k_{HOCl} = k_1$.

The second term in the k_{obs} expression suggests that, in the presence of hydrogen and chloride ions, molecular chlorine is formed, and that it is a much more powerful N-chlorinating agent than HOCl. In a number of chlorination studies of aromatics, molecular chlorine has been found to be an effective chlorinating agent (5–10).

The chlorination reaction proposed is as follows

$$Cl_2 + CH_3CO.NH.CH_3 \xrightarrow{k_{Cl_2}} CH_3CO.N(Cl)(CH_3) + HCl$$

and the rate law expression is

$$\frac{d[CH_3CO.NCl.CH_3]}{dt} = k_{Cl_2}[Cl_2][CH_3CO.NH.CH_3]$$

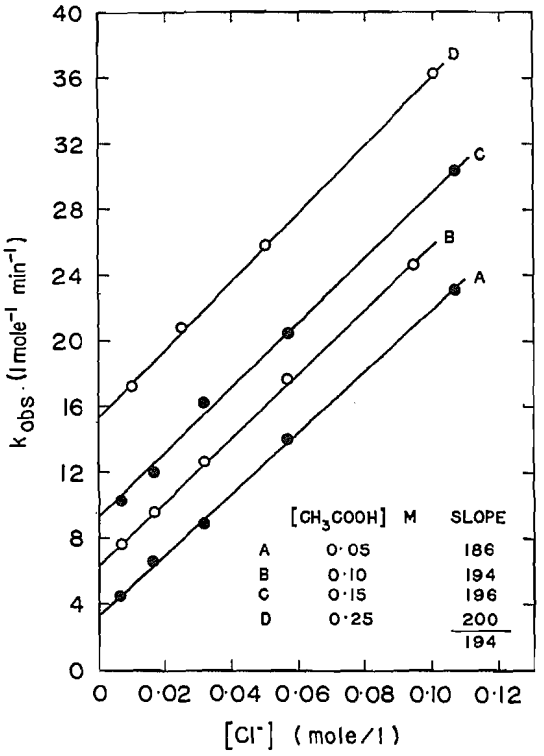

FIG. 4. k_{obs} at pH 5.00, 313 °K.

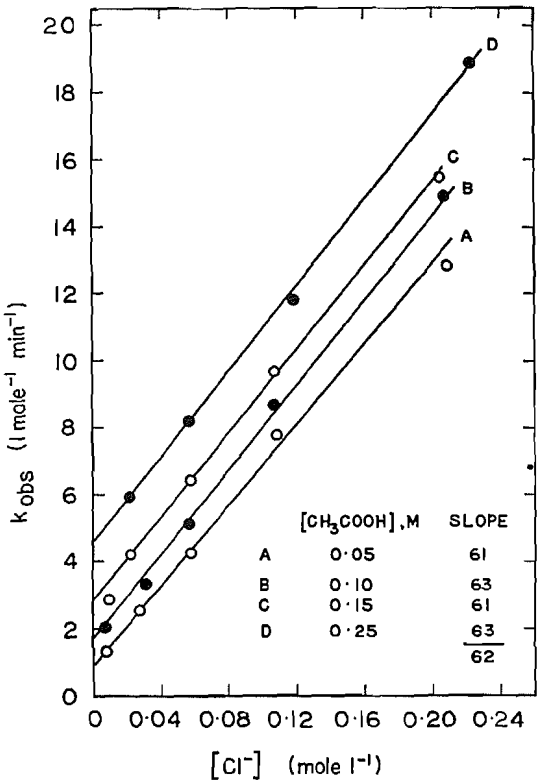

FIG. 5. k_{obs} at pH 5.00, 288 °K.

The chlorine concentration in the reacting mixture is such that it obeys the following equilibrium, which is quickly established

$$H^+ + Cl^- + HOCl \rightleftharpoons Cl_2 + H_2O$$

with the equilibrium constant

$$K_{Cl_2} = \frac{[Cl_2]}{[H^+][Cl^-][HOCl]}$$

By substitution, the above rate law expression becomes

$$\frac{d[CH_3CO.NCl.CH_3]}{dt} = k_{Cl_2}K_{Cl_2}[H^+][Cl^-] \times [HOCl][CH_3CO.NH.CH_3]$$

where

$$k_{Cl_2}K_{Cl_2} = k_2$$

The formation of chlorine has been suggested by de la Mare, Ketley, and Vernon (6) via the following scheme

$$H^+ + HOCl \rightleftharpoons ClOH_2^+$$

$$ClOH_2^+ + Cl^- \rightleftharpoons Cl_2 + H_2O$$

Can. J. Chem. Downloaded from www.nrcresearchpress.com by 210.87.254.5 on 09/05/12
For personal use only.

TABLE II

N-chlorination by molecular chlorine

T (°K)	Slope, $k_{obs}/[Cl^-]$ (l^2 mole^{-2} min^{-1})	$[H^+]$ (mole l^{-1})	K_{Cl_2}* (mole l^{-1})	k_{Cl_2}† (mole l^{-1} min^{-1})
288	62	10^{-5}	3.05×10^3	2.03×10^3
298	103	10^{-5}	2.1×10^3	4.9×10^3
298	1 030	10^{-4}	2.1×10^3	4.9×10^3
298	10 600	10^{-3}	2.1×10^3	5.1×10^3
				Ave. 5.0×10^3
313	194	10^{-5}	1.4×10^3	13.9×10^3

*Data from ref. 11.
†$k_{Cl_2} = k_{obs}/[H^+][Cl^-]\,K_{Cl_2}$.

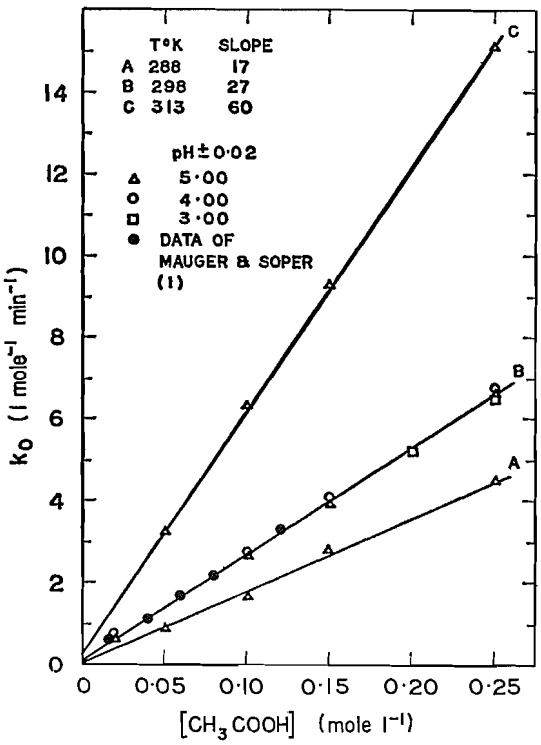

FIG. 6. k_0 vs. [CH_3COOH].

In our work we have no evidence bearing on the species $ClOH_2^+$.

A mass balance on the Cl_2-chlorination process indicates that there is no net change in hydrogen ion concentration. This was found to be so, as the pH of the reacting mixtures remained constant through the course of the reaction, even when the buffer concentration was very low.

The slopes $\Delta k_{obs}/\Delta[Cl^-]$ of the lines in Figs. 1–5 are equal to $k_2[H^+]$. Thus k_{Cl_2} can be calculated by

$$k_{Cl_2} = \frac{k_2}{K_{Cl_2}} = \frac{\dfrac{\Delta k_{obs}}{\Delta[Cl^-]} \Big/ [H^+]}{K_{Cl_2}}$$

The calculated results are presented in Table II.

In Fig. 7, k_{Cl_2} is also plotted against the inverse of temperature. From the slope of the line, the activation energy of the N-chlorination process by molecular chlorine was calculated to be 14.1 kcal/mole.

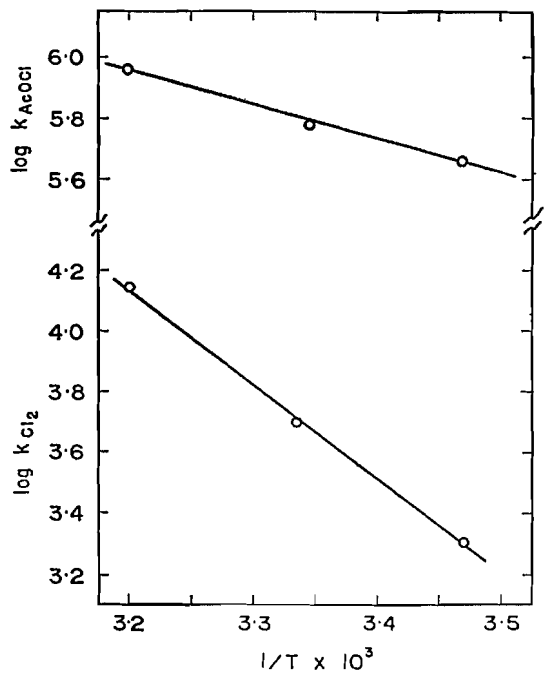

FIG. 7. log k_{Cl_2} and log k_{AcOCl} vs. $1/T$.

Can. J. Chem. Downloaded from www.nrcresearchpress.com by 210.87.254.5 on 09/05/12
For personal use only.

TABLE III

Chlorination by chlorine acetate

T (°K)	Slope, $\Delta k_0/\Delta[AcOH]$ (l^2 mole^{-2} min^{-1})	$[H_2O]$ (mole l^{-1})	K_{AcOCl}	k_{AcOCl}† (mole l^{-1} min^{-1})
288	17	55.5	2.1×10^{-3}	4.6×10^{5}
298	27	55.5	2.5×10^{-3}*	6.0×10^{5}
313	60	55.5	3.4×10^{-3}‡	9.9×10^{5}

*Reference 9.
†$k_{AcOCl}=\Delta k_0/\Delta[AcOH][H_2O]\ K_{AcOCl}$.
‡Extrapolated.

In a mixture of HOCl and acetic acid, an intermediate is formed which serves to be an effective chlorinating agent. Various authors (1, 2, 7, 9, 10) have proposed acetyl hypochlorite (chlorine acetate) formation

$$CH_3COOH + HOCl \rightleftharpoons CH_3CO.OCl + H_2O$$

$$K_{AcOCl} = \frac{[CH_3CO.OCl][H_2O]}{[CH_3COOH][HOCl]}$$

Stanley and Shorter (7) reported that there is considerable combination of HOCl and acetic acid in 75% aqueous acetic acid solutions even though de la Mare and co-workers reported a small K_{AcOCl} value of 0.0025 at 25 °C (9). The present investigation lends support to the chlorination process by chlorine acetate

$$CH_3COOCl + CH_3CO.N(H)(CH_3) \xrightarrow{k_{AcOCl}} CH_3CO.N(Cl)(CH_3) + CH_3COOH$$

with the corresponding rate law expression

$$\frac{d[CH_3CO.NCl.CH_3]}{dt} = k_{AcOCl} \times [CH_3COOCl][CH_3CO.NH.CH_3]$$

By substitution, the preceding rate law expression becomes

$$\frac{d[CH_3CO.NCl.CH_3]}{dt} = k_{AcOCl}K_{AcOCl} \times \frac{[CH_3COOH]}{[H_2O]}[HOCl][CH_3CO.NH.CH_3]$$

where

$$k_{AcOCl}\frac{K_{AcOCl}}{[H_2O]} = k_3$$

It can be seen also that k_3 is equal to the slope $\Delta k_0/\Delta[CH_3COOH]$ of the k_0 vs. $[CH_3COOH]$ lines in Fig. 6, and k_{AcOCl} can be calculated as

$$k_{AcOCl} = \frac{k_3[H_2O]}{K_{AcOCl}} = \frac{\Delta k_0}{\Delta[CH_3COOH]}[H_2O]\Big/K_{AcOCl}$$

At 15 °C, K_{AcOCl} was determined to be 0.0021 in acetic acid medium by employing the methods of de la Mare *et al.* (9). If we can assume that the equilibrium values are independent of acetic acid concentration, then these values can be applied to an aqueous medium. Table III summarizes the values of K_{AcOCl} as well as those of k_{AcOCl}.

The k_{AcOCl} values are also plotted against $1/T$ in Fig. 7. From this curve, it can be seen that the N-chlorination of the amide by chlorine acetate requires a relatively small activation energy of about 5 kcal/mole. While the principal assumption made, namely that the value of K_{AcOCl} determined in concentrated acetic acid is valid in dilute acetic acid, is reasonable, it has not been proved and this calculated activation energy should be regarded with caution.

Thus, the N-chlorination at near room temperatures of the amide in aqueous acetic acid solution by chlorine acetate has a lower apparent activation energy than that by molecular chlorine, and has a rate constant about 100 times as great. Hypochlorous acid is rather unreactive by comparison. Similar conclusions have been reported by de la Mare *et al.* (10) in a study of the chlorination of toluene.

Can. J. Chem. Downloaded from www.nrcresearchpress.com by 210.87.254.5 on 09/05/12
For personal use only.

Acknowledgments

This work was supported in part by the Defence Research Board of Canada (Grant No. 2075–05). One of us (E.W.C.W.T.) would like to thank the National Research Council of Canada for a Scholarship awarded since 1967.

1. R. P. MAUGER and F. G. SOPER. J. Chem. Soc. 71 (1946).
2. C. R. EDMOND and F. G. SOPER. J. Chem. Soc. 2942 (1949).
3. M. WAYMAN, H. SALAMAT, and E. J. DEWER. Can. J. Chem. Eng. **46**, 282 (1968).
4. P. B. D. DE LA MARE, J. T. HARVEY, M. HASSAN, and S. VARMA. J. Chem. Soc. 2756 (1958).
5. P. W. ROBERTSON. J. Chem. Soc. 1267 (1954).
6. P. B. D. DE LA MARE, A. D. KETLEY, and C. A. VERNON. J. Chem. Soc. 1290 (1954).
7. G. STANLEY and J. SHORTER. J. Chem. Soc. 246 (1958).
8. P. B. D. DE LA MARE and M. HASSAN. J. Chem. Soc. 1519 (1958).
9. P. B. D. DE LA MARE, I. C. HILTON, and C. A. VERNON. J. Chem. Soc. 4039 (1960).
10. P. B. D. DE LA MARE, I. C. HILTON, and S. VARMA. J. Chem. Soc. 4044 (1960).
11. A. A. JAKOWIN. Z. Physik. Chem. **29**, 613 (1899).

Can. J. Chem. Downloaded from www.nrcresearchpress.com by 210.87.254.5 on 09/05/12
For personal use only.

Can. J. Chem. Downloaded from www.nrcresearchpress.com by 210.87.254.40 on 09/05/12
For personal use only.

Complexes du germanium(IV) et du bore(III) avec des *o*-diphénols substitués

R. MEILLEUR ET R. L. BENOIT
Département de Chimie, Université de Montréal, Montréal, Québec

Reçu le 5 février 1969

La formation de complexes entre le germanium(IV) et le bore(III) et une série d'*o*-diphénols substitués H_2L a été étudiée par potentiométrie et spectrophotométrie. On a établi des relations linéaires entre les constantes de stabilité des complexes GeL_3^{2-} et $BL(OH)_2^-$ et les constantes d'acidité des diphénols.

Complex formation between germanium(IV) and boron(III) and some substituted *o*-diphenols H_2L has been studied by potentiometric and spectrophotometric methods. Correlations are established between the stability constants of GeL_3^{2-} and $BL(OH)_2^-$ complexes and the acidity constants of the diphenols.

Canadian Journal of Chemistry, 47, 2569 (1969)

Introduction

Les réactions entre le germanium(IV) et quatre *o*-diphénols substitués (H_2L) ont été récemment examinées (1). Dans le but d'élargir le domaine de validité de la relation linéaire obtenue entre les constantes d'acidité des ligands et les constantes de stabilité des complexes GeL_3^{2-}, on a étudié les complexes avec 2 autres catéchols substitués, le chloroacétyl-4 catéchol et le tétrachlorocatéchol (TCC).

On a ensuite examiné le comportement d'un élément voisin, le bore(III), avec 5 des ligands précédents. L'acide borique forme, en effet, des complexes stables avec de nombreux diols, diphénols ou polyols présentant des groupes OH en ortho et en *cis*. Les résultats des recherches antérieures (2–9) indiquent que l'acide borique forme des complexes de stoéchiométrie 1:1 et 1:2 avec les catéchols selon les réactions suivantes

$$[1]\quad B(OH)_3 + H_2L \rightleftarrows BL(OH)_2^- + H^+ + H_2O,\ (\beta_1^0)$$

$$[2]\quad B(OH)_3 + 2H_2L \rightleftarrows BL_2^- + H^+ + 3H_2O,\ (\beta_2^0)$$

On a montré, dans ce travail, que l'équilibre [1] prédomine et déterminé les constantes β_1^0 afin de relier la stabilité des complexes $BL(OH)_2^-$ aux propriétés acides–bases des ligands et à la stabilité des complexes GeL_3^{2-} correspondants.

Partie Expérimentale

A. Réactifs

Les solutions aqueuses de germanium(IV) environ 4×10^{-2} *M* ont été préparées par dissolution du bioxyde (GeO_2 5 *N*, Koch-Light Laboratories) et dosées par titrage potentiométrique avec de la soude non carbonatée en présence de mannitol.

L'acide borique (J. T. Baker Chemical), dosé potentiométriquement avec de la soude non carbonatée en présence de mannitol, donne une pureté de 99.7%.

Le chloroacétyl-4 catéchol (Aldrich Chemical Co.) a été recristallisé dans un mélange eau–éthanol jusqu'à l'obtention d'un produit blanc fondant à 170 °C. Un titrage potentiométrique avec de la soude non carbonatée indique une pureté > 99.5%.

Le TCC (Aldrich Chemical Co.) a été purifié par 2 recristallisations dans un mélange eau–alcool et fond à 189–190 °C (litt. (10) 185–190 °C). Le dosage potentiométrique par de la soude non carbonatée du produit dissous dans un mélange acétone–eau donne une pureté de 98.5%. Les solutions environ 1.5×10^{-4} *M* de ce ligand ont été préparées dans l'eau distillée, bouillie et saturée d'azote. Des solutions fraîchement préparées ont été toujours utilisées.

La purification des autres ligands a été décrite antérieurement (1). Les autres réactifs sont de pureté analytique.

B. Technique expérimentale

Les mesures de densité optique ont été effectuées au moyen des spectrophotomètres Zeiss PMQ II et Bausch and Lomb, munis de cuvettes de quartz dont l'épaisseur varie de 0.20 à 10.0 mm. La concentration des ions H^+ est mesurée avec un appareil Radiometer 22, avec des électrodes de verre et de calomel–KCl saturé.

La linéarité de l'électrode a été vérifiée dans l'intervalle $1.00 < -\log(H^+) < 3.30$ et $3.60 < pH < 12.5$. Le facteur de correction expérimental est négligeable, même pour les valeurs élevées de *pH*, la standardisation étant effectuée avec des tampons recommandés par le N.B.S. Des solutions de concentration (H^+) connue et de force ionique 0.1 (HCl–KCl) ont aussi servi à la standardisation. Toutes les expériences ont été faites à 25.0 ± 0.1 °C, en milieu KCl 0.10 *M* et sous atmosphère d'azote.

C. Méthodes

a. Constantes d'acidité

Les constantes d'acidité K_1 et K_2 du chloroacétyl-4 catéchol et du TCC ont été déterminées par une méthode spectrophotométrique (1) et une méthode potentiométrique reposant sur l'interprétation mathématique de

TABLEAU I

Constantes d'acidité des ligands et constantes de stabilité des complexes

Ligand	pK_1	pK_2	log β_3^0 (GeL_3^{2-})	log β_1^0 ($BL(OH)_2^-$)	log β_1/K_B
Catéchol	9.3	13.1*	−1.45*	−5.13	17.3±0.2
Chloro-4	8.60	12.55*	0.65*	−4.87	16.3±0.1
Chloroacétyl-4	7.45	11.54	2.20	−4.35	14.6±0.2
Nitro-4	6.78*	10.90*	3.90*	−3.91	13.8±0.1
TCC	5.80	10.10	6.67	−3.10	12.8±0.2

*Référence (1).

la courbe de neutralisation de l'acide par de la soude. Cette dernière méthode a aussi permis la détermination de la constante d'acidité de l'acide borique ($pK_B = 9.05 \pm 0.03$ où $K_B = (B(OH)_4^-)(H^+)/(B(OH)_3)$).

b. Constantes de stabilité

Les constantes β_3^0 des complexes du Ge(IV) ont été déterminées par les méthodes spectrophotométriques décrites précédemment (1).

Les constantes de stabilité des complexes du bore(III) ont été déterminées par l'analyse des courbes de dosage potentiométrique de solutions contenant, pour un système donné, une concentration fixe de ligand et des concentrations variables d'acide borique. Pour tous les systèmes, dans le domaine de concentration étudié, ($C_L \simeq 5 \times 10^{-3}$ M et C_M variant entre 5×10^{-2} et 2×10^{-3} M) toutes les courbes sont expliquées par la présence en solution du seul complexe $BL(OH)_2^-$. Les bilans

$$C_L = (H_2L) + (HL^-) + (BL(OH)_2^-)$$
$$C_B = (HL^-) + (BL(OH)_2^-) - (H^+)$$
$$C_M = (B(OH)_3) + (BL(OH)_2^-)$$

(où C_L, C_B et C_M représentent les concentrations molaires totales du ligand, de la base et du métal respectivement) permettent le calcul de β_1^0. Pour toutes les courbes d'un système donné, on obtient la même constante aux limites d'erreurs près. Ces calculs n'ont pas été effectués à pH élevé ($pH > 7.5$) et sur les courbes à forte concentration en acide borique afin de ne pas avoir à tenir compte de l'acidité de l'acide borique et de la stabilité des espèces polyborates.

La constante β_1^0 trouvée par calcul est ensuite affinée par le programme SCOGS (11) et le programme ACEMCA (12) est utilisé pour générer, après l'affinement, une courbe calculée $pH_{cal.} = f(v_{exp.})$. Dans les deux cas, on donne, à l'entrée du programme, les conditions de départ (volume total, concentrations), les coordonnées de chaque point expérimental ($v_{exp.}$, $pH_{exp.}$), ainsi que les constantes des équilibres impliqués dans le système (les constantes d'acidité du ligand et de l'acide borique, la constante de stabilité β_1^0 du complexe, le produit ionique de l'eau ($pK_w = 14.0$) et les constantes d'équilibre des espèces polyborates données par Ingri (13)).

Pour toutes les courbes de dosage, le programme ACEMCA conduit à des résidus $|pH_{cal.} - pH_{exp.}|$ qui n'excèdent pas 0.03, même à pH élevé et dans les cas où la concentration d'acide borique est grande. L'accord entre les courbes expérimentales et les courbes calculées confirme donc le schéma réactionnel [1] et les valeurs des constantes de stabilité. Dans le cas du système acide borique – catéchol, les calculs habituels, effectués sur les courbes de dosage potentiométrique de solutions ayant une concentration élevée de catéchol ($C_L > 0.25$ M), ne donnent pas une valeur constante pour β_1^0. On suppose alors l'existence en solution d'un second complexe BL_2^-. Un bilan d'électroneutralité, des bilans relatifs au ligand et au métal, ainsi que la connaissance de β_1^0 permettent le calcul de β_2^0(log $\beta_2^0 = -4.68$). Le programme ACEMCA a justifié ensuite cette interprétation.

Résultats et Discussion

Les valeurs des constantes obtenues sont résumées au Tableau I, les résultats expérimentaux détaillés étant exposés par ailleurs (14). L'étude des systèmes Ge(IV) – TCC et Ge(IV) – chloroacétyl-4 catéchol permet d'étendre le domaine de validité des relations linéaires entre pK_1 et pK_2 d'une part, et entre les constantes de stabilité des complexes GeL_3^{2-} et les constantes d'acidité des ligands d'autre part (1).

On a aussi relié les constantes de stabilité des complexes du bore(III) aux propriétés acides–bases des ligands. De fait, une relation linéaire satisfaisante est obtenue entre log β_1^0 et la somme des constantes d'acidité ($pK_1 + pK_2$). La pente de la droite est −0.3. Comme dans le cas du germanium(IV) (1), pour que la réaction [1] soit strictement comparable à celle d'un ion métallique M^+, soit $M^+ + L^- \rightleftarrows ML$, on écrit la réaction de formation de $BL(OH)_2^-$

$$B(OH)_2^+ + L^{2-} \rightleftarrows BL(OH)_2^-, (\beta_1)$$

où le cation hypothétique $B(OH)_2^+$ est relié à l'acide borique par l'équilibre

$$B(OH)_2^+ + H_2O \rightleftarrows B(OH)_3 + H^+$$

avec

$$K_B = (B(OH)_3)(H^+)/(B(OH)_2^+)$$

la constante hypothétique K_B inconnue étant extrêmement élevée. La constante de stabilité

Can. J. Chem. Downloaded from www.nrcresearchpress.com by 210.87.254.40 on 09/05/12
For personal use only.

$\beta_1{}^0$ trouvée expérimentalement est reliée à la constante de stabilité β_1 par l'équation

$$\beta_1 = \beta_1{}^0 K_B/K_1K_2$$

Les valeurs de $\log \beta_1/K_B$ données dans la dernière colonne du Tableau I sont portées en fonction de $(pK_1 + pK_2)$ sur la Fig. 1. Une droite de pente positive $0.70 = (1.0 - 0.3)$ est obtenue comme dans le cas des cations M^+ (15).

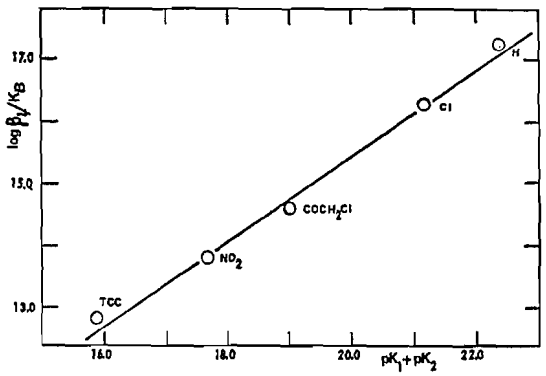

FIG. 1. Les valeurs de $\log \beta_1/K_B$ en fonction de $(pK_1 + pK_2)$ pour les complexes du B(III) avec les dérivés du catéchol: H, catéchol; Cl, chloro-4; NO_2, nitro-4; $COCH_2Cl$, chloroacétyl-4; TCC, tétrachloro-catéchol.

Une comparaison intéressante est aussi faite entre le comportement du germanium(IV) et du bore(III). Les stabilités des complexes $GeL_3{}^{2-}$ et $BL(OH)_2{}^-$ dépendant linéairement des constantes d'acidité des ligands, les valeurs de $\log \beta_3{}^0$ varient aussi linéairement en fonction des valeurs de $\log \beta_1{}^0$ (Fig. 2). Les points sont alignés sur une droite dont la pente est 3.80, ce qui montre la grande similitude de comportement de $Ge(OH)_4$ et $B(OH)_3$. Une étude précédente (1) ayant montré que la stabilité des complexes du Ge(IV) dépendait linéairement de la stabilité des complexes du Si(IV), il en ira donc de même pour les complexes du B(III). L'influence des ligands sur la stabilité des complexes du B(III), du Ge(IV), du Si(IV) étend donc la validité des relations générales entre la stabilité des complexes et la basicité des ligands aux complexes des éléments présents sous forme d'oxydes hydratés en solution aqueuse.

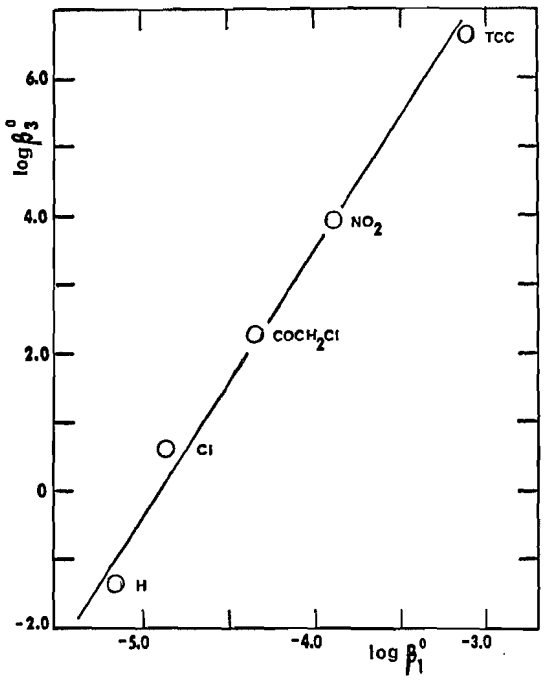

FIG. 2. Les valeurs de $\log \beta_3{}^0$ pour les complexes 1:3 du Ge(IV) en fonction des valeurs de $\log \beta_1{}^0$ pour les complexes 1:1 du B(III) avec les dérivés du catéchol.

Remerciements

Nous remercions le Conseil National de Recherches du Canada pour une subvention et une bourse (R.M.). Nous sommes reconnaissants au Professeur A. L. Beauchamp pour la mise au point des programmes et au Centre de Calcul de l'Université de Montréal pour l'utilisation de l'ordinateur électronique CDC 3400.

1. P. PICHET et R. L. BENOIT. Inorg. Chem. **6**, 1505 (1967).
2. J. BOËSEKEN et A. VAN ROSSEM. Rec. Trav. Chim. **30**, 392 (1911).
3. H. WEIL et M. ADLER. Ber. **57B**, 2091 (1924).
4. J. MEULENHOFF. Rec. Trav. Chim. **44**, 150 (1925).
5. H. SCHÄFER. Z. Anorg. Allgem. Chem. **250**, 126 (1942).
6. J. Y. TUNG et H. L. CHANG. J. Chinese Chem. Soc. **9**, 125 (1942).
7. G. L. ROY, A. L. LAFERRIÈRE et J. O. EDWARDS. J. Inorg. Nucl. Chem. **4**, 106 (1957).
8. P. J. ANTIKAINEN et A. KAUPPILA. Suomen Kemistilehti, **32B**, 141 (1959).
9. L. HAVELKOVA et M. BARTUSEK. Collection Czech. Chem. Commun. **33**, 385 (1968).
10. E. TESTA et L. FONTANELLA. Ann. **660**, 118 (1962).
11. A. L. BEAUCHAMP, J. ISRAELI et H. SAULNIER. Can. J. Chem. **47**, 1269 (1969).
12. A. L. BEAUCHAMP. Communication privée.
13. N. INGRI. Acta Chem. Scand. **17**, 581 (1963).
14. R. MEILLEUR. Thèse de Maîtrise. Université de Montréal, Montréal, Québec. 1968.
15. R. BRUEHLMAN et F. VERHOEK. J. Am. Chem. Soc. **70**, 1401 (1948).

Can. J. Chem. Downloaded from www.nrcresearchpress.com by 210.87.254.40 on 09/05/12
For personal use only.

Can. J. Chem. Downloaded from www.nrcresearchpress.com by 210.87.254.42 on 09/05/12
For personal use only.

Coordination complexes of acetylene diphosphines. II. Diphosphine bridged palladium(II) and platinum(II) derivatives

A. J. Carty and A. Efraty
Chemistry Department, University of Waterloo, Waterloo, Ontario

Received January 28, 1969

Complexes of the type $(MX_2)_2(DPPA)_2$ (M = Pd, Pt; X = Cl, Br, I, SCN; DPPA = bis(diphenylphosphino)acetylene) have been prepared and characterized. Raman, infrared, and molecular weight data have been used to show that the structures are binuclear with bridging bis(diphenylphosphino)-acetylene groups. The infrared spectra of the compounds $[M(SCN)_2]_2(DPPA)_2$ are suggestive of the presence of both N and S bonded thiocyanate within the same molecule.

Les complexes de formule $(MX_2)_2(DPPA)_2$ (M = Pd, Pt; X = Cl, Br, I, SCN; DPPA = bis(diphenylphosphino)acétylène) ont été préparés et caractérisés. Les spectres Raman, infrarouge et les poids moléculaires ont servi à etablir que les groupements bis(diphenylphosphino)acétylène forment des ponts entre les atomes des metaux. Les spectres infrarouges des composés $[M(SCN)_2]_2(DPPA)_2$ semblent indiquer la présence des liaisons M—NCS et M—SCN dans la molécule.

Canadian Journal of Chemistry, 47, 2573 (1969)

Introduction

In several recent publications (1–4) we have described the preparation and characterization of a series of metal halide and carbonyl complexes of the ligand bis(diphenylphosphino)-acetylene, **1** (DPPA). The typical behavior of this disubstituted acetylene is to form bridged binuclear or polymeric complexes in which only the phosphorus atoms of the ligand are coordinated. It was of interest therefore, to investigate the reactions of **1** with platinum(II) and palladium(II) halides since it is well known that these metals form stable acetylene complexes (5) as well as a great many square planar phosphine compounds (6). We describe herein the first binuclear diphosphine bridged palladium(II) and platinum(II) compounds of the type $M_2X_4L_2$ (M = Pd, Pt; X = Cl, Br, I, SCN; L = bis-(diphenylphosphino)acetylene).

Experimental

The ligand **1** was prepared as previously described (see Part I, ref. 1).

Tetrachloro[di-μ-bis(diphenylphosphino)acetylene]diplatinum(II), $(PtCl_2)_2(DPPA)_2$

A solution of K_2PtCl_4 (1.0 g, 2.4 mmoles) in water (10 ml) was added dropwise to a solution of **1** (1.0 g, 2.5 mmoles) in ethanol (120 ml). The reaction mixture

$$Ph_2PC{\equiv}CPPh_2$$

1

was stirred for 35 h at room temperature and the white precipitate filtered off, washed with ethanol, and extracted with dichloromethane. Slow evaporation of solvent on a rotory evaporator gave the crystalline product; yield 1.4 g (96% based on the amount of metal salt used), m.p. 309–315° (decomp.).

Anal. Calcd. for $Pt_2Cl_4(DPPA)_2$ (mol. wt., 1321): C, 47.31; H, 3.05; Cl, 10.74; P, 9.38. Found (mol. wt., osmometric in CH_2Br_2, 1260): C, 47.29; H, 2.91; Cl, 11.01; P, 9.27.

Tetrabromo[di-μ-bis(diphenylphosphino)acetylene]diplatinum(II), $(PtBr_2)_2(DPPA)_2$

A solution of K_2PtCl_4 (1.0 g, 2.5 mmoles) in water (40 ml) was saturated with potassium bromide and an additional amount (2.0 g) of solid potassium bromide added. The mixture was diluted to 400 ml with ethanol and stirred for 3 h. A solution of **1** (1.0 g, 2.5 mmoles) in ethanol was then added dropwise. After stirring for 8 h the pale yellow precipitate was filtered off, stirred thoroughly in water to remove excess potassium bromide, and finally boiled in cyclohexane. Recrystallization from ethanol/dichloromethane afforded pale yellow crystals; yield 1.5 g (84.1%), m.p. 297–300° (decomp.).

Anal. Calcd. for $Pt_2Br_4(DPPA)_2$ (mol. wt., 1499): C, 41.65; H, 2.69; Br, 21.31. Found (mol. wt., CH_2Br_2, 1469): C, 41.90; H, 2.72; Br, 21.60.

Tetraiodo[di-μ-bis(diphenylphosphino)acetylene]diplatinum(II), $(PtI_2)_2(DPPA)_2$

This was prepared from K_2PtCl_4 and **1** in similar fashion to the bromide but with potassium iodide replacing potassium bromide. The m.p. was 275–279° (decomp.).

Anal. Calcd. for $Pt_2I_4(DPPA)_2$: C, 37.02; H, 2.39; I, 30.09. Found: C, 37.38; H, 2.27; I, 29.81.

Tetrathiocyanato[di-μ-bis(diphenylphosphino)acetylene]diplatinum(II), $[Pt(SCN)_2]_2(DPPA)_2$

This was prepared in similar fashion to the bromide using potassium thiocyanate, m.p. 262–268° (decomp.).

Anal. Calcd. for $Pt_2(SCN)_4(DPPA)_2$ (mol. wt., 1411):

TABLE I

Infrared spectra (2200–650 cm^{-1}) of DPPA and complexes

Compound	Frequency (cm^{-1})*								
DPPA	1580 w	1478 m	1433 m	1304 w	1275 vw	1179 vw	1154 w	1090 m	1067 w
	1023 w	998 w	967 vw	913 vw	827 s	752 vs	742 vs	695 vs	
$(PtCl_2)_2(DPPA)_2$	1583 w	1572 vw	1480 sh	1437 s	1334 w	1310 w	1187 w	1161 vw	1095 s
	1070 sh	1028 w	1000 m	974 vw	846 s	826 s	750 s	715 m	694 s
$(PtBr_2)_2(DPPA)_2$	1583 w	1573 vw	1480 sh	1438 s	1335 w	1306 w	1265 vw	1190 w	1160 w
	1095 s	1070 w	1026 w	1000 m	974 vw	920 vw	838 s	825 sh	750 sh
	744 s	714 m	690 s						
$(PtI_2)_2(DPPA)_2$	1585 vw	1575 vw	1478 sh	1437 s	1331 w	1310 w	1225 vw	1185 vw	1155 vw
	1100 s	1026 w	998 m	920 w	840 s	817 s	745 s	713 m	690 s
$[Pt(SCN)_2]_2(DPPA)_2$	2130 ssp	2078 sbr	1584 w	1570 vw	1478 sh	1437 s	1336 w	1310 w	1185 w
	1168 vw	1160 vw	1096 s	1073 sh	1025 w	997 m	975 w	925 vw	844 s
	759 m	747 s	715 s	697 s	693 s				
$(PdCl_2)_2(DPPA)_2$	1584 w	1571 w	1478 sh	1438 s	1333 w	1308 w	1185 w	1161 vw	1095 s
	1070 sh	1024 w	998 m	974 sh	846 s	826 s	750 s	713 m	695 s
$(PdBr_2)_2(DPPA)_2$	1583 w	1573 vw	1480 sh	1439 s	1335 w	1308 w	1185 w	1160 vw	1098 s
	1070 sh	1025 w	999 m	970 vw	846 s	826 s	750 s	713 m	695 s
$(PdI_2)_2(DPPA)_2$	1583 w	1575 w	1478 sh	1437 s	1332 w	1308 w	1230 vw	1187 vw	1155 w
	1100 s	1097 s	1024 w	999 m	920 w	840 s	740 s	710 m	690 s
$[Pd(SCN)_2]_2(DPPA)_2$	2118 ssp	2072 sbr	1582 w	1572 w	1476 sh	1434 s	1331 m	1308 m	1283 w
	1260 w	1098 s	1023 vw	998 m	968 vw	840 s	740 s	711 m	690 s

*w, weak; m, medium; s, strong; sh, shoulder; sp, sharp; br, broad; vw, very weak.

C, 47.66; H, 2.86; N, 3.97. Found (mol. wt., CH_2Br_2, 1436): C, 47.48; H, 3.03; N, 4.14.

Tetrachloro[di-μ-bis(diphenylphosphino)acetylene]dipalladium(II), $(PdCl_2)_2(DPPA)_2$

Reaction of **1** (0.7 g, 1.8 mmoles) in ethanol (75 ml) with a slight excess of Na_2PdCl_4 (0.7 g, 2.4 mmoles) in the same solvent (75 ml) gave the crystalline complex which was washed with boiling cyclohexane and recrystallized from ethanol/dichloromethane; yield 0.75 g (55%), m.p. 263–266° (decomp.).

Anal. Calcd. for $Pd_2Cl_4(DPPA)_2$ (mol. wt., 1143): C, 54.64; H, 3.53; Cl, 12.40; Pd, 18.62. Found (mol. wt., CH_2Br_2, 1159): C, 54.01; H, 3.31; Cl, 12.61; Pd, 19.00.

Tetrabromo[di-μ-bis(diphenylphosphino)acetylene]dipalladium(II), $(PdBr_2)_2(DPPA)_2$

$PdCl_2$ (1.0 g, 5.7 mmoles) and potassium bromide (4.0 g) were boiled together in water for 30 min then stirred for 3 h. Reaction of this solution with **1** (1.3 g, 3.3 mmoles) in ethanol gave, after recrystallization from ethanol/dichloromethane, brown-yellow crystals of the pure product; yield 1.96 g (53%).

Anal. Calcd. for $Pd_2Br_4(DPPA)_2$ (mol. wt., 1321): C, 47.28; H, 3.04; Br, 24.24; Pd, 16.10. Found (mol. wt., CH_2Br_2, 1343): C, 46.50; H, 3.08; Br, 25.10; Pd, 16.40.

Tetraiodo[di-μ-bis(diphenylphosphino)acetylene]dipalladium(II), $(PdI_2)_2(DPPA)_2$

This complex was prepared from either $(PdCl_2)_2(DPPA)_2$ or $(PdBr_2)_2(DPPA)_2$ by metathesis with potassium iodide in ethanol/dichloromethane; m.p. 286–289° (decomp.).

Anal. Calcd. for $Pd_2I_4(DPPA)_2$: C, 41.30; H, 2.68; I, 33.30; Pd, 14.00. Found: C, 41.17; H, 2.63; I, 33.21; Pd, 14.40.

Tetrathiocyanato[di-μ-bis(diphenylphosphino)acetylene]dipalladium(II), $[Pd(SCN)_2]_2(DPPA)_2$

Metathesis of $(PdCl_2)_2(DPPA)_2$ with potassium thiocyanate in acetone followed by normal work-up gave the product as orange crystals, m.p. > 300 °C.

Anal. Calcd. for $Pd_2(SCN)_4(DPPA)_2$ (mol. wt., 1234): C, 54.50; H, 3.02; N, 4.61; Pd, 17.30. Found (mol. wt., CH_2Br_2, 1639): C, 54.19; H, 3.19; N, 4.70; Pd, 17.25.

Physical Measurements

Infrared spectra in the range 4000–600 cm^{-1} were recorded on a Beckmann IR-9 spectrophotometer as Nujol or hexachlorobutadiene mulls between sodium chloride windows. Spectra were calibrated with polystyrene and frequencies are accurate to $\pm 2\ cm^{-1}$. In the region 400–200 cm^{-1} a Beckmann IR-12 spectrophotometer was used. Samples were examined as Nujol mulls between polyethylene plates.

Raman spectra of the solid complexes were measured on a helium/neon gas laser Raman spectrophotometer using the 6328 Å exciting line. In some cases spectra were unobtainable due to the strong fluorescence of the sample. Calibrations were made using the 6518 Å line of carbon tetrachloride and frequencies are accurate to $\pm 2\ cm^{-1}$.

Microanalyses were carried out by A. B. Gygli, Toronto and by Alfred Bernhardt, Mulheim, Germany. Palladium was estimated gravimetrically by direct ignition. Molecular weights were measured osmometrically in dichloromethane and dibromomethane using Mechrolab and Hitachi Perkin–Elmer vapor pressure osmometers.

Can. J. Chem. Downloaded from www.nrcresearchpress.com by 210.87.254.42 on 09/05/12
For personal use only.

TABLE II

Far-infrared spectra (450–200 cm^{-1}) of DPPA and Pt(II) and Pd(II) complexes

Compound	Frequency (cm^{-1})*								
DPPA	447 s	430 s	410 m	370 m	341 w	305 vw	285 vw	238 w	
$Pt_2Cl_4(DPPA)_2$	442 m	388 w	378 w	328 s	302 s	298 sh	274 vw	250 vw	
$Pt_2Br_4(DPPA)_2$	442 s	390 m	370 m	342 vw	305 w	267 vw	237 vw	218 s	
$Pt_2I_4(DPPA)_2$	441 s	390 m	364 m	340 w	309 w	266 w			
$Pt_2(SCN)_4(DPPA)_2$	446 s	415 w	389 m	377 m	339 w	301 m	289 m	272 sh	220 vw
$Pd_2Cl_4(DPPA)_2$	438 m	390 m	375 w	320 s	305 sh	298 s	265 w	210 vw	
$Pd_2Br_4(DPPA)_2$	440 s	390 m	369 m	336 vw	309 w	259 sh	244 m	220 w	
$Pd_2I_4(DPPA)_2$	433 s	420 s	392 vw	380 vw	340 m	305 w	255 w	212 w	
$Pd_2(SCN)_4(DPPA)_2$	436 s	382 w	375 sh	337 w	304 m	280 s	260 sh		

*w, weak; m, medium; s, strong; sh, shoulder; vw, very weak.

Results

The ligand **1** reacts readily with sodium tetrachloropalladate(II) and potassium tetrachloroplatinate(II) to give crystalline, air stable, diamagnetic[1] complexes of empirical formula $MCl_2(DPPA)$. The corresponding bromides, iodides, and thiocyanates can be obtained either by metathesis or by preliminary conversion of the tetrachloro salt into the tetrabromo, tetraiodo, or tetrathiocyanato derivative. The compounds are soluble in dichloromethane (iodides sparingly) but virtually insoluble in the polar solvents nitromethane, acetonitrile, and ethanol, almost certainly ruling out an ionic formulation.

Infrared Spectra

The infrared (i.r.) spectra (2200–650 cm^{-1}) of the ligand and complexes are shown in Table I. Spectra of the complexes are very similar to the free ligand spectrum, the most notable changes being an increase in intensity and frequency of the 1090 cm^{-1} ligand band, a resolution of bands in the 690–850 cm^{-1} region in some complexes, and the appearance of an extra weak absorption in the 1550–1600 cm^{-1} region. The 1090 cm^{-1} absorption is characteristic of the grouping P–phenyl and increases in frequency and intensity for this band are a good diagnostic test for coordination of phenyl phosphines (7 and references therein). For the compounds $[M(SCN)_2]_2(DPPA)_2$ two bands due to $\nu(C{\equiv}N)$ of coordinated thiocyanate appear in each spectrum. The higher of these is strong and sharp whereas the lower is broad. Possible reasons for the appearance of two widely separated $\nu(C{\equiv}N)$ frequencies are discussed later.

The far-infrared spectra (450–200 cm^{-1}) of **1** and the complexes are shown in Table II. The ligand is relatively free from strong absorptions in this region and comparison of analogous complexes allowed ready identification of bands due to $\nu(M{-}X)$. Two platinum–chlorine stretching vibrations were found for $(PtCl_2)_2(DPPA)_2$ at 328 and 302 cm^{-1} in the normal range for $\nu(Pt{-}Cl)$ in square planar complexes (8, 9).

$\nu(Pd{-}Cl)$ modes were similarly identified at 320 and 298 cm^{-1}. Only one $\nu(M{-}Br)$ mode was found at 218 cm^{-1} for M = Pt and at 244 cm^{-1} for M = Pd, the other expected vibration being presumably below the range of the instrument. The compounds $[M(SCN)_2]_2(DPPA)_2$ each exhibit a broad band envelope between 260–310 cm^{-1} consisting of at least 3 strong peaks. This is the region in which $\nu(M{-}S)$ and $\nu(M{-}N)$ occur for complexes containing S-bonded or N-bonded thiocyanate (10, 11).

Raman Spectra

Previous workers on acetylene complexes have used i.r. data almost conclusively to deduce whether the C≡C bond is coordinated (5, 12). Raman data are more useful, however, since $\nu(C{\equiv}C)$ gives rise to a very intense absorption in the Raman effect whereas $\nu(C{\equiv}C)$ for a coordinated triple bond may only appear weakly in the i.r. Using helium/neon excitation, $\nu(C{\equiv}C)$ was readily identified for **1** and the solid complexes which were not highly colored (Table III).

[1]Good quality nuclear magnetic resonance spectra were obtained in deuterochloroform solutions.

Can. J. Chem. Downloaded from www.nrcresearchpress.com by 210.87.254.42 on 09/05/12
For personal use only.

In all cases ν(C≡C) of the complexed ligand is at *higher* frequency than in the free ligand.

TABLE III

ν(C≡C) (cm^{-1}) for DPPA and complexes

Compound	ν(C≡C)
DPPA	2097
$(PtCl_2)_2(DPPA)_2$	2136
$(PtBr_2)_2(DPPA)_2$	2139
$[Pt(SCN)_2]_2(DPPA)_2$	2143
$(PdCl_2)_2(DPPA)_2$	2135

Discussion

Several possible structures (**2**–**7**) can be envisaged for compounds of empirical formula MX_2(DPPA). Although many square planar mononuclear diphosphine complexes of type **2**

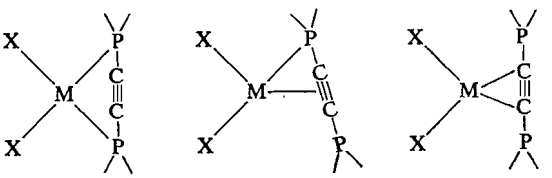

2

3

4

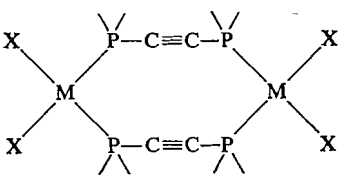

5

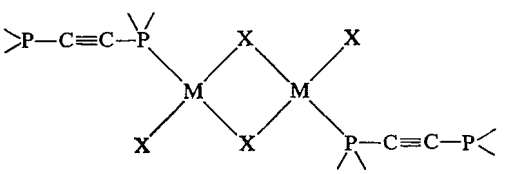

6

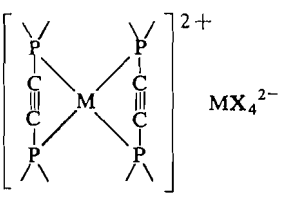

7

are known (6, 13), the molecular weight data in dibromomethane indicate that the compounds MX_2(DPPA) (M = Pd, Pt; X = Cl, Br, I, NCS) are binuclear. Moreover, the linear P—C—C—P skeleton of **1** and the long P—P distance of 4.7 Å (1) prevent chelation. Structures **2** and **7** can therefore be eliminated.

The presence of electronegative substituents on acetylenes markedly increases the ability of the triple bond to coordinate to transition metals (5, 14). Recent calculations (15) have shown that the diphenylphosphino group is strongly electron withdrawing. On this basis the triple bond of **1** might coordinate as in **3** where one phosphorus atom is attached to the metal, or as in **4** by analogy with the known compounds $(Ph_3P)_2Pt$(Ac) (Ac = acetylene) (16). ν(C≡C) is i.r. inactive in symmetrically disubstituted acetylenes but on coordination of the triple bond, a lowering of symmetry occurs and ν(C≡C) appears in the i.r. at a frequency 200–400 cm^{-1} lower than in the free acetylene (12, 16). From Table I, the absence of any band in the region 2200–1600 cm^{-1} assignable to ν(C≡C) of a coordinated triple bond argues convincingly against a formulation as acetylene complexes. Moreover, this is confirmed by the Raman data (Table III) where an increase of 39–50 cm^{-1} for ν(C≡C) occurs on coordination of the ligand.

Spectroscopic evidence also infers that a structure **6** (or similar *cis* isomers) based on bridging halide and monodentate **1** is unlikely. Coordination of only one phosphorus atom of the ligand would certainly cause ν(C≡C) to appear strongly in the i.r.[2] A bridged halide complex of the type shown, exhibits two distinct regions of absorption due to ν(M—X) in the far-infrared. For a chloride complex with a *trans* C_{2h} skeleton one terminal ν(M—Cl) (B_u) mode about 320 cm^{-1} and two bridging ν(M—Cl) (B_u) modes, one above 290 cm^{-1} and the other between 250–290 cm^{-1} are expected (17). The presence of only two ν(M—Cl) modes for the chloride and the absence of a band below 290 cm^{-1} rule out the bridging halide structure.

The only structure consistent with molecular weights, i.r., and Raman data is **5** in which two

[2]An i.r. spectrum of a model compound

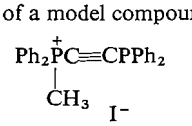

analogous to the case of a monodentate **1** shows ν(C≡C) as an intense absorption in the i.r. at 2108 cm^{-1}.

Can. J. Chem. Downloaded from www.nrcresearchpress.com by 210.87.254.42 on 09/05/12
For personal use only.

Can. J. Chem. Downloaded from www.nrcresearchpress.com by 210.87.254.42 on 09/05/12
For personal use only.

diphosphine molecules symmetrically bridge two MX_2 units. For the D_{2h} planar skeleton two metal–halogen stretching modes (B_{2u} + B_{3u}) are expected in the i.r. in agreement with the two observed ν(M—Cl) bands for $(MCl_2)_2$-$(DPPA)_2$. To confirm this result a Raman spectrum of $(PtBr_2)_2(DPPA)$ was run in the region 400–100 cm^{-1}. Comparison with the Raman spectrum of **1** in the same region shows that ν(Pt—Br) modes appear as one intense and one medium strong band at 232 and 177 cm^{-1}. For D_{2h} symmetry two modes (A_g + B_{1g}) are expected in the Raman and these should be non-coincident with the i.r. modes. Without polarization data a definite assignment is impossible but on the basis of relative intensity the highest band may arise from the symmetric A_g mode. Both i.r. and Raman spectra are therefore nicely interpreted in terms of structure **5**.

Although a number of palladium(II) and platinum(II) diphosphine complexes of the type MX_2 (diphos.) have been prepared (6, 13, 26), these are either monomeric with chelating diphosphine molecules or ionic dimers $[M(diphos)_2][MX_4]$ (6, 26). However, the phosphido bridged dimeric species $M_2X_2(PR_2)_2(PR_3)_2$ (M = Pd, Pt; X = Cl, Br, I; R = CH_3, C_6H_5) are well known (24) and recent work has shown that ethylenediamine bridged platinum(II) complexes exist (25). The preparation of the diphosphine bridged species described herein nevertheless illustrates the importance of ligand geometry in determining the structures of coordination complexes.

The shifts of ν(C≡C) to higher frequency on complexing are worthy of comment. We have recently pointed out (18) that the low ν(C≡C) frequency for **1** is a consequence of pπ–dπ C→P interaction in the linear P—C—C—P skeleton of **1**. On coordination to a transition metal, back donation Mdπ–Pdπ lessens the π electron drift from bonding carbon pπ orbitals to phosphorus dπ orbitals and causes ν(C≡C) to move higher. Comparison of data for copper(I), gold(I), mercury(II), palladium(II), and platinum(II) (18) shows that whereas mercury(II) produces the smallest shift (ca. 20 cm^{-1}), platinum(II) and palladium(II) (Table III) produce a Δν of the order of 40–50 cm^{-1}, indicating extensive π bonding between phosphorus and these metals.

The nature of the bonding of thiocyanate in the complexes $[M(SCN)_2]_2(DPPA)_2$ is of interest, particularly in view of recent X-ray results for compounds thought to contain both N *and* S bonded thiocyanate (19). Infrared correlations have frequently been used with success to predict the occurrence of metal–NCS or metal–SCN bonding in thiocyanate complexes (11, 20, 27). Various authors have used the C—N stretching, C—S stretching, NCS bending, and M—N or M—S stretching regions of the spectra for analytical purposes (20) as well as measurements of the integrated intensity of the ν(C≡N) absorption (21). Two ν(C≡N) absorptions are

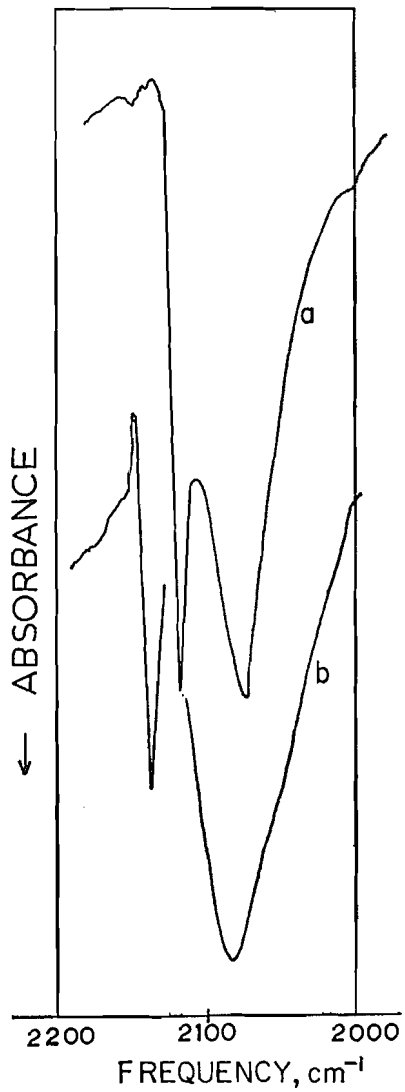

FIG. 1. Infrared spectra in the ν(C—N) region for (*a*) $[Pd(SCN)_2]_2(DPPA)_2$ and (*b*) $[Pt(SCN)_2]_2(DPPA)_2$.

expected for metal–thiocyanate–phosphine complexes of the type *cis* ML_2X_2. However, these are usually separated by $< 20\ cm^{-1}$ and occur above $2100\ cm^{-1}$ for S bonded thiocyanate and below $2100\ cm^{-1}$ for the N bonded isomer (22). Moreover, for M—NCS, $\nu(C{\equiv}N)$ is broad whereas for M—SCN, it is sharp. In $[M(SCN)_2](DPPA)_2$ (M = Pd, Pt), two bands are observed in each case; one is broad and below $2100\ cm^{-1}$ while the other is sharp, and well above $2100\ cm^{-1}$ (Fig. 1). The situation is further complicated by the fact that in phosphine complexes of palladium and platinum thiocyanates, thiocyanate is usually N bonded (22).

Two possible reasons for this behavior can be suggested. Either these compounds belong to a small group having both N and S bonded thiocyanate within the same molecules (23), or two linkage isomers exist for each compound and are difficult to separate by crystallization. Examination of the i.r. spectra in the C—S stretching or N—C—S bending regions provides no further information since the ligand absorbs strongly in these regions and although ν(Pd—N) and ν(Pd—S) are said to absorb in different ranges (11), the absorption for $[Pd(SCN)_2]_2(DPPA)_2$ near $300\ cm^{-1}$ is sufficiently broad and complex that no definite assignments can be made. We are currently attempting to resolve this question by an X-ray crystallographic study of $[Pd(SCN)_2]_2(DPPA)_2$.

Acknowledgments

The financial support of the National Research Council of Canada is acknowledged. We also thank Dr. A. Walker, University of Toronto, for the use of infrared facilities.

1. A. J. Carty and A. Efraty. Inorg. Chem. **8**, 543 (1969).
2. A. J. Carty and A. Efraty. Can. J. Chem. **46**, 1598 (1968).
3. A. J. Carty and A. Efraty. Inorg. Nucl. Chem. Letters, **4**, 427 (1968).
4. A. J. Carty, A. Efraty, and T. W. Ng. Can. J. Chem. **47**, 1429 (1969).
5. F. L. Bowden and A. B. P. Lever. Organometal. Chem. Rev. **3**, 227 (1968).
6. G. Booth. Advan. Inorg. Chem. Radiochem. **6**, 1 (1964).
7. A. J. Carty. Can. J. Chem. **45**, 345 (1967).
8. P. L. Goggin and R. J. Goodfellow. J. Chem. Soc. A, 1462 (1966).
9. R. J. Goodfellow, J. G. Evans, P. L. Goggin, and D. A. Duddell. J. Chem. Soc. A, 1604 (1968).
10. D. Forster and D. M. L. Goodgame. Inorg. Chem. **4**, 715 (1965).
11. R. N. Keller, N. B. Johnson, and L. L. Westmoreland. J. Am. Chem. Soc. **40**, 2729 (1968).
12. J. Chatt, R. G. Guy, and L. A. Duncanson. J. Chem. Soc. 827 (1961).
13. G. Booth and J. Chatt. J. Chem. Soc. A, 634 (1966).
14. M. A. Bennett. Chem. Rev. **59**, 611 (1962).
15. E. N. Tsvetkov, D. L. Lobanov, and M. L. Kabachnik. Theoret. Expt. Chem. **1**, 486 (1965).
16. J. Chatt, G. A. Rowe, and A. A. Williams. Proc. Chem. Soc. 208 (1957).
17. R. J. Goodfellow, P. L. Goggin, and L. M. Venanzi. J. Chem. Soc. A, 1897 (1967).
18. A. J. Carty and A. Efraty. Chem. Commun. 1597 (1968).
19. P. C. Jain and E. C. Lingafelter. J. Am. Chem. Soc. **89**, 724 (1967).
20. I. Bertini and A. Sabatini. Inorg. Chem. **5**, 1025 (1966), and references therein.
21. T. G. Sloan and A. Wojcicki. Inorg. Chem. **7**, 1268 (1968).
22. A. Sabatini and I. Bertini. Inorg. Chem. **4**, 1665 (1965).
23. K. N. Raymond and F. Basolo. Inorg. Chem. **5**, 1633 (1966).
24. J. Chatt and J. M. Davidson. J. Chem. Soc. 2433 (1964).
25. P. C. Kong and T. Theophanides. Can. J. Chem. **45**, 3193 (1967).
26. A. D. Westland. J. Chem. Soc. 3060 (1965).
27. J. L. Burmeister. Coord. Chem. Rev. **3**, 225 (1968).

Can. J. Chem. Downloaded from www.nrcresearchpress.com by 210.87.254.42 on 09/05/12
For personal use only.

Crystal structures of potassium, ammonium, rubidium, and cesium tetrafluoborates

M. J. R. Clark and H. Lynton
Department of Chemistry, University of New Brunswick, Fredericton, New Brunswick

Received January 9, 1969

The crystal structures of potassium, ammonium, and rubidium tetrafluoborates have been redetermined. The structure of cesium tetrafluoborate has also been established. These 4 compounds are isomorphous and show orthorhombic symmetry, space group *Pbnm*. Atomic parameters have been obtained from a block diagonal least squares refinement using anisotropic temperature parameters. The final agreement residuals for observed reflections were KBF_4, $R = 0.072$; NH_4BF_4, $R = 0.075$; $RbBF_4$, $R = 0.064$; and $CsBF_4$, $R = 0.051$.

There are significant differences between some of the B—F bond distances in the $[BF_4]^-$ ions. The shortest N---(H)F distance in NH_4BF_4 is 2.914 Å (estimated standard deviation 0.005 Å) which is long for a hydrogen bond. The positions of the hydrogen atoms in the NH_4^+ ion could not be established.

Canadian Journal of Chemistry, 47, 2579 (1969)

Can. J. Chem. Downloaded from www.nrcresearchpress.com by 210.87.254.42 on 09/05/12
For personal use only.

Introduction

Fluoboric acid and its salts were first characterized by Gay-Lussac and Thénard (1) and by Berzelius (2). Sodium and potassium tetrafluoborates have since been found to occur naturally in volcanic deposits (3, 4).

Interestingly, the alkali metal and ammonium tetrafluoborates have been found to exist in an orthorhombic phase at room temperature (5–15), and in a cubic phase at high temperatures (16–18). In addition, a modification of the orthorhombic phase of NH_4BF_4 has been observed at low temperatures (17, 19).

Crystal structures for the orthorhombic phase have been determined for the sodium (4, 15, 42, 43), potassium (7), rubidium (9), and ammonium (9) salts. The structure determinations of KBF_4, NH_4BF_4, and $RbBF_4$ are inaccurate by present standards. The structure of $CsBF_4$ has not previously been determined.

Crystals of NH_4BF_4, KBF_4, and $RbBF_4$ were obtained by slow evaporation of an aqueous solution formed by the reaction of fluoboric acid on the carbonate, the fluoboric acid being in slight excess. Crystals of $CsBF_4$ were obtained in the same way using the chloride. Crystals of KBF_4 were also prepared by mixing ice-cold concentrated aqueous solutions of boric acid and potassium fluoride, and allowing the resultant solution to stand for several days in an ice bath.

All 4 compounds were analyzed using Dowex 50-X and Dowex 2-X ion exchange resins (20). The boron content was obtained using a Zeiss flame spectrophotometer, the emission line at 521 mμ being examined. The results of these analyses are given in Table I.

Crystallographic Data

The crystal data are given in Table II. All 4 compounds are isomorphous and show orthorhombic symmetry. The systematic absences are compatible with the space groups $Pbn2_1$, and *Pbnm*. The results of the structure analyses confirm the assignment of the space group as *Pbnm*.

Precise cell dimensions were determined using Weissenberg photographs calibrated with aluminium powder. These cell dimensions and those

TABLE I
Analyses

Compound	Theoretical value* anion/cation	Observed value*		% Boron	
		Anion	Cation	Theoretical	Observed
KBF_4	7.942	7.94	7.96	8.59	8.46
NH_4BF_4	9.538	9.59	9.57	10.31	10.31
$RbBF_4$	5.805	5.81	5.81	6.28	6.30
$CsBF_4$	4.551	4.57	4.57	4.92	4.87

*Milliequivalents per gram.

TABLE II

Crystal data*

Parameter	Value in KBF_4	NH_4BF_4	$RbBF_4$	$CsBF_4$
Molecular weight	125.9	104.8.	172.3	219.7
Cell parameter (Å) a	7.03_2	7.27_8	7.29_6	7.64_7
Cell parameter (Å) b	8.67_4	9.07_2	9.10_8	9.67_5
Cell parameter (Å) c	5.49_6	5.67_8	5.63_6	5.88_5
Cell volume (Å^3)	335	375	375	434
D_m(g cm^{-3}), by flotation	2.50	1.86	3.0	3.3
Z	4	4	4	4
D_c(g cm^{-3})	2.50	1.86	3.05	3.36
μ†(cm^{-1})	135.8	24.5	196	654

*System, orthorhombic; space group, *Pbnm*; systematic absence, $h0l$: $h + l = 2n + 1$; $0kl$: $k = 2n + 1$.
†Absorption coefficient for Cu Kα.

TABLE III

Comparison of cell parameters

Compound	Cell parameter a	b	c	Reference
KBF_4	7.38	7.86	5.69	5*
	7.35	7.83	5.67	6
	6.64	8.10	5.18	7
	7.028	8.664	5.480	8
	7.03_2	8.67_4	5.49_6	This paper
NH_4BF_4	7.24	9.08	5.65	9*
	7.22	8.91	5.69	10*
	7.272	9.063	5.686	11
	7.279	9.077	5.679	12
	7.27_8	9.07_2	5.67_8	This paper
$RbBF_4$	7.24	9.09	5.61	9*
	7.29_6	9.10_8	5.63_6	This paper
$CsBF_4$	7.67	9.45	5.84	13*
	7.636	9.658	5.895	14
	7.64_7	9.67_5	5.88_5	This paper

*Cell dimensions converted from kX units to Å by the conversion factor 1.00202.

previously reported in the literature are given in Table III.

The discrepancy that exists between the presently reported cell dimensions for KBF_4, confirmed by the U.S. Bureau of Mines (8), and those published by Pesce (5) and Sharp and Thorley (6), is due to their incorrect interpretation of the X-ray powder pattern for this compound. We are unable to explain the cell dimensions reported by Bellanca and Sgarlata (7), but we note that there are several other errors in their paper. Wyckoff (21) quotes Pesce's cell dimensions but with a list of atomic parameters which are those of Bellanca and Sgarlata with a change of origin.

Intensity Data

The crystals chosen for data collection, with the exception of the KBF_4 a axis crystal, were roughly cube shaped. The average thickness for each crystal is given in Table IV. Absorption corrections were made to these data assuming spherical shape. The KBF_4 a axis crystal was a needle of length 0.35 mm and average cross section of 0.11 mm; absorption corrections for this crystal were made assuming cylindrical shape.

Using the multiple filmpack technique, equi-inclination Weissenberg photographs were taken of all layers accessible on the a and c axes. In addition, the $h0l$ layer for each compound was also obtained.

Can. J. Chem. Downloaded from www.nrcresearchpress.com by 210.87.254.42 on 09/05/12
For personal use only.

TABLE IV
Intensity data

Compound	2/μ(mm)	Axis	Crystal size (mm)	Data collected	Total data within range	Number observed
KBF_4	0.15	*a*	0.11 × 0.35	0*kl*–6*kl*		
		b	0.11	*h*0*l*	401	325
		c	0.13	*hk*0–*hk*4		
NH_4BF_4	0.82	*a*	0.30	0*kl*–6*kl*		
		b	0.30	*h*0*l*	441	346
		c	0.37	*hk*0–*hk*4		
$RbBF_4$	0.10	*a*	0.10	0*kl*–6*kl*		
		b	0.09	*h*0*l*	443	341
		c	0.10	*hk*0–*hk*4		
$CsBF_4$	0.03	*a*	0.08	0*kl*–6*kl*		
		b	0.10	*h*0*l*	520	407
		c	0.12	*hk*0–*hk*5		

The number of permitted independent reflections within the range of photographs taken with Cu Kα radiation is given in Table IV. The number of reflections with intensities above the minimum required for observation is also given in the same table. The intensities of all reflections were estimated by visual comparison with calibration strips prepared using a suitable reflection from each intensity crystal. Lorentz-polarization factors were applied to all intensity data.

Structure Refinement

The structure refinement for all 4 compounds was by successive cycles of block diagonal least squares[1], employing only the observed reflections. The quantity minimized was $\sum w(F_o - F_c)^2$. The matrices used were 3 × 3 for the positional parameters and 6 × 6 for the anistropic thermal parameters of each atom. The weighting scheme $w = 1/a + |F_o| + c|F_o|^2$ was employed with the following values for a and c: KBF_4 a = 5.06, c = 0.028; NH_4BF_4 a = 2.50, c = 0.043; $RbBF_4$ a = 11.04, c = 0.018; and $CsBF_4$ a = 12.50, c = 0.011.

Scattering factor curves used were those given in International Tables (23) for B, N, K^+, and Rb^+. The fluorine scattering curve was for $F^{-1/4}$ obtained by interpolation between F and F^-. Cs^+ was obtained from Cromer and Waber (24).

No correction was made for extinction, and in the last cycle for each compound no parameter shift exceeded 0.3 estimated standard deviations (e.s.d.).

In the case of NH_4BF_4, a difference Fourier evaluated at the end of the last cycle showed no residual electron density near the nitrogen atom that could be associated with the 4 hydrogens.

The final agreement residual, $R = \sum| |F_o| - |F_c| |/\sum|F_o|$, for observed reflections was KBF_4, $R = 0.072$; NH_4BF_4, $R = 0.075$; $RbBF_4$, $R = 0.064$; and $CsBF_4$, $R = 0.051$.

Results

There are 4 molecules in the unit cell. For each molecule, the cation, boron and two fluorine atoms F(1) and F(2) lie in one of the two mirror planes at $Z = 1/4$ and $Z = 3/4$, special positions (4*c*). The two remaining fluorine atoms of the tetrafluoborate ion, F(3) and F(3′), occupy general positions (8*d*) above and below the mirror planes.

The final atomic coordinates are listed in Table V, together with their estimated standard deviations. The temperature parameters are given in Table VI. A detailed analysis of the agreement of individual reflections is summarized in Table VII. The overall agreement residual used in this table included the unobserved reflections.

Tables VIII and IX give the distances and angles in the $[BF_4]^-$ ion together with their e.s.d. A table is also provided listing all the shortest distances between other atoms, Table X. A final set of structure factors for each compound has

[1]All computations were carried out on an IBM 360/50 computer using the programs of Ahmed *et al.* (22).

Can. J. Chem. Downloaded from www.nrcresearchpress.com by 210.87.254.42 on 09/05/12
For personal use only.

Can. J. Chem. Downloaded from www.nrcresearchpress.com by 210.87.254.42 on 09/05/12
For personal use only.

TABLE V

Fractional atomic coordinates, and e.s.d.*

Atom	x	y	z	$\sigma(x)$	$\sigma(y)$	$\sigma(z)$
KBF_4						
K	16 134	18 454	25 000	26	20	
B	68 722	6 332	25 000	134	96	
F(1)	60 250	−8 114	25 000	99	64	
F(2)	55 756	17 860	25 000	88	67	
F(3)	80 416	7 768	4 457	55	41	72
NH_4BF_4						
N	16 420	18 539	25 000	58	51	
B	69 207	6 051	25 000	77	59	
F(1)	61 017	−7 653	25 000	76	45	
F(2)	56 426	17 280	25 000	47	46	
F(3)	80 393	7 559	4 994	33	26	42
$RbBF_4$						
Rb	16 209	18 686	25 000	19	15	
B	69 640	5 894	25 000	219	191	
F(1)	61 792	−8 459	25 000	182	123	
F(2)	56 725	16 224	25 000	137	142	
F(3)	80 056	7 463	4 863	95	75	121
$CsBF_4$						
Cs	16 307	19 174	25 000	13	9	
B	69 140	5 171	25 000	192	192	
F(1)	62 728	−8 385	25 000	172	136	
F(2)	57 227	14 666	25 000	163	138	
F(3)	80 104	7 107	5 772	101	76	152

*All values have been multiplied by 10^5.

TABLE VI

Anisotropic temperature parameters*

Atom	B_{11}	B_{22}	B_{33}	B_{23}	B_{13}	B_{12}
KBF_4						
K	1012	513	2102	67	169	−84
B	1344	456	1972	126	−1552	−732
F(1)	2229	675	3894	209	−184	−1676
F(2)	1311	1139	2545	153	87	948
F(3)	1351	968	1589	143	838	106
NH_4BF_4						
N	1000	586	2083	−30	−216	−96
B	689	533	1286	−235	550	−90
F(1)	2616	961	4406	−67	498	−2030
F(2)	1227	1261	3382	−165	−309	1204
F(3)	1448	1006	1595	42	754	247
$RbBF_4$						
Rb	902	544	2235	97	107	−52
B	593	739	2066	−129	1065	−795
F(1)	2698	940	4352	−302	−159	−1935
F 2)	809	1814	3518	2367	522	844
F(3)	1561	1068	1941	−202	576	−132
$CsBF_4$						
Cs	1100	627	2399	−54	70	−29
B	197	863	2164	818	1052	−122
F(1)	2062	1116	5606	−1651	697	−1683
F(2)	1766	1462	4366	526	−1462	2213
F(3)	1763	1040	2878	−52	1097	24

*All values have been multiplied by 10^5.
$T = \exp -[h^2B_{11} + k^2B_{22} + l^2B_{33} + klB_{23} + hlB_{13} + hkB_{12}]$

TABLE VII

Agreement summary

Category	Limits	KBF_4	NH_4BF_4	$RbBF_4$	$CsBF_4$
Observed reflections					
1	$\lvert\Delta F\rvert \leqslant 1.0\lvert F_{th}\rvert$*, or $\lvert\Delta F\rvert/\lvert F_0\rvert \leqslant 2R$	324	338	340	406
2	$\lvert\Delta F\rvert \leqslant 2.0\lvert F_{th}\rvert$, or $\lvert\Delta F\rvert/\lvert F_0\rvert \leqslant 3R$	1	8	1	1
3	$\lvert\Delta F\rvert \leqslant 3.0\lvert F_{th}\rvert$, or $\lvert\Delta F\rvert/\lvert F_0\rvert \leqslant 4R$	0	0	0	0
4	$\lvert\Delta F\rvert > 3.0\lvert F_{th}\rvert$, or $\lvert\Delta F\rvert/\lvert F_0\rvert > 4R$	0	0	0	0
	Total observed reflections	325	346	341	407
	$\lvert F_0\rvert_{min}$	2.50	1.24	5.60	6.06
	$\lvert F_0\rvert_{max}$	70.74	45.68	112.98	175.08
Unobserved reflections					
1	$\lvert F_c\rvert \leqslant 1.0\lvert F_{th}\rvert$	61	87	87	95
2	$\lvert F_c\rvert \leqslant 1.5\lvert F_{th}\rvert$	10	6	15	18
3	$\lvert F_c\rvert \leqslant 2.0\lvert F_{th}\rvert$	5	1	0	0
4	$\lvert F_c\rvert > 2.0\lvert F_{th}\rvert$	0	1	0	0
	Total unobserved reflections	76	95	102	113
	$\lvert F_c\rvert_{max}$	5.16	4.14	8.38	11.73
	$\lvert F_{th}\rvert_{min}$	2.48	1.15	2.33	6.03
	$\lvert F_{th}\rvert_{max}$	5.05	2.07	6.89	10.10
Overall agreement residual R		0.102	0.100	0.097	0.086

*$\lvert F_{th}\rvert$ = threshold amplitude.

TABLE VIII

Distances in the $[BF_4]^-$ ion, and e.s.d. in parentheses (Å)

Interatomic distance	KBF_4	NH_4BF_4	$RbBF_4$	$CsBF_4$
B—F(1)	1.387(10)	1.379(07)	1.427(21)	1.400(22)
B—F(2)	1.353(11)	1.379(07)	1.332(20)	1.294(21)
B—F(3)	1.402(07)	1.404(04)	1.373(11)	1.421(12)
F(1)—F(2)	2.275(08)	2.286(06)	2.278(17)	2.270(19)
F(1)—F(3)	2.277(07)	2.277(05)	2.273(13)	2.301(14)
F(2)—F(3)	2.247(07)	2.261(04)	2.196(11)	2.208(14)
F(3)—F(3′)	2.258(06)	2.272(03)	2.270(10)	2.263(13)

TABLE IX

Angles, in degrees, in the $[BF_4]^-$ ion, and e.s.d. in parentheses

Bonds	Angle			
	KBF_4	NH_4BF_4	$RbBF_4$	$CsBF_4$
F(1)—B—F(2)	112.21(59)	111.98(37)	111.30(1.10)	114.74(1.17)
F(1)—B—F(3)	109.39(55)	109.79(36)	108.50(1.03)	109.28(1.06)
F(2)—B—F(3)	109.24(56)	108.60(34)	108.55(1.06)	108.78(1.10)
F(3)—B—F(3′)	107.25(53)	107.99(33)	111.46(1.02)	105.59(99)
F(1)—F(2)—F(3)	60.46(20)	60.09(14)	61.03(40)	61.82(44)
F(1)—F(3)—F(2)	60.38(20)	60.52(14)	61.27(40)	60.40(43)
F(1)—F(3)—F(3′)	60.27(19)	60.07(13)	60.05(35)	60.54(39)
F(2)—F(1)—F(3)	59.16(20)	59.39(14)	57.70(38)	57.78(42)
F(2)—F(3)—F(3′)	59.83(19)	59.84(12)	58.88(35)	59.17(40)
F(3)—F(1)—F(3′)	59.46(19)	59.86(13)	59.91(35)	58.93(39)
F(3)—F(2)—F(3′)	60.33(19)	60.33(12)	62.24(36)	61.66(41)

Can. J. Chem. Downloaded from www.nrcresearchpress.com by 210.87.254.42 on 09/05/12
For personal use only.

Can. J. Chem. Downloaded from www.nrcresearchpress.com by 210.87.254.42 on 09/05/12
For personal use only.

TABLE X

Shortest distances, and e.s.d. in parentheses (Å)

Atom pairs*	Interatomic distance			
	KBF_4	NH_4BF_4	$RbBF_4$	$CsBF_4$
M–M	4.513(03)	4.705(07)	4.731(02)	
	4.605(02)	4.762(05)	4.751(02)	4.955(01)
B–B	4.426(12)	4.614(08)	4.621(25)	4.920(26)
	3.961(09)	4.133(06)	4.160(17)	4.269(16)
M–B	3.496(10)	3.618(07)	3.592(16)	3.853(15)
	3.517(05)	3.663(05)	3.656(11)	3.856(12)
	3.648(06)	3.759(05)	3.744(11)	3.930(12)
B–F	3.424(07)	3.594(05)	3.641(13)	3.833(13)
	3.862(08)	4.003(05)	3.962(14)	4.051(15)
	3.420(10)	3.594(07)	3.518(21)	3.789(22)
	3.789(10)	3.939(07)	4.004(21)	4.315(22)
M–F	2.787(07)	2.914(05)	2.965(10)	3.159(13)
	2.906(04)	3.026(05)	3.048(07)	3.211(08)
	2.802(04)	2.926(04)	2.929(07)	3.134(08)
	2.752(07)	2.942(07)	2.917(12)	3.105(13)
	2.808(04)	2.939(04)	2.928(07)	3.108(08)
F–F	3.171(09)	3.284(06)	3.255(17)	3.475(19)
	3.235(06)	3.412(05)	3.358(13)	3.568(15)
	3.088(04)	3.230(03)	3.204(08)	3.370(09)
	3.407(05)	3.544(04)	3.644(11)	3.883(12)
	3.286(07)	3.462(05)	3.488(14)	3.745(14)
	3.204(06)	3.421(04)	3.516(13)	3.878(14)
	3.238(06)	3.406(03)	3.366(10)	3.622(13)
	3.105(05)	3.217(03)	3.259(10)	3.408(11)

*M is K^+, N, Rb^+, and Cs^+.

TABLE XI

Comparison of B—F bonded distances

Compound	Method	Interatomic distance (Å)	Standard deviation (Å)	Reference
$NaBF_4$	X-ray	1.40		15
		1.42		
$NaBF_4$	"	1.377		25
$NaBF_4$	"	1.386	0.002	42
		1.392	0.002	
NH_4BF_4	"	1.406		25
$Cu(pyO)_4(BF_4)_2$	"	1.40		26
		1.36		
		1.35		
		1.30		
$Cu(en)_2(BF_4)_2$	"	1.41	0.03	27
		1.37	0.02	
		1.30	0.03	
		1.38	0.03	
$NaBF_4$	n.m.r.	1.412	±0.015	25
KBF_4	"	1.410	±0.015	25
NH_4BF_4	"	1.382	±0.006	25
$RbBF_4$	"	1.432	±0.015	25
$CsBF_4$	"	1.445	±0.015	25
$H_3N \cdot BF_3$	X-ray	1.36	0.015	30
		1.39	0.015	
		1.38	0.015	
$(CH_3)H_2N \cdot BF_3$	"	1.37	0.015	36
		1.38	0.015	
$(CH_3)_3N \cdot BF_3$	"	1.39	0.03	28
$BF_3 \cdot 2H_2O$	"	1.368	0.01	29
		1.340	0.01	
		1.402	0.01	

TABLE XII

Comparison of shortest distances

Compound	Method	Interatomic distance (Å)	Standard deviation (Å)	Reference
F---F distance				
KBF_4	X-ray	3.088	0.004	This paper
NH_4BF_4	"	3.217	0.003	"
$RbBF_4$	"	3.204	0.008	"
$CsBF_4$	"	3.370	0.009	"
$H_3N \cdot BF_3$	"	3.0		30
$LiSbF_6$	"	2.87	0.01	31
K_3SiF_7	"	2.84		32
K_2NbF_7	"	3.07		33
M^+---F distance				
KBF_4	"	2.752	0.007	This paper
$RbBF_4$	"	2.917	0.012	"
$CsBF_4$	"	3.105	0.013	"
$NaBF_4$	"	2.28		15
Na_2SiF_6	"	2.18		34
K_3SiF_7	"	2.58		32
K_2NbF_7	"	2.64		33
Rb_2ZrF_6/Rb_2HfF_6	"	2.94		35
Cs_2ZrF_6/Cs_2HfF_6	"	3.12		35
N---F distance				
NH_4BF_4	"	2.914	0.005	This paper
$H_3N \cdot BF_3$	"	3.02	0.015	30
$(CH_3)H_2N \cdot BF_3$	"	3.04		36
NH_4F	n.m.r.	2.68	±0.03	37
NH_4F	X-ray	2.69		38
$N_2H_6F_2$	n.m.r.	2.62	±0.03	39
$N_2H_6F_2$	X-ray	2.62	±0.02	40

been placed in the Depository of Unpublished Data[2].

Discussion

An examination of the interatomic distances in the $[BF_4]^-$ ions, Table VIII, shows that there are significant differences between some of the B—F bonds. These results may be compared with some values from the literature, Table XI.

None of the F—B—F bond angles differ greatly from tetrahedral, the largest distortion occuring in $CsBF_4$ where the smallest angle is 105.59° (e.s.d. 0.99°) and the largest 114.74° (e.s.d. 1.17°).

All the distances given in Table X show a change in length with change in cation, in the order

$$K^+ < NH_4^+, Rb^+ < Cs^+$$

The shortest F---F and M^+---F distances are given in Table XII, together with some values from the literature. It can be seen that the cation effect is paralleled in other complex fluorides.

An examination of all the shortest N---(H)F distances in NH_4BF_4 shows that they are long for hydrogen bonds. The shortest distance 2.914 Å (e.s.d. 0.005 Å) compares with 3.02 and 3.04 Å found in $H_3N \cdot BF_3$ (30) and $(CH_3)H_2N \cdot BF_3$ (36) where only very weak hydrogen bonding is suggested. In NH_4F and $N_2H_6F_2$ where strong hydrogen bonding is thought to exist, both nuclear magnetic resonance (n.m.r.) and X-ray studies give internuclear N---(H)F distances in the range 2.6–2.7 Å, see Table XII. In a n.m.r. examination of NH_4BF_4, Pendred and Richards (41) concluded that only very weak hydrogen bonds are present and that the NH_4^+ ion is in motion even at 20 °K. This would account for the absence of localized hydrogen atom positions in our difference synthesis.

Acknowledgments

We acknowledge financial support from the National Research Council of Canada for this work, and we thank Mrs. Brenda Leffen for the

[2]Photocopies may be obtained free of charge, upon request, from the Depository of Unpublished Data, National Science Library, National Research Council of Canada, Ottawa, Canada.

Can. J. Chem. Downloaded from www.nrcresearchpress.com by 210.87.254.42 on 09/05/12
For personal use only.

collection and estimation of the intensity data used in this analysis.

1. J. L. GAY-LUSSAC and J. L. THÉNARD. Ann. Phys. **32**, 1 (1809).
2. J. J. BERZELIUS. Ann. Phys. B, **77**, 1 (1824).
3. F. ZAMBONINI. Rend. Accd. Lincei, Ser. 6, III, 644 (1926).
4. A. BELLANCA. Rend. Soc. Mineral. Ital. **3**, 20 (1946).
5. B. PESCE. Gazz. Chim. Ital. **60**, 936 (1930).
6. D. W. A. SHARP and J. THORLEY. J. Chem. Soc. 3557 (1963).
7. A. BELLANCA and F. SGARLATA. Rend. Soc. Mineral. Ital. **7**, 42 (1951).
8. U. S. Bureau of Mines, Albany, Oregon. A.S.T.M. card 16-378.
9. J. L. HOARD and V. BLAIR. J. Am. Chem. Soc. **57**, 1985 (1935).
10. L. J. KLINKENBERG and J. A. A. KETELAAR. Rec. Trav. Chim. **54**, 959 (1935).
11. H. E. SWANSON, M. C. MORRIS, E. H. EVANS, and L. ULMER. Natl. Bur. Stds. Monogram 25. Sect. 3. U. S. Government Printing Office, Washington. 1964. pp. 6–7.
12. A. P. CARON, J. L. RAGLE, M. E. YORKE, and H. YEH. J. Phys. Chem. **72**, 556 (1968).
13. L. J. KLINKENBERG. Rec. Trav. Chim. **56**, 36 (1937).
14. H. E. SWANSON, N. T. GILFRICH, M. I. COOK, R. STINCHFIELD, and P. C. PARKS. Natl. Bur. Stds. Circ. 539. Vol. 8. U. S. Government Printing Office, Washington. 1959. pp. 22–23.
15. VON E. HÖHNE and L. KUTSCHABSKY. Z. Anorg. Allgem. Chem. **344**, 279 (1966).
16. CHR. FINBAK and O. HASSEL. Z. Physik. Chem. B, **32**, 433 (1936).
17. A. P. CARON, D. J. HUETTNER, J. L. RAGLE, L. SHERK, and T. R. STENGLE. J. Chem. Phys. **47**, 2577 (1967).
18. D. J. HUETTNER, J. L. RAGLE, L. SHERK, T. R. STENGLE, and H. J. C. YEH. J. Chem. Phys. **48**, 1739 (1968).
19. M. STAMMLER, D. ORCUTT, and P. C. COLODNY. Advan. X-ray Anal. **6**, 202 (1962).
20. A. I. VOGEL. A textbook of quantitative inorganic analysis. 3rd ed. Longmans, Green and Co., London. 1961. Chap. IX.
21. R. W. G. WYCKOFF. Crystal structures. Vol. 3. 2nd ed. Interscience Publishers, Inc., New York. 1965. p. 50.
22. F. R. AHMED, C. P. HUBER, M. E. PIPPY, and C. P. SAUNDERSON. N.R.C. Crystallographic Programs for the I.B.M./360 System. Divisions of Pure Physics and Pure Chemistry, National Research Council of Canada, Ottawa, Canada.
23. International tables for X-ray crystallography. Vol. III. The Kynock Press, Birmingham, England. 1962. Table 3.3.1.A.
24. D. T. CROMER and J. T. WABER. Acta Cryst. **18**, 104 (1965).
25. H. J. C. YEH and J. L. RAGLE. J. Phys. Chem. **72**, 3688 (1968).
26. D. S. BROWN, J. D. LEE, and B. G. A. MELSOM. Chem. Commun. 852 (1968).
27. D. S. BROWN, J. D. LEE, and B. G. A. MELSOM. Acta Cryst. **B24**, 730 (1968).
28. J. L. HOARD, S. GELLER, and T. B. OWEN. Acta Cryst. **4**, 405 (1951).
29. W. B. BANG and G. B. CARPENTER. Acta Cryst. **17**, 742 (1964).
30. J. L. HOARD, S. GELLER, and W. M. CASHIN. Acta Cryst. **4**, 396 (1951).
31. J. H. BURNS. Acta Cryst. **15**, 1098 (1962).
32. D. L. DEADMORE and W. F. BRADLEY. Acta Cryst. **15**, 186 (1962).
33. G. M. BROWN and L. A. WALKER. Acta Cryst. **20**, 220 (1966).
34. A. ZALKIN, J. D. FORRESTER, and D. H. TEMPLETON. Acta Cryst. **17**, 1408 (1964).
35. H. BODE and G. TEUFER. Z. Anorg. Allgem. Chem. **283**, 18 (1956).
36. S. GELLER and J. L. HOARD. Acta Cryst. **3**, 121 (1950).
37. L. E. DRAIN. Discussions Faraday Soc. **19**, 200 (1955).
38. R. C. PLUMB and D. F. HORNIG. J. Chem. Phys. **23**, 947 (1955).
39. C. M. DEELEY and R. E. RICHARDS. Trans. Faraday Soc. **50**, 560 (1954).
40. M. L. KRONBERG and D. HARKER. J. Chem. Phys. **10**, 309 (1942).
41. D. PENDRED and R. E. RICHARDS. Trans. Faraday Soc. **51**, 468 (1955).
42. G. BRUNTON. Acta Cryst. **B24**, 1703 (1968).
43. A. WEISS and K. ZOHNER. Phys. Stat. Sol. **21**, 257 (1967).

Can. J. Chem. Downloaded from www.nrcresearchpress.com by 210.87.254.42 on 09/05/12
For personal use only.

Can. J. Chem. Downloaded from www.nrcresearchpress.com by 210.87.254.6 on 09/05/12
For personal use only.

Infrared spectra of adducts of tetrasulfur tetranitride with metal halides

P. J. ASHLEY[1] AND E. G. TORRIBLE[1]
Department of Chemistry, Queen's University, Kingston, Ontario

Received February 3, 1969

New complexes of S_4N_4 with $TiBr_4$, $ZrCl_4$, $NbCl_5$, and $TaCl_5$ have been prepared. The infrared spectra of these complexes together with the spectra of previously reported complexes have been determined. Possible structures for the complexes are discussed.

Canadian Journal of Chemistry, 47, 2587 (1969)

Introduction

The complexes of tetrasulfur tetranitride (S_4N_4) with transition metal halides have not been extensively studied. Adducts of the form $MX_n.S_4N_4$ ($n = 4, 5$) have been formed with $TiCl_4$, VCl_4, WCl_4, $SbCl_5$, $MoCl_5$, and adducts of the form $MX_4.2S_4N_4$ have been formed with $SnCl_4$ (1). Recently Wynne and Jolley reported the preparation of 1:1 adducts with the boron trihalides (2), and Becke-Goehring and Magin have reported the preparation of $2TiCl_4.S_4N_4$ (3). The structures of $SbCl_5.S_4N_4$ (4) and $BF_3.S_4N_4$ (5) have been determined by X-ray crystallographic studies. In this paper we report the preparation and infrared (i.r.) spectra of some new complexes of tetrasulfur tetranitride with transition metal halides, together with the i.r. spectra of the previously known complexes. Possible structures for the complexes are suggested based on the i.r. spectra and on the X-ray data for the antimony pentachloride and boron trifluoride complexes.

Experimental

Special precautions were taken to exclude water from the apparatus and reactants, and all reactions between metal halide and ligand were carried out in a dry nitrogen atmosphere. Solvents were dried by refluxing over sodium or phosphorous pentoxide and then fractionally distilled. Carbon tetrachloride, prepared as solvent for reactions involving niobium and tantalum pentachlorides, was further distilled from those halides and saturated with dry nitrogen. The metal halides were either distilled or sublimed directly into the reaction apparatus immediately prior to use.

Tetrasulfur tetranitride was prepared from ammonia and sulfumonochloride using the conditions described by Villena-Blanco (6), extracted with dioxane from the crude reaction products, and fractionally recrystallized from benzene. The orange crystals melted at 182 °C; lit. 178 °C (7), 184 °C (6).

The complexes were all prepared using the same general method. Either the pure liquid halide or a solution or slurry of solid halide in carbon tetrachloride was added to a refluxing solution of S_4N_4 in carbon tetrachloride. The resulting mixture was refluxed and stirred until reaction was complete; the products, which were all insoluble in carbon tetrachloride, were filtered, washed with hot carbon tetrachloride, and dried in vacuo. All complexes reacted vigorously with water and were hydrolyzed in air. The complexes were non-volatile and appeared insoluble in solvents with which no solvolysis occurred.

Metal, halogen, and nitrogen contents were determined by standard methods. The i.r. spectra were determined as Nujol mulls between KRS-5 plates on a Beckman IR-10 grating instrument.

Results and Discussion

Complexes of S_4N_4 with $TiCl_4$, VCl_4, and $SnCl_4$ were prepared as previously described (1). New complexes with $TiBr_4$, $ZrCl_4$, $NbCl_5$, and $TaCl_5$ were also prepared. Analytical data for these complexes are found in Table I. The i.r. spectra of these complexes and of $2TiCl_4.S_4N_4$, together with the reported spectra (2) of the antimony and boron halide complexes are listed in Table II.

The structural determinations for the BF_3 (5) and $SbCl_5$ (4) complexes gave evidence for S_4N_4 coordinated to the metal atom through one nitrogen atom, as shown in Fig. 1, where MX_n represents the coordinated metal halide. Free

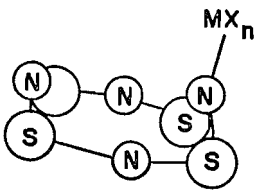

FIG. 1. Structure of S_4N_4 as monodentate ligand to a metal halide.

[1]Present address: Alcan Research and Development Limited, P.O. Box 8400, Kingston, Ontario.

TABLE I

Analytical data for complexes of S_4N_4

Complex	Color	Melting point (°C)	Analysis (%) Theoretical values M	X	N	Found M	X	N
$TiCl_4.S_4N_4$	Red-brown	132	12.81	37.92	14.98	12.74	37.23	14.76
$TiBr_4.S_4N_4$	Red	131	8.68	57.93	10.15	8.62		
$ZrCl_4.S_4N_4$	Brownish pink	244–255*	21.87	33.99	13.44	21.89	34.29	13.65
$SnCl_4.2S_4N_4$	Carmine	215–218	18.88	22.56	17.80	18.79	22.61	17.80
$VCl_4.S_4N_4$	Brown	190	13.52	37.63	14.87	13.52	36.83	15.10
$NbCl_5.S_4N_4$	Green-brown	180	20.45	39.02	12.34	20.45	39.09	12.16
$TaCl_5.S_4N_4$	Brown	180	33.37	32.61	10.33	33.84	32.84	10.16

*Decomposed.

S_4N_4 has a cage-like structure with the 4 nitrogen atoms coplanar and with 2 sulfur atoms above the plane and 2 below. Weak S—S bonding has been postulated (10). As a result of coordination, the configuration of the S_4N_4 molecule changes from the cage-like structure to that of a more open ring type structure in which the sulfur atoms are coplanar (4). Considering the symmetry of the ligand itself, this change in structure would not be expected to alter the number of i.r. active modes of the ligand. However, in the complex, the overall symmetry will govern the number of i.r. active vibrations, and for this reason it was expected that there would be an increase in the number of absorption bands associated with the coordinated ligand over that for the free ligand. Our spectrum for the free ligand shows closer agreement with that of Chapman and Massey (8) than with that of Lippincott and Tobin (9). However, our spectrum does show a weak shoulder at 1040 cm^{-1} in agreement with the weak band at 1040 cm^{-1} reported by Lippincott and Tobin.

From Table II it can be seen that the spectra of the complexes were very similar to those reported for the BF_3 and $SbCl_5$ complexes. The VCl_4 complex spectrum also showed some similarity to the spectrum of $2TiCl_4.S_4N_4$. The spectra were characterized by strong bands at about 1040, 960, 790, 505, and 350 cm^{-1}, respectively. The strong bands at 1040 and 790 cm^{-1} do not appear in the spectrum of S_4N_4 and appear characteristic of the monodentate S_4N_4 ligand.

Only one attempt to assign the frequencies for tetrasulfur tetranitride has so far been reported (9). The model on which the assignments were based has since been shown to be incorrect (10). However, the symmetry of that model has the same D_{2d} symmetry as the presently accepted structure; thus although the assignments made by Lippincott and Tobin are probably incorrect, their symmetry analysis of the i.r. and Raman active modes will apply to the correct structure. On this basis we have tentatively assigned the 920 cm^{-1} band in free S_4N_4 to an S—N stretch of B_2 symmetry. Lippincott and Tobin had previously assigned this band to an N—N stretch. Our assignment of the 920 cm^{-1} to an S—N stretching mode is supported by the results of Banister *et al.* (12) who examined the relationship between S—N stretching frequencies and S—N bond lengths. The S—N bond length of free S_4N_4 has been found to be 1.616 Å (11); Banister's results predict a corresponding stretching frequency of about 940 cm^{-1}. The X-ray studies on the $SbCl_5$ complex (4) indicate that the bond lengths of S_4N_4 are changed on coordination. The S—N distance for the coordinated nitrogen is about 1.75 Å and corresponds to the S—N stretching frequency at 785 cm^{-1} in the $SbCl_5$ complex. Thus the strong band at about 790 cm^{-1} in the complexes can be assigned to the S—N stretching frequency associated with the coordinated nitrogen. Similarly the strong band at around 1020–1040 cm^{-1} can be assigned to S—N stretching of the shortened bonds (13), e.g. 1.55 Å in the $SbCl_5$ complex. The frequency at 960 cm^{-1} in the complexes corresponds to the band at 920 cm^{-1} in free S_4N_4 and can be assigned to the S—N stretch of the bonds unchanged in length from free S_4N_4. The multiple structure of these bands can be attributed to the asymetric nature of the coordinated S_4N_4 ligand (4, 5).

Can. J. Chem. Downloaded from www.nrcresearchpress.com by 210.87.254.6 on 09/05/12
For personal use only.

Can. J. Chem. Downloaded from www.nrcresearchpress.com by 210.87.254.6 on 09/05/12
For personal use only.

TABLE II

Infrared spectra of adducts of S_4N_4 in the 4000–300 cm^{-1} region*

L†	$SbCl_5$.L‡	$NbCl_5$.L	$TaCl_5$.L	$TiCl_4$.L	$TiBr_4$.L	$ZrCl_4$.L	$2TiCl_4$.L	$SnCl_4$.2L	VCl_4.L	BF_3.L‡	BCl_3.L‡
	309 wsh					330 s	320 wsh	304 s	300 mh		
334 s	345 s	330 s	315 s	345 s	355 s	355 s		356 s	335 s		
	364 s	350 s	330 ssh	365 s					385 w		
	371 s			375 s			380 s				
408 vw	413 m	420 w	420 w	410 s	430 m	420 m	400 ssh	404 m	415 s	420 ms	430 m
		460 w			460 w		472 m		460 s	490 wsh	
510 m	513 ms	505 s	500 m	510 s	505 s	505 s		506 s	470 s	502 m	518 ms
521 m					540 w		520 w		500 s	527 s	
545 s		560 w	558 w	545 vw	565 w	550 w	535 w	556 w	560 m	552 w	552 wm
										567 w	614 wsh
619 wsh	625 m	610 w	615 w	625 w	620 w	620 w		619 m	655 ssh	623 ms	627 m
690 s	705 w	680 w	675 w	680 w	675 w	670 w		675 m	670 s	658 ms	660 m
720 ssh				720 wsh	700 w	720 wsh	725 w	715 wsh	720 w	682 w	678 m
757 m	765 wsh	750 m	743 m	760 m	750 wsh	740 w		785 ssh		697 w	695 m
	785 s	785 s			760 wsh			795 ssh		724 w	720 m
795 vw	808 m		791 s	785 s	780 s	790 s	820 s	805 s	840 s	840 mw	736 m
	821 ms	830 w			830 wsh		840 s		850 s	888 s	864 m
920 s		900 w			930 sh				940 s	908 m	
	978 ms	955 s	953 s	950 s	950 s	950 s		960 s	960 msh	949 s	958 s
1000 w			1020 msh	1020 msh	1020 wsh	1020 msh	1020 w	1025 msh	1010 m	1014	982 s
1040 wsh	1040 msh	1040 s	1040 s	1040 s	1040 s	1035 s		1040 s		1040 s	1042 m
1062 w	1060 s	1070 sh				1060 msh				1070 s	1064 s
						1110 w				1117 s	
							1190 w			1138 ms	
						1260 w			1200 w	1171 m	

*Abbreviations: s, strong; m, medium; w, weak; sh, shoulder.
†L = S_4N_4.
‡From ref. 2.

Can. J. Chem. Downloaded from www.nrcresearchpress.com by 210.87.254.6 on 09/05/12
For personal use only.

The spectra of both niobium and tantalum pentachloride complexes were very similar to that of the $SbCl_5 . S_4N_4$ complex, indicating that the structures of these complexes were similar to that of the $SbCl_5$ complex. The bands at 330 and 315 cm^{-1} in the niobium and tantalum complexes respectively are assigned as metal–halide bands, and the values are characteristic of the 6 coordinate metals (14).

The spectra of the titanium and zirconium tetrahalide complexes were also similar to that of the $SbCl_5$ complex. The ligand frequencies indicated a monodentate S_4N_4 ligand which would require a 5 coordinate metal. However, the metal halide bands at 365, 375, and 330 cm^{-1} assigned to the Ti—Cl and Zr—Cl stretching modes, respectively, indicated 6 coordinate metal (14). In such situations it is possible that a 5 coordinate complex forms initially and then achieves 6 coordination by halide bridging, as suggested by Rivest (15). Such a structure has been determined for the $TiCl_4 . POCl_3$ complex (16).

The absence of a terminal and bridging metal–halogen frequency in the spectrum of the $TiCl_4 . S_4N_4$ complex requires explanation. The terminal frequency was assigned as the band at 365–375 cm^{-1}. According to Adams and Chandler (17), bridging frequencies are found about 40 cm^{-1} lower than the terminal frequency, and hence would be expected at 325–335 cm^{-1}. At this frequency the metal–halide bridge absorption will be masked by a strong ligand absorption.

The spectrum of the $SnCl_4$ complex again showed ligand bands indicative of a monodentate ligand. $SnCl_4 . 2L$ complexes have been found to be *cis*-coordinated for small ligands, and *trans*-coordinated for bulky ligands (18). Identification of these two species was based on the number of observed metal–halide absorption bands. For the *cis*-configuration 3 peaks between 360 and 290 cm^{-1} were expected, but only one at about 330 cm^{-1} for the *trans*-configuration. On this basis the single peak at 304 cm^{-1} supported the *trans*-configuration proposed by Weiss (19).

The spectrum of the VCl_4 complex shows some similarity to those of the other tetrahalide complexes but also shows some striking differences. The band at 1010 cm^{-1} in the VCl_4 complex was a singlet, whereas in a complex with monodentate S_4N_4 the band was multiple. Also a strong band system appeared at 840–850 cm^{-1}, about 50 cm^{-1} higher than the corresponding band in complexes containing the monodentate ligand. The band at 670 cm^{-1} was strong whereas for the others it was weak. The i.r. spectrum of a sample of the compound $2TiCl_4 . S_4N_4$ showed a singlet absorption at 1020 cm^{-1}, a strong band system at 820–840 cm^{-1}, but no absorption in the 670 cm^{-1} region. However, a strong band at 472 cm^{-1} in the $2TiCl_4 . S_4N_4$ complex was observed as a doublet in the VCl_4 complex. Becke-Goehring has suggested that in $2TiCl_4 . S_4N_4$, the ligand is bidentate and acts as a bridge between the two $TiCl_4$ molecules which are also halide bridged (3). We suggest that in $VCl_4 . S_4N_4$, the ligand is also bidentate and bridges 2 vanadium atoms. This would give the complex a *trans*-polymeric structure and vanadium a coordination number of 6 (Fig. 2). This is supported by the observed absorption at 385 cm^{-1}, which is reported as characteristic of a V—Cl stretching mode in six-coordinated vanadium complexes (14).

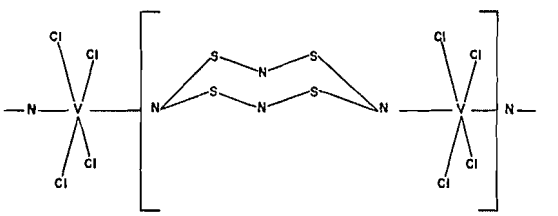

FIG. 2. Polymeric structure of $VCl_4 . S_4N_4$.

Acknowledgments

Grateful acknowledgement is made to the National Research Council of Canada for financial support and to the Government of the Province of Ontario for three Fellowships (to P.J.A.).

The authors are also very grateful to Professor M. Becke-Goehring who generously supplied a sample of the compound $2TiCl_4 . S_4N_4$.

1. D. NEUBAUER, J. WEISS, and M. GOEHRING. Z. Naturforsch. **14B**, 284 (1959).
2. K. WYNNE and W. L. JOLLEY. Inorg. Chem. **6**, 107 (1967).
3. M. BECKE-GOEHRING and G. MAGIN. Z. Anorg. Allgem. Chem. **340**, 125 (1965).
4. D. NEUBAUER and J. WEISS. Z. Anorg. Allgem. Chem. **303**, 28 (1960).
5. M. G. DREW, D. H. TEMPLETON, and A. ZALKIN. Inorg. Chem. **6**, 1906 (1967).
6. M. VILLENA-BLANCO. M.S. Thesis, University of California. 1963.

7. M. BECKE-GOEHRING. Ergebnisse und Problem der chemie du Schwefelstickstoff verbindungen, Scientia Chemica, Band 9. Berlin. 1957.
8. D. CHAPMAN and A. G. MASSEY. Trans. Faraday Soc. **58**, 1291 (1962).
9. E. R. LIPPINCOTT and M. C. TOBIN. J. Chem. Phys. **21**, 1559 (1953).
10. A. G. TURNER and F. S. MORTIMER. Inorg. Chem. **5**, 906 (1966).
11. D. B. SHARMA and J. DONOHUE. Acta Cryst. **16**, 891 (1963).
12. A. J. BANISTER, L. F. MOORE, and J. S. PADLEY. Spectrochim. Acta, **23**, 2705 (1967).
13. T. S. PIPER. J. Am. Chem. Soc. **80**, 30 (1958).
14. R. J. H. CLARK. Spectrochim. Acta, **21**, 955 (1965).
15. R. RIVEST. Can. J. Chem. **40**, 2234 (1962).
16. C. I. BRANDEN and I. LINDQUIST. Acta Chem. Scand. **14**, 726 (1960).
17. D. M. ADAMS and P. J. CHANDLER. Chem. Commun. 69 (1966).
18. I. R. BEATTIE and L. RULE. J. Chem. Soc. 3267 (1964).
19. J. WEISS. Fortschr. Chem. Forsch. **5**. 635 (1966).

Can. J. Chem. Downloaded from www.nrcresearchpress.com by 210.87.254.6 on 09/05/12
For personal use only.

Can. J. Chem. Downloaded from www.nrcresearchpress.com by 210.87.254.40 on 09/05/12
For personal use only.

Calculated R.R.K.M. unimolecular dissociation rate constants for hydrazine[1]

D. W. SETSER[2] AND W. C. RICHARDSON
Department of Chemistry, Kansas State University, Manhattan, Kansas 66502

Received November 26, 1968

Unimolecular rate constants for hydrazine dissociation by thermal and chemical activation have been calculated according to the R.R.K.M. theory. The two activated complex models used in the calculations represent plausible upper and lower bounds to the rate constants. The calculations are mainly directed toward establishing expected decomposition to stablilization ratios of N_2H_4 produced by combination of NH_2 radicals; however, a general comparison to available experimental data for hydrazine dissociation is made.

Canadian Journal of Chemistry, 47, 2593 (1969)

Introduction

During the course of an experimental investigation (1) of NH and NH_2 radical reactions in our laboratory, the stabilization (S) to decomposition (D) ratio at various pressures and temperatures of hydrazine formed by reaction [1] was needed.

$$[1] \qquad NH_2 + NH_2 \rightleftarrows N_2H_4^* \xrightarrow{\omega} N_2H_4(S)$$
$$\xrightarrow{k_a} 2\ NH_2(D)$$

Since experimental information was not available, a Rice Ramsperger Kassel Marcus (R.R.K.M.) (2) theoretical estimate of the S/D ratio (3) was made. The NH_2 radical combination reaction has been suggested to be of importance in many photolysis and pyrolysis systems involving nitrogen–hydrogen compounds, and our calculated results are summarized and compared to the existing experimental data. The calculations suggest that most experiments were done at much too low a pressure to obtain the true rate constant for NH_2 combination due to the occurrence of reverse dissociation. For the models chosen for the activated complex, the calculated results also indicate that the shock tube investigations of N_2H_4 dissociation have been conducted in the fall-off region rather than in the high pressure region.

Reliable experimental information, e.g., entropy of activation, is not available for the formulation of a good model for the activated complex for hydrazine dissociation. Therefore, N_2H_4 decomposition was assumed to belong to the class of dissociation reactions having loose transition states and positive entropies of activation, such as the dissociation of ethane (4). Or in terms of the reverse reaction, NH_2 combination, the assumption is that the combination rate constant is typical for radical combination. R.R.K.M. (2) calculations were performed for two models which are believed to give upper and lower bounds to the rate constants. Only a very general outline of the equations (3, 5) and procedures (1) used in the calculations are presented because they are relatively standard.

We also have done R.R.K.M. calculations for the dissociation of methylamine. The rate constants have values similar to those for acetaldehyde (5). Since CH_3NH_2 is of less general interest than hydrazine, these rate constants are not included here, but they are available upon request (1).

Calculated Results

In order to obtain R.R.K.M. values of the specific rate constants, k_ε, for hydrazine, a model of the molecule, models of the activated complex for reaction [1], and the critical energy for rupture of the $H_2N—NH_2$ bond are needed. The thermochemistry (8), vibrational frequencies (9*a*), and moments of inertia of N_2H_4 (9*b*) are relatively well known. However, despite several shock tube investigations (6, 7) of N_2H_4 dissociation, a reliable value for the high pressure pre-exponential factor is not available and other information was used to obtain an estimate of this pre-exponential factor. We combined calculated values of the equilibrium constant (NH_2, N_2H_4) with values of the NH_2 bimolecular combination rate constant to obtain the pre-exponential factors for the

[1]Abstracted from the thesis of W. C. Richardson, which was submitted in partial fulfillment of the requirements of the Master's Degree, Kansas State University, 1969.

[2]Alfred P. Sloan Foundation Fellow.

TABLE I

Models for N_2H_4 molecule and activated complex

Molecule[a,b]			Complex[a,b]			
Vibrational frequencies[c] (cm^{-1})		I (g cm^2 × 10^{40}) Adiabatic	Vibrational frequencies[d] (cm^{-1})		I (g cm^2 × 10^{40}) Active	I (g cm^2 × 10^{40}) Adiabatic
			Model I			
3282(4)	1549(2)	6.18	3220(2)	150(2)		4.86
1183(2)	860(2)	35.3	3173(2)	80(2)		138.0
780(1)	377(1)	37.0	1499(2)		1.21	134.0
			Model II			
			3220(2)	275(2)		4.86
			3173(2)	200(2)		138.0
			1499(2)		1.21	134.0

[a]The measured torsional frequency of 377 cm^{-1} was used for computation of density of states for N_2H_4 molecule. For the complex the torsional motion was treated as a free internal rotor with a symmetry number of 2.
[b]For both molecule and complex the three overall rotations were treated as adiabatic. The moments of inertia of the complex were obtained by extending the r(N—N) of hydrazine from 1.47 to 3.0 Å and assuming the complex to be planar.
[c]The N_2H_4 frequencies are from ref. 9.
[d]The three high sets of frequencies for the complexes are the same as for NH_2 (12). The two low sets were assigned to obtain the steric factors specified in the text.

unimolecular rate constant which served to define the model of the activated complex.

The thermochemistry of reaction [1] seems well established, and if a 1 kcal $mole^{-1}$ barrier is taken as the activation energy for association of NH_2 radicals, the critical energy for N_2H_4 decomposition becomes 56.8 kcal $mole^{-1}$. The overall rotational degrees of freedom of N_2H_4 were considered to be adiabatic, and all internal degrees of freedom were taken to be active. The torsional motion was treated as a vibration for the computation of the density of states for N_2H_4, although the barrier to internal rotation is only 2.5 kcal $mole^{-1}$ (9*b*). Representing the torsion as a vibration gives a lower limit to the density while using an internal rotor gives an upper limit. The latter would have increased the density of states by about a factor of 3; and hence, the rate constants would be lowered by this amount. For our purpose of estimating a range of rate constants, there is no point in considering anharmonicity (10) or centrifugal stretching (11) effects. The model for N_2H_4 is summarized in Table I.

The N_2H_4, NH_2 equilibrium constant was calculated from the model of N_2H_4, $D(H_2N—NH_2)$ and the molecular parameters of NH_2 (12). The combination reaction of NH_2 radicals has not been thoroughly studied but the available data (13, 14) indicate that it is a "typical" radical combination reaction with a rate constant between 0.1 and 0.01 of the collision number. The pre-exponential factors from these two assumed steric factors correspond to the models of activated complex which are listed in Table I. In terms of partition function ratios and critical energies, the unimolecular high pressure thermal activation rate constants are $k_\infty = 3.35 \times 10^{16} \exp(-56.8 \text{ kcal mole}^{-1}/RT)$ and $2.52 \times 10^{15} \exp(-56.8 \text{ kcal mole}^{-1}/RT)$ at 720 °K. The torsional degree of freedom of the complex was treated as a free rotation; the three overall rotations were taken to be adiabatic as in the molecule. The vibrational frequencies of the activated complex are those of 2 NH_2 radicals (12) with 4 additional low bending frequencies. The latter were arbitrarily adjusted to obtain the two pre-exponential factors defined by the values of the NH_2 combination rate constants. It could be argued that one of the overall rotational degrees of freedom should be active for both the complex and the molecule; this would merely lower the specific rate constants by about a factor of 2 (5).

The specific rate constants and distribution functions, $f(\varepsilon)$, of activated N_2H_4 molecules formed by NH_2 association were computed from standard equations (5) and are shown in Figs. 1 and 2. These rate constants must be matched against a collisional deactivation model and then averaged over the distribution function to obtain quantities (S/D, k_a) which can be compared to

Can. J. Chem. Downloaded from www.nrcresearchpress.com by 210.87.254.40 on 09/05/12
For personal use only.

Can. J. Chem. Downloaded from www.nrcresearchpress.com by 210.87.254.40 on 09/05/12
For personal use only.

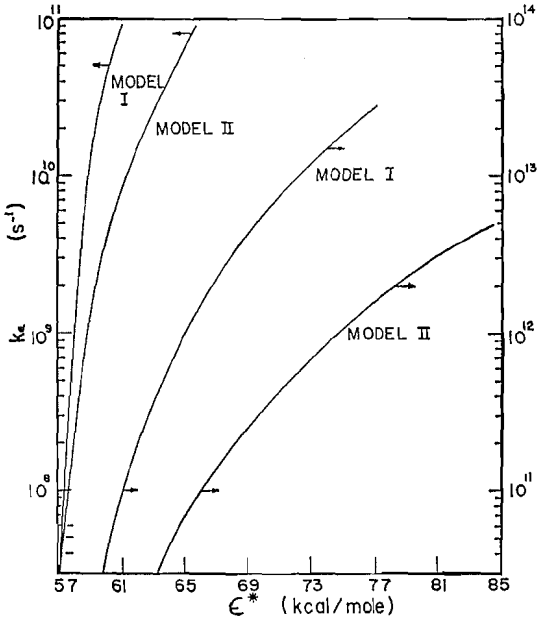

FIG. 1. Hydrazine R.R.K.M. specific rate constants for models I and II as a function of the energy in the molecule; $\varepsilon_0 = 56.8$ kcal mole^{-1}.

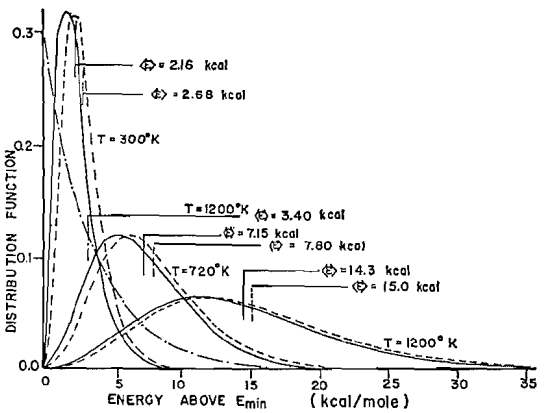

FIG. 2. Distribution functions of activated N_2H_4 molecules in chemical (reaction[1]) and thermal activation. The average energies are specified for each distribution function. –·–, thermal activation at 1200 °K; – – –, chemical activation model I (300, 720, 1200 °K); ——, chemical activation model II (300, 720, 1200 °K).

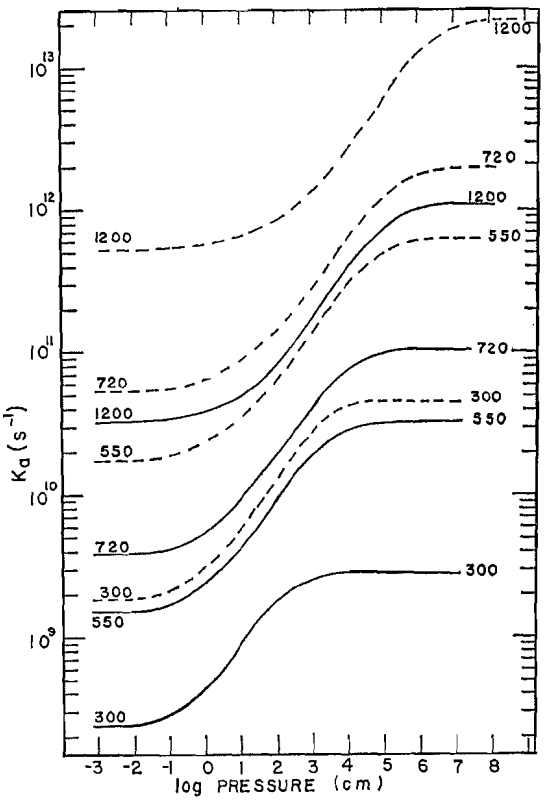

FIG. 3. Values of the chemical activation rate constants at various temperatures (°K) for model I (dotted lines) and model II (solid lines). The k_a values match the S/D values at the indicated pressures of Table II.

experiment. We have used a strong collision formulation with the appropriate equations (3, 5); the S/D results are listed in Table II, and the $k_a = \omega(D/S)$ values are plotted in Fig. 3. The k/k_∞ curves often used in thermal activation studies may be constructed (3) from the S/D values of Table II, i.e., $k/k_\infty = S/(S + D)$. Since some shock tube investigations employ a Kassel s parameter, these values were also extracted from the calculations. Kassel s values were obtained from the average energy of the reacting molecules at high pressure in thermal activation ($s' = \langle\varepsilon\rangle_r\dagger/RT$), which were $s' = 5.4$ and 5.0 at 720 °K and $s' = 6.3$ and 6.0 at 1200 °K for models I and II, respectively. These Kassel parameters were compared to those obtained by matching the shape of the Kassel and R.R.K.M. fall-off curves, and the values were quite similar, as would be expected (15).

Since the distribution functions of N_2H_4 in chemical activation depend upon the model of the association complex (3), the $f(\varepsilon)$ of Fig. 2 are slightly different for models I and II. The exact shape of chemical activation distribution functions is usually not very important. However, it is of interest for hydrazine because the average

Can. J. Chem. Downloaded from www.nrcresearchpress.com by 210.87.254.40 on 09/05/12
For personal use only.

TABLE II

Calculated S/D values for hydrazine

Temperature (°K)	Calculation[a,b,c]	Model	Pressure (cm Hg) 10^6	10^5	10^4	10^3	10^2	10	1.0
300	S/D	I	1.89×10^3	193	22.2	3.48	0.737	0.164	3.15×10^{-2}
		II	3.38×10^4	3.38×10^3	342	37.3	5.28	1.03	0.220
	$\langle\varepsilon\rangle_r$† (kcal/mole)	I	5.00	4.94	4.65	4.00	3.32	2.90	2.73
		II	4.40	4.40	4.37	4.17	3.60	2.91	2.42
550	S/D	I	117	14.2	2.42	0.526	0.114	2.07×10^{-2}	3.06×10^{-3}
		II	2.13×10^3	2.18×10^2	24.7	3.80	0.782	0.170	
	$\langle\varepsilon\rangle_r$† (kcal/mole)	I	10.1	9.29	7.90	6.64	5.94	5.69	5.62
		II	9.61	9.51	8.95	7.67	6.31	5.47	
720	S/D	I	34.4	5.05	1.02	0.227	4.49×10^{-2}	7.24×10^{-3}	9.72×10^{-4}
		II	591	62.9	8.34	1.55	0.343	7.02×10^{-2}	1.16×10^{-2}
	$\langle\varepsilon\rangle_r$† (kcal/mole)	I	13.5	11.8	9.89	8.57	8.00	7.83	7.80
		II	13.5	13.1	11.7	9.75	8.23	7.48	7.24
1200	S/D	I	3.93	0.824	0.184	3.54×10^{-2}	5.51×10^{-3}	7.22×10^{-4}	8.42×10^{-5}
		II	47.3	6.51	1.27	0.284	5.73×10^{-2}	9.38×10^{-3}	1.26×10^{-3}
	$\langle\varepsilon\rangle_r$† (kcal/mole)	I	21.9	18.5	16.2	15.3	15.1	15.0	15.0
		II	24.7	22.2	18.7	16.1	14.8	14.4	14.3

[a]A temperature independent collision cross section of 3.5 Å was used for the calculation of the collision frequency.
[b]$\langle\varepsilon\rangle_r$† is the average internal energy of the reacting molecules above ε_0 (56.8 kcal mole^{-1}).
[c]The average energy of the formed molecules for complex models (I) and (II) is 2.68 and 2.16 kcal mole^{-1} at 300 °K, 5.61 and 5.02 kcal mole^{-1} at 550 °K, 7.80 and 7.15 kcal mole^{-1} at 720 °K, and 15.0 and 14.3 kcal mole^{-1} at 1200 °K.

TABLE III

Reported and calculated Arrhenius rate constants for hydrazine dissociation

Reference	Arrhenius rate constant (s^{-1})	Conditions
(7)	$10^{13.0}$ exp (-54 kcal mole$^{-1}/RT$)	(970–1100 °K, 2.6–8 atm)[a]
(6*a*)	$10^{14.0}$ exp (-60 kcal mole$^{-1}/RT$)	(1100–1500 °K, 2.6–8 atm)[b]
(6*b*)	$10^{12.0}$ exp (-48 kcal mole$^{-1}/RT$)	(1370–1600 °K, 2.3–3.3 atm)[c]
(6*b*)	$10^{12.8}$ exp (-52 kcal mole$^{-1}/RT$)	(1270–1580 °K, 6.8–9.8 atm)[c]
Model I	6.72×10^{17} exp (-61.2 kcal mole$^{-1}/RT$)	1200 °K, ∞ pressure
Model II	3.23×10^{16} exp (-60.5 kcal mole$^{-1}/RT$)	1200 °K, ∞ pressure

[a]The rate under these conditions depended upon $[N_2H_4]$ and the [pressure]$^{1/2}$. The results were "corrected" to the high pressure limit and combined with data from ref. 6*a* to obtain the Arrhenius parameters.
[b]These results were not sufficiently complete for experimental determinations of Arrhenius parameters so the authors used 60 kcal as the activation energy in order to assign a pre-exponential factor.
[c]The experiments were done at constant density which corresponds to the two pressure ranges quoted. The Arrhenius parameters were obtained under conditions where chain reactions were believed to be negligible.

energies of formed molecules differ by about 0.5 kcal mole^{-1} which enhances the difference in k_ε since the broader $f(\varepsilon)$ goes with the higher k_ε values for the calculation of S/D ratios. The distribution functions also give the average energies of reacting molecules at the low and high pressure limits. The distribution function of reacting N_2H_4 molecules at the high pressure limit in the thermal activation system is the same as the distribution function of formed chemically activated molecules, reaction [1], at the same temperature. The difference in average energies of reacting molecules at the low and high pressure limits in thermal activation is 11.6 and 10.9 kcal mole^{-1} for models I and II, respectively. This energy difference at 1200 °K for the chemical activation is similar, 11.3 and 11.1 kcal mole^{-1}. These large values arise from the steep energy dependence of the rate constants and the broad 1200 °K distributions. These are the same factors which cause the large change in the values of the chemical activation rate constants with pressure shown in Fig. 3. Since the difference between the average energies for the two limiting pressures, $\langle\varepsilon\rangle_r^\infty - \langle\varepsilon\rangle_r^0$, decline with decreasing temperature (4.7 and 2.3 kcal mole^{-1} at 550 and 300° for model I), the ratio of k_a^∞ to k_a^0 also diminishes with temperature. However, even at room temperature the ratio is quite large, more than a factor of 10, due to the very steep dependence of k_ε upon energy in the energy range just above ε_0.

Comparison of Calculated Results to Experimental Data

The point of view adopted for these calculations was that our knowledge of radical combination rate constants was more reliable than the existing unimolecular decomposition data for N_2H_4. It is now interesting to compare the results from shock tube studies (6, 7) with the calculated predictions. Table III gives the Arrhenius parameters and shows serious disagreement between the calculated and experimental Arrhenius A factor. Diesen (14) seems to have directly shown that the primary process is reaction [1] and not the less endothermic formation of NH and NH_3, and even at the lower temperatures (1400 °K) the reaction was essentially second order at 0.15 atm pressure. The rate constant at 1400 °K and 0.15 atm was reported (14) as 3×10^3 s^{-1} but the accuracy of these values has been questioned (7). McHale studied the reaction at low temperatures and found that at 2.6–8 atm the rate depended upon the square root of the total pressure (mostly argon). A correction factor was applied to the measured rate constants to give rate constants at $P = \infty$, and these rate constants were combined with other high temperature data (6*a*) to obtain the first set of Arrhenius parameters listed in Table III. The recently reported rate constants of Michel and Wagner (6*b*) show a slight dependence upon gas density but the data are not of great accuracy. The Arrhenius parameters from their first study (6*a*) were merely assigned (see Table III) and are probably not reliable. It should be noted that the experimental rate constants of Table III are numerically about the same at 1200 °K but differ in their temperature coefficients.

The measured pressure dependence of the reaction and the low activation energies from most shock tube investigations point to the hydrazine decomposition reaction being in the

Can. J. Chem. Downloaded from www.nrcresearchpress.com by 210.87.254.40 on 09/05/12
For personal use only.

Can. J. Chem. Downloaded from www.nrcresearchpress.com by 210.87.254.40 on 09/05/12
For personal use only.

fall-off region even at 2–8 atmospheres of pressure. The calculated $k/k_\infty = S(S + D)$ values are in agreement with this. At 1200 °K and for 5 atm pressure of a *unit efficiency* gas, k/k_∞ is 0.018 and 0.12 for models I and II. Since argon was the actual experimental gas which has a collisional efficiency of ~0.1 (16), the experimental rates should be only 10^{-3} and 10^{-2} of the high pressure values of model I and II, respectively. Thus if the degree of fall-off is as great as outlined above, this explains the apparent discrepancy in the pre-exponential factors of Table III. It is worth noting that the calculated limiting low pressure activation energy at 1200 °K would be about 49 kcal/mole. The arguments of this paragraph indicate that the shock tube data do not provide compelling reasons for considering the N_2H_4 dissociation to be different from C_2H_6 (3) or C_2F_6 (16) dissociation[3] reactions. If future data are obtained which show that activated complex models with a tighter structure (smaller pre-exponential factor and smaller steric factor) are appropriate, then those models would not require the experimental data of Table III to be as far into the fall-off region as they presently appear.

Calculated R.R.K.M. unimolecular rate constants have been shown to satisfactorily describe a large variety of unimolecular reaction rate data (18, and recent papers by Rabinovitch) if proper models for the reaction are chosen. The arguments already presented indicate that our calculations for N_2H_4 should encompass the correct description of its unimolecular dissociation. Therefore, it should be possible to use the calculated results with some confidence. The calculations show (for either model) that at temperatures of 300 °K or more, pressures of 100 cm are needed to stabilize a large fraction of N_2H_4* formed by radical association. Most experiments have been done at considerably lower pressures, and reverse dissociation of N_2H_4* should have been important. From a practical point of view, stabilization of N_2H_4* produced by higher energy chemical activation reactions, such as $H + N_2H_3$, would be a slow and strictly pressure dependent reaction (19).

The combination reaction of NH_2 has been suggested in a variety (20) of photolysis and photosensitization studies of NH_3 and N_2H_4 but only a few attempts have been made to extract rate constants. In one such effort Hanes and Bair (13*a*) used a pulsed radio frequency discharge in ammonia and followed the NH_2 concentration by ultraviolet absorption spectroscopy. The data were originally discussed in terms of a simple bimolecular association process. The error of ignoring the NH_2 disproportionation reaction in this treatment was pointed out by Diesen (14)

$$[2] \qquad NH_2 + NH_2 \xrightarrow{k_d} NH_3 + NH \qquad \Delta H_R^\circ = -10 \text{ kcal/mole}$$

In Diesen's (14) shock tube study the rate constant for disproportionation was given as 2.5×10^{13} cc mole^{-1} s^{-1} (2000 °K) and k_d/k_c was estimated as 0.4. A reinvestigation by Salzman and Bair (13*b*) using room temperature NH_3 flash photolysis revealed that the rate of NH_2 disappearance was dependent on total pressure in the pressure range of 5–10 Torr. Extrapolation to low pressure gave the disproportionation rate constant as 0.46×10^{12} cc mole^{-1} s^{-1}, and extrapolation to high pressure gave 2.5×10^{12} cc mole^{-1} s^{-1} as the combination rate constant (k_c). These data give $k_d/k_c = 0.18$, which is a reasonable value by comparison with ethyl radical kinetics. However, some caution should be maintained because the high pressure extrapolation was made from data in the 1–10 Torr region which, according to Table II, are 2 orders of magnitude away from the high pressure limit. A recent investigation (21) of NH_2 kinetics used an ammonia glow discharge flow system as the NH_2 source. The reported k_d/k_c ratio was 1.0, but the absolute values of the rate constants seem impossibly low.

The pressure dependence of the rate of NH_2 combination found by Bair is in qualitative agreement with the calculated results. Further data are required before any discrimination can be made in favor of model I or II.

The decomposition of N_2H_4 was assumed to be a reaction similar to the decomposition of C_2H_6 or CH_3CHO for which R.R.K.M. calcula-

[3] C_2F_6 dissociation (17) has recently been treated by using a Gorin model for the activated complex to obtain a frequency factor of $\sim 5 \times 10^{17}$. The C—C distance was extended by nearly a factor of 4 relative to C_2F_6 which introduced a large centrifugal correction factor. Such a correction is not necessary, if the C—C distance is not extended so much and the high frequency factor is obtained from the large entropy contributions of low frequency bending vibrations, as was done in the N_2H_4* models of Table I.

Can. J. Chem. Downloaded from www.nrcresearchpress.com by 210.87.254.40 on 09/05/12
For personal use only.

tions have been done. It is instructive to compare the results from chemically activated C_2H_6 and CH_3CHO to those of Table II. Similar models should be used for the comparison, and we will compare models that most nearly resemble model I for N_2H_4. The easiest comparison is the half quenching pressures ($S/D = 1$) which are 1, 7, and 1400 Torr, at 300 °K for C_2H_6*, CH_3CHO* and N_2H_4*, respectively. In this series the critical energies are 85.3, 79.0, and 56.8 kcal, and the number of active degrees of freedom successively decline by 3 for each member. Detailed examinations of the relative values of sums and densities of states for these three reactions show that the increase in rate constant for N_2H_4 relative to CH_3CHO is due to both the lower critical energy (about a factor of 15) and to the smaller number of vibrational degrees of freedom. The vibrational frequencies for N_2H_4 are higher than those for CH_3CHO which also enhances the difference in rate constants for N_2H_4 relative to CH_3CHO. Although the models for C_2H_6, CH_3CHO, and N_2H_4 dissociation reactions are not strictly comparable, it is worth noting that CH_3CHO is the anomalous member of the series due to the fact that replacing 2 hydrogen atoms by 1 oxygen atom introduces sufficiently low frequencies in the CH_3CHO molecule, so that the density of states for CH_3CHO is nearly the same as for C_2H_6.

Acknowledgments

This work was supported by the U.S. National Air Pollution Control Administration, Consumer Protection and Environmental Health Service, Public Health Service under contract AP-00391.

1. W. C. RICHARDSON. Master's Thesis, Kansas State University, Manhattan, Kansas. 1969.
2. (*a*) R. A. MARCUS and O. K. RICE. J. Phys. Colloid Chem. **55**, 894 (1951). (*b*) R. A. MARCUS. J. Chem. Phys. **20**, 352 (1952); **43**, 2658 (1965).
3. B. S. RABINOVITCH and D. W. SETSER. Advan. Photochem. **3**, 1 (1964).
4. (*a*) D. W. SETSER and B. S. RABINOVITCH. J. Chem. Phys. **40**, 2427 (1964). (*b*) M. C. LIN and K. J. LAIDLER. Trans. Faraday Soc. **64**, 79 (1968).
5. D. W. SETSER. J. Phys. Chem. **70**, 826 (1966).
6. (*a*) K. W. MICHEL and H. GG. WAGNER. Technical Summary Report No. 3, Contract No. AF61 (514)-1142 (1962). (*b*) K. W. MICHEL and H. GG. WAGNER. 10th Intern. Symp. Comb. Cambridge. 1965. p. 353.
7. E. T. MCHALE, B. E. KNOX, and H. B. PALMER. 10th Intern. Symp. Comb. Cambridge. 1965. p. 341, and Project Squid Technical Report PSU-12-D (1964).
8. JANAF Thermochemical Tables. The Dow Chemical Company, Midland, Michigan. August, 1965; Addendum 1, August, 1966; Addendum 2, August, 1967.
9. (*a*) J. S. ZIOMEK and M. D. ZEIDLER. J. Mol. Spectry. **11**, 163 (1963). (*b*) A. YAMAGUCHI, I. ICHISHIMA, T. SHIMANOUCHI, and S. MIZUSHIMA. Spectrochim. Acta, **16**, 1471 (1960).
10. (*a*) K. A. WILDE. J. Chem. Phys. **41**, 448 (1964). (*b*) Z. PRASIL and W. FORST. J. Phys. Chem. **71**, 3166 (1967).
11. (*a*) W. FORST. J. Chem. Phys. **48**, 3665 (1968). (*b*) E. TSCHUIKOW-ROUX. J. Chem. Phys. **49**, 3115 (1968).
12. D. E. MILLIGAN and M. E. JACOX. J. Chem. Phys. **43**, 4487 (1965).
13. (*a*) M. H. HANES and E. J. BAIR. J. Chem. Phys. **38**, 672 (1963). (*b*) J. D. SALZMAN and E. J. BAIR. J. Chem. Phys. **41**, 3654 (1964), and private communications.
14. R. W. DIESEN. J. Chem. Phys. **39**, 2121 (1963).
15. D. W. PLACZEK, B. S. RABINOVITCH, G. Z. WHITTEN, and E. TSCHUIKOW-ROUX. J. Chem. Phys. **43**, 4071 (1965).
16. F. FLETCHER, B. RABINOVITCH, K. WATKINS, and D. LOCKER. J. Am. Chem. Soc. **70**, 2823 (1966).
17. E. TSCHUIKOW-ROUX. J. Chem. Phys. **43**, 2251 (1965); **49**, 3115 (1968).
18. (*a*) C. W. LARSON, B. S. RABINOVITCH, and D. C. TARDY. **47**, 4570 (1967). (*b*) K. DEES and D. W. SETSER. J. Chem. Phys. **49**, 1193 (1968).
19. P. K. GHOSH and E. J. BAIR. J. Chem. Phys. **45**, 4738 (1966).
20. (*a*) C. C. MCDONALD and H. E. GUNNING. J. Chem. Phys. **23**, 532 (1955). (*b*) D. HUSAIN and R. G. W. NORRISH. Proc. Roy. Soc. London, Ser. A, **273**, 145 (1963).
21. D. C. CARBAUGH, F. J. MUNNO, and J. M. MARCHELLO. J. Chem. Phys. **47**, 5211 (1967).

Electron spin resonance study of γ-irradiated ethyleneimine in the solid state[1]

D. CORDISCHI AND R. DI BLASI
Laboratorio di Chimica delle Radiazioni e Chimica Nucleare del C.N.E.N.
Istituto di Chimica Generale ed Inorganica, Università di Roma, Rome, Italy

Received October 18, 1968

The electron spin resonance (e.s.r.) study of the ethyleneimine in polycrystalline and glassy state shows that the radical 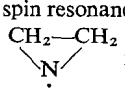 is formed by γ-irradiation at 77 °K. The features of the e.s.r. spectrum of this radical are discussed in terms of the isotropic and anisotropic hyperfine coupling constants of the hydrogen and nitrogen nuclei. The effects of bleaching the γ-irradiated sample with visible and ultraviolet light are also reported.

Canadian Journal of Chemistry, 47, 2601 (1969)

Can. J. Chem. Downloaded from www.nrcresearchpress.com by 210.87.254.42 on 09/05/12
For personal use only.

Various aliphatic amines have been studied by e.s.r. in an attempt to identify the paramagnetic species produced by γ- and ultraviolet (u.v.) irradiation in the solid state (1–4). The low melting points of these compounds make single crystal studies difficult. The published spectra have been obtained from irradiated polycrystalline samples. The anisotropic effects give rise to poorly resolved spectra which are generally difficult to interpret unambiguously. Only in a few cases are fairly clear spectra obtained.

In the present investigation the example of ethyleneimine, which gives a well resolved spectrum, is reported.

Experimental

Ethyleneimine (Fluka reagent) was purified by distillation and dried with a sodium mirror. Ethyleneimine-d_1 was prepared by exchange of ethyleneimine with D_2O. Its isotopic purity, checked by nuclear magnetic resonance, was better than 95%.

Spectrosil quartz tubes filled with about 0.1 g of the substance, were sealed under vacuum at 10^{-4} Torr. Samples were irradiated by γ-rays from a Co^{60} source at −196 °C with a dose rate of 0.23 Mrad/h. A high pressure mercury lamp was used for u.v. irradiation of the samples frozen in liquid nitrogen.

The e.s.r. spectra were recorded at 9.2 GHz using a Hilger and Watts Microspin spectrometer with a TE_{011} cylindrical cavity.

The measurements were performed at —196 °C by keeping the sample tubes in a quartz Dewar filled with liquid nitrogen, or at higher temperatures by using a variable nitrogen flow system.

Small samples of diphenyl picryl hydrazyl (DPPH) were used as g markers. The g value of DPPH was taken as 2.0036.

The field sweep calibration was carried out by a Mn^{2+} doped sample of MgO (5).

Results

Anhydrous ethyleneimine frozen at −196 °C gives an opaque crystalline matrix which after γ-irradiation shows a weak blue color. The product containing about 20% of water gives a transparent glass with an intense blue color after γ-irradiation. The e.s.r. spectrum, recorded at −196 °C, is practically the same in both cases and does not change from −196 to about −90 °C. The only difference is a narrowing of the line-width, from 8 G (peak to peak) at −196 °C to 5.8 G at about −100 °C.

The apparent intensity of the spectrum is of the same order of magnitude in the amorphous and crystalline samples and diminishes continuously with increasing temperature up to about −85 °C, where it disappears. A typical spectrum is reported in Fig. 1*a*. It consists of 5 lines with 30.0 G splitting and of 2 outer weak satellites; the measured g value is 2.0044 ± 0.0004. The spectrum of the deuterated compound (Fig. 1*b*) is practically identical, although slightly better resolved (line width of 5.2 G at −100 °C).

After bleaching the samples with visible or u.v. light the blue color disappears and the e.s.r. spectrum changes, as shown in Figs. 3*a* and 3*b*. The u.v. irradiation of ethyleneimine does not produce any e.s.r. signal without previous γ-irradiation.

[1]This work was supported by Consiglio Nazionale delle Ricerche.

Can. J. Chem. Downloaded from www.nrcresearchpress.com by 210.87.254.42 on 09/05/12
For personal use only.

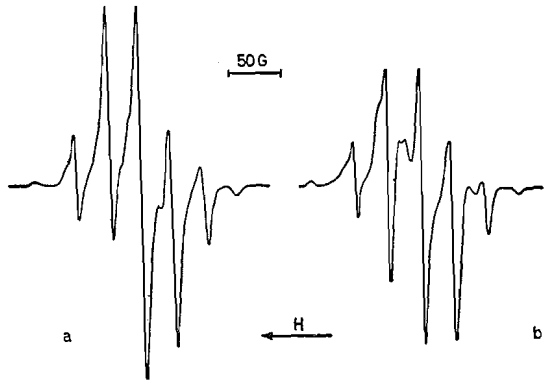

FIG. 1. Electron spin resonance spectra of ethyleneimine γ-irradiated at −196 °C; dose 1.5 Mrads; (*a*) undeuterated sample observed at −140 °C, (*b*) deuterated sample observed at −160 °C.

Discussion

The spectrum of Fig. 1*a* may be assigned to the

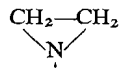

radical. The identical spectrum (Fig. 1*b*) obtained from the N-deuterated compound confirms this assignment. The relative intensities of the 5 lines are near to the theoretical pattern for 4 equivalent protons. The absence of α-protons and the spatial equivalence of the β-protons accounts for the good resolution.

An anisotropic nitrogen hyperfine interaction is expected for this kind of radical. However, at first order, the central line ($M_I = 0$) of the nitrogen hyperfine triplet is isotropic. The other two lines ($M_I = \pm 1$) have an angular dependence and are therefore broadened in a powder sample. Each of these lines is split into 5 components by the hyperfine interaction with the 4 equivalent protons, but only the central quintet is well resolved. An indication of the presence of the 2 unresolved external quintets is provided by the 2 satellite lines.

The anisotropy of the g factor is small, as shown from the linewidth of the quintet. This anisotropy accounts for the different distances of satellites from the central line and for their different broadening (6).

In order to support this interpretation, the theoretical spectrum for a radical where an anisotropic, axially symmetrical interaction with a nitrogen nucleus and an isotropic interaction with 4 equivalent protons are present, was calculated by an I.B.M. 7040 computer.

The method of calculation indicated by Vänngård and Aasa was followed (7). The values of hyperfine parameters for nitrogen were deduced from the data reported in literature, concerning similar radicals in monocrystals (8), while for proton splitting the experimental value was used. An axial g tensor with $\Delta g = 0.002$ and a Lorentzian line shape were also assumed.

Generally, radicals with the unpaired electron on nitrogen exhibit an almost axial hyperfine nitrogen tensor but a completely asymmetrical g tensor; therefore, our assumption about the latter parameter is only a rough approximation. However, on account of the small g anisotropy, the rather simple calculation relative to the axial case has been carried out.

The splitting between satellite lines is given by $2\,A_{\parallel}^{N} + 4\,a^{H}$, where $A_{\parallel}^{N}$ is the principal value of nitrogen coupling tensor parallel to the unpaired electron orbital, and a^{H} is the isotropic coupling constant with protons.

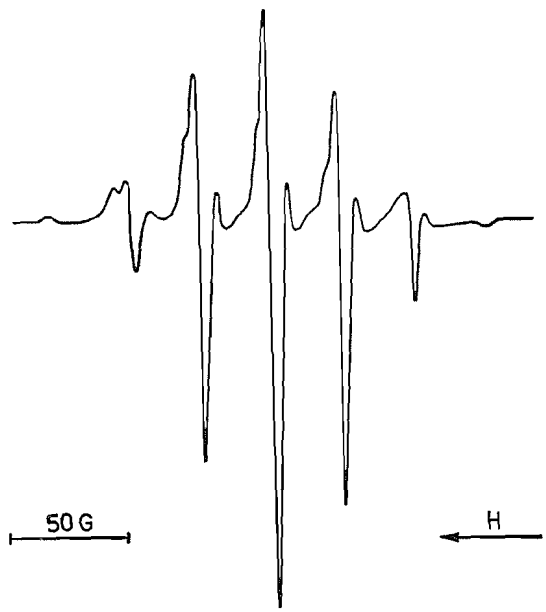

FIG. 2. Calculated spectrum of 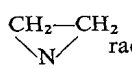 radical in polycrystalline matrix. Values of spin Hamiltonian parameters used for calculation: $g_{\parallel} = 2.003$, $g_{\perp} = 2.005$, $A_{\parallel}^{N} = 33$ G, $A_{\perp}^{N} = 5$ G, $a^{H} = 30$ G, $(\Delta H)_{m.s.} = 2$ G. $g_{\parallel}$ and $g_{\perp}$, $A_{\parallel}^{N}$ and $A_{\perp}^{N}$ are the principal values of g and hyperfine coupling tensor; a^{H} is the isotropic coupling constant with protons. $(\Delta H)_{m.s.}$ is the linewidth at maximum slope.

Can. J. Chem. Downloaded from www.nrcresearchpress.com by 210.87.254.42 on 09/05/12
For personal use only.

As can be seen, the calculated spectrum, shown in Fig. 2, approximates to the experimental ones satisfactorily.

A similar pattern may be observed in the e.s.r. spectrum of the

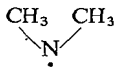

radical. The spectrum of this radical, shows a main septet with a splitting of 28.0 G and an external satellite line (1, 2). This spectrum has been interpreted in terms of equal, isotropic, proton and nitrogen splitting constants (1). However, the asymmetry of the spectrum and the variation of the line shape indicate an anisotropic nitrogen interaction.

The u.v. irradiation of ethyleneimine does not produce any e.s.r. signal without previous γ-irradiation; this suggests that the radical formed by bleaching comes from the

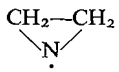

radical. The spectra of Fig. 3*a* and 3*b* are too complex for a straightforward interpretation. The spectrum of the undeuterated sample (Fig. 3*a*) is less resolved but shows the same components as the other spectrum. Their pattern does not change with temperature until they disappear.

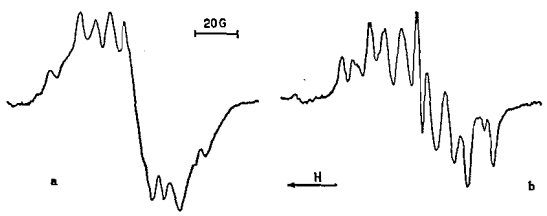

FIG. 3. Electron spin resonance spectra of ethyleneimine γ-irradiated at −196 °C; dose 1.5 Mrads, after 10 min u.v. irradiation; (*a*) undeuterated sample observed at −160 °C, (*b*) deuterated sample observed at −120 °C.

Tentatively these spectra may be assigned to the $CH_2—CH—NH$ or $CH_2—N—CH_2$ radicals. On account of delocalization of the unpaired electron, these allyl-like radicals may have proton and nitrogen splittings lower than that of the

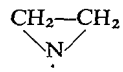

radical.

Unlike ethyleneimine, the dimethylamine gives, by γ-irradiation at −196 °C, two types of radicals (2)

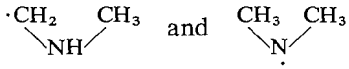

It has also been found that on standing at −196 °C the latter radical converts, by an intramolecular migration of a hydrogen atom, to the former, and by u.v. irradiation the opposite conversion occurs.

In some experiments with the dimethylamine we confirmed these results and we found that these conversions can be done several times with only a small decrease in intensity. The intramolecular migration of hydrogen atom, which probably also takes place in the photolysis of

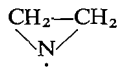

would provoke the ring opening. This fact would explain the lack of reversibility encountered in this case.

The blue color of the irradiated samples is not apparently related to the observed paramagnetic species; no signal from the trapped electron is displayed. The effect of γ-irradiation on ethyleneimine in the solid state is to cleave the N—H bond, in agreement with the reaction of this compound with radicals in the gaseous phase (9, 10).

Acknowledgments

The Consiglio Nazionale delle Ricerche is gratefully acknowledged for a fellowship to R. Di Blasi. The authors are indebted to Dr. C. Giovagnoli for the computer program preparation.

1. S. G. HADLEY and D. H. VOLMAN. J. Am. Chem. Soc. **89**, 1053 (1967).
2. G. V. PUKHAL'SKAYA, A. G. KOTOV, and S. YA PSHEZHETSKII. Dokl. Akad. Nauk SSSR, **171**, 6, 1380 (1966).
3. G. V. PUKHAL'SKAYA, A. G. KOTOV, and S. YA PSHEZHETSKII. Khim. Visok. Energii, **1**, 536 (1967).
4. A. A. REVINA and A. P. PODSOBLAJAEV. Dokl. Akad. Nauk SSSR, **152**, 668 (1963).
5. R. O. LINDBLOM, R. M. LEMMON, and M. CALVIN. J. Am. Chem. Soc. **83**, 2489 (1961).
6. A. S. TENCH and R. L. NELSON. Trans. Faraday Soc. **63**, 2254 (1967).
7. T. VÄNNGÅRD and R. AASA. *In* Proceedings 1st Intern. Conf. Paramagnetic Resonance. Academic Press, Inc., New York. 1963. p. 509.
8. J. R. MORTON. Chem. Rev. **64**, 453 (1964).
9. R. F. KLEMM. Can. J. Chem. **43**, 2633 (1965).
10. P. GREY and A. JONES. Trans. Faraday Soc. **61**, 2161 (1965).

Molecular complexes: effects of multiple equilibria on calculated absorptivities and association constants

C. C. THOMPSON, JR.

Department of Chemistry, Memphis State University, Memphis, Tennessee 38111

Received December 23, 1968

Simulated absorbance data have been used to demonstrate the effects of 2:1 molecular complexes on formation constants and absorptivities calculated for 1:1 donor–acceptor interactions. By systematic variation of associated spectral, thermodynamic, and concentration parameters for these systems, it is found that previous attempts to describe effects produced by the presence of more than one stoichiometric complex species are inadequate. Formation constants and absorptivities calculated with the assumption of a simple 1:1 interaction may be increased or decreased by the occurrence of higher order complexes. These variations depend largely on the ratios of complex absorptivities, relative formation constants, and the range of donor concentrations. Equations incorporating 5 of the experimental variables permit the prediction of formation constants and absorptivities to a high degree of accuracy.

Canadian Journal of Chemistry, 47, 2605 (1969)

Can. J. Chem. Downloaded from www.nrcresearchpress.com by 210.87.254.5 on 09/05/12
For personal use only.

Introduction

In recent years considerable attention has been given to spectroscopic studies of organic molecular complexes involving interactions between electron donor and acceptor molecules (1–3). By means of a variety of mathematical treatments (1, 4), equilibrium constants and absorptivities for these complexes have been calculated from spectral data collected at one or more wavelengths. Among the possible interactions between donor (D) and acceptor (A) molecules we may consider

[1] $$A + D \overset{K_1}{\rightleftharpoons} C_1$$

[2] $$A + 2D \overset{K_2}{\rightleftharpoons} C_2$$

and

[3] $$D + C_1 \overset{K_3}{\rightleftharpoons} C_2$$

where C_1 and C_2 are 1:1 and 2:1 complexes respectively. The corresponding equilibrium constants are given as

[4] $$K_1 = \frac{[C]_1}{([A]_0 - [C]_1 - [C]_2)([D]_0 - [C]_1 - 2[C]_2)}$$

and

[5] $$K_2 = \frac{[C]_2}{([A]_0 - [C]_1 - [C]_2)([D]_0 - [C]_1 - 2[C]_2)^2}$$

Here $[A]_0$ and $[D]_0$ refer to the initial concentrations of acceptor and donor, respectively. Equilibrium constants for the simultaneous (eq. [2]) and consecutive (eq. [3]) mechanisms are very simply related by the expression

$$K_3 = K_2/K_1$$

Although the possible occurrence of higher order complexes has been suggested by several authors (5–8), attempts at complete quantitative treatments of systems containing complexes of more than one stoichiometry have met with only limited success. If, as is usually the case, the presence of a possible 2:1 complex is ignored and computations are carried out for the 1:1 species only, the calculated equilibrium constant, hereafter referred to as K^*, and absorptivity, a_C^*, will differ from the "true" values of K_1 and a_{C_1}. Linear plots obtained from the Benesi–Hildebrand (9) and related procedures generally have been accepted as evidence that higher order complexes are not present. Recently, this conclusion has been shown to be incorrect (8). In addition, equilibrium constants which show a considerable wavelength dependence have been reported (9–13). Variations of K with wavelength cannot be explained by the presence of isomeric 1:1 complexes or by "contact" charge-transfer

Can. J. Chem. Downloaded from www.nrcresearchpress.com by 210.87.254.5 on 09/05/12
For personal use only.

absorptions. It has been pointed out that the presence of 2:1 or other higher order complexes could lead to wavelength variations in equilibrium constants calculated for a 1:1 interaction (8, 14, 15). However, the magnitude of this expected wavelength dependence and the experimental conditions that favor its occurrence have not been fully investigated. Hayman (14) has derived an expression to relate K^* to the true equilibrium constants and absorptivities for 1:1 and 2:1 complexes. Using the terminology of eqs. [1]–[3], Hayman's equation becomes

$$[6] \qquad K^* = K_1 - K_2 a_{C_2}/K_1 a_{C_1}$$

An independent treatment by Jurinski (14) yields a different relationship

$$[7] \qquad K^* = K_1 + K_2[D]_0$$

Since all variables in eqs. [6] and [7] are positive quantities, the two expressions predict reverse trends in K^*. The variations of K^* predicted by these equations have not been verified.

The purpose of this paper is to study systematically the behavior of systems containing both 1:1 and 2:1 complexes by means of computer-generated absorbance data. The principal objectives are threefold: to determine which factors produce significant effects on the calculated absorptivities and equilibrium constants of molecular-complex systems, to evaluate the direction and magnitude of these effects, and to be able to predict K^* and $a_C{}^*$ if the necessary empirical information is available. Two distinct advantages make it highly desirable to use simulated rather than actual experimental data. First, the parameters which define the system under consideration are known exactly and may be varied at will. Secondly, the simulated data are essentially free from experimental errors, unavoidable in real systems, but which frequently make precise analyses impossible.

Methods of Computation

If it is assumed that variables such as temperature, solvent, and path length are suitably controlled, 8 additional factors may be listed which could influence calculated equilibrium constants and absorptivities. These parameters include K_1, K_2, a_{C_1}, a_{C_2}, absorptivities of free donor and acceptor (a_D and a_A), and initial concentrations of D and A ($[D]_0$ and $[A]_0$). The simulated data presented in this paper were calculated by a computer program employing the method outlined below. Computations were carried out on an IBM 1620 computer.

The first phase of the method involved generation of absorbance data using specific values of the above parameters as input information.

Step 1

Assuming initially that $K_2 = 0$, the concentration $[C]_1$ is calculated from eq. [4] which may be rearranged to give

$$[8] \quad [C]_1 = [K_1([A]_0 + [D]_0) + 1 - (K_1{}^2([A]_0 - [D]_0)^2 + 2K_1([A]_0 + [D]_0) + 1)^{\frac{1}{2}}]/2K_1$$

Step 2

First approximations for the equilibrium concentrations of A and D are computed from the relations, $[A] = [A]_0 - [C]_1$ and $[D] = [D]_0 - [C]_1$.

Step 3

Introducing the selected value of K_2, $[C]_2$ is calculated from the relation

$$[9] \qquad [C]_2 = K_2[D][C]_1/K_1$$

Step 4

$[C]_1$ is recalculated by replacing $[A]_0$ and $[D]_0$ of eq. [8] with $[A]'$ and $[D]'$, defined as $[A]' = [A]_0 - [C]_2$ and $[D]' = [D]_0 - 2[C]_2$.

Step 5

Equilibrium concentrations of A and D are computed from the correct expressions

$$[A] = [A]_0 - [C]_1 - [C]_2$$

and

$$[D] = [D]_0 - [C]_1 - 2[C]_2$$

Step 6

A new value of $[C]_2$ is calculated from eq. [9] and steps 3–5 are repeated until $[C]_1$ and $[C]_2$ are unchanged for successive iterations.

Step 7

The simulated absorbance, A_m, is computed from eq. [10] using a convenient path length, b, and selected absorptivities for the various species.

$$[10] \quad A_m = b(a_{C_1}[C]_1 + a_{C_2}[C]_2 + a_A[A] + a_D[D])$$

In phase two, the generated absorbance values and the initial concentrations of A and D are used

Can. J. Chem. Downloaded from www.nrcresearchpress.com by 210.87.254.5 on 09/05/12
For personal use only.

to calculate 1:1 equilibrium constants (K^*) and absorptivities (a_C^*) by a modification of the Benesi–Hildebrand treatment (9) which is outlined below. Specific details of this method have been described previously (10).

Results and Discussion

Approximately 300 different combinations of the 8 input parameters were processed. These combinations were selected systematically in order to determine the combined as well as the separate effect of the various parameters. The total ranges over which the input parameters were varied are listed in Table I. These limits are representative of the usual values encountered in experimental donor–acceptor systems.

TABLE I

Range of input parameters

Parameter	Range	Parameter	Range
K_1	0.2– 50.0	a_A	0.0 –200.0
K_2	0.0– 100.0	a_D	0.0 – 10.0
a_{C_1}	200.0–3600.0	$[A]_0$	0.001– 0.1*
a_{C_2}	0.0–5000.0	$[D]_0$	0.01 – 0.6*

*Concentrations are expressed in moles l^{-1}.

Numerous checks of the results from the absorbance generator program demonstrate conclusively that the method converges to correct values for $[C]_1$ and $[C]_2$. For K_1 and K_2 of the same order of magnitude, convergence to within 0.01% of the absolute concentrations generally requires from 3 to 6 iterations. If K_2 exceeds K_1 by a factor of 10 or more, oscillation may sometimes occur. In this event the calculation is terminated and the offending set of parameters is discarded.

Characteristics of Systems Containing 1:1 and 2:1 Complexes

Results of typical calculations from simulated absorbance data are given in Table II. Columns 2–9 contain "true" equilibrium constants, absorptivities, and concentrations which were used as input parameters. Values of K^* and a_C^* obtained from the method outlined above by treating the absorbance data as though only the 1:1 equilibrium existed, are tabulated in columns 10 and 11.

With reference to specific items in Table II the following generalizations regarding the effects of 2:1 complexes may be inferred[1].

(*a*) When only a 1:1 complex is present, the computational method converges to correct values for K_1 and a_{C_1}. These results are unaffected by absorbance due to free donor and acceptor or by changes in the initial concentrations, $[A]_0$ and $[D]_0$ (lines 1–3).

(*b*) For fixed values of K_1 and K_2 the calculated K^* and relative deviations in absorptivity are dependent only on the *ratio* a_{C_2}/a_{C_1} and not on the absolute magnitudes of these parameters (lines 4 and 5). If absorption bands of the 2 complexes maintain a constant ratio throughout a given wavelength range, the calculated K^* will be numerically incorrect, but will show no wavelength dependence in this region.

(*c*) K^* is greater than K_1 for low a_{C_2}/a_{C_1} ratios, but decreases to considerably smaller values as the absorptivity ratio increases. The behavior of a_C^* follows a reverse pattern (lines 6–10).

(*d*) For a given K_1 and absorptivity ratio, K^* decreases as K_2 increases (lines 11–14).

(*e*) The relative importance of a 2:1 complex is diminished sharply as the absolute value of K_1 increases (lines 15–17). Thus, other factors being equal, the effects of 2:1 species will be minimal in systems containing very strong 1:1 interactions.

(*f*) A 100-fold increase in $[A]_0$ has little effect on K^* and a_C^* (lines 12 and 18).

(*g*) An increase in donor concentration results in a pronounced increase in K^* and an associated decrease in a_C^* (lines 19–21).

(*h*) For non-zero absorptivities of free donor and acceptor, K^* and a_C^* differ only slightly from the case in which $a_A = a_D = 0$ (lines 22 and 23).

It is interesting to note that even a relatively small amount of a 2:1 complex can cause large variations in K^* and a_C^*. This effect can be seen readily by considering the ratio of concentrations of 2:1 to 1:1 complexes for a given set of parameters. From eq. [9], $[C]_2/[C]_1 = K_2[D]/K_1$. Using the parameters of line 10 of Table II, the $[C]_2/[C]_1$ ratio varies from 0.0095 to 0.199 as the total donor concentration is increased from 0.01 to 0.20 mole l^{-1}. Even with these small ratios,

[1]The values reported in Table II were selected from the approximately 300 separate computations in order to illustrate the conclusions noted here. Therefore, each item in this discussion has been fully substantiated through numerous additional calculations.

Can. J. Chem. Downloaded from www.nrcresearchpress.com by 210.87.254.5 on 09/05/12
For personal use only.

TABLE II

Equilibrium constants and absorptivities

	Input parameters								Calculated values†		Predicted values			
											K^*			a_C^*
	K_1	K_2	a_{C_1}	a_{C_2}	a_A	a_D	$[A]_0$‡	$[D]_0$‡	K^*	a_C^*	eq. [6]§	eq. [7]§‖	eq. [23]§	eq. [25]§
1	5.0	0.0	1500	0	0	0	0.001	0.01–0.20	5.000	1500	5.000	5.000	5.000	1500
2	5.0	0.0	1500	0	200	1	0.001	0.01–0.20	5.000	1500	5.000	5.000	5.000	1500
3	0.2	0.0	1500	0	0	0	0.005	0.05–0.50	0.200	1500	0.200	0.200	0.200	1500
4	5.0	5.0	1200	1800	0	0	0.001	0.01–0.20	3.451	1736	3.500	5.525	3.452	1738
5	5.0	5.0	2000	3000	0	0	0.001	0.01–0.20	3.451	2893	3.500	5.525	3.452	2896
6	5.0	5.0	1500	200	0	0	0.001	0.01–0.20	5.905	1293	4.867	5.525	5.806	1303
7	5.0	5.0	1500	600	0	0	0.001	0.01–0.20	5.249	1437	4.600	5.525	5.245	1438
8	5.0	5.0	1500	1000	0	0	0.001	0.01–0.20	4.744	1586	4.333	5.525	4.742	1588
9	5.0	5.0	1500	3000	0	0	0.001	0.01–0.20	2.834	2637	3.000	5.525	2.811	2663
10	5.0	5.0	1500	5000	0	0	0.001	0.01–0.20	1.582	4722	1.667	5.525	1.585**	4728**
11	5.0	0.5	1500	1500	0	0	0.001	0.01–0.20	4.902	1530	4.900	5.053	4.902	1530
12	5.0	1.0	1500	1500	0	0	0.001	0.01–0.20	4.808	1560	4.800	5.105	4.808	1560
13	5.0	5.0	1500	1500	0	0	0.001	0.01–0.20	4.180	1796	4.000	5.525	4.181	1797
14	5.0	20.0	1500	1500	0	0	0.001	0.01–0.20	2.959	2574	1.000	7.100	2.913††	2620††
15	1.0	0.5	1000	1000	0	0	0.001	0.01–0.20	0.548	1824	0.500	1.053	0.548	1826
16	20.0	100.0	1500	1500	0	0	0.001	0.01–0.20	18.076	1696	15.000	30.500	‡‡	‡‡
17	50.0	100.0	1000	1000	0	0	0.001	0.01–0.20	48.416	1034	48.000	60.500	48.523	1034
12§§	5.0	1.0	1500	1500	0	0	0.001	0.01–0.20	4.808	1560	4.800	5.105	4.808	1560
18	5.0	1.0	1500	1500	0	0	0.100	0.01–0.20	4.719	1558	4.800	5.105	4.808	1560
19	5.0	5.0	1500	500	0	0	0.001	0.01–0.20	5.384	1402	4.667	5.525	5.385	1403
20	5.0	5.0	1500	500	0	0	0.001	0.21–0.40	8.516	1158	4.667	6.525	8.495	1158
21	5.0	5.0	1500	500	0	0	0.001	0.31–0.50	11.913	1076	4.667	7.025	11.874	1076
22	5.0	1.0	1500	5000	0	0	0.001	0.01–0.20	3.962	1885	4.333	5.105	3.970	1883
23	5.0	1.0	1500	5000	200	1	0.001	0.01–0.20	3.845	1882	4.333	5.105	3.900	1901

†K^* and a_C^* computed with the assumption that only 1:1 complexes are present.
‡Concentrations in moles l^{-1}.
§Equation numbers correspond to those in the text.
‖K^* computed from average value of [D].
¶Values based on σ computed with $n = 5$ unless otherwise indicated (see text).
**Maximum $\theta = 0.67$; σ computed with $n = 15$.
††Maximum $\theta = 0.80$; σ computed with $n = 50$.
‡‡Maximum $\theta = 1.0$; approximate method not valid.
§§Line 12 repeated to facilitate comparisons with line 18.

Can. J. Chem. Downloaded from www.nrcresearchpress.com by 210.87.254.5 on 09/05/12
For personal use only.

there is a 68% decrease in K^* and a 315% increase in $a_C{}^*$ compared to the values of K_1 and a_{C_1}.

As noted previously, eq. [6] predicts that K^* will always decrease with the occurrence of 2:1 complexes, whereas eq. [7] permits only an increase. However, the results of the present work show that K^* and $a_C{}^*$ may be either *greater than or less than* the true K_1 and a_{C_1} depending upon the specific combination of parameters at each wavelength. Of the 8 parameters studied, 5 are seen to produce significant changes in K^* and $a_C{}^*$. These 5 include the equilibrium constants, K_1 and K_2, absorptivities of the complexes, a_{C_1} and a_{C_2}, and concentrations of the donor. Since for most real systems it is unlikely that a_{C_2}/a_{C_1} will be constant over a wide spectral range, a wavelength dependence of K^* would be expected.

Prediction of Absorptivities and Equilibrium Constants

Applying the conditions, $a_A = a_D = 0$ and $[D]_0 \gg [A]_0$, to eqs. [1] and [2] and choosing a path length of 1 cm, the absorbance is given by

$$A_m = a_{C_1}[C]_1 + a_{C_2}[C]_2$$

and upon substituting for $[C]_2$

$$[11] \quad A_m = [C]_1 a_{C_1}\left(1 + \frac{[D]_0 K_2 a_{C_2}}{K_1 a_{C_1}}\right)$$

Also, since $[D]_0 \simeq [D]$ and $[A]_0 = [A] + [C]_1 + [C]_2$

$$[12] \quad [A]_0[D]_0 = [D]_0([A] + [C]_1 + [C]_2)$$
$$= [C]_1\left(\frac{1}{K_1} + [D]_0 + \frac{K_2[D]_0{}^2}{K_1}\right)$$

Using the present symbols, the Scott (16) form of the Benesi–Hildebrand treatment for a simple 1:1 interaction is

$$[13] \quad \frac{[A]_0[D]_0}{A_m} = \frac{1}{K_1 a_{C_1}} + \frac{[D]_0}{a_{C_1}}$$

For the simultaneous occurrence of both 1:1 and 2:1 complexes eq. [12] can be divided by eq. [11] to yield

$$[14] \quad \frac{[A]_0[D]_0}{A_m} = \frac{\frac{1}{a_{C_1}}\left(\frac{1}{K_1} + [D]_0 + \frac{K_2[D]_0{}^2}{K_1}\right)}{1 + \theta}$$

where θ equals $[D]_0 K_2 a_{C_2}/K_1 a_{C_1}$. If θ is less than unity, the expression can be approximated as

$$[15] \quad \frac{[A]_0[D]_0}{A_m} = \frac{1}{a_{C_1}}\left[\left(\frac{1}{K_1} + [D]_0 + \frac{K_2[D]_0{}^2}{K_1}\right)\sum_{r=0}^{n}(-\theta)^r\right]$$

which can be rearranged to give

$$[16] \quad \frac{[A]_0[D]_0}{A_m} = \frac{1}{K_1 a_{C_1}} + \frac{[D]_0}{a_{C_1}}\left[1 + \frac{K_2[D]_0}{K_1} + \left(1 + \frac{1}{K_1[D]_0} + \frac{K_2[D]_0}{K_1}\right)\sum_{r=1}^{n}(-\theta)^r\right]$$

Designating the term in brackets as σ, eq. [17] is obtained.

$$[17] \quad \frac{[A]_0[D]_0}{A_m} = \frac{1}{K_1 a_{C_1}} + \frac{[D]_0\sigma}{a_{C_1}}$$

Thus, the Scott equation, eq. [13], is a special case of eq. [17] in which $\sigma = 1$ for a simple 1:1 interaction. It is important to note that σ is a function of the 5 parameters which were found to have the greatest effect on K^* and $a_C{}^*$.

In the standard experimental procedure for studying donor–acceptor interactions, spectral measurements are carried out for several solutions of varying donor concentration. Since σ is a function of $[D]_0$, it will vary throughout the series of solutions in which different donor concentrations are used. If we select one of the initial donor concentrations, say $[D]_{0_i}$, then for this solution eq. [17] becomes

$$[18] \quad \frac{[A]_0[D]_{0_i}}{A_{m_i}} = \frac{1}{K_1 a_{C_1}} + \frac{[D]_{0_i}\sigma_i}{a_{C_1}}$$

Equation [18] can be rearranged to give

$$[19] \quad a_{C_1} = \frac{A_{m_i}}{[A]_0}\left(\frac{1}{[D]_{0_i}K_1} + \sigma_i\right)$$

For a different donor concentration within the series, say $[D]_{0_j}$, and with a fixed acceptor concentration, $[A]_0$, another equation of exactly

Can. J. Chem. Downloaded from www.nrcresearchpress.com by 210.87.254.5 on 09/05/12
For personal use only.

the same form as eq. [18] can be written. Rearranging this second equation to give

$$K_1\left(a_{C_i} - \frac{A_{m_j}\sigma_j}{[A]_0}\right) = \frac{A_{m_j}}{[A]_0[D]_{0_j}}$$

and substituting for a_{C_i} from eq. [19], we have

$$[20] \quad K_1 = \frac{[D]_{0_i}A_{m_j} - [D]_{0_j}A_{m_i}}{[D]_{0_i}[D]_{0_j}(A_{m_i}\sigma_i - A_{m_j}\sigma_j)}$$

For calculations in which the 2:1 complex is ignored, it is implicitly assumed that $\sigma_i = \sigma_j = 1$. In that case, eq. [20] will not give K_1, but will yield the value of K^* instead.

$$[21] \quad K^* = \frac{[D]_{0_i}A_{m_j} - [D]_{0_j}A_{m_i}}{[D]_{0_i}[D]_{0_j}(A_{m_i} - A_{m_j})}$$

Upon dividing eq. [21] by eq. [20], we obtain

$$[22] \quad \frac{K^*}{K_1} = \frac{A_{m_i}\sigma_i - A_{m_j}\sigma_j}{A_{m_i} - A_{m_j}}$$

By dividing the numerator and denominator of the right hand side of eq. [22] by A_{m_i} and letting $\xi_{ij} = A_{m_j}/A_{m_i}$, the expression may be solved for K^* to give

$$[23] \quad K^* = K_1\left(\frac{\sigma_i - \xi_{ij}\sigma_j}{1 - \xi_{ij}}\right) = K_1\beta_{ij}$$

where

$$\beta_{ij} = (\sigma_i - \xi_{ij}\,\sigma_j)/(1 - \xi_{ij})$$

A similar procedure can be followed to obtain a relationship for predicting $a_C{}^*$. Again, if the 2:1 complex is ignored, $\sigma_i = 1$ and eq. [19] will become

$$[24] \quad a_C{}^* = \frac{A_{m_i}}{[A]_0}\left(\frac{1}{[D]_{0_i}K^*} + 1\right) = \frac{A_{m_i}}{[A]_0}\left(\frac{1}{[D]_{0_i}K_1\beta_{ij}} + 1\right)$$

Upon dividing eq. [24] by eq. [19] and rearranging, one gets

$$[25] \quad a_C{}^* = \frac{a_{C_i}(1 + K_1\beta_{ij}[D]_{0_i})}{\beta_{ij}(1 + K_1\sigma_i[D]_{0_i})}$$

Thus, K^* and $a_C{}^*$ can be predicted from eqs. [23] and [25], respectively, using values of σ_i, σ_j, and β_{ij} computed from specific combinations of input parameters.

An immediate problem in the evaluation of σ involves the number of terms which must be included in the summation of $(-\theta)^r$ in eq. [16]. Equation [6] was obtained by terminating the series at $n = 1$ and disregarding all but first-power terms of $[D]_0$. However, as mentioned earlier, eq. [6] predicts only negative deviations from K_1. By extending the series to $n \geq 2$ both positive and negative deviations of K^* and $a_C{}^*$ are permitted. Moreover, in the derivation of eq. [16] it has been assumed that θ is less than unity. A comparison of the exact reciprocal of eq. [11] with the approximate summation in eq. [16] shows that termination of the series at $n = 1$ introduces large errors if θ is greater than 0.2. By expanding the summation to $n = 5$, the approximation will be reasonably good up to a value of $\theta = 0.5$; if θ exceeds 1, the entire approximation breaks down.

Columns 11–15 of Table II give K^* predicted by eqs. [6] and [7] as well as K^* and $a_C{}^*$ predicted by eqs. [23] and [25] from values of σ computed with $n = 5$. The close correlation between calculated equilibrium constants and absorptivities, and those predicted by eqs. [23] and [25] illustrates the importance of the 5 parameters included in the evaluation of σ. The absence of a wavelength dependent term in eq. [7] precludes its use for predicting wavelength variations of K^*.

In summary, the presence of even small amounts of 2:1 complexes can have substantial effects on equilibrium constants and absorptivities computed for 1:1 interactions. The ratio of absorptivities for the 2 complex species, their respective association constants, and the range of donor concentrations are the determining factors for the observed variations. These factors are closely interrelated so that a full assessment of their combined effect requires a more elaborate mathematical analysis than has been attempted heretofore.

Acknowledgments

The author would like to thank Professors A. R. Lepley and P. H. Hutcheson for helpful discussions related to this work.

1. G. Briegleb. Elektronen Donator Acceptor Komplexe. Springer-Verlag, Berlin. 1961.
2. R. S. Mulliken and W. B. Person. Ann. Rev.Phys. Chem. **13**, 107 (1962).
3. L. J. Andrews and R. M. Keefer. Molecular complexes in organic chemistry. Holden-Day, San Francisco. 1964.
4. P. A. D. de Maine and R. D. Seawright. Digital computer programs for physical chemistry. Vol. I. The Macmillan Co., New York. 1963.

5. J. LANDAUER and H. MCCONNELL. J. Am. Chem. Soc. **74**, 1221 (1952).
6. R. A. ZINGARO, R. E. MCGLOTHLIN, and E. A. MEYERS. J. Phys. Chem. **66**, 2579 (1962).
7. N. B. JURINSKI and A. F. WAGNER. Abstr. 155th Am. Chem. Soc. Meeting. San Francisco, California. 1968.
8. G. D. JOHNSON and R. E. BOWEN. J. Am. Chem. Soc. **87**, 1655 (1965).
9. H. A. BENESI and J. H. HILDEBRAND. J. Am. Chem. Soc. **71**, 2703 (1949).
10. C. C. THOMPSON, JR. and P. A. D. DE MAINE. J. Am. Chem. Soc. **85**, 3096 (1963).
11. N. B. JURINSKI and P. A. D. DE MAINE. J. Am. Chem. Soc. **86**, 3217 (1964).
12. C. C. THOMPSON, JR. and P. A. D. DE MAINE. J. Phys. Chem. **69**, 2766 (1965).
13. M. J. S. DEWAR and C. C. THOMPSON, JR. Tetrahedron Suppl. No. **7**, 97 (1966).
14. H. J. G. HAYMAN. J. Chem. Phys. **37**, 2290 (1962).
15. N. B. JURINSKI. J. Miss. Acad. Sci. **10**, 74 (1964).
16. R. L. SCOTT. Rec. Trav. Chim. **75**, 787 (1956).

Can. J. Chem. Downloaded from www.nrcresearchpress.com by 210.87.254.5 on 09/05/12
For personal use only.

Can. J. Chem. Downloaded from www.nrcresearchpress.com by 210.87.254.6 on 09/05/12
For personal use only.

Studies of the phosphorodiamidates of alkali metals

Y. N. SADANA
Department of Chemistry, Laurentian University, Sudbury, Ontario

Received November 8, 1968

Phosphorodiamidates of lithium, rubidium, and cesium have been prepared and characterized. The infrared spectra and the X-ray powder diffraction patterns of these and the previously known sodium and potassium salts have been recorded and discussed.

Canadian Journal of Chemistry, 47, 2613 (1969)

Introduction

Even though phosphorodiamidic acid, $HPO_2(NH_2)_2$ has been known since 1894 (1), work on its salts has been rather scanty and only a few phosphorodiamidates have been reported. The earlier work on phosphorodiamidates has been recently reviewed (2, 3). We have now repeated the preparation of the already known sodium (4) and potassium (5) salts and have characterized also the phosphorodiamidates of lithium, rubidium, and cesium. The infrared (i.r.) spectra and the powder diffraction patterns of the new and the previously known alkali metal phosphorodiamidates have been recorded.

Experimental

General

Chemicals used were of C.P. Grade. $POCl_3$ was freshly distilled before use. Liquid ammonia was used directly from a cylinder (Matheson) without further purification. Lithium, rubidium, and cesium hydroxides were purchased from Alfa Inorganics.

Infrared spectra were taken on a Beckman IR-10 spectrophotometer. The spectra were run in Nujol or hexachlorobutadiene mulls or in KBr discs. KRS-5 plates were used for aqueous solutions. Ultraviolet (u.v.) spectra were taken on a Bausch and Lomb SP600 spectrophotometer and X-ray powder diffraction patterns using a Phillips X-ray unit. The samples were charged in Lindemann glass capillary tubes (0.3 and 0.5 mm diameter).

The phosphorodiamidates were prepared by reacting $OP(NH_2)_3$ with an alkali metal hydroxide. $OP(NH_2)_3$ was prepared from freshly distilled $POCl_3$ and liquid ammonia (6), and purified by the method of Klement and Koch (4). $OP(NH_2)_3$ was characterized from its i.r. spectrum and X-ray powder diffraction pattern and by chemical analysis.

Anal. Calcd. for $OP(NH_2)_3$: N, 44.2; P, 32.95. Found: N, 43.8; P, 33.5.

As an example, the preparation of the lithium salt is described in detail.

$OP(NH_2)_3$ (0.237 g) was dissolved in water (20 ml) in 150 ml beaker. To this a solution of LiOH (0.060 g) in water (20 ml) was added. The solution was heated on a water bath (60–65 °C) until the evolution of ammonia had ceased (about 4 h). The solution was then filtered into a 600 ml beaker. Alcohol was added to precipitate the salt, which separated as an oily liquid. The oily liquid changed into a crystalline mass when left aside in a refrigerator.

Chemical Analysis

Nitrogen was determined by the Micro-Kjeldahl method (7). Phosphorus was determined either as phosphomolybdate (8) or by the pH titration method (9). Analyses of the compounds prepared are shown in Table I.

Results and Discussion

The chemical reaction of $OP(NH_2)_3$ with alkali metal hydroxides can be represented by

$$OP(NH_2)_3 + M^+ + OH^- \xrightarrow{H_2O} M^+ + PO_2(NH_2)_2^- + NH_3\uparrow$$

where M = Li, K, Rb, and Cs in the present work, and M = Na in ref. 4.

TABLE I
Chemical analysis

Compound	% N		% P	
	Calculated	Found	Calculated	Found
$LiPO_2(NH_2)_2 \cdot H_2O$	23.40	23.47	25.81	25.51
$NaPO_2(NH_2)_2$	23.72	22.40	26.20	25.51
$NaPO_2(NH_2)_2 \cdot 4H_2O$	14.77	—	16.28	15.98
$KPO_2(NH_2)_2 \cdot H_2O$	18.41	17.97	20.32	20.00
$RbPO_2(NH_2)_2 \cdot H_2O$	14.11	14.58	15.59	—
$CsPO_2(NH_2)_2 \cdot H_2O$	11.39	10.81	12.60	12.46

Can. J. Chem. Downloaded from www.nrcresearchpress.com by 210.87.254.6 on 09/05/12
For personal use only.

The mechanism of the reaction is not immediately obvious but it seems reasonable to assume that $OP(NH_2)_3$ first adds on a molecule of water to form ammonium phosphorodiamidate, which is then decomposed

$$OP(NH_2)_3 + H_2O \rightleftharpoons NH_4^+ + PO_2(NH_2)_2^-$$

$$NH_4^+ + M^+OH^- \rightleftharpoons M^+ + H_2O + NH_3\uparrow$$

The compounds are white crystalline solids, highly soluble in water. The aqueous solutions show a strong absorption band at 215 mμ. The X-ray powder diffraction patterns of the phosphorodiamidates are complex, indicating crystal structures of low symmetry. The three strongest lines of each salt and their corresponding visual intensities are given in Table II.

TABLE II

d-Spacings of the three strongest lines

Compound	d-Spacing I	II	III
$LiPO_2(NH_2)_2 \cdot H_2O$	9.3	3.29	3.25
$NaPO_2(NH_2)_2 \cdot 4H_2O$	3.88	2.68	5.2
$NaPO_2(NH_2)_2$	4.3	3.55	2.7
$KPO_2(NH_2)_2 \cdot H_2O$	3.17	2.48	1.73
$RbPO_2(NH_2)_2 \cdot H_2O$	3.72	2.68	3.42
$CsPO_2(NH_2)_2 \cdot H_2O$	2.75	3.8	3.5

A literature search showed that the i.r. spectra of only zinc (10), barium (11), and silver phosphorodiamidates (12) had been reported by previous workers. In the present study, the i.r. spectra (400–4000 cm^{-1}) of the hydrated phosphorodiamidates of alkali metals and of anhydrous sodium phosphorodiamidate were examined and are recorded in Table III. The assignments of the principal bands in the table are based on the assignments made for silver phosphorodiamidate by Steger and Frei (12). The anion $PO_2(NH_2)_2^-$ has C_{2v} symmetry and possesses 9 fundamentals, out of which 8 are i.r. active (13).

The vibrations involving the PO_2 group are stretching vibrations (ν_{as} and ν_s), a bending vibration (δPO_2), and wagging (ρ_w), twisting (ρ_t) and rocking (ρ_r) vibrations. The last two, viz. ρ_t and ρ_r, would most probably occur below 400 cm^{-1}, the region not covered in the present study. The absorption band at 1680 cm^{-1} is assigned to the bending mode of H_2O and is absent from the spectrum of anhydrous sodium phosphorodiamidate. The asymmetric PO stretch, ν_{as}, assigned to the strong absorption band at 1200 cm^{-1} shifts to a lower frequency (1170 cm^{-1}) in aqueous solution. Similar shifts for the asymmetric PO stretch have been noticed in the i.r. spectra of $H_2PO_2^-$ and $(CH_3O)_2PO_2^-$ ions (14) and ascribed to hydrogen bonding. PN stretching vibrations were, for some unknown reason, not observed in the spectrum of anhydrous sodium phosphorodiamidate.

In a recent paper, the relation of phosphorus–oxygen stretching vibrations to the bond length, bond order, and the force constant of the PO bond has been discussed and important correlations developed (15). PO stretching vibrations in amidophosphates occur at higher wavenumbers than in orthophosphates and this is indeed as expected, because the PO bond order would be expected to increase in the series PO_4^{3-}, PO_3X^{2-}, $PO_2X_2^-$, and POX_3, (15). A comparison of the phosphorus–oxygen stretching vibrations in the fluoro-, chloro-, and amido-derivatives of phosphates is shown in Table IV. It is seen that in fluoro- and chlorophosphates, the successive replacement of oxygen by halogen atoms increases the PO vibration steadily to a maximum value in POX_3 (X = F, Cl) i.e. the PO stretch in POX_3 occurs at a higher wavenumber than the PO stretches in $PO_2X_2^-$ and PO_3X^{2-} (X = F, Cl). In amido-derivatives, on the other hand, the replacement of the first two oxygens by NH_2 groups increases the PO vibrations, but the replacement of the third oxygen does not affect the PO vibration or, if at all, lowers it slightly.

The bonding in phosphates is interesting because of the possibility of phosphorus 3d orbital participation. Commonly used simple valence bond structures for PO_4^{3-}, PO_3X^{2-}, $PO_2X_2^-$, and POX_3 give values of 1.25, 1.33, 1.5, and 2 respectively for the PO bond orders; however, Cruickshank (16) has suggested that in orthophosphates and in substituted phosphates in which phosphorus is tetrahedrally coordinated, the $3d_{x^2-y^2}$ and $3d_{z^2}$ orbitals of phosphorus may take part in d_π–p_π bonding.

On this basis, an average PO bond order of 1.5 is obtained for the orthophosphate ion. In substituted phosphates the prediction of bond order would depend on the nature of the substituent ligand and the extent to which, if any, it takes part in π-bonding with the phosphorus

Can. J. Chem. Downloaded from www.nrcresearchpress.com by 210.87.254.6 on 09/05/12
For personal use only.

TABLE III

Infrared spectra of alkali metal phosphorodiamidates*

Vibration	Frequencies					
	$LiPO_2(NH_2)_2 \cdot H_2O$	$NaPO_2(NH_2)_2 \cdot 4H_2O$	$NaPO_2(NH_2)_2$	$KPO_2(NH_2)_2 \cdot H_2O$	$RbPO_2(NH_2)_2 \cdot H_2O$	$CsPO_2(NH_2)_2 \cdot H_2O$
	3370 s	3400 s	3370 s	3400 s	3400 s	3350 s
ν NH_2	3300 s	3300 s	3300 s	3300 s	3300 s	3270 s
		3190 s	3160 s	3140 s	3140 s	3180 s
δ H_2O	1620 m	1660 m	—	1670	1660 m	1660 m
				1710 m		
δ NH_2	1580 ms	1570 ms	1580 ms	1580 ms	1580 ms	1600 ms
ν_{as} PO_2	1200 s	1200	1205 s	1200 s	1200 s	1200/10 s
	1170 s	1175	1160 sh	1160 s		1170/90 s
ρ_w NH_2	890 m	870 sh	870/40	920 m	870 m	860 m
		850 s		880 m		
$\nu_s PO_2$	1085	1085	1085	1085	1085	
ρ_r NH_2	1075 s	1070 s	1070 s	1070	1065 s	1040 s
ν_{as} PN	800 m	770 m	?	770 w	800 w	?
δ PO_2 }	700 m	680/50 m	?	700 vw	700 vw	700 vw
ν_s PN }						
δ PN_2	530 m	500 m	500 m	500 m	500 m	510 m
δ PO_2	510 m	490 m	480 m	490 m	485 m	490 m

*m, medium; s, strong; v, very; w, weak; sh, shoulder.

TABLE IV

Comparison of P—O vibrations (cm^{-1}) in fluoro-, chloro-, and amido-derivatives of phosphates

	XPO_3^{2-}		$X_2PO_2^-$		X_3PO
X	asym	sym	asym	sym	sym
F	1170	998*	1311	1145*	1415†
Cl	—	—	1258	1147‡	1290†
NH_2	1154	994	1200	1070§	1190§ 1174‖

*Reference 19.
†Reference 20.
‡Reference 31.
§This work.
‖Reference 22.

atom. If the substituent atom does not take part in π-bonding, the d_π–p_π bonding would then involve phosphorus and oxygen atoms only, giving bond orders of 1.67 for PO_3X^{2-}, 2.00 for $PO_2X_2^-$, and 3.00 for POX_3. If, however, the substituent ligand is a good Lewis base, it may take an active part in π-bonding with phosphorus reducing the PO π-bond order and hence the effective PO bond order. In amido-phosphates, the substituent NH_2 group has a lone pair on nitrogen, which is also a good Lewis base, and therefore the PO bond orders would be expected to be less than those mentioned above for the substituted phosphates, in which the substituent was assumed not to take part in π-bonding.

Robinson (15) has shown that for a number of oxygen compounds of phosphorus, the force constant of the PO bond can be estimated from stretching vibrations, by using the Lehmann average rule (17) and the appropriate formula. He has also established an empirical equation relating bond order (n) to force constant. Following his procedure, PO bond order values of 1.80, 1.69, and 1.61 are obtained for $PO(NH_2)_3$, $PO_2(NH_2)_2^-$, and $PO_3(NH_2)^{2-}$ respectively. Assuming, as suggested by Cruickshank (16), that a total of only two π-bonds can be formed by phosphorus, the PN bond orders (n) then are: $PO(NH_2)_3$, $n = 1.40$; $PO_2(NH_2)_2^-$, $n = 1.31$; $PO_3(NH_2)^{2-}$, $n = 1.17$. Thus the averaged PN vibrational frequency and the PN bond force constant would be expected to decrease in the series $PO(NH_2)_3$, $PO_2(NH_2)_2^-$, and $PO_3(NH_2)^{2-}$. In $PO(NH_2)_3$ and $PO(NH_2)_2^-$ the averaged PN stretches, calculated by using Lehmann's rule (17), are respectively 804 and 750 cm^{-1} and the corresponding force constants (dyn/cm) are 3.671×10^5 and 3.194×10^5, which are in the expected order. In $PO_3(NH_2)^{2-}$ the PN stretch has been assigned by Steger (18) to a medium intensity band at 810 cm^{-1} which is higher than that expected from bond order considerations. However, in the spectrum reported by Steger, there is an unassigned band at 700 cm^{-1}, and if this band were to be assigned to the PN stretch, a force constant of 2.783×10^5 dyn/cm would be obtained for the PN bond in $PO_3(NH_2)^{2-}$. By making this assignment, the PN stretches and the PN bond force constants in amidophosphates would follow the pattern expected from the estimated bond orders. The band at 810 cm^{-1} in the published spectrum could possibly be reassigned as ρ_ω NH_2 vibration.

Acknowledgments

The financial support of the National Research Council of Canada is gratefully acknowledged. The author is also thankful to Professor H. C. Clark of the University of Western Ontario for helpful comments and to Dr. R. J. A. Cloutier of Laurentian University for the use of X-ray and infrared machines.

1. H. N. Stokes. Am. Chem. J. **16**, 123 (1894).
2. M. L. Nielsen. *In* Developments in inorganic nitrogen chemistry. *Edited by* Colburn. Vol. 1. Elsevier Publishing Co., Amsterdam. 1966. Chap. 5.
3. E. Fluck. *In* Topics in phosphorus chemistry. *Edited by* Grayson and Griffith. Vol. 4. Interscience Publishers, Inc., New York. 1967. Chap. 6.
4. R. Klement and O. Koch. Chem. Ber. **87**, 333 (1954).
5. R. Klement and G. Biberacher. Z. Anorg. Allgem. Chem. **285**, 75 (1956).
6. M. Becke-Goehring and K. Niedenzu. Chem. Ber. 1768 (1956).
7. A. Steyermark. Quantitative organic microanalysis. 2nd ed. Academic Press, Inc., New York. 1961. Chap. 8.
8. A. I. Vogel. Quantitative inorganic analysis. 3rd ed. Longmans, Green and Co., Ltd., London.
9. W. Rieman III and J. Beukenkamp. *In* Treatise on analytical chemistry. Part II. Vol. 5. *Edited by* Kolthoff and Elving. Interscience Publishers, Inc., New York. 1961. p. 817.
10. J. V. Pustinger Jr., W. T. Cave, and M. L. Nielsen. Spectrochim. Acta, 909 (1959).
11. E. Steger and G. Mildner. Z. Anorg. Allgem. Chem. **333**, 38 (1964).
12. E. Steger and J. Frei. Z. Anorg. Allgem. Chem. **342**, 195 (1966).
13. K. Nakamoto. Infrared spectra of inorganic and coordination compounds. John Wiley and Sons, Inc., New York. 1963. p. 111.
14. M. Tsuboi. J. Am. Chem. Soc. **79**, 1351 (1957).
15. E. A. Robinson. Can. J. Chem. **41**, 3021 (1963).

Can. J. Chem. Downloaded from www.nrcresearchpress.com by 210.87.254.6 on 09/05/12
For personal use only.

16. D. W. J. CRUICKSHANK. J. Chem. Soc. 5486 (1961).
17. W. J. LEHMANN. J. Mol. Spectry. **7**, 26 (1961).
18. E. STEGER. Z. Anorg. Allgem. Chem. **309**, 304 (1961).
19. K. BUEHLER and U. W. BUES. Z. Anorg. Allgem. Chem. **308**, 62 (1961).
20. J. S. ZIOMEK and E. A. PIETROWSKI. J. Chem. Phys. **34**, 1087 (1961).
21. H. MUELLER and K. DEHNICKE. Z. Anorg. Allgem. Chem. **350**, 231 (1967).
22. E. STEGER. Z. Anorg. Allgem. Chem. **310**, 114 (1961).

Can. J. Chem. Downloaded from www.nrcresearchpress.com by 210.87.254.6 on 09/05/12
For personal use only.

Can. J. Chem. Downloaded from www.nrcresearchpress.com by 210.87.254.40 on 09/05/12
For personal use only.

Hydration of the potassium ion in the gas phase: enthalpies and entropies of hydration reactions $K^+(H_2O)_{n-1} + H_2O = K^+(H_2O)_n$ for $n = 1$ to $n = 6$

S. K. Searles and P. Kebarle
Chemistry Department, University of Alberta, Edmonton, Alberta

Received January 31, 1969

The thermodynamic constants $\Delta H^0_{n-1,n}$, $\Delta G^0_{n-1,n}$, and $\Delta S^0_{n-1,n}$ for the reaction $[n-1, n]$: $K^+(H_2O)_{n-1} + H_2O = K^+(H_2O)_n$ proceeding in the gas phase were measured for $n = 1$ to $n = 6$. The equilibria were studied in a reaction chamber containing water vapor at pressures from 0.3 to 6 Torr and at temperatures from −11 to 390 °C. The potassium ions were produced by thermionic emission in a filament chamber and then were equilibrated with the water vapor in the reaction chamber. The relative ionic concentrations were detected with a mass spectrometer. The experimental $\Delta H^0_{n-1,n}$ values are compared with potential energy differences for the reactions $[n-1, n]$ based on simple electrostatic model calculations. The electrostatic calculations produce values in fair agreement with the experimental results. The $\Delta S^0_{0,1}$ calculated on basis of statistical mechanics and energies obtained with the electrostatic model is in very good agreement with the experimental result.

Canadian Journal of Chemistry, **47**, 2619 (1969)

Introduction

In a series of papers published over the past few years (1–5), we have tried to show that important information on the solvation of ions can be obtained by measurement of reaction equilibria involving gaseous ions and molecules of a given "solvent" vapor. An example of such an equilibrium is the gas phase reaction $[n-1, n]$ involving the clustering of water molecules around the potassium ion.

$$K^+(H_2O)_{n-1} + H_2O = K^+(H_2O)_n \qquad [n-1, n]$$

If the equilibrium concentrations of the clustered ions can be measured, and the pressure of the solvent vapor is known, then one can evaluate the equilibrium constant $K_{n-1,n}$. Such equilibrium constants, determined at different temperatures can then be used in Van't Hoff plots for the evaluation of $\Delta H_{n-1,n}$ and thus also $\Delta S^0_{n-1,n}$. The method relies on mass spectrometric determination of the relative ionic concentrations. The primary ions are created by various methods, generally ionizing radiation in a reaction chamber (the ion source) containing the vapor of the solvent. The reaction chamber has a small leak through which the gases and ions bleed out into a high vacuum system where the ions are captured by electric fields and subjected to mass analysis and detection. Conditions in the ion source are so selected that sufficient time is allowed for the establishment of the clustering equilibrium. The measured, mass separated ion currents are assumed proportional to the concentration in the ion sources. Results of the comprehensive investigations of the systems $H^+(H_2O)_n$ (1) and $NH_4^+(NH_3)_n$ (2) have been published, as well as some experiments describing competitive solvation of the proton by methanol and water (3) and of the NH_4^+ ion by water and ammonia (4). The hydration of halide negative ions (F^-, Cl^-, Br^-, and I^-) has also been studied (5). For some time we had wanted to investigate the hydration of the alkali ions. The reasons for this are quite obvious. Since the alkali ions are spherical, one might expect that their hydration energies should be most amenable to classical calculations based on ion dipole interactions. Thus comparisons of experiment with simple theory would be meaningful. The alkali ions have also played an important role in the study of ionic hydration. For example, attempts to evaluate single ion hydration energies, like those of Latimer, Pitzer, and Slanski (6) have been based on the hydration energies of the alkali halide salts. Having succeeded in measuring some hydration energies of the halide ions we became particularly interested in the alkali ions, since interesting comparisons of the hydration of positive and negative ions should be possible when data on both systems become available.

In order to measure hydration equilibria involving the alkali ions one must first find a way of creating these ions in the gas phase under conditions where thermal and clustering equilibrium could be achieved. Ionization by fast

electrons, protons, or α particles, which we had used before, could not be applied, since no compounds containing the alkali atoms and having sufficient vapor pressure could be found. Therefore, a method depending on thermionic emission of positive ions from a filament painted with an alkali salt was developed. The arrangements used are described in the experimental part.

Experimental

Creation of Potassium Ions under Clustering Equilibrium Conditions

The mass spectrometer used for the detection of the potassium hydrates was the instrument formerly connected to a proton generator. This "proton beam" mass spectrometer has been described elsewhere (1) so that no discussion of the gas handling and mass analysis part of the apparatus will be given here. Instead of the proton source, a thermionic source was installed. This new source, and the tests which were made to establish whether clustering equilibrium was established, will be described below.

It is well known that an abundant supply of alkali ions can be obtained by thermionic emission from a heated filament coated with a suitable salt containing the desired ion. Thermionic production is a standard method used in mass spectrometric isotopic determinations of a number of elements. However, for the measurement of hydration equilibria one must meet some special conditions. The ions must be ultimately brought in the presence of water vapor of pressures in the Torr range. Furthermore the ions must be in thermal equilibrium with the surrounding water vapor. Since thermionic emission can be obtained only at elevated temperatures, one must separate the thermionic source from the reaction chamber whose temperature is to be controlled independently. The arrangement used in the present work is shown in Fig. 1. The platinum filament (*5*) coated with the alkali salt preparation is contained in the filament housing (*5a*). The filament housing is attached to the top of the reaction chamber (*1*) and communicates with it by means of an orifice in a polished nichrome disc (*5d*). The disc is in electrical contact with the reaction chamber. A ceramic insulator (*5b*) provided electrical and thermal insulation between the filament housing and the reaction chamber. A positive potential (relative to the reaction chamber) is applied to the filament, filament housing (*5a*), and repeller (*5c*). This field causes the positive ions to drift through the water vapor (which is present in both reaction chamber and filament housing) to the entrance orifice (*5d*) of the reaction chamber. The ions passing through the orifice and into the field free reaction chamber gradually lose their excess energy and become thermalized. Ions diffusing to the exit slit and escaping into the vacuum region are captured by electric fields, accelerated, and then magnetically mass analyzed.

The reaction chamber could be heated by means of electrical heaters placed in heater wells milled out in the chamber block. In the low temperature runs the ion source was cooled by circulating a refrigerated mixture of water and ethylene glycol through channels drilled in the reaction chamber block.

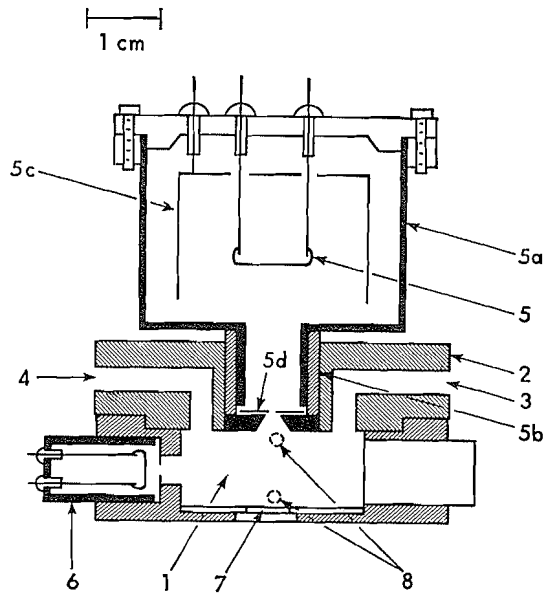

FIG. 1. Reaction chamber for hydration reactions of potassium ions. (*1*) Reaction chamber milled out of solid stainless block; (*2*) chamber lid carrying channels for (*3*) vapor supply and (*4*) pressure measurement; (*5*) potassium ion source consisting of platinum ribbon filament coated by suitable potassium salt (axial filament); (*5a*) filament housing; (*5b*) ceramic insulator between filament housing and reaction chamber; (*5c*) repeller; (*5d*) radiation shield and orifice to reaction chamber backed by copper plate for heat dissipation, diameter of orifice 1.5 mm; (*6*) alternative potassium ion source (right angle filament); (*7*) ion exit slit leading to ion accelerating electrodes and mass analysis; (*8*) thermocouple wells. The reaction chamber also incorporates heaters placed in heater wells which are not shown in the figure.

The coating of the platinum filaments used for the thermionic emission of the potassium ion was a fused mixture of salts which was prepared according to the procedure described by Kunsman (see ref. 7).

To prove that the relative ionic concentrations were not affected by the presence of the filament, whose temperature was about 600 °C and thus some 200–600° higher than the temperature of the reaction chamber, 3 different filament arrangements were used. In the first arrangement the axial filament (*5*) was mounted at only 3 mm distance from the orifice (*5d*). The orifice was also large (5 mm diameter). In later experiments the orifice was closed down to 1.5 mm diameter. A third set of experiments was done with the alternative potassium source (*6*) which was mounted to the side of the reaction chamber such that the ions entering and leaving the reaction chamber were at right angles. A comparison of the results is shown in Fig. 4 which gives the Van't Hoff plots of the equilibrium constants. It can be seen that the equilibrium constants agree for all arrangements so long as the reaction chamber temperature is high. The equilibrium constants (see $K_{2,3}$ Fig. 4) obtained with the larger orifice and the axial filament mounted close are lower than the results obtained with the small orifice

Can. J. Chem. Downloaded from www.nrcresearchpress.com by 210.87.254.40 on 09/05/12
For personal use only.

Can. J. Chem. Downloaded from www.nrcresearchpress.com by 210.87.254.40 on 09/05/12
For personal use only.

and with the right angle filament. This indicates that with the large orifice the effective temperature was higher than the chamber wall temperature measured by the thermocouples. The agreement between the results with the smaller orifice and the right angle filament indicates that with these arrangements the results are not affected by thermal gradients. All further work was done with the axial filament and the small orifice since that geometry gave better sensitivity than the right angle filament. Moving the axial filament further away to the position shown in Fig. 1 produced no change in the observed equilibrium constants (see Fig. 4). As a final test the temperature of the filament was changed by varying the electric power supplying the filament. A change from 22 to 14 W left the equilibrium constants unchanged even when the reaction chamber was in the low temperature range, where the effect of thermal gradients would be most noticeable.

Since an electric field is applied which causes the potassium ions to drift from the filament to the entrance orifice of the reaction chamber, one must show that the ions do have time to reach thermal equilibrium in the field free reaction chamber. To examine this point, the potential between the filament and the reaction chamber was changed. Variation of the electric field strength[1] from 10 to 400 V/cm left the equilibrium constants unchanged even at the lowest reaction chamber pressures (0.4 Torr) used for the equilibria determinations. (These experiments were done at 58 °C.) The usual electric field strength employed was 100 V/cm. The agreement between the determinations with the axial and right angle filaments also suggests that the ions are thermalized. Qualitative calculations (8) based on Wannier's equation also indicate that the excess translational energy of the ions entering the reaction chamber is low and that it is rapidly dissipated through collisions in the reaction chamber.

Results

In Figs. 2 and 3 some representative plots of $K_{0,1}$ and $K_{5,6}$ vs. water pressure are shown. The equilibrium constants $K_{n-1,n}$ were evaluated from the equation

$$K_{n-1,n} = \frac{I_n}{I_{n-1}p}$$

where I_n and I_{n-1} are the measured ion intensities of the ions $K^+(H_2O)_n$ and $K^+(H_2O)_{n-1}$, and p is the directly measured water pressure in Torr. The assumption is made that the measured ion intensities are proportional to the equilibrium ion concentrations in the reaction chamber and that the proportionality constants are identical. The plots in Figs. 2 and 3 illustrate the temperature range (385 to −11 °C) and the pressure range covered in the experiments.

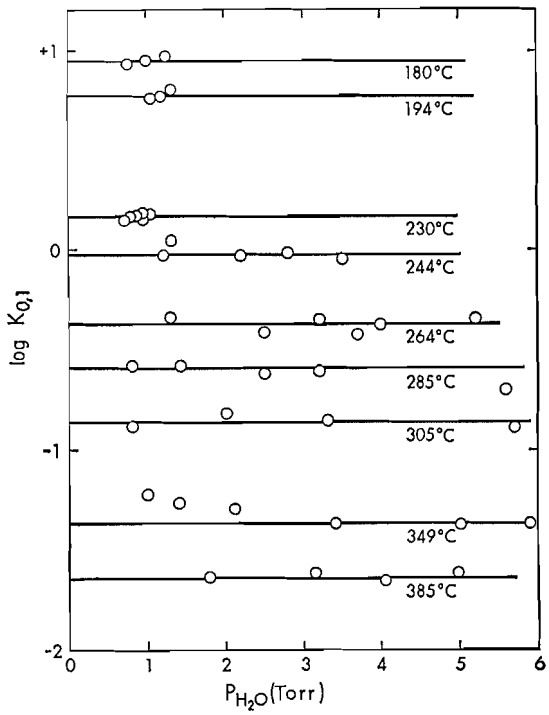

FIG. 2. Plots of $K_{0,1}$ as a function of pressure and temperature of the reaction chamber. Plots illustrate observed constancy of K with water pressure and temperature range covered in experiments. (Standard state for K as given in these plots is 1 Torr.)

Van't Hoff plots of the data are shown in Fig. 4 and the $\Delta H_{n-1,n}$ values obtained from least square fits are given in Table I, together with the values for $\Delta G^0_{n-1,n}$ and $\Delta S^0_{n-1,n}$.

TABLE I

Experimental thermodynamic values for the gas phase reactions: $K^+(H_2O)_{n-1} + H_2O \rightleftarrows K^+(H_2O)_n$ $[n-1, n]$

Reaction	$-\Delta H^0_{n-1,n}$ (kcal/mole)	$-\Delta G^0_{n-1,n}$* (kcal/mole)	$-\Delta S^0_{n-1,n}$* (e.u.)	A†	B†
0,1	17.9	11.4	21.6	3.89	7.57
1,2	16.1	8.9	24.2	3.50	8.14
2,3	13.2	6.3	23.0	2.87	7.88
3,4	11.8	4.4	24.7	2.57	8.26
4,5	10.7	3.2	25.2	2.33	8.35
5,6	10.0	2.3	25.7	2.18	8.46

*At standard state 1 atm. The ΔS values are for temperatures in the temperature range in which each reaction was studied (see Fig. 4). They also are approximately true for 300 °K. The ΔG values are for 298°.

†Constants for the equation $\log (K_{n-1,n}) = (A/T \times 10^3) - B$, data for water pressure in Torr.

[1]The electric field strength quoted above was obtained by dividing the voltage by the distance between the filament and the orifice. Since the electrode geometry is not that of 2 parallel planes, the actual field strength is variable and, for the axial filament in Fig. 1, decreases as the orifice is approached.

Can. J. Chem. Downloaded from www.nrcresearchpress.com by 210.87.254.40 on 09/05/12
For personal use only.

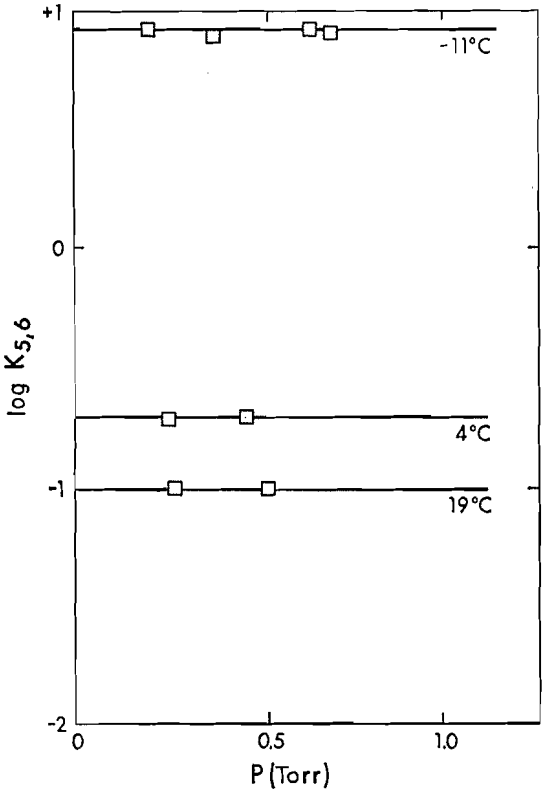

FIG. 3. Plots of $K_{5,6}$ as a function of pressure and temperature of the reaction chamber. Plots illustrate observed constancy of K with water pressure and temperature range covered in experiments. (Standard state for K as given in these plots is 1 Torr.)

The data given in Table I allow the evaluation of the approximate relative equilibrium cluster concentrations over a range widely exceeding the experimental conditions. The relative concentrations given in Fig. 5 illustrate one such calculation made for a temperature of 300 °K. A logarithmic scale was used for the pressure in order to accommodate a wider pressure range. It is interesting to note that the potassium ion is still monohydrated at water pressures as low as 10^{-6} Torr. The simple method by which the calculations of the relative concentrations are made is described in a previous publication (1).

The equilibrium constant $K_{0,1}$ has been obtained in earlier work by Chupka (9). The possibility for determining this equilibrium constant occurred to Chupka while he was measuring the dissociation energies of complex gaseous halide ions. To produce the ions K^+ and $K^+(H_2O)$ he passed water vapor at a pressure of 2×10^{-3} Torr through an oven which was coated with KCl and heated to 570 °C. The resulting ions were detected mass spectrometrically. The value obtained in this manner was $K_{0,1} = 1.2$. The present measurements extend only to 385 °K. However, a reasonably accurate extrapolation can be obtained by means of the Van't Hoff plot constants A and B given in Table I. The extrapolated value obtained in this manner is $K_{0,1} = 0.93$ (both constants are for standard state 1 atm). The very close agreement between Chupka's and the present $K_{0,1}$ is probably fortuitous, considering the widely different experimental conditions. Also Chupka's constant was obtained at a single water pressure which was not directly measured but estimated.

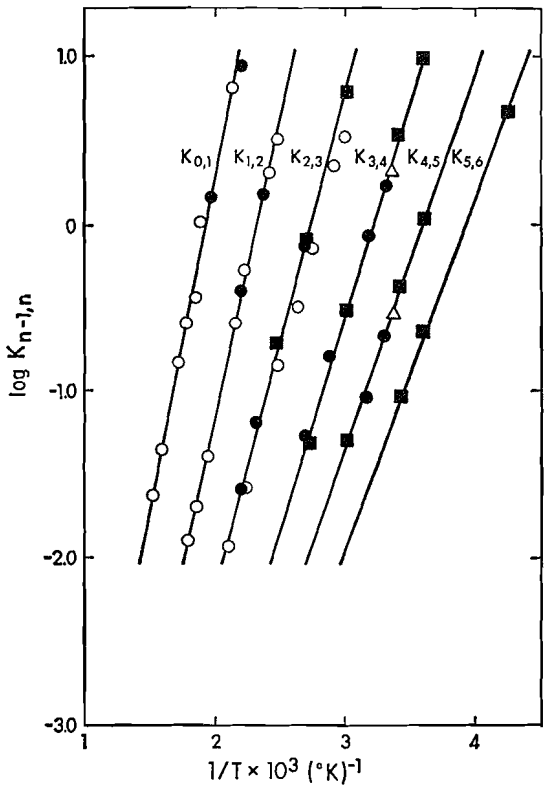

FIG. 4. Van't Hoff plots of equilibrium constants $K_{n-1,n}$. Data illustrate also variation of $K_{n-1,n}$ with different spatial arrangement of filament described in experimental part. ○, axial filament close to reaction chamber and large (5 mm) entrance to reaction chamber; ■, axial filament close to reaction chamber and small (1.5 mm) entrance to reaction chamber; △, axial filament with increased distance from reaction chamber and small (1.5 mm) entrance; ●, right angle filament.

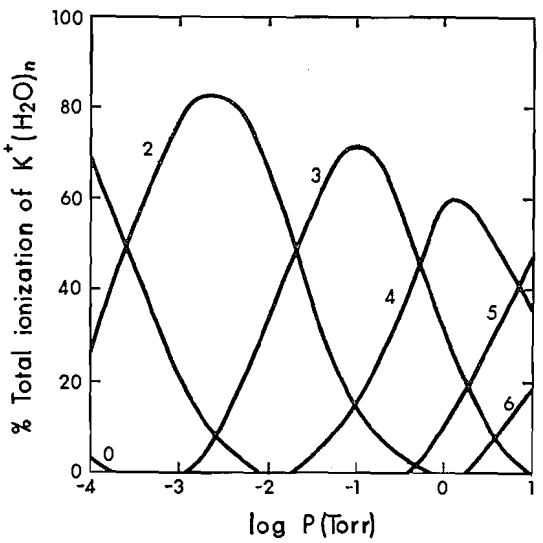

FIG. 5. Equilibrium abundances of $K^+(H_2O)_n$ clusters at different water pressures and 300 °K. Abundances calculated on basis of experimental data by using straight line extrapolation of the Van't Hoff plots in the regions not directly covered by experiment.

Calculations and Comparisons with Experimental Results

Electrostatic Calculations of the Potential Energies of the Complexes $K^+(H_2O)_n$ and Comparison with the Experimental Enthalpy Changes[2]

Many electrostatic calculations of the potential energy changes for attachment of water molecules to ions have been made in the past. In particular, the potential energy of $K^+(H_2O)_6$ (relative to ion and water molecules at infinity) has been calculated by Garrick (10) and that for $K^+(H_2O)_4{}^+$ has been calculated by Muirhead-Gould and Laidler (11). Unfortunately the energies for the other potassium clusters are not available. In order to compare the experimental $\Delta H_{n-1,n}$ with predictions made on the basis of electrostatic attractions we calculated the potential energies of the clusters $K^+(H_2O)_n$ for $n = 1$ to $n = 6$ on the basis of the following models and equations. The total potential energy E_n for a cluster consisting of the potassium ion and n water molecules was expressed by the equation

$$E_n = E_{DIP} + E_{POL} + R_{DIP} + R_{EL}$$

where E_{DIP} is the energy due to ion – permanent dipole attractions, E_{POL} the energy of ion – induced dipole attraction, R_{DIP} is the repulsion of the permanent dipoles, and R_{EL} is the repulsion of the electronic charge clouds of the potassium and oxygen atoms. A point charge model was used for the permanent dipole of the water molecule. The hydrogen atoms were assumed to carry each +0.33 electronic charges (located at the position of the H nuclei) while the oxygen atom carried −0.66 charges located at the O nucleus. The HOH angle in water was taken as 105° and the OH distance as 0.97 Å. The point charge model and other features of the calculation are similar to those used by Doyne and Caldwell (12). The ion – induced dipole attraction energies E_{POL} were calculated on basis of the atomic polarizabilities 0.6 $Å^3$ for oxygen and 0.44 $Å^3$ for hydrogen (13) assumed to be located in the center of the respective atoms. For clusters with $n > 2$ a number of structures are possible. We assumed in all cases structures in which the distances of all oxygen atoms to the potassium ion were equal. The structure for $n = 3$ was of trigonal and planar symmetry. The structure selected for $n = 4$ was tetrahedral, the structure for $n = 5$ was a trigonal bipyramid, and the structure for $n = 6$ was an octahedron. The potassium ion was located in the center, while the water molecules were at the corners of the polyhedra mentioned above. The water molecules were so oriented that the potassium ion was lying on the extension of the bisector of the HOH angle.

The potential energy terms E_{DIP}, E_{POL}, and R_{DIP} for the complex $K^+(H_2O)$ were evaluated for a range of K^+—OH_2 distances by substitution of the above mentioned values in the appropriate equations (8). The numerical computations were performed with an IBM 360 computer. These results are summarized in Fig. 6. The dipole repulsion terms R_{DIP} for $n = 1$ to $n = 6$ and a range of distances were also evaluated with the computer. These results are shown in Fig. 7. The last term R_{EL} in the equation for the total energy E_n accounts for the electronic repulsion between the ion and the water molecules. For this term one uses generally a potential dependence of the form A/R^a where A is a constant, R is the distance, and the power a has a value somewhere between 6 and 12. Neither A nor a is known for the potassium–water pair;

[2]The computer calculations are due to only one of the authors (S.K.S.). These calculations are described in greater detail in ref. 8.

Can. J. Chem. Downloaded from www.nrcresearchpress.com by 210.87.254.40 on 09/05/12
For personal use only.

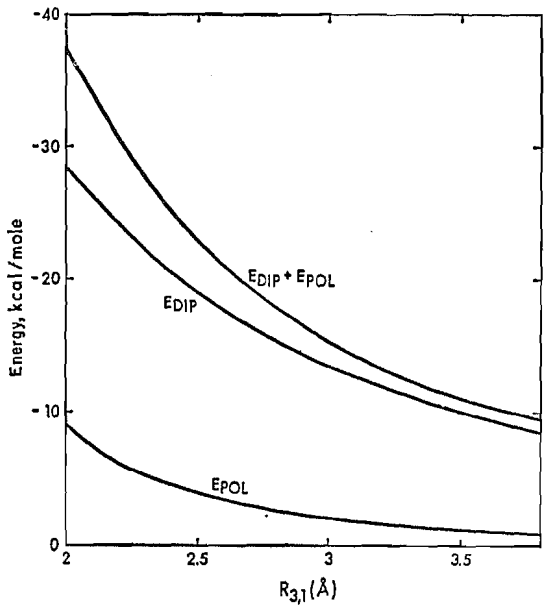

FIG. 6. Plot of calculated electrostatic potential energies for singly charged positive ion – water molecule complex in function of $R_{3,1}$, the distance from the oxygen nucleus to the center of the positive ion. E_{DIP} = ion–dipole attraction; E_{POL} = ion–induced dipole attraction.

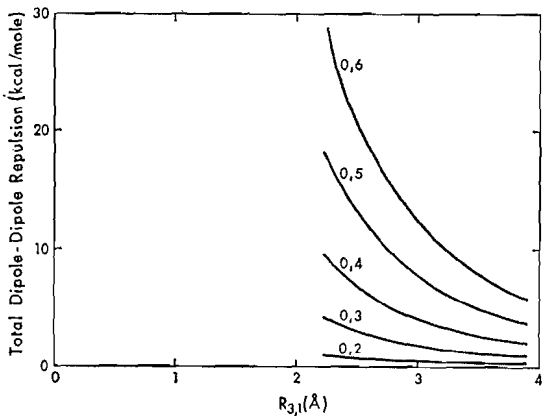

FIG. 7. Plot of dipole–dipole repulsion energies for water molecules around positive ion as functions of $R_{3,1}$, the distance from the oxygen nucleus to the center of the positive ion, 0,n refers to the repulsion of n water molecules around the ion. Geometries of complexes given in text.

however, approximate values could have been selected on the basis of experimentally determined repulsion potentials for the pair Ar—Ne. Since we were more interested in the change of E_n with n rather than in the absolute values, we chose to determine A by setting the (minimized) value for E_1 (K^+—OH_2) equal to the experimental value $\Delta H_{0,1}$. The value of $a = 12$ was used in this calculation. The value for A determined in this way was $A = 3.3 \times 10^5$ kcal/mole^{-1} Å^{12}. R refers to the distance between the potassium and oxygen atom nuclei. The total energies E_n were then evaluated as functions of the distance R. Plots of E_1 and E_6 are shown in Fig. 8. The energy minima E_n^0 in these plots correspond to the total potential energy of the clusters.

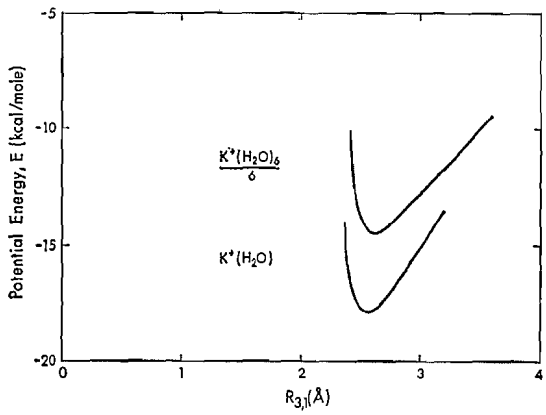

FIG. 8. Plot of calculated potential energy of clusters $K^+(H_2O)$ and $K^+(H_2O)_6$ relative to potassium and water molecules at infinity. The potential energy of $K^+(H_2O)_6$ has been divided by 6 in order to fit on the same scale.

Some calculations were made in which the H_2O molecules in the clusters were rotated around the bisector of the HOH angle. The positions of maximum and minimum energy were found to differ by only a fraction of a kcal. The effect of this rotation was therefore not considered further.

The calculated $E^0_{n-1,n} = E_n^0 - E_{n-1}$ are compared with the experimental $\Delta H_{n-1,n}$ values in Fig. 9. Before considering the meaning of Fig. 9 it is of some interest to compare the results of the present calculations with the quoted calculations of Garrick (10) and Muirhead-Gould and Laidler (11).

Garrick used a point dipole model for the water molecule. Otherwise his approach was very similar except for the ion – oxygen atom electron charge repulsion term for which Garrick used a dependence to the ninth power of the

Can. J. Chem. Downloaded from www.nrcresearchpress.com by 210.87.254.40 on 09/05/12
For personal use only.

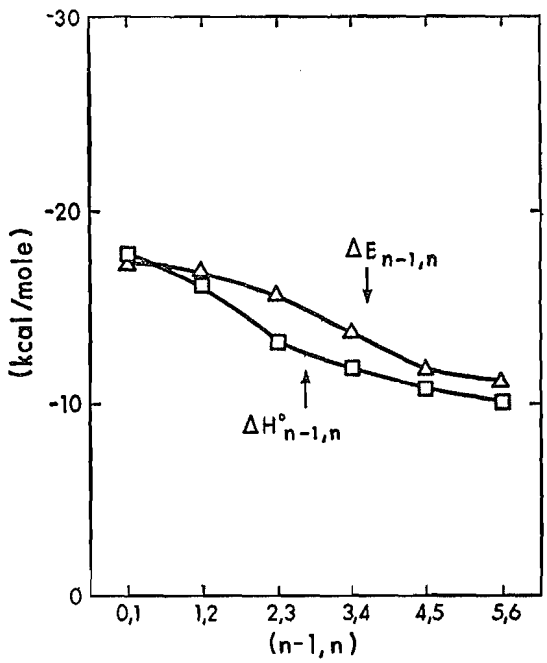

FIG. 9. Comparison of calculated potential energy differences $\Delta E_{n-1,n}$ for reactions $(n-1, n)$ and experimentally determined enthalpy changes, $\Delta H_{n-1,n}$.

radius i.e. AR^{-9}. Garrick used a value for A which was obtained from Lennard–Jones calculations for inert gas repulsions, and a minimization of the total energy. Garrick also included in his calculation a term for the electronic repulsion between water molecules. For the hexahydrate ($n = 6$) Garrick's results gave R_{EL} as +18 kcal/mole and $E_{DIP} + E_{POL} + R_{DIP} = -102$ kcal/mole and the total potential energy $E_6 = -84$ kcal/mole. In comparison the values from this work are +19 kcal/mole for the R_{EL} energy and −86 kcal/mole for the total E_6.

The calculations of Muirhead-Gould and Laidler (11) also involved a point dipole model. These authors did calculations on the $K^+(H_2O)_4$ ion, but unfortunately their results for this ion were presented as a total of a cycle dealing with the heat of hydration of the potassium ion. However, the individual energy contributions to the cycle were given for the ion $Rb^+(H_2O)_4$. Since the ionic radius of Rb is only 0.16 Å larger than the radius of K^+, one would expect the electrostatic energy of formation of $Rb^+(H_2O)_4$ to be slightly smaller than the energy of formation of $K^+(H_2O)_4$. The total potential energy for $Rb^+(H_2O)_4$ by Laidler's calculations is −61 kcal/mole while the corresponding energy for $K^+(H_2O)_4$ by the present calculations is −66 kcal/mole.

On the whole we may conclude that the present calculations give results which are similar to previous calculations based on the electrostatic model and should thus be fairly representative of the predictions of the simple electrostatic theory. The plot in Fig. 9 compared the calculated values $\Delta E^0_{n-1,n}$ with the experimentally determined enthalpy differences. It can be seen that the calculation gives values which qualitatively agree with the experimental results. In comparing the results more closely it is apparent that the $-\Delta H^0_{n-1,n}$ values decrease initially ($n-1,n$ = 1,2; 2,3; and 3,4) considerably more rapidly than the $\Delta E^0_{n-1,n}$ values. The decrease in the electrostatic values is due to dipole–dipole repulsion. Thus dipole–dipole repulsions alone do not seem adequate to explain the initial decrease of the binding energies. Since in initial interactions the primary solvation shell is very uncrowded, the repulsions of the induced dipoles and the electronic repulsions between the water molecules (which were neglected in the electrostatic calculation) are also not likely to provide an explanation for the discrepancy. Thus more recent calculations (14) including these repulsion terms also fail to reproduce the rapid initial drop off in the $\Delta H_{n-1,n}$ terms. A reasonable explanation for the rapid initial drop off would be to invoke a screening effect of the cationic charge by the lone pair oxygen electrons as suggested by Magnusson (15). The presence of the lone pair oxygen electrons in the vicinity of the potassium atom should be due to a certain small amount of covalent (dative bonding) between the oxygen lone pair electrons and empty orbitals of the potassium ion. This covalent effect should be stronger in sodium and lithium. Experimental results for these ions, to be published in the near future (14), confirm this expectation.

The Entropy Changes: $\Delta S^0_{n-1,n}$

The electrostatic calculations described in the previous section are also of help in the comparison of the measured entropy changes $\Delta S^0_{n-1,n}$ (Table I) with theoretical predictions. Thus the entropy change $\Delta S^0_{0,1}$ for the attachment of one water molecule to the potassium ion can be evaluated with fairly good accuracy by standard

Can. J. Chem. Downloaded from www.nrcresearchpress.com by 210.87.254.40 on 09/05/12
For personal use only.

Can. J. Chem. Downloaded from www.nrcresearchpress.com by 210.87.254.40 on 09/05/12
For personal use only.

equations from statistical mechanics. The total entropy change is

$$\Delta S_{0,1} = \Delta S_{tr} + \Delta S_{rot} + \Delta S_{vib}$$

The translational entropy change which is by far the most important term is readily evaluated by means of the Sackur Tetrode equation

$$\Delta S_{tr} = \frac{3}{2} R \ln \frac{M_1}{M_2 \cdot M_3} \frac{3}{2} R \ln T + 2.311$$

where M_1, M_2, and M_3 are the molecular weights of $K^+(H_2O)$, H_2O, and K^+ respectively. Substituting for $T = 570$ °K one obtains $\Delta S^0_{tr} = -36.8$ e.u. The temperature 570 °K corresponds to the average in the temperature range of the Van't Hoff plot from which $\Delta H_{0,1}$ and thus also $\Delta S_{0,1}$ was obtained (see Fig. 4).

To evaluate the rotational entropy change one needs the moments of inertia of the water molecule and the $K^+(H_2O)$ complex. The moments of inertia of water $I_x = 1.91$, $I_y = 1.02$, and $I_z = 2.94 \times 10^{-40}$ g cm^2 are well known. The moments of inertia for the complex were evaluated on the basis of the $K^+—OH_2$ distance of 2.6 Å obtained from the electrostatic calculations in the previous section, and the distances and bond angle of the water molecule. The moments of inertia were found to be equal to: $I_x = 1.91$, $I_y = 1.47$, and $I_z = 1.49 \times 10^{-40}$ g cm^2. Substitution of these values in the equation

$$\Delta S_{rot} = \tfrac{1}{2} R \ln \{(I_x I_y I_z)_2 / (I_x I_y I_z)_1\}$$

leads to $\Delta S_{rot} = 9$ e.u.

To calculate the vibrational entropy change we assume that the vibrations of the water molecule are the same before and after the formation of the complex. In this case the vibrational entropy change is due to 3 new vibrations in the complex. The first of these is a stretching vibration in which the potassium and water molecules are treated as two mass points. The frequency of this vibration was evaluated as $\nu_1 = 8.47 \times 10^{12}$ s^{-1} from the electrostatic potential energy calculation of the $K^+(H_2O)$ complex of the preceding section (see Fig. 8) and the standard equations relating the potential energy to the force constant and thus to the frequency.

The two other assumed vibrations were due to torsional oscillations of the water molecule as a whole around its center of mass. In one oscillation the K, O, and H atoms remain in the same plane, in the other, the O atom moves in the plane perpendicular to the plane.

The potential energy for these motions was evaluated from the electrostatic model and led to the frequencies $\nu_2 = 1.6 \times 10^{13}$ and $\nu_3 = 1.03 \times 10^{13}$ s^{-1}. The corresponding entropies were then obtained from the standard equation for vibrational entropy. The total vibrational entropy change evaluated in this manner was $\Delta S_{vib} = 6.5$ e.u. Combining ΔS_{tr}, ΔS_{rot}, and ΔS_{vib} one obtains $\Delta S^0 = -21.3$ e.u. which is in very good agreement with the experimental value of -21.6 e.u. given in Table I.

A growing number of assumptions would be required for the evaluation of the entropy changes of the reactions leading to the larger potassium–water complexes. Therefore, such calculations were not done. The experimental data in Table I show a gradual increase of $(-\Delta S_{n-1,n})$ with growth of the clusters. This probably reflects the gradual restriction of motion with increased crowding of the water molecules in the first hydration shell. Unfortunately experimental $\Delta S_{n-1,n}$ values could not be obtained for n larger than 6 since at the experimental conditions required to measure these equilibria, condensation of water occurred in the ion source.

Measurements of the hydration of Li^+, Na^+, Cs^+, and Rb^+ by the method described in this paper could be made and will be described in a future publication (14) where a comparison of all the alkali ions will be given also. Measurements of the enthalpies and entropies observed in the hydration of the negative halogen ions are also almost completed. Some interesting differences in the hydration of positive and negative ions will be given in the publication of this work (16).

The $\Delta H_{0,1}$ combined with available thermochemical data permit the evaluation of the proton affinity of KOH. The proton affinities of the alkali hydroxides evaluated from such data are to be found in ref. 17.

Acknowledgments

Dr. A. Zolla contributed significantly to the development of the ion source for potassium

ions in thermal equilibrium with water vapor. The financial assistance of the National Research Council of Canada is gratefully acknowledged.

1. P. KEBARLE, S. K. SEARLES, A. ZOLLA, J. SCARBOROUGH, and M. ARSHADI. J. Am. Chem. Soc. **89**, 6393 (1967).
2. S. K. SEARLES and P. KEBARLE. J. Phys. Chem. **72**, 742 (1968).
3. P. KEBARLE and R. M. HAYNES. J. Am. Chem. Soc. **89**, 5753 (1967).
4. A. M. HOGG and P. KEBARLE. J. Chem. Phys. **43**, 449 (1965).
5. P. KEBARLE, M. ARSHADI, and J. SCHARBOROUGH. J. Chem. Phys. **49**, 817 (1968).
6. W. M. LATIMER, K. S. PITZER, and C. M. SLANSKI. J. Chem. Phys. **7**, 108 (1935).
7. R. O. JENKINS and W. G. TRODDEN. Electron and ion emission from solids. Routledge and Kegan Paul, Ltd., London. 1965. Chap. 7.
8. S. K. SEARLES. Ph.D. Thesis, Chemistry Department, University of Alberta, Edmonton, Alberta. 1968.
9. W. A. CHUPKA. J. Chem. Phys. **30**, 458 (1959).
10. F. J. GARRICK. Phil. Mag. **9**, 131 (1930); **10**, 76 (1930).
11. J. S. MUIRHEAD-GOULD and K. J. LAIDLER. Trans. Faraday Soc. **63**, 944 (1967).
12. G. J. DOYNE and R. G. CALDWELL. Rept. AD 635 522. Stanford Research Institute. 1966.
13. R. R. DREISBACH. Am. Chem. Soc. Advan. Chem. Ser. **15**, 9 (1955).
14. I. DZIDIC and P. KEBARLE. J. Phys. Chem. To be published.
15. L. B. MAGNUSSON. J. Chem. Phys. **39**, 1953 (1963).
16. M. ARSHADI and P. KEBARLE. To be published.
17. S. K. SEARLES, I. DZIDIC, and P. KEBARLE. J. Am. Chem. Soc. To be published.

Can. J. Chem. Downloaded from www.nrcresearchpress.com by 210.87.254.40 on 09/05/12
For personal use only.

Can. J. Chem. Downloaded from www.nrcresearchpress.com by 210.87.254.6 on 09/05/12
For personal use only.

Structural studies on the glycolato, lactato, and mandelato solid complexes of some bivalent iron series metals

ANDREW FISCHINGER, ALLEN SARAPU[1], AND AUDREY COMPANION
Department of Chemistry, Illinois Institute of Technology, Chicago, Illinois 60616

Received July 18, 1968

Electronic absorption spectra, infrared vibrational spectra, and X-ray powder patterns have been measured for anhydrous bis(glycolato), bis(lactato), and bis(mandelato) complexes of bivalent Mn, Co, Ni, Cu, and Zn. Despite indications of considerable differences in crystal structure, the visible spectra of all complexes are quite similar to those of analogous hexaaquo complexes. A ligand field analysis yields as new data a spectrochemical series for the ligands

$$Dq(\text{lactato}) > Dq(\text{glycolato}) > Dq(\text{mandelato})$$

in agreement with the order of proposed metal–oxygen stretch frequencies and previously measured acid pK's of the ligands.

An interesting red to blue color change, observed in all cobalt complexes on heating, is shown to be reversible in the glycolate. A tentative model proposed for the complex appears to be consistent with all the experimental data including the color change phenomena.

Canadian Journal of Chemistry, 47, 2629 (1969)

Introduction

Although considerable effort has been directed toward the study and interpretation of the infrared spectra of the bis(glycolato) (1–4) and bis(lactato) (5) complexes of divalent iron series metal ions, relatively little is known of their structure or of the nature of the reversible color change occurring in the Co(II) complex on gentle heating. In this paper we present the results of investigations of the infrared and visible–near ultraviolet spectra of the anhydrous solid bis(glycolato) metal complexes of composition $M(II)(CH_2OHCOO)_2$ and of similar complexes with lactate ($CH_3CHOHCOO^-$) and mandelate ($C_6H_5CHOHCOO^-$) anions as ligands. Some rough conclusions on comparative crystal structure and the far infrared spectra of lactate and mandelate complexes are presented. For brevity, the glycolate, lactate, and mandelate ions will henceforth be abbreviated G^-, L^-, and M^-, respectively.

Experimental Details

The glycolate and lactate complexes were prepared according to the procedure given by Nast and Ruckemann (2), recrystallized, and heated in vacuo at 50 °C. Mandelate complexes were simply precipitated from aqueous solutions of metal ions of the haloaquo salts by addition of slightly alkaline aqueous mandelic acid. These latter were extremely insoluble in water and common organic solvents and consequently were just washed repeatedly before drying. Results of analysis are shown in Table I.

Samples of the above crystalline solids were ground to a fine powder either by hand or with a Wig-L-Bug mechanical grinder prior to measurement of spectra. When ground mechanically, all three Mn(II) complexes partially decomposed and consequently were powdered carefully by hand. All three Co(II) complexes underwent a gradual color change from red to lavender in the Wig-L-Bug agate capsule and also on gentle heating (up to a temperature of 200 °C) in a vacuum oven. Further heating at 210 °C produced a dramatic color change from lavender to a deep blue first in CoL_2 and much later in CoM_2, but not in CoG_2 which remained lavender. The deep blue color of CoL_2 and CoM_2 as well as the lavender color of CoG_2 persisted from 210 °C to the decomposition temperature, about 240 °C. The color change proved to be rapidly reversible for the lavender form of CoG_2 which totally reverted to the red form in about 30 min as verified by transmission spectra of the two forms and by X-ray powder patterns of the red form before and after reversion. No such definite blue to red reversible change has been observed in the lavender or deep blue forms of CoL_2 and CoM_2.

X-Ray powder patterns were obtained for all samples with a GE XRD-1 diffractometer. Although a thorough crystal structure analysis was not feasible, inspection of the films permitted the following conclusions: (*a*) All compounds were crystalline, with the possible exception of the lavender or blue forms of CoL_2 and CoM_2, which gave no observable lines during the exposure time required by our present equipment (6–8 h). (*b*) Because of the rapidity of the color change in CoG_2 (30 min) relative to exposure time required, no definite evidence could be obtained establishing a structural change with change of color. (*c*) All glycolates with the exception of those of Ni and Zn have distinctly different X-ray patterns. NiG_2 and ZnG_2 appear to be similar in crystal structure but not isomorphous. (*d*) Lactates of Co, Ni, Zn, and Mn appear to be similar in crystal structure, the first three of

[1]Present address: Department of Chemistry, University of Wisconsin, Madison, Wisconsin.

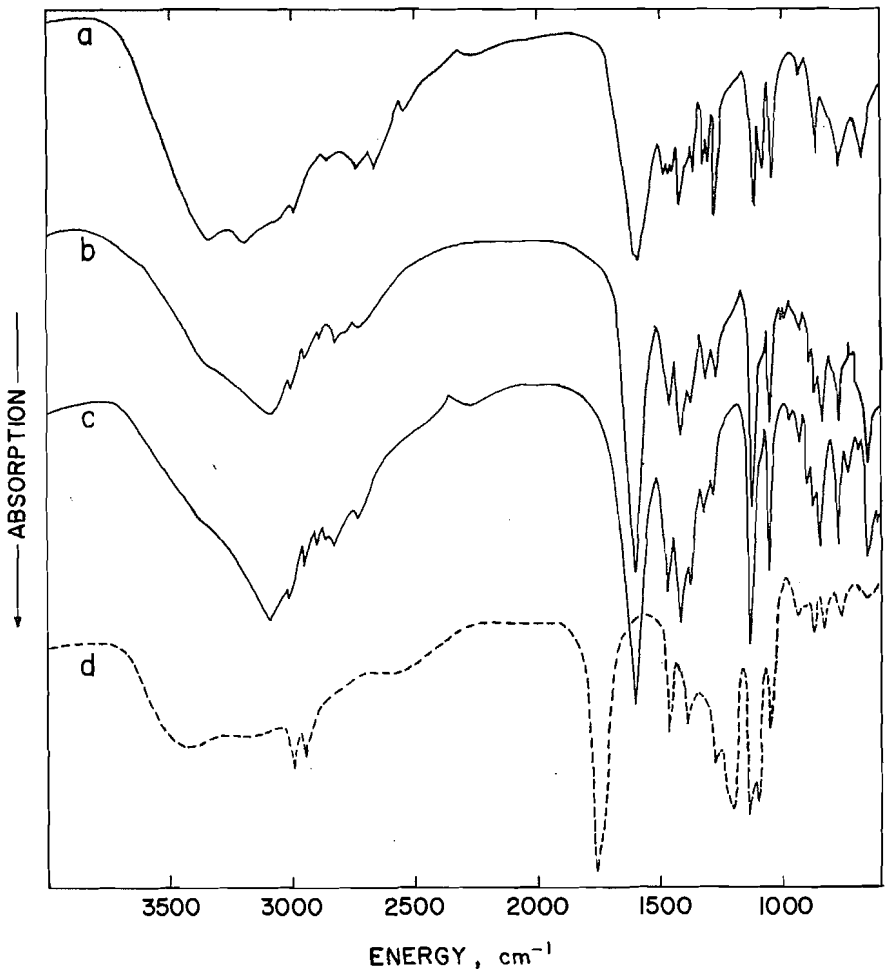

FIG. 1. Infrared spectra of cobalt lactates (4000–600 cm^{-1}): *a*, CoL_2, red form; *b*, CoL_2, lavender form (heated at 168 °C in vacuum oven for 1 day); *c*, CoL_2, deep blue form (heated at 210 °C in vacuum oven for 1 day); *d*, DL-lactic acid, (98% water free but identical to aqueous lactic acid spectrum except for the absence of strong water bands).

these being possibly isomorphous. CuL_2 yields a distinctly different pattern. (*e*) Mandelates of Co, Ni, Zn, and Cu have similar crystal structures, the first three of these being possibly isomorphous. MnM_2 has a distinctly different pattern.

Infrared spectra of the complexes were measured with a Beckman IR 12 spectrophotometer over the region 4000 to 200 cm^{-1}. Figure 1 illustrates tracings obtained for red, lavender, and blue forms of CoL_2 and lactic acid in the region 4000 to 600 cm^{-1}, where evidence supporting coordination is normally found. Table II summarizes for all complexes our proposed energies of the antisymmetric (as) and symmetric (s) stretching modes of the carboxyl group, the alcohol O—H and C—O stretching modes, along with available similar data of other investigators. Figures 2 and 3 reproduce tracings observed for the lactates and mandelates of Cu, Ni, Co (red), Zn, and Mn in the region 600 to 200 cm^{-1}, where metal–oxygen stretching frequencies should be observed. In this region the spectra of blue forms of the cobalt complexes show essentially no shift in peak positions from those of the red forms. The energies of proposed metal–oxygen bands for all complexes are listed in Table III.

The visible, near infrared, and near ultraviolet spectra of the powdered solid complexes were obtained on the Cary Model 14 PMR spectrophotometer with both diffuse reflectance and Nujol mull techniques (7). In general the reflectance spectra agreed quite well with transmission spectra when particles were ground to a sufficiently small size (less than 1 μ in diameter) that contributions from specular reflections were minimal. This small particle size proved to be of critical importance in the case of NiG_2 and NiM_2, both of which exhibited in the hand ground sample a 27 kK peak, which, however, disappeared on prolonged mechanical grinding. X-Ray diffraction studies established that the peak disappearance

Can. J. Chem. Downloaded from www.nrcresearchpress.com by 210.87.254.6 on 09/05/12
For personal use only.

TABLE I

Quantitative analysis

Compound	Metal (%)		C (%)		H (%)	
	Found	Theoretical	Found	Theoretical	Found	Theoretical
MnG_2	26.47	26.80	24.01	23.42	2.95	2.95
CoG_2	27.89	28.19	22.93	22.99	3.02	2.89
NiG_2	28.02	28.12	22.87	23.01	2.94	2.83
CuG_2	29.61	29.74	22.53	22.49	2.78	2.83
ZnG_2	30.05	30.33	22.08	22.30	3.12	2.81
MnL_2	22.44	23.57	30.76	30.91	4.45	4.33
CoL_2	24.73	24.86	30.62	30.39	4.34	4.26
NiL_2	24.74	24.79	30.26	30.42	4.50	4.26
CuL_2	26.16	26.29	29.67	29.82	4.34	4.17
ZnL_2	26.11	26.85	29.41	29.60	4.36	4.15
MnM_2	15.31	15.38	53.96	53.80	3.86	3.95
CoM_2	16.21	16.31	53.20	53.20	3.83	3.91
NiM_2	16.15	16.26	53.11	53.24	3.86	3.91
CuM_2	17.28	17.37	52.68	52.53	4.02	3.86
ZnM_2	17.63	17.78	52.18	52.27	3.98	3.84

TABLE II

Selected carboxyl and hydroxyl frequencies for anhydrous glycolate, lactate, and mandelate complexes in cm^{-1}

Compound	ν(O—H)[a]	ν(COO^-,as)[b]	ν(COO^-,s)[c]	ν(C—OH)[d]
Glycolic acid(HG)	3420[e]	1720	—	1074[e]
ZnG_2	3040[e]	1590[e]	1400[e],1404[f]	1062[e],1067[f]
CoG_2(red)	3090	1595	1402	1062
CoG_2(blue)	3090	1595	1402	1062
CuG_2	3000[e]	1575[e]	1400[e]	1065[e]
NiG_2	3070[e]	1590[e]	1403[e]	1065[e]
MnG_2	3100[e]	1605[e]	1390[e]	1075[e]
Lactic acid(HL)	3420	1753	—	1128
				1098
ZnL_2	3202	1598	1430,1397[f]	1122,1121[f]
				1090,1090[f]
CoL_2(red)	3330	1585	1424	1114
	3180			1085
CoL_2(lavender)	3090	1600	1413	1122
CoL_2(blue)	3097	1600	1416	1122
CuL_2	3240	1582	1412	1125
	2600			1101
NiL_2	3350	1595	1430	1118
	3190			1088
MnL_2	3165	1593	1430	1120
				1088
Mandelic acid(HM)	3406,3450[g]	1722,1710[g]	—	1075
ZnM_2	3250,3260[g]	1595,1600[g]	1410,1410[g]	1006
CoM_2(red)	3250,3270[g]	1580,1570[g]	1414,1310[g]	1005
CoM_2(blue)	3250	1580	1414	1005
CuM_2	3140,3120[g]	1640,1640[g]	1407	1000
NiM_2	3240,3270[g]	1580,1560[g]	1414	1002
MnM_2	3460	1580	1422	1023
	3320	1641		

[a] ν(O—H) is the hydroxyl oxygen–hydrogen stretching frequency.
[b] ν(COO^-, as) is the antisymmetric carboxyl stretching frequency.
[c] ν(COO^-, s) is the symmetric carboxyl stretching frequency.
[d] ν(C—OH) is the carbon–hydroxyl stretching frequency.
[e] Reference 1.
[f] Reference 5.
[g] Reference 6.

Can. J. Chem. Downloaded from www.nrcresearchpress.com by 210.87.254.6 on 09/05/12
For personal use only.

TABLE III

Proposed metal–oxygen stretching frequencies in glycolate, lactate, and mandelate complexes

Metal	Frequencies (cm^{-1})		
	Glycolates[a]	Lactates	Mandelates
Mn	445, 418; 304, 250	466, 426; 382, —	408, 372; 314, 290[b]
Co	459, 427; 343, 307	474, 431; 398, 363[b]	439, 381; 329, 306
Ni	474, 442; 370, 327[b] 317	493, 445; 418[b] 383[b] 483 405 375	449, 392; 339, 319[b]
Cu	484, —; 408, 338	514, 464; 430 396 419[b]	463, 412; 363, —
Zn	468, 435; 327, 284[b] 270	475, 434; 387, 358[b]	435, 374; 310, 286

[a]Data and identification from ref. 1.
[b]Denotes shoulder.

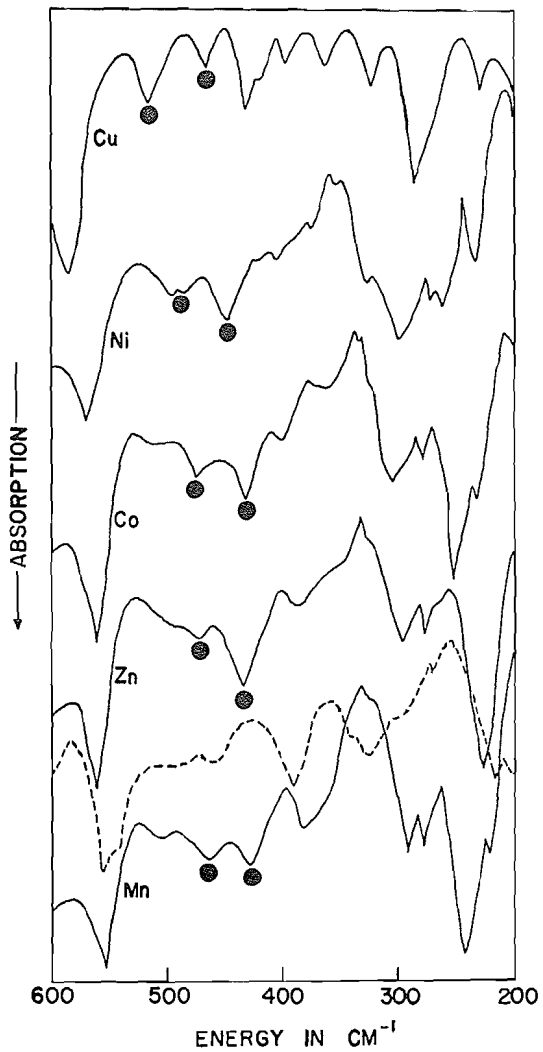

FIG. 2. Infrared spectra of solid lactates (600–200 cm^{-1}). The dots indicate bands attributed to metal–oxygen stretching modes. The dashed line illustrates the spectrum of DL-lactic acid (98% water free).

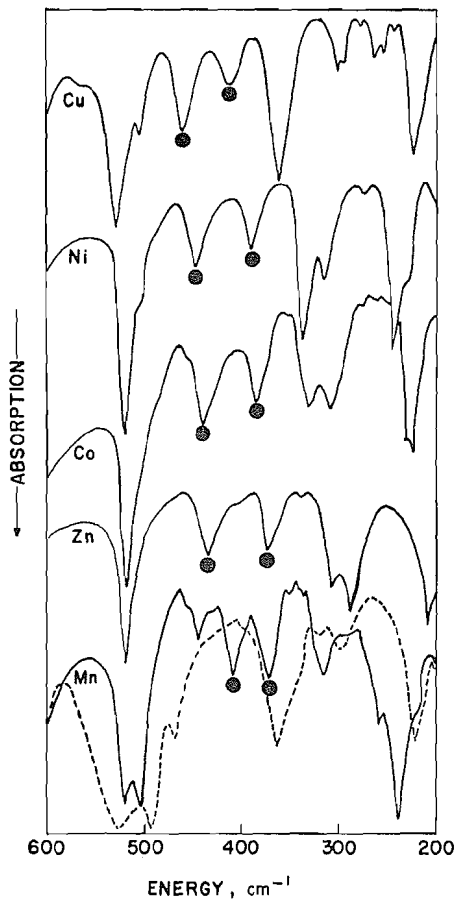

FIG. 3. Infrared spectra of solid mandelates (600–200 cm^{-1}). The dots indicate bands attributed to metal–oxygen stretching modes. The dashed line illustrates the spectrum of solid DL-mandelic acid.

Can. J. Chem. Downloaded from www.nrcresearchpress.com by 210.87.254.6 on 09/05/12
For personal use only.

TABLE IV

Electronic absorption spectral data for glycolato, lactato, and mandelato complexes[a]

Metal	Energy (kK) Glycolates	Lactates	Mandelates	Transition identification
Mn	19.0	18.7	19.1	$^4T_{1g}(G) \leftarrow {}^6A_{1g}$
	23.0	22.6	22.9	$^4T_{2g}(G) \leftarrow {}^6A_{1g}$
	24.6, 24.8	24.6, 24.8	24.4, 24.6	$^4A_{1g}(G), {}^4E_g(G) \leftarrow {}^6A_{1g}$
	27.9	27.8	27.8	$^4T_{2g}(D) \leftarrow {}^6A_{1g}$
	29.3	29.4	28.9, 29.8	$^4E_g(D) \leftarrow {}^6A_{1g}$
	31.9	32.3	30.6	$^4T_{1g}(P) \leftarrow {}^6A_{1g}$
Co(red)	8.88	8.45	8.77	$^4T_{2g}(F) \leftarrow {}^4T_{1g}(F)$
	(16.6)	(16.5)	(16.1)	$^4A_{2g}(F) \leftarrow {}^4T_{1g}(F)$ (?)[b]
	(20.4) 20.8 (21.7)	19.5 (20.5) (21.5)	(20.0) 20.9 21.5	$^4T_{1g}(P) \leftarrow {}^4T_{1g}(F)$
Ni	8.60	8.75	8.45	$^3T_{2g} \leftarrow {}^3A_{2g}$
	14.9	15.0	14.8	$^3T_{1g}(F) \leftarrow {}^3A_{2g}$
	25.1	25.5	25.2	$^3T_{1g}(P) \leftarrow {}^3A_{2g}$
Cu	13.8	13.6	13.5	$^2T_{2g} \leftarrow {}^2E_g$

[a]Numbers in parentheses represent shoulders.
[b]There is some doubt as to the validity of these shoulder peak assignments since the calculated energies for these transitions are considerably higher, being in the range between 18.1 to 18.8 kK.

was not associated with a structural change in the complex. Since, except for strong charge transfer bands in the near ultraviolet, all spectra closely resembled the known spectra of hexaaquo ions, we have simply listed in Table IV the predominant observed peak positions. The spectra for the red and lavender forms of CoG_2 are illustrated in Fig. 4, and for the red, lavender, and deep blue forms of CoL_2 and CoM_2 in Figs. 5 and 6, respectively. All data are reported in terms of kilokaysers (1 kK = 1000 cm^{-1}). The maximum estimated experimental error in these reported peaks is believed to be ± 0.08 kK.

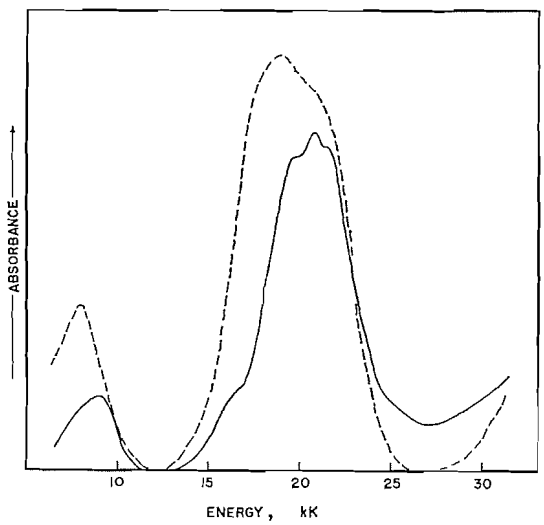

FIG. 4. Visible and near infrared absorption spectra of CoG_2 mulls. The solid curve pertains to the red form while the dashed upper curve describes the lavender form. Relative intensities of absorption are not drawn to scale.

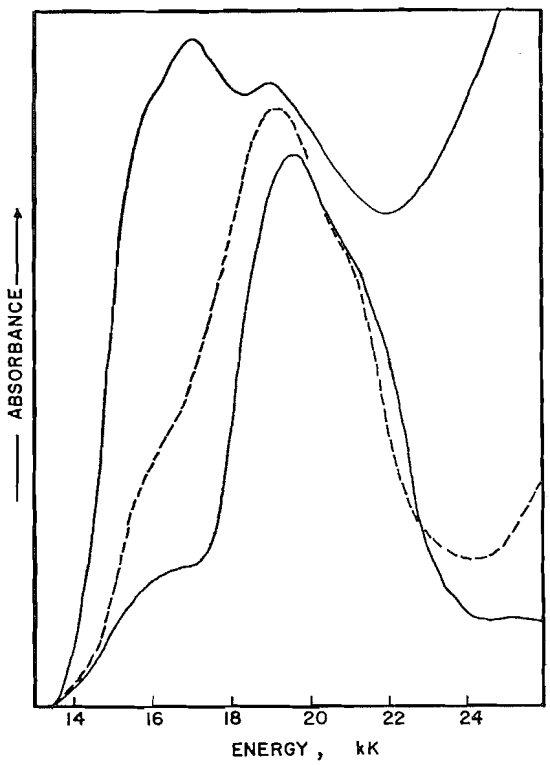

FIG. 5. Visible absorption spectra of CoL_2 mulls. The lower curve refers to the red form, the dashed to the lavender form, and the upper to the deep blue form. Relative intensities are not drawn to scale.

Can. J. Chem. Downloaded from www.nrcresearchpress.com by 210.87.254.6 on 09/05/12
For personal use only.

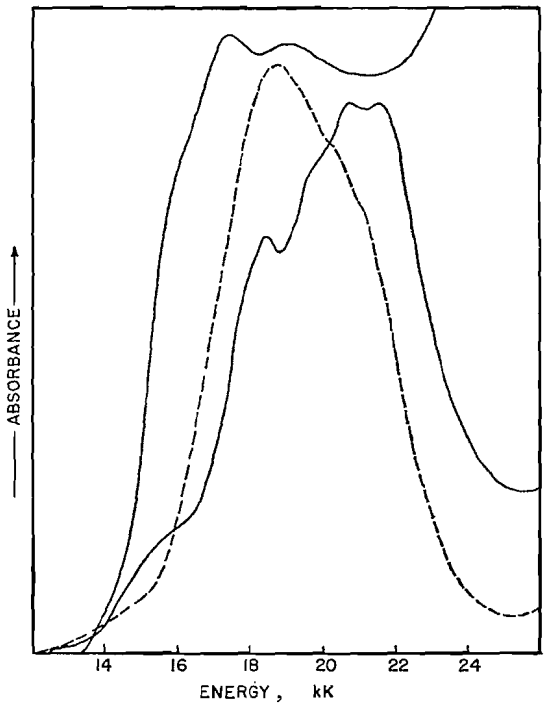

FIG. 6. Visible absorption spectra of CoM_2 mulls. The lower curve refers to the red form, the dashed to the lavender form, and the upper to the deep blue form. Relative intensities are not drawn to scale.

Discussion

Examination of Table II shows that in all complexes studied ν(COO^-, as), ν(O—H), and ν(C—OH) are shifted toward energies lower than those observed in the free acids. Such shifts are generally indicative of coordination of the hydroxyl and carboxyl groups. In some of the lactates, ν(O—H) (which is obscured in the free acid by strong hydrogen bonds) and ν(C—OH) bands are split, yet nevertheless show a definite center-of-gravity shift to lower energy. Similar splitting and shifts are observed in the ν(O—H) and ν(COO^-, as) bands of MnM_2. These splittings may be due to strong hydrogen-bonding between hydroxyl groups with uncoordinated carboxyl groups and other hydroxyl groups, to the presence of both chelate and bridge ligand groups or, particularly in the case of MnM_2, to the presence of some uncoordinated or loosely coordinated ligand groups in the complex. In the red to blue conversion in CoG_2 and CoM_2 no shifts at all occur in the four frequencies listed in Table II. For CoL_2 (Fig. 1), on heating, the separation between the symmetric and antisymmetric COO^- peak positions increases slightly, indicating a possible small increase in the strength of the metal–oxygen bond. Similarly, ν(O—H) shifts strongly toward lower energy as the blue conversion occurs, a shift associable with increased metal–oxygen bond strength or increased hydrogen-bonding in the blue form. The variations shown in Fig. 1 and the lack of variations in the spectra of red and blue CoG_2 and CoM_2 appear consistent with the idea that no chelate bonds are broken in the color conversion process.

Indirect evidence that the ligands are more likely chelates than bridges may be deduced from recent X-ray studies. The structure of anhydrous bis(glycolato)copper(II) has been described (8, 9) as that of a sheet coordination polymer, in which each copper atom is joined in *trans* conformation to two glycolate ligands, forming coplanar rings. The coordination octahedron is completed by carboxy-oxygens of complexes in adjacent layers. No further complete structures have been reported for anhydrous glycolate or lactate compounds. However, structures of related hydrated complexes are known. Aquobis(DL-lactato)copper(II) hemihydrate crystals contain copper atoms *trans* chelated to two lactate ligands in a bow-shaped, almost planar configuration, with the coordination octahedra completed by a water molecule and a weakly interacting neighboring carboxy-oxygen (9). Hydrogen bonds join double ribbons of complexes in sheets, with isolated water molecules in channels between ribbons. It seems reasonable to assume that during loss of water to form the anhydrous lactate the bis-chelate conformation and also the layered structure would be retained.

No X-ray studies have been reported for either anhydrous or hydrated mandelates. However, in diaquobis(phenoxyacetato)copper(II) (9) (in which the ligand differs from mandelate by displacement of the phenyl group from the carbon to the coordinating oxygen), the two *trans* chelate rings and their phenyl groups are almost coplanar, with the complexes hydrogen-bonded to form sheets. Again it seems reasonable that the complex could lose the two water molecules completing the coordination sphere with retention of its bis-chelate and sheet characteristics.

A recent structure determination of isomor-

Can. J. Chem. Downloaded from www.nrcresearchpress.com by 210.87.254.6 on 09/05/12
For personal use only.

Can. J. Chem. Downloaded from www.nrcresearchpress.com by 210.87.254.6 on 09/05/12
For personal use only.

phous $ZnG_2 \cdot 2H_2O$, $CoG_2 \cdot 2H_2O$, and $MnG_2 \cdot 2H_2O$ (10) indicates that both glycolate ligands are chelated in a non-coplanar twisted *cis* configuration with the two water molecules occupying near neighbor positions of the coordination octahedron. The complexes form puckered sheets with pairs of water molecules of neighboring complexes in a channel between the sheets. Since these crystals easily dehydrate in a vacuum at 60–70 °C, one may deduce that if the chelate bonds are not ruptured on dehydration, the molecules will retain the *cis* conformation, with coordination octahedra completed by loosely attracted carboxy-oxygens in adjacent layers. This postulate is in agreement with results of a normal coordinate analysis of the infrared spectrum of anhydrous CoG_2 carried out by Nakamoto, McCarthy, and Miniatas (1), who suggested that the environment around Co(II) should be at most C_{2v}, consistent with a *cis* square-planar configuration.

Although none of the infrared or X-ray evidence definitely precludes the existence of more complicated bridged oligomeric or polymeric structures for the complexes studied, we have assumed as a working model that the compounds contain *cis* or *trans* square-planar 1:2 chelates in layered structures with coordination octahedra completed by oxygen atoms of chelates in neighboring layers, the chelate molecules and layers held together by a network of hydrogen bonds. Such octahedral coordination is consistent with the colors and visible spectra of all freshly prepared complexes.

In line with this model, the visible spectra were analyzed with weak crystal field octahedral matrices of the Orgel type (11), including configuration interaction. Excitation energies for the necessary isolated atom states were calculated by the barricentric method described by Jorgensen (ref. 12, p. 78). The Dq and β values derived are listed in Table V. For all Ni(II) and Mn(II) complexes and the red Co(II) complexes, almost quantitative agreement was obtained between experimental and calculated transition energies.

Despite the observed differences in crystal structures of the complexes, the derived crystal field parameters do exhibit some order. In all complexes the Dq values show that the spectrochemical series of central ions is obeyed for each ligand, i.e.

$$Dq(\text{Cu}) > Dq(\text{Co}) > Dq(\text{Ni}) > Dq(\text{Mn})$$

TABLE V

Octahedral crystal field parameters for complexes

Complex	Dq (cm^{-1})	β
MnG_2	740	0.92
MnL_2	760	0.92
MnM_2	710	0.91
CoG_2(red)	1000	0.89
CoL_2(red)	958	0.84
CoM_2(red)	1000	0.93
NiG_2	860	0.86
NiL_2	875	0.87
NiM_2	845	0.88
CuG_2	1380	—
CuL_2	1360	—
CuM_2	1350	—

Examination of all Mn(II) and Ni(II) complexes indicates the following spectrochemical series for the ligands

$$Dq(\text{L}^-) > Dq(\text{G}^-) > Dq(\text{M}^-)$$

The nephelauxetic series for these ligands cannot be readily established, since the observed β values are essentially invariant in Mn(II) and Ni(II) complexes. For each given ligand, β for the Mn(II) complex is consistently larger than that of the corresponding Ni(II) complex, in agreement with the nephelauxetic series of central ions as advocated by Jorgensen (ref. 12, p. 138).

Except for their position in the spectrochemical series of central ions, the parameters of the red Co(II) complexes appear to be quite erratic in behavior. This may be due to the well-known ambiguities in properly estimating the $^4T_{1g}(P)$ band position in Co(II) complexes, to possible radical deviations from octahedral symmetry (static Jahn–Teller distortions are expected for Co(II) complexes), or to possible presence even in the freshly prepared solid of a small amount of blue form. That the Dq values for the Cu(II) complexes do not obey the expected spectrochemical series of ligands may also be due to Jahn–Teller distortion. It is probable that these Cu(II) complexes are tetragonally distorted (with CuG_2 being least distorted) as some preliminary investigations (13) of electron paramagnetic resonance spectra indicate. Furthermore, the useful "σ ratio" method of Jorgensen (ref. 12, p. 124) yields a value of 1.6 for these compounds, again indicating a strongly tetragonal symmetry.

The lavender or intermediate blue forms of CoG_2, CoL_2, and CoM_2 all have very similar

Can. J. Chem. Downloaded from www.nrcresearchpress.com by 210.87.254.6 on 09/05/12
For personal use only.

spectra with intense peaks near 8.1 and 18.8 kK. The $^4T_{2g}$(F) and $^4T_{1g}$(P) peaks in the corresponding red complexes all undergo a distinct red shift and substantial increase in intensity as the conversion occurs, while the weak $^4A_{2g}$(F) shoulder in the red complexes disappears or is obscured by stronger bands (Figs. 4, 5, 6). As the CoL_2 and CoM_2 samples become increasingly blue, prominent peaks appear near 7.5 and 17.1 kK. These latter correlate well with those observed for known implanted tetrahedral Co(II) species, for example, Co(II) in ZnO (14), for which two main bands are observed at 6.1, 7.0, 7.5 kK and 15.3, 16.4, 17.6 kK. The lavender complexes, however, lie between the theoretical octahedral and tetrahedral peak positions expected for Co(II) coordinated to oxygen atoms. This implies that only a partial conversion to a tetrahedral species has occurred. Since electronic transitions in a tetrahedral molecule are not Laporte forbidden and hence are associated with higher intensities, a relatively small concentration of tetrahedral species may be sufficient to cause the observed color change.

If the postulated structure of these complexes is correct (square-planar species coordinated axially through adjacent layers), on heating, the bonds between layers are most likely weakened or broken, yielding square-planar Co(II) species. For Co(II), weak field square-planar coordination is uncommon (15) and probably less stable than the usual four-coordinated symmetry, tetrahedral. In our series of complexes tetrahedral symmetry may be attained by a 90° twist of one chelate ring with respect to the other. The absence of X-ray diffraction patterns for the lavender to blue forms of CoL_2 and CoM_2 indicates, however, that the postulated twisting must be quite random. In CoG_2 the twisting motion may be relatively unhindered, so that interconversion of red and blue forms occurs readily. In CoL_2, where a methyl group has been introduced on each chelate ring, reversion to tetragonal coordination may be appreciably hindered. Thus a large number of tetrahedral species may accumulate, culminating in the deep blue color never achieved by the glycolate complex. Similar arguments may obtain for CoM_2. Furthermore, the greater steric hindrance caused by the phenyl group possibly makes it more difficult for the twisting to occur in CoM_2, thus explaining why CoM_2 requires a much longer time than CoL_2 to be converted to the deep blue form at 210 °C.

The lower energy (600–200 cm^{-1}) infrared spectra of these complexes appear to substantiate this "twisting" model. The spectra of blue forms of the cobalt complexes show no shift in peak positions from those in the red form in this critical region where metal–oxygen stretching frequencies are to be found. The invariance of all peak positions indicates also that no drastic change in metal–oxygen bond strength occurs on color change; hence the large ν(O—H) shift observed in blue CoL_2 must reflect a change in hydrogen-bonding. Table III lists proposed higher energy metal–oxygen stretching bands for our complexes, deduced by comparison of the spectra with those of the metal glycolates as analyzed by Nakamoto, McCarthy, and Miniatas (1). The positions of these bands are also indicated with dots in Figs. 2 and 3. The magnitude of these frequencies for each given ligand indicates that as the metal ion is varied, the strength of the metal–oxygen bonds decrease in the order

$$Cu(II) > Ni(II) > Co(II) \approx Zn(II) > Mn(II),$$

correlating perfectly with the Irving–Williams stability constant series for metal ions (16). In addition, for each metal ion, these frequencies decrease with change in ligand as

$$\nu(L^-) > \nu(G^-) > \nu(M^-)$$

paralleling exactly the order of oxygen – acidic hydrogen bond strengths in the acids as indicated by their observed pK's (17), HL, 3.86; HG, 3.84; HM, 3.39. Note also that this frequency order is that of the spectrochemical series of these ligands as determined from our Mn(II) and Ni(II) spectra, further evidence of a relation between thermodynamic stability of a complex as reflected in bond strengths and crystal field stabilization.

Further studies on these and related compounds, in search of additional information on their structure, are in progress.

Acknowledgments

The authors are grateful for support of this research in the form of a National Aeronautics and Space Administration Traineeship (to A.F.) and a National Science Foundation Undergraduate Research Participation award (to A.S.).

1. K. NAKAMOTO, P. J. MCCARTHY, and B. MINIATAS. Spectrochim. Acta, **21**, 379 (1965).
2. R. NAST and H. RUCKEMANN. Chem. Ber. **93**, 584 (1960).
3. C. DUVAL and J. LECOMPTE. Bull. Soc. Chim. France, **10**, 180 (1943).
4. R. LARSSON. Acta Chem. Scand. **19**, 783 (1965).
5. J. D. S. GOULDEN. Spectrochim. Acta, **16**, 715 (1960).
6. P. VIELES, A. BONNIOL, and B. LISSORGUES. J. Chim. Phys. **65**, 1482 (1968).
7. K. SHIBATA, A. BENSON, and M. CALVIN. Biochem. Biophys. Acta, **15**, 461 (1954).
8. J. G. FORREST, C. K. PROUT, and F. J. C. ROSSOTTI. Chem. Commun. 658 (1966).
9. C. K. PROUT, R. A. ARMSTRONG, J. R. CARRUTHERS, J. G. FORREST, P. MURRAY-RUST, and F. J. C. ROSSOTTI. J. Chem. Soc. 2791 (1968).
10. A. J. FISCHINGER and L. E. WEBB. Unpublished results.
11. L. E. ORGEL. J. Chem. Phys. **23**, 1004 (1955).
12. C. K. JORGENSEN. Absorption spectra and chemical bonding in complexes. Addison-Wesley, Reading. 1962.
13. J. WASSON and A. J. FISCHINGER. Unpublished results.
14. R. PAPPALARDO, D. L. WOOD, and R. C. LINARES. J. Chem. Phys. **35**, 1460 (1961); **35**, 2041 (1961).
15. F. A. COTTON and G. WILKINSON. Advanced inorganic chemistry. 2nd ed. Interscience Publishers, Inc., New York. 1966. p. 873.
16. H. IRVING and R. WILLIAMS. J. Chem. Soc. 3192 (1953).
17. E. LARSON and B. ADELL. Z. Physik. Chem. **A157**, 342 (1931).

Can. J. Chem. Downloaded from www.nrcresearchpress.com by 210.87.254.6 on 09/05/12
For personal use only.

Diagramme de phase du système $Rb–Rb_2O$: le sous-oxyde de rubidium Rb_3O

PH. TOUZAIN
Département de Chimie, Université de Montréal, Montréal, Québec

Reçu le 21 janvier

Le diagramme de fusion du système $Rb–Rb_2O$ est obtenu par la méthode de l'analyse thermique différentielle. Les échantillons de diverses compositions sont élaborés par combinaison directe de rubidium bidistillé et d'oxygène gazeux. Ce système présente un eutectique fondant vers -10 °C de couleur jaune mordorée pour une composition voisine de $RbO_{0.2}$, et un composé à fusion incongruente (à 48 °C). Ce dernier pouvant être séparé par centrifugation du mélange liquide en cristaux rouges cuivrés est un sous-oxyde de formule Rb_3O. On observe la dismutation de Rb_2O en Rb_2O_2 et Rb à la température de 410 °C.

The $Rb–Rb_2O$ diagram system has been obtained by the technique of differential thermal analysis. The samples of different compositions were prepared by direct synthesis from doubly distilled rubidium and gaseous oxygen. This system shows a golden eutectic which melts at -10 °C for a composition close to $RbO_{0.2}$, and a compound which exhibits incongruent melting (at 48 °C). The latter can be isolated as copper colored crystals by centrifugation of the liquid mixture; it is a sub-oxide with the formula Rb_3O. Dismutation of Rb_2O in Rb_2O_2 and Rb is observed at 410 °C.

Canadian Journal of Chemistry, **47**, 2639 (1969)

Can. J. Chem. Downloaded from www.nrcresearchpress.com by 210.87.254.5 on 09/05/12
For personal use only.

L'étude des sous-oxydes des métaux alcalins commencée par Rengade (1) vers 1909 présente un grand intérêt du point de vue de leurs valences et de leurs structures chimiques.

En traçant le diagramme de phase du système $Cs–Cs_2O$ par analyse thermique, Rengade (2) mis en évidence 4 composés définis du césium: Cs_7O, Cs_4O, Cs_7O_2 et Cs_3O. Brauer (3) détailla une partie de ce diagramme (Cs à Cs_4O) par mesure des coefficients de résistivité des mélanges césium-oxydes en fonction de la température. Les sous-oxydes Cs_7O (3), Cs_4O (3) et Cs_3O (4) examinés aux rayons X présentent en fait des structures cristallines partiellement métalliques. D'ailleurs ces composés conduisent le courant électrique à peu près de la même façon que le césium pur.

Dans le cas des autres métaux alcalins, De Forcrand (5) signale en 1898, le sous-oxyde Na_3O se formant en "arborescences volumineuses grises" au dessus du sodium métallique, mais aucune autre expérience n'a encore confirmé ce résultat.

Rengade (6) observa durant l'oxydation de rubidium par de l'oxygène, la formation d'un liquide jaune roux à éclat métallique et l'apparition au refroidissement de "gros cristaux mordorés". Plus récemment, Herald et Weatherford (7) remarquèrent que l'addition de seulement 1000 p.p.m. d'oxygène au rubidium abaisse son point de fusion de 1 °C. Une mesure très précise de cette température de fusion serait même un critère de pureté du rubidium. Cette dernière méthode, préconisée par Tepper (8), permet de déterminer la concentration en oxygène dans le rubidium avec une précision de 2 p.p.m. tant que cette concentration reste inférieure à 500 p.p.m.

Ayant observé la dissolution des oxydes de rubidium dans le rubidium métallique à des températures même inférieures à 0 °C (9), nous avons pensé étudier le diagramme de phase du systéme $Rb–Rb_2O$, ce qui nous permettrait, en même temps, de prouver l'existence ou l'absence de sous-oxydes de rubidium. Nous avons utilisé pour déterminer les températures de ce diagramme la technique de l'analyse thermique différentielle sur des échantillons de $Rb–Rb_2O$ de l'ordre de 10 mg.

Techniques Expérimentales

Préparation du mélange rubidium–oxygène

Les mélanges $Rb–Rb_2O$ de diverses compositions sont préparés par synthèse directe à partir de rubidium métallique et d'oxygène gazeux.

Le rubidium obtenu par la méthode Hackspill (10) est bidistillé sous vide (10^{-4} mm Hg) suivant une technique déjà décrite (9). Environ 1 g de ce métal est utilisé à chaque expérience.

Un volume précis d'oxygène est alors mis en communication avec le métal. L'absorption de la totalité de l'oxygène par le rubidium est rapide à la température de 70–90 °C tant que la surface en contact entre le gaz et le métal est suffisament grande.

Le poids de métal est déterminé exactement après échantillonnage, par un dosage acidimétrique de la solution aqueuse de rubidine, solution obtenue par attaque ménagée du mélange rubidium–oxyde par l'eau.

Can. J. Chem. Downloaded from www.nrcresearchpress.com by 210.87.254.5 on 09/05/12
For personal use only.

Un calcul simple nous permet de trouver le rapport oxygène/métal du mélange ainsi préparé.

Analyse thermique différentielle (a.t.d.)

(a) Appareillage

La tête semi-micro de l'appareil a.t.d. utilisé dans cette étude et mis au point par Mazières (11), comporte un ensemble de 3 coupelles cylindriques en platine (pour échantillon et références) constituant elles-mêmes la soudure des thermocouples. Ce dernier fait augmente la sensibilité et le pouvoir de résolution de l'appareil. Le volume utilisable des coupelles est de 25 µl.

Un enregistreur à 2 voies galvanométriques est couplé à l'analyseur thermique différentiel. Le signal de température différentielle est enregistré sur une voie particulièrement sensible (62.5 µV échelle).

(b) Préparation des échantillons

Etant très hygroscopiques, les métaux alcalins ou leurs oxydes doivent être introduits à l'abri de l'air, sous vide, à l'intérieur d'un petit tube de verre. Celui-ci sera placé dans la coupelle en platine de l'a.t.d. prévue pour l'échantillon au moment de l'analyse thermique.

La Fig. 1 indique les techniques employées pour introduire du mélange alcalin (environ 10 mg) dans une petite ampoule de verre. Cette ampoule est obtenue par soufflage d'un tube capillaire en verre Pyrex à forte épaisseur et préalablement étiré.

Deux cas se présentent suivant que le point de fusion du mélange est situé en dessous ou au dessus de 50 °C.

Dans le premier cas, le mélange est maintenu à l'état liquide dans un bain thermostaté à 50 °C. Il est homogénéisé par agitation puis on en remplit les ampoules échantillons par gravité. Les ampoules sont alors scellées à l'aide d'une micro-torche, ainsi prêtes pour l'analyse thermique.

Dans le deuxième cas, la température du mélange est d'abord maintenue vers 90 °C pendant plusieurs heures[1]. Refroidi rapidement à la température ordinaire, le mélange y subit sa recuisson qui permet la cristallisation du ou des composés. Ensuite il est réduit en poudre à l'aide d'une masselotte en acier que l'on avait pris soin de placer à l'intérieur du tube laboratoire. Cette opération est conduite à la température de −80 °C pour rendre le mélange alcalin plus brisant. Un peu de cette poudre est introduite dans les ampoules qui sont alors scellées comme dans le premier cas.

L'échantillon de référence pour l'a.t.d. est une petite ampoule de verre identique à celles utilisées pour les échantillons alcalins mais vide de toute substance.

[1]On s'apercevra quand on examinera le diagramme de phase du systéme Rb–Rb_2O sur la Fig. 2 qu'en maintenant la température d'un échantillon au dessus de 50 °C par exemple à 90 °C, au moins une partie du mélange se trouve à l'état liquide. Cette phase liquide réduit en les mouillant les peroxyde ou superoxyde solides qui éventuellement auraient pu se former pendant la période d'oxydation du métal. En fait, maintenir l'échantillon à une température supérieure à celle du liquidus nous conduirait à n'obtenir qu'une seule phase liquide et ainsi une homogénéisation parfaite. Cependant du fait de la température élevée de ce liquidus pour les % d'oxygène proches de celui de Rb_2O, cette méthode occasionnerait à la longue l'attaque du verre Pyrex par le rubidium ou même la dismutation de Rb_2O à partir de 400 °C.

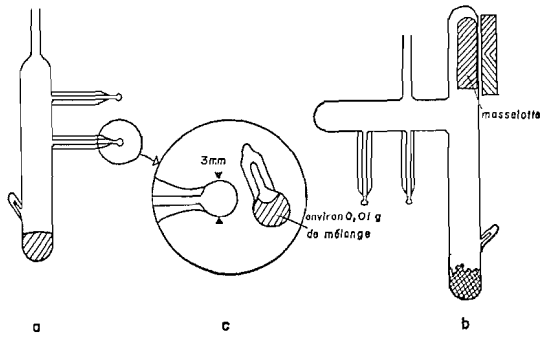

FIG. 1. Préparation des échantillons de Rb–Rb_2O pour l'analyse thermique différentielle. (*a*) Échantillonnage d'un mélange liquide à une température inférieure à 50 °C, (*b*) échantillonnage d'un mélange solide ou en partie solide à 50 °C, (*c*) ampoules-échantillons pour l'a.t.d.

(c) Analyse thermique

Les échantillons alcalins ont tendance à rester en surfusion pendant parfois quelques dizaines de degrés en dessous de leurs points de congélation théorique. Ce phénomène exclut toute précision des mesures que l'on pourrait faire par refroidissement. C'est pourquoi nos courbes d'analyses thermiques $\Delta T = f(T)$ ont été obtenues par chauffage et non par refroidissement du mélange alcalin.

Pour effectuer une analyse thermique, on commence donc par refroidir la tête de l'analyseur aux alentours de −40 °C jusqu'à équilibre thermique puis on procède à l'élévation de température à une vitesse de 3–4 °C par minute.

Les pics des courbes thermiques $\Delta T = f(T)$ ont une hauteur comprise en général entre 1 et 10 µV. Ce sont leurs sommets qui ont permis la détermination la plus reproductible des températures de fusion des échantillons. La calibration des thermocouples (platinel) effectuée par le fabriquant de l'a.t.d. a été utilisée telle quelle. La précision des mesures peut-être fixée à ±2 °C.

Résultats

Le diagramme de phase du système Rb–Rb_2O, obtenu par analyse thermique différentielle, est porté sur la Fig. 2. Ce diagramme présente les points particuliers suivants.

(*a*) Formation d'un eutectique se solidifiant à −10 °C. Le minimum du liquidus correspond au % atomique d'oxygène d'environ 16% (à peu près $RbO_{0.2}$). La couleur jaune dorée du mélange va en s'approfondissant au fur et à mesure que la proportion d'oxygène augmente, allant du blanc argent pour le métal pur au brun doré pour les mélanges de % atomique d'oxygène supérieur à 20.

(*b*) Existence d'un sous-oxyde à fusion incon-

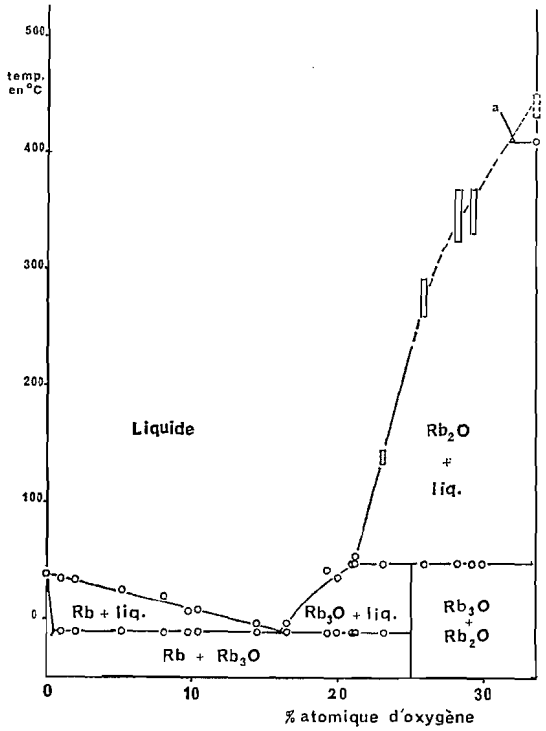

FIG. 2. Diagramme de phase du système Rb–Rb_2O. (*a*) Dismutation de Rb_2O en Rb_2O_2 et Rb.

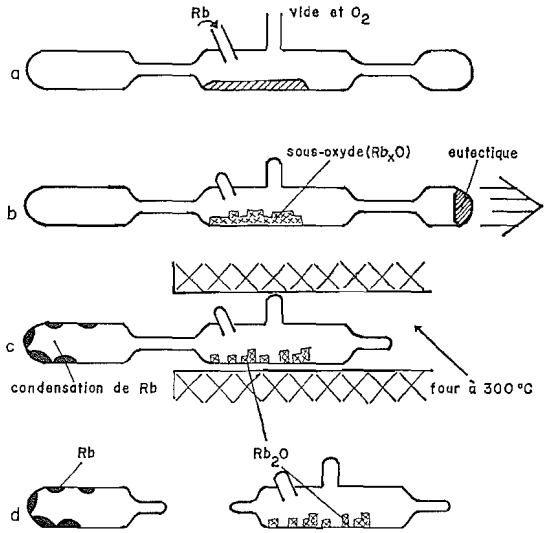

FIG. 3. Préparation et analyse du sous-oxyde de rubidium. (*a*) Introduction de rubidium par distillation et oxydation ménagée de celui-ci par O_2, (*b*) séparation par centrifugation du liquide de la phase solide (le sous-oxyde), (*c*) décomposition thermique à 300 °C du solide Rb_xO (avec $x > 3$) en oxyde Rb_2O et métal qui se condense sur la paroi froide du tube, (*d*) séparation de Rb et Rb_2O. L'analyse se continue par la dissolution dans l'eau de Rb et Rb_2O puis par une acidimétrie de ces deux solutions.

gruente (péritectie à 48 °C) répondant à la formule Rb_3O.

Pour confirmer la formule de ce sous-oxyde, nous l'avons isolé et analysé de la même manière qu'il avait été fait pour un des sous-oxydes de césium (2).

On distille dans un tube en verre de forme particulière (Fig. 3*a*) une certaine quantité de rubidium auquel on ajoute de l'oxygène jusqu'à obtention d'un mélange fondu qui commence à se solidifier vers 45 °C (environ 20% atomique d'oxygène). Ce mélange comporte alors une phase cristallisée (le sous-oxyde) et une phase liquide (l'eutectique). La partie liquide est éliminée grâce à une centrifugation rapide (Fig. 3*b*). Le sous-oxyde reste sous la forme de cristaux rouges à aspect cuivré. Ce composé se dismute à 48 °C selon la réaction :

$$Rb_3O \rightarrow Rb_2O + Rb$$

A 300–320 °C, le rubidium est libéré et se condense sur la partie froide de l'appareil (Fig. 3*c*). Après séparation du tube contenant l'oxyde du tube contenant le métal (Fig. 3*d*), on effectue une mise en solution aqueuse de Rb_2O et de Rb et enfin une analyse acidimétrique de chacune de ces solutions. Le rapport en volume d'acide neutralisant est pour l'oxyde Rb_3O pur :

$$\frac{\text{Rb distillé}}{Rb_2O} = 0.50$$

Expérimentalement, le rapport est trouvé égal à 0.58 ce qui correspond à la formule $Rb_{3.16}O$. La petite quantité de rubidium en excés (5%) s'explique par la couche liquide qui est restée adhérée à la surface des cristaux malgré la centrifugation.

Par analyse thermique différentielle ou par voie chimique, on a donc bien mis en évidence l'existence du sous-oxyde Rb_3O (monooxyde de trirubidium).

(*c*) D'autre part, nous avons essayé de déterminer le point de fusion de Rb_2O qui n'était pas connu avec exactitude. Le monooxyde de dirubidium est préparé par distillation prolongée sous vide, à 300 °C, de rubidium traité par une quantité insuffisante d'oxygène.

L'analyse thermique ainsi que l'observation

Can. J. Chem. Downloaded from www.nrcresearchpress.com by 210.87.254.5 on 09/05/12
For personal use only.

Can. J. Chem. Downloaded from www.nrcresearchpress.com by 210.87.254.5 on 09/05/12
For personal use only.

visuelle du phénoméne dans un tube en verre Pyrex scellé, nous permet seulement de situer la fusion de Rb_2O aux alentours de 430–450 °C. Le verre Pyrex est attaqué à partir de 500 °C.

En fait, il ne semble pas que l'oxyde Rb_2O posséde un point de fusion net car il se décompose d'aprés Rengade (12), déjà vers 400 °C. Nous avons déterminé cette température de dismutation avec plus de précision grâce à une analyse thermogravimétrique sous vide. L'échantillon de Rb_2O d'une vingtaine de mg est placé dans un petit creuset en alumine suspendu au fléau de la thermobalance (électrobalance Cahn). L'élévation de température de l'èchantillon est réglée à 4 °C par minute. On observe une très importante perte de poids due à la volatilisation du rubidium métallique à partir de 405–415 °C. De plus, l'analyse thermique différentielle faite sur un échantillon plus important de Rb_2O nous donne un pic endothermique vers 410 °C également.

Le monooxyde Rb_2O fond donc incongruement à 410 °C selon la réaction :

$$2Rb_2O \rightarrow Rb_2O_2 + 2Rb$$

La précision des températures du liquidus pour les % atomiques d'oxygène supérieurs à 25 est faible car la pente du liquidus est importante. C'est pourquoi, nous avons tracé cette partie du liquidus en pointillés sur le diagramme de la Fig. 2.

Discussion

Le diagramme de phase du système Rb–Rb_2O est comparable par de nombreux points à celui du système Cs–Cs_2O. En effet, il existe, dans les 2 cas, un eutectique respectivement à -10 et à -8 °C pour le même % d'oxygène (16% atomique) bien que ces 2 eutectiques correspondent à 2 réactions différentes (Rb métal + Rb_3O dans un cas et Cs_7O + Cs_4O dans l'autre), un sous-oxyde de formule identique Rb_3O et Cs_3O et enfin un liquidus dont la température s'éléve rapidement quand on s'approche du monooxyde Rb_2O ou Cs_2O. Ces 2 derniers oxydes sont d'ailleurs instables dans les 2 cas avant leurs températures de fusion.

D'autre part, la pente du liquidus du rubidium métallique pour un petit % atomique d'oxygène n_0 permet de calculer l'entropie de fusion du rubidium. La pente linéaire de ce liquidus est

$$\frac{\Delta T}{n_{O(n_0 \rightarrow 0)}} = \frac{\Delta T}{n_0(\text{eut})} = \frac{(39.0 - (-10.0))}{16.0}$$
$$= 3.07\ ^\circ\text{C par \% atomique d'oxygène}$$

et l'entropie est

$$\Delta S_f = \frac{R T_f}{100 \Delta T / n_0} = \frac{2(273 + 39)}{307}$$
$$= 2.03\ \text{cal}\ ^\circ\text{C}^{-1}\ \text{g-atom}^{-1}$$

Les travaux de Tepper (8) permettent également ce calcul d'autant plus qu'ils se rapportent aux très faibles concentrations d'oxygène. L'abaissement cryoscopique est selon lui

$$\Delta T / n_0 = 0.0017\ ^\circ\text{C par p.p.m. d'oxygène}$$

soit 3.18 °C par % atomique d'oxygène et l'entropie de fusion

$$\Delta S_f = \frac{2(273 + 39)}{318} = 1.96\ \text{cal}\ ^\circ\text{C}^{-1}\ \text{g-atom}^{-1}$$

Selon Perel'man (13), la valeur de l'entropie de fusion du rubidium est

$$\frac{\Delta H_f}{T_f} = \frac{540}{(273 + 39)} = 1.73\ \text{cal}\ ^\circ\text{C}^{-1}\ \text{g-atom}^{-1}$$

Notre valeur expérimentale de cette entropie serait donc 17% trop importante et celle de Tepper plus exacte mais encore 13% supérieure.

Avec la vraie valeur de ΔS_f (1.73), on peut calculer le % théorique d'oxygène n_0 pour la composition de l'eutectique à -10 °C

$$100 \times n_0(\text{eut}) = \frac{100 \times \Delta S_f \times \Delta T}{R \times T_f}$$
$$= \frac{100 \times 1.73 \times 49}{2 \times 312}$$
$$= 13.6\%\ \text{atomique d'oxygène}$$

Avec la valeur de ΔS_f de 1.96 de Tepper, le % d'oxygène à la composition de l'eutectique à -10 °C serait

$$100 \times n_0'(\text{eut}) = \frac{100 \times 1.96 \times 49}{2 \times 312}$$
$$= 15.4\%\ \text{atomique d'oxygène}$$

soit 1.8% supérieur à la valeur théorique.

La seule explication de cette différence serait d'admettre une solubilité de 1.8% d'oxygène ou d'oxyde Rb_3O dans le rubidium métallique solide à -10 °C. Cependant, une analyse thermique différentielle faite sur un échantillon de rubidium contenant 1% atomique d'oxygène seulement et recuit pendant 70 h à -10 °C, indique toujours très nettement le pic de fusion

de l'eutectique à −10 °C. Il faudrait donc admettre une légére erreur soit dans les mesures de l'abaissement cryoscopique soit dans la détermination de l'enthalpie de fusion du rubidium. Néanmoins, comme nous l'avons indiqué sur la Fig. 2, il est fort probable qu'il existe une petite zone de solubilité de l'oxygène dans le rubidium solide.

En conclusion, l'étude du diagramme de phase du système Rb–Rb_2O nous a permis de mettre en évidence un sous-oxyde de rubidium (Rb_3O) dont l'existence était insoupçonnée jusqu'à présent. Il sera intéressant d'en examiner la structure cristalline ainsi que les propriétés physiques et chimiques afin de pouvoir le comparer avec les sous-oxydes alcalins déjà connus.

Remerciements

Nous remercions le Conseil National des Recherches du Canada pour l'aide financière apportée à ce travail. Nos remerciements vont également au Professeur Marcel Bourgon de l'Université de Montréal qui a permis la réalisation de ces recherches dans son laboratoire et au Docteur M. A. Bredig (Oak Ridge National Laboratory) pour sa contribution dans la discussion de ce rapport.

1. E. RENGADE. Bull. Soc. Chim. France, **5**, 989 (1909).
2. E. RENGADE. Bull. Soc. Chim. France, **5**, 994 (1909).
3. G. BRAUER. Z. Anorg. Allgem. Chem. **255**, 101 (1947).
4. K. R. TSAI, P. M. HARRIS et E. N. LASSETTRE. J. Phys. Chem. **60**, 345 (1956).
5. DE FORCRAND. Compt. Rend. **127**, 364 (1898).
6. E. RENGADE. Compt. Rend. **143**, 1152 (1906).
7. R. H. HERALD et W. D. WEATHERFORD, JR. IEEE Trans. Aerospace, AS-1(2), 1182 (1963).
8. F. TEPPER. The alkali metals. Chem. Soc. Spec. Publ. **22**, 370 (1967).
9. P. TOUZAIN. Etude cinétique de l'oxydation des métaux alcalins. Rapport CEA. 3301. 1967.
10. L. HACKSPILL. Bull. Soc. Chim. France, **9**, 446 (1911).
11. C. MAZIÈRES. Anal. Chem. **36**, 602 (1964).
12. E. RENGADE. Ann. Chim. Phys. **11**, 348 (1907).
13. F. M. PEREL'MAN. Rubidium and caesium. The Pergamon Press, Ltd., London. 1965. p. 12.

Can. J. Chem. Downloaded from www.nrcresearchpress.com by 210.87.254.5 on 09/05/12
For personal use only.

Can. J. Chem. Downloaded from www.nrcresearchpress.com by 210.87.254.6 on 09/05/12
For personal use only.

Structure of the second coordination sphere of transition metal complexes. I. Co(II) complexes with aniline and pyridine

D. R. EATON
Department of Chemistry, McMaster University, Hamilton, Ontario

Received February 11, 1969

Geometric and thermodynamic parameters relating to the structure of labile second sphere coordination complexes formed between Co(II) chelates and aniline and pyridine molecules in carbon tetrachloride solution have been obtained. The effect of dipolar interactions, resulting from the magnetic anisotropy of the cobalt chelate, on the nuclear magnetic resonance spectra of the complexing molecules has been utilized for this purpose. Both aniline and pyridine show a preferred direction of approach perpendicular to the three fold symmetry axis of the cobalt compound used. In both cases the preferred intermolecular separation corresponds closely to that expected for a second coordination sphere ligand. The preferred orientation of the aniline molecule places the amino group adjacent to the cobalt complex and the pyridine is oriented with the γ hydrogen closest to the chelate. Enthalpy changes of -2.4 ± 0.2 kcal and -2.9 ± 0.3 kcal have been obtained for the formation of the aniline and pyridine complexes, respectively. The effect of averaging tumbling and translational motions on the dipolar shifts has been considered. The meaning of the parameters derived is discussed in the light of the very labile nature of the second coordination sphere complexes. The relevance of these results to the mechanisms of ligand substitution processes and homogeneous catalysis is emphasized.

Canadian Journal of Chemistry, 47, 2645 (1969)

Introduction

The concept of a second coordination sphere of metal complexes has a venerable history dating back to the work of Werner (1, 2). Bjerrum (3*a*) and Beck (3*b*) have recently reviewed this area. For the case of charged metal complexes, outer sphere coordination is synonymous with ion-pairing. A variety of physical techniques has been used to investigate the structure of such ion pairs. Thus Linhard (4) first inferred ion-pairing from studies of charge transfer bands in the ultraviolet and other workers have employed dialysis (5), polarography (6), ion exchange resins (7), and optical rotation techniques (8) to obtain information on this subject. None of these methods have given completely unambiguous answers to such questions as to whether the outer sphere ligands occupy spatially well defined positions and whether forces other than purely electrostatic attraction are involved. Non-ionic outer sphere complexes have received little or no attention.

The idea that the structure of the second coordination sphere is relevant to studies of the mechanisms of reactions involving metal complexes has also been extensively discussed (9, 10). Outer sphere mechanisms for electron transfer reactions have been particularly emphasized. However, the concept has also been invoked to account for ligand substitution processes. Thus Tobe (11), for example, in a discussion of the mechanism of substitution of octahedral cobalt-ammine complexes suggests "that these reactions can be regarded as rearrangement processes of the aggregate whereby an inner sphere ligand changes places with an outer sphere ligand". He points out, though, that such a mechanism is not necessarily general for Co(III) complexes but that the existence of a relatively stable second coordination sphere may depend on hydrogen bonding involving the NH groups of ammine complexes. Our interest in this area derives from speculation regarding the mechanism of homogeneous catalysis involving rhodium complexes (12). It was suggested that a combination of relatively strong binding in the second coordination sphere and relatively weak binding in the first coordination sphere might be particularly favorable for catalytic activity. These complexes are neutral, as are most homogeneous catalysts, so that there is no question of ion pairing. There is at present no firm information bearing on the questions of whether there is a discrete second coordination sphere for neutral molecules, whether molecules in such a sphere have a preferred orientation, what is the nature of the binding forces in the second coordination sphere, and whether it is at all plausible that these binding energies should approach those of first coordination sphere ligands. The present experiments were therefore designed to provide some data pertinent to these questions.

The nuclear magnetic resonance (n.m.r.) technique is particularly suitable for the study

Can. J. Chem. Downloaded from www.nrcresearchpress.com by 210.87.254.6 on 09/05/12
For personal use only.

of solvation effects (13–16) since it provides a sensitive probe for small changes in nuclear environments. In some cases specific interactions such as hydrogen bonding can be identified and some indirect but elegant inferences regarding hydrogen bonding between Co(III) complexes of ethylenediamine and solvent molecules have been reported by Fung (17). The present studies are concerned with interactions in a more general sense and have utilized the enhanced chemical shift effects associated with paramagnetic complexes. It is common to distinguish two such effects (18), namely contact shifts and pseudo-contact shifts. The former demands a finite probability of finding the unpaired electron at the nucleus in question and will probably be negligible in the cases of ion pairing and solvation which do not involve covalent metal–ligand bonds. The latter is a dipolar effect and depends purely on the geometry of the complex. It is, therefore, equally effective for ligands held in the second coordination sphere by electrostatic or other interactions which do not involve admixture of ligand and metal orbitals, as it is for the covalently bonded ligands in the first coordination sphere. It is this effect which we wish to utilize. Pseudo-contact shifts are given by an expression of the form (19)

$$[1] \quad \Delta\nu = -D\frac{(3\cos^2\theta - 1)}{r^3}(g_{\parallel} - g_{\perp})$$

where r is the distance between the metal atom and the nuclear dipole under consideration and θ is the angle between the principal axis of the molecule and the vector joining the metal to the ligand nucleus. D is a constant which depends on the relative values of the electron spin relaxation time, the Zeeman anisotropy energy, and the correlation time for molecular tumbling as has been recently discussed by Jesson (20). It will be noted that the pseudo-contact shift vanishes unless $g_{\parallel} - g_{\perp} \neq 0$, i.e., there must be magnetic anisotropy.

LaMar and others (21–23) have previously utilized pseudo-contact effects to study the geometry of ion pairs in solution. Although the qualitative effect has been clearly demonstrated there has remained some ambiguity in the detailed interpretation of the results. There were two main reasons for this. Firstly, the values of $g_{\parallel}$ and $g_{\perp}$ for the complexes studied were not known so that there is an initial problem in disentangling the geometric factor in eq. [1] from the anisotropy factor. Secondly, counter ions such as $(C_4H_9)_4N^+$ which possess considerable flexibility were utilized so that there is a further problem in averaging over the different conformations resulting from the internal motions of the ion. In the present work these problems have been largely avoided by using rigid ligand molecules and complexes with known g values. A very convenient complex for this purpose is Co(II) trispyrazoyl borate (24) which has the structure shown in Fig. 1. This complex has a very large g value anisotropy ($g_{\parallel} = 8.46$, $g_{\perp} = 0.98$) and the magnetic properties are known in considerable detail from the low temperature electron spin resonance work of Jesson (25). The latter author has also analyzed the isotropic n.m.r. shifts of the pyrazoyl protons (26) and derived an experimental value of D appropriate for use in eq. [1]. On the other hand, the other physical properties (27) of this complex show that it is a typical, almost octahedral, non-labile, Co(II) complex so that the structure of its second coordination sphere should not be greatly dissimilar from that of other stable complexes of Co(II) and neighboring transition metal ions. The magnetic anisotropy merely serves as a convenient probe to locate surrounding molecules. It was initially guessed that polar molecules would participate in the second coordination sphere in preference to non-polar molecules. It is also desirable to have several different sets of protons in the complexing molecule. These considerations lead

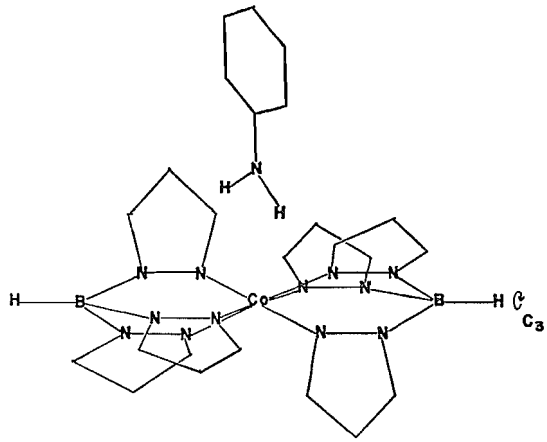

FIG. 1. Structure of Co(II) trispyrazoylborate and preferred direction of approach of aniline molecule.

Can. J. Chem. Downloaded from www.nrcresearchpress.com by 210.87.254.6 on 09/05/12
For personal use only.

to the choice of carbon tetrachloride as a hopefully "inert" solvent and pyridine and aniline as complexing agents. Both of these molecules are rigid (except for rotation of the NH_2 of aniline) and possess comparable dipole moments (aniline = 1.53 D, pyridine = 2.23 D) (28). They differ in that in one case the functional group is the positive end of the dipole (aniline) (29) and in the other case it is the negative end (pyridine).

Results

Figure 2 shows a series of traces of the ^1H spectrum of aniline in the presence of increasing concentrations of Co(II) trispyrazoyl borate (abbreviated $Co[HBpz_3]_2$). Figure 3 shows a similar series for pyridine. Sizable shifts are apparent with those for aniline being greater than those for pyridine. There is broadening of the resonances at higher concentrations of $Co[HBpz_3]_2$, as is expected in a paramagnetic system, but the assignments of individual protons are unambiguous from the spin–spin splittings and intensities. It might next be asked to what extent these shifts are attributable to pseudo-contact interactions. Information on this point can be obtained by carrying out similar experiments with $Zn[HBpz_3]_2$. The Zn and Co complexes are structurally very similar, differing significantly only in the paramagnetism of the latter. From the data in Table I it is apparent that the Zn shifts are very small. Paramagnetic interactions are therefore dominant.

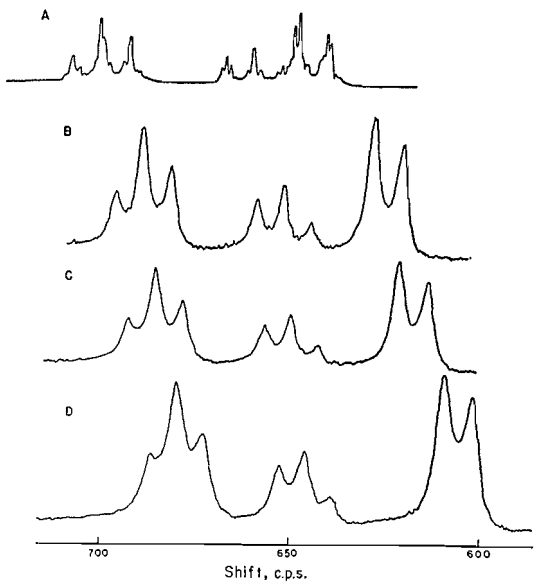

FIG. 2. The n.m.r. spectra of aniline 100 Mc.p.s., CCl_4 solution. A, pure aniline; B, C, D, increasing amounts of $Co[HBpz_3]_2$. Shifts are in c.p.s. to low field of TMS. The lines are assigned as meta, para, and ortho from left to right.

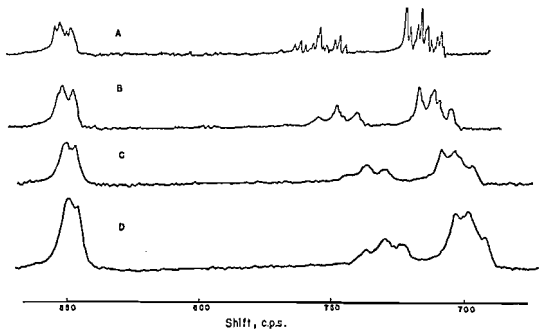

FIG. 3. The n.m.r. spectra of pyridine 100 Mc.p.s., CCl_4 solution. A, pure pyridine; B C, D, increasing amounts of $Co[HBpz_3]_2$. Shifts in c.p.s. to low field of TMS. The lines are assigned as α, γ, and β from left to right.

TABLE I

Chemical shifts* of aniline in the presence of $Zn[HBpz_3]_2$

Concentration of $Zn[HBpz_3]_2$ (M)	Ortho	Meta	Para	NH_2
0	645	700.5	660	337.5
0.026	649	701	659	340
0.039	648.5	701.5	659	340
0.046	647.5	701	658.5	338
0.078	646	700	658.5	336

*Shifts in c.p.s. at 100 Mc.p.s. from TMS, CCl_4 solutions.

A number of qualitative inferences can be drawn immediately. Both aniline and pyridine enter the second coordination shell in preference to carbon tetrachloride, the common solvent. The shifts are uniformly to high field. Since D and $g_{\parallel} - g_{\perp}$ are both positive quantities, eq. [1] determines that $(3\cos^2\theta - 1)$ must be negative and hence that the preferred position of solvation is in a quadrant perpendicular to the symmetry axis of the molecule. This is indicated diagrammatically in Fig. 1. For aniline the shifts decrease in the order NH_2 > ortho > meta > para. The $1/r^3$ dependence of eq. [1] strongly suggests that aniline is oriented with the NH_2 closest to the complex. For pyridine the shifts decrease in the order $\gamma > \beta > \alpha$. Approach of the γ proton to the complex is

indicated. In both cases the orientation of the dipole is with the positive end towards the metal. This is of course the opposite to the situation in the first coordination sphere. Such a double layer structure has obvious mechanistic implications.

Further analysis requires a model for the system. It will be assumed initially that there is rapid exchange (on the n.m.r. time scale) between ligand (L = aniline or pyridine) in solution and in the second coordination sphere of the complex X and that

$$X + L \rightleftharpoons XL$$

with equilibrium constant K. With this assumption it may be easily shown that

$$[2] \qquad \Delta\nu_{obs} = \frac{K[X]\Delta\nu_0}{1 + K[X]}$$

where $\Delta\nu_{obs}$ is the observed shift from the ligand frequency and $\Delta\nu_0$ is the chemical shift of XL relative to the ligand. Hence on this model the shifts are independent of [L]. A number of experiments were carried out to check this point. In these experiments relative concentrations were found by integration of the n.m.r. spectra. Thus in one run in the range of [L]/[X] 0.81–8.31 there was a 2.5 c.p.s. variation in the ortho chemical shift, a 2.0 c.p.s. variation in the meta chemical shift, and a 0.5 c.p.s. variation in the para chemical shift of aniline. The lines were relatively broad and these shifts were only just significant. It was concluded from these experiments that formation of XL_2 or higher complexes is not important at ratios of [L]/[X] of < 5. Subsequent experiments were carried out in this concentration range. From eq. [2] it is also apparent that if $K[X] \ll 1$ a plot of $\Delta\nu_{obs}$ against [X] should be a straight line passing through the origin. Such plots are shown in Figs. 4 and 5 for the ortho and meta protons of aniline and for the β and γ protons of pyridine respectively. The slopes of these lines give values for $K\Delta\nu_0$. Plots for other protons are similar and values of the relative slopes are included in Tables II and III. It might be noted that at room temperature 0.1 M $Co[HBpz_3]_2$ solutions (which are close to the maximum solubility in CCl_4) give shifts of about 50 c.p.s. for the ortho proton of aniline and 30 c.p.s. for the γ proton of pyridine both at 100 Mc.p.s. At room temperature the maximum observed shift for the NH_2 protons is about 55 c.p.s. and at the low concentrations of aniline used, no anomalies in the concentration

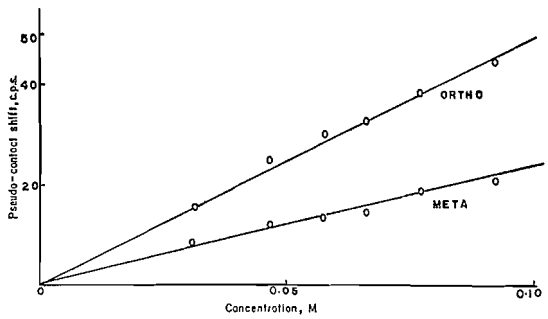

FIG. 4. Plot of the pseudo-contact shifts of the ortho and meta protons of aniline vs. concentration of Co-$[HBpz_3]_2$.

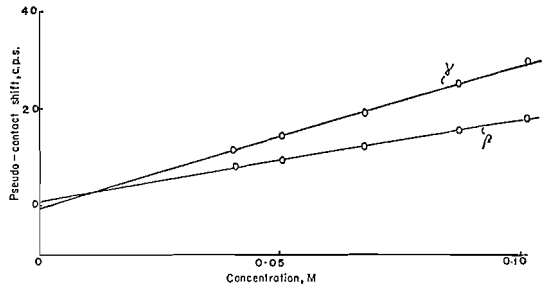

FIG. 5. Plot of the pseudo-contact shifts of the β and γ protons of pyridine vs. concentration of $Co[HBpz_3]_2$.

TABLE II

Calculated relative shifts of aniline protons

Model	r (Å)	Ortho	Meta	Para
$1/r^3$	6	1.0	0.504	0.437
	8	1.0	0.547	0.471
$1/r^4$	6	1.0	0.385	0.305
	8	1.0	0.439	0.348
$1/r^5$	6	1.0	0.295	0.212
	8	1.0	0.352	0.258
Experimental		1.0	0.470	0.320

TABLE III

Calculated relative shifts of pyridine protons

r (Å)	γ	β	α
4.0	1.0	0.202	0.098
6.0	1.0	0.382	0.189
8.0	1.0	0.509	0.274
10.0	1.0	0.598	0.348
12.0	1.0	0.661	0.410
Experimental	1.0	0.57	(0.05)

Can. J. Chem. Downloaded from www.nrcresearchpress.com by 210.87.254.6 on 09/05/12
For personal use only.

Can. J. Chem. Downloaded from www.nrcresearchpress.com by 210.87.254.6 on 09/05/12
For personal use only.

dependence attributable to association were found. Using the relationship

$$-RT \ln K = \Delta H - T\Delta S$$

and assuming as above that $K[X] \ll 1$ it follows that

$$[3] \quad \ln \Delta\nu_{obs} = \frac{-\Delta H}{RT} + \frac{\Delta S}{R} + \ln [X] + \ln \Delta\nu_0$$

However, the pseudo-contact shift $\Delta\nu_0$ will have a temperature dependence of approximately $1/T$ (Curie law) (18) and correction for this effect is necessary before utilizing eq. [3] to obtain ΔH. This correction was applied in the following manner. The shifts of the pyrazoyl protons of $Co[HBpz_3)_2$ relative to $Zn[HBpz_3]_2$ were measured in CCl_4 over the temperature range +60 to −20 °C. These shifts show the expected Curie law dependence. $\Delta\nu_0$ must have exactly this temperature dependence. The aniline shift relative to the zinc complex at temperature T was therefore multiplied by the ratio of the pyrazoyl shift at temperature T to that at 25 °C to give a corrected shift $\Delta\nu_{corr}$. The slope of plots of $\ln \Delta\nu_{corr}$ against $1/T$ then gives ΔH. Such a plot for the meta H of aniline is shown in Fig. 6. In this way values of $\Delta H = -2.4 \pm 0.2$ kcal were obtained for aniline and $\Delta H = -2.9 \pm 0.3$ kcal for pyridine. Values obtained from the temperature dependences of the different protons were in good agreement. It might be noted that in the temperature range +60 to −20 °C there is approximately a 25% increase in the pyrazoyl proton shifts whereas the aniline shifts increase by a factor of 4 and the pyridine shifts by a factor of 5. The temperature dependence of the solvation equilibrium constant is clearly the major factor in determining the variation of the shifts with temperature.

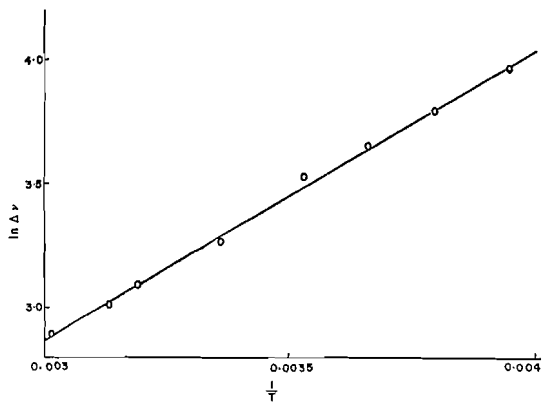

FIG. 6. Plot of $\ln \Delta\nu_{corr}$ vs. $1/T$ for the meta protons of aniline.

In the above manner it is clearly possible to obtain the enthalpy change ΔH for outer sphere coordination without postulating a specific model for the complex. The entropy change ΔS, though, requires a knowledge of $\Delta\nu_0$ and a more detailed discussion of the geometric arrangement of the outer sphere ligands is necesssary.

Discussion

The qualitative considerations of the preceding section have demonstrated that second sphere coodination complexes can be regarded as discrete entities with some degree of geometric structure and with bonding energies of the order of 2 or 3 kcal. However, such complexes are certainly very labile since only the average n.m.r. frequencies for complexed and free ligands are observed. Using the experimental value of D given by Jesson (26), calculation shows that the pseudo contact shift for the ortho proton of an aniline molecule placed on an axis perpendicular to the symmetry axis of $Co[HBpz_3]_2$ with the N atom 7 Å from the Co (a reasonable distance) is +736 c.p.s. at 100 Mc.p.s. Hence the lifetime of the second sphere complex is less than $1/2\pi\Delta\nu \sim 10^{-3}$–$10^{-4}$ s.

It would not be expected that such a loosely bound and transient complex would have a rigid geometry with the well defined bond distances and angles of a conventional chemical compound. The approach adopted in the present discussion will, therefore, be to determine an approximate position for the ligand molecule relative to the complex and then to investigate the effects of various kinds of motion on the pseudo-contact shifts. Three such types of motion may be distinguished: tumbling of the metal complex, tumbling of the ligand, and variation of the intermolecular distance. The absolute pseudo-contact shifts are not available from the experimental data since the entropy changes are unknown. However, the ratios of the shifts for different ligand protons are readily obtained from the slopes of plots such as those of Figs. 4 and 5. These ratios provide the key information needed to determine the geometry. Knowing the geometry, in principle

Can. J. Chem. Downloaded from www.nrcresearchpress.com by 210.87.254.6 on 09/05/12
For personal use only.

$\Delta\nu_0$ can be calculated and the entropy changes obtained.

Consider first the case of aniline. As an initial model the aniline molecule was placed perpendicular to the symmetry axis of the $Co[HBpz_3]_2$ with the amino group directed towards the cobalt complex as suggested by the preliminary interpretation of the pseudo contact shifts. Molecular models suggest that the Van der Waals radius of the chelate is ~5 Å, with the molecule being almost spherical. Values of the geometric factors $(3\cos^2\theta_i - 1)/r_i^3$ were therefore calculated for each type of proton (i) for separations (R) between the Co and the N of the aniline of from 4–12 Å. The ratios of these geometric factors give the relative pseudo-contact shifts for the different protons. These ratios are plotted as a function of R in Fig. 7. Note the different scale for the NH_2 protons. At $R = 7$ Å (approximately the correct distance for close contact of the two molecules) the calculated ratios of NH_2:ortho:meta:para are 3.52:1.00:0.55:0.45 compared with the experimental ratios of 1.07:1.00:0.47:0.32. Values at other distances can be inferred for Fig. 7. Free rotation of the NH_2 group is assumed. At no value of R is the overall agreement of the ratios much better than that quoted above. It is apparent that although this model is qualitatively satisfactory, it by no means reproduces the data to within the experimental accuracy. The largest discrepancy is for the NH_2 protons. Before proceeding further, two possible mechanisms other than the pseudo-contact effect for the NH_2 shifts should be considered. First of all, there could be a deshielding of the amino protons due to hydrogen bonding with the complex resulting in a smaller high field shift. Such bonding has been observed by Fung (17) for ethylenediamine complexes. However, such an effect should be equally effective with the zinc complex and, since this gives shifts of only 2 or 3 c.p.s. from aniline, it seems that hydrogen bonding is unlikely to account for the discrepancies of up to 100 c.p.s. observed. Secondly, it is conceivable that the amino protons could experience a contact shift if the cobalt d orbitals containing the unpaired electrons have a significant density at the proton position. This again would be a downfield shift reducing the observed pseudo-contact shift. A rough calculation using the analytical orbitals of Clementi (30) for Co^{2+} gave a shift 8 orders of magnitude too small for a proton 6 Å from the cobalt.

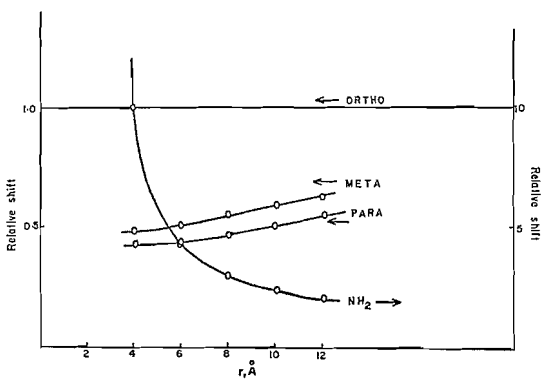

FIG. 7. Calculated pseudo-contact shifts from aniline protons for the model of Fig. 1, r = separation of Co and amino N.

There remains the possibility of a contact shift originating from the spin density on the nitrogen. Such spin density will be much smaller than that on the cobalt but a closer interaction with the amino hydrogens is possible. However, no contact shifts have previously been observed due to spin density transition through even relatively strong hydrogen bonds and Potenza and Poindexter (31) report in a recent paper that they were unable to detect scalar (contact) interactions for solvent protons even by Overhauser effect measurements. It appears, therefore, that the explanation must be sought in terms of the pseudo-contact effect (32)[1].

Before considering motional effects the question might first be asked as to whether a better fit can be obtained with a static model in which the direction of approach is not along the axis perpendicular to the symmetry axis of the molecule. Briefly, the answer to this question is no. The observation of high field shifts restricts the possible directions of approach to a cone of half angle 35° 16′ surrounding the perpendicular to

[1]These authors have attributed proton shifts of chloroform in the presence of ionic Co(II) and Ni(II) phosphine complexes to contact interactions arising from hydrogen bonding. The negative charge on the metal complex makes this perhaps the most favorable situation for observing such an effect. However, their conclusions are not entirely unambiguous since both the detailed geometry of the complex and the g value anisotropies are unknown. In the present case we prefer not to invoke hydrogen bonded contact interactions but would point out that in any event a modest contact contribution to the NH_2 shift would not affect the qualitative conclusions of this paper.

Can. J. Chem. Downloaded from www.nrcresearchpress.com by 210.87.254.6 on 09/05/12
For personal use only.

the symmetry axis. If the approach is not perpendicular all shifts are reduced with para being reduced less than meta < ortho < NH_2. The two ortho protons, for example, become nonequivalent and average values of $(3\cos^2\theta - 1)$ were taken. The effect is rather small, is in the wrong direction to improve the experimental ortho:para ratio, and, although in the right direction to improve the ortho:NH_2 ratio, is not large enough to produce any close agreement. In addition molecular models suggest no reason why there should be any favored angle different from $\theta = \pi/2$.

Consider now a model in which the aniline molecule is fixed in space and the cobalt complex is allowed to tumble. It should first be noted that if the tumbling is entirely free, the angular term in the expression for the average dipolar shift is given by

$$\frac{\int_0^{\pi/2} (3\cos^2\theta - 1)\sin\theta\, d\theta}{\int_0^{\pi/2} d\theta} = 0$$

i.e. the pseudo-contact shifts are averaged to zero. This is clearly not the case. Consider next the situation in which there is a preferred orientation and a distribution of geometries with a maximum probability at $\theta = \pi/2$. For simplicity assume that the distribution function is proportional to $\sin\theta$. The averaged pseudo-contact shift is proportional to

$$\frac{\int_0^{\pi/2} (3\cos^2\theta - 1)\sin^2\theta\, d\theta}{\int_0^{\pi/2} d\theta} = -\frac{1}{4}$$

If the distribution function had been a δ function centered at $\theta = \pi/2$ (i.e. the static model) the angular part of the expression would have had the value -1. Thus the effect of allowing restricted tumbling of the complex is to uniformly reduce the dipolar shifts by a factor equal to 1/4 for a sinusoidal distribution. For other possible forms of the angular dependence this factor will take on values between 0 and 1. In any event such a uniform reduction will merely contribute to the entropy term.

As the opposite extreme to the static model one could consider a very weakly bound pair of molecules with a binding energy ε at a distance of closest approach of a given proton r_0 and with $\varepsilon \ll kT$. There would then be a distribution of molecules with separations varying from $r = r_0$ to $r = \infty$ with the potential energy $u = f(r)$. The average pseudo-contact shift would obviously be less than that of the static model with $r = r_0$ and the variation of this average shift can be investigated as a function of r_0. Thus if the distance of the center of mass of the complexing molecule from the metal atom is x, then the number of molecules at distance x is proportional to $xe^{-u/kT}$. Considering only the radial dependence of the pseudo-contact shift.

$$\Delta\nu \propto \frac{1}{r^3} xe^{-u/kT}$$

For proton a, let $r = x + a$, and for proton b, let $r = x + b$, then

$$\frac{\langle\Delta\nu_a\rangle}{\langle\Delta\nu_b\rangle} = \frac{\int \frac{xe^{-u/kT}}{(x+a)^3}\, dx}{\int \frac{xe^{-u/kT}}{(x+b)^3}\, dx}$$

In general the relative shifts will be a function of u. Taking the particularly simple case for which $u = 0$ if $x > x_0$ and $u = \infty$ if $x < x_0$ i.e. $\varepsilon \ll kT$ and a hard sphere approximation, it is easily shown that

$$\frac{\langle\Delta\nu_a\rangle}{\langle\Delta\nu_b\rangle} = \left(\frac{r_{0b}}{r_{0a}}\right)^4 \left(\frac{r_{0a} + 3x_0}{r_{0b} + 3x_0}\right)$$

where $r_{0a} = x_0 + a$ and $r_{0b} = x_0 + b$. For the case where a and b are small relative to x_0 it is apparent that the shifts are proportional to the inverse fourth power of r_0 rather than the inverse cube. Thus in general a rather faster fall off of shift with distance is expected for a labile complex than for the static model. In Table II are shown the calculated ratios of the ortho, meta, and para shifts for separations of the metal atom and amino nitrogen of 6 and 8 Å and for $1/r^3$, $1/r^4$, and $1/r^5$ dependence of the shifts. The experimental ratios are also given for comparison. It is apparent that the experimental data agrees best with a $1/r^4$ dependence indicating substantial lability.

The final type of motion to be considered is tumbling of the aniline molecule. Averaging of

Can. J. Chem. Downloaded from www.nrcresearchpress.com by 210.87.254.6 on 09/05/12
For personal use only.

this type of motion has been considered by LaMar (21) for the case of freely tumbling tetraalkyl ammonium ions placed on the symmetry axis of the complex. A slight modification of his result gives

$$\left\langle \frac{(3\cos^2\theta - 1)}{R^3} \right\rangle = -\frac{[A^2 - 1.25Q_i^2]}{A^3(A^2 - Q_i^2)}$$

where A is the distance of the center of gravity of the tumbling molecule from the metal ion and Q_i is the radius of rotation of the ith proton, for the case in which the tumbling molecule is situated perpendicular to the axis of symmetry of the complex. Qualitatively the effect of this motion is that when $A \gg Q$ the shifts of all protons in the molecule become equal but when $A \sim Q$ the average shift of protons close to the center of gravity is greater than that of protons further from the center of the molecule. For this reason LaMar observed the shifts of the tetraalkyl ammonium ion protons to diminish in the order $\alpha > \beta > \gamma > \delta$. His analysis led to an interionic distance of 3.8 Å. In the present case the intermolecular distance A is much larger ($\sim$ 10 Å) for a reasonable model and we are much closer to the limit $A \gg Q$. Thus for amino nitrogen – metal distances of 6 and 8 Å we obtain NH_2:ortho:meta:para ratios of 0.987:1.0:0.983:0.975 and 0.992:1.0:0.990:0.985, respectively. Clearly these ratios do not closely resemble those obtained experimentally and a model involving free tumbling of the aniline is inadmissible. It is, however, of interest to compare these results with those from the static molecule. At $r = 8$ Å, the relative shift of the NH_2 protons has been reduced from 2.962 to 0.992 whereas the experimental value is 1.07. A model involving restricted tumbling of the aniline, i.e. where there is a preferred orientation of the aniline molecule with respect to the cobalt complex but other orientations also contribute, could certainly help to account for the observed NH_2 shift.

The qualitative conclusions regarding the effects of non-rigidity of the second sphere complex on the observed pseudo-contact shifts can therefore be summarized as follows. Free tumbling of the transition metal complex averages the shifts to zero. Restricted tumbling with a preferred orientation reduces all the shifts uniformly and does not affect the ratios of NH_2:ortho:meta:para shifts. Free tumbling of the aniline placed in a specified position with respect to the complex tends to equalize the different shifts. Restricted tumbling will tend to make the ratios more nearly equal. A distribution of different intermolecular separations over the range r_0 (the distance of closest approach) to infinity diminishes all the shifts relative to a static model with separation r_0 and accentuates the difference in relative shifts between the closer and farther protons. It is apparent that a combination of these effects will suffice to account for the experimental results. Detailed calculations with a computer would be feasible but it seems doubtful whether they would identify a unique model or whether if such a model was identified it would add significantly to the understanding of second coordination sphere structure.

The considerations for the pyridine case are essentially similar. In Table III calculated ratios for the α, β, and γ pseudo-contact shifts for a static model with the pyridine placed on an axis perpendicular to the symmetry axis of the complex and with different values of the γH to metal distance are shown. For closest approach this distance is expected to be 6–7 Å. The observed ratios are 1.0:0.57:0.05. All the observed shifts are smaller than those for aniline and the α shifts in particular are very small ($\sim$ 2 c.p.s.) so that the last ratio is not very meaningful since it could be affected substantially by effects other than pseudo contact. Qualitatively, however, it is apparent that the pattern is quite similar to that for aniline, in particular in that the relative shift of the closest proton (in this case γH) is somewhat smaller than expected for reasonable values of r, which is taken as evidence for restricted tumbling of the pyridine.

The Structure of the Second Coordination Sphere

It is apparent from the above results that a discussion of the structure of second coordination sphere complexes should not be phrased in the terms usually associated with molecular structure, i.e. well defined bond lengths, bond angles, and bond energies. In terms of the current conventional subdivisions of chemistry, structural and dynamic effects are not separable on the time scale of these experiments. It could be argued that on a sufficiently short time scale the effects would be separable, but since the real

interest of the chemist is in chemical reactions the lifetime of a structure relative to the half life of the chemical rate process of interest is a relevant factor. Thus in the present case we may define an experimentally determined enthalpy change in terms of an equilibrium of the form

$$X + L \rightleftharpoons XL$$

providing it is understood that XL represents the time average of a large number of different geometric structures each appropriately weighted according to its statistical probability of occurrence. ΔH is therefore a rather imprecisely defined quantity in comparison to the changes in enthalpy resulting from well defined chemical reactions but nevertheless it is the correct quantity to use in a discussion of the significance of second coordination sphere complexes in transition metal reactions. The energy of a transient complex is not too useful for this purpose unless it is combined with some measure of the probability of a particular complex ligand arrangement. The point is perhaps illustrated even better by the entropy changes ΔS. Such entropy changes can only be found if a definite model is assumed. Thus the experimental results indicate

(*1*) There is a definite preferred distance of separation of X and L. This distance corresponds rather nicely to a second coordination sphere; the results are not compatible, for example, either with a model in which the aniline molecule is always separated from the complex by a layer of solvent molecules or with one in which the aniline can occupy a position comparable in distance to a first coordination sphere ligand.

(*2*) There is a definite preferred orientation of the complex; the symmetry axis of $Co[HBpz_3]_2$ is perpendicular to the Co–aniline vector.

(*3*) There is a definite preferred orientation of the aniline, with the amino group directed towards the $Co[HBpz_3]_2$ molecule. Using a static model based on these preferences, $\Delta\nu_0$ can be calculated and ΔS found from the slopes of $\Delta\nu_{obs}$ vs. [X] plots since these slopes equal $K\Delta\nu_0$. Results from such a calculation are shown in Table IV. The values obtained for different protons on the same molecule are not the same, i.e. these values of ΔS are not the true entropy changes for a reaction

$$X + L \rightleftharpoons XL$$

but also contain various quantities associated with the internal motions of XL some of which are different for different protons as demonstrated in the discussion. Since such motions contribute to the disorder of the system the "true" entropy change, if measured on a very small time scale, would be more negative than any of the derived values. Consider, however, the virtues of a second coordination sphere complex as an intermediate in a ligand substitution process. If it is to provide a favorable pathway there must be a smaller free energy of activation for the overall process. It could be visualized that this end would be accomplished if the pre-formation of a second sphere complex placed the incoming ligand in the right position for further reaction and hence reduced the entropy requirements of the actual substitution process. If the lifetime of a given second sphere configuration is short compared with the rate of the subsequent substitution step, then a time averaged entropy change for the formation of the outer sphere complex is relevant. Thus it is significant that the values in Table IV are sufficiently large (10–15 e.u.) to make a meaningful impact on a free energy of activation and that they are significantly different for aniline and pyridine. Moreover the ordering of the ligand molecules in the outer sphere is not necessarily entirely helpful from the substitution point of view. Thus the preferred orientation of the pyridine molecule would appear to be unfavorable for further reaction and the advantage of an outer sphere mechanism to be therefore doubtful. It is apparent that the possibilities can be quite subtle and may well help to rationalize some of the rather devious reaction pathways which occur in homogeneous catalysis.

The purpose of the present paper is to demonstrate the utility of this n.m.r. method for studying weak interactions between metal complexes and potential ligands. It is not appropriate to

TABLE IV

Entropy changes for static models

Aniline*	ΔS (e.u.)	Pyridine†	ΔS (e.u.)
Ortho	−8.82	α	—
Meta	−9.04	β	−13.45
Para	−9.51	γ	−14.25
NH_2	−11.19		

*N—Co distance 7 Å.
†γH—Co distance 6 Å.

Can. J. Chem. Downloaded from www.nrcresearchpress.com by 210.87.254.6 on 09/05/12
For personal use only.

draw too many far-reaching conclusions from the two examples studied. Molecular models suggest that the preferred geometry of the complex can be best rationalized in terms of the closest allowed approach of the aniline or pyridine molecule to the negatively charged nitrogen atoms surrounding the cobalt. The ΔH values obtained of course represent a difference between the solvation energies of an aniline or pyridine molecule associated with the cobalt complex or with carbon tetrachloride. The higher ΔH with pyridine may well indicate stronger solvation of aniline by carbon tetrachloride rather than stronger solvation of the cobalt complex by pyridine. The ΔH and ΔS parameters may be strongly influenced by steric as well as electronic factors. These factors will be investigated by using substituted anilines and pyridines as well as a variety of other ligands in experiments of this kind. It is also apparent that in the present case the binding energies for second sphere coordination are considerably less than those for first sphere coordination. This will not necessarily be the case for coordinately non-saturated complexes, e.g. $Rh(P\phi_3)_3Cl$. Investigations aimed at elucidating this situation are also planned and will be reported in subsequent papers in this series.

Experimental

The n.m.r. spectra were obtained on a Varian HA 100 spectrometer. The proton shifts were measured relative to tetramethylsilane used as an internal calibrant. Carbon tetrachloride, aniline, and pyridine were obtained commercially and used without further purification. Cobalt and zinc trispyrazoyl borates were prepared by Dr. S. Trofimenko in a manner described previously (24).

Acknowledgments

The author is indebted to Dr. S. Trofimenko of the Central Research Department, E. I. DuPont Co., Wilmington, Delaware, for gifts of cobalt and zinc trispyrazoyl borates and to the National Research Council of Canada for financial support of this research.

1. A. Werner. Inorganic chemistry. 3rd ed. Vieweg and Sohn. 1913.
2. A. Werner. Ann. **386**, 1 (1912).
3. (a) J. Bjerrum. Advan. Chem. 178 (1967). (*b*) M. P. Beck. Coord. Chem. Rev. **3**, 91 (1968).
4. M. Linhard. Z. Electrochem. **50**, 224 (1944).
5. H. Brintzinger and H. Osswald. Z. Anorg. Allgem. Chem. **225**, 312 (1935).
6. H. A. Laitinen, J. C. Bailar, H. F. Holtzclaw, and J. V. Quagliano. J. Am. Chem. Soc. **70**, 2999 (1948).
7. R. Larsson and I. Tobiason. Acta Chem. Scand. **16**, 1919 (1962).
8. R. Larsson. Acta Chem. Scand. **16**, 2267 (1962).
9. C. H. Langford and H. B. Gray. Ligand substitution processes. W. A. Benjamin, Inc., New York. 1965.
10. F. Basalo and R. G. Pearson. Mechanisms of inorganic reactions. John Wiley and Sons, Inc., New York. 1958.
11. M. L. Tobe. Mechanisms of inorganic reactions. Advan. Chem. **49**, 7 (1965).
12. D. R. Eaton and S. R. Suart. J. Am. Chem. Soc. **90**, 4170 (1968).
13. J. F. Hinton and E. S. Amis. Chem. Rev. **67**, 387 (1967).
14. J. Burgess and M. C. R. Symons. Quart. Rev. London, **22**, 276 (1968).
15. L. S. Frankel, T. R. Stengle, and C. H. Langford. Chem. Commun. **17**, 393 (1965).
16. T. R. Stengle and C. H. Langford. J. Phys. Chem. **69**, 3299 (1965).
17. B. M. Fung. J. Am. Chem. Soc. **89**, 5788 (1967).
18. D. R. Eaton and W. D. Phillips. Advan. Magn. Resonance, **1**, 103 (1965).
19. H. M. McConnell and R. E. Robertson. J. Chem. Phys. **29**, 1361 (1958).
20. J. P. Jesson. J. Chem. Phys. **47**, 579 (1967).
21. G. N. LaMar. J. Chem. Phys. **41**, 2992 (1964); **43**, 235 (1965).
22. W. D. Horrocks, R. H. Fischer, J. R. Hutchison, and G. N. LaMar. J. Am. Chem. Soc. **88**, 2436 (1966).
23. D. W. Larsen and A. C. Wahl. Inorg. Chem. **4**, 1281 (1965).
24. S. Trofimenko. J. Am. Chem. Soc. **88**, 1842 (1966).
25. J. P. Jesson. J. Chem. Phys. **45**, 1049 (1966).
26. J. P. Jesson. J. Chem. Phys. **47**, 582 (1967).
27. J. P. Jesson, S. Trofimenko, and D. R. Eaton. J. Am. Chem. Soc. **89**, 3148 (1967).
28. C. P. Smyth. Dielectric behavior and structure. McGraw Hill Book Co., Inc., New York. 1955.
29. K. Hojendahl. *Quoted in* C. K. Ingold. Structure and mechanism in organic chemistry. Cornell Univ. Press, Ithaca, New York. 1953. p. 102.
30. E. Clementi. Tables of atomic functions. IBM. 1965.
31. J. A. Potenza and E. H. Poindexter. J. Am. Chem. Soc. **90**, 6309 (1968).
32. M. F. Rettig and R. S. Drago. J. Am. Chem. Soc. **88**, 2966 (1966).

Can. J. Chem. Downloaded from www.nrcresearchpress.com by 210.87.254.6 on 09/05/12
For personal use only.

Can. J. Chem. Downloaded from www.nrcresearchpress.com by 210.87.254.40 on 09/05/12
For personal use only.

γ-Radiolysis of cyclohexane with electron scavengers. VII. Perfluorocyclohexane and perfluorobenzene as electron scavengers[1,2]

N. H. SAGERT, J. A. REID[3], AND R. W. ROBINSON
Research Chemistry Branch, Chalk River Nuclear Laboratories, Atomic Energy of Canada Limited, Chalk River, Ontario

Received March 7, 1969

The room temperature, liquid phase radiolysis of cyclohexane has been investigated using perfluorocyclohexane (C_6F_{12}) and perfluorobenzene (C_6F_6) as electron scavengers. Yields of the respective monohydrofluorocarbons were investigated over several orders of magnitude scavenger concentration. The $C_6F_{11}H$ yield from the C_6F_{12}–cyclohexane system has previously been shown to result from electron capture by C_6F_{12}. The data over the extended concentration range were used to calculate a total ion yield of 4.3 ± 0.2 *G* units and a free ion yield of 0.14 ± 0.02 *G* units. With C_6F_6 as an electron scavenger, hydrogen, cyclohexene, and dicyclohexyl yields were all reduced. However, C_6F_5H yields were much lower than the $C_6F_{11}H$ yields from C_6F_{12}. On changing the neutralization step by adding the proton scavenger ethanol, C_6F_5H yields were obtained equal to the $C_6F_{11}H$ yields from C_6F_{12}. Thus C_6F_6 is as efficient an electron scavenger as C_6F_{12}. Since a change in the neutralization process produces a large change in yield, it is likely that C_6F_5H (or C_6F_5) is produced in the neutralization process.

Canadian Journal of Chemistry, 47, 2655 (1969)

Introduction

In recent years, it has been realized that the geminate recombination of ions plays an important part in the radiolysis of non-polar liquids (1). Since they lose energy rapidly, only a small number of electrons escape completely from the fields of their parent ions and become uniformly distributed in the liquid. Typically, the total ion yield for aliphatic hydrocarbons is 4.3 ion pairs for each 100 eV absorbed (4.3 *G* units) (2, 3) and the free ion yield is about 0.1 *G* units (4). One method of studying this phenomenon is to add solutes which react with or scavenge electrons before they can be captured by a positive ion. Theoretical treatments of this electron scavenging have been proposed (5, 6) but one of the most useful treatments is the empirical one of Warman, Asmus, and Schuler (1). This treatment is supported by the theoretical work of Hummel (6), which in turn is largely based on an earlier theoretical paper by Monchick (7).

Rajbenbach (8, 9) has shown that perfluorocyclohexane (C_6F_{12}) and perfluorobenzene (C_6F_6) both reduce hydrogen yields from the radiolysis of liquid hydrocarbons and has argued that they do this by capturing electrons. We have previously used perfluorocycloalkanes as electron scavengers (10), equating the yield of the monohydrofluorocarbon with the electron yield. In the work reported here, we have extended the results for C_6F_{12} to concentrations less than 10^{-5} *M* to allow a comparison with theory. We also wanted to see if C_6F_{12} could effectively scavenge fully thermalized electrons, in order to eliminate the possibility that the production of $C_6F_{11}H$ requires epithermal electrons.

Perfluorobenzene was investigated as an electron scavenger to see if significant C—F bond breaking occurs with aromatic fluorocarbons. As the amount of C—F bond breaking was smaller than with C_6F_{12}, the effect of changing the neutralization process was investigated by adding a proton scavenger such as ethanol (11).

Experimental

Fisher Spectrograde cyclohexane was used as received for experiments at scavenger concentrations greater than 10^{-2} *M*. Phillips Research Grade cyclohexane was also used after treatment overnight with sulfuric acid to remove cyclohexene. For experiments at lower scavenger concentrations, the Fisher cyclohexane was passed through a silica gel column. It was transferred to a vacuum line and pumped on at room temperature until ⅓ of its volume was removed, distilled onto a sodium mirror, and kept in contact with this mirror for several days. It was then distilled into a measuring volume, and pumped on at room temperature until ⅓ of its volume was removed. This procedure was necessary to remove CO_2. A final degassing was done by the freeze – pump – thaw technique. The C_6F_{12} and C_6F_6 (Aldrich) were also pumped on at room temperature for experiments at low scavenger concentrations. The C_6F_{12} had no detectable $C_6F_{11}H$ or C_6F_{10} impurities. The C_6F_6 had a measurable

[1]Issued as A.E.C.L. No. 3317.
[2]Presented in part at 52nd Chemical Institute of Canada Conference, Montreal, Quebec, May 1969.
[3]A.E.C.L. summer student 1968. Present address: Department of Chemistry, University of Waterloo, Waterloo, Ontario.

Can. J. Chem. Downloaded from www.nrcresearchpress.com by 210.87.254.40 on 09/05/12
For personal use only.

amount of C_6F_5H which was allowed for when calculating yields. Absolute ethanol was passed through a silica gel column to remove any traces of benzene.

Solutions of high scavenger concentrations were made up volumetrically or by weighing, as appropriate. Solutions of low scavenger concentrations were made up by measuring out, from a calibrated volume, aliquots of vapor in equilibrium with the thermostated solid or liquid. Vapor pressures as a function of temperature were taken from Reed (12) for C_6F_{12} and from Patrick and Prosser (13) for C_6F_6. Solutions were irradiated in Pyrex cells of 2 ml volume fitted with a breaking device. All sample preparations were carried out on a mercury-free grease-free vacuum line.

Samples were irradiated at 25 °C in a ^{60}Co γ-source at a mean dose rate (in cyclohexane) of 9.7×10^{15} eV/g s as determined by ferrous sulfate dosimetry taking $G(Fe^{3+}) = 15.6$. Appropriate corrections were made to the absorbed dose for the varying electron densities of the solutions.

After irradiation, gases not condensable at 77 °K were measured volumetrically and analyzed mass spectrometrically. Liquid products were determined by gas chromatography (14). The $C_6F_{11}H$ was determined on an XE-60 column at 40 °C and C_6F_5H on a squalane column at 60 °C. For C_6F_6 solutions, cyclohexene was determined on a β,β-oxydipropionitrile – silver nitrate column, as its retention time on the normally more satisfactory 1,2,3-tris(2-cyanoethoxy)propane column was close to that of C_6F_6. Products were identified by retention time and by mass spectrometry (10, 15).

Results

(i) Perfluorocyclohexane in Liquid Cyclohexane

The major features of the γ-radiolysis of liquid cyclohexane in the presence of up to 0.3 M C_6F_{12} have been described (10). Large yields of $C_6F_{11}H$ were noted and were ascribed to the effects of electron capture by C_6F_{12}. In this work, the range of solute concentrations has been extended to below 10^{-5} M C_6F_{12}. The results are shown in Fig. 1. Yields at lower concentrations were quite dose dependent and G values were determined from the initial slopes of plots of the concentration of $C_6F_{11}H$ against the absorbed dose. At the lowest scavenger concentrations, these plots were linear only at doses below 3×10^{17} eV/g, where about 10% of the C_6F_{12} was decomposed. At the highest concentrations the plots were linear to 10^{19} eV/g. At low scavenger concentrations yields of $C_6F_{11}H$ were eliminated by less than 0.1 M of N_2O, SF_6, or CO_2, indicating that electrons are precursors of this yield. Previously, N_2O was shown to compete with C_6F_{12} for electrons in the high scavenger concentration range (10).

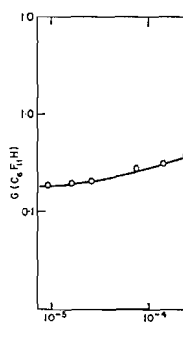

FIG. 1. Yields of $C_6F_{11}H$ as a function of C_6F_{12} concentration on a double logarithmic scale.

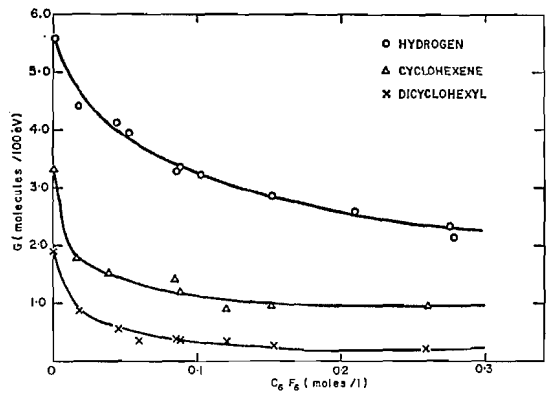

FIG. 2. Hydrogen, cyclohexene, and dicyclohexyl yields from the radiolysis of the C_6F_6 –cyclohexane system. Dose = 1.42×10^{19} eV/g.

(ii) Perfluorobenzene in Liquid Cyclohexane

Perfluorobenzene, (C_6F_6), reduces hydrogen yields from the γ-radiolysis of cyclohexane as has been noted by Rajbenbach (8, 9). The data in Fig. 2 show that dicyclohexyl and cyclohexene yields are reduced as well. In fact, they are reduced well below the limiting yields obtained with relatively uncomplicated electron scavengers such as SF_6 (2) and CO_2 (16). There were a number of unidentified products of both higher and lower molecular weight than dicyclohexyl observed on the XE-60 column at 170 °C, and it is possible that polymers of even higher molecular weight were formed. Polymer formation would account for lower cyclohexene and dicyclohexyl yields. Yields of C_6F_5H are shown in Fig. 3 for a wide range of C_6F_6 concentrations. These yields are all calculated from the initial linear portions of plots of molecules produced against absorbed dose. At the lowest C_6F_6 concentrations these

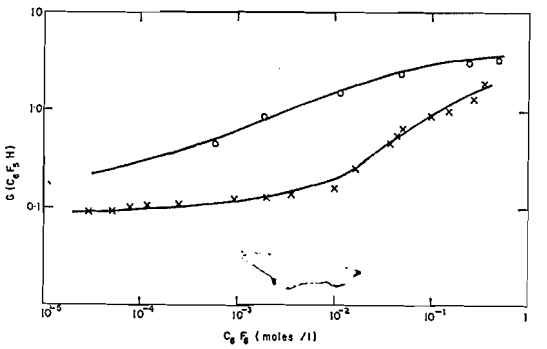

FIG. 3. Yields of C_6F_5H as a function of C_6F_6 concentration on a double logarithmic scale. The crosses (×) represent the C_6F_6 – cyclohexane system. The circles (○) represent yields of the same system with 0.14 *M* ethanol. The upper curve is from Fig. 1.

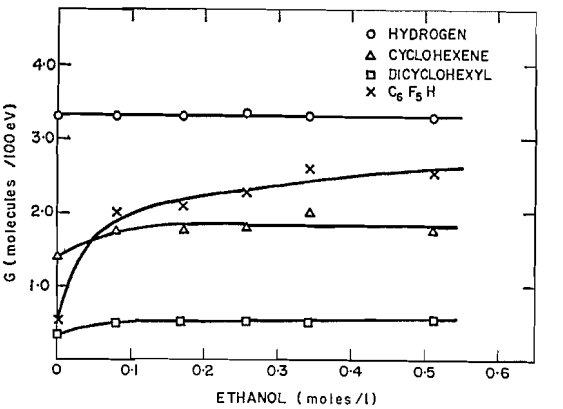

FIG. 4. Hydrogen, cyclohexene, dicyclohexyl, and C_6F_5H yields from the radiolysis of the C_6F_6 – ethanol – cyclohexane system. $C_6F_6 = 0.085_8$ *M*. Dose = $2.1_2 \times 10^{19}$ eV/g.

curves were only linear well below 10^{18} eV/g. Yields of C_6F_5H are much lower than the corresponding yields of $C_6F_{11}H$ from C_6F_{12} shown in Fig. 1. For comparison, the curve from Fig. 1 is shown as the upper curve in Fig. 3. It should be emphasized that the cyclohexane was given the same purification treatment as was given that used for radiolyses with C_6F_{12}. Both N_2O and SF_6 drastically reduced the yield of C_6F_5H, showing that electrons were precursors of this product.

In order to change the neutralization process, ethanol and ammonia, which are known to be efficient proton scavengers (11, 17), were added to the C_6F_6– cyclohexane system. Figure 4 gives yields of the major products of cyclohexane radiolysis with varying amounts of ethanol at a fixed concentration (0.086 *M*) of C_6F_6.

Within experimental error, no significant effect of total dose was noted from $1.0_3 \times 10^{19}$ eV/g to 6.4×10^{19} eV/g. No effect was noted on the hydrogen yield and only small, but significant, increases were noted in the dicyclohexyl and cyclohexene yields. Neither 1-cyclohexyl ethanol nor 2-cyclohexyl ethanol were found in measurable amounts. A large increase was noted in the C_6F_5H yield to a value close to that measured for $C_6F_{11}H$ from C_6F_{12} in cyclohexane at a comparable scavenger concentration.

Yields of C_6F_5H at varying C_6F_6 concentrations in the presence of 0.14 *M* ethanol are given in Fig. 3. These points were obtained at much lower doses, taking care to be always in the linear portion of a plot of C_6F_5H produced against dose. The upper line in Fig. 3 is not drawn through these points, but is the line drawn through the $C_6F_{11}H$ yields in Fig. 1. Except at the highest concentrations, the yield of C_6F_5H from C_6F_6 with ethanol present is equal to the yield of $C_6F_{11}H$ from C_6F_{12}. Unfortunately experimental difficulties prevented us from going to lower C_6F_6 concentrations.

Some work was done with ammonia as a proton scavenger, and increased yields of C_6F_5H were noted in its presence. However, no quantitative results are included since solutions of NH_3 and C_6F_6 in cyclohexane became yellow before irradiation, perhaps due to formation of $C_6F_5NH_2$ and related polymers (18).

Discussion

Rajbenbach (8) was the first to propose that perfluorocycloalkanes affect the radiolysis of liquid hydrocarbons by capturing electrons. Recent work by one of us (10) and by Mittal and Libby (19) support this view. Our work showed that electron capture by C_6F_{12} in cyclohexane (reaction [1])

$$[1] \qquad C_6F_{12} + e^- \rightarrow C_6F_{12}^-$$

leads to an anion which does not produce hydrogen on neutralization and, before or during neutralization, does produce two cyclohexyl radicals, a C_6F_{11} radical, and, as shown by Rajbenbach (9), a molecule of HF. These products could conceivably be produced by dissociation of the $C_6F_{12}^-$ anion (reaction [2])

$$[2] \qquad C_6F_{12}^- \rightarrow C_6F_{11} + F^-$$

Can. J. Chem. Downloaded from www.nrcresearchpress.com by 210.87.254.40 on 09/05/12
For personal use only.

Can. J. Chem. Downloaded from www.nrcresearchpress.com by 210.87.254.40 on 09/05/12
For personal use only.

even though reaction [2] is 1.8 eV endothermic (20) in the gas phase, because of solvation effects. However, we have shown (15) that $C_6F_{11}H$ is produced in the gas phase radiolysis of the cyclohexane – C_6F_{12} system where reaction [2] cannot occur. Hence it now appears that these products are produced mainly in the neutralization step (reaction [3])

$$[3a]\quad C_6F_{12}^- + C_6H_{12}^+ \rightarrow C_6F_{11} + C_6H_{11} + HF$$

$$[3b]\quad \rightarrow C_6F_{11}H + C_6H_{11} + F$$

Although reaction [3*b*] is slightly less favorable thermodynamically, it may occur by proton transfer to $C_6F_{12}^-$ followed by dissociation of the complex (9). Either F or C_6F_{11} would rapidly abstract a hydrogen from cyclohexane.

The results shown in Fig. 1 were fitted to the empirical expression used by Warman, Asmus, and Schuler (1) for electron scavenging

$$[4]\quad G(C_6F_{11}H) = G_{fi} + \frac{G_{gi}\{\alpha_{C_6F_{12}}[C_6F_{12}]\}^{\frac{1}{2}}}{1 + \{\alpha_{C_6F_{12}}[C_6F_{12}]\}^{\frac{1}{2}}}$$

where G_{fi} is the yield of free ions, i.e. the yield of ions which escape the field of their parent ion, and G_{gi} is the geminate ion yield, i.e. the yield of ions which recombine with their parent ion. The $\alpha_{C_6F_{12}}$ is a constant characterizing the reactivity of C_6F_{12} to electrons. This expression was used by its originators to correlate a large number of results with electron scavengers. At low scavenger concentration it reduces to

$$[5]\quad G(C_6F_{11}H) = G_{fi} + G_{gi}\{\alpha_{C_6F_{12}}[C_6F_{12}]\}^{\frac{1}{2}}$$

This same square root dependence is predicted directly by Hummel (6). At scavenger concentrations below 10^{-3} *M*, a plot of $G(C_6F_{11}H)$ against the square root of the scavenger concentration should give a straight line with intercept equal to G_{fi}. Rzad and Warman (21) have applied this method to the determination of the free ion yield from hydrocarbons using $^{14}CH_3Br$ as a scavenger and obtained free ion yields in good agreement with those obtained by other methods. Figure 5 shows our results plotted in this fashion. A free ion yield of 0.14 ± 0.02 *G* units is obtained. This is in good agreement with the 0.12 *G* units obtained by Rzad and Warman using the $^{14}CH_3Br$ scavenging method (21), the 0.14 *G* units obtained by Schmidt and Allen using the clearing field method (4), and the 0.11 *G* units obtained by Tewari and Freeman using the steady state conductivity method (22).

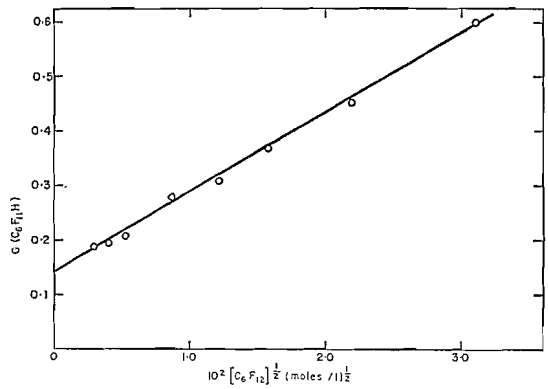

FIG. 5. Determination of free ion yield from the data in Fig. 1.

Over the entire concentration range a plot of $[G(C_6F_{11}H) - G_{fi}]^{-1}$ against $[C_6F_{12}]^{-\frac{1}{2}}$ should be linear. Our results at high concentrations are shown in Fig. 6. This analysis gives a geminate ion yield of 4.2 ± 0.2 *G* units and an $\alpha_{C_6F_{12}}$ of 30 ± 1. Thus the total electron yield is about 4.3 *G* units, close to that predicted from the gas phase *W* values (4, 23), and C_6F_{12} is shown to be a very efficient electron scavenger with one of the highest α's known (1). Furthermore, since C_6F_{12} reacts efficiently with well thermalized electrons to give $C_6F_{11}H$, there is no possibility that excess electron energy is necessary to produce this product, in agreement with conclusions reached previously (10).

Perfluorobenzene is known to attach electrons very rapidly in the gas phase, as the response of an

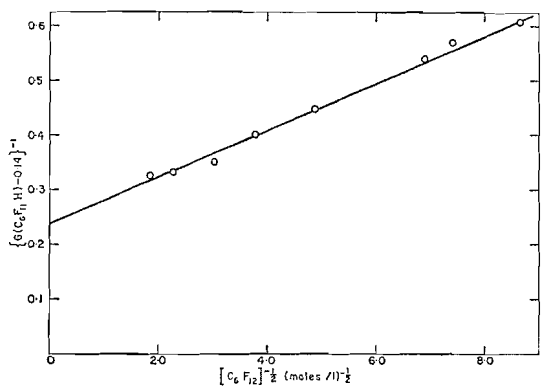

FIG. 6. Determination of the total ion yield and $\alpha_{C_6F_{12}}$ from the data in Fig. 1.

Can. J. Chem. Downloaded from www.nrcresearchpress.com by 210.87.254.40 on 09/05/12
For personal use only.

electron capture detector is very high towards it (24). It captures electrons in liquid hydrocarbons as well, since Rajbenbach (8, 9) has shown that it can reduce nitrogen yields from the radiolysis of N_2O–hydrocarbon systems. The results in Fig. 2 show that the hydrogen yield is reduced as efficiently as with C_6F_{12} (10). In contrast to results with C_6F_{12} (10), cyclohexene, and dicyclohexyl are reduced proportionately more than the hydrogen yield, so that there is a hydrogen surplus of about 1.9 *G* units at 0.05 *M* C_6F_6 and 1 *G* unit at 0.3 *M* C_6F_6. This behavior is similar to that observed with the cyclohexane–benzene system (25), where polymer formation had to be considered to account for a hydrogen surplus of 1 *G* unit at 0.2 *M* C_6H_6.

Some C_6F_5H is formed (Fig. 3) and therefore

[6*a*] $C_6F_6^- + C_6H_{12}^+ \rightarrow C_6F_5 + C_6H_{11} + HF$

[6*b*] $\rightarrow C_6F_5H + C_6H_{11} + F$

reaction [6] occurs to some extent, but the C_6F_5H yields do not fit eq. [4]. One possible complication is the transfer of excitation energy to C_6F_6. Another is the transfer of positive charge to C_6F_6. The gas phase ionization potential of C_6H_{12} is 9.88 eV (26) and that of C_6F_6 is 9.88 (27) to 9.97 eV (28). However, as discussed by Bralsford, Harris, and Price (28), the ionization potential of an aromatic fluorocarbon is a delicate balance between an inductive effect which raises it in saturated fluorocarbons (to 13.2 eV for C_6F_{12} (29)) and resonance effects which lower it by stabilizing the molecular ion. Hence the effects on the ionization potential of the cyclohexane solvent may not be at all equal for cyclohexane and for C_6F_6, and there may be significant charge transfer by reaction [7]

[7] $C_6F_6 + C_6H_{12}^+ \rightarrow C_6F_6^+ + C_6H_{12}$

Neutralization would then be between $C_6F_6^-$ and $C_6F_6^+$, leading to no hydrocarbon products.

In the presence of ethanol, proton transfer to ethanol has been shown to proceed efficiently (11, 30).

[8] $C_6H_{12}^+ + C_2H_5OH \rightarrow C_6H_{11} + C_2H_5OH_2^+$

Neutralization of $C_2H_5OH_2^+$ by an unscavenged electron leads to H_2 formation (reaction [9])

[9] $C_2H_5OH_2^+ + e^- \rightarrow C_2H_5OH + H$

with about the same efficiency as the neutralization of $C_6H_{12}^+$ with e^-, since no large effects of adding ethanol are noted on the hydrogen yield (11).

With C_6F_6 and ethanol both present, neutralization of $C_2H_5OH_2^+$ by $C_6F_6^-$ leads to the efficient formation of C_6F_5H

[10*a*] $C_2H_5OH_2^+ + C_6F_6^- \rightarrow C_6F_5$ + products (C_2H_5OH + HF)

[10*b*] $\rightarrow C_6F_5H$ + products (C_2H_5OH + F)

As the hydrogen yield is not increased, the "products" in reaction [10] do not include H_2 precursors. The actual products of these reactions are not known. The suggestions made in reaction [10] are given to show stoichiometry. Reaction [10*b*] may take place by proton transfer to form a C_6F_6H complex which then eliminates an F atom. A somewhat analogous reaction between protonated methyltetrahydrofuran and the anion of α-methylstyrene has been noted recently (31). Competition between reactions [7] and [8] may account for the fact that C_6F_5H yields are slightly lower than $C_6F_{11}H$ yields from C_6F_{12} at the highest C_6F_6 concentrations. The C_6F_5H yields in Fig. 4 show that a high ratio of ethanol to C_6F_6 is necessary to give the maximum C_6F_5H yield.

The cyclohexyl radicals, produced in reaction [8] and from products formed in reaction [10], are reflected in the small increases in dicyclohexyl and cyclohexene yields, but the hydrogen balance is very poor, so nothing quantitative can be said.

The C_6F_5H yields, in the presence of 0.14 *M* ethanol are very close to those of $C_6F_{11}H$ from the C_6F_{12}–cyclohexane system. Thus, like C_6F_{12}, C_6F_6 is an extremely efficient scavenger for electrons. The large increases on the addition of ethanol imply that C_6F_5H is produced in the neutralization step and not by a unimolecular dissociation of $C_6F_6^-$. In the latter case a change in the neutralization step would not have such a large effect.

Acknowledgment

It is a pleasure to acknowledge useful aid and advice from colleagues Drs. D. A. Armstrong, A. W. Boyd, and C. Willis. We are especially indebted to Dr. J. M. Warman who discussed his results and methods of purifying cyclohexane with us prior to their publication.

1. J. M. Warman, K.-D. Asmus, and R. H. Schuler. Advan. Chem. **82**, 25 (1968).
2. N. H. Sagert and A. S. Blair. Can. J. Chem. **45**, 1351 (1967).

3. G. R. FREEMAN and E. D. STOVER. Can. J. Chem. **46**, 3235 (1968).
4. W. F. SCHMIDT and A. O. ALLEN. J. Phys. Chem. **72**, 3730 (1968).
5. G. R. FREEMAN. J. Chem. Phys. **46**, 2822 (1967).
6. A. HUMMEL. J. Chem. Phys. **48**, 3268 (1968).
7. L. MONCHICK. J. Chem. Phys. **24**, 381 (1956).
8. L. A. RAJBENBACH. J. Am. Chem. Soc. **88**, 4275 (1966).
9. L. A. RAJBENBACH. J. Phys. Chem. **73**, 356 (1969).
10. N. H. SAGERT. Can. J. Chem. **46**, 95 (1968).
11. J. W. BUCHANAN and FF. WILLIAMS. J. Chem. Phys. **44**, 4377 (1966).
12. T. M. REED III. *In* Fluorine chemistry. Vol. V. *Edited by* J. H. Simons. Academic Press, Inc., New York. 1964. p. 139.
13. C. R. PATRICK and G. S. PROSSER. Trans. Faraday Soc. **60**, 700 (1964).
14. J. A. STONE. Can. J. Chem. **42**, 2872 (1964).
15. N. H. SAGERT and A. S. BLAIR. Can. J. Chem. **46**, 3284 (1968).
16. N. H. SAGERT. Can. J. Chem. **46**, 336 (1968).
17. FF. WILLIAMS. J. Am. Chem. Soc. **86**, 3954 (1964).
18. G. M. BROOKE, J. BURDON, M. STACEY, and J. C. TATLOW. J. Chem. Soc. 1768 (1960).
19. J. P. MITTAL and W. F. LIBBY. Nature, **220**, 1027 (1968).
20. M. M. BIBBY and G. CARTER. Trans. Faraday Soc. **62**, 2637 (1966).
21. S. J. RZAD and J. M. WARMAN. J. Chem. Phys. **49**, 2861 (1968).
22. P. H. TEWARI and G. R. FREEMAN. J. Chem. Phys. **49**, 4394 (1968).
23. G. G. MEISELS. J. Chem. Phys. **41**, 51 (1964).
24. C. A. CLEMONS and A. P. ALTSHULLER. Anal. Chem. **38**, 133 (1966).
25. J. A. STONE and P. J. DYNE. Radiation Res. **17**, 353 (1962).
26. K. WATANABE, T. NAKAYAMA, and J. MOTTL. J. Quant. Spectry. Radiative Transfer, **2**, 369 (1962).
27. I. D. CLARK and D. C. FROST. J. Am. Chem. Soc. **89**, 244 (1967).
28. R. BRALSFORD, P. V. HARRIS, and W. C. PRICE. Proc. Roy. Soc. London, Ser. A, **258**, 459 (1960).
29. J. R. MAJER and C. R. PATRICK. Nature, **193**, 161 (1962).
30. J. A. STONE. Can. J. Chem. **46**, 3531 (1968).
31. J. LIN, K. TSUJI, and FF. WILLIAMS. Trans. Faraday Soc. **64**, 2896 (1968).

Can. J. Chem. Downloaded from www.nrcresearchpress.com by 210.87.254.40 on 09/05/12
For personal use only.

Can. J. Chem. Downloaded from www.nrcresearchpress.com by 210.87.254.105 on 09/05/12
For personal use only.

Organic compounds of gallium. III. Reactions of gallium alkoxides with acetylacetone, ethyl acetoacetate, methyl acetoacetate, and methyl salicylate

R. C. MEHROTRA AND S. R. BINDAL
Chemical Laboratories, University of Rajasthan, Jaipur, India

Received November 5, 1968

Derivatives of gallium of the type: $Ga(i\text{-}C_3H_7O)_{3-x}lig_x$ (x = 1, 2, or 3; and H lig = acetylacetone, methyl and ethyl acetoacetate, or methyl salicylate) have been synthesized by reacting gallium alkoxides with ligands in various molar ratios. The compounds are soluble in organic solvents and could be volatilized under reduced pressure. Their molecular weights have been determined ebullioscopically. The infrared spectra of some of the compounds have been studied.

Canadian Journal of Chemistry, 47, 2661 (1969)

Introduction

The reactions of alkoxides of aluminium, lanthanum, neodymium, preseodymium, titanium, niobium, and tantalum (1–7) with bidentate monofunctional ligands like β-diketones and β-ketoesters have recently been studied in these laboratories with interesting results regarding the volatility and coordination number of the products. In the cases of the first 4 elements, all the 3 isopropoxy groups could be replaced by the chelating ligands, but in the cases of the last 3, only partial replacement was possible; e.g. the final end products were $Ti(OR)_2lig_2$ and $Nb(OR)_2lig_3$.

In view of the above studies, it was considered of interest to carry out similar reactions with gallium alkoxides. The synthesis of gallium tris-acetylacetonate was reported as early as 1921 by Morgan and Drew (14). In the present investigation, the acetylacetone and β-ketoester derivatives of gallium have been prepared by the following reactions in benzene solution

$$(i\text{-}C_3H_7O)_3Ga + x\ H\ lig = Ga(i\text{-}C_3H_7O)_{3-x}\ lig + x\ i\text{-}C_3H_7OH$$

where x = 1, 2, or 3; and H lig = acetylacetone, methyl acetoacetate, ethyl acetate, or methyl salicylate.

Isopropanol liberated was fractionated azeotropically and estimated. The products obtained by the above general reactions are soluble in benzene and except those of methyl salicylate can be distilled or sublimed under reduced pressure. All the products obtained in a molar ratio of 1:1 showed dimeric association and the 1:3 derivatives are monomers. However, the compounds obtained in a molar ratio of 1:2 varied in molecular complexity as the ligands were changed; the methyl acetoacetate, the ethyl acetoacetate, and the acetylacetonate derivative showed molecular complexities of 2, 1.3, and 1, respectively.

TABLE I

Infrared analysis of compounds*

$Ga(i\text{-}C_3H_7O)_2$-(acac) (in KBr)	$Ga(i\text{-}C_3H_7O)$-$(acac)_2$ (in $CHCl_3$ soln.)	$Ga(acac)_3$ (in Nujol mull at 4000–400 cm^{-1})
3500 sb	3710 m†	3350 wb
2975 s (A)	2975 s (A)†	2960 s (A)
1950 w	—	2925 sb†
—	—	2850 sb
1600 s (B)	1600 s (B)	1575 sb (B)
1510 w (C)	1545 s (C)	1515 mb (C)
1460 w (D)	1470 w†	1450 s†
—	—	—
1400 sb (E)	1440 m (D)	—
1280 s	1385 w†	1380 s†
1260 m	1335 w (E)	1275 m
1250 w	1295 m	1190 w
1200 w	1270 m	1150 w
1180 w (G)	1180 w (G)	1015 s (F)
1150 s (G)	1130 s (G)	925 s
1100 mb	1050 w (F)†	790 m
1035 s (F)	1035 w (F)	760 s
965 m (G)	935 s†	715 w
935 s	880 m†	670 w (H)
835 w	855 m†	650 w (H)
825 w	680–760 sb†	570 m
805 m		455 w (H)
770 m		430 mb (H)
680 m (H)		

*Modes assigned on the basis of previous measurements are given in parentheses:
(A), ν(C—H); (B), ν(C····C) and chelated ketone —C=O→; (C), ν(C····C); (D), ν(C····O) + CH; (E), δ(C—H); (F), ν(C—O); (G), —CH(CH$_3$)$_2$, skeletal; (H), ν(Ga—O) and ring deformation.
s, strong; m, medium; w, weak; b, broad.
†Bands of the solvent used.

Can. J. Chem. Downloaded from www.nrcresearchpress.com by 210.87.254.105 on 09/05/12
For personal use only.

TABLE II

Reactions of gallium alkoxides with β-ketoesters and acetylacetone

Ligand	Wt. of compound (g)	Wt. of ligand (g)	Molar ratio	Product	Yield (g)	State	Analysis (%) Ga Found	Ga Calcd.	Isopropoxy Found	Isopropoxy Calcd.	Mol. wt. Found	Mol. wt. Calcd.	Wt. of i-C_3H_7OH in azeotrope (g) Found	Wt. of i-C_3H_7OH in azeotrope (g) Calcd.	Boiling point (°C/mm)
Compound = $Ga(i\text{-}C_3H_7O)_3$															
Methyl acetoacetate	2.13	1.00	1:1	$Ga(i\text{-}C_3H_7O)_2(meacac)$	2.61	Yellow liquid	23.06	23.02	37.88	37.98	617	303	0.52	0.52	160/0.6
	2.76	2.62	1:2	$Ga(i\text{-}C_3H_7O)(meacac)_2$	4.5	"	19.35	19.43	17.69	17.48	718	359	1.35	1.36	172/0.4
	1.12	1.58	1:3	$Ga(meacac)_3$	1.87	"	16.79	16.81	—	—	406	413	0.81	0.82	182/2.5
Ethyl acetoacetate	2.70	1.42	1:1	$Ga(i\text{-}C_3H_7O)_2(etacac)$	3.40	Colorless liquid	22.04	22.01	37.17	37.26	632	317	0.65	0.66	136/0.5
	2.03	2.15	1:2	$Ga(i\text{-}C_3H_7O)(etacac)_2$	3.20	"	18.07	18.02	15.37	15.26	504	387	0.99	0.99	170/0.5
	1.23	1.94	1:3	$Ga(etacac)_3$	2.30	White solid	15.23	15.25	—	—	433	457	0.52	0.52	136/0.1
Compound = $Ga(i\text{-}C_3H_7O)(meacac)_2$															
Methyl salicylate	2.14	1.35	1:1	$Ga(i\text{-}C_3H_7O)_2(mesyl)$	2.94	White foamy solid	20.66	20.58	33.70	34.05	680	339	0.51	0.52	285/0.2 (decomp.)
	1.05	1.94	1:3	$Ga(mesyl)_3$	2.26	"	13.26	13.32	—	—	507	523	0.75	0.76	330/0.5 (decomp.)
Acetyl acetone	2.20	0.89	1:1	$Ga(i\text{-}C_3H_7O)_2(acac)$	2.56	Brown liquid	24.33	24.31	38.27	41.25	613	287	0.53	0.54	151/0.8
	2.00	1.62	1:2	$Ga(i\text{-}C_3H_7O)(acac)_2$	2.56	Yellow solid	21.22	21.32	18.68	18.48	324	327	0.97	0.97	171/0.5 (Sublimed)
	1.13	1.39	1:3	$Ga(acac)_3$	1.70	"	18.92	19.00	—	—	352	367	0.81	0.82	197–198 (m.p.)
Acetyl acetone	2.21	1.20	Excess ligand	$Ga(acac)(meacac)_2$	2.30	Yellow liquid	17.69	17.48	—	—	404	399	—	—	170/0.9

Ligand	Wt. of compound (g)	Wt. of ligand (g)	Molar ratio	Product	Yield	State	Analysis (% Ga) Found	Analysis (% Ga) Calcd.	Mol. wt. Found	Mol. wt. Calcd.	Wt. of C_2H_5OH in azeotrope Found	Wt. of C_2H_5OH in azeotrope Calcd.	Boiling point (°C/mm)
Compound = $Ga(OC_2H_5)_3$													
Acetyl acetone	2.37	1.16	1:1	$Ga(OC_2H_5)_2(acac)$	3.01	Brown liquid	27.01	26.95	626	259	0.52	0.53	170/0.9
	1.62	1.58	1:2	$Ga(OC_2H_5)(acac)_2$	2.48	Cream crystals	22.15	22.29	422	313	0.72	0.73	175–176 (m.p.)
	1.76	2.58	1:3	$Ga(acac)_3$	3.16	Yellow crystals	19.13	19.01	377	367	1.18	1.19	190–200/0.2 (Sublimed) 197–198 (m.p.)

Can. J. Chem. Downloaded from www.nrcresearchpress.com by 210.87.254.105 on 09/05/12
For personal use only.

The derivatives could be distilled at higher temperatures compared to gallium isopropoxide indicating that chelation has the expected effect of lowering the volatility.

A mixed ligand product $Ga(acac)(meacac)_2$ was also obtained by reacting $Ga(i\text{-}C_3H_7O)(meacac)_2$ and acetylacetone in excess (acac = acetylacetone, meacac = methyl acetoacetate). The compound is monomeric in benzene.

Infrared spectra of some of the derivatives have been recorded in the range 4000–670 cm^{-1} (2.5–15 μ). The data and the modes assigned on the basis of previous measurements (8–13) are given in Table I. The bands at about 3400–3500 cm^{-1} may be due to slight hydrolysis of isopropoxy derivatives during handling and recording of the spectra.

Experimental

An all-glass apparatus fitted with interchangeable joints was used, special precautions being taken to exclude moisture. All reactions were carried out in a flask under a column packed with Rasching rings and fitted to a total condensation variable take-off stillhead.

Molecular weights were determined ebullioscopically in boiling benzene by means of a semimicro (Gallenkamp) ebulliometer using thermistor sensing. Infrared spectra were recorded on a Perkin–Elmer spectrophotometer model 137B.

Gallium isopropoxide was prepared as previously described (8) and benzene was dried similarly. Methyl acetoacetate, ethyl acetoacetate, and methyl salicylate were distilled over aluminium isopropoxide. Acetylacetone was fractionated over aluminium isopropoxide.

Gallium and isopropanol were estimated as described earlier (8). Isopropoxy in mixed β-diketonate compounds was estimated by liberating the isopropanol with excess of the ligand.

The same synthetic procedure was used in all the cases. Details are, therefore, given for the typical derivatives only; the other reactions are summarized in Table II.

Synthetic Reactions

Reaction of Gallium Isopropoxide and Acetylacetone in Molar Ratio 1:2

Gallium isopropoxide (2.00 g) and acetylacetone (1.62 g) were refluxed in benzene (60 ml) followed by slow distillation of isopropanol azeotropically between 72–80 °C. The remaining solvent was removed under reduced pressure and the product dried at room temperature (35 °C) at 0.5 mm pressure for 2 h. A yellow solid (2.56 g) was obtained.

The analysis of isopropanol in azeotrope required for 2 moles of isopropanol, 0.97 g. Found: 0.97 g.

Anal. Calcd. for $C_{13}H_{21}O_5Ga$: Ga, 21.32; isopropoxy, 18.48. Found: Ga, 21.22; isopropoxy, 18.68.

This compound (2.0 g) was distilled under reduced pressure at 171 °C/0.5 mm as a brown liquid (0.85 g); it solidified after a few minutes on cooling, m.p. 148–149 °C, and this solid was found to be 21.42% Ga.

Reaction of Gallium Ethoxide and Acetylacetone in Molar Ratio 1:2

Gallium ethoxide (1.62 g) and acetylacetone (1.58 g) were refluxed in benzene (55 ml) and ethanol was removed azeotropically between 68–80 °C followed by excess of benzene. On leaving the clear solution overnight, cream colored crystals appeared. The mother liquor was decanted off and the crystals were dried at room temperature (35 °C) at 0.4 mm pressure yielding a crystalline solid (1.58 g). The analysis of ethanol in the azeotrope required for 2 moles of ethanol, 0.73 g. Found: 0.72 g.

The solid was recrystallized from benzene giving crystals (m.p. 175–176 °C) having the same appearance and analysis.

Acknowledgments

The authors are grateful to the Chemical Society, London, for a research grant for chemicals. One of the authors S.R.B. is grateful to the Council of Scientific and Industrial Research, New Delhi, for the award of a Junior Research Fellowship. The authors' thanks are due to Mr. Bhagirath Singh for recording the infrared spectra.

1. R. C. MEHROTRA and R. K. MEHROTRA. Can. J. Chem. **9**, 795 (1961).
2. R. C. MEHROTRA, S. N. MISRA, and T. N. MISRA. Indian J. Chem. **5**, 372 (1967).
3. R. C. MEHROTRA, S. N. MISRA, and T. N. MISRA. Indian J. Chem. **3**, 525 (1965).
4. R. C. MEHROTRA and D. M. PURI. J. Less-Common Metals, **4**, 253 (1961).
5. R. C. MEHROTRA and P. N. KAPOOR. J. Less-Common Metals, **7**, 176 (1964).
6. R. C. MEHROTRA and P. N. KAPOOR. J. Less-Common Metals, **7**, 453 (1964).
7. R. C. MEHROTRA and P. N. KAPOOR. J. Less-Common Metals, **8**, 339 (1965).
8. R. C. MEHROTRA, P. N. KAPOOR, and S. R. BINDAL. Inorg. Chem. **7**, 384 (1968).
9. K. NAKAMOTO, P. J. MCCARTHY, A. RUBY, and A. K. MARTELL. J. Am. Chem. Soc. **83**, 1066, 1272 (1961).
10. R. H. HOLM and F. A. COTTON. J. Am. Chem. Soc. **80**, 5658 (1958).
11. C. DJORDJEVIC. Spectrochim. Acta, **17**, 448 (1961).
12. K. E. LAWSEN. Spectrochim. Acta, **17**, 248 (1961).
13. J. C. BAILAR, L. H. JONES, and J. P. DISMUPES. J. Phys. Chem. **65**, 792 (1961).
14. G. T. MORGAN and H. D. K. DREW. J. Chem. Soc. 1058 (1921).

Can. J. Chem. Downloaded from www.nrcresearchpress.com by 210.87.254.5 on 09/05/12
For personal use only.

Chemistry of metal hydrides[1]. VI. Cationic platinum(II) carbonyls stabilized with tertiary arsines and stibines

W. J. CHERWINSKI AND H. C. CLARK
Department of Chemistry, University of Western Ontario, London, Ontario

Received February 24, 1969

The synthesis of $[Pt_2Cl_2(R_3M)_4][BF_4]_2$, and its cleavage with carbon monoxide to form the cationic carbonyl species $[PtCl(CO)(R_3M)_2]^+$ is described for R = ethyl or phenyl, and M = As or Sb. A comparison of the physical properties and spectroscopic data of these compounds, and the analogues for M = P is made with related complexes of other transition metals.

Only *trans*-$[PtCl(CO)(Et_3As)_2][BF_4]$ reacts with water to give *trans*-$[PtHCl(Et_3As)_2]$ and carbon dioxide. *trans*-$[PtCl(CO)(Ph_3As)_2][BF_4]$ reacts readily with methanol or ethanol to give an alkoxy carbonyl $[PtCl(COOR)(Ph_3As)_2]$, where R = CH_3 or C_2H_5. Unlike their phosphine analogues, these species and the stibine-stabilized cationic carbonyls do not produce the corresponding hydrides on reaction with water in the presence of a salt catalyst. These differences in chemical reactivity are related to the basicity of the ligands.

Canadian Journal of Chemistry, 47, 2665 (1969)

Introduction

An examination of the $[PtCl(CO)(R_3P)_2]^+$ cation (2) has been prompted by the well-known catalytic activity of the isoelectronic species $[RhCl(Ph_3P)_3]$ and *trans*-$[IrCl(CO)(Ph_3P)_2]$ in the homogeneous hydrogenation of olefins (3). Phosphine-stabilized platinum(II) compounds including the dihalo-bridged cationic dimers $[Pt_2X_2(R_3P)_4][BF_4]_2$, the carbonyl cations *trans*-$[PtX(CO)(R_3P)_2][BF_4]$, and the alkoxy carbonyls $[PtX(COOR)(Ph_3P)_2]$ have recently been studied (1, 2). Analogous arsine and stibine complexes have now been prepared, and compared to the former both in physical properties and chemical reactivity. Significant differences have been found, particularly in the ease of formation of the hydrido platinum(II) compounds from the platinum(II) carbonyl cations by the direct reaction with water, and indirectly via alkoxy carbonyl compounds.

Results and Discussion

The synthesis of dihalo-bridged diplatinum cations by reaction of the appropriate dihalo-bisarsine (or stibine) complex with boron trifluoride as previously reported (2), was successful for $[Pt_2Cl_2(R_3M)_4][BF_4]_2$ where M = As or Sb, and R = ethyl. For R = phenyl, a sequence involving silver tetrafluoroborate at room temperature was employed (4).

[1] $2cis\text{-}[PtCl_2(Ph_3M)_2] + 2AgBF_4 \rightarrow [Pt_2Cl_2(Ph_3M)_4][BF_4]_2 + 2AgCl$

[1]For Part V, see ref. (1).

For the resulting two series of compounds, where R = ethyl or phenyl, a marked decrease in melting point and a color change from white to yellow occurs as the ligand donor atom changes down the series P, As, Sb (Table I). A decrease in stability is also apparent since in the series with R = ethyl, both the phosphine- and arsine-stabilized compounds are air-stable, while the stibine analogue decomposes slowly in air; also for R = phenyl and M = Sb, reaction [1] affords a product unstable in solution.

These new dimeric cations, like their phosphine analogues, react in minutes in a chloroform suspension with carbon monoxide at 1 atm pressure, to yield a series of well defined carbonyl platinum(II) salts in the *trans* configuration (2).

[2] $[Pt_2X_2(R_3M)_4][BF_4]_2 + 2CO \rightarrow 2[PtX(CO)(R_3M)_2][BF_4]$

The one step syntheses of $[PtCl(CO)(R_3M)_2]^+$, where M = As or Sb, by (*a*) displacement of chloride ion with carbon monoxide from the complexes $[PtX_2(R_3M)_2]$ in the presence of sodium tetraphenylborate or sodium tetrafluoroborate (5) or, (*b*) reaction of hydrido platinum(II) compounds with aqueous tetrafluoroboric acid and carbon monoxide (2), have also been successful.

For R = ethyl, the carbonyl cations range from the white, crystalline phosphine- and arsine-stabilized complexes to the pale yellow, oily stibine analogue. Similarly, for R = phenyl, the high-melting, lightly-colored compounds for

Can. J. Chem. Downloaded from www.nrcresearchpress.com by 210.87.254.5 on 09/05/12
For personal use only.

TABLE I

Properties of dihalo-bridged cationic, chlorocarbonyl, and alkoxy carbonyl platinum(II) salts

Compound	Melting point (°C)	Color	Recrystallization solvents	Anal. Calcd (%)			Found (%)			$\nu_{C=O}$ (cm^{-1})	
				C	H	Cl	C	H	Cl	Nujol	$CHCl_3$
$[Pt_2Cl_2(Et_3P)_4][BF_4]_2$	250d	White	CH_2Cl_2/Et_2O/pet. ether	*							
$[Pt_2Cl_2(Et_3As)_4][BF_4]_2$	221d	Pale yellow	"	22.5	4.7	5.5	21.7	4.7	5.4		
$[Pt_2Cl_2(Et_3Sb)_4][BF_4]_2$	139d	Yellow	"	19.6	4.1	4.8	19.8	4.2	5.0		
$[Pt_2Cl_2(Ph_3P)_4][BF_4]_2$	300d	White	"	*							
$[Pt_2Cl_2(Ph_3As)_4][BF_4]_2$	260d	Pale yellow	"	46.6	3.3	3.8	47.2	3.6	3.7		
$[Pt_2Cl_2(Ph_3Sb)_4][BF_4]_2$	†	—	—	—	—	—	—	—	—		
$[PtCl(CO)(Et_3P)_2][BF_4]$	168–171	White	Ethyl acetate	*						2100	2098
$[PtCl(CO)(Et_3As)_2][BF_4]$	128–129	White	Ethyl acetate	23.4	4.5	—	23.6	4.6	—	2100	2104
$[PtCl(CO)(Et_3As)_2][BPh_4]$	103–106	White	Ethyl acetate	49.6	5.6	—	49.4	5.6	—		
$[PtCl(CO)(Et_3Sb)_2][BF_4]$	Oil	Yellow	—	20.5	4.0	—	20.3	4.0	—	2080	2082
$[PtCl(CO)(Ph_3P)_2][BF_4]$	270	White	CH_2Cl_2/Et_2O/pet. ether	*						2100	2120
$[PtCl(CO)(Ph_3As)_2][BF_4]$	231–232	Pale yellow	"	46.5	3.2	—	46.3	3.2	—	2105	2138
$[PtCl(CO)(Ph_3Sb)_2][BF_4]$	129–135	Yellow-orange	"	42.3	2.9	—	42.8	2.9	—	2080	2138
$[PtCl(COOMe)(Ph_3P)_2]$	222–227	White	"	*						1664	1637
$[PtCl(COOMe)(Ph_3As)_2]$	234–236	Off-white	"	50.6	3.7	—	50.8	3.7	—	1658	1639
$[PtCl(COOEt)(Ph_3P)_2]$	215–217	White	"	*						1638	1638
$[PtCl(COOEt)(Ph_3As)_2]$	214–216	Pale yellow	"	51.2	3.9	—	50.9	3.9	—	1632	1636

*Previously reported.
†Isolated as impure solid.

M = P or As are in marked contrast to the low-melting, yellow-orange stibine salt (Table I).

Like their phosphine analogues (1), arsine-stabilized carbonyl cations react with pure methanol or ethanol. The reaction of *trans*-$[PtCl(CO)(R_3As)_2][BF_4]$ for R = ethyl gives an unstable, oily alkoxy carbonyl, while for R = phenyl, the products are crystalline, off-white solids.

[3] R^1OH + *trans*-$[PtCl(CO)(R_3As)_2][BF_4]$ $\rightarrow [PtCl(COOR^1)(R_3As)_2] + [HBF_4]$

where R^1 = methyl or ethyl.

Unlike substituted rhodium and iridium carbonyl complexes (6) under basic conditions, the stibine platinum compounds undergo no such reaction.

For the platinum(II) carbonyl cation where M = As or P, and R = ethyl, reaction with water, or aqueous methanol or ethanol takes place quantitatively.

[4] $[PtCl(CO)(R_3M)_2][BF_4] + H_2O$ $\rightarrow$ *trans*-$[PtHCl(R_3M)_2] + CO_2 + [HBF_4]$

This reactivity decreases but is still observed, for M = P and R = phenyl. However, for M = As and R = phenyl, the hydrido platinum(II) complex is not formed, either in this direct fashion, or via the alkoxy carbonyl intermediate species as reported for the triphenylphosphine complex (1). The compounds *trans*-$[PtHCl(R_3Sb)_2]$ where R = ethyl or phenyl are unknown.

The above trends in physical properties of the dihalo-bridged diplatinum cations and of the platinum(II) carbonyl cations are parallel to others reported. For the series of neutral dimeric salts (7) of platinum and palladium, $L_2M_2Cl_4$, stabilities decreased and colors became more intense on changing the donor atom from P to As to Sb. Here also, the stibine-stabilized complex was air-sensitive. Similar gradations of properties have been found for carbonyl complexes of vanadium (8), nickel (9), and rhodium (10). Indeed, it is well-known (11) that, although the differences in electronegativity are not great, the order of co-ordinating affinities of Group V atoms in donor ligands is P > As > Sb > Bi. It has been found more difficult to relate this order to changes in the C—O infrared stretching frequencies of carbonyl complexes, although for nickel carbonyl complexes, small changes in these frequencies have been attributed (12) to differences in the σ-donor and π-acceptor properties between phosphine and arsine ligands. Similarly for these new platinum(II) cationic carbonyl complexes, the changes in $\nu_{C=O}$ are very small; indeed, for R = ethyl, in descending the series P, As, Sb, the frequency changes are negligible, and for R = phenyl, both the arsine and stibine complex show the same carbonyl frequency, only slightly greater than that of the phosphine derivative. The higher frequencies of the carbonyl cations where R = phenyl, compared with those containing R = ethyl are consistent with the less basic character of the former type of ligands.

In interpreting the lesser reactivity of *trans*-$[PtCl(CO)(Ph_3P)_2]$ compared to its triethylphosphine analogue in sequence [4], both the lower stability of the carbonyl, and the greater electron withdrawing ability of the triphenylphosphine ligands lowering the reactivity at carbonyl carbon, have been considered important. When M = As, a similar difference in reactivity occurs for R = ethyl and R = phenyl. Moreover, the chemical reactivity of the carbonyl cations decreases with the order of basicity down the series P > As > Sb. For R = ethyl, only the ligands with M = P and As remain sufficiently basic to support reaction of the carbonyl cation with water to give the corresponding hydride. Sequence [4] is also successful for R = phenyl and M = P, while the more acidic ligands with M = As support conversion only to the intermediate alkoxy carbonyl species. No reaction occurs when M = Sb. Related trends in reactivity have been observed (13) for the series of rhodium compounds, $[RhCl(MPh_3)_3]$ where M = P, As, Sb, although in many of their reactions the tendency is for the arsine and stibine complexes to give more stable derivatives than the phosphine analogue, rather than show a reduced reactivity (14).

Differences in ligand basicity also appear to influence the proton magnetic resonance (p.m.r.) spectra of $[PtCl(COOR)(Ph_3M)_2]$. For R = methyl and M = P, the methyl proton absorption appears as a triplet at 7.6 τ with J_{Pt-H} = 15 c.p.s., while for M = As, this absorption is reduced to a singlet at 7.5 τ, with $J_{Pt-H} < 2$ c.p.s. Similarly for R = ethyl, the methylene proton multiplet at 7.5 τ for M = P appears as a quartet at 7.1 τ for M = As with a corresponding reduction in the platinum–hydrogen coupling constant from 15 to < 2 c.p.s. (Table

Can. J. Chem. Downloaded from www.nrcresearchpress.com by 210.87.254.5 on 09/05/12
For personal use only.

TABLE II

Proton magnetic resonance data of alkoxy carbonyls

Compound	Solvent	Chemical shifts* τ of alkoxy protons (p.p.m.) CH_3	CH_2	Coupling constants (c.p.s.) J_{Pt-H}	J_{H-H}
$[PtCl(COOMe)(Ph_3P)_2]$	CH_2Cl_2	7.6 (t)†	—	15	—
$[PtCl(COOMe)(Ph_3As)_2]$	CH_2Cl_2	7.5 (s)	—	< 2	—
$[PtCl(COOEt)(Ph_3P)_2]$	CH_2Cl_2	9.5 (t)		< 1	15
			7.3 (m)‡	15	15
$[PtCl(COOEt)(Ph_3As)_2]$	CH_2Cl_2	9.5 (t)		< 1	15
			7.1 (q)‡	< 2	15

*(t) = triplet, (s) = singlet, (m) = multiplet, (q) = quartet.
†The methyl protons are split by ^{195}Pt (34% abundance) with $I = \frac{1}{2}$ into a 1:4:1 triplet.
‡The multiplet results from splitting by CH_3 protons and ^{195}Pt.

II). These small decreases in chemical shift and remarkable reductions of J_{Pt-H} may well arise from a depletion of electron density on platinum by the more acidic arsine ligands.

Experimental

Previously described techniques and instrumentation (2) were used. The tertiary arsine and stibine Pt(II) dihalide complexes employed as starting materials were prepared according to established procedures (15). Physical properties and analytical data for prepared derivatives are summarized in Tables I and II.

1. Preparation of $[Pt_2X_2(Et_3M)_4][BF_4]_2$

The reported procedure (2) for the preparation of $[Pt_2X_2(R_3P)_4][BF_4]_2$ proved effective only for the synthesis of the dichloro-bridged species where R = ethyl, and M = As or Sb. Although a range of temperature conditions was employed, compounds with R = phenyl, and M = As or Sb were isolated in poor yield and in an impure condition by this method.

(*a*) *cis*-$[PtCl_2(Et_3As)_2]$ (0.25 g) and boron trifluoride (0.3 g), maintained at 23 °C in a silica Carius tube for 12 h in dried chloroform (5 ml), yielded pale yellow needles of $[Pt_2Cl_2(Et_3As)_4][BF_4]_2$ (0.14 g), which were recrystallized from a methylene chloride – diethyl ether – light petroleum ether mixture. Solubility properties were similar to those of the phosphine analogue (1); prolonged exposure to the atmosphere gave no indication of decomposition.

(*b*) *cis*-$[PtCl_2(Et_3Sb)_2]$ (0.15 g) and BF_3 (0.3 g), after 12 h at 23 °C in dry chloroform (5 ml) yielded yellow crystals of $[Pt_2Cl_2(Et_3Sb)_4][BF_4]_2$ (0.11 g) upon recrystallization as in (*a*). Discoloration was apparent after air-exposure over a period of days.

2. Preparation of $[Pt_2X_2(Ph_3M)_4][BF_4]_2$

(*a*) An acetone solution of silver tetrafluoroborate (0.045 g) was added dropwise with stirring to *cis*-$[PtCl_2(Ph_3As)_2]$ (0.20 g) in a small volume of methylene chloride, and the mixture was maintained at 23 °C for 1 h. When the silver chloride precipitate had been filtered off, crystallization in the clear yellow filtrate was induced by addition of diethyl ether. The off-white solid product was filtered off, washed several times with water, and recrystallized as in (*1*(*a*)), affording pure $[Pt_2Cl_2(Ph_3As)_4][BF_4]_2$ (0.17 g). Characteristic BF_4^- absorptions were prominent in the infrared (i.r.) spectrum, while sensitivity to atmospheric exposure was not observed.

(*b*) The same procedure was employed using *cis*-$[PtCl_2(Ph_3Sb)_2]$; however, the initial filtration yielded a yellow-orange solution which darkened with time. The most successful recrystallization attempts afforded a brown precipitate whose i.r. spectrum was in accord with that anticipated for a charged dimeric species. Its instability in solution prohibited further investigation.

3. Reaction of $[Pt_2Cl_2(R_3M)_4][BF_4]_2$ with Carbon Monoxide

(*a*) The compound $[Pt_2Cl_2(Et_3M)_4][BF_4]_2$ (0.20 g) where M = As or Sb, was stirred for 1 h at 23 °C in degassed chloroform solution (10 ml) under 1 atm of carbon monoxide. The solution was then filtered and the solvent evaporated off. For M = As, white crystalline *trans*-$[PtCl(CO)(Et_3As)_2][BF_4]$ (0.10 g) was recovered by recrystallization from ethyl acetate. For M = Sb, *trans*-$[PtCl(CO)(Et_3Sb)_2][BF_4]$ (0.09 g) was isolated under a carbon monoxide atmosphere from CO-saturated solvents as a pale-yellow oil. Although both compounds slowly discolored on exposure to air, this effect was far more pronounced in the latter case.

(*b*) The procedure above was repeated for $[Pt_2Cl_2(Ph_3M)_4][BF_4]_2$ (0.20 g) where M = As or Sb. After filtration, pale yellow *trans*-$[PtCl(CO)(Ph_3As)_2][BF_4]$ (0.10 g) was isolated by recrystallization from a methylene chloride – diethyl ether – light petroleum ether mixture. Orange *trans*-$[PtCl(CO)(Ph_3Sb)_2][BF_4]$ (0.06 g) was recovered in a similar fashion from reaction of the impure dimeric analogue (see *2*(*b*)).

4. Alternative Preparations of trans-$[PtCl(CO)(R_3M)_2]^+$

(*a*) *trans*-$[PtHCl(Et_3As)_2]$ (0.10 g) in 10 ml benzene was heated with 7 drops aqueous 48% fluoroboric acid in a stainless steel autoclave under a pressure of 5 atm of carbon monoxide at 120° for 48 h. After separation by procedures similar to those previously reported (2), white, solid *trans*-$[PtCl(CO)(Et_3As)_2][BF_4]$ (0.06 g) was obtained and recrystallized from ethyl acetate.

(*b*) *cis*-$[PtCl_2(Et_3M)_2]$ (0.10 g) for M = As, was stirred with sodium tetraphenylborate (0.06 g) in freshly distilled tetrahydrofuran (5 ml) under carbon monoxide (1 atm). The solution became cloudy almost immediately but stirring was continued for 1 h at 23 °C before

Can. J. Chem. Downloaded from www.nrcresearchpress.com by 210.87.254.5 on 09/05/12
For personal use only.

Can. J. Chem. Downloaded from www.nrcresearchpress.com by 210.87.254.5 on 09/05/12
For personal use only.

removal of solvent under vacuum. Extraction of the residues with methylene chloride gave white, solid *trans*-$[PtCl(CO)(Et_3As)_2][BPh_4]$ (0.10 g), while extraction with water, followed by acidification and addition of silver nitrate, yielded silver chloride (0.02 g). A similar reaction sequence for M = Sb, yielded the cationic carbonyl salt as a yellow oil, while products spectroscopically identical to those of preparation *3*(*a*) for M = As and Sb were obtained from reactions using sodium tetrafluoroborate in acetone (Table I).

(*c*) *cis*-$[PtCl_2(Ph_3M)_2]$ (0.10 g) for M = As was similarly treated with $NaBPh_4$ (0.40 g) in dry methylene chloride – acetone solution. Following filtration, work-up was effected in a carbon monoxide atmosphere by addition of the methylene chloride solution to a carbon monoxide saturated diethyl ether – petroleum ether mixture. The resulting yellow solid, *trans*-$[PtCl(CO)(Ph_3As)_2][BPh_4]$ which could not be recrystallized from other solvents without decomposition, showed a prominent carbonyl absorption in the i.r. spectrum. For M = Sb, evaporation of the filtrate afforded a viscous yellow oil whose i.r. spectrum was consistent with expected carbonyl; however, similar work-up procedures yielded an uncharacterized yellow solid lacking the carbonyl i.r. absorption. In both cases, solubility difficulties prohibited the reaction sequence involving $NaBF_4$.

5. Preparation of trans-[PtCl(COOR)(Ph$_3$As)$_2$]

(*a*) For R = methyl, $[PtCl(CO)(Ph_3As)_2][BF_4]$ was stirred in methanol at 23 °C for 1 h. The fine yellow precipitate was filtered, washed with water and methanol, then dried under vacuum.

The reaction was identical where ethanol replaced methanol, (R = ethyl), and both sequences afforded essentially quantitative conversion to the alkoxy species. Solubility properties were identical to those of the Ph_3P analogues, while i.r. assignments, and p.m.r. absorptions were qualitatively similar (Table II).

(*b*) Similar conditions applied to $[PtCl(CO)(Ph_3Sb)_2][BF_4]$ at 23 and at 60 °C yielded only unreacted starting material.

6. Reaction of trans-[PtCl(CO)(Et$_3$M)$_2$][BF$_4$] with Dry Methanol

(*a*) For M = As, *trans*-$[PtCl(CO)(Et_3As)_2][BF_4]$ (0.30 g) in dry methanol (5 ml) was maintained at 90 °C for 12 h in a dried, evacuated Pyrex Carius tube. Volatiles were removed under vacuum leaving a pale yellow oil in quantitative yield, which was then purified by Florisil chromatography with elution with methylene chloride. Proton magnetic resonance absorptions were obscured by arsine peaks in the same region (~2.5 p.p.m.), although for R = ethyl, $—CH_3$ protons were detected at 0.55 p.p.m. The carbonyl cation with M = Sb failed to react under similar conditions. Infrared spectroscopy ($\nu_{C=O}$ at 1601 cm^{-1}) indicated a compound analogous to the reported $[PtCl(COOR)(Et_3P)_2]$ (1), where R = methyl.

7. Reaction of trans-[PtCl(CO)(Et$_3$As)$_2$][BF$_4$] with Water

trans-$[PtCl(CO)(Et_3As)_2][BF_4]$ (0.20 g) was heated at 90 °C for 12 h in degassed methanol (5 ml) with several drops of water in an evacuated Pyrex tube. The volatile products were fractionated under vacuum through −78, −120, and −196 °C traps, and carbon dioxide was collected and identified by i.r. spectroscopy. Extraction of the residue with water afforded a white solid with i.r. absorption characteristic of SiF_6^{2-} and BF_4^- anions. A light petroleum ether extract yielded white, crystalline *trans*-$[PtHCl(Et_3As)_2]$ (0.075 g) characterized by its melting point (89–91 °C), p.m.r. spectroscopy, i.r. spectroscopy, and elemental analysis. Water–methanol mixtures containing greater amounts of water resulted in pronounced decomposition. Similar reactions for M = Sb were unsuccessful.

8. Reactions of trans-[PtCl(COOCH$_3$)(Ph$_3$As)$_2$] with Water

(*a*) *trans*-$[PtCl(COOCH_3)(Ph_3As)_2]$ (0.20 g) was heated with saturated aqueous potassium chloride solution (5 ml) at 110 °C for 12 h in an evacuated Pyrex tube. Extensive decomposition was observed. Carbon dioxide and methanol could not be identified in the volatile products. Extraction of the residue with methylene chloride afforded an uncharacterized oil. No evidence for hydride formation was found.

(*b*) Identical reactions conducted at 80 and 100 °C proceeded with less decomposition, although starting material was the only solid recovered, and carbon dioxide could not be detected in the volatile components.

Acknowledgments

We are grateful to the National Research Council of Canada for financial assistance, and for the award of a 1967 Science Scholarship (to W.J.C.). The loan of platinum compounds from Johnson, Matthey and Company is also gratefully acknowledged.

1. H. C. Clark, K. R. Dixon, and W. J. Jacobs. J. Am. Chem. Soc. **91**, 1346 (1969).
2. H. C. Clark, K. R. Dixon, and W. J. Jacobs. J. Am. Chem. Soc. **90**, 2259 (1968).
3. J. A. Osborn, F. H. Jardine, J. F. Young, and G. Wilkinson. J. Chem. Soc. A, 1711 (1966), and references therein.
4. D. A. Duddell, P. L. Goggin, R. J. Goodfellow, and M. G. Norton. Chem. Commun. 879 (1968).
5. M. J. Church and M. J. Mays. J. Chem. Soc. A, 3074 (1968).
6. W. Hieber and V. Frey. Chem. Ber. **99**, 2614 (1966).
7. J. Chatt and L. M. Venanzi. J. Chem. Soc. 2351 (1957).
8. W. Hieber, J. Peterhans, and E. Winter. Chem. Ber. **94**, 2572 (1961).
9. W. Reppe and W. J. Schweckendiek. Ann. Chem. Liebigs, **560**, 104 (1948).
10. L. Vallarino. J. Chem. Soc. 2287 (1957).
11. G. Booth. Advan. Inorg. Chem. Radiochem. **6**, 1 (1964).
12. J. Chatt and F. A. Hart. J. Chem. Soc. 1378 (1960).
13. J. T. Mague and G. Wilkinson. J. Chem. Soc. A, 1736 (1966).
14. J. T. Mague and G. Wilkinson. Inorg. Chem. 542 (1968).
15. K. A. Jensen. Z. Anorg. Allgem. Chem. **229**, 238 (1936).

Can. J. Chem. Downloaded from www.nrcresearchpress.com by 210.87.254.6 on 09/05/12
For personal use only.

Activities from vapor pressure measurements of lithium and of sodium chlorates in water and water–dioxane solvents

A. N. CAMPBELL AND B. G. OLIVER[1]

Department of Chemistry, University of Manitoba, Winnipeg, Manitoba

Received January 8, 1969

The vapor pressures of solutions of sodium chlorate and of lithium chlorate in water and in solvents consisting of 44.5% dioxane – 55.5% water and of 64.5% dioxane – 35.5% water, at 25 °C, were determined using a differential manometer. The vapor compositions of the dioxane–water solutions were found by the air-saturation method.

The mean molal activity coefficients were calculated from the vapor pressures and compositions. The activity coefficients of the solute were fitted to the theoretical equations of Stokes and Robinson and of Glueckauf, yielding hydration numbers for the cations of the salts.

The minimum dioxanation numbers of sodium and of lithium chlorates in the dioxane–water mixtures were calculated from the experimental activity coefficients by the method of Grunwald. The results show that lithium chlorate is more highly solvated than sodium chlorate and that dioxane plays a major role in the solvation of both electrolytes in the dioxane–water mixtures.

Canadian Journal of Chemistry, 47, 2671 (1969)

Introduction

We had previously determined the conductances of sodium and of lithium chlorates in water and water–dioxane mixtures (1), and it seemed to us appropriate to follow this with an investigation of the activities of the same salts in the same media. The technique chosen was that of vapor pressure and vapor composition. From these data, the partial pressures of the components of the mixed solvents and, by way of the Gibbs–Duhem theorem, the activities of the salts could be obtained.

Experimental

Materials

Salts

Fisher certified sodium chlorate (major impurity 0.01% bromate) was dried at 120° for 48 h or longer, before use. Lithium chlorate was prepared by the method of Campbell and Griffiths (2). The melting point was found to be 127.9°, in agreement with the value of Campbell and Williams (3).

Solvents

Water, of specific conductance 2–5 $\times$ 10^{-7} mhos/cm, was obtained by passing ordinary distilled water through a mixed-resin demineralizing column. Dioxane of spectro quality was further purified by refluxing with sodium, according to the method of Hess and Frahm (4). After purification, the dioxane had a refractive index of $n_D^{25} = 1.4202$ and a density of 1.0278 g/cc at 25°. This is in close agreement with the refractive index of 1.42025 found by Frey and Gilbert (5) and the density of 1.02804 found by Schott (6).

Apparatus

A 3 ft high cylinder was used as one of three thermostats, for work with the differential manometer. Vigorous stirring with a 1/4 hp motor gave a temperature control of $\pm 0.005°$, despite the height of the mass of liquid. The other two thermostats were of conventional type. Temperature was measured with Beckmann thermometers which were calibrated, and frequently re-calibrated, against a platinum resistance thermometer and Mueller bridge. Temperature fluctuations never exceeded $\pm 0.005°$.

Vapor Pressure Measurements

Following Gilson and Adams (7) and Shankman and Gordon (8), a differential manometer was used for the determination of total vapor pressure. A modification of Gilson and Adams' apparatus, introducing glass spirals between the manometer and the three-way cocks to the vacuum line, saved us many breakages. As manometer liquid, we used vacuum pump oil for water solutions, as recommended by Shankman and Gordon (8), but we found it necessary to change the oil after about 5 runs, because of contamination of the oil–glass interface with water. From the densities of oil and mercury and the accuracy of the cathetometer, it would seem that vapor pressures could be measured with an accuracy of ± 0.005 mm of mercury but, as pointed out by McAllan (9), difficulties such as slow drainage time and dissolved gases lead to higher errors than this. We estimate the error of our measurements to be ± 0.01 mm of mercury.

When investigating solutions in water–dioxane mixtures, we found that pump oil, diethyl phthalate, dibutyl phthalate, and other manometric liquids, all dissolve dioxane, and we were therefore forced to use mercury as manometer liquid. The limbs of the manometer were widened to 22 mm so that the capillary depression became negligible. Using mercury, the accuracy of measurement was reduced to ± 0.05 mm. All measurements were reduced to 0° in the usual way.

The solvent was degassed by freezing in dry ice–acetone mixture, pumping down to 1.0 μ, melting, and

---

[1]Present address: Department of Chemistry, Rensselaer Polytechnic Institute, Troy, New York.

repeating the whole process five times. The solvent was then vacuum distilled on to the salt which had previously been placed in one of the manometer flasks. After the determination of vapor pressure, the concentration of the solution was determined by evaporation of a weighed portion to dryness. Separate experiments showed that the composition of the mixed solvent did not change during the manometric experiment.

Vapor Composition

The compositions of the vapors in equilibrium with liquid mixtures of given composition were determined by the air saturation method, using what was essentially the apparatus of Bichowsky and Storch (10). Vapor compositions by this method were reproducible to within 0.1%. The condensed vapor was analyzed refractometrically.

Treatment of Results

As the mathematical treatment is involved, we confine ourselves, for the most part, to referring to published papers, in which this treatment is described.

The activity of the water in the aqueous solutions was calculated from the relation

$$a_1 = p_1/p_1^0$$

where p_1 is the vapor pressure of the water in solution and p_1^0 the vapor pressure of pure water. In what follows subscripts 2 and 3 refer throughout to dioxane and electrolyte, respectively. The activity of the solute was then calculated from the activity of the solvent by using the Gibbs–Duhem equation

$$S\mathrm{d}T - V\mathrm{d}P + \sum N_i \mathrm{d}\bar{G}_i = 0$$

which for constant temperature and pressure, simplifies to

$$\mathrm{d} \ln a_3 = -(N_1/N_3)\mathrm{d} \ln a_1$$

The details of the method are given by Randall and White (11). Because the data were not sufficiently accurate below 0.1 molal, we took the value of $\log \gamma$ at 1 molal as known and integrated to the observed concentration. For sodium chlorate in water at a concentration of 1 molal, we used the figure of Jones (12) for the activity coefficient, viz. 0.589. For lithium chlorate, at 1 molal concentration, we used the value $\gamma = 0.809$ from the freezing point data of Scatchard and Prentiss (13). Scatchard's figure refers necessarily to the freezing point of the solution and, in using the same figure at 25°, we make an assumption that may not be justified. Such an assumption may lead to an error as great as 3% but, when accurate data become available for the dilute region at 25°, our results can be corrected by multiplying by the appropriate factor.

The above simple treatment cannot be used when the solvent is a mixture of water and dioxane. It is now necessary to know both the vapor pressure and the vapor composition in order to calculate the activities of the two components of the solvent. Assuming the applicability of Dalton's law

$$p_i = N_i P$$

and knowing N_i, the mole fraction of the ith component in the vapor, the partial pressure is obtained and the activity of component i in solution results as

$$a_i = p_i/p_i^0$$

The addition of solute to a two-component solvent at constant N_1 can be represented by the equation

$$N_1 \mathrm{d} \ln a_1 + N_2 \mathrm{d} \ln a_2 = -m_3 M_{12} \mathrm{d} \ln a_3/1000$$

where $M_{12} = N_1 M_1 + N_2 M_2$, is the mean molecular weight of the binary solvent. If the solution is not ideal, the equation shows that a_1 and a_2 may alter by different factors. Indeed, where there is strong preferential solvation of the solute by component 1, it is possible for the decrease in a_1 to be so pronounced that a_2 actually increases.

We used the treatment of Grunwald and Baccarella (14). In this treatment, attention is focussed on $\mathrm{d} \ln a_1/a_2$ or, what amounts to the same thing, on the experimental quantity, $\mathrm{d} \ln \alpha_1/\alpha_2$, where $\alpha_1 = p_1/p_1^*$ and $\alpha_2 = p_2/p_2^*$: p_1 and p_2 are the partial pressures of water and of dioxane over the solution containing solute, and p_1^* and p_2^* are the partial pressures of water and of dioxane over the solvent of composition N_1, in the absence of solute.

It is unnecessary to repeat the treatment of Grunwald and Baccarella here. Suffice it that the following equation results for 1–1 electrolytes

$$[1] \quad (1000/M_{12})(N_1 \mathrm{d} \ln \alpha_1 + N_2 \mathrm{d} \ln \alpha_2) = -2\,\mathrm{d}m - 2m\mathrm{d} \ln \gamma_{\pm}$$

Here m is expressed in formula weights of electrolyte per kg of binary solvent. Following

Can. J. Chem. Downloaded from www.nrcresearchpress.com by 210.87.254.6 on 09/05/12
For personal use only.

Can. J. Chem. Downloaded from www.nrcresearchpress.com by 210.87.254.6 on 09/05/12
For personal use only.

Scatchard and Prentiss (13) $\ln \gamma_\pm$ can be expanded in a power series in $m^{1/2}$

$$[2] \quad \ln \gamma_\pm = -Sm^{1/2} + Bm + Cm^{3/2} + Dm^2 + Em^{5/2} + \cdots$$

In eq. [2], S is the Debye-Hückel limiting slope and $B, C, D, E, \cdots$ are adjustable constants. The latter are evaluated from the experimental data as follows. Substitution of [2] in [1] and integration leads to

$$[3] \quad (-1000/M_{12})(N_1 \ln \alpha_1 + N_2 \ln \alpha_2) = 2m - 2/3 Sm^{3/2} + Bm^2 + 6/5 Cm^{5/2} + 4/3\, Dm^3 + 10/7\, Em^{7/2} + \cdots$$

In eq. [3], the terms on the left and the first two terms on the right involve only experimental data and known solvent properties. The adjustable constants in the remainder are evaluated by standard least squares methods, using a computer. Once the constants are obtained, it is a simple matter to insert them in eq. [2] in order to calculate the activity coefficients. In no case were terms higher than Dm^2 found to be necessary.

Results and Discussion

(a) Results in Pure Water (Table I)

At comparable concentrations, the activity coefficients of lithium chlorate in water are considerably larger than those of sodium chlorate. This is consistent with the idea that the smaller lithium ion ($r = 0.68$ Å) is more extensively hydrated in aqueous solutions than the larger sodium ion ($r = 0.97$ Å). The extremely high value attained by the activity coefficient of the lithium salt, ($\gamma = 16.25$ at 43.7577 m) is probably due to the extensive hydration of the lithium ion.

We attempted to treat our results with the theoretical equation of Stokes and Robinson (15) viz.

$$[4] \quad \log \gamma_\pm = \frac{-A|Z_1 Z_2| I^{1/2}}{1 + BaI^{1/2}} - \frac{h}{\nu} \log a_A - \log [1 + 0.001 W_A(\nu - h)m]$$

This eq. contains two adjustable parameters, h, the hydration number, and a, the distance of closest approach. The first term is the well known Debye–Hückel equation. In a more recent paper (16) Stokes and Robinson have developed an equation for the evaluation of a. Assuming that only the cation is hydrated, the parameter a is

$$[5] \quad a = [(\bar{V}_+^{\,0} + 18h)/4.35 \times 10^{24}]^{1/3} + [\bar{V}_-^{\,0}/4.35 \times 10^{24}]^{1/3}$$

The partial molal volumes of the sodium and lithium ions which we introduced into the above eq. were obtained from the data of Mukerjee (17), and that of the chlorate ion from Couture and Laidler (18). These values are $\bar{V}_{Na^+}^{\,0} = -5.7$ cc/mole, $\bar{V}_{Li^+}^{\,0} = -5.2$ cc/mole, and $\bar{V}_{ClO_3^-} = +40.9$ cc/mole. The values of the hydration number h, the 'a' values calculated by the above method, and the calculated activity coefficients are presented in Table I.

Table I shows good agreement between the experimental activity coefficients of sodium chlorate and the theory over the entire concentration range, viz. 4.0–9.4 molal. The results of Jones (12) for the more dilute region when treated in the same way run smoothly into ours. This is to be expected, since sodium chlorate is only slightly hydrated ($h = 1.05$) and there are plenty of free water molecules even at saturation. On the other hand, the theory begins to break down above 2 molal, for lithium chlorate. This also is not surprising, since lithium chlorate is highly hydrated ($h = 6.7$) and there are only a limited number of water molecules available. In fact, Stokes and Robinson (15) have stated that in the majority of cases, the equation breaks down when the product of the hydration number, h, and the molality, m, exceeds 10 or 15. To proceed to higher concentrations it would be necessary to use a hydration number which was a suitably decreasing function of concentration.

We then fitted the experimental activity coefficients to an equation developed by Glueckauf (19).

$$[6] \quad \ln \gamma_\pm = \frac{-A|Z_1 Z_2| I^{\frac{1}{2}}}{1 + BaI^{\frac{1}{2}}} + 0.018mr(r + h - \nu) + \frac{h - \nu}{\nu} \ln (1 + 0.018mr) - \frac{h}{\nu} \ln (1 - 0.018mh)$$

This equation has two adjustable parameters, h and a. The number of adjustable parameters was

TABLE I

Vapor pressures, water activities, and activity coefficients of sodium chlorate and of lithium chlorate in water at 25°C

	Experimental concentration (moles/kg of solvent)	Vapor pressure (mm Hg)	Water activity a_w	Interpolated concentration (moles/kg of solvent)	Molal activity coefficient of salt, γ		
					Experimental	Calculated	
						Stokes–Robinson	Glueckauf
Sodium chlorate						$h=1.05$ $a=3.56$	$h=0.96$ $a=3.50$ $r=1.945$
	3.9724	20.915	0.8804	4.0	0.506	0.505	0.511
	4.9677	20.208	0.8507	5.0	0.501	0.496	0.503
	5.9874	19.513	0.8214	6.0	0.497	0.490	0.499
	7.3200	18.647	0.7849	7.0	0.493	0.485	0.495
	8.0386	18.197	0.7660	8.0	0.489	0.482	0.492
	9.4319	17.279	0.7274	9.0	0.490	0.480	0.491
				9.4319	0.491	0.479	0.490
Lithium chlorate						$h=6.7$ $a=5.09$	$h=3.97$ $a=4.59$ $r=1.976$
	0.9143	22.940	0.9657	1.0	0.809	0.806	0.808
	1.0701	22.778	0.9589	1.2	0.837	0.834	0.836
	1.2630	22.577	0.9504	1.4	0.868	0.866	0.868
	1.4251	22.409	0.9433	1.6	0.905	0.903	0.904
	1.6302	22.196	0.9344	1.8	0.946	0.943	0.942
	1.9650	21.843	0.9194	2.0	0.988	0.988	0.983
	2.2861	21.490	0.9046	2.5	1.088	1.118	1.102
	2.8850	20.814	0.8761	3.0	1.193	1.279	1.242
	3.4305	20.175	0.8492	3.5	1.306	1.478	1.408
	4.1480	19.307	0.8127	4.0	1.428	1.727	1.605
	5.0307	18.205	0.7664	5.0	1.711	2.440	2.119
	6.3738	16.479	0.6937	6.0	2.104	3.614	2.865
	8.5025	13.738	0.5783	7.0	2.472	5.660	3.992
	10.2740	11.680	0.4917	8.0	2.990	9.534	5.788
	11.9558	9.992	0.4206	9.0	3.562	17.39	8.851
	14.3953	8.072	0.3398	10.0	4.161	36.34	14.66
	15.7749	7.159	0.3014	12.0	5.501		
	17.6402	6.083	0.2561	14.0	6.838		
	20.3290	4.838	0.2037	16.0	8.234		
	25.1763	3.637	0.1531	18.0	9.657		
	30.2305	2.779	0.1170	20.0	11.05		
	36.5241	2.145	0.09029	22.0	12.20		
	43.7577	1.380	0.05809	24.0	13.03		
				26.0	13.40		
				28.0	13.68		
				30.0	13.94		
				33.0	14.25		
				36.0	14.41		
				39.0	14.95		
				42.0	15.75		
				43.7577	16.25		

reduced to one by substitution of eq. [5] for a. The values of the hydration number, h, the a values calculated by eq. [5] and the calculated activity coefficients are shown in Table I.

Glueckauf's eq. represents the data as well as that of Stokes and Robinson. In fact, it seems to be valid over the entire concentration range for sodium chlorate, and up to 2.5 molal for lithium chlorate. The hydration numbers found by this method are lower than those obtained by the Stokes and Robinson equation and this agrees with Glueckauf's own findings. Both equations give values for h and a (the distance of closest approach) of the right order of magnitude.

Although Glueckauf's derivation takes into account the size differences between the hydrated ions and the water molecules, both Glueckauf (19) and Stokes and Robinson (15) assume that

Can. J. Chem. Downloaded from www.nrcresearchpress.com by 210.87.254.6 on 09/05/12
For personal use only.

Can. J. Chem. Downloaded from www.nrcresearchpress.com by 210.87.254.6 on 09/05/12
For personal use only.

all the differences between the experimental and the calculated activity coefficients can be ascribed to hydration. It is true that the resulting equations are remarkably useful in describing observed results but this should not obscure the fact that, while hydration is a very important factor, it is not the only one which determines the complicated equilibria in an electrolyte solution. To put it briefly, the secondary hydration has been stretched to cover a number of effects, the quantitative nature of which requires a great deal of investigation.

We attempted to get some information about the behavior of the concentrated lithium chlorate solutions, on the basis of the concept of Stokes and Robinson (15) that the ions adsorb layers of water molecules in accordance with the Brunauer, Emmett, and Teller (B.E.T.) equation (20). Modifying the notation of those authors to suit the present case, their equation is

$$[7] \qquad \frac{ma_w}{55.51(1 - a_w)} = \frac{1}{bg} + \frac{(b - 1)}{bg} a_w$$

where a_w is the water activity of the solution; m is the molality, g is the number of molecules of water in the unimolecular hydration layer when it is complete, and b is a constant related to the heat of adsorption E of the molecules in the layer and is given by the approximate relation $b = \exp (E - E_L)/RT$, E_L being the heat of liquefaction of pure water. Equation [7] may be tested by plotting the left hand side (determined from experimental m and a_w) against a_w. When we did this, we obtained a straight line for lithium chlorate in water at 25° when the water activity of the solution is less than 0.420, i.e. above 12 molal. The best values of b and g were obtained from the slope and intercept of the line, by the method of least squares.

The accuracy of the fit is fairly good over the range 12–44 molal, (a mean deviation in a_w of 0.0032). The value of g, 3.11, is between 3 and 4 in accordance with the values found by Stokes and Robinson (15) for other 1–1 electrolytes. The value of b, 8.75, is also reasonable and corresponds to $E - E_L = 1.29$ kcal/mole of water adsorbed. An unsatisfactory feature of eq. [7] is that it demands a non-integral g value. This can scarcely correspond to any physical reality, and has probably arisen as a result of approximations in the Brunauer, Emmett, and Teller theory and its application to this case. The most drastic of these approximations is that of treating all water molecules beyond the first layer as being held by ordinary liquid forces, with a heat of liquefaction of E_L.

Anderson (21) has introduced a modification of the B.E.T. equation, in which the subsequent layers have a heat of adsorption less than that of water by d. This has the effect of multiplying a_w, wherever it occurs in eq. [7] by a factor $K = e^{-d/RT}$ and leads to the equation

$$[8] \qquad \frac{ma_w}{55.51(1 - Ka_w)} = \frac{1}{bKg} + \frac{(b - 1)}{bg} a_w$$

To test the appropriateness of this equation, the value of g is set at 4. Then eq. [8] is written in the form

$$[9] \qquad b = \left(\frac{1}{K} - a_w\right) \Big/ \left(\frac{gma_w}{55.51(1 - Ka_w)} - a_w\right)$$

and by trial and error, the value of K which leads to a reasonably constant b over the widest possible range of molality is found: this value of K is 0.785.

The average deviation of eq. [8] is the same as that of eq. [7] but the range fitted is slightly smaller (12–37 molal). The value of the parameter b, 6.9, is plausible and corresponds to $E - E_L = 1.14$ kcal/mole of water in the second and subsequent layers. This relatively small energy might easily correspond to a weak ordering effect on the water molecules concerned. The parameter b has a value of 4. This means that lithium chlorate has 4 sites available for occupation by water molecules in the inner layer, each being held with an energy some 1.14 kcal/mole greater than the latent heat of evaporation of water (10.48 kcal/mole at 25°).

The Stokes–Robinson approach used for lower concentrations and the B.E.T. approach used for higher concentrations are not mutually contradictory. As the concentration increases, the hydration number h diminishes and the ions tend to a quasi-crystalline structure with some of the water molecules imbedded in the remnants of crystal lattice (adsorbed water) and some present as "free" solvent. These are the two extremes of a more general theory, which should cover the entire concentration range.

(b) Results in Mixed Water–Dioxane Solvents (Table II)

The properties of solutions in the mixed

solvents will be largely determined by certain physical properties of the mixed solvents, notably the dielectric constant and the viscosity. These, at 25°, are as follows for the three solvents

Solvent	Dielectric constant	Viscosity (cP)
Water	78.3	0.890
44.5% dioxane – 55.5% water	40.6	1.784
64.5% dioxane – 35.5% water	23.4	1.923

Figure 1 gives the change of the water and dioxane activities with addition of sodium chlorate to a solvent consisting of 44.5% dioxane, 55.5% water. It is seen that the water activity decreases upon addition of salt whereas the activity of dioxane increases. These results can be explained on the assumption that sodium chlorate is strongly preferentially solvated by water. As salt is added to the solution, more water than dioxane is bound by the salt, in forming a solvation sheath. Thus the remaining solvent becomes richer in dioxane and the partial pressure and activity of dioxane in the system rises. Similar changes in the water and dioxane activities are observed when sodium chlorate is added to a solvent consisting of 64.5% dioxane – 35.5% water and a similar explanation applies.

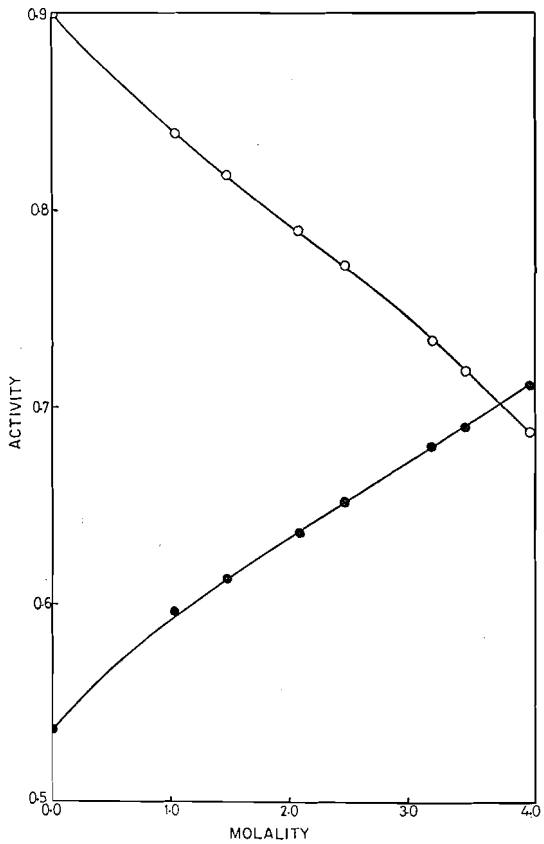

FIG. 1. Water and dioxane activity vs. molality for the system: sodium chlorate – 44.5% dioxane – 55.5% water, at 25°, as determined from vapor pressure and vapor composition; ○, water activity; ●, dioxane activity.

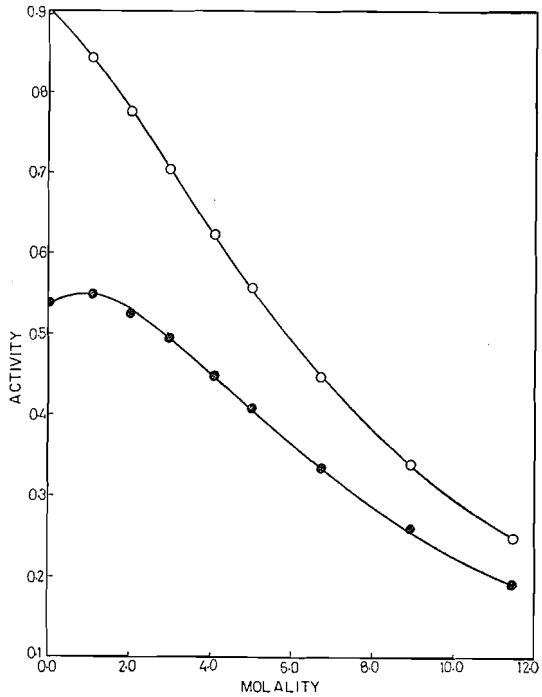

FIG. 2. Water and dioxane activity vs. molality for the system: lithium chlorate – 44.5% dioxane – 55.5% water, at 25°, as determined from vapor pressure and vapor composition; ○, water activity; ●, dioxane activity.

The changes in water and dioxane activity for lithium chlorate in 44.5% dioxane (Fig. 2) and in 64.5% dioxane are quite different from those of sodium chlorate. The water activity in the presence of lithium chlorate decreases to a greater extent than with sodium chlorate, while the dioxane activity at first shows a slight increase and then decreases. The larger decrease in water activity with lithium chlorate is to be expected because of the higher hydration of the lithium ion.

The activity coefficients of sodium and of lithium chlorate in these dioxane–water mixtures were calculated by the method of Grunwald and Bacarella (14) as modified by Scatchard and Prentiss (13) (see "Treatment of Results"). The

Can. J. Chem. Downloaded from www.nrcresearchpress.com by 210.87.254.6 on 09/05/12
For personal use only.

TABLE II

Vapor pressures and composition data*

Solution	Molality (moles/kg of solvent)	Total vapor pressure (mm Hg)	Mole % dioxane in vapor	Partial vapor pressure of dioxane (mm Hg)	α_1†	α_2‡
Sodium chlorate in 44.5% dioxane	0.0	40.57	47.23	19.16	1.0000	1.0000
	1.0332	41.22	51.66	21.29	0.9309	1.1112
	1.4716	41.32	53.00	21.90	0.9071	1.1430
	2.0795	41.47	54.76	22.71	0.8762	1.1853
	2.4637	41.62	55.90	23.27	0.8571	1.2145
	3.2081	41.72	58.23	24.29	0.8141	1.2677
	3.4873	41.72	59.09	24.65	0.7973	1.2865
	4.0314	41.72	60.89	25.40	0.7623	1.3257
Lithium chlorate in 44.5% dioxane	0.0	40.57	47.23	19.16	1.0000	1.0000
	1.0863	39.58	49.50	19.59	0.9337	1.0224
	2.0172	37.14	50.46	18.74	0.8594	0.9781
	3.0094	34.35	51.33	17.63	0.7809	0.9201
	4.1095	30.77	51.98	15.99	0.6903	0.8346
	5.0434	27.78	52.37	14.55	0.6179	0.7594
	6.7324	22.50	52.94	11.91	0.4946	0.6216
	8.9653	17.28	53.40	9.23	0.3760	0.4817
	11.5036	12.65	53.68	6.79	0.2737	0.3544
	14.0631	9.96	53.79	5.36	0.2149	0.2797
Sodium chlorate in 64.5% dioxane	0.0	45.50	56.88	25.88	1.0000	1.0000
	0.8301	46.20	60.75	28.07	0.9241	1.0346
	1.0200	46.23	61.35	28.36	0.9108	1.0958
	1.2800	46.26	62.23	28.79	0.8904	1.1124
	1.4665	46.25	62.83	29.06	0.8761	1.1229
	1.6866	46.30	63.59	29.44	0.8593	1.1376
	2.0000	46.27	64.64	29.91	0.8338	1.1557
	2.3311	46.25	65.82	30.44	0.8058	1.1762
Lithium chlorate in 64.5% dioxane	0.0	45.50	56.88	25.88	1.0000	1.0000
	1.0177	44.91	61.26	27.51	0.8869	1.0630
	1.9613	42.47	63.99	27.18	0.7793	1.0502
	3.0403	38.04	66.92	25.46	0.6412	0.9838
	3.8451	34.60	68.90	23.84	0.5484	0.9212
	5.0592	29.67	70.99	21.06	0.4391	0.8138
	6.2070	25.19	72.20	18.19	0.3568	0.7029
	7.6221	21.36	73.09	15.61	0.2931	0.6032

*Total vapor pressures, vapor compositions, and partial vapor pressures of solutions of sodium chlorate and of lithium chlorate in 44.5% dioxane and in 64.5% dioxane at 25°, together with activity coefficients according to Grunwald and Bacarella (14).

†α_1 is defined as (partial pressure of water over mixed solvent containing salt)/(partial pressure of water over the mixed solvent).

‡α_2 is defined as (partial pressure of dioxane over mixed solvent containing salt)/(partial pressure of dioxane over the mixed solvent).

values of the constants, of eq. [2] calculated by the method of least squares on a computer, are given in Table III. These constants represent the experimental quantity ($N_1 \ln \alpha_1 + N_2 \ln \alpha_2$) of eq. [3] for all systems in mixed solvent, over the entire concentration range, with a maximum deviation of 2%. This means that the activity coefficients are accurate to about the same extent.

Graphs of the activity coefficients of sodium and lithium chlorate in 44.5% dioxane and in 64.5% dioxane are shown as Figs. 3 and 4. The curve for lithium chlorate lies much above that of sodium chlorate, over the entire concentration range. This behavior is similar to that in aqueous solution and can again be explained as due to a higher degree of solvation of the lithium ion. When the activity coefficients of each salt in each solvent (including water) are plotted against salt concentration, it is seen that the activity coefficients of both sodium chlorate and lithium chlorate are greatly reduced on changing the solvent from water to 44.5% dioxane to 64.5% dioxane. Much of the decrease can be ascribed to the large change in dielectric constant, with consequent increased tendency to ion pair formation.

Many inconsistencies appear in the literature as to the nature of solvation in dioxane–water mixtures. Grunwald (22), in a study of a variety of electrolytes in 50% dioxane–water mixtures by

Can. J. Chem. Downloaded from www.nrcresearchpress.com by 210.87.254.6 on 09/05/12
For personal use only.

TABLE III

Constants of the equation of Scatchard and Prentiss (13)
$\ln \gamma_{\pm} = -Sm^{1/2} + Bm + Cm^{3/2} + Dm^2$

System	S	B	C	D
Sodium chlorate in 44.5% dioxane	3.1545	3.67692	−2.14785	0.46257
Deviations	—	—	0.10278	0.03041
Lithium chlorate in 44.5% dioxane	3.1545	2.69531	−0.72993	0.06812
Deviations	—	—	0.03460	0.00635
Sodium chlorate in 64.5% dioxane	7.2091	8.57917	−5.20461	1.22816
Deviations	—	—	0.24878	0.09166
Lithium chlorate in 64.5% dioxane	7.2091	7.71677	−3.07274	0.43970
Deviations	—	—	0.28952	0.06832

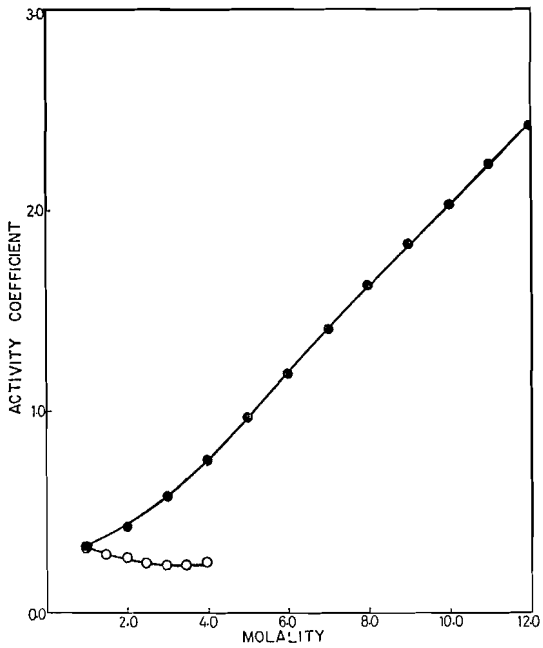

FIG. 3. Mean molal activity coefficients vs. molality for sodium chlorate and for lithium chlorate in the solvent 44.5% dioxane – 55.5% water, at 25°; ○, sodium chlorate; ●, lithium chlorate.

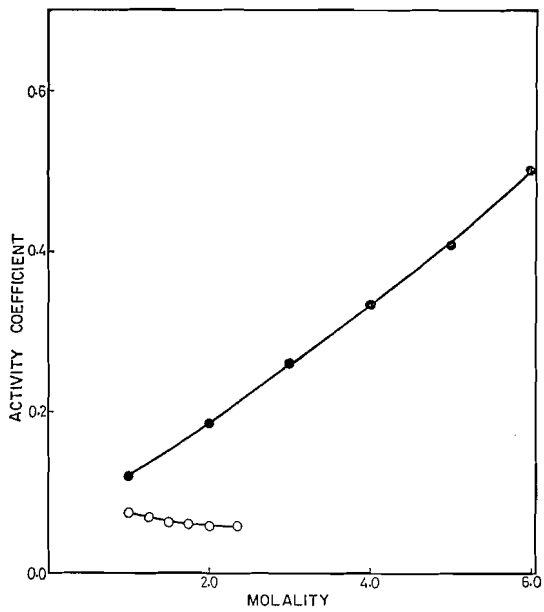

FIG. 4. Mean molal activity coefficients vs. molality for sodium chlorate and for lithium chlorate, in the solvent 64.5 dioxane – 35.5% water at 25°; ○, sodium chlorate; ●, lithium chlorate.

a vapor pressure technique, observed partial solvation of the electrolytes by dioxane. Fratiello and Douglass (23) used nuclear magnetic resonance (n.m.r.) to show that the chlorides of Li, Na, K, Mg, Ca, Zn, and Cd, along with the sodium salts of I, NO_3, ClO_4, and SO_4 are preferentially solvated by water in 50% dioxane – water mixtures: they found no evidence of solvation by dioxane. Other n.m.r. evidence by Hinton *et al.* (24) indicates solvation of aluminium perchlorate by dioxane. Analysis of conductance data by Hyne (25) also indicated interaction between dioxane and electrolyte in similar mixtures.

We attempted to determine the nature of the

Can. J. Chem. Downloaded from www.nrcresearchpress.com by 210.87.254.6 on 09/05/12
For personal use only.

solvation in the mixed solvents by the method of Grunwald (14, 22, 26). His final equation is

$$[10]\quad \frac{1000}{M_{12}}\ln\frac{\alpha_1}{\alpha_2} = \frac{2}{RT}\left(\frac{dG_\pm{}^0}{dN_1}\right)m - m^{3/2}\left(\frac{4}{3}\frac{dS}{dN_1} - \frac{2}{3}Sr\right) + m^2\left(\frac{dB}{dN_1} - Br\right) + m^3\left(\frac{2}{3}\frac{dD}{dN_1} - \frac{4}{3}Dr\right)$$

Here $G_\pm{}^0$ is the mean value of G^0 for cation and anion. The coefficient of the $m^{3/2}$ term was calculated from the Debye–Hückel limiting slope S, along with the slope of the curve of S plotted against N_1. The values of the other coefficients on the right in eq. [10] were obtained by fitting the data by the method of least squares on a computer. The constants that reproduced the experimental quantity $\ln \alpha_1/\alpha_2$ over the entire concentration range, with a maximum deviation of 2%, are presented in Table IV, together with other useful quantities. The values of $dG_\pm{}^0$ were calculated from the values of $2/RT \cdot dG_\pm{}^0/dN_1$ of Table IV. The values of the quantities $d \ln \varepsilon/dN_1$, $d \ln a_1/dN_1$ and $d \ln a_2/dN_1$ were calculated by plotting $\ln \varepsilon$, $\ln a_1$, and $\ln a_2$ against N_1. The required data for the dielectric constants (ε) of various dioxane–water mixtures were obtained from Critchfield *et al.* (27), while the data required for the activities of water and dioxane in water–dioxane mixtures were obtained from Bacarella *et al.* (28).

If it is assumed that the solute is present at extreme dilution and that it exists as an equilibrium mixture of molecular complexes of the type $S \cdot iH_2O \cdot j$dioxane, it is possible to obtain the average solvation numbers h^0 and d^0. The treatment is complex and it is unnecessary to go into it here but suffice it that the following equations are obtained

$$[11]\quad \frac{-Ne^2}{b_\pm \varepsilon}\left(\frac{d \ln \varepsilon}{dN_1}\right) = \frac{dG_\pm{}^0}{dN_1} + h^0RT\frac{d \ln a_1}{dN_1} + d^0RT\frac{d \ln a_2}{dN_1}$$

where $b\pm$ is a harmonic average, defined by the eq.

$$[12]\quad \frac{1}{b_\pm} = \frac{1}{2}\left(\sum_i \sum_{j \text{ cations}} \frac{\phi_{ij}{}^0}{b_{ij}} \cdot \sum_i \sum_{j \text{ anions}} \frac{\phi_{ij}{}^0}{b_{ij}}\right)$$

where $\phi_{ij}{}^0$ is the fraction of total formula weight which exists in the form $S \cdot iH_2O \cdot j$dioxane.

In order to apply eqs. [11] and [12] to our data, it is convenient to represent $b_\pm$ as a function of $r_\pm$, h^0, and d^0. It is assumed that the harmonic average of the b_{ij} values may be approximated by the radius calculated for a hypothetical "average solvate", defined as ion with unsolvated radius $r_\pm$ complexed with $h^0/2$ water molecules and $d^0/2$ dioxane molecules. Assuming spherical molecules and closest packing of spheres, the following eq. results

$$[13]\quad (b_\pm)^3 = 1.351\left[r_\pm{}^3 + \left(\frac{h^0}{2}\right)r_1{}^3 + \left(\frac{d^0}{2}\right)r_2{}^3\right]$$

where r_1 and r_2 were taken as 1.6 and 2.7 Å, respectively. (These radii are computed from the molar volumes of the pure liquids, assuming random packing of spheres, i.e. the actual volume occupied by the molecules is 58% of the total volume.) Using the values quoted in Table IV, eqs. [11] and [13] can be simplified to the form

$$[14]\quad \frac{dG_\pm{}^0}{dN_1} = \frac{-36.7}{b_\pm} - 0.437h^0 + 2.605d^0$$

$$[15]\quad b_\pm = 1.106(r_\pm{}^3 + 2.05h^0 + 9.84d^0)^{1/3}$$

for 44.5% dioxane, while for 64.5% dioxane the following simplified equation can be written

$$[16]\quad \frac{dG_\pm{}^0}{dN_1} = \frac{-59.0}{b_\pm} - 0.264h^0 + 0.613d^0$$

Equations [14], [15], and [16] can now be used to estimate solvation numbers. The first step is to show that d^0 is greater than zero. When $dG_\pm{}^0/dN_1$ for sodium chlorate in 44.5% dioxane is plotted against h^0, the calculated value of $dG_\pm{}^0/dN_1$ is always more negative than the experimental value. Similar behavior is observed with sodium chlorate in 64.5% dioxane and with lithium chlorate in the same solvents. Agreement between the experimental and calculated values is possible only if d^0 is greater than zero. This means that there are two unknown parameters, h^0 and d^0, but since there is only one experimental quantity, $dG_\pm{}^0/dN_1$, it is evidently not

Can. J. Chem. Downloaded from www.nrcresearchpress.com by 210.87.254.6 on 09/05/12
For personal use only.

TABLE IV

Constants for eq. [10] and derived quantities for eq. [11]

System	$\frac{2}{RT}\frac{dG^{\circ}_{\pm}}{dN_1}$	$\left(\frac{4}{3}\frac{dS}{dN_1} - \frac{2}{3}Sr\right)$	$\left(\frac{dB}{dN_1} - Br\right)$	$\left(\frac{2}{3}\frac{dD}{dN_1} - \frac{4}{3}Dr\right)$	$\frac{d \ln \varepsilon}{dN_1}$	$\frac{d \ln a_1}{dN_1}$	$\frac{d \ln a_2}{dN_1}$
$NaClO_3$ in 44.5% dioxane	−20.56456	24.59	−11.00845	0.66085	4.49	0.737	−4.396
$LiClO_3$ in 44.5% dioxane	−22.06514	24.59	− 7.74068	0.19668	4.49	0.737	−4.396
$NaClO_3$ in 64.5% dioxane	−28.03932	48.62	−28.33023	2.85783	4.16	0.445	−1.035
$LiClO_3$ in 64.5% dioxane	−35.78041	48.62	−19.70203	0.85889	4.16	0.445	−1.035

possible to obtain a unique solution. It is possible, however, by substituting all the values of h^0 and d^0 that are consistent with the experimental results, to find the smallest value of d^0 which gives the experimental value for $dG_{\pm}{}^0/dN_1$. Minimum dioxanation numbers, calculated in this way, along with the corresponding values of h^0, are given in Table V.

TABLE V

Minimum values of the average dioxanation number at 25°

Solution	d^0_{min}	h^0
$NaClO_3$ in 44.5% dioxane	2.14	0.0
$LiClO_3$ in 44.5% dioxane	2.08	0.0
$NaClO_3$ in 64.5% dioxane	7.25	0.0
$LiClO_3$ in 64.5% dioxane	5.53	0.0

Thus dioxane plays a major role in the solvation of electrolytes in dioxane–water mixtures. This at first sight may appear unlikely since pure dioxane has such a low dielectric constant (2.21 at 25°) and, therefore, a low dipole moment. Hyne (25), however, has shown that addition of electrolyte to dioxane–water mixtures greatly increases the microdielectric constant above the bulk value. Such an increase is in keeping with the displacement of the boat–chair equilibrium for dioxane in favor of the boat form, under the influence of the Coulombic field of the ionic species. Due to the opposition of the bond moments in the chair form, the preponderance of this form in pure dioxane results in a low dielectric constant, but the preponderance of the boat form, with its bond moments acting together, when electrolyte is added to the system, may explain the strong interaction between dioxane and electrolytes.

1. A. N. CAMPBELL, E. M. KARTZMARK, and B. G. OLIVER. Can. J. Chem. **44**, 925, (1966).
2. A. N. CAMPBELL and J. E. GRIFFITHS. Can. J. Chem. **34**, 1647 (1956).
3. A. N. CAMPBELL and D. F. WILLIAMS. Can. J. Chem. **42**, 1778 (1964).
4. K. HESS and H. FRAHM. Ber. **B 71**, 2627 (1938).
5. P. R. FREY, and E. C. GILBERT. J. Am. Chem. Soc. **59**, 1344 (1937).
6. H. SCHOTT. J. Chem. Eng. Data, **6**, 19 (1961).
7. R. E. GILSON and L. H. ADAMS. J. Am. Chem. Soc. **55**, 2679 (1933).
8. S. SHANKMAN and A. R. GORDON. J. Am. Chem. Soc. **61**, 2370 (1939).
9. J. V. MCALLAN. J. Sci. Instr. **42**, 290 (1965).
10. F. R. V. BICHOWSKY and H. V. STORCH. J. Am. Chem. Soc. **37**, 2696 (1915).
11. M. RANDALL and A. M. WHITE. J. Am. Chem. Soc. **48**, 2514 (1926).
12. J. H. JONES. J. Am. Chem. Soc. **65**, 1353 (1943).
13. G. SCATCHARD and S. S. PRENTISS. J. Am. Chem. Soc. **56**, 1486 (1934).
14. E. GRUNWALD and A. L. BACARELLA. J. Am. Chem. Soc. **80**, 3840 (1958).
15. R. H. STOKES and R. A. ROBINSON. J. Am. Chem. Soc. **70**, 1870 (1948).
16. R. H. STOKES and R. A. ROBINSON. Trans. Faraday Soc. **53**, 301 (1957).
17. P. MUKERJEE. J. Phys. Chem. **65**, 740 (1961).
18. A. M. COUTURE and K. J. LAIDLER. Can. J. Chem. **35**, 207 (1957).
19. E. GLUECKAUF. Trans. Faraday Soc. **51**, 1235 (1955).
20. S. BRUNAUER, P. H. EMMETT, and E. TELLER. J. Am. Chem. Soc. **60**, 309 (1938).
21. R. B. ANDERSON. J. Am. Chem. Soc. **68**, 686 (1946).
22. E. GRUNWALD. Electrolytes. The Pergamon Press, Ltd., New York. 1962. p. 62.
23. A. FRATIELLO and D. C. DOUGLASS. J. Chem. Phys. **39**, 2017 (1963).
24. J. F. HINTON, L. S. MCDOWELL, and E. S. AMIS. Chem. Commun. 776 (1966).
25. J. B. HYNE. J. Am. Chem. Soc. **85**, 304 (1963).
26. E. GRUNWALD, G. BAUGHMAN, and G. KOHNSTAM. J. Am. Chem. Soc. **82**, 5801 (1960).
27. F. E. CRITCHFIELD, J. A. GIBSON, and J. L. HALL. J. Am. Chem. Soc. **75**, 199 (1953).
28. A. L. BACARELLA, A. FINCH, and E. GRUNWALD. J. Phys. Chem. **60**, 573 (1956).

Can. J. Chem. Downloaded from www.nrcresearchpress.com by 210.87.254.6 on 09/05/12
For personal use only.

Diffusion coefficients of sodium and lithium chlorates in water, at 25°

A. N. CAMPBELL AND B. G. OLIVER[1]
Department of Chemistry, University of Manitoba, Winnipeg, Manitoba

Received January 14, 1969

The diffusion coefficients of sodium chlorate and lithium chlorate in water have been determined, using the Stokes' diaphragm technique. The diffusion coefficients of the solutions have been treated by the extended Hartley–Crank analysis to obtain hydration numbers for the electrolytes.

Canadian Journal of Chemistry, 47, 2681 (1969)

Can. J. Chem. Downloaded from www.nrcresearchpress.com by 210.87.254.105 on 09/05/12
For personal use only.

Since we had already studied the conductances of sodium and lithium chlorates in water (1) and the activity coefficients from vapor pressure measurements (2), we thought that a study of diffusion coefficients might add to our knowledge of the structure of these solutions. Janz and Mayer (3) have given a comprehensive treatment of the Stokes' diaphragm technique for diffusion, along with a complete literature survey of the work that has been done on diffusion in electrolyte solutions.

Experimental

The methods of preparation and purification have been given previously (2).

The diffusion coefficients were measured using a magnetically stirred diaphragm cell, as recommended by Stokes (4). One slight modification of the cell was introduced: instead of rubber stoppers, the necks of the cell were closed at the bottom with a capillary bore stopcock and at the top with a fine capillary plug. Both stoppers were lubricated with Dow Corning high vacuum silicone grease; no evaporation of solvent was observed.

The diaphragm cell was calibrated with potassium chloride solutions which were approximately 0.5 M in the lower compartment; pure water was used in the upper compartment. The diffusion coefficients of potassium chloride have been tabulated by Stokes (5). Diaphragm wear by the action of the stirrers and enlargement of the pores from the flow of the solutions causes the cell constant to change with time. Because of this, the cell was calibrated after every 5 runs and the cell constant interpolated for each experimental run. When these precautions are taken and the error of analysis estimated as not more than 0.1%, an accuracy of about $\pm 0.2\%$ in the final measurement can be expected, provided the concentrations of the solutions be kept above 0.05 M; below this concentration, surface transport in the cell leads to significant errors.

Since we had previously determined the conductance of sodium chlorate in water at 25° very accurately (1), we used this method to determine the concentrations of sodium chlorate solutions. It was necessary, however, to dilute some of the more concentrated solutions because the specific conductance passes through a broad maximum beyond 2.5 M. Analyses by this method were accurate to about $\pm 0.1\%$. A volumetric method of analysis, taken from Vogel (6) and Talbot (7) was used for the determination of lithium chlorate because, at the time, sufficiently accurate conductance data were not available.

Our method of determining conductance has been previously described (1). Viscosity was determined with a Cannon and Fenske type viscometer, for which the drainage and kinetic energy corrections are negligible.

Results

Treatment of Results

The theory for calculating the diffusion coefficient for concentration-dependent systems was outlined by Gordon (8) and extended by Stokes (9). It is therefore unnecessary to repeat the treatment here. Computer calculations were used extensively.

The experimental results are given in Tables I and II. The symbols D, $\bar{D}$, and $\bar{D}^0$ mean, respectively, the differential diffusion coefficient, the diaphragm cell integral diffusion coefficient, and the integral diffusion coefficient for a run of vanishingly small duration.

Discussion

The graphs of the differential diffusion coefficients of sodium and lithium chlorates in water vs. the square root of the concentration (in moles/l) are shown in Fig. 1. There is a marked difference between the shapes of the two curves. The differential diffusion coefficient of lithium chlorate is greater than that of sodium chlorate, above 1.23 M. A possible explanation of this is the greater thermodynamic non-ideality of lithium chlorate. Division of the observed D values by the corresponding activity factor, $\mathrm{d} \ln f_{\pm}/\mathrm{d} \ln m$, gives a quantity proportional to the actual mobility of the diffusing solute,

[1]Present address: Department of Chemistry, Rensselaer Polytechnic Institute, Troy, New York.

TABLE I

Diaphragm cell integral diffusion coefficients of sodium chlorate and lithium chlorate in water at 25°

Initial concentration (moles/l)		Final concentration (moles/l)		Diaphragm-cell integral diffusion coefficient
Bottom compartment c_1	Top compartment c_2	Bottom compartment c_3	Top compartment c_4	($\bar{D} \times 10^5$ cm^2 s^{-1})
		a. Sodium chlorate		
0.156	0.0	0.0943	0.0631	1.394
0.435	0.0	0.266	0.174	1.375
0.651	0.0	0.399	0.258	1.358
0.875	0.0	0.536	0.346	1.351
1.423	0.0	0.878	0.557	1.326
2.162	0.0	1.333	0.846	1.305
3.997	0.0	2.505	1.523	1.249
5.775	0.0	3.670	2.140	1.190
4.978	3.010	4.280	3.720	1.102
5.931	4.340	5.410	4.870	0.961
6.491	5.388	6.174	5.711	0.774
		b. Lithium chlorate		
0.114	0.0	0.0708	0.0440	1.225
0.244	0.0	0.154	0.0918	1.208
0.428	0.0	0.269	0.163	1.209
0.867	0.0	0.548	0.326	1.240
1.913	0.0	1.199	0.729	1.271
2.885	0.0	1.787	1.121	1.283
8.126	0.0	4.675	3.504	1.338
13.13	0.0	8.467	4.744	1.104
15.08	6.384	13.51	7.991	0.573
15.15	9.156	14.03	10.31	0.381

TABLE II

Integral diffusion coefficients for runs of vanishingly short duration and differential diffusion coefficients, of sodium chlorate and lithium chlorate in water at 25°

		Integral diffusion coefficient		
$c_{m'} = \frac{c_1 + c_3}{2}$	$c_{m''} = \frac{c_2 + c_4}{2}$	$\bar{D}^0_{(c_{m'})} \times 10^5$ cm^2 s^{-1}	$\bar{D}^0_{(c_{m''})} \times 10^5$ cm^2 s^{-1}	Differential diffusion coefficient $D \times 10^5$ cm^2 s^{-1}
		a. Sodium chlorate		
0.0	0.0	—	—	1.502*
0.125	0.0316	1.404	1.434	1.364
0.351	0.0870	1.385	1.414	1.358
0.525	0.129	1.370	1.406	1.341
0.705	0.173	1.363	1.400	1.325
1.151	0.278	1.341	1.389	1.296
1.747	0.423	1.322	1.378	1.270
3.251	0.762	1.274	1.358	1.167
4.723	1.070	1.225	1.344	1.036
4.629	3.365	1.225	1.272	1.041
5.671	4.605	1.177	1.227	0.865
6.333	5.549	1.135	1.186	0.690
		b. Lithium chlorate		
0.0	0.0	—	—	1.288*
0.0923	0.0220	1.233	1.259	1.212
0.199	0.0459	1.217	1.247	1.205
0.349	0.0815	1.215	1.235	1.218
0.707	0.163	1.235	1.222	1.251
1.556	0.365	1.258	1.216	1.302
2.336	0.561	1.268	1.221	1.341
6.400	1.755	1.317	1.262	1.239
10.80	2.372	1.142	1.278	0.578
14.30	7.187	0.936	1.295	0.143
14.59	9.732	0.921	1.190	0.120

*Nernst limiting value.

Can. J. Chem. Downloaded from www.nrcresearchpress.com by 210.87.254.105 on 09/05/12
For personal use only.

Can. J. Chem. Downloaded from www.nrcresearchpress.com by 210.87.254.105 on 09/05/12
For personal use only.

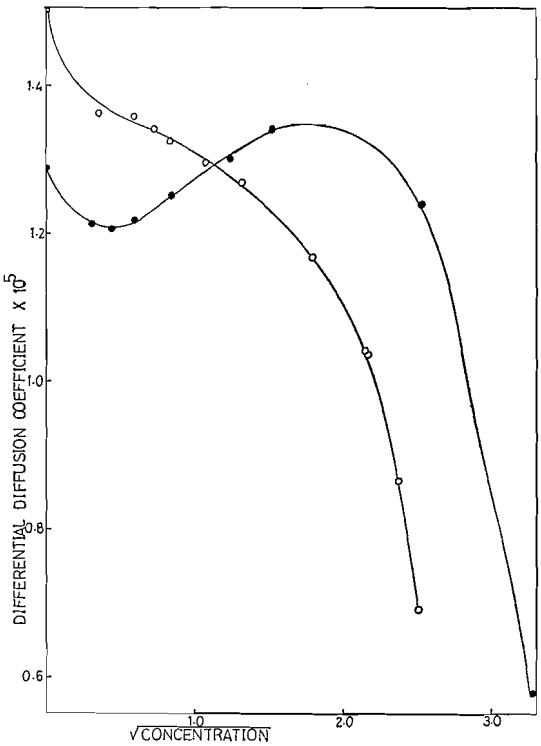

FIG. 1. Differential diffusion coefficients vs. square root of concentration (moles/l) for sodium chlorate (○) and for lithium chlorate (●), in water at 25°.

D_{corr}. The D_{corr} values for lithium chlorate are below the corresponding values for sodium chlorate, over the entire concentration range, indicating that much of the observed change is due to activity coefficient differences.

We attempted to fit the experimental diffusion coefficients to the theoretical equation of Hartley and Crank (10), as extended to electrolytes by Wishaw and Stokes (11). Their two equations are

$$[1] \quad \frac{\eta}{\eta_0} f(D) = 1 + 0.036m[(D^*_{H_2O}/\bar{D}^0) - h]$$

and

$$[2] \quad f(D) = 1 + 0.036[(D^*_{H_2O}/\bar{D}^0) - h']$$

where

$$[3] \quad f(D) = D_{obs}/[(\bar{D}^0 + \Delta_1 + \Delta_2) \times (1 + m \cdot \mathrm{d} \ln \gamma/\mathrm{d}m)]$$

All the quantities, except the hydration numbers, are calculable from experimental limiting mobilities and thermodynamic data; the terms Δ_1 and Δ_2 involve the assumption of some value for the ion size parameter, a, but since this appears only in small correction terms, the exact value chosen is not highly critical (12). The values of the quantities in eqs. [1] and [3] used to fit the experimental data are shown in Tables III and IV.

An examination of eq. [1] shows that the plot of $\eta/\eta_0 f(D)$ vs. m should be a straight line of slope $0.036(D^*_{H_2O}/\bar{D}^0 - h)$. Similarly, from eq. [3], the plot of $f(D)$ vs. m should be a straight line of slope $0.036(D^*_{H_2O}/\bar{D}^0 - h')$. When our figures are plotted, straight lines are obtained below a concentration of 2 molal (Figs. 2 and 3). The values of h and h' are obtained from the slope of these plots by the method of least squares, taking the value of $D^*_{H_2O}$ (the self-diffusion coefficient of water) to be 2.44×10^{-5} cm^2 s^{-1} (13). The hydration numbers calculated in this way, along with the corresponding calculated values of the differential diffusion coefficient are shown in Tables III and IV. It can be seen from

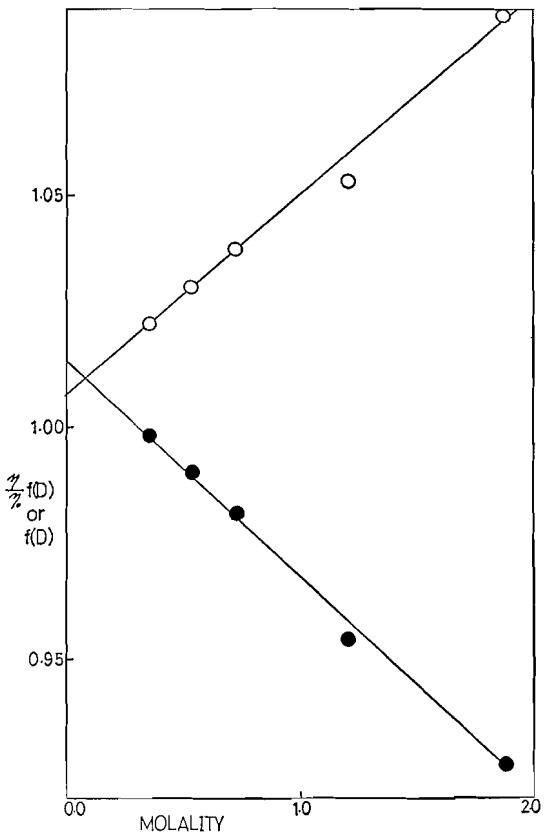

FIG. 2. Function $f(D)\eta/\eta_0$ (○) and the function $f(D)$ (●) vs. molality for sodium chlorate.

TABLE III

Application of eqs. [1] and [2]. Sodium chlorate and lithium chlorate in water at 25°

Concentration (moles/l)	$D_{obs} \times 10^5$	$\Delta_1 \times 10^5$	$\Delta_2 \times 10^5$	$1 + m\frac{d \ln \gamma}{dm}$	η/η_0	$f(D)$ (eq. [2])	$f(D)\eta/\eta_0$
			a. Sodium chlorate				
0.0	1.502	0.000	0.000	1.000	1.000	1.000	1.000
0.125	1.364	−0.003	+0.039	0.905	1.008	0.980	0.988
0.351	1.358	−0.005	+0.055	0.877	1.024	0.998	1.022
0.525	1.341	−0.005	+0.060	0.870	1.040	0.990	1.030
0.705	1.325	−0.005	+0.062	0.866	1.058	0.981	1.038
1.151	1.296	−0.006	+0.065	0.870	1.104	0.954	1.053
1.747	1.270	−0.007	+0.065	0.878	1.175	0.927	1.089
3.251	1.167	−0.007	+0.063	0.931	1.470	0.805	1.183
4.629	1.041	−0.008	+0.060	0.966	1.896	0.693	1.314
4.723	1.036	−0.008	+0.060	0.967	1.932	0.689	1.331
5.671	0.865	−0.008	+0.058	0.978	2.396	0.570	1.366
6.333	0.690	−0.008	+0.057	1.000	2.840	0.445	1.264
			b. Lithium chlorate				
0.0	1.288	0.000	0.000	1.000	1.000	1.000	1.000
0.0923	1.212	−0.010	+0.023	0.937	1.012	0.994	1.006
0.199	1.205	−0.013	+0.028	0.961	1.025	0.962	0.986
0.349	1.219	−0.015	+0.030	0.982	1.042	0.952	0.992
0.707	1.251	−0.018	+0.032	1.074	1.090	0.895	0.975
1.556	1.302	−0.021	+0.031	1.325	1.220	0.757	0.924
2.336	1.341	−0.022	+0.029	1.495	1.360	0.693	0.942
6.400	1.239	−0.025	+0.024	2.478	2.700	0.389	1.049
10.80	0.578	−0.026	+0.020	2.265	8.200	0.199	1.632
14.30	0.143	−0.026	+0.019	1.251	28.9	0.089	2.581
14.58	0.120	−0.026	+0.018	1.308	32.6	0.072	2.337

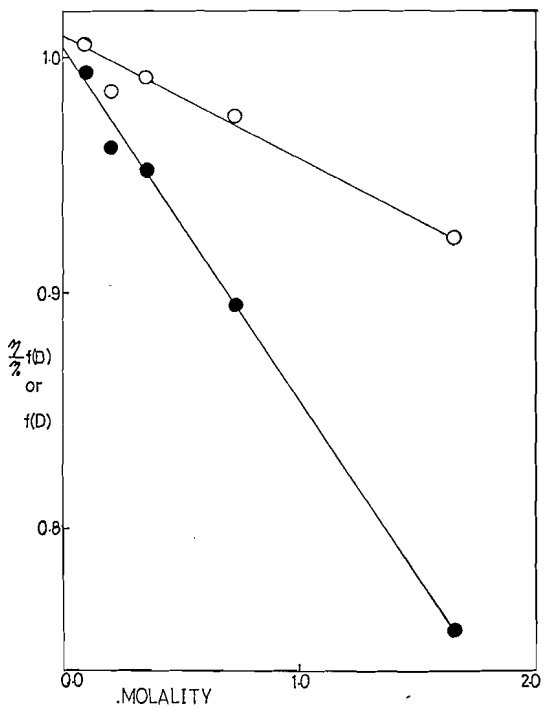

FIG. 3. Function $f(D)\eta/\eta_0$ (○) and the function $f(D)$ (●) vs. molality for lithium chlorate.

the tables that the equations represent the experimental data fairly well, with a maximum deviation of 2%, up to a concentration of 2 *M*.

The values of the hydration numbers obtained by this treatment are reasonable. Lithium chlorate appears more highly hydrated than sodium chlorate, but the viscosity corrected eq. [1] gives very different hydration numbers from those of the uncorrected eq. [2]. A comparison of these hydration numbers with those obtained from activity (2) indicates that the viscosity corrected equation gives values which are too low, while the uncorrected equation gives values which are too high. The determination of hydration by diffusion will be weighted in favor of the firmly bound water molecules, since the ion carries the hydrating water molecules with it through the diaphragm. Thus, diffusion will give a good approximation to the lower limit of the hydration number, i.e. it measures the primary hydration. The determination of hydration from activity, on the other hand (cf. our previous paper (2)) will include secondary hydration, since any interaction between solvent and ions will affect the activity coefficient. Therefore, the viscosity corrected

Can. J. Chem. Downloaded from www.nrcresearchpress.com by 210.87.254.105 on 09/05/12
For personal use only.

TABLE IV

Differential diffusion coefficients of sodium chlorate and lithium chlorate in water at 25°, calculated by eqs. [1] and [2]

Concentration (moles/l) c	Concentration (moles/kg solvent) m	D_{obs} ($cm^2\ s^{-1}$)	D, calculated by eq. [2]	D, calculated by eq. [1]
		a. Sodium chlorate		
			$h' = 2.8$	$h = 0.6$
0.0	0.0	1.502	1.502	1.502
0.125	0.126	1.365	1.384	1.387
0.351	0.356	1.358	1.340	1.347
0.525	0.537	1.341	1.324	1.328
0.705	0.727	1.325	1.308	1.310
1.151	1.207	1.296	1.288	1.285
1.747	1.877	1.270	1.260	1.246
3.251	3.750	1.167	1.219	1.123
4.629	5.699	1.041	1.138	0.957
4.723	5.843	1.036	1.130	0.945
5.671	7.400	0.865	1.041	0.806
6.333	8.594	0.690	0.985	0.718
		b. Lithium chlorate		
			$h' = 6.0$	$h = 3.2$
0.0	0.0	1.288	1.288	1.288
0.0923	0.0929	1.212	1.202	1.199
0.199	0.201	1.205	1.215	1.210
0.349	0.354	1.218	1.213	1.207
0.707	0.729	1.251	1.248	1.239
1.556	1.658	1.302	1.298	1.299
2.336	2.570	1.341	1.200	1.251
6.400	8.575	1.239	Negative	0.767
10.80	19.02	0.578	Negative	0.704
14.30	33.48	0.143	Negative	0.036
14.59	35.01	0.120	Negative	Negative

eq. [1] should give the minimum hydration number, while the Stokes–Robinson equation (cf. our previous paper (2)) should give the maximum hydration number.

Although the theories we have used in this and our preceding paper (2) are useful in predicting the behavior of the activity and the diffusion coefficients and in giving an approximation to the degree of hydration, the results show that the numerical values of the hydration number depend on the equation used to calculate them. This is not surprising because each theory ascribes different importance to solvation and, in some cases, many important factors, such as dielectric constant, viscosity, etc., have been completely omitted. Until a theory has been developed which can predict the effect of dielectric constant, viscosity, ion–ion interaction, ion–solvent interaction, etc., on activity and diffusion, the concept of solvation number will remain vague.

1. A. N. CAMPBELL, E. M. KARTZMARK, and B. G. OLIVER. Can. J. Chem. **44**, 925 (1966).
2. A. N. CAMPBELL and B. G. OLIVER. Can. J. Chem. This issue.
3. G. J. JANZ and G. E. MAYER. United States Department of the Interior Office of Saline Water. Research and Development Progress Report No. 196. 1966.
4. R. H. STOKES. J. Am. Chem. Soc. **72**, 763 (1950).
5. R. H. STOKES. J. Am. Chem. Soc. **73**, 3527 (1951).
6. A. I. VOGEL. A textbook of quantitative inorganic analysis. Longsmans, Green and Co., Ltd., London. 1961.
7. H. P. TALBOT. Quantitative chemical analysis. 11th ed. Macmillan. New York. 1958.
8. A. R. GORDON. Ann. N. Y. Acad. Sci. **46**, 285 (1945).
9. R. H. STOKES. J. Am. Chem. Soc. **72**, 2243 (1950).
10. G. S. HARTLEY and J. CRANK. Trans. Faraday Soc. **45**, 801 (1949).
11. B. F. WISHAW and R. H. STOKES. J. Am. Chem. Soc. **76**, 2065 (1954).
12. D. A. ROBINSON and R. H. STOKES. Electrolyte solutions. 1st ed. Butterworths, London. 1955. p. 317.
13. J. R. PARTINGTON, R. F. HUDSON, and K. W. BAGNALL. Nature, **169**, 583 (1952). J. H. WANG, C. V. ROBINSON, and I. S. EDELMANN. J. Am. Chem. Soc. **75**, 466 (1953).

Can. J. Chem. Downloaded from www.nrcresearchpress.com by 210.87.254.105 on 09/05/12
For personal use only.

Can. J. Chem. Downloaded from www.nrcresearchpress.com by 210.87.254.105 on 09/05/12
For personal use only.

The mechanism of formation of pre-passive films on nickel: a chronoellipsometric study[1]

A. K. N. REDDY[2] AND B. RAO[3]

Electrochemistry Laboratory, University of Pennsylvania, Philadelphia, Pa. 19104

Received February 11, 1969

The authors have previously shown that the anodic passivation of nickel in acid solutions is a two-stage process; the first stage of which involves the formation of a pre-passive film. In this study, the mechanism of formation of the precursor film on nickel in a 0.5 *M* K_2SO_4 (pH = 3.1) solution has been investigated by means of the technique of chronoellipsometry which consists of the ellipsometric *in situ* monitoring of the anode surface during a galvanostatic experiment. The main finding is that, before the pre-passive film forms, there must elapse an induction time which is affected by the current density and mass-transport factors. The nature of the dependence of the induction time upon current density indicates that the pre-passive film is formed by a dissolution–precipitation mechanism. It is proposed that the pre-passive film consists of precipitated $Ni(OH)_2$.

Canadian Journal of Chemistry, 47, 2687 (1969)

Introduction

A steady-state ellipsometric study (1–3) of the mechanism of the anodic passivation of nickel in acid solutions has demonstrated that the process occurs in two stages. The first stage consists of the formation of a precursor or pre-passive film which is transformed in the second stage into a material that is probably a semiconductor. It is the latter material that confers the property of passivity upon the electrode surface.

The object of this paper is to report on a chronoellipsometric study of the mechanism of formation of the pre-passive film. Chronoellipsometry (4–6) permits the continuous *in situ* optical monitoring of the surface of a mirror-like anode, and the registering of the time interval between the imposition of a constant anodic current and the formation of a surface film.

Experimental

(a) Ellipsometer and Cell

A schematic representation of the ellipsometer and cell is shown in Fig. 1. The ellipsometer was a commercial unit (O. Rudolph and Sons) modified to permit adjustment of the polarizer and analyzer azimuths with the quarter-wave plate being fixed with its axes at 45° to the plane of incidence. The cell (4.5 × 2.19 × 4.65 cm^3) was made by the Ultracell Co. of transparent Corning synthetic fused quartz (refractive index $n = 1.458$ at 5461 Å). The cell cover was fabricated out of Teflon, and permitted the introduction of a platinized-platinum counter-electrode, a saturated calomel electrode[4], and an inlet for the bubbling of pre-purified nitrogen.

(b) Electrolyte

In view of the detailed work of Sato and Okamoto (7, 8) on the anodic passivation of nickel, the present experiments were carried out under similar conditions, i.e., at room temperature (~20 °C) in solutions of 0.01 *N* H_2SO_4 plus 0.5 *M* K_2SO_4 (pH = 3.15). Prior to, but not during a chronoellipsometric experiment, pre-purified nitrogen was bubbled through the electrolyte. The polarographer's thumb-rule was followed, i.e., about 1 min of bubbling per ml of electrolyte.

(c) Electrodes

Nickel tape (0.0375 cm thick) of 99.5% purity, obtained from the American Silver Refining Co. was found to have sufficient mirror finish to be used as the reflecting electrode. After degreasing in hot absolute alcohol, the nickel tape was washed in conductivity water, and then for 2 min in a 50–50 mixture of nitric and sulfuric acids to dissolve away air-formed oxides. After another rinse in conductivity water, the nickel was maintained at a potential of −0.15 V (vs. normal hydrogen electrode (n.h.e.)) by means of a Wenking 61-R potentiostat. Under these conditions of potentiostatic control, the nickel could be expected to be thermodynamically immune to surface film formation (cf. the potential–pH diagram for nickel (9)). This expectation was not derived by the ellipsometrically determined optical constants of the nickel (potentiostated at −0.15 V) which were found to be fairly consistent with those given in the literature for a film-free nickel surface.

---

[1]This work was in partial fulfillment of the requirements of the Ph.D. degree awarded to B. Rao in 1966.

[2]Present address: Department of Inorganic and Physical Chemistry, Indian Institute of Science, Bangalore-12, India.

[3]Present address: Department of Chemistry, University of Toronto, Toronto 5, Canada.

[4]The standard calomel electrode (s.c.e.) used in the present study was a Beckman fibrejunction type with a negligible volume flow rate of electrolyte solution, (less than 0.1 ml per 24 h). The fact that passive films were formed (1–3) despite the use of s.c.e. was taken to mean that the efflux of Cl^- ions from the reference electrode, though finite, was too negligible to prevent passivation and obstruct its mechanism.

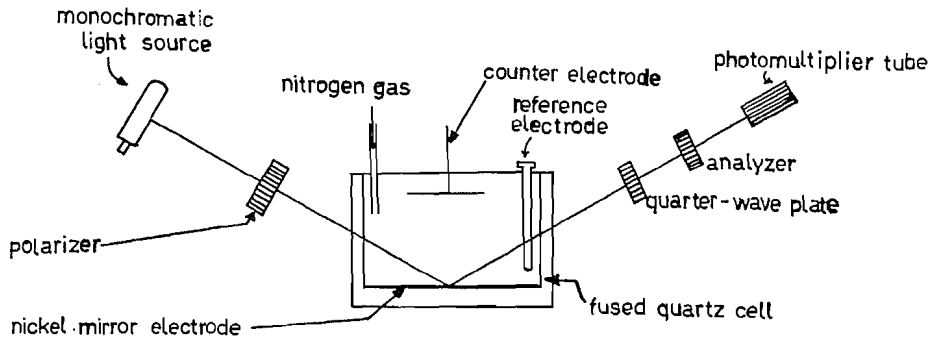

FIG. 1. Schematic representation of ellipsometer cell.

(d) Chronoellipsometric Procedure

While potentiostatically maintaining the nickel mirror electrode under film-free conditions, the azimuths of the polarizer and analyzer (P and A, respectively) were adjusted. The intensity, I_0, of light transmitted by the analyzer can easily be shown, for example by a Poincare sphere derivation (6), to be given by

$$[1] \quad I_0 = \sin^2 \psi_0 + A) - \sin 2\psi_0 \sin 2A \sin^2 \left(\frac{\Delta_0 + P - 90^\circ}{2}\right)$$

where Δ_0 and ψ_0 are the relative phase retardation and amplitude diminution introduced by the film-free metal. If $A = \psi_0$ and $P = 270^\circ - \Delta_0$, then the polarizer and analyzer are in their extinction positions, and $I_0 = 0$.

The initial intensity, I_0, corresponding to film-free conditions was fed via a photomultiplier tube and a preamplifier to one input of a Tektronix RM-35 oscilloscope with a Type CA plug-in. (The other input of the oscilloscope was used to monitor the potential of the nickel electrode relative to the s.c.e.)

The chronoellipsometric experiment consisted of using a fast switch incorporating a Western Electric 275B Relay to switch off the potentiostat used to maintain film-free conditions, and simultaneously (within $< 10\,\mu s$) to impose a constant current across the mirror electrode – solution interface. During such a galvanostatic transient, a simultaneous oscilloscopic record of the electrode potential and ellipsometer intensity were made as a function of time.

The basis of the chronoellipsometric technique is that the formation and growth of a surface film produces a change of the relative phase retardation and amplitude diminution from the "clean surface" values, Δ_0 and ψ_0 to new values, Δ and ψ. The latter change as the film thickens and/or undergoes transformations in composition. Since, during the experiment, the polarizer and analyzer are kept at the initial azimuths P and A respectively, the intensity transmitted by the analyzer during film growth is given by

$$[2] \quad I = \sin^2(\psi + A) - \sin 2\psi \sin 2A \sin^2 \left(\frac{\Delta + P - 90^\circ}{2}\right)$$

From eqs. [1] and [2], it is clear that since $\psi \neq \psi_0$ and $\Delta \neq \Delta_0$ correspond to a film-covered surface, and Δ_0 and ψ_0 to a film-free surface, $I \neq I_0$. In other words, film formation is manifested as a deviation of the intensity from the initial value, I_0. Thus, the onset of film formation can be detected in the transient of ellipsometer intensity vs. time.

An analysis of eqs. [1] and [2] shows that $(I - I_0)$, the change of intensity associated with film formation, depends upon the analyzer azimuth, and is least when $A = \psi_0$, i.e., when $I_0 = 0$. Hence, as stressed in earlier papers on the chronoellipsometric technique (4, 5), film formation can be detected with greater sensitivity and made to reveal itself more distinctly if the polarizer and analyzer are set at off-extinction azimuths when the mirror is in its initial film-free reference state. This means that the initial intensity, I_0, will not be zero. Since, however, the values of P and A are not used in chronoellipsometry to calculate the thickness and optical constants of the film, the actual value of I_0 only serves as an arbitrary "zero."

Results

A typical curve for the variation of ellipsometer intensity with time after imposition of the constant current is shown in Fig. 2. It is obvious from the figure that a time, τ_i, elapses before the ellipsometer intensity, I, changes from the initial value, I_0, corresponding to a film-free nickel anode surface.

The galvanostatic potential–time transient (which is included in Fig. 2) is similar to that obtained by Sato and Okamoto (7, 8). It shows that a plateau potential of +0.04 V vs. n.h.e. is attained by a charging process involving a time X. Thereafter, the potential remains steady until the completion of the induction time, τ_i, at Y. Further, the time taken for the electrode to attain the plateau potential is markedly less than the induction time required for the ellipsometer intensity to deviate from the initial value, I_0. Thus, Fig. 2 shows that the nickel electrode

Can. J. Chem. Downloaded from www.nrcresearchpress.com by 210.87.254.105 on 09/05/12
For personal use only.

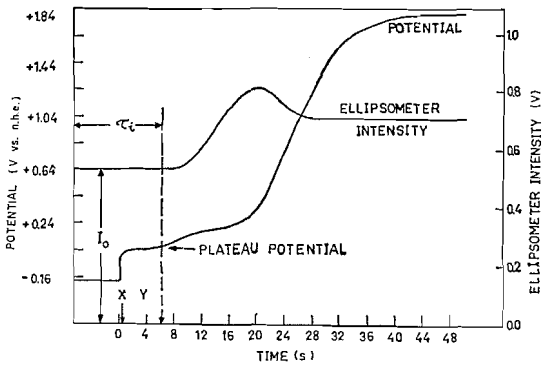

FIG. 2. Potential–time and ellipsometer intensity–time transients obtained with a galvanostatic current density of 1.5 mA cm^{-2}.

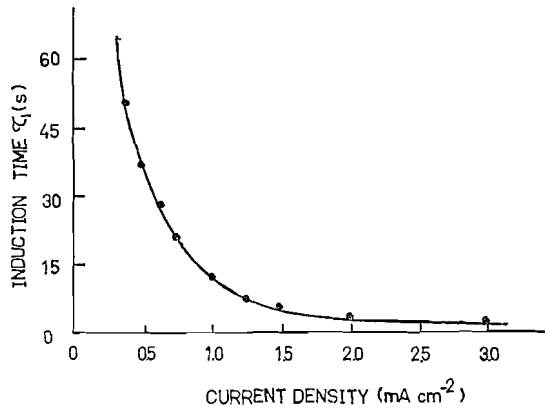

FIG. 3. Induction times observed at various current densities.

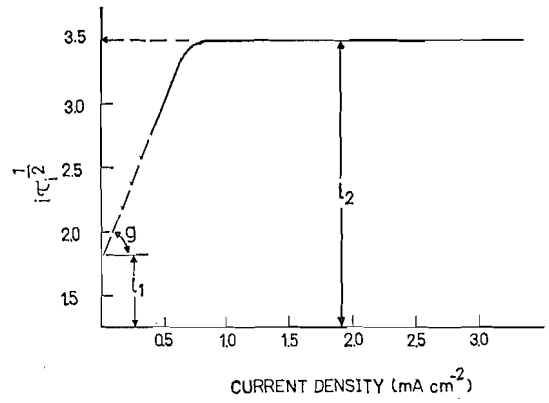

FIG. 4. The function $i\sqrt{\tau_i}$ plotted against current density (the induction times have been taken from the smooth curve of Fig. 3).

potential goes from −0.15 to +0.04 V within 1 s after switching-on the constant current, whereas an induction time of 8 s elapses before the intensity increases.

As observed in the study on calomel (5), the induction time was found to depend upon the magnitude of the constant current density used. A plot of the induction time, τ_i, vs. the galvanostatic current density, i, is given in Fig. 3. From a $i\sqrt{\tau_i}$ vs. i plot (Fig. 4), it is seen that $i\sqrt{\tau_i}$ is independent of i except in the range of low current densities where it increases linearly with i.

An important, though qualitative, result is the fact that the induction time was observed to increase when the electrolyte was stirred (by nitrogen bubbling) during the passage of the galvanostatic stimulus.

Discussion

A possible interpretation of the form of ellipsometer intensity vs. time curve is that the intensity rise (after the induction time) is due to changes in the anolyte refractive index resulting from nickel dissolution. This interpretation, however, is difficult to sustain in view of the fact that between $t = 0$ and $t = \tau_i$ there is a virtually constant intensity despite the occurrence of nickel dissolution. Hence, changes in the refractive index of the solution are obviously inadequate, at least in the case of nickel dissolution, to account for the intensity increase after the induction time. A similar argument can be used to discount the view that the roughening of the nickel surface due to anodic dissolution is responsible for the intensity increase after τ_i. Further confirmation that neither changes of electrolyte refractive index nor changes of surface topography produce the intensity change after τ_i comes from the steady-state work (1–3). There, it was observed that, in the range of potentiostatically-controlled potentials from −0.250 to −0.025 V, the Δ and ψ are constant despite anodic dissolution and its inevitable results, viz., changes of solution refractive index and topography[5].

[5]The above arguments are solely with reference to the present chronoellipsometric experiments on nickel in acid solutions. In the case of other media and/or metals, it may well turn out that solution and/or topographical changes may have to be invoked to interpret small changes in intensity preceding the significant intensity jump associated with the induction time.

Can. J. Chem. Downloaded from www.nrcresearchpress.com by 210.87.254.105 on 09/05/12
For personal use only.

Can. J. Chem. Downloaded from www.nrcresearchpress.com by 210.87.254.105 on 09/05/12
For personal use only.

In view of the discussion just presented, the intensity rise in the ellipsometer intensity–time curve can be interpreted as being due to film formation after an induction time τ_i. Thus, the basic experimental results that need explanation are: (*a*) the existence of an induction time for film formation; (*b*) the attainment of a steady potential in a time significantly less than the induction time (Fig. 2); (*c*) the type of dependence of induction time upon current density revealed in the $i\sqrt{\tau_i}$ vs. i plot (Fig. 4); (*d*) the sensitivity of the induction time to factors (e.g., stirring) that affect mass transfer in the electrolyte.

It has been shown in earlier papers (4–6) that such results are precisely what one would expect if film formation occurs by a dissolution–precipitation mechanism. The essence of such a mechanism is that the anodic dissolution of the metal results in the generation of a soluble species which accumulates in the vicinity of the anode. The accumulation proceeds until the soluble species attains a critical concentration at which stage an insoluble substance precipitates on to the electrode as a film. In unstirred solutions in which natural convection is minimized by appropriate electrode configuration, the accumulation of the species is determined by a diffusion-dependent process. Further, the critical concentration of the soluble species is, to a first approximation[6] decided by the solubility product of the precipitating film-forming substance.

The dependence of the induction time upon the current density has been worked out for the following reaction model

$$[3] \qquad R \xrightarrow{-ne} O$$

$$[4] \qquad O \underset{k^+}{\overset{k^-}{\rightleftharpoons}} Y$$

$$[5] \qquad O + X^- \rightarrow OX\downarrow$$

The general expression for $i\sqrt{\tau_i}$ derived in an earlier paper (4) yields two special cases. At low current densities, i.e., large τ_i

$$[6] \quad i\sqrt{\tau_i} = \frac{\sqrt{(D\pi)nF}}{2}(1 + K_1)C^* + \frac{K_1\sqrt{\pi}}{2\sqrt{Z}}i = l_1 + gi$$

and, at high current densities, i.e., small τ_i

$$[7] \quad i\sqrt{\tau_i} = \frac{\sqrt{(D\pi)nF}}{2}\left(\frac{1 + K_1}{1 - K_1}\right)C^* = l_2$$

where D, Z, n, and F have their usual connotation, $K_1 = k^-/k^+$, $C^* = K_{sp}/C_X^-$ (K_{sp} is the solubility product corresponding to reaction [5]), l_2 is the extrapolated intercept of the i-independent portion of the $i\sqrt{\tau_i}$ vs. i plot, and l_1 and g are the intercept and slope, respectively, of the $i\sqrt{\tau_i}$ vs. i straight line expected at low current densities.

The above precipitations regarding the form of the $i\sqrt{\tau_i}$ vs. i plot expected on the basis of a dissolution–prediction model for film formation are seen to be in excellent agreement with the results of chronoellipsometric experiments on the anodic behavior of nickel in acid solutions. It may be concluded, therefore, that the pre-passive or precursor film in the anodic passivation of nickel in acid solutions is formed by a dissolution–precipitation mechanism.

The next step in the discussion concerns the identity of the species involved in the dissolution–precipitation model (cf. eqs. [1], [2], and reaction [3]). The detailed steady-state, galvanostatic and potentiostatic work of Sato and Okamoto (7, 8) has shown that the initial product of the anodic dissolution of nickel is the species, $NiOH^+$. By analogy with the study of Bockris and co-workers (10) on the dissolution and deposition of iron, in which the species $FeOH^+$ was considered, one can postulate the following reaction sequence

$$[8] \qquad Ni + OH^-_{bulk} \rightarrow Ni + OH^-_{ads}$$

$$[9] \qquad Ni + OH^-_{ads} \rightarrow NiOH_{ads} + e$$

$$[10] \qquad NiOH_{ads} \rightarrow NiOH^+ + e$$

to yield the overall nickel dissolution reaction (cf. eq. [3])

$$[11] \qquad Ni + OH^- \rightarrow NiOH^+ + 2e$$

Thus, the soluble intermediate in the dissolution–precipitation mechanism is suggested to be $NiOH^+$.

The homogeneous chemical equilibrium (cf. reaction [4]) responsible for the two-section $i\sqrt{\tau_i}$ vs. i plot is most probably the breakdown of $NiOH^+$ into the simple aquo-ion and the

[6]In the first approximation version of the theory (4–6), no account has been taken of the kinetics of precipitation of the insoluble substance, in particular of the need for supersaturation.

corresponding reverse reaction

$$[12] \qquad NiOH^+ \underset{k^+}{\overset{k^-}{\rightleftharpoons}} Ni^{2+} + OH^-$$

As to the identity of the precipitate resulting from the accumulation of $NiOH^+$, there are two possibilities: NiO and $Ni(OH)_2$.

Thus, the induction-time analysis must be applied to the following model for the formation of the precursor film in the anodic passivation of nickel

$$[13] \qquad Ni + OH^- \xrightarrow{-2e} NiOH^+ \qquad k^- \Updownarrow k^+ \qquad Ni^{2+} + OH^-$$

followed by either

$$[14] \qquad NiOH^+ \xrightarrow{-H^+} NiO$$

or

$$[15] \qquad NiOH^+ + OH^- \rightarrow Ni(OH)_2$$

Reaction [14] is the one proposed by Sato and Okamoto (7, 8) on the basis of their electrochemical study. Reaction [15] is proposed here as an alternative for the precipitation reaction; it corresponds to the formation of $Ni(OH)_2$ by the two-step addition of OH^- ligands to nickel.

One approach to deciding between the two precipitation reactions [14] and [15] is by calculating the solubility products of NiO and $Ni(OH)_2$ from the induction-time data, and comparing these calculated values with the experimental values published in the literature. The calculation involves the computation of $K_1 = [Ni^{2+}][OH^-]/[NiOH^+]$ by the elimination of C^* from eqs. [6] and [7].

Using the value of Sato and Okamoto (7, 8) of $K_2 = [NiOH^+]/[NiO][H^+] = 10^{2.78}$, the calculated solubility product of NiO, i.e., $K_{sp} = K_1K_2 = [Ni^{2+}][OH^-]/[NiO][H^+]$, turns out to be $10^{2.46}$. To compare this value obtained from the present experiments with the work of previous authors, it is necessary to use a published value of K_1. Unfortunately, the comprehensive compilation (11) contains a spread of values for K_1; the lowest being $10^{-3.1}$ and the average being $10^{-4.9}$. Using the lowest and most favorable value, the solubility product of NiO is $10^{-0.32}$ in contrast to $10^{-2.12}$ based on the average value of K_1. Hence, the chronoellipsometric support for a NiO film is not strong.

In the case of $Ni(OH)_2$, the scatter in the published values for $K'_2 = [NiOH^+][OH^-]/[Ni(OH)_2]$ ranges from the highest value of $10^{-14.98}$ to one of $10^{-11.28}$ calculated from the paper of Pourbaix *et al.* (9). These yield chronoellipsometric values of the solubility product of $Ni(OH)_2$, i.e., $K'_{sp} = [Ni^{2+}][OH^-]^2/[Ni(OH)_2]$, of $10^{-15.1}$ (corresponding to $K'_2 = 10^{-14.98}$) to $10^{-11.60}$ (corresponding to $K'_2 = 10^{-11.28}$), in comparison with the figure of Pourbaix *et al.* (9) of $10^{-15.87}$ and the average value of Sillen (11) of $10^{-14.4}$. Thus, the chronoellipsometric support for a $Ni(OH)_2$ can only be termed fair.

It is seen, therefore, that on the basis of chronoellipsometry and the widely-varying literature values for K_2, K'_2, and K'_{sp}, it is difficult to decide in favor of either NiO or $Ni(OH)_2$ with any degree of certainty. If one chooses favorable values of K_2, K'_2, and K'_{sp}, then the scales appear to be tilted very slightly in favor of reaction [15], viz., the precipitation of $Ni(OH)_2$. In the case of NiO, even favorable values of K_1 do not help to match theory and experiment.

Though the chronoellipsometric evidence is not unambiguously in favor of $Ni(OH)_2$ constituting the precipitated pre-passive film, the formation of $Ni(OH)_2$ rather than NiO is suggested here in view of the following supplementary arguments:

(*a*) All the electrochemical data quoted by Sato and Okamoto (7, 8) as the basis for suggesting NiO can be used to argue equally strongly in favor of $Ni(OH)_2$. This assertion follows naturally from the very small difference (0.310 kcal $mole^{-1}$) in the free energy change associated with the reactions [14] and [15].

(*b*) $Ni(OH)_2$ is thermodynamically more stable than NiO, according to Pourbaix *et al.* (9) the free energy of formation of $Ni(OH)_2$ is -108.300 kcal $mole^{-1}$ in contrast to -107.990 kcal $mole^{-1}$ for NiO + H_2O (see, however, the contrary view of Milner and Thomas (12)). On this basis, $Ni(OH)_2$, which has a lower solubility product than NiO, would be expected to precipitate before NiO. Indeed, Pourbaix *et al.* do not include NiO in the potential–pH diagram for nickel.

(*c*) When the experimental values of the refractive index of the *pre-passive* film are determined by steady-state ellipsometry (1, 2) and then compared with theoretical values calculated for $Ni(OH)_2$, NiO, etc., the comparison favors a pre-passive film of $Ni(OH)_2$. However, these calculations need confirmation because

Can. J. Chem. Downloaded from www.nrcresearchpress.com by 210.87.254.105 on 09/05/12
For personal use only.

they are based on (*a*) the existence of crystalline substances and (*b*) the use of the Lorenz–Lorentz equation for the evaluation of index of refraction, which is not free of shortcomings.

(*d*) The potential–pH diagram for nickel indicates that anodic film formation is impossible at a pH of 3.1. Hence, the observed formation of a pre-passive film shows that the pH in the immediate vicinity of the anode is much higher than in the bulk. In view of this, one would expect the electrochemistry of the nickel oxide electrode in nickel–cadmium and Edison cells to have some bearing on that of anodic passivation. The considerable work (12–14) on the nickel oxide electrode has demonstrated that $Ni(OH)_2$ and not NiO is the starting material for the oxidation to NiOOH. The substance NiO, not only has a face centered cubic lattice dissimilar to the layer lattice of NiOOH, but is electrochemically inert except for the surface layers. $Ni(OH)_2$, on the other hand, has a layer lattice like NiOOH and can be converted into it more easily. The upshot of this comparison with the nickel oxide electrode is the suggestion that, even in the case of the anodic passivation of nickel, the pre-passive film is probably $Ni(OH)_2$.

In conclusion, the present chronoellipsometric experiments and the various auxiliary arguments lend some weight to the suggestion that the precipitation reaction is [15] and leads to the formation of $Ni(OH)_2$. There is no gainsaying the fact, however, that more convincing discriminatory work is required before one can assert that $Ni(OH)_2$, rather than NiO, is formed in the dissolution–precipitation mechanism for the formation of the precursor film in the anodic passivation of nickel in acid solutions.

Acknowledgments

The authors take this opportunity to thank Professor J. O'M. Bockris for the continued interest and encouragement which sustained this work. The final form of this paper was influenced by the thought-provoking critique of Miss Vlasta Brusic (of the Electrochemistry Laboratory, University of Pennsylvania) to whom we express our appreciation. Financial support from the Aeronautical systems command, U.S. Air Force, under contract No. AF 33(616)-8150, and from the National Aeronautical and Space Administration under contract No. NsG-325 is gratefully acknowledged. One of us (A.K.N.R.) thanks the Council of Scientific and Industrial Research, India, for the grant of a leave of absence.

1. B. Rao. Ph.D. Thesis, University of Pennsylvania, Philadelphia, Pennsylvania. 1966.
2. A. K. N. Reddy, M. G. B. Rao, and J. O'M. Bockris. J. Chem. Phys. **42**, 2246 (1965).
3. J. O'M. Bockris, A. K. N. Reddy, and B. Rao. J. Electrochem. Soc. **112**, 1133 (1966).
4. A. K. N. Reddy, M. A. V. Devanathan, and J. O'M. Bockris. J. Electroanal. Chem. **6**, 61 (1963).
5. J. O'M. Bockris, M. A. V. Devanathan, and A. K. N. Reddy. Proc. Royal Soc. London, Ser. A, **279**, 327 (1964).
6. A. K. N. Reddy and J. O'M. Bockris. U.S. Natl. Bur. Std. Misc. Publ. **256**, 229 (1964).
7. N. Sato and G. Okamoto. Trans. Japan Inst. Metals, **2**, 113 (1961).
8. N. Sato and G. Okamoto. J. Electrochem. Soc. **110**, 605 (1963).
9. M. Pourbaix, N. de Zonbov, and E. Deltombe. C. R. de la 71 reunion du C.I.T.C.E., London, 1955, Butterworths Scientific Publications, London. 1957. p. 193.
10. J. O'M. Bockris, D. Drazic, and A. R. Despic. Electrochim. Acta, **4**, 325 (1961).
11. L. G. Sillen. Section I. Inorganic ligands. *In* Stability constants. Special Publication 17. The Chem. Soc. London. 1964. p. 56.
12. P. C. Milner and U. B. Thomas. Advan. Electrochem. Electrochem. Engr. **5**, 27 (1967).
13. G. W. D. Briggs and W. F. K. Wynne-Jones. Trans. Faraday Soc. **52**, 1272 (1956).
14. G. W. D. Briggs and W. F. K. Wynne-Jones. Electrochim. Acta, **7**, 241 (1962).

Can. J. Chem. Downloaded from www.nrcresearchpress.com by 210.87.254.105 on 09/05/12
For personal use only.

Can. J. Chem. Downloaded from www.nrcresearchpress.com by 210.87.254.6 on 09/05/12
For personal use only.

The mechanism of passivation of nickel as determined by an automatic recording ellipsometer[1]

A. K. N. REDDY[2] AND B. RAO[3]

Electrochemistry Laboratory, University of Pennsylvania, Philadelphia, Pa. 19104

Received February 11, 1969

The process of anodic passivation of nickel in acid solutions has been investigated by means of an automatic recording ellipsometer in which the light emerging from a rotating analyzer has been electronically processed to yield a continuous read-out of the changes of polarization state of light reflected from a nickel anode during a galvanostatic transient. Digital computer analysis of the ellipsometric data has revealed: (*a*) the existence of an induction time for film formation; (*b*) a linear growth law for the film during a time interval commencing with the induction time and ending before the passivation time; (*c*) the occurrence of passivation when the absorption coefficient of the film jumps from a near-zero value to a fractional value; and (*d*) continuous changes of the refractive index of the film during the period of film growth. These phenomena are consistent with a model in which (*a*) a pre-passive film forms and thickens by a dissolution–precipitation mechanism, (*b*) the growth of the film is accompanied by its electrochemical oxidation, (*c*) the film growth – oxidation process continues until the pre-passive film is transformed into an electronically-conducting material, and (*d*) the conversion of the pre-passive film into an electronic conductor constitutes the essence of the so-called active–passive transition.

Canadian Journal of Chemistry, 47, 2693 (1969)

Introduction

The techniques (2) of steady-state ellipsometry and chronoellipsometry, developed in the Electrochemistry Laboratory of the University of Pennsylvania, have been used successfully (1–5) to throw light on the mechanism of anodic passivation of nickel in acid solutions.

Steady-state ellipsometry (1, 3, 4) has demonstrated that passivation is a two-stage process. The first stage involves the formation of a non-passivating precursor film, and the second stage involves the transformation of this pre-passive film into a substance, the absorption coefficient of which corresponds to that of an electronic-conductor.

Chronoellipsometry (5) has established that the pre-passive film which has been suggested to be $Ni(OH)_2$, forms by a dissolution–precipitation mechanism.

It must be stressed, however, that both steady-state ellipsometry and chronoellipsometry only reveal partial aspects of the passivation process. The former technique assumes that the steady-state films observed at various steady-state potentials represent the sequence of changes on the anode surface during a non-steady-state dynamic growth process. Chronoellipsometry, by not furnishing quantitative information on film thickness, refractive index, and absorption coefficient, focusses attention on what happens up to the instant of film formation and thus ignores the subsequent events which involve film growth and/or film transformation.

What is needed is a technique which permits *in situ* monitoring and reporting of the changing characteristics of the nickel surface during, for instance, an anodic galvanostatic transient. A technique which fulfills these requirements has been made possible by the development of an automatic recording ellipsometer (1, 6). The object of the present paper is to describe (*a*) the results of a study on the anodic passivation of nickel using an automatic recording ellipsometer and (*b*) the light thrown by these results on the process of formation and growth of pre-passive films and on the conversion of pre-passive to passive films.

Experimental Procedure[4]

The experiments were carried out in a transparent Corning synthetic fused quartz rectangular cell (4.50 × 2.19 × 4.65 cm^3) mounted on the specimen carrier of the

[1]This work was in partial fulfillment of the requirements of the Ph.D. degree awarded to B. Rao in 1966.

[2]Present address: Department of Inorganic and Physical Chemistry, Indian Institute of Science, Bangalore-12, India.

[3]Present address: Department of Chemistry, University of Toronto, Toronto 5, Canada.

[4]To achieve brevity of presentation, those features of the present experimental procedure which are common to steady-state ellipsometry and chronoellipsometry are omitted here. They may be referred to in previous papers (4, 5).

Can. J. Chem. Downloaded from www.nrcresearchpress.com by 210.87.254.6 on 09/05/12
For personal use only.

ellipsometer. The Teflon cell cover was designed to permit (*a*) bubbling of pre-purified nitrogen through the 0.5 *M* K_2SO_4 (pH = 3.1) electrolyte, and (*b*) the introduction of a platinized platinum counter-electrode and a saturated calomel electrode[4]. Commercial nickel tape of adequate reflectivity was held at the bottom of the cell so as to function as an anode and as a mirror.

After pre-treatment[4] of the nickel anode, it was potentiostatically maintained at a cathodic potential of −0.15 V (vs. normal hydrogen electrode (n.h.e.)). Under these film-free conditions, the polarizer and analyzer azimuths, *P* and *A*, respectively, of the conventional ellipsometer (with fixed quarter-wave plate) were adjusted for extinction. Using the relations, $\Delta_0 = 2P - 90°$ and $\psi_0 = A$, the relative phase retardation (Δ_0) and amplitude diminution (ψ_0) introduced by the clean metal surface were calculated.

The ellipsometer was then automated as follows (1, 6). Instead of the quarter-wave plate and analyzer (both of which were removed) a rotating analyzer was mounted as described elsewhere. The modulated light emerging from the rotating analyzer was sensed by a photomultiplier, and the output of this tube was electronically processed for a recorder read-out of the two parameters, azimuth (λ) and ellipticity (ω), characterizing the polarization state of the reflected light[5]. The response time of the instrument was 0.05 (see Appendix I).

After the completion of the steps required for the automation of the ellipsometer, the anodic passivation of the nickel was initiated by means of a constant current. The magnitude of the galvanostatic current was chosen small enough to permit the passivation to proceed far more slowly than the response time of the instrument. The passivation transient was "triggered" by a standard switching circuit which terminated the potentiostatic control of the nickel electrode potential and simultaneously imposed the galvanostatic current across the nickel–solution interface.

The basis of automatic recording ellipsometry is that if any changes on the mirror surface are produced by the constant anodic current, then these changes result in the azimuth (λ) and ellipticity (ω) of the reflected light deviating from the initial pre-transient values characteristic of a film-free nickel anode. Thus, the automated ellipsometer was used to record the changing values of $\lambda(t)$ and $\omega(t)$ during the passivation transient. With the aid of standard transformation formulae (1), these values were converted to give the time-variation of relative phase retardation (Δ) and amplitude diminution (ψ) during the course of the transient. The values of $\Delta(t)$ and $\psi(t)$ were then subjected to digital computer analysis (1, 4) for the elucidation of the thickness, $L_F(t)$, refractive index, $n(t)$, and absorption coefficient, $\kappa(t)$, for times greater than $t = 0$ which marks the switching-on of the constant current.

[5]The actual read-out of the automatic recording ellipsometer was in voltage units. To convert these voltage values into λ and ω in degrees, the instrument was calibrated with Si and Au mirrors as follows: Firstly, the λ–ω values of light reflected from these calibration substrates were determined by the ellipsometer in its conventional form; secondly the ellipsometer was automated; and finally, the calibration values of λ–ω were associated with voltage read-outs resulting from the monitoring of the Si and Au standards by the automatic recording ellipsometer. Within the λ_{Si}–λ_{Au} and ω_{Si}–ω_{Au} range, linearity was assumed.

Results

The galvanostatic anodic passivation of nickel was carried out at three current densities: 1, 0.8, and 0.1 mA cm^{-2}. A typical result showing the

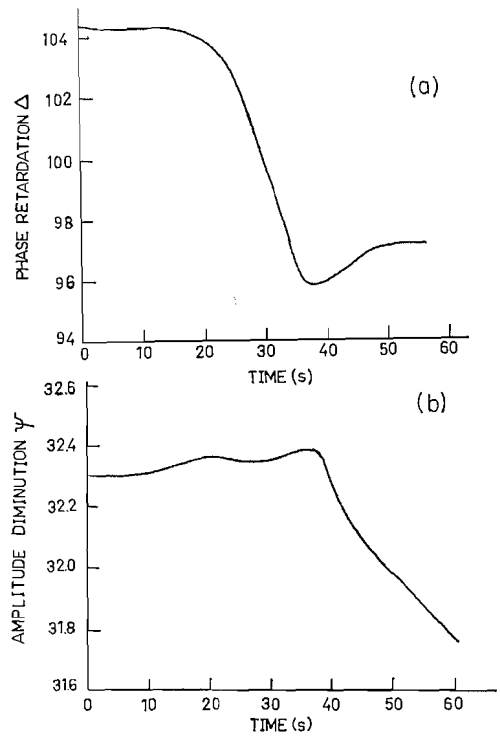

FIG. 1. Variation of *a* the relative phase retardation, Δ, and *b* relative amplitude diminution, ψ, during the anodic passivation of nickel at a galvanostatic current density of 1 mA cm^{-2}.

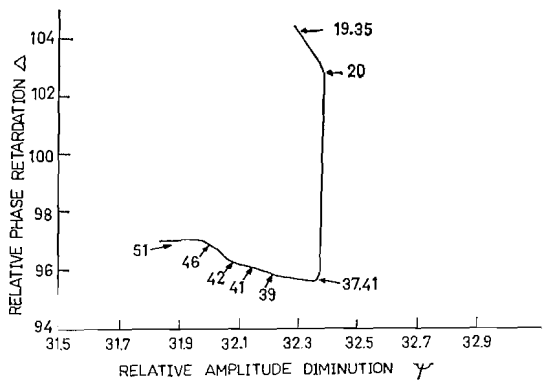

FIG. 2. Ellipsometric Δ–ψ plot corresponding to Fig. 1. The numbers next to the curve represent the time in seconds which has elapsed since $t = 0$, the commencement of the transient.

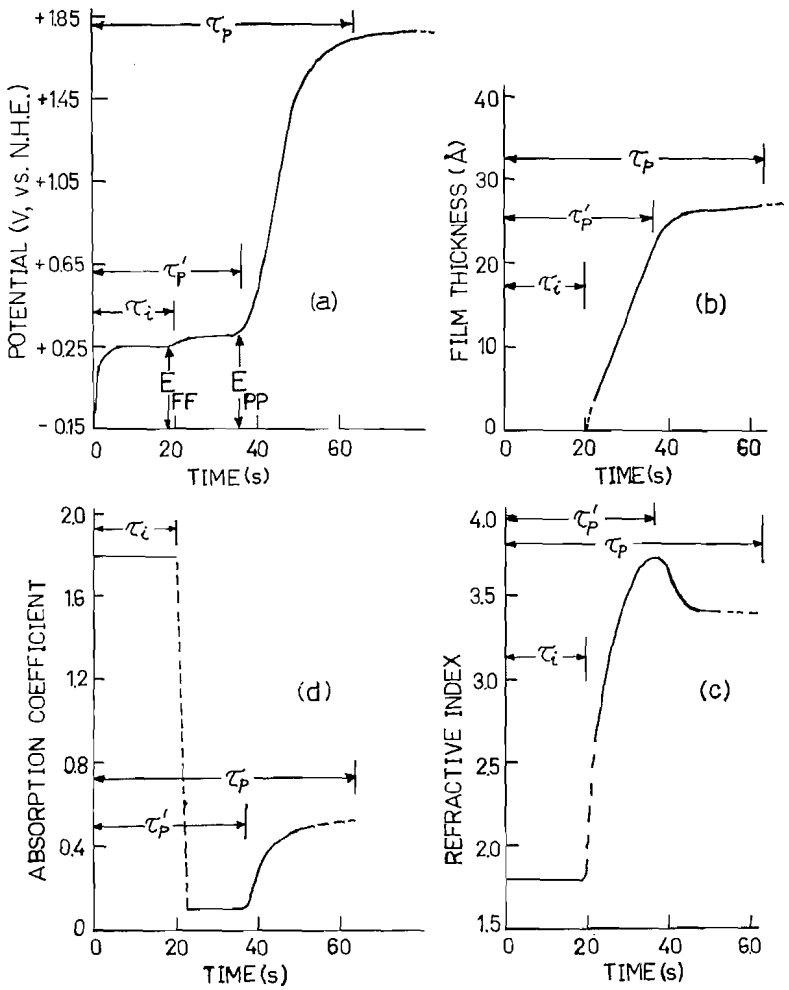

FIG. 3. The time-variation of *a*, nickel electrode potential; *b*, film thickness; *c*, refractive index; and *d*, absorption coefficient in the anodic passivation of nickel at a constant current density of 1 mA cm^{-2}.

variation of Δ and ψ as a function of time is given in Fig. 1. The resulting Δ–ψ plot (Fig. 2) was subject to computer analysis to reveal the time-variation of film thickness (L_F), refractive index (n), and absorption coefficient (κ) during the course of the passivation transient (Fig. 3*b*, *c*, and *d*). Shown for comparison (Fig. 3*a*) is the potential–time transient which was recorded simultaneously with the azimuth–time and ellipticity–time transients.

Several interesting features of the results will now be highlighted.

(*a*) Despite the imposition of a galvanostatic anodic current, the initially film-free nickel surface continues to remain uncovered with an anodic film (cf. Fig. 3*b*) for a time, t, in the range $0 < t < \tau_i$. The time interval after which an anodic film covers the electrode will be referred to as the induction time, τ_i.

(*b*) The lapse of the induction time in the ellipsometrically determined thickness–time plot is reflected in the electrochemically-determined potential–time transient by the occurrence of an inflection at E_{FF} (cf. Fig. 3, *a* and *b*). Thus, the inflection E_{FF} in the potential–time plot denotes film formation.

(*c*) As has been observed in the chronoellipsometric work of the authors, the induction time depends upon the current density used for the transient. The induction times of 16, 20, and 45 s corresponding to current densities of 1, 0.8, and 0.1 mA cm^{-2}, respectively, fit in reasonably

Can. J. Chem. Downloaded from www.nrcresearchpress.com by 210.87.254.6 on 09/05/12
For personal use only.

Can. J. Chem. Downloaded from www.nrcresearchpress.com by 210.87.254.6 on 09/05/12
For personal use only.

well with the τ_i vs. i curve determined by chronoellipsometry.

(*d*) After the lapse of the induction time, the film thickness increases linearly with time for a certain time interval τ'_P subsequent to which the film thickness tapers off to a value which remains virtually constant after the time τ_P.

(*e*) The lapse of time interval τ'_P registered in the thickness–time curve (Fig. 3*b*) is reflected in the potential–time curve (Fig. 3*a*) by the occurrence of an inflection E_{PP} after which the electrode potential climbs rapidly to the oxygen evolution potential.

(*f*) The absorption coefficient, κ, has a value characteristic of clean nickel until the lapse of the induction time, τ_i, after which it falls to a value of almost zero. It remains at that almost zero value until the time τ'_P, then climbs to a value of about 0.4. The time interval (see Fig. 3*c*) after which there is a virtual stabilization of the κ value at about 0.4 is equal to τ_P, i.e., the time interval after which there is cessation of film growth (Fig. 3*b*) and the jump to the oxygen evolution potential (Fig. 3*a*).

(*g*) The refractive index of the film changes continuously during the time interval defined by $\tau_i < t < \tau_P$ with the maximum at τ'_P.

Discussion

In contrast to chronoellipsometry (5) which has yielded inferential and indirect, though powerful, evidence for the existence of an induction time for film formation, the automated ellipsometry results quoted above have directly and unambiguously demonstrated that despite the passage of an anodic current there is no anodic film between $t = 0$ and $t = \tau_i$. Thus, the approximately 20 mC cm^{-2} passed between $t = 0$ and $t = \tau_i$ in the 1 mA cm^{-2} galvanostatic transient are utilized for an anodic process which does *not* involve build-up of material on the nickel surface. Hence, theories requiring or implying the formation of a film (whether crystalline or not) as an immediate and direct consequence of the passage of an anodic current, do not have a *prima facie* case for validity. To claim consideration, a theory must allocate the 20 mC cm^{-2} towards an anodic process in which the product is injected into the electrolyte and not on the surface. By insisting that the immediate product of anodic dissolution is a soluble ionic species, the dissolution–precipitation model, not only allows for the existence of an induction time, but considers its lapse to be a necessary precondition for film formation.

Elsewhere, the authors have stressed that the dissolution–precipitation model predicts certain characteristics of induction times. For example, τ_i should depend upon factors affecting mass transport of the soluble product of anodic dissolution. It should also depend upon the current density in the following way. Provided there is a homogeneous reaction involving the soluble intermediate, $i\sqrt{\tau_i}$ should increase linearly with i at low i's and be independent of i at high i's. These predictions which have been confirmed by the chronoellipsometric experiments (5) are in accord with the present experiments in so far as the values of τ_i determined by automated ellipsometry fit into the τ_i vs. i chronoellipsometric plot.

In addition, however, the present experiments have led to a finding which is of considerable importance to the mechanism of film formation and growth. Reference is made here to the linear increase of thickness with time. Such a linear growth law emerges simply in the following fashion from the dissolution–precipitation model.

From $t = 0$ to $t = \tau_i$, the current is used for the anodic generation of a soluble intermediate. This ionic species which has been argued to be $NiOH^+$ diffuses away from the interface. Thus its accumulation near the anode becomes a diffusion-controlled process. When the concentration of $NiOH^+$ reaches a value corresponding to the solubility product of an insoluble substance which has been suggested to be $Ni(OH)_2$, the precipitation of this material on the anode occurs. It is reasonable to assume that, after the induction time, the region next to the electrode is saturated with $NiOH^+$, so that any further dissolution current, i_d, leads to the generation of fresh $NiOH^+$. Barring a certain fraction, α, of this $NiOH^+$ which diffuses away into the solution, the remainder immediately precipitates on the anode surface by the reaction

$$NiOH^+ + OH^- \rightarrow Ni(OH)_2\downarrow$$

Thus, after the lapse of the induction time, $(\alpha i_d A t)$ coulombs of electricity produce[6] $\alpha i_d A t M/\rho n F = (\rho A L_F)$ grams of $Ni(OH)_2$. The growth

[6]Where ρ is the density and M the molecular weight of the film forming compound.

law for the precipitating film, therefore, turns out to be

$$[1] \qquad L_F = \left(\frac{\alpha i_d M}{\rho n F}\right) t = \text{constant} \times t$$

Hence, according to the dissolution–precipitation model, the film thickness should be zero between $t = 0$ and $t = \tau_i$, and then there should be a linear increase of film thickness with time. Both these predictions are in agreement with the observations. It should perhaps be emphasized here that a unified explanation of the existence of an induction time for film formation followed by a linear growth law does not seem possible on the basis of theories involving discharge followed by simultaneous film build-up.

The increase of film thickness is not the only process occurring between τ_i and τ_P. The ellipsometric results clearly demonstrate that during the period of linear film growth, the refractive index of the film is continuously changing (cf. Fig. 3 *b* and *c*). Thus a chemical transformation of the precipitated film is occurring along with further growth of the film. This variation of refractive index has been observed in steady state experiments too (1, 3, 4), and since it occurs with an increase of the potential in the anodic direction, it has been interpreted as arising from an electrochemical oxidation of the film, in which nickel is oxidized from a Ni^{2+} state in $Ni(OH)_2$, to a higher oxidation state. Whatever the actual identities of the species, it follows that a part of the galvanostatic current is utilized for the electrochemical oxidation of the film, the remainder being utilized for anodic dissolution.

Further work is required before a definitive answer is given to the question of how anodic oxidation of the precipitated film occurs along with metal dissolution and film growth. If, as seems to be the case, the film forms by a dissolution–precipitation mechanism, it is highly likely to be patchy and/or porous, in which case metal dissolution can occur in bare areas and/or through pores. A technique such as electron microscopy ought to throw light on this problem.

That the film formed by the dissolution–precipitation mechanism is not the passive film is clearly proved by the following experimental observations. (*a*) If the jump to the oxygen evolution potential in the potential–time curve is taken to be the electrochemical criterion of passivation, then it is clear that this jump does not occur along with film formation. (*b*) The film growth process which has been explained fairly convincingly on the basis of a dissolution–precipitation model implies that the metal is still corroding and that the surface has not yet been passivated. It must be concluded, therefore, that the surface film formed in the galvanostatic experiment after the induction time and undergoing growth with simultaneous oxidation between τ_i and τ_P, is only a *pre-passive* film which lacks the essential characteristic of the final passivating film. (It must be emphasized here that steady-state ellipsometry too has demonstrated (1, 3, 4) the formation of a pre-passive film as a preliminary step to passivation.)

The nature of the essential characteristic of the final passive film emerges from a consideration of the ellipsometrically revealed plot of absorption coefficient versus time. It is seen that the pre-passive film has an absorption coefficient of almost zero. However, when the absorption coefficient starts rising, the rate of film growth, i.e., dL_F/dt, starts decreasing and in addition the potential starts climbing towards the oxygen evolution potential; and when the absorption coefficient stabilizes at a value of about 0.4, the nickel surface becomes passive as shown not only by the film growth process coming to a virtual stop but by the electrode potential attaining the oxygen evolution value. If, therefore, it is meaningful and legitimate to single out of the complex process of anodic passivation a so-called act of passivation, then one may characterize the active–passive transition by the jump in the absorption coefficient of the film from a near-zero value. On this point too, the present experiments support the conclusions reached by steady-state ellipsometry (1, 3, 4). Thus, by using the latter technique it was shown that the corrosion current starts falling precisely at the potential at which the absorption coefficient starts rising, and that the metal becomes passive when the absorption coefficient stabilizes at a fractional value.

The jump in the film absorption coefficient has been singled out as the essence of passivation because, as stressed earlier, the absorption coefficient is a measure of the electrical conductivity of the film at optical frequencies, and it is invariably, though not always, true that increases in the optical conductivity are paralleled by increases in d.c. electronic conductivity. On this

Can. J. Chem. Downloaded from www.nrcresearchpress.com by 210.87.254.6 on 09/05/12
For personal use only.

Can. J. Chem. Downloaded from www.nrcresearchpress.com by 210.87.254.6 on 09/05/12
For personal use only.

basis, the following model of the active–passive transition is suggested. The pre-passive film is patchy and/or porous because it is formed by precipitation. Even if it were coherent, it is an electronic insulator and ionic conductor ($\kappa_F \approx 0$); hence, it permits ion transport through the film. In other words, corrosion can occur despite the existence of the pre-passive film. When the film becomes electronically conducting (cf. the jump in κ_F), ionic conduction through the film becomes inhibited, film growth by nickel dissolution through the film becomes negligible, and corrosion is drastically reduced, i.e., the surface has become passivated.

Though the automated ellipsometric experiments have demonstrated that passivation is associated with the jump in absorption coefficient, an understanding of why there is a jump in κ_F has not emerged with any degree of certainty. It is clear, however, that this understanding will be based on the electrochemical transformations underlying the changes in refractive index. Some idea of the dimensions of the problem can be gained by realizing that the precipitated and intermediate films are probably porous and hydrated, that the final film is probably a non-stoichiometric oxide semiconductor with electronic conductivity, and that the solid state electrochemistry concerns a very thin film (< 50 Å thick). The problem would have been more straightforward if the refractive indices of thin films of the various oxides, hydrated oxides and hydroxides of nickel were available in the literature. In the absence of such experimental data and pending definitive identification of the chemical compounds involved in the intermediate stages of passivation, the best that can be done is to fall back (*a*) on comparison of the observed refractive index values with those calculated by the Lorenz–Lorentz equation which is not without limitations, and (*b*) on an analogy with the nickel oxide electrode. This is the standpoint from which it is tentatively suggested that the real passivation process consists of the electrochemical oxidation of the pre-passive film, $Ni(OH)_2$, via NiOOH to a non-stoichiometric semiconductor $NiO_{1.7}$.

Acknowledgments

The development and application of the automated ellipsometer was very largely due to the tremendous encouragement from Professor J. O'M. Bockris whom we thank warmly. Financial support from the Aeronautical Systems Command, U.S. Air Force under Contract No. AF 33(616)-8150 and from the National Aeronautical and Space Administration under Contract No. NsG-325 is gratefully acknowledged. One of us (A.K.N.R.) thanks the Council of Scientific and Industrial Research, India, for the grant of leave of absence. We also thank Dr. Mel Benjamin and the staff of Bionic Instruments for their help with the electronics.

Appendix

A brief note on the automated ellipsometer

The fabrication of the automatic recording ellipsometer was based on a rotating analyzer (2) which consisted of a rigid polaroid sheet driven by a well-balanced synchronous motor (600 r.p.m.). The rotating analyzer was placed in the paths of the reflected beam and of the reference beam of linearly polarized light. The two chopped signals at a frequency of 20 c.p.s. were sensed by two separate photomultiplier tubes and the resultant outputs were fed to a phase detector after suitable amplification. The output of this phase detector, which corresponds to the azimuth of the reflected polarized light, was recorded on one channel of a fast strip-chart recorder. A portion of the output from the amplifier handling the chopped reflected beam was fed to electronic circuitry which provided the ratio of the maximum to the minimum of the signal. This ratio which corresponds to the ellipticity of the reflected light under study was recorded on the second channel of the recorder. With the present unit, an accuracy of 0.02° in both azimuth and ellipticity was attained. Further technical details about the design and operation of the automated units are described elsewhere (1).

1. B. Rao. Ph.D. Thesis, University of Pennsylvania, Philadelphia, Pennsylvania. 1966.
2. A. K. N. Ready and J. O'M. Bockris. U.S. Natl. Bur. Std. Misc. Publ. **256**, 229 (1964).
3. A. K. N. Reddy, M. G. B. Rao, and J. O'M. Bockris. J. Chem. Phys. **42**, 2246 (1965).
4. J. O'M. Bockris, A. K. N. Reddy, and B. Rao. J. Electrochem. Soc. **113**, 1133 (1966).
5. A. K. N. Reddy and B. Rao. To be published.
6. B. Rao and A. K. N. Reddy. To be published.

Can. J. Chem. Downloaded from www.nrcresearchpress.com by 210.87.254.5 on 09/05/12
For personal use only.

Complexes of palladium(II) with *cis*- and *trans*-1,2-bis(dimethylarsino)ethylene

G. J. ERSKINE[1]

Chemistry Department, Queen's University, Kingston, Ontario

Received March 10, 1969

Palladium(II) complexes of *cis*- and *trans*-1,2-bis(dimethylarsino)ethylene, **1** and **2**, respectively, in the metal: ligand ratios 1:1 and 1:2 are described. Their structures are discussed in terms of nuclear magnetic resonance, infrared, conductivity, and analytical data, and by comparison with the corresponding platinum(II) complexes (1). The *cis*-isomer, *cis*-ED, is a strong chelating ligand and forms the complexes Pd(*cis*-ED)X_2, **9** (X = Cl^-, Br^-), and Pd(*cis*-ED)$_2X_2 \cdot 3H_2O$, **8** (X = Cl^-, Br^-, ClO_4^-, PF_6^-). The *trans*-isomer, *trans*-ED is a bridging ligand and forms the dimeric complexes, [Pd(*trans*-ED)X_2]$_2$, **10** (X = Cl^-, Br^-), and Pd$_2$(*trans*-ED)$_4X_4 \cdot 3H_2O$, **7** (X = Cl^-, Br^-, ClO_4^-, PF_6^-). All these complexes contain 4-coordinate, square planar palladium(II). The anhydrous form of **7** (X = Cl^-) shows evidence for a Pd—Cl bond, suggesting 5-coordination in the solid state. Room temperature irradiation (with ultraviolet light) of **7** (X = Cl^-), in non-aqueous solvents, causes isomerization of the ligand and the formation of complex **8** (X = Cl^-). No change occurs under these conditions in aqueous solutions. Contrary to the original suggestion for the corresponding platinum(II) derivative, **10** (M = Pt(II), ref. 1) far infrared evidence supports a *cis*-configuration about the metal ion rather than the *trans*-configuration, **6**.

Canadian Journal of Chemistry, 47, 2699 (1969)

Introduction

In a recent publication (1), we reported on the complexes formed between *cis*- and *trans*-1,2-bis(dimethylarsino)ethylene (*cis*-ED, **1**, and *trans*-ED, **2**, respectively) and the salts of platinum(II).

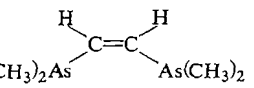

1

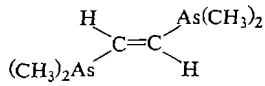

2

These ligands are of interest, first of all, with respect to their coordinating ability relative to similar systems such as *o*-phenylenebisdimethylarsine **3** (2), *cis*-1,2-bis(diphenylphosphino)ethylene **4** (3), 1,2-bis(dimethylarsino)tetrafluorocyclobutene (and its diphenylphosphino analogue) **5** (4).

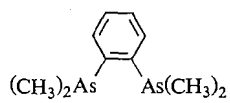

3

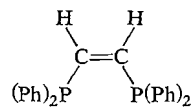

4

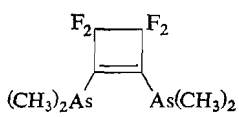

5

The ligand, *cis*-ED, has the advantage of low steric factors compared to the latter ligands and might be expected to show a special coordinating ability where steric considerations are important. *trans*-ED, on the other hand, can act only as a bridging ligand. Second, complexes of *cis*- and *trans*-ED would hold olefinic double bonds in rigid positions relative to the metal ion, and it is of interest to know how the reactivity of these double bonds is affected by this positioning.

In ref. 1 it was shown that the complexes of platinum(II) were of three types, **6**, **7**, and **8**. It

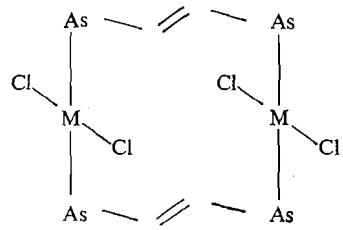

6

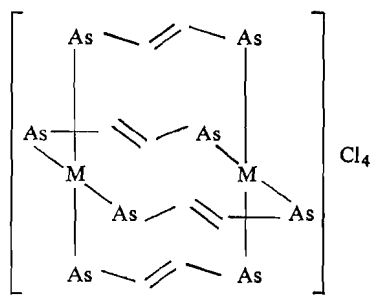

7

[1]Address after September 1, 1969: The Chemistry Department, Silliman University, Dumaguete City, Negros, The Philippines.

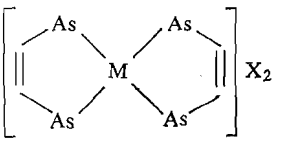

8

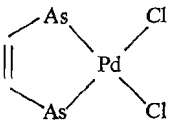

9

(X = Cl^-, ClO_4^-, PF_6^-)

was reported that, at room temperature, conversion of **7** to **8** could be effected in solution with ultraviolet irradiation. In order to make a comparative study of the olefin systems involved here, both from the point of view of this conversion reaction, as well as other reactions of olefins stereochemically fixed relative to metal ions, we have extended the range of complexes to other metals. We now report on the complexes of *cis*- and *trans*-ED with the salts of palladium(II).

Experimental

Cis- and trans-1,2-bis(dimethylarsino)ethylene

These were prepared as described in a previous paper (1). The product is a mixture of isomers (approximately 90% *trans*); attempts to effect a separation of isomers by fractional distillation and gas–liquid chromatography failed. The columns used were Carbowax and SE30 at temperatures of 127 and 167 °C.

Tetrachloro-di-μ-(trans-1,2-bis(dimethylarsino)ethylene)-dipalladium(II)

To the ligand (2.16 g, 1 mole) in ethanol (10 ml) was added concentrated hydrochloric acid (2 ml), and the solution warmed to 60 °C. Potassium tetrachloropalladate(II) (3.00 g, 1 mole) in water (15 ml), was added dropwise. A wine-red solution formed first, followed by the precipitation of a pale orange powder. The mixture was cooled to room temperature, and the orange precipitate was filtered and washed with ethanol and diethyl ether to give a quantitative yield of product. Melting point determination showed that it blackened at 260 °C, and decomposed above 300 °C.

Anal. Calcd. for $C_{12}H_{28}As_4Pd_2Cl_4$: C, 17.4; H, 3.4; Cl, 17.2; Pd, 25.8. Found: C, 17.1; H, 3.3; Cl, 17.6; Pd, 25.7.

Corresponding Tetrabromide Derivative

To a solution of potassium tetrabromopalladate(II) (1 mole) in water, containing excess bromide ion, was added an aqueous solution of Pd_2(*trans*-ED)$_4Cl_4$ (1 mole) (see below). The near quantitative precipitate of red-orange powder was filtered and washed with ethanol and ether.

Anal. Calcd. for $C_{12}H_{28}As_4Pd_2Br_4$: C, 14.4; H, 2.8. Found: C, 14.7; H, 3.3.

Tetra-μ-(trans-1,2-bis(dimethylarsino)ethylene)dipalladium(II) Tetrachloride Trihydrate

Using exactly the conditions described for the 1:1 compound, the ligand (2 moles) was treated with potassium tetrachloropalladate(II) (1 mole). An initial orange precipitate immediately re-dissolved and the product formed as a deep, wine-red solution. Because of oxidation and impurities in the ligand, a slight excess of ligand was used to dissolve the orange precipitate that formed again towards the end of the addition. The solution was cooled to room temperature and left over-night. Filtration and drying under a nitrogen atmosphere yielded red crystals (2.28 g, 73.5%), which melted with decomposition above 260 °C.

Anal. Calcd. for $C_{24}H_{56}As_8Pd_2Cl_4 \cdot 3H_2O$: C, 21.3; H, 4.6; Cl, 10.5; Pd, 15.7. Found: C, 21.0; H, 4.7; Cl, 10.1; Pd, 15.6.

Corresponding Tetrabromide Derivative

To a solution of the chloride complex (0.200 g, 10 ml H_2O) was added excess sodium bromide (3 ml of saturated aqueous solution). An orange powder precipitated from the deep red solution (0.142 g, 63%).

Anal. Calcd. for $C_{24}H_{56}As_8Pd_2Br_4 \cdot 3H_2O$: C, 18.8; H, 4.0. Found: C, 18.6; H, 4.3.

Tetra(hexafluorophosphate) Derivative

To an aqueous solution of the chloride complex was added an excess aqueous ethanol solution of potassium hexafluorophosphate. The yellow-orange powder was filtered and dried.

Anal. Calcd. for $C_{24}H_{56}As_8Pd_2P_4F_{24}$: C, 16.6; H, 3.2; Pd, 12.1. Found: C, 17.0; H, 3.5; Pd, 12.3.

Tetra(perchlorate) Derivative

To an aqueous solution of the chloride complex was added excess 30% perchloric acid. The yellow precipitate was filtered and dried.

Anal. Calcd. for $C_{24}H_{56}As_8Pd_2Cl_4O_{16}$: C, 18.5; H, 3.6. Found: C, 18.3; H, 3.8.

Dichloro(cis-1,2-bis(dimethylarsino)ethylene)palladium(II)

To the filtrate of the reaction yielding Pd_2(*trans*-ED)$_4 \cdot 3H_2O$ (see above), was added potassium tetrachloropalladate(II) (0.4 g), ethanol (30 ml) and concentrated hydrochloric acid (4 ml). The mixture was warmed and held at reflux for 1 h. After filtration of the insoluble dimer, [Pd(*trans*-ED)Cl_2]$_2$, the filtrate was evaporated to dryness on a steam bath and extracted with ethanol. Cooling gave pale yellow crystals (0.47 g, corresponding to approximately 10% *cis*-ED in the original ligand). Melting point determination indicated that it blackened above 260 °C, and left a dry black powder above 300 °C.

Anal. Calcd. for $C_6H_{14}AsPdCl_2$: C, 17.4; H, 3.4; Cl, 17.2; Pd, 25.8. Found: C, 16.9; H, 3.1; Cl, 17.2; Pd, 25.7.

Corresponding Bromide Derivative

To a solution of the chloride complex (0.100 g) in acetonitrile (20 ml) was added excess sodium bromide in acetonitrile solution. The color of the solution darkened immediately and removal of the solvent by a rotary evaporator yielded yellow crystals (0.05 g, 41%).

Anal. Calcd. for $C_6H_{14}AsPdBr_2$: C, 14.4; H, 2.8. Found: C, 14.8; H, 3.1.

Di-(cis-1,2-bis(dimethylarsino)ethylene)palladium(II) Dichloride Trihydrate

The insoluble orange dimer, [Pd(*trans*-ED)Cl_2]$_2$ (0.40 g), suspended in acetonitrile (10 ml) was treated with

Can. J. Chem. Downloaded from www.nrcresearchpress.com by 210.87.254.5 on 09/05/12
For personal use only.

TABLE I

Infrared spectral data (cm^{-1})

Compound	ν(C=C)	δ(=CH)	Far infrared		
trans-ED	—	960	315	—	—
cis-ED	1550	650	—	—	—
[Pd(*trans*-ED)Cl_2]$_2$	—	968	313	284	258
[Pd(*trans*-ED)Br_2]$_2$	—	976	310	—	—
[Pd_2(*trans*-ED)$_4Cl_4$]·$3H_2O$	—	1013	317	—	—
[Pd_2(*trans*-ED)$_4Cl_4$] (anhydrous)		970	311	285	
[Pd_2(*trans*-ED)$_4Br_4$] (anhydrous)		976	311	—	
Pd(*cis*-ED)Cl_2	1560	700	322	293	262
Pd(*cis*-ED)Br_2	1565	703	—	—	—
Pd(*cis*-ED)$_2Cl_2$·$3H_2O$	1575	725	—	296	—
Pd(*cis*-ED)$_2Br_2$·$3H_2O$	1567	713	—	295	—

excess *trans*-ED (containing ca. 10% *cis*-ED). First a red solution was formed, then yellow crystals were deposited and the solution became light yellow. The crude yield was 0.69 g, but included an unknown impurity containing acetonitrile. Washing with dichloromethane removed this impurity. The yield was 0.50 g (76%) and it decomposed above 230 °C.

Anal. Calcd. for $C_{12}H_{28}As_4PdCl_2·3H_2O$: C, 20.5; H, 4.8; Cl, 10.1; Pd, 15.1. Found: C, 21.0; H, 4.8; Cl, 10.3; Pd, 14.8.

Corresponding Bromide Derivative

To the chloride complex (0.100 g) in hot acetonitrile (20 ml) was added excess potassium bromide (in hot acetonitrile). The solution was filtered and the solvent removed at the pump to give yellow crystals. The crystals were filtered and washed several times with acetone to remove any excess potassium bromide (0.050 g, 44%).

Anal. Calcd. for $C_{12}H_{28}As_2PdBr_2$: C, 19.5; H, 3.8. Found: C, 19.4; H, 4.0.

Di(hexafluorophosphate) Derivative

This was prepared as for the corresponding derivative of Pd_2-(*trans*-ED)$_4Cl_4·3H_2O$ and was a pale yellow powder.

Anal. Calcd. for $C_{12}H_{28}As_4PdP_2F_{12}$: C, 16.6; H, 3.2. Found: C, 16.7; H, 3.1.

Diperchlorate Derivative

This was prepared as for the corresponding derivative of Pd_2-(*trans*-ED)$_4Cl_4·3H_2O$ and was a pale orange powder.

Anal. Calcd. for $C_{12}H_{28}As_4PdCl_2O_8$: C, 18.5; H, 3.6. Found: C, 18.4; H, 3.2.

Analyses for metal were carried out by the author. Other analyses were done by the Alfred Bernhardt Analytical Laboratory of West Germany. Precise determination of waters of hydration were not carried out. Where the infrared spectra indicated the presence of water, the number of water molecules was adjusted to give the best fit with the other analyses. It is felt that this is justified where four elements have been determined, but there must remain some uncertainty for the water-containing perchlorate and hexafluorophosphate derivatives. Infrared spectra were recorded on a Beckman IR-10 instrument as Nujol or hexachlorobutadiene mulls. KBr salt plates were employed throughout. Far infrared mull spectra were recorded on a Perkin–Elmer 621 instrument and on a Beckman IR-20 instrument using KRS-5 plates. Conductivity measurements were done using a Phillips Direct Reading conductivity bridge, model PR 9501. Nuclear magnetic resonance (n.m.r.) spectra were recorded on a Varian A60 instrument. Ultraviolet (u.v.) irradiation experiments employed a high pressure mercury lamp, model SOL-608-A-36 from Hanovia Lamp Division of Engelhard Hanovia Inc.

Results and Discussion

The complexes formed between *cis*- and *trans*-ED and palladium(II) salts are structurally similar to those of platinum(II) (1). Thus, the reaction between *trans*-ED and potassium tetrachloropalladate(II), in 1:1 molar ratio, yields an orange powder, insoluble in all common solvents. Its infrared spectrum (Table I) is identical to that of the corresponding platinum(II) complex, **6**, and shows that the ligand retains the *trans*-configuration about the double bond. There is a strong absorption at 968 cm^{-1} due to the out-of-plane (=CH) deformation mode, and no absorption at ca. 1550 cm^{-1}, attributable to the (C=C) stretching vibration. These features are characteristic of symmetrical *trans*-disubstituted ethylenes (5) and agree with the infrared spectrum of the free ligand, *trans*-ED. Far infrared spectra (to be discussed below), however, indicate that the Cl^- ions are *cis* to one another and it is suggested that complex **6** should be given the structure **10**. Molecular models show that structure **10** results in much less ring strain. Whereas in **6** the planes of the metal and ligand donor atoms are parallel, in the *cis*-structure, **10**, these planes spread away from each other at the edges occupied by Cl^- ions.

Mixing *trans*-ED and potassium tetrachloropalladate(II) in a 2:1 molar ratio yields deep orange-red crystals (**7**, M = Pd) whose infrared

Can. J. Chem. Downloaded from www.nrcresearchpress.com by 210.87.254.5 on 09/05/12
For personal use only.

TABLE II
Conductivity data* at 25 °C

Complex	M	Solvent	Λ_M†	Electrolyte type‡
$[Pd_2(trans\text{-}ED)_4]Cl_4 \cdot 3H_2O$	456	H_2O	236	4:1
$[Pd(cis\text{-}ED)_2]Cl_2 \cdot 3H_2O$	246	H_2O	214	2:1
$[Pd(cis\text{-}ED)_2Cl]Cl \cdot 3H_2O$	146	CH_3NO_2	70	1:1
$[Pd(cis\text{-}ED)_2][ClO_4]_2$	425	CH_3NO_2	166	2:1
$[Pd(cis\text{-}ED)_2][Pt_6]_2$	342	CH_3NO_2	152	2:1

*Based on the abbreviated Onsager equation $\Lambda_e = \Lambda_0 - M\sqrt{c}$ where Λ_e is equivalent conductivity, Λ_0 is equivalent conductivity at $c = 0$, and c is the equivalent concentration.
†Solution concentration: 10^{-3} M.
‡Standard slopes from Feltham and Hayter work; H_2O, 4:1 (526); 2:1 (185); CH_3NO_2, 2:1 (420); 1:1 (183).

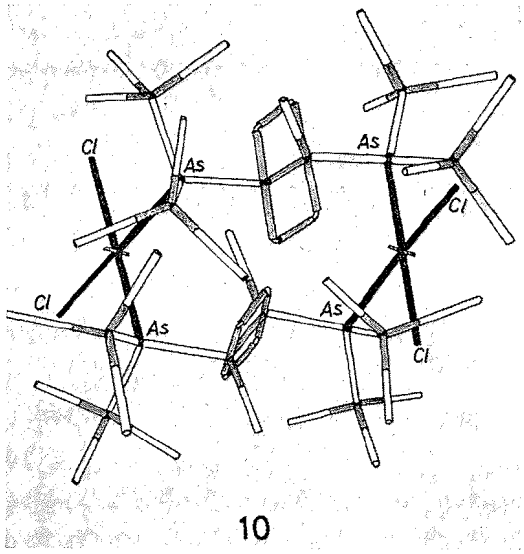

10

spectrum is identical to the platinum(II) complex (7, M = Pt). X-Ray powder photographs of both complexes indicate that they are isomorphous. These complexes are essentially monodentate tertiary arsine complexes of the type, $[M(L)_4]^{2+}$, and as such are extraordinarily stable. In an early paper by Nyholm (6), the addition of excess diphenylmethylarsine to the complex, $PdBr_2(AsMePh_2)_2$, yielded only the complex $[PdBr(AsMePh_2)_3]Br$, which dissociated readily into free arsine and starting material in organic solvents at room temperature. It is clear that stabilization by means of multidentate ligands is not restricted to simple chelation effects. Conductivity measurements (Table II), interpreted by the method of Feltham and Hayter (7), indicate that the palladium complex is a 4:1 electrolyte in aqueous solution. At concentrations above ca. 3×10^{-3} M, significant association occurs, as indicated by non-linear Λ_e vs. $\sqrt{c}$ graphs. Both tetra(perchlorate) and tetra(hexafluorophosphate) derivatives have been prepared, but their low solubilities in nitromethane and acetonitrile have made conductivity measurements impossible. A direct comparison of the conductivity of the palladium and platinum complexes could not be made because the former is very unstable in non-aqueous solutions. The platinum(II) complex, on the other hand, dissolves in water only with some concomitant decomposition, making conductivity measurements meaningless.

The presence of water molecules is very important in these "cage" complexes. Under vacuum, both the palladium and platinum complexes change color, the palladium complex changing from orange to deep scarlet. Upon exposure to the atmosphere, the original color returns, and it has been clearly established that it is water that is being removed and replaced each time. Exposure of the dehydrated complex to an atmosphere of D_2O also produces this reversible color change and the infrared spectrum of the hydrate shows the presence of D_2O. If the hydrate is now re-exposed to the atmosphere (even in the Nujol mull) for only a few seconds, the absorptions due to D_2O disappear and the infrared spectrum is that of the original complex. In the case of the platinum(II) analogue, the water molecules are more firmly held and removal of only a portion of the water is possible. This leads to a change in color of the complex, but the infrared spectrum is unchanged. With the palladium complex almost all the water can be removed and there is a significant change in the infrared spectrum, the (=CH) deformation mode shifting to 970 cm^{-1} (from 1013 cm^{-1}) and the spectrum generally approaching that of the dimer **10**, (M = Pd).

The stability of complex **7**, (M = Pd) depends

Can. J. Chem. Downloaded from www.nrcresearchpress.com by 210.87.254.5 on 09/05/12
For personal use only.

on its water content. In aqueous solution, or under moist air, the complex appears to be stable indefinitely, but under prolonged vacuum, or under conditions of low humidity at atmospheric pressure, the complex gradually loses two molecules of *trans*-ED and the color fades to light orange. The residue is the complex **6**, (M = Pd).

[1]

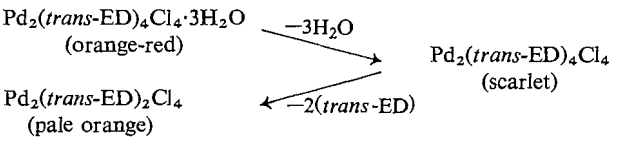

Presumably, oxidation of the escaping *trans*-ED drives the reaction to completion.

Thermogravimetric measurements at atmospheric pressure confirm these observations, showing a smooth elimination of a weight corresponding to two molecules of *trans*-ED at 120–130 °C, followed by a gradual elimination of a further two molecules of *trans*-ED up to 300 °C. The water molecules present are eliminated gradually and do not show a noticeable elimination region. The corresponding platinum(II) derivative shows a similar behavior in the 120–130 °C region, but a more complex behavior at higher temperatures. The significance of the water molecules is discussed below.

Complexes of cis-ED

The ligand, *trans*-ED, as prepared, always contains ca. 10% of the *cis*-isomer, and by-products of the reactions forming the complexes of *trans*-ED are the complexes of *cis*-ED. Because of its favorable stereochemistry, *cis*-ED behaves as a strong bidentate ligand that readily displaces *trans*-ED from its complexes. Thus, by treating either *trans*-ED complex **10** or **7** with excess ligand in acetonitrile solution, pale yellow crystals of a substance analyzing as $Pd(ED)_2Cl_2 \cdot 3H_2O$ are produced. The infrared spectrum of the complex shows strong absorptions at ca. 1640 and 3400 cm^{-1} (H_2O), a sharp strong absorption at 1575 (ν(C=C)), and an intense, rather broader absorption at 725 cm^{-1} (δ(=CH)). The latter two absorptions are characteristic of symmetrical, *cis*-disubstituted ethylenes (5). The band at 970 cm^{-1}, characteristic of the *trans*-ED spectrum, is absent. Conductivity measurements, interpreted by the method of Feltham and Hayter (7), show that in water the complex is a 2:1 electrolyte, but that in nitromethane solution considerable association occurs giving essentially a 1:1 electrolyte. This result is similar to that found for $Pt(cis\text{-}ED)_2Cl_2 \cdot 1.5H_2O$ (1). The perchlorate and hexafluorophosphate derivatives have the formulae, $Pd(cis\text{-}ED)_2X_2$ (X = ClO_4^-, PF_6^-), and conductivity measurements show them to be 2:1 electrolytes in nitromethane solution. These complexes are therefore given the structure **8** (X = Cl^-, PF_6^-, ClO_4^-). (It is interesting to note here the advantage of using the Feltham–Hayter method over that of simply comparing the conductivity of 10^{-3} *M* solutions to determine electrolyte type. For the two complexes, $Pd_2(trans\text{-}ED)_4Cl_4 \cdot 3H_2O$, and $Pd(cis\text{-}ED)_2Cl_2 \cdot 3H_2O$, the molar conductivities of 10^{-3} *M* solutions are 214 and 236 mho cm^2 $mole^{-1}$, respectively, both being in the range quoted for 2:1 electrolytes in aqueous solution (8). The slopes of the Feltham–Hayter plots, however, are 246 and 456, clearly distinguishing the two complexes.)

By treating complex **8** (X = Cl^-) with an equivalent amount of potassium tetrachloropalladate(II), yellow crystals of formula Pd(ED)Cl_2 are obtained. This complex is nonconducting in nitromethane solution, and its infrared spectrum shows bands characteristic of the ligand *cis*-ED. The structure of the complex is therefore assumed to be the neutral species **9**. The corresponding platinum(II) derivative could not be prepared under similar conditions (1). These results are analogous with the behavior of the ligand *o*-phenylenebisdimethylarsine, **3**, which readily gives a complex similar to **9** with palladium(II) (2*a*), but only under special conditions could the corresponding platinum(II) derivative be prepared (9).

Nuclear Magnetic Resonance Spectra

The n.m.r. spectra of the ligands and complexes are summarized in Table III. In each case, the spectrum consists simply of two

Can. J. Chem. Downloaded from www.nrcresearchpress.com by 210.87.254.5 on 09/05/12
For personal use only.

TABLE III

Nuclear magnetic resonance spectral data*

Complex	Vinyl protons (τ)	Methyl protons (τ)
trans-ED	3.23	9.01
cis-ED	3.06	9.02†
Pd(*cis*-ED)Cl_2	2.59	8.23
Pd(*cis*-ED)$_2Cl_2$	2.36	8.10
[Pd(*trans*-ED)Cl_2]$_2$	Insoluble	
Pd_2(*trans*-ED)$_4Cl_4$	2.45	8.05‡

*Data shown are for d_6-dimethylsulfoxide solutions except where indicated. Resonance absorptions are quoted in p.p.m. downfield from TMS = 10.
†Private communication from M. A. Bennett.
‡In D_2O solution. The n.m.r. spectra do not appear to be very solvent dependent and a similar set of data is obtained in d_3-acetonitrile.

resonances (with additional absorptions for attached solvent molecules where relevant) in the ratio 1:6, corresponding to vinyl and methyl protons, respectively. Coordination of the ligands to the metal ion causes a downfield shift of ca. 0.4–1.0 p.p.m. in the proton absorptions relative to those of the free ligands. In the case of the ligand, *cis*-1,2-bis(diphenylphosphino)ethylene, **4**, coordination with the Group VI hexacarbonyl complexes caused a downfield shift in olefinic proton resonances of about 1.3 p.p.m., relative to the free ligand (3). The authors suggested that this shift might reflect a significant amount of ring current in the ring formed between the metal ion and the ligand atoms. Such a delocalization would involve the non-bonding t_{2g} electrons of the metal atom and would help to relieve the build-up of electron density on the metal because of the carbon monoxide groups. This type of "back bonding" is probably not as strong in the d^8 palladium(II) case and might account for the significantly smaller shift in these complexes. It is hoped to explore the question of this ring current in future work by examination of the reactivity of the double bond

Far Infrared Spectra

The absorptions of the complexes in the far infrared region are listed in Table I *trans*-ED has a strong absorption at ca. 315 cm^{-1} which appears in this position in all of its complexes. The *cis*-ED has recently been obtained in a pure state (10), but the far infrared spectrum was not given. However, a sample of *trans*-ED, rich in *cis*-ED, shows a sharp band at 1550 cm^{-1} ($\nu_{C=C}$) and a characteristic strong, sharp absorption at ca. 450 cm^{-1}, both of which appear in all the complexes of *cis*-ED. The δ(=CH) deformation band appears at 650 cm^{-1} in the free ligand and at ca. 700 cm^{-1} in the complexes of *cis*-ED.

The complex, [Pd(*trans*-ED)Cl_2]$_2$, has two absorptions in the far infrared region, at 284 and 258 cm^{-1}, which disappear upon substitution of Cl^- by Br^-. These absorptions are assumed to be associated with metal–halogen stretching frequencies (the infrared spectra are otherwise unaltered by the substitution).

Complexes of the type, *cis*- and *trans*-Pd(AsR_3)$_2X_2$, have been studied in this region (11). *cis*-Isomers show two bands associated with metal–chloride stretching vibrations, at ca. 310–315 cm^{-1} and 280–300 cm^{-1}, while *trans*-isomers show a single absorption at ca. 350 cm^{-1}. For a molecule as complicated as [Pd(*trans*-ED)Cl_2]$_2$ it is difficult to assign structures on the basis of the *number* of metal–halogen vibrations, but both the number and position of the bands are more consistent with a *cis* arrangement of halogens rather than a *trans* arrangement as originally suggested (1). Models confirm that such a structure exhibits less ring strain, and the proposed structure is shown as structure **10**.

The far infrared spectrum of Pd_2(*trans*-ED)$_4$-$Cl_4 \cdot 3H_2O$, **7**, (M = Pd), shows no absorptions that are altered by substitution of Cl^- with Br^-. This suggests that in the solid state, complex **7** (M = Pd) contains no coordinated Cl^- ions. The fact that both the Cl^- and Br^- derivatives are the same color supports this conclusion, because substitution of Cl^- with Br^- in Pd(II) complexes normally results in a deepening color as the charge transfer absorptions move to lower energies. In agreement with this, when water is removed from complex **7** (M = Pd), the color deepens and a new absorption appears at 285 cm^{-1}, suggesting that Cl^- ions have moved into the first coordination sphere.

The complex, Pd(*cis*-ED)$_2Cl_2 \cdot 3H_2O$, shows a single absorption in this region, at 296 cm^{-1}. This band is not altered upon substitution of Cl^- with Br^- and it is concluded that there is no positive evidence for five- or six-coordinate Pd(II) in the solid state. The complex, Pd(*cis*-ED)Cl_2, shows three bands in this region, at 322, 293, and 262 cm^{-1}, none of which appear in Pd(*cis*-ED)Br_2. From the evidence above, the absorption at 293 cm^{-1} could be considered a

Can. J. Chem. Downloaded from www.nrcresearchpress.com by 210.87.254.5 on 09/05/12
For personal use only.

Can. J. Chem. Downloaded from www.nrcresearchpress.com by 210.87.254.5 on 09/05/12
For personal use only.

ligand absorption and it is not clear why it disappears with the removal of Cl^- ions. The number and position of the M—X absorptions, however, do support the structure **9** (11).

Reactions

It was reported (1) that ultraviolet irradiation of solutions of $Pt_2(trans\text{-}ED)_4Cl_4 \cdot 3H_2O$ in a variety of solvents caused a *trans*-to-*cis* conversion of the ligand, to yield the complex, $Pt(cis\text{-}ED)_2Cl_2$. With the complex, $Pd_2(trans\text{-}ED)_4Cl_4 \cdot 3H_2O$, irradiation of an aqueous solution for two days caused no change in the n.m.r. spectrum of that solution, nor in its color. In other solvents (ethanol, acetonitrile), in the presence of excess *trans*-ED to stabilize the starting material, irradiation for 7 h through a Pyrex filter did cause a decoloration of the solution and conversion of the ligand according to the following equation

$$[2]\quad Pd_2(trans\text{-}ED)_4Cl_4 \cdot 3H_2O \xrightarrow{h\nu} 2\,Pd(cis\text{-}ED)_2Cl_2 \cdot 3H_2O$$

(Extra water is picked up during the reaction or during the work-up. Isolation of the product complex in the absence of water yields an extremely hygroscopic yellow powder that is difficult to handle.)

The stability of the complex **7** (M = Pd) in water and its instability in other solvents is evidence for the weaker coordinating power of tertiary arsine and chloride ions for palladium(II) compared to platinum(II). The following points give evidence that in these complexes there is a strong competition between tertiary arsine and Cl^- ion for the metal coordination sites.

(*a*) The ease with which ligands can be removed from solid $M_2(trans\text{-}ED)_4Cl_4 \cdot 3H_2O$ (M = Pd, Pt), i.e.

$$[3]\quad M_2(trans\text{-}ED)_4Cl_4 \cdot 3H_2O \rightleftharpoons M_2(trans\text{-}ED)_2Cl_4 + 2\,trans\text{-}ED + 3H_2O$$

In the case of the palladium derivative, simple loss of water at atmospheric pressure will shift this equilibrium to the right, while for M = Pt(II), heating at high vacuum to 95 °C is required before the internal attack of Cl^- ions causes the M—As bonds to rupture.

(*b*) Stability in non-aqueous solvents. The platinum(II) complex in (*a*) above can be dissolved and recovered unchanged from non-aqueous solvents that are not strongly coordinating (e.g. ethanol). With the corresponding palladium(II) complex, dissolution in solvents in which the halide ion is not strongly solvated causes the immediate elimination of two molecules of ligand and the precipitation of the dimeric, 1:1 complex **6** (M = Pd), see reaction 1. (The process occurs immediately in ethanol, nitromethane, and acetonitrile.) The solvating properties of the solvent favor dissolution of the ligand rather than the chloride ion and this, along with the insolubility of complex **10**, helps to drive the reaction forward.

(*c*) Stability in aqueous solution. Here, the positions of palladium(II) and platinum(II) are reversed. The important equilibrium is

$$[4]\quad M_2(trans\text{-}ED)_4Cl_4(aq) \rightleftharpoons [M_2(trans\text{-}ED)_4]^{(4-x)+}Cl_x(aq) + (4-x)Cl^-(aq)$$

For M = Pd(II), conductivity measurements show that the value of x approaches 0 in dilute solutions, and that there is very little competition between AsR_3 and Cl^- in these solutions. The fact that the corresponding bromide derivative is the same color as the chloride indicates the ionic nature of the halides even in the solid state. The isomerization of *trans*-ED to *cis*-ED requires a rupture of the M—As bond, and in this case the chloride ion is prevented from causing this rupture. For M = Pt(II), however, the complex is much less soluble in water, suggesting that x approaches the value 4 in reaction [4]. Upon exposure to ultraviolet light, the rupture of the M—As bond is greatly assisted by the strongly coordinating chloride ion, and isomerization occurs.

Acknowledgments

The author would like to thank the Salters' Company and the National Research Council of Canada for generously supporting this work. The author is also indebted to Dr. M. A. Bennett of the Australian National University for helpful discussions, to Professor D. W. A. Sharp of the University of Strathclyde for thermogravimetric measurements, and to Miss J. Wong and Mr. N. Darby for technical assistance.

1. M. A. Bennett, G. J. Erskine, and J. D. Wild. Inorg. Chim. Acta, 379 (1968).
2. (*a*) J. Chatt and F. G. Mann. J. Chem. Soc. 611 (1939). (*b*) R. S. Nyholm and G. J. Sutton. J.

Chem. Soc. 575 (1958) and previous papers in this series. (*c*) C. M. HARRIS, R. S. NYHOLM, and D. J. PHILLIPS. J. Chem. Soc. 4379 (1960). (*d*) R. J. H. CLARK, J. LEWIS, and R. S. NYHOLM. J. Chem. Soc. 2460 (1962) and subsequent papers.
3. R. B. KING and C. A. EGGERS. Inorg. Chim. Acta, **2**, 33 (1968).
4. W. R. CULLEN, P. S. DHALIWAL, and C. J. STEWART. Inorg. Chem. **6**, 2256 (1967).
5. L. J. BELLAMY. The infrared spectra of complex molecules. Methuen, London. pp. 45–48. 1958.
6. R. S. NYHOLM. J. Chem. Soc. 848 (1950).
7. R. D. FELTHAM and R. G. HAYTER. J. Chem. Soc. 4587 (1964).
8. R. N. COLLINGS, R. S. NYHOLM, and M. L. TOBE. Nature, **201**, 1322 (1964).
9. M. J. HUDSON, R. S. NYHOLM, and M. H. B. STIDDARD. J. Chem. Soc. A, 40 (1968).
10. R. D. FELTHAM, H. G. METZGER, and W. SILVERTHORN. Inorg. Chem. 2003 (1968).
11. D. M. ADAMS. Metal–ligand and related vibrations. Arnold, London. 1967.

Can. J. Chem. Downloaded from www.nrcresearchpress.com by 210.87.254.5 on 09/05/12
For personal use only.

Calculation of reaction order for the homogeneous pyrolysis of organic vapors

JOHN TOROK[1] AND SAMUEL SANDLER
Department of Chemical Engineering and Applied Chemistry, University of Toronto, Toronto, Ontario
Received November 1, 1968

A method is proposed for the derivation of a mathematical equation that relates the kinetic parameters of the propagation reactions of homogeneous free-radical chain reactions to the overall order of the reaction. The equation may be used in evaluating the predominant chain-termination reaction, provided that the mechanism of propagation of the chain is well understood. Application of the technique is demonstrated for the pyrolysis of *n*-butane. It predicts the predominance of the methyl–methyl radical recombination reaction.

Canadian Journal of Chemistry, 47, 2707 (1969)

Can. J. Chem. Downloaded from www.nrcresearchpress.com by 210.87.254.5 on 09/05/12
For personal use only.

Introduction

Goldfinger, Letort, and Niclause (1) have shown that, for pyrolytic reactions, the overall order of the reaction depends on: (*a*) the order of initiation (first or second order), (*b*) the order of termination (second or third order), and (*c*) the type of radical participating in the chain-termination process. They referred to radicals involved in bimolecular propagation reactions as β radicals, and radicals undergoing unimolecular reactions in the propagating steps as μ radicals. The various possibilities for the overall orders of such reactions are summarized in Table I.

TABLE I

Overall orders of reaction for various types of initiation and termination reactions

First-order initiation		Second-order initiation		
Simple termination	Third-body termination	Simple termination	Third-body termination	Overall order
		ββ		2
ββ		βμ	ββM	3/2
βμ	ββM	μμ	βμM	1
μμ	βμM		μμM	1/2
	μμM			0

Although Goldfinger's rule is helpful in establishing which chain-termination reaction is predominant, it neglects the treatment of the homogeneous reaction phenomena frequently encountered in chain reactions and affecting the overall order of such reactions. These include observations such as: (*a*) the rates of unimolecular initiation, propagation, or bimolecular termination reactions are proportional to a fractional power of the reaction pressure when in their pressure-dependent region, (*b*) some radicals, such as ethyl and isopropyl, may act both as β and as μ radicals, and (*c*) with certain reaction conditions 2 or more chain-termination reactions may have comparable rates.

The present paper is concerned with the mathematical treatment of the above phenomena. One study of the pyrolysis of *n*-butane is used to illustrate the effect of the first 2 points, while the third will be treated in a subsequent publication.

Derivation of Order Equation

Equations permitting the prediction of the overall reaction order for a simple pyrolysis mechanism will be derived first. It will be assumed initially that the initiation and termination reactions are in their pressure-dependent regions in the following generalized scheme.

Initiation

[1] $$a\mathrm{AH} \rightarrow 2 \text{ free radicals} + (a-1)\mathrm{AH}$$

Propagation

[2] $$\mathrm{A}\cdot \rightarrow \mathrm{B}\cdot + \mathrm{C}$$

[3] $$\mathrm{B}\cdot + \mathrm{AH} \rightarrow \mathrm{BH} + \mathrm{A}\cdot$$

Reactions [2] and [3] participate in a cyclic process.

Termination

[4] $$\mathrm{A}\cdot + \mathrm{A}\cdot + b\mathrm{AH} \rightarrow \mathrm{A_2} + b\mathrm{AH}\ (\mu - \mu \text{ termination})$$

[5] $$\mathrm{A}\cdot + \mathrm{B}\cdot + c\mathrm{AH} \rightarrow \mathrm{AB} + c\mathrm{AH}\ (\beta - \mu \text{ termination})$$

[6] $$\mathrm{B}\cdot + \mathrm{B}\cdot + d\mathrm{AH} \rightarrow \mathrm{B_2} + d\mathrm{AH}\ (\beta - \beta \text{ termination})$$

Here A· and B· are free radicals while AH,

[1]Present Address: Norton Research Corporation, Chippawa, Ontario.

Can. J. Chem. Downloaded from www.nrcresearchpress.com by 210.87.254.5 on 09/05/12
For personal use only.

BH, A_2, B_2, AB, and C are organic compounds.

In the following derivation the following assumptions are made.

Assumption 1, the fundamental hypothesis of Bodenstein that the intermediate products of the reaction are of almost stationary concentration is valid.

Assumption 2, the chain lengths are large.

Since the rate of chain initiation is equal to the rate of chain termination

$$[7]\quad k_1[\mathrm{AH}]^a = k_4[\mathrm{A}\cdot]^2[\mathrm{AH}]^b + k_5[\mathrm{A}\cdot][\mathrm{B}\cdot][\mathrm{AH}]^c + k_6[\mathrm{B}\cdot]^2[\mathrm{AH}]^d$$

Based on assumption 2 the rates of the two propagating reactions, [2] and [3], are approximately equal and equivalent to the overall rate of reaction, r, that is

$$[8]\quad r = k_2[\mathrm{A}\cdot] = k_3[\mathrm{B}\cdot][\mathrm{AH}]$$

From eqs. [7] and [8] the steady-state concentration of radical A· is

$$[9]\quad [\mathrm{A}\cdot] = k_1^{1/2}k_3[\mathrm{AH}]^{a/2}/(k_3^2k_4[\mathrm{AH}]^b + k_2k_3k_5[\mathrm{AH}]^{c-1} + k_2^2k_6[\mathrm{AH}]^{d-2})^{1/2}$$

The overall order of the reaction is equivalent to the slope of the ln rate vs. ln pressure relationship, or

$$[10]\quad \text{Order} = \mathrm{d}\ln r/\mathrm{d}\ln[\mathrm{AH}]$$

Substitution of the first part of eq. [8] into eq. [10] results in

$$[11]\quad \text{Order} = \frac{[\mathrm{AH}]}{k_2[\mathrm{A}\cdot]}\cdot\frac{\mathrm{d}(k_2[\mathrm{A}\cdot])}{\mathrm{d}[\mathrm{AH}]} = \frac{[\mathrm{AH}]}{[\mathrm{A}\cdot]}\cdot\frac{\mathrm{d}[\mathrm{A}\cdot]}{\mathrm{d}[\mathrm{AH}]}$$

Equation [9] and its derivative with respect to AH may be substituted into eq. [11]. After rearrangement, one gets

$$[12]\quad \text{Order} = \frac{a-1}{2} + \frac{(0.5 - b/2)k_3^2k_4[\mathrm{AH}]^b + (1.0 - c/2)k_2k_3k_5[\mathrm{AH}]^{c-1} + (1.5 - d/2)k_2^2k_6[\mathrm{AH}]^{d-2}}{k_3^2k_4[\mathrm{AH}]^b + k_2k_3k_5[\mathrm{AH}]^{c-1} + k_2^2k_6[\mathrm{AH}]^{d-2}}$$

By substituting into eq. [12] the rate expressions for reactions [4], [5], and [6], as modified by substitution of the second equality in eq. [8], the following expression is obtained,

$$[13]\quad \text{Order} = \frac{a-1}{2} + \frac{(0.5 - b/2)r_4 + (1.0 - c/2)r_5 + (1.5 - d/2)r_6}{r_4 + r_5 + r_6}$$

where r_i = rate of reaction i. Goldfinger's table (Table I) may be generated from eq. [13] when conditions such that only one of the three possible termination reactions, that is [4], [5], or [6], may be concerned and, when a equals 1 or 2 and either b, c, or d is equal to 0 or 1.

For most pyrolytic reactions the initiation reaction is first order and the predominant termination reactions are second order. Under these circumstances a third assumption may be made.

Assumption 3, the rate constant for the cross combination of free radicals can be calculated from their individual recombination rates. According to the simple collision theory of chemical kinetics

$$[14]\quad k_5 = 2(k_4k_6)^{1/2}$$

Equation [13] then simplifies to the following expression

$$[15]\quad \text{Order} = \frac{(0.5k_4^{1/2}/k_2)[\mathrm{AH}] + 1.5(k_5^{1/2}/k_3)}{(k_4^{1/2}/k_2)[\mathrm{AH}] + (k_5^{1/2}/k_3)}$$

It should be noted that the order in eq. [15] is a function of ratios of rate constants of the form $k_3/k_5^{1/2}$ and $k_2/k_4^{1/2}$. Photolytic investigations of free-radical reactions produce a ratio of rate constants of the form $k_m/k_u^{1/2}$, where k_m is the rate constant of a propagation step involving a free radical as a reactant and k_u is the rate constant of a chain-termination step involving the recombination of two of the same radicals. In the above mechanism $m = 2$ or 3 and $u = 4$ or 5. Thus, a prediction of the overall order may be made if the kinetic parameters for the chain-propagation reactions are known.

Can. J. Chem. Downloaded from www.nrcresearchpress.com by 210.87.254.5 on 09/05/12
For personal use only.

Reaction Order when One of the Radicals Acts both as a β and as a μ Radical, e.g., Pyrolysis of n-Butane

The ethyl radical may act both as a β and as a μ radical. For example, in *n*-butane pyrolysis, it acts as a β radical in the following reaction

[16] $C_2H_5\cdot + C_4H_{10} \rightarrow C_2H_6 + C_4H_9\cdot$

and as a μ radical in

[17] $C_2H_5\cdot \rightarrow C_2H_4 + H\cdot$

According to Purnell and Quinn (2) reaction [17] is in its pressure-dependent region at the conditions of their investigation (420–530 °C). It can more properly be represented by the following reaction

[18] $C_2H_5\cdot + e\,n\text{-}C_4H_{10} \rightarrow C_2H_4 + H\cdot + e\,n\text{-}C_4H_{10}$

where $1 > e > 0$

Derivation of the order equation for *n*-butane pyrolysis will demonstrate the effect of an ambivalent radical such as the ethyl radical on the overall order of reaction.

The following mechanism differs from the ones proposed by previous investigators (2, 3) in that primary (p-$C_4H_9\cdot$) and secondary (s-$C_4H_9\cdot$) butyl radicals are treated separately. Investigations of *n*-butane-2,2,3,3-d_4 pyrolysis (4) and comparison of the kinetic parameters for relative p- and s-hydrogen abstraction from *n*-butane (5, 6) with the kinetic parameters for product distribution in *n*-butane pyrolysis (2) indicate that the rate of isomerization is negligible compared to the rate of decomposition of butyl radicals in the 400–500 °C range. The results of an investigation by Kerr and Trotman-Dickenson (7) in this area indicate an appreciable rate of butyl radical isomerization. However, these results do not agree with the findings of other investigators of butyl radical decomposition kinetics (8–10).

Mechanism of n-Butane Pyrolysis

Initiation

[19] $C_4H_{10} \rightarrow 2C_2H_5\cdot$

Propagation

[20] p-$C_4H_9\cdot \rightarrow C_2H_4 + C_2H_5\cdot$

[21] s-$C_4H_9\cdot \rightarrow C_3H_6 + CH_3\cdot$

[16] $C_2H_5\cdot + C_4H_{10} \rightarrow C_2H_6$ + s- or p-$C_4H_9\cdot$

[22] $CH_3\cdot + C_4H_{10} \rightarrow CH_4$ + s- or p-$C_4H_9\cdot$

[18] $C_2H_5\cdot + eC_4H_{10} \rightarrow C_2H_4 + H\cdot + eC_4H_{10}$

[23] $H\cdot + C_4H_{10} \rightarrow H_2$ + s- or p-$C_4H_9\cdot$

Termination

Assuming that all of the 5 free radicals can participate in recombination and cross-combination reactions and neglecting disproportionation reactions, the following recombination reaction equations may be written

[24] $2CH_3\cdot \rightarrow C_2H_6$

[25] $2C_2H_5\cdot \rightarrow C_4H_{10}$

[26] $2s\text{-}C_4H_9\cdot \rightarrow C_8H_{18}$

[27] $2p\text{-}C_4H_9\cdot \rightarrow C_8H_{18}$

[28] $2H\cdot \rightarrow H_2$

For the free-radical, cross-combination reactions assumption 3 may be applied and the appropriate rates may be expressed in terms of the rates of reactions [24] to [28].

The relative rates of s- and p-butyl radical formation may be obtained from the product distributions

$$[29] \qquad \frac{r_{20}}{r_{21}} = \frac{[C_2H_4] + [C_2H_6]}{[CH_4] + [C_3H_6]} = Q$$

where $Q = f(T)$ only.

Using the three assumptions which were applied to the simple pyrolysis mechanism, the rate of initiation = rate of termination

$$[30] \quad k_{19}C = (k_{24}^{1/2}R1 + k_{25}^{1/2}R2 + k_{26}^{1/2}SR4 + k_{27}^{1/2}PR4 + k_{28}^{1/2}H)^2 = J^2$$

where $R1 = [CH_3\cdot]$, $R2 = [C_2H_5\cdot]$, $SR4 = [s\text{-}C_4H_9\cdot]$, $PR4 = [p\text{-}C_4H_9\cdot]$, $H = [H\cdot]$, $C = [C_4H_{10}]$, and J = a parameter defined as the square root of the rate of initiation (or termination). Since the rate of production of a radical equals the rate of its removal (in propagation reactions only) then

$$r_{21} = r_{22}$$

and

$$[31] \qquad k_{21}SR4 = k_{22}R1C$$

$$r_{20} = r_{16} + r_{18}$$

$$[32] \qquad k_{20}PR4 = k_{16}R2C + k_{18}R2C^e$$

$$r_{18} = r_{23}$$

$$[33] \qquad k_{18}R2C^e = k_{23}HC$$

From eq. [29]

[34] $$k_{20}PR4 = Qk_{21}SR4$$

From eqs. [31]–[34]

[35] $$R1 = (k_{20}/k_{22})(1/CQ)PR4$$

[36] $$R2 = (k_{20}/(k_{16}C + k_{18}C^e))PR4$$

[37] $$SR4 = (k_{20}/k_{21})(1/Q)PR4$$

[38] $$H = (k_{20}/k_{23}C) \times (k_{18}C^e/(k_{16}C + k_{18}C^e))PR4$$

Taking derivatives with respect to C of eqs. [35]–[38], the following relationships are obtained.

---

[39] $$\frac{dR1}{dC} = \frac{k_{20}}{k_{22}}\frac{1}{QC}\frac{dPR4}{dC} - \frac{k_{20}}{k_{22}}\frac{1}{QC^2}PR4$$

[40] $$\frac{dR2}{dC} = \frac{k_{20}}{k_{16}C + k_{18}C^e}\frac{dPR4}{dC} - \frac{k_{16}k_{20} + nk_{18}k_{20}C^{e-1}}{(k_{16}C + k_{18}C^e)^2}PR4$$

[41] $$\frac{dSR4}{dC} = \frac{k_{20}}{k_{21}Q}\frac{dPR4}{dC}$$

[42] $$\frac{dH}{dC} = \frac{k_{20}}{k_{23}C}\frac{k_{18}C^e}{k_{16}C + k_{18}C^e}\frac{dPR4}{dC} - H\frac{e}{C} - \left(\frac{2k_{16} + (n+1)k_{18}C^{e-1}}{k_{16}C + k_{18}C^e}\right)$$

Taking the derivative of eq. [30] with respect to C results in the following expression

[43] $$k_1 = 2J\left(k_{24}^{1/2}\frac{dR1}{dC} + k_{25}^{1/2}\frac{dR2}{dC} + k_{26}^{1/2}\frac{dSR4}{dC} + k_{27}^{1/2}\frac{dPR4}{dC} + k_{28}^{1/2}\frac{dH}{dC}\right)$$

Substitution of eqs. [39], [40], [41], [42], and finally eq. [30] into eq. [43] results in

[44] $$J^2 = 2J^2\frac{C}{PR4}\frac{dPR4}{dC} - 2J\left[k_{24}^{1/2}\frac{k_{20}}{k_{22}}\frac{1}{QC} + k_{25}^{1/2}\left(\frac{k_{16}k_{20} + nk_{18}k_{20}C^{e-1}}{(k_{16}C + k_{18}C^e)^2}\right) + k_{28}^{1/2}H\left(\frac{2k_{16}C + (e+1)k_{18}C^e}{k_{16}C + k_{18}C^e} - e\right)\right]PR4$$

The rate of the overall reaction is equal to the rate of decomposition of butyl radicals.

$$r = r_2 + r_3 = k_2PR4(1 + 1/Q)$$

[45] $$\text{Order} = \frac{d\ln r}{d\ln C} = \frac{C}{r}\frac{dr}{dC} = \frac{C}{PR4}\frac{dPR4}{dC}$$

Substituting eqs. [35], [36], [37], [38], and [45] into eq. [44], then

[46] $$J^2 = 2J^2\,\text{order} - 2J(k_{24}^{1/2}R1 + k_{25}^{1/2}R2U + k_{28}^{1/2}H(U - e + 1))$$

where

[47] $$U = \frac{k_{16}C + ek_{18}C^e}{k_{16}C + k_{18}C^e} = \frac{\text{rate of reaction [16]} + e\ \text{rate of reaction [18]}}{\text{rate of reaction [16]} + \text{rate of reaction [18]}}$$

Can. J. Chem. Downloaded from www.nrcresearchpress.com by 210.87.254.5 on 09/05/12
For personal use only.

Can. J. Chem. Downloaded from www.nrcresearchpress.com by 210.87.254.5 on 09/05/12
For personal use only.

Substitution of eq. [30] into eq. [46] and subsequent rearrangement results in an expression for the order

$$[48]\quad \text{Order} = \frac{\sum_{i=24}^{i=28}\sum_{j=24}^{j=28}(F_i + F_j)(r_i r_j)^{1/2}}{\sum_{i=24}^{i=28}\sum_{j=24}^{j=28}(r_i r_j)^{1/2}}$$

where the values for i, j, $2F_i$, and $2F_j$ are:

Radical	Value	
	i or j	$2(F_{i \text{ or } j})$
$CH_3\cdot$	24	1.5
$C_2H_5\cdot$	25	$0.5 + U$
s-$C_4H_9\cdot$	26	0.5
p-$C_4H_9\cdot$	27	0.5
$H\cdot$	28	$1.5 + U - e$

where $0 < U < 1$ and $0 < e < 1$

Recent investigators (2, 3) of this reaction in the 420–590 °C region have found the overall reaction order to be 1.5. Of the 5 radicals participating in the reactions, the recombination of only the methyl and ethyl radical and hydrogen could result in an order of approximately 1.5. Of these hydrogen is the most reactive since

$$k_{23} \gg k_{16} \text{ or } k_{22}$$

Its steady state concentration is thus expected to be much lower than that of methyl or ethyl radicals. Therefore

$$r_{28} \ll r_{24} \text{ or } r_{25}$$

The termination reaction

$$[49]\quad CH_3\cdot + C_2H_5\cdot \rightarrow C_3H_8$$

would be one of the predominant chain-termination reactions if the two participating radicals were at comparable concentrations. However, Purnell and Quinn (2) did not find propane among the primary reaction products. This indicates that either reaction [24] or reaction [25] is overwhelmingly operative.

It may be seen from eq. [48], that if reaction [24] predominates, the calculated order is 1.5. If, however, reaction [25] predominates then the value of U is needed to calculate the predicted order.

Calculation of the Value of U

From the expressions for the rate of production of ethane and ethylene by reactions [16], [18], and [20] and from eq. [32], the following expression may be derived.

$$[50]\quad \left(\frac{[C_2H_4]}{[C_2H_6]} - 1\right)C = 2\left(\frac{k_{18}C^e}{k_{16}}\right)$$

Purnell and Quinn reported values of the left side of eq. [50] at 518.0 °C between 15 and 120 mm of Hg reaction pressure. They plotted these values as a function of pressure and fitted them with a curve calculated from Kassel's model. This treatment of the data illustrated the pressure dependence of reaction [18].

If natural logarithms of eq. [50] are taken the following relationship is obtained

$$[51]\quad \ln\left[\left(\frac{[C_2H_4]}{[C_2H_6]} - 1\right)C\right] = e \ln C + \ln\left(\frac{2k_{18}}{k_{16}}\right)$$

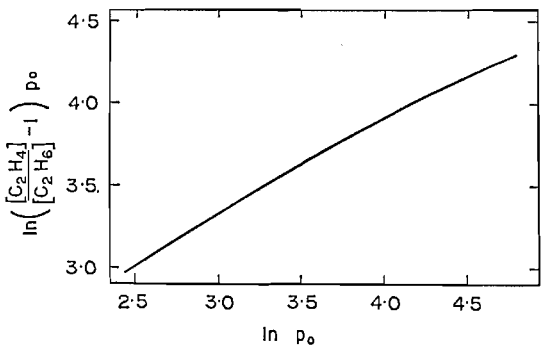

FIG. 1. The variation of the function $\ln\{[C_2H_4]/[C_2H_6]-1\}p_0$ with ln initial pressure, p_0, in the pyrolysis of *n*-butane at 518 °C (from Purnell and Quinn (2)).

Figure 1 shows a plot of $\ln\{[C_2H_4]/[C_2H_6] - 1\}p_0$ vs. $\ln p_0$ calculated from the curve of Purnell and Quinn. Equation [51] indicates that the slope of the curve is equivalent to the value of e. From the values of e, $2(k_{18}C^e/k_{16})$, and C, values of U were calculated and are listed in Table II along with the predicted overall reaction orders (assuming the predominance of the ethyl–ethyl termination reaction).

With an increase in reaction pressure the rate of reaction [16] increases relative to the rate of reaction [18]. This has the effect of increasing the overall order of the reaction. The order of reaction [18] on the other hand decreases with an increase in pressure and thus compensates for the above effect. The predicted overall order is approximately 1.35 and is relatively independent of

TABLE II

Overall reaction orders at 518 °C calculated by assuming reaction [25] as the predominant chain-termination reaction*

Reaction pressure (p_0) mm of Hg	e from Fig. 1	$\frac{[C_2H_4]}{[C_2H_6]}$	U calculated using eq. [47]	Overall reaction order
16	0.63	2.5	0.84	1.34
37	0.58	2.1	0.85	1.35
53	0.55	1.9	0.85	1.35
90	0.47	1.7	0.86	1.36
110	0.44	1.6	0.86	1.36

*Calculations are based on the experimental results of Purnell and Quinn (2).

pressure. However, it is significantly lower than the experimental value of 1.5 reported by Purnell and Quinn (2) and Sagert and Laidler (3).

Based on the pressure dependence of the activation energies for the formation of the major products, Purnell and Quinn (2) predicted the predominance of the ethyl–ethyl radical termination reaction (reaction [25]). On the basis of the overall reaction order and using the results of the same investigators, the above treatment predicts the predominance of the methyl–methyl radical termination reaction. In view of this contradictory evidence, further work is necessary for the establishment of the exact termination mechanism for *n*-butane pyrolysis.

Conclusion

The overall order of a pyrolytic reaction can quite easily be determined in any kinetic study. Its variation with temperature and pressure can be compared with the mathematical analysis outlined above for any proposed mechanism, which then can provide an additional criterion for the proper choice of the chain-termination reaction. Such an analysis of the pyrolysis of *n*-butane has indicated that the methyl–methyl radical recombination is the major chain-termination process.

The validity of a derived order equation hinges on the choice of a correct chain-propagation mechanism. Throughout the above analysis all simple reactions were assumed to be homogeneous. If the experimental order can not be predicted by the calculation procedure outlined, it is likely that some of the simple reactions are partially or completely heterogeneous, or alternatively that incorrect chain-propagation reactions have been assumed.

The method outlined may be quite useful when chain-termination products are identical to the reactant or to products of the propagation reactions, making it necessary to determine the chain-termination process indirectly, as in *n*-butane pyrolysis.

The order equation derived in this publication may also be used for the quantitative interpretation of the order change resulting from a change in the termination mechanism. The results of a study of the kinetics of the thermal decomposition of *n*-butane at low temperatures indicate that, at temperatures below 400 °C, the overall reaction order decreases with a decrease in reaction temperature. This drop in reaction order may be explained by the increasing importance of reaction [26] relative to reaction [24] at lower temperatures. The results of this investigation will be presented in a subsequent publication.

1. P. GOLDFINGER, M. LETORT, and M. NICLAUSE. Contribution a l'étude de la structure moleculaire. Victor Henry Commemorative Volume. Desoer, Liège. 1948. p. 283.
2. J. H. PURNELL and C. P. QUINN. Proc. Roy. Soc. London, Ser. A, **270**, 267 (1962).
3. N. H. SAGERT and K. J. LAIDLER. Can. J. Chem. **41**, 838 (1963).
4. J. R. MCNESBY, C. M. DREW, and A. S. GORDON. J. Chem. Phys. **24**, 1260 (1956).
5. J. G. LARSON and A. KUPPERMAN LONG. Abstracts presented to Am. Chem. Soc. meeting. Washington, D.C., March 21–24, 1962.
6. J. R. MCNESBY and A. S. GORDON. J. Am. Chem. Soc. **78**, 3570 (1956).
7. J. A. KERR and A. F. TROTMAN-DICKENSON. J. Chem. Soc. **323**, 1602 (1960).
8. F. E. FREY and H. J. HEPP. J. Am. Chem. Soc. **55**, 3357 (1933).
9. W. E. MORGANROTH and J. G. CALVERT. J. Am. Chem. Soc. **88**, 5387 (1966).
10. J. T. GRUVER and J. G. CALVERT. J. Am. Chem. Soc. **78**, 5208 (1956).

Can. J. Chem. Downloaded from www.nrcresearchpress.com by 210.87.254.5 on 09/05/12
For personal use only.

Can. J. Chem. Downloaded from www.nrcresearchpress.com by 210.87.254.42 on 09/05/12
For personal use only.

NOTES

Crystal field splitting in the far infrared spectrum of rhombic sulfur

A. ANDERSON AND L. Y. WONG
Department of Physics, University of Waterloo, Waterloo, Ontario

Received February 18, 1969

The infrared (i.r.) spectra of thin polycrystalline samples of orthorhombic sulfur at 95 °K in the range 50–500 cm^{-1} have been recorded. The three i.r. active fundamentals ν_4, ν_5, and ν_6 are observed to be split into 2, 3, and 3 components, respectively, as predicted from a group theoretical analysis of the unit cell symmetry, thus confirming the assignment of ν_4 and ν_6. Several weaker absorptions are assigned by comparison with recent Raman results and a normal coordinate analysis. No peaks assignable to lattice vibrations are observed.

Canadian Journal of Chemistry, 47, 2713 (1969)

Introduction

Of the 11 fundamental vibrations of the S_8 ring molecule only 3 are infrared active. According to Herzberg's notation (1), these are ν_4 (b_2), ν_5 (e_1), and ν_6 (e_1). For many years, incorrect assignments of ν_4 and ν_6 were made on the basis of the early low resolution far infrared studies of Barnes (2), but in 1964 two independent investigations (3, 4) of sulfur in solution established that there are two strong absorptions in the region 175–250 cm^{-1} which should be assigned to these fundamentals. In addition, a normal coordinate analysis (3) based on a modified Urey–Bradley field, showed that the lower frequency band corresponded to the degenerate vibration, ν_6, and the higher one to the non-degenerate ν_4. However, since the separation of the peaks is only about 50 cm^{-1}, an independent check on the assignment of these two modes would seem desirable.

Such a check is possible by consideration of the crystal field splittings expected for the two bands. A recent Raman study (5) of orthorhombic sulfur at liquid nitrogen temperature showed that for the strong Raman peaks, very good agreement is obtained with the predictions of a group theoretical analysis based on the known molecular, site, and unit cell symmetries (6, 7). This suggests that a similar analysis of the strong i.r. spectral features may be confidently used to confirm the assignments. As shown in the previous work (5), the non-degenerate ν_4 should be split into two i.r. components as a result of coupling within the unit cell, whereas ν_5 and ν_6 experience an additional effect, the removal of their degeneracies by the lower site symmetry, resulting in three i.r. active compounds for each. Other molecular vibrations and lattice modes are predicted to have i.r. activity, but should be weak relative to these three fundamentals.

Experimental

Because of low intensity sources and relatively insensitive dectectors in the far i.r. region, coupled with the strong absorption by sulfur, considerable experimental difficulties were experienced before good quality spectra of sufficient resolution to observe the expected fine structure were obtained. Earlier work on sulfur pellets at room temperature was inconclusive in this respect, although some splitting was observed (4). In this research a variety of sampling techniques was tried, including Nujol mulls, KBr pellets, and attenuated total reflection using KRS 5 plates. The most reproducible and reliable spectra were obtained with very thin pressed discs (0.004 in. thick, 0.75 in. diameter) for the region below 400 cm^{-1}, where an RIIC-Beckman 620 Fourier spectrophotometer with direct on-line hook-up to an IBM 360 model 44 computer was used, and a thin uniform layer of finely powdered sulfur on a silver bromide plate for the region 400–500 cm^{-1}, where a Beckman IR-9 instrument was used. The pellet and backing plate were mounted in a conventional glass cryostat with polyethylene windows, and cooled with liquid nitrogen. Sample temperatures in the beam, as measured by a copper–constantan thermocouple, were around 95 °K.

Results

Identical spectra were obtained for sulfur from Fisher (U.S.P. grade) and Gallard–Schlesinger (99.9999% pure). The low-temperature spectra of polycrystalline sulfur are shown in Fig. 1. These differ from those at room temperature in two important respects: the overall width of the strong peaks is reduced, and the fine structure is more apparent, particularly for the ν_5 absorption.

TABLE I

Infrared and Raman spectra of sulfur*

Mode and species	Infrared				Raman, crystal, ref. 5§
	Solution		Crystal		
	Ref. 3	This work	Refs. 3, 4†	This work‡	
$\nu_9(e_2)$	—	—	—	78	77, 79, 85, 91
$\nu_8(e_2)$	—	—	154	149	149, 152, 156, 159
$\nu_6(e_1)$	191	192	186, 197	182, 187, 198	182, 187, 197
$\nu_2(a_1)$	—	—	214	214	214, 218
$\nu_4(b_2)$	243	242	239	240, 243	236
$\nu_{10}(e_3)$	—	—	435	442	441
$\nu_5(e_1)$	471	470.5	465	470, 472.5, 476.5	—‖

*Frequencies of maximum absorption or intensity in cm^{-1}.
†Temperature = 300 °K.
‡Temperature = 95 °K.
§Temperature = 100 °K, only those peaks close to i.r. frequencies are recorded here.
‖Overlaps with strong ν_1 peaks at 470 and 477 cm^{-1}.

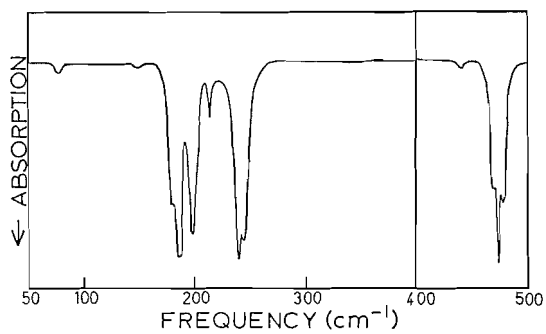

FIG. 1. The i.r. absorption spectrum of orthorhombic sulfur at 95 °K.

The spectral resolution is about 1 cm^{-1} for this band, and 2.5 cm^{-1} for the lower frequency range. Higher resolution (but noisier) spectra were obtained with the interferometer, but no further sharpening was observed. Spectra of sulfur in solution (polyethylene cell, 1 mm thick, saturated solution in CS_2) were also run, under identical resolution conditions. No fine structure was apparent in the strong bands, and the weaker absorptions in the crystal were absent. The frequencies of maximum absorption for crystal and solution are listed in Table I, and are estimated to be accurate to ± 1 cm^{-1}. These are compared with previous values (3, 4) and the relevant Raman data for the crystal at approximately the same temperature (5). Spectra were also obtained for thicker samples, but because of the extent of the wings of the strong bands, these were of poor quality and no reproducible additional features were found. In any case, since there is evidence (8) that orthorhombic sulfur often contains small amounts of S_n chain molecules, the assignment of very weak features is open to question. The region below 75 cm^{-1} was investigated with a thicker beam divider, which is more efficient at low frequencies (9), but no new peaks were found.

Discussion

The predicted numbers of components for the three i.r. fundamentals are observed: ν_4 (2), ν_5 (3), and ν_6 (3). Hence the assignment of Scott *et al.*

Can. J. Chem. Downloaded from www.nrcresearchpress.com by 210.87.254.42 on 09/05/12
For personal use only.

(3) is confirmed, as is the explanation of the splittings in terms of the static and correlation fields. The splittings range from 2.5–11 cm^{-1}, compared to 3–7 cm^{-1} in the Raman spectrum (5). The weaker bands, resulting from activity induced by the perturbing crystal field, are readily assigned by reference to the Raman data and the normal coordinate analysis (3): the sharp symmetric peak at 214 cm^{-1} is the predicted i.r. singlet for ν_2; the other bands are broader, and represent the unresolved triplets of ν_9 (78 cm^{-1}), ν_8 (149 cm^{-1}), and ν_{10} (442 cm^{-1}). The absence of lattice modes indicates that their interaction with the electromagnetic field is a factor of at least 20 less than that of the intramolecular fundamentals, which is not unusual for such a symmetric molecule.

A final point of interest is that a comparison of the frequencies of bands observed in both i.r. and Raman shows evidence for coincidences within experimental error. This is especially noticeable for ν_6, and the only exception is ν_4, where there is a 4 cm^{-1} difference. From spectroscopic evidence alone, one might conclude that the crystal does not possess a center of symmetry, whereas the X-ray data show that the opposite is true (6). Infrared and Raman data are often used to aid in crystal structure determinations, especially of hydrogenic molecules, when X-ray, electron, or neutron diffraction measurements are not available (10). The above result shows that this procedure must be used with extreme caution, if spurious deductions are to be avoided.

Acknowledgments

The authors thank Dr. D. E. Irish, Mr. M. H. Brooker, Mr. F. Grossman, and Mr. J. Beke for their assistance in these experiments. This research was supported, in part, by grants from the National Research Council of Canada and the Ontario Department of University Affairs.

1. G. Herzberg. Infrared and Raman spectra. D. Van Nostrand, New York. 1945. p. 271.
2. R. B. Barnes. Phys. Rev. **39**, 570 (1932).
3. D. W. Scott, J. P. McCullough, and F. H. Kruse. J. Mol. Spectry. **13**, 313 (1964).
4. G. W. Chantry, A. Anderson, and H. A. Gebbie. Spectrochim. Acta, **20**, 1223 (1964).
5. A. Anderson and Y. T. Loh. Can. J. Chem. **47**, 879 (1969).
6. B. E. Warren and J. T. Burwell. J. Chem. Phys. **3**, 6 (1935).
7. C. Lu and J. Donohue. J. Am. Chem. Soc. **66**, 818 (1944).
8. A. T. Ward. J. Phys. Chem. **72**, 4133 (1968).
9. A. Anderson and H. A. Gebbie. Spectrochim. Acta, **21**, 883 (1965).
10. R. Savoie and A. Anderson. J. Chem. Phys. **44**, 548 (1966).

Thermal reactions of O_2^+ and O^- ions in gaseous ammonia

D. K. Bohme[1] and F. C. Fehsenfeld

Environmental Science Services Administration, Research Laboratories, U.S. Department of Commerce, Boulder, Colorado 80302

Received March 10, 1969

The reaction channels and rate coefficients for the reactions of O_2^+ and O^- ions with NH_3 have been determined at 21.4 °C in a flowing afterglow of pure oxygen and a mixture of helium and oxygen. Charge-transfer was found to be the dominant O_2^+ reaction channel whereas hydrogen atom abstraction was found to be the dominant O^- reaction channel. The secondary NH_3^+ ions were found to react further with NH_3 by hydrogen abstraction to yield NH_4^+ ions, which readily associated with NH_3 to yield cluster ions. The further reaction of secondary OH^- ions with NH_3 was not observed suggesting that the electron affinity of NH_2 may be less than 1.10 eV.

Canadian Journal of Chemistry, 47, 2715 (1969)

The flowing afterglow technique developed in the Environmental Science Services Administration Research Laboratories principally for the investigation of thermal ion–molecule reactions of interest on the earth's ionosphere has recently been employed to study the reactions of O_2^+ and O^- ions in gaseous ammonia.

Details of the operation of the flowing afterglow system and the related data analysis have been described elsewhere (1). In the present experiment, pure oxygen or a helium–oxygen

[1]National Research Council of U.S. Postdoctoral Research Associate.

Can. J. Chem. Downloaded from www.nrcresearchpress.com by 210.87.254.42 on 09/05/12
For personal use only.

(3) is confirmed, as is the explanation of the splittings in terms of the static and correlation fields. The splittings range from 2.5–11 cm^{-1}, compared to 3–7 cm^{-1} in the Raman spectrum (5). The weaker bands, resulting from activity induced by the perturbing crystal field, are readily assigned by reference to the Raman data and the normal coordinate analysis (3): the sharp symmetric peak at 214 cm^{-1} is the predicted i.r. singlet for ν_2; the other bands are broader, and represent the unresolved triplets of ν_9 (78 cm^{-1}), ν_8 (149 cm^{-1}), and ν_{10} (442 cm^{-1}). The absence of lattice modes indicates that their interaction with the electromagnetic field is a factor of at least 20 less than that of the intramolecular fundamentals, which is not unusual for such a symmetric molecule.

A final point of interest is that a comparison of the frequencies of bands observed in both i.r. and Raman shows evidence for coincidences within experimental error. This is especially noticeable for ν_6, and the only exception is ν_4, where there is a 4 cm^{-1} difference. From spectroscopic evidence alone, one might conclude that the crystal does not possess a center of symmetry, whereas the X-ray data show that the opposite is true (6). Infrared and Raman data are often used to aid in crystal structure determinations, especially of hydrogenic molecules, when X-ray, electron, or neutron diffraction measurements are not available (10). The above result shows that this procedure must be used with extreme caution, if spurious deductions are to be avoided.

Acknowledgments

The authors thank Dr. D. E. Irish, Mr. M. H. Brooker, Mr. F. Grossman, and Mr. J. Beke for their assistance in these experiments. This research was supported, in part, by grants from the National Research Council of Canada and the Ontario Department of University Affairs.

1. G. Herzberg. Infrared and Raman spectra. D. Van Nostrand, New York. 1945. p. 271.
2. R. B. Barnes. Phys. Rev. **39**, 570 (1932).
3. D. W. Scott, J. P. McCullough, and F. H. Kruse. J. Mol. Spectry. **13**, 313 (1964).
4. G. W. Chantry, A. Anderson, and H. A. Gebbie. Spectrochim. Acta, **20**, 1223 (1964).
5. A. Anderson and Y. T. Loh. Can. J. Chem. **47**, 879 (1969).
6. B. E. Warren and J. T. Burwell. J. Chem. Phys. **3**, 6 (1935).
7. C. Lu and J. Donohue. J. Am. Chem. Soc. **66**, 818 (1944).
8. A. T. Ward. J. Phys. Chem. **72**, 4133 (1968).
9. A. Anderson and H. A. Gebbie. Spectrochim. Acta, **21**, 883 (1965).
10. R. Savoie and A. Anderson. J. Chem. Phys. **44**, 548 (1966).

Thermal reactions of O_2^+ and O^- ions in gaseous ammonia

D. K. Bohme[1] and F. C. Fehsenfeld

Environmental Science Services Administration, Research Laboratories, U.S. Department of Commerce, Boulder, Colorado 80302

Received March 10, 1969

The reaction channels and rate coefficients for the reactions of O_2^+ and O^- ions with NH_3 have been determined at 21.4 °C in a flowing afterglow of pure oxygen and a mixture of helium and oxygen. Charge-transfer was found to be the dominant O_2^+ reaction channel whereas hydrogen atom abstraction was found to be the dominant O^- reaction channel. The secondary NH_3^+ ions were found to react further with NH_3 by hydrogen abstraction to yield NH_4^+ ions, which readily associated with NH_3 to yield cluster ions. The further reaction of secondary OH^- ions with NH_3 was not observed suggesting that the electron affinity of NH_2 may be less than 1.10 eV.

Canadian Journal of Chemistry, 47, 2715 (1969)

The flowing afterglow technique developed in the Environmental Science Services Administration Research Laboratories principally for the investigation of thermal ion–molecule reactions of interest on the earth's ionosphere has recently been employed to study the reactions of O_2^+ and O^- ions in gaseous ammonia.

Details of the operation of the flowing afterglow system and the related data analysis have been described elsewhere (1). In the present experiment, pure oxygen or a helium–oxygen

[1]National Research Council of U.S. Postdoctoral Research Associate.

Can. J. Chem. Downloaded from www.nrcresearchpress.com by 210.87.254.42 on 09/05/12
For personal use only.

TABLE I

Measured rate constants

Reaction	k
$O_2^+ + NH_3 \rightarrow NH_3^+ + O_2$	2.6 (−9)* cm^3/s
$NH_3^+ + NH_3 \rightarrow NH_4^+ + NH_2$	1.6 (−9) cm^3/s
$NH_4^+ + NH_3 + O_2 \rightarrow NH_4^+ \cdot NH_3 + O_2$	1.8 (−27) cm^6/s
$O^- + NH_3 \rightarrow OH^- + NH_2$	1.2 (−9) cm^3/s

*(−9) denotes 10^{-9}.

mixture is introduced into the excitation region of the flow tube. The gas is excited by the energetic electrons from an electron gun producing O^- and O_2^+ by electron impact with O_2. In addition some O_2^+ is produced by reaction of O_2 with O^+ and excited and ionized helium.

In the region following the excitation region the secondary reactions forming O_2^+ go to completion. Also, O_2^+ ions formed in electronically or vibrationally excited states are de-excited. The O^- and O_2^+ ions are carried with the flowing gas past a downstream port where measured quantities of ammonia are added. In the region following this reactant inlet the characteristic reactions between the ions and ammonia take place. This reaction region is terminated by the sampling port of a quadrupole mass spectrometer. The decline of the primary ion signal and the increase of the secondary ions as a function of the rate of addition of the ammonia allows the determination of a reaction rate constant and reaction channel designation. The rates so determined by this technique should possess an absolute accuracy of 30% with a relative accuracy of better than 10%.

Figure 1 shows a sample run of data for the reaction sequence beginning with O_2^+ in reaction with ammonia. This data was taken at a gas temperature of 21.4 °C. Pure oxygen was introduced into the excitation region and the steady state gas pressure was 0.224 Torr. As the ammonia is added the O_2^+ signal declines and there is a corresponding rise in the NH_3^+ signal due to the reaction

[1] $$O_2^+ + NH_3 \rightarrow NH_3^+ + O_2$$

The reaction channel between NH_3 and O_2^+ to produce NH_2^+ and O_2H is endothermic at room temperature for ground state O_2^+ and was not observed.

The NH_3^+ product signal peaks and then declines corresponding to the production of

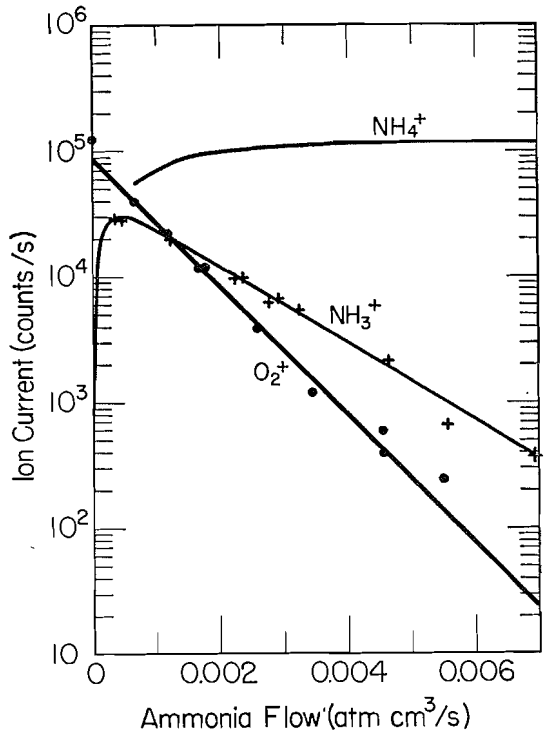

FIG. 1. Ion currents for reactions of O_2^+ and NH_3^+ with NH_3 in an oxygen ion afterglow.

NH_4^+. Since the decline of the NH_3^+ signal is slower than that of the precursor ion O_2^+, a rate coefficient may be determined for the reaction

[2] $$NH_3^+ + NH_3 \rightarrow NH_4^+ + NH_2$$

from the slope of the NH_3^+ signal. With large additions of NH_3 the cluster ions $NH_4^+ \cdot (NH_3)$, $NH_4^+ \cdot (NH_3)_2$, and $NH_4^+ \cdot (NH_4)_3$ were observed, and the rate constant for the first step in the formation of these clusters

[3] $$NH_4^+ + NH_3 + O_2 \rightarrow NH_4^+ \cdot NH_3 + O_2$$

was determined. Table I lists the rate coefficients

Can. J. Chem. Downloaded from www.nrcresearchpress.com by 210.87.254.42 on 09/05/12
For personal use only.

determined for [1], [2], and [3], along with the rate coefficient for the fast reaction between O^- and NH_3 found to proceed by hydrogen abstraction to form OH^-. The product ion OH^- accounted for essentially 100% of the disappearing O^- ions. Electron transfer will not compete since NH_3 has no affinity for electrons (2). Also, there was no indication of a residual signal at $m/e = 16$. This means that no NH_2^- was produced by the reaction and suggests that this channel for the reaction is endothermic at room temperature, implying that the electron affinity of NH_2^- is less than 1.61 eV. This observation is compatible with the electron affinity of NH_2 of 1.21 eV reported by Vedeneyev *et al.* (3). The further reaction of OH^- with NH_3 to yield NH_2^- and H_2O was not observed suggesting that the electron affinity of NH_2 may be less than 1.10 eV.

Gupta *et al.* (4) have measured the thermal (or zero field) rate constant for reaction [2] using a pulsed-beam technique. The rate of 1.0×10^{-9} determined by Gupta *et al.* at 373 °K is somewhat smaller than the value of 1.6×10^{-9} determined in the present experiment at 295 °K. There are no other published rates for the other reactions with which we may compare.

1. E. E. FERGUSON, F. C. FEHSENFELD, and A. L. SCHMELTEKOPF. Advances in atomic and molecular physics. Vol. 5. Academic Press, Inc., New York. 1969; F. C. FEHSENFELD, A. L. SCHMELTEKOPF, P. D. GOLDAN, H. I. SCHIFF, and E. E. FERGUSON. J. Chem. Phys. **44**, 4087 (1966).
2. H. O. PRITCHARD. Chem. Rev. **52**, 529 (1953).
3. V. I. VEDENEYEV, L. V. GURVICH, V. N. KONDRATYEV, V. A. MEDVEDEV, and YE. L. FRANKEVICH. Bond energies, ionization potentials, and electron affinities. St. Martin's Press, Inc., New York. 1966.
4. S. K. GUPTA, E. G. JONES, A. G. HARRISON, and J. J. MYHER. Can. J. Chem. **45**, 3107 (1967).

Thermal reactions of O^- ions with saturated hydrocarbon molecules

D. K. BOHME[1] AND F. C. FEHSENFELD

Environmental Science Services Administration Research Laboratories, U.S. Department of Commerce, Boulder, Colorado 80302

Received March 20, 1969

The thermal energy reactions of O^- ions with saturated hydrocarbon molecules have been investigated in a flowing afterglow of pure oxygen and a mixture of helium and oxygen. Hydrogen atom abstraction was found to be the dominant reaction channel. The reaction probability was found to increase for the higher members of the homologous series. The further reaction of the product OH^- ions with saturated hydrocarbon molecules was not observed. This result was used to estimate an upper limit to the electron affinity of the free radicals CH_3, C_2H_5, C_3H_7, and C_4H_9.

Canadian Journal of Chemistry, 47, 2717 (1969)

The flowing afterglow technique developed in the Environmental Science Services Administration Research Laboratories has been used extensively for the study of thermal energy ion–neutral reactions of interest in aeronomy, and has been employed to investigate the reactions of O^- ions with the homologous hydrocarbon series C_nH_{2n+2}, $n = 1$ to 4. The results suggest a fairly general behavior which is that the reaction of O^- ions with saturated hydrocarbon molecules proceeds by hydrogen atom abstraction

[1] $$O^- + RH \rightarrow OH^- + R$$

and that the reaction probability for this process increases for higher members of the homologous series.

The details of the experimental apparatus, its operation, and the related data analysis have been described in detail elsewhere (1). The flow system is a stainless steel tube about 100 cm long and 8 cm in diameter in which the products of an electron impact ion source are pumped down the tube at a velocity of about 10^4 cm/s. In the present experiments either pure O_2 or O_2 in small fractional quantities in a helium buffer gas is introduced into the excitation region. The O^- ion is then produced by the dissociative ionization reaction, $e + O_2 \rightarrow O^- + O^+ + e$, and, probably to a lesser extent, the dissociative

[1]National Research Council of U.S. Postdoctoral Research Associate.

Can. J. Chem. Downloaded from www.nrcresearchpress.com by 210.87.254.42 on 09/05/12
For personal use only.

determined for [1], [2], and [3], along with the rate coefficient for the fast reaction between O^- and NH_3 found to proceed by hydrogen abstraction to form OH^-. The product ion OH^- accounted for essentially 100% of the disappearing O^- ions. Electron transfer will not compete since NH_3 has no affinity for electrons (2). Also, there was no indication of a residual signal at $m/e = 16$. This means that no NH_2^- was produced by the reaction and suggests that this channel for the reaction is endothermic at room temperature, implying that the electron affinity of NH_2^- is less than 1.61 eV. This observation is compatible with the electron affinity of NH_2 of 1.21 eV reported by Vedeneyev *et al.* (3). The further reaction of OH^- with NH_3 to yield NH_2^- and H_2O was not observed suggesting that the electron affinity of NH_2 may be less than 1.10 eV.

Gupta *et al.* (4) have measured the thermal (or zero field) rate constant for reaction [2] using a pulsed-beam technique. The rate of 1.0×10^{-9} determined by Gupta *et al.* at 373 °K is somewhat smaller than the value of 1.6×10^{-9} determined in the present experiment at 295 °K. There are no other published rates for the other reactions with which we may compare.

1. E. E. FERGUSON, F. C. FEHSENFELD, and A. L. SCHMELTEKOPF. Advances in atomic and molecular physics. Vol. 5. Academic Press, Inc., New York. 1969; F. C. FEHSENFELD, A. L. SCHMELTEKOPF, P. D. GOLDAN, H. I. SCHIFF, and E. E. FERGUSON. J. Chem. Phys. **44**, 4087 (1966).
2. H. O. PRITCHARD. Chem. Rev. **52**, 529 (1953).
3. V. I. VEDENEYEV, L. V. GURVICH, V. N. KONDRATYEV, V. A. MEDVEDEV, and YE. L. FRANKEVICH. Bond energies, ionization potentials, and electron affinities. St. Martin's Press, Inc., New York. 1966.
4. S. K. GUPTA, E. G. JONES, A. G. HARRISON, and J. J. MYHER. Can. J. Chem. **45**, 3107 (1967).

Thermal reactions of O^- ions with saturated hydrocarbon molecules

D. K. BOHME[1] AND F. C. FEHSENFELD

Environmental Science Services Administration Research Laboratories, U.S. Department of Commerce, Boulder, Colorado 80302

Received March 20, 1969

The thermal energy reactions of O^- ions with saturated hydrocarbon molecules have been investigated in a flowing afterglow of pure oxygen and a mixture of helium and oxygen. Hydrogen atom abstraction was found to be the dominant reaction channel. The reaction probability was found to increase for the higher members of the homologous series. The further reaction of the product OH^- ions with saturated hydrocarbon molecules was not observed. This result was used to estimate an upper limit to the electron affinity of the free radicals CH_3, C_2H_5, C_3H_7, and C_4H_9.

Canadian Journal of Chemistry, 47, 2717 (1969)

The flowing afterglow technique developed in the Environmental Science Services Administration Research Laboratories has been used extensively for the study of thermal energy ion–neutral reactions of interest in aeronomy, and has been employed to investigate the reactions of O^- ions with the homologous hydrocarbon series C_nH_{2n+2}, $n = 1$ to 4. The results suggest a fairly general behavior which is that the reaction of O^- ions with saturated hydrocarbon molecules proceeds by hydrogen atom abstraction

[1] $$O^- + RH \rightarrow OH^- + R$$

and that the reaction probability for this process increases for higher members of the homologous series.

The details of the experimental apparatus, its operation, and the related data analysis have been described in detail elsewhere (1). The flow system is a stainless steel tube about 100 cm long and 8 cm in diameter in which the products of an electron impact ion source are pumped down the tube at a velocity of about 10^4 cm/s. In the present experiments either pure O_2 or O_2 in small fractional quantities in a helium buffer gas is introduced into the excitation region. The O^- ion is then produced by the dissociative ionization reaction, $e + O_2 \rightarrow O^- + O^+ + e$, and, probably to a lesser extent, the dissociative

[1]National Research Council of U.S. Postdoctoral Research Associate.

Can. J. Chem. Downloaded from www.nrcresearchpress.com by 210.87.254.40 on 09/05/12
For personal use only.

TABLE I

Calculated reaction probabilities for hydrogen abstraction by O^- ions

Reaction	k (22.5 °C) cm³/s	k_c cm³/s	Reaction probability, k/k_c
$O^- + CH_4 \rightarrow OH^- + CH_3 + 0.26$ eV	1.0 (−10)*	1.3 (−9)	0.08
$O^- + C_2H_6 \rightarrow OH^- + C_2H_5 + 0.46$ eV	7.0 (−10)	1.5 (−9)	0.47
$O^- + C_3H_8 \rightarrow OH^- + C_3H_7 + 0.55$ eV	9.3 (−10)	1.7 (−9)	0.55
$O^- + n\text{-}C_4H_{10} \rightarrow OH^- + C_4H_9 + 0.59$ eV	1.2 (−9)	1.9 (−9)	0.63

*(−10) denotes 10^{-10}.

attachment reaction, $e + O_2 \rightarrow O^- + O$. At the end of the tube the ion composition is sampled, mass analyzed by means of a quadrupole mass spectrometer, and counted. The hydrocarbon reactant gases are added downstream of the excitation region. They had the following minimum purity in mole%: methane, 99.95; ethane, 99.0; propane, 99.5; *n*-butane, 99.5. The decline of the reactant O^- ion signal as a function of hydrocarbon gas addition constitutes the raw data from which rate coefficients are determined with an absolute accuracy of about 30% and a somewhat better relative accuracy. The experiments were performed at 22.5 °C at a total steady state pressure of 0.23 Torr.

A list of the reactions investigated and the measured rate constants are given in Table I. The major product ion in each case was OH^-, indicating that hydrogen abstraction, i.e. reaction [1], is the dominant reaction channel. The reaction energies listed in Table I apply if the products are in their ground states and are given only to show that the reactions are exothermic at 22.5 °C. It is of course not unlikely that the products are formed in vibrationally excited states. Electron affinities of 1.465 and 1.78 eV were used for O and OH respectively (2). Bond energies were taken from Vedeneyev *et al.* (3).

A consideration of the ground state reaction energetics complemented by experimental observations allows an estimation of upper limits to the electron affinity of several hydrocarbon radicals. It is observed in these experiments that the OH^- ions produced by the hydrogen abstraction reactions listed in Table I do not react efficiently with the added hydrocarbon molecules (rate coefficient $\leq 10^{-12}$ cm³/s). This strongly suggests, but does not prove, that the reaction channel

[2] $$OH^- + RH \rightarrow R^- + H_2O$$

is endothermic since most exothermic ion–molecule reactions proceed rapidly with little or no activation energy. Accordingly, an upper limit to the value of the electron affinity of CH_3, C_2H_5, C_3H_7, and C_4H_9 may be estimated. The results are given in Table II together with values reported in the literature.

TABLE II

Estimates of the electron affinity of free radicals

Free radical	Electron affinity: Present result	Reference 4	Reference 5*
CH_3	<1.08	1.08, 1.1†	1.8
C_2H_5	<0.88	0.9†	1.4
C_3H_7	<0.79	0.8†	1.0
C_4H_9	<0.75		

*Calculated values (see ref. 4).
†Provisional results of Hush and Oldham (see ref. 4).

It is instructive to compare the experimentally measured reaction rate constant, k, with the theoretical collision rate constant, k_c. For an ion colliding with a neutral molecule, the theoretical collision rate constant is given by the expression

[3] $$k_c = 2\pi e\left(\frac{\alpha}{\mu}\right)^{\frac{1}{2}}$$

Here μ is the reduced mass of the reactants and α is the polarizability of the neutral reactant. Equation [3] is derived on the assumption that the total collision cross-section is determined solely by the long range ion-induced dipole interaction which results in orbiting or spiralling (6). The ratio k/k_c is a measure of the reaction probability. The calculated reaction probabilities for hydrogen abstraction from saturated hydrocarbon molecules by O^- ions are given in Table I. Polarizabilities for the neutral hydrocarbon

Can. J. Chem. Downloaded from www.nrcresearchpress.com by 210.87.254.40 on 09/05/12
For personal use only.

molecules were taken from Rothe and Bernstein (7). As indicated in Table I, the experimental rate constant for the reaction of O^- with CH_4 is considerably lower than predicted by theory, and accordingly a significant fraction (0.92) of the orbiting collisions does not lead to a reaction. It is also apparent from the reaction probabilities given in Table I that the number of hydrogen abstraction reactions per orbiting collision increases for the reaction of O^- with higher members of the homologous series. Equation [3] neglects the dispersion energy between the two mutually induced dipoles in the ion–molecule collision. Inclusion of such a term in the interaction potential for O^- and the very polarizable hydrocarbon molecules could increase the theoretical collision rate constant, k_c, by as much as 10%. This in turn would decrease the reaction probability by as much as 10%.

1. E. E. FERGUSON, F. C. FEHSENFELD, and A. L. SCHMELTEKOPF. Advances in atomic and molecular physics. Vol. 5. Academic Press, Inc., New York. 1969.
F. C. FEHSENFELD, A. L. SCHMELTEKOPF, P. D. GOLDAN, H. I. SCHIFF, and E. E. FERGUSON. J. Chem. Phys. **44**, 4087 (1966).
2. L. M. BRANSCOMB. Atomic and molecular processes. *Edited by* D. R. Bates. Academic Press, Inc., New York. 1962. Chap. 4.
3. V. I. VEDENEYEV, L. V. GURVICH, V. N. KONDRATYEV, V. A. MEDVEDEV, and YE. L. FRANKEVICH. Bond energies, ionization potentials, and electron affinities. St. Martin's Press, Inc., New York. 1966.
4. H. O. PRITCHARD. Chem. Rev. **52**, 529 (1953).
5. F. A. MATSEN, W. W. ROBERTSON, and R. L. CHUOKE. Chem. Rev. **41**, 273 (1947).
6. G. GIOUMOUSIS and D. P. STEVENSON. J. Chem. Phys. **39**, 1413 (1963).
7. E. W. ROTHE and R. B. BERNSTEIN. J. Chem. Phys. **31**, 1619 (1959).

Photo-initiated reactions of thiols and olefins. IV. Inhibition of butene-2 isomerization by butadiene-1,3

D. M. GRAHAM AND J. F. SOLTYS
Department of Chemistry, University of Western Ontario, London, Ontario

Received December 2, 1968

The kinetics of inhibition of the thiyl radical catalyzed isomerization of *cis*-butene-2 has been investigated. The results yielded the value 6.9×10^7 *l* $mole^{-1}$ s^{-1} for the rate constant for CH_3S attack on butadiene. It is proposed that this technique could be generally useful in determining attack constants for conjugated olefins.

Canadian Journal of Chemistry, 47, 2719 (1969)

Introduction

It was shown previously that the rate constant for thiyl radical attack on butadiene cannot be obtained from the measurement of addition rates (1). The adduct radical produced is not sufficiently reactive for thiol dehydrogenation to compete successfully with termination reactions, and no chain character was observed. This behavior is probably typical of conjugated olefins, and it appeared desirable to find a technique for determining reactivities in such cases. In earlier work on thiyl radical catalyzed isomerization of butene-2, it was found necessary to purify the olefin by gas chromatography in order to obtain consistent kinetic data over the entire concentration range used (2). The effects observed with the non-purified samples were attributed to the presence of very small quantities of butadiene in the olefin. As a result of further investigation of these effects, a new method for determining relative attack constants for conjugated olefins has been obtained.

Experimental

The techniques used were as previously described (1, 2). All results given here were obtained using a quartz reaction cell, 5 cm diameter × 10 cm length.

Results

The isomerization curves given in Fig. 1 show that addition of small amounts of butadiene to *cis*-butene-2 produces an initial retardation in rate which disappears, presumably, when the butadiene is used up. Figure 2 indicates that the initial inhibited rate of isomerization ($R_{ic} = (d[T]/dt)_0$) is inversely proportional to the initial

Can. J. Chem. Downloaded from www.nrcresearchpress.com by 210.87.254.40 on 09/05/12
For personal use only.

molecules were taken from Rothe and Bernstein (7). As indicated in Table I, the experimental rate constant for the reaction of O^- with CH_4 is considerably lower than predicted by theory, and accordingly a significant fraction (0.92) of the orbiting collisions does not lead to a reaction. It is also apparent from the reaction probabilities given in Table I that the number of hydrogen abstraction reactions per orbiting collision increases for the reaction of O^- with higher members of the homologous series. Equation [3] neglects the dispersion energy between the two mutually induced dipoles in the ion–molecule collision. Inclusion of such a term in the interaction potential for O^- and the very polarizable hydrocarbon molecules could increase the theoretical collision rate constant, k_c, by as much as 10%. This in turn would decrease the reaction probability by as much as 10%.

1. E. E. FERGUSON, F. C. FEHSENFELD, and A. L. SCHMELTEKOPF. Advances in atomic and molecular physics. Vol. 5. Academic Press, Inc., New York. 1969. F. C. FEHSENFELD, A. L. SCHMELTEKOPF, P. D. GOLDAN, H. I. SCHIFF, and E. E. FERGUSON. J. Chem. Phys. **44**, 4087 (1966).
2. L. M. BRANSCOMB. Atomic and molecular processes. *Edited by* D. R. Bates. Academic Press, Inc., New York. 1962. Chap. 4.
3. V. I. VEDENEYEV, L. V. GURVICH, V. N. KONDRATYEV, V. A. MEDVEDEV, and YE. L. FRANKEVICH. Bond energies, ionization potentials, and electron affinities. St. Martin's Press, Inc., New York. 1966.
4. H. O. PRITCHARD. Chem. Rev. **52**, 529 (1953).
5. F. A. MATSEN, W. W. ROBERTSON, and R. L. CHUOKE. Chem. Rev. **41**, 273 (1947).
6. G. GIOUMOUSIS and D. P. STEVENSON. J. Chem. Phys. **39**, 1413 (1963).
7. E. W. ROTHE and R. B. BERNSTEIN. J. Chem. Phys. **31**, 1619 (1959).

Photo-initiated reactions of thiols and olefins. IV. Inhibition of butene-2 isomerization by butadiene-1,3

D. M. GRAHAM AND J. F. SOLTYS
Department of Chemistry, University of Western Ontario, London, Ontario

Received December 2, 1968

The kinetics of inhibition of the thiyl radical catalyzed isomerization of *cis*-butene-2 has been investigated. The results yielded the value 6.9×10^7 *l* $mole^{-1}$ s^{-1} for the rate constant for CH_3S attack on butadiene. It is proposed that this technique could be generally useful in determining attack constants for conjugated olefins.

Canadian Journal of Chemistry, 47, 2719 (1969)

Introduction

It was shown previously that the rate constant for thiyl radical attack on butadiene cannot be obtained from the measurement of addition rates (1). The adduct radical produced is not sufficiently reactive for thiol dehydrogenation to compete successfully with termination reactions, and no chain character was observed. This behavior is probably typical of conjugated olefins, and it appeared desirable to find a technique for determining reactivities in such cases. In earlier work on thiyl radical catalyzed isomerization of butene-2, it was found necessary to purify the olefin by gas chromatography in order to obtain consistent kinetic data over the entire concentration range used (2). The effects observed with the non-purified samples were attributed to the presence of very small quantities of butadiene in the olefin. As a result of further investigation of these effects, a new method for determining relative attack constants for conjugated olefins has been obtained.

Experimental

The techniques used were as previously described (1, 2). All results given here were obtained using a quartz reaction cell, 5 cm diameter × 10 cm length.

Results

The isomerization curves given in Fig. 1 show that addition of small amounts of butadiene to *cis*-butene-2 produces an initial retardation in rate which disappears, presumably, when the butadiene is used up. Figure 2 indicates that the initial inhibited rate of isomerization ($R_{ic} = (d[T]/dt)_0$) is inversely proportional to the initial

Can. J. Chem. Downloaded from www.nrcresearchpress.com by 210.87.254.5 on 09/05/12
For personal use only.

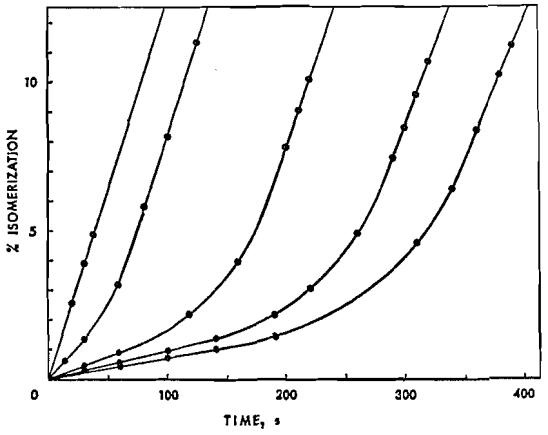

FIG. 1. Inhibition of isomerization. $[CH_3SH] = 1.08 \times 10^{-3}$ mole l^{-1}; [*cis*-butene-2] $= 5.38 \times 10^{-4}$ mole l^{-1}; from left to right, [butadiene] = 0, 2.07, 8.87, 15.5, and 19.9×10^{-7} mole l^{-1}.

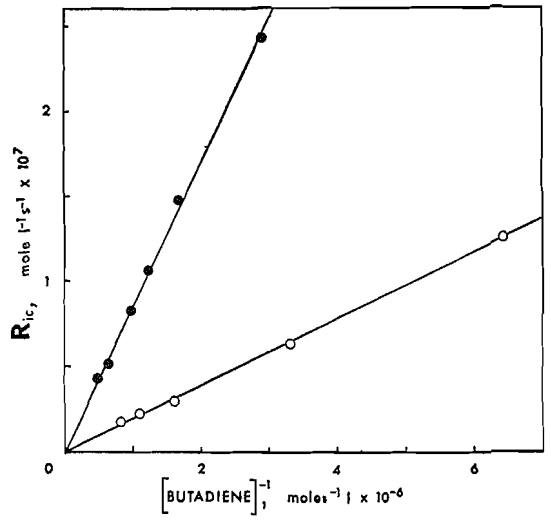

FIG. 2. Dependence of the inhibited rate on butadiene. [*cis*-butene-2] $= 5.38 \times 10^{-4}$ mole l^{-1}; ○, $[CH_3SH] = 2.15 \times 10^{-4}$; ●, 1.08×10^{-3} mole l^{-1}.

butadiene concentration. The slopes of the two lines are approximately in the ratio of the thiol pressures, and, since the rate of thiol photolysis is roughly proportional to the thiol concentration at low pressures, a first order dependence on the rate of generation of CH_3S is indicated. This was confirmed for the higher thiol concentration using calibrated screens to show a first order dependence on incident light intensity.

An inhibition period may be determined by the point of intersection of the extrapolated initial and final rates. This represents the time that would be required for all the butadiene to react if the initial mechanism were continuous to [B] = 0, and then changed abruptly to the uninhibited mechanism. A plot of inhibition periods for the results of Fig. 1 is given in Fig. 3; the constant slope indicates that the rate of disappearance of butadiene is zero order on concentration (a first order plot is not linear).

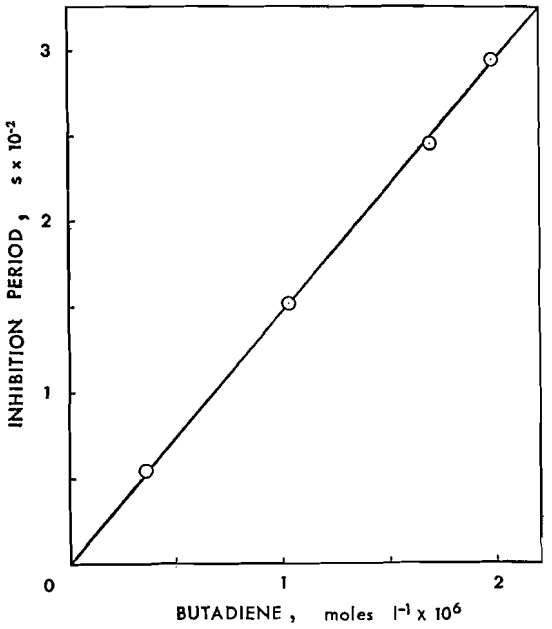

FIG. 3. Dependence of the inhibition period on butadiene. [*cis*-butene-2] $= 5.38 \times 10^{-4}$ mole l^{-1}; $[CH_3SH] = 1.08 \times 10^{-3}$ mole l^{-1}.

Discussion

The initial stages of the thiyl radical catalyzed isomerization of *cis*-butene-2 (C) to the *trans*-form (T) has been treated using the following mechanism (2)

$$CH_3SH \xrightarrow{h\nu} CH_3S \qquad (\text{rate} = r_i)$$

[1*c*] $\quad CH_3S + C \longrightarrow X$

[2] $\quad X + CH_3SH \longrightarrow XH + CH_3S$

[3] $\quad X \longrightarrow CH_3S + \rho_3 T + (1 - \rho_3)C$

[4] $\quad 2CH_3S \longrightarrow CH_3SSCH_3$

X is the adduct radical and ρ_3 is the probability that, when it decomposes, the *trans* isomer is formed. It has been established that the rate of reaction [2] is negligible compared with that of

Can. J. Chem. Downloaded from www.nrcresearchpress.com by 210.87.254.5 on 09/05/12
For personal use only.

reaction [3] over the concentration ranges available to gas phase investigation. Since $[CH_3S] \gg [X]$ over the entire concentration range available to experiment, inhibition by butadiene (B) most probably occurs by competition for thiyl radicals as a result of the following reaction

[1b] $$CH_3S + B \rightarrow Y$$

The allyl-type adduct radical, Y, would be more stable than that obtained from butene by about 13 kcal (3). It is, therefore, very unlikely that the reverse reaction [3] need be considered for butadiene, since, at the pressures used, the radicals would be rapidly thermalized, and the activation energy for decomposition would then be at least 20 kcal.

Photolysis of methanethiol produces initially CH_3S and H almost exclusively; the hydrogen atom may subsequently attack thiol to give $CH_3S + H_2$, or add to olefin. Provided the radical produced by addition to olefin is sufficiently reactive to dehydrogenate thiol rapidly, and does not enter any other reaction, the overall initiation step may be considered to be the generation of two thiyl radicals. On the basis of the earlier study (2), this appears to be valid for the uninhibited reaction at the concentrations used here. Addition of a hydrogen atom to butadiene, however, should be very rapid and, since the resulting radical does not appear to dehydrogenate thiol very effectively (1), the following reactions should also be considered

$$CH_3SH \rightarrow CH_3S + H \qquad (\text{rate} = r_i/2)$$

[a] $$H + CH_3SH \rightarrow H_2 + CH_3S$$

[b] $$H + B \rightarrow Y$$

In terms of these reactions the initial rate of isomerization of *cis*-butene-2 is

[5] $$R_{ic} = \rho_3 k_{1c} [C][CH_3S]$$

This assumes that reaction [3] is the only fate of X. Since the inhibited rate was shown to be proportional to the rate of initiation, and to the inverse butadiene concentration, the steady-state thiyl radical concentration may be written

[6] $$[CH_3S] = \eta r_i/[B]$$

where η is the proportionality factor.

The rate of disappearance of butadiene is

[7] $$-\frac{d[B]}{dt} = \frac{r_i}{2} \cdot \frac{k_b[B]}{k_b[B] + k_a[CH_3SH]} + k_{1b}[B][CH_3S]$$

The second term of this expression must be independent of [B] because of eq. [6], and since it was concluded earlier that the rate of disappearance of butadiene was zero order on butadiene, the first term in eq. [7] must be negligible. This requires that, for these experiments, $k_b[B] \ll k_a[CH_3SH]$, which is not unreasonable since the thiol concentration is about 1000 times that of the butadiene. Omitting the first term and using eq. [6], eq. [7] may be integrated to obtain an expression for the inhibition period, defined as $t_i = t$ at $[B] = 0$

[8] $$t_i = [B]_0/\eta r_i k_{1b}$$

Combining eqs. [5], [6], and [8], one gets

[9] $$t_i R_{ic} = \rho_3 \frac{k_{1c}}{k_{1b}} [C]$$

The rate constant ratios calculated using this equation are given in Table I. The average is 0.0232, and since $\rho_3 k_{1c} = 1.6 \times 10^6$ l mole^{-1} s^{-1} (1), $k_{1b} = 6.9 \times 10^7$ l mole^{-1} s^{-1}.

TABLE I

Inhibition data obtained from Fig. 1

Butadiene mole l^{-1} × 10^7	R_{ic} mole l^{-1} s^{-1} × 10^8	t_i s	$\frac{\rho_3 k_{1c}}{k_{1b}}$
2.07	24.1	54	0.0242
8.87	8.16	152	0.0230
15.5	5.11	246	0.0234
18.9	4.25	294	0.0232

These equations do not depend upon the ultimate fate of the Y radicals; they may disappear by reaction with thiol, or more probably, on the basis of the addition kinetics (1), by termination. The only requirement for the use of this technique for measuring attack constants is that the added species decrease the thiyl radical concentration. This can occur only if decomposition of the resulting adduct radical is very slow. It has been shown, for example, that the presence of a large excess of ethylene has no effect on the rate of isomerization of butene-2, since reaction

Can. J. Chem. Downloaded from www.nrcresearchpress.com by 210.87.254.5 on 09/05/12
For personal use only.

[3] is very rapid for ethylene. It is highly probable that this reaction is negligible at 25 °C for butadiene but until this is experimentally verified, the value of the attack constant given above should perhaps be considered a lower limit.

Acknowledgments

We are grateful to the National Research Council of Canada for the financial support bestowed, and to the Province of Ontario for a Fellowship awarded to J.F.S.

1. D. M. GRAHAM and J. F. SOLTYS. Can. J. Chem. (III). This issue.
2. D. M. GRAHAM, R. L. MIEVILLE, and C. SIVERTZ. Can. J. Chem. **42**, 2239 (1964).
3. K. W. EGGER, D. M. GOLDEN, and S. W. BENSON. J. Am. Chem. Soc. **86**, 5420 (1964).

The use of a saturation narrowed nuclear magnetic resonance spectrum to observe phase transitions in lithium stearate

W. R. JANZEN[1] AND B. A. DUNELL

Chemistry Department, The University of British Columbia, Vancouver 8, British Columbia

Received March 4, 1969

The phase transitions in solid lithium stearate have been observed using saturation narrowed spectra, whose high signal-to-noise ratio is advantageous particularly in cases where unfavorable packing factor for the sample or long T_1 makes the normal unsaturated absorption spectrum difficult to obtain. The saturation narrowed spectra are compared with unsaturated absorption spectra of lithium stearate and are discussed in terms of Provotorov's theory of saturation.

Canadian Journal of Chemistry, 47, 2722 (1969)

The use of broad line nuclear magnetic resonance (n.m.r.) spectra to investigate molecular motion and phase transitions in solids is well known (see, for example, ref. 1), and the method has been used in this laboratory to study a number of long chain fatty acids and their salts (2). During the course of these investigations we observed narrowing and intensification of the n.m.r. line with increasing intensity of the radio frequency (r.f.) field H_1. Our observations are in qualitative agreement with the saturation and line-shape theory of Provotorov (3) for solids at H_1 fields of intermediate intensity. The spectra shown in Fig. 1 were obtained for lithium stearate at room temperature using r.f. fields at 56.4 MHz with intensities of 0.45, 4.5, and 14.3 mG. It can be seen that as the H_1 intensity increases, the observed line shape goes in the direction of the Lorentzian shape, which is predicted by Provotorov theory as the limiting situation for high H_1, in agreement with Redfield's saturation theory (4). The fact that the line shape for lithium stearate at the highest available H_1 at 56.4 MHz is effectively Gaussian is thought to be entirely coincidental. In the strong saturation region the line shape can also be perturbed by absorption of energy by the spin system from the audio modulation field (4, 5). This rotary modulation saturation may account for the difference between the observed saturation narrowed line shape and that predicted by Provotorov. The great improvement in signal-to-noise ratio, which is evident in Fig. 1 as one goes to higher H_1 values, may be of considerable advantage in observing and recording spectra in cases where either an unfavorable packing factor for the sample in the spectrometer probe or a long T_1 makes the normal unsaturated absorption spectrum difficult to obtain.

It was of interest to determine how the saturation narrowed line would behave as one went through phase changes in the solid state of a substance for which such lines were obtainable. Lithium stearate had been observed to have two transitions between room temperature and 200 °C (2, 6). The lower temperature transition, near 115 °C, was attributed to a change from one crystalline form to another, and the higher temperature transition, near 187 °C, to a change from a crystalline to a waxy phase. It was also observed that the thermal history of

[1]Present address: Research Laboratories, Eastman Kodak Co., Rochester, New York 14 650.

Can. J. Chem. Downloaded from www.nrcresearchpress.com by 210.87.254.5 on 09/05/12
For personal use only.

[3] is very rapid for ethylene. It is highly probable that this reaction is negligible at 25 °C for butadiene but until this is experimentally verified, the value of the attack constant given above should perhaps be considered a lower limit.

Acknowledgments

We are grateful to the National Research Council of Canada for the financial support bestowed, and to the Province of Ontario for a Fellowship awarded to J.F.S.

1. D. M. GRAHAM and J. F. SOLTYS. Can. J. Chem. (III). This issue.
2. D. M. GRAHAM, R. L. MIEVILLE, and C. SIVERTZ. Can. J. Chem. **42**, 2239 (1964).
3. K. W. EGGER, D. M. GOLDEN, and S. W. BENSON. J. Am. Chem. Soc. **86**, 5420 (1964).

The use of a saturation narrowed nuclear magnetic resonance spectrum to observe phase transitions in lithium stearate

W. R. JANZEN[1] AND B. A. DUNELL

Chemistry Department, The University of British Columbia, Vancouver 8, British Columbia

Received March 4, 1969

The phase transitions in solid lithium stearate have been observed using saturation narrowed spectra, whose high signal-to-noise ratio is advantageous particularly in cases where unfavorable packing factor for the sample or long T_1 makes the normal unsaturated absorption spectrum difficult to obtain. The saturation narrowed spectra are compared with unsaturated absorption spectra of lithium stearate and are discussed in terms of Provotorov's theory of saturation.

Canadian Journal of Chemistry, 47, 2722 (1969)

The use of broad line nuclear magnetic resonance (n.m.r.) spectra to investigate molecular motion and phase transitions in solids is well known (see, for example, ref. 1), and the method has been used in this laboratory to study a number of long chain fatty acids and their salts (2). During the course of these investigations we observed narrowing and intensification of the n.m.r. line with increasing intensity of the radio frequency (r.f.) field H_1. Our observations are in qualitative agreement with the saturation and line-shape theory of Provotorov (3) for solids at H_1 fields of intermediate intensity. The spectra shown in Fig. 1 were obtained for lithium stearate at room temperature using r.f. fields at 56.4 MHz with intensities of 0.45, 4.5, and 14.3 mG. It can be seen that as the H_1 intensity increases, the observed line shape goes in the direction of the Lorentzian shape, which is predicted by Provotorov theory as the limiting situation for high H_1, in agreement with Redfield's saturation theory (4). The fact that the line shape for lithium stearate at the highest available H_1 at 56.4 MHz is effectively Gaussian is thought to be entirely coincidental. In the strong saturation region the line shape can also be perturbed by absorption of energy by the spin system from the audio modulation field (4, 5). This rotary modulation saturation may account for the difference between the observed saturation narrowed line shape and that predicted by Provotorov. The great improvement in signal-to-noise ratio, which is evident in Fig. 1 as one goes to higher H_1 values, may be of considerable advantage in observing and recording spectra in cases where either an unfavorable packing factor for the sample in the spectrometer probe or a long T_1 makes the normal unsaturated absorption spectrum difficult to obtain.

It was of interest to determine how the saturation narrowed line would behave as one went through phase changes in the solid state of a substance for which such lines were obtainable. Lithium stearate had been observed to have two transitions between room temperature and 200 °C (2, 6). The lower temperature transition, near 115 °C, was attributed to a change from one crystalline form to another, and the higher temperature transition, near 187 °C, to a change from a crystalline to a waxy phase. It was also observed that the thermal history of

[1]Present address: Research Laboratories, Eastman Kodak Co., Rochester, New York 14 650.

Can. J. Chem. Downloaded from www.nrcresearchpress.com by 210.87.254.42 on 09/05/12
For personal use only.

Can. J. Chem. Downloaded from www.nrcresearchpress.com by 210.87.254.42 on 09/05/12
For personal use only.

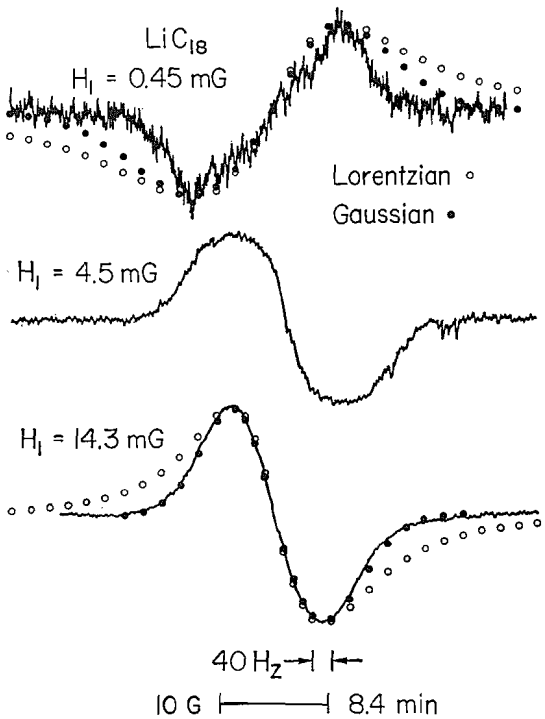

FIG. 1. The development of saturation narrowing with increasing H_1 in solid lithium stearate at room temperature. The observed spectra are compared with calculated Gaussian and Lorentzian line shapes of the same intensity (filled and open points, respectively). Modulation at 40 Hz was of the width indicated. Rate of scanning: 10 G in 8.4 min.

the sample, in particular the number of times the sample had been melted before a spectrum was run, had a strong effect on the line shape as one approached the crystalline to waxy phase transition. The intense, saturation narrowed n.m.r. line of lithium stearate has been observed between room temperature and 200 °C for a sample which was not fused during the course of preparation or subsequently. Preparative details have been given in the paper by Cyr, Janzen, and Dunell (2). Line widths of the saturation narrowed spectra, which were run at $H_1 = 14.3$ mG at 56.4 MHz and with a peak-to-peak modulation varying from 1.8 G at lower temperatures to 0.7 G near 200 °C, are shown in Fig. 2 together with the normal, unsaturated line widths obtained from spectra run at $H_1 = 0.45$ mG.

The line width vs. temperature curves of Fig. 2 show that the lithium stearate phase transitions

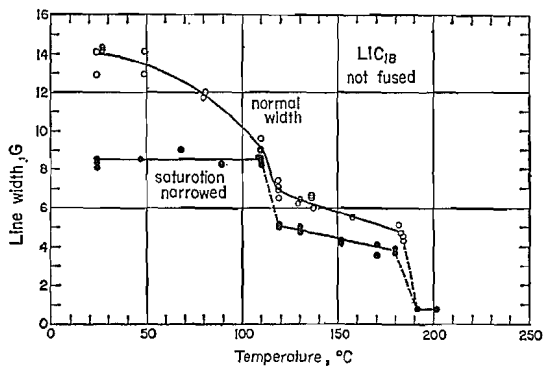

FIG. 2. Line widths of a never fused lithium stearate sample as a function of temperature: open circles, unsaturated, $H_1 = 0.45$ mG; filled circles, saturation narrowed, $H_1 = 14.3$ mG.

are equally observable from the saturation narrowed spectra as from the normal, unsaturated spectra, and that the temperature at which each transition is located is independent of the type of spectrum observed. Provotorov's equation 48 of ref. 3 for the absorption component of magnetic susceptibility can be written as

$$\chi'' = [\gamma^2\hbar\langle I_z\rangle_0\pi g(\Delta)/2][1 + \gamma^2 H_1^2\pi g(\Delta)T_1 \times (1 + T_D\hbar^2\Delta^2/T_1H_D^2)]^{-1}$$

where T_1 and T_D are the spin–lattice relaxation times for energy in the Zeeman system and the dipole–dipole interaction, respectively, $g(\Delta)$ is the unsaturated line shape, $H_D = \gamma\hbar H_L = \gamma\hbar\langle\Delta H^2\rangle^{1/2}/\sqrt{3}$, $\langle\Delta H^2\rangle$ being the second moment and H_L Redfield's local field (4), and $\Delta = \omega - \omega_0$, the distance from resonance. For large enough H_1, in the condition of strong saturation, this expression reduces to

$$\chi'' = (\hbar\langle I_z\rangle_0/2H_1^2T_1)(1 + T_D\hbar^2\Delta^2/T_1H_D^2)^{-1}$$

and we find the absorption line width under strong saturation to be

$$[1] \qquad \Delta H_{as} = (2/3)(T_1/T_D)^{1/2}\langle\Delta H^2\rangle^{1/2}$$

where this is measured from maximum to minimum slope of the absorption. One could expect to find, therefore, under conditions of strong saturation, a rapid change in the width of the saturation narrowed line wherever there is a rapid change in the second moment, $\langle\Delta H^2\rangle$, of the normal line unless there are compensating changes in the ratio of relaxation times T_1/T_D. An estimate of whether we have strong saturation

Can. J. Chem. Downloaded from www.nrcresearchpress.com by 210.87.254.42 on 09/05/12
For personal use only.

can be obtained by considering the quantity $\gamma^2 H_1^2 \pi g(\Delta) T_1$. Saturation is strong at resonance ($\Delta = 0$) if this is large compared to unity. We take $\gamma = 2.68 \times 10^4$ for the proton, $H_1 = 14.3$ mG, and $T_1 = 16.8$ s, a value obtained for this sample by two independent techniques (7). The normalized, unsaturated line shape function at the center of resonance, $g(0)$, can be evaluated by integration of the unsaturated derivative absorption signal (the experimental, lock-in detector signal), called $v_1(\Delta)$ by Goldman (5). Since $g(\Delta)$ is normalized to unity, and $v_1(\Delta) \propto dg(\Delta)/d\Delta$ in the unsaturated condition, one has

$$g(0) = \int_{-\infty}^{\infty} v_1(\Delta)d\Delta/2 \int_{-\infty}^{\infty} \Delta v_1(\Delta)d\Delta$$

An average value of $g(0)$, obtained from three room temperature unsaturated absorption spectra of lithium stearate is 2.90×10^{-6} s (7). We thus obtain $\gamma^2 H_1^2 \pi g(0) T_1 = 22.4$, which is large compared with unity, and we can consider that saturation is strong. As Fig. 3 demonstrates, the second moment of the normal unsaturated spectrum decreases continually in the temperature range 24–110 °C, whereas the saturation narrowed line remains at constant width. Consequently the ratio T_1/T_D must change in this temperature range. Using eq. [1] and values of saturated line width and second moment shown in Figs. 2 and 3, we obtain $T_1/T_D = 7.4$ at 25 °C and 10.8 at 110 °C. Unfortunately this may not be a good method for measuring T_1/T_D ratios because of possible line shape perturbation by rotary modulation saturation mentioned earlier. The ratio can, however, be measured by pulse techniques (see, for example, ref. 8).

One may also note that Fig. 3 shows that the position of even the phase transition between crystalline forms of lithium stearate, as observed by n.m.r., depends on the thermal history of the sample. For the sample never fused the midpoint of the range of rapid decrease in line width and second moment corresponds to approximately 115 °C, which is the temperature of the transition according to dilatometry (9) and differential thermal analysis (10). In the previous experiments on a sample which had been fused during preparation, the transition temperature had been taken as the intersection of the extrapolated straight line portions of the line width or

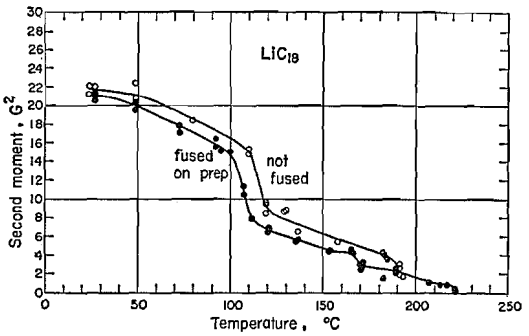

FIG. 3. Second moments for two lithium stearate samples, one never fused (open circles), and the other fused during preparation (filled circles).

second moment vs. temperature curves which lie just above and within the rapid decrease region. For the once melted sample, this corresponded to 114 °C.

The use of saturation narrowed n.m.r. spectra, having excellent signal-to-noise ratio, may be applicable to the examination of phase transitions in other solids. Before placing too much reliance on the method one should, however, investigate the dependence of the T_1/T_D ratio on temperature and on the existence of known phase transitions.

Acknowledgment

The authors thank the National Research Council of Canada for financial support of this work.

1. J. G. POWLES. Arch. Sci. Geneva, **12**, 87 (1959). E. R. ANDREW. J. Phys. Chem. Solids, **18**, 9 (1961). E. R. ANDREW and P. S. ALLEN. J. Chim. Phys. **63**, 85 (1966).
2. T. J. R. CYR, W. R. JANZEN, and B. A. DUNELL. Advan. Chem. Ser. 63. Am. Chem. Soc. 1967. p. 13.
3. B. N. PROVOTOROV. Zh. Eksperim. Teor. Fiz. **41**, 1582 (1961); Soviet Phys. JETP, English Transl. **14**, 1126 (1962).
4. A. G. REDFIELD. Phys. Rev. **98**, 1787 (1955).
5. M. GOLDMAN. J. Phys. **25**, 843 (1964).
6. B. A. DUNELL and W. R. JANZEN. Wiss. Z. Friedrich-Schiller Univ., Jena, Math. Naturwiss. Reihe, **14**, 191 (1965).
7. W. R. JANZEN. Ph.D. Thesis, The University of British Columbia, Vancouver, British Columbia. 1968.
8. J. JEENER, R. DUBOIS, and P. BROEKAERT. Phys. Rev. **139A**, 1959 (1965).
9. D. P. BENTON, P. G. HOWE, R. FARNAND, and I. E. PUDDINGTON. Can. J. Chem. **33**, 1798 (1955).
10. R. D. VOLD and M. J. VOLD. J. Am. Oil Chem. Soc. **26**, 520 (1949).

Thermal decomposition of hydrazoic acid as a possible source of NH radicals[1]

W. C. RICHARDSON AND D. W. SETSER[2]
Department of Chemistry, Kansas State University, Manhattan, Kansas 66502

Received November 26, 1968

The thermal decomposition of hydrazoic acid in the presence of methane, ethane, and propane investigated over the temperature range 285–470 °C gave only N_2, NH_3, and polymer as products. Limited experiments were done with ethene as a substrate, and products were formed which correspond to reactions of nitrogen containing radicals with C_2H_4. The pyrolysis of HN_3 is not a good source of NH radicals due to heterogeneity and complex secondary reactions of radicals with HN_3.

Canadian Journal of Chemistry, 47, 2725 (1969)

Can. J. Chem. Downloaded from www.nrcresearchpress.com by 210.87.254.6 on 09/05/12
For personal use only.

Introduction

Photolysis of HN_3 (1) and photolysis (2), pyrolysis (3), and mercury photosensitization (4) of HNCO have not provided a clean source of NH radicals. Previous work (5) suggested that NH is formed in the primary step in thermal decomposition of HN_3. Also formation of involatile acid–base complexes, a serious problem in HN_3 and HNCO systems, can be avoided because hydrazoic acid complexes are dissociated at temperatures above 100 °C, and complete decomposition of the HN_3 can be achieved before the sample is analyzed. Therefore, we investigated the pyrolysis of HN_3 with hydrocarbons as a source of NH radicals. Unfortunately, due to heterogeneous reactions, polymer formation, and complex secondary reactions, the thermal decomposition of HN_3 proved to be an unsatisfactory source of NH radicals. A brief summary of the results (6) from pyrolysis of HN_3 with CH_4, C_2H_6, C_3H_8, and C_2H_4 is presented.

Experimental

Hydrazoic acid was prepared in two ways: (*a*) by treating sodium azide (Fisher Laboratory Chemical, purified grade) with concentrated sulfuric acid and passing the effluent gas through phosphorous pentoxide, and (*b*) by passing hydrogen chloride gas through an 18 cm column packed with NaN_3. The former preparation contained a trace of SO_2 impurity; the latter preparation gave a poor yield and unreacted HCl had to be removed from the HN_3. The pyrolysis results were the same using HN_3 from either preparation. The hydrocarbons were obtained from standard sources.

Reactions were run by placing 1 cc (at S.T.P.) of HN_3 and 10 cc of substrate in a 10 cc Pyrex bulb. After mixing, the reaction bulb was introduced into a furnace and the temperature was monitored with a calibrated thermocouple. After complete decomposition of HN_3, condensable and noncondensable (−196 °C) products were separated using standard vacuum techniques. Products divided into 2 fractions in this manner were further separated and identified by gas–liquid chromatography (g.l.c.) or in some cases taken directly for mass spectrometric analysis. Using a variety of g.l.c. columns, quantitative analysis could be carried out for NH_3, N_2, CH_4, C_3H_8, C_3H_6, C_4H_{10}, and butenes. Analyses for H_2 and N_2H_4 were made with a Bendix time-of-flight mass spectrometer.

Results

One hundred pyrolyses using a variety of reaction vessels, reaction times, and temperatures from 285–470 °C were carried out with CH_4. In all pyrolyses the total pressure was about 2 atm. No explosions occurred as long as CH_4 was present. The products at complete HN_3 decomposition were nitrogen, ammonia, and nonvolatile polymer and the measured gaseous products were reproducibly the same at complete HN_3 decomposition over the temperature range studied. Within the experimental error, the initial quantity of methane was always recovered. Due to the polymer, direct mass balance could not be achieved. But from the amount of starting material and measurement of N_2 and NH_3 at complete HN_3 decomposition, the polymer was assigned by difference. Starting with 100 molecules of HN_3 the product molecules were 115 N_2, 15 NH_3, and 55 NH. Extensive searches were made for H_2, CH_3NH_2, and N_2H_4 by mass spectrometric and g.l.c. techniques with negative results.

The rate of production of N_2 depended upon the history of the vessel and seemed to be between zero and first order in $[HN_3]$. For example at 355 °C in a freshly cleaned Pyrex vessel

[1]Abstracted from the thesis of W. C. Richardson, which was submitted in partial fulfillment of the requirements of the Master's Degree, Kansas State University, 1969.

[2]Alfred P. Sloan Foundation Fellow.

Can. J. Chem. Downloaded from www.nrcresearchpress.com by 210.87.254.6 on 09/05/12
For personal use only.

the time for half decomposition of HN_3 was 45 min, but in vessels that had been "seasoned" by propene pyrolysis, the half life was too rapid to be measured. At 285 °C in a "seasoned" vessel the half life was 40 min, while at this temperature in a fresh vessel appreciable decomposition did not occur. In contrast at 450 °C, complete decomposition occurred in less than 2 min for both types of vessels[3].

A limited number of experiments were done with C_2H_6 and C_3H_8 as substrates because the lower C—H bond energies relative to CH_4 might have permitted reaction with NH radicals. However, no amine formation could be detected for pyrolysis at 430 °C and the proportions of N_2 and NH_3 formed at complete HN_3 decomposition were similar to the methane system.

From the results described it was not obvious that NH radicals were a significant feature of HN_3 pyrolysis, although other work (5) certainly suggests this. A limited number of experiments with HN_3 and C_2H_4, and HN_3 and C_2D_4 were done because some characteristic products[4] have been reported for the reaction of NH with C_2H_4 (1*b*, 2*a*, 7, 8). Major reaction products (especially CH_3CN) were found which undoubtedly resulted from reaction of C_2H_4 and NH containing radicals. But ammonia was still formed and probably originated from radical reaction with HN_3 which, if true, questions the use of C_2H_4 as an efficient scavenger for NH. Also propane, propene, butane, and butenes were observed as reaction products. Another expected product from NH + C_2H_4 is HCN, but it would not have been detected due to formation of NH_4CN with the NH_3 product. A few experiments were done with C_2D_4. The g.l.c. effluent peaks were trapped and analyzed mass spectroscopically. The mass spectra were very complex, but there was evidence for the presence of H-atoms in fragment ions of propane, propene, and butane.

[3]Assuming a HN_3 diffusion coefficient similar to alkanes, the results at 450 °C imply that decomposition could not occur completely on the surface because, for the pressures of this study, complete diffusion of HN_3 to the surface is impossible in less than 2 min.

[4]Confusion exists in the literature regarding production of HCN and CH_3CN in the reaction of NH with C_2H_4. In some studies both products are observed (1*b*), in others either HCN (2*a*) or CH_3CN (7) or neither (8) has been detected. Careful work is needed to clarify this problem.

Discussion

The severe loss of NH in the overall stoichiometry and the dependence of the decomposition rate on vessel history in the NH_3–CH_4 studies point to a system plagued by heterogeneity. The obvious conclusion of this study is that the thermal pyrolysis of hydrazoic acid is unsuitable as a clean source of NH radicals.

Hydrazoic acid decomposition[5] in the presence of various alkanes gave the same products as those reported for the low temperature pyrolysis work of pure HN_3 (5*a*). No evidence was found for the reaction of NH or other radical intermediates with CH_4, C_2H_6, and C_3H_8, although the formation of CH_3CN in the HN_3–C_2H_4 system implies some gas phase reaction of NH with C_2H_4. Since the reaction of NH with C_2H_4 should be relatively fast, the concomitant formation of NH_3 as a product implies that it arose from an addition reaction (or some other low activation process) of NH with HN_3. The nature of the hydrocarbon products found from the C_2H_4 system, and the isotopic distribution from the C_2D_4 experiments suggest reactions of H-atoms presumably from HN_3. A great deal of further work is necessary before a mechanism (6) can be discussed with any certainty. The results of this work emphasize the need for clean sources of NH and NH_2 radicals so that their elementary reactions can be identified. Then a better understanding of the complex chemistry of nitrogen–hydrogen radical systems should be possible.

Acknowledgments

The authors wish to thank Dr. H. Okabe of the National Bureau of Standards for a generous gift of C_2D_4. This work was supported by the U.S. National Air Pollution Control Administration, Consumer Protection and Environmental Health Service, Public Health Service, under contract AP-00391.

1. (*a*) E. D. MILLER. Ph.D. Thesis. Catholic University of America, Washington, D.C. 1961. (*b*) D. W. CORNELL, R. S. BERRY, and W. LWOWSKI. J. Am. Chem. Soc. **88**, 544 (1966).

[5]The energy separation between the NH ($a^1\Delta$) and ($X^3\Sigma^-$) states has recently been measured (9) as 36 kcal. Hence the homogenous thermal decomposition of HN_3 would be expected to give triplet NH which may explain the lack of reaction with saturated alkanes found in this work.

2. (*a*) W. D. WOOLLEY and R. A. BACK. Can. J. Chem. **46**, 295 (1968). (*b*) J. N. BRADLEY, J. R. GILBERT, and P. SVEJDA. Trans. Faraday Soc. **64**, 911 (1968).
3. R. A. BACK and J. CHILDS. Can. J. Chem. **46**, 1023 (1968).
4. N. J. FRISWELL and R. A. BACK. Can. J. Chem. **46**, 527 (1968).
5. (*a*) R. MEYER and H. J. SCHUMACHER. Z. Physik. Chem. **A170**, 33 (1934). (*b*) P. GRAY and T. C. WADDINGTON. Nature, **179**, 576 (1957). (*c*) F. O. RICE and T. A. LUCKENBACH. J. Am. Chem. Soc. **82**, 2681 (1960). (*d*) H. GUENEBAUT, G. PANNETIER, and P. GOUDMAND. Compt. Rend. **251**, 1166 (1960).
6. W. C. RICHARDSON. Master's Thesis, Kansas State University, Manhattan, Kansas. 1969.
7. A. JONES and F. P. LOSSING. Can. J. Chem. **45**, 1685 (1967).
8. R. F. KLEMM. Can. J. Chem. **45**, 1693 (1967).
9. H. OKABE and M. LENZI. J. Chem. Phys. **47**, 5241 (1967).

Circular dichroism of copper(II) carboxylates

ANTHONY A. SMITH AND ROLAND A. HAINES
Department of Chemistry, University of Western Ontario, London, Ontario

Received December 23, 1968

The circular dichroism (c.d.) spectra of anhydrous copper(II) acetate, copper(II) isobutyrate, and copper(II) allylacetate in *d*-1,2-propanediol are interpreted as showing that all the d → d transitions are contained in a single band envelope with relative energies of the d orbitals being $d_{x^2-y^2} > d_{z^2} > d_{xy} > d_{xz} \simeq d_{yz}$. A possibility for the origin of a c.d. band at ~ 300 mμ is suggested.

Canadian Journal of Chemistry, 47, 2727 (1969)

The crystal structure of copper(II) acetate has been known for some time to be binuclear with the copper atoms joined by 4 bridging carboxylate ligands (1). However, there is still much controversy over the interpretation of its electronic absorption spectrum and that of related compounds. We wish to report a c.d. study of 3 of these compounds in an optically active solvent, *d*-1,2-propanediol, the results of which may give support for a particular assignment of the absorption spectra. The study was carried out on anhydrous copper acetate, copper isobutyrate, and copper allylacetate. The c.d. curves obtained in *d*-1,2-propanediol were virtually the same for all 3 complexes, with very slight differences in peak wavelengths and intensities, and are shown together with the absorption spectra in Fig. 1.

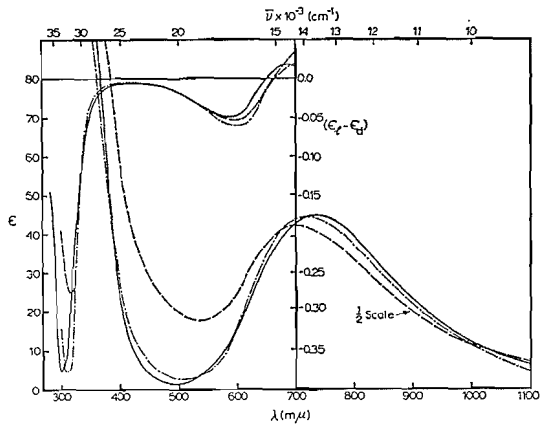

FIG. 1. Circular dichroism and absorption spectra in *d*-1,2-propanediol: (——), copper acetate; (---), copper isobutyrate; (-·-·-), copper allylacetate.

The absorption spectrum of copper acetate at 77 °K has shown 3 bands: a *z*-polarized band at 11 000 cm^{-1}, an *xy*-polarized band at 14 400 cm^{-1}, and another *z*-polarized band at 27 000 cm^{-1} (2). At room temperature, however, the 11 000 cm^{-1} band is seen only as a broadening of the more intense 14 400 cm^{-1} band. The lower energy bands are assigned as d → d transitions, while it is uncertain as to whether or not the high energy band is of this type (2–5). Hansen and Ballhausen (3), using a molecular orbital method of calculation in which the dimeric complex is treated as two weakly coupled chromophores, have assigned the 27 000 cm^{-1} band as a transition to a doubly excited state. On the other hand, Kokoszka, *et al.* (2) have favored the single excitation $d_{z^2} \rightarrow d_{x^2-y^2}$, while Boudreaux (4), and Dubicki and Martin (5) considered it as a charge transfer band.

The close proximity of the Cu atoms (2.64 Å) in each molecule of the complex indicates there is some interaction between them and this may be either a σ or a δ interaction. The σ-bonded

Can. J. Chem. Downloaded from www.nrcresearchpress.com by 210.87.254.6 on 09/05/12
For personal use only.

2. (*a*) W. D. WOOLLEY and R. A. BACK. Can. J. Chem. **46**, 295 (1968). (*b*) J. N. BRADLEY, J. R. GILBERT, and P. SVEJDA. Trans. Faraday Soc. **64**, 911 (1968).
3. R. A. BACK and J. CHILDS. Can. J. Chem. **46**, 1023 (1968).
4. N. J. FRISWELL and R. A. BACK. Can. J. Chem. **46**, 527 (1968).
5. (*a*) R. MEYER and H. J. SCHUMACHER. Z. Physik. Chem. **A170**, 33 (1934). (*b*) P. GRAY and T. C. WADDINGTON. Nature, **179**, 576 (1957). (*c*) F. O. RICE and T. A. LUCKENBACH. J. Am. Chem. Soc. **82**, 2681 (1960). (*d*) H. GUENEBAUT, G. PANNETIER, and P. GOUDMAND. Compt. Rend. **251**, 1166 (1960).
6. W. C. RICHARDSON. Master's Thesis, Kansas State University, Manhattan, Kansas. 1969.
7. A. JONES and F. P. LOSSING. Can. J. Chem. **45**, 1685 (1967).
8. R. F. KLEMM. Can. J. Chem. **45**, 1693 (1967).
9. H. OKABE and M. LENZI. J. Chem. Phys. **47**, 5241 (1967).

Circular dichroism of copper(II) carboxylates

ANTHONY A. SMITH AND ROLAND A. HAINES
Department of Chemistry, University of Western Ontario, London, Ontario

Received December 23, 1968

The circular dichroism (c.d.) spectra of anhydrous copper(II) acetate, copper(II) isobutyrate, and copper(II) allylacetate in *d*-1,2-propanediol are interpreted as showing that all the d → d transitions are contained in a single band envelope with relative energies of the d orbitals being $d_{x^2-y^2} > d_{z^2} > d_{xy} > d_{xz} \simeq d_{yz}$. A possibility for the origin of a c.d. band at ~ 300 mμ is suggested.

Canadian Journal of Chemistry, 47, 2727 (1969)

The crystal structure of copper(II) acetate has been known for some time to be binuclear with the copper atoms joined by 4 bridging carboxylate ligands (1). However, there is still much controversy over the interpretation of its electronic absorption spectrum and that of related compounds. We wish to report a c.d. study of 3 of these compounds in an optically active solvent, *d*-1,2-propanediol, the results of which may give support for a particular assignment of the absorption spectra. The study was carried out on anhydrous copper acetate, copper isobutyrate, and copper allylacetate. The c.d. curves obtained in *d*-1,2-propanediol were virtually the same for all 3 complexes, with very slight differences in peak wavelengths and intensities, and are shown together with the absorption spectra in Fig. 1.

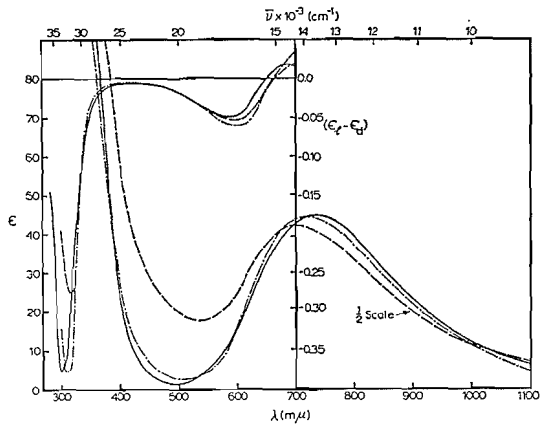

FIG. 1. Circular dichroism and absorption spectra in *d*-1,2-propanediol: (——), copper acetate; (- - -), copper isobutyrate; (—·—·—), copper allylacetate.

The absorption spectrum of copper acetate at 77 °K has shown 3 bands: a *z*-polarized band at 11 000 cm^{-1}, an *xy*-polarized band at 14 400 cm^{-1}, and another *z*-polarized band at 27 000 cm^{-1} (2). At room temperature, however, the 11 000 cm^{-1} band is seen only as a broadening of the more intense 14 400 cm^{-1} band. The lower energy bands are assigned as d → d transitions, while it is uncertain as to whether or not the high energy band is of this type (2–5). Hansen and Ballhausen (3), using a molecular orbital method of calculation in which the dimeric complex is treated as two weakly coupled chromophores, have assigned the 27 000 cm^{-1} band as a transition to a doubly excited state. On the other hand, Kokoszka, *et al.* (2) have favored the single excitation $d_{z^2} \rightarrow d_{x^2-y^2}$, while Boudreaux (4), and Dubicki and Martin (5) considered it as a charge transfer band.

The close proximity of the Cu atoms (2.64 Å) in each molecule of the complex indicates there is some interaction between them and this may be either a σ or a δ interaction. The σ-bonded

Can. J. Chem. Downloaded from www.nrcresearchpress.com by 210.87.254.5 on 09/05/12
For personal use only.

TABLE I

Characteristics of absorption bands for copper acetate

Transition	C_{2v} Polarization	C_{2v} Circular dichroism activity	D_{2h} Polarization	D_{2h} Circular dichroism activity
$d_{z^2} \rightarrow d_{x^2-y^2}$	z	Forbidden	—	Forbidden
$d_{xy} \rightarrow d_{x^2-y^2}$	—	Allowed	—	Allowed
$d_{xz} \rightarrow d_{x^2-y^2}$	x	Allowed	—	Allowed
$d_{yz} \rightarrow d_{x^2-y^2}$	y	Allowed	—	Allowed

system requires that all d → d transitions terminate on the d_{z^2} orbital and all these transitions should thus be solvent sensitive, but this does not seem to be the case (6). For the δ-bonded configuration, the highest energy orbital is the $d_{x^2-y^2}$ level.

Two possibilities exist for this compound in solution, one in which the binuclear species is maintained, and the other in which the dimeric structure is broken down to give the monomer. A close examination of the crystal structure (1) shows that the planes containing the O—Cu—O bonds are not exactly at right angles, but are 7° from orthogonality. This would give a C_{2v} symmetry about each copper atom in the dimeric molecule. The monomer may be considered as a square planar structure with two acetate ligands (7), therefore having D_{2h} symmetry. In each case, a polarization can be predicted for the d → d transitions. Moreover, the c.d. activity of a transition can be predicted, since the requirement for this is met when the direct product of the symmetries of the electronic wave functions belongs to a representation containing a rotation. These predictions are shown in Table I.

The observed c.d. spectrum shows a positive peak around 700 mμ and a broad negative peak centered at ~590 mμ. We propose that the positive c.d. band corresponds to the $d_{xy} \rightarrow d_{x^2-y^2}$ transition and the negative band to the $d_{xz} \rightarrow d_{x^2-y^2}$ and $d_{yz} \rightarrow d_{x^2-y^2}$ transitions. The $d_{z^2} \rightarrow d_{x^2-y^2}$ transition would be at much lower energy and should correspond to the 11 000 cm^{-1} absorption band. It can be seen that this assignment is consistent with both C_{2v} and D_{2h} symmetries, and it is therefore impossible to distinguish which species is in solution from the c.d. spectrum. However, the absorption spectrum of copper acetate in 1,2-propanediol shows a large decrease in the extinction coefficient from that in non-polar solvents, thus suggesting that the species in solution in this case is the monomer. Similar decreases are exhibited by copper allylacetate and copper isobutyrate. The absorption band at 27 000 cm^{-1}, which has been thought to be indicative of dimeric species, is also absent from our spectra (6, 9). Dubicki and Martin (5) have stated that the energy states of the dimer correspond closely to those of the monomer, so it is reasonable that our assignment is also valid for the dimeric molecule.

Our assignment is consistent with the idea that all the d → d transitions are contained in one absorption band envelope (3, 5). Hansen and Ballhausen (3) employed this idea in their calculations using energies of the 3 bands derived from a Gaussian analysis of the absorption spectrum of $CuSO_4 \cdot 5H_2O$ by Holmes and McClure (8). The former authors used C_{4v} symmetry, thus predicting three d → d transitions, while the latter used a model in which 4 such transitions were expected, only 3 of which were indicated as being under the one absorption band. Dubicki and Martin (5), also using C_{4v} symmetry, concurred with the assignment of Hansen and Ballhausen. Our work definitely indicates the presence of all four d → d transitions predicted for both C_{2v} and D_{2h} symmetry under the main absorption band at 700 mμ.

The similarity of the c.d. spectra of copper isobutyrate and copper allylacetate to that of copper acetate indicates that the relative d-orbital energies for all these complexes are the same, i.e., $d_{x^2-y^2} > d_{z^2} > d_{xy} > d_{xz} \simeq d_{yz}$, with the d → d transitions contained in a single absorption envelope.

Edmondson and Lever (6) have noted that if the 14 400 cm^{-1} band is assigned as $d_{xy} \rightarrow d_{x^2-y^2}$, this band should be independent of solvent, but

Can. J. Chem. Downloaded from www.nrcresearchpress.com by 210.87.254.5 on 09/05/12
For personal use only.

such is not the case. Assuming that a direct parallel can be drawn between the energy levels of the monomer and dimer and using our assignment, the solvent dependence could be explained as being due to the presence of the $d_{xz} \rightarrow d_{x^2-y^2}$ and $d_{yz} \rightarrow d_{x^2-y^2}$ transitions, which would be solvent dependent, in the near vicinity of the absorption maximum. Similarly, the *xy* polarization of the 14 400 cm^{-1} band in the dimer may be explained as being due to the polarizations of the underlying $d_{xz} \rightarrow d_{x^2-y^2}$ and $d_{yz} \rightarrow d_{x^2-y^2}$ bands.

The c.d. spectrum of copper acetate also shows a strong negative peak at 305 mμ and an analogous band is observed for the other 2 complexes at slightly higher wavelengths (~ 310 mμ). This band is almost certainly a charge transfer band, most probably one of the $n(s,p) \rightarrow \sigma^*_{x^2-y^2}$ transitions. Due to the large number of charge transfer transitions which could be optically active, however, it is obvious that an unambiguous assignment cannot be made for the c.d. band at 300 mμ.

Experimental

Optically active *d*-1,2-propanediol was obtained from Aldrich Chemical Co., Milwaukee, Wisconsin. The solutions were prepared by weighing both solvent and solute into a weighing bottle and calculating concentrations on the basis of solvent density. The solutions were all $\sim 10^{-2}$ *M* based on the monomeric formula for each complex. Circular dichroism spectra were measured on a Durrum–Jasco ORD-UV-5 spectropolarimeter and absorption spectra on a Beckman DK-1 spectrophotometer. Cupric acetate monohydrate was dried for 34 days at 50° under slight vacuum. If the complex was dried at a higher temperature, acetic acid was given off from the solid and the color changed to a lighter green than that of the monohydrate. Solutions of copper acetate monohydrate in *d*-1,2-propanediol showed evidence of decomposition and gave inconclusive c.d. data.

Acknowledgments

We wish to thank the National Research Council of Canada for financial support of this work. We are also grateful to Dr. A. B. P. Lever for supplying the samples of copper isobutyrate and copper allylacetate.

1. J. N. Van Nierkerk and F. R. L. Schoening. Acta Cryst. **6**, 227 (1953).
2. C. W. Reimann, G. F. Kokoszka, and G. Gordon. Inorg. Chem. **4**, 1082 (1965).
3. A. E. Hansen and C. J. Ballhausen. Trans. Faraday Soc. **61**, 631 (1965).
4. E. A. Boudreaux. Inorg. Chem. **3**, 506 (1964).
5. L. Dubicki and R. L. Martin. Inorg. Chem. **5**, 2203 (1966).
6. B. J. Edmondson and A. B. P. Lever. Inorg. Chem. **4**, 1608 (1965).
7. M. Kato, H. B. Jonassen, and J. C. Fanning. Chem. Rev. **64**, 99 (1964).
8. O. G. Holmes and D. S. McClure. J. Chem. Phys. **26**, 1686 (1957).
9. M. L. Tonnet, S. Yamada, and I. G. Ross. Trans. Faraday Soc. **60**, 840 (1964).

Explosive sensitivity of cobalt(III) ammine complexes

Taylor B. Joyner
Chemistry Division, Naval Weapons Center, China Lake, California 93555

Received February 11, 1969

Unexpected uniformities in the explosive sensitivities of a number of coordination compounds have been observed. These suggest that the kinetics of reaction within the hotspot (as distinct from either generation of the hotspot or propagation from the hotspot to macroscopic proportions) play a critical role in determining the sensitivity of an explosive to initiation by impact.

Canadian Journal of Chemistry, **47**, 2729 (1969)

This note reports unexpected uniformities in the explosive sensitivity of several coordination compounds. Previously, Tomlinson *et al.* reported sensitivities for coordination compounds (1) and we discussed complex azides (2). Of present interest are the perchlorates, chlorates, bromates, and permanganates of Table I. Despite the difficulties inherent in impact testing (Boyars and Levine (3) have recently reviewed the subject) and variations from strong to very weak, underoxidized explosives, the sensitivities of salts of a given anion are quite uniform. Irregularities, shown by nitrates, nitrites, and $[Co(en)_2Cl_2]ClO_4$, were expected. The more surprising uniformities suggest that for these compounds a factor associated with the anion is critical to sensitivity.

Can. J. Chem. Downloaded from www.nrcresearchpress.com by 210.87.254.5 on 09/05/12
For personal use only.

such is not the case. Assuming that a direct parallel can be drawn between the energy levels of the monomer and dimer and using our assignment, the solvent dependence could be explained as being due to the presence of the $d_{xz} \rightarrow d_{x^2-y^2}$ and $d_{yz} \rightarrow d_{x^2-y^2}$ transitions, which would be solvent dependent, in the near vicinity of the absorption maximum. Similarly, the *xy* polarization of the 14 400 cm^{-1} band in the dimer may be explained as being due to the polarizations of the underlying $d_{xz} \rightarrow d_{x^2-y^2}$ and $d_{yz} \rightarrow d_{x^2-y^2}$ bands.

The c.d. spectrum of copper acetate also shows a strong negative peak at 305 mμ and an analogous band is observed for the other 2 complexes at slightly higher wavelengths (~ 310 mμ). This band is almost certainly a charge transfer band, most probably one of the $n(s,p) \rightarrow \sigma^*_{x^2-y^2}$ transitions. Due to the large number of charge transfer transitions which could be optically active, however, it is obvious that an unambiguous assignment cannot be made for the c.d. band at 300 mμ.

Experimental

Optically active *d*-1,2-propanediol was obtained from Aldrich Chemical Co., Milwaukee, Wisconsin. The solutions were prepared by weighing both solvent and solute into a weighing bottle and calculating concentrations on the basis of solvent density. The solutions were all $\sim 10^{-2}$ *M* based on the monomeric formula for each complex. Circular dichroism spectra were measured on a Durrum–Jasco ORD-UV-5 spectropolarimeter and absorption spectra on a Beckman DK-1 spectrophotometer. Cupric acetate monohydrate was dried for 34 days at 50° under slight vacuum. If the complex was dried at a higher temperature, acetic acid was given off from the solid and the color changed to a lighter green than that of the monohydrate. Solutions of copper acetate monohydrate in *d*-1,2-propanediol showed evidence of decomposition and gave inconclusive c.d. data.

Acknowledgments

We wish to thank the National Research Council of Canada for financial support of this work. We are also grateful to Dr. A. B. P. Lever for supplying the samples of copper isobutyrate and copper allylacetate.

1. J. N. Van Nierkerk and F. R. L. Schoening. Acta Cryst. **6**, 227 (1953).
2. C. W. Reimann, G. F. Kokoszka, and G. Gordon. Inorg. Chem. **4**, 1082 (1965).
3. A. E. Hansen and C. J. Ballhausen. Trans. Faraday Soc. **61**, 631 (1965).
4. E. A. Boudreaux. Inorg. Chem. **3**, 506 (1964).
5. L. Dubicki and R. L. Martin. Inorg. Chem. **5**, 2203 (1966).
6. B. J. Edmondson and A. B. P. Lever. Inorg. Chem. **4**, 1608 (1965).
7. M. Kato, H. B. Jonassen, and J. C. Fanning. Chem. Rev. **64**, 99 (1964).
8. O. G. Holmes and D. S. McClure. J. Chem. Phys. **26**, 1686 (1957).
9. M. L. Tonnet, S. Yamada, and I. G. Ross. Trans. Faraday Soc. **60**, 840 (1964).

Explosive sensitivity of cobalt(III) ammine complexes

Taylor B. Joyner
Chemistry Division, Naval Weapons Center, China Lake, California 93555

Received February 11, 1969

Unexpected uniformities in the explosive sensitivities of a number of coordination compounds have been observed. These suggest that the kinetics of reaction within the hotspot (as distinct from either generation of the hotspot or propagation from the hotspot to macroscopic proportions) play a critical role in determining the sensitivity of an explosive to initiation by impact.

Canadian Journal of Chemistry, **47**, 2729 (1969)

This note reports unexpected uniformities in the explosive sensitivity of several coordination compounds. Previously, Tomlinson *et al.* reported sensitivities for coordination compounds (1) and we discussed complex azides (2). Of present interest are the perchlorates, chlorates, bromates, and permanganates of Table I. Despite the difficulties inherent in impact testing (Boyars and Levine (3) have recently reviewed the subject) and variations from strong to very weak, underoxidized explosives, the sensitivities of salts of a given anion are quite uniform. Irregularities, shown by nitrates, nitrites, and $[Co(en)_2Cl_2]ClO_4$, were expected. The more surprising uniformities suggest that for these compounds a factor associated with the anion is critical to sensitivity.

Can. J. Chem. Downloaded from www.nrcresearchpress.com by 210.87.254.105 on 09/05/12
For personal use only.

TABLE I

Impact sensitivities and character of ignition of compounds containing ionic oxidizing anions

Compound	Impact sensitivity, 50% point (cm)	Character of the ignition*
Permanganates		
$[Co(NH_3)_6](MnO_4)_3$	7	s
trans-$[Co(en)_2Cl_2]MnO_4$†	15	w
Perchlorates		
$[Co(NH_3)_6](ClO_4)_3$	19	s
$[Co(NH_3)_5(H_2O)](ClO_4)_3$	21	s
$[Co(NH_3)_4(H_2O)_2](ClO_4)_3$	24	s
$[Co(en)_3](ClO_4)_3$	17	s
$[Co(NH_3)_5Cl](ClO_4)_2$	33	s
trans-$[Co(NH_3)_4Cl_2]ClO_4$	20	w
trans-$[Co(en)_2Cl_2]ClO_4$	180	w
Chlorates		
$[Co(NH_3)_6](ClO_3)_3$	14	s
$[Co(en)_3](ClO_3)_3$	24	s
trans-$[Co(en)_2Cl_2]ClO_3$	16	w
Bromates		
$[Co(NH_3)_6](BrO_3)_3$	12	s
$[Co(en)_3](BrO_3)_3$	15	s
trans-$[Co(en)_2Cl_2]BrO_3$	13	m
Iodates		
$[Co(NH_3)_6](IO_3)_3$	43	w
Nitrates		
$[Co(NH_3)_6](NO_3)_3$	64	m
$[Co(en)_3](NO_3)_3$	> 180	—
$[Co(NH_3)_5Cl](NO_3)_2$	137	w
trans-$[Co(en)_2Cl_2]NO_3$	> 180	—
Nitrites		
$[Co(NH_3)_6](NO_2)_3$	41	w
$[Co(NH_3)_5Cl](NO_2)_2$	141	w

*The reactions were characterized as strong (s), more than 75% of sample consumed, loud report, visible flame; medium (m), 25–75% of sample consumed, audible report, occasionally visible flame; weak (w) less than 25% of sample consumed, usually no audible report, and little or no visible flame.

†Ethylenediamine is represented by "en".

Hotspot theory (4) permits some localization of this factor. Ignition involves: (*1*) generation and concentration of energy in small hotspots, (*2*) growth of reaction within these areas, and (*3*) growth to visible proportions. Failure can result from inadequate energy in (*1*) or the reaction rate during (*2*) or (*3*) not compensating for heat loss. Since the heat of reaction (roughly indicated by oxygen balance and reaction violence) supports propagation through the cool regions of the crystal, the observed independence suggests that the critical factor does not operate during (*3*)[1]. Although the events of (*1*) are complex (crushing, melting, entrapment of gas, etc.), the uniformities again suggest that properties dependent on crystal structure or the nature of the cation are not decisive.

However, during reaction *within* the hotspot the anion, and specifically, the kinetics of its reaction with the ammine, may be decisive. It thus seems reasonable to identify the factor critical to sensitivity with this aspect of the ignition process. This is in encouraging accord with the recent theoretical treatment of Bruckman and Guillet (5) who find that the Arrhenius parameters of the decomposition reaction exercise a dominant effect on the sensitivity of an explosive compound.

The independence of heat of reaction merits brief comment. If impact produces an adequate temperature, decomposition will commence. For success, the rate must be sufficient to maintain the hotspot temperature and reaction. Although growth within the hotspot is relatively easy (compared to the cool surroundings) it still depends on heat of reaction and weaker explosives will require faster rates to overcome heat loss. However, the temperature increase necessary for a two- or three-fold acceleration (a few tens of degrees) is small relative to hotspot temperature (ca. 500°) (4) and the crude tests would be unlikely to differentiate between impacts causing temperature rises of say 500 and 550°. Detailed consideration of the events and reaction mechanisms occurring within the hotspot would, at present, be highly speculative. However, it is hoped that current kinetic studies will permit insight into these problems.

Experimental

Preparations were conventional (6). Some compounds, notably $[Co(NH_3)_6](MnO_4)_3$, are treacherous. The "Type 12" test (3) with a 2 kg hammer and 25 mg of explosive loosely coned on sandpaper was used. The drop heights for 50% successful ignitions based on 20 tests are reported. For purposes of comparison, our machine yields 50% points of 10, 25, and 145 cm for lead azide, RDX, and TNT, respectively.

[1]Presumably, decomposition of a hotspot initiates adequate reactions in even weak explosives. However, propagation failure could explain some of the exceptions.

1. W. R. Tomlinson, K. G. Ottoson, and L. F. Audrieth. J. Am. Chem. Soc. **71**, 375 (1949).
2. T. B. Joyner, A. J. Cohen, and W. S. McEwan. Nature, **196**, 470 (1962).
3. C. Boyars and D. Levine. Pyrodynamics, **6**, 53 (1968).
4. F. P. Bowden and A. D. Yoffe. Initiation and growth of explosion in liquids and solids. Cambridge University Press, Cambridge. 1952.
5. H. J. Bruckman and J. E. Guillet. Can. J. Chem. **46**, 3221 (1968).
6. Gmelin. Handbuch der anorganischen Chemie, Kobalt, Teil B, Die Ammine des Kobalts. System-Nummer 58. Verlag Chemie, Berlin. 1930.

Can. J. Chem. Downloaded from www.nrcresearchpress.com by 210.87.254.105 on 09/05/12
For personal use only.

Spectroscopic and acoustic measurements in relation to the conformation of a cyclic sulfite and a cyclic sulfate

P. C. HAMBLIN AND R. F. M. WHITE
Chemistry Department, Sir John Cass College, Jewry Street, London, E.C.3, England

AND

G. ECCLESTON AND E. WYN-JONES[1]
Department of Pure and Applied Chemistry, University of Salford, Salford 5, Lancashire, England

Received December 16, 1968

In the investigation of certain types of conformational equilibria, the ultrasonic absorption technique can be used to supplement information derived from more conventional spectroscopic techniques, and thereby lead to a more detailed analysis of molecular configuration.

Nuclear magnetic resonance, infrared spectra, and ultrasonic absorption measurements indicate that both 4-methyl trimethylene sulfite and 4-methyl trimethylene sulfate exist as equilibrium mixtures of two chair isomers. In each case one isomer is strongly predominant.

Canadian Journal of Chemistry, 47, 2731 (1969)

Can. J. Chem. Downloaded from www.nrcresearchpress.com by 210.87.254.6 on 09/05/12
For personal use only.

The conformational analysis of heterocyclic molecules has been studied with a variety of physical techniques including nuclear magnetic resonance (n.m.r.), infrared (i.r.), dipole moment (1, and references therein), and more recently the ultrasonic absorption method (2, 3). Spectroscopic and dipole moment studies, together with X-ray investigation of the solid phase (4), have demonstrated that in trimethylene sulfites the chair form is favored with the S=O bond in an axial orientation (5, 6).

The preference for the SO bond axial as against the SO equatorial orientation is estimated to be about 3.5 ± 1 kcal (6). Since the spectroscopic and dipole methods may not be discerning enough to detect conformers present in small percentages in "anancomeric" systems (7), the ultrasonic method (2, 3) constitutes a valuable additional technique since it is sensitive to ~1% of the higher energy rotamer (8).

As a further example of this type of conformational behavior we present spectroscopic and ultrasonic data which have been used to elucidate the conformations of 4-methyl trimethylene sulfite (**1**), and also 4-methyl trimethylene sulfate (**2**). The n.m.r spectra (10) of both **1** and **2** were found to be complex and first order analysis of the spectra gave the values for the coupling constants between the proton at C_4 and the two protons at C_5 as in Table I. A complex n.m.r. spectrum (9) and the above figures (5, 6) are compatible with a chair conformation for

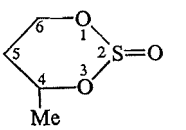

1

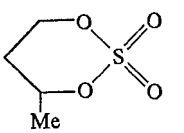

2

TABLE I
Coupling constants between protons

Compound	Coupling constant	Value (Hz)
1	J_{aa}	12
	J_{ae}	2.6
2	J_{aa}	12.3
	J_{ae}	2.5

both molecules with the methyl group in an equatorial position in each case. In addition a strong absorption band at 1190 cm^{-1} in the i.r. spectrum of **1** indicates that the S=O is axial (6). There is no evidence for the corresponding equatorial S=O absorption band in the region 1230–1250 cm^{-1} (6). This combined spectroscopic evidence points to a rigid chair structure for both molecules with the methyl groups in an equatorial position and the S=O bond of **1** being axial. In practice, however, this type of statement can be qualified by postulating an anancomeric chair form for these molecules.

[1]To whom correspondence should be addressed.

Can. J. Chem. Downloaded from www.nrcresearchpress.com by 210.87.254.6 on 09/05/12
For personal use only.

More details about the conformation can be obtained from ultrasonic absorption measurements.

When there is an equilibrium between energetically different conformers in a molecule, this can sometimes be detected by ultrasonic measurements (8). If the appropriate frequency range is chosen, the temperature fluctuations accompanying sound waves can perturb the conformational equilibrium resulting in ultrasonic relaxation. When this occurs the quantity α/f^2 (α is the sound absorption coefficient at frequency f) decreases with increasing frequency (8).

Using a pulse apparatus operating in the frequency range 15–105 MHz we have observed an ultrasonic relaxation in **1**, and also in **2** which was examined as a 30% (wt./v.) solution in two solvents: *p*-xylene and 1,4-dioxan.

The results obtained are shown in Table II and are interpreted in each case as a perturbation of the equilibrium between two chair conformers.

1 $CH_3(e),\ S{=}O(a) \rightleftharpoons CH_3(a),\ S{=}O(e)$

2 $CH_3(e) \rightleftharpoons CH_3(a)$

These conclusions are supported by the following evidence. (*a*) Physico-chemical evidence indicates that in these molecules, the chair conformers are energetically favored compared with other extreme conformations. (*b*) The relaxation frequencies for both solutions of **2** are sensibly the same, indicating that the relaxation is due to an intramolecular mechanism. (*c*) Examination of solutions of **1** produces relaxation frequencies similar to those found in the pure liquid. (*d*) No relaxation (2) was found in solutions of trimethylene sulfate where ring inversion results in chair conformers of equal energy.

TABLE II

Ultrasonic relaxation data

Compound	Relaxation frequency (MHz)	Temperature (°C)
1	40	−10
2 (in *p*-xylene)	13.6	24
(in 1,4-dioxan)	13.3	24

A limitation of the spectroscopic methods is that they are sometimes unable to distinguish between a molecule involved in an anancomeric conformation equilibrium and a rigid molecule. On the other hand the ultrasonic method can detect an equilibrium between conformers differing in energy, in which only ~1% of the higher energy form is present. A preliminary analysis of the ultrasonic data in solutions of **2** in *p*-xylene shows that ΔG (at 298 °K) (axial–equatorial) $\approx$ 2 kcal/mole indicating 97% of the methyl equatorial chair isomer. The ultrasonic relaxation frequencies quoted indicate that the n.m.r. spectra are time averaged spectra.

Acknowledgments

We wish to thank the Science Research Council, London, for a grant for the construction of the ultrasonic apparatus and for a research studentship to P.C.H. G.E. is indebted to the Unilever Company Limited for a Research Studentship.

1. F. Riddell. Quart. Rev. London, **21**, 364 (1967).
2. R. A. Pethrick, E. Wyn-Jones, P. C. Hamblin, and R. F. M. White. J. Mol. Struct. **1**, 333 (1968).
3. P. C. Hamblin, R. F. M. White, and E. Wyn-Jones. Chem. Commun. 1058 (1968).
4. C. Altona, H. J. Geise, and C. Ramers. Rec. Trav. Chim. **85**, 1197 (1966). J. W. L. van Oyen, R. C. D. E. Hasekamp, G. C. Verschoor, and C. Romers. Acta Cryst. **B24**, 1471 (1968).
5. D. G. Hellier, T. G. Tillet, H. F. Van Woerden, and R. F. M. White. Chem. Ind. London, 1956 (1963).
6. H. F. Van Woerden and E. Havinga. Rec. Trav. Chim. **86**, 341 (1967); **86**, 353 (1967).
7. M. Antenius, D. Tavernier, and E. Borremans. Bull. Soc. Chim. Belges, **75**, 396 (1966).
8. J. Lamb. *In* Physical acoustics. Vol. II. Part A. *Edited by* Warren P. Mason. Academic Press, Inc., New York. 1965. Chap. 4. p. 203.
9. J. E. Anderson. Quart. Rev. London, **19**, 426 (1966).
10. P. C. Hamblin and R. F. M. White. Unpublished data.

Can. J. Chem. Downloaded from www.nrcresearchpress.com by 210.87.254.6 on 09/05/12
For personal use only.

Structure of rhodocladonic acid

PAUL M. BAKER AND E. BULLOCK
Department of Chemistry, Memorial University, St. John's, Newfoundland

Received May 26, 1969

The currently accepted formulation of rhodocladonic acid, the red pigment from numerous lichens of the genus *Cladonia*, is revised. The compound is a naphthoquinone derivative, apparently the first isolated from a lichen.

Canadian Journal of Chemistry, 47, 2733 (1969)

Rhodocladonic acid is the characteristic pigment present in the red apothecia of numerous lichens of the genus *Cladonia* (**1**). Shibata (2) proposed a molecular formula $C_{17}H_{12}O_9$ and structure **1** for this substance. Reinvestigation of the compound, obtained from local cladonia species, leads us to propose **2** for the structure of rhodocladonic acid. The compound was isolated by established methods and recrystallized from nitrobenzene (2).

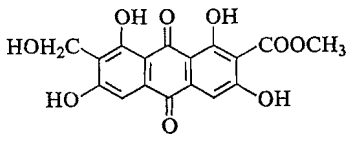

1

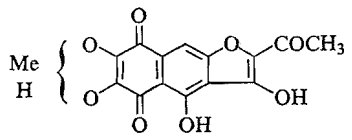

2

Rhodocladonic acid, $C_{15}H_{10}O_8$ (3), (molecular ion at *m/e* 318.0375; calcd. for $C_{15}H_{10}O_8$, 318.0376) has one *O*-methyl group (Zeisel). It gives a trimethyl ether, $C_{18}H_{16}O_8$, m.p. 192–193°, with methanolic diazomethane, and a triacetate, $C_{21}H_{16}O_{11}$, m.p. 210–212°, with acetic anhydride – pyridine. The triacetate can be reductively acetylated to a leucopentaacetate, m.p. 223–225°, with zinc – acetic anhydride. The nuclear magnetic resonance (n.m.r.) spectrum of the trimethyl ether (in $CDCl_3$) shows absorption due to one *C*-methyl group at τ 7.42 and a single aromatic proton at τ 1.98. These data preclude the anthraquinone formula **1**, but support the presence of a trihydroxyquinonoid system in the molecule. The infrared spectrum of the reduced pentaacetate (in $CHCl_3$) has a sharp band at 1690 cm^{-1}; thus the molecule appears to contain an aromatic methyl ketone (cf. 4).

Rhodocladonic acid is readily degraded by refluxing 3% potash solution to a mixture of products. One of these (mol. wt. 236) (**3***a*) gives a trimethyl ether (mol. wt. 278), with alcoholic diazomethane, whose mass spectrum is identical with that of spinochrome B tetramethyl ether (**3***b*).

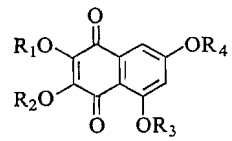

3

a, $R_3 = R_4 = H$; $R_1 = R_2 = H$ or Me
b, $R_1 = R_2 = R_3 = R_4 = Me$
c, $R_1 = R_2 = R_3 = H$; $R_4 = Me$

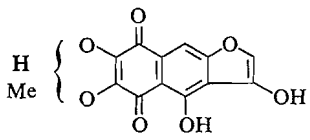

4

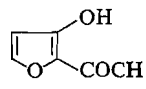

5

A second degradation product, $C_{13}H_8O_7$ (**4**) (molecular ion at *m/e* 276.0264, required *m/e* 276.02701) has formula and properties corresponding to the loss of CH_3CO from rhodocladonic acid. Thus it gives a trimethyl ether (mol. wt. 318) with alcoholic diazomethane, which shows no *C*-methyl absorption in the n.m.r. spectrum ($CDCl_3$), but has 2 low field protons

(τ 2.06 and 2.63), which are not coupled, and 4 methoxyl signals.

Both **3***a* (max. at 311.5, 384.6, and 454.5 mμ) and **4** (max. at 306, 379, and 457 mμ) show typical hydroxy juglone electronic spectra, and give green colors with neutral magnesium acetate solution; hence both possess a free "peri"-hydroxyl group. Further, **3***a* was shown to be different from **3***c*, (obtained from **3***b* by alkaline hydrolysis to demethylate one ether of the quinonoid ring and treatment with ethereal magnesium iodide solution (5) to remove the second methyl from the quinonoid ring and the "peri"-methyl group), and is thus formulated as **3***a*.

The low-field single proton signal observed for rhodocladonic acid trimethyl ether suggests that a peri-aromatic proton is present in the molecule (cf. 6). Thus, rhodocladonic acid may be formulated as arising from addition of a 4 carbon unit at C-6 of **3***a* which, from the hydrogen content of the acid and of **4**, must form a cyclic structure. On the basis of an acetate-type biogenesis, **2** is proposed as the most reasonable formulation. The substituted furan ring in **2** is the analogue of isomaltol ((**5**) (7)). Final assignment of the position of the methyl ether in **2** must await crystallographic analysis, but a characteristic (M-71) peak in the mass spectra of **2**, **3***a*, and **4** supports the presence of a methoxyl substituent adjacent to a quinoid carbonyl (8).

The formulae given are substantiated by accurate mass data or analysis or both and are consistent with all spectroscopic data. This appears to be the first report of a naphthoquinone derivative in a lichen (cf. 9).

Acknowledgments

We are indebted to Dr. W. D. Jamieson of the Atlantic Regional Laboratory, National Research Council of Canada, for accurate mass data, and to Memorial University and the National Research Council of Canada for financial support.

1. W. Zopf. Ber. Dtsch. Bot. Ges. **26**, 51 (1908).
2. S. Shibata. J. Pharm. Soc. Japan, **61**, 320 (1941).
3. O. Hesse. J. Prakt. Chem. **92**, 449 (1915).
4. J. H. Gough and M. D. Sutherland. Australian J. Chem. **20**, 1693 (1967).
5. V. Arkley, J. Attenburrow, G. I. Gregory, and T. Walker. J. Chem. Soc. 1260 (1962).
6. R. E. Moore and P. J. Scheuer. Org. Chem. **31**, 3272 (1966).
7. B. E. Fiaher and J. E. Hodge. J. Org. Chem. **29**, 776 (1964).
8. J. H. Bowie, D. W. Cameron, R. G. F. Giles, and D. H. Williams. J. Chem. Soc. B, 335 (1966).
9. S. Huneck. Progress in phytochemistry. Vol. I. *Edited by* L. Reinhold and Y. Liwschitz. Interscience Publishers, Inc., New York. 1968. p. 334.

A rigorous, purely chemical structure proof for aconitine and delphinine

K. Wiesner, Wen-ling Kao, and Ernest W. K. Jay
Natural Products Research Center, University of New Brunswick, Fredericton, New Brunswick

Received May 20, 1969

A reaction sequence is described which allows the conversion of the aconitine degradation product (**8**) to the previously synthesized compounds **9** and **10** (10), thus providing a complete chemical proof of structures for aconitine **2** and delphinine **1**.

Canadian Journal of Chemistry, 47, 2734 (1969)

Ten years ago we have deduced the structure (**1**) for delphinine (1) and (jointly with the group of Professor G. Büchi) the structure (**2**) for aconitine (2). Shortly after the appearance of our papers in press the structure of desmethanolaconinone (**3**) was derived as a result of an independent crystallographic study (3). This X-ray work, besides corroborating our proposals, helped to orient the substituents in ring A and defined the stereochemistry of all substituents except those located in ring A. Since we have succeeded to correlate (4) aconitine and delphinine, the crystallographic work corroborated the structure of both alkaloids. The orientation and also the configuration of the ring A substituents in aconitine was proved chemically by Professor Büchi (5) and we have derived the configuration of the ring A methoxyl in delphinine (6). Thus the full structure and configuration of both alkaloids may be portrayed by the formulae **4** and **5**. The

Can. J. Chem. Downloaded from www.nrcresearchpress.com by 210.87.254.6 on 09/05/12
For personal use only.

(τ 2.06 and 2.63), which are not coupled, and 4 methoxyl signals.

Both **3***a* (max. at 311.5, 384.6, and 454.5 mμ) and **4** (max. at 306, 379, and 457 mμ) show typical hydroxy juglone electronic spectra, and give green colors with neutral magnesium acetate solution; hence both possess a free "peri"-hydroxyl group. Further, **3***a* was shown to be different from **3***c*, (obtained from **3***b* by alkaline hydrolysis to demethylate one ether of the quinonoid ring and treatment with ethereal magnesium iodide solution (5) to remove the second methyl from the quinonoid ring and the "peri"-methyl group), and is thus formulated as **3***a*.

The low-field single proton signal observed for rhodocladonic acid trimethyl ether suggests that a peri-aromatic proton is present in the molecule (cf. 6). Thus, rhodocladonic acid may be formulated as arising from addition of a 4 carbon unit at C-6 of **3***a* which, from the hydrogen content of the acid and of **4**, must form a cyclic structure. On the basis of an acetate-type biogenesis, **2** is proposed as the most reasonable formulation. The substituted furan ring in **2** is the analogue of isomaltol ((**5**) (7)). Final assignment of the position of the methyl ether in **2** must await crystallographic analysis, but a characteristic (M-71) peak in the mass spectra of **2**, **3***a*, and **4** supports the presence of a methoxyl substituent adjacent to a quinoid carbonyl (8).

The formulae given are substantiated by accurate mass data or analysis or both and are consistent with all spectroscopic data. This appears to be the first report of a naphthoquinone derivative in a lichen (cf. 9).

Acknowledgments

We are indebted to Dr. W. D. Jamieson of the Atlantic Regional Laboratory, National Research Council of Canada, for accurate mass data, and to Memorial University and the National Research Council of Canada for financial support.

1. W. Zopf. Ber. Dtsch. Bot. Ges. **26**, 51 (1908).
2. S. Shibata. J. Pharm. Soc. Japan, **61**, 320 (1941).
3. O. Hesse. J. Prakt. Chem. **92**, 449 (1915).
4. J. H. Gough and M. D. Sutherland. Australian J. Chem. **20**, 1693 (1967).
5. V. Arkley, J. Attenburrow, G. I. Gregory, and T. Walker. J. Chem. Soc. 1260 (1962).
6. R. E. Moore and P. J. Scheuer. Org. Chem. **31**, 3272 (1966).
7. B. E. Fiaher and J. E. Hodge. J. Org. Chem. **29**, 776 (1964).
8. J. H. Bowie, D. W. Cameron, R. G. F. Giles, and D. H. Williams. J. Chem. Soc. B, 335 (1966).
9. S. Huneck. Progress in phytochemistry. Vol. I. *Edited by* L. Reinhold and Y. Liwschitz. Interscience Publishers, Inc., New York. 1968. p. 334.

A rigorous, purely chemical structure proof for aconitine and delphinine

K. Wiesner, Wen-ling Kao, and Ernest W. K. Jay
Natural Products Research Center, University of New Brunswick, Fredericton, New Brunswick

Received May 20, 1969

A reaction sequence is described which allows the conversion of the aconitine degradation product (**8**) to the previously synthesized compounds **9** and **10** (10), thus providing a complete chemical proof of structures for aconitine **2** and delphinine **1**.

Canadian Journal of Chemistry, 47, 2734 (1969)

Ten years ago we have deduced the structure (**1**) for delphinine (1) and (jointly with the group of Professor G. Büchi) the structure (**2**) for aconitine (2). Shortly after the appearance of our papers in press the structure of desmethanolaconinone (**3**) was derived as a result of an independent crystallographic study (3). This X-ray work, besides corroborating our proposals, helped to orient the substituents in ring A and defined the stereochemistry of all substituents except those located in ring A. Since we have succeeded to correlate (4) aconitine and delphinine, the crystallographic work corroborated the structure of both alkaloids. The orientation and also the configuration of the ring A substituents in aconitine was proved chemically by Professor Büchi (5) and we have derived the configuration of the ring A methoxyl in delphinine (6). Thus the full structure and configuration of both alkaloids may be portrayed by the formulae **4** and **5**. The

Can. J. Chem. Downloaded from www.nrcresearchpress.com by 210.87.254.40 on 09/05/12
For personal use only.

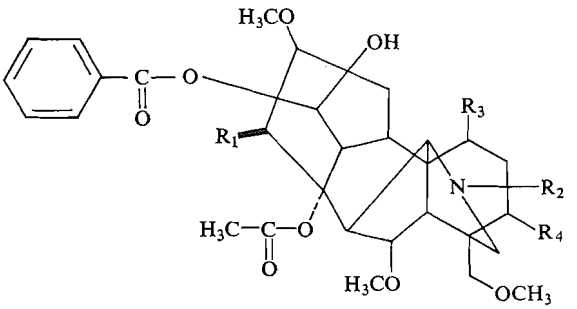

1 $R_1 = H$, $R_2 = CH_3$, R_3,$R_4 = OCH_3$,H
2 $R_1 = OH$, $R_2 = CH_2—CH_3$, R_3,$R_4 = OCH_3$,OH

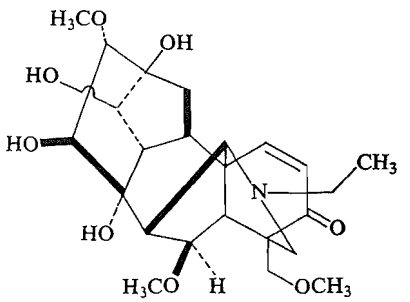

3

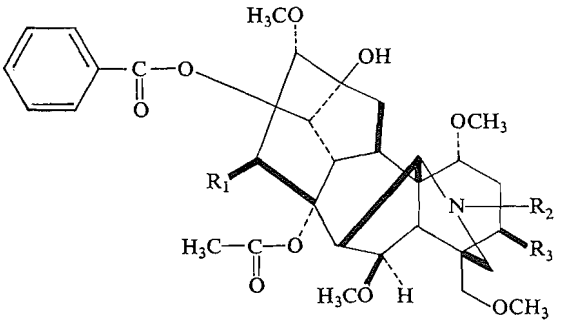

4 $R_1 = H$, $R_2 = CH_3$, $R_3 = H$
5 $R_1 = OH$, $R_2 = CH_2—CH_3$, $R_3 = OH$

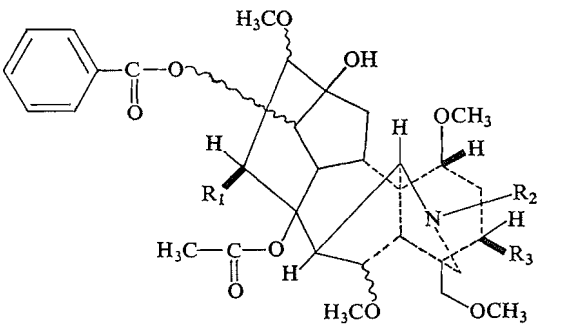

6 $R_1 = H$, $R_2 = CH_3$, $R_3 = H$
7 $R_1 = OH$, $R_2 = CH_2—CH_3$, $R_3 = OH$

chemical evidence for our original structure proposals (1,2,7,8) involved a rigorous proof of the structure and substitution of the C/D ring system and of its relationship to the nitrogen. If we add to this the chemical proof of the orientation and configuration of the ring A substituents in aconitine (5), we can represent the situation, in the chemistry of the two alkaloids, by the formulae **6** and **7**. The partial structure drawn by solid lines in **6** and **7** is rigorously established, while the dotted part of the formulae is in good agreement with a considerable number of experimental data, but not rigidly proved. In fact, this chemically unproved part of the molecule was not difficult to guess. It is common to all known diterpene alkaloids and it was known for a long time since we first proposed this structural feature as a part of the structure of veatchine and atisine (9). Nevertheless, we were interested to provide rigorous purely chemical evidence for the complete structure. Since we wished to accomplish this *via* a total synthesis, this work was simultaneously intended to serve as a stepping stone for the synthesis of the complex diterpene alkaloids themselves.

In our original work on aconitine (2, 8) we have shown that this alkaloid may be simply degraded to the aromatic compound **8**. In this

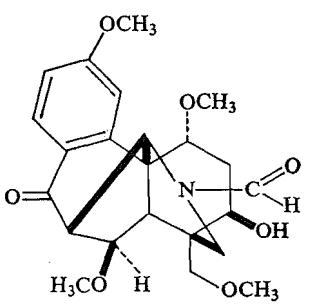

8

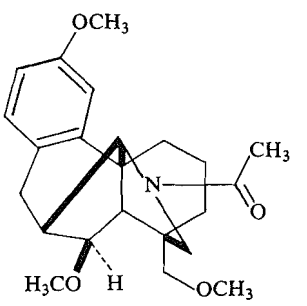

9

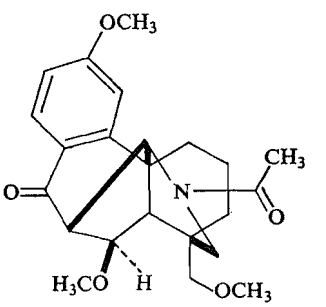

10

Can. J. Chem. Downloaded from www.nrcresearchpress.com by 210.87.254.40 on 09/05/12
For personal use only.

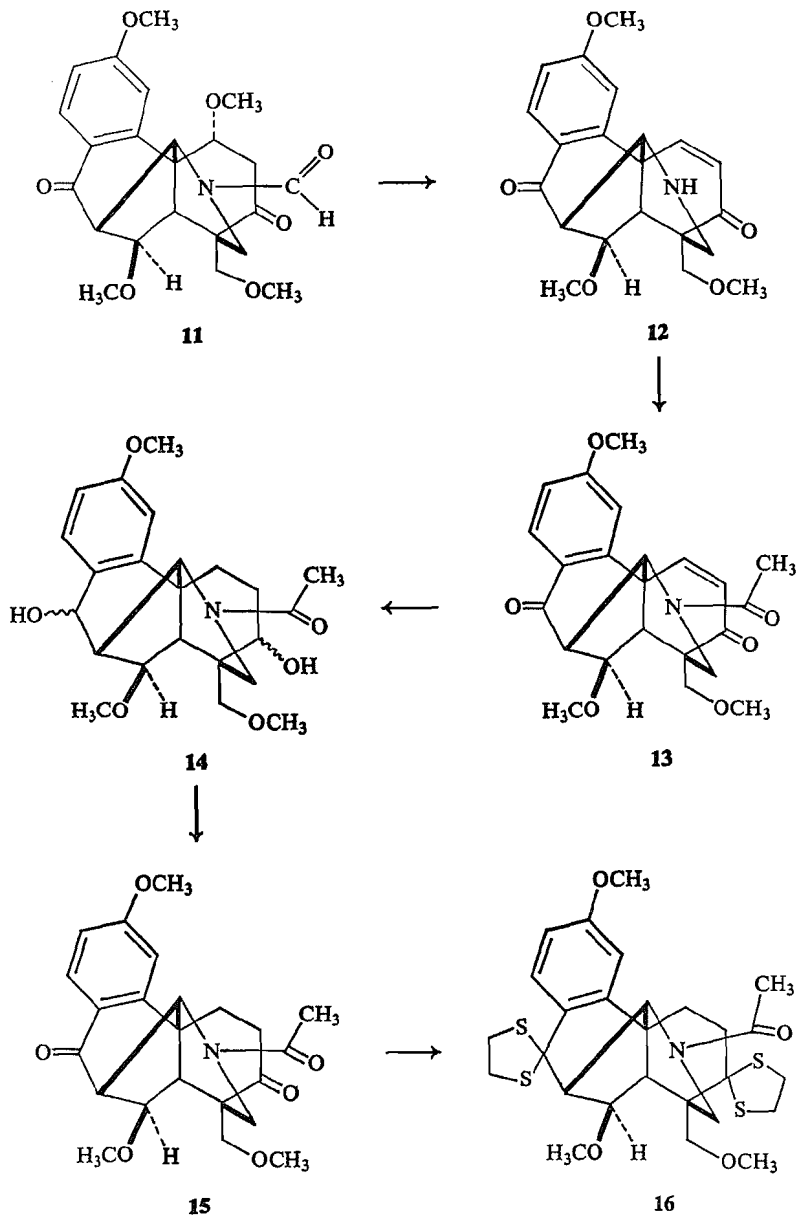

SCHEME 1

derivative the anisole ring originated from the C–D ring system of aconitine, while the rest of the molecule remained completely intact. Recently we have described (10) a total synthesis of the compounds **9** and **10**. In the present communication we wish to disclose the preparation of the optically active form of compounds **9** and **10** from the "natural" aromatization product **8** and a rigorous identification of these materials with the totally synthetic racemates. Since the position and configuration of the ring A substituents in aconitine is fully established by chemistry alone (5) this work represents a rigorous structure proof for aconitine and delphinine. The correlation provides also a chemical proof for the configuration of the ring B methoxyl which is known to be *exo* in the synthetic products (10).

Jones oxidation of compound **8** gave the dike-

Can. J. Chem. Downloaded from www.nrcresearchpress.com by 210.87.254.40 on 09/05/12
For personal use only.

Can. J. Chem. Downloaded from www.nrcresearchpress.com by 210.87.254.40 on 09/05/12
For personal use only.

tone **11** as a chromatographically homogeneous foam in a 91% yield. Infrared (i.r.) (CCl_4): 1720, 1690 cm^{-1} (ketones); nuclear magnetic resonance (n.m.r.): singlets (3H each) τ = 6.14, 6.69, 6.72, 6.80 p.p.m. (4 —OCH_3); *m/e* = 429.

As depicted in Scheme 1, the diketone **11** was heated under reflux with methanolic hydrochloric acid. The basic product **12** was purified by chromatography on alumina and was homogeneous in thin-layer chromatography (t.l.c.). It was obtained in a yield of 75%. Infrared ($CHCl_3$): 3500–3460 cm^{-1} (NH), 1675 cm^{-1} (both ketones); n.m.r.: singlets (3H each) τ = 6.20, 6.68 and 6.76 p.p.m. (3 —OCH_3); *m/e* = 369.1572.

Acetylation of **12** with acetic anhydride and pyridine gave a quantitative yield of the acetyl derivative **13**. It was purified by chromatography and was homogeneous in t.l.c. Infrared (CCl_4): 1700, 1690 cm^{-1} (ketones), 1670 cm^{-1} (N—C—CH_3); n.m.r.: singlets (3H each) τ =

6.14, 6.65, 6.79 p.p.m. (3 —OCH_3), τ = 8.09 p.p.m. (N—C—CH_3); *m/e* = 411.

The acetyl derivative **13** was hydrogenated with platinum oxide in ethanol and the diol **14** thus obtained was immediately oxidized by the Jones reagent to the diketone **15**. After chromatography on alumina compound **15** was homogeneous in t.l.c. and was obtained in a yield of 90%. Infrared (CCl_4): 1720, 1695 cm^{-1} (ketones), 1650 cm^{-1} (N—C—CH_3); n.m.r.: singlets (3H each) τ = 6.18, 6.70, 6.86 p.p.m. (3 —OCH_3), τ = 8.01 p.p.m. (N—C—CH_3); *m/e* = 413.

The diketone **15** was converted quantitatively to the dithioketal **16** by treatment with ethanedithiol and boron trifluoride in glacial acetic acid. The course of this transformation was followed by t.l.c. and by the disappearance of both ketonic absorptions in the i.r. spectrum. Compound **16** was now desulfurized with Raney nickel in alcohol and the product of this reaction was hydrogenated in glacial acetic acid with platinum oxide to reduce a certain amount of material containing a double bond in ring A. Preparative t.l.c. repeated twice yielded the pure "natural" compound **9**. It was homogeneous in six t.l.c. systems using two adsorbents and indistinguishable from the totally synthetic sample (10). The i.r. (CCl_4 and $CHCl_3$), n.m.r. and mass spectra of both materials were superimposable; *m/e* = 385.2252.

Jones oxidation of the "natural" compound **9** yielded the "natural" final product **10** in a 90% yield. It was purified by preparative t.l.c. and it was indistinguishable from the totally synthetic sample (10) of **10** in the same t.l.c. systems used previously. The i.r., mass, n.m.r. and ultraviolet (u.v.) spectra of both materials were identical in every detail; *m/e* = 399.2042.

1. K. Wiesner, F. Bickelhaupt, D. R. Babin, and M. Götz. Tetrahedron Letters, No. 3, 11 (1959).
2. K. Wiesner, M. Götz, D. L. Simmons, L. R. Fowler, F. W. Bachelor, R. F. C. Brown, and G. Büchi. Tetrahedron Letters, No. 2, 15 (1959).
3. M. Przybylska and L. Marion. Can. J. Chem. **37**, 1116 (1959).
4. K. Wiesner, D. L. Simmons, and L. R. Fowler. Tetrahedron Letters, No. 18, 1 (1959).
5. F. W. Bachelor, R. F C. Brown, and G. Büchi. Tetrahedron Letters, No. 10, 1 (1960).
6. K. Wiesner, D. L. Simmons, and R. H. Wightman. Tetrahedron Letters, No. 15, 23 (1960).
7. K. Wiesner, F. Bickelhaupt, D. R. Babin, and M. Götz. Tetrahedron, **9**, 254 (1960).
8. K. Wiesner, M. Götz, D. L. Simmons, and L. R. Fowler. Collect. Czech. Chem. Commun. **28**, 2462 (1963).
9. K. Wiesner, J. R. Armstrong, M. F. Bartlett, and J. A. Edwards. Chem. Ind. 132 (1954).
10. K. Wiesner, Wen-Ling Kao, and J. Šantroch. Can. J. Chem. **47**, 2431 (1969).

Can. J. Chem. Downloaded from www.nrcresearchpress.com by 210.87.254.42 on 09/05/12
For personal use only.

Canadian Journal of Chemistry

Published by The National Research Council of Canada

VOLUME 47 AUGUST 1, 1969 NUMBER 15

Method for the accurate determination of specific rotation. Specific rotation of valine and leucine[1]

J. C. MacDonald

Prairie Regional Laboratory, National Research Council of Canada, Saskatoon, Saskatchewan

Received November 27, 1968

The optical rotation of various concentrations of L-valine and L-leucine, dissolved in glacial acetic acid, or 5 or 6 *M* HCl, was measured with a photoelectric polarimeter at the nominal wavelengths 589, 578, 546, 436, and 365 nm and temperatures of 20, 25, and 30 °C. The specific rotation for any one wavelength, solute, and solvent could be defined by the equation $[\alpha]_\lambda^T = A(1 + D(T - 25)) + BC$, where T is temperature in °C, C is concentration in grams of solute per 100 ml of solution, and A, B, and D are constants. The best fit values of the constants were determined by computer calculation and are listed. Constants are also given for calculating a specific rotation based on grams of solute per 100 g of solution.

Canadian Journal of Chemistry, 47, 2739 (1969)

Introduction

Hayashi and co-workers (1) investigated the specific rotation of amino acids at the sodium D spectral lines (589.3 nm), and the effect of the concentration of solute, molarity of the solvent (aqueous HCl), and temperature on the specific rotation. They found that the specific rotation of leucine and valine increased with increases in the molarity of the HCl and in the concentration of the amino acids. If this is true, few of the specific rotations found in the literature for either of these two compounds can be directly compared, for it is seldom that different workers have used the same temperature, and the same concentrations for HCl and amino acid.

In the work reported here, a formula is developed by which specific rotations of L-valine and L-leucine measured under different conditions can be compared. The solvents used were 5 and 6 *M* HCl, which are frequently employed in optical rotation measurements of amino acids, and glacial acetic acid, which is employed less frequently.

[1]NRCC No. 10648.

Materials and Methods

Solutes

Sucrose was a standard sample obtained from the National Bureau of Standards, Washington, D.C. Amino acid samples were obtained from commercial sources and checked for the content of other amino acids with a Beckman model 120 C amino acid analyzer, using relatively high loads of amino acid. The amino acid samples used in the main part of this work were tested for possible presence of the D-isomer, using a modification of the method of Meister and co-workers (2) and a lyophilized enzyme preparation (3) of D-amino acid oxidase. The modification consisted of the use of 6 ml of buffer instead of 1.5–3.5 ml to dissolve 1 mmole of leucine, because this amount of leucine could not be dissolved in the smaller volume.

Solutions of the amino acids in glacial acetic acid had no appreciable turbidity, and solutions were used directly for optical rotation measurements. Solutions in HCl were slightly hazy at the highest concentration used, so generally the amino acid was recrystallized from ethanol–water prior to making up the stock solution. The weight of material causing the slight haze was found to be negligible in comparison to the weight of amino acid.

A small amount of methionine contaminating the sample of leucine was removed by converting the methionine to the more soluble sulfoxide which was removed by recrystallization. To do this, the leucine was dissolved in water, H_2O_2 added to give a concentration of 0.3%, and the solution allowed to stand overnight. The solution was evaporated *in vacuo* to near dryness

Can. J. Chem. Downloaded from www.nrcresearchpress.com by 210.87.254.42 on 09/05/12
For personal use only.

with a rotary evaporator, the solid washed with ethanol, and recrystallized from water–ethanol.

Solvents

Reagent grade glacial acetic acid was purified by crystallization (4), and used as a solvent for optical rotation measurements. A smaller amount was purified further by drying it for 20 min over one-tenth of its weight of phosphorus pentoxide. The acetic acid was poured off and fractionally distilled until fractions of constant refractive index (measured with a Bausch and Lomb precision refractometer, 25 °C, Na lamp) were obtained. Such fractions of constant refractive index were combined. The refractive index of this standard sample was compared to that of the standard sample plus 0.3% and 0.9% (w/w) water, and to that of the acetic acid used for optical rotations, and the possible content of water in the latter calculated.

Reagent grade HCl was diluted with distilled water, titrated against standard sodium carbonate (5), the concentration readjusted to 5 or 6 M, and the final solutions retitrated.

Concentrations

Stock solutions of solutes in solvents were made up by weight, and dilutions made by weight, to give various values of W (g solute/100 g solution). Densities *in vacuo* were determined as described by Lipkin and co-workers (6) using a thermostatically controlled (±0.05 °C) water bath, and a 5 ml pycnometer modified to give a longer length of capillary below the hook to enable easier filling from a small flask and hence to minimize evaporation. Containers and their contents were equilibrated to balance-room temperature and static charges allowed to dissipate before weighing. All weights of solutes and solvents were corrected to weights *in vacuo* wherever such corrections made a difference of more than 0.05% in the final concentration as compared to uncorrected weights.

The concentration, C, of sucrose solutions in water was calculated from W by eq. [1] (see below), with ρ' values for 20.0, 25.0, and 30.0 °C calculated from Tables 113 and 119 of reference 7 for the appropriate W value. The apparent solution volume, V, of either amino acid in various solvents was calculated from eq. [2] from the density of the solution at the highest W value studied, and checked by appropriate measurements at a lower W value to make sure that it was constant, within experimental error, at differing concentrations. Equation [3] was derived from eqs. [1] and [2], and can be used to calculate C without repeating density determinations for every concentration.

$$[1] \qquad C = \rho' W$$

$$[2] \qquad \frac{1}{\rho'} = \frac{1 - 0.01W}{\rho} + 0.01VW$$

$$[3] \qquad C = \frac{W}{\dfrac{1 - 0.01W}{\rho} + 0.01VW}$$

C = g solute/100 ml solution; W = g solute/100 g solution; ρ' = absolute density of solution (g/ml) at specified temperature; ρ = absolute density of solvent at specified temperature; V = apparent solution volume of solute in solvent (ml/g solute) at specified temperature.

Polarimeter Readings

Optical rotations were measured with a Model 140 Perkin–Elmer photoelectric polarimeter equipped with sodium and mercury lamps and filters to isolate spectral lines at the nominal wavelengths of 589, 578, 546, 436, and 365 nm. The polarimeter cell used was of one-piece glass construction with a length of 1 dcm, a filling volume of 5.7 ml, wide filler ports (0.7 cm diameter) for rapid filling, and a jacket through which water from a thermostatically controlled bath was rapidly circulated. In the experiments with amino acids in glacial acetic acid the temperature of the solution was maintained to ±0.07 °C, and in other experiments the apparatus was improved to give a fluctuation of ±0.03 °C or less. Between different samples, the tube was washed with water and ethanol and dried with an air stream. The outside of the cell windows was wiped with lens tissue moistened with alcohol before each reading.

Amino acid stock solutions were made up by weight, and 5 dilutions made by weight to cover the range of concentrations investigated (Table II). The optical rotation of the stock solution was measured at five wavelengths at a nominal 20 °C (the thermometers were later calibrated against a National Bureau of Standards calibrated thermometer). The rotation with no cell in the light path (instrument blank) was then measured at the 5 wavelengths, and subtracted from the appropriate readings of the solution to obtain observed rotations, α_o The cell blank (i.e., α_o for the cell filled with solvent) was 0.000° for the cell and solvents used, so no corrections for cell blank were necessary. The temperature was readjusted, in turn, to a nominal 25 and 30 °C and the readings were repeated. The whole procedure was repeated for each dilution and all readings were done on the day of preparation of the solutions. The data were transferred to punched cards for computer calculations.

Calculation Methods and Equations

Results were calculated with an I.B.M. 360 computer. W was calculated from weight data, C from eq. [3], and $[\alpha]$ from eq. [4] (see below), using appropriate input data. Then data was separated into sets in which the solvent–solute system and wavelength were constant. From each data set with only C and α_o variable, and eq. [6] (8), which is derived from eqs. [4] and [5], the value of the constants A and B was calculated by a least squares method (eq. [7] and [8]) valid for a polynomial of degree 2 (9). This method gives more exact values of A and B for solutions having low rotations than would a linear regression analysis based on eq. [5]. The polarimeter tube length (0.9999 dcm) was so close to 1.0 dcm that it was treated as such and eliminated from the calculations and equations.

Equation [9] (see below) was found by inspection to fit data with C and T as independent variables, and was combined with eq. [4] to give eq. [10]. In this equation (and eqs. [6] and [13]), α_o has been changed to α_c to distinguish between an observed and calculated rotation. Approximate values of A, B, and D were substituted in

Can. J. Chem. Downloaded from www.nrcresearchpress.com by 210.87.254.42 on 09/05/12
For personal use only.

eq. [10] and varied systematically in a computer program to obtain the best fit between α_0 and α_c values, as calculated from 'weighted degree difference' (w.d.d.) values (see Table II, footnote). The final values of A, B, and D were those which gave the lowest value for the sum of the squares of the w.d.d. values. The weighting of optical rotation values was necessary because the polarimeter had two specified accuracies: $\pm 0.002°$ for readings below 1°, and 0.2% (0.002 parts/degree) for readings greater than 1°.

$$[4] \quad [\alpha] = 100\alpha_0/CL$$

$$[5] \quad [\alpha] = A + BC$$

$$[6] \quad \alpha_c/L = 0.01AC + 0.01BC^2 = \alpha_c \quad (\text{if } L = 1 \text{ dcm})$$

$$[7] \quad a = \frac{\Sigma y \Sigma x^3 - \Sigma xy \Sigma x^2}{\Sigma x \Sigma x^3 - (\Sigma x^2)^2}$$

$$[8] \quad b = \frac{\Sigma y \Sigma x^2 - \Sigma xy \Sigma x}{(\Sigma x^2)^2 - \Sigma x \Sigma x^3}$$

$$[9] \quad [\alpha] = A(1 + D(T - 25)) + BC$$

$$[10] \quad \alpha_c/L = 0.01\,AC\,(1 + D(T - 25)) + 0.01\,BC^2 = \alpha_c \quad (\text{if } L = 1 \text{ dcm})$$

$$[11] \quad [\alpha_w] = 100\alpha_0/WL$$

$$[12] \quad [\alpha_w] = A'(1 + D'(T - 25)) + B'W$$

$$[13] \quad \alpha_c/L = 0.01A'W(1 + D'(T - 25)) + 0.01B'W^2 = \alpha_c \quad (\text{if } L = 1 \text{ dcm})$$

$[\alpha]$ = specific rotation as usually defined; $[\alpha_w]$ = a specific rotation defined by eq. [11]; α_0 = observed rotation of solution; α_c = rotation of solution as calculated from the equation; L = length of polarimeter tube in decimeters; A or A' = constants, the specific rotations at infinite dilution, or intrinsic rotation (8); B or B' = constants, concentration coefficient of specific rotation; D or D' = constants, temperature coefficient of specific rotation. T = temperature at which rotations were measured, °C.

$$a = 0.01A$$

$$b = 0.01B$$

$$y = \alpha_0/L = \alpha_0 \quad (\text{if } L = 1 \text{ dcm})$$

$$x = C$$

C and W have been defined above (see eqs. [1]–[3]).

For some work, a newly-defined specific rotation, $[\alpha_w]$ was calculated by eq. [11], which was used to derive eqs. [12] and [13]. The latter equation was used in the computer programs to find the best fit values of A', D', and B', by procedures similar to those mentioned above.

Results and Discussion

In general, the validity and accuracy of polarimetric results depends on three factors; the purity of the compounds used, the accuracy of the determination of concentration, and the accuracy of the polarimetric readings.

Purity of Compounds

The samples of L-leucine and L-valine used to obtain the data in Tables I, II, and III contained no detectable amount (<0.1%) of D-isomer. The L-valine contained no detectable amount (<0.1%) of any other amino acid but the L-leucine contained a trace (about 0.4%) of L-methionine. To check the validity of data obtained with this L-leucine sample, it was purified to remove methionine, but the rotations obtained in HCl (see below) did not differ significantly from those obtained with the original sample.

Small additions of water to purified acetic acid were found to increase the refractive index in a linear fashion. Analysis by refractive index of the acetic acid used for optical rotation measurements showed that it had a water content of about 0.1%. The acetic acid showed only one peak on gas–liquid chromatography.

Determination of Concentration

Since it is much easier to weigh solutions to an accuracy of 1 mg or better than it is to adjust their volumes to an accuracy of 1 µl or better (which would give comparable accuracy), concentrations were determined by weight and density (see Materials and Methods), and the appropriate factors are given in Table I. The density determinations, as checked with sucrose solutions and tabulated densities (7), were accurate to $\pm 0.02\%$. Good agreement was obtained between the densities of HCl and the data of Akerlof and Teare (10); other published densities for HCl (11, 12) are not so accurate (10). The method used allows for the change of concentration of solute caused by expansion of the solution with change in temperature. There is also a change in the molarity of HCl with change in temperature, but this affects optical rotations to a lesser extent, and may be corrected for as described later.

If an error of 1 mg was made in weighing the solute and solution in making up the stock solutions used to obtain data in Tables II and III,

TABLE I

Factors used in the calculation of concentration C (weight/volume %)

Solvent	Concentration	Temperature °C	Density of solvent, ρ (gm/ml)	Solution volume of solute: V, ml/gm with	
				Leucine	Valine
Acetic acid	99.9%	19.9	1.0495	0.77	0.67
	99.9%	24.9	1.0438	0.77	0.67
	99.9%	29.9	1.0383	0.77	0.67
Aqueous HCl	16.83%=4.99 *M*	19.9	1.0809	0.899	0.862
	16.83%=4.98 *M*	24.9	1.0788	0.902	0.865
	16.83%=4.97 *M*	29.9	1.0767	0.905	0.867
	20.12%=6.06 *M*	19.9	1.0974	0.907	0.869
	20.12%=6.05 *M*	24.9	1.0951	0.910	0.871
	20.12%=6.04 *M*	29.9	1.0928	0.912	0.874

TABLE II

Coefficients for calculation of specific rotations by formula [9]

$$[\alpha]_\lambda^T = A(1 + D(T - 25)) + BC$$

Solvent	Solute and approximate concentration range	λ	A	D	B	Formula fit w.d.d.* −	+
Water	Sucrose	589	66.45	−0.00015	0	0.0005	0.0005
	C=1.0	578	69.18	−0.00014	0	0.0007	0.0010
	to 26.0	546	78.11	−0.00014	0	0.0005	0.0005
		436	128.40	−0.00011	0	0.0015	0.0006
		365	193.01	−0.00007	0	0.0004	0.0002
Acetic acid	L-Leucine	589	25.10	−0.0027	−0.92	0.0011	0.0018
	C=0.5	578	26.28	−0.0028	−0.95	0.0016	0.0016
	to 2.9	546	30.26	−0.0027	−1.09	0.0015	0.0011
		436	55.56	−0.0027	−1.88	0.0014	0.0019
		365	96.91	−0.0027	−3.20	0.0015	0.0031
HCl 4.97 to 4.99 *M*	L-Leucine	589	14.15	0.0053	0.207	0.0013	0.0017
	C=1.3	578	14.83	0.0052	0.223	0.0012	0.0008
	to 7.7	546	17.34	0.0050	0.247	0.0014	0.0014
		436	34.58	0.0038	0.391	0.0013	0.0015
		365	66.30	0.0027	0.608	0.0017	0.0011
HCl 6.04 to 6.06 *M*	L-Leucine	589	14.64	0.0044	0.224	0.0012	0.0009
	C=1.4	578	15.39	0.0044	0.233	0.0016	0.0011
	to 8.4	546	17.97	0.0042	0.260	0.0013	0.0018
		436	35.65	0.0032	0.424	0.0013	0.0016
		365	68.22	0.0022	0.644	0.0024	0.0017
Acetic acid	L-Valine	589	49.42	−0.0041	−1.19	0.0010	0.0009
	C=0.5	578	51.68	−0.0040	−1.23	0.0007	0.0010
	to 1.5	546	59.08	−0.0041	−1.33	0.0005	0.0006
		436	105.30	−0.0040	−2.34	0.0010	0.0012
		365	176.14	−0.0038	−4.22	0.0008	0.0013
HCl 4.97 to 4.99 *M*	L-Valine	589	26.36	−0.0005	0.126	0.0011	0.0014
	C=1.4	578	27.65	−0.0005	0.128	0.0013	0.0012
	to 8.2	546	31.92	−0.0004	0.147	0.0016	0.0013
		436	60.09	−0.0005	0.249	0.0008	0.0010
		365	108.09	−0.0006	0.388	0.0015	0.0010
HCl 6.04 to 6.06 *M*	L-Valine	589	26.96	−0.0007	0.125	0.0009	0.0016
	C=1.4	578	28.28	−0.0007	0.126	0.0016	0.0013
	to 8.2	546	32.63	−0.0007	0.148	0.0014	0.0014
		436	61.34	−0.0008	0.252	0.0008	0.0007
		365	110.27	−0.0008	0.391	0.0012	0.0007

*w.d.d. = weighted degrees-difference = $\alpha_c - \alpha_0$ if $\alpha \leq 1°$ or $(\alpha_c - \alpha_0)/\alpha_0$ if $\alpha_0 > 1°$.

Can. J. Chem. Downloaded from www.nrcresearchpress.com by 210.87.254.42 on 09/05/12
For personal use only.

TABLE III

Coefficients for calculation of weight percent specific rotation by formula [12]

$$[\alpha_w]_\lambda^T = A'(1 + D'(T - 25)) + B'W$$

Solvent	Solute and approximate concentration range	λ	A'	D'	B'	Formula fit w.d.d. −	+
Water	Sucrose	589	66.14	−0.00045	0.280	0.0010	0.0007
	W=1.0	578	68.84	−0.00044	0.293	0.0015	0.0007
	to 23.7	546	77.77	−0.00044	0.327	0.0013	0.0009
		436	127.91	−0.00041	0.531	0.0021	0.0010
		365	192.15	−0.00037	0.811	0.0016	0.0009
HCl	L-Leucine	589	15.27	0.0048	0.245	0.0014	0.0019
16.83%	W=1.2	578	16.02	0.0047	0.261	0.0015	0.0012
	to 7.1	546	18.70	0.0045	0.295	0.0012	0.0016
		436	37.28	0.0034	0.470	0.0016	0.0016
		365	71.51	0.0022	0.731	0.0018	0.0011
HCl	L-Leucine	589	16.02	0.0039	0.271	0.0014	0.0007
20.12%	W=1.4	578	16.87	0.0039	0.277	0.0014	0.0013
	to 7.7	546	19.68	0.0037	0.313	0.0014	0.0021
		436	39.03	0.0027	0.512	0.0013	0.0016
		365	74.69	0.0018	0.778	0.0024	0.0016
HCl	L-Valine	589	28.43	−0.0009	0.168	0.0012	0.0012
16.83%	W=1.3	578	29.80	−0.0009	0.175	0.0016	0.0010
	to 7.6	546	34.42	−0.0009	0.199	0.0011	0.0013
		436	64.81	−0.0009	0.338	0.0009	0.0011
		365	116.57	−0.0010	0.540	0.0017	0.0010
HCl	L-Valine	589	29.51	−0.0012	0.166	0.0010	0.0016
20.12%	W=1.2	578	30.98	−0.0012	0.164	0.0014	0.0013
	to 7.5	546	35.72	−0.0012	0.197	0.0018	0.0015
		436	67.16	−0.0012	0.337	0.0010	0.0007
		365	120.71	−0.0013	0.535	0.0014	0.0009

the maximum error in concentration of the stock solutions would be from 0.07% to 0.19% for the various solvent–solute combinations. Similar small errors in dilutions would have an effect on the fit of data to eq. [10] or [13], but if the errors were random, they would be evened out to some extent in obtaining the best fit to these equations.

Polarimeter Readings

The Perkin–Elmer model 140 polarimeter has a specified accuracy of ±0.2% if $\alpha_0 > 1°$, and ±0.002° if $\alpha_0 < 1°$. The following checks with sucrose solutions of various concentrations from $C = 1.0313$ to $C = 25.974$, indicated that these specifications were correct. The readings were taken at 5 spectral regions, which probably have the effective wavelengths (13): 589.3, 577.9, 546.1, 535.7, and 365.4 nm. The dependence of $[\alpha]_{589.3}^{20}$ on concentration of sucrose can be calculated from the formula (7):

$$[\alpha]_{589.3}^{20} = 66.462 + 0.0087C - 0.000235C^2$$

The $[\alpha]_{589.3}^{20}$ values with the Perkin–Elmer polarimeter agreed within 0.05% with values calculated from this equation for solutions which had $\alpha_0 > 1°$, and within 0.001° where $\alpha_0 < 1°$. Over the range of concentrations studied, the change of specific rotation calculated from the above formula is not large (a maximum difference of 0.11%), which agrees with the finding that there was no significant dependence of specific rotation on concentration of sucrose (B coefficients were 0.000, Table II).

The rotation at other wavelengths can be calculated from the one-term Drude equation (14): $[\alpha]_\lambda^{20} = 21.676/(\lambda^2 - 0.0213)$. This formula is for sucrose in water, $C = 17.218$, and λ is the wavelength in microns. The $[\alpha]_\lambda^{20}$ values obtained with the Model 140 polarimeter at $C = 19.3352$ and the wavelengths mentioned above, were within 0.16% of the calculated values.

Formula for $[\alpha]_\lambda^T$

The formula and constants for specific rotation are shown in Table II. In general, constants were obtained by computer calculation from 18 different readings (6 solutions of different weight percent and 3 temperatures) at each wavelength.

Can. J. Chem. Downloaded from www.nrcresearchpress.com by 210.87.254.42 on 09/05/12
For personal use only.

Can. J. Chem. Downloaded from www.nrcresearchpress.com by 210.87.254.42 on 09/05/12
For personal use only.

The numbers in Table II labeled 'formula fit' show the minimum (−) and maximum (+) w.d.d. values in each set of 18 readings. If $\alpha_0 > 1°$, a figure of 0.002 represents a difference of 0.2% between α_c and α_0, and between calculated and observed specific rotations. If $\alpha_0 < 1°$, a figure of 0.002 represents a difference of 0.002° between α_c and α_0, and a difference of $0.2\%/\alpha_0$ or >0.2% between calculated and observed specific rotations. The accuracy of the polarimeter, as specified by the manufacturer, corresponds to ±0.002 w.d.d., and the above examples show that the best accuracy for specific rotation values is obtained if conditions are chosen so that $\alpha_0 > 1°$. A satisfactory fit to the equation is represented by ±0.002 w.d.d. The maximum absolute value under 'formula fit' in Table II was 0.0031, and the data in general fits the proposed formula and constants very well. In the following discussions the error limits of this formula will be considered to be ±0.003 w.d.d., plus a possible ±0.1% error in determining the concentration of the stock solution from which dilutions were made.

Studies with L-leucine and L-valine in aqueous HCl at one concentration and one temperature (15) showed that a two-term Drude equation (which contains 4 constants) was necessary to describe the variation of specific rotation with wavelength. My results with these compounds cannot usefully be expressed in terms of such an equation, because the range of wavelengths studied does not give sufficient data to evaluate the constants with any certainty.

Specific Rotation of Sucrose in Water

For temperatures near 20 °C, the temperature coefficient, D, of the specific rotation of sucrose in water at 589.3 nm. is known to be −0.00018 (13). This is quite close to the calculated value of D (−0.00015, Table II). The finding that the temperature coefficient 'D' changes with wavelength, if true, requires different constants in the one-term Drude equation at different temperatures. For example, the following equations describe my results quite well:

$$[\alpha]_\lambda^{20°} = 21.676/(\lambda^2 - 0.0213)$$

$$[\alpha]_\lambda^{25°} = 21.653/(\lambda^2 - 0.0214)$$

$$[\alpha]_\lambda^{30°} = 21.627/(\lambda^2 - 0.0215)$$

λ = wavelength in microns.

Specific Rotations of L-Leucine and L-Valine in Glacial Acetic Acid

The specific rotations of L-leucine and L-valine in glacial acetic acid were markedly decreased by the presence of water in the acetic acid. The specific rotation of L-leucine (C = 1.976) was 6.9–8.8% lower (depending on wavelength) in acetic acid containing 1% (w/w) water than in the pure solvent. This result disagrees with those of Greenstein and co-workers (4), who reported that up to 2% water could be present in the acetic acid without appreciably affecting the specific rotation of L-leucine. The specific rotation of L-valine (C = 1.064) was 4.7–5.5% lower in the solvent containing 1% water.

The specific rotation of these amino acids in glacial acetic acid was decreased also by heating. With L-leucine the decrease was about 2%/h at 70 °C and 0.01–0.02%/h at room temperature, and with L-valine was 0.4%/h at 70 °C, and 0.04–0.07%/day at room temperature. To establish the reason for such change, L-leucine was heated in glacial acetic acid for 5 days at 70 °C. After evaporation of the solvent and extraction of the residue with alcohol, a yield of 76% DL-leucine (alcohol-insoluble, identified by infrared spectroscopy) and 24% *N*-acetyl leucine (alcohol-soluble, identified by nuclear magnetic resonance (n.m.r.) spectroscopy) was obtained. The decrease in rotation on heating was therefore due in part to racemization of the amino acid.

For the results in Table II, the heating necessary to dissolve the amino acids was kept to a minimum (at most, 50 min at 50 °C plus 5 min at 60 °C), and the water content of the acetic acid was low (<0.1%). A check of the specific rotation of these amino acids in water-free acetic acid gave results which agreed within 0.54% (0.0028 w.d.d.) with those calculated from Table II, and therefore the results with this solvent can be reproducible. However, acetic acid should not be used where high accuracy is needed, because it may be difficult to obtain and maintain it free of water, and because differing amounts of heating may cause differing amounts of racemization and differing results even with the same sample.

Specific Rotations of L-Leucine and L-Valine in HCl

L-Leucine and L-valine in 5 *M* HCl showed no significant change in optical rotation when heated 1.5 h at 70 °C, or when left for 10 days at room temperature, provided that 5 *M* HCl was

Can. J. Chem. Downloaded from www.nrcresearchpress.com by 210.87.254.42 on 09/05/12
For personal use only.

added to make up for slight evaporation losses. These amino acids are therefore stable in HCl under the conditions used here. The specific rotation results (Table II) agree qualitatively with those of Hayashi and co-workers (1) as outlined in the 'Introduction' section above, but in addition have been extended to other wavelengths and defined in terms of an equation with appropriate constants.

Literature values for specific rotation of these amino acids usually specify 5 or 6 *M* HCl. My results were obtained with HCl which was not exactly 5.00 or 6.00 *M*. One can calculate the specific rotation at exactly these molarities as follows. First find the actual molarities at the desired temperature from Table I (e.g. for 25 °C these were 4.98 and 6.05 *M*) and then calculate the specific rotations at these molarities from the formula and constants of Table II. Next interpolate mathematically to find the specific rotation at either 5.00 or 6.00 *M*, as desired. This linear interpolation is justified by the finding of Hayashi and co-workers (1) that the change of $[\alpha]_D^{20^\circ}$ of these amino acids was approximately linear from 3 to 8 *M* HCl. The interpolation is only over a small range — at most from 6.06–6.00 *M* — and the maximum correction necessary (found for L-leucine $[\alpha]_{589.3}^{20^\circ}$, $C = 8$ in 6.06 *M* HCl as compared to $C = 8$ in 6.00 *M* HCl) was calculated to be 0.24%.

Weight % Specific Rotations $[\alpha_w]$

The determination of concentration on a w/w % basis is undoubtedly more accurate for small amounts of amino acid solutions usually made up for optical rotation measurements than is determination on a w/v % basis. Therefore, it is useful to define a new specific rotation $[\alpha_w]$, eq. [11] on the basis of weight percent, *W*, and eliminate calculations involving density. Some of my data was recalculated with the appropriate equations for $[\alpha_w]$ (see Materials and Methods) to give the results in Table III. The formula fit values (Table III) are within ±0.003 w.d.d. and are satisfactory.

The optical rotations, α_0, of specially purified, methionine-free L-leucine were determined at two concentrations (approximately $W = 7.0$ and 3.5) for the two concentrations of HCl, three temperatures (20, 25, and 30 °C), and the five wavelengths. The results agreed with the α_c values calculated from the constants of Table III and eq. [11] within the range −0.0024 to +0.0028 w.d.d., showing that the optical rotations were not significantly changed by this purification and that the L-leucine used to obtain the data for Tables II and III was pure enough to give reliable results within the accuracy of the method. The rotations of L-valine were checked in a similar way with another commercial sample which contained no detectable amount (<0.1%) of any other amino acid, and satisfactory agreement (−0.0037 to +0.0008 w.d.d.) was obtained also.

Comparison of Specific Rotations with Published Values

Thomas and Nieman (16) reported that the $[\alpha]_D^{25^\circ}$ values for L-leucine in glacial acetic acid increased with a decrease in *C*, and that this increase was more rapid at low *C* values. To check this, the range of concentrations investigated (Table II) was extended by including a measurement at $C = 0.22$. My results showed that the increase of specific rotation with decrease in concentration (*B* constants are negative, Table II) was linear, and the linearity did not change at low *C* values. These authors also reported that the $[\alpha]_D^{25^\circ}$ value for L-leucine in 6.02 *M* HCl was independent of concentration from $C = 2$–5, but this is contradicted both by my results and those of Hayashi and co-workers (1).

Various published specific rotations at the D line of sodium (589.3 nm) for L-valine and L-leucine are compared in Table IV with those calculated from Table II with interpolations to 5.00 or 6.00 *M*, as described above. Greenstein and Winitz (17) stated the concentration for L-valine in acetic acid or in 5 *M* HCl as $C = 1$–2, so the choice of *C* for calculations in comparison with their results is therefore arbitrary. Hayashi and co-workers (1) published specific rotations at what they termed 'optimal conditions of measurement'. Their observed rotations, expressed as α_0/dcm, agree within 0.003° with my calculated values (Table IV), and this agreement is within my experimental error. Because Hayashi and co-workers were aware of the effects of concentration of solute, molarity of HCl, and temperature on the specific rotation of these amino acids, their results are probably much more accurate than those of other investigators, and the other results in Table IV confirm this.

TABLE IV

Comparison of published specific rotations for L-leucine and L-valine with those calculated from Table II

	Published values and conditions						Calculated values	
Solute	Solvent	T, °C	C	$[\alpha]_D$	α_0/dcm	Ref.	$[\alpha]_D$	α_0/dcm
L-Leucine	Acetic acid	25	2	22.5	0.450	17	23.26	0.465
L-Leucine	6 *M* HCl	20	4	15.1	0.604	1	15.17	0.607
L-Leucine	5 *M* HCl	25	2	15.6	0.312	18	15.10	0.302
L-Leucine	5 *M* HCl	25	2	16.0	0.320	17	15.10	0.302
L-Valine	Acetic acid	25	1?	62.0	0.620	17	48.23	0.482
L-Valine	6 *M* HCl	20	8	28.0	2.240	1	28.02	2.242
L-Valine	6 *M* HCl	20	3.4	26.7	0.908	18	27.44	0.933
L-Valine	5 *M* HCl	25	2?	28.3	0.576	17	26.61	0.532

If only a small amount of valine or leucine is available for measurements, so that the observed rotation is small at 589.3 nm, improved accuracy can be obtained by measurements at a lower wavelength where the observed rotation is larger. The data of Tables II or III is useful in evaluating what these rotations should be.

Acknowledgments

I thank Dr. A. J. Finlayson and Mr. D. M. Tenaschuk, Prairie Regional Laboratory, National Research Council of Canada, Saskatoon, Saskatchewan for amino acid analyses and technical assistance, respectively. I also thank Mr. B. Molaro, Computer Centre, University of Saskatchewan, for assistance in programming.

1. K. HAYASHI, Y. FUJII, R. SAITO, H. KANAO, and T. HINO. Agr. Biol. Chem. (Tokyo), **30**, 1221 (1966).
2. A. MEISTER, L. LEVINTOW, R. B. KINGSLEY, and J. P. GREENSTEIN. J. Biol. Chem. **192**, 535 (1951).
3. J. R. PARIKH, J. P. GREENSTEIN, M. WINITZ, and S. M. BIRNBAUM. J. Am. Chem. Soc. **80**, 953 (1958).
4. J. P. GREENSTEIN, S. M. BIRNBAUM, and M. C. OTEY. J. Biol. Chem. **204**, 307 (1953).
5. I. M. KOLTHOFF and E. B. SANDELL. Textbook of quantitative inorganic analysis. The Macmillan Co., New York. 1947. p. 546.
6. M. R. LIPKIN, J. A. DAVISON, W. T. HARVEY, and S. S. KURTZ. Ind. Eng. Chem., Anal. Ed. **16**, 55 (1944).
7. F. J. BATES, and Associates. Polarimetry, saccharimetry, and the sugars. Circular, Nat. Bur. Std., C440. Washington, D.C. 1942. pp. 82, 626, and 648.
8. W. HELLER. Technique of organic chemistry. Physical methods. Vol. I, Pt. 3. A. Weissberger (*Editor*). Interscience Publishers, Inc., New York. 1960. p. 2302.
9. H. L. ALDER and E. B. ROESSLER. Introduction to probability and statistics. 3rd ed. W. H. Freeman and Co., San Francisco. 1964. p. 181.
10. G. AKERLOF, and J. TEARE. J. Am. Chem. Soc. **60**, 1226 (1938).
11. E. W. WASHBURN. (*Editor-in-Chief*). International Critical Tables. McGraw-Hill Book Co., Inc., New York. 1928. Vol. 3. p. 54.
12. R. C. WEAST, and S. M. SELBY. *Editors-in-Chief*. Handbook of chemistry and physics. 47th ed. Chemical Rubber Co., Cleveland, Ohio. 1966. p. D-152.
13. J. FLUGGE. The principles of polarimetry. Carl Zeiss, Oberkochen/Wuertt. 1965. p. 87.
14. T. L. HARRIS, E. L. HIRST, and C. E. WOOD. J. Chem. Soc. 2108 (1932).
15. L. I. KATZIN, and E. GULYAS. J. Am. Chem. Soc. **86**, 1655 (1964).
16. D. W. THOMAS and C. NIEMANN. J. Biol. Chem. **175**, 241 (1948).
17. J. P. GREENSTEIN and M. WINITZ. Chemistry of the amino acids. John Wiley and Sons, Inc., New York. 1961. pp. 2075 and 2368.
18. Specifications and criteria for biochemical compounds. 2nd ed. Publication 1344. National Academy of Sciences, National Research Council. Washington, D.C. 1967. pp. 4, 57, and 79.

Can. J. Chem. Downloaded from www.nrcresearchpress.com by 210.87.254.42 on 09/05/12
For personal use only.

Aminodideoxy sugars. Methyl 3-acetamido-2,3-dideoxy-α-D-*arabino*-hexopyranoside and methyl 2-acetamido-2,3-dideoxy-α-D-*ribo*-hexopyranoside

ALEX ROSENTHAL AND P. CATSOULACOS
Department of Chemistry, University of British Columbia, Vancouver, British Columbia
Received February 26, 1969

Oxidation of methyl 4,6-*O*-benzylidene-3-deoxy-α-D-*arabino*-hexopyranoside (**2**) with methyl sulfoxide and acetic anhydride yielded methyl 4,6-*O*-benzylidene-3-deoxy-α-D-*erythro*-hexopyranosid-2-ulose (**3**) in an 80% yield. Reduction of the oximino derivative of **3** with lithium aluminium hydride in tetrahydrofuran or with diborane afforded, after acetylation, methyl 2-acetamido-4,6-*O*-benzylidene-2,3-dideoxy-α-D-*ribo*-hexopyranoside (**6**) in a 44% yield. The latter was also debenzylidenated with aqueous acetic acid. In a parallel reaction, methyl 4,6-*O*-benzylidene-2,3-dideoxy-3-oximino-α-D-*erythro*-hexopyranoside yielded mainly methyl 3-acetamido-4,6-*O*-benzylidene-2,3-dideoxy-α-D-*arabino*- (and a minor amount of the *ribo*-epimer)-hexopyranoside.

Canadian Journal of Chemistry, 47, 2747 (1969)

Can. J. Chem. Downloaded from www.nrcresearchpress.com by 210.87.254.6 on 09/05/12
For personal use only.

The preparation of methyl 2- and 3-amino-2,3-dideoxy-α-D-glycosides has posed a problem of considerable difficulty. Attempted reduction of methyl 4,6-*O*-benzylidene-2,3-dideoxy-3-oximino-α-D-*erythro*-hexopyranoside with either a palladium or a platinum catalyst, or by zinc and acetic acid, failed (1). On the other hand, methyl 2-deoxy-2-oximino-α-D-glycosides were reduced, to yield 2-amino-2-deoxy glycosides (2). Although methyl 2- and 3-aminodideoxy-α-D-glycosides have been prepared *via* the 2,3-epimine intermediates, this synthesis can not be considered to be attractive owing to the fact that the over-all yield is very low, and furthermore, great difficulty is encountered in separating the mixtures of isomers in the last step (3). For example, methyl 4,6-*O*-benzylidene-2,3-dideoxy-2,3-epimino-α-D allopyranoside afforded syrupy compounds which were assumed to be methyl 3-acetamido (and 2-acetamido)-2,3-dideoxy-α-D-*ribo*-hexopyranoside. 3-Azido derivatives have been successfully reduced with sodium borohydride to afford 3-amino carbohydrates (4). Finally, hydrazino compounds have been cleaved catalytically to yield amino carbohydrates in low over-all yield (5), dideoxyoximino glycosides have been reduced to yield aminodideoxy glycosides (4*c*),[1] and nitro carbohydrates have been used to prepare aminodideoxy carbohydrates (1).

In view of the importance of the amino sugars (6) it was decided to reinvestigate the reduction of the oximino compounds, because the latter can now be readily prepared from ketoses. The latter have now become readily accessible through use of the excellent oxidizing agent methyl sulfoxide in the presence of either acetic anhydride or phosphorus pentoxide.

Reduction of methyl 2,3-anhydro-4,6-*O*-benzylidene-α-D-*manno*-hexopyranoside (**1**) with lithium aluminium hydride in tetrahydrofuran (7, 8)[2] gave an 88% yield of methyl 4,6-*O*-benzylidene-3-deoxy-α-D-*arabino*-hexopyranoside (**2**). Subsequent oxidation of **2** with anhydrous methyl sulfoxide and acetic anhydride afforded methyl 4,6-*O*-benzylidene-3-deoxy-α-D-*erythro*-hexopyranosid-2-ulose (**3**) in 80% yield. Treatment of **3** with hydroxylamine hydrochloride and sodium hydroxide at room temperature gave the oxime **4** in 60% yield. Reduction of **4** with lithium aluminium hydride in tetrahydrofuran or ether followed by acetylation of the amine with acetic anhydride, gave methyl 2-acetamido-2,3-dideoxy-α-D-*ribo*-hexopyranoside (**6**) contaminated with a trace of a compound which was presumed to be the *arabino* isomer. By fractional crystallization of the acetamido derivatives from ether – ethyl acetate, pure **6** was obtained in crystalline form in 44% yield having m.p. 263–264° and $[\alpha]_D = +52°$. Reduction of the 2-acetoximino derivative **5** with diborane in tetrahydrofuran also gave **6**, and in addition, a substance which was presumed to be an un-

[1]These authors reported (after our manuscript was in press) that the lithium aluminium hydride reduction of methyl 4,6-*O*-benzylidene-2,3-dideoxy-3-oximino-α-D-*erythro*-hexopyranoside yields only one substance which was presumed to be the *ribo* isomer.

[2]W. W. Zorbach used lithium aluminium hydride in tetrahydrofuran. Personal communication.

Can. J. Chem. Downloaded from www.nrcresearchpress.com by 210.87.254.6 on 09/05/12
For personal use only.

decomposed complex of the product. Debenzylidenation of **6** with aqueous acetic acid afforded crystalline methyl 2-acetamido-2,3-dideoxy-α-D-*ribo*-hexopyranoside. Buss *et al.* (3) had previously reported the isolation of a syrupy substance which was presumed to be **6** having $[\alpha]_D = +80°$.

The structure of debenzylidenated **6** was deduced from its nuclear magnetic resonance (n.m.r.) spectrum. The axial C-3 hydrogen signals centered at τ 8.56 which appear as a quartet have a total width of 34.5 Hz. This width is practically equal to the sum of the three coupling constants ($J_{3a,3e}$, $J_{3a,2a}$, and $J_{3a,4a}$) with which the axial C-3 hydrogen is coupled to the equatorial C-3 hydrogen and to the two neighboring hydrogens on C-2 and C-4. Thus, the sum of $J_{3a,4a}$ and $J_{3a,2a}$ may be calculated to be approximately 22 Hz. To account for this large value, as well as for the splitting pattern observed, the C-2 hydrogen is assigned an axial configuration as in **6**, and therefore, the acetamido group is equatorially oriented.

Similar consideration of the n.m.r. spectrum of the benzylidene derivative **6** also indicates the presence of an axial hydrogen on C-2. The singlet peak at τ 8.08 also indicates that the acetamido peak is in an equatorial orientation (9). The C-1 anomeric H of **6** appears as a doublet at τ 5.43 having $J_{1,2} = 3.5$ Hz. In general, 4,6-*O*-benzylidene compounds with the α-D-altro and α-D-*manno* configurations give spectra with first-order $J_{1,2} = 1.2$ Hz or less, so that the signal for H-1 frequently appears as a singlet. The fact that $J_{1,2}$ of **6** is much larger than 1.2 Hz indicates that H-2 is probably in an axial orientation. Irradiation experiments confirmed all assignments shown in the Experimental. Finally, indirect additional support for the assignment of structure **6** follows from the fact that methyl 2-acetamido-4,6-*O*-benzylidene-2,3-dideoxy-α-D-*arabino*-hexopyranoside has m.p. 171–173° (3), whereas compound **6** has m.p. 263–264°. Therefore, compound **6** is undoubtedly methyl 2-acetamido-4,6-*O*-benzylidene-2,3-dideoxy-α-D-*ribo*-hexopyranoside.

In an analogous way, methyl 4,6-*O*-benzylidene-α-D-*erythro*-hexopyranoside-3-ulose was oximinated, and the oxime then acetylated to afford the 3-acetoximino derivative. Lithium aluminium hydride reduction of the oximino or acetoximino derivative, followed by acetylation of the amines, gave a mixture of 3-acetamido-4,6-*O*-benzylidene-2,3-dideoxy-α-D-*arabino*-(and *ribo*)-hexopyranoside in 60% yield in the ratio of 3:1, respectively. Fractional crystallization of acetamido derivatives readily afforded crystalline methyl 3-acetamido-4,6-*O*-benzylidene-2,3-dideoxy-α-D-*arabino*-hexopyranoside. The 3-acetamido-α-D-*ribo* derivative was not characterized because of the difficulty of obtaining a pure substance. The n.m.r. and infrared (i.r.) spectra of the major component were similar to those of an authentic sample, kindly furnished by Dr. A.C. Richardson, of methyl 3-acetamido-4,6-*O*-benzylidene-2,3-dideoxy-α-D-*arabino*-hexopyranoside (4), although there is some discrepancy between the physical properties of our compound and those reported previously. It is interesting to note that the n.m.r. spectrum of the crude mixture of 3-acetamido epimers revealed that the equatorial acetamido group resonates at a higher field (about 0.1 p.p.m.) than the corresponding axially oriented counterpart, a finding in agreement with a previous report (9).

Experimental

The melting points were determined on a microstage and are uncorrected. Spectra were measured with a Varian Associates 100 MHz HA spectrometer with deuteriochloroform as a solvent (unless otherwise stated) and tetramethylsilane as the internal standard set at τ = 10. Thin-layer chromatography was performed on silica gel G plates using chloroform – methanol (97:3 v/v) as developer. The optical rotations were measured in a 1 decimeter tubes at the D line of sodium and room temperature (about 22–23°). The microanalyses were carried out by the University of British Columbia Microanalytical Laboratory.

Methyl 4,6-O-Benzylidene-3-deoxy-α-D-arabino-hexopyranoside (2)

Lithium aluminium hydride reduction of **1** in tetrahydrofuran according to a previously described procedure (7) gave **2** in an 88% yield. Compound **2** was recrystallized from ether – petroleum ether (b.p. 35–60°), m.p. 110–112° (lit. (8), m.p. 111–112°).

Methyl 4,6-O-Benzylidene-3-deoxy-α-D-erythro-hexopyranosid-2-ulose (3)

To a solution of 5.74 g of compound **2** in freshly distilled (over calcium hydride) methyl sulfoxide (150 ml) was added anhydrous acetic anhydride (30 ml) and the resulting solution was kept at room temperature for 2 days. The product was worked-up as described previously (7), and recrystallized from ether – petroleum ether b.p. 35–60°), yield 4.6 g (80%), m.p. 114–115°; $[\alpha]_D^{22}$ +109° (*c* 2, in chloroform).

Anal. Calcd. for $C_{14}H_{16}O_5$: C, 63.63; H, 6.06. Found: C, 63.36; H, 6.20.

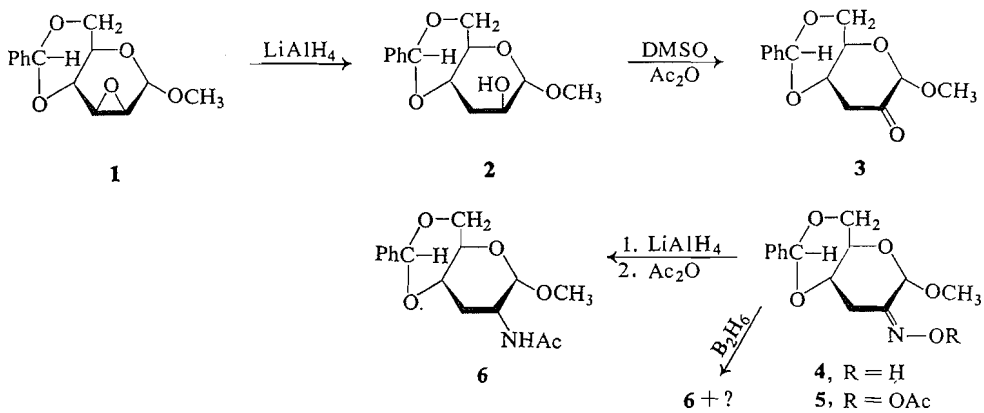

*Methyl 4,6-O-Benzylidene-2,3-dideoxy-2-oximino-α-*D*-erythro-hexopyranoside*

The ketose **3** (0.88 g) was added to an ethanol (75 ml) solution of hydroxylamine hydrochloride (0.240 g) and sodium hydroxide (0.135 g). After the mixture was maintained at room temperature for 24 h with stirring, water was added and the mixture left to stand for 3 h. The oxime was removed by filtration and recrystallized from ether – ethyl acetate to yield pure oxime (0.55 g, 60% yield), m.p. 138–139°; $[\alpha]_D^{22}$ +88° (*c* 1, in chloroform).

Anal. Calcd. for $C_{14}H_{17}NO_5$: C, 60.21; H, 6.09; N, 5.02. Found: C, 60.20; H, 6.32; N, 5.0.

*Reduction of Methyl 4,6-O-Benzylidene-2,3-dideoxy-2-oximino-α-*D*-erythro-hexopyranoside to Yield Methyl 2-Acetamido-4,6-O-benzylidene-2,3-dideoxy-α-*D*-ribo-hexopyranoside (6)*

To a solution of methyl 4,6-*O*-benzylidene-2,3-dideoxy-2-oximino-α-D-*erythro*-hexopyranoside (0.44 g) in 50 ml of anhydrous tetrahydrofuran (or ether) was added lithium aluminium hydride (0.80 g) in portions during a period of 5 min. After the reaction mixture was kept under reflux for 4 h, excess lithium aluminium hydride was destroyed with ethyl acetate followed by water. The flocculent precipitate was separated by centrifugation or removed by filtration and washed several times with chloroform. The combined filtrates were washed twice with water (100 ml), dried over magnesium sulfate, and evaporated to yield 0.41 g of syrup. This syrup was acetylated with a mixture of 3 ml of acetic anhydride and 2 ml of pyridine for 10 h at room temperature. The reaction mixture was poured into a mixture of ice and water, and the product, removed by filtration, was recrystallized from ether – ethyl acetate, yield 0.205 g (44%), m.p. 264–264°; $[\alpha]_D^{22}$ +52° (*c* 1, chloroform). The product was homogeneous by chromatography R_f 0.56, τ ($CDCl_3$) 4.5 (s, CHPh), 5.43 (d, H-1, $J_{1,2}$ = 3.5 Hz), 5.5–6 (m), 6.1–6.5 (m), 6.6 (s, OCH_3), 7.83

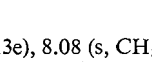

(m, H3e), 8.08 (s, CH_3C—N), 8.16 (q, partly obscured by CH_3CO, total width 34 Hz, $J_{H3a,3e}$ = 11.5 Hz, $J_{H3a,2a}$ = 11 Hz). Irradiation at τ 8.2 collapsed the H-2 signal at τ 5.62. Irradiation at τ 7.8 also collapsed H-2 signal to a doublet. Irradiation at τ 5.70 affected the H-3a and H-3e signals.

Anal. Calcd. for $C_{16}H_{21}NO_5$: C, 62.54; H, 6.84; N, 4.56. Found: C, 62.33; H, 6.92; N, 4.61.

*Methyl 2-Acetamido-2,3-dideoxy-α-*D*-ribo-hexopyranoside*

Compound **6** was debenzylidenated with aqueous acetic acid on the steam bath and the product worked-up in the usual way. Recrystallization of the product from ethanol – ethyl acetate gave pure material, m.p. 204–206°; $[\alpha]_D^{22}$ +80° (*c* 1, in water).

τ (D_2O) 6.60 (s, OCH_3), 8.02 (s, acetyl), 7.8 (m, H-3e, partly obscured by the acetyl peak), 8.56 (q, H-3a, total width 34.5 Hz, $J_{3a,3e}$ = 11.5 Hz, $J_{3a,2a}$ = 11.5 Hz, $J_{3a,4a}$ = 11.5 Hz).

Anal. Calcd. for $C_9H_{17}NO_5 \cdot 1/2H_2O$: C, 47.45; H, 7.87; N, 6.14. Found: C, 47.52; H, 7.42; N, 6.05.

*Methyl 4,6-O-Benzylidene-2,3-dideoxy-3-oximino-α-*D*-erythro-hexopyranoside*

Methyl 4,6-*O*-benzylidene-α-D-*erythro*-hexopyranosid-3-ulose (1.32 g) (7) was converted into the oxime in 74% yield and recrystallized from methanol – ether, m.p. 208–209°, $[\alpha]_D^{22}$ +170° (*c* 1, in chloroform) (lit. (1), m.p. 203°, $[\alpha]_D$ +172°).

Anal. Calcd. for $C_{14}H_{17}NO_5$: C, 60.21; H, 6.14. Found: C, 60.41; H, 6.40.

*Methyl 3-Acetoximino-4,6-O-benzylidene-2,3-dideoxy-α-*D*-erythro-hexopyranoside*

The 3-oxime was acetylated in the usual way, and the product recrystallized from methanol – ethyl acetate, m.p. 201–202° (in agreement with the lit. value (1)).

*Reduction of Methyl 3-Acetoximino (and oximino)-4,6-O-benzylidene-2,3-dideoxy-α-*D*-erythro-hexopyranoside to Yield Methyl 3-Acetamido-4,6-O-benzylidene-2,3-dideoxy-α-*D*-arabino-(and ribo)-hexopyranoside*

(a) With Lithium Aluminium Hydride

The 3-acetoximino derivative (0.200 g) was reduced in a manner analogous to that already described in Experimental, and the syrupy amine was treated with acetic anhydride in ethanol to give the corresponding *N*-acetyl

Can. J. Chem. Downloaded from www.nrcresearchpress.com by 210.87.254.6 on 09/05/12
For personal use only.

derivative; yield 0.115 g (60%); τ (pyridine-d_5) (of crude acetamido compounds) 8.08 (s, equatorial $CH_3C(=O)-N$), 7.98 (s, axial $CH_3C(=O)-N$), in the ratio of 3:1, approximately. Fractional crystallization of the product from methanol – ethyl acetate afforded methyl 3-acetamido-4,6-*O*-benzylidene-2,3-dideoxy-α-D-*arabino*-hexopyranoside, m.p. 284–285°, $[\alpha]_D^{22}$ +64° (*c* 1, in ethanol), R_f 0.5; τ (pyridine-d_5) 4.40 (s, CHPh), 5.15 (NH), 5.23 (q, H-1, $J_{1,2a}$ = 3.5 Hz), 5.65–6.35 (m), 6.78 (s, OCH_3), 7.42 (m, H-2e, $J_{2e,2a}$ = 13 Hz), 8.1 (m, H-2a, partially obscured by CH_3CO), 8.08 (s, *N*-acetyl). Irradiation at τ 7.42 changed the H-1 signal to a doublet having $J_{1,2a}$ = 3.5 Hz. Irradiation at τ 5.23 altered the signals at τ 7.42.

The n.m.r. and i.r. spectra of the above 3-acetamido compound were identical to those of a sample of methyl 3-acetamido-4,6-*O*-benzylidene-2,3-dideoxy-α-D-*arabino*-hexopyranoside furnished by Dr. A.C. Richardson.

Anal. Calcd. for $C_{16}H_{21}NO_5$: C, 62.54; H, 6.84; N, 4.56. Found: C, 62.36; H, 7.04; N, 4.64.

Lithium aluminium hydride reduction of the oximino compound gave approximately the same yield (61%) of amine.

(b) With Diborane

Into an ice-cold solution of methyl 3-acetoximino-4,6-*O*-benzylidene-2,3-dideoxy-α-D-*erythro*-hexopyranoside (0.50 g) in anhydrous tetrahydrofuran (25 ml) was bubbled diborane for 10 min. After the reaction mixture was left to stand at room temperature for 3 h, the solvent was removed under reduced pressure to yield a syrup which was then treated with 10% aqueous sodium hydroxide at 10–15°. The reaction mixture was then extracted twice with chloroform (150 ml), the chloroform extract washed twice with water (100 ml), and dried over magnesium sulfate. After the solvent was removed the product was acetylated with acetic anhydride and pyridine and the product worked-up in the usual way to yield 0.36 g of syrup. This syrup was crystallized from ethanol to give crystalline material (0.09 g), m.p. 150–152°, R_f 0.72 (chloroform). After evaporating off one-half of the solvent, 0.030 g of methyl 3-acetamido-4,6-*O*-benzylidene-2,3-dideoxy-α-D-*arabino*-hexopyranoside, m.p. 284–285°, was obtained. The mother liquor contained about equal amounts of the two fractions. The first fraction was presumed (from its i.r. spectrum) to be an undecomposed borane complex.

Acknowledgments

This work was supported in part by Public Health Service Research Grant No. CA-08382 from the United States National Cancer Institute and by the National Research Council of Canada.

The author (A.R.) wishes to thank Dr. A.C. Richardson for a sample of methyl 3-acetamido-2,3-dideoxy-α-D-*arabino*-hexopyranoside. The technical assistance of Mrs. M. Ong is acknowledged.

1. H. H. Baer and F. Kienzle. Can. J. Chem. **45**, 983 (1967), and references therein to previous papers by H. H. Baer and co-workers.
2. R. U. Lemieux, S. W. Gunner, and T. L. Nagabbushan. Tetrahedron Letters, 2149 (1965).
3. D. H. Buss, L. Hough, and A. C. Richardson. J. Chem. Soc. 2736 (1965).
4. (*a*) A. C. Richardson. Carbohydrate Res. **4**, 422 (1967), and references therein to previous papers by A. C. Richardson and co-workers. (*b*) Y. Ali and A. C. Richardson. Carbohydrate Res. **5**, 441 (1967). (*c*) P. J. Beynon, P. M. Collins, and W. G. Overend. J. Chem. Soc. C, 272 (1969).
5. J. Kovář, V. Dienstbierová, and J. Jary. Collection Czech. Chem. Commun. **32**, 2498 (1967).
6. J. D. Dutcher. Advan. Carbohydrate Chem. **18**, 259 (1963).
7. A. Rosenthal and P. Catsoulacos. Can. J. Chem. **46**, 2868 (1968).
8. D. A. Prins. J. Am. Chem. Soc. **70**, 3955 (1948).
9. F. W. Lichtenthaler and P. Emig. Tetrahedron Letters, 577 (1967).

Can. J. Chem. Downloaded from www.nrcresearchpress.com by 210.87.254.6 on 09/05/12
For personal use only.

Can. J. Chem. Downloaded from www.nrcresearchpress.com by 210.87.254.42 on 09/05/12
For personal use only.

Internal addition of acyl nitrenes to olefins[1]

IVOR BROWN,[2] O. E. EDWARDS, J. M. MCINTOSH,[2] AND D. VOCELLE[2]
Division of Biochemistry and Molecular Biology, National Research Council of Canada, Ottawa, Canada

Received February 24, 1969

Photolysis of cycloheptene-5-carbonyl azide, *endo*-norbornene-5-carbonyl azide and *o*-vinylbenzoyl azide gave very reactive acyl aziridines by internal addition of acyl nitrenes to the olefinic double bonds. Derivatives of 6-azabicyclo-[3,2,2]nonane and 1,2-dihydroisoindol-1-one were prepared. *cis*-2-Vinylcyclopropyl isocyanate, prepared photochemically at −78°, underwent Cope rearrangement at room temperature to 2,3-dihydro-1*H*-azepin-2-one. The mass spectra of a series of lactams are interpreted.

Canadian Journal of Chemistry, 47, 2751 (1969)

The generality of internal CH insertion of what appear to be excited singlet acyl nitrenes, to give lactams, is well documented. Some years ago we undertook to examine the irradiation of molecules containing both an acyl azide group and an olefinic double bond potentially close in space. Previous and subsequent work has shown that azidoformates (alkoxycarbonyl azides) when irradiated in solutions of olefins give the aziridines expected from nitrene addition to the double bond (1). Lwowski and co-workers (2) demonstrated that irradiation of pivaloyl azide in cyclohexene gave 45% of 7-pivaloyl-7-azabicyclo[4,1,0]heptane. Recently Masamune and co-workers (3) have reported intramolecular addition of an acyl nitrene to a carbon–carbon double bond.

Despite the fact that cycloheptene-5-carbonyl azide **1** undoubtedly exists mainly in the conformation illustrated, with the functions remote, its symmetry made it an attractive subject for study.

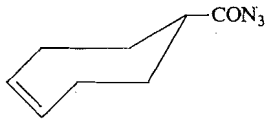

1

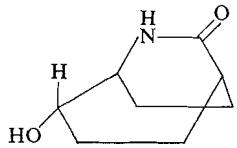

2

Irradiation of hexane solutions of the azide with a high pressure mercury lamp at 0° resulted in its conversion to isocyanate, an insoluble amide polymer (ν_{max} 1650 cm^{-1}) and a soluble substance with ν_{max} 1745 cm^{-1}. When the hexane solution was shaken with water the substance giving the band at 1745 cm^{-1} was destroyed and amides appeared in the water layer. From the latter a crystalline hydroxy lactam analysing correctly for **2** (4-hydroxy-7-oxo-6-azabicyclo[3,2,2]nonane) was isolated in around 12% yield. Its mass spectrum (see below) was consistent with structure **2**. The hydroxy lactam could be oxidized in poor yield to the keto lactam **3**, with ν_{max} 1713 and 1671 cm^{-1}. Again its mass spectrum could be readily reconciled with this structure (see below). The nuclear magnetic resonance (n.m.r.) spectra of the acetate (**4**) of the hydroxy lactam and the keto lactam were also consistent with these structures (see formulas).

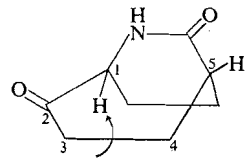

δ 3.82($w_{\frac{1}{2}}$13 c.p.s.)

3

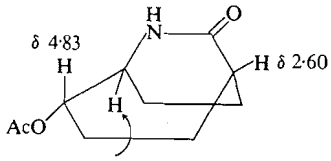

δ 3.50($w_{\frac{1}{2}}$13 c.p.s.)

4

The half-band width of the signal at δ 3.50 in the spectrum of **4** was reduced to 7 c.p.s. when D_2O was added, confirming the assignment to H-1. It follows that the reactive photolysis product is the acylaziridine **5**. The amide resonance in this would be completely suppressed because of

[1]NRCC No. 10700. Presented in part at the Symposium on Reactive Intermediates in Organic Chemistry, Quebec City, Quebec, September, 1964.
[2]NRCC Postdoctorate Fellow.

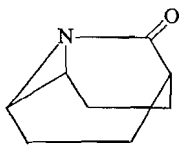

5

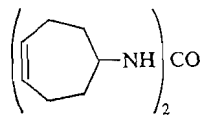

6

orthogonality of the carbonyl π orbitals and the unshared pair on nitrogen. This accounts for the high carbonyl frequency (1745 cm^{-1}). Because of its sensitivity to hydroxylic solvents, and the mixture in which it was formed, we were unable to isolate **5**. As far as we are aware, **2**, **3**, and **4** are the first derivatives of 6-azabicyclo[3,2,2]nonane to be described.

Photolysis of **1** in aqueous dioxane suppressed the polymer formation, but no increase in yields of **2** was noted. Crystals of the urea **6** separated if the solution was allowed to stand overnight.

When the photolysis of **1** was carried out in dry methanol at 0° isocyanate was again the major product (urethane formation was slow). As expected the methoxy lactam **7** (4-methoxy-7-oxo-6-azabicyclo[3,2,2]nonane) was formed, and in addition an isomer of the methyl urethane. The spectra of the latter suggested that it was

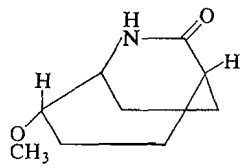

7

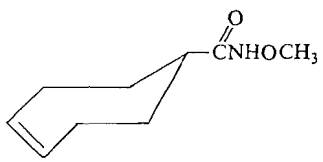

8

N-methoxycycloheptene-5-carboxamide (**8**). This was substantiated by its hydrogenolysis to cycloheptanecarboxamide and confirmed by comparison with a sample synthesized from cycloheptene-5-carbonyl chloride and methoxyamine.

Since considerable cyclization occurred in the case of **1** we expected that *endo*-norbornene-5-carbonyl azide **9**, with the function in close proximity, might give high yields of acyl aziridine. Actually only 20% of aziridine **10** was formed, estimated by the amount of hydroxy lactam produced on its hydrolysis. It again had its CO stretching vibration at very high frequency (ν_{max} 1776 cm^{-1}), accountable for as in the case of

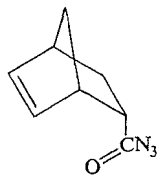

9

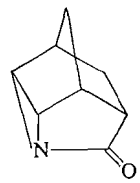

10

5. The structure of the hydroxy lactam could *a priori* have been **11** (5-*exo*-hydroxy-6-*endo*-amino-2-*endo*-norbornane carboxylic acid lactam), **12** or **13** (R = H).

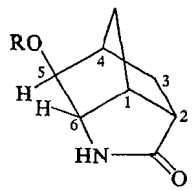

11

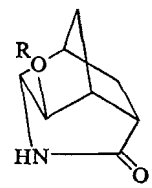

12

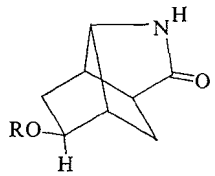

13

We discount the possible structure **12** on the basis of the strain involved. The acetate of the hydroxy lactam was prepared. The signal at lowest field, attributable to the hydrogen on the carbon carrying the acetoxy group at δ 4.33 was fairly sharp ($w_{\frac{1}{2}}$ 3 c.p.s.) whereas the signal for the hydrogen on the carbon carrying the nitrogen was a broad doublet at δ 3.43 and 3.51. These values are only consistent with **11** (R = Ac) in which the coupling of the 5-hydrogen to both the 4- and 6-hydrogens should be very small, while the 6-hydrogen should couple with the 1-hydrogen with $J \simeq 4$.

A minor product of the photolysis reaction had a weak band at 3350 cm^{-1} and strong ones at 1705 and 1600 cm^{-1}. A broad signal centered at

Can. J. Chem. Downloaded from www.nrcresearchpress.com by 210.87.254.42 on 09/05/12
For personal use only.

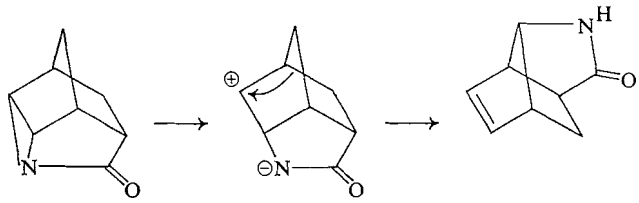

14

δ 6 indicated the presence of olefinic hydrogens. If the photolysis solution was heated prior to hydrolysis the amount of this product increased. It was not further characterized because of the small quantity available, but can tentatively be assigned structure **14.**

To extend the scope of the reaction we next examined the photolysis of *o*-vinylbenzoyl azide **15.** Due to the competitive absorption of light by the aromatic system, the decomposition of the azide was slow relative to the aliphatic examples. Considerable polymer separated as the photolysis proceeded. As the acyl azide bands at 1702 and 2140 cm^{-1} disappeared they were replaced by the isocyanate band at 2280 cm^{-1} and a carbonyl band at 1750 cm^{-1}. The latter seems consistent only with the presence of the aziridine **16.** Part of the material responsible for this absorption was rapidly destroyed when the reaction mixture was shaken with water. From the aqueous phase a

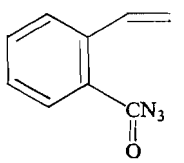

15

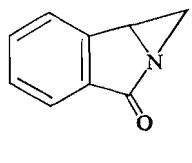

16

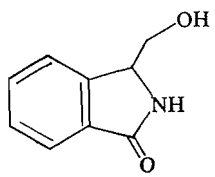

17

10% yield (calculated as hydroxy lactam) of product was obtained. This consisted of two major and three very minor components. The main product (4.5%) had a molecular weight (mass spectrum) of 163 and was a γ-lactam (ν_{max} (Nujol) 1710 cm^{-1}). Its base peak in the mass spectrum was at *m/e* 132 ($M—CH_2OH$) with *m/e* 133 almost as intense ($M—CH_2O$). On this basis we assign with confidence the structure **17** (3-hydroxymethyl-1,2-dihydroisoindolone) to this hydroxy lactam. The fragmentation on electron impact is undoubtedly as illustrated

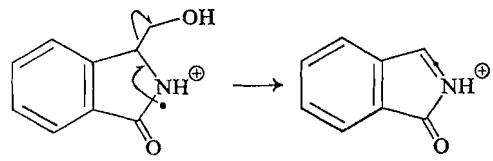

m/e 132

The next most abundant product from the aqueous layer was present in about 1% yield. It was not obtained completely pure. It had ν_{max} 1660 cm^{-1} (δ-lactam) and a molecular weight by mass spectrum of 163. A strong peak at *m/e* 145 (M-18) indicated facile loss of water. On this evidence we consider it probable that it has structure **18** (4-hydroxy-1,2,3,4-tetrahydroisoquinol-1-one) arising from the alternate mode of hydration of the aziridine ring of **16.**

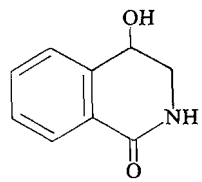

18

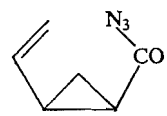

19

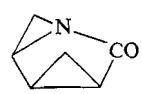

20

Finally, *cis* 2-vinylcyclopropylcarbonyl azide **19** was irradiated in the hope of generating **20** or its rearrangement products. A weak band at

Can. J. Chem. Downloaded from www.nrcresearchpress.com by 210.87.254.42 on 09/05/12
For personal use only.

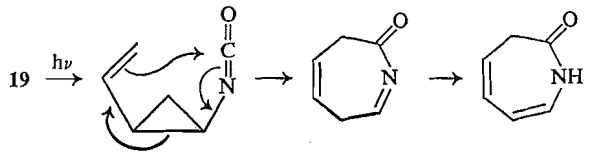

21

1764 cm^{-1} appeared in the infrared (i.r.) spectrum as photolysis proceeded. The compound corresponding to it was destroyed by water, but we were unable to isolate a hydroxy lactam from the mixture of water soluble products. As usual the major product when the photolysis was conducted at −78° was the isocyanate. This gave us a unique opportunity to test the postulate of Vogel *et al.* (4) that the isocyanate underwent Cope rearrangement to 2,3-dihydro-1*H*-azepinone (**21**). When the mixture containing the isocyanate warmed to room temperature, the characteristic i.r. absorption at 2270 cm^{-1} steadily diminished in strength, and a band at 1686 cm^{-1} grew in intensity. The transition was complete in several hours at room temperature, or in 15 min in the i.r. spectrometer beam. The dihydroazepinone was isolated, and proved identical with the product of thermal rearrangement of **19** (4).

Photosensitized decomposition of azide **9** using energy transfer from triplet acetophenone led to an intractable mixture of products. As in a previous study (5), the free radical nature of the process was demonstrated by the presence of cyclohexene and bicyclohexyl derived from the solvent cyclohexane.

Discussion

One of the unanswered questions in the mechanism of the photolytic reaction of acyl azides is whether the reaction with olefins is a nitrene addition (*a*) or involves an intermediate triazoline (*b*)

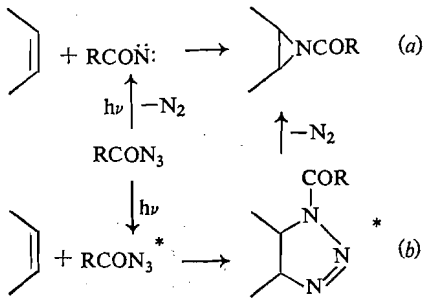

In the cycloheptanecarbonyl azide case a 12% yield of cyclization product was obtained despite the minor fraction of the molecules likely to be in the required conformation for this internal reaction. This suggests that a triazoline is formed, since the nitrene would seem likely to attack solvent or other molecules or rearrange before conformational inversion. However, the yield of cyclized product in the case of **9** was still quite low (20%). Since the triazoline **22** seems strainless while the aziridine is strained, this result leads

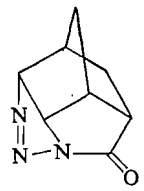

22

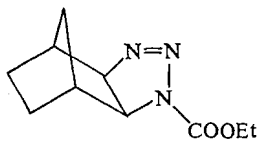

23

to the opposite conclusion, that the low yield is due to direct aziridine formation from the nitrene.

Difference between the product composition on photolysis of triazoline **23** and that of a mixture of norbornylene and ethyl azidoformate (6) also supports the contention that an acyl nitrene is involved in the acyl azide additions to olefins (see also 2).

The ease of solvolytic opening of the acyl aziridines described above is striking. This reactivity can be understood if the transition state for the solvolyses resembles product. In these aziridines the amide resonance is absent as discussed above, while in the product it is completely restored. Since around 20 kcal/mole would be gained on reestablishing the amide resonance, this would markedly accelerate the ring opening.

Mass Spectra

The fragmentation of the various products described above lent some support to the assigned structures. However, some of the ions had complex and obscure origins. Tentative assignments based mainly on single mass unit resolu-

Can. J. Chem. Downloaded from www.nrcresearchpress.com by 210.87.254.42 on 09/05/12
For personal use only.

tion are offered for the most abundant fragments. In the case of ions marked with a dagger (†), however, accurate *m/e* ratios[3] makes the composition certain. The hydroxy lactam **2** gave the following ions

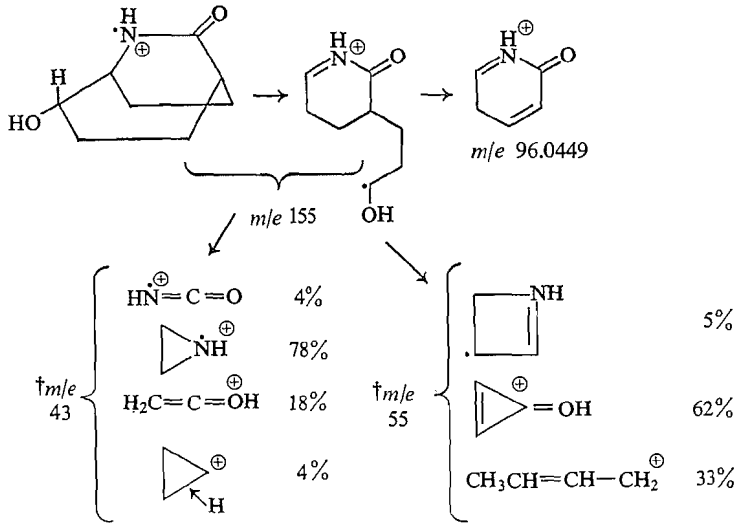

The fragmentation of the acetate of **2** had some interesting features. The base peak was now at *m/e* 96 instead of *m/e* 43, hence the formation of $CH_3C{\equiv}O^{\dagger}$ was not important. The important fragment with *m/e* 56 replaces one at *m/e* 55 in the spectrum of the hydroxy lactam. This suggests transfer of one hydrogen of the acetoxy group to the nucleus with loss of ketene (see also the spectrum of **11** discussed below).

Suggested structures for some of the important ions follow

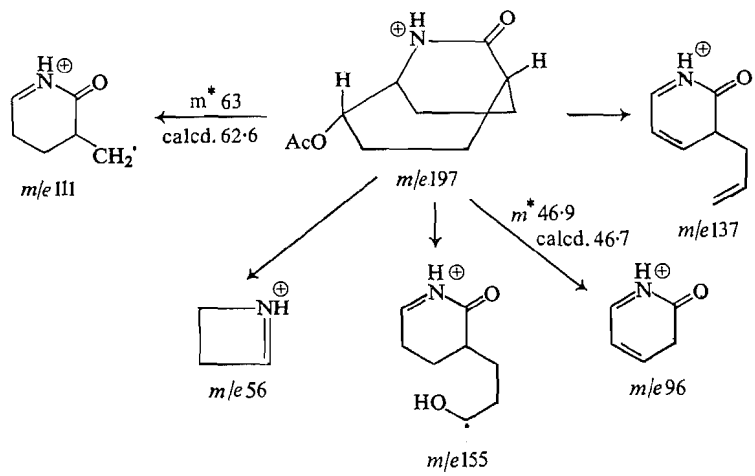

In the methoxy analogue **7**, because of the greater ease of formation of $CH_3\cdot$ over H·, the ion M-15 (*m/e* 154) became an intense peak.

[3]Kindly provided by Dr. W. D. Jamieson, Atlantic Regional Laboratory, National Research Council of Canada, Halifax, Nova Scotia. The cited values are based on *C* = 12.0000.

Can. J. Chem. Downloaded from www.nrcresearchpress.com by 210.87.254.42 on 09/05/12
For personal use only.

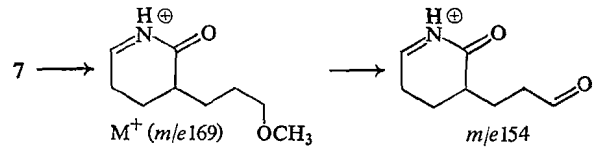

The *m/e* 96 peak was the base peak although *m/e* 43 was still strong.

The ketolactam **3** gave some interesting variations although *m/e* 96, 55, and 43 were still intense. The postulated ions are

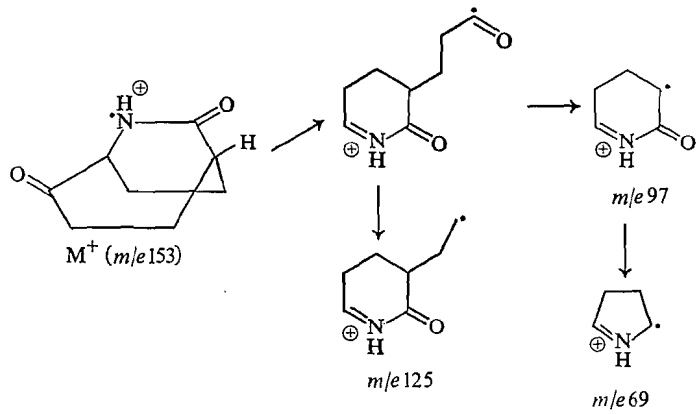

The fragmentation of the *N*-methoxyamide **8** left little doubt about its identity. In this case the metastable peaks were clear and proved very informative.

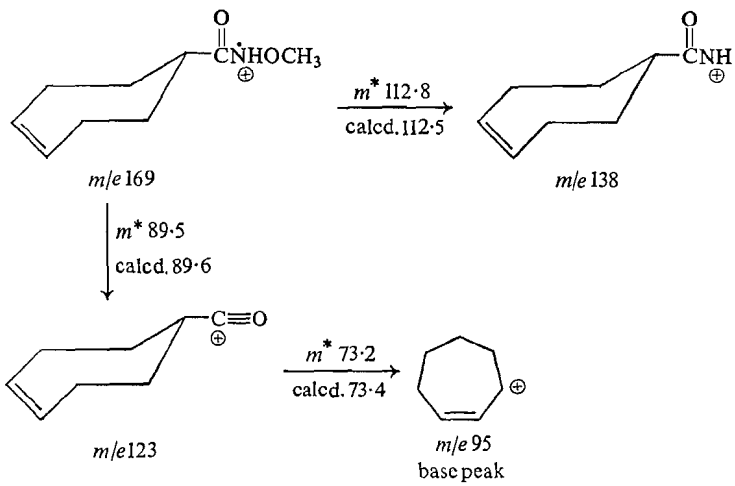

The ions from the hydroxy and acetoxy lactams **11** (R = H or Ac) could be accounted for, but

Can. J. Chem. Downloaded from www.nrcresearchpress.com by 210.87.254.42 on 09/05/12
For personal use only.

not without invoking intramolecular hydrogen transfer (see the analysis of the spectrum of the acetate)

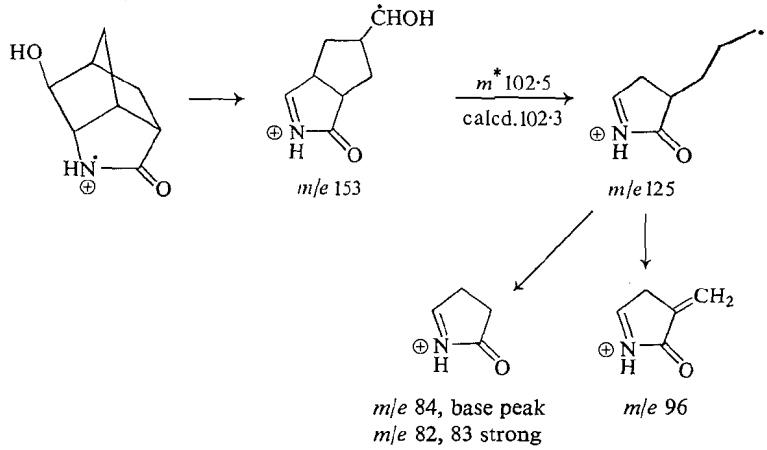

In the case of the acetate (**11**, R = Ac) the ion with *m/e* 84 was again the base peak, and ions at *m/e* 153 and 125 were prominent. The identity of these three ions was established by high resolution mass spectrometry to be $C_4H_6NO^+$, $C_8H_{11}NO_2{}^+$, and $C_7H_{11}NO^+$ respectively. Metastable peaks were found for three transitions, and are consistent with the following fragmentation

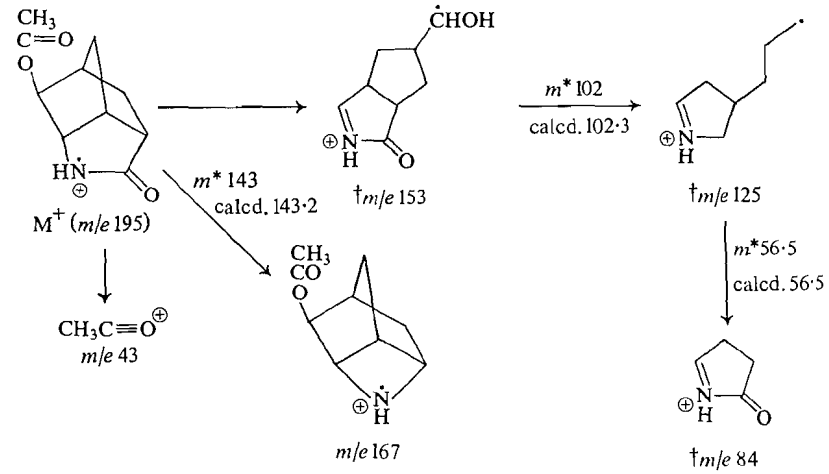

The transitions from *m/e* 153 to *m/e* 125 and from the latter to *m/e* 84 are surprising. The fragmentation of the corresponding trideuterioacetate was examined in an attempt to clarify these. The detail of the transitions is obscure, but the three ions in question probably have the structures illustrated

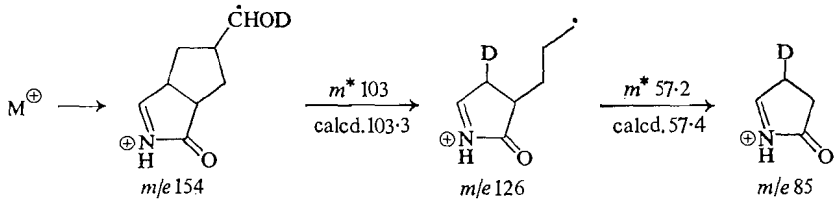

Can. J. Chem. Downloaded from www.nrcresearchpress.com by 210.87.254.42 on 09/05/12
For personal use only.

An additional fragmentation mode for hydroxy lactam **17** led to *m/e* 133. We formulate this as shown

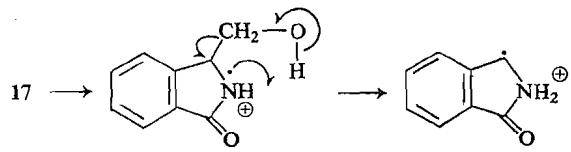

m/e 133

Experimental

Infrared spectra were determined in solution on a Model 257 Perkin–Elmer grating spectrometer or as Nujol mulls using a Model 21 prism spectrometer, and n.m.r. spectra on a Varian A-60A spectrometer. Photolyses were performed, unless otherwise specified, using a 100 W Hanovia high-pressure immersion lamp in a water-jacketed Vycor well surrounded by a thin annular layer of photolyzing solution in a Pyrex container. Analytical thin-layer chromatography (t.l.c.) was done using silica gel G on microscope slides. Mass spectra were obtained using a Hitachi single focusing spectrometer using a direct inlet and a 75 V electron beam. The relative abundance of ions is given in brackets after the *m/e* ratio.

Photolysis of ***1*** *in Aqueous Dioxane*

Oxalyl chloride (3 ml) was added dropwise to a stirred suspension of 2.5 g of powdered, dried (80°, 0.5 mm) sodium salt of cycloheptene-5-carboxylic acid in 20 ml of pentane under a reflux condenser. After 1.5 h of stirring at room temperature, the solid was removed by filtration. The mixture was finally distilled at 80°, 10 mm in a Späth bulb assembly, giving 2.3 g of acid chloride. This had ν_{max} (hexane) 1795 cm^{-1}. The acid chloride was added to an ice-cold solution of 6 g of sodium azide in 20 ml of water. After 1.5 h of stirring at 0° the conversion to azide was complete. Sodium carbonate was added, then the acyl azide was extracted into pentane. The dried pentane solution was evaporated in a rotating evaporator below room temperature at water pump pressure. The oil was allowed to come to room temperature *in vacuo*. The residual colorless oil weighed 2.3 g and had ν_{max} (pentane) 2130, 1715, and 1650 (weak) cm^{-1}. A peak at 2250 cm^{-1} indicated the formation of 5–10% of isocyanate. The azide was dissolved in 40 ml of cold 80% dioxane–20% water and photolyzed at 0°. Gas evolution was complete in 4 h. To the clear solution, 20 ml of water was added. The mixture was then extracted twice with 15 ml portions of pentane and the pentane back-washed with water.

The aqueous dioxane solution was concentrated on a rotating evaporator at 80°, 15 mm pressure, leaving 619 mg of oil. This was dissolved in 5 ml of methylene chloride and seeded with hydroxy lactam. It slowly deposited 233 mg of fairly pure crystals of hydroxy lactam **2**. The methylene chloride soluble products were partially separated by chromatography on a 20-fold ratio of alumina, activity I. However, at least eight readily eluted components were indicated by t.l.c. The methanol in chloroform eluates crystallized in part from methylene chloride giving 32 mg of fairly pure hydroxy lactam. The total yield of hydroxy lactam **2** containing small amounts of components with higher R_f was 265 mg (12% based on azide).

Similar photolysis in 50% aqueous dioxane gave a 9% yield of hydroxy lactam **2**. When the photolysis mixture was allowed to stand overnight crystals of *N,N'*bis(cyclohepten-5-yl)urea **6** were deposited.

Photolysis of ***1*** *in Pentane and Methylene Chloride*

The acid chloride (1.26 g) was prepared from 1.5 g of sodium 4-cycloheptenecarboxylate, and this converted to the azide as described above. The azide was taken up in 350 ml of dry pentane, and photolyzed in an ice-salt bath. After 3.5 h the azide had all reacted. The solution had strong i.r. absorption at 2250 cm^{-1} (isocyanate), 1745 cm^{-1} (acyl aziridine), and broad weak absorption below 1600 cm^{-1} (other lactams). An insoluble solid had separated which had ν_{max} ($CHCl_3$) 1650 cm^{-1}. The filtered solution was extracted three times with distilled water (total 40 ml). The aqueous layer was taken to dryness under reduced pressure, giving 288 mg of residue. This crystallized from chloroform giving 167 mg of quite pure hydroxy lactam **2**, m.p. 220° (13.5% overall yield).

An equivalent experiment was performed using methylene chloride as solvent for the photolysis. At completion the solution had broad i.r. absorption centered at 1695 cm^{-1} with a shoulder near 1720 cm^{-1}, as well as an intense isocyanate band at 2265 cm^{-1}. The aqueous extract of the photolyzed solution gave a 10% yield of crude hydroxy lactam based on the volume of nitrogen evolved.

Hydroxy Lactam ***2*** *and its Acetate (4)*

Hydroxy lactam **2** was purified by chromatography on a 20-fold ratio of neutral alumina, activity III using chloroform and methanol in chloroform as eluting solvents. Fractions with m.p. 205–220° (Pyrex capillary) were recrystallized from benzene — chloroform, giving m.p. 230°. It had ν_{max} 3330, 3190, and 1660 cm^{-1}.

Anal. Calcd. for $C_8H_{13}NO_2$: C, 61.91; H, 8.44; N, 9.03. Found (after sublimation at 150 °C, 5×10^{-4} mm): C, 62.11; H, 8.95; N, 9.11.

Its mass spectrum had strong peaks at *m/e* 28(33), 39(55), 41(63), 43(100), 44(71), 55(57), 56(43), 96(89), 98(69), 99(63), and 155(45).

A solution of 109 mg of the hydroxy lactam in 2 ml of pyridine and 2 ml of acetic anhydride was left for 20 h at room temperature. The reagents were removed under reduced pressure. The residue was dissolved in methylene chloride and the solution washed with dilute sulfuric acid followed by dilute sodium carbonate. The dried solution yielded 140 mg of crystalline solid. After two recrystallizations from acetone – hexane, it melted at

Can. J. Chem. Downloaded from www.nrcresearchpress.com by 210.87.254.42 on 09/05/12
For personal use only.

Can. J. Chem. Downloaded from www.nrcresearchpress.com by 210.87.254.42 on 09/05/12
For personal use only.

120–121° and had ν_{max} ($CHCl_3$) 3420, 1728, and 1675 cm^{-1}.

Anal. Calcd. for $C_{10}H_{15}NO_3$: C, 60.89; H 7.67; N, 7.10. Found: C, 60.91; H, 7.50; N, 7.26.

Its n.m.r. spectrum had signals at δ 7.1(NH), 4.83(1H), 3.50(1H), 2.60(1H), 2.05(CH_3CO) and its mass spectrum had strong peaks at *m/e* 28(76), 55(16), 56(30), 83(20), 96(100), 97(12), 98(19), 99(27), 111(9), 136(8), 137(6), 154(9), 155(25), and 197(2.6).

Keto Lactam 3

Jones' reagent (7) (0.14 ml) was added to a solution of 86 mg (0.55 mmole) of hydroxy lactam **2** in 5 ml of pure acetone at 0°. The small excess of reagent was destroyed using methanol, the mixture filtered, and the filtrate taken to near dryness. The residue was taken up in methylene chloride plus dilute sodium carbonate solution. The aqueous layer was washed twice with methylene chloride. The organic layers were dried and distilled, leaving 22 mg of crystalline residue. After recrystallization and sublimation at 110°, 5×10^{-4} mm, it melted at 128–130° and had ν_{max} (Nujol) 3220, 3100, 1713, and 1672 cm^{-1}. Its n.m.r. spectrum had peaks at δ 7.2(NH) and 3.81(1H)($w_{1/2}$ 13 c.p.s.).

Its mass spectrum had strong peaks at *m/e* 28(100), 32(10), 39(9), 41(12), 42(7), 43(13), 54(5), 55(10), 56(7), 67(6), 68(12.5), 69(24), 82(7), 96(30.5), 97(23), 125(5), and 153(8).

Anal. Calcd. for $C_8H_{12}NO_2$: C, 67.72; H, 7.24. Found: C, 62.88; H, 7,06,

Photolysis of 1 in Methanol

Azide **1** (425 mg) was dissolved in 100 ml of methanol and irradiated for 3 h at 0°. The methanol was distilled under water-pump vacuum, leaving 337 mg of residue. This was adsorbed from hexane onto 6 g of neutral alumina, activity IV. The eluant was examined using t.l.c. on silica gel with ether as developing solvent.

The early eluates (hexane) gave spots on t.l.c. corresponding to cycloheptenyl isocyanate and the methyl urethane of 5-aminocycloheptene. The middle eluates (ether in hexane, ethyl acetate) (148 mg) contained two main components and two minor ones. After distillation at 125°, 0.1 mm, to remove polymer, and separation on a preparative thin layer plate using iodine vapor to locate the bands, the main components and one minor one were obtained pure.

N,N'-bis(cycloheptenyl)urea

The yield was 2% and its R_f was 0.75. After recrystallization from methanol it melted at 228–229° and had ν_{max} (Nujol) 3340, 3025, 1623, and 1573 cm^{-1}.

Anal. Calcd. for $C_{15}H_{24}N_2O$: C, 72.54; H, 9.74; N, 11.28. Found: C, 72.22; H, 10.02; N, 11.43,

Lactam 7

The yield was 7.5% based on the sodium salt used. After recrystallization from ether it changed crystal form to flat needles around 120° and melted at 139–140°. It was sublimed for analysis.

Anal. Calcd. for $C_9H_{15}NO_2$: C, 63.88; H, 8.93. Found: C, 64.41; H, 9.52.

It had ν_{max} ($CHCl_3$) 3430 and 1670 cm^{-1}, and n.m.r. signals at δ 8.05 (NH), 3.32 (OCH_3), ca. 3.4 (broad, N—CH<) 2.52 (broad, CO—CH<). Its mass spectrum had intense peaks at *m/e* 28(9), 39(8), 41(14), 43(13), 44(7.5), 55(12.5), 56(10), 58(15), 82(7.5), 83(6), 96(100), 97(7), 98(31), 136(3), 154(17.5), and 169(M^+) (17).

N-Methoxycycloheptene-5-carboxamide 8

The yield was 5% overall. After crystallization from acetone – hexane it formed needles with m.p. 90–92°. Its n.m.r. spectrum had peaks at δ 8.7(NH), 5.8 (two vinyl H's), 3.74 (OCH_3). A sample was sublimed for analysis.

Anal. Calcd. for $C_9H_{15}NO_2$ (molecular weight 169): C, 63.88; H, 8.93, N, 8.28. Found (molecular weight, (mass spectrum) 169): C, 64.52; H, 9.36; N, 8.58.

An ethanol solution of **8** in the presence of Adam's platinum catalyst rapidly absorbed one mole of hydrogen. The product was hydrogenolyzed slowly in acetic acid over Adam's catalyst. The product was recrystallized from benzene – hexane then sublimed, giving needles with m.p. 195–197°. This proved identical (mixed m.p. and X-ray powder pattern) with an authentic sample of cycloheptanecarboxamide (8). An authentic specimen of *N*-methoxy-cyclohexene-5-carboxamide was prepared from cycloheptene-5-carbonyl chloride and ether solution of methoxyamine. After recrystallization from acetone – hexane it formed needles with m.p. 92–93°. It had ν_{max} ($CHCl_3$) 3400, 3230, 2850, 1680, 1440, 1080, 1040, 935, and 912 cm^{-1}. The i.r. spectrum of the photolysis product was nearly identical to this, and they showed no mixed m.p. depression.

Methyl Urethane of 5-Aminocycloheptene

A methanol solution of cyclohepten-5-yl isocyanate was refluxed for 16 h. The product was recrystallized twice from hexane, filtering from less soluble products. After sublimation at 75°, 1×10^{-3} mm, and further recrystallization from hexane it separated as needles with m.p. 86–87°. It had ν_{max} ($CHCl_3$) 3440, 1712, and 1512 cm^{-1}.

Anal. Calcd. for $C_9H_{15}NO_2$: C, 63.88; H, 8.94; N, 8.28. Found: C, 63.85; H, 9.13; N, 8.46.

Endo-norbornene-5-carbonyl Azide 9

The *endo* acid was prepared following Diels and Alder (9) and purified via the iodolactone (10). Its sodium salt suspended in hexane was converted to the acid chloride using oxalyl chloride, then distilled at 78–80°, 17 mm.

A cold solution of 1.76 g (0.011 mole) of acid chloride in 5 ml of acetone was added to 10 ml of a cold saturated solution of sodium azide in water. More acetone was added until the cloudiness nearly disappeared. The solution was stirred at 0° for 2 h. It was then extracted with three 15 ml portions of cyclohexane and the combined extracts were washed with two 15 ml portions of saturated sodium bicarbonate solution, two 15 ml portions of water, and two 15 ml portions of saturated sodium chloride solution. The cyclohexane solution was then dried for 1 h over magnesium sulphate (large excess) at 0° in the dark. The yield of azide increased if the temperature of all solutions was kept as low as possible.

A 500 μl aliquot of the cyclohexane solution was removed and mixed with 30 μl of chloroform in a n.m.r. tube. Integration of the signals due to the olefinic protons in the azide and the signal due to the proton in the chloroform gave the amount of azide present in the solution. In most cases, this gave approximately 1.25–1.4 g/40 ml of solution. Infrared spectroscopy showed that a

Can. J. Chem. Downloaded from www.nrcresearchpress.com by 210.87.254.42 on 09/05/12
For personal use only.

slight amount of isocyanate had been formed before the photolysis could be started.

Photolysis of endo-Norbornene-5-carbonyl Azide **9**

The photolysis was carried out in a Rayonet apparatus,[4] using a double-walled quartz vessel which contained the solution in the inner chamber and had circulating ice-water in the outer one to minimize thermal reaction of the azide. Lamps with peak radiation at 2537 Å were used.

The photolysis was carried out until the complete disappearance of the i.r. absorption at 2110 cm^{-1} occurred. This required from 3–4 h. As the reaction proceeded, a band at 2250 cm^{-1} developed rapidly. The band at 2110 cm^{-1} decreased more slowly as did the carbonyl absorption at 1700 cm^{-1}. At the same time, a triple peak at 1793, 1776, and 1765 cm^{-1} appeared. Of these, the central band was by far the most intense. This triplet increased steadily and reached a maximum at the disappearance of the azide absorption.

In some cases, a large amount of an amorphous yellow precipitate formed which slowed the photolysis drastically. It was necessary to stop the photolysis and filter the reaction mixture before continuing. Efficient drying of the starting solution eliminated this problem to a major extent.

After completion of the photolysis, the solution was stirred with 5 ml of water for 5 min, the layers were separated, and the procedure was repeated. The combined aqueous extracts were washed with cyclohexane and then poured into 100 ml of methylene chloride. Enough sodium sulfate was added to absorb all the water. This was allowed to stand for 12 h and then, after breaking up the lumps of drying agent, was filtered. The residue was washed well with methylene chloride by decantation (see 'Water-soluble Products').

The combined cyclohexane layers were dried over sodium sulphate. The i.r. spectrum revealed the complete absence of any absorption at 1776 cm^{-1}. Thin-layer chromatography showed one major component and three minor, slower-moving spots. The solution was diluted with 15 ml of anhydrous methanol and heated under vigorous reflux for 24 h. At the end of this period, the fast major spot had disappeared and another slower-moving spot had appeared. None of the three minor components was affected by this treatment.

Evaporation of the cyclohexane – methanol mixture gave a white solid which, after recrystallization from hexane or methanol – water, gave a white solid, m.p. 68–70°, which was identical to methyl 5-*endo*-norborn-2-enyl carbamate (11). The yield of this component based on starting azide was calculated to be 71%. The total amount of the three minor components was estimated to be not more than 2% of the total reaction mixture. By t.l.c. comparison with authentic materials (see below) it was shown that these components were not the amide or *N*-cyclohexylamide of *endo*-norbornylene-5-carboxylic acid.

Water-soluble Products

The methylene chloride solution of the water-soluble products was concentrated to small volume. Hydroxy lactam **11** (R = H) crystallized and proved to be sparingly soluble in methylene chloride or chloroform. The mother liquors contained a complex mixture. More hydroxy lactam was recovered by preparative t.l.c. (R_f 0.3 using 10% methanol in chloroform) but no other component was obtained pure.

Hydroxylactam **11** *(R = H) and its Acetate*

This was sparingly soluble in aprotic solvents. The yield was ca. 20% based on azide. After three recrystallizations from acetone and sublimation at 125°, 5×10^{-4} mm it had m.p. 181–182° and ν_{max} (Nujol) 3215 and 1680 cm^{-1}; n.m.r. signals (in D_2O) at δ 3.80 (1H singlet), 3.74–3.55 (1H, doublet?), 3.51–3.28 (1H multiplet), and 2.75–1.40 (6H multiplet). Its mass spectrum had intense peaks at *m/e* 153(12), 125(32), 96(36), 84(100), 83(41), 82(15), 69(20), 67(15), 41(31), 39(35), and 28(37).

Anal. Calcd. for $C_8H_{11}NO_2$: C, 62.72; H, 7.24. Found: C, 62.58; H, 7.31.

The acetate **11** (R = $COCH_3$) was prepared from the hydroxy lactam using acetic anhydride – pyridine at room temperature. It crystallized from acetone – hexane as hexagonal plates, m.p. 156°. It had ν_{max} 3435, 1720, 1700, and 1240 cm^{-1}. Its n.m.r. spectrum had signals at δ 6.4 (1H, broad), 4.33 (1H, doublet $J = 1$ c.p.s.), 3.54–3.39 (1H, broad doublet), 3.22–2.91 (1H, multiplet), 2.66–1.34 (6H multiplet), and 2.06 (3H, singlet). It was sublimed at 115°, 5×10^{-4} mm, for analysis.

Anal. Calcd. for $C_{10}H_{13}NO_3$: C, 61.52; H, 6.71. Found: C, 61.63; H, 6.79.

Its mass spectrum had strong peaks at *m/e* 28(74), 43(96), 81(92), 83(41), 84(100), 96(4), 124(34), 125(70), 152(5), 153(52), 167(14), and 195(M^+, 28).

Trideuterioacetate **11** *(R = $COCD_3$)*

This was prepared using trideuterioacetic anhydride in pyridine at room temperature. It crystallized from acetone – hexane as hexagonal plates m.p. 155–156°. Its n.m.r. spectrum was identical to that of the acetate except for complete absence of the signal at δ 2.06. Its mass spectrum had the following major peaks displaced from that of the acetate: *m/e* 46, 85, 97, 126, 154, 170, and 198.

Methyl 5-endo-Norborn-2-enyl Carbamate

5-*endo*-Norbornenyl isocyanate prepared by thermal rearrangement of the azide was refluxed in methanol for 24 h. The carbamate was recrystallized from hexane. It had m.p. 68–70° [lit. m.p. 70° (11)]. It had n.m.r. signals at δ 6.50–5.90 (2H, octet), 4.32 (1H, broad) 3.67 (3H, singlet) 3.18–2.72 (2H, broad doublet), 2.47–1.95 (1H, multiplet), 1.35 (2H, multiplet), and 0.9–0.45 (1H, very broad doublet). It had ν_{max} 3440, 1705, and 1510 cm^{-1}.

N-Cyclohexyl-5-endo-norbornenylcarboxamide

A hexane solution of 5-*endo*-norbornenylcarbonyl chloride was added to an ice-cold solution of excess cyclohexyl amine in benzene. The neutral product was recrystallized twice from aqueous ethanol. It had m.p. 170–172° and ν_{max} 3440, 1660, and 1500 cm^{-1}.

Anal. Calcd. for $C_{14}H_{21}NO$: C, 76.66; H, 9.65; N, 6.39. Found: C, 76.42; H, 9.23; N, 6.25.

2-Vinylbenzoyl Azide

2-Vinylbenzoic Acid

This was prepared by carbonation of 2-vinylphenylmagnesium bromide (see ref. 12). It had m.p. 93–96°,

[4]Product of the Southern New England Ultraviolet Company, Middletown, Connecticut.

Can. J. Chem. Downloaded from www.nrcresearchpress.com by 210.87.254.42 on 09/05/12
For personal use only.

ν_{max} ($CHCl_3$) 1690 cm^{-1} and λ_{max} 214(21 000), 246(12 100), and 292(1430) mμ.

Preparation of 2-Vinylbenzoyl Azide

To a slurry of the sodium salt of 2-vinylbenzoic acid (11) (1.0 g, 5.9 mmoles) in 25 ml of dry *n*-hexane was added 2.0 ml of oxalyl chloride. This was stirred at room temperature for 5 h. After filtering, the solution was evaporated to dryness under reduced pressure to give *o*-vinylbenzoyl chloride as a pale yellow oil, i.r. ($CHCl_3$) 1780 and 1740 cm^{-1}.

To a cold saturated aqueous solution of sodium azide (40 ml) was added a cold solution of the acid chloride in 10 ml of dry acetone. The heterogeneous mixture was stirred at 0–5° in the dark for 2 h. The solution was then diluted with 50 ml of cold water and extracted with three 20 ml portions of pure cyclohexane. The combined extracts were washed with two 20 ml portions of saturated sodium bicarbonate solution, two 20 ml portions of water, and two 20 ml portions of saturated sodium chloride solution. The cyclohexane solution was dried over magnesium sulfate at 0–5° in the dark for 2 h. After filtration, the i.r. spectrum of the cyclohexane solution showed no hydroxyl absorption, a clean single peak in the carbonyl region (1702 cm^{-1}), a strong azide absorption (2140 cm^{-1}), and a very small amount of isocyanate absorption (2280 cm^{-1}).

No acid was obtained by acidification of the basic extracts and extraction of these with ether. Therefore, for calculation of yields the conversion to azide was taken as quantitative. It was necessary to maintain the temperature of the solution below 10°. If it was left at 20° for 30 min a large portion of the azide was converted to isocyanate.

Photolysis of 2-Vinylbenzoyl Azide

A cyclohexane solution of azide from 1.0 g of sodium salt was diluted to 80 ml and photolyzed at 0° in a Vycor apparatus using a 450 W Hanovia immersion lamp in a water jacketed well. The polymer which deposited on the immersion unit was removed at intervals. As the photolysis proceeded, the i.r. absorption of the solution at 1702 and 2140 cm^{-1} decreased in intensity and new bands at 2280 and 1750 cm^{-1} appeared. After 7.5 h, i.r. analysis showed that reaction was complete. The solution was filtered and shaken with four 10 ml portions of water for 30 min each. The combined water phases were reduced in volume to ca. 5 ml and poured into 100 ml of methylene chloride. Enough anhydrous sodium sulfate was added to absorb the water. After 2 h, the solution was filtered and the drying agent washed well by grinding with methylene chloride. Evaporation of the solvent gave 90 mg (9.4% as hydroxylactams) of water-soluble material which showed two major spots on t.l.c.

The cyclohexane solution showed only one spot of any intensity on t.l.c. The solution was dried over sodium sulphate, diluted with an equal volume of dry methanol, and heated under reflux for 18 h. Evaporation of the solvent and recrystallization of the residue from *n*-hexane gave white crystals of methyl 2-vinylphenylcarbamate (502 mg, 50%) with m.p. 50.5–52.0. The polymeric material that formed in the reaction was estimated to account for ca. 25–30% of the starting azide.

The separation of the water-soluble products was done by preparative t.l.c. using 10% methanol in chloroform. The plates were developed twice. A total of 130 mg of material from photolyses was spotted. The adsorbent was scraped from the plate and the scrapings were extracted with three 10 ml portions of boiling 50% methanol in chloroform. Evaporation of the extracts gave 20.4 mg of the faster-moving material (**18**?) and 58.3 mg of the slower-moving one (**17**), both of which were slightly brown solids. In addition, several other minor products (weight = less than 5 mg each) were isolated. These were not investigated.

*3-Hydroxymethyl-1,2-dihydroisoindol-1-one (**17**)*

The major slow-moving component (yield 4.5% based on sodium salt) crystallized from methylene chloride. After three recrystallizations from acetone it separated as fine needles, m.p. 148°. It had ν_{max} (Nujol) 3440, 3200, 3080, 1705, 1060, and 740 cm^{-1}. Its mass spectrum had M and M + 1 peaks at *m/e* 163 and 164 and strong peaks at *m/e* 133, 132 (base peak), 104, and 77. After sublimation at 120°, 5×10^{-4} mm, it was analyzed.

Anal. Calcd. for $C_9H_9NO_2$: C, 66.24; H, 5.56. Found: C, 66.06; H, 5.78.

*4-Hydroxy-1,2,3,4-tetrahydroisoquinolin-1-one (**18**?)*

The major faster-moving component could not readily be purified. Its m.p. was 130–135°, and from its i.r. spectrum, it was estimated to be around 75% pure. It had ν_{max} 3420 and 1660 cm^{-1} and its mass spectrum had a prominent parent ion at *m/e* 163 and a strong peak at *m/e* 145 (M-18).

Methyl 2-Vinylphenylcarbamate

A methanol solution of *o*-vinylphenyl isocyanate, produced by thermal decomposition of *o*-vinylbenzoyl azide, was refluxed for 18 h. Removal of the solvent under reduced pressure left the crystalline carbamate. After recrystallization from hexane its m.p. was 50.5–52°; ν_{max} ($CHCl_3$) 3440 and 1740 cm^{-1}; λ_{max} 221 mμ (20 500), 247 mμ (14 200), and 295 mμ (1100).

Anal. Calcd. for $C_{10}H_{11}NO_2$: C, 67.78; H, 6.26; N, 7.91. Found: C, 67.86; H, 6.56; N, 8.02. Its n.m.r. spectrum had bands at 8.0–6.5 (6H, multiplet), 5.50 (2H, sextet), and 3.83 (3H, singlet).

cis-Vinylcylopropane Carboxylic Acid

A mixture of the *cis* and *trans* acids was prepared following Vogel *et al.* (4). The sodium salts were treated with iodine to convert the *cis* acid to iodolactone. The crystalline iodolactone was converted to the *cis* acid by zinc spangles in 95% ethanol. This was converted to its sodium salt using sodium hydroxide in ethanol and then dried *in vacuo*.

*Photolysis of **19***

Sodium salt of *cis*-vinylcyclopropane carboxylic acid (475 mg) was suspended in 5 ml of pentane and 1.5 ml of oxalyl chloride added cautiously. After 2 h of stirring, gas evolution had ceased. The suspension was filtered through cotton wool into a chain of bulbs, using pentane as wash liquid. The acid chloride was distilled at 70°, 25 mm, giving 394 mg of colorless oil.

The acid chloride was added to 10 ml of saturated aqueous sodium azide at 0°. After 1.5 h of vigorous stirring at 0° no acid chloride remained. A little sodium carbonate was added, then the azide extracted into pentane. After drying over sodium sulfate the pentane solution was filtered and made up to 45 ml with cold pentane.

The azide solution (ν_{max} 2150 and 1717 cm^{-1}) was cooled to −78°. A 100 W Hanovia lamp was introduced in a Vycor well, cooled by a stream of dry air through the well and a stream of dry nitrogen through a jacket surrounding the well. After 1.5 h of irradiation at −78°, the azide band was weak. A little polymer was washed off the well, then the irradiation continued for 0.5 h decomposing the remaining azide. The solution now contained isocyanate and carbonyl compounds with i.r. maxima at 1768, 1715, and 1690 cm^{-1}.

The pentane solution of the products was allowed to warm to 0°, then extracted with 2 × 5 ml of ice-water, and dried. It now contained mainly isocyanate (ν_{max} 2275 cm^{-1}). At room temperature this steadily rearranged to amide with ν_{max} 1689 and 1595 cm^{-1} (rapid in the i.r. beam). The solution was left at room temperature overnight, when the isocyanate was all isomerized. On careful distillation the pentane left 93 mg of strong-smelling oil. This was put on a 20 × 20 cm silica gel plate (0.5 mm thick when wet) containing a fluorescent indicator (Merck GF_{254}). When developed with ether 4 bands were detected: zone 1, R_f 0.81, 7 mg with a strong odor; zone 2, R_f 0.64, 5 mg; zone 3, R_f 0.54, 59 mg; zone 4, R_f 0.17, 14 mg.

The 59 mg extracted from zone 3 crystallized when seeded with 2,3-dihydro-1*H*-azepin-2-one. It was distilled at 100°, 1 mm, over a short path, giving a colorless oil which crystallized. When recrystallized from pentane this had a m.p. of 47–48.5°. It had λ_{min} 230 mμ, λ_{max} 255 mμ (ε 4400). It showed no mixed m.p. depression with 2,3-dihydro-1*H*-azepin-2-one (3) and the compound had an i.r. spectrum (ν_{max} ($CHCl_3$) 3400, 3220, 1683 (strong), 1640 (weak), and 1594 (medium) cm^{-1}) identical to that of an authentic sample prepared by refluxing a hexane solution of the isocyanate.

A methylene chloride extract of the above water washings, and of the gum which separated during photolysis gave 65 mg of gum. A hot hexane extract of this gave 10 mg of gum which by its i.r. spectrum and t.l.c. was rich in the dihydroazepinone.

No pure compound was isolated from the water-soluble products.

Acknowledgments

We are grateful to Dr. W. D. Jamieson, Atlantic Regional Laboratory, National Research Council of Canada, Halifax, Nova Scotia, for obtaining accurate masses of many ions and advice on interpretation of mass spectra, to Mr. R. Pilon for mass spectra, and Mr. H. Seguin for microanalyses.

1. W. Lwowski. Angew. Chem. **79**, 922 (1967); International Edition **6**, 897 (1967).
2. G. T. Tisue, S. Linke, and W. Lwowski. J. Am. Chem. Soc. **89**, 6303 (1967).
3. N. C. Castellucci, M. Kato, H. Zendra, and S. Masamune. Chem. Commun. 473 (1967).
4. E. Vogel, R. Erb, G. Lenz, and A. A. Bothner-By. Ann. Chem. **682**, 1 (1965).
5. I. Brown and O. E. Edwards. Can. J. Chem. **45**, 2599 (1967).
6. O. E. Edwards, J. Elder, and M. Lesage. Unpublished observations.
7. K. Bowden, I. M. Heilbron, E. R. H. Jones, and B. C. L. Weedon. J. Chem. Soc. 39 (1946).
8. W. Reppe, O. Schlichting, K. Klager, and T. Toepel. Ann. Chem. **560**, 1 (1948).
9. O. Diels and K. Alder. Ann. Chem. **460**, 98 (1928).
10. J. A. Berson and D. A. Ben-Efraim. J. Am. Chem. Soc. **81**, 4083 (1959).
11. A. C. Cope, E. Ciganek, and N. A. LeBel. J. Am. Chem. Soc. **81**, 2799 (1959).
12. W. J. Dale, L. Starr, and C. W. Strobel. J. Org. Chem. **26**, 2225 (1961).

Can. J. Chem. Downloaded from www.nrcresearchpress.com by 210.87.254.42 on 09/05/12
For personal use only.

Can. J. Chem. Downloaded from www.nrcresearchpress.com by 210.87.254.6 on 09/05/12
For personal use only.

Synthesis of D-*glycero*-D-*gulo*-heptose, D-*glycero*-D-*ido*-heptose, and 2-deoxy-D-*gluco*-heptose from D-glucose[1]

D. T. WILLIAMS[2] AND M. B. PERRY
Division of Biochemistry and Molecular Biology, National Research Council of Canada, Ottawa, Canada

Received March 31, 1969

D-Glucose was condensed with nitromethane to yield 1-deoxy-1-nitro-D-*glycero*-D-*ido*-heptitol and 1-deoxy-1-nitro-D-*glycero*-D-*gulo*-heptitol which were converted *via* the Nef reaction to D-*glycero*-D-*ido*-heptose and D-*glycero*-D-*gulo*-heptose respectively. The acetylated 1-deoxy-1-nitro-D-*glycero*-(D-*ido*- and D-*gulo*-)-heptitols were converted to 3,4,5,6,7-penta-*O*-acetyl-1,2-dideoxy-1-nitro-D-*gluco*-hept-1-enitol and reduction of this derivative afforded 3,4,5,6,7-penta-*O*-acetyl-1,2-dideoxy-1-nitro-D-*gluco*-heptitol which underwent the Nef reaction to give 2-deoxy-D-*gluco*-heptose.

Canadian Journtal of Chemistry, 47, 2763 (1969)

The application of the Sowden–Fischer (1) method for the extension of the carbon chain of glycoses has not, in the case of D-glucose and its derivatives, proved as successful a procedure as in the case of many other glycoses. Sowden and Fischer (2) were able to prepare 3,4,5,6,7-penta-*O*-acetyl-1,2-dideoxy-1-nitro-D-*gluco*-hept-1-enitol in 5% yield from D-glucose but they were unable to isolate the intermediate 1-deoxy-1-nitroheptitol derivatives resulting from the condensation of the D-glucose with nitromethane. 1-Deoxy-1-nitro-D-*glycero*-D-*gulo*-heptitol has been prepared by the mild hydrolysis of 5,7-*O*-benzylidene-1-deoxy-1-nitro-D-*glycero*-D-*gulo*-heptitol prepared in 21% yield by the action of nitromethane on 4,6-*O*-benzylidene-D-glucose (3). In this note we record details of the condensation of nitromethane with D-glucose under modified conditions which leads to the practical synthesis of some derived heptose and heptitol derivatives.

D-Glucose was condensed with nitromethane in the presence of sodium methoxide and the collected insoluble product was composed of at least 24% 1-deoxy-1-nitro-D-*glycero*-D-*gulo*-heptitol and 19% 1-deoxy-1-nitro-D-*glycero*-D-*ido*-heptitol, the remainder being unreacted D-glucose. Fractional crystallization of the decationized product afforded pure crystalline 1-deoxy-1-nitro-D-*glycero*-D-*ido*-heptitol and, 1-deoxy-1-nitro-D-*glycero*-D-*gulo*-heptitol which were converted *via* the Nef reaction (4) to D-*glycero*-D-*ido*-heptose and D-*glycero*-D-*gulo*-heptose in 9 and 10% overall yields respectively.

[1]NRCC No. 10741.
[2]NRCC Postdoctorate Fellow 1967–1969.

The mixed 1-deoxy-1-nitro-D-*glycero*-(D-*ido* and D-*gulo*)-heptitols were acetylated and refluxing the product in benzene in the presence of sodium bicarbonate yielded 3,4,5,6,7-penta-*O*-acetyl-1,2-dideoxy-1-nitro-D-*gluco*-hept-1-enitol which was reduced with hydrogen in the presence of palladium black to yield 3,4,5,6,7-penta-*O*-acetyl-1,2-dideoxy-1-nitro-D-*gluco*-heptitol. The 3,4,5,6,7-penta-*O*-acetyl-1,2-dideoxy-1-nitro-D-*gluco*-heptitol was converted *via* the Nef reaction to crystalline 2-deoxy-D-*gluco*-heptose. The glycose can be readily characterized as its 1,3,4,5,6,7-hexa-*O*-acetyl-2-deoxy-D-*gluco*-heptitol derivative.

Experimental

Paper chromatography was performed by the descending method on Whatman No. 1 filter paper using (*a*) pyridine – ethyl acetate – water (2:5:5 v/v top layer) or (*b*) butan-1-ol – ethanol – water (3:1:1 v/v) as the mobile phase. Compounds were detected with an alkaline silver nitrate spray reagent (5) and their rates of movement are quoted relative to D-glucose (R_G).

Gas–liquid partition chromatography was carried out using a Hewlett–Packard 402 gas chromatograph with a hydrogen flame detector and fitted with glass U tubes (4 ft × 6 mm × 3 mm internal diameter) packed with (A) 10% (w/w) neopentylglycol sebacate polyester on 80–100 mesh acid washed Chromosorb W, (B) 3% (w/w) ECNSS-M (Applied Science Laboratories Inc., Pa.) on 80–100 mesh acid washed Chromosorb W, or (C) a mixture of 1.5% (w/w) GE-XF 1150 (Applied Science Laboratories Inc., Pa.) and 1.5% (w/w) neopentyl–glycol sebacate polyester on 80–100 mesh acid washed Chromosorb W. Retention times are quoted relative to penta-*O*-acetyl-L-arabinitol (T_A).

Melting points were determined on a hot stage and are corrected. Optical rotations were determined at 22 °C with a Perkin–Elmer 141 polarimeter. Solutions were concentrated under reduced pressure below 40 °C.

Can. J. Chem. Downloaded from www.nrcresearchpress.com by 210.87.254.6 on 09/05/12
For personal use only.

*1-Deoxy-1-nitro-*D*-glycero-*D*-gulo-heptitol and 1-Deoxy-1-nitro-*D*-glycero-*D*-ido-heptitol*

Anhydrous D-glucose (100 g) suspended in nitromethane (280 ml) was vigorously stirred and 1.88 *N* sodium methoxide in methanol (630 ml) followed by methanol (125 ml) were added. After stirring for 24 h at room temperature, the precipitated material was collected by filtration, washed with methanol and ether, and dried to leave a light-yellow powder (150 g). The product (150 g) in water (500 ml) was passed down a column of Rexyn 101(H^+) ion-exchange resin (2 l) and the eluate and washings were concentrated to a syrup which was dissolved in ethanol (300 ml) and kept at 0 °C. The first crystalline product obtained was 1-deoxy-1-nitro-D-*glycero*-D-*ido*-heptitol (11 g) which after recrystallization from a methanol – ethanol mixture had m.p. 135–136 °C, $[\alpha]_D$ −1.4° (*c*, 3.3 in water), and on paper chromatography gave a single spot with R_G 1.60 (solvent *b*).

Anal. Calcd. for $C_7H_{15}NO_8$: C, 34.85; H, 6.27; N, 5.80. Found: C, 34.59; H, 6.37; N, 5.65.

The mother liquors on concentration afforded a crystalline mixture of 1-deoxy-1-nitro-D-*glycero*-D-*ido*-heptitol and 1-deoxy-1-nitro-D-*glycero*-D-*gulo*-heptitol (7.2 g). A third crop of crystals proved to be 1-deoxy-1-nitro-D-*glycero*-D-*gulo*-heptitol (13.4 g) which after recrystallization from a methanol – ethanol mixture had m.p. 139–140 °C, $[\alpha]_D$ +2.8° (*c*, 3.1 in water) (lit. (3) m.p. 138–139 °C and $[\alpha]_D$ +3.1°), and on paper chromatography gave a single spot with R_G 1.90 (solvent *b*).

Anal. Calcd. for $C_7H_{15}NO_8$: C, 34.85; H, 6.27; N, 5.80. Found: C, 34.54; H, 6.26; N, 5.70.

A portion of the original nitromethane condensation product (1 g) was treated under the conditions of the Nef reaction and the resulting glycose mixture was reduced with sodium borohydride and acetylated to give the corresponding glycitol acetate derivatives. Following the addition of inositol acetate as an internal standard, the mixture was analyzed by gas–liquid chromatography on column B (189 °C) and showed peaks from hexa-*O*-acetyl-D-glucitol (T_A 3.52), hepta-*O*-acetyl-D-*glycero*-D-*gulo*-heptitol (T_A 8.50), and hepta-*O*-acetyl-D-*glycero*-D-*ido*-heptitol (T_A 9.45). The hexa-*O*-acetyl-D-glucitol arises from unreacted D-glucose present in the crude reaction product and quantitative analysis of the gas chromatograms indicates that it is composed of 24% 1-deoxy-1-nitro-D-*glycero*-D-*gulo*-heptitol and 19% 1-deoxy-1-nitro-D-*glycero*-D-*ido*-heptitol assuming that these derivatives are quantitatively transformed to aldoheptoses in the Nef reaction.

D-*glycero*-D-*ido-Heptose*

1-Deoxy-1-nitro-D-*glycero*-D-*ido*-heptitol (0.5 g), dissolved in *N* sodium hydroxide (5 ml), was added dropwise with stirring to 6 *N* sulfuric acid (6.5 ml) cooled externally with ice. After 30 min the solution was diluted with water (15 ml) and neutralized with barium carbonate. The mixture was filtered and the filtrate was passed down columns of Rexyn 101 (H^+) (20 ml) and Duolite A4(OH^-) (10 ml) ion-exchange resins and the eluate and washing were concentrated to a syrup (0.4 g). Paper chromatographic examination of the product showed a major spot (R_G 1.85, solvent *a*) corresponding with authentic D-*glycero*-D-*ido*-heptose. A portion of the product after reduction with borohydride, on acetylation, gave hepta-*O*-acetyl-D-*glycero*-D-*ido*-heptitol which on gas–liquid chromatography gave a single peak (T_A 9.45, column A, 189 °C) having the same retention time as an authentic sample. A second portion of the D-*glycero*-D-*ido*-heptose (0.2 g) was converted to crystalline D-*glycero*-D-*ido*-heptose dibenzyldithioacetal (0.15 g) which had m.p. 130–131 °C and $[\alpha]_D$ +67° (*c*, 1.6 in pyridine) (lit. (6) m.p. 130–131 °C and $[\alpha]_D$ +71.4° (pyridine)).

D-*glycero*-D-*gulo-Heptose*

1-Deoxy-1-nitro-D-*glycero*-D-*gulo*-heptitol (0.5 g) was converted in the way described above to yield crystalline D-*glycero*-D-*gulo*-heptose (0.26 g) which had m.p. and mixture m.p. 193–194 °C and $[\alpha]_D$ −22° → −18.5° (*c*, 2.5 in water) (lit. (7) m.p. 193 °C and $[\alpha]_D$ −20° (equil. in water)), and gave a single spot on paper chromatograms R_G 0.91 (solvent *a*).

*2-Deoxy-*D*-gluco- heptose*

*3,4,5,6,7-Penta-O-acetyl-1,2-dideoxy-1-nitro-*D*-gluco-hept-1-enitol*

The mixture of 1-deoxy-1-nitro-D-*glycero*-(D-*gulo* and D-*ido*)-heptitol (10.5 g) in acetic anhydride (100 ml) was treated with 2 drops of concentrated sulfuric acid and the mixture was heated for 40 min on a boiling water bath. The cooled reaction mixture was poured into an ice and water mixture (500 ml), and the product was extracted with chloroform in the usual way. The acetylated 1-deoxy-1-nitro-heptitol mixture (21 g) in dry benzene (250 ml) was boiled under reflux for 2.5 h with sodium bicarbonate (25 g). The cooled reaction mixture was filtered and the filtrate was concentrated to a syrup. The syrup was dissolved in ethanol (100 ml) and, when the solution was kept overnight at 0 °C, it gave a crystalline product (15 g) which after recrystallization from ethanol afforded pure 3,4,5,6,7-penta-*O*-acetyl-1,2-dideoxy-1-nitro-D-*gluco*-hept-1-enitol having m.p. 106–107 °C and $[\alpha]_D$ +15° (*c*, 3.55 in chloroform) (lit. (2) m.p. 106–107 °C and $[\alpha]_D$ +18° (in chloroform)).

*3,4,5,6,7-Penta-O-acetyl-1,2-dideoxy-1-nitro-*D*-gluco-heptitol*

3,4,5,6,7-Penta-*O*-acetyl-1,2-dideoxy-1-nitro-D-*gluco*-hept-1-enitol (6 g) in ethanol (400 ml) was shaken with hydrogen at room temperature and pressure in the presence of palladium black (0.5 g). One mole equivalent of hydrogen was absorbed in 30 min and the rate of reduction then became very slow. At this point the reaction mixture was filtered; the filtrate was concentrated to a small bulk and, when cooled to 0 °C, it afforded crystalline 3,4,5,6,7-penta-*O*-acetyl-1,2-dideoxy-1-nitro-D-*gluco*-heptitol (5 g) which after recrystallization from methanol had m.p. 119–120 °C and $[\alpha]_D$ +7.5° (*c*, 3.6 in chloroform).

Anal. Calcd. for $C_{17}H_{25}NO_{12}$: C, 46.89; H, 5.79; N, 3.22. Found: C, 46.51; H, 5.96; N, 3.16.

*2-Deoxy-*D*-gluco-heptose*

3,4,5,6,7-Penta-*O*-acetyl-1,2-dideoxy-1-nitro-D-*gluco*-heptitol (5 g) was dissolved at 36 °C in *N* sodium hydroxide solution (63 ml) and the mixture, after being kept at 20 °C for 1 h, was added dropwise to a cooled stirred solution of sulfuric acid (20 ml) in water (180 ml). After 2 h, the reaction mixture was neutralized with barium carbonate and following centrifugation and filtration, the solution was passed down columns of Rexyn

101(H^+) (150 ml) and Duolite A4(OH^-) (30 ml) ion-exchange resins and the eluate and washings were concentrated to a syrup. The syrup was taken up in a little ethanol and, on cooling, crystalline 2-deoxy-D-*gluco*-heptose was obtained (1.3 g) which after recrystallization from aqueous ethanol had m.p. 174.5–175.5 °C and $[\alpha]_D$ +7.6° (5 min) → +11.1° (30 min equil. value) (*c*, 5 in water).

Anal. Calcd. for $C_7H_{14}O_6$: C, 43.30; H, 7.27. Found: C, 43.16; H, 7.32.

The 2-deoxy-D-*gluco*-heptose gave a single spot on paper chromatograms having R_G 1.67 (solvent *a*) and R_G 2.00 (solvent *b*), and the trimethylsilylated crystalline material on gas chromatography gave a single peak T_A 0.15 (column A, 208 °C) whereas the trimethylsilated product obtained from the glycose, after equilibration in water, on gas–liquid chromatography gave two peaks having T_A 0.15 and 0.20 (very minor).

*1,3,4,5,6,7-Hexa-O-acetyl-2-deoxy-*D*-gluco-heptitol*

2-Deoxy-D-*gluco*-heptose (0.1 g) was reduced with sodium borohydride to 2-deoxy-D-*gluco*-heptitol which on acetylation afforded 1,3,4,5,6,7-hexa-*O*-acetyl-2-deoxy-D-*gluco*-heptitol (0.15 g). The product, after recrystallization from ethanol, had m.p. 106–107 °C and $[\alpha]_D$ +11° (*c*, 2.9 in chloroform).

Anal. Calcd. for $C_{19}H_{28}O_{12}$: C, 50.89; H, 6.29. Found: C, 50.95; H, 6.29.

On gas–liquid chromatography the acetate gave a single peak T_A 4.35 (column C, 209 °C), and T_A 3.64 (column A, 232 °C).

1. J. C. SOWDEN. Advan. Carbohydrate Chem. **6**, 315 (1951).
2. J. C. SOWDEN and H. O. L. FISCHER. J. Am. Chem. Soc. **69**, 1048 (1947).
3. J. C. SOWDEN and H. O. L. FISCHER. J. Am. Chem. Soc. **68**, 1511, (1946).
4. J. U. NEF. Ann. Chem. **280**, 263 (1894).
5. W. E. TREVELYAN, D. P. PROCTER, and J. S. HARRISON. Nature, **166**, 444 (1950).
6. J. W. PRATT, N. K. RICHTMYER, and C. S. HUDSON. J. Am. Chem. Soc. **75**, 4307 (1953).
7. W. N. HAWORTH, E. L. HIRST, and M. STACEY. J. Chem. Soc. 2867 (1931).

Can. J. Chem. Downloaded from www.nrcresearchpress.com by 210.87.254.6 on 09/05/12
For personal use only.

Effect of substituents on the chemical shift of benzylic protons

ROBERT R. FRASER, GURUDATA, ROGER N. RENAUD, CESAR REYES-ZAMORA, AND ROBERT B. SWINGLE
Department of Chemistry, University of Ottawa, Ottawa, Canada

Received December 13, 1968

The chemical shift of the benzylic protons in fifteen series of *para*-substituted toluenes bearing different groups in the alpha position are reported. In each series a plot of the chemical shift in tau units of the benzylic protons against the Hammett σ value of the *para* substituent is linear. The slopes of these plots vary from −0.20 to +0.01 p.p.m./σ. The variation of slopes appears to be conformationally dependent, an observation at odds with current theory. In two rigid systems having the same geometry the slope has been found to vary from −0.12 to −0.18 indicating a dependence on other factors as well. The effect of solvent on the slopes has been determined, and shows no correlation with solvent dielectric properties.

Canadian Journal of Chemistry, 47, 2767 (1969)

Can. J. Chem. Downloaded from www.nrcresearchpress.com by 210.87.254.40 on 09/05/12
For personal use only.

In recent years many examples of correlations between the effect of substituents on the chemical shift (abbreviated to SCS) of a proton on a benzene ring and the Hammett sigma value of the substituents have been found (1–3). In addition similar correlations have been observed for protons in the side chains of toluenes (4–7), phenols (8), anisoles (9), dihydrocinnamic acids (10), cyclopropanes (11), and benzonorbornenes (12). The mechanism by which a substituent exerts its effect is a subject of some contention. It is usually assumed that the substituent alters the electron density of the aromatic ring by both inductive and resonance interactions and that this effect is relayed to the protons on the ring or in the side chain by polarization of the intervening sigma electrons. An alternative explanation involving field and mesomeric effects has been put forward by Dewar and Takeuchi (13). Yet Wittstruck and Trachtenberg examined the shifts in a series of cinnamic and dihydrocinnamic acids and concluded that both field and anisotropy effects of the substituent were negligible (10). Taft has shown that aromatic fluorine shifts correlate well with σ_R^o values (14) and that these parameters can be related by theoretical calculations to the excess π charge density introduced by a substituent (15). While the sensitivity of fluorine and proton nuclei to substituent effects is different, many similarities in their correlations do exist. In the case of aromatic protons, they too are influenced to a large extent by the resonance effect of the substituent as measured by σ_R^o (1).

We wish to report the results of a study of the correlation of SCS with σ for the methylene protons in a series of toluene derivatives. We believe that the observations made on these compounds provide some evidence pertaining to the mechanism by which substituents alter proton shifts. A brief communication of our results has already appeared (16). This paper will provide the details of our communication and will describe additional results on other toluene derivatives.

We have determined the chemical shifts of the benzylic protons in fifteen series of *para*-substituted compounds of the general formula $X—C_6H_5—CH_2—Z$. For each Z, at least four *para* substituents having a range of σ values of 0.95 or more were studied. The extent to which the chemical shifts are correlated by σ is well illustrated by a graph given in our earlier paper (16). Almost all points except that for chlorine fall within 1 Hz of the best straight line.[1] We have presented in Fig. 1 the correlation for the most interesting series of compounds, the *para*-substituted benzyl phenyl sulfoxides. In the sulfoxides the benzylic protons are magnetically non-equivalent and each proton shows a completely different sensitivity to the *para* substituent, X. One of the diastereotopic protons shows a large variation with X, the slope (ρ) of the τ versus σ plot being 0.20 p.p.m./σ and negative.[2]

[1]As has been noted elsewhere (7), the deviations from linearity in one series are usually reproduced in the same way in a second series. For example, a least squares analysis of a plot of the τ values for the *para* substituted benzyl tetrahydropyranyl ethers versus toluenes shows an excellent linear correlation with ρ = .759, r = .993 and s = .0095, less than a 2% uncertainty in ρ. An obvious way to improve the linearity of these σ–τ plots would be to avoid the use of all halogen substituents rather than only chlorine which shows the worst deviations from linearity.

[2]The sigma constants are taken from ref. 40.

Can. J. Chem. Downloaded from www.nrcresearchpress.com by 210.87.254.40 on 09/05/12
For personal use only.

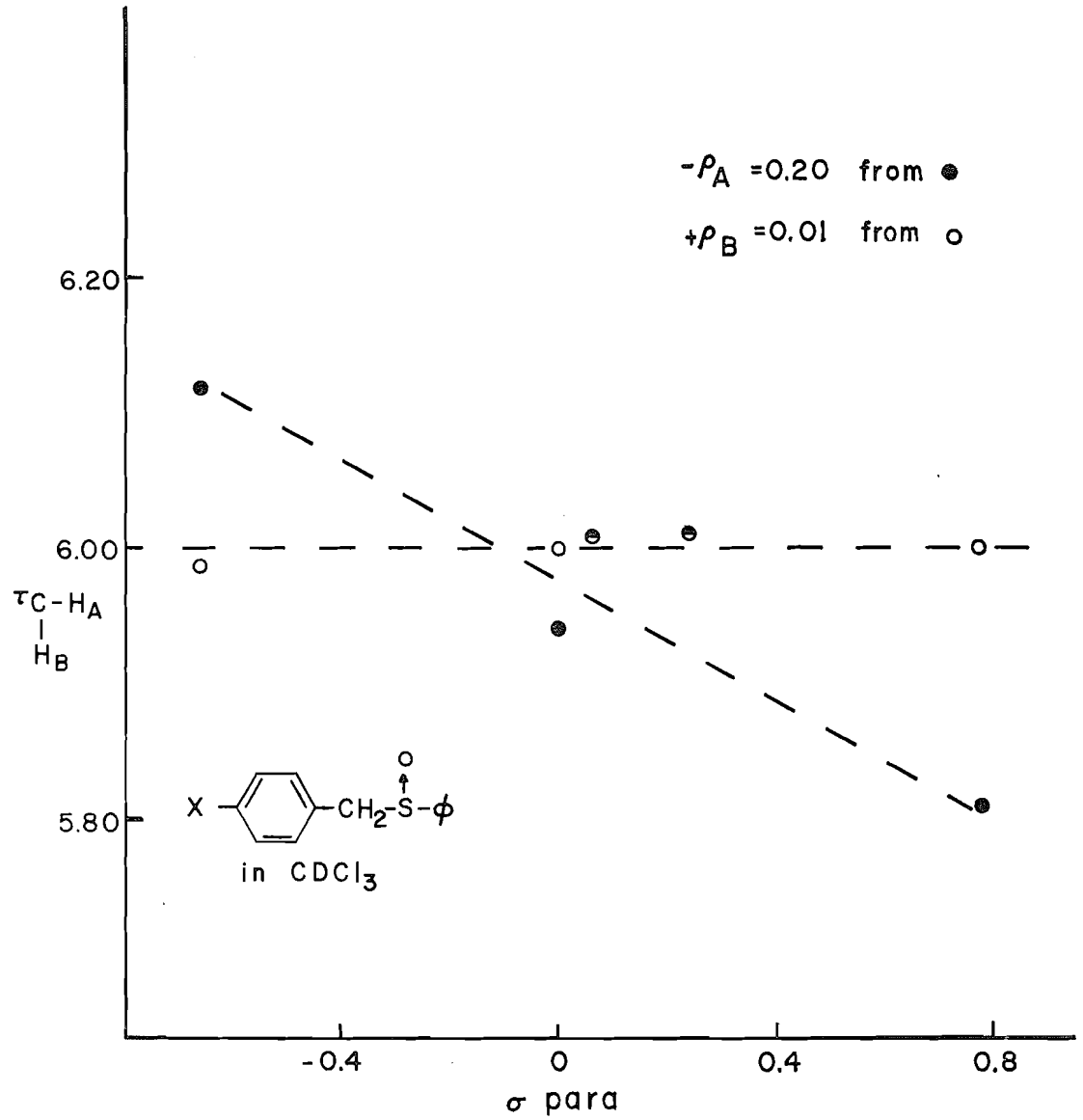

FIG. 1. A plot of the chemical shift of each diastereotopic proton in a series of five *para*-substituted benzyl phenyl sulfoxides versus the Hammett sigma value of the substituent. There is an uncertainty of ±1.5 Hz in the points for fluorine and chlorine since the diastereotopic protons appeared as a broad singlet in these compounds.

The other proton has a ρ or slope of plus 0.01. That the assignments to the diastereotopic protons of the amino derivative are opposite (in terms of relative field strengths) to those in the nitro compound was proven experimentally. A sample of *p*-nitrobenzyl phenyl sulfoxide was partially deuterated (17) by treatment with NaOD in a mixture of chloroform and heavy water.[3] The nuclear magnetic resonance (n.m.r.) spectrum of the product in $CDCl_3$ showed that the low field proton had exchanged more rapidly under these conditions i.e. had less intensity. The sulfoxide was then reduced by stannous

[3]A similar observation of preferential exchange in *p*-chlorophenyl benzyl sulfoxide has been reported (18).

TABLE I

Rho values of SCS-Hammett σ plots for

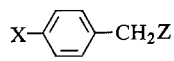

Z	$-\rho^a$	VdW[b]	r^a	s^a	n^c
H	0.21[d]	1.2	.926	.04	9
CH_3	0.20[e]	1.5[t]	.938	.03	9
CH_2COOH	0.20[f]	—	.990	.01	4
COOH	0.18	—	.995	.01	4
CN	0.18	—	.937	.04	7
OH	0.20	1.4	.968	.03	6
$OCOCH_3$	0.17[g]	1.4	.989	.01	5
OCH_3	0.15	1.4	.960	.02	6
OTHP[h]	0.15; 0.15	1.4	.960;.985	.01; .02	8
Cl	0.11	1.8	.975	.01	5
$SOCH_3$	0.12; 0.09	1.85	.943;.978	.02; .02	5
SO_2CH_3	0.16	1.85	.984	.02	5
SC_6H_5	0.07	1.85	.908	.024	5
SOC_6H_5	0.21; −0.01	1.85	.952;.810	.05; .01	5
$SO_2C_6H_5$	0.16	1.85	.984	.02	5
Br	0.01	1.95	.544	.02	5

[a] ρ, *r* and *s* represent the slope in p.p.m./σ, the correlation coefficient and the standard deviation as derived from a least squares treatment of the data (32). The points for chlorine have not been used in the calculations.
[b] Values of the van der Waal's radius of the atom attached to the methylene group are quoted from reference 19.
[c] *n* is the number of compounds studied in each series.
[d] Calculated from the data of Miller *et al.* (4).
[e] Calculated from the data of Williamson (5).
[f] Calculated from the data of Trachtenberg (10).
[g] Calculated from the data in reference 7.
[h] THP stands for tetrahydropyranyl ether.
[i] A van der Waal's radius is, by definition, limited to atoms. For the methyl group we have listed its "interference radius" as estimated from ultraviolet shifts (33).

chloride to the *para*-amino derivative whose n.m.r. in $CDCl_3$ showed that the high field proton had less intensity. There is an uncertainty regarding assignments for the unsubstituted compound in this series, but either assignment would give essentially the same slopes. Chlorine again shows its customary high field deviation. The slopes or ρ values for all series of compounds studied are listed in Table I along with all ρ's reported in the literature. It can be seen that ρ varies widely as Z is altered.

Before discussing these ρ values, it is important to consider the accuracy and reliability of the Hammett correlation. All the data in Table I has been obtained by a least squares analysis of the plots for each series. The correlation is generally good, the criterion of acceptability being that *r*, the correlation coefficient, be greater than 0.90 (32). For our purposes *s* is much more meaningful since *r* decreases as ρ decreases. For instance the plot of the benzyl bromides gives $\rho = 0.01 \pm$ an *s* of 0.02 even though $r = 0.544$. It can be seen that most of the standard deviations are 0.03 or less and this is a reliable limit of accuracy of ρ. It is thus established that the variation in ρ with a change in Z is statistically significant. At the same time the appreciable error in ρ requires that only a qualitative discussion of these initial results is warranted at present.

We wish to assume, as has been done for every Hammett correlation (4, 19), that a *para*-substituent affects only the π electron distribution of the benzene ring, and that no steric factors are involved. Then a change in ρ from series to series must be attributed to a change in some property or properties of Z. It can be seen at a glance that there is no correlation between the size of ρ and the electronegativity of Z. On the other hand, with the exception of the sulfones, there is a reasonably consistent parallel between ρ and the size of Z as estimated by its Van der Waal's radius. We interpret this parallel behavior as evidence that ρ depends, to a significant degree, on the conformation of the methylene group with respect to the benzene ring. This interpretation is strongly supported by the sulfoxide data. Here the two diastereotopic protons have a common Z but will almost certainly possess different orientations with respect to the benzene ring. The most probable conformation, as shown in **1**, should have the bulky phenyls *trans* to one another. The large asymmetric sulfur atom will

Can. J. Chem. Downloaded from www.nrcresearchpress.com by 210.87.254.40 on 09/05/12
For personal use only.

Can. J. Chem. Downloaded from www.nrcresearchpress.com by 210.87.254.40 on 09/05/12
For personal use only.

then prefer to tilt from the symmetrical arrangement in **3** to that shown in **1**. If the substituent effect is maximal when the benzylic C—H bond is colinear with the adjacent p orbital and minimal when perpendicular to it then the results for this sulfoxide and for the decrease in ρ with increasing size of Z can be accounted for.[4] Or, to rephrase the explanation we can say that a decrease in ρ represents a shift of conformational population from that shown in **2** to that shown in **3**. Our previous results on the effect of substituents on geminal coupling constants in the tetrahydropyranyl ethers and sulfoxides led to the same conclusions (20).

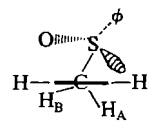

1

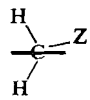

2

3

We have sought some experimental verification for this explanation by determining the ρ values for the benzyl phenyl sulfoxides at 90 °C. At this temperature the ρ values for the protons were −0.02 and −0.18. Unfortunately, this lack of a temperature effect on ρ is neither evidence for nor against our explanation.

Very little data exists at present which bears on the problem of rotation about a benzene to carbon bond. In toluene, the barrier to rotation has not been measured but has been calculated to be about 100 calories (21). A change from a 6-fold to a 2-fold axis of symmetry for benzyl derivatives will undoubtedly raise this barrier. Recently, in two different 2,6-di-substituted benzyl derivatives bearing either *ortho* chlorines or *ortho t*-butyl groups, the barrier was reported to be large enough (15–20 kcal) to have been determined by n.m.r. studies (22, 23). For the compounds in Table I a much smaller barrier will be present, perhaps of the order of a few kcals. The only other system for which experimental evidence on the rotational barrier is available is that of phenyl cyclopropane for which a "bisected" structure has been proposed as the most favorable conformation (24). It is obvious that in order to prove a relation between the CH_2 group's conformation and ρ, these values must be measured in systems of known rigid geometry. Thus far we have obtained data for only two structures of this class, the 6-substituted phthalides and a series of 3-phenyl phthalans. For a series of six phthalides, **4**, ρ was found to be −0.18, a value essentially equivalent to that found in the open chain ethers. For the phthalans, **5**, ρ was −0.12.[5] The similarity in ρ values of the phthalides to the ethers and acetates would indicate that the open chain ethers have **2** as their predominant conformation. The analogous conformation has been found to be the most favorable one in allyl methyl ether (26). However the appreciably lower ρ value for the CH_2 protons of the phthalans lessens the reliability of this conclusion. It indicates that other factors are also influencing the magnitude of ρ. The nature of these factors, electronegativity, strain, etc., cannot be determined at this time. Additional series of benzyl derivatives of fixed geometry are currently being synthesized to provide more evidence about the reliability of using ρ as an indication of conformation.

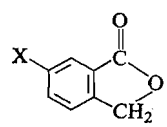

4

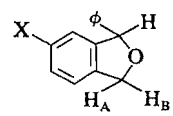

5

As we mentioned previously there does not appear to be any way to explain a conformational dependence of ρ within the present framework of proton shift theory. Three main factors are recognized which determine proton chemical shifts. These are (*a*) the diamagnetic shielding of the electrons which surround the nucleus, (*b*) the anisotropy of other atoms or groups of atoms within the molecule, and (*c*) solvent effects. The diamagnetic shielding of a benzylic proton can be

[4]It is also possible that H_A, because it is *trans* to the sulfoxide oxygen, has a different ρ than H_B which is *gauche* to the oxygen. However this explanation cannot explain the other data in Table I and is therefore less likely.

[5]Details of the preparation, analysis of spectra, and correlation of the data for this series will be described in a separate paper (25).

Can. J. Chem. Downloaded from www.nrcresearchpress.com by 210.87.254.40 on 09/05/12
For personal use only.

influenced through either a field or inductive effect. Neither of these are capable of accounting for the large change in the benzylic shifts. As an example, we have calculated the direct field effect (27) on the benzylic proton shift when a nitro group is substituted for a hydrogen in the *para* position. It amounts to 0.05 p.p.m. and is independent of conformation. Moreover a field effect should correlate with σ_I not σ (28). The inductive effect acting through bonds would not show a conformational dependence. Anisotropy effects are also unable to account for the observed SCS's. Normally the effect is either assumed negligible (29) or variable as Figeys and Flammang propose (30) but much too small. For instance, if one assumes Figeys and Flammang's estimate that $\Delta\chi$ can vary by ten percent from -50×10^{-6} to -45×10^{-6} cm^3/mole, it can be shown that the decrease would alter the screening of a benzylic proton in the plane of the benzene ring by 0.045 p.p.m., and the screening of a benzylic proton as far away from the plane as possible by 0.032 p.p.m. Thus this effect would be far too small, not particularly sensitive to conformation and not related to Hammett σ values. The third factor, solvent effects, has been kept constant throughout the investigation. We must therefore seek a new explanation for our results. It is proposed that either the paramagnetic shielding term in the Ramsay formula is not negligible as normally assumed (31), or that a hyperconjugative interaction between the benzylic hydrogens and the π system of the aromatic ring is responsible for the variations in chemical shifts. A somewhat analogous explanation involving homobenzylic resonance has been proposed by Tanida and co-workers (12) to account for the stereochemical difference between the ρ's for the *syn* and *anti* 7-hydrogens in a series of benzonorbornenes. We hope that additional results will provide further evidence regarding the mechanism by which an SCS is produced.

The subject of solvent effects should be mentioned briefly. We purposefully avoided any change in solvent in the above measurements. We have, nevertheless, studied the solvent effect on ρ in several series including the rigid phthalides. The findings are given in Table II. It is apparent that the solvent can have a large effect on the size of ρ. The data for the phthalides shows that the variation of ρ is not due to an effect of solvent on conformational equilibria. Furthermore in this series, there is no correlation between the solvent effect on ρ and the dielectric constant of the medium. It would appear that specific solvent–solute interactions have a large influence on ρ. We cannot derive any more definitive information from these solvents effects. They do provide the information that ρ is very sensitive to its medium and therefore serve as a warning that the solvent must be kept constant if any meaningful interpretations are to be derived from studies of ρ in different series.

Experimental

Microanalyses were performed by Scandinavian Microanalytical Lab., Herlev, Denmark. The n.m.r. spectra were measured in deuterochloroform on either a

TABLE II

The effect of solvent on ρ values

Series	$-\rho$	Solvent (ε)
p-X—$C_6H_5CH_2OCH_3$	0.15	$CDCl_3$ (5.1)
	0.23	DMSO-d_6 (47)
p-X—$C_6H_5CH_2$—$\overset{\overset{O}{\uparrow}}{S}$—$C_6H_5$	0.00; 0.22	$CDCl_3$
	0.22; 0.33	DMSO-d_6
p-X—$C_6H_5CH_2$—$\overset{\overset{O}{\uparrow}}{S}$—$CH_3$	0.10; 0.14	$CDCl_3$
	0.06; 0.13	D_2O (80)
	0.22; 0.33	DMSO-d_6
Phthalides, **4**	0.19	$CDCl_3$ (5.1)
	0.19	$ClCH_2CH_2Cl$ (10.5)
	0.26	CH_3COCH_3 (21.4)
	0.19	CH_3CN (38.8)
	0.24	DMSO-d_6 (47)

Can. J. Chem. Downloaded from www.nrcresearchpress.com by 210.87.254.40 on 09/05/12
For personal use only.

Varian DA-60 or on a Varian HA-100 spectrometer. Spectra of benzyl derivatives having non-equivalent methylene protons were determined using 0.3 *M* solutions at 60 MHz and using 0.1 *M* solutions at 100 MHz. All other spectra of the benzyl series were run using 0.2 *M* solutions and for at least three compounds in each series 0.1 *M* solutions were also measured, no dilution effect being detectable. In the phthalans and phthalides only 0.1 *M* solutions were studied. All line positions are reported as the average of at least five determinations with a standard deviation of less than 0.2 Hz. The following is a list of the tau values of the methylene protons in each series of benzyl derivatives studied. The values are given in brackets after the *para* substituent, X. For Z = CN; H (6.257), NH_2 (6.390), OH (6.330), CH_3 (6.312), Cl (6.287), Br (6.299), NO_2 (6.111). For Z = COOH; H, (6.361), OCH_3 (6.429), CH_3 (6.405), NO_2 (6.232). For Z = OH; H (5.312), OCH_3 (5.396), F (5.361), Cl (5.351), CN (5.228), NO_2 (5.171). For Z = OCH_3; H (5.544), OCH_3 (5.616), F (5.582), Cl (5.580), CN (5.490), NO_2 (5.439). For Z = OTHP (2-tetrahydropyranyloxy); H_A in H (5.222), NH_2 (5.345), OCH_3 (5.288), CH_3 (5.269), F (5.259), Cl (5.269), CF_3 (5.170), CN (5.162), NO_2 (5.115): H_B in H (5.507), NH_2 (5.623), OCH_3 (5.567), CH_3 (5.553), F (5.544), Cl (5.545), CF_3 (5.454), CN (5.446), NO_2 (5.390). For Z = Cl; H (5.426), CH_3 (5.463), F (5.445), Cl (5.461), NO_2 (5.354). For Z = SCH_3; H (6.344), OCH_3 (6.388), Cl (6.391), NO_2 (6.280). For Z = $SOCH_3$ at 0.3 *M* concentration; H_A in H (5.97), NH_2 (6.06), OCH_3 (6.05), Cl (6.06), NO_2 (5.91): H_B in H (6.10), NH_2 (6.22), OCH_3 (6.14), Cl (6.12), NO_2 (6.02). For Z = $SOCH_3$ at 0.1 *M* concentration; H_A in H (5.942), NH_2 (6.025), OCH_3 (6.009), Cl (6.066), NO_2 (5.907): H_B in H (6.075), NH_2 (6.192), OCH_3 (6.119), Cl (6.066), NO_2 (6.008). J_{AB} was 12.80 in the OCH_3, NH_2 and unsubstituted compounds and 12.95 in the nitro derivative. For Z = SO_2CH_3; H (5.766), NH_2 (5.887), OCH_3 (5.827), Cl (5.799), NO_2 (5.656). For Z = SC_6H_5; H (5.886), NH_2 (5.970), F (5.925), Cl (5.949), NO_2 (5.865). For Z = SOC_6H_5 at 0.3 *M* concentration: H_A in H (5.94), NH_2 (6.12), F (6.02), Cl (6.02), NO_2 (5.80); H_B in H (6.00), NH_2 (5.99), F (6.02), Cl (6.02), NO_2 (5.99). For Z = SOC_6H_5 at 0.1 *M* concentration; H_A in H (5.921), NH_2 (6.110), F (6.005), Cl (6.013), NO_2 (5.811); H_B in H (6.004), NH_2 (5.980), F (6.005), Cl (6.013), NO_2 (6.005). J_{AB} was 12.60 for the unsubstituted and *p*-amino derivative, 12.75 for the *para*-nitro derivative. For Z = $SO_2C_6H_5$; H (5.699), NH_2 (5.828) F (5.734), Cl (5.740), NO_2 (5.599). For Z = Br; H (5.536), OCH_3 (5.519), CH_3 (5.546), CN (5.530), NO_2 (5.505).

The chemical shifts of the benzylic protons in the phthalides **4**, were as follows; H (4.668), NH_2 (4.803), OCH_3 (4.759), F (4.709), Cl (4.711), CN (4.604), NO_2 (4.526).

Preparation of Compounds

The majority of the compounds studied were available commercially. When necessary, the compound was purified by standard techniques until its physical constants were in agreement with literature values. With the exception of the phthalans, **5**, compounds which have been prepared for the first time are described below:

p-Methoxybenzyl Methyl Sulfoxide

This compound was prepared by oxidation of the corresponding sulfide (34) with sodium meta periodate (35). The product was a solid which, after recrystallization from ethyl acetate, had m.p. 60–61° (Previously reported to be 54–55° (37)).

Anal. Calcd. for $C_9H_{12}SO_2$: C, 58.7; H, 6.6. Found: C, 58.7; H, 6.6.

p-Methoxybenzyl Methyl Sulfone

This compound was prepared by oxidation of the sulfoxide with hydrogen peroxide in acetic acid. The sulfone after purification by recrystallization from ethyl acetate was a white solid, m.p. 108–109°.

Anal. Calcd. for $C_9H_{12}SO_3$: C, 54.0; H, 6.0. Found: C, 53.6; H, 6.0.

p-Chlorobenzyl Methyl Sulfoxide

Oxidation (35) of the corresponding sulfide (34, 36) gave a solid which after recrystallization from ethyl acetate had m.p. 98.5–100°.

Anal. Calcd. for C_8H_9ClSO: C, 50.9; H, 4.8. Found: C, 50.9; H, 4.8.

p-Aminobenzyl Methyl Sulfoxide

This sulfoxide was obtained by reduction of the corresponding *p*-nitro sulfoxide (37) in methanol with hydrogen (20 p.s.i.) and palladium (10% on charcoal) for 2 h. The product after recrystallization from ethyl acetate had m.p. 99–101.5°.

Anal. Calcd. for $C_8H_{11}NSO$: C, 56.8; H, 6.6. Found: C, 56.8; H, 6.7.

p-Aminobenzyl Methyl Sulfone

The corresponding *p*-nitro sulfone (35) was reduced with hydrogen and palladium (10% on charcoal) to give the *p*-amino sulfone, m.p. 161.5–162.5.

Anal. Calcd. for $C_8H_{11}NSO_2$: C, 51.9; H, 6.0. Found: C, 51.7; H, 6.0.

p-Aminobenzyl Phenyl Sulfoxide

A solution of 0.5 g of *p*-aminobenzyl phenyl sulfide (39) in 50 ml ethanol was treated dropwise with 0.5 g sodium meta periodate in 50 ml methanol. After stirring overnight the solution was filtered, the solvent evaporated, and chloroform was added. The chloroform solution was washed with water, dried and concentrated. The residue, after recrystallization from ethanol, was a light yellow solid, m.p. 155–156° which oxidized slowly on exposure to the atmosphere.

Anal. Calcd. for $C_{13}H_{13}NOS$: C, 67.5; H, 5.7; N, 6.0. Found: C, 67.0; H, 5.6; N, 5.1.

Acknowledgment

The authors thank the National Research Council of Canada for its generous financial support.

1. R. R. Fraser. Can. J. Chem. **38**, 2226 (1960).
2. H. Spiesecke and W. G. Schneider. J. Chem. Phys. **35**, 731 (1961).
3. J. W. Emsley, J. Feeney, and L. H. Sutcliffe. High resolution nuclear magnetic resonance spectroscopy. Vol. II. The Pergamon Press, Ltd., London. 1966. pp. 749–770.

4. S. H. MARCUS, W. F. REYNOLDS, and S. I. MILLER. J. Org. Chem. **31**, 1872 (1966).
5. K. L. WILLIAMSON. J. Am. Chem. Soc. **86**, 4021 (1964).
6. M. NISHIO. Chem. and Pharm. Bull. Japan, **15**, 1669 (1967).
7. S. ARAKAWA and M. HASHIMOTO. Bull. Chem. Soc. Japan. **41**, 1449 (1968).
8. R. J. OUELLETTE. Can. J. Chem. **43**, 707 (1965).
9. C. J. HEATHCOCK. Can. J. Chem. **40**, 1865 (1962).
10. T. A. WITTSTRUCK and E. N. TRACHTENBERG. J. Am. Chem. Soc. **89**, 3803 (1967).
11. T. A. WITTSTRUCK and E. N. TRACHTENBERG. J. Am. Chem. Soc. **89**, 3810 (1967).
12. N. INAMOTO, S. MASUDA, K. TORI, K. AONO, and H. TANIDA. Can. J. Chem. **45**, 1185 (1967).
13. M. J. S. DEWAR and Y. TAKEUCHI. J. Am. Chem. Soc. **89**, 390 (1967).
14. R. W. TAFT, E. PRICE, I. R. FOX, I. C. LEWIS, K. K. ANDERSEN, and G. T. DAVIS. J. Am. Chem. Soc. **85**, 3146 (1963).
15. R. T. C. BROWNLEE and R. W. TAFT. J. Am. Chem. Soc. **90**, 6537 (1968).
16. R. R. FRASER, GURUDATA, C. REYES-ZAMORA, and R. B. SWINGLE. Can. J. Chem. **46**, 1595 (1968).
17. A. RAUK, E. BUNCEL, R. Y. MOIR, and S. WOLFE. J. Am. Chem. Soc. **87**, 5498 (1965).
18. M. NISHIO. Chem. Commun. 562 (1968).
19. L. N. FERGUSON. The modern structural theory of organic chemistry. Prentice-Hall, Inc., New York. 1962. p. 412.
20. R. R. FRASER, P. HANBURY, and C. REYES-ZAMORA. Can. J. Chem. **45**, 2481 (1967).
21. W. R. WOOLFENDEN and D. M. GRANT. J. Am. Chem. Soc. **88**, 1496 (1966).
22. G. B. NEWSOROFF and S. STERNHELL. Tetrahedron Letters. 2539, (1967).
23. T. SCHAEFER, R. SCHWENK, C. J. MCDONALD, and W. F. REYNOLDS. Can. J. Chem. **46**, 2187 (1968).
24. G. L. CLOSS and H. B. KLINGER. J. Am. Chem. Soc. **87**, 3265 (1965).
25. R. R. FRASER and R. N. RENAUD. To be published.
26. A. A. BOTHNER-BY, S. CASTELLANO, S. J. EBERSOLE, and H. GUNTHER. J. Am. Chem. Soc. **88**, 2466 (1966).
27. A. D. BUCKINGHAM. Can. J. Chem. **38**, 300 (1960).
28. L. N. FERGUSON. The modern structural theory of organic chemistry. Prentice-Hall, Inc., New York. 1962. p. 418.
29. T. K. WU and B. P. DAILEY. J. Chem. Phys. **41**, 2796 (1964).
30. H. P. FIGEYS and R. FLAMMANG. Mol. Phys. **12**, 581 (1967).
31. J. A. POPLE, W. G. SCHNEIDER, and H. J. BERNSTEIN. High resolution nuclear magnetic resonance. McGraw-Hill Book Co. Inc., New York. 1959. p. 170.
32. H. H. JAFFE. Chem. Revs. **53**, 191 (1953).
33. W. F. FORBES and W. A. MUELLER. Can. J. Chem. **34**, 1542 (1956).
34. C. R. JOHNSON and N. J. LEONARD. J. Org. Chem. **27**, 282 (1962).
35. P. MAMALIS. J. Chem. Soc. 4747, (1960).
36. R. MAYER, S. SCHEITBAUER and D. KUNZ. Chem. Ber. **99**, 1393 (1966).
37. I. D. ENTWISTLE, R. JOHNSTONE and B. J. MILLARD. J. Chem. Soc. 302, (1967).
38. C. K. INGOLD, E. H. INGOLD, and F. R. SHAW. J. Chem. Soc. 813, (1927).
39. P. T. S. LAU and G. F. GRILLOT. J. Org. Chem. **28**, 2765 (1963).
40. D. H. MCDANIEL and H. C. BROWN. J. Org. Chem. **23**, 420 (1958).

Can. J. Chem. Downloaded from www.nrcresearchpress.com by 210.87.254.40 on 09/05/12
For personal use only.

Can. J. Chem. Downloaded from www.nrcresearchpress.com by 210.87.254.105 on 09/05/12
For personal use only.

Transmission of polar effects. Part XI[1]. Polar and steric effects in the reactions of arylaliphatic carboxylic acids

KEITH BOWDEN AND R. C. YOUNG
Department of Chemistry, The University of Essex, Wivenhoe Park, Colchester, Essex, England

Received March 28, 1969

The rate coefficients for the reaction with diazodiphenylmethane in ethanol at 30° and the acid-catalyzed esterification with methanol at 60° of a number of arylaliphatic carboxylic acids and their pK_a values in 80% 2-methoxyethanol–water have been measured. Rate coefficients have also been measured for the alkaline hydrolysis in 70% dioxan–water of their 2-diethylaminoethyl esters at 45°. The pK_a values and diazodiphenylmethane esterification rate coefficients were also measured for a series of 2-substituted fluorene-9-carboxylic acids. The latter results have been correlated by Hammett equations and the transmission of polar effects in fluorene is discussed. Polar and steric substituent constants are evaluated for the arylaliphatic systems. These values are used to successfully correlate the hydrolysis and ionization reactions using the Taft–Ingold equation.

Canadian Journal of Chemistry, 47, 2775 (1969)

Introduction

An analysis of the activity of a series of antagonists of acetylcholine and histamine (2) required measurements of the polar and steric effects in the relevant arylaliphatic carboxylic acids. Taft (3) has described a separation of polar and steric effects in the arylaliphatic and aliphatic system using the polar and steric substituent constants, σ^* or σ_I, (4–6) and E_s respectively. Taft instituted the equations [1], [2], and [3] to correlate reactions controlled by polar, steric, or both effects, respectively.

$$[1] \qquad \log (k/k_0) = \rho^*\sigma^* \text{ (or } \rho_I\sigma_I)$$

$$[2] \qquad \log (k/k_0) = \delta E_s$$

$$[3] \qquad \log (k/k_0) = \rho^*\sigma^* \text{ (or } \rho_I\sigma_I) + \delta E_s$$

The relation [3], involving both polar and steric terms, has been called the Taft–Ingold equation (3). Several studies have used these relations successfully to correlate and separate the reactivity of arylaliphatic and aliphatic systems.

The Hammett equation [4] has been used extensively to correlate the reactions of meta- and para-substituents in benzene and similar systems (7). The transmission of polar effects

$$[4] \qquad \log (k/k_0) = \rho\sigma$$

has been investigated by a comparison of the reaction constants of a number of systems undergoing a common reaction (8). Jaffé (9) has adapted the Hammett equation to correlate reactivity in systems where the substituent can be considered formally as having both meta and para orientation with regard to the reaction site. This relation [5] correlates the transmission through the two links X and Y to a reactive site Z (**1**), where σ_X and σ_Y are the appropriate

$$[5] \qquad \log (k/k_0) = \rho_X\sigma_X + \rho_Y\sigma_Y$$

Hammett σ values. Thus, ρ_X and ρ_Y describe the transmission by the links X and Y. A 2-sub-

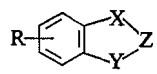

1

stituent in fluorene (**2**, R) can be regarded as being a meta-substituent (direct) and a para-substituent (through the interannular link), with regard to a reactive site at the 9-position (**2**, X).

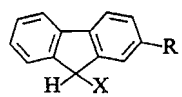

2

In the present study, the polar and steric substituent constants of a number of arylaliphatic groups have been estimated. These have been used to analyze and separate the factors controlling reactivity in other reactions. The transmission of polar effects in fluorene has been examined.

[1]For part X, see reference 1.

Can. J. Chem. Downloaded from www.nrcresearchpress.com by 210.87.254.105 on 09/05/12
For personal use only.

TABLE I

Rate coefficients for reactions and pK_a values of the arylaliphatic carboxylic acids and their esters*

		Esterification of the acids with DDM in ethanol at 30° (k)	pK_a values of the acids in 80% MCS at 25°	Acid-catalyzed esterification of the acids in methanol at 60° (k)	Alkaline hydrolysis of the 2-diethylaminoethyl esters in 70% v/v dioxan–water at 45° (k)
1	Phenylacetic	1.09	6.69	9.43†	8.55‡
2	Diphenylacetic	1.96	6.74	0.774	2.13
3	Triphenylacetic	2.52	6.78	0.000459†	—
4	2,2-Diphenylpropionic	1.37	7.08	0.00627†	0.0265
5	2,2-Diphenylpent-4-enoic	1.59	7.06	0.00103	0.00441
6	Xanthene-10-carboxylic	3.46	6.22	1.12	8.03
7	Thioxanthene-10-carboxylic	2.51	6.60	0.395	2.49
8	9,10-Dihydro-9-anthroic	2.23	6.61	1.13†	2.49
9	Fluorene-9-carboxylic	2.11	6.40	1.77†	—
10	9-Methylfluorene-9-carboxylic	1.42	6.86	0.412†	0.719
11	9-Ethylfluorene-9-carboxylic	1.27	6.97	0.236†	0.321
12	9-Isopropylfluorene-9-carboxylic	1.19	7.08	0.0110†	0.00822
13	9-*n*-Butylfluorene-9-carboxylic	1.35	7.03	0.180	0.214
14	9-*t*-Butylfluorene-9-carboxylic	0.955	7.52	0.00168†	0.00202
15	9-Phenylfluorene-9-carboxylic	3.28	6.56	0.0183†	—
16	9-Benzylfluorene-9-carboxylic	2.18	6.77	0.153	0.631
17	9-Hydroxyfluorene-9-carboxylic	8.32	5.33	2.80	71.3‡
18	2-Bromofluorene-9-carboxylic	3.34	6.08	—	—
19	2-Chlorofluorene-9-carboxylic	3.35	6.12	—	—
20	2-Hydroxyfluorene-9-carboxylic	2.25	6.42	—	—
21	2-Methoxyfluorene-9-carboxylic	2.59	6.37	—	—
22	2-Nitrofluorene-9-carboxylic	5.81	5.60	—	—
23	2-Aminofluorene-9-carboxylic	1.90	6.52	—	—

*Values of k (l mole^{-1} min^{-1}) are accurate to less than ±3% (DDM esterification and alkaline hydrolysis) and ±4% (acid-catalyzed esterification), and of pK_a to ±0.03 unit. Previous workers (6, 10, 11) have found k (DDM esterification) and pK_a for phenylacetic (1.19, 1.08; 6.75, 6.73), diphenylacetic (1.90; 6.76), and triphenylacetic acids (2.56; 6.91), and k (acid-catalyzed esterification) for diphenylacetic acid (0.825).

†Lit. values (11).

‡Values found by extrapolation from those obtained at 0° and 10°, i.e. 1.80, 4.50 (ester 17) and 0.739, 1.36 (ester 1) respectively.

Can. J. Chem. Downloaded from www.nrcresearchpress.com by 210.87.254.105 on 09/05/12
For personal use only.

Results and Discussion

The rate coefficients for the reaction with diazodiphenylmethane (DDM) in ethanol at 30° and the acid-catalyzed esterification with methanol at 60°, and the pK_a values in 80% w/w 2-methoxyethanol–water (80% MCS) at 25° of a series of arylaliphatic carboxylic acids are shown in Table I. The rate coefficients for the alkaline hydrolysis of the 2-diethylaminoethyl esters in 70% v/v dioxan–water at 45° (where measurements could be made) are also shown in this Table.

Effect of 2-Substituents in Fluorene

In 2-substituted fluorene-9-carboxylic acids (Table I, acids 9, 18–23), the 2-substituent, relative to the reaction site, may be regarded as analogous to a meta-substituent in benzene (12). Using meta- σ values (13), good Hammett correlations are obtained for both the ionization and DDM reaction, as shown in Table II. However, the position of the substituent relative to the interannular link is analogous to the para-position in benzene. The extent of transmission by the latter route can be estimated by applying the Jaffé-adapted Hammett equation [5]. Somewhat better correlations are observed as shown in Table II. The much smaller contribution (11–23% of the total) for transmission "via the link" indicates the mainly meta-character of the 2-substituent effect in accord with the findings of earlier workers (12).

It is of interest to calculate the reaction constant ratio, ρ/ρ_0, (8), for the 2-substituted fluorene-9-carboxylic acid compared to the meta- and para-substituted benzoic acid system. This ratio is 0.68 (DDM esterification) and 0.71 (ionization in 80% MCS). The corresponding values for the phenylacetic acid system are 0.43 and 0.56 (in water) respectively (8). The increased transmission in the fluorene-9-carboxylic compared to the phenylacetic acid system could be due to either the extra route through the interannular link or the increased low dielectric cavity of fluorene transmitting the field effect.

Esterification of the Arylaliphatic Carboxylic Acids with Diazodiphenylmethane

The rate coefficients for the esterification of the arylaliphatic carboxylic acids with diazodiphenylmethane in ethanol at 30° are shown in Table I (acids 1–17).

Previous studies (11, 6) have demonstrated the absence of any significant primary steric effects on the rates of this reaction. The Taft equation [1] has been used to correlate the rate coefficients for this reaction of monosubstituted acetic acids with σ_I values very successfully. In this study, this relation [6] (6) has been used to calculate the σ_I values of the

$$[6] \qquad \log k = 2.441\,\sigma_I - 0.227$$

substituents which are shown in Table III. The additivity of similar substitutions has been discussed before (11). Noteworthy points from the present study are that the σ_I value of the 9-xanthene is significantly greater than

TABLE II

Reaction constants*

Reaction	Reaction constant	log k_0	n	r	s
DDM esterification of acids, 2-substituents					
(σ_m)	0.644(ρ)	0.495	7	0.984	0.033
(σ_m,σ_p)	0.532(ρ_X),0.068(ρ_Y)	0.524	7	0.999	0.002
Ionization of acids, 2-substituents					
(σ_m)	1.214(ρ)	−6.519	7	0.978	0.073
(σ_m,σ_p)	0.814(ρ_X),0.243(ρ_Y)	−6.418	7	1.000	0.002
Alkaline hydrolyses of 2-diethylaminoethyl esters					
(σ_I,E_s)	4.390(ρ_I),0.914(δ)	0.749	14	0.999	0.031
Ionization of acids					
(σ_I,E_s)	4.022(ρ_I),0.131(δ)	−7.263	17	1.000	0.015

*n, number of substituents; r, correlation coefficient; s, standard deviation.

TABLE III
Substituent constants

	R*	σ_I	E_s
1	$PhCH_2$	0.11_5†	−0.37†
2	Ph_2CH	0.19†	−1.46
3	Ph_3C	0.25†	−4.68†
4	Ph_2CMe	0.15	−3.55†
5	$Ph_2CCH_2CH{=}CH_2$	0.17_5	−4.33
6	XaCH	0.31_5	−1.29
7	TxCH	0.25_5	−1.75
8	AnCH	0.23_5	−1.29†
9	FlCH	0.22_5	−1.10†
10	FlCMe	0.15_5	−1.73†
11	$FlCCH_2Me$	0.13_5	−1.97†
12	$FlCCHMe_2$	0.12_5	−3.30†
13	$FlC(CH_2)_3Me$	0.14_5	−2.09
14	$FlCCMe_3$	0.08_5	−4.12†
15	FlCPh	0.30_5	−3.08†
16	$FlCCH_2Ph$	0.23	−2.16
17	FlCOH	0.47	−0.90

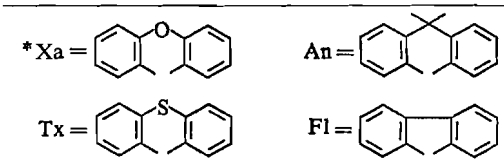

†Lit. values (6, 11).

the 9-thioxanthene system and that both are more electron-withdrawing than the systems (Table III; substituents 2, 8, 9) not having a heteroatom substituent. The first point is possibly due to the planar xanthene having a more favorable disposition of the dipolar substituent with regard to the reaction site. Substituents such as the *para*-MeO and -MeS are normally electron-releasing (13). The effect of insulating the reaction site, as in fluorene, and the symmetrical *ortho*-type substitution of the heteroatom probably easily outweighs any second-order resonance effects.

Acid-catalyzed Esterification of the Arylaliphatic Carboxylic Acids in Methanol

The rate coefficients for the acid-catalyzed esterification of the arylaliphatic carboxylic acids in methanol at 60° are shown in Table I. Steric substituent constants, E can be calculated from these rate coefficients and that for acetic acid (3, 11), as shown below [7], where log k_0 equals 1.34 (11). These steric parameters are shown in Table III and follow closely the pattern of those found previously (11). The small value found for 9-hydroxyfluorene-9-carboxylic acid (−0.90) appears to be due to hydrogen-bonded stabilization or "solvation" of the transition state. This E_s value will probably be applicable to reactions, such as alkaline hydrolysis and ionization, where similar interactions favor the reaction.

$$[7] \qquad E_s = \log (k/k_0)_A$$

Alkaline Hydrolysis of the 2-Diethylaminoethyl Esters of the Arylaliphatic Carboxylic Acids

The rate coefficients for the alkaline hydrolysis of the esters in 70% v/v dioxan–water at 45° are shown in Table I. A correlation of the results with polar and steric substituent constants using the Taft–Ingold equation [3] is very successful as shown in Table II. The polar and steric reaction constants, ρ_I and δ equal to 4.39 and 0.91 respectively, compare closely to those found previously for similar reactions (3, 14, 15). The 2-diethylaminoethyl esters studied here are hydrolyzed more rapidly than their methyl counterparts (14). All the esters in this report can be studied under similar conditions and near to ambient temperature. Only small extrapolations are necessary to obtain rate coefficients at a common temperature. An earlier investigation (14) of a more limited series of methyl esters gave a less well-defined and less general correlation. The present study confirms the Taft separation (3) of polar and steric effects in the alkaline hydrolysis reactions of arylaliphatic carboxylic esters.

Ionization of the Arylaliphatic Carboxylic Acids

The pK_a values of the arylaliphatic carboxylic acids in 80% MCS at 25° are shown in Table I. Our previous study (6) has demonstrated a good correlation of the pK_a values of a series of mono-substituted acetic acids in 80% MCS with σ_I values. A number of workers (16, 14) have shown that bulky groups inhibit the solvation of the carboxylate anions of aliphatic and arylaliphatic carboxylic acids. This causes acid weakening. An earlier investigation (14) indicated that the Taft–Ingold equation [3] could be used to correlate such systems. The more extensive results presented here are correlated excellently by this relation as is shown in Table II. The polar reaction constant, ρ_I equal to 4.02, compares closely with that for the mono-substituted acetic acids where ρ_I equals 4.04 (6). This confirms the meaningful nature of the correlation. The small size of the steric reaction constant, δ equal to 0.13, indicates the small role of steric effects unless the bulk of the substituent is very large.

Can. J. Chem. Downloaded from www.nrcresearchpress.com by 210.87.254.105 on 09/05/12
For personal use only.

Can. J. Chem. Downloaded from www.nrcresearchpress.com by 210.87.254.105 on 09/05/12
For personal use only.

The dominance of polar effects in this reaction is shown by the large ratio of the reaction constants, δ/ρ equal to 0.03, compared to that for the alkaline hydrolysis where δ/ρ equals 0.21.

Experimental

Materials

The acids were commercial samples or were prepared by standard methods. They were purified in order to give physical constants in good agreement with literature values. Neutralization equivalents were determined and were within 2% of the theoretical values, with the exception of 9-phenylfluorene-9-carboxylic acid (see Measurements). The 2-diethylaminoethyl esters of these acids were prepared as their hydrochlorides by reaction of either the acid chloride with 2-diethylaminoethanol or the acid with 2-diethylaminoethyl chloride (2).

Diazodiphenylmethane the solvents and reagents were prepared, purified, and stored as stated previously (6, 17).

Measurements

Rate Coefficients for Diazodiphenylmethane Esterification

These were determined, at 30° (±0.1°), as described previously (6), using a 10-fold excess acid concentration (0.06 *M*). 2-Aminofluorene-9-carboxylic acid was sparingly soluble in ethanol and was studied at equal acid and DDM concentrations (0.006 *M*).

pK_a Values

The pK_a values were determined, at 25° (±0.1°), as described previously (6). 9-Phenylfluorene-9-carboxylic acid was found to decarboxylate on neutralization and could not be measured in the usual manner. Therefore, pH readings were taken in rapid succession in the region of half-neutralization and the pK_a value estimated from the calculated half-neutralization point. This value is thus much more uncertain (±0.07). 9-*t*-Butylfluorene-9-carboxylic acid behaves similarly but at a much higher temperature. These two factors probably caused significant errors in a previous study (14).

Rate Coefficients for Acid-catalyzed Esterification

These were determined, at 60° (±0.1°), by a minor modification of the method described previously (17). The titrimetric apparatus used for the pK_a determinations (6) was used to titrate 1 ml samples of the reaction solution.

Rate Coefficients for Alkaline Hydrolysis of the Esters

These were determined, at 45° (±0.1°), by a titrimetric method using the apparatus described previously (6). The ester hydrochloride (0.02 *M*) was mixed thoroughly with "carbonate-free" sodium hydroxide (0.04 *M*) in 70% v/v dioxan–water at the reaction temperature. Immediately, a 1 ml sample of the reaction solution was withdrawn and placed in the titration vessel at 20°. Timing was commenced at half-addition of the latter and titrated immediately and swiftly with aqueous hydrochloric acid (0.05 *M*) from the micrometer syringe to an end point characterized by a sharp decrease in pH at approximately pH 11.6. Further samples were withdrawn at timed intervals and titrated immediately. This technique required an interval between measurements of approximately 4 min. It was necessary to make measurements at lower temperatures for the two most reactive esters and, also, to thermostat the titration vessel at these temperatures. The rate coefficients can be calculated in the manner previously described (17).

It was found impossible to measure satisfactorily the rates of alkaline hydrolysis of the esters of fluorene-9-carboxylic acids having an unsubstituted 9-position. A competing process produces the corresponding carbanion.

Acknowledgment

One of us (R. C. Y.) is indebted to the Medical Research Council for a Research Scholarship.

1. K. Bowden and D. C. Parkin. Can. J. Chem. **47**, 185 (1969).
2. K. Bowden and R. C. Young. Unpublished results. Partly communicated at the Medicinal Chemistry Symposium, April 1969, Chelsea, England.
3. R. W. Taft. *In* Steric effects in organic chemistry. *Edited by* M. S. Newman. John Wiley and Sons, Inc., New York. 1956. Chap. 13.
4. R. W. Taft and I. C. Lewis. J. Am. Chem. Soc. **80**, 2436 (1958); **81**, 5343 (1959).
5. M. Charton. J. Org. Chem. **29**, 1222 (1964).
6. K. Bowden, M. Hardy, and D. C. Parkin. Can. J. Chem. **46**, 2929 (1968).
7. H. H. Jaffé. Chem. Rev. **53**, 191 (1953).
8. K. Bowden. Can. J. Chem. **41**, 2781 (1963).
9. H. H. Jaffé. J. Am. Chem. Soc. **76**, 4261 (1954).
10. K. Bowden, N. B. Chapman, and J. Shorter. Can. J. Chem. **42**, 1979 (1964).
11. K. Bowden, N. B. Chapman, and J. Shorter. J. Chem. Soc. 5239 (1963).
12. J. D. Dickenson and C. Eaborn. J. Chem. Soc. 3574, 3641 (1959); C. Eaborn, R. C. Golesworthy, and M. N. Lilly. J. Chem. Soc. 3052 (1961); K. D. Warren. J. Chem. Soc. 598 (1963). K. Bowden, A. F. Cockerill, and J. R. Gilbert. Unpublished studies.
13. D. H. McDaniel and H. C. Brown. J. Org. Chem. **23**, 420 (1958); G. B. Barlin and D. D. Perrin. Quart. Rev. (London), **20**, 75 (1966).
14. K. Bowden, N. B. Chapman, and J. Shorter. J. Chem. Soc. 3370 (1964).
15. K. Bowden and M. Hardy. Tetrahedron, **22**, 1169 (1966).
16. J. F. J. Dippy, S. R. C. Hughes and A. Rozanski. J. Chem. Soc. 1441 (1959); G. S. Hammond and D. H. Hogle. J. Am. Chem. Soc. **77**, 338 (1955); M. L. Kilpatrick and E. Fackenthal. J. Electrochem. Soc. **100**, 185 (1953).
17. K. Bowden. Can. J. Chem. **44**, 661 (1966).

Can. J. Chem. Downloaded from www.nrcresearchpress.com by 210.87.254.5 on 09/05/12
For personal use only.

Photochemical behavior of some α,β-unsaturated lactams. Dependence of reaction path on multiplicity

E. CAVALIERI[1] AND S. HOROUPIAN

Department of Chemistry, University of Montreal, Montreal, Quebec

Received November 15, 1968

Whereas direct irradiation (2537 Å) of 5,6-dihydro-4,6,6-trimethyl-2(1*H*)-pyridone **1** (1*a*) produced almost exclusively the cleavage products **2** and **3**, the acetophenone sensitized reaction (3500 Å) gave a single cyclobutane dimer. In contrast, direct (2537 Å) or sensitized (acetophenone, 3500 Å) irradiation of the *homo* derivative **7** of compound **1** gave approximately the same mixture of two cyclobutane dimers. It was thus demonstrated that dimer formation proceeded by way of a triplet excited state and that the cleavage reaction most probably occurred *via* an excited singlet state.

A structure for each cyclobutane dimer in the seven-membered series was proposed on the basis of its spectral properties.

Canadian Journal of Chemistry, 47, 2781 (1969)

Introduction

We have recently shown (1*a*) that irradiation (2537 Å) in water of 5,6-dihydro-4,6,6-trimethyl-2(1*H*)-pyridone **1** produced the amides **2** and **3** together with a small amount of the photohydrate **4**.

The mechanism of this photochemical reaction was demonstrated to occur as depicted below (1*b*):

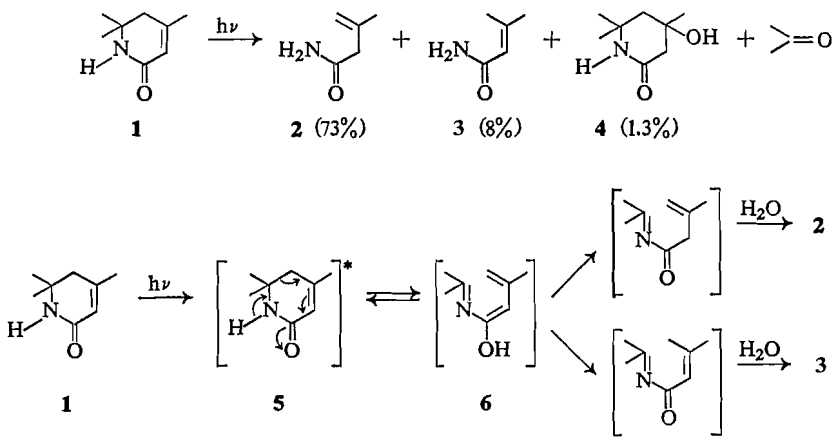

The proposed intermediate **6** was not isolable under the reaction conditions as it was rapidly hydrolyzed to compounds **2** and **3** and acetone. On the other hand, compound **4** was very probably derived from the addition of water to the electronically excited intermediate **5** or a strained ground-state molecule directly derived from it (2). When this photochemical reaction was carried out in dry *t*-butyl alcohol the cleavage reaction occurred very slowly (1*a*, 1*b*). Moreover, no traces of dimer were recovered. Based on the above mechanism it was anticipated that the *homo* derivative **7** would probably not undergo a

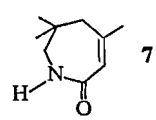

7

photochemical cleavage reaction analogous to that observed for the δ-lactam **1**. Indeed, one might have expected a dimerization of the type observed for carbostyril (3), isophorone (4), and many other α,β-unsaturated carbonyl compounds, or cyclization to a bicyclic β-lactam in a

[1]Present address: University of California, Chemical Biodynamics Laboratory, Lawrence Radiation Laboratory, Berkeley, California 94720.

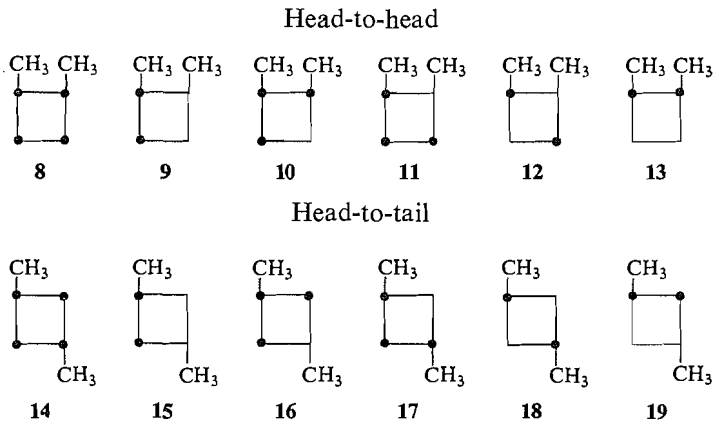

FIG. 1. Possible isomeric forms of dimers.

process similar to that demonstrated to occur on irradiation of certain acrylamides (5).

Results

Unsensitized Irradiation

Irradiation of a dilute (8.7×10^{-2} *M*) aqueous solution of the ε-lactam **7** at 2537 Å for 15 h resulted in the precipitation of an insoluble solid in 82.5% yield which could be separated into two components by virtue of their different solubility in dichloromethane.

The major, soluble product (96%) had m.p. 259–265°.[2] The molecular weight, parent peak at *m/e* 306 in the mass spectrum, and the combustion analysis established the dimeric nature of this compound. The infrared spectrum possessed absorptions at 3450 and 1665 cm^{-1} attributable respectively to the NH and carbonyl vibrations of a lactam.

The nuclear magnetic resonance (n.m.r.) spectrum in deuteriochloroform showed the methyl hydrogens as a complex multiplet centered at δ 1.25, the methylene protons as a series of multiplets absorbing between δ 2.15 and 3.80, the cyclobutane hydrogens as singlets at δ 4.89 and 5.00 ($\Delta\nu$ = 7.0 c.p.s.), and the two NH protons as a broad multiplet centered at δ 6.05. When the solvent was changed to trifluoroacetic acid, the spectrum was largely similar except that the absorptions were shifted by about 0.2 p.p.m. to lower field, the NH protons occurred as two broad singlets at δ 7.4 and 8.0 and the singlets assigned to the cyclobutane protons were now separated by 12.8 c.p.s. At 100 Mc.p.s. in deuteriochloroform the line spacing between the two singlets was 11.6 c.p.s. Furthermore, the expanded scale revealed that the peaks corresponding to each proton were split by 0.5 c.p.s.; a decoupling experiment showed this to be a weak coupling constant.

Given the non-equivalence of and the very weak coupling constant between these protons, all those dimers possessing adjacent cyclobutane hydrogens or symmetry elements can be excluded (6). Consequently only dimers **16** and **17** (see Fig. 1) are thus left for consideration. Inasmuch as *trans*-1,3-protons on a cyclobutane ring are known to be weakly coupled (J = 0.5 c.p.s.) (7), the dimer possessing *cis*-1,3-hydrogens **16** is disregarded over the alternative *trans* formulation **17**.

The minor, dichloromethane insoluble, material, m.p. 346–347° (homogeneous on t.l.c.), was also shown to be dimeric. Its infrared spectrum (Nujol mull) had absorption bands at 3320, 1645, and 1625 cm^{-1} ascribable to the NH and carbonyl moieties respectively of a lactam. The n.m.r. spectrum in trifluoroacetic acid showed the methyl hydrogens as a complicated multiplet centered at δ 1.38, the methylene protons as a series of multiplets between δ 2.40 and 4.00, the cyclobutane protons as two singlets at δ 5.10 and 5.18 ($\Delta\nu$ = 5.2 c.p.s.)[3] and

[2]The melting point remained unchanged after repeated recrystallization. The compound was shown to be homogeneous by thin-layer chromatography (t.l.c.) in alumina using two different solvent systems.

[3]At 100 Mc.p.s., in trifluoroacetic acid, the spacing was 8.4 c.p.s. and the expansion trace showed again the two protons as singlets.

Can. J. Chem. Downloaded from www.nrcresearchpress.com by 210.87.254.5 on 09/05/12
For personal use only.

Can. J. Chem. Downloaded from www.nrcresearchpress.com by 210.87.254.5 on 09/05/12
For personal use only.

the NH protons as two broad absorptions centered at δ 8.40 and 9.28. For the same principle applied above, all those dimer possessing adjacent, cyclobutane hydrogens or symmetry elements can be excluded. Furthermore, considering the lack of a weak coupling constant (7), it follows that only **16** (Fig. 1) remains as a possible structure.

Sensitized Irradiations

The acetophenone (E_T 73.5 Kcal/mole) sensitized photolysis of the ε-lactam (E_T 69 Kcal/mole, see Experimental) in water produced the same two dimers in approximately the same proportion as was obtained in the unsensitized experiment. Whereas in this series, both the sensitized and unsensitized photolysis provided the same products (dimers), in the six-membered series (δ-lactam **1**, E_T 68 Kcal/mole, see Experimental) only the sensitized irradiation (3500 Å, acetophenone sensitizer) provided dimeric material (for the products of the unsensitized photolysis, see Introduction). The rate of sensitized disappearance of the ε-lactam was about ten times greater than that observed for the corresponding δ-lactam (Fig. 2). In the latter case a single dimer, m.p. 343–345°, was isolated in 48% yield.[4] Its infrared spectrum had absorptions at 3380 and 1640 cm^{-1} for the NH and carbonyl vibrations of a lactam. The n.m.r. spectrum showed the *geminal* methyl groups as two closely spaced singlets at δ 1.22 and 1.25, the remaining methyl groups as a singlet at δ 1.57, the methylene protons as a singlet at δ 1.74, the cyclobutane hydrogens as a sharp singlet (even at high resolution) at δ 2.44, and the NH protons at δ 6.23.

If one excludes those dimers with structures **12**, **13**, **18**, and **19** on the basis of strain and **10**, **11**, **16**, and **17** on symmetry principles then the two head-to-head dimers **8** and **9**, and the two head-to-tail dimers **14** and **15** are equally compatible with a singlet absorption for cyclobutane hydrogens (6).

Discussion

Since the sensitized and unsensitized[5] photolysis of the ε-lactam gave the same two dimers in about the same proportion, their formation might have occurred *via* the triplet state. A valid support to this assertion was provided by the lack of fluorescence of the ε-lactam (in the same way as the δ-lactam) at room temperature in absolute ethanol. The non-emitting singlet excited state means that the rate of decay of this state must be higher than 5×10^{10} s^{-1}. Having observed dimerization of the ε-lactam even in very dilute solutions, i.e. 10^{-3} *M*, and considering this reaction to be diffusion-controlled ($K_{dim} \leq 5 \times 10^9$ M^{-1} s^{-1}), it then follows that the maximum quantum yield for dimer formation from the singlet state would be 10^{-4}. In other words, the very short lifetime of the excited singlet makes it an unlikely precursor for the dimer at room temperature because of the longer times required for the monomers to diffuse together. Besides, the relatively high rate of disappearance of this lactam in the unsensitized reaction (see Fig. 3) indicates that singlet–triplet intersystem crossing is probably quite efficient.

On the other hand, the complete lack of dimer formation during direct irradiation of δ-lactam in water and especially in *t*-butyl alcohol (see Introduction) suggested that singlet–triplet intersystem crossing was inefficient as compared to the cleavage reaction observed from the singlet state (see below). The fact that δ-lactam phosphoresced in ethanol at low temperature conflicted

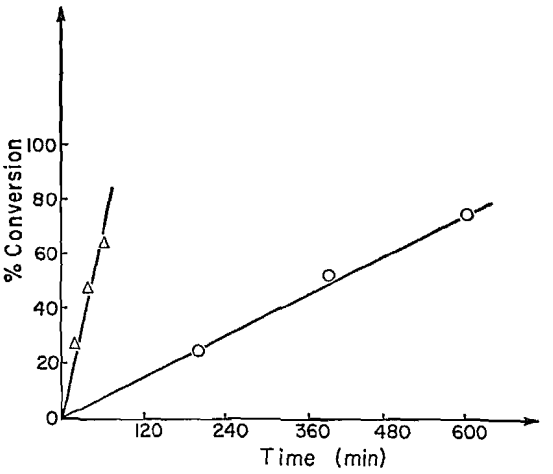

FIG. 2. Rate of acetophenone (2×10^{-2} *M*) sensitized disappearance in water – *t*-butanol 9: 1 at 3500 Å for the ε-lactam **7** (2×10^{-2} *M*, Δ) and δ-lactam **1** (2×10^{-2} *M*, O).

[4]The absence of photoamides **2** and **3** (see Introduction) in the crude product was clearly shown by thin-layer chromatography, and infrared and nuclear magnetic resonance spectroscopy.

[5]The same unsensitized irradiation of the ε-lactam in *t*-butyl alcohol produced dimers at about the same rate as in water.

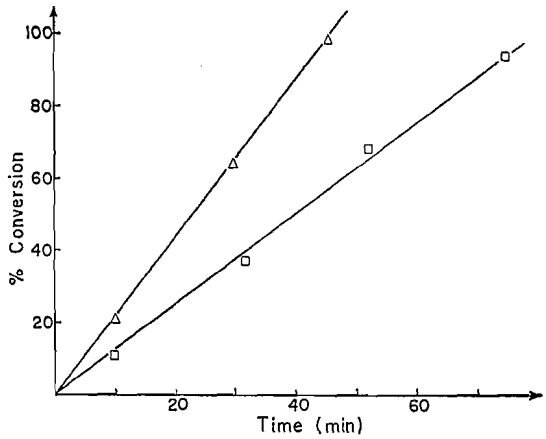

FIG. 3. Rate of disappearance of (2×10^{-2} *M*) lactams **1** (□) and **7** (△) in water.

with this explanation. We therefore think that the cleavage of the C—C bond provides a pathway for radiationless loss of singlet excitation energy which competes successfully with intersystem crossing. At 77 °K in frozen solvent the breaking of the C—C bond might be somehow prevented and the intersystem crossing then becomes a competitive process giving rise to phosphorescence (8). Inasmuch as the sensitized irradiation of the δ-lactam gave exclusively dimer formation, one can conclude that this reaction must proceed through a triplet state. The ring cleavage reaction which occurred upon direct photolysis, therefore must probably involve an excited singlet state.

As previously stated, the spectroscopic properties of the dimers were sufficient to establish the precise stereochemistry in the seven-membered series only. It was indeed found that the two cyclobutane dimers were formed by head-to-tail combination and that both possessed a *cis* (between the seven- and four-membered rings) and a *trans* (between the seven- and four-membered rings) junctions (see **16** and **17**, Fig. 1).[6] A knowledge of the stereochemistry of the dimer in the six-membered series is equally important because it may provide information concerning the nature of triplet state(s) which led to their formation (4). A chemical proof of the structure of the dimers in both series is therefore now in progress.

[6]Other products with *trans*-fused four- and six-membered rings have already been observed in photocycloaddition reactions (9, 10).

Experimental

The ultraviolet spectra were recorded in water using a Cary model 14 recording spectrophotometer.

The fluorescence and phosphorescence spectra were scanned in absolute ethanol at room temperature and at 77 °K respectively using an Aminco–Bowman spectrophotofluorometer (the solvent was distilled twice with a fractionating column and the lactams were sublimated after repeated recrystallizations).

The nuclear magnetic resonance (n.m.r.) spectra were determined on Varian A60 and HR-100 spectrometers using deuteriochloroform (unless otherwise specified) with tetramethylsilane as the internal standard.

The infrared spectra were recorded in chloroform (unless otherwise specified) on a Perkin–Elmer 621 and a Beckman IR-8 spectrophotometer.

The mass spectra were recorded on a Hitachi – Perkin – Elmer RMμ-D mass spectrometer.

The melting points were taken on a Büchi *Schmelzpunktbestimmungapparat* and are uncorrected.

The photolyses were carried out using a Rayonnet photochemical reactor. Prior to irradiation the solutions were flushed with oxygen-free nitrogen for at least 10 min.

The analyses were performed by Dr. C. Daesslé, Organic Microanalyses, Montreal.

5,6-Dihydro-4,6,6-trimethyl-2(1H)-pyridone **1**

This compound was prepared according to the method of Hall (11) and after purification in the manner to be described (sublimation) by Cavalieri and Gravel (1*b*) it had m.p. 118° (reported (11) m.p. 116.5–118°). The ultraviolet spectrum had an absorption maximum at 2128 Å (ε = 15 600) with a shoulder at 2300–2400 Å (ε = ~4300). The phosphorescence spectrum was measured in absolute ethanol at 77 °K and gave a triplet energy (0,0 band maximum) of 68 Kcal/mole.

6,7-Dihydro-4,6,6-trimethyl-2(1,5-H)-azepinone **7**

This lactam was prepared in the manner described by Mazur (12). After three recrystallizations from hexane–acetone and sublimation *in vacuo* at 95°/0.05 mm it had m.p. 109–110° (reported (12), m.p. 112–113°, and (13) m.p. 108.8–109.1°). The infrared spectrum had absorptions at 3440, 1657, and 1616 cm^{-1}. The n.m.r. spectrum showed peaks at δ 0.97 (6H, singlet), 1.92 (3H, doublet, J = 1.2 c.p.s.), 2.04 (2H, singlet), 2.82 and 2.92 (2H, singlets), and 5.74 (1H, quadruplet, J = 1.2 c.p.s.).

The ultraviolet spectrum had a maximum at 2203 Å (ε = 13 000), with no observable shoulder.

The phosphorescence spectrum in absolute ethanol at 77 °K gave a triplet energy (0,0 band maximum) of 69 Kcal/mole.

Irradiation of ε*-Lactam* **7**

(a) Unsensitized

A solution of lactam **7** (4 g) in 300 ml of distilled water was irradiated at 2537 Å for 15 h. A white precipitate of dimeric material separated from the solution during the photolysis. After filtration and drying the residue

Can. J. Chem. Downloaded from www.nrcresearchpress.com by 210.87.254.5 on 09/05/12
For personal use only.

Can. J. Chem. Downloaded from www.nrcresearchpress.com by 210.87.254.5 on 09/05/12
For personal use only.

weighed 3.33 g (82.5%) and had m.p. 256–261°. A small amount (180 mg, 5.5%) of this solid was not soluble in dichloromethane. The soluble portion was obtained on evaporation of the solution *in vacuo*. After two recrystallizations from methanol–water a white solid with m.p. 259–265° was obtained.

Anal. Calcd. for $C_{18}H_{30}N_2O_2$: C, 70.58; H, 9.87; N, 9.14. Found: C, 70.79; H, 9.87; N, 8.90.

The mass spectrum showed the parent peak at *m/e* 306. The infrared spectrum had bands at 3450 and 1665 cm^{-1}. The n.m.r. spectrum possessed absorptions at δ 0.80–1.50 (18 H, methyl hydrogens), 2.15–3.80 (8 H, methylene hydrogens), 4.83 and 5.00 (2H, singlets $\Delta\delta$ = 7.0 c.p.s. methyne hydrogens) and 6.05 p.p.m. (2H, NH, broad multiplet).

The dichloromethane insoluble solid was washed with methanol; it then had m.p. 346–347° (decomp.) and was shown to be homogeneous by thin-layer chromatography, infrared and nuclear magnetic resonance spectroscopy.

Anal. Calcd. for $C_{18}H_{30}N_2O_2$: C, 70.58; H, 9.87; N, 9.14. Found: C, 70.61; H, 10.03; N, 8.94.

The mass spectrum gave the parent peak at *m/e* 306. The infrared spectrum (Nujol mull) showed bands at 3320, 1645, and 1625 cm^{-1}. The n.m.r. spectrum (CF_3COOH) had absorptions at δ 0.97–1.82 (18H, methyl hydrogens), 2.40–4.00 (8 H, methylene hydrogens), 5.10 and 5.18 (2 H, singlet, $\Delta\nu$ = 5.2 c.p.s., methyne hydrogens), 8.40 and 9.28 (2 H, NH broad bands).

(b) Sensitized

A 6.54 × 10^{-2} *M* solution (100 ml: 90 ml of distilled water and 10 ml of distilled *t*-butanol) of the ε-lactam which was 2 × 10^{-2} *M* in acetophenone was irradiated at 3500 Å for 4.33 h.

The precipitated dimeric solid was separated by filtration and after drying it weighed 566 mg. The product was separated into dichloromethane insoluble and soluble fractions as before. The insoluble portion after washing with methanol and drying weighed 30 mg and had m.p. 346–347° (decomp.). The infrared and n.m.r. spectra were identical to that of the minor dimer produced in the unsensitized photolysis.

The dichloromethane soluble fraction after usual work-up gave a solid (536 mg) which had m.p. 259–264°. The infrared and n.m.r. spectra were indistinguishable from that of the major dimer obtained in direct photolysis experiment.

Irradiation of the ε-lactam at 3500 Å in the absence of acetophenone but under otherwise identical conditions resulted in the complete recovery of starting material.

Photosensitized Dimerization of δ-Lactam ***1***

A solution of the δ-lactam **1** (2 g, 1.44 × 10^{-2} moles) in 180 ml of distilled water and 20 ml of distilled *t*-butanol which was 1 × 10^{-2} *M* in acetophenone were irradiated at 3500 Å for 27 h. The *t*-butanol was removed *in vacuo* and the residue was extracted with ether to remove the acetophenone. The aqueous phase was saturated with ammonium sulfate and the product was then extracted into chloroform. The extract was dried over sodium sulfate and on evaporation *in vacuo* 1.725 g of crude product remained.

On recrystallization from dichloromethane ether 0.960 g (48%) of the pure dimer, m.p. 343–345° (decomp.) was obtained.

Anal. Calcd. for $C_{16}H_{26}N_2O_2$: C, 69.02; H, 9.41; N, 10.06. Found: C, 69.09; H, 9.29; N, 10.21.

The infrared spectrum had bands at 3380 and 1640 cm^{-1}. The n.m.r. spectrum had absorptions at δ 1.22 and 1.25 (12 H, 2 singlets, *geminal* methyl protons), 1.57 (6 H, singlet, methyl protons), 1.74 (4 H, methylene protons), 2.44 (2 H, singlets, methyne protons on cyclobutane ring), and 6.23 p.p.m. (NH, relatively sharp).

Measurement of the Rate of Photochemical Disappearance of Lactams ***1*** *and* ***7***

Solutions (2 × 10^{-2} *M*) of the lactams **1** and **7** in distilled water were irradiated in two separate quartz vessels at 2537 Å at near 30°. Aliquots were removed periodically, saturated with ammonium sulfate, extracted with chloroform, and dried over sodium sulfate. The extracts were evaporated *in vacuo* and the residue was dissolved in a standard amount of chloroform and the optical density of the infrared double band absorption (1623 cm^{-1} for **1** and 1616 cm^{-1} for **7**) was determined. The data thus obtained are recorded graphically in Fig. 3.

Measurement of the Rate of Acetophenone Sensitized Disappearance of Lactams ***1*** *and* ***7***

Solutions (2 × 10^{-2} *M*) of lactams ***1*** and ***7*** in distilled water and distilled *t*-butanol (9:1) were irradiated at 3500 Å in separate runs which were both 2 × 10^{-2} *M* in acetophenone. Aliquots were removed periodically and treated the same as above.

The data thus obtained are recorded graphically in Fig. 2.

Acknowledgments

Support of this research by the National Research Council of Canada is gratefully acknowledged. We wish to thank Dr. J. Muchowski for helpful discussions. Thanks are also due to Mlle A. Bossé (B.Sc. III) for valuable assistance and Mr. N. Ness for recording nuclear magnetic resonance spectra.

1. (*a*) E. CAVALIERI and D. GRAVEL. Tetrahedron Letters, 3973 (1967). (*b*) E. CAVALIERI and D. GRAVEL. To be published.
2. (*a*) B. J. RAMEY and P. D. GARDNER. J. Am. Chem. Soc. **89**, 3949 (1967). (*b*) See P. J. KROPP and H. J. KRAUS. J. Am. Chem. Soc. **89**, 5199 (1967), and references cited therein.
3. (*a*) E. C. TAYLOR and W. W. LANDLER. Tetrahedron Letters, 1 (1960). (*b*) O. BUCHARDT. Acta Chem. Scand. **17**, 1461 (1963). (*c*) I. W. ELLIOTT. J. Org. Chem. **20**, 305 (1964).
4. O. L. CHAPMAN, P. J. NELSON, R. W. KING, D. J. TRECKER, and A. A. GRISWOLD. Record Chem. Progr. **28**, 3, 167 (1967).
5. O. L. CHAPMAN and W. R. ADAMS. J. Am. Chem. Soc. **90**, 2333 (1968).
6. P. YATES, S. N. EGĚ, G. BÜCH, and D. KNUTSEN. Can. J. Chem. **45**, 2927 (1967).

7. V. GEORGIAN, L. GEORGIAN, and H. V. ROBERTSON. Tetrahedron, **19**, 1219 (1963).
8. S. MALKIN and E. FISCHER. J. Chem. Phys. **68**, 1153 (1964).
9. H. ZIFFER, N. E. SHAYLESS, and R. O. KAN. Tetrahedron, **22**, 3011 (1966).
10. E. J. COREY, J. D. BASS, R. LEMAHIEU, and R. B. MITRA. J. Am. Chem. Soc. **86**, 5570 (1964).
11. H. K. HALL, JR. J. Am. Chem. Soc. **79**, 5444 (1957).
12. R. H. MAZUR. J. Org. Chem. **26**, 1289 (1961).
13. R. S. MONTGOMERY and G. GOUGHERTY. J. Org. Chem. **17**, 82 (1952).

Can. J. Chem. Downloaded from www.nrcresearchpress.com by 210.87.254.5 on 09/05/12
For personal use only.

Can. J. Chem. Downloaded from www.nrcresearchpress.com by 210.87.254.40 on 09/05/12
For personal use only.

Synthesis of highly hindered diphenyl ethers[1]

GEORGE A. NEVILLE
Research Laboratories, Food and Drug Directorate, Department of National Health and Welfare, Ottawa, Canada

AND

ROBERT Y. MOIR
Department of Chemistry, Queen's University, Kingston, Ontario

Received February 11, 1969

A new modification of the Hems synthesis for diphenyl ethers is reported. The preparation of 11 tetra-ortho-substituted, 12 tri-ortho-substituted, and 4 di-ortho-substituted diphenyl ethers is described for the action of various phenols on *N*-(4′-carbomethoxy-2′,6′-dinitro)phenylpyridinium chloride. Some factors governing product formation are discussed on the basis of the extensive number of successful as well as unsuccessful reactions.

Canadian Journal of Chemistry, 47, 2787 (1969)

Introduction

Highly hindered diphenyl ethers form an admirable series for the study of aromatic conformations (1–3). Since most of the conformational conclusions are reached by difference or by double-difference techniques (2), the synthesis of large numbers of related ethers is required. We have reviewed the available synthetic methods (1), and now draw attention to the ethers of type **1** recently reported by Wright and Jorgensen (4) in which two very bulky groups were placed in the ortho-positions. These were made by the action of phenolates on activated aryl halides in dimethyl sulfoxide.

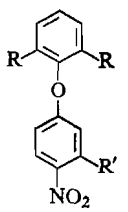

1, R = Me, *i*-Pr, *sec*-Bu, *t*-Bu, R′ = H, Me

In this paper there is described the synthesis of a large number of much more hindered diphenyl ethers by a new modification of the Hems synthesis. In former papers (5, 1, 2) we reported the synthesis of ethers such as **2**, already respectably hindered. By the new modification, it was possible to insert much larger ortho-groups to produce

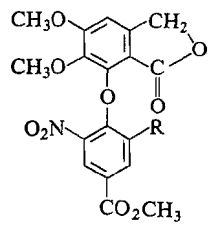

2, R = NO_2, NH_2, NHOAc

compounds of great interest for continuing investigations of the limits of the Hems synthesis, the lifetime of ether enantiomers (1), and the determination of conformation by spectroscopy (2).

Synthesis of Hindered Diphenyl Ethers

The *Hems synthesis* of diphenyl ethers is based on a reaction discovered by Borrows *et al.* (6) which has as its essential step the reaction of a phenol with an activated *N*-phenyl pyridinium salt, e.g. **3***a*. Allen and Moir (1), in discussing the superiority of this synthetic route for the preparation of quadruply ortho-substituted diphenyl ethers, cited many failures of the Ullmann reaction (7, 8) and showed that the lower requirements for activation (6, 5) in the Hems synthesis make it more promising for the preparation of such highly hindered ortho-substituted diphenyl ethers than the well-known reaction of a phenol, a base, and an activated aryl halide (9–11).

A major problem with the Hems synthesis of diphenyl ethers having large steric hindrance in the ortho-positions has occurred when the reaction mixture was poured into ice water. A tar formed from which it was very difficult to extract

[1]The material for this paper is taken from the Ph.D. Thesis of G. A. Neville, Queen's University, Kingston, Ontario, June 1966.

Can. J. Chem. Downloaded from www.nrcresearchpress.com by 210.87.254.40 on 09/05/12
For personal use only.

TABLE I

Various 4′-carbomethoxy-2′,6′-dinitro diphenyl ethers prepared by the Hems synthesis

Compound	Phenolic moiety	Solvent for recrystallization	Melting point (°C)	Yield[a] (%)	Molecular formula	Analysis (%) Found C	Found H	Found N	Calculated C	Calculated H	Calculated N
5*a*	2-Methyl-	Absolute ethanol	135.2–135.7	67	$C_{15}H_{12}N_2O_7$	54.25, 54.40	3.59, 3.74	8.60, 8.66	54.21	3.48	8.43
5*b*	2-*iso*Propyl-	Absolute ethanol	125.5–126.6	82	$C_{17}H_{16}N_2O_7$	56.46, 56.24	4.44, 4.53	8.26, 8.16	56.67	4.48	7.77
5*c*	2-*t*-Butyl-	Absolute ethanol[b]	136.8–137.5	32	$C_{18}H_{18}N_2O_7$	57.47, 57.65	5.08, 4.98	7.55, 7.37	57.75	4.85	7.48
5*d*	2-Allyl-	Absolute ethanol[b]	87.5–88.2	61	$C_{17}H_{14}N_2O_7$	58.14, 58.09	3.90, 4.12	7.72, 7.77	56.98	3.94	7.82
5*e*	2-Phenyl-	Chloroform – diethyl ether (2:1)	188.0–188.4	94	$C_{20}H_{14}N_2O_7$	60.53, 60.74	3.91, 3.79	7.12, 7.16	60.91	3.58	7.10
5*f*	2-(2′′-Hydroxyphenyl)-	Absolute ethanol	157.2–158.3[c]	96	$C_{20}H_{14}N_2O_8$	58.54, 58.42	3.60, 3.48	6.84, 6.97	58.54	3.44	6.83
5*g*	2-(2′′-{4′′′-Carbomethoxy-2′′′,6′′′-dinitro}phenoxy)phenyl-[d]	Acetonitrile	291.8–292.3[e]	88[f]	$C_{28}H_{18}N_4O_{14}$	52.90, 53.14	2.94, 3.04	9.03, 9.07	53.00	2.86	8.83
6*a*	2,6-Dimethyl-	Absolute ethanol	132.2–132.8	77	$C_{16}H_{14}N_2O_7$	55.33, 55.38	4.18, 3.98	8.35, 8.35	55.49	4.07	8.09
6*b*	2-Chloro-6-methyl-	Absolute ethanol[b]	110.0–110.5	56	$C_{15}H_{11}N_2O_7Cl$[g]	49.32, 49.12	3.22, 3.15	7.49, 7.51	49.13	3.02	7.64
6*c*	2-Allyl-6-methyl-	Diethyl ether[b]	93.6–94.5	32	$C_{18}H_{16}N_2O_7$	57.42, 57.23	4.21, 4.05	7.49, 7.42	58.06	4.33	7.52
6*d*	2,6-Dichloro-	Absolute ethanol[b]	123.2–123.8	70	$C_{14}H_8N_2O_7Cl_2$[h]	43.33, 43.10	2.18, 2.12	7.18, 7.06	43.43	2.08	7.24
6*e*	2,6-Dimethoxy-	Absolute ethanol[b]	130.5–131.2	86	$C_{16}H_{14}N_2O_9$	50.85, 50.68	3.83, 3.95	7.28, 7.46	50.80	3.73	7.41
7*a*	2,4,6-Trichloro-	Chloroform – absolute ethanol[b]	147.5–148.5	66	$C_{14}H_7N_2O_7Cl_3$[i]	40.16, 40.12	1.61, 1.51	6.66, 6.73	39.88	1.67	6.65
7*b*	2,4,6-Tribromo-	Absolute ethanol – chloroform[b](1:1)	151.5–152.5	61	$C_{14}H_7N_2O_7Br_3$[j]	30.05, 30.18	1.21, 1.48	4.63, 4.70	30.30	1.27	5.05
7*c*	2,4,6-Trichloro-3-ethyl-5-methyl-	Absolute ethanol – chloroform[b](2:1)	140.4–141.0	71	$C_{17}H_{13}N_2O_7Cl_3$[k]	43.77, 43.87	2.95, 3.03	5.66, 5.51	44.03	2.83	6.04
8*a*	3,4,5-Trimethyl-	Absolute methanol – chloroform[b](1:1)	175.7–176.1	78	$C_{17}H_{16}N_2O_7$	55.98, 56.04	4.27, 4.44	7.62, 7.66	56.66	4.48	7.78
8*b*	4-Chloro-3,5-dimethyl-	Absolute ethanol[b]	153.5–154.6	82	$C_{16}H_{13}N_2O_7Cl$[l]	50.40, 50.39	3.61, 3.49	7.26, 7.18	50.47	3.44	7.36

Can. J. Chem. Downloaded from www.nrcresearchpress.com by 210.87.254.40 on 09/05/12
For personal use only.

TABLE I (*concluded*)

Compound	Phenolic moiety	Solvent for recrystallization	Melting point (°C)	Yield[a] (%)	Molecular formula	Analysis (%) Found C	Found H	Found N	Calculated C	Calculated H	Calculated N
9*a*	2,3,4,6-Tetramethyl-	Absolute ethanol – chloroform[b](2:1)	155.8–156.2	77	$C_{18}H_{18}N_2O_7$	57.82, 57.82	5.27, 5.03	7.49, 7.61	57.75	4.85	7.48
9*b*	2,3,5,6-Tetramethyl-	Absolute ethanol – chloroform	180.5–182.5[m]	79	$C_{18}H_{18}N_2O_7$	57.73, 57.56	5.05, 5.07	7.61, 7.61	57.75	4.85	7.48
10*a*	3,4-Dimethyl-	Absolute ethanol – chloroform	124.5–125.0	84	$C_{16}H_{14}N_2O_7$	55.19, 55.36	4.42, 4.29	7.92, 7.99	55.49	4.08	8.09
10*b*	2-Methoxy-4-methyl-	Absolute ethanol[b]	128.5–129.5	58	$C_{16}H_{14}N_2O_8$	53.14, 53.06	3.97, 3.97	7.73, 7.78	53.04	3.90	7.73
10*c*	2,4-Dimethyl-	Chloroform – absolute ethanol[b](1:4)	138.8–139.0	81	$C_{16}H_{14}N_2O_7$	55.33, 55.46	4.07, 4.16	8.06, 8.11	55.49	4.08	8.09
11	2,5-Dimethyl-	Absolute ethanol	155.8–157.0	85	$C_{16}H_{14}N_2O_7$	55.37, 55.50	4.12, 4.23	8.17, 8.26	55.49	4.08	8.09
12	3-Methyl-2-(4′′-carbomethoxy-2′′,6′′-dinitro)-phenoxy-	Absolute ethanol – chloroform[b](2:1)	181.7–182.3	80	$C_{23}H_{16}N_4O_{14}$	48.13, 48.34	2.92, 3.01	9.92, 9.95	48.26	2.82	9.79
13	4,5-Benzo-2-hydroxy-[e]	Chloroform[b] – pet. ether	171.1–172.0	54	$C_{18}H_{12}N_2O_8$	54.74, 54.84	3.03, 3.16	7.36, 7.48	56.25	3.08	7.29
14	4,5-Benzo-2-(4′′-carbomethoxy-2′′,6′′-dinitro)-phenoxy-[p]	Absolute ethanol – chloroform (1:1)	209.9–210.5[q]	31	$C_{26}H_{16}N_4O_{14}$	50.77, 50.73	2.91, 2.87	9.10, 9.05	51.32	2.65	9.21
15	2-(4′-Carbomethoxy-2′,6′-dinitrophenoxy)-fluorene[r]	Chloroform[b] – absolute ethanol	157.8–158.3	78	$C_{21}H_{14}N_2O_7$	61.89, 62.08	3.58, 3.56	6.97, 6.83	62.07	3.47	6.90

a Yield of once-recrystallized material based on the chloro ester.
b With decolorizing charcoal.
c Initially melting occurred at 154.3–156.2° to form a pasty mass which then melted as above; two crystalline forms appeared to undergo simultaneous melting.
d 2,2′-bis-(4′′-Carbomethoxy-2′′,6′′-dinitrophenoxy)biphenyl.
e Discoloration and shrinkage occurs before melting.
f Yield from 2,2′-dihydroxybiphenyl.
g Anal. Calcd.: Cl, 9.67. Found: Cl, 9.39, 9.50.
h Anal. Calcd.: Cl, 18.32. Found: Cl, 18.24, 18.01.
i Anal. Calcd.: Cl, 25.23. Found: Cl, 25.14, 25.12.
j Anal. Calcd.: Br, 43.20. Found: Br, 43.69, 43.69.
k Anal. Calcd.: Cl, 22.94. Found: Cl, 21.77, 21.88.
l Anal. Calcd.: Cl, 9.31. Found: Cl, 9.34, 9.38.
m A Kofler melting determination showed needles melting at 182–183° and long cube-like crystals melting at 185–186° ;the latter solidified and remelted at 184.0–185.5° (all m.p.s uncorrected).
n 2,3-bis-(4′-Carbomethoxy-2′,6′-dinitrophenoxy)toluene.
o 3-Hydroxy-2-(4′-carbomethoxy-2′,6′-dinitrophenoxy)naphthalene.
p 2,3-bis-(4′-Carbomethoxy-2′,6′-dinitrophenoxy)naphthalene.
q Thermally transformed solid, see Experimental.
r Compound name, not radical.

Can. J. Chem. Downloaded from www.nrcresearchpress.com by 210.87.254.40 on 09/05/12
For personal use only.

any diphenyl ether even when the preferred method (1) of first treating the tar or gum with dilute hydrochloric acid to decompose the pyridinium salts (precursor **3***a* and by-product **3***b*[2]).

By an embarrassingly simple modification to the Hems synthesis, involving addition of the reaction mixture to a mixture of acidified ice–water and chloroform and shaking of the combined mixture for ½ h before separating the phases, the synthesis and ordinarily unrewarding isolation of highly hindered diphenyl ethers has now been transformed into an operation of remarkable ease. Indeed, by this treatment, the product crystallizing from the ethanol–chloroform concentrate[3] (see Experimental) in yields ranging from 32–97% is comparable to a once recrystallized product from the unmodified synthesis.

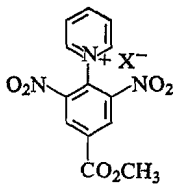

3*a*, $X^- = Cl^-$
3*b*, X^- = anion of 4

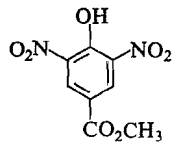

4

Ethers Prepared by the Modified Hems Synthesis and Discussion of Some Factors Affecting Their Synthesis

The diphenyl ethers synthesized may be conveniently classified into six groups **5**, **6**, **7**, **8**, **9**, and **10** by virtue of the substitution derived from the phenolic moiety. In addition, five other diphenyl ethers, **11–15**, were prepared. All of these ethers were prepared using the conditions developed for the modified *Hems synthesis* (except **5***a* which was prepared using the unmodified Hems synthesis), and the percentage yield[4] (Table I) for each diphenyl ether from the chloro

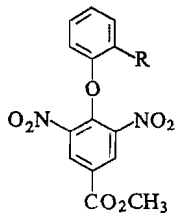

5

5*a*, R = CH_3
5*b*, R = $CH(CH_3)_2$
5*c*, R = $C(CH_3)_3$
5*d*, R = $CH_2CH{=}CH_2$
5*e*, R = C_6H_5
5*f*, R = HO

5*g*, R =

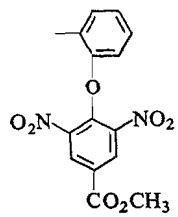

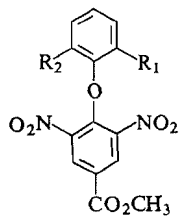

6

6*a*, $R_1 = CH_3$; $R_2 = CH_3$
6*b*, $R_1 = CH_3$; $R_2 = Cl$
6*c*, $R_1 = CH_3$; $R_2 = CH_2CH{=}CH_2$
6*d*, $R_1 = Cl$; $R_2 = Cl$
6*e*, $R_1 = OCH_3$; $R_2 = OCH_3$

[2]Invariably one obtains a small quantity of bright-yellow solid by-product (4 to 9% from the chloro ester) identified as *N*-(4-carbomethoxy-2,6-dinitrophenyl)pyridinium 4′-carbomethoxy-2′,6′-dinitrophenoxide (**3***b*) (1) in the Hems synthesis. Using the modified Hems synthesis we have found that when a reaction gives a good yield of diphenyl ether, a negligible quantity (0.5–1% from chloro ester) of by-product forms, but when no reaction occurs under the standard conditions, an appreciable quantity of the "yellow salt" normally forms.

[3]At the conclusion of our work, we noticed that Zenker and Jorgensen (12) had previously used a similar modification of the Hems synthesis, in which chloroform was introduced with the reactants, rather than at the isolation stage as in the present method. Although the difference may seem trivial at first sight, their method in the preparation of very hindered ethers led, in our hands, to a great decrease in the rate of reaction, with the consequent increased recovery of starting materials and by-products.

[4]Percentage yields varied with conditions in a complex fashion. When heating under reflux was performed with an oil bath instead of with a steam bath, the yield of **6***a* dropped from 77 to 72%, but the yield of **5***c* rose from 32 to 46%. Increasing the scale of the preparation sometimes depressed the yields, and prolonged contact with dilute acid during the isolation procedure had a distinctly deleterious effect.

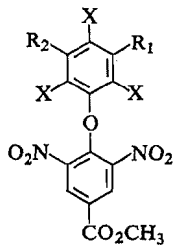

7

7a, X = Cl; $R_1 = R_2 = H$
7b, X = Br; $R_1 = R_2 = H$
7c, X = Cl; $R_1 = CH_3$; $R_2 = CH_2CH_3$

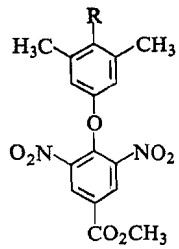

8

8a, R = CH_3
8b, R = Cl

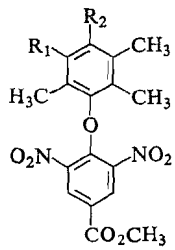

9

9a, $R_1 = H$; $R_2 = CH_3$
9b, $R_1 = CH_3$; $R_2 = H$

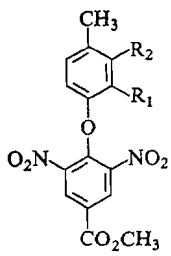

10

10a, $R_1 = H$; $R_2 = CH_3$
10b, $R_1 = OCH_3$; $R_2 = H$
10c, $R_1 = CH_3$; $R_2 = H$

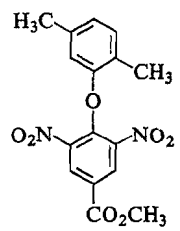

11

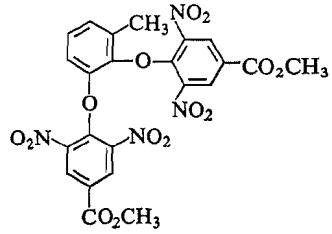

12

ester[5] (except where noted) is that obtained by heating the reaction mixture under reflux for 1 h on a steam-bath.

Effect of Size of the R_1 and R_2 ortho-Substituents

When the size of the R_1 and R_2 ortho-substituents in class **6** diphenyl ethers was large, no isolation of diphenyl ether was possible as found for the following combinations:

TABLE II

Dependence of by-product on the size of the R_1 and R_2 ortho-substituents

R_1	R_2	% By-product (3*b*)
$C(CH_3)_3$	$C(CH_3)_3$	6.2*
$CH(CH_3)_2$	$CH(CH_3)_2$	8.1
CH_3	$C(CH_3)_3$	7.6
CH_3	$CH_2CH_2CH_3$	None
NO_2	NO_2	28†

*11% of the chloro-ester reactant was recovered unchanged.
†40% of the phenolic reactant was recovered unchanged.

Steric factors alone may not provide an explanation for lack of diphenyl ether formation. Steric hindrance from the ortho-substituents of 2-methyl-6-*n*-propylphenol, which may not have reacted,[6] would be little different from that in 2-methyl-6-allylphenol, which did give a product (**6***c*) in moderately low yield. Similarly the steric hindrance of the nitro groups from 2,6-dinitrophenol is not especially large, particularly when these can be easily twisted out of the plane of the benzene ring (13). With ortho-nitro groups, an unfavorable factor seems to be the activation of

[5]The expression "chloro ester" is used for convenience and refers to methyl 4-chloro-3,5-dinitrobenzoate.
[6]No diphenyl ether was isolated from an intractable syrup in great contrast to the ease with which diphenyl ethers crystallized under the conditions of the modified Hems synthesis.

Can. J. Chem. Downloaded from www.nrcresearchpress.com by 210.87.254.40 on 09/05/12
For personal use only.

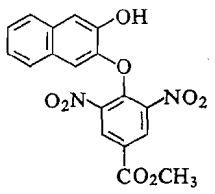

13

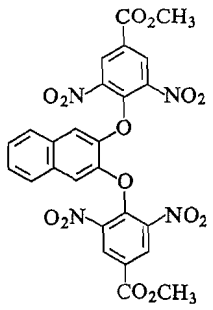

14

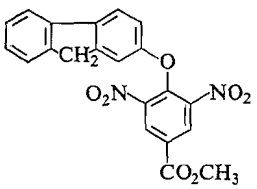

15

the resulting ethers for cleavage. The only example known to us where a report of the synthesis of a diphenyl ether with four ortho-nitro groups is that by Beckwith and Miller (14) for the preparation of 2,2′,4,6,6′-pentanitro-4′-methyldiphenyl ether in 87% yield by heating picryl chloride and potassium 2,6-dinitro-4-methylphenoxide under reflux with 1:1 aqueous acetonitrile for 5 min. In view of our failure to prepare 4-carbomethoxy-2,2′,6,6′-tetranitrodiphenyl ether either by the Hems synthesis or by the method of Barnes *et al.* (15), which is similar to the above method of Beckwith and Miller, it appears puzzling that Beckwith and Miller succeeded in synthesizing this sterically hindered compound; however, its synthesis was achieved by three different methods[7] and its composition was established by scission[8] with pyridine and with sodium methoxide. It is unlikely that the 2,2′,4,6,6′-pentanitro-4′-methyldiphenyl ether could be prepared by the Hems synthesis since the compound is highly activated for cleavage by pyridine. In contrast, diphenyl ethers with three ortho-nitro substituents appear to be insufficiently activated to suffer much competing scission by pyridine since Borrows *et al.* (6) were able to prepare 4-methyl-2,2′,4′,6-tetranitrodiphenyl ether (a yellow oil, b.p. 40–60°/10^{-4} mm Hg) in 38% yield using the Hems synthesis. Later Beckwith and Miller (14) obtained the same compound in solid form (m.p. 160°, 85%) after inducing crystallization of the dark oil resulting from the decomposition of *N*-(2,4-dinitrophenyl)-pyridinium-2′,6′-dinitro-4′-methylphenoxide in boiling anisole. More recently, Chandler[9] prepared 2-nitro-4-carbomethoxy-2′,6′-dinitro-4′-carbomethoxydiphenyl ether in 42% yield using the Hems synthesis.

Effect of para-Electronegative Substituents in the Phenol

Whereas good yields were obtained for class **7** and **8** diphenyl ethers, it appears that the introduction of an electron-withdrawing conjugating substituent in the para-position of the phenols, **16**, **17**, and **18** prevented ether formation. The

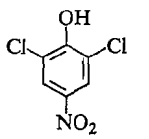

16

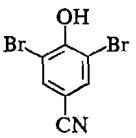

17

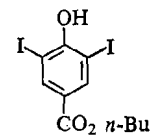

18

high yields of the class **7** diphenyl ethers indicate that neither chlorine nor bromine ortho-substituents provide enough steric hindrance to interfere greatly with synthesis; moreover, the synthesis of 2′,6′-diiodo-4′-methyl-4-carbomethoxy-2,6-dinitrodiphenyl ether in 51% yield by Barnes *et al.* (15) shows that two ortho-iodine substituents can be accommodated with two ortho-nitro groups. Raiford and Colbert (16) have observed that 2,4-dinitrophenol fails to react with any of chlorobenzene, *o*-nitrochlorobenzene, or with *p*-nitrochlorobenzene. Although the combined mesomeric and inductive electron withdrawal by the nitro groups may lower the electron density of the phenolic oxygen to such an extent that 2,4-dinitrophenol is too weakly nucleophilic for the weakly activated chlorobenzenes above, Raiford and Colbert found that diphenyl ethers were always obtained regardless of the substituents on the phenol when 2,4-dinitrochlorobenzene is

[7]2,2′,4,6,6′-Pentanitro-4′-methyldiphenyl ether was prepared by Beckwith and Miller as above; in 21% yield by simply heating the above starting materials together for 30 min at 160° without a solvent, and in 49% yield by decomposition of *N*-picrylpyridinium 2,6-dinitro-4-methylphenoxide in boiling anisole.

[8]Scission with sodium methoxide gave 89% of 3,5-dinitro-*p*-cresol and 78% picryl methyl ether, whereas scission with pyridine gave a 95% yield of *N*-picrylpyridinium 2,6-dinitro-4-methylphenoxide.

[9]W. D. Chandler, personal communication.

Can. J. Chem. Downloaded from www.nrcresearchpress.com by 210.87.254.40 on 09/05/12
For personal use only.

Can. J. Chem. Downloaded from www.nrcresearchpress.com by 210.87.254.40 on 09/05/12
For personal use only.

used, and they cite the synthesis and yields of the following diphenyl ethers: 2,4-dinitro-4′-bromodiphenyl ether (100%), 2,4-dinitro-4′-chlorodiphenyl ether (97%), 2,4,2′-trinitrodiphenyl ether (89%), 2,4,3′-trinitrodiphenyl ether (77%), 2,4,4′-trinitrodiphenyl ether (97%), 2,4-dinitro-2′,4′,6′-tribromodiphenyl ether (28%), 2,4,2′-trinitro-4′-chlorodiphenyl ether (87%), and 2,4,2′-trinitro-4′-bromodiphenyl ether (95%). The synthesis and yield of 2,4,2′,4′-tetranitrodiphenyl ether are conspicuous by their absence from this list; however, Raiford *et al.* (16) may simply have omitted their experimental details since this diphenyl ether had been synthesized many years earlier by Willgerodt (17) by heating 2,4-dinitrochlorobenzene and potassium 2,4-dinitrophenolate together at 180–200°. A reasonable explanation for the lack of diphenyl ether formation from 2,6-dinitrophenol, 2,6-dichloro-4-nitrophenol, and 2,4-dibromo-6-nitrophenol with methyl-4-chloro-3,5-dinitrobenzoate by the Hems synthesis appears to be that any such diphenyl ether formed would be extremely easily cleaved by pyridine or water, due to the combined effects of steric compression and activation of the ethereal linkage for cleavage by the electron withdrawing substituents of both rings. In order to test this hypothesis, an attempt was made to synthesize the corresponding diphenyl ethers by the action of 2,6-dinitrophenol, 2,6-dichloro-4-nitrophenol, *n*-butyl-4-hydroxy-3,5-diiodobenzoate, 5-chloro-8-hydroxy-7-iodoquinoline, and 2,4-dibromo-6-nitrophenol on methyl 4-chloro-3,5-dinitrobenzoate using the mild conditions of Barnes *et al.* (15) which involve refluxing the reactants in methyl ethyl ketone with anhydrous potassium carbonate. In each case, no diphenyl ether was formed, and only the reactants or potassium salts derived from the reactants were recovered. Since the procedure of Barnes *et al.* (15) is successful for the synthesis of 2′,6′-diiodo-4′-methyl-4-carbomethoxy-2,6-dinitrophenyl ether but fails when the CH_3 group of this diphenyl ether is replaced by the carbo-*n*-butoxy group, one can only conclude that synthesis of highly hindered diphenyl ethers from strongly activated aryl halides and moderately activated phenols, either by the Hems synthesis or by the uncatalyzed, mild Ullmann-type condensation, involves a delicate system in which steric, polar, and dipolar factors must be accommodated to result in product formation.

Factors Affecting the Formation of bis-Diphenyl Ethers

It should be noted that even with reactant ratios favoring formation of the mono-ether, 3-methylcatechol gave only the bis-ether **12**. There are two ways to account for exclusive formation of the bis-ether. One explanation consistent with the view that the 2-hydroxyl group should have the greater electron density, is a two-step reaction involving initial rapid attack by the 2-hydroxyl group followed by attack by the 1-hydroxyl group on the pyridinium salt intermediate to give the bis-ether. If nucleophilic attack involved the 1-hydroxyl group first, then steric hindrance of this mono-ether would inhibit further reaction providing no rearrangement could occur. The second explanation rests on the assumption of a facile intranucleophilic attack on the ethereal linkage by the 2-hydroxyl group (Smiles' rearrangement)[10] to form a new ethereal linkage leaving a hydroxyl group in the 1-position with a minimum of steric hindrance (Fig. 1).

Another unexpected finding was that 2,3-dihydroxynaphthalene gave the bis-ether (**14**) exclusively with reactant ratios favoring formation of mono-ether, and gave the mono-ether (**13**) as the major product with reactant ratios favoring formation of the bis-ether. In addition, the bis-ether exhibited marked dimorphism which is of particular interest in view of the recent finding of two crystalline modifications of 1,1′-binaphthyl by Badar *et al.* (18) and of similar phenomena in other diphenyl ethers (2).

Experimental

All melting point (m.p.) determinations, except where noted, were obtained with Anschütz immersion thermometers using an electrically heated precision melting apparatus (19) containing Dow Corning 550 fluid. Thin-walled capillary tubes were drawn from cleaned $\frac{3}{4}$ in. Pyrex tubing. Some m.p. determinations were made using a Kofler hot stage apparatus and are reported uncorrected. Refractive indices were measured on a thermostatted Abbé refractometer, and all readings are reported corrected on the basis of readings of distilled water.

Purification of Phenols

The substituted phenols used in this work were obtained either from the Aldrich Chemical Co., or from Distillation Industries Products (Eastman). Solid phenols, whose

[10]An extensive study of this rearrangement had been made previously in these laboratories by W. D. Chandler.

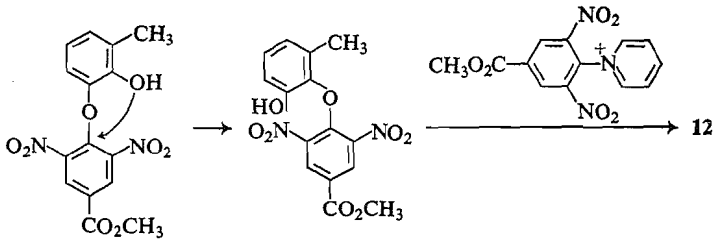

FIG. 1. A rationalization of bis-diphenyl ether formation by the Smiles' rearrangement.

melting range was less than 2°, and liquid phenols whose refractive index agreed with the known n_D by ±0.001, were used as obtained. Other phenols were first purified as follows: 2-chloro-6-methylphenol (80% technical, Aldrich) was fractionated to obtain a liquid, b.p. 81–84°/21 mm Hg, $n_D^{25.0}$ 1.5433; and 2,3,5,6-tetramethylphenol (m.p. 90–100°, Aldrich) was recrystallized twice from aqueous methanol to obtain a solid, m.p. 116.5–117.5°.

General Modified Hems Synthesis

The syntheses of all diphenyl ethers, except where noted, were performed using the following generalized procedure:

Methyl 4-chloro-3,5-dinitrobenzoate[11] (2.00 g, m.p. 104.5–106.0°) was dissolved in dry pyridine (10 ml, Fisher, 0.01% water) stored over anhydrous barium oxide. The stoppered mixture was heated for 5 min on a steam bath to enhance salt formation.

A 1.5 *M* excess of the chosen phenol was then added quantitatively to the pyridinium salt mixture by rinsing it in with minimal chloroform (Fisher spectranalyzed[12]). The mixture was heated for 1 h under reflux (with a $CaCl_2$ guard tube) on the steam bath.

The reaction mixture was cooled under the cold water tap and it was then poured into a conical flask (500 ml) containing ice (handful of chips), water (50 ml), and concentrated hydrochloric acid (15 ml, 12 *N*). Chloroform (25 ml, stock) was added, and the mixture was shaken for ½ h on a mechanical shaker. The mixture was then filtered to remove the insoluble yellow by-product, *N*-(4-carbomethoxy-2,6-dinitro)phenylpyridinium 4′-carbomethoxy-2′,6′-dinitrophenoxide (**3***b*), when present.

The chloroform phase was separated, treated with an equal volume of absolute ethanol, and the solution was reduced to the original volume, or less, by boiling. A copious solid generally crystallized when the concentrate was cooled in a salt–ice bath. The crude solid was collected and washed with petroleum ether (b.p. 30–60°) and dried over P_2O_5 in a desiccator under vacuum. The solid was recrystallized successively, until constancy of melting range was achieved, three recrystallizations normally being required.

All analytical samples received additional drying over P_2O_5 in a drying pistol. Microanalyses were performed by Alfred Bernhardt, 433 Mülheim (Ruhr), West Germany.

[11]Prepared by the method of Borrows *et al.* (6).

[12]Used as a convenient source of dry chloroform. The larger water content of stock chloroform led to increased yields of the by-product **3***b*.

All samples gave nuclear magnetic resonance (n.m.r.) and infrared (i.r.) spectra consistent with the assigned structures.

2-Methyl-4′-carbomethoxy-2′,6′-dinitrodiphenyl Ether (5a)

Freshly distilled *o*-cresol (1.25 g, b.p. 89–90°/13 mm Hg) was added to the pyridinium salt prepared as in general procedure above, and the mixture was heated on a steam bath for 90 min. The cooled mixture was poured onto ice in dilute hydrochloric acid (15 ml of 12 *N* HCl in 50 ml water). The gummy material which formed initially, changed into crystalline solid on standing for 3 h. The solid was recrystallized from acetone – petroleum ether to obtain crude product (1.72 g, 67% from chloro ester) melting mainly 128–133° (uncorrected, Kofler). The solid was recrystallized 4 times from absolute ethanol with successive elevation of the melting range (131.0–132.5, 134.5–135.2, 135.0–135.7, and 135.2–135.7°) before an analytical grade sample was obtained.

The pure compound was observed to turn brown on the surface when exposed to air and sunlight. No color change occurred on standing over sodium hydroxide and concentrated sulfuric acid in the vacuum desiccator. Admixture of the discolored compound with the unchanged compound resulted in a slight lowering of the melting range to 134.2–134.8°, but i.r. spectra of both samples in chloroform solution were identical.

2-(4′-Carbomethoxy-2′,6′-dinitrodiphenoxy)fluorene (**15**) was also observed to be very sensitive to light; the exposed surface of the pale-yellow solid would quickly turn to a pale-orange color.

2,3-bis(4′-Carbomethoxy-2′,6′-dinitrophenoxy)toluene (12)

The reaction was done according to the generalized procedure using 3-methylcatechol (1.43 g, i.e. 1.5 *M* excess over chloro-ester, m.p. 66.4–67.5°, Aldrich). No solid was isolated from this reaction, designed to give the mono-ether, except the unexpected bis-ether. The yield of crude dry solid was 0.20 g or 5% from the chloro-ester, m.p. 174–176°.

The reaction was repeated using conditions designed to favor formation of the bis-ether. A 2.5 *M* excess of the chloro-ester (5.24 g) over 3-methylcatechol (1.00 g) was used. The yield of crude dry product was 3.67 g (or 80% from 3-methylcatechol), m.p. 178.5–180.0°, and negligible **3***b* formed.

3-Hydroxy-2-(4′-carbomethoxy-2′,6′-dinitro)phenoxynaphthalene (13)

Reaction conditions of the generalized procedure

Can. J. Chem. Downloaded from www.nrcresearchpress.com by 210.87.254.40 on 09/05/12
For personal use only.

favorable for synthesis of the bis-phenyl-naphthyl ether were employed, using 2,3-dihydroxynaphthalene (0.49 g, i.e. 1.0–2.5 *M* ratio of phenol to chloro-ester, m.p. 162.0–163.3°, Aldrich).

A small quantity of insoluble yellow solid (0.29 g) was collected from the acid treated reaction mixture. This solid was different from the usual yellow by-product *3b* in that it melted at 95–98° with the melt solidifying around 100° to give feathery crystals which melted at 121–130° (all m.p. determinations were made on a Kofler hot stage). Recrystallization of the solid in chloroform – absolute ethanol (1:1) using decolorizing charcoal gave a solid, m.p. 171.5–175° (Kofler) whose i.r. spectrum showed the presence of O—H stretching. A much larger quantity (1.60 g) of the same compound was obtained from the chloroform–ethanol concentrate by the usual treatment; 2 recrystallizations gave analytical quality material which analyzed for the mono-phenyl-naphthyl ether (**13**).

A small quantity of the bis-phenyl-naphthyl ether was isolated from the residual oil obtained from the chloroform–ethanol concentrate. Crystallization of the oil was induced by treating it with petroleum ether. After recrystallization the crude solid (0.09 g, m.p. 90–95°) was shown to be identical with **14** by comparison of i.r. spectra.

2,3-bis-(4′-Carbomethoxy-2′,6′-dinitrophenoxy)-naphthalene (14)

An attempt was made to synthesize the corresponding mono-naphthyl-phenyl ether by the reaction conditions of the generalized procedure using 2,3-dihydroxynaphthalene (1.85 g, i.e. a 1.5 *M* excess over chloro-ester, m.p. 162.0–163.3°, Aldrich).

A small quantity of the by-product **3b** (0.33 g) was obtained. A dirty yellow solid was obtained from the chloroform–ethanol concentrate with cooling. The crude solid (1.44 g) showed some melting around 110°, but most of the solid melted at 209.5–211.0°. After recrystallization from chloroform – absolute ethanol (2:1) using decolorizing charcoal, the dry solid melted almost completely at 114–116°, then the melt solidified from 151–155° forming feathery crystals which melted completely at 212–215° (Kofler). An i.r. spectrum of the recrystallized solid indicated that it was the bis-phenyl-naphthyl ether.

In view of the remarkable melting behavior of the solid above, a thermal transformation was performed by heating approximately half the recrystallized material in a glass thimble immersed in the vapor of anisole (b.p. 155°). Within 10 min of constant temperature heating, the solid melted and was transformed into a pale-yellow solid which was crusty and porous in nature. A sample of this solid melted at 211.5–214.0° (Kofler) with no melting at lower temperature. After recrystallization from chloroform – absolute ethanol, the thermally transformed solid was found to melt at 212.0–214.5° (Kofler) and 209.9–210.5°; this material was used for the analytical sample.

Acknowledgment

The authors wish to acknowledge the National Research Council of Canada for a grant in support of research and for a studentship awarded to one of us. The Province of Ontario is also gratefully acknowledged for the award of a Graduate Fellowship to one of us.

1. M. Allen and R. Y. Moir. Can. J. Chem. **37**, 1799 (1959).
2. W. D. Chandler, W. MacFarlane Smith, and R. Y. Moir. Can. J. Chem. **42**, 2549 (1964).
3. P. A. Lehman and E. C. Jorgensen. Tetrahedron, **21**, 363 (1965).
4. J. Wright and E. C. Jorgensen. J. Org. Chem. **33**, 1245 (1968).
5. J. A. McRae, R. Y. Moir, J. J. Ursprung, and H. H. Gibbs. J. Org. Chem. **19**, 1500 (1954).
6. E. T. Borrows, J. C. Clayton, B. A. Hems, and A. G. Long. J. Chem. Soc. S190 (1949).
7. F. Ullmann. Ber. **37**, 854 (1904).
8. H. E. Ungnade. Chem. Rev. **38**, 405 (1946).
9. R. W. Bost and F. Nicholson. J. Am. Chem. Soc. **57**, 2368 (1935).
10. J. F. Bunnett and R. E. Zahler. Chem. Rev. **49**, 273 (1951).
11. M. J. Rarick, R. Q. Brewster, and R. B. Dains. J. Am. Chem. Soc. **55**, 1289 (1933).
12. N. Zenker and E. C. Jorgensen. J. Am. Chem. Soc. **81**, 4643 (1959).
13. J. Trotter. Can. J. Chem. **39**, 1638 (1961).
14. A. L. Beckwith and J. Miller. J. Org. Chem. **19**, 1416 (1954).
15. J. H. Barnes, E. T. Borrows, J. Elks, B. A. Hems, and A. G. Long. J. Chem. Soc. 2824 (1950).
16. L. C. Raiford and J. C. Colbert. J. Am. Chem. Soc. **48**, 2652 (1926).
17. C. Willgerodt. Ber. **13**, 887 (1880).
18. Y. Badar, C. C. K. Ling, A. S. Cooke, and M. M. Harris. J. Chem. Soc. 1543 (1965).
19. E. B. Hershberg. Ind. Eng. Chem. Anal. Ed. **8**, 312 (1936).

Can. J. Chem. Downloaded from www.nrcresearchpress.com by 210.87.254.40 on 09/05/12
For personal use only.

Can. J. Chem. Downloaded from www.nrcresearchpress.com by 210.87.254.5 on 09/05/12
For personal use only.

Anomalous acid-catalyzed reactions of cyclobutanones

EDWARD LEE-RUFF AND NICHOLAS J. TURRO
Department of Chemistry, Columbia University, New York, New York 10027

AND

P. AMICE AND J. M. CONIA
Laboratoire d'Etude des Carbocycles-Equipe de Recherche Associée au CNRS, Université de Caen, Caen, France

Received March 10, 1969

The reactions of 2(2-isopropanol)cyclobutanones with phosphorous pentoxide lead to ring opened carboxylic acids. Reaction of 2-isopropylidenecyclobutanones with polyphosphoric acid (PPA) gives ring cleavage rearrangement products. The mechanisms of these reactions are discussed in the light of the observed different reactions of the corresponding cyclopentanones.

Canadian Journal of Chemistry, 47, 2797 (1969)

Anomalous reactions and enhanced reactivities of small ring compounds have recently received considerable interest. The strain involved in bond angular distortions tends to offset "normal" reaction modes so that other pathways are often followed such that relief of this strain occurs. We wish to report some novel acid-catalyzed ring-cleavage and rearrangement of cyclobutanones.

Acid Catalyzed Ring Opening of 2(2-Isopropanol)cyclobutanone

The reaction of 2-isopropylidene-2′(2-isopropanol)cyclobutanone (**1**) with P_2O_5 in C_6H_6 gave the acid **2** (m.p. 50–51°) and an ester **3** in 55 and 35% yields, respectively. A trace amount of **4** was obtained and identified by comparison with an authentic sample (*1*). The structure of carboxylic acid **2** was based on the nuclear magnetic resonance (n.m.r.) spectrum which showed an exchangeable proton signal at 12.64 p.p.m. and vinyl methyl signals at 1.70 p.p.m. (6H), 1.90, and 2.14 p.p.m. The infrared (i.r.) spectrum of **2** showed the characteristic peaks for an α,β-unsaturated carboxylic acid.

Platinum catalyzed hydrogenation of **2** at 1 atmosphere resulted in the sole reduction of the γ–δ unsaturated bond giving **5**, which was also converted to **6** by catalytic hydrogenation at 3 atmospheres. Compound **6** had similar physical constants and spectra with those reported for 2-isopropyl-5-methylhexanoic acid (*2*). Compound **6** was also obtained from the catalytic pressure hydrogenation of 2-isopropylidene-5-methyl-Δ^4-hexenoic acid (**2**).

The structure of **3** was assigned on the basis of spectral and analytical data. Hydrolysis of **3** in a 10% methanolic sodium hydroxide solution gave equimolar amounts of the acid **2** and a mixture of the starting ketone **1** and dienone **4**.

Hydrogenation of 2-isopropylidene-2′(2-isopropanol)cyclobutanone (**1**) at 3 atmospheres yielded an isomeric mixture **7**. Reaction of **7** with P_2O_5 in benzene yielded **8**. The structure of **8** was supported by its spectral data and its ready catalytic hydrogenation at atmospheric pressure giving exclusively the saturated acid **6**.

The reaction of **1** with perchloric acid in benzene yielded the α,β-unsaturated lactone **9** quantitatively. Its structure was supported by spectral data and its synthesis from 2-isopropylidene-5-methyl-Δ^4-hexenoic acid (**2**). Treatment of **2** with 60% perchloric acid in benzene gave exclusively lactone **9** identical in all respects with that obtained from the perchloric acid reaction with **1** (Scheme I).

Rearrangement of 2-Isopropylidenecyclobutanones in PPA

Reaction of 2-isopropylidenecyclobutanone (**10**) with polyphosphoric acid (PPA) at 100° gave 3-methyl-Δ^2-cyclohexenone (**11**) in 82% yield. The n.m.r. and i.r. spectra of **11** were identical with those of an authentic sample. Reaction of 2,2′-diisopropylidenecyclobutanone with polyphosphoric acid at 100° gave piperitenone (**12**) and 3-methyl-Δ^2-cyclohexenone (**11**). The structure of **12** was assigned by comparison of its spectral data with those of an authentic sample (*3*, *4*). An identical mixture of piperitenone (**12**) and **11** was obtained by treating carboxylic

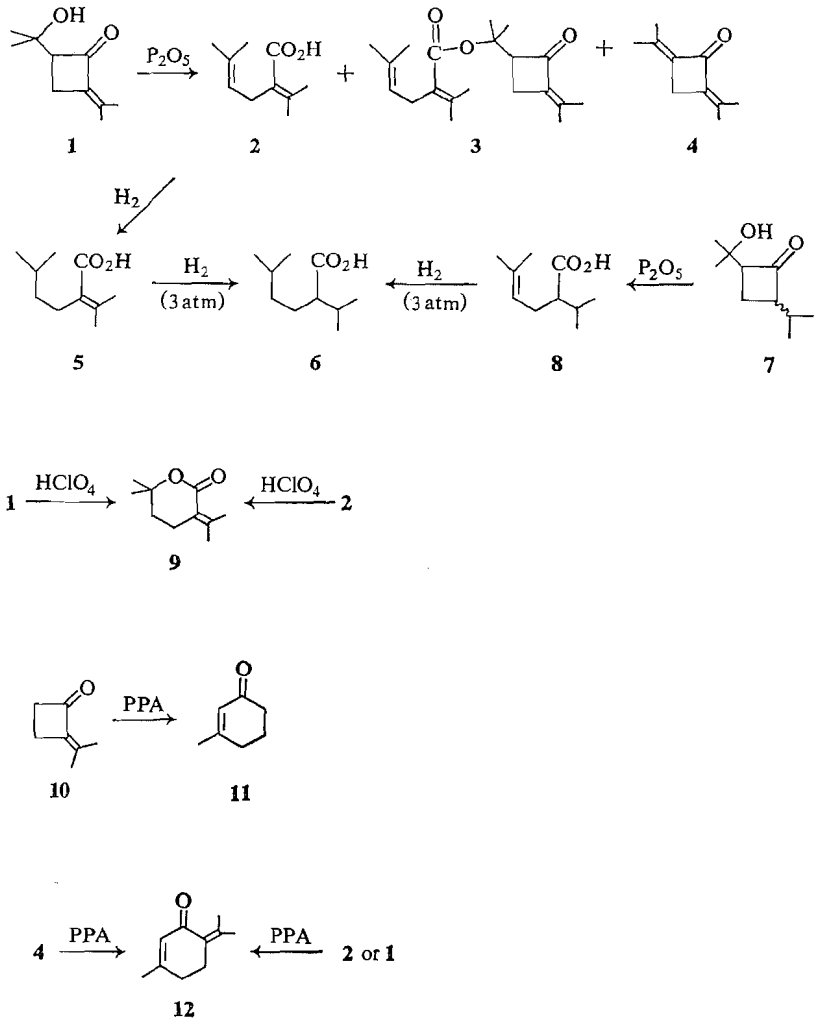

SCHEME I

acid **2** with PPA under the same conditions. Similarly, ketone **1** gave piperitenone **12** with PPA.

Discussion

The acid-catalyzed ring opening of the 2-(2-isopropanol)cyclobutanones can be explained by the following mechanisms (Scheme II). The acylium ion can be generated by direct abstraction of the hydroxyl group by phosphorous pentoxide with subsequent rearrangement or by the initial formation of the phosphate diester **13** (5) with concomitant rearrangement and elimination. On the other hand, phosphate **13** can undergo a cyclic six-centered rearrangement to give the acyl phosphate **14**. The acyl phosphate **14** could also conceivably be formed from the acylium ion **15**. Under the work-up conditions the acyl phosphate would be readily converted to the carboxylic acid **2**. The formation of ester **3** can be envisaged as the reaction of an acylium ion with unreacted ketone **1** or by rearrangement of the phosphate diester **13** as illustrated. The former mechanism is less likely since the reaction of phosphorous pentoxide in a one-tenth dilute benzene solution of **1** gave identical yields of the carboxylic acid **2** and the ester **3**.

In the reaction of **1** with perchloric acid, the carboxylic acid **2** is apparently the precursor of

Can. J. Chem. Downloaded from www.nrcresearchpress.com by 210.87.254.5 on 09/05/12
For personal use only.

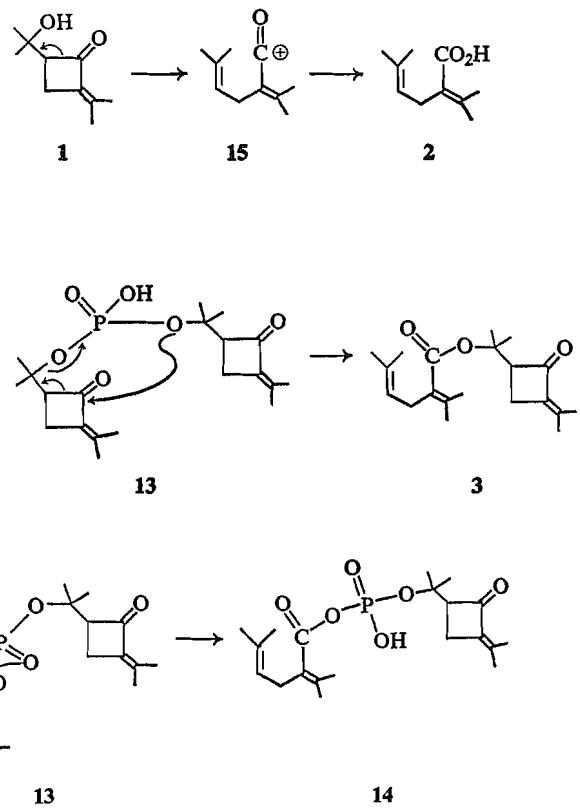

SCHEME II

lactone **9**, since, under the same conditions, **2** was readily converted to **9**. In this particular case only the acylium ion mechanism is tenable.

The phosphorous pentoxide reaction of **1** may proceed in part by the acylium ion mechanism. It was observed that the saturated 2-isopropyl-2(2-isopropanol)cyclobutanone (**7**) reacted much slower than **1**. This is reasonable since the acylium ion **15**, which is derived from **1**, is stabilized by α,β-unsaturation.

Reaction of **16** with phosphorous pentoxide in benzene (Scheme III) results in the normal dehydration products **17** and **18** and reaction of **19** under similar conditions gave **20**, indicating

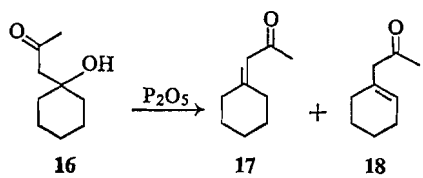

SCHEME III

that the anomalous ring cleavage observed in the cyclobutanones is due to the strain in these derivatives. The polyphosphoric acid reaction of the 2-isopropylidenecyclobutanones may also involve the same acylium ion **15** as shown in the reaction Scheme IV. The acylium ion **15** could tautomerize under the experimental conditions to give acylium ion **21** which could undergo an intramolecular acylation to give ketone **12**. Such tautomerizations have been observed under similar reaction conditions (6). Evidence for the intervention of the acylium ion **15** was found by the observation that carboxylic acid **2** under the same conditions gave an identical mixture of ketones **11** and **12**. The formation of acylium ions from the reaction of α,β-unsaturated carboxylic acids with PPA is well documented (6). The formation of 3-methyl-Δ^2-cyclohexenone (**11**) in the reaction of **4** with PPA appears at first glance to be quite unusual. However, it is possible that phosphate **22** might be formed which could undergo a retro aldol condensation

Can. J. Chem. Downloaded from www.nrcresearchpress.com by 210.87.254.5 on 09/05/12
For personal use only.

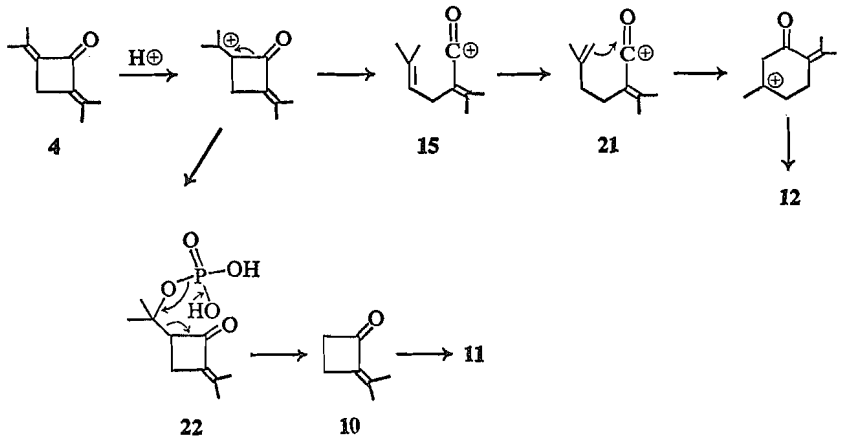

SCHEME IV

as shown, giving rise to 2-isopropylidenecyclobutanone (**10**). Ketone **10** could then be transformed into **11** in the usual manner. Treatment of ketone **1** with base resulted in a 10% yield of 2-isopropylidenecyclobutanone (**10**).

The unusual reactions of the cyclobutanones with PPA appear to be the result of ring strain. It was reported (7) that the reaction of 2-isopropylidene cyclopentanone (**23**) with PPA gave the α,β-conjugated cyclopentenone **24** (Scheme V).

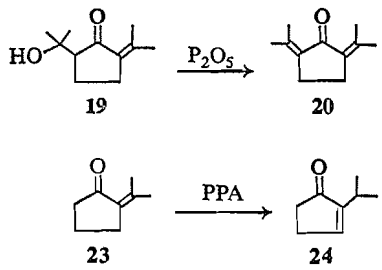

SCHEME V

Experimental

All melting points were obtained on a Buchi melting-point apparatus and are uncorrected. The n.m.r. spectra were run on a Varian A-60A spectrometer (TMS, internal standard). Infrared spectra were run on a Perkin–Elmer model 137 spectrometer. Elemental analyses were obtained from Schwarzkopf Microanalytical Laboratories, Woodside, New York.

Reaction of 1 with Phosphorous Pentoxide

Ketone **1**[1] (800 mg) was dissolved in 15 ml of anhydrous benzene. To this solution was added 1 g of P_2O_5 and the mixture was stirred at room temperature for 3 h. Water was slowly added until all the P_2O_5 was destroyed. The solution was taken up in ether and the ether extract washed neutral with water and then with 25 ml of 10% sodium carbonate solution. The basic extract was acidified with concentrated HCl and washed with 25 ml of ether. The ether layer was washed neutral with water, dried, and evaporated to give 440 mg of carboxylic acid **2**; n.m.r.: (CCl_4, TMS internal) δ 1.70 (6H, s), 1.90 (3H, s), 2.14 (3H, s), 3.00 (2H, A_2X, d, J_{AX} = 7 Hz), 5.01 (1H, t, A_2X, J_{AX} = 7 Hz), 12.64 (1H, s, exchanged with D_2O); i.r.: λ_{max} (CCl_4) 1685 cm^{-1} (carboxylic acid); ultraviolet (u.v.): λ_{max} (pentane) 252 mμ (ε = 1150); (recrystallized from MeOH/H_2O) m.p. 50–51°.

Anal. Calcd. for $C_{10}H_{16}O_2$: C, 71.48; H, 9.52. Found: C, 71.32; H, 9.44.

The neutral ether fraction was dried with anhydrous magnesium sulphate and evaporated to give 340 mg of an oily residue which was chromatographed on 3 thin-layer chromatographic plates (10% ether – benzene). The less polar fraction (20 mg) was assigned structure **4** by comparison with an authentic sample (1). The major fraction was assigned structure **3** (300 mg) based on the following data: n.m.r.: 5.00 (1H, t), 3.1–2.3 (5H, m), 2.2–1.3 (24H, singlets); i.r.: λ_{max} (CCl_4) 3020 (C═C—H), 1725, 1699 (C═O), 1665 (C═C).

Anal. Calcd. for $C_{20}H_{30}O_3$: C, 75.45; H, 9.45. Found: C, 75.36; H, 9.18.

Pressure Hydrogenation of 2

To 500 mg of **2** in 40 ml of ethyl acetate was added 200 mg of PtO_2. This solution was placed in the Parr hydrogenator at 50 lb/in.^{2} for 15 h. The platinum was filtered and the solvent evaporated to give 505 mg of oily **6** (*2a*, *b*). Boiling point (4 mm) 119–121°; lit. (2) b.p. (4 mm) 118–120° (ether pentane); n.m.r.: 0.93 (6H, 2d), 1.09–2.07 (7H, m), 13.04 (1H, s, exchanged with D_2O); i.r.: λ_{max} (neat) 1710 cm^{-1} (carboxylic acid).

Anal. Calcd. for $C_{10}H_{20}O_2$: C, 69.80; H, 11.63. Found: C, 70.04; H, 11.65.

[1]Ketone **1** was obtained by a modified method as described by J. M. Conia (1).

Can. J. Chem. Downloaded from www.nrcresearchpress.com by 210.87.254.5 on 09/05/12
For personal use only.

Can. J. Chem. Downloaded from www.nrcresearchpress.com by 210.87.254.5 on 09/05/12
For personal use only.

The amide of **6** was prepared in the standard way *via* the acyl chloride. The acyl chloride was obtained by reaction of **6** with thionyl chloride. Amide m.p. 111–113°; lit. (2) m.p. 112–114°.

Anal. Calcd. for $C_{10}H_{21}NO$: C, 70.10; H, 12.30; N, 8.20. Found: C, 69.65; H, 12.36; N, 8.02.

Atmospheric Hydrogenation of ***2***

To 102.7 mg of **2** in 10 ml of ethyl acetate was added 35 mg of PtO_2. The mixture was hydrogenated at atmospheric pressure for 6 h. The platinum was filtered off and the solvent evaporated to give 100 mg of oily **5**; n.m.r.: 0.98 (6H, 2 d), 1.29 (3H, m), 1.85 (3H, s), 2.08 (3H, s), 2.30 (2H, m), 12.40 (1H, s, exchanged with D_2O); i.r.: λ_{max} 1695 cm^{-1} (α,β-unsaturated carboxylic acid); *m/e* 170.

Pressure Hydrogenation of ***5***

To 90 mg of **5** in 25 ml of ethyl acetate was added 60 mg of PtO_2. The mixture was hydrogenated at 45 lb/in.^{2} for 10 h. The Pt was filtered off and the solvent evaporated to give 92 mg of **6** identical with a sample previously prepared.

Hydrolysis of Ester ***3***

300 mg of **3** was dissolved in 10 ml of methanol containing 2 ml of water and 1 g of sodium hydroxide. The solution was stirred for 20 min at room temperature. The mixture was taken up in 25 ml of ether, the ether layer washed neutral with water, dried, and evaporated to give 130 mg of an oily residue shown by n.m.r., i.r., and thin-layer chromatography (t.l.c.) to contain a mixture of **1** and **4**. The aqueous layer was acidified with concentrated HCl. This was extracted with 25 ml of ether and worked up in the usual manner to give 135 mg of carboxylic acid **2** identical in all respects with a sample obtained previously.

Pressure Hydrogenation of Ketone ***1***

To 1 g of **1** in 50 ml of ethyl acetate was added 300 mg of PtO_2. The solution was hydrogenated at 45 lb/in.^{2} on a Parr hydrogenator for 6 h. The Pt was filtered off and the solvent evaporated to give 980 mg of oily **7**; n.m.r.: 0.93 (6H, 2 d), 1.14 (3H, s), 1.26 (3H, s); i.r.: λ_{max} 1770 (C=O of cyclobutanone); *m/e* 170.

Phosphorous Pentoxide Reaction of ***7***

500 mg of **7** was dissolved in 5 ml of anhydrous benzene. To the solution was added about 500 mg of P_2O_5 and the mixture was stirred for 4 h. The excess P_2O_5 was quenched by slow addition of water. The mixture was taken up in 25 ml of ether which was washed neutral with water. The ether layer was then extracted with 3 × 8 ml of 10% aqueous sodium carbonate. The aqueous layer was acidified with concentrated HCl and reextracted with 25 ml of ether which was then washed neutral with water, dried over anhydrous $MgSO_4$ and evaporated to give 150 mg of oily carboxylic acid **8**; n.m.r.: 0.98 (6H, d), 1.60 (3H, s), 1.67 (3H, s), 1.80–2.40 (4H, m), 5.10 (1H, t), 13.14 (1H, s, exchanged with D_2O); i.r.: λ_{max} (CCl_4) 1710 (saturated acid C=O).

Anal. Calcd. for $C_{10}H_{18}O_2$: C, 70.50; H, 10.60. Found: C, 70.52; H, 10.74.

Reaction of Ketone ***1*** *with* $HClO_4$

To 200 mg of ketone **1** dissolved in 5 ml of benzene was added 5 drops of concentrated perchloric acid. The solution was stirred at room temperature for 2 h. This was extracted with 25 ml of ether, the ether extract washed netural with water, dried, and evaporated to give 180 mg of **9**; *m/e* 168 (base peak *m/e* 118); n.m.r.: 1.32 (6H, s), 1.84 (3H, broad s), 2.18 (3H, broad s), 1.70 (2H, m), 2.50 (2H, m); i.r.: λ_{max} (CCl_4) 1710 cm^{-1} (C=O), 1630 (C=C), 1275 and 1110 cm^{-1} (C—O—C).

Reaction of Carboxylic Acid ***2*** *with Perchloric Acid*

To 25 mg of **2** in 5 ml of benzene was added 5 drops of concentrated perchloric acid. The solution was stirred at room temperature for 2 h. It was then taken up in 25 ml of ether and worked up in the usual manner to give 25 mg of **9** identical by n.m.r. and t.l.c. with the sample prepared above.

Reaction of Ketone ***10*** *(1) with PPA*

400 mg of **10** (1) was added to 8 g of PPA. The solution was vigorously stirred for 1 h at 100°. The reaction mixture was taken up in 4 ml of water. After cooling, it was extracted with ether and the extract washed with aqueous sodium bicarbonate and water, and dried over sodium sulfate. After evaporation of the solvent under reduced pressure, the residue was analyzed by vapor phase chromatography (v.p.c.) (XF-1150, 5.3 ft, 185°) and shown to consist of one product (retention time 9 min) (82% yield), 3-methylcyclohex-2-enone, **11**, whose i.r. and n.m.r. spectra were compared with those of an authentic sample.

Reaction of Ketone ***4*** *with PPA*

1.5 g of ketone **4** (1) was reacted with 25 g of PPA for 1 h at 100°. After working up in the same way as the procedure above the residue was analyzed by v.p.c. and shown to consist of two products. One was 3-methylcyclohex-2-enone (retention time 9 min) (10%); the other product was found to be piperitenone (**12**) (retention time 18 min) (71%) whose n.m.r. and i.r. spectra were identical with those described in the literature (3, 4).

Reaction of Carboxylic Acid ***2*** *with PPA*

The polyphosphoric acid was prepared by mixing 7 g of P_2O_5 with 3 ml of 85% phosphoric acid and heating at 100° for 12 h. 400 mg of **2** was added and the viscous solution was stirred for 1 h at 100°. 10 ml of water was slowly added and the reaction mixture cooled. This was extracted with 50 ml of ether. The ethereal extract was washed neutral with water, dried over anhydrous magnesium sulfate, and the solvent evaporated to give 320 mg of an oily residue which was separated into two components on v.p.c. (20% FFAP on Chrom W. 3 ft, 150°). The less polar material (retention time 2 min) (20 mg) was identical with 3-methylcyclohex-2-enone (**11**), the more polar product (retention time 4 min) (280 mg) was identical with piperitenone.

Reaction of Ketol ***16*** *with Phosphorous Pentoxide*

To 500 mg of ketol **16**[1] in 5 ml of benzene was added 1 g of P_2O_5. The mixture was stirred at room temperature for 2 h. This was worked-up in the usual manner to give

[1]**16** was obtained from the aldol condensation of acetone and cyclohexenone.

500 mg of an oily residue which showed two peaks (**17** and **18**) on v.p.c. (FFAP, 160°, 3 ft). The mixture showed the following spectral data: n.m.r.: 5.88 (1H, s), 5.50 (1H, m), 2.87 (2H, s), 2.75 (6H, m), 2.02 (3H, s), 1.99 (3H, s), 1.50 (12H, m); i.r. λ_{max} (CCl_4) 1680 (α,β-unsaturated C=O) 1710 (saturated C=O).

*Reaction of Ketol **19** with Phosphorous Pentoxide*

To 100 mg of ketol **19** in 5 ml of benzene was added 500 mg of P_2O_5. The reaction mixture was stirred for 8 h at room temperature. This was extracted with 5 ml of ether and worked up in the usual manner to give 95 mg of oily **20** whose n.m.r. and i.r. spectra were identical with those of an authentic sample (1).

Acknowledgments

The authors at Columbia would like to thank the Air Force Office of Scientific Research (AFOSR-1381) for support of this work. One of us (E.L.R.) would like to thank the National Research Council of Canada for a Post Doctorate Fellowship.

1. J. M. CONIA and J. P. SANDRE. Bull. Soc. Chim. France, 744 (1963).
2. (*a*) R. KOTAOKA. Nippon Kagaku Zasshi, **77**, 627 (1956); (*b*) M. MATSUI. Agr. Biol. Chem. (Tokyo), **27**, 549 (1963).
3. Y. R. NAVES and J. M. CONIA. Bull. Soc. Chim. France, 378 (1960).
4. Y. R. NAVES. Bull. Soc. Chim. France, 1195 (1963).
5. G. M. KOSOLAPOFF. Organophosphorous compounds. J. Wiley and Sons, Inc., New York. 1950. p. 220.
6. F. D. POPP and W. E. MCEWAN. Chem. Rev. **58**, 321 (1958).
7. J. M. CONIA and P. AMICE. Bull. Soc. Chim. France, 3327 (1968).

Can. J. Chem. Downloaded from www.nrcresearchpress.com by 210.87.254.5 on 09/05/12
For personal use only.

Can. J. Chem. Downloaded from www.nrcresearchpress.com by 210.87.254.40 on 09/05/12
For personal use only.

Reaction of thionyl bromide with tropolone and phenol

S. D. SARAF
Defence Science Organization, Chaklala, West Pakistan

Received February 25, 1969

Tropolone and phenol react with thionyl bromide forming 3,7-dibromotropolone and 2,4-dibromophenol respectively.

Canadian Journal of Chemistry, 47, 2803 (1969)

The reported synthesis (1, 2) of 2-chlorotropone from tropolone and thionyl chloride suggested that thionyl bromide might be used for a similar preparation of 2-bromotropone.

The reactions between thionyl bromide and organic compounds have been studied with only a few acids and alcohols. It has been reported (3) that on adding thionyl bromide to heptoic acid, a brisk reaction occured with the evolution of hydrogen bromide and sulfur dioxide and with the formation of acid bromide. It has also been reported (4) that thionyl chloride with tertiary alcohols gives only alkyl halides, whereas with other alcohols, a chlorosulfite is obtained as an intermediate. According to Darzens (4), the reaction of thionyl bromide with alcohols should follow the same course, but the intermediate ROSOBr is so unstable that it decomposes instantly and therefore has never been isolated.

The reaction of phenol with thionyl chloride has attracted a considerable amount of attention, and widely varying results have been obtained according to the experimental conditions chosen. Simply mixing the two reactants in the cold leads to the formation of a number of products, the main one being dihydroxydiphenyl sulfide (**1**) (5, 6). If the reaction takes place in carbon disulfide, dihydroxydiphenyl-*p*-sulfoxide (**2**) is the chief product (7).

Several unsuccessful attempts were made to prepare phenyl chlorosulfinate, but it was eventually obtained by the action of sodium phenoxide on thionyl chloride in toluene (8). This unusual behavior of thionyl chloride with phenol is not unique, since Ebine (9) has reported that 3-bromobenztropolone (**3**) with thionyl chloride gives 3,5-dichlorobenztropolone (**4**).

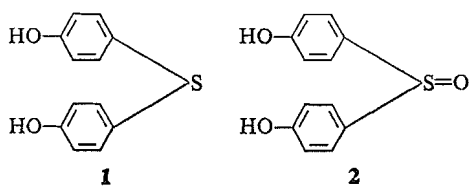

1 **2**

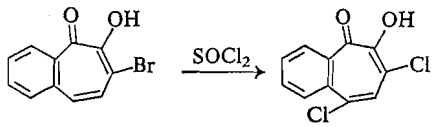

3 **4**

Addition of thionyl bromide to tropolone in dry benzene gave an immediate red precipitate, which redissolved on refluxing for 2 h to give a clear red solution. Work-up in the usual manner followed by sublimation and crystallization from petroleum ether (b.p. 60–80°) gave 3,7-dibromotropolone (**5**) as colorless needles m.p. 160–161° in 45% yield. This structure is based on the following facts.

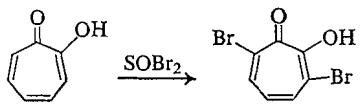

5

The compound analyzed for $C_7H_4Br_2O_2$, a dibromotropolone. The product gave an intense green coloration with ferric chloride, and with sodium hydroxide it formed an insoluble sodium salt. The infrared (i.r.) and ultraviolet (u.v.) spectra were in agreement with the reported spectra of 3,7-dibromotropolone.

The methyl ether of 3,7-dibromotropolone, on treatment with 25% sodium hydroxide solution, rearranged to 2,6-dibromobenzoic acid. Similar treatment of the methyl ether with sodium methoxide gave methyl 2,6-dibromobenzoate. These results are in agreement to those of Nozoe *et al.* (10) and Cook *et al.* (11).

Addition of thionyl bromide to solid phenol at room temperature gave an immediate reaction

with the evolution of hydrogen bromide, sulfur dioxide, and the precipitation of sulfur. Work-up in the usual manner followed by distillation gave 2,4-dibromophenol as colorless needles in an 85% yield. Its structure was confirmed by its i.r. spectrum, melting point, mixed melting point, and by preparing several of its derivatives. The gas–liquid phase chromatography gave the same retention time to that of an authentic 2,4-dibromophenol.

Nothing definite can be said about the mechanism operating in these reactions at the present stage.

Experimental

Thionyl bromide was prepared by the method of Mayes and Partington (3). The product distilled as an orange liquid, b.p. 58–60°/40 mm.

3,7-Dibromotropolone

To a solution of tropolone (200 mg) in dry benzene (50 ml) was added thionyl bromide (0.15 ml) and the mixture was refluxed for 2 h, when a clear red solution was obtained. Removal of the solvent followed by sublimation at 120–125°/0.2–0.3 mm gave a yellow solid, m.p. 142–144°. Crystallization of the crude product from petroleum ether (b.p. 60–80°) gave 3,7-dibromotropolone (200 mg) as long colorless needles, m.p. 160–161°, (lit. (10) 159–160°); i.r. spectrum CH_2Cl_2): 1600 and 1550 cm^{-1}; u.v. spectrum (ethanol): E_{max} 264, 355, 373, and 391 mμ; log ε = 4.4, 3.38, 3.36, and 3.37.

Anal. Calcd. for $C_7H_4Br_2O$: C, 30.0; H, 1.43. Found: C, 29.8; H, 1.5.

3,7-Dibromotropolone Methyl Ether

To a solution of 3,7-dibromotropolone (200 mg) in dry ether (10 ml) was added a dry ethereal solution of diazomethane in small portions until the solution gave no color with ferric chloride. Removal of the solvent under reduced pressure left a yellow crystalline solid, which was crystallized from petroleum ether (b.p. 100–120°) as yellow plates of 3,7-dibromotropolone methyl ether (178 mg, 85%). It melted at 130–131° (lit. (10) 133.5°).

Anal. Calcd. for $C_8H_6Br_2O_2$: C, 32.65; H, 2.04; Br, 54.4. Found: C, 32.35; H, 2.1; Br, 54.7.

Reactions of 3,7-Dibromotropolone Methyl Ether

a) With 25% Sodium Hydroxide

3,7-Dibromotropolone methyl ether (50 mg) and 25% aqueous sodium hydroxide (20 ml) were heated at 60° for 30 min. After acidification and extraction with ether, 2,6-dibromobenzoic acid (23 mg) m.p. 146–148° was isolated. Upon admixture with an authentic specimen of 2,6-dibromobenzoic acid, the melting point remained unchanged.

b) With Sodium Methoxide

A solution of 3,7-dibromotropolone methyl ether (100 mg) in methanol (10 ml) was added to a saturated solution of sodium methoxide and the mixture was refluxed for 3 h. Work-up in the usual manner and recovery of the product in ether afforded methyl 2,6-dibromobenzoate (75 mg, 75%), which melted at 62–63° (lit. (10) 61–62°).

2,4-Dibromophenol

To phenol (5 g) was added thionyl bromide (4.4 ml). A brisk reaction occurred with the evolution of hydrogen bromide and sulfur dioxide. After the reaction had slowed down, the reaction mixture was heated on a steam bath for 30 min. Work-up in the usual manner followed by distillation gave 2,4-dibromophenol (10 g) as a colorless oil, which crystallized from petroleum – ether (b.p. 40–60°) as colorless needles m.p. 35–36°, undepressed with an authentic specimen.

2,4-Dibromo-1-phenoxy Acetic Acid

This compound was prepared by a known procedure (12) from sodium phenate and chloroacetic acid. Crystallization from hot water gave 2,4-dibromo-1-phenoxy acetic acid as colorless needles, m.p. 154–155° (lit. (12) 151.8–153.5°).

Anal. Calcd. for $C_8H_6Br_2O_3$: C, 30.9; H, 1.9; Br, 51.2. Found: C, 30.7; H, 2.0; Br, 51.2.

Acknowledgments

The author is grateful to E. J. Forbes for his guidance and to the Birmingham University for providing the facilities to carry out this work.

1. W. Von E. Doering and L. H. Knox. J. Am. Chem. Soc. **74**, 5683 (1952).
2. B. J. Abadir, D. K. V. Steel, J. D. Loudon, and J. W. Cook. J. Chem. Soc. 2350 (1952).
3. H. A. Mayes and Partington. J. Chem. Soc. 2594 (1926).
4. G. Darzens. Compt. Rend. **152**, 1314, 1601 (1911).
5. P. Tassinari. Gazz. Chim. Ital. **20**, 362 (1890).
6. H. Voswinkel. Pharm. Ztg. Ver. Apotheker-Ztg. **40**, 241 (1895).
7. S. Smiles and A. W. Bains. J. Chem. Soc. 91, 1118 (1907).
8. M. Battergay and L. Denivelle. Compt. Rend. **192**, 492 (1931).
9. S. Ebine. Bull. Chem. Soc. Japan, **35**, 117 (1962).
10. T. Nozoe, Y. Kitahara, and S. Masamune. Proc. Japan Acad. **27**, 649 (1951).
11. J. W. Cook, A. R. M. Gibb, and R. A. Raphael. J. Chem. Soc. 2244 (1951).
12. Z. Steahly. J. Am. Chem. Soc. **69**, 718 (1947).

Can. J. Chem. Downloaded from www.nrcresearchpress.com by 210.87.254.40 on 09/05/12
For personal use only.

Can. J. Chem. Downloaded from www.nrcresearchpress.com by 210.87.254.105 on 09/05/12
For personal use only.

Estimation expérimentale et théorique de l'effet de l'encombrement stérique du groupement *tert*-butyle sur le déplacement chimique des protons aromatiques de nitro-1 naphtalènes substitués

S. ODIOT
Laboratoire de Physique Expérimentale Moléculaire, Faculté des Sciences, Paris, France

ET

J. C. RICHER
Département de Chimie, Université de Montréal, Montréal, Québec

ET

F. TONNARD
Groupe de Physicochimie Structurale, Equipe associée au C.N.R.S., Faculté des Sciences, Rennes, France

Reçu le 5 décembre 1968

Les groupements méthyle, méthoxyle et *tert*-butyle en position-2 dans les nitro-1 naphtalènes, perturbent les valeurs des déplacements chimiques du proton en position-8.

Cette perturbation est évaluée, par défaut à la règle d'additivité.

Par le calcul, on montre que le facteur responsable de cette perturbation est essentiellement lié à la variation de la contribution de l'anisotropie magnétique du groupement NO_2, suivant qu'il est ou non, dans le plan du cycle naphtalénique.

Canadian Journal of Chemistry, 47, 2805 (1969)

Introduction

Au cours d'études sur les substitutions électrophiles, Richer, Pepin, Baskevitch *et al.* (1–5) ont souligné certains effets d'encombrement stérique dûs aux groupements *tert*-butyle, méthoxyle et méthyle. En particulier, ils ont noté que de tels effets peuvent être mis en évidence par la résonance magnétique nucléaire (r.m.n.). Ceux-ci perturbent de façon sensible, les déplacements chimiques de certains protons du cycle naphtalénique. En ce qui concerne le groupe méthyle, Wells et Alcorn (6) sur le nitro-1 naphtalène, ont évalué à 0.64 p.p.m. la variation du déplacement chimique du proton H_8 lors d'une méthylation en 2. Ils attribuent cette différence à une modification de l'anisotropie magnétique du groupe nitro qui, gêné par le méthyle en 2, aurait tourné autour de la liaison CN.

Yamaguchi (7) a préconisé une relation empirique entre le déplacement chimique des protons du méthyle de l'*o*-méthyl-nitrobenzène et l'angle de rotation du groupe nitro. Il note que, pour les protons du méthyle, les variations de l'anisotropie magnétique causées par la rotation de NO_2 l'emportent sur celles d'un effet mésomère puisque, au cours de la rotation, la variation du déplacement chimique des protons du méthyle en *para* est seulement le 1/10 de celle du déplacement chimique des protons du méthyle en *ortho*. Gibbons et Gil (8) sur les mono-dérivés du mésitylène et du tri *tert*-butyl-1,3,5 benzène, concluent également à un effet stérique de ces groupements sur le déplacement chimique des protons du cycle; pour le dérivé nitré, ils observent un effet anormal sur le déplacement chimique du proton en *meta*, qui compenserait l'augmentation de densité électronique au cours de la rotation. Par ailleurs Franck et Williamson (9) ont montré, en série benzénique, que le déplacement chimique des protons aromatiques situés en position-2 par rapport à un groupe nitro est fonction de l'angle de torsion qui lui est imposé par les substituants méthyle, éthyle, propyle et *tert*-butyle situés en position-6. Sur une base d'observation qualitative ils attribuent cette variation de déplacement chimique à une diminution de l'anisotropie magnétique au cours de la rotation. A la suite d'un travail connexe sur la variation, en fonction du solvant, du déplacement chimique des protons aromatiques de nitrobenzènes substitués, Rae (10) a interprété ses résultats en terme d'une augmentation, dans le DMSO, de la grosseur effective du groupe nitro provoquant, dans les cas des produits

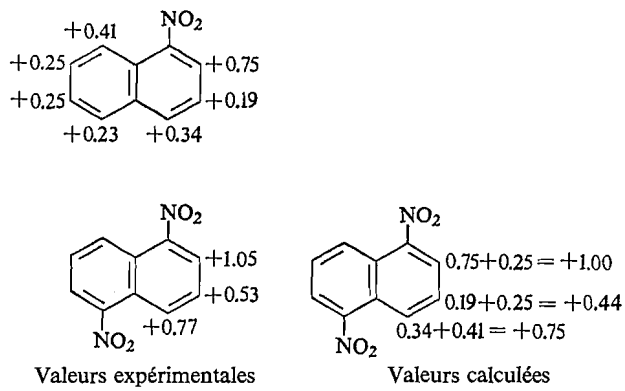

FIG. 1. Comparaison entre les valeurs calculées à l'aide de la loi d'additivité et les valeurs expérimentales (19) des déplacements chimiques par rapport au naphtalène, exprimées en p.p.m.

substitués par des groupes appropriés en *ortho* du groupe nitro, une rotation de ce groupe autour de l'axe Ar—N; cette interprétation tenait aussi compte implicitement d'une variation de l'anisotropie magnétique du groupe NO_2. Dans le cadre d'un travail théorique sur le déplacement chimique et la conformation des molécules, il s'avérait intéressant d'examiner systématiquement les mesures de déplacement chimique des protons des dérivés du nitronaphtalène rassemblés dans ces articles afin tout d'abord, d'estimer l'effet d'encombrement stérique des groupement *tert*-butyle, méthoxyle et méthyle sur la valeur du déplacement chimique δ^H, puis d'en analyser théoriquement le rôle tant du point de vue de l'effet mésomère que de celui de l'anisotropie magnétique.

Estimation de l'effet de l'encombrement stérique sur δ^H

Martin et Dailey (11) ont proposé une loi générale d'additivité des déplacements chimiques, qu'illustre en particulier la Fig. 1 sur les dérivés mono- et di-nitrés du naphtalène. La règle d'additivité suppose que l'apport d'un substituant supplémentaire ne modifie pas la géométrie de la molécule monosubstituée alors que, par effet stérique, le second substituant peut imposer une rotation au premier et rendre non valable l'application de la règle.

Aussi, nous proposons d'estimer l'effet stérique d'un groupement *tert*-butyle, méthoxyle ou méthyle sur le déplacement chimique des protons des dérivés correspondants du naphtalène, à l'aide de la différence entre la valeur expérimentale et celle que donnerait la loi d'additivité.

Dans la Fig. 3, sont rassemblés tous les résultats calculés selon le modèle explicité dans la Fig. 2. Les valeurs inférieures à 0.05 p.p.m. ne sont pas mentionnées.

On constate sur la Fig. 3: (*1*) que pour chaque groupement *tert*-butyle, méthoxyle et méthyle, l'effet est spécifique et prépondérant en position-8; (*2*) que l'effet décroit dans la série avec la dimension du groupement; (*3*) qu'il existe en position-3 un effet non négligeable inhérent au groupe méthoxyle, puisqu'il n'apparait pas pour les autres groupes; (*4*) qu'en position-4 et -5 rien de notable n'est à signaler; et (*5*) enfin, la Fig. 3 illustre assez bien la loi d'additivité lorsque les différents groupements, de par leurs positions relatives, ne peuvent être gênés stériquement.

Il semble que les déplacements chimiques des protons dans les positions 4 et 5 seraient insensibles à une diminution d'effet mésomère, provoquée par la rotation de NO_2. Cet effet devrait intervenir seul, puisqu'en raison de l'éloignement de ces protons du groupe nitro, la variation correspondante d'anisotropie magnétique est négligeable comme le montre le Tableau II.

Par contre, en position-8, contrairement à un proton en 5 ou en 4, une variation d'anisotropie magnétique occasionnée par la rotation, devrait contribuer de façon prépondérante à la variation de déplacement chimique observée.

Interprétation théorique de l'effet stérique du groupement *tert*-butyle sur le déplacement chimique δ^{H_8}

D'après la théorie de Pople (12) du déplacement chimique (dans le cadre de l'approximation des orbitales moléculaires à électrons indépendants,

Can. J. Chem. Downloaded from www.nrcresearchpress.com by 210.87.254.105 on 09/05/12
For personal use only.

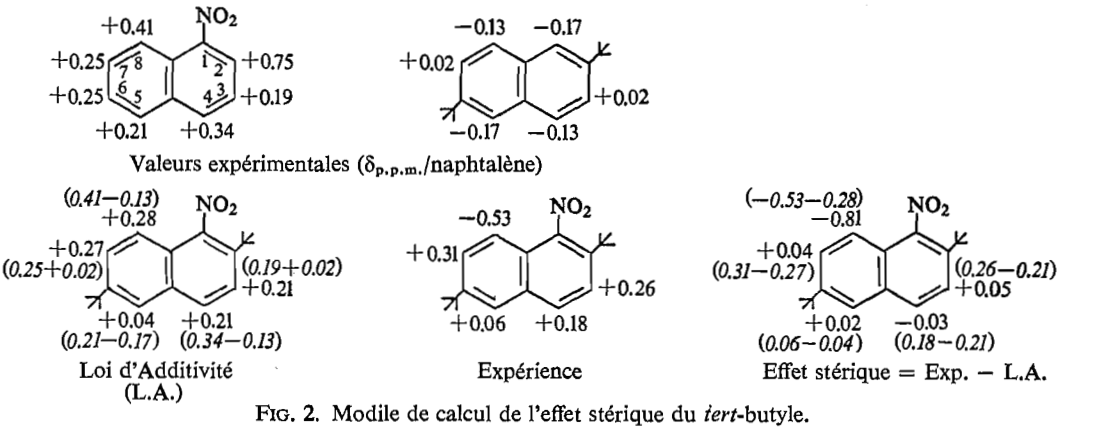

FIG. 2. Modile de calcul de l'effet stérique du *tert*-butyle.

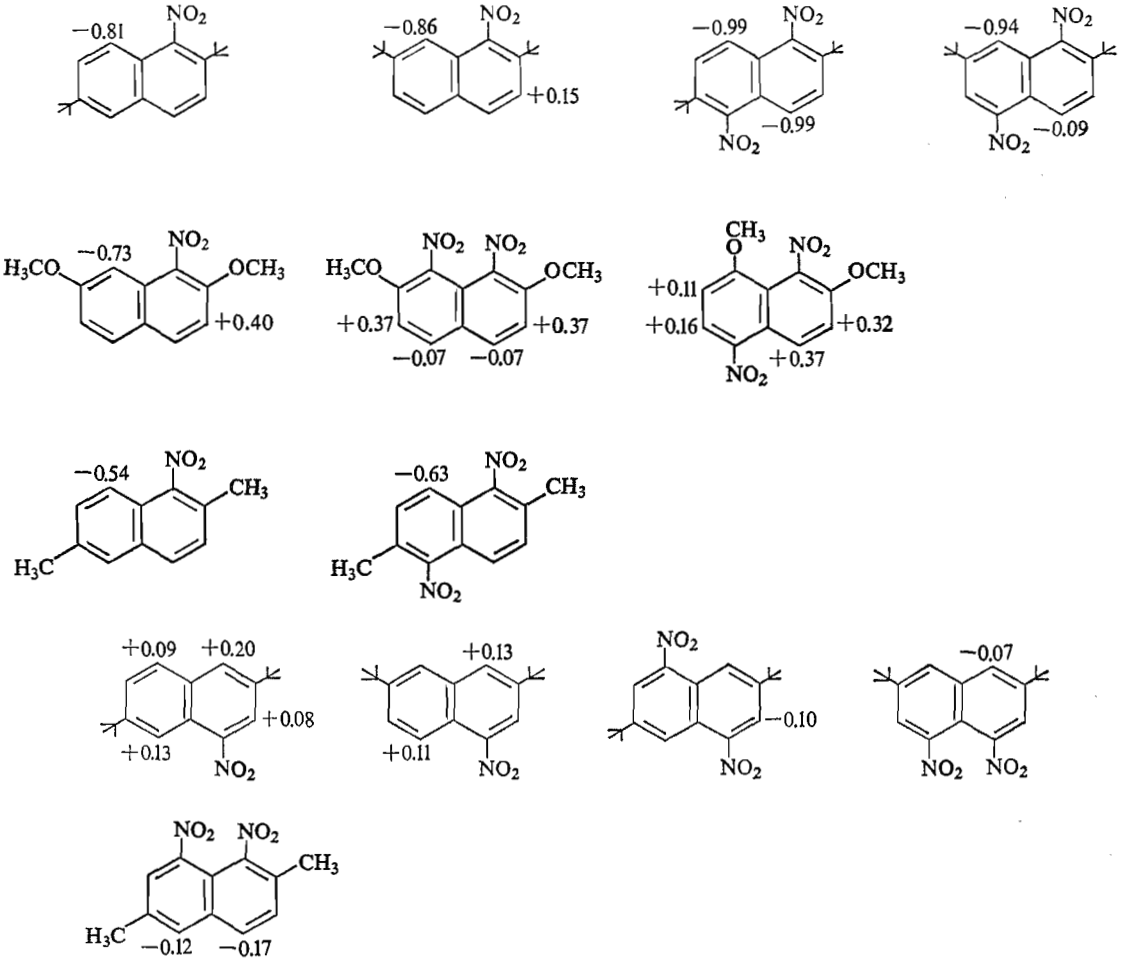

FIG. 3. Estimation des effet stériques.

NOTE: Les résultats expérimentaux nécessaires à ces estimations proviennent: pour les dérivés nitrés de la référence (10); pour les di-*tert*-2,6 (ou 2,7) diméthyl-2,6 et dimethoxy-2,7 (ou 2,8) naphtalènes et leurs dérivés nitrés des références (1–5). Les valeurs inférieures à 0.05 p.p.m. ne sont pas mentionnées.

Can. J. Chem. Downloaded from www.nrcresearchpress.com by 210.87.254.105 on 09/05/12
For personal use only.

TABLEAU I

Determination du parametre inductif (h_c) du *tert*-butyle comme function de δ^{H_i}.

	$\delta^{H_i} = -\Delta\sigma^{H_iH_i}$ Calc. (p.p.m/naphtalène)		
$h_2=h_6$	$i=1$	$i=3$	$i=4$
	Di-*tert*-butyl-2,6 naphtalène		
+0.10	+0.04≃0	−0.02≃0	+0.04≃0
−0.05	−0.02≃0	+0.01≃0	−0.02≃0
−0.10	−0.04≃0	+0.01≃0	−0.04≃0
−0.20	−0.08	+0.03≃0	−0.08
−0.30	−0.12	+0.05	−0.12
−0.40	−0.15	+0.07	−0.16
−0.50	−0.18	+0.09	−0.19
−0.70	−0.24	+0.14	−0.27
$\delta^{H_i}{}_{exp}$	−0.17	+0.02≃0	−0.13
	Di-*tert*-butyl-2,7 naphtalène		
+0.10	+0.05	−0.01≃0	+0.04≃0
−0.05	−0.01≃0	+0.01≃0	−0.02≃0
−0.10	−0.04≃0	+0.01≃0	−0.04≃0
−0.20	−0.08	+0.03≃0	−0.07
−0.30	−0.12	+0.05	−0.11
−0.40	−0.16	+0.06	−0.15
−0.50	−0.19	+0.08	−0.19
$\delta^{H_i}{}_{exp}$	−0.13	−0.04≃0	−0.19

TABLEAU II

Calcul de la contribution de l'anisotropie magnétique du groupe NO_2, à la constante d'écran des protons du nitro-1 naphtalène selon les deux modèles plan et non plan.

	$\sigma^{NO_2 plan}$	$\sigma^{NO_2 \perp plan}$
$\sigma^{H_3-NO_2}$	−0.05	−0.01≃0
$\sigma^{H_4-NO_2}$	−0.04≃0	−0.01≃0
$\sigma^{H_5-NO_2}$	−0.002=0	−0.01≃0
$\sigma^{H_8-NO_2}$	−0.65	+0.10

pour expliciter la fonction d'onde moléculaire) la constante d'écran σ^H d'un proton engagé dans une molécule cyclique, résulte de la contribution de trois termes: σ^{HH}, diamagnétique lié à la distribution électronique autour du proton; $\Sigma_X\sigma^{HX}$, anisotropie magnétique des atomes ou groupes d'atomes X, voisins; et σ^H_{CC} courant cyclique.

Si l'on prend le naphtalène comme référentiel dans la série de molécules étudiées, on peut négliger la variation de la contribution du courant cyclique vis à vis des deux autres et écrire:

$$[1] \qquad \delta^H = \sigma^H_{ref} - \sigma^H_{ech} = -\Delta\sigma^H = -(\Delta\sigma^{HH} + \Sigma_X\Delta\sigma^{HX})$$

Comme il l'a été mentionné, un groupe *tert*-butyle, au voisinage immédiat du groupe nitro doit avoir tendance à faire tourner d'un angle α le groupement NO_2 autour de la liaison C—N.

Quelle peut être alors la conséquence de cette rotation respectivement sur $\Delta\sigma^{H_8-H_8}$ et sur $\Delta\sigma^{H_8-NO_2}$? (Ce dernier terme est celui auquel on peut réduire la somme: $\Sigma_X\Delta\sigma^{H_8-X}$ lorsque l'on cherche à prévoir la variation de δ^{H_8} au cours de la rotation de NO_2.)

(*i*) *Influence de la rotation de NO_2 sur le terme diamagnétique* $\Delta\sigma^{H_8-H_8}$

Nous avons établi (13) théoriquement une relation qui permet le calcul de la variation du terme diamagnétique d'un proton indicé par *i* en fonction de la variation correspondante des charges π: Δq_i du carbone *i*, lié au proton *i*, $\Delta q_{i\pm1}$ des carbones voisins $i \pm 1$ et de l'indice de valence libre ΔF_i du carbone *i*.

$$[2] \quad \Delta\sigma^{H_iH_i} = 5\Delta q_i - 2\Delta F_i + 2(\Delta q_{i+1} + \Delta q_{i-1})$$

La détermination des charges et de l'indice de valence libre, résulte d'un calcul Hückel de fonction d'onde π. Pour ce calcul, les paramètres de l'azote et de l'oxygène sont connus; par contre, ceux du groupement *tert*-butyle, sont à déterminer.

D'après les travaux de Heilbronner (14) sur les spectres u.v., d'Ingold (15) sur les vitesses de nitration du toluène et du *tert*-butyl-benzène et de Gibbons et Gil (16) sur une étude comparée des déplacements chimiques des protons dans les 2 séries des méthyl- et *tert*-butyl-benzènes, le groupe *tert*-butyle semble interagir avec le cycle, par effet inductif, de la même façon que le groupe méthyle. Nous traitons l'effet inductif du *tert*-butyle en choisissant pour paramètre h_c du carbone qui lui est chimiquement lié, celui qui rend le mieux compte des déplacements chimiques, par rapport au naphtalène, des protons du cycle des 2,6- et 2,7-di-*tert*-butyl-naphtalènes. L'ajustement sur l'expérience se fait, en considérant l'anisotropie du *tert*-butyle comme négligeable, à l'aide de la formule [1]:

$$\delta^{H_i} = -\Delta\sigma^{H_i} = -\Delta\sigma^{H_iH_i}$$

et de la formule [2] pour le calcul de $\Delta\sigma^{H_iH_i}$. Les résultats rassemblés dans le Tableau I montrent qu'une valeur de h_c comprise entre −0.3 et −0.5 peut être retenue, ce qui confirme le caractère électro-donneur du *tert*-butyle comparable

Can. J. Chem. Downloaded from www.nrcresearchpress.com by 210.87.254.105 on 09/05/12
For personal use only.

Can. J. Chem. Downloaded from www.nrcresearchpress.com by 210.87.254.105 on 09/05/12
For personal use only.

au méthyle. En effet, l'effet inductif du méthyle se traite habituellement avec un paramètre h_c égal à -0.5 (17), (dans le cadre de la méthode de Hückel).

Nous avons effectué le calcul Hückel de la fonction d'onde du di-*tert*-butyl-2,6 nitro-1 naphtalène en utilisant les paramètres suivants (17), $h_2 = h_6 = -0.3, h_{\dot{N}} = 1.5$, $h_{\dot{O}} = 1.00$, et $K_{CN} = 1.00 \cos\alpha$, avec $\cos\alpha = 1$ pour le modèle plan et $\cos\alpha = 0$ pour le modèle non plan.

Pour le proton en 8, il résulte du calcul sur les deux modèles plan et non plan, une différence de variation de constante d'écran diamagnétique, par rapport au naphtalène:

$$\Delta\sigma^{H_8H_8}_{\text{non plan}} - \Delta\sigma^{H_8H_8}_{\text{plan}} = +0.12 - 0.04 = +0.08 \text{ p.p.m.}$$

La rotation du groupement NO_2 induit donc une variation de la contribution diamagnétique au déplacement chimique du proton en 8 de l'ordre de:

$$(a) \quad \delta^{H_8H_8}_{\text{non plan}} - \delta^{H_8H_8}_{\text{plan}} = -0.12 - (-0.04) = -0.08 \text{ p.p.m.}$$

(ii) Influence de la rotation de NO_2 sur le terme d'anisotropie $\sigma^{H_8-NO_2}$

En adoptant la technique proposée par Pople (18) pour le calcul du terme d'anisotropie, nous avons calculé la contribution à la constante d'écran du proton en 8 de l'anisotropie du groupement NO_2 dans les deux cas où, NO_2 est dans le plan du cycle ou perpendiculaire à ce plan.

Le calcul, détaillé dans l'appendice, conduit aux résultats suivants:

$$\sigma^{H_8-NO_2}_{\text{plan}} = -0.65 \quad \text{et} \quad \sigma^{H_8-NO_2}_{\text{non plan}} = +0.10$$

soit

$$\Delta\sigma^{H_8-NO_2} = \sigma^{H_8-NO_2}_{\text{non plan}} - \sigma^{H_8-NO_2}_{\text{plan}} = +0.75$$

d'où

$$(b) \quad \delta^{H_8-NO_2}_{\text{non plan}} - \delta^{H_8-NO_2}_{\text{plan}} = -\Delta\sigma^{H_8-NO_2} = -0.75 \text{ p.p.m.}$$

En additionnant les deux contributions (*a*) et (*b*), l'effet d'une rotation de 90° du groupement NO_2 (gêné par le groupe voisin du *tert*-butyle), sur le déplacement chimique du proton H_8 est théoriquement égal à:

$$(c) \quad \delta^{H_8}_{\text{non plan}} - \delta^{H_8}_{\text{plan}} = -0.83 \text{ p.p.m.}$$

C'est l'ordre de grandeur de l'effet stérique estimé empiriquement dans la première partie. Il faut remarquer que ce chiffre calculé, est une borne supérieure de l'effet réel puisque l'on a supposé l'angle de rotation égal à 90°.

Conclusion

Cette analyse souligne le rôle important que peut jouer l'anisotropie magnétique d'un groupe d'atomes en vue de l'élaboration d'un modèle moléculaire. Elle est, en grande partie, responsable des variations de déplacement chimique, vers les champs forts, du proton, en position péri du groupement nitro, dans le cycle naphtalénique, lorsque —NO_2 se place hors du plan, sous la contrainte de l'encombrement stérique du groupe *tert*-butyle. Cette conclusion basée sur des calculs semi-empiriques rejoint précisément les observations qualitatives faites par Franck et Williamson (9).

C'est aussi l'anisotropie magnétique qui, dans certains cas, met en défaut la relation linéaire entre le déplacement chimique et la charge (au sens L.C.A.O.O.M.). Une telle relation n'est en effet valable, qu'appliquée à des séries de molécules pour lesquelles les termes d'anisotropie sont comparables ou nuls; le seul terme sensiblement variable d'une molécule à l'autre, se réduit alors au terme diamagnétique explicité par la formule [2].

Partie expérimentale

Les spectres r.m.n. ont été déterminés à la température ambiante pour des solutions diluées (environ 5% ou saturées lorsque la solubilité n'était pas suffisamment élevée) dans la diméthyl-acétamide et à l'aide de spectromètres Varian A-60 et Jeolco JNM-4H-100; le tetraméthylsilane a été utilisé comme référence interne.

Appendice

Calcul de l'anisotropie du groupement NO_2 pour le proton H_8

Pour ce calcul nous avons utilisé la méthode proposée par Pople (18) basée sur l'approximation dipolaire. Pour un atome A situé à la distance R du proton étudié, l'anisotropie est donnée par la formule:

$$\sigma^{H-A} = \frac{2}{3NR^3}\left[(\chi^A_P)_{xx} - \tfrac{1}{2}(\chi^A_P)_{yy} - \tfrac{1}{2}(\chi^A_P)_{zz}\right]$$

à condition que l'axe des x soit orienté dans la

direction HA. N est le nombre d'Avogadro; χ_P^A est la susceptibilité paramagnétique de l'atome A. Si χ_P admet une symétrie axiale, la formule précédente se réduit à:

$$\sigma^{H-A} = \frac{1}{3NR^3}(\chi_{\parallel}^A - \chi_{\perp}^A)(1 - 3\cos^2\Theta)$$

où Θ est l'angle formé par l'axe de symétrie et la direction HA. La susceptibilité paramagnétique se calcule à l'aide de la formule proposée par Pople (18).

$$\chi_P^A = \frac{Ne^2\hbar^2}{4m^2c^2}\frac{1}{\Delta E}\sum_B Q_{AB}$$

avec

$$Q_{AB} = P_{x_Ax_B}(2\delta_{AB} - P_{y_Ay_B}) + P_{y_Ay_B}(2\delta_{AB} - P_{x_Ax_B}) + 2P_{x_Ay_B}P_{y_Ax_B}$$

Premier cas: *NO_2 est dans le plan des cycles*

On prend l'axe des x dans la direction H_8O_1 et on obtient: $(\chi_P^{O_1})_{xx} = 6.48 \times 10^{-6}$, $(\chi_P^{O_1})_{yy} = 3.30 \times 10^{-6}$, $(\chi_P^{O_1})_{zz} = 4.31 \times 10^{-6}$, d'où $\sigma^{H_8O_1} = -0.59$.

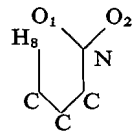

Anisotropie de O_2—On prend maintenant l'axe des x dans la direction H_8O_2, ce qui donne: $(\chi_P^{O_2})_{xx} = 2.76 \times 10^{-6}$, $(\chi_P^{O_2})_{yy} = 7.03 \times 10^{-6}$, $(\chi_P^{O_2})_{zz} = 4.31 \times 10^{-6}$, et $\sigma^{H_8-O_2} = +0.07$.

Anisotropie de N—L'axe des y étant dirigé suivant C—N, on obtient: $(\chi_P^N)_{xx} = 9.91 \times 10^{-6}$, $(\chi_P^N)_{yy} = 9.72 \times 10^{-6}$, $(\chi_P^N)_{zz} = 6.44 \times 10^{-6}$. On voit que χ_P^N est pratiquement symétrique par rapport à l'axe des z. On peut utiliser la deuxième formule, ce qui donne: $\sigma^{H_8N} = -0.13$, d'où finalement $\sigma^{H-NO_2} = -0.65$.

Deuxième cas: *NO_2 perpendiculaire au plan de la molécule*

Dans ce cas le groupement NO_2 n'est plus conjugué avec le reste de la molécule et on doit alors recalculer les indices P_{zz} pour ce groupement. Dans ce but, nous avons utilisé les paramètres suivants: $k_{NO} = 0.70$, $h_N = 1.50$ et $h_O = 1.00$ et on obtient: $P_{z_Nz_N} = 1.245$, $P_{z_Oz_O} = 1.378$ et $P_{z_Nz_O} = 0$.

Pour les deux atomes d'oxygène qui sont maintenant à la même distance de H_8, on prendra l'axe des y parallèle à la liaison C—N et l'axe des x dans le plan de NO_2. On obtient ainsi: $(\chi_P^O)_{xx} = 4.43 \times 10^{-6}$, $(\chi_P^O)_{yy} = 5.24 \times 10^{-6}$, $(\chi_P^O)_{zz} = 4.31 \times 10^{-6}$.

Ici encore on peut admettre qu'il y a symétrie axiale, autour de Oy, d'où: $\sigma^{H_8O} = +0.013$.

Pour l'atome d'azote nous avons pris les mêmes axes que pour l'oxygène et nous avons obtenu les résultats suivants: $(\chi_P^N)_{xx} = (\chi_P^N)_{yy} = 6.46 \times 10^{-6}$, $(\chi_P^N)_{zz} = 5.38 \times 10^{-6}$, d'où $\sigma^{H_8N} = +0.078$ et $\sigma^{H_8NO_2} = +0.10$.

Remerciements

Les auteurs sont reconnaissants à Madame Blain pour sa participation fructueuse à l'élaboration des calculs.

Simone Odiot et François Tonnard remercient l'O.T.A.N. pour sa contribution financière n° 296 qui leur a donné la possibilité de cette collaboration avec Jean Claude Richer, lors de leur séjour à l'Université de Montréal.

Jean Claude Richer remercie vivement le Conseil National de Recherches du Canada pour l'aide financière apportée sous forme de bourse et d'octrois de recherches.

1. J. C. Richer et C. Lamarre. Can. J. Chem. **43**, 715 (1965).
2. J. C. Richer et Y. Pepin. Can. J. Chem. **43**, 3443 (1965).
3. L. Erichomovitch, M. Menard, F. L. Chubb, Y. Pepin et J. C. Richer. Can. J. Chem. **44**, 2305 (1966).
4. J. C. Richer et N. Baskevitch. Can. J. Chem. **46**, 2975 (1968).
5. J. C. Richer, N. Baskevitch, L. Erichomovitch et F. L. Chubb. Can. J. Chem. **46**, 3363 (1968).
6. P. R. Wells et P. G. E. Alcorn. Australian J. Chem. **16**, 1108 (1963).
7. I. Yamaguchi. Mol. Phys. **6**, 105 (1963).
8. W. A. Gibbons et V. M. S. Gil. Mol. Phys. **9**, 167 (1965).
9. R. W. Franck et M. A. Williamson. J. Org. Chem. **31**, 2420 (1966).
10. I. D. Rae. Australian J. Chem. **20**, 2381 (1967).
11. J. S. Martin et B. P. Dailey. J. Chem. Phys. **39**, 1722 (1963).
12. J. A. Pople. J. Chem. Phys. **37**, 53 (1962).
13. S. Odiot et F. Tonnard. Compt. Rend. **262B**, 1181 (1966).
14. E. Heilbronner. Tetrahedron, **12**, Suppl. 2, 289 (1963).
15. C. K. Ingold. Structure and mechanism in organic chemistry. G. Bell and Sons, London. 1953.
16. W. A. Gibbons et V. M. S. Gil. Mol. Phys. **9**, 163 (1965).
17. A. Streitwieser. Molecular orbital theory for organic chemists. John Wiley and Sons, Inc., New York. 1961. p. 135.
18. J. A. Pople. J. Chem. Phys. **38**, 1276 (1963).
19. P. R. Wells. J. Chem. Soc. 1967 (1963).

Can. J. Chem. Downloaded from www.nrcresearchpress.com by 210.87.254.105 on 09/05/12
For personal use only.

Can. J. Chem. Downloaded from www.nrcresearchpress.com by 210.87.254.42 on 09/05/12
For personal use only.

Reactions of nitro sugars. XI. Formation of 2,3-unsaturated hexonolactones by denitration of methyl deoxynitroglycosides[1,2]

HANS H. BAER AND WERNER RANK
Department of Chemistry, University of Ottawa, Ottawa, Canada

Received February 20, 1969

Treatment of methyl 4,6-*O*-benzylidene-3-deoxy-3-nitro-β-D-glucopyranoside (**1**) and its α-anomer (**3**), as well as of methyl 4,6-*O*-benzylidene-2,3-dideoxy-3-nitro-β-D-*erythro*-hex-2-enopyranoside (**2**) and its α-anomer (**4**), with basic aluminum oxide in refluxing toluene, leads to loss of the nitro and glycosidic methoxyl groups. As a common product an α,β-unsaturated lactone, 4,6-*O*-benzylidene-2,3-dideoxy-D-*erythro*-hex-2-enono-1,5-lactone (**5**), was isolated in crystalline form. The β-D-*manno* isomer (**6**) of **1** incurs epimerization to **1** and partial conversion to **5**. Methyl 4,6-*O*-benzylidene-3-deoxy-3-nitro-β-D-galactopyranoside (**7**) and methyl 4,6-*O*-benzylidene-2,3-dideoxy-3-nitro-β-D-*threo*-hex-2-enopyranoside (**8**) similarly yield a crystalline lactone, 4,6-*O*-benzylidene-2,3-dideoxy-D-*threo*-hex-2-enono-1,5-lactone (**9**). The mechanism of this novel reaction is discussed, and certain differences in reactivity in the *gluco* and *galacto* series are pointed out. Base-catalyzed additions of methyl alcohol, ethyl alcohol, and piperidine to **8** afford methyl 4,6-*O*-benzylidene-3-deoxy-2-*O*-methyl-3-nitro-β-D-galactopyranoside (**10**), its 2-*O*-ethyl analogue (**11**), and methyl 4,6-*O*-benzylidene-2,3-dideoxy-3-nitro-2-piperidino-β-D-galactopyranoside (**12**), respectively.

Canadian Journal of Chemistry, 47, 2811 (1969)

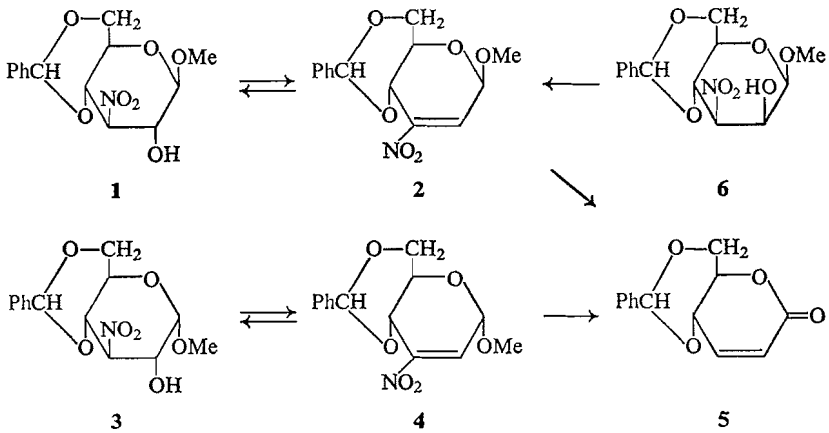

As has been shown earlier in this series (2), the treatment of methyl 4,6-*O*-benzylidene-3-deoxy-3-nitro-β-D-glucopyranoside (**1**) with basic aluminum oxide in the presence of alcohols or amines leads to an exchange of the C-2 hydroxyl for an alkoxy or amine function. The reaction, which is carried out in refluxing toluene, is considered to be an elimination–addition proceeding via an intermediate nitroalkene, methyl 4,6-*O*-benzylidene-2,3-dideoxy-3-nitro-β-D-*erythro*-hex-2-enopyranoside (**2**). We now wish to report that action of basic aluminum oxide upon **1** as well as **2** in the *absence* of nucleophilic addends furnished a hitherto unknown, unsaturated sugar lactone, namely 4,6-*O*-benzylidene-2,3-dideoxy-D-*erythro*-hex-2-enono-1,5-lactone (**5**). The same lactone (**5**) was also obtained from the α-anomers of **1** and **2** (**3** and **4**).

The structure of **5** followed from elemental analysis which agreed with the formula $C_{13}H_{12}O_4$, and from spectral data. The infrared (i.r.) spectrum exhibited a strong carbonyl band and lacked nitro and hydroxyl absorptions. The nuclear magnetic resonance (n.m.r.) spectrum (Fig. 1) revealed that the product had lost the glycosidic methoxyl but retained the benzylidene group. The latter gave a 5-proton multiplet centered at τ 2.6 and a 1-proton singlet at τ 4.38.

[1]For Part X in this series, see ref. 1.
[2]Presented at the 155th National Meeting of the American Chemical Society, April 1968, San Francisco, California.

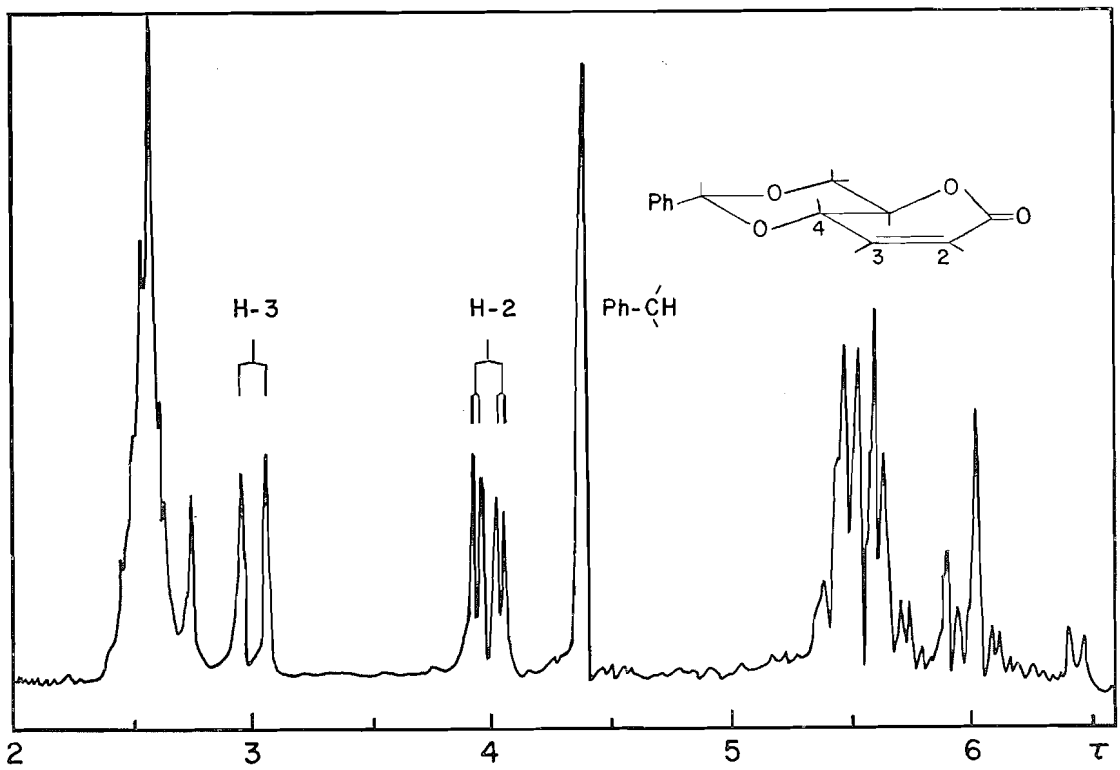

FIG. 1. Nuclear magnetic resonance spectrum (100 MHz) of 4,6-*O*-benzylidene-2,3-dideoxy-D-*erythro*-hex-2-enono-1,5-lactone (**5**).

Two 1-proton signals at τ 3.01 and 4.00 were assigned to the olefinic hydrogens at C-3 and C-2, respectively. The lower-field signal (H-3) appeared as a doublet due to vicinal coupling with H-2 ($J_{2,3}$ = 10 Hz); no vicinal coupling between H-3 and H-4 was observable, and this was not unexpected since, as a Dreiding model shows, the dihedral bond angle is close to 90° and coupling must therefore be at a minimum. The H-2 signal was a quartet exhibiting the 10 Hz vicinal coupling with H-3 and indicating allylic coupling with H-4 ($J_{2,4}$ = 2 Hz). The relatively large allylic coupling seen here is in line with a nearly perpendicular orientation of the bonds (3). Overlapping multiplets with a total intensity corresponding to four protons occurred in the region τ 5.3–6.3 (H-4, H-5, H-6, and H-6′).

With yields in crystalline **5** being about 30% the reactions evidently were incomplete under the conditions investigated. When the hydroxy compounds **1** and **3** were used as starting materials, appreciable proportions of them seemed to remain unaffected. On the other hand, the nitroalkenes **2** and **4** were consumed completely as far as could be judged from thin-layer chromatography (t.l.c.). However, they were in part hydrated to **1** and **3**, respectively, and no increase in yields of **5** resulted. The partial hydration of **2** and **4** was ascertained by the isolation of crystalline **1** and **3** from crude reaction mixtures that contained **5**. The β-D-*gluco* compound (**1**) was also formed, and isolated in 24% yield along with 30% of the lactone (**5**), when methyl 4,6-*O*-benzylidene-3-deoxy-3-nitro-β-D-mannopyranoside (**6**) was subjected to the reaction. Obviously **6** was dehydrated to give intermediate **2** which was then partly converted into **5** and partly rehydrated, not to **6** but to thermodynamically more stable **1**[3].

[3]It may be recalled that *acetylation* of **6** with hot acetic anhydride and sodium acetate led to the 2-*O*-acetyl derivative of **1** rather than to that of **6** (4). Further studies concerning the base-catalyzed epimerization of **6** to **1** and the hydration of **2** to **1** are reported in Part XII of this series. The fact that conversion of **1** and **3** into **5** was incomplete was due, we believe, to deactivation of the alumina during the reaction.

Can. J. Chem. Downloaded from www.nrcresearchpress.com by 210.87.254.42 on 09/05/12
For personal use only.

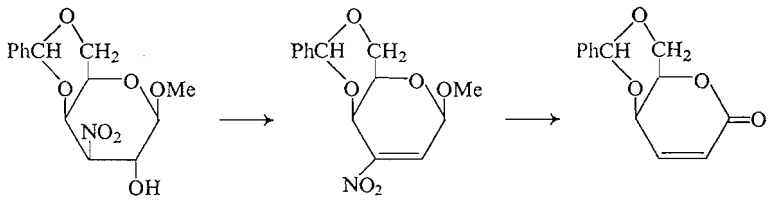

7 8 9

Analogous experiments were performed with methyl 4,6-*O*-benzylidene-3-deoxy-3-nitro-β-D-galactopyranoside (**7**) and with the nitroolefin derived from it, namely methyl 4,6-*O*-benzylidene-2,3-dideoxy-3-nitro-β-D-*threo*-hex-2-enopyranoside (**8**). Both compounds furnished the unsaturated lactone, 4,6-*O*-benzylidene-2,3-dideoxy-D-*threo*-hex-2-enono-1,5-lactone (**9**), which was isolated in crystalline form in yields of about 50%.

Elemental analysis of **9** agreed with the formula $C_{13}H_{12}O_4$, and the i.r. spectrum showed a prominent carbonyl peak and indicated the absence of nitro and hydroxyl groups. The n.m.r. spectrum (Fig. 2) exhibited the same general features as that of the D-*erythro* isomer (**5**). A 1-proton quartet attributed to H-3 occurred at τ 3.10 ($J_{2,3}$ = 10 Hz, $J_{3,4}$ = 6 Hz), the vicinal coupling with the quasi-equatorial H-4 being of the expected order. A 1-proton doublet for H-2 was at τ 3.76 (splitting, 10 Hz). In agreement with the bond orientation of H-4, the H-2 signal of **9** showed no allylic coupling (3) and in this respect differed from the analogous signal in isomeric **5**.

The carbonyl frequency in the i.r. spectrum of

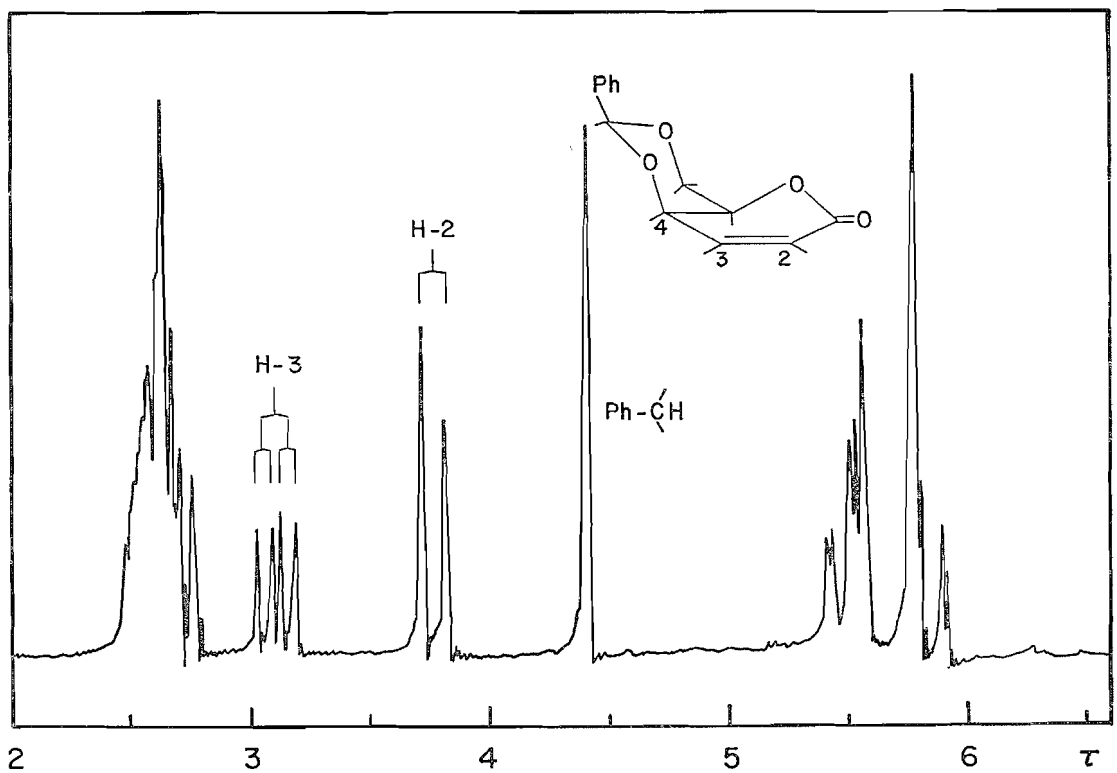

FIG. 2. Nuclear magnetic resonance spectrum (100 MHz) of 4,6-*O*-benzylidene-2,3-dideoxy-D-*threo*-hex-2-enono-1,5-lactone (**9**).

Can. J. Chem. Downloaded from www.nrcresearchpress.com by 210.87.254.42 on 09/05/12
For personal use only.

Can. J. Chem. Downloaded from www.nrcresearchpress.com by 210.87.254.42 on 09/05/12
For personal use only.

9 was at 1725 cm^{-1} in accord with the α,β-unsaturated, δ-lactone structure. The corresponding peak in stereoisomeric **5** occurred at 1755 cm^{-1}. This surprisingly high value can, we believe, be reconciled with the structure by assuming the presence of some strain in the molecule due to the *trans* junction between the chair and half-chair rings. The assumption received support when hydrolytic removal of the benzylidene group caused the carbonyl frequency to shift to 1725 cm^{-1}.

It could be shown by t.l.c. and other means (see below) that **8** is indeed an intermediate in the conversion of **7** into **9**. In interesting contrast to the behavior of the D-*gluco* compounds described in the preceding section, the D-*galacto* compound (**7**) disappeared entirely from the reaction mixture within 1 h, and when the nitroalkene (**8**) was employed as starting material, no hydration to **7** was observed. This is reminiscent of the behavior of **7** under conditions of sodium acetate - catalyzed acetylation, which resulted (4) in a facile dehydration to **8** rather than production of the 2-acetate[4]. It is considered that transformation of the pyranoside chair conformation of **7** into the half-chair of **8** is attended with relief of strain on account of an outward movement by the axial C-4 oxygen atom; the reverse transformation would involve a corresponding strain increase. This steric factor (6), which is absent in the systems with equatorial C-4 oxygen (**1** ⇄ **2** and **3** ⇄ **4**), is thought to explain the observed differences in reactivity.

However, the steric effect just invoked is obviously not powerful enough to prevent the nitroalkene **8** from adding nucleophiles under more favorable conditions. We have recently reported the preparative addition to **8** of nitroalkanes (7) and of ammonia (8). In the present work, use was made of similar additions to demonstrate the intermediacy of **8** in the reaction **7** → **9**. When the progress of the action of basic aluminum oxide upon **7** was monitored by t.l.c., it was seen that **8** arose as an intermediate showing maximum spot intensity after about 30–40 min; this spot then receded while the lactone (**9**) was slowly engendered, eventually becoming the sole spot (Fig. 3). When the process was interrupted after 40 min by cooling followed by the addition of sodium methoxide, sodium ethoxide, or piperidine, crystalline addition products from intermediate **8** and these nucleophiles could be isolated. They were methyl 4,6-*O*-benzylidene-3-deoxy-2-*O*-methyl-3-nitro-β-D-galactopyranoside (**10**), its 2-*O*-ethyl analogue (**11**), and methyl 4,6-*O*-benzylidene-2,3-dideoxy-3-nitro-2-piperidino-β-D-galactopyranoside (**12**). Identical products were obtained from pure **8** directly[5]. The β-D-*galacto* configuration, which on the basis of previous experiences (7, 8) could be predicted as most likely for **10**, **11**, and **12** but required proof nonetheless, was ascertained by n.m.r. spectroscopy. This was possible by analysis of the ring proton signals (see Experimental), and reference is here made to relevant discussions in earlier work (2, 7) on analogous compounds.

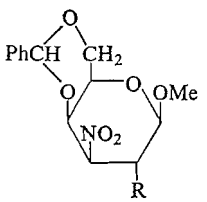

10 R = OMe
11 R = OEt
12 R = $N(CH_2)_5$

Concerning the mechanism of formation of the unsaturated lactones we envisage a sequence of acid–base catalyzed reactions as exemplified in Scheme I. The essential steps in that scheme are abstraction of the anomeric (and here, allylic) proton in the starting nitroolefin (**2**), protonation of the resulting nitronate (**13**) followed by hydrolysis of the ketene acetal (**14**), and finally β-elimination of nitrous acid from the nitro lactone (**15**). No intermediates have been isolated so far, but unidentified chromatographic spots, observed in the reactions that furnished **5** from **2** and **4**, are possibly attributable to such intermediates.

The results of the present investigation will remind the reader of two recent studies which

[4]A similar dehydration, leading to the α-anomer of **8**, has been found to take place in the acetylation of the α-D-*talo* isomer of **7** (5).

[5]An attempt to produce **12** from **7** by allowing piperidine to be present from the outset (i.e. during the initial period of heating with aluminum oxide) did not succeed but resulted in decomposition, although an analogous experiment in the D-*gluco* series (2) was successful. It is believed that this failure was caused by the greater sensitivity toward base of the 4,6-*O*-benzylidene blocking group in 3-deoxy-3-nitro-D-galactose derivatives (7, 8).

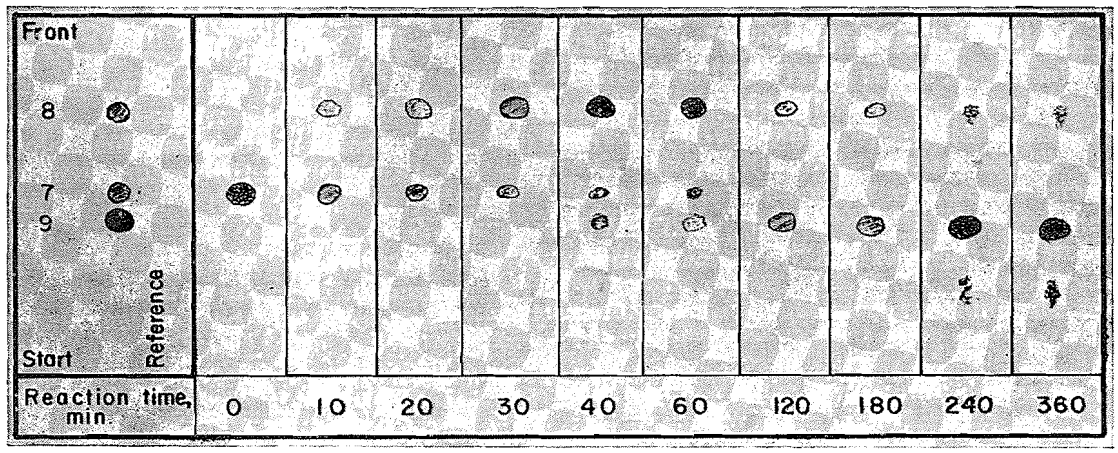

FIG. 3. Thin-layer chromatography of the reaction **7** → **9**.

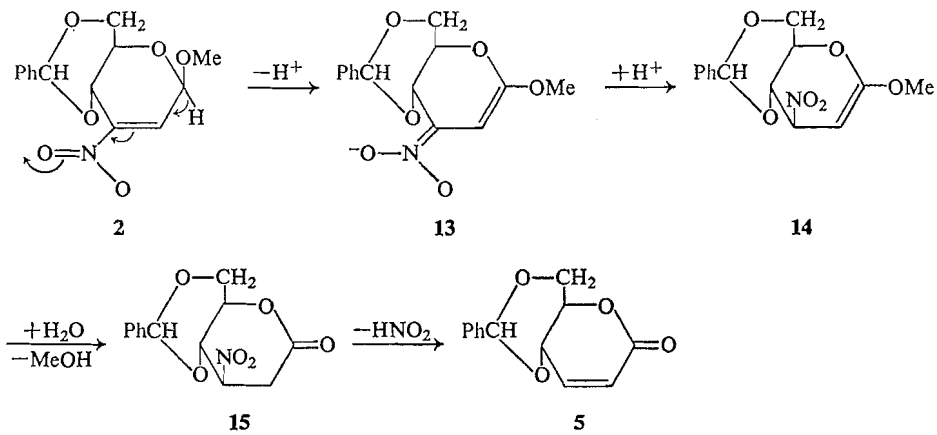

SCHEME I

revealed some related features in other nitro sugar reactions. Firstly, the formation of 4,5-unsaturated glycoside nitronates (9) from glycosides of type **16** in aqueous medium is explained in terms of abstraction of an allylic hydrogen (H-5) in intermediate nitroolefins (**17**); whereas the reaction products proved stable as sodium nitronates (**18**), they rapidly decomposed upon acidification or deionization, evidently as a consequence of hydrolysis of the enol ether linkage in liberated **19** (Scheme II). Although the details of the fate of **19** could not be ascertained, a kinship of the reactions portrayed in Schemes I and II is, nevertheless, quite obvious. Secondly, the facile elimination of the elements of nitrous acid that occurred in a tricyclic Diels–Alder product derived from a nitro

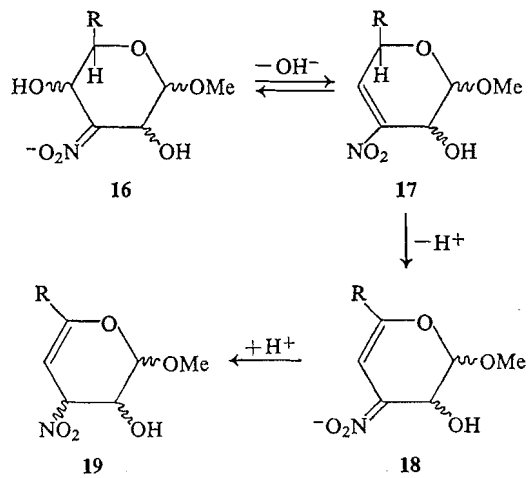

SCHEME II

Can. J. Chem. Downloaded from www.nrcresearchpress.com by 210.87.254.42 on 09/05/12
For personal use only.

glycoside (10) constituted a first, if only formally related, example of such an elimination in this field[6].

Experimental

Thin-layer chromatography (t.l.c.) was performed on silica gel G (E. Merck A.G., Darmstadt) with butanone–*n*-heptane (6:4, v/v) as solvent and ceric sulfate–sulfuric acid as spray indicator. Nuclear magnetic resonance (n.m.r.) spectra (100 MHz) were obtained on a Varian HA-100 spectrometer using chloroform-*d* solutions with internal tetramethylsilane standard, unless indicated otherwise. Infrared (i.r.) spectra were taken from Nujol mulls on a Beckman IR-8 instrument. Petroleum ether refers to the fraction with boiling range 30–60°.

*4,6-O-Benzylidene-2,3-dideoxy-*D*-erythro-hex-2-enono-1,5-lactone (5)*

All reactions were performed by heating the nitro glycosides and basic aluminum oxide (hereafter for simplicity referred to as Al_2O_3)[7] under reflux in toluene in the amounts and for the periods of time specified. The toluene had been dried over anhydrous calcium sulfate, and the reflux condenser was equipped with a drying tube. Efficient magnetic stirring was maintained. For work-up the hot mixtures were filtered, the oxide was washed on the filter with benzene, and the filtrates were evaporated after being clarified with activated charcoal if necessary. The crude reaction products so obtained were dry, usually crystalline, and almost colorless substances.

*(a) From Methyl 4,6-O-Benzylidene-3-deoxy-3-nitro-*β*-*D*-glucopyranoside (1)*

The reaction of nitro glycoside **1** (12) (300 mg) and Al_2O_3 (1.2 g) in toluene (30 ml) was monitored by t.l.c. Visually estimated ratios of starting material (**1**) to faster moving product (**5**) were approximately 1:1, 1:2, and 1:3 after 2, 4, and 12 h respectively. Work-up after 24 h gave a crude product which still contained some **1**, according to t.l.c. Recrystallization from ethyl acetate – petroleum ether furnished colorless **5** (65 mg, 29%), m.p. 121–123°. Infrared and n.m.r. spectra proved the substance to be virtually the same as the preparations of **5** described below, although the low melting point and a (weak) i.r. peak at 1550 cm^{-1} revealed the presence of a minor impurity.

*(b) From Methyl 4,6-O-Benzylidene-2,3-dideoxy-3-nitro-*β*-*D*-erythro-hex-2-enopyranoside (2)*

The nitro glycoside **2** (12) (300 mg) and Al_2O_3 (900 mg) were allowed to react in toluene (30 ml) for 8 h. During this period the appearance on t.l.c. plates of a strong, light-brown spot (**5**) with slightly lower R_f-value than dark-brown **2** was observed. In addition, two blackish brown spots, one faster and the other slower than **5**, were seen. The slower spot corresponded to the hydroxy compound **1**. Work-up gave a crystalline mass (253 mg) which was chromatographed on a column (1.2 × 20 cm) of silica gel G using ethyl acetate–petroleum ether (2:15, v/v) as irrigant. The lactone (**5**), which was eluted first, was once recrystallized from ethyl acetate – petroleum ether and was then pure according to t.l.c. The yield was 79 mg (33%), m.p. 134–135°. A mixture melting point with **5** obtained under (*d*) was undepressed, and i.r. spectra were identical.

Continued elution of the column gave about 85 mg of crystals, m.p. 181–182°, identified with **1** by t.l.c. and i.r. spectrum.

*(c) From Methyl 4,6-O-Benzylidene-3-deoxy-3-nitro-*β*-*D*-mannopyranoside (6)*

The nitro glycoside **6** (4) (300 mg) and Al_2O_3 (900 mg) were allowed to react in toluene (30 ml) for 6 h. It was revealed by t.l.c. that after 1 h all the mannoside (**6**) had disappeared and glucoside (**1**) was present along with lactone (**5**) in a ratio of about 3:1. The ratio appeared to be about 3:2 after 3 h and did not seem to change significantly thereafter. Stirring was continued at room temperature overnight, and work-up then yielded a crystalline residue (204 mg) which was subjected to column chromatography as described under (*b*). There was obtained, first, 67 mg (30%) of the lactone (**5**) in colorless crystals that were identified by t.l.c. and an i.r. spectrum. Continued elution gave crystalline **1** (72 mg) which was found to be identical with an authentic sample (12) by t.l.c. and i.r. comparison.

*(d) From Methyl 4,6-O-Benzylidene-2,3-dideoxy-3-nitro-*α*-*D*-erythro-hex-2-enopyranoside (4)*

The nitro glycoside **4** (5) (200 mg) and Al_2O_3 (600 mg) were refluxed in toluene (20 ml) for 5 h. Prior pilot experiments using t.l.c. for monitoring the reaction course had indicated the occurrence of three products within 3 min. They were represented by a light-brown spot (**5**) traveling slightly more slowly than the starting glycoside (**4**) which gave a dark-brown spot, and by a black double spot of even lower mobility. The slower (and stronger) portion of the double spot corresponded to the hydroxy compound **3**; the faster portion was unidentified. Inspection of the run in 15-min intervals showed clearly a gradual disappearance of **4** with concomitant increase of spot intensity for the three products until, after 1 h, the growing spot of **5** overlapped what was left of **4**. The three reaction products remained visible without significant changes after 3, 5, and 22 h. An i.r. spectrum taken after 1 h showed a strong carbonyl peak at 1750 cm^{-1} and a strong nitroalkane peak at 1555 cm^{-1} in addition to a weaker nitroalkene peak at 1530 cm^{-1} (of remnant **4**). There also was a broad hydroxyl band (ca. 3400 cm^{-1}). After 3 h the carbonyl peak had grown stronger and the nitroalkene absorption was reduced to a small shoulder to the nitroalkane peak.

Work-up of the preparative run (after 5 h) gave a syrupy residue which was chromatographed on a column as described under (*b*). The first fractions containing solid material were evaporated to give a crystalline product. Recrystallization from acetone–water yielded 45 mg (29%) of the lactone (**5**), m.p. 134–135°, $[\alpha]_D$ +26.5° (*c*, 1 in chloroform). The i.r. spectrum was

[6]During this writing, a communication (11) appeared describing a natural sugar (evernitrose) and its structural elucidation, in the course of which there was effected an elimination quite analogous to that depicted above (**15** → **5**).

[7]"$Al_2O_3 + H_2O$, reagent grade, suitable for chromatographic adsorption, pH (slurry 10:100) 10.0–10.5", manufactured by Shawinigan Chemical Co., and distributed by McArthur Chemical Co. Ltd., Montreal.

Can. J. Chem. Downloaded from www.nrcresearchpress.com by 210.87.254.42 on 09/05/12
For personal use only.

Can. J. Chem. Downloaded from www.nrcresearchpress.com by 210.87.254.42 on 09/05/12
For personal use only.

devoid of hydroxyl and nitro absorption but showed a strong carbonyl band at 1755 cm^{-1}. A C=C stretching vibration expected in the 1600 cm^{-1} region was not detectable, possibly owing to ring strain (13). A sample of **5** was debenzylidenated with 90% trifluoroacetic acid (14); it then exhibited hydroxyl absorption in the 3400–3200 cm^{-1} region and ν_{max} 1725 cm^{-1} for the carbonyl band, broadened to smaller frequencies.

Anal. Calcd. for $C_{13}H_{12}O_4$ (232.2): C, 67.20; H, 5.21. Found: C, 67.04; H, 5.34.

Continued elution of the column furnished colorless crystals (38 mg) of the nitro glycoside **3**. Identity with an authentic sample of **3** (4) was established by t.l.c. and by comparison of i.r. spectra.

Another preparative run was worked up without column chromatography. The crude reaction residue was crystallized from cyclohexane–benzene to give fine needles (48 mg, single spot on t.l.c.) of the nitro glycoside **3** melting at 166° and showing $[\alpha]_D$ +85° (*c*, 0.8 in ethanol). (Lit. (4) m.p. 167°, $[\alpha]_D$ +87.2° (*c*, 1 in ethanol)). The mother liquor gave two crops of crystals that were inhomogeneous in t.l.c., both showing the three spots referred to above. The second crop was recrystallized from ethyl acetate – pentane which removed remnant **3** and afforded crystals of m.p. 125–126°. This material consisted largely of the lactone (**5**), but the presence of a by-product (possibly the nitro lactone (**15**)) was indicated by a weak nitro band at 1560 cm^{-1} and by retention of the unidentified (see above) t.l.c. spot. Nearly pure crystals of **5** (m.p. 132°) were obtained by acetamide fusion (10) of the product (5 min on the steam bath), recovery of **5** by trituration with water, and recrystallization from benzene–cyclohexane.

(e) From Methyl 4,6-O-Benzylidene-3-deoxy-3-nitro-α-D-glucopyranoside (3)

The reaction of nitro glycoside **3** (4) (50 mg) and Al_2O_3 (150 mg) in toluene (10 ml) was monitored by t.l.c. A strong spot of **5** arose within 1 h, and simultaneously the spot that was due to remnant **3** acquired a weak front halo indicating the presence of an intermediate or by-product (**15**?).

4,6-O-Benzylidene-2,3-dideoxy-D-threo-hex-2-enono-1,5-lactone (9)

For the conduct of the reactions that are described hereunder, reference is made to the general remarks preceding the description of **5**.

(a) From Methyl 4,6-O-Benzylidene-3-deoxy-3-nitro-β-D-galactopyranoside (7)

The nitro glycoside **7** (4) (300 mg) and Al_2O_3 (900 mg) were refluxed in toluene (50 ml) for 8 h. After that time, t.l.c. revealed the absence of starting material. Filtration and evaporation gave a colorless, crystalline residue (107 mg, 51%) which exhibited a single t.l.c. spot representing the lactone **9** (interestingly, **9** was found to move somewhat *more slowly* than **7**, in contrast to the relative mobilities of **5** and **1**). The product, which was already nearly pure according to its i.r. spectrum, was recrystallized from ethyl acetate–petroleum ether and then melted at 156–157° and showed $[\alpha]_D$ −256° (*c*, 1.1 in chloroform). It lacked hydroxyl and nitro group absorptions in the i.r. and possessed a strong band at 1726 cm^{-1} (C=O) and a weak band at 1633 cm^{-1} (C=C).

Anal. Calcd. for $C_{13}H_{12}O_4$ (232.2): C, 67.20; H, 5.21. Found: C, 67.10; H, 5.16.

Several experiments using varying ratios of **7** and Al_2O_3 were performed. It was found that a reduction in the amount of Al_2O_3 caused a slow reaction whereas an increase in the amount, while accelerating the reaction, was disadvantageous in that it diminished the yield, owing perhaps to more extensive losses by adsorption.

(b) From Methyl 4,6-O-Benzylidene-2,3-dideoxy-3-nitro-β-D-threo-hex-2-enopyranoside (8)

Nitro glycoside **8** (4) (100 mg) and Al_2O_3 (300 mg) were refluxed in toluene (10 ml) for 6 h. It was seen by t.l.c. that a large amount of **9** was formed but also, that some starting material (**8**) and an unidentified, slow-moving substance were present, each at an estimated 10%. Work-up gave crystalline **9** which after recrystallization from ethyl acetate – petroleum ether weighed 38 mg (48%) and melted at 157–158°. Its i.r. spectrum was identical with that of **9** obtained under (*a*).

Generation of 8 from 7, and Addition Reactions of 8

(a) General Procedure

Samples of the nitro glycoside **7** (4) (300 mg) and Al_2O_3 (600 mg) were refluxed in toluene (30 ml). Having observed by means of t.l.c. in pilot experiments that **8** was formed and disappeared as depicted in Fig. 3, we arrested the reactions by cooling and filtering the solutions after 40–45 min. In one experiment the solution was evaporated to dryness and the solid residue recrystallized from ethyl acetate – petroleum ether to give impure **8** (205 mg). The i.r. spectrum was very similar to that of authentic **8**, but weak carbonyl and nitroalkane peaks suggested the presence of **9** and **7**, as did a chromatogram. For the addition reactions described subsequently, the filtered toluene solutions were used directly without isolation of **8**.

(b) Methyl 4,6-O-Benzylidene-3-deoxy-2-O-methyl-3-nitro-β-D-galactopyranoside (10)

To the toluene solution (see (*a*), above) was added, at 25°, a solution of sodium (5 mg) in methanol (5 ml). After 30 min, the mixture was deionized and evaporated to furnish a crystalline residue. Recrystallization from methanol–water gave **10** (144 mg, 46%) in 2 crops of m.p. 170–171° and 169–170°; ν_{max} 1555 cm^{-1} (nitroalkane).

Anal. Calcd. for $C_{15}H_{19}NO_7$ (325.3): C, 55.39; H, 5.89; N, 4.31. Found: C, 55.25; H, 5.76; N, 4.29.

Treatment of an authentic sample of **8** (100 mg) in methanol (10 ml) with a few drops of 0.2 *N* sodium methoxide solution for 20 min at 23° followed by deionization, evaporation, and recrystallization gave **10** (98 mg, 88%) as fine needles, m.p. 171°, $[\alpha]_D$ +35.1 (*c*, 1 in dimethylformamide). Infrared and n.m.r. spectra established its identity with the previous product.

Nuclear magnetic resonance data. The substituent signals were τ 2.65 (5H multiplet, $-C_6H_5$); τ 4.52 (1H singlet, benzylidene hydrogen); τ 6.42 and 6.45 (two 3H singlets, $-OCH_3$). The chain hydrogen signals were centered at τ 5.39 (quartet, H-4, with $J_{4,5}$ = 1 Hz and $J_{4,3}$ = 4 Hz); τ 5.51 (quartet, H-3, with $J_{3,4}$ = 4 Hz and $J_{3,2}$ = 9.5 Hz); τ 5.65 (quartet, H-6, with $J_{6,6'}$ = 12.5 Hz and $J_{6,5}$ = 1.5 Hz); τ 5.75 (doublet, H-1, with $J_{1,2}$ = 7.5 Hz); τ 5.98 (two partially overlapping quartets, H-6′ and H-2, with $J_{6,6'}$ = 12.5 Hz, $J_{6',5}$ = 1.5 Hz,

$J_{2,1}$ = 7.5 Hz, and $J_{2,3}$ = 9.5 Hz); τ 6.55 (narrow quartet, H-5, with width at half-height = 4 Hz). In *acetonitrile solution*, the chemical shift difference between H-6 and H-6′ was strongly reduced so that their signals moved together giving a narrow, apparent triplet situated between and not overlapped by the H-1 doublet and the H-2 quartet; the narrow H-4 signal overlapped the upfield portion of the H-3 quartet, and the H-5 signal was displaced slightly downfield of the OCH_3 peaks.

(c) Methyl 4,6-O-Benzylidene-3-deoxy-2-O-ethyl-3-nitro-β-D-galactopyranoside (11)

Starting from the glycoside **7** (as in (*a*), above) and proceeding as in (*b*) except for the use of sodium ethoxide instead of sodium methoxide, we obtained a crude product that was recrystallized from ethanol–water to give colorless needles (168 mg, 53%) of **11** in 2 crops, m.p. 174–176° and 176–178°, which upon further, joint recrystallization melted at 186°; ν_{max}, doublet 1553–1563 cm^{-1} (nitroalkane).

Anal. Calcd. for $C_{16}H_{21}NO_7$ (339.3): C, 56.63; H, 6.24; N, 4.13. Found: C, 56.46; H, 6.09; N, 4.01.

Authentic **8** and sodium ethoxide in ethanol (30 min at 23°) produced **11** in a yield of 95% (crude; 84% after recrystallization). It melted at 186°, showed $[\alpha]_D$ +37.7° (*c*, 0.9 in chloroform), and it was identical with the previous product according to t.l.c., i.r., and n.m.r. spectroscopy.

Nuclear magnetic resonance data. The spectrum showed the same general features as that of **10**, except that there was only one OCH_3 peak (τ 6.45). The OC_2H_5 group gave a 3H triplet centered at τ 8.88 and a 2H quartet at τ 6.23.

(d) Methyl 4,6-O-Benzylidene-2,3-dideoxy-3-nitro-2-piperidino-β-D-galactopyranoside (12)

The nitro glycoside **7** was treated as described in (*a*), above. To the filtered solution was then added piperidine (0.5 ml) at room temperature. After 15 min the solvent was removed, and the residue was evaporated twice with ethyl acetate and twice with ethanol and was then recrystallized from ethanol–water. Compound **12** (139 mg, 38%) was obtained in two crops, m.p. 141–142° and 139–141°; ν_{max} 1558 cm^{-1} (nitroalkane).

Anal. Calcd. for $C_{19}H_{26}N_2O_6$ (378.4): C, 60.30; H, 6.93; N, 7.48. Found: C, 60.50; H, 7.08; N, 7.46.

A solution of authentic **8** (100 mg) and piperidine (0.05 ml) in benzene (3 ml) was allowed to stand at 23° for 15 min. The yellow solution was evaporated with several successive additions of benzene, ethyl acetate, and ethanol. The residue was recrystallized from a small amount of cold ethanol by careful addition of water, to give **12** (85 mg, 70%) of m.p. 140° (decomposition). Another recrystallization using warm ethanol but avoiding prolonged heating gave felt-like needles of m.p. 140–141° (decomposition); $[\alpha]_D$ + 72.5° (*c*, 1 in chloroform).

Nuclear magnetic resonance data. The substituent signals were at τ 2.69 (5H multiplet, $-C_6H_5$); τ 4.55 (1H singlet, benzylidene hydrogen); τ 6.51 (3H singlet, $-OCH_3$); τ 7.3 (broad 4H multiplet, α-CH_2 groups of $-NC_5H_{10}$); τ 8.59 (6H singlet, β- and γ-CH_2 groups of $-NC_5H_{10}$). The chain hydrogen signals were centered at τ 5.33 (quartet, H-3, with $J_{3,4}$ = 4 Hz and $J_{3,2}$ = 11.5 Hz); τ 5.48 (quartet, H-4, with $J_{4,3}$ = 4 Hz and $J_{4,5}$ = 1.5 Hz); τ 5.63 (doublet, H-1, with $J_{1,2}$ = 8.5 Hz); τ 5.70 (quartet, H-6, with $J_{6,6'}$ = 12.5 Hz and $J_{6,5}$ = 1.5 Hz); τ 5.94 (quartet, H-6′, with $J_{6',6}$ = 12.5 Hz and $J_{6',5}$ = 1.5 Hz); τ 6.66 (narrow quartet, H-5); H-2 gave a quartet centered at τ 6.53, and although one of the lines was obscured by the OCH_3 peak, the spacings of 8.5 Hz ($J_{1,2}$) and 11.5 Hz ($J_{2,3}$) could still be verified. Assignments were confirmed by deuterium exchange at C-3 which was accomplished by prolonged stirring of a solution of **12** in $CDCl_3$ with two successive portions of D_2O and drying of the organic phase over magnesium sulfate. The H-3 quartet disappeared, the H-4 quartet collapsed to a narrow doublet, and the H-2 signal changed to two lines (spaced by 8.5 Hz) straddling the OCH_3 peak.

Acknowledgment

We thank the National Research Council of Canada for financial support of this work.

1. H. H. Baer and I. Furić. J. Org. Chem. **33**, 3731 (1968).
2. H. H. Baer, T. Neilson, and W. Rank. Can. J. Chem. **45**, 991 (1967).
3. E. W. Garbisch, Jr. J. Am. Chem. Soc. **86**, 5561 (1964).
4. H. H. Baer, F. Kienzle, and T. Neilson. Can. J. Chem. **43**, 1829 (1965).
5. H. H. Baer and F. Kienzle. Can. J. Chem. **45**, 983 (1967).
6. E. L. Eliel, N. L. Allinger, S. J. Angyal, and G. A. Morrison. Conformational analysis. John Wiley and Sons, Inc., New York. 1965. p. 111.
7. H. H. Baer and K. S. Ong. Can. J. Chem. **46**, 2511 (1968).
8. H. H. Baer and K. S. Ong. J. Org. Chem. **34**, 560 (1969).
9. H. H. Baer and F. Kienzle. Ann. Chem. **695**, 192 (1966); H. H. Baer, F. Kienzle, and F. Rajabalee. Can. J. Chem. **46**, 80 (1968).
10. H. H. Baer and F. Kienzle. J. Org. Chem. **33**, 1823 (1968).
11. A. K. Ganguly, O. Z. Sarre, and H. Reimann. J. Am. Chem. Soc. **90**, 7129 (1968).
12. H. H. Baer and T. Neilson. Can. J. Chem. **43**, 840 (1965).
13. H. B. Henbest, G. D. Meakins, B. Nicholls, and R. A. L. Wilson. J. Chem. Soc. 997 (1957).
14. J. E. Christensen and L. Goodman. Carbohydrate Res. **7**, 510 (1968).

Can. J. Chem. Downloaded from www.nrcresearchpress.com by 210.87.254.42 on 09/05/12
For personal use only.

Reactions of nitro sugars. XII. A novel type of disaccharide synthesis[1]

HANS H. BAER AND FRANK KIENZLE
Department of Chemistry, University of Ottawa, Ottawa 2, Canada
Received February 20, 1969

Nitro disaccharide methyl glycosides were obtained by base-catalyzed addition of partially blocked sugar derivatives having one free hydroxyl group, across the ethylenic bond in methyl 4,6-*O*-benzylidene-2,3-dideoxy-3-nitro-β-D-*erythro*-hex-2-enopyranoside (**1**) and its α-anomer (**2**). Thus, the addition of 2,3,4,6-tetra-*O*-acetyl-β-D-glucopyranose (**3**) gave blocked derivatives of sophorose, namely methyl 2-*O*-(2,3,4,6-tetra-*O*-acetyl-β-D-glucopyranosyl)-4,6-*O*-benzylidene-3-deoxy-3-nitro-β-D-glucopyranoside (**4**) and -α-D-glucopyranoside (**5**). Similarly, the use of methyl 4,6-*O*-benzylidene-3-deoxy-3-nitro-β-D-glucopyranoside (**10**) and its α-anomer (**13**) as addends led to 2 → 2 linked bisglycosidyl ethers; these were the methyl 4,6-*O*-benzylidene-3-deoxy-2-*O*-(methyl 4,6-*O*-benzylidene-2,3-dideoxy-3-nitro-D-glucopyranosid-2-yl)-3-nitro-D-glucopyranosides with the anomeric configurations β,β, α,α, and α,β (**11**, **14**, and **15**, respectively). Methyl 4,6-*O*-benzylidene-3-deoxy-3-nitro-β-D-mannopyranoside (**12**) was found to epimerize to **10** under the reaction conditions; therefore, interaction of **12** and **1** also gave the bis-β-D-glucosidyl ether (**11**). The L-enantiomer of **12** gave with **1** an optically inactive *meso* compound (**16**) possessing a β-L- and a β-D-glucosidyl moiety.

Canadian Journal of Chemistry, 47, 2819 (1969)

Only one disaccharide that contains a nitro sugar has been described in the literature (1): a trehalose-type compound composed of α-D-glucopyranose and 4-deoxy-4-nitro-β-D-*gluco*-heptulopyranose, which was obtained by nitromethane cyclization of the dialdehyde arising in a partial lead tetraacetate oxidation of sucrose. We now wish to report the synthesis of several disaccharide methyl glycosides derived from 3-deoxy-3-nitro-D-glucose. The new compounds were prepared by a method not common in disaccharide synthesis, namely, by nucleophilic addition of one monosaccharide component across an activated double bond in a second component. This article represents a continuation of our recent work on the preparation of nitro sugar ethers (2–4) and branched-chain dinitro sugars (5), in which the same principle of nucleophilic addition was employed.

Methyl 4,6-*O*-benzylidene-2,3-dideoxy-3-nitro-β-D-*erythro*-hex-2-enopyranoside (**1**) as well as its α-anomer (**2**) were allowed to react with 2,3,4,6-tetra-*O*-acetyl-β-D-glucopyranose (**3**) in refluxing benzene for 3 h. Although the reactions, which were catalyzed by a small amount of solid potassium hydroxide (3), did not go to completion, crystalline disaccharide derivatives (**4** and **5**) could be isolated in yields of 51 and 36%, respectively. They were methyl 2-*O*-(2,3,4,6-tetra-*O*-acetyl-β-D-glucopyranosyl)-4,6-*O*-benzylidene-3-deoxy-3-nitro-β-D-glucopyranoside (**4**) and -α-D-glucopyranoside (**5**). Acid debenzylidenation furnished the corresponding, partially acetylated compounds **6** and **7**, and subsequent acetylation gave the hexaacetates **8** and **9**. The disaccharide glycosides may be regarded as derivatives of sophorose (2-*O*-β-D-glucopyranosyl-D-glucose). Proof of configuration will be presented below.

While the synthesis of 1,2-linked disaccharides as just described was a logical extension of our previous work concerning the introduction of various substituents into position-2 of 3-deoxy-3-nitro sugars, there was a second reason that prompted the present investigation. As was reported in 1965, the unsaturated nitro glycoside **1** can be prepared readily by dehydroacetylation of methyl 2-*O*-acetyl-4,6-*O*-benzylidene-3-deoxy-3-nitro-β-D-glucopyranoside with dry sodium bicarbonate in anhydrous benzene (6); the α-anomer **2** is made analogously (7). We now wish to communicate that, although compound **1** in particular has since been prepared in this laboratory numerous times without difficulty, on some occasions there was encountered an unidentified, high-melting by-product (m.p. 295–299°). Its infrared (i.r.) spectrum suggested a saturated nitro sugar structure devoid of acetyl or hydroxyl functions. The formation of this by-product occurred erratically and seemed to be favored when moisture was not rigorously excluded in the operation. For a working hypothesis it was considered that a small part of **1** may become hydrated to methyl 4,6-*O*-benzylidene-3-deoxy-3-nitro-β-D-glucopyranoside (**10**) which could then react with excess **1** to form the bisglycosidyl ether **11**. The spectral and analytical

[1]For part XI in this series see ref. 4.

Can. J. Chem. Downloaded from www.nrcresearchpress.com by 210.87.254.6 on 09/05/12
For personal use only.

Can. J. Chem. Downloaded from www.nrcresearchpress.com by 210.87.254.6 on 09/05/12
For personal use only.

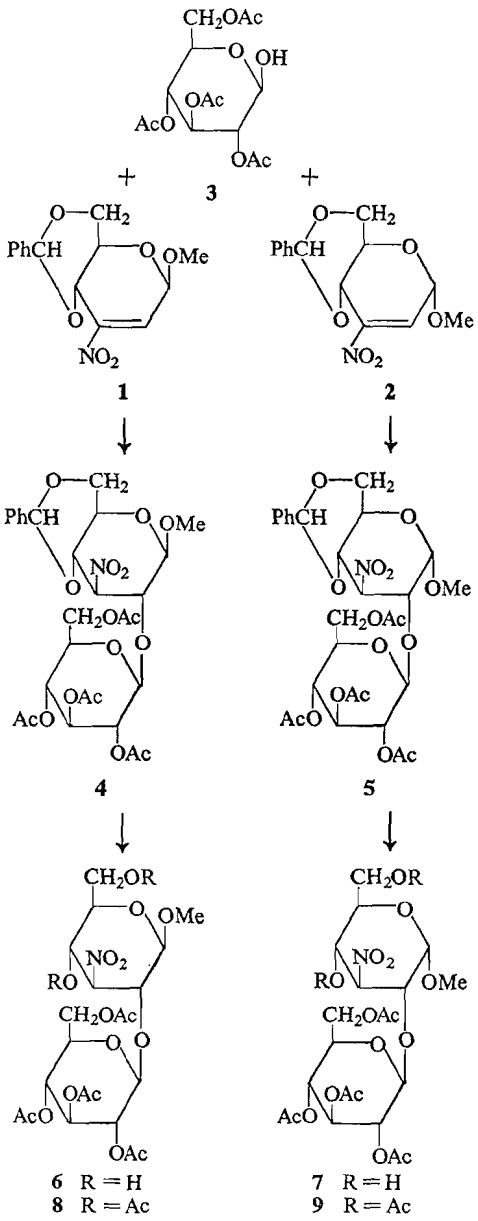

data of the unknown product were in keeping with structure **11**.

This concept has been substantiated by an experiment showing that water can indeed be added with ease (even without provision of a catalyst) across the double bond of **1** to give **10**. Final proof for the by-product to possess structure **11** was obtained through its synthesis in 65% yield by the interaction of equimolar amounts of **1** and **10**. The compound, whose configurational elucidation will be discussed in a subsequent paragraph, is named methyl 4,6-*O*-benzylidene-3-deoxy-2-*O*-(methyl 4,6-*O*-benzylidene-2,3-dideoxy-3-nitro-β-D-glucopyranosid-2-yl)-3-nitro-β-D-glucopyranoside. As far as we are aware, **11** is the first example of a derivative of a 2 → 2 linked aldose disaccharide[2].

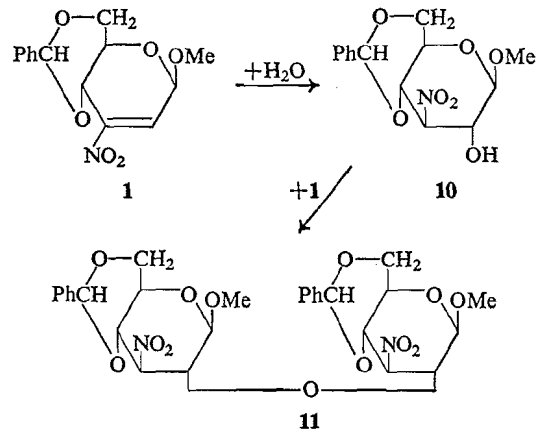

When methyl 4,6-*O*-benzylidene-3-deoxy-3-nitro-β-D-mannopyranoside (**12**) was substituted for **10** in the above synthesis, the product was the same bis-glucoside **11**, not a stereoisomer thereof. It was verified in a separate experiment that epimerization of **12** to **10** takes place under the reaction conditions. Evidently **10**, with its equatorial hydroxyl group, combines with **1** more readily than does **12** with its axial hydroxyl group. Epimerization in the same sense, undoubtedly proceeding via intermediate **1**, has already been mentioned in the foregoing paper (4) and in earlier work cited there.

A number of stereoisomers of **11** were synthesized as follows. Methyl 4,6-*O*-benzylidene-3-deoxy-3-nitro-α-D-glucopyranoside (**13**, the α-anomer of **10**) was added to **2** (the α-anomer of **1**), to produce the bis-α-glycosidyl ether, methyl 4,6-*O*-benzylidene-3-deoxy-2-*O*-(methyl 4,6-*O*-benzylidene-2,3-dideoxy-3-nitro-α-D-glucopy-

[2]Actually, **11** is a (bis-benzylidenated) intermolecular anhydride of a glycoside. It could be named also as bis(methyl 4,6-*O*-benzylidene-2,3-dideoxy-3-nitro-β-D-glucopyranosid-2-yl) ether, but such a name ceases to be shorter than one of the type given above when the two moieties are nonidentical, as is the case in some of the analogues to be described. We are obliged to Dr. R. S. Tipson, Washington, D.C., for his kind advice on the nomenclature.

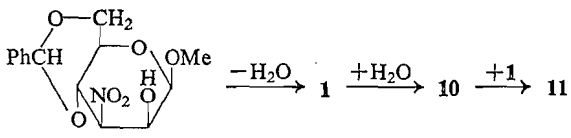

12

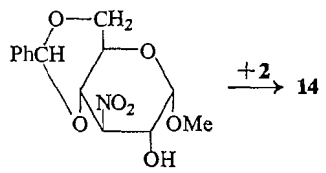

13

ranosid-2-yl)-3-nitro-α-D-glucopyranoside (**14**). Combination of the nitroolefin **2** and the nitro alcohol **10** furnished the mixed ether, methyl 4,6-*O*-benzylidene-3-deoxy-2-*O*-(methyl 4,6-*O*-benzylidene-2,3-dideoxy-3-nitro-β-D-glucopyranosid-2-yl)-3-nitro-α-D-glucopyranoside (**15**)[3]. Finally we synthesized a stereoisomer in which one moiety possesses the β-D-*gluco* configuration and the other, the β-L-*gluco* configuration. This optically inactive *meso* compound, methyl

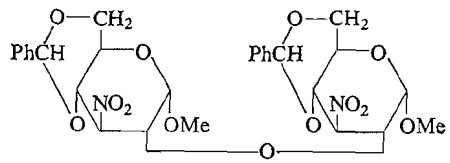

14

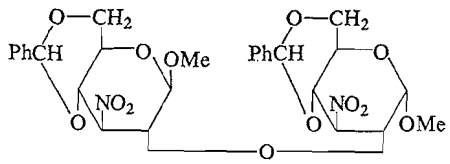

15

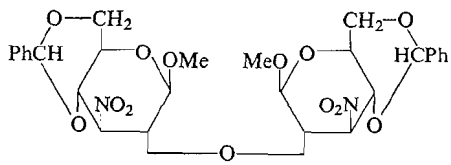

16

[3]The same ether would be expected to arise from an addition of **13** to **1**. The α and β prefixes in the name of **15** are interchangeable.

[4]A sample of the β-L-mannoside (enantiomer of **12**) happened to be on hand, but the β-L-glucoside (enantiomer of **10**) would have afforded the same product. As shown above for the D-series, *manno* to *gluco* epimerization precedes the disaccharide formation.

4,6-*O*-benzylidene-3-deoxy-2-*O*-(methyl 4,6-*O*-benzylidene-2,3-dideoxy-3-nitro-β-D-glucopyranosid-2-yl)-3-nitro-β-L-glucopyranoside (**16**), was obtained from **1** and the optical antipode of **12**[4].

Mild acid hydrolysis of the disaccharides **11**, **14**, and **15** gave the corresponding, debenzylidenated compounds **17**, **18**, and **19**, and these were acetylated with acetic anhydride and boron trifluoride to yield the tetraacetates **20**, **21**, and **22**.

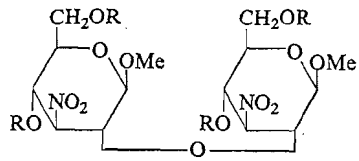

17 R=H
20 R=Ac

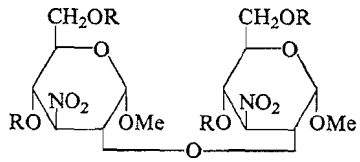

18 R=H
21 R=Ac

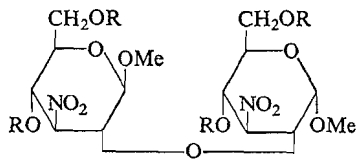

19 R=H
22 R=Ac

Concerning the stereochemistry of the new disaccharide synthesis it is to be noted that bond formation between the nucleophilic donor and the unsaturated acceptor molecules resulted, in all instances, in 2,3-diequatorial substituent orientation and, therefore, D-*gluco* configuration in the latter component. This was in line with what had been observed earlier in similar addition reactions using various other nucleophiles (2–5). Configurational proof was afforded, as in the previous studies (2, 4, 5), by the character of the nuclear magnetic resonance (n.m.r.) signals from the protons at nitro-substituted C-3. In the acetates **8**, **9**, **20**, **21**, and **22** these signals, which occurred at lowest fields near τ 4.6, were symmetrical triplets with large splittings (10 Hz)

Can. J. Chem. Downloaded from www.nrcresearchpress.com by 210.87.254.6 on 09/05/12
For personal use only.

Can. J. Chem. Downloaded from www.nrcresearchpress.com by 210.87.254.6 on 09/05/12
For personal use only.

indicating triaxial proton arrangement at C-2, C-3, and C-4. The H-3 triplets of the mononitro compounds **8** and **9** showed the required, one-proton intensity. In the symmetrical dinitro ethers **20** and **21**, all the signals given by one half of the molecule coincided with the corresponding ones of the other half, according to expectation. Thus, the spectra showed one H-3 triplet, one methoxyl singlet, and two separate *O*-acetyl singlets in an intensity ratio 1:3:3:3, although each signal was caused by a double number of protons. By contrast, the molecule halves of the unsymmetrical dinitro ether **22** gave corresponding signals that differed in chemical shift. There were two partially overlapping H-3 triplets, two methoxyl peaks, and four *O*-acetyl peaks (for details see Experimental).

A final point to be considered was the anomeric configuration of the disaccharide linkages in **4** and **5**. It was assumed that no anomerization of 2,3,4,6-tetra-*O*-acetyl-β-D-glucopyranose (**3**) took place during its addition to **1** and **2**, respectively, and consequently, that the linkages were of the β-type. Owing to crowding of the pertinent n.m.r. signals this feature could not be verified unambiguously by means of the spectra. However, the optical rotations of **4** and **5** and their derivatives listed in Table I clearly established the β-disaccharide linkages. The moderate levorotations of the methyl β-glycosides **4**, **6**, and **8**, and the relatively low dextrorotations of the methyl α-glycosides **5**, **7**, and **9**, are comparable in magnitude with the values recorded in the literature for anomeric derivatives of β-D-glucopyranosyl-D-glucoses (sophorose, laminaribiose, cellobiose, gentiobiose), whereas the corresponding derivatives of α-D-glucopyranosyl-D-glucoses (kojibiose, nigerose, maltose, isomaltose) show much higher dextrorotations (8).

Also included in Table I are physical constants of the new 2 → 2 linked disaccharides.

Experimental

The starting compounds **1** (6), **2** (7), **3** (9), **10** (6), **12** (10), the L-enantiomer of **12** (11), and **13** (10) were prepared as previously reported. Melting points were taken in capillaries in an electric aluminium block apparatus. Petroleum ether refers to the fraction of boiling range 30–60°. Thin-layer chromatography (t.l.c.) was performed on silica gel G with ethyl acetate – petroleum ether in the ratio (v/v) 1:1 (solvent *a*) or 1:2 (solvent *b*). Optical rotations (Table I) were determined at about 25° using a Perkin–Elmer 141 photoelectric polarimeter. Infrared spectra were obtained by the Nujol mull technique on a Beckman IR-8 instrument. Nuclear magnetic resonance spectra were taken in chloroform-*d* solution, with internal tetramethylsilane standard, on a 100 MHz Varian spectrometer.

Methyl 2-O-(2,3,4,6-Tetra-O-acetyl-β-D-glucopyranosyl)-4,6-O-benzylidene-3-deoxy-3-nitro-β-D-glucopyranoside (4)

The nitroolefin **1** (293 mg, 1 mmole) and β-D-glucopyranose 2,3,4,6-tetraacetate (**3**) (348 mg, 1 mmole) were refluxed in dry, reagent grade benzene (50 ml) in the presence of a small chip of potassium hydroxide (ca. 5 mg). Monitoring by t.l.c. (solvent *a*) revealed that the slow-moving (**3**) and fast-moving (**1**) starting materials were gradually replaced by a reaction product (**4**) of inter-

TABLE I

Physical constants of disaccharides

Compound	Anomeric configuration	Melting point, °C	$[\alpha]_D^{25°}$	(*c*, solvent)
4	β,β	218	−39.0	(0.6, Chloroform)
6	β,β	164–165	−12.5	(0.7, Ethanol)
8	β,β	97–98	−4.6	(0.8, Chloroform)
5	α,β	267	+13.3	(0.8, Chloroform)
7	α,β	197	+43.8	(0.8, Ethanol)
9	α,β	175–176	+44.5	(0.6, Chloroform)
11	β,β	299 decomp.	−22.0	(1.0, Dimethylformamide)
17	β,β	205–206 decomp.	−11.7	(0.6, Ethanol)
20	β,β	237 decomp.	−1.8	(1.0, Chloroform)
14	α,α	348 decomp.	+117.0	(0.55, Dimethylformamide)
18	α,α	250–251 decomp.	+201.0	(0.9, Ethanol)
21	α,α	202–203 decomp.	+167.0	(0.75, Chloroform)
15	α,β	325 decomp.	+70.0	(0.7, Dimethylformamide)
19	α,β	240–241 decomp.	+122.0	(0.8, Ethanol)
22	α,β	201–203 decomp.	+90.6	(0.4, Chloroform)
16	β,β	325 decomp.	0.0	(0.7, Dimethylformamide)

Can. J. Chem. Downloaded from www.nrcresearchpress.com by 210.87.254.6 on 09/05/12
For personal use only.

mediate mobility. Refluxing was discontinued after 3 h although residual **1** and **3** were still present. (Prolonged reaction times allowed in preliminary experiments failed to increase the yield). The solution was treated with activated charcoal, filtered, and evaporated to leave a solid residue which after one recrystallization from ethyl acetate – petroleum ether gave colorless **4** (329 mg, 51%) melting at 216°. The m.p. was raised to 218° by another recrystallization from the same solvents and then remained unchanged.

Infrared bands were at 1745 (strong, C=O) and 1555 cm^{-1} (medium strong, NO_2), and at 765 and 705 cm^{-1} (medium strong, C_6H_5); there was no hydroxyl absorption.

Nuclear magnetic resonance data: τ 2.65 (5 H) and 4.51 (1 H), C_6H_5CH; τ 6.42 (3 H), OCH_3; τ 7.92, 7.95, 8.00, 8.03 (12 H), 4 $OCOCH_3$. The 14 sugar chain protons gave complicated signals in the region τ 4.8–6.6.

Anal. Calcd. for $C_{28}H_{35}NO_{16}$ (mol. wt., 641.6): C, 52.42; H, 5.50; N, 2.18. Found: C, 52.64; H, 5.40; N, 2.20.

Methyl 2-O-(2,3,4,6-Tetra-O-acetyl-β-D-glucopyranosyl)-3-deoxy-3-nitro-β-D-glucopyranoside (6)

The benzylidene compound **4** (300 mg) and 70% acetic acid (25 ml) were heated on a steam bath for 30 min. Complete conversion of **4** into a non-migrating product was revealed by t.l.c. (solvent *a*). Evaporation of the solution, followed by three co-evaporations with water and two with ethanol, gave a solid which upon recrystallization from aqueous ethanol yielded **6** (163 mg, 63%) of m.p. 159–160°, raised to 164–165° by recrystallization from the same solvents. The i.r. spectrum exhibited broad hydroxyl absorption with ν_{max} 3380 and 3200 cm^{-1}, and bands attributable to C_6H_5 were lacking. A strong ester peak was at 1740 cm^{-1}, and a nitro peak at 1553 cm^{-1}.

Anal. Calcd. for $C_{21}H_{31}NO_{16}$ (mol. wt., 553.5): C, 45.58; H, 5.65; N, 2.53. Found: C, 45.71; H, 5.72; N, 2.36.

Methyl 4,6-Di-O-acetyl-2-O-(2,3,4,6-tetra-O-acetyl-β-D-glucopyranosyl)-3-deoxy-3-nitro-β-D-glucopyranoside (8)

Compound **6** (175 mg) was dissolved in acetic anhydride (2 ml), and *one* drop of boron trifluoride etherate was added. The mixture was allowed to stand at ambient temperature for 10 min. Ethanol (5 ml) was then added, and the solution was evaporated to a syrup which was co-evaporated thrice with toluene and twice with ethanol. The residue was dissolved in a small amount of ethyl acetate, petroleum ether was added to incipient cloudiness, and the hexaacetate **8** separated in the course of 2 weeks at 5° as a gel-like material. Filtration, washing with petroleum ether, and drying in a high vacuum gave a white powder (141 mg, 70%) that melted at 97–98°. It showed strong i.r. bands at 1740 (C=O) and 1563 cm^{-1} (NO_2) but lacked hydroxyl absorption.

Nuclear magnetic resonance data: τ 4.64 (triplet, 1 H, J = 9.7 Hz), H-3; τ 4.85–5.95 and ca. 6.3 (compli cated pattern of total intensity 13 H), sugar chain protons; τ 6.44 (singlet, 3 H), OCH_3; τ 7.92, 7.92, 7.96, 7.98, 8.00, 8.03 (singlets, 18 H), 6 $OCOCH_3$.

Anal. Calcd. for $C_{25}H_{35}NO_{18}$ (mol. wt., 637.6): C 47.10; H, 5.53; N, 2.19. Found: C, 47.29; H, 5.48; N, 2.29.

Methyl 2-O-(2,3,4,6-Tetra-O-acetyl-β-D-glucopyranosyl)-4,6-O-benzylidene-3-deoxy-3-nitro-α-D-glucopyranoside (5)

The reaction between the nitroolefin **2** and the tetraacetate **3** was carried out precisely as described above for the preparation of **4**, except for a reflux time of 2.5 h. There was obtained, after recrystallization, 232 mg (36%) of **5** as fine, colorless needles with m.p. 267° (unchanged on further recrystallization). Characteristic i.r. bands were at 1745 (with satellite at 1773) (C=O), 1568 (NO_2), and 773 and 705 cm^{-1} (C_6H_5).

Nuclear magnetic resonance data: τ 2.64 (5 H) and 4.50 (1 H), C_6H_5CH; τ 6.55 (3 H), OCH_3; τ 7.91, 7.98, 7.98, 8.02 (12 H), 4 $OCOCH_3$. The 14 sugar chain protons gave complicated signals in the region τ 4.7–6.3.

Anal. Calcd. for $C_{28}H_{35}NO_{16}$ (mol. wt., 641.6): C, 52.42; H, 5.50; N, 2.18. Found: 52.60; H, 5.47; N, 2.30.

Methyl 2-O-(2,3,4,6-Tetra-O-acetyl-β-D-glucopyranosyl)-3-deoxy-3-nitro-α-D-glucopyranoside (7)

The debenzylidenation of compound **5** (110 mg), performed as that of **4**, afforded **7** (89 mg, 93%) as beautiful needles, m.p. 197°, from aqueous ethanol. The i.r. spectrum showed broad hydroxyl absorption with ν_{max} 3570, 3510, and 3250 cm^{-1}, as well as strong peaks at 1740 (C=O) and 1553 cm^{-1} (NO_2).

Anal. Calcd. for $C_{21}H_{31}NO_{16}$ (mol. wt., 553.5): C, 45.58; H, 5.65; N, 2.53. Found: C, 45.48; H, 5.56; N, 2.41.

Methyl 4,6-Di-O-acetyl-2-O-(2,3,4,6-tetra-O-acetyl-β-D-glucopyranosyl)-3-deoxy-3-nitro-α-D-glucopyranoside (9)

Compound **7** (55 mg) was treated with acetic anhydride (2 ml) and 1 drop of boron trifluoride etherate as described for the acetylation of **6**. The hexaacetate **9** was obtained as needles (44 mg, 69%) from 50% ethanol. It melted at 166° (rapid heating) or at 175–176° (very slow heating). The i.r. spectrum showed strong bands at 1740 (C=O) and 1560 cm^{-1} (NO_2); hydroxyl absorption was absent.

Nuclear magnetic resonance data: τ 4.60 (triplet, 1 H, J = 10 Hz), H-3; τ 4.8 – 5.2 (overlapping signals corresponding to 5 chain protons); τ 5.50 (doublet, 1 H, J = 8 Hz), H-1′; τ 5.65–ca. 6.4 (overlapping signals corresponding to 7 chain protons); τ 6.56 (singlet, 3 H), OCH_3; τ 7.91–8.02 (partially overlapping singlets, 18 H), 6 $OCOCH_3$.

Anal. Calcd. for $C_{25}H_{35}NO_{18}$ (mol. wt., 637.6): C, 47.10; H, 5.53; N, 2.19. Found: C, 47.26; H, 5.42; N, 2.22.

Hydration of Nitroolefin 1

A solution of compound **1** (90 mg) in tetrahydrofuran (10 ml) and water (10 ml) was gently refluxed on a steam bath. Inspection at intervals by t.l.c. (solvent *b*) revealed that the fast-moving **1** was largely converted into a slow-moving product (**10**) within 3.5 h. Removal of the solvents *in vacuo* gave a white solid which upon recrystallization from aqueous ethanol furnished crude **10** (41 mg), m.p. 171–173°. Once more recrystallized from ethyl acetate – petroleum ether, the product (24 mg) melted at 180–181°, showed $[\alpha]_D$ −73.2° (*c*, 0.5 in

Can. J. Chem. Downloaded from www.nrcresearchpress.com by 210.87.254.6 on 09/05/12
For personal use only.

ethanol), and gave an i.r. spectrum identical with that of authentic **10**. Reported (6): m.p. 181–182°, $[\alpha]_D$ −72.5° (in ethanol).

Epimerization of the Nitro Mannoside ***12***

Compound **12** (20 mg) was refluxed in dry benzene (10 ml) in the presence of a chip of potassium hydroxide (ca. 5 mg). The conversion into the nitro glucoside **10** was monitored by t.l.c. with solvent *b* (in which **10**, moving somewhat faster, clearly separates from **12**) and was found to be nearly complete after 1 h. Evaporation of the solvent left a solid which was recrystallized from ethyl acetate – petroleum ether to give 14 mg (70%) of chromatographically pure **10**, m.p. 179–180°. A mixture melting point with authentic **10** (6) was undepressed, and the i.r. spectra were identical.

Methyl 4,6-O-Benzylidene-3-deoxy-2-O-(methyl 4,6-O-benzylidene-2,3-dideoxy-3-nitro-β-D-glucopyranosid-2-yl)-3-nitro-β-D-glucopyranoside ***(11)***

(a) From ***1*** *and* ***10***

The nitroolefin **1** (586 mg, 2 mmole) and nitro glucoside **10** (622 mg, 2 mmole) were refluxed in dry benzene (100 ml) together with a piece (about 20 mg) of solid potassium hydroxide. Thin-layer chromatography with solvent *b* indicated that the starting compounds **1** and **10** (R_f approximately 0.8 and 0.3, respectively) gradually diminished with concurrent formation of a product that did not migrate. (Traces of a very fast by-product were also noticed.) The reaction was stopped after 5 h when it had progressed far, though not quite to completion. The brown solution was decolorized with activated charcoal and evaporated to give a white solid. Recrystallization from ethyl acetate – petroleum ether gave crude **11** (795 mg, 66%) melting at 272–275° decomp. Another recrystallization from the same solvents afforded virtually pure needles (610 mg) of m.p. 295–296° decomp. An analytical sample (twice more recrystallized) had m.p. 299° decomp. The most prominent i.r. bands were at 1555 (nitroalkane), 1105, and 987 cm^{-1} (strong), and at 1168, 1070, 1045, 755, 732, 705, and 665 cm^{-1} (medium strong). Hydroxyl absorption was absent.

Anal. Calcd. for $C_{28}H_{32}N_2O_{13}$ (mol. wt., 604.6): C, 55.62; H, 5.34; N, 4.63. Found: C, 55.73; H, 5.47; N, 4.77.

(b) From ***1*** *and* ***12***

Nitroolefin **1** (50 mg) and nitro mannoside **12** (55 mg) were allowed to react in benzene (25 ml) as described under (*a*) and yielded 28 mg of pure **11**, m.p. 295° decomp. (raised to 299° by further recrystallization). The i.r. spectrum was superimposable with that of **11** as prepared under *(a)* and with that of the high-melting by-product that has occasionally been encountered in the synthesis (6) of **1**.

An experiment in which 1 drop of pyridine was substituted for the potassium hydroxide catalyst failed to produce **11**. According to t.l.c., the starting materials did not seem to change during 24 h of refluxing.

Methyl 3-Deoxy-2-O-(methyl 2,3-dideoxy-3-nitro-β-D-glucopyranosid-2-yl)-3-nitro-β-D-glucopyranoside ***(17)***

A suspension of **11** (430 mg) in 85% acetic acid (30 ml) was heated on the steam bath until dissolution was complete (4 h). Evaporation *in vacuo*, followed by three evaporations with water and one each with ethanol and ethyl acetate, gave a solid which was dissolved in ethyl acetate (5 ml). Addition of a small amount of petroleum ether and cooling (2 h at 0°) induced crystallization of fine needles (247 mg, 81%) which were isolated and washed with ethyl acetate – petroleum ether (1:2); m.p. 205–206° decomp., unchanged after another recrystallization. (This m.p. was observed when the sample was introduced at 200°; slow temperature raise caused decomposition without melting). Compound **17** showed strong, broad hydroxyl absorption with ν_{max} 3400 and 3200 cm^{-1}.

Anal. Calcd. for $C_{14}H_{24}N_2O_{13}$ (mol. wt., 428.4): C, 39.26; H, 5.65; N, 6.54. Found: C, 39.40; H, 5.72; N, 6.65.

Methyl 4,6-Di-O-acetyl-3-deoxy-2-O-(methyl 4,6-di-O-acetyl-2,3-dideoxy-3-nitro-β-D-glucopyranosid-2-yl)-3-nitro-β-D-glucopyranoside ***(20)***

The compound **17** (90 mg) was treated with acetic anhydride (2 ml) and boron trifluoride etherate (2 drops) for 10 min at room temperature. Excess anhydride was removed by several co-evaporations with toluene. The crystalline residue was once evaporated with added ethanol and then recrystallized from ethyl acetate – petroleum ether; from these solvents the tetraacetate (**20**) crystallized as big prisms (65 mg) of m.p. 237° decomp. Precipitation by water from solution in DMF or DMSO produced fine needles of the same melting point and with a closely similar i.r. spectrum. There were strong peaks at 1750 and 1737 cm^{-1} (acetate C=O) and at 1555 cm^{-1} (NO_2), and hydroxyl absorption was absent.

In addition to the (constant) specific rotation in *chloroform* (Table I), the rotation in *dimethylformamide* (*c*, 0.85) was taken: $[\alpha]_D$ +24.7° (initial) → +9.9° (5 min) → −23.5° (25 min, constant). The cause of the mutarotation is not clear but could possibly be *aci* – salt formation due to dimethylamine present in the DMF. Compound **20** was recovered unchanged by precipitation with water.

Nuclear magnetic resonance data: τ 4.52 (triplet, J = 10 Hz), H-3; τ 5.39 (triplet, J = 10 Hz), H-4; τ 5.58 (doublet, J = 7.5 Hz), H-1; τ 5.65–6.00 (series of poorly resolved signals due to C-6 methylene and H-2); τ 6.4 (multiplet, extending beneath OCH_3 signal), H-5; τ 6.52 (singlet), OCH_3; τ 7.92 and 7.97 (singlets), $OCOCH_3$.

Anal. Calcd. for $C_{22}H_{32}N_2O_{17}$ (mol. wt., 596.5): C, 44.30; H, 5.41; N, 4.70. Found: C, 44.42; H, 5.34; N, 4.61.

Methyl 4,6-O-Benzylidene-3-deoxy-2-O-(methyl 4,6-O-benzylidene-2,3-dideoxy-3-nitro-α-D-glucopyranosid-2-yl)-3-nitro-α-D-glucopyranoside ***(14)***

Compound **14** was obtained from nitroolefin **2** (425 mg) and nitro glycoside **13** (440 mg) by the procedure (*a*) given for the preparation of **11**. Because of increasing discoloration of the solution, the reaction was stopped after 1.5 h although t.l.c. (solvent *b*) showed considerable spots of **2** and **13** besides a predominant spot of nonmigrating **14** at that stage. The residue of evaporation was dissolved

Can. J. Chem. Downloaded from www.nrcresearchpress.com by 210.87.254.6 on 09/05/12
For personal use only.

in ethyl acetate from which, on addition of petroleum ether and cooling (2 h at 5°), colorless crystals of **14** (210 mg, 24%) separated. They decomposed at about 340°. Recrystallization from benzene – ethyl acetate – petroleum ether (5:1:5) gave fine needles, m.p. 348° decomp. The i.r. spectrum was similar to that of **11**, but was distinguished by a strong band at 1060 cm^{-1}.

Anal. Calcd. for $C_{28}H_{32}N_2O_{13}$ (mol. wt., 604.6): C, 55.62; H, 5.34; N, 4.63. Found: C, 55.49; H, 5.15; N, 4.73.

Methyl 3-Deoxy-2-O-(methyl 2,3-dideoxy-3-nitro-α-D-glucopyranosid-2-yl)-3-nitro-α-D-glucopyranoside (18)

Compound **14** (200 mg) was debenzylidenated with acetic acid as described for **11** → **17**. The crude reaction product was dissolved in ethanol and ethyl acetate (7 ml each), the solution clarified with charcoal, and slow crystallization (3 days at 5°) was induced by adding petroleum ether. The product **18** (57 mg, 40%) melted with decomposition at 248–250°, and at 250–251° after another recrystallization from the same solvents, when introduced at 240°. Slow heating caused decomposition without melting. According to t.l.c. the mother liquor still contained much **18** which did not crystallize. The i.r. spectrum of **18** showed strong, broad hydroxyl adsorption (ν_{max} 3380 cm^{-1}) and no phenyl bands in the 700 cm^{-1} region.

Anal. Calcd. for $C_{14}H_{24}N_2O_{13}$ (mol. wt., 428.4): C, 39.26; H, 5.65; N, 6.54. Found: C, 39.45; H, 5.69; N, 6.40.

Methyl 4,6-Di-O-acetyl-3-deoxy-2-O-(methyl 4,6-di-O-acetyl-2,3-dideoxy-3-nitro-α-D-glucopyranosid-2-yl)-3-nitro-α-D-glucopyranoside (21)

Compound **18** (28 mg) was acetylated as described for the acetylation of **17**. The tetraacetate **21** (30 mg, 77%) crystallized as fine needles, m.p. 202–203°, from 95% ethanol. It exhibited strong i.r. bands at 1735 (ester C=O) and 1550 cm^{-1} (NO_2) and lacked hydroxyl absorption.

Nuclear magnetic resonance data: τ 4.65 (triplet, J = 10 Hz), H-3; τ 5.13 (triplet, J = 10 Hz), H-4; τ 5.22 (doublet, J = 3 Hz), H-1; τ 5.6–6.2 (series of poorly resolved signals due to C-6 methylene, H-2, and H-5); τ 6.62 (singlet), OCH_3; τ 7.91 and 7.96 (singlets), $OCOCH_3$.

Anal. Calcd. for $C_{22}H_{32}N_2O_{17}$ (mol. wt., 596.5): C, 44.30; H, 5.41; N, 4.70. Found: C, 44.56; H, 5.57; N, 4.58.

Methyl 4,6-O-Benzylidene-3-deoxy-2-O-(methyl 4,6-O-benzylidene-2,3-dideoxy-3-nitro-β-D-glucopyranosid-2-yl)-3-nitro-α-D-glucopyranoside (15)

Compound **15** was obtained from nitroolefin **2** (720 mg) and nitro glycoside **10** (765 mg) by the procedure (*a*) given for the preparation of **11**. The reaction time was 3 h, and 570 mg (38.5%) of **15**, m.p. 315–316° decomp., was obtained. Recrystallization from ethyl acetate–petroleum ether raised the melting point to 325° decomp. The i.r. spectrum was very similar to those of **11** and **14**, with small differences in band positions and intensities.

Anal. Calcd. for $C_{28}H_{32}N_2O_{13}$ (mol. wt., 604.6): C, 55.62; H, 5.34; N, 4.63. Found: C, 55.67; H, 5.20; N, 4.55.

Methyl 3-Deoxy-2-O-(methyl 2,3-dideoxy-3-nitro-β-D-glucopyranosid-2-yl)-3-nitro-α-D-glucopyranoside (19)

A sample of **15** (100 mg) was debenzylidenated as described for **11** → **17**, except that 70% instead of 85% acetic acid was used; a reaction time of 7 h was required to effect complete dissolution of the sample. Work-up gave 28 mg (39.5%) of crystalline **19**, m.p. 240–241° decomp. (from ethanol – ethyl acetate – petroleum ether).

Another sample of **15** (45 mg) was treated at room temperature with 1 ml of 90% trifluoroacetic acid (12) in which it dissolved within 10 min. After 45 min the solution was concentrated *in vacuo* (bath temperature, 30°) to 0.5 ml. The concentrate was twice evaporated with excess ether whereby **19** crystallized. The crystals were isolated and washed with ether, and melted at 240.5–241.5° decomp. (yield, 18 mg, 57%). They showed strong, broad hydroxyl absorption (ν_{max} 3370 cm^{-1}) and a strong nitro band at 1553 cm^{-1}.

Anal. Calcd. for $C_{14}H_{24}N_2O_{13}$ (mol. wt., 428.4): C, 39.26; H, 5.65; N, 6.54. Found: C, 39.24; H, 5.89; N, 6.38.

Methyl 4,6-Di-O-acetyl-3-deoxy-2-O-(methyl 4,6-di-O-acetyl-2,3-dideoxy-3-nitro-β-D-glucopyranosid-2-yl)-3-nitro-α-D-glucopyranoside (22)

Compound **19** (17 mg) was treated with acetic anhydride (1 ml) and boron trifluoride etherate (1 drop) for 15 min at room temperature. The mixture was then poured into ice cold methanol and evaporated with several additions of methanol and finally with toluene. The residue was recrystallized from chloroform – petroleum ether to give fine needles (19 mg, 89%) of **22**, m.p. 201–203° decomp. (with sintering from 199°).

Nuclear magnetic resonance data: τ 4.55 and 4.65 (two triplets, J = 10 Hz for each, combined intensity 2 H), H-3β and H-3α; τ 5.0–6.4 (complicated pattern of signals of total intensity 12 H), the remaining sugar chain protons; τ 6.47 (singlet, 3 H), β-OCH_3; τ 6.66 (singlet, 3 H), α-OCH_3; τ 7.91, 7.93, 7.96, 7.97 (singlets, 12 H total), 4 $OCOCH_3$. The substance apparently contained an impurity, as the α-OCH_3 peak was accompanied by a weak, unidentified signal (τ 6.62).

Anal. Calcd. for $C_{22}H_{32}N_2O_{17}$ (mol. wt., 596.6): C, 44.30; H, 5.41. Found: C, 44.47; H, 5.52.

Methyl 4,6-O-Benzylidene-3-deoxy-2-O-(methyl 4,6-O-benzylidene-2,3-dideoxy-3-nitro-β-D-glucopyranosid-2-yl)-3-nitro-β-L-glucopyranoside (16)

The nitroolefin **1** (160 mg) and methyl 4,6-*O*-benzylidene-3-deoxy-3-nitro-β-L-mannopyranoside (170 mg) were refluxed for 3 h in dry benzene (25 ml) in the presence of a chip of potassium hydroxide (ca. 10 mg). The solution was filtered with activated charcoal and evaporated to give a solid which was recrystallized from ethyl acetate – petroleum ether. There was obtained 84 mg of **16** having m.p. 292–293° decomp., raised to 325° decomp. by further recrystallization from the same

solvents. The i.r. spectrum was quite similar to those of the stereoisomeric disaccharides, but the optical rotation was 0.0° (*c*, 0.7 in dimethylformamide).

Anal. Calcd. for $C_{28}H_{32}N_2O_{13}$ (mol. wt., 604.6): C, 55.62; H, 5.34; N, 4.63. Found: C, 55.55; H, 5.21; N, 4.56.

Acknowledgment

The authors are grateful to the National Research Council of Canada for the support of their work. F. Kienzle thanks the Ogilvie Flour Mills Co. for a postgraduate fellowship.

1. H. H. Baer and A. Ahammad. Can. J. Chem. **44**, 2893 (1966).
2. H. H. Baer, T. Neilson, and W. Rank. Can. J. Chem. **45**, 991 (1967).
3. H. H. Baer and F. Kienzle. J. Org. Chem. **32**, 3169 (1967).
4. H. H. Baer and W. Rank. Can. J. Chem. This issue.
5. H. H. Baer and K. S. Ong. Can. J. Chem. **46**, 2511 (1968).
6. H. H. Baer and T. Neilson. Can. J. Chem. **43**, 840 (1965).
7. H. H. Baer and F. Kienzle. Can. J. Chem. **45**, 983 (1967).
8. J. Staněk, M. Černý, and J. Pacák. The oligosaccharides. Academic Press, Inc., New York. 1965. Tables 33–36, 49, and 55.
9. C. M. McCloskey and G. H. Coleman. Org. Syntheses, Coll. **3**, 434 (1955).
10. H. H. Baer, F. Kienzle, and T. Neilson. Can. J. Chem. **43**, 1829 (1965).
11. H. H. Baer and F. Kienzle. Can. J. Chem. **43**, 3074 (1965).
12. J. E. Christensen and L. Goodman. Carbohydrate Res. 7, 510 (1968).

Can. J. Chem. Downloaded from www.nrcresearchpress.com by 210.87.254.6 on 09/05/12
For personal use only.

Transannular reactions in the dibenzo[*a*,*d*]cycloheptene series. IV. 10,5 Ketone–amide interactions

M. A. DAVIS, T. A. DOBSON, AND J. M. JORDAN
Ayerst Laboratories, Ayerst, McKenna and Harrison Ltd., Montreal, Quebec

Received January 3, 1969

10-Ketodibenzocycloheptene-5-carboxamides undergo transannular interactions to form carbinolamides. This approach has been used to prepare a number of 11-substituted and -unsubstituted-10,11-dihydro-10,5-(iminomethano)-5*H*-dibenzo[*a*,*d*]cycloheptenes. The ketolactone **3** was a convenient starting material for the substituted compounds. It reacted readily with primary amines to give the carbinolamides **7** or **8**, and underwent equally rapid transformations with secondary amines or alkali to furnish products derived from aerial oxidation, decarboxylation, ring contraction, and/or dimerization. The epoxynitrile **20** was converted by a 5-step sequence to the ketocarboxamide **27** which cyclized at once to the 11-unsubstituted carbinolamide **28**. A modification of this sequence gave the carbinolamine **31**.

Canadian Journal of Chemistry, 47, 2827 (1969)

Can. J. Chem. Downloaded from www.nrcresearchpress.com by 210.87.254.40 on 09/05/12
For personal use only.

We have previously described methods for the preparation of a number of substituted 10,11-dihydro-10,5-(iminomethano)-5*H*-dibenzo[*a*,*d*]-cycloheptenes (**1**) (1). In principle, these methods utilize the ready transannular reaction of a 10-substituted dibenzocycloheptene-5-carboxamide or -carboxylate derivative. The present paper describes a related preparation of the ring system which relies on a 10,5 ketone–amide interaction to form a carbinolamide. The generality of such interactions in linear (2) and alicyclic amides (3), amino acids and peptides (4), alkaloids (5), and steroids (6) has been discussed. The method has been used for a synthesis of atisine (7) and for an analogue of a degradation product of aconitine (8).

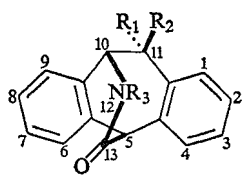

1

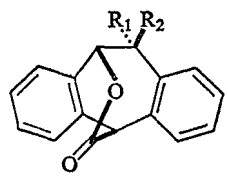

2*a*, R_1 = H, R_2 = OH
b, R_1 = OH, R_2 = H
c, $R_1 = R_2$ = H

Chromic acid oxidation of the readily available mixture of hydroxylactones **2***a*,*b* gave the corresponding ketolactone **3** (9). This served as starting material for several of the carbinolamides by way of its varied reactions with nucleophilic reagents. On treatment with ammonia or methylamine in the absence of air it furnished the carbinolamides **7***a*,*b* in which the secondary hydroxyl group was assigned the *syn*-configuration (see below). When the reactions were carried out in the presence of air the corresponding ketocarbinolamides **8***a*,*b* were obtained. The products were obviously formed from the intermediate *o*,*o*′-disubstituted benzoins **4** which could readily be oxidized by air to the corresponding benzils **5** *via* enediol formation (10) (Scheme I). This mechanism was supported by the observation that analytically pure **7***a* underwent aerial oxidation to **8***a* only in the presence of a base, such as ammonium hydroxide.

Several reactions were investigated which supported the structures of the carbinolamides. The action of chromic acid on **7***a* furnished **8***a*. The ketone group of **8***a* was catalytically reduced to the corresponding alcohol **7***a* which in turn was treated with lithium aluminum hydride to give the basic carbinol **6** of known geometry (1). Although **7***a* was unaffected by sodium borohydride, **8***a* gave the *anti*-hydroxylactone **2***b*, presumably by base-promoted ring opening to the 10,11-dione followed by reduction to a *trans*-diol and subsequent lactone formation on acidification. The action of sodium in liquid ammonia removed both hydroxy groups from **7***a* with concomitant ring scission to give the unsubstituted carboxamide **10**. In contrast to this result, ring cleavage did not occur when the 10-desoxy analogue of **7***a* (**1**, $R_1 = R_3 =$ H; $R_2 =$ OH) was treated with sodium in ammonia (1). The action of warm, dilute mineral acid converted **7***a* to the original ketolactone **3**. The tertiary hydroxyl group was unreactive and could not be esterified; acetylation of **7***a*,*b* under various conditions resulted only in acylation of the secondary hydroxyl group to form **9***a*,*b*. The

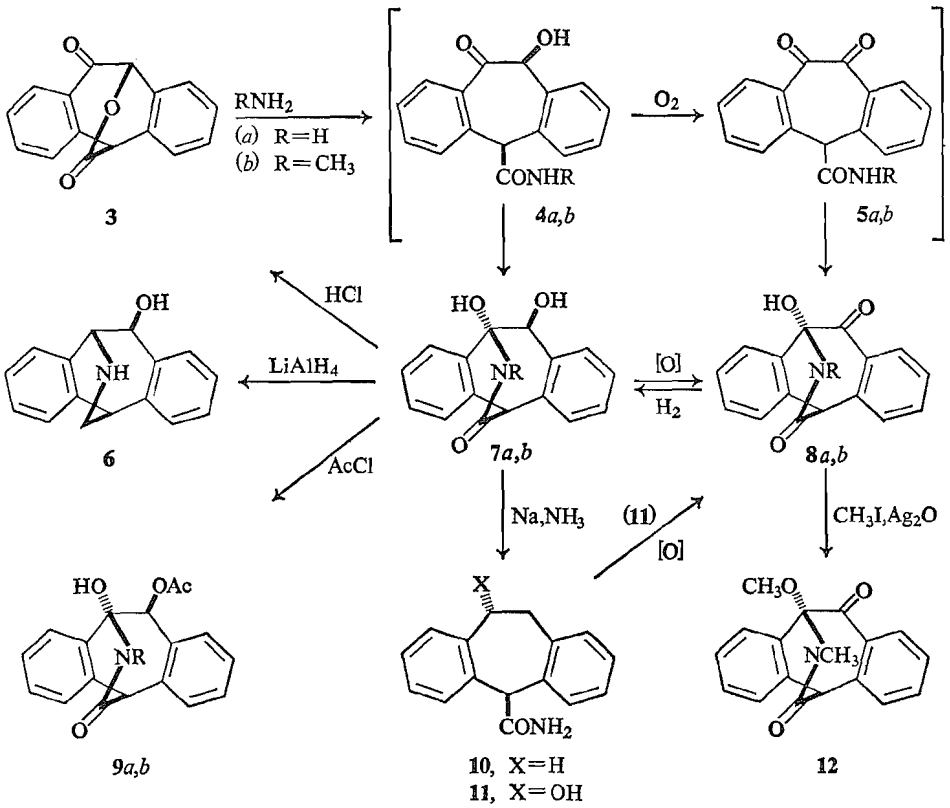

SCHEME I

hydroxyl group of **8***b* could, however, be etherified: the methyl ether **12** was obtained by the action of methyl iodide and silver oxide. Under similar conditions, the same compound was obtained from **7***b* by simultaneous oxidation of the secondary alcohol. The ketone group of **8***a* was unaffected by treatment with either *p*-toluenesulfonylhydrazine or 1,2-ethanedithiol.

Reactions of the ketolactone **3** with secondary amines were investigated; here carbinolamide formation would not be expected. On treatment with either dry diethylamine or morpholine in the presence of air, the lactone ring was opened and the intermediate 10,11-ketohydroxyamides **13***a,b* were rapidly oxidized to the corresponding 10,11-diones **14***a,b*. Once formed, the latter resisted further attack. When the reactions were carried out in the presence of added water, some hydrolytic opening of the lactone occurred and the resulting carboxylic acid **13***c* was oxidized to the dione **14***c*. This vinylogous β-ketoacid decarboxylated and the product (**15**), under the basic conditions of the reaction, dimerized to give the known compound **16** (11). The yield of this dimer depended on the water content of the reaction medium and became the principal product when the reactions were carried out in 30% aqueous dioxane. Similar paths were followed when the ketolactone was treated with dilute aqueous sodium hydroxide, as shown in Scheme II. Here, the 10,11-dione system could undergo a benzilic acid rearrangement under the influence of the stronger base. In agreement with the results of other workers (12), the intermediate dione **15** formed 9-anthroic acid (**19**) *via* ring contraction and dehydration. In one instance the dione carboxylic acid **14***c* rearranged before decarboxylation could occur and the dicarboxylic acid **18** was isolated. Evidence for enediol formation was obtained by the isolation of the dimeric enediol diacetate **17** on treatment of the ketolactone with sodium hydroxide followed by acetyl

Can. J. Chem. Downloaded from www.nrcresearchpress.com by 210.87.254.40 on 09/05/12
For personal use only.

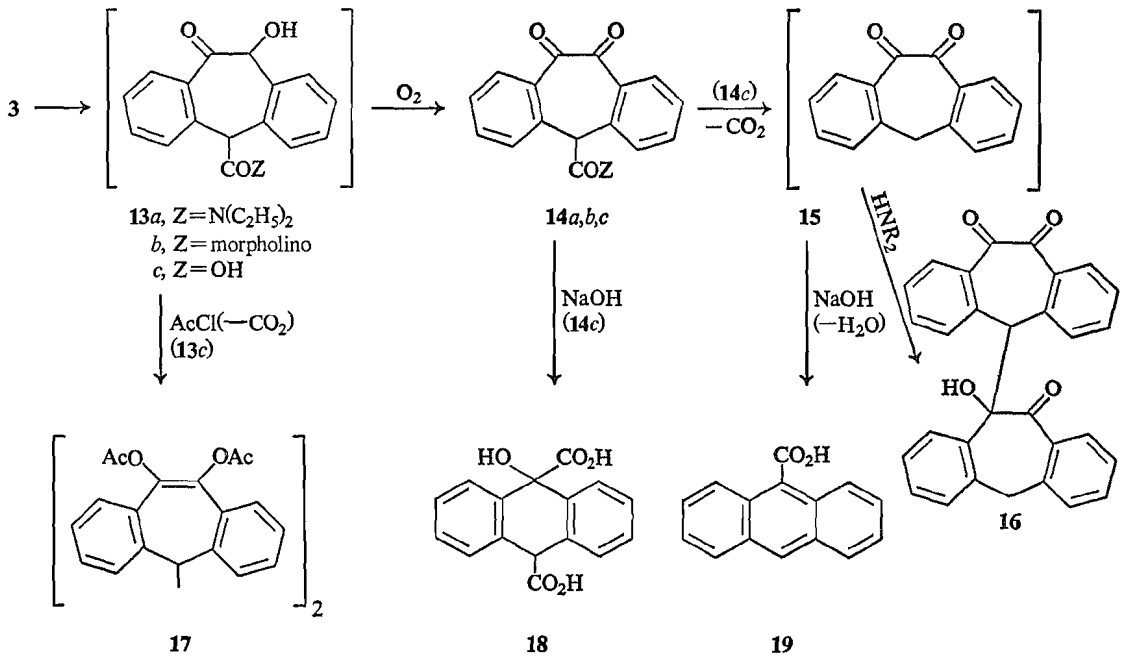

SCHEME II

chloride in the absence of air. Other 5,5′-dimerizations of the dibenzocycloheptene nucleus have been noted (13).

A different route was employed for the preparation of an 11-unsubstituted carbinolamide (Scheme III). Oxidation of 5*H*-dibenzo[*a*,*d*]-cycloheptene-5-carbonitrile with 3-chloroperbenzoic acid gave an apparently homogeneous epoxynitrile **20** of unassigned geometry. Whereas the related 5-keto- (14), 5-hydroxy (15), and 5-unsubstituted epoxides (16) are known to react normally with amines to give the corresponding 10,11-aminoalcohols, the reaction of **20** with diethylamine gave the 9-anthronitrile derivative **23**. This presumably arose by a base-promoted rearrangement of the epoxide (1) to 10-cyano-9,10-dihydro-9-anthraldehyde followed by condensation with the secondary amine and aromatization. Catalytic hydrogenation of the epoxynitrile gave a mixture of epimeric hydroxynitriles **21***a*,*b*, possibly formed by partial epimerization of **20** during the reduction. In one of these epimers, ready interaction of the functional groups occurred. Thus, the iminolactone **22** or its hydrochloride salt were obtained when the *syn*-epimer **21***a* was treated with either aqueous sodium hydroxide or anhydrous hydrogen chloride. Similar behavior has been reported for other hydroxynitriles (6*c*, 17) and the method has been used for a synthesis of aldosterone (18) and steroids bearing an 8β-substituent (19) or a bridged lactone group (20). Chromic acid oxidation of the mixture of alcohols gave the ketonitrile **24**. As with other 10-ketodibenzocycloheptenes (21), the carbonyl group of **24** was markedly enolized and readily formed enol ethers (**25***a*–*c*) rather than ketals on treatment with alcohols in acidic media. Hydration of the nitrile group of **25***a*, using hydrogen peroxide and potassium carbonate (22), gave the corresponding carboxamide **26**. Treatment of this with hydrochloric acid hydrolyzed the enol ether and the resulting 10-ketone **27** cyclized to the desired carbinolamide **28**. A related attempt to obtain **28** by chromic acid oxidation of the *anti*-hydroxyamide **11** gave the ketocarbinolamide **8***a* as the only isolable product.

Since ketone–amide interactions had been shown to proceed with considerable facility, it was of interest to study the behavior of the related ketoamine **30**. Cyclizations of ketoamines are well-known in the alkaloid field (23) and the chemistry of pseudobasic carbinolamines has been reviewed (24). Catalytic hydrogenation of

Can. J. Chem. Downloaded from www.nrcresearchpress.com by 210.87.254.40 on 09/05/12
For personal use only.

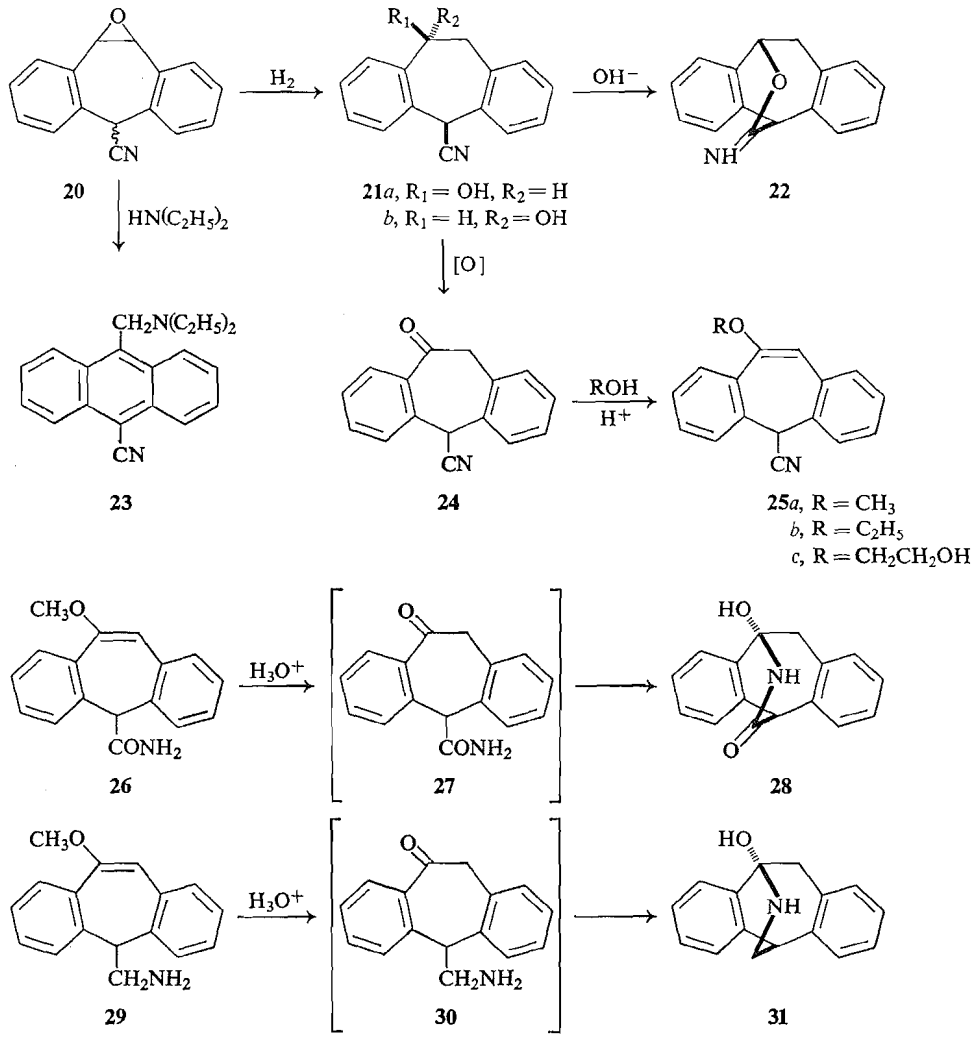

SCHEME III

the nitrile group of **25***a* gave the corresponding 5-aminomethyl compound **29**. The enol ether was hydrolyzed as before to give the 10-ketone **30** which spontaneously formed the carbinolamine **31**. Spectral data indicated that the compound existed as the cyclic form in either neutral or acidic media.

Experimental

Nuclear magnetic resonance (n.m.r.) spectra in the indicated solvents were determined using a Varian A-60A instrument; melting points were recorded on Thomas–Hoover Uni-melt apparatus.

10,11-Dihydro-10,11-dihydroxy-10,5-(iminomethano)-5H-dibenzo[a,d]cyclohepten-13-one (7a)

A solution of ketolactone **3** (8.0 g, 0.03 mole) in dioxane (40 ml) was treated with ammonium hydroxide (*d* 0.88, 250 ml) and the mixture was stirred for 2 h under argon. The precipitated product (4.2 g, 49%) was filtered off and washed with water; m.p. 175–177°, unchanged on recrystallization from chloroform–hexane or from 1,2-dimethoxyethane–ether; ν_{max} (Nujol) 3510, 3430, 3200, 3070 cm^{-1} (NH, OH); 1690 cm^{-1} (lactam); λ_{max} (EtOH) 263 mμ (ε 418); n.m.r. (DMSO), τ: 2.59 (8-H aromatic, m); 5.52 (1-H, s); 5.58 (1-H, s); 6.43 (NH + 2-OH, s).

Anal. Calcd. for $C_{16}H_{13}NO_3$ (267): C, 71.90; H, 4.90; N, 5.24. Found (*m/e* 267): C, 71.53; H, 4.91; N, 5.10.

10,11-Dihydro-10,11-dihydroxy-12-methyl-10,5-(iminomethano)-5H-dibenzo[a,d]cyclohepten-13-one (7b)

A saturated solution of methylamine in anhydrous ether (100 ml) was added to **3** (10.0 g, 0.04 mole) dissolved in dry 1,2-dimethoxyethane (125 ml). The mixture was

Can. J. Chem. Downloaded from www.nrcresearchpress.com by 210.87.254.40 on 09/05/12
For personal use only.

Can. J. Chem. Downloaded from www.nrcresearchpress.com by 210.87.254.40 on 09/05/12
For personal use only.

stirred for 1.5 h under argon, diluted with hexane (50 ml), and the precipitate was filtered off. Recrystallization from acetone–hexane or dimethoxyethane gave 4.5 g (40%), m.p. 170–171°.

Anal. Calcd. for $C_{17}H_{15}NO_3$: C, 72.58; H, 5.37; N, 4.98. Found: C, 72.73; H, 5.16; N, 4.95.

From the mother liquors 1.4 g of the corresponding ketone **8***b* was obtained, m.p. 219–224° (see below).

10-Hydroxy-10,5-(iminomethano)-5H-dibenzo[a,d]cycloheptene-11,13(10H)-dione (8a)

a) A solution of **3** (10.0 g) in dioxane (50 ml), ammonium hydroxide (200 ml), and water (100 ml) was stirred and a stream of air was passed through for 3 h. Recrystallization of the precipitated product from dioxane–ether gave 7.4 g (69%) of **8***a*, m.p. 244–245°; ν_{max} (Nujol) 3420 cm^{-1} (OH); 3140, 3050 cm^{-1} (NH); 1695 cm^{-1} (ketone); 1683 cm^{-1} (lactam); λ_{max} (EtOH) 263 mμ (ε 7610); n.m.r. (DMSO), τ: 1.90 (1-H aromatic, m); 2.67 (7-H aromatic, m); 5.15 (1-H at C-5, s); 6.51 (NH + OH, s).

Anal. Calcd. for $C_{16}H_{11}NO_3$ (265): C, 72.44; H, 4.18; N, 5.28. Found (*m/e* 265): C, 72.68; H, 4.34; N, 5.29.

b) Jones' reagent (25)(2 ml) was added dropwise to a stirred solution of 10,11-dihydro-*anti*-11-hydroxy-5*H*-dibenzo[*a,d*]cycloheptene-5-carboxamide (9) (**11**, 200 mg) in acetone (25 ml). The mixture was filtered through Celite, the filtrate diluted with water and extracted with dichloromethane. The organic layer was washed with water and evaporated. Several recrystallizations of the residue from ethanol gave a sample (25 mg) of **8***a*, m.p. 210–216°, whose spectral properties were essentially identical to those of the material obtained above.

10-Hydroxy-12-methyl-10,5-(iminomethano)-5H-dibenzo[a,d]cycloheptene-11,13(10H)-dione (8b)

A saturated solution of methylamine in chloroform (150 ml) was added to **3** (6.0 g, 0.024 mole) dissolved in the same solvent (100 ml) and a stream of air was passed through the mixture for 15 min. It was kept overnight, then evaporated and the residue was recrystallized from ethanol to give 3.5 g (52%) of product, m.p. 225–227°.

Anal. Calcd. for $C_{17}H_{13}NO_3$: C, 73.11; H, 4.69; N, 5.02. Found: C, 73.07; H, 4.84; N, 5.20.

Reactions of Carbinolamides 7

Oxidation

a) A solution of **7***a* (1.0 g) in acetone (25 ml) was treated with Jones' reagent (2.9 ml) and the mixture was processed in the usual manner to give **8***a* (0.1 g), identified by m.p. and mixed m.p.

b) A solution of **7***a* (0.2 g), ammonium hydroxide (5 ml), dioxane (5 ml), and water (10 ml) was kept in an open vessel and the ultraviolet (u.v.) spectrum was taken at intervals. The percentage conversion was 25% (0.5 h), 50% (2 h), 70% (4 h), and 100% (25 h; chromatographically pure **8***a*). A similar reaction with **7***a* (0.1 g), NH_4OH (4 ml), dioxane (1 ml), and water (4 ml) gave 0.03 g of **8***a*, m.p. 233–235°.

Reduction

A suspension of **7***a* (1.0 g, 0.004 mole) and lithium aluminium hydride (0.8 g, 0.004 mole) in dioxane (30 ml) was heated under reflux for 20 h. The complex was hydrolyzed with aqueous sodium hydroxide and the filtered solution was evaporated. The residue was triturated with a little ether and recrystallized from ethanol to give 10,11-dihydro-*syn*-11-hydroxy-10,5-(iminomethano)-5*H*-dibenzo[*a,d*]cycloheptene (1) (**6**, 0.23 g), m.p. and mixed m.p. 190–191°.

Hydrogenolysis

Sodium was added in small portions to a solution of **7***a* (0.5 g, 0.002 mole) in redistilled liquid ammonia (25 ml) until the blue color persisted for 10 min. An excess of ammonium chloride was added and the mixture was allowed to evaporate. The residue was triturated with water and recrystallized from ethanol to give 10,11-dihydro-5*H*-dibenzo[*a,d*]cycloheptene-5-carboxamide (26) (**10**, 0.03 g), m.p. and mixed m.p. 190–192°.

Hydrolysis

A solution of **7***a* (0.5 g) and 1 *N* HCl (20 ml) in dioxane (4 ml) and methanol (5 ml) was heated on the steam bath for 1 h. The cooled mixture was diluted with water and extracted with dichloromethane. Evaporation and recrystallization of the residue from ethanol–hexane gave the ketolactone **3** (0.1 g), m.p. and mixed m.p. 162–163°.

Acetylation

a) A solution of **7***a* (1.0 g, 0.004 mole) and pyridine (7 ml) in dioxane (10 ml) was cooled in an ice bath and treated dropwise with acetyl chloride (3 ml). The solution was kept in the cooling bath for 1 h and then at room temperature for an additional 0.5 h. Water (10 ml) was added and the precipitated product was recrystallized from chloroform–hexane to give 11-acetoxy-10,11-dihydro-10-hydroxy-10,5-(iminomethano)-5*H*-dibenzo-[*a,d*]cyclohepten-13-one (**9***a*; 0.4 g, 36%), m.p. 225–226°; ν_{max} (Nujol) 3230 cm^{-1} (broad, intense; NH + OH); 1730 cm^{-1} (ester); 1663 cm^{-1} (lactam); λ_{max} (EtOH) 256, 262 mμ (596, 596); n.m.r. (DMSO), τ: 1.53 (NH, s); 2.45 (1-H aromatic, m); 2.80 (7-H aromatic, m); 4.12 (1-H at C-11, s); 5.45 (1-H at C-5, s); 6.68 (OH, s); 7.83 (CH_3, s).

Anal. Calcd. for $C_{18}H_{15}NO_4$: C, 69.89; H, 4.89; N, 4.53. Found: C, 69.76; H, 5.18; N, 4.65.

b) A mixture of calcium hydride (2.0 g) and acetic anhydride (27) (20 ml) was heated under reflux for 2 h with stirring. It was cooled to room temperature and a solution of **7***a* (1.0 g) in dry dioxane (20 ml) was added. The mixture was then heated under reflux for 2 h, left overnight and treated successively with ethanol and water. The product was extracted into benzene and the organic layer was extracted with water, dried, and evaporated. Recrystallization gave 0.3 g (27%) of monoacetate **9***a*, m.p. 217–218°.

c) Acetylation of **7***b* (1.0 g, 0.004 mole) with acetyl chloride (5 ml) and pyridine (10 ml) as described above gave 11-acetoxy-10,11-dihydro-10-hydroxy-12-methyl-10,5-(iminomethano)-5*H*-dibenzo[*a,d*]cyclohepten-13-one (**9***b*, 0.06 g), m.p. 200–201° (from ethanol–hexane); n.m.r. (DMSO), τ: 6.95 (NCH_3, s); remainder similar to that of **9***a*.

Anal. Calcd. for $C_{19}H_{17}NO_4$: C, 70.57; H, 5.30; N, 4,33. Found: C, 70.03; H, 5.50; N, 4.32.

Reactions of Carbinolamides 8

Reduction

a) A solution of **8***a* (1.5 g, 0.006 mole) in absolute ethanol (25 ml) and dioxane (15 ml) was hydrogenated

Can. J. Chem. Downloaded from www.nrcresearchpress.com by 210.87.254.40 on 09/05/12
For personal use only.

at 1 atmosphere and 25° for 6.5 h using 10% palladium-on-charcoal (0.2 g). The filtered solution was evaporated and the residue was recrystallized from chloroform to give 7*a* (0.5 g), m.p. and mixed m.p. 173–174°.

b) A solution of 8*a* (0.7 g, 0.003 mole) and sodium borohydride (0.1 g, 0.003 mole) in ethanol (60 ml) was kept at room temperature overnight. The excess of hydride was destroyed by the addition of acetic acid, water was added, and the ethanol was removed *in vacuo*. The product was extracted into chloroform and the solution was dried and evaporated. Recrystallization of the residue from ethanol–hexane gave *anti*-11-hydroxy-10,11-dihydro-10,5-(epoxymethano)-5*H*-dibenzo[*a,d*]-cyclohepten-13-one (9) (2*b*, 0.02 g), m.p. and mixed m.p. 188–190°.

Methylation

Silver oxide (0.3 g) was added to a solution of 8*b* (0.5 g, 0.002 mole) and methyl iodide (5 ml) in acetone (75 ml) and the suspension was stirred for 18 h. The filtered solution was evaporated and the residue was recrystallized from chloroform–hexane to give 10-methoxy-12-methyl-10,5-(iminomethano)-5*H*-dibenzo[*a,d*]cyclo-heptene-11,13(10*H*)-dione (**12**, 0.2 g), m.p. 202–203°; ν_{max} (Nujol) 1695 cm^{-1} (ketone); 1675 cm^{-1} (lactam); 1090 cm^{-1} (ether); λ_{max} (EtOH) 268 mμ (ε 6740); n.m.r. (DMSO), τ: 2.00 (1-H aromatic, m); 2.52 (7-H aromatic, m); 4.97 (1-H at C-5, s); 6.56 and 7.12 (OCH_3 and NCH_3, s).

Anal. Calcd. for $C_{18}H_{15}NO_3$: C, 73.70; H, 5.15; N, 4.78. Found: C, 73.69; H, 5.06; N, 4.67.

Replacing 8*b* by 7*b* also gave the same product, m.p. 195–198°.

N,N-Diethyl-10,11-dioxo-5H-dibenzo[a,d]cycloheptene-5-carboxamide (14a)

Diethylamine (redistilled, 60 ml) was added to the ketolactone **3** (6.0 g, 0.024 mole) dissolved in dry dioxane (60 ml) and the yellow solution was kept for 6 days in an open vessel. The precipitated product was recrystallized from acetonitrile to give 3.2 g (42%) of the amide as yellow crystals, m.p. 271–272°; ν_{max} (Nujol) 1690, 1670 cm^{-1} (ketone); 1613 cm^{-1} (amide); λ_{max} (EtOH) 259 mμ (ε 11 400); $\lambda_{max}(CH_3CN)$ 256 mμ (ε 11 200) (spectra unchanged on addition of HCl).

Anal. Calcd. for $C_{20}H_{19}NO_3$ (321): C, 74.74; H, 5.96; N, 4.36. Found (*m/e* 321): C, 74.91; H, 6.25; N, 4.26.

Keeping a solution of the amide (0.5 g), diethylamine (5 ml), and water (20 ml) in dioxane (75 ml) for 5 days gave unchanged starting material, identified by m.p. and spectral data.

The quinoxaline derivative was prepared by heating the amide with an excess of *O*-phenylenediamine in acetic acid under reflux for 1 h; m.p. 207–208° (from ethanol).

Anal. Calcd. for $C_{26}H_{23}N_3O$: C, 79.36; H, 5.90; N, 10.68. Found: C, 79.41; H, 5.93; N, 10.75.

5-Morpholinocarbonyl-5H-dibenzo[a,d]cycloheptene-10,11-dione (14b)

The interaction of **3** (0.02 mole) and morpholine (undistilled, 20 ml) in dioxane (25 ml) gave the morpholide (1.1 g, 16%), m.p. 288–292° (from acetonitrile); n.m.r. (DMSO), τ: 2.35 (8-H aromatic, m); 4.03 (1-H at C-5, s); 6.08 (2-H, m); 6.53 (6-H, m).

Anal. Calcd. for $C_{20}H_{17}NO_4$: C, 71.63; H, 5.11; N, 4.18. Found: C, 71.74; H, 5.24; N, 4.49.

10′-Hydroxy-{5,10′-bi-5H-dibenzo[a,d]cycloheptene}-10,11,11′-trione (16)

The crude filtrate from the preceding reaction was diluted with water to afford 1.1 g of the dimer. Recrystallization of a portion from acetonitrile gave a sample m.p. 290–295° decomp. (reported (11) m.p. 285° decomp.). As previously observed (11), the compound dissociated to the monomer on heating; the mass spectrum contained a strong peak at *m/e* 222 but on introduction of the sample by direct inlet at temperatures below 150°, a weak peak for the dimer at *m/e* 444 was seen.

Anal. Calcd. for $C_{30}H_{20}O_4$: C, 81.06; H, 4.54. Found: C, 81.41; H, 4.77.

The dimer was formed as the principal product on interaction of the ketolactone with secondary amines in the presence of 30% aqueous dioxane.

The quinoxaline derivative of monomer **15** was prepared from **16** as described (11); m.p. 234–235° (from acetonitrile) (reported m.p. 234°).

Reaction of 3 with sodium hydroxide

a) Finely ground *3* (2.0 g) was added to 1 *N* NaOH (200 ml) and the mixture was stirred overnight in an open vessel. As the reaction proceeded a purple color developed which was quickly discharged on contact with the air. A small quantity of unreacted ketolactone was filtered off and the chilled solution was adjusted to pH 4 with 10% HCl. The precipitated 9-anthroic acid (0.6 g), m.p. 215–217°, was identified by comparison with an authentic specimen.

In a similar experiment, the ketolactone (1.0 g) and 1 *N* NaOH (100 ml) were stirred together for 1 h. The product (0.5 g) was 9,10-dihydro-9-hydroxyanthracene-9,10-dicarboxylic acid (**18**), m.p. 207–209°. Recrystallization from ethanol–ethyl acetate, avoiding undue heating, gave a sample m.p. 217–218°; ν_{max}(Nujol) 3525, 3385, and envelope around 2900 cm^{-1} (OH); 1680 cm^{-1}, broad (carboxyl); λ_{max}(EtOH) 253, 262 mμ (ε 465, 407); n.m.r. (DMSO), τ: 2.33–2.75 (8-H aromatic, m); 4.99 (1-H, s); on the addition of D_2O, 3 exchanged protons were observed.

Anal. Calcd. for $C_{16}H_{12}O_5$: C, 67.59; H, 4.26. Found: C, 67.22; H, 4.26.

b) A solution of **3** (5.0 g, 0.02 mole) in dioxane (75 ml) was kept under purified nitrogen. A 50% NaOH solution which had been freed from air by prior boiling under nitrogen (6.0 ml), was added dropwise. The deeply colored reaction mixture was stirred for 10 min and then treated dropwise with acetyl chloride (4.7 g, 0.06 mole). The gummy precipitate was removed and triturated with a little methanol to afford 2.4 g of material, m.p. > 250°. Recrystallization of a portion from acetonitrile gave a sample of 5,5′bis(5*H*-dibenzo[*a,d*]cycloheptene-10,11-diol)-tetracetate (**17**), m.p. 335–340° (decomp.); ν_{max}(Nujol) 1750 cm^{-1} (enol acetate); 1763, 1205, 1190 cm^{-1} (inflections); $\lambda_{max}(CH_3CN)$ 248 mμ (ε 23 200).

Anal. Calcd. for $C_{38}H_{30}O_8$ (614): C, 74.25; H, 4.92. Found (*m/e* 614, weak; 307, strong): C, 73.77; H, 5.10.

10,11-Dihydro-10,11-epoxy-5H-dibenzo[a,d]cycloheptene-5-carbonitrile (20)

A solution of 5*H*-dibenzo[*a,d*]cycloheptene-5-carbonitrile (26) (100 g, 0.46 mole) and 85% 3-chloroperbenzoic acid (115 g, 0.56 mole) in ethyl acetate (1100 ml) was kept at room temperature for 9 days at which time the reaction

Can. J. Chem. Downloaded from www.nrcresearchpress.com by 210.87.254.40 on 09/05/12
For personal use only.

was judged from optical density measurements to be complete. Hexane (800 ml) was added with cooling and the long, needle-like crystals (45.3 g, m.p. 160–161°) were filtered off. An additional amount was obtained by evaporation of the solvent and addition of chloroform to the residue. The insoluble 3-chlorobenzoic acid was removed and the filtrate was extracted successively with aqueous sodium bisulfite and sodium bicarbonate. Evaporation of the solvent and recrystallization from chloroform–hexane gave 26.6 g (total yield 67%), m.p. 157–158°. An analytical sample had m.p. 162–163°; ν_{max}(CHCl$_3$) 2250 cm^{-1} (C≡N); λ_{max}(EtOH) 268 mμ (ε 812); n.m.r. (CDCl$_3$), τ: 2.33 (2-H aromatic, m); 2.70 (6-H aromatic, m); 3.20 (1-H at C-5, s); 5.74 (1-H each at C-10 and C-11, s).

Anal. Calcd. for $C_{16}H_{11}NO$: C, 82.38; H, 4.75; N, 6.01. Found: C, 82.12; H, 4.62; N, 6.05.

10-Diethylaminomethyl-9-anthronitrile (23)

A solution of the epoxynitrile **20** (10.0 g, 0.04 mole) and diethylamine (5.8 g, 0.08 mole) in toluene (100 ml) was heated under reflux for 7 h. The solvent was evaporated and the residue was recrystallized from 2-propanol to give 5.5 g of the anthracene derivative, m.p. 127–128°; ν_{max}(CHCl$_3$) 2215 cm^{-1} (C≡N); λ_{max}(EtOH) 259, 369, 388 mμ (ε 137 000, 7940, 10 140); n.m.r. (CDCl$_3$), τ: 1.50, 2.48 (4-H + 4-H aromatic, m); 5.62 (CH$_2$, s); 7.46 (q) and 8.98 (t; 2-C$_2$H$_5$ groups).

Anal. Calcd. for $C_{20}H_{20}N_2$: C, 83.29; H, 6.99; N, 9.71. Found: C, 83.07; H, 6.81; N, 9.58.

The hydrochloride had m.p. 255–256° (from methanol-2-propanol).

Anal. Calcd. for $C_{20}H_{21}ClN_2$: C, 73.96; H, 6.52; Cl, 10.38; N, 8.62. Found: C, 74.20; H, 6.55; Cl, 10.68; N, 8.73.

10,11-Dihydro-10-hydroxy-5H-dibenzo[a,d]cycloheptene-5-carbonitrile (21)

A solution of **20** (100 g) in absolute ethanol (1000 ml) was hydrogenated over 10% palladium-on-carbon (8 g) at room temperature and atmospheric pressure until the theoretical amount of hydrogen was consumed (2 h). The catalyst was filtered off and the solution was chilled to give 56.0 g of hydroxynitrile, m.p. 150–151°. An additional 21.2 g (m.p. 151–152°) was obtained by evaporation of the solvent, dissolution of the residue in chloroform, and addition of hexane. Further recrystallizations from chloroform afforded a sample of the *syn*-epimer (**21***a*), m.p. 160°; ν_{max}(Nujol) 3500, 3270 cm^{-1} (assoc. OH); 2250, 2240 cm^{-1} (split C≡N); λ_{max}(EtOH) 263 mμ (ε 480); n.m.r. (DMSO), τ: 2.55 (8-H aromatic, m); 3.87 (1-H at C-5, s); 4.31 (OH, d); 4.78 (1-H at C-10, q); 6.65 (CH$_2$, m).

Anal. Calcd. for $C_{16}H_{13}NO$: C, 81.68; H, 5.57; N, 5.95. Found: C, 81.64; H, 5.87; N, 5.92.

The chloroform–hexane filtrate was diluted with a further quantity of hexane to afford an impure sample (4.2 g), m.p. 128–137° of the *anti*-epimer (**21***b*). Recrystallization of material obtained from a similar experiment (m.p. 123–130°) from ether–hexane gave the pure form, m.p. 118–120°; ν_{max}(Nujol) 3510 cm^{-1} (OH): 2225 cm^{-1} (C≡N) (both singlets); λ_{max}(EtOH) 262 mμ (ε 509); n.m.r. (DMSO) τ: 2.55 (8-H aromatic, m); 3.87 (1-H at C-5, s); 4.70 (1-H at C-10, q); 6.72 (CH$_2$, m); 6.68 (OH, s).

Anal. Found: C, 81.51; H, 5.79; N, 5.79.

Carrying out the hydrogenation of **20** (5.0 g) in ethyl acetate (125 ml) under similar conditions (4 h, 0.4 g catalyst) gave mainly **21***b* (3.6 g), m.p. 124–127° after one recrystallization from chloroform–hexane.

10,11-Dihydro-10,5-(epoxymethano)-5H-dibenzo[a,d]cyclohepten-13-imine (22)

A solution of the *syn*-hydroxynitrile **21***a* (11.9 g) in methanol (475 ml) was treated with 10% aqueous NaOH (10 ml) and kept overnight at room temperature. The methanol was removed *in vacuo* and the product was extracted into chloroform. The extracts were washed with water, dried, and evaporated to give the iminolactone (11.6 g, 97%), m.p. 150–152°. An analytical sample had m.p. 153–154° (from chloroform–hexane); ν_{max}(CHCl$_3$) 3280 cm^{-1} (NH); 1660 cm^{-1} (C=N); λ_{max}(EtOH) 265 mμ (ε 574); n.m.r. (DMSO), τ: 2.68 (8-H, aromatic, m); 4.35 (1-H at C-10, q); 5.13 (1-H at C-5, s); 6.65 (CH$_2$, m); 6.67 (NH, s).

Anal. Calcd. for $C_{16}H_{13}NO$: C, 81.68; H, 5.57; N, 5.95. Found: C, 81.58; H, 5.49; N, 5.71.

Treatment of **21***a* (1.0 g) in methanol (40 ml) with 10% NaOH (1 ml) for 45 min furnished 1.0 g of crude iminolactone, m.p. 151–152°. The use of **21***b* under these conditions similarly gave **22** (0.99 g, m.p. 151–153°) although the reaction mixture was discolored by the presence of side-products.

The hydrochloride of **22** was obtained by treating a solution of **21***a* (0.5 g) in anhydrous tetrahydrofuran (25 ml) with ethereal HCl (10 ml). The solution was kept at room temperature for 4 h and the precipitated salt (0.33 g) was filtered off; m.p. 190–191°. Dilution of the filtrate with ether gave an additional 0.11 g (total yield 76%), m.p. 188–190°.

Anal. Calcd. for $C_{16}H_{14}ClNO$: C, 70.71; H, 5.19; Cl, 12.93; N, 5.15. Found: C, 70.62; H, 5.30; Cl, 13.09; N, 5.19.

The *anti*-epimer **21***b* was recovered largely unchanged after similar treatment with HCl.

A solution of the hydrochloride of **22** (0.1 g) in water (20 ml) was kept at 50° for 10 min and the precipitated 10,11-dihydro-10,5-(epoxymethano)-5*H*-dibenzo[*a*,*d*]-cyclohepten-13-one **2***c* (9) (0.07 g) was filtered off; m.p. and mixed m.p. 169–170°.

10-Oxo-5H-dibenzo[a,d]cycloheptene-5(11-H)-carbonitrile (24)

A solution of **21***a*,*b* (32.6 g, 0.14 mole) in acetone (650 ml) was cooled to 0° in an ice–salt bath and Jones' reagent (41.5 ml) was added dropwise with stirring. The precipitate was filtered off (Celite) and the solution was evaporated *in vacuo* to about one-half volume. Water was added and the precipitated product was collected and dissolved in chloroform. The solution was thoroughly extracted with water to remove the last traces of mineral acid. It was dried and evaporated and the residue was recrystallized once from chloroform–hexane to give 26.8 g (83%), m.p. 128–130°; ν_{max}(CHCl$_3$) 2245 cm^{-1} (C≡N); 1672 cm^{-1} (C=O); λ_{max}(CHCl$_3$) 260, 288 mμ (ε 10 550, 1770); λ_{max}(EtOH) 240, 290 mμ (ε 8180, 5200); n.m.r. (CDCl$_3$), τ: 1.95 (1-H aromatic, m); 2.53 (7-H aromatic, m); 4.38 (1-H at C-5, s); 5.75 (CH$_2$, s).

Anal. Calcd. for $C_{16}H_{11}NO$: C, 82.38; H, 4.75; N, 6.01. Found: C, 82.33; H, 4.80; N, 5.78.

Can. J. Chem. Downloaded from www.nrcresearchpress.com by 210.87.254.40 on 09/05/12
For personal use only.

Enol Ethers of ***24***

a) The ketonitrile (24.0 g) was added to a saturated solution of HCl in methanol (600 ml) with sufficient warming to effect dissolution. The reaction mixture was kept at room temperature for 1 h and then chilled. The precipitated product was filtered off and washed with ether–hexane to give 10-methoxy-5*H*-dibenzo[*a*,*d*]cycloheptene-5-carbonitrile (***25a***, 21.9 g, 86%), m.p. 145–146°, unchanged on recrystallization from chloroform–hexane or methanol; ν_{max}(Nujol) 2235 cm^{-1} (C≡N); 1562 cm^{-1} (C=C); 1241, 1090 cm^{-1} (C—O); λ_{max}(EtOH) 288 mμ (ε 12 430).

Anal. Calcd. for $C_{17}H_{13}NO$: C, 82.57; H, 5.30; N, 5.66. Found: C, 82.30; H, 5.30; N, 5.92.

A solution of the enol ether (1 g) in dioxane (25 ml) containing concentrated HCl (1 ml) was kept at room temperature for 24 h; regeneration of the ketonitrile (m.p. 116–120°) was almost complete.

b) Absolute ethanol (0.8 ml) was cooled in an ice–salt bath and treated with thionyl chloride (1.0 ml), followed by the ketonitrile (0.5 g) An additional 3 ml of ethanol was added to effect dissolution and the mixture was left at room temperature for 3 days. Recrystallization of the precipitated product (0.35 g) from ethanol gave the ethyl enol ether ***25b***, m.p. 157–158°; ν_{max}(Nujol) 2235 cm^{-1} (C≡N); 1560 cm^{-1} (C=C); 1240, 1135 cm^{-1} (C—O); λ_{max}(EtOH) 287 mμ (ε 12 280).

Anal. Calcd. for $C_{18}H_{15}NO$: C, 82.73; H, 5.79; N, 5.36. Found: C, 83.01; H, 5.77; N, 5.35.

c) A solution of the ketonitrile (0.5 g), ethylene glycol (0.6 g), and *p*-toluenesulfonic acid (0.1 g) in benzene (100 ml) was heated under reflux for 20 h using a Dean–Stark trap to remove the entrained water. The solution was extracted with aqueous sodium bicarbonate and then dried and evaporated. The residue was triturated with a little chloroform–hexane to give 0.3 g of the 2-hydroxyethyl enol ether ***25c***, m.p. 148–150°. An analytical sample had m.p. 152–153° (from ethanol); ν_{max}(Nujol) 3260 cm^{-1} (OH); 2240 cm^{-1} (C≡N); 1563 cm^{-1} (C=C); 1070 cm^{-1} (C—O); λ_{max}(EtOH) 288 mμ (ε 11 460).

Anal. Calcd. for $C_{18}H_{15}NO_2$: C, 77.96; H, 5.45; N, 5.05. Found: C, 78.18; H, 5.29; N, 5.06.

*10-Methoxy-5H-dibenzo[a,d]cycloheptene-5-carboxamide (****26****)*

A solution of the enol ether ***25a*** (31.8 g) in acetone (1350 ml) was chilled in an ice bath and 30% hydrogen peroxide (450 ml) was added, followed by 10% aqueous potassium carbonate (540 ml). The mixture was stirred in the cold for 10 min and then heated to the boiling point during 40 min, at which time an exothermic reaction ensued. The heating mantle was removed, the mixture was left at ambient temperature for 18 h, and the acetone was removed *in vacuo*. The precipitated product was recrystallized from dioxane–ether to give 15.1 g (44%) of the amide, m.p. 224–225°; ν_{max}(Nujol) 3430, 3330 cm^{-1} (NH); 1660 cm^{-1} (amide); 1560 cm^{-1} (C=C); 1250, 1096 (C—O); λ_{max}(EtOH) 286 mμ (ε 12 740).

Anal. Calcd. for $C_{17}H_{15}NO_2$: C, 76.96; H, 5.70; N, 5.28. Found: C, 76.63; H, 6.00; N, 5.42.

*10,11-Dihydro-10-hydroxy-10,5-(iminomethano)-5H-dibenzo[a,d]cyclohepten-13-one (****28****)*

A solution of the preceding amide (6.5 g) in dioxane (200 ml) was treated with concentrated HCl (3 ml) and left at room temperature overnight. It was diluted with water (150 ml) and the dioxane was removed *in vacuo*. The product was extracted into chloroform and this solution was washed with water, dried, and evaporated. Recrystallization of the residue from acetonitrile–ether gave the carbinolamide (3.3 g, 54%), m.p. 213–214° decomp.; ν_{max}(Nujol) 3450, 3200 cm^{-1} (OH, NH); 1662 cm^{-1} (lactam); λ_{max}(EtOH) 260, 272 mμ (ε 886, 698); n.m.r. (DMSO), τ: 1.67 (NH, s); 2.67 (8-H, aromatic, m); 5.50 (1-H at C-5, s); 6.65 (OH, s); 6.70 (CH_2, q).

Anal. Calcd. for $C_{16}H_{13}NO_2$: C, 76.47; H, 5.22; N, 5.57. Found: C, 76.25; H, 5.23; N, 5.72.

*10-Methoxy-5H-dibenzo[a,d]cycloheptene-5-methylamine hydrochloride (****29****)*

a) A solution of ***25a*** (58.0 g) in methanol (600 ml) was saturated with ammonia and hydrogenated over Raney nickel (6 g) at 1100 p.s.i. and 75° for 7 h. The filtered solution was evaporated, taken into ether, and treated with hydrogen chloride. Recrystallization of the precipitate from ethanol–ether gave 39.5 g (58%) of the product, m.p. 241–242°. An analytical sample had m.p. 244–245° (from 2-propanol); ν_{max}(Nujol) 1560 cm^{-1} (C=C); 1210, 1120 cm^{-1} (C—O); λ_{max}(EtOH) 228, 292 mμ (ε 13 100, 12 600); n.m.r. (D_2O), τ: 3.00 (8-H, aromatic, m); 4.10 (1-H at C-11, s); 5.45 (3-H exch, s); 5.96 (1-H at C-5, m); 6.54 (OCH_3, s); 6.96 (CH_2, d).

Anal. Calcd. for $C_{17}H_{18}ClNO$: C, 70.94; H, 6.30; Cl, 12.32; N, 4.87. Found: C, 70.87; H, 6.40; Cl, 12.62; N, 4.97.

From the neutral fraction 21.3 g of unchanged nitrile was obtained, m.p. 142–144°.

b) A solution of ***25a*** (1.0 g) in dry tetrahydrofuran (40 ml) was treated with 1 *M* diborane in tetrahydrofuran (20 ml) and kept overnight. It was then heated under reflux for 1 h to complete the reaction, treated with water, and the solvent removed *in vacuo*. The amine was extracted into chloroform and the solution was washed with water, dried, and evaporated. The crude hydrochloride could not be adequately purified and was reconverted to the free amine. This in turn furnished a hydrochloride, m.p. 244–245° (60 mg).

*10,11-Dihydro-10-hydroxy-10,5-(iminomethano)-5H-dibenzo[a,d]cycloheptene (****31****)*

A solution of the preceding salt (5.0 g) in water (300 ml) and concentrated HCl (6 ml) was kept for 24 h at room temperature. Neutralization with sodium bicarbonate gave a precipitate which was recrystallized from ethanol or nitromethane to furnish 1.8 g (42%), m.p. 180–181°; ν_{max}(Nujol) 3300, 2900 cm^{-1} (NH, OH assoc.); λ_{max}(CH_3CN) 273, 290 mμ (ε 684, 223); λ_{max}(CH_3CN+HCl) 271 (infl.), 293 mμ (ε 828, 773); n.m.r. (DMSO), τ: 2.24 (1-H, aromatic, m); 2.83 (7-H, aromatic, m); 6.00 (1-H at C-5, m); 6.70 (2-CH_2, m).

Anal. Calcd. for $C_{16}H_{15}NO$: C, 80.98; H, 6.37; N, 5.90. Found: C, 80.71; H, 6.36; N, 5.94.

Acknowledgments

We wish to thank Dr. G. S. Myers and his group for furnishing several intermediates in

quantity. Spectral data were recorded by Mrs. J. Jachner and Mr. M. Boulerice, and microanalyses were carried out by Mr. W. J. Turnbull. The mass spectra were determined by Morgan–Schaffer Corp., Montreal.

1. T. A. DOBSON, M. A. DAVIS, and A.-M. HARTUNG. Can. J. Chem. **46**, 3391 (1968).
2. A. QUEEN and A. REIPAS. J. Chem. Soc. (C). 245 (1967). N. H. CROMWELL and K. E. COOK. J. Am. Chem. Soc. **80**, 4573 (1958).
3. F. H. BOTTOM and F. J. MCQUILLIN. Tetrahedron Letters, 459 (1968).
4. (*a*) L. A. COHEN and B. WITKOP. *In* Molecular rearrangements. Part 2. *Edited by* P. de Mayo. Interscience Publishers, Inc., New York. 1964. pp. 996–998. (*b*) O. YONEMITSU, B. WITKOP, and I. L. KARLE. J. Am. Chem. Soc. **89**, 1039 (1967).
5. E. W. WARNHOFF. *In* Molecular rearrangements. Part 2. *Edited by* P. de Mayo. Interscience Publishers, Inc., New York. 1964. p. 895.
6. (*a*) A. BOWERS. J. Org. Chem., **26**, 2043 (1961). (*b*) W. NAGATA, S. HIRAI, H. ITAZAKI, and K. TAKEDA. J. Org. Chem. **26**, 2413 (1961). (*c*) A. T. GLEN, W. LAWRIE, and J. MCLEAN. J. Chem. Soc. (C). 661 (1966).
7. W. NAGATA, T. SUGASAWA, M. NARISADA, T. WAKABAYASHI, and T. HAYASE. J. Am. Chem. Soc. **89**, 1483 (1967).
8. K. WIESNER and J. SANTROCH. Tetrahedron Letters, 5939 (1966).
9. T. A. DOBSON, M. A. DAVIS, A.-M. HARTUNG, and J. M. MANSON. Can. J. Chem. **46**, 2843 (1968).
10. S. H. HARPER *in* Chemistry of carbon compounds. Vol. III. Part B. *Edited by* E. H. Rodd. Elsevier Publ. Co., Inc., Amsterdam. 1956. p. 1163.
11. J. RIGAUDY and L. NÉDÉLEC. Bull. Soc. Chim. France, 643 (1959).
12. J. RIGAUDY and L. NÉDÉLEC. Bull. Soc. Chim. France, 638 (1959).
13. I. MORITANI, S.-I. MURAHASHI, K. YOSHINAGA, and H. ASHITAKA. Bull. Chem. Soc. Japan, **40**, 1506 (1967). S.-I. MURAHASHI, I. MORITANI, and M. NISHINO. J. Am. Chem. Soc. **89**, 1257 (1967).
14. F. W. HOFFMAN-LAROCHE. A.-G. South African Patent No. 65/6869 (1966); Derwent Farmdoc No. 22076.
15. N. L. BAULD and Y. S. RIM. J. Am. Chem. Soc, **89**, 179 (1967).
16. S. KIMOTO and S. OHTA. Yakugaku Zasshi, **8.7** 861 (1967).
17. J. ATTENBURROW, J. ELKS, B. A. HEMS, and K. N. SPEYER. J. Chem. Soc. 510 (1949).
18. W. NAGATA, M. NARISADA, and T. SUGASAWA. J. Chem. Soc. (C). 648 (1967).
19. W. NAGATA, T. TOMITA, and H. ITASAKI. Japanese Patent No. 3166/67; Derwent Farmdoc No. 25495.
20. W. NAGATA. Proceedings Intern. Symp. on Drug Res., Chemical Institute of Canada, Ottawa. 1967. p. 188. A. KASAL and V. CERNY. Collection Czech. Chem. Commun. **32**, 3733 (1967). M.-M. JANOT, X. LUSINCHI, and R. GOUTAREL. Bull. Soc. Chim. France, 1566 (1964). K. G. HOLDEN and J. F. KERWIN. U.S. Patent No. 3 272 799 (1966); Chem. Abstr. **65**, 20195^e (1966).
21. J. RIGAUDY and L. NÉDÉLEC. Bull. Soc. Chim. France, 659 (1959). J. O. JÍLEK, V. SEIDLOVÁ, E. SVÁTEK, and M. PROTIVA. Monatsh. Chem. **96**, 182 (1965). M. PROTIVA. Farmaco, (Pavia), Ed. Sci. **21**, 76 (1966). G. J. B. CORTS and W. TH. NAUTA. Rec. Trav. Chim. **85**, 389 (1966).
22. J. V. MURRAY and J. B. CLOKE. J. Am. Chem. Soc. **56**, 2749 (1934).
23. E. W. WARNHOFF. *In* Molecular rearrangements. Part 2. *Edited by* P. de Mayo. Interscience Publishers, Inc., New York. 1964. pp. 901–961. Y. INUBUSHI, H. ISHII, T. HARAYAMA, R. H. BURNELL, W. A. AYER, and B. ALTENKIRK. Tetrahedron Letters, 1069 (1967). W. A. AYER, B. ALTENKIRK, S. VALVERDE-LOPEZ, B. DOUGLAS, R. F. RAFFAUF, and J. A. WEISBACH. Can. J. Chem. **46**, 15 (1968).
24. D. BEKE. *In* Advances in heterocyclic chemistry. Vol. 1. *Edited by* A. R. Katritzky. Academic Press, Inc., New York. 1963. p. 167.
25. C. DJERASSI, R. R. ENGLE, and A. BOWERS. J. Org. Chem. **21**, 1547 (1956).
26. M. A. DAVIS, S. O. WINTHROP, R. A. THOMAS, F. HERR, M.-P. CHAREST, and R. GAUDRY. J. Med. Chem. **7**, 88 (1964).
27. R. V. OPPENAUER. Monatsh. Chem. **97**, 62 (1966).

Can. J. Chem. Downloaded from www.nrcresearchpress.com by 210.87.254.40 on 09/05/12
For personal use only.

Can. J. Chem. Downloaded from www.nrcresearchpress.com by 210.87.254.40 on 09/05/12
For personal use only.

Cycloalkylation d'aryloléfines par le trifluorure de bore. Synthèse d'hydrocarbures aromatiques polyméthylés[1]

P. CANONNE ET A. REGNAULT[2]
Département de Chimie, Université de Laval, Québec, Québec

Reçu le 23 janvier 1969

L'examen d'ensemble des résultats de nos travaux sur la cyclisation des aryl-4 oléfines nous permet de conclure que le trifluorure de bore est le catalyseur d'élection pour les aryl-4 oléfines ne possédant pas de groupement fonctionnel.

Son utilisation est illustrée par la synthèse du tétraméthyl-1,3,6,8 triphénylène non encore décrit dans la littérature et par une nouvelle méthode rapide de préparation du diméthyl-1,5 naphtalène.

A survey of the results obtained by us in the course of cyclizations of 4-arylolefins indicates that boron trifluoride is the most satisfactory catalyst in the case of otherwise non-functionalized substrates. Its use is illustrated by the synthesis of the heretofore unknown 1,3,6,8-tetramethyltriphenylene and by an improved preparation of 1,5-dimethylnaphthalene.

Canadian Journal of Chemistry, 47, 2837 (1969)

Dans une série de publications (1–4) nous avons développé une nouvelle méthode de synthèse de systèmes polycycliques à partir d'acides aryloléfiniques. L'étude comparative de la cyclisation de diverses aryloléfines possédant des groupements fonctionnels variés ($(COOC_2H_5)_2$, COOH, $COOCH_3$, CH_2OH, CH_3) en β de la double liaison fait l'objet du présent mémoire.

Cyclisation des acides éthyléniques

L'intérêt d'effectuer la cyclisation à cette étape réside dans le fait que seul le carbométhoxy-2 tétrahydro-1,2,3,4 naphtalène peut être aromatisé avec un bon rendement, sans élimination ou transformation du groupement fonctionnel (5). Nous avons ainsi préparé des naphtalènes possédant un groupement réactionnel en position β, lesquels sont difficilement accessibles par d'autres voies (schéma 1). Nous nous sommes aperçus (schéma 1) que les acides benzyl-2 pentène-4 oïques (1) et naphtylméthyl-2 pentène-4 oïques (3) avaient un comportement identique vis à vis des acides protoniques: concurrence entre cyclisation et lactonisation. Afin d'éviter cette dernière réaction parasite (lactonisation) nous nous sommes tournés vers d'autres catalyseurs de cyclisation. Le chlorure d'aluminum nous permet de cycliser quantitativement l'acide **7** lorsque l'on opère à reflux de CS_2, mais si l'on travaille à 0°, on recueille un mélange d'acide cyclisé **8** et de lactone **9** (84:16). Pour expliquer cette différence de comportement suivant la température, nous avons cherché à définir les conditions dans lesquelles la lactone **9** s'isomérisait en acide **8** et nous avons vu que cette transformation s'effectuait totalement dans les conditions employées pour la cyclisation de l'acide éthylénique **7** (schéma 2). Il est bien connu qu'en présence de chlorure d'aluminum les γ-olides se scindent et se conduisent comme des réactifs alkylants.

Cyclisations d'ester éthyléniques

Comme l'on pouvait s'y attendre, la cyclisation du benzyl-2 pentène-4 carboxylate de méthyle (**10**) par les acides protoniques s'accompagne de lactonisation mais par contre le chlorure d'aluminum cyclise cet ester sans lactonisation (schéma 3). Cependant cette réaction n'est pas applicable aux homologues méthylés sur le cycle aromatique ni aux naphtylméthyl-2 pentène-4 oates de méthyle, en raison des inconvénients inhérents à ce catalyseur (transposition intramoléculaire des groupements méthyles du cycle aromatique dans le premier cas, résinification dans le second cas).

Des essais de cyclisation effectués sur l'ester malonique **21**, en présence d'un grand excès de chlorure d'aluminum, n'ont fourni que de faibles rendements en ester cyclisé **22** (schéma 4).

Cyclisation d'alcools éthyléniques

La cyclisation de l'alcool éthylénique **12** est réalisée par chauffage à reflux dans un mélange d'acides sulfurique et acétique (5:95); on

[1]Ce mémoire constitue une partie de la thèse de doctorat de A. Regnault.

[2]Adresse actuelle: Département de Chimie, Faculté des Sciences, Université de Montréal, Montréal, Québec.

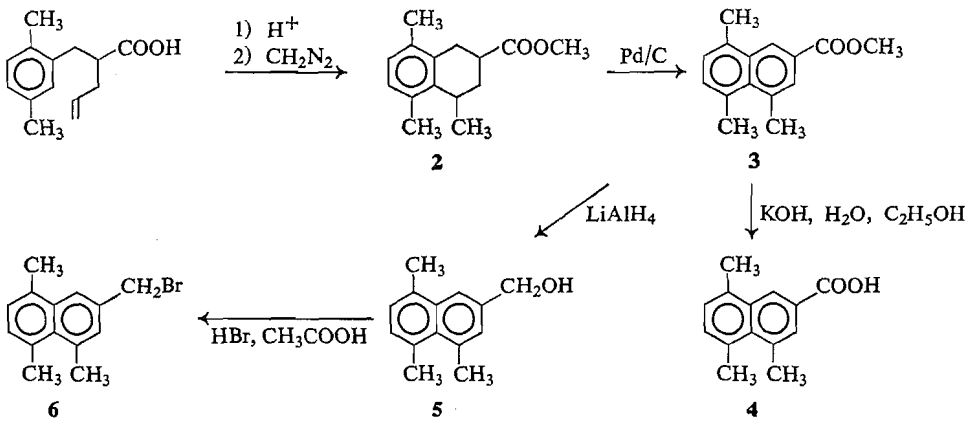

SCHÉMA 1

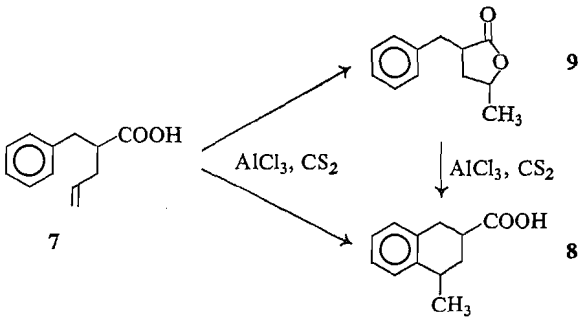

SCHÉMA 2

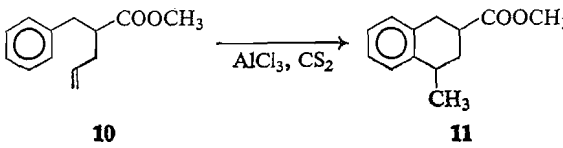

SCHÉMA 3

recueille l'acétate de l'alcool cyclisé **13** (schéma 5). Effectuer la cyclisation à cette étape permet de conserver le groupement fonctionnel tout en évitant une réaction secondaire (lactonisation des acides éthyléniques). Cependant la cyclisation d'oléfines ne possédant pas de groupement fonctionnel, comme méthode de synthèse de certains hydrocarbures aromatiques polyméthylés, nous a semblé mériter une étude plus détaillée.

Cyclisation d'oléfines

La cyclisation de l'oléfine **14**, préparée à partir de l'acide éthylénique **7**, s'effectue avec un excellent rendement sous l'action de BF_3, en solution benzénique (schéma 6). Pour illustrer cette méthode nous avons mis au point une nouvelle synthèse du diméthyl-1,5 naphtalène (schéma 7). L'oléfine **16** produit de la condensa-

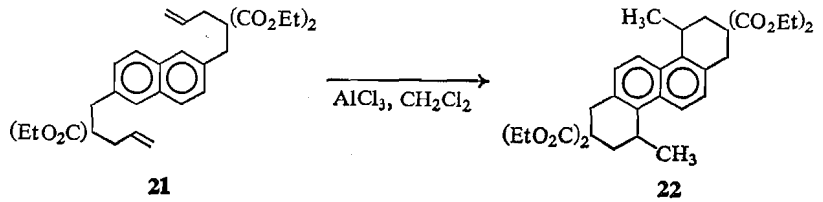

SCHÉMA 4

Can. J. Chem. Downloaded from www.nrcresearchpress.com by 210.87.254.40 on 09/05/12
For personal use only.

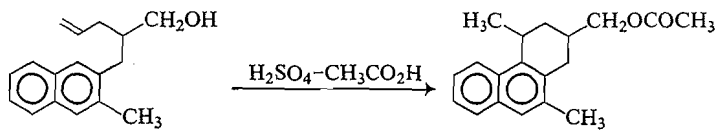

12 **13**

SCHÉMA 5

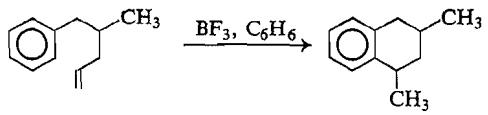

14 **15**

SCHÉMA 6

tion du bromure de crotyle sur le chlorure de (méthyl-2) benzylmagnésium, est cyclisée par BF_3 en diméthyl-1,5 tétrahydro-1,2,3,4 naphtalène (**17**) lequel est aromatisé, en diméthyl-1,5 naphtalène (**18**). Ce naphtalène était auparavant préparé au terme d'une longue synthèse qui impliquait le passage par la méthyl-5 tétralone (6). Les enseignements tirés à l'étude de la cyclisation des bis(pentène-4)yl benzènes (2, 3) ne sont pas applicables aux bis(pentène-4)yl naphtalènes, car le chlorure d'aluminum ne donne pas des résultats satisfaisants dans la cycloalkylation d'aryloléfines contenant un reste naphtalénique. Lors de la cyclisation des acides naphtylméthyl-2 pentène-4 oïques (3), nous avions surmonté cet inconvénient en utilisant les acides protoniques, au prix d'une certaine lactonisation, mais cet artifice ne peut pas être utilisé avec des composés possédant deux chaînes oléfiniques car l'on recueillerait un mélange de diacide, de dilactone, et d'acide–lactone (3). En l'absence de catalyseur capable d'effectuer avec de bons rendements la cyclisation de bis(pentène-4)yl naphtalènes possédant un groupement dicarbéthoxyle ou carboxyle sur la chaîne oléfinique, nous avons réduit ce groupement fonctionnel en méthyle et utilisé le trifluorure de bore à l'étape de cyclisation.

Le tétraméthyl-1,3,6,8 triphénylène est synthétisé par cyclisation de 2 enchaînements oléfiniques portés par un noyau naphtalénique (schéma 8). Le bisbromométhyl-2,3 naphtalène réagit avec 2 molécules d'allylmalonate d'éthyle sodé pour donner le bis(dicarbéthoxy-2,2 pentène-4)yl-2,3 naphtalène (**20**). Le bis(méthyl-2 pentène-4)yl-2,3 naphtalène (**27**) est obtenu par transformation des groupements dicarbéthoxyles en méthyles selon la suite de réactions habituelles.[1] La cyclisation de l'oléfine **27** en tétraméthyl-1,3,6,8 octahydrotriphénylène (**28**) nécessite 2 h de réaction à température ambiante, sous l'action de BF_3 en solution benzénique. L'aromatisation de l'hydrocarbure **28** en présence de Pd/C conduit au tétraméthyl-1,3,6,8 triphénylène

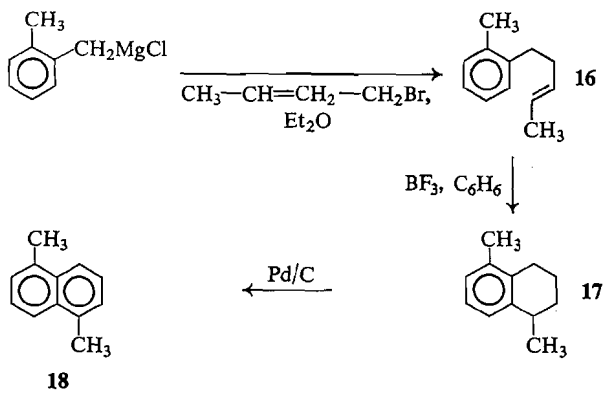

SCHÉMA 7

[1]Une partie de cette synthèse fut réalisée en collaboration avec J. L. Riendeau que nous tenons à remercier.

Can. J. Chem. Downloaded from www.nrcresearchpress.com by 210.87.254.40 on 09/05/12
For personal use only.

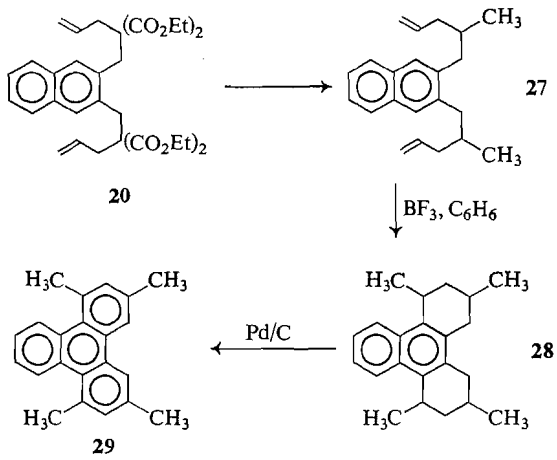

SCHÉMA 8

(**29**). La synthèse d'hydrocarbures aromatiques polycycliques à partir d'aryloléfines semble générale car nous avons montré que l'utilisation du trifluorure de bore pouvait s'appliquer à tous les cas envisageables (4): simple, double, et triple cyclisation sur un substrat benzénique ou naphtalénique. Les rendements des cyclisations sont toujours supérieurs à 80%.

Partie expérimentale

Les spectres infrarouges (i.r.) ont été pris sur un spectrophotomètre Beckman, modèle IR-4, et les spectres de résonance magnétique nucléaire (r.m.n.) sur un spectromètre Varian, modèle A-60, dans $CDCl_3$, sauf indication contraire. Les points de fusion ont été déterminés dans les tubes capillaires sur un appareil Thomas–Hoover et ne sont pas corrigés. Les analyses élémentaires ont été effectués par Organic Microanalysis (Montréal).

Triméthyl-4,5,8 carbométhoxy-2 naphtalène (3)

L'acide triméthyl-4,5,8 tétrahydro-1,2,3,4 naphtoique-2 (**1**) (p.f. 123–124°) est préparé selon Cannone et Regnault (1). L'ester méthylique **2** correspondant est préparé par action d'une solution éthérée de diazométhane. Dix grammes d'ester **2** et 2.0 g de Pd/C à 5% sont portés pendant 3 h à 320 °C. Après lavage du catalyseur avec 100 ml de méthanol bouillant, on recueille par recristallisation 5.9 g d'ester **3** (p.f. 83–84°).

Spectre i.r.; ν (C=O) 1735 cm^{-1} (CCl_4).

Anal. calc. pour $C_{15}H_{16}O_2$: C, 78.92; H, 7.06; O, 14.02. Trouvé: C, 78.98; H, 7.14.

Acide triméthyl-4,5,8 naphtoique-2 (4)

Obtenu par hydrolyse à la potasse hydroalcoolique de l'ester **3**, p.f. 271–272° (éthanol–benzène).

Anal. calc. pour $C_{14}H_{14}O_2$: C, 78.48; H, 6.59; O, 14.93. Trouvé: C, 78.52; H, 6.51.

Triméthyl-4,5,8 naphtalèneméthanol-2 (5)

La réduction par $LiAlH_4$ de l'ester **3** fournit l'alcool **2**, p.f. 88–89° (éthanol).

Triméthyl-4,5,8 bromométhyl-2 naphtalène (6)

On ajoute à température ambiante une solution de 12.8 g d'alcool **5** dans 100 ml d'acide acétique à 50 ml d'acide acétique saturés en HBr. On laisse réagir 20 min à 50°, et verse sur 200 g de glace pilée. Le bromure **6** précipite, on l'extrait à l'éther, lave les extraits éthérés au bicarbonate et à l'eau, sèche sur $MgSO_4$. On recueille 15.0 g de dérivé bromé **6**, p.f. 70–75° (brut). La réduction d'un échantillon par l'hydrogène en présence de Pd/C et en solution dans l'acétone, fournit le tétraméthyl-1,3,5,8 naphtalène (p.f. 56–57°) identique à celui préparé par aromatisation du tétraméthyl-1,3,5,8 tétrahydro-1,2,3,4 naphtalène (1). Les déplacements chimiques des protons aromatiques et des protons des méthyles sont résumés dans le Tableau I.

Cyclisation de l'α-benzyl-γ-valérolactone (9)

La lactone **9** (p.é. 130–131° sous 0.6 mm Hg, n_D^{25} 15 210) est préparée par lactonisation de l'acide benzyl-2 pentène-4 oïque 7 (1). A une solution de 1.9 g (0.01 mole) de lactone **9** dans 50 ml de CS_2, on ajoute par petites portions 2 g (0.015 mole) de chlorure d'aluminum anhydre. Une fois l'addition de catalyseur terminée, on porte à reflux 1.5 h. On hydrolyse, traite de façon habituelle et recueille 1.75 g d'acide méthyl-4 tétrahydro-1,2,3,4 naphtoique-2 (**8**) (p.f. 115–119°) identique à un échantillon du même acide obtenu par cyclisation de l'acide 7 (spectres i.r. et de r.m.n. superposables). L'acide **8** (p.f. 115–119°) brut, obtenu à partir de l'acide **7** ou de la lactone **9** est un mélange des deux isomères possibles, où le méthyle peut occuper une position quasi axiale (doublet centré à 74 Hz, (J = 7 Hz) ou une position quasi équatoriale (doublet centré à 77.5 Hz, J = 7 Hz). Deux cristallisations dans l'éthanol dilué donnent un isomère pur (p.f. 120–121°); son spectre de r.m.n. ne montre plus qu'un seul doublet à 77.5 Hz.

Anal. calc. pour $C_{14}H_{18}O_2$: C, 77.03; H, 8.31; O, 14.66. Trouvé: C, 77.10; H, 8.38.

Cyclisation du benzyl-2 pentène-4 carboxylate de méthyle (10)

On opère sur 0.01 mole d'ester **10** en suivant le mode opératoire précédent. Après traitement habituel et chromatographie sur alumine (grade 1, éther-éther de pétrole), on recueille 1.80 g de méthyl-4 tétrahydro-1,2,3,4

TABLEAU I

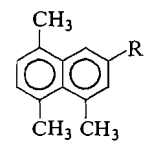

	Méthyles			Protons aromatiques			
R	4	5	8	1	3	6, 7	R
CH_3	169	169	153	453	421	421	145(CH_3)
$COOCH_3$	170	166	155	504	459	421	232(CH_3)
COOH*	170	167	154	499	457	427	
CH_2OH	167	167	152	455	423	419	277(CH_2)
CH_2Br	168	165	152	459	427	419	268(CH_2)

*DMSO - d_6

Can. J. Chem. Downloaded from www.nrcresearchpress.com by 210.87.254.40 on 09/05/12
For personal use only.

Can. J. Chem. Downloaded from www.nrcresearchpress.com by 210.87.254.40 on 09/05/12
For personal use only.

carboxylate de méthyle (**11**) (p.é. 96° sous 0.08 mm Hg). Le méthyle cyclanique apparaît en r.m.n. sous forme de deux doublets d'intensité égale centrés à 73 et 76 Hz (J = 7 Hz).

Anal. calc. pour $C_{15}H_{20}O_2$: C, 77.55; H, 8.68; O, 13.77. Trouvé: C, 77.60; H, 8.62.

*Cyclisation du (méthyl-3)naphtyl-2 méthyl-2 pentène-4 ol-1 (**12**)*

L'alcool **12** provient de la réduction par $LiAlH_4$ de l'acide (méthyl-3)naphtyl-2 méthyl-2 pentène-4 oïque (p.f. 109–111°, préparé selon (3)). On chauffe à reflux pendant 1 h une solution de 1.0 g d'alcool **12** dans 20 ml d'un mélange (5:95) d'acides sulfurique concentre et acétique concentre. Après dilution à l'eau et extraction au benzène, on obtient 0.92 g d'acétate **13** (liquide visqueux incristallisable).

Spectre i.r.; 1230 et 1750 cm^{-1} (acétate).

Spectre de r.m.n. CH_3 cyclanique:76 Hz (d, J = 7 Hz) et 80 Hz (d, J = 7 Hz); CH_3 acétate:122 Hz (s); CH_3 aromatique:140 Hz (s); $—CH_2—O—CO—$:246 Hz (d, J = 6 Hz); H_5, H_6, H_7, H_8:massif complexe (435–485 Hz); H_9:445 Hz (s).

*Cyclisation du benzyl-4 pentène-1 (**14**)*

Cette oléfine est préparée par réduction du groupement carboxyle en méthyle de l'acide 7 (1), p.é. 118–120° sous 20 mm Hg. On fait barboter lentement BF_3 dans une solution de 2.00 g d'oléfine **14** dans 50 ml de benzène jusqu'à apparition d'une couleur rouge-orangée (5–10 min). On abandonne ensuite en flacon bouché pendant 1 h à température ambiante, puis on ajoute 50 ml d'eau et décante la couche benzénique. Après évaporation du solvant, on filtre sur colonne d'alumine et on élue à l'éther de pétrole 1.85 g de diméthyl-1,3 tétrahydro-1,2,3,4 naphtalène (**15**) identique au même hydrocarbure obtenu par réduction du groupement carboxyle en méthyle de l'acide **8** (1).

*Préparation du (méthyl-2) phényl-5 pentène-2 (**16**)*

On prépare, sous atmosphère d'azote, une solution éthérée de chlorure de (méthyl-2) benzylmagnésium à partir de 12 g (0.50 atmospheric g) de magnésium en tournure, 70 g (0.50 mole) de chlorométhyl-1 méthyl-2 benzène (préparée par chloration de l'*O*-xylène au moyen de SO_2Cl_2, selon (7)) et 400 ml d'éther anhydre, en maintenant la température en dessous de −10 °C, ainsi qu'une vigoureuse agitation mécanique. On filtre l'excès de magnésium et ajoute goutte à goutte une solution de 67.5 g (0.50 mole) de bromure de crotyle dans 100 ml d'éther anhydre. On laisse réagir quelques heures à température ambiante, hydrolyse avec une solution aqueuse de chlorure d'ammonium, et on décante la couche éthérée. On évapore le solvant et rectifie l'oléfine **16** sur une colonne de Vigreux: 53.5 g, rdt 67%, p.é. 108–110° sous 20 mm Hg, n_D^{25} 1.5120.

Anal. calc. pour $C_{12}H_{16}$; C, 89.44; H, 10.06. Trouvé: C, 89.99; H, 10.01.

*Cyclisation du (méthyl-2) phényl-5 pentène-2 (**16**)*

L'oléfine **16** est cyclisé par BF_3 en suivant le mode opératoire de la cyclisation de **14** ou **15**, rdt 95%. Spectre r.m.n.: CH_3 cyclanique: 73 Hz (d, J = 7 Hz); CH_3 aromatique: 126 Hz (s), H aromatiques (3): multiplet étroit centré à 418 Hz.

*Diméthyl-1,5 naphtalène (**17**)*

L'aromatisation de 5.0 g de tétraline **16** fournit, après chromatographie sur alumine, 4.2 g de diméthyl-1,5 naphtalène, p.f. 81° (méthanol), (litt. (6) p.f. 81 °C) picrate p.f. 131–132.5°.

Préparation des bis(dicarbéthoxy-2,2 pentène-4)yl naphtalènes

Les bisbromométhyl-2,3 naphtalène (**18**) et bisbromométhyl-2,6 naphtalène **19** sont préparés par bromation des diméthylnaphtalènes correspondants au moyen de deux équivalents de NBS selon Ried et Bodem (8). Dibromure **18**, p.f. 144–145° (litt. (8) p.f. 145°, rdt 66%); dibromure **19**, p.f. 175–180° (litt. (8) p.f. 182°, rdt 72%).

A une solution de 0.30 mole d'allylmalonate d'éthyle sodé dans 300 ml d'éthanol anhydre, on ajoute une solution de 31.4 g de dibromure **18** en solution dans 600 ml de benzène. On laisse réagir une nuit à température ambiante, évapore le maximum de solvants, ajoute 100 ml d'eau, et extrait l'ester malonique à l'éther (4 fois). Le bis(dicarbéthoxy-2,2 pentène-4)-2,3 naphtalène (**20**) est distillé sous pression réduite (206–210° sous 0.08 mm Hg) puis il cristallise lentement (72–73°, méthanol); rdt 74%.

Anal. calc. pour $C_{32}H_{40}O_8$: C, 69.55; H, 7.30; O, 23.16. Trouvé: C, 69.63; H, 7.27.

Après distillation des solvants, le bis(dicarbéthoxy-2,2 pentène-4)-2,6 naphtalène (**21**) se présente sous forme d'une masse pâteuse qui est lavée à l'eau afin d'éliminer le bromure de sodium, puis dissoute dans le méthanol bouillant; l'ester **21** précipite et est recueilli par filtration, p.f. 119–120°, rdt 76%.

Anal. calc. pour $C_{32}H_{40}O_8$: C, 69.55; H, 7.30; O, 23.16. Trouvé: C, 69.64; H, 7.26.

*Cyclisation de l'ester (**21**)*

A une suspension de 11.7 g (0.08 mole) de chlorure d'aluminum anhydre dans 250 ml de CH_2Cl_2, on ajoute lentement une solution de 5.50 g (0.01 mole) d'ester **21** dans 100 ml de CH_2Cl_2. Après 5 h de réaction à température ambiante, on hydrolyse et extrait à l'éther 5.0 g d'une huile brune qui est triturée dans le méthanol. Par filtration on recueille 0.8 g de cristaux fondant à 168–172°. Après plusieurs cristallisations dans un mélange de méthanol–benzène (75:25) le p.f. se stabilise à 179–180°. L'examen du spectre r.m.n. permet d'affirmer que l'on a isolé l'ester **22**. CH_3 (6H): superposition de plusieurs doublets (J = 7 Hz) centrés entre 70 et 82 Hz; H arom: (4H) les protons 6 (et 12) et 5 (et 11) sortent sous forme de deux doublets respectivement centrés à 485 et 488 Hz (J = 6.5 Hz). Les protons allyliques et les protons aromatiques H-1 et H-5 de l'ester **21** ont totalement disparu.

*Préparation des bis(méthyl-2 pentène-4)yl-2,3 naphtalène (**27**)*

L'ester **20** est hydrolysé par la potasse hydroalcoolique en acide malonique **23** (incristallisable), lequel est décarboxylé par reflux dans la pyridine. Les groupements carboxyles du diacide éthylénique **24** (p.f. 129–131°, méthanol sont réduits en méthyles, via dialcool **25** et ditosylate **26** (3)). Le rendement de cette transformation est de 37–39%. L'oléfine **27** est un liquide dont l'examen du spectre de r.m.n. permet de confirmer sa structure; CH_3 (6H):52 Hz (d, J = 6.5 Hz); $=CH_2$ (4H):291 Hz (m) et 304 Hz (m); $—CH=$ (2H):345 Hz (m); H-1 et

H-4:448 Hz (s); H-5, H-6, H-7, H-8:forment un système A_2B_2 centré à 447 Hz. (p.é. 350 °C, 760 mm de Hg).

Tétraméthyl-1,3,6,8 triphénylène (29)

On fait barboter BF_3 pendant 15 min dans une solution de 1.00 g d'oléfine **27** et 25 ml de benzène. Après 3 h de réaction à température ambiante, on hydrolyse, décante la couche benzénique, extrait la couche aqueuse à l'éther de pétrole. On sèche sur $MgSO_4$, évapore les solvants et recueille 0.93 g de tétraméthyl-1,3,6,8 octahydrotriphénylène (**28**). Cet hydrocarbure est aromatisé en présence de 0.50 g de Pd/C à 5%. Après chromatographie, on élue (éther de pétrole–benzène 90:10) 0.81 g de tétraméthyl-1,3,6,8 triphénylène (**29**), p.f. 137–137.5° (éthanol–benzène): *m/e* 284.

Anal. calc. pour $C_{22}H_{20}$: C, 92.91; H, 7.09. Trouvé: C, 92.91; H, 7.13.

Spectre de résonance magnétique nucléaire du triphénylène **29**; méthyles 1 et 8:173 Hz (s); méthyles 3 et 6: 147 Hz (s); protons 2 et 7:433 Hz (large singulet); protons 4 et 5:488 Hz (large singulet); protons 9,10,11,12: forment un système A_2B_2 centré à 474 Hz, dont la partie la plus déblindée (498–512 Hz) est attribuée aux protons 9 et 12 et la partie la plus blindée (440–454 Hz), aux protons 10 et 11. Ces valeurs sont conformes à celles données par Bartle *et al.* (9).

Remerciements

Les auteurs expriment leur gratitude au Conseil National de Recherches du Canada pour l'aide financière apportée sous forme de subventions et au Conseil des Arts du Canada pour une bourse d'études.

1. P. Canonne et A. Regnault. Can. J. Chem. **45**, 1267 (1967).
2. A. Regnault, P. Canonne, et L. C. Leitch. Tetrahedron Letters, 355 (1968).
3. A. Regnault et P. Canonne. Tetrahedron, Sous presse.
4. P. Canonne et A. Regnault. Tetrahedron Letters, 243 (1969).
5. M. S. Newman et J. R. Maugham. J. Am. Chem. Soc. **71**, 3342 (1950).
6. C. S. Marvel et B. C. Wilson. J. Org. Chem. **23**, 1483 (1958).
7. P. Canonne et L. C. Leitch. Can. J. Chem. **45**, 1761 (1967).
8. W. Ried et H. Bodem. Chem. Ber. **91**, 1981 (1958).
9. K. D. Bartle, H. Heaney, D. W. Jones, and P. Lees. Spectromchim. Acta, **22**, 941 (1966).

Can. J. Chem. Downloaded from www.nrcresearchpress.com by 210.87.254.40 on 09/05/12
For personal use only.

Can. J. Chem. Downloaded from www.nrcresearchpress.com by 210.87.254.105 on 09/05/12
For personal use only.

Heterocyclic system containing bridgehead nitrogen atom. Part III. 3-Substituted-, 2,3-disubstituted-5,6-dihydro-4*H*-imidazo[2,1-*b*]thiazoles and 3-substituted-, 2,3-disubstituted-4,5,6,7-tetrahydrothiazolo[3,2-*a*]pyrimidines

VIJAY K. CHADHA AND H. K. PUJARI
Department of Chemistry, Kurukshetra University, Kurukshetra, India

Received December 17, 1968

The syntheses of 3-substituted-, 2,3-disubstituted-5,6-dihydro-4*H*-imidazo[2,1-*b*]thiazoles and 3-substituted-, 2,3-disubstituted-4,5,6,7-tetrahydrothiazolo[3,2-*a*]pyrimidines have been achieved by reacting ketones with 2-mercaptoimidazoline and 2-mercapto-3,4,5,6-tetrahydropyrimidine respectively in the presence of iodine. The condensation has also been affected by replacing iodine with bromine.

Canadian Journal of Chemistry, 47, 2843 (1969)

In view of the broad spectrum anthelmintic activity of *dl*-6-phenyl-2,3,5,6-tetrahydro-4*H*-imidazo[2,1-*b*]thiazole hydrochloride (tetramisole-HCl) (1–3), it was thought of considerable interest to improve upon the methods of synthesizing condensed thiazoles. The present communication reports the synthesis of two such systems.

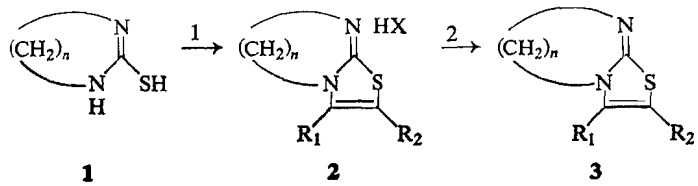

1. $R_1COCH_2R_2$, I_2 or Br_2.
2. K_2CO_3 or Et_3N.

Imidazo-thiazoles (**3**, $n = 2$) have been synthesized by condensing 2-mercaptoimidazoline (**1**, $n = 2$) with α-haloketones (4, 5). The observation of King (6) that ketones and halogens can be used in place of α-haloketones in the synthesis of 2-aminothiazoles, has been utilized in the present investigations for the synthesis of imidazo–thiazoles (**3**, $n = 2$) and thiazolo-pyrimidines (**3**, $n = 3$). The method adopted here has a distinct advantage in dispensing with the difficultly available α-haloketones by using ketone and halogens and should also be applicable to the preparation of other condensed thiazoles. Thiazolo-pyrimidines (**3**, $n = 3$) were prepared by three methods. In the first method, 2-mercapto-3,4,5,6-tetrahydropyrimidine (**1**, $n = 3$) was condensed with ketones in the presence of iodine. The resulting hydroiodide salt (**2**, $n = 3$, X = iodine) on treatment with potassium carbonate, yielded the desired base **3**, ($n = 3$). Iodine was replaced by bromine in the second method. The compound **3** ($n = 3$, $R_1 = C_6H_5$, $R_2 = H$) prepared by both of the methods was identical with that obtained by condensing **1** ($n = 3$) with phenacylbromide followed by basification of the hydrobromide (**2**, $n = 3$, X = Br) with potassium carbonate. The structure of **3** ($n = 3$, $R_1 = C_6H_5$, $R_2 = H$; $R_1 = p\text{-}O_2N\text{—}C_6H_4$, $R_2 = H$) was characterized by the infrared (i.r.) spectrum (vide Experimental). Imidazo-thiazoles (**3**, $n = 2$) were also prepared by the above methods.

Fungicidal Tests

For fungicidal assay, the method of Aytoun *et al.* (7) was used. *Aspergillus*, *fusarium*, *penicillium*, and *rhizopus* species were used as test fungi. None of the compounds was found to be active at 1:1000 concentration.

Bactericidal Tests

The Rideal–Walker (8) serial drop dilution method was used for the comparative antibacterial activity. The test organisms were 24 h culture of *Staphylococcus aureus* and *E. coli*.

Can. J. Chem. Downloaded from www.nrcresearchpress.com by 210.87.254.105 on 09/05/12
For personal use only.

TABLE I

Vide structure **3** ($n = 3$)
3-Substituted-, 2,3-disubstituted-4,5,6,7-tetrahydrothiazolo[3,2-*a*]pyrimidines

									Picrate			
		Melting point	Yield		% calcd		% found		Melting point		% sulphur	
R_1	R_2	°C	%	Formula	S	N	S	N	°C	Formula	Calcd.	Found
(*p*)Br—C_6H_4	H	133–135	59	$C_{12}H_{11}N_2SBr$	10.85	9.49	10.72	9.27	196–197	$C_{18}H_{14}N_5O_7SBr$	6.10	5.87
(*p*)Cl—C_6H_4	H	140–141	50	$C_{12}H_{11}N_2SCl$	12.77	11.18	12.51	10.90	181–182	$C_{18}H_{14}N_5O_7SCl$	6.67	6.41
(*p*)NH_2—C_6H_4	H	200–201	33	$C_{12}H_{13}N_3S$	13.86	18.18	13.61	17.99	190–191	$C_{18}H_{16}N_6O_7S$	6.95	6.73
CH_3	C_6H_5	165–166	44	$C_{13}H_{14}N_2S$	13.91	12.17	13.75	11.95	190–192	$C_{19}H_{17}N_5O_7S$	6.97	6.75
C_6H_5	CH_3	154	49	$C_{13}H_{14}N_2S$	13.91	12.17	13.74	11.89	198–199	$C_{19}H_{17}N_5O_7S$	6.97	6.69
(*p*)C_6H_5—C_6H_4	H	150	35	$C_{18}H_{16}N_2S$	10.96	9.59	10.65	9.42	231–232	$C_{24}H_{19}N_5O_7S$	6.14	5.92
(*p*)CH_3—C_6H_4	H	Gummy, not analyzed							185–186	$C_{19}H_{17}N_5O_7S$	6.97	6.71
(*p*)HO—C_6H_4	H	270	64.5	$C_{12}H_{12}N_2SO$	13.79	12.07	13.67	11.89				

TABLE II

Vide structure **3** ($n = 3$)
3-Substituted-, 2,3-disubstituted-4,5,6,7-tetrahydrothiazolo[3,2-a]pyrimidines

				HBr Salt					
						% Calcd.		% Found	
R_1	R_2	Melting point °C	Yield %	Melting point °C	Formula	S	N	S	N
(*p*)NO_2—C_6H_4	H	168–169	48	250 (decomp.)	$C_{12}H_{12}N_3O_2SBr$	9.35	12.28	9.12	12.01
(*p*)Br—C_6H_4	H	135	72	285	$C_{12}H_{12}N_2SBr_2$	8.50	7.44	8.41	7.12
(*p*)Cl—C_6H_4	H	140	45	265	$C_{12}H_{12}N_2SClBr$	9.65	8.44	9.42	8.23
(*p*)C_6H_5—C_6H_4	H	149–150	32	>300	$C_{18}H_{17}N_2SBr$	8.57	7.50	8.45	7.26
(*p*)HO—C_6H_4	H	267	50	248–250 (decomp.)	$C_{12}H_{13}N_2SOBr$	10.22	8.94	10.17	8.64

Among all the compounds tested, compound **3** ($n = 3, R_1 = p\text{-}BrC_6H_4, R_2 = H$) showed maximum activity at 1:4000 concentration.

Experimental[1]

3-Phenyl-4,5,6,7-tetrahydrothiazolo[3,2-a]pyrimidine

(*a*) A mixture of 2-mercapto-3,4,5,6-tetrahydropyrimidine (9) (5 g, 0.431 mole), and phenacylbromide (8.6 g, 0.431 mole) in anhydrous ethanol (50 ml) was heated on a water bath under reflux for 7–8 h. The residue obtained, after distilling off the solvent, was dissolved in boiling water and purified by charcoal treatment. Neutralization of the filtrate with potassium carbonate solution gave an oily substance which solidified on standing. It was filtered, washed with water, and finally recrystallized from aqueous ethanol giving colorless crystals, m.p. 110–111° (7.0 g, 75%); ν_{max} (KBr) 760, 1080, 1135 (monosubstituted benzene ring), 1428 (CH_2 deformation), 1475 (C—N stretching), 1590 (C=N and C=C), 2835, 2910 cm^{-1} (C—H stretching in CH_2). Lack of absorption in the region 1680–1700 cm^{-1} shows the absence of carbonyl group.

Anal. Calcd. for $C_{12}H_{12}N_2S$: S, 14.81; N, 12.07. Found: S, 14.68; N, 11.82.

The picrate had a m.p. 168–169°.

Anal. Calcd. for $C_{18}H_{15}N_5O_7S$: S, 7.19. Found: S, 7.02.

(*b*) A mixture containing 2-mercapto-3,4,5,6-tetrahydropyrimidine (9.3 g, 0.08 mole), acetophenone (4.8 g, 0.04 mole), iodine (10.2 g, 0.04 mole), and anhydrous benzene (30 ml) was heated, under reflux, for 20 h on a water bath and again for 10 h without a condenser. The reaction mixture was kept in contact with ether for 48 h with occasional shaking to remove unchanged ketone. The residual iodine was removed by treatment with sodium thiosulfate solution. The resulting solid was dissolved in boiling water and purified by charcoal treatment. The filtrate on cooling gave hydroiodide salt which was dissolved in water, and basification with potassium carbonate solution yielded the base. Crystallization from aqueous ethanol gave colorless crystals, m.p. 111–112° (6 g, 69%), undepressed with the sample obtained above.

(*c*) Bromine (6.4 g, 0.04 mole) was added dropwise, with constant shaking and cooling under running water, to a mixture of 2-mercapto-3,4,5,6-tetrahydropyrimidine (9.38 g, 0.08 mole) and acetophenone (4.8 g, 0.04 mole) in anhydrous ethanol (30 ml). The reaction mixture was then heated on a water bath for 20 h, under reflux and again for 10 h, after removal of the condenser. The crude product was kept in contact with ether for 24 h with occasional shaking. Last traces of bromine were removed by very dilute thiosulfate solution. The solid thus obtained, was dissolved in water on boiling and purified by charcoal treatment. The filtrate on cooling gave hydrobromide salt which on treatment with potassium carbonate solution yielded the base. (In some cases the salt was obtained on concentration of the filtrate and then on cooling in a fridge.) Crystallization of the base from aqueous ethanol gave colorless crystals, m.p. 110–111° (5 g, 57%), undepressed with the sample obtained above.

3-p-Nitrophenyl-4,5,6,7-tetrahydrothiazolo[3,2-a]-pyrimidine

This compound was prepared by heating 2-mercapto-3,4,5,6-tetrahydropyrimidine with *p*-nitroacetophenone in the presence of iodine, under reflux, on a water bath. The rest of the procedure was followed as in (*b*) above. Crystallization from aqueous ethanol gave yellow crystals, m.p. 168° (43%); ν_{max} (KBr) 850 (1:4-disubstituted benzene ring), 1340 (NO_2), 1430 (CH_2 deformation), 1500 (C—N stretching), 1592 (C=N and C=C), 2840, 2920 cm^{-1} (C—H stretching). The absence of a carbonyl group was indicated by the lack of absorption in the region 1680–1700 cm^{-1}.

Anal. Calcd. for $C_{12}H_{11}N_3O_2S$: S, 12.26; N, 16.09. Found: S, 12.05; N, 15.82.

The picrate had a m.p. 200–201°.

Anal. Calcd. for $C_{18}H_{14}N_6O_9S$: S, 6.53. Found S, 6.38.

The properties and analysis of other thiazolo-pyrimidines prepared by using iodine and bromine are described in Tables I and II respectively.

3-Biphenyl-5,6-dihydro-4H-imidazo[2,1-b]thiazole

(*a*) A mixture of 2-mercaptoimidazoline (9) (2 g, 0.019

[1]All melting points are uncorrected.

Can. J. Chem. Downloaded from www.nrcresearchpress.com by 210.87.254.105 on 09/05/12
For personal use only.

Can. J. Chem. Downloaded from www.nrcresearchpress.com by 210.87.254.105 on 09/05/12
For personal use only.

TABLE III

Vide Structure **3** ($n = 2$)
3-Substituted-, 2,3-disubstituted-5,6-dihydro-4*H*-imidazo[2,1-b]thiazoles

R_1	R_2	Melting point °C	Yield %	Formula	% calcd. S	% calcd. N	% found S	% found N	Picrate Melting point °C	Picrate Formula	Picrate % sulphur Calcd.	Picrate % sulphur Found
C_6H_5	H	111*	55	$C_{11}H_{10}N_2S$	15.84		15.71		200	$C_{17}H_{13}N_5O_7S$	7.42	7.12
(*p*)NO_2—C_6H_4	H	214–216†	40	$C_{11}H_9N_3O_2S$	12.95		12.84		236	$C_{17}H_{12}N_6O_9S$	6.72	6.38
(*p*)Br—C_6H_4	H	145‡	30	$C_{11}H_9N_2SBr$	11.39		11.28		197–198	$C_{17}H_{12}N_5O_7SBr$	6.27	6.05
(*p*)Cl—C_6H_4	H	113–114§	35	$C_{11}H_9N_2SCl$	13.53		13.21		198–199	$C_{17}H_{12}N_5O_7SCl$	6.87	6.59
CH_3	C_6H_5	122‖	45	$C_{12}H_{12}N_2S$	14.81		14.52		200	$C_{18}H_{15}N_5O_7S$	7.19	7.02
C_6H_5	CH_3	88–90**	50	$C_{12}H_{12}N_2S$	14.81		14.64		172–175	$C_{18}H_{15}N_5O_7S$	7.19	6.95
(*p*)CH_3—C_6H_4	H			Gummy, not analyzed					184	$C_{18}H_{15}N_5O_7S$	7.19	7.02
(*p*)NH_2—C_6H_4	H	181	30	$C_{11}H_{11}N_3S$	14.74	19.35	14.55	19.07	191	$C_{17}H_{14}N_6O_7S$	7.17	6.91
(*p*)HO—C_6H_4	H	250	65	$C_{11}H_{10}N_2SO$	14.68	12.84	14.33	12.61				

*Lit. (6) m.p. 111–113.
†Lit. (7) m.p. 216–218.
‡Lit. (7) m.p. 145–146.
§Lit. (7) m.p. 113–114.
‖Lit. (6) m.p. 121–124.
**Lit. (6) m.p. 90.5–91.5.

TABLE IV

Vide Structure 3 ($n = 2$)
3-Substituted-, 2,3-disubstituted-5,6-dihydro-4*H*-imidazo[2,1-b]thiazoles

				HBr Salt					
						% calcd		% found	
R_1	R_2	Melting point °C	Yield %	Melting point °C	Formula	S	N	S	N
C_6H_5	H	110–112	35	246*	$C_{11}H_{11}N_2SBr$	10.99	9.62	10.76	9.31
(*p*)NO_2—C_6H_4	H	214–116	38	285†	$C_{11}H_{10}N_3O_2SBr$	9.75	12.80	9.72	12.62
(*p*)Br—C_6H_4	H	144–145	55	295–296‡	$C_{11}H_{10}N_2SBr_2$	8.83	7.73	8.52	7.52
(*p*)Cl—C_6H_4	H	113–114	42	272–273§	$C_{11}H_{10}N_2SBrCl$	10.08	8.81	9.85	8.64
C_6H_5	CH_3			236–238‖	$C_{12}H_{13}N_2SBr$	10.77	9.42	10.58	9.31
(*p*)HO—C_6H_4	H	250	58	>290	$C_{11}H_{11}N_2SOBr$	10.70	9.36	10.53	9.24
(*p*)CH_3—C_6H_4	H			264–265	$C_{12}H_{13}N_2SBr$	10.77	9.42	10.59	9.22

*Lit. (6) m.p. 248–250.
†Lit. (7) m.p. 287–290.
‡Lit. (7) m.p. 290–300.
§Lit. (7) m.p. 272–274.
‖Lit. (6) m.p. 236–239.

mole), *p*-phenylphenacylbromide (10) (5.5 g, 0.019 mole) in anhydrous ethanol (50 ml) was heated under reflux, on water bath for 4½ h. The solvent was then distilled off and the hydrobromide salt (m.p. above 290°) thus obtained, was suspended in ethanol and triethylamine was added dropwise until akaline. The mixture was refluxed for another 10 min and then poured into iced water, yielding cream-colored shiny leaflets. The solid was recrystallized from benzene – petroleum ether (60–80°), m.p. 154–155° (3.3 g, 60%).

Anal. Calcd. for $C_{17}H_{14}N_2S$: S, 11.51; N, 10.07. Found: S, 11.37, N. 9.78.

The picrate had a m.p. 208°.

Anal. Calcd. for $C_{23}H_{17}N_5O_7S$: S, 6.31. Found: S, 6.07.

(*b*) It was prepared by condensation of 2-mercapto-imidazoline (8 g, 0.074 mole) with *p*-phenylacetophenone (10) (7.84 g, 0.037 mole) in the presence of iodine (10.2 g, 0.037 mole). The procedure adopted was the same as in the case of thiazolo-pyrimidine except that triethylamine was used in place of potassium carbonate. It was recrystallized from benzene – petroleum ether (60–80°), m.p. 154–155° (4.54 g, 40%). The mixed m.p. with that obtained by method (*a*) remained undepressed. The picrate had a m.p. 208°, undepressed with the sample obtained above.

(*c*) It was also prepared by condensing 2-mercapto-imidazoline (8 g, 0.074 mole), *p*-phenylacetophenone (7.848 g, 0.037 mole) in presence of bromine (6.4 g, 0.037 mole). The procedure followed was the same as in case of thiazolo-pyrimidine. HBr salt had a m.p. above 290°.

Anal. Calcd. for $C_{17}H_{15}N_2SBr$: S, 8.91. Found: S, 8.62.

The base had a m.p. 155–156° (4 g, 30%), the mixed m.p. remaining undepressed. The picrate had a m.p. 208–209°, undepressed with the sample obtained above.

The properties and analysis of other imidazo-thiazoles prepared by using iodine and bromine are described in Tables III and IV respectively.

Acknowledgments

The authors are thankful to Prof. L.N. Mohapatra, Professor of Microbiology, All India Institute of Medical Sciences, New Delhi, for biological screening; to Mr. C. S. Panda, Indian Institute of Technology; Kanpur for i.r. spectra; and to the authorities of Kurukshetra University, Kurukshetra for providing a fellowship to one of them (V.K.C.).

1. A. H. M. Raeymaekers, F. T. N. Allewijin, J. Vandenberk, P. J. A. Demon, T. T. T. Van Offenwent and P. A. J. Jansen. J. Med. Chem. 9, 545 (1966).
2. E. F. Elslager. *In* Annual reports in medicinal chemistry, 1965. *Edited by* C. K. Cain. Academic Press, Inc., New York. 1966. p. 146. E. F. Elslager. *In* Annual reports in medicinal chemistry, 1967. *Edited by* C. K. Cain. Academic Press, Inc., New York. 1968. p. 141.
3. D. R. Hoff. *In* Annual reports in medicinal chemistry, 1965. *Edited by* C. K. Cain. Academic Press, Inc., New York. 1966. p. 150. D. R. Hoff. *In* Annual reports in medicinal chemistry, 1967. *Edited by* C. K. Cain. Academic Press, Inc., New York. 1968. p. 149.
4. W. Wilson and R. Woodger. J. Chem. Soc. 2943 (1955).
5. M. Fefer and L. C. King. J. Org. Chem. **26**, 828 (1961).
6. R. M. Dodson and L. C. King. J. Am. Chem. Soc. **67**, 2242 (1945). L. C. King and R. J. Hlavacek. J. Am. Chem. Soc. **72**, 3722 (1950).
7. R. S. C. Aytoun, A. H. Campbell, E. J. Napier, and D. A. L. Sciler. Arch. Dermatol. **81**, 650 (1960).
8. S. Rideal and J. F. A. Walker. J. Roy. Sanit. Insti. (London), **24**, 424 (1903).
9. C. F. H. Allen, C. O. Edens, and J. VanAllan. Org. Syn. Coll. Vol. III, 394 (1955).
10. A. I. Vogel. A text book of practical organic chemistry. Longmans, Green and Co., London. 1962, p. 962.

Can. J. Chem. Downloaded from www.nrcresearchpress.com by 210.87.254.105 on 09/05/12
For personal use only.

Structures of bahia-I and bahia-II: two new guaianolides[1]

A. ROMO DE VIVAR AND A. ORTEGA
Instituto de Química de la Universidad Nacional Autónoma de México, México 20, D.F., México

Received November 5, 1968

Two new guaianolides bahia-I and bahia-II were isolated from Bahia pringlei.[2] Their structures are shown to be **1***a* and **1***b*.

Canadian Journal of Chemistry, 47, 2849 (1969)

Can. J. Chem. Downloaded from www.nrcresearchpress.com by 210.87.254.5 on 09/05/12
For personal use only.

As part of our search for sesquiterpene lactones we studied *Bahia pringlei,* a small Composita which grows not far from Mexico City. We report herein the isolation of two sesquiterpenes which we propose to name bahia-I and bahia-II.

Bahia-I (**1***a*) $C_{15}H_{18}O_4$, m.p. 209–210°, $[\alpha]_D^{28}$ +4° possesses a free hydroxyl group as shown by the infrared (i.r.) band at 3500 cm^{-1} and by the formation of a monoacetate (**2**). It has two double bonds (i.r. bands at 1670 and 1600 cm^{-1}), one of them being an exocyclic double bond conjugated with a γ-lactone (1–3), as indicated by the i.r. band at 1765 cm^{-1}, the ultraviolet (u.v.) absorption (λ_{max} 207 mμ; ε = 10 370), and the characteristic low field doublets in the nuclear magnetic resonance (n.m.r.) spectrum at 6.26 and 5.69 p.p.m. (J = 3.2 c.p.s.). Aluminum amalgam reduction saturated the exocyclic methylene yielding dihydrobahia-I (**6**) whose n.m.r. spectrum showed a new methyl group signal as a doublet at 1.20 p.p.m. (J = 7 c.p.s.). The signals for the exocyclic double bond are not present and the high intensity u.v. absorption has also disappeared.

The second double bond in bahia-I should be trisubstituted since its n.m.r. spectrum showed signals at 5.57 p.p.m. (1H, s) and 1.85 p.p.m. (3H, s) due to the proton at C-3 and to the methyl group at C-4, respectively. The trisubstituted double bond in dihydrobahia-I was further hydrogenated in the presence of platinum oxide, leading to the oily tetrahydrobahia-I (**10**).

Dehydrogenation with palladium on charcoal of the lithium aluminum hydride reduction product of bahia-I afforded chamazulene (**3**),

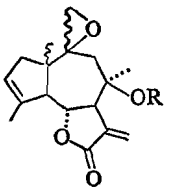

1*a*, R = H

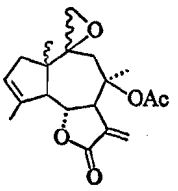

2

1*b*, R = —O—CO—C(H)=C(HOCH$_2$)(CH$_2$OH)

linderazulene (**4**), and artemazulene (**5**). From these results we can infer that bahia-I is a guaianolide.

The lactone group in bahia-I should be closed to C-6 since the hydrogen on this carbon produces a triplet at 4.42 p.p.m. (1H) (J = 9 c.p.s.), arising from the interaction with the hydrogens at C-7 and C-5.

The methyl present at C-10 in the majority of the guaianolides is absent in bahia-I. However there appeared a singlet at 2.71 p.p.m. (2H) which we attribute to a spiroepoxide. Euparotin (4) containing the same functional group gives a similar signal.

When dihydrobahia-I (**6**) was hydrogenated in acetic acid with Adams' catalyst, the product obtained was the diol (**11**) whose n.m.r. spectrum shows a singlet at 1.30 due to a tertiary methyl group attached to a carbon atom bearing a hydroxyl group; such a grouping must have been formed by hydrogenolysis of the spiroepoxide, since the signal at 2.71 has disappeared.

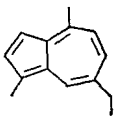

3

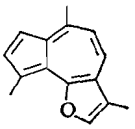

4

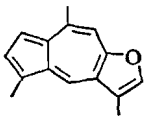

5

[1]Contribution number 288 from the Instituto de Química de la Universidad Nacional Autónoma de México.

[2]We are grateful to Dr. A. Gómez Pompa for the identification of this plant (Voucher AR-6 of the Instituto de Biología de la Universidad Nacional Autónoma de México).

Can. J. Chem. Downloaded from www.nrcresearchpress.com by 210.87.254.5 on 09/05/12
For personal use only.

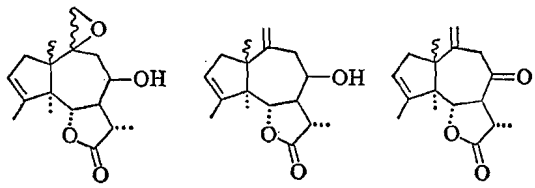

6 7 8

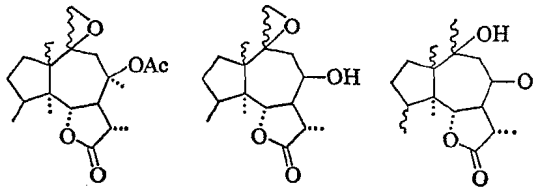

9 10 11

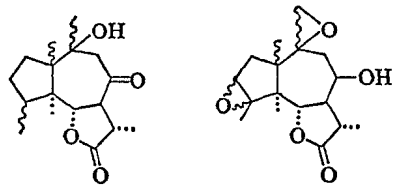

12 13

Oxidation of the diol (**11**) afforded a ketone (**12**) which still contains the tertiary hydroxyl group (i.r. band at 3550 cm^{-1}). The n.m.r. spectrum of (**12**) shows a singlet at 1.35 p.p.m. due to the tertiary methyl group linked at C-10, the singlet at 2.80 p.p.m. (2H) is attributed to the C-9 hydrogens.

Further evidence for the presence of a spiro-epoxide in bahia-I was obtained by aluminum amalgam reduction of **1***a*. This reaction gave rise to dihydrobahia-I (**6**), together with the product (7) which did not show the epoxide signal in the n.m.r. spectrum. Instead, it showed two singlets at 4.99 and 5.09 p.p.m. with apparent long-range coupling attributed to a new exocyclic methylene group formed by reductive elimination of the spiroepoxide.

Compound (7) was also obtained by $CrCl_2$ treatment of dihydrobahia-I (**6**). This reagent has been reported to produce reductive elimination in other isolated epoxides (5).

Epoxidation of dihydrobahia-I (**6**) afforded the diepoxide (**13**). An attempt to obtain the same product from compound (7) resulted in a di-epoxide with the same gross structure but differing in stereochemistry, probably at C-10.

The secondary alcohol (7) and its oxidation product (**8**) were identified as dihydroligustrin (6) and dihydrodehydroligustrin (6), respectively. This correlation establishes the structure of bahia-I and its stereochemistry at positions C-5, C-6, and C-7 as shown in **1***a*. This correlation also indicates the configuration of the methyl group attached to the lactone ring of dihydro-bahia-I.

The orientation of the secondary hydroxyl group at C-8 was established by the method developed by Horeau (7, 8).

The α-phenylbutyric acid recovered from the esterification of bahia-I with α-phenylbutyric anhydride was dextrorotatory, therefore the C-8 hydroxyl group must have the absolute configuration R (β orientation).

The second and more polar component of *Bahia pringlei*, bahia-II, $C_{20}H_{24}O_7$, m.p. 133–134°, $[\alpha]_D^{28}$ +47.7, contains two hydroxyl groups (i.r. bands at 3620 and 3500 cm^{-1}), and a γ-lactone group conjugated with an exocyclic methylene group as indicated by the i.r. bands at 1765 and 1655 cm^{-1}. The u.v. absorption λ_{max} 212 mμ (ε = 19 500) is the result of the absorption of the conjugated exocyclic methylene group and another chromophore.

Bahia-II is an ester of bahia-I (i.r. band at 1725 cm^{-1}), since reduction of bahia-II with aluminum amalgam followed by hydrolysis produced dihydrobahia-I (**6**) identical in all respects with an authentic sample.

The acid which esterifies bahia-I must be α,β-bis-(hydroxymethyl)-acrylic acid in order to account for the elemental anaylsis of bahia-II, its correlation with bahia-I, and its spectroscopic features. This acid has been found in eupatoriopicrin (9) and cnicin (10). We could not identify the acid chemically. Nevertheless, high resolution n.m.r. (100 M c.p.s.) confirmed the structure **1***b* for bahia-II. It showed a triplet at 6.90 p.p.m. (J = 3 c.p.s.) attributed to the vinylic hydrogen of the α,β-unsaturated ester, a doublet at 4.39 (2H) (J = 3 c.p.s.) is due to a hydroxymethyl group with an allylic double bond. As the coupling constant is similar to that of the vinyl proton in the ester, they should be at vicinal positions (O—CO—C=$CHCH_2$—OH). The second hydroxymethyl group appeared as a singlet at 4.29 p.p.m.

The hydrogen bonded to the carbon bearing the ethereal oxygen of the lactone produces a triplet at 4.68 p.p.m. (J = 4.5 c.p.s.).

Can. J. Chem. Downloaded from www.nrcresearchpress.com by 210.87.254.5 on 09/05/12
For personal use only.

The hydrogen at C-8, where the ester is attached is responsible for a multiplet at 5.72 p.p.m.

The structure **1***b* for bahia-II was confirmed by spin decoupling. When bahia-II was irradiated at 6.9 p.p.m., the doublet at 4.39 p.p.m. (—O—CO—C=CH—CH_2—OH) collapsed to a singlet, thus confirming the structure for the ester as shown in (**1***b*).

Irradiation of the triplet at 3.25 p.p.m. (H at C-7) transforms the multiplet at 5.72 p.p.m. into a triplet proving the relative position of the ester and the lactone groups. The chemical shift of the vinylic hydrogen of the ester is characteristic of a tiglate (approximately 6.7 p.p.m.) rather than of an angelate (approximately 6 p.p.m.) (11, 12). Hence, the more probable stereochemistry for the ester should be the *cis*, as depicted in **1***b*.

Experimental

Melting points were carried out in a Koffler apparatus and are uncorrected. Analyses were by Dr. F. Pascher, Bonn, Germany. Infrared spectra were run in chloroform in a Perkin–Elmer double beam spectrophotometer unless otherwise specified. Ultraviolet spectra were run in 95% ethanol and rotation was in chloroform. Nuclear magnetic resonance spectra were run by Mr. Eduardo Díaz on a Varian A-60A n.m.r. spectrometer, in deuterio–chloroform with tetramethylsilane as internal standard unless otherwise specified.

Isolation of bahia-I (1a) and bahia-II (1b)

Bahia pringlei was collected 90 km north of Mexico City along the highway Mexico–Laredo in November, 1966. The whole plant was dried, and ground to a fine powder (3.7 kg), which was extracted with ethanol and worked out in the usual manner, leaving 52 g of a syrup. This was dissolved in benzene and chromatographed on 1 kg of alumina Alcoa F-20, washed previously with ethyl acetate. Benzene ethyl acetate 2:1 eluted 650 mg of bahia-I, m.p. 200°; recrystallization from acetone – isopropyl ether raised the m.p. to 209–210°; ν_{max} 3600, 3500, 1765, 1670, 1600, and 870 cm^{-1}; λ_{max} 207 mμ; $\varepsilon = 10\,370$; $[\alpha]_D^{28}$ +4° (*c* 0.96); n.m.r.: δ 1.85 (3H, s), 2.71 (2H, s), 4.42 (1H, t), (*J* = 9 c.p.s.), 5.57 (1H, s), 5.69 (1H, d), and 6.26 (1H, d) (*J* = 3.2 c.p.s.).

Anal. Calcd. for $C_{15}H_{18}O_4$: C, 68.68; H, 6.92; O, 24.40. Found: C, 68.79; H, 6.87; O, 24.38.

Chloroform containing 5% methanol eluted 11.8 g bahia-II, m.p. 126–127°. Further crystallization from ethyl acetate–isopropyl ether raised the m.p. to 134–137°; $[\alpha]_D^{28}$ +47.7° (*c* 1); ν_{max} 3500, 1765, 1725, and 1665 cm^{-1}; λ_{max} 212 mμ; $\varepsilon = 19\,500$; n.m.r. (100 M c.p.s.): δ 1.95 (3H, s), 2.7 (2H, s), 4.29 (2H, s), 4.39 (2H, d) (*J* = 3 c.p.s.), 4.68 (1H, t) (*J* = 4.5 c.p.s.), 5.6 (1H, d) (*J* = 2 c.p.s.), 6.31 (1H, d) (*J* = 2 c.p.s.), 6.90 (1H, t) (*J* = 3 c.p.s.), 5.72 p.p.m. (2H, m).

Anal. Calcd. for $C_{20}H_{24}O_7$: C, 63.82; H, 6.43; O, 29.75. Found: C, 63.93; H, 6.20; O, 29.55.

Dehydrogenation of bahia-I

A solution of crude bahia-I (2.5 g) in anhydrous ethyl ether containing a little THF was added slowly over a slurry of LAH (4 g) in 100 ml of anhydrous ethyl ether and then refluxed for ½ h. The excess of LAH was destroyed with a small amount of water, the mixture filtered, and the filtrate concentrated. The residue (2 g) was treated with 4 g 10% Pd/C in 10 ml of Nujol. The mixture was heated at 300° for 35 min, dissolved in hexane, and chromatographed on 60 g of alumina Alcoa F-20. Hexane eluted, in the first fractions, 45 mg of chamazulene; hexane–benzene 9:1 eluted a little artemazulene and in the last fractions, linderazulene. The 3 aromatization products were identified as the TNB adducts which were compared with authentic samples.

Tetrahydrobahia-I Acetate (9)

Bahia-I (100 mg) was acetylated with acetic anhydride–pyridin in the usual manner, affording 80 mg of an oily product. This was hydrogenated in 15 ml of ethyl acetate with 20 mg 10% $Pd/CaCO_3$, affording 20 mg of tetrahydrobahia-I acetate, m.p. 160–162°. The pure sample was obtained after several recrystallizations from ethyl acetate – isopropyl ether, m.p. 165–167°. The same product was obtained by acetylation of the oily tetrahydrobahia-I (**10**), obtained by hydrogenation of dihydrobahia-I with platinum oxide; n.m.r.: δ 0.95 (3H, d) (*J* = 7 c.p.s.), 1.2 (3H, d) (*J* = 7 c.p.s.), 2.08 (3H, s), 4.75 (1H, t) (*J* = 9.5 c.p.s.), 5.17 (1H, complex signal).

Anal. Calcd. for $C_{17}H_{24}O_5$: C, 66.25; H, 7.85; O, 25.94. Found: C, 66.45; H, 7.76; O, 26.06.

Dihydrobahia-I (6)

A solution of 2 g of bahia-I in 100 ml ethanol was treated with freshly prepared aluminum amalgam (from 5 g Al and 3.5 g Hg_2Cl_2). The reaction mixture was refluxed for 8 h, filtered, and concentrated. Crystallization of the residue afforded 650 mg of a mixture of two substances which were separated by chromatography on silica gel (30 g). The first substance was eluted with a mixture of benzene – ethyl acetate (90:10), yielding 325 mg of product (6), m.p. 144–145°; $[\alpha]_D^{28}$ +62.2°; ν_{max} 3600, 1770, and 1645 cm^{-1}; n.m.r.: δ 1.20 (3H, d) (*J* = 7 c.p.s.), 1.92 (3H, d) (*J* = 1 c.p.s.), 2.69 (2H, s), 4.08 (1H, complex signal), 4.58 (1H, t) (*J* = 9 c.p.s.), 5.5 (1H, s).

Anal. Calcd. for $C_{15}H_{20}O_4$: C, 68.16; H, 7.63; O, 24.21. Found: C, 68.23; H, 7.55; O, 24.10.

The substance (7) was eluted with ethyl acetate (155 mg, m.p. 167–169°). The m.p. of the mixture with dihydrodehydroligustrin (6) showed no depression and the i.r. spectra were superimposable; $[\alpha]_D^{28}$ +92.1°; ν_{max} 3500, 1770, and 1645 cm^{-1}.

Anal. Calcd. for $C_{15}H_{20}O_3$: C, 72.55; H, 8.12; O, 19.33. Found: C, 72.36; H, 8.02; O, 19.55.

Hexahydrobahia-I (11)

A solution of 200 mg of dihydrobahia-I in 15 ml of AcOH was hydrogenated in the presence of 20 mg of PtO_2 until the absorption of hydrogen ceased. The solution was filtered and the solvent evaporated *in vacuo*; the product crystallized on addition of isopropyl ether, yielding 200 mg of hexahydrobahia-I, m.p. 144–146°; ν_{max} 3500 and 1765 cm^{-1}; $[\alpha]_D^{27}$ +5.5° (*c* 1); n.m.r.: δ 0.97 (3H, d) (*J* = 7 c.p.s.), 1.2 (3H, d) (*J* = 7 c.p.s.), 1.30 (3H, s), 4.01 (1H, complex signal), 4.82 (t) (*J* = 10 c.p.s.).

Can. J. Chem. Downloaded from www.nrcresearchpress.com by 210.87.254.5 on 09/05/12
For personal use only.

Anal. Calcd. for $C_{15}H_{24}O_4$: C, 67.13; H, 9.02; O, 23.85. Found: C, 67.10; H, 8.98; O, 23.81.

Ketone (8)

A solution of 100 mg of (7) in acetone (3 ml) was oxidized by the Bowers' method (13). Yield: 85 mg, m.p. 108–110°. The analytical sample was obtained by recrystallization from acetone – isopropyl ether; m.p. 114–116°. The m.p. of the mixture with dihydroligustrin (6) was also 114–116° and the i.r. spectra were superimposable; λ_{max} 205 mμ; ε = 10 723.

Anal. Calcd. for $C_{15}H_{18}O_3$: C, 73.14; H, 7.37; O, 19.49. Found: C, 72.93; H, 7.39; O, 20.06.

Oxidation of the Diol (11)

A solution of 50 mg of (**11**) in 3 ml of acetone was oxidized with Jones' reagent (13), and the reaction was completed in 4 min at room temperature. The mixture was diluted with a little water and was cooled; the crystalline product so formed was collected, yielding 50 mg of (**12**), m.p. 174–175°; ν_{max} 1770 and 1725 cm^{-1}; $[\alpha]_D^{28}$ −82.3 (*c* 1.045); n.m.r.: δ 0.95 (3H, d) (*J* = 7 c.p.s.), 1.2 (3H, d) (*J* = 6.5 c.p.s.), 1.35 (3H, s), 2.8 (2H, s), 4.59 (1H, t) (*J* = 8.5 c.p.s.).

Anal. Calcd. for $C_{15}H_{22}O_4$: C, 67.64; H, 8.33; O, 24.03. Found: C, 67.82; H, 8.27; O, 24.07.

Epoxidation of Dihydrobahia-I

A solution of 90 mg of dihydrobahia-I in 25 ml of chloroform was treated with 90 mg of *m*-chloroperbenzoic acid. The mixture was refluxed for 8 h, washed with an $NaHCO_3$ solution and water, dried with anhydrous sodium sulfate, and evaporated to dryness. Yield: 12 mg of 11-dihydro-3-epoxybahia-I (**13**); m.p. 175–178°; a recrystallization from acetone – isopropyl ether raised the m.p. to 178–180°; ν_{max} 3500 and 1780 cm^{-1}; n.m.r.: δ 1.27 (3H, d) (*J* = 7 c.p.s.), 1.64 (3H, s), 4.08 (1H, complex signal), 4.43 (1H, t).

Anal. Calcd. for $C_{15}H_{20}O_5$: C, 64.27; H, 7.19; O, 28.54. Found: C, 64.32; H, 7.12; O, 28.64.

Epoxidation of (7)

A solution of 90 mg of the unsaturated alcohol (7) in 25 ml of chloroform was treated with 90 mg of *m*-chloroperbenzoic acid and worked-up as in the previous case. The substance (**13**) isolated from the oily residue melted at 183–185°; ν_{max} 3500, 1780 cm^{-1}; n.m.r.: δ 1.22 (3H, d) (*J* = 7 c.p.s.), 1.61 (3H, s), 2.65 (s), 4.4 (1H, complex signal), 4.42 (1H, t) (*J* = 9 c.p.s.).

Anal. Calcd. for $C_{15}H_{20}O_5$: C, 64.27; H, 7.19; O, 28.54. Found: C, 64.39; H, 7.09; O, 28.60.

Dihydrobahia-I from Bahia-II

A solution of 1 g of bahia-II in 150 ml of ethanol was treated with 5 g of freshly prepared aluminum amalgam, the reaction mixture refluxed for 8 h, filtered, and taken to dryness. The oily residue (1 g) was dissolved in 30 ml of methanol and treated with 1 g of potassium carbonate in 6 ml of water for 15 h at room temperature. The solution was concentrated at reduced pressure, diluted with water, and extracted with ethyl ether. The organic layer was washed, dried, and evaporated, the residue crystallized from isopropyl ether, affording 300 mg of crude product, m.p. 158–160°. Further recrystallizations from the same solvents raised the m.p. to 169–170°. The product was identified as dihydrobahia-I, as the mixed m.p. showed no depression and the i.r. spectra were identical (superimposable) on a comparison with an authentic sample.

Chromous Chloride Treatment of Compound 6

A solution of 200 mg of dihydrobahia-I in 8 ml of acetone was treated in a CO_2 atmosphere with a solution of chromous chloride in 4 ml of acetic acid. The reaction was completed in 20 min. The mixture was concentrated at reduced pressure and diluted with ethyl acetate.

The organic layer was washed with a sodium bicarbonate solution and with water, dried, and evaporated leaving an oily residue which, after chromatography on alumina, afforded 20 mg of the compound (7) m.p. 167–168°.

Determination of the Configuration at C-8

Esterification of Bahia-I

Racemic α-phenylbutyric anhydride (472.7 mg, 1.287 mmole) and dihydrobahia-I (133 mg, 0.500 mmole) were dissolved in 5 ml pyridine, and the mixture was allowed to stand overnight at room temperature. The reaction mixture was diluted with water and extracted with ethyl acetate. The ethyl acetate extract was washed with water, with a 5% sodium bicarbonate solution, and again with water. The ethyl acetate solution was dried with anhydrous sodium sulfate, and evaporated *in vacuo* to a constant weight of 200.5 mg.

The sodium bicarbonate extract was acidified with HCl and extracted with chloroform. The chloroform was eliminated leaving a residue of 208.5 mg of pure α-phenylbutyric acid. The acid and the ester were identified by n.m.r. spectroscopy. The acid was dissolved in 10 ml of chloroform and the specific rotation was determined: $[\alpha]_D^{25}$ +8.4°.

The optical yield is 36% of dextrorotatory acid.

1. F. Šorm, M. Suchy, and V. Herout. Coll. Czech. Chem. Commun. **24**, 1548 (1959).
2. G. Büchi and D. Rosenthal. J. Am. Chem. Soc. **78**, 3860 (1956).
3. W. Herz, R. B. Mitra, and P. Jayaraman. J. Am. Chem. Soc. **81**, 6061 (1959).
4. S. Morris Kupchan, Jane C. Hemingway, John M. Cassady, John R. Knox, A. T. McPhail, and G. A. Sim. J. Am. Chem. Soc. **89**, 465 (1967).
5. C. W. L. Bevan, A. H. Rees, and D. A. H. Taylor. J. Chem. Soc. 983, (1963).
6. J. Romo, T. Ríos, and L. Quijano. Tetrahedron, **24**, 6087 (1968).
7. A. Horeau. Tetrahedron Letters, **15**, 506 (1961).
8. Werner Herz and H. B. Kagan. J. Org. Chem. **32**, 216 (1967).
9. Dolejs L. and V. Herout. Coll. Czech. Chem. Commun. **27**, 2654 (1962).
10. Suchy M., V. Beresová, V. Herout, and F. Šorm. Chem. Ber. **93**, 2449 (1960).
11. W. Herz and M. V. Lakshmikantham. Tetrahedron, **21**, 1711 (1965).
12. R. R. Fraser. Can. J. Chem. **38**, 549 (1960).
13. A. Bowers, T. G. Halsall, E. R. H. Jones, and A. J. Lemin. J. Chem. Soc. 2548 (1953).

Can. J. Chem. Downloaded from www.nrcresearchpress.com by 210.87.254.6 on 09/05/12
For personal use only.

Etude de la décomposition des diazo-2 dicétones-1,3. II. Cas du diazo-2 diphényl-4,5 cyclohexanedione-1,3

WILLIAM D. BARKER, ROLAND GILBERT, JEAN-PAUL LAPOINTE, HENRI VESCHAMBRE,[1] ET DANIEL VOCELLE[2]

Département de Chimie, Université de Montréal, Montréal, Québec

Reçu le 29 octobre, 1968

L'étude des décompositions thermique et photochimique du diazo-2 diphényl-4,5 cyclohexanedione-1,3 dans différents solvants a été réalisée. Les résultats obtenus sont analogues à ceux fournis par le diazo-2 diméthyl-5,5 cyclohexanedione-1,3 dans les mêmes conditions. A savoir: formation de **2***a* au cours de la thermolyse dans le xylène, de **5** dans la photolyse dans le tétrachlorure de carbone, de **6** et **7** dans le méthanol et finalement de **4** dans l'éthanol. Il a été noté que la présence d'un groupement phényle en β du carbène oriente la contraction de cycle.

Canadian Journal of Chemistry, 47, 2853 (1969)

Au cours d'une étude précédente (1) nous avons montré que la décomposition photochimique du diazo-2 diméthyl-5,5 cyclohexanedione-1,3 se faisait selon deux modes principaux de réaction: *1*) par contraction de cycle et *2*) par réduction du carbène.

Dans le but de vérifier la généralité de ces modes réactionnels et en vue de préciser le mécanisme réactionnel de la contraction de cycle, nous avons effectué une étude analogue sur le diazo-2 diphényl-4,5 cyclohexanedione-1,3 (**1**).

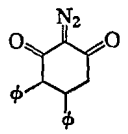

1

Ce diazo n'avait jamais été préparé jusqu'ici. Nous l'avons obtenu à partir de la diphényl-4,5 cyclohexanedione-1,3 selon une méthode inspirée de celle décrite par Rosenberg *et al.* (2) pour préparer d'autres composés diazoïques.

Afin de pouvoir comparer le comportement du diazo **1** avec celui du diazo-2 diméthyl-5,5 cyclohexanedione-1,3 nous avons refait les mêmes expériences: à savoir décomposition thermique dans le xylène, décompositions photochimiques dans le tétrachlorure de carbone, dans l'alcool méthylique et dans l'alcool éthylique.

Résultats

(1) Thermolyse

Par décomposition thermique dans le xylène à 140 °C, le diazo-2 diphényl-4,5 cyclohexanedione-1,3 conduit au composé **2***a*.

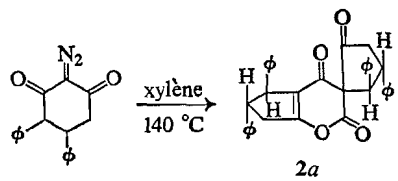

2*a*

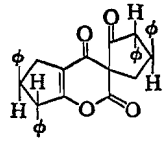

2*b*

Ce composé est du même type que celui obtenu lors de la décomposition thermique du diazo de la dimédone (1). En particulier, les caractéristiques spectrales sont analogues. De plus, l'analyse est en accord avec la formule brute de **2***a* soit $C_{36}H_{28}O_4$. L'ensemble de ces données permet donc d'attribuer à **2***a* la formule du tétraphényl-6,7,4′,5′ trioxo-2,4,2′ hexahydro-2,3,4,5,6,7 spiro (cyclopenta (*b*) pyran-3,1′ cyclopentane).

Ce composé admet plusieurs isomères. Toutefois l'attribution de la structure, telle que décrite ci-dessus, semble raisonnable et repose sur les arguments suivants.

La cyclisation de **3** en présence de base (schéma

[1]Congé du CNRS (1967–1968). Etudiant post-doctoral du Conseil National de Recherches du Canada. Adresse actuelle: Laboratoire de Chimie Organique 3, Faculté des Sciences, 17 ter rue Paul Collomp, 63 Clermont-Ferrand, France.

[2]Attaché de recherche (1966–68). Adresse actuelle: Collège Sainte-Marie, 1180 rue Bleury, Montréal, Québec et à qui toute demande d'information devra être adressée.

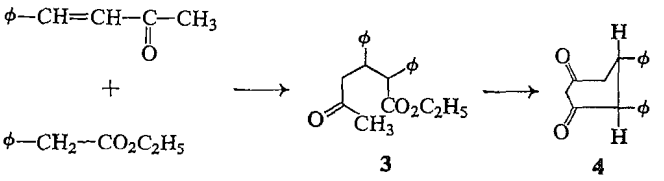

SCHÉMA 1

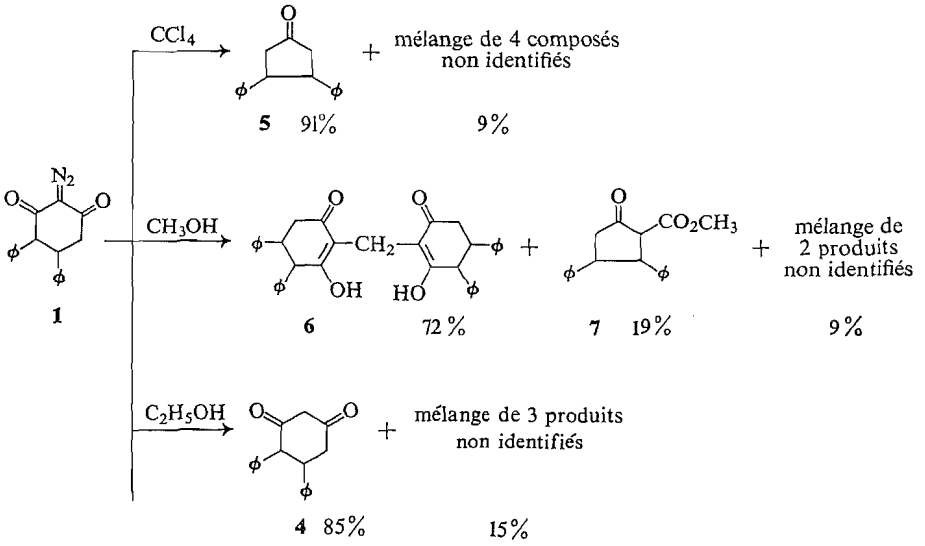

SCHÉMA 2

1) devrait donner la dicétone **4** (phényles *trans* di-équatoriaux) plutôt que l'isomère *cis* (3).

Il sera montré plus loin que le diazo **1**, par décomposition photochimique dans le tétrachlorure de carbone, fournit la *trans*-diphényl-3,4 cyclopentanone. Nonobstant un réarrangement profond de la molécule, la position *trans* des deux groupes phényles dans la cyclopentanone implique un arrangement *trans* dans le diazo **1**.

Finalement un composé isomérique à **2***a* peut être aussi formé. En effet, le composé **2***b* est aussi possible par la réaction de deux molécules de cétène **9**.

Que ce composé ne se forme pas, a été montré par le fait que la thermolyse de **1** dans le xylène et en présence d'une trace de méthanol n'a donné que le céto–ester **7**. Par hydrolyse, ce dernier a donné qu'un seul produit, la *trans*-diphényl-3,4 cyclopentanone.

(2) Photolyse

L'ensemble des résultats, obtenus au cours des décompositions photochimiques du diazo-2 diphényl-4,5 cyclohexanedione-1,3, est rassemblé dans le schéma 2.

Toutes les photolyses ont été réalisées avec une lampe Hanovia de 450 watts sous atmosphère d'azote et pendant 1 h dans presque tous les cas. Après distillation du solvant, le résidu solide a été analysé par chromatographie sur couches minces. Des chromatographies sur colonne ont permis d'isoler purs les principaux produits réactionnels. Les pourcentages paraissant au schéma 2 sont des pourcentages de récupération.

a) Photolyse dans le tétrachlorure de carbone

La photolyse a été effectuée pendant 1 h et 30 min avec un filtre Pyrex.

Le principal produit de la réaction (91%) s'avéra être la *trans*-diphényl-3,4 cyclopentanone (**5**). Elle fut identifiée par comparaison avec un échantillon authentique obtenu selon le mode réactionnel décrit au schéma 3.

Il fut également obtenu, dans un rendement de 9%, un mélange d'au moins quatre produits

Can. J. Chem. Downloaded from www.nrcresearchpress.com by 210.87.254.6 on 09/05/12
For personal use only.

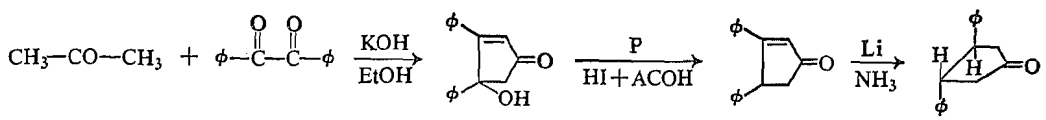

SCHÉMA 3

(chromatographie sur couches minces) qui ne furent pas identifiés.

b) Photolyse dans les alcools méthylique et éthylique

Les photolyses dans les alcools méthylique et éthylique ont été faites pendant 1 h, sans filtre.

Dans le cas du méthanol, la chromatographie sur colonne permit d'isoler un mélange de deux produits qui furent séparés par recristallisation fractionnée dans le méthanol aqueux. Il fut ainsi obtenu 72% de bis (diphényl-4,5 cyclohexèn-1 ol-2 oxo-6 yl) méthane (**6**) et 19% de diphényl-2,3 oxo-5 cyclopentanecarboxylate de méthyle (**7**).

Le composé **6** a été identifié par comparaison avec un échantillon authentique obtenu par réaction de la diphényl-4,5 cyclohexanedione-1,3 sur le formaldéhyde selon la méthode utilisée pour préparer les dérivés dimédoniques des aldéhydes (4).

Le composé **7** a été identifié par ses caractéristiques spectrales:

Infrarouge: bandes à 1755, 1720, et 1600 cm^{-1}.

Résonance magnétique nucléaire: bandes à 2.79 τ (10H, singulet); 6.28 τ (3H, singulet); de 6.1–7.3 τ (5H, multiplet).

Spectre de masse: pic parent à 294 (valeur calculée 294.6) et par son analyse qui est en accord avec la formule brute de **7** soit $C_{19}H_{18}O_3$. En outre, la structure de 7 a été confirmée par une hydrolyse acide; celle-ci conduisit à la *trans*-diphényl-3,4 cyclopentanone (**5**).

Un mélange d'au moins deux produits (chromatographie sur couches minces) fut également obtenu. Ils ne furent pas identifiés.

La photolyse dans l'éthanol a fourni comme principal produit réactionnel la diphényl-4,5 cyclohexanedione-1,3 (**4**) dans un rendement de 85%. Elle fut identifiée par comparaison avec un échantillon authentique. Cette photolyse a également conduit à un mélange d'au moins 3 composés qui ne purent être séparés et qui ne furent pas identifiés.

Discussion

Les résultats des décompositions thermique et photochimiques du diazo-2 diphényl-4,5 cyclohexanedione-1,3 montrent que celui-ci se comporte de la même façon que le diazo-2 diméthyl-5,5 cyclohexanedione-1,3 (1). Les mécanismes permettant d'expliquer la formation des différents composés obtenus sont donc les mêmes. Cependant le diazo-2 diphényl-4,5 cyclohexanedione-1,3 ayant une structure dissymétrique, la contraction de cycle pouvait conduire à deux cétènes différents **8** et **9** selon que la liaison a ou la liaison b se transposait (schéma 4).

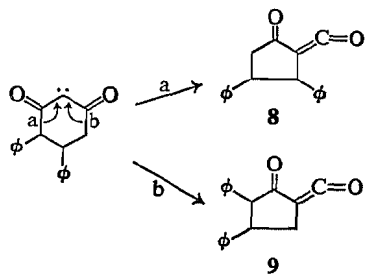

SCHÉMA 4

Les résultats montrent, sans l'ombre d'un doute, que seul la transposition selon a, pour donner **8** intervient. Ce réarrangement unique pourrait s'expliquer par une plus grande stabilité de la charge négative (due à la présence d'un groupement phényle en α) qui doit se développer dans l'état de transition.

Le schéma 5 montre les mécanismes proposés pour expliquer la formation des différents composés obtenus au cours des décompositions thermique et photochimiques du diazo-2 diphényl-4,5 cyclohexanedione-1,3.

Il est à noter que le composé **10** ne se forme pas, au cours de la photolyse du diazo-2 diphényl-4,5 cyclohexanedione-1,3 dans l'alcool éthylique; contrairement à ce qui se passe avec le diazo de la dimédone où un composé similaire est obtenu (1). La réaction entre la dimédone et l'acétaldéhyde selon la méthode de Horning et Horning (4) est très facile et conduit rapidement au composé attendu. Il n'en est pas de même avec la diphényl-4,5 cyclohexanedione-1,3. En

Can. J. Chem. Downloaded from www.nrcresearchpress.com by 210.87.254.6 on 09/05/12
For personal use only.

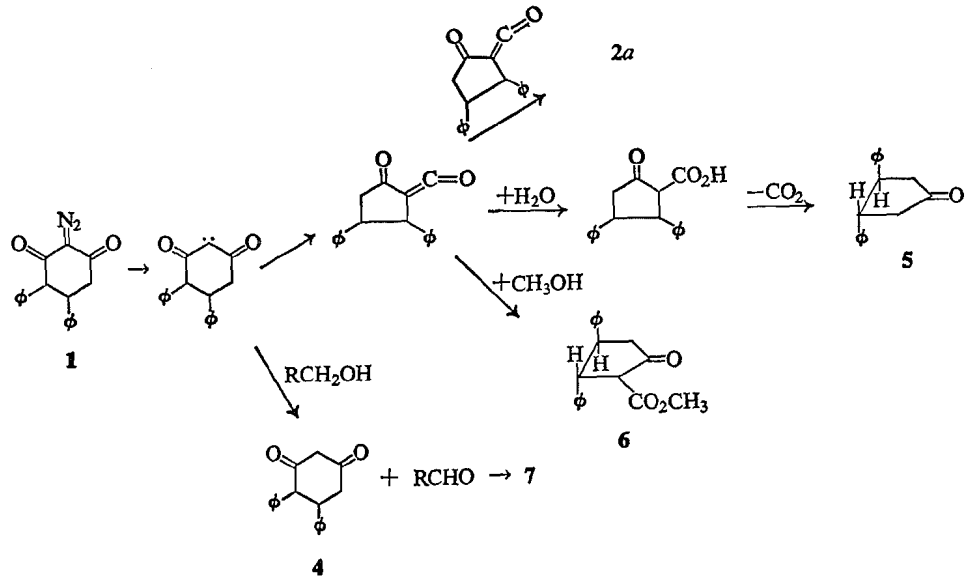

SCHÉMA 5

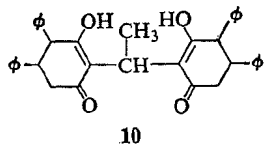

10

effet, celle-ci ne réagit pas avec l'acétaldéhyde dans les conditions décrites par Horning. On la retrouve inchangée à la fin de la réaction.

Cependant la présence de diphényl-4,5 cyclohexanedione-1,3 implique la réduction du carbène et l'oxydation de l'éthanol en acétaldéhyde. La formation de ce dernier, au cours de la photolyse, a d'ailleurs été vérifiée par l'obtention de son dérivé dinitro-2,4 phénylhydrazone (voir Partie expérimentale).

Conclusion

Les résultats obtenus, au cours des décompositions thermique et photochimiques du diazo-2 diphényl-4,5 cyclohexanedione-1,3, montrent que celui-ci se comporte de la même manière que le diazo de la dimédone (1). Les deux modes réactionnels rencontrés au cours de l'étude précédente se retrouvent ici.

De plus, cette étude a permis de montrer que la présence d'un groupement phényle en β du carbène oriente la contraction de cycle. Celle-ci se fait, en effet, uniquement du côté de la molécule contenant le groupement phényle.

Partie expérimentale

Les points de fusion ont été déterminés sur un appareil Büchi Modèle Dr. Tottoli et sont donnés sans correction. Les spectres infrarouges ont été enregistrés sur un spectrophotomètre Beckman IR 8 et les spectres ultraviolets sur un Spectronic 505 de Bausch et Lomb. Les spectres de résonance magnétique nucléaire ont été réalisés sur un appareil Jéol type C60H dans du chloroforme deutérié avec du TMS comme référence interne. Les spectres de masse on été pris sur un appareil Hitachi Perkin–Elmer type RMU-6D. Les microanalyses ont été effectuées par Schwarzkopf Microanalytical Laboratory, Woodside, New York, USA. Les chromatographies sur couches minces ont été faites sur chromagram Eastman–Kodak No 6060 en utilisant le mélange cyclohexane–acétate d'éthyle 75/25 en volume comme éluant.

Synthèse de la diphényl-4,5 cyclohexanedione-1,3 (4)

Elle fut préparée selon la méthode de Zimmerman et Schuster (5) à partir de phénylacétate d'éthyle et de *trans*-phényl-4 buten-3 one-2 p.f. 160–162 °C (litt. p.f. 160–165 °C (5)).

Synthèse du diazo-2 diphényl-4,5 cyclohexanedione-1,3 (1)

Une solution de 21 g (0.08 *M*) de diphényl-4,5 cyclohexanedione-1,3 et de 14 g (0.08 *M*) d'azoture de tosyle dans 1400 ml d'éther anhydre et 25 ml d'alcool éthylique, est refroidie sous agitation. Lorsque la température est inférieure à 5 °C, 10 ml de diéthylamine sont ajoutés rapidement. Le mélange est laissé sous agitation 15 min à froid et 2 h 30 min à température ambiante. La solution éthérée est lavée plusieurs fois avec une solution de soude à 10%, puis à l'eau jusqu'à neutralité. Après séchage sur sulfate de sodium anhydre, le solvant est éliminé et le résidu solide, recristallisé dans l'alcool à 95%. Rendement 45–50%: p.f. 130–132 °C.

Can. J. Chem. Downloaded from www.nrcresearchpress.com by 210.87.254.6 on 09/05/12
For personal use only.

Can. J. Chem. Downloaded from www.nrcresearchpress.com by 210.87.254.6 on 09/05/12
For personal use only.

Spectre infrarouge: 2165, 2140, et 1645 cm^{-1}.

Spectre ultraviolet (EtOH 95%): λ_{max} = 230 mμ ε_{max} = 15 114; λ_{max} = 259 mμ ε_{max} = 9175.

Spectre de résonance magnétique nucléaire: multiplet centré à 2.85 τ (10H); multiplet entre 6 et 6.6 τ (2H), doublet à 7.15 τ (2H).

Anal. calc. pour $C_{18}H_{14}N_2O_2$ (290.3): C, 74.47; H, 4.86; N, 9.65. Trouvé: C, 74.37; H, 4.97; N, 9.43.

Décomposition thermique du diazo-2 diphényl-4,5 cyclohexanedione-1,3

Trente ml de xylène ont été placés dans un ballon de 100 ml à 2 tubulures muni d'un réfrigérant, d'une ampoule à brome et plongé dans un bain d'huile. Lorsque la température du bain d'huile atteint 140°, une solution de 1 g de diazo-2 diphényl-4,5 cyclohexanedione-1,3 dans 50 ml de *m*-xylène est ajoutée goutte à goutte. Le dégagement gazeux s'arrête 15 min après la fin de l'addition de la solution de diazo. La solution encore chaude est traitée par du charbon actif et filtrée. Le *m*-xylène est éliminé sous pression réduite. Le résidu jaune pâle huileux est repris par une petite quantité d'éther. En chassant rapidement l'éther sous vide, un produit solide est obtenu. Il est purifié par une chromatographie sur colonne de silicagel (éluant cyclohexane–acétate d'éthyle 75/25).

Par comparaison avec le composé obtenu dans le cas du diazo de la dimédone, ce produit fut identifié comme étant le tétraphényl-6,7,4′,5′ trioxo-2,4,2′ hexahydro-2,3,4,5,6,7 spiro (cyclopenta (*b*) pyran-3,1′ cyclopentane) (**2***a*): p.f. 79–80 °C.

Spectre infrarouge: 1780, 1750, 1678, et 1645 cm^{-1}.

Spectre ultraviolet: (EtOH) λ_{max} = 292 mμ ε_{max} = 11 000.

Spectre de masse: pic parent à 524 (valeur calculée 524.6).

Résonance magnétique nucléaire: 2.75 τ (singulet large, 20H) 5.9–7.7 τ (multiplet, 8H).

Anal. calc. pour $C_{36}H_{28}O_4$ (524.6): C, 82.42; H, 5.38. Trouvé: C, 82.06; H, 5.52.

Selon les mêmes conditions, mais en présence d'une trace de méthanol anhydre, le céto–ester **7** a été obtenu. Ce dernier présentait exactement les mêmes caractéristiques que le céto–ester obtenu par photolyse de **1** dans le méthanol: à savoir: p.f. 127–129 °C i.r. et r.m.n. rigoureusement identiques. L'hydrolyse donna une cétone présentant un p.f. 175–177 °C et un dérivé dinitro-2,4 phénylhydrazone p.f. 172–174 °C en plus d'avoir des caractéristiques spectrales rigoureusement identiques à la *trans*-diphényl-3,4 cyclopentanone de synthèse.

Décompositions photochimiques du diazo-2 diphényl-4,5 cyclohexanedione-1,3.

a) Photolyse dans le tétrachlorure de carbone.

1 g de diazo-2 diphényl-4,5 cyclohexanedione-1,3 dissout dans 800 ml de tétrachlorure de carbone (Anachemia reagent) est soumis à la photolyse. Une lampe Hanovia de 450 w avec filtre de Pyrex est utilisée. Après 1 h et 30 min de photolyse sous courant d'azote, le tétrachlorure de carbone est éliminé par distillation. Une chromatographie sur couches minces montra que le résidue contenait au moins 4 produits, dont l'un en très forte majorité. Une chromatographie sur colonne de silicagel (100 g Baker Analyzed, acétate d'éthyle–cyclohexane 25/75) permet d'isoler un composé pur (0.73 g). Celui-ci s'avéra être la *trans*-diphényl-3,4 cyclopentanone (**5**). Elle présente les caractéristiques suivantes: p.f. 175–177 °C (litt. p.f. 177 °C (6)).

Spectre infrarouge: 1740 et 1600 cm^{-1}.

Résonance magnétique nucléaire: singulet très large centré à 2.80 τ (10H); multiplet entre 6.3 et 6.9 τ (2H); multiplet entre 7.1 et 7.7 τ (4H).

Spectre de masse: pic parent à 236 (valeur calculée 236.3). Ces caractéristiques sont rigoureusement identiques à celles obtenues pour un échantillon authentique synthétisé à partir d'acétone et de benzoïne (voir à la fin de la Partie expérimentale). En particulier le point de fusion mixte ne donna lieu à aucune dépression.

Il ne fut pas possible, par chromatographie sur colonne, de séparer les autres constituants du mélange; ils furent toujours obtenus en petites quantités et impurs.

b) Photolyse dans l'alcool méthylique

2.5 g de diazo-2 diphényl-4,5 cyclohexanedione-1,3 sont dissouts dans 500 ml d'alcool méthylique purifié selon la méthode de Lund et Bjerum (7) et soumis à la photolyse. Celle-ci est effectuée pendant 1 h sous courant d'azote et avec une lampe Hanovia 450 W et sans filtre. Le solvant est ensuite éliminé par distillation. Le résidu, analysé par chromatographie sur couches minces contient au moins 4 produits dont 2 sont nettement majoritaires. Une chromatographie sur colonne de silicagel (éluant cyclohexane–acétate d'éthyle 75/25) permet d'isoler le mélange des deux produits majoritaires. Ceux-ci furent séparés par une recristallisation fractionnée dans le méthanol aqueux. Le premier composé qui précipite au cours de cette recristallisation est le bis (diphényl-4,5 cyclohexèn-1 ol-2 oxo-6 yl) méthane (**6**) obtenu dans un rendement de 72%. Ses caractéristiques sont les suivantes: p.f. 114–117 °C.

Infrarouge: 1600 et 1590 cm^{-1}.

Résonance magnétique nucléaire: pic très large entre −2.5 et 1.5 τ (2H); singulet large centré à 2.9 τ (20H); série de bandes entre 6 et 7.3 τ (10H).

Ces caractéristiques sont rigoureusement identiques à celles obtenues pour un échantillon authentique synthétisé à partir de diphényl-4,5 cyclohexanedione-1,3 et de formaldéhyde selon la méthode utilisée pour obtenir les dérivés dimédoniques des aldéhydes (4) (voir à la fin de la Partie expérimentale).

En augmentant la quantité d'eau dans le solvant de recristallisation, 19% de diphényl-2,3 oxo-5 cyclopentane –carboxylate de méthyle (**7**) sont obtenus. Ce composé présente les caractéristiques suivantes: p.f. 127–129 °C.

Infrarouge: 1750, 1725, et 1600 cm^{-1}.

Résonance magnétique nucléaire: singulet large centré à 2.78 τ (10H); singulet à 6.28 τ (3H); multiplet de 6 à 7.3 τ (5H).

Spectre de masse: pic parent à 294 (valeur calculée 294.6).

Anal. calc. pour $C_{19}H_{18}O_3$ (294.6): C, 77.53; H, 6.16. Trouvé: C, 77.93; H, 6.28.

La structure de ce céto–ester a également été confirmée par une hydrolyse acide: 60 mg de **7**, en suspension dans 5 ml d'acide chlorhydrique (1/1), sont chauffés à reflux pendant 2 h. Après refroidissement et dilution de la solution, celle-ci est extraite à l'éther. La solution éthérée est lavée avec de la soude 10%, puis avec de l'eau

Can. J. Chem. Downloaded from www.nrcresearchpress.com by 210.87.254.6 on 09/05/12
For personal use only.

et séchée par sulfate de sodium anhydre. Après évaporation du solvant, le solide restant est recristallisé dans du méthanol aqueux. Il fut identifié comme étant la *trans*-diphényl-3,4 cyclopentanone (**5**) par comparaison avec un échantillon authentique. Le point de fusion mixte ne donna aucune dépression. Il en fut de même avec les dérivés dinitro-2,4 phénylhydrazones.

Les deux derniers composés (9%) furent obtenus en mélange et ne furent pas identifiés.

c) Photolyse dans l'alcool éthylique.

2.5 g de diazo-2 diphényl-4,5 cyclohexanedione-1,3 sont dissouts dans 500 ml d'alcool éthylique purifié selon la méthode de Lund et Bjerum et soumis à la photolyse pendant une heure, sous courant d'azote. Une lampe Hanovia de 450 w, sans filtre, fut utilisée pour réaliser cette photolyse. Après avoir distillé le solvant, une huile jaune est obtenue, elle cristallise en partie au bout d'un certain temps. La filtration fournit dans un rendement de 85%, la diphényl-4,5 cyclohexanedione-1,3 (**4**). Celle-ci fut caractérisée par comparaison avec un échantillon authentique.

L'huile jaune (15%) obtenue lors de la filtration contient au moins 3 produits. Ceux-ci ne purent pas être séparés par une chromatographie sur colonne et ne furent pas identifiés. La résonance magnétique nucléaire de ce mélange indique qu'il n'y a pas incorporation d'un groupement éthyle.

Nous avons également mis en évidence la formation d'acétaldéhyde au cours de cette photolyse. De la même façon que dans le cas du diazo de la dimédone, l'azote, à la sortie de l'appareil de photolyse a barbotté dans une solution acide de dinitro-2,4 phénylhydrazine. A la fin de la photolyse, un précipité jaune-orangé s'était formé. Il fut identifié comme étant la dinitro-2,4 phénylhydrazone de l'acétaldéhyde par comparaison avec un échantillon authentique.

Synthèse de la trans-diphényl-3,4 cyclopentanone

La diphényl-3,4 cyclopenten-2 ol-4 one fut d'abord préparée par l'action de l'acétone sur la benzoïne en présence de potasse alcoolique selon la méthode de Japp et Knox (8).

Puis la diphényl-3,4 cyclopenten-2 ol-4 one a été traitée par du phosphore rouge en présence d'acide iodhydrique et d'acide acétique selon le procédé de Geissman et Koelsch (9). La diphényl-3,4 cyclopenten-2 one, ainsi obtenue, fut réduite par le lithium dans l'ammoniac pour fournir la *trans*-diphényl-3,4 cyclopentanone: p.f. 175–177 °C (litt. p.f. 177 °C (6)). Dinitro-2,4 phénylhydrazone: p.f. 172–174 °C (litt. p.f. 173 °C (10)).

Infrarouge: 1740 et 1600 cm^{-1}.

Résonance magnétique nucléaire: singulet très large centré à 2.86 τ (1H); multiplet entre 6.3 et 6.7 τ (2H); multiplet entre 7.1 et 7.7 τ (4H).

Synthèse du bis [diphényl-4,5 cyclohexèn-1 ol-2 oxo-6 yl] méthane

700 mg de diphényl-4,5 cyclohexanedione-1,3 sont dissouts dans le minimum d'alcool éthylique 87%. 5 ml d'une solution aqueuse à 37% de formaldéhyde sont ensuite ajoutés. Le mélange est chauffé à reflux pendant 5 min au bain-marie.

Par refroidissement, un abondant précipité se forme, il est filtré et recristallisé dans le méthanol aqueux: p.f. 116–119 °C.

Spectre infrarouge: 1600 et 1590 cm^{-1}.

Résonance magnétique nucléaire: pic très large entre −2.5 et 0.5 τ (2H); singulet large centré à 2.9 τ (20H) série de bandes entre 6 et 7.5 τ (10H).

Anal. calc. pour $C_{37}H_{32}O_4$ (560.7): C, 82.20; H, 5.97. Trouvé: C, 81.92; H, 5.85.

Remerciements

Nous remercions Monsieur le Professeur H. Favre qui a gracieusement mis son laboratoire à notre disposition et sans qui ce travail n'aurait pu avoir lieu. Nos remerciements vont également à Monsieur R. Mayer pour les spectres de résonance magnétique nucléaire et à Monsieur J.C. Regenass pour les spectres de masse. Nous tenons également à remercier le Conseil National de Recherches du Canada pour l'aide financière accordée et pour une bourse de recherches post-doctorale (Subvention A-14).

1. H. Veschambre et D. Vocelle. Can. J. Chem. Sous presse.
2. M. Rosenberg, P. Yates, J. B. Hendrickson, et W. Wolf. Tetrahedron Letters, **33**, 2285 (1964).
3. Organic Reactions. Roger Adams et al., éd. Vol. 15. John Wiley and Sons, Inc., New York. p. 1.
4. H. C. Horning et M. G. Horning. J. Org. Chem. **11**, 95 (1946).
5. H. E. Zimmerman et D. I. Schuster. J. Am. Chem. Soc. **84**, 4527 (1962).
6. H. A. Weidlich. Chem. Ber. 1601 (1938).
7. A. I. Vogel. A text-book of practical organic chemistry. John Wiley and Sons, Inc., New York. 1966. p. 167.
8. F. R. Japp et J. Knox. J. Chem. Soc. **87**, 673 (1905).
9. J. A. Geissman et C. F. Koelsch. J. Org. Chem. 485 (1938).
10. J. W. Lynn et J. English, Jr. J. Org. Chem. 1546 (1951).

Can. J. Chem. Downloaded from www.nrcresearchpress.com by 210.87.254.42 on 09/05/12
For personal use only.

Diterpene chemistry III. Chemistry of some epoxides derived from methyl pimarate

J. W. ApSimon and H. Krehm
Department of Chemistry, Carleton University, Ottawa, Canada

Received January 13, 1969

Some chemistry of the α- and β-epoxides derived from a methyl pimarate degradation product (vinyl group transformed into a methoxycarbonyl) is described. The α-epoxide was found to be a very reactive species leading, by an intramolecular process, to a hydroxy-γ-lactone even on standing in hexane solution. A possible explanation for the reactivity is given, based on a conformational argument. The β-epoxide undergoes a cleavage reaction with Lewis acid to give a 'backbone' rearrangement product, although a non-rearranged compound was observed in minor yield.

Canadian Journal of Chemistry, 47, 2859 (1969)

In Part II of this series (1) we described the formation of an epoxide **1** during the Lemieux oxidation (2) of methyl pimarate **2**. In this paper we describe some chemistry of the decarbonylated esterified derivative of **1**, i.e. epoxide **3**, and of its α-epoxy isomer ***4a*** synthesized previously (1) in our structural studies. We also present further evidence for the structural assignments for these compounds.

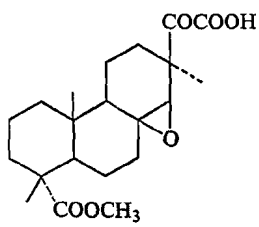

1

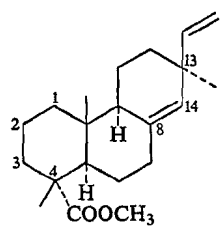

2

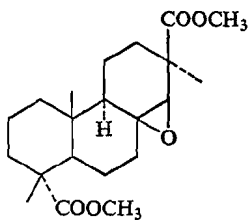

3

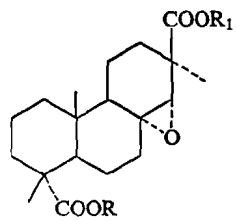

4a R = R_1 = CH_3
b R = CH_3, R_1 = C_2H_5

Some Reactions of α-Epoxide 4a

In our earlier work (1) we proposed the structure of **3** derived from **1** on the basis of a synthesis from a methyl pimarate degradation product and by comparison to the α-epoxide ***4a***. This last compound was obtained by epoxidation of the corresponding olefinic material assuming that the approach of epoxidizing agent was from the least hindered side of the molecule. It is interesting to compare the nuclear magnetic resonance (n.m.r.) spectra of **3** and **4** where the signals for the C-14 protons appear at 2.75 and 3.25 δ respectively. Inspection of models shown here in the perspective drawings **5** and **6** reveal that in the α-oxide **6**≡***4a***, the 14β-proton is always adjacent to the ester group, and would thus be subject to an extra

5

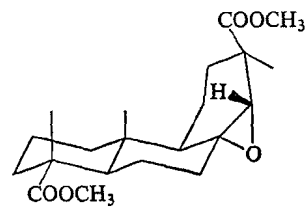

6

deshielding effect by this group, a juxtaposition not possible in **5** (≡**3**).[1]

Epoxide ***4a*** is a very labile compound and rearranges even on warming in hexane to a new material m.p. 215 °C analyzing for $C_{20}H_{30}O_5$.

[1]The conformation **6** representing the α-epoxide is only that which we considered in our early n.m.r. assignments since it seemed the most logical at the time. However, as the chemistry described here has led us to propose that this compound exists as **9** the n.m.r. arguments could be in question. But examination of Dreiding models indicates that, regardless of the conformations taken up by the B and C rings, there still exists a difference in the degree of eclipsing of the C-14 C—H bond and the methoxycarbonyl grouping sufficient to distinguish between the α- and β-epoxides.

Can. J. Chem. Downloaded from www.nrcresearchpress.com by 210.87.254.42 on 09/05/12
For personal use only.

This compound was best obtained by boiling a hexane solution of **4***a* when direct crystallization from this solvent gave a substantially pure sample. Its infrared (i.r.) spectrum suggested a hydroxy-γ-lactone with $\nu_{max}(CCl_4)$ 3620, 3450 (OH), 1785 (γ-lactone) and 1730 cm^{-1} (ester). The n.m.r. spectrum indicated the loss of one methoxyl group with the appearance of a slightly broadened one proton singlet (half height width = 4 c.p.s.) at 3.5 δ attributable to a single methine proton. This singlet became sharp on addition of D_2O when the loss of a similar singlet at 2.70δ was also noticed. This information suggested structure **7** arising from intramolecular attack on the epoxide by the C-13 ester grouping possibly catalyzed by traces of *m*-chlorobenzoic acid still present in the reaction mixture.[2]

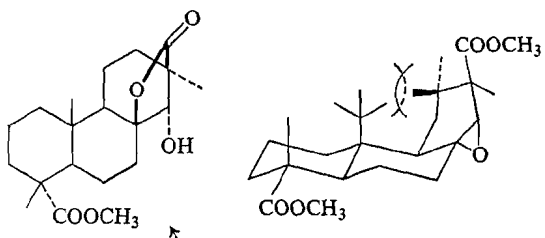

7 **8**

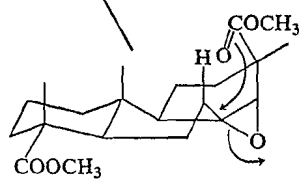

9

An examination of Dreiding models of the α-epoxides in this type of molecule is revealing and possibly gives a clue as to their lability. The B–C *cis* ring fusion, combined with the distorting effect on the epoxide ring, brings the 12β-hydrogen atom very close to the C-10 methyl group leading to a destabilization of conformation **8**. A flip of ring C to relieve this interaction leads to a worse situation between the 13β-methoxycarbonyl group and the C-10 methyl group whilst intermediate conformations of ring C appear equally unfavorable. Thus we suggest that the preferred conformation of epoxide **4** is with ring B in a boat form (3) as shown in **9**. The unfavorable flagpole–flagpole interaction between the C-10 methyl group and H-7 can be relieved somewhat by a flattening of ring B. This, however, is not a perfect situation and the ready rearrangement to **7** is doubtless a reflection of this conformational dilemma, the product being formed as indicated (arrows in **9**).

If **7** does in fact have the structure proposed, then an alternate synthesis of the β-epoxide **3** suggests itself analogous to that already performed (1). Thus the mesylate of **7** was prepared with methane sulfonyl chloride in pyridine which without further purification was dissolved in 50% methanolic potassium hydroxide. After 30 min at room temperature, work-up gave a high yield of **3**. In this manner a ready conversion of the α-epoxide **4***a* to the β-epoxide **3** was accomplished via the route indicated in Scheme 1 and supporting our structural assignments of **3** and **4***a*.

Earlier in our studies on **9** we had some thoughts on structure **10** for this hydroxylactone, although such a structure would have to arise in a stepwise manner by deprotonation–protonation steps (4) to give an 8β—H, and thus account for the low coupling constant with the 14β-proton (5) (n.m.r. shows a singlet). This possibility

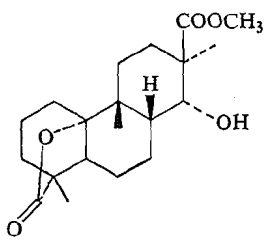

10

was readily eliminated as follows. The ethyl methyl diester epoxide **4***b* was made by esterification of the parent olefinic acid with diazoethane (6). On epoxidation with *m*-chloroperoxybenzoic acid and allowing the product to stand in hexane for several days, the same hydroxylactone **7** was obtained indicating that it is the C-13 ester grouping that is involved in the lactonization, and not that at C-4.

Lewis Acid Cleavage of β-*Epoxide* **3**

We had hoped to use β-epoxide **3** as a source of

[2]In many epoxidations with *m*-chloroperoxybenzoic acid we have often experienced difficulty in removing all *m*-chlorobenzoic acid even with many bicarbonate washings.

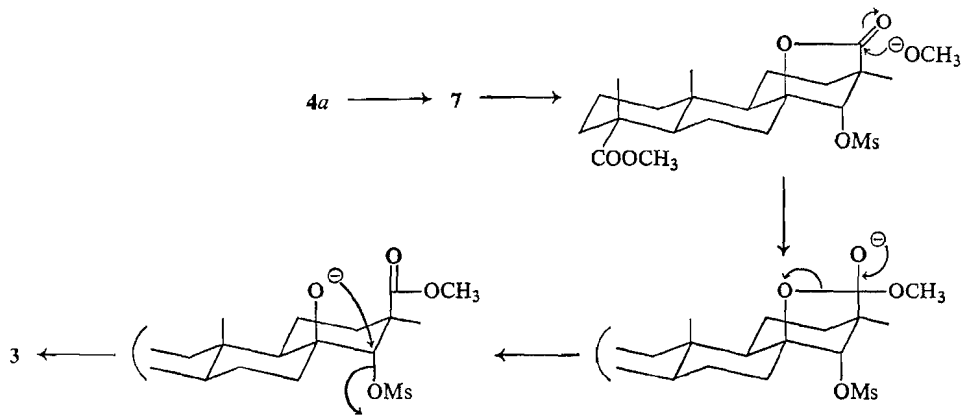

SCHEME 1

a 14-keto precursor to lead to novel steroids and thus we examined its reaction with Lewis acids (7). Reaction of **3** with either stannic chloride or BF_3–etherate in benzene led to a high yield of an alcohol m.p. 128 °C analyzing for $C_{21}H_{32}O_5$. The i.r. and n.m.r. spectra indicated the presence of both ester groups and probably a secondary alcohol. This last observation was made difficult since the methine proton signal was buried under the methoxyl signals; however, integration of this region indicated 7 protons. A possible formulation for this compound is **11** (partial structure) arising from cleavage of the epoxide followed by deprotonation of the C-8 carbonium ion leading to the tetrasubstituted double bond (no ethylenic signals in n.m.r.). This, however, proved to be

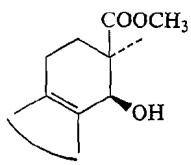

11

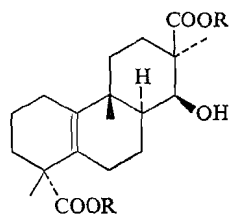

12*a* R = CH_3
b R = H

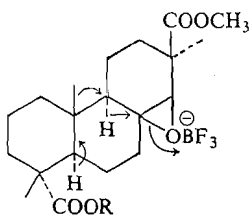

13

incorrect since oxidation of **11** with Jones' reagent (8) gave a saturated ketone and it was inert to manganese dioxide (9), either of which would have been expected to lead to an α,β-unsaturated ketone.

Therefore, it appears that this cleavage product has the 'backbone' rearranged structure **12***a* (4, 10) arising from the concerted anti-peri-planar movement of the migrating groups on cleavage of the β-oxide as shown in **13**. Further support for this structure was obtained by hydrolysis of **12***a* with dilute base to give the diacid **12***b*. The n.m.r. spectrum of this acid revealed the 14α methine proton signal at 4.18 δ as a broadened singlet of half height width 4 c.p.s. This small coupling is indicative of a dihedral angle of about 60° for the vicinal 8 and 14 protons (5) alternate formulations requiring a dihedral angle of 180° or no adjacent protons at all (cf. **11**). Treatment of the diacid **12***b* with concentrated sulfuric acid at 0° afforded a mixture of γ and δ lactones as indicated by i.r. spectroscopy. These lactones could not be successfully separated but their formation is indicative of the β,γ-unsaturated nature of one of the carboxyl groups of **12***b* (4). Having shown that the double bond is tetrasubstituted and is not at the BC ring junction (Δ 8, 9), there only remains the AB junction of a rearranged structure such as proposed[3] in **12***b*.

At one stage in our studies we required a further sample of diester epoxide **3** and therefore

[3]A ring expansion–contraction opening of the oxide would give either a tri-substituted double bond or a ketone neither of which fit the above data.

Can. J. Chem. Downloaded from www.nrcresearchpress.com by 210.87.254.42 on 09/05/12
For personal use only.

Can. J. Chem. Downloaded from www.nrcresearchpress.com by 210.87.254.42 on 09/05/12
For personal use only.

chromatographed some residues from earlier crystallizations which had remained untouched for about 1 year. After elution of **3** on a silica gel column, 50 mg (3% of residues) of another compound were obtained, m.p. 162–164 °C, which analyzed for $C_{21}H_{32}O_5$, whose i.r. spectrum indicated hydroxyl (3500 cm^{-1}) and ester (1725 cm^{-1}) absorption and whose n.m.r. spectrum exhibited an extra proton buried under the methoxyl region (integration). Oxidation with Jones' reagent (7) gave an α,β-unsaturated ketone (λ_{max} 248 nm, ε 9000; ν_{max} 1660, 1620 cm^{-1}). This information leads us to structures **14** and **15** for the alcohol and its oxidation product. Thus **14** represents an intermediate stage in the re-

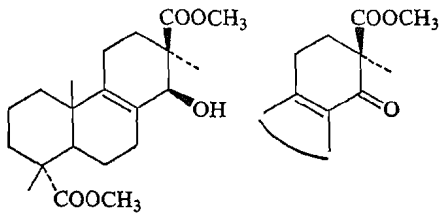

14 **15**

arrangement pathway of **3** to **12***a*. It is interesting to speculate whether, in fact, **12***a* and **14** represent different reaction pathways (concerted vs stepwise) or whether **14** is merely an intermediate in the rearrangement pathway (11). Lack of starting material terminated our studies at this stage.

Experimental

Infrared spectra were determined on a Perkin–Elmer Infracord 237B spectrophotometer. Nuclear magnetic resonance spectra were determined at 60 MHz on a Jeolco C-60 or a Varian A-60 spectrometer; chemical shifts are given in δ units relative to tetramethylsilane as an internal standard (s is used to signify singlets). Only those signals deemed to be of interest in assigning structures have been quoted. Sample concentrations were approximately 10% (w/v) in deuteriochloroform as solvent. All optical rotations were of 1% solutions in absolute ethanol at room temperatures unless otherwise stated. Ultraviolet spectra were determined in absolute ethanol on a Perkin–Elmer 202 spectrophotometer. Melting points are corrected and were determined on a Köfler hot stage, except for mixed melting points which were done in capillary tubes. Thin-layer chromatography (t.l.c.) was carried out on either silica gel G plates or Eastman Kodak chromatogram sheets. Mass spectra were obtained on the Perkin–Elmer–Hitachi instrument of McMaster University through the kindness of Professors D. B. McLean and R. A. Bell.

Hydroxylactone 7

α-Epoxide **4***a* was very labile, changing even on recrystallization from hexane to another compound m.p. 215 °C; $[\alpha]_D = +7°$ purified by crystallization from hexane and identified as hydroxy-γ-lactone **7**; $\nu_{max}(CCl_4)$, 3620, 3450 (hydroxyl), 1785 (lactone), and 1730 cm^{-1} (ester); n.m.r. signals at 3.70 (3H, s, methyl ester), 3.50 (1H, s, C-14 methine proton), 2.70 (1H, broad s, hydroxyl, D_2O exchange), and 1.30, 1.20, 0.95 δ (3 × 3H, s, angular methyl groups).

Anal. Calcd. for $C_{20}H_{30}O_5$: C, 68.55; H, 8.63. Found: C, 68.46; H, 8.65.

Synthesis of β-Epoxide 3 from Hydroxylactone 7

To a solution of 55 mg (0.151 mmole) of the hydroxy-γ-lactone **7** in 1 ml pyridine was added 0.02 ml of methane sulfonyl chloride; crystals (pyridine·HCl) appeared after several minutes. The mixture was allowed to stand overnight and poured into ice water. Ether extraction followed by drying over magnesium sulfate and evaporation gave 72 mg of an oil, exhibiting little hydroxyl in the i.r. but did show a lactone band (1785 cm^{-1}) and sulfonate bands at 1450 cm^{-1} (film). This compound was dissolved in 2 ml dry methanol and treated with 2 ml of 50% methanolic potassium hydroxide. After 30 min water (5 ml) was added and when the solution was left at room temperature colorless needles separated m.p. 135–137 °C. Recrystallization from methanol gave the epoxy diester **3** identical (melting point, mixture melting point, i.r., and n.m.r. spectra) with that obtained on methylation of the oxidation product of methyl pimarate (1).

Hydroxy-γ-lactone 7 via Ethyl, Methyl Diester Epoxide 4b

The Lemieux oxidation product of methyl pimarate **2**, (carboxyl group for C-13 vinyl) (1) (50 mg) in dry ether was treated with an ethereal solution of diazoethane (5) until a yellow color persisted. After evaporation of the ether, **4***b* was obtained as an oil (52 mg) n.m.r. 5.35 (1H, s, C-14 olefinic proton), 4.12 δ (2H, quartet of ethyl group) and no acid proton signal. This was directly epoxidized with *m*-chloroperoxybenzoic acid in ether (0° for 3 days). The reaction mixture was poured into sodium carbonate solution and extracted with ether, dried, and evaporated to yield an oil (no olefinic protons in n.m.r., signal at 3.2 δ for 14β-proton). This oil was allowed to stand in hexane for several days when, after evaporation of one half of the hexane, crystals of the hydroxy-γ-lactone **7** (20 mg) appeared, identical in all respects to those obtained from **4***a*.

Rearrangement of β-Epoxide 3 to 12a

(a) Boron Trifluoride Etherate Method

To 110 mg (0.32 mmole) of epoxide **3** dissolved in 10 ml dry benzene was added 0.10 ml of freshly distilled boron trifluoride etherate. After 24 h the solution was diluted with 100 ml water and ether extracted. Washing and drying the ethereal extracts in the usual manner yielded 119 mg of a greasy crystalline solid m.p. 115 °C. Repeated crystallization from hexane raised this to 127–128 °C (80 mg) $[\alpha]_D = -30°$; $\nu_{max}(CCl_4)$ 3500 (hydroxyl), 1725 cm^{-1} (diester); n.m.r. signals at 3.74, 3.68 (2 × 3H, s, two methyl esters), 2.65 (1H, s, C-14 hydroxyl, disappearing on D_2O exchange), and 1.25, 1.22, and 1.09 δ (3 × 3H, s, angular methyl groups); ultraviolet (u.v.), λ_{max}208 nm, ε 3480.

Can. J. Chem. Downloaded from www.nrcresearchpress.com by 210.87.254.42 on 09/05/12
For personal use only.

Anal. Calcd. for $C_{21}H_{32}O_5$: C, 69.20; H, 8.85. Found (mol. weight: 364 (mass spectral)): C, 69.17; H, 8.58.

(b) Stannic Chloride Method

The above experiment was repeated using 0.2 ml $SnCl_4$ in place of the boron trifluoride etherate. The product obtained was identical with the former (m.p., mixed m.p., t.l.c., and superimposable spectra).

Treatment of an ethanolic solution of alcohol **12***a* with 10% aqueous potassium hydroxide at reflux afforded the diacid **12***b* m.p. 205 °C, ν_{max}(Nujol) 3500 cm^{-1} (hydroxyl), 3300–3050, 1700 cm^{-1} (diacid); n.m.r. signals at 7.0 (3H, broad s, two acids, hydroxyl), 4.18, $J_{1/2}$ band width = 4 c.p.s. (1H, s, methine proton), 1.3, 1.3, and 1.1 δ (3 × 3H, s, angular methyls). The *bis* cyclohexylamine salt of this acid had a melting point of 174–176 °C.

Treatment of 50 mg of this acid in 1 ml chloroform with 1 ml concentrated sulfuric acid at 0 °C gave a mixture of δ- and γ-lactones $\nu_{max}(CCl_4)$ 1780 (γ-lactone), 1750 (δ-lactone) 1700 cm^{-1} (C-13 carboxyl).

Oxidation of **12***a*

(a) With Jones' Reagent (8)

Two drops of Jones' reagent (permanent orange tinge persisted) were added to 40 mg of alcohol **12***a* dissolved in 1 ml acetone. Dilution with water followed by ether extraction gave 30 mg of an oil which appeared to be two compounds by t.l.c. analysis (benzene–trace ether). An i.r. spectrum of this oil (film) showed the absence of hydroxyl absorption, with peaks at 1740, 1730 (diester), and 1720 cm^{-1} (6-membered ketone), *but no bands characteristic of an α,β-unsaturated ketone.* Similarly the u.v. spectrum revealed only the ester absorption λ_{max}218 nm; ε 2900. The oil could not be induced to crystallize from either hexane or aqueous ethanol solution, and was therefore treated with a base in an effort to equilibrate what was presumably a mixture of two ketones. Examination by t.l.c., however, showed the original two spots to be unchanged. The oil was not characterized further.

(b) With Manganese Dioxide (9).

To 60 mg of alcohol **12***a* dissolved in 3 ml chloroform was added an excess of freshly prepared MnO_2 and stirred for 24 h. Thin-layer chromatography analysis (benzene–2% ether) showed only unchanged starting material.

Allylic Alcohol **14** *and α,β-Unsaturated Ketone* **15**

Fifty milligrams (3%) of needles were obtained by column chromatography on silica gel of 1.6 g of diester epoxide, **3**, residues. This material was eluted after the epoxide fraction by 10% ethyl acetate in benzene. Several recrystallizations from hexane raised the m.p. to 162–164 °C, $[\alpha]_D = 107°$; ν_{max} (Nujol) 3500 cm^{-1} (hydroxyl); 1725 cm^{-1} (diester); n.m.r. showed no protons in the olefinic region, and peaks at 3.7, 3.6 (2 × 3H singlets methoxyls); 2.4, 1H broad singlet (angular methyl groups).

Anal. Calcd. for $C_{21}H_{32}O_5$: C, 69.20; H, 8.85. Found (mol. weight 364 (mass spectral)): C, 69.61; H, 8.78.

The above alcohol (10 mg) **16** dissolved in 1 ml acetone was treated with two drops Jones' reagent (8). After 10 min the mixture was diluted with 2 ml water and chilled overnight. Filtration afforded 5 mg of short needles, m.p. 106–108 °C; ν_{max} (KBr), 1740, 1725 cm^{-1} (diester) and 1660 cm^{-1} (α,β-unsaturated ketone); u.v., λ_{max} 248 nm; ε 9900, (endocyclic α,β-unsaturated ketone). A mass spectrum of this compound showed a parent peak *m/e* 362. Insufficient material was available for elemental analysis.

Acknowledgments

We thank the National Research Council of Canada for continued generous financial support. J. W. ApSimon expresses his appreciation to the Administrators of the C.D. Howe Memorial Foundation for the award of a Fellowship during the tenure of which this manuscript was written; he also thanks Professor G. Ourisson, Institut de Chimie, Strasbourg for his hospitality during this time. H. Krehm expresses his thanks to the British American Oil Research and Development Company, Sheridan Park, Ontario for the use of instrumental and laboratory facilities during the final phases of this work.

1. J. W. ApSimon, A. S. Y. Chau, W. G. Craig, and H. Krehm. Can. J. Chem. **45**, 1439 (1967).
2. R. U. Lemieux and E. von Rudloff. Can. J. Chem. **33**, 1701, 1710, 1714 (1955).
3. E. L. Eliel, N. L. Allinger, S. J. Angyal, and G. A. Morrison. Conformational analysis. John Wiley and Sons, Inc., New York. 1965. p. 476.
4. W. Herz and H. J. Wahlborg. J. Org. Chem. **30**, 1881 (1965), and references therein.
5. M. Karplus. J. Am. Chem. Soc. **85**, 2870 (1963); K. L. Williamson and W. S. Johnson. J. Am. Chem. Soc. **83**, 4623 (1961).
6. E. A. Werner. J. Chem. Soc. **115**, 1093 (1919).
7. H. B. Henbest and T. I. Wrigley. J. Chem. Soc. 4596 (1957).
8. L. F. Fieser and M. Fieser. Reagents for organic synthesis. John Wiley and Sons, Inc., New York. 1967. p. 142.
9. L. F. Fieser and M. Fieser. Reagents for organic synthesis. John Wiley and Sons, Inc., New York. 1967. p. 636.
10. J. W. Blunt, J. M. Coxon, M. P. Hartshorn, and D. N. Kirk. Tetrahedron, **23**, 1811 (1967); J. C. Jacquesy, J. Levisalles, and J. Wagnon. Chem. Commun. 25 (1967); M. Fetizon and P. Foy. Chem. Commun. 1005 (1967).
11. J. F. King and P. de Mayo. *In* Molecular rearrangements. Vol. II. *Edited by* P. de Mayo. John Wiley and Sons, Inc., New York. 1964. p. 816.

Can. J. Chem. Downloaded from www.nrcresearchpress.com by 210.87.254.6 on 09/05/12
For personal use only.

Diterpene chemistry. IV. The oxymercuration–demercuration of methyl pimarate and methyl sandaracopimarate[1]

J. W. ApSimon and H. Krehm
Department of Chemistry, Carleton University, Ottawa, Canada

Received January 13, 1969

The oxymercuration–demercuration procedure was explored for methyl pimarate and methyl sandaracopimarate. In the first case a dimercurial-monoether was obtained yielding a cyclic ether on demercuration. In the second, a monomercurial was obtained arising from attack on the vinyl group only, and demercuration gave a mixture of alcohols which were oxidized to a methyl ketone, which on hypoiodite degradation yielded a known degradation product of methyl sandaracopimarate. The difference in behavior between the two series is attributed to the proximity of the double bonds in methyl pimarate.

Canadian Journal of Chemistry, 47, 2865 (1969)

As part of our studies on pimaric **1***a* and sandaracopimaric acid **2***a* (1, 2) we were interested in two aspects of their chemistry. Firstly we wished to epoxidize the vinyl groups preferentially in order to study their cleavage in the vicinity of the nuclear double bonds, and secondly we were intrigued by the interaction of the double

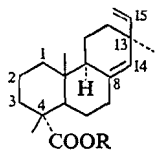

1*a* R=H
b R=CH_3

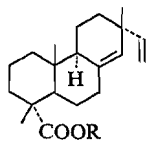

2*a* R=H
b R=CH_3

bonds in pimaric acid as compared with sandaracopimaric acid, as evidenced by unusual oxidation products (1).

Normal epoxidation of the parent acids or their methyl esters led exclusively to epoxidation of the nuclear double bond (3, 4), and attempts at bromohydrin formation (5) were inconclusive. Thus we felt that perhaps the oxymercuration procedure (6) would lead to preferential vinyl attack, and this process might also provide us some further information on the spatial interaction of the two double bonds in **1** (7).

Oxymercuration–demercuration of Methyl Pimarate 1b

Reaction of methyl pimarate **1***b* with one equivalent of mercuric nitrate or mercuric acetate in aqueous *t*-butyl alcohol resulted in about 50% conversion to an oxymercurial isolated at its chloroderivative (see Experimental). When two equivalents of mercuric nitrate were used, about 90% conversion was observed.

The crystalline chloromercurial analyzed for $C_{21}H_{32}O_3Hg_2Cl_2$ m.p. 176°, its infrared (i.r.) spectrum indicating no hydroxyl absorption but ester absorption was evident at 1726 cm $^{-1}$. The nuclear magnetic resonance (n.m.r.) spectrum showed no signals for olefinic protons. Assuming Markofinikov-type addition of the mercury salts (6) then these facts are best accommodated by structure **3**. The n.m.r. spectrum of **3** supported the structural assignment as follows.

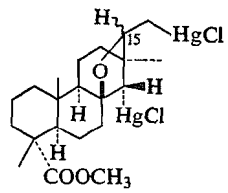

3

Centered at 3.9 δ was a doublet of doublets characteristic of the X branch of an ABX system with J_{AX} 6 Hz and J_{BX} 11 Hz which we assign to the H-15 proton of **3**. At 3.0 δ there was a weakly coupled singlet (*J* 0.2 Hz) which we assign to H-14β appearing at a lower field than the C-16 protons since it is both tertiary and will be affected somewhat by the proximate ether bridge. The coupling observed is probably due to W-plan coupling (8) with the 12β proton.

The stereochemistry at C-14 is assumed since the intramolecular attack on a mercurinium ion (6, 9) at C-8 and C-14 must come from the opposite face than the mercury (10), and the stereochemistry of pimaric acid fixes the direction of attack from the β face by the two carbon

[1]For Part III see ref. 2.

chain of the original vinyl group, thus necessitating an α oriented mercury at C-14 in the final product. There is one position in the product, C-15, where isomers could arise, yet all our evidence points to the formation on only one stereoisomer as inferred from sharp m.p., thin-layer chromatography (t.l.c.) in several solvent systems, and sharp n.m.r. signals.

The stereospecificity of the above process is further supported by the obtention of only one product on reduction of **3** with basic sodium borohydride in tetrahydrofurane or dioxane (7, 11). This product, m.p. 132 °C, analyzed for $C_{21}H_{34}O_3$ and its n.m.r. spectrum exhibited a new methyl group signal as a doublet, 1.2 δ, $J = 8$ Hz, and a one hydrogen quartet centered at 3.76 δ, $J = 8$ Hz. No other low field signals apart from the methoxyl proton signals were evident. On the basis of the structure assigned to **3** and the above data, this reduction product is assigned structure **4**. The stereochemistry at C-15 must remain unassigned at present since, to us at least, conformational arguments appear too tenuous. The mode for formation of **3** is

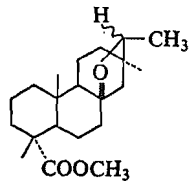

4

probably as shown in Scheme 1, *via* a very reactive monohydroxymercurial **5**, the intramolecular step being faster than the initial step, otherwise with one equivalent of mercuric salt, the mono-organomercurial **5** might have been

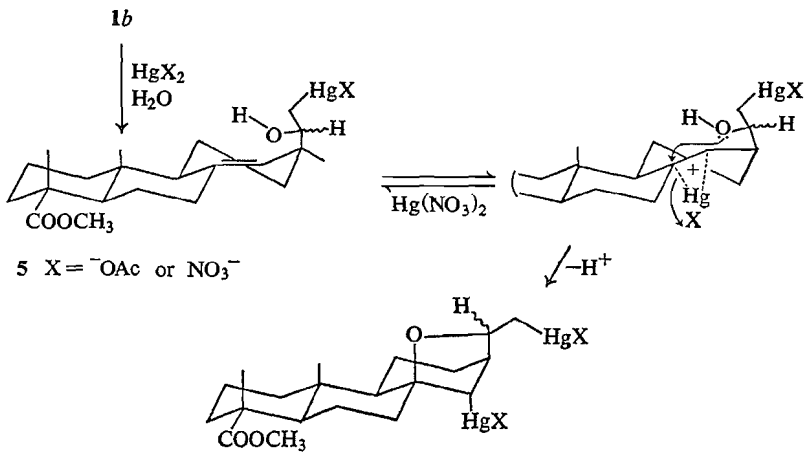

5 X = $^-$OAc or NO_3^-

3 Isolated as X = Cl^-

SCHEME

expected. In none of our experiments were we ever able to detect such an intermediate stage.[2]

Reduction of **3** with borohydride in ethanol/tetrahydrofurane (7, 12) yielded methyl pimarate indicating that no skeletal rearrangements had occurred in the formation of the organomercurial.

[2]Attempts at quenching the reaction after short periods in order to isolate **5** were unsuccessful. This is in agreement with earlier work (13) which indicates a rapid reaction, essentially complete in 30 s.

Oxymercuration–demercuration of Methyl Sandaracopimarate 2b

Oxymercuration of methyl sandaracopimarate, **2***b*, gave a crystalline product, m.p. 164°, analyzing for $C_{21}H_{33}O_3HgCl$, showing hydroxyl absorption at 3420 cm^{-1} in its i.r. spectrum. The n.m.r. spectrum indicated that the vinyl group had reacted, but not the nuclear double bond. The signal for the C-14 olefinic proton was at first puzzling since it appeared as a doublet centered at 5.42 δ; however, it became evident

Can. J. Chem. Downloaded from www.nrcresearchpress.com by 210.87.254.6 on 09/05/12
For personal use only.

Can. J. Chem. Downloaded from www.nrcresearchpress.com by 210.87.254.6 on 09/05/12
For personal use only.

from the demercuration step that a mixture of diastereoisomers at C-15 was present in the product for which we assign structure **6**. This inhomogeneity escaped us at first since the rest of the n.m.r. spectrum showed very sharp signals (e.g. for C-13β methyl group) and the product had a sharp m.p. and showed only one spot on t.l.c. in a number of solvent systems. On basic borohydride reduction (7, 11), a mixture of three compounds was obtained. One was methyl sandaracopimarate, whilst the other two were more polar by t.l.c. and appeared as overlapping spots in a number of solvent systems. It would appear that these reduction products were the epimeric alcohols **7**, although all our attempts at separation failed. Oxidation of this mixture with Jones' reagent (14) gave one compound **8** with a new strong carbonyl absorption of 1710 cm^{-1} in its i.r. spectrum. This ketone was subjected to the iodoform reaction (15), which was

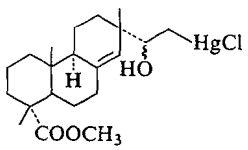

6

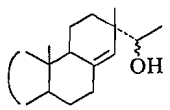

7

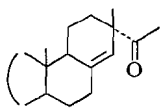

8

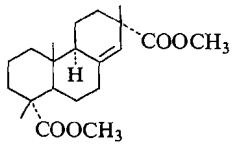

9

positive, and acidification of the reaction mixture followed by extraction and chromatography after methylation with diazomethane gave the dimethyl ester **9**, identical in all respects to an authentic sample previously obtained from our oxidation studies on methyl sandaracopimarate (1). Reduction of the mercurial, **6**, with borohydride in ethanol gave methyl sandaracopimarate. The ease with which methyl sandaracopimarate forms a mono-mercurial[3] and that with which methyl pimarate forms a dimercurial *via* intramolecular attack on the nuclear double bond, again emphasizes the interesting chemistry arising from closely spaced non-conjugated double bonds in a molecule. The results described here reinforce the observation (16) that the oxymercuration–demercuration procedure could be a useful synthetic route to cyclic ethers (17).

[3]Reaction with excess $Hg(OAc)_2$ or $Hg(NO_3)_2$ did not give any evidence of a dimercurial.

Experimental

Infrared spectra were determined on a Perkin-Elmer infracord 237-B spectrophotometer. Nuclear magnetic resonance spectra were determined at 60 MHz on a JEOLCO C-60 or Varian A-60 spectrometer; chemical shifts are given in δ units relative to tetramethylsilane as an internal standard (s is used to signify singlets). Only those signals deemed to be of interest in assigning structures have been quoted. Sample concentrations were approximately 10% in deuteriochloroform as solvent. All optical rotations were of 1% solutions in absolute ethanol at room temperature, unless otherwise stated. Ultraviolet spectra were determined in absolute ethanol on a Perkin-Elmer 202 spectrophotometer. Melting points are corrected and were determined on a Köfler hot stage except for mixed melting points which were done in capillary tubes. Thin-layer chromatography was carried out on either silica gel G plates or Eastman Kodak Chromatogram sheets. Mass spectra were obtained on the Perkin-Elmer-Hitachi instrument of McMaster University through the courtesy of Professors D. B. McLean and R. A. Bell.

Oxymercuration of Methyl Pimarate

(*a*) To 110 mg (0.348 mmole) methyl pimarate in 5 ml *tert*-butyl alcohol, was added a solution of 100 mg (0.312 mmole) mercuric acetate in 6 ml of water. The solution was left for 30 min and at the end of this period gave a negative spot test for mercuric ion with base. The addition of 25 ml of water containing a slight excess of sodium chloride caused the formation of a white precipitate (240 mg, 46%), m.p. 89–100 °C. Several recrystallizations from ethyl acetate – hexane afforded the analytical sample m.p. 176–177 °C; i.r.: $\nu_{max}(CHCl_3)$ 1725 (ester), 1250, 915, and 835 cm^{-1} (ether bands), and no hydroxyl absorption; n.m.r. bands at 3.9 (1H, doublet of doublets, C-15 methine), J = 6 Hz and 0.98 δ (3 × 3H, s, angular methyl groups).

Anal. Calcd. for $C_{21}H_{32}O_3Hg_2Cl_2$: C, 31.30; H, 4.02; Cl, 8.83. Found: C, 31.13; H, 4.02; Cl, 8.97.

The above dimercurial also formed an alcoholate on crystallization from ethyl alcohol, m.p. 100–150 °C, the i.r. spectrum (Nujol) showing strong hydroxyl absorption at 3625 and 3400 cm^{-1}. A satisfactory analysis for this compound was not obtained.

Work-up of the mother liquors by hexane extraction yielded about 40% unchanged starting material (i.r., n.m.r., and t.l.c.).

(b) Two Equivalents of Mercuric Salt

When the above oxymercuration was repeated with two equivalents of mercuric nitrate or acetate, the yield of crude chloromercurial was 90%.

Reduction of Chloromercurial Obtained from Methyl Pimarate

(a) With Sodium Borohydride

To 107 mg (0.133 mmole) of the above mercurial dissolved in absolute ethyl alcohol (5 ml) and tetrahydrofuran (5 ml) at 0 °C was added portionwise sodium

Can. J. Chem. Downloaded from www.nrcresearchpress.com by 210.87.254.6 on 09/05/12
For personal use only.

borohydride (26 mg) when a vigorous reaction occurred depositing metallic mercury. The solution was left overnight and then filtered and acidified. Extraction with methylene chloride and subsequent work-up yielded 45 mg (90%) of methyl pimarate (i.r., n.m.r., and comparative t.l.c.).

(b) In Basic Dioxane

To a solution of 0.590 g (0.734 mmole) of mercurial dissolved in dioxane (40 ml) and 10% KOH solution (10 ml) was added portionwise solid sodium borohydride (100 mg) at room temperature. After 12 h the mercury was filtered off and the filtrate acidified and extracted with ether. Work-up of the ethereal extracts afforded 232 mg (95%) of a greasy solid. Crystallization from methanol gave colorless needles, m.p. 130–132 °C of ether **4**, $[\alpha]_D$ −18.6°; i.r.: ν_{max}(Nujol) 1723 (ester) 1250, 915, and 835 cm^{-1} (ether) and no hydroxyl absorption; n.m.r.: 3.76, 1H A_3X quartet $J_{AX} = 6$ Hz (C-15 methine) 3.7, s, (methoxyl) and a new methyl doublet centered at 2.2, $J = 6$ Hz in addition to the angular methyls at 1.2, 1.04, and 0.87 δ.

Anal. Calcd. for $C_{21}H_{34}O_3$: C, 75.41; H, 10.25. Found: C, 75.34; H, 10.00.

Oxymercuration of Methyl Sandaracopimarate 2b

To a solution of 200 mg (0.634 mmole) of methyl sandaracopimarate in 6 ml *tert*-butyl alcohol (peroxide-free) was added a solution of 218 mg (0.637 mmole) mercuric nitrate monohydrate and 1 drop of concentrated nitric acid in 12 ml water. The solution cleared immediately on swirling and after standing for 30 min, the reaction mixture was poured into 75 ml water containing a small excess of sodium chloride. The white precipitate so formed was filtered (391 mg), m.p. 151–159 °C. Recrystallization from methanol raised this to 164–165 °C; i.r.: ν_{max}(Nujol) 3420 broad, (hydroxyl), 1725 cm^{-1} (ester); n.m.r.: 5.5 (1H, s), 5.35 (1H, s, C-14 olefinic protons), 4.0 (1H broadened triplet, C-15 methine), 3.65 (3H, s, methoxyl), 1.2, 1.05, and 0.81 δ (3 × 3H, s, angular methyl groups), but no vinyl protons.

Anal. Calcd. for $C_{21}H_{33}O_3HgCl$: C, 44.29; H, 5.80. Found: C, 44.39; H, 5.88.

Reduction of Chloromercurial 6 Obtained from Methyl Sandaracopimarate

(a) With Sodium Borohydride

To a solution of 159 mg (0.266 mmole) of the above chloromercurial in 10 ml tetrahydrofuran at 0 °C was added portionwise, sodium borohydride (20 mg). The reaction mixture turned gray immediately. After 1 h, more reducing agent was added but no further reaction was observed. The mercury was filtered off and the clear filtrate acidified (2 *N* HCl). Ether extraction and subsequent work-up afforded methyl sandaracopimarate (76 mg, 86%) (i.r., n.m.r., and comparative t.l.c.).

(b) With Sodium Borohydride in Basic Dioxane

To a solution of 650 mg (1.14 mmole) of chloromercurial 6 in 40 ml dioxane and 10 ml 10% sodium hydroxide, were added portionwise ca. 200 mg solid sodium borohydride. The reaction was extremely slow (2–4 days) compared to the non-basic reduction. After filtration of the metallic mercury the filtrate was acidified and ether extracted. Work-up gave 300 mg (79%) of a greasy solid showing three compounds by t.l.c. analysis, two polar spots very close together (diastereomeric alcohols), and some methyl sandaracopimarate, i.r. ($CHCl_3$) 3400 cm^{-1} broad (hydroxyl), and 1725 cm^{-1} (ester). Chromatography on silica gel separated the methyl sandaracopimarate but no separation of the alcohols was obtained. This material crystallized slowly from aqueous methanol to give a low melting solid which was oxidized with Jones' reagent (14). The product (250 mg) **8** after ether extraction showed no hydroxyl in the i.r., (film from ether solution), a new carbonyl peak at 1710 cm^{-1}, and ester absorption at 1725 cm^{-1}. An analytical sample was obtained, by sublimation (90°/10^{-3} mm), m.p. 73–75°, $[\alpha]_D$ −18.4°.

Anal. Calcd. for $C_{21}H_{32}O_3$: C, 75.86; H, 9.70. Found: C, 75.77; H, 9.62.

An iodoform reaction on 144 mg (15) was positive. This confirmed the presence of an acyl group. Extraction of the acidified reaction mixture after this test gave 80 mg (53%) of an acid: i.r.: ν_{max} (Nujol) 3400 broad, 1700 cm^{-1} (acid), and 1725 cm^{-1} (ester). Treatment of this oil with diazomethane gave diester 9, m.p. 71 °C, a mixture m.p. with the authentic sample (1) was not depressed, i.r., t.l.c. were identical.

Acknowledgments

We thank the National Research Council of Canada for continued generous financial support. J. W. ApSimon expresses his appreciation to the Administrators of the C. D. Howe Memorial Foundation for the award of a Fellowship during the tenure of which this manuscript was written; he also thanks Professor G. Ourisson, Institut de Chimie, Strasbourg, for his hospitality during this time. H. Krehm expresses his thanks to the British American Oil Research and Development Company, Sheridan Park, Ontario, for the use of instrumental and laboratory facilities during the final phases of this work.

1. J. W. ApSimon, A. S. Y. Chau, W. G. Craig, and H. Krehm. Can. J. Chem. **45**, 1439 (1967).
2. J. W. ApSimon and H. Krehm. Can. J. Chem. This issue.
3. O. E. Edwards and R. S. Rosich. Private communication.
4. J. W. ApSimon and H. Krehm. Unpublished observations.
5. E. E. Van Tamelen, A. Storni, E. J. Hessler, and M. Schwartz. J. Am. Chem. Soc. **85**, 3295 (1963); J. Fried and E. F. Sabo. J. Am. Chem. Soc. **75**, 2273 (1953); **76**, 1455 (1954).
6. W. Kitching. Organometal. Chem. Rev. **3**, 61 (1968); J. Chatt. Chem. Rev. **48**, 1 (1951); N. S. Zefitov. Russ. Chem. Rev. (English Transl.), **34**, 527 (1965).
7. F. G. Bordwell and M. L. Douglass. J. Am. Chem. Soc. **88**, 993 (1966).
8. N. S. Bhacca and D. H. Williams. Applications of nuclear magnetic resonance spectroscopy in or-

ganic chemistry. Holden-Day Inc., San Francisco. 1964. p. 115.
9. H. J. LUCAS, F. R. HEPNER, and S. WINSTEIN. J. Am. Chem. Soc. **61**, 3102 (1939) but cf. J. HALPERN and H. B. TINKER. J. Am. Chem. Soc. **89**, 6427 (1967).
10. S. WOLFE and P. G. C. CAMPBELL. Can. J. Chem. **43**, 1184 (1965).
11. H. C. BROWN and P. GEOGHEGAN, JR. J. Am. Chem. Soc. **89**, 1522 (1967), also ref. 8 therein.
12. J. H. ROBSON and G. F. WRIGHT. Can. J. Chem. **38**, 21 (1960); T. G. TRAYLOR and A. W. BAKER. J. Am. Chem. Soc. **85**, 2746 (1963).
13. H. KREHM. M.A. Thesis, University of Toronto, Toronto 5, Ontario. 1962.
14. L. F. FIESER and M. FIESER. Reagents for organic synthesis. John Wiley and Sons, Inc., New York. 1967. p. 142.
15. A. I. VOGEL. A text-book of practical organic chemistry. Longmans, Green and Co., Ltd., London. 1954. p. 930.
16. H. B. HENBEST and B. NICHOLLS. J. Chem. Soc. 227 (1959).
17. J. M. COXON, M. P. HARTSHORN, J. W. MITCHELL, and K. E. RICHARDS. Chem. Ind. London, 652 (1968); H. STRETTER, H. J. MEISSNER, and W. D. LAST. Chem. Ber. **101**, 2889 (1968); J. S. MILLS. J. Chem. Soc. C, 2514 (1967).

Can. J. Chem. Downloaded from www.nrcresearchpress.com by 210.87.254.6 on 09/05/12
For personal use only.

Can. J. Chem. Downloaded from www.nrcresearchpress.com by 210.87.254.105 on 09/05/12
For personal use only.

Synthesis of 8-deoxy-D-*erythro*-D-*galacto*-octose. Determination of the configuration of two octenoses

D. G. LANCE, W. A. SZAREK, J. K. N. JONES, AND G. B. HOWARTH
Department of Chemistry, Queen's University, Kingston, Ontario

Received March 3, 1969

The preparation of 8-deoxy-1,2:3,4-di-*O*-isopropylidene-D-*erythro*-α-D-*galacto*-octopyranose (**2**) from two octenoses is described. The structure of **2** was established by degradation of its di-*O*-methyl derivative to 1-deoxy-2,3-di-*O*-methyl-L-erythritol. This work permits the assignment of configuration to the octenoses. Acid-catalyzed hydrolysis of **2** gave a new higher-carbon sugar, 8-deoxy-D-*erythro*-D-*galacto*-octose (**4**). The synthesis of 1-deoxy-2,3-di-*O*-methyl-L-threitol and 1-deoxy-2,3-di-*O*-methyl-D-erythritol is reported.

Canadian Journal of Chemistry, 47, 2871 (1969)

Introduction

In a recent publication (1) the preparation of 6,7,8-trideoxy-1,2:3,4-di-*O*-isopropylidene-α-D-*galacto*-oct-6-enose (**1**) by the reaction of ethylidenetriphenylphosphorane with 1,2:3,4-di-*O*-isopropylidene-α-D-*galacto*-hexodialdo-1,5-pyranose was reported. At that time the configuration of the double bond had not been established. Compound **1** is of particular interest to us since it may be suitable for conversion, by way of a pseudohalogen addition reaction (2), to the carbohydrate moiety in the antibiotic lincomycin (3, 4). In the present paper we describe some experiments which permit the assignment of the *cis* stereochemistry to compound **1**. This work has led also to the synthesis of a new higher-carbon sugar, 8-deoxy-D-*erythro*-D-*galacto*-octose (**4**).

During the course of our synthetic studies related to lincomycin (4), vinylmagnesium bromide was added to 1,2:3,4-di-*O*-isopropylidene-α-D-*galacto*-hexodialdo-1,5-pyranose to give a mixture of allylic alcohols. The preponderant epimer was obtained pure in crystalline form. It has now been established that this compound is 7,8-dideoxy-1,2:3,4-di-*O*-isopropylidene-D-*glycero*-α-D-*galacto*-oct-7-enopyranose (**3**).

Results and Discussion

Treatment of the crude Wittig product (1), from the reaction of ethylidenetriphenylphosphorane with 1,2:3,4-di-*O*-isopropylidene-α-D-*galacto*-hexodialdo-1,5-pyranose, with aqueous potassium permanganate gave predominantly a crystalline *vic*-diol. The structure of 8-deoxy-1,2:3,4-di-*O*-isopropylidene-D-*erythro*-α-D-*galacto*-octopyranose (**2**) has been assigned to this dihydroxylation product as follows.

Methylation of the crystalline diol gave the di-*O*-methyl derivative, which was obtained as a chromatographically homogeneous and analytically pure syrup. This compound was degraded by removal of the isopropylidene residues with acid, followed by oxidation of the product with sodium metaperiodate. Reduction of the resultant aldehyde with sodium borohydride gave a 1-deoxy-2,3-di-*O*-methyltetritol. The nuclear magnetic resonance (n.m.r.) spectrum of this tetritol was identical with that of authentic 1-deoxy-2,3-di-*O*-methyl-D-erythritol (Fig. 1), and the two compounds were indistinguishable by gas–liquid chromatography (g.l.c.). A comparison of specific rotations (Table I) shows that the two compounds are enantiomers. Thus, the isolation of 1-deoxy-2,3-di-*O*-methyl-L-erythritol establishes the D-*erythro* configuration at C-7 and C-6 in the crystalline diol. Moreover, this work permits the assignment of the *cis* stereochemistry to the predominant octenose (**1**) formed in the Wittig reaction (1), since it is well-known that in the dihydroxylation of alkenes by

TABLE I

Retention times (*T*) and specific rotations of tetritol derivatives*

Compound	*T*	$[\alpha]_D$	$[\alpha]_{546}$
1-Deoxy-2,3-di-*O*-methyl-L-threitol	3.69	−10.7	−12.7
1-Deoxy-2,3-di-*O*-methyl-D-erythritol	3.50	+18.3	+21.4
Degradation product	3.50	−21.5	−23.9

*See Experimental for details. Retention times given here are relative to 2-methoxyethanol (1.00).

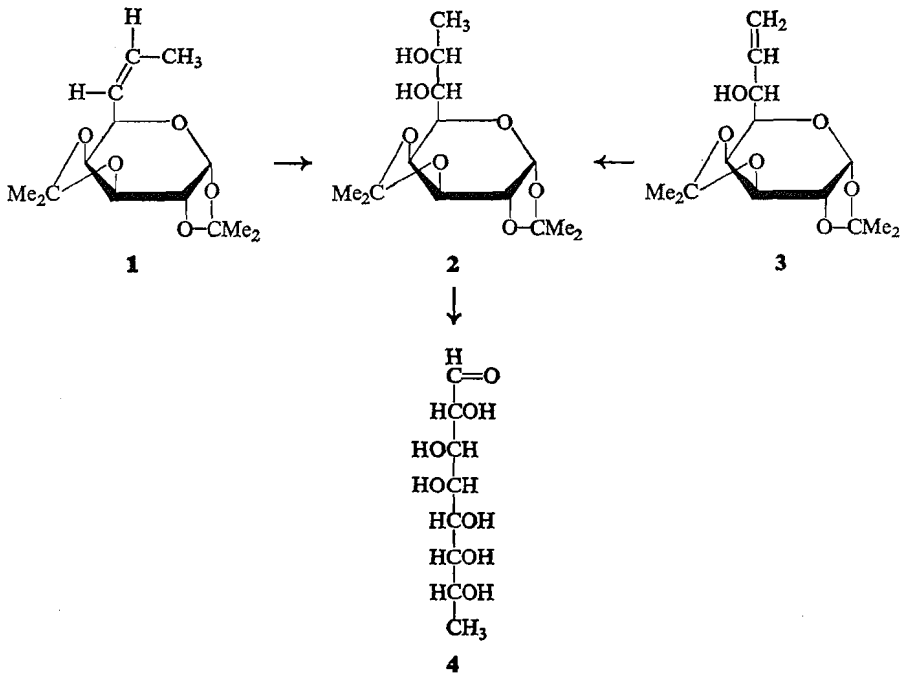

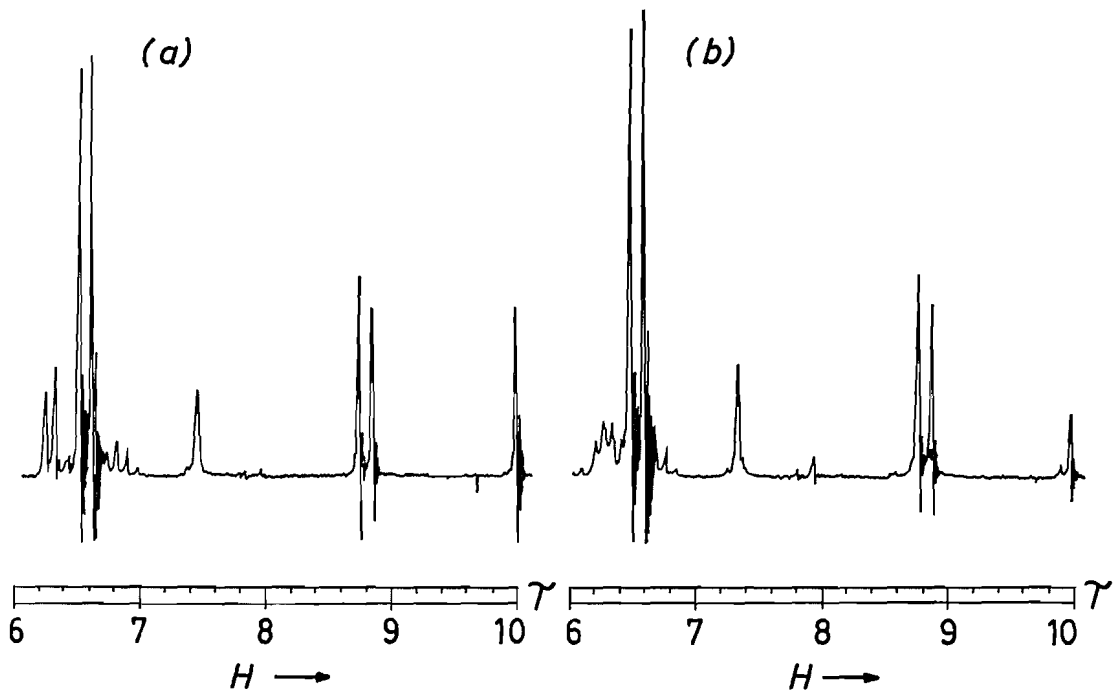

FIG. 1. (*a*) Nuclear magnetic resonance spectrum of 1-deoxy-2,3-di-*O*-methyl-D-erythritol. (*b*) Nuclear magnetic resonance spectrum of 1-deoxy-2,3-di-*O*-methyl-L-threitol.

Can. J. Chem. Downloaded from www.nrcresearchpress.com by 210.87.254.105 on 09/05/12
For personal use only.

Can. J. Chem. Downloaded from www.nrcresearchpress.com by 210.87.254.105 on 09/05/12
For personal use only.

permanganate, the mode of addition of the hydroxyl groups is *cis*.

The synthesis of 8-deoxy-1,2:3,4-di-*O*-isopropylidene-D-*erythro*-α-D-*galacto*-octopyranose (**2**) has been achieved also from the preponderant allylic alcohol obtained by the addition of vinylmagnesium bromide to 1,2:3,4-di-*O*-isopropylidene-α-D-*galacto*-hexodialdo-1,5-pyranose (4). Compound **2** was obtained by the Markovnikov hydration of the carbon–carbon double bond using the oxymercuration–demercuration procedure of Brown and Geoghegan (5). This result establishes the D-*glycero* configuration at C-6 in the octenose; the compound is, therefore, 7,8-dideoxy-1,2:3,4-di-*O*-isopropylidene-D-*glycero*-α-D-*galacto*-oct-7-enopyranose (**3**).

Acid-catalyzed hydrolysis of compound **2** gave, in crystalline form, a new higher-carbon sugar, 8-deoxy-D-*erythro*-D-*galacto*-octose (**4**), which to our knowledge is the first example of an 8-deoxyoctose.

For the degradative work described above, authentic samples of 1-deoxy-2,3-di-*O*-methylerythritol and -threitol were required. These were readily prepared as follows. 1-Deoxy-2,3-di-*O*-methyl-L-threitol was obtained from 2,3-di-*O*-methyl-D-xylose diethyl dithioacetal (6) by its desulfurization with Raney nickel followed by oxidation of the product with sodium metaperiodate and reduction of the resultant aldehyde with sodium borohydride. A homogeneous liquid was isolated by preparative g.l.c. 1-Deoxy-2,3-di-*O*-methyl-D-erythritol was prepared similarly from 1-deoxy-2,3-di-*O*-methyl-D-ribitol (7). The n.m.r. spectra of the two tetritol derivatives are shown in Fig. 1, and some physical data are given in Table I.

Experimental

Melting points were determined on a Fisher–Johns melting point apparatus and are uncorrected. Optical rotations were measured with a Perkin–Elmer Model 141 automatic polarimeter at 29°. Thin-layer chromatography (t.l.c.) was performed with Silica Gel G as the adsorbent. The term "petroleum ether" refers to the fraction of b.p. 60–80°. Paper chromatography was carried out by the descending method at room temperature on Whatman No. 1 filter paper in butan-1-ol:ethanol:water, 3:1:1 (v/v). Sugars were detected on paper chromatograms by the *p*-anisidine hydrochloride spray reagent (8); rates of movement of the sugars are given relative to that of glucose (R_{glu}). Gas–liquid chromatography (F and M chromatograph, Model 402) was carried out at a carrier gas (helium) flow rate of ca. 75 ml/min on a column of 20% octylphenoxypoly(oxyethylene)ethanol supported on 100–120 mesh acid washed Chromosorb W at 175°. The chromatograph was adapted for preparative separations as described previously (9), using a column of 1% (w/w) Apiezon L supported on 50–60 mesh DMCS treated Chromosorb W at 120°. Nuclear magnetic resonance spectra were measured on a Varian T-60 spectrometer in chloroform-*d* and tetramethylsilane as internal standard. Infrared (i.r.) spectra were measured on a Beckman-IR5A spectrophotometer.

*8-Deoxy-1,2:3,4-di-O-isopropylidene-*D*-erythro-α-*D*-galacto-octopyranose (2)*

*(a) From 6,7,8-Trideoxy-1,2:3,4-di-O-isopropylidene-α-*D*-galacto-oct-6-enose (1)*

To a solution in ethanol (20 ml) of the crude Wittig product (2.0 g) (1), from the reaction of ethylidenetriphenylphosphorane with 1,2:3,4-di-*O*-isopropylidene-α-D-*galacto*-hexodialdo-1,5-pyranose, was added a solution of potassium permanganate (1.5 g) in water (45 ml) dropwise, with stirring, over a period of 30 min. The mixture was then filtered through Celite; the residue was washed with hot ethanol. The colorless filtrate and washings were concentrated to dryness, and the residue was extracted with several portions of hot ethyl acetate. The dried (magnesium sulfate) extracts were concentrated under reduced pressure to a residue, which was crystallized from chloroform – petroleum ether; yield 1.40 g. Compound **2** was obtained pure by sublimation at 130°/0.1 Torr; m.p. 151–152°, $[\alpha]_D$ −57° (*c*, 1.4 in chloroform); λ_{max}(KBr) 2.85 (OH), 7.20, 7.25 μm (CMe_2); n.m.r. data: τ 4.53 (1-proton doublet, $J_{1,2}$ = 5 Hz, H-1), τ 8.50, 8.56, 8.67, 8.72 (3-proton singlets, CMe_2), τ 8.80 (3-proton doublet, J = 6 Hz, C-7 Me).

Anal. Calcd. for $C_{14}H_{24}O_7$: C, 55.2; H, 7.9. Found: C, 55.5; H, 7.8.

Thin-layer chromatographic examination (3:2 ethyl acetate – petroleum ether) of the mother liquors above showed the presence of a component with the same mobility as **2** and material which moved very close to the base line. The faster-moving component was separated by column chromatography on silica gel; it then yielded a small amount of crystalline **2** from chloroform – petroleum ether. Removal of the solvent gave a syrup (0.12 g) which could not be induced to crystallize.

*(b) From 7,8-Dideoxy-1,2:3,4-di-O-isopropylidene-*D*-glycero-α-*D*-galacto-oct-7-enopyranose (3)*

Compound **3** (0.286 g) was added with stirring to a mixture of mercuric acetate (0.319 g) in water (1 ml) and tetrahydrofuran (1 ml). The reaction mixture was stirred for 15 min at room temperature, and then 3 *M* sodium hydroxide (1 ml) followed by a solution of 0.5 *M* sodium borohydride in 3 *M* sodium hydroxide (1 ml) were added. The mercury was allowed to settle, and the supernatant liquid was separated and extracted with chloroform. The extracts were washed with water, dried over magnesium sulfate, and concentrated to a syrup. Thin-layer chromatographic examination (ethyl acetate) showed the presence of two new components, R_f 0.89 and 0.61, and a small amount of starting material, R_f 1.0. The major component (R_f 0.89) was obtained pure by fractional crystallization from ether – petroleum ether as fine needles (0.105 g, 42%), whose physical constants were in agreement with those obtained for compound **2** above.

8-Deoxy-D-erythro-D-galacto-octose (4)

A solution of compound **2** (0.25 g) in 1 *M* sulfuric acid (10 ml) was heated at 100° for 5 h. It was then passed through a column of Duolite A-4 (OH form) anion exchange resin and concentrated to a syrup, which was crystallized from ethanol. Compound 4 was obtained pure on further recrystallization from ethanol; yield 0.126 g, m.p. 118–122°; $[\alpha]_D$ +58.4 ± 0.5° (45 min), +57.4 ± 0.5° (final) (*c*, 2.1 in water); R_{glu} 0.87 (yellow-brown spot with *p*-anisidine hydrochloride spray reagent).

Anal. Calcd. for $C_8H_{16}O_7$: C, 42.9; H, 7.2. Found: C, 42.9; H, 7.3.

8-Deoxy-1,2:3,4-di-O-isopropylidene-6,7-di-O-methyl-D-erythro-α-D-galacto-octopyranose

To solution of compound **2** (0.50 g) in tetrahydrofuran (25 ml) containing powdered sodium hydroxide (5.0 g) was added dimethyl sulfate (5.0 ml) with stirring and over a period of 3 h. More sodium hydroxide (5.0 g) was then added, and the mixture was heated at reflux temperature while dimethyl sulfate (5.0 ml) was added over a period of 1 h. The excess of dimethyl sulfate was destroyed with aqueous ammonia solution, and the product was isolated as a syrup, which was chromatographed on silica gel, with 2:3 ethyl acetate – petroleum ether as eluent. The dimethyl ether was obtained as a syrup (0.40 g), $[\alpha]_D$ −60.5 ± 1° (*c*, 1.0 in ethyl acetate); n.m.r. data: τ 4.53 (1-proton doublet, $J_{1,2}$ = 5 Hz, H-1), τ 6.47, 6.64 (3-proton singlets, OMe), τ 8.50, 8.53, 8.63, 8.69 (3-proton singlets, CMe_2), τ 8.87 (3-proton doublet, J = 7 Hz, C-7 Me).

Anal. Calcd. for $C_{16}H_{28}O_7$: C, 57.8; H, 8.5. Found: C, 57.7; H, 8.7.

Degradation of 8-Deoxy-1,2:3,4-di-O-isopropylidene-6,7-di-O-methyl-D-erythro-α-D-galacto-octopyranose to 1-Deoxy-2,3-di-O-methyl-L-erythritol

A solution of 8-deoxy-1,2:3,4-di-*O*-isopropylidene-6,7-di-*O*-methyl-D-*erythro*-α-D-*galacto*-octopyranose (0.39 g) in methanol (20 ml) containing 2 *M* hydrochloric acid (6 ml) was boiled under reflux for 1.5 h, and then concentrated to dryness under reduced pressure. The syrup (R_{glu} 3.7) was dissolved in 0.1 *M* hydrochloric acid (5 ml) and stirred for 9 h with sodium metaperiodate (1.6 g). The solution was extracted with chloroform (4 × 3 ml), and the combined extracts were stirred vigorously with a solution of sodium borohydride (0.05 g) in water (1 ml) for 15 min. The aqueous phase was extracted with chloroform (2 × 2 ml). Since g.l.c. examination of the combined chloroform solutions showed the presence of only a small amount of a component with *T* 3.5 (Table I), they were then concentrated to a syrup, which was dissolved in 2 *M* hydrochloric acid (5 ml), and heated at 100° for 1 h. The acid was neutralized with an excess of sodium carbonate, and the solution was treated with sodium metaperiodate (0.70 g) for 0.5 h. The solution was extracted with chloroform, and the extracts were treated with sodium borohydride as before. 1-Deoxy-2,3-di-*O*-methyl-L-erythritol was isolated as a homogeneous liquid (25 mg) by preparative g.l.c. Its n.m.r. spectrum was identical with that of 1-deoxy-2,3-di-*O*-methyl-D-erythritol (Fig. 1); specific rotations (±1.3°) (*c*, 1.1 in ethyl acetate) are given in Table I.

1-Deoxy-2,3-di-O-methyl-L-threitol and 1-Deoxy-2,3-di-O-methyl-D-erythritol

A solution of 2,3-di-*O*-methyl-D-xylose diethyl dithioacetal (6) (1.75 g) in ethanol was heated in the presence of freshly prepared Raney nickel (10) (6 g) for 8 h at reflux temperature. The product was treated with sodium metaperiodate and then with sodium borohydride as described above. 1-Deoxy-2,3-di-*O*-methyl-L-threitol was isolated as a homogeneous liquid (45 mg) by preparative g.l.c. 1-Deoxy-2,3-di-*O*-methyl-D-erythritol was prepared similarly from 1-deoxy-2,3-di-*O*-methyl-D-ribitol (7). The n.m.r. spectra of the two tetritol derivatives are shown in Fig. 1, and retention times and specific rotations (±1.0°) (*c*, 1.3 and 1.6 in ethyl acetate, respectively) are given in Table I.

Acknowledgments

The authors thank the National Research Council of Canada and the Department of University Affairs in the Province of Ontario for financial support of this research.

1. D. G. LANCE and W. A. SZAREK. Carbohyd. Res. To be published.
2. W. A. SZAREK, D. G. LANCE, and R. L. BEACH. Chem. Commun. 356 (1968).
3. W. SCHROEDER, B. BANNISTER, and H. HOEKSEMA. J. Am. Chem. Soc. **89**, 2448 (1967).
4. G. B. HOWARTH, D. G. LANCE, W. A. SZAREK, and J. K. N. JONES. Can. J. Chem. **47**, 75 (1969).
5. H. C. BROWN and P. GEOGHEGAN, JR. J. Am. Chem. Soc. **89**, 1522 (1967).
6. D. G. LANCE and J. K. N. JONES. Can. J. Chem. **45**, 1533 (1967).
7. D. G. LANCE, W. A. SZAREK, and J. K. N. JONES. Can. J. Chem. **47**, 2889 (1969).
8. L. HOUGH, J. K. N. JONES, and W. H. WADMAN. J. Chem. Soc. 1702 (1950).
9. D. G. LANCE and G. B. HOWARTH. Lab. Pract. **17**, 1351 (1968).
10. A. I. VOGEL. Textbook of practical organic chemistry. Longmans, Green and Co., Inc., New York. 1951.

Can. J. Chem. Downloaded from www.nrcresearchpress.com by 210.87.254.105 on 09/05/12
For personal use only.

Can. J. Chem. Downloaded from www.nrcresearchpress.com by 210.87.254.105 on 09/05/12
For personal use only.

α,β-Epoxy sulfones. The Darzens condensation with α-halosulfones[1]

PETER F. VOGT[2] AND DONALD F. TAVARES
Department of Chemistry, University of Calgary, Calgary, Alberta

Received June 3, 1968

Darzens type condensation of chloromethyl *p*-tolyl sulfone with benzaldehyde, acetaldehyde, acetone, benzophenone, and cyclohexanone, with potassium *tert*-butoxide as base, gave good to excellent yields of the corresponding α,β-epoxy sulfones (**1**). The condensation of α-chloroethyl *p*-tolyl sulfone and bromomethyl *p*-tolyl sulfone with benzaldehyde also gave excellent yields. With the aldehydes only the *trans*-epoxides were formed, which is shown by nuclear magnetic resonance spectroscopy. The mechanism and stereochemistry are discussed.

Canadian Journal of Chemistry, 47, 2875 (1969)

The preparation and reactions of α,β-unsaturated sulfones have commanded much attention in the last 15 years (1). The behavior of saturated sulfones as they compare with ketones has also been investigated and it has been found that the hydrogen adjacent to the sulfonyl group is very acidic (2). This has led to the use of sulfones in many aldol-type condensations.

However, to this date, there have been no reports in the literature on the epoxidation of α,β-unsaturated sulfones, or on other methods for the preparation of α,β-epoxy sulfones, except that of Ballester (3), who mentioned in a review article that he had obtained an α,β-epoxy sulfone by a Darzens type condensation of benzaldehyde with chloromethyl *p*-tolyl sulfone. No further details have ever been published. The only epoxy sulfones described, so far then, are the β,γ-epoxy sulfones (4).

The aim of the present study was the synthesis of α,β-epoxy sulfones of the following type

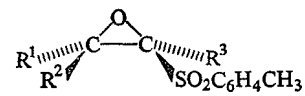

1

R^1: CH_3, C_6H_5, $-(CH_2)_5-$; R^2: H, CH_3, C_6H_5, $-(CH_2)_5-$; R^3: H, CH_3

From the great variety of conditions employed in the Darzens condensation, it has been shown that the use of potassium *tert*-butoxide as base resulted in excellent yields (5). In this investigation, therefore, potassium *tert*-butoxide was chosen as the condensing base, in a method similar to that described by Hunt *et al.* (6) and Johnson *et al.* (5).

When a solution of potassium *tert*-butoxide in *tert*-butyl alcohol was added slowly to a solution of chloromethyl *p*-tolyl sulfone (**2**) and benzaldehyde in *tert*-butyl alcohol – ether mixture (2:1, v/v) at 10–15°, the epoxide was formed in 95% yield (eq. [1]).

$$CH_3C_6H_4SO_2CH_2Cl + C_6H_5CHO + t\text{-BuOK} \xrightarrow[10\text{–}15^\circ]{t\text{-BuOH}}$$

2

[1]

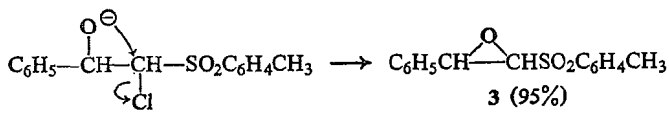

3 (95%)

The anhydrous ether in the solvent was used to prevent crystallization of the *tert*-butyl alcohol when the reaction mixture was cooled.

Besides benzaldehyde, acetaldehyde, benzophenone, acetone, and cyclohexanone also gave good to excellent yields of the corresponding epoxide (Table I).

The lower yield using acetaldehyde agrees with the observation of previous workers in the Darzens condensation using aliphatic aldehydes. The obvious explanation is that the aldehyde undergoes aldol condensation more readily than

[1]Taken from the Ph.D. thesis of P. F. Vogt.
[2]Present address: GAF (Canada) Ltd., 2403 Stanfield Rd., Cooksville, Ontario.

TABLE I

α,β-Epoxy sulfones prepared by Darzens condensation

Experiment	α-Halosulfone	Carbonyl compound	Epoxy sulfone (yield)*		Melting point
1	$CH_3C_6H_4SO_2CH_2Cl$	C_6H_5CHO	**3**	(95%)	157–159° dec.
2	$CH_3C_6H_4SO_2CH_2Cl$	C_6H_5CHO	**3**	(20%)†	157–159° dec.
3	$CH_3C_6H_4SO_2CH_2Cl$	CH_3CHO	**4**	(53%)	83–84°
4	$CH_3C_6H_4SO_2CH_2Cl$	CH_3COCH_3	**5**	(80%)	93.5–94°
5	$CH_3C_6H_4SO_2CH_2Cl$	$C_6H_5COC_6H_5$	**6**	(57%)	106–107°
6	$CH_3C_6H_4SO_2CH_2Cl$	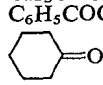	**7**	(77%)	54–55°
8	$CH_3C_6H_4SO_2CHClCH_3$	C_6H_5CHO	**8**	(92%)	113–115° dec.
9	$CH_3C_6H_4SO_2CH_2Br$	C_6H_5CHO	**3**	(91%)	157–159° dec.
10	$CH_3C_6H_4SO_2CH_2Br$	CH_3COCH_3	**5**	(77%)	93.5–94°

*Using potassium *tert*-butoxide as base.
†Using sodium methoxide as base.

the Darzens condensation reaction, as shown by Field and Carlile (7). The lower yield using benzophenone might be explained by steric hindrance, and therefore a slower reaction.

However, the reaction of acetophenone with **2** resulted only in the isolation of a white crystalline product which was shown to be 2-phenyl-2-(*p*-tolylsulfonyl)propanal (**9**). The formation of this aldehyde is suggested by a rearrangement of the intermediate epoxide[3] (eq. [2])

$$CH_3C_6H_4SO_2CH_2Cl + CH_3COC_6H_5 + t\text{-BuOK} \xrightarrow[10\text{-}15°]{t\text{-BuOH}}$$

[2]

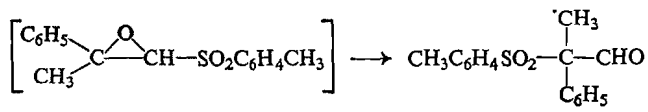

9

Besides chloromethyl *p*-tolyl sulfone, α-chloroethyl *p*-tolyl sulfone (**10**) also gave satisfactory reaction with benzaldehyde, the epoxide **8** being isolated in excellent yield (eq. [3])

$$CH_3C_6H_4SO_2\underset{\displaystyle Cl}{\underset{|}{C}}HCH_3 + C_6H_5CHO + t\text{-BuOK} \xrightarrow[10\text{-}15°]{t\text{-BuOH}}$$

10

[3]

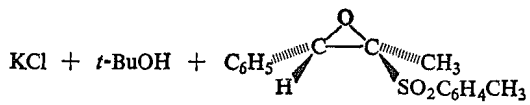

8 (92%)

The Ramberg–Baecklund rearrangement (8), with the formation of an episulfone and subsequent decomposition to the olefin by the action of base, imposes a limitation in the use of other α-chlorosulfones. Therefore, only α-halosulfones of the general formula can be used, where R^1 is bonded to the sulfonyl group with a carbon atom which bears no hydrogen.

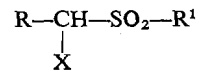

R.... H, alkyl, aryl

R^1... phenyl, aryl or *tert*-alkyl

[3]W. E. Truce (private communication) reports the formation of *p*-nitrophenacyl phenyl sulfone by treatment of *p*-nitrobenzaldehyde and chloromethyl phenyl sulfone with sodium ethoxide, also implying the formation of an epoxy sulfone as an intermediate.

Can. J. Chem. Downloaded from www.nrcresearchpress.com by 210.87.254.105 on 09/05/12
For personal use only.

Can. J. Chem. Downloaded from www.nrcresearchpress.com by 210.87.254.105 on 09/05/12
For personal use only.

An attempt to use sodium methoxide in methanol as the condensing agent in the reaction of **2** and benzaldehyde gave only 20% of epoxide **3**, the halosulfone being recovered in 80% yield.

Although the yields from α-bromocarbonyl compounds are not as high as those from α-chlorocarbonyl compounds in the Darzens condensation, due mostly to the competing alkylation reaction (9), the use of α-bromosulfones such as bromomethyl *p*-tolyl sulfone (**11**), gave in the reaction with benzaldehyde and acetone, the same yields as the corresponding chlorosulfone (Table I).

In contrast to the known retarding effect of an α-sulfonyl group on an intermolecular S_N2 displacement of a halogen atom, the intramolecular S_N2 displacement is facile, and there is no sign of diminished reactivity. This might be explained by the fact that in an intramolecular S_N2 displacement the attacking nucleophile is already close to the reaction center, whereas the nucleophile in the intermolecular attack must overcome the repulsion of the negative charges on the oxygen atoms of the sulfonyl group to get as close. Thus, the difference between bromide and chloride as leaving groups appears to be insignificant.

Mechanism and Stereochemistry

The stereochemistry of the isolated epoxides was established by n.m.r. spectroscopy to be exclusively of the *trans* configuration; no *cis*-epoxide could be detected.

Lyle and Keefer (10) showed, in a series of *cis* and *trans* oxirane compounds, that the coupling constants of the protons for the *cis*-isomers were significantly larger than those of the isomeric *trans*-epoxides. For the coupling constants, they found a range of 2.2–5.2 Hz for the *cis* protons and 1.4–2.6 Hz for the *trans* protons.

Comparing these values for the coupling constants with the coupling constants of 1.5 and 2.0 Hz for epoxides **3** and **4**, respectively (Table II), it seems reasonable to propose that these epoxides are of the *trans* configuration.

A deuterium exchange experiment on **3**, with sodium methoxide in methanol-*d* (eq. [4]), shows that the α-hydrogen has a chemical shift of 5.86 τ while the β-hydrogen is at 5.48 τ, and not the reverse, as was first expected.

No epimerization was observed in this experiment and no other compound was found by either thin-layer chromatography or n.m.r. spectroscopy. Since the β-hydrogen in **12** has the same chemical shift as in **3**, it is in the same environment.

From the position of the epoxymethine protons in **3** it must be inferred that the β-hydrogen is in the paramagnetic region of the β-phenyl ring and therefore the phenyl ring is in a plane perpendicular to the plane of the epoxide ring; this is necessary to obtain any conjugation of the epoxide ring with the phenyl group.

In the case of 2,2-diphenyl-1-(*p*-tolylsulfonyl)-1,2-epoxyethane (**6**), the phenyl groups cannot be

TABLE II

Chemical shifts and coupling constants for the epoxide ring protons in α,β-epoxy sulfones*

	Compound			Chemical shift (τ)†		Coupling constant
	R^1	R^2	R^3	H_α	H_β	$J(H_\alpha, H_\beta)$ in Hz
3	C_6H_5	H	H	5.86	5.48	1.5
4	CH_3	H	H	6.14	6.38	2.0
5	CH_3	CH_3	H	6.22	—	—
6	C_6H_5	C_6H_5	H	5.60	—	—
7	$-(CH_2)_5-$		H	6.45	—	—
8	C_6H_5	H	CH_3	—	5.16	—
12	C_6H_5	H	D	—	5.48	—

*In $CDCl_3$ as 10% (w/w) solution.
†On the τ-scale with $(CH_3)_4Si$ as internal reference.

Compounds of structure 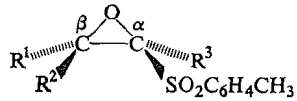

[4] 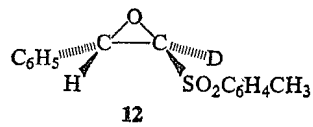

12

perpendicular to the plane of the epoxide ring, and are probably twisted (steric hindrance) so that the α-hydrogen of the epoxide ring is more in the paramagnetic region of the *cis*-β-phenyl ring. Therefore, the α-hydrogen exhibits a further downfield shift over that observed in epoxide **3** where it is more in the diamagnetic region. Reference (21) gives an interesting discussion concerning the difference in the chemical shift of *cis* and *trans* 1,2-diphenyl compounds.

The determination of the β-hydrogen in epoxide **4** was facilitated by its being split into a quartet by the adjacent methyl group.

Thus, the n.m.r. spectra are in good agreement with the proposed structures for the α,β-epoxy sulfones.

It is not unreasonable to suppose that the mechanism for the formation of α,β-epoxy sulfones might be the same as has been proposed for the general Darzens condensation (3, 11), with some differences caused by the sulfonyl group in the place of the carbonyl group (eqs. [5]–[7]).

[5] 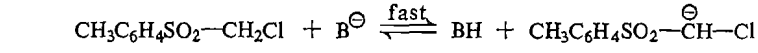

[6] 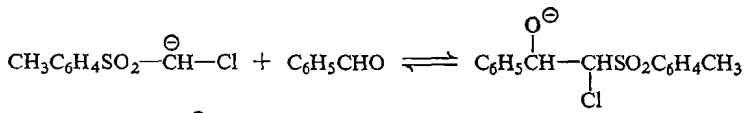

[7] 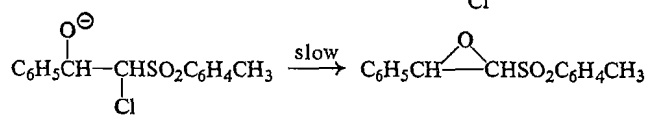

The initial nucleophilic attack upon the aldehyde or ketone is probably rapidly reversible, thus leading only to the preferred transition state, as otherwise two isomers should be found.

Since there is little or no angular dependence for effective π-overlap involving 3d orbitals, because of cylindrical symmetry of 3d atomic orbitals, rotation about a 3d–2p π-bond should not then result in diminished overlap (12). Therefore "overlap control," as proposed by Zimmerman and Ahramjian (13) in the Darzens condensation with carbonyl compounds, cannot be considered to have any significant influence on the stereochemistry of the cyclization step. For facile ring closure, however, steric effects are of more importance, and the energy of transition state **B** must be considerably higher than that of **A**.

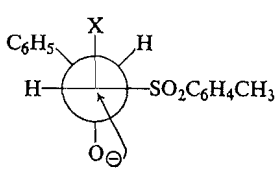

A

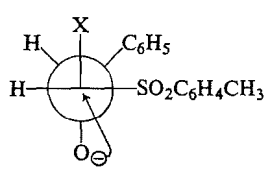

B

Also, solvation of the sulfonyl group with its negative charges on oxygen, should be an important factor which holds the oxygen in an outward position, pointing the *p*-tolyl group toward the *cis*-substituent on the other carbon atom. Thus, the preferred transition state would have the following structure

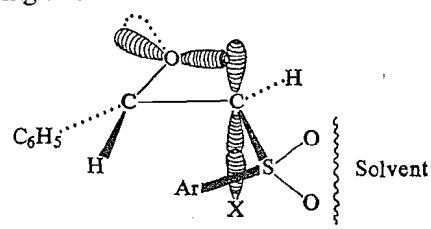

Considering that a wide variety of α-chlorosulfones can be prepared easily by the method of Boehme *et al.* (14), and also the fact that the α-bromosulfones give the same good yields, the Darzens condensation seems an excellent method for the preparation of α,β-epoxy sulfones in large quantities.

Experimental

All melting points were determined on a Kofler hot

Can. J. Chem. Downloaded from www.nrcresearchpress.com by 210.87.254.105 on 09/05/12
For personal use only.

Can. J. Chem. Downloaded from www.nrcresearchpress.com by 210.87.254.105 on 09/05/12
For personal use only.

stage and are corrected; infrared (i.r.) spectra were determined with a Perkin–Elmer model 337 spectrophotometer by the potassium bromide pellet method, unless otherwise indicated; n.m.r. spectra were measured at 60 MHz in deuteriochloroform (10–20%, by weight), with tetramethylsilane as internal standard ($\tau = 10$); microanalyses, except for sulfur, were performed by S. J. Bagley, University of Calgary; sulfur analyses were performed by C. Daesslé, Montreal.

Reagents

The benzaldehyde used was purified (15) and stored under nitrogen. Reagent-grade benzophenone from Fisher Scientific, m.p. 47.8–48.8°, reagent-grade acetophenone from British Drug Houses, m.p. 18–20°, spectrograde acetone from Matheson, Coleman, and Bell, reagent-grade acetaldehyde from British Drug Houses, and cyclohexanone from Eastman Kodak were used without further purification. Anhydrous ethyl ether was freshly distilled from lithium aluminum hydride.

General Procedure

In a 100 ml 3-necked flask, equipped with thermometer, addition funnel, drying tube (silica gel), and a magnetic stirrer, was placed a solution of 0.016 mole of an α-halosulfone and 0.016 mole of an aldehyde or ketone dissolved in a mixture of 30 ml of *tert*-butyl alcohol (reagent-grade from British Drug Houses, m.p. 24–25.5°) and 15 ml anhydrous ethyl ether. The resulting solution was cooled to 10° in a water bath. Then 1.80 g (0.016 mole) of potassium *tert*-butoxide (from K and K Laboratories), dissolved in 20 ml of *tert*-butyl alcohol, were added slowly so that the temperature did not exceed 15°. After all the base was added, the solution was allowed to warm to room temperature. After being stirred for 3 h, the reaction mixture was poured into 400 ml of water. The solids were separated by filtration and washed with water, and the liquids were extracted with ether. Purification of the crude products by recrystallization gave analytical samples.

Reactions of Chloromethyl p-Tolyl Sulfone (2)

Compound **2** was prepared by a method based on that of Ziegler and Connor (16). Sodium *p*-toluenesulfinate (17) (71.2 g, 0.4 mole) and bromochloromethane (104 g, 0.8 mole; from Eastman Kodak) were heated at reflux in 100 ml of ethanol for 7 days. The sodium bromide which had precipitated out was separated by filtration and the filtrate was evaporated at reduced pressure. Crude **2** was recrystallized from methanol to give 57.3 g (71%) of white crystals, m.p. 81–82° (lit. (18) m.p. 84°).

With Benzaldehyde. trans-2-Phenyl-1-(p-tolylsulfonyl)-1,2-epoxylethane (3)

From benzaldehyde (1.69 g, 0.016 mole) and compound **2** (2.75 g, 0.016 mole). Crude **3** was recrystallized from *n*-hexane – carbon tetrachloride to give 4.1 g (95%) of fine white needles, m.p. 157–159° (with decomposition). The i.r. spectrum showed epoxide ring absorption at 1228, 909, 790, and 828 cm^{-1}, epoxymethine absorption at 3010 cm^{-1}, and sulfonyl absorption at 1315 cm^{-1} (ν_{as}) and 1146 cm^{-1} (ν_s). The n.m.r. spectrum showed three methyl protons at 7.55 τ, one methinyl proton (doublet) at 5.86 τ (α-proton) with $J = 1.5$ Hz, one methinyl proton (doublet) at 5.48 τ (β-proton) with $J = 1.5$ Hz, five phenyl protons at 2.71 τ, and four aromatic protons at 2.52 and 2.16 τ with $J = 8.0$ Hz.

Anal. Calcd. for $C_{15}H_{14}O_3S$: C, 65.69; H, 5.14; S, 11.70. Found: C, 65.54; H, 5.16; S, 11.87.

With Benzaldehyde. Using Sodium Methoxide as Base to form 3

Using sodium methoxide (0.9 g, 0.016 mole) in methanol (20 ml) as the condensing base and methanol (30 ml) as solvent gave, after being stirred for 9 h, only 0.85 g (20%) of **3**, and 2.2 g (80%) of **2** was recovered unchanged.

With Acetaldehyde. trans-1-p-Tolylsulfonyl-1,2-epoxypropane (4)

From acetaldehyde (0.67 g, 0.016 mole) and compound **2** (2.75 g, 0.016 mole). Compound **4** was obtained as a yellow oil, which became solid on standing. Recrystallization from *n*-hexane – carbon tetrachloride gave 1.8 g (53%) of light-yellow crystals, m.p. 60–66°. Three further recrystallizations from *n*-hexane – carbon tetrachloride, using decolorizing charcoal in the last one, gave small white plates, m.p. 83–84°. The i.r. spectrum showed epoxide ring absorptions at 1226, 820, 803, and 828 cm^{-1}, epoxymethine absorption at 3020 cm^{-1}, and sulfonyl absorption at 1318 cm^{-1} (ν_{as}), and 1155 cm^{-1} (ν_s). The n.m.r. spectrum showed three methyl protons at 7.56 τ (CH_3Ar), three methyl protons (doublet) at 8.60 τ with $J = 5.2$ Hz, one methinyl proton (β-proton) at 6.38 τ, consisting of a quartet ($J = 5.2$ Hz) split into doublets ($J = 2.0$ Hz), one methinyl proton (doublet) at 6.14 τ (α-proton) with $J = 2.0$ Hz, and four aromatic protons at 2.65 and 2.33 τ with $J = 8.0$ Hz.

Anal. Calcd. for $C_{10}H_{12}O_3S$: C, 56.58; H, 5.70; S, 15.10. Found: C, 56.35; H, 5.85; S, 15.19.

With Acetone. 2-Methyl-1-(p-tolylsulfonyl)-1,2-epoxypropane (5)

From acetone (0.93 g, 0.016 mole) and **2** (2.75 g, 0.016 mole). Crude **5** was recrystallized from *n*-hexane – carbon tetrachloride to give 2.9 g (80%) of a white crystalline product, m.p. 93.5–94.0°. The i.r. spectrum showed epoxide ring absorptions at 1238, 925, 830, and 749 cm^{-1}, epoxymethine absorption at 3010 cm^{-1}, and sulfonyl absorption at 1316 cm^{-1} (ν_{as}), and 1148 cm^{-1} (ν_s). The n.m.r. spectrum showed three methyl protons at 8.63 τ, three methyl protons at 8.23 τ, three methyl protons (CH_3Ar) at 7.57 τ, one methinyl proton at 6.22 τ, and four aromatic protons at 2.67 and 2.20 τ with $J = 8.0$ Hz.

Anal. Calcd. for $C_{11}H_{14}O_3S$: C, 58.37; H, 6.23; S, 14.19. Found: C, 58.35; H, 6.37; S, 13.99.

With Benzophenone. 1,1-Diphenyl-2-(p-tolylsulfonyl)-1,2-epoxyethane (6)

From benzophenone (2.73 g, 0.016 mole) and **2** (2.75 g, 0.016 mole). Crude **6** was recrystallized from *n*-hexane – carbon tetrachloride to give 3.0 g (57%) of small needles, m.p. 106–107°. The i.r. spectrum showed epoxide ring absorptions at 1250, 945, 795, and 756 cm^{-1}, epoxymethine absorption at 3000 cm^{-1}, and sulfonyl absorption at 1330 cm^{-1} (ν_{as}), and 1150 cm^{-1} (ν_s). The n.m.r. spectrum showed three methyl protons at 7.66 τ, one methinyl proton at 5.60 τ, and fourteen aromatic protons at 2.3–2.8 τ.

Anal. Calcd. for $C_{21}H_{18}O_3S$: C, 71.97; H, 5.18; S, 9.15. Found: C, 71.73; H, 5.27; S, 9.24.

Can. J. Chem. Downloaded from www.nrcresearchpress.com by 210.87.254.105 on 09/05/12
For personal use only.

With Cyclohexanone. 1,1-Pentamethylene-2-(p-tolylsulfonyl)-1,2-epoxyethane (7)

From cyclohexanone (1.57 g, 0.016 mole) and **2** (2.75 g, 0.016 mole). Crude **7** was recrystallized from *n*-hexane – carbon tetrachloride to give a fine white powder (3.3 g, 77%), which at first melted at 54–55°, and then formed needles which melted at 69–70°. The i.r. spectrum showed epoxide ring absorptions at 1267, 1210, 940, 849, and 760 cm^{-1}, epoxymethine absorption at 3010 cm^{-1}, and sulfonyl absorption at 1321 cm^{-1} (ν_{as}), and 1149 cm^{-1} (ν_s). The n.m.r. spectrum showed three methyl protons at 7.58 τ, one methinyl proton at 6.45 τ, ten methylene protons (multiplets) at 7.7–8.7 τ, and four aromatic protons at 2.70 and 2.27 τ with $J = 8.0$ Hz.

Anal. Calcd. for $C_{14}H_{18}O_3S$: C, 63.12; H, 6.82; S, 12.04. Found: C, 62.95; H, 6.98; S, 11.94.

With Acetophenone. 2-Phenyl-2-(p-tolylsulfonyl)-propanal (9)

From acetophenone (1.92 g, 0.016 mole) and **2** (2.75 g, 0.016 mole). The product was a yellow oil; this material solidified when left for two days. On recrystallization from carbon tetrachloride compound **9** was obtained as white needles (4.1 g, 89%), m.p. 125–125.5°. The i.r. spectrum showed carbonyl absorption at 1730 cm^{-1}, and sulfonyl absorption at 1310 cm^{-1} (ν_{as}), and 1140 cm^{-1} (ν_s). The n.m.r. spectrum showed three methyl protons at 8.18 τ, three methyl protons (CH_3Ar) at 7.61 τ, five phenyl protons at 2.62 τ, four aromatic protons at 2.83 and 2.60 τ with $J = 8.0$ Hz, and one aldehydic proton at −0.21 τ.

Anal. Calcd. for $C_{16}H_{16}O_3S$: C, 66.66; H, 5.58; S, 11.12. Found: C, 66.81; H, 5.48; S, 10.96.

The 2,4-dinitrophenylhydrazone of compound **9**, prepared in the usual way, melted at 197–198° (with decomposition).

Reactions of α-Chloroethyl p-Tolyl Sulfone (10)

Compound **10** was prepared by a method based on that of Ziegler and Connor (16). A mixture of sodium *p*-toluenesulfinate (17) (36.3 g, 0.204 mole) and chloroiodoethane (19) (38.7 g, 0.204 mole) in 100 ml of ethanol (95%) was heated at reflux for 5 days. Yield, 17.8 g (40%), m.p. 84° (lit. (20) m.p. 84°).

With Benzaldehyde. trans-1-Phenyl-2-(p-tolylsulfonyl)-1,2-epoxypropane (8)

From benzaldehyde (1.69 g, 0.016 mole) and **10** (3.5 g, 0.016 mole). Crude **8** (4.25 g, 92%) was recrystallized from *n*-hexane – carbon tetrachloride to give 3.4 g (78%) of a product with m.p. 113–115° (with decomposition). The i.r. spectrum showed epoxide ring absorption at 1211, 870, and 760 cm^{-1}, epoxymethine absorption at 3020 cm^{-1}, and sulfonyl absorption at 1316 cm^{-1} (ν_{as}), and 1143 cm^{-1} (ν_s). The n.m.r. spectrum showed three methyl protons at 8.65 τ, three methyl protons (CH_3Ar) at 7.53 τ, one methinyl proton at 5.16 τ, five phenyl protons at 2.69 τ, and four aromatic protons at 2.62 and 2.13 τ with $J = 8.0$ Hz.

Anal. Calcd. for $C_{16}H_{16}O_3S$: C, 66.66; H, 5.58; S, 11.12. Found: C, 66.43; H, 5.66; S, 11.00.

Reactions of Bromomethyl p-Tolyl Sulfone (11)

Compound **11** was prepared from sodium *p*-toluenesulfinate (17) and methylene bromide by the method of Ziegler and Connor (16) in 71% yield, m.p. 90–91° (lit. (16) m.p. 89–90°; 90–91°).

With Benzaldehyde to form 3

Benzaldehyde (1.69 g, 0.016 mole) and **11** (4.0 g, 0.016 mole) gave 4.0 g (91%) of **3**, which was identical in every respect with the **3** obtained with **2**.

With Acetone to form 5

Acetone (0.93 g, 0.016 mole) and **11** (4.0 g, 0.016 mole) gave 2.8 g (77%) of **5**, which was identical in every respect with the **5** obtained with chloromethyl *p*-tolyl sulfone.

Deuterium Exchange Experiment. trans-2-Phenyl-1-(p-tolylsulfonyl)-1,2-epoxyethane-1-d (12)

0.1 g (2 mmole) of sodium methoxide was added to a sample of 0.5 g (2 mmole) of **3**, dissolved in 10 ml of methanol-*d* (prepared from sodium methoxide and deuterium oxide) and 10 ml of anhydrous benzene. After standing at room temperature for 36 h, the mixture was diluted with water, the benzene layer was separated, washed with water, dried with anhydrous magnesium sulfate, and the benzene evaporated at reduced pressure. The residue was recrystallized from *n*-hexane – carbon tetrachloride to give 0.45 g (90%) of **12**, m.p. 157–159°; mixed m.p. with **3**, 157–159°. The i.r. spectrum showed epoxide ring absorptions at 1248, 966, 935, and 783 cm^{-1}, epoxymethine absorption at 3010 cm^{-1}, deuterium absorption at 2255 cm^{-1}, and sulfonyl absorption at 1315 cm^{-1} (ν_{as}) and 1146 cm^{-1} (ν_s). The n.m.r. spectrum showed three methyl protons at 7.55 τ, one methinyl proton at 5.48 τ, five phenyl protons at 2.71 τ, and four aromatic protons at 2.52 and 2.16 τ with $J = 8.0$ Hz.

Acknowledgment

We thank the National Research Council of Canada for financial support for this research.

1. (*a*) W. E. Truce and J. A. Simms. J. Am. Chem. Soc. **78**, 2756 (1956); (*b*) W. E. Truce and V. V. Badiger. J. Org. Chem. **29**, 3277 (1964); (*c*) M. F. Shostakovskii, E. P. Gracheva, and N. K. Kul'-Bovskaya. Usp. Khim. **30**, 493 (1961).
2. H. E. Zimmerman and B. S. Thyagarajan. J. Am. Chem. Soc. **82**, 2505 (1960).
3. M. Ballester. Chem. Rev. **55**, 283 (1955).
4. (*a*) W. R. Sorensen. J. Org. Chem. **24**, 1796 (1959); (*b*) B. Loev. J. Org. Chem. **26**, 4394 (1961); (*c*) W. Dittmann and F. Stuerzenhofecker. Ann. Chem. **699**, 177 (1966); (*d*) W. Dittmann and H. Stock. Ger. Patent No. 1 210 889 (1966) (Chem. Abstr. **64**, 17605*a* (1966)) and Ger. Patent No. 1 224 326 (1966) (Chem. Abstr. **65**, 20128*g* (1966)).
5. W. S. Johnson, J. S. Belew, L. J. Chinn, and R. H. Hunt. J. Am. Chem. Soc. **75**, 4995 (1953).
6. R. H. Hunt, L. J. Chinn, and W. S. Johnson. Org. Synth. **34**, 54 (1954).
7. L. Field and C. G. Carlile. J. Org. Chem. **26**, 3170 (1961).
8. (*a*) D. J. Cram. Fundamentals of carbanion chemistry *In* Organic chemistry. Vol. 4. *Edited by* A. T. Blomquist. Academic Press, Inc., New York. 1965. Chap. I; (*b*) N. P. Neureiter. J. Am. Chem. Soc. **88**, 558 (1966); (*c*) N. P. Neureiter and F. G. Bordwell. J. Am. Chem. Soc. **85**, 1209 (1963);

(*d*) F. G. BORDWELL and G. D. COOPER. J. Am. Chem. Soc. **73**, 5187 (1951).
9. M. S. NEWMAN and B. J. MAGERLEIN. Org. Reactions, **5**, 413 (1949).
10. G. G. LYLE and L. K. KEEFER. J. Org. Chem. **31**, 3921 (1966).
11. M. BALLESTER and P. D. BARTLETT. J. Am. Chem. Soc. **75**, 2042 (1953).
12. (*a*) M. C. CASERIO, R. E. PRATT, and R. J. HOLLAND. J. Am. Chem. Soc. **88**, 5747 (1966); (*b*) C. C. PRICE and S. OAE. Sulfur bonding. The Ronald Press Co., New York. 1962. p. 106.
13. H. E. ZIMMERMAN and L. AHRAMJIAN. J. Am. Chem. Soc. **82**, 5459 (1960).
14. (*a*) H. BOEHME and H. J. GRAN. Ann. Chem. **577**, 68 (1952); (*b*) H. BOEHME, H. FISCHER, and R. FRANK. Ann. Chem. **563**, 54 (1949).
15. A. I. VOGEL. Practical organic chemistry. Longmans, Green and Co., Inc., Toronto. 1962. p. 694.
16. W. M. ZIEGLER and R. CONNOR. J. Am. Chem. Soc. **62**, 2596 (1940).
17. L. FIELD and R. D. CLARK. Org. Synth. **38**, 62 (1958).
18. N. OTTO. J. Prakt. Chem. [2] **40**, 528 (1889); cited in Beilstein, "Organische Chemie," **6**, 421 (1923).
19. N. SIMPSON. Bull. Soc. Chim. France, **31**, 411 (1879); cited in Beilstein, "Organische Chemie," **1**, 98 (1918).
20. N. OTTO. J. Prakt. Chem. [2] **40**, 515 (1889); cited in Beilstein, "Organische Chemie," **6**, 421 (1923).
21. (*a*) Y. CURTIN, H. GRUEN, Y. G. HENDRICKSON, and H. E. KNIPMEYER. J. Am. Chem. Soc. **83**, 4838 (1961); (*b*) D. Y. CURTIN, H. GRUEN, and B. A. SHOULDERS. Chem. Ind. London, 1205 (1958).

Can. J. Chem. Downloaded from www.nrcresearchpress.com by 210.87.254.105 on 09/05/12
For personal use only.

Can. J. Chem. Downloaded from www.nrcresearchpress.com by 210.87.254.105 on 09/05/12
For personal use only.

Galactomannan from *Cassia absus* seed. I. Nature of sugars present, methylation, and periodate oxidation studies

V. P. KAPOOR AND S. MUKHERJEE
Department of Organic Chemistry, National Sugar Institute, Kanpur, India

Received March 3, 1969

A galactomannan composed of D-galactose (1 mole) and D-mannose (3 moles) was isolated from the seed of *Cassia absus*. Methylation and hydrolysis of the galactomannan produced 2,3,4,6-tetra-*O*-methyl-D-galactose (2 moles), 2,3,6-tri-*O*-methyl-D-mannose (4.2 moles), 2,3-di-*O*-methyl-D-mannose (1 mole), and 4,6-di-*O*-methyl-D-mannose (1 mole). Periodate consumption was 1.09 moles for each hexose unit with concomitant liberation of 0.26 mole of formic acid. The periodate oxidized and the reduced galactomannan afforded, on hydrolysis, glycerol (1.94 moles), erythritol (5 moles), and D-mannose (1.08 moles).

On the basis of the above findings, a structure for the galactomannan can be proposed in which mannose units form the main chain and the galactose units are present as branches, the former being attached mostly through $1 \rightarrow 4$ (ca. 85%) and the rest which is nearly half the branch points through $1 \rightarrow 3$ or $1 \rightarrow 2$, and branches of single galactose units are attached through $1 \rightarrow 6$ (ca. 50%) and the rest through $1 \rightarrow 2$ or $1 \rightarrow 3$.

Canadian Journal of Chemistry, 47, 2883 (1969)

Cassia absus belongs to the N.O. Leguminosae. The endosperm of leguminous seeds is usually mucilaginous and galactomannan is its main component (1). Many such seeds e.g. guar (2, 3), fenugreek (4), carob (5, 6), lucerne and clover (7), and Kentucky coffee bean (8) have been studied and the structure of galactomannan worked out. It would be interesting to study other seeds of this family and find out the relationship between their polysaccharide material. *Cassia absus* seed, which is medically important (9) and easily available, was taken up for the study. It will be seen that endosperm of this seed, which is about 55% of the total weight, is chiefly a galactomannan.

Isolation of the galactomannan from the seeds was carried out by the usual procedure of extraction with hot water and precipitation with ethanol. This crude polysaccharide formed an insoluble complex when treated with a saturated barium hydroxide solution. The barium complex, containing pure polysaccharide material (10) yielded two fractions, A (soluble) and B (insoluble) when stirred with dilute acetic acid. The two fractions were in the ratio of 3:1. The major fraction A was taken up for the present study. It was taken to be homogeneous since (*i*) almost all of it precipitated from an aqueous solution over a narrow concentration range of ethanol, and (*ii*) the precipitated material displayed the same physical properties as the product regenerated from the acetyl derivative of the original fraction. Complete acid hydrolysis of the purified polysaccharide afforded D-galactose (1 mole), D-mannose (3 moles), and xylose (0.17 mole) (11).

The purified polysaccharide was converted into its fully methylated derivative and fractionated. Hydrolysate of the main fraction showed three spots on paper which were separated on Whatman No. 3 MM sheets. The sugar which moved fastest was 2,3,4,6-tetra-*O*-methyl-D-galactose. It was followed by 2,3,6-tri-*O*-methyl-D-mannose. An unusually elongated spot of the slowest moving component suggested the possibility of its being a mixture of at least two sugars. The common solvent systems failed to resolve this mixture. It could be finally separated with butanone – ethyl acetate – water – ammonia (80:20:8:1 v/v, upper phase), a new solvent composition. These two sugars were 2,3-di-*O*-methyl-D-mannose and 4,6-di-*O*-methyl-D-mannose. The four sugars were in the molar ratio 2:4.2:1:1.

Since 2,3,6-tri-*O*-methyl-D-mannose is the major component, the main chain must be composed of $1 \rightarrow 4$ linkages. The mannose units giving rise to 2,3-di-*O*-methyl-D-mannose would also be $1 \rightarrow 4$ linked, one of the galactose end units being linked to it at C-6. The remaining mannose unit makes its appearance as a 4,6-di-*O*-methyl derivative suggesting linkages through its C-1, C-2, and C-3. Such a combination of linkages is not reported in any of the seed galactomannans. Bishop *et al.* (12) have, however, reported mannose unit similarly linked in a

Can. J. Chem. Downloaded from www.nrcresearchpress.com by 210.87.254.105 on 09/05/12
For personal use only.

dermatophyte (Trichophyton granulosum) galactomannan. This mannose unit may be attached to its adjacent mannose unit through $1 \rightarrow 3$ and to the terminal galactose unit through $1 \rightarrow 2$; the linkages may also be attached otherwise, the proof of which cannot be afforded at this stage. The exact nature of these linkages will be clear only from the isolation of such an oligosaccharide from the galactomannan in which a mannose unit is attached to another mannose unit or a galactose unit is attached to a mannose unit through $1 \rightarrow 2$ or $1 \rightarrow 3$ linkage. Such an attempt will be made in future. The simplest symmetrical structure which can accommodate the above findings is shown in Formula I.

Most of the seed galactomannans have a main chain of $1 \rightarrow 4$ linked mannose units. The side chains are linked at C-6 and are composed of galactose and mannose (8, 13) or only the former (2–7, 14). It will be seen that the *Cassia absus* galactomannan is essentially similar to other seed galactomannans: the major difference being the attachment of half of the galactose side units to C-2 or C-3 of the hexose units in the main chain. In this respect it bears similarity to galactomannans from microorganisms (15–17). In these cases the branches have been shown to be attached at C-2.

The structure shown below would consume 1.125 moles of periodate per hexose unit and would liberate 0.25 mole of formic acid. In actual practice 1.09 moles of periodate were consumed, with the liberation of 0.26 mole formic acid. The periodate-oxidized polysaccharide was reduced with sodium borohydride and hydrolyzed according to the method of Abdel-Akher *et al.* (18). The hydrolysate was resolved on Whatman No. 3 MM sheets using butan-1-ol – ethanol – water (31:11:9 v/v, upper phase) mixture. The components were glycerol (1.94 moles), erythritol (5 moles), D-mannose (1.08 moles), and traces of galactose. The results are in substantial agreement with the expected values, but no satisfactory explanation can yet be given for the detection of traces of galactose.

The infrared (i.r.) spectrum of the galactomannan showed absorption bands at 817 and 874 cm^{-1} thus indicating the presence of α-linked D-galactopyranose units and β-linked D-mannopyranose units respectively (19). The fact that galactomannan has a majority of β-linkages is further confirmed by low positive rotations of the polysaccharide $[\alpha]_D^{20}$ +23.8 (H_2O), its acetate $[\alpha]_D^{24}$ +25.6 (acetone), and its methyl ether $[\alpha]_D^{27}$ +28.3 ($CHCl_3$). Such glycosidic configuration is reported in most seed galactomannans.

Experimental

Methods

Unless otherwise stated all evaporations were carried out at 40–50° under reduced pressure. All specific rotations are equilibrium values and melting points are uncorrected. The i.r. spectra were recorded on a Perkin–Elmer model 137-B either in chloroform solutions in sodium chloride cells or in potassium bromide pellets. Paper chromatographic analysis was carried out by descending method on Whatman No. 1 paper using non-aqueous phases of the following solvent systems (by volume): (*a*) butan-1-ol – acetic acid – water (4:1:5); (*b*) benzene – ethanol – water (167:47:15); (*c*) butanone – water azeotrope; (*d*) butanone – ethyl acetate – water – ammonia (80:20:8:1); (*e*) butan-1-ol – ethanol – water (31:11:9). Silver nitrate–sodium hydroxide and *p*-anisidine phosphate were used as spray reagents. Sugar mixtures were separated on Whatman No. 3 MM sheets and columns of Whatman cellulose powder. Deionization was done with Amberlite IR-120 (H^+) and IR-45 (OH^-).

Isolation, Fractionation, and Purification of the Galactomannan

The seeds were cleaved in a low speed grinder when the seedcoat together with the embryo attached to it broke off from the light yellow-colored cotyledons. The cotyledons were separated by winnowing and rejected. The remaining material (100 g) containing the endosperm was soaked in water (3 l) overnight followed by heating at 100° for 4 h. The swollen material was then blended with additional quantities of water. The resulting viscous solution (8 l) was filtered through a muslin cloth and

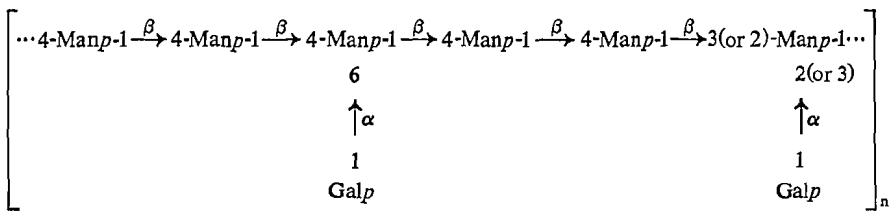

Formula I. A probable structure of Cassia absus seed galactomannan.
LEGEND: Gal*p*, D-galactopyranose; Man*p*, D-mannopyranose.

Can. J. Chem. Downloaded from www.nrcresearchpress.com by 210.87.254.105 on 09/05/12
For personal use only.

centrifuged at 25 000 r.p.m. in a supercentrifuge when most of the suspended matter was removed and an almost clear solution resulted. Addition of ethanol (14 l) to this solution precipitated the polysaccharide in the form of a coarse powder (12.5 g). It was redissolved in water (5 l) with constant mechanical stirring for 5 h. To this solution was added saturated barium hydroxide solution (10 l) when the polysaccharide precipitated out as its barium complex. It was allowed to settle and isolated by decantation followed by filtration. The solid material was stirred with 2 *N* acetic acid (2 l) for 30 h when it partially dissolved. After removal of the insoluble fraction by filtration, the soluble fraction was isolated by precipitation with ethanol (4 l). The two fractions were successively stirred in 2 l each of 50, 80, 90, and 95% ethanol. The washed fractions were free from acetic acid; yield, soluble 7.2 g; insoluble, 2.5 g.

The acetic acid soluble polysaccharide was deionized. The ash-free product (6 g) was stirred for 4 h with water (1 l) and ethanol was added to the solution in stages. After each addition the solution was allowed to stand overnight. Addition of the first 150 ml had no effect but the next 100 ml produced a turbidity which was centrifuged out. Another 75 ml resulted in a slight precipitate (340 mg) which was removed by filtration. Finally, addition of 60 ml more resulted in copious precipitation of the polysaccharide (5.4 g). At this stage alcohol concentration had increased from 19 to 23% (weight of ethanol/weight of solution).

The polysaccharide which was in the form of white amorphous powder had $[\alpha]_D^{20}$ +23.8° (*c*, 1.0 H_2O) and did not reduce Fehling's solution. Nitrogen, sulfur, halogens, methoxyl, and uronic acid were absent. Its preliminary analysis gave sulfated ash (0.12%) and pentosans (6.61%).

Acetylation of the Galactomannan (8)

The polysaccharide (0.8 g) was finely ground and shaken at room temperature with formamide (50 ml) for 24 h. Anhydrous pyridine (12 ml) was added to the above suspension and it was followed by dropwise addition of acetic anhydride (10 ml) during 4 h when a brown viscous solution resulted. It was kept overnight and the acetylated product was precipitated from it as a greyish-white powder by stirring into water. It was washed with water, followed by ethanol, and finally with petroleum ether to dry it. The dried acetyl derivative was dissolved in acetone (50 ml). A small amount of undissolved material was centrifuged out. The pure derivative was then reprecipitated and dried as above; yield, 0.79 g; $[\alpha]_D^{24}$ +25.6 (*c*, 0.5 acetone).

Regeneration of the Galactomannan from its Acetate

The acetate (0.7 g) was dissolved in acetone (25 ml) and refluxed with potassium hydroxide (45%, 25 ml). The lower viscous layer, containing alkali and polysaccharide, was separated and poured into acidified ethanol. A further precipitation in the same manner with neutral ethanol afforded purified galactomannan which was dried by solvent exchange; yield, 0.29 g; $[\alpha]_D^{25}$ +24.7 (*c*, 1.0 H_2O).

Identification and Estimation of Sugars from the Galactomannan

The polysaccharide (1 g) was kept with sulfuric acid (72%, 4 ml) overnight, cooled in a freezing mixture, diluted with water (108 ml), and hydrolyzed at 100°. Hydrolysis was complete after 10 h as shown by iodometric titrations. The resulting solution was neutralized (barium carbonate), deionized, and evaporated to a thin syrup. Paper chromatography in solvent *a* revealed the presence of D-galactose (strong spot), D-mannose (strong spot), and xylose (faint spot). The sugar mixture was resolved on cellulose column using butan-1-ol half saturated with water as eluent. Appropriate fractions of eluate containing single pure sugar were mixed and concentrated. They yielded (*i*) D-galactose, m.p. and mixed m.p. 163–165°; $[\alpha]_D^{34}$ +81.0 (*c*, 0.5 H_2O); *p*-nitro-*N*-phenyl-D-galactosylamine, m.p. and mixed m.p. 216–219°; $[\alpha]_D^{30}$ −247° (*c*, 0.2 pyridine); (*ii*) D-mannose, m.p. and mixed m.p. 132°; $[\alpha]_D^{35}$ +14.2 (*c*, 0.5 H_2O); *p*-nitro-*N*-phenyl-D-mannosylamine, m.p. and mixed m.p. 216–219°; $[\alpha]_D^{32}$ −325° (*c*, 0.5 pyridine).

To estimate the component sugars in the polysaccharide, it (0.2 g) was heated at 100° with 1 *N* sulfuric acid (10 ml) in a sealed tube and finally processed as usual. The sugars were separated on paper. Areas of the paper containing single sugar component were cut out, eluted, and estimated by oxidizing the sugar with periodate (20) and titrating the liberated formic acid with standard alkali. Ratio of galactose, mannose, and xylose was 1:3:0.17.

Methylation of the Galactomannan

The polysaccharide (5 g) was subjected to methylation by Haworth's method by five successive treatments with dimethyl sulfate and sodium hydroxide solution (45%) yielding a light-yellow product (3.95 g). The i.r. spectrum of this polysaccharide in chloroform still had a prominent hydroxyl peak (3400–3600 cm^{-1}).

The partially methylated product was dissolved in dimethyl sulfoxide (150 ml) (21) and to the resulting solution, sodium hydroxide pellets (35 g) and dimethyl sulfate (20 ml) were added during a period of 6 h with constant stirring at 20° under an atmosphere of nitrogen. The reaction mixture was stirred overnight and excess of dimethyl sulfate was decomposed by heating at 95° for 1 h. It was diluted with water to dissolve residual sodium hydroxide, cooled in freezing mixture, and neutralized (sulfuric acid). The solution was dialyzed in running distilled water for 7 days to remove dimethyl sulfoxide and inorganic salts. The solution was concentrated to 100 ml and extracted with chloroform which on evaporation yielded a clear yellow glassy solid (4 g); $[\alpha]_D^{27}$ +28.3 (*c*, 1.5 H_2O). This product showed no hydroxyl absorption in the i.r. spectrum. Further methylations with Purdie reagents did not increase its methoxyl content.

Anal. Found: OCH_3, 43.3.

Fractionation of the Methylated Galactomannan

The methylated polysaccharide (3.8 g) was successively extracted with petroleum ether (40–60°) and chloroform mixture (100 ml) containing increasing proportions of the latter. During every stage the methylated residue was refluxed with solvent mixture for 2 h. Fractions 4, 5, and 6, which were analytically similar and together formed the major component (3.6 g), were combined and further study was carried out only on this material.

Can. J. Chem. Downloaded from www.nrcresearchpress.com by 210.87.254.105 on 09/05/12
For personal use only.

Sugars from the Methylated Galactomannan, their Characterization, and Estimation

A solution of methylated polysaccharide (1.5 g) in methanolic hydrogen chloride (4%, 125 ml) was refluxed for 10 h, cooled, neutralized (silver carbonate), filtered, and concentrated. The syrupy residue was then taken up in 1 *N* hydrochloric acid (125 ml) and heated for 8 h at 100°. The cooled solution was neutralized (silver carbonate) and filtered. Silver ions in the filtrate were removed by precipitation with hydrogen sulfide. The filtered solution was deionized and evaporated to a syrup. Paper chromatography in solvent *b* and *c* of this syrup showed three spots. But in the newly devised solvent *d*, the syrup showed four discrete spots which could be separated quantitatively on paper. The additional spot in this case was due to the resolution of the former slowest moving component into two. Table I shows the nature of different sugars.

Fraction I, 2,3,4,6-Tetra-O-methyl-D-galactose

The syrupy product had $[\alpha]_D^{30}$ +110° (*c*, 0.5 H_2O). Its demethylation gave galactose. Treatment of the syrup with aniline in the usual way yielded fine needles of *N*-phenyl-2,3,4,6-tetra-*O*-methyl-D-galactosylamine, m.p. and mixed m.p. 194° after recrystallization from ethyl acetate; lit. m.p. 192° (22).

Anal. Calcd. for tetramethyl hexose: OCH_3, 52.5. Found: OCH_3, 52.2.

Fraction II, 2,3,6-Tri-O-methyl-D-mannose

This component had $[\alpha]_D^{26}$ −7.6 (*c*, 1.0 H_2O). On demethylation it gave mannose with traces of galactose. Attempts to separate the two methylated sugars did not succeed. A portion of the syrup was oxidized with bromine water, lactonized in the usual way, and crystallized from acetone – petroleum ether. The resulting crystals of 2,3,6-tri-*O*-methyl-D-mannono-γ-lactone had m.p. 83–85°; lit. m.p. 84–85° (6). *N*-Phenyl-2,3,6-tri-*O*-methyl-D-mannosylamine prepared from another portion of the syrup had m.p. 130°; lit. m.p. 127–128° (23).

Anal. Calcd. for trimethyl hexose: OCH_3, 41.8. Found: OCH_3, 41.5.

Fraction III, 2,3-Di-O-methyl-D-mannose

The syrup had $[\alpha]_D^{25}$ −15.5 (*c*, 0.5 H_2O) and $[\alpha]_D^{25}$ +6.1 (*c*, 0.5 MeOH). Upon demethylation this component gave mannose only. On treatment with *p*-nitrobenzoyl chloride, the sugar yielded 2,3-di-*O*-methyl-D-mannose-1,4,6-tri-*p*-nitrobenzoate m.p. 192–194°; lit. m.p. 192–194° (14).

Anal. Calcd. for dimethyl hexose: OCH_3, 29.8. Found: OCH_3, 29.5.

Fraction IV, 4,6-Di-O-methyl-D-mannose

This component was obtained as glassy solid $[\alpha]_D^{25}$ +23.7 (*c*, 1.0 H_2O) and it gave mannose only on demethylation. It was characterized through its crystalline isopropylidine derivative, m.p. 77°, after recrystallization with petroleum ether; lit. m.p. 76–77° (24).

Anal. Calcd. for dimethyl hexose: OCH_3, 29.8. Found: OCH_3, 29.6.

The mixture of methylated sugars was separated on Whatman No. 1 paper in solvent *d* and the different zones containing methylated sugars were cut out and eluted. The eluted sugars were estimated by hypoiodite titrations (25) and fractions I, II, III, and IV were found to be in the molar ratio of 2:4.2:1:1.

Periodate Oxidation of the Galactomannan

The polysaccharide (141 mg) was dissolved in water (70 ml) and the solution cooled to 0°. A cold solution of 0.12 *M* sodium metaperiodate (30 ml) was added to it and reaction was carried out at 5°. The periodate consumption was determined (26) by treating the solution with excess of potassium iodide after buffering it with borax–boric acid and titrating the liberated iodine equivalent to unreacted periodate with 0.12 *N* sodium arsenite. After destroying the excess of periodate with ethylene glycol, the liberated formic acid was titrated with 0.01 *N* sodium hydroxide solution. The two estimations were done at different time intervals. Titre values became constant after 93 h which corresponded to 1.09 moles of periodate and 0.26 mole of formic acid per hexose unit.

Periodate Degradation of the Galactomannan (18)

The polysaccharide (1.5 g) was oxidized with sodium metaperiodate as mentioned above. The excess periodate was destroyed, solution was dialyzed in running distilled water for 5 days and concentrated to 400 ml. To this solution was added sodium borohydride (1.3 g) to effect reduction of polyaldehyde to corresponding polyalcohol. After standing at room temperature for 20 h, the solution was neutralized (acetic acid), deionized, and evaporated to dryness. After removing boric acid by repeated evaporations with methanol, the residue was hydrolyzed with 1 *N* sulfuric acid (150 ml) for 12 h at 95°. The hydrolysate was neutralized (barium carbonate), filtered, deionized, and evaporated to a syrup. The chromatographic examination in solvent *e* revealed the presence of glycerol, erythritol, D-mannose, and traces of galactose. The alcohols gave very prominent spots if the developed chromatogram passed through silver nitrate and was sprayed with 1% aqueous alcoholic sodium metaperiodate before the final sodium hydroxide spray. The mixture was

TABLE I

Hydrolysis products from methylated galactomannan

Fraction number	Methylated sugar	Yield (mg)	R_G in solvent *b*	R_G in solvent *d*
I	2,3,4,6-tetra-*O*-Methyl-D-galactose	348	0.95	0.92
II	2,3,6-tri-*O*-Methyl-D-mannose	691	0.62	0.67
III	2,3-di-*O*-Methyl-D-mannose	160	0.27	0.34
IV	4,6-di-*O*-Methyl-D-mannose	152	0.27	0.24

R_G values are with reference to 2,3,4,6-tetra-*O*-methyl-D-glucose.

resolved into its components using solvent *e* and Whatman 3 MM papers.

Identification and Estimation of Glycerol, Erythritol, and D-*mannose*

Fraction 1 (140 mg) was glycerol, identified by the preparation of its tri-*p*-nitrobenzoate, m.p. and mixed m.p. 185–186°; lit. m.p. 186–188° (13). Fraction 2 (370 mg) which was erythritol had m.p. and mixed m.p. 121°; lit. m.p. 120–122° (27). It was converted into tetra-*O*-tosyl-erythritol, m.p. and mixed m.p. 164–165°; lit. m.p. 165–166° (27). Fraction 3 (78 mg) on chromatographic examination was found to be D-mannose containing ca. 5–10% galactose. D-mannose was separated on paper in solvent *a* and had $[\alpha]_D^{22}$ +14.1 (*c*, 0.4 H_2O) and was converted into its crystalline *p*-nitroaniline derivative, m.p. and mixed m.p. 217–218°.

The mixture was separated on paper in solvent *e*, the strips corresponding to different components were cut out and eluted. Glycerol and erythritol were estimated by periodate – chromotropic acid method (28) and mannose by phenol–sulfuric acid method (29). The ratio of glycerol, erythritol, and mannose was 1.94:5:1.08.

Acknowledgments

The authors express their sincere thanks to Shri S. C. Gupta, Director, for his kind interest in this investigation. One of the authors (V.P.K.) is also grateful to the Ministry of Education, Government of India, for the award of a senior research scholarship.

1. E. ANDERSON. Ind. Eng. Chem. **41**, 2887 (1949).
2. J. W. SWANSON. J. Am. Chem. Soc. **71**, 1510 (1949).
3. Z. F. AHMED and R. L. WHISTLER. J. Am. Chem. Soc. **72**, 2524 (1950).
4. P. ANDREWS, L. HOUGH, and J. K. N. JONES. J. Chem. Soc. 2744 (1952).
5. E. L. HIRST and J. K. N. JONES. J. Chem. Soc. 1278 (1948).
6. F. SMITH. J. Am. Chem. Soc. **70**, 3249 (1948).
7. P. ANDREWS, L. HOUGH, and J. K. N. JONES. J. Am. Chem. Soc. **74**, 4029 (1952).
8. E. B. LARSON and F. SMITH. J. Am. Chem. Soc. **77**, 429 (1955).
9. B. N. SHASTRI (*Editor*). The wealth of India—raw materials. Vol. II. Council of Scientific and Industrial Research, New Delhi, 1950. p. 93.
10. H. MEIER. *In* Methods in carbohydrate chemistry. Vol. V. *Edited by* R. L. Whistler. Academic Press, Inc., New York. 1965. p. 45.
11. V. P. KAPOOR and S. MUKHERJEE. Current Sci. (India), **38**, 38 (1969).
12. C. T. BISHOP, F. BLANK, and M. HRANSAVLEVIC-JACOVLJEVIC. Can. J. Chem. **40**, 1816 (1962).
13. A. M. UNRAU. J. Org. Chem. **26**, 3097 (1961).
14. A. S. CEREZO. J. Org. Chem. **30**, 924 (1965).
15. F. BLANK and M. B. PERRY. Can. J. Chem. **42**, 2862 (1964).
16. C. T. BISHOP, M. B. PERRY, F. BLANK, and F. P. COOPER. Can. J. Chem. **43**, 30 (1965).
17. P. A. J. GORIN and J. F. T. SPENCER. Can. J. Chem. **46**, 2299 (1968).
18. M. ABDEL-AKHER, J. K. HAMILTON, R. MONTGOMERY, and F. SMITH. J. Am. Chem. Soc. **74**, 4970 (1952).
19. S. A. BARKER, E. J. BOURNE, and D. H. WHIFFEN. Methods Biochem. Analy. **3**, 213 (1956).
20. E. L. HIRST and J. K. N. JONES. J. Chem. Soc. 1659 (1949).
21. H. C. SRIVASTAVA, P. P. SINGH, S. N. HARSHE, and K. VIRK. Tetrahedron Letters, 493 (1964).
22. I. EHRENTHAL, M. C. RAFIQUE, and F. SMITH. J. Am. Chem. Soc. **74**, 1341 (1952).
23. W. N. HAWORTH, E. L. HIRST, and H. R. L. STREIGHT. J. Chem. Soc. 1349 (1931).
24. R. G. AULT, W. N. HAWORTH, and E. L. HIRST. J. Chem. Soc. 1012 (1935).
25. E. L. HIRST, L. HOUGH, and J. K. N. JONES. J. Chem. Soc. 928 (1949).
26. A. N. SHRIVASTAVA. Ph.D. Thesis. Agra University, Agra, India. 1959. p. 93.
27. J. K. HAMILTON and F. SMITH. J. Am. Chem. Soc. **78**, 5907 (1956).
28. M. LAMBERT and A. C. NEISH. Can. J. Res. **28B**, 83 (1950).
29. M. DUBOIS, K. A. GILLES, J. K. HAMILTON, R. A. REBERS, and F. SMITH. Anal. Chem. **28**, 350 (1956).

Can. J. Chem. Downloaded from www.nrcresearchpress.com by 210.87.254.105 on 09/05/12
For personal use only.

Can. J. Chem. Downloaded from www.nrcresearchpress.com by 210.87.254.40 on 09/05/12
For personal use only.

NOTES

Some *O*-isopropylidene derivatives of D-ribose diethyl dithioacetal

D. G. LANCE, W. A. SZAREK, AND J. K. N. JONES
Department of Chemistry, Queen's University, Kingston, Ontario

Received December 19, 1968

Acetonation of D-ribose diethyl dithioacetal using anhydrous copper sulfate as catalyst gives predominantly 2,4- and 4,5-*O*-isopropylidene derivatives. The structures of the compounds were established by chemical and nuclear magnetic resonance spectroscopic methods.

L'acétonation du D-ribose diethyl dithioacetal, utilisant le sulfate de cuivre anhydre comme catalyseur, conduit essentiellement aux donnés 2,4- et 4,5-*O*-isopropylideniques. Les structures de ces composés ont été vérifiées par des méthodes chimiques et spectroscopiques (résonance magnétique nucléaire).

Canadian Journal of Chemistry, 47, 2889 (1969)

The acetonation of aldose dithioacetals has been studied by a number of investigators (1, 2). In a previous paper (3) from this laboratory, the formation of 2,3:4,5-di-*O*-isopropylidene-D-xylose diethyl dithioacetal from D-xylose diethyl dithioacetal and acetone was described, with either a strongly acidic ion-exchange resin or anhydrous copper sulfate as catalyst; partial acetonation yields the 4,5-, 3,4-, 2,3-, and 2,4-*O*-isopropylidene derivatives. We report now the preparation of some *O*-isopropylidene derivatives of D-ribose diethyl dithioacetal.

Acetonation of D-ribose diethyl dithioacetal using anhydrous copper sulfate as catalyst gives predominantly two mono-*O*-isopropylidene derivatives. These were isolated by column chromatography, and characterized as 4,5- and 2,4-*O*-isopropylidene-D-ribose diethyl dithioacetals.[1] The evidence for these assignments is given below. Thin-layer chromatographic (t.l.c.) examination of the reaction mixture showed, in addition, the presence of small amounts of two compounds with mobilities expected of di-*O*-isopropylidene derivatives. The structures of these compounds have not been investigated in this work. It has been reported (4), however, that D-ribose diethyl dithioacetal gives the 2,3:4,5-di-*O*-isopropylidene derivative on reaction with acetone in the presence of anhydrous copper sulfate and concentrated sulfuric acid.

[1]The 4,5-*O*-isopropylidene derivative was required for the synthesis of 1-deoxy-2,3-di-*O*-methyl-D-erythritol, a compound which we have used in some structural studies.

4,5-O-Isopropylidene-D-ribose Diethyl Dithioacetal

The 4,5-*O*-isopropylidene derivative was the preponderant product formed in the acetonation reaction; it was obtained as a chromatographically homogeneous and analytically pure syrup (65%). The nuclear magnetic resonance (n.m.r.) spectrum of the compound, measured in methyl sulfoxide-d_6, showed signals of the hydroxyl protons as 1-proton doublets, and hence the two hydroxyl groups are both secondary (5). Methylation of the compound with subsequent desulfurization with Raney nickel and acid-catalyzed hydrolysis gave a 1-deoxy-di-*O*-methyl-D-ribitol. This derivative rapidly consumed periodate, and was shown to possess a primary hydroxyl group by n.m.r. spectroscopy in methyl sulfoxide-d_6. The above observations for a mono-*O*-isopropylidene derivative of D-ribose diethyl dithioacetal are consistent only with the 4,5-isomer; the 1-deoxy-di-*O*-methyl-D-ribitol is, therefore, the 2,3-isomer.

2,4-O-Isopropylidene-D-ribose Diethyl Dithioacetal

The 2,4-*O*-isopropylidene derivative was obtained also as a syrup (12%). Its n.m.r. spectrum, measured in methyl sulfoxide-d_6, showed signals of two hydroxyl protons as a doublet and a triplet, indicating that a secondary and a primary hydroxyl group are present. Reductive desulfurization gave a crystalline 1-deoxy-mono-*O*-isopropylidene-D-ribitol, which was resistant to oxidation with sodium periodate. The crystalline

compound was methylated and then hydrolyzed to give a 1-deoxy-di-*O*-methyl-D-ribitol, which was also resistant to periodate oxidation, and whose n.m.r. spectrum showed the presence of two secondary hydroxyl groups. Thus, the 2,4-*O*-isopropylidene substitution in D-ribose diethyl dithioacetal is established, and the 1-deoxy-di-*O*-methyl-D-ribitol, in this case, is the 3,5-isomer.

Experimental

Melting points were determined on a Fisher–Johns melting point apparatus and are uncorrected. Optical rotations were measured with a Perkin–Elmer Model 141 automatic polarimeter at 24 ± 2° in ethyl acetate unless otherwise stated. Thin-layer chromatography (t.l.c.) was performed with Silica Gel G as the adsorbent. The developed plates were air-dried, sprayed with 5% ethanolic sulfuric acid, and heated at about 150°. The term "petroleum ether" refers to the fraction of b.p. 60–80°. Nuclear magnetic resonance (n.m.r.) spectra were measured on a Varian T-60 spectrometer in methyl sulfoxide-d_6 and tetramethylsilane as external standard unless otherwise stated; the assignment of peaks to the protons of hydroxyl groups was confirmed by the addition of deuterium oxide. Vacuum distillations were carried out with a Gallenkamp microdistillation apparatus at 70–100°/~ 0.1 Torr.

*2,4- and 4,5-O-Isopropylidene-*D*-ribose Diethyl Dithioacetals*

D-Ribose diethyl dithioacetal (6) (2.0 g) in dry acetone (50 ml) was stirred with anhydrous copper sulfate (5 g) for 3 h at room temperature. The mixture was filtered, and the filtrate was concentrated to dryness. The syrupy residue was dissolved in chloroform, and the solution was washed with water, dried, and concentrated to give an almost colorless syrup. Thin-layer chromatography (2:3 ethyl acetate – petroleum ether) showed the presence of two main components, R_f 0.50 and 0.30, and small amounts of two other components, R_f 0.95 and 0.97. The syrup was chromatographed on silica gel, with the same solvent as eluent. 4,5-*O*-Isopropylidene-D-ribose diethyl dithioacetal was obtained as a syrup (1.52 g, 65%), $[\alpha]_D$ +9.8 ± 0.3° (*c*, 2.8 in chloroform); R_f 0.50 (t.l.c.); n.m.r. data (internal tetramethylsilane standard): τ 4.93, 5.12 (1-proton doublets, J = 6 Hz, secondary OH's), τ 5.5–7.0 (6 protons, sugar-chain H's), τ 7.1–7.5 (4-proton quartet, J = 7 Hz, thioethyl CH_2's), τ 8.6–9.0 (12 protons, CMe_2 and thioethyl Me's).

Anal. Calcd. for $C_{12}H_{24}O_4S_2$: C, 48.6; H, 8.2. Found: C, 48.5; H, 8.4.

2,4-*O*-Isopropylidene-D-ribose diethyl dithioacetal was obtained also as a syrup (0.29 g, 12%), $[\alpha]_D$ −16.7 ± 0.5° (*c*, 1.23); R_f 0.30 (t.l.c.); n.m.r. data: τ 4.80 (1-proton doublet, J = 6 Hz, secondary OH), τ 5.39 (1-proton triplet, J = 5 Hz, primary OH), τ 5.5–6.6 (6 protons, sugar-chain H's), τ 6.9–7.5 (4-proton quartet, J = 7 Hz, thioethyl CH_2's), τ 8.3–8.8 (12 protons, CMe_2 and thioethyl Me's).

Anal. Calcd. for $C_{12}H_{24}O_4S_2$: C, 48.6; H, 8.2. Found: C, 48.3; H, 8.2.

*4,5-O-Isopropylidene-2,3-di-O-methyl-*D*-ribose Diethyl Dithioacetal*

4,5-*O*-Isopropylidene-D-ribose diethyl dithioacetal (1.4 g) was methylated at room temperature by a modification (3) of the method of Falconer and Adams (7). The product was purified by chromatography on silica gel, with 1:4 ethyl acetate – petroleum ether as eluent, to give a mobile oil (1.0 g, 65%), $[\alpha]_D$ +24.0 ± 0.5° (*c*, 1.25); R_f 0.7 (t.l.c.).

Anal. Calcd. for $C_{14}H_{28}O_4S_2$: C, 51.9; H, 8.6. Found: C, 52.2; H, 8.9.

*1-Deoxy-2,3-di-O-methyl-*D*-ribitol*

A solution of 4,5-*O*-isopropylidene-2,3-di-*O*-methyl-D-ribose diethyl dithioacetal (1.0 g) in ethanol (50 ml) was heated in the presence of freshly prepared Raney nickel (8) (~ 6 g) for 8 h at reflux temperature. The product was purified by chromatography on silica gel, with 1:4 ethyl acetate – petroleum ether as eluent, to give an oil (0.30 g, 54%), $[\alpha]_D$ +16.4 ± 0.3° (*c*, 1.65); R_f 0.4 (t.l.c., 1:5 ethyl acetate – petroleum ether). This material (0.28 g) was hydrolyzed overnight at room temperature in methanol (20 ml) and *N* sulfuric acid (5 ml). The product (0.20 g, 92%) was purified by vacuum distillation to give 1-deoxy-2,3-di-*O*-methyl-D-ribitol as a colorless oil, $[\alpha]_D$ +38.6 ± 0.5° (*c*, 1.0); n.m.r. data: τ 5.25 (1-proton, secondary OH), τ 5.48 (1-proton triplet, J = 5.5 Hz, primary OH), τ 6.43, 6.55 (3-proton singlets, OMe's), τ 8.75 (3-proton doublet, J = 6 Hz, CMe). Thin-layer chromatographic analysis revealed only one component, with R_f 0.4 in ethyl acetate; a spot appeared within 1 min with sodium periodate – potassium permanganate spray (9). An aqueous solution of the compound (~ 5 mg) and sodium periodate (~ 25 mg) was left to stand at room temperature. After 30 min, t.l.c. showed that the starting material had all reacted.

*1-Deoxy-2,4-O-isopropylidene-*D*-ribitol*

2,4-*O*-Isopropylidene-D-ribose diethyl dithioacetal (0.23 g) was treated with Raney nickel as described above. The product crystallized from ethyl acetate – petroleum ether. Recrystallization from chloroform – petroleum ether gave the analytically pure desulfurized compound (0.08 g, 58%), m.p. 132.5–133°, $[\alpha]_D$ +12.0 ± 1° (*c*, 0.7); R_f 0.6 (t.l.c., ethyl acetate); n.m.r. data: τ 4.90 (1-proton doublet, J = 6.5 Hz, secondary OH), τ 5.40 (1-proton triplet, J = 5 Hz, primary OH), τ 8.36, 8.50 (3-proton singlets, CMe_2), τ 8.65 (3-proton doublet, J = 6 Hz, CMe). No spot appeared on a thin-layer chromatogram with sodium periodate – potassium permanganate spray, and the compound was unaffected by a sodium periodate solution.

Anal. Calcd. for $C_8H_{16}O_4$: C, 54.6; H, 9.1. Found: C, 54.5; H, 9.2.

*1-Deoxy-3,5-di-O-methyl-*D*-ribitol*

1-Deoxy-2,4-*O*-isopropylidene-D-ribitol (20 mg) was methylated (3), and the product was hydrolyzed by heating a solution in methanol (1 ml) and *N* sulfuric acid (0.25 ml) for 1 h at reflux temperature. The resulting syrup was purified by vacuum distillation to give 1-deoxy-3,5-di-*O*-methyl-D-ribitol as a colorless oil, $[\alpha]_D$ +9.1 ± 1° (*c*, 0.75 in chloroform); R_f 0.5 (t.l.c., ethyl acetate); n.m.r. data: τ 5.24, 5.48 (1-proton doublets, J = 5 Hz, secondary OH's), τ 6.57, 6.65 (3-proton singlets, OMe's), τ 8.89 (3-proton doublet, J = 6 Hz, CMe). No spot appeared

Can. J. Chem. Downloaded from www.nrcresearchpress.com by 210.87.254.40 on 09/05/12
For personal use only.

on a thin-layer chromatogram with sodium periodate – potassium permanganate spray, and the compound was unaffected by a sodium periodate solution.

Acknowledgment

The authors thank the National Research Council of Canada for financial support of this research.

1. H. ZINNER and J. MILBRADT. Carbohydrate Res. **3**, 389 (1967), and references therein.
2. P. A. J. GORIN. Can. J. Chem. **43**, 2078 (1965), and references therein.
3. D. G. LANCE and J. K. N. JONES. Can. J. Chem. **45**, 1533 (1967).
4. M. A. BUKHARI, A. B. FOSTER, J. LEHMANN, J. M. WEBBER, and J. H. WESTWOOD. J. Chem. Soc. 2291 (1963).
5. O. L. CHAPMAN and R. W. KING. J. Am. Chem. Soc. **86**, 1256 (1964).
6. G. W. KENNER, H. J. RODDA, and A. R. TODD. J. Chem. Soc. 1613 (1949); D. T. WILLIAMS and J. K. N. JONES. Can. J. Chem. **44**, 412 (1966).
7. E. L. FALCONER and G. A. ADAMS. Can. J. Chem. **34**, 338 (1956).
8. A. I. VOGEL. Textbook of practical organic chemistry. Longmans, Green and Co., Inc., New York. 1951.
9. R. U. LEMIEUX and H. F. BAUER. Anal. Chem. **26**, 920 (1954).

Can. J. Chem. Downloaded from www.nrcresearchpress.com by 210.87.254.40 on 09/05/12
For personal use only.

Synthesis of 3-*O*-α-D-glucopyranosyl-D-ribose and 3-*O*-α-D-glucopyranosyl-D-arabinose by the nitromethane method[1]

I. FURDA[2] AND M. B. PERRY
Biochemistry Laboratory, National Research Council of Canada, Ottawa, Canada

Received March 31, 1969

2-*O*-α-D-Glucopyranosyl-D-erythrose condensed with nitromethane in the presence of sodium methoxide to yield a mixture of 1-deoxy-3-*O*-α-D-glucopyranosyl-1-nitro-D-ribitol and 1-deoxy-3-*O*-α-D-glucopyranosyl-1-nitro-D-arabinitol which were converted *via* the Nef reaction to 3-*O*-α-D-glucopyranosyl-D-ribose and 3-*O*-α-D-glucopyranosyl-D-arabinose.

Canadian Journal of Chemistry, 47, 2891 (1969)

Methods for the synthesis of oligosaccharides involving lengthening of the carbon chain at the reducing end-group of known oligosaccharides have usually employed the addition of hydrogen cyanide (1–6) followed by reduction of the resulting acids to their corresponding reducing glycose derivatives. It was considered that the Fischer–Sowden (7) method of chain extension, if experimentally feasible, might provide a more convenient procedure for the synthesis of oligosaccharides which could possibly be extended to the synthesis of derivatives having 2-amino-2-deoxyglycose or 2-deoxyglycose reducing end-groups. This note records the application of the nitromethane method to 2-*O*-α-D-glucopyranosyl-D-erythrose.

2-*O*-α-D-Glucopyranosyl-D-erythrose condensed with nitromethane in the presence of sodium methoxide to yield a mixture of 1-deoxy-3-*O*-α-D-glucopyranosyl-1-nitro-D-ribitol and 1-deoxy-3-*O*-α-D-glucopyranosyl-1-nitro-D-arabinitol which could not be separated by fractional crystallization. The mixture, on treatment with dilute sulfuric acid, gave 3-*O*-α-D-glucopyranosyl-D-ribose and 3-*O*-α-D-glucopyranosyl-D-arabinose which were separated by cellulose column chromatography to yield pure samples of each oligosaccharide in approximately equal amounts and in a 52% overall yield from 2-*O*-α-D-glucopyranosyl-D-erythrose.

The two oligosaccharides were reduced to their corresponding 3-*O*-α-D-glucopyranosyl-pentitol derivatives which when oxidized with periodate

[1]NRCC No. 10739.
[2]NRCC Postdoctorate Fellow 1968–1969. Present address: Department of Chemistry, Trent University, Peterborough, Ontario.

on a thin-layer chromatogram with sodium periodate – potassium permanganate spray, and the compound was unaffected by a sodium periodate solution.

Acknowledgment

The authors thank the National Research Council of Canada for financial support of this research.

1. H. ZINNER and J. MILBRADT. Carbohydrate Res. **3**, 389 (1967), and references therein.
2. P. A. J. GORIN. Can. J. Chem. **43**, 2078 (1965), and references therein.
3. D. G. LANCE and J. K. N. JONES. Can. J. Chem. **45**, 1533 (1967).
4. M. A. BUKHARI, A. B. FOSTER, J. LEHMANN, J. M. WEBBER, and J. H. WESTWOOD. J. Chem. Soc. 2291 (1963).
5. O. L. CHAPMAN and R. W. KING. J. Am. Chem. Soc. **86**, 1256 (1964).
6. G. W. KENNER, H. J. RODDA, and A. R. TODD. J. Chem. Soc. 1613 (1949); D. T. WILLIAMS and J. K. N. JONES. Can. J. Chem. **44**, 412 (1966).
7. E. L. FALCONER and G. A. ADAMS. Can. J. Chem. **34**, 338 (1956).
8. A. I. VOGEL. Textbook of practical organic chemistry. Longmans, Green and Co., Inc., New York. 1951.
9. R. U. LEMIEUX and H. F. BAUER. Anal. Chem. **26**, 920 (1954).

Can. J. Chem. Downloaded from www.nrcresearchpress.com by 210.87.254.42 on 09/05/12
For personal use only.

Synthesis of 3-*O*-α-D-glucopyranosyl-D-ribose and 3-*O*-α-D-glucopyranosyl-D-arabinose by the nitromethane method[1]

I. FURDA[2] AND M. B. PERRY
Biochemistry Laboratory, National Research Council of Canada, Ottawa, Canada

Received March 31, 1969

2-*O*-α-D-Glucopyranosyl-D-erythrose condensed with nitromethane in the presence of sodium methoxide to yield a mixture of 1-deoxy-3-*O*-α-D-glucopyranosyl-1-nitro-D-ribitol and 1-deoxy-3-*O*-α-D-glucopyranosyl-1-nitro-D-arabinitol which were converted *via* the Nef reaction to 3-*O*-α-D-glucopyranosyl-D-ribose and 3-*O*-α-D-glucopyranosyl-D-arabinose.

Canadian Journal of Chemistry, 47, 2891 (1969)

Methods for the synthesis of oligosaccharides involving lengthening of the carbon chain at the reducing end-group of known oligosaccharides have usually employed the addition of hydrogen cyanide (1–6) followed by reduction of the resulting acids to their corresponding reducing glycose derivatives. It was considered that the Fischer–Sowden (7) method of chain extension, if experimentally feasible, might provide a more convenient procedure for the synthesis of oligosaccharides which could possibly be extended to the synthesis of derivatives having 2-amino-2-deoxyglycose or 2-deoxyglycose reducing end-groups. This note records the application of the nitromethane method to 2-*O*-α-D-glucopyranosyl-D-erythrose.

2-*O*-α-D-Glucopyranosyl-D-erythrose condensed with nitromethane in the presence of sodium methoxide to yield a mixture of 1-deoxy-3-*O*-α-D-glucopyranosyl-1-nitro-D-ribitol and 1-deoxy-3-*O*-α-D-glucopyranosyl-1-nitro-D-arabinitol which could not be separated by fractional crystallization. The mixture, on treatment with dilute sulfuric acid, gave 3-*O*-α-D-glucopyranosyl-D-ribose and 3-*O*-α-D-glucopyranosyl-D-arabinose which were separated by cellulose column chromatography to yield pure samples of each oligosaccharide in approximately equal amounts and in a 52% overall yield from 2-*O*-α-D-glucopyranosyl-D-erythrose.

The two oligosaccharides were reduced to their corresponding 3-*O*-α-D-glucopyranosyl-pentitol derivatives which when oxidized with periodate

[1]NRCC No. 10739.
[2]NRCC Postdoctorate Fellow 1968–1969. Present address: Department of Chemistry, Trent University, Peterborough, Ontario.

at pH 3 released almost immediately 2 moles of formaldehyde per mole of glycitol, followed by a much slower release of a third mole of formaldehyde. This result is consistent with an oligosaccharide having a 3-*O*-substituted pentitol end-group (8, 9).

Experimental

Paper chromatography was performed by the descending method on Whatman No. 1 filter paper using pyridine – ethyl acetate – water (2:5:5 v/v, top layer) as the mobile phase. Glycose derivatives were detected with alkaline silver nitrate (10) or *p*-anisidine hydrochloride (11) and their rates of movement are quoted relative to D-galactose (R_{gal}).

Melting points were determined on a Fisher–Johns apparatus and are corrected. Optical rotations were determined at room temperature using a Perkin–Elmer 141 polarimeter. Solutions were concentrated under reduced pressure and below 40 °C.

3-O-α-D-Glucopyranosyl-D-ribose and 3-O-α-D-Glucopyranosyl-D-arabinose

To a solution of 2-*O*-α-D-glucopyranosyl-D-erythrose (12) (14 g) in methanol (200 ml) was added nitromethane (55 ml) followed by a solution of sodium (2.5 g) in methanol (100 ml), and the mixture was shaken at room temperature for 18 h. Following the addition of ether (500 ml) the precipitated product was collected, washed with light petroleum (b.p. 30–60 °C), and dried (20.6 g). The mixed 1-deoxy-3-*O*-α-D-glucopyranosyl-1-nitro-D-ribitol and 1-deoxy-3-*O*-α-D-glucopyranosyl-1-nitro-D-arabinitol (19 g) was dissolved in 2 *N* sodium hydroxide (200 ml) and the solution was added dropwise with stirring to 6 *N* sulfuric acid (250 ml) cooled externally in an ice-bath. After 1 h the solution was allowed to stand at 20 °C for 2 h and following neutralization with barium carbonate, the filtered mixture was passed down a column of Rexyn 101(H^+) (250 ml) and Duolite A4(OH^-) (50 ml) ion-exchange resins and the eluate and washings were concentrated to a syrup (13 g).

The syrup was fractionated on a cellulose column (7 × 85 cm) using acetone – water mixture (7:1 v/v) as the mobile phase to yield first 3-*O*-α-D-glucopyranosyl-D-ribose (4.0 g) followed by 3-*O*-α-D-glucopyranosyl-D-arabinose (4.1 g).

3-O-α-D-Glucopyranosyl-D-ribose

The syrup of 3-*O*-α-D-glucopyranosyl-D-ribose gave a single spot on paper chromatography (R_{gal} 1.05), having $[\alpha]_D$ +90.5° (*c*, 3 in water), and on hydrolysis (2 *N* H_2SO_4 for 4 h at 98 °C) it gave D-glucose and D-ribose.

Anal. Calcd. for $C_{11}H_{20}O_{10}$: C, 42.31; H, 6.46. Found: C, 42.22; H, 6.50.

A portion of the oligosaccharide (0.6 g) was acetylated at room temperature with acetic anhydride (15 ml) containing zinc chloride (0.35 g) afforded a hepta-*O*-acetyl derivative as a syrup having $[\alpha]_D$ +77.2° (*c*, 1.2 in chloroform).

Anal. Calcd. for $C_{25}H_{34}O_{17}$: C, 49.50; H, 5.65. Found: C, 48.86; H, 5.64.

3-*O*-α-D-glucopyranosyl-D-ribose (10 mg) in water (10 ml) was reduced for 48 h at room temperature with sodium borohydride (50 mg) and after decationization with Rexyn 101(H^+) ion-exchange resin (15 ml), the concentrated product was evaporated from methanol solution (5 × 30 ml) to remove boric acid. The residue was dissolved in 0.2 *M* acetate buffer pH 3.0 and following the addition of 0.3 *M* sodium metaperiodate (4 ml), the mixture was made up to 50 ml with more acetate buffer. The mixture was analyzed at intervals for formaldehyde using the colorimetric chromotropic acid method (13). 1.98 moles of formaldehyde per mole of oligosaccharide were liberated almost immediately (3 min) followed by a slow release of 0.78 mole of formaldehyde (28 h).

3-O-α-D-Glucopyranosyl-D-arabinose

The syrup of 3-*O*-α-D-glucopyranosyl-D-arabinose gave a single spot on paper chromatography (R_{gal} 0.67), having $[\alpha]_D$ +51.4° → +46° (*c*, 2.7 in water) (lit. (14) $[\alpha]_D$ +57° → +47°) and on hydrolysis (2 *N* H_2SO_4 for 5 h at 98 °C) it gave D-glucose and D-arabinose.

Anal. Calcd. for $C_{11}H_{20}O_{10}$: C, 42.31; H, 6.46. Found: C, 41.80; H, 6.42.

A portion of the disaccharide (0.7 g), acetylated as described above, afforded hepta-*O*-acetyl-3-*O*-α-D-glucopyranosyl-(α-D-arabinose) which after recrystallization from methanol afforded the pure derivative (0.58 g) which had m.p. 192 °C and $[\alpha]_D$ +15.1° (*c*, 1.6 in chloroform). (Nuclear magnetic resonance H-1(arabinose) τ 3.73 spacing 3.7 c.p.s.)

Anal. Calcd. for $C_{25}H_{34}O_{17}$: C, 49.50; H, 5.65. Found: C, 49.42; H, 5.47.

Periodate oxidation of 3-*O*-α-D-glucopyranosyl-D-arabinitol, prepared, and treated as described above, resulted in the rapid release of 1.92 moles of formaldehyde per mole of glycitol (5 min) followed by the slow release of a further 0.69 mole of formaldehyde (22 h).

1. E. FISCHER. Chem. Ber. **23**, 932 (1890).
2. O. REINBRECHT. Ann. **272**, 197 (1892).
3. R. M. HANN and C. S. HUDSON. J. Am. Chem. Soc. **56**, 1390 (1934).
4. M. UENAKA. Chem. Abstr. **46**, 8883 (1952).
5. H. L. FRUSH and H. S. ISBELL. J. Res. Natl. Bur. Std. **50**, 133 (1953).
6. H. S. ISBELL and R. SCHAFFER. J. Am. Chem. Soc. **78**, 1887 (1956).
7. J. C. SOWDEN. Advan. Carbohydrate Chem. **6**, 315 (1951).
8. L. HOUGH and M. B. PERRY. Chem. and Ind. (London), 768 (1956).
9. L. HOUGH, B. M. WOODS, and M. B. PERRY. Chem. and Ind. (London), 1100 (1957).
10. W. E. TREVELYAN, D. P. PROCTER, and J. S. HARRISON. Nature, **166**, 444 (1950).
11. L. HOUGH, J. K. N. JONES, and W. H. WADMAN. J. Chem. Soc. 2511 (1949).
12. A. J. CHARLSON and A. S. PERLIN. Can. J. Chem. **34**, 1200 (1956).
13. J. F. O'DEA and R. A. GIBBONS. Biochem. J. **55**, 580 (1953).
14. R. L. WHISTLER and K. YAGI. J. Org. Chem. **26**, 1050 (1961).

Can. J. Chem. Downloaded from www.nrcresearchpress.com by 210.87.254.42 on 09/05/12
For personal use only.

Synthesis of 3-deoxy-D-*galacto*-octulosonic acid[1]

M. B. PERRY AND ANN C. WEBB
Division of Biochemistry and Molecular Biology, National Research Council of Canada, Ottawa, Canada

Received March 27, 1969

3-Deoxy-D-*galacto*-octulosonic acid was prepared by oxidation of 3-deoxy-D-*glycero*-L-*manno*-octonic acid, and 3-deoxy-D-*glycero*-L-*gluco*-octonic acid made by the action of sodium cyanide on 2-deoxy-D-*galacto*-heptose. Gas–liquid chromatographic procedures for the detection and quantitative analysis of the 3-deoxy-D-*galacto*-octulosonic acid are described.

Canadian Journal of Chemistry, 47, 2893 (1969)

Can. J. Chem. Downloaded from www.nrcresearchpress.com by 210.87.254.40 on 09/05/12
For personal use only.

The important role of 3-deoxy-D-*manno*-octulosonic acid as a component of the cell wall lipopolysaccharides of gram negative bacteria is well established (1–5). A recent investigation of the hydrolyzates of several lipopolysaccharide preparations in this laboratory (6) in some cases suggested that an additional 3-deoxyoctulosonic acid was also present, and this prompted us to devise a general synthetic method for the preparation of reference 3-deoxyoctulosonic acids involving the use of 2-deoxyheptoses of known configuration as starting materials.

The chemical synthesis of 3-deoxy-D-*manno*-octulosonic acid has been made by the condensation of D-arabinose with oxalacetic acid (4, 7) or di-*tert*-butyl oxalacetate (8), and Kochetkov *et al.* (9) has described a new synthetic approach in which a monosaccharide is transformed by the Wittig reaction into a 3,4-dideoxyglyculos-3-enoic acid with subsequent lactonization. The present work involving the addition of sodium cyanide to a 2-deoxyheptose to yield epimeric 3-deoxyoctonic acids, which undergo oxidation to yield a 3-deoxyoctulosonic acid derivative having the same configuration of the hydroxyl groups as those present in the starting 2-deoxyheptose, appears to give a general route to the practical synthesis of standard 3-deoxyoctulosonic acids.

On treatment with sodium cyanide, 2-deoxy-D-*galacto*-heptose (10) was converted in almost quantitative yield to a mixture of 3-deoxy-D-*glycero*-L-*manno*-octonic acid and 3-deoxy-D-*glycero*-L-*gluco*-octonic acid, and the mixed acids after conversion to their potassium salts were oxidized with a vanadium chloride – potassium chlorate catalyst, developed by Sprinson *et al.* (11), to yield 3-deoxy-D-*galacto*-octulosonic acid in a 60% overall yield from the 2-deoxy-D-*galacto*-heptose.

The reduction of 3-deoxy-D-*galacto*-octulosonic acid with sodium borohydride gave 3-deoxy - D - *glycero* - L - *manno* - octonic acid and 3-deoxy-D-*glycero*-L-*gluco*-octonic acid, whose lactone derivatives were indistinguishable on paper chromatograms from the lactones of the acids prepared by the addition of cyanide to 2 - deoxy - D - *galacto* - heptose. Similarly the trimethylsilylated 3-deoxyoctonolactones (12, 13) from reduced 3-deoxy-D-*galacto*-octulosonic acid on gas chromatography gave two peaks corresponding in retention times with the trimethylsilyl derivatives of the lactones from the cyanide addition to the 2-deoxy-D-*galacto*-heptose. The 3-deoxy-D-*galacto*-octulosonate after reduction was degraded with ceric sulfate (4, 14) to give 2-deoxy-D-*galacto*-heptose. The above evidence indicates that the catalytic oxidation occurred exclusively at C-2 of the 3-deoxyoctonic acid derivatives, and that the hydroxyl groups of the 3-deoxy-octulosonic acid had the D-*galacto* configuration.

Trimethylsilylation of either free 3-deoxy-D-*galacto*-octulosonic acid or its ammonium salts with bis(trimethylsilyl)trifluoroacetamide containing 1% trimethylchlorosilane gave a product, which on gas–liquid chromatography gave a single peak. The procedure could be extended to the quantitative analysis of the acid using D - *glycero* - D - *gulo* - heptono - 1,4 - lactone or α-androstane as an internal standard in the trimethylsilylating mixture. The standards give an equal molar response to the octulosonic acid derivative, thus providing a convenient method for the quantitative analysis of 3-deoxy-D-*galacto*-octulosonic acid. The gas–liquid chromatographic

[1]NRCC No. 10746.

Can. J. Chem. Downloaded from www.nrcresearchpress.com by 210.87.254.40 on 09/05/12
For personal use only.

method demonstrated that 3-deoxy-D-*galacto*-octulosonate was not a component of any lipopolysaccharide preparation examined so far in this laboratory (6).

Experimental

Paper chromatography was performed by the descending method on Whatman No. 1 filter paper using the solvent systems: (*a*) pyridine – ethyl acetate – water (2:5:5 v/v, top layer) and (*b*) butan-1-ol – pyridine – 0.1 *N* hydrochloric acid (5:3:2 v/v). Compounds were detected on the chromatograms with either (*a*) alkaline silver nitrate (15), or (*b*) periodate – 2-thiobarbiturate (16) spray reagents, and their rates of movement are quoted relative to D-galactose (R_{gal}).

Gas–liquid chromatography was performed using a Hewlett–Packard 402 gas chromatograph with a hydrogen flame detector and fitted with glass U tubes (4 ft × 6 mm × 3 mm internal diameter) packed with either (*a*) 2.5% (w/w) SE-30 on 80–100 mesh acid washed Chromosorb W, (*b*) 10% (w/w) neopentylglycol sebacate polyester on 80–100 mesh acid washed Chromosorb W, or (*c*) a mixture of 1.5% (w/w) neopentylglycol sebacate polyester and 1.5% (w/w) GE–XF 1150 (Applied Science Laboratories Inc., Pa.) on 80–100 mesh acid washed Chromosorb W. Development was made with dry helium at a flow rate of 100 ml per min and samples were injected directly onto the column packing material without the use of the flash heating system. Retention times are quoted relative to penta-*O*-acetyl-L-arabinitol (T_A).

Optical rotations were determined at 20 °C using a Perkin–Elmer 141 polarimeter. Infrared (i.r.) spectra were obtained by the potassium bromide disk technique using a Perkin–Elmer Infracord 237B. Solutions were concentrated under reduced pressure and below 40 °C.

Synthesis of 3-Deoxy-D-galacto-octulosonic Acid

To 2-deoxy-D-*galacto*-heptose (10) (0.3 g) dissolved in water (2.3 ml) and cooled in ice was added a fresh cold solution of sodium cyanide (0.15 g) in water (1.2 ml) and the mixture was left at 0 °C for 4 days. The mixture was aerated and kept at 70 °C for 4 h and the cooled solution was then passed down a column of Rexyn 101(H^+) ion-exchange resin (8 ml). The eluate and washings were concentrated to a syrup (0.36 g) which was shown by paper chromatography to have two components having R_{gal} 1.68 and 1.84 (solvent *a*), R_{gal} 1.13 and 1.26 (solvent *b*). The trimethylsilylated (12, 13) 3-deoxyoctonolactones on gas–liquid chromatography again indicated the presence of two products having retention times expected of 3-deoxy-octono-1,4-lactones T_A 0.74 (33%) and 0.83 (67%) (column *b*, 198 °C), and T_A 0.86 (34%) and 0.97 (66%) (column, *c*, 200 °C). The i.r. spectrum of the mixed lactones showed a strong carbonyl absorption at 1770 cm^{-1} indicative of 1,4-lactone structure.

The mixture of 3-deoxy-D-*glycero*-(L-*manno*- and L-*gluco*)-octono-1,4-lactone (0.32 g) was neutralized with 0.5 *N* potassium hydroxide to the phenolphthalein end-point. A suspension (3.2 ml) of the oxidation catalyst, prepared by dissolving vanadium pentoxide (75 mg) in concentrated hydrochloric acid (4.5 ml) and adding pyridine (4.5 ml) followed by adjustment to pH 3.2 with HCl or pyridine (11), was added, followed by potassium chlorate (0.11 g). The mixture was stirred at room temperature for 8 h and was then neutralized with ammonium hydroxide to the phenolphthalein end-point and the free pyridine was extracted with chloroform. The residual aqueous solution was lyophilized to give a yellow powder (1.4 g) which was subjected to cellulose column chromatography (3.5 × 25 cm) using 75% aqueous acetone as the mobile phase. The portion of the eluant giving a positive reaction with the periodate–thiobarbiturate reagent was collected and concentrated to a small volume. After passage through Rexyn 101 (H^+) ion-exchange resin (5 ml) the eluate was neutralized with ammonium hydroxide and lyophilized to give ammonium 3-deoxy-D-*galacto*-octulosonate (0.25 g), which failed to crystallize from aqueous ethanol and had $[\alpha]_D$ −43° (*c*, 0.3 in water).

Anal. Calcd. for $C_8H_{19}O_9N$: C, 34.78; H, 6.88; N, 5.07. Found: C, 34.5; H, 6.5; N, 4.9.

The i.r. spectrum of ammonium 3-deoxy-D-*galacto*-octulosonate was almost identical with that of lyophilized ammonium 3-deoxy-D-*manno*-octulosonate exhibiting peaks at 3350, 1600 (strong), 1430, 1205, 1143, 1052, 1025, 970, 924, 883, 840, and 775 cm^{-1}.

On paper chromatography the ammonium 3-deoxy-D-*galacto*-octulosonate gave a single spot having R_{gal} 0.27 (solvent *a*) and 0.26 (solvent *b*). The ammonium salt or free 3-deoxyoctulosonic acid after trimethylsilylation in acetonitrile at 80 °C for 2 h with bis(trimethylsilyl)trifluoroacetamide containing 1% trimethylchlorosilane (REGISIL™ – TMCS, Regis Chemical Co., Chicago, Ill.) on gas–liquid chromatography gave a single peak T_A 3.50 (column A, 200 °C). It was readily distinguished from the peaks at T_A 2.60 and 3.00 arising for the trimethylsilylated product of 3-deoxy-D-*manno*-octulosonate analyzed under the same conditions.

Synthetic mixtures of ammonium 3-deoxy-D-*galacto*-octulosonate (ca 30–100 μg) and either D-*glycero*-D-*gulo*-heptono-1,4-lactone or α-androstane were trimethylsilylated as described above. On gas–liquid chromatography using column *a* at 200 °C, it was found that the areas of the peaks of the internal standards D-*glycero*-D-*gulo*-heptono-1,4-lactone (T_A 3.30) and α-androstane (T_A 1.57) gave a 1:1 molar response to the 3-deoxy-D-*galacto*-octulosonate peak area. The procedure affords a convenient method of its analysis with an accuracy of ±3%.

Reduction of 3-Deoxy-D-galacto-octulosonic Acid

Ammonium 3-deoxy-D-*galacto*-octulosonate (20 mg) in water (4 ml) was stirred for 1 h with barium carbonate (0.1 g) and, after filtration, the filtrate was treated with sodium borohydride (40 mg) at room temperature for 3 h. Excess borohydride was destroyed by acidification with acetic acid and the mixture, after passage down a column of Rexyn 101 (H^+) ion-exchange resin (5 ml), was concentrated to dryness and the residue was again concentrated from methanol solution (5 × 12 ml) to remove boric acid. The residue when examined on paper chromatography showed two spots having R_{gal} 1.68 and 1.84 (solvent *a*) and R_{gal} 1.13 and 1.26 (solvent *b*) corresponding to the 3-deoxy-octono-1,4-lactones derived from the addition of cyanide to 2-deoxy-D-*galacto*-

heptose. The trimethylsilylated (12, 13) residue on gas chromatography showed only two peaks having T_A 0.74 (56%) and 0.83 (44%) (column *b*, 198 °C) and T_A 0.86 (55%) and 0.97 (45%) (column *c*, 200 °C) corresponding in retention times with the trimethylsilylated 3-deoxy-octono-1,4-lactones obtained directly from 2-deoxy-D-*galacto*-heptose.

*Ceric Sulfate Degradation of 3-Deoxy-*D*-galacto-octulosonic Acid*

Ammonium 3-deoxy-D-*galacto*-octulosonate (40 mg) was reduced with borohydride and the product was oxidized with ceric sulfate as described by Ghalambor *et al.* (4). The product was fractionated on paper chromatograms and the component having R_{gal} 1.40 (solvent *a*) corresponding to 2-deoxy-D-*galacto*-heptose was collected (8 mg). The heptose (8 mg) was reduced with borohydride and was acetylated to yield 1,3,4,5,6,7-hexa-*O*-acetyl-2-deoxy-D-*galacto*-heptitol (5 mg) which had m.p. and mixture m.p. 118 °C and $[\alpha]_D$ +10° (0.05 in methanol) and on gas chromatography it gave a single peak having T_A 4.41 (column *b*, 200 °C) having the same retention time as an authentic specimen.

1. E. C. HEATH, and M. A. GHALAMBOR. Biochem. Biophys. Res. Commun. **10**, 340 (1963).
2. M. J. OSBORN. Proc. Natl. Acad. Sci. U.S. **50**, 499 (1963).
3. R. D. EDSTROM and E. C. HEATH. Biochem. Biophys. Res. Commun. **16**, 576 (1964).
4. M. A. GHALAMBOR, E. M. LEVINE, and E. C. HEATH. J. Biol. Chem. **241**, 3207 (1966).
5. Molecular Biology of Gram-negative Lipopolysaccharides. Ann. N.Y. Acad. Sci. **133**, Art. 2 (1966).
6. D. T. WILLIAMS and M. B. PERRY. Can. J. Biochem. **47**, 691 (1969).
7. C. HERSHBERGER, M. DAVIS, and S. B. BINKLEY. J. Biol. Chem. **243**, 1585 (1968).
8. C. HERSHBERGER and S. B. BINKLEY. J. Biol. Chem. **243**, 1578 (1968).
9 N. K. KOCHETKOV, B. A. DIMITRIEV, and L. V. BASCKINOWSKY. Carbohydrate Res. **5**, 399 (1967).
10. M. B. PERRY and A. C. WEBB. Can. J. Chem. **46**, 789 (1967).
11. D. B. SPRINSON, J. ROTHSCHILD, and M. SPRECHER. J. Biol. Chem. **238**, 3170 (1963).
12. M. B. PERRY and R. K. HULYALKAR. Can. J. Biochem. **43**, 573 (1965).
13. I. M. MORRISON and M. B. PERRY. Can. J. Biochem. **44**, 1115 (1966).
14. M. B. PERRY and G. A. ADAMS. Biochem. Biophys. Res. Commun. **26**, 417 (1967).
15. W. E. TREVELYAN, D. P. PROCTER, and J. S. HARRISON. Nature, **166**, 444 (1950).
16. L. WARREN. Nature, **186**, 237 (1960).

Nuclear magnetic resonance studies of cyanide ion–2,4,6-trinitroanisole σ-complexes

A. R. NORRIS
Department of Chemistry, Queen's University, Kingston, Ontario

Received February 12, 1969

Nuclear magnetic resonance studies at −30 °C reveal that the cyanide ion reacts with 2,4,6-trinitroanisole to form σ-complexes by attachment of the cyanide ion at both the C-1 and C-3 positions on the ring. In contrast to the methoxide ion adducts of 2,4,6-trinitroanisole, the cyanide ion adduct resulting from attack of the cyanide at the C-3 position is the more stable species.

Canadian Journal of Chemistry, 47, 2895 (1969)

The interactions of neutral or anionic bases with 1-R-2,4,6-trinitrobenzenes (R = CH_3, CHO, Cl, CH_3O, NH_2, CH_3NH) can lead to a variety of products including the σ-complexes **1** and **2** resulting from addition of the base at either the C-1 or the C-3 position (1).

In both chloroform and acetone, the cyanide ion reacts with 2,4,6-trinitrotoluene to form complexes of type **2** (R = CH_3; Y = CN) while with 2,4,6-trinitrobenzaldehyde in the same solvents, complexes of type **1** (R = CHO; Y = CN) are formed (2). In each of these systems, attack of the cyanide ion is either specific at the ring carbon indicated, or the isomeric complex, if formed, rearranges too rapidly to be detected at the temperature of observation (−30 °C).

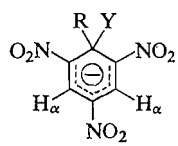

1

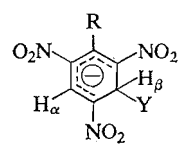

2

Can. J. Chem. Downloaded from www.nrcresearchpress.com by 210.87.254.40 on 09/05/12
For personal use only.

heptose. The trimethylsilylated (12, 13) residue on gas chromatography showed only two peaks having T_A 0.74 (56%) and 0.83 (44%) (column *b*, 198 °C) and T_A 0.86 (55%) and 0.97 (45%) (column *c*, 200 °C) corresponding in retention times with the trimethylsilylated 3-deoxy-octono-1,4-lactones obtained directly from 2-deoxy-D-*galacto*-heptose.

*Ceric Sulfate Degradation of 3-Deoxy-*D*-galacto-octulosonic Acid*

Ammonium 3-deoxy-D-*galacto*-octulosonate (40 mg) was reduced with borohydride and the product was oxidized with ceric sulfate as described by Ghalambor *et al.* (4). The product was fractionated on paper chromatograms and the component having R_{gal} 1.40 (solvent *a*) corresponding to 2-deoxy-D-*galacto*-heptose was collected (8 mg). The heptose (8 mg) was reduced with borohydride and was acetylated to yield 1,3,4,5,6,7-hexa-*O*-acetyl-2-deoxy-D-*galacto*-heptitol (5 mg) which had m.p. and mixture m.p. 118 °C and $[\alpha]_D$ +10° (0.05 in methanol) and on gas chromatography it gave a single peak having T_A 4.41 (column *b*, 200 °C) having the same retention time as an authentic specimen.

1. E. C. HEATH, and M. A. GHALAMBOR. Biochem. Biophys. Res. Commun. **10**, 340 (1963).
2. M. J. OSBORN. Proc. Natl. Acad. Sci. U.S. **50**, 499 (1963).
3. R. D. EDSTROM and E. C. HEATH. Biochem. Biophys. Res. Commun. **16**, 576 (1964).
4. M. A. GHALAMBOR, E. M. LEVINE, and E. C. HEATH. J. Biol. Chem. **241**, 3207 (1966).
5. Molecular Biology of Gram-negative Lipopolysaccharides. Ann. N.Y. Acad. Sci. **133**, Art. 2 (1966).
6. D. T. WILLIAMS and M. B. PERRY. Can. J. Biochem. **47**, 691 (1969).
7. C. HERSHBERGER, M. DAVIS, and S. B. BINKLEY. J. Biol. Chem. **243**, 1585 (1968).
8. C. HERSHBERGER and S. B. BINKLEY. J. Biol. Chem. **243**, 1578 (1968).
9 N. K. KOCHETKOV, B. A. DIMITRIEV, and L. V. BASCKINOWSKY. Carbohydrate Res. **5**, 399 (1967).
10. M. B. PERRY and A. C. WEBB. Can. J. Chem. **46**, 789 (1967).
11. D. B. SPRINSON, J. ROTHSCHILD, and M. SPRECHER. J. Biol. Chem. **238**, 3170 (1963).
12. M. B. PERRY and R. K. HULYALKAR. Can. J. Biochem. **43**, 573 (1965).
13. I. M. MORRISON and M. B. PERRY. Can. J. Biochem. **44**, 1115 (1966).
14. M. B. PERRY and G. A. ADAMS. Biochem. Biophys. Res. Commun. **26**, 417 (1967).
15. W. E. TREVELYAN, D. P. PROCTER, and J. S. HARRISON. Nature, **166**, 444 (1950).
16. L. WARREN. Nature, **186**, 237 (1960).

Nuclear magnetic resonance studies of cyanide ion–2,4,6-trinitroanisole σ-complexes

A. R. NORRIS
Department of Chemistry, Queen's University, Kingston, Ontario

Received February 12, 1969

Nuclear magnetic resonance studies at −30 °C reveal that the cyanide ion reacts with 2,4,6-trinitroanisole to form σ-complexes by attachment of the cyanide ion at both the C-1 and C-3 positions on the ring. In contrast to the methoxide ion adducts of 2,4,6-trinitroanisole, the cyanide ion adduct resulting from attack of the cyanide at the C-3 position is the more stable species.

Canadian Journal of Chemistry, 47, 2895 (1969)

The interactions of neutral or anionic bases with 1-R-2,4,6-trinitrobenzenes (R = CH_3, CHO, Cl, CH_3O, NH_2, CH_3NH) can lead to a variety of products including the σ-complexes **1** and **2** resulting from addition of the base at either the C-1 or the C-3 position (1).

In both chloroform and acetone, the cyanide ion reacts with 2,4,6-trinitrotoluene to form complexes of type **2** (R = CH_3; Y = CN) while with 2,4,6-trinitrobenzaldehyde in the same solvents, complexes of type **1** (R = CHO; Y = CN) are formed (2). In each of these systems, attack of the cyanide ion is either specific at the ring carbon indicated, or the isomeric complex, if formed, rearranges too rapidly to be detected at the temperature of observation (−30 °C).

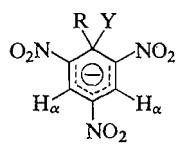

1

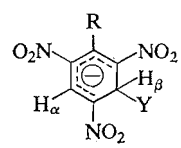

2

Can. J. Chem. Downloaded from www.nrcresearchpress.com by 210.87.254.42 on 09/05/12
For personal use only.

Can. J. Chem. Downloaded from www.nrcresearchpress.com by 210.87.254.42 on 09/05/12
For personal use only.

Servis (3) has shown that the reaction of 2,4,6-trinitroanisole with methoxide ion in dimethylsulfoxide – methanol at room temperature yields initially the type **2** complex (R = Y = OCH_3). This complex undergoes a rapid conversion to the thermodynamically more stable **1** product (R = Y = OCH_3), the nuclear magnetic resonance (n.m.r.) characteristics of which are reported by Crampton and Gold (4). With sulfite ion in dimethylsulfoxide – water, 2,4,6-trinitroanisole forms only complex **2** (R = OCH_3; Y = SO_3^-) (5), while with azide ion in acetone-d_6 and acetonitrile-d_3 at −40 °C only σ-complexes of type **1** (R = OCH_3; Y = N_3) have been observed (6).

We wish to report that the cyanide ion also reacts with 2,4,6-trinitroanisole to form two types of σ-complexes. In contrast to the methoxide ion adducts, the cyanide ion σ-complex of type **2** is more stable than the σ-complex of type **1**.

The proton n.m.r. spectrum of 2,4,6-trinitroanisole (TNA) in deuteriochloroform at −30 °C shows resonance absorptions at 9.08 and 4.27 p.p.m. (sharp singlets, relative band areas 2:3)[1]. A deuteriochloroform solution containing 2,4,6-trinitroanisole (0.6 *M*) and tetraphenylarsonium cyanide (0.4 *M*) shows, in addition to the parent TNA peaks now shifted to 9.09 and 4.26 p.p.m. and the multiplet in the 7.8 p.p.m. region due to the tetraphenylarsonium group, new resonances at 8.90 (singlet), 8.64 (doublet), 5.73 (doublet), 3.98 (singlet), and 3.73 (singlet) p.p.m. The absorptions at 8.64, 5.73, and 3.98 p.p.m. have relative areas of 1:1:3 while the absorptions at 8.90 and 3.13 p.p.m. have areas in the ratio of 2:3. The splitting of both the 8.64 and the 5.73 absorption bands is 0.80 c.p.s. The complete spectrum is developed immediately on mixing and both the band positions and the band intensities remain unchanged even after several hours at −30 °C.

The appearance of these new absorptions is consistent with the formation of both σ-complexes **1** and **2** (R = OCH_3; Y = CN). The absorptions at 8.90 and 8.64 p.p.m. are assigned to the H_α hydrogens of **1** and **2** respectively while the absorption at 5.73 is assigned to the H_β hydrogen in complex **2**. The assignments are made on the basis of the chemical shifts observed in the cyanide ion complexes of 1,3,5-trinitrobenzene and 2,4,6-trinitrotoluene (2) and the methoxide ion complexes of 2,4,6-trinitroanisole (3, 4, 7–9). Representative data for these systems are listed in Table I. As in the case of the methoxide ion adducts, the methoxyl group hydrogens in the **1** complex absorb further upfield than the methoxyl group hydrogens in the **2** complex, while the H_α protons in the **1** complex absorb further downfield than the H_α proton in the **2** complex (3).

For the cyanide ion-2,4,6-trinitroanisole system in deuteriochloroform, the integrated areas of the bands due to both the ring and the methyl hydrogens indicate that approximately 70% of the added TNA has been converted to complex under the stated reaction conditions. Of the total complex generated, 80 ± 2% is in the form of complex **2** and 20 ± 2% is in the form of complex **1**. On warming the solution to −6.5 °C, one finds that 60% of the added TNA is now in the form of complex and that of the total complex present, 85 ± 2% is in the form of complex **2** and 15 ± 2% is in the form of complex **1**. The observations suggest that the heat of formation of complex **1** is more negative than the heat of formation of complex **2**.

Irreversible reactions occur when the solutions are warmed to room temperature. Complex **1** disappears rapidly followed by a much slower disappearance of **2**. The solutions which result after several hours possess very complex spectra which suggests that a number of reaction products have been formed. Unlike the spectra obtained in the case of the cyanide–1,3,5-trinitrobenzene and cyanide–2,4,6-trinitrotoluene reactions, the resulting bands in this case are still very sharp.

If deuteriochloroform solutions containing TNA and tetraphenylarsonium cyanide are prepared at room temperature and their spectra recorded as soon as possible after mixing, only the absorption pattern characteristic of complex **2** is observed. This pattern is slowly replaced by that characteristic of the reaction products.

Both types of complex are also formed when 2,4,6-trinitroanisole and tetraphenylarsonium cyanide are allowed to react at −30 °C in

[1]Chemical shifts are quoted relative to a 6% solution of tetramethylsilane in $CHCl_3$ as external standard. Spectra were recorded on Varian A-60 and HA60 instruments.

TABLE I

Chemical shifts of anions from 1-substituted 2,4,6-trinitrobenzenes

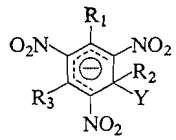

R_1	R_2	R_3	Y	Solvent	T(°C)	R_1	R_2	R_3	Y	Reference
H	H	H	CN	$CDCl_3$	−30	8.42	5.48	8.42	—	2
H	H	H	CN	CD_3COCD_3	30	8.30	5.58	8.30	—	This work
H	H	H	SO_3^-	CH_3SOCH_3: H_2O (70/30)	31	8.30	6.00	8.30*	—	4
H	H	H	OCH_3	CH_3SOCH_3	33.5	8.52	6.22	8.52	—	6, 7
H	OCH_3	H	CN	$CDCl_3$	−30	8.90	3.13	8.90	—	This work
H	OCH_3	H	CN	CD_3COCD_3	−30	8.71	3.01	8.71	—	This work
H	OCH_3	H	OCH_3	CH_3SOCH_3: CH_3OH(90/10)	31	8.67	3.06	8.67	3.06	3
H	OCH_3	H	N_3	CD_3COCD_3	−40	8.66	3.03	8.66	—	5
H	OCH_3	H	$(C_2H_5)_2N$	CD_3SOCD_3	—	8.65	3.08	8.65	—	3
H	CHO	H	CN	$CDCl_3$	−30	8.55	10.14	8.55	—	2
H	CHO	H	CN	CD_3COCD_3	−32	8.35	10.09	8.35	—	This work
H	CHO	H	CN	$CDCl_3$	35	8.42	10.03	8.42	—	This work
OCH_3	H	H	CN	$CDCl_3$	−30	3.98	5.73	8.64†	—	This work
OCH_3	H	H	CN	CD_3COCD_3	−30	3.82	5.68	8.46‡	—	This work
OCH_3	H	H	OCH_3	CH_3SOCH_3: CH_3OH(90/10)	31	3.85	6.17	8.42§	3.20	3
OCH_3	H	H	SO_3^-	CH_3SOCH_3: H_2O(70/30)	31	3.85	6.03	8.35‖	—	4
CH_3	H	H	CN	$CDCl_3$	−30	2.74	5.76	8.65	—	2
CH_3	H	H	CN	$CDCl_3$	30	2.68	5.67	8.52	—	This work

NOTE: Coupling constants quoted for the cyanide adducts were obtained from spectra recorded on a Varian HA-60 spectrometer.
*Ring protons are coupled, $J \sim 1.5$ c.p.s.
†Ring protons coupled, $J = 0.8$ c.p.s.
‡Ring protons coupled, $J = 0.95$ c.p.s.
§Ring protons coupled, J not quoted.
‖Ring protons coupled, $J \sim 1.5$ c.p.s.

acetone-d_6. Once again the type **2** complex predominates at −30 °C and is the complex which disappears the least rapidly as the temperature of the solution is raised to room temperature. The chemical shift data (relative to tetramethylsilane internal standard) characteristic of these two cyanide ion complexes of 2,4,6-trinitroanisole in deuterioacetone are given in Table I.

Further studies relating to the effect of solvent on the stabilities and rates of formation and decay of these two types of cyanide ion–2,4,6-trinitroanisole complex are planned.

Acknowledgments

Financial support by the National Research Council of Canada is gratefully acknowledged. The author is indebted to Dr. Art Grey, National Research Council of Canada, Ottawa, for recording a number of the spectra on the Varian HA-60 spectrometer.

1. E. Buncel, K. E. Russell, and A. R. Norris. Quart. Rev. (London), **22**, 123 (1968).
2. E. Buncel, A. R. Norris, and W. Proudlock. Can. J. Chem. **46**, 2759 (1968).
3. K. L. Servis. J. Am. Chem. Soc. **89**, 1508 (1967).
4. M. R. Crampton and V. Gold. J. Chem. Soc. 4293 (1964); J. Chem. Soc. B, 893 (1966).
5. M. R. Crampton. J. Chem. Soc. B, 1341 (1967).
6. P. Caveng and H. Zollinger. Helv. Chim. Acta, **50**, 861 (1967).
7. R. Foster and C. A. Fyfe. Tetrahedron, **21**, 3363 (1965).
8. R. Foster, C. A. Fyfe, P. H. Emslie, and M. I. Foreman. Tetrahedron, **23**, 227 (1967).
9. P. Caveng, P. B. Fischer, E. Heilbronner, A. L. Miller, and H. Zollinger. Helv. Chim. Acta, **50**, 848 (1967).

Can. J. Chem. Downloaded from www.nrcresearchpress.com by 210.87.254.42 on 09/05/12
For personal use only.

Reaction of *m*-methoxyphenol with trichloromethanesulfenyl compounds. A novel route to sulfines

G. DENIS THORN
Research Institute, Canada Department of Agriculture, London, Ontario

Received March 11, 1969

The reaction of *m*-methoxyphenol with various compounds containing the trichloromethanesulfenyl moiety gives 3,6-dimethoxyxanthione-*S*-oxide.

Canadian Journal of Chemistry, 47, 2898 (1969)

Can. J. Chem. Downloaded from www.nrcresearchpress.com by 210.87.254.6 on 09/05/12
For personal use only.

The standard method of analysis of captan (*N*-trichloromethanesulfenyl-4-cyclohexene-1,2-dicarboximide) is based on a yellow color produced on heating the test material with resorcinol at 140 °C (1). We have found that *m*-methoxyphenol can be substituted advantageously for resorcinol in the analytical procedure. The structure of the main reaction product on which the analysis is based is proposed to be 3,6-dimethoxyxanthione-*S*-oxide **1**.

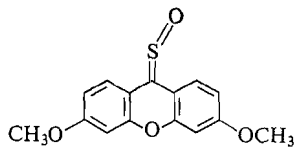

1

The assignment of structure **1** is based on elemental analyses and the following considerations. The intense absorption peak at 420 mμ, log ε 4.54 (ethanol) is characteristic of xanthione-*S*-oxides. (Zwanenburg *et al.* (2) give for xanthione-*S*-oxide, λ_{max} 410 mμ, log ε 4.02 (cyclohexane) and for 10-thiaxanthene-9-thione-*S*-oxide, λ_{max} 420 mμ, log ε 3.85.) Characteristic infrared (i.r.) absorptions for the sulfine[1] group (2, 4) are given at 1125 and 1015 cm^{-1} ($CHCl_3$). The proton magnetic resonance spectrum (CF_3COOH) indicates a symmetrical molecule with one *O*-methyl group to three aromatic H showing an ABX pattern almost identical with that given by 3,6-dimethoxyxanthione.

Attempted oxidation with perphthalic acid (2) of 3,6-dimethoxyxanthione to the sulfine yielded in our hands only the corresponding xanthone and unchanged starting material. Spectroscopic monitoring of the reaction, however, indicated transient existence of the sulfine.

[1]Sheppard and Diekmann (3) suggested the name sulfines for thioketone-*S*-oxides.

The same sulfine **1** is obtained by fractionation and methylation (diazomethane) of the reaction product of resorcinol and captan heated at 140 °C, and also, in about the same yield, by reacting *m*-methoxyphenol with various other compounds containing the trichloromethanesulfenyl moiety, including perchloromethylmercaptan, folpet (*N*-trichloromethanesulfenylphthalimide), *N*-trichloromethanesulfenylmorpholine, *N*,*N*-dimethyltrichloromethanesulfenamide, and *N*,*N*-diethyltrichloromethanesulfenamide. The sulfine is not obtained on reaction of thiophosgene and *m*-methoxyphenol under the above conditions.

The low yields obtained are explicable in part by other colored compounds formed in the macro reaction, none of which, however, shows the intense absorption in the 420 mμ region displayed by the isolated sulfine. In the micro, analytical, reaction, the sulfine is formed in yields of 65–85%, depending on the trichloromethanesulfenyl compound involved.

Experimental

Melting points were determined on a Büchi melting point apparatus and are uncorrected. Elemental analyses were performed by C. Daesslé, Montreal. The mass spectrum was determined by the Morgan–Schaffer Corp., Montreal. Infrared spectra were recorded on a Perkin–Elmer 21 spectrophotometer and the nuclear magnetic resonance spectra obtained with the Varian A-60A spectrophotometer.

3,6-Dimethoxyxanthione-S-oxide (*I*)

Captan (1.0 g) was heated in an open test tube with 2.0 ml of *m*-methoxyphenol at 140–145 °C for 20 min. The dark-red product was dissolved in 5 ml of glacial acetic acid and the solution poured into 100 ml of water. The resulting solid was removed by filtration and dried *in vacuo*. The portion soluble in methylene chloride was fractionated by passing through a column of Woelm acid alumina, methylene chloride being used as eluting solvent. The first fraction consisted of brilliant yellow needles, (55 mg) with m.p. 255–256 °C from ethanol – ethyl acetate (1:1).

Anal. Calcd. for $C_{15}H_{12}O_4S$ (mol. wt., 288): C, 62.5;

H, 4.19; S, 11.11; OCH_3, 21.5. Found (M^+, 288): C, 62.7; H, 4.34; S, 11.11; OCH_3, 21.4.

3,6-Dimethoxyxanthone

3,6-Dihydroxyxanthone, prepared according to Grover *et al.* (5), was methylated in methanol – diethyl ether with diazomethane. The product was crystallized from ethanol, m.p. 189.5–190 °C.

Anal. Calcd. for $C_{15}H_{12}O_4$: C, 70.3; H, 4.68. Found: C, 70.1; H, 4.73.

3,6-Dimethoxyxanthione

3,6-Dimethoxyxanthone (1.0 g) and 1.25 g P_2S_5 were intimately mixed and heated in a test tube at 145–150 °C for 1 h. The reaction mixture was extracted with benzene and with ethyl acetate, the solvents removed on a rotary evaporator, and the residue crystallized from ethanol to give 0.40 g of orange product. It was recrystallized from benzene – ethanol to a m.p. of 212.5–213 °C.

Anal. Calcd. for $C_{15}H_{12}O_3S$: C, 66.2; H, 4.42; S, 11.7. Found: C, 66.5; H, 4.32; S, 11.9.

1. Official methods of analysis of the association of official agricultural chemists. 9th ed. *Edited by* W. Horwitz. Washington, D. C. 1960. p. 340.
2. B. Zwanenburg, L. Thijs, and J. Strating. Rec. Trav. Chim. **86**, 577 (1967).
3. W. A. Sheppard and J. Diekmann. J. Am. Chem. Soc. **86**, 1891 (1964).
4. C. W. Pluijgers, J. Berg, A. Kaars Sijpesteijn, A. Tempel, and A. Verloop. Rec. Trav. Chim. **87**, 833 (1968).
5. P. K. Grover, G. D. Shah, and R. C. Shah. J. Chem. Soc. 3982 (1955).

Can. J. Chem. Downloaded from www.nrcresearchpress.com by 210.87.254.6 on 09/05/12
For personal use only.

Synthesis of D-chalcose

B. T. Lawton, D. J. Ward, W. A. Szarek, and J. K. N. Jones
Department of Chemistry, Queen's University, Kingston, Ontario

Received January 31, 1969

A facile synthesis of 4,6-dideoxy-3-*O*-methyl-D-*xylo*-hexose (D-chalcose) is described, which involves the preparation of methyl 4,6-dichloro-4,6-dideoxy-3-*O*-methyl-D-galactopyranoside (**2**) by a reaction with sulfuryl chloride, and its reduction to the dideoxy sugar by hydrogenation over Raney nickel.

Canadian Journal of Chemistry, 47, 2899 (1969)

Chalcose (lankavose) is a constituent of the antibiotics chalcomycin (1), lankamycin (2), and neutramycin (3). On the basis of nuclear magnetic resonance (n.m.r.) and chemical evidence (1, 4), the structure of 4,6-dideoxy-3-*O*-methyl-D-*xylo*-hexose (**3**) was assigned to the sugar. The stereochemical assignment has been corroborated by a number of syntheses of chalcose (5–7). In continuation of our syntheses of branched-chain and deoxy sugars, we have now prepared D-chalcose, in high yield, by a route that is considerably more facile than those employed by other workers. Two salient features of this work are the preparation of a methyl 4,6-dichloro-4,6-dideoxy-hexoside by reaction with sulfuryl chloride, and its reduction to the dideoxy sugar by hydrogenation over Raney nickel.

Treatment of 1,2:5,6-di-*O*-isopropylidene-3-*O*-methyl-α-D-glucofuranose with methanolic hydrogen chloride gave syrupy methyl 3-*O*-methyl-D-glucopyranoside (**1**), presumably as a mixture of α- and β-anomers. Reaction of **1** with sulfuryl chloride, by the general method of Jennings and Jones (8), and dechlorosulfation of the product using sodium iodide afforded methyl 4,6-dichloro-4,6-dideoxy-3-*O*-methyl-D-galactopyranoside (**2**). The stereochemistry at C-4 was assigned on the basis of work with methyl α-D-glucopyranoside (9, 10); C-4 was substituted by a chlorine atom with inversion of configuration.

It is known that the ease of reductive dehalogenation decreases markedly in the order I > Br > Cl > F. Thus, although several examples of the use of bromo- and iodo-deoxy sugars as intermediates in the synthesis of deoxy sugars are known (11), the reduction of chlorodeoxy sugars is rare (12). In the present work, however, we have found that such reductions can be readily achieved by hydrogenation over a W-4 Raney nickel catalyst, prepared by the procedure described by Pavlic and Adkins (13). It is essential that stirring is maintained during this procedure, since catalysts prepared without stirring were not sufficiently active to effect the reduction of chlorodeoxy sugars. Thus, compound **2** was reduced

H, 4.19; S, 11.11; OCH_3, 21.5. Found (M^+, 288): C, 62.7; H, 4.34; S, 11.11; OCH_3, 21.4.

3,6-Dimethoxyxanthone

3,6-Dihydroxyxanthone, prepared according to Grover *et al.* (5), was methylated in methanol – diethyl ether with diazomethane. The product was crystallized from ethanol, m.p. 189.5–190 °C.

Anal. Calcd. for $C_{15}H_{12}O_4$: C, 70.3; H, 4.68. Found: C, 70.1; H, 4.73.

3,6-Dimethoxyxanthione

3,6-Dimethoxyxanthone (1.0 g) and 1.25 g P_2S_5 were intimately mixed and heated in a test tube at 145–150 °C for 1 h. The reaction mixture was extracted with benzene and with ethyl acetate, the solvents removed on a rotary evaporator, and the residue crystallized from ethanol to give 0.40 g of orange product. It was recrystallized from benzene – ethanol to a m.p. of 212.5–213 °C.

Anal. Calcd. for $C_{15}H_{12}O_3S$: C, 66.2; H, 4.42; S, 11.7. Found: C, 66.5; H, 4.32; S, 11.9.

1. Official methods of analysis of the association of official agricultural chemists. 9th ed. *Edited by* W. Horwitz. Washington, D. C. 1960. p. 340.
2. B. Zwanenburg, L. Thijs, and J. Strating. Rec. Trav. Chim. **86**, 577 (1967).
3. W. A. Sheppard and J. Diekmann. J. Am. Chem. Soc. **86**, 1891 (1964).
4. C. W. Pluijgers, J. Berg, A. Kaars Sijpesteijn, A. Tempel, and A. Verloop. Rec. Trav. Chim. **87**, 833 (1968).
5. P. K. Grover, G. D. Shah, and R. C. Shah. J. Chem. Soc. 3982 (1955).

Synthesis of D-chalcose

B. T. Lawton, D. J. Ward, W. A. Szarek, and J. K. N. Jones
Department of Chemistry, Queen's University, Kingston, Ontario

Received January 31, 1969

A facile synthesis of 4,6-dideoxy-3-*O*-methyl-D-*xylo*-hexose (D-chalcose) is described, which involves the preparation of methyl 4,6-dichloro-4,6-dideoxy-3-*O*-methyl-D-galactopyranoside (**2**) by a reaction with sulfuryl chloride, and its reduction to the dideoxy sugar by hydrogenation over Raney nickel.

Canadian Journal of Chemistry, 47, 2899 (1969)

Chalcose (lankavose) is a constituent of the antibiotics chalcomycin (1), lankamycin (2), and neutramycin (3). On the basis of nuclear magnetic resonance (n.m.r.) and chemical evidence (1, 4), the structure of 4,6-dideoxy-3-*O*-methyl-D-*xylo*-hexose (**3**) was assigned to the sugar. The stereochemical assignment has been corroborated by a number of syntheses of chalcose (5–7). In continuation of our syntheses of branched-chain and deoxy sugars, we have now prepared D-chalcose, in high yield, by a route that is considerably more facile than those employed by other workers. Two salient features of this work are the preparation of a methyl 4,6-dichloro-4,6-dideoxy-hexoside by reaction with sulfuryl chloride, and its reduction to the dideoxy sugar by hydrogenation over Raney nickel.

Treatment of 1,2:5,6-di-*O*-isopropylidene-3-*O*-methyl-α-D-glucofuranose with methanolic hydrogen chloride gave syrupy methyl 3-*O*-methyl-D-glucopyranoside (**1**), presumably as a mixture of α- and β-anomers. Reaction of **1** with sulfuryl chloride, by the general method of Jennings and Jones (8), and dechlorosulfation of the product using sodium iodide afforded methyl 4,6-dichloro-4,6-dideoxy-3-*O*-methyl-D-galactopyranoside (**2**). The stereochemistry at C-4 was assigned on the basis of work with methyl α-D-glucopyranoside (9, 10); C-4 was substituted by a chlorine atom with inversion of configuration.

It is known that the ease of reductive dehalogenation decreases markedly in the order I > Br > Cl > F. Thus, although several examples of the use of bromo- and iodo-deoxy sugars as intermediates in the synthesis of deoxy sugars are known (11), the reduction of chlorodeoxy sugars is rare (12). In the present work, however, we have found that such reductions can be readily achieved by hydrogenation over a W-4 Raney nickel catalyst, prepared by the procedure described by Pavlic and Adkins (13). It is essential that stirring is maintained during this procedure, since catalysts prepared without stirring were not sufficiently active to effect the reduction of chlorodeoxy sugars. Thus, compound **2** was reduced

Can. J. Chem. Downloaded from www.nrcresearchpress.com by 210.87.254.40 on 09/05/12
For personal use only.

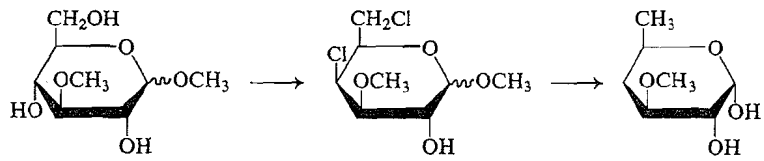

1 2 3

using the active catalyst and a hydrogen pressure of 45 p.s.i.g. to give a product, which on acid-catalyzed hydrolysis afforded crystalline 4,6-dideoxy-3-*O*-methyl-D-*xylo*-hexose (D-chalcose) (**3**).

Experimental

Melting points were determined on a Fisher–Johns melting point apparatus and are uncorrected. Optical rotations were measured with a Perkin–Elmer model 141 automatic polarimeter at 23 ± 2°. Thin-layer chromatography (t.l.c.) was performed with Silica Gel G as the adsorbent in the following solvent systems (v/v): (*a*) ethyl acetate – light petroleum (b.p. 60–80°), 2:1; (*b*) chloroform – methanol, 17:3. Sugars were detected by spraying the developed, air-dried plates with 5% ethanolic sulfuric acid, and heating at about 150°.

Methyl 3-O-Methyl-α,β-D-glucopyranoside (1)

1,2:5,6-Di-*O*-isopropylidene-3-*O*-methyl-α-D-glucofuranose was prepared by treatment of 1,2:5,6-di-*O*-isopropylidene-α-D-glucofuranose (1.85 g) with methyl iodide (15 ml) and silver oxide (1 g) at reflux temperature for 16 h. The syrupy product (1.91 g) was heated at reflux temperature in 3% methanolic hydrogen chloride (20 ml) for 4 h to give a chromatographically homogeneous (t.l.c.) syrup (1.46 g). The absence of furanosides was indicated by the fact that no spot was detected when a thin-layer chromatogram was sprayed with sodium periodate – potassium permanganate reagent (14).

Methyl 4,6-Dichloro-4,6-dideoxy-3-O-methyl-α,β-D-galactopyranoside (2)

To a cooled (dry ice – acetone) solution of **1** (1.4 g) in dry pyridine (5.5 ml) and chloroform (14 ml) was added sulfuryl chloride (3.6 ml) dropwise, with stirring. Cooling was continued for an additional 2 h, and then the reaction mixture was stirred at room temperature for a further 6 h. The mixture was diluted with chloroform (25 ml) and washed with 3 *N* hydrochloric acid, sodium hydrogen carbonate solution, and water. Concentration of the dried (Na_2SO_4) chloroform solution gave a syrup, which showed two spots by t.l.c. in solvent *a*. Only the faster-moving component was detected with aniline–pyridine in *n*-butanol (15), a spray reagent for sugars containing a chlorosulfate group.

The syrup was dissolved in methanol (50 ml), and a 10% solution of sodium iodide in 1:1 methanol – water was added dropwise, with stirring, until iodine was no longer observed to be produced. The solution was neutralized with sodium hydrogen carbonate, filtered, and concentrated to a residue, which was partitioned between chloroform and water. The dried (Na_2SO_4) chloroform solution was concentrated to a syrup, which partially crystallized on standing (1.69 g, 99%), $[\alpha]_D$ +128° (*c*, 2.03 in chloroform). Only the slower-moving component observed above, R_f 0.38, was detected by t.l.c. in solvent *a*; no spots were visible with aniline – pyridine spray.

Anal. Calcd. for $C_8H_{14}Cl_2O_4$: C, 39.2; H, 5.8; Cl, 28.9. Found: C, 39.2; H, 6.0; Cl, 29.0.

4,6-Dideoxy-3-O-methyl-D-xylo-hexose (D-Chalcose) (3)

A solution of compound **2** (1.0 g) in absolute ethanol (30 ml) containing potassium hydroxide (0.9 g) and W-4 Raney nickel catalyst (13) (2 g) was subjected to a hydrogen pressure of 45 p.s.i.g. for 4 h. The solution was filtered free of catalyst, and the filtrate was neutralized with *N* hydrochloric acid and concentrated to a residue, which was partitioned between chloroform and water. The dried (Na_2SO_4) chloroform solution was concentrated to a syrup (0.53 g).

A portion of the syrupy product (0.32 g) in water (5 ml) containing Rexyn-101 (H form) resin was heated at reflux temperature for 5 h. Thin-layer chromatography in solvent *b* showed the presence of only one component. The resin was removed and the solution was concentrated to a syrup (0.29 g, 72%), which was distilled at 65–75° (bath)/0.1 Torr; the distillate crystallized on standing. Recrystallization from ether – light petroleum gave D-chalcose (**3**) as needles, m.p. 90–93°, $[\alpha]_D$ +132° (1.5 min) → +76° (final) (*c*, 0.52 in water). The physical constants are in agreement with those published for the sugar by other workers (4–7).

Acknowledgments

The authors thank the National Research Council of Canada and the Committee on Scientific Research at Queen's University for financial support for this research.

1. P. W. K. Woo, H. W. Dion, and Q. R. Bartz. J. Am. Chem. Soc. **83**, 3352 (1961).
2. W. Keller-Schierlein and G. Roncari. Helv. Chim. Acta, **45**, 138 (1962); **47**, 78 (1964).
3. M. P. Kunstmann and L. A. Mitschev. Experientia, **21**, 372 (1965).
4. P. W. K. Woo, H. W. Dion, and L. F. Johnson. J. Am. Chem. Soc. **84**, 1066 (1962).
5. N. K. Kochetkov and A. I. Usov. Tetrahedron Letters, 519 (1963); Izv. Akad. Nauk SSSR, Ser. Khim. 492 (1965).
6. A. B, Foster, M. Stacey, J. M. Webber, and J. H. Westwood. Proc. Chem. Soc. 279 (1963).
7. S. McNally and W. G. Overend. Chem. Ind. (London), 2021 (1964).

Can. J. Chem. Downloaded from www.nrcresearchpress.com by 210.87.254.40 on 09/05/12
For personal use only.

8. H. J. JENNINGS and J. K. N. JONES. Can. J. Chem. **40**, 1408 (1962).
9. P. D. BRAGG, J. K. N. JONES, and J. C. TURNER. Can. J. Chem. **37**, 1412 (1959). J. K. N. JONES, M. B. PERRY, and J. C. TURNER. Can. J. Chem. **38**, 1122 (1960).
10. R. HOGE and J. TROTTER. J. Chem. Soc. Ser. A. To be published.
11. S. HANESSIAN. *In* Deoxy sugars. Advances in Chemistry Series, No. 74. American Chemical Society, Washington, D.C. 1968. Chap. 9.
12. T. TSUSHIYA and S. UMEZAWA. Bull. Chem. Soc. Japan, **38**, 1181 (1965). L. VARGHA and J. KUSZMANN. Chem. Ber. **96**, 411 (1963).
13. A. A. PAVLIC and H. ADKINS. J. Am. Chem. Soc. **68**, 1471 (1946).
14. R. U. LEMIEUX and H. F. BAUER. Anal. Chem. **26**, 920 (1954).
15. G. CRANK. M.Sc. Thesis, Queen's University, Kingston, Ontario. 1960.

Can. J. Chem. Downloaded from www.nrcresearchpress.com by 210.87.254.40 on 09/05/12
For personal use only.

Non-equivalence of *gem*-dimethyl protons in some bi- and tricyclic compounds. Stereochemical assignments in the khusenic, isokhusenic, and chamigrene series

GEORGE A. NEVILLE AND ISHWAR C. NIGAM[1]

Research Laboratories, Food and Drug Directorate, Department of National Health and Welfare, Ottawa, Canada

Received September 23, 1968

The non-equivalence of *gem*-dimethyl protons in two novel series of tricyclic sesquiterpenes, khusenic (**1**) and isokhusenic (**2**), is discussed in terms of anisotropy effects and compared with that found in the analogous monoterpenic compounds, fenchone (**8**), pinocamphone (**9**), camphene (**10***a*), methylenenorbornane (**10***b*), camphenilone (**11**), and dimethylnorcampholide (**12**). The stereochemistry of the *gem*-dimethyl groups has been assigned in the above compounds. The chemical shift data and the stereochemistry of the above compounds has been used to make stereochemical assignments in the novel chamigrene series **13**, **15**, **17**, and **19**.

Canadian Journal of Chemistry, 47, 2901 (1969)

In recent years, the isolation and characterization of two novel series of tricyclic sesquiterpenes from Oil of Vetiver, khusenic (**1**) and isokhusenic (**2**), were reported from these laboratories by the late Dr. Nigam[2] and his co-workers (1). About the same time Kido, *et al.* (2) reported similar structural findings for zizanoic acid (= khusenic acid **1***b*) and recorded physicochemical data on the related compounds **1***d*, **3***a*, and **3***b*. Later Kido *et al.* (3) established the stereochemistry of **4** (R = CO_2H) for zizanoic acid which is also applicable to structures **1**, **2**, **3**, and **5**. More recently, our elucidation of long-range couplings in the khusenic (**1**) and isokhusenic (**2**) series (4) has provided additional evidence in support of these tricyclic sesquiterpenic skeletons. We now wish to discuss examples of non-equivalence of *gem*-dimethyl protons found in the khusenic (**1**) and isokhusenic (**2**) series in relation to similar phenomena in the monoterpenic compounds **8**–**12**. The chemical shift data and experience gained from structural analysis of the above compounds proved helpful in assigning the stereochemistry of some recently reported, unique, spiro-bicyclic sesquiterpenes (chamigrene series).

gem-Dimethyl in the Khusenic Series

Non-equivalence of the *gem*-dimethyl protons in the khusenic series (**1**, **5**, and **6**) arises from a combination of anisotropic effects, i.e. from both the carbonyl or olefinic groups and from the proximate C—C and C—H bonds. Undoubtedly, it is the extra anisotropic shielding and deshielding effect on the axial and equatorial methyl substituents respectively, having its origin in the anisotropy of C=C (5) and C=O (6, 7), that accounts for the small, but noticeable non-equivalence of these protons. Dreiding models show **1** and **5** to be rigid molecules in which the cyclohexane ring (stereochemistry of **4**) has the chair configuration. For this configuration, we would assign the low field singlets from **1***a*, **1***b*, **1***c*, **1***d*, **5**, and **6** at 1.05, 1.07, 1.07, 1.06, 1.18, and

[1]Deceased.

[2]The widely recognized work of Dr. I.C. Nigam in the field of terpene chemistry was tragically terminated by an automobile accident on August 19, 1968. For a leading reference to Dr. Nigam's extensive series of publications on 'Essential Oils and their Constituents', see ref. 20.

8. H. J. JENNINGS and J. K. N. JONES. Can. J. Chem. **40**, 1408 (1962).
9. P. D. BRAGG, J. K. N. JONES, and J. C. TURNER. Can. J. Chem. **37**, 1412 (1959). J. K. N. JONES, M. B. PERRY, and J. C. TURNER. Can. J. Chem. **38**, 1122 (1960).
10. R. HOGE and J. TROTTER. J. Chem. Soc. Ser. A. To be published.
11. S. HANESSIAN. *In* Deoxy sugars. Advances in Chemistry Series, No. 74. American Chemical Society, Washington, D.C. 1968. Chap. 9.
12. T. TSUSHIYA and S. UMEZAWA. Bull. Chem. Soc. Japan, **38**, 1181 (1965). L. VARGHA and J. KUSZMANN. Chem. Ber. **96**, 411 (1963).
13. A. A. PAVLIC and H. ADKINS. J. Am. Chem. Soc. **68**, 1471 (1946).
14. R. U. LEMIEUX and H. F. BAUER. Anal. Chem. **26**, 920 (1954).
15. G. CRANK. M.Sc. Thesis, Queen's University, Kingston, Ontario. 1960.

Can. J. Chem. Downloaded from www.nrcresearchpress.com by 210.87.254.6 on 09/05/12
For personal use only.

Non-equivalence of *gem*-dimethyl protons in some bi- and tricyclic compounds. Stereochemical assignments in the khusenic, isokhusenic, and chamigrene series

GEORGE A. NEVILLE AND ISHWAR C. NIGAM[1]

Research Laboratories, Food and Drug Directorate, Department of National Health and Welfare, Ottawa, Canada

Received September 23, 1968

The non-equivalence of *gem*-dimethyl protons in two novel series of tricyclic sesquiterpenes, khusenic (**1**) and isokhusenic (**2**), is discussed in terms of anisotropy effects and compared with that found in the analogous monoterpenic compounds, fenchone (**8**), pinocamphone (**9**), camphene (**10***a*), methylenenorbornane (**10***b*), camphenilone (**11**), and dimethylnorcampholide (**12**). The stereochemistry of the *gem*-dimethyl groups has been assigned in the above compounds. The chemical shift data and the stereochemistry of the above compounds has been used to make stereochemical assignments in the novel chamigrene series **13**, **15**, **17**, and **19**.

Canadian Journal of Chemistry, 47, 2901 (1969)

In recent years, the isolation and characterization of two novel series of tricyclic sesquiterpenes from Oil of Vetiver, khusenic (**1**) and isokhusenic (**2**), were reported from these laboratories by the late Dr. Nigam[2] and his co-workers (1). About the same time Kido, *et al.* (2) reported similar structural findings for zizanoic acid (= khusenic acid **1***b*) and recorded physicochemical data on the related compounds **1***d*, **3***a*, and **3***b*. Later Kido *et al.* (3) established the stereochemistry of **4** (R = CO_2H) for zizanoic acid which is also applicable to structures **1**, **2**, **3**, and **5**. More recently, our elucidation of long-range couplings in the khusenic (**1**) and isokhusenic (**2**) series (4) has provided additional evidence in support of these tricyclic sesquiterpenic skeletons. We now wish to discuss examples of non-equivalence of *gem*-dimethyl protons found in the khusenic (**1**) and isokhusenic (**2**) series in relation to similar phenomena in the monoterpenic compounds **8**–**12**. The chemical shift data and experience gained from structural analysis of the above compounds proved helpful in assigning the stereochemistry of some recently reported, unique, spiro-bicyclic sesquiterpenes (chamigrene series).

gem-Dimethyl in the Khusenic Series

Non-equivalence of the *gem*-dimethyl protons in the khusenic series (**1**, **5**, and **6**) arises from a combination of anisotropic effects, i.e. from both the carbonyl or olefinic groups and from the proximate C—C and C—H bonds. Undoubtedly, it is the extra anisotropic shielding and deshielding effect on the axial and equatorial methyl substituents respectively, having its origin in the anisotropy of C=C (5) and C=O (6, 7), that accounts for the small, but noticeable non-equivalence of these protons. Dreiding models show **1** and **5** to be rigid molecules in which the cyclohexane ring (stereochemistry of **4**) has the chair configuration. For this configuration, we would assign the low field singlets from **1***a*, **1***b*, **1***c*, **1***d*, **5**, and **6** at 1.05, 1.07, 1.07, 1.06, 1.18, and

[1]Deceased.

[2]The widely recognized work of Dr. I.C. Nigam in the field of terpene chemistry was tragically terminated by an automobile accident on August 19, 1968. For a leading reference to Dr. Nigam's extensive series of publications on 'Essential Oils and their Constituents', see ref. 20.

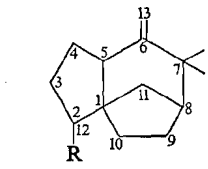

1

a: R = CO_2CH_3
b: R = CO_2H
c: R = CH_2OH
d: R = CH_3

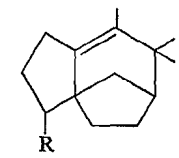

2

a: R = CO_2CH_3
b: R = CO_2H

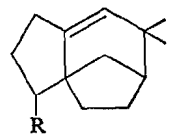

3

a: R = CO_2CH_3
b: R = CH_3

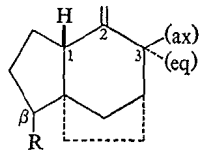

4

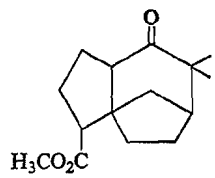

5

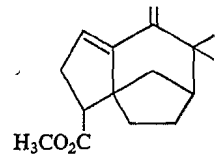

6

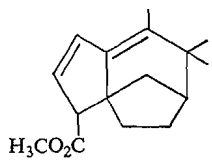

7

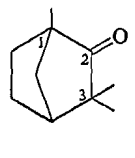

8

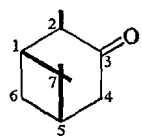

9

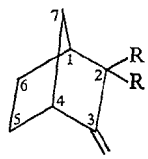

10

a: R = CH_3
b: R = H

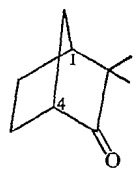

11

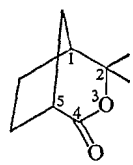

12

1.07 δ, respectively, to the C-7 equatorial methyl protons (cf. **4**). These chemical shift values are in excellent agreement with the chemical shift (1.15 δ) for the C-1 methyl group of fenchone (**8**) whose protons would be exposed to anisotropic deshielding by the vicinal carbonyl group on the basis of the older and commonly accepted anisotropy model (8*a*). In terms of the newly proposed anisotropy model (7) for the carbonyl group, it must be concluded that both the C-1 methyl protons of fenchone (**8**) and the C-7 equatorial methyl protons of **5** are exposed to weak anisotropic shielding from the vicinal carbonyl group while the C-7 axial methyl protons of **5** are exposed to relatively stronger anisotropic shielding.

It is also noteworthy that the frequency of the equatorial *gem*-methyl protons in the cyclohexanone **5** (1.18 δ) and of the C-2 *endo*-methyl protons in pinocamphone (**9**) (1.15 δ, CCl_4) (9) lies within the range (1.15–1.20 δ, CCl_4) reported for the quasi-equatorial, C-2 methyl protons of variously substituted (C-3) cyclobutanones (10). For the khusenic diene methyl ester **6**, the additional unsaturation ($\Delta^{4,5}$) results in no appreciable change in the deshielding of the C-7 equatorial methyl protons from that observed for the methyl ester **1***a* (Table I).

From Table I, it is seen that the C-7 axial methyl protons of the khusenic series (**1**, **5**, and **6**) are shielded relative to the equatorial *gem*-methyl protons and show nearly constant chemical shift. The assignment of the more shielded *gem*-methyl signal to the axial conformation is also in accor-

Can. J. Chem. Downloaded from www.nrcresearchpress.com by 210.87.254.6 on 09/05/12
For personal use only.

TABLE I

gem-Dimethyl chemical shift data for the khusenic and isokhusenic series (δ in p.p.m. downfield from TMS internal reference)*

Compound	Solvent	Reference	*gem*-$(Me)_2$
		Khusenic Series	
1*a*†	$CDCl_3$		1.055(3H, equatorial); 1.042(3H, axial)
1*b*†	$CDCl_3$		1.073(3H, equatorial); 1.047(3H, axial)
1*c*†	$CDCl_3$		1.073(3H, equatorial); 1.046(3H, axial)
1*d*	CCl_4	(2)	1.06(3H, equatorial); 1.04(3H, axial)
5‡§	$CDCl_3$		1.18(3H, equatorial); 1.05(3H, axial)
6‡§	$CDCl_3$	(1*c*)	1.07(3H, equatorial); 0.97(3H, axial)
		Isokhusenic Series	
2*a*†	$CDCl_3$		0.986(3H, *exo*); 0.973(3H, *endo*)
2*b*§‖	$CDCl_3$		0.986(3H, *exo*); 0.973(3H, *endo*)
3*a*	CCl_4	(2)	0.97(6H, *endo* and *exo*)
3*b*	CCl_4	(2)	0.95(6H, *endo* and *exo*)
7‡§	$CDCl_3$	(1*c*)	1.03(6H, *endo* and *exo*)

*The chemical shifts measured in $CDCl_3$ solution (10–15% solute) showed no variation with dilution. Chemical shifts were calibrated by the side-band technique for the 100 MHz spectra and are considered accurate to ± 0.005 p.p.m.; the accuracy for the 60 MHz spectra is considered to be ± 0.02 p.p.m.
†Chemical shifts measured at 100 MHz on the 250 Hz sweep width of a Varian HA-100 spectrometer.
‡Chemical shifts measured at 60 MHz with a Varian A-60A spectrometer.
§Compound not available when 100 MHz spectra were recorded.
‖The 60 MHz spectra of 2*a* and of 2*b* gave unresolved peaks with identical chemical shifts.

dance with the generalization for cyclohexane rings that axial protons absorb at higher field than their equatorial counterparts (8*b*). Constancy of chemical shift for axial methyl protons (1.02–1.05 δ, CCl_4) has also been observed in the cyclobutane ring system (9, 10); however, in contrast to the cyclohexane ring system, axial methyl protons are deshielded relative to equatorial methyl protons in the cyclobutane system. Similarly in the khusenic series (stereochemistry **4**) it appears that the axial methyl protons at C-7 in **1***a*, **1***b*, **1***c*, **1***d*, and **5** (Table I) are also insensitive to changes in anisotropy effects from β-substituents (carbomethoxy, etc.) at C-2. The axial methyl protons of the khusenic diene methyl ester **6**, however, are more deshielded (4–5 Hz) than those in **1***a* due to the additional unsaturation ($\Delta^{4,5}$).

gem-Dimethyl in the Isokhusenic Series

While equivalence of the C-7 *gem*-dimethyl protons might have been expected in the isokhusenic series[3] (**2**) due to the symmetrical arrangement of these methyl groups about the planar olefinic group in the molecule, small non-equivalence has been detected. From inspection of models, it is seen that the *endo*-methyl group in these compounds is much closer to the ethano bridge than the *exo*-methyl group is to the methylene bridge. This factor would, therefore, account for the small non-equivalence found in the *gem*-dimethyl protons of **2***a* by a 100 MHz proton magnetic resonance (p.m.r.) spectrometer. In the isokhusenic series, the *endo*-methyl group at C-7 is assigned to the signal at higher field since these protons are more proximate to the majority of C—C bonds than are the *exo*-methyl protons at C-7. The *endo*-methyl protons should be more shielded also by analogy with the finding that the C-1 proton in camphene[4] (**10***a*) is shielded by 0.41 p.p.m. relative to that in methylenenorbornane (**10***b*) (11).

gem-Dimethyl in Some Bicyclic Monoterpenes

The non-equivalence of the *gem*-dimethyl protons at C-2 in camphene (**10***a*) (1.03 and 1.06 δ, CCl_4) (12) and in camphenilone (**11**) (0.97 and 1.00 δ, CCl_4) appears to arise from the same combination of anisotropy factors operative in the isokhusenic series. Although the *gem*-dimethyl groups of **10** and **11** are symmetrically oriented about the C=C and C=O group respectively, the *endo*-methyl protons are much closer to the ethano bridge than the *exo*-methyl protons are to the methylene bridge; consequently, we would assign the more shielded *gem*-methyl signal in

[3]It would appear from the chemical shift data currently available for other members of the khusenic series (**3** and **7**) (Table I) that *gem*-dimethyl protons are equivalent. It is most likely that small non-equivalence will be detected between these *gem*-dimethyl protons when the above compounds are examined by a high resolution proton magnetic resonance spectrometer.

[4]It also follows from this analogy that the C-1 and C-4 protons of camphenilone (**11**) can be assigned to 2.20 and 2.47 δ (CCl_4) respectively.

Can. J. Chem. Downloaded from www.nrcresearchpress.com by 210.87.254.6 on 09/05/12
For personal use only.

Can. J. Chem. Downloaded from www.nrcresearchpress.com by 210.87.254.6 on 09/05/12
For personal use only.

each (1.03 and 0.97 δ) to the *endo*-conformation. It is interesting to note, therefore, that introduction of a methyl substituent at C-4 in **11** and introduction of a carboxyl group at C-4 of camphene (**10***a*) results in equivalent *gem*-dimethyl protons for fenchone (**8**) (6H, 1.03 δ, CCl_4) and for the carboxy-derivative of **10** (6H, 1.12 δ, CCl_4) (13) respectively, the *endo*-methyl protons in each derivative being more strongly deshielded than the *exo*-methyl protons relative to the parent molecules.

In dimethylnorcampholide (**12**), the perbenzoic acid oxidation product of **11**, non-equivalence of the *gem*-dimethyl protons (1.35 and 1.30 δ, CCl_4) is also seen. In view of considerable evidence for δ-lactones possessing a planar C—OCO—C group in a half-chair type ring configuration (14), this non-equivalence must arise from the same anisotropy effects as proposed above for camphene (**10***a*) and camphenilone (**11**). Likewise we would assign the *endo*-methyl protons of **12** to the signal at higher field (1.30 δ) and the C-1 and C-5 proton signals to 2.05 and 2.67 δ respectively.

Stereochemical Assignments in the Novel Chamigrene Series

A new, sesquiterpenic hydrocarbon, chamigrene (**13***a*), with a unique spiro-ring system was recently isolated from the leaves of *Chamaecyparis taiwanensis* Masam. and characterized by Itô and his colleagues (15). Tanaka *et al.* (16) have synthesized 5,5,9-trimethyspiro(5,5)undec-8-en-1-one (**15***a*) and derivatives (e.g. **15***b*) as convenient precursors for the synthesis of chamigrene (**13***a*). More recently Ohta and Hirose (17) isolated chamigrene from the oil of the fruits of *Schisandra chinensis* together with two new compounds of the same carbon skeleton, namely, chamigrenal (**13***c*) and α-chamigrene (**19**). In addition, γ-chamigrene (**17**) was obtained by Ohta and Hirose as the minor product from the Wolff–Kishner reduction of the semicarbazone of **13***c*. Since only the gross structure has been reported for the above compounds, it is most appropriate to employ the reported p.m.r. data in conjunction with the deductions made above for the tri- and bi-cyclic terpenic systems, to assign the stereochemistry in these remarkable compounds. This objective appears all the more desirable since the chamigrene system constitutes the first instance of a spiro (5,5)undecane skeleton being found in a sesquiterpenoid (13).

From a study of models, it is seen that chamigrene may have two conformations[5]; "*endo-gem*-dimethyl" (**13***a*), or "*endo*-(*exo*-)methyleno" (**14***a*) by virtue of inversion of the half-chair cyclohexane ring about C-7 and C-11. Conformation **14***a* would appear to be prohibited by a large non-bonded interaction between one of the *exo*-methylene hydrogen atoms and the cyclohexene ring; moreover, the *exo*-cyclic vinylic protons (4.47, 1H, J = 2 Hz; 4.82 δ, 1H, J = 2 and 1 Hz; CCl_4) do not show the shielding which would arise in conformation **14***a* from the double bond of the cyclohexene ring. In addition the *gem*-dimethyl protons appear at much higher field (0.82 and 0.87 δ, CCl_4) than the axial *gem*-methyl protons in the khusenic series (**1**) indicative of conformation **13***a* in which the *gem*-dimethyl protons of chamigrene would be subjected to anisotropic shielding by the double bond of the cyclohexene ring. The same preferred conformation (**13**) must hold for the chamigrene derivatives **13***b* and **13***c* since the *exo*-cyclic vinylic proton signals (4.49, 4.88, and 4.34, 4.84 δ, CCl_4, respectively) appear in the same range as those of **13***a*. The small variation in the chemical shifts for the *gem*-dimethyl protons of **13***b* and **13***c* in the "*endo-gem*-dimethyl" conformation (0.83, 0.88, and 0.87, 0.90 δ, CCl_4, respectively) from those of **13***a* merely reflect the expected change in anisotropy of the cyclohexene ring with variation of the substituent R.

Similarly, for the cyclohexanone analogues (**15**), the preferred conformation is that for the "*endo-gem*-dimethyl" orientation. The fact that the allylic methyl protons of **15***a* (1.58 δ, CCl_4) are not greatly deshielded relative to the allylic methyl protons of **13***a* (1.55 δ, CCl_4), as they would have to be in conformation **16***a*, is evidence for the preferred conformation **15***a*. Moreover, the shielding of the *gem*-dimethyl protons in the "*endo-gem*-dimethyl" conformation **15** is very similar to that found for **13** (Table II), and replacement of R = CH_3 by R = OEt has negligible effect in agreement with conformation **15***b*.

In contrast, γ-chamigrene appears to prefer the conformation **17**. In this compound, the two sets of *exo*-cyclic protons show abnormal chemical shifts (4.46 δ, 2H; and 4.73,5.09 δ, 1H each;

[5]For each stable conformation, a pair of optical antipodes is possible because of the asymmetry about the "spiro" carbon atom.

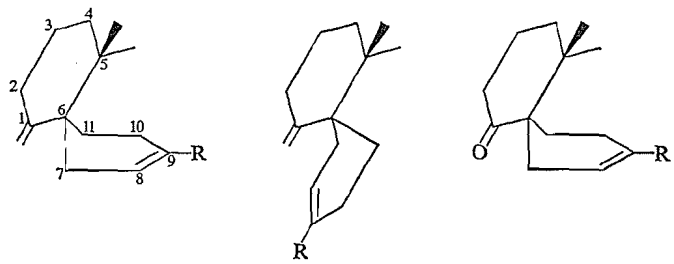

13

a: R = CH_3
b: R = CH_2OH
c: R = HC=O

14

a: R = CH_3
b: R = CH_2OH
c: R = HC=O

15

a: R = CH_3
b: R = OEt

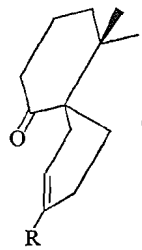

16

a: R = CH_3
b: R = OEt

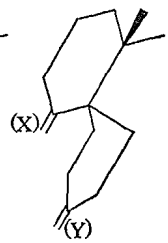

17

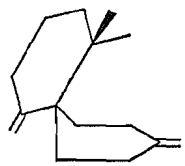

18

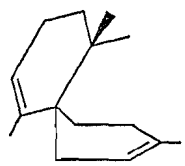

19

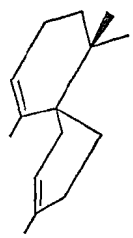

20

CCl_4), one set at higher field and the other set at lower field than found for those of **13***a*. Since such a mutually shielding and deshielding effect is only possible in conformation **17**, this must be the preferred conformation in which the *exo*-cyclic methylene protons (X) are shielded by the double bond (Y) and the *exo*-cyclic protons (Y) are deshielded by the double bond (X).

Finally, α-chamigrene must prefer the "*endo*-gem-dimethyl" conformation (**19**) since both sets of allylic methyl protons are equivalent (Table II). If α-chamigrene preferred conformation **20**, then the allylic methyl protons would be non-equivalent by virtue of the mutual shielding and deshielding effects of the double bonds in each cyclohexene ring. The *gem*-dimethyl protons of α-chamigrene also show chemical shifts typical for methyl protons shielded by the double bond of the other ring and consistent with conformation **19**.

Concluding Comment

The variety of chemical shift data together with the many stereochemical assignments should prove useful for testing mathematical models designed to predict proton shifts from anisotropy effects. Caution must be exercised not to extrapolate too much from available anisotropy data in treating such compressed ring systems, since poor agreement between calculated and found shifts has been experienced to date in similar bicyclic systems (18). Improved anisotropy data,

Can. J. Chem. Downloaded from www.nrcresearchpress.com by 210.87.254.6 on 09/05/12
For personal use only.

TABLE II

Selected chemical shift data for the chamigrene series (δ in p.p.m. downfield from TMS in CCl_4)

Compound	*gem*-$(Me)_2$	Allylic Me	*exo*-Cyclic vinylic	Reference
13*a*	0.82(3H), 0.87(3H)	1.55(3H)	4.47(1H), 4.82(1H)	15
13*b*	0.83(3H), 0.88(3H)	—	4.49(1H), 4.88(1H)	17
13*c*	0.87(3H), 0.90(3H)	—	4.34(1H), 4.84(1H)	17
15*a*	0.80(3H), 0.93(3H)	1.58(3H)	—	16
15*b*	0.82(3H), 0.93(3H)	—	—	16
17	0.85(6H)	—	4.46(2H); 4.73(1H), 5.09(1H)	17
19	0.84(3H), 0.89(3H)	1.63(6H)	—	17

applicable to these systems, was recently reported by Homer and Callaghan (19).

Acknowledgment

The author gratefully acknowledges the interest and assistance of Dr. Robert R. Fraser, University of Ottawa, Canada for obtaining the 100 MHz spectra.

1. (*a*) I. C. NIGAM and H. KOMAE. J. Pharm. Sci. **56**, 1299 (1967); (*b*) I. C. NIGAM, H. KOMAE, G. A. NEVILLE, C. RADECKA, and S. K. PAKNIKAR. Tetrahedron Letters 2497 (1968); (*c*) H. KOMAE and I. C. NIGAM. J. Org. Chem. **33**, 1771 (1968); (*d*) I. C. NIGAM, C. RADECKA, and H. KOMAE. J. Pharm. Sci. **57**, 1029 (1968).
2. F. KIDO, H. UDA, and A. YOSHIKOSHI. Tetrahedron Letters, 2815 (1967).
3. F. KIDO, H. UDA, and A. YOSHIKOSHI. Tetrahedron Letters, 1247 (1968).
4. G. A. NEVILLE and I. C. NIGAM. Tetrahedron Letters, 837 (1969).
5. J. W. APSIMON, W. G. CRAIG, P. V. DEMARCO, D. W. MATHIESON, L. SAUNDERS, and W. B. WHALLEY. Tetrahedron, **23**, 2357 (1967).
6. J. W. APSIMON, W. G. CRAIG, P. V. DEMARCO, D. W. MATHIESON, A. K. G. NASSER, L. SAUNDERS, and W. B. WHALLEY. Chem. Commun. 754 (1966).
7. G. J. KARABATSOS, G. C. SONNICHSEN, N. HSI, and D. J. FENOGLIO. J. Am. Chem. Soc. **89**, 5067 (1967).
8. L. M. JACKMAN. Applications of nuclear magnetic resonance spectroscopy in organic chemistry. The Pergamon Press, Ltd., London. 1959. Chap. 7. (*a*) p. 124; (*b*) p. 116.
9. N. NAKAGAWA, S. SAITO, A. SUZUKI, and M. ITOH. Tetrahedron Letters, 1003 (1967).
10. L. R. SUBRAMANIAN and G. S. KRISHNA RAO. Tetrahedron Letters, 3693 (1967).
11. J. A. CLAISSE and D. I. DAVIES. J. Chem. Soc. B, 679 (1967).
12. R. B. BATES. Nuclear magnetic resonance spectral collection of terpenes. Private communication.
13. R. R. SOBTI and S. DEV. Tetrahedron Letters, 2893 (1967).
14. R. C. SHEPPARD and S. TURNER. Chem. Commun. 77 (1968).
15. S. ITÔ, K. ENDO, T. YOSHIDA, M. YATAGAI, and M. KODAMA. Chem. Commun. 186 (1967).
16. A. TANAKA, H. UDA, and A. YOSHIKOSHI. Chem. Commun. 188 (1967); 56 (1968).
17. Y. OHTA and Y. HIROSE. Tetrahedron Letters, 2483 (1968).
18. J. W. APSIMON. Personal communication.
19. J. HOMER and D. CALLAGHAN. J. Chem. Soc. A, 439 (1968).
20. I. C. NIGAM and L. LEVI. Can. J. Chem. **46**, 1944 (1968).

Phospholipids. Part I. Synthesis of phosphatidyl ethanolamines

S. RAKHIT, J. F. BAGLI, AND R. DEGHENGHI

Ayerst Research Laboratories, Montreal, Quebec

Received February 24, 1969

This paper deals with a simple and general method of preparation of polyunsaturated 1,2-diacyl glycerol-3-phosphate and the synthesis of phosphatidyl ethanolamines. Dilinolenyl phosphatidyl ethanolamine was found to inhibit *in vitro* production of angiotensin **1** by renin from renin substrate.

Canadian Journal of Chemistry, 47, 2906 (1969)

Introduction

Recent publication by Sen *et al.* (1) on the isolation of a phospholipid from the kidney and its inhibitory action on the renin–angiotensin system, prompted us to investigate the synthesis and biological activity of phosphatidyl ethanolamines containing various fatty acids. Two main routes for the synthesis of optically active

Can. J. Chem. Downloaded from www.nrcresearchpress.com by 210.87.254.6 on 09/05/12
For personal use only.

TABLE II

Selected chemical shift data for the chamigrene series (δ in p.p.m. downfield from TMS in CCl_4)

Compound	*gem*-$(Me)_2$	Allylic Me	*exo*-Cyclic vinylic	Reference
13*a*	0.82(3H), 0.87(3H)	1.55(3H)	4.47(1H), 4.82(1H)	15
13*b*	0.83(3H), 0.88(3H)	—	4.49(1H), 4.88(1H)	17
13*c*	0.87(3H), 0.90(3H)	—	4.34(1H), 4.84(1H)	17
15*a*	0.80(3H), 0.93(3H)	1.58(3H)	—	16
15*b*	0.82(3H), 0.93(3H)	—	—	16
17	0.85(6H)	—	4.46(2H); 4.73(1H), 5.09(1H)	17
19	0.84(3H), 0.89(3H)	1.63(6H)	—	17

applicable to these systems, was recently reported by Homer and Callaghan (19).

Acknowledgment

The author gratefully acknowledges the interest and assistance of Dr. Robert R. Fraser, University of Ottawa, Canada for obtaining the 100 MHz spectra.

1. (*a*) I. C. NIGAM and H. KOMAE. J. Pharm. Sci. **56**, 1299 (1967); (*b*) I. C. NIGAM, H. KOMAE, G. A. NEVILLE, C. RADECKA, and S. K. PAKNIKAR. Tetrahedron Letters 2497 (1968); (*c*) H. KOMAE and I. C. NIGAM. J. Org. Chem. **33**, 1771 (1968); (*d*) I. C. NIGAM, C. RADECKA, and H. KOMAE. J. Pharm. Sci. **57**, 1029 (1968).
2. F. KIDO, H. UDA, and A. YOSHIKOSHI. Tetrahedron Letters, 2815 (1967).
3. F. KIDO, H. UDA, and A. YOSHIKOSHI. Tetrahedron Letters, 1247 (1968).
4. G. A. NEVILLE and I. C. NIGAM. Tetrahedron Letters, 837 (1969).
5. J. W. APSIMON, W. G. CRAIG, P. V. DEMARCO, D. W. MATHIESON, L. SAUNDERS, and W. B. WHALLEY. Tetrahedron, **23**, 2357 (1967).
6. J. W. APSIMON, W. G. CRAIG, P. V. DEMARCO, D. W. MATHIESON, A. K. G. NASSER, L. SAUNDERS, and W. B. WHALLEY. Chem. Commun. 754 (1966).
7. G. J. KARABATSOS, G. C. SONNICHSEN, N. HSI, and D. J. FENOGLIO. J. Am. Chem. Soc. **89**, 5067 (1967).
8. L. M. JACKMAN. Applications of nuclear magnetic resonance spectroscopy in organic chemistry. The Pergamon Press, Ltd., London. 1959. Chap. 7. (*a*) p. 124; (*b*) p. 116.
9. N. NAKAGAWA, S. SAITO, A. SUZUKI, and M. ITOH. Tetrahedron Letters, 1003 (1967).
10. L. R. SUBRAMANIAN and G. S. KRISHNA RAO. Tetrahedron Letters, 3693 (1967).
11. J. A. CLAISSE and D. I. DAVIES. J. Chem. Soc. B, 679 (1967).
12. R. B. BATES. Nuclear magnetic resonance spectral collection of terpenes. Private communication.
13. R. R. SOBTI and S. DEV. Tetrahedron Letters, 2893 (1967).
14. R. C. SHEPPARD and S. TURNER. Chem. Commun. 77 (1968).
15. S. ITÔ, K. ENDO, T. YOSHIDA, M. YATAGAI, and M. KODAMA. Chem. Commun. 186 (1967).
16. A. TANAKA, H. UDA, and A. YOSHIKOSHI. Chem. Commun. 188 (1967); 56 (1968).
17. Y. OHTA and Y. HIROSE. Tetrahedron Letters, 2483 (1968).
18. J. W. APSIMON. Personal communication.
19. J. HOMER and D. CALLAGHAN. J. Chem. Soc. A, 439 (1968).
20. I. C. NIGAM and L. LEVI. Can. J. Chem. **46**, 1944 (1968).

Phospholipids. Part I. Synthesis of phosphatidyl ethanolamines

S. RAKHIT, J. F. BAGLI, AND R. DEGHENGHI

Ayerst Research Laboratories, Montreal, Quebec

Received February 24, 1969

This paper deals with a simple and general method of preparation of polyunsaturated 1,2-diacyl glycerol-3-phosphate and the synthesis of phosphatidyl ethanolamines. Dilinolenyl phosphatidyl ethanolamine was found to inhibit *in vitro* production of angiotensin **1** by renin from renin substrate.

Canadian Journal of Chemistry, 47, 2906 (1969)

Introduction

Recent publication by Sen *et al.* (1) on the isolation of a phospholipid from the kidney and its inhibitory action on the renin–angiotensin system, prompted us to investigate the synthesis and biological activity of phosphatidyl ethanolamines containing various fatty acids. Two main routes for the synthesis of optically active

Can. J. Chem. Downloaded from www.nrcresearchpress.com by 210.87.254.105 on 09/05/12
For personal use only.

Can. J. Chem. Downloaded from www.nrcresearchpress.com by 210.87.254.105 on 09/05/12
For personal use only.

phosphatidyl ethanolamines developed in recent years by Baer and co-workers (2) and Daemen and co-workers (3) involved phosphorylation of 1,2-diglycerides and 1,2-diacyl 3-iodopropanediols. The main difficulty in the above syntheses has been the suitable protection of the amino group. The phthaloyl group used for the protection of amino group must be removed by hydrazinolysis, a procedure that attacks the lipid to produce considerable amounts of impurities, extremely difficult to separate from the phosphatides. The first method also suffers from the drawback that poly-unsaturated 1,2-diacyl glycerols cannot be synthesized by the described method, thus limiting its use as a general procedure. In a later synthesis, Daemen and coworkers (4, 10) have used the *t*-butyloxycarbonyl group and Billimoria and Lewis (5) used the trityl group as a protective group for the amino nitrogen. The above two methods involved several step syntheses and the use of silver dibenzyl phosphate as phosphorylating agent.

The present work describes a very convenient method for the preparation of polyunsaturated 1,2-diacyl glycerol.[1] Protection of the amino nitrogen by *t*-butyloxycarbonyl was quite suitable because this group seemed to be rather versatile in the preparation of a wide variety of alkanolamines needed for our future studies.

The removal of the protective group did not offer any difficulty, since the by-products produced could be separated easily from the desired product.

The use of the new protecting group β,β,β-trichloroethoxycarbonyl (6) in lipid chemistry provided a suitable and convenient method for the preparation of optically active 1,2-diacyl-*sn*-glycerol-3-phosphate.[2] The facile removal of the protective group by zinc and acetic acid enabled us to synthesize polyunsaturated, 1,2-diacyl-*sn*-glycerol-3-phosphate that was hitherto unknown.

Reaction of **1** obtained from D-mannitol (7) with β,β,β-trichloroethyl chloroformate (6) gave in almost quantitative yield the corresponding carbonate **2**. When this was passed through a column of Dowex 50 (H^+)ion exchange resin in 90% aqueous methanol, the isopropylidine group was cleaved with the formation of **3** in a very high yield. Subsequently the diol **3** was acylated with 2 moles of the appropriate acylchloride to give the corresponding 1,2-diacyl carbonate **4** that was purified by silica gel chromatography. The trichloroethoxycarbonyl group was removed from **4** very conveniently by treating it with zinc and acetic acid, to give 1,2-diacyl glycerol **5**. Now these diacyl glycerols could be phosphorylated by phosphorous oxychloride to give the 1,2-diacyl-*sn*-3-glycerol phosphate **6** or phosphorylated and coupled with *N*-*t*-butyloxycarbonylethanolamine to give 1,2-diacyl-*sn*-glycerol-3-(*N*-*t*-butyloxycarbonyl-aminoethyl)-phosphate **7**. Alternatively the glycerophosphoric acid **6** could be converted into **7** by treating it in acetonitrile with trichloroacetonitrile and *N*-*t*-butyloxycarbonyl ethanolamine. Phosphorylation of alcohols by treating with phosphoric acid monoester in presence of trichloroacetonitrile is known to proceed in high yield (7).

The protective *t*-butyloxycarbonyl group was removed from **7** by treating it with HCl gas in anhydrous chloroform or ether to give the phosphatidyl ethanolamines **8** (10).

Experimental

The nuclear magnetic resonance (n.m.r.) spectra were taken on a Varian A-60 instrument using trimethylsilane as internal standard. Silica gel G was used as adsorbent for thin-layer chromatography (t.l.c.).

sn-Glycerol 1,2-Isopropylidine-3-(β,β,β-trichloro Ethyl)-carbonate (2)

A solution of 1 g of β,β,β-trichloroethoxy carbonyl chloride (6) in 5 ml of dry ether was added slowly with vigorous stirring to an ice-cooled solution of 500 mg of 1,2-isopropylidine-*sn*-glycerol prepared from D-mannitol (8) and 1 ml of dry pyridine in 5 ml of dry ether. Stirring was continued for 1 h at room temperature, more ether was added, and the precipitated pyridine hydrochloride was filtered off. The ether solution was washed with iced 2 *N* HCl and water and dried over sodium sulfate. Removal of solvent gave 1.125 g of an oil (yield 96%) that showed only one spot on t.l.c. (10% ethyl acetate in benzene). Nuclear magnetic resonance ($CDCl_3$) δ 4.75 (singlet, 2H, CH_2CCl_3) $[\alpha]_D^{25}$ −1.8 (*c*, 1.0 in $CHCl_3$).

Anal. Calcd. for $C_9H_{13}Cl_3O_5$: C, 35.12; H, 4.2; Cl, 34.63. Found: C, 34.98; H, 4.15; Cl, 35.14.

1,2,Dilinolenyl-3-(β,β,β-trichloro Ethoxy)-sn-glycerol (4)

A solution of 1.1 g of **2** in 100 ml of 90% aqueous methanol was percolated through a column (2.5 × 20 cm) containing Dowex 50 resin in H^+ form at the rate of 60 drops per min. The eluate was evaporated to

[1]When the present work was already completed, essentially the same procedure for the preparation of 1,2-diacyl glycerols was disclosed by Pfeiffer *et al.* (12).

[2]Nomenclature conforms to tentative rules proposed by IUPAC-IUB Commission on Biochemical Nomenclature.

dryness under reduced pressure and finally traces of water were removed by azeotropic distillation with benzene. The resulting oil **3** [n.m.r. ($CDCl_3$) δ 4.75 singlet 2H, $CH_2{\cdot}CCl_3$, no CH_3 protons] was used directly for acylation. Linolenyl chloride 2.1 g was added to a solution of 900 mg of **3** in 10 ml of dry DMF and 5 ml of dry pyridine, and the mixture was stored at room temperature for 24 h. The solution was poured into iced 2 *N* HCl and extracted with ether. The ether extract was washed with iced 2 *N* HCl, water, cold $NaHCO_3$ solution and water. It was dried over sodium sulfate. Removal of solvent gave 2.3 g of oil. This was chromatographed over 50 g silica gel. Elution of the column with pure benzene gave 1.2 g of pure oil **4** (yield 48%) showing a single spot on t.l.c. (benzene); n.m.r. ($CDCl_3$) δ 5.35 (4H olefinic), 4.75 (2H singlet $CH_2{\cdot}CCl_3$).

Anal. Calcd. for $C_{42}H_{65}O_7Cl_3$: C, 64.0; H, 8.25. Found: C, 64.3; H, 8.64.

In a similar manner, distearoyl, dioleoyl, and dilinoleoyl derivatives were prepared. 1,2-Distearoyl-3-(β,β,β-trichloroethoxy)-*sn*-glycerol, m.p. 54–55°.

Anal. Calcd. for $C_{42}H_{77}O_7Cl_3$: C, 63.04; H, 9.62. Found: C, 63.01; H, 9.80.

1,2-Dioleoyl-3-(β,β,β-trichloroethoxy)-*sn*-glycerol(oil).

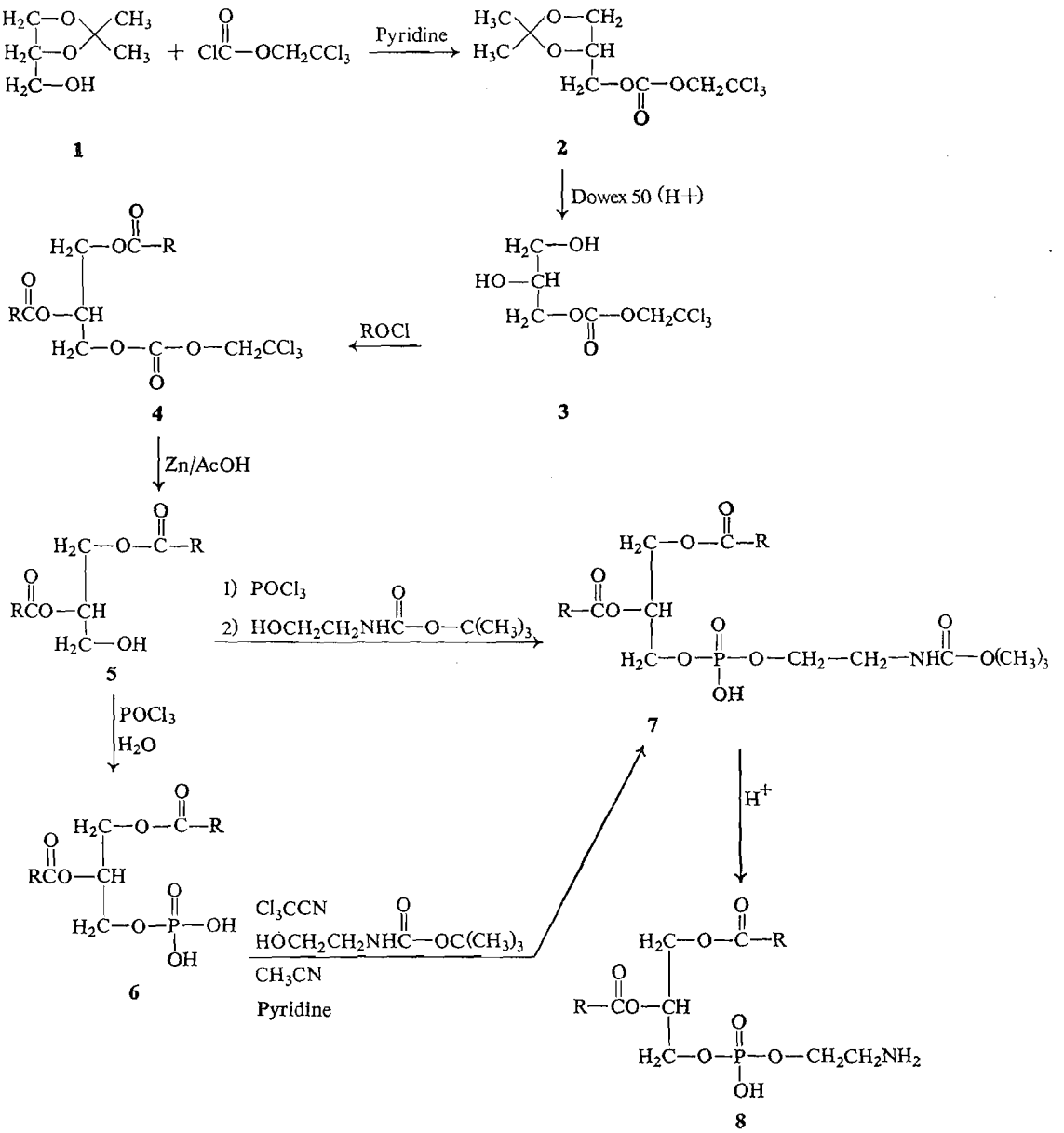

1 **2** **3** **4** **5** **6** **7** **8**

R = Stearoyl, Oleoyl, Linoleoyl, Linolenyl.

Can. J. Chem. Downloaded from www.nrcresearchpress.com by 210.87.254.105 on 09/05/12
For personal use only.

Can. J. Chem. Downloaded from www.nrcresearchpress.com by 210.87.254.105 on 09/05/12
For personal use only.

Anal. Calcd. for $C_{42}H_{73}O_7Cl_3$: C, 63.52; H, 9.19. Found: C, 63.71; H, 9.35.

1,2-Dilindeoyl-3-(β,β,β-trichloroethoxy)-*sn*-glycerol-(oil).

Anal. Calcd. for $C_{42}H_{69}O_7Cl_3$: C, 63.72; H, 8.72. Found: C, 63.58; H, 8.95.

1,2-Dilinolenyl-sn-glycerol (5)

To a solution of 650 mg of **4** in 8 ml of glacial acetic acid, 700 mg of powdered zinc was added and the mixture was shaken at room temperature for 2½ h. After this, benzene was added and the zinc was filtered off. The solution was washed with cold water and cold $NaHCO_3$ solution and water. It was dried over sodium sulfate. Removal of solvent yielded 410 mg of oily 1,2-dilinolenyl-*sn*-glycerol **5** (yield 82%); $[\alpha]_D^{20}$ −2.1° (*c*, 3 in $CHCl_3$).

Anal. Calcd. for. $C_{39}H_{64}O_5$: C, 76.42; H, 10.52. Found: C, 76.56; H, 10.81.

Similarly 1,2,distearoyl, 1,2,dioleoyl, and 1,2-dilinoleoyl-*sn*-glycerols were obtained.

1,2-Distearoyl-*sn*-glycerol, m.p. 68–69°. $[\alpha]_D^{20}$ −2.3° (*c*, 3 in $CHCl_3$), (lit. (9) $[\alpha]_D$ −2.7°).

Anal. Calcd. for $C_{39}H_{76}O_5$: C, 74.95; H, 12.26. Found: C, 74.80; H, 11.89.

1,2-Dilinoleyl-*sn*-glycerol (oil). $[\alpha]_D$ −2.5° (*c*, 3.0 in $CHCl_3$), (lit. (11) $[\alpha]_D^{20}$ −2.8°).

Anal. Calcd. for $C_{39}H_{72}O_5$: C, 75.43; H, 11.69. Found: C, 75.25; H, 11.58.

1,2-Dilinolenyl-*sn*-glycerol (oil). $[\alpha]_D$ −2.1° (*c*, 4.0 in $CHCl_3$).

Anal. Calcd. for $C_{39}H_{68}O_5$: C, 75.92; H, 11.11. Found: C, 76.10; H, 11.25.

1,2-Dilinolenyl-sn-glycerol-3-phosphate (6)

A solution of 3.00 g of 1,2-dilinolenyl-*sn*-3-glycerol in 15 ml dry benzene containing 0.4 g dry pyridine was added over a period of 10 min to a cooled solution of 0.77 g of distilled phosphorous oxychloride in 20 ml dry benzene. The solution was stirred at room temperature under nitrogen for 2 h, diluted with 100 ml of benzene, and washed with cold water, iced 2 *N* HCl and water, and was dried over sodium sulfate. Removal of solvent gave an oily product that showed essentially one spot on t.l.c. (chloroform, methanol, water; 95:35:6). $[\alpha]_D^{20}$ 3.1° (*c*, 3.5 in $CHCl_3$).

Anal. Calcd. for $C_{39}H_{65}PO_8$: C, 67.62; H, 9.39; P, 4.5. Found: C, 67.85; H, 9.28; P, 4.8.

1,2-Dilinolenyl-sn-glycerol-3-(N-t-butyloxy Carbonyl-aminoethyl)-phosphate (7)

Method A

A solution of 1,2,dilinolenyl-*sn*-glycerol **5** 1.836 g and 0.43 g of dry quinoline in 10 ml dry methylene chloride was added slowly under nitrogen over a period of 30 min to a stirred solution of 0.46 g of freshly distilled phosphorous oxychloride in 10 ml dry methylene chloride cooled to 0°. After this the reaction mixture was kept at room temperature under nitrogen for 2 h. It was recooled to 0° and a solution of 0.483 g of *N-t*-butyloxy carbonyl ethanolamine (4) and 0.8 g pyridine in 10 ml dry methylene chloride was added over a period of 30 min. The reaction mixture was stored at room temperature under nitrogen for 18 h, water (0.05 ml) was added and mixture was stirred for 1 h. It was then diluted with 200 ml of methylene chloride and washed with ice 2 *N* HCl and water. It was dried over sodium sulfate. Removal of solvent gave 2.4 g of an oil. This was chromatographed on silicic acid. Elution with 5% methanol in benzene yielded 2.0 g of the desired product as an oil (yield 80%). This showed only one spot on t.l.c. ($CHCl_3$:MeOH:H_2O ratio is 95:35:6); i.r. ν_{max} ($CHCl_3$) 3400–3500 (broad —OH), 1745 (ester carbonyl) 1690 cm^{-1} (amide).

Anal. Calcd. for $C_{46}H_{86}O_9NP$: C, 66.74; H, 10.39; N, 1.69; P, 3.74. Found: C, 66.85; H, 10.61; N, 1.80; P, 3.40.

Method B

A solution of 1.2 g of *N-t*-butyloxycarbonyl ethanolamine in 3.6 g trichloroacetonitrile and 10 ml of acetonitrile was added to a solution of 1.8 g of 1,2-dilinolenyl-*sn*-glycerol-3-phosphate **6** in 10 ml of dry pyridine, and the mixture was heated in a closed flask under nitrogen at 100° for a period of 4 h. After this, it was cooled and acidified with cold 2 *N* HCl and extracted with ether. Ether solution was washed several times with cold 2 *N* HCl and water, dried over sodium sulfate, and taken to dryness under vacuum. The dark brown oily residue was chromatographed over silicic acid. Elution with 5% methanol in benzene yielded 180 mg of an oily product identical to **7** as obtained by Method A.

1,2-Dilinolenyl-sn-glycerol-3-phosphoryl-ethanolamine (8)

To a solution of 2.1 g of **7** in dry ether, cooled to 0°,

TABLE I

In vitro—renin inhibitory action of various phosphatides

Samples tested	Amount of samples (mg)	Angiotensin formed (ng/4 h)	% inhibition
1. Dilinolenyl-phosphatidyl ethanolamine	3.5 1.1	34 54	43 10
2. Dilinoleoyl-phosphatidyl ethanolamine	8.0	56	7
3. Dioleoyl-phosphatidyl ethanolamine	9.0	61	—
4. Distearoyl-phosphatidyl ethanolamine	3.5	62	—
5. Natural renin inhibitor	3.5	32	48
6. Control	—	60	—

a stream of dry HCl gas was passed for 2 h. The solvent was removed under reduced pressure at 30°. The residue was dissolved in 1 ml of chloroform and chromatographed over 60 g silicic acid. Elution of the column with 5–10% methanol in chloroform yielded 350 mg of the desired product (yield 17.5%); i.r. ν_{max} ($CHCl_3$) 3500–3100 (—OH, phosphate and —NH_2), 1735 (ester carbonyl), 1650 cm^{-1} (—C—NH_2); $[\alpha]_D$ 6.1 (*c*, 2.0 in $CHCl_3$).

Anal. Calcd. for $C_{41}H_{70}O_8NP$: C, 66.93; H, 9.52; N, 1.9; P, 4.21. Found: C, 67.15; H, 9.81; N, 1.69; P, 4.02.

Biological activity

Preliminary studies on various phosphatidyl ethanolamines in an *in vitro* assay of renin inhibition (1) are indicated in Table I. Dilinolenyl phosphatidyl ethanolamine was found to be almost as active as the natural renin inhibitor isolated by Sen *et al.* (1). These observations indicate that for renin-inhibiting action, phosphatidyl ethanolamines should contain fatty acids with more than two double bonds. Other factors, such as positional requirements of the fatty acids are under investigation.

Acknowledgments

The authors wish to acknowledge technical assistance of Mr. A. Malik and thank Dr. G. Schilling and his associates for analytical data. *In vitro* assays were kindly performed by Dr. R. Smeby and his associates of Cleveland Clinic, Cleveland, Ohio. Continuous encouragement by Dr. D.A. Buyske throughout this work is highly appreciated.

1. S. Sen, R. P. Smeby, and F. M. Bumpus. Biochem **6**, 1572 (1967).
2. E. Baer, D. Buchnea, and A. G. Newcombe. J. Am. Chem. Soc. **78**, 232 (1956).
3. F. J. M. Daemen, G. H. De Haas, and L. L. M. Van Deenen. Rec. Trav. Chim. **81**, 348 (1962).
4. F. J. M. Daemen, G. H. De Haas, and L. L. M. Van Deenen. Rec. Trav. Chim. **82**, 487 (1963).
5. J. D. Billimoria and K. O. Lewis. J. Chem. Soc. 1404 (1968).
6. T. B. Windholz and D. B. R. Johnston. Tetrahedron letters, 2555 (1967).
7. F. Cramer and G. Weimann. Chem. Ber. **94**, 996 (1961).
8. E. Baer and H. O. L. Fischer. J. Biol. Chem. **128**, 463 (1939).
9. J. C. Sowden and H. O. L. Fischer. J. Am. Chem Soc. **63**, 3244 (1941).
10. F. J. M. Daemen. Chem. Phys. Lipids, **1**, 476 (1967).
11. E. Baer and D. Buchnea. J. Biol. Chem. **230**, 447 (1958).
12. F. R. Pfeiffer and S. R. Cohen. Tetrahedron Letters, 3549 (1968).

Can. J. Chem. Downloaded from www.nrcresearchpress.com by 210.87.254.105 on 09/05/12
For personal use only.

Can. J. Chem. Downloaded from www.nrcresearchpress.com by 210.87.254.105 on 09/05/12
For personal use only.

COMMUNICATION

The barrier to the conformational interconversion of 1,4-dimethylenecyclohexane and related compounds

MAURICE ST-JACQUES AND MICHEL BERNARD
Department of Chemistry, University of Montreal, Montreal, Quebec

Received May 20, 1969

The proton magnetic resonance spectra of 1,4-cyclohexanedione, 1,4-dimethylenecyclohexane, and 1,4-difluoromethylenecyclohexane have been studied at various temperatures; the spectra of the last two compounds were found to be temperature dependent. ΔF^{+} values of 7.5 and 6.5 kcal/mole, respectively, were estimated from the spectral changes.

Canadian Journal of Chemistry, 47, 2911 (1969)

Recent communications (1, 2) have shown that the replacement of the carbonyl group in cyclohexanone by a methylene group markedly raises the energy barrier to ring inversion. We wish to report that similar chemical transformations of 1,4-cyclohexanedione (**1**) also result in an increased barrier to conformational interconversion.

The proton magnetic resonance (p.m.r.) spectra of **1**, 1,4-dimethylenecyclohexane (**2**), and 1,4-difluoromethylenecyclohexane (**3**) have been investigated at various temperatures. Compound **2** was prepared from **1** by a Wittig reaction using the procedure of Corey and co-workers (3); **3** was also prepared from **1** by the method developed by Fugua and co-workers (4).

The p.m.r. spectrum[1] of **1** consists of a single line at 2.74 p.p.m. from TMS; it showed no peak separation on lowering the temperature to -160 °C. At this temperature, the peak was broader than that of TMS and both were appreciably broad due to an increase in the viscosity of the solution.

The p.m.r. spectrum of **2** has been reported as temperature independent down to -120 °C (5). Our results (Fig. 1) show that a change takes place at lower temperature. At room temperature, the spectrum consists of two singlets centered at

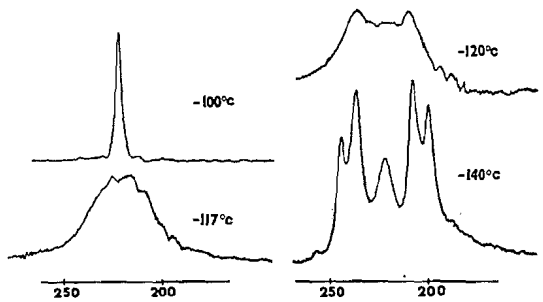

FIG. 1. The ring proton portion of the 100 MHz p.m.r. spectrum of 1,4-dimethylenecyclohexane. The scale is in Hz relative to internal TMS.

4.74 p.p.m. (vinyl protons, relative area 1) and 2.27 p.p.m. (ring protons, relative area 2). As the sample temperature is lowered, the upfield peak broadens and at -118 °C changes into a complex pattern whose symmetric appearance at -140 °C identifies it basically as an AA'BB' (6) for which many lines are not resolved. The quality of the spectra did not improve at lower temperatures. The vinyl proton peak remains a singlet throughout this temperature interval.

A similar change takes place for **3**. At ambient temperature, the ring protons appear as a quintuplet (splitting = 1.3 Hz) at 2.18 p.p.m. owing to coupling with the fluorine atoms. Below -134 °C, a pattern emerges which eventually can be identified basically as an AA'BB' exhibiting overlapping lines and appreciable coupling with the fluorine atoms.

The rate constant, k (in units of s^{-1}), for the conformational interconversions detected were estimated at the coalescence temperature, T_c,

[1]Spectra were recorded with a JEOL JNM-4H-100 spectrometer using a 2% solution of **1** in chlorodifluoromethane and a 7% solution of each **2** and **3** in vinyl chloride containing 10% of chlorodifluoromethane for locking purpose. Temperatures were determined with a thermocouple inside a dummy nuclear magnetic resonance tube.

Can. J. Chem. Downloaded from www.nrcresearchpress.com by 210.87.254.105 on 09/05/12
For personal use only.

from the equation (7) $k = \pi(6J_{AB}^2 + \Delta\nu^2)^{1/2}/\sqrt{2}$. This equation is strictly applicable only for an AB spectrum where $\Delta\nu$ is the chemical shift difference (in Hz) between the A and B protons and J_{AB} is the coupling constant. But since the most intense lines of an AA'BB' can be treated as an AB spectrum (6) with an apparent coupling constant equal to N, setting N equal to J_{AB} in the above equation should provide a reasonable approximation for k and subsequently for $\Delta F^{\ddagger}$. Thus from the four most intense lines of the spectrum of **2** (Fig. 1, -140 °C) one obtains $\Delta\nu \approx 35$ Hz and $N \approx 8.5$ Hz; these values give $k = 90\ s^{-1}$ at -118 °C corresponding to a free energy of activation of about 7.5 kcal/mole using a transmission coefficient of 1. Similar calculations for **3** yield $k = 180\ s^{-1}$ and $\Delta F^{\ddagger} = 6.5$ kcal/mole at -134 °C. The uncertainty in $\Delta F^{\ddagger}$ is probably about ± 0.5 kcal/mole. Arguments analogous to Jensen's (1) indicate that $\Delta F^{\ddagger}$ for **1** is probably less than 5 kcal/mole.

It is firmly established that **1** exists as a twist-boat (t.b.) conformation (8) in the solid state (9) and in solution (10), and it has been reported that the coupling constants in the p.m.r. spectrum of **2** at ambient temperature are consistent with that of a twist boat, although a flattened chair conformation could not be excluded (11). The AA'BB' appearance of the low temperature spectra is equally compatible with either the t.b. or the chair (c.) form as the most predominant for **2** and **3**. Only a consideration of the interconversion mechanisms available to both conformations allows a selection to be made.

If it is assumed that the t.b. form is predominant, then two basic modes of interconversion are available, namely, a symmetrical mode and a pseudorotation (12). Both processes have the property of averaging an AA'BB' spectrum into an A_4 singlet as illustrated in Fig. 2, where it is shown that "axial" and "equatorial" protons exchange environments in both interconversion itineraries. Calculations carried out by Allinger and co-workers (13) suggest that the pseudorotation of **2** should have a relatively small energy barrier (about 2.4 kcal/mole); therefore, if **2** existed in the t.b. form, it should still undergo rapid pseudorotation on the nuclear magnetic resonance (n.m.r.) time scale at -140 °C and its p.m.r. spectrum should consist of a singlet instead of a complex pattern. It seems that if the calculations are reasonably accurate, **2** does not exist in the t.b. form.

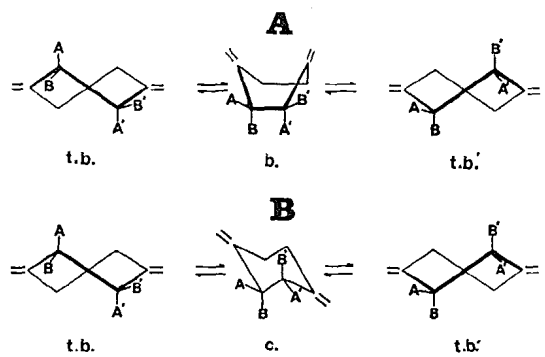

FIG. 2. Interconversion modes for the twist-boat (t.b.) conformation of compounds **1**, **2**, and **3**: (A), pseudorotation; (B), symmetrical mode.

The $\Delta F^{\ddagger}$ determined for **2** is most reconcilable with the chair form as the predominant conformation. The interconversion itinerary is probably analogous to the ring inversion in cyclohexane (12) and involves the symmetrical c. $\rightleftarrows$ t.b. pathway. It is evident from Fig. 2 that this process averages the AA'BB' spectrum expected for c. to a singlet. Calculations have not been carried out for **3** but its behavior appears to be analogous to that of **2**.

The differences in $\Delta F^{\ddagger}$ observed for **1**, **2**, and **3** appear in part to be analogous to the barrier to internal rotation for acetaldehyde (14), propene (14), and 1,1-difluoropropene (15) and the change in nature of the predominant conformation of **1** and **2** reflect in part the greater stability associated with an eclipsed arrangement between α-protons and the exo double bonds of **2**. Studies on other related compounds are planned to define more precisely the factors involved.

Acknowledgments

We wish to thank D. F. Williams for recording the n.m.r. spectra, the National Research Council of Canada for financial support, and Quebec Ministry of Education for a fellowship (France-Québec) to M. B.

1. F. R. JENSEN and B. H. BECK. J. Am. Chem. Soc. **90**, 1067 (1968).
2. J. T. GERIG. J. Am. Chem. Soc. **90**, 1065 (1968).
3. R. GREENWALD, M. CHAYKOVSKY, and E. J. COREY. J. Org. Chem. **28**, 1128 (1963).
4. S. A. FUQUA, W. F. DUNCAN, and R. M. SILVERSTEIN. J. Org. Chem. **30**, 2543 (1965).
5. F. LAUTENSCHLAEGER and G. F. WRIGHT. Can. J. Chem. **41**, 1972 (1963).
6. J. W. EMSLEY, J. FEENEY, and L. H. SUTCLIFFE. High resolution nuclear magnetic resonance spectros-

copy. Vol. 1. The Pergamon Press, Ltd., New York. 1966. p. 399.
7. R. J. KURLAND, M. B. RUBIN, and W. E. WISE. J. Chem. Phys. **40**, 2426 (1964).
8. E. L. ELIEL, N. L. ALLINGER, S. J. ANGYAL, and G. A. MORRISON. Conformational analysis. Interscience Publishers, Inc., New York. 1965. p. 473.
9. *a* P. GROTH and O. HASSEL. Acta Chem. Scand. **18**, 923 (1964). *b* A. MOSSEL and C. ROMERS. Acta Cryst. **17**, 1217 (1964).
10. *a* C. Y. CHEN and R. J. W. LEFÈVRE. Aust. J. Chem. **16**, 917 (1963). *b* N. L. ALLINGER, H. M. BLATTER, L. A. FREIBERG, and F. M. KARKOWSKI. J. Am. Chem. Soc. **88**, 2999 (1966).
11. J. B. LAMBERT. J. Am. Chem. Soc. **89**, 1836 (1967).
12. J. B. HENDRICKSON. J. Am. Chem. Soc. **89**, 7047 (1967).
13. N. L. ALLINGER, J. A. HIRCH, M. A. MILLER, and I. J. TYMINSKY. J. Am. Chem. Soc. **90**, 5773 (1968).
14. D. J. MILLEN. Progr. Stereochem. **3**, 144 (1962).
15. V. W. WEISS, P. BEAK, and W. H. FLYGARE. J. Chem. Phys. **46**, 981 (1967).

Can. J. Chem. Downloaded from www.nrcresearchpress.com by 210.87.254.105 on 09/05/12
For personal use only.

Can. J. Chem. Downloaded from www.nrcresearchpress.com by 210.87.254.5 on 09/05/12
For personal use only.

Canadian Journal of Chemistry

Published by THE NATIONAL RESEARCH COUNCIL OF CANADA

VOLUME 47 AUGUST 15, 1969 NUMBER 16

Infrared spectra, rotational correlation functions, band moments, and intermolecular mean squared torques of methane dissolved in liquid noble gases[1]

A. CABANA, R. BARDOUX, AND A. CHAMBERLAND

Département de Chimie, Université de Sherbrooke, Sherbrooke, Québec

Received January 24, 1969

Extensive measurements of the infrared (i.r.) absorption spectra of liquid methane and of methane dissolved in liquid argon, krypton, and xenon have been carried out. Band profiles for the ν_3 and ν_4 modes of CH_4 and CD_4 are reported. From these profiles the rotational correlation functions have been calculated. Comparison of the experimental functions with the functions calculated for the free rotators at the appropriate temperatures reveals that each molecule rotates freely for only 1.3×10^{-13} s before it undergoes a hard collision; the same result was obtained for all the systems investigated. Difficulties in obtaining accurate values of the band moments are discussed and suggestions for overcoming them are presented. Values ranging from 6.9 to 8.2×10^4 cm^{-2} have been obtained for the mean squared torques acting on methane in the various solutions.

Canadian Journal of Chemistry, 47, 2915 (1969)

Introduction

The vibrational bands of methane in the liquid state have been studied in a number of laboratories (1). However, very little information on the molecular motions in the liquids has been extracted from them because of a lack of a suitable method of interpretation. Until Gordon (2) introduced what he called "the Heisenberg picture of spectroscopy", spectra were analyzed using the conventional method which he referred to as "the Schröedinger approach". In the conventional interpretation of spectroscopic information, knowledge about the molecular motions is obtained from the assignment of various features in the spectrum to the allowed quantum states of the system. In the liquid state, the closely spaced rotational levels blend together to form a continuous band such that no information on molecular rotation can be obtained from such an analysis. However, the Heisenberg picture of spectroscopy makes the interpretation possible by focussing attention on the time development of the system rather than on the energy states. The absorption spectrum may thus be considered as a Fourier transform of an appropriate time correlation function. This paper will discuss the experimental difficulties encountered in the application of this method to the analysis of the i.r. absorption bands of methane both as a pure liquid and in solutions with liquid noble gases. The calculation of the time correlation functions will first be carried out and will yield information on the nature of the motions. It will then be shown that, in order to obtain accurate values of the band moments, unattainable accuracy in the base line position is necessary. In the systems of present interest, it appears that the moments can be calculated to within a factor of about 2 and that reasonable estimates of the intermolecular torques are thus obtained. These torques are a measure of the hindrance to rotation. A similar paper dealing with high pressure gaseous samples has been published recently (3).

Experimental

The vibrational spectra of methane dissolved in liquid noble gases were recorded on a Perkin–Elmer Model 125 prism-grating spectrophotometer calibrated with gaseous methane or hydrogen chloride, using IUPAC tables (4), with a frequency accuracy of ± 0.5 cm^{-1}. Spectral slit widths were of the order of 0.5–1.0 cm^{-1}. The width at half height of the bands investigated was always at least

[1]Work supported, in part, by the Defence Research Board of Canada Grant No. 9511-67.

Can. J. Chem. Downloaded from www.nrcresearchpress.com by 210.87.254.5 on 09/05/12
For personal use only.

an order of magnitude greater. The accuracy of the frequency, limited by the broadness of the observed bands, was ± 2 cm^{-1}.

The cooling was provided by a commercially available cryostat equipped with a variable pressure gas exchanger (obtained from Andonian Associates, Waltham, Mass.) that permits a temperature control; fine control was done by means of electrical heating. The temperatures, readily kept constant to within ± 1 °K, were measured with a copper–constantan thermocouple embedded in the sample cell.

The sample cell, a properly machined copper block, was equipped with either sapphire or irtran-2 windows spaced 2 mm apart. Initially indium wires 0.030 in. diameter, squeezed between the cell body and the windows, were used as seals; it was later found that irtran-2 windows, which were rather fragile, were more easily sealed with wires 0.010 in. diameter.

Research grade noble gases and methane were obtained from Matheson; CD_4 with a stated purity of 99% was purchased from Merck, Sharp and Dohme of Canada, Ltd. In order to ensure complete mixing, the solutions investigated were solidified, evaporated, and heated to 150 °C several times.

In a typical experiment, pure solvent gas was liquefied into the cell, the spectrum recorded, and the gas re-evaporated into the storage bulb. Only then was it mixed with methane in a ratio of at least 500:1 and liquefied again in the sample cell.

In order to minimize absorbance error, the spectra were recorded at a maximum rate of 3 cm^{-1} per min; the slits were kept constant and as wide as consistent with adequate resolution. The gain was set low enough to maintain the noise level within ± 0.2%, yet high enough to ensure proper response.

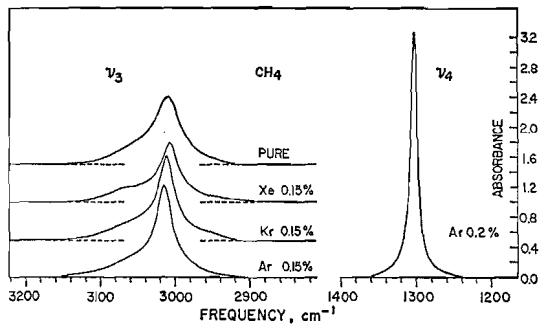

FIG. 1. The ν_3 and ν_4 i.r. absorption bands of CH_4 at various temperatures in various solvents. Pure CH_4, 117 °K; 0.15% CH_4 in xenon, 163 °K; 0.15% CH_4 in krypton, 135 °K; 0.15 and 0.2% CH_4 in argon, 91 °K.

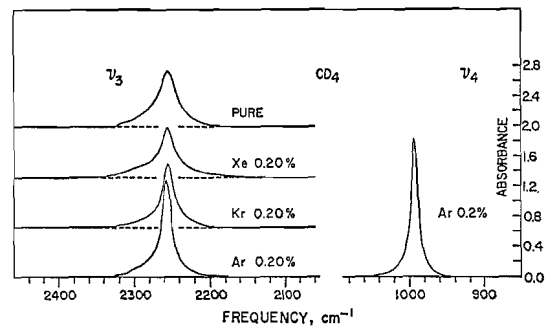

FIG. 2. The ν_3 and ν_4 i.r. absorption bands of CD_4 at various temperatures in various solvents. Pure CD_4, 120 °K; 0.20% CD_4 in xenon, 163 °K; 0.20% CD_4 in krypton, 121 °K; 0.20% CD_4 in argon, 91 °K.

Results and Discussion

Infrared Spectra

An extensive series of i.r. absorption spectra of liquid methane and of methane dissolved in liquid argon, krypton, or xenon has been recorded and analyzed. Representative examples of the profiles of the ν_3 and ν_4 absorption bands of CH_4 are given in Fig. 1 while those of CD_4 are given in Fig. 2. The Coriolis coupling constants for the two CH_4 modes are $\zeta_3 = 0.04$ and $\zeta_4 = 0.46$ (5); the constants for CD_4 are $\zeta_3 = 0.16$ and $\zeta_4 = 0.34$ (6). The effect of a greater constant for the ν_4 modes with respect to the ν_3 modes is clearly seen in both sets of spectra through a narrowing of the bands attributable to the bending modes. The applicability of the Coriolis coupling correction for the liquid state may be questioned since the ζ_i will certainly be affected by the potential fields. The greater moment of inertia for CD_4 with respect to CH_4 is reflected in the spectra by a relative narrowing of the CD_4 bands. For reasons to be discussed later, only the ν_3 bands of CH_4 will be completely analyzed. Remnants of the R branch appear on the high frequency side of every spectrum but more strikingly in the cases of xenon solutions.

Calculation of the Dipole Correlation Functions and Relaxation Rates

An i.r. correlation function is given by $\langle \mu(0)\cdot\mu(t)\rangle$, where $\mu(0)$ and $\mu(t)$ are the appropriate components of the Heisenberg dipole moments at times 0 and t respectively, and the brackets denote the equilibrium ensemble average (2). For convenience $\langle \mu(0)\cdot\mu(t)\rangle$ will be replaced by $C(t)$. The classical theoretical function for a freely rotating top is given by (7)

$$C_{C1}(t) = \frac{1}{3}\left\{1 + 2\left[1 + \left(\frac{kT}{I}\right)i^2\right]\exp\left(-\frac{kT}{2I}\right)t^2\right\}$$

Thus only the temperature and the moment of inertia determine the correlation function of freely rotating molecules. These functions were calculated for CH_4 at 75 and 100 °K and are

Can. J. Chem. Downloaded from www.nrcresearchpress.com by 210.87.254.5 on 09/05/12
For personal use only.

illustrated in Fig. 3. Also shown on the same figure is the theoretical function obtained from a "stick spectrum" calculated at 75 °K; the latter function is then also a function for the free molecules but now quantum effects are somehow taken into account. At short times ($t < 0.3 \times 10^{-12}$ s), both functions are superimposed.

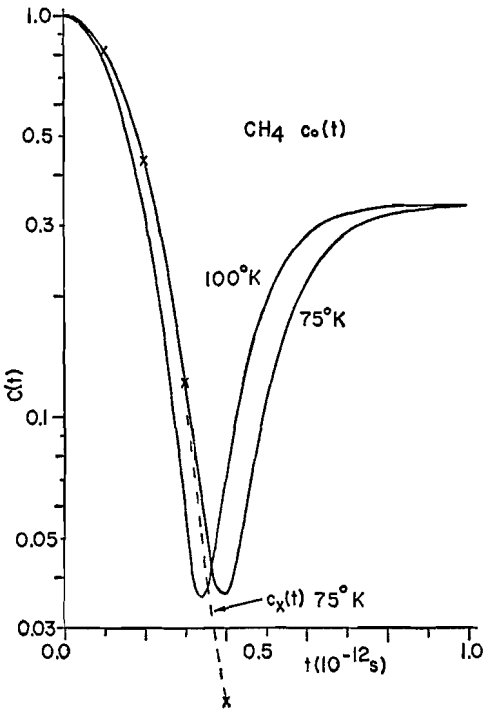

FIG. 3. Theoretical correlation functions for freely rotating methane: full lines, classical functions; dashed line, obtained from a stick spectrum using the method outlined by Gordon. At short times both curves are superimposed.

The experimental dipole correlation functions were calculated (2) from the following expressions

$$C(t) = \int_{\text{band}} \hat{I}(\omega) e^{i\omega t} d\omega$$

In the above relationship the spectrum is normalized to unit area by defining

$$\hat{I}(\omega) = I(\omega) \Big/ \int_{\text{band}} I(\omega) d\omega$$

where ω is the circular frequency measured from the maximum value of $I(\omega)$, $I(\omega)$ is the absorbance, and the summation is carried out over the complete frequency spectrum.

In the actual calculations the following function was evaluated

$$C(t) = \frac{\int_{\text{band}} \log (I_0/I) \cos (\omega t) d\omega}{\int_{\text{band}} \log (I_0/I) d\omega}$$

It may be useful to note that, in a recent paper (8), another form of this relation was given; that relation should be used with caution since a factor of 2 has been omitted from the denominator.

Those vibrational modes which are strongly coupled with the rotational motions cannot be adequately treated using the expressions reproduced above, because for such modes the dipole correlation functions cannot be factorized into vibrational and rotational parts. Both i.r. active vibrations of CD_4 and the ν_4 vibration of CH_4 have large Coriolis coupling constants and consequently the present method is not strictly applicable to them. However, in order to illustrate the influence of the coupling, correlation functions have been obtained for some of those bands and are reproduced in Figs. 4 and 5. Further discussion will be restricted to the ν_3 vibration of CH_4 whose functions are given in

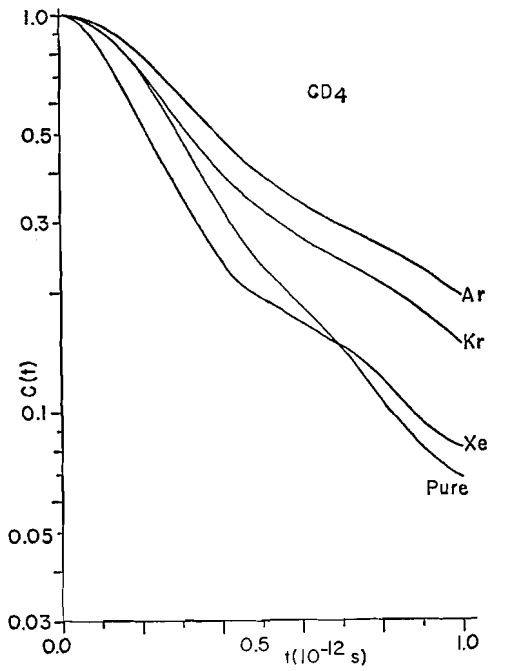

FIG. 4. Rotational correlation functions for CD_4 obtained from the frequency spectra reported in Fig. 2.

Can. J. Chem. Downloaded from www.nrcresearchpress.com by 210.87.254.5 on 09/05/12
For personal use only.

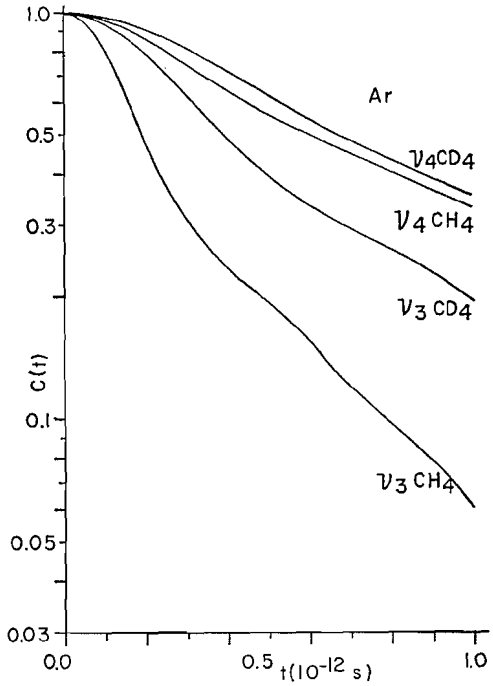

FIG. 5. Rotational correlation functions for CH_4 and CD_4 obtained from frequency spectra shown in Figs. 1 and 2.

Fig. 6. On each absorption spectrum, between 200–300 values of the absorbance were read and carefully subtracted from the corresponding readings of the blank spectrum. The average values of 3 different sets of tracings were used for the calculations. The interval of integration was always chosen to be at least 10 times the width-at-half-height and contained the complete region where measurable absorption occurred. We could not carry out an error calculation because there is no precise way of measuring the uncertainty in absorbance at each wavelength. Moreover, as pointed out by Favelukes and co-workers (9), only an upper limit could be computed. In order to get an estimate of the errors, 3 correlation functions were obtained for 3 different mixtures of the same pair of gases (methane–argon); at short times, the resulting curves were perfectly superimposable but at longer times, when oscillations developed, the dispersion was evident but never large enough to modify the meaning of our results. In some preliminary experiments when the interval of integration was inadvertently truncated or the base line shifted, very large oscillations appeared. There is a simple mathematical reason for these oscillations: when an absorption band is truncated or when the base line is displaced from its exact position, a small rectangle is either added or subtracted from the real band. The Fourier transform of that small rectangle is a function of the form $\sin x/x$ which is either added or subtracted from our real function. Any error in the base line position will thus cause oscillations. It may be possible to avoid such errors by recording an additional spectrum with an increased path length (say 10–20 times) and using this spectrum to obtain more reliable values of the absorbance in the wings. However, in spectra of rather complex molecules, this procedure is in general not applicable since overtones or combination bands overlap the fundamentals. In the ν_3 region of CH_4 for example, $2\nu_2$ or $\nu_2 + \nu_4$ are extremely weak but their presence excludes the possibility of using the method suggested above. Comparison of the experimental curves with those obtained for freely rotating methane (Figs. 6 and 3) reveals that the experimental functions follow the free rotator functions for times shorter than about 1.2×10^{-13} s, and that

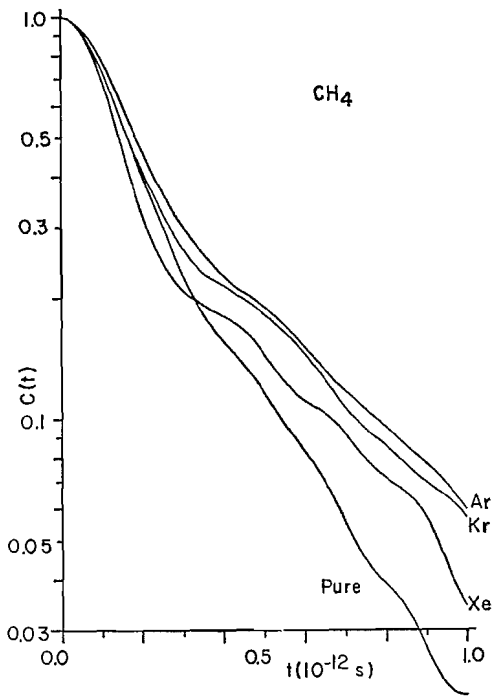

FIG. 6. Rotational correlation functions for CH_4 obtained from frequency spectra shown in Fig. 1.

Can. J. Chem. Downloaded from www.nrcresearchpress.com by 210.87.254.5 on 09/05/12
For personal use only.

molecular rotation in pure methane is very similar to molecular rotation of methane in any of the liquid noble gases. At intermediate times, the intermolecular interactions cause the experimental function to decay more slowly than the theoretical function; by that time the molecules will have undergone a hard collision with their neighbors. The semilogarithmic plots illustrate well the exponential decay at long times. The relaxation rates τ_0^{-1} are obtained from the slopes of the straight lines drawn to approximate the long time behavior; Table 1 summarizes the results.

TABLE I

Relaxation rates for CH_4 in various solvents

System	τ_0^{-1} (± 0.2) $\times 10^{12}$ s^{-1}
Pure CH_4	3.5
0.15% CH_4 in Ar	2.4
0.15% CH_4 in Kr	2.5
0.15% CH_4 in Xe	2.4

In the gas phase it has already been shown (3) that the relaxation rate increases with the gas density, and it should be noted that the relaxation rate in a liquid is of the same order of magnitude as that measured in the gas at comparable densities. The relaxation rate of CH_4 in the pure liquid is definitely longer than that of methane mixed with liquid noble gases; the same qualitative behavior is also clearly observed in the CD_4 correlation functions (Fig. 4). The relaxation rates are rather insensitive to base line errors.

Calculation of Band Moments and Torques from Observed Absorption Spectra

The mean squared torque (3) is given by

$$\left[[M(4) - (5/2)M(2)^2]\frac{3}{2}I^2 = \langle\tau^2\rangle\right.$$

In this expression $M(2)$ and $M(4)$ are respectively the 2nd and 4th moments of the i.r. band, I is the moment of inertia, and $\langle\tau\rangle$ is the torque on the radiating molecule; the brackets denote a classical configurational average.

The calculated experimental torques are extremely sensitive to the position of the background level. The background trace was matched to the absorption trace outside the region of measurable absorption. In some experiments, after calculating the moments with the best "visual fit" we searched with the computer to find what shift in the base line would be necessary to obtain a 2nd moment which would have the theoretical classical value. The classical 2nd moment is dependent on the temperature and the moment of inertia but independent of the intermolecular forces. Thus it can be used to augment the accuracy on the fit in the wings. The adjustments necessary to match the experimental 2nd moments to the classical 2nd moments were always small (within the combined errors on both traces) but they had a large effect on the 4th moments and consequently on the mean squared torques. Table II illustrates these effects with a typical example where the base line was deliberately shifted from its real position. We wish to point out that, except for slight modifications of the oscillations observed at long times, these adjustments did not alter the correlation functions; at short times all the curves were superimposable. Table III gives selected values of the 2nd and 4th moments, and of the mean squared torques, for pure methane and methane dissolved in 3 different noble gases. The theoretical classical 2nd moments are also included. The reported moments and torques are the average values obtained from several experiments; sets of band moments where $M(2)$ was too far from the theoretical value were discarded. It was observed that

TABLE II

Typical effects of base line uncertainty on the 2nd and 4th band moments and on the torques

System	$M(2)$ (10^{26} s^{-2})	$M(4)$ (10^{52} s^{-4})	$\langle\tau^2\rangle$ (10^4 cm^{-2})	P.H.R. (10^2 cm^{-1})
0.15% CH_4 in Ar*	0.483	0.987	4.36	2.1
0.15% CH_4 in Ar†	0.528	1.24	5.87	2.4
0.15% CH_4 in Ar‡	0.579	1.57	7.92	2.8

*Obtained with the best "visual fit" between the absorption spectrum and the background trace.
†Background trace lowered about 0.4% of maximum absorption.
‡Background trace lowered a further 0.4% of maximum absorption.

TABLE III

Selected values of 2nd and 4th band moments and the corresponding torques

System	T (°K)	ν (cm^{-1})	$M(2)$* (10^{26} s^{-2})	$M(2)$† (10^{26} s^{-2})	$M(4)$† (10^{52} s^{-4})	$\langle\tau^2\rangle$ (10^4 cm^{-2})
Pure CH_4	117	3010	0.61	0.63	1.76	8.2
0.15% CH_4 in Ar	111	3015	0.58	0.58	1.57	7.9
0.15% CH_4 in Kr	135	3011	0.73	0.66	2.05	6.9
0.20% CH_4 in Xe	163	3007	0.84	0.77	2.20	7.8

*Theoretical values.
†Experimental values.

the experimental torques for methane, in the 4 solutions studied, are all about the same. When great care was exercised in recording and reading the spectra, successive values of the mean squared torques computed from different sets of spectra have shown an uncertainty of $\pm 35\%$; this figure may be considerably larger if insufficient care is taken. It would appear that the uncertainty may be minimized by insisting that the 2nd moments obtained from spectral data have the theoretical classical values. The square root of the mean squared torques should provide a fair idea of the average potential hindering rotation; even if it is not exact, such calculations were carried out and the values obtained were compared to those reported in the literature. For pure methane we have found an average barrier of 2.8×10^2 cm^{-1} and surprisingly enough about the same value was obtained for the noble gases. Values reported in the literature include 63 cm^{-1} for pure liquid methane (1), 165–330 cm^{-1} for pure solid methane (10), and 83 cm^{-1} (11) and 348–533 cm^{-1} (12) for methane dissolved in the solid noble gases. Although these measurements of the average potential hindering rotation were obtained using widely different assumptions, it is interesting to note that they are all within an order of magnitude.

Acknowledgments

The authors benefited from discussions with R. G. Gordon, W. B. Person, and Bryce Crawford, Jr. Their interest in this problem is greatly appreciated.

Generous financial assistances from the National Research Council of Canada and from the "Ministère de l'Education de la Province de Québec" are gratefully acknowledged.

1. GEORGE E. EWING. J. Chem. Phys. **40**, 179 (1964); M. F. CRAWFORD, H. L. WELSH, and J. H. HARROD. Can. J. Phys. **30**, 81 (1952); M. O. BULANIN and N. D. ORLOVA. Opt. i Spektroskopiya, **4**, 569 (1958); J. LASCOMBE, P. VAN HUONG, and M. L. JOSIEN. Bull. Soc. Chim. France, **50**, 1175 (1959).
2. R. G. GORDON. J. Chem. Phys. **43**, 1307 (1965).
3. R. L. ARMSTRONG, S. M. BLUMENFELD, and C. G. GRAY. Can. J. Phys. **46**, 1331 (1968).
4. Tables of wavenumbers. Butterworth Inc., Washington, D.C. 1961.
5. R. S. MCDOWELL. J. Mol. Spectry. **21**, 280 (1966).
6. J. HERRANZ, J. MORCILLO, and A. GÓMEZ. J. Mol. Spectry. **19**, 226 (1966).
7. W. A. STEELE. J. Chem. Phys. **38**, 2411 (1963).
8. J. T. SHIMOZAWA and M. K. WILSON. Spectrochim. Acta, **22**, 1609 (1966).
9. C. E. FAVELUKES, A. A. CLIFFORD, and BRYCE CRAWFORD, JR. J. Phys. Chem. **72**, 962 (1968).
10. G. B. SAVITSKY and D. F. HORNIG. J. Chem. Phys. **36**, 2634 (1962).
11. A. CABANA, G. B. SAVITSKY, and D. F. HORNIG. J. Chem. Phys. **39**, 2942 (1963).
12. FRANKLIN H. FRAYER and GEORGE E. EWING. J. Chem. Phys. **48**, 781 (1968).

Can. J. Chem. Downloaded from www.nrcresearchpress.com by 210.87.254.5 on 09/05/12
For personal use only.

Can. J. Chem. Downloaded from www.nrcresearchpress.com by 210.87.254.42 on 09/05/12
For personal use only.

Nuclear charge dispersion in the fission of ^{233}U by protons of medium energy[1]

I. TOMITA[2] AND L. YAFFE

Radiochemistry Laboratory, Department of Chemistry, McGill University, Montreal, Quebec

Received February 11, 1969

Independent yields and excitation functions have been determined for the formation of cesium isotopes with masses $129 \leqslant A \leqslant 138$ in the fission of ^{233}U with protons of energies between 20 and 80 MeV. The energies at which the various excitation functions reach their maxima have been compared with those obtained for the same isotopes from fissioning systems with targets of different neutron-to-proton (N/Z) ratios. The neutron-deficient species have a higher probability of being produced at lower energies from targets with lower N/Z ratios. Charge dispersion curves have been obtained and these show the familiar broadening and displacement of Z_p, the most probable charge, towards stability with increase in bombardment energy. Values of $Z_A - Z_p$ have been compared with those obtained from other fissioning systems, and predictions made for values of Z_p in the fission of systems yet unstudied, e.g. ^{235}U and ^{239}Pu. In addition Z_p values were calculated for ^{233}U fission, assuming compound nucleus formation up to a proton energy of 50 MeV, assuming pre- and post-fission neutron evaporation on the equal charge displacement and unchanged charge division postulates. Experimental values were found to lie between the two predictions.

Canadian Journal of Chemistry, 47, 2921 (1969)

Introduction

Considerable information has been published by workers in this laboratory regarding the charge dispersion of fission products with mass numbers A between 130 and 143, formed in the fission of ^{232}Th (1–3) and ^{238}U (4–6) bombarded by protons of energies 10–85 MeV. Friedlander *et al.* (7) reported a detailed study of excitation functions and nuclear charge dispersion in this fission product mass region in the fission of ^{238}U by protons of energies 0.1–6.2 GeV.

No data for the nuclear charge dispersion in the proton-induced fission of ^{233}U have been published hithertofore. In this paper we report a study of cross sections for the independent and cumulative formation of cesium isotopes (A = 129–128) in the interaction of protons of kinetic energies between 20–85 MeV with ^{233}U. Charge dispersion data are then deduced from these cross sections.

Experimental

1. Targets and Irradiation

The targets were irradiated with protons in the internal beam of the McGill Synchrocyclotron. The target material was finely powdered uranium oxide[3], $^{233}U_3O_8$. The oxide was uniformly mixed with "spec-pure" copper oxide which served as a beam monitor. The mixture (10–15 mg containing about 5 mg uranium oxide) was loaded into a thin (10 mg/cm^2) aluminium tube which had been clamped at one end. The tube was now sealed, flattened by rolling, and clamped to an aluminium holder, which was fastened to a water-cooled probe and positioned in the cyclotron tank at a radius corresponding to the desired proton energy. The time of irradiation varied from 5 to 15 min and the beam intensity was monitored by the reaction $^{65}Cu(p,pn)^{64}Cu$.

2. Chemical Separations

The general procedure for cesium purification was similar to that of Friedlander *et al.* (7). The aluminium tube, containing the uranium and copper oxides, was dissolved in 12 N HCl along with a drop of concentrated nitric acid. Carriers for Cs (20 mg), Ba (50 mg), Rb (5 mg), and La (2 mg) had been added to the centrifuge tube in which the target was dissolved. When it was necessary to separate Ba, barium chloride was precipitated from the concentrated solution by bubbling gaseous hydrogen chloride, and cooling the solution.

The solution containing the cesium was diluted to 6 N HCl, and silicotungstic acid was added to precipitate cesium silicotungstate. The precipitate was centrifuged, washed with 6 N HCl, and dissolved in a minimal volume of sodium hydroxide. The solution was cooled with ice, acetic acid and rubidium hold-back carrier was added, and $Cs_3Bi_2I_9$ was precipitated by the addition of BiI_3–HI reagent. The precipitate was dissolved in concentrated HCl under gentle heat, rubidium hold-back carrier was added, and $Cs_3Bi_2I_9$ was reprecipitated from the cooled solution by further addition of the BiI_3–HI reagent. The final precipitate was washed with 0.1 N HCl, filtered, and mounted for activity measurements. The chemical yield of cesium in this procedure was of the order of 20 to 30%.

The copper was separated from the supernate of the cesium silicotungstate precipitation by anion exchange. The supernate was evaporated to a small volume and made to 10 N in HCl. The solution was adsorbed on a Dowex 1 (x8) anion exchange column. The column was treated successively with 10 and 4 N HCl to remove

[1]This research was supported by the National Research Council of Canada.

[2]Present Address: Department of Chemistry, Tokyo Kyoiku University, Otsuka, Tokyo, Japan.

[3]The authors are grateful to Atomic Energy of Canada Ltd. for the loan of this material. The isotopic analysis was given as 97.75% ^{233}U, 2.25% ^{238}U.

TABLE I

Nuclides measured and modes of detection used

Nuclide	Half-life	Mode of decay	Radiation measured	Branch abundance	Instrument used
^{129}Cs	32.0 h	e.c.	X	1.0	NaI spectrometer
^{130}Cs	30 min	β^+, e.c., β^-	β^+	0.46	511–511 coincidence
^{131}Cs	9.7 days	e.c.	X	1.0	NaI spectrometer
^{132}Cs	6.5 days	e.c., (γ)	X 670 keV γ	0.97 0.99	NaI spectrometer
^{134}Cs	2.1 years	β^- (γ)	800 keV γ	0.99	NaI spectrometer
^{134}Cs^m	2.9 h	i.t.	128 keV γ e^-, β^-	0.14 1.0	NaI spectrometer End-window proportional counter
^{136}Cs	12.9 days	β^- (γ)		1.0	End-window proportional counter
^{138}Cs	32.2 min	β^- (γ)		1.0	NaI spectrometer End-window proportional counter

impurities and copper was finally eluted with 2 *N* HCl. The final solution was made up to 2 ml in a standard vial for γ-ray measurements. The chemical yield of copper was determined by titration with the disodium salt of ethylenediamine tetraacetic acid with PAN indicator (8).

In some cases barium was purified (7) and timed extractions of cesium were made.

3. Activity Measurements

The decay characteristics of the radionuclides and their method of assay are given in Table I.

An end-window gas-flow proportional counter was used to measure the counting rates of ^{136}Cs, ^{138}Cs, and in some cases, ^{134}Cs^m. The decay curves were resolved by means of the CLSQ least-square computer program (9). The activities due to ^{138}Cs (32.2 min) and ^{130}Cs (30 min) were initially analyzed as one component. The contribution due to ^{130}Cs was later subtracted when it had been obtained by positron measurements as described later.

In one experiment uranium foil, of normal isotopic composition, was irradiated with 45 MeV protons. Cesium was separated and purified as described, and the radioactivities used to calibrate the end-window counter relative to a $4\pi\beta$-proportional counter. Empirical self-absorption curves for ^{136}Cs and ^{134}Cs^m in $Cs_3Bi_2I_9$ were also constructed.

Gamma rays and K X-rays emitted by the cesium isotopes were measured by a 3 in. × 3 in. NaI(Tl) crystal linked to a 400-channel pulse-height analyzer. Counting efficiencies were determined by the use of radioactive standards whose γ-ray disintegration rates were known. The decay curve from the X-ray data was resolved into half-life components of 32 h (^{129}Cs), 6.5 days (^{132}Cs), 9.7 days (^{131}Cs), 12.9 days (^{136}Cs), and a longer-lived tail. The error in the computer analysis was highest for the 9.7-day component, undoubtedly caused by the presence and interference from the 6.5- and 12.9-day components. Since the 6.5-day ^{132}Cs emits a 670-keV γ-ray, this was also measured and the cross sections calculated in this way compared with those determined from the X-ray data. The agreement was reasonably good. No interference was found from the 660 keV γ-ray from ^{137}Cs (30 years) since its contribution was negligible. A fluorescence yield of 0.87 and an L/K capture ratio (7) were used to convert the measured K X-ray emission rates to K-electron capture disintegration rates.

Positron emission rates of ^{130}Cs (30 min) were determined by means of coincidence measurements of the 511 keV annihilation radiation. The cesium sample was mounted between two copper absorbers 1/16 in. thick. The annihilation radiation was detected by two 1½ in. × 1 in. NaI(Tl) crystals placed at 180° to the source and connected to a single-channel pulse-height analyzer gated to accept the 511 keV photopeak. The contribution to the coincidence rate from nuclear γ-radiation was monitored simultaneously using a third detector placed at 90° to the main assembly. The accidental rate was of the order of 40 and 10% at bombarding energies of 45 and 85 MeV, respectively, during the first hour of measurement, with intermediate values in between. The accidental rate was subtracted from the 180° rate to obtain the true annihilation coincidence rate. The efficiency of the assembly was calibrated by a standard source of ^{22}Na, mounted in a manner similar to that of the ^{130}Cs source.

The ^{64}Cu activity was measured as a liquid source using the γ-ray spectrometer.

Results and Discussion

1. Treatment of Data

The measured counting rates, either at the end of the irradiation, or at time of separation from the parent, were converted to disintegration rates by correcting for counter efficiencies, self-absorption, branching ratio, and chemical yield. The relationships given below to transform these into formation cross sections are essentially those given by Friedlander *et al.* (7) and are summarized and given here for ready reference.

Can. J. Chem. Downloaded from www.nrcresearchpress.com by 210.87.254.42 on 09/05/12
For personal use only.

Can. J. Chem. Downloaded from www.nrcresearchpress.com by 210.87.254.42 on 09/05/12
For personal use only.

In those experiments which did not require consideration of parent–daughter relationships (e.g. shielded or effectively-shielded nuclides), the cross section, σ, was obtained from the disintegration rate, D^0, at the end of the irradiation by means of the equation

[1] $$\sigma = D^{\infty} \cdot F$$

where

$$F = \frac{W_{Cu}}{W_U} \cdot \frac{A_U}{A_{Cu}} \cdot \frac{\sigma_{Cu}}{D_{Cu}{}^{\infty}}$$

$$D^{\infty} = D^0/[1 - \exp(-\lambda t_0)]$$

and

$$D_{Cu} = D^0{}_{64_{Cu}}/[1 - \exp(-\lambda_{64_{Cu}} t_0)]$$

where λ is the decay constant of the nuclide in question, t_0 is the length of irradiation, W_{Cu} and W_U are the weights of ^{65}Cu and ^{233}U in the target, respectively, A_{Cu} and A_U are the atomic weights of ^{65}Cu and ^{233}U, respectively, and σ_{Cu} is the appropriate formation cross section of ^{64}Cu in copper at various energies. The latter have been interpolated from the excitation functions reported by Meghir (10) and are given in Table II.

TABLE II

Monitor cross section values (10) for the reaction $^{65}Cu(p,pn)\,^{64}Cu$

E_p (MeV)	σ(mb)
20	320
30	325
40	262
45	240
50	223
60	190
70	170
80	150
85	140

Although ^{131}Cs grows from a ^{131}Ba parent with half-life of 12 days, ^{131}Cs was considered to be shielded from β-decay since the separation of cesium from barium was effectively complete within 30 min after irradiation. In the case of ^{129}Cs, the contribution from the parent (2.4 h ^{129}Ba) would be most pronounced at higher energies. A check was made at an irradiation energy of 70 MeV to see how great this contribution was. The cross sections of parent and daughter were determined from a single irradiation followed by 2 successive separations of the daughter product. The daughter activity obtained in the second extraction was used to find the parent cross section in standard fashion, and the daughter cross section was then determined by means of eq. [2] described below from the daughter activity obtained in the first extraction. The result showed that the cross section of ^{129}Cs was about 10 times larger than that of ^{129}Ba at this energy. If the contribution from ^{129}Ba were ignored, and ^{129}Cs treated as a shielded nuclide, the error would be less than 2%, well within experimental error. The independent yield of ^{129}Cs was therefore calculated in terms of eq. [1] in this experiment.

However, for the ^{138}Xe–^{138}Cs pair (half-lives of 14 and 32.2 min, respectively), the contribution from the parent to the yield of the daughter, because of the decay in the period between the end of irradiation and chemical separation, is no longer negligible.

When both members of the pair are produced independently (7) with cross sections σ_p and σ_d, respectively, in an irradiation of duration t_0, the distintegration rate D_d' of the daughter at a time t_1 after the end of irradiation is given by

[2] $$D_d' = (\lambda_d/F)(K_1\sigma_p + K_2\sigma_d)$$

where F is as defined previously, and

$$K_1 = \frac{e^{-\lambda_p t_1}(1 - e^{-\lambda_p t_0}) - (\lambda_p/\lambda_d)e^{-\lambda_d t_1}(1 - e^{-\lambda_d t_0})}{\lambda_d - \lambda_p}$$

$$K_2 = \frac{e^{-\lambda_d t_1}(1 - e^{-\lambda_d t_0})}{\lambda_d}$$

and λ_d and λ_p are the decay constants of the daughter and parent, respectively.

The values of the formation cross sections of ^{138}Xe and ^{138}Cs were determined from two separate irradiations with appropriately chosen times t_0 and t_1, each leading to an equation of the form of eq. [2]. In one irradiation, for example, the target was dissolved as soon as possible after the end of irradiation, and in the second an interval of about 1 h was allowed to elapse before dissolution.

2. Cross Sections and Excitation Functions

The formation cross sections for the nuclides investigated are given in Table III. All results quoted, with the exception of those for ^{138}Xe are independent formation cross sections. The numbers in parentheses following each cross

Can. J. Chem. Downloaded from www.nrcresearchpress.com by 210.87.254.42 on 09/05/12
For personal use only.

TABLE III

Formation cross sections (mb)*

E_p (MeV)	Formation cross sections								
	^{129}Cs	^{130}Cs	^{131}Cs	^{132}Cs†	^{134}Cs^m	^{134}Cs^{m+g}	^{136}Cs	^{138}Cs	^{138}Xe(*C*)*‡
20					7.2±0.2 (2)	10.1±1.5 (1)	30.5±1.4 (2)	17.3±3.8 (1)	6.0±1.3 (1)
30			2.5±0.8 (1)	2.7±0.4 (1) 2.3±0.4 (1)	10.3±1.5 (1)	15.9±2.4 (1)	28.3±1.7 (2)	17.9±3.9 (1)	2.1±0.5 (1)
40					16.1±2.4 (1)	21.0±3.2 (1)	31.4±3.4 (2)		
45		1.8±0.3 (1)		10.8±0.3 (3) 10.8±2.5 (1)	23.1±0.3 (2)	29.5±4.4 (1)	35.0±2.5 (4)	18.0±3.9 (1)	9.5±2.1 (1)
50	0.8±0.2 (1)	2.1±0.3 (2)	5.0±1.8 (1)	12.7±1.9 (1) 12.1±1.0 (1)	20.2±0.7 (2)	26.3±4.0 (1)	33.1±1.2 (3)		
55				13.5±0.4 (2)			30.2±1.3 (3)	19.5±4.3 (1)	5.5±1.2 (1)
60	1.0±0.2 (1)	3.7±0.4 (1)	5.7±1.8 (1)	12.6±1.9 (1) 13.5±1.8 (1)	16.3±2.5 (1)	21.3±3.2 (1)	25.6±4.0 (3)		
65	1.6±0.3 (1)	5.1±0.6 (1)	10.2±2.3 (1)	12.9±1.9 (1) 11.7±1.7 (1)	15.9±2.4 (1)	20.2±3.0 (1)	26.1±3.0 (1)		
70	1.8±0.3 (1)	4.5±0.5 (1)	8.0±1.4 (2)	15.0±0.8 (2) 14.3±1.6 (1)	16.4±2.5 (1)	20.3±3.0 (1)	26.1±3.0 (1)	17.0±3.7 (1)	7.1±1.6 (1)
80	2.7±0.3 (1)	7.6±0.8 (1)	9.9±1.2 (1)	14.5±0.8 (3) 15.3±1.6 (1)	16.2±2.5 (1)	20.8±3.1 (1)	27.4±3.0 (1)	12.2±2.7 (1)	8.0±1.8 (1)
85	2.8±0.7 (1)	7.7±0.8 (1)	9.6±2.5 (1)	16.4±2.5 (1) 16.7±2.2 (1)	16.7±2.5 (1)	20.1±3.0 (1)	27.0±3.0 (1)		

*The numbers in brackets give the number of determinations.
†The upper and lower rows give cross sections obtained by γ-ray and X-ray measurements respectively. The value at 55 MeV was obtained by γ-ray measurements.
‡(*C*) = cumulative yield.

Can. J. Chem. Downloaded from www.nrcresearchpress.com by 210.87.254.42 on 09/05/12
For personal use only.

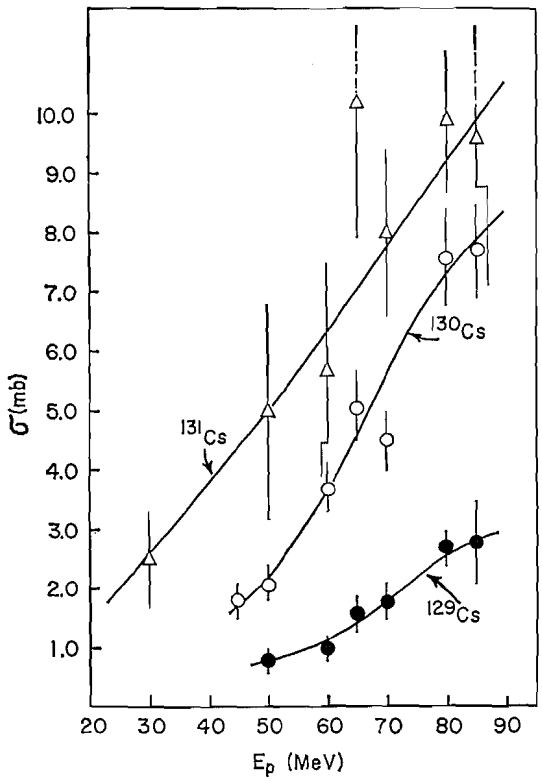

FIG. 1. Excitation functions for the independent yields of ^{129}Cs, ^{130}Cs, and ^{131}Cs.

section value indicate the number of determinations. Errors for individual results were estimated from the uncertainties in decay curve analyses, counting efficiencies, chemical yields, photopeak area estimation (for γ-measurements), and self-absorption (for β-measurements). Where more than one determination was made the average value is given along with the mean deviation.

Excitation functions for the various products are shown in Figs. 1–4. In Table IV the independent formation cross sections of ^{133}Cs, ^{135}Cs, and ^{137}Cs have been interpolated from charge dispersion curves, and these are shown in Fig. 5. The excitation functions of some of the nuclides studied exhibit maxima in this energy region. In Fig. 6, the energy at which the excitation function reaches its maximum is plotted against the neutron-to-proton ratio (N/Z) of the nuclide. The interpolated data have also been included. Corresponding data obtained by others for ^{232}Th (3) and natural uranium (4) targets have also been included for comparison. It has been

TABLE IV

Independent formation cross sections (mb) interpolated from charge dispersion curves

E_p (MeV)	Cross section ^{133}Cs	^{135}Cs	^{137}Cs
20	6	23	27
30	9	25	26
45	20	33	30
50	20	31	27
60	20	25	24
70	20	25	22
80	21	24	19

pointed out previously (3–6) that the energies, at which the excitation functions for the independent formation of various fission products reach their maxima, increase with decreasing neutron-to-proton ratio of the product. That this is also true for ^{233}U is evident from Fig. 6. However, the slope of the curve is a function of the N/Z ratio of the target (1.587, 1.578, and 1.533 for ^{238}U, ^{232}Th, and ^{233}U, respectively).

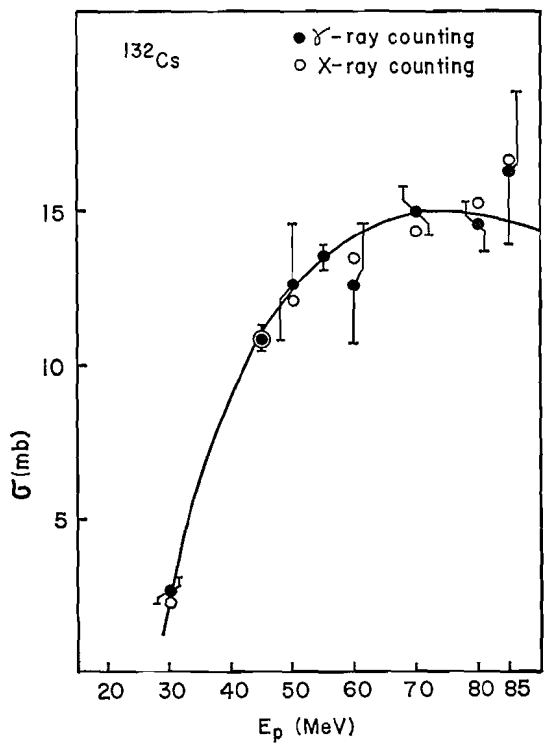

FIG. 2. Excitation function for the independent yield of ^{132}Cs.

Can. J. Chem. Downloaded from www.nrcresearchpress.com by 210.87.254.42 on 09/05/12
For personal use only.

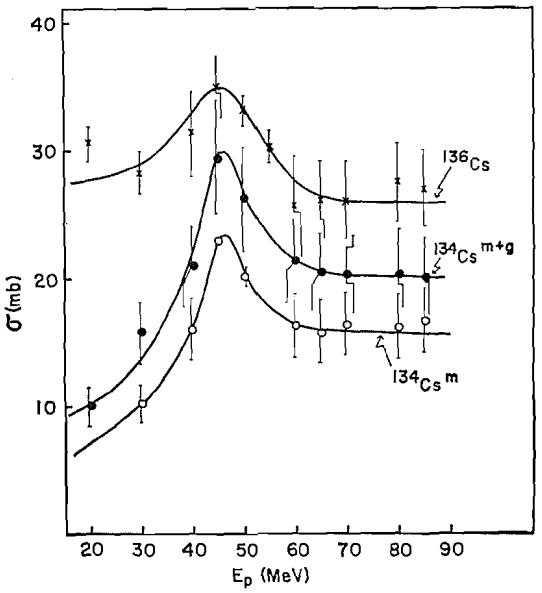

FIG. 3. Excitation functions for the independent yields of $^{134}Cs^{m}$, $^{134}Cs^{m+g}$, and ^{136}Cs.

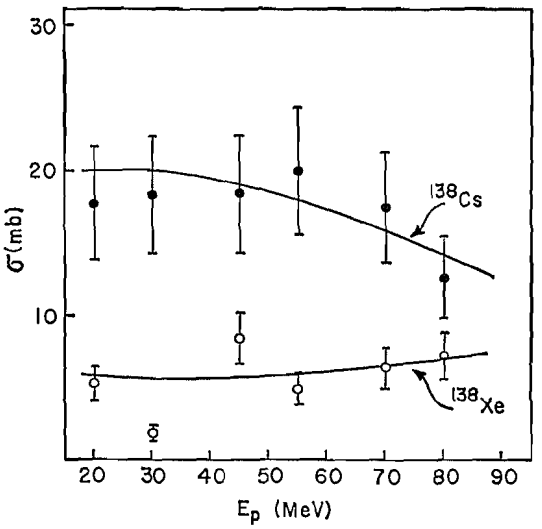

FIG. 4. Excitation functions for the independent yield of ^{138}Cs and the cumulative yield of ^{138}Xe.

More data are needed to give quantitative relations. However, it is obvious that, even though ^{233}U and ^{238}U differ only by 0.054 N/Z units, yet it takes 310 MeV more for ^{132}Cs to be a highly probable fission product in the latter case than the former. Highly neutron-deficient products, normally occurring in relatively high abundance at GeV energies in the case of ^{238}U will be expected at energies that are factors of 10 less in the case of ^{233}U. For example, Friedlander *et al.* (7) found a negligible yield of ^{129}Cs at 100 MeV and only 1.5 mb at 200 MeV bombarding energy in the fission of ^{238}U. The present data for ^{233}U show a yield of 1.5 mb at 65 MeV and the excitation function is rising very steeply. The excitation function would be expected to reach its maximum at about 95 MeV bombardment energy, to be contrasted with the value of 900 MeV, found by Friedlander *et al.* (7) for ^{238}U fission. The role in the fission of the neutron-to-proton ratio of the target is thus quite obvious.

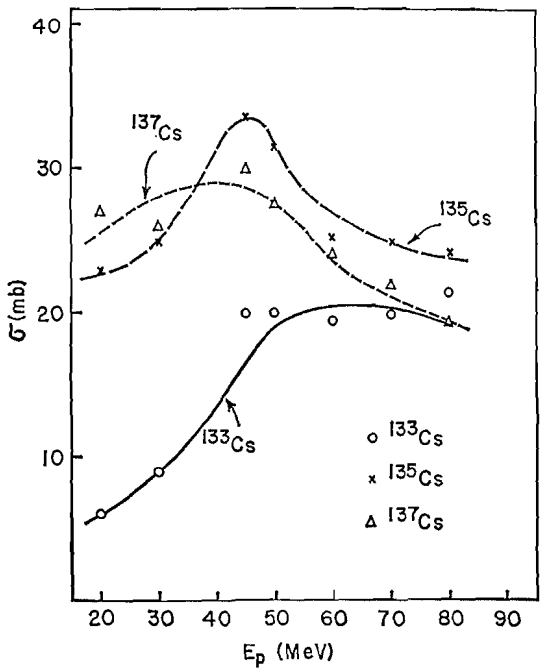

FIG. 5. Excitation functions for the independent yields of ^{133}Cs, ^{135}Cs, and ^{137}Cs, interpolated from charge dispersion curves.

Another feature of the excitation functions is that the independent cross sections for ^{138}Cs do not vary much in the energy region studied, and are relatively small compared to those for ^{136}Cs, the closest shielded isotope. This is not the case for ^{238}U fission (4) and indicates that, in the present case, Z_p, the most probable charge, is considerably displaced relatively towards β-stability. This is also clearly observed in the charge dispersion curves.

Can. J. Chem. Downloaded from www.nrcresearchpress.com by 210.87.254.42 on 09/05/12
For personal use only.

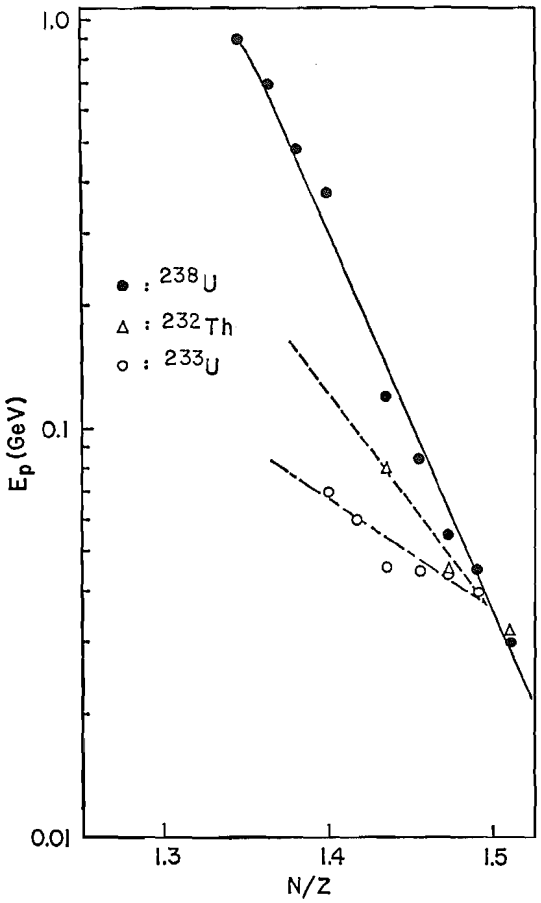

FIG. 6. Energies at which excitation functions reach their maxima.

3. Charge Dispersion

If one assumes that the mass–yield curve is essentially flat in the region $129 \leq A \leq 138$, the cross section data given in Table III can be used to construct charge dispersion curves. These are given in Figs. 7–13 inclusive. The cumulative cross sections of ^{138}Xe were used to define the shape of the neutron-excess sides of the curves where only a few independent yield data were available. The curves, plotted as a function of N/Z, as done by Friedlander *et al.* (7), were drawn in such a fashion that the sum of the interpolated independent yields equalled the experimentally-determined cumulative yields.

As the bombardment energy increases from 20 to 80 MeV the curves become broader, and the peak position, Z_p, moves to smaller N/Z ratios. The relevant parameters of the charge

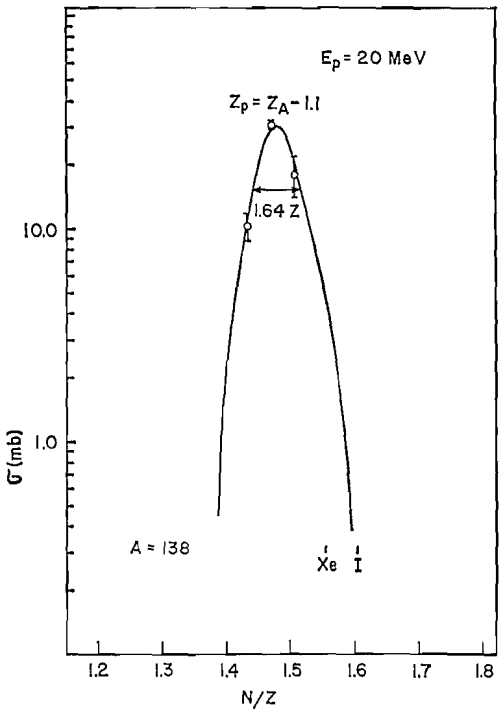

FIG. 7. Charge dispersion at 20 MeV.

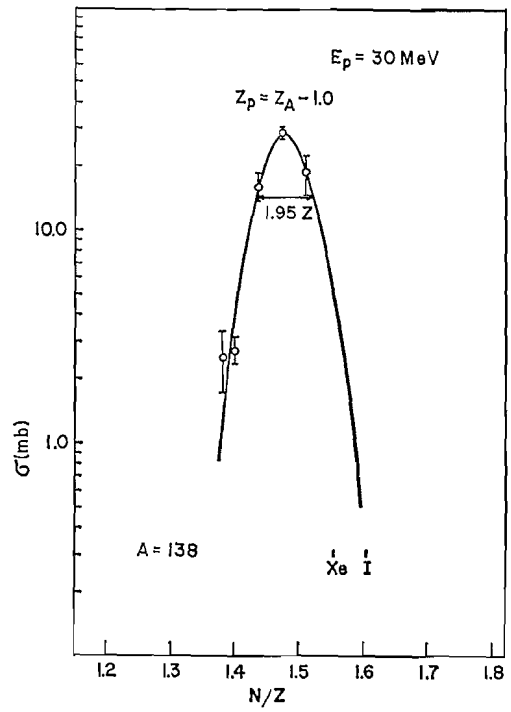

FIG. 8. Charge dispersion at 30 MeV.

TABLE V

Parameters of charge dispersion curves

Proton energy (MeV)	Full-width at half-maximum		Peak position	
	N/Z	ΔZ	N/Z	$Z_A - Z_p$
20	0.074	1.6	1.480	1.1
30	0.090	2.0	1.475	1.0
45	0.112	2.5	1.467	0.8
50	0.110	2.5	1.466	0.8
60	0.132	3.0	1.466	0.8
70	0.134	3.0	1.460	0.6
80	0.141	3.1	1.451	0.4

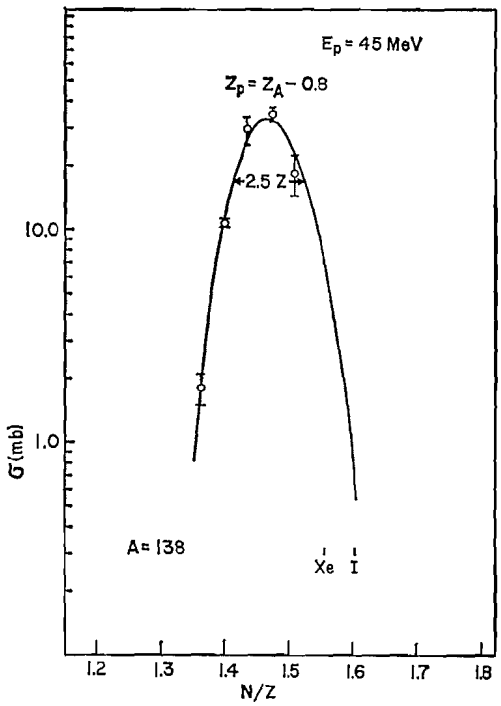

FIG. 9. Charge dispersion at 45 MeV.

dispersion curves are given in Table V and the trends are shown graphically in Fig. 14 together with similar data for ^{238}U (4) and ^{232}Th (3). The appropriate values of Z were obtained from the charge dispersion curves in the same way as in ref. 5. The most stable charge for a given A value, Z_A, was taken from Coryell (11). The full-widths at half-maximum seem to be similar for the 3 target nuclei. However, the displacement towards β-stability in the case of ^{233}U relative to both ^{238}U and ^{232}Th is quite apparent. In Fig. 15 the values of $Z_A - Z_p$ at different energies

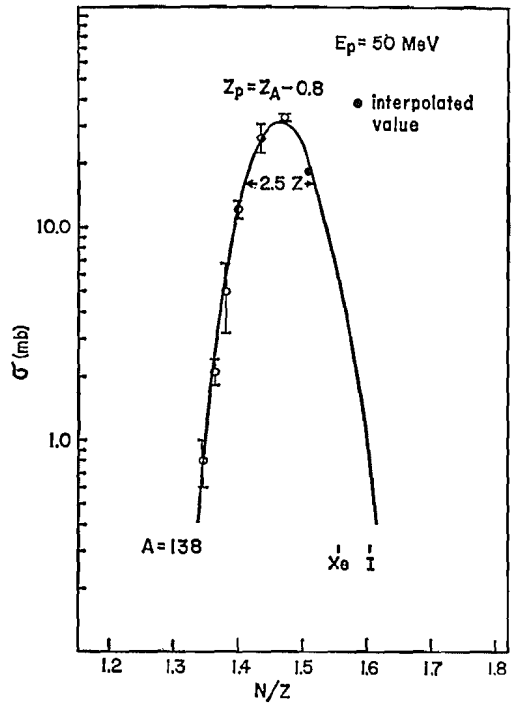

FIG. 10. Charge dispersion at 50 MeV.

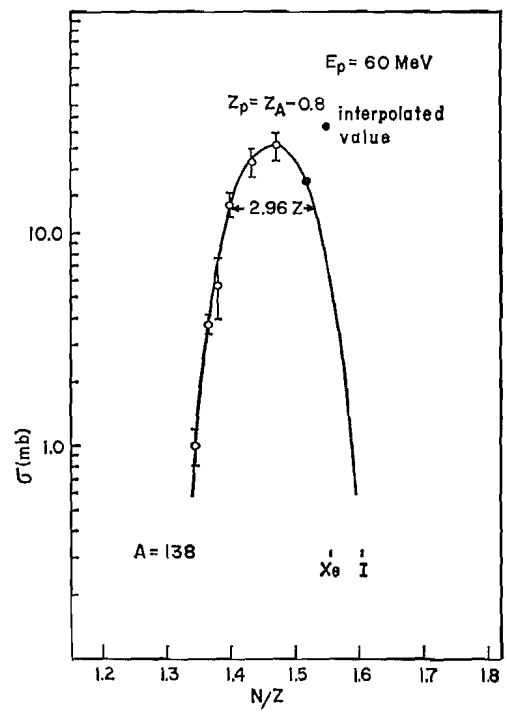

FIG. 11. Charge dispersion at 60 MeV.

Can. J. Chem. Downloaded from www.nrcresearchpress.com by 210.87.254.42 on 09/05/12
For personal use only.

Can. J. Chem. Downloaded from www.nrcresearchpress.com by 210.87.254.42 on 09/05/12
For personal use only.

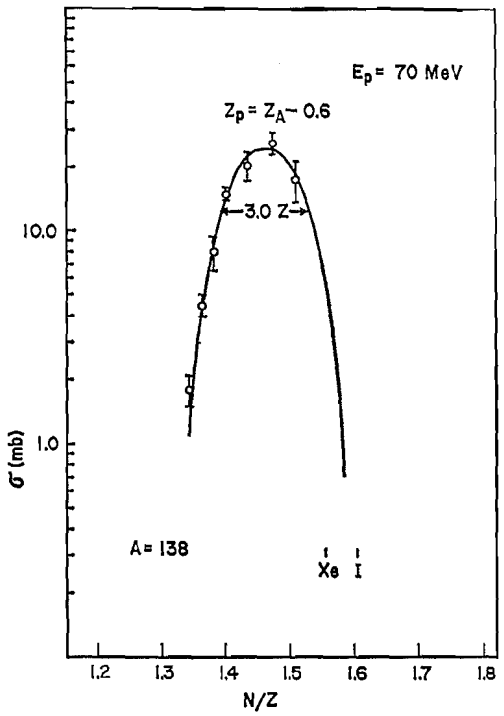

FIG. 12. Charge dispersion at 70 MeV.

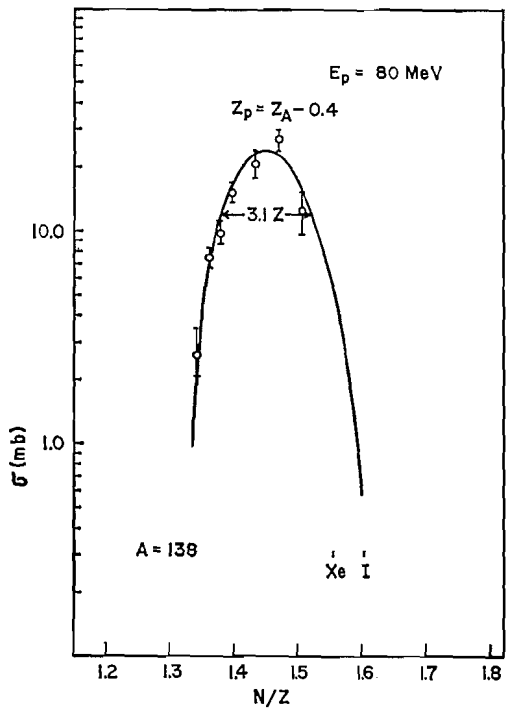

FIG. 13. Charge dispersion at 80 MeV.

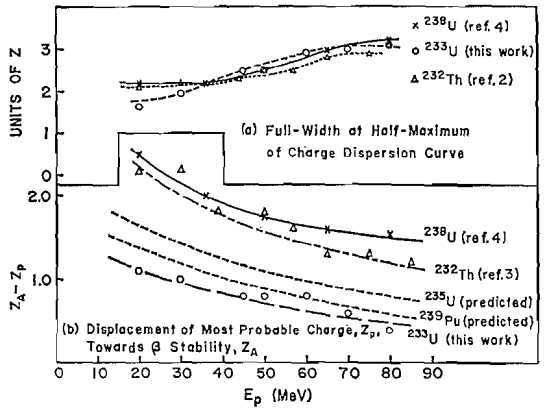

FIG. 14. Charge dispersion parameters: (*a*) full-width at half-maximum; (*b*) displacement of most probable charge, Z_p, towards stability, Z_A.

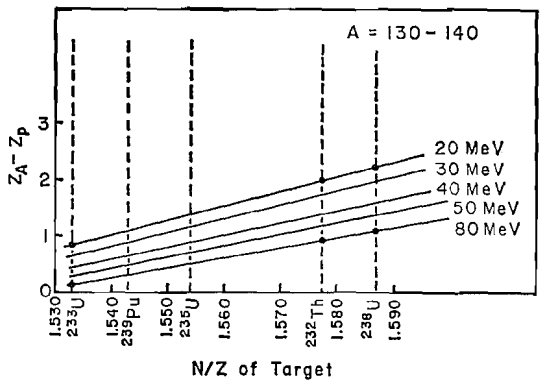

FIG. 15. Plot of $Z_A - Z_p$ at various energies as a function of neutron-to-proton (N/Z) ratio of target.

are plotted against N/Z of the target nuclei. The displacement of the most probable charge from that corresponding to stability for ^{235}U and ^{239}Pu was then read off these curves and the predictions shown in Fig. 14. These target nuclei are now being studied in our laboratory and results should be available shortly.

The total formation cross section for $A = 136$ was estimated as a function of energy from the charge dispersion curves and plotted in Fig. 16 along with data obtained by Davies and Yaffe (4) for ^{238}U. The total isobaric cross section for mass 136 is greater for ^{233}U than for ^{238}U. There is a peak at about 50 MeV in each case, but it is very much more pronounced in ^{233}U.

4. Z_p *Values*

An approximate estimation of Z_p values has been made for bombardment energies up to 50

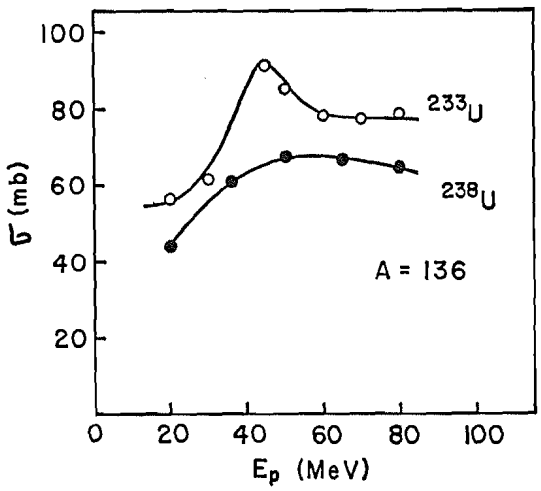

FIG. 16. Total isobaric cross section for $A = 136$.

MeV by means of the postulates of equal charge displacement (e.c.d.) (12) or unchanged charge division (u.c.d.) (13). Compound nucleus formation was assumed in this energy range. The excitation energies given to the compound nucleus were estimated initially as full energy transfer, i.e. 20, 30, and 50 MeV, plus the Q value for the reaction. Then the residual energies were calculated at each stage after neutron emission until the residual excitation energy reached a value below the neutron-binding energy. In each case an average kinetic energy for neutron emission of $2T$ was taken, T being the nuclear temperature. The masses of the fissioning nuclei are shown in Table VI. The

TABLE VI

Estimated fissioning nuclei and initial mass of fission fragment (final $A = 136$) at several bombardment energies

Proton energy (MeV)	Fissioning nuclei		Initial mass of fission fragment (final $A = 136$)
	Z	A	
20	93	234	139
	93	233	138
	93	232	138, 137
30	93	234	139
	93	233	139, 138
	93	232	138
	93	231	137
50	93	234	141, 140
	93	233	140
	93	232	139
	93	231	139, 138
	93	230	138

residual excitation energy of each nucleus was assumed to be divided into two fragments in the ratio of their masses when fissioning. In the next step, several fission processes leading to Cs isotopes were checked for each fissioning nucleus to find out which isotope contributes to the final fission product (^{136}Cs) as a result of post-fission neutron emission.

Z_p values were estimated according to the 2 postulates

$$Z_p = Z_{A_1} - 1/2(Z_{A_1} + Z_{A_2} - Z_f)$$

for e.c.d. where Z_{A_1} and Z_{A_2} are the Z_A values for the complementary fragments of masses A_1 and A_2, and Z_f is the nuclear charge, 93, of the compound nucleus.

Similarly

$$Z_p = (Z_f/A_f)A_1$$

for u.c.d., where A_f is the mass of the fissioning nucleus. Where 2 initial masses for a given fissioning nucleus had to be considered, as shown in Table VI, the average value of separately calculated Z_p values was taken. This is admittedly a crude approximation, but has no appreciable effect on the results.

In order to obtain the actual value of Z_p, to be compared with the experimental value, the formation and fission probabilities for a given fissioning nucleus have to be taken into account. The emission of charged particles can be disregarded in this low-energy region (14).

The probability, G, for the fission of a given nucleus is

$$G = \Gamma_f/(\Gamma_n + \Gamma_f)$$

where Γ_n and Γ_f are neutron evaporation and fission widths, respectively. Values of G were estimated from the data of Vandenbosch and Huizenga (15), assuming that the value of Γ_n/Γ_f is independent of excitation energy (16). The formation probability for the compound nucleus ^{234}Np was assumed to be unity and that for the product resulting from neutron evaporation was the neutron evaporation probability for the precursor.

The Z_p values, calculated on the basis of the e.c.d. and u.c.d. postulates were now weighted by the product of formation and fission probabilities for each fissioning nucleus and the weighted average Z_p value was determined. The calculated and experimental values are given in Table VII.

Can. J. Chem. Downloaded from www.nrcresearchpress.com by 210.87.254.42 on 09/05/12
For personal use only.

TABLE VII

Comparison of calculated and experimental Z_p values ($A = 136$)

E_p (MeV)	Z_p e.c.d.	Z_p u.c.d.	Z_p Experimental
20	54.0	55.2	54.8
30	54.0	55.2	54.9
50	54.6	55.8	55.1

The experimental values fall between those predicted by the 2 postulates.

Pappas (17) has suggested that e.c.d. and u.c.d. depict the asymmetric and symmetric modes of fission, respectively. In general, with increasing bombardment energy the yields corresponding to symmetric fission increase rapidly, but the relative yield of very asymmetric fission also increases (18). Thus the two-mode fission hypothesis would predict that the overall fission product distribution be interpreted as the superposition of an asymmetric and symmetric mode. If this is correct, the results given here would indicate that the 2 modes contribute roughly equally to the fission process at these energies.

It has also been shown by others (19, 20) that at low and medium energies, the u.c.d. postulate predicts Z_p values for the heavy mass chains which are higher than those experimentally determined. If one assumes this postulate, lower limits of the average total number of neutrons can be roughly estimated (6). An exact formulation of the u.c.d. postulate should of course involve an exact knowledge of the yields of pre- and post-fission neutrons. Failing that, the simplified expression given below can be used

$$(Z_p)_{fp} = A_{fp}\frac{Z_t + Z_{pr}}{A_t + A_{pr} - \bar{\nu}_T}$$

where fp, t, and pr refer to fission product, target, and projectile, respectively. This simplification makes the gross assumption that all the neutrons emitted are pre-fission neutrons. However, this is equivalent to the assumption that the mass of the fission product is the same as that of the fission fragment (before post-fission neutron emission) and introduces an error of only a few % into the calculations. Average $\bar{\nu}_T$ values estimated on this basis for $A_{fp} = 136$ are 3.2, 3.6, 4.0, and 4.5 neutrons for bombardment energies of 20, 30, 40, and 50 MeV, respectively. Although lower limits, the agreement with values deduced from the data in Table VI is quite good. These data have been extended to 80 MeV, where admittedly the assumption of compound nucleus formation is not so certain, and are compared with data obtained in a similar fashion from the work of Benjamin *et al.* (3) and Davies and Yaffe (4) for ^{232}Th and ^{238}U, respectively. The results are shown in Fig. 17.

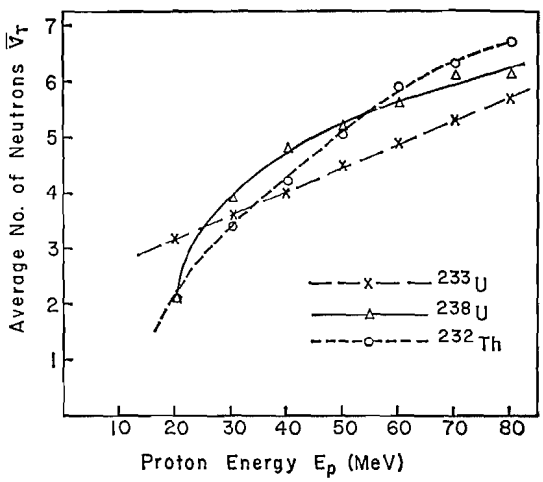

FIG. 17. Average number of neutrons ($\bar{\nu}_T$) as a function of bombardment energy as a lower limit, calculated on the basis of u.c.d.

Acknowledgments

The authors wish to thank Professor R. E. Bell, Director of the Foster Radiation Laboratory, for his ready permission to use the McGill Synchrocyclotron and Mr. R. H. Mills who cheerfully performed the irradiations.

1. B. D. PATE, J. S. FOSTER, and L. YAFFE. Can. J. Chem. **36**, 1691 (1958).
2. A. KJELBERG, H. TANIGUCHI, and L. YAFFE. Can. J. Chem. **39**, 635 (1961).
3. P. P. BENJAMIN, D. A. MARSDEN, N. T. PORILE, and L. YAFFE. Can. J. Chem. **47**, 301 (1969).
4. J. H. DAVIES and L. YAFFE. Can. J. Phys. **41**, 762 (1963); Can. J. Chem. **41**, 1836 (1963).
5. S. S. PARIKH, D. A. MARSDEN, N. T. PORILE, and L. YAFFE. Can. J. Chem. **45**, 1863 (1967).
6. J. H. FORSTER, N. T. PORILE, and L. YAFFE. Can. J. Chem. **44**, 2951 (1966).
7. G. FRIEDLANDER, L. FRIEDMAN, B. GORDON, and L. YAFFE. Phys. Rev. **129**, 1809 (1963).
8. F. J. WELCHER. The analytical uses of ethylenediaminetetraacetic acid. D. Van Nostrand Co., Inc., Princeton, New Jersey. 1958. p. 242.
9. J. B. CUMMING. Brookhaven Natl. Lab. Rept. BNL 6470, 1962.

Can. J. Chem. Downloaded from www.nrcresearchpress.com by 210.87.254.42 on 09/05/12
For personal use only.

10. S. MEGHIR. Ph.D. Thesis, Department of Chemistry, McGill University, Montreal, Quebec. 1962.
11. C. D. CORYELL. Ann. Rev. Nucl. Sci. **2**, 305 (1953).
12. L. E. GLENDENIN, C. D. CORYELL, and R. R. EDWARDS. The fission products. Natl. Nucl. Energy Ser. Vol. 9, Div. IV. McGraw-Hill Book Co., Inc., New York. 1951. Paper 52.
13. R. H. GOECKERMANN and I. PERLMAN. Phys. Rev. **76**, 628 (1949).
14. I. DOSTROVSKY, Z. FRAENKEL, and G. FRIEDLANDER. Phys. Rev. **116**, 683 (1959).
15. R. VANDENBOSCH and J. R. HUIZENGA. Proc. 2nd Intern. Conf. Peaceful Uses Atomic Energy. Paper P/688, U.N., Geneva. **15**, 284 (1958).
16. M. LINDNER and A. TURKEVICH. Phys. Rev. **119**, 1632 (1960).
17. A. C. PAPPAS. Z. Naturforsch. **21***a*, 995 (1966).
18. E. K. HYDE. UCRL-9065, Feb. 1960. The nuclear properties of the heavy elements III. Prentice Hall Inc., Englewood Cliffs, New Jersey. 1964.
19. J. A. MCHUGH, JR. Ph.D. Thesis, Univ. Calif. Radiation Lab. Rept. UCRL-10673, 1963.
20. A. C. WAHL. Symp. Phys. Chem. Fission. I.A.E.A. Salzburg. 1965. Paper SM-60/22.

Can. J. Chem. Downloaded from www.nrcresearchpress.com by 210.87.254.42 on 09/05/12
For personal use only.

Can. J. Chem. Downloaded from www.nrcresearchpress.com by 210.87.254.40 on 09/05/12
For personal use only.

Chemisorption of hydrogen on nickel–magnesia catalysts. Part I. General kinetic characteristics

N. S. VISWANATHAN[1] AND L. M. YEDDANAPALLI
Loyola College, Madras 34, India

Received August 19, 1968

A detailed study of the kinetics of hydrogen chemisorption on 3 different nickel catalysts, supported on magnesia and prepared by coprecipitation, has been made over a wide range of pressures and temperatures. The results have been analyzed in the light of the Elovich equation. Experimental data obtained by variations of pressure and temperature indicate the existence of a number of stages in the chemisorption process and support the multiple kinetic stage hypothesis suggested by Low. The effect of temperature on the parameters has been studied, and relations obtained which have been used to calculate activation energies for each of the stages.

Canadian Journal of Chemistry, 47, 2933 (1969)

The kinetics of chemisorption of gases on solids has been represented by various types of equations. A logarithmic relation, often referred to as the Elovich equation, probably has the widest applicability in accounting for the kinetic data in at least a semiquantitative way, as has been shown by Low (1). It has, however, been criticized quite often as being not much more than an empirical relation. Very recently Allen and Scaife (2) have attempted a modification of the Elovich equation and have indicated its usefulness in explaining commonly encountered experimental observations. They have employed a method based on linear regression analysis and claim a high order of precision in their evaluation of the Elovich parameters (3, 4).

In this paper, we report the experimental results of the chemisorption of hydrogen on nickel–magnesia catalysts, analyzed in the light of the Elovich equation. Not only a more thorough study of the kinetic characteristics of the adsorption than an earlier investigation from this laboratory has been made, but also a detailed study of the temperature effect on the adsorption process has been carried out in view of the conflicting reports on the activation energy of the process.

The Elovich equation is used in the form

$$dq/dt = a \exp(\alpha q)$$

as suggested by Low (1) and in the original paper by Roginskii and Zeldowich (5), a and α being constants.

[1]Present address: Components Division, IBM East Fishkill, Hopewell Junction, New York 12533.

Experimental

The adsorption measurements were made in a constant volume system, provided with a McLeod gauge and accurately calibrated oil and mercury manometers. The dead spaces used in the experiments were 27.97 ml with mercury manometers and 87.97 ml with the Apiezon oil manometers. The adsorption was followed by the decrease in pressure in the constant volume system. In the cases of low initial pressure experiments, limitations were due mainly to noting small changes in pressure of gas remaining in the system after long adsorption times. The oil manometer was of the differential type with Apiezon B oil (ABO) which had been thoroughly degassed and which permitted accurate measurements of low initial pressures (equivalent to 1 mm Hg).

The nickel–magnesia adsorbent was prepared by coprecipitation of the mixed hydroxides from a solution of the 2 nitrates in about 250 ml of distilled water by the addition of 1 *N* sodium hydroxide solution. The precipitates were washed for 48 h with distilled water, dried for 12 h at 110 °C, and finally the dried hydrated oxides were reduced in a stream of purified hydrogen at measured flow rates.

Nickel nitrate, (British Drug Houses) Analar quality was of purity better than 99.94%, magnesium nitrate (Sarabhai Merck) was of guaranteed Reagent quality with purity better than 99.98%, and sodium hydroxide (E. Merck) was of analytical grade.

The amount of nickel in the catalysts was estimated by wet methods. The degree of reduction was estimated by the methods described by Schuit and de Boer (6). The method using HCl was found to give satisfactory results when compared with the sulfur vapor method described by these authors. The data reported in Table I were obtained by the HCl method. The dimethylglyoxime method was crosschecked by an electrochemical method based on the outline by Furman (7). Dead space measurements were made with helium and nitrogen according to the method described by Loebenstein (8). Surface area measurements were made by the Brunauer–Emmett–Teller (B.E.T.) method at −183 °C with nitrogen as the adsorbate. In a few cases krypton was used at −196 °C. There was a variation of 10% in the values of the B.E.T. areas by these gases. All the B.E.T. areas mentioned in

TABLE I

Specifications of the catalysts used in the experiments

Specification	Catalyst **1**	Catalyst **2**	Catalyst **3**
Weight (g)*	4.5094	4.0141	4.2385
Nickel %†	36.56	14.56	14.56
Reduction time (h)‡	24	30	48
BET area (m^2)§	196.8	105.9	113.7
Degree of reduction (%)‖	90	55	78

*Weight of the catalyst after the completion of the experiments.
†Estimated by a wet analysis of the oxides, base MgO = 100.
‡At a constant flow rate of hydrogen 4 l/h at 475 ± 5 °C, except in the case of catalyst **1**, where the flow rate was 8 l/h.
§B.E.T. surface area with nitrogen at −183 °C. (Catalyst **1**, using krypton at −196 °C.)
‖Estimate based on hydrogen adsorption at low temperatures.

this paper were made using nitrogen, except in the case of catalyst **1** for which experimental evidence of possible nitrogen chemisorption precluded any B.E.T. measurements with nitrogen as the adsorbate gas.

Hydrogen was purified by passage over platinized asbestos at 450 °C, then through a drying tower, and finally through a cold trap maintained at −183 °C. The flow rates were controlled by Hoke valves and measured by soap bubble flowmeters. Nitrogen was purified by passage over hot copper at 350 °C, dried over drierite, and passed through a dry ice – acetone trap before being allowed into the system. Helium was purified by passing it over reduced copper turnings at 400 °C and then through an activated charcoal trap at −195 °C.

Temperature control better than 1 °C during adsorption experiments was achieved by a Fisher–Serfass relay in conjunction with a Gallenkamp contact thermometer as the sensor in the heating circuit of the furnace. Low temperature measurements were made with appropriate baths, suitably thermostated. For measurements at 100 and 0 °C, boiling water and melting ice were used.

Between adsorption measurements, the adsorbents were degassed for 8 h at 380 ± 4 °C at 10^{-6} mm Hg. This pressure was obtained by a Cenco Megavac and a mercury diffusion pump along with cold traps. Helium flushing was resorted to for a few experiments but this procedure did not seem to lead to any significant improvement over the normal degassing method which was adopted in general. The reproductibility of the surface was checked by making adsorption measurements at standard conditions.

A summary of the properties of the catalysts and some relevant data of interest are given in Table I.

Results and Discussion

For the evaluation of the Elovich parameters, the integrated form of the Elovich equation has been used in the form (9)

$$[1] \qquad q_{nt} - q_{mt} = \frac{2.303}{\alpha} \log n/m$$

where q_{nt} and q_{mt} are the volumes of gas adsorbed at N.T.P. at times nt and mt respectively. In the present study the values of $a\alpha$ were very large and the linearizing constant t_0 for the $q - \log t$ plots was found to be small. Hence the algebraic method suggested by Low and Saramousakis was used entirely for the evaluation of the parameters. α was calculated by eq. [1] and a by using the known values of q according to the relation

$$[2] \qquad q_1 = \frac{2.303}{\alpha_1} \log a_1\alpha_1$$

where q_1 = volume adsorbed at time t = 1 min. This method was found to be superior to using the slopes of Elovich plots.

By an exhaustive study of the adsorption kinetics of a number of gas–solid systems, Low found that the slopes of the Elovich $q - \log t$ plots showed changes both in magnitude and direction. In the case of hydrogen on rhodium and palladium he could detect several kinetic stages (10) in a single adsorption experiment, and on this basis suggested the possibility of multiple kinetic stages in terms of which the experimental data of earlier investigations could be explained. Our own preliminary experiments with catalyst **1** and the earlier work from this laboratory (11) seemed to indicate, in fact, the occurrence of more than one kinetic stage in the same adsorption experiment. Figure 1 represents a typical series of adsorption plots for catalyst **1** at an initial pressure of 60 cm Hg. Curves A and C represent the data for 208 and 30 °C respectively, and show breaks at different times with slopes of different magnitude. In the case of curve A, the slope of the first position is lower than that of the second position whereas the reverse is the case with curve C. Curve B is a straight line; this is being considered for discussion in a later section. In the case of catalyst **3** of a different nickel content, a similar behavior was observed.

Can. J. Chem. Downloaded from www.nrcresearchpress.com by 210.87.254.40 on 09/05/12
For personal use only.

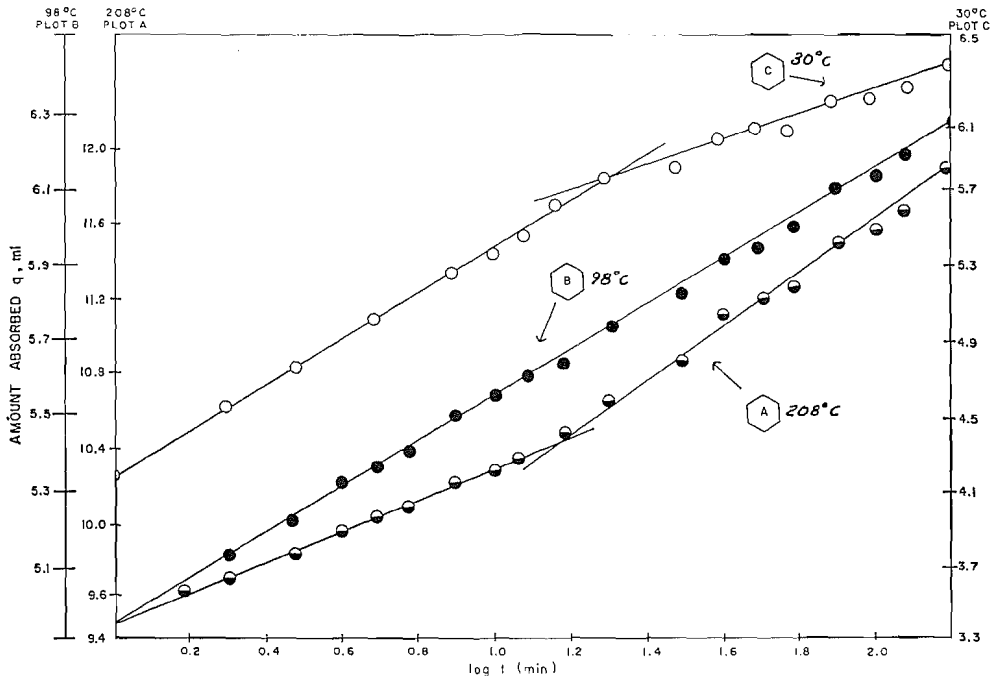

FIG. 1. Elovich plots at 60 cm Hg; effect of temperature. Catalyst 1: *A* at 208 °C, ◒; *B* at 98 °C, ●; *C* at 30 °C, ○.

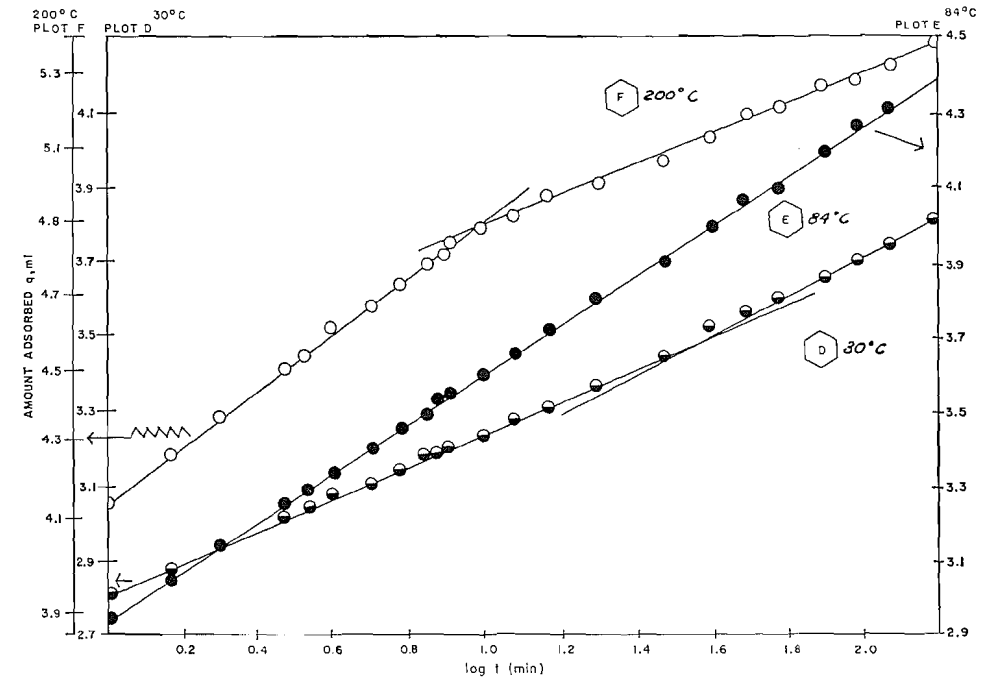

FIG. 2. Elovich plots at 60 cm ABO; effect of temperature. Catalyst 2: *D* at 30 °C, ◒; *E* at 84 °C, ●; *F* at 200 °C, ○.

Can. J. Chem. Downloaded from www.nrcresearchpress.com by 210.87.254.40 on 09/05/12
For personal use only.

TABLE II

Effect of temperature on the Elovich parameters, at high pressures

Temperature °C	α_1	α_2	log $a_1\alpha_1$	log $a_2\alpha_2$	a_1	a_2	t_b
*Catalyst 1**							
208	2.773	1.849	11.440	8.437	9.931×10^{10}	1.479×10^{8}	12
180	3.005	2.204	10.760	8.812	1.915×10^{10}	2.943×10^{8}	14
140	3.481	2.958	9.820	9.588	1.898×10^{10}	1.309×10^{9}	19
100	3.893	3.651	8.360	9.210	5.886×10^{7}	4.442×10^{8}	21
Catalyst 3†							
200	2.783	3.396	6.6071	7.9167	1.454×10^{6}	2.431×10^{7}	7
180	3.210	4.280	7.0390	8.0824	3.408×10^{6}	2.891×10^{7}	8
160	3.904	5.062	7.6080	8.5065	1.039×10^{7}	6.342×10^{7}	8
120	5.804	6.800	9.0070	9.7978	1.991×10^{8}	9.231×10^{8}	10
100	6.419	7.352	10.5400	11.8359	5.401×10^{9}	9.322×10^{10}	12

*Initial pressure 60.00 ± 1.5 cm Hg.
†Initial pressure 60.00 ± 1.21 cm Hg.

Figure 2 gives the results obtained with catalyst **2** and for initial pressures of hydrogen less than 60 cm ABO, that is, less than 4 cm Hg. Plot *D* represents the data at 30 °C, *F* at 200 °C, and *E* at 84 °C. This last plot is a straight line. A similar type of plot at a constant temperature and varying pressures was obtained, although the data at low pressures were not very quantitative due to difficulty in measuring small volumes of hydrogen.

Having established experimentally that the variation of pressure and temperature bring about variations in the nature of Elovich plots, and knowing that the slope of the plot is equal to $2.303/\alpha$, the quantity of gas adsorbed at time t is given by

$$[3] \qquad q_t = \frac{2.303}{\alpha} \log (1 + a\alpha t)$$

It was of interest to study the effects of temperature and pressure on the Elovich constants which indirectly define the adsorption behavior of the catalyst.

Effect of Temperature

An attempt has been made to examine the Elovich plots at a fixed initial pressure over a range of temperatures on catalysts **1** and **3**. Table II contains the data for these 2 catalysts at the high pressure of 60 cm Hg, and Table III the data for low pressure of 60 cm ABO on catalyst **2**. In both the tables, the values of α_1 and α_2 are for the first and second portions of the plots. Columns 3 and 4 show the values of log $a_1\alpha_1$ and log $a_2\alpha_2$ for the two portions of the curves. It is to be noted that the parameters for the second portion of the curve after the break were evaluated on the assumption that the value of q at the time of the break is equal to q_0 for this portion. q_1 is the q value of the adsorbed gas from the graph at time 1 min plus the time of appearance of the break. Thus, if the break appears at time 20 min, the value of q at time 21 min is taken as the value for the evaluation of a_2. Columns 5 and 6 list the values of a_1 and a_2 evaluated in this manner. The last column shows the time of occurrence of the break in minutes. Table III lists the data obtained similarly on catalyst **2** at low pressures.

Examination of Table II reveals that both α and $a\alpha$ decrease gradually with increasing temperatures. In the case of catalyst **1**, log $a_1\alpha_1$, and a_1 show an increase with temperature but log $a_2\alpha_2$ and hence a_2 show inconsistencies. The data presented for catalyst **3** show that α_1, α_2 log $a_1\alpha_1$, log $a_2\alpha_2$, and a_2 show a decrease with increasing temperature. It is to be noted that an examination of the data available in the literature (1) shows that this is the behavior expected for the hydrogen–nickel system. Catalyst **1** showed some peculiar adsorption data and gave indications of adsorbing nitrogen at low temperatures (12).

Catalyst **2** provides some interesting information as seen from the data in Table III. In the range 200–127 °C, the α values for the first portion of the curve listed in column 2, while decreasing with increasing temperatures, are consistently smaller than the α values for the second portion of the curve. But within the range 70–0 °C the reverse holds true, the α_2 values being smaller than α_1 values. This means that the comparison of the parameters should be made within a restricted range of temperature.

In the range 0–70 °C the values of α_1, α_2, and

Can. J. Chem. Downloaded from www.nrcresearchpress.com by 210.87.254.40 on 09/05/12
For personal use only.

TABLE III

Effect of temperature on the Elovich parameters, at low pressures for catalyst **2***

Temperature °C	α_1	α_2	log $a_1\alpha_1$	log $a_2\alpha_2$	a_1	a_2	t_b
200	3.042	5.333	5.468	11.400	9.661×10^{4}	5.930×10^{10}	11
181	3.830	6.419	5.981	11.560	2.500×10^{5}	5.636×10^{10}	14
160	4.444	6.933	6.611	12.770	9.187×10^{5}	3.460×10^{11}	23
140	5.501	7.536	7.261	12.770	3.315×10^{5}	7.816×10^{11}	23
127	5.975	8.352	7.731	12.600	9.007×10^{6}	6.001×10^{11}	24
70	4.202	3.747	4.901	6.212	1.891×10^{4}	4.348×10^{5}	16
57	4.780	4.387	5.105	5.835	2.727×10^{4}	1.570×10^{5}	19
30	5.174	4.612	6.284	7.352	3.331×10^{5}	4.876×10^{6}	30
0	6.540	5.777	7.516	7.952	5.017×10^{6}	1.550×10^{7}	29

*Initial pressure: 60 ± 1.50 cm ABO.

t_b show the expected decrease with temperature. A similar behavior is seen in the case of the values in the temperature range 127–200 °C. The magnitudes of all the constants change drastically in the region 70–127 °C. The error in the earlier observations reported from this laboratory was due to associating the values of parameters with the kinetic plot itself, assuming that the same kinetic stages were present and could be detected in all the temperature ranges. By this assumption it has not been possible to explain the drastic increase in the α values with an increase in temperature.

In the case of catalyst **1**, in Table II, it is seen that at 100 °C the values of α_1 and α_2 are very close, 3.893 and 3.651 respectively, and these decrease with increasing temperature. Extending this tendency one might say that there should be a temperature at which the values should be equal and the Elovich plot should show no breaks, and be a straight line with $t_b = 0$. By graphical extrapolation of the plot of α values with temperature, the critical temperature was found to be around 96 °C. Runs at 94 ± 4 °C showed that there was no break till 160 min at an initial pressure of 60 cm Hg. This plot is given in Fig. 1 as plot *B*.

It might be of interest to note that from the data in Table III for catalyst **2** it has been possible to estimate the temperature at which the Elovich plot would be a straight line to be 90 °C and the value α to be 3.500. The actual plot obtained at 84 °C with initial pressure of 60 cm ABO is given by *E* in Fig. 2, the experimental α value being 3.519. Utilizing this value the data in Table III can be grouped into those of two temperature ranges, 0–84 °C and 127–200 °C. The results in the latter range show some inconsistency only in the case of a_1 and a_2 values. In the range 84–127 °C, the kinetic data failed to show any regularity. No satisfactory explanation of this is at present available. However, within the temperature ranges mentioned above, the general behavior of adsorption of hydrogen on various catalysts studied seems to be perfectly in line with the results reported by Low (1).

Effect of Pressure

In order to examine the effect of pressure on the adsorption kinetics at constant temperature, catalysts **1** and **3** were used for the high pressure range 10–60 cm Hg and catalyst **2** for the low pressure range 15–60 cm ABO (1–4 cm Hg). Table IV contains the data for catalyst **1** and catalyst **3**. The α values show an increase with decrease in pressure, whereas all other values decrease with decrease in pressure. The decrease in the values of a_1 was found to be quantitative in the case of experiments on catalyst **3** in the sense that a plot of log P_0 (initial pressure) vs. log a_1 gave a straight line. Such a linear relationship has been reported by Kubakowa for hydrogen on chromia gel (13) and by Low (1).

The results on catalyst **1** given in Table V for 30 and 200 °C show that α_1 and α_2 increase with decrease in pressure. The same trend was observed at other temperatures too. However, the changes in the α values at lower pressures are much more marked. Thus, at 200 °C for a variation of pressure from 40 to 30 cm ABO the value changes from 3.650 to 4.461, whereas for a pressure change from 19.96 to 15.05 cm ABO, the α value goes up from 9.001 to 14.040. Experimental limitations prevented accurate measurements at initial pressures less than 10 cm ABO, although these could be of interest.

Figure 3 represents the Elovich plots at 30 °C,

Can. J. Chem. Downloaded from www.nrcresearchpress.com by 210.87.254.40 on 09/05/12
For personal use only.

TABLE IV

Effects of initial pressure on the Elovich parameters: high pressure range

P_0 (cm Hg)	α_1	α_2	log $a_1\alpha_1$	log $a_2\alpha_2$	a_1	a_2	t_b
Catalyst 1, temperature 100 °C							
60.08	3.893	3.651	8.3500	8.7391	5.886×10^7	1.498×10^8	29
50.41	4.441	3.955	8.2209	8.5931	3.745×10^7	9.906×10^7	20
39.93	5.000	4.121	8.1007	8.4542	2.523×10^7	6.905×10^7	16
29.97	5.800	4.599	7.9080	8.4354	1.395×10^7	5.984×10^7	12
22.00	6.421	5.501	7.8961	8.1688	1.226×10^7	2.680×10^7	10
15.65	7.491	6.432	7.8699	7.7570	9.895×10^6	8.886×10^6	8
Catalyst 3, temperature 220 ± 2 °C							
60.04	2.543	3.128	5.4659	6.8241	1.832×10^5	2.132×10^6	29
50.02	2.684	3.498	5.4826	6.8835	1.798×10^5	2.186×10^6	24
39.98	3.145	4.692	5.4746	6.1761	1.509×10^5	3.196×10^5	19
21.21	3.283	4.829	5.3480	6.2862	1.060×10^5	4.002×10^5	12
10.01	6.194	7.286	5.4839	6.5978	7.086×10^4	5.409×10^5	10

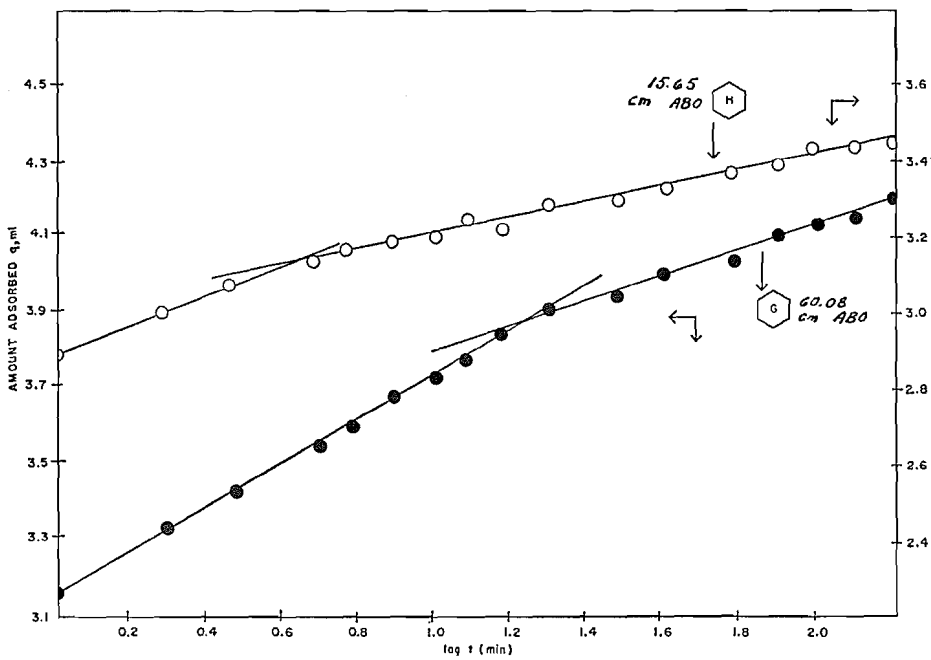

FIG. 3. Effect of pressure on the Elovich plots. Catalyst **2** at 30 °C: *G* at 60.08 cm ABO, ●; *H* at 15.65 cm ABO, ○.

G and *H* being for pressures 60.08 and 15.65 cm ABO respectively. Figure 4 illustrates changes in α values for catalyst **1** at 208 °C for the high pressure region and Fig. 5 for catalyst **2** at 127 °C in the low pressure region. The changes in this last case are drastic, as demonstrated also by Low's data on many systems at low pressure.

From the experimental results presented so far, some general conclusions may be drawn about the nature of the plots. At a constant pressure the break in the $q - \log t$ curve appears earlier with increasing temperature.

At constant temperature, the break appears early with decreasing pressures. Also, the changes in α values seem to depend on the temperature range in question.

Some of our results on catalyst **2** and those of Low on platinum group metals, lend support to his hypothesis of multiple kinetic stages. For instance, α_2 for catalyst **2** in the range 0–70 °C is

Can. J. Chem. Downloaded from www.nrcresearchpress.com by 210.87.254.40 on 09/05/12
For personal use only.

TABLE V

Effects of initial pressure on the Elovich parameters: low pressure region*

P_0	α_1	α_2	log $a_1\alpha_1$	log $a_2\alpha_2$	a_1	a_2	t_b
(A) at 200 °C							
60.00	3.041	5.533	5.468	11.400	9.666×10^{4}	5.930×10^{10}	11
40.04	3.650	6.640	5.295	13.170	5.404×10^{4}	2.227×10^{12}	10
30.02	4.461	7.402	5.004	10.160	2.798×10^{4}	1.998×10^{9}	8
19.96	9.001	11.190	4.632	6.753	4.762×10^{3}	5.060×10^{5}	6
15.03	14.040	18.100	4.013	6.288	1.340×10^{2}	1.073×10^{5}	6
(B) at 30 °C							
60.50	5.174	4.612	6.284	7.352	3.331×10^{5}	4.876×10^{6}	30
40.00	5.800	5.200	5.950	6.616	1.537×10^{5}	7.943×10^{5}	24
30.04	6.400	5.784	5.800	6.371	9.709×10^{4}	4.059×10^{3}	20
20.20	14.040	12.070	5.400	6.346	1.785×10^{4}	2.314×10^{5}	10
14.90	20.100	16.400	4.800	4.699	3.952×10^{4}	3.049×10^{4}	8

*Pressures in cm ABO.

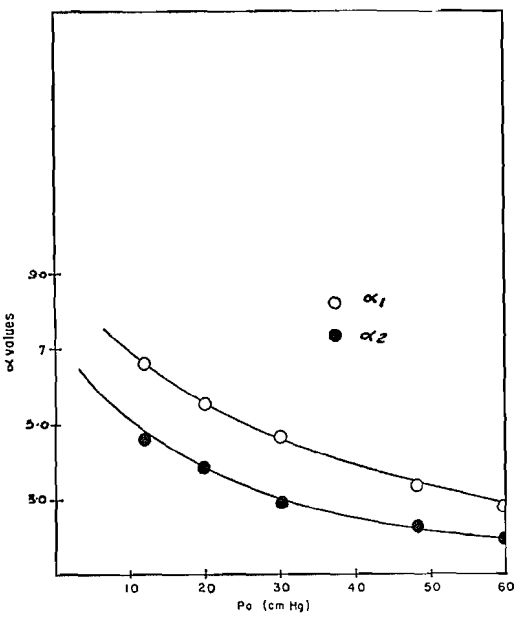

FIG. 4. Effect of initial pressure on the α values. Catalyst **1** at 208 °C: α_1, ○; α_2, ●.

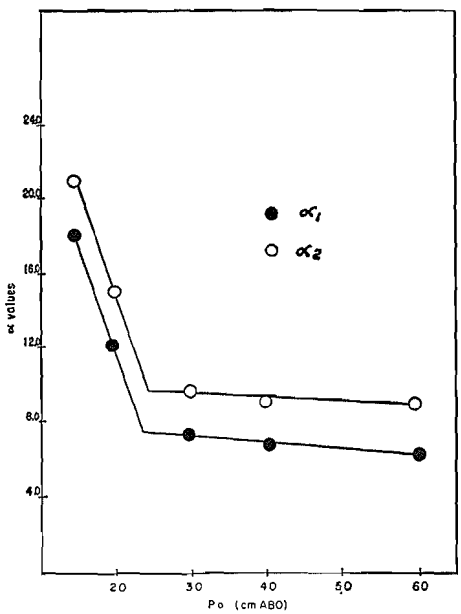

FIG. 5. Effect of initial pressure on the α values. Catalyst **2** at 127 °C: α_1, ●; α_2, ○.

less than α_1 of Table III, but in the high temperature range α_1 is less than α_2. In other words, α values show a regular variation only within a definite temperature range. At 84 °C this temperature variation disappears and there is no break in the Elovich plots. Following Low, one might say that the portions of the plots within the temperature range 0–84 °C are analogous to portion *A* of the Low's idealized curve. Our kinetic data above 84 °C represent portion *B*, and the data at higher temperatures, portion *C* of Low's curve. Actually, this last point has not been verified by our results, since due to experimental difficulties, low enough pressures could not be attempted, and at higher temperatures desorption from the metal surface was noticeable. It is as well to note that Low was successful in detecting all these breaks only in a few cases. However, it seems to be reasonable to postulate the occurrence of stepwise adsorption, each step characterized by its own Elovich parameters. In the case of high temperature experiments, our

Can. J. Chem. Downloaded from www.nrcresearchpress.com by 210.87.254.40 on 09/05/12
For personal use only.

Can. J. Chem. Downloaded from www.nrcresearchpress.com by 210.87.254.40 on 09/05/12
For personal use only.

results would suggest the occurrence of stages II and III, stage I being submerged in the first portion of the plots and experimentally not detectable.

A complete physical explanation of the multiple kinetic stages as mentioned by Low, is not available at present. An excellent parallelism seems to exist between chemisorption stages and the well-established kinetic stages in the oxidation of metals. It may be of interest that our observations made in 1964 (14), were the first to be reported in this connection and that the recent adsorption data reported by Allen and Scaife seem to be in agreement with the multiple stage hypothesis. Our present experiments (15) on variation of support material might throw added light on to this matter.

Energies of Activation

Activation energies have been calculated according to the expression suggested by Leibowitz *et al.* (18)

$$[4] \qquad E = RVq\left(\frac{e^{\alpha q}}{e^{\alpha q} - 1}\right) - RY$$

which, when $e^{\alpha q} \gg 1$ as in the present case, yields $E = RVq - RY$, where R is the gas constant; V and Y are evaluated by the following relationships

$$[5] \qquad \alpha = V/T - U$$

$$[6] \qquad \ln a\alpha = Y/T - X$$

V and Y were evaluated by a least square analysis of experimental data. Substituting these values, we get for stage I, the relationships

$$[7] \qquad \alpha_1 = \frac{3.504 \times 10^3}{T} - 6.290$$

$$[8] \qquad \ln a_1\alpha_1 = \frac{2.450 \times 10^3}{T} - 1.457$$

the expression for E being:

$$[9] \quad E = 1.987\,(3.504 \times q - 2.450 \times 2.303)$$

For this stage at temperatures less than 84 °C, the minimum and maximum values of q are 2.211 and 3.451 ml. On substitution of these values, E is found to be between 4 and 13 kcal.

Stage II, as was suggested earlier, might occur at both temperature ranges below and above 84 °C (as the second portion and the first portion of the Elovich plots) and using q values of 3.452 and 4.972 ml, the value of E is between 7–15 kcal at the low temperature region. In the case of temperatures above 84 °C, the value of E lies between the extremes of 7 to 34 kcal (q being 2.979 to 5.002 ml).

For stage III, calculations show E to have limits of 36 to 60 kcal.

In all the stages considered, E values are positive and seem to fit in the multiple stage hypothesis of Low. The value 4–13 kcal for stage I is well within the range of 7–34 kcal of stage II so that the first portion of the Elovich plot at higher temperatures is in fact a combination of stages I and II. Similarly, the final portions of stage II seem to be in close agreement with the values of E calculated for stage III.

The range of activation energies seems to indicate the actual merger of one stage into the next one. The high values of E for stage II in the final portions and those of stage III from the initial portions are not easy to account for.

The experimental data presented in this paper offer support to the multiple kinetic stage hypothesis suggested by Low. This hypothesis, which is in accordance with his observations on a number of systems, is based on results from our laboratory on the hydrogen–nickel system (10, 15–17) and very recently on the reports of Allen and Scaife (2–4) on a different system. Catalyst **1** used in the present study, however, shows different adsorption behavior than that reported earlier. It has to be stressed here that the catalyst used in the earlier reports had different surface properties (surface area 21.30 m^2 as against 196.8 m^2 in the present case) and the degree of reduction of the surface can be different. The multiple kinetic stages can be caused by the nature of the surface. In their paper, Allen and Scaife offer an explanation based on the interaction of adsorbed particles with the surrounding sites, and use the Elovich equation with an additional term γ. However, the lack of mathematical foundation casts doubt on the universal applicability of this approach to explain the multiple kinetic stages.

The Taylor–Thon model (19) and the Gundry–Tompkins model (20) have enjoyed a wide applicability in the case of a number of gas–solid systems, especially in explaining the effects of temperature on chemisorption kinetics. Special mention should be made of the former model, which is probably the only one which takes the

occurrence of breaks in the Elovich plots into account.

Low, by using the Taylor–Thon model, derives the Elovich equation in the form

$$[10] \qquad \frac{dq}{dt} = K[V_0]\, e^{-(K_d/K)q}$$

giving the values

$$[11] \qquad a = KV_0$$

and

$$[12] \qquad \alpha = \frac{K_d}{K}$$

where K_d is the rate of chain termination (by which free valences terminate on the surface). K is the rate constant for the overall adsorption process, and V_0 is the initial site density. This derivation seems to account for all the relations involving the constants, except in the case of α variations with initial pressure. The following explanation may be considered valid for this phenomenon. α is calculated to be equal to K_d/K. The site destruction process is governed by K, while the formation of sites themselves, as suggested by the Taylor–Thon hypothesis, depends on the adsorbate concentration; this, in a constant volume system, is completely controlled by initial pressure of the gas. This makes K smaller, due to the non-availability of sites making α higher at low pressure regions. It has to be noted that in this treatment, the Elovich constants show the expected variation with the initial pressure. The effect of ambient pressure changes on these is to be reported later.

The model proposed by Allen and Scaife suffers from the drawback that it fails to show any variations of α with pressure and temperature. This is in complete disagreement with all the data available on chemisorption kinetics.

The Gundry–Tompkins model, based on the mobility of adsorbate from sites of strong adsorption to those of weak adsorption, is well supported by the now widely accepted type C adsorption states suggested by Dowden (21), and by a recent tracer experiment by Takeuchi and Miyatani (22). Low temperature experiments should be of real significance in explaining some of the kinetic characteristics.

Acknowledgments

We wish to thank the Council of Scientific and Industrial Research for financial help. One of us (N.S.V.) thanks the Ministry of Education, Government of India, for the award of a research fellowship during the tenure of which this work was done.

1. M. J. D. Low. Chem. Rev. **60**, 267 (1960).
2. J. A. Allen and P. H. Scaife. Australian J. Chem. **19**, 2015 (1966).
3. J. A. Allen and P. H. Scaife. Australian J. Chem. **20**, 399 (1967).
4. J. A. Allen and P. H. Scaife. Australian J. Chem. **20**, 409 (1967).
5. Y. A. Zeldowich and S. Roginskii. Acta Physicochem. URSS, **1**, 554 (1934).
6. G. C. Schuit and N. H. de Boer. Rec. Trav. Chim. **70**, 1067 (1951).
7. N. Harrell Furman (*Editor*). Standard methods of chemical analysis. Vol. 1. D. Van Nostrand Co., New Jersey. 1964. pp. 696–713.
8. W. V. Loebenstein. J. Chem. Phys. **29**, 236 (1958).
9. J. N. Saramousakis and M. J. D. Low. J. Chem. Phys. **25**, 178 (1956).
10. M. J. D. Low. Can. J. Chem. **38**, 588 (1960).
11. N. Ramasubramanian. Ph.D. Thesis, Madras University, India. 1959.
12. N. S. Viswanathan. Ph.D. Thesis, Madras University, India. 1965.
13. Y. Kubakowa. Bull. Chem. Soc. Japan, **33**, 734 (1960).
14. N. S. Viswanathan and L. M. Yeddanapalli. Symposium on Catalysis. 41st Annual Meeting of the Indian Chemical Society, Allahabad. 1964.
15. S. Narayanan and L. M. Yeddanapalli. Unpublished results.
16. N. Ramasubramanian and L. M. Yeddanapalli. J. Phys. Chem. **66**, 1222 (1962).
17. N. Ramasubramanian and L. M. Yeddanapalli. Can. J. Chem. **41**, 1588 (1963).
18. L. Leibowitz, M. J. D. Low, and H. A. Taylor. J. Phys. Chem. **63**, 471 (1958).
19. H. A. Taylor and N. Thon. J. Am. Chem. Soc. **74**, 4169 (1952).
20. P. M. Gundry and F. C. Tompkins. Trans. Faraday Soc. **52**, 1609 (1956).
21. D. A. Dowden. Bull. Chem. Soc. Belges, **67**, 439 (1958).
22. T. Takeuchi and D. Miyatani. Bull. Chem. Soc. Japan, **40**, 58 (1967).

Can. J. Chem. Downloaded from www.nrcresearchpress.com by 210.87.254.40 on 09/05/12
For personal use only.

The existence of salts of the oxyfluoborate ion $[BF_3O]^{2-}$

M. J. R. CLARK AND H. LYNTON
Chemistry Department, University of New Brunswick, Fredericton, New Brunswick

Received January 29, 1969

The soluble hydrated oxyfluoborates previously reported as "$CuBF_3O \cdot 5H_2O$" and "$ZnBF_3O \cdot 7H_2O$" are now believed to be the fluosilicates $CuSiF_6 \cdot 4H_2O$ and $ZnSiF_6 \cdot 6H_2O$. The insoluble anhydrous oxyfluoborates of Sr, Ba, and Pb could not be prepared.

Canadian Journal of Chemistry, 47, 2943 (1969)

Can. J. Chem. Downloaded from www.nrcresearchpress.com by 210.87.254.105 on 09/05/12
For personal use only.

Introduction

The existence of salts of the oxyfluoborate ion, $[BF_3O]^{2-}$, was first reported in a series of papers by Ray and Mitra (1–6). In these papers, they give the preparation and chemical analysis of the soluble, hydrated oxyfluoborate salts of Cu, Zn, Cd, Co, and Ni; and of the insoluble anhydrous salts of Sr, Ba, and Pb. They also report X-ray powder diffraction patterns for the copper, barium, and lead salts.

Ray and Mitra's claim to have established this new family of salts is supported by two later papers, the preparation and examination of $ZnBF_3O \cdot 7H_2O$ by Long and Bailey (7); and the determination of the structure of $BaBF_3O$ from its X-ray powder diffraction pattern by Chackraburtty (8), using a sample supplied by Mitra.

In this paper, we report that the compounds previously identified as $CuBF_3O \cdot 5H_2O$ and $ZnBF_3O \cdot 7H_2O$ are the fluosilicates: $CuSiF_6 \cdot 4H_2O$ and $ZnSiF_6 \cdot 6H_2O$. We were unable to repeat Ray and Mitra's preparation of the insoluble, anhydrous oxyfluoborate salts of Sr, Ba, and Pb.

Experimental

"$CuBF_3O \cdot 5H_2O$"

This compound was prepared by the reaction of basic copper carbonate, boric acid, hydrofluoric acid, and nitric acid as described by Ray and Mitra. The product was recrystallized from aqueous solution. X-Ray powder diffraction patterns taken before and after recrystallization established that no decomposition had occurred. An identical copper salt was also obtained when the procedure of Ray and Mitra was followed, with the exception that boric acid and nitric acid were not added to the reaction mixture.

"$ZnBF_3O \cdot 7H_2O$"

This salt was prepared by reacting zinc carbonate, boric acid, hydrofluoric acid, and nitric acid as described by Ray and Mitra.

$CuSiF_6 \cdot 4H_2O$

A 25% aqueous solution of HF was allowed to stand over excess silica for several days. The resulting solution was decanted and added to a paste of basic copper carbonate and water. After reaction, the solution was filtered and evaporated to a smaller volume in a hot water bath at 45 °C. The blue crystals obtained were then recrystallized from aqueous solution at the same temperature.

$ZnSiF_6 \cdot 6H_2O$

This compound was prepared by a procedure similar to that for $CuSiF_6 \cdot 4H_2O$.

All compounds were analyzed as follows: copper and zinc gravimetrically by thermal decomposition to the oxides; copper was also determined by electrodeposition; boron by flame spectrophotometer using the emission line at 521 mμ; fluorine by titration with standard base; silicon by using sodium carbonate to precipitate H_2SiO_3 from an aqueous solution of controlled pH and the precipitate analyzed by thermal decomposition to SiO_2.

Table I gives the results of the analyses together with those reported by Ray and Mitra and by Long and Bailey.

Results and Discussion

The analyses and X-ray powder patterns, Tables I, II, and III, establish the identity of both the copper and zinc compounds prepared by us as the fluosilicates $CuSiF_6 \cdot 4H_2O$ and $ZnSiF_6 \cdot 6H_2O$. The powder pattern for "$CuBF_3O \cdot 5H_2O$" published by Ray and Mitra contains relatively few lines. This pattern corresponds, within the limits of probable experimental error, with the strongest lines of $CuSiF_6 \cdot 4H_2O$. The line given at 2.38 Å must be our line at 2.27 Å.

A single crystal examination of both "$CuBF_3O \cdot 5H_2O$" and $CuSiF_6 \cdot 4H_2O$ by oscillation and Weissenberg photography, confirms the powder identification and gives the space group as $P2_1/c$, with cell dimensions $a = 5.36$ Å, $b = 9.64$ Å, $c = 7.22$ Å, $\beta = 105.2°$. These cell dimensions agree with the optical results given by Mellor (9) for $CuSiF_6 \cdot 4H_2O$, ratio $a:b:c = 0.5519:1:0.7604$, $\beta = 105.6°$; and allow the powder patterns to be indexed unambiguously, as shown in Table II.

TABLE I
Analyses

Compound	Reference	Amount (%) Cu	B	Si	F	Zn
"$CuBF_3O \cdot 5H_2O$"	Ray and Mitra	26.84	4.50		23.90	
"$CuBF_3O \cdot 5H_2O$"	This paper	22.3	Nil	10.0	40.5	
$CuBF_3O \cdot 5H_2O$	Theoretical	26.75	4.55		24.00	
$CuSiF_6 \cdot 4H_2O$	This paper	22.6		10.1	40.8	
$CuSiF_6 \cdot 4H_2O$	Theoretical	22.88		10.12	41.05	
"$ZnBF_3O \cdot 7H_2O$"	Ray and Mitra		3.92		20.53	23.80
"$ZnBF_3O \cdot 7H_2O$"	Long and Bailey		3.61			21.62
"$ZnBF_3O \cdot 7H_2O$"	This paper		Nil	8.8	35.9	20.6
$ZnBF_3O \cdot 7H_2O$	Theoretical		3.93		20.70	23.75
$ZnSiF_6 \cdot 6H_2O$	This paper			8.8	36.0	20.6
$ZnSiF_6 \cdot 6H_2O$	Theoretical			8.90	36.13	20.72

TABLE II
X-Ray powder patterns of copper compounds*

"$CuBF_3O \cdot 5H_2O$"				$CuSiF_6 \cdot 4H_2O$		
Ray and Mitra		This paper		This paper		
d (Å)	Intensity	d (Å)	Intensity	d (Å)	Intensity	hkl
4.75	vs	4.83	vs	4.80	s	020
4.36	vs	4.26	vs	4.29	vs	$11\bar{1}$
3.48	vs	3.47	vs	3.45	vs	002
		3.04	vw	3.00	vw	121
		2.89	vw			031
		2.82	w	2.81	w	$02\bar{2}$
		2.72	vw	2.72	vw	$12\bar{2}$
2.69	m	2.66	m	2.66	m	$13\bar{1}$
		2.58	vw	2.57	vw	102
		2.50	w	2.49	w	112
		2.32	w	2.33	w	$22\bar{1}$
2.38	m	2.27	m	2.27	m	$13\bar{2}$
		2.18	w	2.17	vw	140
2.16	s	2.14	m	2.14	m	$22\bar{2}$
		2.03	vw			$23\bar{1}$
		2.01	vw	2.01	vw	$13\bar{2}$
1.91	vs	1.90	s	1.90	m	$13\bar{3}$
		1.85	w	1.85	vw	051, 202
		1.79	w	1.79	vw	$15\bar{1}$
		1.76	w	1.76	vw	240
		1.73	vw	1.73	vw	222
1.71	m	1.70	m	1.69	m	$24\bar{2}$
		1.67	vw	1.66	vw	$15\bar{2}$, 133
		1.64	w	1.64	vw	024
		1.60	vw	1.60	vw	060
1.57	m	1.58	w	1.58	vw	$31\bar{3}$
		1.56	w	1.55	vw	$33\bar{1}$

*s = strong, m = medium, w = weak, v = very.

We have no explanation to offer for the results of the chemical analyses given by Ray and Mitra for both compounds. The analysis of the zinc compound by Long and Bailey does not have a fluorine assay and the boron and zinc content differ from the theoretical values by almost 8%.

The absorption frequencies in the infrared (i.r.) region reported by Long and Bailey can all be accounted for by a mixture of zinc nitrate and zinc tetrafluoborate. The components for these compounds are present in Ray and Mitra's procedure. $ZnSiF_6 \cdot 6H_2O$ shows three absorption frequencies in this i.r. region, none of which coincide with those reported by Long and Bailey, as shown in Table IV.

Neither Ray and Mitra, nor Long and Bailey

Can. J. Chem. Downloaded from www.nrcresearchpress.com by 210.87.254.105 on 09/05/12
For personal use only.

Can. J. Chem. Downloaded from www.nrcresearchpress.com by 210.87.254.105 on 09/05/12
For personal use only.

TABLE III

X-Ray powder patterns of zinc compounds*

"$ZnBF_3O \cdot 7H_2O$"		$ZnSiF_6 \cdot 6H_2O$				
This paper		This paper		Swanson *et al.* (10)		
d (Å)	Intensity	*d* (Å)	Intensity	*d* (Å)	Intensity	*hkl*
6.22	vw	6.24	vw	6.22	2	101
4.69	vs	4.68	vs	4.68	100	110
4.16	s	4.16	s	4.16	46	012
3.12	m	3.11	m	3.11	5	202
2.93	m	2.93	m	2.922	10	211
2.66	m	2.66	m	2.660	5	113
2.59	s	2.59	s	2.590	27	122
2.33	vw	2.33	vw	2.321	2	104
2.20	w	2.19	w	2.191	2	131
2.08	m	2.08	m	2.080	6	024
				2.074	4	303
2.04	vw	2.04	vw	2.040	2	312
1.99	w	1.98	w	1.9835	4	401
1.90	m	1.90	m	1.9008	10	214
1.88	w	1.87	w	1.8706	5	042
1.83	vw	1.83	vw	1.8270	3	321
1.77	w	1.77	w	1.7694	4	410
1.74	w	1.74	w	1.7372	4	232
1.65	m	1.65	m	1.6488	7	134
1.60	vw	1.60	vw	1.5999	1	051
1.56	vw	1.56	vw	1.5603	2	330
1.54	vw	1.53	vw	1.5271	2	116
1.48	w	1.48	w	1.4754	2	324

*s = strong, m = medium, w = weak, v = very.

TABLE IV

Infrared absorption spectra of zinc compounds*

Infrared absorption frequency (μ)			
Long and Bailey	$Zn(NO_3)_2 \cdot 6H_2O$	$Zn(BF_4)_2 \cdot 6H_2O$	$ZnSiF_6 \cdot 6H_2O$
			2.90 s
		2.95 w	
	3.15 w		
	3.70 vw		
	4.40 w		
	5.84 w		
		6.22 m	
	6.35 w		
7.12	7.12 m		
7.21	7.21 m		
7.33	7.33 s		
7.36	7.36 s		
	7.50 m		
		7.71 w	
8.89 m		8.87 m	
9.22 vs		9.19 vs	
		9.31 w	
9.62 w	9.61 vw	9.59 w	
11.93 w	11.97 w		
12.09 s	12.09 s		
			12.80 vs
		12.97 w	
			13.50 vs
18.59	Beyond range of our instrument		
18.98 m			

*s = strong, m = medium, w = weak, v = very.

examined their preparation for silicon content, as silicon was not intentionally added to the reaction mixture. We believe, however, that silicon enters the reaction mixture at the point in the Ray and Mitra procedure (4) when the mixture is stored in a glass desiccator. We observed that the glass was subject to chemical attack during this storage period and a white deposit was left on the inner surface. This deposit was identified by X-ray analysis as $NaBF_4$. The silicon probably moves into the reaction mixture through the formation of SiF_4 by fluoride attack on the glass. SiF_4 readily reacts with water to form H_2SiF_6.

Attempts to prepare the insoluble oxyfluoborates $BaBF_3O$, $SrBF_3O$, and $PbBF_3O$ by the procedure of Ray and Mitra were unsuccessful. However, we did obtain a small yield of barium salt whose X-ray diffraction pattern is different to that reported for $BaBF_3O$. The powder pattern for this compound identifies it as $BaSiF_6$ (Table V).

Ray and Mitra state that $BaBF_3O$ and $PbBF_3O$ are isomorphous with the corresponding sulfates. Our inability to prepare these compounds, their similarity to the sulfates, and the presence of sulfuric acid as a desiccant in the storage stage of the Ray and Mitra procedure suggest that they may have prepared the sulfates, rather than the oxyfluoborates.

TABLE V

X-Ray powder patterns of $BaSiF_6$*

This paper		Swanson *et al.* (11)		
d (Å)	Intensity	*d* (Å)	Intensity	*hkl*
4.63	w	4.650	30	101
3.58	vs	3.593	100	110
3.04	m	3.055	60	012
2.83	vw	2.845	11	021
2.32	m	2.336	42	003
		2.327	27	202
2.23	s	2.230	58	211
2.07	w	2.075	9	300
1.97	s	1.958	29	113
		1.953	62	122
1.80	w	1.796	13	220
1.68	vw	1.686	5	104
		1.676	4	131
1.55	w	1.550	6	303
		1.548	9	312
1.52	w	1.5269	7	024
		1.5187	7	401

*s = strong, m = medium, w = weak, v = very.

Acknowledgment

We acknowledge the financial support of the National Research Council of Canada for this work.

1. G. MITRA. Sci. Cult. Calcutta, **19**, 106 (1953).
2. D. DASGUPTA, A. RAY, and G. MITRA. J. Indian Chem. Soc. **35**, 185 (1958).
3. A. RAY and G. MITRA. J. Indian Chem. Soc. **35**, 677 (1958).
4. A. RAY and G. MITRA. J. Indian Chem. Soc. **35**, 690 (1958).
5. G. MITRA and A. RAY. Proc. Symp. Chem. Coord. Compds. Agra, India, 1959. pp. 48–54.
6. A. RAY. J. Indian Chem. Soc. **35**, 874 (1958).
7. D. A. LONG and R. T. BAILEY. Spectrochim. Acta, **19**, 1607 (1963).
8. D. M. CHACKRABURTTY. Acta Cryst. **10**, 199 (1957).
9. J. W. MELLOR. A comprehensive treatise on inorganic and theoretical chemistry. Vol. VI. Longmans, Green and Co., London. 1925. p. 950.
10. H. E. SWANSON, N. T. GILFRICH, M. I. COOK, R. STINCHFIELD, and P. C. PARKS. Natl. Bur. Std. U.S. Circ. 539. **8**, 70 (1959).
11. H. E. SWANSON, M. C. MORRIS, and E. H. EVANS. Natl. Bur. Std. Monograph 25. **4**, 7 (1966).

Can. J. Chem. Downloaded from www.nrcresearchpress.com by 210.87.254.105 on 09/05/12
For personal use only.

Can. J. Chem. Downloaded from www.nrcresearchpress.com by 210.87.254.105 on 09/05/12
For personal use only.

On the characteristic vibrations of the NH_2 group

B. R. CAIN, J. M. FREEMAN, AND T. HENSHALL[1]

Department of Chemistry and Applied Chemistry, University of Salford, Salford M5 4WT, Lancashire, England

Received February 18, 1969

The group frequency factorization procedure developed by King and Crawford (1) for the reduction in size of a vibrational secular determinant, by factorizing from it those frequencies that are characteristic of a constituent group, and subsequently extended by us (2), has now been successfully applied to NH_2 group vibrations.

The method is exemplified by the skeletal vibrations of methylamine, for which satisfactory results are obtained on factorization from the secular determinant of frequencies that are characteristic of both NH_2 and CH_3 groups.

Canadian Journal of Chemistry, 47, 2947 (1969)

The NH_2 group in both primary amines and amides is associated with three characteristic infrared (i.r.) absorption bands. Two, with frequencies around 3500 and 3300 cm^{-1}, are identified respectively with the antisymmetric and symmetric NH stretching vibrations. In the third, in the range 1590–1650 cm^{-1}, the $H\hat{N}H$ bending mode is considered to predominate (3). The NH_2 group can also engage in inter- and intramolecular hydrogen bonds, but no attempt is made to account for these effects in our considerations.

Analysis of the NH_2 group vibrations involves the consideration of a "standard molecule", NH_2—R, with the geometry of Fig. 1, and in

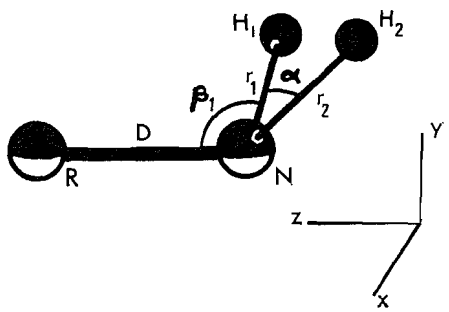

FIG. 1. The "standard molecule" RNH_2: r = 1.014 Å, D = 1.474 Å, α = 106°, β = 112°.

which R is assigned infinite mass (actually 10^6 a.m.u.). This "standard molecule" belongs to the symmetry point group C_s; and the symmetry coordinates chosen for the A′ and A″ vibrational species are given in Table I.

[1]To whom correspondence should be addressed.

TABLE I

Symmetry coordinates in C_s for the "standard molecule"

Species	Coordinate	
A′	$S_1 = (r_1 + r_2)/\sqrt{2}$ $S_2 = \alpha$ $S_3 = D$ $S_4 = (\beta_1 + \beta_2)/\sqrt{2}$	Group coordinates
A″	$S_5 = (r_1 - r_2)/\sqrt{2}$ $S_6 = (\beta_1 - \beta_2)/\sqrt{2}$	Group coordinate

The calculations of the frequencies in NH_2R reported here constitute an extension and improvement of those first reported by King (4) and use the same values for the force constants (Table III), and the valence force field of Table II. In Table III, the constant K_D is representative

TABLE II

Valence force field for NH_2R*

$2V$	r_1	r_2	D	α	β_1	β_2
r_1	K_r	F_r	0	0	0	0
r_2		K_r	0	0	0	0
D			K_D	0	$rF_{D\beta}$	$rF_{D\beta}$
α				r^2H_α	0	0
β_1					r^2H_β	r^2F_β
β_2						r^2H_β

*$r = r(\text{N—H})_{eq}$.

TABLE III

Force constants for "standard molecule" NH_2R (mdyn $Å^{-1}$)

Force constant	Value	Force constant	Value
K_r	6.40	F_r	0.00
K_D	4.80	$F_{D\beta}$	0.14
H_α	0.65	F_β	−0.03
H_β	0.47		

Can. J. Chem. Downloaded from www.nrcresearchpress.com by 210.87.254.105 on 09/05/12
For personal use only.

of an N—C bond, with the intention to extend the calculation to organic molecules.

The calculations were performed on an English-Electric KDF-9 computer. The calculated frequencies are listed in Table IV, and the normal coordinate matrices, taken with experimental evidence, indicate that ν_1 and ν_2 in A′, and ν_5 in A″ are group vibrations. The orthogonal transformation matrices **A** relating new displacement coordinates **D** to symmetry coordinates **S** through $\mathbf{D} = \mathbf{A}^*\mathbf{S}$, and which are required in the group factorization procedure (1), are given in Table V. Since the leading elements in the **A** matrices greatly exceed the off-diagonal entries, the success of the NH_2 group frequency factorization procedure was assured, and the submatrix $\bar{\mathbf{H}}_{gf}$ was null as required by the method.

The corrections, $\mathbf{\Phi}_{ff}$, which are to be made to the force field of a framework to which the NH_2 group is attached are given in Table VI; those in the A″ species are so small as to be negligible.

The effective-mass tensor, $(\mathbf{M}^{-1})^+_{NN}$, of the NH_2 group whose elements are the effective inverse masses in $(\text{a.m.u.})^{-1}$ of the nitrogen atom required in the construction of a reduced kinetic matrix $\mathbf{G}^+_{ff}$, is given in Table VII.

TABLE IV

Calculated frequencies of "standard molecule" NH_2R (cm^{-1})

Species	Mode	Frequency	Species	Mode	Frequency
A′	ν_1	3371	A″	ν_5	3432
	ν_2	1630		ν_6	967
	ν_3	688			
	ν_4	786			

TABLE VI

The corrections, Φ_{ff}, to the force constants for framework vibrations (mixed units)

$\Phi_{ff}(A')$	S_3	S_4
S_3	0.0278	−0.0382
S_4	−0.0382	0.0641
$\Phi_{ff}(A'')$	S_6	
S_6	0.0004	

TABLE VII

Effective mass tensor $(M^{-1})^+_{NN}$ for the nitrogen atom in the NH_2 group

$(M^{-1})^+_{NN}$ (a.m.u.$^{-1}$)	X_N	Y_N	Z_N
X_N	0.06529	0	0
Y_N		0.06758	0
Z_N	(symmetrical)		0.06561

The coordinates S_4 and S_6 which describe respectively the symmetric and antisymmetric $\hat{HNR}$ angular deformation frequencies, and which are coupled to the vibrations of the framework to which the NH_2 group is attached, involve the displacements of both N and H atoms. The complete effective mass matrix $(\mathbf{M}^{-1})^+$ which is required for the factorization of the NH_2 group frequencies will hence contain cross-terms involving these atoms. The diagonal elements $(\mathbf{G}^+)_{ii}$ $(i = 4, 6)$, of the reduced kinetic matrix $\mathbf{G}^+_{ff}$ require effective inverse hydrogen masses for their calculation. Following the methods described in (1) with the molecular geometry of Fig. 1, and the assumption that the expressions for μ^+_H are relatively insensitive to

TABLE V

The orthogonal transformation matrix, **A**, for NH_2 group frequency factorization

A (A′)	D_1	D_2	D_3	D_4
S_1	−0.9995	−0.0168	−0.0260	0.0013
S_2	0.0124	−0.9403	0.1464	0.3071
S_3	0.0284	−0.1755	−0.9815	−0.0706
S_4	−0.0005	0.2912	−0.1203	0.9490
A (A″)	D_5	D_6		
S_5	0.9999	−0.0083		
S_6	−0.0083	−0.9999		

changes in geometry, the following results were obtained

$$\mathbf{G}^+_{44} = \mu^+_{H(2)}/r^2(2m^2/\sin^2\beta)(1/D - \cos\beta/r)^2\mu_{Ny} + [2(1 + n\cos\beta)^2/r^2\sin^2\beta]\mu_{Nz} + (2m^2/D^2\sin^2\beta)\mu_R$$

where

$$\mu^+_{H(2)} = 0.4973 + 0.0450a$$

$$\mathbf{G}^+_{66} = \mu^+_{H(1)/r^2} + (2l^2/\sin^2\beta)(\cos\beta/r - 1/D)^2\mu_{Nx} + (2l^2/D^2\sin^2\beta)\mu_R$$

where $\mu^+_{H(1)} = 0.9917 - 0.0015a$, $a = r/D$, and l, m, n are the direction cosines of the N—R bond.

For the off-diagonal elements of $\mathbf{G}^+$ involving the interactions of S_i ($i = 4, 6$), with any framework coordinate S_j, and for which $(\mathbf{G}^+)_{ij} = \boldsymbol{B}_i(\mathbf{M}^{-1})^+\boldsymbol{B}^*_j$, the required row vectors $\boldsymbol{B}_i(\mathbf{M}^{-1})^+$ are given in Table VIII. It is therefore to be noted that when the terms $(1/D - \cos\beta/r)$ and $(1 + n\cos\beta)$ arise in the elements of the $\mathbf{G}$ matrix of the A′ vibrational species of molecules with NH_2 groups, then on taking account in the $\mathbf{G}^+_{ff}$ matrix for vibrational interaction between ν_4 and the group vibrations in such molecules, these terms are to be modified respectively to

$$(1/D - \cos\beta/r + 0.6453/r)$$

and

$$(1 + n\cos\beta - 0.4026 + 0.0319a)$$

Similarly, in considering the vibrations of species A″, when the term $(1/D - \cos\beta/r)$ arises in $\mathbf{G}$, it must be replaced in $\mathbf{G}^+_{ff}$ by $(1/D - \cos\beta/r - 0.0076/r)$ to account for the interaction of ν_6 and the NH_2 group vibrations.

Application of first-order perturbation theory (1) leads to the following approximation equations for the NH_2 group frequencies.

Species A′

$$\lambda_1 = 6.6948 + 1.0434\Delta F_{11} + 0.0147\Delta F_{22} + 0.0016\Delta F_{33} + 0.0006\Delta F_{44} - 0.0020\Delta F_{34}$$

[1] $$\lambda_2 = 1.5648 + 0.0004\Delta F_{11} + 2.0120\Delta F_{22} + 0.0042\Delta F_{33} + 0.4623\Delta F_{44} + 0.0881\Delta F_{34}$$

[2] $$\lambda_5 = 6.9376 + 1.0831\Delta F_{11} + 0.0115\Delta F_{22}$$

$\Delta F_{ij} = F_{ij} - F^0_{ij}$, wherein F^0_{ij} refers to the "standard molecule", and F_{ij} is the corresponding force constant in the molecule bearing the NH_2 group. $\lambda_i = 4\pi^2c^2\nu_i^2/N_0$, where N_0 = Avogadro's number.

When applied to the methylamine molecule (with the notational changes of Tables I and X and with the force constants of Table XII), eqs. [1] and [2] give the encouraging results of Table IX.

It was then decided to attempt the factorization from the vibrational secular equations for methylamine of both the methyl and amino group frequencies. The methylamine molecule has 15 modes of vibration, and in C_s point symmetry, these may be subdivided as in:

characteristic group modes: $6A' + 3A''$

framework modes : $3A' + 3A''$

One of the A″ framework modes involves the relative internal rotation of the NH_2 and CH_3

TABLE VIII

Row vectors, $\boldsymbol{B}_i(\mathbf{M}^{-1})^+$, for the calculation of $\mathbf{G}^+$ involving the interaction of group and framework coordinates*

Vector	N			R		
$\boldsymbol{B}_1(\mathbf{M}^{-1})^+$	x	y	z	x	y	z
$\boldsymbol{B}_4(\mathbf{M}^{-1})^+$	0	b	c	0	$(-\sqrt{2}m/D\sin\beta)\mu_R$	0
$\boldsymbol{B}_6(\mathbf{M}^{-1})^+$	e	0	0	$(\sqrt{2}l/D\sin\beta)\mu_R$	0	0

*Wherein $b = (\sqrt{2}m/\sin\beta)(1/D - \cos\beta/r + 0.6453/r)\mu_{Ny}$
$c = (\sqrt{2}/r\sin\beta)(1 + n\cos\beta - 0.4026 + 0.0319a)\mu_{Nz}$
$e = (-\sqrt{2}l/\sin\beta)(1/D - \cos\beta/r - 0.0764/r)\mu_{Nx}$
l, m, n are direction cosines of the N—R bond, and are respectively $\sin\alpha/2$, $-\cos\beta$, $(\cos^2\alpha/2 - \cos^2\beta)^{\frac{1}{2}}$.

Can. J. Chem. Downloaded from www.nrcresearchpress.com by 210.87.254.105 on 09/05/12
For personal use only.

TABLE IX

Application of NH_2 group frequency eqs. [1] and [2] to methylamine

Vibrational species in C_s		Approximate description	NH_2 frequencies (cm^{-1}) Complete solution	Approximate solution
A′	ν_1	ν_s (N—H)	3366	3366
	ν_4	δ (HNH)	1641	1635
A″	ν_{10}	ν_a (N—H)	3464	3464

TABLE X

Symmetry coordinates for methylamine

Species	Coordinate		Approximate description of mode
A′	$S_1 = (r_1+r_2)/\sqrt{2}$	Group coordinates	N—H sym. stretch
	$S_2 = (2d_3-d_4-d_5)/\sqrt{6}$		C—H antisym. stretch
	$S_3 = (d_3+d_4+d_5)/\sqrt{3}$		C—H sym. stretch
	$S_4 = \alpha$		HN̂H deformation
	$S_5 = (2\phi_3-\phi_4-\phi_5)/\sqrt{6}$		CH_3 antisym. deformation
	$S_6 = (\theta_3-\phi_3+\theta_4-\phi_4+\theta_5-\phi_5)/\sqrt{6}$		CH_3 sym. deformation
	$S_r = (\theta_3+\phi_3+\theta_4+\phi_4+\theta_5+\phi_5)/\sqrt{6}$		Redundant coordinate
	$S_7 = (2\theta_3-\theta_4-\theta_5)/\sqrt{6}$	Framework coordinates	Methyl rock
	$S_8 = D$		C—N stretch
	$S_9 = (\beta_1+\beta_2)/\sqrt{2}$		Sym. HN̂C deformation
A″	$S_{10} = (r_1-r_2)/\sqrt{2}$	Group coordinates	N—H antisym. stretch
	$S_{11} = (d_4-d_5)/\sqrt{2}$		CH antisym. stretch
	$S_{12} = (\phi_4-\phi_5)/\sqrt{2}$		CH_2 antisym. deformation
	$S_{13} = (\theta_4-\theta_5)/\sqrt{2}$	Framework coordinates	Methyl rock
	$S_{14} = (\beta_1-\beta_2)/\sqrt{2}$		Antisym. HN̂C deformation

TABLE XI

Valence force field* for methylamine

$2V$	r_1	r_2	D	d_3	d_4	d_5	α	β_1	β_2	θ_3	θ_4	θ_5	ϕ_3	ϕ_4	ϕ_5
r_1	K_r	F_r													
r_2		K_r													
D			K_D							$dF_{D\theta}$	$dF_{D\theta}$	$dF_{D\theta}$			
d_3				K_d	F_d	F_d									
d_4					K_d	F_d									
d_5						K_d									
α							r^2H_α								
β_1								r^2H_β	r^2F_β						
β_2									r_2H_β						
θ_3										d^2H_θ	d^2F_θ	d^2F_θ			
θ_4											d^2H_θ	d^2F_θ			
θ_5												d^2H_θ			
ϕ_3													d^2H_ϕ		
ϕ_4														d^2H_ϕ	
ϕ_5															d^2H_ϕ

*$r = r(\text{N—H})_{eq}$; $d = r(\text{C—H})_{eq}$.

Can. J. Chem. Downloaded from www.nrcresearchpress.com by 210.87.254.105 on 09/05/12
For personal use only.

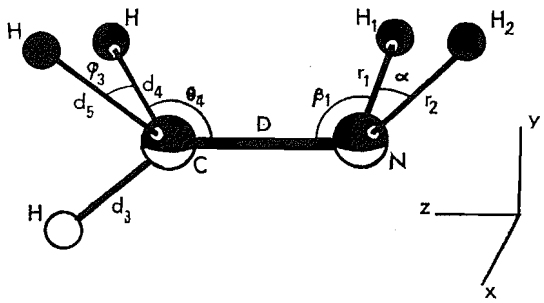

FIG. 2. The methylamine molecule: $r = 1.014$ Å, $d = 1.093$ Å, $D = 1.474$ Å, $\alpha = 106°$, $\beta = 112°$, $\theta = \phi = 109° 27'$.

TABLE XII

Valence force constants for methylamine (mdyn Å^{-1})

Force constant	Value	Force constant	Value	Force constant	Value
K_r	6.45	H_α	0.64	F_r	−0.07
K_D	4.70	H_β	0.40	F_d	0.08
K_d	4.71	H_θ	0.67	F_β	0.07
		H_ϕ	0.44	F_α	−0.04
				$F_{D\theta}$	0.31

groups; this has been assumed to be free, and is omitted from the discussion. The remaining 14 modes were treated in terms of the symmetry coordinates of Table X, the molecular geometry of Fig. 2, and the force field and force constants of Tables XI and XII.

The reduced kinetic matrices $\mathbf{G}^+_{ff}$ for the framework vibrations and corrected for interactions with both CH_3 and NH_2 groups, are presented in Table XIII, whilst Table XIV gives the reduced force constant matrices $\mathbf{F}^+_{ff}$ including the corrections $\mathbf{\Phi}_{ff}$ for the NH_2 group from Table VI and for the CH_3 group from refs. (1) and (2*a*).

Solution of the reduced secular equation,

$$|\mathbf{G}^+_{ff}\mathbf{F}^+_{ff} - \lambda\mathbf{E}_{ff}| = 0$$

gave the vibrational frequencies which are compared in Table XV with those obtained from a complete solution by us, and based on the assignment and force constants reported by King (4). A more recent, and somewhat different

TABLE XIII

Reduced kinetic matrices, $\mathbf{G}^+_{ff}$, for framework vibrations of methylamine

$\mathbf{G}^+_{ff}(A')$	S_7	S_8	S_9
S_7	$[\mu^+_{H(3)/d^2}+(3/2d^2)(a+1/3)^2\mu_{Cy}$ $+(3a^2/2d^2\mu_{Ny}]$	0	$[-(\sqrt{3}ma/d\sin\beta)(1/D-\cos\beta/r+0.6453/r)\mu_{Ny}$ $-(\sqrt{3}m/dD\sin\beta)(a+1/3+g)\mu_{Cy}]$
S_8	(symmetrical)	$[\mu_{Nz}+\mu_{Cz}]$	$[-(\sqrt{2}/r\sin\beta)(1+n\cos\beta-0.4026$ $+0.0319a)\mu_{Nz}]$
S_9			$[\mu^+_{H(2)/r^2}+(2m^2/\sin^2\beta)(1/D-\cos\beta/r)^2\mu_{Ny}$ $+[2(1+n\cos\beta)^2/r^2\sin^2\beta]\mu_{Nz}+(2m^2/D^2\sin^2\beta)\mu_{Cy}]$
$\mathbf{G}^+_{ff}(A'')$	S_{13}		S_{14}
S_{13}	$[\mu^+_{H(3)/d2}+(3/2d^2)(a+1/3)^2\mu_{Cx}$ $+(3a^2/2d^2)\mu_{Nz}]$		$[-(\sqrt{3}al/d\sin\beta)(1/D-\cos\beta/r-0.0076/r)-(\sqrt{3}/D\sin\beta)(a$ $+1/3+g)\mu_{Cx}]$
S_{14}	(symmetrical)		$[\mu^+_{H(1)/r2}+(2l^2/\sin^2\beta)(\cos\beta/r-1/D)^2\mu_{Nx}$ $+(2l^2/D^2\sin^2\beta)\mu_{Cx}]$

NOTES: $g = 0.2523$; $\mu^+_{H(3)}$, $\mu^+_{H(1)}$, and $\mu^+_{H(2)}$ refer to the reduced hydrogen masses in CH_3 and NH_2, respectively.

TABLE XIV

The reduced symmetry force fields, $\mathbf{F}^+_{ff}$, for framework vibrations of methylamine (mixed units)

$\mathbf{F}^+_{ff}(A')$	S_7	S_8	S_9
S_7	$d^2(H_\theta-F_\theta+0.0781)$	0	0
S_8	(symmetrical)	$K_D-0.0158$*	-0.0382
S_9			$r^2(H_\beta+F_\beta)+0.0641$
$\mathbf{FF}^+_{ff}(A'')$	S_{13}		S_{14}
S_{13}	$d^2(H_\theta-F_\theta+0.0781)$		0
S_{14}	(symmetrical)		$r^2(H_\beta-F_\beta)+0.0004$

*Average of corrections for NH_2 and CH_3.

Can. J. Chem. Downloaded from www.nrcresearchpress.com by 210.87.254.105 on 09/05/12
For personal use only.

TABLE XV

Framework vibration frequencies in methylamine (cm^{-1})

Species	Mode	Frequencies		
		Complete solution	Approximate solution	Observed (ref. 4)
A′	ν_7	1142	1147	1145
	ν_8	1036	1048	1041
	ν_9	754	748	779
A″	ν_{13}	1142	1145	1145
	ν_{14}	784	782	779

vibrational assignment for methylamine has been reported by Gray and Lord (5), but clearly since our aim was simply to provide an approximation method, having used King's force field, then comparison must be made with the frequencies on which it is based.

Acknowledgments

The authors thank the Science Research Council for the award of a Studentship to B.R.C., the Council of the University of Salford for the award of a Demonstratorship to J.M.F., and the staff of the Computations Laboratory for assistance with the calculations.

1. W. T. KING and B. L. CRAWFORD, JR. J. Mol. Spectry. **5**, 421 (1960); **8**, 58 (1962).
2. (*a*) J. H. CARTER, J. M. FREEMAN, and T. HENSHALL. J. Mol. Spectry. **20**, 402 (1966); **22**, 18 (1967). (*b*) J. M. FREEMAN and T. HENSHALL. J. Mol. Structure, **1**, 31 (1967); Can. J. Chem. **46**, 2131 (1968); **46**, 2135 (1968); **46**, 2175 (1968); 1969. In press.
3. L. J. BELLAMY. The infrared spectra of complex molecules. Methuen and Co., London. 1956.
4. W. T. KING. Ph.D. Thesis, University of Minnesota, Minneapolis, Minnesota. 1956.
5. A. P. GRAY and R. C. LORD. J. Chem. Phys. **26**, 690 (1959).
6. Tables of interatomic distances and configurations in molecules and ions. Chem. Soc. Spec. Publ. No. 11 (1959), supplement. Chem. Soc. Publ. No. 18 (1959).

Can. J. Chem. Downloaded from www.nrcresearchpress.com by 210.87.254.105 on 09/05/12
For personal use only.

Two linear correlations of pK_a vs. solvent composition

JOAN A. GOWLAND[1] AND GEORGE H. SCHMID
Department of Chemistry, University of Toronto, Toronto 5, Ontario

Received February 18, 1969

The dissociation constants, pK_a, of pyridine, *n*-pentylamine, triethanolamine, and benzylamine were studied in a series of ethanol–water and dimethyl sulfoxide – water solvent systems. Linear correlations were found between the pK_a of these amines and Kosower's Z values and weight % water content of the solvent.

Canadian Journal of Chemistry, 47, 2953 (1969)

Can. J. Chem. Downloaded from www.nrcresearchpress.com by 210.87.254.6 on 09/05/12
For personal use only.

Introduction

Many studies have been carried out to determine the dissociation constants of acids and bases in mixed solvent systems containing water and a miscible organic solvent. Michaelis and Mizutani (1–3), early workers in this field, studied benzoic acids, amines, amino acids, lower weight carboxylic acids, and hydroxycarboxylic acids in ethanol–water and methanol–water solvent systems. Their plots of pK_a vs. % volume alcohol gave non-linear lines of various shapes. Later workers, Hall and Sprinkle, obtained similar results (4).

In time, correlations were attempted which would give linear plots with changing pK_a, and which would lead to some explanation for the change of pK_a with changing solvent composition. One of the first was the correlation between changing pK_a and the inverse of the dielectric constant (5). Again non-linear plots were obtained. Added refinements such as Schwarzenbach's work (6, 7) combining the effects of dielectric constant and changing radius of the species with changing solvent gave only slightly improved results. It was felt (ref. 8, p. 193) that this treatment broke down because the dielectric constant measures a property of the solution in general and takes no account of specific solvent–solute effects.

In light of this, Grunwald and co-workers proposed Y_- and Y_0 activity functions (9–11) for pK_a correlations in the ethanol–water system. Their results were satisfactory for carboxylic acids but less satisfactory for amines, and were limited because the work was confined to the ethanol–water solvent system.

Another recent approach by Glover (12, 13) was to include the molal concentration of the solvent promoting ionization in the K_a equilibrium expression. Difficulties were encountered here in determining the exact structure of the mixed solvent and in deciding which portion of it participated in the ionization process. However, solvation effects do seem to be important in these studies. It was felt that a better understanding of the change in pK_a with changing solvent lay in finding some indication of the nature of the solvent in the immediate vicinity of the molecules involved in the dissociation.

Since none of these correlations gave satisfactory results in all cases, it became of interest to find a linear relation between the changing pK_a of an amine in the mixed solvent systems ethanol–water and dimethyl sulfoxide – water. Since most of the work reported has been concerned with a property of the solvent as a whole, it seemed, then, that some parameter which was a measure of the change of the solvent in the immediate vicinity of the ions might prove a useful correlation.

In 1958, Kosower (14) discovered that the charge transfer band in the ultraviolet (u.v.) spectrum of 1-ethyl-4-carbomethoxypyridinium iodide was very sensitive to solvent changes. The energy calculated from the wavelength of the charge transfer band gave an empirical measure of the ionizing ability of the solvent system and was defined as the Z value of the solvent. It was felt that the solvent environment in this electron transfer might be similar enough to the charge transfer from the protonated base to the free proton, to give a useful correlation. Therefore, in order to test this idea, pK_a values were determined for pyridine, triethanol–amine, benzylamine, and *n*-pentylamine in ethanol–water and dimethyl sulfoxide – water mixtures.

[1]Holder of a Province of Ontario Government Fellowship, 1966–1967.

Can. J. Chem. Downloaded from www.nrcresearchpress.com by 210.87.254.6 on 09/05/12
For personal use only.

Experimental

A. Preparation and Purification of Materials

All melting points and boiling points are uncorrected. Ultraviolet spectra were taken on a Bausch and Lomb 505 spectrometer equipped with a thermostated cell block with temperature 25.15 ± 0.05°. Refractive indices were measured on a Bausch and Lomb "Abbe" Refractometer.

(a) Solvents

Ethanol. Technical grade absolute ethanol was purified according to a modification of the method of Vogel (15).

Dimethyl Sulfoxide (Fisher Certified Reagent) was distilled with slight modification according to the procedure of Schlafer (16). Because of decomposition at higher temperatures, fractions were collected for use only if the boiling point was less than 55° and the pressure of the system less than 5 mm Hg. The criteria of purity were (*a*) resistance > 9900 Ω, (*b*) freezing point > 18.50°, (*c*) $n_D^{25} = 1.4778$.

Water. Doubly distilled water which was boiled just prior to use, was used to prepare all solutions.

(b) Bases

A value of pK_a in water in good agreement with literature values was considered a good criterion of purity for these bases.

Pyridine (British Drug House Ltd., Analar Grade) was purified by distillation from calcium hydride: b.p. 113.4° (lit. (17) 115.5°); $n_D^{26.5}$, 1.5066 (cf. ref. 18); and $\lambda_{max}^{95\%}$ EtOH, 257 mμ (ε 2862); $\lambda_{max}^{95\%}$ EtOH, 251 mμ (ε 2550, lit. (19)); $\lambda_{max}^{95\%}$ EtOH, 257 mμ (ε 2610); $\lambda_{max}^{95\%}$ EtOH, 251 mμ (ε 2370).

Benzylamine (Eastman Kodak Practical 579). About 25 ml of benzylamine was distilled from calcium hydride through a 20 cm column at reduced pressure, b.p. 83–84° at 23 mm Hg, (lit. (17), b.p. 84° at 24 mm Hg).

n-Pentylamine (Matheson, Coleman and Bell PX 308) was distilled from calcium hydride prior to use, b.p. 104° (lit. (17) b.p. 103°).

Triethanolamine (Fisher Certified Reagent) was distilled under vacuum, b.p. 137° at 150 μ Hg (lit. (17) b.p. 206.2° at 15 mm Hg).

(c) Compounds for Spectroscopy

Pyridine-N-oxide (Eastman Organic Chemicals) was distilled at 1 mm Hg and 75° to give colorless to white crystals.

1-Methyl-4-carbomethoxy-pyridinium-iodine. Isonicotinic methyl ester was prepared from isonicotinic acid (Kodak) according to the method of Levine and Sneed (20). Then, the isonicotinic methyl ester (4 g) and methyl iodide (4 g) were heated together in 6 ml of acetone to give bright orange crystals. The product was recrystallized from methanol, m.p. 174–176° decomp. (lit. (14) m.p. 176–179°).

B. Preparation of Solutions

(a) Ethanol–water solutions were made up by weight % and thus could be duplicated quite precisely. Stock solutions (1000 g) were prepared using absolute ethanol and water as described previously.

(b) Dimethyl sulfoxide – water solutions were prepared just before use with freshly distilled dimethyl sulfoxide (DMSO) in 250 g quantities because solutions did not seem stable over long periods of time. Refractive indices were used to compare different solutions of the same composition.

(c) Hydrochloric acid (approximately 1 *M*) was prepared by diluting C-I-L c.p. reagent concentrated HCl with boiled doubly-distilled water. NaOH, 1.0 *M* (standardized with potassium hydrogen phthalate just prior to use), was used to standardize the acid.

(d) N.B.S. buffers 185*c* (pH = 4.01 at 25.0°), 187*a* (pH = 9.18 at 25.0°), and 186*b* (pH = 6.86 at 25.0°) were prepared according to the instructions of the National Bureau of Standards supplied with the buffers.

C. pK_a Measurements

The general technique used to determine pK_a is that suggested by Albert and Sergeant (21).

(a) Apparatus. A Radiometer Type PHM 4b pH meter was used. It is calibrated to 0.01 pH units and thus pH readings can be made to ±0.002 pH units. Radiometer calomel (K4025) and glass (G2025B) electrodes were used. A Haake Thermostat type "F" bath was used and it maintained the temperature to within ±0.05° of the desired temperature.

The pK_a determinations were made in a jacketed vessel of approximately 125 ml volume. A ground glass top was fitted with ground glass openings for the electrodes, thus insuring the same geometry for the system at all times. An inlet and an outlet for nitrogen were also provided. A Hamilton microliter syringe No. 710 with a Chaney adapter was used to add the HCl. The volume delivered was determined by standardization with distilled water at 25°.

The pH values for triethanolamine and *n*-pentylamine determinations were fairly high and in these cases, the solutions were blanketed with nitrogen during the complete run to prevent contamination by CO_2. Further specific details for each amine are given in the results.

D. Determination of Z Values

Z values were determined according to the method of Kosower (14). In ethanol–water solutions 1-methyl-4-carbomethoxy-pyridinium-iodide was used as the primary standard from 0 to 40% water–ethanol. Because the charge transfer band becomes a poorly defined shoulder at this point, pyridine-N-oxide was used as a secondary standard for the remaining solutions. In a manner similar to Kosower, an equation linearly relating to *Z* values (energy of the charge transfer for the alkyl salt) and the energy, E_t, of the charge transfer for pyridine-N-oxide, $Z = 2.999E_t - 243.67$, was obtained by least squares calculation. In dimethyl sulfoxide – water, *Z* values could only be determined in pure DMSO, 5, 10% DMSO, and pure water (from Kosower's work (14)). These values were used to find the linear correlation between *Z* and E_t of $Z = 2.37E_t - 172.99$.

Results

All pK_a values were obtained by extrapolation to zero ionic strength and are thermodynamic values.

pK_a values for pyridine showed a definite increasing trend with increasing ionic strength as

TABLE I

pK_a of amines in the mixed solvent systems at 25 °C

% Solvent	pK_a			
	Pyridine	Triethanol-amine	*n*-Pentyl-amine	Benzyl-amine
100% H_2O	5.152	7.774	10.64	9.348
95% H_2O–EtOH	5.027	7.747	10.59	9.293
90% H_2O–EtOH	4.967	7.715	10.52	9.278
85% H_2O–EtOH	4.929	7.679	10.49	9.230
80% H_2O–EtOH	4.830	7.644	10.44	9.152
75% H_2O–EtOH	4.751	7.607	10.38	9.088
70% H_2O–EtOH	4.684	7.588	10.27	9.025
60% H_2O–EtOH	4.413	7.490	10.13	8.933
50% H_2O–EtOH	4.218	7.872	10.01	8.830
40% H_2O–EtOH	4.025	7.325	9.885	
30% H_2O–EtOH	3.809	7.222		
100% H_2O	5.152			
95% H_2O–DMSO	5.148			
90% H_2O–DMSO	5.092			
85% H_2O–DMSO	5.032			
80% H_2O–DMSO	4.976			
75% H_2O–DMSO	4.905			
70% H_2O–DMSO	4.851			
60% H_2O–DMSO	4.733			
50% H_2O–DMSO	4.521			

illustrated in Fig. 1. Therefore, the pK_a values for pyridine have been obtained from least squares calculations of the best line for pK_a vs. the ionic strength. No concentrations greater than 0.007 *M* were used since plots began to curve quite badly at higher ionic strengths. This curvature has been noted by other workers (22).

pK_a values for triethanolamine, benzylamine, and *n*-pentylamine were found to have random deviations smaller than those arising from experimental error and no trends were evident with increasing ionic strength. Therefore, the pK_a values for these three amines are taken to be thermodynamic values. The values obtained at 25° are summarized in Table I.

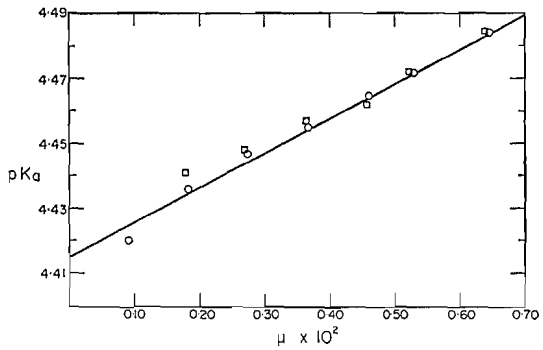

FIG. 1. pK_a of pyridine at different ionic strengths (μ) in 60% H_2O–EtOH at 24.97 °C: ○, no added salt; □, concentration of added LiCl is 0.0883×10^{-2} moles/l.

The validity of pH measurements in aqueous solvent mixtures has been established in other studies (22, 9). Bates (ref. 8, p. 222) has pointed out that many glass electrodes display nearly theoretical response to the hydrogen ion concentration to 10% water concentration.

The *Z* values for water–ethanol solutions are given in Table II and in Table III for water – dimethyl sulfoxide.

In this work, the methyl salt was used instead of the ethyl salt used by Kosower. However, λ_{max} usually differs by 0.5 mμ from the ethyl salt, that is, *Z* for the methyl salt is 0.0 to 0.4 kcal/mole higher than the ethyl salt (14). These differences fall within experimental error and thus the methyl salt energies may be called *Z* values.

To calculate *Z*, where it was not possible to measure λ_{max} for the methyl salt, an equation relating E_t and *Z* in the solutions where λ_{max} for both compounds used could be measured, was obtained by least squares measurements. Then λ_{max} for pyridine-N-oxide was measured, E_t was calculated, and *Z* was determined in the remaining

Can. J. Chem. Downloaded from www.nrcresearchpress.com by 210.87.254.6 on 09/05/12
For personal use only.

Can. J. Chem. Downloaded from www.nrcresearchpress.com by 210.87.254.6 on 09/05/12
For personal use only.

TABLE II

Z values for water–ethanol solutions

Compound*	Weight % H_2O–EtOH	λ_{max} (mμ)	E_t (kcal/mole)	*Z* (kcal/mole)
A	0.0	360.6		79.28
A	5.0	355.6		80.40
A	10	352.3		81.15
A	15	346.6		82.49
A	20	346.2		82.58
A	25	340.9		83.87
A	30	337.6		84.69
A	40	330.1		86.61
B	0.0	265.1	107.85	
B	5.0	263.6	108.46	
B	10	263.1	108.67	
B	15	262.0	109.12	
B	20	261.5	109.33	
B	25	261.1	109.50	
B	30	260.6	109.70	
B	40	259.6	110.13	
B	50	258.6	110.56	87.90
B	60	257.6	110.99	89.19
B	70	256.6	111.42	90.48
B	75	256.1	111.64	91.14
B	80	255.6	111.85	91.77
B	85	255.1	112.07	92.47
B	90	254.6	112.29	93.09
B	95	254.1	112.51	93.75
B	100	253.6	112.74	94.46

*A is 1-methyl-4-carbomethoxy-pyridinium-iodide, B is pyridine-N-oxide.

TABLE III

Z values for water–DMSO solutions

Compound*	Weight % H_2O–DMSO	λ_{max} (mμ)	E_t (kcal/mole)	*Z* (kcal/mole)
A	0.0	401.3		71.24
A	5.0	388.5		73.59
A	10	377.3		75.78
B	0.0	277.3	103.10	
B	5.0	275.1	103.93	
B	10	273.1	104.69	
B	20	269.0	106.28	79.11
B	30	256.1	107.85	82.83
B	40	263.5	108.50	84.35
B	50	260.3	109.83	87.53
B	60	258.6	110.58	89.31
B	70	257.3	111.12	90.58
B	75	256.3	111.55	91.61
B	80	255.9	111.72	92.01
B	85	255.5	111.90	92.44
B	90	255.0	112.12	92.96
B	95	254.3	112.43	93.69
B	100	253.6	112.74	94.42

*A is 1-methyl-4-carbomethoxy-pyridinium-iodide, B is pyridine-N-oxide.

solutions by substituting E_t into the equation, for both ethanol–water and dimethyl sulfoxide – water. In both cases a *Z* value for water (given as 94.4 kcal/mole by Kosower (28)) was included in the data for find the best straight line.

As can be seen from Tables II and III, the change in the wavelength of λ_{max} for pyridine-N-oxide with changing solvent is quite small. However, measurements made over a period of 2 days on one solvent mixture, and duplicate or more measurements made at the same time on all other solvent mixtures indicate that the peak maximum occurred at a reproducible wavelength in all cases. Thus, the experimental error is estimated to be ± 0.1 mμ for pyridine-N-oxide maxima.

Because the peaks for the methyl salt are not symmetrical, and because there is some change with changing salt concentration in λ_{max}, the error in the wavelength of the maxima is ± 0.5 mμ.

Plots were made of the pK_a of all the amines studied in this work at 25°, vs. *Z* and all were found to be linear. They are shown in Fig. 2.

The data in this figure suggest a good correlation between pK_a and *Z*. However, once the values of pK_a and *Z* had been determined, it was found that plots of *Z* vs. weight % water are also linear from 100 to 40% water by weight for water–ethanol and from 100 to 65% water by weight for water – dimethyl sulfoxide. Although earlier workers suggested that plots against % solvent were not linear, these pK_a values were

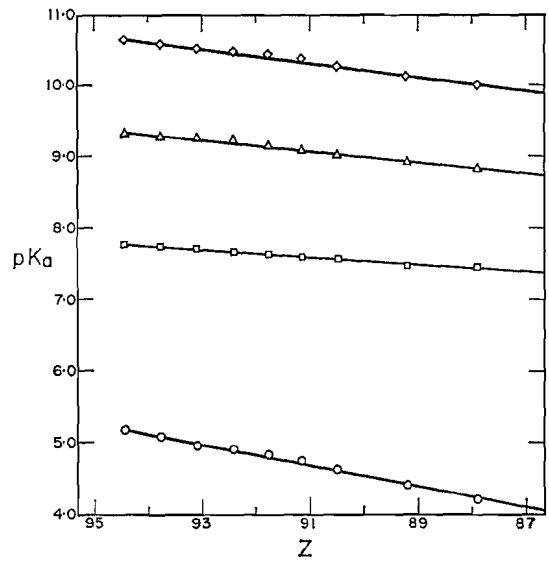

FIG. 2. pK_a of amines at 24.97 °C with changing *Z* values; ○, pyridine; □, triethanolamine; △, benzylamine; ◇, *n*-pentylamine.

Can. J. Chem. Downloaded from www.nrcresearchpress.com by 210.87.254.6 on 09/05/12
For personal use only.

TABLE IV

Comparison of experimental and calculated pK_a from literature results

Compound	Experimental pK_a in H_2O	Reference	Calcd. pK_a in H_2O from "vs. H_2O"	Deviation from exp. value	Calcd. pK_a in H_2O from "vs. Z"	Deviation from exp. value
Formic acid	3.75	9	3.58	0.17	3.60	0.15
Acetic acid	4.76	9	4.63	0.13	4.66	0.10
Benzoic acid	4.20	9	4.15	0.05	4.19	0.01
p-Methoxybenzoic acid	4.492	23	4.432	0.06	4.440	0.05
ϕ-CH_2—CH_2CO_2H	4.708	24	4.573	0.135	4.601	0.10
ϕ-O—CH_2CO_2H	3.182	24	3.045	0.14	3.071	0.11
ϕ-S—CH_2CO_2H	3.564	24	3.408	0.15	3.434	0.13
Aniline	4.64	10	4.65	0.01	4.65	0.01
Methylaniline	4.84	10	4.91	0.07	4.91	0.07
Dimethylaniline	5.01	10	5.11	0.10	5.11	0.10
Pyridine*	5.167	This work	5.199	0.03	5.12	0.05
Pyridine†	5.167	This work	5.189	0.02	5.18	0.01
n-Pentylamine†	10.64	This work	10.66	0.02	10.64	0.00
Benzylamine†	9.348	This work	9.36	0.01	9.38	0.03
Triethanolamine†	7.774	This work	7.769	0.005	7.788	0.01
Pyridine‡	5.167	This work	5.217	0.05	5.177	0.01

*To 30% H_2O–EtOH.
†To 50% H_2O–EtOH.
‡To 50% H_2O–DMSO.

plotted against weight % water and found to be linear for all the experimental data obtained, as illustrated in Fig. 3.

The results for plots of pK_a vs. weight % water for the amines studied tend to indicate that this correlation is sufficient and a secondary correlation such as against Z is not necessary.

Since only 4 amines were studied the correlations could not be assumed to hold generally. Therefore, it was of interest to take literature values of pK_a in ethanol–water (since no corresponding work has been reported in dimethyl sulfoxide – water) and see how linear correlations against weight % solvent and against Z would be.

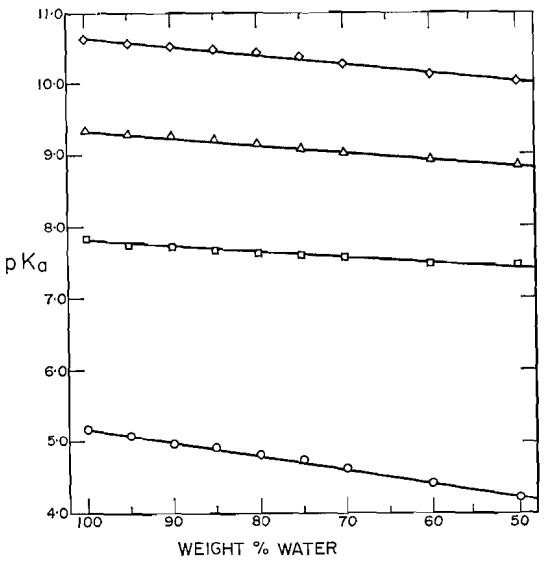

FIG. 3. pK_a of amines at 24.97 °C with changing concentrations of water–ethanol; ○, pyridine; □, triethanolamine; △, benzylamine; ◇, *n*-pentylamine.

Calculations were made on formic, acetic, and benzoic acids (9), *p*-methoxybenzoic acid (23), ϕ-$CH_2CH_2CO_2H$, ϕ-OCH_2CO_2H, and ϕ-SCH_2-CO_2H (24), aniline, methaniline, and dimethylaniline (10). The composition varied from pure water to approximately 20% water. In Table IV, the experimental and calculated pK_a values are given of compounds studied in this work.

As can be seen from Table IV, the results for amines are better than those for acids for the most part. The results from this work are generally in very good agreement (in most cases within experimental error) with the experimental pK_a values. The pK_a results calculated from equations vs. Z are as good as or often better than, results vs. weight % solvent.

The success of the correlation with carboxylic acids seems to depend unfortunately on the nature of the carboxylic acid. In view of the extra work needed to determine the values of Z for the various solvent systems, the correlation of pK_a with weight % water is to be preferred.

Correlation of the experimental data with Grunwald's Y_- (10) values would be of interest. However, only three of the reported Y_- values

are for solvent compositions used in this work. Therefore, it was felt that since other Y_- values were not available, a meaningful correlation with the experimental data was not possible.

Discussion

The plots of pK_a of pyridine vs. weight % water are good straight lines with good correlation coefficients as noted, except in H_2O–DMSO at 25° where the correlation coefficient for the plot against Z is slightly better.

The fact that the slope of the lines for pyridine is smaller in H_2O–DMSO would suggest that this solvent system affects the equilibrium in a different way and certainly to a lesser extent than does water–ethanol.

The two primary amines studied, benzylamine and *n*-pentylamine, both have similar slopes of approximately 0.01 for the plots of pK_a vs. weight % water–ethanol. Thus, they are affected similarly by the changing solvent composition. However, this slope is only about one-half that of pyridine in the same solvent. If the change in solvation of the protonated base affects the equilibrium, then these slopes are strange, for it is generally acknowledged (e.g. ref. 25) that primary amines and ammonium ions are more strongly solvated than tertiary amines. Hence, a greater change in pK_a in mixed solvents would be expected for primary amines than tertiary if the above assumption is correct. Since the opposite result was obtained, it can be suggested that, at least for the amines studied, either changing solvation for the protonated amine does not affect the equilibrium, or, solvation effects are seen only in variations of ΔH^0 and ΔS^0, and because of compensating effects, the variation is not seen in ΔG^0 (and therefore pK_a). For triethanolamine, the lines for pK_a vs. % solvent have slopes which are smaller than those for pyridine, thus indicating again that solvent changes do not affect the triethanolamine equilibrium as greatly.

It is most likely that the changing solvent system is affecting the activity coefficients of the amine, the protonated amine, and the proton. It would seem feasible that the change in the activity coefficients of the amine and protonated amine are either negligible or cancel one another out. Therefore, it is likely that the change in the activity of the proton as another solvent is added to water is affecting the pK_a of the amine. The exact nature of this change is complex and as Franks and Ives point out (26), great difficulty has been encountered in interpreting the data available from studies in alcohol–water systems.

Acknowledgment

We wish to thank Imperial Oil Limited for financial support.

1. L. Michaelis and M. Mizutani. Z. Physik. Chem. **116**, 135 (1925).
2. M. Mizutani. Z. Physik. Chem. **116**, 350 (1925).
3. M. Mizutani. Z. Physik. Chem. **118**, 318 (1925).
4. N. F. Hall and M. R. Sprinkle. J. Am. Chem. Soc. **54**, 3469 (1932).
5. W. L. Bright and H. T. Briscoe. J. Phys. Chem. **38**, 745 (1933).
6. G. Schwarzenbach. Helv. Chim. Acta, **16**, 522 (1933).
7. G. Schwarzenbach. Helv. Chim. Acta, **13**, 870 (1930).
8. Roger G. Bates. Determination of pH theory and practice. John Wiley and Sons, Inc., New York. 1964.
9. E. Grunwald and B. J. Berkowitz. J. Am. Chem. Soc. **73**, 4939 (1951).
10. B. Gutbezahl and E. Grunwald. J. Am. Chem. Soc. **75**, 559 (1953).
11. B. Gutbezahl and E. Grunwald. J. Am. Chem. Soc. **75**, 565 (1953).
12. D. J. Glover. J. Am. Chem. Soc. **87**, 5275 (1965).
13. D. J. Glover. J. Am. Chem. Soc. **87**, 5279 (1965).
14. E. M. Kosower. J. Am. Chem. Soc. **80**, 3253 (1958).
15. A. I. Vogel. A textbook of practical organic chemistry. Longmans, Green and Co., Ltd., London. 1961. p. 167.
16. H. F. Schlafer and W. Schaafernicht. Angew. Chem. **72**, 618 (1960).
17. C. D. Hodgman (*Editor-in-Chief*). Handbook of physics and chemistry. 44th ed. The Chemical Rubber Co., Cleveland, Ohio.
18. R. B. Helm, W. J. Lanum, C. L. Cook, and J. S. Ball. J. Phys. Chem. **62**, 858 (1958).
19. W. K. Miller, S. B. Knight, and A. Roe. J. Am. Chem. Soc. **72**, 1629 (1950).
20. R. Levine and J. K. Sneed. J. Am. Chem. Soc. **73**, 5614 (1951).
21. A. Albert and E. P. Sergeant. Ionization constants of acids and bases. Methuen and Co., Ltd., London. 1962.
22. A. Patterson and W. A. Felsing. J. Am. Chem. Soc. **64**, 1480 (1942).
23. E. E. Sager and V. E. Bower. J. Res. Natl. Bur. Stds. A, Phys. Chem. **64a**, 351 (1960).
24. D. J. Pasto and R. Kent. J. Org. Chem. **30**, 2684 (1965).
25. H. K. Hall, Jr. J. Am. Chem. Soc. **79**, 5441 (1957).
26. F. Franks and D. J. G. Ives. Quart. Rev. **20**, 37 (1966).

Can. J. Chem. Downloaded from www.nrcresearchpress.com by 210.87.254.6 on 09/05/12
For personal use only.

Can. J. Chem. Downloaded from www.nrcresearchpress.com by 210.87.254.40 on 09/05/12
For personal use only.

Carbonyl stretching frequencies and force constants in cyclopentadienylmolybdenum tricarbonyl derivatives

R. B. KING[1] AND L. W. HOUK[2]
Department of Chemistry, University of Georgia, Athens, Georgia

Received January 20, 1969

The infrared spectra of compounds of the type $RM(CO)_3C_5H_5$ (M = Mo or W; R = $(CH_3)_3Sn$, σ-alkyl groups, halides, etc.) exhibit the expected three ν(CO) frequencies (2A′ + A″). The relative positions of the A″ and the lower A′ frequencies interchange upon variation of the electronegativity of the R group. Values for the Cotton–Kraihanzel stretching force constants k_1 and k_2 have been calculated from these ν(CO) frequencies assuming the ratio $k_d/k_s = 2$ for the interaction force constants. From these force constants the σ and π parameters of Graham were calculated. The σ and π parameters were found to be very similar for analogous $RM(CO)_3C_5H_5$ and $RMn(CO)_5$ compounds.

Canadian Journal of Chemistry, 47, 2959 (1969)

Recently we have been studying the relationship between the π-cyclopentadienyl proton nuclear magnetic resonance (n.m.r.) chemical shifts and the carbon–oxygen stretching force constants in cyclopentadienylmetal carbonyls in an attempt to investigate the π-cyclopentadienyl n.m.r. chemical shift as a possible indicator of the negative charge on the metal atom (1). Evaluation of the carbon–oxygen stretching force constants in monocarbonyl and dicarbonyl derivatives from the ν(CO) infrared (i.r.) frequencies is a very simple problem. This paper discusses the much more difficult problem of evaluating the carbon–oxygen force constants from the ν(CO) frequencies in compounds of the type $C_5H_5M(CO)_3X$ (**1**: M = Mo or W; R = one-electron donor (2)).

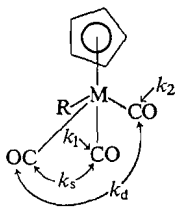

1

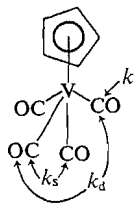

2

These $C_5H_5M(CO)_3X$ compounds, **1**, have C_s symmetry. A group theoretical analysis predicts three ν(CO) frequencies (2A′ + A″) which are related to the four force constants (k_1, k_2, k_d, and k_s) by the following secular equations

$$2A': \quad \begin{vmatrix} \mu(k_2 + k_d) - \lambda & \sqrt{2}\mu k_s \\ \sqrt{2}\mu k_s & \mu k_1 - \lambda \end{vmatrix} = 0$$

$$A'': \quad \mu(k_2 - k_d) - \lambda = 0$$

Since there are four force constants but only three ν(CO) frequencies, a solution of the secular equations is only possible if one additional relationship between two of the force constants is used. This additional relationship requires an additional assumption and/or approximation. Since the stretching force constants k_1 and k_2 are both larger and of greater interest than the interaction force constants k_d and k_s, the additional relationship used was an assumption of a constant value for the ratio k_d/k_s.

The constant value of 2 for k_d/k_s was selected for the following reasons: (1) The metal orbitals required for bonding in $C_5H_5MX_4$ were first considered. The five metal orbitals s, p_x, p_y, p_z, and $d_{x^2-y^2}$ are used for the forward σ-bonding of the metal atom to the π-C_5H_5 ligand and the four X groups. The two metal orbitals d_{xz} and d_{yz} are used for the two orthogonal forward π-bonds of the metal atom to the π-C_5H_5 ring. This leaves the two metal orbitals d_{z^2} and d_{xy} available for retrodative bonding. Linear combinations of these two metal orbitals can form the following two hybrid orbitals

$$\psi^+ = 2^{-\frac{1}{2}}[\phi(d_{z^2}) + \phi(d_{xy})]$$

$$\psi^- = 2^{-\frac{1}{2}}[\phi(d_{z^2}) - \phi(d_{xy})]$$

The lobes of one of these hybrid orbitals will be of suitable symmetry to engage in retrodative

[1]Fellow of the Alfred P. Sloan Foundation, 1967–1969.
[2]Postdoctoral Fellow, 1967–1968. Present address: Department of Chemistry, Memphis State University, Memphis, Tennessee.

Can. J. Chem. Downloaded from www.nrcresearchpress.com by 210.87.254.40 on 09/05/12
For personal use only.

π-bonding with two X groups in mutually diagonal[3] positions of the $C_5H_5MX_4$ derivative. Similarly the lobes of the other of these hybrid orbitals can engage in retrodative π-bonding with the two remaining X groups which are also in mutually diagonal positions. However, X groups in lateral[3] positions do not use the same hybrid orbitals for retrodative π-bonding. These theoretical considerations thus suggest that the diagonal interaction force constant (k_d) is appreciably greater than the lateral interaction force constant (k_s) and hence that the ratio k_d/k_s is appreciably greater than 1. Indeed the metal orbitals available for retrodative π-bonding in $C_5H_5MX_4$ derivatives resemble those available for such bonding in the octahedral MX_6 compounds in that X groups in diagonal positions of $C_5H_5MX_4$ derivatives can interact through the same (hybrid) orbital as is the case with the X groups in *trans* positions of the octahedral complexes MX_6, whereas the X groups in lateral positions of $C_5H_5MX_4$ compounds do not interact directly through the same (hybrid) orbital, as is the case with X groups in *cis* positions of the octahedral complex MX_6. The successful approximation $k_t/k_c \approx 2$ for octahedral metal carbonyl complexes (3) suggests a similar approximation $k_d/k_s \approx 2$ for $C_5H_5Mo(CO)_3R$ complexes (2). Empirical evidence has been obtained supporting the approximation $k_d/k_s \approx 2$ for the $C_5H_5M(CO)_3R$ complexes. The related $C_5H_5MX_4$ compound, $C_5H_5V(CO)_4$, **2**, has only three force constants (k, k_d, and k_s) and exhibits the three ν(CO) frequencies A_1 (i.r. and Raman active), B_1 (Raman active), and E (i.r. and Raman active). The ratio k_d/k_s for $C_5H_5V(CO)_4$ can thus be calculated from its ν(CO) frequencies *without any approximations*. Such calculations (4) from Raman data on $C_5H_5V(CO)_4$ for the ratio k_d/k_s gave 1.53 (cyclohexane solution) and 1.73 (solid state). Similarly the ratio k_d/k_s for the acetylcyclopentadienyl derivative $CH_3COC_5H_4V(CO)_4$ was found to be 2.68 for the solid state (4). These experimentally determined values for k_d/k_s in cyclopentadienylvanadium tetracarbonyl derivatives support the assumption, $k_d/k_s \approx 2$, made for the $C_5H_5M(CO)_3R$ derivatives.

Previous studies on the infrared spectra of $C_5H_5M(CO)_3R$ derivatives indicate the observation of the expected three ν(CO) frequencies for some compounds of this type such as organotin derivatives (5) of the type $R_3SnM(CO)_3C_5H_5$ and the halides $C_5H_5M(CO)_3X$ (6). However, in previous work (5, 6) only two ν(CO) bands were observed for the σ-alkyl derivatives $RM(CO)_3C_5H_5$ (e.g. $CH_3Mo(CO)_3C_5H_5$) with metal-carbon bonds to the R group. The lower ν(CO) frequency was considerably more intense than the upper ν(CO) frequency. We have now found that the lower ν(CO) frequency in $RM(CO)_3C_5H_5$ compounds (R = σ-alkyl group) can be split into two closely separated bands by running the spectra under optimum conditions (cyclohexane solution (7) and a grating spectrometer). However, the infrared spectrum of the hydride $C_5H_5W(CO)_3H$ exhibited only two ν(CO) bands even under our optimum conditions.

Having obtained the three ν(CO) frequencies for the compounds of interest, the next problem was the assignment of these frequencies to the two A′ and one A″ modes. Data on related compounds, particularly $M(CO)_3L_2L'$ derivatives (8), indicated the highest and most widely separated ν(CO) frequency to be one of the two A′ modes. The two lowest and relatively close ν(CO) frequencies are then the remaining A′ mode and the A″ mode. Force constant calculations were made using both possible assignments of the two lowest ν(CO) frequencies. Decisions between the two possible assignments were then made using the following criteria:

(1) $k_1 < k_2$

The stretching force constant k_1 represents that of a carbonyl group diagonal to the R group whereas the stretching force constant k_2 represents that of a carbonyl group diagonal to another carbonyl group. Since all of the R groups in the $RM(CO)_3C_5H_5$ compounds investigated are weaker π-acceptors than the carbonyl group (3,

[3]The relative positions of the four X ligands in $C_5H_5MX_4$ complexes are conveniently designated by terms relating to their positions on the square with vertices corresponding to the four atoms of the four X groups which are directly bonded to the metal atom. *Diagonal* positions refer to positions at diagonally opposite corners of this square corresponding to the interaction constants k_d in structures **1** and **2**. Lateral positions refer to positions on one side of this square corresponding to the interaction constants k_s in structures **1** and **2**. Both diagonal and lateral positions are geometrically *cis* positions when considered relative to the metal atom. This paper suggests that diagonal positions in $C_5H_5MX_4$ complexes are electronically similar to *trans* positions in octahedral complexes and lateral positions in $C_5H_5MX_4$ complexes are electronically similar to *cis* positions in octahedral complexes.

Can. J. Chem. Downloaded from www.nrcresearchpress.com by 210.87.254.40 on 09/05/12
For personal use only.

7), the bond between the central metal atom and a carbonyl group diagonal to the R group is expected to be stronger than the bond between the central metal atom and a carbonyl group diagonal to another carbonyl group. This weakens the carbon–oxygen bond in carbonyl groups diagonal to the R group relative to that in carbonyl groups diagonal to another carbonyl group. For this reason, a requisite for a satisfactory assignment for the ν(CO) frequencies in the $RM(CO)_3C_5H_5$ compounds was $k_1 < k_2$. Implicit in this reasoning is the assumption of stronger interaction across diagonal positions than across lateral positions in $C_5H_5MX_4$ derivatives; this assumption is supported by both the theoretical considerations and the experimental data on $C_5H_5V(CO)_4$ given above.

(2) Comparison of π and σ parameters calculated for the $RM(CO)_3C_5H_5$ compounds with those previously (9) reported for $RMn(CO)_5$ derivatives with the same R group

In some cases a clear decision between the two possible assignments could be made by calculating the π and σ parameters of Graham (9) from the force constants for both possible assignments and selecting the assignment which gave π and σ parameters closest to those reported (9) for the analogous $RMn(CO)_5$ derivative. This was particularly useful for making the assignments in the cases of the trimethyltin derivatives $(CH_3)_3SnM(CO)_3C_5H_5$ (M = Mo or W) and the halides $C_5H_5M(CO)_3X$.

Table I indicates the assignments for the $RM(CO)_3C_5H_5$ compounds investigated in this work. Of particular interest is the assignment of the lowest ν(CO) frequency in the trimethyltin derivatives $(CH_3)_3SnM(CO)_3C_5H_5$ (M = Mo or W) to the unique A″ mode but the assignment of the middle ν(CO) frequency in the halides $C_5H_5M(CO)_3X$ (M = Mo or W, X = Cl or Br) to the unique A″ mode[4]. The relative positions of the A″ and lower A′ modes thus appear to interchange upon going from the relatively electropositive tin atom to the relatively electronegative halogens in $RM(CO)_3C_5H_5$ compounds. In cases where the $C_5H_5M(CO)_3$ group is bonded to an atom of intermediate electronegativity (carbon or hydrogen) the A″ and lower A′ ν(CO) frequencies are very close together[5]. In the case of the hydride $C_5H_5W(CO)_3H$ the A″ and the lower A′ mode could not be resolved even under our optimum conditions.

Table I also lists the force constants calculated for the $RM(CO)_3C_5H_5$ compounds on the basis $k_d/k_s = 2$. The stretching force constants k_1 and k_2 are all lower for $RM(CO)_3C_5H_5$ compounds than for the analogous $RM(CO)_5$ compounds. This is another example of the lowering of carbon–oxygen stretching force constants in metal carbonyls upon the replacement of carbonyl groups with more weakly retrodative bonding ligands (in this case the π-C_5H_5 ring). The general pattern of changes in k_1 and k_2 with changes in the R group for the $RM(CO)_3C_5H_5$ compounds resembles that previously reported for changes in k_1 and k_2 with changes in the R group for the $RM(CO)_5$ compounds. However, the difference $k_2 - k_1$ is much less with $RM(CO)_3C_5H_5$ compounds than with analogous $RM(CO)_5$ compounds. Changes in the value assumed for k_d/k_s have some effect on the value found for $k_2 - k_1$ with increases in k_d/k_s increasing the difference $k_2 - k_1$. However, even if k_d/k_s is assumed to be 3.33, the values calculated for $k_2 - k_1$ of the $RM(CO)_3C_5H_5$ compounds are still much less than the reported (7, 9) $k_2 - k_1$ values for $RM(CO)_5$ compounds. This means that the effect of a given change in the π-acceptor strength of the R group is less in a formally 7-coordinate $RM(CO)_3C_5H_5$ derivative than in an octahedral $RM(CO)_5$ derivative. This may arise

[4]The opposite assignment for $(CH_3)_3SnMo(CO)_3C_5H_5$ (middle ν(CO) frequency = unique A″ mode) gives the values $\sigma = 0.15$ and $\pi = -0.44$. The opposite assignment for $C_5H_5Mo(CO)_3Cl$ (lowest ν(CO) frequency = unique A″ mode) gives the values $\sigma = 0.10$ and $\pi = 0.29$. In the cases of these compounds as well as their tungsten analogues the σ and π parameters obtained from these "opposite" assignments are radically different from those of the analogous $RMn(CO)_5$ compounds (9).

[5]In the cases of $RM(CO)_3C_5H_5$ derivatives where R is a σ-alkyl group bonded to the metal atom by a metal–carbon bond, the positions of the two lowest ν(CO) frequencies were so close that a reversal in their assignments did not change the force constants enough to permit an unambiguous decision between the two alternatives by the criteria discussed above. In the absence of more definite criteria the assignments of the two lowest ν(CO) frequencies in the $RM(CO)_3C_5H_5$ derivatives with a metal-carbon bond to the R group were taken to be similar to the tin derivatives $(CH_3)_3SnM(CO)_3C_5H_5$ rather than the halides, on the basis of the greater similarity of carbon to tin than to halogen. This made the unique A″ mode the lowest ν(CO) frequency in these $RM(CO)_3C_5H_5$ derivatives with metal-carbon bonds to the R group.

TABLE I

ν(CO) frequencies, force constants, and Graham parameters for $RM(CO)_3C_5H_5$ and related compounds

	ν(CO) frequencies*			Force constants†			Graham parameters‡	
R	A′		A″	k_1	k_2	k_d	σ	π
$RMo(CO)_3C_5H_5$ compounds								
$(CH_3)_3Sn$	1994	1931	1907	15.27	15.26	0.58	−0.86	0.33
$—CO(CF_2)_3CO$	2036	1979	1969	15.96	16.13	0.47	0.17	0.14
CH_3SCH_2	2023	1959	1948	15.65	15.85	0.52	−0.06	0.11
n-C_3F_7	2049	1985	1975	16.07	16.28	0.52	0.38	0.10
$C_6H_5CH_2$	2014	1951	1942	15.51	15.73	0.50	−0.16	0.09
CF_3CO	2039	1977	1971	15.92	16.17	0.48	0.31	0.06
$CH_3CO_2CH_2$	2027	1961	1955	15.67	15.94	0.51	0.10	0.04
$C_2H_5CO_2CH_2$	2027	1960	1954	15.66	15.93	0.52	0.09	0.04
$Br(CH_2)_4$	2013	1945	1938	15.42	15.69	0.53	−0.15	0.04
CF_3	2049	1984	1978	16.04	16.31	0.51	0.47	0.04
n-C_3F_7CO	2039	1976	1972	15.90	16.18	0.48	0.35	0.03
CH_3	2018	1950	1946	15.49	15.80	0.51	0§	0§
Br	2045	1968	1989	15.72	16.39	0.42	0.95	−0.36
Cl	2050	1969	1991	15.74	16.45	0.44	1.05	−0.40
$RW(CO)_3C_5H_5$ compounds								
$(CH_3)_3Sn$	1992	1924	1902	15.16	15.21	0.60	−0.77	0.30
$Br(CH_2)_4$	2012	1940	1931	15.34	15.62	0.56	−0.11	0.07
C_3F_7CO	2036	1966	1961	15.75	16.06	0.53	0.34	0.04
$NC_5H_4CH_2$	2012	1938	1932	15.32	15.63	0.56	−0.09	0.04
$CH_2=CHCO$	2015	1939	1934	15.34	15.67	0.57	−0.03	0.02
$Br(CH_2)_3$	2014	1940	1935	15.34	15.68	0.56	−0.01	0.01
CH_3	2015	1939	1935	15.33	15.68	0.56	0§	0§
H	2021	1942	1942	15.37	15.79	0.56	0.18	−0.07
Cl	2045	1958	1983	15.56	16.34	0.46	1.11	−0.43

	ν(CO) frequencies*			Force constants†		
Compound	A′		A″	k_1	k_2	k_d
Substituted π-cyclopentadienyl derivatives						
$CH_3Mo(CO)_3(\pi\text{-}C_9H_7)$	2016	1949	1941	15.49	15.74	0.53
$[CH_3Mo(CO)_3C_{10}H_8]_2$	2011	1946	1943	15.42	15.73	0.48
$CH_3Mo(CO)_3[\pi\text{-}C_5(CH_3)_5]$	2004	1931	1931	15.19	15.57	0.51
$HW(CO)_3[\pi\text{-}C_5(CH_3)_5]$	2006	1928	1928	15.14	15.56	0.55

*These frequencies (in cm^{-1}) were obtained from cyclohexane solutions using a Perkin–Elmer Model 621 spectrometer with grating optics. The spectra were calibrated against the 1601.4 cm^{-1} band of polystyrene. The reported frequencies are averages of values obtained from two different spectra.
†These force constants are reported in mdyn/Å. The assumption $k_d/k_s = 2$ was made.
‡These are reported in mdyn/Å and were obtained by the procedure described in ref. 9.
§The methyl derivatives were taken as the zero points.

from the availability of only two metal *d* orbitals for retrodative bonding to π-acceptor ligands in the $RM(CO)_3C_5H_5$ system as contrasted with the availability of three metal *d* orbitals for retrodative bonding to π-acceptor ligands in the $RM(CO)_5$ system.

The σ and π parameters of Graham (9) were also compared for some analogous $RM(CO)_3C_5H_5$ and $RM(CO)_5$ systems (Table II). These parameters were very similar for the same R group in both types of systems indicating the expected independence of σ and π bonding of the ligand on the nature of the metal atom to which the ligand is bonded. In order to test the importance of the assumption $k_d/k_s = 2$, the σ and π parameters found for several complexes were compared as the value of k_d/k_s was varied from 1.54 to 2.00 to 2.70. These calculations were made using the generalized Graham (9) equations $\Delta k_1 = \Delta\sigma + (k_d/k_s)\Delta\pi$ and $\Delta k_2 = \Delta\sigma + \Delta\pi$. The range 1.54 to 2.70 was selected as being the range of k_d/k_s values empirically found from the infrared and Raman studies on $C_5H_5V(CO)_4$ and $CH_3COC_5H_4C(CO)_4$ (4). Varying the k_d/k_s ratio in this manner did not alter significantly the relative σ and π parameters for the different R groups in the $RM(CO)_3C_5H_5$ complexes; instead, varying this ratio merely expanded or contracted the numerical range of the σ and π parameters. For this reason, possible errors

Can. J. Chem. Downloaded from www.nrcresearchpress.com by 210.87.254.40 on 09/05/12
For personal use only.

Can. J. Chem. Downloaded from www.nrcresearchpress.com by 210.87.254.40 on 09/05/12
For personal use only.

TABLE II

A comparison of Graham parameters for analogous $RMn(CO)_5$ and $RM(CO)_3C_5H_5$ compounds and for different values of k_d/k_s

	$RMn(CO)_5$		$RMo(CO)_3C_5H_5$						$RW(CO)_3C_5H_5$					
			σ			π			σ			π		
R	$\sigma =$ 2.00	$\pi =$ 2.00	1.54	2.00	2.70	1.54	2.00	2.70	1.54	2.00	2.70	1.54	2.00	2.70
$(CH_3)_3Sn$	−0.84	0.51	−1.28	−0.86	−0.68	0.72	0.32	0.16	−1.13	−0.77	−0.61	0.65	0.30	0.15
H	−0.09	0.20							0.26	0.18	0.14	−0.15	−0.07	−0.04
CF_3CO	0.28	0.13	0.28	0.31	0.48	0.09	0.06	0.02						
CH_3*	0	0	0	0	0	0	0	0	0	0	0	0	0	0
CF_3	0.56	−0.04	0.44	0.47	0.48	0.07	0.04	0.02						
Br	1.03	−0.44	1.39	0.95	0.77	−0.78	−0.36	−0.19						
Cl	1.25	−0.57	1.52	1.05	0.94	−0.85	−0.40	−0.22	1.33	1.11	0.86	−0.76	−0.43	−0.22

*Arbitrarily selected as the zero point.

introduced by the assumption $k_d/k_s = 2$ do not affect the assignments and other significant conclusions of this paper.

Experimental

The $RM(CO)_3C_5H_5$ compounds used for this study were samples which had been prepared by published methods[6,7] (10). The infrared spectra in the 2100–1600 cm^{-1} region were run on a Perkin–Elmer Model 621 spectrometer with grating optics. Cyclohexane solutions were used. The spectra were calibrated against the 1601.4 cm^{-1} band of a polystyrene film. The frequencies reported in Table I were the average of frequencies obtained from two different spectra; frequencies observed from the different spectra of the same compound differed by less than 2 cm^{-1}.

The force constants were calculated from the ν(CO) frequencies on the University of Georgia IBM 7094 computer using a previously developed program (11). These calculations were performed for both possible assignments of the two lowest ν(CO) frequencies. In these calculations the *reciprocal* of k_d/k_s was made to vary in the range 0.30 to 0.75 in steps of 0.01. The calculations of force constants for different k_d/k_s ratios (see Table II) indicated that this ratio can deviate appreciably from the assumed value of 2 without having a significant effect on the conclusions of this paper.

[6]For a general discussion of many of the preparative techniques in the chemistry of $RM(CO)_3C_5H_5$ compounds see ref. 6. This reference also gives suitable preparations of methyl, hydride, and halide derivatives.

[7]For acyl, perfluoroacyl, and perfluoroalkyl derivatives, see ref. 10*a*; $CH_3SCH_2Mo(CO)_3C_5H_5$, ref. 10*b*; derivatives from π-indenyl and azulene (dimer) systems, ref. 10*c*; $ROCOCH_2Mo(CO)_3C_5H_5$ derivatives, ref. 10*d*; $NC_5H_4CH_2W(CO)_3C_5H_5$, ref. 10*e*; $C_6H_5CH_2Mo(CO)_3C_5H_5$, ref. 10*f*; $Br(CH_2)_nM(CO)_3C_5H_5$ derivative, ref. 10*g*; pentamethylcyclopentadienyl derivatives, ref. 10*h*; trimethyltin derivatives, ref. 5.

Acknowledgment

We are indebted to the Sloan Foundation for partial financial support of this work.

1. R. B. KING. Inorg. Chim. Acta, **2**, 454 (1968).
2. R. B. KING. Advan. Chem. Ser. 62, Am. Chem. Soc. Washington, D.C. 1967. p. 203.
3. F. A. COTTON and C. S. KRAIHANZEL. J. Am. Chem. Soc. **84**, 4432 (1962).
4. J. R. DURIG, R. B. KING, L. W. HOUK, and A. L. MARSTON. J. Organometal. Chem. Amsterdam, **16**, 425 (1969).
5. H. R. H. PATIL and W. A. G. GRAHAM. Inorg. Chem. **5**, 1401 (1966).
6. T. S. PIPER and G. WILKINSON. J. Inorg. Nucl. Chem. **3**, 104 (1956).
7. J. B. WILFORD and F. G. A. STONE. Inorg. Chem. **4**, 389 (1965).
8. L. W. HOUK and G. R. DOBSON. J. Chem. Soc. A, 317 (1966).
9. W. A. G. GRAHAM. Inorg. Chem. 7, 315 (1968).
10. (*a*) R. B. KING and M. B. BISNETTE. J. Organometal Chem. Amsterdam, **2**, 15 (1964); (*b*) R. B. KING and M. B. BISNETTE. Inorg. Chem. **4**, 486 (1965); (*c*) R. B. KING and M. B. BISNETTE. Inorg. Chem. **4**, 475 (1965); (*d*) R. B. KING, M. B. BISNETTE, and A. FRONZAGLIA. J. Organometal. Chem. Amsterdam, **5**, 341 (1966); (*e*) R. B. KING and M. B. BISNETTE. Inorg. Chem. **5**, 293 (1966); (*f*) R. B. KING and A. FRONZAGLIA. J. Am. Chem. Soc. **88**, 709 (1966); (*g*) R. B. KING and M. B. BISNETTE. J. Organometal. Chem. Amsterdam, **7**, 311 (1967); (*h*) R. B. KING and M. B. BISNETTE. J. Organometal. Chem. Amsterdam, **8**, 287 (1967).
11. L. W. HOUK. Ph.D. Dissertation, University of Georgia, Athens, Georgia. 1967.

Can. J. Chem. Downloaded from www.nrcresearchpress.com by 210.87.254.40 on 09/05/12
For personal use only.

Photolysis of thiophene vapor

H. A. WIEBE AND JULIAN HEICKLEN

Department of Chemistry and Center for Air Environment Studies, The Pennsylvania State University, University Park, Pennsylvania 16802

Received February 11, 1969

Thiophene vapor was photoexcited with 2139 and 2288 Å radiation as well as by mercury sensitization at 2537 Å. Experiments were done at 25, 200, and 305 °C at various pressures and light intensities as well as in the presence of CO_2, C_2H_4, butenes, and O_2. In all cases the products were C_2H_2, CH_2CCH_2, CH_3CCH, CS_2, CH_2CHCCH, and polymer. When O_2 was present CO_2, COS, SO_2, and CO were also produced. The product quantum yields dropped as the pressure was raised. A mechanism was deduced and is given by the lettered reactions in the text. The initially formed excited state, Th* (where Th stands for thiophene), as well as the excited intermediate leading to CH_2CCH_2 production, I*, decomposed at a rate dependent only on the total energy content, regardless of whether thermal or photolytic. The efficiencies for energy removal from both Th* and I* decrease along the series: thiophene, C_2H_4, CO_2, O_2. Appropriate rate constant ratios for all the gases were obtained and are listed in Table IX. Experiments in the presence of olefins showed that sulfur atoms were not intermediates. The experiments with O_2 further eliminated a number of possibilities. The hydrocarbons are all produced in primary processes with additional CH_2CHCCH and C_2H_2 coming respectively from the postulated intermediates ·CHCHCHCHS· and C_2H_2S. Along with the C_3 hydrocarbons, excited CS species are produced. They can either react with the above intermediates to produce CS_2 or be deactivated to eventually form polymer (or oxidation products in the presence of O_2).

Canadian Journal of Chemistry, 47, 2965 (1969)

Can. J. Chem. Downloaded from www.nrcresearchpress.com by 210.87.254.6 on 09/05/12
For personal use only.

Introduction

The photochemistry of various arylthiophenes in solution has recently been extensively examined (1, and references therein). A number of 2-arylthiophenes were found to undergo clean, irreversible photoisomerizations to 3-arylthiophenes. While 3-arylthiophenes failed to revert to the 2-substituted isomer upon photolysis, rearrangement of carbon atoms in the thienyl ring was observed.

It was suggested (2) that the photoreorganization proceeds by an excited singlet state intermediate, which may have a valene-type structure (1). Concerted rearrangement of this species would then account for the observed isomerizations. A mechanism involving ring-contracted thioaldehydes or thioketones as intermediates was considered to be unlikely.

On the other hand, furan, the oxygen analogue of thiophene, undergoes decarbonylation as the principal process when photolyzed (3–7). From chemical and kinetic evidence it was inferred that ring-contracted cyclopropene carboxaldehydes were formed as intermediates before loss of carbon monoxide. Photoisomerization of 2-alkylfurans to yield 3-alkylfurans (7) was also postulated to proceed through the ring-contracted intermediate.

Whereas $Hg(^3P_1)$ sensitization of furan gave carbon monoxide and cyclopropene as the principal products, direct photolysis (6) resulted in the formation of CO, allene, and methylacetylene, with cyclopropene present in only trace amounts. A pressure dependence on the quantum yield for CO production was observed in the $Hg(^3P_1)$ sensitized reaction, but was absent in direct photolysis. Since $Hg(^3P_1)$ sensitization should give triplet furan, these results suggested that direct irradiation produces an excited singlet state of furan which does not cross over to the triplet.

The present investigation was carried out to extend the photochemistry of thiophenes to the vapor phase. The effects of temperature, various additives, absorbed intensity, and energy of radiation on the photodecomposition of thiophene were examined. A kinetic analysis of the pressure dependence on the photodecomposition was made to determine if the presence of an intermediate is required to explain the mechanism of the reaction.

Experimental

Thiophene (Sharples Chemical Inc.) was purified by gas chromatography on a 20 ft long column packed with 10% tricresyl phosphate on chromosorb G. The column temperature was 100° with helium as the carrier gas at a flow rate of 60 cc/min. All gases were from the Matheson Co. C.P. grade C_2H_2, iso-C_4H_8, *trans*-2-C_4H_8, and bone dry grade CO_2 were used after degassing at −196°. HBr was distilled in vacuo at −130° after degassing at −196°. Extra dry grade O_2 was introduced into the reaction cell directly.

Cylindrical (50 × 100 mm) quartz reaction cells were used for all irradiations. These were incorporated into a

Can. J. Chem. Downloaded from www.nrcresearchpress.com by 210.87.254.6 on 09/05/12
For personal use only.

grease-free vacuum system which utilized Teflon stopcocks with Viton "O" rings. For the temperature studies a reaction cell was mounted in an aluminium block furnace with quartz windows. The temperature variation during an individual experiment was $\pm 0.5°$.

The radiation sources for direct photolyses were Phillips 25 W cadmium and zinc resonance lamps. The effective emissions of these lamps were the spectral lines at 2139 Å (zinc) and 2288 Å (cadmium). The cadmium lamp also emitted at 2265 Å (about 25% as intense as the 2288 Å line) and at 2144 Å (about 20% as intense as the 2288 Å line). For mercury-photosensitized reactions a Hanovia flat spiral low-pressure mercury-arc in conjunction with a Corning 9-54 filter was used. The filter removed all radiation below 2200 Å. Since the absorption by thiophene vapor is very weak above 2475 Å, direct photolysis by the 2537 Å mercury resonance line was negligible.

After irradiation the products were analyzed by gas chromatography on a 20 ft long column packed with 10% dimethyl sulfolane on chromosorb P and operated at 0 °C with a helium flow rate of 65 cc/min. Samples of the products were obtained from the gas chromatographic effluent and identified on a Nuclide 12-90 mass spectrometer. Further identification came from comparison of the gas chromatographic retention times of the products with authentic commercial samples.

Products from the experiments with added olefin were also analyzed by gas chromatography on a 10 ft long column packed with 10% tricresyl phosphate on chromosorb G operated at room temperature and a helium flow rate of 50 cc/min. No compounds other than those observed with thiophene alone were found.

Since polymer formation was observed during long irradiations (1 h), air was admitted to the cell and heated with an oxygen torch to ca. 500° after each experiment to remove the polymer.

Quantum yields of the gaseous products were measured utilizing HBr as an actinometer at 2288 and 2139 Å (where $\Phi\{H_2\} = 1.00$ for conversions below 1% (8, p. 782)) and N_2O as an actinometer for the mercury-sensitized studies at 2537 Å (where $\Phi\{N_2\} = 1.00$). With 2537 Å radiation, all the light was absorbed and actinometry was straightforward. At the other wavelengths, equal optical densities of reagent and actinometer gases were used to avoid errors due to the uncertain path length of light. Room temperature extinction coefficients (to base 10) at 2139 and 2288 Å were found on a Cary 15 spectrophotometer to be, respectively, 5.40×10^{-3} and 1.17×10^{-3} $Torr^{-1}$ cm^{-1} for HBr and 0.198 and 0.258 $Torr^{-1}$ cm^{-1} for thiophene. The extinction coefficients at elevated temperatures were assumed to be the room temperature values. Thus optical densities are matched at elevated temperatures only if the ratio of extinction coefficients for thiophene and HBr is invariant with temperature. If the ratio is not invariant with temperature, then some error exists in our absolute quantum yields for elevated temperatures at the lower pressures. However, above about 0.8 Torr pressure, absorption is essentially complete, and uncertainties in the extinction coefficients are irrelevant.

Results

Thiophene vapor has a weak absorption band starting at about 2600 Å, but the absorption becomes very strong below 2400 Å (9). We have photodecomposed the vapor with 2139 and 2288 Å radiation as well as by mercury sensitization using 2537 Å radiation. Under all experimental conditions the gas phase products were C_2H_2, $CH_2{=}C{=}CH_2$, $CH_3C{\equiv}CH$, CS_2, and $CH_2{=}CHC{\equiv}CH$ even at elevated temperatures. Also produced was a brown, sulfur-containing polymer. The products were routinely analyzed by gas chromatography. Initially a combination thermal conductivity and hydrogen-flame detector was used; 10% of the sample was passed through the hydrogen flame and 90% was passed through the thermal conductivity cell which was needed for CS_2 analysis. Later a thermistor detector was used to obtain more accurate analyses. The polymer was not identified, but the following inequalities always held

$$[1] \quad \Phi\{CS_2\} \leqslant \Phi\{CH_2CCH_2\} + \Phi\{CH_3CCH\}$$

and

$$\Phi\{CS_2\} \leqslant (1/2)\Phi\{C_2H_2\} + \Phi\{CH_2CHCCH\}$$

The former inequality shows that CS groups were in the polymer, whereas the latter inequality indicated that additional sulfur (i.e., beyond that from CS groups) was also present.

The values reported for I_a are average values assuming uniform absorption in the reaction vessel. Actually the absorption is very nonuniform, and the effective intensity is much higher than the average intensity. All the quantum yields are correct, but relative rate constant ratios of processes first order in intermediates to those second order in intermediates will be lower limits. If the intermediates diffused completely through the cell before reaction then the average intensity goes over to the effective intensity and the computations are correct; otherwise they are not. In this system the intermediates proposed are CS, C_2H_2S, and $\cdot CHCHCHCHS\cdot$, all of which probably are long-lived and diffusion may be complete before reaction. In any case it happens that intensity effects are quite minor. Uncertainties introduced because of the variation in intensity throughout the cell cannot be much greater than the uncertainty due to experimental errors.

The effect of extent of conversion on product yields is shown in Table I for two conditions where it was thought the effect might be greatest.

TABLE I

Effect of extent of conversion on product yields

Irradiation time, min	$\Phi\{C_2H_2\}$	$\Phi\{CH_2CCH_2\}$	$\Phi\{CH_3CCH\}$	$\Phi\{CS_2\}$	$\Phi\{CH_2CHCCH\}$
$\lambda = 2139$ Å, $T = 25 \pm 5$ °C, $I_a = 16.0 \times 10^{11}$ quanta/cc s, [Th] = 0.30 Torr					
5	0.265	0.095	0.045	0.046	0.253
10	0.290	0.104	0.049	0.071	0.244
10	0.268	0.098	0.044	0.059	0.221
20	0.277	0.094	0.042	0.070	0.195
40	0.259	0.077	0.036	0.058	0.116
60	—	0.069	0.031	0.050	0.075
$\lambda = 2288$ Å, $T = 305 \pm 5$ °C, $I_a = 150 \times 10^{11}$ quanta/cc s, [Th] = 1.22 ± 0.07 Torr					
2.0	0.246	0.094	0.039	0.124	0.241
4.0	0.256	0.096	0.042	0.147	0.220
8.0	0.243	0.084	0.039	0.143	0.172
16.0	0.244	0.071	0.034	0.145	0.113

The ± values reported in the table headings for all the tables do not reflect uncertainties in measurement, but rather variations in the experimental parameters. Product analysis was made utilizing the thermistor detector. For short irradiation times the product yields are all independent of time, but $\Phi\{CH_2CHCCH\}$ falls noticeably as the extent of conversion increases. This falloff is attributed to polymerization of the $CH_2{=}CHC{\equiv}CH$. The other product yields drop slightly as the irradiation time is lengthened at room temperature, but are unaffected at elevated temperatures. The room-temperature drop is an artifact caused by a diminishing intensity as polymer deposits on the windows and absorbs some of the light. This was verified by performing an actinometer run before and after a 30 min irradiation of 10 Torr of thiophene; I_a dropped by 25%. At elevated temperatures, the polymer does not deposit in the cell but rather on the inlet line (which is cold); thus the product yields, except for $CH_2{=}CHC{\equiv}CH$, are independent of extent of conversion. All experiments reported in subsequent tables were for small conversions, and the quantum yields reported are true initial values.

Tables II and III give the results of the photolysis of thiophene at 2139 and 2288 Å, respectively, as a function of pressure and light intensity for various temperatures. At 305 °C, a dark run showed no decomposition. To check that the products were not decomposing, some samples were permitted to remain at this temperature for ½ h after irradiation; the product yields were unaffected. As can be seen from Tables II and III the low pressure limiting value for $\Phi\{C_2H_2\}$ is about 0.31, independent of wavelength or temperature. The quantum yield of each of the products drops measurably as the pressure is enhanced. This effect is shown for C_2H_2 in Fig. 1. In spite of the scatter of the data, the Stern–Volmer plots in Fig. 1 give reasonable straight lines with a common intercept but different slopes for different temperatures and exciting wavelengths.

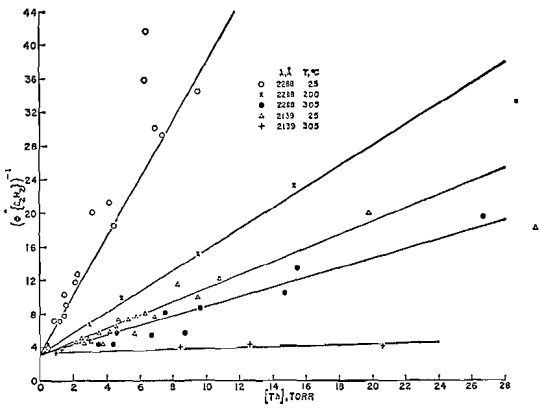

FIG. 1. Plots of the reciprocal acetylene quantum yield vs. thiophene pressure in the photolysis of thiophene vapor.

The quantum yields of the products other than C_2H_2 are presented as ratios, so that less important secondary effects can be discerned more easily. There is no effect of I_a on the hydrocarbon ratios under any conditions even when I_a was altered by a factor of 30. For the CS_2/C_2H_2 ratio there is also little if any dependence on I_a within the scatter of the data except for the room

Can. J. Chem. Downloaded from www.nrcresearchpress.com by 210.87.254.6 on 09/05/12
For personal use only.

TABLE II

Photolysis of thiophene at 2139 Å

[Th], Torr	$I_a \times 10^{-11}$ quanta/cc s	Irradiation time, min	$\Phi\{C_2H_2\}$	$\frac{\Phi\{CH_2CCH_2\}}{\Phi\{C_2H_2\}}$	$\frac{\Phi\{CH_3CCH\}}{\Phi\{C_2H_2\}}$	$\frac{\Phi\{CS_2\}}{\Phi\{C_2H_2\}}$	$\frac{\Phi\{CH_2CHCCH\}}{\Phi\{C_2H_2\}}$
			$T = 25 \pm 5$ °C				
0.103	7.9	6.0	0.30	0.36	0.178	—	0.68
0.115	8.5	10.0	0.34	0.34	0.161	0.215	0.77
0.240	12.2	3.0	0.42	0.33	0.182	0.148	0.94
0.37	31.2	5.0	0.32	0.26	0.137	0.155	0.68
0.45	15.4	20.0	0.41	0.33	0.145	0.204	0.64
0.47	2.80	40.0	0.24	0.38	0.126	0.189	0.81
0.62	3.00	40.0	0.31	0.34	0.138	0.218	0.84
0.89	34.5	5.0	0.32	0.30	0.155	—	0.85
0.92	19.3	20.0	0.35	0.33	0.153	0.229	0.81
0.92	83	2.0	0.30	0.28	0.133	0.167	0.86
1.05	3.00	40.0	0.29	0.36	0.147	0.178	0.92
1.36	100	2.0	0.31	0.30	0.139	0.158	0.87
1.45	38.5	5.0	0.30	0.29	0.158	—	0.94
1.48	20.3	20.0	0.30	0.36	0.163	0.218	0.97
1.73	38.5	5.0	0.27	0.32	0.158	0.090*	0.95
1.80	100	2.0	0.31	0.32	0.158	0.162	0.97
1.80	3.00	40.0	0.28	0.37	0.139	—	0.97
1.88	3.00	40.0	0.28	0.39	0.143	0.324	1.01
2.13	21.0	20.0	0.22	0.38	0.170	0.217	1.04
2.52	100	2.0	0.20	0.27	0.130	0.115*	0.90
2.63	100	2.0	0.22	0.27	0.150	0.127*	1.00
2.88	3.00	40.0	0.20	0.37	0.142	0.298*	1.04
3.07	3.00	40.0	0.21	0.36	0.124	0.132*	0.96
3.54	100	2.0	0.176	0.28	0.139	0.150*	0.94
3.77	38.5	5.0	0.23	0.28	0.138	0.138*	0.94
4.18	21.0	25.0	0.167	0.35	0.178	0.141	1.24
4.60	100	2.0	0.153	0.28	0.140	0.087*	1.07
4.76	3.00	40.0	0.137	0.35	0.130	0.045*	1.04
5.30	100	2.0	0.136	0.26	0.136	—	1.00
5.66	38.5	5.0	0.18	0.26	0.122	0.076*	0.98
5.82	100	2.0	0.130	0.25	0.131	0.045*	1.00
6.3	21.0	31.0	0.124	0.34	0.157	0.169	1.13
6.9	21.0	25.0	0.130	0.33	0.161	0.127	1.16
8.3	21.0	42.0	0.086	0.33	0.154	0.133	1.14
9.5	21.0	22.0	0.100	0.33	0.160	0.108	1.21
10.8	100	2.0	0.082	0.32	0.146	—	1.19
19.8	100	2.0	0.050	0.28	0.140	—	1.14
29.8	100	2.0	0.055	0.22	0.127	—	1.04
39.7	100	2.0	0.024	0.31	0.20	—	1.54
					Ave. 0.147 ± 0.013		Ave. 1.06 ± 0.08†
			$T = 305 \pm 5$ °C				
0.95	58	5.0	0.30	0.31	0.194	0.52	0.87
1.31	63	6.0	0.26	0.33	0.224	0.63	0.96
8.4	61	6.0	0.25	0.35	0.249	0.51	1.39
12.6	36	6.0	0.23	0.35	0.252	0.46	1.38
20.6	10.8	6.0	0.24	0.34	0.228	0.56	1.48
					Ave. 0.229 ± 0.017		Ave. 1.42 ± 0.04†

*Thermocouple detection, analysis of CS_2 is very crude.
†Average of runs with more than 2 Torr thiophene.

temperature runs. At room temperature, $\Phi\{CS_2\}/\Phi\{C_2H_2\}$ drops as I_a falls, especially at the higher pressures.

The pressure effects are somewhat more complex. $\Phi\{CH_2CHCCH\}/\Phi\{C_2H_2\}$ initially rises with the pressure and then levels off for all temperatures and incident wavelengths. $\Phi\{CH_3CCH\}/\Phi\{C_2H_2\}$ is invariant with changes in pressure but increases from 0.13 to 0.23 as the energy content is augmented. $\Phi\{CS_2\}/\Phi\{C_2H_2\}$ drops about a factor of 2 as the pressure rises from 0.1 to 40 Torr except for the lowest energy series of runs (i.e. 25 °C, 2288 Å) where the falloff is more pronounced and the highest energy series

Can. J. Chem. Downloaded from www.nrcresearchpress.com by 210.87.254.6 on 09/05/12
For personal use only.

TABLE III

Photolysis of thiophene at 2288 Å

[Th], Torr	$I_a \times 10^{-11}$ quanta/cc s	Irradiation time, min	$\Phi\{C_2H_2\}$	$\frac{\Phi\{CH_2CCH_2\}}{\Phi\{C_2H_2\}}$	$\frac{\Phi\{CH_3CCH\}}{\Phi\{C_2H_2\}}$	$\frac{\Phi\{CS_2\}}{\Phi\{C_2H_2\}}$	$\frac{\Phi\{CH_2CHCCH\}}{\Phi\{C_2H_2\}}$
			$T = 25 \pm 5$ °C				
0.103	66	3.0	0.31	0.42	0.142	0.062	0.64
0.115	70	3.0	0.32	0.43	0.145	0.085	0.63
0.145	4.1	60.0	0.29	0.44	0.150	0.114	0.68
0.178	4.8	90.0	0.27	0.42	0.138	0.137	0.62
0.240	100	3.0	0.31	0.41	0.139	0.101	0.68
0.340	165	10.0	0.26	0.32	0.102	0.246	0.42
0.450	113	5.0	0.25	0.40	0.138	0.100	0.68
0.88	6.3	60.0	0.14	0.42	0.131	0.075	0.81
0.90	206	10.0	0.14	0.36	0.129	0.246	0.71
0.92	137	7.0	0.16	0.39	0.134	0.090	0.76
1.18	213	10.0	0.14	0.36	0.165	0.206	0.71
1.48	6.7	120.0	0.097	0.35	0.108	0.052	0.77
1.48	139	10.0	0.129	0.35	0.129	0.101	0.76
1.55	213	10.0	0.11	0.31	0.142	0.249	0.82
2.13	140	11.0	0.085	0.34	0.133	0.099	0.86
2.24	213	10.0	0.079	0.34	0.157	0.157	0.87
3.16	6.7	180.0	0.050	0.31	0.102	0.029	0.81
4.18	145	16.0	0.047	0.32	0.123	0.043	0.92
4.39	213	10.0	0.054	0.30	0.118	0.104	0.88
6.3	145	20.0	0.028	0.28	0.116	0.054	0.78
6.37	6.7	180.0	0.024	0.22	0.097	~0	0.70
6.9	145	10.0	0.033	0.27	0.117	0.037	0.84
7.32	213	10.0	0.034	0.26	0.120	0.065	0.94
8.3	145	25.0	0.0187	0.24	0.109	0.040	0.74
9.5	145	10.0	0.029	0.25	0.115	0.025	0.84
10.8	6.7	180.0	0.0081	0.19	0.17	~0	1.2
					Ave. 0.128±0.014		Ave. 0.83±0.06†
			$T = 200 \pm 5$ °C				
0.141	54	3.0	0.300	0.39	0.138	0.48	0.71
0.370	83	3.0	0.338	0.39	0.150	0.49	0.78
0.850	112	3.0	0.235	0.39	0.147	0.50	0.85
1.76	118	3.0	0.164	0.40	0.150	0.43	0.92
1.86	120	3.0	0.166	0.39	0.149	0.40	0.98
2.94	109	3.0	0.150	0.38	0.157	0.40	0.99
4.90	109	3.0	0.101	0.37	0.150	0.40	1.06
9.5	109	3.0	0.066	0.32	0.118	0.27	1.02
15.3	117	3.0	0.043	0.27	0.121	0.24	0.86
28.7	109	3.0	0.030	0.22	0.065	0.086	0.79
					Ave. 0.142±0.011		Ave. 0.94±0.10†
			$T = 305 \pm 5$ °C				
0.285	68	3.0	0.273	0.37	0.149	0.58	0.76
0.68*	77	3.0	0.352	0.38	0.167	0.58	0.88
0.77	90	3.0	0.293	0.39	0.174	0.64	0.92
0.85	138	2.0	0.285	0.39	0.159	0.54	0.83
0.91	18.3	30.0	0.304	0.37	0.163	0.57	0.78
0.96*	83	3.0	0.327	0.41	0.171	0.61	0.94
0.96	142	2.0	0.291	0.39	0.163	0.56	0.94
1.10	18.7	15.0	0.297	0.40	0.178	0.58	0.94
1.11	98	3.0	0.281	0.37	0.159	0.55	0.89
1.32*	97	3.0	0.279	0.39	0.174	0.57	0.96
1.68	142	1.5	0.276	0.40	0.161	0.47	1.06
2.32	100	3.0	0.282	0.39	0.159	0.53	0.98
3.5	18.3	15.0	0.227	0.40	0.167	0.40	1.03
4.36	104	3.0	0.227	0.40	0.150	0.45	1.05
4.6	157	2.0	0.174	0.37	0.161	0.40	1.06
6.72	108	3.0	0.181	0.38	0.159	0.45	1.05
7.5	157	2.0	0.124	0.37	0.170	0.36	1.09
8.7	17.7	10.0	0.174	0.36	0.182	0.32	1.09
9.6	96	3.0	0.112	0.36	0.160	0.36	1.13
14.8	156	2.0	0.094	0.32	0.151	0.39	1.10
15.5	97	3.0	0.074	0.34	0.161	0.35	1.12
26.7	96	3.0	0.051	0.30	0.161	0.28	1.07
					Ave. 0.164±0.007		Ave. 1.07±0.03†

*Sample left in reaction cell for ½ h after irradiation.
†Average of runs with more than 2 Torr thiophene.

Can. J. Chem. Downloaded from www.nrcresearchpress.com by 210.87.254.6 on 09/05/12
For personal use only.

TABLE IV

Photolysis of thiophene in the presence of CO_2

$[CO_2]$, Torr	Irradiation time, min	$\Phi\{C_2H_2\}$	$\frac{\Phi\{CH_2CCH_2\}}{\Phi\{C_2H_2\}}$	$\frac{\Phi\{CH_3CCH\}}{\Phi\{C_2H_2\}}$	$\frac{\Phi\{CS_2\}}{\Phi\{C_2H_2\}}$	$\frac{\Phi\{CH_2CHCCH\}}{\Phi\{C_2H_2\}}$
$\lambda = 2139$ Å, $T = 25 \pm 5$ °C, $I_a = (22 \pm 4) \times 10^{11}$ quanta/cc s, [Th] = 0.31 ± 0.03 Torr						
0.0	15.0	0.28	0.33	0.145	—	0.65
0.0	6.0	0.33	0.37	0.158	0.256	0.85
1.37	10.0	0.266	0.36	0.176	0.284	0.85
2.42	10.0	0.249	0.34	0.148	0.238	0.73
3.38	10.0	0.244	0.33	0.144	0.245	0.73
6.41	10.0	0.165	0.33	0.151	0.218	0.79
6.75	15.0	0.15	0.28	0.119	—	0.69
10.0	10.0	0.108	0.31	0.154	0.157	0.77
10.1	10.0	0.143	0.29	0.138	0.171	0.74
39.2	15.0	0.058	0.21	0.115	—	0.70
76.0	15.0	0.028	0.154	0.113	—	0.80
				Ave. 0.142 ± 0.014		Ave. 0.75 ± 0.05
$\lambda = 2288$ Å, $T = 25 \pm 5$ °C, $I_a = (126 \pm 6) \times 10^{11}$ quanta/cc s, [Th] = 0.32 ± 0.02 Torr						
0.0	3.0	0.232	0.41	0.130	0.113	0.67
1.24	5.0	0.148	0.38	0.130	0.092	0.67
2.15	10.0	0.105	0.32	0.109	0.103	0.52
3.75	6.0	0.070	0.33	0.099	0.047	0.60
7.37	5.0	0.046	0.29	0.109	0.050	0.69
8.80	10.0	0.042	0.23	0.097	0.060	0.52
				Ave. 0.112 ± 0.012		Ave. 0.61 ± 0.06
$\lambda = 2288$ Å, $T = 25 \pm 5$ °C, $I_a = 159 \times 10^{11}$ quanta/cc s, [Th] = 0.95 ± 0.03 Torr						
0	5	0.153	0.38	0.128	0.141	0.83
0	10	0.154	0.36	0.122	0.148	0.73
6.45	10	0.052	0.27	0.123	0.090	0.77
8.20	15	0.046	0.27	0.110	0.110	0.71
15.7	20	0.028	0.21	0.119	0.122	0.72
27.7	22	0.012	0.20	0.146	0.062	1.02
				Ave. 0.125 ± 0.012		Ave. 0.80 ± 0.09
$\lambda = 2288$ Å, $T = 305 \pm 5$ °C, $I_a = (78 \pm 2) \times 10^{11}$ quanta/cc s, [Th] = 0.83 ± 0.05 Torr						
2.00	3.0	0.271	0.39	0.166	0.54	0.98
3.63	3.0	0.221	0.38	0.153	0.46	0.98
5.10	3.0	0.193	0.38	0.167	0.52	0.98
6.90	3.5	0.163	0.36	0.168	0.51	1.00
10.00	3.0	0.127	0.37	0.156	0.42	1.08
				Ave. 0.162 ± 0.006		Ave. 1.00 ± 0.03

of runs (i.e. 305 °C, 2139 Å) where there is no falloff. The ratio $\Phi\{CH_2CCH_2\}/\Phi\{C_2H_2\}$ is invariant to pressure changes at 0.31 ± 0.05 for 2139 Å radiation, but shows a falloff with increasing pressure at 2288 Å. The values range from 0.42 to 0.24 at 25 °C, 0.39 to 0.22 at 200 °C, and 0.38 to 0.30 at 305 °C.

To find out whether the pressure effects involved chemical reactions with the thiophene or whether they were inert gas effects, a number of experiments were done with CO_2. The results are listed in Table IV. For those runs in which CS_2 was not reported, product analysis was by hydrogen flame ionization. For the other runs the thermistor was used. In most respects the variations with CO_2 pressure are similar to but less pronounced than with thiophene, as would be expected for a less efficient inert gas. The quantum yields drop with increasing CO_2 pressure, and almost identical effects to those with thiophene are observed for $\Phi\{CH_2CCH_2\}/\Phi\{C_2H_2\}$, $\Phi\{CH_3CCH\}/\Phi\{C_2H_2\}$, and $\Phi\{CS_2\}/\Phi\{C_2H_2\}$. A minor difference is that $\Phi\{CH_2CCH_2\}/\Phi\{C_2H_2\}$ drops from 0.34 to 0.15 as the CO_2 pressure is raised to 76 Torr at 2139 Å and 25 °C. However, a significant difference occurs in $\Phi\{CH_2CHCCH\}/\Phi\{C_2H_2\}$ in that no enhancement occurs with the addition of

Can. J. Chem. Downloaded from www.nrcresearchpress.com by 210.87.254.6 on 09/05/12
For personal use only.

TABLE V

Photolysis of thiophene in the presence of C_2H_4 at 25 ± 5 °C and [Th] = 0.31 ± 0.04 Torr

$[C_2H_4]$, Torr	Irradiation time, min	$\Phi\{C_2H_2\}$	$\frac{\Phi\{CH_2CCH_2\}}{\Phi\{C_2H_2\}}$	$\frac{\Phi\{CH_3CCH\}}{\Phi\{C_2H_2\}}$	$\frac{\Phi\{CS_2\}}{\Phi\{C_2H_2\}}$	$\frac{\Phi\{CH_2CHCCH\}}{\Phi\{C_2H_2\}}$
		$\lambda = 2139$ Å, $I_a = (21 \pm 3) \times 10^{11}$ quanta/cc s				
0.0	6.0	0.33	0.37	0.158	0.256	0.85
0.0	20.0	0.32	0.36	0.155	0.273	0.80
1.37	20.0	0.23	0.31	0.154	0.102	0.68
1.47	10.0	0.25	0.34	0.147	0.181	0.78
3.43	10.0	0.176	0.30	0.121	0.121	0.80
4.00	20.0	0.186	0.30	0.144	0.088	0.74
5.39	10.0	0.158	0.29	0.128	0.096	0.80
7.01	10.0	0.141	0.27	0.138	0.108	0.86
10.4	10.0	0.115	0.25	0.125	0.095	0.77
				Ave. 0.144±0.011		Ave. 0.79±0.04
		$\lambda = 2288$ Å, $I_a = (128 \pm 5) \times 10^{11}$ quanta/cc s				
0.0	3.0	0.232	0.41	0.130	0.113	0.67
1.30	5.0	0.109	0.35	0.118	0.058	0.60
3.09	5.0	0.067	0.31	0.103	0.030	0.72
4.92	10.0	0.053	0.26	0.092	0.035	0.60
6.27	10.0	0.043	0.23	0.098	0.0172	0.56
9.17	10.0	0.030	0.20	0.104	0.025	0.64
				Ave. 0.108±0.011		Ave. 0.63±0.05

CO_2. Consequently the enhancement caused by increases in thiophene pressure must be a chemical rather than an inert gas effect.

The data in Tables V and VI show the results in the presence of C_2H_4 and O_2, respectively. Those runs of 20 min duration were analyzed by hydrogen flame and thermal conductivity detection, whereas the other runs were analyzed by the thermistor.

Ethylene acts like an inert gas, the effects being similar to those with CO_2. These results surprised us as we expected to trap sulfur atoms and find episulfides and possibly thiols (10). A careful search was made for these compounds but the results were negative. Runs were also done at 2139 Å, 25 °C, and 0.3 Torr of thiophene using 14.5 Torr C_2H_4, 7 Torr iso-C_4H_8, 0.31 Torr *trans*-2-C_4H_8, or 1.67 Torr *trans*-2-C_4H_8. The latter two compounds are respectively, 57 and 22 times more efficient than C_2H_4 in trapping sulfur atoms (10). Yet episulfides and thiols were definitely absent, clearly demonstrating that no free sulfur atoms were in the system.

Oxygen also did not behave much differently than CO_2 or C_2H_4. However, CO_2 and COS were produced, as well as SO_2 and CO. Our analysis procedure did not provide quantum yield information for the latter two products. One result which was different with O_2 was the value for $\Phi\{CH_2CHCCH\}/\Phi\{C_2H_2\}$ which dropped to 0.5 even with only 0.12 Torr of O_2 and remained at that value as $[O_2]$ was raised to 92 Torr.

The results of the Hg sensitized photolyses are in Tables VII and VIII. In Table VII the relative quenching efficiency between thiophene and N_2O was measured from the reduction in $\Phi\{N_2\}$. The C_2H_6 was present to scavenge the oxygen atoms; its cross section for quenching Hg6($^3P_1$) is too small (8, p. 74) to be of consequence. The reactions of pertinence are

[*a*] $\quad Hg^* + N_2O \rightarrow Hg + N_2 + O$

[*b*] $\quad Hg^* + Th \rightarrow$ removal of Hg*

where Hg* is the 6($^3P_1$) state of Hg. The expression for $\Phi\{N_2\}$ is

$$[2] \quad (\Phi\{N_2\})^{-1} = 1 + k_b[Th]/k_a[N_2O]$$

The data give a best estimate of 1.52 for k_b/k_a.

Table VIII lists the results of the Hg sensitized decomposition of thiophene. The gaseous products are the same as for the direct irradiation and even their relative importance is not much different. However the absolute quantum yields are much reduced and there is little, if any, falloff with increasing pressure except for C_2H_2 and CS_2. Extensive amounts of polymer were produced and this interfered with obtaining good

Can. J. Chem. Downloaded from www.nrcresearchpress.com by 210.87.254.6 on 09/05/12
For personal use only.

Can. J. Chem. Downloaded from www.nrcresearchpress.com by 210.87.254.6 on 09/05/12
For personal use only.

TABLE VI

Photolysis of thiophene in the presence of O_2 at 25 ± 5 °C and [Th] = 0.33 ± 0.03 Torr

$[O_2]$, Torr	Irradiation time, min	$\Phi\{C_2H_2\}$	$\frac{\Phi\{CH_2CCH_2\}}{\Phi\{C_2H_2\}}$	$\frac{\Phi\{CH_3CCH\}}{\Phi\{C_2H_2\}}$	$\frac{\Phi\{CS_2\}}{\Phi\{C_2H_2\}}$	$\frac{\Phi\{CH_2CHCCH\}}{\Phi\{C_2H_2\}}$	$\frac{\Phi\{CO_2\}}{\Phi\{C_2H_2\}}$	$\frac{\Phi\{COS\}}{\Phi\{C_2H_2\}}$	$\frac{\Phi\{COS + CS_2\}}{\Phi\{CH_2CCH_2 + CH_3CCH\}}$
				$\lambda = 2139$ Å, $I_a = (23 \pm 4) \times 10^{11}$ quanta/cc s					
0.0	6.0	0.33	0.36	0.158	0.256	0.85	—	—	—
0.0	20.0	0.32	0.36	0.155	0.273	0.79	—	—	—
0.125	20.0	0.32	0.28	0.117	0.154	0.42	—	—	—
0.410	20.0	0.30	0.28	0.151	0.160	0.43	—	—	—
1.59	10.0	0.31	0.29	0.151	0.165	0.60	0.213	0.064	0.52
1.78	20.0	0.28	0.24	0.136	0.056	0.31	—	—	—
4.97	11.0	0.29	0.27	0.148	0.096	0.53	0.131	0.069	0.48
9.65	10.0	0.27	0.27	0.152	0.086	0.57	0.154	0.094	0.42
28.2	15.0	0.171	0.23	0.140	0.056	0.48	0.274	0.128	0.50
34.0	20.0	0.127	0.23	0.132	—	0.48	—	—	—
45.5	10.0	0.171	0.22	0.133	0.070	0.48	0.316	0.123	0.54
92.0	20.0	0.081	0.189	0.143	—	0.54	—	—	—
				Ave. 0.144±0.009		Ave. 0.48±0.06			
				$\lambda = 2288$ Å, $I_a = (129 \pm 6) \times 10^{11}$ quanta/cc s					
0.0	3.0	0.232	0.41	0.130	0.113	0.67	—	—	—
1.43	5.0	0.196	0.37	0.139	0.125	0.62	0.029	0.060	0.36
1.78	5.0	0.168	0.33	0.129	0.102	0.58	0.037	0.044	0.26
3.96	5.0	0.128	0.33	0.123	—	—	0.059	0.112	—
4.32	5.0	0.125	0.31	0.123	0.072	0.60	0.068	0.104	0.39
4.41	5.0	0.115	0.32	0.133	0.080	0.60	0.073	0.110	0.42
7.90	5.0	0.092	0.29	0.125	0.060	0.55	0.115	0.154	0.51
8.65	5.0	0.088	0.28	0.125	0.063	0.52	0.148	0.172	0.58
9.34	5.0	0.081	0.27	0.120	0.072	0.54	0.118	0.148	0.56
9.65	5.0	0.079	0.26	0.121	0.064	0.58	0.139	0.135	0.52
23.0	10.0	0.053	0.187	0.113	0.084	0.41	0.36	0.223	1.03
24.7	5.0	0.047	0.210	0.137	—	0.50	0.29	0.213	—
53.8	5.0	0.031	0.140	0.132	0.055	0.56	0.52	0.181	0.87
				Ave. 0.127±0.006		Ave. 0.55±0.04			

TABLE VII

Relative quenching efficiencies of thiophene and N_2O for $Hg6(^3P_1)$ at 27 ± 2 °C and $I_a = 1.00 \times 10^{14}$ quanta/cc s

[Th], Torr	[N_2O], Torr	[C_2H_6], Torr	$\Phi\{N_2\}$
7.6	77.7	8.0	0.79
10.5	66.2	6.8	0.64
33.1	16.4	1.7	0.205
28.6	11.5	1.2	0.200
59.1	8.62	0.88	0.091

quantitative data. In the presence of O_2, the product quantum yields were not much affected though CO_2 and COS, as well as CO and SO_2, were produced. The CO and SO_2 quantum yields increased with exposure time, and they may be secondary products.

Discussion

The absorption of radiation leads to a π–π^* transition

[c] $\quad Th + h\nu \rightarrow Th^*$

where Th stands for thiophene and Th* is the vibrationally excited, upper singlet state. The Stern–Volmer plots in Fig. 1 show that quenching competes with photodissociation from a state which varies with the energy input to the molecule; this state must be Th*. Furthermore the results in Fig. 1 show that thermal and photolytic energy are equivalent.

Thiophene has 21 oscillators. In the classical limit these would provide 10.3 and 15.7 kcal/mole additional energy at 200 and 305 °C, respectively, over that at 25 °C. However, all the oscillators will not be classical. From Kassel theory computations, the number of effective classical oscillators usually corresponds to 1/2 to 2/3 of the actual number of oscillators. Then the additional thermal energy available at 305 °C would be reduced to 8–11 kcal/mole; at 205 °C, 5–7 kcal/mole. The 2139 Å line is more energetic than the 2288 Å line by 8.7 kcal/mole. Thus if thermal and photolytic energy are equivalent, the room temperature results at 2139 Å should lie between those at 200 and 305 °C at 2288 Å and very near to those at 305 °C and 2288 Å, which indeed they do.

The quenching and decomposition steps are included as follows

[d] $\quad Th^* + M \rightarrow Th + M$

[e] $\quad Th^* \rightarrow I^*$

[f] $\quad \rightarrow Th\ (+h\nu)$

[g] $\quad \rightarrow C_2H_2 + C_2H_2S$

[h] $\quad \rightarrow \cdot CHCHCHCHS\cdot$

[i] $\quad \rightarrow CH_3CCH + CS^*$

Reaction [d] is the normal quenching step, and either reaction [d] or reaction [f] might also lead to triplet thiophene, if that state does not decompose extensively. Reaction [d] could also lead to polymer if the quenching gas is thiophene itself.

The energized intermediate I* is needed as a precursor to $CH_2{=}C{=}CH_2$ formation in order to explain the pressure effect on $\Phi\{CH_2CCH_2\}/\Phi\{C_2H_2\}$. The intermediate I might be the valene intermediate suggested in the studies on arylthiophenes (1). Presumably it is not the triplet state which should be scavenged by O_2, nor the ring-contracted cyclopropene intermediate which should lead to cyclopropene (or propyne if the cyclopropene were formed "hot").

Reactions [f–i] are parallel processes and may proceed through some common precursor, but there is no kinetic need to invoke such a precursor. Steps [g] and [h] are responsible for C_2H_2 and

TABLE VIII

$Hg6(^3P_1)$ sensitized decomposition of thiophene at 25 ± 5 °C and $I_a = 0.92 \times 10^{14}$ quanta/cc s

[Th], Torr	Irradiation time, min	$\Phi\{C_2H_2\} \times 10^3$	$\frac{\Phi\{CH_2CCH_2\}}{\Phi\{C_2H_2\}}$	$\frac{\Phi\{CH_3CCH\}}{\Phi\{C_2H_2\}}$	$\frac{\Phi\{CS_2\}}{\Phi\{C_2H_2\}}$	$\frac{\Phi\{CH_2CHCCH\}}{\Phi\{C_2H_2\}}$
0.45	5.0	12.9	0.053	0.071	0.24	0.41
1.15	10.0	7.8	0.080	0.13	0.26	0.75
2.98	15.0	6.2	0.166	0.23	0.29	1.03
6.0	10.0	6.2	0.23	0.26	0.31	1.49
12.3	11.5	6.6	0.192	0.23	0.23	1.35
26.2	10.0	4.6	0.25	0.28	0.20	1.75
51.3	10.0	3.0	0.26	0.27	0.147	1.57
49.7*	2.0	5.0	0.152	0.172	0.175	1.04

*$[O_2] = 5.27$ Torr, $I_a = 2.35 \times 10^{14}$ quanta/cc s, $\Phi\{CO_2\}/\Phi\{C_2H_2\} = 0.76$, $\Phi\{COS\}/\Phi\{C_2H_2\} = 0.155$, CO and SO_2 are also produced.

Can. J. Chem. Downloaded from www.nrcresearchpress.com by 210.87.254.6 on 09/05/12
For personal use only.

Can. J. Chem. Downloaded from www.nrcresearchpress.com by 210.87.254.6 on 09/05/12
For personal use only.

CH_2CHCCH production, respectively, even though our results with added olefins clearly indicate that sulfur atoms are not produced. The product of reaction [*h*] might be a contracted cyclic compound rather than a biradical, but mechanistic simplicity recommends the latter in the absence of any conclusive evidence. The C_2H_2 cannot come from "hot" CH_2CHCCH, for if it did, then $\Phi\{CH_2CHCCH\}/\Phi\{C_2H_2\}$ would vary with $[CO_2]$ and $[C_2H_4]$ as these quenchers thermalized the "hot" species. The variation of the ratio with [Th] must be interpreted by a chemical reaction rather than an inert gas effect. The subsequent discussion requires that the CS intermediate produced in step [*i*] must be energetic when initially formed and this is designated by the asterisk. Some excitation might also occur by absorption of the radiation by CS, which has a long lifetime and a large extinction coefficient in this region (11).

The intermediate I can either decompose to allene or be deactivated, thus explaining the pressure effect on $\Phi\{CH_2CCH_2\}/\Phi\{C_2H_2\}$.

[*j*] $\quad I^* \rightarrow CH_2CCH_2 + CS^*$

[*k*] $\quad I^* + M \rightarrow Th + M$

Again the CS intermediate is initially energized, the excess energy probably not being the same as from reaction [*i*]. However, for simplicity we shall consider all CS* identical. As before, reaction [*k*] could lead to triplet thiophene or polymer if thiophene is the quenching gas.

CS_2 must come from CS. Since there is an inert gas effect on CS_2 production, presumably the precursor is CS* which can be deactivated and removed as polymer.

[*l*] $\quad CS^* + M \rightarrow CS + M$

[*m*] $\quad nCS \rightarrow (CS)_n$

Reaction [*m*] might occur either in the gas phase or on the wall. The steps leading to CH_2CHCCH production are

[*n*] $\quad CS^* + \cdot CHCHCHCHS\cdot \rightarrow CS_2 + CH_2CHCCH$

[*o*] $\quad 2\cdot CHCHCHCHS\cdot \rightarrow 2CH_2CHCCH + S_2$

[*p*] $\quad Th + \cdot CHCHCHCHS\cdot \rightarrow 2CH_2CHCCH + S_2$

Reaction [*p*] is needed to explain the effect of [Th] on $\Phi\{CH_2CHCCH\}/\Phi\{C_2H_2\}$. These processes require ·CHCHCHCHS· to have a sufficiently long life time for reaction with thiophene. Other sulfur containing biradicals, such as thiodimethylene (12) and thiotetramethylene (13) have long lifetimes as shown by their addition across the double bond of olefins. Hence it is not unreasonable to assume that ·CHCHCHCHS· is also long-lived.

There are two possibilities for the C_2H_2S species. Either it polymerizes all the time or it yields C_2H_2 all the time. The two possibilities are kinetically indistinguishable. We choose the latter by analogy with the ·CHCHCHCHS· species. There is good supporting evidence for this choice. Strausz *et al.* (14) photolyzed $\overline{CH{=}CH{-}N{=}N{-}S}$ and found C_2H_2 and N_2 as the sole gas phase products. The decomposition was shown to proceed through a C_2H_2S intermediate by adding $CF_3C{\equiv}CCF_3$; the C_2H_2 formation was repressed and the adduct of C_2H_2S and $CF_3C{\equiv}CCF_3$ was found. Strausz *et al.* concluded that the structure of C_2H_2S was $\overline{CH{=}CHS}$. The thioketene structure $CH_2{=}C{=}S$ was eliminated since they should have been able to observe it by kinetic absorption spectroscopy in their system, and they did not. (Thioketene is stable as a monomer at -80 °C but polymerizes on warming (15).) The reactions of C_2H_2S become

[*q*] $\quad CS^* + C_2H_2S \rightarrow CS_2 + C_2H_2$

[*r*] $\quad 2C_2H_2S \rightarrow 2C_2H_2 + S_2$

[*s*] $\quad C_2H_2S + \cdot CHCHCHCHS\cdot \rightarrow C_2H_2 + CH_2CHCCH + S_2$

The invariance of $\Phi\{CH_3CCH\}/\Phi\{C_2H_2\}$ with [Th] requires that C_2H_2S does not react with thiophene.

The presence of even small amounts of O_2 drastically reduces CS_2 and CH_2CHCCH. Since this effect cannot possibly be a quenching effect, chemical scavenging of the intermediates must be involved.

[*t*] $\quad O_2 + \cdot CHCHCHCHS\cdot \rightarrow SO_2 + CH_2CHCCH$

[*u*] $\quad O_2 + C_2H_2S \rightarrow SO_2 + C_2H_2$

The COS results from oxidation of CS (16).

[*v*] $\quad CS + O_2 \rightarrow COS + O$

The oxygen atoms may further react to produce CO_2, though this cannot account for all the CO_2. Other photooxidation processes are probably occurring also.

TABLE IX
Summary of rate constant data

Ratio	Value	Units	T, °C	λ, Å	M	Source
k_b/k_a	1.52	None	25	2537	—	Equation [2]
$k_\phi/2k_g$	3.1	None	—	—	—	Equation [3], Fig. 1
$k_d/2k_g$	3.5	$Torr^{-1}$	25	2288	Th	Equation [3], Fig. 1
"	1.24	"	200	2288	"	"
"	0.86	"	25	2139	"	"
"	0.57	"	305	2288	"	"
"	0.064	"	305	2139	"	"
"	2.25*	"	25	2288	CO_2	Equation [3], Figs. 2, 3
"	1.87†	"	25	2288	"	"
"	0.53	"	25	2139	"	"
"	0.41	"	305	2288	"	"
"	3.2	"	25	2288	C_2H_4	Equation [3], Fig. 3
"	0.59	"	25	2139	"	"
"	0.85	"	25	2288	O_2	Equation [3], Figs. 2, 3
"	0.093	"	25	2139	"	"
$k_i/2k_g$	0.128	None	25	2288	Th	Equation [4], Table III
"	0.112*	"	"	"	CO_2	Equation [4], Table IV
"	0.125	"	"	"	CO_2	Equation [4], Table IV
"	0.108	"	"	"	C_2H_4	Equation [4], Table V
"	0.127	"	"	"	O_2	Equation [4], Table VI
"	0.142	"	200	2288	Th	Equation [4], Table III
"	0.147	"	25	2139	Th	Equation [4], Table II
"	0.142	"	"	"	CO_2	Equation [4], Table IV
"	0.144	"	"	"	C_2H_4	Equation [4], Table V
"	0.144	"	"	"	O_2	Equation [4], Table VI
"	0.164	"	305	2288	Th	Equation [4], Table III
"	0.162	"	"	"	CO_2	Equation [4], Table IV
"	0.229	"	305	2139	Th	Equation [4], Table II
k_h/k_g	0.83	None	25	2288	Th	Equation [5], Table III
"	1.10	"	"	"	O_2	Equation [6], Table VI
"	0.94	"	200	2288	Th	Equation [5], Table III
"	1.06	"	25	2139	Th	Equation [5], Table II
"	0.96	"	"	"	O_2	Equation [6], Table VI
"	1.07	"	305	2288	Th	Equation [5], Table III
"	1.42	"	305	2139	Th	Equation [5], Table II
$k_e/2k_g$	0.43	None	25	2288	—	Equation [7], Fig. 4
"	0.40	"	200	2288	—	Equation [7], Fig. 4
"	0.36	"	25	2139	—	Equation [7], Table II
"	0.39	"	305	2288	—	Equation [7], Table III
"	0.34	"	305	2139	—	Equation [7], Table II
k_k/k_j	0.122	$Torr^{-1}$	25	2288	Th	Equation [7], Fig. 4
"	0.030	"	200	2288	"	Equation [7], Fig. 4
"	0.087*	"	25	2288	CO_2	Equation [7], Fig. 5
"	0.064†	"	25	2288	"	Equation [7], Fig. 5
"	0.0183	"	25	2139	"	Equation [7], Fig. 5
"	0.127	"	25	2288	C_2H_4	Equation [7], Fig. 6
"	0.053	"	25	2139	"	Equation [7], Fig. 6
"	0.062	"	25	2288	O_2	Equation [7], Fig. 7
"	0.0068	"	25	2139	"	Equation [9], Fig. 7
k_w/k_j	~0	None	25	2288	O_2	Equation [8], Fig. 7
"	0.33	"	25	2139	O_2	Equation [8], Fig. 7

*[Th] = 0.32 Torr.
†[Th] = 0.95 Torr.

The mechanism outlined above leads to numerous quantitative predictions. The C_2H_2 yield should obey the equation

$$[3] \quad (\Phi\{C_2H_2\})^{-1} = k_\phi/2k_g + k_d[M]/2k_g$$

where $k_\phi \equiv k_e + k_f + k_g + k_h + k_i$. Figure 1 shows plots based on eq. [3] when M is thiophene. The intercepts of all 5 plots are essentially the same and give $k_\phi/2k_g = 3.1$. It is only fortuitous that this ratio is independent of conditions since both k_ϕ and k_g should increase with the energy content of Th*. Apparently they increase proportionately. The slopes of the graphs give $k_d/2k_g$ and these are listed in Table IX. Since k_g

Can. J. Chem. Downloaded from www.nrcresearchpress.com by 210.87.254.6 on 09/05/12
For personal use only.

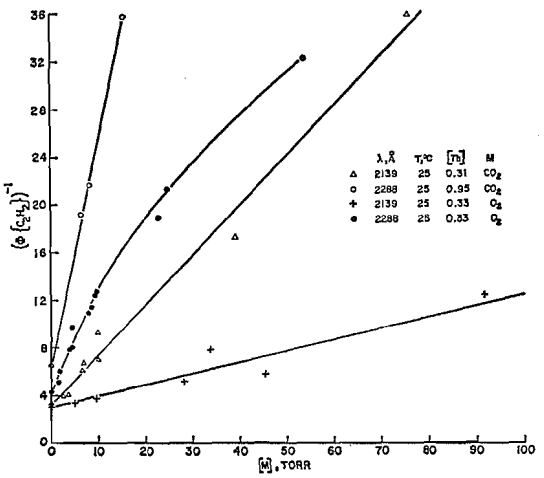

FIG. 2. Plots of the reciprocal acetylene quantum yield vs. the pressure of a foreign gas in the photolysis of thiophene vapor in the presence of foreign gases.

increases with the energy content of Th*, $k_d/2k_g$ drops. Figures 2 and 3 give the Stern–Volmer plots for other chaperone gases. The plots are linear except at low energy content (i.e., 2288 Å and 25 °C) with O_2. Here the falloff in $\Phi\{C_2H_2\}$ is not as rapid as expected at high pressures which suggests that additional oxidation processes are occurring (perhaps of I* or the triplet state) which lead to additional C_2H_2. The low pressure part of the graph is expanded in Fig. 3, and it is linear. The intercepts of each of the plots are different and correspond to the value for the thiophene pressure used at the respective conditions. The slopes give $k_d/2k_g$ and they are also

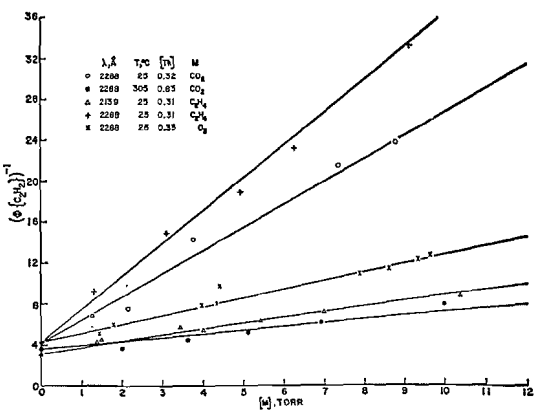

FIG. 3. Plots of the reciprocal acetylene quantum yield vs. the pressure of a foreign gas in the photolysis of thiophene vapor in the presence of foreign gases.

tabulated in Table IX. As with the thiophene, the ratio drops as the energy content of Th* is augmented. The two values for different [Th] at 2288 Å and 25 °C with CO_2 as a chaperone should be the same; within the experimental uncertainty, they are. The relative quenching efficiencies of thiophene, C_2H_4, CO_2, and O_2 are 1.1:1:0.7:0.26 at 25 °C and 2288 Å and 1.5:1:0.9:0.16 at 25 °C and 2139 Å. The quenching efficiencies are in the order expected, i.e. the efficiency increases with the complexity of the quenching molecule. Also it is to be expected that the quenching efficiencies should not be a strong function of the energy content of Th*. Even though $k_d/2k_g$ changes by a factor of 4 to 10 for the two conditions, the relative quenching efficiencies change less than a factor of 2. Finally if quenching occurs with each gas kinetic collision, then the values for $\log k_\phi$ (s^{-1}) vary between about 7 and 8.5, which are reasonable values.

The relative importance of the various decomposition paths [*g*], [*h*], and [*i*] can be obtained directly from the results. The mechanism predicts that

$$[4] \qquad \Phi\{CH_3CCH\}/\Phi\{C_2H_2\} = k_i/2k_g$$

The ratio k_h/k_g can be obtained in two ways. For high values of [Th]

$$[5] \qquad \Phi\{CH_2CHCCH\}/\Phi\{C_2H_2\} \rightarrow k_h/k_g$$

In the presence of O_2, the relationship is

$$[6] \qquad \Phi\{CH_2CHCCH\}/\Phi\{C_2H_2\} = k_h/2k_g$$

The values of $k_i/2k_g$ as obtained from the average value of $\Phi\{CH_3CCH\}/\Phi\{C_2H_2\}$ at each set of conditions are listed in Table IX. The values are independent of the nature of the chaperone gas, as they should be. They increase with the energy content of Th*, indicating that CH_3CCH is energetically more difficult to produce than C_2H_2. This conforms with expectations since CH_3CCH production requires a complex rearrangement of the parent molecule. Table IX also lists the values of k_h/k_g as determined from eqs. [5] and [6] and the data in Tables II–VI. The discrepancy in the values obtained from the two equations is rather large, but probably within the experimental uncertainty. If we accept the values obtained by using eq. [5] then k_h/k_g rises monotonically with the energy content of Th*. This result is somewhat surprising in that it indicates that reaction

Can. J. Chem. Downloaded from www.nrcresearchpress.com by 210.87.254.6 on 09/05/12
For personal use only.

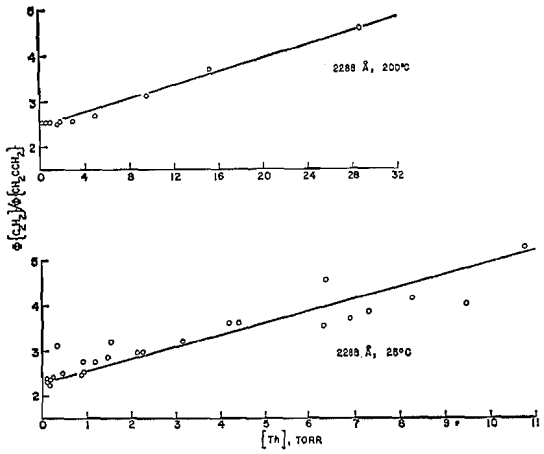

FIG. 4. Plots of the acetylene to allene ratio vs. thiophene pressure in the photolysis of thiophene vapor.

[g] is more favorable, energetically, than reaction [h]; one would have expected the opposite. Incidentally the ratio k_i/k_h rises slightly with energy content of Th*.

Information about the reactions involving the intermediate I* can be obtained from the relationship

$$[7]\quad \Phi\{C_2H_2\}/\Phi\{CH_2CCH_2\} = (2k_g/k_e)(1 + k_k[M]/k_j)$$

Figure 4 is the appropriate plot based on eq. [7] for the two low energy series with no foreign gas. The plots are reasonably linear and the intercepts give $2k_g/k_e$. For the three high-energy series, pressure quenching was too small for plots to be meaningful; however, averages of the low-pressure results for $\Phi\{CH_2CCH_2\}/\Phi\{C_2H_2\}$ give $k_e/2k_g$. The values for $k_e/2k_g$ are listed in Table IX. They diminish as the energy content of I* increases. The fourth entry is about 10% higher than it should be to fit in the progression, but this is probably within the experimental uncertainty. The ratios of slope to intercept for the lines in Fig. 4 give k_k/k_j for the two low-energy series. As expected the value drops from 0.122 $Torr^{-1}$ at 25 °C to 0.030 $Torr^{-1}$ at 200 °C. For higher energy conditions the ratios are so small that accurate values cannot be deduced.

Plots based on eq. [7] are shown in Figs. 5–7, when foreign gases are present. The intercept values do not give $2k_g/k_e$, but rather the value expected for the appropriate pressure of thiophene. The slopes give $(2k_g/k_e)(k_k/k_j)$. With the

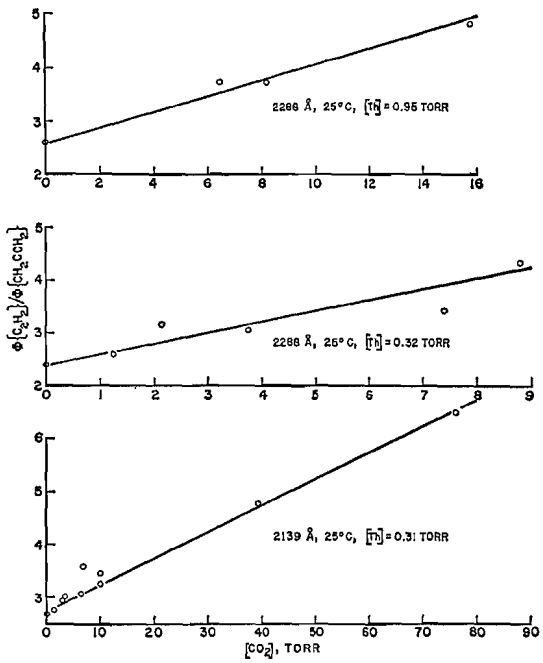

FIG. 5. Plots of the acetylene to allene ratio vs. the pressure of carbon dioxide in the photolysis of thiophene vapor in the presence of carbon dioxide.

values of $2k_g/k_e$ already deduced, values for k_k/k_j can be obtained and they are listed in Table IX. There are abnormalities in the plots for O_2 in Fig. 7. At 25 °C and 2288 Å, the plot deviates from linearity at high pressure though a good straight line prevails at low pressure, as indicated in the expanded plot of the low-pressure portion. The same abnormality was found for quenching

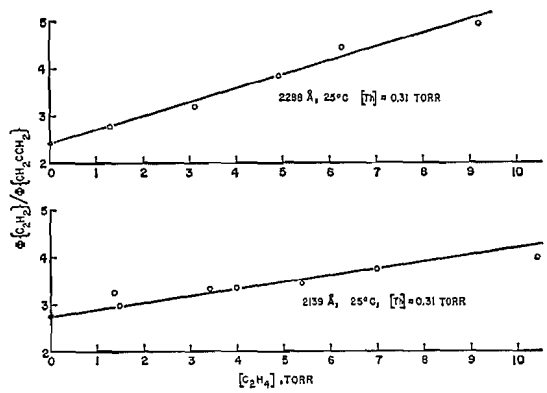

FIG. 6. Plots of the acetylene to allene ratio vs. the pressure of ethylene in the photolysis of thiophene vapor in the presence of ethylene.

Can. J. Chem. Downloaded from www.nrcresearchpress.com by 210.87.254.6 on 09/05/12
For personal use only.

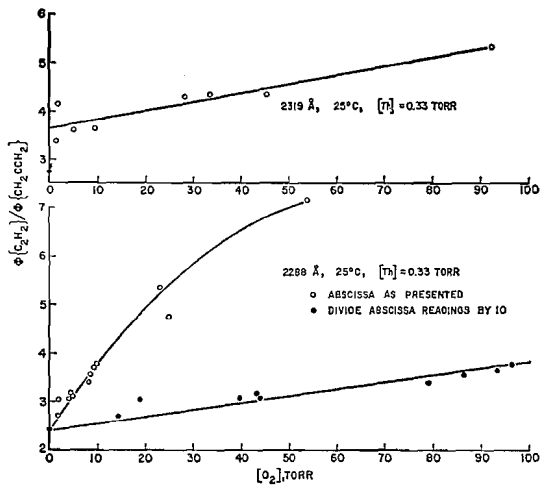

FIG. 7. Plots of the acetylene to allene ratio vs. the pressure of oxygen in the photolysis of thiophene vapor in the presence of oxygen.

of Th* under the same conditions (see Fig. 2); presumably these effects are coupled. An even more serious anomaly exists at 25 °C and 2139 Å. The plot is linear, but the intercept does not correspond to the value in the absence of O_2. Apparently even trace amounts of O_2 inhibit some of the allene production; this must be a scavenging effect rather than a chaperone quenching effect. The proposed mechanism does not explain this scavenging effect. To do so it is necessary to introduce additional steps

$$[w] \qquad I^* \rightarrow B^*$$

$$[x] \qquad B^* \rightarrow CH_2CCH_2 + CS^*$$

$$[y] \qquad B^* + O_2 \rightarrow Th + O_2$$

where B is some other intermediate, perhaps a triplet. Reaction [w] is too slow to be apparent with 2288 Å radiation, but occurs with 2139 Å radiation. From the intercept of Fig. 7, k_w/k_j can be deduced to be 0.33 from the expression

$$[8] \quad k_w/k_j = \Phi_0\{CH_2CCH_2\}/\Phi_0'\{CH_2CCH_2\} - 1$$

where $\Phi_0\{CH_2CCH_2\}$ and $\Phi_0'\{CH_2CCH_2\}$ are $\Phi\{CH_2CCH_2\}$ at zero thiophene pressure in the absence of any foreign gas; $\Phi_0\{CH_2CCH_2\}$, being the true value, and $\Phi_0'\{CH_2CCH_2\}$ being the value obtained from the extrapolation of Fig. 7. In the presence of O_2, these steps lead to the expression

$$[9] \quad \Phi\{C_2H_2\}/\Phi\{CH_2CCH_2\} = (2k_g/k_e)(1 + k_w/k_j + k_k[M]/k_j)$$

The slope of the graph based on eq. [9] multiplied by $k_e/2k_g$ gives k_k/k_j.

The values for k_k/k_j are summarized in Table IX. The two values for CO_2 at 25 °C and 2288 Å should be the same. The discrepancy represents a measure of the experimental uncertainty. As with thiophene, the values for k_k/k_j drop as the energy content rises. As quenchers C_2H_4 and thiophene are equally efficient, CO_2 is less efficient, and O_2 is the least efficient. The relative efficiencies for quenching I* are about the same as for quenching Th*.

The system is too complex to provide a quantitative explanation for CS_2 formation. However since $\Phi\{CS_2\} \leqslant \Phi\{CH_2CCH_2\} + \Phi\{CH_3CCH\}$, all the CS_2 can be explained as coming from CS as a precursor. Nevertheless, at room temperature the equality never holds even at the lowest pressures. Thus all of the CS* cannot have sufficient energy to produce CS_2, even if not deactivated. Presumably the fraction of CS* with sufficient energy should rise with the energy content of Th*, but even this is not so. At 200 °C with 2288 Å radiation $\Phi\{CS_2\}$ at small pressures exceeds that at 25 °C and 2139 Å. Apparently an additional thermal reaction can produce CS_2 at elevated temperatures even from collisionally de-energized CS species or from C_2H_2S (17).

In the presence of O_2, the initial sharp drop in CS_2 formation can be attributed to the scavenging of ·CHCHCHCHS· by O_2. The slower diminution as additional O_2 is added can be caused by deactivation of CS* or scavenging of C_2H_2S or both. However, even at large $[O_2]$, some CS_2 remains; this is difficult to explain.

Some of the CS species react with O_2 to produce COS via reaction [v]. The ratio of COS + CS_2 to CH_2CCH_2 + CH_3CCH is given in Table VI. It never exceeds unity, and is often much less, indicating that other processes may also be occurring, possibly to produce CO_2 or CO.

The results of the mercury sensitized experiments are remarkably similar to those from the direct photolysis. The same products are formed. Also $\Phi\{CS_2\}/\Phi\{C_2H_2\}$ and $\Phi\{CH_2CHCCH\}/\Phi\{C_2H_2\}$ are similar to those values from direct irradiation. Furthermore the addition of O_2 has

Can. J. Chem. Downloaded from www.nrcresearchpress.com by 210.87.254.6 on 09/05/12
For personal use only.

the same effect in both cases; COS, SO_2, CO, and CO_2 are produced, but otherwise nothing much happens. The differences are threefold with Hg sensitization: all the quantum yields are much smaller, the pressure quench is much smaller, and $\Phi\{CH_2CCH_2\}/\Phi\{C_2H_2\}$ and $\Phi\{CH_3CCH\}/\Phi\{C_2H_2\}$ rise with pressure. The first difference is consistent with the fact that less energy is put into the thiophene. The second difference can be explained if there is a small residual decomposition from the vibrationally deactivated excited electronic state. This decomposition would be insignificant for the higher energy radiation but would reduce the pressure quench for the low energy input. Finally the third difference can be explained if the vibrationally thermalized excited electronic state decomposes to the C_3 compounds by a unimolecular process in the second order regime.

We conclude that there is every reason to believe that the same excited electronic levels are involved regardless of the method of excitation. The first state, Th*, is presumably the excited singlet state since it is not scavenged by O_2. For the intermediate I we favor the valene intermediate by analogy with the results on substituted thiophenes, and the fact that cyclopropene is not formed. The state B to which I reverts part of the time is presumably a triplet since it is scavenged by O_2. However, whether it is triplet I or triplet Th has not been resolved.

Acknowledgments

The authors wish to thank Professor O. P. Strausz for suggestions. This work was supported by the U.S. Public Health Service under Grant No. 1 RO1 AP00718-01, for which we are grateful.

1. H. Wynberg, R. M. Kellogg, H. van Driel, and G. E. Beekhuis. J. Am. Chem. Soc. **89**, 3501 (1967).
2. R. M. Kellogg and H. Wynberg. Tetrahedron Letters, **56**, 5895 (1968).
3. R. Srinivasan. J. Am. Chem. Soc. **89**, 1758 (1967).
4. R. Srinivasan. J. Am. Chem. Soc. **89**, 4812 (1967).
5. R. Srinivasan. Pure Appld. Chem. **16**, 65 (1968).
6. H. Hiraoka and R. Srinivasan. J. Chem. Phys. **48**, 2185 (1968).
7. H. Hiraoka and R. Srinivasan. J. Am. Chem. Soc. **90**, 2720 (1968).
8. J. G. Calvert and J. N. Pitts, Jr. Photochemistry. John Wiley and Sons, Inc., New York. 1966.
9. G. Herzberg. Molecular spectra and structure. III. Electronic spectra and electronic structure of polyatomic molecules. D. van Nostrand Co., Inc., Princeton, N.J. 1966. p. 549.
10. H. E. Gunning and O. P. Strausz. Advan. Photochem. **4**, 143 (1966).
11. M. de Sorgo, O. P. Strausz, and H. E. Gunning. Can. J. Chem. **43**, 1886 (1965).
12. H. E. Gunning. Trans. Roy. Soc. Can. **2**, 293 (1964).
13. K. S. Sidhu. Ph.D. Thesis, University of Alberta, Edmonton, Alberta. 1965.
14. O. P. Strausz, J. Font, E. L. Dedio, P. Kebarle, and H. E. Gunning. J. Am. Chem. Soc. **89**, 4805 (1967).
15. H. G. Hammond. U.S. Patent No. 3,035,030. 1962; as reported in Chem. Abstr. **57**, 13617*f* (1962).
16. W. Wood. Unpublished results.
17. E. L. Dedio. Ph.D. Thesis, University of Alberta, Edmonton, Alberta. 1967.

Can. J. Chem. Downloaded from www.nrcresearchpress.com by 210.87.254.6 on 09/05/12
For personal use only.

Can. J. Chem. Downloaded from www.nrcresearchpress.com by 210.87.254.42 on 09/05/12
For personal use only.

Activity coefficients of aqueous thiocyanic acid solutions from electromotive force, transference number, and freezing-point depression measurements

H. E. BARTLETT, A. JURRIAANSE, AND K. DE HAAS
National Nuclear Research Centre, Pelindaba, Private Bag 256, Pretoria, South Africa

Received February 25, 1969

Accurate values of the activity coefficients of thiocyanic acid in aqueous solution have been obtained for concentrations of up to 0.1 molal at 25 °C by combining results for transference-number experiments with those for cells with transport. The transference-number experiments were done with the moving-boundary method, the transference-number at infinite dilution being calculated from measured conductivities of the thiocyanic acid. For the electromotive force (e.m.f.) measurements, conventional glass electrodes were used in conjunction with a high input-impedance electrometer.

The results obtained electrochemically were checked by determining activity coefficients from freezing-point depression measurements which also extended the range of concentrations to 1 molal.

The results of the two types of measurement are in good agreement.

Canadian Journal of Chemistry, 47, 2981 (1969)

Introduction

In earlier work (1), it was found that there was a need for activity coefficients of aqueous thiocyanic acid to be determined over a wide concentration range. This present work describes the determination of these coefficients by electrochemical and freezing-point depression methods.

For the electrochemical determination, a cell with transport had to be used because the only electrode found to be reproducible in the aqueous thiocyanic acid was a glass electrode. Among other electrodes tried were the standard hydrogen electrode (2) and the silver/silver thiocyanate electrode of Vanderzee and Smith (3), but neither of these was satisfactory because the platinum for the hydrogen electrode was poisoned by the thiocyanic acid and the thiocyanate electrode was not sufficiently reproducible in acid media.

Calculation of activity coefficients from e.m.f. data on cells with transport requires a knowledge of accurate transference-number data and, as none of these were available, the transference-numbers of the hydrogen ion and the conductance of the thiocyanic acid had to be determined.

As a check on the electrochemical method, and to extend the range of concentrations, the activity coefficients were also determined by a freezing-point depression method.

Experimental

Reagents

The methyl isobutyl ketone (MIBK) was of B.D.H. laboratory reagent grade and the sodium thiocyanate was Merck pure grade, while all other reagents were of analytical reagent grade.

Procedure

The water used throughout had been triply distilled through quartz apparatus and had a specific conductivity of less than 0.7×10^{-6} mho cm^{-1}.

Preparation of the Thiocyanic Acid

Thiocyanic acid solutions were prepared by mixing equal volumes of 5 *M* sodium thiocyanate and of 5 *M* sulfuric acid with MIBK which extracted the thiocyanic acid from the aqueous phase (1). After 2 or 3 washings of the MIBK with small volumes of water which, it was found, removed all the sulfate and all but a few p.p.m. of the sodium from the organic phase, the thiocyanic acid was back-extracted from the organic phase into water. Any ketone dissolved in the acid was removed by 3 extractions with small volumes of benzene which, in turn, was removed by filtration and by bubbling oxygen-free nitrogen through the acid.

Finally the concentrated acid was diluted to the concentration required and degassed with oxygen-free nitrogen. The concentrations were determined by titration of the acid with sodium hydroxide solutions, regularly standardized against potassium hydrogen phthalate. At the higher concentrations, bromocresol green indicator was used while, at the lower concentrations, titrations were conducted with a pH meter.

Conversions of the concentrations from molarity to molality were effected using the expression

$$\rho = 0.99707 + 0.017\, m$$

This was based on the densities (ρ) of thiocyanic acid solutions as determined at 25 °C with a pycnometer.

It was found necessary to make a fresh sample of acid daily because hydrogen sulfide could be detected above an aqueous solution of the acid that had been left overnight. During the course of 1 day, however, there was no detectable odor over the acid but, with the transference-number experiments in contrast to the other measurements, the acid could not be kept for more than about 3 h before decomposition became evident from the experimental results.

Transference-Numbers

The transference-numbers were determined by the

Can. J. Chem. Downloaded from www.nrcresearchpress.com by 210.87.254.42 on 09/05/12
For personal use only.

moving-boundary method with the sheared rising boundary cell as used by Allgood, Le Roy, and Gordon (4). The tube in which the boundary was formed was about 2.3 mm internal diameter and was marked with a diamond cutter at 1 cm intervals over its entire length of 21 cm.

The tube was calibrated by doing a number of experiments on hydrochloric acid, using KCl solutions as indicators and a silver/silver chloride electrode as described below. The transference-numbers and the data necessary for calculation of the volume correction at the silver/silver chloride cathode were obtained from Longsworth (5).

A number of experiments were also done on hydrochloric acid which had been treated with organic solvents in the same way as the thiocyanic acid had been, but it was found that any solvent that may have remained after degassing with the nitrogen had no measurable effect on the transference-number.

The boundary between the indicator solution (a potassium thiocyanate solution) and the acid was observed by means of the optical system described by Spiro (6), and the cell was immersed in a wide glass tube containing water which was thermostated to 25 °C.

The cathode consisted of a platinum spiral at the end of a ground-glass stopper closing off the one side of the cell. Before the start of an experiment, the platinum spiral was repeatedly dipped into molten silver chloride, thus forming a silver/silver chloride electrode. This electrode was sufficiently deeply immersed in the thiocyanic acid so that no chloride ions reached the boundary between the hydrogen and potassium ions.

The voltage to the cell was supplied either by a d.c. power supply or by a bank of dry batteries. The current was kept only approximately constant and was passed through a standard resistor. The voltage developed across this resistor was converted to a frequency by means of a Dymec Hewlett-Packard voltage-to-frequency converter and the frequency thus generated was integrated on a Hewlett-Packard digital frequency meter. During the experiment, one person observed the motion of the boundary while a second noted down the reading on the digital meter as the boundary passed one of the gradation marks.

By passing a fixed current through a standard resistor for known lengths of time, it was found that this method of current integration described was accurate to within 0.06%.

Before the cell was filled at the start of an experiment, each compartment was rinsed at least 3 times with the acid or the indicator respectively. After being filled, the cell was allowed to stand in the thermostat bath for at least 20 min before the tap shearing the boundary was turned and the potential applied.

Conductivity Measurements

The conductivity of the thiocyanic acid solutions was determined in a Jones' cell, thermostated to 25 °C in an oil bath, using a Wayne Kerr Model B221 impedance bridge which is accurate to 0.1%.

The cell constant was calculated from the measured conductivities of KCl solutions ranging in concentration from 0.2 to 0.01 *M*, using the literature values for the KCl specific conductivities (7).

Electromotive Force Measurements

The electrochemical cell, its method of being filled, and the transferring of the electrodes from one compartment to the other to eliminate the effects of the asymmetry potentials were as described by Covington and Prue (8). However, as electrodes with a resistance sufficiently low to be measured directly with a potentiometer were not available, the potential between two Polymetron type M201 electrodes (resistance about 6 MΩ at 25 °C) was fed into a Keithley Model 610BR electrometer. The scale reading on the electrometer was not sufficiently precise for potential differences greater than 3 mV and so, on the higher ranges, the output from the electrometer recorder points was measured with a Pye Universal Precision potentiometer (Model 7565) which made it possible to attain a higher precision. This output was accurately calibrated against known input potentials from a potentiometer. With this system it was possible to measure any potential up to 30 mV to within a precision of 0.01 mV.

Initially a water-thermostat bath was used but it was found that, on turning the taps isolating the two halves of the transport cell, a leakage path to earth was formed and the measurements of the potentials between the two electrodes were erroneous. This difficulty was obviated by the substitution of a light paraffin for the water.

Freezing-point Measurements

For the freezing-point depression measurements, about 100 ml of the acid in a glass vessel about 5 cm diameter and about 13 cm deep were placed in a Dewar of liquid nitrogen and vigorously stirred so that about 10% of the liquid was frozen into fine ice crystals. The vessel was then transferred to a second Dewar containing a freezing mixture. The top of the vessel was closed with an expanded polystyrene stopper through which passed a Beckmann thermometer and a circular, motor-driven, reciprocating stirrer.

Temperature changes for solutions above 0.1 molal were recorded with a 5 °C Beckmann thermometer graded in 0.01 °C intervals, while for the lower concentrations a 1 °C thermometer graded to 0.002 °C was used. With the 5 °C thermometer, temperatures were estimated to 0.002 °C and with the 1 °C thermometer, to 0.0005 °C.

The temperature was recorded every minute during the course of each experiment, which took between 30 and 50 min, the length of time being controlled by keeping the temperature of the surrounding freezing mixture at 0.1 °C above that of the thiocyanic acid. At the end of the experiment, the differences between the temperatures measured and that of the melting point of pure ice, separately determined with the appropriate thermometer, were plotted as a function of time. The resultant curves were extrapolated according to the method of Sidorova and Baiteryakova (9) to obtain the freezing-point depression at the particular concentration.

Results and Discussion

Transference-Numbers

From the number of coulombs q needed to move the boundary through successive 10 cm lengths, and from the volume V of the tube over

Can. J. Chem. Downloaded from www.nrcresearchpress.com by 210.87.254.42 on 09/05/12
For personal use only.

TABLE I

Results of e.m.f. measurements*

m_2 (moles kg^{-1})	E (mV)	t^-	$\log \frac{\gamma_2}{\gamma_1}$	$\log \frac{\gamma_2}{\gamma_1} - \Delta \log \gamma^{st}$
0.09343	0.49	0.1504	0.0043	+0.0009
0.08672	1.07	0.1505	0.0042	−0.0025
0.08074	1.58	0.1506	0.0066	−0.0033
0.06545	3.05	0.1509	0.0154	−0.0035
0.04612	5.60	0.1513	0.0247	−0.0080
0.03559	7.45	0.1517	0.0340	−0.0079
0.03033	8.59	0.1519	0.0400	−0.0072
0.02940	8.86	0.1520	0.0387	−0.0095
0.01947	11.86	0.1526	0.0510	−0.0094
0.01425	14.13	0.1532	0.0610	−0.0075
0.00854	18.01	0.1545	0.0703	−0.0095
0.00502	22.09	0.1556	0.0782	−0.0111

*$m_1 = 0.1006$ moles kg^{-1}, $t_1 = 0.1503$.

the particular length, the transference numbers t^+ were calculated from the equation

$$t^+ = 96\,488 \times c \times \frac{V}{q}$$

where c is the molar concentration of the acid.

Because of the instability of the thiocyanic acid, it was not possible to prepare sufficient acid for a number of determinations at one particular concentration. Hence the acid, after preparation, was diluted to approximately the concentration required, the experiment carried out, and the result tabulated for the nearest round-number concentration. This procedure is justified as the variation of the transference-number with concentration is not rapid.

From weight changes of the cathode it was established that, under the experimental conditions, the electrode functioned as a silver/silver chloride electrode. Hence, the volume corrections for transference-numbers were calculated from the data given by Longsworth (5) for the partial molar volume for hydrochloric acid and for the molar volumes of silver and of silver chloride. However, the calculated corrections were negligible and have not been taken into consideration.

No solvent corrections were made as it was assumed that the conductivity of the water used could be attributed to carbonic acid, the ionization of which would be suppressed by the thiocyanic acid.

The results of the transference-number experiments are presented in Fig. 1 and Table I.

Conductivity Measurements

The results of the conductivity measurements

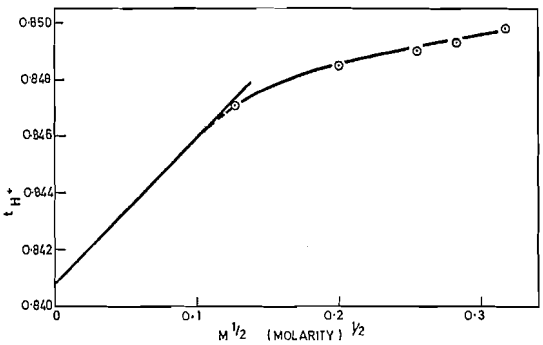

FIG. 1. Variation of the transference-number of the hydrogen ion at 25 °C in an aqueous thiocyanic acid (t_{H^+}) as a function of the square root of the molarity ($M^{\frac{1}{2}}$). The straight line is calculated from the Onsager limiting law.

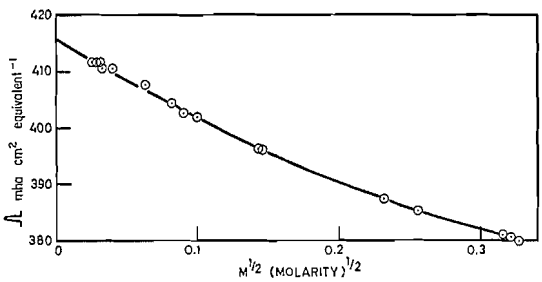

FIG. 2. The equivalent conductance of thiocyanic acid at 25 °C as a function of the square root of the molarity.

are presented graphically in Fig. 2, where the equivalent conductance of the acid is plotted as a function of the square root of the molarity.

The variation in the equivalent conductance Λ as a function of concentration, c, can be expressed

Can. J. Chem. Downloaded from www.nrcresearchpress.com by 210.87.254.42 on 09/05/12
For personal use only.

by the relationship proposed by Robinson and Stokes (10)

$$\Lambda = \Lambda^0 - \frac{B_1\Lambda^0 + B_2\sqrt{c}}{1 + Ba\sqrt{c}}$$

where Λ^0 is the equivalent conductance at infinite dilution, B_1, B_2, and B are constants, while a is the mean diameter of the ions in the thiocyanic acid (in Å). Numerical values chosen for the constants at 25 °C are (from Robinson and Stokes (10)): $B_1 = .2300$ mole$^{-\frac{1}{2}}$ $1^{\frac{1}{2}}$; $B_2 =$ 60.65 cm^2 ohm^{-1} equivalent^{-1}(l/mole)$^{\frac{1}{2}}$; $B =$ 0.3291 Å^{-1} mole$^{-\frac{1}{2}}$ $1^{\frac{1}{2}}$. It was found, by an iterative method with an IBM 360 computer, that the values for a and Λ^0 that best fitted the equation were $a = 3.8$ Å and $\Lambda^0 = 416.0 \pm 0.5$ ohm^{-1}cm^2 equivalent^{-1}.

From this value for the equivalent conductance at infinite dilution and from a value of 349.8 ohm^{-1} cm^2 equivalent^{-1} (10) for the limiting equivalent conductance of the hydrogen ion at 25 °C, the value for the limiting transference-number of the hydrogen ion in thiocyanic acid at 25 °C is 0.8409. This value is plotted on Fig. 1 and the line of slope given by the Onsager limiting law (6) is drawn through this point.

Activity Coefficients from E.M.F. Data

After elimination of the effects of the asymmetry potentials of the electrodes, the e.m.f. of the cell

glass electrode |HSCN(m_1)|HSCN(m_2)| glass electrode

is given by the expression

$$E = \frac{2RT}{F}\int_{m_1}^{m_2} t^- \, \mathrm{d} \ln m\gamma$$

where γ is the mean ionic activity coefficient of the thiocyanic acid at molality m and t^- is the value of the transport number of the thiocyanate ion.

Putting $t^- = t_1 + \Delta t$, where t_1 is the transport number of the thiocyanate ion at a fixed molality m_1 (at 25 °C)

$$\log\frac{\gamma_2}{\gamma_1} = \frac{-E}{t_1 \times 0.1183} - \log\frac{m_2}{m_1} - \frac{1}{t_1}\int_{m_1}^{m_2}\Delta t \, \mathrm{d} \log m - \frac{1}{t_1}\int_{\gamma_1}^{\gamma_2}\Delta t \, \mathrm{d} \log \gamma$$

The values of the integrals are obtained by numerical integration, the last term, which is very small, being elucidated by using preliminary values for γ_2 and γ_1 obtained from the expression, with the fourth term eliminated.

Covington and Prue (8) have shown that γ can be given by a Debye-Hückel expression

$$\log\gamma = -\frac{Am^{\frac{1}{2}}}{1 + m^{\frac{1}{2}}} + bm$$

where A is the Debye-Hückel constant taken as having a value of 0.5115 at 25 °C, and b is an empirical constant. Hence

$$\log\frac{\gamma_2}{\gamma_1} = -\frac{Am_2^{\frac{1}{2}}}{1 + m_2^{\frac{1}{2}}} + \frac{Am_1^{\frac{1}{2}}}{1 + m_1^{\frac{1}{2}}} + b(m_2 - m_1)$$

The quantity $-Am_2^{\frac{1}{2}}/(1 + m_2^{\frac{1}{2}}) + Am_1^{\frac{1}{2}}/(1 + m_1^{\frac{1}{2}})$ is defined as $\Delta \log \gamma^{st}$ and therefore

$$\log\frac{\gamma_2}{\gamma_1} - \Delta \log \gamma^{st} = b(m_2 - m_1)$$

In Table I the results of the e.m.f. measurements are given, and in Fig. 3 the values of $\log\gamma_2/\gamma_1 - \Delta \log\gamma^{st}$ against $(m_2 - m_1)$ are plotted. The line in Fig. 3 does not pass through the origin but this is probably due to small errors in the preparation of the solution m_1 of fixed molality.

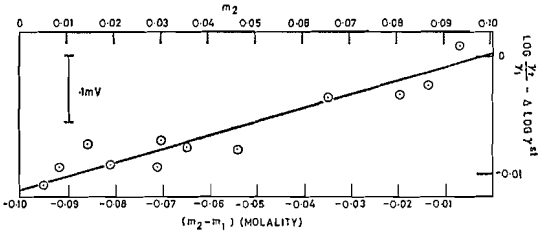

FIG. 3. $\log\gamma_2/\gamma_1 - \Delta \log\gamma^{st}$ as a function of $(m_2 - m_1)$.

From the gradient of the line in Fig. 3, the value of b was determined by least squares analysis as 0.12 ± 0.05. This is the value used in the calculation of the mean activity coefficients at round-number concentrations shown in Table II.

Activity Coefficients from Freezing-point Depression Data

For calculation of γ from the freezing-point depression, θ, for solutions of molality m, the

TABLE II

Mean activity coefficients of aqueous thiocyanic acid from e.m.f. measurements at 25 °C and from freezing-point depression data

Concentration (moles kg^{-1})	Mean activity coefficients	
	At 25 °C	At freezing point
0.001	0.965	—
0.005	0.926	—
0.01	0.901	0.902
0.02	0.869	0.870
0.03	0.848	0.849
0.04	0.831	0.833
0.05	0.818	0.820
0.06	0.807	0.810
0.07	0.797	0.800
0.08	0.788	0.793
0.09	0.781	0.786
0.10	0.775	0.779
0.20	—	0.745
0.30	—	0.734
0.40	—	0.730
0.50	—	0.730
0.60	—	0.730
0.70	—	0.732
0.80	—	0.734
0.90	—	0.736
1.00	—	0.739

Randall and Vanselow expression (11)

$$[1] \quad \log \gamma = \int_0^m -j \, \mathrm{d} \log m - \frac{j}{2.303} + \frac{0.00025}{\nu} \int_0^m \frac{\theta}{m} \, \mathrm{d}\theta$$

was used, j being defined by the equation

$$j = 1 - \frac{\theta}{\nu \lambda m}$$

where λ is the molal lowering of the freezing point and has a value of 1.860 and ν is the number of ions into which the molecule ionizes in solution.

The first expression on the right hand side of the eq. [1] is not directly integrable as there is no exact analytical expression for the variation of j with $\log m$. Furthermore, a numerical integration between the limits m and 0 is not possible as $\log m$ is indeterminate at $m = 0$. However, up to a concentration of 0.01 molal, Randall and Vanselow (11) have shown that an equation

$$[2] \quad \log j = \log \beta + \alpha \log m$$

holds for uni-univalent electrolytes with the constant α equal to approximately 0.5.

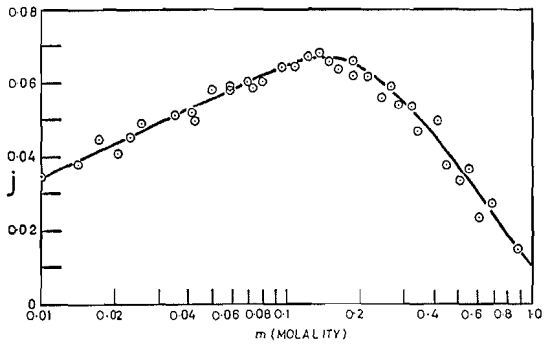

FIG. 4. Values of j plotted as a function of log molality.

Hence, in this work, below a concentration of 0.01 M a straight line with a slope of 0.5 (α) was fitted to a plot of $\log j$ vs. $\log m$ and β obtained as the intercept at $\log m = 0$.

Therefore, elucidation of the integral over the whole concentration range was achieved by use of eq. [2] up to 0.01 molal and numerical integration thereafter.

The value of the third term on the right hand side of eq. [1] was also numerically integrated but it was found that this term only became significant at concentrations above 0.1 molal.

The results are presented in Fig. 4 where the values of j are plotted against $\log m$, and in Table II, the values of the mean activity coefficients are presented at round-number concentrations.

From this Table it can be seen that the results from the freezing-point depression data are marginally higher than those from the e.m.f. measurements. However, it is estimated that the calculated error in b, which is the greatest source of uncertainty in the calculation of the values of the activity coefficients, makes a difference of about 1% to the activity coefficients at 0.1 molal but only about 0.1% at 0.01 molal. These are about the differences between the activity coefficients as determined electrochemically and from the freezing-point depression data. Hence, nothing can be said about the significance of the difference between the data obtained at the two different temperatures.

Acknowledgment

We are indebted to Mr. H. C. Ridderhof for his fabrication of the glass apparatus.

1. A. JURRIAANSE and D. M. KEMP. Talanta, **15**, 1287 (1968).

Can. J. Chem. Downloaded from www.nrcresearchpress.com by 210.87.254.42 on 09/05/12
For personal use only.

2. G. J. HILLS and D. J. G. IVES. *In* Reference electrodes. *Edited by* Ives and Janz. Academic Press, Inc., New York. 1961. Chap. 2.
3. C. E. VANDERZEE and W. E. SMITH. J. Am. Chem. Soc. **78**, 721 (1956).
4. R. W. ALLGOOD, D. J. LE ROY, and A. R. GORDON. J. Chem. Phys. **8**, 418 (1940).
5. L. G. LONGSWORTH. J. Am. Chem. Soc. **54**, 2741 (1932).
6. M. SPIRO. Technique of organic chemistry. Vol. I. Part IV. *Edited by* A. Weissberger. Interscience Publishers, Inc., New York. 1960. Chap. 46.
7. G. W. C. KAYE and T. H. LABY. Tables of physical and chemical constants. 12th ed. Longmans, Green and Co., Ltd., London. 1958.
8. A. K. COVINGTON and J. E. PRUE. Chem. Soc. 3701 (1955).
9. E. E. SIDOROVA and L. KH. BAITERYAKOVA. Russ. J. Phys. Chem. English Transl. **39**, 1521 (1965).
10. R. A. ROBINSON and R. H. STOKES. Electrolyte solutions. Butterworths, London. 1959.
11. M. RANDALL and A. P. VANSELOW. J. Am. Chem. Soc. **46**, 2418 (1924).

Can. J. Chem. Downloaded from www.nrcresearchpress.com by 210.87.254.42 on 09/05/12
For personal use only.

Can. J. Chem. Downloaded from www.nrcresearchpress.com by 210.87.254.105 on 09/05/12
For personal use only.

Reaction of methyl radicals with *cis*-butene-2

NOBUO YOKOYAMA AND R. K. BRINTON[1]
Department of Chemistry, University of California, Davis, California
Received February 3, 1969

Methyl radicals generated by di-*t*-butylperoxide pyrolysis interact at comparable rates with *cis*-butene-2 in the gas phase by both addition and hydrogen atom abstraction. The determination of the rate of these reactions was simplified by the addition of a large concentration of acetaldehyde to the system. The additive, a source of low activation energy abstractable hydrogen atoms, was effective in suppressing polymerization reactions, and in addition, maintained a high steady state methyl radical concentration as a result of the carbonyl radical decomposition. The rate constants, k_5 and k_6 for the reactions [5] and [6], were determined to be $4.5 \times 10^{10} \exp(-7000/RT)$ and $1.8 \times 10^{10} \exp(-7300/RT)$

[5] $CH_3^{\cdot} + \text{C}_4\text{H}_8 \longrightarrow \text{C}_5\text{H}_{11}^{\cdot}$

[6] $\text{C}_5\text{H}_{11}^{\cdot} \longrightarrow CH_4 + \text{C}_4\text{H}_7^{\cdot}$

$cm^3\ mole^{-1}\ s^{-1}$, respectively, over the temperature range 126–163 °C. The butenyl radical formed in reaction [6] isomerizes much faster than its interaction with other species in the system, and the distribution of the various conformations is similar to the equilibrium distribution of the butenes at a similar temperature.

Canadian Journal of Chemistry, 47, 2987 (1969)

Introduction

The study of the vapor phase reaction of methyl radicals with ethylene (1*a*) and propylene (1*b*) is herein extended to the analogous reaction with *cis*-butene-2. Although a number of studies have been made on the reaction between methyl radicals and butenes (2–7), none has dealt in detail with the complicated sequence of radical reactions which occurs in the interaction. In addition, quantitative treatment of the experimental data to obtain kinetic parameters for the methyl radical addition to the butene molecule depends, in all these studies, on various simplifying assumptions as to the relative importance of certain reactions in the total mechanism scheme. The validity of such assumptions cannot, in general, be definitely established experimentally, and the best measure for the significance of the absolute magnitude of the addition parameters evaluated is a correspondence between the values obtained by rather widely different experimental techniques involving dissimilar types of assumptions. For this reason the present study involving a somewhat different technique to that used in previous investigations should offer an important check on the interconsistency of the kinetic data.

The major complication in all studies of the addition of radicals to olefins is produced by the formation of an adduct radical rather than a stable molecule in the primary step. These adduct radicals may add again to the olefin in a chain type polymerization or interact at any stage of the polymerization, in a very complicated fashion, with any of the many types of radicals in the system. In this investigation, a simplification of the reaction mechanism was attained by adding large quantities of acetaldehyde to a di-*t*-butyl peroxide (methyl radical source)/*cis*-butene-2 gaseous system. This technique is similar to the "aldehyde method" used by Trotman-Dickenson and co-workers (8) to study the addition of various alkyl radicals to multiple bonds. Under such conditions, addition polymerization is minimized by the active competition for all radicals in the system by acetaldehyde which furnishes opportunity for a low activation energy hydrogen abstraction of the carbonyl hydrogen. In addition, the methyl radical steady state concentration is maintained at a high level by the decomposition of the acetyl radical formed in the abstraction process, and as a consequence, combination reactions of all radicals with methyl radicals are enhanced. Such combinations lead to easily

[1]Author to whom request for reprints should be addressed.

identified and analyzed products which allow a much easier assessment of the total products resulting from the pentyl radical formed in the primary methyl radical to *cis*-butene-2 addition.

Experimental

The reaction system and procedure for its use were similar to those described earlier (1). The two component system, di-*t*-butyl peroxide (DTBP) + *cis*-C_4H_8-2, or the three component system, DTBP + *cis*-C_4H_8-2 + CH_3CHO, were formed by pressure–volume measurement of the gaseous components followed by thorough mixing in a 2 l glass bulb. Reaction was initiated by expansion of a mixture into a 1 l glass reaction bulb contained in a silicone oil thermostat. Reaction was terminated by a subsequent expansion into a calibrated sample bulb at room temperature.

In many of the early experiments a large amount of the CH_3CHO contained in the three component products was removed by a condensation and polymerization on moist KOH pellets, but this step was eliminated in later work when it was found that on the proper gas chromatographic column, CH_3CHO did not interfere with any step of the analytical procedure. The products were separated by temperature fractionation using a vacuum system with Ward still-traps and a gas buret. These fractions were analyzed, for the most part, using gas chromatographic techniques wherein the evaluation was made from previously prepared standard curves. Details of the analysis of the various fractions follow.

−210 °C

This fraction consisted of CH_4 with CO additionally present when CH_3CHO was added. It was measured by gas buret and analyzed by temperature fractionation after the CO had been converted to CO_2 in a CuO furnace. Analysis was checked on some samples by mass spectrometric methods.

−145 °C

This fraction consisting of C_2 and C_3 hydrocarbons (mainly C_2H_6) was effectively temperature separated from C_4 and higher hydrocarbons as well as from oxygenated products. The fraction was analyzed on an alumina column at 80 °C.

−78 °C

The C_4–C_6 hydrocarbons, CH_3CHO, $(CH_3)_2CO$, and a part of the $CH_3COC_2H_5$, $(CH_3)_3COH$, and a small amount of DTBP were contained in this fraction. Analysis was made by use of an adiponitrile on firebrick column at 0 °C. Oxygen containing compounds, for which no quantitative measure was made, were retained sufficiently to effect the separation of most of the hydrocarbons. In cases where hydrocarbons were not sufficiently separated to allow quantitative estimation, the effluent was condensed at −196 °C and reanalyzed at 25 °C on a dinonylphthalate column which produced separation approximately in order of the boiling points.

Residue

This fraction consisted of DTBP, the remainder of the $(CH_3)_2CO$, $(CH_3)_3COH$, and $CH_3COC_2H_5$ as well as C_8–C_{10} hydrocarbons. Analysis was accomplished at 80 °C on a 0.75 mm inner diameter by 150 m stainless steel capillary column coated with didecylphthalate. Analysis of this fraction was not regularly carried out on the pyrolysis products because of the difficulty of identification and calibration.

The *cis*-butene-2 used in this study was Phillip's research grade of specified 99.87% purity. The impurity, mainly *trans*-C_4H_8-2, was not removed, but proportionate correction was always made for the contamination in the product analyses. Eastman Organic Chemicals' CH_3CHO contained two impurities of the order of 0.01–0.001%, probably polymerization inhibitors, as well as a number of hydrocarbons in very low concentration (3–600 p.p.m.). In initial experiments an attempt was made to correct for those substances in the reaction products. This procedure was unsatisfactory, and CH_3CHO used in the later pyrolyses was purified by gas chromatography on an adiponitrile–firebrick preparative column, a procedure which eliminated all detectable impurities. The CH_3CHO was stored and handled using all due precaution to eliminate formation of paraldehyde as well as the low temperature polymer formed when CH_3CHO is cooled below its freezing point. Di-*t*-butyl peroxide from K and K Laboratories contained trace impurities of CH_3COCH_3, $CH_3COC_2H_5$, and $(CH_3)_3COH$, presumably from gradual decomposition of DTBP. Inasmuch as the rates of formation of these substances were not followed in the present investigation, their presence was considered to have negligible effect, and no serious attempt at their removal was made except a bulb-to-bulb distillation with only center fraction retention. Matheson C. P. grade (99.0% minimum purity) *trans*-C_4H_8-2 and C_4H_8-1 were used as received. Correction for small quantities of isomeric butene impurities was made in the reaction products.

The data for the studies made at 125.8, 136.8, 150.2, and 163.0 °C are shown in Table I. Rates and calculated kinetic data listed are based on average rates ($\Delta C/\Delta t$) and average concentration of a component during the course of the reaction. *cis*-Butene-2 disappearance was always small, ca. 1–3% so the average concentration approximation could cause little error. Decomposition of DTBP (ca. 10–15%) and CH_3CHO reaction (ca. 5–20%) was, however, appreciable. An exact analysis of the errors made in using average rates and concentrations in the treatment of a complicated reaction mechanism is quite difficult. It was concluded, at least in the case of somewhat simplified mechanisms, that concentration changes up to 25–30% caused errors no larger than 2–3% in the values of reaction constants so evaluated. Time of pyrolysis was 320 min at 125.8 °C, 80 min at 136.8 °C, 20 min at 150.2 °C, and 5 min at 163.0 °C except for exp. 331 (25 min), exp. 332 (12.5 min), and exp. 431 (400 min).

Results and Discussion

The pyrolysis of DTBP in the gas phase is described by the following mechanism

[1] $(CH_3)_3COOC(CH_3)_3 \rightarrow 2(CH_3)_3CO^{\bullet}$

Can. J. Chem. Downloaded from www.nrcresearchpress.com by 210.87.254.105 on 09/05/12
For personal use only.

Can. J. Chem. Downloaded from www.nrcresearchpress.com by 210.87.254.105 on 09/05/12
For personal use only.

[2] $(CH_3)_3CO^{\cdot} \rightarrow CH_3COCH_3 + CH_3^{\cdot}$

[3] $2CH_3^{\cdot} \rightarrow C_2H_6$

[4] $CH_3^{\cdot} + (CH_3)_3COOC(CH_3)_3 \rightarrow CH_4 + (CH_3)_3COO(CH_3)_2CH_2^{\cdot}$

In presence of *cis*-C_4H_8-2, $CH_3^{\cdot}$ reacts at about comparable rates by addition and H atom abstraction

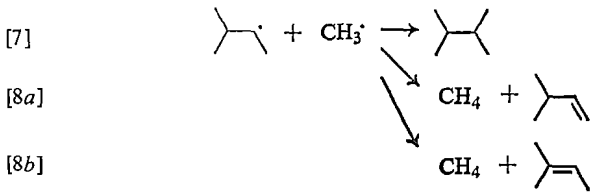

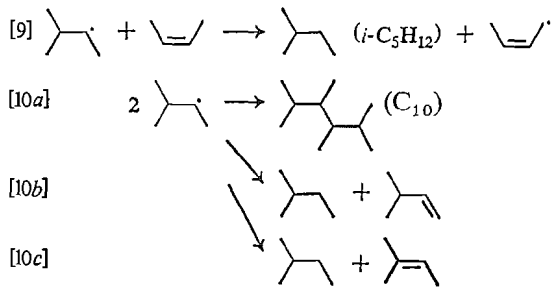

Other minor reactions, some leading to the same products, also occur and discussion concerning such possibilities will be given in later sections of this paper.

The butenyl radical, But$^{\cdot}$, from reactions [6] and [9], is capable of an allylic type resonance and, in addition, rotation may occur about the central bond.

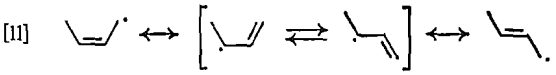

These species may be treated as if three isomeric forms were available for subsequent reaction, and isomeric products result from their interaction with other radicals present in the system, e.g.

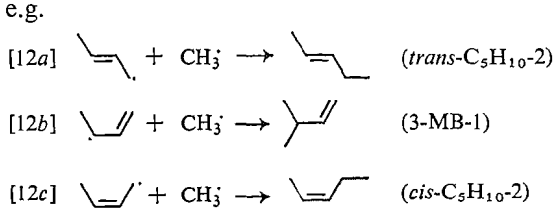

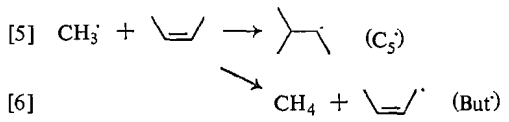

An alternate to reaction [6], hydrogen abstraction from the vinyl position, was not observed to any significant extent. The fate of the pentyl radical, $C_5^{\cdot}$, from reaction [5] can be summarized by

and by H atom abstraction

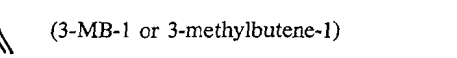

and [13*b*] and [13*c*] analogously.

However, this latter process with *cis*-butene-2 as RH leads to no net change in But$^{\cdot}$ concentration or distribution if the butenyl radical isomerization is much faster than the abstraction process. Combination reactions of butenyl radicals among themselves as well as with the $C_5^{\cdot}$ radical lead to many C_8–C_9 hydrocarbons. Although the $C_5^{\cdot}$ radicals showed a ready ability to disproportionate with loss of an H atom, e.g. reactions [8*a*, *b* – 10*b*, *c*], a careful inspection of the pyrolysis products for butadienes-1,2 and -1,3 indicated that an analogous reaction of But$^{\cdot}$ either did not occur at all, or at most, certainly occurred only to an extent of a few % of the comparable $C_5^{\cdot}$ disproportionation.

The assessment of the rates of reactions [5] and [6], which is necessary for the determination of the activation energies of these two reactions, is possible by determining all products resulting from $C_5^{\cdot}$ and But$^{\cdot}$ interaction with active species in the system. As pointed out above, the many C_8–C_9 hydrocarbon products are not negligible and are, in addition, difficult to analyze. Furthermore, addition of any radical in the system to the *cis*-butene-2 substrate is possible, and the result of such addition reactions is to form products of high molecular weight which further complicate the analytical procedures. As pointed out earlier,

Can. J. Chem. Downloaded from www.nrcresearchpress.com by 210.87.254.105 on 09/05/12
For personal use only.

TABLE I

Rates of formation of products in DTBP–*cis*-C_4H_8-2–CH_3CHO pyrolyses*

Experiment No.	201	211	212	213	214	215	216	217	218	221	222	223
Temperature (°C)	150.2	150.2	150.2	150.2	150.2	150.2	150.2	150.2	150.2	150.2	150.2	150.2
[DTBP]	5.37	4.11	4.11	4.21	4.29	1.36	1.30	1.46	1.41	4.21	3.06	1.35
[*cis*-C_4H_8-2]	0	2.00	8.09	12.70	4.26	2.00	6.24	14.0	11.0	2.10	5.44	4.07
[CH_3CHO]	0	0	0	0	0	0	0	0	0	40.6	59.4	59.8
Rates	Values											
R_{CH_4}	29.0	53.7	154.5	214	67.9	28.6	58.8	106.7	88.7	5150	6040	4010
R_{CO}										6060	6850	4860
$R_{C_2H_6}$	990	728	544	500	717	238	162	114.5	132	619	393	179
$R_{i\text{-}C_5H_{12}}$				13.1		0.587	3.39	9.79	7.76	13.55	41.2	23.6
$R_{trans\text{-}C_4H_8\text{-}2}$				3.39		0.742	1.42	1.03	3.59	2.57	5.75	3.04
R_{C_6}				97.8		15.4	27.3	42.7	42.3	10.8	15.7	5.98
$R_{trans\text{-}C_5H_{10}\text{-}2}$				61.0		8.38	17.3	27.6	24.8	13.2	24.6	11.4
$R_{cis\text{-}C_5H_{10}\text{-}2}$				48.8		6.57	13.9	21.8	19.4	10.4	18.1	8.25
$R_{2\text{-MB-}2}$				6.68		1.09	1.96	3.73	3.04		1.90	0.589
$R_{3\text{-MB-}1}$				49.6		5.06		22.2	16.0		12.4	7.81
$R_{3\text{-MB-}1[But\cdot]}$				35.8		4.91	10.15	16.2	14.4	7.75	14.4	6.69
$R_{3\text{-MB-}1[C_5\cdot]}$				13.8		0.15		6.0	1.6		0	1.12
$R_{High[C_5\cdot]}$				23.8		1.14	5.85	20.2	16.1	0.367	1.46	0.540
$R_{High[But\cdot]}$				35.5		1.47	8.83	31.0	23.1	1.07	5.16	2.38
$R_{C_5\cdot}$				155.2		18.4	40.5	82.4	70.8	24.7	60.3	31.8
$R_{But\cdot}$				186.5		22.5	52.5	98.3	87.4	36.5	71.5	33.6
$R_{CO}/R_{CH_4[CH_3CHO]}$										1.19	1.15	1.23

Can. J. Chem. Downloaded from www.nrcresearchpress.com by 210.87.254.105 on 09/05/12
For personal use only.

TABLE I (*Continued*)

Experiment No.	224	225	226	227	228	231	213′	213″	301	311	312	313
Temperature (°C)	150.2	150.2	150.2	150.2	150.2	150.2	150.2	150.2	163.0	163.0	163.0	163.0
[DTBP]	1.35	1.30	0.392	4.06	1.48	1.32	4.21	2.08	5.85	1.43	1.37	1.35
[*cis*-C_4H_8-2]	4.08	14.0	0.760	12.3	8.41	8.14	13.2	6.81	0	6.35	9.80	3.39
[CH_3CHO]	33.8	59.5	59.4	61.1	63.0	0	0	63.5	0	0	0	0
Rates	Values											
R_{CH_4}	2330	3390	2180	6040		88.8			100	204	2.53	113
R_{CO}	2770	3720	2490	7470								
$R_{C_2H_6}$	176	150	52.4	408	145	140			4400	878	6.62	905
$R_{i\text{-}C_5H_{12}}$	19.2	65.3	3.27	86.5	54.1	10.4				8.10	14.7	3.61
$R_{trans\text{-}C_4H_8\text{-}2}$	2.84	8.92	0.62	12.4	7.50	1.31				4.15	6.24	2.32
R_{C_6}	9.80	9.84		41.0	9.72	38.0				105	135	57.2
$R_{trans\text{-}C_5H_{10}\text{-}2}$	12.9	23.3	0.85	53.5	19.5	23.1				47.0	61.5	29.4
$R_{cis\text{-}C_5H_{10}\text{-}2}$	8.08	18.8	0.64	41.8	14.2	17.9				38.7	47.2	24.2
$R_{2\text{-}MB\text{-}2}$	0.708	1.72	0	2.26	0.956	2.60				5.85	7.53	3.47
$R_{3\text{-}MB\text{-}1}$		15.5	0.50	32.6	11.2	14.5				39.0	43.4	22.6
$R_{3\text{-}MB\text{-}1[But\cdot]}$	7.57	13.7	0.502	31.4	11.4	13.6				29.5	38.6	18.5
$R_{3\text{-}MB\text{-}1[C_5\cdot]}$		1.8	0.	1.2	0	0.90				9.5	4.8	4.1
$R_{High[C_5\cdot]}$	1.07	2.15	0	8.41	1.84	12.5				13.2	28.8	4.09
$R_{High[But\cdot]}$	3.11	12.2	0.0371	26.0	8.55	17.9				14.5	31.4	5.15
$R_{C_5\cdot}$	31.5	80.8	3.27	139.4	66.6	64.4				141.6	190.8	72.5
$R_{But\cdot}$	36.2	86.3	3.03	172.5	65.7	74.5				136.4	188.8	81.1
$R_{CO}/R_{CH_4[CH_3CHO]}$	1.21	1.15	1.15	1.28								

Can. J. Chem. Downloaded from www.nrcresearchpress.com by 210.87.254.105 on 09/05/12
For personal use only.

TABLE I (*Continued*)

Experiment No.	321	322	323	324	331	332	401	411	412	413	421	422
Temperature (°C)	163.0	163.0	163.0	163.0	163.0	163.0	136.8	136.8	136.8	136.8	136.8	136.8
[DTBP]	1.30	0.370	0.288	2.65	0.280	0.302	4.65	0.565	2.10	0.950	0.563	0.926
[*cis*-C_4H_8-2]	10.1	0.970	0.590	12.4	0.584	0.576	0	1.73	8.26	4.92	1.72	3.88
[CH_3CHO]	63.4	64.9	61.0	64.1	67.3	65.3	0	0	0	0	61.5	46.9
Rates	Values											
R_{CH_4}	9500	6310	4980	14650	4040	4210	7.35	3.94	33.5	12.1	866	800
R_{CO}	11300	7490	5830	17500	4710	5440					984	896
$R_{C_2H_6}$	576	218	155	989	109	136	191	15.5	48.1	20.1	15.6	21.2
$R_{i\text{-}C_5H_{12}}$	145	10.9	6.26	200	5.67	5.65		0.204	3.21	1.16	2.73	5.75
$R_{trans\text{-}C_4H_8\text{-}2}$	22.3	3.06	1.49	31.2	1.58	1.62		0.254	0.953	0.421	0.626	1.33
R_{C_6}	34.1	0.795	0.443	78.0	0.424	0.162		1.98	12.6	6.04	0.135	1.07
$R_{trans\text{-}C_5H_{10}\text{-}2}$	77.4	3.20	1.22	98.9	1.51	1.26		1.44	9.34	3.95	0.833	2.56
$R_{cis\text{-}C_5H_{10}\text{-}2}$	55.9	2.45	0.916	73.8	1.13	0.929		1.04	6.42	2.83	0.617	1.86
$R_{2\text{-}MB\text{-}2}$	2.41	0.127	0	4.82	0.0668	0		0.141	1.10	0.545	0	0.175
$R_{3\text{-}MB\text{-}1}$	54.0		0.760	60.4	0.570	0.800		1.09	6.76	3.08	0.484	2.05
$R_{3\text{-}MB\text{-}1[But\cdot]}$	48.6	2.01	0.766	62.0	0.949	0.790		0.844	5.46	2.31	0.487	1.50
$R_{3\text{-}MB\text{-}1[C_5\cdot]}$	5.4		0	0	0	0.01		0.246	1.3	0.77	0	0.55
$R_{High[C_5\cdot]}$	6.38	0.0154	0.00478	12.33	0.00779	0.00185		0.339	4.44	2.27	0.0090	0.178
$R_{High[But\cdot]}$	34.0	0.148	0.0313	37.0	0.0660	0.0324		0.569	7.44	3.42	0.129	0.978
$R_{C_5\cdot}$	193.3	11.9	6.71	285.2	6.17	5.82		2.91	22.7	10.8	2.88	7.72
$R_{But\cdot}$	252.3	12.8	5.36	322.6	6.23	5.65		4.30	30.1	13.2	3.06	9.00
$R_{CO}/R_{CH_4[CH_3CHO]}$	1.23	1.19	1.19	1.24							1.14	1.15

Can. J. Chem. Downloaded from www.nrcresearchpress.com by 210.87.254.105 on 09/05/12
For personal use only.

TABLE I (*Concluded*)

Experiment No.	423	431	501	511	512	521	522	523	531	232	233
Temperature (°C)	136.8	136.8	125.8	125.8	125.8	125.8	125.8	125.8	125.8	150.2	150.2
[DTBP]	0.361	0.302	4.50	4.40	4.18	3.42	0.751	0.395	0.410	1.32	1.36
[*cis*-C_4H_8-2]	2.12	0.582	0	17.0	8.39	5.68	2.42	1.80	0.821	11.2†	11.1‡
[CH_3CHO]	54.4	62.1	0	0	0	62.5	61.8	61.5	62.6	0	0
Rates						Values					
R_{CH_4}	537	465	1.87	28.4	15.3	700	344	247	229	737	71.1
R_{CO}	597	575				880	425	318	306		
$R_{C_2H_6}$	9.55	6.93	41.1	15.6	21.5	18.2	3.61	1.78	2.12	69.8	104
$R_{t\text{-}C_5H_{12}}$	2.49	0.714		4.10	2.23	6.40	1.39	0.717	0.379		11.9
$R_{trans\text{-}C_4H_8\text{-}2}$	0.775	0.103		0.714	0.336	1.18	0.489	0.300	0.153	16.8	
R_{C_6}	0.177	0.0133		8.30	6.15	0.930	0.0860	0.0324	0.0101		54.5
$R_{trans\text{-}C_5H_{10}\text{-}2}$	0.670	0.127		6.17	4.28	2.53	0.411	0.185	0.158		18.6
$R_{cis\text{-}C_5H_{10}\text{-}2}$	0.490	0.126		4.84	3.22	1.89	0.312	0.140	0.119	17.3	14.3
$R_{2\text{-}MB\text{-}2}$	0.0552	0		0.991	0.565	0.152	0.0342		0		4.21
$R_{3\text{-}MB\text{-}1}$	0.383	0.0746		4.32	2.83	1.62	0.266	0.106	0.0925		
$R_{3\text{-}MB\text{-}1[But\cdot]}$	0.392	0.0744		3.62	2.50	1.43	0.241	0.108	0.0925		
$R_{3\text{-}MB\text{-}1[C_5\cdot]}$	0	0.002		0.70	0.33	0.19	0.025	0	0		
$R_{High[C_5\cdot]}$	0.0159	0.00031		6.08	2.31	0.174	0.0124	0.00425	0.00090		
$R_{High[But\cdot]}$	0.140	0.00839		10.8	3.76	1.09	0.140	0.0566	0.0331		
$R_{C_5\cdot}$	2.74	0.729		20.2	11.6	7.85	1.55	0.754	0.390		
$R_{But\cdot}$	2.91	0.499		26.5	14.3	8.78	1.87	0.958			
$R_{CO}/R_{CH_4[CH_3CHO]}$	1.13					1.28	1.24	1.29			

*All rates in units of mole cm^{-3} s^{-1} × 10^{13}. All initial concentrations in units of mole cm^{-3} × 10^7.
†C_4H_8-1 instead of *cis*-C_4H_8-2.
‡*trans*-C_4H_8-2 instead of *cis*-C_4H_8-2.

Can. J. Chem. Downloaded from www.nrcresearchpress.com by 210.87.254.105 on 09/05/12
For personal use only.

it should be possible to minimize the occurrence of such complicating reactions if large amounts of acetaldehyde, a source of easily abstractable H atom, were added to the system. With this objective in view, a detailed investigation of the effect of acetaldehyde on the *cis*-butene-2/DTBP system was undertaken.

A. The Reactivities of Pentyl and Butenyl Radicals with CH_3CHO

In the two component system the major reaction of both $C_5^{\cdot}$ and But$^{\cdot}$ is combination with $CH_3^{\cdot}$ by reactions [7] and [12], respectively, leading to C_6 and the three corresponding pentenes. In presence of appreciable amounts of CH_3CHO, hydrogen abstraction from the aldehyde

[14] 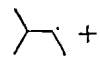 + $CH_3CHO \rightarrow i\text{-}C_5H_{12} + CH_3CO^{\cdot}$

[15*a*] 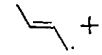 + $CH_3CHO \rightarrow trans\text{-}C_4H_8\text{-}2 + CH_3CO$

and [15*b*, *c*] (analogous reactions involving other butenyl radical forms) lead to an increase in $i\text{-}C_5H_{12}$ as well as isomeric butenes and a relative decrease in C_6 and pentenes. However, it is readily seen from the data of Table I that the ratio, $i\text{-}C_5H_{12}/C_6$, increases rapidly with increase in CH_3CHO added, while the increase in *trans*-C_4H_8-2/*trans*-C_5H_{10}-2 is rather insensitive to change in CH_3CHO. This behavior indicates that $C_5^{\cdot}$ and But$^{\cdot}$ abstract H atoms with greatly differing facility. To obtain an estimate of the abstraction rate constants it is to be observed that C_6 is formed by a single process, reaction [7], while $i\text{-}C_5H_{12}$ is formed not only through interaction with CH_3CHO, reaction [14], but also by reaction [9] and other radical–radical interactions. As CH_3CHO concentration is increased, reaction [14] becomes predominant, reaction [7] is still significant because of the high $CH_3^{\cdot}$ concentration from $CH_3CO^{\cdot}$ decomposition, but other reactions contributing to $i\text{-}C_5H_{12}$ formation become relatively unimportant. Thus

$$[16]\quad R_{i\text{-}C_5H_{12}} \approx k_{14}[C_5^{\cdot}][CH_3CHO] + k_9[C_5^{\cdot}][cis\text{-}C_4H_8\text{-}2]$$

$$[17]\quad R_{C_6} = k_7[C_5^{\cdot}][CH_3^{\cdot}]$$

$$[18]\quad R_{C_2H_6} = k_3[CH_3^{\cdot}]^2$$

and

$$[19]\quad \frac{R_{i\text{-}C_5H_{12}}R_{C_2H_6}^{1/2}}{R_{C_6}[cis\text{-}C_4H_8\text{-}2]} \approx \frac{k_{14}k_3^{1/2}[CH_3CHO]}{k_7[cis\text{-}C_4H_8\text{-}2]} + \frac{k_9k_3^{1/2}}{k_7}$$

In this case an average value of $[CH_3CHO]$ is used based on the assumption that all $CH_3CO^{\cdot}$ produced decomposed to $CH_3^{\cdot}$ and CO, an approximation which may be justified in the temperature range above 120 °C by the results of several previous investigations (9). Thus

$$[20]\quad [CH_3CHO]_{ave} = [CH_3CHO]_{initial} - \tfrac{1}{2}R_{CO}\Delta t$$

A similar treatment for the production of *trans*-C_4H_8-2 gives

$$[21]\quad \frac{R_{trans\text{-}C_4H_8\text{-}2}R_{C_2H_6}^{1/2}}{R_{trans\text{-}C_5H_{10}\text{-}2}[cis\text{-}C_4H_8\text{-}2]} \approx \frac{k_{15a}k_3^{1/2}[CH_3CHO]}{k_{12a}[cis\text{-}C_4H_8\text{-}2]} + \frac{k_{13a}k_3^{1/2}}{k_{12a}}$$

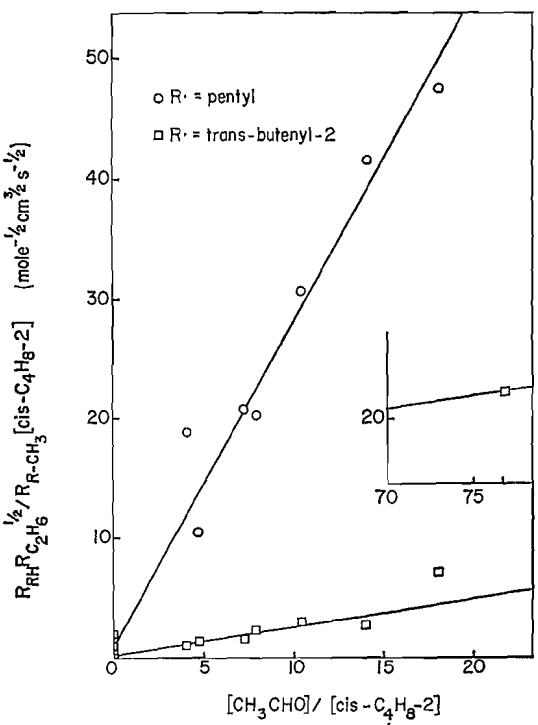

FIG. 1. The reactivities of pentyl and butenyl radicals with CH_3CHO.

Can. J. Chem. Downloaded from www.nrcresearchpress.com by 210.87.254.105 on 09/05/12
For personal use only.

In Fig. 1 the quantities on the left of eqs. [19] and [21] are plotted vs. $[CH_3CHO]/[cis\text{-}C_4H_8\text{-}2]$. The slopes $k_{14}k_3^{1/2}/k_7$ and $k_{15a}k_3^{1/2}/k_{12a}$ are found to be 2.7 and 0.22 $(cm^3\ mole^{-1}\ s^{-1})^{1/2}$, respectively, at 150.2 °C. The intercepts on the ordinate would evaluate $k_9k_3^{1/2}/k_7$ and $k_{13a}k_3^{1/2}/k_{12a}$ to be 0.8 and 0.3, but the extrapolation is subject to large errors so that these latter values are of doubtful significance. If it is further assumed that $CH_3^{\cdot}$ combination rates with $C_5^{\cdot}$ and But$^{\cdot}$ are about equal

$$[22] \qquad k_7 \approx k_{12a}$$

then $k_{14}/k_{15a} \approx 12.5$ and, for what it is worth, $k_9/k_{13a} \approx 2.5$. These relationships indicate that H atom abstraction from both CH_3CHO and *cis*-C_4H_8-2 is considerably faster by $C_5^{\cdot}$ than by But$^{\cdot}$. Support for the assumption shown in reaction [22] is indicated by the equivalence of the ratio, C_6/*trans*-C_5H_{10}-2, in the three component system to the ratio of the formation of $C_5^{\cdot}$ to But$^{\cdot}$ in the two component system evaluated in a later section.

B. The Origin of 3-Methylbutene-1

The 3-MB-1 was formed both from $C_5^{\cdot}$ through reaction [8*a*] and other similar disproportionations as well as from But$^{\cdot}$ through reaction [12*b*]. This may be represented as

$$[23] \qquad R_{3\text{-MB-1}} = R_{3\text{-MB-1}[C_5^{\cdot}]} + R_{3\text{-MB-1}[But^{\cdot}]}$$

As seen in the previous discussion, the reactivity of the two radicals with CH_3CHO differs widely. Hence, when the concentration of CH_3CHO is increased sufficiently, the $C_5^{\cdot}$ steady state concentrations could be expected to be reduced to the point where $R_{3\text{-MB-1}[C_5^{\cdot}]}$ becomes negligibly small but $R_{3\text{-MB-1}[But^{\cdot}]}$ is still significant. Thus in the presence of sufficiently large enough amounts of CH_3CHO, But$^{\cdot}$ reactions furnish the only measurable source of 3-MB-1.

$$[24] \qquad R_{3\text{-MB-1}} \approx R_{3\text{-MB-1}[But^{\cdot}]}$$

Inasmuch as the ratio, $R_{3\text{-MB-1}[C_5^{\cdot}]}/R_{2\text{-MB-2}}$, is controlled by k_{8a}/k_{8b} and analogous disproportionation ratios, when $R_{2\text{-MB-2}} = 0$, so should $R_{3\text{-MB-1}[C_5^{\cdot}]}$. In exps. 226, 323, 332, 421, and 531 (Table I), $R_{2\text{-MB-2}}$ was indeed reduced to zero, and eq. [24] should apply. In addition, it is clear according to reactions [11] and [12], that $R_{3\text{-MB-1}[But^{\cdot}]}/R_{trans\text{-}C_5H_{10}\text{-}2}$ should remain constant at a given temperature regardless of the relative concentration of reagents as long as the equilibrium between the various forms of the But$^{\cdot}$ is maintained. Then

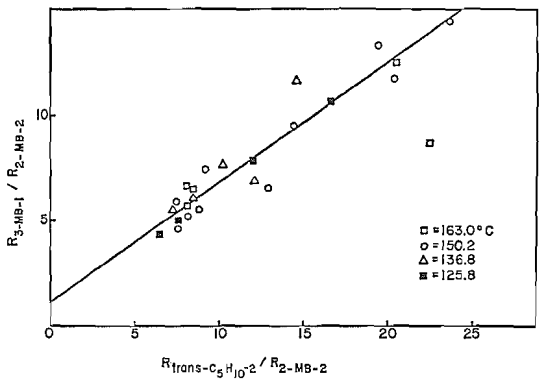

FIG. 2. The origin of 3-methylbutene-1.

$$[25] \qquad \gamma = R_{3\text{-MB-1}[But^{\cdot}]}/R_{trans\text{-}C_5H_{10}\text{-}2}$$

may be obtained when $R_{2\text{-MB-2}} = 0$, and γ thus obtained under these special conditions should apply to all experiments at a similar temperature. By arrangement of eqs. [23] and [25]

$$[26] \qquad \frac{R_{3\text{-MB-1}}}{R_{2\text{-MB-2}}} = \frac{R_{3\text{-MB-1}[C_5^{\cdot}]}}{R_{2\text{-MB-2}}} + \gamma\frac{R_{trans\text{-}C_5H_{10}\text{-}2}}{R_{2\text{-MB-2}}}$$

when $R_{2\text{-MB-2}} \neq 0$. The ratio, $R_{3\text{-MB-1}}/R_{2\text{-MB-2}}$ is plotted vs. $R_{trans\text{-}C_5H_{10}\text{-}2}/R_{2\text{-MB-2}}$ in Fig. 2 for data at various temperatures. The slopes and ordinate intercepts of Fig. 2 obtained by a least squares method are tabulated in Table II. It is seen that the value of γ is essentially independent of temperature, and the variation in the value obtained for the intercept at the various temperatures probably merely indicates the extent of the error in determining this parameter. Nevertheless, the corresponding intercept and γ value were used at each temperature to divide the total

TABLE II

Parameters for the origin of 3-MB-1

Temperature (°C)	Slope(*a*)	Ordinate intercept	γ
163.0	0.56	1.07	0.63
150.2	0.58	0.76	0.59
136.8	0.68	0.55	0.59
125.8	0.62	0.40	0.56

Can. J. Chem. Downloaded from www.nrcresearchpress.com by 210.87.254.105 on 09/05/12
For personal use only.

3-MB-1 yield according to eqs. [23] and [25] into amounts attributable to each type of origin. These data are included in Table I. In certain cases involving small overall yields of 3-MB-1 the values of $R_{3\text{-MB-1}[C_5\cdot]}$ calculated from $R_{trans\text{-}C_5H_{10}\text{-}2}$ and a corresponding γ came out with negative values. Such irregularities result from the quantities involved being of the same order as the accuracy of the analytical methods. For these experiments the values of $R_{3\text{-MB-1}[C_5\cdot]}$, certainly small, were assumed to be zero.

C. The Disproportionation Behavior of the $C_5\cdot$ Radical

The data of Table II indicate that the intercepts of Fig. 2, $R_{3\text{-MB-1}[C_5\cdot]}/R_{2\text{-MB-2}}$, do not have a consistent trend with temperature, and as already suggested, could best be interpreted as a single value ca. 0.8 ± 0.3 independent of temperature. It is seen from the possible disproportionation mechanism for the $C_5\cdot$ radical and methyl radical, as in reactions [8*a*, *b*], that $C_5\cdot$ is capable of giving up a hydrogen atom in two different ways. Although other radicals may disproportionate with $C_5\cdot$ in a manner similar to the interaction with $CH_3\cdot$, the transfer of H atom by $C_5\cdot$ in these cases is strictly analogous to the exchange with the $CH_3\cdot$ radical. Thus

$$[27] \qquad R_{3\text{-MB-1}[C_5\cdot]}/R_{2\text{-MB-2}} \approx k_{8a}/k_{8b}$$

There have been many reports on the disproportionation–combination ratio for various pairs of radicals (10, 11) in order to understand the relationship of disproportionation to the bond involved. However, such ratios, because of the wide variation in the absolute value of the combination rate constants (12), may lead to misleading conclusions concerning relative disproportionation tendencies. In the present study the relative split of the $C_5\cdot$ radical between two competing disproportionation mechanisms is unambiguously given by the value of the Fig. 2 intercept, although, to be sure, not with high precision. Calvert and co-workers (13, 14) proposed, from a study of disproportionation between the various butyl radical isomers, that the split would occur in a manner proportional to the number of available H atoms on the carbon atoms adjacent to the radical site. This rule would predict $R_{3\text{-MB-1}[C_5\cdot]}/R_{2\text{-MB-2}} = 3$ for the $C_5\cdot$ disproportionation instead of the 0.8 obtained. Data collected subsequent to Calvert and co-worker's original postulate indicate strongly that the rule is certainly qualitative in nature, and the present test involving a competition for a single tertiary H atom or three primary H atoms indicates a complete lack of conformity.

D. Pentene Formation from Butenyl–Methyl Radical Combination

The combination of $CH_3\cdot$ and $But\cdot$ results in the formation of three pentene isomers as indicated in reactions [12*a*, *b*, *c*]. If the internal rotation of $But\cdot$ about the central bond is much faster than the radical–radical combination, the three pentenes should be produced, at a single temperature, in constant ratio independent of reaction conditions. In addition, if the activation energies of reactions [12*a*, *b*, *c*] are zero or all equal to each other, the constancy of pentene isomer ratio should persist in spite of changes in temperature as well. In the previous analysis of the 3-MB-1 formation, it was shown that $\gamma = R_{12b}/R_{12a} = 0.59$ independent of temperature over the range 126–163 °C. In Fig. 3 is plotted $R_{cis\text{-}C_5H_{10}\text{-}2}$ vs. $R_{trans\text{-}C_5H_{10}\text{-}2}$. Here again the data are consistent with a similar interpretation, and $R_{12c}/R_{12a} = 0.76$ independent of temperature over a similar range. Further support for the rapid rotational equilibrium of the butenyl radical is shown by the results of exp. 233 which involves the reaction of *trans*-C_4H_8-2 and DTBP. The ratio, $R_{cis\text{-}C_5H_{10}\text{-}2}/R_{trans\text{-}C_5H_{10}\text{-}2}$ has the same value, 0.78, even though the original butenyl radical was of opposite steric configuration. Con-

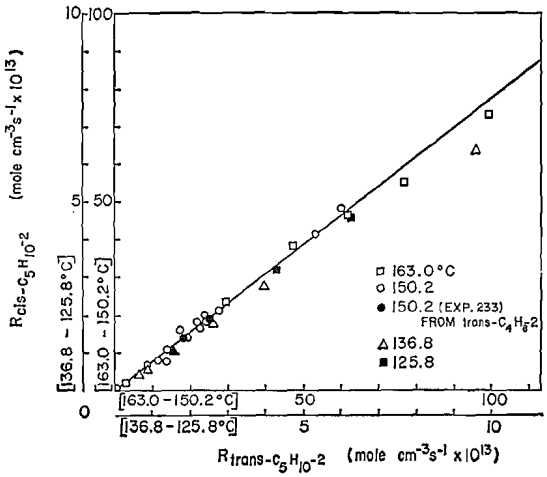

FIG. 3. The formation of *cis*- and *trans*-pentene-2.

Can. J. Chem. Downloaded from www.nrcresearchpress.com by 210.87.254.105 on 09/05/12
For personal use only.

trary evidence concerning butenyl radical isomerization was obtained by Walling and Thaler (15) who reported complete retention of the *cis–trans* configuration of But· in the liquid phase at 40 °C. Holroyd and Klein (16) reported a similar result at −88 °C. It seems probable within the range 40–125 °C that a region exists wherein the rotation rate may be effectively measured by a kinetic study.

E. Combination of Butenyl and Pentyl Radicals

Combination of C_5· and the three isomeric But· radicals should form a decane, three nonenes, and six octadienes. Search was made for these products in exps. 213, 213′, and 213″. Three of the octadiene isomers were positively identified and the presence of the other seven products was tentatively established by the retention times. In view of the difficulty entailed in carrying out such analyses on a quantitative basis, it was decided to calculate the rates of formation of these products for their use in calculations to be made in the next section. These evaluations are based on the premise that the cross combination ratio (12), $R_{ab}/R_{aa}^{1/2}R_{bb}^{1/2} = k_{ab}/k_{aa}^{1/2}k_{bb}^{1/2} = 2$, a result justified by fairly extensive experimental evidence, but not easily predicted quantitatively by a priori theory. Although no direct confirmation is available that this relationship is valid for the radicals under consideration, the results of the calculations do agree quite well with the limited experimental data of exps. 213, 213′, and 213″. By use of the rates of formation of C_2H_6, C_6, *cis*- and *trans*-C_5H_{10}-2, and 3-MB-1 [But·], the quantity of C_5· and But· radicals which disappeared by formation of these C_8–C_{10} hydrocarbons could be estimated.

$$[28] \quad \text{High } C_5\cdot = \sum_{C_9C_{10}} C_5\cdot = 2C_{10} + \sum \text{nonenes}$$

$$[29] \quad \text{High But}\cdot = \sum_{C_8C_9} \text{But}\cdot = \sum \text{nonenes} + 2\sum \text{octadienes}$$

Results of these calculations are also included in Table I.

F. The Rates of the Primary Reactions

Maintenance of a steady state concentration of C_5· in the system allows the rate of C_5· formation to be evaluated in terms of its product formation rates,

$$[30] \quad R_{C_5\cdot} = k_5[CH_3][cis\text{-}C_4H_8\text{-}2] = R_{C_6} + R_{i\text{-}C_5H_{12}} + R_{2\text{-MB-2}} + R_{3\text{-MB-1}[C_5\cdot]} + R_{\text{High } C_5\cdot}$$

The values of $R_{C_5\cdot}$, calculated from the individual terms of eq. [30] given in Table I, are plotted vs. $R_{C_2H_6}{}^{1/2}[cis\text{-}C_4H_8\text{-}2]$ in Figs. 4 and 5. In order to make it clear that the last term of eq. [30] is merely calculated according to the postulate of the preceding section, this portion of the rate is indicated by a vertical line for the 150.2 °C data displayed in Fig. 4. In the reactions containing no CH_3CHO, this portion amounts to as much as 25% of the total (exp. 217). The corrections for those experiments which contain added CH_3CHO are in almost all cases very minor. The corrected values, both with and without CH_3CHO, lie to within the limits of experimental error on a single line, an indication that the correction procedure is valid.

Ignored in the above expression is the second step addition of C_5· to the *cis*-C_4H_8-2 substrate to yield a nonyl radical (C_9·). This radical could in turn combine and disproportionate with CH_3·

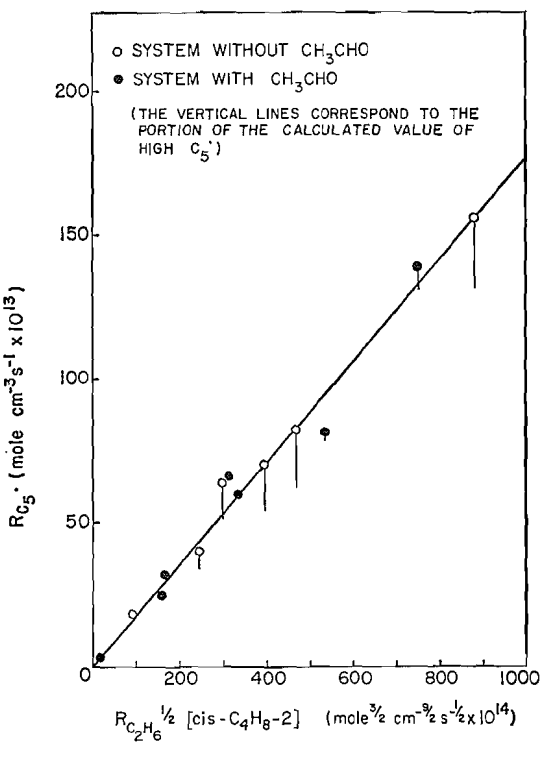

FIG. 4. Pentyl radical formation at 150.2 °C.

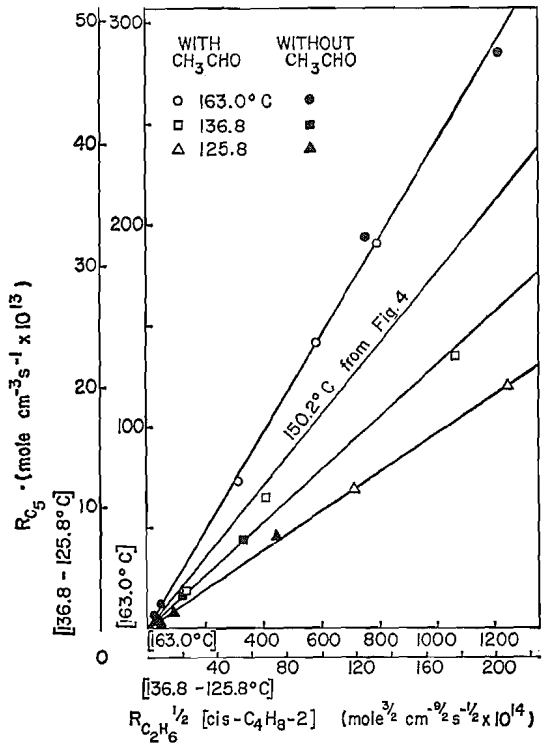

FIG. 5. Pentyl radical formation at other temperatures.

and other radicals in the system. The relative rates of formation of pentyl and nonyl radical, $R_{C_5\cdot}/R_{C_9\cdot}$ may be shown to be approximately equal to $R_{C_2H_6}/R_{C_6}$ if the rates of addition of the two radicals to *cis*-C_4H_8-2 are equal. Furthermore, this result would represent a minimum value of this rate, since it is to be predicted that $C_5\cdot$ would add more slowly than $CH_3\cdot$. Calculation of the values of $R_{C_2H_6}/R_{C_6}$ from the data of Table I shows the very strong influence of added CH_3CHO in minimizing the second stage addition to *cis*-C_4H_8-2. In general, experiments without CH_3CHO showed calculated $C_5\cdot$ addition to be of significant magnitude, ~15–40% as great as the comparable $CH_3\cdot$ addition. Experiments conducted with added CH_3CHO had almost negligible $C_5\cdot$ addition, ~0–3%. Conditions most favorable for minimizing second step addition are low concentrations of DTBP and *cis*-C_4H_8-2, and high CH_3CHO concentration. Inspection of the curves of Figs. 4 and 5 does not indicate the kind of difference between the two and three component systems that is predicted in the above argument. It must be concluded that $C_5\cdot$ radicals are much less active than $CH_3\cdot$ in adding to *cis*-C_4H_8-2.

The rate of But· formation may be formulated analogously as

$$[31]\quad R_{But\cdot} = R_{trans\text{-}C_5H_{10}\text{-}2} + R_{cis\text{-}C_5H_{10}\text{-}2} + R_{3\text{-}MB\text{-}1[But\cdot]} + R_{Butenes} + R_{High\ But\cdot}$$

$R_{Butenes}$ represents the formation of three butene isomers by H atom abstraction reactions of But· reactions [13*a*, *b*, *c*], from molecules such as *cis*-C_4H_8-2 and CH_3CHO as well as disproportionation reactions between But· and other radicals, mainly $C_5\cdot$. Of these three isomers *trans*-C_4H_8-2 was regularly measured; C_4H_8-1 was partially separated and identified, but could not be quantitatively determined by gas chromatography because of its small magnitude and incomplete separation from *i*-C_5H_{12}. It was possible to identify *cis*-C_4H_8-2 in the products from exps. 232 and 233, reactions conducted with C_4H_8-1 and *trans*-C_4H_8-2, but again quantitative estimation was unsuccessful. Consequently the distribution of butenes was calculated from the amount of *trans*-C_4H_8-2 experimentally determined combined with the corresponding thermodynamic equilibrium distribution data for the butenes recently reported by Golden, Egger, and Benson (17).

$$[32]\quad R_{Butenes} = \alpha R_{trans\text{-}C_4H_8\text{-}2}$$

α = 1.63(163.0 °C), 1.60(150.2 °C), 1.58(136.8 °C), 1.56(125.8 °C)

Although such an approximation probably leads to small errors in the amounts of the butene isomers so calculated, their total amount is generally not appreciable and no great differences result in the overall But· formation rate.

Unlike the expression developed for $R_{C_5\cdot}$, eq. [30], the above expression for $R_{But\cdot}$, eq. [31], does not directly apply to a single process for the formation of But·, $R_6 = k_6[CH_3][cis\text{-}C_4H_8\text{-}2]$, but also includes But· generated by H atom abstraction by other radicals, mainly $C_5\cdot$ and But·, from *cis*-C_4H_8-2. Thus $R_{But\cdot}$ represents a maximum value possible for R_6. In addition, the effect of a second step addition of But· to *cis*-C_4H_8-2 is again ignored. An argument similar to the one used for the second step $C_5\cdot$ addition would apply here also, and in this case the addition would produce an octenyl radical (Oct·). The minimum value of the ratio of rates of formation

Can. J. Chem. Downloaded from www.nrcresearchpress.com by 210.87.254.105 on 09/05/12
For personal use only.

Can. J. Chem. Downloaded from www.nrcresearchpress.com by 210.87.254.105 on 09/05/12
For personal use only.

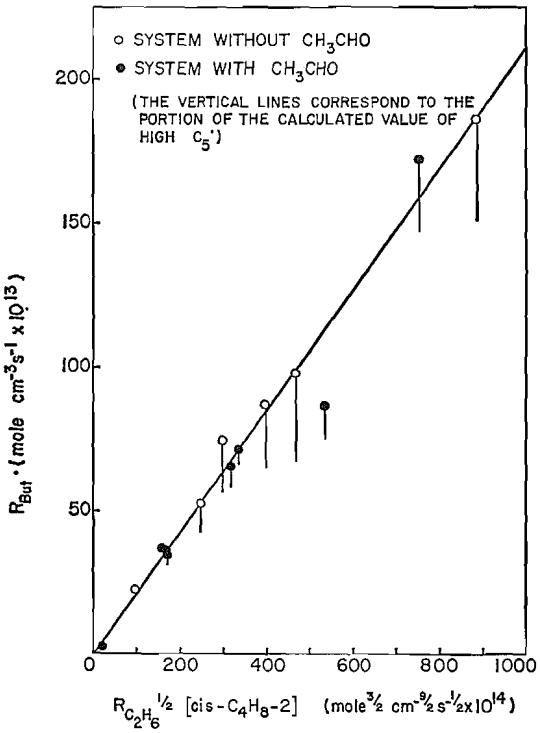

FIG. 6. Butenyl radical formation at 150.2 °C.

of But· and Oct·, $R_{But\cdot}/R_{Oct\cdot} \approx R_{C_2H_6}/R_{C_5H_{10}}[But\cdot]$. Although the addition of CH_3CHO also minimizes the second step addition of But·, the effect is not as pronounced as with the C_5· radical because of the inability of But· to react rapidly with CH_3CHO by H atom abstraction. However, reasonably high concentrations of CH_3CHO do cause the formation of Oct· to be almost negligible.

The data for $R_{But\cdot}$ is shown in Figs. 6 and 7. In spite of the prediction that the corrected value of $R_{But\cdot}$ determined in the absence of CH_3CHO might differ appreciably from its value in the experiments with CH_3CHO, it is seen that no significant deviation is apparent. This may be due to counteracting errors, those tending toward high $R_{But\cdot}$ because of But· formed by processes other than reaction [6] and those leading to low $R_{But\cdot}$ because of the neglect of products of the second step But· addition. In any event the results of the experiments with CH_3CHO may be expected to give valid results due to the high CH_3· steady state concentration which minimizes the complicating factors of the R_6 determination. The Arrhenius plot of the data contained in Figs. 4, 5, 6, and 7 is given in Fig. 8. Rate constants evaluated from the best lines are

$$k_5/k_3^{1/2} = 9.5 \times 10^3 \exp(-7000/RT) \quad (\text{cm}^3\ \text{mole}^{-1}\ \text{s}^{-1})^{1/2}$$

$$k_6/k_3^{1/2} = 3.9 \times 10^3 \exp(-7300/RT) \quad (\text{cm}^3\ \text{mole}^{-1}\ \text{s}^{-1})^{1/2}$$

or if the value of Shepp (18) is used for $k_3 = 2.2 \times 10^{13}$ cm^3 mole^{-1} s^{-1}, $k_5 = 4.5 \times 10^{10} \exp(-7000/RT)$, and $k_6 = 1.8 \times 10^{10} \exp(-7300/RT)$ cm^3 mole^{-1} s^{-1}. These values compare favorably with the corresponding k_5 and k_6 determined by Cvetanović and Irvin (6) of $9.0 \times 10^{10} \exp(-7500/RT)$ and $1.3 \times 10^{11} \exp(-7600/RT)$, respectively.

G. CH_4 Formation

In the absence of CH_3CHO, CH_4 is formed by abstraction from DTBP, reaction [4], and *cis*-butene-2, reaction [6], as well as by CH_3· disproportionation with other radicals present, a source for the most part represented by reactions

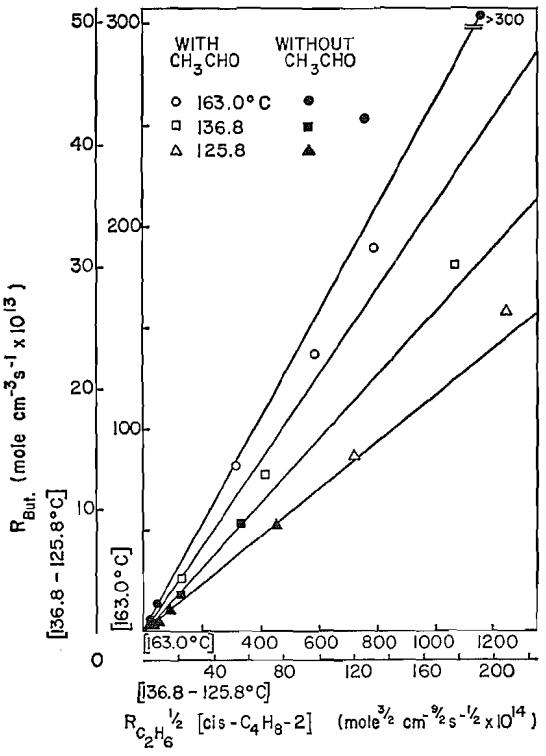

FIG. 7. Butenyl radical formation at other temperatures.

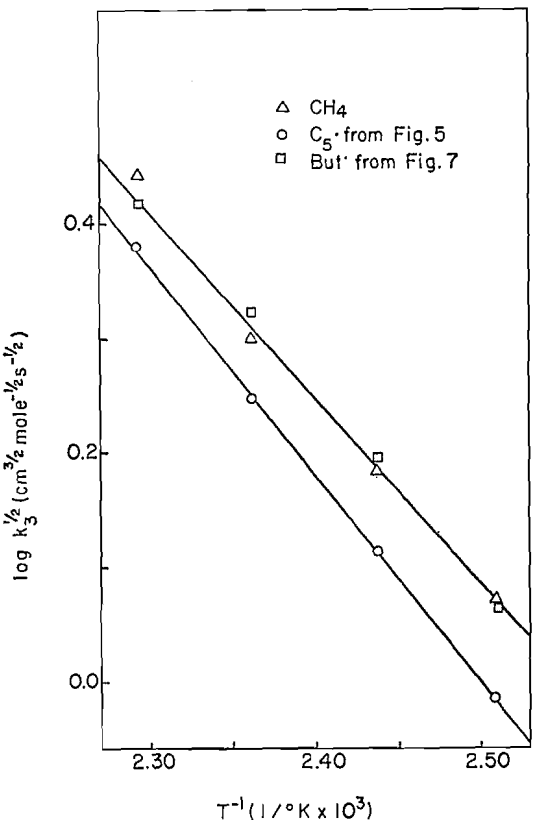

FIG. 8. The formation of methane, pentyl and butenyl radicals as a function of temperatures.

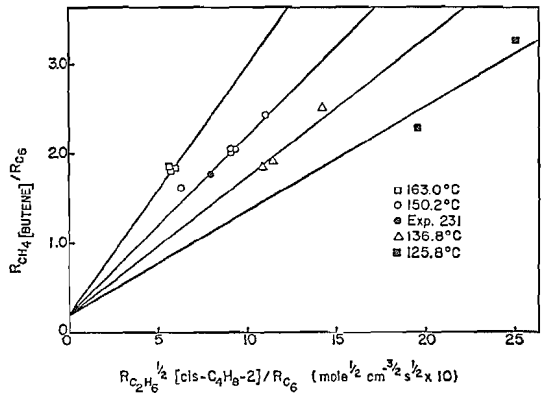

FIG. 9. The formation of methane from *cis*-butene-2.

[8*a*, *b*]. The portion attributable to reaction [4] may be estimated similarly to the method used by Miyoshi and Brinton (1*b*). Split of the CH_4 between reactions [6] and [8*a*, *b*] may be evaluated by plotting of the easily derived function

$$[33]\quad \frac{R_{CH_4[Butene]}}{R_{C_6}} = \frac{k_6 R_{C_2H_6}{}^{1/2}}{k_3{}^{1/2} R_{C_6}}[cis\text{-}C_4H_8\text{-}2] + \frac{k_{8a} + k_{8b}}{k_7}$$

where $R_{CH_4[Butene]}$ represents the CH_4 arising solely through butene interaction, i.e. R_{CH_4} corrected for $R_{CH_4[DTBP]}$. The plot shown in Fig. 9 is not a critical test of eq. [33] because the spread of the variables is limited in extent at most temperatures. The intercept, $k_{8a} + k_{8b}/k_7$, ≈ 0.2 is a very rough evaluation of the disproportionation–combination ratio of the CH_3–$C_5{}^{\cdot}$ interaction. However, the 0.2 intercept is not inconsistent with any of the curves, and the slopes, $k_6/k_3{}^{1/2}$, which are much more accurately given from the curves than the intercepts, are included in Fig. 8. It is seen that points evaluating $k_6/k_3{}^{1/2}$ from quite different procedures, CH_4 formation as contrasted to But$^{\cdot}$ radical formation, are quite consistent and a single line may be drawn through the two sets of data. This correspondence gives confidence that the value of $k_6/k_3{}^{1/2}$ given earlier is a reasonable one. However, the check of the But$^{\cdot}$ formation data may well be fortuitous as discussed previously.

In presence of CH_3CHO large quantities of CH_4 and CO are formed by the following chain mechanism

$$[34]\quad CH_3{}^{\cdot} + CH_3CHO \rightarrow CH_4 + CH_3CO^{\cdot}$$

or more generally

$$[35]\quad R^{\cdot} + CH_3CHO \rightarrow CH_4 + CH_3CO^{\cdot}$$

and

$$[36]\quad CH_3CO^{\cdot} \rightarrow CH_3{}^{\cdot} + CO$$

The % of the total CH_4 formed by reactions associated with *cis*-C_4H_8-2 and $CH_3{}^{\cdot}$ interaction was quite small in all cases when appreciable CH_3CHO was present. Plots of $R_{CH_4[CH_3CHO]}$ vs. $R_{C_2H_6}{}^{1/2}[CH_3CHO]$ gave good lines at single temperatures. An Arrhenius plot of these data evaluated $k_{34}/k_3{}^{1/2} = 8.5 \times 10^4 \exp(-7200/RT)$ (cm^3 mole^{-1} s^{-1})$^{1/2}$. Volman and Brinton (19) reported $E_{34} = 7500 \pm 300$ cal mole^{-1} for the system containing only DTBP and CH_3CHO. Kerr and Calvert (20), from a composite Arrhenius plot of the data of a number of studies involving quite different systems, determined E_{34} as 6800 cal mole^{-1}.

Can. J. Chem. Downloaded from www.nrcresearchpress.com by 210.87.254.105 on 09/05/12
For personal use only.

Acknowledgment

The authors express their appreciation to the National Science Foundation for a grant-in-aid which partially supported this research, as well as for funds contributed toward the purchase of a mass spectrometer used in some of the analytical procedures of the investigation.

1. (*a*) R. K. BRINTON. J. Chem. Phys. **29**, 781 (1958). (*b*) M. MIYOSHI and R. K. BRINTON. J. Chem. Phys. **36**, 3019 (1962).
2. F. F. RUST, F. H. SEUBOLD, and W. E. VAUGHN. J. Am. Chem. Soc. **70**, 95 (1948).
3. F. A. RAAL and C. J. DANBY. J. Chem. Soc. 2222 (1949).
4. A. F. TROTMAN-DICKENSON and E. W. R. STEACIE. J. Chem. Phys. **19**, 169 (1951).
5. S. A. RYCE and W. A. BRYCE. Trans. Faraday Soc. **57**, 943 (1961).
6. R. J. CVETANOVIĆ and R. S. IRVIN. J. Chem. Phys. **46**, 1694 (1967).
7. R. P. BUCKLEY, A. REMBAUM, and M. SZWARC. J. Polymer Sci. **24**, 135 (1957).
8. (*a*) J. A. KERR and A. F. TROTMAN-DICKENSON. Trans. Faraday Soc. **55**, 572 (1959). (*b*) J. A. GARCIA DOMINGUEZ and A. F. TROTMAN-DICKENSON. J. Chem. Soc. 940 (1962). (*c*) R. R. GETTY, J. A. KERR, and A. F. TROTMAN-DICKENSON. J. Chem. Soc. A, 979 (1967); 1361 (1967).
9. (*a*) J. G. CALVERT and J. G. GRUVER. J. Am. Chem. Soc. **80**, 1313 (1958). (*b*) H. E. O'NEAL and S. W. BENSON. J. Chem. Phys. **36**, 2196 (1962). (*c*) J. A. KERR and J. G. CALVERT. J. Phys. Chem. **69**, 1022 (1965).
10. P. J. BODDY and J. C. ROBB. Proc. Roy. Soc. London, Ser. A, **249**, 547 (1959).
11. S. W. BENSON and W. B. DEMORE. Ann. Rev. Phys. Chem. **16**, 397 (1965).
12. A. D. STEPUHOVICH and V. A. ULITZKII. Uzbeksk. Khim. Zh. XXXV 487 (1966).
13. J. W. KRAUS and J. G. CALVERT. J. Am. Chem. Soc. **79**, 5921 (1957).
14. D. H. SLATER, S. S. COLLIER, and J. G. CALVERT. J. Am. Chem. Soc. **90**, 268 (1968).
15. C. WALLING and W. THALER. J. Am. Chem. Soc. **83**, 3877 (1961).
16. R. A. HOLROYD and G. W. KLEIN. J. Phys. Chem. **69**, 194 (1965).
17. D. M. GOLDEN, K. W. EGGER, and S. W. BENSON. J. Am. Chem. Soc. **86**, 5416 (1964).
18. A. SHEPP. J. Chem. Phys. **24**, 939 (1956).
19. D. H. VOLMAN and R. K. BRINTON. J. Chem. Phys. **20**, 1764 (1952).
20. J. A. KERR and J. G. CALVERT. J. Phys. Chem. **69**, 1022 (1965).

Can. J. Chem. Downloaded from www.nrcresearchpress.com by 210.87.254.105 on 09/05/12
For personal use only.

Can. J. Chem. Downloaded from www.nrcresearchpress.com by 210.87.254.6 on 09/05/12
For personal use only.

Preparation and properties of σ-bonded picryl platinum compounds

A. R. Norris and M. C. Baird
Department of Chemistry, Queen's University, Kingston, Ontario

Received March 4, 1969

The compounds *cis*-PtCl(pic)(EPh_3)$_2$ (pic = 2,4,6-trinitrophenyl; E = P, As) have been prepared by the oxidative addition of picryl chloride to the zero valent platinum compounds, $Pt(PPh_3)_3$ and $Pt(AsPh_3)_4$. Both new compounds react with cyanide ion to give intensely colored red complexes.

Canadian Journal of Chemistry, 47, 3003 (1969)

Introduction

In recent years a number of σ-bonded organoplatinum compounds have been prepared by the oxidative addition of active halides such as methyl iodide, allylchloride, and acyl and sulfonyl halides to the zero valent platinum compounds $Pt(PPh_3)_{3,4}$ (1). The method has proven to be extremely useful in preparing compounds of the general formula $PtRCl(PPh_3)_2$, where R is an organic moiety for which the Grignard or lithium derivative cannot be prepared.

We have now found that picrylchloride (1-Cl-2,4,6-trinitrobenzene) readily adds to both $Pt(PPh_3)_3$ and $Pt(AsPh_3)_4$ to form the stable new compounds PtCl(pic)(EPh_3)$_2$ (E = P, As; pic = 2,4,6-trinitrophenyl). The infrared and proton nuclear magnetic resonance (n.m.r.) spectra of these compounds and their interactions with cyanide ion are described.

Observations

A solution of $Pt(PPh_3)_3$ (2) in benzene treated with an excess of picryl chloride rapidly turns deep red-brown. By refluxing for 15 min, concentrating, adding ethanol, and cooling, a virtually quantitative yield of pale orange-yellow crystals of Pt(pic)Cl(PPh_3)$_2$ was obtained. The yellow triphenylarsine analogue PtCl(pic)($AsPh_3$)$_2$ was similarly obtained by treating $Pt(AsPh_3)_4$ (2) with excess picryl chloride. Both compounds are very stable, soluble in chloroform (0.10 *M*) and benzene, and virtually insoluble in alcohols, ether, and acetone.

In addition to bands which can be assigned to the triphenylphosphine or arsine, the infrared (i.r.) spectra (Nujol mull, KBr disk) of both compounds contain bands assignable to the picryl group at 1590 (strong, C—C stretch), 1515 (strong, ν_{asym}-NO_2), 1330 (strong, ν_{sym}-NO_2) and 730 cm^{-1} (medium, in-plane deformation, NO_2). The frequencies of the first three bands are significantly lower than the average values of these same vibrations in 17 picryl compounds, in which R is the more conventional substituent (Cl, Br, I, CH_3, etc.) (3). In both compounds the band at 755 cm^{-1}, characteristic of the C—Cl stretch in picryl chloride, is absent. The phosphine compound has a band at 306 cm^{-1} which can be assigned to the platinum–chlorine stretching mode. This region is obscured in the i.r. spectrum of the arsine complex by a triphenylarsine band and ν_{Pt-Cl} cannot be assigned in this case.

The proton n.m.r. spectrum ($CDCl_3$, 37 °C) of PtCl(pic)(PPh_3)$_2$ contains a number of intense bands at about 2.6τ (relative intensity 30) which may be assigned to triphenylphosphine resonances and a triplet of doublets centered at 1.43τ (relative intensity 2) which may be assigned to the two picryl protons. This spectrum is compatible only with *cis* square planar coordination about the platinum, the triplet structure being due to coupling with ^{195}Pt ($J = \frac{1}{2}$, 34% abundance, J_{Pt-H} = 9.6 c.p.s.) and the doublets being due to coupling with one of the phosphorus atoms (J_{P-H} = 1.6 c.p.s.). Only a single sharp line at 1.52τ can be assigned to the picryl protons in the n.m.r. spectrum of the arsine derivative; no satellites due to coupling with the platinum could be observed. In both the triphenylarsine and triphenylphosphine complexes the resonance absorptions of the picryl hydrogens are considerably upfield compared to the resonance absorbances of the ring hydrogens in 1,3,5-trinitrobenzene (0.67τ) and 1-R-2,4,6-trinitrobenzenes, where R = CH_3 (1.00τ), OCH_3 (0.95τ) and COH (~0τ) (4).

Attempts to replace the chlorine in PtCl(pic)-(PPh_3)$_2$ by refluxing with excess tetraethylammonium bromide in acetonitrile for ½ h were unsuccessful, the chloro complex being reisolated

Can. J. Chem. Downloaded from www.nrcresearchpress.com by 210.87.254.6 on 09/05/12
For personal use only.

in good yield. The absence of substitution in this reaction is in direct contrast with the ease of similar metathetical reactions in other arylplatinum compounds (5, 6).

Reactions of $Pt(PPh_3)_3$ with 1,3,5-trinitrobenzene (TNB), *m*-dinitrobenzene, 2,4,6-trinitrotoluene, and 1-chloro-2,4-dinitrobenzene all gave deeply colored solutions. However, only the first reaction appeared promising, yielding a black crystalline compound which analyzed as $Pt(TNB)(PPh_3)_2$ and which has been reported separately (7).

Both $PtCl(pic)(PPh_3)_2$ and $PtCl(pic)(AsPh_3)_2$ interact with cyanide ion (introduced as the tetraphenylarsonium salt) in a wide range of protic and dipolar aprotic solvents to yield intensely colored red solutions which possess two absorption maxima in the range 350 to 850 mμ. The shorter wavelength absorption is always the more intense by a factor of 1.1 to 1.3. The positions of maximum absorption vary to a slight extent in different solvents but the general form of the visible absorption bands is the same in all the solvents investigated. A similar behavior has been noted for the σ-complex formed between cyanide ion and 1,3,5-trinitrobenzene (8).

The molar extinction coefficients (ε) of the colored species at the wavelength of maximum absorption and the equilibrium constants (K) associated with their formation were evaluated in several solvents from absorbance studies of a series of solutions in which the $PtCl(pic)(PPh_3)_2$ concentration was held constant (usually near 1.0×10^{-4} M) and the concentration of tetraphenylarsonium cyanide varied over the range 1.0×10^{-4} to 5.0×10^{-3} M. The results indicate that complexes of 1:1 stoichiometry are formed in acetone (λ_{max}, 458 mμ), chloroform (461 mμ), dichloromethane (459 mμ) and acetonitrile (455 mμ) with, in all cases, a molar extinction coefficient of $1.9 \pm 0.5 \times 10^4$ l mole^{-1} cm^{-1} at the absorption maximum. The equilibrium constant for complex formation is strongly solvent dependent, being $3.0 \pm 0.5 \times 10^2$ in chloroform and $1.5 \pm 0.5 \times 10^4$ in acetone.

Very little could be learned about the structure of the cyanide complex from the n.m.r. spectrum of the red solution in $CDCl_3$. As the ratio CN^-:Pt was increased, the absorptions at 1.43τ (in the case of the phosphine complex) remained at the same position but decreased in intensity. However, no new resonance absorptions could be detected in the range 10 to 0τ. Since the addition of cyanide ion to a C-3 position on the picryl group would be expected to lead to resonance absorptions of equal intensity at ca. 2.4 and 4τ (4), the absence of the latter absorption strongly suggests that cyanide adds at the C-1 position. In this case the resonance absorptions of the two picryl protons in the complex would be buried under the very intense phenyl resonances of the tetraphenylarsonium ion (4). The infrared spectra of the products obtained after long standing of the solutions used in the n.m.r. studies indicate that cyanide eventually replaces the picryl group in the inner coordination sphere of the platinum.

Experimental

Infrared spectra were run on a Beckman IR-10 spectrophotometer, n.m.r. spectra on a Varian T-60 using internal TMS as a standard and visible spectra on Unicam SP800 and Cary 14 spectrophotometers. Determinations of K and ε were carried out using spectro-grade solvents, matched silica cells of 1.0 cm path length and with the cell compartments of the spectrophotometers maintained at 25.0 ± 0.1 °C. Molecular weights were determined using a Mechrolab vapor pressure osmometer. Melting points (uncorrected) were obtained using a Gallenkamp melting point apparatus. Analyses were carried out by A. Bernhardt, Max Planck Institut, Mulheim, Ruhr, West Germany.

Chloropicrylbistriphenylphosphineplatinum(II)

Treatment of 1.805 g $Pt(PPh_3)_3$ with 1.38 g picryl chloride in 40 ml benzene solution under nitrogen at room temperature gave a dark-colored solution. On refluxing for 15 min, the color of the solution turned lighter, and on concentrating, adding excess ethanol, and cooling, 1.73 g (92% yield) of the crude *complex* precipitated. Recrystallization from benzene–ethanol gave pale orange-yellow crystals, m.p. 264–265 °C (decomp.).

Anal. Calcd. for $C_{42}H_{32}ClN_3O_6P_2Pt$: C, 52.15; H, 3.34; Cl, 3.67; N, 4.34; M, 967. Found: C, 51.17; H, 3.25; Cl, 3.33; N, 4.30; M, 1200 (chloroform).

Chloropicrylbistriphenylarsineplatinum(II)

The compound was prepared from $Pt(AsPh_3)_4$ and picryl chloride by a method similar to that used for the phosphine analogue. Recrystallized from benzene–ethanol, the compound formed pale yellow crystals, m.p. 238–239 °C.

Anal. Calcd. for $C_{42}H_{32}As_2ClN_3O_6Pt$: C, 47.81; H, 3.06; M, 1055. Found: C, 48.21; H, 3.26; M, 1340 (chloroform).

Discussion

Oxidative addition reactions of active halocarbons to $Pt(PPh_3)_3$ are well-known, platinum compounds containing methyl (6), acetyl (9), and benzoyl (10) groups having been reported previously. Although addition of an alkyl or aryl

Can. J. Chem. Downloaded from www.nrcresearchpress.com by 210.87.254.6 on 09/05/12
For personal use only.

halide to a metal atom presumably yields a *cis*-adduct initially, isomerization to the more stable *trans*-isomer usually occurs very readily, especially in the presence of free phosphine (6). On this basis the stable *cis*-configuration of PtCl(pic)-$(PPh_3)_2$, as shown unequivocally by the n.m.r. spectrum, seems surprising. However, *cis-trans* isomerization would undoubtedly occur via attack on the platinum atom by free phosphine, a process which would be sterically hindered by the ortho nitro groups of the picryl ring. The failure to substitute the chloride by bromide, a reaction which normally proceeds rapidly, is also presumably hindered by steric interactions.

The position of ν_{Pt-Cl} (306 cm^{-1}) of PtCl(pic)-$(PPh_3)_2$ lies within the range normally found for chloride *trans* to tertiary phosphines in platinum compounds (11). X-Ray powder diffraction patterns of the two picryl compounds reported here indicate that the compounds are not isomorphous, and thus nothing can be said about the structure of the arsine compound.

Aside from determining the stereochemistry, the n.m.r. spectrum of $PtCl(pic)(PPh_3)_2$ is of great interest because of the large long-range interactions which are observed. The platinum–hydrogen coupling constant (9.6 c.p.s.) is much greater than coupling constants through four bonds in several other organometallic compounds (12), while the phosphorus–hydrogen coupling constant (1.6 c.p.s.) extends through five bonds involving four different elements. It is generally agreed (12) that *trans* couplings in square complexes are larger than *cis* couplings, and therefore it is likely that the coupling observed here is with the *trans* phosphine. The fact that such long-range coupling is observed suggests that π-electron delocalization via platinum–carbon d_π–p_π bonding and platinum–phosphorus d_π–d_π bonding must be important. Parshall has demonstrated extensive back-donation from platinum(II) to fluorophenyl groups (13); it is to be expected that the highly electronegative nitro-groups would also facilitate such back-donation.

In this respect, it is interesting to note, as mentioned above, that the NO stretching modes in the i.r. spectrum of the platinum compounds are lower than normal, suggesting that a platinum atom donates greater electron density to an aromatic ring than do ordinary organic functional groups. Similarly the resonances of the protons on the picryl group appear at much higher fields in the n.m.r. spectra of the platinum compounds than is found for other picryl compounds. Indeed, the positions of resonance are approximately the same as for the cyanide adducts of other picryl compounds (4). Again extensive delocalization of electron density from the metal atom into the ring is implied.

Acknowledgments

The authors acknowledge financial assistance from the National Research Council of Canada and experimental assistance from Mr. A. Drinkwalter.

1. R. Ugo. Coord. Chem. Rev. **3**, 319 (1968).
2. L. Malatesta and C. Cariello. J. Chem. Soc. 2323 (1958).
3. T. N. Hall and J. P. Haberman. NOL TR 64-62. 1964.
4. E. Buncel, A. R. Norris, and W. Proudlock. Can. J. Chem. **46**, 2759 (1968).
5. F. Basolo, J. Chatt, H. B. Gray, R. G. Pearson, and B. L. Shaw. J. Chem. Soc. 2207 (1961).
6. J. Chatt and B. L. Shaw. J. Chem. Soc. 705 (1959).
7. M. C. Baird. J. Organometal. Chem. Amsterdam, **16**, 16 (1969).
8. A. R. Norris. Can. J. Chem. **45**, 2703 (1967).
9. C. D. Cook and G. S. Jauhal. Can. J. Chem. **45**, 301 (1967).
10. M. C. Baird and G. Wilkinson. J. Chem. Soc. A, 865 (1967).
11. D. M. Adams. Metal–ligand and related vibrations. Edward Arnold Publishers, London. 1967. p. 75.
12. E. O. Greaves, R. Bruce, and P. M. Maitlis. Chem. Commun. 860 (1967).
13. G. W. Parshall. J. Am. Chem. Soc. **88**, 704 (1966).

Can. J. Chem. Downloaded from www.nrcresearchpress.com by 210.87.254.40 on 09/05/12
For personal use only.

Primary yields and mechanism in the radiolysis of gaseous ammonia[1]

C. WILLIS, A. W. BOYD, AND O. A. MILLER

Research Chemistry Branch, Atomic Energy of Canada Limited, Chalk River Nuclear Laboratories, Chalk River, Ontario

Received March 10, 1969

Ammonia vapor has been irradiated with single pulses of electrons at a very high dose rate (10^{27} eV g^{-1} s^{-1}) with a Febetron 705. At this dose rate radical–product reactions are not significant. In pure ammonia, hydrogen, nitrogen, and hydrazine are produced and the yields[2] found at 10^{27} eV g^{-1} s^{-1} are: $G(H_2) = 3.58 \pm 0.08$; $G(N_2) = 1.00 \pm 0.05$; $G(N_2H_4) = 0.58 \pm 0.05$. The yields are independent of pressure from 1 to 5 atm and of temperature between 20 and 200 °C. Above 250 °C the yields of all three products increase significantly and this is due to reaction [1] competing with radical–radical reactions.

[1] $$H + NH_3 \rightarrow H_2 + NH_2$$

A rate constant for this reaction has been determined,

$$k_1 = 4 \pm 2 \times 10^9 \exp(-10\,000 \pm 1\,500/RT) \quad 1\ \text{mole}^{-1}\ \text{s}^{-1}$$

Product yields have been measured for ammonia–propene mixtures. These yields have allowed determination of the primary radiation yields $G_{NH} = 0.74$; $G_{H_2} = 0.74$; $G_{NH_2} = 4.8$; $G_H = 4.8$; and $G(-NH_3) = 5.4$.

Canadian Journal of Chemistry, 47, 3007 (1969)

Introduction

It has long been known (1) that the products of ammonia radiolysis are hydrogen, nitrogen, and hydrazine and that under static conditions only hydrogen and nitrogen are found. It is clear that hydrogen atoms and NH_2 radicals are formed and product yields depend upon the reaction of these radicals with each other and with hydrazine. Only recently have radical yields been measured and primary mechanisms proposed.

A non-scavengeable or direct yield of hydrogen has been determined to be $G(H_2) = 0.74 - 0.75$ by the addition of ethylene (2–4). There is considerable disagreement in the value for the yield of hydrogen atoms. Jones and Sworski (2) obtained $G_H = 12.5$ from the formation of HD in D_2–ammonia mixtures and from the formation of hydrogen in hydrazine–ammonia mixtures. Johnson and Simic (3) found $G_H = 7.2$ from the addition of propane. Nishikawa *et al.* (4) also used propane but found $G_H = 5.1$ by extrapolating to zero concentration of propane.

At low dose rates, 10^{16}–10^{20} eV g^{-1} s^{-1}, the yield of hydrogen in pure ammonia ranges from $G(H_2) \sim 5$ at room temperature to $G(H_2) \sim 15$ above 200 °C. This temperature dependence has been accounted for by reaction [1] becoming increasingly important with temperature (2).

[1] $$H + NH_3 \rightarrow H_2 + NH_2$$

Johnson and Simic (3) rejected this because of the low apparent activation energy (~2 kcal $mole^{-1}$) for the increase in yields and suggested competition between reactions [2] and [3]

[2] $$H + NH_2 + M \rightarrow NH_3 + M$$

[3] $$H + N_2H_4 \rightarrow H_2 + N_2H_3$$

Anderson and Winter (5) proposed that the increase is due to changes in the clustering of ions with temperature, resulting in different yields of hydrogen atoms on neutralization.

Because of the disagreement in radical yields and the proposed mechanisms a further investigation of ammonia radiolysis seemed worthwhile. In previous papers (6, 7) we have reported on results obtained at very high dose rates (10^{27} eV g^{-1} s^{-1}) from a Febetron pulsed electron accelerator and have done liquid (8) and gas (9–11) phase dosimetry for these dose rates. At very high dose rates radical–radical reactions become dominant and it is possible to measure yields with no interference from radical–product reactions.

We have irradiated ammonia and ammonia mixed with propene at temperatures from 20–450 °C with single electron pulses from the Febetron. From the effects of propene and the variation of yields with temperature we have

[1]Issued as A.E.C.L. No. 3325

[2]G_x is the primary yield of species x, $G(x)$ is the observed yield of species x.

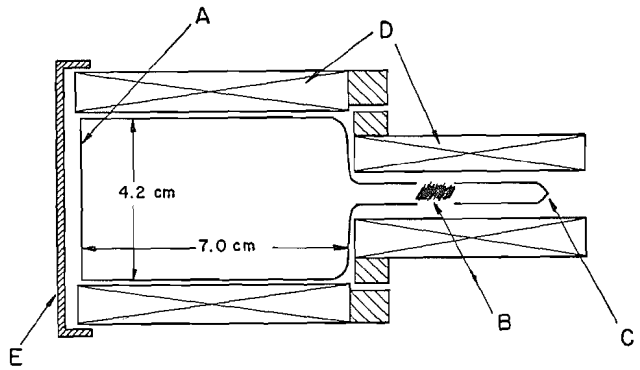

FIG. 1. Quartz irradiation cell and furnace; A, electron window ≈ 0.05 cm; B, graded seal; C, ground glass joint and break seal; D, interlocking annular furnace; and E, removable transite cover.

derived values for the yields of primary species and have proposed a mechanism for the radiolysis of ammonia under "zero dose" conditions.

Experimental

Pulsed Electron Accelerator and Dosimetry

The pulsed electron accelerator[3] was a Febetron 705 which gives ~100 ns pulses of 1.0–1.7 MeV electrons with a maximum current of ~5000 A. Details have been given previously (6–9).

The dosimetry was based on a nitrogen yield of $G(N_2) = 12.4 \pm 0.2$ for the radiolysis of nitrous oxide at 1 atm. This value was obtained by comparing the yields from nitrous oxide with the dose per pulse measured by adiabatic calorimetry (9). This yield is independent of temperature from 20–200 °C (10). The dosimetry at low pressures, below 600 Torr, is very uncertain. The yield of nitrogen from nitrous oxide increases by a factor of 2 between 600 and 15 Torr. This increase, which is thought to be due to transient electric fields, is discussed elsewhere (12). The dose absorbed in the ammonia was calculated from the measured dose in nitrous oxide using standard electron stopping parameters (9).

Gas samples were contained in quartz cells with ~0.5 mm quartz electron windows. The actual pulse shape and duration in these cells are uncertain. The voltage range of the transmitted pulse is estimated to be 0.4–1.1 MeV and its duration to be 30–50 ns. We have no detailed knowledge of the homogeneity of the irradiation field over the cell volume, however, variations should be less than a factor of 3.

Irradiation Cells

The irradiation cells and the furnace are shown in Fig. 1. The cells are quartz with a Pyrex break seal (C). The electron window (A) was made by pulling down quartz tubing to make a thin membrane ~0.5 mm thick. The windows were not uniform in thickness. Variations of dose from cell to cell were kept to ±10%. The dose in each cell was determined several times with nitrous oxide. Typically a cell could withstand 2.5 atm pressure.

For irradiations at elevated temperatures the cells were placed in the annular furnace shown in Fig. 1. This gave good temperature uniformity over the cell volume. The cells were placed in the preheated furnace for 15 min before irradiation (with the removable transite cover (E) in place) to allow temperature to be attained. Above 250 °C some pyrolysis of samples occurred. The irradiation yields reported are corrected for the contribution of pyrolysis. The corrections were generally small but above 450 °C could be as much as 10%. No results are given for experiments conducted above this temperature.

Each sample was quenched in liquid nitrogen within 20 s of irradiation. Unquenched samples gave low hydrazine yields and high nitrogen and hydrogen yields. This was almost certainly due to pyrolysis of the hydrazine formed by radiolysis. However, even at 400 °C, provided quenching was performed within 60 s after irradiation, reproducible results were obtained.

Sample Preparation and Gas Analysis

The ammonia used was Matheson anhydrous grade. The propene was Phillip's research grade hydrocarbon. All gases were used directly from the cylinder and subjected to several freeze–pump–thaw cycles to remove non-condensible impurities. Samples were frozen into the cell and the cell was closed by collapsing the Pyrex break seal under vacuum.

Analysis of the gaseous products was achieved by immersing the irradiated cell in liquid nitrogen and pumping off the non-condensible product gases into a McLeod gauge. After the volume of the gas had been measured its composition was determined by mass spectrometry.

Early experiments involved distillation of the residual ammonia and hydrazine into a cold trap followed by flaming of the cell to ensure no errors due to adsorbed products. Flaming did contribute about 20% more gas, but this arose from a non-radiation process. Some ammonia seemed to have been irreversibly adsorbed on to the quartz walls and, when the cell was flamed, pyrolyzed to give nitrogen and hydrogen. Identical

[3]Manufactured by the Field Emission Corporation, McMinnville, Oregon.

Can. J. Chem. Downloaded from www.nrcresearchpress.com by 210.87.254.40 on 09/05/12
For personal use only.

"flaming" yields were obtained from irradiated and unirradiated samples. The yields reported in this paper are those obtained without flaming.

Hydrazine Analysis

The hydrazine yield was measured using the spectrophotometric method of Watt and Crisp (13). The method is based on the yellow color developed upon the addition of *p*-dimethylaminobenzaldehyde to hydrazine in dilute hydrochloric acid solution. The irradiated ammonia sample was frozen in the cell and after the break seal was opened, dilute hydrochloric acid was added to neutralize the ammonia and to dissolve the hydrazine. The solution was then mixed with *p*-dimethylaminobenzaldehyde reagent solution and left at least 15 min for the color to develop. The % transmittancy of the solution was read at 455 nm and the hydrazine concentration read from calibration curves. Normally duplicate ammonia samples were irradiated; one being used to measure the gas yield and the other to measure the hydrazine yield.

Results

(a) Pure Ammonia

The amounts of nitrogen, hydrogen, and hydrazine produced at 24 °C as a function of absorbed dose are shown in Fig. 2. These were obtained by pulsing the same sample with more than one electron pulse. The amounts of all three products are linear with absorbed dose up to at least six pulses.

The effect of pressure on product yields is shown in Fig. 3. The yields are constant from 1–2.25 atm. Irradiations in stainless steel cells (9) showed the independence of yields on pressure up to 5 atm. Below 700 Torr the yields increase with decreasing pressure.

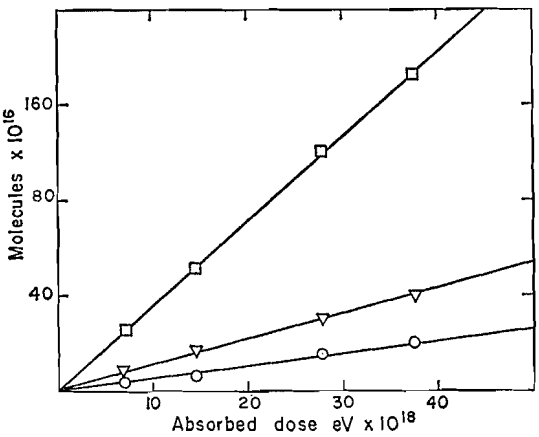

FIG. 2. Product yields as a function of dose; □, hydrogen yield; ▽, nitrogen yield; and ○, hydrazine yield.

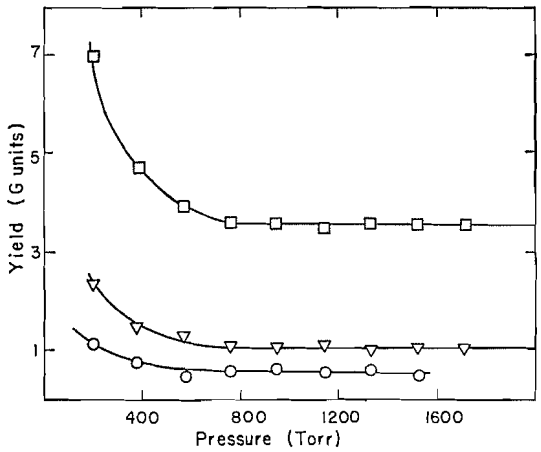

FIG. 3. Product yields as a function of pressure; □, hydrogen; ▽, nitrogen; and ○, hydrazine.

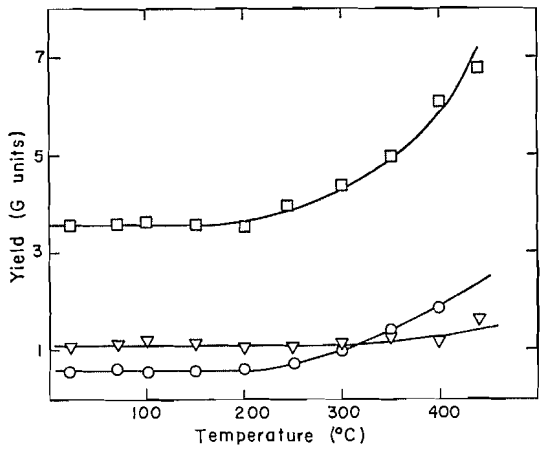

FIG. 4. Product yields as a function of temperature; □, hydrogen; ▽, nitrogen; and ○, hydrazine. Yields are corrected for pyrolysis.

The effect of temperature on the product yields is shown in Fig. 4. The results are for a dose of 1.7 Mrads (1 pulse) for pure ammonia at 760 Torr.

(b) Ammonia–Propene Mixtures

The product yields from ammonia–propene mixtures are shown in Figs. 5 and 6. The yields are calculated using the dose absorbed in the ammonia. Initially the hydrogen yield rapidly decreases and then decreases more slowly as more propene is added. The nitrogen yield decreases slowly with increasing propene. The hydrazine yield rapidly increases to a maximum and then decreases as more propene is added.

Can. J. Chem. Downloaded from www.nrcresearchpress.com by 210.87.254.40 on 09/05/12
For personal use only.

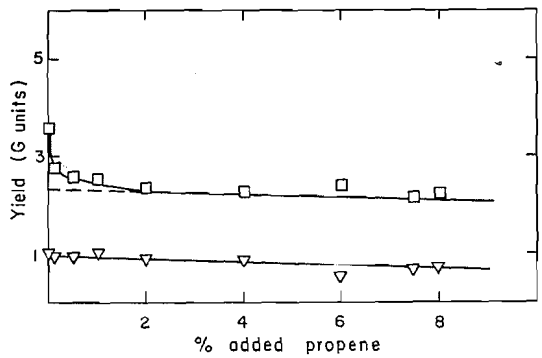

FIG. 5. Gas yields in presence of added propene; □, hydrogen and ▽, nitrogen.

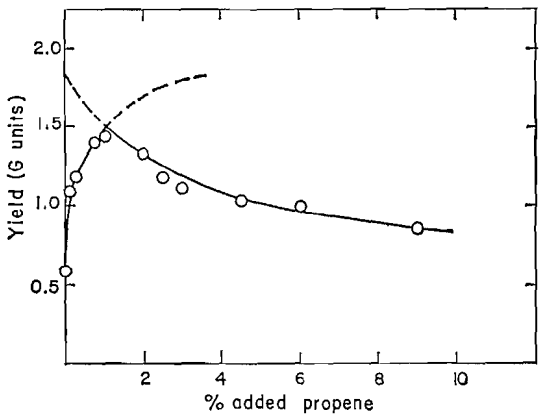

FIG. 6. Hydrazine yield in presence of added propene.

Discussion

(a) Pure Ammonia

At the dose rates used in the present experiments the product yields in the radiolysis of ammonia are: $G(H_2) = 3.58 \pm 0.08$; $G(N_2) = 1.00 \pm 0.05$; and $G(N_2H_4) = 0.58 \pm 0.05$. These yields are independent of dose over at least a factor of 5; of temperature from 20–200 °C; and of pressure from 1–5 atm.

At lower dose rates, up to 10^{19} eV g^{-1} s^{-1}, no hydrazine is found in static systems, and the yields of hydrogen and nitrogen are markedly temperature dependent in the range 0–200 °C (2, 3, 5).

At Febetron dose rates of 10^{27} eV g^{-1} s^{-1}, primary ion–molecule reactions[4]–[6] should not be affected.

[4] $NH_3 \rightarrow NH_3^+ + e$

[5] $NH_3^+ + NH_3 \rightarrow NH_4^+ + NH_2$

[6] $NH_4^+ + e \rightarrow NH_3 + H$

At very high dose rates, it is possible that the NH_3^+ ion may be neutralized as in reaction [7] before it undergoes reaction [5].

[7] $NH_3^+ + e \rightarrow NH_3^*$

However, this can be eliminated for the dose rates of the present experiments. Although the rate constant[4] for reaction [7] is 10^3 that of reaction [5], the maximum concentration of NH_3^+ ions that can be obtained during the pulse is less than 10^{-5} of the ammonia concentration.

The reactions of radicals, however, will change at 10^{27} eV g^{-1} s^{-1}. At this dose rate radical–radical reactions can compete with radical–hydrazine reactions. For example, reaction [2]

[2] $NH_2 + H + M \rightarrow NH_3 + M$

at 1 atm pressure is $\sim 10^4$ times faster than reaction [3].

[3] $H + N_2H_4 \rightarrow H_2 + N_2H_3$

The total hydrazine concentration even after several pulses (e.g. 10 Mrads total dose and assuming $G(N_2H_4) \sim 3$) is 2×10^{19} molecules g^{-1} whereas the total NH_2 radical concentration immediately after a single 1 Mrad pulse is 2×10^{18} molecules g^{-1}, giving

$$k_3[N_2H_4]/k_2[NH_2] = 10^{-3}$$

The linearity of the amount of hydrazine produced with absorbed dose (Fig. 2) confirms that reaction [3] does not compete with reaction [2] and further, it demonstrates that no radical–hydrazine reactions occur.

The radiolysis yields, therefore, can largely be considered to be a result of competition between the following radical–radical reactions

[8] $NH_2 + NH_2 + M \rightarrow N_2H_4 + M$

[9] $NH_2 + NH_2 (+ M) \rightarrow \cdots \rightarrow N_2 + 2H_2 + M$

[10] $NH_2 + NH_2 \rightarrow NH + NH_3$

[2] $NH_2 + H + M \rightarrow NH_3 + M$

[11] $NH_2 + H (+ M) \rightarrow \cdots \rightarrow \frac{1}{2}N_2 + \frac{3}{2}H_2$

[12] $H + H + M \rightarrow H_2 + M$

Above 200 °C, it is suggested that the increase in

[4]All rate constants and their references are collected in Table IV and generally will not be referred to in the text.

Can. J. Chem. Downloaded from www.nrcresearchpress.com by 210.87.254.40 on 09/05/12
For personal use only.

Can. J. Chem. Downloaded from www.nrcresearchpress.com by 210.87.254.40 on 09/05/12
For personal use only.

yields of hydrogen, nitrogen, and hydrazine is due to reaction [1] and that below this temperature it does not occur for the present conditions.

[1] $$NH_3 + H \rightarrow NH_2 + H_2$$

Reaction [9], the bimolecular disproportionation of NH_2 radicals to give nitrogen and hydrogen, may occur as written. A similar reaction has been observed in the photochemistry of hydrazine (14). However, this may involve an electronically

[13] $$N_2H_4 + h\nu \rightarrow N_2H_2 + H_2 \rightarrow N_2 + 2H_2$$

excited hydrazine molecule which is different from the transition state for reaction [9]. Thus reaction [9] should only be taken as a formalism for the overall reaction of hydrogen and nitrogen production, initiated by a bimolecular reaction between NH_2 radicals. Similarly, reaction [11] is a formalism for gas production from reaction of a hydrogen atom with an NH_2 radical. This may involve an NH radical intermediate but no definite evidence can be presented at present.

Reaction [2] shows a three body pressure dependence between 10–1000 Torr (15). As the pressure is reduced in this range, recombination of hydrogen atoms and NH_2 radicals is decreased, resulting in a net increase in yields. As can be seen in Fig. 3 the yields of all products do increase with decreasing pressure. The increase is far too large to be quantitatively explained by changes in reaction [2]. The reasons for increases of yields of this type for intense electron beam radiolysis are discussed elsewhere (12).

(b) Ammonia–Propene Mixtures

At low dose rates, the addition of olefins removes both H atoms and NH_2 radicals from the system. The effects of propene addition at 10^{27} eV g^{-1} s^{-1} are shown in Figs. 5 and 6. These are most simply explained by reactions [14] and [15]

[14] $$H + C_3H_6 \rightarrow C_3H_7$$

[15] $$NH_2 + C_3H_6 \rightarrow \text{Products}$$

Reaction [14] accounts for the initial increase in $G(N_2H_4)$ and decrease in $G(H_2)$ at low olefin concentrations. Initially reaction [14] competes with reaction [12] and then with reactions [2] and [11] so as to allow the NH_2 radicals to take part in reactions [8], [9], and [10]. The more gradual decrease in yields at higher propene concentrations can be due both to reaction [15] withdrawing NH_2 radicals from the system and to reaction [16] withdrawing NH radicals from the system.

[16] $$NH + C_3H_6 \rightarrow \text{Products}$$

Using the known rate constants for reactions [14], [2], [11], and [12], it is possible to extrapolate the yields in the presence of propene to eliminate scavenging of the NH_2 and NH radicals and to maximize the H atom scavenging as shown in Figs. 5 and 6. The extrapolated yields for this low propene condition are: $G(N_2H_4) = 1.8_2$, $G(N_2) = 0.9_5$, and $G(H_2) = 2.3_0$.

These yields result only from NH_2 radicals reacting either by reactions [8] or [9] plus the direct yields. The hydrazine yield directly gives the contribution of reaction [8]. The contribution of reaction [9] is estimated from the measured nitrogen yield less the direct yield. Therefore, the total yield of NH_2 radicals is $G_{NH_2} = 2 \times G(N_2H_4) + 2\{G(N_2) - G_{N_2}\text{ (direct)}\}$. The "direct" yield of nitrogen included in this expression is more properly the yield of nitrogen from processes not involving NH_2 radicals. A "direct" yield usually refers to the direct elimination of a stable product from a substrate molecule. Obviously this cannot be the case for nitrogen from ammonia and this direct yield should perhaps be called the "pseudo-direct" yield. It will be referred to as such.

At low dose rates, in the presence of olefin, a "molecular" yield of hydrogen has been determined (2–4) to be $G(H_2\text{ molecular}) = 0.74$. This yield has been demonstrated to have no ionic precursor (16), eliminating reactions of the type

[17] $$NH_4^+ + e \rightarrow NH_2 + H_2$$

The most obvious origin of this direct hydrogen yield is dissociation of an excited ammonia molecule as suggested by Okabe and co-workers (17, 18).

[18] $$NH_3^* \rightarrow NH + H_2$$

In the presence of olefin at low dose rates the NH radical will be scavenged, leaving only the direct yield of hydrogen. It is evident, therefore, that $G_{NH} = G_{H_2} = 0.74$.

Now for conditions where the NH radical is not scavenged by some additive (as is the case for the present high dose rate studies) it can react to give nitrogen and hydrogen by reaction either

TABLE I

The mechanism of high dose rate radiolysis: contributions of reactions in pure ammonia

	Reaction	Radicals used G_H	Radicals used G_{NH_2}	Yields $G(H_2)$	Yields $G(N_2)$	Yields $G(N_2H_4)$
	Pseudo-direct			1.11	0.37	
[8]	$NH_2 + NH_2 \rightarrow N_2H_4$	—	1.16	—	—	0.58
[9]	$NH_2 + NH_2 \rightarrow N_2 + 2H_2$	—	0.37	0.37	0.19	—
[11]	$NH_2 + H \rightarrow \frac{1}{2}N_2 + \frac{3}{2}H_2$	0.88	0.88	1.32	0.44	—
[2]	$NH_2 + H \rightarrow NH_3$	2.39	2.39	—	—	—
[12]	$H + H \rightarrow H_2$	1.53	—	0.77	—	—
	Totals	4.80	4.80	3.57	1.00	0.58

with itself as in reaction [19], or with NH_2 radicals, or with hydrogen atoms. Because we do

[19] $NH + NH \rightarrow N_2H_2 \rightarrow N_2 + H_2$

not have a detailed knowledge of the reactions of the NH radical, it will be assumed that all NH radicals react via reaction [19]. Although this is an approximation if the NH yield is 0.74 G units then it will not seriously affect the calculation of yields of the other radicals. The yields of nitrogen and hydrogen by reaction [19] will be $G(N_2) = G(H_2) = \frac{1}{2}G_{NH} = 0.37$. The total values for the pseudo-direct yields that should be used for conditions where the NH radical is not scavenged then, are $G(H_2) = 0.74 + 0.37 = 1.11$ and $G(N_2) = 0.37$. Such will be the case for extrapolation to low propene addition with Febetron irradiations.

Therefore, $G_{NH_2} = 2 \times 1.8_2 + 2(0.95 - 0.37) = 4.8$. The above values can be used to give the ratio of reaction [8] to reaction [9] of $k_8/k_9 = 1.8_2/0.5_8 = 3.1$.

Considering the results for pure ammonia at room temperature the contributions to the yields of reactions [2], [11], and [12] can be obtained. The total nitrogen yield from pure ammonia with the Febetron is $G(N_2) = 1.0$. This is the pseudo-direct yield ($G(N_2) = 0.37$) plus contributions from reactions [9] and [11]. The contribution of reaction [9] is that of reaction [8] times k_9/k_8. The contribution of reaction [8] is given directly by the hydrazine yield, $G(N_2H_4) = 0.58$. Therefore the contribution of reaction [9] to the nitrogen yield is equal to $1.00 - 0.37 - 0.58 \times (1/3.1) = 0.44$. This neglects the contribution of reaction [10]. The significance of reaction [10] will be discussed later.

In the same way the contributions of reactions [2] and [12] can be assessed and the contributions of all the reactions are summarized in Table I. The contribution of reaction [12] uses the value of $G_H = 4.8$, which is implicit in the mass balance.

The ratio of reactions [2] to [11] is determined to be $k_2/k_{11} = 2.71$.

Assuming initially equal concentrations of H atoms and NH_2 radicals, the ratio of total rate constants for the disappearance of NH_2 radicals by reaction with H atoms to disappearance by reaction with itself, i.e. $(k_2 + k_{11})/2(k_8 + k_9)$ is 4.4.

The yields extrapolated to low propene concentration are consistent with the above values. The net yields of hydrogen and nitrogen, $G(H_2) = 2.30 - 1.11 = 1.19$ and $G(N_2) = 0.95 - 0.37 = 0.58$, are very close to a ratio of 2:1. This implies that these yields originate from NH_2 radicals rather than NH radicals and that reaction [10] is not significant.

In the foregoing we have neglected reaction of propyl radicals with NH_2 radicals

[20] $C_3H_7 + NH_2 \rightarrow C_3H_7NH_2$ and/or $C_3H_6 + NH_3$

This has been suggested to occur in the photochemistry of ammonia in the presence of propane by Groth *et al.* (19). This would leave our yield of $G_{NH_2} = 4.8$ as a minimum. The importance of reaction [20] cannot be assessed at the present time due to the lack of rate data. Considering the rate of disappearance of propyl radicals by dimerization (20), it is perhaps not significant.

[21] $C_3H_7 + C_3H_7 \rightarrow C_6H_{14}$ and $C_3H_6 + C_3H_8$

Also the agreement of the present work with both other yield data and kinetic data suggests that the effect of propyl radical reaction with NH_2 radicals is not important.

Can. J. Chem. Downloaded from www.nrcresearchpress.com by 210.87.254.40 on 09/05/12
For personal use only.

TABLE II

Product yields in the radiolysis of NH_3 at 10^{27} eV g^{-1} s^{-1}, dose 1.7 Mrads

Temperature °C	$G(N_2H_4)$	$G(H_2)$	$G(N_2)$ Calculated*	$G(N_2)$ Observed
24	0.58	3.58	1.00	1.06
200	0.63	3.53	0.97	1.08
250	0.78	3.97	1.06	1.09
300	1.04	4.32	1.10	1.14
350	1.37	4.49	1.21	1.27
400	1.88	6.05	1.34	1.32
440	2.33	6.79	1.49	1.53

*$G(N_2) \equiv [G(H_2) - G(N_2H_4)]/3$.

(c) Effect of Temperature

At low temperatures in pure ammonia we have proposed that reactions [2], [12], [8], [9], and [11] (plus the pseudo-direct contributions) account for the hydrogen, nitrogen, and hydrazine yields at 10^{27} eV g^{-1} s^{-1}. As the temperature increases above 200 °C, the hydrogen, nitrogen, and hydrazine yields increase.

This increase in yields with temperature is most simply explained by reaction [1]

[1] $$H + NH_3 \rightarrow NH_2 + H_2$$

If all of the H atoms react with ammonia in this way the limiting yields of the products would be $G(H_2) = 8.30$; $G(N_2) = 1.55$; and $G(N_2H_4) = 3.60$.

It is apparent from Fig. 4 that the limiting conditions have not been reached at 400–450 °C, but the observed product yields are not inconsistent with the above values. Table II shows the mass balance calculations for the results obtained as a function of temperature. Calculated nitrogen yields may be compared to the measured values. Good agreement is found at all temperatures.

In order to calculate an activation energy for reaction [1] it is necessary to relate the increase in reaction [1] with absolute temperature. Now although the increase in the hydrogen and hydrazine yields are related to an increase in reaction [1], since there is no linear correlation between these, it is not useful to plot either ln $\Delta G(H_2)$ or ln $\Delta G(N_2H_4)$ against the reciprocal temperature. The quantity which does directly correlate is the increase in NH_2 yield with temperature. Using the ratios of reactions obtained above and the G values given in Table II, $\Delta G(NH_2)$ has been calculated at various temperatures and is given in Table III. The Arrhenius plot of these values is given in Fig. 7. The slope of the line gives E_a/RT where E_a is the activation energy of reaction [1]. The value obtained is $E_a = 10.0 \pm 1.5$ kcal $mole^{-1}$.

TABLE III

Total yield of NH_2 as a function of temperature

Temperature, °C	$G(NH_2)$	$\Delta G(NH_2)$
24	4.80	—
250	5.30	0.50
300	5.70	0.90
350	6.64	1.84
400	7.70	2.90
440	9.10	4.30

When $\Delta G(NH_2) = \frac{1}{2}G_H = 2.4$, reaction [1] will account for half of the H atoms in the system. This occurs at ~380 °C (see Fig. 7). If we assume that the other H atoms react with NH_2 radicals by reactions [2] and [11], as is suggested by the mechanism, then

$$\frac{k_1[NH_3]}{(k_2 + k_{11})[NH_2]} = 1$$

Now for a pulse of 1.7 Mrads, assuming no decay of NH_2 radicals during the pulse, the NH_2 radical concentration is $\sim 5.5 \times 10^{18}$ molecules g^{-1}. Using the value of 1.1×10^{10} l $mole^{-1}$ s^{-1} for $(k_2 + k_{11})$ (see Table IV), k_1 at 380 °C = 1.7×10^6 l $mole^{-1}$ s^{-1}

$$\therefore \quad k_1 = 4 \pm 2 \times 10^9 \exp\left(-\frac{10\,000 \pm 1\,500}{RT}\right) \text{ l mole}^{-1}\ \text{s}^{-1}$$

(d) Comparison with Previous Work

Some reactions and rate constants that might be important in irradiated ammonia are given in Table IV.

Can. J. Chem. Downloaded from www.nrcresearchpress.com by 210.87.254.40 on 09/05/12
For personal use only.

TABLE IV

Reactions and rate constants for possible processes in irradiated ammonia*

	Reaction	Rate constant 1 mole^{-1} s^{-1}	Reference
[1]	$NH_3 + H \rightarrow NH_2 + H_2$	Estimated 10^4 at 150 °C	21
[2]	$NH_2 + H + M \rightarrow NH_3 + M$	$(k_2 + k_{11}) = 1.1 \pm 0.1 \times 10^{10}$	15
[3]	$H + N_2H_4 \rightarrow H_2 + N_2H_3$	$3.5 \times 10^8 \exp(-2000/RT)$	22
[4]	$NH_3 \rightarrow NH_3^+ + e$	—	—
[5]	$NH_3^+ + NH_3 \rightarrow NH_4^+ + NH_2$	$5 \pm 2 \times 10^{11}$	23,24
[6]	$NH_4^+ + e \rightarrow NH_3 + H$	$> 5 \times 10^{13}$	Estimated
[7]	$NH_3^+ + e \rightarrow NH_3^*$	$> 5 \times 10^{13}$	Estimated
[8]	$NH_2 + NH_2 + M \rightarrow N_2H_4 + M$	$(k_8 + k_9) = 2.3 \times 10^9$	15
[9]	$NH_2 + NH_2 + M \rightarrow N_2 + 2H_2 + M$	See [8]	—
[10]	$NH_2 + NH_2 \rightarrow NH + NH_3$	$\sim 4 \times 10^8$	15,25–27
[11]	$NH_2 + H (+ M) \rightarrow \frac{1}{2}N_2 + \frac{3}{2}H_2$	See [2]	—
[12]	$H + H + M \rightarrow H_2 + M$	1.6×10^8	28
[14]	$H + C_3H_6 \rightarrow C_3H_7$	1.6×10^8	22,29
[15]	$NH_2 + C_3H_6 \rightarrow$ Products	—	—
[16]	$NH + C_3H_6 \rightarrow$ Products	—	30,31
[17]	$NH_4^+ + e \rightarrow NH_2 + H_2$	see [6]	5
[18]	$NH_3^* \rightarrow NH + H_2$	—	17,18
[19]	$NH + NH \rightarrow N_2H_2 \rightarrow N_2 + H_2$	$< 10^{11}$	25,26,31
[20]	$NH_2 + C_3H_7 \rightarrow C_3H_7NH_2$	—	19
[21]	$C_3H_7 + C_3H_7 \rightarrow C_6H_{14}$	$\sim 1.8 \times 10^{10}$	20
[22]	$NH_2^+ + NH_3 \rightarrow NH_3^+ + NH_2$	1×10^{12}	24
[23]	$NH_2^+ + NH_3 \rightarrow NH_4^+ + NH$	—	32
[24]	$N_2H_3 + N_2H_3 \rightarrow N_2 + 2NH_3$	3×10^9	33

*The rate constants for reactions [8] + [9] and [2] + [11] are for the high pressure two body limit. This occurs ~ 1.0 Torr for reactions [8] + [9] and at ~ 1000 Torr for reactions [2] + [11] (15). Other three body reactions are calculated out for 1 atm.

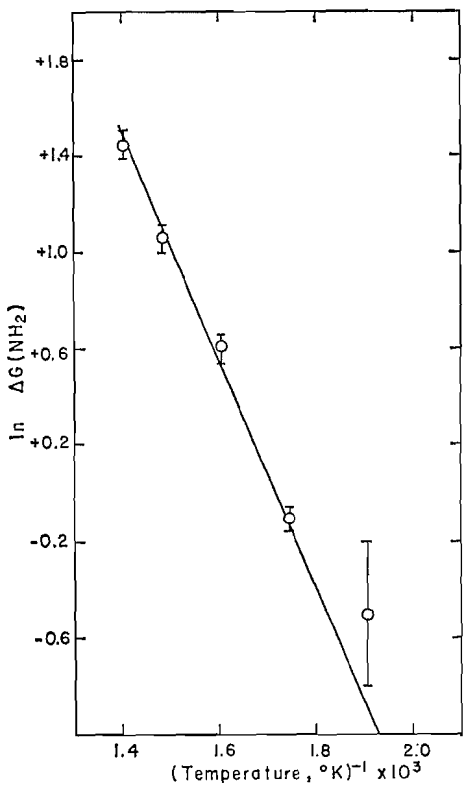

FIG. 7. Arrhenius plot of $\Delta G(NH_2)$.

The rate of disappearance of NH_2 radicals by reaction with H atoms compared to the rate of reaction with themselves, $[k_2 + k_{11}]/[k_8 + k_9 (+ k_{10})]$ is given by Hanes and Bair (15) to be $1.1 \times 10^{10}/2.3 \times 10^9 = 4.8$ at 1000 Torr pressure. This compares very well to the value calculated by us to be 4.4 (equals $(k_2 + k_{11})/2(k_8 + k_9)$).

The value of k_1 estimated by Schiavello and Volpi (21) to be 10^4 l mole^{-1} s^{-1} at 150 °C from mass spectrometric evidence is in good agreement with a value of 2.4×10^4 l mole^{-1} s^{-1} at 150 °C, obtained by using the rate constant determined from the temperature effect. The value for k_1 compares to known H atom transfer rate constants (22).

The only work directly comparable to the present work is that of Meaburn and Gordon (31). These workers irradiated ammonia vapor with a Febetron type device. They stressed the importance of the NH radical in the radiation chemistry of gaseous ammonia. Qualitatively their observations agree with the general mechanism we have proposed. The yields measured by these workers do not agree with the present work, however; their data are rather sparse and their experimental conditions are not well defined. They estimate $G(NH) \simeq 0.53$, which is comparable with the direct yield expected to be $G_{NH} = 0.74$.

Can. J. Chem. Downloaded from www.nrcresearchpress.com by 210.87.254.40 on 09/05/12
For personal use only.

Can. J. Chem. Downloaded from www.nrcresearchpress.com by 210.87.254.40 on 09/05/12
For personal use only.

Our value of $G_{NH_2} = G_H = 4.8$ is in very good agreement with the work of Nishikawa *et al.* (4). These workers report $G_H = 5.1$. The validity of this low value compared to the higher values of Jones and Sworski (2) and Johnson and Simic (3) has already been adequately discussed (4).

It seems very unlikely that the temperature effect observed by other workers at low dose rates (3) is due to competition between reaction [2] and reaction [3]

[2] $$NH_2 + H + M \rightarrow NH_3 + M$$

[3] $$N_2H_4 + H \rightarrow H_2 + N_2H_3$$

This conflicts with the rate data given in Table IV. The coincidence of activation energies for the increase of hydrogen yields with temperature with that of reaction [3] is meaningless without a clear knowledge of the mechanism involved. There are a large number of possibilities for reaction of N_2H_3 type radicals that might show a temperature dependence to give the hydrogen yield increases observed. It is also possible that there is indeed a competition between reaction [1] and reaction [3] as the temperature increases, as has been tentatively suggested (2).

Anderson and Winter have suggested that clustering of the NH_4^+ ion is important in the radiation chemistry of ammonia (5), and that neutralization of an unclustered NH_4^+ ion could yield two H atoms, whereas neutralization of a clustered ion is thermodynamically capable of producing only one H atom.

Clustering of NH_4^+ ions has been demonstrated by Hogg and Kebarle (34) and Searles and Kebarle (35). They found that there can be up to 20 ammonia molecules around the ion with 4 molecules in the inner shell, and an energy of about 80 kcal $mole^{-1}$ associated with the clustering. However, Johnson and Simic (3) have shown that the neutralization yield of H atoms is $\sim$ 3.9 G units and is independent of temperature. The W value of ammonia is $\sim$ 26 eV/ion pair (36), G(ion pair) $\simeq$ 3.8. This suggests that only one H atom is produced on neutralization and that any change in clustering with temperature is not significant in the radiation chemistry of ammonia. Some confirmation of the yield of one H atom per neutralization of NH_4^+ is a total G_H value of 5.1 given by Nishikawa *et al.* (4)

The equivalence of this low yield (4) for low dose rates with our high dose rate value implies either that significant clustering is complete before neutralization at 10^{27} eV g^{-1} s^{-1} or that clustering does not significantly affect the radiation chemistry yields. The lifetime of NH_4^+ ions with respect to neutralization at these dose rates is $\sim 2 \times 10^{-9}$ s (11). Kinetic data on the rate of clustering is not presently available but Dugan and Magee (37) have calculated some cross-sections for clustering. From their calculations it is unlikely that ions would neutralize before being clustered, even at our dose rates.

Conclusions

We have defined a possible primary mechanism for the radiolysis of gaseous ammonia. It is consistent with the initial primary yields being $G_{H_2} = 0.74$; $G_{NH} = 0.74$; $G_H = 4.8$; and $G_{NH_2} = 4.8$. If the W value for ammonia (36) is a reliable measure of G(ion pair) and if all ion pairs eventually lead to one H atom and one NH_2 radical, as has been suggested, then G(ionization) = 3.8; G(excitation) = 1.6; and $G(-NH_3) = 5.4$; where G(excitation) refers to dissociative excitation. This implies that H atoms and NH_2 radicals arise predominantly by ion–molecule reactions rather than by excited state dissociation. This conclusion is supported by the observations of Marx and Mauclaire (38). These authors have bombarded ammonia vapor with electrons of well defined energies and observed the generation of NH_2 radicals as a function of electron energy. The large proportion of radicals are produced by electrons with 8–11 eV, very close to the first ionization potential of ammonia at 10.4 eV (39). This should be compared with the energy loss impact spectrum (40).

The mechanism defined for the radiolysis of ammonia from the present study is only applicable to lower dose rates for very low absorbed doses (i.e. "zero dose" condition). As soon as the concentration of hydrazine becomes sufficient to compete with the radicals the mechanism will change.

The rate constant for the reaction of hydrogen atoms with ammonia has been estimated to be

$$k_1 = 4 \pm 2 \times 10^9 \exp\left(-\frac{10\,000 \pm 1\,500}{RT}\right) \text{ l mole}^{-1}\ \text{s}^{-1}$$

this indicates that reaction [1] is important in the room temperature radiolysis of ammonia vapor at low dose rates.

We have omitted detailed discussion of the reaction of NH radicals and of propyl radicals in

the ammonia propene mixture. It is possible that reactions of these radicals could change the estimated yields given. Such changes would probably not be significant for the reasons already given.

The effect of both of these omissions could be corrected by a measurement of the yields from pure ammonia in the high temperature plateau region, where all H atoms react with ammonia molecules. In order to carry out these measurements at temperatures where pyrolysis is not a problem a slightly lower dose rate must be used (about 1/20th of the present value to give the plateau at ~ 200 °C). We are presently attempting to make these measurements.

Acknowledgments

We would like to thank Mr. D. R. Leeder and Mr. R. Cyr for some of the preliminary experimental work. We should also like to thank Dr. R. S. Dixon of WNRE and Drs. D. R. Smith and W. A. Seddon of CRNL for their critical reading of the manuscript and their useful comments.

1. S. C. Lind. Radiation chemistry of gases. Reinhold Publishing Corp., New York. 1961. p. 92.
2. F. T. Jones and T. J. Sworski. Trans. Faraday Soc. **63**, 2411 (1967).
3. G. R. A. Johnson and M. Simic. Advan. Chem. **82**, 197 (1968).
4. M. Nishikawa, K. Kuroda, and N. Matsuura. Bull. Chem. Soc. Japan, **41**, 1276 (1968).
5. A. R. Anderson and J. A. Winter. The chemistry of ionization and excitation. Taylor and Francis Ltd., London. 1967. p. 197.
6. A. W. Boyd, C. Willis, O. A. Miller, and A. E. Rothwell. Advan. Chem. **82**, 456 (1968).
7. C. Willis, A. W. Boyd, A. E. Rothwell, and O. A. Miller. Intern. J. Radiation Phys. Chem. To be published.
8. C. Willis, O. A. Miller, A. E. Rothwell, and A. W. Boyd. Radiation Res. **35**, 428 (1968).
9. C. Willis, O. A. Miller, A. E. Rothwell, and A. W. Boyd. Advan. Chem. **81**, 539 (1968).
10. A. W. Boyd, C. Willis, and O. A. Miller. Can. J. Chem. **47**, 351 (1969).
11. D. A. Armstrong, C. Willis, and A. W. Boyd. J. Chem. Phys. To be published.
12. A. W. Boyd, D. A. Armstrong, C. Willis, and O. A. Miller. Radiation Res. To be published.
13. G. W. Watt and J. D. Crisp. Anal. Chem. **24**, 2006 (1952).
14. L. J. Stief and V. J. DeCarlo. J. Chem. Phys. **49**, 100 (1968).
15. M. H. Hanes and E. J. Bair. J. Chem. Phys. **38**, 672 (1963).
16. M. Nishikawa, N. Shinohara, and N. Matsuura. Bull. Chem. Soc. Japan, **40**, 1993 (1967).
17. J. R. McNesby, I. Tanaka, and H. Okabe. J. Chem. Phys. **36**, 605 (1962).
18. H. Okabe and M. Lenzi. J. Chem. Phys. **47**, 5241 (1967).
19. W. E. Groth, U. Schurath, and R. N. Schindler. J. Phys. Chem. **72**, 3914 (1968).
20. A. Shepp and K. O. Kutschke. J. Chem. Phys. **26**, 1020 (1957).
21. M. Schiavello and G. G. Volpi. J. Chem. Phys. **37**, 1510 (1962).
22. B. A. Thrush. Prog. Reaction Kinetics, **3**, 65 (1965).
23. L. M. Dorfman and P. C. Noble. J. Phys. Chem. **63**, 980 (1959).
24. G. A. W. Derwish, A. Galli, A. Giardini-Guidoni, and G. G. Volpi. J. Chem. Phys. **39**, 1959 (1963).
25. K. A. Mantei and E. J. Bair. J. Chem. Phys. **49**, 3248 (1968).
26. R. W. Diesen. J. Chem. Phys. **39**, 2121 (1963).
27. D. C. Carbaugh, F. J. Munro, and J. M. Marchello. J. Chem. Phys. **47**, 5211 (1967).
28. K. Schofield. Planetary Space Sci. **15**, 743 (1967).
29. R. Cvetanović. Advan. Photo. Chem. **1**, 115 (1963).
30. J. L. Brash and R. A. Back. Can. J. Chem. **43**, 1778 (1965).
31. G. M. Meaburn and S. Gordon. J. Phys. Chem. **72**, 1592 (1968).
32. A. G. Harrison and J. C. J. Thynne. Trans. Faraday Soc. **62**, 2804 (1966).
33. L. J. Stief and V. J. DeCarlo. J. Phys. Chem. **71**, 2350 (1967).
34. A. M. Hogg and P. Kebarle. J. Chem. Phys. **43**, 449 (1965).
35. S. K. Searles and P. Kebarle. J. Phys. Chem. **72**, 742 (1968).
36. R. Cooper and R. M. Mooring. Australian J. Chem. **21**, 2417 (1968) and references therein.
37. J. V. Dugan and J. L. Magee. J. Chem. Phys. **47**, 3103 (1967).
38. R. Marx and G. Mauclaire. Advan. Chem. **82**, 212 (1968).
39. D. C. Forst, C. A. McDowell, and D. A. Vroom. Can. J. Chem. **45**, 1343 (1967).
40. A. Skerbele and E. N. Lassettre. J. Chem. Phys. **42**, 395 (1965).

Can. J. Chem. Downloaded from www.nrcresearchpress.com by 210.87.254.40 on 09/05/12
For personal use only.

Can. J. Chem. Downloaded from www.nrcresearchpress.com by 210.87.254.40 on 09/05/12
For personal use only.

Absolute rate constants for hydrocarbon autoxidation. XIII. Aldehydes: photo-oxidation, co-oxidation, and inhibition[1]

G. E. ZAIKOV[2], J. A. HOWARD, AND K. U. INGOLD
Division of Applied Chemistry, National Research Council of Canada, Ottawa, Canada

Received March 24, 1969

The oxidations of acetaldehyde, heptanal, octanal, cyclohexanecarboxaldehyde, pivaldehyde, and benzaldehyde in chlorobenzene at 0 °C have been studied. These aldehydes oxidize at similar rates under similar conditions because there are compensating changes in the rate constants for chain propagation (k_p) and chain termination ($2k_t$). The termination rate constants increase from $\sim 7 \times 10^6\ M^{-1}\ s^{-1}$ for pivaldehyde and cyclohexanecarboxaldehyde to $\sim 2 \times 10^9\ M^{-1}\ s^{-1}$ for benzaldehyde. The propagation rate constants increase from $\sim 1 \times 10^3\ M^{-1}\ s^{-1}$ for pivaldehyde to $\sim 1 \times 10^4\ M^{-1}\ s^{-1}$ for benzaldehyde.

The rate of oxidation of the aldehydes was decreased by the addition of 1,4-cyclohexadiene, tetralin, tetralin hydroperoxide, cumene, cumene hydroperoxide, *t*-butyl hydroperoxide, and 2,6-di-*t*-butyl-4-methylphenol. As a result of product analysis and absolute rate constant measurements, it is concluded that the peroxy radicals derived from aldehydes are considerably more reactive in hydrogen atom abstraction from hydrocarbons than are the peroxy radicals derived from the hydrocarbons. In the abstraction from cyclohexadiene, the acylperoxy radicals appear to be from 15 to 70 times as reactive, and the benzoylperoxy radicals about 800–900 times as reactive, as the hydroperoxy radical. The differences in reactivity are very much less pronounced in the abstraction from 2,6-di-*t*-butyl-4-methylphenol.

The great ease of oxidation of all aldehydes, and particularly benzaldehyde, is due at least in part to the high reactivity of the peroxy radicals formed in these reactions.

Canadian Journal of Chemistry, 47, 3017 (1969)

Introduction

The thermal or photochemically initiated autoxidation of aldehydes in the liquid phase was shown by Bäckström (1) to be a chain reaction yielding, as the initial product, a peracid. At the oxygen pressures normally used in the kinetic studies of aldehyde oxidation (0.2–1.0 atm) the following mechanism is generally accepted

Initiation

[1] $\mathrm{RCHO} \rightarrow \mathrm{R\dot{C}{=}O}$

Propagation

[2] $\mathrm{R\dot{C}{=}O + O_2 \rightarrow RC(=O)OO\cdot}$

[3] $\mathrm{RC(=O)OO\cdot + H\text{-}C(=O)R \xrightarrow{k_p} RC(=O)OOH + R\dot{C}{=}O}$

Termination

[4] $\mathrm{RC(=O)OO\cdot + RC(=O)OO\cdot \xrightarrow{2k_t}}$ Inactive products

A subsequent polar reaction between the peracid and aldehyde forms the final product of autoxidation, the carboxylic acid

[5] $\mathrm{RC(=O)OOH + H\text{-}C(=O)R \rightarrow RC(=O)OH + RC(=O)OH}$

In the 1950's a number of workers provided information about many details of aldehyde oxidations (see e.g. refs. 2–11). By carrying out competitive oxidations of ring-substituted benzaldehydes, Walling and McElhill (2) were able to compare the relative reactivities of the different aldehydes towards a particular peroxy radical. They found that electron supplying groups on the ring facilitated, and electron withdrawing groups retarded the attack by the peroxy radical on the aldehyde. Furthermore, *n*-butyraldehyde was found to be twice as reactive towards *p*-chlorobenzoylperoxy radicals as benzaldehyde, which suggests that polar effects rather than C—H bond strengths are of primary importance in determining the rate of reaction [3]. A more direct approach to the determination of aldehyde reactivities was the measurements by Melville and co-workers of the absolute rate constants for propagation (reaction [3]) and termination (reaction [4]) in the oxidation of *n*-decanal (4), benzaldehyde (6), and mixtures of the two aldehydes (5).

[1]NRCC No. 10 740.

[2]Visiting Scientist 1968. Present address: Moscow V-334, Vorob'evskoe Shausse 2b, Institute of Chemical Physics, Academy of Science of the USSR.

Can. J. Chem. Downloaded from www.nrcresearchpress.com by 210.87.254.40 on 09/05/12
For personal use only.

The work of Walling and of Melville leaves two major questions unanswered, viz. (*a*) do acylperoxy, aroylperoxy, and alkylperoxy radicals have similar reactivities (towards hydrogen atom abstraction)? and (*b*) are the termination rate constants reported by Melville typical for aldehyde autoxidations?

With regard to the first question, Bateman and Morris (12) have pointed out that aldehydes are produced as scission products of olefin autoxidations and are found as such in significant yield, despite their oxidizability separately being so much greater than the olefin. They suggest that this is due to the greater reactivity of acylperoxy radicals relative to alkenylperoxy radicals. That is, both types of peroxy radicals attack the olefin more readily than they attack the aldehyde, so that the olefin is oxidized preferentially. A similar suggestion was made earlier by Wittig (13) who found that the self-initiated oxidation of benzaldehyde was inhibited by a number of olefins. Retardation of benzaldehyde autoxidation by cyclohexene (14), cumene, and tetralin (15) has also been reported. However, in none of these works was the rate of chain initiation known or controlled. If retardation by hydrocarbons is due to their effect on the propagation step rather than the initiation or termination step, it would certainly suggest that the perbenzoate radical has an unusually high reactivity.

With regard to the second question, Melville reported termination rate constants of $7.5 \times 10^6\ M^{-1}\ s^{-1}$ for *n*-decanal, 3.4×10^7 for *n*-decanal in *n*-decane, and 2.1×10^8 for benzaldehyde in *n*-decane. These values appear high in relation to the values found for tertiary peroxy radicals[3] (10^3–$10^6\ M^{-1}\ s^{-1}$ (16, 17)). High termination constants have also been reported for the gas phase oxidation of acetaldehyde and propionaldehyde (8.9×10^{10} and $2.7 \times 10^{10}\ M^{-1}\ s^{-1}$, respectively (21)). In the gas phase, it has been shown by means of $^{18}O_2$ labeling of peroxyacetyl radicals that the molecular oxygen evolved in termination comes from both radicals (22). Even if the same holds true for the liquid phase, it does not allow a distinction to be made between a concerted process analogous to the Russell mechanism for secondary peroxy radicals (19), i.e.

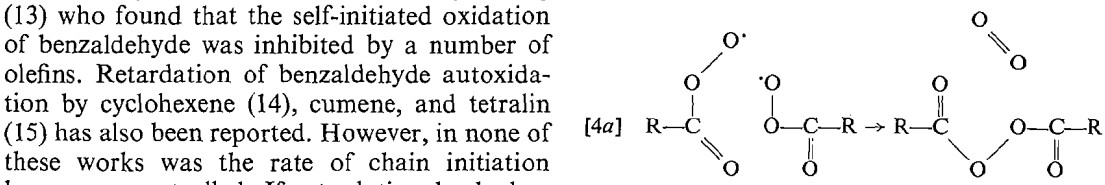

and a process (possibly involving the reversible formation of a tetroxide intermediate) analogous to that for tertiary peroxy radicals (see e.g. ref. 23), i.e.

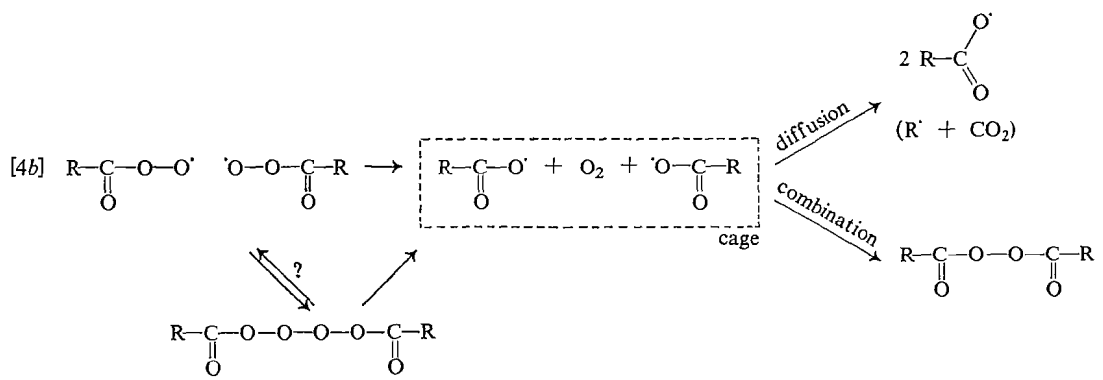

According to the second mechanism, a significant fraction of peroxy radical interactions may be non-terminating because of the diffusion of acyloxy (and, presumably, alkyl radicals) from the cage. Such a process has been demonstrated for some *t*-alkylperoxy radicals by showing that the corresponding *t*-alkyl hydroperoxides can undergo a radical induced chain decomposition (24). Our attempts to induce similar decomposi-

[3]Rate constants for the self-reactions of primary and secondary alkylperoxy radicals are generally higher than those of tertiary peroxy radicals (16, 18), apparently because of the availability for transfer between the reactants of a hydrogen atom on the α-carbon (19, 20).

Can. J. Chem. Downloaded from www.nrcresearchpress.com by 210.87.254.40 on 09/05/12
For personal use only.

tions of perbenzoic acid, *m*-chloroperbenzoic acid, and per-octanoic acid with azo-bis-isobutyronitrile and *t*-butyl hyponitrite (TBH) in carbon tetrachloride at 30 °C were unsuccessful. That is, the rate of loss of peroxide, as measured by iodometric titration, was essentially unaffected by the addition of the initiators. It is possible that the per-acids are relatively unreactive towards free radicals because the acidic hydrogen is intramolecularly bonded, i.e.

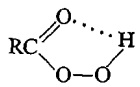

Intermolecular hydrogen bonds have been shown to have a very large retarding effect on the analogous transfer reaction between a peroxy radical and a hydroperoxide (25)

[6] $$ROO^{\cdot} + R'OOH \rightleftarrows ROOH + R'OO^{\cdot}$$

We have utilized reaction [6] to determine the absolute reactivities of different alkylperoxy radicals towards the same substrate by oxidizing the substrate in the presence of the different hydroperoxides. This technique cannot be applied to acylperoxy radicals because the transfer between alkylperoxy radicals and per-acids is too slow. The potential alternative procedure involving the addition of alkyl hydroperoxides to aldehydes did not look particularly promising because of the well known equilibrium

[7] 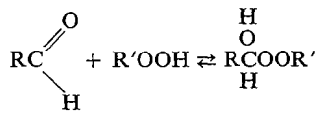

The present paper describes our preliminary attempt to answer the questions posed above. Propagation and termination rate constants have been measured for the oxidation of six aldehydes in chlorobenzene at 0 °C. The question of acylperoxy radical reactivity has been approached in two ways. Firstly, by the co-oxidation composition procedure in which the aldehydes were oxidized in the presence of a very reactive hydrocarbon (1,4-cyclohexadiene) and the relative consumptions of the two reactants were determined (see ref. 26 for a critical discussion of this method). Secondly, by the co-oxidation kinetic procedure in which the rates and some of the rate constants were measured for the co-oxidation of the aldehydes with one or two representative hydrocarbons. The aldehydes were also oxidized in the presence of the hindered phenol 2,6-di-*t*-butyl-4-methylphenol, "Ionol", (InH). Under ideal conditions, chain termination then occurs (27) by the reactions

[8] 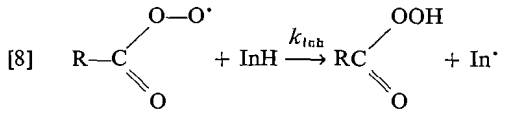

[9] 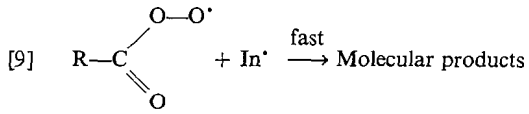

The ratio of the rate constants for propagation and hydrogen abstraction from the phenol, i.e., k_p/k_{inh} can be determined from the inhibited rates of oxidation.

Experimental

Preliminary experiments at our usual temperature of 30 °C confirmed the observation of Cooper and Melville (3) that thermally initiated oxidations are important even with carefully purified aldehydes. We followed their general procedure for decreasing the importance of the thermal reaction relative to the photochemical reaction by working with dilute aldehyde solutions at 0 °C. Chlorobenzene was used as the inert diluent rather than *n*-decane (3) because it has been the principal solvent in our work with hydrocarbons. The thermal reaction was always less than 10% of the photo reaction.

Our general procedure for determining absolute rate constants for autoxidations has been described in previous papers in this series (18, 28). In each oxidation experiment the absolute rate constants were determined from averages of at least 4 and generally 6–10 consecutive measurements of the ratio of the rate under steady illumination to the rate with the optimum frequency of intermittent light. The rate constants showed no systematic variation with aldehyde concentration nor with the extent of aldehyde consumption (between 2 and 20%).

Oxidation rates were measured with a Dynisco pressure transducer (DPT 85-2). Rates could be measured with greater accuracy on smaller samples and at lower extent of oxidation than was possible in Melville and Cooper's experiments. In the kinetic work, the aldehyde was rarely oxidized beyond 5–10%. Under these conditions the yield of per-acid, as determined by iodometric titration, was 98–100% based on the absorbed oxygen provided the titration was performed without delay. That is, reaction [5] is of little importance under our experimental conditions.

The photochemical oxidation of the aldehydes does not require the addition of an azo photo-initiator. The rates of chain initiation were determined by the inhibitor method using hydroquinone (4) and, less satisfactorily, 2,6-di-*t*-butyl-4-methoxyphenol. The efficiency of photoinitiation at full light intensity for each aldehyde is reasonably constant at different aldehyde concentrations (i.e. R_i/[aldehyde] ≈ constant, see Table I). There is, however, a pronounced increase in efficiency along the

Can. J. Chem. Downloaded from www.nrcresearchpress.com by 210.87.254.40 on 09/05/12
For personal use only.

series, octanal ~ heptanal < cyclohexanecarboxaldehyde < pivaldehyde ≪ benzaldehyde. The greater photoinitiating efficiency of benzaldehyde relative to *n*-decanal has been noted previously (6) and has been attributed to its stronger absorption of the incident light. Cyclohexanecarboxaldehyde also appears to absorb slightly more strongly than *n*-alkanals at the initiating wavelengths (3500–3800 Å).

In the co-oxidation experiments the analyses were performed by vapor phase chromatography (v.p.c.) on a silicone rubber column using a saturated hydrocarbon as the internal standard. All analytical results are averages of at least 3 separate measurements.

Cyclohexanecarboxaldehyde, *n*-octanal, and pivaldehyde were obtained from the J. T. Baker Chemical Co., benzaldehyde from Anachemia Chemicals Ltd., and acetaldehyde and *n*-heptanal from Eastman Organic Chemicals. They were dried and purified by distillation on a vacuum line. Samples only came in contact with the air immediately before an oxidation.

All the work described in this paper was done at 0 °C.

Results

Absolute Rate Constants

Under 1 atm of oxygen the overall rates of oxidation of the six aldehydes are given by[4]

$$-\frac{d[O_2]}{dt} = R_s = \frac{k_p[RCHO]R_i^{1/2}}{(2k_t)^{1/2}}$$

and the absolute rate constants for their oxidation are given in Table I. The values of $k_p/(2k_t)^{1/2}$ are quite similar for the different aldehydes (0.3–1.0 $M^{-1/2}$ $s^{-1/2}$) but there is a wide variation in the absolute values of k_p (1–12 × 10^3 M^{-1} s^{-1}) and $2k_t$ (7–1800 × 10^6 M^{-1} s^{-1}).

The propagation and termination rate constants for heptanal and octanal are in reasonably good agreement with Melville's values of 2.7 × 10^3 and 3.4 × 10^7 M^{-1} s^{-1} for a 30% solution of decanal in decane at 5 °C (4). The present termination constant for benzaldehyde (~ 2 × 10^9 M^{-1} s^{-1}) is an order of magnitude greater than that reported by Ingles and Melville (6). We believe that our value is more likely to be correct because of the more accurate method used to measure the rates (see above) and the ratios of rates (28). Incidentally, there was a small contribution to termination from a kinetically first order process in all but one of the benzaldehyde oxidations. The effect of the first order process was allowed for in the usual way (28). If the first order process was ignored the calculated values of $2k_t$ would have been about 10^{10} M^{-1} s^{-1}.

Propagation and termination rate constants for the oxidation of 1,4-cyclohexadiene and tetralin at 0 °C are also included in Table I. The values obtained for tetralin are in good agreement with those estimated from our previous measurements in the temperature range 13–50 °C (29).

Composition Co-oxidations

A primary purpose of this work was to determine whether the peroxy radicals derived from aldehydes have similar reactivities to the peroxy radicals involved in hydrocarbon oxidations. The aldehydes (except acetaldehyde) were co-oxidized with 1,4-cyclohexadiene which was chosen because of its high propagation rate constant and because its oxidation product, benzene, could be analyzed easily. This diene suffers the minor disadvantage that the oxidation chain is carried by a hydroperoxy radical rather than by an alkylperoxy radical (30), i.e.

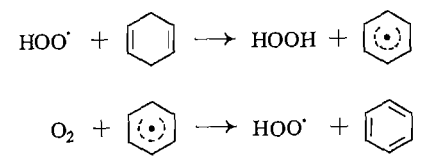

However, it seems likely that the reactivities of HOO· and ROO· radicals will be rather similar.

There was a slow reaction between cyclohexadiene and the per-acids in the dark at 0 °C, amounting to about 1% conversion of diene to benzene per hour under typical experimental conditions. For this reason the products were analyzed immediately after oxidation. The results given in Table II show that only with very extensive oxidation is the absorbed oxygen not equal to the yield of titratable peroxide. This implies that for low extents of oxidation, the aldehyde and diene are consumed in the primary chain process, i.e., by reaction with peroxy radicals. The benzene yield is generally in good agreement with the amount of diene consumed.

[4]In the range of oxygen pressures from 200–760 mm only pivaldehyde showed any dependence of the rate on the oxygen pressure. Over this 3–4 fold change in pressure the rate of oxidation of pivaldehyde decreased by about 20%. Decreasing the oxygen pressure to 80 mm decreased the rate by about 50%. These results indicate that termination processes involving $(CH_3)_3CCO$ (or $(CH_3)_3C^{\cdot}$) radicals play a role in the reaction at low oxygen pressures. However, the effect of these processes on the overall reaction under 1 atm of oxygen is small enough to be ignored for the purpose of the present work.

Can. J. Chem. Downloaded from www.nrcresearchpress.com by 210.87.254.40 on 09/05/12
For personal use only.

TABLE I

Rate constants for the oxidation of some aldehydes in chlorobenzene at 0 °C (in M s units)

Concentration, M	$R_i \times 10^8$	$\frac{R_i \times 10^8}{[RCHO]}$	$R_s \times 10^5$	$k_p/(2k_t)^{1/2}$	$k_p \times 10^{-3}$	$2k_t \times 10^{-6}$
Acetaldehyde						
0.078	0.18	2.4	0.12	0.30	3.4	130
0.144	0.31	2.1	0.24	0.30	3.9	170
0.37	0.9	2.4	0.81	0.23	1.6	52
0.57	1.4	2.4	1.55	0.23	1.9	66
Heptanal						
0.09	0.27	3.0	0.16	0.35	2.7	58
0.34	1.0	3.0	1.4	0.40	3.9	53
1.7	5.3	3.1	16	0.42	3.0	52
1.7	5.3	3.1	15	0.38	2.8	54
Octanal						
0.13	0.24	1.8	0.36	0.57	4.5	61
0.20	0.53	2.7	0.67	0.46	3.3	52
0.43	1.59	3.7	1.9	0.35	2.7	61
0.58	1.56	2.7	3.7	0.51	5.1	100
1.4	3.9	2.8	13	0.48	4.0	70
Cyclohexanecarboxaldehyde						
0.10	1.0	10	0.38	0.37	0.95	6.4
0.21	2.0	9.5	1.3	0.46	1.4	9.5
0.21	2.0	9.5	1.4	0.50	1.3	6.5
0.77	4.5	5.8	6.6	0.41	0.9	4.7
Pivaldehyde						
0.045	1.4	31	0.50	0.95	2.4	6.3
0.22	2.7	12	4.5	1.2	3.4	8.1
0.22	3.6	16	4.9	1.1	2.8	6.3
0.84	7.0	8.3	13.4	0.6	1.4	5.6
Benzaldehyde						
0.08	34	425	2.4	0.52	—	—
0.99	420	425	104	0.51	—	—
0.04*	2.1	53	0.17	0.30	10	1200
0.08*	3.1	39	0.42	0.30	17	3100
0.08*	3.1	39	0.42	0.30	13	1800
0.08*	3.1	39	0.44	0.31	14	2000
0.24*	13	54	2.8	0.32	12	1500
0.50*†	18	36	4.2	0.2	6	930
1,4-Cyclohexadiene‡						
0.16	19	—	0.037	0.0053	0.05	100
0.66	19	—	0.25	0.0088	0.09	100
1.06	4.75	—	0.205	0.0090	0.09	100
1.06	4.75	—	0.20	0.0087	0.08	80
3.3	19	—	1.2	0.0087	0.10	140
Tetralin‡						
4.3	19	—	0.146	0.00078	0.0012	2.3
1.7–7.3	—	—	—	0.00069§	0.0013§	3.1§

*With 10% light intensity.
†The termination was entirely second order for this run.
‡With azo-bis-cyclohexylnitrile as photo-initiator.
§From data in ref. 29.

Can. J. Chem. Downloaded from www.nrcresearchpress.com by 210.87.254.40 on 09/05/12
For personal use only.

TABLE II

Photochemically initiated co-oxidation* of aldehydes and 1,4-cyclohexadiene in chlorobenzene at 0 °C

$[RCHO]_0$	$[C_6H_8]_0$	$R_s \times 10^6$	$\Delta[O_2]$	[ROOH]	$\Delta[RCHO]$	$\Delta[C_6H_8]$	$\Delta[C_6H_6]$	$R = \frac{[RCHO]_{ave}}{[C_6H_8]_{ave}}$	$\rho = \frac{\Delta[RCHO]}{\Delta[C_6H_8]}$
Heptanal									
0.835	2.56	—	0.265	0.270	0.045	0.22	0.22	0.332	0.205
1.00	0.97	2.4	0.215	0.215	0.085	0.13	0.13	1.06	0.650
1.00	0.97	2.6	1.00	0.90	0.40	0.64	0.64	1.23	0.625
2.30	0.805	—	0.30	0.31	0.20	0.10	0.10	2.92	2.0
Octanal									
0.835	2.56	—	0.36	0.36	0.06	0.30	0.30	0.333	0.20
1.00	0.97	2.4	0.255	0.26	0.10	0.16	0.16	1.07	0.625
1.00	0.97	2.5	0.21	0.21	0.08	0.13	0.13	1.06	0.615
1.91	0.88	—	0.32	0.33	0.19	0.13	0.13	2.23	1.46
2.43	0.805	—	0.295	0.29	0.21	0.10	0.10	3.08	2.1
Cyclohexanecarboxaldehyde									
0.77	2.26	—	0.36	0.36	0.13	0.23	0.23	0.328	0.565
0.835	2.56	—	0.305	0.31	0.11	0.20	0.195	0.317	0.55
1.00	0.97	7.1	0.255	0.26	0.145	0.105	0.101	1.01	1.38
1.00	0.97	—	1.00	0.75	0.56	0.48	0.58	0.99	1.17
2.25	0.805	—	0.305	0.31	0.24	0.08	0.08	2.78	3.00
Pivaldehyde									
0.835	2.56	7.2	0.41	0.41	0.18	0.23	0.23	0.306	0.785
0.835	2.56	7.2	0.275	0.28	0.12	0.16	0.16	0.313	0.75
1.00	0.97	5.65	0.102	0.102	0.07	0.03	0.03	1.01	2.33
1.00	0.97	5.65	0.10	0.10	0.07	0.03	0.03	1.01	2.33
1.00	0.97	6.0	0.40	0.40	0.28	0.12	0.12	0.95	2.33
2.37	0.805	8.5	0.18	0.18	0.155	0.025	0.025	2.9	6.17
Benzaldehyde									
0.835	2.56	112	0.295	0.30	0.02	0.28	0.28	0.34	0.072
1.00	0.97	50	0.255	0.26	0.045	0.22	0.215	1.13	0.204
1.00	0.97	56	0.255	0.26	0.045	0.21	0.215	1.13	0.213
1.00	0.97	50	1.00	0.77	0.35	0.84	0.65	1.5	0.42
2.50	0.805	44	0.255	0.26	0.11	0.16	0.17	3.37	0.69

*Full light intensity; concentrations in *M*.

TABLE III
Rate constant ratios for co-oxidations

AH	BH	r_a	r_b	$r_a r_b$
Heptanal	Cyclohexadiene	0.64	1.65	1.06
Octanal	Cyclohexadiene	0.64	1.65	1.06
Cyclohexanecarboxaldehyde	Cyclohexadiene	0.95	0.44	0.42
Pivaldehyde	Cyclohexadiene	2.15	0.36	0.77
Benzaldehyde	Cyclohexadiene	0.17	4.75	0.81
Heptanal	Benzaldehyde	~10	~0.1	~1.0

The propagation reactions for the co-oxidation of an aldehyde, AH, and cyclohexadiene, BH, can be represented by

$$A^{\cdot} + O_2 \longrightarrow AOO^{\cdot}$$

$$B^{\cdot} + O_2 \longrightarrow HOO^{\cdot} + C_6H_6$$

$$\left.\begin{aligned} AOO^{\cdot} + AH &\xrightarrow{k_p^{aa}} AOOH + A^{\cdot} \\ AOO^{\cdot} + BH &\xrightarrow{k_p^{ab}} AOOH + B^{\cdot} \end{aligned}\right\} r_a = k_p^{aa}/k_p^{ab}$$

$$\left.\begin{aligned} HOO^{\cdot} + BH &\xrightarrow{k_p^{hb}} HOOH + B^{\cdot} \\ HOO^{\cdot} + AH &\xrightarrow{k_p^{ha}} HOOH + A^{\cdot} \end{aligned}\right\} r_b = k_p^{hb}/k_p^{ha}$$

At long chain lengths and relatively low conversions r_a and r_b can be obtained by applying the copolymer composition equation (31) to these co-oxidations. That is

$$\rho = \frac{\Delta[AH]}{\Delta[BH]} = \frac{r_a[AH]/[BH] + 1}{r_b[BH]/[AH] + 1}$$

where $\Delta[AH]$ and $\Delta[BH]$ are the amounts of AH and BH consumed. In the present work, the r values were determined by the method of Fineman and Ross (32). That is, if $(\rho - 1)/R$ is plotted against ρ/R^2, a straight line should be obtained with intercept r_a and slope $-r_b$, the quantity R being the average value of [AH]/[BH] during the reaction. The data from Table II are plotted in this way in Fig. 1, rather good straight lines are obtained in all cases. The values of r_a and r_b are given in Table III. If the relative reactivity of AH and BH towards $AOO^{\cdot}$ is the same as towards $HOO^{\cdot}$, then $r_a = 1/r_b$ and $r_a r_b = 1$. Values of $r_a r_b$ less than 1.0 may be due to polar or to steric factors (26). However, Mayo *et al.* (26) have pointed out that in co-oxidations, all $r_a r_b$ products less than 0.5 or greater than 1.0 should be considered suspect unless unusual care has been taken to confirm them. The $r_a r_b$ products obtained with aldehydes and cyclohexadiene in the present work are reasonably satisfactory according to this criterion.

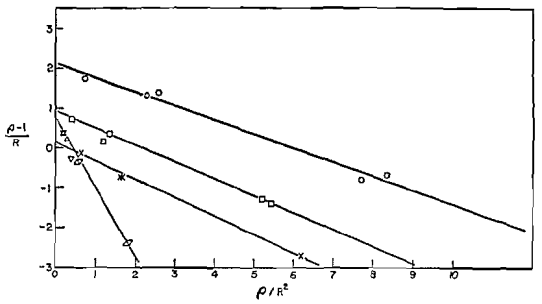

FIG. 1. Fineman–Ross plot of the co-oxidation of 1,4-cyclohexadiene with pivaldehyde, ○; cyclohexanecarboxaldehyde, □; octanal, △; heptanal, ▽; and benzaldehyde, ×. (The abscissa for the cyclohexadiene-benzaldehyde co-oxidation is 1/10 of that shown.) Data are from Table II.

The r_a and r_b values in Table III imply that saturated aldehydes and cyclohexadiene have rather similar reactivities towards acylperoxy and hydroperoxy radicals. However, benzaldehyde would appear to be quite a bit less reactive than the diene. This was not entirely unexpected in view of previous work on benzaldehyde co-oxidations (2, 5). The low reactivity of benzaldehyde was confirmed by its co-oxidation with *n*-heptanal. In these reactions so little benzaldehyde was consumed that errors in the analyses made it impossible to determine r_a and r_b with much accuracy even after repeated experiments. The estimated values of r_a (~ 10) and r_b (~ 0.1) given in Table III are subject to considerable error. They are, however, in reasonable agreement with the values reported for the butanal, *p*-chlorobenzaldehyde co-oxidation ($r_a = 10.7$, $r_b = 0.28$ (2)) and for the decanal, benzaldehyde co-oxidation ($r_a = 8.6$, $r_b = 0.2$ (5)).

Co-oxidation Kinetics

A comparison of the oxidation rates listed in Tables I and II show that the aldehydes oxidize

Can. J. Chem. Downloaded from www.nrcresearchpress.com by 210.87.254.40 on 09/05/12
For personal use only.

Can. J. Chem. Downloaded from www.nrcresearchpress.com by 210.87.254.40 on 09/05/12
For personal use only.

much more rapidly in the absence of cyclohexadiene. In quantitative terms, the values of $R_s/[RCHO]R_i^{1/2}$ for the aldehydes and for their 1.0:0.97 M mixtures with cyclohexadiene are 0.39 and 0.02 for heptanal, 0.47 and 0.018 for octanal, 0.44 and 0.027 for cyclohexanecarboxaldehyde, 0.96 and 0.018 for pivaldehyde, and 0.31 and 0.03 for benzaldehyde. In principle, this inhibition might be due solely to the fact that chain terminations involving HOO· radicals occur very rapidly. However, the absolute rate constants found for benzaldehyde, heptanal, and octanal relative to cyclohexadiene (Table I) rule out this explanation.

The photochemically initiated oxidation of benzaldehyde (0.5 M) is also retarded by the addition of other fairly readily oxidized hydrocarbons and by the addition of hydroperoxides. Thus tetralin, tetralin hydroperoxide, *t*-butyl hydroperoxide, and cumene hydroperoxide reduce the rate of oxidation of benzaldehyde by a factor of 10–50 and cumene reduces the rate by a factor of 5 (see Table IV and Fig. 2). The hydroperoxide concentrations in Table IV and Fig. 2 represent, of course, the amount of hydroperoxide added. It is not clear what role, if any, the hydroperoxide–aldehyde addition product (reaction [7]) plays in retarding the oxidation.

TABLE IV

The retardation of the photochemically initiated oxidation of benzaldehyde (0.5 M) by hydrocarbons and hydroperoxides*

Hydrocarbon or hydroperoxide	Concentration, M	Rate of oxidation $\times 10^5\ M\ s^{-1}$
—	—	8.75
Tetralin hydroperoxide	0.005	1.6
,,	0.0125	0.72
,,	0.025	0.49
,,	0.05	0.32
,,	0.13	0.15
Tetralin	0.025	0.77
,,	0.05	0.45
,,	0.5	0.4
Cumene hydroperoxide	0.01	2.0
,,	0.05	0.9
,,	0.1	0.54
Cumene	0.01	7.0
,,	0.025	5.7
,,	0.05	4.2
,,	0.5	1.9
t-Butyl hydroperoxide	0.016	0.57
	0.031	0.44

*$R_i = 3.4 \times 10^{-7}\ M\ s^{-1}$

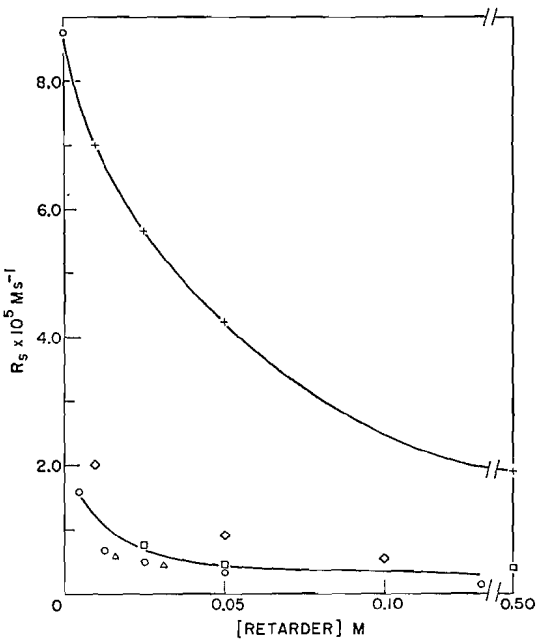

FIG. 2. The oxidation of benzaldehyde (0.5 M) in the presence of tetralin, □; tetralin hydroperoxide, ○; cumene, ×; cumene hydroperoxide, ◇; and *t*-butyl hydroperoxide, △. Data are from Table IV.

The rate constants for the oxidation of benzaldehyde (0.5 M) in the presence of tetralin (0.5 M) are $k_p/(2k_t)^{1/2} = 0.011\ M^{-1/2}\ s^{-1/2}$, $k_p = 23\ M^{-1}\ s^{-1}$, and $2k_t = 4.5 \times 10^6\ M^{-1}\ s^{-1}$, and in the presence of tetralin hydroperoxide (0.13 M) $k_p/(2k_t)^{1/2} = 0.0053\ M^{-1/2}\ s^{-1/2}$, $k_p = 13\ M^{-1}\ s^{-1}$, and $2k_t = 6.0 \times 10^6\ M^{-1}\ s^{-1}$. These termination rate constants are about 1/400 of the value found for pure benzaldehyde in chlorobenzene. They are, in fact, similar to the value for pure tetralin which suggests that tetralylperoxy radicals are by far the most abundant peroxy radical species present in these reactions. Tetralin and tetralin hydroperoxide reduce the rate of oxidation of benzaldehyde in spite of the fact that they reduce the termination rate constant. The propagation rate constant is, therefore, much lower in the oxidation of the mixtures than in the oxidation of pure benzaldehyde. The retarding effect that hydrocarbons and their hydroperoxides have on the oxidation of benzaldehyde must be due to the participation of alkylperoxy radicals in the oxidation chain. Alkylperoxy radicals must therefore be considerably less reactive than the benzoylperoxy radical.

TABLE V

Thermal oxidation of aldehydes and their co-oxidation with tetralin and cumene*

Aldehyde	Concentration, M	$R_s \times 10^5\ M\ s^{-1}$	Tetralin (0.5 M) $R_s \times 10^5\ M\ s^{-1}$	Cumene (0.5 M) $R_s \times 10^5\ M\ s^{-1}$
Heptanal	0.5	0.86	0.18	0.76
Cyclohexanecarboxaldehyde	0.45	1.13	0.44	1.12
Pivaldehyde	0.5	2.0	0.47	1.61
Benzaldehyde	0.5	0.51	0.024	0.11

*[TBH] = 0.2 M; $R_i = 2.6 \times 10^{-9}\ M\ s^{-1}$.

Tetralin and cumene also retard the oxidations of heptanal, cyclohexanecarboxaldehyde, and pivaldehyde (Table V). Tetralin reduces the rate of oxidation of these three aldehydes by a factor of 3–4 which is considerably less than its retarding effect on benzaldehyde ($\sim$ 20). Cumene is a rather weak retarder for the oxidation of these aliphatic aldehydes. Its effect on them is much less than its effect on benzaldehyde. The rate constants for the co-oxidation of heptanal (0.5 M) – tetralin (0.5 M) are $k_p/(2k_t)^{1/2} = 0.07\ M^{-1/2}\ s^{-1/2}$, $k_p = 700\ M^{-1}\ s^{-1}$, and $2k_t = 1 \times 10^8\ M^{-1}\ s^{-1}$. The termination rate constant is reasonably close to the value for pure heptanal. The retarding effect of tetralin on the oxidation of heptanal is, therefore, due to a decrease in the rate constant for the propagation of the chain. The chain is probably carried by both acylperoxy radicals and tetralylperoxy radicals, with the former predominating.

The TBH thermally initiated aldehyde oxidations were also inhibited with 2,6-di-*t*-butyl-4-methylphenol (Ionol). The rates were inversely proportional to the Ionol concentration and the kinetics are similar to those of hydrocarbon oxidations inhibited with this phenol (27). The rate controlling step for chain termination involves abstraction of the phenolic hydrogen by a peroxy radical (reaction [8]). The inhibited rate is given by

$$R_{inh} = \frac{k_p[\mathrm{RCHO}]R_i}{2k_{inh}[\mathrm{InH}]}$$

The values of k_p/k_{inh} and k_{inh} are given in Table VI. This table also summarizes the absolute rate constants determined from the photo-initiated reactions and the values of $k_p/(2k_t)^{1/2}$ obtained from the TBH thermally initiated oxidations (Table V, column 2).

Discussion

Termination

The aldehydes studied in the present work oxidize at similar rates under similar experimental conditions. That is, the values of $k_p/(2k_t)^{1/2}$ only differ slightly from one aldehyde to another. The absolute rate constants summarized in Table VI show that this is due to compensating changes in k_p and $2k_t$. The termination rate constants increase from $\sim 7 \times 10^6$ for pivaldehyde and cyclohexanecarboxaldehyde, to $\sim 6 \times 10^7$ for heptanal and octanal, $\sim 1 \times 10^8$ for acetaldehyde, and to $\sim 2 \times 10^9$ for benzaldehyde. The propagation rate constants increase from $\sim 1 \times 10^3$ for pivaldehyde to $\sim 1 \times 10^4$ for benzaldehyde.

The termination rate constant for benzaldehyde is close to the diffusion controlled limit for a bimolecular reaction. This implies that the aroyl tetroxide, $PhC(O)O_4C(O)Ph$ (whether a true intermediate or merely a transition state), is not formed reversibly. Moreover, if this tetroxide decomposes to give benzoyloxy radicals (reaction [4*b*]), the majority of these radicals must combine in the cage.

The lower termination constants for the alkanals may arise partly from the rapid decarboxylation of the acyloxy radicals formed in the tetroxide homolysis. That is, the radical centers will be separated by a greater distance if CO_2 loss occurs concurrently with, or immediately after, oxygen loss, e.g.

[4*c*] $Me_3CCOOOOCCMe_3 \rightarrow$ (O, O) $Me_3C^{\cdot} + CO_2 + O_2 + CO_2 + {}^{\cdot}CMe_3$

Carbon dioxide is, in fact, formed in these oxidations. Under the usual experimental conditions, acetaldehyde and pivaldehyde gave one

Can. J. Chem. Downloaded from www.nrcresearchpress.com by 210.87.254.40 on 09/05/12
For personal use only.

Can. J. Chem. Downloaded from www.nrcresearchpress.com by 210.87.254.40 on 09/05/12
For personal use only.

TABLE VI

Summary of rate constants, in units of M s, for the oxidation of aldehydes at 0 °C

Substrate	Thermal $k_p/(2k_t)^{\frac{1}{2}}$	Photo $k_p/(2k_t)^{\frac{1}{2}}$	$k_p \times 10^{-3}$	$2k_t \times 10^{-6}$	k_p/k_{inh}	$k_{inh} \times 10^{-3}$	$k_p^{ha} \times 10^{-1}$*	$k_p^{ab} \times 10^{-3}$†
Acetaldehyde	—	0.265	2.7	104	—	—	—	—
Heptanal‡	0.34	0.39	3.1	54	0.64	4.8	5.0	4.8
Octanal‡	—	0.47	3.9	69	0.95	4.1	5.0	6.1
Cyclohexanecarboxaldehyde	0.49	0.44	1.1	6.8	0.68	1.6	18.6	1.2
Pivaldehyde	0.80	0.96	2.5	6.6	1.6	1.6	22.8	1.2
Benzaldehyde‡	0.20	0.29	12	1760	0.13	92	1.7	70.6
1,4-Cyclohexadiene	0.008	0.0081	0.082	104	0.034	2.4	(8.2)	(0.082)
Tetralin	0.0008	0.00078	0.0012	2.3	0.000556	2.2	—	—

*$k_p^{ha} = (k_p)_{C_6H_8}/r_b$; i.e., k_p for $HOO^{\cdot} + RCHO$.
†$k_p^{ab} = (k_p)_{RCHO}/r_a$; i.e., k_p for $RC(O)OO^{\cdot} + C_6H_8$.
‡At 5 °C, Melville reports $k_p/(2k_t)^{\frac{1}{2}} = 0.45$, $k_p = 2.7 \times 10^3$, $2k_t = 34 \times 10^6$ for decanal and $k_p/(2k_t)^{\frac{1}{2}} = 0.13$, $k_p = 1.9 \times 10^3$, $2k_t = 210 \times 10^6$ for benzaldehyde (4–6).

Can. J. Chem. Downloaded from www.nrcresearchpress.com by 210.87.254.40 on 09/05/12
For personal use only.

molecule of carbon dioxide per chain initiated, but benzaldehyde gave only 0.1. Although Kiefer and Traylor (33) have shown that the presence of one or two small molecules (O_2, N_2, CO_2) in the cage separating a *t*-butoxy radical pair has only a relatively small effect on the percentage of geminate combination in the cage, it is possible that three molecules would have a significant effect on this percentage.

A possible additional reason for the slower termination of acylperoxy radicals compared with benzoylperoxy radicals is that the acyltetroxides are formed reversibly and decompose more slowly than the aroyltetroxide. A parallel may perhaps be drawn with the tertiary peroxy radicals for which it has been found that *t*-alkylperoxy radicals terminate oxidation chains more slowly than *t*-aralkylperoxy radicals, apparently because the *t*-alkyltetroxides are more stable than the *t*-aralkyltetroxides (34).

A contributing factor to the low termination rate constants of the alkanals may be the presence of alkylperoxy radicals in the reaction. Since these radicals have a much lower reactivity in propagation than acylperoxy radicals, their steady-state concentration might rise to the point where they contributed significantly to termination even though they do not themselves terminate chains particularly rapidly[5]. If alkylperoxy radicals do play a role in the reaction, the alkyl radicals may be formed by the non-terminating interactions of acylperoxy radicals (reactions [4*b*] and [4*c*]) or, with the linear alkanals, by intramolecular hydrogen abstraction by the acylperoxy radical. Alkylperoxy radicals are not formed by decarbonylation of the acyl radical (35) at 0 °C since carbon monoxide is virtually absent in the gaseous products of the oxidation of 0.2 *M* pivaldehyde to 20% conversion. The fact that alkylperoxy radicals cannot be present in large amounts in this pivaldehyde oxidation was confirmed by the fact that *t*-butanol was not detected when the peroxidic products of the reaction were reduced with triphenylphosphine.

Propagation

The propagation rate constants for aldehyde oxidation can best be understood in terms of the variations in the reactivity of the aldehyde and the variations in the reactivity of the attacking peroxy radical. The reactivities of the aldehydes towards a single peroxy radical (HOO·) are given by the k_p^{ha} values in Table VI. These rate constants decrease by an order of magnitude along the series pivaldehyde > cyclohexanecarboxaldehyde > heptanal[6] ~ octanal > benzaldehyde[6]. While not too much reliance should be put on the absolute values of k_p^{ha}, this order can best be understood in terms of the inductive effect of the group R attached to the CHO group, increased electron donation increasing the rate of hydrogen abstraction by a peroxy radical (cf. 2, 36, 37). It is perhaps worth noting that alkyl radicals also abstract hydrogen more rapidly from alkanals than from benzaldehyde (35).

The variation in the reactivity of the various acylperoxy radicals is clearly demonstrated by the absolute rate constants for their attack on cyclohexadiene, i.e., k_p^{ab} (Table VI, last column). The peroxy radicals from pivaldehyde and cyclohexanecarboxaldehyde are about 15 times as reactive as the hydroperoxy radical, those from heptanal and octanal are about 70 times as reactive, and the benzoylperoxy radicals about 860 times as reactive as HOO·. The high reactivity of benzoylperoxy radicals relative to arylperoxy radicals is also indicated by the greater sensitivity to inhibition by hydrocarbons of the oxidation of benzaldehyde compared with the other aldehydes. Moreover, if tetralylperoxy radicals are in fact dominant in the benzaldehyde–tetralin co-oxidation and the benzaldehyde–tetralin hydroperoxide oxidation, as is suggested by the termination rate constants, then the propagation rate constant for these reactions (~ 13–23 M^{-1} s^{-1}) represents the rate constant for attack of tetralylperoxy radicals on benzaldehyde. Since benzoylperoxy radicals attack benzaldehyde with a rate constant of 12 000 M^{-1} s^{-1}, the benzoylperoxy radical is 12 000/23 to 12 000/13 ≈ 520–920 times as reactive as tetralylperoxy in abstraction from benzaldehyde.

The differences in reactivity between the various acylperoxy radicals are probably due mainly to polar effects. Acylperoxy radicals must be considerably more electrophilic species than

[5]The rate constants for the self reactions of *t*-butylperoxy and cyclohexylperoxy radicals at 30 °C are 1.3×10^3 and 2.0×10^6 M^{-1} s^{-1} (17, 18, 20).

[6]The co-oxidation of heptanal and benzaldehyde (Table III) indicates that the former is about ten times as reactive as the latter towards the two corresponding acylperoxy radicals.

Can. J. Chem. Downloaded from www.nrcresearchpress.com by 210.87.254.40 on 09/05/12
For personal use only.

alkylperoxy radicals[7] and polar effects must play an important role in their reactions. Electron releasing groups will decrease the electrophilicity of the radical and hence decrease the importance of polar contributions of the following type to the transition state

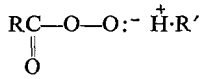

Electron releasing groups will therefore decrease the reactivity of an acylperoxy radical and electron attracting groups will increase its reactivity, and hence the radical reactivity increases along the aldehyde series from pivaldehyde to benzaldehyde. Since this polar effect works in the opposite direction from that influencing the intrinsic reactivity of the aldehyde, the two effects tend to cancel each other out in determining the reactivity of the aldehyde towards its own peroxy radical (i.e. the k_p values).

The Ionol Inhibited Reaction

The rate constants for attack on Ionol by the acylperoxy and benzoylperoxy radicals (k_{inh}, Table VI) are roughly equal to the values found for their attack on cyclohexadiene (k_p^{ab}). In contrast, the hydroperoxy radical attacks Ionol about 30 times as fast as it attacks cyclohexadiene, the rate constant for the Ionol reaction (and for the tetralylperoxy–Ionol reaction) being similar to the values for the acylperoxy–Ionol reaction. Only the benzoylperoxy radicals are noticeably more reactive towards Ionol than the other radicals. The reason for (what appears to be) an unexpectedly low reactivity of Ionol towards acylperoxy and benzoylperoxy is not at all obvious. Conceivably, the rate of hydrogen atom transfer from the phenol might be reduced by the bonding of the phenolic hydrogen to the carbonyl oxygen of the acylperoxy radical, i.e.

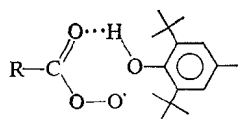

Conclusion

Although excessive reliance on any of the individual rate constants or rate constant ratios obtained in this work is unjustified, the overall picture leaves little doubt that acylperoxy radicals are considerably more reactive in hydrogen atom abstraction than alkylperoxy radicals. The main reason for this must be that acylperoxy radicals form stronger bonds to hydrogen than alkylperoxy radicals, i.e. $D(RC(O)OO—H) > D(ROO—H)$[8]. A greater O—H bond strength in the per-acid is to be expected both because of strong polar contributions to the bond[9] and because of the intramolecular hydrogen bond to the carbonyl oxygen. Perbenzoic acid is a slightly stronger acid than alkyl per-acids which could mean that its O—H bond strength is also greater, thus accounting for the higher reactivity of benzoylperoxy radicals relative to acylperoxy radicals.

The enhanced reactivity of acylperoxy and benzoylperoxy radicals provides a ready explanation for the inhibition of aldehyde oxidations by hydrocarbons (see Tables IV and V and ref. 39). That is, by its attack on the hydrocarbon the acylperoxy radical is converted to an alkyl peroxy radical of much lower reactivity. The overall propagation rate constant is therefore decreased. This was confirmed by the actual measurement of the propagation rate constants in the benzaldehyde–tetralin and heptanal–tetralin mixtures.

1. H. L. J. Bäckström. J. Am. Chem. Soc. **49**, 1460 (1927); Z. Physik. Chem. **B25**, 99 (1934).
2. C. Walling and E. A. McElhill. J. Am. Chem. Soc. **73**, 2927 (1951).
3. H. R. Cooper and H. W. Melville. J. Chem. Soc. 1984 (1951).
4. H. R. Cooper and H. W. Melville. J. Chem. Soc. 1994 (1951).
5. T. A. Ingles and H. W. Melville. Proc. Roy. Soc. London, Ser. A, **218**, 163 (1953).
6. T. A. Ingles and H. W. Melville. Proc. Roy. Soc. London, Ser. A, **218**, 175 (1953).
7. W. A. Waters and C. Wickham-Jones. J. Chem. Soc. 812 (1951).
8. P. Fillet, M. Niclause, and M. Letort. Compt. Rend. **236**, 1489 (1953); J. Chim. Phys. **53**, 8 (1956).
9. M. F. R. Mulcahy and I. C. Watt. J. Chem. Soc. 2971 (1954).
10. J. R. McNesby and T. W. Davis. J. Am. Chem. Soc. **76**, 2148 (1954).
11. J. Lemaire, M. Niclause, and M. Dzierzynski. J. Chim. Phys. **62**, 1249 (1965).
12. L. Bateman and A. L. Morris. Trans. Faraday Soc. **49**, 1026 (1953).
13. G. Wittig. Ann. Chem. **558**, 201 (1947).
14. T. Ikawa, T. Fukushima, M. Muto, and T. Yanagihara. Can. J. Chem. **44**, 1817 (1966).

[7]It is worth noting that *p*-chlorobenzoylperoxy radical attack on substituted benzaldehydes (2) when correlated by the Hammett equation using σ^+ constants gives $\rho^+ \approx -0.65$, while cumylperoxy radicals attacking substituted cumenes (37) give a much smaller $\rho^+ \sim -0.29$.

[8]$D(ROO—H) \approx D(HOO—H) \approx 90$ kcal/mole (38).

[9]The O—H bond strength in organic acids is about 10 kcal/mole greater than in alcohols (38).

15. T. IKAWA, M. MUTO, and T. SHINTANI. Bull. Japan Petrol. Inst. **7**, 41 (1965).
16. J. A. HOWARD and K. U. INGOLD. Can. J. Chem. **45**, 793 (1967).
17. J. A. HOWARD and K. U. INGOLD. Can. J. Chem. **46**, 2655 (1968).
18. J. A. HOWARD and K. U. INGOLD. Can. J. Chem. **46**, 2661 (1968).
19. G. A. RUSSELL. J. Am. Chem. Soc. **79**, 3871 (1957).
20. J. A. HOWARD and K. U. INGOLD. J. Am. Chem. Soc. **90**, 1056, (1968); **90**, 1058 (1968).
21. C. A. MCDOWELL and L. K. SHARPLES. Can. J. Chem. **36**, 268 (1958).
22. C. A. MCDOWELL and S. SIFNIADES. Can. J. Chem. **41**, 300 (1963).
23. K. U. INGOLD. Accounts Chem. Res. **2**, 1 (1969).
24. R. HIATT, J. CLIPSHAM, and T. VISSER. Can. J. Chem. **42**, 2754 (1964).
25. J. A. HOWARD, W. J. SCHWALM, and K. U. INGOLD. Advan. Chem. Ser. **75**, 6 (1968).
26. F. R. MAYO, M. G. SYZ, T. MILL, and J. K. CASTLEMAN. Advan. Chem. Ser. **75**, 38 (1968).
27. J. A. HOWARD and K. U. INGOLD. Can. J. Chem. **40**, 1851 (1962); **41**, 1744 (1963); **47**, 2800 (1963); **42**, 2324 (1964); **43**, 2724 (1965).
28. J. A. HOWARD and K. U. INGOLD. Can. J. Chem. **43**, 2729 (1965).
29. J. A. HOWARD and K. U. INGOLD. Can. J. Chem. **44**, 1119 (1966).
30. J. A. HOWARD and K. U. INGOLD. Can. J. Chem. **45**, 785 (1967).
31. F. R. MAYO and C. WALLING. Chem. Revs. **46**, 191 (1950).
32. M. FINEMAN and S. D. ROSS. J. Polymer Sci. **5**, 259 (1950).
33. H. KIEFER and T. G. TRAYLOR. J. Am. Chem. Soc. **89**, 6667 (1967).
34. K. ADAMIC, J. A. HOWARD, and K. U. INGOLD. Unpublished results.
35. C. WALLING. Free radicals in solution. John Wiley and Sons, Inc., New York. 1957. pp. 277–278.
36. G. A. RUSSELL. J. Am. Chem. Soc. **78**, 1047 (1956).
37. J. A. HOWARD, K. U. INGOLD, and M. SYMONDS, Can. J. Chem. **46**, 1017 (1968).
38. S. W. BENSON. J. Am. Chem. Soc. **87**, 972 (1965). S. W. BENSON and R. SHAW. Advan. Chem. Ser. **75**, 288 (1968).
39. T. G. TRAYLOR and N. CLINTON. Division of Petroleum Chemistry Preprints, 157th National Meeting of the Am. Chem. Soc., Minneapolis. April 13–18, 1969. p. A99 and private communication.

Can. J. Chem. Downloaded from www.nrcresearchpress.com by 210.87.254.40 on 09/05/12
For personal use only.

Can. J. Chem. Downloaded from www.nrcresearchpress.com by 210.87.254.105 on 09/05/12
For personal use only.

Thermal decomposition of barium perchlorate

R. J. Acheson and P. W. M. Jacobs
Department of Chemistry, University of Western Ontario, London, Ontario

Received February 20, 1969

The thermal decomposition of anhydrous barium perchlorate to barium chloride and oxygen has been studied by pressure measurements, or by weight loss, in vacuo, under the accumulated gaseous products (0–3 Torr oxygen), under dry air or nitrogen, and mixed with added barium chloride. The plots of fractional decomposition (α) against time (t) are complex, as would be expected for a reaction proceeding via unstable intermediates. The most pronounced features of the $\alpha(t)$ curves are an initial acceleratory period, which is succeeded by an approximately linear period and then, after a sharp break (reduction in rate), by a deceleratory period which conforms to the contracting-volume kinetic law. The latter stage is associated with the decomposition of barium chlorate and has an activation energy of 59 kcal/mole. The first two stages comprise the decomposition of perchlorate to chlorate with the approximate stoichiometry $3ClO_4^- \rightleftharpoons 2ClO_3^- + Cl^- + 3O_2$. A chain reaction sequence, which involves O atoms as chain carriers, is proposed for these stages. The effect of the removal of products, of increasing the ambient pressure of inert gas, and of the addition of barium chloride, can all be explained on this model.

Canadian Journal of Chemistry, 47, 3031 (1969)

The thermal decomposition of barium perchlorate (BP) yields barium chloride and oxygen (1). Barium perchlorate trihydrate may be dehydrated, without decomposition *in vacuo*, but in air, hydrolysis of the perchlorate accompanies dehydration. Dehydration to the monohydrate occurs on pumping at room temperature and subsequent dehydration occurs at temperatures well below that of the thermal decomposition of the anhydrous salt (435–495 °C).

Barium perchlorate is known to undergo two crystalline phase transitions (2). The transition from α-BP to β-BP occurs at 284 °C and that from β-BP to γ-BP at 360 °C. At the time this work was performed no complete study of the thermal decomposition of BP had been reported although one incomplete study (3) had yielded an activation energy of 61.6 kcal/mole. When this paper had been written in manuscript form, a series of papers (4–8) by Solymosi and his collaborators, which overlaps our work, appeared. Our manuscript has therefore been rewritten to take account of these new data. The principal experimental differences are that Solymosi (8) used only pressure measurements to investigate the thermal decomposition of BP, whereas we used thermogravimetric measurements as well, but he also studied the decomposition of $Ba(ClO_2)_2$ (4) and $Ba(ClO_3)_2$ (5). There are also considerable differences in the kinetic analyses and in the interpretation of the results.

Thermal Decomposition of Anhydrous Barium Perchlorate

The thermal decomposition of anhydrous BP *in vacuo* was studied by measurement, with McLeod gauges, of the pressure increase as a function of time in a constant volume system. The isothermal decomposition of single crystals, pellets, and crushed reactant was followed in this way. Weight loss measurements in a dynamic vacuum were also made. The percentage residue obtained from 4 determinations was $62.75 \pm 1.05\%$ which may be compared with a theoretical value 61.76% for complete decomposition to $BaCl_2$. Thus decomposition of BP to $BaCl_2$ under our experimental conditions is $97.4 \pm 1.5\%$ complete to $BaCl_2$, in substantial agreement with the results from ref. 1, thus vindicating the use of pressure–time measurements to follow the kinetics.

Plots were made of the fractional decomposition (α) against time. In all runs the general form of $\alpha(t)$ was acceleratory up to $\alpha = 0.52 \pm 0.02$ (but see later for more specific comments). The rate of this reaction was independent of the mechanical pre-treatment of the reactant, or of the ambient gas atmosphere. The kinetics of thermal decomposition ($\alpha \lesssim 0.52$) of crystals, pellets, or powder samples, in a dynamic vacuum, in the accumulated reaction products (volatile at −195 °C), or in 160 Torr dry air, were identical within experimental error.

Representative $\alpha(t)$ plots are shown in Fig. 1. At $\alpha = 0.52 \pm 0.02$ a distinct break occurred and thereafter the reaction was slower by a factor of ~ 10. This break occurred when the decomposition was carried out in N_2, in air, or in the gaseous reaction products, though not when BP was decomposed in a dynamic vacuum. Above $\alpha = 0.52 \pm 0.02$ the reaction was always deceleratory throughout. As the ambient pressure was

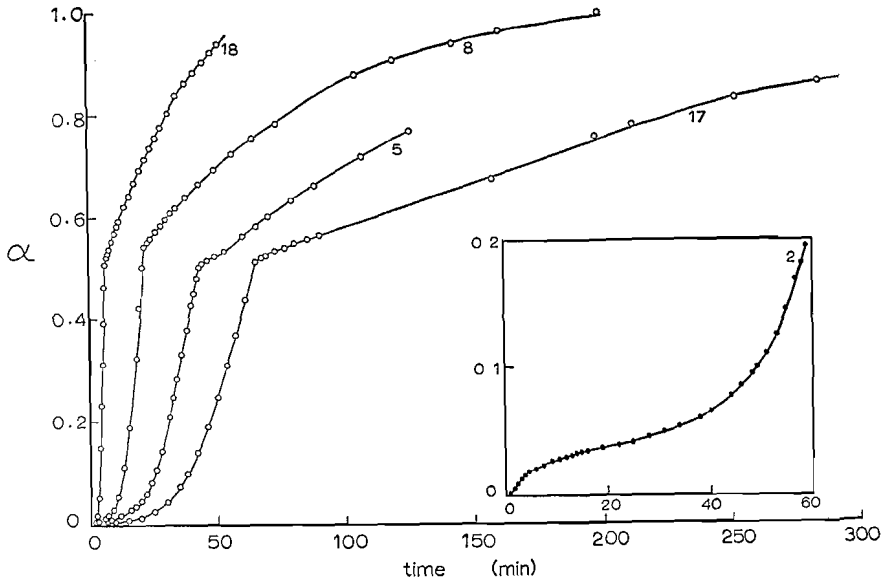

FIG. 1. Plots of fractional decomposition α against time for the thermal decomposition of anhydrous BP in vacuo. Run 18, 487 °C; run 8, 467.5 °C; run 5, 459.6 °C; run 17, 451.6 °C.

decreased, the rate of the reaction for $\alpha \gtrsim 0.52$ increased markedly and in a vacuum of better than 10^{-3} Torr no distinct change was seen in the $\alpha(t)$ plot and the reaction continued without a break. This effect is displayed in Fig. 2 where curve *a* shows "normal" behavior when BP decomposes under its own reaction products (i.e. oxygen, which reaches a pressure of $\sim$ 1–3 Torr at the break), curve *b* shows the effect of reduced pressure, and curve *c* shows an $\alpha(t)$ plot in a dynamic vacuum of $\sim 10^{-3}$ Torr, with the break just distinguishable.

Solymosi (8) followed the reaction only by measuring the pressure of the accumulated products and his results (see Fig. 1 of ref. 8) are similar to ours under these conditions. Reaction of those samples of crystals or pelleted reactant which contained a small percentage of water, due to incomplete dehydration prior to heating to the reaction temperature, was initially deceleratory, but following the completion ($\alpha < 0.05$) of this reaction, decomposition continued in a manner identical to that of the anhydrous reactant. This effect is illustrated in the inset diagram in Fig. 1.

Four preparations of BP were used in this investigation. These were (*a*) Analytical Grade barium perchlorate from Alfa Inorganics Inc., (*b*) anhydrous barium perchlorate, (*c*) once recrystallized BP, and (*d*) twice recrystallized BP. No differences in the behavior or kinetics of decomposition of the 4 samples were observed. The hydrated salts were dehydrated, normally *in situ*, at $\sim$ 250 °C prior to reaction (except for commercial "anhydrous" BP, which nevertheless contained a substantial amount of water). Melting did not appear to occur since the shape of the original sample, whether pellet or single crystal, was usually retained throughout the experiment (corresponding differential thermal analysis results presented later). One experiment was interrupted at $\alpha = 0.4$, the reactant was cooled to room temperature, exposed to air, re-evacuated, reheated to the original reaction temperature, and decomposition continued. This procedure resulted in no significant deviation of the kinetics of the subsequent reaction ($0.4 < \alpha < 0.96$) from those expected for an uninterrupted experiment.

Kinetics of Thermal Decomposition for $0 < \alpha < 0.5$

No significant differences were detected between the thermal decomposition of BP, in the temperature range 435–495 °C, when this was followed by (*a*) pressure measurements, or (*b*) weight-loss measurements. The reaction was

Can. J. Chem. Downloaded from www.nrcresearchpress.com by 210.87.254.105 on 09/05/12
For personal use only.

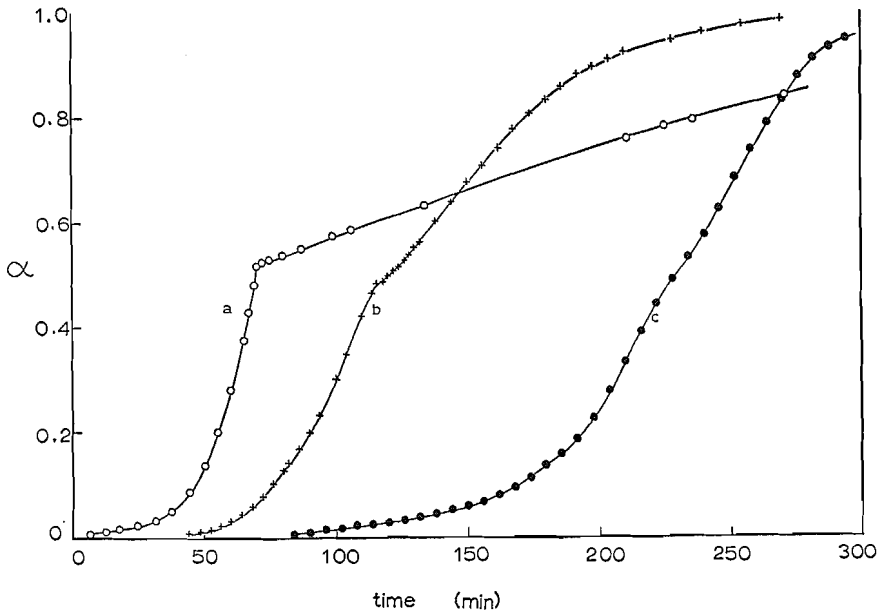

FIG. 2. Effect of pressure on the kinetics of the reaction for $\alpha > 0.52$. (*a*) ○, Decomposition at 446.6 °C under accumulated reaction products volatile at −195 °C (i.e. oxygen); (*b*) +, decomposition at 441.1 °C under reduced pressure; (*c*) ●, decomposition at 437.5 °C at $P < 10^{-3}$ Torr.

acceleratory $0 < \alpha < 0.25$. For $0.25 < \alpha < 0.5$, the reaction generally continued at an approximately linear rate, although in a significant number of experiments the reaction either became somewhat decelerating or continued in a slightly acceleratory fashion. Clearly, therefore, the kinetics cannot obey a single rate equation, even over the range $0 < \alpha < 0.5$.

It is evident from Fig. 1 that $t_{0.1}$, the time taken to reach $\alpha = 0.1$, is a measure of the induction period for the reaction. Accordingly $\log (t_{0.1} - \tau)$ where τ is the heat-up time ($\tau = 1$ min for pressure measurements, 4 min for weight-loss measurements) was plotted against T^{-1} whence the parameters $E = 83.5$ kcal/mole, $\log (A/s^{-1}) = 21.72$ were derived by least mean squares (l.m.s.) fit to the Arrhenius equation. The rate during the roughly linear portion of the $\alpha(t)$ curve was obtained by calculating the slopes, $S(0.25)$, of the $\alpha(t)$ plots at $\alpha = 0.25$. This method was adopted in order to include those runs which displayed an acceleratory or deceleratory character. The least squares values for the Arrhenius parameters derived from $S(0.25)$ were $E = 80.0$ kcal/mole, $\log (A/s^{-1}) = 20.52$.

Because of the predominantly acceleratory kinetics at small α, extensive use was made initially of the Avrami–Erofeev equation

$$[1] \qquad [-\ln (1 - \alpha)]^{\frac{1}{n}} = k_1 t$$

However, both the range of α over which this relationship was obeyed and the value of n varied significantly for different experiments, the full range of n being $2 \leq n \leq 5$. Rate-constants k_1 were therefore extracted from the relationship

$$[1'] \quad \log [-\ln (1 - \alpha)] = n \log k_1 + n \log t$$

and a least squares fit to the Arrhenius equation for k_1 yielded values for the activation energy and pre-exponential factor of $E = 76.7$ kcal/mole and $\log (A/s^{-1}) = 19.54$, respectively. However, because of the large variations in n, this analysis was not considered satisfactory, although the value of the activation energy $E = 76.7$ kcal/mole for $0.05 < \alpha < 0.36$ may be of some significance (see later).

Despite the unsatisfactory representation of the data by eq. [1'], a simple power law

$$[2] \qquad \alpha^{\frac{1}{2}} = k_2(t - t_0)$$

fitted the kinetics quite well. Plots of $\alpha^{\frac{1}{2}}$ against t

Can. J. Chem. Downloaded from www.nrcresearchpress.com by 210.87.254.105 on 09/05/12
For personal use only.

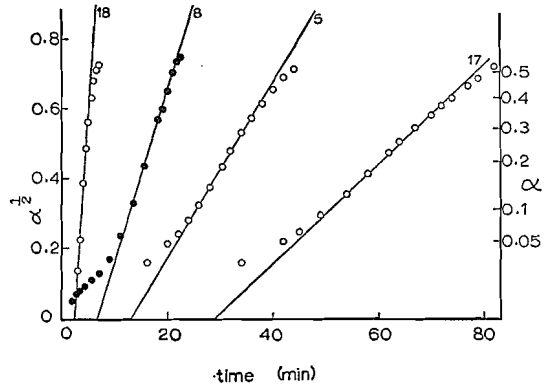

FIG. 3. Plots of $\alpha^{\frac{1}{2}}$ against t for the data shown in Fig. 1.

for the runs depicted in Fig. 1 are given in Fig. 3. The fit seems to improve somewhat with temperature but covers the range $0.06 < \alpha < 0.4$–0.5, in general. The least mean squares Arrhenius parameters for k_2 were $E = 80.9$ kcal/mole and $\log (A/s^{-1}) = 20.72$. The values of t_0, which represent the induction period before eq. [2] is obeyed, were also fitted to the Arrhenius equation and yielded the l.m.s. parameter-values $E = 69.7$ kcal/mole, $\log (A/s^{-1}) = 17.91$.

Effect of Additives

(a) Ammonium Perchlorate (AP)

The thermal decomposition of an intimately crushed mixture of BP with 3.86% AP showed an initial deceleratory reaction for $0 < \alpha < 0.03$. A first order rate plot using $\alpha' = \alpha/0.03$ was linear and the rate constant obtained (0.382 min^{-1} at 450 °C) was in close agreement with that found for the thermal decomposition of pure AP at this temperature (9). For $\alpha > 0.03$ the reaction was acceleratory, the rate being a factor of ~ 1.7 faster than that for pure BP at this temperature. Apparently AP and BP decompose essentially independently at this temperature with only a marginal change in the rate of decomposition of the BP. This might easily arise from the changes in porosity, etc., brought about by the distillation of the products from the AP decomposition of the reactant matrix.

(b) Barium Chloride

The thermal decomposition of an intimate mixture of anhydrous BP and excess anhydrous barium chloride is shown in Fig. 4. If the gaseous products are allowed to accumulate in the reaction zone, the decomposition is deceleratory throughout. (The kinetics of this reaction are described later, along with those for $\alpha > 0.52$, which they

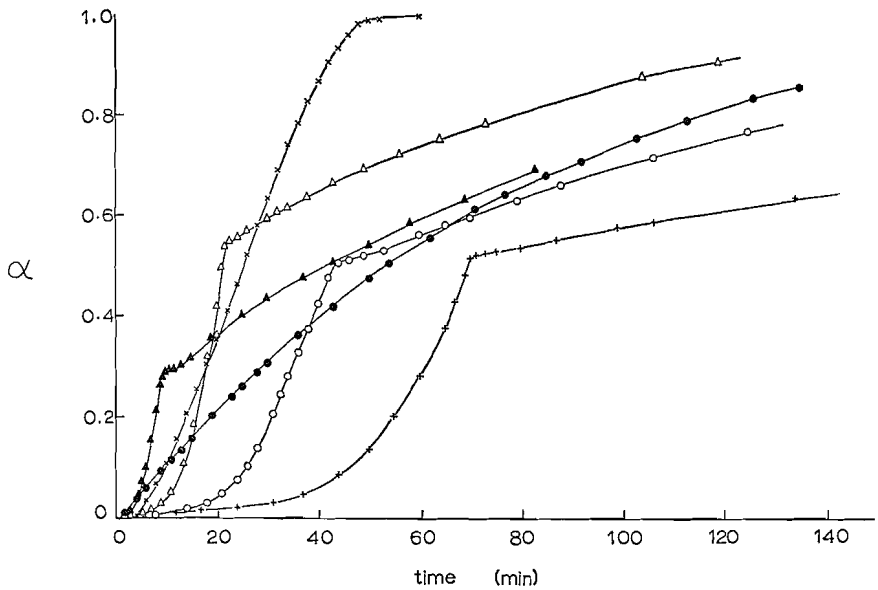

FIG. 4. Effect of $BaCl_2$ on the decomposition of BP. ○, Normal reactant at 459.6 °C; ●, BP with excess $BaCl_2$ at 459.4 °C; △, normal reactant at 467,5 °C; ▲, BP plus 31 mole % $BaCl_2$ at 466.0 °C; +, normal reactant at 446.6 °C; ×, BP with excess $BaCl_2$ at 445 °C in a vacuum of $< 10^{-3}$ Torr.

Can. J. Chem. Downloaded from www.nrcresearchpress.com by 210.87.254.105 on 09/05/12
For personal use only.

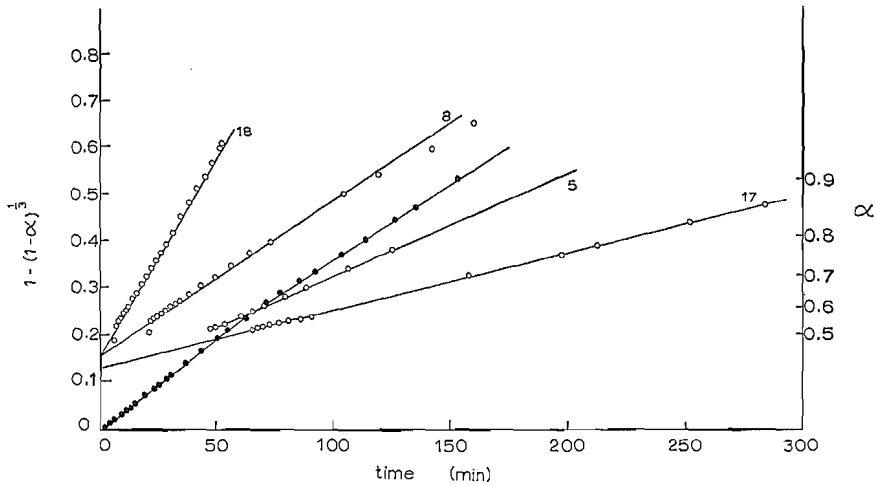

FIG. 5. Plots of the function $1 - (1 - \alpha)^{\frac{1}{3}}$ against t to test eq. [3]. ○, Normal reactant, run numbers as in Fig. 1; ●, BP with excess $BaCl_2$, 459.4 °C.

resemble.) In a dynamic vacuum, however, an acceleratory period was noted. The thermal decomposition of an intimate mixture of 0.69 mole fraction BP with 0.31 mole fraction $BaCl_2$ was acceleratory in the range $0 < \alpha < 0.29$ even though gaseous products were allowed to accumulate. It is apparent from these experiments that the sharp change to deceleratory kinetics (Figs. 1 and 4) is associated with a composition equivalent to equimolar proportions of BP and $BaCl_2$. For the decomposition of pure BP this occurs at $\alpha = 0.52$. The addition of excess $BaCl_2$ is therefore expected to suppress the acceleratory reaction, as is indeed observed. Further, a reaction mixture containing initially 0.31 mole fraction of $BaCl_2$ is predicted to show the discontinuity at $\alpha = 0.29$, exactly as observed. The acceleratory portion of the reaction of BP, containing excess $BaCl_2$, *in vacuo* obeyed the power law, eq. [2], in the range $0.01 < \alpha < 0.50$ but the rate constant was 3.8 times faster than that of pure BP.

(c) Thermal Decomposition of BP in Air or Nitrogen

The plot of α against t for a single experiment in which BP was decomposed under a pressure of 160 Torr of dry air was identical in form to that for reaction under the accumulated gaseous products, but started *in vacuo*, with the discontinuity occurring at $\alpha = 0.52$, as usual. For decomposition under 250 Torr dry nitrogen, the $\alpha(t)$ curve was again similar to that under 160 Torr dry air.

Kinetics of Thermal Decomposition for $\alpha > 0.52$

The thermal decomposition of BP for $0.54 < \alpha < 0.90$ obeys the contracting volume formula

$$[3] \qquad R_3(\alpha) \equiv 1 - (1 - \alpha)^{\frac{1}{3}} = k_3 t$$

as found previously (3), when the reaction occurs (*i*) in air, (*ii*) in nitrogen and, (*iii*) in the accumulated product gases. Representative plots of $R_3(\alpha)$ against t are shown in Fig. 5. The least squares values of the Arrhenius parameters corresponding to k_3, measured for decomposition under product gases, are $E = 59.1$ kcal/mole, $\log (A/s^{-1}) = 13.16$. Reaction under air or nitrogen was a factor of 1.4 times slower. Reaction in a dynamic vacuum was much faster than (*iii*). For example, at a steady state pressure of 10^{-3} Torr the reaction was ~ 12 times faster than under the accumulated reaction products. These facts are illustrated in Fig. 6.

Effect of Added Barium Chloride

It will be recalled that the kinetics of the thermal decomposition of BP in the presence of excess $BaCl_2$ are deceleratory throughout when reaction occurs under the accumulated product gases. Under these conditions $\alpha(t)$ obeys the contracting volume equation throughout the range $0 < \alpha < 0.9$, Fig. 5. The rate constants determined under these conditions are plotted in Fig. 6, where the least mean squares line shown was calculated for k_3 determined for the decomposition of BP,

Can. J. Chem. Downloaded from www.nrcresearchpress.com by 210.87.254.105 on 09/05/12
For personal use only.

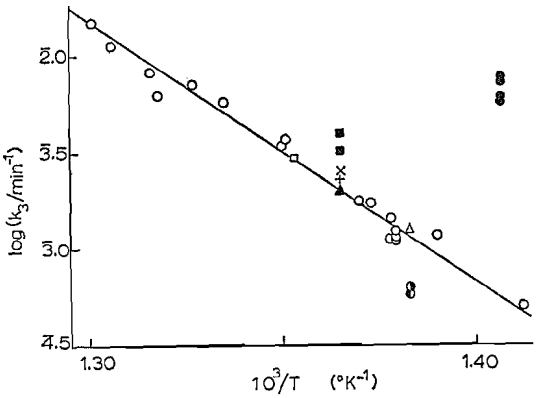

FIG. 6. Arrhenius plot for the rate constant k_3 obtained by fitting the data to eq. [3]. ○, BP decomposed under the accumulated gaseous products; △, BP containing 3.86 mole % AP; ◐, BP under 250 Torr N_2; ◑, BP under 160 Torr air; ●, $P < 10^{-3}$ Torr; □, BP plus 31 mole % $BaCl_2$; ■, BP plus excess $BaCl_2$; ▲, $P = 0.25$ Torr; + , $P = 0.048$ Torr; × , $P = 0.025$ Torr.

without added $BaCl_2$, under the accumulated product gases in the range $0.54 < \alpha < 0.90$. The rate constant in the range $0 < \alpha < 0.5$ with $BaCl_2$ is somewhat greater than, but clearly similar to, the rate constant in the range $0.54 < \alpha < 0.90$ without added $BaCl_2$. The variation (decrease) in k_3 during the course of the decomposition is perhaps explained in part by the dependence of the reaction kinetics on the ambient pressure (Figs. 2 and 6) which is, of course, "zero" at the start of the reaction and increases with α. This pressure-dependence of the kinetics is illustrated by (see Fig. 6) the variation of k_3 for pure BP with product-gas pressure in the range 0.25–0.025 Torr at 459.5 °C ($10^3/T = 1.365$), by the increase in k_3 by a factor of around 12 when the ambient pressure is decreased to $< 10^{-3}$ Torr (4 points at 437.5 °C, or $10^3/T = 1.407$), and by the decrease in k_3 when the ambient pressure is increased (160 Torr air or 250 Torr nitrogen, 449.9 °C or $10^3/T = 1.383$). The fact that adding $BaCl_2$ alters the range of the last part of the reaction, which usually begins at $\alpha > 0.52$ in pure BP (Figs. 1 and 5), but not the mechanism or rate constant, is emphasized by the point in Fig. 6 which corresponds to a mixture of BP containing 0.31 mole fraction $BaCl_2$ and which lies right on the least squares line (from data for pure BP) even though the break occurs at $\alpha = 0.29$ and eq. [3] holds from $\alpha > 0.36$ (466.0 °C or $10^3/T = 1.353$). The least mean squares line in Fig. 6 was calculated for data from "normal" runs in which the pressure of the accumulated products lay in the range 1–2.5 Torr at $\alpha = 0.52$.

Differential Thermal Analysis

A differential thermal analysis (d.t.a.) trace for crushed barium perchlorate is shown in Fig. 7. The first endotherm commencing at around 60 °C represents loss of water and corresponds to dehydration from $3H_2O$ to $1H_2O$, the two stages not being clearly separated. The second broad endotherm in the range 150–220 °C corresponds to loss of the final 1 mole of water. This is preceded by a peak with a sharp leading edge which probably represents a phase change in the monohydrate. The next two endotherms commencing at 282 and 358 °C correspond to the $\alpha \rightarrow \beta$ and $\beta \rightarrow \gamma$ phase transitions of anhydrous BP (2). The single exotherm with its first major peak at 486 °C corresponds to thermal decomposition of anhydrous BP. There is no evidence of melting, in agreement with our visual observations.

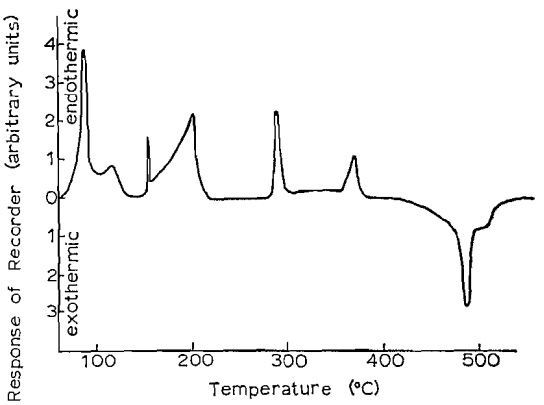

FIG. 7. Differential thermal analysis trace for crushed barium perchlorate showing dehydration and phase transition endotherms and the decomposition exotherm.

Discussion

The Gibb's free energy of formation of $BaCl_2$(c) is more negative than that of BaO(c) by −31.8 kcal/mole at 427 °C (10). Thus decomposition of BP to $BaCl_2$ rather than to the oxide is predicted and this is confirmed both by previous work and by the present study. Decomposition of BP to the chloride appears to be 97.5 ± 1.5% complete. The $\alpha(t)$ plots (Fig. 1) are complicated, indicating at least 2, and probably 3, stages to the reaction. Of many possible intermediates the likely ones,

Can. J. Chem. Downloaded from www.nrcresearchpress.com by 210.87.254.105 on 09/05/12
For personal use only.

Can. J. Chem. Downloaded from www.nrcresearchpress.com by 210.87.254.105 on 09/05/12
For personal use only.

on the basis of the limited thermodynamic data available, are $Ba(ClO_3)_2$ and $Ba(ClO_2)_2$. Since oxygen is the only gaseous product, the break which occurs at $\alpha \simeq 0.52$ corresponds stoichiometrically to formation of $Ba(ClO_2)_2$. However, Solymosi and Bánsági (4) have shown that $Ba(ClO_2)_2$, in the presence of equimolar amounts of Al_2O_3, NiO, $Ba(ClO_3)_2$, or $BaCl_2$, is transformed completely into $Ba(ClO_3)_2$ and $BaCl_2$.

[4] $$3ClO_2^- \leftrightharpoons 2ClO_3^- + Cl^-$$

We conclude, therefore, that the break corresponds to the complete decomposition of $Ba(ClO_4)_2$ into $Ba(ClO_3)_2$ and $BaCl_2$ in the mole ratio of 2:1 and that, because of the precise and reproducible value of α at which this occurs, the reaction involves $Ba(ClO_2)_2$ as an unstable intermediate. The first half of the reaction therefore corresponds to

[5] $$3ClO_4^- \rightarrow 2ClO_3^- + Cl^- + 3O_2$$

with little decomposition ($\sim$ 4%) of ClO_3^- having occurred prior to this point. The second half of the reaction then corresponds to the decomposition of barium chlorate into barium chloride and oxygen.

Mechanism of Decomposition for $\alpha > 0.52$

According to our model the reaction after the break corresponds to the decomposition of ClO_3^-. The kinetics fit eq. [3] so that a contracting interface is indicated. The activation energy (Table I) is 59.1 kcal/mole and this is reasonably close to, although lower than, that expected for the splitting of a single Cl—O bond, D(Cl—O) = 64.2 kcal/mole (11). We conclude, therefore, that the first step is

[6] $$ClO_3^- \rightarrow ClO_2^- + O$$

Since the transition state involves the loss of one vibrational degree of freedom only, the pre-exponential factor is expected to be "normal", i.e. about 10^{13} s^{-1}. The experimental value is 1.5×10^{13} s^{-1}. One knows from the work of Solymosi and Bánsági (4, 5) that ClO_2^- and ClO^- are less stable than ClO_3^-, and that ClO_2^- disproportionates into $ClO_3^- + Cl^-$, eq. [4]. Thus we propose the mechanism

[6] $$ClO_3^- \rightleftharpoons ClO_2^- + O$$

[7] $$ClO_2^- \rightleftharpoons ClO^- + O$$

[8] $$ClO^- \rightleftharpoons Cl^- + O$$

[9] $$O + O + M \rightarrow O_2$$

The effect of the pressure and nature of the ambient gas are only explicable if the combination of O atoms (reaction [9]) is relatively inefficient so that O atoms produced in reactions [6] – [8] have the choice of either diffusing away through the gas phase or of reacting with $Cl^- \rightarrow ClO^-$, or with $ClO^- \rightarrow ClO_2^-$, or with ClO_2^-. Although data for ΔG_f^0 for $Ba(ClO)_2$ and $Ba(ClO_2)_2$ are not available, there is no evidence that we know of that O_2 reacts with Cl^-. The most direct evidence for reaction of ClO_2^- with O *atoms* is that the rate of decomposition of ClO_3^- increases about 12 times in a pumping vacuum. If the retardation observed under 1–3 Torr of oxygen were due to a back-reaction with O_2 molecules

[10] $$ClO_2^- + O_2 \rightarrow ClO_3^- + O$$

this would have to mean that $k_{10} \gg k_6$ and so complete decomposition under oxygen would never be observed. Furthermore, air and nitrogen are equally effective in retarding the reaction, thus proving that the retardation is competitive with diffusion. Thus reaction [6] has to be reversible. Evidence for reactions [7] and [8] being reversible comes from the effect of $BaCl_2$ on the reaction, to be discussed in the next section. Reactions [6]–[8] are consistent with Solymosi and Bánsági's findings on the disproportionation of $Ba(ClO_2)_2$ into $Ba(ClO_3)_2$ and $BaCl_2$. An approximate order of rate constants is: $k_{\bar{8}} > k_8 > k_{\bar{6}} > k_{\bar{7}} > k_7 > k_6$.

TABLE I

Activation parameters for the thermal decomposition of barium perchlorate

Method	α-Range	E (kcal/mole)	log (A/s^{-1})
Equation [2], t_0	0–0.035	69.7	17.91
$t_{0.1}$	$\alpha = 0.1$	83.5	21.72
$S(0.25)$	$\alpha = 0.25$	80.0	20.52
Equation [1′]	0.05–0.36	76.7	19.54
Equation [2], k_2	0.06–0.45	80.9	20.72
Equation [3]	$\alpha > 0.52$	59.1	13.16

Mechanism of Decomposition for $\alpha < 0.52$

The decomposition of Na, K, Rb, and Cs perchlorates has recently been studied at low fractional decompositions ($\alpha < 0.035$) by Cordes and Smith (12) using a mass spectrometric method. Their data thus refer to the reaction

[11] $$2ClO_4^- \rightarrow 2ClO_3^- + O_2$$

Can. J. Chem. Downloaded from www.nrcresearchpress.com by 210.87.254.105 on 09/05/12
For personal use only.

without complications arising from secondary reactions. The activation energies found, 44.6 kcal/mole for $CsClO_4$, 46.0 kcal/mole for $RbClO_4$, and 50.2 kcal/mole for $KClO_4$, are similar, indicating little dependence of the anion decomposition (reaction [11]) on the cation, and being all markedly less than D(Cl—O). A bimolecular reaction, with the transition state O_3Cl^-—O---O—ClO_3^-, is therefore indicated (12) and this is confirmed by the low value of the pre-exponential factor $\sim 10^8$ s^{-1}, since the reactants will be freely rotating but the complex will have restricted rotation about the O---O bond because of the value of the Cl—O---O dihedral angle (cf. H_2O_2).

The kinetic analysis of the BP decomposition for $\alpha < 0.52$ is complicated by the fact that a number of reactions are going on simultaneously. That which has been achieved is recognizably empirical; nevertheless the activation energies (Table I) will be at least qualitatively meaningful. That referring to the lowest extent of decomposition is the value from t_0, the induction period before the empirical square law, eq. [2], starts to describe the data. This value is 69.7 kcal/mole which is not much greater than D(Cl—O); in fact one anticipates a high value because all the E values referring to higher values of α are much higher than 64 kcal/mole, so that any admixture of secondary reactions with the primary process

[12] $$ClO_4^- \rightarrow ClO_3^- + O$$

will tend to raise E. The pre-exponential factor is high, almost 10^{18} s^{-1}, but not much outside the range, $10^{18} - 10^{17}$ s^{-1}, which is considered appropriate for unimolecular solid state reactions (13, 14). The remaining 4 activation energies determined in different ways at higher α are all around 80 kcal/mole and so are either composite or refer to a different process than reaction [12].

The effect of $BaCl_2$ provides a clue to the other reactions occurring. The break in the $\alpha(t)$ curves is a linear function of the initial $BaCl_2$:BP ratio, r. Furthermore, the effect of $BaCl_2$ when $r < 1$ is to shorten the induction period, but leave the subsequent linear rate unchanged. When $r > 1$, the induction period, as well as the approximately linear portion of the reaction, are removed completely and the decomposition of BP is decelerator throughout (Fig. 4) under the accumulated product gases. The reaction rate for $\alpha > 0.3$ with 0.29 mole fraction $BaCl_2$ is identical with that for $\alpha > 0.52$ with no added $BaCl_2$ (both under product oxygen). This shows that the added $BaCl_2$ is converted to $Ba(ClO)_2$, and thence to $Ba(ClO_3)_2$ + $BaCl_2$, by reacting with the oxygen atoms produced in reaction [12] with great efficiency. As the $BaCl_2$ and BP are particulate, and not a solid solution, diffusion of O atoms is prerequisite.

In the absence of $BaCl_2$ the initial reaction is much slower than with $BaCl_2$ present ($r < 1$, or $r > 1$ in a pumping vacuum). This shows that when the O atoms are not trapped by Cl^- (and ClO^-) they react partly with ClO_3^- to reform ClO_4^- thus slowing down the production of O_2. Finally, the fact the reaction is acceleratory means that autocatalysis must be involved. We thus arrive at the following reaction scheme

[13]	$ClO_4^- \rightarrow ClO_3^- + O$	initiation
[14]	$O + ClO_4^- \rightarrow ClO_3^- + O_2$	propagation
[6]	$ClO_3^- \rightarrow ClO_2^- + O$	
[4]	$3ClO_2^- \rightarrow 2ClO_3^- + Cl^-$	
[9]	$O + O + M \rightarrow O_2 + M$	termination
[13]	$O + ClO_3^- \rightarrow ClO_4^-$	

For $\alpha < 0.52$, ClO_2^- is the *effective* end of the chain because of the ease with which it undergoes the disproportionation reaction [4], the mechanism of which involves reactions [7], [8], and [$\bar{6}$]. The induction period is explained by the importance of reaction [13], and the apparent stability of ClO_3^-, while any ClO_4^- remains, is due to the fact that its production from reactions [13], [14], [$\bar{6}$], and [4] just balances its loss by reaction [6] and [$\bar{13}$].

This scheme is consistent with all the experimental facts. Being a chain reaction it is acceleratory at first. The acceleratory period is removed practically completely (Fig. 4) by adding Cl^- since these react with O atoms with high efficiency, thus reducing the importance of the back reaction [$\bar{13}$] and also reaction [14]. In the presence of excess Cl^- the following (fast) reactions occur

[13]	$ClO_4^- \rightarrow ClO_3^- + O$
[6]	$ClO_3^- \rightarrow ClO_2^- + O$
[$\bar{8}$]	$O + Cl^- \rightarrow ClO^-$
[$\bar{7}$]	$O + ClO^- \rightarrow ClO_2^-$
[4]	$3ClO_2^- \rightarrow 2ClO_3^- + Cl^-$

so that the whole reaction appears as the decomposition of ClO_3^- (equal in amount to $1\frac{1}{3}$ times

Can. J. Chem. Downloaded from www.nrcresearchpress.com by 210.87.254.105 on 09/05/12
For personal use only.

the number of moles of BP initially present, if $r > 1$), Fig. 4. For $r = 0.31$, the induction period is reduced because the trapping of O atoms by the added Cl^- (reactions [8] and [7]) competes successfully with reaction [13], but the amount of Cl^- added is insufficient to provide for complete rapid conversion of ClO_4^- to ClO_3^-. Thus the remaining 0.38 mole fraction of ClO_4^- (equivalent to $\alpha = 0.29$) decomposes to ClO_3^- by the usual route.

As explained above, the preservation of $\frac{2}{3}$ mole of ClO_3^- in the reaction without added Cl^- is a classic example of a steady-state situation and this explains the almost linear kinetics in the range $0.2 < \alpha < 0.52$. There is evidently a delicate balance between the various contributing processes, since both acceleratory and decelera-tory rates are sometimes observed.

The activation energy for $0.05 < \alpha < 0.45$ has not been determined very accurately but is evidently about 80 ± 4 kcal/mole, with a corresponding pre-exponential factor of $\sim 3 \times 10^{20}$ s^{-1}. These parameters do not refer to a single rate constant but rather to the temperature-dependence of a complex expression involving many rate constants. While this reaction scheme is certainly capable of explaining the experimental results in a qualitative fashion, it is too complicated for the time-dependent problem to be readily solved in a general way.

One of the simplest representations of chain kinetics is the Prout–Tompkins (P–T) equation (15). It is based on assumptions (16) that are hardly likely to apply in this complicated situation but nevertheless, containing as it does the essential features of branching and termination, it might be expected to represent the kinetics of BP decomposition tolerably well. In fact, the P–T equation describes the course of the decomposition at least as well as the other equations tried (eq. [2], eq. [3]) and the activation energies deduced $E = 58.4$ kcal/mole, for $\alpha > 0.52$ and $E = 86.4$ kcal/mole, for $0.02 < \alpha < 0.40$, are consistent with those found by the other methods. Solymosi (8) used only the P–T equation and the first order law to analyze his kinetic results. The activation energies he reports are $E = 60.2$ kcal/mole ($\alpha < 0.52$) and $E = 52.2$ kcal/mole ($\alpha > 0.52$) from the P–T equation and $E = 46.7$ kcal/mole from the first order law, which can clearly only apply after the break. He states that the contracting volume eq. [3] also fits the decay period ($0.45 < \alpha < 0.9$) but no examples of this were shown, nor was an activation energy quoted.

Acknowledgment

We are indebted to the National Research Council of Canada for financial support of this work.

1. A. A. Zinov'ev and L. I. Cludinova. Z. Neorg. Khim. **1**, 1772 (1956).
2. A. A. Zinov'ev, L. I. Cludinova, and L. P. Smolina. Z. Neorg. Khim. **1**, 1850 (1956).
3. F. Solymosi and Gy. Braun. Acta Chim. Acad. Sci. Hung. **52**, 1 (1967).
4. F. Solymosi and T. Bánsági. Acta Chim. Acad. Sci. Hung. **56**, 251 (1968).
5. F. Solymosi and T. Bánsági. Acta Chim. Acad. Sci. Hung. **56**, 337 (1968).
6. F. Solymosi. Z. Physik. Chem. N.F. **57**, 1 (1968).
7. F. Solymosi. Acta Chim. Acad. Sci. Hung. **57**, 11 (1968).
8. F. Solymosi. Acta Chim. Acad. Sci. Hung. **57**, 35 (1968).
9. A. K. Galwey. Ph.D. Thesis, University of London, London, England. 1958.
10. M. M. Markowitz. J. Inorg. Nucl. Chem. **25**, 407 (1963).
11. D. D. Wagman, W. H. Evans, I. Halow, V. B. Parker, S. M. Bailey, and R. H. Schumm. Selected values of chemical thermodynamic properties. Natl. Bur. Stds. NBS Tech. Note 270–1. October 1965.
12. H. F. Cordes and S. R. Smith. J. Phys. Chem. **72**, 2189 (1968).
13. H. F. Cordes. J. Phys. Chem. **72**, 2185 (1968).
14. R. D. Shannon. Trans. Faraday Soc. **60**, 1902 (1964).
15. E. G. Prout and F. C. Tompkins. Trans. Faraday Soc. **40**, 488 (1944).
16. P. W. M. Jacobs and F. C. Tompkins. *In* Chemistry of the solid state. *Edited by* W. E. Garner. Butterworths, London. 1955.

Can. J. Chem. Downloaded from www.nrcresearchpress.com by 210.87.254.5 on 09/05/12
For personal use only.

Raman spectra of liquid and crystalline HCN and DCN

M. PÉZOLET AND R. SAVOIE
Chemistry Department, Laval University, Quebec, Quebec

Received March 27, 1969

Raman spectra of liquid and crystalline HCN and DCN have been recorded at various temperatures down to 77 °K. The spectra of the liquids are characteristic of hydrogen-bonded compounds. The two solid phases have very similar spectra, in which each fundamental is complicated by an anomalous shoulder on the high-frequency side. Possible explanations for these are given.

Les spectres Raman de HCN et DCN liquides et solides ont été enregistrés à diverses températures entre 77 et 290 °K. Les spectres des liquides mettent en évidence les effets dus aux liaisons hydrogène. Les deux phases solides présentent dans chaque cas des spectres à peu près identiques, où chacune des fondamentales est compliquée par un épaulement du côté des hautes fréquences. On suggère quelques explications pour ces anomalies.

Canadian Journal of Chemistry, 47, 3041 (1969)

Introduction

The structure of the free HCN molecule has been accurately determined from its microwave (1) and vibration–rotation (2) spectra. Hydrogen cyanide forms unexpectedly strong hydrogen bonds, given the C—H donor group and the N acceptor. This results in some association in the vapor phase (3) and in the exceptionally high dielectric constant of the liquid, which has been explained by the formation of polymeric linear chains (4, 5).

Specific-heat measurements (3) on solid HCN (m.p. 259.86 °K) have indicated a phase transition at 170.37 °K. The very small entropy change (0.022 e.u.) associated with this process was interpreted in terms of a rearrangement involving large groups of hydrogen cyanide molecular units. This was later confirmed by an X-ray diffraction study (6) which showed that both crystalline phases are composed of infinite linear chains with all the molecules and the chains oriented in the same direction. The high-temperature modification, described by the space group $C_{4v}{}^{9}$-*I*4*mm*, is tetragonal with unit-cell dimensions: $a = 4.63$, $c = 4.34$ Å. In the orthorhombic low-temperature phase ($C_{2v}{}^{20}$-*Imm*), the *a* and *b* dimensions of the unit-cell are slightly different ($a = 4.13$ and $b = 4.85$ Å).

The mid-infrared spectrum of solid HCN has been obtained by Hornig and co-workers (7, 8) and the measurements were recently extended to the far-infrared (9). An infrared study of HCN and DCN isolated in various solid matrices has also been published (10). Our main purpose in undertaking the present study was to determine whether the Raman spectra of HCN in its two solid phases were consistent with the reported crystal structures. The liquid also seemed worth studying in view of its unusual properties. Finally, it was hoped that the Raman bands of crystalline HCN and DCN would help to explain the marked asymmetry of the Raman components of the H—X stretching doublets of HCl and HBr in their low-temperature modification (11).

Experimental

The hydrogen cyanide used in our experiments was obtained by the method of Ziegler (12), slightly modified in that the evolved gas was transferred under reduced pressure (1/2 atm) rather than by a flow of dry nitrogen gas. Diluted aqueous H_2SO_4 (1:1 per volume) was slowly added to a solution containing 200 g NaCN in 500 ml water. The evolved HCN was then passed through drying columns (P_2O_5 and $CaCl_2$) and condensed in a trap at liquid-nitrogen temperature. The ~ 75 ml of sample thus collected was then distilled several times, the middle portion only being retained at each distillation. A mass spectrum of the final product indicated traces of water present as an impurity (0.1%). The deuterated acid was obtained in a similar manner by reacting a 1:1 D_2SO_4/D_2O solution with 30 g NaCN in 50 g D_2O. The D_2SO_4 was produced by distilling SO_3 from 30% fuming sulfuric acid into D_2O (99.7% isotopic purity, Merk Sharpe Dohme of Canada, Ltd.). In order to prevent any undue isotopic contamination, the DCN sample was purified by passing it through thoroughly dried $CaCl_2$ only. The percentage of deuteration of the sample was estimated at 85%, from the relative intensity of an HCN impurity band in the Raman spectrum.

The 10–15 ml samples were studied in 19 mm diameter cylindrical Pyrex cells. The solids were obtained by slowly (usually over a 12 h period) lowering the cell into a constant-temperature bath maintained at approximately −20 °C. The polycrystalline solids thus obtained were not completely transparent and cracked upon cooling.

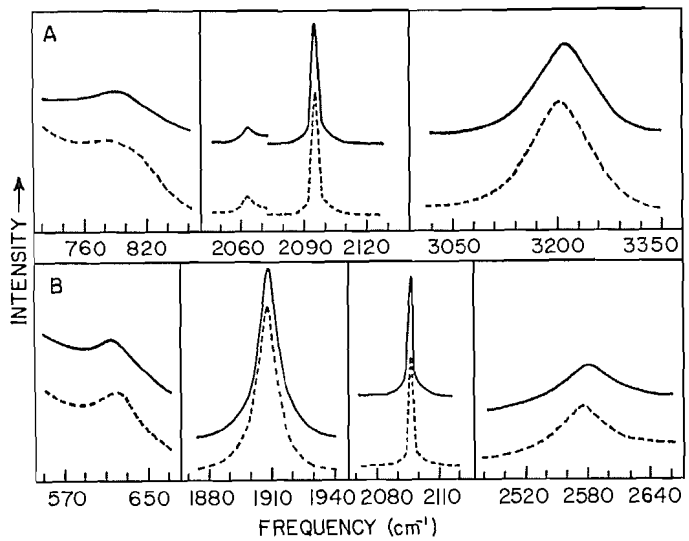

FIG. 1. Raman spectra of liquid (A) HCN and (B) DCN at 19 (—) and −12 °C (· · · · ·).

TABLE I

Observed frequencies in gaseous and liquid HCN and DCN

Frequencies (cm^{-1})						
HCN			DCN			
Gas (i.r.) Reference 2	Liquid (Raman) 19 °C	Liquid (Raman) −12 °C	Gas (i.r.) Reference 2	Liquid (Raman) 19 °C	Liquid (Raman) −12 °C	Assignment
3311.4	3215	3207 (95)*	2630.3	2581	2575 (50)*	ν_3
3295	—	—	2589	—	—	ν_3 ($H^{13}CN$)
2096.7	2096	2097 (3)	1928.0	1909	1908 (11)	ν_1
	2097	2097 (2.5)				ν_1 HCN in DCN
712.1	~794	~798 (~55)	569.1	~615	~622 (~30)	ν_2

*Numbers in parentheses refer to band width at half-intensity.

The low-temperature spectra were recorded with the sample cell placed inside a Pyrex Dewar and cooled by a flow of cold nitrogen gas, as previously described (13).

The spectra were obtained on a Cary 81 Raman spectrometer equipped with a Toronto-arc source. The instrument was calibrated with various discharge lamps (Ne, Na, and Hg) and the frequencies cited later are believed to be accurate to ± 1 cm^{-1} for sharp peaks. The spectral slit width was adjusted between 0.5 to 5 cm^{-1}, so as to obtain reasonable intensity in each region of the spectra. A background run in the low-frequency region indicated ghost bands at ca. 90, 145, and 175 cm^{-1}, that at 145 cm^{-1} being the sharpest and the most intense.

Results and Discussion

(A) Raman Spectra of Liquid HCN and DCN

The Raman spectra of liquid HCN and DCN at −12 and 19 °C are reproduced in Fig. 1. Observed frequencies are collected in Table I, which also includes the width at half intensity and the infrared frequencies in the gas phase. Since the ν_3 (C—H or C—D stretch) and ν_2 (H—C—N or D—C—N bend) bands of liquid HCN and DCN are very weak, large slit widths (~ 5 cm^{-1}) had to be used to obtain reasonable intensity. However, in the ν_1 (C—N stretch) region, a slit width of ~ 1 cm^{-1} was usually sufficient.

On the whole, the spectra of liquid HCN and DCN are those which might be expected for hydrogen-bonded compounds. The ν_3 band appears at a frequency lower than that in the gas, in both HCN and DCN, while the bending vibration is shifted to higher frequency. The C—N

Can. J. Chem. Downloaded from www.nrcresearchpress.com by 210.87.254.5 on 09/05/12
For personal use only.

TABLE II

Symmetry correlation diagrams for crystalline HCN and DCN

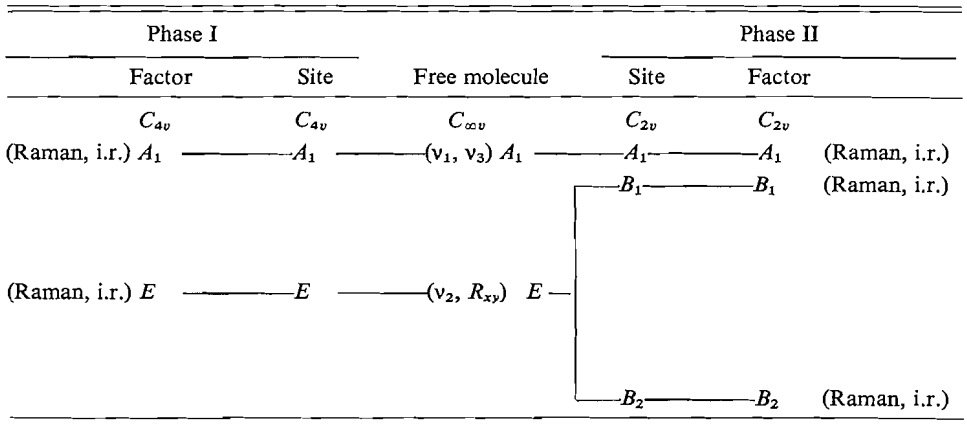

stretching mode on the other hand is only slightly shifted, indicating that the strong C—N bond is weakly perturbed by molecular interactions. Band widths in both spectra are proportional to gas–liquid frequency shifts.

The appreciable blue shift of the bending mode of hydrogen cyanide upon condensation is unique in that it is almost as large as that of the ν_3 mode. This is probably because the atomic masses in HCN are such that a bending of the molecule involves mostly a displacement of the hydrogen atom, which is most influenced by hydrogen-bonding. The fact that the ν_1 band of DCN is almost 4 times as broad as the corresponding band of HCN is also peculiar. This does not imply that hydrogen bonds are stronger in DCN, since the gas–liquid frequency shifts of ν_3 in HCN and DCN are comparable. Rather, it is likely that the breadth of ν_3 (in both HCN and DCN) is partly transmitted to ν_1 through intramolecular coupling. Since the ν_3–ν_1 frequency difference is greater in HCN than in DCN, we can expect the coupling to be less in the first case. This would therefore explain why the ν_1 band of HCN is sharper than that of DCN, even when HCN is present as an impurity in liquid DCN.

The temperature effects on the Raman spectra of liquid HCN and DCN are small, as can be seen by comparing the spectra at −12 and 19 °C. (The normal boiling point of HCN is 25.7 °C.) Small frequency shifts occur for those bands which are more sensitive to hydrogen-bond formation, but these variations are not accompanied by any significant changes in band widths. Furthermore, all the bands have symmetrical shapes suggesting that the polymeric units in the liquid are rather long. Were monomers and dimers present in appreciable concentrations, a high-frequency tail should be observed alongside ν_3, contrary to our findings.

(B) Raman Spectra and Crystal Structures of the Solids

Hydrogen cyanide has very simple crystal structures in both its solid phases (6). Since there is only one molecule per primitive cell in each case (although there are two per crystallographic unit-cell), no translational lattice mode should be observed in the vibrational spectra of the pure solid. This is because acoustic modes have vanishing frequency at the center of the Brillouin zone ($\boldsymbol{k} = 0$), where optical transitions occur. The site and coupling effects in the crystal are easily taken into account by the use of a correlation diagram (Table II) which is straightforwardly obtained from standard group-theoretical procedures (14, 15). It is thus seen that the two stretching modes (ν_1 and ν_3) should not be split in either solid phase. The bending (ν_2) and librational modes, however, although they should appear as singlets in phase I, are predicted to yield two components (B_1 and B_2) in phase II. Physically, this comes about because of the anisotropy of the static crystalline field (in the x and y directions) in the low-temperature modification of the crystal. This results in different

Can. J. Chem. Downloaded from www.nrcresearchpress.com by 210.87.254.5 on 09/05/12
For personal use only.

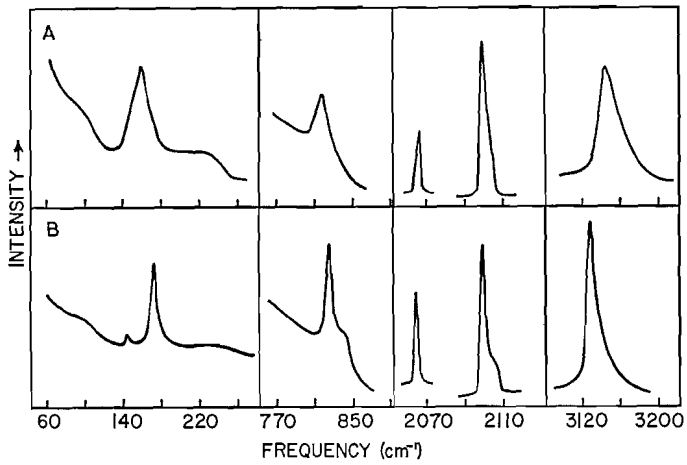

FIG. 2. Raman spectra of HCN in (A) phase I at −90 °C and (B) phase II at −195 °C.

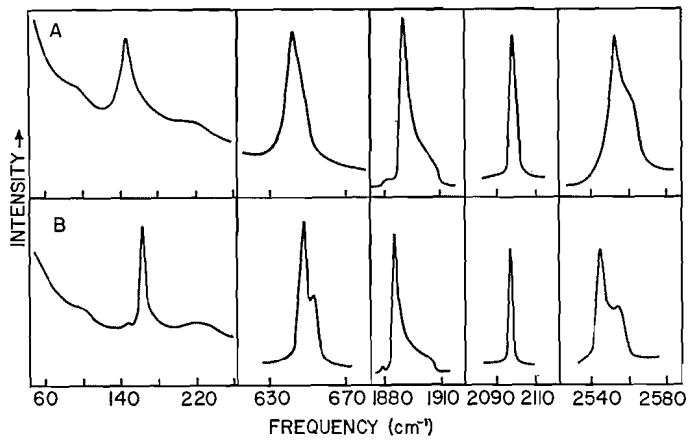

FIG. 3. Raman spectra of DCN in (A) phase I at −90 °C and (B) phase II at −195 °C.

frequencies for the two perpendicular motions involved in the otherwise doubly degenerate E modes.

The Raman spectra of crystalline HCN and DCN in their two solid phases are reproduced in Figs. 2 and 3. Observed frequencies are given in Table III. The spectra differ appreciably from those predicted above on the basis of the accepted crystal structures. In particular, the C—N and C—H (C—D) stretching vibrations (ν_1 and ν_3) are complicated by high-frequency shoulders, whereas the bending mode yields an asymmetric peak, even in the high-temperature phase. In the lattice region, the only predicted active mode is most probably responsible for the sharp peak at 161 cm^{-1} in the spectrum of HCN at −90 °C. The corresponding band appears at 149 cm^{-1} in DCN, with an appropriate (0.93) isotopic frequency shift. The predicted site splitting of this band in the low-temperature phase is not observed, which raises the question as to whether the two components in the ν_2 region arise from a site splitting. The broad band in the Raman spectra of both HCN and DCN at $\sim$ 220 cm^{-1} cannot be assigned to a component of the librational mode arising from a site splitting, since it is also present in phase I spectra. We do not believe that the present results are in contradiction with the crystal structures obtained from X-ray diffraction. Rather, it seems that all fundamentals (including the librational mode) are complicated by anomalous high-frequency shoulders, which may appear as separate components at low temperature because of band sharpening. Possible

Can. J. Chem. Downloaded from www.nrcresearchpress.com by 210.87.254.5 on 09/05/12
For personal use only.

TABLE III
Observed frequencies in crystalline HCN and DCN

Frequencies (cm^{-1})						
HCN			DCN			
Phase I	Phase II		Phase I	Phase II		
Raman*	Raman*	i.r.†	Raman*	Raman*	i.r.†	Assignment
		112			105	Disorder?
		127			117	
		149			146	
		158			—	
161	173	186	149	163	171	Libration
		205			—	
~230	~240	228	~210	~220	224	
819	827	828	643	648		ν_2
	~840	838		653		
2064	2064	2063		1878		ν_1 (^{13}C)
2098	2098	2097	1890	1885		ν_1
~2104	~2104		~1900	~1900		
			2097	2097		ν_1 HCN in DCN
				2528		$\nu_1 + \nu_2$ or ^{13}C (ν_3)
3047	3046					Impurity?
3145	3129	3132	2553	2545		ν_3
~3180	~3150		~2560	~2555		

*Raman results were obtained at −90 (phase I) and −195 °C (phase II).
†The far- (ref. 9) and mid-infrared (ref. 7) data were obtained at approximately −180 °C.

explanations for these anomalies will be given below (see section *D*). The similarity of the crystal structures of the two solid phases is such that very little change is seen in the spectra at the phase transition. However, temperature dependence studies have shown that some frequency shifts occur at the transition temperature.

(C) Force-constant Calculations

A puzzling characteristic of the high-frequency shoulders observed alongside the fundamentals of crystalline hydrogen cyanide is their anomalous shapes, which suggest a whole frequency distribution rather than a separate component with a normal band shape. This is especially noticeable in the shape of the shoulder alongside the band at 1885 cm^{-1} in the spectrum of DCN at −195 °C (Fig. 3). We first thought that transitions at $\boldsymbol{k} \neq 0$, possibly induced by crystalline disorder, could be responsible for the above anomalies. This prompted us to calculate the force constants and obtain the frequency dispersion curves for the vibrations taking place along the chains in crystalline HCN and DCN.

In order to simplify the problem, the approximation of a linear triatomic chain of infinite length was used. This is particularly well justified in this case because molecular interactions within a chain are much greater than those between adjacent chains. The calculations of the fundamental frequencies, in the harmonic oscillator approximation, are quite simple for the $\boldsymbol{k} = 0$ case. The procedure described by Shimanouchi *et al.* (16) was followed and four force constants were used: f_0, f_1, and f_2 were related to the variations of the N · · · H, H—C, and C—N distances, respectively, whereas f_{12} took into account the coupling of the C—H and C—N stretching motions. The normal frequencies were obtained from the secular equation

$$\begin{vmatrix} f_0(\mu_1 + \mu_3) - \omega^2 & -f_1\mu_1 - f_{12}\mu_3 & -f_{12}\mu_1 - f_2\mu_3 \\ -f_0\mu_1 & f_1(\mu_1 + \mu_2) - f_{12}\mu_2 - \omega^2 & f_{12}(\mu_1 + \mu_2) - f_2\mu_2 \\ -f_0\mu_3 & -f_1\mu_2 + f_{12}(\mu_2 + \mu_3) & -f_{12}\mu_2 + f_2(\mu_2 + \mu_3) - \omega^2 \end{vmatrix} = 0$$

Can. J. Chem. Downloaded from www.nrcresearchpress.com by 210.87.254.5 on 09/05/12
For personal use only.

Can. J. Chem. Downloaded from www.nrcresearchpress.com by 210.87.254.5 on 09/05/12
For personal use only.

where ω is the angular frequency ($\omega = 2\pi\nu$ c.p.s.) and μ_1, μ_2, and μ_3 are the inverses of the H, C, and N atomic masses. Expansion of the determinant yields the following equation

$$\omega^6 - \omega^4[\mu_1 X + \mu_2(X + Y - 2Z) + \mu_3 Y] + \omega^2[(\mu_1\mu_2 + \mu_1\mu_3 + \mu_2\mu_3)(XY - Z^2)] = 0$$

where
$$X = f_0 + f_1$$
$$Y = f_0 + f_2$$
$$Z = f_0 + f_{12}$$

One possible solution of this equation is $\omega = 0$. This is expected since the acoustic branch has zero frequency at $\boldsymbol{k} = 0$, in which case the motion corresponds to a displacement of the whole chain. It is also seen from the above equation that the force constants cannot be individually calculated, although the three parameters X, Y, and Z can be obtained for both HCN and DCN from three observed frequencies (C—H, C—N, and ^{13}C—N stretching). This procedure applied separately to HCN and DCN yields two sets of values which differ appreciably because of anharmonicity. However, it was found that the following set of force constants can reproduce the observed stretching frequencies of both HCN and DCN to better than 2% (at −195 °C)

$$f_0 + f_1 = 4.95$$
$$f_0 + f_2 = 19.28$$
$$f_0 + f_{12} = -0.37 \text{ mdyn/Å}$$

These values, when compared to the corresponding force constants of the free molecule ($f_1 = 5.62, f_2 = 18.85$, and $f_{12} = -0.44$ mdyn/Å (8)), points to the weakening of the C—H bond in the solid and allows f_0 to be estimated at ~ 0.3 mdyn/Å. This intermolecular force constant could be obtained directly from the frequency of the H bond stretching of a HCN dimer isolated in a solid matrix. Such a dimer should also yield two doubly degenerate libration-like modes. In the far-infrared spectrum of HCN isolated in a solid N_2 matrix, King and Nixon (10) have observed three bands at 96, 137, and 144 cm^{-1}. If the dimer is regarded as a diatomic oscillator, the lowest of these frequencies yields a force constant of 0.074 mdyn/Å, which is rather low. If on the other hand, the stretching motion is taken to have a frequency of 144 cm^{-1}, a more reasonable value of 0.19 mdyn/Å is obtained.

The calculations involved in obtaining the frequency dispersion curves for a linear triatomic chain will not be given here, since it is only an extension of the well-known case of the diatomic linear chain, which is treated by the Born–von Kármán approach in most textbooks on solid state physics (see, for example, refs. 17–19). The acoustic and optical frequencies were obtained as a function of the wave vector $\boldsymbol{k}$ from the equation

$$\omega^6 - \omega^4[\mu_1(f_0 + f_1) + \mu_2(f_2 + f_1 - 2f_{12}) + \mu_3(f_0 + f_2)] + \omega^2[(\mu_1\mu_2 + \mu_2\mu_3)(f_0f_1 + f_0f_2 + f_1f_2 - 2f_0f_{12} - f_{12}^2) + (\mu_1\mu_3)(f_0f_1 + f_0f_2 + f_1f_2 - 2f_0f_{12}\cos \boldsymbol{k}d - f_{12}^2)] + 2(f_0f_1f_2 - f_0f_{12}^2)(\cos \boldsymbol{k}d - 1)(\mu_1\mu_2\mu_3) = 0$$

where d is the primitive unit-cell dimension along the chain axis. The frequency dispersion curves obtained from this equation, with f_0 arbitrarily fixed at 0.2 mdyn/Å, are given in Fig. 4.

(D) Anomalies in Raman Spectra

The possible causes for the anomalous shoulders observed on the high-frequency side of the fundamentals in the Raman spectra of crystalline HCN and DCN are numerous and only the more plausible ones will be discussed.

(a) Incorrect Crystal Structure

The X-ray study on crystalline HCN (6) has unambiguously established the parallel-linear-chain structure of this solid. However, given the

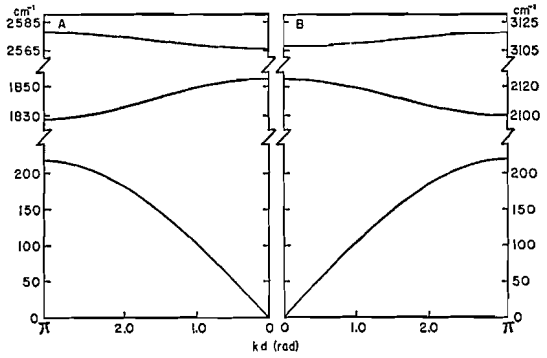

FIG. 4. Dispersion curves for motions along linear chains of (*A*) DCN and (*B*) HCN molecules.

Can. J. Chem. Downloaded from www.nrcresearchpress.com by 210.87.254.5 on 09/05/12
For personal use only.

cylindrical shape of the HCN molecule and the small scattering cross section of the hydrogen atom, it could be argued that the X-ray study has failed to recognize the exact molecular orientation in the solid. The strongest point against this hypothesis is the pyroelectric nature of the crystal in phase II, which is only possible if the crystal is non centro-symmetric. Furthermore, because of the low heat of transition between the two solid phases (3) and their similar Raman spectra, it is most likely that phase I is also non centro-symmetric. The coincidence of Raman and infrared (7) frequencies of the internal modes at low temperature and the simplicity of the Raman spectra in the lattice region are in agreement with this conclusion. It should also be pointed out that a centro-symmetric structure would not lead to a splitting of the ν_1 and ν_3 bands in the crystal, and cannot therefore explain the observed anomalies.

(b) Disorder

Although crystalline HCN should have a well-ordered structure, positional and orientational disorder could be introduced in the crystal through bad crystallization. This could possibly explain the large number of bands in the far-infrared spectrum of crystalline HCN and DCN (9). In these experiments, the samples had to be deposited from the vapor onto a cold window maintained at approximately -100 °C, because of the high vapor pressure of the solid. Subsequent annealing of the sample was not possible for the same reason. It is clear that such a drastic process is not the ideal way to obtain a good crystal. If the weaker peaks in the far-infrared spectra of HCN and DCN are ascribed to disorder, one is left with a very intense band complicated by a high-frequency shoulder, which is exactly what we observe in the Raman spectra. The frequencies differ somewhat in the two types of spectra contrary to what can be predicted on the basis of a non centro-symmetric crystal structure, but this can be explained by the strong overlapping of the infrared bands.

There is both experimental and theoretical evidence that the anomalies observed in the Raman spectra are not caused by the above type of disorder. In particular, improving the quality of the solid samples, by extending the time of crystallization to one week, failed to produce any significant change in the Raman band shapes. Also, attempts to induce disorder by rapid crystallization (1/2 h) or by filling the sample cell with capillary tubes led to the same results. Theoretically, disorder should broaden the vibrational bands by allowing the observation of part of the exciton spectrum. Consequently, the frequency spread of the anomalous shoulders alongside the stretching bands in the Raman spectra would be expected to bear a rough proportionality to the variation in frequency of the optical vibrations between the center and the edge of the Brillouin zone. This is not the case, as can be seen from the dispersion curves (Fig. 4). Furthermore, there is no reason for disorder to cause a broadening of the bands on the high-frequency side only.

(c) Piezoelectric-crystal Anomalies

We have pointed out in a recent note (20) that the type of anomaly discussed here could well be related to the piezoelectric nature of the crystals studied. Frequencies of Raman bands of piezoelectric uniaxial (or biaxial) crystals should vary with the angle of incidence of the exciting light with respect to the optic axis of the crystal (21, 22). Theoretically, the frequency spread for a given band should be approximately limited by the transverse (ν_t) and longitudinal (ν_l) frequencies. Furthermore, it has been shown (22) that

$$\nu_l^2 - \nu_t^2 \propto \left(\frac{\partial \mu}{\partial Q}\right)^2 \propto I$$

where I is the intensity of the corresponding infrared absorption band. Although this relation is open to some theoretical question (23), it should hold approximately in the case of HCN and the hydrogen halides, the spectra of which contain but a small number of relatively well separated bands.

Assuming that ν_t corresponds to the band maximum and that ν_l is given by the high-frequency cutoff of the anomalous shoulder, for any particular band in a Raman spectrum, it should be possible to calculate the relative intensity of the infrared bands from Raman data alone. The above relation applied to the ν_3 and ν_1 bands of crystalline HCN yields $I(\nu_3)/I(\nu_1) = 7.2$, which agrees reasonably well with the value of 5.7 measured experimentally (7). If the high-frequency shoulder alongside ν_2 is used to calculate $I(\nu_2)$, one obtains $I(\nu_2)/I(\nu_1) = 1.2$, which is quite close to the experimental value of 1.4. This suggests that the asymmetric shape of ν_2 does not arise from a site splitting, and is more

consistent with the absence of splitting of the librational mode (in phase II). Calculations based on our Raman results for DCN indicate that ν_1 and ν_3 should have equal infrared intensities, the ν_2 band being about 6 times weaker. We intend to do complementary infrared studies on HCN and DCN and check if this prediction is verified. Also planned is a study of the reflection spectra of these compounds. If the interpretation given above is correct, reflection bands should be seen in the infrared where anomalous shoulders appear in Raman spectra.

As further evidence for the correctness of our assignment of the high-frequency tails in the Raman spectra of HCN and DCN, we turn to the case of HCl and HBr where such shoulders were first observed (11). The H—X stretching region of the Raman spectra of HCl and HBr in their low-temperature modification consists of two sharp peaks, each complicated by a high-frequency tail. These shoulders were first interpreted as arising from a factor-group splitting, and a model with four molecules per primitive cell was proposed for these crystals. However, a recent neutron-diffraction study (24) has shown that orthorhombic crystalline HCl consists of zigzag planar chains, with two molecules per cell, in which case we predict only a doublet in the H—X stretching region. If the shoulders are taken to be analogous to those observed in HCN, we can use the same procedure as above to calculate the infrared intensity ratio of the two components of the doublets. The calculated values (1.55 for HCl and 1.16 for HBr) are almost identical to those measured experimentally (ref. 25, 1.54 for HCl and 1.14 for HBr). Such a close agreement is probably accidental, given the somewhat uncertain choice of ν_1 and the approximate nature of the formula used. Nevertheless, it is a good indication that our interpretation of the anomalous Raman shoulders is correct.

Anomalous shoulders have also been observed in Raman spectra of SO_2 (26) and ICN (27). The fact that these crystals are piezoelectric adds some support to our conclusions, since $\nu_1 \neq \nu_t$ only if $\partial\mu/\partial Q \neq 0$, which is only possible for non centro-symmetric (piezoelectric) crystals. It is expected that anomalies such as those discussed here should be observable in Raman spectra of many piezoelectric molecular crystals. It is therefore advisable in these cases to check the intensity of the corresponding infrared bands, in order to properly assign these "anomalous" features.

Acknowledgments

We gratefully acknowledge financial support of this work by the National Research Council of Canada. We also wish to thank Professor J. R. Durig, Dr. F. G. Baglin, and Mr. G. L. Coulter (Department of Chemistry, University of South Carolina) for communication of their unpublished far-infrared results. Stimulating discussions with Professor W. B. Person and Professor G. Andermann were much appreciated. Finally, one of us (M.P.) is indebted to the National Research Council of Canada for a Graduate Studentship.

1. J. W. Simmons, W. E. Anderson, and W. Gordy. Phys. Rev. 77, 77 (1950).
2. D. H. Rank, G. Skorinko, D. P. Eastman, and T. A. Wiggins. J. Opt. Soc. Am. **50**, 421 (1960). H. C. Allen, Jr., E. D. Tidwell, and E. K. Plyler. J. Chem. Phys. **25**, 302 (1956). W. S. Richardson. J. Chem. Phys. **19**, 1213 (1951).
3. W. F. Giauque and R. A. Ruehrwein. J. Am. Chem. Soc. **61**, 2626 (1939).
4. G. E. Coates and J. E. Coates. J. Chem. Soc. 77 (1944).
5. R. H. Cole. J. Am. Chem. Soc. 77, 2012 (1955).
6. W. J. Dulmage and W. N. Lipscomb. Acta Cryst. **4**, 330 (1951).
7. R. E. Hoffman and D. F. Hornig. J. Chem. Phys. **17**, 1163 (1949).
8. G. E. Hyde and D. F. Hornig. J. Chem. Phys. **20**, 647 (1952).
9. F. G. Baglin, G. L. Coulter, and J. R. Durig. Private communication.
10. C. M. King and E. R. Nixon. J. Chem. Phys. **48**, 1685 (1968).
11. R. Savoie and A. Anderson. J. Chem. Phys. **44**, 548 (1966).
12. K. Ziegler. Organic syntheses. Vol. I. John Wiley and Sons, Inc., New York. 1932. p. 307.
13. R. Savoie and M. Pézolet. Can. J. Chem. **45**, 1677 (1967).
14. D. F. Hornig. J. Chem. Phys. **16**, 1063 (1948).
15. H. Winston and R. S. Halford. J. Chem. Phys. **17**, 607 (1949).
16. T. Shimanouchi, M. Tsuboi, and T. Miyazawa. J. Chem. Phys. **35**, 1597 (1961).
17. M. Born and K. Huang. Dynamical theory of crystal lattices. 2nd ed. Oxford Univ. Press, London. 1956.
18. J. De Launay. Solid State Phys. **2**, 220 (1956).
19. C. Kittel. Introduction to solid state physics. 3rd ed. John Wiley and Sons, Inc., New York. 1968.
20. R. Savoie and M. Pézolet. J. Chem. Phys. **50**, 2781 (1969).
21. J. A. A. Ketelaar, C. Haas, and J. Fahrenfort. Physica, **20**, 1259 (1954).
22. C. Haas and D. F. Hornig. J. Chem. Phys. **26**, 707 (1957).
23. G. Andermann and D. A. Dows. J. Phys. Chem. Solids, **28**, 1307 (1967).
24. E. Sandor and R. F. C. Farrow. Nature, **171**, 171 (1967).
25. H. B. Friedrich and W. B. Person. J. Chem. Phys. **39**, 811 (1963).
26. A. Anderson and R. Savoie. Can. J. Chem. **43**, 2271 (1965).
27. M. Pézolet and R. Savoie. Unpublished results.

Can. J. Chem. Downloaded from www.nrcresearchpress.com by 210.87.254.5 on 09/05/12
For personal use only.

Can. J. Chem. Downloaded from www.nrcresearchpress.com by 210.87.254.6 on 09/05/12
For personal use only.

Solubility of some iodides in non-polar solvents

S. K. SURI AND V. RAMAKRISHNA[1]

Department of Chemistry, Indian Institute of Technology, New Delhi-29, India

Received February 20, 1969

The solubilities of SnI_4, AsI_3, SbI_3, and BiI_3 in carbon tetrachloride, cyclohexane, benzene, and dioxane have been determined at different temperatures (30–55 °C). The entropy of solution of these iodides at 25 °C has been calculated from the data, and compared with the calculated entropy of fusion. The solubility parameters of these iodides have been computed and their spectral behavior in the solvents studied in the near ultraviolet region. On the basis of these data, the nature of the solutions of the iodides in the non-polar solvents has been compared.

Canadian Journal of Chemistry, 47, 3049 (1969)

In the course of their investigations on the solubility of non-electrolytes, Hildebrand and Scott (1); and Smith and Walkley (2) determined the solubility of several solutes, including I_2 and SnI_4, in a large number of solvents. They showed that the entropy of dissolution of the solutes could be predicted in those solvents where complexing tendency did not exist, on the basis of the "regular solution theory". The fundamental assumptions of the theory are: (*i*) a random distribution of molecules in solutions of non-polar liquids, leading to an entropy of mixing term from liquid state, of value $-R\ln X_i$; and (*ii*) a geometric mean for the cohesive energy density i.e. $C_{12} = (C_{11}C_{22})^{\frac{1}{2}}$, where $C_{ii} = \Delta E_i^{vap}/V_i$ and ΔE_i^{vap} = energy of vaporization and V_i = molar volume of the liquid. Given these assumptions, the regular solution theory can predict thermodynamic properties of solutions within 10–20% of those calculated from thermal data. Hildebrand and Scott (1) and Smith and Walkley (2) demonstrated the remarkable usefulness of this approach in dealing with a variety of solutions of non-electrolytes, in comparison to the more limited applicability of the other elaborate theoretical treatments.

While the solubility of SnI_4 has been studied to some extent (1), other covalently bonded iodides have received considerably less attention. It would be interesting to compare the solutions of other covalently bonded iodides, particularly those of Group V elements, for which thermochemical properties have become available in recent years (3, 4). Also, the solvent properties of dioxane have not been studied in this manner previously. With this in view, we have studied the solubilities of the iodides of As, Sb, Bi, and Sn, in four solvents; viz. carbon tetrachloride, cyclohexane, benzene, and dioxane, and also determined their spectroscopic behavior in the near ultraviolet (u.v.) region.

Experimental Procedure

The solvents used were purified according to standard procedures (5). Some of the physical properties determined showed good agreement with literature values (6).

Stannic iodide was prepared in lots of 40–50 g by the method described by Dorfmann and Hildebrand (7). Arsenic, antimony, and bismuth tri-iodides were prepared and purified according to methods described by Cubicciotti and Eding (3, 4) in lots of $\sim$ 30 g.

The technique we used for the determination of solubilities was similar to that of Glew and Hildebrand (8). In the place of a teflon bearing for the stirring shaft, we used the conventional mercury seal. We did not observe any chemical action on mercury during these experiments with the iodides. The temperature of the circulating water was controlled to ± 0.01 °C and the difference between inlet and outlet temperature was not greater than 0.02 °C at the highest temperature of determination. The solubility was measured by taking out a known weight (approximately 15 ml) of the solution into a tared dish, then carefully evaporating the solution under slightly reduced pressure and finally under a good vacuum. Constancy of weight fraction of iodides over three successive determinations at a temperature was taken as indicative of the final equilibrium value. These results were also checked by the chemical analysis of the residue left. SnI_4 gave a precipitate in concentrated solutions of dioxane. BiI_3 was found to be sparingly soluble in carbon tetrachloride, cyclohexane, and benzene. Hence, no solubility data could be obtained for these systems.

Spectroscopic measurements were carried out using a Unicam SP-500 manually operated spectrophotometer with 1 cm quartz cells. The concentrations of the solutes in these measurements were kept at $\sim 5 \times 10^{-5}$ *M*.

Results

The melting points and the determined

[1]To whom all correspondence should be addressed.

TABLE I

Melting point and composition of iodides used

Iodide	Melting point (°C) This work	Melting point (°C) Refs. 3, 4, 12	% iodine This work	% iodine Calculated value
SnI_4	143.0	144.5	80.97*	81.05
AsI_3	141.0	140.4	83.41†	83.56
SbI_3	170.0	171.0	75.75†	75.77
BiI_3	—	408.7	64.45‡	64.56

*Tin estimated as tin oxide (7).
†Estimated volumetrically (13).
‡Bismuth estimated as bismuth oxide (13).

composition of the iodides have been recorded in Table I and the solubilities over the temperature range 30–55 °C in Table II. The results are shown as log X_2 (subscript 2 denoting the solute) vs. log T plots in Fig. 1. Our values for the solubility of SnI_4 in benzene and CCl_4 extrapolated to 25 °C are in good agreement with those reported by Smith and Walkley (2) and Dorfmann and Hildebrand (7). The solubility plots given in Fig. 1 yield good straight lines in all cases, similar to the results of previous workers (1, 2), and permitting accurate determination of entropy (1). Further, it is seen that the solubility of all the iodides, determined in the present investigations, increases in the order: cyclohexane, carbon tetrachloride, benzene, and dioxane. In the first three solvents, the same order has been observed for the solubility of other solutes in earlier investigations (vide 1, 2). The solubility of the iodides in dioxane is much larger than in other conventional solvents.

In Table III, the known thermochemical properties for the iodides (1, 3, 4) are recorded. Other values presented in Table III, have been estimated as follows.

Since $\Delta C_p(= C_p(\mathrm{l}) - C_p(\mathrm{s}))$, is known for these iodides (vide column 4, Table III), and is not close to zero, the following equation has

TABLE II

Solubility data for some metal iodides in four solvents at various temperatures

Components Solvent (1)	Components Solute (2)	Temperature °C	X_2 (sat)	Components Solvent (1)	Components Solute (2)	Temperature °C	X_2 (sat)
CCl_4	AsI_3	36.8	1.296×10^{-3}	C_6H_6	SbI_3	30.1	2.265×10^{-3}
		43.8	1.732			41.9	3.225
		46.5	1.949			45.1	3.539
		50.2	2.234			49.0	3.960
		54.1	2.680			52.5	4.444
c-C_6H_{12}	AsI_3	37.5	1.072×10^{-3}	Dioxane	SbI_3	30.1	6.069×10^{-3}
		41.1	1.255			39.6	7.324
		44.8	1.478			44.9	7.829
		49.2	1.790			49.9	9.963
		53.9	2.139			54.6	10.649
C_6H_6	AsI_3	40.3	5.342×10^{-3}	Dioxane	BiI_3	30.1	6.777×10^{-3}
		44.2	5.868			39.3	9.058
		48.8	6.907			43.0	10.136
		49.7	7.123			46.4	11.152
		54.3	8.580			53.7	13.915
Dioxane	AsI_3	40.1	7.740×10^{-3}	CCl_4	SnI_4	38.9	2.279×10^{-2}
		42.4	8.574			42.4	2.530
		44.8	9.280			47.5	2.986
		49.5	11.598			50.4	3.239
		53.6	12.631			54.7	3.701
CCl_4	SbI_3	36.1	2.265×10^{-4}	c-C_6H_{12}	SnI_4	30.1	1.639×10^{-2}
		41.1	3.036			36.6	2.058
		46.9	4.054			40.1	2.318
		51.1	5.104			43.0	2.547
		54.7	6.168			50.1	3.176
c-C_6H_{12}	SbI_3	36.6	1.828×10^{-4}	C_6H_6	SnI_4	40.1	3.605×10^{-2}
		41.4	2.426			43.6	3.972
		45.0	2.559			45.1	4.225
		47.4	3.514			48.9	4.739
		51.9	4.119			52.9	5.303

Can. J. Chem. Downloaded from www.nrcresearchpress.com by 210.87.254.6 on 09/05/12
For personal use only.

TABLE III

Thermochemical properties of the iodides

Compound	T_f (m.p.) (°K)	ΔH_f at T_f (kcal/mole)	ΔC_p (C_p(l) − C_p(S)) (cal/deg/mole)	ΔH^{vap} at 25 °C (kcal/mole)	log a_2‡ at 25 °C	ΔS_f‡ at 25 °C (e.u.)	V_2‡ at 25 °C (ml)
SnI_4*	417.5	4.60	5.7	19.63	−0.948	9.1	151.0
AsI_3†	413.4	5.21	3.5	18.29	−1.022	11.42	104.0
SbI_3†	444.0	5.44	7.9	20.13	−1.155	9.53	109.5
BiI_3†	681.7	9.35	8.5	26.67	−3.004	6.69	115.0

*From Hildebrand and Scott (1).
†From Cubicciotti and Eding (3, 4).
‡See text for the method of estimation.

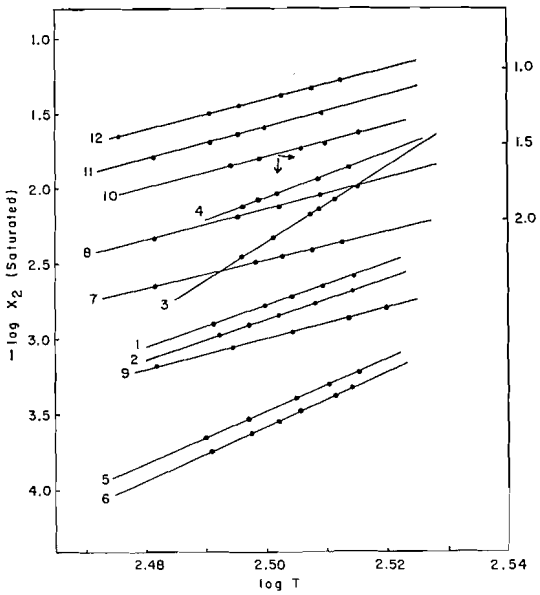

FIG. 1. Solubility of some iodides in four solvents. 1, AsI_3 in carbon tetrachloride; 2, AsI_3 in cyclohexane; 3, AsI_3 in benzene; 4, AsI_3 in dioxane; 5, SbI_3 in carbon tetrachloride; 6, SbI_3 in cyclohexane; 7, SbI_3 in benzene; 8, SbI_3 in dioxane; 9, BiI_3 in dioxane; 10, SnI_4 in carbon tetrachloride; 11, SnI_4 in cyclohexane; 12, SnI_4 in benzene.

been used for estimating log a_2, a_2 being the activity of the iodides

$$[1] \quad \log a_2 = -\frac{\Delta H_f}{2{\cdot}303R}\left[\frac{T_f - T}{T T_f}\right] + \frac{\Delta C_p}{2{\cdot}303R}\left[\frac{T_f - T}{T}\right] - \frac{\Delta C_p}{R}\log\frac{T_f}{T}$$

In the above equation ΔH_f = heat of fusion and T_f = temperature of fusion of the iodides, and the other symbols have their usual significance.

The entropy of fusion of the iodides at 25 °C has been obtained by extrapolation from their melting points by the aid of ΔH_f and ΔC_p data given in Table III. It is estimated that the error in log a_2 values so obtained would be of the order of 3–5%. The molar volumes in the liquid state for these iodides (except for SnI_4), as far as we know, are not available in literature. We have proceeded, therefore, to estimate them by comparing with the corresponding bromides, for which the requisite data are available (9). The assumption we have made in this estimation is that the % volume expansion upon change of state from solid to liquid for the iodides and bromides of the same elements are equal. In the case of SnI_4, for which molar volume data are available, the error caused by our estimation procedure is observed to be ~ 2%. With the data thus estimated, it has been possible to calculate the Hildebrand solubility parameters of the iodides (1) from the following equation

$$[2] \quad \log a_2 = \log X_2 + \frac{V_2\phi_1^2(\delta_2 - \delta_1)^2}{2{\cdot}303RT}$$

where ϕ_1 = volume fraction of solvent, δ_i = solubility parameter = $(C_{ii})^{\frac{1}{2}} = (\Delta E_i^{vap}/V_i)^{\frac{1}{2}}$. The δ's so calculated are tabulated in Table VII, along with the values obtained from $[(\Delta H^{vap} - RT)/V]^{\frac{1}{2}}$. The value of ΔH^{vap} used here involves extrapolation over a fairly wide range of temperature, from the melting point of the solids to 25 °C. The data reported in Table VII are probably in error to the extent of 5–10%.

From the slope of the straight lines of Fig. 1, the term, $R(\partial \ln X_2/\partial \ln T)_{sat}$ has been calculated and recorded in Table IV, together with the corresponding $(-R \ln X_2)$ values at 25 °C, at which temperature most of the earlier solubility

Can. J. Chem. Downloaded from www.nrcresearchpress.com by 210.87.254.6 on 09/05/12
For personal use only.

Can. J. Chem. Downloaded from www.nrcresearchpress.com by 210.87.254.6 on 09/05/12
For personal use only.

TABLE IV

Estimated entropy of solution and solubility of the iodides in four solvents at 25 °C

Solute	Solvent	$\Delta\bar{S}_2$ (cal/deg mole)	$-R \ln X_2$
AsI_3	CCl_4	26.37	13.79
	c-C_6H_{12}	27.70	14.70
	C_6H_6	24.24	11.77
	Dioxane	23.74	10.79
SbI_3	CCl_4	34.10	17.95
	c-C_6H_{12}	33.78	19.22
	C_6H_6	18.41	12.55
	Dioxane	20.47	10.96
BiI_3	Dioxane	18.88	14.80
SnI_4	CCl_4	19.61	8.42
	c-C_6H_{12}	20.47	8.50
	C_6H_6	19.45	7.55

data have been reported (1). The entropy of solution at saturation is related to the term $R(\partial \ln X_2/\partial \ln T)_{sat}$ by means of the following equation

$$[3] \quad \Delta\bar{S}_2 = \bar{S}_2 - S_2^S = R(\partial \ln X_2/\partial \ln T)_{sat,P} \times (\partial \ln a_2/\partial \ln X_2)_{P,T}$$

The factor $(\partial \ln a_2/\partial \ln X_2)_T$ in eq. [3], which is the "Henry's Law" factor, is not far from unity when X_2 is small. Hence the values recorded in Table IV can be taken to represent $(\bar{S}_2 - S_2^S)$, the entropy of solution of the iodides in the solvents.

Discussion

The first point to observe is that the values recorded for SnI_4 solutions in benzene and carbon tetrachloride agree very well with those of Smith and Walkley (2), and serve as a check on our determinations. The $\Delta\bar{S}_2$ value for SnI_4 solution in cyclohexane recorded in Table IV is higher than in other solvents. Cyclohexane has given similar higher values for other solutes studied by earlier workers (vide 1). According to the regular solution theory, the entropy of dissolution of a solid, $(\bar{S}_2 - S_2^S)$, obeys the linear relationship: $(\bar{S}_2 - S_2^S) = -R \ln X_2 + \Delta S$(fusion). That is, a plot of entropy of dissolution vs. $-R \ln X_2$ is expected to have a slope of unity and an intercept of ΔS (fusion). When the entropy measurements are made at constant pressure, as in our systems, the slope of the above line would be expected to be higher than unity, depending on the term $(\partial P/\partial T)_{v,1} \cdot \bar{V}_2^E$. The slopes obtained by us for various solutions

TABLE V

Slope of the lines joining ΔS (fusion) of iodides with $\Delta\bar{S}_2$ in various solvents

	Slopes			
Iodides	CCl_4	c-C_6H_{12}	C_6H_6	Dioxane
AsI_3	1.08	1.11	1.09	1.14
SbI_3	1.37	1.26	0.71	1.00
BiI_3	—	—	—	0.82
SnI_4	1.25	1.34	1.37	—

are given in Table V. It will be observed that for SnI_4 solutions in all the solvents studied, and for SbI_3 in CCl_4 and c-C_6H_{12} the slopes are 25–37% larger than unity. This is to be expected when the large value of $\bar{V}_2^E$ for the solutes is taken into consideration, anticipated on the basis of the value for SnI_4 (vide 1). However, all other values in Table V are smaller than expected, particularly for solutions of SbI_3 and BiI_3 in benzene and dioxane, indicating the possibility of complexing in solution, which reduces the number of independent molecules. In the case of I_2 and SnI_4 solutions, Hildebrand and Scott (1) and Smith and Walkley (2) found that the degree of complexing could be related to the departure of solubility from what it would be if the solution were regular. Applying this concept to our data (Table V), it would appear that the solutions of

TABLE VI

Absorption maxima for the iodides in the four solvents*

Iodide	Solvent	Absorption maxima λ (mμ)	Peak separation (cm^{-1})
AsI_3	CCl_4	*282*, *384*	9 400
	c-C_6H_{12}	230, *282*, *384*	9 400
	C_6H_6	*282*, *384*, 490	9 400
	Dioxane	*260*, *370*, 450	11 400
	Vapor†	*276*, *384*	10 200
SbI_3	CCl_4	288	—
	c-C_6H_{12}	233, *285*, *345*	6 100
	C_6H_6	280	—
	Dioxane	*260*, *345*	9 500
	Vapor†	*273*, *343*	7 500
BiI_3	CCl_4	—	—
	c-C_6H_{12}	—	—
	C_6H_6	—	—
	Dioxane	*250*, *332*, 400	9 900
	Vapor†	*281*, *338.6*, 415	6 050
SnI_4	CCl_4	*285*, *365*	7 700
	c-C_6H_{12}	245, *282*, *365*	8 100
	C_6H_6	*292*, *370*	7 200
	Dioxane	250, *292*, *362*	6 600

*Values in italics in column 3 have been used for calculating data in column 4.
†From ref. 10.

TABLE VII

Solubility parameter (cal/ml)$^{\frac{1}{2}}$ of the iodides at 25 °C

	Solubility parameter				
	Calculated from eq. [2]*				Calculated from
Iodides	CCl_4	c-C_6H_{12}	C_6H_6	Dioxane	$[(\Delta H^{vap} - RT)/V]^{\frac{1}{2}}$
AsI_3	13.72	13.56	13.72	14.21	13.05
SbI_3	14.47	14.36	13.65	13.95	13.35
BiI_3	—	—	—	11.67	15.00
SnI_4	11.50	11.12	11.82	—	11.70

*δ, values obtained from ΔH^{vap} of solvent (1).

SbI_3 in benzene and dioxane and of BiI_3 in dioxane have undergone considerable complexing, while the solutions of AsI_3 show this tendency to a smaller extent. This also explains the greater solvation of BiI_3 in dioxane, while it is only sparingly soluble in the other three solvents.

In this context, it is of interest to examine the electronic spectra of these systems. There are generally two characteristic absorption maxima, for which the separation has been calculated in wave numbers (Table VI). For these iodides in CCl_4 and c-C_6H_{12} solutions, the higher frequency absorption peak occurs at 282–285 mμ, while the other falls in a wider range from 345–384 mμ, depending on the solute. We will use the first two solvents as a reference for comparison. For SnI_4 in benzene and dioxane, the lower frequency peak is more or less unchanged, while the other is shifted to 292 mμ, in agreement with earlier observations (1). For AsI_3, there is no change in the absorption maxima in benzene. In the case of SbI_3 only one peak at 280 mμ is observed in benzene compared to 288 mμ in CCl_4, the lower frequency peak being absent from both solutions. A similar observation has recently been made by Mishra and Ramakrishna (14) in our laboratories in chloroform and t-BuOH solutions, contrary to reports available in literature (10, 11). On this aspect, further investigations are underway. However, it will be noted in Table VI that both the absorption peaks for AsI_3, SbI_3 (except 345 mμ), and BiI_3 in dioxane solutions shift to a higher frequency. The electronic spectra of these iodides therefore generally support complexation in dioxane solutions.

Finally, attention is drawn to the solubility parameters for the solutes (Table VII), which have been calculated from the solutions on the basis of eq. [2]. The values thus obtained are in strikingly good agreement with those calculated from the enthalpy of vaporization given in the last column. The value of δ_2 obtained for SbI_3 in benzene and dioxane is much lower than the corresponding values for AsI_3; and the value for BiI_3 is exceptionally low, corroborating again that in these solutions specific solute–solvent interactions occur.

1. J. H. HILDEBRAND and R. L. SCOTT. Regular solutions. Prentice-Hall, Inc., New York. 1962.
2. E. B. SMITH and J. WALKLEY. Trans. Faraday Soc. **56**, 220 (1960).
3. D. CUBICCIOTTI and H. EDING. J. Phys. Chem. **69**, 2743 (1965).
4. D. CUBICCIOTTI and H. EDING. J. Phys. Chem. **69**, 3621 (1965).
5. A. WEISSBERGER. Technique of organic chemistry. Vol. VII. 3rd ed. Interscience Publishers, Inc., New York. 1959.
6. J. TIMMERMANS. Physicochemical constants of pure organic compounds. Elsevier Publ. Co., Inc., Amsterdam. 1950.
7. N. E. DORFMANN and J. H. HILDEBRAND. J. Am. Chem. Soc. **49**, 729 (1927).
8. D. N. GLEW and J. H. HILDEBRAND. J. Phys. Chem. **60**, 616 (1956).
9. E. W. WASHBURN (*Editor*). International critical tables. Vol. 3. 1928.
10. L. I. KATZIN. J. Chem. Phys. **23**, 2055 (1955).
11. R. H. POTTERILL and O. S. WALKER. Trans. Faraday Soc. **33**, 363 (1937).
12. R. F. ROLSTEN. Iodide metals and metal iodides. John Wiley and Sons, Inc., New York, 1961.
13. W. F. HILLEBRAND, G. E. F. LUNDELL, H. A. BRIGHT, and J. I. HOFFMAN. Applied inorganic analysis. 2nd ed. John Wiley and Sons, Inc., New York. 1953.
14. B. MISHRA and V. RAMAKRISHNA. Unpublished data.

Can. J. Chem. Downloaded from www.nrcresearchpress.com by 210.87.254.6 on 09/05/12
For personal use only.

Can. J. Chem. Downloaded from www.nrcresearchpress.com by 84.22.46.98 on 09/08/12
For personal use only.

Electrochemistry of copper, silver, gold, gallium, indium, and thallium in fused $AlCl_3$–NaCl–KCl eutectic[1]

UDO ANDERS AND JAMES A. PLAMBECK
Department of Chemistry, University of Alberta, Edmonton, Alberta

Received March 3, 1969

The electrochemistry of copper, silver, gold, gallium, indium, thallium, and their ions, and of chlorine and bromine in fused $AlCl_3$–NaCl–KCl was investigated by electromotive force (e.m.f.) and voltammetric techniques. Univalent oxidation states were observed for all the metals. In addition, copper was further oxidized to the divalent species while gallium and indium were oxidized to trivalent species. The standard potentials for the above couples were established in the $AlCl_3$–NaCl–KCl eutectic at 135 °C.

Canadian Journal of Chemistry, **47**, 3055 (1969)

Introduction

It has been shown by electrochemical and spectroscopic methods (1–3) that molten salt systems containing $AlCl_3$ have a tendency to stabilize low valence states of metal ions. The presence of Bi(I) has been established in $NaAlCl_4$ (3), as has that of Cd(I) (4). A recent electrochemical study (2) of the Group IIB elements has demonstrated the enhanced stability of lower valence states in the fused ternary $AlCl_3$–NaCl–KCl (66:20:14 mole %, respectively) eutectic. The present paper extends that study to the Group IB and IIIA elements.

Some of these metals have been investigated by Yntema and co-workers (6–9) in this solvent. The primary objective of these studies was deposition of the metals from their solutions in the eutectic, and little attention was paid to other effects. Thus when Ga(III) was added to the melt and gallium electrodeposited at the cathode, the presence of Ga(I) was not recognized although the polarization curve displayed one additional break. Indium was not investigated. No electrochemical activity was found when TlCl was added to the melt, and it was concluded that thallous chloride was therefore insoluble. The present study shows, however, that the oxidation and reduction potentials of Tl(I) are beyond the melt range and so no electrochemical activity should be observed. Yntema reported his studies of gallium 25 years ago when the chemistry of gallium was not well understood. It is now known that gallium metal reacts with gallium trichloride to form $Ga(GaCl_4)$, a complex containing equal amounts of Ga(I) and Ga(III). Excess gallium metal does not undergo further reaction with this complex unless aluminum trichloride is added (5); under these circumstances the $GaCl_4^-$ ion reacts until all Ga(III) is reduced to Ga(I). The resulting complex has the formula $Ga(AlCl_4)$.

Experimental

The electronic instrumentation and electrochemical cell used have been described previously (2). The metals for the electrodes were obtained in wire form from A.D. MacKay (New York) and were of 99.99% purity. Anhydrous $GaCl_3$ and $InCl_3$ were produced from the pure metals and chlorine gas (10). Anhydrous InCl was purchased from Alfa Inorganics (Beverly, Mass.). Reagent grade $AlCl_3$, NaCl, and KCl (Fisher Scientific Co.) were used. The purification procedure used for the aluminum chloride in this investigation was less cumbersome than that previously reported (2) and allowed the preparation of a new melt for each experiment. In this procedure, 250 g of aluminum chloride were placed in a closed-end Pyrex tube 40 cm long and 5 cm in diameter, which was fitted with a 6 cm O-ring joint. The aluminum chloride was covered with a 1 cm thick layer of granular aluminum metal (reagent grade 30 mesh, Fisher Scientific Co.). The tube was flushed with nitrogen and closed with a Pyrex cap which had a 4 mm stopcock on top; this was open to a mercury pressure relief valve during the sublimation. The vertical tube was heated by an external heating mantle and heating tape which extended to the height of the aluminum layer. A tubular ring with pin holes pointing inwards fitted loosely over the sublimation tube. Compressed air was blown through it to cool the tube and prevent condensation of subliming aluminum chloride in the upper half of the tube. It was positioned approximately 10 cm down from the glass joint. The aluminum chloride condensed over a length of 7–10 cm as a colorless, crystalline solid. After nearly complete sublimation, the closed tube was cooled and transferred into a glove box filled with dry nitrogen. The glass tube

[1]Taken from the Thesis of U. Anders submitted to the Faculty of Graduate Studies, University of Alberta, Edmonton, in partial fulfillment of the requirements for the degree of Doctor of Philosophy.

Can. J. Chem. Downloaded from www.nrcresearchpress.com by 84.22.46.98 on 09/08/12
For personal use only.

was then broken to obtain the solid aluminum chloride. The lower part of the crystallized aluminum chloride cylinder was generally discarded due to baked-in granular aluminum.

The aluminum chloride obtained by the above procedure was a crystalline material, pure white in color. It was ground, transferred into a tightly stoppered flask, removed from the glove box, weighed, and returned to the glove box in which all further work was done. After addition of the appropriate amounts of sodium chloride and potassium chloride, the mixture was melted in a round bottomed flask and transferred into the electrochemical cell previously described (2). It was observed that the color of the melt varied with the temperature employed during this initial melting process, from a faint yellow to light-brown. The cause of the coloration is unknown. It has been suggested that it is due to carbon from organic material (11, 12) or dissolved silicon compounds (13). An aluminum wire spiral was added to the melt for 1 h in order to reduce any metal ion impurities.

Reference Electrode

All potentials were measured with respect to an aluminum wire inserted into the melt. The use and nonpolarizability of this reference electrode have been described (2). All measurements were made at 135 ± 1 °C rather than at 150 °C (2), to keep evaporation of the aluminum chloride to a minimum during the experiments.

Metal–Metal Ion Electrodes

The compartments consisted of 10C sealing tubes (Ace Glass Inc., Vineland, N.J.) which were inserted into the melt and allowed to fill to the melt level. The metals were inserted as wires except in the case of gallium which is a liquid at this temperature. Here a spoon-like Pyrex cup attached to the end of a glass tube was used. A platinum wire which did not come in contact with the melt led to the bottom of the cup, which was filled with liquid gallium metal and then inserted into the compartment.

Gas Electrodes

The chlorine electrode employed a compartment consisting of a 10D sealing tube extended to 20 cm and closed on top. A tungsten wire was sealed through the top and reached to the frit, parallel to a glass tube, 5 mm outer diameter, which served as a feed-in tube for chlorine gas and which also entered the compartment near the top. A second tube on top of this half cell was used as a gas outlet. The chlorine gas was dried over phosphorus pentoxide before being fed through Teflon tubing to the electrode.

Chlorine gas was first bubbled through the melt rapidly to saturate the melt and displace the nitrogen above it. Then time was allowed for the melt to reach thermal equilibrium, until the potential became stable within 1 mV. It was ascertained by several more small additions of chlorine and successive equilibrations that the melt was truly saturated with chlorine gas.

The bromine cell differed from the above by an additional 10/35 standard taper joint on top, into which a small dropping funnel containing liquid bromine was fitted. At first a total of 5 ml of bromine was added in small portions to saturate the melt with bromine, as well as to replace the nitrogen above it by bromine vapor. Bromide ion was produced by coulometric reduction of bromine in the compartment at a tungsten electrode operated at low current densities. The melt was occasionally checked for bromine saturation by addition of small amounts of bromine as described above for the chlorine electrode.

Results and Discussion

The standard states used in this work are those defined previously (2, 14). The reference electrode used for all standard or measured potentials is Al(III)/Al(0), for which the standard and measured potentials are the same. The standard potentials calculated for all couples are given in Table I.

Chlorine

To establish the potential span of the melt in terms of standard potentials, the e.m.f. of the Cl_2/Cl^- couple was measured precisely. Wade *et al.* (6) reported a value of 2.09 ± 0.04 V for this couple at 156 °C. Treadwell and Terebesi (15) found 2.062 V at 721 mm Hg and 135 °C in a slightly different ternary system (62 mole % $AlCl_3$, 26 mole % NaCl, and 12 mole % KCl). The temperature dependence at a platinum electrode, as measured against an Al(III)/Al(0) reference electrode, was − 0.72 mV/°C.

The present study reports a standard potential of 2.064 ± 0.002 V at 135 °C and 1 atm, the standard and measured potentials for this couple being the same. The temperature dependence of the electrode from 120 to 180 °C was −0.65 ± 0.03 mV/°C. No hysteresis was observed.

Identical potentials were obtained for chlorine in the $AlCl_3$–NaCl–KCl melt with carbon and tungsten electrodes. It must be noted that the carbon electrodes disintegrated slowly upon contact with the melt to give carbon powder. This, however, did not give rise to an observable change in potential. Apparently this disintegration, which also occurs in the melt in the absence of chlorine, is due to the high content of aluminum trichloride since carbon electrodes have been used successfully in the $NaAlCl_4$ melt (1).

Bromine

The molal standard potential of the Br_2/Br^- couple was found to be 1.785 ± 0.002 V at 135 °C and 1 atm. The temperature dependence of this couple was measured as −0.16 ± 0.03 mV/°C from 120 to 170 °C.

TABLE I

Electromotive force series in $AlCl_3$–NaCl–KCl at 135 °C

Couple	E^0_{molar}	E^0_{molal}	$E^0_{mole\ fraction}$	Standard deviation
Al(III)/Al(0)	0.000	0.000	0.000	Defined*
Ga(I)/Ga(0)	0.199	0.222	0.276	0.002
Zn(II)/Zn(0)	0.254†	0.263†	0.304†	0.002
Ga(III)/Ga(0)	0.577‡	0.585‡	0.603‡	0.002
Cu(I)/Cu(0)	0.689	0.710	0.745	0.002
Ag(I)/Ag(0)	0.695	0.719	0.802	0.001
Ag(I)/Ag(0)	0.740†	0.759†	0.832†	0.001
Ga(III)/Ga(I)	0.766	0.766	0.766	0.002
Hg(I)/Hg(0)	1.028†	1.037†	1.077†	0.001
In(III)/In(I)	1.1	1.1	1.1	0.15
Hg(II)/Hg(0)	1.222†‡	1.231†‡	1.271	0.002
Cu(II)/Cu(0)	1.278‡	1.288‡	1.306	0.002
Hg(II)/Hg(I)	1.415†	1.424†	1.464†	0.002
Br_2/Br^-	1.768	1.785	1.631	0.002
Cu(II)/Cu(I)	1.866	1.866	1.866	0.001
Au(I)/Au(0)	2.022	2.046	2.119	0.002
Cl_2/Cl^-	2.064	2.064	2.064	0.002

*Defined as 0.000 at all temperatures in this melt.
†Measured at 150 °C; ref. 2.
‡Calculated from free energies of experimentally measured couples.

Gallium

Gallium metal was anodized at low current densities to form Ga(I) (Fig. 1). The Nernst plot indicated a slope of 81 mV/log unit for this process, corresponding to 1.0 ± 0.1 electrons. The molal standard potential was 0.222 ± 0.002 V. Voltammetry with an inert tungsten electrode indicated the presence of an anodic wave corresponding to the oxidation of Ga(I). Quantitative coulometric oxidation at a platinum electrode at 5 mA/cm^2 showed this to be a two-electron process. The plot of log (Ga(I)/Ga(III)) vs. e.m.f. (Fig. 2) resulted in a straight line whose slope corresponded to 2.2 ± 0.1 electrons. A

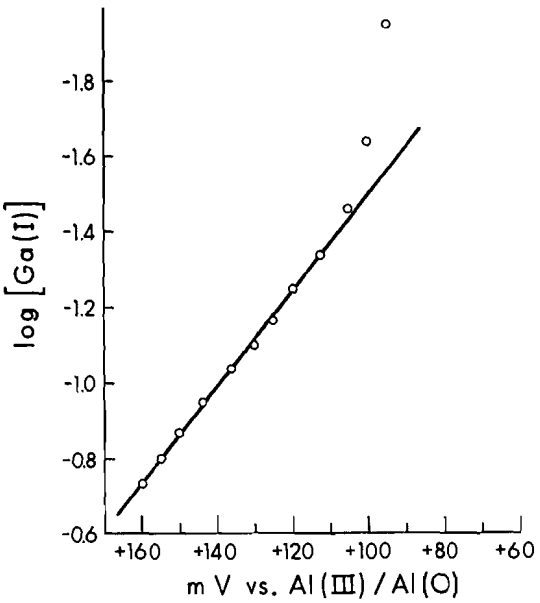

FIG. 1. Nernst plot for the Ga(I)/Ga(0) couple. Typical run, concentration on molal basis.

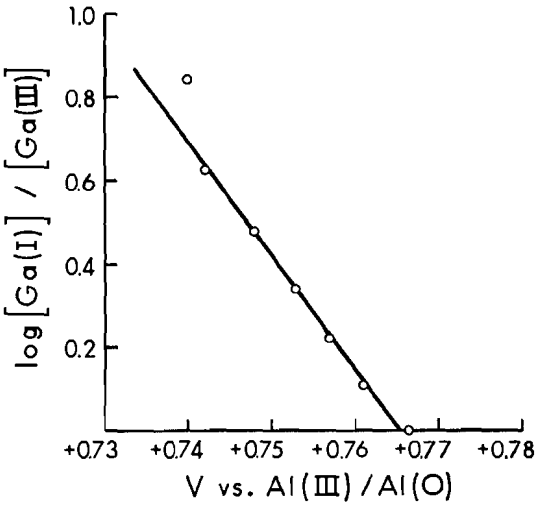

FIG. 2. Nernst plot for the Ga(III)/Ga(I) couple. Typical run, concentration on molal basis, obtained by coulometric reduction of Ga(III) at the platinum electrode.

Can. J. Chem. Downloaded from www.nrcresearchpress.com by 84.22.46.98 on 09/08/12
For personal use only.

TABLE II

Equilibrium constants for Group IB, IIB, and IIIA elements

Reactions	Equilibrium constant		
	$AlCl_3$–NaCl–KCl	LiCl–KCl (450 °C)*	H_2O (25 °C)
Cu(II) + Cu(0) ⇄ 2Cu(I)	2.1×10^{14}	7.1×10^{6}	5.9×10^{-7}‡
Ag(II) + Ag(0) ⇄ 2Ag(I)	$>3 \times 10^{12}$	$>3 \times 10^{7}$	1×10^{20}‡
1/2Au(III) + Au(0) ⇄ 3/2Au(I)	$>2 \times 10^{-20}$	$>4 \times 10^{-1}$	3.4×10^{-2}‡
Zn(II) + Zn(0) ⇄ 2Zn(I)	Very small	Very small	Very small
Cd(II) + Cd(0) ⇄ 2Cd(I)	2.6×10^{1}	Very small	Very small
Hg(II) + Hg(0) ⇄ 2Hg(I)	3.6×10^{4}	—	1.6×10^{2}‡
1/2Ga(III) + Ga(0) ⇄ 3/2Ga(I)	5.0×10^{6}	—	3.0×10^{-10}†
1/2In(III) + In(0) ⇄ 3/2In(I)	$>4 \times 10^{13}$	—	1.9×10^{-6}†
1/2Tl(III) + Tl(0) ⇄ 3/2Tl(I)	$>4 \times 10^{25}$	—	2.3×10^{27}†

*Reference 14.
†Reference 17.
‡Reference 18.

standard potential of 0.766 ± 0.002 V was measured at equal concentrations of Ga(I) and Ga(III). The voltammetric value of 0.77 ± 0.02 V is in good agreement (Fig. 3).

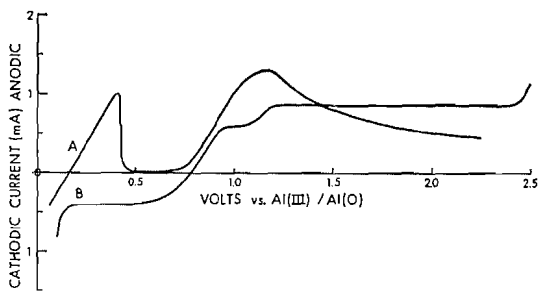

FIG. 3. Voltammetry of gallium ions. A, 0.1 molal Ga(I), 0.04 V/s; B, 0.05 molal Ga(I), 0.05 molal Ga(III), 0.02 V/s. Tungsten microelectrodes, scan direction toward the positive potential.

With these data it is possible to calculate the equilibrium constant. If the equilibrium reaction is defined as 1/2Ga(III) + Ga(0) ⇄ 3/2Ga(I), which involves a change of one electron, $K = 5.0 \times 10^{6}$ (Table II). The equilibrium constant is in molal units and is given by $K = [Ga(I)]^{3/2}/[Ga(III)]^{1/2}$.

Figure 3 shows two voltammetric curves of gallium solutions which were obtained with a tungsten microelectrode. Curve A represents the result of a scan of a solution approximately 0.1 molal in Ga(I) while curve B was obtained at equal concentrations of Ga(I) and Ga(III), about 0.05 molal. The peak of curve A is slightly broader than is usual in fused salts (16); this is due to the high IR drop across the cell resistance (250 Ω, primarily in the frit of the compartment). Curve B shows waves rather than peaks. The first anodic wave in curve B is followed by a second, suggesting further oxidation of Ga(III). However, a voltammetric scan of a solution of pure $GaCl_3$ shows no such second anodic wave, and the cathodic wave observed on attempted reduction of Ga(III) to Ga(I) appears at the expected potential. The shapes of the second anodic wave (curve B) and the cathodic reduction wave are not simple; the significance of this is not clearly understood and may be due to slow kinetic steps in the oxidations and reductions involved.

Indium

Indium metal in contact with the melt reacts with it completely to give aluminum metal. From the amount of indium metal put into the melt and, in the case of a complete reaction, of aluminum metal obtained, it was ascertained that In(I) was formed in solution by the reaction Al(III) + 3In(0) → Al(0) + 3In(I). The In(I)/In(0) couple must therefore be more negative in potential than the Al(III)/Al(0) couple. Monovalent indium can be further oxidized within the melt range; a voltammetric scan indicates oxidation at 1.2 ± 0.1 V. Likewise, the addition of $InCl_3$ and subsequent scanning results in a cathodic wave at 1.1 ± 0.1 V. More precise potentiometric measurements could not be made because $InCl_3$ scarcely dissolves into the melt even if the temperature is raised to 220 °C, while In(I) could not be quantitatively oxidized at higher In(I) concentrations. The waves seen in voltammetry must, however, correspond to the oxidation of In(I) to In(III) and the reduction from In(III) to In(I).

Can. J. Chem. Downloaded from www.nrcresearchpress.com by 84.22.46.98 on 09/08/12
For personal use only.

Can. J. Chem. Downloaded from www.nrcresearchpress.com by 84.22.46.98 on 09/08/12
For personal use only.

The data obtained allow estimation of the lower limit of K for the reaction 1/2In(III) + In(0) $\rightleftarrows$ 3/2In(I) as 4×10^{13}.

Thallium

Thallium metal also reacts with the melt with production of aluminum. It was shown, by the method described above for indium, that thallium exists as Tl(I) in the melt. It is, however, not possible to further oxidize Tl(I) to Tl(III) inside the melt range. The lower limit of the equilibrium constant for 1/2Tl(III) + Tl(0) $\rightleftarrows$ 3/2Tl(I) can then be estimated as 4×10^{25}.

Copper

Wade *et al.* (6) measured the decomposition potential of Cu(I) from which a value of $E^0 = 0.81 \pm 0.03$ V was calculated (14) on the mole fraction scale. He made no attempt to oxidize Cu(I) to Cu(II). In the present study, potentials of both the Cu(I)/Cu(0) and Cu(II)/Cu(I) couples were measured accurately, which allowed the determination of their standard potentials and equilibrium constants. A value of 0.710 ± 0.002 V was obtained for the molal standard potential of the Cu(I)/Cu(0) couple. Cu(I) was then oxidized coulometrically at inert electrodes in the same manner as Ga(I).

Plotting the coulometric data as log [Cu(I)]/[Cu(II)] vs. e.m.f. resulted in a straight line with a slope corresponding to 1.0 ± 0.1 electrons. The standard potential was measured at equal concentrations of Cu(I) and Cu(II) as 1.866 ± 0.001 V. The solution of Cu(II) in this melt shows the well-known green color of chloride-solvated Cu(II) while the solution of Cu(I) is colorless. The equilibrium value for the reaction Cu(II) + Cu(0) $\rightleftarrows$ 2Cu(I), with K defined using molal concentrations, is $K = 2.1 \times 10^{14}$ which is much larger than the aqueous value of 5.9×10^{-7} (18); the equilibrium in acetonitrile, however, is favored by an even larger constant of 2.5×10^{25} (19).

Silver

The couple Ag(I)/Ag(0) has been measured previously (2) at 150 °C and a value of 0.795 ± 0.001 V was reported. In the present study the molal standard potential obtained was 0.719 ± 0.001 V at 135° with a temperature dependence of -0.44 ± 0.03 mV/°C from 120 to 170 °C. The temperature vs. e.m.f. plot did not show any hysteresis. The Nernst slope corresponded to 1.0 ± 0.1 electrons. Anodizing silver in another experiment at 150 °C resulted in a value of 0.729 V for the standard potential with $n = 1.1$. The experimental conditions such as concentration and current densities during anodization were identical to the ones of the previous runs at 135 °C. However, weighing the silver wire before and after the experiment disclosed that more silver metal was lost than corresponded to the faradaic process. Reducing the amount of melt inside the compartments in another run resulted in a molal standard potential of 0.736 V with $n = 0.97$. The amount of silver lost was always significantly larger than corresponded to the faradaic process. This, together with the consistent value of one electron, seems to suggest a complex silver species, e.g. Ag_q^{p+} with q and p depending on the experimental conditions. Although complex silver ions have not thus far been observed in fused salts, species like Bi_5^{3+} are known (20) in chloroaluminate melts. It should therefore not be assumed that the potential measured for this couple corresponds to the simple reaction $Ag^+ + e^- \rightleftarrows Ag$. The matter is discussed in more detail in the Thesis of the junior author.

Gold

Gold was anodized into solution at low current densities with a slope corresponding to 1.1 ± 0.1 electrons. Several of the earlier anodization runs were unsuccessful in that no stable potentials could be obtained. Inspection of the gold wire after these experiments showed that anodization had occurred only in a few spots where it had resulted in the formation of deep pin holes. The holes showed the crystalline structure of the metal wire. It was found that remelting the wire before use tended to prevent deep holes although dissolution was still not uniform. Stable potentials were thus obtained, however, and a molar standard potential of 2.046 ± 0.002 V was calculated for the Au(I)/Au(0) couple. This value is much higher than those for Cu(I)/Cu(0) and Ag(I)/Ag(0). The solution containing Au(I) is orange in color while those of Cu(I) and Ag(I) are colorless, which may indicate that the solvation of Au(I) is different from that of the other two ions.

Conclusion

As Table II clearly shows, chloroaluminate melts favor the existence of lower-valence ionic species more strongly than water or chloride melts. This appears to be a general phenomenon

in which the chlorides, strongly polarized by aluminum, are unable to donate as much electron density toward stabilization of the higher valence state, rather than a specific characteristic of the elements studied. The nature of the actual chloroaluminate species and its effect on other metal ions are being investigated.

Acknowledgments

The authors are grateful to the National Research Council of Canada for financial assistant in the form of a Scholarship (U.A.) and Operating Grant (J.A.P.). This work was also supported in part by the Defence Research Board of Canada, Grant No. 5412-09.

1. T. C. F. MUNDAY and J. D. CORBETT. Inorg. Chem. **5**, 1263 (1966).
2. D. A. HAMES and J. A. PLAMBECK. Can. J. Chem. **46**, 1727 (1968).
3. N. J. BJERRUM, C. R. BOSTON, G. P. SMITH, and H. L. DAVIS. Inorg. Nucl. Chem. Letters, **1**, 141 (1965).
4. R. A. POTTS, R. D. BARNES, and J. D. CORBETT. Inorg. Chem. **7**, 2558 (1968).
5. B. R. SUNDHEIM (*Editor*). Fused salts. McGraw-Hill Book Co., Inc., New York. 1964. p. 378.
6. W. H. WADE, G. O. TWELLMEYER, and L. F. YNTEMA. Trans. Electrochem. Soc. **78**, 77 (1940).
7. E. MARSHALL and L. F. YNTEMA. J. Phys. Chem. **46**, 353 (1942).
8. R. G. VERDIECK and L. F. YNTEMA. J. Phys. Chem. **46**, 344 (1942).
9. R. WEHRMANN and L. F. YNTEMA. J. Phys. Chem. **48**, 259 (1944); **48**, 268 (1944).
10. G. BRAUER. Handbook of preparative inorganic chemistry. Academic Press, Inc., New York. 1965. pp. 843 and 858.
11. M. A. FRISCH, M. A. GREENBAUM, and M. FABER. J. Phys. Chem. **69**, 300 (1965).
12. J. R. MORREY. Inorg. Chem. **2**, 163 (1963).
13. W. FISCHER and A. L. SIMON. Z. Anorg. Allgem. Chem. **306**, 10 (1960).
14. J. A. PLAMBECK. J. Chem. Eng. Data, **12**, 77 (1967).
15. W. D. TREADWELL and L. TEREBESI. Helv. Chim. Acta, **18**, 103 (1935).
16. P. DELAHAY. New instrumental methods in electrochemistry. Interscience Publishers, Inc., New York. 1954. p. 139.
17. D. D. WAGMAN W. H. EVANS, V. B. PARKER, I. HALOW, S. M. BAILEY, and R. H. SCHUMM. U.S. Nat. Bur. Std. Tech. Note 270-3, U.S. Govt. Printing Office, Washington, D.C. 1968.
18. W. M. LATIMER. Oxidation potentials. Prentice-Hall, Inc., New York. 1961. Chaps. 9 and 11.
19. I. M. KOLTHOFF and J. F. COETZEE. J. Am. Chem. Soc. **79**, 1852 (1957).
20. N. J. BJERRUM, C. R. BOSTON, and G. P. SMITH. Inorg. Chem. **6**, 1162 (1967).

Can. J. Chem. Downloaded from www.nrcresearchpress.com by 84.22.46.98 on 09/08/12
For personal use only.

Can. J. Chem. Downloaded from www.nrcresearchpress.com by 210.87.254.105 on 09/05/12
For personal use only.

Relaxations of molecular charge distributions and the vibrational force constants in diatomic hydrides

R. F. W. BADER AND J. L. GINSBURG
Department of Chemistry, McMaster University, Hamilton, Ontario
Received February 24, 1969

The force constants for LiH, HF, NaH, and HCl are calculated from Hartree–Fock wavefunctions by a polynomial fit of the forces exerted on the nuclei as a function of the internuclear separation. The magnitude of the force constant is interpreted in terms of the relaxation of the molecular charge distribution induced by the nuclear displacement. In LiH or NaH, for which the molecular charge distribution exhibits the characteristics of ionic binding, two distinct relaxations are evident: a relaxation in the region of the cationic core and a relaxation of the density localized on the proton. The relaxation of the charge density in the vicinity of the Li^+ or Na^+ core opposes the motion of either nucleus while the relaxation of the density localized on the proton facilitates the displacement of the nuclei. In HF or HCl the relaxation of the molecular charge distribution is dominated by one continuous region of charge increase (for bond contraction) or decrease (for bond extension) over the whole of the binding region, a relaxation which facilitates the motion of the nuclei. Thus the relaxation of a molecular charge distribution and its effect in determining the magnitude of the force constant is dominated by the same features of the static charge distribution which serve to distinguish ionic from covalent binding.

Canadian Journal of Chemistry, 47, 3061 (1969)

I. Introduction

In a previous paper (1) we presented an interpretation of the vibrational force constant in terms of the relaxation of the molecular charge distribution. The study was concerned with the origin and variation in the magnitude of the force constants through the two series of molecules N_2, CO, BF and BeO, LiF. The present paper extends this study to the diatomic hydrides, specifically to the molecules LiH, HF, NaH, and HCl. The force constants for hydride molecules have been the subject of numerous theoretical investigations, most of them based on assumed models of the charge distribution and employing simplifying assumptions regarding the manner in which the charge density changes during a vibrational motion (2–5). In this work the force constants are calculated from and interpreted in terms of charge distributions obtained from Hartree–Fock (H.F.) wavefunctions, functions which are known to give the charge density and its dependent properties correct to second-order (6).

Previous publications have presented an interpretation of chemical binding in terms of the molecular charge distribution, the density difference distribution $\Delta\rho_{SA}(r)$, and the forces which the charge distribution exerts on the nuclei (7–10). The $\Delta\rho_{SA}(r)$ distribution is obtained by subtracting from the molecular charge distribution the distribution obtained from the overlap of the component atomic densities with the nuclei situated at the same internuclear separation as found in the molecule. These studies provide detailed knowledge of the spatial distribution and polarizations (relative to the atomic densities via the $\Delta\rho_{SA}(r)$ distributions) of molecular charge densities covering the spectrum of possible bond types from the covalent to the ionic extremes. A knowledge of the properties of the equilibrium charge distributions is a necessary prerequisite for the understanding of the force constant since the dominant characteristic of the relaxation of a charge distribution caused by a nuclear motion, whether it opposes or facilitates the motion of the nuclei, is directly determined by the polarizations present in the static charge distribution of the undistorted molecule (1). The initial study determined the nature of the relaxation of the molecular charge distribution associated with the motions of nuclei of first-row atoms in the two extremes of binding, ionic and covalent. The terms ionic and covalent as used here are defined in terms of the properties of the molecular charge distribution (7–10). In the present work the dominant characteristics of the relaxation of the charge distribution accompanying the motion of a proton in the two binding situations are to be determined. The four hydride molecules considered will make possible both intra- and inter-row comparisons of the relaxation characteristics.

TABLE I

Forces and force constants for hydrides at R_e (H.F.)*

AH or HA	R_e Exp.	R_e H.F.	K_2 Exp.	K_2 Calcd. from Force	K_2 Calcd. from Energy	K_3 Exp.	K_3 Calcd.	$K_3{}^e$†	Force‡ On A nucleus	Force‡ On H nucleus
LiH	3.015	3.034	0.0654	0.0722	0.0685	−0.123	−0.129	0.0855	−0.007	
HLi				0.0684			−0.125	0.0888		−0.001
NaH	3.566	3.616	0.0507	0.0465	0.0515	−0.0886	−0.128	0.258	−0.056	
HNa				0.0531			−0.0871	0.299		−0.002
FH	1.7328	1.696	0.620	0.791	0.723	−2.59	−3.55	2.98	−0.047	
HF				0.731			−2.81	3.72		−0.001
ClH	2.4087	2.389	0.331	0.179	0.375	−0.967	−0.708	2.42	0.165	
HCl				0.386			−1.10	2.03		−0.003

*All quantities are in atomic units; length, 1 a.u. $= a_0 = 0.52917 \times 10^{-8}$ cm; K_2, 1 a.u. $= e^2/a_0{}^3 = 15.568 \times 10^5$ dyn/cm; K_3, 1 a.u. $= e^2/a_0{}^4 = 2.9421 \times 10^{14}$ dyn/cm².
†$K_3{}^e$ denotes the electronic contribution to the cubic potential constant.
‡A negative force implies a force of attraction.

II. Calculation of the Force Constants

In what follows we give a brief summary of the methods used in the calculation and interpretation of the force constant (1). The force on nucleus A in a diatomic molecule AH is given by (11)

$$[1] \quad F_A = \frac{-dE}{dR} = \frac{\partial E}{\partial X_A} = \frac{Z_A Z_H}{R^2} - Z_A \int \rho(r) \frac{\cos\theta_A}{r_A{}^2} dr$$

where $\rho(r)$ is the molecular charge distribution expressed in terms of space-fixed coordinates r, and r_A and θ_A are polar coordinates centered on nucleus A. A change in the nuclear positions causes a change in the charge distribution and hence a change in the forces acting on the nuclei. Thus the electrostatic interpretation of binding in terms of the forces exerted on the nuclei afforded by eq. [1] may be extended to the interpretation of the vibrational potential constants as well. In particular, the second-order potential constant is given by

$$[2] \quad K_{2A} = K_A = \left(\frac{d^2E}{dR^2}\right)_{R_e} = \left(\frac{\partial^2 E}{\partial X_A{}^2}\right)_{R_e} = \frac{2Z_A Z_H}{R_e{}^3} - Z_A \frac{\partial}{\partial X_A} \int \rho(r) \frac{\cos\theta_A}{r_A{}^2} dr$$

A corresponding equation may be written for K_H.

The wavefunctions employed in this investigation were obtained by Cade and Huo (12) and are claimed to be close to the Hartree–Fock limit. From these functions, the forces on each nucleus were calculated at seven values of R. The points other than R_e (the Hartree–Fock value) were regularly situated with respect to R_e. The potential constants were then determined from a Dunham expansion of the force curve. The coefficients of the expansion were obtained by a five-term Tchebycheff polynomial best fit, which was at all times checked against a least-squares fit of the same degree in order to ensure consistency of the method. In Table I, we present the harmonic force constants and the cubic constants K_3 obtained from a fitting of the force curves for the A and H nuclei in the four hydride molecules. These results are compared with the experimental values and with the values of K_2 obtained by Cade and Huo (12) by a Dunham analysis of the potential energy curve.

The values of K_2 calculated from the force curves for the proton K_H are in fair agreement with experiment, the values for the hydrides LiH and NaH being in error by 4 and 6%, while the values for HF and HCl are in error by 18 and 17%, respectively. The values of K_H are in agreement with the values of K_2 calculated from the curvature of the potential energy curves. The agreement with experiment of the K_2 values determined by the force curves for the A nuclei

Can. J. Chem. Downloaded from www.nrcresearchpress.com by 210.87.254.105 on 09/05/12
For personal use only.

Can. J. Chem. Downloaded from www.nrcresearchpress.com by 210.87.254.105 on 09/05/12
For personal use only.

is less satisfactory[1]. Kern and Karplus (6) have shown that it is a requirement of the true Hartree–Fock wavefunction that $F_A = F_H$ for all values of R. From this it follows that $K_A = K_H$, the equality of the force constants providing an even more stringent test of how closely a given wavefunction approaches the Hartree–Fock limit. The value of K_2 as determined by an energy fit should also equal the value determined by a fitting of the force curve for an exact Hartree–Fock result. Table I shows that the condition $F_A = F_H$ (= 0 at R_e(H.F.)) is most closely met for the first-row hydrides. There is a larger discrepancy between F_A and F_H for the second-row results, including a difference in sign. The calculated values of F_A and hence K_A are expected to deteriorate as Z_A increases. It should be pointed out that the force and force constant criteria given above for the true Hartree–Fock limit are very stringent and perhaps impossible to attain from any analytical expansion of the wavefunction with the coefficients of the basis orbitals given to only five or six significant figures.

The values of K_A and K_H are accurate enough to warrant the interpretive analysis which follows. The important quantities for this analysis are the polarizations present in the charge distributions, and comparison of the Hartree–Fock results with more accurate functions (13, 14) indicates that the Hartree–Fock functions provide excellent representations of the overall distribution of the charge densities.

III. Interpretation of the Force Constant

Schwendeman (15) has shown that when the charge distribution is expanded in terms of a coordinate system which is centered on A and which *translates with center A*, denoted by $\rho(\alpha,r_A)$, the entire electronic contribution to K_A may be expressed as

$$[3] \quad \frac{\partial}{\partial X_A}\int \rho(\alpha,r_A)\frac{\cos\theta_A}{r_A^2}\,d\tau = \int \frac{\partial\rho(\alpha,r_A)}{\partial X'_A}\frac{\cos\theta_A}{r_A^2}\,d\tau_A = K_A^e$$

The prime on the X-coordinate of nucleus A in the differentiation implies that the derivative of $\rho(\alpha,r_A)$ is to be taken only through the parameters α in $\rho(\alpha,r_A)$ which change as the internuclear distance is changed.

$$\frac{\partial\rho(\alpha,r_A)}{\partial X'_A} = \sum_\alpha \frac{\partial\alpha}{\partial X_A}\frac{\partial\rho(\alpha,r_A)}{\partial\alpha}$$

In the present expressions for $\rho(\alpha,r_A)$, the parameters α refer to orbital coefficients and exponents, which because of the fixed nucleus approximation, depend parametrically on the internuclear separation. Equation [3] states that any portion of the charge density which moves rigidly with nucleus A does not contribute to the force constant; only a change in the charge distribution, a polarization or a change in polarization, i.e., a "relaxation" of the charge density can contribute to the force constant governing the motion of nucleus A. The "relaxation" of a molecular charge distribution for the motion of nucleus A as defined by $\partial\rho(\alpha,r_A)/\partial X'_A \neq 0$ may be presented pictorially by subtracting the charge distribution for $R = R_e$ from that obtained for $R \neq R_e$, and at the same time holding the position of nucleus A fixed in space. Since

$$\partial\rho(\alpha,r_A)/\partial X'_A = -\partial\rho(\alpha,r_A)/\partial X_B$$

and

$$\partial r_A/\partial X_B = 0$$

the only contributions to a density difference map obtained by holding A fixed and moving B will arise from those parts of the charge density which do not remain rigidly attached to nucleus A. Such a map thus exhibits the relaxation of the charge density with respect to the motion of nucleus A and represents the entire electronic contribution to the force constant. For interpretive purposes, however, a breakdown of the total relaxation effect is necessary and is indeed suggested by the following analysis. When the charge density is expanded about and tied to center A, any density which remains rigidly

[1]In the previous paper dealing with the force constants in N_2, CO, BF, BeO, and LiF, substantially better agreement was obtained between the calculated and theoretical values of the force constants when the forces were expanded about R_e (exp.) rather than about R_e (H.F.). A rationalization of this observation was given based on the fact that for all the above molecules R_e (H.F.) < R_e(exp.) as is indeed expected. This latter inequality is true for HF and HCl as well and the errors in the value of K_H using R_e(exp.) for these two molecules are reduced to 1 and 11%, respectively. However, for some reason, R_e(H.F.) > R_e(exp.) for LiH and NaH. Not surprisingly, the error in K_H is increased for these molecules (to 8 and 14%, respectively) if R_e(exp.) is employed rather than R_e(H.F.) in the expansion of the forces.

Can. J. Chem. Downloaded from www.nrcresearchpress.com by 210.87.254.105 on 09/05/12
For personal use only.

bound to the second nucleus, inner shell density, for example, will appear to relax with respect to a motion of the A nucleus, since it remains fixed to B as A is displaced. If we wish to reserve the term relaxation for changes in the density distribution which do not include rigid following of either nucleus, then the contribution to K_A^e from density which remains rigidly attached to B as A is moved should be treated separately. We have, in fact, previously shown that there is no real distinction between a relaxation with respect to A and a static field gradient contribution from density rigidly fixed to B (1). That is,

$$[4] \quad -\int \frac{\partial \rho_B(\alpha, r_A)}{\partial X_A} \frac{\cos\theta_A}{r_A^2} \, dr_A = (4\pi/3)\rho_B(A) - \int \rho_B(\beta, r_B) \frac{3\cos^2\theta_A - 1}{r_A^3} \, dr$$

Equation [4] states that the contribution to the relaxation integral from density bound rigidly to B, but expanded from center A, is equal to $(4\pi/3)$ times the amount of charge density which ρ_B places at the position of the A nucleus $\rho_B(A)$, plus the electronic field gradient which ρ_B exerts at A. The former term is small relative to the latter and actual calculations show that the difference between the electronic force constant contribution from ρ_B and its static field gradient is very small, of the order of a few %.

The approach outlined above requires a partitioning of the total charge density into atomic components on B, ρ_B, and on A, ρ_A, leaving a delocalized component, ρ_{AB}. While there is no unique way in which such a partitioning may be carried out, the identification of ρ_A, ρ_B, and ρ_{AB} with the usual atomic and overlap populations obtained from the wavefunctions used in this study does, in general, yield physically meaningful results. The molecular Hartree–Fock wavefunctions used in the present study were obtained by starting with a consistent set of accurate atomic basis sets sufficient in size to yield Hartree–Fock solutions for the atoms, to which are added the minimum number of orbitals with higher l values required to adequately describe the polarizations and distortions encountered in forming the molecule from atoms (12). All orbital exponents were then reoptimized. In this way the best orbital description of the atoms is built into the molecular basis set with a minimum of alterations. Since this procedure is followed consistently for all the hydrides, comparisons between molecules of quantities based on the derived populations should be meaningful.

The total electronic contribution to the force constant is partitioned into a contribution K_A^{AA} from the atomic density ρ_A, K_A^{AB} from the delocalized or overlap density ρ_{AB}, and K_A^{BB} from the atomic density ρ_B. Each of these quantities has in turn been multiplied by $R_e^3/2$, a factor which converts their values into an equivalent number of charges. These contributions were determined by separate polynomial fits of the corresponding atomic and overlap contributions to the forces on the A or H nuclei.

The final working expression for the force constant for the displacement of the A nucleus with the proton held fixed in space is

$$[5] \quad K_A = \frac{2Z_A}{R_e^3}[(Z_H - K_A^{HH}) - K_A^R]$$

where $K_A^R = (K_A^{AA} + K_A^{AH})$ represents the total relaxation contribution. The first term in brackets $(Z_H - K_A^{HH})$ is the *net* unshielded nuclear charge on the proton. As discussed above, the contribution to K_A from the atomic charge density on the proton may be interpreted as a field gradient effect and $(Z_H - K_A^{HH})$, when multiplied by $2/R_e^3$, is the static field gradient contribution to K_A from the proton and its associated charge density. Its value may be less than or greater than zero depending on whether charge density is transferred to or removed from the proton in the formation of the molecule. The relaxation contribution K_A^R is different from zero only if ρ_A and ρ_{AH} do not rigidly follow the displacement of the A nucleus. For example, if the relaxation of the charge density corresponds to a polarization or transfer of charge density in the direction of motion of nucleus A, thereby facilitating the nuclear motion, $-K_A^R$ is negative in sign and hence, by eq. [5], will decrease the force constant. If, on the other hand, the relaxation corresponds to a transfer of charge density in a direction counter to the motion of nucleus A, the effect of the relaxation will be to oppose the motion of the nucleus. The value of $-K_A^R$ will be greater than zero and the magnitude of the force constant will be increased. An equation corresponding to [5] may be written for K_H expressed in terms of K_H^R and $(Z_A - K_H^{AA})$.

The contributions to the force constants for a displacement of the A nuclei are given in Table

TABLE II

Contributions to the force constants K_A

AH	$-K_A^R$	$-K_A^{HH}$	$Z_H - K_A^{HH}$
LiH	0.219	−0.885	0.115
NaH	0.497	−1.397	−0.397
FH	−0.711	−0.075	0.925
ClH	−0.344	−0.583	0.417

II, and Fig. 1 gives a pictorial representation of the accompanying relaxations when the displacement corresponds to a bond extension. These contour maps were constructed in the manner outlined in Section II. They do not, however, include the atomic density on the proton since its contribution to the force constant is primarily that of a static field gradient.

The contour maps of the total charge distribution of LiH and NaH show the charge density in each case to be almost totally localized in near spherical contours centered on the Li or Na and hydrogen nuclei (8, 10). The amount of charge in these localized components and their radii are consistent with those expected for Li^+, Na^+, and H^- ions. These properties of the charge distributions and an analysis of the forces which they exert on the nuclei indicate that the binding in LiH and NaH is ionic. The relaxation maps for the LiH and NaH molecules in Fig. 1 reflect this localization of the total charge densities. Both maps exhibit two distinct relaxations: a relaxation in the regions of the Li^+ and Na^+ ion cores[2] and a relaxation of the density localized on the proton.

It is clear from the presence of the term $\cos\theta_A$ in the relaxation integral, eq. [3], that only the dipolar component of the charge relaxation contributes to K_2. Both relaxations indicated in the contour maps for LiH and NaH exhibit large dipolar characteristics, but the relaxation in the regions of the cationic cores will, in each case, dominate the relaxation because of the $1/r_A^2$ dependence of the relaxation integral. The core relaxations in both LiH and NaH correspond to a flow of charge in a direction counter to the direction of the displacement of the cationic nucleus, therefore opposing nuclear displacement. The relaxation of the density around the proton is in the same direction as that in the regions of the cores, resulting in a transfer of charge density from the binding to the antibinding region of the proton and thereby facilitating displacement of the Li or Na nucleus. The total relaxation effect is, however, dominated by the relaxation in the region of the Li^+ and Na^+ cores and the net effect of the relaxation in both molecules is to impede the motion of the displaced nucleus. As seen from Table II, $-K_A^R$ is positive for both LiH and NaH in accordance with the above conclusions. A positive contribution to K_2 from the relaxation of the charge density was also found for a displacement of the Li nucleus in LiF and the Be nucleus in BeO, and is a characteristic feature of ionic binding (1).

The molecular charge distributions of HF and HCl exhibit contours of high value which encompass both nuclei and large, continuous concentrations of charge density in the region between the nuclei. Unlike the LiH and NaH molecules in which both nuclei are bound by the charge density transferred to and localized on the proton, the nuclei in HF and HCl are bound by the density which is accumulated and shared in the region between the two nuclei. The binding is covalent (8, 10). The differences in the disposition of the total charge density between the hydrides from the two extremes of the periodic table are reflected in their respective relaxation densities. Thus the relaxation of the charge densities in HF and HCl for a displacement of the heavy nucleus is characterized by one continuous region of charge depletion between the nuclei[3]. Charge density is removed from the antibinding regions of the F and Cl nuclei as well but not to as great an extent as from the binding region. The charge increase at the F and Cl nuclei is restricted to a belt-like region perpendicular to the bond axis at the positions of these nuclei. Since the relaxations result in a more extensive loss of charge density from the binding regions than from the antibinding regions of the F and Cl nuclei, the relaxation facilitates outward displacements of these

[2]The relaxation of the Na^+ "KL core" actually exhibits three polarizations, a reflection of the more complex static polarizations of the core density found in the second-row molecules compared to that found in the first-row. This feature will be discussed more fully below. The outermost and dominant polarization induced in the region of the Na^+ core is, however, in the same direction as that found for the Li^+ core and the initial discussion will be concerned with this particular polarization.

[3]The "KL" core of Cl exhibits a polarization as well, but the relaxation of the valence density is similar in form to that observed for HF.

Can. J. Chem. Downloaded from www.nrcresearchpress.com by 210.87.254.105 on 09/05/12
For personal use only.

Can. J. Chem. Downloaded from www.nrcresearchpress.com by 210.87.254.105 on 09/05/12
For personal use only.

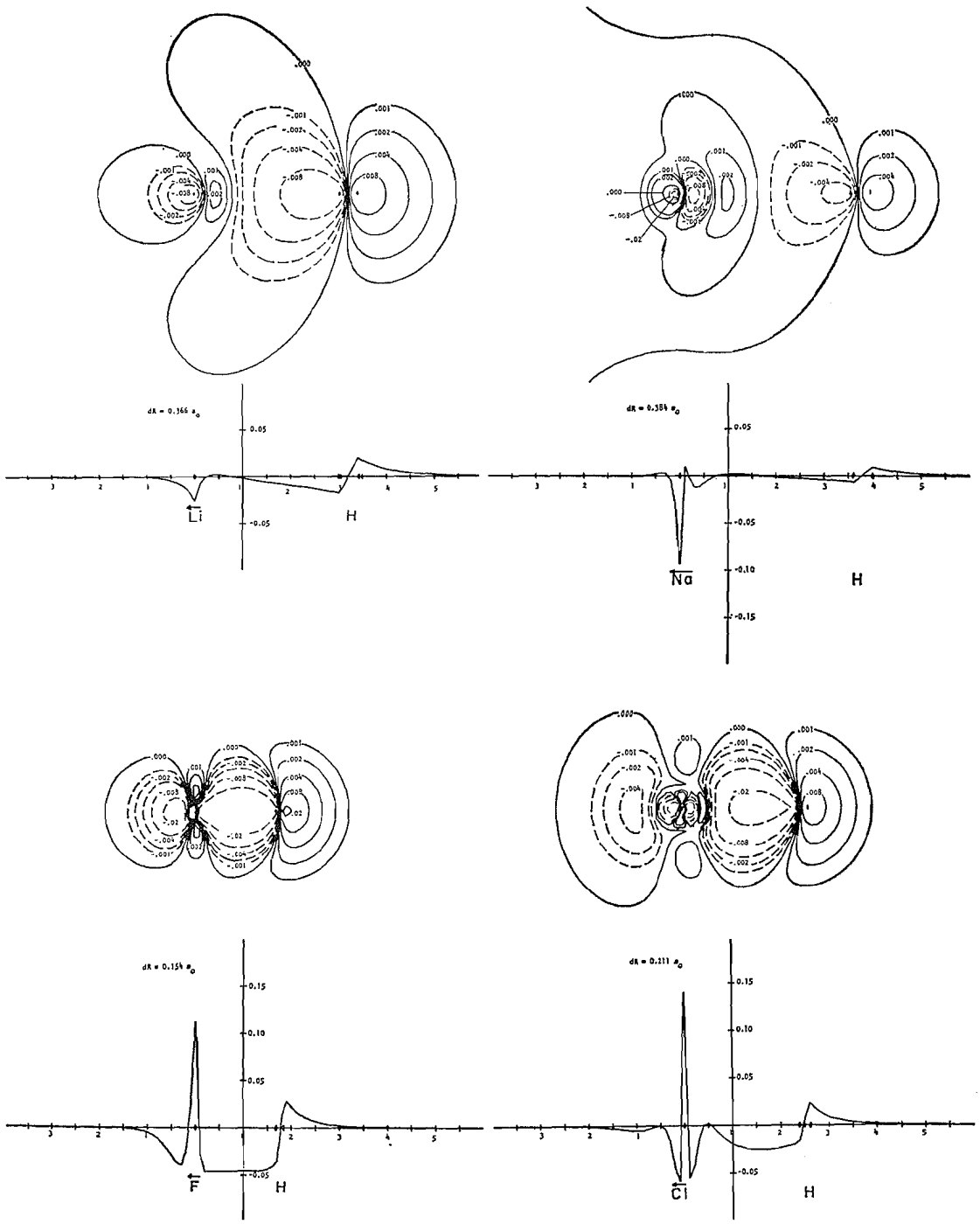

FIG. 1. Contour maps and profiles of the relaxation of the molecular charge distribution for an outward displacement of the A nuclei in AH. The quantity dR is the amount by which the H nucleus is displaced to obtain the relaxation.

Can. J. Chem. Downloaded from www.nrcresearchpress.com by 210.87.254.105 on 09/05/12
For personal use only.

nuclei. Thus, as seen from Table II, the values of $-K_A{}^R$ for the covalently bound hydrides HF and HCl are large and negative and the relaxations decrease the force constants. A relaxation which facilitates the motions of the nuclei is characteristic of covalent binding (1). The magnitude of $K_F{}^R$ is greater than that of $K_{Cl}{}^R$ since the principal relaxation, that of the valence density, is excluded from the immediate region of the Cl nucleus by the presence of the large "KL" core density on this nucleus. The relaxation of the core itself results in a more symmetrical redistribution of the charge as can be seen most clearly from the profile of the relaxation diagram. Consequently its contribution to $-K_{Cl}{}^R$ is relatively small.

In summary, the relaxation of the charge distribution of a diatomic hydride is such as to oppose the displacement of the heavy nucleus when the binding is ionic and to facilitate the motion when the binding is covalent. In spite of the relaxation contributions favoring a larger force constant for the ionic molecules, the force constants for the covalently bound molecules are greater than those for molecules with ionic binding. The reason for this is to be found in the much larger positive field gradient contributions to K_A (or K_H) in the covalent as opposed to the ionic cases. It is characteristic of covalent binding that the charge density in the regions of *both* nuclei are considerably decreased (7) thereby giving rise to large unshielded nuclear charges and hence to large net field gradient contributions $2(Z_H - K_A{}^{HH})/R_e{}^3$ and $2(Z_A - K_H{}^{AA})/R_e{}^3$. In ionic binding, the shielding of one nucleus is increased and the other decreased by the transfer of charge density from one center to the other in the formation of the molecule. However, as shown below, the deshielding of the Li or Na nucleus in the ionic hydrides does not approach in magnitude the deshielding of the F or Cl nuclei in the covalent hydrides.

The values of $K_A{}^{HH}$ in Table II may be interpreted as the number of electronic charges which when placed at the position of the proton exert the same field gradient at the A nuclei as do the atomic charge populations on the protons in these molecules. As expected, this number is least for HF, where the charge equivalent of the field gradient exerted at F by the atomic charge density on the proton is only -0.075, and the charge equivalent of the net positive field gradient exerted at F, $+0.925$, is close to that exerted by a bare proton. The deshielding of the proton in HCl is much less severe and the net field gradient at Cl corresponds to approximately 2/5 of the protonic charge. The strength of the "A nucleus + core" electric field is reduced in the second-row hydrides because of the increased size of the KL-shell core relative to that of the K-shell core. In fact, the reduction in the effective field which the A nuclei of the second-row exert on the valence density is largely responsible for the differences between the binding of the proton in the first- and second-row hydrides (10). A direct consequence of the reduced field exerted by the Cl nucleus + core compared to that exerted by the F nucleus + core is the reduction in the extent to which the proton is deshielded in HCl compared to HF. The quantity $Z_H - F_A{}^{HH}$ is the charge equivalent of the net *field* exerted at the A nucleus by the proton and its associated charge density at R_e. In HCl this field is equivalent to $+0.463$ charges while in HF its value is $+0.876$. It is the *gradient* of this repulsive field which determines the value of the field gradient contribution $Z_H - K_A{}^{HH}$ to the force constant. If the atomic density on the proton, which is approximately spherical in its distribution, remained completely rigid during a displacement of the A nucleus, the *charge equivalents* for the field and field gradients at A would be identical. The two values differ by only 5% of a unit charge for both HF and HCl.

In NaH the net field gradient at the Na nucleus is *negative* because of the transfer of charge density to the proton. Surprisingly, the net field gradient contribution at Li in LiH is slightly positive[4]. This is, however, simply a case where the population analysis does not yield a valid description of the charge distribution. The ρ and $\Delta\rho$ maps (and separate maps for the individual populations) indicate that the overlap population in this molecule is, in fact, almost totally localized on the proton. The atomic nature of the overlap population is reflected in the relaxation map for LiH as well. If the positive and negative contours of the relaxation in the vicinity of the proton, a

[4]The almost complete rigidity of the atomic densities on the protons in LiH and NaH is evidenced by the near equality of the charge equivalents of the net fields and field gradients which they exert at the A nuclei. The charge equivalent of the field $Z_H - F_A{}^{HH}$, is $+0.110$ in LiH and -0.354 in NaH.

Can. J. Chem. Downloaded from www.nrcresearchpress.com by 210.87.254.105 on 09/05/12
For personal use only.

relaxation which arises from the overlap population, were exact mirror images of one another, the relaxation would correspond to the density remaining rigidly bound to the proton. Figure 1 shows that this is nearly the case in LiH, and to a lesser extent in NaH. In both cases the extent of charge removal exceeds slightly the charge increase in the region of the proton. An examination of the separate relaxation maps for the overlap populations indicates that the charge density lost from the region of the proton is transferred back to the cation. Thus, a small amount of valence charge density is transferred from H to Li or Na as the bond is extended. In LiH the transferred charge is placed in a tight, near spherical distribution centered on Li with an essentially zero dipolar component. In NaH on the other hand, the valence density transferred to Na is primarily responsible for the large diffuse charge accumulation on the bonded side in the region of the Na core. Thus in LiH the major contribution from the overlap density is a static field gradient effect and is, therefore, more suitably included with contribution from the atomic population or the proton. The addition of $-K_{Li}^{LiH}$ to $-K_{Li}^{HH}$ yields a net static field gradient of -0.341, and a relaxation contribution (which then equals $-K_{Li}^{LiLi}$) of $+0.675$.

Regardless of the imperfect nature of the breakdown of the contributions to the force constant, the following clear distinctions may be made between the ionic and covalent cases. The net field gradients exerted at the Li and Na nuclei arising from the proton and the charge density which moves rigidly with it, are negative. Thus the whole of the *positive* restoring force acting on the Li and Na nuclei when they are displaced from their equilibrium positions originates in a relaxation of the charge density in the core regions, a relaxation which results in a transfer of charge density in a direction opposite to the direction of the displacement. In contrast, the relaxation of the charge density in HF and HCl is such as to facilitate the motion of the nuclei as charge density is shifted in the same direction as that of the nuclear displacement. The large force constants for the covalently bound hydrides (relative to the ionic cases) are a result of the large gradient of the repulsive field exerted by the unshielded proton.

The fundamental difference which exists between the relaxation of an ionic and a covalent charge distribution is very clearly illustrated in Fig. 2. This figure illustrates the relaxation of the *total* charge densities for a displacement of Li and F nuclei in LiH and HF, as described[5] in Section II. In LiH the density on the proton follows its motion with almost complete rigidity as can be judged from the essentially complete antisymmetry of the relaxation with respect to a plane through the proton (see, in particular, the profile map for LiH). This justifies our ascribing the major contribution from the density localized on the proton in LiH to a field gradient effect. In HF the area of charge depletion extends over the whole of the binding region. The relaxation with respect to the proton is particularly unsymmetrical, with an obvious net loss of charge density. In this case the major contribution to the total relaxation integral arises from a non-rigid relaxation of the charge density. The opposite effects which the relaxations in the vicinities of Li and F have on the motions of these nuclei is clearly evident in these diagrams. Note that the spike-like charge increase at F also facilitates the outward motion of the F nucleus.

The forms of the relaxations are readily understood in terms of the static polarizations present in the equilibrium charge densities. The $\Delta\rho_{SA}(r)$ maps for LiH and NaH show that the densities localized on A and H are polarized in a direction *counter* to the direction of charge transfer from A to H (8, 10). These polarizations[6] are a necessary requirement for the attainment of electrostatic equilibrium in the face of an almost complete transfer of one electronic charge from Li to H or Na to H. Thus the relaxation of the charge density in LiH for bond extension represents a simple reversal of the static polarizations present in the equilibrium charge distribution. Since bond extension is the reverse of bond formation, the relaxation map should exhibit a reversal of (i.e., a decrease in) the polarizations present in the $\Delta\rho_{SA}(r)$ map, as this

[5]Such maps are meaningful only when the position of a proton is not held fixed in their construction. In any other case, the amount of charge density shifted with the nucleus displaced in the construction of the diagram is so great that it dominates the entire map.

[6]The transfer of valence density results in a net negative field and an attractive force on the Li or Na nucleus, and in a net positive field and a force of repulsion on the proton. These forces are balanced by the core densities of Li or Na being polarized away from the proton and the density localized on the proton being polarized towards the Li or Na.

Can. J. Chem. Downloaded from www.nrcresearchpress.com by 210.87.254.105 on 09/05/12
For personal use only.

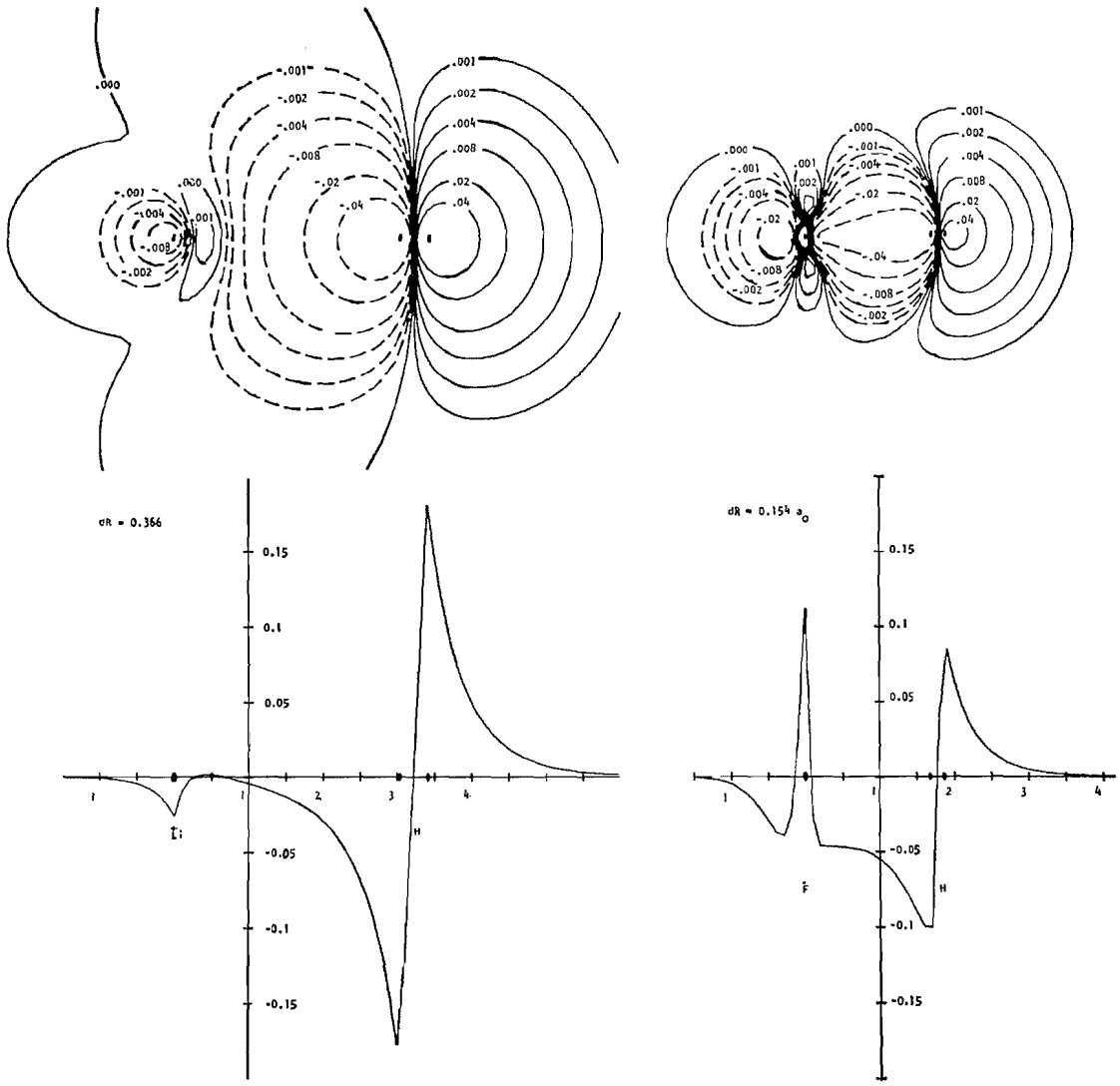

FIG. 2. Contour maps and profiles of the *total* electronic relaxations as seen from the A nuclei in LiH and HF for a bond extension.

latter map represents the total change in density on forming the bond from the separated atoms. A relaxation diagram for bond contraction would be of the same form as shown in Fig. 1, but with all signs reversed. A bond contraction thus *enhances* the polarizations depicted in the $\Delta\rho_{SA}(r)$ map, a bond extension *diminishes* them. The $\Delta\rho_{SA}(r)$ maps for HF and HCl exhibit large accumulations of charge density in the internuclear region. In addition, the density remaining on the A and H nuclei (as opposed to the molecules with ionic binding) is strongly polarized in the direction of charge transfer from H → A. The charge removal in the vicinity of either the F or Cl is restricted to a belt-like region perpendicular to the bond axis at the position of the A nucleus. Thus the dominant polarization induced in the valence densities of F and Cl by bond formation is quadrupolar, an increase in charge density along the bond axis on both the bonded and nonbonded sides of the A nucleus and a decrease from a torus-like region

Can. J. Chem. Downloaded from www.nrcresearchpress.com by 210.87.254.105 on 09/05/12
For personal use only.

perpendicular to the axis (16). The relaxation maps for a bond extension in HF and HCl represent a simple reversal of the polarizations present in the $\Delta\rho_{SA}(r)$ maps, including a reversal of the quadrupolar polarization in the regions of the F and Cl nuclei. Note that the polarizations of the charge densities in the vicinities of the H, Li, and Na nuclei are predominantly dipolar in character in both their $\Delta\rho_{SA}(r)$ and relaxation maps, a characteristic of atoms which employ principally s-type orbitals in forming chemical bonds (16).

Just as the dipolar components of the charge relaxation determines K_2, so the cubic constant K_3 is determined by the quadrupolar component (15). The much larger values of K_3 and their electronic contributions listed in Table I for HF and HCl compared to those for LiH and NaH are thus readily explained in terms of the polarizations evident in the relaxation maps (or the $\Delta\rho_{SA}(r)$ maps). In HF and HCl the binding is primarily the result of the participation of p-type orbitals and only in these two molecules is there a large quadrupole component in the charge reorganization accompanying a displacement of the nuclei.

The "KL" cores of Na and Cl require special comment (10). The transfer of valence density from around the Na^+ core to around the proton on bond formation induces an opposing polarization in the $2\sigma^2 \sim 2s^2$ and $1\pi^4 \sim 2p\pi^2$ densities in the direction ($\bar{A}$—H), which in turn is countered to a slight extent by a deeper axial attractive polarization of the $3\sigma^2 \sim 2p\sigma^2$ density (A—H), which is opposed by a back-polarization of the $1\sigma^2 \sim 1s^2$ density ($\bar{A}$—H) in the immediate vicinity of the Na nucleus. Unlike LiH, the residual "tail" of valence density in the region of Na is polarized in the direction ($\vec{A}$—H) in opposition to the back-polarized core (10). However, the net polarization of the atomic density on sodium is still the direction ($\bar{A}$—H).

As determined from both the separate relaxation maps for ρ_{Na} and from the negative sign of $-K_{Na}^{NaNa}$, the net relaxation of ρ_{Na} is not dominated by a reversal of the statically dominant core polarization which would oppose nuclear motion but by a relaxation of the valence "tail" which facilitates nuclear displacement. The total relaxation contribution, $-K_{Na}^{R}$, is positive because, as mentioned previously, the density transferred back from H^- to Na^+ builds up in front of and strongly opposes displacement of the Na nucleus. This rather more complex relaxation, compared to LiH, is mirrored in Fig. 1 and is especially clear in the profile. The sharp deficit at the nucleus (and unsymmetrically placed with respect to it) and the increase immediately adjacent to the nucleus represent a reversal of the $1s^2$ polarization. This is bounded by an increase of charge density on the nonbonded side and a decrease on the bonded side. This mostly represents a reversal of the residual $4\sigma^2$ polarization. Finally, the outermost deficit in density (so shallow that it is difficult to illustrate on the profile) is a reversal of the polarization of the $2s^2$ (and $2p\pi^4$ off the axis) density while the outermost increase on the bonded side of the Na nucleus is both a reversal of the $2s^2$ polarization and, more important, a result of charge transfer from H^- back to Na^+. Thus we see that the subtle dynamic interplay between core and valence densities complicates the simple connection between the static and dynamic picture which exists for LiH.

As the direction and extent of charge transfer changes in the formation of HA from HNa → HCl, the response of the core density changes. Thus in HCl, the outermost core polarization is now directed *towards* the proton in response to the transfer of valence density from H to Cl, the axial polarization is directed away from H and the inner $1\sigma^2$ ($\sim 1s^2$) polarization is directed towards H. The reversal of these polarizations and hence of their corresponding relaxations and their more evenly balanced nature compared to those of the Na core are evident in the profile diagram in Fig. 1. Note that the core, as well as the valence density of Cl, exhibits a quadrupolar-type relaxation.

Figure 3 illustrates the relaxation encountered in the four molecules for a displacement of the proton and the contributions K_H^R and K_H^{AA} are given in Table III. In both LiH and NaH there is a loss of charge from the vicinity of the proton[7]. The loss of charge is unsymmetrically placed

[7]These relaxation maps and those for the displacement of the A nuclei are self-consistent even though the maps in Fig. 1 indicate a charge increase in the antibinding region of the proton. Figure 1 depicts the change in density observed from an A nucleus as it recedes from a proton; Fig. 3 depicts the change in density as viewed from a proton as it recedes from an A nucleus. Any overlap density rigidly tied to the proton appears in Fig. 1 but not in Fig. 3. The striking extent to which the relaxation maps represent a reversal of the static polarizations in the $\Delta\rho_{SA}(r)$ maps can be seen by comparing the two distributions for LiH. (See ref. (8) for the $\Delta\rho_{SA}(r)$ plot for LiH.)

Can. J. Chem. Downloaded from www.nrcresearchpress.com by 210.87.254.105 on 09/05/12
For personal use only.

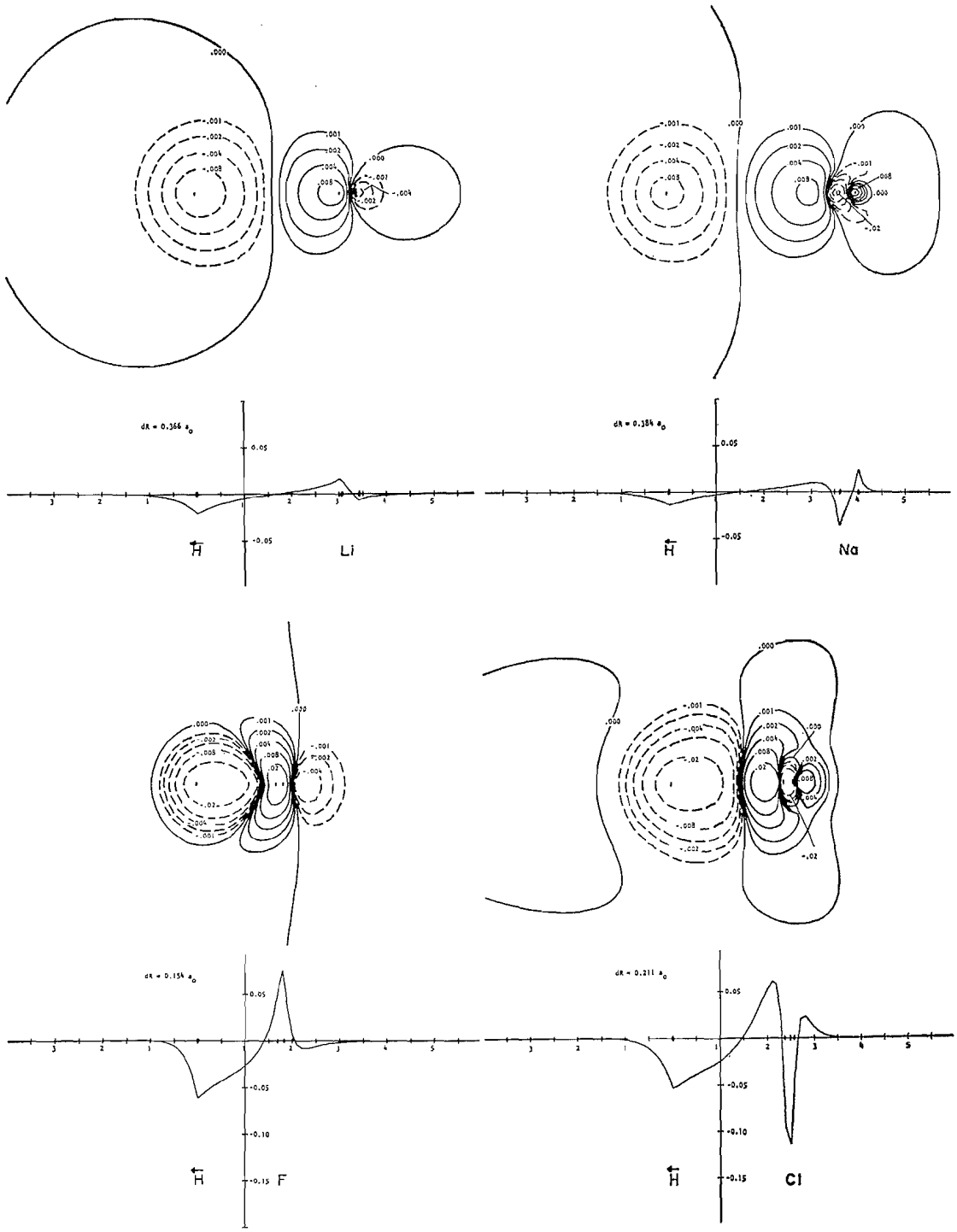

FIG. 3. Contour maps and profiles of the relaxation of the molecular charge distribution for an outward displacement of the proton.

TABLE III

Contributions to the force constants K_H

HA	$-K_H^R$	$-K_H^{AA}$	$Z_A - K_H^{AA}$
HLi	−0.121	−1.923	1.077
HNa	0.148	−9.893	1.107
HF	−0.850	−6.366	2.634
HCl	−1.667	−12.702	4.298

with respect to the proton such that less charge is removed from the region into which the proton moves than from the region it moves from. This relaxation thus facilitates the displacement of the proton in both LiH and NaH. Countering this, however, is the dipolar relaxation of the densities in the vicinities of the Li and Na nuclei, relaxations which concentrate charge density on the bonded side of the proton and oppose its outward displacement. (Note that both relaxations in LiH or NaH are in the same direction for a displacement of A or H. The relaxation in the vicinity of the Li or Na nuclei opposes the motion of either A or H, while that on the proton facilitates either motion.) The two opposing relaxations are more evenly balanced for a displacement of the proton than they are for a motion of the A nuclei and the magnitude of the relaxation contribution to K_H is small in both LiH and NaH. In LiH the net effect is to facilitate the displacement of the proton, while in NaH it opposes the motion. Figure 3 clearly indicates that the charge removal from the proton in NaH is much more symmetrically placed with respect to the proton than in LiH and hence it has a smaller dipolar component, while the induced polarization in the region of the Na core is greater than that in the region of the Li core.

The static field gradient contributions to K_H in LiH and NaH, $Z_A - K_H^{AA}$, are both nearly equivalent to a charge of +1.00 situated at the Li or Na nuclei, values corresponding to the presence of Li^+ or Na^+ ions. Because of the near cancellation of the opposing relaxations generated by a motion of the proton, the force constants in LiH and NaH are both approximately equal to the nuclear charge of the proton multiplied by the field gradient obtained from a *single positive charge* located a distance R_e away; $K_H \sim Z_H \times 2/R_e^3 = 2/R_e^3$. The present results regarding the differing behavior of the relaxations in the two molecules predict that for LiH, $K_2 < 2/R_e^3$ while in NaH, $K_2 > 2/R_e^3$. These are indeed the experimental results as the values of K_2 for LiH and NaH in units of $2/R_e^3$ are 0.896 and 1.41, respectively. The relationship $K_2 \sim 2/R_e^3$ for the ionic hydrides was first noticed by Bratož *et al.* (5). Salem (4) has shown how the result can be rationalized in terms of a simple charge model corresponding to A^+H^- with *rigid*, spherical, nonoverlapping charge distributions on both A^+ and H^-. With no relaxation effects whatsoever, it is clear from the present formulation of K_2 as well, that a simple ionic charge distribution will yield $K_2 = 2/R_e$. In actual fact, the relationship is not that closely obeyed and the relaxations in the vicinities of A^+ and H^- are important. It is interesting to note that of all the alkali metal diatomic hydrides, only for LiH is $K_2 < 2/R_e^3$. For the remaining members NaH to CsH, $K_2 > 2/R_e^3$ (4). Thus the relaxation of the charge density in the vicinity of the cationic core must be the dominant one in KH → CsH as in NaH. That the relaxation of the charge distribution is essential to the understanding of the force constants in the ionic hydrides is further illustrated by the fact that Salem's rigid ionic model predicts a *negative* force constant for a displacement of the cation, equal to $-2/R_e^3$. Furthermore, as shown above, the relaxation of the charge distribution provides the whole of the restoring force when the force constant of an ionic molecule is viewed from a displacement of the cationic nucleus.

It is interesting to note that in ionic fluorides and oxides, the contribution from the relaxation of the charge density localized on the anionic nucleus is considerably greater in magnitude than that of the H^--like distribution in the ionic hydrides and is always dominant (1). Thus the force constants in the ionic fluorides and oxides are all substantially less than the values anticipated on the basis of static field gradients of $2/R_e^3$ (for the fluorides) and $4/R_e^3$ (for the oxides). The relaxation in the fluorides, $-K_F^R$, reduces the unit positive charge contribution from the cation by approximately 2/3 in LiF → CsF and similarly in the oxides, $-K_O^R$, has the almost constant value of −1.35, more than halving the nuclear charge equivalent of +2.00 on the cation in BeO → BaO.

The relaxation contribution for a displacement of the proton in HF or HCl is large in magnitude and negative in value. The relaxation is very

Can. J. Chem. Downloaded from www.nrcresearchpress.com by 210.87.254.105 on 09/05/12
For personal use only.

Can. J. Chem. Downloaded from www.nrcresearchpress.com by 210.87.254.105 on 09/05/12
For personal use only.

unsymmetrical with respect to the proton in both cases with a much larger removal of charge density from the binding region than from the antibinding region of this nucleus. In HF the principal charge increase occurs in a belt-like region perpendicular to the bond at the position of the F nucleus. In HCl this same charge increase is shifted towards the proton. There is an additional counter polarization induced in the Cl core density. The relaxations in the regions of F and Cl mimic the reverse of the quadrupolar polarizations shown in the respective $\Delta\rho_{SA}(r)$ maps.

The $\Delta\rho_{SA}(r)$ maps for HF and HCl indicate that relative to the separated atom densities, a considerable amount of charge is removed from the antibinding region of the proton and transferred primarily to the binding region. One might anticipate that an outward displacement of the proton would result in a return of charge density to the proton and thus to a region of positive contours on the side of the proton in the direction of the displacement. Instead the relaxation maps indicate that the charge density in the vicinity of the proton is decreased in both the binding and antibinding regions and the dipolar nature of the polarization is reflected only in the unsymmetrical removal from the two sides of the proton. In fact, there is less charge density in the vicinity of the proton for values of R slightly larger than R_e than when $R = R_e$, as an examination of the molecular charge density as a function of R shows. For example, the $\Delta\rho_{SA}(r)$ map for HF at $R = 2.00$ a.u. ($> R_e$) indicates a loss of charge from the general region of the proton, from both the bonded and nonbonded sides. The charge lost by the proton is transferred to the F and accumulated along the bond axis in both its binding and antibinding regions with the typical quadrupolar-type polarization. As R is further decreased to R_e the proton *penetrates* the charge build-up in the binding region of F and the area of charge deficit remaining in the antibinding region of the proton is decreased in magnitude and extent. Thus the outward displacement of the proton from its equilibrium position does not result in a transfer of charge density from F $\rightarrow$ H, a phenomenon which does occur at larger R values, but instead in a reorganization of charge density in the vicinity of the F via a reduction in its quadrupole polarization. The relaxation map for HF in Fig. 3 clearly illustrates the removal of charge from the binding and antibinding regions of the F and its accumulation in a torus-like region at the F nucleus perpendicular to the bond. The equilibrium charge distribution in HF and its relaxation are both dominated by the field of the F nucleus.

The considerable penetration of the charge density localized on the F and Cl nuclei by the proton in HF and HCl is reflected in the large positive field gradients exerted at the proton by these nuclei and their associated atomic densities. The field gradients are equivalent to 2.6 and 4.3 nuclear charges at the positions of the F and Cl nuclei, respectively, and thus far exceed the corresponding values of approximately unity observed in LiH and NaH, values which correspond to the stripping of the valence density from Li and Na, leaving the cores intact. Thus when viewed from either a displacement of the proton or the A nuclei, the large force constants in HF and HCl compared to those in the ionic hydrides are a result of the large positive gradients of the repulsive forces, which result from the deshielding of both the A and H nuclei in formation of a covalently bound hydride. The relaxation of the charge density in such a situation always facilitates the motion of the nuclei as it is dominated by the accumulation (for a bond contraction) or removal (for a bond extension) of charge density from the binding region between the nuclei.

The simplest model for predicting K_2 of polar (in the sense $A^{\delta-}H^{\delta+}$) diatomic hydrides is that of Platt (2). In Platt's model the charge distribution in the hydride is taken as that of the corresponding united atom with $Z_A + 1$ electrons. The proton is assumed to penetrate the spherical charge distribution on A up to a separation R_e such that the sphere of volume $(4/3)\pi R_e^3$ contains Z_A electrons. This results in a zero force on the proton (but not on A). A simple electrostatic calculation then shows that if the charge distribution is assumed to remain rigidly bound to A as H is displaced, the force constant is equal to $4\pi\rho(H)$. The quantity $\rho(H)$ is the density at the position of the proton predicted by the united atom density distribution. The model thus predicts both R_e and K_2 and successfully mimics the variations in K_2 across the rows in the periodic table. Platt's result is easily derived in the present formulation. *Assuming a rigid spherical charge distribution* which remains tied

Can. J. Chem. Downloaded from www.nrcresearchpress.com by 210.87.254.105 on 09/05/12
For personal use only.

to the A nucleus as the proton is displaced, and applying to this distribution the theorem previously proved (1) and expressed in eq. [4], we find

$$K_H = Z_H\left(\frac{2Z_A}{R_e^3} - \int \rho_A \frac{3\cos^2\theta_H - 1}{r_H^3}\,d\tau + \tfrac{4}{3}\pi\rho(H)\right)$$

However, the static field gradient at H of a spherical charge distribution centered on A and containing Z_A electronic charges in the sphere defined by R_e is given by

$$-\int \rho_A \frac{3\cos^2\theta_H - 1}{r_H^3}\,d\tau = -\frac{2Z_A}{R_e^3} + \tfrac{8}{3}\pi\rho(H)$$

Thus the nuclear field gradient is cancelled and the result for K_H is that obtained by Platt.

In actual fact the charge density of HA is not well approximated by the united atom density. We have previously presented diagrams of the density difference distribution

$$\Delta\rho_{UA}(r) = \rho_{HA}(r) - \rho_{UA}(r)$$

for the first- and second-row hydrides (8, 10) where $\rho_{HA}(r)$ and $\rho_{UA}(r)$ are the Hartree–Fock density distributions for HA and the corresponding united atom, respectively. The $\Delta\rho_{UA}(r)$ maps indicate that the density in the region of the proton is greatly underestimated by $\rho_{UA}(r)$ and in particular the value of $\rho(H)$, the important quantity in Platt's model, is in error by approximately 90%. The assumption regarding the rigidity of the charge distribution during displacement of the proton is, of course, also incorrect. However, the two assumptions lead to a cancellation of errors.

Following Clinton (17) we may investigate Platt's model in more detail by expressing the exact density distribution of the hydride as

$$\rho_{HA}(r_H) = \rho_{UA}(r_H) + \Delta\rho_{UA}(r_H)$$

Platt's result that $K_H = 4\pi\rho_{UA}(H)$ will be obtained (not necessarily at the correct value of R_e) if

$$\int \frac{\partial\Delta\rho_{UA}(r_H)}{\partial X'_H}\frac{\cos\theta_H}{r_H^2}\,dr_H = 0$$

that is, if the relaxation of the density difference distribution $\Delta\rho_{UA}(r_H)$ exhibits no dipolar component with respect to the proton. We have investigated the relaxation of $\Delta\rho_{UA}(r)$ for HF using a Hartree–Fock wavefunction for Ne. Platt's model, in this case[8], yields $R_e = 1.52$ and $K_H = 0.98$ a.u. A contour map of the relaxation of $\Delta\rho_{UA}(r)$ for HF indicates that its contribution might be expected to be small. The proton is encompassed by an unsymmetrical region of charge removal, one which facilitates the motion of the proton. Immediately adjacent to this region on the bonded side of the proton, however, is an even larger increase in charge density, an increase which opposes the motion of the proton. The net contribution from the relaxation of $\Delta\rho_{UA}(r)$ should be small. Thus Platt's model yields values for K_H of the right order of magnitude *not* because ρ_{HA} resembles or behaves as does a rigid ρ_{UA} but rather because $\rho(H)$ is greatly underestimated by ρ_{UA} and the relaxation contribution from the error in the density $\Delta\rho_{UA}(r)$ is small.

1. R. F. W. Bader and A. D. Bandrauk. J. Chem. Phys. **49**, 1666 (1968).
2. J. R. Platt. J. Chem. Phys. **18**, 932 (1950).
3. H. C. Longuet-Higgins and D. A. Brown. J Inorg. Nucl. Chem. **1**, 60 (1955).
4. L. Salem. J. Chem. Phys. **38**, 1227 (1963).
5. S. Bratož and G. Bessis. J. Chim. Phys. **56**, 1042 (1959). S. Bratož, R. Daudel, M. Roux, and M. Allovena. Rev. Mod. Phys. **32**, 412 (1960).
6. C. W. Kern and M. Karplus. J. Chem. Phys. **40**, 1374 (1964).
7. R. F. W. Bader, W. H. Henneker, and P. E. Cade. J. Chem. Phys. **46**, 3341 (1967).
8. R. F. W. Bader, I. Keaveny, and P. E. Cade. J. Chem. Phys. **47**, 3381 (1967).
9. R. F. W. Bader and A. D. Bandrauk. J. Chem. Phys. **49**, 1653 (1968).
10. P. E. Cade, R. F. W. Bader, W. H. Henneker, and I. Keaveny. J. Chem. Phys. In press.
11. R. P. Feynman. Phys. Rev. **56**, 340 (1939).
12. P. E. Cade and W. M. Huo. J. Chem. Phys. **47**, 614 (1967); **47**, 649 (1967).
13. E. R. Davidson and C. F. Bender. J. Chem. Phys. **47**, 360 (1967).
14. R. F. W. Bader and A. K. Chandra. Can. J. Chem. **46**, 953 (1968).
15. R. H. Schwendeman. J. Chem. Phys. **44**, 556 (1966).
16. R. F. W. Bader, I. Keaveny, and G. Runtz. Can. J. Chem. **47**, 2308 (1969).
17. W. L. Clinton. J. Chem. Phys. **33**, 1603 (1960).

[8]It should be pointed out that when a Hartree–Fock wavefunction is used in Platt's model for the united atom the results obtained are not as satisfactory as those obtained originally by Platt who used Hartree (self-consistent field without exchange) or simple Slater functions.

Can. J. Chem. Downloaded from www.nrcresearchpress.com by 210.87.254.6 on 09/05/12
For personal use only.

Complexing between palladium(II) halides and p-$NOC_6H_4NMe_2$ and p-$NOC_6H_4NEt_2$

I. BATTEN[1]
Department of Chemistry, Sir John Cass College, London, E.C.3, England

AND

K. E. JOHNSON
Division of Natural Sciences, University of Saskatchewan, Regina, Saskatchewan

Received January 16, 1969

The complexes PdL_2X_2 (L = p-nitrosodimethylaniline, p-nitrosodiethylaniline; X = Cl, Br, I) have been prepared. The principal absorption band in the visible spectra of the complexes has been identified as a π–π^* transition centered primarily on the ligands on the basis of its high oscillator strength, the similarity of the latter to that of the free organic ligand, and the insensitivity of the band position to the nature of the halide. Infrared data indicate that palladium is bonded through the NO group.

Canadian Journal of Chemistry, 47, 3075 (1969)

p-Nitrosodialkylanilines have been used for the colorimetric determination of palladium and platinum for many years (1–3). Solid products were isolated from the reaction mixtures and formulated as PdL_2Cl_2 (L = p-$NOC_6H_4NH_2$, p-$NOC_6H_4N(Me)_2$, p-$NOC_6H_4NEt_2$) (1) and $Pt(p\text{-}NOC_6H_4NMe_2)_4Cl_2$ (2).

In this paper we report the isolation, ultraviolet–visible spectra, and infrared spectra of the complexes PdL_2X_2 (L = p-$NOC_6H_4NMe_2$, p-$NOC_6H_4NEt_2$; X = Cl, Br, I) and conclude that Pd is bonded to the NO group.

Experimental

Starting Materials

p-Nitrosodimethylaniline and p-nitrosodiethylaniline, obtained from Hopkin and Williams, Ltd., were twice recrystallized from diethyl ether. $PdCl_2$ and K_2PdBr_4 were obtained from Johnson Matthey, Ltd. K_2PdCl_4 was made as described in the literature (4).

Preparation of Complexes

The procedure of Overholser and Yoe (2) gave poor results and was modified to remove the traces of unreacted ligand believed to be contaminating the product. For PdL_2Cl_2 (L = nitrosodimethylaniline) the recommendation is: dilute 20 ml of palladium(II) chloride solution containing 20 mg of palladium to 500 ml with water. Add 40 ml of a filtered alcoholic solution containing 100 mg of p-nitrosodimethylaniline. Allow the bright red suspension to stand for several hours and then filter through a G4 sintered-glass crucible. Wash the precipitate with three 5 ml portions of water and then three 5 ml portions of diethyl ether. Dry at 110 °C for 3 h and then under vacuum over anhydrous calcium chloride for several days.

The procedures for the other complexes are the same except that the iodide complexes should not be heated. The microanalytical figures obtained appear in Table I. Decomposition temperatures were determined with a simple electric melting point apparatus.

The complexes were only readily soluble in chloroform, tetrachloroethane, tetrahydrofuran, and acetone. The solutions in chloroform were stable (for several weeks) and the original compounds were recoverable from them.

Spectral Measurements

Ultraviolet–visible spectra were recorded on a Beckman DK2A spectrophotometer using 1 cm quartz cells.

Infrared (i.r.) spectra were recorded by means of a Hilger H900 Infrascan spectrometer over the region 4000–700 cm^{-1} and a Hilger H800 spectrometer equipped with cesium iodide optics over the region 1000–280 cm^{-1}. The latter instrument was thermostated at 25 °C and flushed with dry dust-free air during operations below 400 cm^{-1}. The H900 was calibrated by the polystyrene film method and the H800 against polythene film and water vapor. The i.r. spectral bands of the complexes and organic ligands were recorded on mulls in Nujol and hexachlorobutadiene.

Results and Discussion

The electronic spectra of p-$NOC_6H_4NEt_2$ and the complex $Pd(p\text{-}NOC_6H_4NEt_2)_2Cl_2$, both in chloroform solution, appear in Fig. 1. Changing

[1]Present address: Borough Road College of Education, Isleworth, Middlesex, England.

TABLE I

Analytical data for Pd complexes, PdL_2X_2 (L = p-$NOC_6H_4NMe_2$, L′ = p-$NOC_6H_4NEt_2$)

	PdL_2Cl_2		PdL_2Br_2		PdL_2I_2		PdL'_2Cl_2		PdL'_2Br_2		PdL'_2I_2	
Element	Calcd.	Found	Calcd.	Found	Calcd.	Found	Calcd.	Found	Calcd.	Found	Calcd.	Found
C	40.20	39.94	33.91	33.90	31.01	29.09	44.98	44.73	38.61	36.26	33.52	33.40
H	4.22	4.36	4.08	3.93	3.74	3.00	5.31	5.44	4.54	4.47	3.92	3.90
N	11.72	11.52	9.88	10.32	6.51	8.48	10.49	10.38	9.01	9.02		
Pd											14.88	14.65
X	14.84	14.69	28.19	28.16	38.55	38.42	13.28	12.74	25.69	26.65	35.41	35.20
Decomp. temp. (°C)	259		257		213		230		226		180	

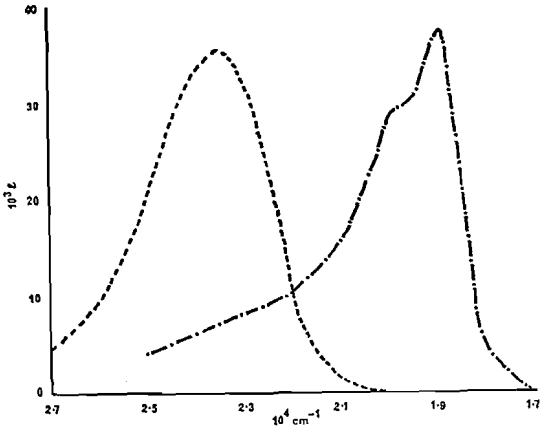

FIG. 1. Ultraviolet-visible spectra of p-$NOC_6H_4NEt_2$ (left hand line) and $Pd(p\text{-}NOC_6H_4NEt_2)_2Cl_2$ (right hand line).

the halogen in the complex did not change the band positions but with bromide and, to a greater extent iodide, the high energy band became more, and the low energy bands less, intense. Complexes with p-$NOC_6H_4NMe_2$ gave essentially the same spectra as those with p-$NOC_6H_4NEt_2$.

The electronic transition of the *C*-nitrosodialkylanilines responsible for their green color has been assigned as a π–π^* transition (5). Its oscillator strength[2], defined as $4.32 \times 10^{-9} \int \varepsilon dv$, was found to be 0.485 in the case of L′ = p-$NOC_6H_4NEt_2$. The spectrum of the complex, $PdCl_2L'_2$, although showing some overlap with that of the ligand L′, is primarily shifted to lower energy and split into at least 2 components. The total oscillator strength of the bands of the complex[2] is 0.48. This intensity is about 100 times too large for d–d transitions of Pd(II) and the frequency (ν_{max} = 19 000 cm^{-1}) too low for Pd^{2+}–Cl^- charge transfer transitions (6). The constancy of oscillator strength and the insensitivity of band position and shape to the change from Cl to Br to I, suggest that we are still seeing the π–π^* transition of the ligand but lowered in energy and split through complexing. Reference to the molecular orbital scheme of Ballhausen and Gray (6) for square planar complexes of metals with π-bonding ligands—those with relatively low π^* levels—indicates the likelihood of the energy shift and, if we note that the scheme is for D_{4h} symmetry, the splitting of the degenerate π^* levels in $PdCl_2L'_2$ is not unreasonable. (We are dealing with Pd(II) and L′ orbitals, not Cl orbitals.)

It is usual for complexes PdX_2Y_2 to have a *trans* structure unless there is considerable Pd—Y π-bonding. The arguments above then, raise the possibility of a *cis* structure for $PdCl_2L'_2$.

The i.r. spectra of the free ligands are in accord with previous studies (7–9). Bands in the region 1500–1550 cm^{-1}, attributed to the N—O stretching vibration are altered in the complexes. Further, new bands appear on complexing in the 780 cm^{-1} region. This would be consistent with bonding from palladium to the N—O group and activation of a N—O deformation mode at 780 cm^{-1}. The 510 cm^{-1} band of L and the 505 cm^{-1} band of L′ drop by 15 cm^{-1} in the chloride and bromide complexes and are not discernible in the iodide complexes. This is the expected region of Pd—O and Pd—N stretching vibrations (10) and one might tentatively assign them at $\sim$ 490 cm^{-1} but the evidence is not conclusive. Finally, both chloride complexes show an intense band at 340 cm^{-1} with shoulders on the low frequency side. This

[2]The spectral limits for L′ were $\nu_1 = 2.0 \times 10^4$ and $\nu_2 = 2.7 \times 10^4$ cm^{-1}, and for PdL_2Cl_2, $\nu_1 = 1.7 \times 10^4$ and $\nu_2 = 2.5 \times 10^4$ cm^{-1}.

Can. J. Chem. Downloaded from www.nrcresearchpress.com by 210.87.254.6 on 09/05/12
For personal use only.

is clearly the Pd—Cl stretching vibration (11). For *trans*-PdX_2Y_2 only one Pd—X band is expected and this at 353–359 cm^{-1}, but for *cis*-PdX_2Y_2 2 bands, separated by 10–30 cm^{-1}, are expected in the 270–335 cm^{-1} region. For the complexes in question one cannot be too definite; although the band structure is complex and occurs below 350 cm^{-1}, a ligand vibration also occurs in this region as shown in the spectra of bromide and iodides. The general impression is of one very strong and one moderate band in line with a *cis* structure.

Since palladium has a greater affinity for nitrogen than for oxygen we would expect the bonding sequence Pd—N—R but the data do

not preclude Pd—O—N—R. If bonding to palladium were through the amino-nitrogen then the N—O vibration and the π–π^* transition, which is primarily concerned with the N—O group, should not be noticeably affected.

Acknowledgment

We are indebted to Dr. D. B. Powell (University of East Anglia, Norwich, Norfolk, England) for discussions of the infrared work.

1. L. G. Overholser and J. H. Yoe. J. Am. Chem. Soc. **63**, 3224 (1941).
2. J. J. Kirkland and J. H. Yoe. Anal. Chem. **26**, 1340 (1954).
3. J. H. Yoe and J. J. Kirkland. Anal. Chem. **26**, 1335 (1954).
4. P. Pascal. Noveau traite de chimie minerale. Vol. XIX. Masson et Cie, Paris. 1958. p. 636.
5. H. Labhart and G. Wagniere. Helv. Chim. Acta, **46**, 1314 (1963).
6. C. J. Ballhausen and H. B. Gray. J. Am. Chem. Soc. **85**, 260 (1963).
7. P. Tarte. Bull. Soc. Chim. Belges, **63**, 525 (1954).
8. W. Luttke. Z. Elektrochem. **61**, 302 (1957).
9. D. Birca-Galateanu, L. Arcan, and C. Lupu. Acad. Rep. Populare Romine, Studii Cercetari Fiz. **10**, 417 (1959).
10. D. M. Adams. Metal–ligand and related vibrations. Edward Arnold and Co., London, 1967. Chap. 5 and 6.
11. G. E. Coates and C. Parkin. J. Chem. Soc. 421 (1963).

Radiation induced dimerization of 2- and 3-methyl-2-pentenes

J. L. Brash and M. A. Golub[1]
Stanford Research Institute, Menlo Park, California 94025

Received March 12, 1969

The dimers formed in the electron irradiation of 2- and 3-methyl-2-pentenes were found to have average unsaturations of 1.53 and 1.35 double bonds per dimer molecule, respectively, and were formed with *G* values of 2.6 and 1.8, respectively. The dimers were considered to form by both ion-molecule and radical mechanisms.

Canadian Journal of Chemistry, **47**, 3077 (1969)

Introduction

The radiation induced dimerization of terminal olefins is known to proceed largely through a mechanism involving rapid condensation of an electron-deficient molecule with a neighboring olefin molecule, followed by intramolecular hydride transfer and electron recombination (1–5). The dimers resulting from this ion–molecule mechanism are exclusively mono-olefinic. To account for the formation of other dimer structures from terminal olefins, a second ionic mechanism is invoked which involves hydrogen transfer from the parent olefin to the molecule-ion, leading to a carbonium ion and an alkenyl radical, followed by ion–molecule condensation as well as radical coupling. The latter mechanism yields mixtures of saturated, mono-olefinic and diolefinic dimers but with an *average* unsaturation of just one double bond per dimer molecule. This, in combination with the former mechanism, is compatible with the observed overall mono-olefinic character of the total dimeric product obtained from a terminal olefin. Both of these ionic mechanisms, designated [I*a*] and [I*b*], respectively (6), or just [I*b*] itself, have been considered to account for part of the radiation induced dimerization of several non-terminal olefins (4, 6), the remaining part being

[1]Present address: Ames Research Center, National Aeronautics and Space Administration, Moffett Field, California 94035.

Can. J. Chem. Downloaded from www.nrcresearchpress.com by 210.87.254.6 on 09/05/12
For personal use only.

is clearly the Pd—Cl stretching vibration (11). For *trans*-PdX_2Y_2 only one Pd—X band is expected and this at 353–359 cm^{-1}, but for *cis*-PdX_2Y_2 2 bands, separated by 10–30 cm^{-1}, are expected in the 270–335 cm^{-1} region. For the complexes in question one cannot be too definite; although the band structure is complex and occurs below 350 cm^{-1}, a ligand vibration also occurs in this region as shown in the spectra of bromide and iodides. The general impression is of one very strong and one moderate band in line with a *cis* structure.

Since palladium has a greater affinity for nitrogen than for oxygen we would expect the bonding sequence Pd—N—R but the data do

not preclude Pd—O—N—R. If bonding to palladium were through the amino-nitrogen then the N—O vibration and the π–π^* transition, which is primarily concerned with the N—O group, should not be noticeably affected.

Acknowledgment

We are indebted to Dr. D. B. Powell (University of East Anglia, Norwich, Norfolk, England) for discussions of the infrared work.

1. L. G. Overholser and J. H. Yoe. J. Am. Chem. Soc. **63**, 3224 (1941).
2. J. J. Kirkland and J. H. Yoe. Anal. Chem. **26**, 1340 (1954).
3. J. H. Yoe and J. J. Kirkland. Anal. Chem. **26**, 1335 (1954).
4. P. Pascal. Noveau traite de chimie minerale. Vol. XIX. Masson et Cie, Paris. 1958. p. 636.
5. H. Labhart and G. Wagniere. Helv. Chim. Acta, **46**, 1314 (1963).
6. C. J. Ballhausen and H. B. Gray. J. Am. Chem. Soc. **85**, 260 (1963).
7. P. Tarte. Bull. Soc. Chim. Belges, **63**, 525 (1954).
8. W. Luttke. Z. Elektrochem. **61**, 302 (1957).
9. D. Birca-Galateanu, L. Arcan, and C. Lupu. Acad. Rep. Populare Romine, Studii Cercetari Fiz. **10**, 417 (1959).
10. D. M. Adams. Metal–ligand and related vibrations. Edward Arnold and Co., London, 1967. Chap. 5 and 6.
11. G. E. Coates and C. Parkin. J. Chem. Soc. 421 (1963).

Radiation induced dimerization of 2- and 3-methyl-2-pentenes

J. L. Brash and M. A. Golub[1]
Stanford Research Institute, Menlo Park, California 94025

Received March 12, 1969

The dimers formed in the electron irradiation of 2- and 3-methyl-2-pentenes were found to have average unsaturations of 1.53 and 1.35 double bonds per dimer molecule, respectively, and were formed with *G* values of 2.6 and 1.8, respectively. The dimers were considered to form by both ion-molecule and radical mechanisms.

Canadian Journal of Chemistry, **47**, 3077 (1969)

Introduction

The radiation induced dimerization of terminal olefins is known to proceed largely through a mechanism involving rapid condensation of an electron-deficient molecule with a neighboring olefin molecule, followed by intramolecular hydride transfer and electron recombination (1–5). The dimers resulting from this ion–molecule mechanism are exclusively mono-olefinic. To account for the formation of other dimer structures from terminal olefins, a second ionic mechanism is invoked which involves hydrogen transfer from the parent olefin to the molecule-ion, leading to a carbonium ion and an alkenyl radical, followed by ion–molecule condensation as well as radical coupling. The latter mechanism yields mixtures of saturated, mono-olefinic and diolefinic dimers but with an *average* unsaturation of just one double bond per dimer molecule. This, in combination with the former mechanism, is compatible with the observed overall mono-olefinic character of the total dimeric product obtained from a terminal olefin. Both of these ionic mechanisms, designated [I*a*] and [I*b*], respectively (6), or just [I*b*] itself, have been considered to account for part of the radiation induced dimerization of several non-terminal olefins (4, 6), the remaining part being

[1]Present address: Ames Research Center, National Aeronautics and Space Administration, Moffett Field, California 94035.

Can. J. Chem. Downloaded from www.nrcresearchpress.com by 210.87.254.6 on 09/05/12
For personal use only.

attributed to a radical process [R] which yields additional diolefinic dimers (7).

As an extension of our earlier work on the radiolysis of hexene-1, -2, and -3 (6), the present note reports results on the radiation induced dimerization of 2-methyl-2-pentene and 3-methyl-2-pentene.

Experimental

3-Methyl-2-pentene (3MP2) was prepared by dehydration of 3-methylpentanol-3 with *p*-toluenesulfonic acid, and purified by bulb-to-bulb distillation on the vacuum line. The resulting product was a mixture of the geometric isomers, 29.2% *cis*; 70.8% *trans*. 2-Methyl-2-pentene (2MP2) (Phillips technical grade) was purified by bulb-to-bulb distillation.

Irradiations were carried out *in vacuo* at ~20 °C using 1 MeV electrons as described previously (6).

The yield of dimer was obtained from gas–liquid chromatography (g.l.c.) measurements using a 3 ft silicone column (G.E. SF-96) at 155 °C. Partial resolution of dimer components from the irradiated methylpentenes was carried out with the same column at 100 °C. The dimers, and various dimer components, were collected as they emerged from the g.l.c. and characterized by nuclear magnetic resonance (n.m.r.) and infrared spectroscopy, as before (6).

Results and Discussion

Dimerization of Methylpentenes

The *G*(dimer) values obtained in this work for 2MP2 and 3MP2 (2.6 and 1.8, respectively) are comparable to the values obtained (2.4–2.6) for the structurally related compound, dihydromyrcene (8), but considerably lower than those obtained for the nonterminal *n*-hexenes (4.6 and 4.1 for hexene-2 and -3, respectively (6)). Evidently, the trisubstituted double bond is less prone to take part in ion–molecule condensation than is the disubstituted double bond; on the other hand, the trisubstituted double bond apparently favors a relatively larger contribution from the radical mechanism [R]. Thus, the total dimeric products obtained from 2MP2 and 3MP2 had average unsaturations of 1.53 and 1.35 double bonds per dimer molecule, respectively, whereas the total dimers from hexene-2 and -3 both had average unsaturations of 1.2 double bonds per dimer molecule. The dimer yield reported here for 3MP2 (at 20 °C) is very similar to the *G*(dimer) values of 1.7 and 2.2 obtained by Wagner (9) for *cis*- and *trans*-3MP2, respectively (at −196 °C).

(a) 2-Methyl-2-pentene

The silicone chromatogram for 2MP2 dimer showed three peaks which could not be fully resolved and which, following collection, yielded very similar infrared and n.m.r. spectra. Accordingly, the observations on the 2MP2 dimer were based on a careful analysis of the spectra of the total dimeric product, including a thorough quantitative reconcilement of all the n.m.r. spectral features with one another and with the proposed assortment of dimeric structures.

The infrared spectrum of the whole dimer revealed the presence of the following unsaturation: trisubstituted, or isoprenic, double bonds (at 11.9 μ), *trans*-vinylene (at 10.4 μ), vinylidene (at 11.3 μ), probable *cis*-vinylene (at ~13.6 μ), and negligible vinyl (at 11.0 μ). The isoprenic/vinylidene ratio was ~4.8:1, and the *trans*-vinylene/vinylidene ratio was 1.23:1. The n.m.r. spectrum showed the presence of 43.9% of the protons as $CH_3-\overset{|}{C}-$, 24.4% as $CH_3-\overset{|}{C}=$, 3.1% as $-CH=CH-$ (*cis* and *trans*), 4.1% as $-\overset{|}{C}=CH-$, 2.0% as $CH_2=\overset{|}{C}-$, 10.5% as $-CH_2-\overset{|}{C}=$, and 12.0% as $-CH_2-\overset{|}{C}-$. From these spectroscopic data, it was deduced that the 2MP2 dimer had an *average* unsaturation of 1.53 double bonds per dimer molecule, consisting of 0.95 isoprenic, 0.35 vinylene, and 0.23 vinylidene units.

Since the overall unsaturation is well below 2.0 double bonds per molecule, the dimerization cannot proceed exclusively by the radical mechanism [R] but must also involve an important contribution from some ionic process. In terms of an effective 1,5 hydride transfer (5), mechanism [I*a*] could account for some of the vinylene and vinylidene units formed, while mechanism [I*b*], to the extent that various isomers of the 2MP2 allylic radical are formed, could give rise to dimers having these same double bonds and isoprenic units as well.

(b) 3-Methyl-2-pentene

As with 2MP2, the chromatogram of the 3MP2 dimer showed three peaks which could not be adequately separated, and so the spectroscopic analysis was again based on the whole dimeric product.

The infrared spectrum showed the presence of isoprenic double bonds (at 12.15 μ), and vinylidene and vinyl double bonds in the ratio of

Can. J. Chem. Downloaded from www.nrcresearchpress.com by 210.87.254.6 on 09/05/12
For personal use only.

$\sim$1.6:1, but no vinylene units. The n.m.r. spectrum showed the following distribution of protons: 42.4% as $CH_3-\overset{|}{C}-$, 23.4% as $CH_3C=$, 1.9% as $CH_2=\overset{|}{C}-$, 5.9% as olefinic protons in $-CH=CH-$ and $CH_2=CH-$, 15.1% as $-CH_2C=$, and 11.3% as $-CH_2-\overset{|}{C}-$. From these spectroscopic results, it was deduced that the 3MP2 dimer had an *average* unsaturation of 1.35 double bonds per dimer molecule, consisting of 0.99 isoprenic, 0.22 vinylidene, and 0.14 vinyl units.

Once again, both ionic and radical processes must be invoked to account for the radiation induced dimerization of 3MP2. Mechanism [I*a*] would be compatible with the formation of isoprenic and vinyl units, while [I*b*] could yield these double bonds and vinylidene units as well.

1. P. C. Chang, N. C. Yang, and C. D. Wagner. J. Am. Chem. Soc. **81**, 2060 (1959).
2. C. D. Wagner. Tetrahedron, **14**, 164 (1961).
3. E. Collinson, F. S. Dainton, and D. C. Walker. Trans. Faraday Soc. **57**, 1732 (1961).
4. P. C. Kaufman. J. Phys. Chem. **67**, 1671 (1963).
5. C. D. Wagner. Trans. Faraday Soc. **64**, 163 (1968).
6. J. L. Brash and M. A. Golub. Can. J. Chem. **46**, 593 (1968).
7. M. S. Kharasch, D. Schwartz, and W. Nudenberg. J. Org. Chem. **18**, 337 (1953).
8. J. L. Brash and M. A. Golub. Can. J. Chem. **45**, 101 (1967).
9. C. D. Wagner. J. Phys. Chem. **71**, 3445 (1967).

On the absence of triplet ketene in ketene excited in the region 2800–3660 Å

M. Grossman, G. P. Semeluk, and I. Unger

Department of Chemistry, University of New Brunswick, Fredericton, New Brunswick

Received March 12, 1969

The sensitized biacetyl emission technique was used in an attempt to detect triplet ketene molecules, which might be formed when ketene is excited by light ranging in wavelength from 2800 to 3600 Å. No sensitized emission was observed in this exciting wavelength region thus confirming the recent results of Voisey (1) which also show that triplet ketene is not produced when ketene is excited by light between 2800 and 3200 Å, and that the triplet CH_2 found in such systems must arise from some source other than triplet ketene.

Canadian Journal of Chemistry, **47**, 3079 (1969)

Introduction

The photolysis of ketene was first examined by Norrish and co-workers (2) in 1933. Since then, this molecule has received much attention (3–6, and for a recent review see ref. 7). In 1964, Simons and Rabinovitch (8) showed that both singlet and triplet CH_2 are produced when ketene is excited by radiation of 3130 Å. It has been shown by several authors (9, 10) that the ratio of singlet to triplet CH_2 produced in the photolysis of ketene is wavelength dependent. The ratio of triplet CH_2 increases with increasing wavelength. It has been suggested (11) that the precursor of triplet CH_2 is triplet ketene.

Recently, Voisey (1) examined the photolysis of ketene and diazomethane in the presence of ethyl methyl ether and concluded that triplet CH_2 was formed from singlet CH_2 by collisional processes, although he did acknowledge the possibility of triplet ketene formation at the irradiating wavelengths greater than 3200 Å.

We have attempted to detect triplet ketene, using the sensitized biacetyl emission technique (12), in ketene–biacetyl mixtures irradiated by wavelengths ranging from 2800 to 3660 Å.

Experimental

The ketene was prepared, according to a method described by Ho and Noyes (11), in a mercury free vacuum system equipped mostly with teflon stop-cocks, and stored at -196 °C until needed.

The biacetyl was obtained from the Aldrich Chemical Company and was used without further purification. Research grade *cis*-butene-2 was obtained from the Phillips Petroleum Company. Vapor phase chromatography shows this material to be essentially pure.

The emission data were obtained on a modified Aminco–Bowman spectrophoto-fluorometer (s.p.f.) which

Can. J. Chem. Downloaded from www.nrcresearchpress.com by 210.87.254.6 on 09/05/12
For personal use only.

$\sim$1.6:1, but no vinylene units. The n.m.r. spectrum showed the following distribution of protons: 42.4% as $CH_3-\overset{|}{\underset{|}{C}}-$, 23.4% as $CH_3C=$, 1.9% as $CH_2=\overset{|}{C}-$, 5.9% as olefinic protons in $-CH=CH-$ and $CH_2=CH-$, 15.1% as $-CH_2C=$, and 11.3% as $-CH_2-\overset{|}{C}-$. From these spectroscopic results, it was deduced that the 3MP2 dimer had an *average* unsaturation of 1.35 double bonds per dimer molecule, consisting of 0.99 isoprenic, 0.22 vinylidene, and 0.14 vinyl units.

Once again, both ionic and radical processes must be invoked to account for the radiation induced dimerization of 3MP2. Mechanism [I*a*] would be compatible with the formation of isoprenic and vinyl units, while [I*b*] could yield these double bonds and vinylidene units as well.

1. P. C. Chang, N. C. Yang, and C. D. Wagner. J. Am. Chem. Soc. **81**, 2060 (1959).
2. C. D. Wagner. Tetrahedron, **14**, 164 (1961).
3. E. Collinson, F. S. Dainton, and D. C. Walker. Trans. Faraday Soc. **57**, 1732 (1961).
4. P. C. Kaufman. J. Phys. Chem. **67**, 1671 (1963).
5. C. D. Wagner. Trans. Faraday Soc. **64**, 163 (1968).
6. J. L. Brash and M. A. Golub. Can. J. Chem. **46**, 593 (1968).
7. M. S. Kharasch, D. Schwartz, and W. Nudenberg. J. Org. Chem. **18**, 337 (1953).
8. J. L. Brash and M. A. Golub. Can. J. Chem. **45**, 101 (1967).
9. C. D. Wagner. J. Phys. Chem. **71**, 3445 (1967).

On the absence of triplet ketene in ketene excited in the region 2800–3660 Å

M. Grossman, G. P. Semeluk, and I. Unger

Department of Chemistry, University of New Brunswick, Fredericton, New Brunswick

Received March 12, 1969

The sensitized biacetyl emission technique was used in an attempt to detect triplet ketene molecules, which might be formed when ketene is excited by light ranging in wavelength from 2800 to 3600 Å. No sensitized emission was observed in this exciting wavelength region thus confirming the recent results of Voisey (1) which also show that triplet ketene is not produced when ketene is excited by light between 2800 and 3200 Å, and that the triplet CH_2 found in such systems must arise from some source other than triplet ketene.

Canadian Journal of Chemistry, **47**, 3079 (1969)

Introduction

The photolysis of ketene was first examined by Norrish and co-workers (2) in 1933. Since then, this molecule has received much attention (3–6, and for a recent review see ref. 7). In 1964, Simons and Rabinovitch (8) showed that both singlet and triplet CH_2 are produced when ketene is excited by radiation of 3130 Å. It has been shown by several authors (9, 10) that the ratio of singlet to triplet CH_2 produced in the photolysis of ketene is wavelength dependent. The ratio of triplet CH_2 increases with increasing wavelength. It has been suggested (11) that the precursor of triplet CH_2 is triplet ketene.

Recently, Voisey (1) examined the photolysis of ketene and diazomethane in the presence of ethyl methyl ether and concluded that triplet CH_2 was formed from singlet CH_2 by collisional processes, although he did acknowledge the possibility of triplet ketene formation at the irradiating wavelengths greater than 3200 Å.

We have attempted to detect triplet ketene, using the sensitized biacetyl emission technique (12), in ketene–biacetyl mixtures irradiated by wavelengths ranging from 2800 to 3660 Å.

Experimental

The ketene was prepared, according to a method described by Ho and Noyes (11), in a mercury free vacuum system equipped mostly with teflon stop-cocks, and stored at −196 °C until needed.

The biacetyl was obtained from the Aldrich Chemical Company and was used without further purification. Research grade *cis*-butene-2 was obtained from the Phillips Petroleum Company. Vapor phase chromatography shows this material to be essentially pure.

The emission data were obtained on a modified Aminco–Bowman spectrophoto-fluorometer (s.p.f.) which

Can. J. Chem. Downloaded from www.nrcresearchpress.com by 210.87.254.40 on 09/05/12
For personal use only.

TABLE I

Relative biacetyl emission intensity from ketene/biacetyl mixtures and *cis*-butene-2/biacetyl mixtures at various exciting wavelengths

λ_{ex} (Å)	Pressure (Torr)			% Light absorbed by BiA	Relative biacetyl emission intensity
	ketene	*cis*-butene-2	biacetyl		
2800	273	0	23.4	1.9	37.5
2800	0	271	25.8		150.7
2860	273	0	23.4	1.8	33.0
2860	0	271	25.8		108.5
2910	273	0	23.4	9.7	97.8
2910	0	271	25.8		321.5
2960	273	0	23.4	8.05	366.0
2960	0	271	25.8		965.0
3010	273	0	23.4	2.1	384.0
3010	0	271	25.8		801.0
3060	273	0	23.4	1.4	177.0
3060	0	271	25.8		351.0
3130	273	0	23.4	21.8	1 050.0
3130	0	271	25.8		2 067.0
3160	273	0	23.4	2.1	277.0
3160	0	271	25.8		566.0
3210	273	0	23.4	≤ 0.5	30.5
3210	0	271	25.8		61.0
3360	273	0	23.4	≤ 0.2	68.3
3360	0	271	25.8		171.5
3510	273	0	23.4	≤ 0.5	80.3
3510	0	271	25.8		224.7
3560	273	0	23.4	≤ 0.3	210.3
3560	0	271	25.8		441.0
3610	273	0	23.4	≤ 0.3	748.0
3610	0	271	25.8		1 460.0
3660	273	0	23.4	2.8	9 021.0
3660	0	271	25.8		17 200.0

has been described previously (13). A mercury and grease free high vacuum system, equipped with Hoke Packless Diaphragm (stainless steel) metal valves was used to handle the compounds.

Mixing was accomplished by means of flash vaporization and by circulating the vapors through the s.p.f. cell by means of an all glass circulating pump constructed at the National Research Council of Canada in Ottawa.

All experiments were carried out at room temperature ($\sim$ 27 °C).

Results and Discussion

Two types of experiments were performed. Mixtures of ketene and biacetyl were irradiated and the intensity of the biacetyl emission (as an area under a curve) was noted. Then, similar mixtures were prepared containing *cis*-butene-2 instead of ketene, irradiated at the same wavelength, and the intensity of the biacetyl emission was again noted. The *cis*-butene-2 experiments were performed as a control, since biacetyl absorbs in the spectral region used in this study and exhibits a weak emission which can be enhanced by the addition of vibrational quenchers (14). Thus, the amount of light absorbed by the biacetyl was approximately the same for each comparison pair of mixtures. The results of these experiments are given in Table I. The major requirement for the successful use of the biacetyl sensitized emission technique is that the triplet of the donor be higher in energy than the triplet of biacetyl (15). The triplet of ketene has been given as 61 kcal (16), while the triplet of biacetyl has been given as 55 kcal (17). Thus, if ketene triplets are produced in the presence of biacetyl, one would expect to observe an enhanced emission from biacetyl due to the reaction

$$^3K + BiA \rightarrow {}^3BiA + K$$

Our data indicate that biacetyl emission is reduced in the presence of ketene. One is thus forced to the conclusion that either (*a*) ketene

Can. J. Chem. Downloaded from www.nrcresearchpress.com by 210.87.254.40 on 09/05/12
For personal use only.

reacts chemically with excited biacetyl, or (*b*) that triplet ketene is not produced in this irradiation wavelength region. Voisey's work, the relatively small energy separation between triplet and singlet methylene (18), and the evidence of Ring and Rabinovitch (19) which disputes the reliability of the conventional method of diagnosing singlet and triplet methylene, leads us to suggest the latter conclusion to be the more likely.

Acknowledgments

The authors gratefully acknowledge financial assistance from the Associated Alumni of the University of New Brunswick and from the National Research Council of Canada. We also wish to thank Mr. S. Stevens for his help with some of the experiments.

1. M. A. Voisey. Trans. Faraday Soc. **64**, 3058 (1968).
2. R. G. W. Norrish, H. G. Crone, and O. D. Saltmarsh. J. Chem. Soc. 1533 (1933).
3. G. B. Kistiakowsky and T. A. Walter. J. Phys. Chem. **72**, 3952 (1968).
4. H. E. Avery and R. J. Cvetanović. J. Chem. Phys. **48**, 380 (1968).
5. J. W. Powell-Wiffen and R. P. Wayne. Photochem. Photobiol. **8**, 131 (1968).
6. P. G. Bowers. J. Chem. Soc. A, 466 (1967).
7. J. G. Calvert and J. N. Pitts. Photochemistry. John Wiley and Sons, Inc., New York. 1966. p. 391.
8. J. W. Simons and B. S. Rabinovitch. J. Phys. Chem. **68**, 1322 (1964).
9. S. Y. Ho, I. Unger, and W. A. Noyes, Jr. J. Am. Chem. Soc. **87**, 2297 (1965).
10. R. W. Carr, Jr. and G. B. Kistiakowsky. J. Phys. Chem. **70**, 118 (1966).
11. S. Y. Ho and W. A. Noyes, Jr. J. Am. Chem. Soc. **89**, 5091 (1967).
12. H. Ishikawa and W. A. Noyes, Jr. J. Chem. Phys. **37**, 583 (1962).
13. J. L. Durham, G. P. Semeluk, and I. Unger. Can. J. Chem. **46**, 3177 (1968).
14. H. Ishikawa and W. A. Noyes, Jr. J. Am. Chem. Soc. **84**, 1502 (1962).
15. W. A. Noyes Jr. and I. Unger. Advan. Photochem. **4**, 49 (1966).
16. A. N. Strachan and D. E. Thornton. Can. J. Chem. **46**, 2353 (1968).
17. W. G. Herkstroeter, A. A. Lamola, and G. S. Hammond. J. Am. Chem. Soc. **86**, 4537 (1964).
18. M. L. Halberstadt and J. R. McNesby. J. Am. Chem. Soc. **89**, 3417 (1967).
19. D. F. Ring and B. S. Rabinovitch. J. Phys. Chem. **72**, 191 (1968).

Effect of chain length on storage stability and hydrolytic reversion of sodium polyphosphate glasses

Robert J. Fuchs and Charles W. Lutz

Inorganic Research and Development Department, FMC Corporation, Carteret, New Jersey 07008

Received February 14, 1969

At low concentrations in hard water, the polyphosphates revert to orthophosphate at rates which are not predictable from data obtained at higher concentrations. A reversal in the effect of pH on reversion rate at lower concentrations appears to be due to complex formation between the polyphosphate and the hard water metal ions. A minimum in the rate of reversion of polyphosphate glasses to orthophosphate occurs at an average chain length between about 13 and 40 under the low concentration hard water conditions. Phosphate glasses having an average chain length below 30 show good storage stability but longer-chain glasses undergo a decrease in chain length under normal "dry" storage conditions, with the rate of degradation increasing with increasing chain length.

Canadian Journal of Chemistry, **47**, 3081 (1969)

Most of the published work on hydrolytic degradation, or reversion, of polyphosphates (1) has overlooked the effect of phosphate concentration or has treated it over a very limited range. Bell (2) studied the reversion of commercially available phosphates at concentrations of 1 and 10% and showed a relatively small effect of concentration. However, at the low (p.p.m.) phosphate concentration levels used in such applications as industrial water treatment, the published reversion data for higher concentrations are of little value. At these low concentrations the effects of water hardness and other materials dissolved in the water become highly significant. In the presence of microorganisms, enzyme catalysis can increase the rate of reversion of the polyphosphates by a factor of 10^5–10^6 (3) but these enzymes are deactivated or destroyed in high temperature systems or by the use of biocides. Green (4) studied the reversion

Can. J. Chem. Downloaded from www.nrcresearchpress.com by 210.87.254.40 on 09/05/12
For personal use only.

reacts chemically with excited biacetyl, or (*b*) that triplet ketene is not produced in this irradiation wavelength region. Voisey's work, the relatively small energy separation between triplet and singlet methylene (18), and the evidence of Ring and Rabinovitch (19) which disputes the reliability of the conventional method of diagnosing singlet and triplet methylene, leads us to suggest the latter conclusion to be the more likely.

Acknowledgments

The authors gratefully acknowledge financial assistance from the Associated Alumni of the University of New Brunswick and from the National Research Council of Canada. We also wish to thank Mr. S. Stevens for his help with some of the experiments.

1. M. A. Voisey. Trans. Faraday Soc. **64**, 3058 (1968).
2. R. G. W. Norrish, H. G. Crone, and O. D. Saltmarsh. J. Chem. Soc. 1533 (1933).
3. G. B. Kistiakowsky and T. A. Walter. J. Phys. Chem. **72**, 3952 (1968).
4. H. E. Avery and R. J. Cvetanović. J. Chem. Phys. **48**, 380 (1968).
5. J. W. Powell-Wiffen and R. P. Wayne. Photochem. Photobiol. **8**, 131 (1968).
6. P. G. Bowers. J. Chem. Soc. A, 466 (1967).
7. J. G. Calvert and J. N. Pitts. Photochemistry. John Wiley and Sons, Inc., New York. 1966. p. 391.
8. J. W. Simons and B. S. Rabinovitch. J. Phys. Chem. **68**, 1322 (1964).
9. S. Y. Ho, I. Unger, and W. A. Noyes, Jr. J. Am. Chem. Soc. **87**, 2297 (1965).
10. R. W. Carr, Jr. and G. B. Kistiakowsky. J. Phys. Chem. **70**, 118 (1966).
11. S. Y. Ho and W. A. Noyes, Jr. J. Am. Chem. Soc. **89**, 5091 (1967).
12. H. Ishikawa and W. A. Noyes, Jr. J. Chem. Phys. **37**, 583 (1962).
13. J. L. Durham, G. P. Semeluk, and I. Unger. Can. J. Chem. **46**, 3177 (1968).
14. H. Ishikawa and W. A. Noyes, Jr. J. Am. Chem. Soc. **84**, 1502 (1962).
15. W. A. Noyes Jr. and I. Unger. Advan. Photochem. **4**, 49 (1966).
16. A. N. Strachan and D. E. Thornton. Can. J. Chem. **46**, 2353 (1968).
17. W. G. Herkstroeter, A. A. Lamola, and G. S. Hammond. J. Am. Chem. Soc. **86**, 4537 (1964).
18. M. L. Halberstadt and J. R. McNesby. J. Am. Chem. Soc. **89**, 3417 (1967).
19. D. F. Ring and B. S. Rabinovitch. J. Phys. Chem. **72**, 191 (1968).

Effect of chain length on storage stability and hydrolytic reversion of sodium polyphosphate glasses

Robert J. Fuchs and Charles W. Lutz

Inorganic Research and Development Department, FMC Corporation, Carteret, New Jersey 07008

Received February 14, 1969

At low concentrations in hard water, the polyphosphates revert to orthophosphate at rates which are not predictable from data obtained at higher concentrations. A reversal in the effect of pH on reversion rate at lower concentrations appears to be due to complex formation between the polyphosphate and the hard water metal ions. A minimum in the rate of reversion of polyphosphate glasses to orthophosphate occurs at an average chain length between about 13 and 40 under the low concentration hard water conditions. Phosphate glasses having an average chain length below 30 show good storage stability but longer-chain glasses undergo a decrease in chain length under normal "dry" storage conditions, with the rate of degradation increasing with increasing chain length.

Canadian Journal of Chemistry, 47, 3081 (1969)

Most of the published work on hydrolytic degradation, or reversion, of polyphosphates (1) has overlooked the effect of phosphate concentration or has treated it over a very limited range. Bell (2) studied the reversion of commercially available phosphates at concentrations of 1 and 10% and showed a relatively small effect of concentration. However, at the low (p.p.m.) phosphate concentration levels used in such applications as industrial water treatment, the published reversion data for higher concentrations are of little value. At these low concentrations the effects of water hardness and other materials dissolved in the water become highly significant. In the presence of microorganisms, enzyme catalysis can increase the rate of reversion of the polyphosphates by a factor of 10^5–10^6 (3) but these enzymes are deactivated or destroyed in high temperature systems or by the use of biocides. Green (4) studied the reversion

Can. J. Chem. Downloaded from www.nrcresearchpress.com by 210.87.254.6 on 09/05/12
For personal use only.

TABLE I

Reversion of polyphosphates to orthophosphate in aqueous solutions at 100 °C

Concentration	pH	H_2O hardness	Reversion (as % orthophosphate after 1.5 h)†					
			TSPP ($\bar{n}$ = 2)	STPP ($\bar{n}$ = 3)	Glass 6 ($\bar{n}$ = 6)	Glass 13 ($\bar{n}$ = 13)	Glass 21 ($\bar{n}$ = 21)	Glass 40 ($\bar{n}$ = 40)
1%	8	Distilled	9	14	30	22	15	9
1%	6	Synth. hard*	64	54	57	39	25	16
	8	" "	9	14	31	21	15	10
	10	" "	0.5	7	27	21	12	9
0.2%	9	Synth. hard				20	16	
0.05%	6	Distilled				33	20	
	8	"				15	10	
	9	"				13	9	
0.05%	6	Synth. hard				31	26	
	8	" "				26	25	
	9	" "				26	26	
40 p.p.m.	6	Distilled	68			34	23	22
	8	"	10			15	10	12
	9	"	5			10	8	—
40 p.p.m.	6	Synth. hard	13	35	44	34	33	38
	7	" "	—	—	—	35	33	—
	8	" "	27	41	49	40	37	51
	9	" "	32	59	56	58	58	63

*Synthetic hard water = 40 p.p.m. Ca (as $CaCO_3$), 20 p.p.m. Mg (as $CaCO_3$), and 12 p.p.m. Cl.
†TSPP = tetrasodium pyrophosphate, STPP = sodium tripolyphosphate, glasses are designated by their number average chain length.

of some commercially-available sodium polyphosphates at phosphate concentrations of 5 and 50 p.p.m., under typical water-treatment conditions. The work described in this paper is intended to supplement his work and give more insight into the effects of chain length on reversion, both in dilute aqueous systems and under "dry" storage conditions. Like Green we used the ultimate hydrolyzed-phosphate species, orthophosphate, as our measure of reversion in aqueous systems.

In the use of polyphosphates for inhibition of corrosion or scale formation, all of the chain polyphosphate species are effective and the rate of formation of orthophosphate is usually the determining factor in selecting a polyphosphate for a specific use. The formation of ring phosphates, such as sodium trimetaphosphate, during hydrolysis of long-chain phosphates (5, 6) is also important, since these species are not effective in water treatment, but they are subsequently hydrolyzed to useful chain phosphates.

Experimental

Five sodium polyphosphate glasses of varying average chain length, from 6–400, were tested for reversion in aqueous systems and several additional glasses of intermediate chain length were evaluated for dry storage stability. For comparison, two crystalline polyphosphates, tetrasodium pyrophosphate (TSPP) and sodium tripolyphosphate (STPP), were tested. All samples were well below 1% in orthophosphate content. Tests were run in distilled water and in a "synthetic hard water" which contained a calcium hardness of 40 p.p.m. $CaCO_3$, a magnesium hardness of 20 p.p.m. $CaCO_3$, and 12 p.p.m. chloride.

In the 100 °C tests, the samples were added to boiling water and the pH adjusted immediately and periodically as required. Initially, samples were analyzed by paper chromatography (7, 8) to determine the change in composition with time. In subsequent tests samples were analyzed for orthophosphate using the Martin and Doty method (9).

In the 63 °C tests, the pH was checked and adjusted twice daily. The validity of this procedure was established using a pH-stat (Stat Model B-1, JKM Instrument Co.) in which the sample was kept at a constant pH by automatic introduction of acid or base when the pH changed slightly.

Average chain lengths ($\bar{n}$) were determined using the method of Van Wazer *et al.* (10).

Results and Discussion

The 100 °C reversion test was used to determine the effects of chain length, concentration, pH, and the presence of multivalent cations under conditions in which there would be no contribution from enzymes or microorganisms.

Can. J. Chem. Downloaded from www.nrcresearchpress.com by 210.87.254.6 on 09/05/12
For personal use only.

TABLE II

Reversion of polyphosphates to orthophosphate in aqueous solution at 63 °C

Concentration	pH	H_2O hardness	Reversion (as % orthophosphate after 5 days)†					
			TSPP ($\bar{n}$ = 2)	STPP ($\bar{n}$ = 3)	Glass 6 ($\bar{n}$ = 6)	Glass 13 ($\bar{n}$ = 13)	Glass 21 ($\bar{n}$ = 21)	Glass 40 ($\bar{n}$ = 40)
1%	6	Synth. hard*	56			27	21	—
	8	" "	4			15	11	
	10	" "	0.5			12	8	
40 p.p.m.	6	Distilled	71	62	43	24	21	20
	7	"	45			17	14	
	8	"	17			13	11	
	10	"	7			9	7	
40 p.p.m.	6	Synth. hard	36	52	47	34	29	28
	7	" "	14	37	41	31	28	27
	8	" "	14	37	43	35	33	33
	10	" "	46	69	88	77	78	79
12 p.p.m.	6	Distilled	73	62	41	30	26	22
12 p.p.m.	6	Synth. hard	31	40	40	29	25	21

*Synthetic hard water = 40 p.p.m. Ca (as $CaCO_3$), 20 p.p.m. Mg (as $CaCO_3$), and 12 p.p.m. Cl.
†TSPP = tetrasodium pyrophosphate, STPP = sodium tripolyphosphate, glasses are designated by their number average chain length.

In the initial tests, the change in composition with time was followed by paper chromatography. Figure 1 shows a typical distribution curve for a glass of average chain length 13. No attempt was made to separate the species longer than chain length 3. A 21 chain length glass gave a distribution curve that was almost identical to Fig. 1 in all species except orthophosphate, which increased to only 38% in 3 h instead of 55%, and in the content of chains longer than 3, which was higher by the corresponding amount.

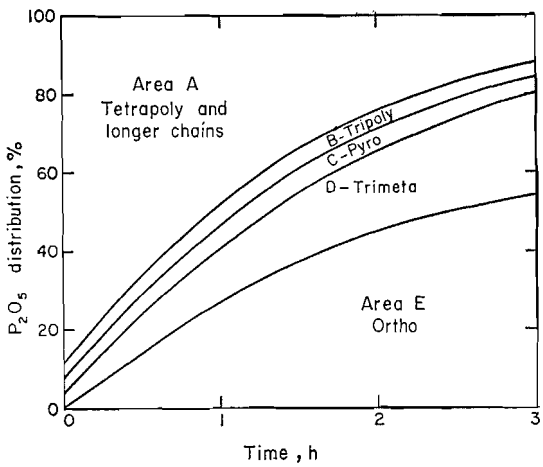

FIG. 1. Change in distribution of phosphate species with time for sodium polyphosphate glass of average chain length 13 in 1% solution at pH 6 at 100 °C.

Results at 100 p.p.m. concentration were very similar to those at 1%.

On the basis of these initial results, it was decided to standardize on a 1.5 h test, since the increase in orthophosphate and decrease in chain phosphate content are close to linear up to this point. Similar tests at 63 °C gave about the same change in composition in 5 days as the 100 °C tests did in 1.5 h, so this time interval was selected as a standard.

Results of the 100 °C tests in Table I show very little change in reversion rate with concentration, over the range of 1% to 40 p.p.m., in distilled water. However, in synthetic hard water there was a significant shift in behavior, with the effect of pH in the 40 p.p.m. tests being reversed from that at 1%. All of the glasses as well as TSPP and STPP showed greater reversion at pH 9 than at pH 6 or 7 in the 40 p.p.m. tests in synthetic hard water. The cross-over point (between increasing and decreasing reversion with increased pH) for the 13 and 21 chain length glasses appears to occur at about 500 p.p.m. concentration under these test conditions. At this concentration a substantial portion (of the order of one-half) of the polyphosphate should be present as a complex with the calcium and magnesium ions of the standard hard water.

Table II shows results of tests at 63 °C, a temperature more typical of industrial water treatment applications. Results show a similar

Can. J. Chem. Downloaded from www.nrcresearchpress.com by 210.87.254.6 on 09/05/12
For personal use only.

pattern to those at 100 °C, indicating that enzymatic hydrolysis did not contribute significantly to reversion at the low concentrations. A sodium polyphosphate glass having an average chain length of about 400 was tested at 12 p.p.m. concentration under the conditions shown in Table II and gave exactly the same amount of reversion to orthophosphate as that of the 40 chain length glass in each test.

The combined data from the distilled water tests show a general trend towards reduced reversion with increase in average chain length which is in qualitative agreement with the combined data of Griffith and Buxton (11) and of Wieker (12) who found an increase in reversion rate with increasing chain length up to 8 and a decreasing rate with increasing chain length above 24. Our data indicate that the maximum reversion rate must lie between 8 and 13, probably close to chain length 8. However, our data show that at low concentrations of phosphate in hard water there is a minimum in rate of reversion between a chain length of about 13 and 40.

In the course of this work, some of the "dry" phosphate glass samples which were stored in the laboratory in screw capped jars were reanalyzed after a period of several months and found to have decreased in average chain length. All of the stored glass samples were reanalyzed and it was found that none of the samples having an average chain length of less than 30 had changed significantly on storage while all samples above 30 had degraded. Both groups contained samples which had been stored for periods ranging from 3 to 12 months. Storage conditions were not closely controlled (heated laboratory in winter, air-conditioned in summer) but all samples were stored in the same manner.

Figure 2 shows the rate of decrease in average chain length for the various stored samples. Glasses having an average chain length between 30 and 90 show a linear increase in rate of degradation with increasing chain length. Because of the wide range of storage times and storage conditions represented by the data, only qualitative conclusions can be drawn, but the excellent fit of the experimental data to a straight line graph attests to its reliability.

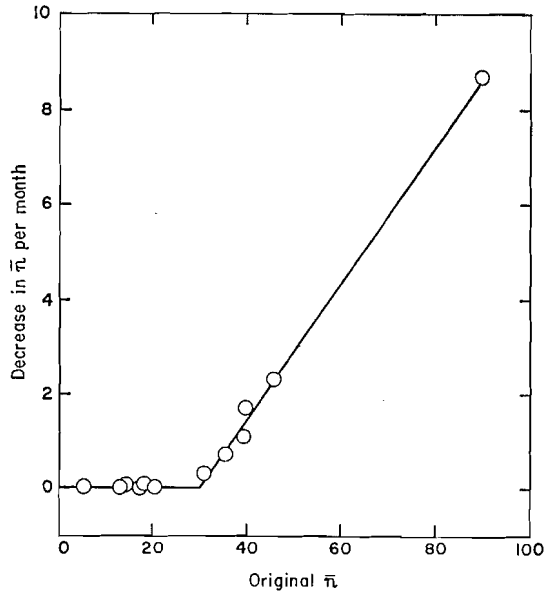

FIG. 2. Rate of reduction in average chain length of sodium polyphosphate glasses under "dry" storage conditions as a function of initial average chain length.

Acknowledgment

The authors thank J. D. Mowell for assistance in the experimental work.

1. J. R. VAN WAZER (*Editor*). Phosphorus and its compounds. Vol. I. Interscience Publishers, Inc., New York. 1958. Chap. 8.
2. R. N. BELL. Ind. Eng. Chem. **39**, 136 (1947).
3. N. L. CLESCERI and G. F. LEE. Intern. J. Air Water Pollution, **9**, 723 (1965).
4. J. GREEN. Ind. Eng. Chem. **42**, 1542 (1950).
5. J. F. MCCULLOUGH, J. R. VAN WAZER, and E. J. GRIFFITH. J. Am. Chem. Soc. **78**, 4528 (1956).
6. E. THILO, G. SCHULTZ, and E. WICHMAN. Z. Anorg. Allgem. Chem. **272**, 182 (1953).
7. E. KARL KROUPA. Anal. Chem. **28**, 1093 (1956).
8. R. J. FUCHS and F. W. CZECH. Anal. Chem. **35**, 769 (1963).
9. J. B. MARTIN and D. M. DOTY. Anal. Chem. **21**, 965 (1949).
10. J. R. VAN WAZER, E. J. GRIFFITH, and J. F. MCCULLOUGH. Anal. Chem. **26**, 1755 (1954).
11. E. J. GRIFFITH and R. L. BUXTON. J. Am. Chem. Soc. **89**, 2884 (1967).
12. W. WIEKER. Z. Anorg. Allgem. Chem. **313**, 309 (1961).

Can. J. Chem. Downloaded from www.nrcresearchpress.com by 210.87.254.6 on 09/05/12
For personal use only.

Can. J. Chem. Downloaded from www.nrcresearchpress.com by 210.87.254.105 on 09/05/12
For personal use only.

Canadian Journal of Chemistry

Published by THE NATIONAL RESEARCH COUNCIL OF CANADA

VOLUME 47 SEPTEMBER 1, 1969 NUMBER 17

Studies in ferrocene derivatives. VII[1]. The synthesis of ferrocenyl ethylenes via an abnormal Grignard reaction[2]

W. H. HORSPOOL

Department of Chemistry, The University, Dundee, Scotland

AND

R. G. SUTHERLAND[3] AND J. R. SUTTON

Department of Chemistry and Chemical Engineering, The University of Saskatchewan, Saskatoon, Saskatchewan

Received February 27, 1969

RMgBr reacts normally with acylferrocenes to give the corresponding alcohols. RMgI gives good yields of the most highly substituted ferrocenyl ethylene. In solutions of moderate acid strength, α-ferrocenyl carbonium ions lose a proton to form the substituted alkene rather than undergo nucleophilic attack by water to give the corresponding alcohol. Since the alcohols are more basic than the alkenes, it is possible to devise a general synthesis of ferrocenyl ethylenes by the reaction of any Grignard reagent with an acylferrocene.

Canadian Journal of Chemistry, 47, 3085 (1969)

Ferrocenyl ethylenes have been synthesized previously by the facile dehydration of ferrocenyl alcohols (3–6), the reaction of acyl ferrocenes with alkyl lithium reagents (5), and, more recently, by the Wittig reaction (7, 8). In connection with other work on ferrocenophanes (9), we required several ferrocenyl-1,1′-diols of the general structure **1**. These compounds had been prepared previously by reaction of the 1,1′-diacyl ferrocene with the appropriate Grignard reagent followed by conventional work-up. The synthesis of **1**; $R_1 = R_2 = CH_3$) was accomplished as described in the literature (10). Preliminary examination of the crude product showed that there were two major products and chromatographic work-up gave the diol (**1**; $R_1 = R_2 = CH_3$) in a 56% yield and the bis alkene (**2**; $R_1 = CH_3$, $R_2 = R_3 = H$) in 32% yield. This constitutes a useful synthesis of 1,1′-bis isopropenyl ferrocene since alternative syntheses involve the prior formation of 6,6-dimethyl fulvene (11) or methylene triphenyl phosphorane (7, 8).

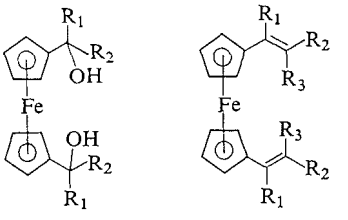

1 **2**

Examination of the literature (10, 12), showed that in many cases where alkyl magnesium iodides had been used in the synthesis of ferrocenyl alcohols, the yields were somewhat lower than would be expected in a Grignard reaction; the yields obtained from alkyl magnesium bromides were usually much higher. Accordingly, we examined the reaction of several acyl ferrocenes with RMgI and RMgBr. The former gave good yields of alkenes whereas the latter usually gave high yields of the corresponding alcohol. Since the work-up conditions were identical for both iodides and bromides it appears likely that

[1]See ref. 1 for Part VI of this series.
[2]See ref. 2.
[3]The author to whom correspondence may be addressed.

the elimination occurs during the reaction, and not during the work-up procedure. The elimination of HOMgI is not without precedent (13) in Grignard reactions, but the conditions employed are usually severe, involving the use of acids and/or refluxing solvents. It appears likely that this reaction involves the ionization of the magnesium alcoholate to give an intermediate α-ferrocenyl carbonium ion which then loses a proton to form the ferrocenyl ethylene (eq. [1]).

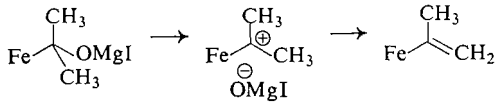

Eq. [1]

Support for this hypothesis comes from the reaction of 2-ferrocenyl-propan-2-ol (**4**) with an excess of methyl magnesium iodide in refluxing benzene – ether overnight. Chromatography of the crude product gave 2-ferrocenyl propene in 44% conversion with 36% of the alcohol being recovered. Although the work-up conditions used in these reactions were identical for the Grignard reagents derived from alkyl iodides and alkyl bromides, it was necessary to prove convincingly that the alkenes were present in the RMgI reactions before hydrolysis. This was normally done by thin-layer chromatographic (t.l.c.) examination of the crude reaction mixture. In the case of the reaction between acetylferrocene and methyl magnesium iodide, the reaction mixture was chromatographed without the hydrolysis step. The alkene (**5**) was obtained in yields of greater than 80% whether the alumina was used as received or after drying to Brockman Activity I. This constitutes strong support for the mechanism outlined in eq. [1]. Our results, together with these in the literature, are summarized in Table I.

Acyl ferrocenes which yield secondary alcohols react normally with alkyl magnesium iodides, whereas the formation of tertiary magnesium alcoholates gives rise to substantial quantities of alkene. The greater the degree of substitution of the double bond, the more likely is alkene formation. Branching of the carbon chain of the acyl ferrocene e.g. pivaloyl ferrocene decreases the amount of alkene formed. In fact no ferrocenyl ethylene was found in the reaction between pivaloyl ferrocene and methyl magnesium iodide, the only product isolated being the endo

TABLE I

Synthetic results: effect of X in RMgX on product proportions.

Acyl ferrocene	RMgI % alkene	RMgI % alcohol	RMgBr % alcohol
		R = CH_3	
1. Formyl	6	90	
2. Acetyl	75	16	58*
3. Pivaloyl	—	74	
4. Benzoyl			32†
5. 1,1′-Diacetyl	32	56	
6. 1,1′-Dipropionyl	49	47	
		R = C_2H_5	
7. Formyl			89†
8. Acetyl	68	20	50†
9. 1,1′-Diacetyl	41	56	88
10. 1,1′-Dipropionyl	26	62	
		R = C_3H_7	
11. Benzoyl			60*

*See reference 17.
†See reference 4.

alcohol (**3**) where the hydroxyl group is strongly hydrogen bonded to the iron atom, as shown by the sharp OH stretch at 3560 cm^{-1} (14) and the fact that it sublimes readily. It showed the chromatographic behavior normally associated with a ferrocenyl ethylene. It would appear, therefore, that where possible ferrocenyl alcohols should be synthesized either by reaction with alkyl magnesium bromides or the corresponding lithium reagent, to avoid the dehydration problems encountered with the corresponding iodides. In many cases, reaction with alkyl magnesium iodides leads to synthetically useful yields of the most highly substituted alkene.

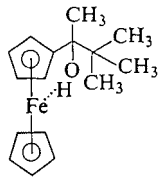

3

It would be useful if the abnormal Grignard reaction could be modified to give the alkene as the sole product. In connection with our work on α-ferrocenyl carbonium ions (15), we have compared the basicity of 2-ferrocenyl propan-2-ol (**4**) and 2-ferrocenyl propene (**5**), both compounds forming the dimethyl ferrocenyl carbonium ion (**6**) (eq. [2]). The alcohol is 1/2 protonated in 37%

458946

Can. J. Chem. Downloaded from www.nrcresearchpress.com by 210.87.254.105 on 09/05/12
For personal use only.

TABLE II

A. Monosubstituted ferrocenes (7)

R_1	R_2	OH	Substituted ring	Unsubstituted ring
1. $R_1 = R_2 = H$	5.8 s (2)	8.59 s (1)	5.91 s (9)	
2. CH_3 8.62 d (3) $J = 6.5$ Hz	H 5.6 m* (1)	8.2 m (1)	5.92 m (4)	5.87 s (5)
3. $R_1 = R_2 = CH_3$	8.57 s (6)	8.25 (1)	5.92 m (4)	5.88 s (5)
4. CH_3 8.43 s (3)	t. Bu 9.19 s (9)	8.33 s (1)	5.6–6.1 m (4)	5.85 s (5)

B. Disubstituted ferrocenes (1)			Ring protons
5. $R_1 = R_2 = CH_3$	8.5 s (12)	5.8 bs (10)†	
6. CH_3 8.44 q (10)‡	CH_3—CH_2‡ 9.24 t (6) $J = 7.5$ Hz	4.99 s (2)	5.63, 5.93, 6.1 bt (8)
7. CH_3 8.2 s (6)	Phenyl 2.8 m (10)		5.75, 5.85† m (10)
8. $R_1 = R_2 = C_2H_5$ CH_3 9.2 t (12)	CH_2 8.3 m (8)	6.95 s (2)	5.90 s (8)

NOTE: Spectra are reported in τ, and are recorded in CCl_4. s, singlet; d, doublet; m, multiplet; bs, broad singlet; q, quartet; t, triplet.
*After treatment with D_2O, the multiplet collapsed to a quartet, $J = 6.5$ Hz.
†D_2O treatment showed that the OH resonance occurred under the multiplet due to the ring protons.
‡The resonance of the methylene group of the CH_3CH_2— substituent overlapped that of the CH_3— group.

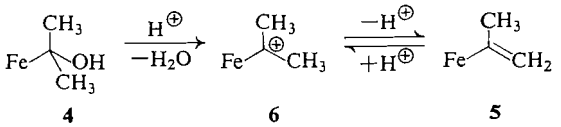

4 6 5

EQ. [2]

sulfuric acid and the alkene in 44% sulfuric acid. The carbonium ion formed deprotonates to give the alkene much faster than it undergoes solvolytic attack to form the alcohol. Accordingly by working-up the Grignard reaction mixture by treatment with dilute acid ca. 20% H_2SO_4 in a two-phase system, the alkene formed is removed into the organic layer. A two-phase system of carbon tetrachloride – 20% H_2SO_4 gave a 95% conversion of (**4**) to (**5**).

We have discussed the nuclear magnetic resonance (n.m.r.) spectra of ferrocenyl ethylenes previously (8) in some detail. Most of the alcohols described in this work have all been prepared previously without mention of their n.m.r. spectra. These are unexceptional and the observed spectra are recorded in Table II.

The mass spectra of the alcohols have been recorded and in most instances the molecular ion is not observed in the mass spectrometer, the major peak being attributable to the corresponding alkene. The same is also true of vapor phase chromatography (v.p.c.) of the alcohols where injection of the alcohol leads to formation of the olefin.

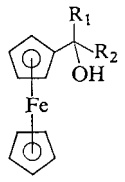

7

Experimental

The acyl ferrocenes used were synthesized by standard methods (12*b*). Nuclear magnetic resonance spectra were recorded on a Perkin–Elmer R10 (60 Mc.p.s.) spectrometer or a Varian A60 spectrometer in CCl_4 solution. Mass spectra were recorded on an M.S. 12 instrument.

Pivaloyl ferrocene was prepared essentially as described by Leigh (16). The crude product had to be chromatographed several times on alumina (Fisher A540) to remove several other products e.g. 1-*t*-butyl-1′-pivaloyl ferrocene which were formed during the Friedel-Crafts reaction.

1-Ferrocenyl-3,3-dimethyl Butan-2-ol (3)

Pivaloyl ferrocene (2.7 g; 10 mmole) in dry benzene (15 ml) was added to a refluxing solution CH_3MgI (from Mg (0.72g)) and CH_3I (1.8 ml) in anhydrous ether (25 ml). The mauve solution was refluxed for 3½ h and the reaction terminated by pouring the cooled solution into water (200 ml). The precipitated magnesium salts were dissolved using 20% H_2SO_4. The organic layer was separated and the ether washings of the aqueous layer

Can. J. Chem. Downloaded from www.nrcresearchpress.com by 210.87.254.105 on 09/05/12
For personal use only.

added. The combined extracts were washed (water) till neutral and dried (Na_2SO_4). Removal of solvent (rotary evaporator) gave a yellow crystalline solid, m.p. 70–80°. Chromatography on alumina (Fisher 540H) using skellysolve F:benzene (1:1) gave **3** as yellow plates m.p. 85–87° (2.1 g, 73.4%). An analytical sample was obtained by sublimation at 100 °C/2 mm as golden-yellow plates, m.p. 91–92°.

Anal. Calcd. for $C_{16}H_{22}FeO$ (mol. wt. (mass spectra) 286): C, 67.20; H, 7.70. Found: C, 67.17; H, 7.8.

Synthesis of Ferrocenyl Ethylenes

(i) 2-Ferrocenyl Prop-2-ene

Acetyl ferrocene (10 mmole) in benzene (10 ml) was added over 30 min to a refluxing solution of methyl magnesium iodide (100 mmole) in ether (15 ml). The reaction mixture was refluxed for 20 min, cooled, and quenched in ice water (100 ml). The organic phase was separated, washed with water, dried (Na_2SO_4), and solvent removed. The semi-crystalline residue was chromatographed on alumina (Fisher 540A) and the olefin eluted with skellysolve F. The yield of olefin varied from 62–75%. Further elution with benzene – ether (1:4) gave 2-ferrocenyl propan-2-ol in ca. 15% yield.

(ii) 2-Ferrocenyl But-2-ene

Acetyl ferrocene (20 mmole) in benzene (25 ml) was added to a stirred solution of ethyl magnesium iodide (30 mmole) over 30 min and the mixture stirred overnight. The reaction mixture was worked-up in the usual manner and the crude product chromatographed on alumina (Spence, H). Elution with petrol gave the ferrocenyl ethylene as a red oil in a 68.4% yield.

Synthesis of Ferrocenyl Alcohols

(iii) Bis-1,1'-(2-hydroxy-1-methyl propyl) Ferrocene (***1***; $R_1 = CH_3$, $R_2 = C_2H_5$)

1,1'-Diacetyl ferrocene (25 mmole) in benzene (40 ml) was added to a stirred solution of ethyl magnesium bromide (100 mmole) in ether (100 ml) and the reaction mixture stirred overnight. Conventional work-up gave the product as an oil which was chromatographed on alumina. Elution with benzene – ether (1:4) gave the diol as yellow plates, m.p. 100–101° (10) in an 88% yield.

Dehydration of Ferrocenyl Alcohols Using a Two-Phase System of 20% H_2SO_4–CCl_4

2-Ferrocenyl-2-propanol (1 g) was dissolved in carbon tetrachloride (20 ml) and 20% H_2SO_4 (20 ml) added. The two-phase system was shaken mechanically for 3½ h and the reaction followed by t.l.c. The CCl_4 layer was separated, washed with water till neutral, dried (Na_2SO_4), and solvent removed. The residue was pure (by v.p.c.) 2-ferrocenyl prop-2-ene (0.89 g, 95%) m.p. 61–62°.

Acknowledgments

We thank the University of Saskatchewan for the award of a research assistantship (J.R.S.) and the National Research Council of Canada for generous financial assistance.

1. W. M. Horspool, R. G. Sutherland, and B. J. Thomson. Tetrahedron Letters, 6045 (1968).
2. W. M. Horspool and R. G. Sutherland. Tetrahedron Letters, 4165 (1967).
3. F. S. Arimoto and A. C. Haven. J. Am. Chem. Soc. **77**, 6295 (1955).
4. K. Schlogl and A. Mohar. Monatsh. Chem. **92**, 219 (1961).
5. W. P. Fitzgerald. Ph.D. Thesis, Purdue University, Lafayette, Indiana. 1963.
6. M. D. Rausch and A. Siegel. J. Organometal. Chem. **11**, 317 (1968).
7. W. M. Horspool and R. G. Sutherland. Chem. Commun. 456 (1966).
8. W. M. Horspool and R. G. Sutherland. Can. J. Chem. **46**, 3453 (1968).
9. W. M. Horspool and R. G. Sutherland. Chem. Commun. 240 (1967).
10. R. Reimschneider and D. Helm. Chem. Ber. **89**, 155 (1956).
11. G. R. Knox and P. L. Pauson. J. Chem. Soc. 4610 (1961).
12. *a*) M. Dub. *In* Organometallic compounds. Vol. 1. 2nd. ed. Springer-Verlag, Berlin. 1966. *b*) M. Rosenblum. *In* Chemistry of the iron group metallocenes. John Wiley and Sons, Inc., New York. 1965. p. 1.
13. M. S. Karasch and O. Reinmuth. Grignard reactions of non-metallic substances. Prentice-Hall, Inc., New York. 1954.
14. E. A. Hill and J. H. Richards. J. Am. Chem. Soc. **83**, 3840 (1961).
15. W. M. Horspool and R. G. Sutherland. Chem. Commun. 786 (1967).
16. T. Leigh. J. Chem. Soc. 3294 (1964).
17. WuKuan-Li, E. B. Sokolova, I. E. Chlenov, and A. D. Petrov. Dokl. Akad. Nauk SSSR, **137**, 111 (1961).

Can. J. Chem. Downloaded from www.nrcresearchpress.com by 210.87.254.105 on 09/05/12
For personal use only.

Nuclear magnetic resonance studies. XVI.[1] Oxygen-17 shieldings of some substituted acetophenones

D. J. SARDELLA[2] AND J. B. STOTHERS
Department of Chemistry, University of Western Ontario, London, Ontario
Received February 25, 1969

The ^{17}O spectra of some *ortho*- and *para*-substituted acetophenones were determined to examine the effect of substituent polarity and steric hindrance on the acetyl oxygen shieldings. The results are compatible with proposals previously advanced on the basis of the ^{13}C shielding data for these compounds.

Canadian Journal of Chemistry, 47, 3089 (1969)

Can. J. Chem. Downloaded from www.nrcresearchpress.com by 210.87.254.5 on 09/05/12
For personal use only.

Introduction

An examination of the ^{13}C magnetic resonance (c.m.r.) spectra of an extensive series of substituted acetophenones (1) and alkyl phenyl ketones (2) revealed that the shielding of the carbonyl carbon is insensitive to substituent polarity for a wide range of *meta*- and *para*-substituted compounds. Although there is ample evidence from reactivity studies (3) and infrared spectra (4) to show that the carbonyl bond is perturbed by polar substituents, the ^{13}C results indicate that the electron density about the carbonyl carbon is not significantly altered even with the change, *p*-NMe_2 → *p*-NO_2. This behavior is in direct contrast with that exhibited by the fluorine nucleus in *p*-substituted fluorobenzenes for which the ^{19}F shieldings vary by ca. 28 p.p.m. for the same change in substituent. An interpretation of the ^{13}C results was advanced (1) in terms of the resonance forms contributing to the structures of these compounds in which it was suggested that the location of a nucleus within the aryl system could be an important factor governing substituent effects on its shielding. In the fluorobenzenes the fluorine nucleus is at the end of the resonance system while the carbonyl carbon in the aryl ketones is one atom from the end. Polarization of the π-cloud governed by the electronic character of a substituent could, it was suggested, be expected to cause appreciable changes in the electron density at the end of the system but these would be much less pronounced at nuclei within the system, e.g. the carbonyl carbon. Some support for this proposal was subsequently obtained from the c.m.r. spectra of a series of substituted styrenes (5). The vinyl carbon shieldings in these materials were measured and found to differ in their response to a variety of polar substituents. The absorption of the β-carbon of the vinyl groups shifts to lower field with electron-withdrawing substituents. A total change of −10 p.p.m. was found for the change, *p*-NMe_2 → *p*-NO_2. On the other hand, the α-carbon shieldings for the same series appear over a total range of only 1.6 p.p.m. Although this variation is just greater than the experimental uncertainty, the trend, if any, is in the opposite direction to that exhibited by the β-carbons. Although it was gratifying to find that the styrene results offered some confirmation of our proposal regarding polar effects on side-chain carbons of substituted aromatics, the vinyl group differs substantially from a carbonyl group and further evidence to support our interpretation is desirable. To this end we have measured the ^{17}O shieldings of the carbonyl oxygen in some of the acetophenones for which we have the ^{13}C data and these results are presented in this paper. For this work, the compounds chosen were enriched with ^{17}O to aid the determination of their shieldings.

Experimental

Spectra

The ^{17}O spectra were obtained at 8.13 MHz with a Varian DP-60 spectrometer using a V-4210A variable frequency oscillator. The audio side-band technique was employed to calibrate the spectra and chemical shifts were measured relative to external ^{17}O-enriched water. The audio and radio frequencies were measured with an HP-5245L counter. The samples were examined in a concentric cell arrangment having an outer spherical cavity containing ca. 1 ml of the sample and an inner sphere ca. 0.2 ml in volume containing enriched water. Acetone solutions of the labelled acetophenones were employed in concentrations of ca. 1:3 (v/v). A more dilute solution (1:6) of acetophenone in acetone was

[1]Part XV. G. W. Buchanan, J. B. Stothers, and S-t Wu, Can. J. Chem. **45**, 2955 (1967).
[2]NRCC Postdoctorate Fellow, 1966–1967. Present address: Department of Chemistry, Boston College, Chestnut Hill, Massachusetts.

Can. J. Chem. Downloaded from www.nrcresearchpress.com by 210.87.254.5 on 09/05/12
For personal use only.

examined to check for the absence of an appreciable solvent effect.

Proton and infrared spectra of all samples of the ^{17}O-enriched acetophenones were obtained to ensure the absence of impurities. Ultraviolet spectra of these acetophenones were recorded on a Cary 14 spectrophotometer to measure the position of the $n \rightarrow \pi^*$ transitions in n-hexane solutions. The infrared spectra, (i.r.), provided a measure of the ^{18}O content, after exchange, from which the ^{17}O enrichment was determined. To test the reliability of the infrared analysis, the ^{18}O content of 4-bromoacetophenone was also determined by mass spectrometry.[3] Comparison of the intensities of peaks, m/e = 202 and 198 for $^{81}Br^{18}O^{12}C_8H_7$ and $^{79}Br^{18}O^{12}C_8H_7$, respectively, gave, after correction for the background due to mercury isotopes and the $^{79}Br/^{81}Br$ ratio (1.021), the ^{18}O enrichment. The results of the isotopic analyses are included in Table I. The $^{18}O/^{17}O$ ratio for the water used to enrich the ketones was provided by the supplier, Yeda Research and Development Co.

TABLE I

^{17}O-Enriched acetophenones

Substituent	Method of preparation*	^{17}O Content† (%)	$\bar{\nu}$ C=^{18}O cm^{-1}
H	*a*	1.7	1660
4-Me	*a*	1.5	1657
4-Br	*a*	1.6‡	1660
4-NO_2	*b*	1.5	1667
4-MeO	*b*	1.0	1650
2-Me	*a*	1.7	1657
2,6-Me_2	*a*	1.7	1659
2,4,6-Me_3	*b*	0.5	1667

*(*a*) Hydrolysis of corresponding anil; (*b*) acid-catalyzed exchange.
†Estimated from ^{18}O content measured by i.r. absorption.
‡By mass spectrometry, 1.5% ^{17}O.

Materials

The ^{17}O-labelled acetophenones were prepared following either of two routes: (*a*) by hydrolysis of the corresponding anil or (*b*) by acid-catalyzed exchange with ^{17}O-enriched water (6). The general procedures are described and the specific method employed for each case is indicated in Table I.

Method (a)

A solution of the ketone (0.02 mole) in aniline (15 ml) was placed in a Dean–Stark apparatus and 0.05 g of an aniline – zinc chloride complex was added. The mixture was heated under reflux for 4 h.

The catalyst was obtained by mixing aniline (50 ml) with anhydrous zinc chloride (3.5 g) in a flask protected from atmospheric moisture by a drying tube. After the initial reaction subsided the flask was shaken and left to stand with occasional shaking. The resulting suspension was filtered and the filtrant washed thoroughly with dry ether to remove all traces of aniline. After storage overnight under vacuum the complex was ready for use.

After cooling, the reaction mixture was distilled to remove the excess aniline, the residue was shown to be mainly the desired anil (ca. 80%) containing some of the original ketone (ca. 20%). Since the i.r. and ^1H spectra showed the absence of impurities this mixture was used directly in the next step.

The crude anil was dissolved in CCl_4 (ca. 1 ml) and ^{17}O-enriched water (0.12 g) added. Hydrogen chloride was bubbled through the mixture for a few minutes and then the mixture was shaken. This was repeated until no further reaction was evident. After the addition of more solvent, the solids were removed by filtration and the solution dried over magnesium sulfate. Removal of the solvent yielded a product shown to be essentially pure ketone by i.r. and nuclear magnetic resonance (n.m.r.) spectroscopy with the presence of an additional carbonyl band in the former.

Method (b)

To a solution of the ketone (0.04 mole) in dioxane (12 ml) containing ^{17}O-enriched water (0.3 ml) was added two drops of concentrated HCl and the solution heated under reflux overnight. After cooling, the water was removed with 4A molecular sieves and the solvent removed by distillation under vacuum. The residue was examined by i.r. and ^1H spectroscopy to ensure the absence of impurities.

Results and Discussion

Five members of the *para*-substituted series were examined and the data are listed in Table II. The total range of these ^{17}O shieldings was found to be 19 p.p.m. for the substituent change *para*-methoxyl to *para*-nitro. We have found acetophenone itself to absorb at −555 p.p.m. (from external water) in these acetone solutions and, furthermore, the shielding was unchanged at the two dilutions examined, 33 and 15% (v/v). Earlier, Christ and Diehl (7) reported that neat acetophenone absorbs at −546 p.p.m. This difference is larger than the combined experimental uncertainty and may be due, in part, to a medium effect. We feel, however, that the present set of data is internally consistent. The trend exhibited by the *para*-substituted derivatives is in agreement with expectations since a progressive increase in electron-withdrawing power tends to shift the ^{17}O absorption to lower field, a paramagnetic shift. This trend was found earlier (7) in a comparison of the ^{17}O shieldings of *p*-anisaldehyde and benzaldehyde which differ by 24 p.p.m. with *p*-anisaldehyde at the higher field.

It has been established that the paramagnetic contribution, σ_p, to the total screening constant, σ, dominates ^{17}O nuclear shieldings (7, 8) and

[3]We wish to thank Mr. John Krause for kindly performing these analyses.

Can. J. Chem. Downloaded from www.nrcresearchpress.com by 210.87.254.5 on 09/05/12
For personal use only.

TABLE II

^{17}O Shifts of *para*-substituted acetophenones

Substituent	δ (^{17}O)	λ (n $\rightarrow \pi^*$)
4-MeO	-548 ± 4	~308 mμ
4-Me	-555 ± 6	320
Nil	-554 ± 7	320
4-Br	-552 ± 5	323
4-NO_2	-567 ± 5	~335
2-Me	-586 ± 4	319
2,6-Me_2	-608 ± 5	~310
2,4,6-Me_3	-593 ± 15	~313

the present results may be considered qualitatively in terms of this contribution which has the form

$$\sigma_p \alpha - \frac{1}{\Delta E}\langle r^{-3}\rangle_{2p}$$

where ΔE represents the excitation energy to the low lying excited state, and $\langle r^{-3}\rangle_{2p}$, is the mean inverse cube radius for the 2p orbitals. The latter term accounts for the charge density effect in the paramagnetic term since increasing charge density leads to an expansion of the orbitals and thereby a reduction in σ_p. Comparing a carbonyl oxygen in a saturated ketone with one in a conjugated system would lead to the prediction that σ_p should be less for the latter *if the* $\langle r^{-3}\rangle_{2p}$ *term dominates* since there is a greater contribution from the polarized forms such as **2** and **3** in conjugated systems.

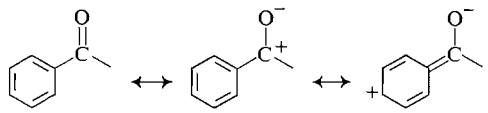

1 **2** **3**

It has been shown by Figgis *et al.* (8) that organic carbonyl oxygen shieldings correlate approximately with $\lambda_{max}^{n\rightarrow\pi^*}$ values (i.e. the inverse of the excitation energy for the lowest electronic transition), if the series including several different types of carbonyl compound is considered. Within specific families, such as the aliphatic ketones, however, the correlation does not hold. For the *para*-substituted derivatives in the present study, a correlation of the δ_0 with λ_{max} may exist but the interdependence between these two parameters is quite different from that of Figgis *et al.* in which a shielding change of ca. -3 p.p.m./mμ was found while our series shows a change of only ca. -0.6 p.p.m./mμ. Furthermore, the δ_0 values for the *ortho*-substituted cases (see Table II) exhibit the opposite trend with the $\lambda_{max}^{n\rightarrow\pi^*}$ data. Clearly a consistent explanation of the present results in terms of a dominant $1/\Delta E$ contribution does not exist. A reason for this may be the fact that the ΔE term represents a summation extending over all ground to excited state transitions and the exclusion of all but the n $\rightarrow \pi^*$ transition is too drastic an approximation for aryl ketones since the $\pi \rightarrow \pi^*$ transitions are relatively close. An indication that this is the case is provided by the observation that the shielding difference between acetone and acetophenone of -17 p.p.m. bears no relation to the value of ca. -120 p.p.m. predicted by the original δ_0 vs. $\lambda_{max}^{n\rightarrow\pi^*}$ correlation. It is interesting, however, that the solvent dependence of the oxygen shielding for acetone correlates rather nicely with $1/\Delta E$ for the n $\rightarrow \pi^*$ transition energies as shown in Fig. 1, in which the shielding data reported by Christ and Diehl (7) are plotted vs. $\lambda_{max}^{n\rightarrow\pi^*}$ for five solvents (9). In fact the slope, δ_0/λ_{max}, is essentially the same as that found by Figgis *et al.* (8).

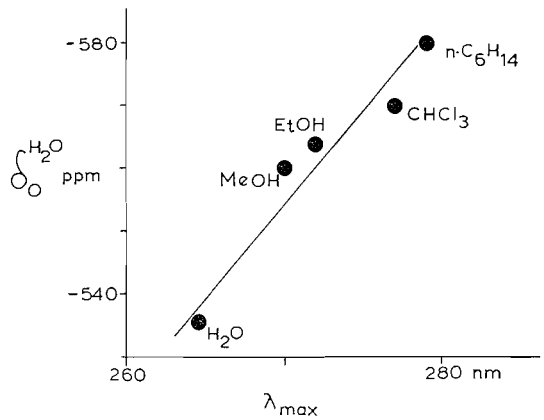

FIG. 1. A plot of acetone oxygen shieldings (7) vs. $\lambda_{max}^{n\rightarrow\pi^*}$ (9) in the indicated solvents.

In terms of the relative contribution of forms akin to **2** and **3** to the electronic distribution about the carbonyl oxygen nuclei, however, a certain consistency appears to hold throughout the present series. The polarized form will be more important in those cases in which an electron-releasing substituent is present at the *para* position and less important for electron-withdrawing substituents. In other words the $\langle r^{-3}\rangle_{2p}$ term will increase along the series *p*-MeO

$\rightarrow p$-NO_2 and, consequently, σ_p will increase. Thus δ_0 will be expected to decrease, i.e. a shift to lower field, since σ_p is negative. Another mechanism by which the polarization of the carbonyl bond may be decreased is through steric inhibition of resonance. Thus, substitution of the *ortho* protons with methyl groups should result in a shift of δ_0 to lower field if the $\langle r^{-3} \rangle$ term dominates. This is the observed trend. The fact that the ^{17}O nucleus in the *ortho*-substituted cases absorbs at even lower field than that in aliphatic systems suggests the presence of an additional perturbation. This may be a contribution due to a dispersion or van der Waals effect owing to the close approach of the methyl protons of the *ortho*-groups. In any event, it appears that the ^{17}O shieldings in these aryl ketones can be satisfactorily interpreted in terms of a charge transfer effect which is manifested in the $\langle r^{-3} \rangle_{2p}$ term of the paramagnetic term, σ_p. This trend is in general agreement with that found earlier in these laboratories from the c.m.r. spectra of substituted styrenes (5) in which the variation of the β-vinyl carbon shieldings exhibit similar variations. The previous c.m.r. and the present ^{17}O magnetic resonance data are plotted in Fig. 2 to illustrate the similarities.

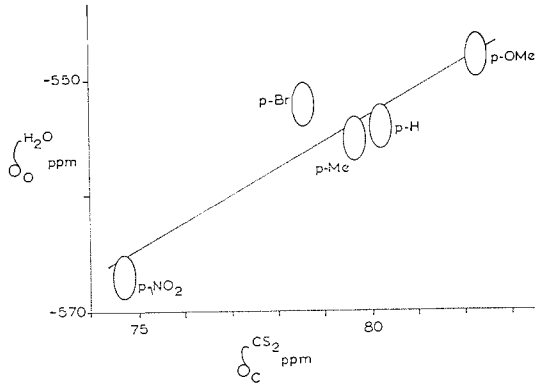

FIG. 2. A plot of the ^{17}O shieldings of some substituted acetophenones vs. the β-vinyl ^{13}C shieldings of the corresponding styrenes.

Acknowledgments

This work was supported by the National Research Council of Canada whose aid we gratefully acknowledge. We also thank Prof. R. G. Kidd for valuable discussions and some assistance with the experimental problems associated with ^{17}O studies.

1. J. B. STOTHERS and P. C. LAUTERBUR. Can. J. Chem. **42**, 1563 (1964). K. S. DHAMI and J. B. STOTHERS. Tetrahedron Letters, 631 (1964). K. S. DHAMI and J. B. STOTHERS. Can. J. Chem. **43**, 479 (1965).
2. K. S. DHAMI and J. B. STOTHERS. Can. J. Chem. **43**, 498 (1965).
3. J. E. LEFFLER and E. GRUNWALD. Rates and equilibria of organic reactions. John Wiley and Sons, Inc., New York. 1963. p. 181f.
4. R. STEWART and K. YATES. J. Am. Chem. Soc. **80**, 6355 (1958). H. H. FREEDMAN. J. Am. Chem. Soc. **82**, 2454 (1960).
5. K. S. DHAMI and J. B. STOTHERS. Can. J. Chem. **43**, 510 (1965).
6. M. GORODETSKY, A. LUZ, and Y. MAZUR. J. Am. Chem. Soc. **89**, 1183 (1967).
7. H. A. CHRIST and P. DIEHL. Helv. Phys. Acta, **36**, 170 (1963).
8. B. N. FIGGIS, R. G. KIDD, and R. S. NYHOLM. Proc. Roy. Soc. (London), Ser. A, **269**, 469 (1962).
9. H. H. JAFFE and M. ORCHIN. Theory and applications of ultraviolet spectroscopy. John Wiley and Sons, Inc., New York. p. 187.

Can. J. Chem. Downloaded from www.nrcresearchpress.com by 210.87.254.5 on 09/05/12
For personal use only.

Can. J. Chem. Downloaded from www.nrcresearchpress.com by 210.87.254.42 on 09/05/12
For personal use only.

Stereochemistry of some olefins $R_fCH{=}CHI$ and the preparation of some new cyclopropenes

W. R. CULLEN AND M. C. WALDMAN
Chemistry Department, University of British Columbia, Vancouver, British Columbia

Received April 9, 1969

The light induced additions of CF_3I and C_2F_5I to acetylene yield the *trans* 1:1 adducts predominantly [$CF_3CH{=}CHI$ (*trans*:*cis* = 6.7:1) and $C_2F_5CH{=}CHI$ (*trans*:*cis* = 9:1)]. The addition of *i*-C_3F_7I to acetylene gives a 1:1 adduct consisting of a higher proportion of the *cis* isomer (*trans*:*cis* = 1.78:1). The *i*-C_3F_7I-acetylene adduct can be dehydrohalogenated to produce *i*-$C_3F_7C{\equiv}CH$. Difluorocarbene (from $(CH_3)_3SnCF_3$) does not add to the olefinic 1:1 adducts but does add to the polyfluoroalkyl acetylenes $R_fC{\equiv}CH$ to produce the cyclopropenes $R_fC{=}CHCF_2$ (R_f = CF_3, C_2F_5, *i*-C_3F_7).

Canadian Journal of Chemistry, 47, 3093 (1969)

Introduction

The light induced free radical addition of perfluoroalkyl iodides to acetylenes has been reported by several authors.

[1] $RC{\equiv}CH + R_fI \rightarrow RCI{=}CHR_f$
R = H, R_f = CF_3 (1), C_2F_5 (2); R = CH_3, R_f = CF_3 (3, 4);
R = CF_3, R_f = CF_3, C_2F_5, *n*-C_3F_7 (3);
R = C_6H_5, R_f = CF_3 (5);
R = CD_3, R_f = CF_3 (6).

Trifluoroiodomethane also adds to hexafluorobut-2-yne and *N*,*N*-bis(trifluoromethyl)amine under the influence of heat, probably by a radical mechanism (7, 8).

[2] $CF_3I + CF_3C{\equiv}CCF_3 \rightarrow (CF_3)_2C{=}CICF_3$

[3] $CF_3I + (CF_3)_2NC{\equiv}CH \rightarrow (CF_3)_2NCI{=}CHCF_3$

Stereochemical information about the vinyl iodide products is limited. The zinc – hydrochloric acid reduction of 1,1,1,4,4,4-hexafluoro-2-iodobut-2-ene produced a 70% yield of *trans*-1,1,1,4,4,4-hexafluorobut-2-ene; and a similar reduction using magnesium gave a 78% yield of the same butene (3). The *trans* nature of the iodobutene (implying *cis* addition) was inferred from these results. The product of eq. [3] was found by vapor phase chromatography (v.p.c.) to be a 1:1 mixture of isomers (8).

In the course of preparing 3,3,4,4,4-pentafluorobutyne and 3,4,4,4-tetrafluoro-3-(trifluoromethyl)butyne for our studies on sigma bonded fluorocarbon alkynyl derivatives of metals (9–11), we have isolated and studied the stereochemistry of the intermediate vinyl iodides produced by the radical addition of R_fI to acetylene (eq. [1]: R = H; R_f = CF_3, C_2F_5, and *i*-C_3F_7).

In keeping with our interest in difluorocarbene additions to unsaturated systems (9–11) we have reacted the olefins $R_fCH{=}CHI$ and the acetylenes $R_fC{\equiv}CH$ (R_f = CF_3, C_2F_5, and *i*-C_3F_7) with the carbene source, $(CH_3)_3SnCF_3$, in the gas phase.

Experimental

Volatile reactants and products were manipulated in a vacuum system. All reactions were carried out in sealed Pyrex tubes. Infrared (i.r.) spectra were recorded using Perkin–Elmer models 21 and 457 instruments and nuclear magnetic resonance (n.m.r.) spectra were run using Varian A-60 and HA-100 spectrometers. Chemical shifts are given in p.p.m. with respect to external tetramethylsilane (^1H spectra) and either internal or external $CFCl_3$ (^{19}F spectra), negative values being to low field. Analytical and spectroscopic data are listed in Tables I–IV and in diagrams **4–15**. Microanalyses were done by Mr. Peter Borda of this Department.

The perfluoroalkyl iodides were obtained from Peninsular ChemResearch Inc. and $CF_3CCl{=}CCl_2$ from Columbia Organic Chemicals. Acetylene was purchased from Matheson of Canada Ltd. and the acetone solvent was removed by trap-to-trap distillation. 3,3,3-Trifluoropropyne was prepared from $CF_3CCl{=}CCl_2$ by the method of Finnigan and Norris (12) with two slight modifications. The amount of fused zinc chloride was increased from 0.025 to 0.3 moles and the reaction temperature was maintained at 140–150° instead of 100° during the addition of the propene. Using these modifications a 77% yield of the propyne was obtained. 3,3,4,4,4-Pentafluorobutyne was prepared in 51.2% yield as described by Haszeldine and Leedham (2).

Preparation of 3,3,3-Trifluoro-1-iodopropene

3,3,3-Trifluoro-1-iodopropene (**1**) was prepared from acetylene and trifluoroiodomethane as described by Haszeldine (1). The reactants were irradiated for 14 days (100 W lamp).[1] The product **1** (69% yield) was purified by distillation at atmospheric pressure, b.p. 70.5°–73.0°

[1]A Hanovia lamp, 608A-36 or 679A-36 (100 or 450 W), was placed 10 cm from the reaction tube.

TABLE I
Analytical data for olefins and acetylenes

Compound	Boiling point*, °C	Yield (%)	Found (%) (Calculated (%)) C	H	I
$CF_3CH{=}CHI$ (**1**)	70.5–73	69	16.19 (16.21)	0.850 (0.895)	57.01 (57.70)
$C_2F_5CH{=}CHI$ (**2**)	89	82‡	17.67 (17.64)	0.875 (0.735)	34.52‖ (34.92)
i-$C_3F_7CH{=}CHI$ (*trans*) (**8**)§	97.8†	85	18.69 (18.65)	0.635 (0.620)	39.12 (39.45)
i-$C_3F_7CH{=}CHI$ (*cis*) (**9**)§	109.7†		18.79 (18.65)	0.69 (0.62)	39.38 (39.45)
$C_2F_5CH{=}CH{-}CH{=}CHI$	97 (48 mm)		23.95 (24.16)	1.48 (1.34)	
i-$C_3F_7C{\equiv}CH$ (**12**)§	23	42	30.71 (30.92)	0.515 (0.60)	

*Boiling points are recorded at atmospheric pressure unless otherwise noted.
†Micro boiling points.
‡Average of two experiments.
§New compound.
‖Fluorine analysis.

(lit. value 70.2° (1)) and was further identified by microanalysis (Table I). The ^1H n.m.r. spectrum of **1** was unaltered after distillation. The isomer ratio *trans*:*cis* = 6.7:1 was determined from the ^{19}F n.m.r. spectrum. The i.r. spectrum of a very small, higher boiling fraction (< 1 g) showed double bonds at 1662 and 1630 cm^{-1}. It was presumably the known diene $CF_3CH{=}CH{-}CH{=}CHI$ (1) and was not further studied.

Preparation of 3,3,4,4,4-Pentafluoro-1-iodobutene

3,3,4,4,4-Pentafluoro-1-iodobutene (**2**) was also prepared as previously described (2). In two separate experiments the reactants were irradiated with 100 and 450 W lamps for 14 days each. The former produced an 87% yield of **2**, the latter, a 78% yield, b.p. 89° (lit. value 84.4° (2)). The ^{19}F n.m.r. spectrum of **2** produced by irradiation under the 450 W lamp showed an isomer ratio of *trans*:*cis* = 9:1. A higher boiling fraction (0.35 g, b.p. 97° (48 mm)) analyzed (Table I) for the known 5,5,6,6,6-pentafluoro-1-iodohexa-1,3-diene (b.p. lit. value 104° (46 mm) (2)). The i.r. spectrum showed absorptions at 1642 and 1573 cm^{-1}.

Preparation of 3,4,4,4-Tetrafluoro-3-(trifluoromethyl)-1-iodobutene (3)

1,1,1,2,3,3,3-Heptafluoro-2-iodopropane (122.67 g) and acetylene (13.06 g) in six Carius tubes, were irradiated for 14 days (100 W lamp). A small amount (0.4 g) of unreacted acetylene was isolated. The major distillation fraction, b.p. 92°–120°, was found by v.p.c. (Kel-F grease at 70°) to be a mixture of isomers of 3,4,4,4-tetrafluoro-3-(trifluoromethyl)-1-iodobutene (**3**) (85% yield), (*trans*:*cis* = 1.78:1) (b.p. *trans*, 97.8°, b.p. *cis*, 109.7° (micro boiling points)). Two small, higher boiling fractions, 110°–114° (285 mm) and 113°–114.5° (151 mm) were obtained which had the same i.r. spectrum with double bond absorptions at 1648 and 1578 cm^{-1}.

Ultraviolet Irradiation of cis- and trans-3,4,4,4-Tetrafluoro-3-(trifluoromethyl)-1-iodobutene

In two separate experiments pure samples of the *cis* and *trans* **3** were irradiated for 15 days under a 450 W lamp. A v.p.c. examination of the material in both tubes after irradiation showed that the same ratio of isomers, *trans*:*cis* = 1.49:1, had been established.

Preparation of 3,4,4,4-Tetrafluoro-3-(trifluoromethyl)-butyne

The butyne was prepared using Haszeldine's method for the preparation of 3,3,4,4,4-pentafluorobutyne (1).

In two separate experiments **3** was added to a large excess of finely powdered KOH and heated under reflux (1 h). The resultant acetylene (26.2 g, 42%) was purified by trap-to-trap distillation and dried for one day over KOH.

The extrapolated vapor pressure curve gave a boiling point of 23.0° (ΔH_{vap} = 6.28 kcal/mole; Trouton's constant = 21.2 cal/mole deg).

Addition of Difluorocarbene to the Olefins and Acetylenes

Trimethyl(trifluoromethyl)tin did not react with the olefins **1**, **2**, and **3** in the gas phase at 150° (24 h) to produce cyclopropanes.

The gas phase reaction of trimethyl(trifluoromethyl)tin with each of the acetylenes $R_fC{\equiv}CH$ ($R_f = CF_3$, C_2F_5, and *i*-C_3F_7) at 150° (24 h) did produce the expected cyclopropene $R_fC{=}CHCF_2$ (Table IV). The cyclopropenes were condensed in a trap cooled to −78° and characterized by their ^1H, ^{19}F, and i.r. spectra.

Results and Discussion

Stereochemistry of the Addition Reactions

3,3,3-Trifluoro-1-iodopropene (**1**) and 3,3,4,4,4-pentafluoro-1-iodobutene (**2**) were prepared

Can. J. Chem. Downloaded from www.nrcresearchpress.com by 210.87.254.42 on 09/05/12
For personal use only.

Can. J. Chem. Downloaded from www.nrcresearchpress.com by 210.87.254.42 on 09/05/12
For personal use only.

TABLE II

Infrared absorption for olefins, acetylenes, and cyclopropenes*

$CF_3CH{=}CHI$ (*trans*)	3098		1638			1314	1309	1289	1225	1160br	1145br				951
$CF_3CF_2CH{=}CHI$ (*trans*)	3095		1638	1618	1345		1296		1219	1125		1097			942
$(CF_3)_2CFCH{=}CHI$ (*trans*)	3101		1629		1333		1295		1209			1055	993		949
					1329		1251			1186					
							1245								
$(CF_3)_2CFCH{=}CHI$ (*cis*)	3089		1632		1338		1289			1182			1048	991	
					1329		1269			1160					
							1244								
$CF_3C{\equiv}CH$	3329	2162					1261			1180					
							1252								
							1243								
$CF_3CF_2C{\equiv}CH$	3339	2160		1348				1237		1205	1150				
$(CF_3)_2CFC{\equiv}CH$	3340	2155				1319	1282	1259		1189		1079	990		
										1160					
$CF_3\overset{\frown}{C{=}CH}\overset{\frown}{CF_2}$	3115		1730	1353				1264		1189					
$CF_3CF_2\overset{\frown}{C{=}CH}\overset{\frown}{CF_2}$	3165		1737	1347				1231		1172		1046			
										1126					
$(CF_3)_2CF\overset{\frown}{C{=}CH}\overset{\frown}{CF_2}$	3162		1732	1360	1318			1252		1190		1059	992		
										1125					

*Main bands only in cm^{-1}.

Can. J. Chem. Downloaded from www.nrcresearchpress.com by 210.87.254.42 on 09/05/12
For personal use only.

TABLE III

Summary of chemical shifts*

Structure	H_a	H_b	CF_3	CF_2	CF	CF_2(bridge)
4	−6.57‡	−7.29‡	65.85			
5			61.95			
6	−6.59‡	−7.33‡	85.7	116.1		
7			85.85	114.5		
8	−6.53‡	−7.21‡	77.7		196.3	
9	−6.61‡	−7.24‡	77.6		189.4	
10†	−1.88		55.55			
11†	−2.23		88.7	105.9		
12†	−2.35		90.7		171.8	
13	−7.37		63.3			102.8
14	−7.80		85.85	115.8		104.6
15	−7.95		77.05		128.9	104.9

*With respect to internal $CFCl_3$ except where indicated by†.
‡Middle of appropriate doublet of basic AB quartet.

in good yield by the known ultraviolet (u.v.) induced (presumably free radical) reactions of trifluoroiodomethane and pentafluoroiodoethane with acetylene (1, 2). The ^1H n.m.r. spectrum of **1**, because of peak overlap, shows the presence of the *trans* adduct only (Table III, (**4**)); however, the ^{19}F n.m.r. spectrum does show both isomers **5**. The assignments are based on the now well-established results for substituted trifluoromethyl compounds: $J_{CF_3-H(trans)}$ ~0, $J_{CF_3-H(cis)}$ ~2, and $J_{CF_3-H(gem)}$ ~8 (13–15). The integrated ^{19}F n.m.r. spectrum gives the ratio *trans*:*cis* = 6.7:1.

First-order analysis of the ^1H and ^{19}F n.m.r. spectra of **2** gives the couplings shown in **6** and **7**. The *cis* isomer is again seen only in the ^{19}F n.m.r. spectrum due to overlapping peaks in the ^1H spectrum. Because the H—H couplings could not be established, the assignments are based on the finding that $J_{F-H(gem)}$ in the *cis* isomer > $J_{F-H(gem)}$ in the *trans* isomer (13); this is also seen in **4** and **5**. This assignment gives consistent values for the other couplings, especially the $J_{H-H(trans)}$ of 15 c.p.s. which is the same as in **4**. Confirmation of the predominantly *trans* structure comes from the i.r. spectrum which shows the characteristic band at 942 cm^{-1} (16). The isomer distribution, *trans*:*cis* = 9:1, was determined from the integrated ^{19}F n.m.r. spectrum.

3,4,4,4-Tetrafluoro-3-(trifluoromethyl)-1-iodobutene (**3**) can be prepared by reacting heptafluoroisopropyl iodide with acetylene under u.v. light. The reaction gives an 85% yield of a mixture of the *trans* and *cis* isomers of **3** which

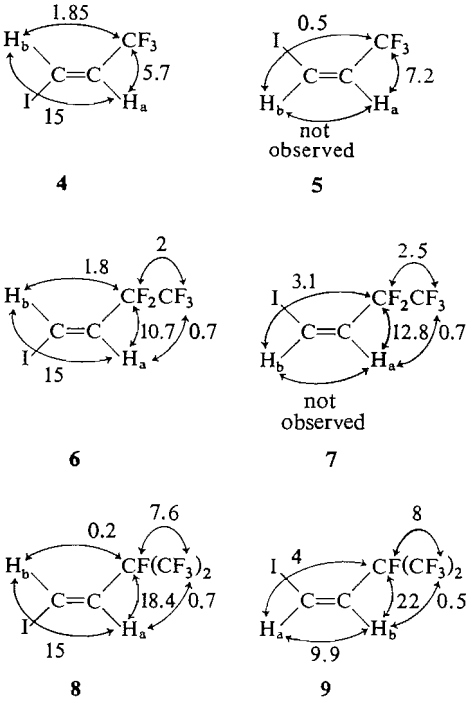

4 **5** **6** **7** **8** **9**

can be separated by v.p.c. Two smaller higher boiling fractions are also obtained which have almost identical i.r. spectra with double bond absorptions at 1648 and 1578 cm^{-1}. These are, presumably, mixtures of isomers of the diadduct, *i*-$C_3F_7CH{=}CH{-}CH{=}CHI$ (1, 2). The assignments for the two isomers of **3** (Table III, (**8**) and (**9**)) are based on the now generally accepted rule that for olefins $J_{H-H(trans)} > J_{H-H(cis)}$. The assigned coupling constants are of the same

TABLE IV

Difluorocarbene reactions with polyfluoroacetylenes

Reactants	Conditions	Products identified	Yield (%)
$CF_3C{\equiv}CH$ (1.119 g, 11.9 mmole) $(CH_3)_3SnCF_3$ (2.634 g, 11.3 mmole)	150° (24 h)	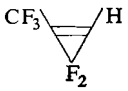	15.2
$C_2F_5C{\equiv}CH$ (0.830 g, 5.75 mmole) $(CH_3)_3SnCF_3$ (1.985 g, 8.52 mmole)	150° (24 h)	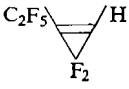	23.6
$(CF_3)_2CFC{\equiv}CH$ (0.683 g, 3.52 mmole) $(CH_3)_3SnCF_3$ (1.142 g, 4.91 mmole)	150° (24 h)	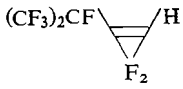	8.25

order of magnitude as those found for *trans* and *cis* i-$C_3F_7CH{=}CHF$ (17). The isomer distribution, *trans*:*cis* = 1.78:1, was determined by v.p.c.

Interconversion of **8** and **9** occurs readily under u.v. irradiation to give an equilibrium mixture of **8** to **9** equal to 1.49:1. The ratio present in the product mixture (**3**) is greater than this, namely, 1.78:1 indicating that the *trans* isomer (**8**) is formed preferentially by *trans* addition as it is in the reactions giving **1** and **2**. As mentioned in the Introduction *cis* addition of trifluoroiodomethane to 3,3,3-trifluoropropyne seems to take place (3).

Although, with respect to the double bond, $J_{F-H(cis)}$ (**4**) > $J_{F-H(trans)}$ (**5**), the reverse is true for the same couplings shown in **6** and **7** and in **8** and **9**. Bothner-By and co-workers (15) found that as fluorine atoms are substituted by hydrogen, $J_{F-H(trans)}$ decreases from +0.03 to −0.89 c.p.s. and $J_{F-H(cis)}$ decreases from −2.22 to −4.32 c.p.s. in going from 3,3,3-trifluoropropene to 3-fluoropropene. It is possible that our results have a similar explanation. However, a complete explanation lies in a determination of the relative populations of the most preferred rotamers and the relative signs and contributions of the couplings of each rotamer to the observed averaged coupling constant. This, however, is beyond the scope of the present investigation.

The dehydrohalogenation of **3** produced a 42% yield of the isopropyl acetylene i-$C_3F_7C{\equiv}CH$ (**12**). The new acetylene has the expected ^1H n.m.r., ^{19}F n.m.r., and i.r. spectra (Tables I–III, (**12**)) and the formula is confirmed by analysis (Table I). The i.r. spectrum shows the strong C≡C stretching frequency at 2155 cm^{-1}.

The spectra of 3,3,4,4,4-pentafluorobutyne have also been recorded for the first time (Tables II and III and Diagrams (**10**–**12**)).

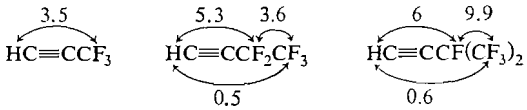

10 **11** **12**

The coupling constant J_{F-H} for 3,3,3-trifluoropropyne is 3.5 c.p.s. (**10**). This same coupling constant increases as the fluorine atoms are replaced by the less electronegative trifluoromethyl groups in **11** and **12**. Similar electronegative effects have been found by Abraham and Cavalli (18).

Difluorocarbene Additions

Difluorocarbene from trimethyl(trifluoromethyl)tin (19) does not add in the gas phase at 150° to any of the olefins **1**, **2**, or **3**. This carbene does add, under the same conditions, to 2-dimethylarsino-1,1,1,4,4,4-hexafluorobutene to give the expected cyclopropane (9) although it does not add to the analogous trimethylsilyl compound. Seyferth and co-workers (20) have added difluorocarbene to a number of olefins using the same tin compound as the carbene source. These reactions, however, were done in solution.

Difluorocarbene from various sources has been added to several acetylenes to produce

Can. J. Chem. Downloaded from www.nrcresearchpress.com by 210.87.254.42 on 09/05/12
For personal use only.

cyclopropenes (9–11, 21, 22). We have added difluorocarbene (from $(CH_3)_3SnCF_3$) in the gas phase at 150° to the acetylenes $R_fC{\equiv}CH$ (R_f = CF_3, C_2F_5, and *i*-C_3F_7) to produce the cyclopropenes $R_fC{=}CHCF_2$ in low yield. Be-

[4] $R_fC{\equiv}CH + (CH_3)_3SnCF_3 \rightarrow$ 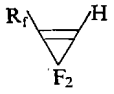 $+ (CH_3)_3SnF$

cause of difficulties in separating these novel compounds from trace impurities, the cyclopropenes have been characterized on the basis of their spectroscopic properties. The i.r. spectra of

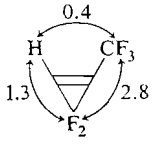

13

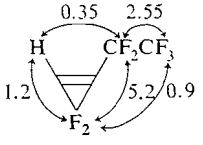

14

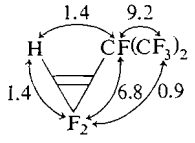

15

all three compounds show the characteristic high frequency double bond absorption, and the spectrum of the trifluoromethyl compound in the CF stretching region is very similar to those of related and fully characterized compounds (9, 11). The best confirmation of their structure comes from their n.m.r. spectra (Table III); the structures **13**, **14** and **15** which can be assigned on a first-order basis, give couplings which are again consistent with those of known cyclopropenes (9–11).

Acknowledgment

The authors wish to thank the National Research Council of Canada for financial assistance.

1. R. N. Haszeldine. J. Chem. Soc. 3037 (1950).
2. R. N. Haszeldine and K. Leedham. J. Chem. Soc. 3483 (1952).
3. K. Leedham and R. N. Haszeldine. J. Chem. Soc. 1634 (1954).
4. B. Bak, L. Hansen, and J. Rastrup-Anderson. J. Chem. Phys. **21**, 1612 (1953).
5. J. F. Helling, S. C. Rennison, and A. Merijan. J. Am. Chem. Soc. **89**, 7140 (1967).
6. B. Bak, D. Christensen, L. Hansen-Wygard, and E. Tannenbaum. J. Chem. Phys. **26**, 241 (1957).
7. C. G. Krespan. J. Am. Chem. Soc. **83**, 3434 (1961).
8. J. Freear and A. E. Tipping. J. Chem. Soc. C, 1096 (1968).
9. W. R. Cullen and W. R. Leeder. Inorg. Chem. **5**, 1004 (1966).
10. W. R. Cullen and M. C. Waldman. Inorg. Nucl. Chem. Letters, **4**, 205 (1968).
11. W. R. Cullen and M. C. Waldman. To be published.
12. W. G. Finnigan and W. P. Norris. J. Org. Chem. **28**, 1139 (1963).
13. W. R. Cullen, D. S. Dawson, and G. E. Styan. Can. J. Chem. **43**, 3392 (1965).
14. D. A. Harbourne and F. G. A. Stone. J. Chem. Soc. A, 1765 (1968).
15. A. A. Bothner-By, S. Castellano, and H. Günther. J. Am. Chem. Soc. **87**, 2439 (1965).
16. L. J. Bellamy. Infrared spectra of complex molecules. 2nd ed. Methuen, London. 1958.
17. N. Boden, J. W. Emsley, J. Feeney, and L. H. Sutcliffe. Proc. Roy. Soc. Ser. A, **282**, 559 (1964).
18. R. J. Abraham and L. Cavalli. J. Mol. Phys. **9**, 67 (1965).
19. H. C. Clark and C. J. Willis. J. Am. Chem. Soc. **82**, 1888 (1960).
20. D. Seyferth, H. Dertouzos, R. Suzuki, and J. Y.-P. Mui. J. Org. Chem. **32**, 2980 (1967).
21. W. Mahler. J. Am. Chem. Soc. **84**, 4600 (1962).
22. P. Anderson, P. Crabbé, A. D. Cross, J. H. Fried, L. H. Knox, J. Murphy, and E. Velarde. J. Am. Chem. Soc. **90**, 3888 (1968).

Can. J. Chem. Downloaded from www.nrcresearchpress.com by 210.87.254.42 on 09/05/12
For personal use only.

Some reactions of 2,4-dimethoxytetrahydropyrans[1]

M. J. BALDWIN[2] AND R. K. BROWN
Department of Chemistry, University of Alberta, Edmonton, Alberta

Received January 13, 1969

Acid-catalyzed elimination of methanol from 2,4-dimethoxytetrahydropyran (**1**) produces 2-methoxy-5,6-dihydro-2*H*-pyran (**3**) rather than the expected olefin 4-methoxy-3,4-dihydro-2*H*-pyran (**2**).

The reaction of 1,3-dibromo-5,5-dimethylhydantoin with **3** in ether – methanol gives a 2:1 mixture of the isomers 3β-bromo-2α,4α-dimethoxytetrahydropyran (**5***a*) and 3α-bromo-2α,4β-dimethoxytetrahydropyran (**5***b*) respectively. A rationale is given to explain the preponderance of **5***a* over **5***b* and the highly selective attack of the bromine of the hydantoin and the methanol on C-3 and C-4 respectively of the double bond of **3**. Reduction of **5***ab* with zinc in ethanol provides only compound **3**.

The room temperature reaction of **1** in a mixture of water and 1,2-dimethoxyethane containing Amberlite IR-120, produces 2-hydroxy-4-methoxytetrahydropyran (**6**) as an equilibrium mixture of *cis* and *trans* isomers in the ratio 1:1. This gave a value of 0.9 kcal/mole for the anomeric effect in **6**. Pyrolysis of the derivative, 2-acetoxy-4-methoxytetrahydropyran failed to produce the olefin **2** and resulted only in extensive decomposition.

Canadian Journal of Chemistry, 47, 3099 (1969)

Can. J. Chem. Downloaded from www.nrcresearchpress.com by 84.22.46.98 on 09/08/12
For personal use only.

Introduction

A recent communication from this laboratory described the preparation of *cis*- and *trans*-2,4-dimethoxytetrahydropyran (1). Since then, we have explored the utility of these isomers as intermediates for the preparation of 3-alkyl (or aryl) thio-2,4-dimethoxytetrahydropyrans. Although in our hands the 2,4-dimethoxytetrahydropyrans could not be converted to 3-alkyl (or aryl) thio-2,4-dimethoxytetrahydropyrans, a number of interesting reactions and properties of the dimethoxy compounds was discovered. This paper describes the results of these findings.

Results and Discussion

Since it has been shown that 3,4-dihydro-2*H*-pyran reacts with ethanesulfenyl chloride and then with methanol to produce 3-ethylthio-2-methoxytetrahydropyran (2, 3), it is quite possible that 4-methoxy-3,4-dihydro-2*H*-pyran (**2**, Scheme 1) might react in the same manner to provide the 3 - alkylthio - 2,4 - dimethoxytetrahydropyran. Accordingly, attempts were made to convert 2,4-dimethoxytetrahydropyran, (**1**), into **2**. This appeared to be feasible since both 2-*n*-butoxy-4-methyltetrahydropyran (4) and the 2-ethoxy homologue (5) have been successfully converted to 4-methyl-3,4-dihydro-2*H*-pyran by treatment with phosphorus pentoxide and *p*-toluenesulfonic acid respectively.

A *cis–trans* mixture of 2,4-dimethoxytetrahydropyran (**1**) (1) was heated at 180° with a catalytic amount of phosphorus pentoxide (4). Only extensive decomposition occurred. At a lower temperature (130° for 1.5 h), only unchanged **1** was obtained in an 88% yield (by distillation). When **1** was heated at 150° with a catalytic amount of *p*-toluenesulfonic acid (5), only 2-methoxy-5,6-dihydro-2*H*-pyran (**3**, Scheme 1) was obtained in an 86% yield. This product was identical in all respects with an authentic sample (6).

The formation of **3** is somewhat surprising since of the two methoxy groups in **1**, that at the anomeric carbon (C-2) is undoubtedly the more readily removed by acid catalysts because it is part of an acetal structure. It is quite likely that compound **3** was formed by a route such as the reverse of eq. *a*, Scheme 2 in the previous report (1).

A second route to 4-methoxy-3,4-dihydro-2*H*-pyran (**2**) was attempted, based upon the knowledge that reductive removal of halogen and an alkoxy group from a β-haloether leads to the formation of an olefin (7). The necessary intermediate, 3 - bromo - 2,4 - dimethoxytetrahydropyran was prepared by the reaction of 1,3-dibromo-5,5-dimethylhydantoin with 2-methoxy-5,6-dihydro-2*H*-pyran (**3**) in the solvent ether – methanol, a technique for bromomethoxylation of olefins employed by van de Sande and Kopecky (8). This route provided in a

[1]Taken from the Thesis of M. J. Baldwin submitted to the Faculty of Graduate Studies as part of the requirements for the Ph.D. degree.

[2]Present address: The Dow Chemical Company, Midland, Michigan 48640, U.S.A.

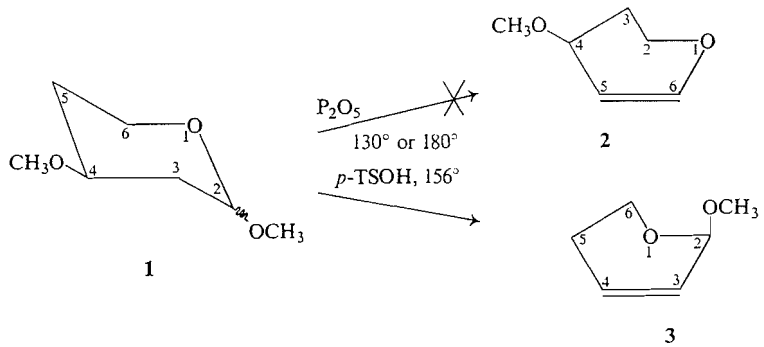

(p-TSOH = p-$CH_3C_6H_4SO_3H$)

SCHEME 1

72% yield an isomeric mixture which was composed essentially of the two compounds, 3β-bromo - 2α,4α - dimethoxytetrahydropyran (**5***a* in Scheme 2) and 3α-bromo-2α,4β-dimethoxytetrahydropyran (**5***b*), in the proportion 2:1 respectively.

That the 2:1 mixture of **5***a* and **5***b* did not arise from an equilibration process stemming from acid catalyzed isomerization of the acetal linkage during the bromomethoxylation reaction, is strongly supported by the finding (9) that 2α-ethoxy - 3α,4β - dibromotetrahydropyran and 2α - ethoxy - 3β,4α - dibromotetrahydropyran, heated separately for 12 h in refluxing absolute ethanol containing some p-toluenesulfonic acid, failed to show evidence of isomerization. It is well-known that electron-withdrawing groups attached to the carbon adjacent to the anomeric center of an acetal, strongly retard hydrolysis of the acetal. Since both **5***a* and **5***b* are closely similar to the 2-ethoxy-3,4-dibromotetrahydropyrans both in structure and nature of the substituents, it can be concluded that under the low temperature conditions of bromomethoxylation (−50°), and during the short time required for the reaction, no significant isomerization would have occurred.

The structures and preferred conformations of the isomers **5***a* and **5***b* were determined by the following methods. Catalytic hydrogenation of this mixture, with palladium, gave a 2:1 mixture of *cis*- and *trans*-2,4-dimethoxytetrahydropyran whose nuclear magnetic resonance (n.m.r.) spectrum, refractive index, and infrared (i.r.) spectrum were identical to those of an authentic 2:1 mixture of these compounds (1). Thus, bromomethoxylation of **3** has occurred with highly selective attack of the methanol and bromine on C-4 and C-3 respectively of the double bond in **3**. The 100 MHz n.m.r. spectrum of the isomeric mixture (**5***a* and **5***b*) in $CDCl_3$ showed two doublets in the anomeric proton region, at τ 5.21 ($J_{2,3}$ = 2.6 Hz) and at τ 5.62 $J_{2,3}$ = 7.5 Hz). The magnitudes of the couplings permit the assignment of the former signal (τ 5.21) to the C-2 proton in a structure in which the C-3 bromine and C-2 methoxy groups are either *cis* to each other (axial–equatorial) or *trans* diaxial, while the latter signal (at τ 5.62) can be assigned to the C-2 proton of a structure in which these two groups are *trans* diequatorial (10).

Experience has shown that bromomethoxylation of olefins occurs such that the bromine and methoxy groups attack the double bond *trans* to each other (11). As well, in the absence of strong 1,3-diaxial interaction, the anomeric effect (12) favors that conformer in the 2-alkoxytetrahydropyrans in which the alkoxy group is axial. On the basis of these two observations and the information given above, a definite structural and preferred conformational assignment of **5***a* and **5***b* can be made. These are shown in Scheme 2.

The following rationale is given to explain both the 2:1 predominance of isomer **5***a* in which the C-3 bromine and C-2 methoxy groups are *trans* to each other, and the highly selective attack of the bromine atom on C-3 of compound **3**. Because of the anomeric effect (12), the preferred conformation of compound **3** is no doubt that in which the anomeric methoxy group is *quasi* axial (9). Accordingly, attack by the bulky

Can. J. Chem. Downloaded from www.nrcresearchpress.com by 84.22.46.98 on 09/08/12
For personal use only.

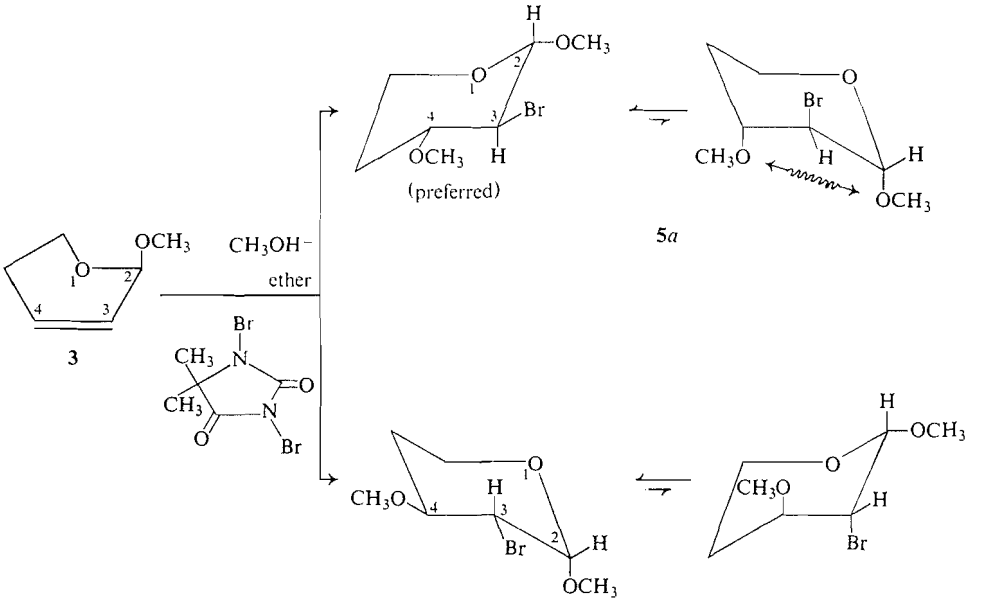

SCHEME 2

1,3-dibromo-5,5-dimethylhydantoin then must be preferably by a route *trans* to the C-2 methoxy group of **3** to avoid its bulk steric opposition (route (*a*), Scheme 3). However, the formation of a substantial amount of isomer **5***b* in which the C-3 bromine is *cis* to the C-2 methoxy group, clearly shows that the double bond is reasonably accessible from the side on which the C-2 methoxy group is located. This could occur by way of the alternative conformer of **3** in which the C-2 methoxy group is *quasi* equatorial (route (*b*), Scheme 3), since in such a position it would offer less steric resistance. However, previous work (9) has indicated that compound **3** exists to the extent of 80% in the conformation in which the anomeric methoxy group is *quasi* axial. In view of this, and the fact that there is no hindrance to approach by the brominating agent via route (*a*) *trans* to the anomeric methoxy group, one should expect an even greater proportion of **5***a* to **5***b* than 2:1. It appears then that there is some other factor which promotes attack by the *N*-bromohydantoin from the same side as the *quasi* axial anomeric methoxy group. Our recent work (9), concerning the preferred attack of bromine on the C-3 position of compound **3** and also *cis* to the C-2 methoxy group, has suggested the possibility that the brominating agent could transfer the species $Br^{\oplus}$ to the double bond by association of the bromine with the anomeric methoxy group's oxygen atom. In the present case, the extent to which such association (route (*c*), Scheme 3) is involved in the bromination reaction would depend upon the ability of the oxygen atom to compete for the $Br^{\oplus}$ with the resonance stabilized hydantoin anion which liberates the $Br^{\oplus}$. Such a directive effect of the anomeric methoxy group, possibly assisted to some extent by a similar association with the ring oxygen when the *quasi* equatorial conformer is attacked, might well play a part in this reaction and thus account at least in part for the 33% proportion of isomer **5***b*.

Both the above mentioned directions of attack on the double bond of **3** by the brominating agent would lead to the transient formation of the 3-membered ring bromonium ion (Scheme 3), which is then attacked by the methanol from the side *trans* to the bromine atom (13, 14). The factors which determine the direction of opening of such 3-membered halonium rings have been discussed previously (13, 14). It is clear that the reaction of the *trans* bromonium ion (obtained by route (*a*)) with methanol should (*and does*)

Can. J. Chem. Downloaded from www.nrcresearchpress.com by 84.22.46.98 on 09/08/12
For personal use only.

Can. J. Chem. Downloaded from www.nrcresearchpress.com by 84.22.46.98 on 09/08/12
For personal use only.

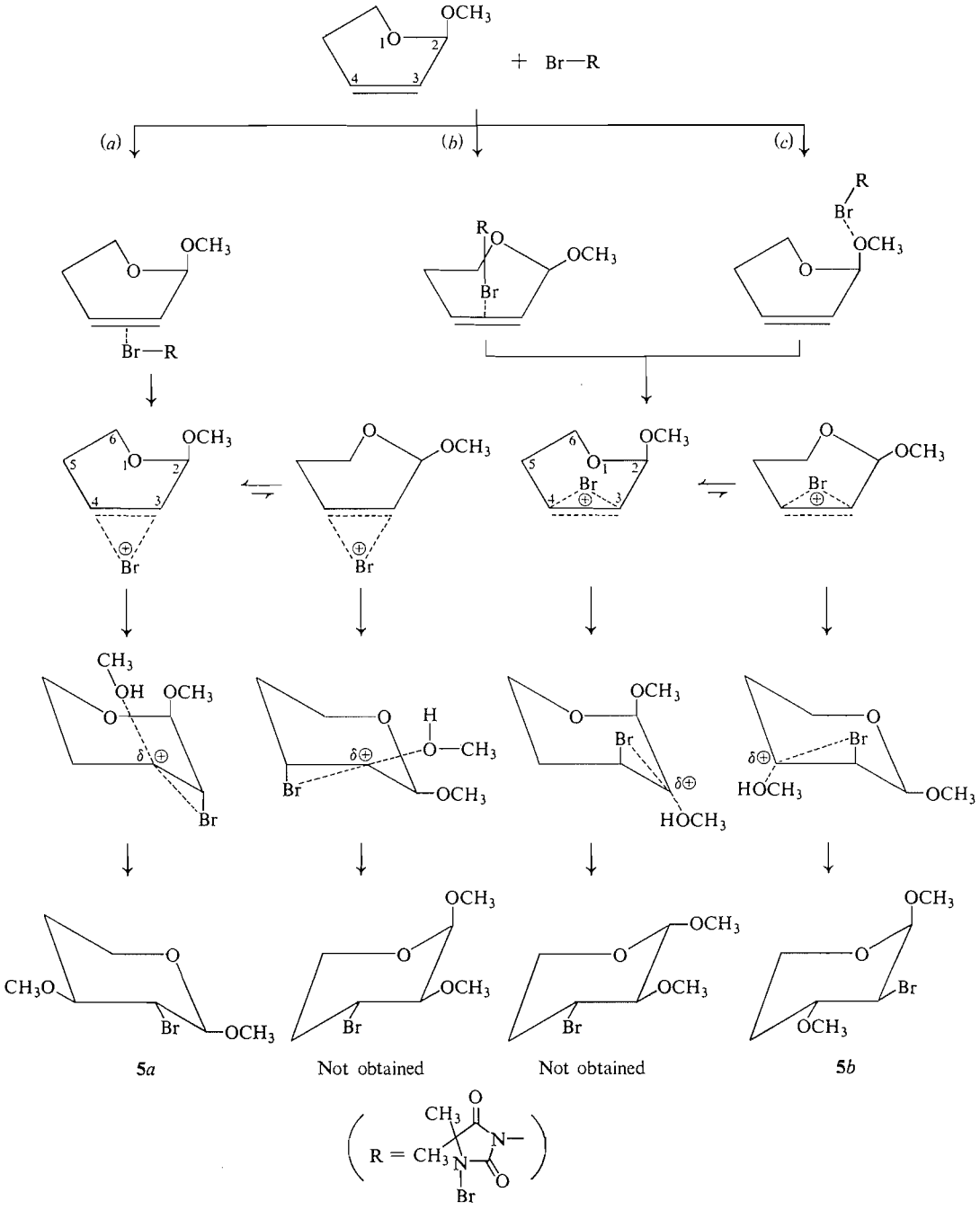

SCHEME 3

Can. J. Chem. Downloaded from www.nrcresearchpress.com by 84.22.46.98 on 09/08/12
For personal use only.

occur preferentially at C-4, since by this path, the bulk steric and the polar repulsion of the C-2 methoxy group is minimal. As well, C-4 — Br bond breaking to form an incipient carbonium ion at C-4 is less inhibited by the electron-withdrawing effect of the geminal dioxy group on C-2, than is carbonium ion formation at C-3 (9, 15). Attack at C-4 would also permit the opening of the 3-membered ring so that the substituents at C-3 and C-4 are *trans* diaxial, with the tetrahydropyran ring in the favored chair form (16). For this same type of favored ring opening to occur by attack of methanol at C-3, a conformational change in the bromonium ion structure must occur in opposition to the anomeric effect.

With respect to the *cis* bromonium ion obtainable via route (*b*) and/or (*c*) (Scheme 3), the experimental evidence shows that attack by methanol is essentially at C-4. For this to occur in agreement with the view that preference is given to the pathway in which the entering and "leaving" groups of the 3-membered ring are *trans* diaxial and the 6-membered ring is in the chair form (16), a conformational change must also take place in the bromonium ion structure so that the C-2 methoxy group is *quasi* equatorial. This must occur in opposition to the anomeric effect and hence such a reaction should be retarded. It is not sufficient to say that a reaction involving the less favored conformation would occur because the alternative route (attack of methanol at C-3, with attendant *trans* diaxial opening and maintenance of chair form) would have all three substituents axially disposed, hence resulting in sufficient 1,3-diaxial repulsion to prevent this alternative route, since similar 1,3-diaxial repulsion of all three substituents was not prohibitive in route (*a*). A factor which may be very important in promoting C-4 — Br bond breaking and successful attack by the methanol at C-4 is the electronic effect of the C-2 geminal dioxy group, which would retard incipient carbonium ion formation less at C-4 than at C-3. This factor is present in both the *trans* (route (*a*)) and the *cis* (route (*b*), (*c*)) species and hence may be the dominant factor which determines that **5***a* and **5***b* be formed.

Separation of the isomers **5***a* and **5***b* was not attempted. When this 2:1 mixture was treated with zinc in refluxing ethanol according to Boord's method (7), there was obtained only unchanged starting material (~50%) and 2-methoxy-5,6-dihydro-2*H*-pyran, (**3**) (in a 44% yield). None of the expected olefin, **2**, was detected.

A final attempt to synthesize 4-methoxy-3,4-dihydro-2*H*-pyran (**2**) was made using the method of ester pyrolysis to produce olefins. The advantage of such a method is that it provides a product free from isomers (17). The pyrolysis of carbonate esters (18) has the added advantage that they decompose at lower temperatures than do the acetate esters, and produce the innocuous products carbon dioxide and an alcohol rather than acetic acid.

For the preparation of such esters, the compound 2 - hydroxy - 4 - methoxytetrahydropyran (**6**) was required. This was readily made in a 74% yield by treatment of a solution of 2,4-dimethoxytetrahydropyran (**1**) in the mixed solvent, water, and 1,2-dimethoxyethane (DME), with Amberlite IR-120 (Scheme 4). This distillable material was found to be a 1:1 equilibrium mixture of the *cis* and *trans* isomers as shown by the 100 MHz n.m.r. spectrum in D_2O. The signals for the anomeric protons were at τ 4.80 (triplet, $J_{2,3a} = J_{2,3e} = 3.7$ Hz) and at τ 5.28 (quartet, $J_{2,3a} = 7.5$ Hz, $J_{2,3e} = 2.0$ Hz).

It has been shown that in the compounds *cis*- and *trans*-2,4-dimethoxytetrahydropyran, the C-4 methoxy group prefers to adopt the equatorial position (1). Accordingly, the *cis*- and *trans*-2-hydroxy - 4 - methoxytetrahydropyrans most likely exhibit the same preference in conformation. On this basis, the magnitudes of the couplings stated above permit the indentification of the *cis* and *trans* isomers. These isomers, **6**, and their preferred conformations are shown in Scheme 4. From the integrated area of the anomeric proton signals we know that the ratio of *cis*:*trans* is 1:1, and since this is an acid catalyzed equilibrium mixture, it is clear that in D_2O the free energy difference between the two isomers is ~0 kcal/mole. Inspection of the preferred conformers of *cis*- and *trans*-2-hydroxy-4-methoxytetrahydropyran (Scheme 4) suggests that the *cis* isomer, possessing an equatorial hydroxyl group at C-2, should be preferred over the *trans* isomer with the axial hydroxyl group at C-2 by ~0.9 kcal/mole as a result of the interaction of the axial hydroxyl group in the latter isomer with the two *syn*- axial hydrogen atoms at C-4 and C-6 (19). The equilibrium composition of 1:1 for

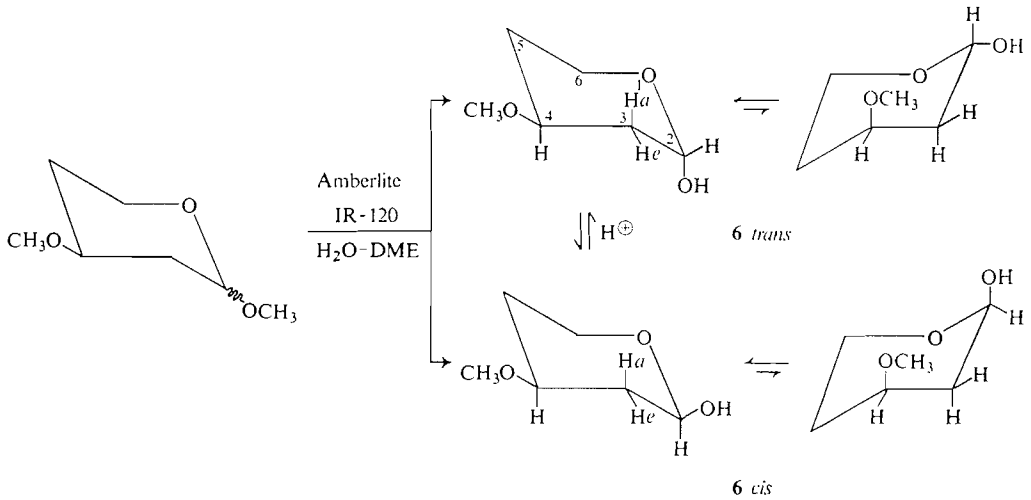

SCHEME 4

the two isomers shows that the magnitude of the anomeric effect present in 2-hydroxy-4-methoxytetrahydropyran in D_2O must then be ~0.9 kcal/mole. The anomeric effect for the compounds *cis*- and *trans* - 2,4 - dimethoxytetrahydropyran, on the basis of their spectra in $CDCl_3$, has been calculated to be ~1.4 kcal/mole (1). The smaller value (0.9 kcal/mole) observed for 2 - hydroxy - 4 - methoxytetrahydropyran is not surprising since it is known that the anomeric effect decreases as the solvent becomes more polar (19, 20).

Treatment of the isomeric mixture of **6** with acetic anhydride in pyridine provided a 61% yield of a mixture of *cis*- and *trans*-2-acetoxy-4-methoxytetrahydropyran in the expected 1:1 ratio, as shown by the 60 MHz n.m.r. spectrum in $CDCl_3$. The magnitude of the couplings agrees with the preferred conformation in which the C-4 methoxy group is equatorial. The signals at τ 3.88 (triplet, $J_{2,3a} = J_{2,3e} = 3.0$ Hz) and at τ 4.34 (quartet, $J_{2,3a} = 7.5$ Hz, $J_{2,3e} = 3.0$ Hz were assigned to the anomeric protons of the *trans* and *cis* isomers respectively.

Room temperature treatment of the 1:1 mixture of 2-acetoxy-4-methoxytetrahydropyran in glacial acetic acid, with a catalytic amount of *p*-toluenesulfonic acid, in an attempt to achieve equilibrium, as had been done by Anderson and Sepp (21) with 2-acetoxy-4-methyltetrahydropyran, in order to determine the influence of the acetoxy group in determining the magnitude of the anomeric effect, was unsuccessful. Within 1 h the solution had darkened, and an n.m.r. analysis of the crude reaction product in $CDCl_3$ showed complete absence of the signals at τ 3.88 and τ 4.34 due to the anomeric protons of the two isomers. Apparently, a simple anomerization had not occurred. The nature of this change was not investigated further.

Pyrolysis of 2-acetoxy-4-methoxytetrahydropyran at either 180° or 290° gave only extensive decomposition. No evidence was found for the formation of either 4-methoxy-3,4-dihydro-2*H*-pyran (**2**) or its isomer 2-methoxy-5,6-dihydro-2*H*-pyran (**3**).

Attempts to prepare the carbonate ester of **6** by treatment with methyl chloroformate in pyridine (18) gave only unchanged **6** in high yield.

Experimental

All boiling points and melting points are uncorrected.

Infrared spectra were recorded on Perkin–Elmer instruments, models 21 and 421.

The n.m.r. spectra were obtained with a Varian Associates model A-60 (60 MHz) spectrometer or a Varian Associates HA-100 (100 MHz) spectrometer. Unless otherwise stated, the n.m.r. spectra were obtained from samples dissolved in $CDCl_3$. Tetramethylsilane was used as internal reference.

Solvents were removed by a rotary evaporator under reduced pressure unless otherwise stated.

Elemental analyses and molecular weight determinations were carried out by Mrs. Darlene Mahlow of the Chemistry Department of the University of Alberta, Edmonton, Alberta.

Can. J. Chem. Downloaded from www.nrcresearchpress.com by 84.22.46.98 on 09/08/12
For personal use only.

Can. J. Chem. Downloaded from www.nrcresearchpress.com by 84.22.46.98 on 09/08/12
For personal use only.

2-Methoxy-5,6-dihydro-2H-pyran (3)

It was prepared by a modification of the procedure of Woods and Sanders (6). To a stirred solution of sodium methoxide (29.7 g, 0.55 mole) in 300 ml of anhydrous dimethylsulfoxide was added dropwise 97 g (0.5 mole) of 3-bromo-2-methoxytetrahydropyran (15). An exothermic reaction ensued and the rate of addition was controlled so that the reaction temperature did not exceed 60°. When the addition was completed, the mixture was stirred for a further 15 min, and then subjected to fractional distillation under reduced pressure. All material in the boiling range 62° at 700 mm to 90° at 23 mm was collected in a dry ice–acetone cooled receiver. This material was redistilled under reduced pressure in a Nestor–Faust spinning band column and afforded 44 g (77%) of 2-methoxy-5,6-dihydro-2*H*-pyran, b.p. 66° at 67 mm, n_D^{23} 1.4430 (lit. b.p., 136–138° at 700 mm, n_D^{25} 1.4425 (6)).

2,4-Dimethoxytetrahydropyran (1)

It was prepared according to published directions (1).

Attempted Acid Catalyzed Removal of Methanol from 1 to Produce 4-Methoxy-3,4-dihydro-2H-pyran (2)

The published procedure (5) provided no detailed directions. Accordingly, those employed here are described below. A solution of 100 mg of *p*-toluenesulfonic acid in 20 g (0.137 mole) of 2,4-dimethoxytetrahydropyran (1) was heated to 150° for 2 h. Distillation of the reaction mixture under reduced pressure afforded 13.5 g (86%) of 2-methoxy-5,6-dihydro-2*H*-pyran, boiling at 69° at 70 mm. This was identical to authentic material (6) as shown by its i.r. and n.m.r. spectra.

3-Bromo-2,4-dimethoxytetrahydropyran (5)

1,3-Dibromo-5,5-dimethylhydantoin (7.0 g, 0.025 mole) (Matheson, Coleman and Bell) was added in small portions to a cold (−50°) stirred solution of 2-methoxy-5,6-dihydro-2*H*-pyran (5.7 g, 0.05 mole) in a mixture of 10 ml of dry ether and 10 ml of dry methanol. When the addition was completed, the reaction mixture was allowed to warm to room temperature and then poured into ice-cold, saturated sodium bicarbonate solution. The resulting mixture was extracted with ether, and the ether extract washed with saturated aqueous sodium bisulfite solution and then with saturated aqueous sodium bicarbonate solution. The dried ($MgSO_4$) ether solution was separated from the drying agent and freed from ether. The residual oil was distilled under vacuum and provided 8.0 g (72%) of 3-bromo-2,4-dimethoxytetrahydropyran, b.p., 63° at 0.05 mm, n_D^{22} 1.4832.

Anal. Calcd. for $C_7H_{13}BrO_3$ (mol. wt. 225): C, 37.36; H, 5.82; Br, 35.50. Found (mol. wt. (mass spectrum) 225): C, 37.35; H, 5.77; Br, 35.78.

The n.m.r. spectrum was consistent with the structure. The significant details of the n.m.r. spectrum are given in the Discussion.

To 3-bromo-2,4-dimethoxytetrahydropyran (5.2 g, 0.023 mole) in 50 ml of anhydrous methanol containing 1.7 g (0.03 mole) of sodium methoxide, was added 500 mg of 5% palladium on charcoal. The resulting mixture was shaken for 24 h with hydrogen at 55 p.s.i. in a Parr hydrogenator. The solids were then separated by filtration and the solvent removed from the filtrate. An ether solution of the residual paste was washed with water, dried ($MgSO_4$), and freed from solvent by fractional distillation. The product (2.2 g, 67%) was 2,4-dimethoxytetrahydropyran whose refractive index, n.m.r., and i.r. spectra were identical with those of an authentic sample (1). The n.m.r. spectrum showed it to be a mixture of *cis* and *trans* isomers in the ratio 2:1 (integrated areas of the anomeric proton signals).

2-Hydroxy-4-methoxytetrahydropyran (6)

A solution of 2,4-dimethoxytetrahydropyran (1) (7 g, 0.454 mole) in 75 ml of water containing 25 ml of DME and 1.5 g of Amberlite IR-120 ion exchange resin, was stirred at room temperature for 24 h. The solution was then filtered and the filtrate freed from solvents. Toluene (10 ml) was added towards the end of the solvent removal to effect complete elimination of water by azeotropic distillation. Fractional distillation of the residual oil under reduced pressure gave 4.7 g (74%) of 2-hydroxy-4-methoxytetrahydropyran as a (1:1) mixture of *cis* and *trans* isomers, b.p., 65° at 0.1 mm; n_D^{23} 1.4573.

Anal. Calcd. for $C_6H_{12}O_3$: C, 54.53; H, 9.15. Found: C, 54.61; H, 9.37.

The i.r. absorption spectrum in CCl_4 showed a broad absorption band at 3400 cm^{-1} (OH). The n.m.r. spectrum was consistent with the assigned structure and the analysis of its significant features is described in the Discussion.

2-Acetoxy-4-methoxytetrahydropyran

A solution of 2-hydroxy-4-methoxytetrahydropyran (8 g, 0.06 mole) and acetic anhydride (10.2 g, 0.1 mole) in 50 ml of dried (KOH) pyridine was heated under reflux for 15 min. The cooled reaction mixture was diluted with 125 ml of water and then treated with solid sodium bicarbonate until evolution of carbon dioxide ceased. An ether extract (3X) was washed successively with ice-cold 10% hydrochloric acid, with saturated aqueous sodium bicarbonate, and then with water. The dried ($MgSO_4$) ether solution was freed from solvent and the residue distilled under reduced pressure to give 6.4 g (61%) of 2-acetoxy-4-methoxytetrahydropyran. This was a 1:1 mixture of *cis* and *trans* isomers as shown by integration of the anomeric proton signal areas of the n.m.r. spectrum. The salient features of the n.m.r. spectrum are presented in the Discussion. It had b.p., 67° at 0.05 mm; n_D^{22} 1.4447.

Anal. Calcd. for $C_8H_{14}O_4$: C, 55.16; H, 8.10. Found: C, 55.07; H, 7.91.

Acknowledgments

The authors wish to thank the National Research Council of Canada for financial assistance for a part of this work. One of us (M.J.B.) gratefully acknowledges a scholarship from Canadian Industries Limited.

The assistance of Mr. Glen Bigham and Mr. Robert Swindlehurst in obtaining the n.m.r. and i.r. spectra is gratefully acknowledged.

1. F. SWEET and R. K. BROWN. Can. J. Chem. **46**, 1543 (1968).
2. M. J. BALDWIN and R. K. BROWN. Can. J. Chem. **45**, 1195 (1967).

3. M. J. BALDWIN and R. K. BROWN. Can. J. Chem. **46**, 1093 (1968).
4. W. E. PARHAM and H. E. HOLMQUIST. J. Am. Chem. Soc. **73**, 913 (1951).
5. M. JULIA and B. JACQUET. Bull. Soc. Chim. France, 1983 (1963).
6. G. F. WOODS and H. SANDERS. J. Am. Chem. Soc. **68**, 2484 (1946).
7. H. B. DYKSTRA, J. F. LEWIS, and C. E. BOORD. J. Am. Chem. Soc. **52**, 3396 (1930).
8. J. H. VAN DE SANDE and K. R. KOPECKY. Department of Chemistry, University of Alberta, Edmonton, Alberta. Private communication.
9. R. M. SRIVASTAVA, F. SWEET, and R. K. BROWN. Unpublished results.
10. R. U. LEMIEUX, R. K. KULLNIG, H. J. BERNSTEIN, and W. S. SCHNEIDER. J. Am. Chem. Soc. **80**, 6090 (1958).
11. M. D. JOHNSON. *In* Bromine and its compounds. *Edited by* Z. E. Jolles. Academic Press, Inc., New York. 1966. p. 256.
12. E. L. ELIEL, N. L. ALLINGER, S. J. ANGYAL, and G. A. MORRISON. Conformational analysis. John Wiley and Sons, Inc., New York. 1965. p. 375–377.
13. E. J. LANGSTAFF, E. HAMANAKA, G. A. NEVILLE, and R. Y. MOIR. Can. J. Chem. **45**, 1907 (1967).
14. R. A. B. BANNARD, A. A. CASSELMAN, and L. R. HAWKINS. Can. J. Chem. **43**, 2398 (1965).
15. F. SWEET and R. K. BROWN. Can. J. Chem. **46**, 707 (1968).
16. S. J. ANGYAL. Chem. Ind. London, 1230 (1954).
17. R. B. WAGNER and H. D. ZOOK. Synthetic organic chemistry. John Wiley and Sons, Inc., New York. 1953. p. 41.
18. W. J. BAILEY and R. A. BAYLOUNY. J. Org. Chem. **27**, 3476 (1962).
19. S. J. ANGYAL and D. J. MCHUGH. Chem. Ind. London, 1147 (1956).
20. G. O. PIERSON and O. A. RUNQUIST. J. Org. Chem. **33**, 2572 (1968).
21. C. B. ANDERSON and D. T. SEPP. Chem. Ind. London, 2054 (1964).

Can. J. Chem. Downloaded from www.nrcresearchpress.com by 84.22.46.98 on 09/08/12
For personal use only.

Mechanism of formation of trimethylisoxazole and intermediates upon alkaline hydrolysis of nitroethane

R. W. LOCKHART, K. W. NG, P. E. NOTT, AND A. M. UNRAU
Department of Chemistry, Simon Fraser University, Burnaby 2, British Columbia

Received March 6, 1969

Nitroethane and higher homologous primary nitroalkanes undergo a base-catalyzed condensation yielding the corresponding 2,3,4-trialkyisoxazoles. Basic hydrolysis of nitroethane to acetaldehyde is the key initial step followed by a series of condensation and elimination reactions. Through the use of appropriately ^{14}C-labelled intermediates and acetaldehyde-d_4, a relatively simple mechanism is indicated which will satisfactorily account for all observed intermediates indicated in a summary of the reaction sequence.

1) nitroethane → acetaldehyde + nitrite

2) acetaldehyde + nitroethane → nitroalcohol → nitroolefin

3) nitroolefin + nitroethane → 2,4-dinitro-3-methylpentane → 3-methylpentan-2,4-dioxime → 3,4,5-trimethylisoxazole

Canadian Journal of Chemistry, 47, 3107 (1969)

Can. J. Chem. Downloaded from www.nrcresearchpress.com by 210.87.254.5 on 09/05/12
For personal use only.

Discussion

Primary and secondary nitroparaffins usually dissolve in aqueous or aqueous alcoholic solutions of strong alkali due to the formation of the corresponding salt of the aci-form, e.g.

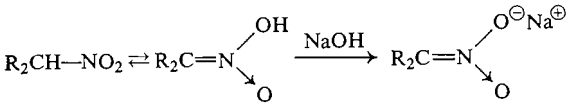

Other reactions of such nitroparaffins with alkali and/or other reagents have been reported (1–6) and most have been considered to involve the aci-forms. One particularly common product of prolonged action of alkali on nitroethane is trimethylisoxazole. By treating nitroethane with a concentrated solution of potassium carbonate, Dunstan *et al.* (2, 3) identified acetonitrile, trimethylisoxazole, and nitrite ions. An aldehyde was also found in the reaction mixture of alcoholic KOH and nitroethane. Nitropropane gave under similar conditions propionitrile, triethylisoxazole, and nitrite ion (2).

In considerably more recent work, Lippincott (1) has shown that using an organic base such as propylamine in aqueous solution in conjunction with nitroethane, facilitates the isolation of crystalline 3-methyl-2,4-pentanedionedioxime, which upon subsequent heating in aqueous medium gives trimethylisoxazole. The 1,3-dioximes have long been known as suitable precursors in the preparation of isoxazoles (7). In the mechanism proposed by Lippincott (1), the aci-nitroethane was considered as the key starting compound.

It has been found that 2-methyl-2-nitro-1,3-propanediol decomposes in alkali to give nitrite in variable yields (8), with the reverse aldol reaction becoming increasingly important as the alkali concentration is increased. Even in the absence of a base, 2-methyl-2-nitro-1,3-propanediol and 2-ethyl-2-nitro-1,3-propanediol were found to generate formaldehyde when heated under reflux in water (ca. 30%). The resulting solution became acidic, whereupon no further formation of formaldehyde and only a trace of nitrite (0.5 %) could be detected in the decomposition mixture. In the absence of a base, the decomposition does not go to completion due to the acidity of the resulting solution, since the nitroparaffin may behave as a pseudo acid,

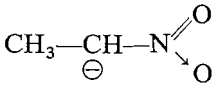

Treatment of nitroethane with saturated potassium carbonate resulted in the formation of a red-colored oil, which accumulated on the surface of the mixture on warming or upon storage at room temperature for several days. It was shown by gas chromatography to be composed of acetonitrile, acetaldoxime, and trimethylisoxazole (Fig. 1). The nitrite ion, up to 35% based on the nitroethane, could be detected in the aqueous solution. When a mixture of

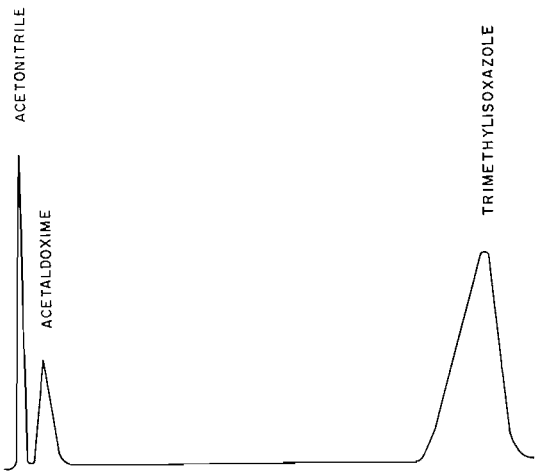

FIG. 1. Gas chromatography of product from nitroethane in potassium carbonate solution, silicone gum rubber column at 100 °C helium flow 30 ml/min.

nitroethane in carbonate solution was distilled prior to the appearance of the red oil, the distillate was shown to contain acetaldehyde which was identified as its 2,4-dinitrophenylhydrazone.

The conversion of primary and secondary nitroparaffins to aldehydes and ketones, respectively, by acidifying the aci-salts was discovered by Nef and has been extensively investigated (9). Oxidation of some nitroparaffins in basic media to the corresponding carbonyl compounds has also been reported (4, 10, 11). However, the isolation of acetaldehyde from a mixture of nitroethane in aqueous potassium carbonate solution has apparently not been reported before. To explain the formation of these reaction products, we formulate the reaction as follows (cf. 12).

(1) Conversion of nitroethane to acetaldehyde and nitrite ion in the following sequence

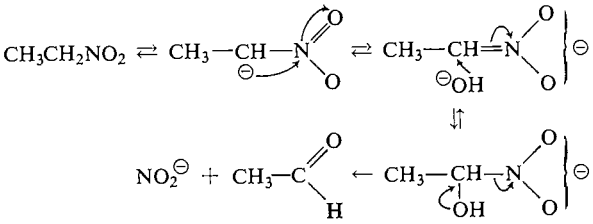

It has been suggested (4, 10) that an oxidative process involving free radical intermediates may be involved in this conversion. We have found little or no change in the rate of formation of the nitrite ion under nitrogen, and hence the hydrolytic mechanism involving the initial carbanion formation is favored.

(2) A condensation of acetaldehyde and nitroethane in the presence of a base, followed by facile elimination of water giving rise to a nitro-olefin.

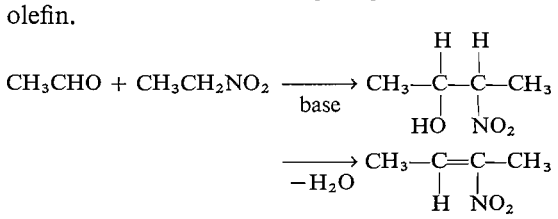

The formation of a nitro-olefin from the corresponding nitro-alcohol is not uncommon. For example, Reasenberg and Smith (13) have isolated 2-nitro-2-butene from a mixture of acetaldehyde and nitroethane in alcoholic solution with a trace of sodium hydroxide. With high base concentrations such as in our experiment, the elimination reaction would be very much enhanced.

(3) Condensation of nitroethane with 2-nitro-2-butene gives rise to 2,4-dinitro-3-methylpentane. Analogous reactions between primary or secondary aliphatic nitro compounds with

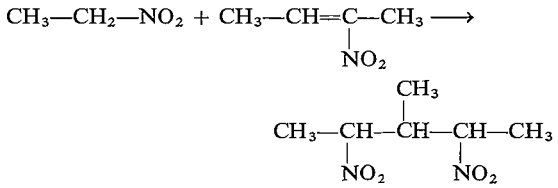

α-nitro-olefins have been described (14, 15) and this forms the basis of the preparation of 1,3-dinitroparaffins, although yields are reported to be variable.

(4) The γ-dinitroparaffin is converted to the corresponding dioxime. Lippincott (1) has shown that the dioxime is an isolable intermediate in the reaction of nitroethane with an

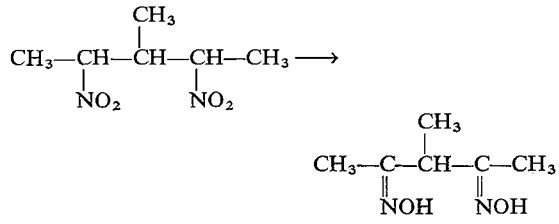

organic base. The exact mechanism of the conversion of the dinitro compound to the

Can. J. Chem. Downloaded from www.nrcresearchpress.com by 210.87.254.5 on 09/05/12
For personal use only.

Can. J. Chem. Downloaded from www.nrcresearchpress.com by 210.87.254.5 on 09/05/12
For personal use only.

dioxime is as yet not clear. The possibility exists that acetaldehyde may serve as a reducing agent since some ^{14}C-labelled acetate was found when acetaldehyde-1-^{14}C was used. More likely, acetate is formed in the competitive alkaline oxidation of the corresponding aldehyde or via oxidation by the nitrite. Alternatively, the dinitroparaffin may be converted to the dioxime via a hydrolytic process either involving the carbanion or hydration of the nitro form. Detailed experimentation would be necessary to illucidate the exact mechanism involved in this particular step.

(5) The 2,4-dioxime, on hydrolysis with or without an acid or base, will give the expected trimethylisoxazole together with hydroxylamine (1).

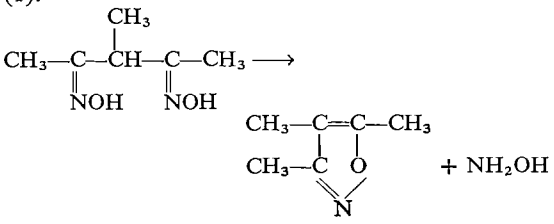

(6) The formation of acetaldoxime and acetonitrile as by-products can be accounted for by the reaction between an aldehyde and hydroxylamine while acetonitrile results from

$$CH_3CHO + NH_2OH \longrightarrow$$

$$CH_3{-}CH{=}NOH \xrightarrow{-H_2O} CH_3CN$$

a dehydration of the oxime. In the preparation of heptaldoxime in the presence of a strong sodium carbonate solution, the corresponding nitrile has been identified (16).

The isolation of the intermediates indicated above has been accomplished either in our laboratory or reported by others and particularly, we have now isolated for the first time the intermediate 1,3-dioxime in the aqueous, basic reaction medium. The identity of the dioxime (3-methyl-acetylacetone-2,4-dioxime) was provided by nuclear magnetic resonance (n.m.r.) and by comparison of physical properties (melting point) with those of the corresponding dioxime provided by direct synthesis. Further proof of identity of the dioxime was its facile transformation in slightly basic aqueous media to form the expected 3,4,5-trimethylisoxazole.

We have obtained supporting evidence for the above mechanism by the reaction of nitroethane with formaldehyde, acetaldehyde-1-^{14}C, formaldehyde-^{14}C, and deuterated (d_4) acetaldehyde. When the reaction was carried out in the presence of formaldehyde, the products were 3,4,5-trimethylisoxazole and 3,5-dimethylisoxazole as predicted from the mechanism. Reactions carried out in the presence of acetaldehyde-1-^{14}C and formaldehyde-^{14}C resulted in radioactivity incorporation of a high percentage into the respective isoxazole. Decomposition of the labelled isoxazole and positive positioning of the radioactive carbon gave further proof for the suggested mechanism. Finally, deuterated (d_4) acetaldehyde was also incorporated in the predicted fashion as shown by n.m.r. The n.m.r. spectrum of 3,4,5-trimethylisoxazole consists of three singlet peaks with τ values of 8.2, 7.95, and 7.8. These peaks have been ascribed to the methyl groups on the 4, 3, and 5 positions, respectively.

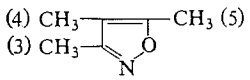

The singlet at τ 7.95 has a maximum intensity while the other two have equivalent intensities but the intensity of each individually is about two-thirds of that at 7.95. Deuterated acetaldehyde was incorporated into trimethyl isoxazole with the D_3C-group appearing in the predicted 4 position since the intensity of the peak at τ 8.2 was reduced to about two-thirds its usual intensity, while the intensity ratio of the other peaks did not change.

Experimental

Analytical Methods

(1) Estimation of Nitrite Ions

The standard colorimetric method of determination of nitrite ion by diazotizing sulfanilic acid followed by coupling with α-naphthylamine was employed (17).

(2) Estimation of Formaldehyde

The colorimetric determination by complex formation with chromotropic acid was employed (18).

(3) Identification of Products by Gas Chromatography

Reaction products were separated by gas chromatography, on a column (5 ft long, 0.25 in. diameter) packed with 60–80 Chromosorb W containing 20% silicone gum rubber SE-30 as liquid phase. The helium flow rate was 30 ml/min. and the temperature adjusted to 100 °C. Each component in a mixture was identified by comparing its retention time with that of a known compound from other sources except for trimethylisoxazole. Trimethylisoxazole was separated from the rest of the product mixture by treating the mixture with a saturated aqueous solution of mercuric chloride. The grayish precipitate was collected,

Can. J. Chem. Downloaded from www.nrcresearchpress.com by 210.87.254.5 on 09/05/12
For personal use only.

washed with cold water, and dried between filter papers. This double salt of trimethylisoxazole was suspended in water and distilled. The distillate was extracted with petroleum ether (30–60°) and the extract dried with sodium sulfate. The residue of the extract, after evaporating off the solvent, was an oil of pyridine-like odor. This oil was shown to be the component having the longest retention time on gas chromatography and gave the expected n.m.r. spectrum with singlets of τ 8.2, 7.95, and 7.8.

Preparative Experiments

(1) Synthesis of 3,4,5-Trimethylisoxazole

To a saturated aqueous solution (100 ml) of potassium carbonate was added with thorough mixing, 3-methylpentane-2,4-dione (12 g) and hydroxylamine hydrochloride (16 g) and the mixture heated at 60–70° for 4 h. The reddish oil that formed was separated and excess saturated aqueous mercuric chloride added to yield the water insoluble mercury complex. The gray precipitate was suspended in water and the mixture distilled. The distillate was extracted with chloroform, the extract dried with sodium carbonate, and evaporation of the solvent left a pale yellow oil. Distillation under reduced pressure gave a clear oil the n.m.r. of which showed the three expected methyl singlets at τ 8.2 (C-4), 7.95 (C-5), and 7.8 (C-3).

Anal. Calcd. for C_6H_9NO: C, 64.86; H, 8.18; N, 12.61. Found: C, 64.86; H, 8.21; N, 12.75.

(2) Synthesis of 3,5-Dimethylisoxazole

This isoxazole was synthesized as described above from pentane-2,4-dione (11 g) and hydroxylamine hydrochloride (16 g) as described for 3,4,5-trimethylisoxazole. The n.m.r. spectrum showed the two expected methyl singlets with τ 7.82 (C-5) and 7.68 (C-3) with a vinylic proton singlet (C-4) at τ 4.15.

Anal. Calcd. for C_5H_7NO: C, 61.84; H, 7.21; N, 14.43. Found: C, 61.83; H, 7.29; N, 14.52.

(3) Synthesis of 3,4,5-Trimethylisoxazole from Nitroethane

Nitroethane (15 ml, 0.2 mole) was introduced to a saturated aqueous solution of potassium carbonate (138 g, 1 mole) and thoroughly mixed. The mixture was either heated gently to about 60–70 °C or left at room temperature for several days until a red oil (ca. 5 ml) separated at the surface. The oil was separated, followed by drying with potassium carbonate and by gas chromatography (Fig. 1). Alternatively, the cooled two phase mixture was extracted with chloroform and the chloroform extract was washed with water and evaporated under vacuum. Addition of an excess of a saturated aqueous solution of mercuric chloride to the residue gave a gray-brown precipitate which was filtered off and washed with cold water. The precipitate was suspended in water (300 ml) and the mixture distilled. The distillate was extracted with chloroform and the chloroform extract was evaporated to leave a pale yellow oil. Distillation of the oil under reduced pressure gave trimethylisoxazole with physical characteristics identical to trimethylisoxazole prepared from 3-methylpentane-2,4-dione.

(4) Isolation of 3-Methylpentane-2,4-dione Dioxime from Nitroethane – K_2CO_3 Reaction Mixtures

Reaction mixtures of nitroethane (15 ml) in saturated aqueous potassium carbonate solution (100 ml) were stored at room temperature for extended time periods (4–7 days). A white, crystalline solid that slowly collected at the interface of the reddish oil (trimethylisoxazole) and the aqueous phase, was collected, washed with ether, and recrystallized from acetone – ether, m.p. 130–131 °C, undepressed upon admixture with dioxime obtained from 3-methylpentane-2,4-dione. The n.m.r. spectrum was also identical to that of the dioxime synthesized from the dione (C-1 and C-5 methyl singlet, τ 8.25, C-3 proton quartet, τ 7.3, 3-methyl doublet, τ 8.9, and the N—O—H proton singlet downfield, τ −0.8 to −1.0).

Anal. Calcd. for $C_6H_{12}N_2O_2$: C, 50.00; H, 8.33; N, 19.44. Found: C, 50.09; H, 8.27; N, 19.32.

(5) Synthesis of Dioxime of 3-Methylpentane-2,4-dione

To an ethanolic solution (20 ml) of the dione (5.0 g) was added a neutral alcoholic solution (20 ml) containing a 2.2 molar equivalent of hydroxylamine. The mixture was gently heated (50–60°) for 30 min after which the volume of the solution was reduced and upon storage at 5 °C, a white, crystalline solid separated. Upon recrystallization from acetone – ether, it had m.p. 131–132 °C. The n.m.r. spectrum showed the expected singlet for the C-1 and C-5 methyl protons, τ 8.2, C-3 proton quartet, τ 7.3, 3-methyl doublet, τ 8.9, and the N—O—H proton singlet downfield, τ −0.7 to −1.0.

Anal. Calcd. for $C_6H_{12}N_2O_2$: C, 50.00; H, 8.33; N, 19.44. Found: C, 50.05; H, 8.30; N, 19.51.

(6) Incorporation of ^{14}C-Formaldehyde

To a solution (200 ml) of potassium carbonate (138 g) was added nitroethane (15 ml) and ^{14}C-formaldehyde (5 ml aqueous solution containing 5.25×10^6 d.p.m.) and the mixture refluxed for 4 h. Steam distillation followed by extraction of the distillate with chloroform, and evaporation, yielded a light yellow oil which upon gas chromatographic analysis showed the presence of trimethylisoxazole (main component) and 3,5-dimethylisoxazole. Collection of the components in the scintillator liquid showed no radioactivity in the trimethylisoxazole while 3,5-dimethylisoxazole was highly active (see Table I). Total activity (5.094×10^6 d.p.m.) in the mixture showed only a 3% loss of added ^{14}C-formaldehyde. Authentic 3,5-dimethylisoxazole was added to the reaction product and the mixture separated on a preparative vapor phase chromatographic (v.p.c.) column (XF-1150 liquid phase, 6 ft × 1/2 in., operating temperature 120 °C). The specific activity of 3,5-dimethylisoxazole was 73.6×10^6 d.p.m./mole.

(7) Degradation of Radioactive 3,5-Dimethylisoxazole

Label positioning was accomplished as follows: aliquots of dimethylisoxazole (DMI) in dry ethylacetate were subjected to ozone treatment. The ozonide was decomposed with water (10 ml) containing 6 *N* H_2SO_4 (3 ml). Nitrogen was passed through the reaction mixture for 20 min after which $KMnO_4$ solution (15 ml, 2 mmoles) was added. The CO_2 evolved was trapped in either barium hydroxide solution or ethanolamine (5 ml). Control experiments with pyruvic acid indicated about 80% decarboxylation under these conditions. Addition of acetate-1-^{14}C showed insignificant degradation (1–3%). The recoveries of $^{14}CO_2$ from C-1 of pyruvate (corresponding to the 4 position of 3,5-dimethylisoxazole) are summarized below in Table I.

Can. J. Chem. Downloaded from www.nrcresearchpress.com by 210.87.254.5 on 09/05/12
For personal use only.

TABLE I

Label positioning of radioactive 3,5-dimethylisoxazole

	d.p.m. of DMI	d.p.m. in CO_2	% recovery
1.	80 300	60 700	75
2.	4 620	3 690	80
3.	8 160	7 150	88
4.	6 010	5 520	91

(8) Incorporation of Acetaldehyde-1-^{14}C into 3,4,5-trimethylisoxazole

To a solution (200 ml) of potassium carbonate (45 g) and nitroethane (15 ml) was added aqueous (5 ml) acetaldehyde-1-^{14}C (11.1×10^6 d.p.m.) and the solution heated (70–80 °C) for 5 h, after which the reaction mixture was stored at room temperature overnight. A v.p.c. analysis of the red oil appearing at the surface indicated, as before, the presence of acetonitrile, acetaldoxime (both minor peaks appearing in that order), and trimethylisoxazole (major peak). Trapping of these components in the scintillator liquid showed minor radioactivity in acetonitrile and acetaldoxime while trimethylisoxazole was highly radioactive. Separate collections of acetonitrile and acetaldoxime were diluted with the cold compound followed by alkaline oxidation to acetate. The resulting acetate was degraded to CO_2 and the methylamine by the Schmidt procedure (19) (see Table II).

TABLE II

Label positioning of radioactive acetonitrile and acetaldoxime

d.p.m. in:	d.p.m. in CO_2	% recovery
Acetonitrile		
1. 75	73	97
2. 85	81	95
3. 105	101	97
Acetaldoxime		
1. 175	170	97
2. 140	135	96
3. 210	190	91

The alkaline reaction was exhaustively extracted with chloroform and the extract evaporated to yield a reddish oil, which upon v.p.c. analysis indicated almost pure 3,4,5-trimethylisoxazole (3.2 g, 9.1×10^6 d.p.m.). Total recovery of radioactivity in trimethylisoxazole was about 90%. The aqueous alkaline solution was acidified with sulfuric acid (8 *N*) and the acid solution extracted exhaustively with ether. Evaporation to a small volume (3 ml) and v.p.c. analysis indicated the presence of acetic acid containing some radioactivity. Glacial acetic acid (1.0 ml) was added and the solution neutralized with sodium carbonate followed by evaporation to dryness. The sodium salt was consequently degraded (in triplicate) to CO_2 and methylamine by the Schmidt procedure (19) (see Table III).

(9) Degradation of Radioactive Trimethylisoxazole

To aliquots of radioactive 3,4,5-trimethylisoxazole dissolved in water saturated ether was added metallic sodium. A typical run would involve about 100 mg of isoxazole (2845 d.p.m.) in 200 ml water saturated ether. Upon completion of refluxing (2 h), 2-butanone (5 ml) was added and the butanone fraction (4.5 ml) recovered by fractional distillation. The total radioactivity recovered was between 200 and 300 d.p.m. The butanone fraction was treated with alkaline hypoiodite, the iodoform which formed being collected and found to be inactive while the sodium propionate contained all the radioactivity. Propionate was decarboxylated to acetate via a Hoffman reaction (ethylamine being oxidized to acetate with permanganate) in the usual manner. All radioactivity remained in acetate. Acetate was degraded by the Schmidt procedure (see Table IV).

TABLE III

Label positioning in radioactive acetate

	d.p.m. in acetate	d.p.m. in CO_2	% recovery
1.	275	260	95
2.	350	340	97
3.	310	195	93

TABLE IV

Label positioning in methylethylketone from trimethylisoxazole

	d.p.m. in original MEK sample	d.p.m. in CO_2 from acetate	% recovery
1.	215	185	86
2.	275	255	93

(10) Incorporation of Acetaldehyde-d_4

To a solution (100 ml) of nitroethane (15 ml) and potassium carbonate (30 g) was added acetaldehyde-d_4 (5 ml) and the solution heated (80 °C) for 4 h followed by storage at room temperature for a further 16 h. The reaction mixture was worked up as described above and the 3,4,5-trimethylisoxazole formed analyzed by n.m.r. spectroscopy. A reduction (ca. 40%) in the intensity of the C-4 methyl singlet (τ, 8.2) was noted.

Acknowledgment

Continued financial support from the National Research Council of Canada is gratefully acknowledged.

1. S. B. LIPPINCOTT. J. Am. Chem. Soc. **62**, 2604 (1940).
2. W. R. DUNSTAN and E. GOULDING. J. Chem. Soc. **77**, 1262 (1900).
3. W. R. DUNSTAN and T. S. DYMOND. J. Chem. Soc. **59**, 410 (1891).
4. H. SHECHTER and R. B. KAPLAN. J. Am. Chem. Soc. **75**, 3980 (1953).
5. W. R. DUNSTAN and T. S. DYMOND. Proc. Chem. Soc. 117 (1888).
6. P. T. SPEAKMAN and W. A. WATERS. J. Chem. Soc. 40 (1955).
7. A. QUILICO. *In* The chemistry of heterocyclic compounds. Vol. VII. *Edited by* R. H. Wiley.

Interscience Publishers, Inc., New York. 1962. Chapter on Isoxazoles and related compounds.
8. A. M. UNRAU. Can. J. Chem. **42**, 1741 (1964).
9. W. E. NOLAND. Chem. Rev. **55**, 137 (1955).
10. G. A. RUSSELL. J. Am. Chem. Soc. **76**, 1595 (1954).
11. H. SHECHTER and F. T. WILLIAMS, JR. J. Org. Chem. **27**, 3699 (1962).
12. H. FEUER and S. MARKOFSKY. J. Org. Chem. **29**, 935 (1964).
13. J. R. REASENBERG and G. B. L. SMITH. J. Am. Chem. Soc. **66**, 993 (1944).
14. A. LAMBERT and H. A. PIGGOTT. J. Chem. Soc. 1489 (1947).
15. H. B. HASS. Ind. Eng. Chem. **35**, 1151 (1943).
16. E. W. BOUSQUET. *In* Organic synthesis. Collective Vol. II. *Edited by* A. H. Blatt. John Wiley and Sons, Inc., New York. 1963. p. 313.
17. A. J. CLEAR and M. ROTH. *In* Treatise on analytical chemistry. Part II. Vol. 5. *Edited by* I. M. Kolthoff, P. J. Elving, and E. B. Sandell. Interscience Publishers, Inc., New York. 1961. p. 303.
18. N. D. CHERONIS and T. S. MA. *In* Organic functional group analysis by micro and semimicro methods. Interscience Publishers, Inc., New York. 1964. p. 504.
19. S. ARONOFF. Techniques of radiobiochemistry. Iowa State College Press, Ames, Iowa. 1956.

Can. J. Chem. Downloaded from www.nrcresearchpress.com by 210.87.254.5 on 09/05/12
For personal use only.

Can. J. Chem. Downloaded from www.nrcresearchpress.com by 210.87.254.105 on 09/05/12
For personal use only.

^{13}C Nuclear magnetic resonance studies. XII. Conformational effects on ^{13}C shieldings in alicyclic oxygenated compounds[1,2]

G. W. BUCHANAN,[3] J. B. STOTHERS, AND SIU-TZYY WU
Department of Chemistry, University of Western Ontario, London, Ontario

Received February 25, 1969

The ^{13}C shieldings of the primary carbinyl carbons in cyclohexylmethanol, its acetate and methyl ether as well as those for the corresponding carbon in their 4-*t*-butyl derivatives have been measured at 15.1 MHz using the 'proton-decoupling' method. Similar data for the 1-methyl-4-*t*-butylcyclohexylcarbinols and their acetates were obtained to examine the influence of the additional methyl substituent. Possible origins of the observed conformational effects on ^{13}C nuclear shieldings are considered. The ^{1}H results for the methylene protons in these carbinyl groups are also presented and discussed. These results, which permit estimations of the conformational free energies ($-\Delta G°$) of the $—CH_2OR$ groupings (R = H, Ac, Me), are presented to illustrate the ^{13}C approach to conformational analysis.

Canadian Journal of Chemistry, 47, 3113 (1969)

Introduction

From the results now available, it is clear that ^{13}C nuclear shieldings are affected by molecular conformation (1–4) and, therefore, these parameters should yield information regarding conformational preferences for a variety of functional groups in a manner similar to that exhibited by the nuclear magnetic resonance data for several other nuclei. This has been demonstrated for the hydroxyl, methoxyl, and acetoxyl groups in cyclohexanes (3) and the fact that axial and equatorial carbon atoms on cyclohexane ring systems experience different shielding influences has been confirmed in the case of the methylcyclohexanes (4). To examine these differences for carbons bearing oxygenated functional groups we have prepared as model compounds, the *cis*- and *trans*-4-*t*-butyl derivatives of cyclohexylmethanol (**1**), its acetate (**2**) and ether (**3**) and of (1-methylcyclohexyl)-methanol (**4**) and the corresponding acetate (**5**) and determined the ^{13}C shielding of the carbinyl carbon ($—CH_2OR$) nucleus in each of these as well as in those of the parent compounds. The shieldings for the methylene protons of these carbinyl groups were also measured. In this paper we present these results and examine their utility for the determination of the conformational free energies of the $—CH_2OR$ groups (R=H, Me, Ac). A preliminary report of this work has already appeared (6).

[1]For Pt. XI see reference 6; for Pt. X see reference 20.
[2]These results were presented in part at the 2nd International nuclear magnetic resonance Symposium, Sao Paulo, Brazil, July, 1968.
[3]Holder of NRCC Studentships 1966–1968. Present address: Dept. of Chemistry, UCLA, Los Angeles, California.

Experimental

Spectra

The natural abundance ^{13}C spectra were obtained at 15.1 MHz on a dual-purpose Varian spectrometer utilizing a NMR Specialties SD-60 spin-decoupler operating at a nominal frequency of 60 MHz. The irradiating frequencies were monitored directly with a Hewlett-Packard 5245L counter. The 'proton-decoupling' technique developed by Paul and Grant (5) was employed for the ^{13}C shielding measurements and the results are reported relative to CS_2.

The proton spectra were recorded with a Varian A60 spectrometer using the usual audio side-band technique to measure the position of the proton absorptions relative to internal TMS to better than 0.5 Hz.

The alcohols were examined in carbon disulfide solution (5 *M*) while the esters and ethers were studied as neat liquids.

Materials

Cyclohexylmethanol, its acetate and methyl ether were prepared by standard methods and their physical constants agreed well with the published data (7). Reduction with lithium aluminum hydride was employed to prepare 1-methylcyclohexylcarbinol from 1-methylcyclohexane carboxylic acid, which was obtained by the reaction of 2-methylcyclohexanol with formic acid (8).

cis- and trans-4-t-Butyl Cyclohexylmethanols (1)

Hydrogenation of *p-t*-butylbenzoic acid to yield a mixture of the isomeric 4-*t*-butylcyclohexane carboxylic acids was done according to the published method (9) except that less catalyst was found necessary (1 g PtO_2 for 37 g acid). After separation by fractional crystallization, each of the acids gave the desired carbinol in 98% yield upon reduction with lithium aluminum hydride.

cis- and trans-4-t-Butylcyclohexylmethyl Acetates (2)

These materials were prepared from the corresponding alcohols by heating with acetic anhydride and sodium

TABLE I

^{13}C and ^{1}H Shieldings for $—CH_2OR$ groups in some 4-*t*-butylcyclohexanols and derivatives

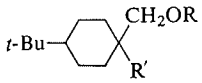

Structures				Shielding data			
				^{13}C		^{1}H	
No.	R	R′	Orientation of CH_2OR	Γ_i	δ_c (p.p.m. from CS_2)	ν	δ (p.p.m. from TMS)
1*	H	H	*cis*	3.97669129	128.38±0.12	210.8	3.51_4
			trans	3.97667212	123.74±0.08	199.4	3.32_7
2	Ac	H	*cis*	3.97669181	127.99±0.05	242.2	4.03_7
			trans	3.97667212	123.26±0.05	228.8	3.81_3
3	Me	H	*cis*	3.97664906	117.99±0.08	197.5	3.29_2
			trans	3.97662844	113.01±0.07	185.3	3.08_9
4*	H	Me	*cis*	3.97667723	124.99±0.15	202.8	3.38_0
			trans	3.97664953	118.25±0.10	189.0	3.15_0
5	Ac	Me	*cis*	3.97667875	124.80±0.07	237.0	3.95_0
			trans	3.97664872	117.48±0.10	223.0	3.71_1

*5 *M* in CS_2.

acetate for 1 h at 120 °C. After dilution with water the acetate was extracted with ether and isolated by distillation.

cis-Acetate: b.p. 94–95/1.5 mm; n_D^{25} 1.4565.

Anal. Calcd. for $C_{13}H_{24}O_2$: C, 73.54; H, 11.39. Found: C, 73.55; H, 11.16.

trans-Acetate: b.p. 79–80/0.2 mm; n_D^{25} 1.4520.

Anal. Calcd. for $C_{13}H_{24}O_2$: C, 73.54; H, 11.39. Found: C, 73.53; H, 11.16.

cis- and trans-4-t-Butylcyclohexylmethyl Methyl Ethers (3)

The cyclohexylmethanols were allowed to react with sodium in ether until hydrogen evolution ceased. Excess methyl iodide was slowly added and the mixture refluxed gently for 2 h. The product was isolated by distillation.

cis-Ether: b.p. 104.6/16 mm., n_D^{25} 1.4520.

Anal. Calcd. for $C_{12}H_{24}O$: C, 78.19; H, 13.13. Found: C, 78.06; H, 13.07.

trans-Ether: b.p. 102.3/16 mm. n_D^{25} 1.4508.

Anal. Calcd. for $C_{12}H_{24}O$: C, 78.19; H, 13.13. Found: C, 77.92; H, 12.89.

cis- and trans-1-Methyl-4-t-butylcyclohexyl Carbinols (4)

The mixture of the isomeric 1-methyl-4-*t*-butylcyclohexanols obtained by the reaction of 4-*t*-butylcyclohexanone with methyl magnesium iodide was treated with zinc chloride and hydrochloric acid to give a mixture of the corresponding cycloalkyl chlorides. Reaction of these chlorides in ether solution with magnesium, followed by carbonation of the resulting Grignard reagent, afforded a mixture of the 1-methyl-4-*t*-butylcyclohexane carboxylic acids in 30% yield. This mixture was reduced with lithium aluminum hydride. The alcohol product was separated by chromatography on alumina to yield a first fraction of *cis*-1-methyl-4-*t*-butylcyclohexyl carbinol, m.p. 76–78°, while later fractions gave the *trans*-isomer, m.p. 73.5–75°.

Anal. Calcd. for $C_{12}H_{24}O$: C, 78.19; H, 13.13.

cis-Isomer; Found: C, 78.10; H, 12.99.

trans-Isomer: Found: C, 78.09; H, 13.20.

cis- and trans-(1-Methyl-4-t-butylcyclohexyl) Methyl Acetates (5)

These materials were prepared on a small scale by reaction of the carbinols with acetic anhydride and sodium acetate in the usual fashion. Their structures were confirmed by infrared and proton spectra. The *cis*-isomer has n_D^{28} = 1.4519, while n_D^{28} = 1.4527 for the *trans*-isomer.

Results and Discussion

The ^{13}C and ^{1}H shielding values for the carbinyl carbons and the protons bonded thereto are collected in Tables I–III. The results for the compounds having essentially fixed conformations because of the 4-*t*-butyl substituent are listed in Table I, the results for the *trans*-isomers, **1–3**, are compared with those for isobutyl alcohol, isobutyl acetate and isobutyl methyl ether in Table II while the data for the conformationally mobile systems appear in Table III. As noted above, the ^{13}C results were obtained by the 'proton-decoupling' method (5) wherein the proton frequency required to obtain an optimum ^{13}C signal is determined as carefully as possible and the ratio of this frequency to that employed to irradiate the ^{13}C nucleus, Γ_i, measured. Having a reference Γ_0 value for a standard substance, the ^{13}C shielding value, δ_c,

Can. J. Chem. Downloaded from www.nrcresearchpress.com by 210.87.254.105 on 09/05/12
For personal use only.

Can. J. Chem. Downloaded from www.nrcresearchpress.com by 210.87.254.105 on 09/05/12
For personal use only.

TABLE II

^{13}C and ^{1}H Shieldings for $—CH_2OR$ groups in iso-butyl alcohol, *trans*-4-*t*-butylcyclohexylmethanol and their derivatives

Compound	Shielding results	
	^{13}C(p.p.m. from CS_2)	^{1}H(p.p.m. from TMS)
iso-Butyl alcohol	123.4	3.30
trans-**1**	123.7	3.33
iso-Butyl methyl ether	112.7	3.07
trans-**3**	113.0	3.09
iso-Butyl acetate	122.4	3.81
trans-**2**	123.3	3.81
neo-Pentyl alcohol	119.5	3.14
trans-**4**	118.3	3.15
neo-Pentyl acetate	118.9	3.73
trans-**5**	117.5	3.72

is computed using the expression (5):

$$\delta_c = 1 - \frac{\Gamma_0}{\Gamma_i}(1 + \delta_H)$$

where δ_H is the shielding difference between the protons of the standard and those of the compound measured on the δ-scale (TMS = 0 p.p.m.). In this case we have used methyl iodide as our standard, $\Gamma_0 = 3.97702300$, and converted the data to the CS_2 scale using the value 213.10 p.p.m. as the shift difference between methyl iodide and CS_2 (10).

From Table I it is clear that the axial carbinyl carbons are significantly shielded relative to the corresponding equatorial nuclei for each pair of *cis–trans* isomers, **1–5**. The differences appear to fall into two groups, 4.8 ± 0.2 p.p.m. for **1–3** and 7.0 ± 0.3 p.p.m. for **4** and **5**, which may be contrasted to the difference of −0.21 ± 0.02 p.p.m. found for the methylene protons bonded to these carbinyl carbons. It is especially interesting that the shifts for the methylene protons in the two orientations change in the direction opposite to that exhibited by the ^{13}C nuclei in that the protons on axial carbinyl carbons are deshielded relative to their equatorial counterparts. Furthermore, the difference in magnitude of the ^{1}H and ^{13}C shifts by a factor of ca. 25 is remarkably similar to the difference in their sensitivities to electron density changes (11, 12). These trends suggest that polarization effects may be principally responsible for the observed changes.

Of the two stable rotamers, **11** and **12**, available to the *cis*-isomers, **1–5**, the former will be much more highly populated because of the destabilizing interaction in **12** between the oxygen atom and the axial ring protons on C-3 and C-5. In **11**, however, one of the methylene

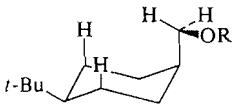

11

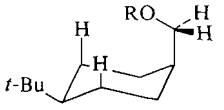

12

protons is within ca. 2 Å of these axial protons and a relatively strong repulsive force will act between these nuclei. The net result will be a perturbation of the local electron clouds which can be expected to reduce their shielding

TABLE III

^{13}C and ^{1}H Shieldings for the $—CH_2OR$ groups in cyclohexylmethanol and derivatives

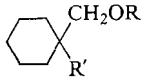

Compound			Shielding data			
			^{13}C		^{1}H	
No.	R	R′	Γ_i	δ_c (p.p.m. from CS_2)	ν	δ (p.p.m. from TMS)
6*	H	H	3.97667384	124.17±0.10	200.0	3.33_3
7	Ac	H	3.97667298	123.48±0.05	229.3	3.82_2
8	Me	H	3.97663029	113.46±0.07	186.1	3.10_2
9*	H	Me	3.97665940	120.64±0.12	194.3	3.23_8
10	Ac	Me	3.97666045	120.33±0.10	229.0	3.81_7

*5 *M* in CS_2.

Can. J. Chem. Downloaded from www.nrcresearchpress.com by 210.87.254.105 on 09/05/12
For personal use only.

relative to that of a proton in a similar chemical environment but lacking this steric perturbation, as in the corresponding *trans*-isomers having equatorial carbinyl groups. It seems reasonable to assume that this dispersion effect at the carbinyl proton will tend to polarize the electrons of the C—H bond such that the electron density at the carbinyl carbon is increased. Consequently this carbon will be shielded relative to that in the *trans*-isomer. Dalling and Grant (4) have presented their measurements of the ^{13}C shieldings in several methylated cyclohexanes and have discussed the observed trends on the basis of steric perturbation of the electron distributions. Grant and Cheney (13) have described a theoretical approach for the estimation of this effect which attributes the changes entirely to polarization. The difference of 3.9 p.p.m. found for the shieldings of isolated axial and equatorial methyl carbons is comparable to the differences observed in the present series. It is interesting that the corresponding change for the methyl protons is ca. 0.1 p.p.m. which is approximately 50% of that found in the present series (Table I) and is consistent with the assumption that rotamer **11** will be more highly populated than **12**. It seems unlikely that the introduction of the 1-methyl group in *cis*-**4** and *cis*-**5** will alter the situation as far as rotamer populations are concerned.

In the *trans*-series, there are two different rotamers, **13** and **14** available to the equatorial carbinyl groups of which **13** should be favored,

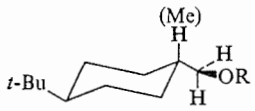

13

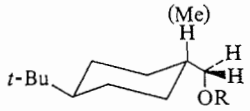

14

both statistically and energetically. In the 1-methyl substituted cases, however, **13** will be destabilized to some degree due to methyl H---O non-bonded interactions. It follows, therefore, that the rotamer populations for the equatorial cases may be different for the two types, **1–3** and **4–5**. Perhaps this is the reason that the ^{13}C shielding difference between the *cis*-pairs **1**, **4** and **2**, **5** is 3.3 ± 0.1 p.p.m. while that between the *trans*-pairs **1**, **4** and **2**, **5** is 5.5 ± 0.2 p.p.m. For alkyl groups it is well established (1, 4, 12) that replacement of a proton with a methyl group tends to deshield the β-carbon by several p.p.m.

i.e. 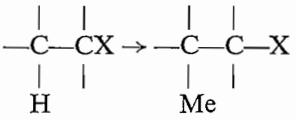

In hydrocarbons with X=C or H this change is ca. 9 p.p.m. Clearly the effect is markedly attenuated with X=O, a trend that was reported previously in the case of carbonyl compounds (14). A recent theoretical interpretation of alkyl substituent effects on ^{13}C shieldings in hydrocarbons failed to predict the β-effect (15) and its origin remains obscure.

Since the distances of closest approach between non-bonded atoms are all appreciably larger in the series of *trans*-isomers, **1–5**, it seems reasonable to propose that the major factor contributing to the shielding differences between axial and equatorial carbinyl nuclei in these systems is a steric perturbation of the local electron distributions in the axial orientation. Support for this conclusion is provided by ^{1}H and ^{13}C shielding data for the carbinyl nuclei in *iso*-butyl alcohol, its acetate and methyl ether and in *neo*-pentyl alcohol and acetate. These results are listed in Table II together with those for the *trans*-isomers, **1–5**. Presumably, rotamer populations will be similar in the acyclic and cyclic systems and it is clear that the shieldings are remarkably similar for each pair of compounds. It follows, therefore, that the different shieldings observed for the *cis*-isomers, **1–5**, are primarily due to steric effects acting on the axial carbinyl groups.

The fact that the shielding differences for the carbinyl carbons in the alcohols are comparable to those exhibited by the ethers and acetates indicates that hydrogen-bonding is not a major factor. Dalling and Grant (4) have already suggested that a basic difference in the electronic structure of axial and equatorial methyls probably exists which precludes precise characterization of the steric effects on their shieldings by direct comparison of the observed values. If this be the case, the same difficulty arises in the present cases. In any event, the effect of medium on ^{13}C shieldings has not been adequately investigated, although there are indications that these can be significant (14, 16). Because of the polar nature of the compounds examined in this study, it appears necessary to investigate medium effects in detail before attempting even a semi-

Can. J. Chem. Downloaded from www.nrcresearchpress.com by 210.87.254.105 on 09/05/12
For personal use only.

quantitative interpretation of the observed trends.

Although a detailed analysis of the trends exhibited by these *cis–trans* isomers cannot be offered, the use of these compounds as model systems to estimate conformational preferences of the —CH_2OR groups merits consideration. For this purpose, we have determined the shieldings of the protons and carbons in the carbinyl groups of these systems in the "mobile" forms (i.e. lacking the 4-*t*-butyl group). These data, listed in Table III, permit one to estimate K_e for the conformational equilibrium, **15** ⇄ **16**, assuming that the data for the *cis*-isomers, **1–5**, are characteristic of the axial forms, **15**,

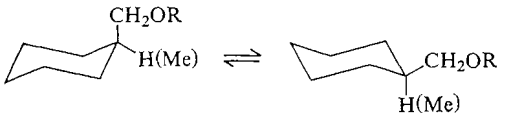

15 **16**

and those for the *trans*-series, **1–5**, for the equatorial conformation, **16**, for the compounds, **6–10** respectively.

Using the expressions

$$K_e = (\delta_{cis} - \delta)/(\delta - \delta_{trans})$$

where δ is the observed shielding for the mobile systems, **6–10**, and $-\Delta G^0 = RT\ln K_e$, values for $-\Delta G^0$, the conformational free energy, for the —CH_2OR groups (R = H, Me, Ac) have been estimated. Both ^{1}H and ^{13}C data were employed to obtain independent assessments. The results are collected in Table IV and the estimated precision of the individual values is indicated. There are rather large discrepancies apparent between the $-\Delta G^0$ values obtained from each set of shielding results, but there is an indication that $-\Delta G^0_{CH_2OAc} > -\Delta G^0_{CH_2OMe} \approx -\Delta G^0_{-CH_2OH}$. In fact, the close agreement between the latter values indicates that hydrogen bonding is a minor factor contributing to these equilibria.

TABLE IV

Conformational free energies ($-\Delta G^0_x$) of —CH_2OR groups (in kcal/mole)

X	Method of estimation	
	^{13}C	^{1}H
—CH_2OH	1.42±0.30*	1.77±0.15*
—CH_2OMe	1.40±0.24	1.65±0.15
—CH_2OAc	1.87±0.35	1.94±0.15
—CH_2OH—Me	0.37±0.07*	0.29±0.10*
—CH_2OAc—Me	0.28±0.05	0.18±0.10

*5 *M* in CS_2.

Perhaps the more reliable data, however, are those obtained for the 1-methyl substituted cases because the shieldings observed for **9** and **10** are mid-way between the absorption positions of the "fixed" systems, **4** and **5**. The experimental error is therefore reduced as indicated in Table IV. In the simpler systems, **6–8**, the —CH_2OR group heavily biases the equilibrium toward the equatorial forms, **16**, and the differences between their shielding values and those for the *trans*-isomers, **1–3**, are small, leading to a proportionately larger error in $-\Delta G^0$. Assuming that the better data are those for the methyl substituted systems, it would appear that the CH_2OH and CH_2OAc groups have comparable $-\Delta G^0$ values. In combination with the value $-\Delta G^0_{Me}$ = 1.56 kcal/mole (17), the present results indicate that $-\Delta G^0_{CH_2OH}$ and $-\Delta G^0_{CH_2OAc}$ are 1.90 and 1.79 kcal/mole, respectively.

Eliel, Nielsen and Gilbert (18) have recently reported results of measurements of $-\Delta G^0$ for the hydroxymethyl group by the equilibration method. Their determinations lead to the values 1.65 and 2.06 kcal/mole in the solvents, cyclohexane and isopropyl alcohol, respectively, at 80° using Raney nickel as the catalyst. These results serve to support our conclusion that ^{13}C nuclear magnetic resonance offers an alternative approach to conformational analysis, at least in a semi-quantitative fashion. The pronounced sensitivity of ^{13}C shieldings to steric perturbations is apparent and it is conceivable that these parameters may offer a more reliable approach for stereochemical studies than proton data, since the contribution of other factors may be much less significant. Jensen (19) has clearly demonstrated the error associated with estimations of $-\Delta G^0$ values from proton results employing the 4-*t*-butyl derivatives as models for the axial and equatorial forms. In view of his findings, it is highly probable that the results obtained from the proton parameters are, at best, a first approximation. The reliability of the ^{13}C results herein remains to be demonstrated. To this end, we are in the course of investigating the ^{13}C spectra of the series, **1–3**, which have been enriched in ^{13}C at the carbinyl carbon. With these models, the study can be extended to include the effect of medium at low concentration and the effect of temperature.

Acknowledgments

Support of this investigation from the Petroleum Research Fund, administered by the American Chemical Society and from the National Research Council of Canada is gratefully acknowledged. We thank Dr. D. J. Sardella for recording some of the proton spectra.

1. D. M. GRANT and E. G. PAUL. J. Am. Chem. Soc. **86**, 2584 (1964).
2. W. R. WOOLFENDEN and D. M. GRANT. J. Am. Chem. Soc. **88**, 1496 (1966).
3. G. W. BUCHANAN, D. A. ROSS, and J. B. STOTHERS, J. Am. Chem. Soc. **88**, 4301 (1966).
4. D. K. DALLING and D. M. GRANT. J. Am. Chem. Soc. **89**, 6612 (1967).
5. E. G. PAUL and D. M. GRANT. J. Am. Chem. Soc. **86**, 2977 (1964).
6. G. W. BUCHANAN and J. B. STOTHERS. Chem. Commun. 1250 (1967).
7. J. H. STOCKTON. J. Org. Chem. **27**, 2288 (1962).
8. E. J. COREY. Org. Syn. **46**, 72 (1966).
9. M. TICHY, J. JONAS, and J. SICHER. Collection Czech. Chem. Comm. **24**, 3434 (1959).
10. L. F. JOHNSON. Pitt. Conf. on Anal. Chem. and App. Spectry. March, 1967. Pittsburg, Pa.
11. G. FRAENKEL, R. E. CARTER, A. MCLACHAN, and J. H. RICHARDS. J. Am. Chem. Soc. **82**, 5846 (1960).
12. P. C. LAUTERBUR. Tetrahedron Letters, 274 (1961); J. Am. Chem. Soc. **83**, 1838 (1961).
13. D. M. GRANT and B. V. CHENEY. J. Am. Chem. Soc. **89**, 5315 (1967).
14. J. B. STOTHERS and P. C. LAUTERBUR. Can. J. Chem. **42**, 1563 (1964).
15. B. V. CHENEY and D. M. GRANT. J. Am. Chem. Soc. **89**, 5319 (1967).
16. G. E. MACIEL and G. C. RUBEN. J. Am. Chem. Soc. **85**, 3903 (1963); G. E. MACIEL and J. J. NATTERSTAD. J. Chem. Phys. **42**, 2752 (1965); G. E. MACIEL and R. V. JAMES. J. Am. Chem. Soc. **86**, 3893 (1964).
17. E. L. ELIEL and T. J. BRETT. J. Am. Chem. Soc. **87**, 5039 (1965).
18. E. L. ELIEL, D. G. NEILSON, and E. C. GILBERT. Chem. Commun. 360 (1968).
19. F. R. JENSEN and B. H. BECK. J. Am. Chem. Soc. **90**, 3251 (1968).
20. K. S. DHAMI and J. B. STOTHERS. Can. J. Chem. **45**, 233 (1967).

Can. J. Chem. Downloaded from www.nrcresearchpress.com by 210.87.254.105 on 09/05/12
For personal use only.

Composition of the leaf wax of Little Club wheat[1]

A. P. TULLOCH AND R. O. WEENINK[2]
Prairie Regional Laboratory, National Research Council of Canada, Saskatoon, Saskatchewan

Received January 27, 1969

Leaf wax of Little Club wheat is composed of: hydrocarbons (8–15%); esters (20–26%); alcohols (25–42%); acids (2%); β-diketone (6–10%); hydroxy β-diketones (9–16%); and unidentified material (9–12%). The esters are mainly octacosanol esters of C_{14} to C_{32} fatty acids but lesser amounts of esters of *trans* 2-tetracosenoic and *trans* 2-docosenoic acids also occur. The free alcohols are almost entirely octacosanol. The β-diketone is hentriacontane-14,16-dione and the hydroxy-β-diketones are a 1:1 mixture of 8- and 9-hydroxyhentriacontane-14,16-diones.

Canadian Journal of Chemistry, 47, 3119 (1969)

Can. J. Chem. Downloaded from www.nrcresearchpress.com by 210.87.254.42 on 09/05/12
For personal use only.

During investigations of the spores of wheat stem rust, spores were collected by washing infected wheat plants with light petroleum (1). It was then found that a good yield of wheat leaf wax could be recovered from the petroleum washings. This extraction procedure was applied to a number of wheat varieties and the yield of wax varied from 0.2 to 0.45% of the dry weight depending on the variety and maturity of the plants.

Apparently only one previous investigation of wheat leaf wax has been made. Pollard *et al.* (2) extracted an unspecified variety of wheat and reported that the principal component of saponified wax was octacosanol. Since large amounts of straw are potentially available in Western Canada, it seemed worthwhile to determine the composition of the wax and to find out whether or not it contained any useful components.

Horn and Lamberton (3) showed that β-diketones are major components of a number of plant waxes and that they can be detected and estimated by infrared (i.r.) and ultraviolet (u.v.) spectroscopy. We have found that they can also be readily detected by thin-layer chromatography (t.l.c.) since they rapidly give yellow spots on exposure to iodine vapor. Hydrocarbons, esters, free alcohols, and other hydroxy compounds can also be detected by t.l.c.

Waxes from 6 varieties of wheat were examined spectroscopically and by t.l.c., and that of Little Club (*Triticum compactum* Host.) contained the most even distribution of the different components. Though Little Club is not a commercial wheat variety it was convenient to examine wax from it, since most of the components could be isolated in reasonable yield, rather than waxes from some other varieties which contained major proportions of just one or two components.

The approximate composition of Little Club wax collected in 1964 and 1965 is shown in Table I along with the yields and u.v. absorption characteristics. The 1965 wax, though harvested at approximately the same stage of growth, contained more alcohols and less β-diketones than the 1964 wax. It has been suggested recently (4) that some varieties of wheat produce wax containing alcohols in place of β-diketones, but growing conditions and maturity apparently must also be taken into account.

Separation of Components

β-Diketones were removed from the wax (1965) as copper complexes (3, 5) but part of the alcohols crystallized at the same time. The resulting mixture of β-diketones, alcohols, and hydroxy-β-diketones was separated chromatographically. Free acids were lost, presumably as copper salts. However, they were isolated in earlier experiments with 1964 wax (6).

Wax remaining after the above removal of β-diketones and part of the alcohols was separated into 20 fractions by a combination of column chromatography and crystallization as shown in Fig. 1. Similar fractions were combined and examined by gas–liquid chromatography (g.l.c.). The composition of the hydrocarbons (fraction 1) is shown in Table II; the principal components were saturated C_{27}–C_{33} hydrocarbons with an odd number of carbon atoms.

Esters, Free Acids, and Free Alcohols

Analysis, by g.l.c., of esters obtained by combining fractions 6, 13, and 18 (Fig. 1),

[1]NRCC No. 10 723.
[2]NRCC Postdoctorate Fellow 1964–1965.

Can. J. Chem. Downloaded from www.nrcresearchpress.com by 210.87.254.42 on 09/05/12
For personal use only.

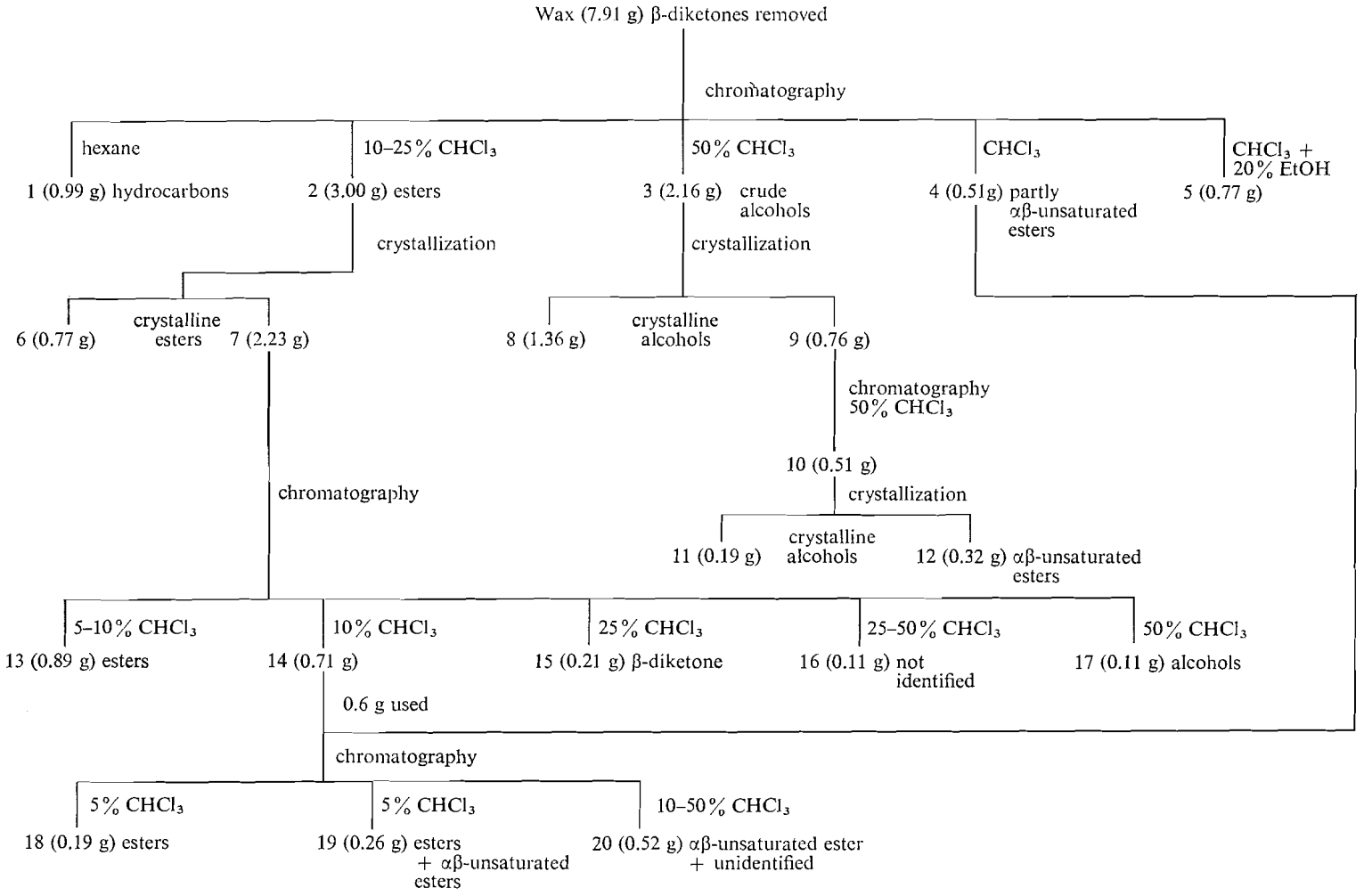

FIG. 1. Separation of wax after removal of β-diketones. Percentages refer to chloroform in hexane and crystallizations were from chloroform. Fractions were identified by thin-layer chromatography and nuclear magnetic resonance spectroscopy.

Can. J. Chem. Downloaded from www.nrcresearchpress.com by 210.87.254.42 on 09/05/12
For personal use only.

TABLE I

Approximate composition and yields of wax samples

Date of harvest	20–7–64	21–8–64	6–7–65
Yield (% of dry weight)	0.45	0.37	0.43
Ultraviolet absorption ($E^{1\%}_{1cm}$ at 273 mμ)	63	46	39
Hydrocarbons	15	*	8
Esters	20		26
Free alcohols	25		42
Free acids	2		†
β-Diketone	10		6
Hydroxy-β-diketone	16		9
Unidentified	12		9

*Composition of this sample was not determined.
†Could not be determined by the method used with this sample.

TABLE II

Composition of wax fractions

Number of C atoms	Hydrocarbons %	Esters %	Hydrolysis products of esters		Free* acids	Free alcohols
			Acids %	Alcohols %		
14	—	—	0.2	—	2.8	—
16	—	—	8.6	—	34.7	—
18	—	—	5.4	—	5.6	—
20	—	—	18.2	1.3	1.8	—
21	0.7	—	—	0.4	—	—
22	0.1	—	38.4†	5.7	21.4†	—
23	1.2	—	—	0.2	—	—
24	0.1	—	13.1‡	4.6	14.9‡	0.9
25	3.1	—	—	0.2	—	—
26	—	—	3.2	6.9	5.1	4.6
27	9.9	—	—	0.4	—	0.2
28	—	—	11.1	79.4	7.5	93.4
29	31.9	—	—	—	—	—
30	—	—	1.6	0.9	3.9	0.9
31	34.7	—	—	—	—	—
32	—	—	0.2	—	2.0	—
33	16.6	—	—	—	—	—
34	—	—	—	—	0.3	—
35	1.7	—	—	—	—	—
40	—	1.2	—	—	—	—
42	—	3.9	—	—	—	—
44	—	19.2	—	—	—	—
46	—	14.4	—	—	—	—
48	—	18.8	—	—	—	—
50	—	23.5	—	—	—	—
52	—	5.5	—	—	—	—
54	—	3.9	—	—	—	—
56	—	9.6	—	—	—	—

*From wax collected in 1964.
†Includes cf. 1% of *trans* 2-docosenoic acid.
‡Includes cf. 4.5 of *trans* 2-tetracosenoic acid.

showed that they consisted of C_{44}–C_{56} monoesters. The major hydrolysis products were C_{16}–C_{30} fatty acids and octacosanol (Table II), showing that the original esters were octacosanol esters of these acids.

Small percentages of *trans* 2-tetracosenoic and docosenoic acids were observed in the above acids during g.l.c. analysis, but much larger proportions of the two acids were present in the hydrolysis products of fractions 12, 19, and 20 (Table III). The structures of these acids were deduced from their g.l.c. retention times, the

TABLE III

Composition of hydrolysis products of fractions containing *trans* αβ-unsaturated esters

Number of C atoms	Fraction 12		Fraction 19		Fraction 20	
	Acids %	Alcohols %	Acids %	Alcohols %	Acids %	Alcohols %
14	0.2	—	—	2.9	3.6	—
16	0.5	—	1.4	0.7	13.4	—
18	0.2	—	0.6	6.9	3.6	—
20	0.2	0.7	1.4	41.1	3.0	4.3
21	—	0.1	—	—	—	—
22	5.3	9.7	2.1	25.1	17.8	11.4
trans 22:1	39.6	—	18.0	—	15.2	—
23	—	0.1	—	—	—	—
24	4.5	24.9	3.0	7.7	6.5	5.7
trans 24:1	49.5	—	39.8	—	15.5	—
25	—	0.2	—	—	—	—
26	0.2	26.0	1.4	2.3	3.9	7.6
27	—	0.5	—	—	—	2.1
28	—	36.9	13.4	11.4	13.6	66.9
30	—	0.9	2.8	1.9	3.0	2.0
32	—	—	1.1	—	0.9	—
Unidentified	—	—	15.0(4)*	—	—	—
Yield on hydrolysis (as % of fraction weight)	45	36	47	15	60	12

*Number in parentheses refers to number of components.

nuclear magnetic resonance (n.m.r.) signals at 5.7 and 6.8 p.p.m., characteristic of acids with *trans* 2,3-unsaturation (7, 8), and the fact that oxidation with the permanganate–periodate reagent (9) yielded saturated C_{20} and C_{22} acids. *trans* 2-Tetracosenoic and docosenoic acids do not seem to have been isolated from natural sources before though a number of *trans* αβ-unsaturated C_{10} acids have been isolated from bees (7, 10).

Fractions 12, 19, and 20, which were eluted just after the monoesters or along with the alcohols (Fig. 1), appeared from t.l.c. to be mixtures of several components. The hydrolysis products are listed in Table III. Difunctional components such as diols or hydroxy acids, the presence of which could account for the low yields of alcohols, were not detected. The structures of the parent compounds could not be completely elucidated, but part probably consists of esters of *trans* 2-tetracosenoic and docosenoic acids with C_{20}–C_{28} alcohols.

It is of interest that the *trans* αβ-unsaturated acids are found only as C_{22} and C_{24} compounds whereas the acids of the other ester fractions range from C_{14} to C_{32}. When all ester fractions are considered together, the approximate % of esters containing *trans* 2-docosenoic acid is 5% and of esters containing *trans* 2-tetracosenoic acid is 10%.

The free fatty acids in Table II are similar to those of the esters except that palmitic acid is the major component. These acids were isolated from wax collected in 1964 whereas the other analyses were made on material collected in 1965. However, hydrolysis of the total ester fraction of the 1964 wax gave acids with the composition: C_{14} 2.4; C_{16} 9.8; C_{18} 4.5; C_{20} 9.9; C_{22} 20.1; *trans* $C_{22:1}$ 10.2; C_{24} 8.4; *trans* $C_{24:1}$ 15.5; C_{26} 3.1; C_{28} 8.4; C_{30} 4.5; C_{32} 2.8; C_{34} 0.4%, which is not very different from that of the 1965 esters.

The composition of the free alcohols is similar to that of the alcohols of the esters but an even higher proportion of octacosanol is present (Table II).

β-*Diketone*

Only one β-diketone, hentriacontane-14,16-dione, was present. The chain length was established by reduction to hentriacontane (3). Alkaline hydrolysis gave equal amounts of pentadecan-2-one and heptadecan-2-one and of myristic and palmitic acids. This diketone has not previously been isolated in the pure state though it occurs as a minor component of the mixed β-diketones of leaf wax of two species of

Can. J. Chem. Downloaded from www.nrcresearchpress.com by 210.87.254.42 on 09/05/12
For personal use only.

Can. J. Chem. Downloaded from www.nrcresearchpress.com by 210.87.254.42 on 09/05/12
For personal use only.

Eucalyptus (5). Wax of the grass *Festuca glauca* contained mainly tritriacontane-12,14-dione (5).

Hydroxy-β-diketones

These components also gave only hentriacontane on reduction. The n.m.r. spectrum showed that a secondary hydroxyl group was present which was at least 4 methylene groups removed from the diketone group (11). The neutral fraction obtained by alkaline hydrolysis was a mixture of heptadecan-2-one and hydroxypentadecan-2-ones, which were separated on a silicic acid column. The acidic fraction was shown by g.l.c. to be a mixture of palmitic and hydroxymyristic acids, which as methyl esters, were also separated chromatographically.

Oxidation of the hydroxy esters with chromium trioxide at 25° (12) gave an oxomyristate which appeared to be a mixture of 6- and 7-oxomyristates (g.l.c. using QF-1 column (13)). Oxidation with chromium trioxide at 100° (12), when cleavage occurs on both sides of the oxygenated carbon atom, gave the monocarboxylic acids heptanoic, octanoic, and nonanoic approximately in the ratio 1:2:1, and the dicarboxylic acids glutaric, adipic, and pimelic also in the ratio 1:2:1, showing that an approximately equimolar mixture of 6- and 7-hydroxymyristates had been oxidized.

The n.m.r. spectrum of the hydroxymyristates in quinoline was indistinguishable from that of a 1:1 mixture of synthetic 6- and 7-hydroxymyristates. It was shown previously (11) that, using quinoline as solvent, the center of the α-CH_2 signal of 6-hydroxystearate appears at ca. 0.1 p.p.m. downfield from the corresponding signal of 7-hydroxystearate. The hydroxymyristates showed signals at both positions and the rest of the spectrum also agreed with the proposed structure. This was confirmed by the mass spectrum of the hydroxymyristates which showed peaks at *m/e* 145 (also shown by methyl 6-hydroxymyristate) and at *m/e* 159 (also shown by methyl 7-hydroxymyristate). Mass spectra of the corresponding hydroxystearates (14) show that the peak at *m/e* 145 is due to the ion $^{+}CHOH(CH_2)_4CO_2CH_3$ and at *m/e* 159 is due to the ion $^{+}CHOH(CH_2)_5CO_2CH_3$. The hydroxymyristates have a positive rotation suggesting the L-configuration (15, 16).

We conclude that the hydroxy-β-diketone fraction of Little Club wax consists of an approximately 1:1 mixture of 8- and 9-hydroxyhentriacontane-14,16-diones.

Hydrolysis of the most polar wax fraction (5, Fig. 1) gave palmitic acid as 15% of the fraction and a brown gum from which no definite compounds could be isolated. No diols or hydroxy acids could be detected. The unidentified portion of the wax consists of material of indefinite composition from fraction 5 above and of materials not recovered from the chromatographic columns.

The compositions of the wax components have certain features of interest. The hydrocarbons are composed mainly of 4 chain lengths C_{27}–C_{33}, whereas the other components with an odd number of carbon atoms, the β-diketones, have a chain length of 31 carbons only. The lack of relation between chain length of hydrocarbons and β-diketones was also observed with waxes of *Eucalyptus* species (5). The compositions of the free acids and free alcohols are fairly similar to those of the acids and alcohols of the esters. In many studies of waxes these pairs of components have not been examined separately. However, the acids contain a wide variety of chain lengths but the alcohols are composed largely of octacosanol. These differences and also the finding of unsaturated C_{22} and C_{24} acids, suggest the operation of several different biosynthetic pathways. Diols and hydroxy acids, which are frequently isolated from plant waxes (17) are apparently absent. Hydroxy-β-diketones have not previously been found in waxes, though hydroxy-ketones are present in cabbage wax (18).

Experimental

Silicic acid (Bio-Sil A from Bio-Rad Laboratories) was used for column chromatography, after activation at 120° for 18 h, and silica gel G for t.l.c. Typical *R* values found by t.l.c. of representative compounds in benzene and chloroform respectively were: triacontane 0.86, 0.74; octadecanol octadecanoate 0.68, 0.70; methyl octacosanoate 0.40, 0.49; β-diketone 0.38, 0.45; octacosanol 0.07, 0.15; hydroxy-β-diketones 0.02, 0.06; octacosanoic acid 0.00, 0.00. Chloroform was the most satisfactory solvent for t.l.c. although it sometimes did not separate hydrocarbons and wax esters. Iodine vapor was used to detect β-diketones, which rapidly gave dark orange spots, and the other components were detected by spraying with 50% sulfuric acid and heating.

Nuclear magnetic resonance spectra were measured at 100 Mc.p.s. using a Varian HA-100 spectrometer. Chemical shifts are in parts per million (p.p.m.) from tetramethylsilane (internal standard). Carbon tetrachloride was used as solvent except where otherwise

Can. J. Chem. Downloaded from www.nrcresearchpress.com by 210.87.254.42 on 09/05/12
For personal use only.

stated. Specific rotations were measured at 25° using a Perkin Elmer model 141 polarimeter. Infrared spectra were recorded in carbon tetrachloride (5% solution) in a 0.1 mm cell. Mass spectra were determined by the Morgan–Schaffer Corporation, Montreal.

Gas–Liquid Chromatography

Gas–liquid chromatography (g.l.c.) was carried out using: (*A*) an F and M model 402 gas chromatograph with flame ionization detectors fitted with 3 ft × 1/4 in. glass columns packed with 20–30 mesh glass beads coated with 0.3% silicone SE 30 and having a flow rate of 45 ml of helium/min, with the temperature programmed at 2°/min from various temperatures between 100 and 200° to 325° depending on the samples being analyzed; (*B*) an F and M model 5750 gas chromatograph with a flame ionization detector fitted with an 8 ft × 1/4 in. stainless steel column packed with 5% w/w 1,3-propanediol succinate (prepared by Dr. B. M. Craig) on 60–80 mesh acid washed chromosorb W operated isothermally at 215° with a flow rate of 40 ml/min; and (*C*) a unit of conventional design with thermal conductivity detectors and a 3 ft × 1/4 in. copper column packed with 5% silicone SE 30 on 60–80 mesh acid washed celite.

When synthetic, even numbered long chain alcohol esters of long chain acids were analyzed by unit (*A*) and the temperature programmed from 200–325°, a plot of retention temperature against carbon number (19) was almost a straight line making possible the measurement of the carbon numbers of the wax esters. The results were confirmed by re-analysis after addition of synthetic esters of various chain lengths to the mixture. Also, analysis of mixtures of synthetic esters showed that correction factors were not required to calculate composition. Unit (*A*) programmed from 100 to 275° was used to analyze hydrocarbons, alcohols, and methyl esters. Hydrocarbons and methyl esters were also analyzed using units (*B*) and (*C*); alcohols and their acetates were also analyzed on unit (*C*); carbon numbers were determined from isothermal analyses.

Synthesis of Octacosanol and Other Model Compounds

13-Oxooctacosanoic acid (19.8 g) was synthesized from 1-morpholino-1-cyclododecene (20) (17.5 g) and hexadecanoyl chloride (13.7 g) by the method previously used to prepare 13-oxodocosanoic acid (21). After crystallization from ethyl acetate, the m.p. was 100.5–101.5 (lit. (22), 99.5°). Wolf–Kishner reduction of the oxo acid (18 g) and crystallization of the product from chloroform gave octacosanoic acid (10 g), m.p. 89.5–90.5 (lit. (22), 90.2°). Reduction of octacosanoic acid with lithium aluminum hydride in tetrahydrofuran gave octacosanol in high yield. The alcohol was crystallized from chloroform, m.p. 82.5–83.5 (lit. (22), 82.5°); the acetate had a m.p. 64°.

Other long chain alcohols were prepared by reduction of the corresponding acids which were commercial products. Even-numbered hydrocarbons with 26 and 34 carbons were prepared by the method previously used to prepare tetracosane (23). The synthesis and properties of long chain wax-like esters will be described elsewhere.

Isolation and Properties of the Wax

Plants of *Triticum compactum* Host. var. Little Club were grown outdoors and collected 4–6 weeks before maturity (generally just before the heads appeared and when green leaf formation was greatest). One sample was also collected from mature straw. The plants were swirled in light petroleum b.p. 40–60° for about 10 s (cf. 1) and the extract filtered and evaporated to dryness.

Further washings generally yielded only a small amount of wax with a composition similar to that of the first extract, though sometimes later extracts seemed to contain higher proportions of polar, pigmented material. Purdy and Truter (24) found that repeated extraction of cabbage leaves with different solvents gave wax samples which all had similar compositions. Some wax components, as pure compounds, were poorly soluble in light petroleum but, as mixtures in the wax, were quite soluble.

The melting point of the wax was 42–62°. The i.r. spectra had a broad peak at ca. 1600 cm^{-1} (β-diketone), a small shoulder at 1655 cm^{-1} (double bond of αβ-unsaturated ester), broad carbonyl absorption at 1705–1730 cm^{-1}, and a small OH peak at 3670 cm^{-1}; the peak at 1655 cm^{-1} was most pronounced in the spectrum of wax from mature straw. Thin layer chromatography indicated the presence of hydrocarbons, esters, β-diketone, alcohols, hydroxy β-diketones, and a trace of free acids.

Separation of Components

β-Diketones were separated from the wax (14.2 g, collected 6-7-65) as copper complexes, as described by Horn *et al.* (5), but some alcohols also crystallized with the complex. The mixture (4.6 g) obtained after decomposition of the complex was chromatographed on silicic acid giving β-diketone (0.73 g) (elution with hexane – chloroform 3:1), alcohols (1.61 g), and a mixture of alcohols and hydroxy-β-diketones (2.0 g) (elution with hexane – chloroform 1:1). The mixed fraction gave alcohols (0.3 g) on crystallization from chloroform and the mother liquors, after two further chromatographic separations, gave alcohols (0.64 g) and hydroxy-β-diketones (0.98 g).

When wax collected on 20-7-64 was separated on a column without removing diketones first (6), free acids were found in the alcohol fraction. Treatment with diazomethane and rechromatography on silicic acid (elution with hexane – chloroform 3:1) gave methyl esters of the free acids (0.044 g from 5.7 g wax).

Determination of Structure of Components of Wax

Hydrocarbons

Analysis of fraction 1 (Fig. 1) by g.l.c. and examination by n.m.r. spectroscopy showed that the principal components were saturated, straight chain compounds (25). Chromatography on a silver nitrate – silicic acid column (26) gave only a small fraction (4% of total hydrocarbons) which appeared (by n.m.r.) to be partly unsaturated hydrocarbons.

Saturated esters

Fractions 6, 13, and 18 (Fig. 1) were combined and analyzed by g.l.c. using unit (*A*) and programming from 250–325°. By adding eicosanol eicosanoate as internal standard (27), components found by g.l.c. were shown to compose 91% of the combined fractions. Esters (1.746 g) were refluxed for 22 h with ethanol (125 ml) containing 5% hydrogen chloride; the mixture was then poured into water, extracted with chloroform and dried over sodium

Can. J. Chem. Downloaded from www.nrcresearchpress.com by 210.87.254.42 on 09/05/12
For personal use only.

sulfate. The product (1.852 g) was examined by t.l.c. and showed only traces of unhydrolyzed material; there were no spots corresponding to diols or hydroxy esters.

The product was chromatographed on silicic acid (200 g) and elution with hexane – 10% chloroform gave hydrocarbons (0.057 g) and unhydrolyzed esters (0.068 g). Elution with hexane – 25% chloroform gave ethyl esters (0.685 g) and with hexane – 50% chloroform, first an unidentified component (0.065 g) with R_f 0.3 (chloroform) and then alcohols (0.956 g). Ethyl esters were converted to methyl esters by refluxing with methanolic hydrogen chloride (6%) for 20 h. Methyl esters and alcohols were analyzed by g.l.c. giving the results shown in Table II. A portion of the alcohols was acetylated and the relative intensities of the n.m.r. signals (in chloroform, with chloroform proton as lock signal) confirmed that they were straight chain, saturated, primary alcohols.

Fraction 5 was hydrolyzed, after ethanolysis, and gave acids (0.104 g) consisting mainly of palmitic acid but no other definite compounds were isolated.

αβ-Unsaturated esters

Fraction 12

Analysis by t.l.c. showed a major spot with R_f 0.18 (benzene) and 0.55 (chloroform) and a minor spot in the free alcohol region. Analysis by g.l.c. showed small C_{22} to C_{28} alcohol peaks and a single very broad peak in the C_{52} to C_{62} ester region. The n.m.r. spectrum showed signals for free primary alcohols (triplet 3.5 p.p.m., *c* 1 proton), acylated primary alcohols (triplet 4.00 p.p.m., *c* 2 protons), and for 2 protons of a *trans* double bond αβ to an ester group (H-2, doublet, 5.70 p.p.m.; $J = 16$ c.p.s.; H-3, 2 triplets, 6.82 p.p.m., $J = 16$ c.p.s.).

Fraction 19

Analysis by t.l.c. (benzene) showed a major spot at R_f 0.65 and a minor spot at 0.40; in chloroform there were spots at R_f 0.70 and 0.50. Analysis by g.l.c. showed peaks with retention times of C_{42}, C_{44}, and C_{46} esters. The n.m.r. spectrum was similar to that of fraction 12 except that the free alcohol —CH_2OH signal was missing and the other signals were weaker and less well-defined.

Fraction 20

Analysis by t.l.c. (chloroform) showed 6 ill-defined spots, 4 of which had R_f's intermediate between those of wax ester and of alcohol and the other two were slower. No peak was obtained by g.l.c. using unit (*A*) at 350°. The n.m.r. spectrum was similar to that of fraction 19.

On ethanolysis, as above, fraction 12 (0.280 g) gave esters (0.130 g) and alcohols (0.104). The i.r. spectrum of the methyl esters was very similar to that of methyl *trans* 2-octadecenoate. The carbon numbers of the two principal components of the methyl esters were 22.4 and 24.4 (silicone column) and 23.35 and 25.4 (polyester column). Methyl *trans* 2-octadecenoate had carbon numbers 18.4 and 19.35 using the same two columns.

Oxidation of the methyl esters of fraction 12 with the permanganate–periodate reagent (9, 28) gave a mixture of monocarboxylic acids with the composition C_{20}, 39.3%; C_{22}, 56.7%; and C_{24}, 4.0% (g.l.c. analysis as methyl esters using two different columns).

On ethanolysis, fraction 19 (0.250 g) gave esters (0.117 g) and alcohols (0.037 g) and an unidentified product (0.042 g) (R_f 0.3 ($CHCl_3$)). Ethanolysis of fraction 20 (0.510 g) gave esters (0.300) and alcohols (0.060 g) and unidentified gum (0.104 g). The compositions of methyl ester and alcohol fractions are given in Table III.

β-Diketone

The β-diketone was crystallized from ethyl acetate and had m.p. 58–59° and u.v. absorption maximum at 273 mμ (ε 12 125). The i.r. spectrum had a strong band at 1605 cm^{-1}. Nuclear magnetic resonance: terminal CH_3 0.87 (6 protons); methylene groups, 1.25; α-CH_2 (triplet, 2.19 (4 protons)); CH of enolic form (singlet, 5.31 (0.9 protons)).

Anal. Calcd. for $C_{31}H_{60}O_2$: C, 80.10; H, 13.01. Found: C, 79.92; H, 12.80.

β-Diketone (1.0 g) was refluxed with 4% ethanolic potassium hydroxide for 18 h when water was added; extraction with hexane gave neutral product (0.53 g). The aqueous layer was then acidified and the acidic product (0.52 g) extracted with ether. Analysis by g.l.c. (unit (*C*)) showed that the neutral product consisted of equal amounts of pentadecan-2-one and heptadecan-2-one and the acidic product of equal amounts of myristic and palmitic acids.

The ketones were separated in batches by g.l.c. (unit (*C*) at 180°) and gave equal weights of pentadecan-2-one, m.p. 37.5–38.5°, the mixed m.p. with synthetic ketone (m.p. 37.5–38.5, lit. (29) gives 39°) was 38.0–38.5°, and heptadecan-2-one, m.p. 47.5–48.5°, the mixed m.p. with synthetic ketone (m.p. 48–48.5°, lit. (29) gives 48°) was 47.5–48.5°. Authentic methyl ketones were synthesized by alkaline hydrolysis of methyl 3-oxohexadecanoate and 3-oxooctadecanoate (30, 31). The acids were converted to methyl esters and separated in the same way giving equal weights of methyl myristate and methyl palmitate. Hydrolysis yielded myristic acid, m.p. and mixed m.p. 51.5–53°, and palmitic acid, m.p. and mixed m.p. 62–63°.

Reduction of the β-diketone (3, 32) gave only hentriacontane (g.l.c. using unit (*C*) at 250°).

Free Alcohols

Fractions 8, 11, and 17 (Fig. 1) were combined with alcohols separated from the β-diketone fraction and analyzed by g.l.c.; a portion was also acetylated and reanalyzed. Crystallization from chloroform gave almost pure octacosanol (99% by g.l.c.), the m.p. was 81.5–82.5° and mixed m.p. with synthetic octacosanol (m.p. 82.5–83.5°) was 82–83°.

Hydroxy-β-diketones

Hydroxy-β-diketones were crystallized from ethyl acetate and had m.p. 70–72° and $[\alpha]_D$ +0.99°, $[\alpha]_{546}$ +1.19, $[\alpha]_{436}$ +1.94, $[\alpha]_{365}$ +2.91 (*c*, 9.3 in chloroform). The u.v. absorption maximum was at 273 mμ (ε 12 410) and the i.r. spectrum had bands at 1602 (s) and 3660 (w) cm^{-1}. Nuclear magnetic resonance: CH of CHOH (multiplet) 3.43, CH of enolic form (singlet) 5.30 and one hydroxylic proton removed by D_2O.

Anal. Calcd. for $C_{31}H_{60}O_3$: C, 77.44; H, 12.58. Found: C, 77.39; H, 12.47.

On hydrolysis as before, hydroxy-β-diketones (0.76) gave acidic (0.39 g) and neutral (0.40) fractions. After conversion of acids to methyl esters, g.l.c. analysis (unit (*C*), 220°) showed only one peak for each fraction

Can. J. Chem. Downloaded from www.nrcresearchpress.com by 210.87.254.42 on 09/05/12
For personal use only.

but after acetylation both fractions showed 2 approximately equal peaks differing by 2 carbon numbers (cf. 12 and 13).

The acidic fraction, as methyl esters, was chromatographed on a silic acid column. Elution with hexane – 4% ether gave methyl palmitate (0.19 g) which on hydrolysis gave palmitic acid, m.p. and mixed m.p. with authentic acid 61–62°. Elution with hexane – 5% acetone yielded methyl hydroxymyristates. After crystallization from hexane these esters had m.p. 31–33° and $[\alpha]_D$ +1.33, $[\alpha]_{546}$ +1.51, $[\alpha]_{436}$ +2.54 and $[\alpha]_{365}$ +3.86 (*c*, 7.4 in chloroform). Nuclear magnetic resonance (quinoline): the signal in the α CH_2 region contained peaks at 2.38 and 2.30 corresponding to the central portion of the α CH_2 signal in spectra of 6- and 7-hydroxymyristates respectively. The rest of the spectrum was indistinguishable from that of a 1:1 mixture of synthetic methyl 6- and 7-hydroxymyristates (13).

Anal. Calcd. for $C_{15}H_{30}O_3$: C, 69.72; H, 11.70. Found: C, 69.39; H, 11.47.

Hydrolysis gave hydroxymyristic acids which, after crystallization from hexane had m.p. 61.5–62.5 (neutralization equiv. 247; calcd. for $C_{14}H_{28}O_3$, 244).

Chromic acid oxidation at 25° (12) gave oxo acids with m.p. 53–53.5° which was unchanged by repeated crystallization from hexane (6-oxotetradecanoic acid has m.p. 70.5–71.5 and 7-oxotetradecanoic acid has m.p. 67.5–68° (13)). When analyzed by g.l.c. using a QF-1 column (conditions used with methyl oxooctadecanoates (13)), two partly resolved peaks of equal size with retention times of 21.4 and 22.3 min were obtained (methyl 6-oxo and 7-oxotetradecanoates had retention times of 21.5 and 22.3 min respectively).

The mixed oxo esters were oxidized with chromic oxide at 100° (12) and the product converted to methyl esters. Analysis by g.l.c. (QF-1 column) showed the presence of C_7, C_8, and C_9 monocarboxylic esters (retention times 1.65, 2.4, and 3.3 min) and C_5, C_6, and C_7-dicarboxylic esters (retention times 4.8, 7.0, and 9.9 min). The molar percentages were C_7 26.7; C_8 46.7; C_9 26.6 and C_5 25.0; C_6 50.6; C_7 24.4. When the oxidation product was saponified, steam distilled, and mono- and dicarboxylic acids analyzed separately, the same acids were found as before showing that decanoic and succinic acids, which have retention times (as methyl esters), close to those of glutaric and nonanoic acids respectively, were absent.

The neutral fraction isolated on hydrolysis of the hydroxy β-diketones was separated into two approximately equal fractions as above. The first, heptadecan-2-one, was crystallized from methanol and had m.p. and mixed m.p. 47–48°. The second, 7- and 8-hydroxypentadecan-2-ones, had m.p. 39–53°, and $[\alpha]_D$ +1.06°, $[\alpha]_{546}$ +1.22°, $[\alpha]_{436}$ +2.10°, $[\alpha]_{365}$ +3.12° (*c*, 7.5 in chloroform).

Anal. Calcd. for $C_{15}H_{30}O_2$: C, 74.32; H, 12.48. Found: C, 74.56; H, 12.45.

Reduction of the hydroxy-β-diketones as before gave only hentriacontane.

Acknowledgments

The authors wish to thank Mr. L. L. Hoffman for experimental assistance, Mr. M. Mazurek for nuclear magnetic resonance measurements, and Mr. W. C. Haid for microanalyses and infrared measurements.

1. A. P. Tulloch and G. A. Ledingham. Can. J. Microbiol. **6**, 425 (1960).
2. A. Pollard, A. C. Chibnall, and S. H. Piper. Biochem. J. **27**, 1889 (1933).
3. D. H. S. Horn and J. A. Lamberton. Chem. and Ind. (London), 2036 (1962).
4. H. N. Barber and A. G. Netting. Phytochem. **7**, 2089 (1968).
5. D. H. S. Horn, Z. H. Kranz, and J. A. Lamberton. Australian J. Chem. **17**, 464 (1964).
6. A. P. Tulloch and R. O. Weenink. Chem. Commun. 255 (1966).
7. S. A. Barker, A. B. Foster, D. C. Lamb, and L. M. Jackman. Tetrahedron, **18**, 177 (1962).
8. C. Y. Hopkins. *In* Progress in the chemistry of fats and other lipids. Vol. VIII. *Edited by* R. T. Holman. The Pergamon Press, Ltd., Oxford. 1965. p. 213.
9. E. von Rudloff. Can. J. Chem. **34**, 1413 (1956).
10. R. K. Callow, J. R. Chapman, and P. N. Paton. J. Apicult. Res. **3**, 77 (1964).
11. A. P. Tulloch. J. Am. Oil Chemists' Soc. **43**, 670 (1966).
12. A. P. Tulloch. Can. J. Chem. **43**, 415 (1965).
13. A. P. Tulloch. J. Am. Oil Chemists' Soc. **41**, 833 (1964).
14. R. Ryhage and E. Stenhagen. Arkiv. Kemi, **15**, 545 (1960).
15. G. J. Schroepfer and K. Bloch. J. Biol. Chem. **240**, 54 (1965).
16. A. P. Tulloch. Can. J. Chem. **46**, 3727 (1968).
17. G. Eglinton and R. J. Hamilton. Science, **156**, 1322 (1967).
18. S. J. Purdy and E. V. Truter. Proc. Roy. Soc. London, Ser. B, **158**, 553 (1963).
19. W. E. Harris and H. W. Hapgood. Programmed temperature gas chromatography. J. Wiley and Sons, Inc., New York, 1966. pp. 141–168.
20. H-J. Buysch. Ph.D. Thesis. Julius–Maximilian University, Würzburg, Germany. 1963.
21. A. P. Tulloch, J. F. T. Spencer, and M. H. Deinema. Can. J. Chem. **46**, 345 (1968).
22. A. Watanabe. Bull Chem. Soc. Japan, **34**, 398 (1961).
23. A. P. Tulloch, J. F. T. Spencer, and P. A. J. Gorin. Can. J. Chem. **40**, 1326 (1962).
24. S. J. Purdy and E. V. Truter. Proc. Roy. Soc. London, Ser. B, **158**, 536 (1963).
25. J. Cason and G. L. Lange. J. Org. Chem. **29**, 2107 (1964).
26. M. Streibl, K. Stránský, and F. Sǒrm. Fette, Seifen Anstrichmittel, **68**, 799 (1966).
27. R. B. Iden and E. J. Kahler. J. Am. Oil Chemists' Soc. **39**, 171 (1962).
28. A. P. Tulloch and B. M. Craig. J. Am. Oil Chemists' Soc. **41**, 322 (1964).
29. F. Krafft. Chem. Ber. **12**, 1668 (1879).
30. S. Stallberg-Stenhagen. Arkiv. Mineral. Geol. **20**, 1 (1945).
31. B. Helferich and H. Köster. Chem. Ber. **56**, 2088 (1923).
32. D. T. Downing, Z. H. Kranz, and K. E. Murray. Australian J. Chem. **13**, 80 (1960).

Can. J. Chem. Downloaded from www.nrcresearchpress.com by 210.87.254.40 on 09/05/12
For personal use only.

A new direct synthesis of equilin from equilenin. Potassium–ammonia reduction of some non-conjugated double bonds[1]

DAVID J. MARSHALL AND ROMANO DEGHENGHI
Ayerst Research Laboratories, Montreal, Quebec

Received March 18, 1969

It is shown that the reduction of equilenin ethylene ketal with alkali metals in ammonia can be controlled to yield equilin ketal as the major product. With potassium at −33°, equilenin and equilin ketals are readily reduced to afford 8α-estrone ketals in good yield. Analogous reactions were observed with 2-naphthol.

Canadian Journal of Chemistry, 47, 3127 (1969)

Only one of the known syntheses of equilin (1–4), uses equilenin as starting material. Equilenin methyl ether and derivatives (**1**) on prolonged reduction with lithium and *t*-butanol in ammonia afforded tetrahydro compounds (**2**) which underwent bromination–dehydrobromination in ring A to give estra-1,3,5(10),7-tetraenes (**3**, R = H or Me) in rather low overall yields (4).

The work to be described here started with the assumption that a naphthol-type molecule such as equilenin in the presence of alkali metal in liquid ammonia would rapidly form a naphthoxide anion. If the oxygen at C-17 was protected so that no other negative charge could develop, the addition of electrons which is necessary for reduction should take place most readily (at least from an electrostatic point of view) in ring B, which could lead to a direct synthesis of equilin.

Experiments in which equilenin ethylene ketal (**4**) was allowed to react with alkali metals in ammonia without an added proton source and preferably at −70° showed that equilin (**5**) could indeed be obtained as the major product (except with potassium at −33°; see below), after hydrolysis of the intermediate ketal. Slightly better yields were obtained if the naphthoxide anion was formed by reaction of the ketal with sodium hydride in tetrahydrofuran before addition to a solution of the metal in ammonia. Analysis by gas–liquid chromatography (g.l.c.) of the total crude product of a reaction carried out in this way with lithium as the metal showed the presence of 76% of equilin. Purification by crystallization afforded a 55% yield of equilin, identified by melting point and mixture melting point with an authentic sample.

Analysis by g.l.c. of crude reaction products showed that the major by-products were a pair of closely related compounds, one of which was identical (by g.l.c. and thin-layer chromatography (t.l.c.)) with 3β-hydroxyestra-5,7,9-trien-17-one (5). The other member of the pair was presumably the 3-epimer. Infrared (i.r.) spectra indicated the presence of the 3-ketone (**6**) (band at 1715 cm^{-1}) in the product of some runs.[2]

At −70°, the yield of equilin as determined by g.l.c. was affected only to a minor extent on changing the metal from lithium to sodium to potassium. With calcium, however, the major product was the mixture of ring A-reduced alcohols **7**. If the oxygen at C-17 was in the form of a free hydroxyl or carbonyl group, and hence not protected against reaction with the metal, lower yields of estra-1,3,5(10),7-tetraenes resulted. When the starting material was a 3-methyl or 3-tetrahydropyranyl ether, complex mixtures of products were obtained.

At −33°, the major product of reduction of equilenin ethylene ketal with sodium and lithium followed by acid hydrolysis was equilin, but the

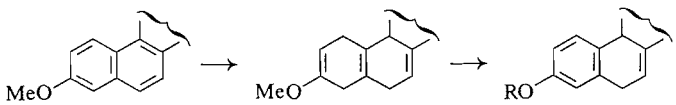

1 2 3

[1]This work was presented at the 51st Annual Conference of the Chemical Institute of Canada, Vancouver, British Columbia, June 3, 1968.

[2]The formation of the pair of ring A-reduced compounds **7** may be analogous to the formation of estr-5(10)-ene-3α,17β-diol by Birch reduction of estrone (6).

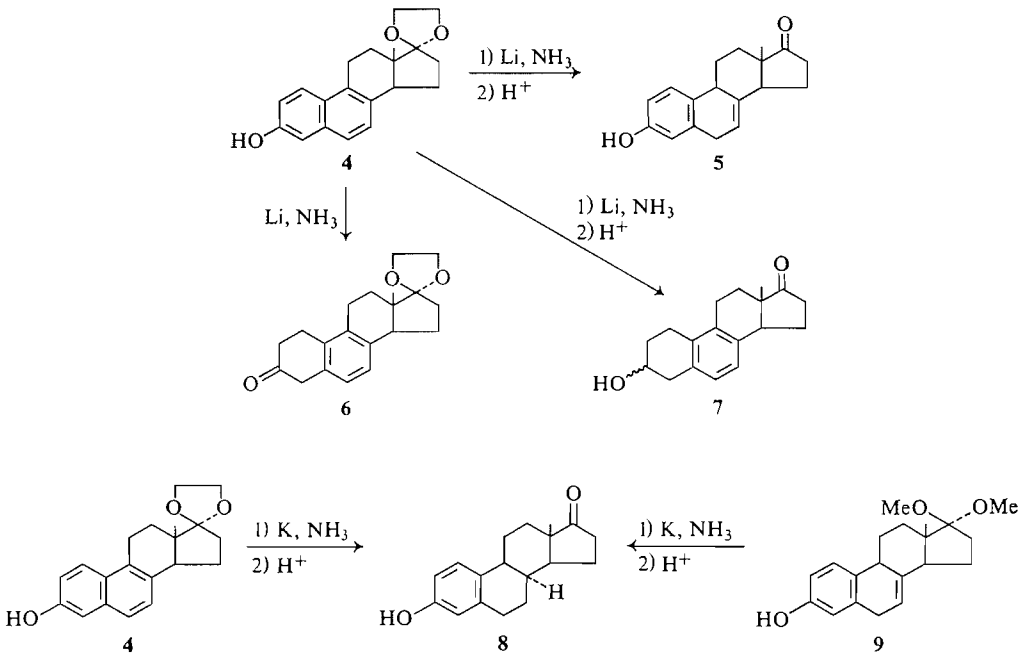

4 5 6 7 4 8 9

yield was inferior to that obtained at −70°. On the other hand, with potassium at −33°, no equilin at all was obtained. Instead a tetrahydro derivative of equilenin formed which was shown to be 8α-estrone (**8**). The same product could be obtained in high yield on reduction of equilin (as the dimethyl ketal **9**) with potassium at −33°. The structure was established by comparison of physical constants with those recorded (7,8) for 8α-estrone and by conversion to the methyl ether which was identical spectroscopically with a sample of totally synthetic *dl*-8α-estrone methyl ether (9).

The reduction of the double bond of equilin with potassium in ammonia was quite unexpected. Isolated non-terminal double bonds are not normally reduced by this method unless the intermediate radical–anion can be stabilized by the presence of a suitably situated double bond, as in the case of norbornadiene, which is reduced to norbornene by sodium or lithium in ammonia (10).

It could be shown that the formation of 8α-estrone under our conditions was not the result of amide-catalyzed rearrangement to the conjugated 8-dehydro isomer. Equilin dimethyl ketal, on contact with potassium amide in ammonia for 2 h, underwent rearrangement to the 8-dehydro isomer to the extent of only about 30%. In addition, 8-dehydroestrone ketal gave no 8α-estrone on reduction with potassium in ammonia. The reduction of equilin methyl ether dimethyl ketal with potassium at −33° afforded a mixture consisting of 55% starting material, 45% 8β-estrone methyl ether and, at most, traces of 8α-estrone methyl ether.[3]

Since the behavior of these related compounds towards potassium in ammonia is different from that of equilin ketal, we appear to be dealing with a direct reduction of the 7,8-double bond in the case of the latter compound. The fact that a 3-methyl ether does not undergo the same reaction shows that the negative charge of the anion formed on contact of the phenol with the metal must be participating in the reduction, perhaps by resonance stabilization of the radical anion **10**: The addition of the second electron and proton (e.g., **11** → **12**) might well be a fast, kinetically-controlled process taking place from the less hindered α-side of the molecule, resulting in the formation of the *cis*-fused 8α,9α-system.

[3]The 8β-estrone methyl ether probably was formed via the conjugated 8-dehydroestrone derivative, since metal–ammonia reduction of 8-dehydroestrone methyl ether is known to result in the formation of the *trans*-8β,9α-system (9).

Can. J. Chem. Downloaded from www.nrcresearchpress.com by 210.87.254.40 on 09/05/12
For personal use only.

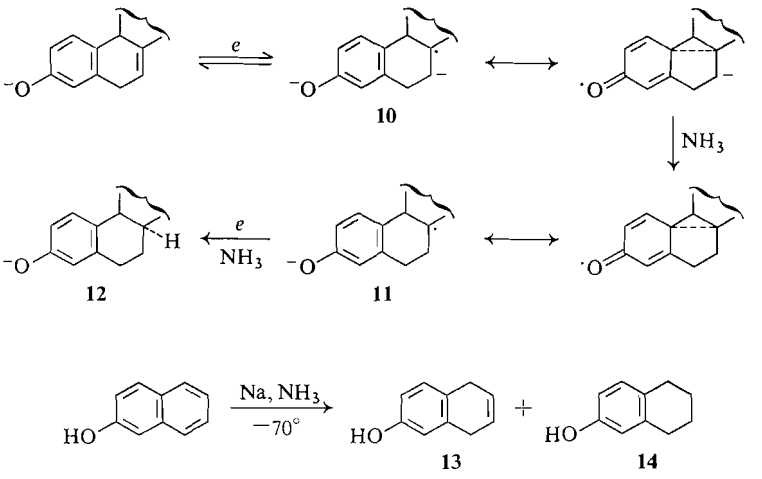

The nature of the oxygen–metal bond may account for the unique effectiveness of potassium in this reaction. This metal would be expected to form a more ionic bond to oxygen than would sodium or lithium. The negative charge on oxygen might, therefore, be more "available" for stabilization of the radical anion **10** in the presence of potassium than it would be in the presence of the more covalently bound sodium or lithium.

Since Birch (11) has shown that 2-naphthol is reduced to 2-tetralone by sodium and *t*-amyl alcohol in refluxing ammonia, it was of interest to determine how this simple analogue of the steroid system would behave under our reducing conditions. It was found that with sodium at −70° and in the absence of alcohol, 2-naphthol gave a 56% yield of a 3:2 mixture (as determined by g.l.c.) of 5,8-dihydro-2-naphthol (**13**) and 5,6,7,8-tetrahydro-2-naphthol (**14**). The dihydro compound **13** could not be obtained completely free of tetrahydro compound **14**, but its structure was evident from its ultraviolet (u.v.) spectrum (λ_{max} 282 mμ, ε 2220) and its nuclear magnetic resonance (n.m.r.) spectrum which showed multiplets centered at δ 3.40 (C-5, C-8 protons) and δ 5.93 p.p.m. (C-6, C-7 olefinic protons). Catalytic reduction of the impure **13** with palladium-on-charcoal gave a mixture consisting of 86% **14** and 13% 2-naphthol, as determined by g.l.c. The ratio of **13** to **14** obtained in the sodium–ammonia reduction of 2-naphthol was not a function of the length of time the reaction was allowed to proceed; hence, it is unlikely that **14** arises by rearrangement of **13** to a styrenoid isomer followed by reduction.

The formation of the tetrahydro derivative **14** under these conditions, in contrast to the case of naphthalene which affords only the1,4-dihydro derivative with sodium at −70° (12,13), perhaps reflects a destabilization of the resonance structure **15** relative to **16** due to the influence of the

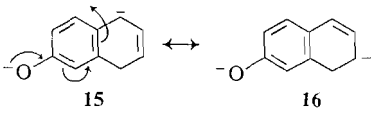

negatively charged oxygen-bearing ring (cf. **15**, arrows). However, the same effect is not seen in the steroid series, since very little, if any, tetrahydro derivative is formed (as judged by g.l.c.) in the reduction of equilenin ethylene ketal at −70°.

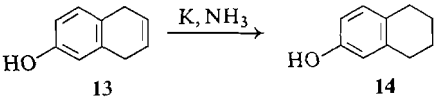

The dihydronaphthol **13** was rapidly reduced to the tetrahydro derivative **14** by potassium in ammonia at −33° but not by sodium. As in the case of the analogous reaction in the steroid series, it appeared that this reduction was not taking place via conjugation of the double bond, since, on contact with potassium amide under the same conditions, **13** underwent rearrangement to the extent of only 20%. Thus, here again, reduction of the double bond apparently occurs with the participation of the oxygen-bearing ring with its associated negative charge.

Can. J. Chem. Downloaded from www.nrcresearchpress.com by 210.87.254.40 on 09/05/12
For personal use only.

Can. J. Chem. Downloaded from www.nrcresearchpress.com by 210.87.254.40 on 09/05/12
For personal use only.

Experimental

Melting points were determined on a Thomas Hoover apparatus and are uncorrected. Nuclear magnetic resonance spectra were taken on a Varian A-60A instrument with tetramethylsilane as internal standard. Microanalyses were performed by W. J. Turnbull and associates. Gas–liquid chromatography was carried out on trimethylsilyl ethers of steroids on an F and M model 402 instrument on 6 ft columns of 3.75% DEGS on Gaschrom Q, 80–100 mesh, at 200°. In the case of naphthols, analyses by g.l.c. were done on a Perkin-Elmer model 800 instrument on 6 ft columns of 15% QF-1 on Gaschrom Q at 150°. Liquid ammonia was distilled from a commercial cylinder into reaction flasks fitted with dry ice condensers. Except where otherwise indicated, "usual work-up" of a reaction in liquid ammonia means that excess ammonium chloride was added, the ammonia was allowed to evaporate, usually under a stream of nitrogen, ether and water were added, and the product was extracted with ether. The ether extracts were washed several times with water, dried, and the solvent was removed under reduced pressure.

Equilin (8)

A mixture of 8.7 g of equilenin, 0.70 g of *p*-toluenesulfonic acid, and 70 ml of ethylene glycol in 600 ml of benzene was stirred and heated under reflux using a water separator for 7 h. The cooled benzene solution was washed with $NaHCO_3$ solution and water and, after removal of solvent, crystallization from methylene chloride–hexane yielded 7.2 g of equilenin ethylene ketal, m.p. 161–163°.

Sodium hydride (1.54 g of a 50% dispersion in mineral oil) was washed three times by decantation with petroleum ether. The adhering solvent was blown off by a stream of nitrogen, 25 ml of tetrahydrofuran (THF) was added, and a solution of 7.00 g of equilenin ethylene ketal in 75 ml of THF was added dropwise with stirring under nitrogen. The solution was stirred for 1 h at room temperature and was then transferred to a dropping funnel attached to a 3-necked flask containing a solution of 2.65 g of lithium in 250 ml of ammonia (previously prepared by stirring at the b.p. of ammonia for 1 h). The lithium solution was cooled to −70° with a dry ice–acetone bath and the steroid solution was added dropwise with stirring over a period of 30 min. Stirring was continued at −70° for 2 h. A small sample of the crude ketal obtained after the usual work-up was hydrolyzed with dilute HCl and the product was found to contain 76% equilin by g.l.c. analysis. The remainder of the crude ketal was dissolved in 75 ml of methanol and 5 ml of 10% HCl were added. After 2 h at room temperature, the mixture, containing precipitated product, was cooled and filtered, and the solid was washed with cold 1:1 methanol–water. The product (3.6 g, m.p. 229–233°) was crystallized once from isopropanol to yield 3.28 g of equilin, m.p. 234–237°, undepressed on admixture with an authentic sample.

8α-Estrone (8)

a) From Equilenin

To a solution of 10.2 g of potassium in 250 ml of ammonia under reflux was added dropwise a solution of 1.00 g of equilenin ethylene ketal in 20 ml of THF. After stirring for 3 h, ethanol was added to decolorize the solution, the ammonia was allowed to evaporate, and the product was extracted with ether. A solution of the crude product in 10 ml of acetone and 1 ml of 10% HCl was kept at 40–50° for 1 h, concentrated, and extracted with ethyl acetate. The product (545 mg) was chromatographed on 40 g of deactivated silica gel. Elution with ether–benzene 5:95 gave 436 mg of 8α-estrone which, after crystallization from methanol, had m.p. 246–247° (decomp.), λ_{max} 278.5 mμ (ε 2340). This product was identical (by mixture melting point) with the 8α-estrone prepared from equilin (see below).

b) From Equilin

To a stirred suspension of 5.00 g of equilin in 25 ml of methanol and 25 ml of trimethyl orthoformate were added 2.5 ml of a solution of 0.2 ml of concentrated H_2SO_4 in 4 ml of trimethyl orthoformate. The steroid rapidly dissolved and the product precipitated slowly. After 2 h, the mixture was neutralized with a few drops of pyridine, cooled, and filtered to yield 4.63 g of equilin dimethyl ketal, m.p. 199–200°. The i.r. spectrum showed the absence of carbonyl absorption and the presence of ether bands at 1105–1110 cm^{-1}. The compound decomposed on prolonged standing and on attempted crystallization.

To a solution of 20.4 g of potassium in 300 ml of refluxing ammonia was added dropwise a solution of 2.00 g of equilin dimethyl ketal in 20 ml of THF. After stirring for 3 h, the reaction mixture was worked up as usual. A solution of the crude product in 20 ml of acetone was treated with 0.5 ml of 10% HCl and kept for 1 h at room temperature. Dilution with 25 ml of water and filtration yielded 1.7 g of 8α-estrone, m.p. 242–244° (decomp.). Recrystallization from methanol and then from ethyl acetate gave an analytical sample, m.p. 247–249° (decomp.), $[\alpha]_D$ +101° (dioxane) (lit. (7) m.p. 242–244°, $[\alpha]_D$ +105° (EtOH)).

Anal. Calcd. for $C_{18}H_{22}O_2$: C, 79.96; H, 8.20. Found: C, 79.97; H, 8.10.

Methylation with dimethyl sulfate and aqueous KOH in ethanol gave 8α-estrone methyl ether, m.p. 92.5–95.5° (from hexane) (lit. (7) m.p. 93–94°).

Anal. Calcd. for $C_{19}H_{24}O_2$: C, 80.24; H, 8.51. Found: C, 80.50; H, 8.60.

This compound was identical spectroscopically (by i.r., n.m.r.) and by g.l.c. with *dl*-8α-estrone methyl ether (8).

Reaction of Equilin Dimethyl Ketal with Potassium Amide

To a suspension of potassium amide made from 440 mg of potassium and a trace of ferric chloride hydrate in 50 ml of ammonia under reflux was added dropwise a solution of 500 mg of equilin dimethyl ketal in 10 ml of THF. The resulting orange suspension was stirred for 2 h. After the usual work-up and hydrolysis of the ketal grouping with dilute HCl in methanol at room temperature, a solid (375 mg) was obtained with λ_{max} 275–281 mμ (ε 5460). Analysis by g.l.c. and n.m.r. showed this product to consist essentially of a 2:1 mixture of equilin and 8-dehydroestrone.

Reduction of 8-Dehydroestrone Ethylene Ketal

A mixture of 480 mg of *dl*-8-dehydroestrone (8), 35 mg of *p*-toluenesulfonic acid, and 3 ml of ethylene glycol in 35 ml of benzene was stirred and heated under reflux for 8 h using a water separator. After washing with $NaHCO_3$

Can. J. Chem. Downloaded from www.nrcresearchpress.com by 210.87.254.40 on 09/05/12
For personal use only.

solution and water followed by drying and removal of solvent, a pale-yellow foam was obtained whose i.r. spectrum showed no carbonyl absorption.

A solution of 490 mg of this material in 8 ml of THF was added to a solution of 3.4 g of potassium in 50 ml of ammonia under reflux. After stirring for 4 h, the usual work-up gave a yellow foam with λ_{max} 271 mμ (ε 12 100). Analysis by n.m.r. and g.l.c. (after hydrolysis of the ketal group with dilute HCl in methanol) showed the product to be a mixture of 27% 8-dehydroestrone, 34% estrone, and 19% 9(11)-dehydroestrone.[4]

Reduction of Equilin Methyl Ether Dimethyl Ketal

To a suspension of 1.00 g of equilin methyl ether in 3 ml of methanol and 3 ml of trimethyl orthoformate was added 0.3 ml of a solution of 0.1 ml of concentrated H_2SO_4 in 2 ml of trimethyl orthoformate. The ketal began to precipitate after 10 min. After stirring for 3 h, a few drops of pyridine and 3 ml of water were added and the product was filtered and washed with cold methanol. The yield of dimethyl ketal was 1.10 g, m.p. 106–109°, showing no carbonyl absorption in its i.r. spectrum.

A solution of 570 mg of this ketal in 5 ml of THF was added to a refluxing solution of 3.4 g of potassium in 50 ml of ammonia. After a reaction time of 2 h followed by the usual work-up and hydrolysis of the ketal with dilute HCl in methanol, 365 mg of a crystalline solid was obtained, m.p. 152–158°. Analysis by n.m.r. spectrum and g.l.c. (the latter performed on the 17-alcohol formed by reduction with $NaBH_4$ in methanol) showed the product to consist essentially of a 55:45 mixture of starting material and 8β-estrone methyl ether possibly containing a very small amount of 8α-estrone methyl ether.

Reduction of 2-Naphthol

A solution of 2.77 g of sodium in 80 ml of ammonia was cooled to −70° and a solution of 5.00 g of 2-naphthol in 20 ml of ether was added dropwise over a period of 10 min. After stirring for 1 h at −70°, ammonium chloride was added and the ammonia was allowed to evaporate under a stream of nitrogen. Ether and dilute HCl were added, and an ether extract of the crude product was extracted six times with cold 5% NaOH solution. Acidification of the alkaline extracts with dilute HCl followed by ether extraction gave 3.9 g of a dark brown oil. Shortpath distillation at 0.1 mm yielded 2.8 g of a colorless solid with m.p. 71–73°. Analysis by g.l.c. and n.m.r. spectrum showed this to be a 3:2 mixture of 5,8-dihydro-2-naphthol (**13**) and 5,6,7,8-tetrahydro-2-naphthol (**14**). Repeated recrystallization from ether–petroleum ether gave **13** with m.p. 78–79° which still contained 7% of tetrahydro compound; λ_{max} 282 mμ (ε 2220); n.m.r. ($CDCl_3$) δ 1.76, 2.72 (multiplets, tetrahydro compound impurity), 3.40 (multiplet, C-5, C-8 H), 5.10 (singlet, O—H), 5.93 (multiplet, C-6, C-7 H), and 6.60–7.18 p.p.m. (multiplet, aromatic H).

Anal. Calcd. for $C_{10}H_{10}O$: C, 82.16; H, 6.89. Found: C, 82.06; H, 6.88.

A solution of 1.51 g of **13** which contained 21% of **14** in 30 ml of benzene was shaken with hydrogen in the presence of 300 mg of 5% palladium-on-charcoal. When hydrogen absorption ceased after 1.5 h, the mixture was filtered and the solvent was evaporated to give a colorless oil. Analysis by g.l.c. showed this product to be a mixture containing 86% **14**, 13% 2-naphthol, and 0.5% **13**.

Reduction of 5,8-Dihydro-2-naphthol (13) with Potassium in Ammonia

To a stirred refluxing solution of 4.4 g of potassium in 50 ml of ammonia was added dropwise over a period of 2 min a solution of 500 mg of a 65:35 mixture of **13** and **14** in 5 ml THF. After stirring for 15 min, the reaction mixture was worked up in the usual way to give an oil which solidified. Analysis by g.l.c. showed this product to be pure tetrahydro compound **14**. Crystallization from hexane gave **14** with m.p. 59–60° (lit. m.p. 58–59° (14)).

With sodium, under the same conditions, no reduction of **13** took place. A sample of **13** which was allowed to react with potassium amide in ammonia for 15 min was found by g.l.c. to have undergone rearrangement to the extent of about 20%.

[4]The 9(11)-dehydroestrone was probably formed by isomerization during the ketal formation (cf. (8)) and the estrone could have arisen from either the 8- or 9(11)-dehydroestrone.

Acknowledgments

We are indebted to Dr. G. Schilling and associates for n.m.r. data and for numerous g.l.c. analyses. We are extremely grateful to J. Schmid for enthusiastic and skilled technical assistance.

1. J. A. Zderic, H. Carpio, A. Bowers, and C. Djerassi. Steroids, **1**, 233 (1963).
2. J. F. Bagli, P. F. Morand, K. Wiesner, and R. Gaudry. Tetrahedron Letters, 387 (1964).
3. R. P. Stein, G. C. Buzby, Jr., and H. Smith. Tetrahedron Letters, 5015 (1966).
4. E. J. Bailey, A. Gale, G. H. Phillipps, P. T. Siddons, and G. Smith. Chem. Commun. 1253 (1967).
5. R. D. H. Heard and M. M. Hoffman. J. Biol. Chem. **138**, 651 (1941).
6. J. Fried, N. A. Abraham, and T. S. Santhanakrishnan. J. Am. Chem. Soc. **89**, 1044 (1967).
7. A. Serini and W. Logemann. Chem. Ber. **71**, 186 (1938).
8. C. Rufer, E. Schroeder, and H. Gibian. Ann. Chem. **705**, 211 (1967).
9. G. H. Douglas, J. M. H. Graves, D. Hartley, G. A. Hughes, B. J. McLoughlin, J. Siddall, and H. Smith. J. Chem. Soc. 5072 (1963).
10. B. R. Ortiz de Montellano, B. A. Loving, T. C. Shields, and P. D. Gardner. J. Am. Chem. Soc. **89**, 3365 (1967).
11. A. J. Birch. J. Chem. Soc. 430 (1944).
12. W. Hückel and H. Bretschneider. Ann. Chem. **540**, 157 (1939).
13. H. Smith. Organic reactions in liquid ammonia. John Wiley and Sons, Inc., New York. 1963. p. 237.
14. S. Goodwin and B. Witkop. J. Am. Chem. Soc. **79**, 179 (1957).

Can. J. Chem. Downloaded from www.nrcresearchpress.com by 210.87.254.42 on 09/05/12
For personal use only.

Fragmentation reactions promoted by cyanogen bromide

A. F. Casy, M. M. A. Hassan, and A. P. Parulkar
Faculty of Pharmacy and Pharmaceutical Sciences, University of Alberta, Edmonton, Alberta

Received December 23, 1968

The fragmentation of α-4-dimethylamino-3-methyl-1,2-diphenylbutan-2-ol to *cis* H/Ph 3-methyl-1,2-diphenylprop-2-ene, normally induced by treating the corresponding 2-chloro derivative with a base, also results when the alcohol itself is treated with cyanogen bromide; related γ-hydroxy acyclic tertiary amines similarly undergo fragmentation in this reaction. In contrast, cyclic analogues such as β-1,3-dimethyl-4-phenyl-4-piperidinol are not cleaved by cyanogen bromide (corresponding *N*-cyano derivatives are formed in low yield) even though β-4-chloro-1,3-dimethyl-4-phenylpiperidine is fragmented by potassium cyanide to *trans* H/Ph 5(*N*-cyanomethyl-*N*-methylamino)-3-phenylpent-2-ene.

Canadian Journal of Chemistry, 47, 3133 (1969)

As part of a study of the von Braun *N*-demethylation procedure (1), the aminoalcohols **1***a*, **2***a*, and **2***b* were treated with cyanogen bromide. These compounds were chosen as reaction substrates because of the previous finding (1) that bases with oxygen functions delta to a dimethylamino group (e.g. methadone) are converted to cyclic products by cyanogen bromide (NCBr) instead of to *N*-cyano-*N*-methyl derivatives, the normal products of the von Braun reaction. An abnormal reaction course was also seen in the present experiments, the alcohols **1***a*, **2***a*, and **2***b* (OH γ- to NMe_2) being fragmented by NCBr at room temperature. Products isolated from the α-(±)-diastereoisomer of **1***a*, of known configuration (2), were *cis* H/Ph 3-methyl-1,2-diphenylprop-2-ene **3** (3) [ultraviolet (u.v.) and proton

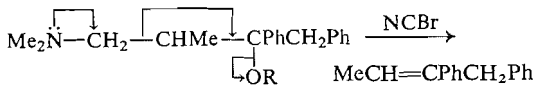

1 *a*) R = H; *b*) R = OCOMe — **3**

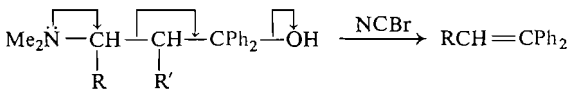

2 *a*) R = H, R′ = Me; *b*) R = Me, R′ = H — **4** *a*) R = Me; *b*) R = H

magnetic resonance (p.m.r.) spectra were identical with those of an authentic sample obtained from the 2-chloro analogue of **1***a* and sodium methoxide or pyridine] and α-**1***a* hydrobromide. No attempt was made to isolate the fragment complementary to the propene **3**. The diphenylpropan-1-ols **2***a* and **2***b* gave 1,1-diphenylprop-1-ene **4***a* and 1,1-diphenylethylene **4***b* respectively together with the corresponding substrate hydrobromides. No *N*-cyano derivatives were detected in any of the reaction products. The α-acetate **1***b* was also fragmented by NCBr giving *cis* **3**, but in this case the non-basic fraction contained the *N*-cyano-*N*-methyl acetate **5** in comparable amount (proton magnetic resonance evidence). Reaction between NCBr and the β-(±) diastereoisomer of **1***a* again gave the *cis* propene **3** as the major non-basic product. Hence, reaction of both α- and β-**1***a* appears to proceed through a common intermediate. This is probably a carbonium ion since if NCBr is regarded as analogous to an acyl halide, its reaction upon the tertiary benzylic alcohols **1** and **2** would be expected to give a reaction species of this nature.[1] The intermediate is represented in **6** by a conformer which satisfies the stereoelectronic requirements of fragmentation (4) and accounts for the exclusive or preponderant formation of the *cis* H/Ph

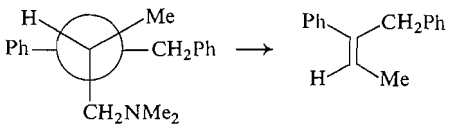

6

alkene **3**. Recovery of the α- rather than the β-**1***a* hydrobromide when β-**1***a* is treated with NCBr further supports the above interpretation of the reaction course. The β-ester **1***b* with NCBr gave a solid *N*-cyano-*N*-methyl ester **5** as the sole non-basic reaction product.

Some related reactions of the cyclic γ-hydroxy-tertiary amine **7** (β-prodinol, *cis* 3-Me/4-Ph) were next investigated. The 4-chloro analogue **7***b*, obtained by treating **7***a* with thionyl chloride (5), has

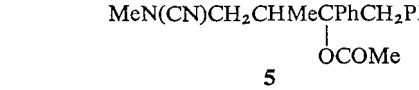

5

[1]Thanks to a referee for this suggestion.

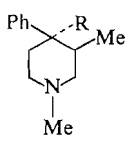

7 *a*) R = OH,
b) R = Cl

the same configuration as the parent alcohol since its 3-methyl p.m.r. signal suffers a pronounced downfield shift (base, 52 Hz; HCl, 68 Hz from TMS in $CDCl_3$ at 60 MHz) when the basic center is protonated [the 3-methyl chemical shifts of α-isomers (*trans* 3-Me/4-Ph) of this type are little changed after *N*-protonation] (6). When **7***b* was treated with potassium cyanide in ethanol–water at the reflux temperature, a fragmentation reaction[2] occurred (cf. reaction between 3-β-chlorotropane and potassium cyanide) (7), the major product being 5-(*N*-methyl-*N*-cyanomethylamino)-3-phenylpent-2-ene **8**; this structure is substantiated by spectroscopic evidence (see Ex-

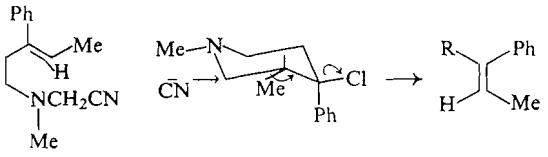

8 **9**

perimental). The predicted stereochemistry of **8**, based on reaction proceeding via the intermediate **9**, consistent with the stereoelectronic requirements of fragmentation (4) and the *cis* 3-Me/4-Ph configuration of **7***b*, is *trans* H/Ph. Support for this assignment is provided by the higher field chemical shift of the vinylic proton of **8** (336 Hz from TMS, base in $CDCl_3$) compared with that of the *cis* analogue **3** (365 Hz from TMS in $CDCl_3$) and comparative u.v. characteristics (**8** λ_{max} 231 mμ, ε 7600; **3** λ_{max} 245 mμ, ε 10 850 both in ethanol); these differences are consistent with a reduced degree of aromatic ring double bond coplanarity in the *trans* H/Ph derivative. β-Prodinol **7***a* and the tetrahydropyridine **10** were minor products of this reaction.

In view of the proneness of **7***b* to fragmentation, it was felt that NCBr should induce the cleavage of the precursor alcohol itself (**7***a*) by analogy with experiments upon the acyclic amino–alcohol

[2]The two fragments are, of necessity, linked together because of the ring system and no loss of carbon occurs.

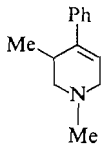

10

$Me_2NCH_2CMe{=}CPh_2$ **11**

$BrCH_2CMe{=}CPh_2$ **12**

1*a* and its chloro derivative. When β-prodinol was treated with NCBr in chloroform or benzene, however, the alcohol was recovered in high yield as the hydrobromide salt together with a small amount of the *N*-cyano-4-piperidinol (**7***a*, N—Me replaced by N—CN). The absence of a vinylic signal in the p.m.r. spectrum of the total hydrobromide showed that no fragmentation product formed. A similar result was obtained when 1-methyl-4-phenyl-4-piperidinol was used in this reaction, except that a small yield of the dehydrated alcohol also resulted. The process by which hydrogen bromide is generated in these reactions is not clear. The relative inertness of β-prodinol **7***a* (and the 3-desmethyl analogue) towards NCBr is possibly due to the highly hindered nature of its hydroxyl function (axial in preferred conformation and geminal to phenyl) (6).

Reaction of NCBr with the aminoalkene **11** gave 3-bromo-2-methyl-1,1-diphenylprop-1-ene **12**. This appears to be a normal tertiary-amino NCBr reaction in that one of the groups attached to nitrogen is cleaved, but is unusual in that the largest rather than the smallest *N*-substituent is lost.

Experimental

The p.m.r. spectra were recorded on a Varian A-60 spectrometer using $CDCl_3$ or DMSO-d_6 as solvent. Chemical shifts are expressed in τ units with TMS as standard. Infrared (i.r.) spectra of salts were recorded as Nujol mulls. The previously described (1) method for the reaction of tertiary amino substrates with NCBr was used. In the following specific cases, weight of substrate, reaction period, and temperature are given in parentheses after each example. Salts were crystallized from ethanol–ether.

(*a*) The α-butan-2-ol **1***a* (2) (11.2 g, 2 h, room) and NCBr (4.2 g) in $CHCl_3$ (40 ml) gave α-**1***a* hydrobromide (6.5 g), m.p. 235–237°, lit. (8) 235–236°, and 3-methyl-1,2-diphenylprop-2-ene (3.4 g) b.p. 104°/0.05 mm. Characteristics of the latter's u.v. and p.m.r. spectra were the same as those of the authentic *cis* H/Ph propene **3** (3).

(*b*) The α-acetate **1***b* (2) (14.6 g, 3 h, room) and NCBr (4.8 g) in $CHCl_3$ (40 ml) gave α-**1***b* hydrobromide, (7.5 g), ν_{max} 2650 ($\overset{+}{N}H$), 1735 (C=O) and 3350 cm^{-1} (H_2O), and the *cis* H/Ph propene **3** (4 g) b.p. 104°/0.05 mm.

Can. J. Chem. Downloaded from www.nrcresearchpress.com by 210.87.254.42 on 09/05/12
For personal use only.

Can. J. Chem. Downloaded from www.nrcresearchpress.com by 210.87.254.42 on 09/05/12
For personal use only.

Anal. Calcd. for $C_{21}H_{28}BrNO_2 \cdot H_2O$: C, 59.4; H, 7.1. Found: C, 60.0; H, 7.05.

The p.m.r. spectrum of the total non-basic fraction in $CDCl_3$ displayed signals due to the *N*-cyanomethyl derivative of **1***b* [singlets 7.33 (NMe) and 8.1 (OCOMe) and doublet 8.95 τ, *J* 6.5 Hz (3-Me)] as well as those due to the *cis* propene **3**.

(*c*) The β-butan-2-ol **1***a* (2) (3 g, 12 h, room) and NCBr (1 g) in $CHCl_3$ (20 ml) have **1***a* hydrobromide (2 g), m.p. 234–236° established as the α-diastereoisomer since its i.r. spectrum showed bands at 3080 and 3240 cm^{-1}, typical of the α-form and absence of β-bands (9). The major component of the non-basic product (0.5 g) was the *cis* propene **3** (p.m.r. comparisons).

(*d*) The β-acetate **1***b* (2) (1.5 g, 2 h, room) and NCBr (0.5 g) in $CHCl_3$ (20 ml) gave 2-acetoxy-4-*N*-cyano-*N*-methylamino-3-methyl-1,2-diphenylbutane (0.4 g), m.p. 131–132° from ether, ν_{max} 2195 (NCN) and 1730 cm^{-1} (C=O); p.m.r. characteristics in $CDCl_3$: singlets 7.23 (NMe) and 7.97 (COMe), doublet 8.95 τ, *J* 6.5 Hz (3-Me).

Anal. Calcd. for $C_{21}H_{24}N_2O_2$: C, 75.0; H, 7.2; N, 8.3. Found: C, 75.2; H, 7.3; N, 8.3.

(*e*) β-Prodinol **6***a* (10) (10.2 g, 2 h, room) and NCBr (5.3 g) in $CHCl_3$ (50 ml) or benzene (50 ml) gave **6***a* hydrobromide (6.5 g), m.p. 203–205°.

Anal. Calcd. for $C_{13}H_{20}BrNO$: C, 52.9; H, 7.1. Found: C, 52.5; H, 7.1.

1-Cyano-3-methyl-4-phenyl-4-piperidinol (0.18 g), m.p. 106–108° from hexane–methanol, was also isolated.

Anal. Calcd. for $C_{13}H_{16}N_2O$: C, 72.1; H, 7.45; N, 13.9. Found: C, 72.2; H, 7.6; N, 13.85.

The total hydrobromide had a p.m.r. spectrum in DMSO-d_6 very similar to that of β-**6***a* hydrochloride and lacked signals in the vinylic region.

The same treatment of 1-methyl-4-phenyl-4-piperidinol (1.6 g) gave 1-cyano-4-phenyl-4-piperidinol (40 mg), m.p. 138–140° from hexane–methanol.

Anal. Calcd. for $C_{12}H_{14}N_2O$: C, 71.2; H, 7.0; N, 14.85. Found: C, 71.0; H, 7.0; N, 14.7.

The piperidinol hydrobromide (0.5 g) and 1-methyl-4-phenyl-1,2,5,6-tetrahydropyridine, isolated as a hydrochloride m.p. 252–253°, lit. (11) 251–253°, were also obtained.

(*f*) The amino-propanol **2***a* (10.8 g, 2 h, room) and NCBr (4.2 g) in $CHCl_3$ (40 ml) gave **2***a* hydrobromide (6.5 g), m.p. 228–230°, ν_{max} 2650 cm^{-1} ($\overset{+}{N}$—H).

Anal. Calcd. for $C_{18}H_{24}BrNO$: C, 61.7; H, 6.9. Found: C, 61.4; H, 6.9.

The non-basic product of this reaction, 1,1-diphenylprop-1-ene (2 g), m.p. 46–48° from ethanol, lit. (12) b.p. 143–145°/11 mm, had u.v. and p.m.r. characteristics similar to those reported (12).

Anal. Calcd. for $C_{15}H_{14}$: C, 92.7; H, 7.3. Found: C, 92.85; H, 7.3.

(*g*) The amino-propanol **2***b* (10.8 g, 3 h, room) and NCBr (4.3 g) in $CHCl_3$ (40 ml) gave **2***b* hydrobromide (7 g), m.p. 229–231°. Anal. Found: C, 61.6; H, 6.7.

The non-basic product of this reaction, 1,1-diphenylethylene (2.2 g), b.p. 102°/0.5 mm, lit (12) b.p. 128°/10 mm, had u.v. and p.m.r. characteristics similar to those reported (12).

(*h*) The amino-alkene **10** (obtained by dehydrating the propanol **2***a* with HCl–acetic acid) (4 g, 3 h, room) and NCBr (1.7 g) in $CHCl_3$ (20 ml) gave 3-bromo-2-methyl-1,1-diphenylprop-1-ene (3.5 g), b.p. 118°/0.05 mm, m.p. 45–47°, λ_{max} 252 mμ, ε 13 200 in ethanol; p.m.r. characteristics in $CDCl_3$: multiplet 2.8 (10 aryl protons), singlets 5.97 (2-methylene protons) and 8.08 τ (*t*-methyl).

Anal. Calcd. for $C_{16}H_{15}Br$: C, 66.9; H, 5.3; Br, 28.5. Found: C, 66.9; H, 5.1; Br, 28.55.

Reaction of β-4-chloro-1-methyl-4-phenylpiperidine with KCN.

A mixture of the 4-chloropiperidine (6), (1.8 g), freshly liberated from the hydrochloride salt, KCN (0.6 g), ethanol (15 ml), and water (2.8 ml) was heated under reflux for 11 h. The product was concentrated, diluted with water, and extracted with ether. The ether (dried, Na_2SO_4) was evaporated and the residue (1.7 g) acidified with ethanol–HCl when the cyanomethylamino-alkene **7** hydrochloride (0.6 g) m.p. 125.5–126.5° after recrystallization, separated; ν_{max} 2245 cm^{-1} (CN, base, band obscured in the salt), λ_{max} 231 mμ, ε 7600 in ethanol; p.m.r. characteristics in $CDCl_3$; quartet 4.2 *J* 7 Hz (base 4.4, vinylic proton), broad singlet 4.72 (base 6.62, NCH_2CN), singlet 7.08 (base 7.78, NMe), and doublet 8.4 *J* 7 (base 8.45, τ MeCH=).

Anal. Calcd. for $C_{14}H_{19}ClN_2$: C, 67.1; H, 7.6; N, 11.2. Found: C, 67.6; H, 7.6; N, 11.6.

β-Prodinol hydrochloride (0.2 g), m.p. 214–214.5°, was isolated from the mother liquors.

Anal. Calcd. for $C_{13}H_{20}ClNO$: C, 64.5; H, 8.3; N, 5.8. Found: C, 64.3; H, 8.25; N, 6.1. The p.m.r. spectrum of the total reaction product (base in $CDCl_3$) had signals characteristic of β-prodinol (3-Me doublet at 9.23) (7) and the tetrahydropyridine **9** (vinylic band at 4.17 and Me doublet at 9.02 τ) (13).

Acknowledgments

The authors thank Dr. J. Lee of Roche (Nutley, N.J.) for a sample of β-prodinol, and the Medical Research Council of Canada for financial support.

1. A. F. Casy and M. M. A. Hassan. Tetrahedron, **23**, 4075 (1967).
2. A. Pohland and H. R. Sullivan. J. Am. Chem. Soc. **75**, 4458 (1953); H. R. Sullivan, J. R. Beck, and A. Pohland. J. Org. Chem. **28**, 2381 (1963).
3. A. F. Casy, J. L. Myers, and P. Pocha. Tetrahedron, **22**, 1001 (1966).
4. C. A. Grob, H. R. Kiefer, H. Lutz, and H. Wilkens. Tetrahedron Letters, 2901 (1964).
5. A. F. Casy. J. Chem. Soc. 5057 (1961).
6. A. F. Casy. Tetrahedron, **22**, 2711 (1966).
7. S. Archer, T. R. Lewis, and B. Zenitz. J. Am. Chem. Soc. **80**, 958 (1958).
8. P. Pocha. Ph.D. Thesis, University of London. 1966.
9. A. F. Casy and P. Pocha. J. Chem. Soc. B. 1160 (1966).
10. A. Ziering and J. Lee. J. Org. Chem. **12**, 911 (1947).
11. C. J. Schmidle and R. C. Mansfield. J. Am. Chem. Soc. **77**, 5698 (1955).
12. A. Jung and M. Brini. Bull. Soc. Chim. (France), 693 (1964).
13. A. F. Casy, A. H. Beckett, M. A. Iorio, and H. Z. Youssef. Tetrahedron, **21**, 3387 (1965).

Can. J. Chem. Downloaded from www.nrcresearchpress.com by 210.87.254.105 on 09/05/12
For personal use only.

Conformation and configuration of some α,β-unsaturated carbonyl compounds from their nuclear magnetic resonance spectra

W. M. PHILLIPS AND D. J. CURRIE
Chemistry Section, Defence Research Establishment, Suffield, Ralston, Alberta

Received February 21, 1969

Nuclear magnetic resonance spectra were recorded for 95 styrenes with two functional groups (A and B) on the β-carbon atom where A, B are $COCH_3$, $COCH_3$; $COCH_3$, $CO_2C_2H_5$; $CO_2C_2H_5$, $COCH_3$; $CO_2C_2H_5$, $CO_2C_2H_5$; $CO_2C_2H_5$, CN; and $CO_2C_2H_5$, H. The chemical shifts of the ethylenic hydrogen and the hydrogens of the functional A and B groups were examined in detail to determine the effects of ring substituents. The configuration of the unsymmetrical styrenes and the conformation of the A and B groups as deduced from the spectra are discussed.

Canadian Journal of Chemistry, 47, 3137 (1969)

Introduction

Nuclear magnetic resonance (n.m.r.) spectra have been used by Timmons (1) to assign *S-cis* or *S-trans* conformations to α,β-unsaturated ketones and by Hayashi (2) to deduce the configuration of β-alkyl-α-cyanocinnamic esters. In this work the n.m.r. spectra of a number of ethyl α-cyanocinnamates or ethyl benzalcyanoacetates, **1**(A = $CO_2C_2H_5$, B = CN), ethyl benzalacetoacetates,

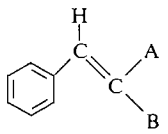

1

1(A = $COCH_3$, B = $CO_2C_2H_5$ or A = $CO_2C_2H_5$, B = $COCH_3$), diethyl benzalmalonates, **1**(A = B = $CO_2C_2H_5$), and 3-benzal-2,4-pentanediones, **1**(A = B = $COCH_3$), were used to assign configuration to the compounds with different A and B groups and to deduce the conformation of the A and B groups. The electronic environment of the ethylenic hydrogen and the hydrogens of the functional ester and ketone groups were monitored and changes in the conformation of these functional groups with substitution on the phenyl ring were examined.

Experimental

The preparation, properties, and analyses of the compounds used in this work have been described by Silver *et al.* (3). Solutions of the compounds, 10–20% w/v in $CDCl_3$ containing tetramethylsilane as the internal reference were used to record the spectra on a Varian A-60 spectrometer.

Results

Nuclear magnetic resonance spectral evidence indicates that all the compounds examined are geometrically homogeneous except the 2-methyl-, 3-methyl-, 3-fluoro-, 2-chloro-, 3-chloro-, 2-methoxy-, 4-methoxy-, 3,*n*-propoxy-, 2,6-dichloro-, 2,3-dimethoxy-, 2,4-dimethoxy-, and 3,4-methylenedioxy- derivatives of ethyl benzalacetoacetate, **1**(A or B = $COCH_3$ or $CO_2C_2H_5$). The τ values for the ethylenic proton and for those of the ketone and ester groups are tabulated in Tables I–VI. Displacements for similarly located protons in analogous members of different series

TABLE I

Chemical shifts in some 3-benzal-2,4-pentanediones*

X	Y	CH_3(B)	CH_3(A)	C=CH
H	H	7.75	7.60	2.51
2-CH_3	H	7.94	7.62	2.27
4-CH_3	H	7.74	7.61	2.55
4-F	H	7.72	7.59	2.60†
2-Cl	H	7.83	7.57	2.23
3-Cl	H	7.74	7.60	2.58
4-Cl	H	7.73	7.59	2.59
4-Br	H	7.73	7.59	2.59
2-CH_3O	H	7.79	7.60	2.18
3-CH_3O	H	7.76	7.61	2.55
4-CH_3O	H	7.71	7.62	2.59†
2-Cl	6-Cl	7.80	7.52	2.57
2-CH_3O	4-CH_3O	7.77	7.62	2.23
2-CH_3	6-CH_3			
4-methyl derivative		8.07	7.58	2.30

*Compounds of structure 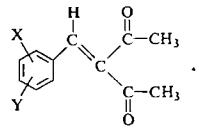 .

†Phenyl absorptions also occur in this region.

TABLE II

Chemical shifts in some ethyl benzalacetoacetates (ketone A)*

X	Y	CH_3(ketone)	CH_3(ester)	CH_2(ester)	C=CH
H	H	7.58	8.74	5.66	2.42
2-CH_3	H†	7.60	8.85	5.82	2.25
3-CH_3	H†	7.60	8.74	5.66	2.46
4-CH_3	H	7.62	8.72	5.66	2.48
3-F	H†	7.60	8.74	5.65	2.50
2-Cl	H†	7.54	8.83	5.78	2.13
3-Cl	H†	7.59	8.73	5.65	2.49
4-Cl	H	7.59	8.71	5.65	2.48
2-CH_3O	H†	7.58	8.78	5.74	2.04
3-CH_3O	H	7.60	8.73	5.67	2.48
4-CH_3O	H†	7.64	8.72	5.66	2.50
3-C_2H_5O	H	7.62	8.74	5.68	2.48
3,*n*-C_3H_7O	H†	7.62	8.74	5.68	2.50
3,*n*-C_4H_9O	H	7.61	8.72	5.67	2.48
2-Cl	4-Cl	7.57	8.81	5.75	2.24
2-Cl	6-Cl†	7.51	9.01	5.91	2.38
3-Cl	4-Cl	7.61	8.71	5.65	2.48
2-CH_3O	3-CH_3O†	7.57	8.79	5.74	2.13
2-CH_3O	4-CH_3O†	7.61	8.75	5.69	2.11
3-CH_3O	4-CH_3O	7.62	8.69	5.64	2.50
CH_2 (O—3†, O—4)		7.63	8.69	5.65	2.56

*Compounds of structure 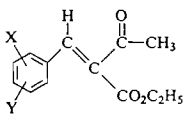 .

†These compounds were initially geometrically non-homogeneous.

relative to the unsubstituted parent compounds are virtually identical except when substitution occurs at C-2 and C-6 of the phenyl group. These average displacements appear in Table VII.

Substituted ethyl cinnamates[1], **1**(A = $CO_2C_2H_5$, B = H), (5, 6) (Table VI) were used as reference for assigning configuration to the unsymmetrical difunctional styrenes, **1**. The chemical shifts of the methyl triplet and the methylene quartet in these compounds are virtually independent of the position and nature of the substituent on the phenyl group. For the substituted diethyl benzalmalonates, **1**(A = B = $CO_2C_2H_5$), (Table IV) the chemical shifts of one of the two sets of methyl and of the methylene protons[2] likewise are virtually independent of the substituent on the phenyl group and therefore were assigned to the A position. The alternative set of absorptions which exhibit marked dependence upon substitution in the benzene ring were associated with the ester in the B position.

Chemical shifts for the ester group of the geometrically homogeneous ethyl benzalacetoacetates (Table II) are dependent upon phenyl substituents so the ester must be in the B position of **1**(A = $COCH_3$, B = $CO_2C_2H_5$). These compounds are unstable in solution and isomerize to approximately equimolar mixtures of the two geometric isomers. The chemical shifts for the ester protons of the new geometric isomers, **1**(A = $CO_2C_2H_5$, B = $COCH_3$), like those for the ethyl cinnamates, were independent of ring substituents (Table III). For those ethyl benzalacetoacetates that were mixtures of geometric isomers prior to recording the spectra (Tables II and III), it was possible to assign the two sets of absorption bands to the respective A and B ester groups by comparing the chemical shifts with those of the analogous diethyl benzalmalonates. Where overlap of the two sets of absorption bands occurred, the relative intensities of the methylene and methyl absorption peaks materi-

[1]The coupling constant for the ethylenic hydrogens of ethyl cinnamate is 16.3 ± 0.2 c.p.s. For the methyl and methylene protons in all ethyl ester derivatives of **1**, the coupling constant is 7.1 ± 0.2 c.p.s.

[2]For diethyl dihydrobenzalmalonate, only single absorptions (τ (CH_3) 8.84, τ (CH_2) 5.89) were observed.

Can. J. Chem. Downloaded from www.nrcresearchpress.com by 210.87.254.105 on 09/05/12
For personal use only.

TABLE III

Chemical shifts in some ethyl benzalacetoacetates (ketone B)*

X	Y	CH_3(ketone)	CH_3(ester)	CH_2(ester)	C=CH
H	H†	7.66	8.68	5.68	2.32
2-CH_3	H	7.83	8.67	5.69	2.19
3-CH_3	H	7.67	8.69	5.70	2.36
4-CH_3	H†	7.66	8.70	5.72	2.38
3-F	H	7.66	8.68	5.68	2.40
2-Cl	H	7.76	8.65	5.65	2.11
3-Cl	H	7.66	8.68	5.68	2.40
4-Cl	H†	7.65	8.66	5.67	2.40
2-CH_3O	H	7.71	8.67	5.72	2.04
3-CH_3O	H†	7.67	8.69	5.70	2.37
4-CH_3O	H	7.64	8.72	5.74	2.41
3-C_2H_5O	H†	7.68	8.69	5.71	2.38
3,*n*-C_3H_7O	H	7.69	8.71	5.72	2.39
3,*n*-C_4H_9O	H†	7.67	8.68	5.71	2.38
2-Cl	4-Cl†	7.75	8.67	5.68	2.16
2-Cl	6-Cl	7.68	8.64	5.64	2.40
3-Cl	4-Cl†	7.66	8.68	5.65	—
2-CH_3O	3-CH_3O	7.72	8.67	5.70	2.10
2-CH_3O	4-CH_3O	7.69	8.70	5.72	2.11
3-CH_3O	4-CH_3O†	7.63	8.69	5.72	2.41
CH_2(O—3, O—4)		7.63	8.69	5.72	2.47

*Compounds of structure 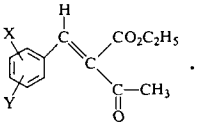 .

†These compounds were formed by isomerization in $CDCl_3$.

ally assisted in associating the bands with each of two geometrically positioned ester groups. Characterization of the A and B carbethoxyl groups of the isomeric ethyl benzalacetoacetates permitted the assignment of τ values to the A and B methyl ketone singlets. Assignment of the twin singlets for the A and B methyl ketones of the 3-benzal-2,4-pentanediones, **1**(A = B = $COCH_3$), followed (Table I). The positions of the methyl absorption for the A ketone of the 3-benzal-2,4-pentanediones and the ethyl benzalacetoacetates, like those of A ester groups, were independent of ring substituents while the positions of bands for the methyl protons of the B ketone groups were quite variable. If this approach to configuration is valid the methyl ketone protons of benzalacetone, **1**(A = $COCH_3$, B = H), should absorb at ~ 7.60 τ. The observed absorption was at 7.58 τ.

Similar arguments lead to the conclusion that the ester group in the ethyl benzalcyanoacetates, **1**(A = $CO_2C_2H_5$, B = CN), (Table V) is in the A position and that these compounds are not susceptible to isomerization in solution.

The positions of the methyl singlets in the phenyl substituted methyl and methoxyl derivatives of these styrenes are listed in Table VIII.

Discussion

The probable conformation of the difunctional conjugated heteroenoid compound is revealed in the relative positions of the various absorption bands of the C-2 -substituted derivatives. The aplanarity of the styrene moiety in C-2 -substituted ethyl cinnamates, **1**(A = $CO_2C_2H_5$, B = H), due to interference of the substituent with the B hydrogen atom[3] is reflected in a large downfield shift of the ethylenic hydrogen vicinal to the benzene ring, relative to that for the analogous hydrogen atom of the parent unsubstituted ethyl cinnamate. The orientation of this hydrogen in the deshielding field of the benzene ring, by itself, is not sufficient to account for the magnitude of

[3]Any discussion of the variation in the displacements of B hydrogen atoms with substitution on the phenyl group must await further data from similar systems.

Can. J. Chem. Downloaded from www.nrcresearchpress.com by 210.87.254.105 on 09/05/12
For personal use only.

Can. J. Chem. Downloaded from www.nrcresearchpress.com by 210.87.254.105 on 09/05/12
For personal use only.

TABLE IV

Chemical shifts in some diethyl benzalmalonates*

X	Y	CH_3(B)	CH_3(A)	CH_2(A)	CH_2(B)	C=CH
H	H	8.74	8.69	5.69	5.67	2.26
2-CH_3	H	8.85	8.68	5.69	5.79	2.05
3-CH_3	H	8.74	8.70	5.71	5.69	2.32
2-F	H	8.75	8.68	5.69	5.69	2.10
3-F	H	8.72	8.67	5.68	5.65	2.32
4-F	H	8.72	8.69	5.70	5.67	2.32
2-Cl	H	8.82	8.67	5.68	5.77	2.01
3-Cl	H	8.72	8.69	5.68	5.65	2.34
4-Cl	H	8.72	8.69	5.71	5.68	2.34
4-Br	H	8.74	8.69	5.69	5.66	2.34
2-CH_3O	H	8.79	8.69	5.70	5.74	1.93
3-CH_3O	H	8.74	8.70	5.70	5.67	2.32
4-CH_3O	H	8.70	8.70	5.70	5.65	2.34
3-C_2H_5O	H	8.73	8.69	5.71	5.68	2.31
3,*n*-C_3H_7O	H	8.72	8.69	5.69	5.66	2.30
3,*n*-C_4H_9O	H	8.72	8.69	5.70	5.67	2.31
2-NO_2	H	8.98	8.66	5.66	5.91	1.81†
3-NO_2	H	8.68	8.65	5.65	5.61	2.23†
4-NO_2	H	8.72	8.66	5.65	5.65	2.25
2-Cl	4-Cl	8.78	8.67	5.67	5.75	2.10
2-Cl	6-Cl	8.99	8.64	5.64	5.89	2.27
3-CH_3O	4-HO	8.69	8.69	5.71	5.65	2.34
3-CH_3O	4-CH_3O	8.69	8.69	5.67	5.63	2.34

*Compounds of structure 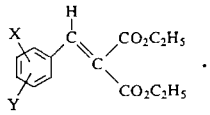 .

†Phenyl absorptions occur in this region.

the shift (4) and moreover, the hydrogen probably moves along an isoshielding line (5) as the phenyl group is rotated. Resonance will be damped as soon as the styrene moiety is forced into an aplanar conformation, and the carbon atom attached to the benzene ring thereby acquires a more positive character resulting in less shielding of the attached hydrogen atom. The magnitude of the downfield displacement for this hydrogen in C-2 -substituted derivatives relative to that in ethyl cinnamate is therefore a function of the size of the C-2 -substituent; the bulkier the substituent the less the overlap of π orbitals between the benzene ring and those of the styrenic double bond. Displacements of the bands for this hydrogen in the C-2 -substituted 3-benzal-2,4-pentanediones, **1**(A = B = $COCH_3$), the ethyl benzalacetoacetates, **1**(A or B = $COCH_3$ or $CO_2C_2H_5$), and the diethyl benzalmalonates, **1**(A = B = $CO_2C_2H_5$), are similar to those for similarly substituted ethyl cinnamates. Enhanced displacements are observed for these members of the ethyl benzalcyanoacetates, **1**(A = $CO_2C_2H_5$, B = CN),

TABLE V

Chemical shifts in some ethyl benzalcyanoacetates*

X	Y	CH_3	CH_2	C=CH
H	H	8.62	5.62	1.74
2-CH_3	H	8.62	5.62	1.45
4-CH_3	H	8.63	5.64	1.82
3-F	H	8.61	5.61	1.80
2-Cl	H	8.60	5.59	1.31
3-Cl	H	8.62	5.61	1.84
4-Cl	H	8.62	5.62	1.83
2-CH_3O	H	8.62	5.62	1.28
3-CH_3O	H	8.62	5.64	1.84
4-CH_3O	H	8.63	5.64	1.87
3,*n*-C_4H_9O	H	8.63	5.63	1.82
3-NO_2	H	8.59	5.56	1.67
4-CN	H	8.60	5.58	1.75
2-Cl	4-Cl	8.60	5.59	1.41
2-Cl	6-Cl	8.58	5.59	1.73
2-CH_3O	4-CH_3O	8.64	5.65	1.34
3-CH_3O	4-CH_3O	8.61	5.62	1.87

*Compounds of structure 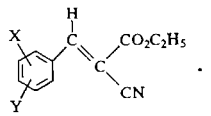 .

TABLE VI
Chemical shifts in some ethyl cinnamates*

X	Y	CH_3	CH_2	α-H	β-H(B)
H	H	8.69	5.75	3.57	2.33
2-CH_3	H	8.67	5.73	3.65	2.04
4-CH_3	H	8.69	5.75	3.62	2.36
4-F	H	8.67	5.73	3.63	2.36
2-Cl	H	8.67	5.72	3.58	1.92
4-Cl	H	8.69	5.74	3.59	2.37
4-Br	H	8.67	5.73	3.57	2.38
2-CH_3O	H	8.69	5.75	3.48	2.03
3-CH_3O	H	8.69	5.75	3.59	2.37
4-CH_3O	H	8.69	5.76	3.71	2.38
3-C_2H_5O	H	8.69	5.76	3.60	2.38
3,*n*-C_3H_7O	H	8.69	5.75	3.60	2.37
2-NO_2	H	8.65	5.73	3.64	1.91
3-NO_2	H	8.67	5.71	3.44	2.28
4-NO_2	H	8.68	5.73	3.46	2.33
2-Cl	4-Cl	8.65	5.71	3.59	2.01
2-CH_3O	4-CH_3O	8.71	5.78	3.69	2.05
2-CH_3O	5-CH_3O	8.68	5.75	3.51	2.05
3-CH_3O	4-CH_3O	8.68	5.76	3.69	2.40
CH_2(O—3, O—4)		8.70	5.77	3.76	2.43

*Compounds of structure 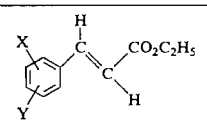 .

and benzalcyanoacetamides[4], **1**(A = $CONH_2$, B = CN), and are similar to those already reported for the benzalmalononitriles, **1**(A = B = CN), (4). While the conjugative effect of the A group governs the extent of the chemical shift, the conformation of the B group appears to be a decisive factor as well.

Substituents on the phenyl group, especially at C-2, cause a marked variation in the chemical shift of the methyl of a B ketone and the methyl and methylene of similarly located ester groups, while the effect on the corresponding protons of A groups is small. Since the functional group at A is undoubtedly involved in conjugation, stabilization of the molecule would dictate planarity of this group over that of an angular B group (6). Moreover, repulsion between the phenyl group and the negative charge on the polarized B carbonyl group would favor a predominantly *S-trans* configuration[5] for this carbonyl group. This being the case, the methyl group of the ketone at B and the ethyl group of the ester at B will be in the field of the phenyl ring (5) (see Figs. 1, 2). The small displacements of τ (CH_3) (ketone or ester) and τ (CH_2) (ester) upon introduction of substituents at C-3 or C-4 (Table VII) arise then from small changes in the anisotropy of the ring due to the electronic effects of the substituent. The marked effect of C-2 -substituents, on the other hand, supports the *S-trans* configuration for the B functional group and the orientation of the phenyl ring (2) must outweigh the electronic effects of the substituent in positioning the proton bands of the neighboring ester or ketone. In accord with this, the downfield shifts of these protons increase with increasing dimensions of the C-2 -substituent in the order CH_3O < Cl < CH_3 < NO_2.

The τ value for the ethylenic hydrogen vicinal to the benzene ring in 2-benzal-1,3-indanedione, **1**(A, B = —CO—C_6H_4—CO—), supports the premise that the conformation of the B functional group governs in part, the chemical shift for this proton. For 3-benzal-2,4-pentanedione, with the B carbonyl in an *S-trans* configuration, τ(CH=C) is 2.51 while for 2-benzal-1,3-indanedione which has a B carbonyl with an unambiguous *S-cis* configuration, τ is 1.93. The linear B cyano group of ethyl benzalcyanoacetate, benzalcyanoacetamide,

[4]Unpublished work, this laboratory.
[5]These geometric configurations will be referred to the styrene ethylene.

Can. J. Chem. Downloaded from www.nrcresearchpress.com by 210.87.254.105 on 09/05/12
For personal use only.

Can. J. Chem. Downloaded from www.nrcresearchpress.com by 210.87.254.105 on 09/05/12
For personal use only.

TABLE VII

Average displacements ($\tau_X - \tau_H$) for similarly located protons in compounds with the generalized formula **1** relative to the unsubstituted parent compound

X	Ester or ketone CH_3(B)	Ester CH_2(B)	CH=C	Ester or ketone CH_3(A)	Ester CH_2(A)	H(B)
2-CH_3	+0.14	+0.14	−0.19	0.00	0.00	+0.08
3-CH_3	0.00	+0.02	+0.05	+0.01	+0.01	—
4-CH_3	−0.01	0.00	+0.05	+0.02	+0.02	+0.05
2-F	+0.01	+0.02	−0.17	−0.01	0.00	—
3-F	−0.01	−0.01	+0.07	−0.01	−0.01	—
4-F	−0.03	−0.01	+0.08	−0.01	−0.01	+0.06
2-Cl	+0.09	+0.11	−0.27	−0.02	−0.02	+0.01
3-Cl	−0.01	−0.01	+0.08	0.00	−0.01	—
4-Cl	−0.02	+0.01	+0.08	−0.01	0.00	+0.02
4-Br	−0.01	0.00	+0.09	−0.01	−0.02	0.00
2-CH_3O	+0.04	+0.08	−0.34	0.00	+0.01	−0.09
3-CH_3O	0.00	+0.02	+0.05	+0.01	+0.01	+0.02
4-CH_3O	−0.04	−0.01	+0.08	+0.01	+0.03	+0.14
3-C_2H_5O	−0.01	+0.03	+0.06	0.00	+0.01	+0.03
3,*n*-C_3H_7O	−0.01	+0.02	+0.06	+0.01	0.00	+0.03
3,*n*-C_4H_9O	−0.02	+0.02	+0.06	0.00	+0.01	—
2-NO_2	+0.24	+0.24	−0.46	−0.04	−0.03	+0.07
3-NO_2	−0.06	−0.04	−0.04	−0.03	−0.05	−0.14
4-NO_2	−0.02	−0.04	−0.02	−0.02	−0.02	−0.12
2,3-$(CH_3O)_2$	+0.06	+0.08	−0.27	−0.01	−0.02	—
2,4-$(CH_3O)_2$	+0.03	+0.03	−0.28	+0.02	+0.03	+0.12
3,4-$(CH_3O)_2$	−0.04	−0.03	+0.08	+0.02	+0.01	+0.12
2,5-$(CH_3O)_2$	—	—	−0.29	−0.01	0.00	−0.06
2,4-Cl_2	+0.04	+0.09	−0.18	−0.02	−0.02	+0.02
2,6-Cl_2	+0.27*	+0.23	+0.02	−0.04	−0.04	—
3,4-Cl_2	−0.02	−0.01	+0.06	−0.03	+0.02	—
CH_2(O—3, O—4)	−0.04	−0.01	+0.13	+0.02	+0.03	+0.19
4-CN	—	—	+0.01	−0.02	−0.04	—
3-CH_3O, 4-HO	−0.05	−0.02	+0.06	0.00	−0.02	—

*This value is only applicable to compounds in which the ester is *cis* to the phenyl ring.

TABLE VIII

Chemical shifts of ring substituents*

X	A = $COCH_3$ B = $COCH_3$	A = $COCH_3$ B = $CO_2C_2H_5$	A = $CO_2C_2H_5$ B = $CO_2C_2H_5$	A = $CO_2C_2H_5$ B = CN	A = $CO_2C_2H_5$ B = H
2-CH_3	7.54	7.64	7.66	7.58	7.59
3-CH_3	—	7.67	7.69	—	—
4-CH_3	7.64	—	—	7.60	7.66
2-CH_3O	6.13	6.15	6.18	6.11	6.15
3-CH_3O	6.21	6.22	6.26	6.19	6.21
4-CH_3O	6.18	6.18	6.19	6.13	6.20
2-CH_3O }	6.15	6.20	—	6.13	—
4-CH_3O }	6.19	6.20	—	6.13	—
2-CH_3]	7.83	—	—	—	—
4-CH_3 }	7.72	—	—	—	—
6-CH_3]	7.83	—	—	—	—

*Compounds of structure 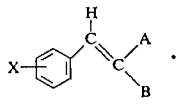

.

Can. J. Chem. Downloaded from www.nrcresearchpress.com by 210.87.254.105 on 09/05/12
For personal use only.

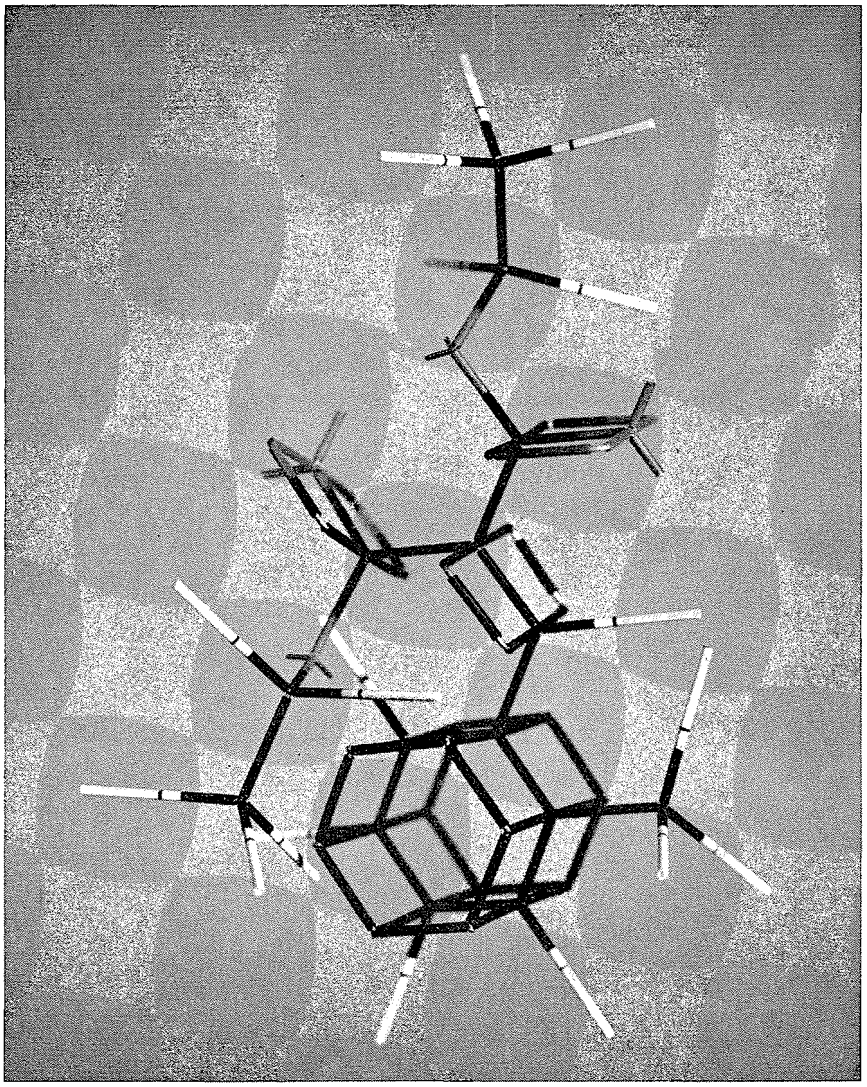

FIG. 1. The Prentice–Hall framework molecular model of diethyl 2-methylbenzalmalonate, **1**(A = B = $CO_2C_2H_5$).

and benzalmalononitrile apparently functions similarly to a B ketone group with an *S-cis* configuration since the ethylenic hydrogen is downfield compared to that in related *S-trans* ketone compounds. The effect of steric arrangement of these groups is also manifest in increased reactivity of *S-cis* B carbonyl compounds and B cyano compounds with thiols (7, 8).

In contrast to the chemical shifts for the methyl protons of the A ester of the diethyl benzalmalonates and ethyl benzalacetoacetates, those for the methylene protons are displaced downfield compared to those for the analogous ethyl cinnamates. For the compounds to which an *S-trans* configuration has been assigned to the B carbonyl group, an *S-cis* configuration for the A ester would place the methylene protons in the field of the B carbonyl group. In accord with the *S-cis* character of the cyano group in the ethyl benzalcyanoacetates, both the methyl and methylene protons, as expected, are deshielded (see Fig. 3).

Unusual chemical shifts were observed for 2,6-disubstituted conjugated heteroenoid compounds. With chlorine atoms in these positions

Can. J. Chem. Downloaded from www.nrcresearchpress.com by 210.87.254.105 on 09/05/12
For personal use only.

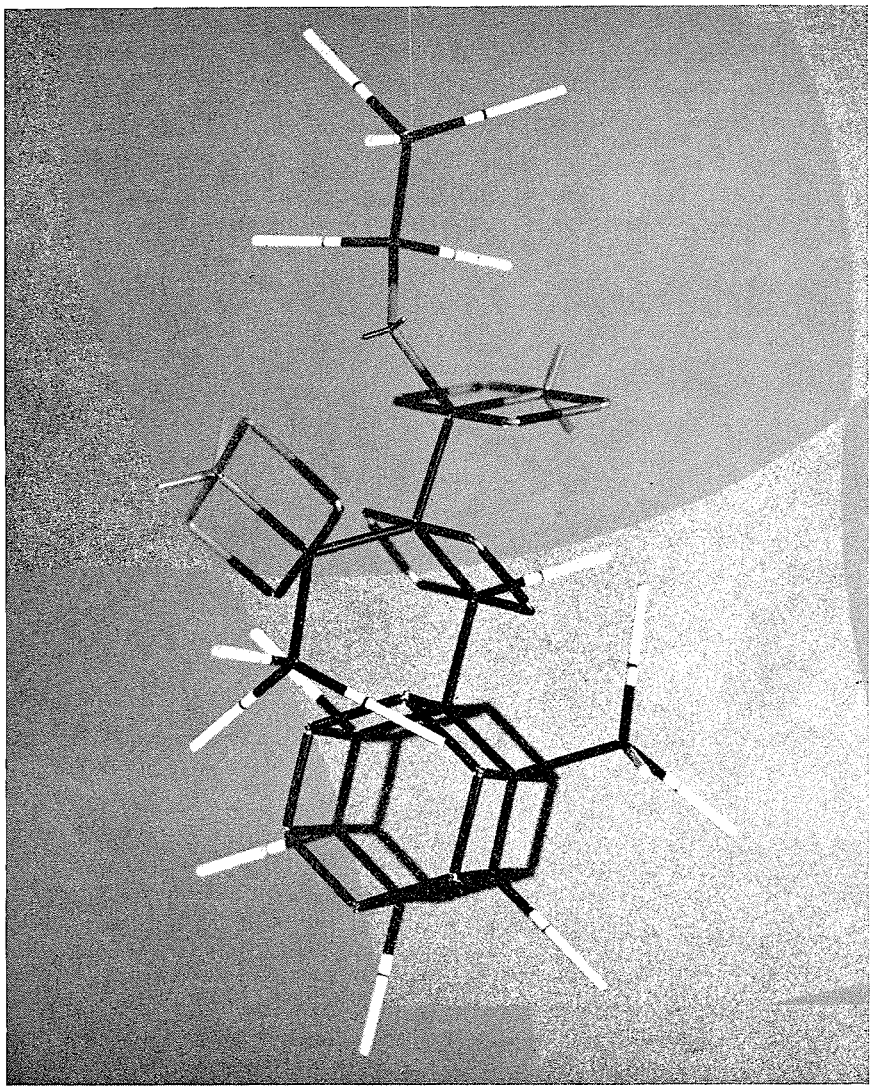

FIG. 2. The Prentice–Hall framework molecular model of ethyl 2-methylbenzalacetaocetate, **1**(A = $CO_2C_2H_5$, B = $COCH_3$).

the absorption of the ethylenic proton is variable and displaced slightly upfield relative to the parent compound and dramatically upfield from that of the 2-chloro derivative. However, with methyl groups in the same positions the ethylenic proton is downfield relative to the parent compound. Lapine's Stewart–Briegleb models indicate that the ethylenic hydrogen is locked in a position intermediate between the C-2 - and C-6 -substituents. The ethylenic bond, then, is virtually at right angles to the plane of the phenyl group and a maximal downfield displacement for this hydrogen would be anticipated. In the case of the 2,6-dichloro-derivatives, the field effects of these chlorines counteract the deshielding influence of the ring.

The positions of the B ketone–methyl absorption bands in the 2,6-dichloro-derivatives are only slightly upfield relative to those in 3-benzal-2,4-pentanedione and ethyl benzalacetoacetate, while the positions of the B methyl ester in the 2,6-dichloro-derivatives exhibit the expected signif-

Can. J. Chem. Downloaded from www.nrcresearchpress.com by 210.87.254.105 on 09/05/12
For personal use only.

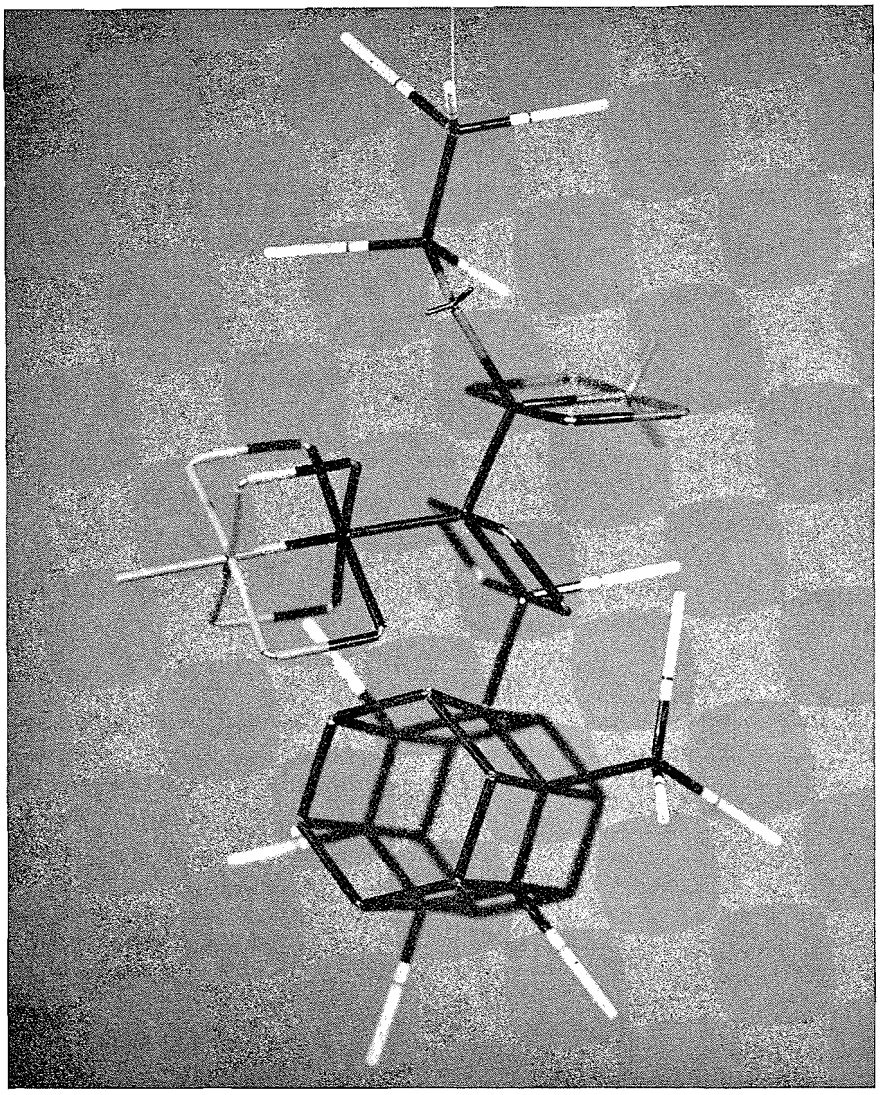

FIG. 3. The Prentice–Hall framework molecular model of ethyl 2-methylbenzalcyanoacetate, **1**(A = $CO_2C_2H_5$, B = CN).

icant displacements compared with those of ethyl benzalacetoacetate and diethyl benzalmalonate. The smaller bulk of the ethoxy–oxygen of the ester relative to that of the methyl group of the methyl ketone permits a normal *S-trans* conformation for the B ester function but requires an abnormal *S-cis* conformation for the analogous methyl ketone function. In this way the methyl protons of the methyl ketone are outside the field of the benzene ring. Downfield shifts for the protons of the A ketone in 2′,6′-dichloro-3-benzal-2,4-pentanedione and the A ester in ethyl 2,6-dichlorobenzalacetoacetate suggest a similar reversal to the *S-trans* conformation for these functional groups. The chemical shift for the B methyl ketone protons in 2′,4′,6′-trimethyl-3-benzal-2,4-pentanedione indicates that the normal *S-trans* configuration obtains for this functional group. Electronic repulsion of the B carbonyl group by the trimethylphenyl group may account

for this. The upfield shifts of the ring-methyl protons in this trimethylphenyl derivative relative to those of an analogous C-2 or C-4 monomethylphenyl derivative attest to the highly negative character of this ring.

The conformations assigned to the A and B functional groups in these compounds accord with those deduced from infrared spectral data (10). A study of n.m.r. solvent shifts should provide additional evidence for *S-trans* and *S-cis* conformations (9).

Acknowledgments

The authors thank Dr. H. L. Holmes for supplying samples of the compounds used in this study, members of the Chemistry Section for helpful discussions, and Mr. J. B. Richardson, Mr. H. S. Johnson, and Mr. C. E. Lough for technical assistance.

1. C. J. TIMMONS. Chem. Commun. **22**, 576 (1965).
2. T. HAYASHI. J. Org. Chem. **31**, 3253 (1966).
3. R. F. SILVER, K. ANN KERR, PEGGY D. FRANDSEN, SHEILA J. KELLEY, and H. L. HOLMES. Can. J. Chem. **45**, 1001 (1967).
4. M. A. WEINBERGER, R. M. HEGGIE, and H. L. HOLMES. Can. J. Chem. **43**, 2585 (1965).
5. J. J. BLOOMFIELD and R. FUCHS. J. Org. Chem. **26**, 2991 (1961).
6. D. J. CURRIE, C. E. LOUGH, R. F. SILVER, and H. L. HOLMES. Can. J. Chem. **45**, 1567 (1967).
7. C. E. LOUGH, D. J. CURRIE, and H. L. HOLMES. Can. J. Chem. **46**, 771 (1968).
8. R. B. PRITCHARD, C. E. LOUGH, D. J. CURRIE, and H. L. HOLMES. Can. J. Chem. **46**, 775 (1968).
9. F. H. COTTEE and C. J. TIMMONS. J. Chem. Soc. (B), 326 (1968).
10. D. J. CURRIE, C. E. LOUGH, F. K. MCCLUSKY, and H. L. HOLMES. Can. J. Chem. This issue.

Can. J. Chem. Downloaded from www.nrcresearchpress.com by 210.87.254.105 on 09/05/12
For personal use only.

Can. J. Chem. Downloaded from www.nrcresearchpress.com by 210.87.254.40 on 09/05/12
For personal use only.

Effect of functional group conformation on the infrared spectra of some gem difunctional phenylethylene derivatives

D. J. Currie, C. E. Lough, F. K. McClusky, and H. L. Holmes
Chemistry Section, Defence Research Establishment Suffield, Ralston, Alberta

Received February 21, 1969

Except for the benzalmalononitriles, two functional group stretching vibrations occur in the infrared (i.r.) spectra of the β,β-difunctional-styrenes with similar functional groups. For geometrically homogeneous compounds with dissimilar functional groups only one absorption band occurs for each functional group. The two bands for similar functional groups have been ascribed to *S-cis*- and *S-trans*-conformations of the carbonyl groups with respect to the ethylene and variation in the frequencies of each of these oriented carbonyls to rotation of the functional group or groups out of the plane of the ethylene by steric factors.

Frequencies for ethylenic C—H out of plane deformation bands for β-monofunctional styrenes accorded with those already assigned to this vibration. A similar assignment could not be made for the difunctional analogues.

Canadian Journal of Chemistry, 47, 3147 (1969)

Introduction

Demonstration of a relationship of stimulatory activity on the hind legs of pithed frogs (1) and bacterial growth inhibitory activity (2) of conjugated heteroenoid compounds, **1**, with rates of reaction with nucleophiles and the

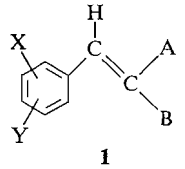

1

dependence of these rates upon the functional groups, A and B,[1] has necessitated an extensive study of the conformations of A and B in these compounds. An insight has been gained from nuclear magnetic resonance (n.m.r.) spectral work into the orientation of the B group (3) while a parallel i.r. study has now shed light upon the conformation (*S-cis* or *S-trans* to the ethylene (4)) of the A group.

Models of **1** where A and B are angular groups ($COCH_3$, $CO_2C_2H_5$, $CONH_2$, CONHR, $CONR_2$, etc.) indicate the presence of considerable steric restraint due to spatial congestion between A, B, and the phenyl group, and Shubert and Sweeney (5) have shown that inhibition of molecular planarity in the armethylacetophenones has a pronounced influence upon their i.r. spectra. The spectra of compounds with structure **1** have been similarly ascribed by Zabicky (6) to aplanarity of the molecule. Hayes and Timmons have demonstrated recently that, depending upon the bulk of the alkyl group of the alkylstyryeketone, the conformation of the planar conjugated system in solution may be either *S-cis*, **2**, or *S-trans*, **3**, while in potassium bromide disc spectra, one conformation may be favored to the exclusion of the other (4). The

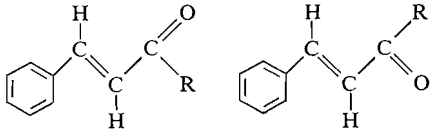

2 **3**

large number of compounds, **1**, that were prepared for the biological program and which have *S-cis* and *S-trans* arrangements of the —CH=C(B) moiety of the molecule[2] have been examined spectrally in the i.r. region, and an interpretation is advanced for the observed frequencies in the ethylenic and functional group stretching regions.

Experimental

The preparation of the compounds used in this work, and their purity are described in Silver *et al.* (7). The

[1]The A and B groups will always refer respectively to the functional groups *trans* and *cis* to the phenyl group.

[2]See the previous paper (3) for nuclear magnetic resonance evidence.

TABLE I

Frequencies for functional group and ethylenic stretching vibrations of some conjugated heteroenoid compounds

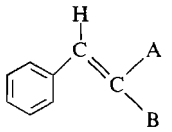

Functional groups		ν carbonyl (cm^{-1})		ν CN and ν NO_2 (cm^{-1})	ν C=C* (cm^{-1})
A	B	*S-cis*	*S-trans*		
$COCH_3$		1691	1669	—	1610†
	H	—	—	—	1628
$COCH_3$		1711	—	—	1658
	$COCH_3$	—	1691	—	—
$CO_2C_2H_5$		—	1715	—	1638
	H	—	—	—	—
$CO_2C_2H_5$		~1727	—	—	1630
	$CO_2C_2H_5$	—	1727	—	—
$CO_2C_6H_5$		1728	1690‡	—	1638
	H	—	—	—	—
$CO_2C_6H_5$		1756	—	—	1625
	$CO_2C_6H_5$	—	1735	—	—
$CONH_2$		—	1661	—	1632
	H	—	—	—	—
$CONH_2$		1690	—	—	1642
	$CONH_2$	—	1660	—	—
$CON(CH_3)_2$		—	1645	—	1635‡
	H	—	—	—	—
$CON(CH_3)_2$		—	1640	—	1628
	$CON(CH_3)_2$	1650‡	—	—	—
$CONHC_6H_5$		1678	1660	—	1625
	H	—	—	—	1614†‡
$CONHC_6H_5$		1670	—	—	1645
	$CONHC_6H_5$	—	1670	—	—
CN		—	—	2220	1618
	H	—	—	—	—
CN		—	—	2214	1591
	CN	—	—	—	—
$COCH_3$		1696	—	—	1660
	$CO_2C_2H_5$	—	1729	—	—
$CO_2C_2H_5$		1731	—	—	1608
	CN	—	—	2228	—
$CONH_2$		1692	—	—	1595
	CN	—	—	2220	—
$CONHCH_3$		—	1656	—	1619
	H	—	—	—	—
$CONHCH_3$		1675	—	—	1603
	CN	—	—	2215	—
$CON(CH_3)_2$		—	1648	—	1600
	CN	—	—	2215	—
$CONHC_6H_5$		1680	—	—	1595
	CN	—	—	2220	—
NO_2		—	—	1512	1634
	H	—	—	1347	—
NO_2		—	—	1520	1658
	CH_3	—	—	1324	—
NO_2		—	—	1520	1650
	C_2H_5	—	—	1330	—

*See text.
†Assigned to the *S-cis* ethylenic stretching vibration.
‡This is a shoulder on another absorption band.

Can. J. Chem. Downloaded from www.nrcresearchpress.com by 210.87.254.40 on 09/05/12
For personal use only.

Can. J. Chem. Downloaded from www.nrcresearchpress.com by 210.87.254.40 on 09/05/12
For personal use only.

spectra[3] were recorded on a model 621 Perkin–Elmer spectrophotometer using potassium bromide pellets for solids and contact films for liquids. The spectra of chloroform solutions of a number of these compounds were also recorded.

Results

A number of absorption bands occur in the region of the spectra between 2500 and 1380 cm^{-1} and their positions are summarized in Table I. At least two, and in most cases, three bands appear in the carbonyl region of the spectra of the 3-benzal-2,4-pentanediones, **1**(A = B = $COCH_3$) and of the benzalmalonamides, **1**(A = B = $CONH_2$). The band with the lowest frequency, however, falls in the ethylenic stretching vibration region (8). A similar multiplicity of bands is also observed in the carbonyl region of the diphenyl benzalmalonates, **1**(A = B = $CO_2C_6H_5$). In the analogous spectra of the diethyl benzalmalonates, **1**(A = B = $CO_2C_2H_5$), the contiguous carbonyl bands are fused into one broad band.

In contrast to the carbonyl stretching region only a single band appears in the cyano stretching region, irrespective of whether A or B = CN, and its position is relatively insensitive to structural changes. The limited steric restraint of the cyano group (9) affords the greatest opportunity for a planar molecule in these gem-difunctional compounds. When the conjugative effect (9) of the A group differs but slightly, e.g., $CO_2C_2H_5$, from that of the cyano group in the B position, then electromeric shifts in the *cis*–cinnamonitrile moiety should contribute materially to the resonance stabilization of the molecule as a whole. When the conjugative effect of the A group, e.g. COC_6H_5 in α-cyano-*trans*-benzalacetophenone, markedly exceeds that of the cyano group at B, then the cyano group might be expected to function more like a non-conjugated cyano group to i.r. light than that in ethyl benzalcyanoacetate. For equimolar solutions of these two compounds in chloroform, the absorbance of the former was somewhat greater than in the latter but the area under the two peaks was about the same.

Analysis of the 1670–1550 cm^{-1} spectral region proved difficult because the diagnosis of these bands as either ethylenic stretch vibrations or skeletal aromatic ring vibrations could not be made with certainty especially in the vicinity of 1600 cm^{-1}. Two bands at 1500 and 1440 cm^{-1} which are common to most of the spectra are undoubtedly due to skeletal aromatic ring vibrations and, in most cases, were accompanied by other bands. While some consider absorption at ~ 1600 cm^{-1} to be aromatic in origin Hayes and Timmons (4) have assigned bands between 1616 and 1604 cm^{-1} in alkylstyrylketones, **1**(A = COR, B = H) to cisoid ethylenic stretch vibrations.

Discussion

Functional Group Stretching Vibrations

The multiplicity of bands appearing in the 1750–1500 cm^{-1} region of the spectra of conjugated heteroenoid compounds with *gem* difunctional groups, **1**, might be ascribed, on steric grounds, to conjugated A and non-conjugated B groups as was done in the derivation of numerical values for the steric, conjugative, and inductive effects for the groups around the ethylene in these compounds and which provides long wavelength ultraviolet (u.v.) absorption maxima in accord with those observed (9). This band multiplicity could equally well arise from the presence of *S-trans* and *S-cis* conformations of the A- and B-carbonyl groups resulting from steric restraints imposed by the A, B, and phenyl groups. This tacitly implies that the molecules of these compounds are planar or nearly so. A combination of these two hypotheses appears to more adequately accommodate the facts.

The two carbonyl absorptions (1669 and 1691 cm^{-1}) in the spectrum of benzalacetone, **1**(A = $COCH_3$, B = H), have been ascribed (4) to the existence of *S-trans* and *S-cis* carbonyl groups in this compound while steric factors have favored the existence of only an *S-cis* carbonyl group (1678 cm^{-1}) in 4,4-dimethyl-1-phenyl-1-pentene-3-one, **2**(R = $(CH_3)_3C$) (4). There are then four possible combinations for the conformation of the A(*S-cis* or *S-trans*) and B(*S-cis* and *S-trans*) groups in 3-benzal-2,4-pentanedione, **1**(A = B = $COCH_3$). Only two of the four requisite bands are apparent and have frequencies of 1691 and 1711 cm^{-1}. Two of the possible conformations either do not occur or their absorption bands are superimposed upon the two already described. If each of these bands

[3]Photocopies of the pellet or liquid contact spectra of some 300 compounds recorded on a model 21 Perkin–Elmer spectrophotometer may be obtained, upon request, from the Depository of Unpublished Data, National Science Library, National Research Council of Canada, Ottawa, Canada.

Can. J. Chem. Downloaded from www.nrcresearchpress.com by 210.87.254.40 on 09/05/12
For personal use only.

represents single absorptions then from n.m.r. data (3) the first one must be associated with the *S-trans* B-carbonyl group and the remaining *S-cis* carbonyl absorption band must arise from the carbonyl group of the A-acetyl group. The hypsochromic shifts of $\sim 20\ cm^{-1}$ from the position of the analogous bands in benzalacetone must then be ascribed to rotation of the A- and B-acetyl groups out of the plane of the ethylene.

The spectrum of ethyl cinnamate, **1**(A = $CO_2C_2H_5$, B = H), has one band at 1715 cm^{-1} in the carbonyl region while that of diethyl benzalmalonate, **1**(A = B = $CO_2C_2H_5$), has a broad band[4] at 1727 cm^{-1}. Nuclear magnetic resonance evidence (3) associates an *S-trans* conformation with the B-ester carbonyl of diethyl benzalmalonate. If, as above, the distortion from planarity accounts for the frequency shift in the bands of diethyl benzalmalonate relative to ethyl cinnamate, then the broad band at 1727 cm^{-1} must be associated with both the *S-trans* B group and the *S-cis* A group. The smaller deviation ($\sim 12\ cm^{-1}$) between the frequencies for the *S-trans* carbonyl group in ethyl cinnamate and diethyl benzalmalonate, compared to that for their ketone analogues ($\sim 20\ cm^{-1}$), probably stems from less steric interference by the ethoxyl in the ester group compared to that of the methyl in the acetyl group.

The hypothesis ascribing the magnitude of the hypsochromic shifts, observed above, to the extent of steric restraint finds added support in the spectra of phenyl cinnamate, **1**(A = $CO_2C_6H_5$, B = H) and diphenyl benzalmalonate, **1**(A = B = $CO_2C_6H_5$). Bands at 1728 and 1690 cm^{-1} in the spectrum indicate the presence of both *S-cis* and *S-trans* conformers in phenyl cinnamate. The corresponding bands in the spectrum of diphenyl benzalmalonate are at 1756 and 1735 cm^{-1}. The larger shifts in going from the monoester to the diester (28 and 45 cm^{-1}) are in the direction expected for the greater steric effects of the phenoxy group in these esters.

The carbonyl group of cinnamamide, **1**(A = $CONH_2$, B = H) absorbs at 1661 cm^{-1} while those of benzalmalonamide, **1**(A = B = $CONH_2$) absorb at 1660 and 1690 cm^{-1}. The carbonyl group in benzalmalonamide associated with the 1660 cm^{-1} band probably has the same conformation as that in cinnamamide and in analogy with the previous cases, it is surmised that this is the B-carboxyamide group.[5] In any event the two carboxyamides have opposite conformations. If the conformation of the carbonyl of cinnamamide is the same as that of ethyl cinnamate and benzalacetone then the picture is consistent throughout.

Using a similar approach, the 1660 cm^{-1} band has been assigned to the *S-trans* carbonyl group of cinnamanilide, **1**(A = $CONHC_6H_5$, B = H), and benzalmalonanilide, **1**(A = B = $CONHC_6H_5$) and the 1678 cm^{-1} band to the *S-cis* carbonyl of both compounds. The carbonyl absorption in benzalcyanoacetanilide at 1680 cm^{-1} is at the same frequency as the *S-cis* carbonyl groups in the above mono- and diamides. By similar reasoning the absorption for *S-trans* carbonyl of *N*-alkylcarboxyamides occurs at 1656 cm^{-1} while that for the *S-cis* carbonyl occurs at 1675 cm^{-1}. The absence of steric influences upon the position of carbonyl absorption of carboxyamides and their *N*-alkyl derivatives demonstrates that hydrogen bonding can exert a pronounced influence upon the planarity of the conjugated system.

Steric factors and the absence of hydrogen bonding alter the conformation of the *N,N*-dialkylbenzalcyanoacetamides, as it did in 4,4-dimethyl-1-phenyl-1-pentene-3-one. The carbonyl group in *N,N*-dimethylbenzalcyanoacetamide, **1**(A = $CON(CH_3)_2$, B = CN) appears to be restricted to the *S-trans* (1645 cm^{-1})[6] conformation since it absorbs at a frequency similar to that (1648 cm^{-1}) for that in *N,N*-dimethylcinnamamide, **1**(A = $CON(CH_3)_2$, B = H).

The linear cyano group, by its very nature, minimizes steric effects (9) and favors a coplanar molecule with the result that only a single

[4]A small shoulder, present at $\sim 1705\ cm^{-1}$, which was present in the parent compound was absent in about one third of the substituted derivatives.

[5]Limited solubility in $CDCl_3$ precluded the n.m.r. conformational analysis of the B-carbonyl group in the benzalmalonamides. The conformations assigned throughout to the amide carbonyl group are, however, in accord with their observed rates of reaction with *n*-butanethiol.

[6]A less likely explanation for the 1645 cm^{-1} band for the *N,N*-dialkylbenzalcyanoacetamides is that the *N*-methyl groups rotate the *S-cis* A-carboxyamide group out of the plane of the molecule. With properties more like that of a non-conjugated amide group the carbonyl absorption would be shifted to a lower frequency (10). The assignment for compound **1** (A = B = $CON(CH_3)_2$) is tentative.

Can. J. Chem. Downloaded from www.nrcresearchpress.com by 210.87.254.40 on 09/05/12
For personal use only.

absorption is observed for this functional group whether located at A and/or B.

Combinations of different functional groups in the same molecule present no spectral complications, however, the ethyl benzalacetoacetates, **1**(A = $COCH_3$, B = $CO_2C_2H_5$) geometrically isomerize slowly in chloroform solution. The initial conformation of the carbonyl group of the B-ester, on n.m.r. spectral evidence[7] has been diagnosed as *S-trans*. Using the same inductive argument as above the conformation of the A-ketone carbonyl would be expected to be *S-cis*. The observed absorption bands at 1696 and 1729 cm^{-1} are in accord with this concept. The decreased spatial congestion between A($COCH_3$) and B = $CO_2C_2H_5$ relative to that when B = $COCH_3$ (9) accounts for the bathochromic shift (15 cm^{-1}) for the *S-cis* A-ketone carbonyl of ethyl benzalacetoacetate compared with that in 3-benzal-2,4-pentanedione. The *S-trans* B-ester carbonyl group of ethyl benzalacetoacetate absorbs at 1729 cm^{-1} as does the B-ester carbonyl of diethyl benzalmalonate.

Absorption at 1731 cm^{-1} in the spectra of the ethyl benzalcyanoacetates, **1**(A = $CO_2C_2H_5$, B = CN), is ascribed to the carbonyl with an *S-cis* conformation which then must be the counterpart of the 1692 cm^{-1} band in benzalcyanoacetamide, **1**(A = $CONH_2$, B = CN).

Based upon the above arguments the conformations of all these gem difunctional compounds are given by **4** and **5**.

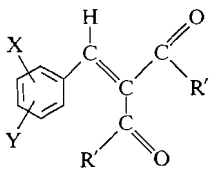

R′ = CH_3, OC_2H_5, OC_6H_5, NH_2, NHC_6H_5

4

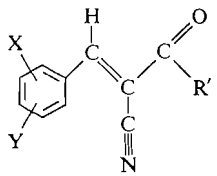

R′ = OC_2H_5, NH_2, NHR

5

Ethylenic Stretching Vibrations

Hayes and Timmons (4) have shown that the position of the ethylenic stretching vibration in the spectra of the ac-alkylbenzalacetones is intimately associated with the conformation of the ketone carbonyl group. The ethylenic stretch vibration associated with an *S-cis* ketone carbonyl has intense absorption between 1616 and 1604 cm^{-1} while the absorption of that associated with an *S-trans* ketone carbonyl is less intense and occurs from 1630 to 1620 cm^{-1}. In gem difunctional compounds, **1**, with similar angular functional groups the ethylene is cisoid with respect to the A-carbonyl but transoid to the B-carbonyl. A band appearing between 1660 and 1620 cm^{-1} in the spectra of these compounds has been diagnosed as an ethylenic stretching vibration and if a second band is present it is masked by the phenyl doublet at about 1600 cm^{-1}. The frequency of the clearly defined ethylenic stretching vibration is intimately associated with degree of substitution around the ethylene and the nature of the substituents. This is not the only factor influencing the frequency of this vibration since attempts to account for their position on steric grounds alone have been only partially successful. The position of this band is summarized in Table I.

The ethylene (1628 cm^{-1}) of benzalacetone, **1**(A = $COCH_3$, B = H) absorbs at a much lower frequency than that (1658 cm^{-1}) of the more hindered 3-benzal-2,4-pentanedione, **1**(A = B = $COCH_3$). Similarly the analogous band for cinnamamide, **1**(A = $CONH_2$, B = H), is at a lower wavenumber (1632 cm^{-1}) than it is in benzalmalonamide (1642 cm^{-1}). The same is true for the *N*-phenylated derivatives, cinnamanilide (1625 cm^{-1}) and benzalmalonanilide (1645 cm^{-1}) as would be expected on steric grounds.[8] On the other hand, the ethylene of ethyl cinnamate and of phenyl cinnamate absorb at frequencies 10–15 cm^{-1} greater than those of the analogous gem difunctional compounds. Furthermore the frequency of the absorption band for this group in ethyl benzalacetoacetate, **1**(A = $COCH_3$, B = $CO_2C_2H_5$) is at a very high frequency (1660 cm^{-1}) although the hinderance to coplanarity should be intermediate between that of 3-benzal-2,4-pentanedione and of diethyl benzalmalonate.

[7]See previous paper. Only 2,6-dichloro-3′-benzal-2′4′-pentanedione and one isomer of ethyl 2,6-dichlorobenzalacetoacetate, **1**(A = $CO_2C_2H_5$, B = $COCH_3$) had *S-cis* B-carbonyl groups.

[8]On the same grounds the ethylenic stretch vibration for β-nitrostyrene, **1**(A = NO_2, B = H) should, and does, absorb (1634 cm^{-1}) at a lower frequency than that of β-nitropropenylbenzene, **1**(A = NO_2, B = CH_3) (1659 cm^{-1}) or of β-nitrobutenylbenzene (1650 cm^{-1}).

In general, when only *S-cis* carbonyl groups are possible, as in 2-benzal-1,3-indanedione, or when B is a cyano group the ethylenic stretch vibration is either absent or is masked by phenyl absorptions at $\sim$ 1600 cm^{-1}.

The 975 cm^{-1} region of the spectra has been examined for evidence for an ethylenic C—H out of plane deformation band for the monofunctional compounds, **1**(B = H), and the 850–790 cm^{-1} region (11) scanned for a similar band in the difunctional compounds, **1**. The former diagnosis is confirmed by this work but such is not the case for the latter.

The dramatic differences in rates of reaction of thiols with difunctional compounds of type **1** and the extent to which they proceed may be intimately associated with the conformation of the A and/or B groups. If this is the case, then the evidence presented herein suggests that the *S-cis* B-ketone carbonyl of the 2-benzal-1,3-indanediones is involved in the rapid attainment of equilibrium in the *n*-butanethiol addition reaction (12). All evidence points to the conclusion that the B-cyano group of the cyano-containing compounds, **1**, (B = CN), fulfills the same role.

1. H. L. HOLMES and D. J. CURRIE. Unpublished work, this laboratory.
2. H. L. HOLMES, J. R. MALTMAN, and D. J. CURRIE. Unpublished work, this laboratory.
3. W. M. PHILLIPS and D. J. CURRIE. Can. J. Chem. This issue.
4. W. P. HAYES and C. J. TIMMONS. Spectrochim. Acta, **24A**, 323 (1968).
5. W. M. SHUBERT and W. A. SWEENEY. J. Am. Chem. Soc. **77**, 4172 (1955).
6. J. ZABICKY. J. Chem. Soc. 683 (1961).
7. R. F. SILVER, K. A. KERR, P. D. FRANDSEN, S. J. KELLEY, and H. L. HOLMES. Can. J. Chem. **45**, 1001 (1967).
8. L. J. BELLAMY. The infrared spectra of complex molecules. 2nd ed. John Wiley and Sons, Inc., New York. 1958. pp. 71, 72.
9. D. J. CURRIE, C. E. LOUGH, R. F. SILVER, and H. L. HOLMES. Can. J. Chem. **45**, 1567 (1967).
10. M. YAMAGUCHI. Nippon Kagaku Zasshi, **78**, 1236 (1957); Chem. Abstr. **52**, 13 540 (1958).
11. C. N. R. RAO. Chemical applications of infrared spectroscopy. Academic Press, Inc., New York. 1963. p. 151.
12. R. B. PRITCHARD, C. E. LOUGH, D. J. CURRIE, and H. L. HOLMES. Can. J. Chem. **46**, 775 (1968).

Can. J. Chem. Downloaded from www.nrcresearchpress.com by 210.87.254.40 on 09/05/12
For personal use only.

Free radical hydrobromination of propargyl bromide and bromoallene[1]

KARL R. KOPECKY AND SHIMA GROVER[2]
Department of Chemistry, University of Alberta, Edmonton, Alberta
Received November 22, 1968

Rearrangement is observed in the free-radical hydrobromination of propargyl bromide. Between −20 and +30 °C in *n*-pentane or ether solution, 1,2-dibromopropene is the major product. A detailed stereochemical and kinetic study of the reaction indicates that the 1,2-dibromopropene is formed via bromoallene which results from the loss of a bromine atom from the first formed 1,3-dibromo-2-propenyl radical. Only 1/3 to 1/2 of the bromoallene diffuses away from its bromine atom partner. The remainder of the bromoallene recombines within the solvent cage with its bromine atom partner at a rate which is competitive with its rate of rotation with respect to the bromine atom. When the free radical hydrobromination of propargyl bromide is carried out at −78° in liquid hydrogen bromide, the 1,3-dibromo-2-propenyl radical can be trapped to a large extent by the hydrogen bromide to form *cis*-1,3-dibromopropene. The stereochemistry of this addition reaction > 99% *trans*. A small amount of 1,2-dibromopropene which is 77% *trans* is also formed. Under the same conditions a 3:1 mixture of 1,2- and 1,3-dibromopropenes is produced from bromoallene. The 1,3-dibromopropene produced from bromoallene is > 95% *cis*, while the 1,2-dibromopropene consists of a 49:51 *cis*:*trans* mixture of isomers.

Canadian Journal of Chemistry, **47**, 3153 (1969)

Can. J. Chem. Downloaded from www.nrcresearchpress.com by 210.87.254.42 on 09/05/12
For personal use only.

In connection with another problem in these laboratories a large amount of 1,3-dibromopropene was required. The free radical hydrobromination of propargyl bromide appeared to be a more convenient route to this compound than

[1] $HC{\equiv}CCH_2Br + HBr \rightarrow CHBr{=}CHCH_2Br$

those already available (1–3). Free radical hydrobromination of terminal acetylenes has been shown to give anti-Markovnikov products (4–6). However, when hydrogen bromide was bubbled through propargyl bromide containing benzoyl peroxide at 0 °C, only ca. 15% of 1,3-dibromopropene was formed. The major product was 1,2-dibromopropene which was isolated in 54% yield. A rearrangement, presumably migration of a bromine atom, has clearly occurred in this transformation. In view of the interest in bromine migrations (7, 8) and the mechanism of free radical addition of hydrogen bromide to unsaturated systems (7–16), the course of this reaction was examined in detail.

Products and Nature of Reaction

It was found that up to 7 compounds can be present in reaction mixtures from the hydrobromination of propargyl bromide. These are *cis*- and *trans*-1,2-dibromopropene, *cis*- and *trans*-1,3-dibromopropene, 2-3-dibromopropene, bromoallene, and propargyl bromide. Clean separation by gas–liquid chromatography of all these compounds could be achieved using a 9.5 ft × 1/4 in. column of 10% UCON 50HB5100 on Chromosorb W. All analyses reported were obtained by gas–liquid chromatography using this column. The identification of these compounds is described in the Experimental.

Some preliminary experiments were carried out in order to confirm that the formation of 1,2-dibromopropene from the hydrobromination of propargyl bromide was the result of a free radical process. These are summarized in Table I.

High yields of 1,2-dibromopropene were obtained only in the presence of benzoyl peroxide or under illumination. Addition of the free radical inhibitors hydroquinone and ferrous chloride to the reaction mixtures resulted in the formation of considerable amounts of 1,3- and 2,3-dibromopropenes, presumably by an ionic process or processes. Reaction in the dark is very slow in the absence of initiators. This evidence confirms that hydrobromination of propargyl bromide under free radical conditions results in almost exclusive formation of a product of a rearrangement, 1,2-dibromopropene, at 0 °C.

No evidence was found for the formation of any 3,3-dibromopropene by either the free radical or ionic addition of hydrogen bromide to

---

[1](*a*) Presented in part at the 48th Chemical Conference of the Chemical Institute of Canada, Montreal, Quebec, May, 1965. Abstracts, p. 61. (*b*) Abstracted from a Thesis submitted by S. Grover to the Faculty of Graduate Studies of the University of Alberta in partial fulfillment of the requirements for the M.Sc. Degree, May, 1966.

[2]Holder of a Province of Alberta Scholarship 1963–1964 and 1964–1965 and a NRCC Studentship 1965–1966.

TABLE I

Product distribution from preliminary hydrobrominations of propargyl bromide at 0 °C*

Run	Solvent	Conditions and additives	% Dibromopropene† 1,2-	2,3-	1,3-
1	None	Benzoyl peroxide	54‡	0‡	15‡
2	None	$FeCl_3$ + hydroquinone	59	26	15
3	Pentane	Benzoyl peroxide	98	0.1	2
4	Ether	Dark, $FeCl_3$ + hydroquinone	21	79	0
5	Acetic acid§	$FeCl_2$ + hydroquinone	64	25	11
6	Pentane	Dark, no additive	91¶	5¶	4¶

*Except for run 5 reactions were carried out by passing HBr gas into the reaction mixture. Reactions were complete after 2–8 h.
†Analysis by g.l.c. except for run 1. Yields are relative yields at the end of the reaction except for runs 1 and 6. Total absolute yield of products > 98%, except in run 1.
‡Isolated yield from a preparative run.
§Propargyl bromide added to solution of 30% HBr in acetic acid containing the additives.
¶More than 95% starting material left after 48 h.

propargyl bromide. Product balances of 95–100% were obtained indicating that little, if any, polymer or tribromide was formed in either the ionic or free radical reactions and that these reactions stopped cleanly at the dibromide stage.

The 1,2- and 1,3-dibromopropenes produced in these reactions are mixtures of *cis* and *trans* isomers. It was shown that these mixtures are equilibrium mixtures. The equilibrium compositions of the 1,2- and 1,3-dibromopropenes were determined by irradiating with a sun lamp, the pure geometric isomers in pentane solution saturated with hydrogen bromide until no further change in isomer composition was observed. These results are shown in Table II.

TABLE II

Equilibration of isomers of 1,2- and 1,3-dibromopropene at 0 °C.

Starting compound	Equilibrium composition
cis-1,2-Dibromopropene	76.8% *trans*
trans-1,2-Dibromopropene	77.1% *trans*
cis-1,3-Dibromopropene	84.5% *cis*
trans-1,3-Dibromopropene	83.1% *cis*

Bromoallene was detected in reactions which were interrupted before completion. Continuous monitoring of several hydrobromination reactions in pentane containing benzoyl peroxide as initiator revealed that the concentration of bromoallene always increases to a maximum of about 10% of the initial propargyl bromide concentration at about 20 to 40% reaction, and then slowly decreases as the reaction progresses further. The amount of propargyl bromide smoothly decreases and that of 1,2-dibromopropene smoothly increases as the reaction progresses. This behavior is independent of the rate of hydrogen bromide addition and of the initial propargyl bromide and benzoyl peroxide concentrations. The propargyl bromide initially contained less than 0.5% bromoallene. These observations, coupled with the observation that no bromoallene is produced in the dark in the absence of benzoyl peroxide under otherwise identical conditions (run 6, Table I), show that formation of bromoallene from propargyl bromide also is a free radical process under these conditions.

When pure bromoallene is hydrobrominated at 0° in pentane solution in the presence of benzoyl peroxide, a mixture of 95% 1,2-dibromopropene and 5% 1,3-dibromopropene is formed. This product composition is essentially identical to that obtained from propargyl bromide under these conditions (run 3, Table I). Only trace amounts of propargyl bromide are formed during the hydrobromination of bromoallene under these conditions.

Attempts to Trap Radical Intermediate

It seemed possible that all the dibromide produced from the free radical hydrobromination of propargyl bromide is formed from bromoallene after a prior isomerization of the propargyl bromide to bromoallene under the reaction conditions, eqs. [2]–[5]. The bromoallene could be formed from propargyl bromide by addition of a bromine atom to the terminal carbon atom of the acetylene, followed by loss of the bromine atom originally present, see

Can. J. Chem. Downloaded from www.nrcresearchpress.com by 210.87.254.42 on 09/05/12
For personal use only.

[2] 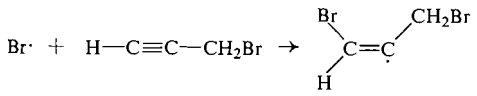

[3] 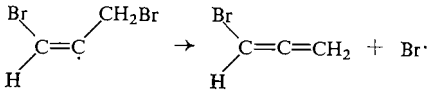

[4] 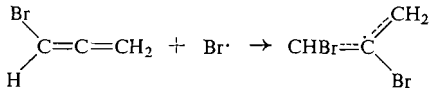

[5] 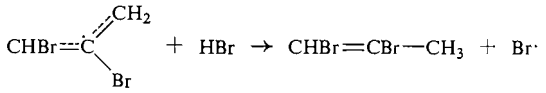

reactions [2] and [3]. In the free radical hydrobromination of propyne to form *cis*-1-bromopropene (6) the bromine atom adds to the terminal carbon atom, and it has been shown that a bromine atom is readily lost from a carbon atom adjacent to a radical center (17). Addition of a bromine atom to the center carbon atom of bromoallene would give a long-lived allylic radical, reaction [4], which would react with hydrogen bromide to form 1,2-dibromopropene.

Several attempts were made to trap the postulated intermediate *cis*-1,3-dibromo-2-propenyl radical with hydrogen bromide at 25° in solution, reaction [6*a*]. Increasing the rate of introduction of hydrogen bromide into hydrobromination reactions of propargyl bromide in pentane solution did not result in any change in product composition. The maximum concentration of hydrogen bromide in pentane which could have been attained under these conditions is ca. 0.6 *M* (18). More concentrated hydrogen bromide solutions can be prepared in ether. A hydrobromination under illumination by a sun lamp of propargyl bromide in ether saturated with hydrogen bromide (ca. 40% HBr) did result in formation of significant amounts of 1,3-dibromopropene. The distribution of dibromides formed was 1,2-dibromopropene (11%), 2,3-dibromopropene (19%), and 1,3-dibromopropene (70%). The presence of a considerable quantity of 2,3-dibromopropene in the product mixture indicates that a significant amount of ionic reaction had occurred. This makes uncertain what amount of 1,3-dibromopropene was formed by trapping of any intermediate radical. A hydrobromination under illumination of propargyl bromide in ether solution 1.3 *M* in hydrogen bromide resulted in the formation of a 90:10 mixture of 1,2-:1,3-dibromopropene and only traces of 2,3-dibromopropene. This product composition is not significantly different from those of numerous runs carried out in ether solution 0.32 *M* in hydrogen bromide at 25° (see below) or in one run at −20°. Hydrobromination under illumination of propargyl bromide in ether solution more concentrated than about 1.3 *M* in hydrogen bromide always resulted in formation of significant amounts of 2,3-dibromopropene. The intermediate radical cannot be trapped to any significant extent by hydrogen bromide at hydrogen bromide concentrations of up to 1.3 *M* at 25°. Above this concentration ionic reactions begin to interfere.

An earlier attempt to carry out free radical addition of hydrogen bromide to unsaturated systems in ether solution failed (10). In the present study free radical hydrobrominations in ether solution occurred only if ether was carefully treated prior to reaction (see Experimental).

The intermediate 1,3-dibromo-2-propenyl radical would be expected to have a longer life at lower temperatures and experiments designed to trap it at −78° were carried out.

Attempts to carry out free radical hydrobromination of propargyl bromide in ether or pentane solution at low temperature were

[6*a*] 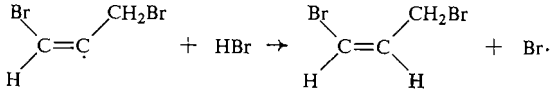

Can. J. Chem. Downloaded from www.nrcresearchpress.com by 210.87.254.42 on 09/05/12
For personal use only.

TABLE III

Product distribution and stereochemistry of free radical hydrobromination of propargyl bromide and bromoallene in liquid hydrogen bromide at −78°

		% Dibromopropene	
Conversion (%)	Bromoallene (%)	1,2- (% *trans*)	1,3- (% *cis*)
	From propargyl bromide		
0	0.3	—	—
1.8	0.5	0.1 (77.0)	1.5 (98.8)
10.7	2.0	0.7 (77.1)	8.3 (97.5)
27.7	1.4	2.0 (77.2)	24.6 (96.0)
	From bromoallene		
9.3	—	6.8 (51.4)	2.5 (95.5)
48.0	—	36.1 (50.8)	11.9 (92.6)

frustrated by the formation of solid phases. When a 0.32 *M* solution of hydrogen bromide in ether was cooled to −78° a large amount of white precipitate formed. A pentane solution 0.32 *M* in hydrogen bromide was homogeneous at −78°. However, introduction of even small amounts of propargyl bromide resulted in immediate formation of a precipitate.

Both bromoallene and propargyl bromide form homogeneous solutions with hydrogen bromide at −78°. A number of free radical hydrobrominations of bromoallene and propargyl bromide were carried out in degassed liquid hydrogen bromide solution at this temperature. Reactions were initiated by illumination from a sun lamp. Similar conditions have previously been used for the free radical hydrobromination of propyne (6). No addition or isomerization occurred in the absence of illumination. No reaction products with molecular weight higher than that of dibromopropene were detected. Results from a number of experiments are summarized in Table III. Propargyl bromide and bromoallene gave different product distributions under these conditions and product distributions from both were different from those observed in reactions at room temperature in solution. The ratio 1,2-:1,3-dibromopropene formed in the radical hydrobromination of either bromoallene or propargyl bromide in solution at room temperature is always in the range 10:1 to 30:1. In reactions at −78° the 1,2-:1,3-dibromopropene ratio obtained from propargyl bromide was ca. 1:12 and that obtained from bromoallene was ca. 3:1. Radical hydrobromination of propargyl bromide can yield either 1,2-dibromopropene almost exclusively or 1,3-dibromopropene almost exclusively depending upon reaction conditions. The very predominant formation of 1,3-dibromopropene at low temperature shows that the bromine atom adds at the terminal acetylenic carbon atom of propargyl bromide. That only small amounts of bromoallene and 1,2-dibromopropene are formed from propargyl bromide in these reactions can be explained by postulating that in liquid hydrogen bromide at −78° (*a*) the intermediate *cis*-1,3-dibromo-2-propenyl radical, if formed, abstracts a hydrogen atom from hydrogen bromide much more rapidly than it loses a bromine atom to form bromoallene, or (*b*) the bromine atom reacts with a propargyl bromide–hydrogen bromide complex and hydrogen atom transfer is rapid (10).

Stereochemistry of Hydrogen Bromide Addition at −78°

The proportion of the *cis*-isomer in the 1,3-dibromopropene mixture decreases somewhat as the reaction proceeds. This appears to be due to a slow isomerization catalyzed by hydrogen bromide. Extrapolation of a plot of % *cis*-1,3-dibromopropene vs. % conversion to 0% conversion gives an intercept of 99.2% *cis*. This value is significantly different from the equilibrium value which is calculated to be ca. 90% *cis* at −78°. The radical hydrobromination of propargyl bromide under these conditions is a stereospecific *trans* addition reaction. The hydrobromination of propyne has also been shown to be a stereospecific *trans* addition reaction under the same conditions (6).

Unexpectedly, the 1,3-dibromopropene formed from bromoallene under these conditions is also

Can. J. Chem. Downloaded from www.nrcresearchpress.com by 210.87.254.42 on 09/05/12
For personal use only.

Can. J. Chem. Downloaded from www.nrcresearchpress.com by 210.87.254.42 on 09/05/12
For personal use only.

mainly the *cis*-isomer. Extrapolation to 0% conversion indicates that the proportion of *cis*-isomer formed initially in this reaction is > 96%.

The radical addition of hydrogen bromide to olefins at low temperature has been shown to be a stereospecific *trans*-process (11, 12, 19) and there is no obvious reason why addition of a bromine atom could not occur equally well at either side of the bromoallene molecule to give a mixture of *cis*- and *trans*-1,3-dibromo-2-propenyl radicals, at least in incipient form, reactions [6*a*] and [6*b*]. Perhaps hydrogen transfer

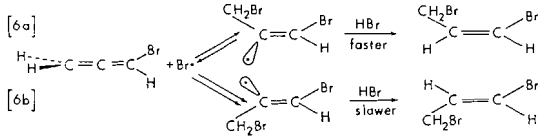

from hydrogen bromide to the *trans*-radical is sterically hindered. Inspection of Fisher–Hirschfelder–Taylor molecular models indicates that there may be some interference by the vinyl bromine atom to approach of hydrogen bromide to the adjacent vinylic radical center in the *trans* radical. In the case of the reaction involving a hydrogen bromide–allene complex, the hydrogen bromide would have to shift from a symmetrical position between the terminal and central carbon atoms toward the central carbon atom before hydrogen atom transfer could occur, and this shift would also be more difficult in the process leading to the *trans*-dibromide.

The 1,2-dibromopropene produced from bromoallene has a different isomer composition from that produced from propargyl bromide. At −78° the equilibrium mixture is calculated to contain ca. 82% of the *trans*-isomer. In neither reaction is the equilibrium mixture formed. The isomer ratio of 1,2-dibromopropene remains essentially constant during both reactions, so that 1,2-dibromopropene is isomerized much more slowly than 1,3-dibromopropene under these reaction conditions.

Kinetic Evidence for Radical Intermediate in Solution

The results of the low temperature hydrobrominations of propargyl bromide show that the initial point of attack of the bromine atom is at the terminal carbon atom of the acetylernic group. This would indicate that in ether and pentane solution bromoallene is formed by way of the *cis*-1,3-dibromo-2-propenyl radical, reactions [2] and [3]. In order to obtain kinetic evidence for the formation of this intermediate, several runs were made in ether with known concentrations of reactants and were continuously monitored.

Oxygen-free solutions of propargyl bromide and hydrogen bromide in ether were irradiated at room temperature. These reactions were homogeneous. As was observed in the more qualitative runs carried out in pentane, the bromoallene concentration increased to ca. 10–12% of the initial propargyl bromide concentration and then decreased as the reaction progressed further. No variation in behavior was observed when the initial hydrogen bromide concentrations were varied from 0.32 to 1.3 *M*. Results from two runs at the extremes of hydrogen bromide concentration used are shown in Fig. 1. No reaction was observed in the absence of illumination.

Although the 1,2-dibromopropenes formed in hydrobromination reactions carried out in pentane solution were always equilibrated, this was not the case when the reactions were carried out in ether solution. Here the isomer ratio varied during the course of a reaction and always contained less than the equilibrium amount of the *trans*-isomer.

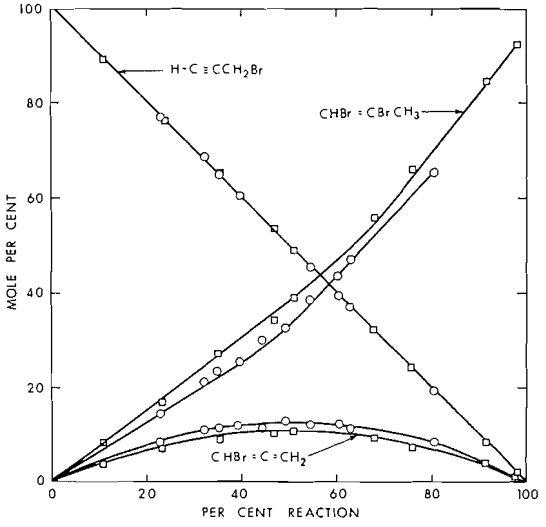

FIG. 1. Disappearance of starting material and formation of products in radical hydrobromination of propargyl bromide in ether at 25°. □, run 8, $[HBr]_0$ = 1.32 *M*, $[PB]_0$ = 0.032 *M*, 6% 1,3-dibromopropene present at 80% reaction; ○, run 10, $[HBr]_0$ = 0.32 *M*, $[PB]_0$ = 0.032 *M*, 5% 1,3-dibromopropene present at the end of the reaction.

Can. J. Chem. Downloaded from www.nrcresearchpress.com by 210.87.254.42 on 09/05/12
For personal use only.

The equilibrium ratio was determined in ether by irradiating a solution of pure *trans*-1,2-dibromopropene and hydrogen bromide in this solvent. Equilibration proceeded much more slowly than did the equilibration in pentane, but afforded essentially the same isomer composition as formed in pentane: 77.8% *trans*- and 22.2% *cis*-1,2-dibromopropene.

It appeared at first that the 1,2-dibromopropene formed initially contained more of the *cis*-isomer than the equilibrium mixture and that equilibration occurred slowly as the reaction progressed. However, when the isomer composition was monitored early in the reaction, it was found that the reaction was more complex. The upper curve of Fig. 2 shows the variation of the % of *trans*-isomer in the 1,2-dibromopropenes formed from propargyl bromide during ca. the first 30% of reaction. Extrapolation of the curve to 0% reaction gives an intercept of ca. 74% *trans*-1,2-dibromopropene. The % of *trans*-isomer present actually decreases from near the equilibrium % early in the reaction, to 67%, and only later beings to increase again.

The lower curve of Fig. 2 shows the variation during approximately the first 30% of reaction of the % of the *trans*-isomer of the 1,2-dibromopropenes formed in hydrobromination of bromoallene under illumination in ether. The results are entirely different from those obtained with propargyl bromide. Initially, nearly equal amounts of *cis*- and *trans*-isomers are present. As the reaction progresses the proportion of *trans*-isomer increases slowly.

It is clear that mechanism of formation of 1,2-dibromopropene in the radical hydrobromination of propargyl bromide is more complex than is indicated by reactions [2]–[5]. In ether solution at 25° a significant portion of the product must arise by a process not involving free bromoallene.

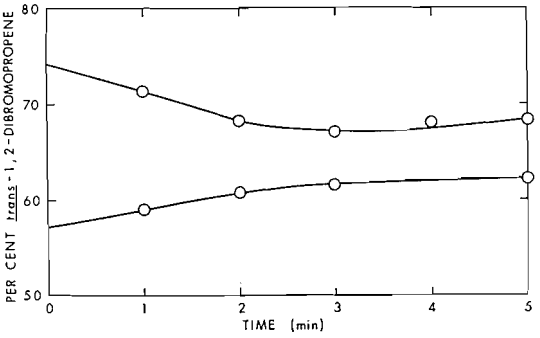

FIG. 2. Variation of isomer composition of 1,2-dibromopropene with time in radical hydrobromination of propargyl bromide (upper curve) and bromoallene (lower curve) in ether at 25°.

Further support for this conclusion is obtained from the kinetic analysis of the reaction. If all the product were formed via free bromoallene then the reactions may be formulated as in reactions [2]–[5]. Since the loss of a bromine atom from the 1,3-dibromo-2-propenyl radical is fast and the amount of bromoallene present in the reactions is independent of hydrogen bromide concentration, Fig. 1, rate-determining steps may be represented as

$$[7] \qquad PB + Br\cdot \xrightarrow{k_1} BA + Br\cdot$$

$$[8] \qquad BA + Br\cdot \xrightarrow{k_2} DB$$

where PB = propargyl bromide, BA = bromoallene, and DB = 1,2-dibromopropene. The following expressions may now be written

$$[9] \qquad \frac{-d[PB]}{dt} = k_1[PB][Br\cdot]$$

$$[10] \qquad \frac{-d[BA]}{dt} = k_2[BA][Br\cdot] - k_1[PB][Br\cdot]$$

$$[11] \qquad \frac{d[BA]}{d[PB]} = \frac{k_2[BA] - k_1[PB]}{k_1[PB]}$$

$$[12] \qquad \frac{d[BA]}{d[PB]} - \frac{k_2[BA]}{k_1[PB]} = -1$$

This expression may be integrated (20) using $[PB_0]$ and [0] as the initial limits, and [PB] and [BA] as the final limits of the variables to give

$$[13] \qquad [BA] = \frac{[PB]}{1 - k_2/k_1}\left[\left(\frac{[PB]}{[PB_0]}\right)^{k_2/k_1 - 1} - 1\right]$$

This result is identical to that obtained by McMillan (21) using a somewhat different method. The ratio k_2/k_1 may be determined from the maximum concentration of bromoallene.

$$[14] \qquad \frac{-d[BA]}{dt} = 0 = k_2[BA][Br\cdot] - k_1[PB][Br\cdot]$$

$$[15] \qquad k_2/k_1 = [PB]/[BA] \text{ at maximum BA}$$

Can. J. Chem. Downloaded from www.nrcresearchpress.com by 210.87.254.42 on 09/05/12
For personal use only.

Unfortunately the concentration of bromoallene passes through a broad maximum and the concentration of propargyl bromide varies considerably, while the concentration of bromoallene varies but little. In each of a number of runs the ratio k_2/k_1 calculated in this manner varied from about 5 at the beginning of the broad maximum to about 3.5 at the end of the broad maximum. The ratios used for calculations were taken from concentrations at the estimated midpoint of the broad maximum and were 4.0 for three runs and 4.7 for one run. Using eq. [13] the upper curve of Fig. 3 was calculated for the concentration of bromoallene during run 10. This curve is clearly different from the experimental curve. Bromoallene is neither being formed as rapidly nor consumed as rapidly as required were all the intermediate *cis*-1,3-dibromo-2-propenyl radicals converted to free bromoallene. It appears that only a portion of the intermediate radicals formed yields free bromoallene.

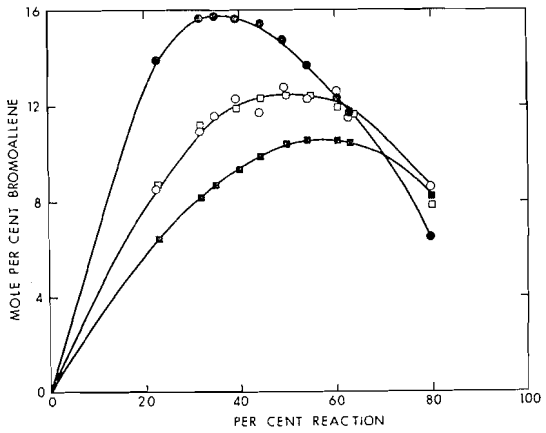

FIG. 3. Variation of bromoallene concentration with time in hydrobromination of propargyl bromide in ether at 25° in run 10. ○, Observed; ●, calculated using eq. [13]; □, calculated using eq. [16] with $F = 1/2$; ■, calculated using eq. [16] with $F = 1/3$. The middle curve is drawn through the experimental points.

If only a fraction, F, of the intermediate *cis*-1,3-dibromo-2-propenyl radicals formed is diverted to free bromoallene, the following equation may be derived to represent the concentration of bromoallene during the course of the reaction

$$[16] \quad [BA] = \frac{F[PB]}{1 - k_2/k_1}\left[\left(\frac{[PB]}{[PB_0]}\right)^{k_2/k_1 - 1} - 1\right]$$

A series of curves was calculated for each run using various values of F. The ratio k_2/k_1 in these cases is given by

$$[17] \quad k_2/k_1 = F\,[PB]/[BA] \text{ at maximum BA}$$

Figure 3 shows curves obtained using eq. [16] for run 10 using different values of F. The curve calculated using $F = 1/2$ gives a very close fit to the experimental curve. For four runs very close agreement between the calculated and experimental curves was obtained, with the values of F and k_2/k_1 shown in Table IV. These results indicate that about 50% of the reaction proceeds by a process not involving free bromoallene.

TABLE IV

Values of F and k_2/k_1 for hydrobrominations of propargyl bromide in ether at 25°

Run	$[PB]_0$, * M	$[HBr]_0$, M	F	k_2/k_1
7	0.354	0.354	1/2	2.0
8	0.032	0.324	1/3	1.6
9	0.100	0.324	1/2	2.0
10	0.032	1.30	1/2	2.0

*Propargyl bromide contained less than 0.5% bromoallene initially.

Reactions of the Radical Intermediate

There appear to be two possible processes which could account for that part of the reaction which does not form free bromoallene. One process involves an intramolecular bromine atom migration, Fig. 4, to form the allylic 1,2-dibromopropenyl radical. The other process could be a

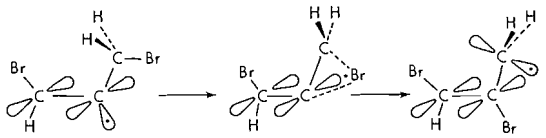

FIG. 4. Stereochemistry of bromine atom migration.

cage reaction between bromoallene and its bromine atom partner which results from loss of a bromine atom from the 1,3-dibromo-2-propenyl radical, Fig. 5. A choice can be made between these two processes by considering the stereochemistry of the reaction in ether solution at short reaction times, Fig. 2, and the geometric requirements of the two processes.

As Fig. 4 shows, bromine atom migration must produce the 1,2-dibromopropenyl radical with the bromine atoms *trans*. This would also

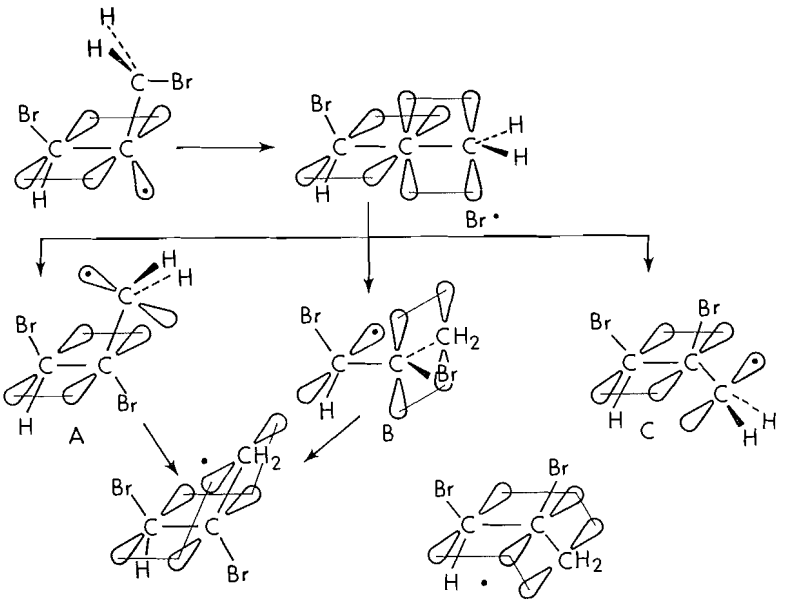

FIG. 5. Stereochemistry of bromine atom elimination followed by recombination.

be so if the initial radical were a bridged radical instead of a vinyl radical as depicted. However, it is difficult to account for the formation of bromoallene from a bridged radical without first opening it to *cis*-1,3-dibromo-2-propenyl radical, and it is not required to account for any of the results. From the stereochemical results illustrated in Fig. 2, it can be concluded that the 1,2-dibromopropenyl radicals must maintain their geometry under these reaction conditions. It has already been shown that other types of allylic radicals are geometrically stable (22). Thus, any 1,2-dibromopropene formed via bromine atom migration must be completely *trans*. The stereochemistry of the first formed 1,2-dibromopropene can be determined by reference to Fig. 2. The intercept at 0% reaction of the upper curve gives the stereochemistry of the initial product before isomerization and before any reaction of bromoallene. The result is 74% *trans*. It can be shown in another way from the data illustrated in Fig. 2 that the initial stereochemistry cannot be 100% *trans*. The lower curve in Fig. 2 shows that isomerization of the products (to 78% *trans*) is very slow under these conditions and that at reaction times of 2–5 min the stereochemistry of the 1,2-dibromopropenes formed from bromoallene is about 60% *trans*. Assuming that 50% of the 1,2-dibromopropenes produced in the hydrobromination of propargyl bromide under these conditions arises via free bromoallene (a maximum amount based on the kinetic results) and the other 50% arises via a process giving 74% *trans*, then the net isomer distribution during this time should be about 67% *trans*. This agrees well with the value of 68–69% *trans* shown by the upper curve of Fig. 2. Were the other 50% to arise via a process giving 100% *trans* rather than 74% *trans*, then the net isomer distribution would be about 80% *trans* during the first 2–5 min of reaction. This is not observed. Clearly the stereochemistry of the first formed 1,2-dibromopropenes must be quite different from 100% *trans* which indicates that a bromine atom migration cannot be involved. This is not unexpected as the initial radical formed upon bromine atom migration would not be the stabilized allyl radical but one in which the odd electron is localized in an atomic p orbital which is perpendicular to the plane of the adjacent π-orbital. There is no driving force for the migration as the primary radical formed would not be expected to show stability over the initial vinyl radical.

This leaves the cage reaction as the only alternative for the ca. 50% of the reaction which does not proceed via bromoallene. The cage

Can. J. Chem. Downloaded from www.nrcresearchpress.com by 210.87.254.42 on 09/05/12
For personal use only.

Can. J. Chem. Downloaded from www.nrcresearchpress.com by 210.87.254.42 on 09/05/12
For personal use only.

reaction must be stereoselective since the initial stereochemistry of the 1,2-dibromopropene formed from bromoallene is different from that of the 1,2-dibromopropene formed from propargyl bromide. Loss of a bromine atom from the 1,3-dibromo-2-propenyl radical must occur from a conformation in which the carbon–bromine bond that is breaking is parallel to the orbital containing the odd electron. The conformation of lower energy is shown in Fig. 5. The other conformation in which the bromomethyl group has rotated by 180° with respect to the conformation shown is seen by inspection of Fisher–Hirschfelder–Taylor models to be severely strained due to steric interference between the bromine atoms. In fact, that conformation cannot be made with the models. When initially formed the bromoallene molecule and the bromine atom have the steric relationship shown in Fig. 5 in which the bromine atom is on the opposite side of the molecule from the bromine atom in the molecule and in the plane defined by the bromomethylene group. Radical A, formed by recombination of the bromine atom with the p orbital in the plane of the bromomethylene group on the side opposite to the bound bromine, will give the *trans*-1,2-dibromopropenyl radical upon rotation of the methylene group and will finally give *trans*-1,2-dibromopropene. Reaction at the same orbital at the side *cis* to the bound bromine will give radical C which will then give the *cis*-1,2-dibromopropenyl radical and thus *cis*-1,2-dibromopropene. Reaction with the other p orbital will give radical B. Rotation of the bromomethylene group in either direction will give a stable allylic radical so that one would expect radical B to give approximately equal amounts of *cis*- and *trans*-1,2-dibromopropenyl radicals, and hence equal amounts of *cis*- and *trans*-1,2-dibromopropene. Since the cage recombination gives more *trans*-1,2-dibromopropene than does recombination outside the cage, the cage recombination to give radical A must compete with rotation of the bromoallene molecule with respect to its bromine atom partner. This is, then, an example of a stereoselective atom–molecule cage recombination reaction.

Relaxation times for molecular rotation of a number of small molecules in the liquid phase are near 10^{-11} s (23–25). This corresponds to the time that two particles will be confined to a solvent cage (26). It is thus reasonable that a reaction which can compete with diffusion can also compete with molecular rotation. Cage recombination of radicals derived from optically active azo compounds is a stereoselective process (27).

The addition of a bromine atom to bromoallene must have a very low activation energy if it is to compete with diffusion and molecular rotation. It has been suggested that the addition of a bromine atom to allene requires little or no activation energy (28). The energetic requirements for the bromine atom – bromoallene addition reaction are expected to be very similar. An atom–molecule cage recombination appears to occur in the radical chlorination of *t*-butyl bromide by *t*-butyl hypochlorite (29).

In an excellent study of the radical hydrobromination of allene it was shown that bromine atoms add to the terminal and central carbon atoms of allene at equal rates, and that the radical resulting from addition to the central carbon has a longer lifetime with respect to loss of the bromine atom than the radical resulting from terminal addition (28). As a result only products resulting from an initial addition of a bromine atom at the central carbon of allene are isolated when the concentration of hydrogen bromide is low or at high temperatures (30–32), while products resulting from initial addition at the terminal carbon are observed only at high hydrogen bromide concentrations and lower temperatures. It was suggested that a bromine-bridged radical was not required to account for these results (28). The results of the present study are in complete agreement with these conclusions, and provide stereochemical evidence against the intervention of bromine-bridged radicals in allenic systems.

The significance of the results obtained in the present study with respect to other systems in which bromine-bridged radicals or bromine atom migrations have been postulated (6–8, 33–35) is unclear. As was pointed out above there appears to be little, if any, driving force for bromine atom migration in the 1,3-dibromo-2-propenyl radical. In most of the other systems migration would lead directly to a more stable radical. Also, in the present system the orbital bearing the odd electron is directed more away from the adjacent carbon–bromine bond than is the case in a saturated system, Fig. 6. Both factors would make either bridging or migration in the 1,3-dibromo-2-propenyl radical less favorable than in the saturated systems. Thus, although the present

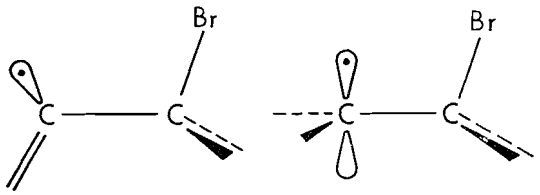

FIG. 6. Geometry of the 3-bromo-2-propenyl and the 1-bromo-2-propyl radicals.

study provides additional evidence that the loss of a bromine atom adjacent to a radical center is very rapid (17, 29) and that recombination at a different carbon atom is very rapid, the present system does not serve as a good model for an analogous process in the saturated systems.

The ratio of terminal to center addition of a bromine atom to bromoallene observed in liquid hydrogen bromide in this study, 1:3, differs from the ratio of 1:1 to be expected from the limiting ratio found in the case of allene (28). It is difficult to tell if the difference is significant as no effort was made in the present study to determine whether the ratio found was the limiting ratio.

Gas Phase Reactions

The gas phase hydrobromination of propargyl bromide was also briefly studied in an attempt to confirm that a considerable amount of the bromoallene formed in solution from propargyl bromide is consumed by a cage recombination reaction. There can be no cage reaction in the gas phase and in the absence of bromine atom migration; all the 1,2-dibromopropene formed should result from free bromoallene. If bromine atom migration is occurring in solution it should also occur in the gas phase, and there would be, as in solution, two routes to 1,2-dibromopropene. Reactions were carried out in an oxygen-free system at room temperature under illumination. All the reactions had an inhibition period of ca. 5 min. No reaction was observed in the dark. In contrast to the reactions in solution, bromoallene was always formed much more rapidly than was 1,2-dibromopropene. The isomer composition of the 1,2-dibromopropene formed initially is ca. 54% *trans*, Fig. 7. Isomerization is rapid and the equilibrated mixture was present after only 2.6% 1,2-dibromopropene had been formed. About 35% bromoallene was present by this time. No structurally isomeric dibromopropenes were detected at these amounts of conversions. At higher conversions a thin film

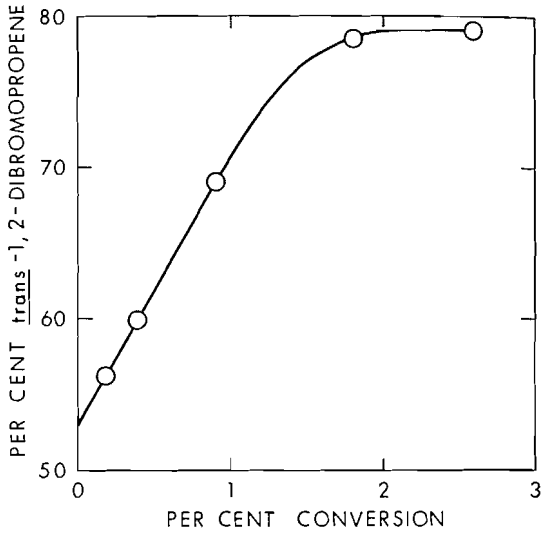

FIG. 7. Variation of isomer composition of 1,2-dibromopropene with conversion in the gas phase hydrobromination of propargyl bromide at 25°.

deposited on the walls of the reaction vessel so the reaction was not investigated at higher conversions. The stereochemistry of the 1,2-dibromopropenes formed is quite similar to that found from hydrobromination of bromoallene in solution. This indicates that in the gas phase the 1,2-dibromopropenes are formed entirely from free bromoallene and that bromine atom migration is unimportant.

A recent report describes the equilibration of propargyl bromide and bromoallene catalyzed by hydrogen bromide under illumination at 135–200° (36). Equilibrium could be reached starting with either component and propargyl bromide was found to be more stable than bromoallene by 0.83 kcal at 400 °K. No more than traces of propargyl bromide were observed in any of the radical hydrobrominations of bromoallene in solution in the present study, even though at 25° the equilibrium mixture should consist of about 80% propargyl bromide. The route to propargyl bromide from bromoallene would be the reverse of reaction [3] followed by the reverse of reaction [2]. That this process does not occur at 25° indicates that the activation energy for the loss of the vinyl bromine atom from the 1,3-dibromo-2-propenyl radical to give propargyl bromide, reaction [2], is significantly greater than is that for loss of the allylic bromine atom to give bromoallene, reaction [3]. This is

Can. J. Chem. Downloaded from www.nrcresearchpress.com by 210.87.254.42 on 09/05/12
For personal use only.

[18–19] $$H{-}C{\equiv}C{-}CH_2Br + Br\cdot \rightleftarrows HBr + \left[\begin{array}{c} H{-}C{\equiv}C\dot{C}HBr \\ \updownarrow \\ HC{=}C{=}CHBr \end{array}\right] \rightleftarrows Br\cdot + H_2C{=}C{=}CHBr$$

to be expected as aryl bromides, and, therefore, quite probably, vinyl bromides, have much stronger carbon bromine bonds than do allylic bromides (37).

The mechanism proposed for the propargyl bromide–bromoallene equilibration (36) consists of reversible hydrogen atom abstractions by bromine atoms, reactions [18–19]. From the results of the present study it is clear that propargyl bromide can be converted to bromoallene simply by addition and subsequent elimination of bromine atoms, reactions [2] and [3]. These steps should be reversible at the temperatures used in the equilibration studies (36) and such a reversible addition–elimination sequence surely contributes significantly to the equilibration process and may well account for almost all the equilibration.

Hydrogen chloride was also reported to catalyze the equilibration and a reversible hydrogen abstraction reaction by chlorine atoms was invoked to account for it. However, an addition–elimination sequence probably contributes in this case also. Such a sequence would initially produce chloroallene and bromine atoms, reactions [20] and [21]. After only a few per cent conversion to chloroallene there would be enough bromine atoms produced, so that they would then become the exclusive chain carriers.

Experimental

Boiling points are uncorrected values. Infrared (i.r.) spectra were recorded on a Perkin–Elmer recording infrared spectrophotometer, model 421, equipped with sodium chloride optics. Nuclear magnetic resonance (n.m.r.) spectra were recorded on a Varian analytical spectrophotometer, Model A-60. Tetramethylsilane was used as internal standard.

Analytical gas–liquid chromatography (g.l.c.) was carried out with an Aerograph 202 fractometer using a 9.5 ft × 1/4 in. stainless steel column packed with 10% Ucon-50-HB5100 (Polyglycol) on Chromosorb W. For preparative g.l.c. an Aerograph Autoprep equipped with a 20 ft × 3/8 in. stainless steel column packed with 10% Ucon-50-HB280X (Polyglycol) on Diaport W.A.W. was used. The order of elution was the same on both columns and was bromoallene, propargyl bromide, *trans*-1,2-dibromopropene, *cis*-1,2-dibromopropene, 2,3-dibromopropene, *cis*-1,3-dibromopropene, and *trans*-1,3-dibromopropene. Heptane was used as internal standard. Areas were measured by peak height × width at half-peak height. Controls using authentic mixtures showed that the thermal response factors of all the above materials were within 2% of the internal standard and no corrections were applied.

Reactions carried out under irradiation were irradiated with a General Electric sun lamp. Solutions were dried with anhydrous magnesium sulfate. Matheson 99.8% hydrogen bromide was used without further purification.

Pentane was purified by shaking 500 ml technical grade material with 50 ml portions of concentrated sulfuric acid until the sulfuric acid layer remained colorless. The pentane was then shaken several times with water, dried, and distilled through a 40 cm vigreaux column. Heptane was purified in the same manner.

Diethyl ether used as solvent for photoinitiated hydrobrominations was purified in the following way. Mallinckrodt absolute reagent grade material was distilled, anhydrous hydrogen bromide added to the distillate, and the resulting solution irradiated for 1 h. The ether was then washed with saturated salt solution until the aqueous layer was neutral, dried, distilled, and stored over sodium. Photoinitiated hydrobrominations in ether which was not purified in this manner had very long induction periods and produced impurities which interfered with product analysis by g.l.c.

Propargyl bromide was prepared according to the method of Jacobs and Brill (38), b.p. 79° (695 mm), n_D^{25} 1.4906; reported b.p. 81.8° (750 mm), n_D^{20} 1.4929 (38). This material always contained less than 0.5% bromoallene according to g.l.c. analysis.

Bromoallene was prepared according to a modification of the method of Jacobs and Brill (38). The crude product

[20] $$Cl\cdot + H{-}C{\equiv}C{-}CH_2Br \rightarrow \begin{array}{l} Cl \\ \quad\diagdown \\ \quad\quad C{=}\dot{C} \\ \quad\diagup \\ \quad H \end{array} \quad \begin{array}{l} \\ \diagup CH_2Br \\ \\ \\ \end{array}$$

[21] $$\begin{array}{l} Cl \\ \quad\diagdown \\ \quad\quad C{=}\dot{C} \\ \quad\diagup \\ \quad H \end{array} \quad \begin{array}{l} \\ \diagup CH_2Br \\ \\ \\ \end{array} \rightarrow \begin{array}{l} Cl \\ \quad\diagdown \\ \quad\quad C{=}C{=}CH_2 \\ \quad\diagup \\ \quad H \end{array} + Br\cdot$$

Can. J. Chem. Downloaded from www.nrcresearchpress.com by 210.87.254.42 on 09/05/12
For personal use only.

Can. J. Chem. Downloaded from www.nrcresearchpress.com by 210.87.254.42 on 09/05/12
For personal use only.

was purified by preparative g.l.c. to give material containing less than 0.5% propargyl bromide, n_D^{25} 1.5182, reported n_D^{20} 1.5200 (38).

Hydrobromination Reactions at Room Temperature

Reactions in pentane were carried out by bubbling hydrogen bromide through a stirred solution of 5 g propargyl bromide or bromoallene and 5 g heptane in 20 ml pentane in a 3-necked round bottomed flask fitted with a dry ice condenser. Peroxide-initiated runs were carried out using 0.5 g benzoyl peroxide as additive. Dark reactions were carried out in a darkened hood in apparatus wrapped with aluminium foil. Before g.l.c. analysis the reaction mixtures were poured into ice water. The organic layer was washed twice more with ice water, once with sodium bicarbonate solution, and dried. Results are summarized in Table I.

Ionic reactions in ether were carried out in the dark by adding 0.6 g propargyl bromide or bromoallene to 10 ml of an ether solution saturated with hydrogen bromide and containing 0.5 g of hydroquinone and/or 0.5 g ferrous chloride. Before analysis, solutions were freed from hydrogen bromide as described for the reactions in pentane.

Free radical reactions in ether were carried out in a 3-necked flask attached to a vacuum line using as solvent ether purified as described above. The system was purged with nitrogen by several cycles of evacuating and filling with purified nitrogen before each run. Ether and hydrogen bromide which had been stored under nitrogen were distilled into the flask. Propargyl bromide or bromoallene were introduced through a serum cap with a hypodermic syringe and the solution was irradiated. The reactions had induction periods of 1–2 min and were complete in about 1 h. Samples were withdrawn through the serum cap periodically, freed of hydrogen bromide as described above, and analyzed.

One run was carried out in ether solution at −20° with propargyl bromide. The product distribution was the same as in the runs carried out at room temperature. Homogeneous hydrobrominations of propargyl bromide at −78° in pentane and ether solution could not be carried out. When propargyl bromide was added to a solution of hydrogen bromide in pentane at −78° a white precipitate formed immediately. This presumably was a complex of hydrogen bromide and propargyl bromide (39). A 1 *M* solution of hydrogen bromide in ether formed white crystals on cooling to −40°.

Hydrobromination Reactions in Liquid Hydrogen Bromide

A 10 ml pear-shaped flask was charged with 0.83 g (0.01 *M*) hydrogen bromide and 1.25 g (0.01 *M*) propargyl bromide. A homogeneous solution formed. The solution was degassed with two freeze–thaw cycles, −195° to −78°, before irradiation. The flask was then irradiated from 20 cm while immersed in a bath at −78°. After irradiation the flask was evacuated and the contents distilled twice from flask to flask under 2 mm pressure before analysis. Extensive *cis–trans* isomerization occurred when analyses were performed without prior distillation of the reaction mixture.

Gas Phase Hydrobromination of Propargyl Bromide

Hydrogen bromide and propargyl bromide were introduced into a 200 ml evacuated flask to partial pressures of 34 and 49 mm respectively. The contents were stirred for 5 min with a magnetic stirrer. The flask and its contents were irradiated after which a 5 ml portion of anhydrous ether was injected into the flask. The ether solution was freed of hydrogen bromide as described previously, before analysis. All the reactions had an inhibition period of ca. 5 min and formed a thin film on the wall of the flask after ca. 7 min of irradiation. Irradiations were not carried on beyond this point.

Product Identification

The products of the hydrobromination reactions were identified by comparison of their retention times on the g.l.c. column used and by comparison of n.m.r and i.r. spectra of samples collected from the effluent of the g.l.c. with those of authentic samples, with the exception of 2,3-dibromopropene.

trans-1,2-Dibromopropene was prepared by the slow addition of bromine to a solution of propyne in methylene chloride at −78°. The product was 99% *trans*-1,2-dibromopropene, b.p. 124–125° (688 mm), n_D^{25} 1.5323; reported b.p. 125.9°, $n_D^{17.4}$ 1.5369 (40). The n.m.r. spectrum (neat) showed absorption at τ 3.58 (multiplet) and τ 7.67 (doublet, J = 1.1 c.p.s.) with relative areas 1.0:3.0.

cis-1,2-Dibromopropene was prepared by isomerization of the *trans*-compound. *trans*-1,2-Dibromopropene was dissolved in pentane containing some hydrogen bromide and the solution was irradiated for 1 h. The solution was then washed several times with ice water, dried, and distilled. The fraction boiling at 45° at 18.5 mm was collected and contained 77% *trans*- and 23% *cis*-1,2-dibromopropene. A sample of the *cis*-isomer was collected by preparative g.l.c., b.p. 133–134° (688 mm), n_D^{25} 1.5290; reported b.p. 135.2°, $n_D^{17.4}$ 1.5337 (40). The n.m.r. spectrum (neat) showed absorption τ 3.91 (multiplet) and τ 7.66 (doublet, J = 1.1 c.p.s.) with relative areas of 1.0:3.0.

A mixture of *cis*- and *trans*-1,3-dibromopropene prepared by the method of Hatch (1) was separated into the two components by g.l.c. The n.m.r. spectrum (neat) of the *cis*-isomer, n_D^{25} 1.5519, reported n_D^{25} 1.5516 (41), liquid at −78°, showed absorption at τ 3.6 (multiplet) and τ 5.95 (multiplet) with relative areas 1.0:1.0. The n.m.r. spectrum of the *trans*-isomer, n_D^{25} 1.5572, reported n_D^{25} 1.5570 (41), solid at −78°, showed absorption at τ 3.6 (multiplet) and τ 6.15 (multiplet) with relative areas of 1.0:1.1. Hatch reports that *cis*-1,3-dibromopropene is a liquid at −78° while *trans*-1,3-dibromopropene is a solid at −78° (1).

The material with retention time between those of *cis*-1,2-dibromopropene and *trans*-1,3-dibromopropene was identified only on the basis of its n.m.r. spectrum (neat) which showed absorption at τ 3.91 (multiplet), τ 4.32 (doublet, J = 2.2 c.p.s.), and τ 5.75 (doublet, J = 1.0 c.p.s.) with relative areas 1.0:1.0:2.0. The data are in agreement with those reported for 2,3-dibromopropene (42).

No evidence was obtained in any of the reactions for the formation of 3,3-dibromopropene.

Determination of cis–trans Equilibria

A stirred solution of 0.29 g of a pure isomer of dibromopropene in 125 ml pentane was irradiated while a very slow stream of hydrogen bromide was slowly

bubbled into the solution. Aliquots were withdrawn periodically and analyzed directly by g.l.c. Irradiation was continued until there was no further change in isomer composition.

Acknowledgments

We wish to thank Professors D. Darwish and D. D. Tanner for helpful discussions.

1. L. F. HATCH and K. HARWELL. J. Am. Chem. Soc. **75**, 6002 (1953).
2. M. R. LESPIEAU. Ann. chim. et phys. [7] **11**, 232 (1897).
3. F. STITZ. Öester. Chemiker Zg. **48**, 186 (1947).
4. P. L. HARRIS and J. C. SMITH. J. Chem. Soc. 1572 (1935).
5. C. A. YOUNG, R. R. VOGT, and J. A. NIEUWLAND. J. Am. Chem. Soc. **58**, 1807 (1936).
6. P. S. SKELL and R. G. ALLEN. J. Am. Chem. Soc. **80**, 5997 (1958).
7. P. S. SKELL, R. G. ALLEN, and N. D. GILMOUR. J. Am. Chem. Soc. **83**, 504 (1961).
8. P. S. SKELL, D. L. TULEEN, and P. D. READIO. J. Am. Chem. Soc. **85**, 2849 (1963).
9. H. L. GOERING, P. I. ABELL, and B. F. AYCOCK. J. Am. Chem. Soc. **74**, 3588 (1952).
10. H. L. GOERING and L. L. SIMS. J. Am. Chem. Soc. **77**, 3465 (1955).
11. H. L. GOERING and D. W. LARSEN. J. Am. Chem. Soc. **81**, 5937 (1959).
12. P. S. SKELL and R. G. ALLEN. J. Am. Chem. Soc. **81**, 5883 (1959).
13. P. I. ABELL and C. CHIAO. J. Am. Chem. Soc. **82**, 3610 (1960).
14. N. A. LEBEL. J. Am. Chem. Soc. **82**, 623 (1960).
15. L. D. BERGEL'SON. Izvest. Akad. Nauk S.S.S.R. Otdel. Khim. Nauk, 887 (1960); Chem. Abstr. **57**, 24334*g* (1962).
16. L. D. BERGEL'SON. Izvest. Akad. Nauk S.S.S.R. Otdel. Khim. Nauk, 1499 (1958); Chem. Abstr. **53**, 7969*f* (1959).
17. H. STEINMETZ and R. M. NOYES. J. Am. Chem. Soc. **74**, 4141 (1952).
18. E. R. BOEDEKER and C. C. LYNCH. J. Am. Chem. Soc. **72**, 3234 (1950).
19. P. S. SKELL and P. FREEMAN. J. Org. Chem. **29**, 2524 (1964).
20. A. L. NELSON, K. W. FOLLEY, and M. CORAL. Differential equations. D. C. Heath and Co., Boston, Massachusetts. 1952. p. 39.
21. W. G. MCMILLAN. J. Am. Chem. Soc. **79**, 4838 (1957).
22. C. WALLING and W. THALER. J. Am. Chem. Soc. **83**, 3877 (1961).
23. W. P. PURALL, K. FISH, and C. P. SMYTH. J. Am. Chem. Soc. **82**, 6299 (1960).
24. A. J. CURTIS, P. L. MCGEER, G. B. RATHMAN, and C. P. SMYTH. J. Am. Chem. Soc. **74**, 644 (1952).
25. K. HIGASI, K. BERGMANN, and C. P. SMYTH. J. Phys. Chem. **64**, 880 (1960).
26. R. M. NOYES. J. Am. Chem. Soc. **77**, 2042 (1955).
27. (*a*) K. R. KOPECKY, T. GILLAN, and T. W. MOJELSKI. 51st Ann. Conf. Chemical Institute of Canada, Vancouver, British Columbia. June, 1968. Abstracts. p.57. (*b*) F. D. GREENE and M. A. BERWICK. 156th Meeting of the American Chemical Society, Atlantic City. September, 1968. Abstracts. ORGN, No. 112.
28. E. I. HEIBA and W. O. HAAG. J. Org. Chem. **31**, 3815 (1966).
29. W. D. HAAG and E. I. HEIBA. Tetrahedron Letters, 3683 (1965).
30. D. KOVACHIC and L. C. LEITCH. Can. J. Chem. **39**, 3636 (1961).
31. K. GRIESBAUM, A. A. OSWALD, and D. M. HALL. J. Org. Chem. **29**, 2404 (1964).
32. P. I. ABELL and R. S. ANDERSON. Tetrahedron Letters, 3727 (1964).
33. P. S. JUNEJA and E. M. HODNETT. J. Am. Chem. Soc. **89**, 5685 (1967).
34. W. THALER. J. Am. Chem. Soc. **85**, 2607 (1963).
35. P. S. SKELL and P. D. READIO. J. Am. Chem. Soc. **86**, 3334 (1964).
36. H. G. MEUNIER and P. I. ABELL. Tetrahedron Letters, 3633 (1967).
37. T. L. COTTRELL. The strengths of chemical bonds. 2nd ed. Butterworths, London. 1958. p. 205.
38. T. L. JACOBS and W. F. BRILL. J. Am. Chem. Soc., **75**, 1314 (1953).
39. O. MAAS and J. RUSSELL. J. Am. Chem. Soc. **43**, 1227 (1921).
40. H. VAN RISSEGHEM. Bl. Soc. Chim. Belg. **28**, 379 (1919).
41. A. T. BOTTINI, B. J. KING, and J. M. SNEAS. J. Org. Chem. **27**, 3688 (1962).
42. F. B. WHIPPLE, J. H. GOLDSTEIN, and G. R. MCCLURE. J. Am. Chem. Soc. **82**, 3811 (1960).

Can. J. Chem. Downloaded from www.nrcresearchpress.com by 210.87.254.42 on 09/05/12
For personal use only.

Magnetic nonequivalence in asymmetric phosphorus compounds

L. FRANKEL, J. CARGIOLI, H. KLAPPER, AND R. DANIELSON
Physical Chemistry Department, Chemical Research Laboratory, Edgewood Arsenal, Maryland, 21010

Received April 17, 1969

The nuclear magnetic resonance (n.m.r.) spectra of seven compounds of the type $(CH_3)P(O)(SCH_2SR)(OR')$ have been examined as a function of solvent. The resonance pattern of the methylene protons, SCH_2S, is strongly solvent dependent. In solvents of low dielectric constant, the methylene protons are magnetically nonequivalent and are observed as the AB part of an ABX spin system, where X is the phosphorus atom. In high dielectric constant medium (DMSO d_6) only a well-resolved doublet is obtained indicating magnetic equivalence. When $R' = CH(CH_3)_2$, nonequivalent methyl groups which show analogous solvent effects are observed.

Eight compounds of the type $(CH_3)P(O)(OCH(CH_3)_2)(X)$ have been studied. The chemical shift between the magnetically nonequivalent isopropyl methyl groups does not correlate with any simple property of X.

Canadian Journal of Chemistry, 47, 3167 (1969)

Can. J. Chem. Downloaded from www.nrcresearchpress.com by 210.87.254.6 on 09/05/12
For personal use only.

Introduction

Several n.m.r. studies have been reported on the effect of asymmetric carbon atoms in causing magnetic nonequivalence (1). An asymmetric phosphorus atom may also cause magnetic nonequivalence in nearby methylene protons (2, 3) and methyl groups (4–6). The origin of the magnetic nonequivalence is strictly due to symmetry effects (7) which may be further augmented by the effect of conformational preference. For all previously reported systems rapid intramolecular rotation occurs. The experimental parameters observed are averages over all conformers (7).

$$[1] \qquad \delta = \sum_i X_i(\nu_{A,i} - \nu_{B,i})$$

$$J_K = \sum_i X_i J_{K,i}$$

where X_i is the mole fraction of a particular conformer and the sum is over all conformers. $J_{K,i}$ and $\nu_{X,i}$ are the coupling constants and frequencies of a particular conformer. It has been previously pointed out that chemical shift differences are usually of questionable use for investigating conformer preference, because individual conformer frequencies are generally expected to be both temperature and solvent dependent to a much greater degree than $J_{K,i}$ coupling constants (8).

We wish to report our findings on the organophosphorus compounds in Tables I and V. Comparisons are made with the factors (solvent, temperature, and substituent effects) that influence the spectra of asymmetric carbon atoms.

TABLE I

Compounds of the type $(CH_3)P(O)(SCH_2SR)(OR')$ have been investigated

No.	R	R′
1	CH_3	Cyclopentyl
2	CH_3	$CH(CH_3)_2$
3	$(CH_2)_2CH_3$	$CH(CH_3)_2$
4	$(CH_2)_3CH_3$	$CH(CH_3)_2$
5	$(CH_2)_4CH_3$	$CH(CH_3)_2$
6	$CH(CH_3)_2$	Cyclopentyl
7	$CH(CH_3)_2$	$CH(CH_3)_2$

Experimental

Spectra were obtained on a Varian HA-100 spectrometer. When required, supplementary spectra were obtained on a Varian A-60 spectrometer. All the compounds reported are liquids. Their spectra were obtained in a 10% by volume solution which contained less than 5% by volume of TMS.

The compounds in Tables I and V were supplied by Mr. Ray Irino (Organic Chemistry Department of this laboratory) or obtained from commercial sources. General characterizations of those compounds not commercially available will be reported at a later date. The n.m.r. spectra were in consonance with the proposed structures.

Results and Discussion

The SCH_2S methylene protons of the compounds in Table I form the AB part of an ABX spin system where X is the phosphorus atom. A typical spectrum is shown in Fig. 1 (the second peak from the right contains two overlapping peaks). The spectra were analyzed as previously described (3). The coupling constants J_{AX} and J_{BX} may be of like or unlike sign. A comparison of the 100 and 60 Mc.p.s. spectra definitively shows that the coupling constants have the same relative sign (3). The magnitude of the coupling constants

Can. J. Chem. Downloaded from www.nrcresearchpress.com by 210.87.254.6 on 09/05/12
For personal use only.

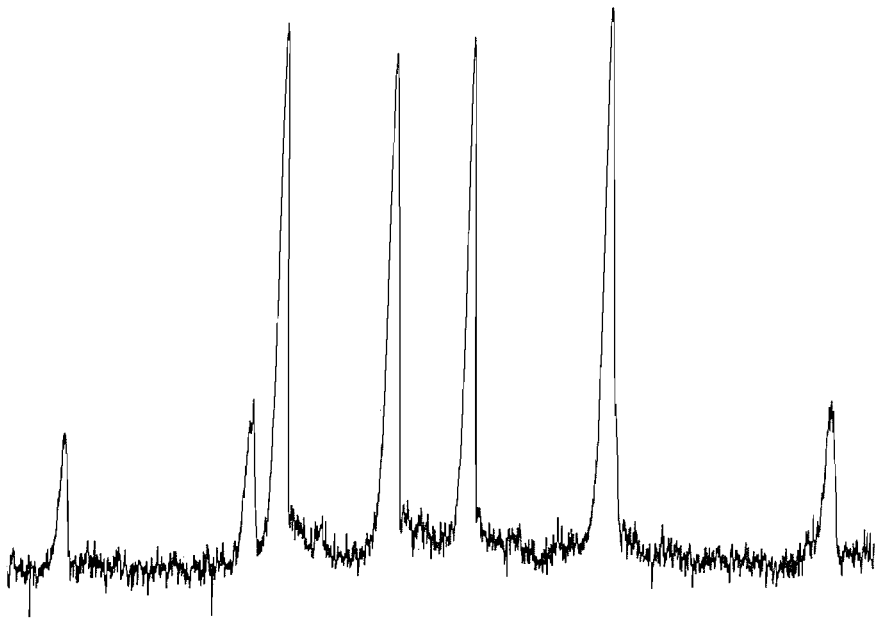

FIG. 1. The 100 Mc.p.s. spectra of the SCH_2S methylene protons of compound **3** (Table I) in benzene.

TABLE II

Nuclear magnetic resonance data for $(CH_3)P(O)(SCH_2SCH_3)(OCH(CH_3)_2)$ as a function of solvent

No.	Solvent	ε*	$\lvert J_{AX} + J_{BX}\rvert$ c.p.s.	J_{AX} c.p.s.	δ_{CH_2} p.p.m.†	δ_{CH_3} p.p.m.‡
1	Cyclohexane d_{12}	2.05	24.5	13.5	0.147	0.074
2	CCl_4	2.24	24.9	13.4	0.135	0.072
3	Benzene d_6	2.28	24.3	13.3	0.216	0.147
4	C_2Cl_4	2.30	24.4	13.4	0.140	0.068
5	CS_2	2.64	24.8	13.5	0.139	0.057
6	CCl_3D	5.05	24.5	12.9	0.108	0.063
7	CD_3I	7.0	24.1	13.1	0.097	0.045
8	Neat		23.8	12.6	0.071	0.048
9	Acetone d_6	21.4	23.1	12.6	0.065	0.039
10	CD_3OD	33.1	24.7	13.0	0.066	0.041
11	DMF d_7	36.7	22.7	12.0	0.02	0.031
12	CD_3NO_2	37.5	23.0	12.1	0.059	0.025
13	DMSO d_6	48.9	22.4§	11.2	<0.01	0.029

NOTE: The following parameters show only a ±0.2 c.p.s. variation with solvent $J_{PCH_3} = 15.9$ c.p.s., $J_{AB} = 13.2$ c.p.s., $J_{CH_{3(A)},H} = J_{CH_{3(B)},H} = 6.3$ c.p.s.

*Dielectric constant of protonated solvents.
†The chemical shift between nonequivalent methylene protons.
‡The chemical shift between nonequivalent methyl groups.
§Assumed to be twice J_{AX}.

J_{HX} (Tables II and III), $9 < J_{HX} < 14$ c.p.s., is within the expected range (3, 9). Assignment of different signs would lead to one unusually large value for J_{HX}. Since the errors in J_{AX} and J_{BX} can be large while the errors in their sum is small, only the latter quantity is considered.

From a detailed analysis of the AB part of the ABX spectrum, one obtains three manifestations of the nonequivalence of the methylene protons. These parameters are listed in Tables II and IV. They are: (*1*) proton coupling between nonequivalent methylene protons, J_{AB}; (*2*) a chemical shift difference between nonequivalent methylene protons, δ_{CH_2}; (*3*) heteronuclear proton phosphorus coupling which in general is different for different protons, $J_{H(A),X} \neq J_{H(B),X}$.

TABLE III

Summary of variable temperature results in CCl_3D

T °C	$\lvert J_{AX} + J_{BX}\rvert$ c.p.s.	J_{AX} c.p.s.	δ_{CH_2} p.p.m.	δ_{CH_3} p.p.m.
	*(1) $(CH_3)P(O)(SCH_2SCH_3)(OCH(CH_3)_2)$**			
57	23.8	12.5	0.098	0.060
30	24.5	12.9	0.108	0.063
− 5	24.8	13.4	0.125	0.069
−21	25.3	13.7	0.138	0.072
−36	25.8	14.2	0.148	0.074
−48	26.2	14.5	0.155	0.076
−62	26.4	14.8	0.165	0.077
	(2) $(CH_3)P(O)(SCH_2S(CH_2)_3CH_3)(OCH(CH_3)_2)$†			
56	23.5	12.5	0.082	
30	23.8	12.9	0.088	
− 4	24.4	13.2	0.099	
−14	24.6	13.3	0.104	
−26	24.7	13.6	0.111	
−45	25.3	13.9	0.121	
−62	26.0	14.4	0.129	

*As the temperature is lowered, J_{AB} increases from 13.2 c.p.s. (57 °C) to 13.6 c.p.s. (−62 °C) and J_{BX} increases from 11.3 c.p.s. (57 °C) to 11.7 c.p.s. (−62 °C).
†As the temperature is lowered, J_{AB} increases from 13.3 c.p.s. (56 °C) to 13.6 c.p.s. (−62 °C), and J_{BX} increases from 11.0 c.p.s. (56 °C) to 11.6 c.p.s. (−62 °C).

TABLE IV

Summary of results for compounds in Table I

Compound*	Solvent	J_{PCH_3} c.p.s.	J_{AB} c.p.s.	$\lvert J_{AX} + J_{BX}\rvert$ c.p.s.	δ_{CH_2} p.p.m.	δ_{CH_3} p.p.m.
1	CCl_4	16.2	13.1	24.4	0.133	
3	CCl_4	15.8	13.2	24.1	0.100	0.075
	C_6D_6	15.7	13.1	23.9	0.157	0.137
4	CCl_4	16.0	13.2	23.9	0.101	0.076
	C_6D_6	16.0	13.2	24.0	0.158	0.134
5	CCl_4	15.8	13.2	23.9	0.099	0.077
	C_6D_6	15.7	13.3	23.5	0.158	0.134
6	CCl_4	15.8	13.4	23.7	0.079	
	C_6D_6	15.8	13.3	23.4	0.132	
	Neat	15.9	†	22.4	<0.02	
	DMSO	15.7	‡	21.8§	<0.01	
7	CCl_4	16.0	13.3	24.5	0.080	0.074
	C_6D_6	16.2	13.1	23.2	0.128	0.134
	Neat	16.0	13.1	23.2	<0.03	†
	DMSO	16.0	‡	22.2§	<0.01	0.034

*See Table I for identification of compounds.
†The spectrum is not sufficiently resolved to permit calculations.
‡The methylene protons are equivalent in DMSO.
§Assumed to be twice J_{AX}.

The n.m.r. data for the SCH_2S methylene protons of compound **2** (Table I) as a function of solvent are summarized in Table II. Figure 2 clearly shows that $\lvert J_{AX} + J_{BX}\rvert$ and δ_{CH_2} depend on common factors. In DMSO d_6 the methylene protons appear as a well-resolved doublet with a line width at half height which is identical to that of the PCH_3 methyl group (0.5 c.p.s.). Previously it had been suggested that a primary prerequisite for magnetic nonequivalence to be observable in an asymmetric phosphorus compound was that one of the substituents be a benzene ring (4). Our data as well as that of Rowsell (5) clearly show this need not be the case.

The R′ group of compound **2** also contains a magnetically nonequivalent set of methyl groups. The spectrum of these methyl groups is two doublets separated by an internal chemical shift δ_{CH_3}. The data for the methyl groups are included in Table II.

Can. J. Chem. Downloaded from www.nrcresearchpress.com by 210.87.254.6 on 09/05/12
For personal use only.

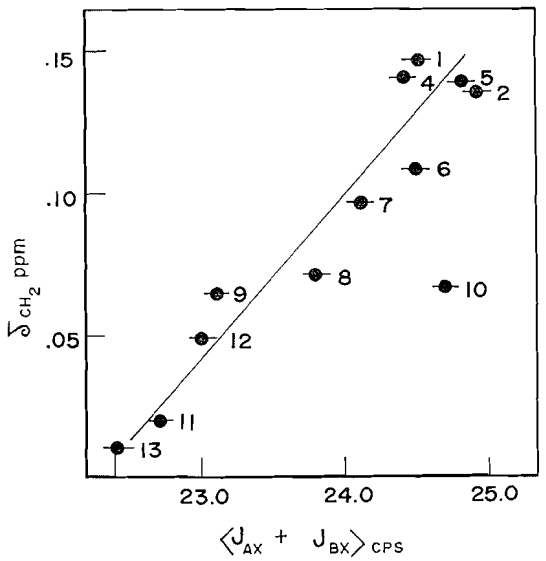

FIG. 2. A plot of δ_{CH_2} vs. $|J_{AX} + J_{BX}|$ of the SCH_2S methylene protons of $(CH_3)P(O)(SCH_2SCH_3)(OCH(CH_3)_2)$ in various solvents. The experimental points are numbered by solvents according to Table II.

Assuming $J_{K,i}$ is constant for the same compound in different solvents, the extent of conformer preference of the SCH_2S protons may be examined. The small variation of J_{PCH_3} with solvent supports this assumption.

As the temperature is increased the degree of conformer preference, determined by the relative values of X_i (eq. [1]), decreases. The results of a variable temperature study summarized in Table III suggest that the smaller values of $|J_{AX} + J_{BX}|$ are associated with reduced conformer preference. Intervening groups between the asymmetric phosphorus atom and the nonequivalent protons do not allow a simple representation of the conformers. The solvents in Table II are arranged with regard to increasing dielectric constant. $|J_{AX} + J_{BX}|$ shows decreasing conformer preference with increasing dielectric constant. Similar solvent effects have been observed in symmetry restricted phosphorus (3) and carbon analogues (10–12). The degree of conformer preference follows an inverse dependence with the dielectric constant of the solvent in agreement with the predictions of an electrostatic model (12).

Previous explanations of similar results have generally considered two major factors, (*1*) solvent dielectric constant effects and (*2*) solvent anisotropy effects. The latter can be included within (*1*) by taking a more cognizant picture of the microscopic dielectric medium which may be primarily governed by solvent anisotropy. While it is not readily possible to separate micro–macro dielectric effects, attention is called to the fact that the above views are not necessarily divergent (12, 13).

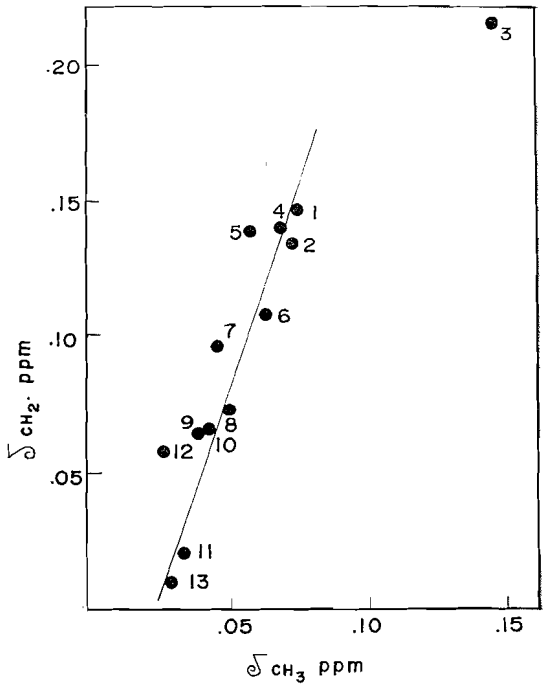

FIG. 3. The chemical shift of the methylene protons SCH_2S vs. the chemical shift of the isopropyl methyl groups of $(CH_3)P(O)(SCH_2SCH_3)(OCH(CH_3)_2)$ in various solvents. The experimental points are numbered by solvent according to Table II.

The spectra of the isopropyl methyl groups are relatively insensitive to temperature (Table III). Figure 3 shows that the degree of magnetic nonequivalence of δ_{CH_2} and δ_{CH_3} are related. Apparently the medium dielectric constant is a primary factor in determining the magnitude of the magnetic nonequivalence.

Some exceptions to the trends discussed are noted. Both δ_{CH_3} and δ_{CH_2} are unusually large in benzene as is typical of aromatic solvents (11, 12). In Fig. 2, the values for methanol clearly deviate from the general trend. A reasonable explanation for this is that hydrogen bonding between the phosphoryl group and/or the lone pair sulfur electrons and methanol is responsible.

Can. J. Chem. Downloaded from www.nrcresearchpress.com by 210.87.254.6 on 09/05/12
For personal use only.

Can. J. Chem. Downloaded from www.nrcresearchpress.com by 210.87.254.6 on 09/05/12
For personal use only.

An interesting feature of the data in Table II is that in solvents of low dielectric constant $\delta_{CH_2} > \delta_{CH_3}$ while in high dielectric media, the reverse may hold.

The results for the other compounds in Table I, summarized in Table IV, show similar solvent effects.

In benzene the methyl protons on R of compounds **6** and **7** (Table I) are observed as a sharp doublet due to coupling with the methine proton. No evidence for long range magnetic nonequivalence is observed. Roberts *et al.* (1) have reported nonequivalent methyl groups seven bonds removed from an asymmetric carbon atom.

An attempt was made to see if the degree of magnetic nonequivalence of the isopropyl methyl groups could be correlated to the nature of one of the substituents at the asymmetric center (11).

TABLE V

A comparison of the degree of magnetic nonequivalence of the isopropyl methyl groups of $(CH_3)P(O)(OCH(CH_3)_2)(X)$ in benzene

X	δ_{CH_3} p.p.m.
SCH_2S	0.166–0.128*
S-phenyl	0.125
H	0.108
SH	0.080
$OCH(CH_3)_2$	0.010
F	<0.010†
OH	<0.010‡
OCH_3	<0.010‡

*Range of results reported in Tables II and IV.
†For X = F, δ_{CH_3} is too small to be measured accurately.
‡No evidence of magnetic nonequivalence is observed for X = OH or OCH_3.

Compounds of the following type were examined, $(CH_3)P(O)(OCH(CH_3)_2)(X)$, in benzene and the results summarized in Table V. Although δ_{CH_3} shows large variations as X is varied, there is no obvious effect such as steric hindrance or electronegativity that can account for the observed variation of δ_{CH_3}.

The pseudo asymmetric compound listed in Table V, $(CH_3)P(O)(OCH(CH_3)_2)_2$, is the methyl analogue of a compound reported by Finegold (14) which has been discussed by Waugh and Cotton (15). The compounds $(H)P(O)(OCH(CH_3)_2)_2$ ($\delta_{CH_3} = 0.029$ p.p.m.) and $(phenyl)P(O)(OCH(CH_3)_2)_2$ ($\delta_{CH_3} = 0.107$ p.p.m.) also show magnetic nonequivalent methyl groups.

1. G. M. WHITESIDES, D. HOLTZ, and J. D. ROBERTS. J. Am. Chem. Soc. **86**, 2628 (1964).
2. T. H. SIDDALL III. J. Phys. Chem. **70**, 2249 (1966).
3. L. S. FRANKEL, H. KLAPPER, and J. CARGIOLI. J. Phys. Chem. **73**, 91 (1969).
4. T. H. SIDDALL III and C. A. PROHASKA. J. Am. Chem. Soc. **84**, 2502, 3467 (1962).
5. D. G. ROWSELL. J. Mol. Spectry. **23**, 32 (1967).
6. R. KEAT and W. SIM. Chem. Commun. **4**, 191 (1968).
7. J. A. POPLE. Mol. Phys. **1**, 1 (1958).
8. H. S. GUTOWSKY, G. G. BELFORD, and P. E. MCMAHON. J. Chem. Phys. **36**, 3353 (1962).
9. J. W. EMSLEY, J. FEENEY, and L. H. SUTCLIFFE. High resolution nuclear magnetic resonance. Vol. 2. The Pergamon Press, Ltd., London. 1966. Table 12.62.
10. R. V. MOEN and W. H. MUELLER. J. Org. Chem. **31**, 1971 (1966).
11. G. M. WHITESIDES, J. J. GROCKI, D. HOLTZ, H. STEINBERG, and J. D. ROBERTS. J. Am. Chem. Soc. **87**, 1058 (1965).
12. E. I. SNYDER. J. Am. Chem. Soc. **85**, 2624 (1963).
13. S. SELTZER and S. G. MYLONAKIS. J. Phys. Chem. **72**, 754 (1968).
14. H. FINEGOLD. J. Am. Chem. Soc. **82**, 2641 (1960).
15. J. S. WAUGH and F. A. COTTON. J. Phys. Chem. **65**, 562 (1961).

Can. J. Chem. Downloaded from www.nrcresearchpress.com by 210.87.254.5 on 09/05/12
For personal use only.

π-Electronic structure and reactivity of phenoxazine (1), phenothiazine (2), and phenoxthiin (3)

H. H. MANTSCH[1]
Institute of Chemistry, Cluj, Rumania

AND

J. DEHLER
Study Group of Structural Chemistry, Technische Hochschule, Munich, Germany

Received March 7, 1969

The ultraviolet, fluorescence, and phosphorescence spectra as well as the corresponding polarized excitation spectra were recorded for phenoxazine, phenothiazine, and phenoxthiin at 80 °K and discussed in terms of a number of theoretical transitions, calculated by a configuration interaction π-electron approximation.

The computed transition energies and the reactivity indices (π-electronic charge, mobile bond order, free-valence index, superdelocalizability index, and localization energy) are in good agreement with experimental data and chemical evidence.

Canadian Journal of Chemistry, 47, 3173 (1969)

Introduction

In connection with current investigations on the π-electronic structure and reactivity of heterocyclic systems (1, 2), we have examined the three heterocycles mentioned in the title which are of both theoretical and practical interest, since many of their derivatives are pharmacologically highly important substances (e.g. phenothiazine drugs). As it has been pointed out elsewhere, a better knowledge of their physical properties might be important for understanding the way these systems interact with living organisms.

The reactivity indices calculated in this paper are within the limits of the accuracy which can be achieved by considering the π-electrons only, yet with all the known limitations in mind, they still should be successful in covering the order of reactivity of individual positions mainly for electrophilic substitutions.

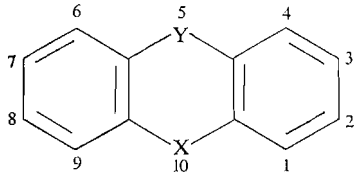

1, X = NH; Y = O
2, X = NH; Y = S
3, X = S; Y = O

[1]All inquiries should be addressed to: H. H. Mantsch, Division of Pure Chemistry, National Research Council of Canada, Room 2150, Sussex Drive, Ottawa, Canada.

Parameterization

The present calculations were performed by a self-consistent field (s.c.f.) method within the Pariser–Parr–Pople (PPP) approximation (zero differential-overlap), and the semi-empirical parameters U_μ, $\gamma_{\mu\mu}$, and $\beta_{\mu\nu}$ have been compiled by testing s.c.f. calculations on monosubstituted benzene derivatives containing the heteroatoms oxygen, sulfur, and nitrogen, to achieve optimum fit to the electronic spectra. The transfer ability of the established parameters to greater molecules like those investigated in this paper was assured by calculating the energy, the intensity pattern, and the direction of polarization for the corresponding $\pi^* \leftarrow \pi$-transitions up to 50 000 cm^{-1} which are compared with the experimental ultraviolet and polarized excitation spectra in Figs. 1–3 (*vide infra*).

The one-center repulsion integrals $\gamma_{\mu\mu}$ and the U_μ integrals for heteroatoms were evaluated as follows: $\gamma_{CC} = 11$ eV; $\gamma_{SS} = 11$ eV; $\gamma_{NN} = 13$ eV and $\gamma_{OO} = 15$ eV; $U_S - U_C = -9$ eV; $U_N - U_C = -11$ eV and $U_O - U_C = -16$ eV, while the two-center repulsion integrals $\gamma_{\mu\nu}$ ($\mu \neq \nu$) have been approximated by the already classical method of Nishimoto and Mataga (3). All resonance integrals $\beta_{\mu\nu}$ are taken to be -2.3 eV, except for the CS bond which should be lowered slightly i.e. $\beta_{CS} = 0.6\beta_{CC}$.

The π-electronic system of these molecules consists of a number of 16 π-electrons on 14

centers and although they are not rigorously planar, (roughly speaking they are slightly folded along their short axis) the calculations we carried out assumed a common "aromatic" length of 1.4 Å and an angle of 120° throughout for the initial guessed input values, which later are refined by an iterative process. By considering a few folded structures for input values, we actually found that the geometry is not too critical as far as the reproduction of the electronic transitions is concerned.

An initial set of orthogonalized eigenvectors obtained from a Hückel approximation was used to construct the starting molecular orbitals, while the molecular orbitals obtained from Pople's s.c.f. procedure were then used as the basis for a configuration interaction treatment which included all possible configurations arising from single electron excitations between the 5 highest occupied and the 4 lowest empty orbitals.

From the various proposed bond order (p_{rs}), bond length (r_{rs}) relationships for CC bonds, we have used the linear one of Coulson and Golebiewski (4) which is particularly suitable for benzenoid bonds. The CN and CO bond lengths have been evaluated by two similar relations compiled by Nishimoto and Forster (5), assuming that the differences between a double bond and the hypothetical single bond with sp^2-hybridization distances are all 0.180 Å. As a similar relation was lacking for carbon–sulfur bonds, we have compiled it in a similar manner by using the values of 1.61 Å for a CS double bond and 1.82 Å for a corresponding single bond (6), i.e. 1.79 Å after correcting it for sp^2-hybridization.

$$r_{CC} = 1.517 - 0.180p_{CC}\ (Å)$$

$$r_{CN} = 1.451 - 0.180p_{CN}\ (Å)$$

$$r_{CO} = 1.410 - 0.180p_{CO}\ (Å)$$

$$r_{CS} = 1.790 - 0.180p_{CS}\ (Å)$$

The actual computations were carried out on a Telefunken TR-4 computer with a closed shell s.c.f.-CI computer program written in Algol.

Experimental

The $\pi^* \leftarrow \pi$-transitions calculated by this procedure are shown as vertical lines under the experimental absorption spectra (curves A) in Figs. 1–3 while their height is chosen as $\log f + 4$ (where f represents the oscillator strength calculated from the dipole strength of the transition). This allows for a better comparison between calculated and experimental intensities.

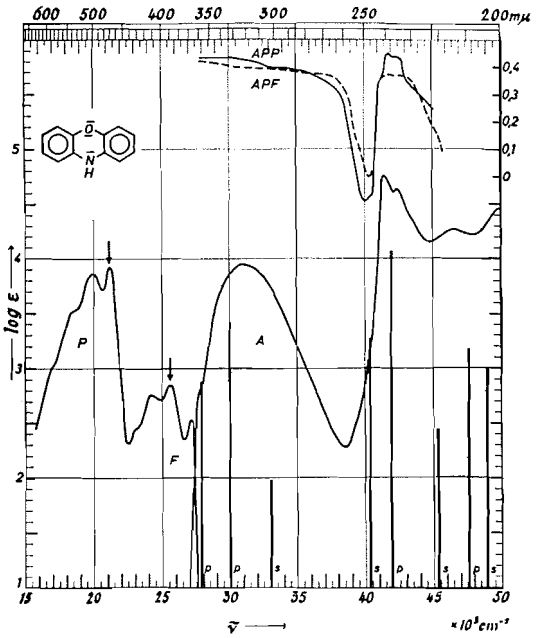

FIG. 1. Phenoxazine in ethanol at 80 °K. A, Absorption spectrum; F, fluorescence spectrum; P, phosphorescence spectrum; APF, polarized excitation spectrum based on the fluorescence; APP, polarized excitation spectrum based on the phosphorescence; vertical lines, calculated $\pi^* \leftarrow \pi$-transitions (p, parallel, s, perpendicularly polarized).

Besides these two parameters i.e. energy and intensity, an additional quite valuable criteria for testing theoretical calculations is provided by the direction of polarization of the $\pi^* \leftarrow \pi$-transitions. Therefore we have measured the polarized excitation spectra either based on the fluorescence spectrum (F), or based on the phosphorescence spectrum (P) and they are shown in the upper part of Figs. 1–3 as APF and APP spectra; the polarizations have been measured relative to the most intense vibronic band, marked by an arrow. The experimental technique for recording polarized excitation spectra has been described extensively by Dörr (7). In the line diagrams, the calculated direction of polarization is marked as p for parallel and s for perpendicular orientation of the transition moments in relation to the long axis of the molecular framework.

By considering these calculations, the electronic spectra of **1**, **2**, and **3** may now be discussed briefly as follows. The broad absorption band at the longest wavelength consists of three closely situated $\pi^* \leftarrow \pi$-transitions, with two strong parallel polarized transitions which yield high positive APF and APP values for the corresponding polarized excitation spectra in this region. The most intense transition at about 41 500 cm^{-1} (**1** and **3**) and 39 000 cm^{-1} (**2**) is also parallel polarized in agreement with the strong maximum in the polarized excitation

Can. J. Chem. Downloaded from www.nrcresearchpress.com by 210.87.254.5 on 09/05/12
For personal use only.

Can. J. Chem. Downloaded from www.nrcresearchpress.com by 210.87.254.5 on 09/05/12
For personal use only.

spectra; this strong transition is preceded by a perpendicular polarized transition about ten fold less intense and which is marked by the strong minimum (especially for **1** and **3**) at about 40 000 cm^{-1} in the APF and APP spectra. The PPP calculations in agreement with the decrease of the APF and APP curves, predict another perpendicularly polarized transition between 43 000–45 000 cm^{-1} where the experimental limit of APF and APP spectra is reached.

Results and Discussion

As shown in the previous section, the assumed model on which the PPP calculations are resting is successful, within the expected limits, in reproducing the experimental transition energies, intensities, and polarization, and hence it should allow for at least qualitative reactivity calculations.

The reactivity indices i.e. the π-electronic charge (q_r), the mobile bond order (p_{rs}), and the free-valence index (F_r), as well as the superdelocalizability index (S_r) and the localization energy (L_r), were obtained on expanding the corresponding coefficients and orbital energies (8) and are shown in Figs. 4–6.

The chemical reactivity of these three molecules, governed primarily by their excellent electron-donor properties, is evidenced by the particularly easy formation of charge-transfer

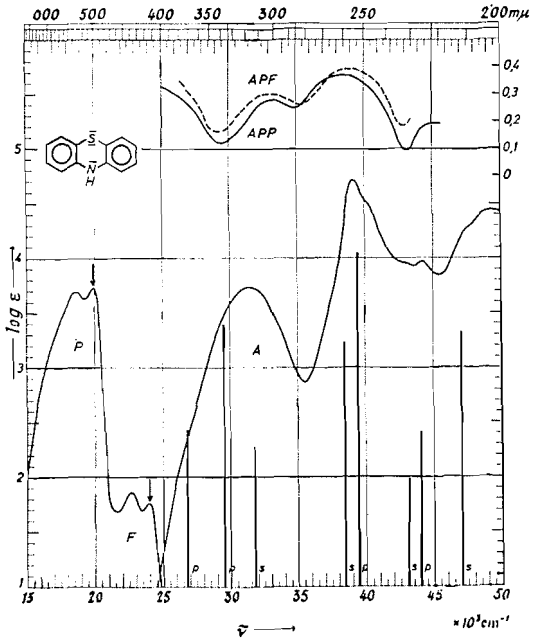

FIG. 2. Phenothiazine in ethanol at 80 °K. For notation see Fig. 1.

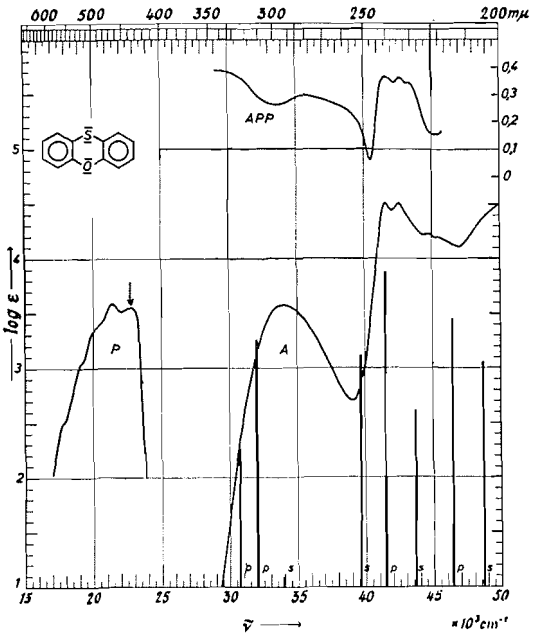

FIG. 3. Phenoxthiin in ethanol at 80 °K. For notation see Fig. 1.

complexes and by their enhanced reactivity towards electrophilic reagents. Indeed, the following molecular diagrams show that there is an excess of charge at all carbon atoms in the ground state configuration (see Fig. 4).

In discussing the chemical reactivity, the peculiarities of their ring structure should be considered first. These heterocyclic systems, which are not strictly heteroaromatic, consist of two benzenoid rings linked together by two *ortho* located bridges. The two groups which constitute these bridges (i.e. imino, sulfide or oxide) may slightly interact with each other through the two rings, yet the main influence exerted by these heteroatoms is directed towards the π-electronic distribution and hence to the reactivity within the carbocyclic rings.

Insofar as the chemical reactivity of phenoxazine and phenothiazine is concerned, it appears that the nitrogen plays the key role, in only a very few cases is the directing influence of the oxygen or sulfur important. The highest π-electron density, excepting the S or O atoms, is located at the nitrogen atom where some electrophilic reagents attack the heterocyclic ring, whereas with **2** and **3**, sulfoxides are formed quite easily by an electrophilic attack of the oxidant at the sulfur atom.

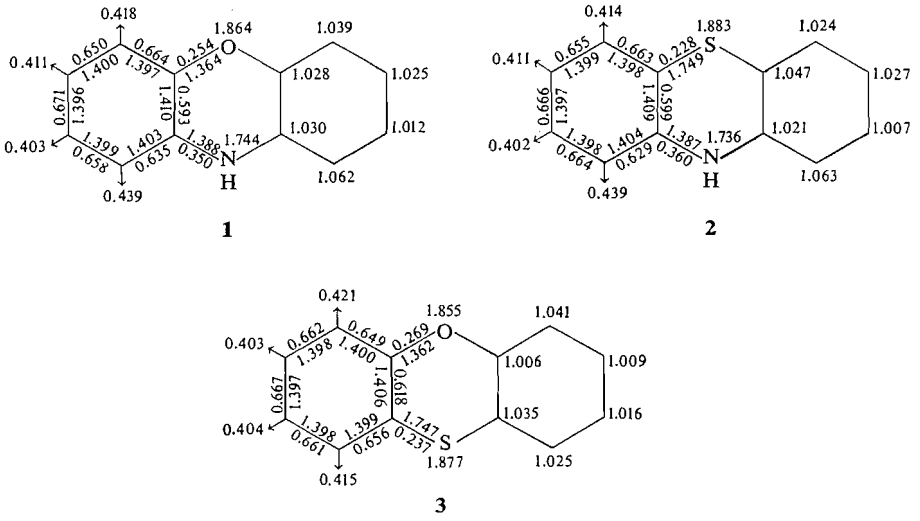

FIG. 4. Molecular diagrams for phenoxazine (**1**), phenothiazine (**2**), and phenoxthiin (**3**). π-Electronic charge (q_r), at the atomic centers; bond orders (p_{rs}), on the corresponding bonds (outside); bond lengths in Å (r_{rs}), on the corresponding bonds (inside); free-valence index (F_r), at the arrows.

Nevertheless the most important electrophilic reactions are associated with C-substitution. Indeed with phenoxazine (9) and phenothiazine (10), positions 3 and 7 are preferentially attacked by electrophilic reagents; reactions such as nitration, halogenation, Friedel–Crafts acylation, Vilsmeier formylation, sulfonation, or thiocyanation yield firstly 3 or 7-mono, or 3,7-disubstituted products and under more rigorous conditions, the 1,3,7,9-tetrasubstituted derivatives.

These experimental results are in good agreement with the calculated S_r and L_r values of these two compounds (see Figs. 5 and 6) which show that all positions in the carbocyclic rings are suitable for electrophilic substitution ($L_r < 1$ eV) and that positions 3 and 1 (or 7 and 9) are favored strongly over positions 2 and 4 (or 8 and 6), supporting the conclusions drawn in ref. 9, p. 101 and ref. 10, p. 431, that the reactivity of the carbon atoms of the phenoxazine and phenothiazine ring systems during electrophilic substitution decreases in the following order: $3 \geq 1 \gg 2 \geq 4$. This confirms that mainly the nitrogen is determining the reactivity of these two compounds, whereas the influence of the oxygen or sulfur is relatively small.

A different situation is encountered with the phenoxthiin ring system (**3**) which possesses two similar activating and competing heteroatoms to direct the substitution. According to the S_r and L_r values, there is no strongly favored position for electrophilic substitution and the L_r values are relatively high compared with positions 3 and 1 in **1** and **2**. Yet the experimental results (the chemistry of this heterocyclic system has been reviewed by Maior (11)) showed that a number of electrophilic substitutions like bromination, formylation, or chloromethylation actually occur at position 2 or 8 i.e. *para* to the oxygen. Now it has been proved that the bromination for instance occurs via an isolable phenoxthiin–dibromide complex, but no definite structure has been assigned to it (σ- or π-complexes). If one admits that the electrophilic substitution of **3** is preceded by the formation of a more or less stable complex with the electrophile, one could possibly understand the directing influence of the oxygen atom because the sulfur is more involved in the complex formation and should be deactivated slightly.

The nucleophilic substitution of these three ring systems should be very difficult as indicated by the high localization energy values (Fig. 6), yet unfortunately there are no reliable experimental results concerning nucleophilic substitutions of the unsubstituted ring systems **1**, **2**, and **3**. However it is interesting to mention that the metalation of these ring systems (9, 10) with butyllithium (observed experimentally), follows the order of the free-valence index i.e. availability of π-electrons for radical substitution, whereas

Can. J. Chem. Downloaded from www.nrcresearchpress.com by 210.87.254.5 on 09/05/12
For personal use only.

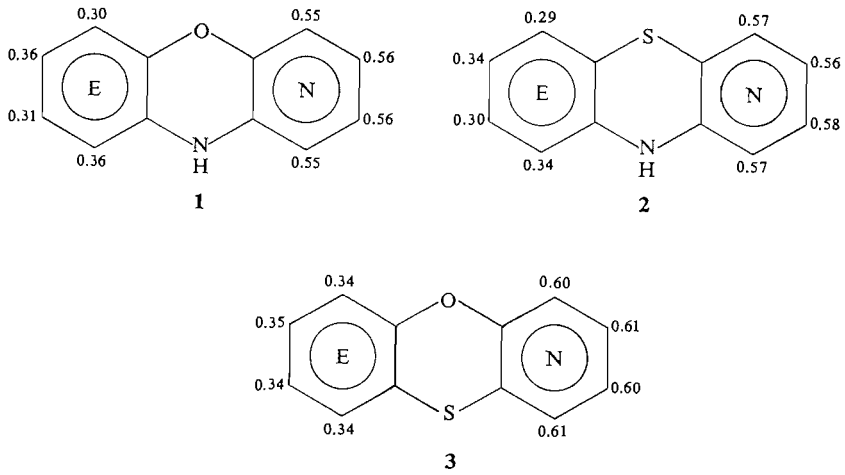

FIG. 5. The calculated superdelocalizability index (S_r) for phenoxazine (**1**), phenothiazine (**2**), and phenoxthiin (**3**) shown on the left side rings (E) for electrophilic and on the right side rings (N) for nucleophilic substitution. The larger the magnitude of S_r, the easier the reaction, considered separately for electrophilic and nucleophilic substitutions.

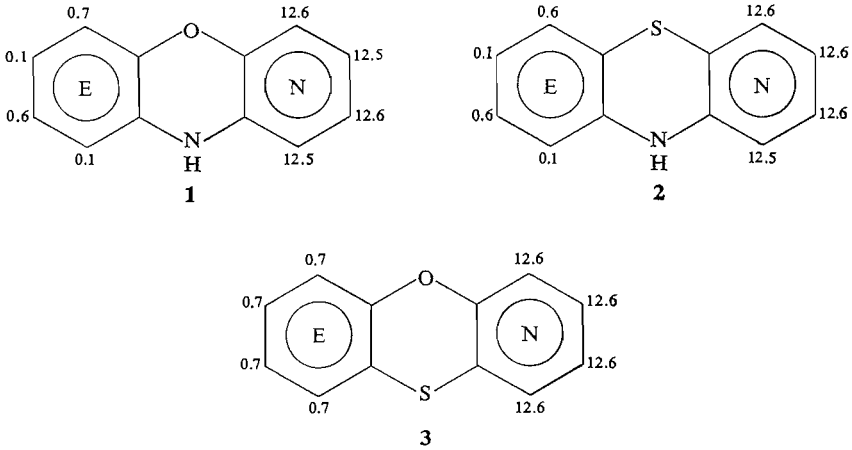

FIG. 6. Calculated localization energies (L_r) in eV, shown for electrophilic substitutions on the left side rings (E) and for nucleophilic substitutions on the right side rings (N). The smaller the magnitude of L_r, the easier the reaction.

the calculated reactivity indices S_r for nucleophilic substitution do not greatly favor any particular position.

The computed interatomic distances shown in Fig. 4 indicate a rather small interaction of the two carbocyclic rings through the central heteroring, which itself shows little aromatic character; indeed the carbocyclic rings do not show the strong bond order alternation which is found for instance with the carbocyclic rings in acridine (1). As indicated by these calculations, the two carbocyclic rings within the three compounds investigated are quite independent and the chemical behavior of the molecule resembles the chemistry of the corresponding *ortho*-disubstituted benzene derivatives; perhaps to explain other peculiarities of these ring systems one has also to invoke steric considerations, imposed by the two fixed heteroatom bridges.

Acknowledgments

We are grateful to the Bavarian Academy of Science for the use of the digital computer TR-4, to K. Fritz for experimental help, and to the

Can. J. Chem. Downloaded from www.nrcresearchpress.com by 210.87.254.5 on 09/05/12
For personal use only.

Humboldt Foundation and the Deutsche Forschungsgemeinschaft for support.

1. W. SEIFFERT, V. ZANKER, and H. H. MANTSCH. Tetrahedron Letters, **30**, 3437 (1968); **40**, 4303 (1968); **54**, 5655 (1968).
2. H. H. MANTSCH, V. SEIFFERT, and V. ZANKER. Revue Roumaine de Chimie, **14**, 125 (1969).
3. K. NISHIMOTO and N. MATAGA. Z. physik. Chem. Frankfurt, **12**, 335 (1957); **13**, 140 (1957).
4. C. A. COULSON and A. GOLEBIEWSKI. Proc. Phys. Soc. London, **78**, 1310 (1961).
5. K. NISHIMOTO and L. S. FORSTER. Theoret. Chim. Acta, Berlin, **4**, 155 (1966).
6. W. A. PRYOR. Mechanisms of sulfur reactions. McGraw-Hill Book Co., Inc., N.Y. 1962. p. 23.
7. F. DÖRR. Z. Angew. Chem. **78**, 457 (1966); Z. Angew. Chem. Intern. Ed., **5**, 478 (1966).
8. L. SALEM. The molecular orbital theory of conjugated systems. W. A. Benjamin, Inc., New York. 1966.
9. M. IONESCU and H. H. MANTSCH. Phenoxazines. *In* Advances in heterocyclic chemistry. Vol. 8. *Edited by* A. R. Katritzky. Academic Press, Inc., New York. 1967.
10. C. BODEA and I. SILBERG. Recent advances in the chemistry of phenothiazines. *In* Advances in heterocyclic chemistry. Vol. 9. *Edited by* A. R. KATRITZKY. Academic Press, Inc., New York. 1968.
11. O. MAIOR. Contributions to the chemistry of phenoxthiin. Ph.D. Thesis, University of Bucharest, Rumania. 1965.

Can. J. Chem. Downloaded from www.nrcresearchpress.com by 210.87.254.5 on 09/05/12
For personal use only.

Can. J. Chem. Downloaded from www.nrcresearchpress.com by 210.87.254.6 on 09/05/12
For personal use only.

Réactions des acides aminés avec l'épithiocyclohexane

KRZYSZTOF JANKOWSKI, ROGER GAUTHIER, ET CASIMIR BERSE
Département de Chimie, Université de Montréal, Montréal, Québec

Reçu le 16 septembre 1968

L'ouverture de l'épithiocyclohexane (**1**) a été effectuée avec le glycinate d'éthyle et le sarcosinate d'éthyle. Les produits d'ouverture simple ont été isolés dans les deux cas. De plus, des produits de "disubstitution" (attaque du produit formé sur une deuxième molécule de l'épithiocyclohexane) ont été observés. Les structures des mercaptoesters formés sont discutées. Leur fragmentation en spectroscopie de masse a été étudiée et comparée avec celle des produits modèles.

Canadian Journal of Chemistry, 47, 3179 (1969)

L'ouverture des époxydes par les acides aminés à déjà été étudiée (1–4). Il nous a semblé intéressant d'observer le comportement des épisulfures face aux mêmes réactifs, de façon à établir les différences de réactivité entre les deux cycles. De plus les ouvertures des épisulfures ont été très peu étudiées (5) comparativement aux époxydes, ce qui présente un intérêt supplémentaire.

Il a été impossible d'utiliser les acides aminés libres ou les sels sodés des acides aminés comme réactifs; en effet, les acides aminés libres ne donnent pas de produits d'ouverture, ce qui est en accord avec les résultats obtenus avec les époxydes (2). Quant aux sels sodés, ils conduisent, avec de très bas rendements, à des mélanges de produits difficilement séparables et identifiables. Nous avons donc utilisé les esters éthyliques de la glycine et de la sarcosine comme réactifs.

Les produits obtenus sont des mercaptoesters, qui sont plus stables que leurs analogues hydroxylés obtenus par ouverture des époxydes. En effet, dans le cas des époxydes alicycliques, les produits primaires d'ouverture sont instables et se réarrangent en dicéto-2,5 pipérazines ou morpholones substituées, ce qui n'arrive pas avec les épisulfures. La réaction du glycinate d'éthyle sur **1** mène à deux produits d'ouverture, que l'on peut appeler monosubstitué et disubstitué: le *N*-(mercapto-2 cyclohexyl) glycinate d'éthyle (**2**) et le *N*-[(mercapto-2′ cyclohexylthio)-2 cyclohexyl] glycinate d'éthyle (**3**).

L'influence du solvant sur la réaction a été étudiée, ainsi que celle de la concentration. Comme on voit par le tableau I, la réaction sans solvant est de loin celle qui donne le meilleur rendement, et ce pour les deux produits obtenus. Toutes les valeurs sont données pour 2 h de chauffage à reflux. Les rendements ont été déterminés par chromatographie préparative sur couche mince.

TABLEAU I

Influence du solvant sur le rendement des produits **2** et **3**

Solvant	Rapport épithiocyclohexane acide aminé	Rendement de **2** (%)	Rendement de **3** (%)
—	1:1	16	2
	2:1	7	11
Benzène*	1:1	4	—
	2:1	3	2
Chloroforme*	1:1	8	Trace
	2:1	3	4

*Concentration ~ 10%.

Les produits **2** et **3** peuvent être séparés soit par distillation sous pression réduite, soit par chromatographie sur colonne. Les structures des deux produits ont été déterminées à l'aide des spectres et par synthèse. Pour le produit **2**, le spectra infrarouge indique la présence des groupements NH, SH et C=O (ester); les spectres de r.m.n. et de masse concordent aussi parfaitement avec la structure proposée (la fragmentation en spectrométrie de masse est donnée à la fin pour tous les produits d'ouverture).

Le produit **2** a aussi été synthétisé à partir de l'amino-2 cyclohexanethiol (**4**) (voir le Schéma 1). La réaction de ce dernier produit—connu dans la littérature (6) mais obtenu cette fois par l'action de l'ammoniaque sur l'épithiocyclohexane (**1**)—avec le chloroacétate d'éthyle a donné le chlorhydrate de *N*-(mercapto-2 cyclohexyl) glycinate d'éthyle (**5**). Le même produit a été obtenu par saturation avec HCl *gazeux* du composé **2**. Les deux produits ont des spectres i.r. et r.m.n. identiques et présentent de plus le même R_f en chromatographie sur couche mince.

Can. J. Chem. Downloaded from www.nrcresearchpress.com by 210.87.254.6 on 09/05/12
For personal use only.

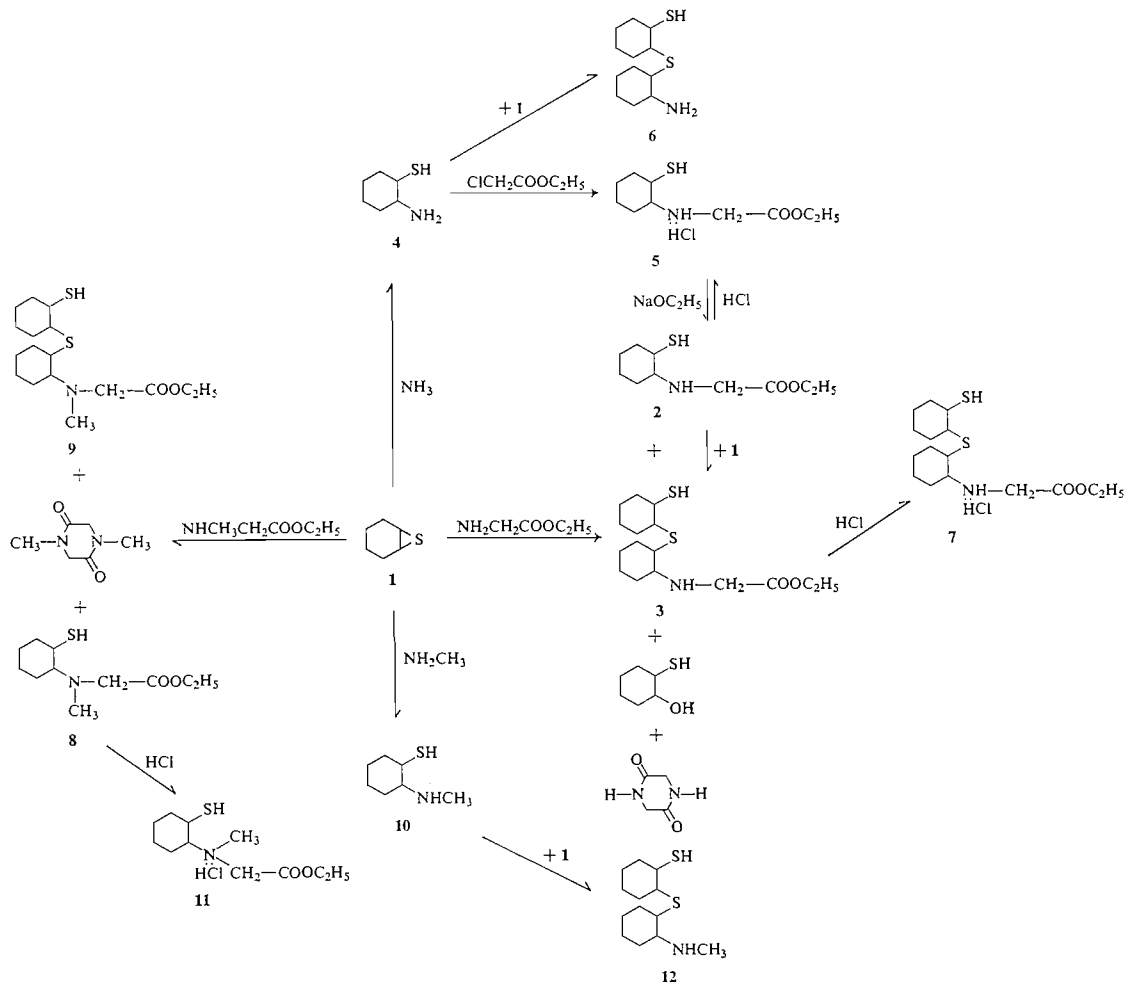

SCHÉMA 1

Le produit **5** synthétique a été libéré de son chlorhydrate avec l'éthanolate de sodium en donnant le produit **2** avec un bon rendement. L'identité de ce produit avec le produit d'ouverture **2**, a été prouvée par les spectres r.m.n. et i.r. ainsi que par un test chimique démontrant la présence de —SH.

Pour le deuxième produit d'ouverture deux structures peuvent être proposées: *N*-[(mercapto-2′ cyclohexylthio)-2 cyclohexyl] glycinate d'éthyle (**3**) ou *N*,*N*-bis (mercapto-2 cyclohexyl) glycinate d'éthyle (**3***a*).

L'examen des différentes données spectrales montre toutefois que seule la structure **3** est possible; le spectre infrarouge présente les bandes NH et SH et dans le spectre de r.m.n., il y a échange de NH avec D_2O. De plus la structure **3** a été vérifiée par comparaison avec le produit

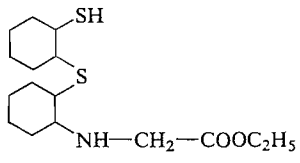

3

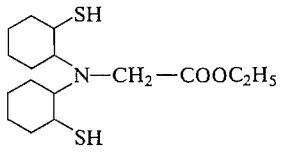

3*a*

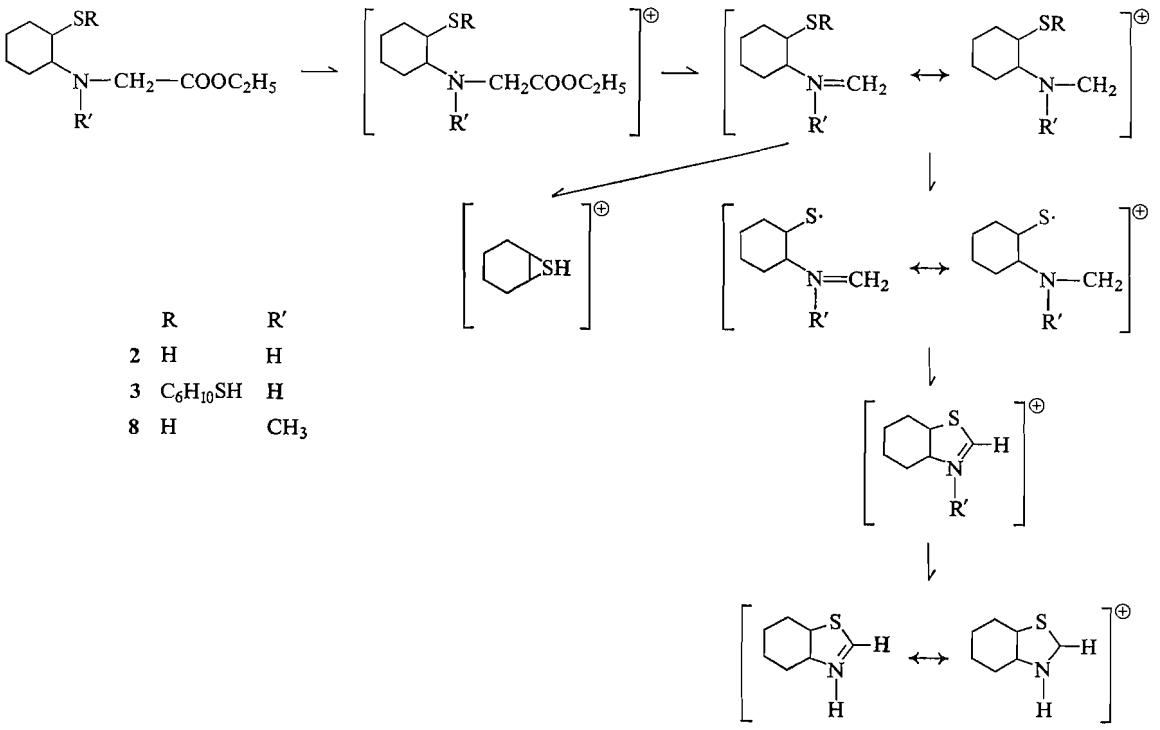

	R	R′
2	H	H
3	$C_6H_{10}SH$	H
8	H	CH_3

SCHÉMA 2

modèle: la (mercapto-2′ cyclohexylthio)-2 cyclohexylamine (**6**) a été obtenue par l'action de **4** sur l'épithiocyclohexane (**1**). Le chlorhydrate du *N*-[(mercapto-2′ cyclohexylthio)-2 cyclohexyl] glycinate d'éthyle (**7**) a été obtenu par saturation avec HCl de l'ester libre **3.**

Les arguments justifiant la structure du produit **6** sont les suivants: échange de deux hydrogènes dans le spectre de r.m.n. avec D_2O (présence de NH_2) et discussion du spectre de masse.

De plus, le produit **3** a été obtenu directement par réaction de l'épithiocyclohexane (**1**) sur l'ester libre **2** obtenu du produit **5**, ce qui justifie indirectement la structure du produit **6.**

Avec le sarcosinate d'éthyle, deux produits ont été obtenus, correspondant au *N*-(mercapto-2 cyclohexyl) sarcosinate d'éthyle (**8**) et *N*-[(mercapto-2′ cyclohexylthio)-2 cyclohexyl] sarcosinate d'éthyle (**9**) (Schéma 1). La structure du produit **8** a été établie à l'aide des spectres et des produits modèles. L'épithiocyclohexane (**1**) avec la méthylamine produit soit le méthylamino-2 cyclohexanethiol (**10**) soit, si on travaille avec un excès de **1**, la *N*-[(mercapto-2′ cyclohexylthio)-2 cyclohexyl] méthylamine (**12**). Le chlorhydrate du *N*-(mercapto-2 cyclohexyl) sarcosinate d'éthyle (**11**) a été obtenu par saturation de l'ester **8** avec le HCl *gazeux*.

La structure du produit **9** n'ext basée que sur les spectres infrarouge et de r.m.n. ainsi que les données analytiques, à cause de la très faible quantité de produit obtenu.

La fragmentation en spectrométrie de masse des produits **2**, **3**, **6**, **8** et **12** a été étudiée. Les esters **2**, **3** et **8** (voir Fig. 1, 2, et 3) se fragmentent par perte de $—COOC_2H_5$ suivie de la perte de H_2 pour donner l'ion le plus intense—l'ion cyclohexyl-[*b*]-dihydro-4,5 thiazolonium tel qu'indiqué dans le Schéma 2.

De plus on peut observer la présence des pics très intenses *m/e* 115 (114), 98 (112) et 81 correspondant aux structures suivantes:

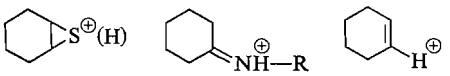

2 R = H
8 R = CH_3

Les deux dernières structures peuvent être obtenues à partir d'une deuxième route de

Can. J. Chem. Downloaded from www.nrcresearchpress.com by 210.87.254.6 on 09/05/12
For personal use only.

Can. J. Chem. Downloaded from www.nrcresearchpress.com by 210.87.254.6 on 09/05/12
For personal use only.

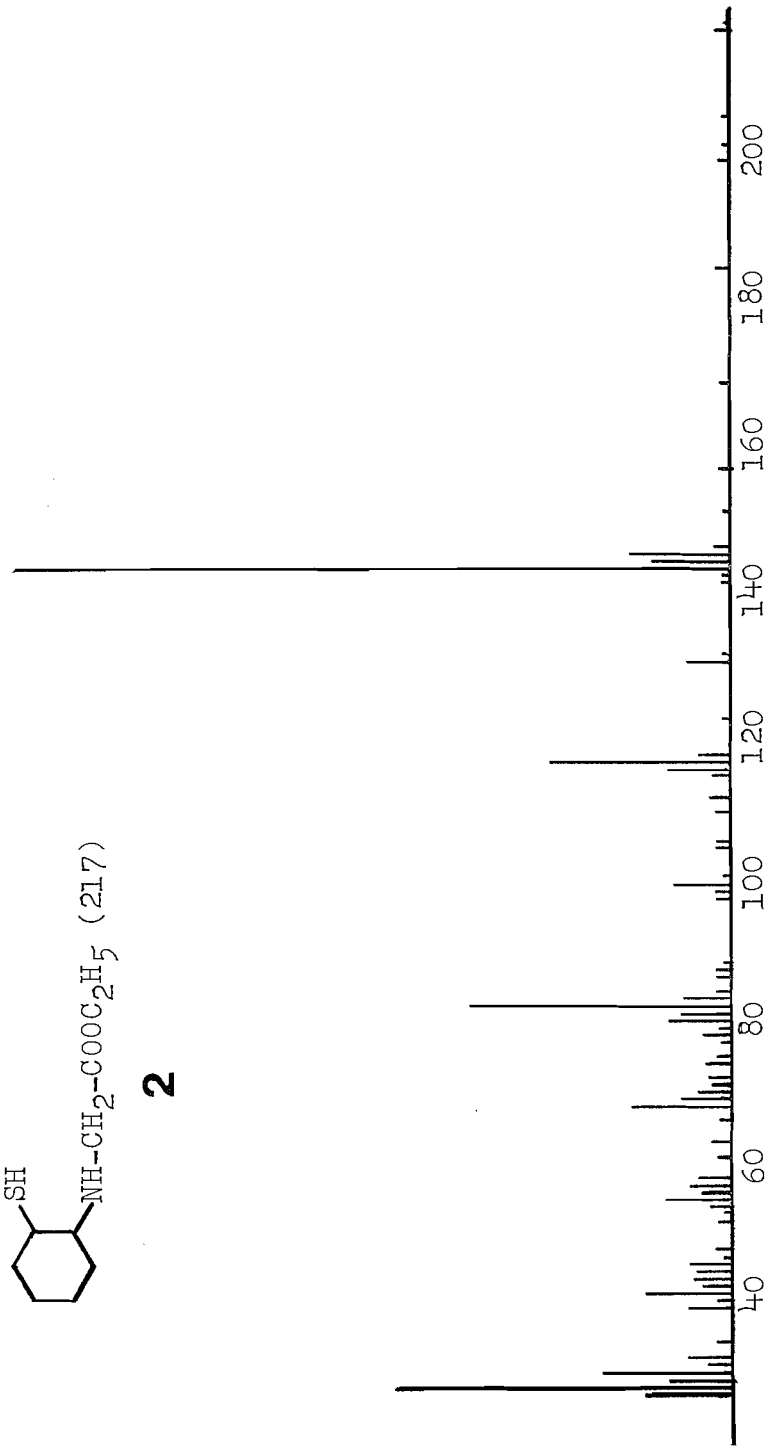

FIG. 1. Spectre de masse de **2**.

Can. J. Chem. Downloaded from www.nrcresearchpress.com by 210.87.254.6 on 09/05/12
For personal use only.

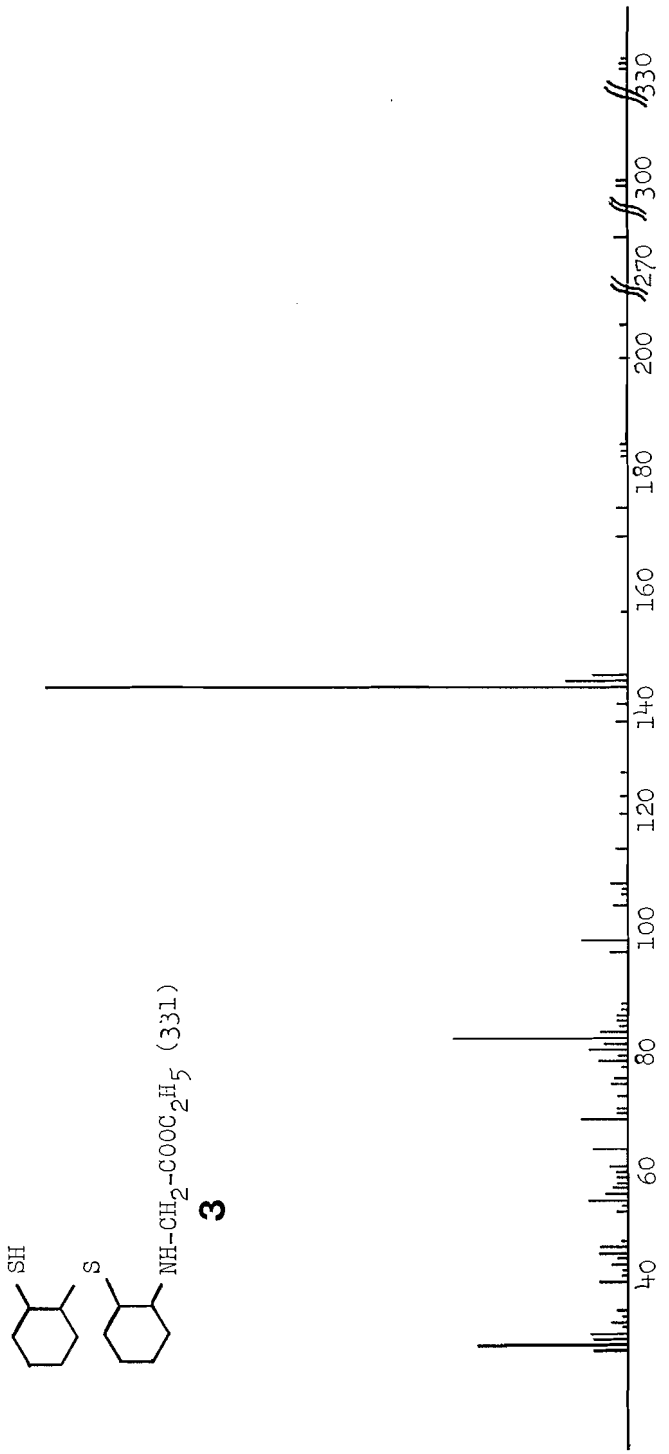

FIG. 2. Spectre de masse de **3**.

Can. J. Chem. Downloaded from www.nrcresearchpress.com by 210.87.254.6 on 09/05/12
For personal use only.

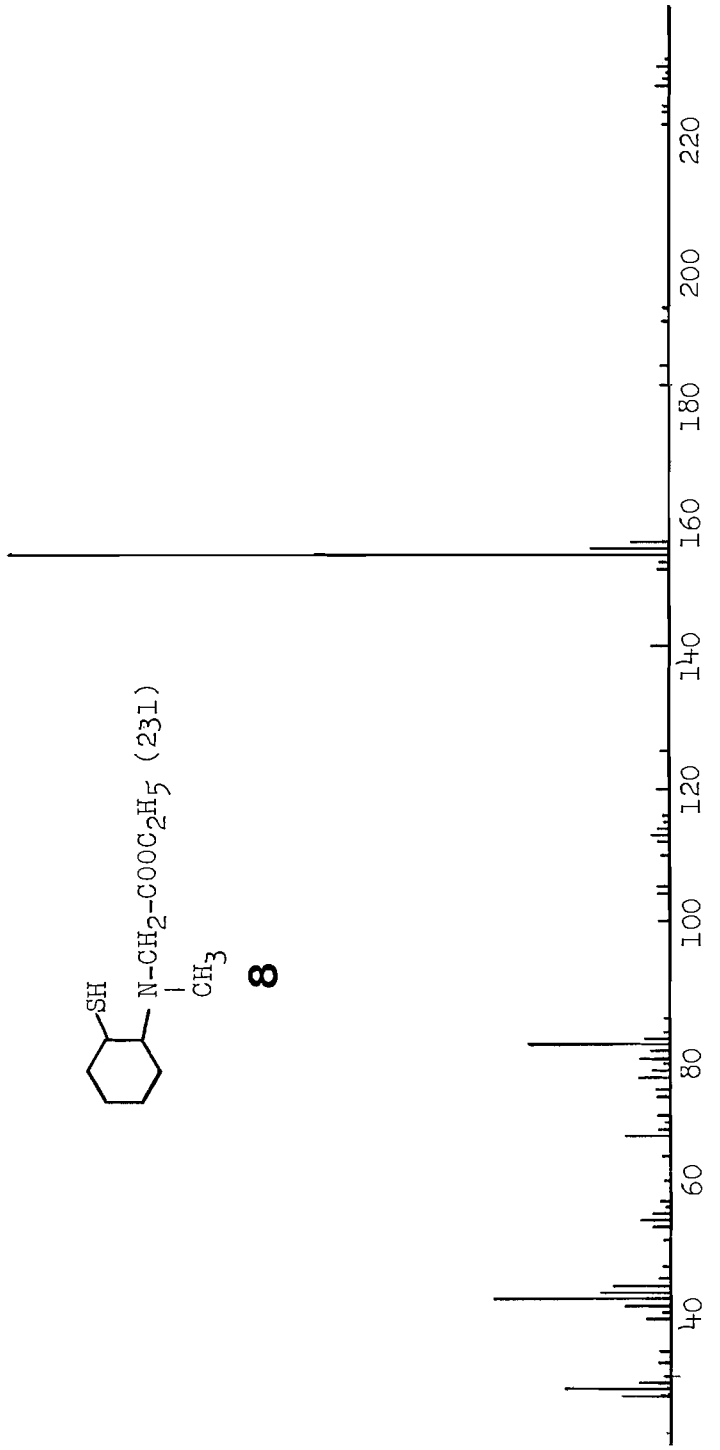

FIG. 3. Spectre de masse de **8**.

Can. J. Chem. Downloaded from www.nrcresearchpress.com by 210.87.254.6 on 09/05/12
For personal use only.

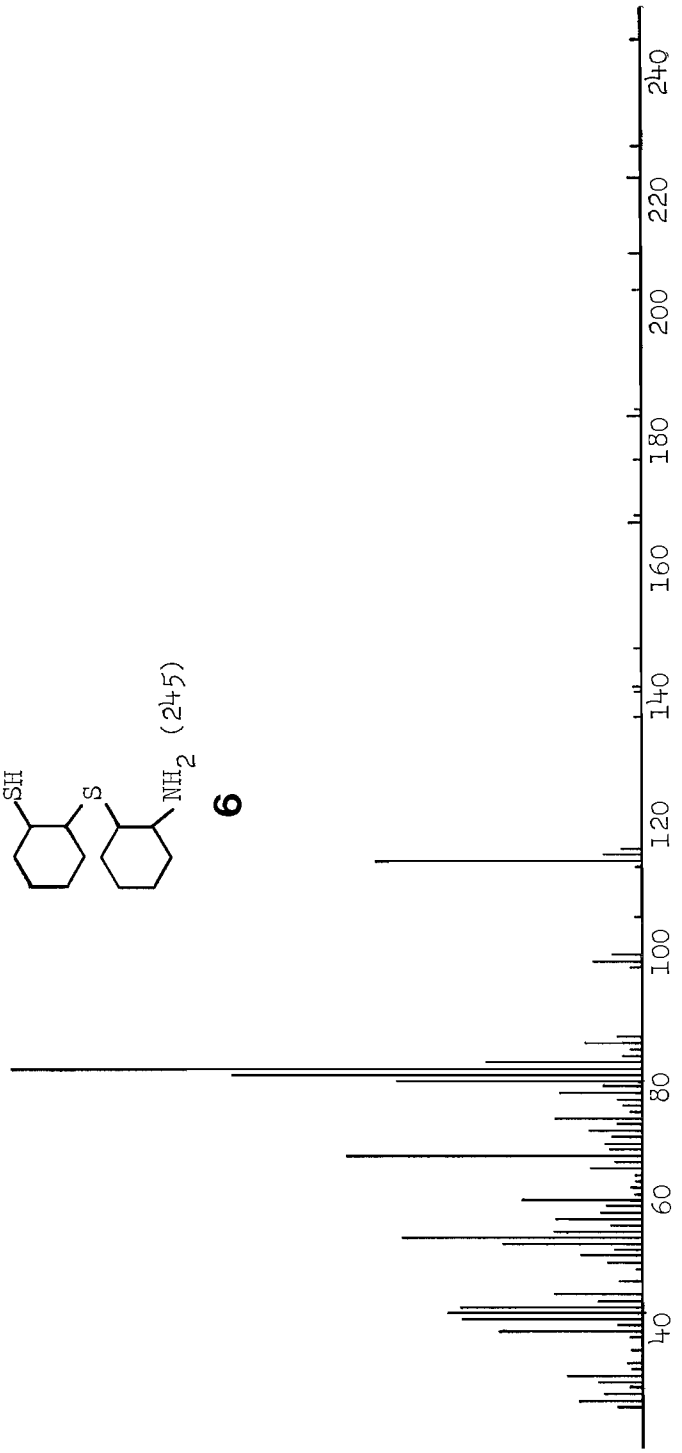

FIG. 4. Spectre de masse de **6**.

Can. J. Chem. Downloaded from www.nrcresearchpress.com by 210.87.254.6 on 09/05/12
For personal use only.

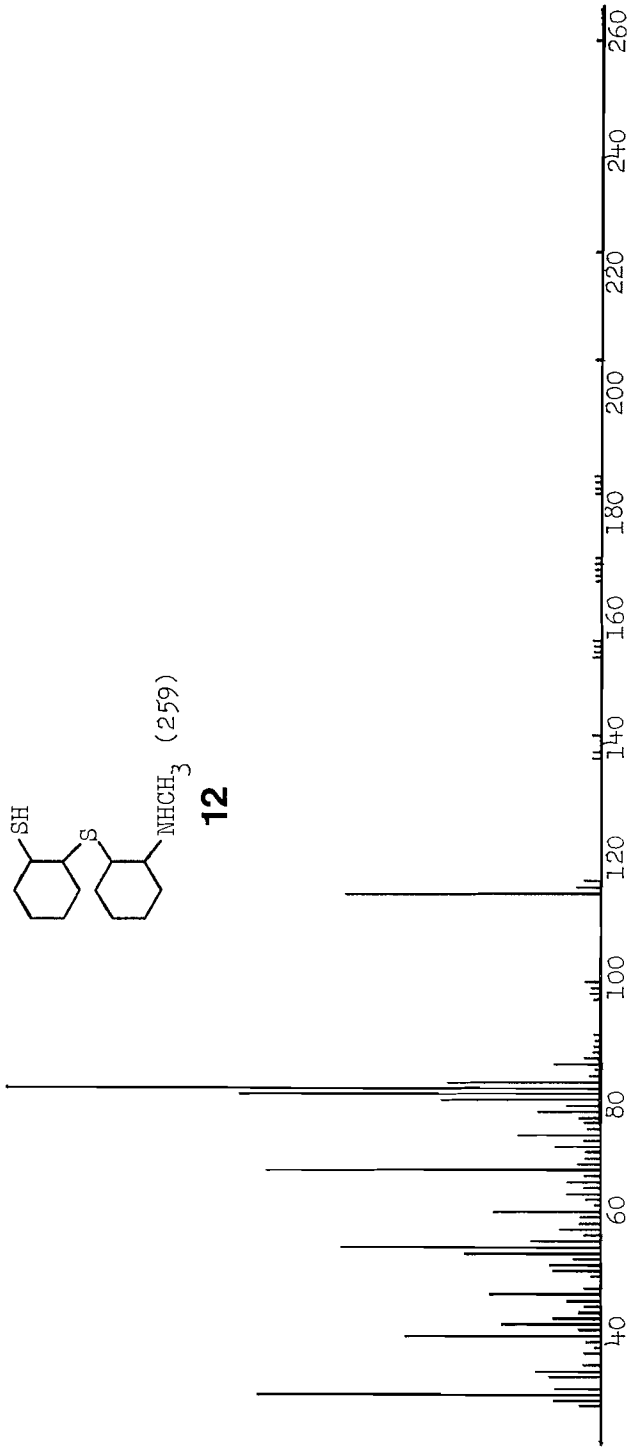

FIG. 5. Spectre de masse de **12**.

Can. J. Chem. Downloaded from www.nrcresearchpress.com by 210.87.254.6 on 09/05/12
For personal use only.

fragmentation possible commençant par la perte de SH. D'ailleurs, le spectre de masse pris à 70° met en évidence ce processus de fragmentation. Cependant, vu la faible intensité du fragment *m/e* 184 pour le produit **2**, cette deuxième route est beaucoup moins importante.

La présence des pics 142 et 98 dans le spectre du produit **3** est un argument supplémentaire en faveur de la structure proposée pour ce produit. En effet, il est difficile d'obtenir ces 2 pics à partir de la structure **3***a*. Si le produit **3** avant la structure **3***a*, on devrait très probablement trouver un pic assez intense à *m/e* 256:

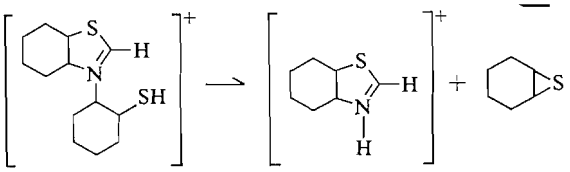

m/e 256 *m/e* 142

L'absence de ce pic dans le spectre de masse de **3** constitue un argument supplémentaire pour le rejet de la structure **3***a*.

Les spectres des deux produits modèles **6** et **12** (voir Fig. 4 et 5) ont également été étudiés pour vérifier la présence éventuelle d'un ion bicyclohexylthio ou mercapto-2 bicyclohexylthio. L'absence de ces deux fragments à la fois dans les spectres des produits **3**, **6** et **12** supporte l'exactitude du mécanisme proposé ainsi que la structure du produit **3**.

Dans les deux cas la réaction a donné aussi les dérivés de la dicéto-2,5 pipérazine et l'hydroxy-2 cyclohexanethiol.

Partie expérimentale

Les spectres infrarouges ont été pris sur un spectrophotomètre Beckman IR-8 à double réseau. Les spectres de résonance magnétique nucléaire ont été pris à l'aide d'un spectrophotomètre modèle A-60 de la compagnie Varian. Les déplacements chimiques δ sont exprimés en p.p.m. et le tétraméthylsilane est utilisé comme référence interne. Les spectres de masse ont été enregistrés sur un appareil Hitachi RMU-6D (température de 25 °C et 70 °C, 70 eV).

Les points de fusion et d'ébullition ne sont pas corrigés.

Les analyses élémentaires ont été faites par C. Daesslé, Organic Microanalysis à Montréal, et par nous-même (micro Kjeldahl).

L'épithiocyclohexane (**1**) a été obtenu d'après la méthode de E. van Tamelen (7).

Les esters éthyliques de la glycine et de la sarcosine ont été obtenus selon la méthode de Fischer (8).

L'amino-2 cyclohexanethiol (**4**), p.é. 115–117°/40 mm Hg a été obtenu par l'ouverture du produit **1** avec un excès d'ammoniaque concentré dans l'éthanol avec un rendement de 40%. Le méthylamino-2 cyclohexanethiol (**10**) p.é. 97°/1 mm Hg (9) a été obtenu par l'action de la méthylamine sur le produit **1** avec un rendement de 25–27%. (Les deux composés ont été obtenus par l'ouverture de **1** pour la première fois.)

Ouverture de l'épithiocyclohexane (1) par le glycinate d'éthyle

Un mélange de l'épithiocyclohexane (**1**) et du glycinate d'éthyle[1] a été porté à reflux pendant 2 h. La chromatographie du mélange sur silice a donné les quatre produits suivants: (*a*) dicéto-2,5 pipérazine, p.f. 260°, identifié par comparaison des spectres i.r., et point de fusion mixte (10). Rendement ~40%. (*b*) mercapto-2 cyclohexanol, p.éb. 137°/45 mm identifié par les spectres i.r. et r.m.n. (11), et comparé avec le produit d'ouverture de **1** avec H_2O. Rendement ~10%.

Anal. Calc. pour $C_6H_{12}OS$ (132.2): C, 54.53; H, 9.15. Trouvé: C, 54.60; H, 8.60. (*c*) *N*-(mercapto-2 cyclohexyl) glycinate d'éthyle (**2**) (voir tableau II). (*d*) *N*-[(mercapto-2 cyclohexylthio)-2 cyclohexyl] glycinate d'éthyle (**3**) (voir tableau II).

Ouverture de l'épithiocyclohexane (1) par le sarcosinate d'éthyle

Un mélange de quantités équimoléculaires l'épithiocyclohexane (1) avec le sarcosinate d'éthyle a été porté à reflux pendant 2 h. Les trois produits formés ont été séparés par chromatographie sur silice: (*a*) diméthyl-1,4 dicéto-2,5 pipérazine, p.f. 144–146° (12) identifiée par comparaison des spectres i.r. et r.m.n. Rendement ~20%. (*b*) *N*-(mercapto-2 cyclohexyl) sarcosinate d'éthyle (**8**). (Voir tableau II), rendement: 13%. (*c*) *N*-[(mercapto-2' cyclohexylthio)-2 cyclohexyl] sarcosinate d'éthyle (**9**). (Voir tableau II), rendement: ~20%.

Préparation des produits 6 et 12

Une solution éthanolique des produits **4** ou **10** (~10%) a été portée à reflux pendant 2 h avec 60% d'une quantité équimoléculaire d'épithiocyclohexane. La solution a été évaporée sous vide, le résidu dissous dans l'éthanol absolu et le 40% restant d'épithiocyclohexane a été ajouté; le mélange a été porté à reflux pendant 2 h. Le solvant a été évaporé sous vide et distillé sous pression réduite. Le rendement brut est de 60%. Les rendements après distillation pour les produits **6** et **12** sont de 23% et 31% respectivement (tableau II).

N-[(*Mercapto-2' cyclohexylthio*)-*2 cyclohexyl glycinate d'éthyle (3)*

Une solution du *N*-(mercapto-2 cyclohexyl) glycinate d'éthyle (**2**) (50 mg, 0.25 mmole) dans l'éthanol absolu (5 ml) a été chauffé à reflux avec l'épithiocyclohexane (25 mg, ~0.25 mmole) pendant 2 h. Le solvant a été évaporé *in vacuo* et le produit a été dissous dans l'éther anhydre et la solution éthérée a été décantée, séchée sur carbonate de potassium anhydre. Le solvant a été évaporé *in vacuo*. Le produit formé a été identifié au produit **3** obtenu précédemment, à l'aide des spectres de

[1]Pour les quantités, les conditions et les rendements, voir tableau I.

Can. J. Chem. Downloaded from www.nrcresearchpress.com by 210.87.254.6 on 09/05/12
For personal use only.

TABLEAU II*

Resultats spectroscopiques et analytiques

Nom		p.é. °C/mm Hg	Infrarouge [cm⁻¹]			Résonance magnétique nucléaire δ[p.p.m.] $CDCl_3$ (~10%)							Analyses					
													Calculé			Trouvé		
			C=O	—N—H	SH	CH_2—CO	N—H	SH	CH_2 CH_2 †	CH_2 † CH_2	Autres		Pour le composé	C	H	N	C	H	N
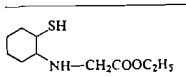	2	77°/0.5 mm	1740	3340	2560	3.48	2.3	2.7	1.5	2.3	CH_3 CH_2—CH_3	1.28 4.22	$C_{10}H_{19}NO_2S$ (217.2)	55.30	8.82	6.09	55.33	9.02	6.45
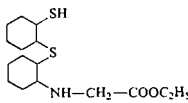	3	98–100°/0.3 mm	1745	3320	2580	3.45	2.20	2.7	1.5	2.3	CH_3 CH_2—CH_3	1.25 4.20	$C_{16}H_{29}NO_2S_2$ (331.4)	57.98	8.79	4.23	57.47	9.15	4.11
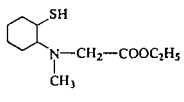	8	80–82°/0.3–0.4 mm	1743	—	2560	3.10	—	2.6	1.55	2.25	N—CH_3 CH_3 CH_2—CH_3	2.41 1.28 4.20	$C_{11}H_{21}NO_2S_2$ (231.3)	57.12	9.15	6.06	56.81	8.54	5.90
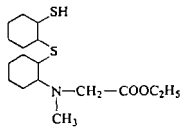	9	—	1738	—	~2570	3.20	—	2.5	1.5	2.30	N—CH_3 CH_3 CH_2—CH_3	2.42 1.25 4.25	$C_{17}H_{31}NO_2S_2$ (345.4)	—	—	4.05	—	—	3.70
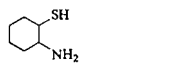	4	115–117°/40 mm	—	3320 1580	2580	—	2.20	2.93	1.55	2.18	—		$C_6H_{13}NS$ (131.2)	—	—	10.86	—	—	10.77
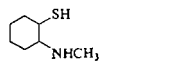	10	97°/1 mm‡	—	3300	2590	—	2.70	2.90	1.50	2.25	N—CH_3	2.40	$C_7H_{15}NS$ (145.2)	—	—	9.65	—	—	9.70
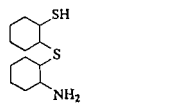	6	85–87°/0.3 mm	—	3300 1570	2560	—	2.22	2.88	1.45	2.20	—		$C_{12}H_{23}NS_2$ (245.3)	—	—	5.71	—	—	5.47
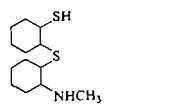	12	90–92°/0.3 mm	—	3300	2600	—	2.68	2.92	1.52	2.25	N—CH_3	2.42	$C_{13}H_{23}NS_2$ (259.3)	—	—	5.40	—	—	5.21

*La présence de SH rend l'analyse de ces produits difficile.
†Centre.
‡Le chlorhydrate p.f. 125–127° (11).

Can. J. Chem. Downloaded from www.nrcresearchpress.com by 210.87.254.6 on 09/05/12
For personal use only.

TABLEAU III

Résultats analytiques des chlorhydrates des esters

		Analyses								Migration sur couche mince du produit obtenu par			Rendement (%)	
		Calculé				Trouvé								
	Pour le composé	C	H	N	HCl*	C	H	N	HCl*	Synthèse	Saturation	Solvant	Synthèse	Saturation
5	$C_{10}H_{20}NO_2SCl$ (253.6)	47.35	7.95	5.52	14.37	46.63	8.39	5.11	14.00	0.88	0.90	benzène–méthanol 1:1	40	55
7	$C_{11}H_{22}NO_2SCl$ (267.6)	49.37	8.28	5.23	13.62	49.15	7.94	5.00	12.88	—	0.92	‾‖‾	—	~35
11	$C_{16}H_{30}NO_2S_2Cl$ (367.8)	—	—	3.80	9.91	—	—	3.42	9.60	—	0.83	‾‖‾	—	~30

*0.1 *N* $AgNO_3/K_2CrO_4$.

r.m.n. et infrarouge, ainsi que par migration sur couche mince; rendement 17%.

Anal. Calc. pour $C_{16}H_{29}NO_2S_2$ (331.4): N, 4.23. Trouvé: N, 4.02.

Chlorhydrates des esters

Méthode a (par saturation)

On a fait barbotter HCl gazeux dans une solution éthanolique de l'ester (environ 20%) jusqu'à saturation. La solution a été évaporée *in vacuo* et le résidu a été redissous dans l'éthanol absolu et saturé à nouveau avec HCl. L'évaporation du solvant a donné un résidu huileux, qui a été dissous dans l'éther anhydre. La solution éthérée contenant l'ester libre a été décantée et le résidu séché sous vide. Il a été impossible d'obtenir les produits sous forme cristalline à cause de leur caractère hygroscopique. Les chlorhydrates **5**, **7** et **11** ont été obtenus par cette méthode (tableau III).

Méthode b (synthèse)

Une solution éthanolique (~10%) de l'aminothiol **4**, (500 mg) a été portée à reflux avec une quantité équimoléculaire de chloroacétate d'éthyle pendant 5 h. Le solvant a été évaporé sous vide, puis le résidu a été dissous dans l'éther anhydre (50 ml) et agité pendant 30 min. La solution éthérée a été décantée, et le résidu séché *in vacuo*. Le produit huileux a été comparé avec celui obtenu précédemment.

Trois produits ont été indentifiés: les deux produits de départ, et le chlorhydrate de l'ester **5**. De plus, la présence d'un quatrième produit a été décelée par migration sur couche mince, mais il n'a pas été identifié.

Libération du chlorhydrate 5

Une solution du chlorhydrate de *N*-(mercapto-2 cyclohexyl) glycinate d'éthyle **5** (50 mg, 0.2 mmole) dans l'éthanol absolu a été traitée avec quelques gouttes d'éthanolate de sodium 10%, et le mélange a été chauffé pendant 20 min au bain-marie. Après refroidissement, le NaCl a été filtré. La solution éthanolique a été évaporée *in vacuo* et le résidu distillé (70–74%/0.4 mm Hg); rendement 42%. Le produit obtenu **2** est identique avec celui obtenu par l'ouverture du produit **1** avec le glycinate d'éthyle (spectre de r.m.n. et i.r.).

Remerciements

Nous remercions le Conseil National de Recherches du Canada de son appui financier qui a rendu ce travail possible.

1. C. Berse et K. Jankowski. Can. J. Chem. **44**, 1513 (1966).
2. K. Jankowski et C. Berse. Can. J. Chem. **45**, 2865 (1967).
3. K. Jankowski et C. Berse. Can. J. Chem. **46**, 1835 (1968).
4. K. Jankowski et C. Berse. Can. J. Chem. **46**, 1939 (1968).
5. C. C. Culvenor, W. Davies et N. S. Health. J. Chem. Soc. 278, 282 (1949).
   D. D. Reynolds et D. L. Fields. (A. Weissberger, *Editeur*) Heterocyclic compounds with three- and four-membered rings. Pt. 1. Interscience Publishers, New York. 1964. p. 602.
6. S. D. Turk, R. P. Louthan, R. L. Cobb et C. R. Bresson. J. Org. Chem. **27**, 2846 (1962).
   R. P. Louthan, C. R. Bresson et R. L. Cobb. U.S. Patent 3,257,301, June 21, 1966 d'après Chem. Abstr. **65**, 13574*a* (1966).
   H. Yoshikara. Nippon Igaku Hoshasen Gakkai Zasshi, **23**, 1 (1963).
   M. Mousseron, F. Winternitz et R. Dennilauler. Compt. Rend. **239**, 278 (1954).
7. E. van Tamelen. Organic Syntheses. Coll. Vol. IV, 232 (1963). J. Wiley and Sons, Inc., New York.
8. E. Fisher. Ber. **34**, 436 (1901).
9. M. Mousseron, F. Winternitz et R. Dennilauler. Compt. Rend. **241**, 805 (1955).
   F. L. Carroll, J. D. White et M. E. Wall. J. Org. Chem. **28**, 1236 (1963).
10. H. Schott, J. Larkin, L. Rockland et M. Dunn. J. Org. Chem. **12**, 490 (1949), voir aussi la bibliographie des articles 1 et 4.
11. F. G. Bordwell et H. M. Anderson. J. Am. Chem. Soc. **75**, 4959 (1953).
    M. Mousseron, R. Jacquier, M. Mousseron-Canet et R. Zagdun. Bull. Soc. Chim. France 1042 (1952).
12. C. A. Bischoff et A. Hausdörfer. Ber. **25**, 2270 (1892).

Can. J. Chem. Downloaded from www.nrcresearchpress.com by 210.87.254.6 on 09/05/12
For personal use only.

Liquid-phase oxidation of 2-butene in the presence of benzaldehyde

FUJIO TSUCHIYA AND TSUNEO IKAWA
Tokyo Institute of Technology, O-Okayama, Meguro-ku, Tokyo, Japan
Received February 7, 1969

The co-oxidation of *cis*- and *trans*-2-butene and benzaldehyde at 110 °C has been carried out in benzene and the mechanism of epoxide formation has been investigated by examining the ratio of *cis*- to *trans*-epoxides. The results indicate that epoxides were formed by two mechanisms, one involving the benzoylperoxy radical to give about half *cis* and half *trans* epoxides and the other by stereospecific epoxidation with perbenzoic acid. Experimental results show that the stereospecific character of epoxidation increases with the reaction time and the concentration of benzaldehyde, but does not depend on the concentration of 2-butene.

Canadian Journal of Chemistry, 47, 3191 (1969)

Can. J. Chem. Downloaded from www.nrcresearchpress.com by 210.87.254.42 on 09/05/12
For personal use only.

Introduction

It has been reported that various olefins trap acylperoxy radicals which are formed from aldehydes in the liquid-phase oxidation of aldehydes at room temperature, and react as a retarder (1, 2), and also that much epoxide was formed in the co-oxidation of cyclohexene with benzaldehyde at 70 and 110 °C. Two major processes of epoxidation have been proposed by the study of products (1), the first being the reaction of the benzoylperoxy radical, formed from benzaldehyde with cyclohexene, the second being the reaction of perbenzoic acid, formed from benzaldehyde with cyclohexene.

It has been shown that the stereochemistry is preserved during the epoxidation of olefins by per-acids (3). In this paper we will examine the mechanism of epoxidation in the co-oxidation of olefins with aldehydes by means of the stereochemical character of epoxides, using *cis*- and *trans*-2-butene as olefins and benzaldehyde.

Experimental

The reactions were conducted in a 200 cc autoclave, equipped with a reservoir and a magnetic stirrer. The volume of the reaction solution was kept constant at 100 cc, the total pressure 15 kg/cm^2, the partial pressure of oxygen 3 kg/cm^2, and the reaction temperature 110 °C. Benzene was used as solvent. The reaction time and concentration of the 2-butenes and benzaldehyde were changed. Oxygen was supplied from an oxygen accumulator to maintain a constant pressure during the course of the reaction.

The epoxidation of *cis*-2-butene by perbenzoic acid was performed, using authentic perbenzoic acid prepared from benzoyl chloride by the method of Moyer and Manley (4).

Benzene and acetonitrile were purified as usual, and benzaldehyde was distilled under a reduced nitrogen pressure in the dark. *cis*-2-Butene and *trans*-2-butene were 99.0% pure grade. Oxygen and nitrogen were 99.8% pure.

Gas chromatography was used to analyze the reacted and unreacted substances: *cis*- and *trans*-2,3-butyleneoxides, methylvinylcarbinol, crotonaldehyde, and acetaldehyde by a 2 m column of polyethyleneglycol-(PEG) 20 *M* at 60 °C, and unreacted benzaldehyde by the same column at 150 °C, *cis*- and *trans*-butenes by a 1 m column of DMF and 6 m of benzyl cyanide at room temperature, with a hydrogen flow rate of 40 cc/min. The total acids were measured by a titration with alcoholic potassium hydroxide, and most of the acid was found to be benzoic acid (m.p. 121 °C) by an elemental analysis after distillation of the products. Peroxide was measured by iodometry. *cis*- and *trans*-2,3-Butyleneoxides were isolated by the gas chromatography, and identified by infrared absorption spectra at 777 cm^{-1} (*cis*) and 812 cm^{-1} (*trans*), which are assigned to the epoxide rings (5).

Results

A series of runs with 1.6 moles/l of *cis*- and *trans*-2-butene and 2.3 moles/l of benzaldehyde was carried out in benzene at 110 °C with reaction times varying from 4 to 80 min. The results are summarized in Table I. Moreover the results of co-oxidation of 1.6 moles/l of *cis*-2-butene and 2.7 moles/l of benzaldehyde are tabulated in Table I. Table I shows that there is no difference between the rate of co-oxidation for the 2-butene isomers and also that the selectivity of epoxide, which is defined as the mole percent of epoxide based on consumed 2-butene, increases in accordance with the increase in the conversion of 2-butene. In these experiments 2,3-butyleneoxide was the main product. Other products were acetaldehyde and carbon dioxide. Oily products, having high boiling points higher than 180 °C at 60 mm Hg, were found but not analyzed. The absolute amount of benzoic acid was equal to that of butyleneoxide. Methylvinylcarbinol and

Can. J. Chem. Downloaded from www.nrcresearchpress.com by 210.87.254.42 on 09/05/12
For personal use only.

TABLE I

Co-oxidation of *cis*- and *trans*-2-butene and benzaldehyde at 110 °C: effect of conversion on epoxide

Run no.	Reaction time (min)	Conversion (mole%) 2-C_4H_8	Conversion (mole%) C_6H_5CHO	Oxygen absorbed (moles)	Mole percent of products‡ c-C_4H_8O	t-C_4H_8O	CH_3CHO	CO_2	$C_6H_5CO_2H$	Peroxide	Molar ratio of epoxide isomers (*cis*/*trans*)
					*cis**						
1	60	17.5	15.4	0.019	40.1	30.0	4.2	4.8	51.4	13.6	1.3
2	30	13.7	11.5	0.014	37.0	31.1	5.7	3.2	33.7	9.4	1.2
3	20	9.9	7.4	0.011	31.0	27.0	4.7	3.3	50.0	13.5	1.1
4	7	8.2	6.7	0.008	27.2	26.1	4.7	2.5	41.0	18.2	1.0
5	4.5	7.2	4.9	0.007	25.9	26.1	5.1	2.0	41.6	27.3	0.99
					*trans**						
6	80	32.3	15.4	0.041	9.5	44.1	4.3	4.9	48.1	13.0	0.22
7	60	19.9	10.9	0.015	8.9	34.4	4.7	3.3	44.0	18.0	0.26
8	40	18.1	9.6	0.013	9.6	33.5	4.1	2.8	40.2	15.0	0.29
9	20	9.8	7.4	0.009	10.1	32.6	4.7	3.4	34.6	20.3	0.31
					cis†						
10	5	5.8	2.8	0.009	34.5	28.4	6.2	2.9	60.5	24.6	1.2
11	20	10.9	6.0	0.015	34.9	27.7	3.8	3.0	56.3	17.0	1.3
12	25	23.8	8.1	0.035	42.8	31.7	4.8	1.9	58.9	16.1	1.4

**cis*- and *trans*-2-Butene were 1.6 mole/l and benzaldehyde was 2.3 mole/l.
†*cis*-2-Butene was 1.6 mole/l and benzaldehyde 2.7 mole/l.
‡Mole percent of products calculated from consumed 2-butene except for benzoic acid and peroxide which were based on consumed benzaldehyde.

Can. J. Chem. Downloaded from www.nrcresearchpress.com by 210.87.254.42 on 09/05/12
For personal use only.

crotonaldehyde, which are the primary products after the abstraction of hydrogen from 2-butene were not observed. Traces of methylformate and acetic acid were found on gas chromatograms.

The molar ratios of *cis*-epoxide to *trans*-epoxide against 2-butene conversion are plotted in Fig. 1. These show that the stereospecific character increases with the increase in conversion. Figure 1 also shows that the concentration of benzaldehyde affects the stereochemical character of the formed epoxide.

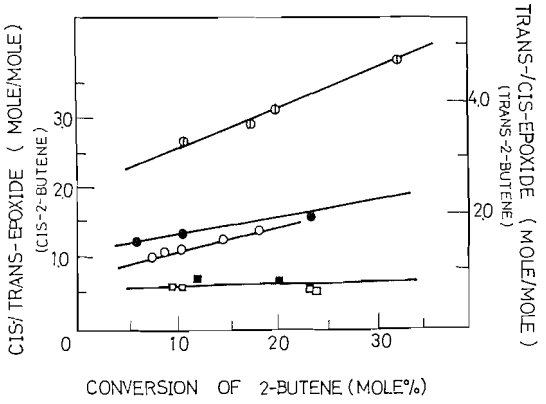

FIG. 1. Molar ratio of stereoisomers of epoxide versus conversion of 2-butene. *cis*-2-Butene, 1.6 moles/l: ○ benzaldehyde, 2.3 moles/l; ● benzaldehyde, 2.7 moles/l; □ benzaldehyde, 2.3 moles/l, $Co(OCOCH_3)_2$, 0.2 g; ■ benzaldehyde, 2.3 moles/l in acetonitrile. *trans*-2-Butene, 1.6 moles/l: ⓘ benzaldehyde, 2.3 moles/l.

A series of runs with 1.6 moles/l of *cis*- and *trans*-2-butenes was carried out in benzene at 110 °C for 20 min during which time the concentration of benzaldehyde was varied from 0 to 3.1 mole/l. The results are summarized in Table II. Molar ratios of *cis*- to *trans*-epoxide are plotted against the concentration of benzaldehyde in Fig. 2. It is apparent that the stereospecific character increases with an increase in concentration of aldehyde. The same result was obtained using *trans*-2-butene, as shown in Fig. 2.

The concentration of *cis*-2-butene was varied while the concentration of benzaldehyde and the reaction time were kept constant at 2.3 moles/l and 20 min, respectively. The results are tabulated in Table III.

With the increase in the concentration of butene, the amount of the reacted butene decreased and also the amount of absorbed oxygen decreased, as shown in Table III. These

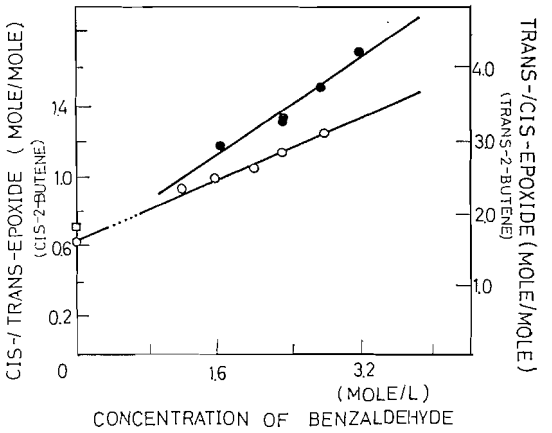

FIG. 2. Molar ratio of stereoisomers of epoxide versus concentration of benzaldehyde. ○ *cis*-2-Butene, 1.6 moles/l; □ Brill's result; ● *trans*-2-butene, 1.6 moles/l.

facts indicate that *cis*-2-butene reacts as a retarder of the reaction. The variation in the concentration of *cis*-2-butene caused a very large change in the conversion in the same reaction time. Therefore, the molar ratios of *cis*- to *trans*-epoxide formed in various concentrations of butene were plotted against the conversion of benzaldehyde, and found to be on the same line, as shown in Fig. 3. This means that the molar ratio of the stereoisomer does not depend on the concentration of *cis*-2-butene.

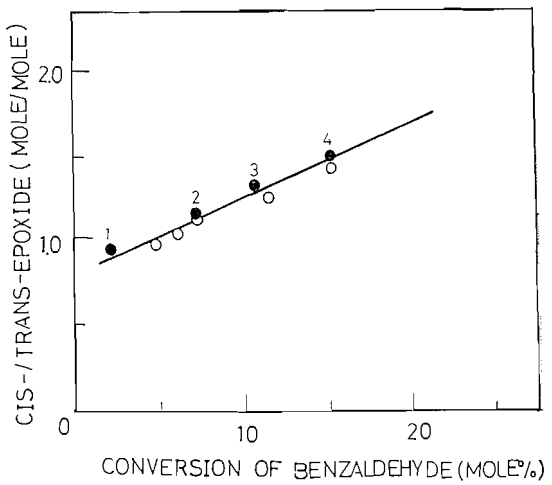

FIG. 3. Molar ratio of stereoisomers of epoxide versus conversion of benzaldehyde. ○ Value from Table I. ● *cis*-2-butene (moles/l) varied: (1) 3.1, (2) 1.6, (3) 1.2, (4) 0.96.

Can. J. Chem. Downloaded from www.nrcresearchpress.com by 210.87.254.42 on 09/05/12
For personal use only.

TABLE II

Co-oxidation of *cis*- and *trans*-2-butene and benzaldehyde at 110 °C: effect of the concentration of benzaldehyde

Run no.	Initial conc. of C_6H_5CHO (mole/l)	Conversion (mole %) 2-C_4H_8	Conversion (mole %) C_6H_5CHO	Oxygen absorbed (moles)	Mole percent of products‡ c-C_4H_8O	t-C_4H_8O	CH_3CHO	CO_2	$C_6H_5CO_2H$	Peroxide	Molar ratio of epoxide isomers (*cis*/*trans*)
					*cis**						
13	2.7	10.9	6.0	0.015	35.0	27.0	3.9	3.5	56.1	17.0	1.3
14	2.3	8.6	5.5	0.008	28.1	24.4	4.5	3.1	50.6	22.2	1.2
15	1.9	6.2	4.6	0.006	24.7	23.6	4.1	2.8	50.8	17.4	1.1
16	1.6	4.5	5.0	0.005	23.2	24.3	4.5	2.5	42.5	16.7	0.96
17	1.2	3.1	4.0	0.002	18.5	21.1	7.7	3.1	40.8	32.4	0.90
18†	0	4.3	—	0.002	12.5	19.4	26.1	1.8	—	—	0.64
19§	0	18.6	—	—	19.5	28.7	17.3	—	—	—	0.68
					*trans**						
20	3.1	18.6	6.5	0.023	17.8	58.5	4.0	4.1	53.4	13.7	0.23
21	2.7	14.3	6.5	0.014	13.9	50.9	4.0	2.2	51.3	13.7	0.27
22	2.3	10.7	6.0	0.011	9.6	31.8	5.5	1.8	43.8	25.9	0.30
23	2.3	9.8	5.7	0.009	10.2	33.4	3.8	3.5	43.9	23.4	0.31
24	1.6	6.8	3.4	0.006	8.0	23.2	4.5	1.2	40.9	16.5	0.34

*cis- and *trans*-2-Butenes were 1.6 mole/l.
†Reaction time was 480 min, others, 20 min.
‡Mole percent of products calculated from consumed 2-butene except for benzoic acid and peroxide which were based on consumed benzaldehyde.
§Referred from Brill's report (6).

TABLE III

Co-oxidation of *cis*-2-butene and benzaldehyde at 110 °C: effect of the concentration of *cis*-2-butene

Run no.	Initial conc. of C_4H_8 (mole/l)	Conversion* (mole %) c-2-C_4H_8	Conversion* (mole %) C_6H_5CHO	Oxygen absorbed (moles)	Mole percent of products† c-C_4H_8O	t-C_4H_8O	CH_3CHO	CO_2	$C_6H_5CO_2H$	Peroxide	Molar ratio of epoxide isomers (*cis*/*trans*)
25	3.1	4.1	2.2	0.007	22.9	24.2	5.4	2.5	33.7	16.0	0.95
26	1.2	13.5	10.5	0.019	28.8	22.0	7.6	1.6	46.0	12.3	1.3
27	1.0	32.7	14.8	0.032	45.5	30.9	5.0	2.6	52.6	14.0	1.5
28	0.8	66.7	33.6	0.053	45.2	27.0	2.5	7.3	60.6	28.6	1.7

*The initial concentration of benzaldehyde were 2.3 mole/l.
†Mole percent of products calculated from consumed *cis*-2-butene except for benzoic acid and peroxide, which were based on benzaldehyde.

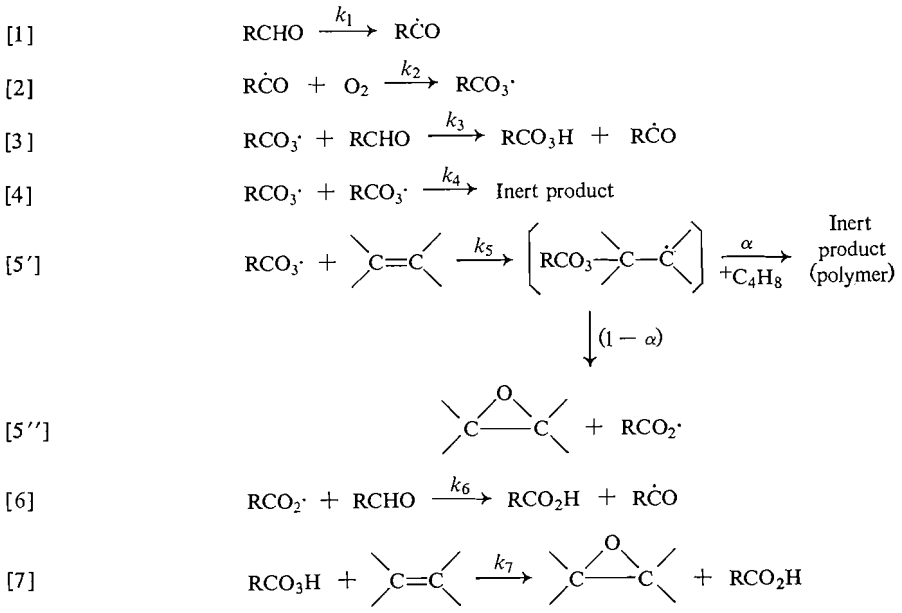

REACTION SCHEME 1.

The epoxide formed from the reaction of *cis*-2-butene and perbenzoic acid was only *cis*-2,3-butyleneoxide.

It is known that the decomposition of perbenzoic acid by cobalt – acetate is faster than the epoxidation of olefin (1), and also that acetonitrile forms a complex with per-acid to prevent the epoxidation by per-acid (7). Thus, if cobalt – acetate is added under the reaction conditions to the reaction mixture of 1.6 moles/l of *cis*-2-butene and 2.3 moles/l of benzaldehyde at 110 °C, or if acetonitrile instead of benzene is used as a solvent under the same reaction conditions, the epoxidation by per-acid will be prevented and the stereospecificity will be reduced. The results are summarized in Table IV. The behaviors of the molar ratios of the stereoisomer are shown in Fig. 1. Molar ratios of *cis*- to *trans*-epoxide were significantly reduced. It suggests that the major process of epoxidation with cobalt – acetate or in acetonitrile is the addition of the benzoylperoxy radical to 2-butene.

Discussion

The authors have proposed the reaction scheme for the co-oxidation of benzaldehyde and olefins (1, 2). In the case of this experiment, the hydrogen abstraction from 2-butene by radicals may be neglected, since only traces of methylvinylcarbinol and crotonaldehyde have been found. The decomposition of per-acid will be small (8) in comparison with the epoxidation by per-acid (9). The rate of the epoxidation is larger than the Baeyer-Villiger reaction by per-acid (10). Consequently, epoxides seem to be formed by reactions [5″] and [7], as shown in Reaction scheme 1.

In this experiment, the conversions of 2-butene were fairly large, and the concentrations of 2-butene and aldehyde varied during the course of reaction. However, applying the stationary state method to the elementary radical reactions, we kinetically speculate the epoxidation mechanism, comparing with the experimental results.

The consideration of the factors that affect the molar ratio of *cis*- to *trans*-epoxide is as follows. The rate of epoxide formation by reaction [5″] is

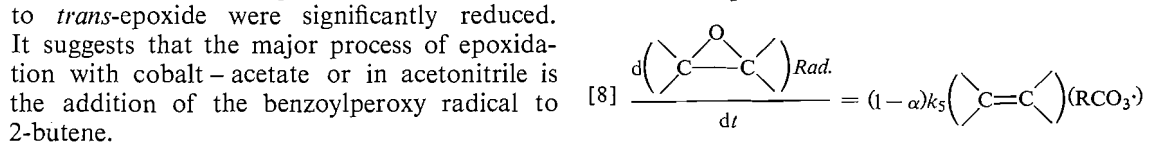

The rate of epoxide formation by reaction [7] is

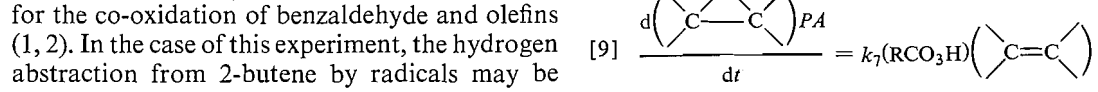

Can. J. Chem. Downloaded from www.nrcresearchpress.com by 210.87.254.42 on 09/05/12
For personal use only.

Can. J. Chem. Downloaded from www.nrcresearchpress.com by 210.87.254.42 on 09/05/12
For personal use only.

TABLE IV

The Co-oxidation in the presence of cobaltacetate and in acetonitrile as solvent

Run no.	Reaction time (min)	Conversion* (mole %)		Oxygen absorbed (mole)	Mole percent of products†						Molar ratio of epoxide isomers (*cis*/*trans*)
		c-2-C_4H_8	C_6H_5CHO		*c*-C_4H_8O	*t*-C_4H_8O	CH_3CHO	CO_2	$C_6H_5CO_2H$	Peroxide	
					with cobaltacetate of 0.2 g						
29	1.5	9.8	9.0	0.006	18.3	33.8	5.9	2.4	43.0	7.7	0.54
30	4.0	11.6	9.5	0.009	18.2	33.5	4.7	3.9	46.0	11.2	0.54
31	10.0	24.3	14.0	0.023	17.3	31.2	3.8	3.1	47.6	3.7	0.57
32	20.0	23.8	17.6	0.024	18.2	33.0	6.1	2.8	74.5	3.8	0.56
					in acetonitrile						
33	9.0	12.3	‡	0.011	27.6	48.9	8.5	7.8	‡	‡	0.66
34	30.0	20.5	‡	0.020	27.9	39.3	7.2	4.0	‡	‡	0.71

*Initial concentration of cis-2-butene and benzaldehyde were 1.6 and 2.3 mole/l, respectively.
†Mole percent of products calculated from consumed cis-2-butene except for benzoic acid and peroxide, which were based on consumed benzaldehyde.
‡Did not analyze.

Can. J. Chem. Downloaded from www.nrcresearchpress.com by 210.87.254.42 on 09/05/12
For personal use only.

The concentration of per-acid will be calculated by the rate of per-acid formation as follows

$$[10] \qquad \frac{d(RCO_3H)}{dt} = k_3(RCO_3\cdot)(RCHO)$$

Moreover, we may write the next approximation assuming the steady state of radicals and the low conversion of reactants

$$[11] \qquad (RCO_3H) \doteqdot k_3(RCO_3\cdot)(RCHO)t$$

where t is the reaction time.

It is reasonable to consider that the epoxidation [5″] does not preserve a stereochemical character of the reactant olefin and the epoxides formed are a mixture of *cis*- and *trans*-epoxides, while the epoxide formed by reaction [7] preserves a stereochemical character of the reactant olefin. Then, the following relation can be obtained by the integration of eqs. [8], [9], and [11], assuming the steady state of radicals and the low conversion of reactants

$$[12] \qquad \frac{cis\text{-epoxide}}{trans\text{-epoxide}} = \beta + \frac{1}{2}\frac{1+\beta}{1-\alpha}\frac{k_3}{k_5} \times k_7(RCHO)t$$

where, β is the molar ratio of *cis*- to *trans*-epoxide formed by radical attack, that is, eq. [8], and the value of β seems to be a constant, about 0.6. We shall discuss this in more detail in the following section.

This equation indicates that the molar ratio of stereoisomers depends on the concentration of aldehyde and the reaction time, i.e., conversion of the reactants, but does not depend on the concentration of olefin.

These results derived kinetically are consistent qualitatively with the trend of the experimental results, shown in Figs. 1–3.

It is shown in Table I that the distribution of *trans*-epoxide formed from *cis*-2-butene has not changed, while *cis*-epoxide has increased with conversion. This fact indicates that the reaction [7] of *cis*-epoxide formation is the successive reaction. The same behavior has been observed in the case of *trans*-2-butene.

It is clear in Table III that olefin reacts as a scavenger of peroxy radical, i.e., as in reaction [5], and gives a mixture of epoxides, or reacts further with 2-butene to form inert products such as polymers or esters. These will correspond to the brownish oily products having high boiling points. Adding cobalt – acetate, which decomposes per-acid, or using acetonitrile as a solvent instead of benzene (which makes a complex to prevent the epoxidation by reaction [7]), the amount of *cis*-epoxide formed from *cis*-2-butene has been decreased. These experimental results, shown in Fig. 1, indicate epoxidation by per-acid and peroxyradical. The value of the molar ratio of *cis*- to *trans*-epoxide formed from *cis*-2-butene is about 0.6, when the epoxidation by per-acid is completely prevented, and this value agrees with that when only *cis*-2-butene has been oxidized without aldehyde, the value by Brill and Baronr (6), and also the value extrapolated to zero concentration of aldehyde, as shown in Fig. 2. These facts mean that the value of the molar ratio (β) of *cis*- to *trans*-epoxide formed from *cis*-2-butene by radical attack is about 0.6.

From the above discussion on the value of the molar ratio of stereoisomers by a radical process, and the epoxidation by per-acid being a successive reaction, the increase in the molar ratio with the concentration of benzaldehyde (Fig. 2) and with the conversion of benzaldehyde (Fig. 3) is thought to be due to the contribution of epoxidation by per-acid. The amount of *cis*-epoxide in excess of 0.6 of the *trans*-epoxide results from the epoxidation by per-acid in the experiment using *cis*-2-butene. Therefore, the relative proportion of non-radical epoxidation to radical epoxidation is $(N - 0.6)/0.6$, where N is the molar ratio of *cis*- to *trans*-epoxide in the products.

1. T. Ikawa, T. Fukushima, M. Muto, and T. Yanagihara. Can. J. Chem. **44**, 1817 (1966); Can. J. Chem. **45**, 1900 (1967).
2. H. Tomizawa, D. Tanaka, and T. Ikawa. Preprint of Annual Meeting of the Chemical Soc. of Japan, No. 3, 2102 (1968).
3. B. M. Lynch and K. H. Pausacker. J. Chem. Soc. 1525 (1955).
4. J. R. Moyer and N. C. Manley. J. Org. Chem. **29**, 2099 (1964).
5. T. Shimanouchi. Infrared absorption spectrum. Kagaku-no-ryoiki, zōkan, **37**, Nankodo, Tokyo. 1963. p. 88.
6. W. Brill and B. J. Baronr. J. Org. Chem. **29**, 140 (1964).
7. N. N. Schwartz and J. H. Blumberg. J. Org. Chem. **29**, 1976 (1964).
8. G. Giacometti and A. Iliceto. Ric. Sci. **27**, 743 (1957), C.A. **51**, 12612e.
9. D. Swern. J. Amer. Chem. Soc. **69**, 1692 (1947).
10. Y. Ogata, I. Tabushi, and H. Akimoto. J. Org. Chem. **26**, 4803 (1961).

Can. J. Chem. Downloaded from www.nrcresearchpress.com by 210.87.254.42 on 09/05/12
For personal use only.

Permanganate oxidation of aromatic alcohols in acid solution[1]

FARIZA BANOO[2] AND ROSS STEWART
Department of Chemistry, University of British Columbia, Vancouver 8, British Columbia

Received March 13, 1969

The mechanism of the permanganate oxidation of di- and tri-arylcarbinols has been studied in aqueous sulfuric acid. With both kinds of alcohols the rate-controlling step in solutions more acidic than H_0 −0.50 was found to be the ionization of the carbinol to give the carbonium ion followed, it is believed, by rapid reaction with permanganate ion to form the ester which decomposes rapidly to products. In the case of the tertiary alcohols the decomposition probably proceeds via a 1,2-aryl shift. The effect of substituents is correlated with σ^+ in both cases, ρ^+ being −1.02 and −1.39 for the secondary and tertiary series. The acidity function which governs both reactions is H_0. Tri(*p*-tolyl)carbinol is exceptional in that its oxidation in solutions more acidic than H_R −2.6 is second-order and is governed by the H_R acidity function.

Canadian Journal of Chemistry, 47, 3199 (1969)

Introduction

The permanganate oxidation of primary and secondary alcohols has previously been studied in basic and weakly acidic solution (1–4). The reaction is strongly accelerated by base and this has been shown to be due to the ready transfer of hydrogen (either as a hydride ion or as a hydrogen atom) from the alkoxide ion to the permanganate ion.

$$R_2CHOH + OH^- \rightleftarrows R_2CHO^- + H_2O$$

$$R_2CHO^- + MnO_4^- \rightarrow \begin{cases} R_2C{=}O + Mn(V) \xrightarrow{Mn(VII)} \\ R_2\dot{C}{-}O^- + Mn(VI) \xrightarrow{Mn(VII)} \end{cases} R_2C{=}O + Mn(VI)$$

Little is known about the way in which strongly acidic permanganate reacts with alcohols, although it has been shown that aldehyde hydrates (which are gem diols) undergo much more rapid oxidation in acidic than in neutral solution, because of the increased reactivity of the permanganate acid formed in this region (5). Furthermore, virtually nothing is known about the way tertiary alcohols are oxidized by permanganate. These compounds lack a hydrogen atom on the alcoholic carbon and any oxidation must produce carbon–carbon bond cleavage, possibly via aryl migration. It seemed worthwhile to study these reactions and accordingly, a series of diarylcarbinols and triarylcarbinols were prepared and subjected to permanganate oxidation over a wide acidity range. The results have been analyzed in terms of mechanism.

[1]Part IX of the series, Mechanisms of Permanganate Oxidation. Taken in part from the Ph.D. Thesis of Fariza Banoo, University of British Columbia, 1968.

[2]Colombo Plan Scholar, on leave of absence from the East Regional Laboratories, P.C.S.I.R., Pakistan.

Experimental

Materials

The substituted benzhydrols were prepared by standard methods usually involving the reduction of the corresponding ketone (1). The triarylcarbinols were, with one exception (4-nitrotriphenylcarbinol (6)) prepared by the Grignard procedure. The physical properties of those compounds that have previously been prepared agreed in all cases with the literature values. The following two compounds have not been previously reported.

(1) 3-Trifluoromethyl-4′-methyltriphenylcarbinol: from 4-methylbenzophenone and 3-trifluoromethylphenylmagnesiumbromide. Yield 41%, b.p. 184°/0.8 mm.

Anal. Calcd. C, 73.7; H, 4.97; F, 16.7. Found: C, 73.5; H, 5.11; F, 16.9.

(2) 3-Trifluoromethyltriphenylcarbinol: from benzophenone and 3-trifluoromethylphenylmagnesiumbromide. (We thank Mr. I. Beheshti for the preparation of this compound.) Yield, 61%, b.p. 120°/0.2 mm.

Anal. Calcd. C, 73.17; H, 4.57; F, 17.37. Found: C, 73,14; H, 4.87; F, 17.14.

Reaction Products

The following benzhydrols were oxidized (listed in the order in which they appear in Fig. 8, left to right: 4,4′-dimethoxy, 2,4,6,2′,4′,6′-hexamethyl (σ^+ value calculated from pK_{R+} of the diarylcarbinol (9), 4-methoxyl 4,4′-dimethyl, 4-methyl, unsubstituted, 4-chloro, 4,4′-dichloro, 4-carboxy. Isolation experiments

Can. J. Chem. Downloaded from www.nrcresearchpress.com by 210.87.254.42 on 09/05/12
For personal use only.

were performed in the cases of benzhydrol and 4-methoxybenzhydrol. The former gave a 99.2% yield of benzophenone, m.p. 49°, 2,4-dinitrophenylhydrazone, m.p. 238°. The latter gave a 98.1% yield of crystalline 4-methoxybenzophenone, m.p. 62°. The reaction products of all the other alcohols contained strong carbonyl peaks in their infrared spectra.

The following triphenylcarbinols were oxidized (listed in the order which they appear in Fig. 9, left to right): 3,3′,3″-trichloro, 4,4′,4″-trichloro, 4,4′-dichloro, 3-trifluoromethyl-4′-methyl, 4-chloro, unsubstituted, 4-fluoro, 4-methyl, 4,4′-dimethyl, 4,4′,4″-trimethyl. The ketonic products have been identified in the case of triphenylcarbinol and two of its derivatives (Table II). Triphenylcarbinol was shown to produce benzophenone and carbon dioxide when an excess of permanganate was employed. The carbon dioxide was swept out of the reaction mixture and trapped in barium hydroxide solution. The increase in weight of this system corresponded to the production of 6 moles of carbon dioxide. We conclude that phenol is the other product of reaction and that it has been completely degraded by the acidic permanganate, the known fate of phenol under these conditions (4).

Kinetics

The kinetics of the reaction were followed by two procedures; titration of unreacted permanganate and observation of the disappearance of the 526 mμ permanganate peak in the visible spectrum, essentially as previously described (1, 5, 7).

A spectrophotometric method was used to follow the rate of ionization of 4-methoxybenzhydrol by observing the increase in absorption of the corresponding carbonium ion at 466 mμ. Because of the low solubility of the carbinol in water, 70% methanol (by volume) in water was taken as the reaction medium. In a typical experiment 2 ml of 18.0 *M* sulfuric acid was taken in a 10 ml volumetric flask and made up to the mark with the aqueous methanol; 2.5 ml of this solution was taken in a cell and placed in the thermostatted cell compartment of a Cary 16 spectrophotometer. Next 50 μl of a 2.5 *M* solution of 4-methoxybenzhydrol were injected to the cell from a syringe. The increase in optical density at 466 mμ showed the extent of ionization. The values for the acidity functions, H_0 and H_R, for the solutions were determined by the standard Hammett indicator technique (8). The results are given in Table I.

TABLE I

H_0 and H_R values for 70 vol% aqueous methanol

M(H_2SO_4)	H_0*	H_R†	(H_R)‡
1.80	−0.15 (−0.14)	−0.58	−0.63
2.16	−0.38	−0.98	−0.89
2.31	−0.50	−1.25	−1.02
2.88	−0.64	−1.65	−1.78
3.60	−0.82	−1.94	−2.01

*4-Chloro-2-nitroaniline was used as indicator except for the value in parentheses which was obtained using 2-nitroaniline (8).
†4,4′-Dimethoxytriphenylchloromethane was used as indicator (9).
‡Calculated from the final absorbance of the 4-methoxybenzhydryl cation (9).

Results and Discussion

The stoichiometry of both reactions, the oxidation to the ketone in the case of the secondary alcohols, and the oxidative cleavage in the case of the tertiary alcohols, requires a 3:2 molar ratio of alcohol to permanganate

$$3Ar_2CHOH + 2MnO_4^- + 2H^+ \rightarrow 3Ar_2C{=}O + 2MnO_2 + 4H_2O$$

$$3Ar_3COH + 2MnO_4^- + 2H^+ \rightarrow 3Ar_2C{=}O + 3ArOH + 2MnO_2 + H_2O$$

Although the permanganate–alcohol reaction in basic and in mildly acidic solution is cleanly second-order (1), the reaction that becomes dominant as more acidic conditions are reached ($H_0 < -0.50$) is first-order in alcohol and zero-order in permanganate. Figure 1 shows a typical first-order plot for the oxidation of benzhydrol. Doubling the permanganate concentration has no effect on the rate at which it is consumed.

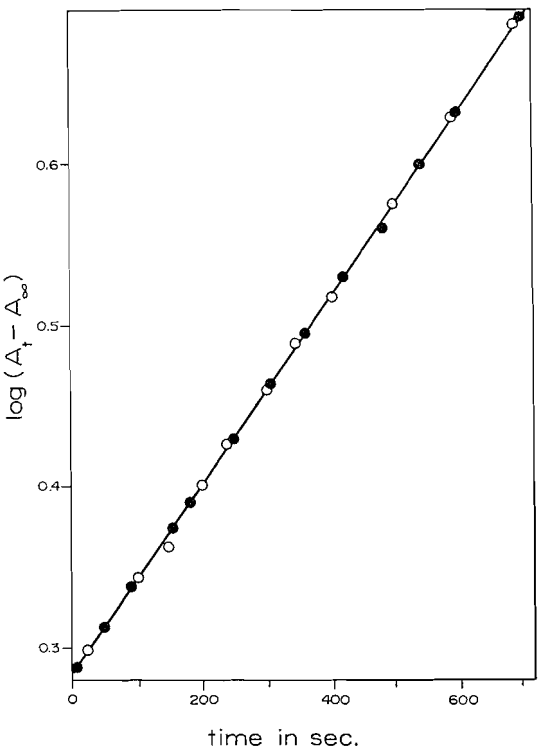

FIG. 1. First-order rate plots of the permanganate oxidation of benzhydrol, $H_0 = -0.69$, $T = 25°$, [benzhydrol] = 3.65×10^{-4}; [MnO_4^-] = 4.87×10^{-4} (open circles), [MnO_4^-] = 2.43×10^{-4} (closed circles); $k_1 = 2.00 \times 10^{-3}$ s^{-1}.

TABLE II

Analysis of permanganate oxidation product of triarylcarbinols

Substituted triphenylcarbinols	Melting point of ketone derivative* (°)		λ_{max} of conc. H_2SO_4 soln. of products (mμ)	Identified benzophenones
	Obs.	Lit. (12)		
4-Me	238	239	344†	Unsubstituted
4-Cl	184	185	299, 367‡	4-Cl

*2,4-Dinitrophenylhydrazone.
†The conjugate acid of benzophenone absorbs at 344 mμ (13).
‡The conjugate acid of 4-chlorobenzophenone absorbs at 300 and 367 mμ (13).

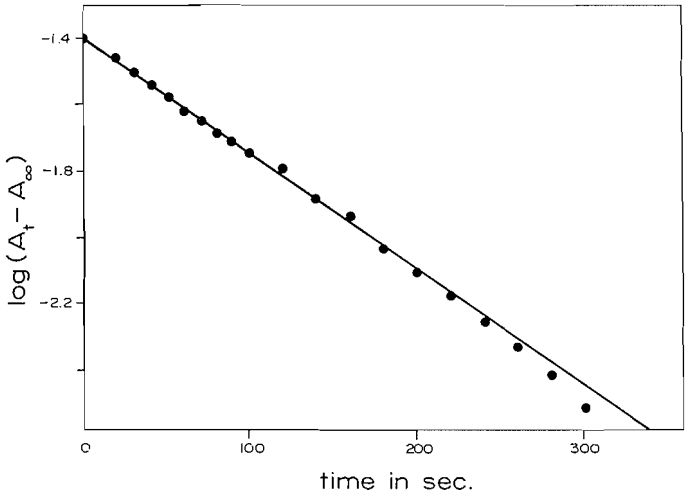

FIG. 2. First-order rate plot of the permanganate oxidation of triphenylcarbinol, $H_0 = -1.50$, $T = 25°$, $k_1 = 1.14 \times 10^{-2}\ s^{-1}$.

Most of the tertiary alcohols also gave good first-order plots up to about 50–60% reaction, after which serious deviations began to appear, presumably because of degradation of the phenolic products (Fig. 2). In the case of tri(*p*-tolyl)carbinol a second-order reaction reappeared at higher acidities ($H_R < -2.6$).

The effect of acidity on the rate of the permanganate oxidation of benzhydrol and triphenylcarbinol is shown in Figs. 3 and 4. In both cases, reasonably linear plots are obtained when the logarithm of the first-order rate constant is plotted against H_0 (8) and the slopes are found to be close to unity. When the acidity function H_R is used (9), somewhat less linear plots are obtained and, more significantly, the slopes are found to deviate greatly from unity (0.58 for benzhydrol and 0.45 for triphenylcarbinol). Only for tri(*p*-tolyl)carbinol did H_R appear to govern the rate of the oxidation reaction. Between H_R values of -2.5 and -3.6, a straight line of unit slope was obtained when the logarithm of the second-order rate constant for the oxidation of this alcohol is plotted against H_R (Fig. 5).

Rate-controlling Step

The first-order dependence of the rate on the concentration of alcohol, the zero-order dependence on permanganate, and the first-order dependence on the acidity means that the rate can be expressed by the equation

$$\text{rate} = k[\text{alcohol}]h_0 \quad \text{where } h_0 = -\text{antilog } H_0$$

This suggests that the rate-controlling step is the ionization of the alcohol to give the carbonium ion

$$ROH + H^+ \rightleftarrows ROH_2^+ \quad \text{fast}$$
$$ROH_2^+ \rightarrow R^+ + H_2O \quad \text{slow}$$
$$R^+ + MnO_4^- \rightarrow \text{products} \quad \text{fast}$$

Can. J. Chem. Downloaded from www.nrcresearchpress.com by 210.87.254.42 on 09/05/12
For personal use only.

Can. J. Chem. Downloaded from www.nrcresearchpress.com by 210.87.254.42 on 09/05/12
For personal use only.

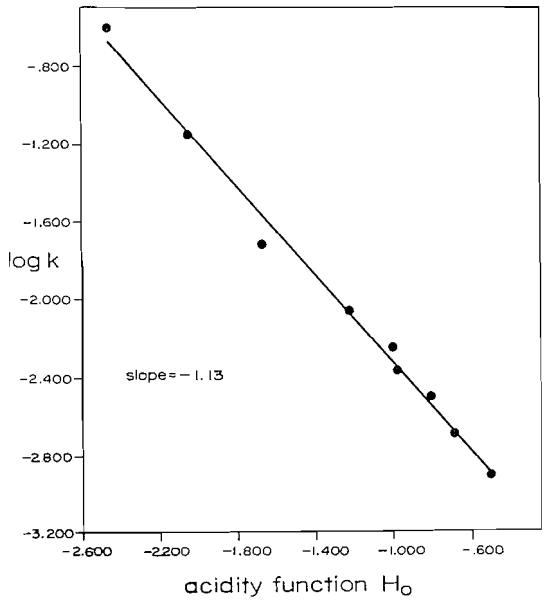

FIG. 3. Variation of the rate of permanganate oxidation of benzhydrol as a function of H_0; correlation coefficient, 0.996.

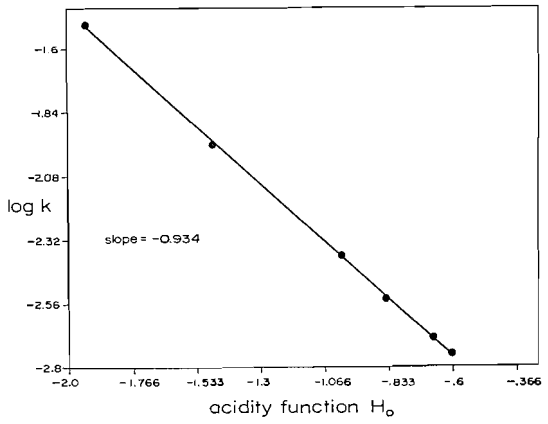

FIG. 4. Variation of the rate of permanganate oxidation of triphenylcarbinol as a function of H_0; correlation coefficient, 0.999.

Although the rate-controlling step above involves the formation of a carbonium ion, it is not surprising that the operative acidity function is H_0 rather than H_R. The latter governs the *equilibrium* of the alcohol–carbonium ion reaction and differs in form from H_0 by containing a water activity term. It seems unlikely that the activity of water in the medium will alter the *rate* at which a water molecule is expelled

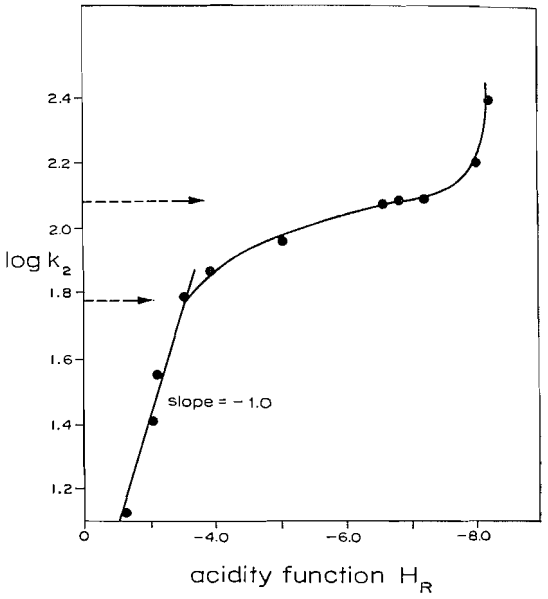

FIG. 5. Variation of the rate of permanganate oxidation of tri(*p*-tolyl) carbinol with H_R.

although it will clearly affect the equilibrium position of the system. In this connection Rocek (10) has shown that the rate of carbonium ion formation from 1-methylcyclohexanol is governed by H_0. Further information on this point was obtained by measuring the rate of ionization of *p*-methoxybenzhydrol under conditions that were as close as possible to those used for the oxidation process. Unfortunately the high concentration of alcohol required to measure the rate and degree of ionization of this alcohol at acidities so far from its pK_{R+} value, precluded the use of a purely aqueous system. The rates of ionization of 4-methoxybenzhydrol were accordingly determined in 70 vol% aqueous methanol containing sulfuric acid ranging from 1.8 to 3.6 *M*. The reaction was found to be of first-order in carbinol concentration. The following first-order rate expression was used to obtain the rate constants

$$kt = 2.303 \log \frac{A_\infty}{A_\infty - A_t}$$

where A_∞ = absorbance at infinite time, and A_t = absorbance at time t, at the wavelength maximum for the carbonium ion, 466 mμ. Log $(A_\infty - A_t)$ was plotted against time and the rate constants calculated from the slopes of the lines. A typical rate plot is shown in Fig. 6.

Can. J. Chem. Downloaded from www.nrcresearchpress.com by 210.87.254.42 on 09/05/12
For personal use only.

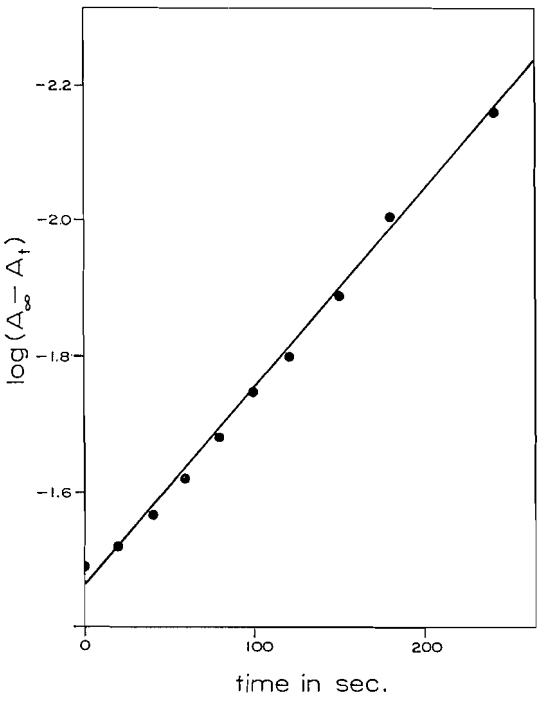

FIG. 6. Rate of ionization of *p*-methoxybenzhydrol in 70 vol% aqueous methanol containing sulfuric acid, 25°. $H_0 = -0.38$, $[H_2SO_4] = 2.16$, [*p*-methoxybenzhydrol] = 6.0. $k_1 = 5.99 \times 10^{-3}\ s^{-1}$.

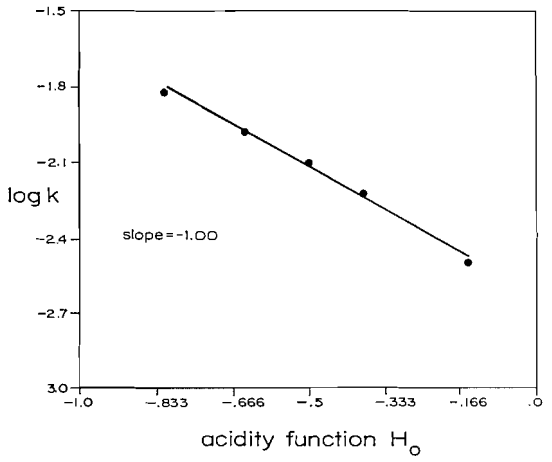

FIG. 7. The variation of the rate of ionization of *p*-methoxybenzhydrol with H_0; correlation coefficient, 0.998.

In Fig. 7 the logarithm of the ionization rate for *p*-methoxybenzhydrol in 70 vol% aqueous methanol is plotted against the acidity function H_0. A straight line of slope −1.00 with a correlation coefficient of 0.998 is obtained by this means whereas the use of the function H_R gives a considerably less satisfactory relation (slope = −0.48, correlation coefficient 0.990). The rate of ionization of 4-methoxybenzhydrol is close to this compound's rate of oxidation by permanganate when these measurements are made in solutions of the same acidity. For an H_0 of −0.81 the two rates are $1.55 \times 10^{-2}\ s^{-1}$ for the ionization (in 70 vol% aqueous methanol) and $1.79 \times 10^{-2}\ s^{-1}$ for the oxidation (in water).

The isotope effect for the permanganate oxidation of $(C_6H_5)_2CDOH$ at 25° is 7.3 at pH 7.00 (where the reaction is second-order) (1), but is only 1.08 in the region between $H_0 = -0.50$ and −1.22 (where the reaction is first-order). This, too, is consistent with the ionization reaction being the rate-controlling step of the oxidation.

Overall Reaction Path

The following path accounts for the oxidation of secondary aromatic alcohols by permanganate in aqueous sulfuric acid

$$Ar_2CHOH + H^+ \rightarrow Ar_2CH^+ + H_2O \quad \text{slow}$$

$$Ar_2CH^+ + MnO_4^- \rightarrow \text{products} \quad \text{fast}$$

A permanganate ester, $Ar_2CH—O—MnO_3$, is likely the first intermediate formed in the fast steps that lead to product.

The tertiary alcohols follow a similar course with the decomposition of the permanganate ester probably involving rearrangement of an aryl group, followed by hydrolysis

$$Ar_3C—O—MnO_3 \longrightarrow \left[Ar_2C{=}\overset{\diagdown\ \diagup}{O}{\cdots}MnO_3\right]^{\ddagger} \longrightarrow Ar_2C{=}\overset{+}{O}—Ar + MnO_3^-$$

$$Ar_2C{=}\overset{+}{O}—Ar \xrightarrow{H_2O} Ar_2\overset{OH}{\overset{|}{C}}—OAr \longrightarrow Ar_2C{=}O + ArOH$$

Can. J. Chem. Downloaded from www.nrcresearchpress.com by 210.87.254.42 on 09/05/12
For personal use only.

It is conceivable that the permanganate esters of secondary aromatic alcohols also decompose by a 1,2-rearrangement step in which hydride ion is transferred from carbon to oxygen or in which hydrogen is transferred to the oxygen of the ester via a cyclic 5-membered transition state. Alternatively, the decomposition may proceed by proton loss to a water molecule and expulsion of MnO_3^-. This general question is discussed in greater detail in the accompanying paper on chromium(VI) oxidations. A 1-equivalent step has been considered distinctly possible in the base-promoted permanganate oxidation of alcohols (3, 4) and for the secondary alcohols, at least, it cannot be ruled out for the acid-promoted reaction. Four possibilities, three 2-equivalent and one 1-equivalent routes, are given below. (Since this step follows the rate-controlling step it is difficult to distinguish between these possibilities.)

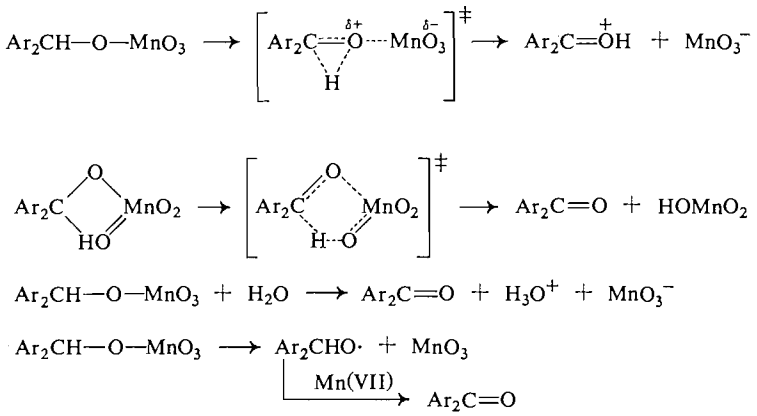

Effect of Substituents

The effect of substituents on the oxidation of the secondary alcohols is shown by the plot in Fig. 8 in which σ^+ substituent constants are used (11). The Hammett rho value of -1.02 and the excellent correlation with σ^+ support the idea that the rate-controlling step is ionization of the carbinol.

The effect of substituents on the rate of oxidation of the tertiary aromatic alcohols is shown in Fig. 9. As in the case of the secondary alcohols an excellent correlation is obtained when σ^+ is used. The rho value of -1.39 is also consistent with an ionization process, the larger value probably reflecting a higher degree of bond-breaking in the transition state.

In the case of tri(*p*-tolyl)carbinol the ionization step at intermediate acidities is faster than the decomposition of the ester as shown by the observations that the reaction is first-order in both alcohol and permanganate and is governed by the H_R acidity function (Fig. 5). The pK_{R+} of this alcohol is -3.56 (9) and the levelling-off of the rate above $H_R = -4$ doubtless reflects the fact that the ionization equilibrium has moved towards completion, although the curve shown in Fig. 5 does not duplicate exactly the ionization curve expected for this alcohol. The sharp rise in rate beyond an H_R of -7.2 (52% sulfuric acid) is

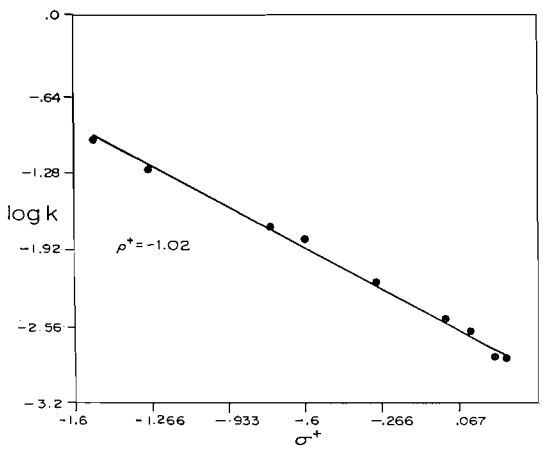

FIG. 8. The effect of substituents on the rate of the permanganate oxidation of diarylcarbinols, $H_0 = -0.81$; correlation coefficient, 0.998.

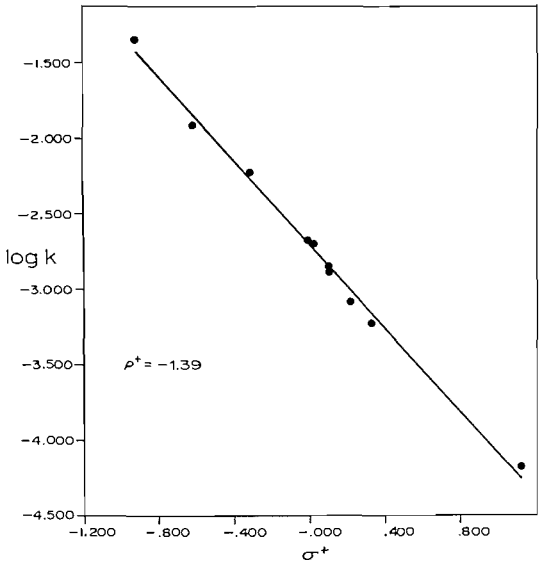

FIG. 9. The effect of substituents on the rate of the permanganate oxidation of triarylcarbinols, $H_0 = -0.65$; correlation coefficient, 0.998.

probably caused by formation of the powerful oxidant, permanganic acid, which is half-ionized in 61% sulfuric acid (5).

In the case of triphenylcarbinol the activation parameters for the oxidation at an H_0 of -1.00 are $\Delta H\dagger = 17.2$ kcal/mole and $\Delta S\dagger = 11.7$ e.u. The temperature range over which these measurements were conducted was 15–40°.

Acknowledgments

The financial support of the National Research Council of Canada and the External Aid Office, Government of Canada, is gratefully acknowledged.

1. R. STEWART. J. Amer. Chem. Soc. **79**, 3057 (1957).
2. R. STEWART and R. VAN DER LINDEN. Discuss. Faraday Soc. 211 (1960).
3. R. STEWART. Oxidation mechanisms. W. A. Benjamin, Inc., New York. 1964. Chap. 5.
4. R. STEWART. *In* Oxidation in organic chemistry. K. B. Wiberg, *Editor*. Academic Press, Inc., New York. 1965. Chap. 1.
5. R STEWART and M. M. MOCEK. Can. J. Chem. **41**, 1160 (1963).
6. W. H. STARNES, JR. J. Amer. Chem. Soc. **89**, 3368 (1967); J. Amer. Chem. Soc. **90**, 1807 (1968).
7. M. M. WEI and R. STEWART. J. Amer. Chem. Soc. **88**, 1974 (1966).
8. M. A. PAUL and F. A. LONG. Chem. Rev. **57**, 1 (1957).
9. N. C. DENO, H. E. BERKHEIMER, W. L. EVANS, and H. L. PETERSON. J. Amer. Chem. Soc. **81**, 2344 (1959). N. C. DENO, J. J. JARUZELSKI, and A. SCHRIESHEIM. J. Org. Chem. **19**, 155 (1954).
10. J. ROCEK. Colloq. Czech. Chem. Commun. **25**, 375 (1960).
11. H. C. BROWN and Y. OKAMOTO. J. Amer. Chem Soc. **80**, 4979 (1950).
12. A. I. VOGEL. Practical organic chemistry. Long mans, Green and Co., Ltd., London. 1964.
13. R. STEWART, M. R. GRANGER, R. B. MOODIE, and L. J. MUENSTER. Can. J. Chem. **41**, 1065 (1963).

Can. J. Chem. Downloaded from www.nrcresearchpress.com by 210.87.254.42 on 09/05/12
For personal use only.

Can. J. Chem. Downloaded from www.nrcresearchpress.com by 210.87.254.5 on 09/05/12
For personal use only.

Chromic acid oxidation of aromatic alcohols[1]

ROSS STEWART AND FARIZA BANOO[2]
Department of Chemistry, University of British Columbia, Vancouver 8, British Columbia

Received March 13, 1969

The mechanism of the chromic acid oxidation of di- and tri-aryl carbinols has been studied in 80 wt% acetic acid containing sulfuric acid. The reactions are cleanly second-order and give benzophenones in the case of the secondary alcohols and benzophenones plus phenols in the case of the tertiary alcohols. Electron-donating substituents in the tertiary alcohol appear predominantly in the phenol component and the rate-controlling step is believed to be a 1,2-aryl shift. The reaction constant for the migration is $\rho^+ = -1.44$ and that for the overall reaction is $\rho^+ = -0.879$. The presence of manganous ions does not alter these values although it lowers the overall rate of reaction. Although an analogous 1,2-hydride shift mechanism can be written for the oxidation of the secondary alcohols, there are enough points of difference between the oxidations of the secondary and tertiary systems to make this appear unlikely.

Canadian Journal of Chemistry, 47, 3207 (1969)

Introduction

The chromic acid oxidation of primary and secondary alcohols has been very extensively studied and is believed by most workers in the field to proceed via a chromate ester whose decomposition may proceed either by proton loss to the solvent or by an internal hydrogen shift (1–4). Tertiary alcohols which can be dehydrated to alkenes often suffer oxidation via the alkenes. Those which cannot be dehydrated undergo oxidative cleavage, triphenylcarbinol producing benzophenone. Bartlett and Cotman (5) showed that *p*-nitrotriphenylcarbinol gives *p*-nitrobenzophenone and they considered the reaction pathway to involve rearrangement of a phenyl group to electron deficient oxygen. Cleavage products also appear in the case of the secondary alcohol, phenyl *t*-butyl carbinol (6, 7) which gives a 60–70% yield of benzaldehyde and *t*-butyl alcohol, phenyl *t*-butyl ketone being the minor product.

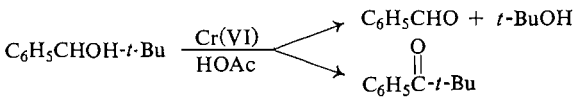

The cleavage reaction can be virtually eliminated, however, by the addition of manganous or cerous ions to the system. These ions scavenge chromium(IV) and chromium(V) intermediates (1, 6–8) and it is clear that the cleavage is not caused by chromium(VI).

In order to learn more about the mode of the chromic acid cleavage of tertiary aromatic alcohols we have examined the reaction kinetics, the effect of substituents, and the product distribution in a series of triarylcarbinols. A similar study of an analogous series of diarylcarbinols was made for the purposes of comparison.

Experimental

The preparation of the alcohols is described elsewhere (9*a*). The reaction rates were followed spectrophotometrically, essentially as previouly described (9*b*). A 3:2 ratio of alcohol to Cr(VI) was used for the secondary alcohols. Because of the lower acidities used with the tertiary alcohols and because of the production of phenol, which is subject to some degradation, a considerable excess of tertiary alcohol was used and the second-order rate constants obtained by correction. The extinction coefficient of Cr(VI) at 350 mμ is 3.33×10^3 whereas that of $(C_6H_5)_3C^+$ at the same wavelength is 1.03×10^2; hence the change of concentration of $(C_6H_5)_3C^+$ (and the other triaryl cations) will have only a small effect on the decrease in absorbance at 350 mμ. In a typical run, 10 μl of 0.14 *M* potassium dichromate was added by syringe to 2 ml of a solution made by mixing 80 wt% acetic acid and the required quantity of 99.9% sulfuric acid and containing 2.3×10^{-3} *M* benzhydrol.

Product Analysis

The secondary alcohols gave nearly quantitative yields of ketones. In the case of 4-methylbenzhydrol a yield of 96.4% of ketone was obtained and the small amount of oily residue showed no absorption bands characteristic of benzaldehyde, the product that would be formed if aryl migration occurred instead of hydrogen loss.

With the tertiary alcohols a weighed quantity (0.001 mole) of the carbinol under investigation was dissolved in 85 ml of 80 wt% aqueous acetic acid and 15 ml of 99.9% sulfuric acid was added slowly and with stirring. This gave a solution containing approximately 23% sulfuric acid. Next, 0.10 g potassium dichromate (a slight excess) dissolved in 3 ml of 80 wt% acetic acid in water

[1]Taken in part from the Ph.D. Thesis of Fariza Banoo, University of British Columbia, 1968.
[2]Colombo Plan Scholar, on leave of absence from the East Regional Laboratories, P.C.S.I.R., Pakistan.

TABLE I

Analysis of chromic acid oxidation products

Substituted triphenylcarbinols	Benzophenones	Molar ratio of benzophenones (*a*) without Mn^{++} (*b*) with Mn^{++}
A 4,4′-diMe	(*i*) 4,4′-diMe (*ii*) 4-Me	(*ii*)/(*i*) (*a*) 6.60 (*b*) 6.55
B 4-Me	(*i*) 4-Me (*ii*) Unsubstituted	(*ii*)/(*i*) (*a*) 1.70 (*b*) 1.72
C 4-Cl	(*i*) 4-Cl (*ii*) Unsubstituted	(*ii*)/(*i*) (*a*) 0.38 (*b*) 0.37
D 4-NO_2	(*i*) 4-NO_2 (*ii*) Unsubstituted	(*ii*)/(*i*) (*a*) 0.039 (*b*) 0.031
E 3-CF_3	(*i*) 3-CF_3 (*ii*) Unsubstituted	(*ii*)/(*i*) (*a*) 0.18 (*b*) 0.17
F 3-CF_3-4′-CH_3	(*i*) 3-CF_3 (*ii*) 3-CF_3-4′-CH_3 (*iii*) 4-CH_3	(*i*):(*ii*):(*iii*) (*a*) 3.1:1:0.34 (*b*) 3.0:1:0.35

containing 0.5 ml of 99.9% sulfuric acid was added. After standing for several days the mixture was diluted with water and extracted several times with ligroin. The extract was treated with dilute sodium bicarbonate solution to remove acid and then with 10% sodium hydroxide solution to remove the phenols. The ligroin extract was evaporated to dryness and the infrared (i.r.) spectrum of the residue was taken. The residue was then dissolved in a measured quantity of ether and the ether solution was analyzed by vapor-phase chromatography (v.p.c.). The exact quantities of each component of the products were determined by measuring the areas of the peaks and comparing them with those obtained from known quantities of the corresponding compounds.

The alkali washings of the ligroin extract were acidified with dilute hydrochloric acid and extracted with ether. The ether extract was analyzed for phenols by preparing the corresponding bromo-derivatives.

Acidity Functions

The solvent used for the oxidations and for the acidity function determinations was made by adding a known weight of 80 wt% aqueous acetic acid (80 g acetic acid and 20 g water) to a given weight of 99.99% sulfuric acid. The concentrations are expressed as wt% sulfuric acid and refer to that % of the solution weight that is contributed by the sulfuric acid. (A consequence of this procedure is that the % of acetic acid in the system varies somewhat as the sulfuric acid concentration changes.)

The H_0 and H_R values were determined by standard techniques using previously established values of pK_{BH}^+ and pK_R^+ of the indicators (10, 11). The results are given in Table II.

TABLE II

Acidity functions in 80 wt% acetic acid containing various concentrations of sulfuric acid

$\%H_2SO_4$	H_0*	H_R†
0.34	0.73	
0.85	0.46	
1.80	−0.02	
4.20	−0.27	
5.90	−0.75	−2.50
8.30	−1.12	−2.80
12.9	−1.68	−3.58
15.9		−4.08
18.0	−2.18	−4.40
22.7	−2.78	−4.83
26.7		−5.50
29.3	−3.38	−6.01
35.6	−4.03	−7.03
37.7		−7.26
39.6		−7.48
41.0	−4.50	
46.8	−5.25	
51.8	−5.67	

*Indicators: 4-nitroaniline, 3-methoxydiphenylamine, 3,4′-dichlorodiphenylamine, 3-nitrodiphenylamine, 4-nitrodiphenylamine, 2-nitrodiphenylamine.

†Indicators: tri(4-tolyl)carbinol, 4,4′-dimethoxytriphenylcarbinol, triphenylcarbinol, tri(4-chlorophenyl)carbinol.

Results and Discussion

Acidity Dependence

As with other alcohol–chromic acid systems that have been examined the kinetics are cleanly second-order, first-order in each of the alcohol and oxidant. (In the case of the tertiary alcohols deviations were apparent beyond 60% reaction; this is presumably due to some degradation of the phenol produced in the reaction.) The acid-catalysis of the oxidation of benzhydrol was similar to that found previously with isopropyl alcohol (9) i.e. a linear relation of unit slope between log k and H_0 up to an H_0 of approximately −1, fol-

Can. J. Chem. Downloaded from www.nrcresearchpress.com by 210.87.254.5 on 09/05/12
For personal use only.

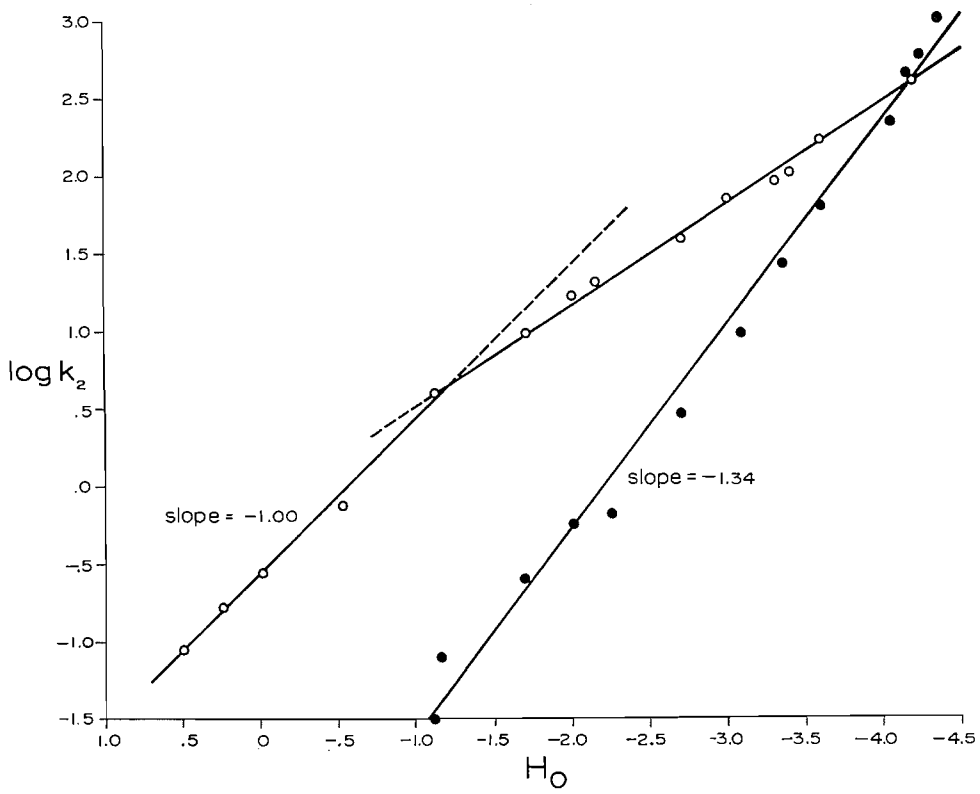

FIG. 1. Effect of acidity on the rate of the chromic acid oxidation of diphenylcarbinol (open circles) and triphenylcarbinol (closed circles).

lowed by a more gradual increase in rate as the acidity of the solution was increased (Fig. 1). The source of this effect, which is believed to be connected with ligand substitution on chromium, has been discussed previously (9). Curiously enough this effect is not present in the case of the tertiary alcohol, triphenylcarbinol. Indeed, the greater dependence of rate on acidity in this case causes the tertiary alcohol to be oxidized faster than the secondary alcohol at high acidities. (When H_R is used instead of H_0 a somewhat better straight line of slope -0.92 is obtained for triphenyl carbinol.)

Substituent Effects

Analysis of products showed that both the secondary and tertiary alcohols produced high yields of ketones, with phenols also being formed in the latter case. The cleavage which occurs with the tertiary alcohols produces mixtures of products when substituted triarylcarbinols are used and Table I gives the distribution of these products with various substituents. The tendency for electron-withdrawing substituents to be retained in the ketone, which is clearly apparent from the results in the table, suggests that a 1,2-shift to an electron-deficient atom is occurring in agreement with the early suggestion of Bartlett and Cotman (5). (In contrast, homolytic rearrangements of these systems have quite different migration aptitudes (5, 12).) On this basis the migration aptitudes for the various rings were calculated, with appropriate statistical corrections being made, and the results are given in Table III and plotted against σ^+ (13) in Fig. 2. The ρ^+ value for migration is -1.44 and this was not affected appreciably by the addition of manganous ions.

The effect of substituents on the overall rate of oxidation of diarylcarbinols is similar to that found with other secondary alcohols except that the reaction constant is lower, being -0.54 (Fig. 3). In the case of the tertiary alcohols the effect of substituents was best correlated with σ^+ (Fig. 4). The reaction constant for the oxidation, ρ^+, was found to be -0.879. In the presence of added

Can. J. Chem. Downloaded from www.nrcresearchpress.com by 210.87.254.5 on 09/05/12
For personal use only.

Can. J. Chem. Downloaded from www.nrcresearchpress.com by 210.87.254.5 on 09/05/12
For personal use only.

TABLE III

Migration aptitude of aryl groups in the chromic acid oxidation of triaryl carbinols

Aryl group	Relative migration aptitude, y	log y
C_6H_5-	1.00	0.000
4-$CH_3C_6H_4$-	3.35*	0.525
4-ClC_6H_4-	0.76	−0.143
3-$CF_3C_6H_4$-	0.36†	−0.444
4-$NO_2C_6H_4$-	0.078	−1.102

*Average of the values obtained with compounds A and B in Table I; 3.30 and 3.40, respectively. Compound F gave a value of 3.1.
†Compound F gave a value of 0.34.

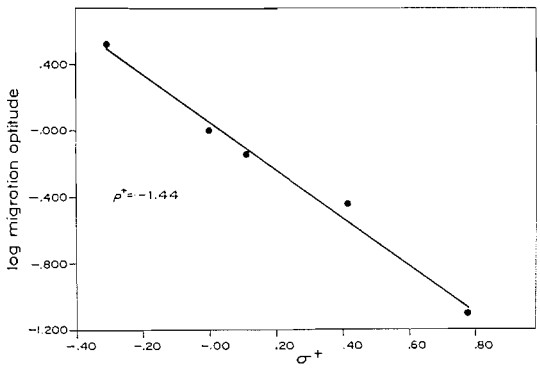

FIG. 2. Effect of substituents on the migration aptitude of aryl rings in the chromic acid oxidation of triarylcarbinols.

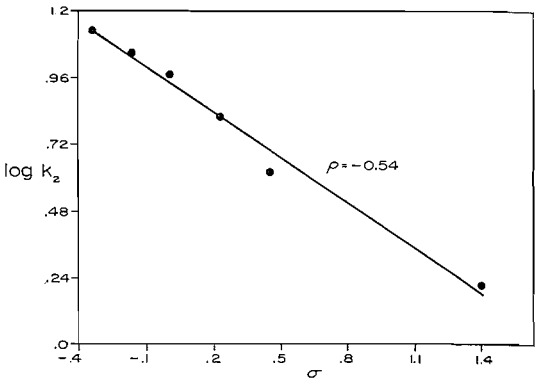

FIG. 3. Effect of substituents on the rate of the chromic acid oxidation of diarylcarbinols in 80 wt% aqueous acetic acid at 25°, $H_0 = -1.70$, correlation coefficient, 0.993. Substituents are from upper left to lower right: 4,4′-dimethyl, 4-methyl, none, 4-chloro, 4,4′-dichloro, 2,4,6,2′,4′,6′-hexamethyl. The latter's σ was calculated using the pK_{HA} of mesitoic acid.

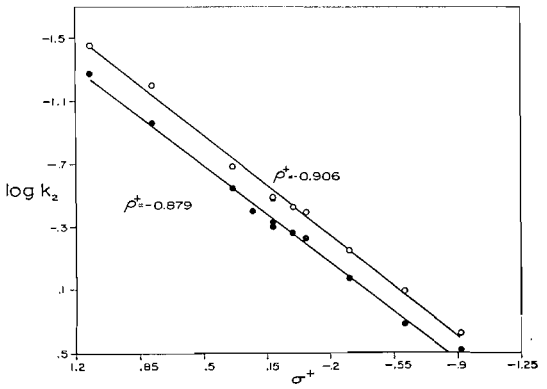

FIG. 4. Effect of substituents on the rate of the chromic acid oxidation of triarylcarbinols. Open circles, manganous ion present; closed circles, manganous ion absent.

manganous ions, an almost uniform reduction in rate was observed for all the tertiary alcohols (Table IV), the ρ^+ value, −0.906, being almost identical with that found in the absence of manganous ions. The cleavage reaction, which evidently occurs via a 1,2-shift of an aryl group, thus takes place in the same way whether chromium(VI) or chromium ions of intermediate valence are the active oxidants.

Mechanism

The mechanism of the chromium(VI) oxidation of triarylcarbinols to substituted benzophenones and phenols can be written as follows

$$Ar_3COH + H_2CrO_4 + H^+ \rightleftarrows Ar_3C{-}O{-}CrO_3H_2^+ + H_2O$$

$$Ar_3C{-}O{-}CrO_3H_2^+ \rightarrow \left[Ar_2C\overset{\delta+}{\underset{Ar}{\cdots}}O\cdots CrO_3H_2^{\delta+}\right] \rightarrow Ar_2C{=}\overset{+}{O}{-}Ar + H_2CrO_3$$

transition state

$$Ar_2C{=}\overset{+}{O}{-}Ar + H_2O \rightarrow Ar_2C{=}O + ArOH + H^+$$

Can. J. Chem. Downloaded from www.nrcresearchpress.com by 210.87.254.5 on 09/05/12
For personal use only.

The effects of substituents and acidity on the rate of the oxidation are in agreement with the above path. Preferential migration of rings containing electron-donating substituents is expected and is found, although the influence of substituents on migration aptitude[3] is somewhat smaller than that found in the analogous acid-catalyzed rearrangement of triarylmethyl hydroperoxides (14)

$$Ar_3C{-}O{-}OH + H^+ \rightleftarrows Ar_3C{-}O{-}\overset{+}{O}H_2 \rightarrow$$
$$Ar_2C{=}\overset{+}{O}Ar + H_2O \rightarrow Ar_2C{=}O + ArOH + H^+$$

The possibility that secondary and primary alcohols are oxidized by a similar mechanism, i.e. a 1,2-hydride shift to give the conjugate acid of benzophenone, should be considered. Such shifts occur with ease in many other systems (15).

TABLE IV

Chromic acid oxidation of triphenylcarbinol. Effect of substituents. $H_R = -3.95$, $T = 25°$

Substituent	$10^2 \times k_2$ 1 mole^{-1}s^{-1}	Mn^{2+} Present*
H	54.8	37.8
4-Me	108.2	71.4
4,4′-diMe	209.6	129.0
4,4,4′′-triMe	306.3	237.2
4-F	59.9	41.2
4-Cl	47.0	32.2
4,4′-diCl	39.8	
4,4′,4′′-triCl	28.6	20.7
3,3′,3′′-triCl	5.34	3.5
4-NO_2	11.1	8.0
3-CF_3,4′-Me	50.4	32.9

*3.045×10^{-4} M manganous acetate added.

$$Ar_2CHOH + H_2CrO_4 + H^+ \rightleftarrows Ar_2CH{-}O{-}CrO_3H_2^+ + H_2O$$

$$Ar_2CH{-}O{-}CrO_3H_2^+ \rightarrow Ar_2C\overset{\delta+}{\underset{H}{\cdots}}O\cdots CrO_3H_2 \rightarrow Ar_2C{=}\overset{+}{O}H + H_2CrO_3$$

Over most of the acidity range examined, benzhydrol is oxidized considerably faster than triphenylcarbinol and if the two pre-equilibrium steps are comparable, this would require a hydride shift to be faster than a phenyl shift. There is evidence that this order prevails in some, though not all, 1,2-shifts (15). On the whole, however, the weight of evidence is against a 1,2-hydride shift mechanism. First, a careful examination of the products of the oxidation of 4-methylbenzhydrol revealed no trace of 4-methylphenol. It seems unlikely that a hydride shift would be that much more facile than a 4-methylphenyl shift. (It was not possible to study alkoxybenzhydrols under the same conditions as were used for the other carbinols because complex formation between the alkoxy group and chromium(VI) occurs.) Second, the dependence of the oxidation rate on acidity is sufficiently different for secondary and tertiary aromatic alcohols (Fig. 1) as to suggest different reaction paths. (The effect of substituents also shows an important difference—the secondary alcohols follow ρ and the tertiary alcohols follow ρ^+—but this may simply be due to the participation of the substituent in the migrating ring in the latter case.) Third, the activation parameters are rather different for the chromic acid oxidation of the two kinds of alcohol. At an H_R of -3.95, the activation parameters for the oxidation of triphenylcarbinol are $\Delta H\dagger = 11.8$ kcal mole^{-1} and $\Delta S\dagger = -25.1$ e.u., whereas for benzhydrol at $H_R = -2.62$ the values are $\Delta H\dagger = 5.9$ kcal mole^{-1} and $\Delta S\dagger = -37.1$ e.u. (The weight to be attached to this factor is uncertain since significant variations in these quantities can occur even with secondary alcohols (16).)

We conclude that tertiary aromatic alcohols are oxidized by means of a 1,2-aryl shift (5) but that primary and secondary alcohols undergo some other form of carbon–hydrogen bond rupture involving, we would suggest, the 5-membered transition state that has been previously favored (2, 3, 17). The two transition states are shown below

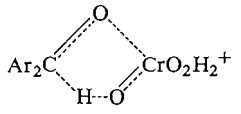

2° alcohol

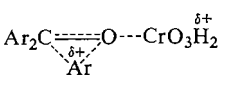

3° alcohol

[3]A referee has made the interesting suggestion that the higher ρ^+ for migration than for reaction may be due to partial equilibration of bridged ions after the rate-controlling step.

Acknowledgments

The financial support of the National Research Council of Canada and the External Aid Office, Government of Canada, is gratefully acknowledged.

1. K. B. WIBERG. *In* Oxidation in organic chemistry. *Edited by* K. B. Wiberg. Academic Press, Inc., New York. 1965. Chap. 2.
2. R. STEWART. Oxidation mechanisms. W. A. Benjamin, Inc., New York. 1964. Chap. 4.
3. D. G. LEE and R. STEWART. J. Org. Chem. **32**, 2868 (1967).
4. K. B. WIBERG and H. SCHAFER. J. Amer. Chem. Soc. **89**, 455 (1967).
5. P. D. BARTLETT and J. D. COTMAN. J. Amer. Chem. Soc. **72**, 3095 (1950).
6. J. J. CAWLEY and F. H. WESTHEIMER. J. Amer. Chem. Soc. **85**, 1771 (1963).
7. J. HAMPTON, A. LEO, and F. H. WESTHEIMER. J. Amer. Chem. Soc. **78**, 306 (1956).
8. J. ROCEK and A. E. RADKOWSKY. J. Amer. Chem. Soc. **90**, 2986 (1968).
9. (*a*) F. BANOO and R. STEWART. Accompanying paper. (*b*) D. G. LEE and R. STEWART. J. Amer. Chem. Soc. **86**, 3051 (1964).
10. D. DOLMAN and R. STEWART. Can. J. Chem. **45**, 903 (1967).
11. N. C. DENO, J. J. JARUZELSKI, and A. SCHRIESHEIM. J. Amer. Chem. Soc. **77**, 3044 (1955).
12. W. H. STARNES, JR. J. Amer. Chem. Soc. **90**, 1807 (1968).
13. H. C. BROWN and Y. OKAMOTO. J. Amer. Chem. Soc. **80**, 4979 (1958).
14. D. E. BISSING, C. A. MATUSZAK, and W. E. MCEWEN. J. Amer. Chem. Soc. **86**, 3824 (1964).
15. C. J. COLLINS. Quart. Rev. **14**, 357 (1960).
16. J.-C. RICHER and CLAUDE GILARDEAU. Can. J. Chem. **43**, 538 (1965).
17. R. STEWART and D. G. LEE. Can. J. Chem. **42**, 439 (1964).

Can. J. Chem. Downloaded from www.nrcresearchpress.com by 210.87.254.5 on 09/05/12
For personal use only.

Can. J. Chem. Downloaded from www.nrcresearchpress.com by 210.87.254.105 on 09/05/12
For personal use only.

Large heterocyclic rings from carbohydrate precursors

J. F. STODDART, W. A. SZAREK, AND J. K. N. JONES
Department of Chemistry, Queen's University, Kingston, Ontario

Received April 2, 1969

Periodate oxidation of cycloheptaamylose and cyclohexaamylose, followed by borohydride reduction and acetylation, yields 2*s*,4*S*,5*R*,7*s*,9*S*,10*R*,12*s*,14*S*,15*R*,17*s*,19*S*,20*R*,22*s*,24*S*,25*R*,27*s*,29*S*,30*R*,32*s*,34*S*,-35*R*-heneicosaacetoxymethyl-1,3,6,8,11,13,16,18,21,23,26,28,31,33-tetradecaoxacyclopentatriacontane (**2**) and 2*s*,4*S*,5*R*,7*s*,9*S*,10*R*,12*s*,14*S*,15*R*,17*s*,19*S*,20*R*,22*s*,24*S*,25*R*,27*s*,29*S*,30*R*-octadecaacetoxymethyl-1,3,6,8,11,13,16,18,21,23,26,28-dodecaoxacyclotriacontane (**5**), respectively. Both molecules are achiral.

L'oxydation périodique du cycloheptaamylose et du cyclohexaamylose, suivie de réduction au borohydrure, puis d'acétylation, conduit respectivement au 2*s*,4*S*,5*R*,7*s*,9*S*,10*R*,12*s*,14*S*,15*R*,17*s*,19*S*,20*R*,-22*s*,24*S*,25*R*,27*s*,29*S*,30*R*,32*s*,34*S*,35*R*-heneicosaacetoxymethyl-1,3,6,8,11,13,16,18,21,23,26,28,31,33-tetradecaoxacyclopentatriacontane (**2**) et au 2*s*,4*S*,5*R*,7*s*,9*S*,10*R*,12*s*,14*S*,15*R*,17*s*,19*S*,20*R*,22*s*,24*S*,25*R*,-27*s*,29*S*,30*R*-octadecaacetoxymethyl-1,3,6,8,11,13,16,18,21,23,26,28-dodecaoxacyclotriacontane (**5**). Ces deux molécules sont achirales.

Canadian Journal of Chemistry, 47, 3213 (1969)

Recently, it has been shown (1) that periodate oxidation of di-β-D-ribofuranose 1,5′:1′,5-dianhydride (1–5), followed by borohydride reduction and acetylation yields 2*R*,4*S*,7*R*,9*S*-tetraacetoxymethyl-1,3,6,8-tetraoxacyclodecane. During this investigation, it was appreciated that the same sequence of reactions employed on the Schardinger dextrins (6)[1] would provide a route to the synthesis of large heterocyclic rings.

When cycloheptaamylose (**1**) was subjected to periodate oxidation (7), followed by borohydride reduction and acetylation (1, 8), a crystalline compound was obtained in 11% yield. The expected product from this reaction sequence is a cyclic acetal (**2**) with 14 oxygen atoms and 21 carbon atoms in a 35-membered ring. Examination of the symmetry properties of **2** shows that it has seven σ planes which intersect at a C_7 axis. Thus, the molecule belongs to point group $\mathbf{C}_{7v}$ and is achiral. The observation that the crystalline compound is optically inactive suggests that it is indeed 2*s*,4*S*,5*R*,7*s*,9*S*,-10*R*,12*s*,14*S*,15*R*,17*s*,19*S*,20*R*,22*s*,24*S*,25*R*,27*s*,-29*S*,30*R*,32*s*,34*S*,35*R*-heneicosaacetoxymethyl-1,3,6,8,11,13,16,18,21,23,26,28,31,33-tetradecaoxacyclopentatriacontane (**2**). In addition, elemental analysis, acetyl content, molecular weight, and infrared (i.r.) and proton magnetic resonance (p.m.r.) spectral data are all consistent

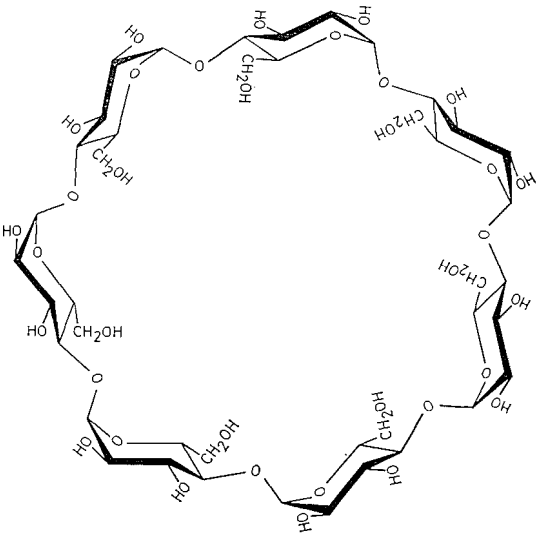

1

with this structural formulation. A low field 7-proton triplet in the p.m.r. spectrum between τ 4.63–5.04 (*J* 4.0 Hz) was assigned to the equivalent acetal protons at C-2,7,12,17,22,27, and 32. De-*O*-acetylation of **2** yielded 2*s*,4*S*,5*R*,7*s*,9*S*,-10*R*,12*s*,14*S*,15*R*,17*s*,19*S*,20*R*,22*s*,24*S*,25*R*,27*s*,-29*S*,30*R*,32*s*,34*S*,35*R*-heneicosahydroxymethyl-1,3,6,8,11,13,16,18,21,23,26,28,31,33-tetradecaoxacyclopentatriacontane (**3**), which was also optically inactive and gave a satisfactory elemental analysis. Mild acid hydrolysis of **3**, followed by

[1]The Schardinger dextrins provide additional examples (11) of molecules having $\mathbf{C}_n$ symmetry of an order higher than two. For example, cyclohexaamylose and cycloheptaamylose belong to point groups $\mathbf{C}_6$ and $\mathbf{C}_7$, respectively.

Can. J. Chem. Downloaded from www.nrcresearchpress.com by 210.87.254.105 on 09/05/12
For personal use only.

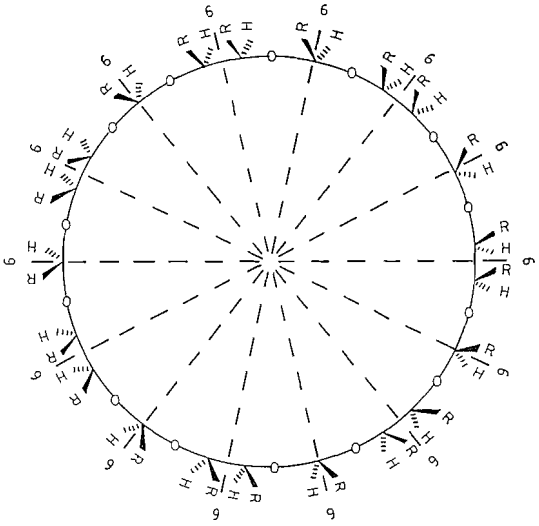

2 R = CH_2OAc
3 R = CH_2OH

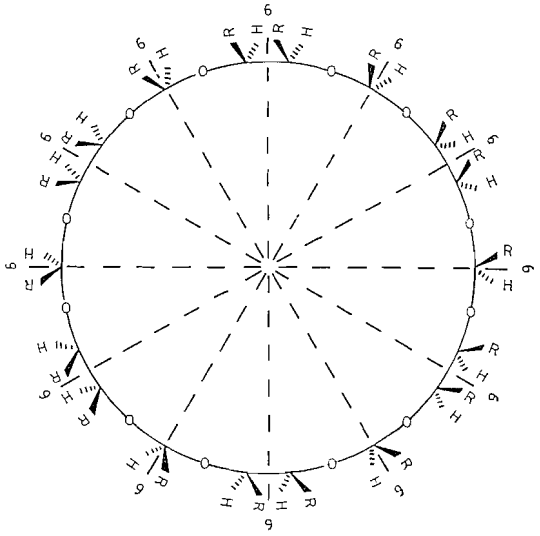

5 R = CH_2OAc

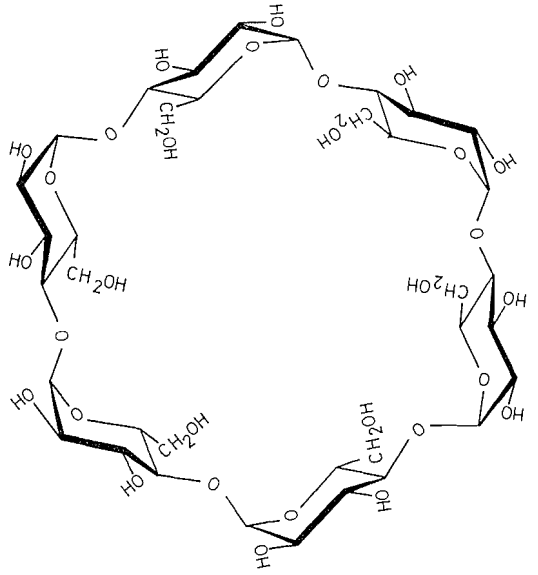

4

borohydride reduction of the products gave erythritol and ethylene glycol.

Examination of the symmetry properties of the cyclic acetal (**5**) with 12 oxygen atoms and 18 carbon atoms in a 30-membered ring, obtained after borohydride reduction and acetylation of periodate-oxidized (7) cyclohexaamylose (**4**), shows that it has six σ planes which intersect at a C_6 axis (point group $\mathbf{C}_{6v}$) and is therefore achiral. Indeed, the crystalline product (**5**) is optically inactive. All other physical and analytical data are consistent with the formulation of the structure as 2*s*,4*S*,5*R*,7*s*,9*S*,10*R*,12*s*,14*S*,15*R*,17*s*, 19*S*, 20*R*, 22*s*, 24*S*, 25*R*, 27*s*, 29*S*, 30*R*-octadecaacetoxymethyl-1,3,6,8,11,13,16,18,21,23,26,28-dodecaoxacyclotriacontane (**5**).

Experimental

Melting points are uncorrected and were determined with a Fisher–Johns apparatus. Optical rotations were measured using a Perkin–Elmer model 141 automatic polarimeter at 23 ± 2°. Molecular weights were determined in chloroform using a Mechrolab vapor pressure osmometer model 301A. Solvent calibration (9) was achieved using tetra-*O*-acetyl-β-D-ribofuranose 1,5′:1′,5-dianhydride (mol. wt. 432) (1–5) and tetra-*O*-benzoyl-β-D-ribofuranose 1,5′:1′,5-dianhydride (mol. wt. 681).[2] Paper chromatography was carried out on Whatman No. 1 paper using the following solvent systems (v/v):

[2]The tetrabenzoate was prepared[3] from di-β-D-ribofuranose 1,5′:1′,5-dianhydride in the usual manner. Recrystallization from ethanol yielded needle-shaped crystals, m.p. 219–220°, $[\alpha]_D$ +12.0° (*c*, 1.12 in chloroform). Elemental analysis and i.r. and p.m.r. spectroscopic data were consistent with the compound being tetra-*O*-benzoyl-β-D-ribofuranose 1,5′:1′,5-dianhydride.

[3]P. A. Lockwood, J. F. Stoddart, and W. A. Szarek. Unpublished results.

Can. J. Chem. Downloaded from www.nrcresearchpress.com by 210.87.254.105 on 09/05/12
For personal use only.

(*a*) benzene – butan-1-ol–pyridine–water (1:5:3:3, upper layer); (*b*) butan-1-ol–ethanol – water (4:1:5, upper layer). Sugars were detected with the periodate–permanganate spray reagent (10). Thin-layer chromatography (t.l.c.) was carried out on glass microplates (40 × 90 mm) coated with silica gel (Camag) using the following solvent systems (v/v): (*c*) chloroform – methanol (19:1); (*d*) ethyl acetate – petroleum ether (b.p. 60–80°) (1:1). The developed plates were air-dried and heated at about 150°. Infrared spectra were recorded on a Beckman-IR5A spectrophotometer. Proton magnetic resonance spectra were measured at 60 MHz in chloroform-*d* with tetramethylsilane (τ 10.00) as internal standard.

2s,4S,5R,7s,9S,10R,12s,14S,15R,17s,19S,20R,22s,24S,-25R,27s,29S,30R,32s,34S,35R-Heneicosaacetoxymethyl-1,3,6,8,11,13,16,18,21,23,26,28,31,33-tetradecaoxacyclopentatriacontane (2)

Cycloheptaamylose (**1**) (4 g) was dissolved in water (125 ml) and a solution of sodium metaperiodate (5.8 g) in water (125 ml) was added. The reaction mixture was allowed to stand at 26° for 60 h. After excess of periodate and iodate had been precipitated by addition of a 10% aqueous barium chloride solution, sodium borohydride (2 g) was added to the filtered solution and the reaction mixture was allowed to stand at 26°. After 48 h, excess of borohydride was destroyed by addition of dry ice and the solution was concentrated to dryness. The residue was extracted twice (200 ml and then 100 ml) with boiling ethanol and the combined extracts were concentrated to a syrup, which was acetylated in the usual manner with acetic anhydride (60 ml) and pyridine (60 ml). After 18 h, the acetylation mixture was poured into ice water (1000 ml) and allowed to stand for 1 h before being extracted several times with chloroform. The chloroform extracts were combined, washed with water, dried over anhydrous sodium sulfate, filtered, and the filtrate concentrated to a syrup, which migrated as one spot on t.l.c. in solvents (*c*) and (*d*). On addition of ethanol, the syrup crystallized. Recrystallization from the same solvent yielded needle-shaped crystals of the title compound (**2**) (813 mg, 11%), m.p. 106–109°, $[\alpha]_D$ 0 ± 1° (*c*, 2.0 in chloroform); λ_{max} (Nujol) 5.75 μm (OAc), no absorption attributable to OH; p.m.r. data: τ 4.63–5.04 (7-proton triplet, *J* 4.0 Hz, H-2,7,12,17,22,27,32), τ 7.64–8.04 (63-proton multiplet, OAc groups on C-2,4,5,7,9,-10,12,14,15,17,19,20,22,24,25,27,29,30,32,34,35).

Anal. Calcd. for $C_{84}H_{126}O_{56}$ (mol. wt. 2032): C, 49.65; H, 6.25; CH_3CO, 43.2. Found (mol. wt. 2000 ± 50): C, 49.37; H, 6.19; CH_3CO, 42.6.

2s,4S,5R,7s,9S,10R,12s,14S,15R,17s,19S,20R,22s,24S,-25R,27s,29S,30R,32s,34S,35R-Heneicosahydroxymethyl-1,3,6,8,11,13,16,18,21,23,26,28,31,33-tetradecaoxacyclopentatriacontane (3)

The heneicosaacetate (**2**) (500 mg) was dissolved in chloroform (25 ml) and methanol (25 ml), and 2 drops of a 7% solution of sodium methoxide were added. The de-*O*-acetylation was followed by t.l.c. in solvent (*c*) and was complete after 3 h. Dry ice was added to the reaction mixture, the solution was filtered, and the filtrate was concentrated to a crystalline product. Recrystallization from ethanol yielded the title compound (**3**) (230 mg, 81%), m.p. 125–132°, $[\alpha]_D$ 0 ± 1° (**c**, 2.0 in water); λ_{max} (Nujol) 2.75–4.25 μm (OH), no absorption attributable to OAc.

Anal. Calcd. for $C_{42}H_{84}O_{35}$: C, 43.9; H, 7.37. Found: C, 43.5; H, 7.24.

The heneicosaalcohol (**3**) (50 mg) was hydrolyzed with 0.1 *N* sulfuric acid (20 ml) on a steam bath for 6 h. The cooled solution was neutralized with barium carbonate, filtered, and allowed to stand for 36 h after addition of sodium borohydride (50 mg). Excess of borohydride was destroyed by treatment with Amberlite IR-120 (H form) resin, followed by filtration, and concentration of the filtrate to a syrup after removal of borate ions as methyl borate. Paper chromatographic examination of the syrup in solvents (*a*) and (*b*) indicated the presence of erythritol and ethylene glycol. No glucose was detected.

2s,4S,5R,7s,9S,10R,12s,14S,15R,17s,19S,20R,22s,24S,-25R,27s,29S,30R-Octadecaacetoxymethyl-1,3,6,8,-11,13,16,18,21,23,26,28-dodecaoxacyclotriacontane (5)

Cyclohexaamylose (**4**) (2.84 g) was subjected to the same sequence of reactions as described for cycloheptaamylose (**1**) to yield the title compound (**5**) (35 mg, 0.6%), m.p. 162–164°, $[\alpha]_D$ 0 ± 1° (*c*, 2.0 in chloroform); λ_{max} (Nujol) 5.75 μm (OAc), no absorption attributable to OH; p.m.r. data: τ 4.65–5.03 (6-proton triplet, *J* 4.5 Hz, H-2,7,12,17,22,27), τ 7.70–8.06 (54-proton multiplet, OAc groups on C-2,4,5,7,9,10,12,14,15,17,19,20,22,24,-25,27,29,30).

Anal. Calcd. for $C_{72}H_{108}O_{48}$ (mol. wt. 1742): C, 49.65; H, 6.25; CH_3CO, 43.2. Found (mol. wt. 1760 ± 40): C, 49.26; H, 6.22; CH_3CO, 43.2.

Acknowledgments

These investigations were supported by grants from the National Research Council of Canada. The authors wish to express their thanks to Dr. D. French of Iowa State University for providing a sample of cycloheptaamylose and to Dr. A. G. Harrison of the University of Toronto for his attempts to obtain mass spectrometric data for **2**.

1. J. F. Stoddart and W. A. Szarek. Can. J. Chem. **46**, 3061 (1968).
2. H. Bredereck, M. Köthing, and E. Berger. Chem. Ber. **73**, 956 (1940).
3. G. R. Barker and M. V. Lock. J. Chem. Soc. 23 (1950).
4. R. W. Jeanloz, G. R. Barker, and M. V. Lock. Nature, **167**, 42 (1951).
5. H. B. Wood, Jr., H. W. Diehl, and H. G. Fletcher, Jr. J. Am. Chem. Soc. **78**, 4715 (1956).
6. D. French. Advan. Carbohydrate Chem. **12**, 189 (1957).
7. D. French and R. L. McIntyre. J. Am. Chem. Soc. **72**, 5148 (1950).
8. J. K. Hamilton, G. W. Huffman, and F. Smith. J. Am. Chem. Soc. **81**, 2173, 2176 (1959).
9. R. H. Müller and H. J. Stolten. Anal. Chem. **25**, 1103 (1953).
10. R. U. Lemieux and H. F. Bauer. Anal. Chem. **26**, 920 (1954).
11. K. Mislow. Introduction to stereochemistry. W. A. Benjamin, Inc., New York. 1966. p. 26.

Can. J. Chem. Downloaded from www.nrcresearchpress.com by 210.87.254.105 on 09/05/12
For personal use only.

Study of the exchange rates of ethanol and water on ferriprotoporphyrin IX by n.m.r. line broadening

N. S. ANGERMAN, B. B. HASINOFF, H. B. DUNFORD, AND R. B. JORDAN
Department of Chemistry, University of Alberta, Edmonton, Alberta

Received January 6, 1969

The nuclear magnetic resonance (n.m.r.) line broadening technique has been used to determine the rate of solvent exchange from the first coordination sphere of ferriprotoporphyrin IX (hemin) in aqueous ethanol. The line broadenings of the methyl and methylene protons of ethanol and the water protons have been studied as a function of solvent composition at 35° and of temperature in 48.8 mole % ethanol.

The average values of the kinetic parameters for ethanol molecule exchange, taken from the CH_3 and CH_2 proton broadening are $\Delta H^{\ddagger} = 6.2 \pm 1.0$ kcal mole^{-1} and $\Delta S^{\ddagger} = -9.1 \pm 4.4$ cal mole^{-1} deg^{-1}. Both proton transfer and water molecule exchange contribute to the water proton line broadening with a net value of $\Delta H^{\ddagger} = 6.3 \pm 0.5$ kcal mole^{-1} and $\Delta S^{\ddagger} = -3.8 \pm 2.0$ cal mole^{-1} deg^{-1}.

From the n.m.r. study at varying solvent composition, it is concluded that monomeric and dimeric hemin undergo solvent exchange at the same rate. The equilibrium constant for formation of the mono-ethanol solvated hemin from hydroxyhemin is determined as 8.7 at 35° from this study.

A comparison of the rate of ethanol exchange (1.8×10^6 s^{-1} at 25°) and the rate of imidazole binding to hemin (from a separate temperature jump study) indicates that the imidazole substitution occurs through an S_N1 ion pair mechanism.

Canadian Journal of Chemistry, 47, 3217 (1969)

Introduction

Ferriprotoporphyrin IX (Fig. 1) is the prosthetic group of a number of heme proteins including hemoglobin, myoglobin, horseradish peroxidase and catalase. We shall henceforth use the simpler name hemin for ferriprotoporphyrin IX. Four of the coordination positions of iron(III) in hemin are occupied by the dianionic porphyrin ring so that there is a formal charge of +1 on the ferric ion. Because of the two propionate side chains the net charge on the molecule is −1. The remaining fifth and sixth coordination positions, which are *trans* to each other above and below the plane of the porphyrin ring, are occupied by solvent molecules. It should be noted that X-ray crystallographic studies (1) have shown that the iron atom (high spin) in porphyrins is above the plane of the four nitrogen atoms and is five coordinate. However the fact that dimidazole (2) and dipyridine (3, 4) complexes are formed by hemin indicates that in solution, the iron atom in hemin is best considered as six coordinate.

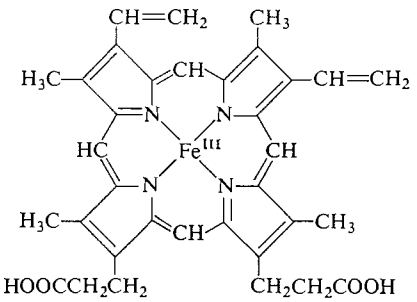

FIG. 1. Ferriprotoporphyrin IX or hemin.

It has been shown previously by Maehly and Akeson (5) that hemin exists as a dimer in aqueous solution. The same authors found that addition of ethanol causes the dimer to dissociate and that the complex is almost completely monomeric in 50 volume % ethanol. These observations have been confirmed by the polarographic study of Davis and Martin (4). Thus complications due to dimer formation may be avoided by working in ethanol – water solutions.

In connection with a recent temperature jump study (2) of the exchange rate of imidazole on hemin, it became of interest to study the linewidths of the solvent n.m.r. resonances as a function of solvent composition and temperature. The n.m.r. results may be used to characterize the solvated species and to determine the exchange rate of the solvent molecules from the paramagnetic iron center in hemin.

The ethanol – water solvent system has been used in this and the temperature jump work (2). The n.m.r. line broadenings of water and the methyl and methylene proton resonances of ethanol have been studied. The linewidths were observed as a function of solvent composition at 35° and the temperature dependence of the

line broadening was measured in 48.8 mole % ethanol between −40° and 70°. The results indicate that the monomer and dimer are kinetically indistinguishable, and the solvent exchange rates have been determined.

Experimental

In order to dissolve ferriprotoporphyrin IX (Eastman Organic Chemicals) it was necessary to wet the complex first with concentrated sodium hydroxide and then dilute the solution to the required volume and pH*[1]. The n.m.r. spectra were run on 5 samples in the concentration range $1.2_5 \times 10^{-3}$ to $5.0_0 \times 10^{-3}$ *M*. The line broadenings were found to vary linearly with the concentration of hemin. Shifts were measured from internal sodium 3-(trimethylsilyl)-1-propanesulfonate, (Eastman Organic Chemicals) which was dissolved at the minimum concentration for detection of the methyl resonance signal. The data were obtained at pH* 11, but it was found that the linewidths were independent of hydroxide ion concentration over the range 10^{-6} to 0.1 *M*.

The n.m.r. spectra were run on a Varian model A-56/60 spectrometer equipped with a standard variable temperature probe and temperature controller. All full linewidths at half height and chemical shifts were reproducible to ±2 Hz. A DuPont 310 curve resolver was used to separate the contribution of the water and ethanol to the hydroxy proton resonance.

Spectrophotometric measurements were made on a Cary Model 14 spectrophotometer equipped with variable temperature cell holders. The temperature was controlled to ±1° by rapidly flowing water from an external temperature bath.

Results

A spectrophotometric study was carried out to determine the monomer–dimer equilibrium constant. The extinction coefficients for the dimer and monomer were determined in a 1.0×10^{-5} *M* solution of hemin at 400 mμ at 5 and 64.8 mole % ethanol. The equilibrium constant K_1 for dimerization was then calculated from the spectrum in a 48.8 mole % ethanol solution (the solvent for the n.m.r. temperature study) containing 5×10^{-3} *M* hemin

$$[1] \qquad 2M \rightleftharpoons D$$

where M represents monomer and D represents dimer and $K_1 = [D]/[M]^2$. The values for K_1 at 25.0° and 34.8° are 25 and 34 M^{-1}. Therefore there is about 10% of the dimer present in the 48.8 mole % solution used in the n.m.r. temperature study. For the more dilute solutions used in the accompanying kinetic study, the dimer concentration is insignificant (2).

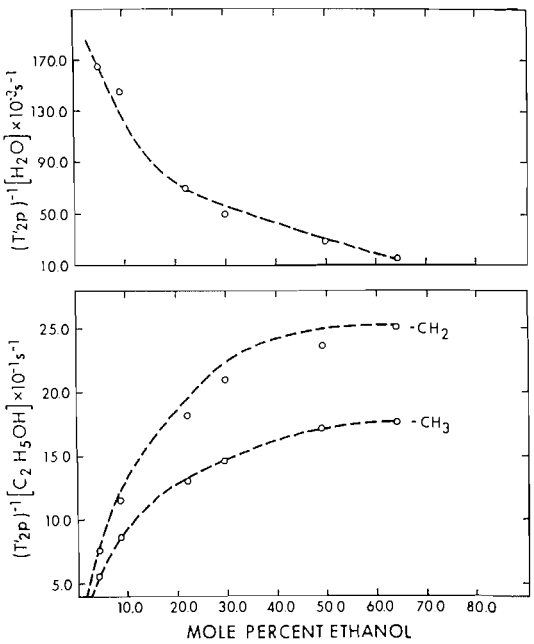

FIG. 2. Variation of solvent proton $(T_{2p'})^{-1}$ with solvent composition at 35°.

The results of a study of the n.m.r. linewidths at various ethanol concentrations at 35 °C are shown in Fig. 2. The full linewidths at half height of the line in the presence of hemin ($\Delta\nu_{obs}$) and in the pure solvent ($\Delta\nu_s$) are related to the transverse relaxation time, T_{2p} by

$$[2] \qquad (T_{2p'})^{-1} = \frac{(T_{2p})^{-1}}{[M]_T} = \frac{\pi(\Delta\nu_{obs} - \Delta\nu_s)}{[M]_T}$$

where $[M]_T$ is the total hemin concentration.

The full width at half height of the methyl proton resonance was determined from the center peak of the triplet, and that of the methylene protons from the average width of the two center peaks of the quartet. It is somewhat more difficult to analyze the hydroxy proton resonance because it consists of contributions from the water protons and the hydroxy proton of ethanol. To separate these two contributions, it was assumed that the peak due to the hydroxy proton on ethanol has an area corresponding to one proton and that it has the same width as the methylene proton resonance. The latter assumption is not necessarily valid but has little effect on the results,

[1]We use the term pH* as defined by Bates *et al.* (15) for a mixed solvent system.

Can. J. Chem. Downloaded from www.nrcresearchpress.com by 210.87.254.105 on 09/05/12
For personal use only.

Can. J. Chem. Downloaded from www.nrcresearchpress.com by 210.87.254.105 on 09/05/12
For personal use only.

because of the small contribution of the hydroxy proton to the total signal.

In order to discuss the results in Fig. 2, it is necessary to anticipate the conclusions of the temperature study. From the latter study it is concluded that at 35° the relaxation time is given by limiting conditions [10*b*] and [10*d*] of Swift and Connick (6). Then

$$[3] \quad (T_{2p})^{-1} = P_m\{(T_{2m})^{-1} + \tau_m\Delta\omega_m{}^2\}$$

where P_m is the ratio of solvent bound to the metal ion to the free solvent concentration, τ_m is the lifetime of the solvent molecule in the first coordination sphere of the metal ion, T_{2m} is the transverse relaxation time of the protons in the first coordination sphere of the paramagnetic ion, and $\Delta\omega_m$ is the chemical shift of the same protons from their position in the bulk solvent. At 35° the $T_{2m}{}^{-1}$ term constitutes about 50 and 30% of $(T_{2p'})^{-1}$ for the methyl and methylene protons and about 30% of $(T_{2p'})^{-1}$ for the water protons. Therefore, the results in Fig. 2 might be interpreted qualitatively as being due to the change from dimer to monomer with a longer T_{2m} for ethanol protons in the dimer. However, the T_{2m} relaxation mechanism should be the same for both the water and alcohol protons and, therefore, a parallel change in T_{2mw} and T_{2ma} would be expected on going from monomer to dimer. The subscripts "w" and "a" refer to water and alcohol. Aside from these qualitative arguments, the monomer–dimer equilibrium constant K_1 may be calculated at 48.8 mole % ethanol using limiting values at 0 and 64 mole % ethanol. The values obtained are 2.12×10^{-2}, 3.90×10^{-2}, and 1.46 M^{-1} from the methyl, methylene, and water protons. These values for K_1 do not agree with the value of 34 M^{-1} obtained by the spectrophotometric method, nor with each other. Therefore, it is concluded that the dimer–monomer equilibrium is not the process causing the variation in linewidth shown in Fig. 2.

The curves in Fig. 2 may be explained by the replacement of water or hydroxide by ethanol or ethoxide in the first coordination sphere of the iron, as represented by eqs. [4] and [4*a*].

$$[4] \quad HOFe(OH_2) + C_2H_5OH \overset{K_4}{\rightleftharpoons} HOFe(C_2H_5OH) + H_2O$$

$$[4a] \quad HOFe(OH) + C_2H_5OH \rightleftharpoons HOFe(OC_2H_5) + H_2O$$

The subsequent treatment assumes that the monomer and dimer give the same n.m.r. line broadening per iron atom, at 35°. This assumption is consistent with the fact that the line broadening was directly dependent on the hemin concentration and gives internal consistency between the two studies in which solvent composition and temperature were varied. Therefore there is no justification for making further complicating assumptions. The apparent similarity in line broadening properties of monomer and dimer are most easily rationalized if dimerization involves hydrophobic bonding between the hemin ring systems or its substituents as proposed by Gallagher and Elliott (7). However it is not necessarily inconsistent with an oxide ion bridged dimer. In the latter case the above assumption requires that the electron spin relaxation times of the Fe and the solvent exchange rate are unaffected by changing the hydroxide ion ligand in $(HO)Fe(OH_2)$ for an $(H_2O)FeO$ ligand in the dimer $(H_2O)Fe—O—Fe(OH_2)$.

Consideration of the equilibrium properties of the system represented by eq. [4] or [4*a*] and [3] shows that

$$[5] \quad (T_{2p'})_a{}^{-1}[C_2H_5OH] = \frac{K_4[C_2H_5OH]}{[H_2O] + K_4[C_2H_5OH]} \times \{T_{2ma}{}^{-1} + \tau_{ma}\Delta\omega_{ma}{}^2\}$$

$$[6] \quad (T_{2p'})_w{}^{-1}[H_2O] = \frac{[H_2O]}{[H_2O] + K_4[C_2H_5OH]} \times \{T_{2mw}{}^{-1} + \tau_{mw}\Delta\omega_{mw}{}^2\}$$

Initially the $—CH_2—$ and CH_3 proton data in Fig. 2 will be considered. The value of τ_{ma} may or may not depend on the water and ethanol concentrations. If the latter condition holds then consideration of eq. [5] shows that a plot of $(T_{2p'})_a[C_2H_5OH]^{-1}$ vs. $[H_2O]/[C_2H_5OH]$ should be linear with an intercept of $(T_{2ma}{}^{-1} + \tau_{ma}\Delta\omega_{ma}{}^2)^{-1}$ and a slope of $[K_4(T_{2ma}{}^{-1} + \tau_{ma}\Delta\omega_{ma}{}^2)]^{-1}$. The value of $[T_{2ma}{}^{-1} + \tau_{ma}\Delta\omega_{ma}{}^2]$ can be determined from the temperature study in 48.8 mole % ethanol for comparison to the intercepts on Fig. 3. Also the values of K_4 obtained from the $—CH_2—$ protons should be

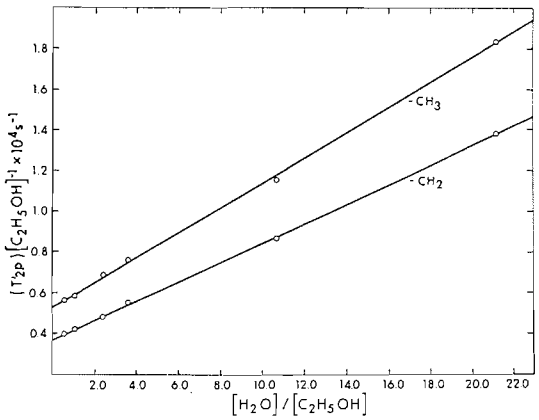

FIG. 3. Dependence of the transverse relaxation time of the methyl (—CH_3) and methylene (—CH_2—) ethanol protons on solvent composition; temperature 35°.

equal. Although these ideals are not completely achieved, the agreement is good. For the CH_3 protons the values of $[T_{2ma}^{-1} + \tau_{ma}\Delta\omega_{ma}^2]$ from the intercept of Fig. 3 and from the temperature study are 1.89×10^4 and 1.75×10^4 s^{-1}. The value of K_4 from Fig. 3 is 8.7_5. The analogous values for the —CH_2— protons are 2.7×10^4, 2.4×10^4 s^{-1}, and 7.7_9 respectively[2]. It should be pointed out that for the methyl protons $\tau_{ma}\Delta\omega_{ma}^2$ is 6.40×10^3 s^{-1} compared to T_{2ma}^{-1} of 11.1×10^3 s^{-1}. Therefore the $\tau_{ma}\Delta\omega_{ma}^2$ term is contributing significantly to the sum. The observed discrepancies between the temperature study and solvent variation study are within the errors of the temperature study values (see Table II). It is concluded that τ_{ma} is zero-order in ethanol and water concentrations.

A similar analysis may be made of the water proton data in Fig. 2. Equation [6] indicates that a plot of $(T_{2p'})_w[H_2O]^{-1}$ vs. $[C_2H_5OH]/[H_2O]$ should be linear with the intercept and slope yielding values analogous to those for the ethanol protons. However, in this case the plot is not linear. This result might be expected from examination of Fig. 2 because the water line broadening does not decrease to zero as predicted if τ_{mw} is independent of water concentration, but rather seems to level off at the high ethanol concentrations. It is found empirically that the water broadening data may be represented by

$$[7] \quad (T_{2p'})_w^{-1}[H_2O] = \frac{[H_2O]}{[H_2O] + K_4[C_2H_5OH]} \times \left\{T_{2mw}^{-1} + \frac{1.50 \times 10^{-6}}{13.5 + [H_2O]}\Delta\omega_{mw}^2\right\}$$

using the values for T_{2mw}^{-1} and $\Delta\omega_{mw}$ of 1.90×10^5 s^{-1} and 1.34×10^6 radians s^{-1}, as obtained from the temperature study in 48.8 mole % ethanol. The observed and calculated results are compared in Table I. It should be noted that a considerable range of values around 13.5 in eq. [7] would still give a reasonable fit to the experimental data.

TABLE I

Water proton relaxation time as a function of solvent composition at 35°

Mole% C_2H_5OH†	$10^{-5} \times (T_{2p'})_w^{-1} \times [H_2O]$	
	Observed	Calculated*
4.5	1.65	1.65
8.6	1.47	1.30
21.8	0.70	0.68
29.5	0.50	0.56
48.8	0.29	0.31
64.0	0.15	0.15

*Calculated from eq. [7] using K_4, 8.7; $(T_{2mw})^{-1}$, 1.90×10^5 s^{-1}; $\Delta\omega_{mw}$, 1.34×10^6 radians s^{-1}.

†The molar ethanol concentrations for the solvent compositions listed in the order shown in the table are 2.28; 4.03; 8.22; 9.93; 13.1, and 14.7. The corresponding water molarities are 48.3; 42.8; 29.4; 23.7; 13.9, and 8.3.

The variation of $(T_{2p'})^{-1}$ with temperature for the water and ethanol protons is shown in Figs. 4 and 5, respectively. The kinetic parameters for this system were determined by fitting the data in Figs. 4 and 5 to the general eq. [8] developed by Swift and Connick (6), using a non-linear least squares computer program (IBM SHARE Library, 1964 Program SDA 3094).

$$[8] \quad (T_{2p})^{-1} = \frac{P_m}{\tau_m}\left\{\frac{(T_{2m}\tau_m)^{-1} + T_{2m}^{-2} + \Delta\omega_m^2}{[T_{2m}^{-1} + \tau_m^{-1}]^2 + \Delta\omega_m^2}\right\}$$

In treating the temperature dependence of $(T_{2p})^{-1}$ it was assumed that τ_m^{-1} was represented by the usual transition state theory expression. The temperature dependence of $\Delta\omega_m$ and its

[2]In the subsequent analysis a somewhat arbitrary value of 8.7 has been used for K_4, giving more weight to the methyl proton value since these data seem in better agreement with the temperature study.

Can. J. Chem. Downloaded from www.nrcresearchpress.com by 210.87.254.105 on 09/05/12
For personal use only.

Can. J. Chem. Downloaded from www.nrcresearchpress.com by 210.87.254.105 on 09/05/12
For personal use only.

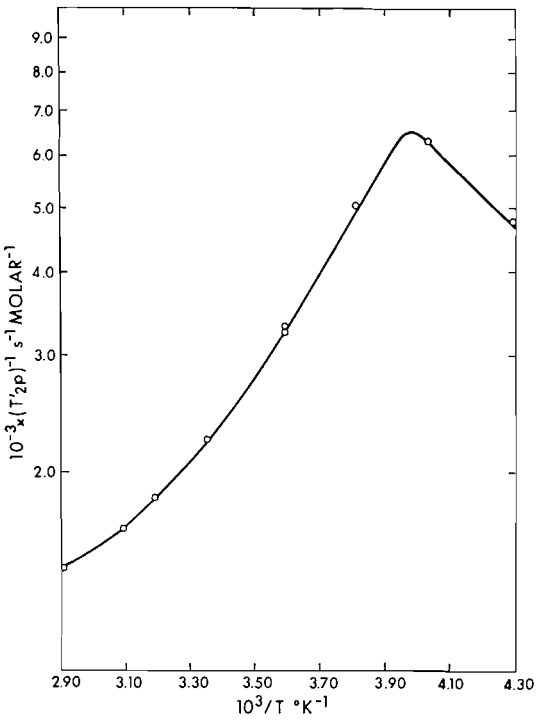

FIG. 4. Dependence of $-\log (P_m T_{2p'})$ for water protons on the reciprocal of the absolute temperature for solutions of hemin in 48.8 mole % ethanol.

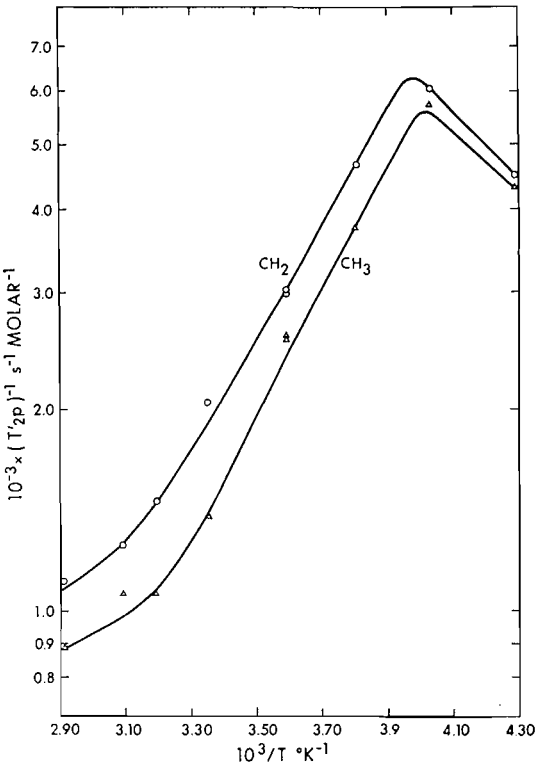

FIG. 5. Dependence of $-\log (P_m T_{2p'})$ on the reciprocal of the absolute temperature for the methyl and methylene protons of solvent ethanol in solutions of hemin in 48.8 mole % ethanol.

relationship to the hyperfine coupling constant are given by eq. [9].

$$[9] \qquad \Delta\omega_m = \frac{\omega_o(S)(S+1)(A/h)h\gamma_e}{3kT\gamma_I}$$

where ω_o is the operating frequency, h is Planck's constant, k is Boltzman's constant, γ_e and γ_I are the magnetogyric ratios of the electron and proton, respectively, S is the spin quantum number for the paramagnetic ion, and (A/h) is the electron–nuclear hyperfine coupling constant (8). In eq. [9] the spin only magnetic moment for the paramagnetic ion is assumed.

Preliminary calculations indicated that T_{2m} was controlled by the electron–nuclear hyperfine interaction, rather than the dipole–dipole interaction, and that the condition $\omega_s^2\tau^2 \gg 1$ would apply, where τ is the correlation time for the interaction and ω_s is the resonance frequency of the free electron. The expression for (T_{2m}^{-1}) under these conditions is (9)

$$[10] \qquad (T_{2m})^{-1} = \frac{1}{3}(S)(S+1)\left(\frac{A}{\hbar}\right)^2\tau_e$$

In the subsequent treatment the temperature dependence of the correlation time is assumed to have the form

$$[11] \qquad \tau_e = \tau_o \exp(E_a/RT)$$

In the non-linear least squares program the values of $\Delta H^{\ddagger}$, $\Delta S^{\ddagger}$, A/h, τ_o and E_a were used as adjustable parameters. The initial estimates of these parameters, necessary for the computation, were obtained by the usual graphical procedure using the limiting conditions [10a], [10b], and [10d] of Swift and Connick (6). The resulting least squares parameters for the water and ethanol protons are given in Table II, along with their standard errors determined from the computer best fit to the data. The results in Table II show that the values of $\Delta H^{\ddagger}$, $\Delta S^{\ddagger}$, τ_o, and E_a for the methyl and methylene protons are the same within their standard errors from the fit, as is necessary for whole ethanol molecule exchange.

TABLE II

Best fit parameters for n.m.r. line broadening

Parameters	Ethanol		Water
	CH_3	CH_2	
$\Delta H^{\ddagger}$ kcal mole^{-1}	6.3 ± 0.9	6.1 ± 1.0	6.3 ±0.5
$\Delta S^{\ddagger}$ cal mole^{-1} deg^{-1}	−8.9 ± 4.1	−9.3 ± 4.7	−3.8 ±2.0
$\tau_0 \times 10^{-12}$ s	44 ±86	99 ±16	1.77±1.1
E_a kcal mole^{-1}	0.12± 1.3	1.0 ± 0.5	0.73±0.43
$A/h \times 10^{-6}$ Hz	1.16± 0.06	1.22± 0.05	11.9 ±0.03

The values in Table II are calculated assuming that K_4 is temperature independent. In 48.8 mole % ethanol the water or hydroxide solvated species makes up 10.8% of the total hemin concentration. Therefore, if K_4 were not essentially temperature independent, the concentration of ($HOFeOH_2$) or ($HOFeOH^-$) would change considerably over the wide temperature range of the study, and some rather unusual effects would be noted in the plot of $(T_{2p'})_w^{-1}$ [H_2O] vs. $(T)^{-1}$ °K^{-1}. Since this is not the case the results are consistent with the assumed temperature independence of K_4. This assumption is also consistent with the studies of Kemp and King (10) on the solvated chromium ion in ethanol – water solutions.

The hyperfine coupling constants in Table II may be used to calculate the chemical shift which should be observed in the solutions. Although the coupling constants are large, the small concentration of hemin ($< 5 \times 10^{-3}$ *M*) results in a calculated shift of less than 5 Hz in all cases. A downfield shift was observed generally but its magnitude was too small and the error in the measurement too large to permit any quantitative analysis. The downfield direction of the shift indicates a positive value for the coupling constants.

It has also been observed that the solvent n.m.r. resonances have their natural linewidths when imidazole is added to the hemin solution in a mole ratio of 100:1. This result confirms that imidazole binds to the paramagnetic center and displaces solvent molecules from the coordination sphere of the metal ion.

A study was also made of the effect of hydroxide ion on the linewidths in 48.8 mole % ethanol at 35°. No change in the linewidths was observed between 10^{-6} and 0.1 *M* hydroxide ion.

Discussion

In the previous analysis to obtain the results, the exact nature of the solvated species causing the n.m.r. line broadening was not specified. The results are consistent with the assumption that the dimeric and monomeric forms of hemin have the same kinetic properties. The study of the linewidth dependence on ethanol and water concentration has shown that in the mixed ethanol – water solvent there is an equilibrium between water or hydroxide and ethanol or ethoxide solvated hemin. These species may be represented by the formulae [H_2OFeOH], [$HOFeOH]^-$, [$C_2H_5OHFeOH$], and [$C_2H_5OFeOH]^-$ where the porphyrin ring structure is omitted.

Hasinoff *et al.* (2) have measured an acid dissociation constant for hemin of 1.4×10^{-7} *M*. This equilibrium might be represented by eqs. [12*a*] or [12*b*]

[12*a*] $$H_2OFeOH_2 \rightleftharpoons H_2OFeOH + H^+$$

or

[12*b*] $$HOFeOH_2 \rightleftharpoons HOFeOH + H^+$$

Then at pH* 11 the water solvated species may be either (H_2OFeOH) or $(HOFeOH)^-$. A reexamination by Phillips (3) of the data of Schack and Clark (11) gives a pK_a of 7.3 for proton dissociation from the dimeric diaquo species, $(H_2OFeOH_2)_2^{2+}$, to give the hydroxy–aquo dimer, $(H_2OFeOH)_2$, in water. This pK is reasonably close to the value of 6.8_5 obtained by Hasinoff *et al.* (2) for the monomer in ethanol – water solution, indicating that the same process [12*a*] is being observed in both studies. This is also consistent with the potentiometric work of Davis and Martin (4) in ethanol – water mixtures. It is therefore, assumed in the subsequent discussion that the solvated species are (H_2OFeOH) and ($C_2H_5OHFeOH$).

In interpreting the water proton exchange rates there is a further difficulty because the water protons may exchange with the whole water molecule or by proton transfer. Since the activa-

Can. J. Chem. Downloaded from www.nrcresearchpress.com by 210.87.254.105 on 09/05/12
For personal use only.

Can. J. Chem. Downloaded from www.nrcresearchpress.com by 210.87.254.105 on 09/05/12
For personal use only.

tion parameters for water and ethanol exchange are the same, within their error limits, it is tempting to propose that entire water molecules are exchanging. However, the term directly dependent on water concentration in the rate law for water proton exchange indicates that these protons may be exchanging by a different process from the ethanol molecule exchange.

A possible pathway for water proton transfer is represented by

$$[13]\quad (H_2OFeOH) + H_2O \underset{k_{-13}}{\overset{k_{13}}{\rightleftharpoons}} (H_2OFeOH_2)^+ + OH^-$$

$$\frac{1}{\tau_m} = k_{13}[H_2O] = \frac{[H_2O]}{1.5 \times 10^{-6}}$$

The value for τ_m is given in eq. [7]. It can be shown by using the value of 1.4×10^{-7} determined in ref. (3) for the dissociation constant of $[H_2OFeOH_2]^+$, that

$$[14]\qquad \frac{k_{13}}{k_{-13}} = \frac{K_w}{1.4 \times 10^{-7}}$$

Therefore, $k_{-13} = 0.93 \times 10^{13}$. This value of k_{-13} is several orders of magnitude larger than the usually accepted diffusion controlled limit. Therefore, proton transfer cannot be occurring by reaction [13].

A similar analysis shows that the reaction

$$[15]\quad (HOFeOH_2) + H_2O \rightleftharpoons (HOFeOH)^- + H_3O^+$$

cannot be contributing to proton exchange unless the coordinated water is a moderately weak acid, a conclusion which is inconsistent with the pH titrations and the analysis of Phillips (3).

A reaction such as

$$[16]\quad (HOFeOH_2) + OH^- \rightleftharpoons (HOFeOH)^- + H_2O$$

cannot be contributing to proton exchange because the exchange lifetime, τ_m^{-1}, is independent of hydroxide ion.

One transition state for proton transfer might be pictured as

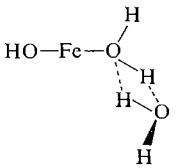

where the dotted lines represent hydrogen bonds between the free and coordinated solvent. Proton transfer might take place by a concerted interchange of the hydrogen-bonded hydrogens. It is difficult to judge the likelihood of such a mechanism. There appears to be no evidence for this type of transfer in the studies of proton exchange in simple hydrated metal cations. However, in these systems the hydrated ion is a weak acid and exchange by a process analogous to reaction [15] usually predominates. It is also unlikely that these cations will be solvated with the hydrogen end of the solvent water molecule. The mechanism pictured for the proton transfer is similar in some ways to that proposed for proton exchange in methanolic solutions of benzoic acids (12, 13) and for proton exchange between trimethylamine and the trimethylammonium ion in aqueous solution (14). It should be noted that this mechanism for water proton exchange has been proposed because other seemingly reasonable possibilities are not consistent with the acid–base properties of the hemin.

The results on the ethanol proton line broadening are free from the ambiguities of the water protons because there is no possibility for the methyl or methylene protons to exchange independently. Therefore, the values for $\Delta H^{\ddagger}$ and $\Delta S^{\ddagger}$ given in Table II are for the exchange of a whole ethanol molecule from the coordination sphere of iron (III) in hemin. If average parameters, from the $-CH_2-$ and $-CH_3-$ protons, of 6.2_0 kcal mole^{-1} for $\Delta H^{\ddagger}$ and -9.1_0 cal mole^{-1} deg^{-1} for $\Delta S^{\ddagger}$ are used, then the average rate constant for ethanol exchange is 1.8×10^6 s^{-1} at 25°.

The solvent-independent term in the water exchange rate is presumably due to whole water molecule exchange. The rate constant for water exchange is 9×10^5 s^{-1} at 35°, and if an activation energy of 6.2 kcal mole^{-1} is assumed, based on the ethanol value, then the exchange rate is 6×10^5 s^{-1} at 25°. If a limiting S_N1 mechanism is assumed for the solvent exchange, then the mechanism may be represented by the following equation

$$(HOFeOH_2) \underset{k_{-1}}{\overset{k_1}{\rightleftharpoons}} \{HOFe\} + \underset{H_2O}{C_2H_5OH} \underset{k_2}{\overset{k_{-2}}{\rightleftharpoons}} (HOFeC_2H_5OH)$$

Therefore

$$\frac{k_1 k_{-2}}{k_2 k_{-1}} = K_4 = 8.7$$

The values of k_1 and k_2 are 6×10^5 and 1.8×10^6 s^{-1}; therefore $k_{-2}/k_{-1} \approx 25$. This value indicates that ethanol is 25 times more nucleophilic than water, a result which is not consistent with the expected nucleophilic order of water and ethanol. The high ratio of k_{-2}/k_{-1} may be due to preferential solvation by ethanol in the second coordination sphere of the hemin and also to the neglect of the solvent activity ratios in calculating K_4 (5).

The relative rates of solvent exchange and imidazole substitution (2) on hemin seem most consistent with an ion pair substitution mechanism. The imidazole study was carried out under conditions where the hemin is about 70% in the ethanol form, therefore the rather uncertain value for the water exchange rate does not affect these conclusions. If protonated imidazole (HIm^+) and imidazole (Im) are the binding species then the binding rate constants are 4×10^6 and 3×10^4 $M^{-1}s^{-1}$ respectively. The larger rate constant for HIm^+ substitution may be accounted for by an ion pair formation constant of about 3 for HIm^+ and 0.02 for Im. This and other mechanisms are discussed more fully by Hasinoff *et al.* (2).

1. J. L. Hoard, M. J. Hamor, T. A. Hamor, and W. S. Caughey. J. Amer. Chem. Soc. **87**, 2312, (1965).
2. B. B. Hasinoff, H. B. Dunford, and D. G. Horne. Can. J. Chem. This issue.
3. J. N. Phillips. Rev. Pure Appl. Chem. **10**, 35 (1960).
4. D. G. Davis and R. F. Martin. J. Amer. Chem. Soc. **88**, 1365 (1966).
5. A. C. Maehly and A. Akeson. Acta. Chem. Scand. **12**, 1254 (1958).
6. T. J. Swift and R. E. Connick. J. Chem. Phys. **37**, 307 (1962).
7. W. A. Gallagher and W. B. Elliott. Biochem. J., **108**, 131 (1968).
8. N. Bloembergen. J. Chem. Phys. **27**, 595 (1957).
9. I. Solomon and N. Bloembergen. J. Chem. Phys. **25**, 261 (1956).
10. D. W. Kemp and E. L. King. J. Amer. Chem. Soc. **89**, 3433 (1967).
11. J. Schack and W. M. Clark. J. Biol. Chem. **171**, 143 (1947).
12. E. Grunwald, C. F. Jumper, and S. Meiboom. J. Amer. Chem. Soc. **85**, 522 (1963).
13. E. Grunwald and S. Meiboom. J. Amer. Chem. Soc. **85**, 2047 (1963).
14. E. Grunwald and A. Y. Ku. J. Amer. Chem. Soc. **90**, 29 (1968).
15. R. G. Bates, M. Paabo, and R. A. Robinson. J. Phys. Chem. 67, 1833, 1963.

Can. J. Chem. Downloaded from www.nrcresearchpress.com by 210.87.254.105 on 09/05/12
For personal use only.

Temperature jump kinetics of the binding of imidazole to ferriprotoporphyrin IX

BRIAN B. HASINOFF, H. BRIAN DUNFORD, AND DALE G. HORNE
Department of Chemistry, University of Alberta, Edmonton, Alberta

Received January 6, 1969

The kinetics of binding of imidazole to ferriprotoporphyrin IX (hemin) in aqueous ethanol has been studied at 25° using the temperature jump technique. The reaction was studied quantitatively as a function of acid concentration using the pH scale developed by Bates *et al.* for mixed solvent systems. The results can be explained by a mechanism in which the imidazolium ion binds to hemin with a specific rate constant of $(4 \pm 2) \times 10^6\ M^{-1}\ s^{-1}$ and imidazole binds with a rate constant of $(3 \pm 0.3) \times 10^4\ M^{-1}\ s^{-1}$. The dissociation constant for the imidazolium ion was determined by acid–base titration to be $1.8 \times 10^{-7}\ M$, and a dissociation constant for the hemin of $2.3 \times 10^{-7}\ M$ was determined by spectrophotometric titration in a solvent containing 44.5 weight % of ethanol. The latter dissociation involves the proton on a solvent ligand.

Canadian Journal of Chemistry, 47, 3225 (1969)

Can. J. Chem. Downloaded from www.nrcresearchpress.com by 210.87.254.5 on 09/05/12
For personal use only.

Introduction

Some equilibrium studies have been carried out on the coordination of various ligands to ferriprotoporphyrin IX (hemin) in a variety of solvents (1, 2). Neutral or acidic aqueous solutions of hemin are prone to precipitation. At high pH in aqueous solution, hemin tends to dimerize or polymerize (3). Maehly and Akeson have shown that a solvent composed of about 50 volume % ethanol stabilizes a dilute solution of monomeric hemin (4). For this reason the present study of the kinetics of imidazole binding was conducted in 44.5 weight % ethanol.

Experimental

The kinetic measurements were conducted on a temperature jump apparatus constructed in this laboratory and based on the concepts put forth by Eigen (5, 6). The detection circuit, monochromator, light source, and light power supply were identical to those described elsewhere (7). The temperature jump was obtained by triggering the discharge of a high voltage capacitor (Plastic Capacitors, Inc. LK500-104ZND, 0.1 μF, 50 kV) through a spark gap in series with the temperature jump cell. The trigger module (TM-11) was obtained from EG and G Inc. The voltage for charging the capacitor was supplied by a Spellman high voltage power supply Model 2040. The cell, constructed of Plexiglass with cylindrical quartz lenses, was designed so that approximately 1 ml of the solution was heated. It was possible to perform experiments on a minimum of 5 ml of solution. The cell fitted snugly into a brass thermostatting jacket enclosed in a light-tight canister. The heating time constant of the cell and the response time constant of the photomultiplier circuit were negligibly small compared to the measured chemical relaxations.

Association constants of the imidazole–hemin complex were determined by measuring absorbances with a Beckman DU spectrophotometer with a cell compartment thermostatted at 25.0°. Imidazole and hemin of White Label grade were obtained from Eastman Organic Chemicals and were used without further purification. The solvent, 44.5 weight % ethanol, was prepared from distilled, filtered, deionized water and reagent grade 95% ethanol. A stock hemin solution was prepared by dissolving hemin in 0.1 *M* NaOH and diluting until the stock was $1.0 \times 10^{-3}\ M$ in hemin and $1.0 \times 10^{-2}\ M$ in NaOH. This stock was stored in a refrigerator and from it freshly diluted solutions, $4.00 \times 10^{-5}\ M$ in hemin, were prepared for each day's experiments. Kinetic and equilibrium measurements were conducted on $4.00 \times 10^{-6}\ M$ hemin solutions within minutes of their preparation. For all experiments the imidazole concentrations were at least 50 times larger than the hemin concentrations.

An operational pH scale was established using the method described by Bates *et al.* (8). We shall follow their nomenclature in which the term pH* is used for pH in a mixed aqueous solvent. An accurate measure of pH* can be obtained with an aqueous glass electrode in a mixed aqueous solvent. The glass electrode (a Beckman long thin probe combination 38183) was stored in a solution of composition, pH*, and ionic strength similar to that used in the experiments, and was standardized with a triethanolammonium chloride – triethanolamine buffer of pH* 7.05 (8). This electrode was used in combination with a Beckman expanded scale pH meter. All solutions contained a buffer contributing 0.01 to the total ionic strength of 0.11 with the remainder contributed by KNO_3. In the pH* range 4.5–6.0 acetate buffer was used, 6.2–7.5 maleate buffer, 6.3–8.3 phosphate buffer, and 8.8–10.3 borate buffer.

The temperature jump cell was thermostatted at 19.0° and a voltage of 20.5 kV was applied which was sufficient to give a 6° rise in temperature. A monochromator setting of 413 mμ was employed which corresponded to the maximum of the difference spectrum of the two absorbing species in solution. Changes in absorbance caused by the temperature perturbation were observed by monitoring the output voltage of a photomultiplier on an oscilloscope with a differential high gain d.c. amplifier. The relaxation curve was photographed and the single observed relaxation time, τ, was determined by use of a photographic enlarger to match the negative of the oscilloscope trace with one of a series of exponential curves specially

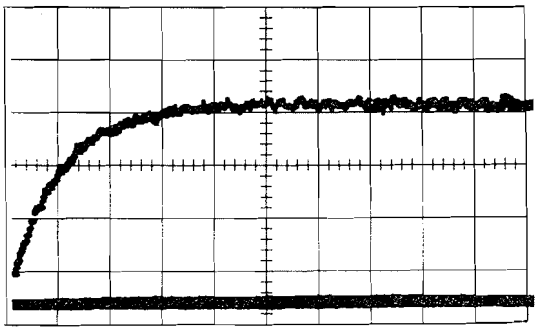

FIG. 1. Oscilloscope trace of voltage *vs.* time. Concentration of hemin was 4.0×10^{-6} *M* and of imidazole 1.2×10^{-3} *M*. The pH* was 7.5 and ionic strength 0.11 with 0.01 contributed by maleate buffer. The horizontal scale is 1 ms/cm and the vertical scale 100 mV/cm. Monochromator setting was 413 mμ.

constructed for this purpose. A typical trace is shown in Fig. 1.

Results

At a constant pH* the hemin solutions were found to obey Beer's law for a single absorbing species over an appreciable range of hemin concentrations, indicating that the hemin species did not change as a function of concentration. From the studies of Maehly and Akeson this species is known to be monomeric hemin (4).

Studies were made of spectral changes as a function of pH*. Hemin solutions with pH* ranging from 8 to 3.6 *M* with respect to NaOH showed no significant spectral changes. From pH* 8 to 5.5 significant spectral changes were observed at 400 mμ, where the maximum absorption in the Soret region occurs. Upon standing 24 h or more, solutions of hemin at pH* less than 5.8 were observed to precipitate. Hence it was difficult to obtain accurate absorbance readings corresponding to complete conversion to the acid form of the hemin. Nevertheless, using the absorbance of the alkaline solutions as reference, it was possible using the method of Coward and Kiser (9) to show that the absorbance changes corresponded to a single proton dissociation with a p*K* of 6.6_3. The titration results, shown as the fraction of protonated species, α, *vs.* pH*, are shown in Fig. 2. No attempt was made to measure possible p*K*'s which might be observed in more acid solutions and kinetic experiments were not conducted below pH* 6.0.

The acid dissociation constant of imidazolium ion in 44.5 weight % ethanol was measured at a constant ionic strength of 0.11 and a temperature of 25.0°, by titrating a solution of 0.1 *M* imidazole with concentrated HNO_3 so that the volume change over the course of the titration was negligibly small. The inflection point of the sigmoid titration curve (plot of pH* *vs.* volume of HNO_3 added) indicated the acid dissociation constant of imidazolium ion, K_{ImH}, to be 1.8×10^{-7} *M*.

When imidazole is added to a solution of hemin, large changes in the spectrum occur as shown in Fig. 3. There are 4 well-defined isosbestic points indicating the presence of two absorbing species in solution which, as discussed below,

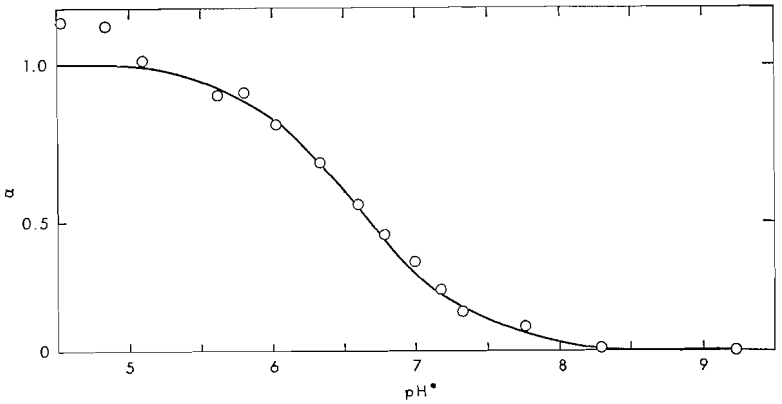

FIG. 2. Plot of α, the fraction of hemin present, *vs.* pH*. The solid line is a theoretical sigmoid curve for the dissociation of a single proton from an acid group with a p*K* of 6.63 and the circles represent experimental points.

Can. J. Chem. Downloaded from www.nrcresearchpress.com by 210.87.254.5 on 09/05/12
For personal use only.

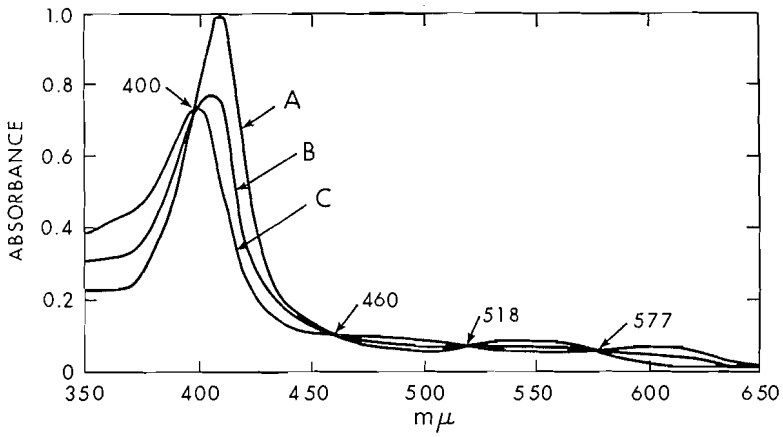

FIG. 3. Plot of absorbance *vs.* wavelength in mμ. Concentration of hemin was 8.0×10^{-6} *M* and concentrations of imidazole for curves A, B, and C were 1×10^{-2}, 1×10^{-3}, and 0 *M*. The pH* was 7.6 and the ionic strength 0.11. Curve A is the spectrum of fully complexed diimidazole hemin.

appear to be hemin and diimidazole hemin. No spectral evidence could be obtained for the existence of an intermediate species. If the state of ionization of the various species is neglected, the association of imidazole and hemin may be represented as[1]

[1] $$M + 2Im \rightleftarrows MIm_2$$

The corresponding apparent association constant is

[2] $$K_{app} = \frac{[\overline{MIm_2}]}{[\overline{M}][\overline{Im}]^2}$$

The slope of a plot of log $[(A_r - A_s)/(A_s - A_\infty)]$ *vs.* log $[\overline{Im}]$, shown in Fig. 4, indicates the number of molecules of imidazole that are binding to a molecule of hemin (2). The slope of our plot is 1.9 which, within experimental error, confirms the validity of eqs. [1] and [2]. From eq. [2], it can be shown that a plot of $\Delta A/[\overline{Im}]^2$ *vs.* ΔA should be linear with the absolute value of the slope equal to the association constant, K_{app} (9). Linear plots were obtained over the entire pH* range; a typical example is shown in Fig. 5. This type of plot is particularly useful when a large excess of ligand is required for complete formation of the complex. The K_{app} data as a function of pH* are listed in column 3 of Table I and are plotted in Fig. 6.

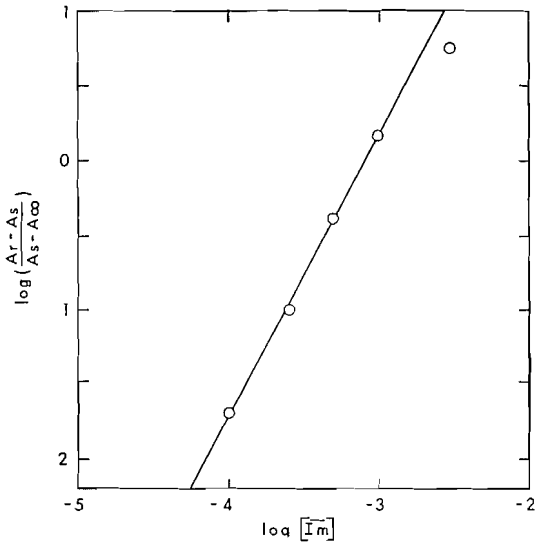

FIG. 4. Plot of log $[(A_r - A_s)/(A_s - A_\infty)]$ *vs.* log $[\overline{Im}]$. The concentration of hemin was 4.0×10^{-6} *M*. The pH* was 7.5. The slope of 1.9 indicates that 2 molecules of imidazole coordinate per molecule of hemin.

[1]Abbreviations used: M or $M(H_2O)$ is the metalloporphyrin ferriprotoporphyrin IX or hemin; M(OH), hydroxyhemin or hematin; MIm, monoimidazole hemin; MIm_2, diimidazole hemin; Im, imidazole; ImH, imidazolium ion. The bracketed quantities which have bars or subscript zero represent equilibrium concentrations or total initial concentrations. The absorbances of hemin solutions in a 1 cm cuvette with no added imidazole (reference), a known amount of imidazole added (sample), and an excess of imidazole added such that the diimidazole hemin complex is completely formed, are designated A_r, A_s, and A_∞; ΔA is $A_s - A_r$; α is the fraction of the hemin present as $M(H_2O)$.

Can. J. Chem. Downloaded from www.nrcresearchpress.com by 210.87.254.5 on 09/05/12
For personal use only.

TABLE I

Apparent rate and equilibrium constants for the binding of imidazole to hemin at 25° and ionic strength 0.11 M*

pH*	Spectrophotometric k_{1app} $\times 10^{-6}$, $(M^{-1}\ s^{-1})$	Spectrophotometric K_{app} $\times 10^{-6}$, (M^{-2})	k_{-2app} (s^{-1})	$\frac{k_{2app}}{k_{-1app}}$ (M^{-1})	Kinetic K_{app} $\times 10^{-6}$, (M^{-2})
6.00	0.75 ±0.15	0.76 ±0.08	570±260	220±340	1.6 ±0.6
6.20	0.92 ±0.09	1.2 ±0.1	580±40	330±80	1.1 ±0.9
6.40	1.12 ±0.11	1.6 ±0.2	710±50	640±120	0.7 ±0.6
6.62	1.40 ±0.14	2.4 ±0.2	650±20	510±50	1.4 ±0.4
6.70	1.44 ±0.14	2.8 ±0.3	650±70	620±180	1.0 ±0.4
6.70	1.44 ±0.14	2.6 ±0.3	760±70	880±220	0.7 ±1.1
6.80	1.46 ±0.15	2.8 ±0.3	480±100	90±260	0.15 ±0.13
6.90	1.34 ±0.13	3.2 ±0.3	720±50	1370±170	6.5 ±7.5
7.12	1.40 ±0.14	3.5 ±0.3	640±90	720±290	1.0 ±0.6
7.30	1.15 ±0.11	2.0 ±0.2	580±70	440±160	0.36 ±0.04
7.53	0.88 ±0.09	1.5 ±0.1	550±10	510±30	2.0 ±0.6
7.76	0.74 ±0.07	1.2 ±0.1	550±40	520±90	1.3 ±1.0
7.79	0.64 ±0.06	1.0 ±0.1	440±80	400±210	1.1 ±3.6
8.32	0.26 ±0.03	0.35 ±0.03	510±20	650±60	0.9 ±0.2
8.82	0.12 ±0.01	0.11 ±0.01	340±30	270±40	0.23 ±0.27
9.72	0.042±0.004	0.0095±0.001	290±30	26±10	0.024 ±0.043
10.30	0.028±0.003	0.0069±0.001	359±100	70±30	0.0012±0.011

*Error limits given are the standard errors. Error limits on the k_{1app} and the spectrophotometric K_{app} are estimated at ±10%.

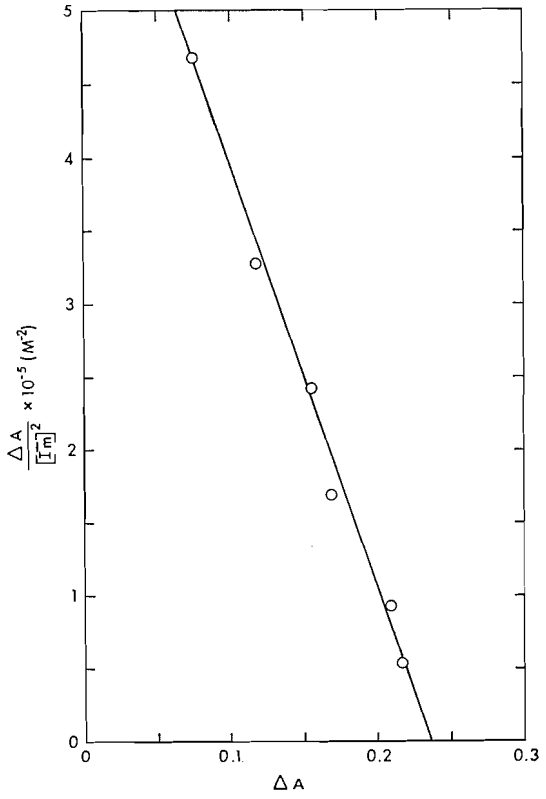

FIG. 5. Plot of $\Delta A/[\overline{Im}]^2$ *vs.* ΔA. Concentration of hemin was 4.0×10^{-6} M. The pH* was 6.7. K_{app} from the slope of the line is 2.8×10^6 M^{-2}.

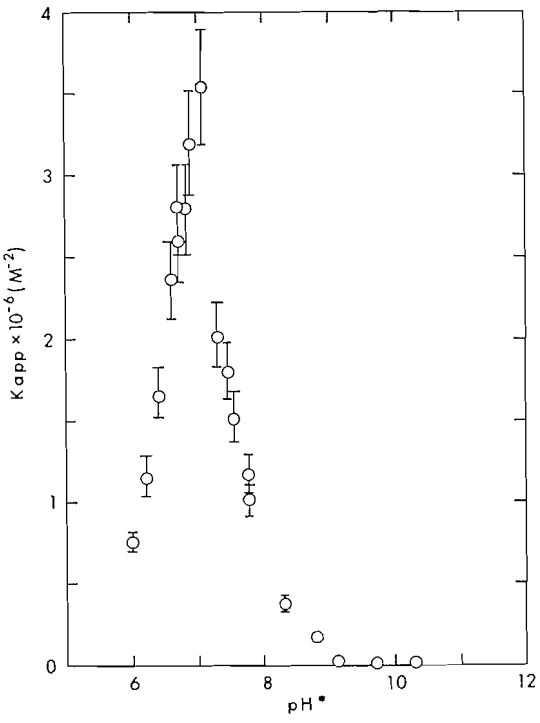

FIG. 6. Plot of K_{app} *vs.* pH*. Error limits given are estimates.

Can. J. Chem. Downloaded from www.nrcresearchpress.com by 210.87.254.5 on 09/05/12
For personal use only.

Can. J. Chem. Downloaded from www.nrcresearchpress.com by 210.87.254.5 on 09/05/12
For personal use only.

The overall reaction represented in eq. [1] can be written in two steps

$$\mathrm{M} + \mathrm{Im} \underset{k_{-1\mathrm{app}}}{\overset{k_{1\mathrm{app}}}{\rightleftharpoons}} \mathrm{MIm} \qquad [3]$$

$$\mathrm{MIm} + \mathrm{Im} \underset{k_{-2\mathrm{app}}}{\overset{k_{2\mathrm{app}}}{\rightleftharpoons}} \mathrm{MIm_2}$$

The relation between the association constant, K_{app}, and the apparent rate constants is

$$K_{app} = \frac{k_{1\,app}k_{2\,app}}{k_{-1\,app}k_{-2\,app}} \qquad [4]$$

In all temperature jump experiments only one relaxation time, τ, was observed. The values of τ, which are dependent upon the concentration of added imidazole, ranged from about 0.1 to 2 ms. The single relaxation time and lack of any spectroscopically observable intermediate provides evidence that the steady state approximation

$$\frac{d[\mathrm{MIm}]}{dt} = 0 \qquad [5]$$

is valid. Without the steady state condition two relaxation times would be expected (10). The reciprocal of the relaxation time, based on eqs. [3]–[5] is given by

$$\frac{1}{\tau} = \frac{k_{-2\,app}(1 + K_{app}[\overline{\mathrm{Im}}]^2)}{1 + \frac{k_{2\,app}}{k_{-1\,app}}[\overline{\mathrm{Im}}]} \qquad [6]$$

where $[\overline{\mathrm{Im}}] = [\mathrm{Im}]_0 \gg [\mathrm{M}]_0$. It is possible to show that for large $[\overline{\mathrm{Im}}]$, eq. [6] is reduced to $1/\tau = k_{1app}[\overline{\mathrm{Im}}]$ and for small $[\overline{\mathrm{Im}}]$, it becomes $1/\tau = k_{-2app}$. Therefore from plots of $1/\tau$ *vs.* $[\overline{\mathrm{Im}}]$, the limiting slopes at large $[\overline{\mathrm{Im}}]$ yield k_{1app} data. A typical limiting slope plot is shown in Fig. 7. Values of k_{1app} as a function of pH*, obtained by the limiting slope method, are listed in column 2 of Table I and are plotted in Fig. 8. Values of k_{-2app} and k_{2app}/k_{-1app} were computed from eq. [6] using K_{app}, from the spectrophotometric titrations, and τ and $[\overline{\mathrm{Im}}]$ values as input data for a non-linear least squares program (11). They are listed in columns 4 and 5 of Table I. Finally, in order to obtain values of K_{app}, solely from kinetic data, as a check on the spectrophotometric titration results, all three quantities K_{app}, k_{-2app}, and k_{2app}/k_{-1app} were treated as unknowns and best-fit values were obtained from eq. [6] using the same computer program (11). The results for K_{app} are listed in column 6 of Table I.

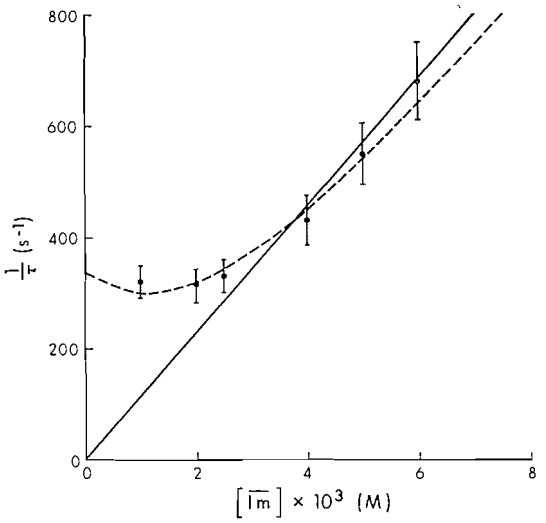

FIG. 7. Plot of $1/\tau$ *vs.* $[\overline{\mathrm{Im}}]$ for imidazole binding to hemin at pH* 8.82. The solid line is an estimated limiting slope and the dashed line was computed from eq. [6] using K_{app} determined spectrophotometrically and best-fit values for k_{-2app} and k_{2app}/k_{-1app}.

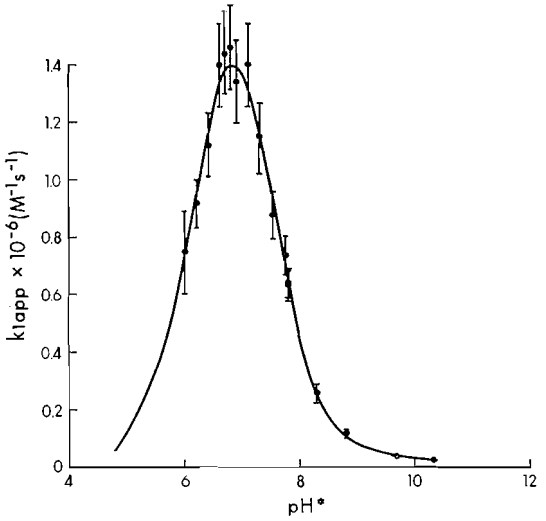

FIG. 8. Plot of k_{1app} *vs.* pH*. The solid line is that predicted using the best four-parameter fit to eq. [10]. The circles are experimental points and error limits are estimated.

Discussion

There are two kinetically indistinguishable mechanisms which can explain the pH* dependence of the k_{1app} data. In one, imidazole is

Can. J. Chem. Downloaded from www.nrcresearchpress.com by 210.87.254.5 on 09/05/12
For personal use only.

TABLE II

Best-fit parameters to explain the pH* dependence of k_{1app} data. Standard errors are obtained from the non-linear least squares program

Equation number	$k_1 \times 10^{-6}$ (M^{-1} s^{-1})	$k_2 \times 10^{-4}$ (M^{-1} s^{-1})	$k_3 \times 10^{-6}$ (M^{-1} s^{-1})	$k_4 \times 10^{-4}$ (M^{-1} s^{-1})	K_{ImH} (M)	K_a (M)	% Standard error of fit
[10]	2.4±0.2	2.7±0.2	—	—	(4.1±0.5) × 10^{-8}	(4.8±0.8) × 10^{-7}	6.2
[10]	5.5±0.3	3.2±0.5	—	—	—	—	22.9
[11]	—	—	2.4±0.2	2.7±0.2	(4.8±0.8) × 10^{-7}	(4.1±0.5) × 10^{-8}	6.2
[11]	—	—	7.0±0.4	3.2±0.5	—	—	22.9

Can. J. Chem. Downloaded from www.nrcresearchpress.com by 210.87.254.5 on 09/05/12
For personal use only.

postulated to bind to two forms of hemin differing by a single ionizable proton

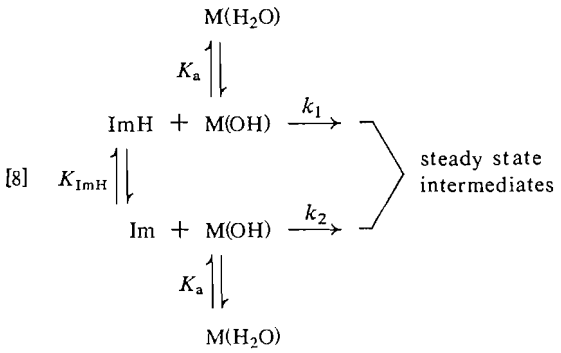

where K_a and K_{ImH} are the acid dissociation constants of hemin and imidazolium ion. The vertical arrows indicate fast proton transfer reactions in buffered solutions and the horizontal arrows slower bimolecular association reactions. The other mechanism is

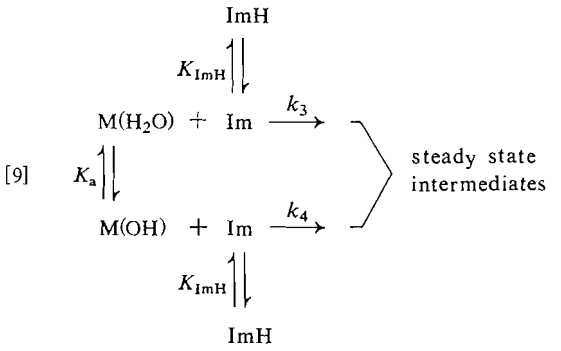

According to eq. [8] the apparent forward rate constant, k_{1app} is given by

$$[10]\quad k_{1app} = \left[\frac{k_1}{1 + K_{ImH}/[H^+]} + \frac{k_2}{1 + [H^+]/K_{ImH}}\right] \times \left[\frac{1}{1 + [H^+]/K_a}\right]$$

and from eq. [9] one obtains

$$[11]\quad k_{1app} = \left[\frac{k_3}{1 + K_a/[H^+]} + \frac{k_4}{1 + [H^+]/K_a}\right] \times \left[\frac{1}{1 + [H^+]/K_{ImH}}\right]$$

It can be shown that $k_3 = k_1K_a/K_{ImH}$ whereas $k_2 = k_4$. Equations [10] and [11] are readily tested using a non-linear least squares program (11). The program was modified to minimize the sum of the squares of the relative residuals rather than the sum of the squares of the absolute residuals. The results of two different approaches are summarized in Table II. In the first approach, 4 parameters from eq. [10], k_1, k_2, K_{ImH}, and K_a and 4 from eq. [11], k_3, k_4, K_{ImH}, and K_a, were regarded as unknowns and best-fit values were obtained. In the second approach, the values of K_{ImH} and K_a, 1.8×10^{-7} and 2.3×10^{-7} M, obtained independently by titration, were treated as constants and the best-fit values of the other two parameters to each of eqs. [10] and [11] were obtained. The agreement between the four- and two-adjustable-parameter fits is somewhat better for eq. [10] than for eq. [11]. This does not provide sufficient evidence to exclude the mechanism represented in eqs. [9] and [11] however.

From an examination of the equilibrium data one can write two pairs of equations

$$[12]\quad M(OH) + ImH + Im \overset{K'}{\rightleftarrows} M(Im)_2 + H_2O$$

$$[13]\quad K_{app} = K'\left[\frac{K_a}{K_a + [H^+]}\right]\left[\frac{K_{ImH}}{K_{ImH} + [H^+]}\right] \times \left[\frac{[H^+]}{K_{ImH} + [H^+]}\right]$$

as well as

$$[14]\quad M(H_2O) + 2Im \overset{K''}{\leftrightarrows} M(Im)_2 + H_2O$$

$$[15]\quad K_{app} = K''\left[\frac{K_{ImH}}{K_{ImH} + [H^+]}\right]^2\left[\frac{[H^+]}{K_a + [H^+]}\right]$$

Both pairs of equations provide equally reasonable approximations to the observed equilibrium data, and therefore offer no clue as to a preferred mechanism.

From independent evidence, reviewed in the accompanying nuclear magnetic resonance (n.m.r.) study of solvent exchange of hemin (12), it appears likely that the $M(H_2O)$ is an equilibrium mixture of diaquohemin and aquoethanol hemin, whereas M(OH) is an equilibrium mixture of hydroxyaquo hemin and hydroxyethanol hemin. From the n.m.r. data, the rate constant for the dissociation of ethanol from hydroxyethanol hemin was determined to be 2×10^6 s^{-1}, whereas for the water from hydroxyaquo hemin it was 6×10^5 s^{-1} at 25° (12).

Can. J. Chem. Downloaded from www.nrcresearchpress.com by 210.87.254.5 on 09/05/12
For personal use only.

From simple electrostatic consideration, the OH^- ligand should labilize other ligands. Thus the water exchange rate on $Fe(OH_2)_5OH^{2+}$ is faster than on $Fe(OH_2)_6{}^{3+}$ (13). On this basis the reaction scheme outlined in eq. [8] appears more plausible. From the results of Table II, the value of k_1 is $(4 \pm 2) \times 10^6\ M^{-1}\ s^{-1}$ and for k_2 $(3.0 \pm 0.2) \times 10^4\ M^{-1}\ s^{-1}$.

If an S_N1 limiting mechanism is considered (14), then the first reaction in eq. [8] becomes

$$[16]\qquad M(C_2H_5OH)^{2-} \underset{k_b}{\overset{k_a}{\rightleftarrows}} M'^{2-} + C_2H_5OH$$

$$M'^{2-} + ImH^+ \underset{k_d}{\overset{k_c}{\rightleftarrows}} MIm^{2-} + H^+$$

where M'^{2-} represents a pentacoordinated hemin intermediate and $M(C_2H_5OH)^{2-}$ is hydroxyethanol hemin with only its most labile ligand shown. For eqs. [16] and [17] total charges on the ionic species are shown. Since no inhibition at large [Im] is observed, $k_1 = k_a k_c / k_b$[EtOH] (15). The value of k_a is $2 \times 10^6\ s^{-1}$ from the n.m.r. results (12), and $k_1 = 4 \times 10^6/0.7 = 6 \times 10^6\ M^{-1}\ s^{-1}$. The correction is applied to k_1 since the n.m.r. results indicate that the hemin is about 70% in its ethanol form. The concentration of EtOH is about 8.2 M so that $k_c/k_b \approx 25$, or in words, the imidazolium ion is predicted to be 25 times better as a nucleophile than ethanol. Furthermore since $k_1 \gg k_2$, the imidazolium ion is predicted to be a better nucleophile than imidazole. Both of these predictions appear highly questionable.

On the other hand, if an ion pair mechanism is considered, the first reaction in eq. [8] becomes

$$[17]\qquad M(C_2H_5OH)^{2-} + ImH^+ \overset{K}{\rightleftarrows} M(C_2H_5OH)(ImH)^-$$

$$M(C_2H_5OH)(ImH)^- \overset{k_e}{\rightleftarrows} MIm^{2-} + H^+ + C_2H_5OH$$

It would appear plausible that the imidazolium ligand transfers its acid proton to the solvent molecule which it replaces. From the comparison of eqs. [8] and [17], $k_1 = Kk_e$, where K is the ion pair formation constant (15). If the rate of solvent exchange is not affected by ion pair formation, then $k_e = 2 \times 10^6\ s^{-1}$ and since $k_1 = 6 \times 10^6\ M^{-1}\ s^{-1}$, then $K = 3\ M^{-1}$ which appears quite reasonable. If the ion pair accelerates solvent removal then this value of K represents an upper limit. On a similar basis the "ion pair" constant for Im is about $0.02\ M^{-1}$ and a decrease in K is expected when a cation is replaced by a neutral ligand.

Fleischer *et al.* have studied ligand binding to cobalt(III) and iron(III) hematoporphyrin IX presumably in monomeric form in aqueous solution (16). Hematoporphyrin IX has two $CH_3CH(OH)$— substituents in place of the two vinyl groups in protoporphyrin IX. It can be shown that their measured specific rate constant for the overall pseudo first-order binding reaction is identical to our $1/\tau$, so that when their k_{obs} is plotted *vs.* ligand concentration, the behavior exhibited in Fig. 8 might be expected. However, they operated with a much larger excess of ligand than in our temperature jump experiments, so that detection of a finite intercept in the plot is more difficult. With the large excess of ligand they were able to obtain evidence for an S_N1 ligand substitution mechanism for the cobalt system but not for the iron system.

Acknowledgment

This work was supported by a grant from the National Research Council. One of us (B.B.H.) is also indebted for a National Research Council Scholarship.

1. J. E. Falk. Porphyrins and metalloporphyrins. Elsevier Publishing Company, New York. 1964.
2. W. Scheler. Biochem. Z. **332**, 542 (1960).
3. J. Shack and W. M. Clark. J. Biol. Chem. **171**, 143 (1947).
4. A. C. Maehly and A. Akeson. Acta Chem. Scand. **12**, 1259 (1958).
5. M. Eigen and L. de Maeyer. *In* Techniques in organic chemistry. S. L. Friess, E. S. Lewis, and A. Weissberger. *Editors*. Vol. 8. Part II. 2nd ed. Interscience Publishers Inc., New York. 1963. p. 895.
6. W. F. Diven, D. E. Goldsack, and R. A. Alberty. J. Biol. Chem. **240**, 2437 (1965).
7. W. D. Ellis and H. B. Dunford. Biochem. **7**, 2054 (1968).
8. R. G. Bates, M. Paabo, and R. A. Robinson. J. Phys. Chem. **67**, 1833 (1963).
9. N. A. Coward and R. W. Kiser. J. Phys. Chem. **70**, 213 (1966).
10. R. A. Alberty, G. Yagil, W. F. Diven, and M. Takahashi. Acta Chem. Scand. **17**, S34 (1963).
11. IBM SHARE Library, Program SDA 3094 (modified for use in the University of Alberta IBM 360 Computer) (1964).
12. N. S. Angerman, B. B. Hasinoff, H. B. Dunford, and R. B. Jordan. This issue.
13. M. Eigen and R. G. Wilkinson. *In* Mechanisms of inorganic reactions. ACS Monograph Series. 1965. p. 64.
14. D. Seewald and N. Sutin. Inorg. Chem. **2**, 643 (1963).
15. N. Sutin. Ann. Rev. Phys. Chem. **17**, 119 (1966).
16. E. B. Fleischer, S. Jacobs, and L. Mestichelli. J. Am. Chem. Soc. **90**, 2527 (1968).

Can. J. Chem. Downloaded from www.nrcresearchpress.com by 210.87.254.105 on 09/05/12
For personal use only.

Les acétates énoliques des *tert*-butyl-6α et 7α décalones-2 *cis*[1]

H. Favre et A. J. Liston[2]
Département de Chimie, Université de Montréal, Montréal, Québec

Reçu le 2 avril 1969

Les *tert*-butyl-6α et 7α décalones-2 *cis*, respectivement *cis a* et *cis e*, ont été préparées. A l'équilibre, les acétates énoliques Δ^1, Δ^2 en série *cis a* sont dans le rapport 35–65; en série *cis e*, un seul acétate énolique est présent, l'isomère Δ^1. Ces faits invalident la règle de l'énolisation préférentielle des décalones-2 *cis* vers la position 1. Une comparaison de ces résultats avec ceux obtenus à partir des décalones-2 *cis* diméthylées en 6,6 et 7,7 permet de dégager quelques conclusions au sujet des interactions non liées qui représentent un facteur important dans la direction de l'énolisation.

Canadian Journal of Chemistry, 47, 3233 (1969)

Les acétates énoliques sont particulièrement appropriés pour apporter des éclaircissements sur la direction de l'énolisation de cétones cyclohexaniques (1), polycyclohexaniques (2,3) et stéroïdiques, (4,5). Il nous a paru intéressant d'étendre notre étude préliminaire dans la série décalinique *cis*. Il conviendrait d'avoir en mains plusieurs cas types, de manière à mieux asseoir les faits sur lesquels se fondent les études, qui, par calcul, déterminent les énergies conformationnelles (6,7) et qui, en dernier ressort apporteront les précisions indispensables à notre compréhension de la direction de l'énolisation.

Ce travail rapporte l'étude des acétates énoliques de la *tert*-butyl-6α décalone-2 *cis* (**1**) et de la *tert*-butyl-7α décalones-2 *cis* (**2**). Elles présentent l'avantage sur les décalone-2 diméthylées en 6,6 et 7,7 d'avoir une bonne stabilité conformationnelle stéroïde et non stéroïde respectivement, et de ne posséder aucun substituant axial, source d'interactions entre atomes non liés. Les décalones-2 *cis tert*-butylées peuvent ainsi être considérées comme les véritables représentants des deux systèmes fondamentaux, les décalones-2 *cis a* et *cis e* (nomenclature de Klyne (8)).

La conformation double chaise des décalones-2 *cis* est ajourd'hui bien établie (9,10).

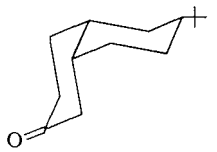

1

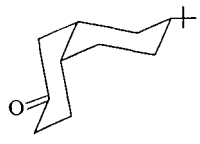

2

[1]Ce mémoire est tiré de la thèse de doctorat de A. J. Liston.

[2]Adresse actuelle: Research Laboratories, Food and Drug Directorate, Department of National Health and Welfare, Ottawa, Canada.

Synthèse de la tert-butyl-6α décalone-2 cis (1)

La *tert*-butyl-4 cyclohexanone est le composé de départ. Une annellation à la manière de Stork (11) par l'intermédiaire de l'ènepyrrolidine correspondante, conduit à un mélange brut contenant entre autres, les octalones **3** et **4** (bandes infrarouges (i.r.) à 1675 cm^{-1} et 1710 cm^{-1}). Par distillation, on obtient un mélange des octalones **3** et **4**, les proportions étant 60–40 environ par dosage par résonance magnétique nucléaire (r.m.n.). Ce mélange 60–40 traité, par l'acide *p*-toluènesulfonique dans le benzène, s'isomérise en un mélange formé de 83% de l'octalone **3** et de 17% de l'isomère **4**; une distillation dans une colonne munie d'une bande tournante permet d'obtenir l'octalone pure **3**.

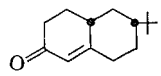

3

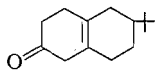

4

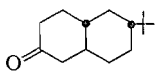

5

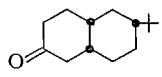

1

D'une manière générale, les $\Delta^{1(9)}$-octalones-2 se réduisent par le lithium dans l'ammoniac en décalone-2 *trans* (12,13) et catalytiquement en décalone *cis*. Traitée par le lithium et l'ammoniac, l'octalone **3** conduit à une décalone de point de fusion 55.5°. Réduite catalytiquement (palladium sur charbon) en solution alcoolique contenant de l'acide chlorhydrique (14), l'octalone **3** conduit à une décalone liquide homogène en chromatographie en phase gazeuse (c.p.g.) différente de celle obtenue par la réduction par le lithium et l'ammoniac. Il est raisonnable de conclure que la réduction chimique conduit à l'isomère *trans* **5** tandis que la réduction catalytique conduit à

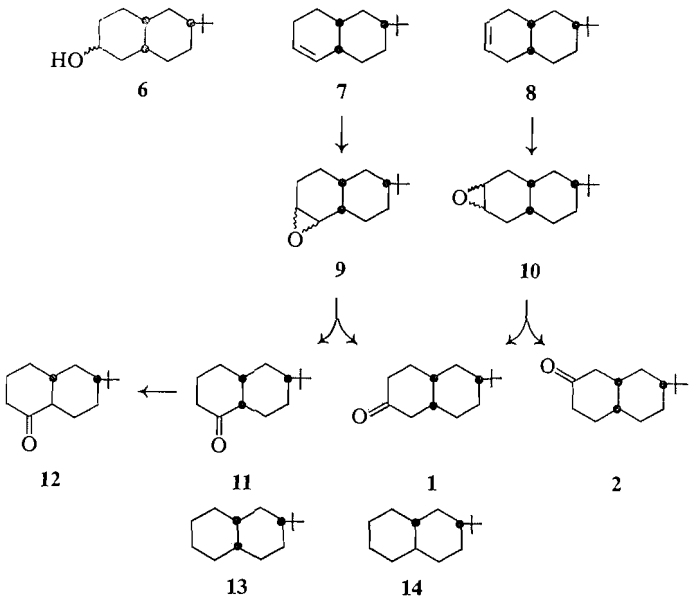

SCHÉMA 1. Synthèse de la décalone **2**.

l'isomère *cis a* (**1**). L'isomérisation que subit le mélange des octalones **3** et **4** en milieu acide donne certainement la configuration **3**, configuration *cis* pour le groupe *tert*-butyle (équatorial) et la liaison 4 (10) (équatoriale). Voir (11) pour les résultats de l'annellation de la décalone-2 *trans*. Cette octalone se réduit catalytiquement en engendrant une liaison 1 (9) axiale, comme c'est le cas pour la nor-19 testostérone qui donne un composé 5β, 10β (15). Nous apportons plus loin une autre preuve de la configuration *cis a*.[3]

Synthèse de la tert-butyl-7 décalone-2 cis (2)

La synthèse de la décalone **2** se fait à partir de la décalone **1** par une méthode qui s'inspire du travail de Church, Ireland, et Shridhar (16).

La décalone **1** réduite catalytiquement sur nickel de Raney, engendre un mélange des deux alcools, dont les configurations n'ont été déterminées, est de **3** à **2** comme le montre une analyse par c.p.g.[4] Le mélange des deux alcools est déshydraté pour donner un mélange des deux octalines **7** et **8**: la méthode de Chugaev conduit à un rapport **7**–**8** de 1–1 tandis que le rapport est de 61–39 lorsque l'agent de déshydratation est le bisulfate de potassium. La structure octalinique découle du fait que la méthode de Chugaev ne s'accompagne d'aucune transposition (17). Les deux octalines se séparent aisément en c.p.g. préparative et s'obtiennent pures. Leur preuve de structure, qui constitue en même temps la synthèse de la décalone **2** est la suivante.

Chacune des oléfines **7** et **8** est traitée par l'acide perbenzoïque, les époxydes sont réduits par l'hydrure de lithium et d'aluminium et les alcools oxydés par l'anhydride chromique.

De cette manière, l'une des octalines conduit à 90% environ de décalone **1** connue et à 10% environ de deux décalones auxquelles nous attribuons les formules **11** et **12**: en effet, le mélange brut s'isomérise en présence d'hydroxyde de potassium en un mélange qui ne contient plus que deux décalones, **1** et **12**; une réduction de Clemmensen confirme la présence de la décalone-2 *trans* (**12**) dans le mélange, en conduisant à un mélange des décalines **13** et **14** dans le rapport de 86 à 14; ces décalines s'obtiennent pures à partir des décalones-2 *cis* et *trans* **1** et **5**. L'autre octaline conduit à 60% de décalone **1** connue et à 40% de la décalone désirée **2** que l'on retire du mélange

[3]Maes, Ottinger, Reisse, et Chiurdoglu (29) ont préparé la cétone **1** par réduction catalytique de la cétone **3**. Ils lui attribuent la conformation *cis a* à la suite d'une étude en r.m.n.

[4]Selon la théorie générale (30), l'alcool prépondérant sera axial.

Can. J. Chem. Downloaded from www.nrcresearchpress.com by 210.87.254.105 on 09/05/12
For personal use only.

TABLEAU I

Pourcentages d'acétates énoliques

	Commande cinétique				Equilibre			
			Rapport des acétates				Rapport des acétates	
Décalone-2 *cis*	% —OAc	% C=O	Δ^1	Δ^2	% —OAc	% C=O	Δ^1	Δ^2
tert-Butyl-6 (**1**)	100	0	59	41	92	8	35	65
tert-Butyl-7 (**2**)	100	0	50	50	98	2	100	0
Diméthyl-6,6	100	0	57	43	92	8	60	40
Diméthyl-7,7	100	0	59	41	94	6	74	26

par c.p.g. préparative. Ce mélange 60–40 ne s'isomérise pas en présence d'hydroxyde de potassium. Il est donc évident que la première des octalines doit recevoir la structure Δ^1 (**7**), seule capable de donner naissance à une décalone *trans*.

Le fait d'obtenir un mélange des décalines *cis* et *trans*, en plus d'établir la position Δ^1 de la double liaison dans l'octaline de départ, permet de confirmer la conformation *cis a* de la décalone **1**. Si la décalone avait été *cis e* le groupe carbonyle en 1 serait sur un embranchement équatorial et aucune isomérisation ne se produirait, comme on l'a observé en série polycyclique (18). Le fait d'obtenir deux alcools pour chaque double liaison semble être une caractéristique de la série décalinique *cis* (16). En série stéroïde 5β, on rapporte la formation d'un seul époxyde à partir de double liaison Δ^2 et Δ^3 (19,20) et la réduction de ces époxydes en un seul alcool (19–21) selon la règle d'ouverture diaxiale de Fürst et Plattner (22). Nous étudions la question de savoir: *a*) si deux époxydes se forment à partir de chaque double liaison au lieu des époxydes **9** et **10**; pour des raisons d'encombrement stérique sur la face α, les époxydes isomères ne doivent pas se former; ou *b*) si les époxydes **9** et **10** peuvent, pour des raisons stériques (23), engendrer deux alcools contrairement à la règle de Fürst et Plattner: cette règle souffre en effet quelques exceptions (23–25).

Les acétates énoliques des décalones 1 et 2

Selon notre travail antérieur (1) nous avons soumis les deux décalones **1** et **2** à l'action de l'acétate d'isopropényle et de l'acide sulfurique concentré (réaction à commande cinétique) et la décalone **1**, à l'action de l'anhydride acétique et de l'acide perchlorique aqueux (formation d'acétates énoliques à l'équilibre); le mélange cinétique obtenu de la décalone **2** a été mis en équilibre par l'anhydride acétique et l'acide perchlorique aqueux (1). Les résultats apparaissent au Tableau I. Les mélanges d'acétates énoliques ont été dosés par c.p.g.

Le schéma 2 montre comment les acétates énoliques des décalones **1** et **2**, comme dans notre travail antérieur (2), sont transformés en diéthers méthyliques que l'on compare en c.p.g. à ceux que l'on obtient à partir de composés connus, en l'occurrence **7** et **8**. C'est ainsi que le mélange 59/41 issu de la décalone **1** conduit à un mélange de **19** et de **20** dans les proportions de 65/35 ce qui fait de l'acétate énolique prépondérant l'acétate **15**. Le seul acétate énolique obtenu à partir de la décalone **2**, par la méthode à l'anhydride acétique acide perchlorique, engendre un éther qui ne correspond ni à **19** ni à **20**; nous lui attribuons la formule **21** correspondant à l'acétate énolique **18**. Antérieurement (1), nous avions converti les diols en diéthers méthyliques par la méthode de Williamson; dans ce travail nous avons mis en œuvre la méthode au diazométhane et à l'acide fluoborique (26).

Discussion

Nous ramènerons les acétates énoliques **15**, **16**, **17** et **18** aux trois octalines A, B, C, respectivement Δ^1, Δ^2 et Δ^3. Les récents calculs et estimations de Bucourt et Hainaut (6) indiquent une différence de 0.15 kcal/mole en faveur d'une Δ^2-octaline *cis* par rapport à ses isomères Δ^1 et Δ^3 (A,B,C:R,R′=H), lorsqu'on ne considère que le point de vue conformationnel, c'est à dire que l'on ne fait entrer en ligne de compte que les énergies de déformation des deux anneaux de la molécule. Il faut cependant combiner à cette énergie conformationnelle les résultats des effets stériques des interactions non liées, H3-H5 dans A et H1-H5, H1-H7 dans B et C. Bucourt et

Can. J. Chem. Downloaded from www.nrcresearchpress.com by 210.87.254.105 on 09/05/12
For personal use only.

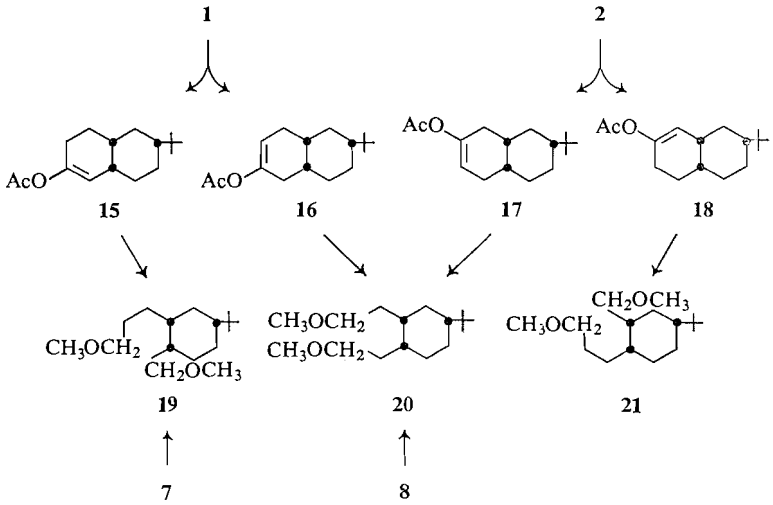

SCHÉMA 2. Preuves de structures des acétates énoliques.

Hainaut estiment alors que les effets stériques deviendront plus importants que les effets conformationnels et que les enthalpies des isomères Δ^1 et Δ^3 seront finalement plus petites que celle de l'isomère Δ^2. D'un autre côté Allinger et ses collaborateurs (7) ont calculé que la différence d'enthalpie entre les Δ^1 et Δ^2-octalines est de 0.8 kcal/mole en faveur de l'isomère Δ^1.

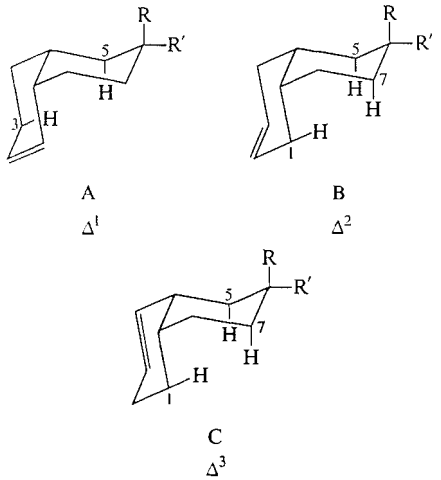

Le Tableau I montre que si l'accord est bon entre les pourcentages des acétates énoliques à l'équilibre et les calculs et les estimations dans la série diméthylée, il n'en va plus de même dans la série *tert*-butylée. D'une part, la présence du seul acétate énolique Δ^1 (**18**) dans le mélange à l'équilibre **17**⇌**18** en série *cis e* indique une forte différence d'énergie entre ces isomères. D'autre part, le fait que l'isomère Δ^2 (**16**) soit plus stable que l'isomère Δ^1 en série *cis a* est d'autant plus significatif qu'il est imprévu et contraire au calculs et aux estimations. Il est vrai que la différence d'énergie libre n'est pas grande entre les deux isomères **15** et **16** et qu'une comparaison des acétates énoliques (ΔF) et des octalines (ΔH) n'est pas possible, en raison du facteur entropique (6) et de la présence dans ces molécules d'éléments dissemblables, un hydrogène et un groupe —OAc, volumineux et polaire. La comparaison des acétates énoliques entre eux peut être plus profitable. L'effet du groupe *gem*-diméthyles se fait sentir par rapport au groupe *tert*-butyle, de façon opposée dans la série *cis a* et dans la série *cis e*. Le pourcentage d'isomère Δ^1 augmente dans la série *cis a* et diminue dans la série *cis e*. Le groupe *gem*-diméthyles cause des interactions non liées entre le méthyle axial et les hydrogènes axiaux. Nous postulons que la décompression stérique qui résulte des interactions CH_3-H8 et CH_3-H10 se fera surtout sentir en position 8 et peu en position 10, car dans cette dernière position toute déformation entraine des perturbations directes dans les angles dièdres de jonction. En série *cis e* l'interaction CH_3-H8 se traduit par un effet réflexe (27) qui fera que H1 se rapprochera de H5 et s'éloignera de H7. Comme l'interaction la plus forte est H1-H5 dans C et H1-H7 dans B, l'effet réflexe diminuera les interactions non liées

Can. J. Chem. Downloaded from www.nrcresearchpress.com by 210.87.254.105 on 09/05/12
For personal use only.

Can. J. Chem. Downloaded from www.nrcresearchpress.com by 210.87.254.105 on 09/05/12
For personal use only.

dans B et les augmentera dans C: le résultat est une augmentation de l'isomère Δ^2, lorsqu'on passe de *tert*-butyle à diméthyle. En série *cis a* l'effet réflexe diminuera les énergies d'interaction des deux isomères A et B: le résultat net doit toutefois être une plus grande diminution dans A que dans B, car dans A une seule interaction est en jeu, elle diminue, tandis que dans B deux interactions interviennent, l'une diminue, l'autre augmente.

En définitive, ce travail justifie les conclusions de Bucourt et Hainaut, à savoir que les interactions métadiaxiales régissent finalement la direction de l'énolisation en série *cis*. Il n'en reste pas moins qu'il faudra expliquer la nature précise des interactions non liées dans les octalines A, B et C et la forme exacte du squelette de ces molécules. Il devrait alors être possible de remplacer les règles simples de l'énolisation préférentielle vers la position 1 (6) ou vers 1 en série *cis a* et vers 2 en série *cis e* (28), qui ne se justifient plus, par une règle fondée sur la variation des interactions non liées en prenant comme base les trois octalines A, B et C, stabilisées par un groupe *tert*-butyle.

Partie expérimentale

Les points de fusion ont été déterminés en tubes capillaires, au moyen d'un thermomètre étalonné avec des substances de points de fusion connu. Les analyses sont de C. Daesslé, Organic Microanalyses, Montréal. Les chromatographies en phase gazeuse (c.p.g.) ont été réalisées à l'aide d'un appareil Kromo-Tog K-2 de Burrell Corporation. Les spectres infrarouges (i.r.) ont été mesurés sur un appareil Perkin–Elmer modèle 21, optique de NaCl. Les spectres de résonance magnétique nucléaire (r.m.n.) ont été mesurés au moyen d'un appareil Varian A-60 avec référence au tétraméthylsilane.

1 Synthèse de la tert-butyl-6α décalone-2 cis (1)

1.1 tert-Butyl-6α $\Delta^{1(9)}$-octalone-2 (3)

L'ènepyrrolidine correspondant à la *tert*-butyl-4 cyclohexanone a été préparée avec un rendement de 93% selon (11). On en condense 566 g selon la méthode II, 2 de Stork *et al.* (11) avec 228 ml de méthyl-vinyl-cétone: après distillation en atmosphère d'azote on recueille 120 g de *tert*-butyl-4 cyclohexanone et 494 g de produit brut contenant les octalones **3** et **4** avec des cétols p.éb. 125 à 140° sous 0.3 mm. Une distillation fractionnée donne 240 g (42.5%) d'un mélange de 60% de l'isomère $\Delta^{1(9)}$ (**3**) (pic à δ 5.62 équivalent à 0.6 H dans le spectre r.m.n.). On chauffe 10 g du mélange à reflux pendant 20 h dans 100 ml de benzène en présence de 100 mg d'acide *p*-toluènesulfonique. On isole à la manière habituelle 5.0 g du mélange des deux octalones contenant par dosage r.m.n. 83% de l'isomère $\Delta^{1(9)}$ (**3**). Le mélange 83/17 est distillé à l'aide d'une colonne à bande tournante (longueur 400 mm, diamètre 8 mm). On fait distiller une fraction de tête équivalent à 45% en poids du mélange brut. Le résidu de distillation, 2.8 g consiste en l'octalone **3** pure qui après distillation dans un ballon de Claisen présente les constantes suivantes: p.éb. 108° sous 0.07 mm, $n_D^{24.5} = 1.5140$: spectre i.r. (CCl_4) 1675 cm^{-1}, C=O; 1625 cm^{-1}, C=C.

Anal. calc. pour $C_{14}H_{22}O$: C, 81.50; H, 10.75. Trouvé: C, 81.77; H, 10.67.

Dinitro-2,4 phénylhydrazone, aiguilles rouges (chloroforme–méthanol) p.def. 179°.

Anal. calc. pour $C_{20}H_{26}N_4O_4$: C, 62.16; H, 6.78; N, 14.50. Trouvé: C, 62.33; H, 6.68; N, 14.50.

Semicarbazone de p.def. 217° (méthanol).

Anal. calc. pour $C_{15}H_{25}N_3O$: C, 68.40; H, 9.57; N, 15.95. Trouvé: C, 68.50; H, 9.53; N, 15.71.

1.2 tert-Butyl-6α décalone-2 cis (1)

On agite en atmosphère d'hydrogène 2.4 g de *tert*-butyl-6α $\Delta^{1(9)}$-octalone-2 pure, 10 ml d'éthanol 95%, 1.0 ml d'acide chlorhydrique 3 *N* et 0.1 g de catalyseur (palladium 10% sur charbon actif), à 25° et pression atmosphérique, jusqu'à absorption de la quantité calculée d'hydrogène, soit pendant 17 h. On essore le catalyseur, évapore l'éthanol. Le résidu est repris par de l'éther; on lave avec une solution de bicarbonate de sodium puis avec une solution aqueuse saturée de chlorure de sodium. On sèche sur sulfate de sodium anhydre, évapore l'éther et distille le résidu. La décalone **1** présente les constantes suivantes: p.éb. 93° sous 0.1 mm; $n_D^{24.5} = 1.4874$; bande i.r. (CCl_4) à 1715 cm^{-1}, C=O. Temps de rétention de 57 min en c.p.g. sur colonne de 2.5 m, 20% de polyester succinique de Craig sur Chromat FB, température de la colonne 195°, hélium 60 ml par min.

Anal. calc. pour $C_{14}H_{24}O$: C, 80.71; H, 11.61. Trouvé: C, 80.38; H, 11.34.

Anal. calc. pour $C_{20}H_{27}N_4O_4$ (dinitro-2,4 phénylhydrazone, p.def. 167°): C, 61.84; H, 7.27; N, 14.42. Trouvé: C, 61.76; H, 7.08; N, 14.46.

Anal. calc. pour $C_{15}H_{27}N_3O$ (semicarbazone p.def. 205.5°): C, 67.88; H, 10.25; N, 15.83. Trouvé: C, 68.01; H, 10.37; N, 15.92.

Par réduction de 240 g du mélange 60–40 des octalones **3** et **4** décrit en 1.1 plus haut, on obtient la décalone **1** pure, homogène en c.p.g. dans les conditions décrites en 1.2.

1.3 tert-Butyl-6α décalone-2 trans (5)

On suit fidèlement les indications opératoires données dans un mémoire précédent (31), soit deux réductions successives et une oxydation de l'alcool saturé formé. Ainsi, 10.0 g d'octalone **3** donnent 3.0 g de décalone *trans* **5**, p.éb. 105° sous 0.6 mm; le distillat cristallise lentement pour donner des aiguilles p.def. 55.5°; bande i.r. (CCl_4) 1720 cm^{-1} (C=O); homogène en c.p.g. dans les conditions décrites en 1.2 plus haut avec temps d'ébullition de 38 min.

Anal. calc. pour $C_{14}H_{24}O$: C, 80.71; H, 11.61. Trouvé: C, 80.43; H, 11.33.

Anal. calc. pour $C_{20}H_{28}N_4O_4$ (dinitro-2,4 phénylhydrazone (chloroforme-méthanol) p.def. 175.5°): C, 61.84; H, 7.27; N, 14.42. Trouvé: C, 61.31; H, 7.27; N, 14.72.

Anal. calc. pour $C_{15}H_{27}N_3O$ (semicarbazone (méthanol) p.def. 214.5°): C, 67.88; H, 10.25; N, 15.83. Trouvé: C, 67.63; H, 10.34; N, 15.58.

Can. J. Chem. Downloaded from www.nrcresearchpress.com by 210.87.254.105 on 09/05/12
For personal use only.

2 tert-Butyl-7α décalone-2 cis (2)

2.1 tert-Butyl-6α Δ^1-octaline cis (7) et tert-butyl-6α Δ^2-octaline cis (8)

On dissout 175.0 g de *tert*-butyl-6α décalone-2 *cis* (**1**) dans 500 ml d'éthanol 95%; on y ajoute 25 ml d'une suspension de nickel de Raney préparé selon (32); on agite à 25° et à pression atmosphérique jusqu'à cessation de l'absorption d'hydrogène. On essore le catalyseur, évapore l'éthanol et distille le résidu; on obtient 170 g (97%) d'une huile, p.éb. 116° sous 0.8 mm qui cristallise lentement. En c.p.g. on distingue deux pics, dans le rapport 3 à 2 (2.5 m, 20% Tergitol sur brique 225°) qui sont les alcools **6**. On place 20.0 g des alcools bruts **6** dans un ballon de Claisen en mélange avec 8.0 g de bisulfate de potassium fraîchement fondu et pulvérisé. On chauffe sur un bain de sable à 290° en faisant passer un léger courant d'azote dans le ballon. Les octalines brutes distillent à 195°. Elles contiennent environ 15% de décalols non entrés en réaction. On répète l'opération plusieurs fois, de telle sorte que 170 g de décalols donnent naissance à 155 g d'octalines brutes. Les décalols qu'elles contiennent se mettent à précipiter; au bout de quelques jours, on les essore. Le mélange brut des octalines est dosé en c.p.g.: 61%–39%, **7** et **8**, temps de rétention respectivement de 9.5 et 8.5 min, en utilisant une colonne de 2.5 m, 20% de polyester succinique de Craig sur brique, 195°, hélium 60 ml/min. On fractionne ce mélange au moyen d'un appareil Fisher Prep Partitioner de c.p.g. préparative. On injecte dans une première colonne de 45 × 5 cm, suivie de 5 colonnes de 45 × 3 cm, 20% polyester de Craig sur brique; température de l'injecteur 250° et des colonnes 180°, azote comme éluant, 0.91 kg/cm^2. Le temps de rétention sont les suivants: octaline Δ^1, 45 min et Δ^2, 35 min, si l'on injecte des prises de 2 ml; des prises de 3 ml, ou supérieures provoquent un recouvrement des bandes préjudiciables à une bonne séparation. Dans ces conditions 138 g de mélange des octalines Δ^1 et Δ^2 conduit à 33 g de l'isomère Δ^1 (**7**) et à 15 g de l'isomère Δ^2 (**8**) purs.

La *tert*-butyl-6α Δ^1-octaline *cis* (**7**) présente les constantes suivantes: p.éb. 70.5° sous 0.45 mm; $n_D^{24} = 1.4878$; bandes i.r. à 658 et 1658 cm^{-1}.

Anal. calc. pour $C_{14}H_{24}$: C, 87.42; H, 12.58. Trouvé: C, 87.90; H, 12.23.

La *tert*-butyl-6α Δ^2-octaline *cis* (**8**) présente les constantes suivantes: p.éb. 70.5° sous 0.5 mm; $n_D^{24} = 1.4878$; bandes i.r. à 664 et 1648 cm^{-1}.

Anal. calc. pour $C_{14}H_{24}$: C, 87.42; H, 12.58. Trouvé: C, 87.70; H, 12.31.

Préparation des alcènes 7 et 8 par la méthode de Chugaev

On dissout 1.5 g du mélange des décalols **6** dans 40 ml de toluène anhydre et chauffe à l'ébullition à reflux pendant 18 h en présence de 0.21 g de sodium métallique, sous atmosphère d'azote. On refroidit, enlève l'excès de sodium et ajoute 50 ml d'éther anhydre contenant 0.93 g de bisulfure de carbone. On agite pendant quelques minutes et ajoute 6.0 g d'iodure de méthyle; on chauffe à l'ébullition à reflux pendant 4 h. On distille le solvant, ajoute 10 ml d'éther, filtre. Le xanthogénate cristallisant, on ajoute de l'éther jusqu'à obtention d'une solution limpide. On pyrolyse, en atmosphère d'azote, en laissant tomber goutte à goutte, la solution éthérée dans un ballon qui contient du verre concassé, maintenu à 295°. Le distillat de la pyrolyse est traité par du noir animal et distillé: p.éb. 115–118° sous 20 mm, rendement de 68%. La c.p.g. et le spectre i.r. indiquent un mélange 1–1 des deux octalines **7** et **8**.

2.2 tert-Butyl-7α décalone-2 cis (2)

En refroidissant par un bain de glace, on ajoute à 10.5 g de *tert*-butyl-6α Δ^2-octaline *cis* (**8**) dans un ballon à fond rond, 158 ml d'une solution chloroformique d'acide perbenzoïque contenant 10.5 g d'acide ou 50% d'excès. Il faut ajouter la solution chloroformique lentement car la réaction est fortement exothermique. On ajoute ensuite 10 g de sulfate de sodium anhydre et abandonne le tout à 3° pendant 48 h, en munissant le ballon d'un tube contenant du chlorure de calcium comme protection contre l'humidité. On filtre la solution, on la lave avec une solution aqueuse à 10% d'hydroxyde de sodium pour éliminer les acides organiques, puis avec une solution aqueuse saturée de sulfate de sodium jusqu'à neutralité. On sèche sur sulfate de sodium anhydre, évapore le solvant et recueille le résidu (10.2 g) qui est sans autre soumis à l'action de l'hydrure de lithium et d'aluminium.

L'époxyde brut (10.2 g) est dissous dans 100 ml d'éther anhydre: la solution est ajoutée goutte à goutte, avec agitation, à une suspension de 5.0 g d'hydrure de lithium et d'aluminium dans 250 ml d'éther. On chauffe à l'ébullition à reflux pendant 2 h, détruit l'excès d'hydrure en ajoutant de l'eau goutte à goutte ajoute ensuite 100 ml d'eau et 50 ml d'acide chlorhydrique aqueux 3 *N*. On extrait la couche aqueuse par trois portions de 100 ml d'éther. Les solutions éthérées sont réunies, lavées avec une solution aqueuse à 5% de bicarbonate de sodium, puis avec une solution saturée de chlorure de sodium jusqu'à neutralité. On sèche sur sulfate de sodium anhydre, évapore l'éther et recueille le résidu (10.0 g) qui est immédiatement oxydé.

On dissout 10.0 g des alcools bruts dans 100 ml de pyridine anhydre on y ajoute à température de 25° une suspension de 15.0 g de trioxyde de chrome dans 150 ml de pyridine anhydre. On agite pendant 20 h en protégeant bien de l'humidité. On ajoute alors 500 ml d'eau et 500 ml d'éther; on extrait, sépare la couche aqueuse qu'on extrait encore par trois portions d'éther (3 × 500 ml). On réunit les solutions éthérées, on lave à l'acide chlorhydrique 3 *N*, à l'eau, au bicarbonate de sodium puis avec une solution saturée de chlorure de sodium jusqu'à neutralité. On sèche sur sulfate de sodium anhydre, évapore l'éther et distille le résidu: 9.2 g, p.éb. 104–112° sous 0.4 mm, bande i.r. (CCl_4) à 1715 cm^{-1}; c.p.g.: décalone **1**, 57.3%, décalone **2**, 42.7%, à 35 et 47.5 min respectivement, colonne de 2.5 m polyester succinique de Craig, 20% sur brique, température de la colonne 95°, hélium 60 ml/min. La décalone **1** connue (voir plus haut en 2) a servi à l'identification par la méthode du rehaussement de pic.

Le mélange brut des décalones **1** et **2** est chromatographié en phase gazeuse au moyen d'un appareil préparatif Fisher Prep Partitioner. On injecte le mélange dans une première colonne de 45 × 5 cm, suivie de 7 colonnes de 45 × 3 cm, 20% de polyester succinique de Craig sur brique. Les temps de rétention sont alors de 80 min pour **1**, 100 min pour **2**. La séparation est aisée; il convient toutefois de repasser la *tert-butyl-7 décalone-2 cis* (**2**) sur la colonne pour l'obtenir pure; p.def. 69.5°

Can. J. Chem. Downloaded from www.nrcresearchpress.com by 210.87.254.105 on 09/05/12
For personal use only.

après cristallisation dans l'éther de pétrole (p.éb. 38°), bande i.r. (CCl_4) à 1715 cm^{-1}, C=O; on obtient 1.1 g.

Anal. calc. pour $C_{14}H_{24}O$: C, 80.71; H, 11.61. Trouvé: C, 80.89; H, 11.38.

Anal. calc. pour $C_{20}H_{28}N_4O_4$ (dinitro-2,4 phénylhydrazone (chloroforme/éthanol) p.def. 202.5°): C, 61.84; H, 7.27; N, 14.42. Trouvé: C, 61.96; H, 7.24; N, 14.39.

Le mélange brut des décalones **1** et **2** reste inchangé par traitement par une solution alcoolique d'hydroxyde de potassium à 2%.

*3 Décalones **1**, **11**, et **12** à partir de l'octaline **7**.*

En suivant les modes opératoires décrits dans la section 2.2 plus haut, 5.0 g de *tert*-butyl-6α Δ^1-octaline *cis* (**7**) sont transformés en époxyde (4.79 g), qui est réduit en alcools (4.5 g) par l'hydrure de lithium et d'aluminium, qui sont à leur tour oxydés en décalones (4.3 g) p.éb. 104–107° sous 0.7 mm. Ce mélange donne un chromatogramme en c.p.g. (2.5 m, 15% de polyester succinique de Craig, 225°, hélium 60 ml/min) montrant un pic principal à 18 min, flanqué de deux épaulements, l'un à 16 min, l'autre à 19 min. Le pic principal, qui représente 90% environ du total, est rehaussé par adjonction de *tert*-butyl-6α décalone-2 *cis* (**1**) au mélange.

Le mélange des trois décalones est isomérisé dans les conditions suivantes: 446 mg du mélange sont dissous dans 10 ml de méthanol contenant 200 mg d'hydroxyde de sodium; on abandonne le tout à 25° pendant 24 h, puis chauffe à 55° pendant 1 h. On ajoute après refroidissement, 250 ml d'éther, on lave avec de l'acide chlorhydrique 3 *N*, puis avec une solution aqueuse saturée de chlorure de sodium jusqu'à neutralité.

On sèche sur sulfate de sodium anhydre, évapore l'éther et distille le résidu; on recueille 322 mg distillant à 105° sous 0.7 mm. On chromatographie en phase gazeuse, dans les conditions décrites pour le mélange avant isomérisation; le chromatogramme montre un pic principal à 18 min, l'épaulement à 16 min a augmenté tandis que celui à 19 min a disparu.

4 Réduction de Clemmensen.

*4.1 tert-Butyl-2α décaline trans (**14**)*

On dissout 200 mg de *tert*-butyl-6 décalone-2 *trans*, pure (**5**) dans 1 ml d'acide acétique glacial; on y ajoute un mélange de 0.2 ml d'eau et 0.1 ml d'éthanol, 0.5 ml d'acide chlorhydrique concentré et 700 mg de zinc traité par 36 mg de chlorure mercurique; (le traitement de ce zinc s'effectue en agitant pendant 5 min, dans 1.0 ml d'eau et 0.3 ml d'acide chlorhydrique concentré les quantités indiquées de zinc et de chlorure mercurique puis en pipettant le liquide surnageant). On chauffe à reflux pendant 17 h, en ajoutant après 5 h 0.5 ml d'acide chlorhydrique concentré. Le reflux terminé, on dilue la solution avec un égal volume d'eau; on extrait par 25 ml d'éther; on répète cette opération 5 fois. Les solutions éthérées réunies, lavées avec une solution à 5% de bicarbonate de sodium jusqu'à neutralité. On évapore l'éther. Le résidu est distillé: on recueille 120 mg de *tert-butyl-2α décaline trans* (**14**), p.éb. 134° sous 0.35 mm, $n_D^{25} = 1.4722$. Le spectre i.r. (CCl_4) montre l'absence de bande carbonyle. Le chromatogramme en c.p.g. montre un seul pic à 60 min (2.5 m, 25% d'huile de silicone 550 sur brique 143°, hélium 70 ml/min).

Anal. calc. pour $C_{14}H_{26}$: C, 86.52; H, 13.48. Trouvé: C, 85.93; H, 13.57.

*4.2 tert-Butyl-2α décaline cis (**13**)*

On réduit selon les indications opératoires données en 4.1, 1.0 g de *tert*-butyl-6α décalone-2 *cis* (**1**) en 600 mg de *tert-butyl-2α décaline cis* (**13**), p.éb. 120° sous 28 mm, $n_D^{23} = 1.4887$. Le spectre i.r. (CCl_4) ne montre pas de bande carbonyle. Le chromatogramme montre un seul pic à 67 min, dans les conditions décrites en 4.1.

Anal. calc. pour $C_{14}H_{26}$: C, 86.52; H, 13.48. Trouvé: C, 86.51; H, 13.36.

*4.3 Réduction du mélange des décalones **1** et **12***

On réduit 300 mg du mélange des décalones **1** et **12** obtenu à la section 3 plus haut, selon les données opératoires décrites en 4.1. Le chromatogramme c.p.g. montre 86% de *tert*-butyl-2 décaline *cis* (**13**) et 14% de *tert*-butyl-2 décaline *trans* (**14**), dont la présence est corroborée par rehaussement des pics avec les échantillons des décalines authentiques préparées dans les sections 4.1 et 4.2.

5 Préparation des acétates énoliques

5.1 Première méthode (acétate d'isopropényle, acide sulfurique concentré)

5.11 Mode opératoire général

On suit les indications données dans un mémoire précédent (2).

*5.12 Acétates énoliques de la tert-butyl-6α décalone-2 cis (**1**)*

On obtient, à partir de 2.0 g de décalone, 1.9 g du mélange des acétates énoliques Δ^1 et Δ^2, (**15**) et (**16**), p.éb. 98° sous 0.45 mm $n_D^{27} = 1.4940$. Bandes i.r. (CCl_4) à 1758 et 1695 cm^{-1}, aucune bande carbonyle cétonique à 1715 cm^{-1}.

Anal. calc. pour $C_{16}H_{26}O_2$: C, 76.75; H, 10.47. Trouvé: C, 77.01; H, 10.35.

Le chromatogramme c.p.g. (2.5 m, 20% de polyester succinique de Craig sur Chromat FB 195°, hélium 60 ml/min), montre deux pics: acétate énolique Δ^2, 41% à 35 min et acétate énolique Δ^1, 59% à 46 min.

Anal. calc. pour $C_{16}H_{26}O_2$: C, 76.75; H, 10.47. Trouvé: C, 77.01; H, 10.35.

*5.13 Acétates énoliques de la tert-butyl-7α décalone-2 cis (**2**)*

On obtient, à partir de 249 mg de décalone, 266 mg du mélange des acétates énoliques Δ^1 et Δ^2, p.éb. 106° sous 0.3 mm, $n_D^{26} = 1.4872$, bandes i.r. (CCl_4) à 1715 et 1680 cm^{-1}; analyse c.p.g. comme en 5.12, indique un mélange 50–50% pour des temps de rétention de 26.7 min (isomère Δ^2) et 33.0 min (isomère Δ^1).

Anal calc. pour $C_{16}H_{26}O_2$: C, 76.75; H, 10.47. Trouvé: C, 76.92; H, 10.33.

5.2 Deuxième méthode (anhydride acétique–acide perchlorique)

*5.21 Acétates de la tert-butyl-6α décalone-2 cis (**1**)*

En suivant les indications données dans un mémoire précédent (2), on obtient, à partir de 478 mg de décalone, 100 mg du mélange des acétates énoliques Δ^1 et Δ^2, qui contient par dosage i.r. de 5 à 8% de décalones de départ et de 92 à 95% d'acétates énoliques dans le rapport de 35.5–64.5, Δ^1 et Δ^2 respectivement, avec des élutions à 46 et 35 min, déterminé par c.p.g. comme plus haut en 5.12.

Can. J. Chem. Downloaded from www.nrcresearchpress.com by 210.87.254.105 on 09/05/12
For personal use only.

5.22 Mise à l'équilibre des acétates ***17*** *et* ***18***

On suit le mode opératoire décrit dans un article précédent (1) section 1.4. Le mélange obtenu plus haut à la section 5.13 (200 mg) est mis à l'équilibre et donne 130 mg d'acétate énolique Δ^1 contenant 1–2% de décalone de départ, comme le montrent la c.p.g. et l'i.r.

6 Preuves de structure des acétates énoliques ***15***, ***16***, ***17*** *et* ***18***

*6.1 tert-Butyl-4 bis-(méthoxy-2 éthyl)-1,2 cyclohexane cis, cis (**20**)*

On dissout 2.5 g de *tert*-butyl-6α Δ^2-octaline *cis* (**8**) dans 150 ml d'éther de pétrole (p.éb. 38–40°); on fait passer un courant d'oxygène chargé de 1.8% d'ozone dans la solution refroidie par un bain de CO_2–acétone, jusqu'à coloration bleue persistante. On évapore le solvant en faisant passer un courant d'azote dans le ballon, en laissant revenir le tout à la température de 25°. On reprend l'ozonide par 20 ml d'acétate d'éthyle, 18 ml d'acide acétique glacial, 10 ml d'eau et 15 ml de peroxyde d'hydrogène (30% en volume). On agite 12 h à 25°. On détruit l'excès de peroxyde d'hydrogène en ajoutant du bioxyde de manganèse jusqu'à que cesse l'effervescence. On évapore les solvants sur le bain-marie, reprend le résidu par une solution de NaOH à 10% aqueuse; on filtre; le filtrat est acidifié par adjonction de HCl 10% aqueux jusqu'à pH 2, l'acide brut est extrait par de l'éther; les solutions éthérées sont lavées avec une solution saturée de chlorure de sodium; on sèche sur du sulfate de sodium anhydre, évapore l'éther, on reprend par de l'éther anhydre et ajoute une solution de diazométhane jusqu'à coloration jaune persistante. On évapore l'éther et l'excès de diazométhane et recueille 2.0 g de diester brut.

Le diester brut, 2.0 g, est dissout dans 200 ml d'éther anhydre; cette solution est ajoutée goutte à goutte à une suspension de 2.0 g d'hydrure de lithium et d'aluminium dans 200 ml d'éther. On chauffe à reflux pendant 45 min, détruit l'excès d'hydrure par de l'eau, ajoute de l'acide chlorhydrique concentré jusqu'à disparition de tout précipité et extrait d'une manière continue à l'éther. En évaporant la solution éthérée on recueille le diol brut, que l'on sèche sur P_2O_5 jusqu'à poids constant.

Pour l'éthérification du diol brut on suit la méthode (26). On prépare une solution de catalyseur en mélangeant 1.3 ml d'acide fluoborique 16 *N* dans 20 ml d'éther. On ajoute 3 ml de la solution de catalyseur à 1.6 g de diol brut dans 20 ml d'éther et 50 ml de solution de diazométhane dans l'éther. On garde à 0°; la coloration jaune disparaît en 2–3 min; on rajoute alors 3 ml de la solution de catalyseur et 50 ml de la solution de diazométhane. Au bout de 5 min, on filtre. Le filtrat est lavé avec une solution saturée de chlorure de sodium, on sèche sur sulfate de sodium anhydre et évapore l'éther. On recueille 0.7 g de diéther **20** que l'on distille: p.éb. 98° sous 0.5 mm; $n_D^{23} = 1.4592$.

Anal. calc. pour $C_{16}H_{32}O_2$: C, 74.94; H, 12.58. Trouvé: C, 75.14; H, 12.32.

Un pic en c.p.g., 2.5 m, 20% de Tergitol NPX sur Chromat FB 215°, hélium 60 ml/min: temps de rétention 26.2 min.

*6.2 tert-Butyl-4 méthoxyméthyl-1 (méthoxy-3 propyl)-2 cyclohexane cis,cis (**19**)*

A partir de 1.0 g de *tert*-butyl-6α Δ^1-octaline *cis* (**7**) on obtient comme plus haut en 6.1, 0.23 g de diéther **19**, p.éb. 95° sous 0.3 mm, $n_D^{21} = 1.4605$, pic unique en c.p.g. à 29 min.

Anal. calc. pour $C_{16}H_{32}O_2$: C, 74.94; H, 12.58. Trouvé: C, 74.72; H, 12.31.

*6.3 tert-Butyl-5 méthoxyméthyl-1 (méthoxy-3 propyl)-2 cyclohexane cis,cis (**21**).*

On ozonise l'acétate énolique obtenu plus haut en 5.2 en dissolvant 126 mg dans 20 ml d'éther de pétrole (p.éb. 38–40°), en faisant barboter un courant d'oxygène chargé de 1.8% d'ozone dans la solution plongée dans un bain de CO_2–acétone jusqu'à coloration bleue persistante. On évapore ensuite l'éther de pétrole en faisant passer un courant d'azote dans le ballon, à 0°. Le résidu huileux est séché sous vide (1/20 mg).

On réduit l'ozonide par l'hydrure de lithium et d'aluminium comme décrit précédemment (2) et on éthérifie le diol brut comme en 6.1. On obtient 78 mg de diéther **21**, p.éb. 95° sous 0.3 mm, $n_D^{22} = 1.4562$, pic unique en c.p.g. à 38 min dans les conditions décrites plus haut en 6.1. Ce diéther n'est pas superposable en c.p.g. au diéther **19** et au diéther **20** décrits en 6.2 et 6.1.

Anal. calc. pour $C_{16}H_{32}O_2$: C, 74.94; H, 12.58. Trouvé: C, 75.08; H, 12.42.

6.4 Ozonolyse des acétates énoliques obtenus en 5.12

Comme en 6.1 on ozonise 1.0 g du mélange des acétates énoliques obtenu plus haut en 5.12, on réduit le mélange des ozonides par $LiAlH_4$ (voir (2)), et on éthérifie comme en 6.1 pour obtenir 0.59 g d'un mélange consistant en 35% de diéther **20** pic à 26 min en c.p.g. et 65% de diéther **19**, pic à 29 min en c.p.g. Il y a recouvrement de pics en mélange avec les diéthers purs décrits en 6.1 et 6.2.

Remerciements

Nous remercions le Conseil National de Recherches du Canada de son aide financière (subvention T-14) et les Etablissements Dow Chemical of Canada Ltd., Montréal, pour la quantité généreuse de *tert*-butyl-4 cyclohexanols-1 mise à notre disposition.

1. J. Champagne, H. Favre, D. Vocelle et I. Zbikowski. Can. J. Chem. **42**, 212 (1964).
2. H. Favre et A. J. Liston. Can. J. Chem. **42**, 268 (1964).
3. H. O. House et B. M. Trost. J. Org. Chem. **30**, 1341 (1965).
4. A. J. Liston et M. Howarth. J. Org. Chem. **32**, 1034 (1967).
5. R. Villotti, H. J. Ringold et C. Djerassi. J. Am. Chem. Soc. **82**, 5693 (1960).
6. R. Bucourt et D. Hainaut. Bull. Soc. Chim. France, 1366 (1965).
7. N. L. Allinger, J. A. Hirsch, M. A. Miller et I. J. Tyminski. J. Am. Chem. Soc. **90**, 5773 (1968).
8. W. Klyne. Experientia, **12**, 119 (1956).
9. D. R. Elliott, M. J. T. Robinson et F. G. Riddell. Tetrahedron Letters, 1693 (1965).
10. N. L. Allinger, J. A. Hirsch, M. A. Miller et I. J. Tyminski. J. Am. Chem. Soc. **91**, 336 (1969).
11. G. Stork, A. Brizzolara, H. Landesman, J. Szmuszkovicz et R. Terrell. J. Am. Chem. Soc. **85**, 207 (1963).

12. G. STORK et S. D. DARLING. J. Am. Chem. Soc. **86**, 1761 (1964).
13. M. J. T. ROBINSON. Tetrahedron, **21**, 2475 (1965).
14. R. L. AUGUSTINE et A. D. BROOM. J. Org. Chem. **25**, 802 (1960).
15. R. E. COUNSELL. Tetrahedron, **15**, 202 (1961).
16. R. F. CHURCH, R. E. IRELAND et D. R. SHRIDHAR. J. Org. Chem. **27**, 707 (1962).
17. J. M. BILLY, H. FAVRE et J. M. LALANCETTE. Can. J. Chem. **39**, 835 (1961).
18. W. S. JOHNSON, E. R. ROGIER et J. ACKERMAN. J. Am. Chem. Soc. **78**, 6322 (1956).
19. C. DJERASSI et J. FISHMAN. J. Am. Chem. Soc. **77**, 4291 (1955).
20. K. TAKEDA, T. OKANISHI, H. OSAKA, A. SHIMAOKA et N. MAESONO. Chem. Pharm. Bull. Tokyo, **9**, 388 (1961).
21. H. OSAKA. Chem. Pharm. Bull. Tokyo, **10**, 404, 413, 417 (1962).
22. A. FÜRST et PL. A. PLATTNER. Helv. Chim. Acta, **32**, 275 (1949).
23. J. C. RICHER et C. FREPPEL. Can. J. Chem. **46**, 3709 (1968).
24. E. J. COREY et R. L. DAWSON. J. Am. Chem. Soc. **85**, 1782 (1963).
25. B. RICKBORN et W. E. LAMKE, II. J. Org. Chem. **32**, 537 (1967).
26. M. NEEMAN, M. C. CASERIO, J. D. ROBERTS et W. S. JOHNSON. Tetrahedron, **6**, 36 (1959).
27. C. SANDRIS et G. OURISSON. Bull. Soc. Chim. France, 1524 (1958).
28. A. S. DREIDING. Chem. Ind. London, 1419 (1954).
29. N. MAES, R. OTTINGER, J. REISSE et G. CHIURDOGLU. Tetrahedron Letters, 335 (1969).
30. R. J. WICKER. J. Chem. Soc. 2165 (1956).
31. H. BRUDERLEIN, N. DUFORT, H. FAVRE et A. J. LISTON. Can. J. Chem. **41**, 2908 (1963).
32. H. FAVRE, M. LEFEBVRE et J. C. RICHER. Can. J. Chem. **37**, 403 (1959).

Can. J. Chem. Downloaded from www.nrcresearchpress.com by 210.87.254.105 on 09/05/12
For personal use only.

Can. J. Chem. Downloaded from www.nrcresearchpress.com by 210.87.254.105 on 09/05/12
For personal use only.

Barriers to rotation in *ortho*-alkylphenyl substituted 1,3-benzoxazines[1]

S. BROWNSTEIN, E. C. HORSWILL, AND K. U. INGOLD
Division of Applied Chemistry, National Research Council of Canada, Ottawa, Canada

Received April 25, 1969

Four 3,4-dihydro-3-*ortho*-alkylphenyl-2*H*-1,3-benzoxazines have been synthesized. Enthalpies and entropies of activation for rotation about the phenyl–nitrogen bond have been calculated from the temperature dependence of the proton resonance spectra for the *o*-isopropyl ($\Delta S‡ = -4$ e.u., $\Delta H‡ = 10.8$ kcal/mole) and *o*-*t*-butyl ($\Delta S‡ = 0.4$ e.u., $\Delta H‡ = 16.9$ kcal/mole) derivatives. The barrier to rotation for the *o*-methyl and 2,6-dimethyl derivatives was too low to be measured by this procedure.

Canadian Journal of Chemistry, **47**, 3243 (1969)

Introduction

There have been many high resolution magnetic resonance studies of hindered rotation about nominally single bonds (1–5). In most cases reported for hindered rotation about a carbon–nitrogen single bond the magnitude of the barrier to rotation has been attributed to partial double bond character. Thus far no studies have been reported in which changes in the barrier to rotation along a homologous series have been attributed solely to steric effects. In the present investigation proton resonance spectra were obtained for a series of substituted benzoxazines of the following general formula.

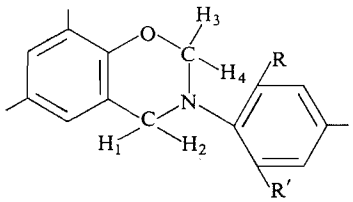

It was found that when R′ is a bulky substituent H-1 and H-2, and H-3 and H-4 were not equivalent on the nuclear magnetic resonance time scale.

In principle the non-equivalence of H-1 through H-4 could arise either by hindered rotation about the aryl carbon–nitrogen bond or by a barrier to inversion of the non-planar benzoxazine ring. Provided that R and R′ are not identical, H-1 through H-4 should remain non-equivalent even when ring inversion is rapid, provided that rotation about the carbon–nitrogen bond is slow. The non-equivalence arises from the closer proximity to R′ of, say, H-2 and H-4, compared with H-1 and H-3. If R = R′ this non-equivalence is removed.

When both hindered inversion and hindered rotation occur two different sets of non-equivalent proton signals can be expected. One set would arise from the isomer in which R′ is closest to H-1 and H-3 and the other set when R′ is closest to H-2 and H-4. However, if one of the R groups is more bulky than the other, one of the conformers may be present at a much lower concentration because steric repulsion between R and the benzoxazine ring will raise its potential energy. Therefore, although in principle two sets of non-equivalent proton signals can be expected, in fact only one set may be observable. If R = R′ the existence of two unique isomers would be removed and only one set of non-equivalent proton resonance signals would be observed. The possible situations are summarized in Table I.

In the preceding discussion it is implicitly assumed that there can be rapid inversion about the nitrogen atom. Because of the asymmetry of the benzoxazine ring, H-1 through H-4 will remain non-equivalent when inversion about nitrogen is fast, provided that ring inversion is slow. If ring inversion is rapid but rotation about the phenyl–nitrogen bond is slow, then ring inversion will probably be accompanied by nitrogen inversion to place the *o*-alkylphenyl ring in the conformation with minimum steric strain.

Experimental

Proton resonance spectra were obtained at 100 MHz on a "Varian Associates" HR 100 spectrometer. Probe temperatures were calibrated with a copper–constantan thermocouple in a dummy sample tube and should be accurate within 1 °C. Low temperature spectra were obtained using carbon disulfide as solvent while for the high temperature studies the solvent was *s*-tetrachloroethane. Tetramethylsilane was used as internal reference, and

[1]Issued as NRCC No. 10811.

TABLE I

Relationship between motional freedoms and equivalency of benzoxazine ring protons

Inversion	Rotation	R = R′	R ≠ R′
Hindered	Hindered	Protons different	Two sets of different protons
Hindered	Free	Protons different	Protons different
Free	Hindered	Protons equivalent	Protons different
Free	Free	Protons equivalent	Protons equivalent

chemical shifts are reported as p.p.m. to low field. All melting points were determined on a Kofler hot stage using factory-calibrated thermometers. Infrared (i.r.) spectra were measured in carbon tetrachloride solution on a Perkin–Elmer model 621 spectrophotometer. The i.r. spectra of all the compounds showed no absorption in the 3700–3100 cm^{-1} region. The mass spectra were recorded on an Atlas CH 4 spectrometer. Microanalyses were carried out by Mr. J. R. H. Seguin of these laboratories.

*6-tert-Butyl-3,4-dihydro-3-o-tolyl-2H-1,3-benzoxazine (**1**)*

A solution of 1.5 g of barium hydroxide octahydrate in 25 ml (0.33 mole) of formalin was added to a mixture of 10.9 g (0.073 mole) of 4-*tert*-butylphenol and 7.8 g (0.073 mole) of *o*-toluidine and the mixture shaken at room temperature for 6 h. After the aqueous phase was decanted, the solid was dissolved in benzene and the solution washed with water. Benzene was removed after drying to give 18.8 g of crystalline product which recrystallized from 95% ethanol to produce 12.6 g of colorless crystals, m.p. 88–90°. An analytical sample was recrystallized from pentane, m.p. 90.9–92.0°. The i.r. spectrum showed no absorption in the 3700–3100 cm^{-1} region.

Anal. Calcd. for $C_{19}H_{23}ON$ (mol. wt., 281): C, 81.10; H, 8.24; N, 4.98. Found (mol. wt., mass spectroscopy, 281): C, 81.02; H, 8.21; N, 4.89.

*6-tert-Butyl-3,4-dihydro-3-(2,6-xylyl)-2H-1,3-benzoxazine (**2**)*

Treatment of 3.0 g of 4-*tert*-butylphenol and 2.4 g of 2,6-xylidine with alkaline formalin gave a product containing some starting materials (by thin-layer chromatography). The benzene solution was extracted with 2 *N* hydrochloric acid, with 10% sodium hydroxide solution, and then water. Drying and concentration left 3.8 g of yellow syrup, n_D^{25} 1.5592, pure by thin-layer chromatography.

Anal. Calcd. for $C_{20}H_{25}NO$: C, 81.31; H, 8.53; N, 4.74. Found: C, 81.08; H, 8.51; N, 4.89.

*6-tert-Butyl-3-o-cumyl-3,4-dihydro-8-methyl-2H-1,3-benzoxazine (**3**)*

The use of 4-*tert*-butylphenol with 2-*iso*-propylaniline in the reaction above produced a strongly acidic phenolic compound rather than a benzoxazine.

When 3.3 g of 4-*tert*-butyl-*o*-cresol and 2.7 g of purified 2-*iso*-propylaniline (n_D^{25} 1.5458) were condensed with alkaline formaldehyde the only product was the benzoxazine. After solution in hexane, extraction and concentration, the colorless crystals (2.8 g) melted 91–97°. Recrystallization from ethanol gave 2.4 g of a compound of melting point 93–96°. An analytical sample was obtained from pentane, m.p. 97.5–99.0°.

Anal. Calcd. for $C_{22}H_{29}NO$ (mol. wt., 323): C, 81.69; H, 9.04; N, 4.33. Found (mol. wt., mass spectroscopy, 323): C, 81.39; H, 9.11; N, 4.05.

*6,8-Di-tert-butyl-3-(2,4-di-tert-butylphenyl)-3,4-dihydro-2H-1,3-benzoxazine (**4**)*

A mixture of 0.56 g of 2,4-di-*tert*-butylaniline, 0.56 g of 2,4-di-*tert*-butylphenol and 10 ml of 37% formalin solution (no catalyst) was stirred and heated in a bath at 95° for 2 h. The cooled suspension was filtered, washed with water, and vacuum dried. The colorless crystalline product (1.08 g) after recrystallization from absolute ethanol gave 0.72 g of colorless felted needles, m.p. 173–175.6°. Further recrystallization gave an analytical sample, m.p. 174.7–176.0°.

Anal. Calcd. for $C_{30}H_{45}NO$ (mol. wt., 435): C, 82.70; H, 10.41; N, 3.21. Found (mol. wt., mass spectroscopy, 435): C, 82.24; H, 10.23; N, 3.46.

Results and Discussion

The structural formulae of the compounds studied and chemical shifts for the various types of protons are given in Fig. 1. Theoretical spectra were calculated by computer using a previously reported program (6). To utilize this program for an AB system it is necessary to specify the position, intensity and transition probability for each line. In all the compounds H-1 and H-2 gave significantly broadened lines both at the limits of rapid rotation and slow rotation. This is attributed to long range spin coupling to a proton or protons on the adjacent aromatic ring. To correct for this line broadening a convolution integral was introduced into the computer program to broaden the theoretical spectra by a Gaussian function whose width could be adjusted to that of the experimental line widths in the absence of exchange broadening. In Fig. 2 experimental spectra for H-1 and H-2 of compound **3** are presented along with approximately equivalent theoretical spectra. The rate constant for rotation at a given temperature was obtained by interpol-

Can. J. Chem. Downloaded from www.nrcresearchpress.com by 210.87.254.105 on 09/05/12
For personal use only.

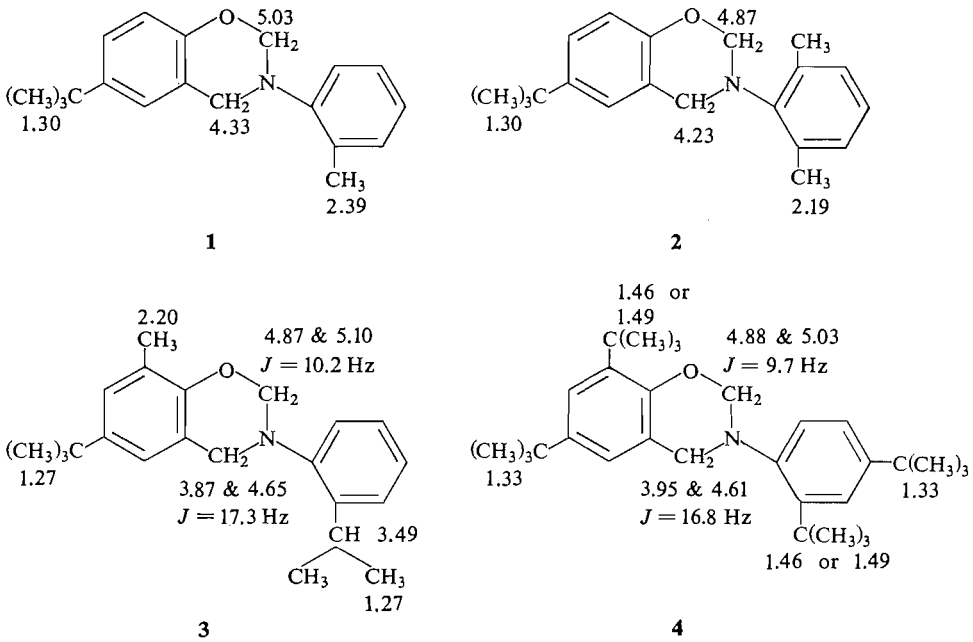

FIG. 1. Structural formulae and chemical shifts of some benzoxazines.

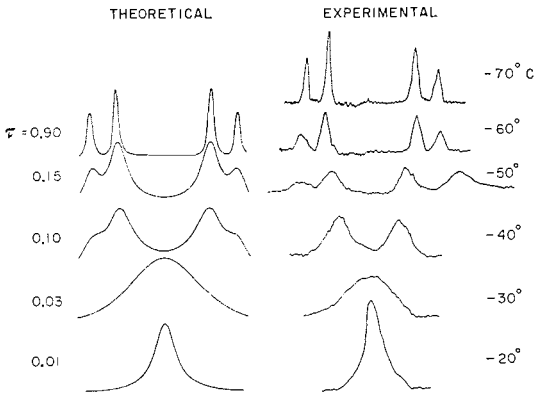

FIG. 2. Theoretical and experimental spectra for H-1 and H-2 of compound **3**.

ation of line widths and peak to trough ratios between theoretical spectra closely matching the experimental spectrum.

At room temperature the benzoxazine ring protons are equivalent, in pairs, for compounds **1**, **2**, and **3** but are non-equivalent in **4**. Lowering the temperature below 0 °C causes an observable non-equivalence in the proton resonance spectra for **3** but the protons in **1** and **2** remain equivalent down to the lowest temperatures studied (−60 °C). From the behavior of the proton resonance spectra of **3** and **4** it can be concluded that there is rapid inversion but that rotation about the carbon–nitrogen bond is slow on the n.m.r. time scale. Further evidence for this conclusion is obtained from the methyl resonances of R in compounds **3** and **4**. If ring inversion is slow there should be two different environments for R, i.e. with the *o*-alkyl substituted phenyl axial or equatorial, regardless of the rate of rotation about the carbon–nitrogen bond. Examination of a space filling molecular model suggests that there is considerable steric hindrance about the nitrogen of the benzoxazine ring. For a given conformation of the ring only one configuration of the benzene ring, relative to nitrogen, can be constructed. Therefore, the averaging effect of inversion about nitrogen alone need not be considered. Since only a single sharp signal is observed for R under conditions that yield non-equivalent benzoxazine ring protons, it is quite likely that ring inversion is a rapid process.

In Fig. 3 the logarithm of the rate constant for rotation about the carbon–nitrogen bond of compound **4**, averaged for results from *both* sets of ring protons, is plotted against the reciprocal temperature. From a least squares analysis of this

Can. J. Chem. Downloaded from www.nrcresearchpress.com by 210.87.254.105 on 09/05/12
For personal use only.

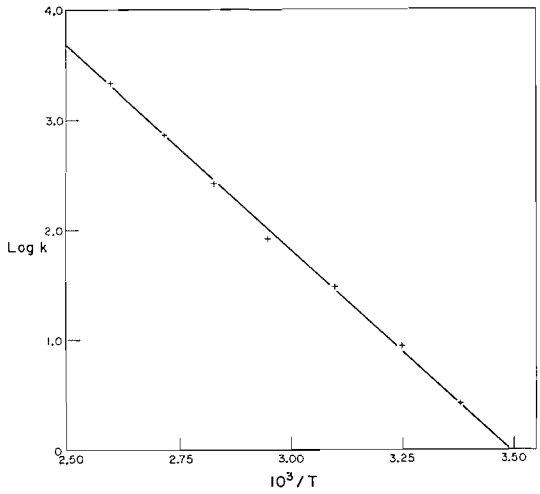

FIG. 3. The variation of rate of rotation with temperature for compound **4**.

data and similar data for compound **3** the following activation parameters were obtained.

$$\text{Compound } \mathbf{3}\ \Delta H^{\ddagger} = 10.8 \pm 0.6 \text{ kcal/mole}$$
$$\Delta S^{\ddagger} = -4 \pm 2 \text{ e.u.}$$
$$\text{Compound } \mathbf{4}\ \Delta H^{\ddagger} = 16.9 \pm 0.3 \text{ kcal/mole}$$
$$\Delta S^{\ddagger} = 0.4 \pm 0.2 \text{ e.u.}$$

The activation entropies are normal suggesting no unusual conformational requirement in the transition state for rotation. The failure to observe any line broadening arising from non-equivalent protons in compound **1** even at -60 °C implies that the rate constant for rotation in this compound is greater than 3.3×10^3 s^{-1} if we assume that all compounds have similar chemical shift differences. If we make the further assumption that $\Delta S^{\ddagger} = 0$ for compound **1** it can be calculated that $\Delta H^{\ddagger}$ for an *o*-methyl substituent is less than 8.9 kcal/mole. The barrier to rotation about the phenyl–nitrogen bond therefore increases by more than 1.9 kcal/mole on changing the *ortho* substituent from methyl to isopropyl and by 6.1 kcal/mole on changing from isopropyl to *t*-butyl.

1. D. S. THOMPSON, R. A. NEWMARK, and C. H. SEDERHOLM. J. Chem. Phys. **37**, 411 (1962).
2. T. D. ALGER, H. S. GUTOWSKY, and R. L. VOLD. J. Chem. Phys. **47**, 3130 (1967).
3. J. W. EMSLEY, J. FEENEY, and L. H. SUTCLIFFE. High resolution nuclear magnetic resonance spectroscopy. Vol. I. Pergamon Press, Oxford. 1965. p. 551.
4. B. J. PRICE, J. A. EGGLESTON, and I. O. SUTHERLAND. J. Chem. Soc. B 922 (1967).
5. A. MANNSCHRECK and H. MUENSCH. Tetrahedron Letters, 3227 (1968).
6. S. BROWNSTEIN and J. BORNAIS. Can. J. Chem. **46**, 225 (1968).

Can. J. Chem. Downloaded from www.nrcresearchpress.com by 210.87.254.105 on 09/05/12
For personal use only.

Can. J. Chem. Downloaded from www.nrcresearchpress.com by 210.87.254.6 on 09/05/12
For personal use only.

Etudes stereochimiques. VIII.[1] Sur la serie *exo*-maleopimarique

C. MACIEJEWSKI, M. GILLARD, N. LANGLOIS[2], ET B. GASTAMBIDE
Laboratoire de Chimie Organique, Faculté des Sciences, 51, Reims, France

Reçu le 25 mars 1969

L'action de l'anhydride maléique sur les esters résiniques conduit non seulement à l'adduit classique **3***a* mais aussi à l'*exo*-anhydro-maléopimarate de méthyle (**3***b*) dont la structure est prouvée par des mesures physiques et des transformations chimiques.

Canadian Journal of Chemistry, 47, 3247 (1969)

Le lévopimarate de méthyle (**1**), cela est classique, réagit avec l'anhydride maléique, à la température ordinaire, pour donner un composé d'addition de Diels–Alder dénommé anhydro-maléopimarate de méthyle (**3***a*). Parmi les quatre isomères susceptibles de se former dans la réaction, seul l'adduit **3***a*, de configuration *endo* bien établie (1–3) a été décrit dans la littérature. Cette synthèse diénique était donc considérée jusqu'à présent comme tout à fait stéréospécifique et utilisable par exemple pour la détermination quantitative de l'acide lévopimarique dans les résines (1). On doit signaler, cependant, que Sandermann (4), en titrant par acidimétrie l'adduit formé, a envisagé la formation possible dans la réaction d'un deuxième isomère; cette hypothèse n'a pas été prise jusqu'à présent en considération.

Nous avons donc décidé d'examiner la stéréospécificité de cette réaction et avons isolé un deuxième adduit **3***b* de structure *exo*; ceci est en accord avec les travaux effectués par deux d'entre nous (5) en série citraconopimarique où trois adduits ont été obtenus, l'un de ceux-ci possédant l'inhabituelle configuration *exo*.

Lorsqu'on opère sur de grosses quantités de produits initiaux, la réaction de Diels–Alder est effectuée, non pas avec le lévopimarate de méthyle, mais en traitant à 160° un mélange de résinates de méthyle préparé à partir de la gemme de pin d'Alep selon une méthode mise au point par Mme Carnero (6, 7). La chromatographie sur couche mince montre la présence du composé **3***b* dans les eaux-mères de cristallisation de l'adduit **3***a*: par ordre de vitesses de migration décroissantes, on trouve les résinates de méthyle, l'adduit **3***b*, puis l'isomère **3***a*, et enfin un mélange de composés acides. Nous avons tout d'abord cherché à éliminer les quantités assez considérables de résinates de méthyle n'ayant pas réagi. Après divers essais, seule la chromatographie sur colonne de florisil du produit issu de l'évaporation des eaux-mères semble satisfaisante; on peut ainsi obtenir un mélange des composés **3***a* et **3***b* qui sont ensuite isolés par chromatographie d'élution sur gel de silice. L'*exo*-anhydro-maléopimarate de méthyle (**3***b*) est ainsi obtenu avec un rendement de 8%.

La réaction de Diels–Alder, effectuée d'une manière similiaire à 160° avec de l'abiétate de méthyle commercial ou du palustrate de méthyle, montre la constance du rapport des quantités d'isomères **3***a* et **3***b* formés. Ce rapport varie cependant avec la température utilisée. Des synthèses diéniques effectuées avec le lévopimarate de méthyle et l'anhydride maléique dans l'acétone à 25° et sans solvant à 160° conduisent à des rapports **3***a*/**3***b* respectivement égaux à 77 et 8 d'après la chromatographie gazeuse ou les quantités obtenues.

Ces résultats pourraient s'expliquer par une épimérisation **3***a* → **3***b*, épimérisation du type *endo* → *exo* qui se produirait pour une température élevée de réaction de Diels–Alder. D'après la littérature (8, 9) une isomérisation *endo* → *exo* peut s'effectuer selon deux voies différentes: un mécanisme dit "externe" où l'adduit *endo* par rétroréaction se transforme peu à peu en l'autre isomère avec passage par les composés de départ et une voie dite "interne" où l'épimérisation s'effectue directement sans qu'il y ait

[1]Partie VII voir réf. 5.
[2]Institut de Chimie des Substances Naturelles, 91, Gif-sur-Yvette, France.

Can. J. Chem. Downloaded from www.nrcresearchpress.com by 210.87.254.6 on 09/05/12
For personal use only.

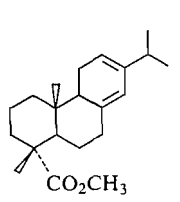

1

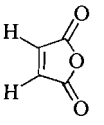

2

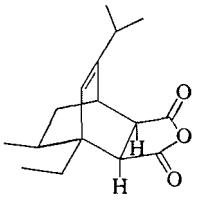

3*a*

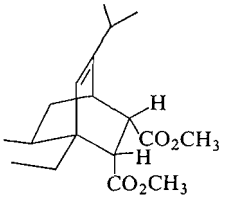

7

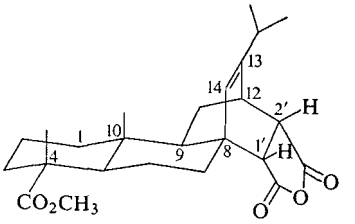

3*b*

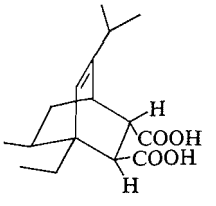

4

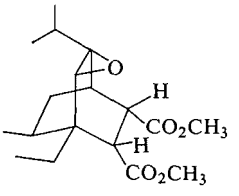

6

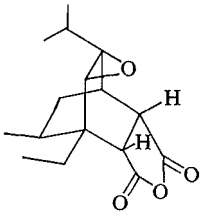

5

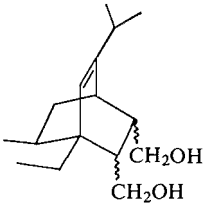

8

scission. Cependant nous avons observé que l'adduit **3***a* chauffé à 160° ou 220° en présence ou non d'anhydride maléique ne s'épimérise pas comme d'ailleurs à 195° l'adduit **3***b*. De l'ensemble des résultats obtenus, on peut en déduire que, pour la synthèse diénique étudiée, une température de réaction élevée semble améliorer le rendement en isomère **3***b* sans que celui-ci provienne toutefois d'une isomérisation *endo* → *exo*.

La structure de l'adduit **3***b* a été déterminée tout d'abord par voie chimique: ce composé, traité à la température ordinaire par de la soude alcoolique durant six heures, se transforme en fumaropimarate de monométhyle **4**. Les caractéristiques physiques du produit ainsi obtenu sont identiques à celles du composé provenant de l'épimérisation de l'adduit **3***a* (7). Ce résultat ne peut être concevable que si **3***b* a une configuration *exo* et provient de l'attaque du diène par le face α.

On peut d'autre part considérer comme arguments en faveur de la structure **3***b* les observations suivantes: si l'on fait agir sur ce composé l'acide *p*-nitroperbenzoïque, on obtient un époxyde dont la stéréochimie **5** est attribuée par analogie (7) et qui se transforme en époxydetriester **6** sous l'action du diazométhane méthanolique. En traitant **5** par de l'acide sulfurique et du méthanol, on aboutit notamment au composé **6** sans apparition d'aucune substance lactonique comme en série *endo*-maléopimarique. De même le triester **7**, provenant du traitement de **3***b* par du diazométhane en solution méthanolique, est transformé par action de l'acide *p*-nitroperbenzoïque en époxyde (**6**) sans formation, comme en série *endo*, d'un quelconque composé lactonique. Une configuration *exo* est compatible avec les résultats ainsi obtenus.

Des études de résonance magnétique nucléaire permettent de confirmer la structure du composé **3***b*. Celui-ci, en solution dans le deutériochloroforme, donne un pic à δ 0.61 p.p.m. qui correspond au méthyle porté par le carbone-10. Cette valeur de résonance située vers les champs forts s'explique (2) par l'anisotropie magnétique de la

Can. J. Chem. Downloaded from www.nrcresearchpress.com by 210.87.254.6 on 09/05/12
For personal use only.

double liaison *ou* des carbonyles du groupement anhydride. Or la réduction de **3***b* par le borohydrure de sodium (5, 10, 11) conduit au diol **8** qui malgré la disparition de la fonction anhydride donne cependant un pic à 0.59 p.p.m. attribué au méthyle angulaire. Cet effet d'écran confirme la position de la double liaison et se retrouve chez les composés **4** et **7**. Par contre, chez les époxydes **5** et **6**, le méthyle en C-10 donne une résonance à 0.84, valeur tout à fait normale.

En conclusion, on peut affirmer que la série *exo*-maléopimarique est accessible à l'aide d'une réaction de Diels–Alder effectuée à haute température.

Partie expérimentale

Sauf mentionné, les chromatoplaques analytiques (0.25 mm) et préparatives (0.5–0.75 mm) sont confectionnées avec du gel de silice HF 254 + 366; les points de fusion corrigés ont été déterminés à l'aide d'un microscope Leitz; les pouvoirs rotatoires sont mesurés avec un polarimètre Jouan–Roussel en solution chloroformique et à des concentrations exprimées en g/100 ml. Les spectres infrarouge (i.r.) et de résonance magnétique nucléaire (r.m.n.) ont été enregistrés sur des appareils Perkin–Elmer 521 et Varian A60 (δ; t.m.s. interne; *J* en c.p.s.).

Isolement de 3b

La réaction de Diels–Alder est effectuée comme décrite (7) sur 50 g de résinates de méthyle. Le filtrat provenant de la précipitation de l'adduit **3***a* (23 g) est évaporé, puis traité plusieurs fois par de l'eau chauffée préalablement à la température de 50°. Après extraction à l'éther et séchage sur sulfate de sodium, on obtient une huile jaune orangée (45 g) contenant des résinates de méthyle, les deux adduits et des produits acides.

Ce produit brut (8 g) est chromatographié sur 500 g de florisil (diamètre 125 mm, hauteur 200 mm): les résinates de méthyle sont élués par du tétrachlorure de carbone et les deux adduits (2.8 g) par du chloroforme. La séparation des deux adduits (500 mg) est effectuée par chromatographie sur un mélange de gel silice Mallinckrodt célite (2/1) (75 g; 30 × 300 mm) avec contrôle du fractionnement sur chromatoplaques (benzène–méthyl éthyl cétone 9/1). L'adduit **3***b* (170 mg; Rdt total 8%) est élué par du benzène contenant 1% de chloroforme. L'anhydride du (dicarboxy-1′α,2′α éthano)-8α,12α abiétène-13 oate-18 de méthyle (*exo*-anhydro-maléopimarate de méthyle) est recristallisé dans cinq volumes d'éthanol absolu: $F = 193°$; $[\alpha]_D = -42°$ (2.4); i.r. ($CHCl_3$): 1855, 1783 (anhydride) 1725; r.m.n. ($CDCl_3$): 0.61 (CH_3-10), 1.03 (isopropyle, $J = 7$), 1.12 (CH_3-4), 3.60 (CO_2CH_3), 5.42 (H—C═); malgré l'utilisation de plusieurs solvants non n'avons pu mettre en évidence que la moitié de l'octet dû à l'hydrogène 2′β: (quadruplet, $J_{2'\beta\,11\beta} \sim 2$, $J_{2'\beta 12} \sim 4$).

Anal. calc. pour $C_{25}H_{34}O_5$: C, 72.43; H, 8.27. Trouvé: C, 72.31; H, 8.14.

Préparation du composé 4

Une solution de 50 mg d'adduit **3***b* dans 2 ml de soude 2 *N* alcoolique à 80% est agitée pendant 6 h à la température ordinaire. Le mélange réactionnel est jeté dans 15 ml d'eau et extrait par 3 × 3 ml d'éther. Les phases alcalines sont ensuite acidifiées par de l'acide chlorhydrique 6 *N*, puis extraites par du benzène–éther (1/1). Les couches organiques, réunies, sont traitées deux fois par 5 ml d'une solution de carbonate de sodium à 5%, les phases alcalines étant acidifiées puis extraites par du benzène–éther. Le produit brut (49 mg) après plusieurs recristallisations dans cinq volumes, alternativement, de benzène–dioxanne (2/1) et d'éthanol, conduit à 56% de (dicarboxy-1′β,2′α éthano)-8α,12α abiétène-13 oate-18 de méthyle (fumaropimarate de méthyle) **3***b*: $F = 297°$; $[\alpha]_D = +35°$ ($c = 0.6$; éthanol); i.r. (KBr): 3220, 1730, 1710, 1690 (épaulement); r.m.n. (CF_3COOH): 0.76 (CH_3-10), 1.17 (isopropyle, $J = 7$), 1.26 (CH_3-4), 5.48 (H—C═).

Anal. calc. pour $C_{27}H_{40}O_6$: C, 69.42; H, 8.39. Trouvé: C, 69.13; H, 8.44.

Ces constantes sont identiques à celles du produit résultant de l'action de la soude alcoolique sur l'adduit **3***a*.

Epoxyde 5

En opérant comme décrit (7) et à partir de 20 mg de **3***b*, on obtient 92% de produit brut. Après trois recristallisations dans du chloroforme–oxyde d'isopropyle (1/1) l'anhydride de l'époxy-13α,14α (dicarboxy-1′α,2′α éthano)-8α,12α abiétanoate-18 de méthyle (11 mg) présente les caractéristiques suivantes: $F = 298°$; $[\alpha]_D = -11°$ (2); i.r. ($CHCl_3$): 1850, 1783, 855 (époxyde); r.m.n. ($CDCl_3$): 0.84 (CH_3-10), 0.71 et 1.05 (2d isopropyle $J = 7$), 1.19 (CH_3-4).

Anal. calc. pour $C_{25}H_{34}O_6$: C, 69.74; H, 7.96. Trouvé: C, 69.58; H, 7.80.

Action du diazométhane ou de l'acide sulfurique–méthanol sur l'époxyde 5

Une solution de 100 mg de **5** dans du benzène–méthanol (1/7) est traitée une nuit à −20° par un excès de diazométhane éthéré. Par chromatographie préparative sur couche mince, on isole 80 mg d'époxy-13α,14α (diméthoxycarbonyl-1′α,2′α éthano)-8α,12α abiétanoate-18 de méthyle (**6**) huileux: $[\alpha]_D = +11°$ (1.4); i.r. ($CHCl_3$): 3035, 1740, 890, 870.

Anal. calc. pour $C_{27}H_{40}O_7$ (sur 2.3 mg distillé): C, 68.04; H, 8.46. Trouvé: C, 68.41 H, 8.39.

L'action de l'acide sulfurique–méthanol sur 50 mg de **5** selon (7) conduit à 48 mg d'huile (pas de bande i.r. caractéristique d'une γ-lactone) donnant sur chromatoplaque au moins quatre taches. Le composé **6** est isolé (49%) par chromatographie préparative sur couche mince.

$[\alpha]_D = +8°$ (1.5); r.m.n. ($CDCl_3$): 0.74 et 1.06 (2d isopropyle $J = 7$), 0.83 (CH_3-10), 1.11 (CH_3-4), 3.07 (H-14), 3.59 (9H).

Action du diazométhane sur l'adduit 3b

Le composé **3***b* (50 mg) dissous dans 5ml de méthanol est traité à −10° par une solution éthérée de diazométhane. On distille à $85°/10^{-2}$ mm le (diméthoxycarbonyl-1′α, 2′α éthano)-8α,12α abiétène-13 oate-18 de méthyle **7**, composé huileux: $[\alpha]_D = -6°$ (2.4); i.r. ($CHCl_3$): trois bandes vers 1730; r.m.n. ($CDCl_3$): 0.62 (CH_3-10), 1.09 (isopropyle $J = 7$), 1.15 (CH_3-4), 3.52 (6H), 3.65 (3H), 5.43 (H—C═).

Anal. calc. pour $C_{27}H_{40}O_6$: C, 70.41; H, 8.75. Trouvé: C, 70.62; H, 8.71.

L'action du méthanol sulfurique sur **3***b* conduit au même triester huileux.

Action de l'acide p-nitroperbenzoïque sur **7**

En opérant comme pour l'époxydation de **3***b*, le produit brut obtenu (pas de bande i.r. caractéristique d'une γ-lactone) donne cinq taches sur chromatoplaque, dont la plus intense correspond au composé **6**, isolé par chromatographie sur couche épaisse. Les spectres i.r. et de r.m.n. montrent que ce produit est identique aux échantillons obtenus par action du diazométhane ou du méthanol sulfurique sur le composé **5**.

Réduction par le borohydrure de sodium du composé **3***b*

Selon le mode opératoire décrit (5) et à partir de 50 mg de **3***b*, on obtient 45 mg d'un mélange de deux composés séparés sur chromatoplaques préparatives.

La γ-lactone du [carboxy-1′α (ou 2′α) hydroxyméthyl-2′α (ou 1′α) éthano]-8α,12α abiétène-13 oate-18 de méthyle (33%) est recristallisée dans cinq volumes de méthanol: $F = 159°$; i.r. ($CHCl_3$): 1755 (lactone), 1718; r.m.n. ($CDCl_3$): 0.60 (CH_3-10), 1.03 (isopropyle $J = 7$), 1.13 (CH_3-4).

Anal. calc. pour $C_{25}H_{36}O_4$: C, 74.96; H, 9.06. Trouvé: C, 75.13; H, 8.96.

Le (dihydroxyméthyl-1′ξ,2′ξ éthano)-8α,12α abiétène-13 oate-18 de méthyle (47%) est recristallisé dans cinq volumes d'acétate d'éthyle: $F = 155°$; $[\alpha]_D = +5°$ (2.6); i.r. ($CHCl_3$): 3610, 3410, 1720; i.r. (CCl_4 1‰): 3632 (OH libre), 3490 (OH lié); r.m.n. ($CDCl_3$): 0.59 (CH_3-10), 1.01 (isopropyle $J = 7$), 1.15 (CH_3-4), 5.46 (H—C=).

Anal. calc. pour $C_{25}H_{40}O_4$: C, 74.21; H, 9.97. Trouvé: C, 74.19; H, 9.94.

Remerciements

Monsieur Poudeybat et les Anciens Etablissements Granel Frères, 40-Lesperon ont eu l'amabilité de nous fournir à plusieurs reprises des échantillons d'acides résiniques purs.

1. W. D. Lloyd et G. W. Hedrick. J. Org. Chem. **26**, 2029 (1961).
2. W. L. Meyer et R. W. Huffman. Tetrahedron Letters, **16**, 691 (1962).
3. W. A. Ayer, C. E. McDonald, et J. B. Stothers. Can. J. Chem. **41**, 1113 (1963).
4. W. Sanderman. Chem. Ber. **71B**, 2005 (1938).
5. B. Gastambide et N. Langlois. Helv. Chim. Acta, **51**, 2048 (1968).
6. P. Carnero et B. Gastambide. D'être publié.
7. N. Langlois et B. Gastambide. Bull. Soc. Chim. France, 2966 (1965).
8. V. A. Mironov, T. M. Fadewa, A. V. Stepaniantz, et A. A. Akhrem. Tetrahedron Letters, **47**, 5823 (1966).
9. H. Kwart et K. King. Chem. Rev. **68**, 415 (1968).
10. S. W. Chaikin et G. Brown. J. Am. Chem. Soc. **71**, 122 (1949).
11. N. Langlois et B. Gastambide. Compt. Rend. **264**, 1878 (1967).

Photolysis and mass spectra of *trans*-cinnamimide[1]

Robert T. LaLonde and Curry B. Davis

Department of Chemistry, State University College of Forestry, Syracuse University, Syracuse, New York 13210

Received March 25, 1969

Using Pyrex filtered light, irradiation of *trans*-cinnamimide in 1,2-dimethoxyethane solution gave β-truxinimide (48% yield), *cis*-cinnamamide and *trans*-cinnamamide. Both *trans*-cinnamimide and β-truxinimide undergo fragmentation in the mass spectrometer to give $C_{16}H_{14}+$, $C_{16}H_{13}+$, $C_{16}H_{12}+$, and $C_{14}H_{12}+$.

Canadian Journal of Chemistry, 47, 3250 (1969)

The solution photolysis of cinnamic acids, esters, and amides is capable of producing under widely varying conditions cyclobutanes, hydrogen abstraction reactions, *cis–trans* isomerizations and internal cyclizations. The following may be given as examples. Coumarin undergoes dimerization affording cyclobutane isomers, the geometry of which is solvent and sensitizer dependent (1, 2). Ethyl *trans*-cinnamate, ethyl *trans*-α-methylcinnamate and analogous lactones undergo isomerization and hydrogen abstraction reactions (3). A different mode of reactivity has been observed for α-phenylcinnamic acid and α-phenylcinnamamide (4). The acid and amide in each case give a β-lactone and a β-lactam and their formation have been viewed as cyclization reactions belonging to the general class of electrocyclic processes.

In connection with a study of the chemistry of α,β-unsaturated *N*-acylimides and imides we have explored the solution photochemistry of *trans*-cinnamimide (**1**).

A carefully degassed 1,2-dimethoxyethane solution of **1** was irradiated in a Pyrex tube

[1]Acknowledgement is made to the donors of the Petroleum Research Fund, administered by the American Chemical Society for support of this work.

Can. J. Chem. Downloaded from www.nrcresearchpress.com by 210.87.254.6 on 09/05/12
For personal use only.

L'action du méthanol sulfurique sur **3***b* conduit au même triester huileux.

Action de l'acide p-nitroperbenzoïque sur **7**

En opérant comme pour l'époxydation de **3***b*, le produit brut obtenu (pas de bande i.r. caractéristique d'une γ-lactone) donne cinq taches sur chromatoplaque, dont la plus intense correspond au composé **6**, isolé par chromatographie sur couche épaisse. Les spectres i.r. et de r.m.n. montrent que ce produit est identique aux échantillons obtenus par action du diazométhane ou du méthanol sulfurique sur le composé **5**.

Réduction par le borohydrure de sodium du composé **3***b*

Selon le mode opératoire décrit (5) et à partir de 50 mg de **3***b*, on obtient 45 mg d'un mélange de deux composés séparés sur chromatoplaques préparatives.

La γ-lactone du [carboxy-1′α (ou 2′α) hydroxyméthyl-2′α (ou 1′α) éthano]-8α,12α abiétène-13 oate-18 de méthyle (33%) est recristallisée dans cinq volumes de méthanol: $F = 159°$; i.r. ($CHCl_3$): 1755 (lactone), 1718; r.m.n. ($CDCl_3$): 0.60 (CH_3-10), 1.03 (isopropyle $J = 7$), 1.13 (CH_3-4).

Anal. calc. pour $C_{25}H_{36}O_4$: C, 74.96; H, 9.06. Trouvé: C, 75.13; H, 8.96.

Le (dihydroxyméthyl-1′ξ,2′ξ éthano)-8α,12α abiétène-13 oate-18 de méthyle (47%) est recristallisé dans cinq volumes d'acétate d'éthyle: $F = 155°$; $[\alpha]_D = +5°$ (2.6); i.r. ($CHCl_3$): 3610, 3410, 1720; i.r. (CCl_4 1‰): 3632 (OH libre), 3490 (OH lié); r.m.n. ($CDCl_3$): 0.59 (CH_3-10), 1.01 (isopropyle $J = 7$), 1.15 (CH_3-4), 5.46 (H—C=).

Anal. calc. pour $C_{25}H_{40}O_4$: C, 74.21; H, 9.97. Trouvé: C, 74.19; H, 9.94.

Remerciements

Monsieur Poudeybat et les Anciens Etablissements Granel Frères, 40-Lesperon ont eu l'amabilité de nous fournir à plusieurs reprises des échantillons d'acides résiniques purs.

1. W. D. Lloyd et G. W. Hedrick. J. Org. Chem. **26**, 2029 (1961).
2. W. L. Meyer et R. W. Huffman. Tetrahedron Letters, **16**, 691 (1962).
3. W. A. Ayer, C. E. McDonald, et J. B. Stothers. Can. J. Chem. **41**, 1113 (1963).
4. W. Sanderman. Chem. Ber. **71B**, 2005 (1938).
5. B. Gastambide et N. Langlois. Helv. Chim. Acta, **51**, 2048 (1968).
6. P. Carnero et B. Gastambide. D'être publié.
7. N. Langlois et B. Gastambide. Bull. Soc. Chim. France, 2966 (1965).
8. V. A. Mironov, T. M. Fadewa, A. V. Stepaniantz, et A. A. Akhrem. Tetrahedron Letters, **47**, 5823 (1966).
9. H. Kwart et K. King. Chem. Rev. **68**, 415 (1968).
10. S. W. Chaikin et G. Brown. J. Am. Chem. Soc. **71**, 122 (1949).
11. N. Langlois et B. Gastambide. Compt. Rend. **264**, 1878 (1967).

Photolysis and mass spectra of *trans*-cinnamimide[1]

Robert T. LaLonde and Curry B. Davis

Department of Chemistry, State University College of Forestry, Syracuse University, Syracuse, New York 13210

Received March 25, 1969

Using Pyrex filtered light, irradiation of *trans*-cinnamimide in 1,2-dimethoxyethane solution gave β-truxinimide (48% yield), *cis*-cinnamamide and *trans*-cinnamamide. Both *trans*-cinnamimide and β-truxinimide undergo fragmentation in the mass spectrometer to give $C_{16}H_{14}+$, $C_{16}H_{13}+$, $C_{16}H_{12}+$, and $C_{14}H_{12}+$.

Canadian Journal of Chemistry, 47, 3250 (1969)

The solution photolysis of cinnamic acids, esters, and amides is capable of producing under widely varying conditions cyclobutanes, hydrogen abstraction reactions, *cis–trans* isomerizations and internal cyclizations. The following may be given as examples. Coumarin undergoes dimerization affording cyclobutane isomers, the geometry of which is solvent and sensitizer dependent (1, 2). Ethyl *trans*-cinnamate, ethyl *trans*-α-methylcinnamate and analogous lactones undergo isomerization and hydrogen abstraction reactions (3). A different mode of reactivity has been observed for α-phenylcinnamic acid and α-phenylcinnamamide (4). The acid and amide in each case give a β-lactone and a β-lactam and their formation have been viewed as cyclization reactions belonging to the general class of electrocyclic processes.

In connection with a study of the chemistry of α,β-unsaturated *N*-acylimides and imides we have explored the solution photochemistry of *trans*-cinnamimide (**1**).

A carefully degassed 1,2-dimethoxyethane solution of **1** was irradiated in a Pyrex tube

[1]Acknowledgement is made to the donors of the Petroleum Research Fund, administered by the American Chemical Society for support of this work.

Can. J. Chem. Downloaded from www.nrcresearchpress.com by 84.22.46.98 on 09/08/12
For personal use only.

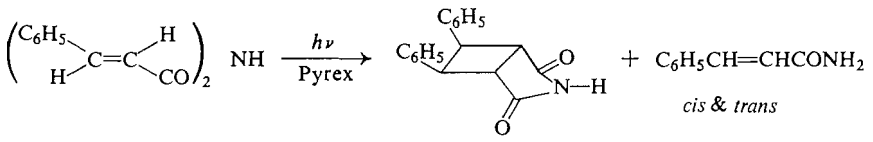

1 2

immersion apparatus. The disappearance of **1** was monitored by observing the decreasing intensity of the 300 mμ absorption maximum. After 113 h, at least 96% of **1** had been transformed. A thin-layer chromatogram (t.l.c.) of the crude product mixture indicated the presence of three new materials, one present in excess of the other two. The chromatogram also revealed the presence of a very small amount of unconverted **1**.

The predominating product was isolated in 48% yield. Its mass spectrum[2] revealed a molecular ion peak at *m/e* 277. Other features of the mass spectra of this product are discussed in another section of this note. That the predominating product possessed a five-membered imide was suggested by the strong infrared (i.r.) carbonyl bands at 1710 and 1770 cm^{-1}. The basis for this suggestion was the appearance of bands at 1710 and 1760 cm^{-1} in the five-membered imide, cyclobutane-*cis*-1,2-dicarboximide[3]. On the other hand, the six-membered imide 1,3-dimethylcyclobutane-1,3-dicarboximide revealed bands at 1710 and 1730 cm^{-1} (5). The absence of a band in the region of 1650 cm^{-1} indicated the loss of carbon–carbon double bonds in the formation of the predominating photo-product. The nuclear magnetic resonance (n.m.r.) spectrum displayed a ten proton aromatic absorption at 2.93 τ and a four proton A_2B_2 pattern centered at 6.11 τ. No signals in the vinyl proton region were observed.

Strong base hydrolysis of the predominating photo-product gave a dicarboxylic acid which on admixture with authentic β-truxinic acid gave no depression in melting point[4]. The dicarboxylic acid was converted to a dimethyl ester. This likewise showed no depression in melting point on admixture with authentic dimethyl β-truxinate.

The two minor products of photolysis were isolated and identified as *cis*- and *trans*-cinnamamide by comparison i.r. spectra.

The evidence presented above attests to the formation of the cyclobutane photoisomer (**2**), by intramolecular cyclization and *cis*- and *trans*-cinnamamide, presumably by nitrogen–carbonyl fission and hydrogen abstraction from solvent. Interestingly, only a single isomer of the truxinimide–truxillimide series was produced. Its formation is consistent with a photochemically allowed *cis,cis* mode of cyclization (6). Possibly this result could mean that the isomerization of a *trans*- to *cis*-cinnamoyl moiety occurs at the amide rather than the imide (**1**) stage. Isomerization of *trans*- to *cis*-cinnamamide under photolysis conditions does occur. Should *trans* to *cis* isomerization occur at the amide stage during the photolysis of **1**, it follows that cyclobutane formation and carbonyl–nitrogen bond fission are faster than is *trans* to *cis* isomerization in **1**. Alternatively, should *trans* to *cis* isomerization occur in **1**, then the absence of other truxinimide isomers could mean that the formation of these isomers from either a *trans* or *cis* excited state is much slower than the bond fission process or the formation of β-truxinimide from a *trans* excited state.

The course of the photolysis of **1** is also of interest in relation to the mass spectrum of **1**. This spectrum displayed two prominent sets of triads among several other peaks. The first of these triads was located at *m/e* 206, 205 (base peak), and 204 and the second at 180, 179, and 178. High resolution mass spectrometry (h.r.m.s.) showed the peaks of the first triad corresponded to $C_{16}H_{14}$ +, $C_{16}H_{13}$ +, and $C_{16}H_{12}$ +. This manner of fragmentation at first was interpreted in terms of either the five-membered imide **2***a* or the six-membered imide **3**, but later identification of *m/e* 180 as $C_{14}H_{12}$ + ($C_6H_5CH{=}CHC_6H_5$ +, by h.r.m.s.), the i.r. spectral characteristics, and conversion to β-truxinic acid eliminated **3** from consideration. However, the

[2]The authors wish to thank Prof. Carl Djerassi for making the mass spectrometry facilities at Stanford University available for this work during the sabbatical leave of R.T.L.

[3]H.D. Scharf, Organish-Chemisches Institut, Der Universität Bonn, private communication.

[4]An authentic sample of β-truxinic acid was obtained from Drs. G. M. J. Schmidt and M. Cohen, Weizman Institute of Science, Rehovoth, Israel. We wish to thank Drs. Schmidt and Cohen for this sample.

Can. J. Chem. Downloaded from www.nrcresearchpress.com by 84.22.46.98 on 09/08/12
For personal use only.

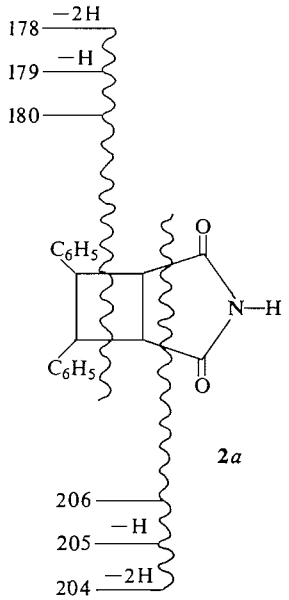

2a

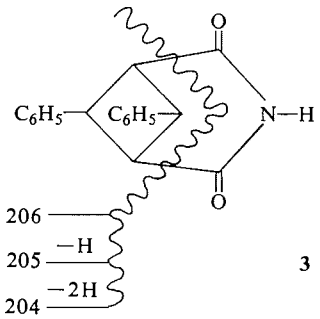

3

mass spectra of the imide **1** (*m/e* 43, base peak) was similar to the spectrum of **2**. The spectra in the region *m/e* 100-M^+ are reproduced in Fig. 1. The h.r.m.s. of **1** revealed the fragments $C_{16}H_{14}$ +, $C_{16}H_{13}$ +, $C_{16}H_{12}$ +, and $C_{14}H_{12}$ + as did the spectrum of **2**. Thus the use of mass spectra for structure information was of questionable value since it was reasoned that if both **1** and **2** could produce $C_{14}H_{12}$ + then it might be possible also for **3** to undergo bond rupture in the mass spectrometer to give a charged species structurally similar to **1** which subsequently would give $C_{14}H_{12}$ +. Though the mass spectral results were not of great utility in determining the structure of **2**, they were of interest nonetheless since they indicated the occurrence of an isomerization in the mass spectrometer which was similar to that observed in the photolysis of **1**.

Experimental

Spectra were obtained as follows: nuclear magnetic resonance (n.m.r.) in solution as indicated, 2% TMS, Varian A60A; i.r. Baird-Atomic Spectrometer; mass spectra, Atlas CH-4 direct inlet, and determined by Dr. John MacLeod and Mr. Robert Ross; ultraviolet (u.v.) Cary model 14, in 1,2-dimethoxyethane and ethanol; melting points were determined on a Köfler micro hot stage and are uncorrected.

trans-Cinnamimide (1)

The procedure of Thompson (7) was used to prepare **1**: m.p. 198–200° (lit. 198.5–199°); mass spectra M^+ *m/e* 277, base peak *m/e* 43; h.r.m.s., *m/e* 206, 206.10916 (calcd. for $C_{16}H_{14}$, 206.10955), *m/e* 205, 205.10148 (calcd. for $C_{16}H_{13}$, 205.10172), *m/e* 204, 204.09372 (calcd. for $C_{16}H_{12}$, 204.09390), *m/e* 180, 180.09409 (calcd. for $C_{14}H_{12}$, 180.09390); u.v. λ_{max}(DME) = 300 mμ, ε = 39 000.

Photolysis of trans-Cinnamimide (1)

The photolysis vessel consisted of a 500 ml round bottom flask fitted with a 19 mm (I.D.) Pyrex, concentric well which accommodated the lamp. The vessel also was equipped with a 12 mm side arm which was fitted with a 2 mm quartz cell containing a 1.90 mm spacer.

The light source was a General Electric AH-4 medium pressure mercury vapor lamp modified for water cooling by sealing the quartz bulb in a 16 mm (O.D.) Pyrex tube. This modified lamp was placed in the concentric Pyrex well. Tap water was circulated between inner Pyrex tube and outer well and was effective in maintaining the reaction temperature between 10–15°. The lamp was operated at a primary input of 275 W.

A 1.01 g sample of *trans*-cinnamimide (3.6 mmoles) was dissolved in 400 ml of anhydrous 1,2-dimethoxyethane in the photolysis flask. The solution was degassed and the flask sealed at reduced pressure. Periodically the light source was turned off, the flask was inverted and the optical densities at 300 and 262 mμ were determined. Optical densities after various time intervals of irradiation are given as follows:

Photolysis time (h)	O.D. λ_{max} 300 mμ	O.D. λ_{max} 265 mμ
0.0	3.5	—
21.0	3.2	—
69.0	1.6	0.1
113.0	0.15	0.55

After irradiation for 113.0 h, the solvent was distilled off on the vacuum line and thereby 1.18 g of crude product

Can. J. Chem. Downloaded from www.nrcresearchpress.com by 84.22.46.98 on 09/08/12
For personal use only.

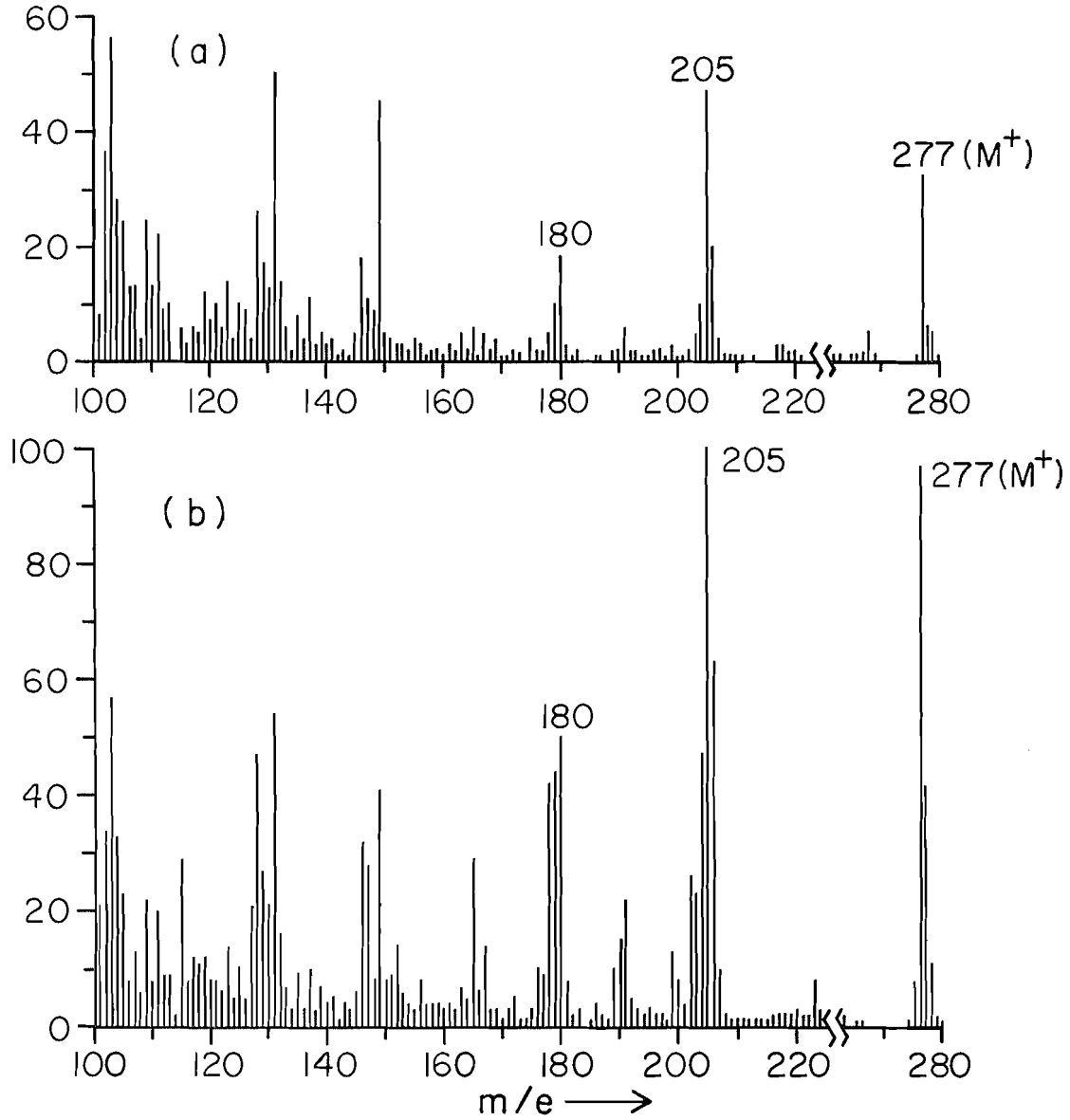

FIG. 1. The mass spectrum in the region *m/e* 100-M^+ of: (*a*) *trans*-cinnamimide; (*b*) β-truxinimide.

was recovered as an oil. This showed four spots on t.l.c. (unactivated 0.25 mm Silica Gel, GF-254, 5% methanol in chloroform). Several recrystallizations from cyclohexane–acetone afforded 202 mg of pure β-truxinimide: m.p. 225–227°; i.r. (KBr) 1770 (sh) and 1710 cm^{-1} (s); n.m.r. (hexachloroacetone) 2.93 τ (singlet, 10H), 6.11 (symmetrical A_2B_2 multiplet, 4H); u.v. λ_{max}(DME) 262 mμ, ε = 700; mass spectrum, M^+ *m/e* 277, base peak *m/e* 205; h.r.m.s., *m/e* 277, 277.11001 (calcd. for $C_{18}H_{15}NO_2$, 277.11028), *m/e* 206, 206.10974 (calcd. for $C_{16}H_{14}$, 206.10955), *m/e* 205, 205.10187 (calcd. for $C_{16}H_{13}$, 205.10172), *m/e* 204, 204.09410 (calcd. for $C_{16}H_{12}$, 204.09390), *m/e* 180, 180.09375 (calcd. for $C_{14}H_{12}$, 180.09390).

The filtrates from recrystallization were combined and the mixture separated on a column of 20 g of activated Silica Gel eluted with a linear gradient of 2-butanol in chloroform. The first material eluted was 32 mg of *trans*-cinnamimide: m.p. 199–200°. The second material eluted (1% methanol in chloroform) was 266 mg of β-truxinimide. Continued elution with about 10% 2-butanol in chloroform produced a total of 450 mg in several fractions. The last four fractions contained 47 mg whose t.l.c. and i.r. spectral properties were identical with those

Can. J. Chem. Downloaded from www.nrcresearchpress.com by 84.22.46.98 on 09/08/12
For personal use only.

Can. J. Chem. Downloaded from www.nrcresearchpress.com by 84.22.46.98 on 09/08/12
For personal use only.

of *trans*-cinnamamide. The several fractions preceding *trans*-cinnamamide were rich in an unidentified product as shown by t.l.c. Preparative t.l.c. (0.50 mm Silica Gel GF-254, 5% methanol in chloroform) of a portion of the combined fractions afforded an 8 mg sample of t.l.c. homogeneous (R_f 0.25, 5% methanol in chloroform) *cis*-cinnamamide: i.r. ($CHCl_3$) 3570 (m), 3460 (m), 1680 (s), 1630 (m), and 1590 cm^{-1} (m).

Hydrolysis of β-Truxinimide

An 89 mg sample of pure β-truxinimide (0.3 mmole) was dissolved in 30 ml of Claisen's alkali and the reaction mixture was refluxed, under nitrogen, for 24 h. Concentrated hydrochloric acid was added to bring the mixture to pH 2, and the aqueous phase was extracted continuously with ether. The ether extract was dried over anhydrous magnesium sulfate and the solvent evaporated under vacuum to afford 129 mg of a residue. Two recrystallizations from benzene–acetic acid afforded 40 mg (45% yield) of pure β-truxinic acid: m.p. 190–202°. No melting point depression was observed when mixed with an authentic sample of β-truxinic acid[4]: i.r. (KBr) 3000 (very broad), 2300 (broad) and 1700 cm^{-1}; n.m.r. (acetone-d_6) 6.09 τ (cyclobutane methine multiplet, 2H, B_2 of A_2B_2), 5.58 τ (cyclobutane methine multiplet, 2H, A_2 of A_2B_2) and 2.95 τ (aromatic hydrogen singlet, 10H).

A 40 mg sample of β-truxinic acid (0.13 mmoles) was treated with diazomethane. The white crystalline solid was recrystallized to a constant melting point from hexane. An authentic sample of dimethyl β-truxinate was prepared from a sample of the authentic β-truxinic acid. The i.r. spectra of both esters were identical. Dimethyl β-truxinate: m.p. 69–70°; i.r. 1730 cm^{-1} (strong); n.m.r. 6.28 τ (methoxyl singlet, 6H), 6.05 τ (cyclobutane methine multiplet, 2H, B_2 of A_2B_2), 5.63 τ (cyleobutane methine multiplet, 2H, A_2 of A_2B_2) and 2.92 τ (aromatic hydrogen singlet, 10H).

Synthesis of cis-Cinnamamide

Phenylpropiolic acid (m.p. 132–136°) was prepared by the method of Reimer (8) and converted to phenylpropiolyl chloride (b.p. 63–66° at 0.6 mm) through a 2 h treatment with a threefold excess of thionyl chloride at room temperature. A 6.5 g sample of phenylpropiolyl chloride was dissolved in 50 ml of anhydrous ether and excess ammonia gas was bubbled into the solution. The solvent was evaporated from the heterogeneous reaction mixture and the solid washed with 25 ml of water and extracted with chloroform (3 × 30 ml). The chloroform extracts were combined and dried over anhydrous magnesium sulfate. When the solvent was removed on the rotary evaporator, phenylpropiolamide (m.p. 108–109°) was afforded in nearly quantitative yield.

A 1.53 g sample of phenylpropiolamide (0.01 moles), dissolved in 50 ml of methanol, was shaken in an atmosphere of hydrogen at standard pressure along with 2% palladium on barium sulfate catalyst, poisoned with 170 mg of reagent grade quinoline. A total of 259 ml of hydrogen was absorbed over 2.7 h (258 ml calculated for 0.01 mole). No further hydrogen uptake was observed after an additional 30 min of hydrogenation. Removal of the catalyst by filtration, and the solvent on a rotary evaporator produced a residue which was then redissolved in chloroform. The resulting solution was washed consecutively with 30 ml of 1 *N* hydrochloric acid, water and dried over anhydrous magnesium sulfate. Removal of the solvent at the rotary evaporator gave the crude product. One recrystallization from cyclohexane afforded 1.0 g (70% yield) of analytically pure *cis*-cinnamamide: m.p. 83–87°; u.v. λ_{max}(EtOH) 255 mμ, ε = 10 600; i.r. ($CHCl_3$) 3570, 3460, 1680, 1630, and 1590 cm^{-1}; n.m.r. 4.07 τ (vinyl hydrogen doublet, J = 12 Hz, 1H), 3.23 τ (vinyl hydrogen doublet, J = 12 Hz, 1H) and 2.6 τ (aromatic hydrogen multiplet, 5H).

Anal. Calcd. for C_9H_9NO: C, 73.46; H, 6.12; N, 9.53. Found: C, 73.38; H, 6.36; N, 9.24.

1. H. Morrison, H. Curtis, and T. McDowell. J. Am. Chem. Soc. **88**, 5415 (1966).
2. G. S. Hammond, C. A. Stout, and A. A. Lamola. J. Am. Chem. Soc. **86**, 3103 (1964).
3. N. Baumann, M. Sung, and E. F. Ullman. J. Am. Chem. Soc. **90**, 4157 (1968).
4. O. L. Chapman and W. R. Adams. J. Am. Chem. Soc. **90**, 2333 (1968).
5. R. I. Aksentijevich, M.S. Thesis, State University College of Forestry, Syracuse University, Syracuse, New York. 1964. p. 15.
6. R. Hoffmann and R. B. Woodward. Accounts Chem. Res. **1**, 17 (1968).
7. Q. E. Thompson. J. Am. Chem. Soc. **73**, 5841 (1951).
8. M. Reimer. J. Am. Chem. Soc. **64**, 2510 (1942).

1,2,3,4,5-Pentaphenylimidazolium benzoate

James G. Smith and Hazem M. H. Ghonima
University of Waterloo, Department of Chemistry, Waterloo, Ontario

Received February 24, 1969

The compound reported to be *N,N'*-dibenzoyl-*N,N'*-diphenylstilbene-α,α'-diamine is shown to be 1,2,3,4,5-pentaphenylimidazolium benzoate.

Canadian Journal of Chemistry, 47, 3254 (1969)

In connection with other work (1) the synthesis of *N*-benzoyl-*N,N'*-diphenylstilbene-α,α'-diamine (**1**), reported by Everest and McCombie (2), was repeated. The synthesis proceeds by the initial preparation and subsequent alkaline hydrolysis of a compound whose structure was considered

Can. J. Chem. Downloaded from www.nrcresearchpress.com by 210.87.254.5 on 09/05/12
For personal use only.

of *trans*-cinnamamide. The several fractions preceding *trans*-cinnamamide were rich in an unidentified product as shown by t.l.c. Preparative t.l.c. (0.50 mm Silica Gel GF-254, 5% methanol in chloroform) of a portion of the combined fractions afforded an 8 mg sample of t.l.c. homogeneous (R_f 0.25, 5% methanol in chloroform) *cis*-cinnamamide: i.r. ($CHCl_3$) 3570 (m), 3460 (m), 1680 (s), 1630 (m), and 1590 cm^{-1} (m).

Hydrolysis of β-Truxinimide

An 89 mg sample of pure β-truxinimide (0.3 mmole) was dissolved in 30 ml of Claisen's alkali and the reaction mixture was refluxed, under nitrogen, for 24 h. Concentrated hydrochloric acid was added to bring the mixture to pH 2, and the aqueous phase was extracted continuously with ether. The ether extract was dried over anhydrous magnesium sulfate and the solvent evaporated under vacuum to afford 129 mg of a residue. Two recrystallizations from benzene–acetic acid afforded 40 mg (45% yield) of pure β-truxinic acid: m.p. 190–202°. No melting point depression was observed when mixed with an authentic sample of β-truxinic acid[4]: i.r. (KBr) 3000 (very broad), 2300 (broad) and 1700 cm^{-1}; n.m.r. (acetone-d_6) 6.09 τ (cyclobutane methine multiplet, 2H, B_2 of A_2B_2), 5.58 τ (cyclobutane methine multiplet, 2H, A_2 of A_2B_2) and 2.95 τ (aromatic hydrogen singlet, 10H).

A 40 mg sample of β-truxinic acid (0.13 mmoles) was treated with diazomethane. The white crystalline solid was recrystallized to a constant melting point from hexane. An authentic sample of dimethyl β-truxinate was prepared from a sample of the authentic β-truxinic acid. The i.r. spectra of both esters were identical. Dimethyl β-truxinate: m.p. 69–70°; i.r. 1730 cm^{-1} (strong); n.m.r. 6.28 τ (methoxyl singlet, 6H), 6.05 τ (cyclobutane methine multiplet, 2H, B_2 of A_2B_2), 5.63 τ (cyleobutane methine multiplet, 2H, A_2 of A_2B_2) and 2.92 τ (aromatic hydrogen singlet, 10H).

Synthesis of cis-Cinnamamide

Phenylpropiolic acid (m.p. 132–136°) was prepared by the method of Reimer (8) and converted to phenylpropiolyl chloride (b.p. 63–66° at 0.6 mm) through a 2 h treatment with a threefold excess of thionyl chloride at room temperature. A 6.5 g sample of phenylpropiolyl chloride was dissolved in 50 ml of anhydrous ether and excess ammonia gas was bubbled into the solution. The solvent was evaporated from the heterogeneous reaction mixture and the solid washed with 25 ml of water and extracted with chloroform (3 × 30 ml). The chloroform extracts were combined and dried over anhydrous magnesium sulfate. When the solvent was removed on the rotary evaporator, phenylpropiolamide (m.p. 108–109°) was afforded in nearly quantitative yield.

A 1.53 g sample of phenylpropiolamide (0.01 moles), dissolved in 50 ml of methanol, was shaken in an atmosphere of hydrogen at standard pressure along with 2% palladium on barium sulfate catalyst, poisoned with 170 mg of reagent grade quinoline. A total of 259 ml of hydrogen was absorbed over 2.7 h (258 ml calculated for 0.01 mole). No further hydrogen uptake was observed after an additional 30 min of hydrogenation. Removal of the catalyst by filtration, and the solvent on a rotary evaporator produced a residue which was then redissolved in chloroform. The resulting solution was washed consecutively with 30 ml of 1 *N* hydrochloric acid, water and dried over anhydrous magnesium sulfate. Removal of the solvent at the rotary evaporator gave the crude product. One recrystallization from cyclohexane afforded 1.0 g (70% yield) of analytically pure *cis*-cinnamamide: m.p. 83–87°; u.v. λ_{max}(EtOH) 255 mμ, ε = 10 600; i.r. ($CHCl_3$) 3570, 3460, 1680, 1630, and 1590 cm^{-1}; n.m.r. 4.07 τ (vinyl hydrogen doublet, J = 12 Hz, 1H), 3.23 τ (vinyl hydrogen doublet, J = 12 Hz, 1H) and 2.6 τ (aromatic hydrogen multiplet, 5H).

Anal. Calcd. for C_9H_9NO: C, 73.46; H, 6.12; N, 9.53. Found: C, 73.38; H, 6.36; N, 9.24.

1. H. Morrison, H. Curtis, and T. McDowell. J. Am. Chem. Soc. **88**, 5415 (1966).
2. G. S. Hammond, C. A. Stout, and A. A. Lamola. J. Am. Chem. Soc. **86**, 3103 (1964).
3. N. Baumann, M. Sung, and E. F. Ullman. J. Am. Chem. Soc. **90**, 4157 (1968).
4. O. L. Chapman and W. R. Adams. J. Am. Chem. Soc. **90**, 2333 (1968).
5. R. I. Aksentijevich, M.S. Thesis, State University College of Forestry, Syracuse University, Syracuse, New York. 1964. p. 15.
6. R. Hoffmann and R. B. Woodward. Accounts Chem. Res. **1**, 17 (1968).
7. Q. E. Thompson. J. Am. Chem. Soc. **73**, 5841 (1951).
8. M. Reimer. J. Am. Chem. Soc. **64**, 2510 (1942).

1,2,3,4,5-Pentaphenylimidazolium benzoate

James G. Smith and Hazem M. H. Ghonima
University of Waterloo, Department of Chemistry, Waterloo, Ontario

Received February 24, 1969

The compound reported to be *N,N'*-dibenzoyl-*N,N'*-diphenylstilbene-α,α'-diamine is shown to be 1,2,3,4,5-pentaphenylimidazolium benzoate.

Canadian Journal of Chemistry, 47, 3254 (1969)

In connection with other work (1) the synthesis of *N*-benzoyl-*N,N'*-diphenylstilbene-α,α'-diamine (**1**), reported by Everest and McCombie (2), was repeated. The synthesis proceeds by the initial preparation and subsequent alkaline hydrolysis of a compound whose structure was considered

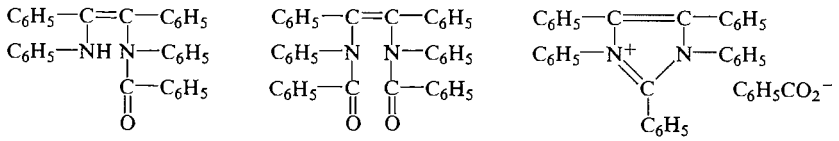

1 2 3

to be *N,N'*-dibenzoyl-*N,N'*-diphenylstilbene-α,α'-diamine (**2**). This structure (**2**) was indicated by the conversion of the compound with aqueous alkali to **1** plus benzoic acid.

It has been found that the infrared (i.r.) spectrum (Fig. 2) of the compound is incompatible with structure **2** since no amide carbonyl band appears in the 1630–1650 cm^{-1} region. Furthermore, the remarkably easy hydrolysis of one *N*-benzoyl group appears unlikely for a compound of structure **2**. Structure **3** was felt to be compatible with the i.r. spectrum, with the ready formation of **1** by alkaline hydrolysis (6), and with the fact that both **1** and **3** gave the same picrate; however, at the time, no convenient way of firmly establishing this structure was available.

Recently, the synthesis of a related compound, 1,2,3,4,5-pentaphenylimidazolium chloride (**4**), has been described (3). With this as a starting point, the proposed structure **3** has been confirmed. The imidazolium chloride (**4**) underwent facile hydrolysis to **1** in alcoholic alkali. Treatment of the chloride (**4**) with silver benzoate produced the benzoate (**3**) and treatment of the benzoate with excess lithium chloride in *N,N*-dimethylacetamide produced the chloride (**4**). Thionyl chloride also effected this last conversion, although the conversion of **1** to **4** by this means was not successful.

In view of the above results, the structure **5** assigned by McCombie to products from similar reactions are suspect. While a detailed structure proof has not been performed, the fact that both these compounds lack carbonyl bands in their i.r. spectra and both are obtained under reaction conditions similar to those producing **3**, strongly indicates that their true structure is **6**. McCombie's reaction conditions thus provide a convenient, although inefficient, means of preparing these pentaarylimidazolium salts.

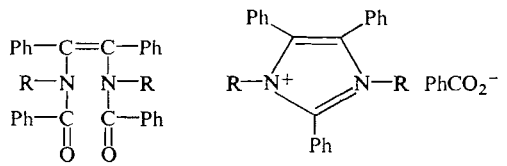

5 6

R = *m*-tolyl or *m*-chlorophenyl

Experimental

Infrared spectra were recorded on a Beckmann IR-10 spectrophotometer using Nujol mulls. The spectra reported in Fig. 1 and 2 were recorded on a Beckmann IR-9 spectrophotometer using either a Nujol mull (Fig. 1) or a split Fluorolube–Nujol mull (Fig. 2).

1,2,3,4,5-Pentaphenylimidazolium Benzoate (3)

The compound was prepared according to McCombie's directions (2) in 11% crude yield. In accordance with these directions, purification was effected by a lengthy extraction with diethyl ether. A simpler purification method was recrystallization from *N,N*-dimethylacetamide (27 ml/g). Infrared spectra of both samples were identical and the absence of a carbonyl absorption band is evident from Fig. 2.

Alternatively, the benzoate (**3**) can be prepared from the chloride (**4**). The chloride (**4**) (0.400 g, 0.00083 moles) was dissolved in a boiling mixture of 15 ml of *N,N*-dimethylacetamide and 4 ml of water. Silver benzoate (5) (0.195 g, 0.00085 moles) dissolved in 10 ml of hot *N,N*-dimethylacetamide was then added. After boiling briefly, the mixture was filtered, the filtrate was evaporated, and the brownish crystalline residue (0.415 g, 86% crude yield) recrystallized from 15 ml of *N,N*-dimethylacetamide to give 0.262 g of 1,2,3,4,5-pentaphenylimidazolium benzoate (**3**). The infrared spectra of the crude and the purified benzoate (**3**) were identical with that of the material prepared using McCombie's method.

1,2,3,4,5-Pentaphenylimidazolium Chloride (4)

A reference sample was prepared according to the published procedure (3). Purification was effected by recrystallization from ethanol or from *N,N*-dimethylacetamide containing 20% water (26 ml/g).

Alternatively, 0.570 g (.001 mole) of the benzoate (**3**) and 0.212 g (.005 mole) of lithium chloride were heated in 10 ml of *N,N*-dimethylacetamide to reflux for 5 min. The mixture was cooled and filtered to give 0.472 g (97% yield) of the chloride (**4**). Recrystallization was effected from 15 ml of *N,N*-dimethylformamide containing 10% water. The i.r. spectra of both the crude and recrystallized material were identical with that of the reference sample (**4**).

The benzoate (**3**) (0.150 g, 0.00026 moles) was refluxed

Can. J. Chem. Downloaded from www.nrcresearchpress.com by 210.87.254.5 on 09/05/12
For personal use only.

Can. J. Chem. Downloaded from www.nrcresearchpress.com by 210.87.254.5 on 09/05/12
For personal use only.

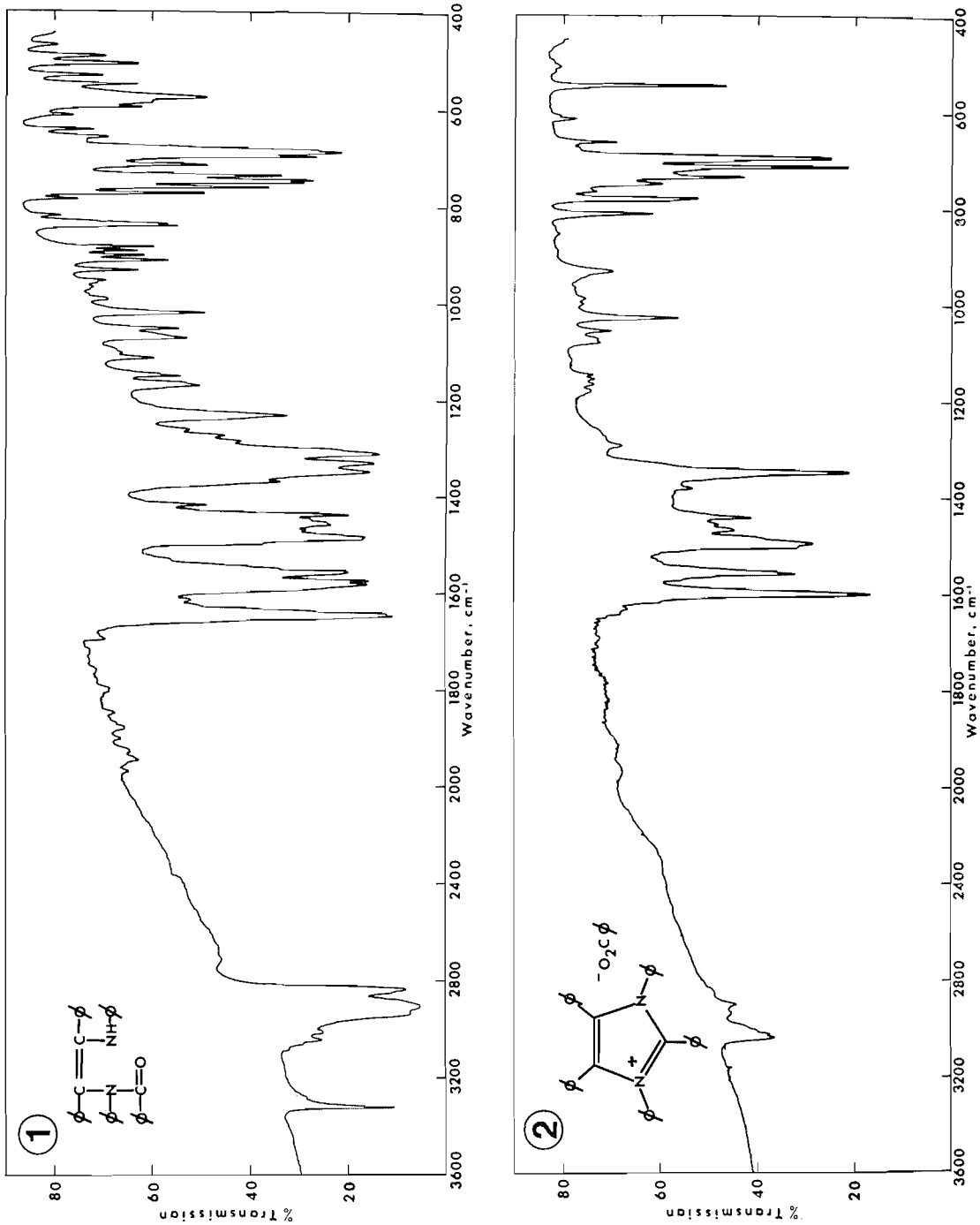

FIG. 1. Infrared spectrum of *N*-benzoyl-*N*,*N*′-diphenylstilbene-α,α′-diamene (**1**).
FIG. 2. Infrared spectrum of 1,2,3,4,5-pentaphenylimidazolium benzoate (**3**).

with 6 ml of thionyl chloride for 45 min. The clear solution was poured onto ice and the precipitate which separated was filtered, washed with water, and dried; weight: 0.097 g (76% yield). This material was recrystallized from 6 ml of *N,N*-dimethylacetamide containing 10% water to give 0.034 g of solid having an i.r. spectrum identical with that of the chloride (**4**). The i.r. spectrum of the crude material contained a strong band in the 1200–1300 cm^{-1} region which was attributed to sulfate or sulfite impurities.

Hydrolysis of 1,2,3,4,5-Pentaphenylimidazolium Chloride

The chloride (**4**) (0.25 g, 0.00056 moles) was dissolved in 20 ml of hot ethanol and 0.25 g of sodium hydroxide in 10 ml of ethanol was added. A yellow color developed and after boiling for 5 min the solution was treated with 50 ml of water. A yellow solid separated and was filtered, washed with water, and dried; weight 0.183 g (70% yield). This solid had a m.p. of 210–215° (with decomposition) and an i.r. spectrum identical to *N*-benzoyl-*N,N'*-diphenylstilbene-α,α'-diamine (**1**) prepared by a similar hydrolysis (2) of 1,2,3,4,5-pentaphenylimidazolium benzoate (**3**).

1,3-Diaryl-2,4,5-triphenylimidazolium Benzoate

These were prepared by the method described by Bailey and McCombie (4) in rather poor yields: 1,3-di-*m*-tolyl-, 0.7% yield, m.p. 370–375°, 1,3-di-*m*-chlorophenyl-, 4% yield. Both were purified by dissolving in boiling benzene containing sufficient methanol to solubilize the compound, filtering with decolorizing charcoal, and boiling the filtrate so as to distill off the methanol and precipitate the imidazolium salt. Neither the crude nor the purified products showed a carbonyl band in their i.r. spectra.

Acknowledgment

The financial support of the National Research Council of Canada is gratefully acknowledged.

1. J. G. Smith. Can. J. Chem. **44**, 59 (1966).
2. A. E. Everest and H. McCombie. J. Chem. Soc. **99**, 1752 (1911).
3. J. Heinze, H. Baumgärtel, and H. Zimmermann. Chem. Ber. **101**, 3504 (1968).
4. C. W. Bailey and H. McCombie. J. Chem. Soc. **101**, 2272 (1913).
5. L. F. Fieser and M. Fieser. Reagents for organic synthesis. John Wiley and Sons, Inc., New York. 1967. p. 1004.
6. D. R. Robinson. Tetrahedron Letters 5007 (1968).

Azaindoles. Part II. The proton magnetic resonance spectra of 5-azaindoles[1]

P. G. Riley and B. Robinson
Department of Pharmacy, University of Manchester, Manchester 13, England

Received March 27, 1969

The proton magnetic resonance (p.m.r.) spectra of 5-azaindole and 5-aza-1- and 3-methylindoles have been recorded and analyzed. It has been shown that in the spectrum of 5-azaindole, 3,7- coupling occurs but 1,3- coupling is not observed. In none of the spectra were any 2,6- or 4,6- couplings observed.

Canadian Journal of Chemistry, 47, 3257 (1969)

The p.m.r. spectra of 5-aza-2,3-dimethylindole (**1**; R = H, R' = R'' = Me) (1) and 5-azaindole (**1**; R = R' = R'' = H) (2) have been reported.

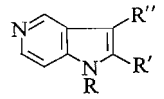

1

The doublet of doublets centered at 3.30 τ in the spectrum of 5-azaindole has been assigned (2) to the 3-proton (H-3) which, it is suggested (2), is coupled with H-2 ($J_{2,3}$ = 3.2 Hz) and the *N*-proton ($J_{1,3}$ = 1.0 Hz). The possibility that this latter fine coupling was not caused by 1,3- but by 3,7- coupling was not considered, probably because the H-7 signal was detected (2) only as a doublet of doublets centered at 2.61 τ ($J_{7,4}$ = 1.0 Hz, $J_{7,6}$ = 5.6 Hz). However, such 3,7- coupling or its equivalent is well-established in indole and many other polynuclear aromatic systems (3, 4). Also, the spectrum of 5-azaindole in DCl/D_2O (in which the *N*-proton will be completely exchanged for deuterium) still shows such coupling (2), and in the spectrum of 7-azaindole such coupling is absent (2, 5). We have now reinvestigated the p.m.r. spectrum of 5-azaindole (6) and have also analyzed the p.m.r. spectrum of its 1- and 3-methyl derivatives (**1**; R = Me, R' = R'' = H and R = R' = H, R'' = Me, respectively). The results of these studies have established that in the 5-azaindole

[1]For Part I, see reference 8.

Can. J. Chem. Downloaded from www.nrcresearchpress.com by 210.87.254.5 on 09/05/12
For personal use only.

with 6 ml of thionyl chloride for 45 min. The clear solution was poured onto ice and the precipitate which separated was filtered, washed with water, and dried; weight: 0.097 g (76% yield). This material was recrystallized from 6 ml of *N,N*-dimethylacetamide containing 10% water to give 0.034 g of solid having an i.r. spectrum identical with that of the chloride (**4**). The i.r. spectrum of the crude material contained a strong band in the 1200–1300 cm^{-1} region which was attributed to sulfate or sulfite impurities.

Hydrolysis of 1,2,3,4,5-Pentaphenylimidazolium Chloride

The chloride (**4**) (0.25 g, 0.00056 moles) was dissolved in 20 ml of hot ethanol and 0.25 g of sodium hydroxide in 10 ml of ethanol was added. A yellow color developed and after boiling for 5 min the solution was treated with 50 ml of water. A yellow solid separated and was filtered, washed with water, and dried; weight 0.183 g (70% yield). This solid had a m.p. of 210–215° (with decomposition) and an i.r. spectrum identical to *N*-benzoyl-*N,N'*-diphenylstilbene-α,α'-diamine (**1**) prepared by a similar hydrolysis (2) of 1,2,3,4,5-pentaphenylimidazolium benzoate (**3**).

1,3-Diaryl-2,4,5-triphenylimidazolium Benzoate

These were prepared by the method described by Bailey and McCombie (4) in rather poor yields: 1,3-di-*m*-tolyl-, 0.7% yield, m.p. 370–375°, 1,3-di-*m*-chlorophenyl-, 4% yield. Both were purified by dissolving in boiling benzene containing sufficient methanol to solubilize the compound, filtering with decolorizing charcoal, and boiling the filtrate so as to distill off the methanol and precipitate the imidazolium salt. Neither the crude nor the purified products showed a carbonyl band in their i.r. spectra.

Acknowledgment

The financial support of the National Research Council of Canada is gratefully acknowledged.

1. J. G. Smith. Can. J. Chem. **44**, 59 (1966).
2. A. E. Everest and H. McCombie. J. Chem. Soc. **99**, 1752 (1911).
3. J. Heinze, H. Baumgärtel, and H. Zimmermann. Chem. Ber. **101**, 3504 (1968).
4. C. W. Bailey and H. McCombie. J. Chem. Soc. **101**, 2272 (1913).
5. L. F. Fieser and M. Fieser. Reagents for organic synthesis. John Wiley and Sons, Inc., New York. 1967. p. 1004.
6. D. R. Robinson. Tetrahedron Letters 5007 (1968).

Azaindoles. Part II. The proton magnetic resonance spectra of 5-azaindoles[1]

P. G. Riley and B. Robinson
Department of Pharmacy, University of Manchester, Manchester 13, England

Received March 27, 1969

The proton magnetic resonance (p.m.r.) spectra of 5-azaindole and 5-aza-1- and 3-methylindoles have been recorded and analyzed. It has been shown that in the spectrum of 5-azaindole, 3,7- coupling occurs but 1,3- coupling is not observed. In none of the spectra were any 2,6- or 4,6- couplings observed.

Canadian Journal of Chemistry, 47, 3257 (1969)

The p.m.r. spectra of 5-aza-2,3-dimethylindole (**1**; R = H, R' = R'' = Me) (1) and 5-azaindole (**1**; R = R' = R'' = H) (2) have been reported.

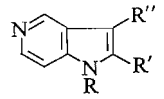

1

The doublet of doublets centered at 3.30 τ in the spectrum of 5-azaindole has been assigned (2) to the 3-proton (H-3) which, it is suggested (2), is coupled with H-2 ($J_{2,3}$ = 3.2 Hz) and the *N*-proton ($J_{1,3}$ = 1.0 Hz). The possibility that this latter fine coupling was not caused by 1,3- but by 3,7- coupling was not considered, probably because the H-7 signal was detected (2) only as a doublet of doublets centered at 2.61 τ ($J_{7,4}$ = 1.0 Hz, $J_{7,6}$ = 5.6 Hz). However, such 3,7- coupling or its equivalent is well-established in indole and many other polynuclear aromatic systems (3, 4). Also, the spectrum of 5-azaindole in DCl/D_2O (in which the *N*-proton will be completely exchanged for deuterium) still shows such coupling (2), and in the spectrum of 7-azaindole such coupling is absent (2, 5). We have now reinvestigated the p.m.r. spectrum of 5-azaindole (6) and have also analyzed the p.m.r. spectrum of its 1- and 3-methyl derivatives (**1**; R = Me, R' = R'' = H and R = R' = H, R'' = Me, respectively). The results of these studies have established that in the 5-azaindole

[1]For Part I, see reference 8.

Can. J. Chem. Downloaded from www.nrcresearchpress.com by 210.87.254.42 on 09/05/12
For personal use only.

TABLE I

Analysis of the p.m.r. spectrum of 1-methyl-5-azaindole

Proton	Signal	Center of signal (τ)	Coupling constants (Hz)	Effect of double irradiation of signal
H-2	d	2.98*	$J_{2,3} = 3.0$	d^2(H-3) → d ($J = 0.8$ Hz)
H-3	d^2	3.46*	$J_{3,2} = 3.0, J_{3,7} = 0.8$	d (H-2) → s,d^3(H-7) → d^2 ($J = 6.0$ and 0.8 Hz)
H-4	d	1.11	$J_{4,7} = 0.8$	d^3(H-7) → d^2 ($J = 6.0$ and 0.8 Hz)
H-6	d	1.70	$J_{6,7} = 6.0$	d^3(H-7) → d^2 ($J = 0.8$ and 0.8 Hz)
H-7	d^3	2.83	$J_{7,6} = 6.0, J_{7,4} = J_{7,3} = 0.8$	d^2(H-3) → d ($J = 3.0$ Hz), d(H-4) and d(H-6) → s
NCH_3	s	6.27		

NOTE: s, singlet; d, doublet; d^2, doublet of doublets; d^3, doublet of doublets of doublets.
*cf. the signals of the 2- and 3-protons in the p.m.r. spectrum of 1-methylindole which are doublets centered at 3.18 and 3.52 τ, respectively (9).

system 3,7- coupling occurs and 1,3- coupling is absent.

The spectrum of 5-azaindole has a doublet centered at 1.02 τ ($J_{4,7} = 1.0$ Hz) (H-4), a doublet centered at 1.72 τ ($J_{6,7} = 6.0$ Hz) (H-6), a doublet of doublets centered at 3.38 τ ($J_{3,2} = 3.1$ Hz, $J_{3,7} = 0.9$ Hz) (H-3) and a broad singlet between −2.40 and −1.40 τ (NH). The signals caused by the H-2 and H-7 protons were superimposed to give a 2-proton multiplet between 2.56 and 2.78 τ. The chemical shifts for all these protons are in keeping with those previously (2) reported. Both they and the assigned couplings were verified by double irradiation of the (H-2 + H-7) multiplet, which caused the H-3, H-4, and H-6 signals to collapse to singlets, and by exchange of the *N*-proton with deuterium which had no observable effect on the spectrum other than eliminating the NH-signal.

Further evidence that 1,3- coupling was not contributing to the doublet of doublets signal of H-3, but that the couplings in this signal are caused by 3,2- and 3,7- couplings, was obtained by analysis (Table I) of the spectrum of 5-aza-1-methylindole, prepared by the reaction of 5-azaindole (6) with sodamide followed by methyl iodide (7, 8).

The H-7 signal in the spectrum of 5-aza-3-methylindole (8) appears as a doublet of doublets centered at 2.75 τ ($J_{7,6} = 5.7$ Hz, $J_{7,4} = 0.8$ Hz), as would be expected since now 3,7- coupling has been eliminated. The H-4 and H-6 protons give rise to doublets centered at 1.09 and 1.73 τ ($J_{4,7} = 0.8$ Hz, $J_{6,7} = 5.7$ Hz), respectively, as does the H-2 proton whose doublet signal is centered at 2.96 τ ($J = 0.8$ Hz). This latter doublet is caused by coupling of H-2 with the *N*-proton (a broad signal between −0.98 and −0.58 τ), since after exchange of this proton with deuterium the H-2 doublet collapses to a singlet.

Surprisingly, in spectra recorded in $CDCl_3$, 1,2- coupling is not observed in 7-azaindole (2) although it is observed (2) in 4-, 5-, and 6-azaindoles. The reason why such coupling should still be observed (2) in the spectra of 5- and 6-azaindoles recorded in DCl/D_2O solution remains obscure and is worthy of further investigation.

In none of the spectra described in the present studies were any 2,6- (4) (cf. ref. 2) or 4,6- (2) couplings observed.

Experimental

Proton magnetic resonance spectra were recorded in deutero-chloroform solution on a Varian HA 100 spectrometer, tetramethylsilane being used as internal standard; unless otherwise stated, all signals referred to integrated for one proton. Exchanges of *N*-protons for deuterium were effected by shaking the deutero-chloroform solutions with D_2O.

5-Azaindole and 5-Aza-3-methylindole

These were prepared as described in the literature (refs. 6 and 8, respectively).

5-Aza-1-methylindole

To liquid ammonia (20 ml) was added sodium (1 g) and a few crystals of anhydrous ferric chloride. After stirring for 1¼ h the original blue color of the mixture disappeared. Finely powdered 5-azaindole (5) (1.0 g) was then added, stirring continued for 1½ h, methyl iodide (2.5 ml) added, and stirring continued a further 4½ h. The excess ammonia and methyl iodide were then allowed to evaporate at room temperature overnight, and the residual traces of these reagents removed by heating on a steam-bath. The residue was shaken with water, strongly basified by the addition of sodium hydroxide and the liberated oil extracted with chloroform (3 × 25 ml). The combined chloroform extracts were washed with water (2 × 25 ml), dried (magnesium sulfate), and evaporated to afford a yellow-green oil which after distillation [b.p. 180–190 °C (bath temperature)/0.1 mm] gave a colorless oil which rapidly crystallized.

Recrystallization of the product could not be satisfactorily effected and therefore it was subjected to column chromatography in ether on grade "H" alumina. Upon evaporation of the ether eluates, colorless crystals were

Can. J. Chem. Downloaded from www.nrcresearchpress.com by 210.87.254.42 on 09/05/12
For personal use only.

obtained, which after recrystallization from ether afforded 305 mg (27%) of white needles, m.p. 78–80 °C.

Anal. Calcd. for $C_8H_8N_2$: C, 72.73; H, 6.06; N, 21.22. Found: C, 73.01; H, 5.72; N, 21.37.

Acknowledgment

One of us (P. G. Riley) acknowledges the award of a research scholarship by the Science Research Council, London, England.

1. P. A. Crooks and B. Robinson. Chem. Ind. London, 547 (1967).
2. R. E. Willette. Advan. Heterocyclic Chem. **9**, 27 (1968).
3. J. A. Elvidge and R. G. Foster. J. Chem. Soc. 981 (1964).
4. M. Martin-Smith, S. T. Reid, and S. Sternhell. Tetrahedron Letters, 2393 (1965).
5. P. J. Black and M. L. Heffernan. Australian J. Chem. **18**, 353 (1965).
6. R. R. Lorenz, B. F. Tullar, C. F. Koelsch, and S. Archer. J. Org. Chem. **30**, 2531 (1965).
7. K. T. Potts and J. E. Saxton. J. Chem. Soc. 2641 (1954).
8. P. A. Crooks and B. Robinson. Can. J. Chem. **47**, 2061 (1969).
9. L. A. Cohen, J. W. Daly, H. Kny, and B. Witkop. J. Am. Chem. Soc. **82**, 2184 (1960). R. V. Jardine and R. K. Brown. Can. J. Chem. **41**, 2067 (1963).

Nuclear magnetic resonance spectrum and deuteration of porphobilinogen lactam and its derivatives[1]

Y. C. Kim[2]

Division of Pure Chemistry, National Research Council of Canada, Ottawa, Canada

Received May 21, 1968

Derivatives of porphobilinogen are distinguished from those of its lactam in that the C_4- and C_7-protons of the latter show homoallylic coupling, $J_{4,7} = 2.5$–3.0 Hz (150°) and the C_4-protons are exchangeable in alkaline solution.

Canadian Journal of Chemistry, 47, 3259 (1969)

As will be reported elsewhere (1), the very labile dipyrryl-methane **1** was synthesized for biogenetic studies as a reasonably stable potassium salt. As obtained by the hydrolysis of **8**, it was difficult to characterize, and the usual methods did not clearly show that the lactam ring had been opened. We now report an examination of model porphobilinogen derivatives **2–10** (1–3) showing that, in lactam but not in open forms, the C_4- and C_7-protons show homoallylic coupling, $J_{4,7} = 2.5$–3.0 Hz (150°) and the C_4-protons are exchangeable; in alkaline D_2O, this exchange is faster than ring-opening.

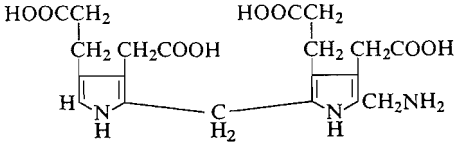

1

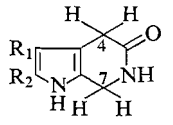

	R_1	R_2
2	CH_2CH_2COOEt	COOEt
3	CH_2CH_2COOEt	H
4	CH_2CH_2COOH	COOH
5	CH_2CH_2COOH	H

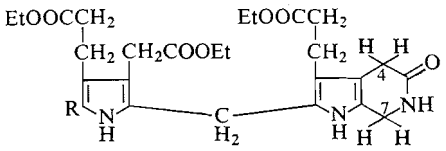

6 R = $COOCH_2C_6H_5$
7 R = COOH
8 R = H

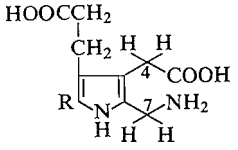

9 R = COOH
10 R = H (porphobilinogen)

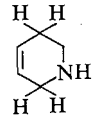

11

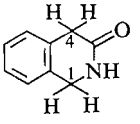

12

[1]NRCC No. 10750.

[2]NRCC Postdoctorate Fellow, 1965–1967. Present address: Frank W. Horner Ltd., Town of Mount Royal, Quebec.

Can. J. Chem. Downloaded from www.nrcresearchpress.com by 210.87.254.42 on 09/05/12
For personal use only.

obtained, which after recrystallization from ether afforded 305 mg (27%) of white needles, m.p. 78–80 °C.

Anal. Calcd. for $C_8H_8N_2$: C, 72.73; H, 6.06; N, 21.22. Found: C, 73.01; H, 5.72; N, 21.37.

Acknowledgment

One of us (P. G. Riley) acknowledges the award of a research scholarship by the Science Research Council, London, England.

1. P. A. Crooks and B. Robinson. Chem. Ind. London, 547 (1967).
2. R. E. Willette. Advan. Heterocyclic Chem. **9**, 27 (1968).
3. J. A. Elvidge and R. G. Foster. J. Chem. Soc. 981 (1964).
4. M. Martin-Smith, S. T. Reid, and S. Sternhell. Tetrahedron Letters, 2393 (1965).
5. P. J. Black and M. L. Heffernan. Australian J. Chem. **18**, 353 (1965).
6. R. R. Lorenz, B. F. Tullar, C. F. Koelsch, and S. Archer. J. Org. Chem. **30**, 2531 (1965).
7. K. T. Potts and J. E. Saxton. J. Chem. Soc. 2641 (1954).
8. P. A. Crooks and B. Robinson. Can. J. Chem. **47**, 2061 (1969).
9. L. A. Cohen, J. W. Daly, H. Kny, and B. Witkop. J. Am. Chem. Soc. **82**, 2184 (1960). R. V. Jardine and R. K. Brown. Can. J. Chem. **41**, 2067 (1963).

Nuclear magnetic resonance spectrum and deuteration of porphobilinogen lactam and its derivatives[1]

Y. C. Kim[2]

Division of Pure Chemistry, National Research Council of Canada, Ottawa, Canada

Received May 21, 1968

Derivatives of porphobilinogen are distinguished from those of its lactam in that the C_4- and C_7-protons of the latter show homoallylic coupling, $J_{4,7} = 2.5$–3.0 Hz (150°) and the C_4-protons are exchangeable in alkaline solution.

Canadian Journal of Chemistry, 47, 3259 (1969)

As will be reported elsewhere (1), the very labile dipyrryl-methane **1** was synthesized for biogenetic studies as a reasonably stable potassium salt. As obtained by the hydrolysis of **8**, it was difficult to characterize, and the usual methods did not clearly show that the lactam ring had been opened. We now report an examination of model porphobilinogen derivatives **2–10** (1–3) showing that, in lactam but not in open forms, the C_4- and C_7-protons show homoallylic coupling, $J_{4,7} = 2.5$–3.0 Hz (150°) and the C_4-protons are exchangeable; in alkaline D_2O, this exchange is faster than ring-opening.

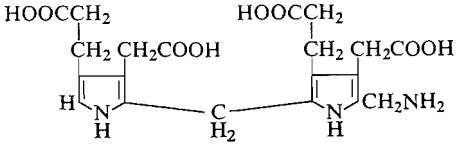

1

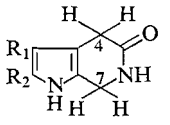

	R_1	R_2
2	CH_2CH_2COOEt	COOEt
3	CH_2CH_2COOEt	H
4	CH_2CH_2COOH	COOH
5	CH_2CH_2COOH	H

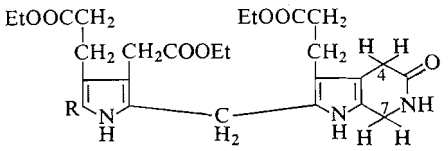

6 R = $COOCH_2C_6H_5$
7 R = COOH
8 R = H

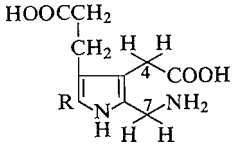

9 R = COOH
10 R = H (porphobilinogen)

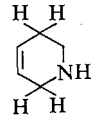

11

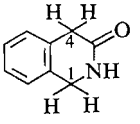

12

[1]NRCC No. 10750.
[2]NRCC Postdoctorate Fellow, 1965–1967. Present address: Frank W. Horner Ltd., Town of Mount Royal, Quebec.

Can. J. Chem. Downloaded from www.nrcresearchpress.com by 210.87.254.105 on 09/05/12
For personal use only.

TABLE I

The chemical shifts (τ) of some protons in compounds **2–8**

Compound	$J_{4,7}$(Hz)* at 150° (DMSO-d_6)	DMSO-d_6			CF_3COOH			$CDCl_3$			D_2O†		
		P-H‡	C_4-H	C_7-H	P-H‡	C_4-H	C_7-H	P-H‡	C_4-H	C_7-H	P-H‡	C_4-H	C_7-H
2	2.5	7.30	6.73	5.67	6.95	6.03	5.08	—	—	—	—	—	—
3	3.0	7.45	6.82	5.74	—	—	—	—	—	—	—	—	—
4§	3.0	7.30	6.70	5.68	6.90	6.02	4.97	—	—	—	7.40	6.76	5.86
5‖	3.0	7.50	6.80	5.70	6.89	6.00	4.87	—	—	—	7.60	6.92	5.93
6	3.0	7.46	6.90	5.82	—	—	—	7.32	6.70	5.66	—	—	—
7	3.0	7.50	6.87	5.80	—	—	—	—	—	—	—	—	—
8	3.0	7.58	6.90	5.80	—	—	—	7.46	6.76	5.70	—	—	—

*All signals were triplets.
†The chemical shift of the HOD signal (assigned 5.30) was used as an internal standard.
‡Protons on the propionic methylenes.
§Potassium salt in D_2O.
‖Sodium salt in D_2O.

The nuclear magnetic resonance (n.m.r.) spectra of the lactams **2–8** suggested homoallylic coupling between the C_4- and C_7-protons. These appear as broad singlets, $w_{1/2}$ = 7–9 Hz at 35°, and as well-resolved triplets, $J_{4,7}$ = 2.5–3.0 Hz at 150° (Table I). Analogous homoallylic coupling had been noted (4,5), particularly in **11** (6) which had $J_{2,5}$ = 3.0 Hz. In contrast to these signals for the C_4- and C_7-protons in **4** and **5**, those for the corresponding protons in the open forms **9** (K salt in D_2O: C_4- and C_7-protons at τ 6.63 and τ 5.90) and **10** (Na salt in D_2O: C_4- and C_7-protons at τ 6.80 and τ 6.49) were all sharp singlets indicating no homoallylic coupling.

After the lactam **2** had stood for one week in DMSO-d_6/KOBu^t at 50°, its spectrum at 150° showed no C_4-proton signal at τ 6.73 and the triplet at τ 5.67 for the C_7-protons had collapsed to a singlet. As this could only be ascribed to deuteration at C_4, it established both the assignments for the C_4- and C_7-protons and also the homoallylic coupling. Again the open analogues **9** and **10** differed, showing no exchange in alkaline D_2O.

In 2 *N* KOD/D_2O, **4** was rapidly deuterated at C_4 and more slowly hydrolyzed to largely C_4-deuterated **9**. Here the C_4-proton signal at τ 6.90 was largely eliminated in 7 min, completely in 1 h, and the appearance of a small sharp singlet at τ 6.75 indicated some hydrolysis to **9** prior to the deuteration. Concurrently, the C_7-proton signal of **4** at τ 6.02 first sharpened, then was replaced by the sharp singlet at τ 6.52 representing C_7-protons of **9**, whether or not deuterated at C_4. At the same time, the signal for the propionic methylenes of **4**, a poorly-resolved multiplet at τ 7.57, became a well-resolved multiplet at τ 7.45, identical with that observed in the spectrum of the potassium salt of **9**. The spectrum of the recovered deuterated **9** in CF_3COOH was identical with that of **9** except that the 2H singlet at τ 6.02 (C_4-protons) had almost disappeared. Here the C_7-protons of **9** appear as a quartet (τ 5.33, J = 5.5 Hz) in CF_3COOH but as a singlet in CF_3COOD; evidently the quartet arises from coupling of the C_7-protons with those of the protonated amino group.

In 1 *N* NaOD/D_2O, **5** behaved analogously. Within 15 min it was deuterated on C_4 then converted into C_4-deuterated **10**, a little undeuterated **10** being formed also.

The same homoallylic coupling and deuterium exchange was found in the less closely related lactam **12**, which was prepared for the purpose. Its n.m.r. spectrum in $CDCl_3$ showed the C_4-protons as a poorly resolved triplet (τ 6.47, J = 1.5 Hz) and the C_1-protons as a broad singlet (τ 5.57, $w_{1/2}$ = 5.0 Hz). The spectrum in DMSO-d_6 at 130° was no better resolved. After **12** was deuterated by leaving it in CH_3ONa/CH_3OD for 3 days at 20°, its spectrum showed no signal at τ 6.47 and that at τ 5.57 was sharper ($w_{1/2}$ = 3.3 Hz).

Experimental

Compounds **2,4,5** and **10** (2), **3** (3) and **6–8** (1) were obtained by literature methods.

1,4-Dihydro-3[2H]-isoquinolone (12)

In a 250 ml flask fitted with a magnetic stirrer, condenser and drying tube, were placed 150 ml of THF and 1 g of 2-thiohomophthalimide (7). Two teaspoons of Raney Nickel (Grace No. 28) were added as a slurry in 50 ml of THF and the mixture was stirred and refluxed for 3 h. The nickel was filtered off within an hour for, if the mixture first stood overnight, an unidentified com-

Can. J. Chem. Downloaded from www.nrcresearchpress.com by 210.87.254.105 on 09/05/12
For personal use only.

pound m.p. 300° containing nickel was the only product obtained. The filtrate was evaporated and the residue was crystallized from aqueous acetone (Darco) as greenish-yellow crystals (0.54 g, 65%), m.p. 150–152° (lit. (8): colorless crystals, m.p. 149.5–150.5°); infrared spectrum (Nujol): 3330 cm^{-1}, 3200 cm^{-1} (ν_{NH}), 3050 cm^{-1} (ν_{CH} aromatic), 1665 cm^{-1} (ν_{CO} amide), 1606 cm^{-1} ($\nu_{C:C}$), 748 cm^{-1} (δ_{CH} aromatic); n.m.r. spectrum ($CDCl_3$): τ 6.47 (C_4-H) (on expanding the spectrum, this signal became a poorly-resolved triplet, J = 1.5 Hz), τ 5.57 (s, C_1-H), τ 2.89 (aromatic), τ 2.00 (NH); mass spectrum, m/e = 147 (mol. wt., 147.18).

Anal. Calcd. for C_9H_9NO: C, 73.45; H, 6.16; N, 9.52. Found: C, 73.53; H, 5.98; N, 9.34.

Acknowledgment

The author gratefully acknowledges a personal grant during 1967–1968 from G. D. Searle and Company, Skokie, Illinois.

1. J. M. Osgerby, J. Pluščec, Y. C. Kim, and S. F. MacDonald. To be published.
2. A. H. Jackson and S. F. MacDonald. Can. J. Chem. **35**, 715 (1957).
3. G. P. Arsenault and S. F. MacDonald. Can. J. Chem. **39**, 2043 (1961).
4. S. Sternhell. Rev. Pure Appl. Chem. **14**, 15 (1964).
5. K. Katari, K. Tori, Y. Kimura, T. Yoshida, T. Nakasaki, and H. Minato. J. Med. Chem. **10**, 1149 (1967).
6. J. N. Shoolery. Discussions Faraday Soc. **34**, 104 (1962).
7. P. A. S. Smith and R. O. Kan. Org. Syn. **44**, 91 (1964).
8. R. Huisgen and J. Reinertshofer. Ann. **575**, 197 (1952).

Reissert compound studies. XXI. Arylation reactions[1]

Robert Piccirilli[2] and Frank D. Popp

Department of Chemistry, Clarkson College of Technology, Potsdam, New York 13676

Received March 18, 1969

The anions derived from both the isoquinoline and the quinoline Reissert compounds have been arylated by use of nitro and dinitro arylhalides. *p*-Fluorobenzaldehyde reacts preferentially at the carbonyl group and does not lead to arylation.

Canadian Journal of Chemistry, 47, 3261 (1969)

A variety of reactions have been reported for the anions **1** and **2** derived from the isoquinoline and quinoline Reissert compounds (2). We now wish to report on the arylation of these anions.

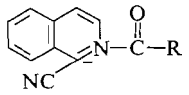

1

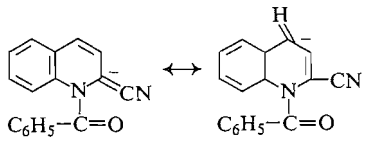

2

Reaction of the anion **1** (R = CH_3 or C_6H_5) derived from the appropriate isoquinoline Reissert compound and sodium hydride in dimethylformamide (3) with 2,4-dinitrofluorobenzene gave **3** (R = CH_3 or C_6H_5; Ar = 2,4-$(NO_2)_2C_6H_3$) which could be hydrolyzed to **4** (Ar = 2,4-$(NO_2)_2C_6H_3$). Reaction of **1** (R = CH_3 or C_6H_5) under the same conditions with 2-bromo-3-nitropyridine proceeded in a similar manner to give **3** (R = CH_3 or C_6H_5; Ar = 2-(3-$NO_2C_5H_3N$)) which could be hydrolyzed to 1-(3-nitro-2-pyridyl) isoquinoline (**4**, Ar = 2-(3-$NO_2C_5H_3N$)). For unexplained reasons the

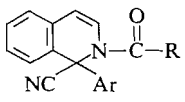

3

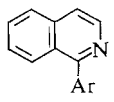

4

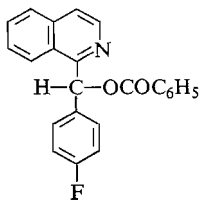

5

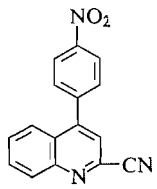

6

[1]For Part XX, see Reference 1.
[2]N.S.F. Undergraduate Research Participant.

Can. J. Chem. Downloaded from www.nrcresearchpress.com by 210.87.254.105 on 09/05/12
For personal use only.

pound m.p. 300° containing nickel was the only product obtained. The filtrate was evaporated and the residue was crystallized from aqueous acetone (Darco) as greenish-yellow crystals (0.54 g, 65%), m.p. 150–152° (lit. (8): colorless crystals, m.p. 149.5–150.5°); infrared spectrum (Nujol): 3330 cm^{-1}, 3200 cm^{-1} (ν_{NH}), 3050 cm^{-1} (ν_{CH} aromatic), 1665 cm^{-1} (ν_{CO} amide), 1606 cm^{-1} ($\nu_{C:C}$), 748 cm^{-1} (δ_{CH} aromatic); n.m.r. spectrum ($CDCl_3$): τ 6.47 (C_4-H) (on expanding the spectrum, this signal became a poorly-resolved triplet, J = 1.5 Hz), τ 5.57 (s, C_1-H), τ 2.89 (aromatic), τ 2.00 (NH); mass spectrum, m/e = 147 (mol. wt., 147.18).

Anal. Calcd. for C_9H_9NO: C, 73.45; H, 6.16; N, 9.52. Found: C, 73.53; H, 5.98; N, 9.34.

Acknowledgment

The author gratefully acknowledges a personal grant during 1967–1968 from G. D. Searle and Company, Skokie, Illinois.

1. J. M. Osgerby, J. Pluščec, Y. C. Kim, and S. F. MacDonald. To be published.
2. A. H. Jackson and S. F. MacDonald. Can. J. Chem. **35**, 715 (1957).
3. G. P. Arsenault and S. F. MacDonald. Can. J. Chem. **39**, 2043 (1961).
4. S. Sternhell. Rev. Pure Appl. Chem. **14**, 15 (1964).
5. K. Katari, K. Tori, Y. Kimura, T. Yoshida, T. Nakasaki, and H. Minato. J. Med. Chem. **10**, 1149 (1967).
6. J. N. Shoolery. Discussions Faraday Soc. **34**, 104 (1962).
7. P. A. S. Smith and R. O. Kan. Org. Syn. **44**, 91 (1964).
8. R. Huisgen and J. Reinertshofer. Ann. **575**, 197 (1952).

Reissert compound studies. XXI. Arylation reactions[1]

Robert Piccirilli[2] and Frank D. Popp

Department of Chemistry, Clarkson College of Technology, Potsdam, New York 13676

Received March 18, 1969

The anions derived from both the isoquinoline and the quinoline Reissert compounds have been arylated by use of nitro and dinitro arylhalides. *p*-Fluorobenzaldehyde reacts preferentially at the carbonyl group and does not lead to arylation.

Canadian Journal of Chemistry, 47, 3261 (1969)

A variety of reactions have been reported for the anions **1** and **2** derived from the isoquinoline and quinoline Reissert compounds (2). We now wish to report on the arylation of these anions.

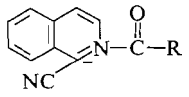

1

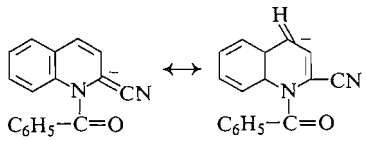

2

Reaction of the anion **1** (R = CH_3 or C_6H_5) derived from the appropriate isoquinoline Reissert compound and sodium hydride in dimethylformamide (3) with 2,4-dinitrofluorobenzene gave **3** (R = CH_3 or C_6H_5; Ar = 2,4-$(NO_2)_2C_6H_3$) which could be hydrolyzed to **4** (Ar = 2,4-$(NO_2)_2C_6H_3$). Reaction of **1** (R = CH_3 or C_6H_5) under the same conditions with 2-bromo-3-nitropyridine proceeded in a similar manner to give **3** (R = CH_3 or C_6H_5; Ar = 2-(3-$NO_2C_5H_3N$)) which could be hydrolyzed to 1-(3-nitro-2-pyridyl) isoquinoline (**4**, Ar = 2-(3-$NO_2C_5H_3N$)). For unexplained reasons the

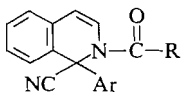

3

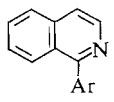

4

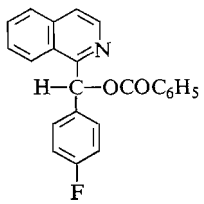

5

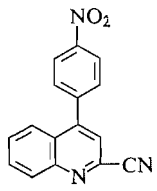

6

[1]For Part XX, see Reference 1.
[2]N.S.F. Undergraduate Research Participant.

Can. J. Chem. Downloaded from www.nrcresearchpress.com by 210.87.254.42 on 09/05/12
For personal use only.

TABLE I

Arylation of isoquinoline Reissert compounds*

R	Ar	Yield	Melting point	Analyses Calcd C	Calcd H	Calcd N	Found C	Found H	Found N
C_6H_5	2,4-$(NO_2)_2C_6H_3$	97	163–164	64.78	3.30	13.14	64.63	3.38	13.06
CH_3	2,4-$(NO_2)_2C_6H_3$	90	193–195	59.34	3.32	15.38	59.38	3.36	15.38
C_6H_5	3-$NO_2C_5H_3N$	56	230–231	69.10	3.69	14.65	68.87	3.66	14.55
CH_3	3-$NO_2C_6H_3N$	74	227–228	63.74	3.77	17.49	63.20	3.77	17.51

*Compounds with the structure 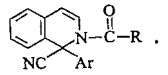 .

reaction of **1** (R = CH_3 or C_6H_5) under the same conditions with *p*-nitrofluorobenzene proceeded directly to **4** (Ar = *p*-$NO_2C_6H_4$) and none of the normal product (3) of the type **3** could be isolated.

The reaction of **1** (R = C_6H_5) with *p*-fluorobenzaldehyde gave the ester **5**, the type of product normally obtained from the reaction of an aldehyde with **1**, indicating that the formyl group did not activate the halogen sufficiently to allow arylation to take place in preference to the reaction of **1** at the carbonyl carbon. The halogen was also not sufficiently activated in 2-bromopyridine and the only product from the reaction of this compound with **1** (R = C_6H_5) was 1-benzoylisoquinoline, the normal base-catalyzed rearrangement product of **1**.

Extension of this arylation to the quinoline series through reaction of **2** with *p*-nitrofluorobenzene gave 2-cyano-4-(*p*-nitrophenyl)quinoline (**6**). It is of interest to note that the use of *p*-fluoronitrobenzene in the isoquinoline series led to complete hydrolysis in the reaction or reaction work up to yield **4** and not **3** while the similar reaction in the quinoline series led to partial hydrolysis with the removal of the benzoyl group but not the cyano group. The reaction might be expected to take place in the 2-position of **2**, as is the case with aldehydes or in the 4-position of **2** as is the case with methyl iodide (2). That the product had the structure indicated, (**6**), and was not 2-cyano-2-(*p*-nitrophenyl)-1,2-dihydroquinoline was indicated by the mass spectra which had a strong molecular ion at 275 indicating the structure **6** and not the dihydro structure which would have arisen from reaction at the 2-position.

Experimental[3]

Arylation of Isoquinoline Reissert Compounds

To a mixture of 0.01 mole of the benzoyl or acetyl isoquinoline Reissert compound and 0.01 mole of 2,4-dinitrofluorobenzene or 3-nitro-2-bromopyridine dissolved in dimethylformamide was added 0.80 g (0.01 mole) of sodium hydride (30% in oil). The mixture was stirred for 1.5 h, poured over 500 g of ice, filtered, and recrystallized from ethanol to give the materials in Table I.

Use of *p*-nitrofluorobenzene with either of the Reissert compounds in the above procedure gave a quantitative yield of 1-(*p*-nitrophenyl)isoquinoline (**4**, Ar = *p*-$NO_2C_6H_4$), m.p. 151–152° (reported (4) m.p. 155°).

Anal. Calcd. for $C_{15}H_{10}N_2O_2$: C, 71.99; H, 4.03; N, 11.20. Found: C, 71.87; H, 4.04; N, 11.08.

Use of *p*-fluorobenzaldehyde with the benzoyl isoquinoline Reissert compound in the above procedure gave a 31% yield of **5**, m.p. 150–151°.

Anal. Calcd. for $C_{23}H_{16}FNO_2$: C, 77.30; H, 4.51; N, 3.92. Found: C, 77.47; H, 4.47; N, 3.84.

Hydrolysis of Arylated Reissert Compound

In a typical experiment 1.7 g of **3** (R = C_6H_5; Ar = 2-(3-$NO_2C_5H_3N$)) was dissolved in 25 ml of ethanol and 25 ml of water containing 8.0 g of potassium hydroxide and refluxed for 2 h. The ethanol was removed *in vacuo* and the precipitate was subjected to dry column chromatography on alumina with chloroform. The first fraction was recrystallized from ethanol to give 0.48 g of **4** (Ar = 2-(3-$NO_2C_5H_3N$)), m.p. 169–171°. The same product was also obtained from the acetyl Reissert adduct.

Anal. Calcd. for $C_{14}H_9N_3O_2$: C, 66.93; H, 3.61; N, 16.73. Found: C, 66.99; H, 3.68; N, 16.82.

In a similar manner, **3** (R = CH_3 or C_6H_5; Ar = 2,4-$(NO_2)_2C_6H_3$) gave **4** (Ar = 2,4-$(NO_2)_2C_6H_3$), m.p. 222–223°.

Anal. Calcd. for $C_{15}H_9N_3O_4$: C, 61.02; H, 3.07; N, 14.23. Found: C, 61.12; H, 3.10; N, 14.08.

[3]All melting points are corrected and taken in capillaries. Analyses were determined by Spang Microanalytical Lab., Ann Arbor, Mich; mass spectra were performed by Morgan–Schaffer Co., Montreal.

Can. J. Chem. Downloaded from www.nrcresearchpress.com by 210.87.254.42 on 09/05/12
For personal use only.

Arylation of Quinoline Reissert Compound

As described above for the isoquinoline Reissert compound, equimolar quantities of 1-benzoyl-1,2-dihydroquinaldonitrile, *p*-nitrofluorobenzene, and sodium hydride in dimethylformamide gave after dry column chromatography on alumina with benzene and recrystallization from ethanol a 47% yield of **6**, m.p. 253–255°. Mass spectra 275 (100%), 259 (2%), 245 (8%), 229 (42%), 228 (28%), 216 (11%), 203 (5%), 202 (27%), 201 (23%), 176 (17%), 175 (13%), 151 (12%), 149 (4%).

Anal. Calcd. for $C_{16}H_9N_3O_2$: C, 69.81; H, 3.30; N, 15.27. Found: C, 69.57; H, 3.38; N, 15.17.

1. F. D. POPP and C. W. KLINOWSKI. J. Chem. Soc. C, 741 (1969).
2. F. D. POPP. Advan. Heterocyclic Chem. **9**, 1 (1968), and leading references therein.
3. F. D. POPP and J. M. WEFER. J. Heterocyclic Chem. **4**, 183 (1967).
4. H. GILMAN and G. C. GAINER. J. Am. Chem. Soc. **69**, 1946 (1947).

Branched-chain sugar nucleosides. II. 9-(3-Deoxy-3-*C*-hydroxymethyl-β-D-glucopyranosyl)-adenine[1]

ALEX ROSENTHAL, M. SPRINZL, AND H. J. KOCH
Department of Chemistry, University of British Columbia, Vancouver 8, British Columbia

Received March 17, 1969

Application of the oxo reaction to 1,2,4,6-tetra-*O*-acetyl-3-deoxy-α-D-*erythro*-hex-2-enopyranose (**1**), followed by acetylation of the oxo products, gave crystalline 1,2,3′,4,6-penta-*O*-acetyl-3-deoxy-3-*C*-(hydroxymethyl)-α-D-glucopyranose (**2**) in about 30% yield. Conversion of **2** into the branched-chain sugar bromide, followed by condensation of the latter with 6-benzamidochloromercuripurine afforded a blocked branched-chain sugar nucleoside (**5**) in 67% yield based on **2**. The nucleoside (**5**) was deblocked with methanolic sodium methoxide to afford 9-(3-deoxy-3-*C*-hydroxymethyl-β-D-glucopyranosyl)-adenine (**6**) in 75% yield.

Canadian Journal of Chemistry, **47**, 3263 (1969)

Can. J. Chem. Downloaded from www.nrcresearchpress.com by 210.87.254.42 on 09/05/12
For personal use only.

From 1966 to the present a number of reports have appeared (1–8) dealing with branched-chain sugar nucleosides. Most of these unusual nucleosides contain the furanosyl moiety (1–5), but a few have the pyranosyl ring system (6–8). The fact that some of the synthetic branched-chain sugar nucleosides (1–3) have been found to exhibit biological activity has helped to focus further attention on these interesting compounds. In this communication we wish to report complete details of a facile synthesis of the branched-chain deoxy sugar 3-deoxy-3-*C*-hydroxymethyl-D-glucopyranose and its conversion into the branched-chain deoxy sugar nucleoside (8).

When 1,2,4,6-tetra-*O*-acetyl-3-deoxy-α-D-*erythro*-hex-2-enopyranose (**1**) (9) was allowed to react with a mixture of carbon monoxide and hydrogen (oxo synthesis) in the presence of preformed dicobalt octacarbonyl at 150–160° for 2 h, a mixture of oxo products was obtained (8). After the products were freed from catalyst, they were fully acetylated using acetic anhydride and pyridine. An attempt to separate the mixture by column chromatography using alumina as adsorbent and ether as developer gave a partial separation of the products. Preparative vapor phase chromatography (v.p.c.) of the mixture of acetates gave compound (**2**) (having the longest retention time), in about 30% yield. A suggested mechanism of the reaction has already been discussed (8). A parallel reaction of **1** with carbon monoxide and deuterium followed by acetylation gave the partially deuterated analogue, namely, 1,2,3′,4,6-penta-*O*-acetyl-3-deoxy-3-*C*-(hydroxymethyl)-α-D-glucopyranose-2,3′,3′,-$^2H_3$ (*cis*) (**7**). The structures of **2** and **7** were readily ascertained from their nuclear magnetic resonance (n.m.r.) spectra and have already been described (8).

The branched-chain sugar (**2**) was converted into 2,3′,4,6-tetra-*O*-acetyl-3-deoxy-3-*C*-(hydroxymethyl)-D-glucopyranosyl bromide (**4**) by the usual method (not isolated because of instability) and immediately condensed with 6-benzamidochloromercuripurine in the presence of cadmium carbonate to afford the crystalline blocked branched-chain sugar nucleoside (**5**) in 67% yield based on the acetate (**2**). Although a

[1]For part I, see reference 13.

Arylation of Quinoline Reissert Compound

As described above for the isoquinoline Reissert compound, equimolar quantities of 1-benzoyl-1,2-dihydroquinaldonitrile, *p*-nitrofluorobenzene, and sodium hydride in dimethylformamide gave after dry column chromatography on alumina with benzene and recrystallization from ethanol a 47% yield of **6**, m.p. 253–255°. Mass spectra 275 (100%), 259 (2%), 245 (8%), 229 (42%), 228 (28%), 216 (11%), 203 (5%), 202 (27%), 201 (23%), 176 (17%), 175 (13%), 151 (12%), 149 (4%).

Anal. Calcd. for $C_{16}H_9N_3O_2$: C, 69.81; H, 3.30; N, 15.27. Found: C, 69.57; H, 3.38; N, 15.17.

1. F. D. POPP and C. W. KLINOWSKI. J. Chem. Soc. C, 741 (1969).
2. F. D. POPP. Advan. Heterocyclic Chem. **9**, 1 (1968), and leading references therein.
3. F. D. POPP and J. M. WEFER. J. Heterocyclic Chem. **4**, 183 (1967).
4. H. GILMAN and G. C. GAINER. J. Am. Chem. Soc. **69**, 1946 (1947).

Branched-chain sugar nucleosides. II. 9-(3-Deoxy-3-*C*-hydroxymethyl-β-D-glucopyranosyl)-adenine[1]

ALEX ROSENTHAL, M. SPRINZL, AND H. J. KOCH
Department of Chemistry, University of British Columbia, Vancouver 8, British Columbia

Received March 17, 1969

Application of the oxo reaction to 1,2,4,6-tetra-*O*-acetyl-3-deoxy-α-D-*erythro*-hex-2-enopyranose (**1**), followed by acetylation of the oxo products, gave crystalline 1,2,3′,4,6-penta-*O*-acetyl-3-deoxy-3-*C*-(hydroxymethyl)-α-D-glucopyranose (**2**) in about 30% yield. Conversion of **2** into the branched-chain sugar bromide, followed by condensation of the latter with 6-benzamidochloromercuripurine afforded a blocked branched-chain sugar nucleoside (**5**) in 67% yield based on **2**. The nucleoside (**5**) was deblocked with methanolic sodium methoxide to afford 9-(3-deoxy-3-*C*-hydroxymethyl-β-D-glucopyranosyl)-adenine (**6**) in 75% yield.

Canadian Journal of Chemistry, **47**, 3263 (1969)

Can. J. Chem. Downloaded from www.nrcresearchpress.com by 210.87.254.105 on 09/05/12
For personal use only.

From 1966 to the present a number of reports have appeared (1–8) dealing with branched-chain sugar nucleosides. Most of these unusual nucleosides contain the furanosyl moiety (1–5), but a few have the pyranosyl ring system (6–8). The fact that some of the synthetic branched-chain sugar nucleosides (1–3) have been found to exhibit biological activity has helped to focus further attention on these interesting compounds. In this communication we wish to report complete details of a facile synthesis of the branched-chain deoxy sugar 3-deoxy-3-*C*-hydroxymethyl-D-glucopyranose and its conversion into the branched-chain deoxy sugar nucleoside (8).

When 1,2,4,6-tetra-*O*-acetyl-3-deoxy-α-D-*erythro*-hex-2-enopyranose (**1**) (9) was allowed to react with a mixture of carbon monoxide and hydrogen (oxo synthesis) in the presence of preformed dicobalt octacarbonyl at 150–160° for 2 h, a mixture of oxo products was obtained (8). After the products were freed from catalyst, they were fully acetylated using acetic anhydride and pyridine. An attempt to separate the mixture by column chromatography using alumina as adsorbent and ether as developer gave a partial separation of the products. Preparative vapor phase chromatography (v.p.c.) of the mixture of acetates gave compound (**2**) (having the longest retention time), in about 30% yield. A suggested mechanism of the reaction has already been discussed (8). A parallel reaction of **1** with carbon monoxide and deuterium followed by acetylation gave the partially deuterated analogue, namely, 1,2,3′,4,6-penta-*O*-acetyl-3-deoxy-3-*C*-(hydroxymethyl)-α-D-glucopyranose-2,3′,3′,-$^2H_3$ (*cis*) (**7**). The structures of **2** and **7** were readily ascertained from their nuclear magnetic resonance (n.m.r.) spectra and have already been described (8).

The branched-chain sugar (**2**) was converted into 2,3′,4,6-tetra-*O*-acetyl-3-deoxy-3-*C*-(hydroxymethyl)-D-glucopyranosyl bromide (**4**) by the usual method (not isolated because of instability) and immediately condensed with 6-benzamidochloromercuripurine in the presence of cadmium carbonate to afford the crystalline blocked branched-chain sugar nucleoside (**5**) in 67% yield based on the acetate (**2**). Although a

[1]For part I, see reference 13.

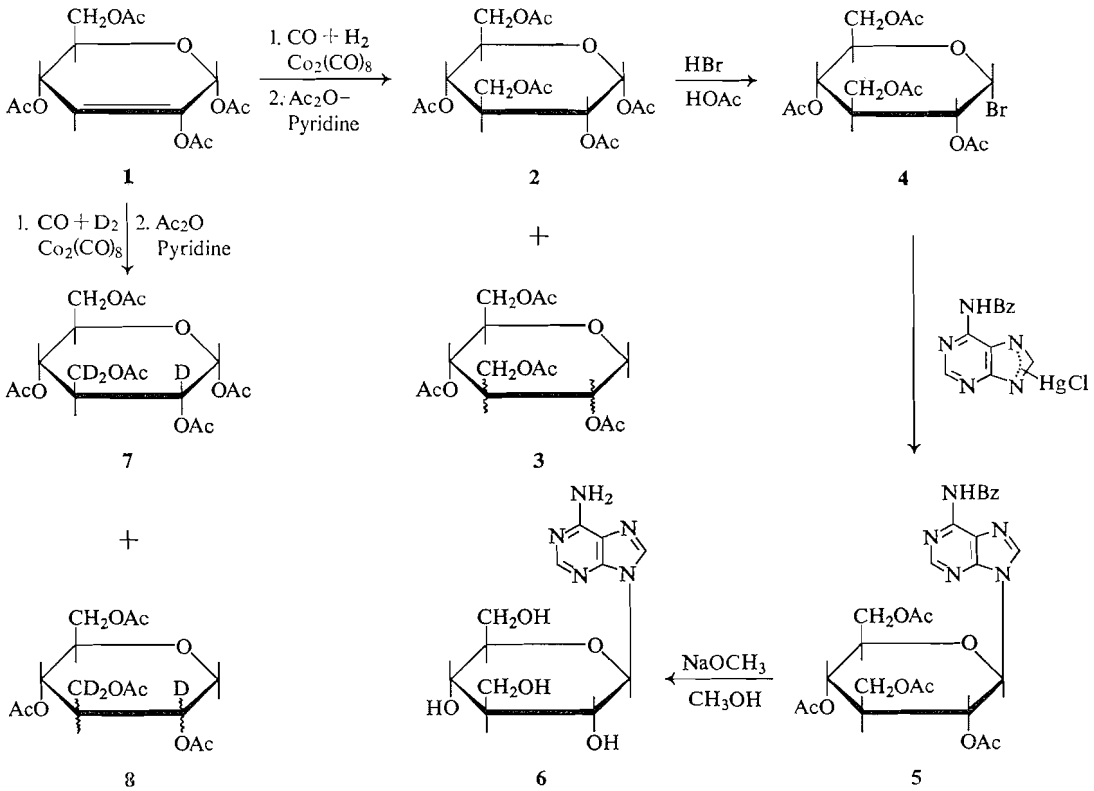

trace of impurity could not be removed from the blocked nucleoside, its analysis (by nitrogen and n.m.r. data) was compatible with the suggested structure. The trace of impurity was readily removed on unblocking **5** using methanolic sodium methoxide to afford the unsubstituted branched-chain sugar nucleoside (**6**) in 75% yield.

The assignment of the structure of **6** was based on the following: (*a*) ultraviolet (u.v.) absorption data of **6** substantiate the site of glycosylation at N-9 (10), (*b*) the *trans* rule (11) indicates that **6** has a β-configuration, (*c*) n.m.r. evidence (H-1′ gave a doublet with $J_{1',2'} = 9$ Hz) clearly corroborates the β-anomeric configuration of **6**.

Experimental

General Considerations

The oxo reaction (8) was performed in an Aminco autoclave. Dicobalt octacarbonyl was purchased from Alfa Inorganics, Inc., Beverley, Massachusetts. Nuclear magnetic resonance spectra were performed on a 100-HMz HA spectrometer, using tetramethylsilane (unless otherwise stated) as the internal standard set at $\tau = 10$. Mass spectra were measured with an A.E.I. M.S.9 spectrometer. Vapor phase chromatography was performed on a Varian Aerograph model 1525 instrument operated at 280° using a 12 ft column of Chromosorb W carrying 10% (by weight) silicone gum rubber SE-52. Detection of nucleosides was performed using a short wave u.v. filter (mineralicht) lamp.

*Reaction of 1,2,4,6-Tetra-O-acetyl-3-deoxy-α-D-erythro-hex-2-enopyranose (**1**) with Carbon Monoxide and Hydrogen to Yield 1,2,3′,4,6-Penta-O-acetyl-3-deoxy-3-C-(hydroxymethyl)-α-D-glucopyranose (**2**)*

A solution of 1,2,4,6-tetra-*O*-acetyl-3-deoxy-α-D-*erythro*-hex-2-enopyranose (8 g) (9) and dicobalt octacarbonyl (3 g) in dry purified benzene (35 ml) was shaken with carbon monoxide (800 p.s.i.) and hydrogen (1400 p.s.i.) in a high-pressure autoclave at a temperature of 150–160° for 2 h. After the gases were vented, 100 ml of petroleum ether (b.p. 35–60°) was added to the reaction mixture. The brown syrup which precipitated was separated from the solution and dissolved in benzene. The benzene solution was decolorized with activated charcoal, filtered, and evaporated under reduced pressure to yield an amber colored syrup (7.7 g). The syrup was acetylated using pyridine (50 ml) and acetic anhydride (50 ml). The acetylation mixture was evaporated to dryness and dissolved in chloroform. The chloroform solution was washed with aqueous sodium bicarbonate followed by water. The dried organic layer was evaporated

Can. J. Chem. Downloaded from www.nrcresearchpress.com by 210.87.254.105 on 09/05/12
For personal use only.

Can. J. Chem. Downloaded from www.nrcresearchpress.com by 210.87.254.105 on 09/05/12
For personal use only.

under reduced pressure to yield a syrup (8.8 g). Preparative v.p.c. of the product (in 200 ml of toluene) at 280° gave two major zones, A and B, and traces of five minor zones. The loss due to aerosol formation was considerable. One of the major zones (A) (0.530 g), which had the longest retention time (15.4 min), was readily recrystallized from ethyl ether – light petroleum ether (b.p. 30–60°); m.p. 100°, $[\alpha]_D^{22}$ +58° (*c*, 4 in benzene). The n.m.r. of **2** has been reported previously (8).

Anal. Calcd. for $C_{17}H_{24}O_{11}$ (mol. wt. 404): C, 50.47; H, 5.98. Found (mol. wt. 404 (added 43 to parent peak) (*m/e* 361, loss of CH_3CO)): C, 50.41; H, 5.98.

The second major zone (B) (compound **3**) (1.6 g) was a syrup and had a retention time of 11 min. The v.p.c. rerun of zone B at 180° showed the presence of two zones (never separated in 100% purity); τ ($CDCl_3$) 4.9–5.5 (overlapping multiplets, equal to 2 hydrogens attributed to H-2 and H-4), 5.6 to 6.6 (overlapping multiplets equal to 5 hydrogens, assigned to 2H-6, 1H-5, and 2H-3′) 7.55 (t, assigned to a single H-3a methine hydrogen, with J_{3-4} = 12 Hz), 7.36 (m, assigned to H-3e, 8 (12 acetyl H)). There was no signal that corresponded to the H-1 anomeric proton.

Two mobile zones (retention time 5 min) isolated in low yield (about 5%) were directly compared by v.p.c. with products obtained by carrying out a platinum-catalyzed hydrogenation in ethanol of **1**, whereby two main zones (exhibiting no anomeric hydrogens in their n.m.r. spectra) were obtained with retention times identical with those of the two fast moving minor components in the fully acetylated oxo product of **1**.

*Reaction of **1** with Carbon Monoxide and Deuterium to Yield 1,2,3′,4,6-Penta-O-acetyl-3-deoxy-3-C-(hydroxymethyl)-α-D-glucopyranose-2,3′,3′-$^2H_3$ (cis) (7)*

The unsaturated sugar (**1**) was allowed to react with carbon monoxide and deuterium and the product worked up as described above.

Anal. Calcd. for $C_{17}H_{21}D_3O_{11}$ (mol. wt. 407): C, 50.10; H and D, 6.68. Found (mol. wt. 407 (added 43 to parent peak) (*m/e* 364, loss of CH_3CO)): C, 50.26; H and D, 6.56. The nuclear magnetic resonance spectrum of 7 has been shown previously (8).

The branched-chain anhydroalditols (**8**) were not characterized.

3-Deoxy-3-C-(hydroxymethyl)-α(β)-D-glucopyranose-2,3′,3′-$^2H_3$(cis)

Compound (7) was deacetylated with sodium methoxide in methanol and the product worked up in the usual way. Recrystallization of the product from aqueous methanol gave crystalline 3-deoxy-3-*C*-(hydroxymethyl)-α(β)-D-glucopyranose-2,3′,3′-$^2H_3$(*cis*); m.p. 169–170°, $[\alpha]_D^{22}$ +44° (*c*, 1 in water), R_{G1} 1.65 (ethyl acetate, pyridine, water 5:2:7). Too little compound was available for reliable chemical analysis.

Anal. Calcd. for $C_7H_{11}D_3O_6$: C, 42.64; H, 8.63. Found: C, 41.68; H, 7.24.

6-Benzamido-9-(2,3′,4,6-tetra-O-acetyl-3-deoxy-3-C-hydroxymethyl-α-D-glucopyranosyl)-purine (5)

1,2,3′,4,6-Penta-*O*-acetyl-3-deoxy-3-*C*-hydroxymethyl-α-D-glucopyranose (0.146 g, 0.36 mmole) was allowed to react with 18% hydrogen bromide in glacial acetic acid (1 ml) at room temperature for 2 h under anhydrous conditions. After the solvent was removed under reduced pressure (anhydrous conditions), the residue was treated thrice with 3 ml of freshly distilled anhydrous xylene and the solvent then distilled to remove the hydrogen bromide. To a mixture of 0.24 g of 6-benzamidochloromercuripurine (12), 0.24 g of Celite, and 0.10 g of cadmium carbonate in 15 ml of anhydrous xylene (first dried by distilling off 5 ml under anhydrous conditions and normal pressure) was added a solution of the sugar bromide (0.140 g) in xylene (3 ml). The reaction mixture was heated at 60° for 0.5 h and then refluxed for 5 h. The hot reaction mixture was then filtered, and the precipitate washed with 20 ml of chloroform. After the solvent was removed under reduced pressure, the residue was extracted with 20 ml of chloroform. The chloroform solution was washed with 7 ml of 30% potassium iodide and with 7 ml of water. Concentration of the dried ($MgSO_4$) chloroform layer gave 0.20 g of product which was extracted with 10 ml of petroleum ether (b.p. 60–90°) to remove non-nucleoside material. The remaining solid residue in 5 ml of methanol was decolorized with charcoal, filtered, and the solvent removed under reduced pressure; yield, 0.14 g (67%); the crystalline product was recrystallized from methanol; m.p. 102–104°; $[\alpha]_D^{22}$ +18° (*c*, 2 in chloroform). The substance contained a trace of impurity which could not be removed by thin layer chromatography on silica gel using ethyl acetate–benzene (2:1); R_f = 0.25. τ ($CDCl_3$) 7.9 (12 acetyl hydrogens), 7.65 (H-3′, $J_{3',2'}$ = 12 Hz, $J_{3',4'}$ = 12 Hz), 5.6–6.3 (m, assigned to branched-chain CH_2 and to 2H-6′, H-5′), 4.4–4.9 (m, assigned to H-2′ and H-4′), 4.06 (d, H-1′, $J_{1',2'}$ = 9.0 Hz), 2.5 and 2.0 assigned to phenyl, 1.75 and 1.2 assigned to H-2 and H-8.

Anal. Calcd. for $C_{27}H_{29}N_5O_{10}$: N, 11.98. Found: N, 11.62.

9-(3-Deoxy-3-C-hydroxymethyl-β-D-glucopyranosyl)-adenine (6)

The blocked nucleoside (**5**) (0.53 g) (first dried by azeotroping with anhydrous benzene) was allowed to react with 0.05 *N* methanolic sodium methoxide (5 ml) at 50° for 2 h. The cooled solution was added to a column (1 cm diameter) containing 5 ml of freshly activated Rexyn 102 (H^+) resin and the resin then eluted with 10 ml water. The combined eluate was evaporated to dryness and the residue extracted with ether. The resin was further eluted with 50 ml of 0.7 *N* ammonium hydroxide and the eluate evaporated under reduced pressure. The resulting residue was combined with the residue remaining after the ether extraction (total yield, 0.041 g), and separated by paper chromatography using 1-butanol–ethanol–water (40:19:11) as developer; yield of **6**, 0.021 g (75%) amorphous substance which could not be crystallized from methanol or water. The solid nucleoside appeared to lose water at about 100° and decomposed at 230–235°, $[\alpha]_D^{22}$ +7° (*c*, 2 in water); $\lambda_{max}(H_2O)$ (mμ) 258 (ε 12 600); R_f 0.31; τ (D_2O) (DDS as internal standard) 8.2 (H-3′ signal overlapping with DSS signal), 6.15–6.4 (m, 2H-6′, H-5′, H-4′), 6.05 (d, branched-chain CH_2, *J* = 3 Hz), 5.75 (two d, assigned to H-2′, $J_{2',1'}$ = 9 Hz and $J_{2',3'}$ = 9 Hz), 5.3 (DOH), 4.42 (d, H-1′, $J_{1',2'}$ = 9.0 Hz), 1.9 (s, H-8), 1.75

(s, H-2). Irradiation at τ 8.3 changed the doublet at τ 6.05 to a singlet and altered the multiplet at τ 6.15–6.4. Irradiation at τ 4.4 altered the H-2′ signal.

For analysis compound (**6**) was dried at 60° under reduced pressure for 1 h.

Anal. Calcd. for $C_{12}H_{17}N_5O_5 \cdot H_2O$: C, 43.70; H, 5.75; H, 21.20. Found: C, 43.40; H, 5.60; N, 21.41.

Acknowledgments

The authors gratefully acknowledge financial assistance from the U.S. Public Service Research Grant No. CA-08382, National Cancer Institute, and from the National Research Council of Canada.

1. E. WALTON, S. R. JENKINS, R. F. NUTT, M. ZIMMERMAN, and F. W. HOLLY. J. Am. Chem. Soc. **88**, 4524 (1966).
2. R. F. NUTT and E. WALTON. J. Med. Chem. **11**, 151 (1968).
3. R. F. NUTT, M. J. DICKINSON, F. W. HOLLY, and E. WALTON. J. Org. Chem. **33**, 1789 (1968).
4. E. J. REIST. Chem. Ind. London, 1957 (1967).
5. E. J. REIST, D. F. CALKINS, and L. GOODMAN, J. Am. Chem. Soc. **90**, 3852 (1968).
6. S. OKUDA, N. SUZUKI, and S. SUZUKI. J. Biol. Chem. **242**, 958 (1967).
7. G. B. HOWARTH. W. A. SZAREK, and J. K. N. JONES. Can. J. Chem. **46**, 3691 (1968).
8. (*a*) A. ROSENTHAL and H. J. KOCH. J. Am. Chem. Soc. **90**, 2181 (1968); (*b*) A. ROSENTHAL. Advan. Carbohydrate Chem. **23**, 59 (1968).
9. (*a*) R. U. LEMIEUX, D. R. LINEBACK, M. L. WOLFROM, F. B. MOODY, E. G. WALLACE, and F. KOMITSKY, JR. J. Org. Chem. **30**, 1092 (1965); (*b*) R. J. FERRIER, W. G. OVEREND, and G. H. SANKEY. J. Chem. Soc. 2830 (1965).
10. J. M. GULLAND and E. R. HOLIDAY. J. Chem. Soc. 765 (1936).
11. B. R. BAKER. Ciba Found. Symp., Chem. Biol. Purines. Little, Brown and Co., Boston, Mass. 120 (1957).
12. J. PROKOP and D. H. MURRAY. J. Pharm. Sci. **54**, 359 (1965).
13. A. ROSENTHAL and L. NGUYEN. J. Org. Chem. **34**, 1029 (1969).

Ring enlargement through acyloin condensation of cycloalkane-1,2-dicarboxylic esters

T. MORI, T. NAKAHARA, AND H. NOZAKI

Department of Industrial Chemistry, Kyôto University, Kyôto, Japan

Received March 26, 1969

Cycloalkane-1,2-dicarboxylic esters of 11-, 12-, and 13-membered rings were prepared from cyclododecanone. Acyloin condensation of these esters in the presence of trimethylchlorosilane followed by acidic hydrolysis afforded 13-, 14-, and 15-membered cycloalkane-1,2-diones in 71–74% yields. The diketones were reduced by treatment with triethyl phosphite and alkali hydroxide into corresponding acyloins.

Canadian Journal of Chemistry, 47, 3266 (1969)

Acyloin condensation in the presence of trimethylchlorosilane was first reported by Schräpler and Rühlmann (1) and later extended to the preparation of four membered cyclic acyloins by Rühlmann (2) and Bloomfield (3). Bloomfield further discussed thermal ring-opening of intermediary cyclobutene-1,2-diol disilyl ethers being controlled by the Woodward–Hoffmann rule.[1]

We now wish to report that this procedure, when applied to large ring cycloalkane-1,2-dicarboxylic esters, constitutes a convenient method for ring enlargement affording cycloalkane-1,2-diones under the incorporation of two side-chain carbons into the rings.[2,3]

Experiments were conducted with 11-, 12-, and 13-membered cycloalkane-1,2-dicarboxylic esters (**6***a–c*), all of which were hitherto unknown compounds and prepared from cyclododecanone (**1**) as a common starting material as shown in Scheme 1. The 11-membered unsaturated ester **2** (7) and the 12-membered unsaturated nitrile **3** (8*b*) have already been obtained from cyclo-

[1]For the valence-isomerization of cyclobutenes, see ref. 4.

[2]Brannock *et al.* (5) and Scharf *et al.* (6) reported similar ring enlargements through thermal ring-opening of bicyclic cyclobutene derivatives.

[3]Dr. Bloomfield kindly suggested to us that the application of this procedure to the diester available from cycloalkanone enamine and dimethyl acetylenedicarboxylate (5) can add four carbon atoms into the starting ring.

Can. J. Chem. Downloaded from www.nrcresearchpress.com by 210.87.254.105 on 09/05/12
For personal use only.

(s, H-2). Irradiation at τ 8.3 changed the doublet at τ 6.05 to a singlet and altered the multiplet at τ 6.15–6.4. Irradiation at τ 4.4 altered the H-2′ signal.

For analysis compound (**6**) was dried at 60° under reduced pressure for 1 h.

Anal. Calcd. for $C_{12}H_{17}N_5O_5 \cdot H_2O$: C, 43.70; H, 5.75; H, 21.20. Found: C, 43.40; H, 5.60; N, 21.41.

Acknowledgments

The authors gratefully acknowledge financial assistance from the U.S. Public Service Research Grant No. CA-08382, National Cancer Institute, and from the National Research Council of Canada.

1. E. WALTON, S. R. JENKINS, R. F. NUTT, M. ZIMMERMAN, and F. W. HOLLY. J. Am. Chem. Soc. **88**, 4524 (1966).
2. R. F. NUTT and E. WALTON. J. Med. Chem. **11**, 151 (1968).
3. R. F. NUTT, M. J. DICKINSON, F. W. HOLLY, and E. WALTON. J. Org. Chem. **33**, 1789 (1968).
4. E. J. REIST. Chem. Ind. London, 1957 (1967).
5. E. J. REIST, D. F. CALKINS, and L. GOODMAN, J. Am. Chem. Soc. **90**, 3852 (1968).
6. S. OKUDA, N. SUZUKI, and S. SUZUKI. J. Biol. Chem. **242**, 958 (1967).
7. G. B. HOWARTH. W. A. SZAREK, and J. K. N. JONES. Can. J. Chem. **46**, 3691 (1968).
8. (*a*) A. ROSENTHAL and H. J. KOCH. J. Am. Chem. Soc. **90**, 2181 (1968); (*b*) A. ROSENTHAL. Advan. Carbohydrate Chem. **23**, 59 (1968).
9. (*a*) R. U. LEMIEUX, D. R. LINEBACK, M. L. WOLFROM, F. B. MOODY, E. G. WALLACE, and F. KOMITSKY, JR. J. Org. Chem. **30**, 1092 (1965); (*b*) R. J. FERRIER, W. G. OVEREND, and G. H. SANKEY. J. Chem. Soc. 2830 (1965).
10. J. M. GULLAND and E. R. HOLIDAY. J. Chem. Soc. 765 (1936).
11. B. R. BAKER. Ciba Found. Symp., Chem. Biol. Purines. Little, Brown and Co., Boston, Mass. 120 (1957).
12. J. PROKOP and D. H. MURRAY. J. Pharm. Sci. **54**, 359 (1965).
13. A. ROSENTHAL and L. NGUYEN. J. Org. Chem. **34**, 1029 (1969).

Ring enlargement through acyloin condensation of cycloalkane-1,2-dicarboxylic esters

T. MORI, T. NAKAHARA, AND H. NOZAKI

Department of Industrial Chemistry, Kyôto University, Kyôto, Japan

Received March 26, 1969

Cycloalkane-1,2-dicarboxylic esters of 11-, 12-, and 13-membered rings were prepared from cyclododecanone. Acyloin condensation of these esters in the presence of trimethylchlorosilane followed by acidic hydrolysis afforded 13-, 14-, and 15-membered cycloalkane-1,2-diones in 71–74% yields. The diketones were reduced by treatment with triethyl phosphite and alkali hydroxide into corresponding acyloins.

Canadian Journal of Chemistry, 47, 3266 (1969)

Acyloin condensation in the presence of trimethylchlorosilane was first reported by Schräpler and Rühlmann (1) and later extended to the preparation of four membered cyclic acyloins by Rühlmann (2) and Bloomfield (3). Bloomfield further discussed thermal ring-opening of intermediary cyclobutene-1,2-diol disilyl ethers being controlled by the Woodward–Hoffmann rule.[1]

We now wish to report that this procedure, when applied to large ring cycloalkane-1,2-dicarboxylic esters, constitutes a convenient method for ring enlargement affording cycloalkane-1,2-diones under the incorporation of two side-chain carbons into the rings.[2,3]

Experiments were conducted with 11-, 12-, and 13-membered cycloalkane-1,2-dicarboxylic esters (**6***a–c*), all of which were hitherto unknown compounds and prepared from cyclododecanone (**1**) as a common starting material as shown in Scheme 1. The 11-membered unsaturated ester **2** (7) and the 12-membered unsaturated nitrile **3** (8*b*) have already been obtained from cyclo-

[1]For the valence-isomerization of cyclobutenes, see ref. 4.

[2]Brannock *et al.* (5) and Scharf *et al.* (6) reported similar ring enlargements through thermal ring-opening of bicyclic cyclobutene derivatives.

[3]Dr. Bloomfield kindly suggested to us that the application of this procedure to the diester available from cycloalkanone enamine and dimethyl acetylenedicarboxylate (5) can add four carbon atoms into the starting ring.

Can. J. Chem. Downloaded from www.nrcresearchpress.com by 210.87.254.105 on 09/05/12
For personal use only.

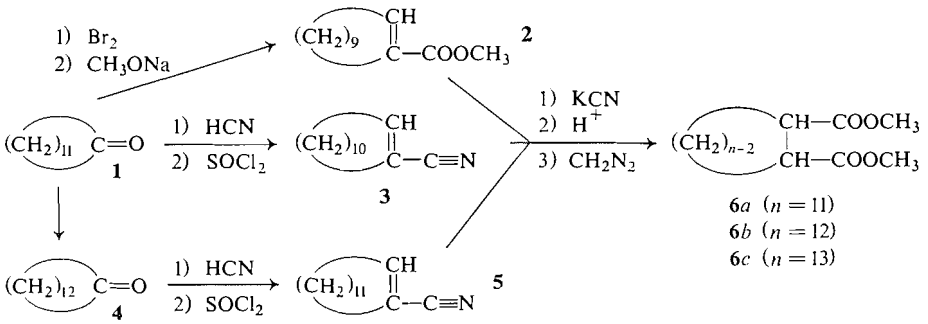

SCHEME 1

dodecanone (**1**) in good yields. Cyclotridecanone (**4**) required in the preparation of 13-membered nitrile **5** is now readily accessible from **1** or its precursor 1,5,9-cyclododecatriene (8).

The α,β-unsaturated ester and nitriles were all converted into corresponding diesters (**6***a–c*) by hydrocyanation, acidic hydrolysis, and final esterification with diazomethane. The diesters (**6**) were characterized by correct elemental analyses, infrared (i.r.) absorption spectra, and nuclear magnetic resonance (n.m.r.) spectra (see Experimental). Each diester would naturally form a mixture of *cis* and *trans* isomers but the separation has not been attempted. As described below, both of the *cis* and *trans* isomers of the intermediates **7** derived from the respective isomers of **6** should be able to undergo ring-opening to **8** to give the same products after hydrolysis, when *n* is sufficiently large.

The acyloin condensation of **6** (see Scheme 2) was performed by following the procedure of Bloomfield (3) in the presence of trimethylchlorosilane in xylene at 110–120°. The reaction was completed by heating to reflux in order to ensure the ring-opening of intermediary cyclobutenes **7** into 1,3-dienes (**8**). Acidic hydrolysis of the reaction mixture gave 1,2-diketones (**9**) in 71–74% yields. The structures of the diketones **9** were ascertained by elemental analyses, i.r., visible absorption spectra, n.m.r., and by reduction to the known cyclic acyloins (**10**).

Reduction of **9** was attained by alkaline hydrolysis of the adducts of **9** with triethyl phosphite in 74–79% yields.

Since the cyclic acyloins (**10**) can be easily reduced to cycloalkanones (9) this reaction sequence would constitute another route to larger ring ketones including cyclotetradecanone and exaltone that are useful as musk odor substances.

Experimental

All temperatures are uncorrected. Nuclear magnetic resonance spectra were obtained on JOEL C-60-H spectrometer in CCl_4 solutions with tetramethylsilane as an internal reference. Chemical shifts are given in p.p.m. from this reference, together with the multiplicity of signals indicated in an abbreviated form: s for singlet, t for triplet, and m for multiplet, respectively. Gas–liquid chromatography was conducted on SE-30 on Chromosorb W (10%) with hydrogen as a carrier gas at 150–190°.

Dimethyl Cycloundecane-1,2-dicarboxylate (6a)

A solution of methyl cycloundecene-1-carboxylate (**2**) (7) (105 g, 0.5 mole) in ethanol (500 ml) was added to potassium cyanide (97.5 g, 1.5 mole) dissolved in water (225 ml) and the whole mixture was heated at reflux for

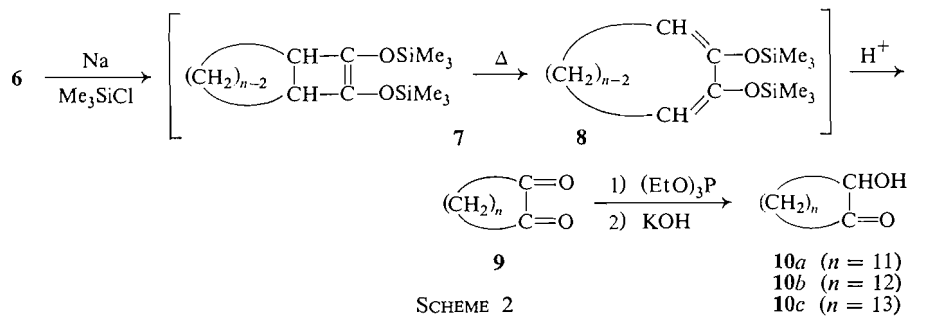

SCHEME 2

Can. J. Chem. Downloaded from www.nrcresearchpress.com by 210.87.254.105 on 09/05/12
For personal use only.

Can. J. Chem. Downloaded from www.nrcresearchpress.com by 210.87.254.105 on 09/05/12
For personal use only.

40 h. After cooling, the mixture was diluted with water (300 ml) and washed with ether. The aqueous layer was acidified with dilute hydrochloric acid and extracted with ether. The organic layer was washed with water, dried (Na_2SO_4), and concentrated *in vacuo*. The residual semisolid was dissolved in acetic acid (830 ml) and concentrated hydrochloric acid (450 ml) and the solution was heated at reflux for 40 h. After cooling and dilution with water, the mixture was extracted with ether several times. The extracts were combined, washed with water, and concentrated *in vacuo*. The resulting solid was immediately esterified with diazomethane to give dimethyl ester (**6***a*). Vacuum distillation gave pure **6***a* (47.3 g, 35% yield based on **2**) as a colorless oil, b.p. 128–134°/0.2 mm Hg. Gas–liquid chromatography showed a single peak. Infrared (neat): 1740, 1190, 1160 cm^{-1} ($COOCH_3$). Nuclear magnetic resonance: δ 3.60 s (6 H), 2.75 m (2 H), 2.0–1.0 m (18 H, a peak at 1.45).

Anal. Calcd. for $C_{15}H_{26}O_4$: C, 66.6; H, 9.7. Found: C, 66.4; H, 9.8.

Dimethyl Cyclododecane-1,2-dicarboxylate (6b)

To a solution of cyclododecene-1-carbonitrile (**3**) (8*b*) (50 g, 0.26 mole) in ethanol (500 ml) was added potassium cyanide (80 g, 1.23 mole) dissolved in water (200 ml) and the whole mixture was heated at reflux for 42 h. After cooling, the reaction mixture was diluted with water. Acidification with dilute hydrochloric acid and salting-out gave white powdery precipitates which were separated by filtration and dissolved in acetic acid (1100 ml) and concentrated hydrochloric acid (750 ml). The resulting solution was heated at reflux for 16 h, cooled, diluted with water, and extracted with ether several times. The extracts were, combined, washed with water, dried (Na_2SO_4), and concentrated *in vacuo* to give solid cyclododecane-1,2-dicarboxylic acid which was esterified with diazomethane without further purification into dimethyl ester (**6***b*). Distillation *in vacuo* afforded pure **6***b* as a colorless solid (57.3 g, 77% yield based on **3**), b.p. 116–118°/0.03 mm Hg, m.p. 54–56°. Gas–liquid chromatography gave a single peak. Infrared (Nujol): 1740, 1190, 1160 cm^{-1} ($COOCH_3$). Nuclear magnetic resonance: δ 3.60 s (6 H), 2.70 m (2 H), 2.0–1.0 m (20 H, a peak at 1.40).

Anal. Calcd. for $C_{16}H_{28}O_4$: C, 67.6; H, 9.9. Found: C, 67.4; H, 9.9.

Cyclotridecene-1-carbonitrile (5)

Hydrocyanic acid (35 ml) was added to a mixture of cyclotridecanone (**4**) (8) (27.5 g, 0.14 mole), triethylamine (3 ml), and ether (50 ml) under stirring in the course of 1 h at room temperature. After stirring at room temperature for 3 h, the mixture was heated at reflux for 1 h. The reaction mixture was cooled, acetic acid (4 ml) added, and the whole washed with water, dried (Na_2SO_4), and concentrated *in vacuo* to give crude cyclotridecanone cyanohydrine (33 g) as a pale-yellow solid. Thionyl chloride (50 g, 0.41 mole) was added dropwise to the crude cyanohydrine dissolved in benzene (70 ml) under stirring at 60° during 2 h. Then the reaction temperature was raised to 75–80° and stirring was continued until no evolution of hydrogen chloride was observed. Vacuum distillation of the reaction mixture gave **5** (24 g, 83% yield based on **4**) as a yellow oil. Redistillation afforded an analytically pure sample as an almost colorless oil, b.p. 102–107°/0.2 mm Hg. Infrared (neat): 2240 cm^{-1} C≡N). Nuclear magnetic resonance: δ 6.05 t (1 H), 2.6–1.9 m (4 H), 1.9–1.1 m (18 H, a peak at 1.30).

Anal. Calcd. for $C_{14}H_{23}N$: C, 81.9; H, 11.3; N, 6.8. Found: C, 81.6; H, 11.2; N, 6.4.

Dimethyl Cyclotridecane-1,2-dicarboxylate (6c)

The unsaturated nitrile **5** was converted into dimethyl ester **6***c* in the same way as described for the preparation of **6***b*. The ester **6***c* was obtained in 56% yield as a colorless solid, b.p. 137–142°/0.08 mm Hg, m.p. 95–97°. Infrared (Nujol): 1740, 1190, 1160 cm^{-1} ($COOCH_3$). Nuclear magnetic resonance: δ 3.65 s (6 H), 2.7 m (2 H), 2.0–1.0 m (22 H, a peak at 1.40).

Anal. Calcd. for $C_{17}H_{30}O_4$: C, 68.4; H, 10.1. Found: C, 68.3; H, 10.2.

Cycloalkane-1,2-diones (9a–c)

General Procedure

A mixture of dimethyl cycloalkane-1,2-dicarboxylate (**6**) (0.04 mole), trimethylchlorosilane (21.7 g, 0.2 mole), and xylene (20 ml) was added dropwise to metallic sodium (5.7 g, 0.24 mole) dispersed in xylene (60 ml) with vigorous stirring at 110–120° under nitrogen atmosphere in the course of 3 h. Stirring was continued at 110–120° for 6 h, and then at reflux temperature for 3 h. After cooling and filtration of inorganic substances, the filtrate was concentrated *in vacuo* to give a viscous oil, which was dissolved in ethanol (140 ml). The resulting solution was added with water (25 ml) and with concentrated hydrochloric acid (4 ml) and the mixture was heated at reflux for 15 min under nitrogen atmosphere. After cooling and dilution with water, the mixture was extracted with ether. The extracts were combined, washed with water, dried (Na_2SO_4), and distilled *in vacuo* to afford **9** as a golden yellow oil or solid. The yields and physical properties were as follows. There was no spectral evidence indicating the presence of enol tautomer.

Cyclotridecane-1,2-dione (9a)

Product was obtained in 71% yield, b.p. 94–97°/2 mm Hg, infrared (neat): 1710 cm^{-1} (C=O), nuclear magnetic resonance: δ 2.70 diffused t (4 H), 2.0–1.0 m (18 H, a peak at 1.25), visible and ultraviolet absorption spectra (in *n*-hexane): log ε_{max} 1.33 (446 mμ), 3.22 (267 mμ). The abnormal absorption in the ultraviolet region might possibly be ascribed to the presence of a trace of inseparable impurity. Biacetyl and cyclodecane-1,2-dione show absorptions of log ε_{max} 1.2 (276 mμ, in cyclohexane) and 1.43 (270 mμ, in ethanol), respectively (10).

Anal. Calcd. for $C_{13}H_{22}O_2$: C, 74.2; H, 10.5. Found: C, 74.4; H, 10.6.

Cyclotetradecane-1,2-dione (9b)

Product was obtained in 73% yield, b.p. 88–93°/0.03 mm Hg, m.p. 37–38° (from *n*-hexane), infrared (Nujol): 1710 cm^{-1} (C=O), nuclear magnetic resonance: δ 2.70 diffused t (4 H), 2.0–1.0 m (20 H, a peak at 1.25), visible and ultraviolet absorption spectra (in *n*-hexane): log ε_{max} 1.37 (443 mμ), 1.53 (278 mμ).

Anal. Calcd. for $C_{14}H_{24}O_2$: C, 75.0; H, 10.8. Found: C, 75.2; H, 10.8.

Cyclopentadecane-1,2-dione (9c)

Product was obtained in 74% yield, b.p. 86–92°/0.02 mm Hg, m.p. 35–37° (from *n*-hexane), infrared (Nujol): 1710 cm^{-1} (C=O), nuclear magnetic resonance: δ 2.75

diffused t (4 H), 2.0–1.0 m (22 H, a peak at 1.25), visible and ultraviolet absorption spectra (in *n*-hexane): log ε_{max} 1.31 (442 mμ), 1.58 (276 mμ).

Anal. Calcd. for $C_{15}H_{26}O_2$: C, 75.6; H, 11.0. Found: C, 75.3; H, 11.0.

*2-Hydroxycycloalkanones (**10a–c**)*

General Procedure

1,2-Diketones (**9**) (0.03 mole) dissolved in benzene (20 ml) was added to a stirred mixture of triethyl phosphite (6.1 g, 0.04 mole) and benzene (16 ml) in the course of 15 min at room temperature under nitrogen atmosphere. The whole mixture was then heated at reflux for 1 h, and concentrated *in vacuo*. The residual oil was mixed with ethanol (75 ml), water (60 ml), and potassium hydroxide (6.7 g, 0.12 mole) and the mixture was stirred at room temperature for 3 h. After dilution with water, the mixture was extracted with chloroform. The extracts were combined, washed, dried and concentrated. Purification of the residual solid by vacuum distillation and recrystallization from *n*-hexane gave analytically pure samples of acyloins **10**. The yields, melting points, etc. were as follows.

*2-Hydroxycyclotridecanone (**10a**)*

Product was obtained in 79% yield, m.p. 44–45° (reported (11) m.p. 45–46°), infrared (Nujol): 3400 (OH), 1710 cm^{-1} (C=O).

Anal. Calcd. for $C_{13}H_{24}O_2$: C, 73.5; H, 11.4. Found: C, 73.5; H, 11.4.

*2-Hydroxycyclotetradecanone (**10b**)*

Product was obtained in 78% yield, m.p. 82–83° (reported (11) m.p. 84–85°), infrared (Nujol): 3530 (OH), 1705 cm^{-1} (C=O).

Anal. Calcd. for $C_{14}H_{26}O_2$: C, 74.3; H, 11.6. Found: C, 74.4; H, 11.5.

*2-Hydroxycyclopentadecanone (**10c**)*

Product was obtained in 74% yield, m.p. 55–56° (reported (11) m.p. 57–58°), infrared (Nujol): 3450 (OH), 1710 cm^{-1} (C=O).

Anal. Calcd. for $C_{15}H_{28}O_2$: C, 75.0; H, 11.7. Found: C, 75.1; H, 11.8.

Acknowledgment

The authors are thankful to Prof. K. Sisido for generous help and encouragement. This work was partially supported by The Scientific Research Grant, Ministry of Education, Japanese Government.

1. U. Schräpler and K. Rühlmann. Chem. Ber. **97**, 1383 (1964).
2. K. Rühlmann, H. Seefluth, and H. Becker. Chem. Ber. **100**, 3820 (1967).
3. J. J. Bloomfield. Tetrahedron Letters, 587 (1968).
4. R. Criegee, D. Seebach, R. E. Winter, B. Börretzen, and H-A. Brune. Chem. Ber. **98**, 2339 (1965).
5. K. C. Brannock, R. D. Burpitt, V. W. Goodlett, and J. G. Thweatt. J. Org. Chem. **28**, 1464 (1963).
6. H-D. Scharf, M. Gallus, and F. Korte. Angew. Chem. **79**, 1015 (1967).
7. E. W. Garbish, Jr. and J. Wohllebe. J. Org. Chem. **33**, 2157 (1968).
8. (*a*) H. Nozaki, S. Kato, and R. Noyori. Can. J. Chem. **44**, 1021 (1966); (*b*) W. Kirchhof, W. Stumpf, and W. Franke. Ann. Chem. **681**, 32 (1965); (*c*) M. Mühlstädt and J. Graefe. Chem. Ber. **100**, 223 (1967); (*d*) W. E. Parham and R. J. Sperley. J. Org. Chem. **32**, 926 (1967).
9. V. Prelog, L. Frenkiel, M. Kobelt, and P. Barman. Helv. Chim. Acta, **30**, 1741 (1947).
10. (*a*) K. Alder, H. K. Schäfer, H. Esser, H. Krieger, and R. Reubke. Ann. Chem. **593**, 23 (1955); (*b*) E. A. Braude and B. F. Gofton. J. Chem. Soc. 4720 (1957).
11. M. Stoll and A. Rouvé. Helv. Chim. Acta, **30**, 1822 (1947).

Separation and identification of methyl ethers of D-glucose and D-glucitol by gas–liquid chromatography[1]

H. G. Jones and J. K. N. Jones

Department of Chemistry, Queen's University, Kingston, Ontario

Received May 5, 1969

The separation by gas–liquid chromatography of the methyl ethers of D-glucose and of D-glucitol is described.

Canadian Journal of Chemistry, **47**, 3269 (1969)

In view of the importance of methyl ether derivatives in the determination of polysaccharide structure it is considered of value to publish details of their separation by gas–liquid chromatography as methyl glycosides and glycitol ethers, and as their acetyl derivative. Details of the separation of methyl ethers of arabinose (1) and of xylose have already been given (2). We now publish details of the separation of the methyl ethers of D-glucose and of D-glucitol.

All separations were made on a Pye–Argon

[1]Abstracted from the Ph.D. thesis of H. G. Jones, Queen's University, Kingston, Ontario, 1964.

Can. J. Chem. Downloaded from www.nrcresearchpress.com by 210.87.254.105 on 09/05/12
For personal use only.

diffused t (4 H), 2.0–1.0 m (22 H, a peak at 1.25), visible and ultraviolet absorption spectra (in *n*-hexane): log ε_{max} 1.31 (442 mμ), 1.58 (276 mμ).

Anal. Calcd. for $C_{15}H_{26}O_2$: C, 75.6; H, 11.0. Found: C, 75.3; H, 11.0.

*2-Hydroxycycloalkanones (**10a–c**)*

General Procedure

1,2-Diketones (**9**) (0.03 mole) dissolved in benzene (20 ml) was added to a stirred mixture of triethyl phosphite (6.1 g, 0.04 mole) and benzene (16 ml) in the course of 15 min at room temperature under nitrogen atmosphere. The whole mixture was then heated at reflux for 1 h, and concentrated *in vacuo*. The residual oil was mixed with ethanol (75 ml), water (60 ml), and potassium hydroxide (6.7 g, 0.12 mole) and the mixture was stirred at room temperature for 3 h. After dilution with water, the mixture was extracted with chloroform. The extracts were combined, washed, dried and concentrated. Purification of the residual solid by vacuum distillation and recrystallization from *n*-hexane gave analytically pure samples of acyloins **10**. The yields, melting points, etc. were as follows.

*2-Hydroxycyclotridecanone (**10a**)*

Product was obtained in 79% yield, m.p. 44–45° (reported (11) m.p. 45–46°), infrared (Nujol): 3400 (OH), 1710 cm^{-1} (C=O).

Anal. Calcd. for $C_{13}H_{24}O_2$: C, 73.5; H, 11.4. Found: C, 73.5; H, 11.4.

*2-Hydroxycyclotetradecanone (**10b**)*

Product was obtained in 78% yield, m.p. 82–83° (reported (11) m.p. 84–85°), infrared (Nujol): 3530 (OH), 1705 cm^{-1} (C=O).

Anal. Calcd. for $C_{14}H_{26}O_2$: C, 74.3; H, 11.6. Found: C, 74.4; H, 11.5.

*2-Hydroxycyclopentadecanone (**10c**)*

Product was obtained in 74% yield, m.p. 55–56° (reported (11) m.p. 57–58°), infrared (Nujol): 3450 (OH), 1710 cm^{-1} (C=O).

Anal. Calcd. for $C_{15}H_{28}O_2$: C, 75.0; H, 11.7. Found: C, 75.1; H, 11.8.

Acknowledgment

The authors are thankful to Prof. K. Sisido for generous help and encouragement. This work was partially supported by The Scientific Research Grant, Ministry of Education, Japanese Government.

1. U. Schräpler and K. Rühlmann. Chem. Ber. **97**, 1383 (1964).
2. K. Rühlmann, H. Seefluth, and H. Becker. Chem. Ber. **100**, 3820 (1967).
3. J. J. Bloomfield. Tetrahedron Letters, 587 (1968).
4. R. Criegee, D. Seebach, R. E. Winter, B. Börretzen, and H-A. Brune. Chem. Ber. **98**, 2339 (1965).
5. K. C. Brannock, R. D. Burpitt, V. W. Goodlett, and J. G. Thweatt. J. Org. Chem. **28**, 1464 (1963).
6. H-D. Scharf, M. Gallus, and F. Korte. Angew. Chem. **79**, 1015 (1967).
7. E. W. Garbish, Jr. and J. Wohllebe. J. Org. Chem. **33**, 2157 (1968).
8. (*a*) H. Nozaki, S. Kato, and R. Noyori. Can. J. Chem. **44**, 1021 (1966); (*b*) W. Kirchhof, W. Stumpf, and W. Franke. Ann. Chem. **681**, 32 (1965); (*c*) M. Mühlstädt and J. Graefe. Chem. Ber. **100**, 223 (1967); (*d*) W. E. Parham and R. J. Sperley. J. Org. Chem. **32**, 926 (1967).
9. V. Prelog, L. Frenkiel, M. Kobelt, and P. Barman. Helv. Chim. Acta, **30**, 1741 (1947).
10. (*a*) K. Alder, H. K. Schäfer, H. Esser, H. Krieger, and R. Reubke. Ann. Chem. **593**, 23 (1955); (*b*) E. A. Braude and B. F. Gofton. J. Chem. Soc. 4720 (1957).
11. M. Stoll and A. Rouvé. Helv. Chim. Acta, **30**, 1822 (1947).

Separation and identification of methyl ethers of D-glucose and D-glucitol by gas–liquid chromatography[1]

H. G. Jones and J. K. N. Jones

Department of Chemistry, Queen's University, Kingston, Ontario

Received May 5, 1969

The separation by gas–liquid chromatography of the methyl ethers of D-glucose and of D-glucitol is described.

Canadian Journal of Chemistry, **47**, 3269 (1969)

In view of the importance of methyl ether derivatives in the determination of polysaccharide structure it is considered of value to publish details of their separation by gas–liquid chromatography as methyl glycosides and glycitol ethers, and as their acetyl derivative. Details of the separation of methyl ethers of arabinose (1) and of xylose have already been given (2). We now publish details of the separation of the methyl ethers of D-glucose and of D-glucitol.

All separations were made on a Pye–Argon

[1]Abstracted from the Ph.D. thesis of H. G. Jones, Queen's University, Kingston, Ontario, 1964.

Can. J. Chem. Downloaded from www.nrcresearchpress.com by 210.87.254.40 on 09/05/12
For personal use only.

Can. J. Chem. Downloaded from www.nrcresearchpress.com by 210.87.254.40 on 09/05/12
For personal use only.

TABLE I

The retention times of methyl *O*-acetyl-*O*-methyl-D-glucopyranosides relative to methyl 4,6-di-*O*-acetyl-2,3-di-*O*-methyl-α-D-glucoside (1.0)

Methyl D-glucopyranoside	Retention time 190°
Methyl 2,3,4,6-tetra-*O*-methyl-α-D-glucoside	0.114
Methyl 2,3,4,6-tetra-*O*-methyl-β-D-glucoside	0.085
Methyl 6-*O*-acetyl-2,3,4-tri-*O*-methyl-α-D-glucoside	0.350
Methyl 6-*O*-acetyl-2,3,4-tri-*O*-methyl-β-D-glucoside	0.250
Methyl 4-*O*-acetyl-2,3,6-tri-*O*-methyl-α-D-glucoside	0.390
Methyl 4-*O*-acetyl-2,3,6-tri-*O*-methyl-β-D-glucoside	0.276
Methyl 3-*O*-acetyl-2,4,6-tri-*O*-methyl-α-D-glucoside	0.575
Methyl 3-*O*-acetyl-2,4,6-tri-*O*-methyl-β-D-glucoside	0.38
Methyl 2-*O*-acetyl-3,4,6-tri-*O*-methyl-α-D-glucoside	0.245
Methyl 2-*O*-acetyl-3,4,6-tri-*O*-methyl-β-D-glucoside	0.355
Methyl 4,6-di-*O*-acetyl-2,3-di-*O*-methyl-α-D-glucoside	1.00 (15 min)
Methyl 4,6-di-*O*-acetyl-2,3-di-*O*-methyl-β-D-glucoside	0.725
Methyl 3,6-di-*O*-acetyl-2,4-di-*O*-methyl-α-D-glucoside	0.825
Methyl 3,6-di-*O*-acetyl-2,4-di-*O*-methyl-β-D-glucoside	0.655
Methyl 3,4-di-*O*-acetyl-2,6-di-*O*-methyl-α-D-glucoside	0.890
Methyl 3,4-di-*O*-acetyl-2,6-di-*O*-methyl-β-D-glucoside	0.600
Methyl 2,6-di-*O*-acetyl-3,4-di-*O*-methyl-α-D-glucoside	0.695
Methyl 2,6-di-*O*-acetyl-3,4-di-*O*-methyl-β-D-glucoside	1.08
Methyl 2,4-di-*O*-acetyl-3,6-di-*O*-methyl-α-D-glucoside	0.690
Methyl 2,4-di-*O*-acetyl-3,6-di-*O*-methyl-β-D-glucoside	1.05
Methyl 2,3-di-*O*-acetyl-4,6-di-*O*-methyl-α-D-glucoside	0.685
Methyl 2,3-di-*O*-acetyl-4,6-di-*O*-methyl-β-D-glucoside	0.755
Methyl 2,3,4-tri-*O*-acetyl-6-*O*-methyl-α-D-glucoside	1.10
Methyl 2,3,4-tri-*O*-acetyl-6-*O*-methyl-β-D-glucoside	1.39
Methyl 3,4,6-tri-*O*-acetyl-2-*O*-methyl-α-D-glucoside	2.33
Methyl 3,4,6-tri-*O*-acetyl-2-*O*-methyl-β-D-glucoside	1.56
Methyl 2,4,6-tri-*O*-acetyl-3-*O*-methyl-α-D-glucoside	1.80
Methyl 2,4,6-tri-*O*-acetyl-3-*O*-methyl-β-D-glucoside	2.66
Methyl 2,3,6-tri-*O*-acetyl-4-*O*-methyl-α-D-glucoside	2.05
Methyl 2,3,6-tri-*O*-acetyl-4-*O*-methyl-β-D-glucoside	2.28
Methyl 2,3,4,6-tetra-*O*-acetyl-α-D-glucoside	2.84
Methyl 2,3,4,6-tetra-*O*-acetyl-β-D-glucoside	3.58

TABLE II

The retention times of acetylated methylated glucitols relative to 1,4,5,6-tetra-*O*-acetyl-2,3-di-*O*-methyl-D-glucitol (1.0)

Acetylated methylated glucitol	Retention time
1,5-Di-*O*-acetyl-2,3,4,6-tetra-*O*-methyl-D-glucitol	0.244
1,2,5-Tri-*O*-acetyl-3,4,6-tri-*O*-methyl-D-glucitol	0.390
1,3,5-Tri-*O*-acetyl-2,4,6-tri-*O*-methyl-D-glucitol	0.412
1,5,6-Tri-*O*-acetyl-2,3,4-tri-*O*-methyl-D-glucitol	0.468
1,4,5-Tri-*O*-acetyl-2,3,6-tri-*O*-methyl-D-glucitol	0.477
1,3,4,5-Tetra-*O*-acetyl-2,6-di-*O*-methyl-D-glucitol	0.750
1,2,3,5-Tetra-*O*-acetyl-4,6-di-*O*-methyl-D-glucitol	0.795
1,2,4,5-Tetra-*O*-acetyl-3,6-di-*O*-methyl-D-glucitol	0.821
1,2,5,6-Tetra-*O*-acetyl-3,4-di-*O*-methyl-D-glucitol	0.973
1,3,5,6-Tetra-*O*-acetyl-2,4-di-*O*-methyl-D-glucitol	1.00
1,4,5,6-Tetra-*O*-acetyl-2,3-di-*O*-methyl-D-glucitol	1.00 (29 min)
1,2,3,4,5-Penta-*O*-acetyl-6-*O*-methyl-D-glucitol	1.14
1,3,4,5,6-Penta-*O*-acetyl-2-*O*-methyl-D-glucitol	1.60
1,2,4,5,6-Penta-*O*-acetyl-3-*O*-methyl-D-glucitol	1.81
1,2,3,5,6-Penta-*O*-acetyl-4-*O*-methyl-D-glucitol	2.00
1,2,3,4,5,6-Hexa-*O*-acetyl-D-glucitol	2.66

Chromatograph at 190 °C and with a gas flow of 190 ml per min. The methyl glucosides were separated on a column (120 × 0.5 cm I.D.), the packing of which was composed of LAC-4R-886[2] (15%) polyester wax on Chromosorb W(60–80 mesh). The glucitols were separated on a similar column containing LAC-4R-886[2] (10%) polyester wax. Experimental details are given in reference (1).

[2]Chromatographic Specialities, Brockville, Ontario.

Acknowledgment

The authors thank the National Research Council of Canada for a grant (A-19).

1. S. C. WILLIAMS and J. K. N. JONES. Can. J. Chem. **45**, 275 (1967).
2. D. G. LANCE and J. K. N. JONES. Can. J. Chem. **45**, 1995 (1967).

Can. J. Chem. Downloaded from www.nrcresearchpress.com by 210.87.254.40 on 09/05/12
For personal use only.

New synthesis of *S*-alkyl-DL-homocysteines

HAROLD M. KOLENBRANDER
Department of Chemistry, Central College, Pella, Iowa 50219

Received March 27, 1969

A simple method for the synthesis of *S*-alkyl-DL-homocysteines is described. The method involves the reaction of homocysteine thiolactone with a primary alkyl halide in sodium methoxide solution.

Canadian Journal of Chemistry, 47, 3271 (1969)

Ethionine, *S*-ethyl homocysteine, has long been known to be a methionine antagonist in biological systems (1). More recently it has been found capable of lowering the level of activity of rat liver urocanase (2–4). Because we desired to learn whether the effect on liver urocanase could also be produced by other *S*-alkyl homocysteines, it was necessary to prepare these commercially unavailable compounds.[1]

Previously published methods for the synthesis of the homologous series of alkyl homocysteines require the use of liquid ammonia and/or hydrogen cyanide (5, 6). In an attempt to avoid the use of these reagents, we have developed a simple method for the synthesis of alkyl homocysteines giving yields of 75–95%. The method involves the reaction of homocysteine thiolactone[2] (**1**) with a primary alkyl halide[3] (**2**) in sodium methoxide solution. The reaction sequence is outlined in Scheme 1, using the synthesis of methionine as an example.

[1]Recent experiments conducted in our laboratory have demonstrated that the higher alkyl homologues do not affect the level of urocanase activity in rat liver.
[2]Obtained from the Aldrich Chemical Company.
[3]We found that a secondary alkyl iodide can be used, but the yield of final product was significantly reduced. Using 2-iodopropane, we synthesized *S*-isopropyl homocysteine in 20% yield.

Experimental

The purity of each compound whose synthesis is reported was assayed by: *1*) melting points; *2*) thin-layer chromatography (t.l.c.); *3*) infrared (i.r.) spectroscopy; and *4*) nuclear magnetic resonance (n.m.r.) spectroscopy.

Melting points were determined using a Hoover–Thomas capillary melting point apparatus at a heating-rate setting of 7. Each compound was recrystallized until its melting point was constant.

The compounds were examined by t.l.c. on Bio-Sil A[4] using three solvent systems: *1*) $CHCl_3$/methanol/17% NH_4OH (2:2:1, v/v); *2*) *n*-propanol/water (64:36, w/w); and *3*) *n*-butanol/glacial acetic acid/water (60:20:20, w/w). Each compound was chromatographically pure in all three solvent systems. The modified ninhydrin solution described by Moffat and Lytle (7) was used to detect the presence of the amino acids on the thin-layer plates.[5]

The i.r. spectra were obtained with a Perkin–Elmer 337 spectrophotometer using KBr pellets. The spectra were very similar to one another showing strong absorption bands near 1420, 1345, 1282, 1078, 547, and 435 cm^{-1}. The spectra of the DL-methionine and of the DL-ethionine, prepared by using the method outlined below, were identical with those obtained from the respective commercial compounds. The other *S*-alkyl homocysteines are not commercially available.

The absence of absorption bands at 840 and 904 cm^{-1} in the spectra of each compound indicates that neither

[4]Silicic acid, available from Bio–Rad Laboratories.
[5]We also sprayed identical chromatograms with concentrated sulfuric acid in order to detect any non-amino acid impurities. None were found.

Chromatograph at 190 °C and with a gas flow of 190 ml per min. The methyl glucosides were separated on a column (120 × 0.5 cm I.D.), the packing of which was composed of LAC-4R-886[2] (15%) polyester wax on Chromosorb W(60–80 mesh). The glucitols were separated on a similar column containing LAC-4R-886[2] (10%) polyester wax. Experimental details are given in reference (1).

[2]Chromatographic Specialities, Brockville, Ontario.

Acknowledgment

The authors thank the National Research Council of Canada for a grant (A-19).

1. S. C. WILLIAMS and J. K. N. JONES. Can. J. Chem. **45**, 275 (1967).
2. D. G. LANCE and J. K. N. JONES. Can. J. Chem. **45**, 1995 (1967).

Can. J. Chem. Downloaded from www.nrcresearchpress.com by 210.87.254.40 on 09/05/12
For personal use only.

New synthesis of *S*-alkyl-DL-homocysteines

HAROLD M. KOLENBRANDER
Department of Chemistry, Central College, Pella, Iowa 50219

Received March 27, 1969

A simple method for the synthesis of *S*-alkyl-DL-homocysteines is described. The method involves the reaction of homocysteine thiolactone with a primary alkyl halide in sodium methoxide solution.

Canadian Journal of Chemistry, 47, 3271 (1969)

Ethionine, *S*-ethyl homocysteine, has long been known to be a methionine antagonist in biological systems (1). More recently it has been found capable of lowering the level of activity of rat liver urocanase (2–4). Because we desired to learn whether the effect on liver urocanase could also be produced by other *S*-alkyl homocysteines, it was necessary to prepare these commercially unavailable compounds.[1]

Previously published methods for the synthesis of the homologous series of alkyl homocysteines require the use of liquid ammonia and/or hydrogen cyanide (5, 6). In an attempt to avoid the use of these reagents, we have developed a simple method for the synthesis of alkyl homocysteines giving yields of 75–95%. The method involves the reaction of homocysteine thiolactone[2] (**1**) with a primary alkyl halide[3] (**2**) in sodium methoxide solution. The reaction sequence is outlined in Scheme 1, using the synthesis of methionine as an example.

[1]Recent experiments conducted in our laboratory have demonstrated that the higher alkyl homologues do not affect the level of urocanase activity in rat liver.
[2]Obtained from the Aldrich Chemical Company.
[3]We found that a secondary alkyl iodide can be used, but the yield of final product was significantly reduced. Using 2-iodopropane, we synthesized *S*-isopropyl homocysteine in 20% yield.

Experimental

The purity of each compound whose synthesis is reported was assayed by: *1*) melting points; *2*) thin-layer chromatography (t.l.c.); *3*) infrared (i.r.) spectroscopy; and *4*) nuclear magnetic resonance (n.m.r.) spectroscopy.

Melting points were determined using a Hoover–Thomas capillary melting point apparatus at a heating-rate setting of 7. Each compound was recrystallized until its melting point was constant.

The compounds were examined by t.l.c. on Bio-Sil A[4] using three solvent systems: *1*) $CHCl_3$/methanol/17% NH_4OH (2:2:1, v/v); *2*) *n*-propanol/water (64:36, w/w); and *3*) *n*-butanol/glacial acetic acid/water (60:20:20, w/w). Each compound was chromatographically pure in all three solvent systems. The modified ninhydrin solution described by Moffat and Lytle (7) was used to detect the presence of the amino acids on the thin-layer plates.[5]

The i.r. spectra were obtained with a Perkin–Elmer 337 spectrophotometer using KBr pellets. The spectra were very similar to one another showing strong absorption bands near 1420, 1345, 1282, 1078, 547, and 435 cm^{-1}. The spectra of the DL-methionine and of the DL-ethionine, prepared by using the method outlined below, were identical with those obtained from the respective commercial compounds. The other *S*-alkyl homocysteines are not commercially available.

The absence of absorption bands at 840 and 904 cm^{-1} in the spectra of each compound indicates that neither

[4]Silicic acid, available from Bio–Rad Laboratories.
[5]We also sprayed identical chromatograms with concentrated sulfuric acid in order to detect any non-amino acid impurities. None were found.

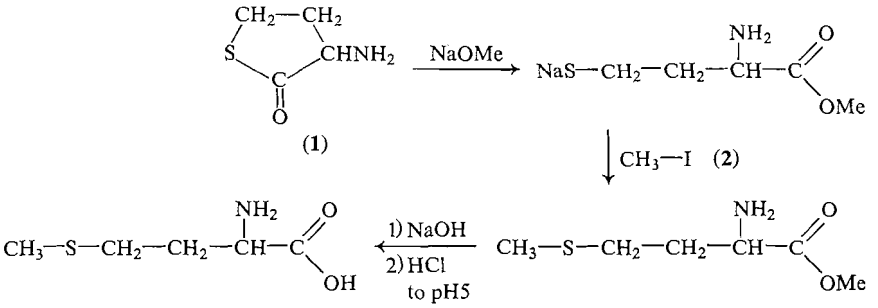

SCHEME 1

TABLE I

Nuclear magnetic resonance spectra of the *S*-alkyl-DL-homocysteines (τ, parts per million)*

S-Alkyl substituent	Homocysteine protons		*S*-Alkyl protons
	C-2 proton	Methylene protons	
Methyl	5.79t	7.07–8.00m	7.88s
Ethyl	5.76t	7.07–8.05m	8.79t
Propyl	5.76t	7.05–8.01m	8.17–8.75m and 8.75–9.30m
Butyl	5.78t	7.08–8.00m	8.15–8.90m and 8.90–9.33m
Pentyl	5.79t	7.06–8.00m	8.10–8.95m and 8.95–9.42m
Hexyl	5.79t	7.08–8.06m	8.06–9.00m and 9.00–9.42m
Benzyl	5.71t	7.05–7.95m	2.58s and 6.16s

*The notations m, s, and t refer to multiplets, singlets, and triplets respectively.

homocysteine nor its thiolactone are significant contaminants of any of the compounds synthesized. Furthermore, none of the spectra had absorption bands in the 1070–1030 cm^{-1} and the 1160–1120 cm^{-1} regions indicating the absence of sulfoxides and sulfones respectively.

The n.m.r. spectra were obtained using a Varian A-60 spectrometer and were entirely consistent with the assigned structures. The spectra of commercial DL-methionine and DL-ethionine could be superimposed exactly on those of the corresponding compounds obtained using the synthetic method described below. Analysis of the integration data indicated that deviations from the expected number of hydrogens relative to the C-2 proton were within ±3%. The data obtained from the n.m.r. spectra are presented in Table I.

Synthesis of DL-*Methionine*

DL-Homocysteine thiolactone hydrochloride (50 mmoles, 7.65 g) was added to a cold solution, 0°, of sodium methoxide in methanol (2.7 g of sodium metal in 210 ml of methanol). After stirring at room temperature for 0.5 h, 50 mmoles (3.11 ml) of iodomethane were added dropwise during 5 min and the stirring continued for 1.25 h. The reaction mixture was then filtered and the filtrate concentrated to 20 ml under reduced pressure. The concentrate was taken up in 300 ml of 1 *N* sodium hydroxide and the resulting solution was heated under reflux for 1.5 h. Following concentration to 40 ml under reduced pressure, the reaction mixture was cooled to 0° and brought to pH 5 by the dropwise addition of concentrated hydrochloric acid with vigorous stirring. The resulting thick suspension was stirred at 0° for 15–20 min and filtered. The precipitate was dissolved in a minimum volume of boiling water and filtered. Four volumes of absolute ethanol were added to the filtrate which was cooled to 0° for 2 h to give 7.05 g of crystals, m.p. 268–270° with decomposition.

*Synthesis of Other S-Alkyl-*DL-*homocysteines*

The ethyl, propyl, butyl, pentyl, and hexyl homocysteines were synthesized by similar procedures. *S*-Benzyl-DL-homocysteine was synthesized by the same procedure except that benzyl chloride was used as the alkylating agent rather than benzyl iodide.

The melting points and other data pertaining to the preparation of DL-methionine and the other *S*-alkyl-DL-homocysteines are recorded in Table II.

Acknowledgments

This work was supported by Grant No. AM-09847 from the National Institutes of Health, United States Public Health Service.

Can. J. Chem. Downloaded from www.nrcresearchpress.com by 210.87.254.40 on 09/05/12
For personal use only.

TABLE II

Data concerning the purification of the *S*-alkyl-DL-homocysteines

S-Alkyl substituent	Melting point observed* °C	Recrystallization solvent	% yield after recrystallization
Methyl	268–270	Ethanol:water†	95
Ethyl	267–268	Ethanol:water†	96
Propyl	258–260	Water	75
Butyl	250–252	Water	82
Pentyl	247–248	1.5 *N* HCl‡	80
Hexyl	246–248	1.5 *N* HCl‡	85
Benzyl	252–253	1.5 *N* HCl‡	86

*All melting points were accompanied by decomposition.
†See text for details.
‡The compounds were precipitated from this solvent by the addition of concentrated ammonium hydroxide.

The author wishes to thank Dr. Robert Barker, at the University of Iowa, for his help in obtaining and interpreting the nuclear magnetic resonance spectra.

1. H. M. DYER. J. Biol. Chem. **124**, 519 (1938).
2. M. SILVERMAN, R. C. GARDINER, and H. A. BAKERMAN. Arch. Biochem. Biophys. **87**, 306 (1960).
3. P. D. SPOLTER and R. C. BALDRIDGE. Proc. Soc. Exp. Biol. Med. **113**, 436 (1963).
4. H. M. KOLENBRANDER and C. P. BERG. Arch. Biochem. Biophys. **119**, 110 (1967).
5. J. P. GREENSTEIN and M. WINITZ. Chemistry of the amino acids. John Wiley and Sons, Inc., New York, N.Y. 1961. pp. 2137–2145.
6. M. D. ARMSTRONG and J. D. LEWIS. J. Org. Chem. **16**, 749 (1951).
7. E. D. MOFFAT and R. I. LYTLE. Anal. Chem. **31**, 926 (1959).

Partition coefficients of some *N*-alkyl-and *N,N*-dialkyl-derivatives of some cinnamamides and benzalcyanoacetamides in the system cyclohexane–water

A. D. DELANEY[1], D. J. CURRIE, AND H. L. HOLMES
Chemistry Section, Defence Research Establishment Suffield, Ralston, Alberta

Received August 14, 1968

Substituent constants, π, and substituent interaction constants, π interaction, for the groups —CONHR and —CONRR[1] have been derived which allow the calculation of the partition coefficients of the title compounds.

Canadian Journal of Chemistry, 47, 3273 (1969)

A series of *N*-alkyl and *N,N*-dialkyl derivatives of cinnamamide and α-cyanocinnamamide and their 4-chloro-, 4-methoxy-, and 3,4-methylenedioxy-derivatives, **1**, have been synthesized and

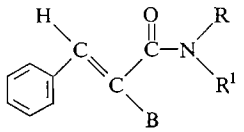

1 *a*) B = H
b) B = CN

their partition coefficients, *K*, determined in the system cyclohexane–water. From these values and eq. [1] (1,2) substituent constants, π, and substituent interaction constants, π interaction, have been determined for the functional groups —CONHR and —CONRR[1]. For —CONHR, π = −4.65 and π interaction = +2.00[2] while for −CONRR[1], π = −4.00 and π interaction = +0.95.

$$[1] \qquad \log K = \Sigma\pi + \Sigma\pi \text{ interaction} - 1.30$$

For cinnamamides and α-cyanocinnamamides with large alkyl groups (e.g. *N*-cyclohexyl, *N,N*-pentamethylene, *N,N*-dipentyl, and *N,N*-dicyclohexyl) the calculated partition coefficients are more positive than those observed. These lower observed values probably result from intramolecular solvation. In contrast to this, the partition coefficients calculated for the *N,t*-butyl derivatives are less positive than those measured indicating that solvation of the nitrogen atom is sterically hindered by the *t*-butyl group.

After excluding these few anomalies, the following correlations were obtained. For 41 *N*-alkyl- and *N,N*-dialkyl-cinnamamides log *K* observed =

[1]Summer student: present address McGill University, Montreal, Quebec.

[2]These values replace those reported (1) for NHCOR.

Can. J. Chem. Downloaded from www.nrcresearchpress.com by 210.87.254.40 on 09/05/12
For personal use only.

TABLE II

Data concerning the purification of the *S*-alkyl-DL-homocysteines

S-Alkyl substituent	Melting point observed* °C	Recrystallization solvent	% yield after recrystallization
Methyl	268–270	Ethanol:water†	95
Ethyl	267–268	Ethanol:water†	96
Propyl	258–260	Water	75
Butyl	250–252	Water	82
Pentyl	247–248	1.5 *N* HCl‡	80
Hexyl	246–248	1.5 *N* HCl‡	85
Benzyl	252–253	1.5 *N* HCl‡	86

*All melting points were accompanied by decomposition.
†See text for details.
‡The compounds were precipitated from this solvent by the addition of concentrated ammonium hydroxide.

The author wishes to thank Dr. Robert Barker, at the University of Iowa, for his help in obtaining and interpreting the nuclear magnetic resonance spectra.

1. H. M. DYER. J. Biol. Chem. **124**, 519 (1938).
2. M. SILVERMAN, R. C. GARDINER, and H. A. BAKERMAN. Arch. Biochem. Biophys. **87**, 306 (1960).
3. P. D. SPOLTER and R. C. BALDRIDGE. Proc. Soc. Exp. Biol. Med. **113**, 436 (1963).
4. H. M. KOLENBRANDER and C. P. BERG. Arch. Biochem. Biophys. **119**, 110 (1967).
5. J. P. GREENSTEIN and M. WINITZ. Chemistry of the amino acids. John Wiley and Sons, Inc., New York, N.Y. 1961. pp. 2137–2145.
6. M. D. ARMSTRONG and J. D. LEWIS. J. Org. Chem. **16**, 749 (1951).
7. E. D. MOFFAT and R. I. LYTLE. Anal. Chem. **31**, 926 (1959).

Partition coefficients of some *N*-alkyl-and *N,N*-dialkyl-derivatives of some cinnamamides and benzalcyanoacetamides in the system cyclohexane–water

A. D. DELANEY[1], D. J. CURRIE, AND H. L. HOLMES
Chemistry Section, Defence Research Establishment Suffield, Ralston, Alberta

Received August 14, 1968

Substituent constants, π, and substituent interaction constants, π interaction, for the groups —CONHR and —CONRR[1] have been derived which allow the calculation of the partition coefficients of the title compounds.

Canadian Journal of Chemistry, 47, 3273 (1969)

A series of *N*-alkyl and *N,N*-dialkyl derivatives of cinnamamide and α-cyanocinnamamide and their 4-chloro-, 4-methoxy-, and 3,4-methylenedioxy-derivatives, **1**, have been synthesized and

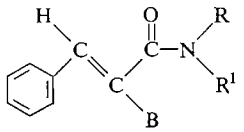

1 *a*) B = H
b) B = CN

their partition coefficients, *K*, determined in the system cyclohexane–water. From these values and eq. [1] (1,2) substituent constants, π, and substituent interaction constants, π interaction, have been determined for the functional groups —CONHR and —CONRR[1]. For —CONHR, π = −4.65 and π interaction = +2.00[2] while for −CONRR[1], π = −4.00 and π interaction = +0.95.

$$[1] \qquad \log K = \Sigma\pi + \Sigma\pi \text{ interaction} - 1.30$$

For cinnamamides and α-cyanocinnamamides with large alkyl groups (e.g. *N*-cyclohexyl, *N,N*-pentamethylene, *N,N*-dipentyl, and *N,N*-dicyclohexyl) the calculated partition coefficients are more positive than those observed. These lower observed values probably result from intramolecular solvation. In contrast to this, the partition coefficients calculated for the *N,t*-butyl derivatives are less positive than those measured indicating that solvation of the nitrogen atom is sterically hindered by the *t*-butyl group.

After excluding these few anomalies, the following correlations were obtained. For 41 *N*-alkyl- and *N,N*-dialkyl-cinnamamides log *K* observed =

[1]Summer student: present address McGill University, Montreal, Quebec.

[2]These values replace those reported (1) for NHCOR.

Can. J. Chem. Downloaded from www.nrcresearchpress.com by 210.87.254.40 on 09/05/12
For personal use only.

TABLE I

Characterization of and partition coefficients for some *N*-alkyl- and *N*,*N*-dialkyl-cinnamamides

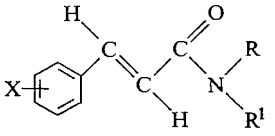

X	R	R[1]	Melting (boiling) point (°C)*	Analytical figures %N, Calcd	Analytical figures %N, Found	log Partition coefficient Found	log Partition coefficient Calcd†
H	CH_3	H	111.8–112.4(16)	—	—	−1.27	−1.25
H	C_2H_5	H	95.2–95.6 (4)	—	—	−0.58	−0.60
H	n-C_3H_7	H	80.0–81.0	7.40	7.40	0.01	0.05
H	i-C_3H_7	H	102.0–103.0(17)	7.40	7.38	0.01	0.05
H	n-C_4H_9	H	79.2–80.2 (6)	—	—	0.66	0.70
H	i-C_4H_9	H	112.0–113.0(7)	—	—	0.53	0.70
H	t-C_4H_9	H	142.8–143.8(8)	—	—	1.12	0.70
H	n-C_5H_{11}	H	85.4–86.4	6.45	6.50	1.38	1.35
H	i-C_5H_{11}	H	101.4–101.8(9)	6.45	6.50	1.29	1.35
H	C_6H_{11}(cyclo)	H	179.2–180.2(10)	—	—	1.39	2.00
H	CH_3	CH_3	100.0–100.8(4)	—	—	0.05	0.05
H	C_2H_5	C_2H_5	68.0–69.0 (4)	—	—	1.28	1.35
H	n-C_3H_7	n-C_3H_7	51.0–52.0 (4)	—	—	2.60	2.65
H	i-C_3H_7	i-C_3H_7	(173–174/4 mm (4))	—	—	2.59	2.65
H	n-C_4H_9	n-C_4H_9	(165–166/1 mm (4))	—	—	2.70	3.95
H	n-C_5H_{11}	n-C_5H_{11}	(175–176/1 mm (4))	—	—	3.43	5.25
H	i-C_5H_{11}	i-C_5H_{11}	(160–161/0.2 mm)	4.87	4.89	3.79	5.25
H	—$(CH_2)_5$—		119.0–120.0(11)	—	—	1.44	2.00
4-Cl	CH_3	H	169.0–169.4	7.15	7.09	−0.58	−0.80
4-Cl	C_2H_5	H	149.0–149.6	6.68	6.72	0.06	−0.15
4-Cl	n-C_3H_7	H	138.8–139.2	6.26	6.35	0.74	0.50
4-Cl	i-C_3H_7	H	180.5–181.5	6.26	6.29	0.79	0.50
4-Cl	n-C_4H_9	H	119.5–120.0	5.89	5.84	1.45	1.15
4-Cl	i-C_4H_9	H	138.6–139.2	5.89	5.94	1.28	1.15
4-Cl	t-C_4H_9	H	186.5–187.5	5.89	5.95	1.92	1.15
4-Cl	n-C_5H_{11}	H	125.2–125.6	5.56	5.54	2.08	1.80
4-Cl	i-C_5H_{11}	H	115.0–115.4	5.56	5.61	2.01	1.80
4-Cl	CH_3	CH_3	125.2–125.6	6.68	6.65	0.70	0.50
4-Cl	C_2H_5	C_2H_5	44.2–44.8 (12)	5.89	5.82	2.05	1.80
4-CH_3O	CH_3	H	129.0–129.6(13)	7.32	7.23†	−1.43	−1.35
4-CH_3O	C_2H_5	H	126.8–127.4	6.82	6.77	−0.70	−0.70
4-CH_3O	n-C_3H_7	H	111.6–112.2	6.39	6.35	−0.13	−0.05
4-CH_3O	i-C_3H_7	H	128.0–128.6	6.39	6.32	−0.12	−0.05
4-CH_3O	n-C_4H_9	H	83.0–83.6	6.00	6.00	0.53	0.60
4-CH_3O	i-C_4H_9	H	109.5–110.5	6.00	5.97	0.45	0.60
4-CH_3O	t-C_4H_9	H	120.8–121.2	6.00	5.96	1.00	0.60
4-CH_3O	n-C_5H_{11}	H	113.0–113.6	5.66	5.59	1.23	1.35
4-CH_3O	i-C_5H_{11}	H	81.6–82.4	5.66	5.66	1.06	1.35
4-CH_3O	C_6H_{11}(cyclo)	H	171.2–172.0	5.40	5.36	1.26	2.00
4-CH_3O	CH_3	CH_3	100.0–100.8	6.82	6.75	−0.13	−0.05
4-CH_3O	C_2H_5	C_2H_5	(158/0.10 mm)	6.00	5.75	1.01	1.25
4-CH_3O	n-C_3H_7	n-C_3H_7	32.0–33.0	5.36	5.29	2.03	2.55
O-3 / CH_2 \ O-4	n-C_3H_7	H	(173/0.10 mm) 117.8–118.4	6.00	6.09	−0.29	−0.35
O-3 / CH_2 \ O-4	n-C_4H_9	H	95.8–96.2	5.67	5.83	0.32	0.30
O-3 / CH_2 \ O-4	i-C_4H_9	H	118.0–119.0(14)	—	—	0.24	0.30

Can. J. Chem. Downloaded from www.nrcresearchpress.com by 210.87.254.40 on 09/05/12
For personal use only.

TABLE I (*concluded*)

X	R	R^1	Melting (boiling) point (°C)*	Analytical figures %N, Calcd	%N, Found	log Partition coefficient Found	Calcd
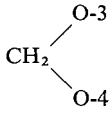	t-C_4H_9	H	136.6–137.2	5.67	5.63	0.78	0.30
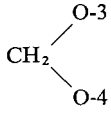	i-C_5H_{11}	H	98.0–99.0 (9)	—	—	0.94	0.95
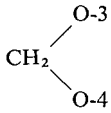	C_6H_{11}(cyclo)	H	185.2–186.0	5.12	5.05	1.08	1.60
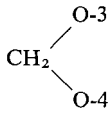	n-C_3H_7	n-C_3H_7	84.8–85.4	5.09	5.07	2.20	2.25
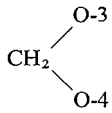	n-C_4H_9	n-C_4H_9	(180/0.05 mm)	4.77	4.57	~3.22‡	3.55
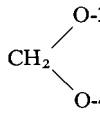	i-C_4H_9	i-C_4H_9	54.5–55.5 (175/0.1 mm)	4.77	4.67	3.40	3.55
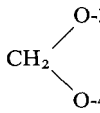	—$(CH_2)_5$—		83.4–84.6	5.44	5.61	1.12	1.60

*All melting points are corrected.
†Anal. Calcd. for $C_{11}H_{13}O_2N$: C, 69.09; H, 6.85. Found: C, 68.96; H, 6.70.
‡The sign "~" indicates that the variation in the measured log K values exceeded 0.06 log unit.

0.91 log K calculated +0.05. The correlation coefficient, r, is 0.98, the standard error of r, Δr, is 0.03 and the standard error of the estimate, Δ estimate, is 0.24. For 41 N-alkyl- and N,N-dialkyl-α-cyanocinnamamides, log K observed = 0.98 log K calculated +0.04: $r = 0.98$, $\Delta r = 0.04$ and Δ estimate = 0.23.

Benzalcyanoacetic acid (m.p. 181.5–181.8 °C) and its 4-chloro (m.p. 198.0–198.3 °C)-, 4-methoxy (m.p. 228.6–229.4 °C)- and 3,4-methylenedioxy (m.p. 229.8–230.4 °C)-derivatives as well as their acid chlorides were prepared by the method of Synerholm and Hartzell (3). The preparation of these new N-substituted cinnamamides and α-cyanocinnamamides from amines followed established procedures (3, 4) as did the preparation from amine hydrochlorides (5).

The partition coefficients were determined as in the earlier papers (1, 2). Each determination was done at least twice, the phases remaining in contact for 10 and 15 min with periods of shaking of 5 and 10 min respectively. The difference between the log K values from the two determinations rarely exceeded 0.06 log units. The averages of these log K values are listed in Tables I and II. Changes with time in the log K values of the N-alkyl- and N,N-dialkyl-derivatives of 4-methoxy- and 3,4-methylenedioxy – benzalcyanoacetamide were eliminated by partitioning these compounds in the absence of light.

Melting and/or boiling points of the amides and their analytical figures are given in Tables I and II.

Acknowledgment

The authors wish to acknowledge the suggestion of Dr. J. B. Reesor that this research be

Can. J. Chem. Downloaded from www.nrcresearchpress.com by 210.87.254.40 on 09/05/12
For personal use only.

TABLE II

Characterization of and partition coefficients for some *N*-alkyl- and *N,N*-dialkyl-derivatives of some benzalcyanoacetamides

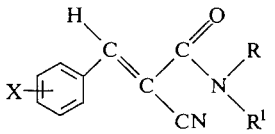

X	R	R^1	Melting point (°C)*	Analyses		log Partition coefficient	
				Calcd	Found	Found	Calcd
H	CH_3	H	98.0–99.5(15)	—	—	−0.11	0.25
H	C_2H_5	H	67.0–68.0	C,71.97; H,6.04; N,13.99	C,72.24; H,5.99; N,13.79	0.81	0.90
H	*n*-C_3H_7	H	88.0–88.2	C,72.87; H,6.58	C,73.23; H,6.65	1.50	1.55
H	*n*-C_4H_9	H	91.5–92.0	C,73.65; H,7.06	C,73.53; H,6.83	2.26	2.20
H	*i*-C_4H_9	H	89.6–90.0	C,73.65; H,7.06	C,73.42; H,7.09	2.09	2.20
H	*t*-C_4H_9	H	88.5–89.5	C,73.65; H,7.06	C,73.78; H,7.01	2.85	2.20
H	*n*-C_5H_{11}	H	81.5–82.0	C,74.35; H,7.49	C,74.06; H,7.50	2.80	2.85
H	*i*-C_5H_{11}	H	98.0–98.5	C,74.35; H,7.49	C,74.45; H,7.50	3.02	2.85
H	C_6H_{11}(Cyclo)	H	147.5–148.8	C,75.56; H,7.13	C,75.21; H,7.17	~3.11‡	3.50
H	CH_3	CH_3	37.0–38.0	C,71.97; H,6.04; N,13.99	C,71.89; H,5.96; N,13.82	0.40	0.50
H	C_2H_5	C_2H_5	Oil†	C,73.65; H,7.06; N,12.27	C,73.58; H,7.09; N,12.08	1.42	1.80
H	*n*-C_3H_7	*n*-C_3H_7	43.0–44.0	C,74.96; H,7.86; N,10.93	C,75.11; H,7.94; N,10.93	2.79	3.10
4-Cl	CH_3	H	174.8–175.4	C,59.87; H,4.11	C,59.71; H,4.05	0.73	0.70
4-Cl	C_2H_5	H	152.6–153.2	C,61.40; H,4.73	C,61.27; H,4.66	1.47	1.35
4-Cl	*n*-C_3H_7	H	137.8–138.4	C,62.77; H,5.27	C,62.78; H,5.40	2.17	2.00
4-Cl	*i*-C_3H_7	H	155.0–155.5	C,62.77; H,5.27	C,62.82; H,5.17	2.20	2.00
4-Cl	*n*-C_4H_9	H	126.6–127.5	C,64.00; H,5.75	C,63.81; H,5.74	2.70	2.65
4-Cl	*i*-C_4H_9	H	133.8–134.7	C,64.00; H,5.75	C,63.97; H,5.77	2.68	2.65
4-Cl	*t*-C_4H_9	H	173.5–174.5	C,64.00; H,5.75	C,64.06; H,5.51	3.50	2.65
4-Cl	*n*-C_5H_{11}	H	124.8–125.0	C,65.10; H,6.19	C,65.00; H,5.98	~3.44	3.30
4-Cl	*i*-C_5H_{11}	H	156.0–156.8	C,65.10; H,6.19	C,65.02; H,6.05	3.43	3.30
4-Cl	C_6H_{11}(cyclo)	H	157.5–158.2	C,66.50; H,5.93	C,66.31; H,5.81	3.41	3.95
4-Cl	CH_3	CH_3	84.0–84.5	C,61.40; H,4.72; N,11.93; Cl,15.10	C,61.40; H,4.65; N,11.88; Cl,15.10	1.10	0.95
4-CH_3O	CH_3	H	148.7–149.6(15)	C,66.64; H,5.60	C,66.56; H,5.57	0.13	0.15
4-CH_3O	C_2H_5	H	115.8–117.0	C,67.81; H,6.12	C,67.84; H,5.90	0.87	0.80
4-CH_3O	*n*-C_3H_7	H	93.2–94.0	C,68.82; H,6.60	C,68.79; H,6.31	1.50	1.45
4-CH_3O	*i*-C_3H_7	H	98.2–99.0	C,68.82; H,6.60	C,68.74; H,6.25	—	—
4-CH_3O	*n*-C_4H_9	H	100.6–100.8	C,69.74; H,7.02	C,69.55; H,6.96	2.27	2.10
4-CH_3O	*i*-C_4H_9	H	111.5–112.0	C,69.74; H,7.02	C,69.91; H,6.64	2.23	2.10
4-CH_3O	*t*-C_4H_9	H	104.0–104.5	C,69.74; H,7.02	C,69.87; H,6.90	3.00	2.10
4-CH_3O	*n*-C_5H_{11}	H	93.6–94.3	C,70.55; H,7.40	C,70.68; H,7.38	3.03	2.75
4-CH_3O	*i*-C_5H_{11}	H	126.6–127.6	C,70.55; H,7.40	C,70.44; H,7.42	2.86	2.75
4-CH_3O	C_6H_{11}(cyclo)	H	181.9–182.8	C,71.80; H,7.05	C,71.67; H,6.87	3.09	3.40
4-CH_3O	CH_3	CH_3	85.2–86.0	C,67.81; H,6.12	C,67.67; H,5.96	0.41	0.40
4-CH_3O	C_2H_5	C_2H_5	87.8–88.2	C,69.74; H,7.02	C,69.63; H,6.76	1.86	1.70
4-CH_3O	*n*-C_3H_7	*n*-C_3H_7	46.0–47.0	C,71.29; H,7.74; N,9.78	C,71.49; H,7.73; N,9.66	2.64	3.00
4-CH_3O	*i*-C_3H_7	*i*-C_3H_7	70.5–71.5	C,71.29; H,7.74; N,9.78	C,71.33; H,7.70; N,9.96	2.62	3.00
4-CH_3O	C_6H_{11}(cyclo)	C_6H_{11} (cyclo)	125.4–126.8	C,75.37; H,8.27	C,75.46; H,8.14	~4.02	6.90
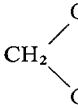	*n*-C_4H_9	H	130.4–130.8	N,10.29	N,10.28	2.00	1.80
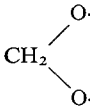	*i*-C_4H_9	H	156.9–157.4	N,10.29	N,10.23	1.97	1.80

Can. J. Chem. Downloaded from www.nrcresearchpress.com by 210.87.254.40 on 09/05/12
For personal use only.

TABLE II (*concluded*)

X	R	R[1]	Melting point (°C)*	Analyses		log Partition coefficient	
				Calcd	Found	Found	Calcd
CH_2(O-3, O-4)	*t*-C_4H_9	H	141.0–141.4	N,10.29	N,10.45	2.66	1.80
CH_2(O-3, O-4)	*i*-C_5H_{11}	H	114.8–115.4(3)	—	—	2.57	2.45
CH_2(O-3, O-4)	C_6H_{11}(cyclo)	H	178.4–179.0(3)	—	—	2.87	3.10
CH_2(O-3, O-4)	*n*-C_3H_7	*n*-C_3H_7	78.4–79.0	N,9.34	N,9.62	2.66	2.70
CH_2(O-3, O-4)	*n*-C_4H_9	*n*-C_4H_9	104.4–104.7(3)	—	—	≥4.40	4.00
CH_2(O-3, O-4)	*i*-C_4H_9	*i*-C_4H_9	89.8–90.3	N,8.54	N,8.58	3.26	4.00
CH_2(O-3, O-4)	—$(CH_2)_5$—		138.4–138.8(3)	—	—	1.57	2.05

*All melting points are corrected.
†This oil was purified by chromatographing on alumina, $n_D = 1.5696$.
The sign "~" indicates that the variation in the measured log K values exceeded 0.06 log unit.

initiated. Mr. C. E. Lough determined the partition coefficients and assisted in the calculation of the new substituent constants. Some of these compounds were prepared by Mr. R. F. Silver and the microanalyses were done by Mr. R. P. Hicken.

1. D. J. Currie, C. E. Lough, R. F. Silver, and H. L. Holmes. Can. J. Chem. **44**, 1035 (1966).
2. C. E. Lough, R. F. Silver, and F. K. McClusky. Can. J. Chem. **46**, 1943 (1968).
3. M. E. Synerholm and A. Hartzell. Contribs. Boyce Thompson Inst. **14**, 79 (1945).
4. D. Papa, E. Schwenk, F. Villani, and E. Klinsberg. J. Am. Chem. Soc. **72**, 3885 (1950).
5. A. J. Speziale and P. C. Hamm. J. Am. Chem. Soc. **78**, 2556 (1956).
6. H. Pacheco, M. Dreux, and A. Beauvillain. Bull. Soc. Chim. France, 1379 (1962); Chem. Abstr. **58**, 7933 (1963).
7. C. R. Hauser, R. S. Yost, and B. I. Ringler. J. Org. Chem. **14**, 261 (1949).
8. H. Plaut and J. J. Ritter. J. Am. Chem. Soc. **73**, 4076 (1951).
9. S. Kaneo and S. Inakawa. J. Pharm. Soc. Japan. **58**, 261 (1938); Chem. Abstr. **32**, 4141 (1938).
10. I. L. Knunyants and N. P. Gambaryan. Izvest. Akad. Nauk SSSR, Otdel. Khim. Nauk. 834 (1957); Chem. Abstr. **52**, 3816 (1958).
11. N. H. Cromwell and J. A. Caughlan. J. Am. Chem. Soc. **67**, 903 (1945).
12. E. T. McCabe, W. F. Barthel, S. I. Gertler, and S. A. Hall. J. Org. Chem. **19**, 493 (1954).
13. R. E. Corbett and C. L. Davey. J. Chem. Soc. 296 (1955).
14. J. A. Goodson. Biochem. J. **15**, 123 (1921); Chem. Abstr. **15**, 2468 (1921).
15. H. Boehme and S. Ebel. Chem. Ber. **98**, 1819 (1965).
16. L. H. Briggs, G. C. DeAth, and S. R. Ellis. J. Chem. Soc. 61 (1942).
17. J. A. Domínguez, G. L. Díaz, and M. A. Vinales D. Ciencia (Mex.) **17**, 213 (1957); Chem. Abstr. **52**, 18198 (1958).

Can. J. Chem. Downloaded from www.nrcresearchpress.com by 210.87.254.40 on 09/05/12
For personal use only.

Functional group and substituent effects, both steric and electronic, upon the ultraviolet absorption spectra of some *N*-alkyl- and *N,N*-dialkyl-derivatives of some cinnamamides and benzalcyanoacetamides

A. D. DELANEY,[1] D. J. CURRIE, AND H. L. HOLMES
Chemistry Section, Defence Research Establishment Suffield, Ralston, Alberta

Received August 14, 1968

Conjugative and steric constants for *N*-substituted carboxyamide groups have been derived which allow the calculation of the long wavelength absorption maxima of *N*-alkyl- and *N,N*-dialkyl-derivatives of cinnamamide and benzalcyanoacetamide. Deviations between calculated and observed values indicate that there may be steric interference between bulky *N,N*-dialkylcarboxyamide groups and the benzylic hydrogen atom.

Canadian Journal of Chemistry, 47, 3278 (1969)

Can. J. Chem. Downloaded from www.nrcresearchpress.com by 210.87.254.42 on 09/05/12
For personal use only.

Ultraviolet (u.v.) absorption spectra have been recorded for a number of *N*-alkyl- and *N,N*-dialkyl-derivatives of cinnamamide and benzalcyanoacetamide and their 4-chloro-, 4-methoxy-, and 3,4-methylenedioxy derivatives. The constancy of the long wavelength absorption maxima for the *N*-alkylcinnamamides, **1**(A = CONHR, B = H), and for the *N*-alkyl-benzal-

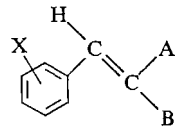

1

cyanoacetamides, **1**(A = CONHR, B = CN), and the close approximation of these (Tables I and II) to the respective values for the cinnamamides, **1**(A = $CONH_2$, B = H), and the benzalcyanoacetamides, **1**(A = $CONH_2$, B = CN), indicate that the *N*-alkyl group does not influence significantly the polarization of the conjugated system in these compounds. The effect of two alkyl groups on the carboxyamide nitrogen atom upon polarization of the conjugated system, on the other hand, is much more pronounced especially for bulky alkyl groups. For example, the absorption maximum of *N,N*-diisopropylcinnamamide is at a wavelength 5 mμ shorter than that of the *N,N*-di-*n*-propyl analogue. This probably results from interference between the isopropyl groups and the hydrogen atom on the β carbon atom rotating the *N,N*-diisopropylcarboxyamide group out of the plane of the styrene moiety, thus reducing overlap of the π orbitals. The assumption is made above that, in analogy with the configuration of benzalcyanoacetamide, the CONHR and $CONRR^1$ groups of these compounds are *trans* to the phenyl group.

Equation [1] was developed earlier in these laboratories (1) for calculating the long wavelength absorption maxima for conjugated heteroenoid compounds with the generalized structure **1**.

$$[1]\quad \lambda(X{-}C_6H_4{-}CH{=}C(A)(B)) = \lambda(C_6H_5{-}CH{=}CH_2) + \Delta\lambda_A + \Delta\lambda^1{}_B + \Sigma\Delta\lambda^{11} + D$$

The term $\Delta\lambda_A$ is the conjugative effect (mμ units) of the *trans* group, $\Delta\lambda^1{}_B$ is the inductive effect of the *cis* group in the same units, while $\sum\Delta\lambda^{11}$ is the sum of the steric effects of the A, B, and phenyl groups. *D* quantitates the effect (mμ units) of phenyl substituents, X, upon the absorption maximum (1, 3).

This equation has now been applied to these *N*-alkyl- and *N,N*-dialkyl-derivatives and for CONHR, $\Delta\lambda_A$ is +24 mμ and $\Delta\lambda^{11}$ is −10 mμ, while for $CONRR^1$, $\Delta\lambda_A$ is +31 mμ and $\Delta\lambda^{11}$ is −20 mμ.[2] Using these values, long wavelength absorption maxima have been calculated for the cinnamamides (Table I) and benzalcyanoacetamides (Table II) and compared with the observed

[1]Summer student; present address: McGill University, Montreal, Quebec.

[2]The spectra of cinnamic acid, benzalcyanoacetic acid, and benzalmalonic acid (Table XI) provided values for the carboxyl group of $\Delta\lambda_A = +25.5$ mμ, $\Delta\lambda^1{}_B = +30.5$ mμ, and $\Delta\lambda^{11} = -9.0$ mμ. The conjugative effect ($\Delta\lambda_A \simeq +46.5$ mμ) and the steric effect ($\Delta\lambda^{11} \simeq -7.5$ mμ) for —C(O)Cl are obtained similarly from cinnamoyl chloride and benzalcyanoacetylchloride.

TABLE I

Calculated and average observed absorption maxima for some *N*-alkyl- and *N,N*-dialkyl-cinnamamides* in ethanol

X	R†	R¹†	Number of compounds	λ_{max} (mμ) Average obs. value	Calculated value
H	H	H	1	272.5	272
	Alkyl	H	10	274±1	273.5
	Alkyl	Alkyl	7	279±1‡	280
4-Cl	H	H	1	303	—
				~277	277
	Alkyl	H	9	304	—
				~294	—
				~284	—
				277±0.5	278.5
	Alkyl	Alkyl	2	~305	—
				~295	—
				286	285
				~282	—
4-CH_3O	H	H	1	~305	306.5
				~297	—
				292	—
	Alkyl or cycloalkyl	H	10	~305	308
				291.5	—
	Alkyl	Alkyl	3	310±0.5	315
				299	—
O-3 / CH_2 \ O-4	H	H	1	322.5	320.5
				290	—
				~283	276.5
	Alkyl or cycloalkyl	H	6	321±0.5	322
				290±0.5	—
				~283	278
	Alkyl	Alkyl	4	326±0.5	329.5
				292.5±0.5	—
				~287	284.5

*General formula:

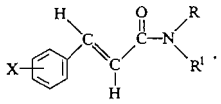

†The R and R¹ groups are those listed in Tables III–VI.
‡When R = R¹ = *i*–C_3H_7, λ_{max} = 275.5 mμ.

values (Tables III–VI and Tables VII–X respectively).[3] For all the compounds listed λ observed = 0.98λ calculated + 6.3. The correlation coefficient, *r*, is 0.99 and the standard errors of *r* and the estimate are 0.01 and 2.7 respectively.

Substituent X wavelength increments or *D* values (1, 3) were useful in predicting the positions of the long wavelength absorption bands of phenyl-substituted derivatives of the *N*-alkyl- and *N,N*-dialkyl-derivatives of the benzalcyanoacetamides. These *D* values, however, only provided one or two of the multiple absorption bands of 4-chloro-, 4-methoxy-, and 3,4-methylenedioxy-cinnamamides and their *N*-alkyl- and *N,N*-dialkyl-derivatives (Table I). A similar inadequacy of *D* values has been noted for other unifunctional styrene derivatives, e.g. 4-chloro-derivatives of ethyl cinnamate, cinnamanilide and β-nitropropenylbenzene.

The preparation of these compounds is described by Delaney *et al.* (2). Their spectra were determined with a Cary model 15 spectrophotometer using 10^{-3} *M* ethanolic solutions of the

[3]Photocopies of Tables III–XI may be obtained free of charge, upon request, from The Depository of Unpublished Data, National Science Library, National Research Council of Canada, Ottawa, Canada.

Can. J. Chem. Downloaded from www.nrcresearchpress.com by 210.87.254.42 on 09/05/12
For personal use only.

TABLE II

Calculated and average observed absorption maxima for some *N*-alkyl- and *N,N*-dialkyl-benzalcyanoacetamides* in ethanol

X	R†	R¹†	Number of compounds	λ_{max} (mμ) Average obs. value	λ_{max} (mμ) Calculated value
H	H	H	1	299	302
	Alkyl or cycloalkyl	H	9	298±1.5	298.5
	Alkyl	Alkyl	3	295±6	295
4-Cl	H	H	1	307	307
	Alkyl or cycloalkyl	H	10	305±1.5	303.5
	CH_3	CH_3	1	301	300
4-CH_3O	H	H	1	336	340
	Alkyl or cycloalkyl	H	9	335±0.5	336.5
	Alkyl or cycloalkyl	Alkyl or cycloalkyl	4	328.5±0.5‡	332
O-3 / CH_2 \ O-4	H	H	1	355.5	355.5
				309	307
	Alkyl or cycloalkyl	H	5	355±2	351.5
				308±1	303.5
	Alkyl	Alkyl	4	349±0.5	347.5
				303	300

*General formula:

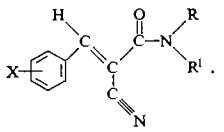

†The R and R¹ groups are those listed in Tables VII–X.
‡When R = R¹ = *i*-C_3H_7 or C_6H_{11}, λ_{max} = 326.5 mμ.

compounds.[4] Light isomerization of the *N*-alkyl and *N,N*-dialkyl derivatives of 4-methoxy- and 3,4-methylenedioxy-benzalcyanoacetamides required that the spectra of these compounds be determined as quickly as possible and in the absence of sunlight. The absorption maxima and the extinction coefficients of the cinnamamide- and benzalcyanoacetamide-derivatives are listed in Tables III to X.

[4]A hypsochromic shift of 3–3.5 mμ was observed for the maxima when cyclohexane was the solvent.

Acknowledgment

The authors thank Mr. C. E. Lough for valuable discussions and for recording the ultraviolet spectra.

1. D. J. Currie, C. E. Lough, R. F. Silver, and H. L. Holmes. Can. J. Chem. **45**, 1567 (1967).
2. A. D. Delaney, D. J. Currie, and H. L. Holmes. Can. J. Chem. This issue.
3. D. J. Currie and H. L. Holmes. Can. J. Chem. **47**, 863 (1969).

Can. J. Chem. Downloaded from www.nrcresearchpress.com by 210.87.254.42 on 09/05/12
For personal use only.

Solvolyse des tosylates des *tert*-butyl-4 diméthyl-2,2 cyclohexanols *cis* et *trans*[1]

JEAN-CLAUDE RICHER ET PATRICE BELANGER[2]
Département de Chimie, Université de Montréal, Montréal, Québec

Reçu le 29 novembre 1968

La solvolyse des tosylates des *tert*-butyl-4 diméthyl-2,2 cyclohexanols a été effectuée dans diverses conditions expérimentales et la nature des produits obtenus a été établie. Les vitesses de solvolyse dans l'acide acétique ont été déterminées à différentes températures; les facteurs thermodynamiques qui en découlent ont été calculés. Les résultats sont discutés en fonction de la stéréochimie des produits de départ.

Canadian Journal of Chemistry, 47, 3281 (1969)

Can. J. Chem. Downloaded from www.nrcresearchpress.com by 210.87.254.42 on 09/05/12
For personal use only.

Introduction

Plusieurs auteurs (voir réf. 1) se sont penchés sur le problème de la solvolyse des tosylates des *tert*-butyl-4 alkyl-2 cyclohexanols. Dans le cadre de nos travaux (voir réf. 2) sur la *tert*-butyl-4 diméthyl-2,2 cyclohexanone (**1**) et ses dérivés (**2***a* et **3***a*) nous avons examiné les vitesses et la nature des produits de solvolyse des tosylates **2***b* et **3***b*; ces produits pourraient être considérés comme conformationnellement semblables aux dérivés des diméthyl-4,4 stéroïdes examinés entre autres par Levisalles et Pete (3). Les résultats obtenus au cours de cette étude font l'objet de la présente communication.

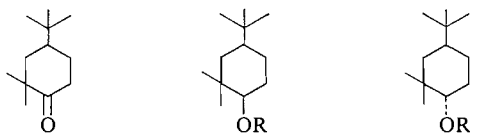

1 **2** **3**

a) R = H
b) R = SO_2—C_6H_4—CH_3 *p*
c) R = $COCH_3$

Partie expérimentale

Les spectres infrarouges (i.r.) ont été déterminés sur un spectrophotomètre Perkin–Elmer, modèle 21 à double faisceaux avec prisme de chlorure de sodium. Les analyses en chromatographie en phase gazeuse (c.p.g.) sont effectuées sur un appareil KROMO-TOG K-2 de la Compagnie Burrell. Les points de fusion sont pris dans des tubes capillaires à l'aide d'un appareil muni d'un thermomètre calibré avec des standards du bureau de Washington. Les spectres de résonance magnétique nucléaire (r.m.n.) ont été pris avec un spectrophotomètre modèle A-60 de la Compagnie Varian; les déplacements chimiques, δ, sont exprimés en p.p.m. du champ total et se réfèrent au tétraméthylsilane utilisé comme standard interne. Les mesures cinétiques sont faites dans un bain maintenu à température constante, grâce à un thermostat Haake–Universal de la Compagnie Gebruger Haake A. G.

1 Tosylates

1.1 Tosylate 3b du tert-butyl-4 diméthyl-2,2 cyclohexanol trans

Obtenu à la manière habituelle (4) par réaction de 5 g d'alcool **3***a* (5) avec 9 g de chlorure de *p*-toluenesulfonyle, ce dérivé fond à 83–84 °C; son spectre i.r. montre des bandes caractéristiques à 1170 et 1190 cm^{-1} et son spectre r.m.n. présente des pics à 0.82 p.p.m. (*tert*-butyle), à 0.88 p.p.m. (*gem*-diméthyle) et à 4.25 p.p.m. (proton carbinolique).

Anal. calculé pour $C_{19}H_{30}O_3S$: C, 67.86; H, 8.88; S, 9.36. Trouvé: C, 67.41; H, 8.94; S, 9.50.

1.2 Tosylate 2b du tert-butyl-4 diméthyl-2,2 cyclohexanol cis

Obtenu à la manière habituelle (4) par réaction de 5 g d'alcool **2***a* pur par c.p.g., (5) avec 9 g de chlorure de *p*-toluenesulfonyle, ce dérivé fond à 93–94 °C; son spectre i.r. montre des bandes caractéristiques à 1170 et 1190 cm^{-1} et son spectre r.m.n. présente des pics à 0.82 p.p.m. (*tert*-butyle), à 0.80 et 0.90 p.p.m. (*gem*-diméthyle) et à 4.25 p.p.m. (proton carbinolique). L'instabilité de ce dérivé n'a pas permis d'obtenir d'analyses centésimales satisfaisantes.

2 Mesures cinétiques

Les vitesses de solvolyse des tosylates ont été effectuées dans l'acide acétique anhydre et en tubes scellés; la procédure expérimentale de Winstein et ses collaborateurs (6) a été fidèlement suivie. Dans tous les cas les constantes de vitesse de l'acétolyse sont du premier ordre pour plus de 70% de la réaction. Les résultats obtenus sont rapportés au Tableau I, en regard des facteurs thermodynamiques qui peuvent en être déduits utilisant les méthodes décrites par Laidler (7).

3 Solvolyse et identification des produits obtenus au cours de ces réactions

3.1 Dans l'acide acétique

3.11 En présence d'acétate de sodium—D'une manière générale, 500 mg de tosylate et 2 g d'acétate de sodium anhydre dissous dans 15 ml d'acide acétique anhydre sont

[1]Les résultats rapportés dans cette communication sont extraits en partie du mémoire de maîtrise de P. Bélanger, Faculté des Sciences, Université de Montréal, 1963.

[2]Adresse actuelle: Laboratoires Merck. Frosst, 365, rue Selby, Montréal, Québec.

TABLEAU I

Cinétique de l'acétolyse des tosylates des *tert*-butyl-4 diméthyl-2,2 cyclohexanols

Tosylates	$T(\pm 0.05$ °C)	10^2C (mole/l)	$10^6 k_1$ (s^{-1})	$\Delta H^{\neq}$ (kcal/mole)†	$\Delta S^{\neq}$ (cal deg^{-1} $mole^{-1}$)§	$\Delta F^{\neq}$ (kcal/mole)†
cis **2b**	49.85	1.811	5.66			
		1.550	5.72			
		1.858	5.65			
			5.68			
	64.90	1.472	38.0			
		1.118	36.9			
		1.585	37.5	27.6	2.3	26.83
			37.5			
	79.70*	1.109	217			
		1.413	218			
		1.295	219			
			218			
trans **3b**	49.85	2.323	4.47			
		2.365	4.49			
		3.564	4.49	27.1	1.2	26.71
			4.48			
	64.90	1.372	30.3			
		1.509	30.1			
		1.087	30.2			
			30.2			
	79.70*	1.206	179			
		1.596	178			
		1.541	180			
			179			

*Dans ces conditions il a été mesuré que les constantes de vitesses d'acétolyse des *tert*-butyl-4 cyclohexanols *cis* et *trans* sont respectivement de 153 et 56.5.
†Les erreurs moyennes sur ces valeurs sont de ±0.2 kcal/mole.
§Les erreurs moyennes sur ces valeurs sont de ±0.2 u.c.

maintenus à 65 °C pendant 9 jours. Le mélange réactionnel est alors neutralisé par une solution glacée de NaOH 20% et extrait à l'éther. La couche éthérée est lavée par de l'eau salée, séchée sur Na_2SO_4 anhydre et évaporée au travers une colonne de Widmer. Le résidu est analysé par c.p.g. à l'aide d'une colonne de 2.5 m contenant 20% de Ucon Polar adsorbé sur du Kromat F.B. L'analyse est effectuée à 150 °C utilisant un débit de 90 ml/min d'hélium. Les pics sont identifiés par leur temps de rétention et par superposition à l'aide de produits authentiques (8). Les résultats obtenus sont résumés au Tableau II. Les pourcentages relatifs qui sont rapportés ont été évalués en faisant l'hypothèse (9) que les surfaces relatives sous les pics peuvent être assimilées aux pourcentages relatifs de produits présents.

3.12 En présence d'acétate de tétrabutylammonium—Les opérations sont comme précédemment (section 3.11) excepté que l'acétate de sodium est remplacé par de l'acétate de tétrabutylammonium.

3.13 Sans base additionnée—Les opérations sont telles que décrites dans la section 3.11 excepté que l'acétate de sodium est omis.

3.2 Dans la N-méthylpyrollidone en présence de l'acétate de tétrabutylammonium

3.21 A 65 °C—La réaction est effectuée sur 500 mg de tosylate, 390 mg d'acétate de tétrabutylammonium dans 15 ml de *N*-méthylpyrollidone dans les conditions décrites dans la section 3.11.

3.22 A 160 °C—La réaction est effectuée comme décrite dans la section 3.21 excepté que le mélange réactionnel est chauffé à 160 °C pendant 4 h plutôt qu' à 65 °C pendant 9 jours.

Discussion

Si l'on examine les vitesses de réactions portées dans le Tableau I, on observe que l'introduction de deux substituants en position adjacente du site réactionnel provoque une accélération de la vitesse de réaction; cette observation est formellement en accord avec la suggestion de Winstein et Hollness (10) qui

Can. J. Chem. Downloaded from www.nrcresearchpress.com by 210.87.254.42 on 09/05/12
For personal use only.

Can. J. Chem. Downloaded from www.nrcresearchpress.com by 210.87.254.42 on 09/05/12
For personal use only.

TABLEAU II

Produits obtenus lors de la solvolyse des tosylates des *tert*-butyl-4 diméthyl-2,2 cyclohexanols

		Conditions									
		A*		B*		C*		D*		E*	
Produits	T_R (min)	**2***b*	**3***b*	**2***b*	**3***b*	**2***b*	**3***b*	**2***b*	**3***b*	**2***b*	**3***b*
4	4	2.9		16.1		10.3		83.7		77.2	
5	4		27.1		10.3		9.3		37.6		12.3
6	5		13.6		13.3		9.3		16.8		21.0
7	5.5	3.2		5.5		8.1		6.6		15.8	
8	6.5		25.9		41.1		56.0		31.3		56.7
9	7	85.7	2.7	74.4	9.2	71.0	9.3		2.2		4.3
Acétate inconnu	15		17.1		25.6		15.6		6.9		4.7
Acétate inconnu	16	4.5		2.9		6.4		1.4		1.7	
Acétate inconnu	19	1.5	2.1			1.7		2.9		1.4	1.0
Acétate inconnu	23	2.2		1.1		2.5		5.4		3.9	
Acétate inconnu	24		11.5		0.5		0.5		5.2		1.0

*Conditions décrites A (section 3.13), B (section 3.11), C (section 3.12), D (section 3.21), E (section 3.22).

Can. J. Chem. Downloaded from www.nrcresearchpress.com by 210.87.254.42 on 09/05/12
For personal use only.

attribuent ces différences de vitesse à la compression stérique. Toutefois l'utilisation des valeurs k_{Me}/k_H rapportées par Sicher et ses collaborateurs (1) permettrait de prévoir, si l'additivité des compressions joue un rôle, que les vitesses de solvolyse des tosylates **2***c* et **3***c* relatives à celle du tosylate dérivé du *tert*-butyl-4 cyclohexanol *trans* devraient être respectivement de 35 et 11; or les vitesses relatives observées sont de l'ordre de 3.8 pour **2***c* et 3.2 pour **3***c*, ce qui indiquerait que les effets de compression ne sont pas les seules causes influençant les vitesses relatives de solvolyse et nous rejoignons alors les conclusions de Sicher et ses collaborateurs (1). Il peut aussi être envisagé que les états de transition des réactions étudiées au cours du présent travail diffèrent de ceux impliqués dans les réactions de solvolyses plus rapides (composés de la série "*cis*") examinées par Sicher et ses collaborateurs (1); en effet des formes non chaises ayant été postulées (1) pour expliquer ces résultats il n'est pas certain qu'il soit nécessaire dans notre cas de faire intervenir ces conformations.

Les résultats rapportés dans le Tableau II font ressortir que les solvolyses des tosylates examinés conduisent principalement aux produits d'élimination plutôt qu'aux produits de substitution et ce, quelles que soient les conditions expérimentales; à la suite des travaux de Henbest et Jackson (11), il avait été espéré que les réactions conduites dans la *N*-méthylpyrollidone conduiraient à des quantités importantes d'acétates **2***c* et **3***c*. Des conclusions importantes peuvent toutefois être tirées de la nature des oléfines produites au cours des solvolyses:

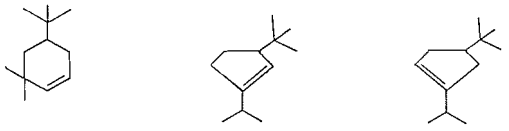

4

5

6

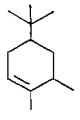

7

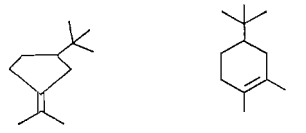

8

9

1. Le fait que le tosylate *cis*, **2***b*, ne conduit à aucun produit de contraction de cycle indiquerait que dans l'état de transition, le produit est sous forme chaise et que l'élimination directe (conduisant à **4**) ou le réarrangement (conduisant à **7** et **9**) impliquent respectivement l'hydrogène axial en position-6 et le méthyle axial (*trans* et coplanaire, antiparallèle ou antipériplanaire) en position-2; cette conclusion serait en accord d'une part avec les propositions formulées par Campbell et ses collaborateurs (12) et selon lesquelles "il n'y a aucune preuve expérimentale que la réaction de solvolyse du tosylate du *tert*-butyl-4 cyclohexanol *cis* se produise par l'intermédiaire d'une forme autre que la conformation chaise" et d'autre part avec les hypothèses de Levisalles et Pete (3) et selon lesquelles il est inutile, pour expliquer les réactions de tosylates dérivés du diméthyl-4,4 cholestanol-3α de faire intervenir des conformations différentes de la conformation chaise.

2. Considérant que la solvolyse du tosylate **3***b* conduit à des fortes proportions de produits provenant d'une contraction de cycle, il peut en être déduit que l'état de transition de ces réactions est aussi presque complètement sous forme chaise; toutefois la formation de faibles quantités de l'oléfine **9** permettrait de suggérer à la suite de Shiner et Jewett (13) et Campbell et ses collaborateurs (12) que cette réaction peut procéder par l'intermédiaire d'un état de transition qui n'impliquerait pas une chaise parfaite. Pour expliquer les résultats obtenus avec les tosylates du diméthyl-4,4 cholestanol-3β, Levisalles et Pete (3) invoquent aussi l'intervention de conformations non-chaise.

L'ensemble des résultats rapportés dans le présent travail, tout en montrant que des différences existent entre les réactions de solvolyse des tosylates des méthyl-2 d'une part et diméthyl-2,2 *tert*-butyl-4 cyclohexanols d'autre part, met en évidence un accord général entre les réactions de solvolyse des tosylates **2***c* et **3***c* et les dérivés correspondants dans le domaine des diméthyl-4,4 stéroïdes (3, 14).

Remerciements

Les auteurs remercient sincèrement le Conseil National de Recherches du Canada et le Ministère de la Jeunesse de la Province de Québec pour l'aide financiaire apportée sous forme de subvention de recherche et de bourse de perfectionnement. Les auteurs remercient aussi la Compagnie Dow Chemicals of Canada Ltd.,

pour un généreux échantillon de *tert*-butyl-4 cyclohexanone utilisé au cours de ce travail.

1. M. PANKOVA, J. SICHER, M. TICHY et M. C. WHITING. J. Chem. Soc. B, 365 (1968).
2. J.-C. RICHER et C. LAMARRE. Can. J. Chem. **47**, 2349 (1969).
3. J. LEVISALLES et J. P. PETE. Bull. Soc. Chim. France, 3747 (1967).
4. R. L. SHRINER, R. C. FUSON et D. Y. CURTIN. The systematic identification of organic compounds. John Wiley and Sons, Inc., New York. 1964.
5. J.-C. RICHER et G. PERRAULT. Can. J. Chem. **43**, 18 (1965).
6. S. WINSTEIN, E. GRUNWALD et C. HANSON. J. Am. Chem. Soc. **70**, 812 (1948).
7. K. J. LAIDLER. Chemical kinetics. McGraw-Hill Book Co., Inc., New York. 1950.
8. J.-C. RICHER et P. BÉLANGER. Can. J. Chem. **42**, 2398 (1964).
9. L. S. ETTRE. J. Chromatog. **8**, 525 (1962).
10. S. WINSTEIN et N. J. HOLLNESS. J. Am. Chem. Soc. **77**, 5562 (1955).
11. H. B. HENBEST et W. R. JACKSON. J. Chem. Soc. 954 (1961).
12. N. C. G. CAMPBELL, D. M. MUIR, R. R. HILL, J. H. PARISH, R. M. SOUTHAM et M. C. WHITING. J. Chem. Soc. B, 355 (1968).
13. V. J. SHINER et J. G. JEWETT. J. Am. Chem. Soc. **87**, 1387 (1965).
14. J. F. BIELLMAN, D. KUCAN, M. RAJIC, P. WIST et G. OURISSON. Bull. Soc. Chim. France, 330 (1962).

Sur la stéréochimie de la réduction des alkyl-2 cyclohexanones par les organomagnésiens[1]

GÉRARD CHAUVIÈRE ET ZOLTAN WELVART
Groupe de Laboratoires du CNRS, Thiais-94, France

ET

DENIS EUGÈNE ET JEAN-CLAUDE RICHER
Département de Chimie, Université de Montréal, Montréal, Québec

Reçu le 13 mars 1969

La stéréochimie de la réduction d'alkyl-2 cyclohexanones par des organomagnésiens a été établie. Les résultats obtenus montrent que l'encombrement stérique présenté par le groupe alkyle en position-2 vis à vis du réducteur est tout à fait comparable à celui des substituants du carbone-3 du noyau cyclohexanique.

Canadian Journal of Chemistry, **47**, 3285 (1969)

Introduction

Dans le cadre de nos travaux (1, 2) sur la stéréochimie des additions nucléophiles sur des dérivés cyclohexaniques substitués, il s'avérait intéressant d'examiner la réduction par des organomagnésiens, d'alkyl-2 cyclohexanones; en effet trois hypothèses ont déjà été formulées pour apprécier l'importance du substituant en position-2 sur la stéréochimie de la réduction du groupement carbonyle. Pour Dauben et ses collaborateurs (3), ce groupement ne devrait pratiquement pas influencer la stéréochimie des réductions puisqu'il se trouve approximativement dans le plan du carbonyle et de ce fait opposerait le même empêchement à une attaque axiale qu'à une attaque équatoriale. Landor et Regan (4) considèrent que la formation de deux alcools *cis* et *trans* résulte uniquement d'une attaque équatoriale soit sur la forme flexible de la cyclohexanone en conduisant à l'alcool *trans* soit sur la forme chaise en conduisant à l'alcool *cis* (Schéma 1);

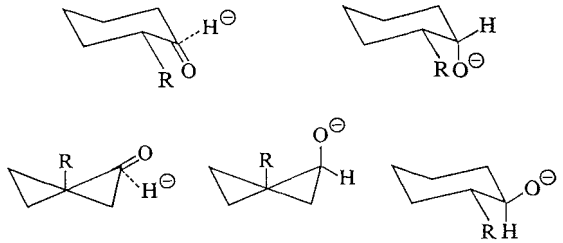

SCHÉMA 1

le groupement alkyle en position-2 devrait aussi être considéré comme ayant une influence négligeable sur la stéréochimie de la réduction puisque

[1]Les résultats rapportés dans ce mémoire sont extraits en parties de la Thèse de Doctorat ès-Sciences de Gérard Chauvière et du mémoire soumis par Denis Eugène en vue de l'obtention du grade de Maitre ès-Sciences (Faculté des Sciences, Université de Montréal, Août 1968).

Can. J. Chem. Downloaded from www.nrcresearchpress.com by 210.87.254.42 on 09/05/12
For personal use only.

pour un généreux échantillon de *tert*-butyl-4 cyclohexanone utilisé au cours de ce travail.

1. M. PANKOVA, J. SICHER, M. TICHY et M. C. WHITING. J. Chem. Soc. B, 365 (1968).
2. J.-C. RICHER et C. LAMARRE. Can. J. Chem. **47**, 2349 (1969).
3. J. LEVISALLES et J. P. PETE. Bull. Soc. Chim. France, 3747 (1967).
4. R. L. SHRINER, R. C. FUSON et D. Y. CURTIN. The systematic identification of organic compounds. John Wiley and Sons, Inc., New York. 1964.
5. J.-C. RICHER et G. PERRAULT. Can. J. Chem. **43**, 18 (1965).
6. S. WINSTEIN, E. GRUNWALD et C. HANSON. J. Am. Chem. Soc. **70**, 812 (1948).
7. K. J. LAIDLER. Chemical kinetics. McGraw-Hill Book Co., Inc., New York. 1950.
8. J.-C. RICHER et P. BÉLANGER. Can. J. Chem. **42**, 2398 (1964).
9. L. S. ETTRE. J. Chromatog. **8**, 525 (1962).
10. S. WINSTEIN et N. J. HOLLNESS. J. Am. Chem. Soc. **77**, 5562 (1955).
11. H. B. HENBEST et W. R. JACKSON. J. Chem. Soc. 954 (1961).
12. N. C. G. CAMPBELL, D. M. MUIR, R. R. HILL, J. H. PARISH, R. M. SOUTHAM et M. C. WHITING. J. Chem. Soc. B, 355 (1968).
13. V. J. SHINER et J. G. JEWETT. J. Am. Chem. Soc. **87**, 1387 (1965).
14. J. F. BIELLMAN, D. KUCAN, M. RAJIC, P. WIST et G. OURISSON. Bull. Soc. Chim. France, 330 (1962).

Sur la stéréochimie de la réduction des alkyl-2 cyclohexanones par les organomagnésiens[1]

GÉRARD CHAUVIÈRE ET ZOLTAN WELVART
Groupe de Laboratoires du CNRS, Thiais-94, France

ET

DENIS EUGÈNE ET JEAN-CLAUDE RICHER
Département de Chimie, Université de Montréal, Montréal, Québec

Reçu le 13 mars 1969

La stéréochimie de la réduction d'alkyl-2 cyclohexanones par des organomagnésiens a été établie. Les résultats obtenus montrent que l'encombrement stérique présenté par le groupe alkyle en position-2 vis à vis du réducteur est tout à fait comparable à celui des substituants du carbone-3 du noyau cyclohexanique.

Canadian Journal of Chemistry, **47**, 3285 (1969)

Introduction

Dans le cadre de nos travaux (1, 2) sur la stéréochimie des additions nucléophiles sur des dérivés cyclohexaniques substitués, il s'avérait intéressant d'examiner la réduction par des organomagnésiens, d'alkyl-2 cyclohexanones; en effet trois hypothèses ont déjà été formulées pour apprécier l'importance du substituant en position-2 sur la stéréochimie de la réduction du groupement carbonyle. Pour Dauben et ses collaborateurs (3), ce groupement ne devrait pratiquement pas influencer la stéréochimie des réductions puisqu'il se trouve approximativement dans le plan du carbonyle et de ce fait opposerait le même empêchement à une attaque axiale qu'à une attaque équatoriale. Landor et Regan (4) considèrent que la formation de deux alcools *cis* et *trans* résulte uniquement d'une attaque équatoriale soit sur la forme flexible de la cyclohexanone en conduisant à l'alcool *trans* soit sur la forme chaise en conduisant à l'alcool *cis* (Schéma 1);

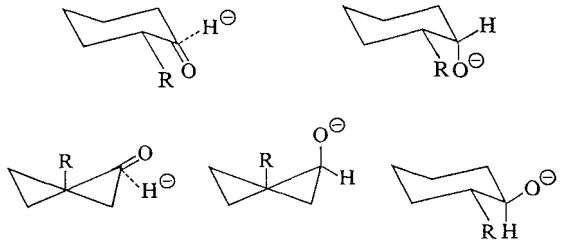

SCHÉMA 1

le groupement alkyle en position-2 devrait aussi être considéré comme ayant une influence négligeable sur la stéréochimie de la réduction puisque

[1]Les résultats rapportés dans ce mémoire sont extraits en parties de la Thèse de Doctorat ès-Sciences de Gérard Chauvière et du mémoire soumis par Denis Eugène en vue de l'obtention du grade de Maitre ès-Sciences (Faculté des Sciences, Université de Montréal, Août 1968).

Can. J. Chem. Downloaded from www.nrcresearchpress.com by 210.87.254.6 on 09/05/12
For personal use only.

TABLEAU I

Pourcentages normalisés d'alcools *cis* obtenus lors de la réduction d'alkyl-2 cyclohexanones par des organomagnésiens

	RMgCl			
Cyclohexanone	$(CH_3)_3C$—	$(CH_3)_2CH$—	C_6H_{11}—	$(CH_3)_2CH$—CH_2—
Méthyl-2*	36†	38	50	83‡
tert-Butyl-2*	73	68	78	95

*Les pourcentages d'alcools de réduction par rapport au total des produits (réduction, addition et énolisation) de la réduction sont d'environ 50% dans le cas de la méthyl-2-cyclohexanone et d'environ 10% dans le cas de la *tert*-butyl-2 cyclohexanone.
†Un travail de Cornubert (7) d'une époque antérieure à la c.p.g. indiquait la formation exclusive de l'alcool *trans*.
‡Cornubert (7) indiquait la formation exclusive de l'alcool *cis*.

les attaques équatoriales sont peu sensibles à l'empêchement stérique (5, 6). Par contre Kamernitzky et Akhrem (5) considèrent que dans la forme chaise de la cyclohexanone le carbone α, adjacent au carbone-2, des alkyl-2 cyclohexanones joue un rôle comparable à celui des carbones-3 et -5 du noyau cyclohexanique (Schéma 2); on introduit ainsi une nouvelle intéraction 1:3 diaxiale qui défaboriserait les attaques axiales donc la formation de l'alcool *trans*.

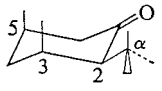

SCHÉMA 2

C'est afin de pouvoir choisir entre ces trois interprétations que nous avons examiné la stéréochimie de la réduction des méthyl-2 et *tert*-butyl-2 cyclohexanones par les magnésiens. Les résultats obtenus font l'objet de la présente communication.

Résultats et Discussion

Les résultats obtenus lors de la réduction des alkyl-2 cyclohexanones par les chlorures d'alkylmagnésium sont consignés dans le Tableau I; ils expriment le pourcentage normalisé d'alcool *cis* (attaque équatoriale) présent dans le mélange réactionnel et sont indépendants de la concentration et de la stoechiométrie des réactifs utilisés.

Ce tableau montre d'une part que la stéréosélectivité de la réduction est beaucoup plus grande pour la *tert*-butyl-2 cyclohexanone. D'autre part, il ressort très bien que la stéréochimie de la réduction dépend beaucoup de l'encombrement présenté par le carbone-2 de l'organomagnésien; ce résultat, en opposition avec les prévisions qui peuvent être formulées grâce aux hypothèses de Dauben (3), nous permet d'écarter ces dernières.

Examinons maintenant les suggestions de Landor et Regan (4). Premièrement, les résultats obtenus par Stolow (8) suggèrent que dans leur état fondamental la *tert*-butyl-2 et la methyl-2 cyclohexanone sont comparables et possèdent la conformation chaise; il est légitime de penser que dans l'état de transition de la réduction ces cétones se comporteront de la même façon. Le parallélisme qui existe entre les résultats obtenus lors de la réduction des deux alkyl-2 cyclohexanone appuie bien cette prévision et permet par ailleurs d'exclure l'hypothèse selon laquelle la méthyl-2 cyclohexanone pourrait être réduite dans sa conformation portant le groupe méthyle axial. Deuxièmement d'après l'hypothèse de Landor et Regan (4), la formation de l'alcool *trans* implique une conformation croisée; cette conformation, d'après les calculs d'Allinger (9) doit être beaucoup plus favorisée pour la *tert*-butyl-2 cyclohexanone que pour la méthyl-2 cyclohexanone ce qui laisserait prévoir que la première cétone devrait conduire à plus d'alcool *trans* que la seconde. Les résultats obtenus sont contraires à cette prévision. Finalement on devrait s'attendre de plus à ce que la stéréochimie des réductions soit indépendante de l'encombrement du réactif réducteur puisque l'attaque équatoriale dépend peu des facteurs stériques (5, 6). Nos résultats sont encore une fois en opposition avec ces prévisions; l'ensemble de cette argumentation tend donc à démontrer que l'hypothèse de Landor et Regan (4) doit être écartée.

Si l'on examine enfin l'interprétation de Kamernitzky et Akhrem (5) pour qui le groupement méthyle en position-2 est équivalent à l'un des carbones-3 ou -5 de la cyclohexanone, on introduit donc avec le méthyle une intéraction 1:3 diaxiale supplémentaire qui va ralentir l'attaque axiale; ce ralentissement sera encore plus accen-

Can. J. Chem. Downloaded from www.nrcresearchpress.com by 210.87.254.6 on 09/05/12
For personal use only.

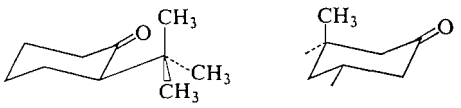

SCHÉMA 3

tué pour la *tert*-butyl-2 cyclohexanone car dans cette molécule le groupement *tert*-butyle amène une intéraction 1:3 diaxiale comparable à celle d'un groupement méthyle axial en position-3 (Schéma 3). Comme l'attaque axiale est sensible à l'encombrement stérique présenté par l'agent réducteur, cette attaque devrait donc diminuer en passant premièrement de la méthyl-2 à la *tert*-butyl-2 cyclohexanone et deuxièmement lorsqu'on augmente le nombre de substituants sur le carbone-2 de l'organomagnésien; c'est effectivement ce qui est observé. Il en ressort donc que la stéréochimie de ces réductions peut être rationalisée en ne faisant intervenir que des facteurs stériques (2, 5) affectant les états de transition.

Le fait que les chlorures de *tert*-butyle et d'*iso*-propyle donnent, comme il a été mis en évidence précédemment (1), une stéréochimie sensiblement la même est compatible avec le mécanisme cyclique de Whitmore (voir Schéma 4) et montre que les substituants du carbone-1 de l'organomagnésien n'ont qu'une influence faible sur la stéréochimie de la réduction.

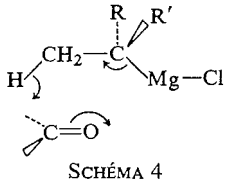

SCHÉMA 4

L'importance de l'encombrement présenté par l'agent réducteur ne se limite pas seulement aux organomagnésiens. En effet la très grande stéréospécificité de la réduction de la méthyl-2 et de la *tert*-butyl-2 cyclohexanone par les dicyclohexyl- et *diiso*pinocamphenylboranes (10 et 11) qui peuvent être rapprochés des additions de borane (12) et de peracides (13) au *tert*-butyl-3 cyclohexène montrent que le groupement alkyle sur le carbone adjacent au site réactionnel ralentit notablement l'attaque axiale.

Partie experimentale

Alcools de références et analyse

Méthyl-2 cyclohexanols

Ces alcools ont été identifiés par c.p.g. à l'aide de témoins préparés par réduction (14, 15) de la méthyl-2 cyclohexanone; ils constituaient un mélange contenant 75% d'alcool *trans* et 25% d'alcool *cis*. Lors de la chromatographie en phase gazeuse à 85 °C, avec un débit d'hélium de 20 ml/min et à l'aide d'une colonne de 1/8 po. × 3 m contenant 20% de glycérol déposé sur du chromosorb W 80/100, les temps de rétention sont de 13 min pour l'alcool *cis* et de 18 min pour l'alcool *trans*.

tert-Butyl-2 cyclohexanols

L'alcool *cis* est préparé à partir de l'acétate correspondant alors que l'alcool *trans* (contenant 10% de son isomère) est obtenu par réduction de la cétone correspondante par le sodium et l'éthanol. Lors de la c.p.g. à 110 °C, avec un débit d'hélium de 35 ml/min et une colonne de 1/4 po. par 8 pi. contenant 15% de diglycérol et 2% d'eau déposés sur du chromosorb W, les temps de rétention des alcools *cis* et *trans* sont respectivement de 9.5 min et de 13 min.

Tous les pourcentages relatifs d'épimères qui sont rapportés ont été déterminés en faisant l'hypothèse qui a été vérifiée pour de nombreux alcools épimères (16) que dans le cas de composés épimères, les surfaces relatives sous les pics peuvent être assimilées aux pourcentages relatifs de produits présents.

Réductions

Les réactifs de Grignard ont été préparés de la façon classique et titrés par iodométrie (17, 18). Les réactions de réduction ont été effectuées sur des quantités de cétone variant de 0.1 à 1 g. L'hydrolyse de ces milieux réactionnels est effectuée par NH_4Cl 10% et les produits bruts, obtenus par extraction à la manière habituelle avec de l'éther, sont examinés par c.p.g. Les résultats obtenus sont rapportés dans le Tableau I; chaque valeur représente la moyenne d'au moins trois expériences.

Remerciements

Les auteurs remercient vivement le Centre National de la Recherche Scientifique (CNRS) de France, le Conseil National de Recherches du Canada et le service de la Coopération avec l'extérieur du Ministère de l'Education de la province de Québec pour l'aide financière apportée sous forme d'octrois de recherches et de bourses d'étude. L'un de nous (J.C.R,) tient â exprimer sa profonde gratitude au Dr. Pierre Maroni et à Mlle Marthe Benoit de la Faculté des Sciences de Toulouse pour l'accueil et l'aide qui lui ont été accordés durant la préparation de ce manuscrit.

1. D. CABARET, G. CHAUVIÈRE et Z. WELVART. Tetrahedron Letters, 549 (1968).
2. J. C. RICHER. J. Org. Chem. **30**, 324 (1965).
3. W. G. DAUBEN, G. J. FONKEN et D. S. NOYCE. J. Am. Chem. Soc. **78**, 2579 (1956).
4. S. R. LANDOR et J. P. REGAN. J. Chem. Soc. (C) 1159 (1967).
5. A. V. KAMERNITSKY et A. A. AKHREM. Tetrahedron, **18**, 705 (1962).

Can. J. Chem. Downloaded from www.nrcresearchpress.com by 210.87.254.6 on 09/05/12
For personal use only.

6. M. CHEREST et H. FELKIN. Tetrahedron Letters, 2205 (1968).
7. P. ANZIANI, A. N. AUBRY, G. BARRAUD, M. M. CLAUDON et R. CORNUBERT. Bull. Soc. Chim. France, 408 (1955).
8. R. D. STOLOW, T. GROOM et M. GERACE. J. Am. Chem. Soc. **90**, 3290 (1968).
9. N. L. ALLINGER, H. B. BLATTER, A. FREIBERG et F. M. KARKOWSKI. J. Am. Chem. Soc. **88**, 2999 (1966).
10. H. C. BROWN et D. B. BIGLEY. J. Am. Chem. Soc. **83**, 3166 (1961).
11. H. C. BROWN et V. VARMA. J. Am. Chem. Soc. **88**, 2871 (1966).
12. D. J. PASTO et F. M. KLEIN. J. Org. Chem. **33**, 1468 (1968).
13. J. C. RICHER et C. FREPPEL. Can. J. Chem. **46**, 3709 (1968).
14. H. C. BROWN et H. R. DECK. J. Am. Chem. Soc. **87**, 5620 (1965).
15. W. G. DAUBEN et R. E. BOZACK. J. Org. Chem. **24**, 1596 (1959).
16. E. L. ELIEL, S. H. SCHROETER, T. J. BRETT, F. J. BIROS et J. C. RICHER. J. Am. Chem. Soc. **88** 3327 (1966).
17. R. D. HOLLANDER et M. ANTEUNIS. Bull. Soc. Chem. Belg. **74**, 71 (1965).
18. C. COURTOT. *Dans* Traité de chimie organique de V. Grignard. Vol. 5. Masson et Cie, Paris. 1937. p. 188.

Erratum: Identification of di-*O*-, tri-*O*-, and tetra-*O*-methylmannoses by gas–liquid chromatography

S. S. BHATTACHARJEE AND P. A. J. GORIN
Prairie Regional Laboratory, National Research Council of Canada, Saskatoon, Saskatchewan

Received May 9, 1969

(Ref.: Can. J. Chem. **47**, 1207 (1969))

Canadian Journal of Chemistry, **47**, 3288 (1969)

On page 1212, Table I, the retention time of the trimethylsilyl derivative of methyl 2,4,6- tri-*O*-methylmannoside at 136° should read 28.4 min, not 17.2 min.

Can. J. Chem. Downloaded from www.nrcresearchpress.com by 210.87.254.6 on 09/05/12
For personal use only.

Can. J. Chem. Downloaded from www.nrcresearchpress.com by 210.87.254.5 on 09/05/12
For personal use only.

Canadian Journal of Chemistry

Published by THE NATIONAL RESEARCH COUNCIL OF CANADA

VOLUME 47 SEPTEMBER 15, 1969 NUMBER 18

N-Chlorination of secondary amides. II. Effects of substituents on rates of N-chlorination

E. W. C. W. THOMM AND M. WAYMAN

Department of Chemical Engineering and Applied Chemistry, University of Toronto, Toronto 5, Ontario

Received February 18, 1969

Various secondary amides have been N-chlorinated, at high and at low pH. The reactivity of the chlorinating reagents with all the amides investigated was found to have the sequence

$$CH_3COOCl > Cl_2 > OCl^- > HOCl$$

The substituent groups R_1 and R_2 of the amide $R_1\overset{\overset{O}{\|}}{C}NHR_2$ were found to have large effects on the rate of chlorination. With the three molecular chlorinating agents, the reactivity of the amides was found to be in the order

$$CH_3\overset{\overset{O}{\|}}{C}NHCH_3 > CH_3\overset{\overset{O}{\|}}{C}ClNHCH_3 > CH_3CH_2\overset{\overset{O}{\|}}{C}NHCH_3 > CH_3\overset{\overset{O}{\|}}{C}NHCH_2CH_3 >$$
$$CH_3\overset{\overset{O}{\|}}{C}NHCH_2CH_2OH > CH_3\overset{\overset{O}{\|}}{C}NHCH_3 > H\overset{\overset{O}{\|}}{C}NHCH_2CH_3 > H\overset{\overset{O}{\|}}{C}NHCH_3 > CH_3\overset{\overset{O}{\|}}{C}NHC_6H_5$$

With hypochlorite ion the reverse order of reactivity was observed. These results are discussed and reaction mechanisms proposed. It is proposed that, when a hypochlorite ion is a chlorinating agent, the primary reaction is hydrogen bond formation between the amido hydrogen and the hypochlorite oxygen atom, but that the donation of electrons from the amido N to the Cl atom is the primary reaction with the molecular chlorinating agents.

Canadian Journal of Chemistry, 47, 3289 (1969)

Introduction

This paper is part of a series intended to shed light on the mechanism of N-chlorination of secondary amides. Interest in this group of compounds arose as a result of the development of chlorine exchange resins (1), which contain amide functional groups of which the nitrogen atoms take up positive chlorine reversibly. The first paper of this series (2) reported rate studies which suggested that the active species in the chlorination of N-methyl acetamide, in acetate buffered hypochlorous acid solutions and in the pH range 3.0 to 6.0, are CH_3COOCl, Cl_2, and HOCl, in order of decreasing reactivity. The apparent activation energy of the N-chlorination of N-methyl acetamide was found to be very low near room temperature, the secondary amide group of N-methyl acetamide being very sensitive to a chlorinating environment. Since secondary amide groups are common in many polymers, including proteins, it was decided to investigate the effects of substituents upon the rates and energies of these reactions. In the present paper 7 other amides were chlorinated, in the pH range 3 to 10.5.

Experimental

Reagents

All of the following amides were purchased from the Eastman Kodak Co.: N-methyl formamide, N-ethyl formamide, N-methyl acetamide, N-ethyl acetamide, N-methyl propionamide, N,N′-dimethyl urea, and

Can. J. Chem. Downloaded from www.nrcresearchpress.com by 210.87.254.5 on 09/05/12
For personal use only.

TABLE I

N-Chlorination of secondary amides at 25 °C

Amide R_1CONHR_2		Acidic chlorination					Alkaline chlorination		
				Rate constant for chlorinating species $(mole/l\ s)^{-1}$					
R_1	R_2	pH	$[CH_3COOH]$ in buffer (mole/l)	Hypochlorous acid (k_{HOCl})	Molecular chlorine (k_{Cl_2})	Chlorine acetate (k_{AcOCl})	pH	$[Na_2HPO_4]$ in buffer (mole/l)	Rate constant, hypochlorite ion $(mole/l\ s)^{-1}$ (k_{OCl^-})
CH_3NH	CH_3	5.30	0.05–0.10	$\sim 8.2\times10^{-1}$	4.50×10^{5}	8.58×10^{7}	10.0	0.15	$<8.3\times10^{-3}$
CH_3NCl	CH_3	5.0–5.85	0.05–0.25	7.5×10^{-2}	7.84×10^{2}	1.13×10^{5}	—	—	
CH_3CH_2	CH_3	5.0	0.05–0.25	1.7×10^{-2}	1.47×10^{2}	1.45×10^{4}	10.0	0.15	9.2×10^{-3}
CH_3	CH_2CH_3	5.0	0.05–0.25	5.0×10^{-2}	1.05×10^{2}	1.03×10^{4}	10.0–11.0	0.05–0.25	1.1×10^{-2}
CH_3	CH_3	3.0–6.0	0.05–0.25	1.7×10^{-3}	8.33×10*	1.00×10^{4}**	10.0–10.5	0.01–0.25	1.82×10^{-2}
CH_3	CH_2CH_2OH	5.0	0.05–0.25	—	4.36×10	3.25×10^{3}	10.0	0.10	2.88×10^{-2}
H	CH_2CH_3	5.0	0.05–0.50	1.7×10^{-3}	2.96	3.37×10^{2}	10.0–10.5	0.05–0.25	1.15×10^{-1}
H	CH_3	5.0	0.05–0.50	1.7×10^{-3}	1.95	2.56×10^{2}	10.0–10.5	0.05–0.25	2.1×10^{-1}
CH_3	C_6H_5				0.916†				5.63‡

*Reference 2.
†Reference 7.
‡Reference 4.

Can. J. Chem. Downloaded from www.nrcresearchpress.com by 210.87.254.5 on 09/05/12
For personal use only.

N-(hydroxyl ethyl) acetamide. These were of the purest commercial grade. They were further purified by precipitation from ethanol solutions using ethyl acetate as the non solvent.

Hypochlorous acid was obtained by acidifying sodium hypochlorite solutions (Fisher Scientific Co.) to the appropriate pH.

Experimental Procedure

The kinetic runs were carried out as outlined previously (2). The buffer used at low pH was acetic acid – sodium acetate, and at high pH, disodium hydrogen phosphate – sodium hydroxide. Sodium chloride was added to the reaction mixture in most runs. The working pH ranges were so chosen that in the absence of other additives, either undissociated HOCl or OCl^- ion was the main chlorinating species present (3).

As previously reported (2) in the low pH region 4–6, the pH of the reaction medium did not alter. However, in the high pH region, 10 or above, the pH increased as the reaction proceeded. As an example, in the reaction medium containing 12 m*M* $CH_3CH_2\overset{O}{\overset{\|}{C}}—NH\cdot CH_3$ and 3 m*M* OCl^- initially, the change in pH is shown below.

Buffer concentration $[Na_2HPO_4]$, *M*	pH	
	Initial	Final
0.05	10.0	10.5
0.10	10.0	10.3
0.15	10.0	10.2
0.25	10.0	10.1

Treatment of Data

All results fit the following rate expression

$$\frac{d[R_1CONClR_2]}{dt} = k_{obs}[R_1CONHR_2][ROCl]$$

where R_1CONHR_2 denotes a secondary amide, $R_1CONClR_2$ denotes the corresponding chlorinated amide, and ROCl denotes hypochlorous acid in the pH range 4–6, or the hypochlorite ion at pH 10 or above.

The observed rate constant, k_{obs}, was calculated from the best straight line of the plot of log $[R_1CONHR_2]/[ROCl]$ vs. time. Although in the high pH region, where OCl^- is the dominating species, the pH of the reaction mixture increased as the chlorination reaction proceeded, no deviation from the observed rate law was found.

Results

In our previous communication (2), we found that for N-methyl acetamide chlorination, the observed rate constant, k_{obs}, could be expressed as the sum of three terms. This was also true in acid medium for the secondary amides under study in the present work. In general, in the absence of other additives, the following relationship holds for N-chlorination in acid medium

$$\begin{aligned} k_{obs} &= k_1 + k_2[H^+][Cl^-] + k_3[CH_3COOH] \\ &= k_{HOCl} + k_{Cl_2}K_{Cl_2}[H^+][Cl^-] \\ &\quad + k_{AcOCl}K_{AcOCl}\frac{[CH_3COOH]}{[H_2O]} \end{aligned}$$

where k_{HOCl}, k_{Cl_2}, and k_{AcOCl} are specific rate constants of N-chlorination involving HOCl, Cl_2, and CH_3COOCl, respectively, as the chlorinating species, and the *K*'s are the equilibrium constants of the formation of the subscript species by reacting HOCl and either HCl or HOAc.

As can be noted in Table I, the rate of N-chlorination of secondary amides due to undissociated hypochlorous acid is small, being significant only for the ureas. Various reports (4–6) have confirmed that hypochlorous acid is a rather poor agent for C-chlorination of aromatics. Table I shows that molecular chlorine and chlorine acetate are much more powerful chlorinating agents than HOCl. The k_{Cl_2} values are, however, smaller than the k_{AcOCl} values by a factor of about 100 for all the amides studied. This observation was also made by Mauger and Soper (4) in their study of N-chlorination of N-methyl acetamide and by de la Mare and Hassan (7) for C-chlorination of aromatics. Schilov and Kaniaev (8) noted that the rate of addition of molecular chlorine to carbon–carbon double bonds was some 10^5 times that of HOCl. In the present work, the ratio of the N-chlorination reactivity of chlorine and hypochlorous acid varied within a range of 10^3–10^4, depending on the amide, with the exception that the ratio for the N,N'-dimethyl urea is about 5×10^5.

The order of reactivity of the various amides with molecular chlorine and chlorine acetate was observed as follows

$$\begin{aligned} &\overset{O}{\overset{\|}{C}}H_3NHCNHCH_3 > CH_3N\overset{Cl}{}\overset{O}{\overset{\|}{C}}NHCH_3 > CH_3CH_2\overset{O}{\overset{\|}{C}}NHCH_3 > CH_3\overset{O}{\overset{\|}{C}}NHCH_2CH_3 \\ &> CH_3\overset{O}{\overset{\|}{C}}NHCH_3 > CH_3\overset{O}{\overset{\|}{C}}NHCH_2CH_2OH > H\overset{O}{\overset{\|}{C}}NHCH_2CH_3 > H\overset{O}{\overset{\|}{C}}NHCH_3 \end{aligned}$$

TABLE II

Activation energies of N-chlorination

Chlorinating species	Amide	Temperature °C	Rate constant (mole/l s)	E_a (kcal/mole)
Cl_2	$CH_3\overset{\overset{O}{\|}}{C}NHCH_3$*	0		
		15	3.34×10	
		25	8.33×10	14.1
		40	23.2×10	
	$CH_3NCl\overset{\overset{O}{\|}}{C}NHCH_3$	0	1.95×10	
		15	50.0×10	9
		25	78.5×10	
		40		
AcOCl	$CH_3\overset{\overset{O}{\|}}{C}NHCH_3$*	0		
		15	0.78×10^4	
		25	1.0×10^4	5
		40	1.58×10^4	
	$CH_3NCl\overset{\overset{O}{\|}}{C}NHCH_3$	0	7.8×10^4	
		15	10.2×10^4	2.5
		25	11.3×10^4	
		40		

*Reference 2.

The literature value (7) for k_{Cl_2} for acetanilide is less than that for methyl formamide. The order of reactivity of these amides with HOCl is essentially the same, although the smallest rate constants shown in Table I are not accurate enough to distinguish between the two formamides and N-methyl acetamide.

The activation energies of Cl_2-chlorination and CH_3COOCl-chlorination of two amides are shown in Table II. The activation energy of N-chlorination by chlorine acetate was found to be lower than that of the reaction with molecular chlorine. Our activation energies are in qualitative agreement with the generally low values found for chlorination of organic compounds. The following activation energies of chlorination were reported by de la Mare and his co-workers.

Compound	Chlorinating species	E_a (kcal/mole)	Reference
Benzene	Cl_2	17	9
Toluene	Cl_2	13	6
Naphthalene	Cl_2	7.5	9
Anisole	HOCl	10	10

The effects of additives on the observed rate constant are presented in Table III. It is obvious from the table that the chloride ion, which participates in the formation of molecular chlorine, has the greatest catalytic effect, while the phosphate and sulfate ions increase the N-chlorination rate only slightly. The nitrate ion exhibits no catalytic activity. Our data are consistent with those of Mauger and Soper (4).

Thus far, we have been reporting data obtained from weakly acidic medium, where the dominant species is undissociated hypochlorous acid. In

TABLE III

Effect of additives on the rate of N-chlorination of N-methyl acetamide in 0.10 *M* acetic acid buffer, at pH 5 and 25 °C

Additive concentration (mole/l)	$10^2 \times k_{obs}$ (mole/l s)$^{-1}$			
	NaCl	NaH_2PO_4	Na_2SO_4	$NaNO_3$
0.00	4.50	4.50	4.50	4.50
0.01	6.0			
0.02	7.75			
0.05	12.9	4.90	4.64	4.50
0.10	21.6	5.15	4.91	4.55
0.15				
0.25		6.25	5.35	4.50
0.50		7.95	6.35	4.55
$10^2 \times \Delta k_{obs}$ / Δ concentration	105	4.2	2.2	0

Can. J. Chem. Downloaded from www.nrcresearchpress.com by 210.87.254.5 on 09/05/12
For personal use only.

Can. J. Chem. Downloaded from www.nrcresearchpress.com by 210.87.254.5 on 09/05/12
For personal use only.

an alkaline medium, the acid dissociates according to the following equilibrium

$$HOCl \rightleftharpoons H^+ + OCl^-$$

with the equilibrium constant $K_{OCl^-} = 4.1 \times 10^{-8}$ mole/l at 25 °C (11). At pH higher than 9, practically all the acid is ionized. The N-chlorination of amides would thus involve the hypochlorite ion OCl^- and it was assumed in the present work that the primary chlorinating agent at high pH was the hypochlorite ion

$$R_1\overset{\overset{O}{\|}}{C}NHR_2 + OCl^- \xrightarrow{k_{OCl^-}} R_1\overset{\overset{O}{\|}}{C}NClR_2 + OH^-$$

with the rate law expression

$$\frac{d\left[R_1\overset{\overset{O}{\|}}{C}NClR_2\right]}{dt} = k_{OCl^-}\left[R_1\overset{\overset{O}{\|}}{C}NHR_2\right][OCl^-] = k_{OCl^-}\frac{[OCl^-]}{[HOCl]}\left[R_1\overset{\overset{O}{\|}}{C}NHR_2\right][HOCl]$$

This reaction results in the formation of hydroxyl ion. Indeed, this was observed, as the pH of the reaction medium increased in all cases studied. It was observed that the pH, in the alkaline range studied, did not have any effect on the hypochlorite ion rate constant k_{OCl^-}. Thus, to the general expansion of the observed rate constant, k_{obs}, we must add the term $k_{OCl^-} \cdot [OCl^-]/[HOCl]$ to account for N-chlorination by the hypochlorite ion.

The k_{OCl^-} values for the various amides under study are presented in Table I. Mauger and Soper reported an estimated k_{OCl^-} value of 1.54×10^{-2} (mole/l s)$^{-1}$ for N-methyl acetamide at 25 °C (4). The present determined value was 1.82×10^{-2} (mole/l s)$^{-1}$, in reasonable agreement.

It was noted that the buffer concentration did not influence the specific hypochlorite rate constant, k_{OCl^-}, for all the amides studied. The addition of sodium chloride had no noticeable effect either (Table IV). It is obvious that buffer concentration and the sodium chloride addition would affect the ionic strength of the reaction medium.

TABLE IV

Effect of sodium chloride on the rate of N-chlorination of N-methyl acetamide by hypochlorite ion in 0.15 *M* phosphate buffer at pH 10 and 25 °C

Added NaCl (mole/l)	$10^2 \times k_{OCl^-}$ (mole/l s)$^{-1}$
0.00	1.82
0.01	1.82
0.13	1.78
0.50	1.82
	Mean 1.82

The order of reactivity of the various amides studied with OCl^- is the reverse of that for the molecular chlorinating species hypochlorous acid, chlorine, and chlorine acetate.

The specific rate constants of the various N-chlorinating species are in the order

$$CH_3COOCl > Cl_2 > OCl^- > HOCl$$

with the exception that the two lowest constants were in the reverse order for N-methylpropionamide and N,N′-dimethyl urea. In the chlorination of toluene, de la Mare and co-workers (6) found the same reactivity sequence.

Discussion

Ionic Strength Dependence

For an ionic reaction, the reaction rate constant is related to the ionic strength of the medium by the following expression (12)

$$\log k_I = \log k_{0I} + 1.018 Z_A Z_B I^{1/2}$$

where k_I and k_{0I} are the rate constants at ionic strength I and zero respectively, and Z_A and Z_B are the ionic charges of the ions A and B that enter into the reaction.

The absence of dependence of the reaction rate on ionic strength, both at low and at high pH, leads to the conclusion that at least one of the amide and the chlorinating species is uncharged. Since in the high pH region the dominant chlorinating species is the hypochlorite ion, ClO^-, it can be deduced that the amide or its intermediate remains molecular and uncharged.

Chlorination

(a) Acidic Medium

In an acid medium, where hypochlorous acid exists mainly undissociated, in the absence of buffer or other additives, the rate of N-chlorination of amides was slight. The chlorinating

Can. J. Chem. Downloaded from www.nrcresearchpress.com by 210.87.254.5 on 09/05/12
For personal use only.

species may be the hypochlorous acid itself or an intermediate. It was proposed by de la Mare and his co-workers (13, 14) that the electropositive chloronium ion, Cl^+, was a possible chlorinating agent. However, the addition of electrolytes should reduce the Cl^+ concentration

$$Cl^+ + Cl^- \rightarrow Cl_2$$
$$Cl^+ + HPO_4^{2-} \rightarrow ClHPO_4^-$$
$$Cl^+ + SO_4^{2-} \rightarrow ClSO_4^-$$

It is inconceivable that such species as $ClHPO_4^-$ and $ClSO_4^-$ should be more reactive than Cl^+ itself, and should increase the reaction rate, as observed, instead of decreasing it. No doubt, Cl^+ would be highly reactive. However, its concentration must be negligibly small. Anbar and Dostrovsky (15) suggested the protonated hypochlorous acid, $ClOH_2^+$, as a likely chlorinating agent

$$H^+ + HOCl \rightarrow ClOH_2^+$$

The absence of dependence of the HOCl reaction rates on pH argues against this formulation. We propose that in the absence of additives, and in the pH region of undissociated hypochlorous acid, the active N-chlorinating species is the acid itself. The absence of influence of changes of pH in this range and of electrolytes upon k_{HOCl} lends support to the molecular HOCl N-chlorination hypothesis.

In the presence of chloride ions, molecular chlorine is generated by the following reaction

$$HOCl + H^+ + Cl^- \rightleftharpoons Cl_2 + H_2O$$

In the presence of acetic acid, chlorine acetate is formed by the following reaction

$$HOCl + CH_3COOH \rightleftharpoons CH_3COOCl + H_2O$$

The protonated chlorine acetate does not exist to any appreciable extent

$$CH_3COOCl + H^+ \rightleftharpoons CH_3.CO^+H.OCl$$

as the N-chlorination reaction involving chlorine acetate was not noticeably affected by the pH of the reaction medium. Again, we are led to the conclusion that the active chlorinating species are molecular chlorine and chlorine acetate.

In general, active N-chlorinating species are generated from hypochlorous acid by reaction either with chloride ion in acidic medium, as follows

[1] $$HOCl + H^+ + Cl^- \rightleftharpoons Cl_2 + H_2O$$

or with a molecular species such as acetic acid, as follows

[2] $$HOCl + HOAc \rightleftharpoons AcOCl + H_2O$$

The catalytic action of phosphates and sulfates, and of other organic acids described by Mauger and Soper (4) appears to result from reactions similar to [1] or [2].

(b) Alkaline Medium

In an alkaline medium, hypochlorous acid reacts to form OCl^- as follows

$$HOCl + OH^- \rightleftharpoons OCl^- + H_2O$$

Neither chloride ion concentration nor hydrogen ion concentration affected the chlorination rate in the ranges studied. We are led to the conclusion that the OCl^- ion takes part directly in the N-chlorination process.

Effect of Substituent Groups

It was suggested in the first part of this discussion that the amide reacts primarily as a molecular entity. The present discussion illustrates the effects of substituents R_1 and R_2 on the reactivity

$$R_1{-}\overset{\overset{O}{\|}}{C}{-}NHR_2$$

of the secondary amides towards the different chlorinating agents. Following Mauger and Soper (4) the reaction may be written

$$R_1{-}\overset{\overset{O}{\|}}{C}{-}\underset{\underset{R_2}{|}}{N}\cdots\overset{\overset{H}{|}}{Cl}\leftarrow X$$

where X may be Cl, HO, AcO, or O^-. Mauger and Soper suggested hydrogen bond formation between the amido hydrogen and the X group. The rate of reaction of the chlorinating agent and the amide is seen as dependent upon the ease of formation of such a bond. It is evident that readiness with which such bonds form would depend on the properties of R_1 and R_2, which determine the electron density about the amide N, and thus the strength of the NH bond, and the chlorinating agent.

The carbonyl group has a high electron affinity. When other effects are equal, the electron-donor properties of the R_1 and R_2 groups would determine the electron density about the amide N. The higher the electron-donating power, the more electronegative the amide N, the stronger the NH bond, and the lower the expected rate of reaction. If the electron-donating power of the

Can. J. Chem. Downloaded from www.nrcresearchpress.com by 210.87.254.5 on 09/05/12
For personal use only.

On p. 3295, the footnote ‡ of Table V should read "In amide series $R_1\overset{\overset{O}{\|}}{C}NHR_2$", not "In amide series $R_1\overset{\overset{O}{|}}{C}NHCH_3$".

Can. J. Chem. Downloaded from www.nrcresearchpress.com by 210.87.254.5 on 09/05/12
For personal use only.

R_1 or R_2 groups of the amides is measured as the inverse of K_a, the dissociation constants of the corresponding acids, the following order for $1/K_a$ is observed

$$CH_3CH_2COOH > CH_3COOH > HCOOH$$

The specific rate constants for the corresponding amides and the various N-chlorinating species are then expected to be in the reverse order, that is

$$HCNHR_2 > CH_3CNHR_2 > CH_3CH_2CNHR_2$$

and

$$R_1CNHCH_3 > R_1CNHC_2H_5$$

This order is that observed for k_{OCl^-}. The suggestion of Mauger and Soper appears then to be consistent with the observations when the chlorinating agent is hypochlorite ion.

The observed order of reactivity of the amides with the molecular chlorinating agents is just the reverse, that is, the reactions are most rapid when there is the greatest electron density about the amide N atom. In this case it is suggested that the primary reaction is the donation of electrons from the N to the Cl atom, as follows

$$R_1—C(=O)—N(H\ldots X)—R_2 \rightarrow Cl$$

where X is Cl, HO, or AcO. Such a reaction would appear to be most likely if the molecular chlorinating agent were somewhat polarized, with a partial positive charge on the Cl atom, as follows

$$X^{\delta-}—Cl^{\delta+}$$

In this case the order of reactivity would be the same as the degree of such polarization. A measure of such polarization may be the rate or extent of reaction with Cl^- in a slightly acid medium, as follows

[3] $$HOCl + Cl^- + H^+ \rightleftharpoons Cl_2 + H_2O$$

[4] $$Cl_2 + Cl^- \rightleftharpoons Cl_3^-$$

[5] $$CH_3—C(=O)—OCl + Cl^- + H^+ \rightleftharpoons Cl_2 + CH_3COOH$$

At pH near 5, in the presence of low concentrations of Cl^-, very little reaction takes place between HOCl and Cl^-, the equilibrium being far to the left and the equilibrium constant (16) being given as

$$K = \frac{[H^+][Cl^-][HOCl]}{[Cl_2]} = 4.75 \times 10^{-4} \text{ (mole/l)}^2 \text{ at } 25\,^\circ\text{C}$$

The equilibrium constant for the reaction between Cl_2 and Cl^- is given (17) as 1.91×10^{-1} $(\text{mole/l})^{-1}$ at 25 °C.

While again the equilibrium lies to the left, at pH 5 there would be more reaction between Cl_2 and Cl^- than between HOCl and Cl^-.

The equilibrium constant (16, 14) for reaction [5] is

$$K = \frac{[Cl_2][AcOH]}{[AcOCl][Cl^-][H^+]} = \frac{[Cl_2][H_2O]}{[HOCl][Cl^-][H^+]} \times \frac{[AcOH][HOCl]}{[AcOCl][H_2O]}$$

$$= 2.1 \times 10^3 \times 4.0 \times 10^2 \times [H_2O] = 8.4 \times 10^5 \times [H_2O] \text{ (mole/l)}^{-1}$$

The large equilibrium constant suggests a high fraction of positive charge on the Cl of the acetyl hypochlorite, which is consistent with its high reactivity. If we can extend the Hammett equation to the present systems

$$\log (k/k_0) = \sigma\rho$$

where k is the specific rate constant, k_0 is a reference rate constant, σ is the substituent constant independent of the reaction, and ρ is the proportionality constant, then the slope of the

TABLE V

Substituent constants, σ_p

Substituent	σ_p*	σ_I†	$\sigma_R = \sigma_p - \sigma_I$†
R_1‡			
CH_3NH	−0.592		
CH_3CH_2	−0.151	−0.05	
CH_3	−0.170	−0.05	−0.13
H	0.0	0.0	0.0
X§			
OH	−0.357	+0.25	−0.61
Cl	0.227	+0.47	−0.24
CH_3COO	0.50	+0.27	+0.25

*Reference 19.
†References 20 and 21.
‡In amide series R_1CNHCH_3.
§In chlorinating agent series XCl.

FOR ERRATA SEE
Vol. 47 #24 1969 p. 4713

plot log k vs. σ, i.e., ρ, would indicate the electronic interaction between the amide and the chlorinating species. If the substituent groups are electron-withdrawing, ρ should have a positive value; on the other hand, a negative ρ value would indicate facilitation of reaction by electron-releasing substituents.

Taft (18) proposed that σ is made up of two components, the inductive effect σ_I and the resonance effect σ_R, such that

$$\sigma_p = \sigma_I + \sigma_R$$

where σ_p is the σ value for *p*-substituted benzene rings. Table V lists the σ values for R_1 of the amide series

$$R_1\overset{\overset{O}{\|}}{C}NHCH_3$$

and for X of the molecular chlorinating species X—Cl. As can be seen from the X—Cl series, the reactivity is not a function of the inductive effect alone. If it were so, the reactivity of the chlorinating species should be in the order $Cl_2 > CH_3COOCl > HOCl$. However, this was not the observed order.

Figure 1 plots the specific rate constants of the amides against the σ_p values of the substituent X of the chlorinating species. Figure 2 shows the rate constants plotted against σ_p of the substituent R_1 of the amide $R_1\overset{\overset{O}{\|}}{C}NHCH_3$. Both plots exhibit remarkable linearity. It appears that resonance plays an important role in the reaction. It is the combined inductive and resonance effects of the substituents that determine the reactivities of both the amides and the chlorinating species.

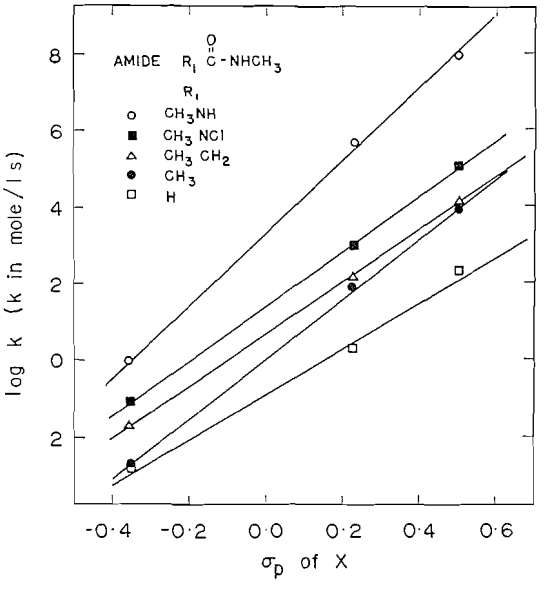

FIG. 1. Effects of the substituents of the chlorinating species X—Cl on the reaction rate constants.

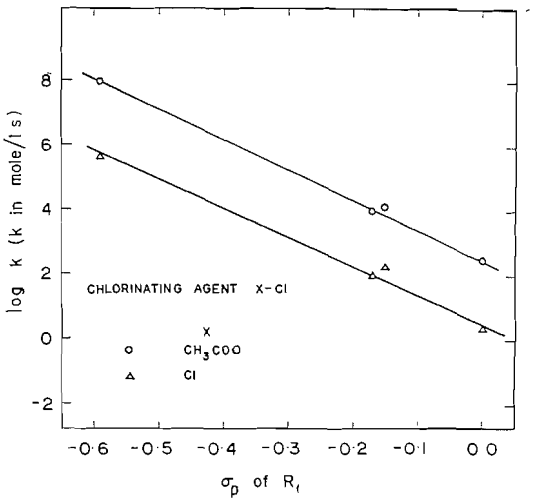

FIG. 2. Effects of the substituents of the amides $R_1\overset{\overset{O}{\|}}{C}NHCH_3$ on the reaction rate constants.

Pauling (22) suggested that amides have two main resonance structures

$$R_1-\overset{\overset{O}{\|}}{C}-N\begin{matrix}H\\ \diagdown\\ \diagup\\ CH_3\end{matrix} \rightleftharpoons R_1-\overset{\overset{O^-}{|}}{C}=N^+\begin{matrix}H\\ \diagdown\\ \diagup\\ CH_3\end{matrix}$$

It is reasonable to suggest that there are similar inductive and resonance effects by the substituent R_1 on the structure of the amide as on the benzene ring.

The positive slopes of Fig. 1 lend support to our hypothesis that the higher the electron-withdrawing power of X, the more reactive the chlorinating species. The negative slopes of Fig. 2 suggest that higher electron density of the amide N facilitates the up-take of positive chlorine. These two observations clearly supplement each other.

Thus, it would appear reasonable to suggest

FOR ERRATA SEE
v. 47 #24 1969 ..... p. 4713.

Can. J. Chem. Downloaded from www.nrcresearchpress.com by 210.87.254.5 on 09/05/12
For personal use only.

that the specific rate constants for the reactions between these molecular chlorinating agents and the amides are in the order of the magnitude of the partial positive charge on the Cl atom of the chlorinating species and also of the electron density on the N atom of the amide.

Acknowledgments

This work was supported in part by the Defence Research Board of Canada (Grant No. 2075-05). One of us (E.W.C.W.T.) would like to thank the National Research Council of Canada for a Scholarship.

1. M. WAYMAN, H. SALAMAT, and E. J. DEWAR. Can. J. Chem. Eng. **46**, 282 (1968).
2. M. WAYMAN and E. W. C. W. THOMM. Can. J. Chem. **47**, 2561 (1969).
3. W. O. HISEY and C. M. KOON. Paper Trade J. **103**, 36 (1936).
4. R. P. MAUGER and F. G. SOPER. J. Chem. Soc. 71 (1946).
5. G. STANLEY and J. SHORTER. J. Chem. Soc. 256 (1958).
6. P. B. D. DE LA MARE, I. C. HILTON, and S. VARMA. J. Chem. Soc. 4044 (1960).
7. P. B. D. DE LA MARE and M. HASSAN. J. Chem. Soc. 1519 (1958).
8. E. A. SCHILOV and N. P. KANIAEV. J. Phys. Chem. Russ. **5**, 654 (1934).
9. P. B. D. DE LA MARE and P. W. ROBERTSON. J. Chem. Soc. 279 (1943).
10. P. B. D. DE LA MARE, A. D. KETLEY, and C. A. VERNON. J. Chem. Soc. 1290 (1954).
11. International critical tables. Vol. V. p. 176.
12. S. GLASSTONE. Textbook of physical chemistry. 2nd ed. D. Van Nostrand Co., Inc., New York. 1950. p. 1116.
13. P. B. D. DE LA MARE, J. T. HARVEY, M. HASSAN, and S. VARMA. J. Chem. Soc. 2756 (1958).
14. P. B. D. DE LA MARE, I. C. HILTON, and C. A. VERNON. J. Chem. Soc. 4039 (1960).
15. M. ANBAR and I. DOSTROVSKY. J. Chem. Soc. 1094 (1954).
16. A. A. JAKOWIN. Z. Phys. Chem. Leipzig, **29**, 613 (1899).
17. G. ZIMMERMAN and F. C. STRONG. J. Amer. Chem. Soc. **79**, 2063 (1957).
18. R. W. TAFT, JR. *In* Steric effects in organic chemistry. John Wiley and Sons, Inc., New York. 1956. Chap. 13.
19. H. H. JAFFE. Chem. Rev. **53**, 191 (1953).
20. R. W. TAFT, JR. J. Amer. Chem. Soc. **79**, 1045 (1957).
21. R. W. TAFT, JR. and I. C. LEWIS. J. Amer. Chem. Soc. **80**, 2436 (1958).
22. L. PAULING. The nature of the chemical bond. 3rd ed. Cornell Univ. Press, Ithaca, N.Y. 1960. p. 181.

Can. J. Chem. Downloaded from www.nrcresearchpress.com by 210.87.254.5 on 09/05/12
For personal use only.

Can. J. Chem. Downloaded from www.nrcresearchpress.com by 210.87.254.5 on 09/05/12
For personal use only.

Etude du coefficient d'expansion linéaire de polymères en solution par sédimentation et par viscosimétrie

NGA HO-DUC ET HUBERT DAOUST
Département de Chimie, Université de Montréal, Montréal, Québec

Reçu le 7 mars 1969

Les coefficients d'expansion linéaire de polyméthacrylate de méthyle en solution dans du tétrachlorure de carbone à 45 °C, dioxanne, benzène et chloroforme à 25 °C et de polyisobutylène en solution dans du caprylate d'éthyle à 10.8 °C, triméthyle-2,2,4 pentane, cyclohexane et heptane à 25 °C ont été étudiés à partir de données expérimentales de sédimentation et de viscosimétrie. Les valeurs des coefficients d'expansion linéaire α_η et α_f sont comparées entre elles et le rapport α_η/α_f trouvé pour les différents systèmes étudiés se situe entre 0.9 et 1.0. Une correction proposée pour la constante de sédimentation, S^0, tenant compte de la variation de α avec la concentration, nous permet de rapprocher davantage les valeurs expérimentales et théoriques de l'exposant δ de la relation entre la viscosité intrinsèque $[\eta]$ et le coefficient de frottement intrinsèque $[f]$. Les valeurs trouvées pour δ se situent entre 2.4 et 3.0 en accord avec la valeur proposée par Stockmayer et Albrecht (2), soit 2.8 et la valeur de 2.7 tirée de la théorie de Ptitsyn (7).

Canadian Journal of Chemistry, 47, 3299 (1969)

Introduction

L'ultracentrifugation offre, en principe, une méthode pour l'étude des dimensions des macromolécules en solution (1). Le coefficient de frottement des particules de soluté à concentration nulle est défini par

$$[1] \qquad f_0 = M(1 - \bar{v}_2\rho)/N_A S_0{}^0$$

où M est la masse moléculaire du soluté, $\bar{v}_2$, son volume spécifique partiel, ρ, la densité du solvant, N_A, le nombre d'Avogadro, et $S_0{}^0$, le coefficient de sédimentation du soluté à concentration nulle et sous 1 atm de pression. Le coefficient de frottement intrinsèque $[f]$ défini par f_0/η_0, η_0 étant la viscosité du solvant, est relié au coefficient d'expansion linéaire d'une chaîne de polymère en solution infiniment diluée α_f, par la relation

$$[2] \qquad [f] = K_f M^{1/2}\alpha_f$$

où K_f est une constante pour un polymère donné. Cette constante est définie par la relation

$$[3] \qquad K_f = P_0(R_0{}^2/M)^{1/2}$$

où P_0 est une constante universelle dont la valeur limite pour un polymère homogène est 5.11 (2); R_θ est la racine carrée de la distance quadratique moyenne entre les bouts d'une chaîne en solvant thêta à concentration nulle. Il existe donc une relation directe entre $[f]$ et la dimension moyenne d'une chaîne de polymère dans un solvant quelconque à concentration nulle définie par R_0. Evidemment, le calcul de R_0 repose sur la détermination de $S_0{}^0$. Cette détermination peut se faire à l'aide de la méthode décrite par Billick (3) dans laquelle le coefficient de sédimentation apparent à une concentration particulière est défini par

$$[4] \qquad S = \frac{\ln (r/r_0)}{\omega^2 t} = S^0\left\{1 - \frac{[m(2a + 1) - a]}{(1 + a)} S^0\omega^2 t - \cdots\right\}$$

où r est la distance radiale de la frontière solvant–solution au temps t, r_0, la valeur au temps zéro, ω, la vitesse angulaire du rotor, S^0, la valeur de S sous 1 atm de pression, m, un paramètre reflétant l'effet de la pression sur la sédimentation et a, un paramètre reflétant l'effet de la concentration. La valeur de $S_0{}^0$ s'obtient par l'extrapolation de la droite obtenue du graphique $1/S^0 = f(c)$.

Une autre méthode grandement utilisée à la détermination des dimensions des macromolécules en solution est la viscosité. La relation classique de Fox et Flory (1) entre la viscosité intrinsèque $[\eta]$ d'un polymère dans un solvant donné et la dimension de la chaîne s'écrit

$$[5] \qquad [\eta] = KM^{1/2}\alpha_\eta{}^3$$

La constante K étant définie par

$$[6] \qquad K = \Phi(R_0{}^2/M)^{3/2}$$

où Φ est un paramètre dont la valeur varie en fonction de la nature du solvant (4).

Les équations données ci-haut pour les deux méthodes de caractérisation reposent sur le

TABLEAU I

Résultats pour le PMM

Solvant	t °C	$[\eta]$	α_η	$1/S_0^0$ ($\times 10^{-13}$)	α_f	α_η/α_f
Tétrachlorure de carbone	45*	0.38	1.00	0.082	1.00	
Dioxanne	25	0.98	1.44	0.340	1.40	1.03
Benzène	25	0.91	1.41	0.088	1.39	1.02
Chloroforme	25	1.17	1.56	0.162	1.63	0.96

*Température thêta (12).

TABLEAU II

Résultats pour le PIB

Solvant	t °C	$[\eta]$	α_η	$1/S_0^0$ ($\times 10^{-13}$)	α_f	α_η/α_f
Caprylate d'éthyle	10.8*	1.18	1.00	0.810	1.00	
Heptane	25	2.75	1.39	0.048	1.46	0.96
Cyclohexane	25	3.90	1.56	0.220	1.72	0.91
Triméthyle-2,2,4 pentane	25	2.14	1.28	0.057	1.34	0.96

*Température thêta (9).

même modèle physique mais la théorie prévoit une différence entre les valeurs de α_η et α_f (2, 4–7). Dans ce travail, nous avons fait une étude comparative des deux méthodes sur des solutions de polyméthacrylate de méthyle (PMM) et de polyisobutylène (PIB).

Partie Expérimentale

La fraction de PMM utilisée est la septième d'un fractionnement simple d'un échantillon préparé d'après la méthode décrite par Fox *et al.* (8). Sa masse moléculaire déterminée par viscosimétrie est 3.91×10^5. La fraction de PIB utilisée vient d'un fractionnement double d'un échantillon commercial connu sous le nom de Vistanex L-100 de Enjay Co., Inc., ayant pour masse moléculaire viscosimétrique 1.17×10^6 (9). Les solvants utilisés sont de qualité réactif analytique.

Les mesures de sédimentation sont effectuées à l'aide d'une ultracentrifugeuse analytique "Spinco" modèle E-HT. La vitesse du rotor est fixée à 59 780 t/min pour tous les systèmes étudiés, soient: PMM–dioxanne, –benzène, –chloroforme, PIB–heptane, –cyclohexane, –triméthyle-2,2,4 pentane à 25 °C, PMM–tétrachlorure de carbone à 45 °C, et PIB–caprylate d'éthyle à 10.8 °C. La température du rotor est maintenue stable à ± 0.2 °C. Le dépouillement des plaques photographiques se fait à l'aide d'un microcomparateur de Nippon Kogaku; la précision de la platine de cet appareil est de ± 0.01 mm. La détermination du "temps zéro" se fait suivant la méthode d'estimation du temps zéro à accélération constante (10). Les graphiques $\ln r = f(t)$ permettent ensuite la détermination précise du temps zéro i.e. à quelques secondes près. Les coefficients de sédimentation S^0 à différentes concentrations sont calculés graphiquement à partir de l'éq. [4] et la valeur de S_0^0 est déduite à partir du graphique $(1/S^0) = f(c)$.

La viscosité intrinsèque est calculée pour chaque système à partir de mesures effectuées, à l'aide d'un viscosimètre Ubbelhode modifié (11), aux températures correspondantes.

Résultats et Discussion

Les Tableaux I et II représentent les valeurs de $1/S_0^0$, α_f et α_η des différents systèmes. Afin d'éliminer les valeurs de M, P_0 et de la constante structurale (R_0^2/M) dans les calculs, nous avons utilisé les relations suivantes

$$[7] \quad \alpha_\eta = ([\eta]\Phi_0/[\eta]_0\Phi)^{1/3}$$

$$[8] \quad \alpha_f = [f]/[f]_0 = (1 - \bar{v}_2\rho)\eta_{00}(S_0^0)_0/(1 - \bar{v}_2\rho)_0\eta_0 S_0^0$$

Nous avons négligé dans ces calculs l'effet de la température sur la valeur de la constante structurale et nous avons utilisé la valeur de 2.48×10^{21} pour la constante Φ pour les bons solvants et 2.87×10^{21} pour les solvants thêta (4). Les différentes constantes physiques des polymères et des solvants sont données dans le Tableau III.

L'analyse des Tableaux I et II permet de constater que le rapport entre α_η et α_f varie entre 0.91 et 1.03, tandis que Kurata et Stockmayer prévoient une valeur de 0.97 (4). Tout le long des études théoriques du coefficient de sédimentation, les auteurs ont tenu compte de l'effet de concentration seulement au point de vue hydrodynamique ou autrement dit de l'effet de

Can. J. Chem. Downloaded from www.nrcresearchpress.com by 210.87.254.5 on 09/05/12
For personal use only.

Can. J. Chem. Downloaded from www.nrcresearchpress.com by 210.87.254.5 on 09/05/12
For personal use only.

TABLEAU III

Constantes physiques utilisées dans les calculs

Système	t °C	$\bar{v}_2$	ρ‡	η_0‡ ($\times 10^3$)
PMM–benzène	25	0.8069*	0.8736	5.97
PMM–chloroforme	25	0.7942*	1.479	5.47
PMM–dioxanne	25	0.818*	1.027	12.6
PMM–tétrachlorure de carbone	45	0.829†	1.546	7.28
PIB–heptane	25	1.094†	0.6795	3.86
PIB–cyclohexane	25	1.094†	0.7739	8.88
PIB–triméthyle-2,2,4 pentane	25	1.094†	0.6878	4.7
PIB–caprylate d'éthyle	10.8	1.084†	0.8758	18.34

*Référence 19.
†Référence 20.
‡Référence 21.

frottement. D'autre part, si on suppose que le coefficient de diffusion est indépendant de la concentration, cela signifie que la dimension de la chaîne est définie par R_0 à toute concentration. Alors, l'éq. [4] suppose que la dimension de la sphère équivalente au volume d'encombrement des chaînes ne change pas avec la concentration. Cependant, il a été démontré théoriquement que le coefficient d'expansion linéaire varie avec la concentration de la solution (13–15). Ainsi, nous pensons qu'il est nécessaire de tenir compte de cet effet et d'apporter une correction sur chaque valeur de S^0. Cette correction pourrait se faire en considérant que le rayon quadratique moyen de la chaîne des polymères est une fonction de la concentration dans la déduction mathématique des équations. Cette nouvelle fonction complique énormément la résolution mathématique de l'équation différentielle de base de la sédimentation.

Pour ne pas se heurter à des difficultés presqu'insurmontables, nous proposons la relation suivante en partant de la loi de Stokes

$$[9] \qquad (1/S_0{}^0)_0 = (1/S^0)_c(\alpha_0/\alpha_c)$$

Cette relation assez rudimentaire amène la valeur de S^0, obtenue à une concentration c pour laquelle le coefficient d'expansion linéaire est α_c, à celle correspondant à la dimension moyenne des chaînes de polymères à concentration nulle comme le suppose la dérivation de l'éq. [4].

La valeur de α à une concentration donnée peut être calculée à l'aide de la relation suivante (13)

$$[10] \qquad \alpha_c = \alpha_0 \exp(-Ac)$$

avec

$$[11] \qquad A = 0.0794(N_A n^2 \beta/2M)\varphi_2(z_0)]$$

où n est le nombre de segments par chaîne, β, l'intégrale obtenue lors du couplage des segments pour former les chaînes de polymères et $\varphi_2(z_0)$ est une fonction dépendant de α_0.

Les Figs. 1 et 2 représentent les courbes moyennes calculées par la méthode des moindres carrés à partir des données expérimentales. Les courbes en traits brisés représentent les pentes limites à dilution infinie de la relation $(1/S^0) = f(c)$ ou en d'autres termes, elles représentent l'allure de cette relation lorsque les dimensions des chaînes sont définies par R_0 à toute concentration. Les courbes en traits continus représentent l'allure des résultats expérimentaux et il est d'usage de définir $1/S_0{}^0$ par l'extrapolation linéaire à concentration nulle des résultats obtenus à des concentrations allant de 0.1 à 1 %. En principe, les deux séries de courbes devraient donner les mêmes valeurs pour $1/S_0{}^0$ mais

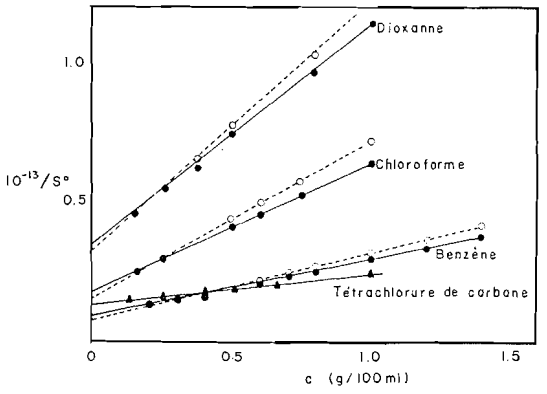

FIG. 1. Variation de $1/S^0$ en fonction de la concentration pour le PMM; traits continus, sans correction; traits brisés, avec correction.

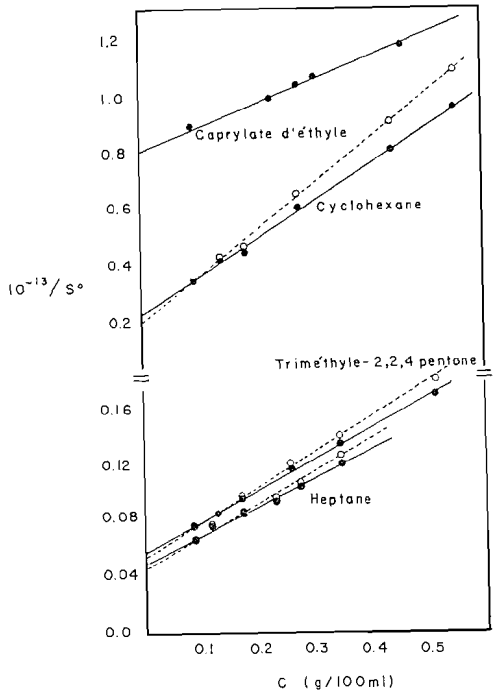

FIG. 2. Variation de $1/S^0$ en fonction de la concentration pour le PIB; traits continus, sans correction; traits brisés, avec correction.

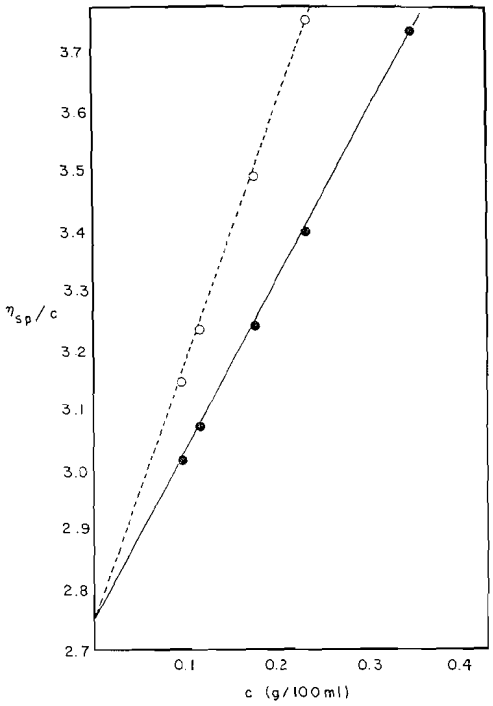

FIG. 3. Variation de la viscosité spécifique réduite en fonction de la concentration pour le système PIB–heptane à 25 °C; trait continu, sans correction; trait brisé, avec correction.

l'imprécision des données expérimentales ne permet pas de conclure à un changement d'allure de la relation $(1/S^0) = f(c)$ à très faibles concentrations. Nous devons donc recourir à la méthode que nous avons utilisée pour arriver au calcul de $1/S_0{}^0$ dans le cas de bons solvants.

Nous avons groupé les résultats finals dans le Tableau IV. Nous constatons qu'avec la correction proposée, la comparaison des valeurs du coefficient d'expansion linéaire calculées à partir des données de l'ultracentrifugation et celles de la viscosimétrie est très avantageuse. Notons que cette conclusion n'est pas du tout justifiée pour les systèmes PMM–benzène et PMM–dioxanne. Nous croyons que ces exceptions pourraient être dues à la différence entre la polarité du polymère et celle du solvant. En effet, il a été démontré (16, 17) que lorsqu'un polymère polaire est en solution dans un solvant de polarité comparable, la polarité n'entre pas en ligne de compte, mais lorsque le solvant possède un moment dipolaire beaucoup plus faible que celui du polymère, alors le paramètre d'interaction polymère–solvant χ_1 augmente avec la dilution. Cette augmentation de χ_1 entraîne une diminution de α avec la dilution et alors la correction suggérée devient difficile à réaliser ou peut-être n'a plus de raison d'être à cause de la cancellation des deux effets opposés.

Nous voudrions faire remarquer qu'en réalité il faut apporter le même genre de correction pour les résultats obtenus à partir des données viscosimétriques car les deux théories traitant de la sédimentation et de la viscosité des polymères en solution sont basées sur le même modèle physique. Nous avons effectué les mêmes calculs afin de corriger le coefficient d'expansion linéaire α_η. Les résultats de ces calculs pour le système PIB–heptane sont représentés dans la Fig. 3 comme exemple afin de montrer que la correction est vraiment négligeable dans le cas de la viscosimétrie. Le changement de la pente est plus accentué que dans le cas de la sédimentation à cause de l'exposant trois de α_η mais l'extrapolation reste pratiquement la même.

Le paramètre δ dont les valeurs sont données dans le Tableau IV vient de la relation

$$[12] \qquad [\eta]/[\eta]_0 = ([f]/[f]_0)^\delta$$

Can. J. Chem. Downloaded from www.nrcresearchpress.com by 210.87.254.5 on 09/05/12
For personal use only.

TABLEAU IV

Résumé des résultats finals

Système	A	$1/S_0^0$ ($\times 10^{-13}$) corr.	α_f corr.	α_η/α_f corr.	δ	δ corr.
PMM–dioxanne	8.70	0.330	1.36	1.06	2.8	3.0
PMM–benzène	7.74	0.086	1.36	1.04	2.6	2.8
PMM–chloroforme	13.31	0.156	1.57	0.99	2.3	2.6
PIB–heptane	11.95	0.046	1.37	1.01	2.3	2.7
PIB–cyclohexane	23.5	0.202	1.56	1.00	2.3	2.7
PIB–triméthyle-2,2,4 pentane	6.95	0.053	1.28	1.00	2.1	2.4

Une étude récente de Noda *et al.* (6) a montré que $\delta = 2.4$ pour une série de fractions de poly-α-méthyle-styrène en solution dans le toluène et dans le cyclohexane (solvant thêta). Cette valeur se compare très bien avec celles rapportées dans le présent travail. Cependant, les valeurs de δ corrigées sont plutôt en accord avec la valeur théorique de 2.8 telle que suggérée par Stockmayer et Albrecht (2) et celle de 2.7 tirée du travail de Ptitsyn (7). La correction semi-empirique proposée pour $S_0{}^0$ nous permet ainsi de rapprocher les résultats expérimentaux de ceux prédits par la théorie.

L'application des relations [7] et [8] suppose que les fractions utilisées dans ce travail sont de faible polydispersité, ce qui nous permet d'utiliser les valeurs limites de Φ et de P_0. Dans le cas de la fraction de PIB, des calculs théoriques (18) permettent de prévoir une valeur pour le facteur de polydispersité $h > 10$ donc suffisamment monodisperse (4). Par ailleurs, une valeur de $h = 4$ peut être prévue dans le cas de PMM, ce qui amène une correction due à la polydispersité inférieure à 2% sur le rapport α_η/α_f.

Remerciements

Nous remercions le Conseil National de Recherches du Canada pour son aide financière au cours de ce travail.

1. P. J. FLORY. Principles of polymer chemistry. Cornell Univ. Press, Ithaca, N.Y. 1953.
2. W. H. STOCKMAYER et A. C. ALBRECHT. J. Polym. Sci. **32**, 215 (1958).
3. I. H. BILLICK. J. Phys. Chem. **66**, 1941 (1962).
4. M. KURATA et W. H. STOCKMAYER. Fortschr. Hochpolym. Forsch. **3**, 196 (1963).
5. M. KURATA et H. YAMAKAWA. J. Chem. Phys. **32**, 1852 (1960).
6. I. NODA, S. SAITO, T. FUJIMOTO et M. NAGASAWA. J. Phys. Chem. **71**, 4048 (1967).
7. O. B. PTITSYN. Vysokomol. Soedin. **3**, 1673 (1963).
8. T. G. FOX, J. B. KINSINGER, H. F. MASON et E. M. Schuele. Polymer, **3**, 71 (1962).
9. J. DURANCEAU. Thèse de Doctorat. Université de Montréal, Montréal, Québec. 1966.
10. H. K. SCHACHMAN. Ultracentrifugation, diffusion, and viscometry, *Dans* methods of enzymology. Vol. IV. Academic Press, Inc., New York. 1951.
11. D. A. HENDERSON et N. R. LEGGE. J. Polym. Sci. **19**, 215 (1956).
12. N. HO-DUC et H. DAOUST. Can. J. Chem. **46**, 2456 (1968).
13. H. YAMAKAWA. J. Chem. Phys. **43**, 1334 (1963).
14. M. FIXMAN. J. Polym. Sci. **47**, 91 (1960).
15. M. FIXMAN. Ann. N.Y. Acad. Sci. **89**, 659 (1961).
16. R. CORNELIUSSEN, S. A. RICE et H. YAMAKAWA. J. Chem. Phys. **38**, 1768 (1963).
17. H. DAOUST et A. HADE. Polymer, **9**, 48 (1968).
18. Y. SICOTTE. A paraître.
19. G. V. SCHULZ et M. HOFFMAN. Makromol. Chem. **23**, 220 (1957).
20. T. G. FOX, JR. et P. J. FLORY. J. Phys. Colloid Chem. **55**, 221 (1951).
21. J. TIMMERMANS. Physico-chemical constants of pure organic compounds. Elsevier Publ. Co., Inc., Amsterdam. 1950.

Can. J. Chem. Downloaded from www.nrcresearchpress.com by 210.87.254.5 on 09/05/12
For personal use only.

Arrhenius parameters for the reaction of propyl radicals with propane

R. E. BERKLEY, G. N. C. WOODALL, O. P. STRAUSZ, AND H. E. GUNNING
Department of Chemistry, University of Alberta, Edmonton, Alberta

Received March 19, 1969

The reaction of *n*-propyl radicals from the photolysis of azo-*n*-propane with propane has been studied and Arrhenius parameters for hydrogen atom abstraction relative to the recombination of *n*-propyl radicals determined. From the Arrhenius parameters obtained and the available thermodynamic data, the Arrhenius parameters of the reverse reaction, the hydrogen atom abstraction from propane by *iso*-propyl radicals, have been calculated.

Some complicating factors in the photolysis of azopropane are discussed.

Canadian Journal of Chemistry, 47, 3305 (1969)

Can. J. Chem. Downloaded from www.nrcresearchpress.com by 210.87.254.40 on 09/05/12
For personal use only.

The hydrogen abstraction reactions of methyl radicals from alkanes have been extensively studied, but information on the analogous reactions of higher alkyl radicals is scant (1). It has generally been assumed that the reactions of the higher alkyl radicals are very similar to those of methyl except that the activation energy of abstraction would progressively increase as the C—H bond energy of the abstracting radical decreases. This expectation, though trivial, still lacks proof of general validity. The most abundant data for comparison of methyl with higher alkyl radicals are for abstraction of hydrogen from aldehydes. Here, however, the data, if trustworthy, appear to favor an opposite trend. Abstraction of hydrogen for example by Me and *t*-Bu from *t*-BuCHO has activation energies of 10.2 and 4.3 kcal, respectively. For abstraction from *s*-BuCHO by Me and *s*-Bu, the values are 10.4 and 4.9, and from *i*-BuCHO by Me and *i*-Bu 8.4 and 6.5 kcal, respectively (1). The abstraction from *n*-BuCHO and EtCHO by Me, *n*-Bu, and Me and Et exhibits the same trend. On the other hand, abstraction of hydrogen from paraffins (for example from *n*- and *iso*-butane and *cyclo*-hexane) by methyl and ethyl shows the expected trend in that abstraction by ethyl has activation energies about 0.8 kcal larger than by methyl (1).

Hydrogen abstractions by propyl radicals from hydrocarbons have not been reported in the literature. In conjunction with another study, we have determined the Arrhenius parameters for the *n*-propyl-propane reaction.

n-Propyl radicals were generated by the 3660 Å photolysis of azo-*n*-propane. It is generally accepted that photolysis of azo-alkanes in their first absorption band leads to an $n \rightarrow \pi^*$ excitation. The excited molecules may either undergo decomposition into nitrogen and two alkyl radicals or suffer collisional deactivation to the ground state. The decomposition evidently has a small activation energy, and the radicals produced are thermally equilibrated (2–14).

The photolysis of azo-*n*-propane has been carried out in the presence of propane and propane-1,1,1,3,3,3-d_6, and rate constants for the reaction of *n*-propyl radicals with propane relative to the recombination of *n*-propyl have been measured. In the kinetic treatment allowance has been made for the reactions of propyl radicals with the parent azo compound.

Experimental

Small portions of azo-*n*-propane (Merck) were purified by gas chromatography before each run, using the method described below for separation of components of the "heavy fraction". *n*-Propane-azo-isopropane was synthesized according to the method of Spialter and coworkers (15) and was purified in the same manner as the azo-*n*-propane. The propane (Phillips Research Grade) was distilled under vacuum at −131 °C and degassed at −196 °C. It was shown by gas chromatography to contain less than 0.1% ethane and no other detectable impurities. *n*-Hexane, 2,3-dimethylbutane, 2-methylpentane, and propylene used as calibration samples were also shown by chromatography to contain negligible impurities.

Photolyses were carried out in a cylindrical quartz cell equipped with a cold finger and attached to a high vacuum system. The cell was mounted inside an aluminum block furnace. Light was isolated from a Hanovia Utility medium pressure mercury arc by a Kodak Wratten 18A filter. Product analyses were accomplished by low temperature distillation and gas chromatography. The fraction volatile at −210 °C was measured in a gas burette. It was occasionally analyzed by gas chromatography (10 ft 13X molecular sieves, 0 °C) or by mass spectrometry. It consisted of pure nitrogen with the exception of the 232 °C run which showed a trace of methane. The fraction volatile at −131 °C was measured in a gas burette and then analyzed by gas chromatography (15 ft

Can. J. Chem. Downloaded from www.nrcresearchpress.com by 210.87.254.40 on 09/05/12
For personal use only.

medium activity silica gel, 50 °C). This fraction consisted of propane, propylene, and, occasionally, traces of ethylene. In runs with added propane this fraction was simply discarded. The components of the heavy fraction were separated on a 20 ft 20% SE-30 silicone gum rubber on Chromosorb W.A.W. column at 100 °C. The hexanes were trapped and quantitatively analyzed (24 ft 10% dimethylsulfolane on Chromosorb W.A.W., 0 °C). The dimethylsulfolane column would not resolve 2,3-dimethylbutane and 2-methylpentane, so the proportions of each were calculated, assuming $R_{ab}/(R_{aa}R_{bb})^{\frac{1}{2}} = 2$, where R_{ab} is the rate of cross combination of *n*-propyl and isopropyl radicals and R_{aa} and R_{bb} are the respective rates of autocombination. In the latter part of the investigation the hexanes were analyzed at 25 °C on a 20 ft column packed with 40% isoquinoline on Chromosorb W.A.W. which resolved all three hexane isomers.

Results

Photolyses of pure azo-*n*-propane at 25 °C afforded N_2, propane, propylene, and *n*-hexane, as reported by Calvert and Kerr (4). Upon addition of propane to the system small quantities of 2-methylpentane could be detected. Use of d_6-propane resulted in formation of 2-methylpentane-d_6.

With increasing temperature, many products of lower vapor pressure than azo-*n*-propane began to appear, and the mass balance as calculated from the hydrocarbon products decreased steadily. The heavy products were eluted from the column as very broad peaks with long retention times when the column was operated under conditions optimal for separation of hydrocarbon products, and it was therefore impractical to attempt quantitative analysis of them. Instead account of these products has been taken in the kinetic treatment in terms of the mass balance defect.

The nature of the reactions between alkyl radicals and azoalkanes has been briefly examined in an auxiliary study and the result will be described in another communication (16).

In the azopropane system only the four lightest of the heavy products were trapped, and their identification attempted. One product proved to be propanal propylhydrazone, an isomer of azo-*n*-propane. It was identified by mass spectrometry and nuclear magnetic resonance (n.m.r.). Only mass spectra were obtained for the other three products, since it was too time-consuming to obtain enough sample for n.m.r. spectra. An exact mass measurement indicated that the lightest of these products was a hydrocarbon, or mixture of hydrocarbons, C_9H_{20}. The cracking pattern did not match closely the known cracking pattern of any individual isomer. The other two products both had molecular formula $C_9H_{20}N_2$. The two cracking patterns were virtually identical, except that the product with the shorter retention time had a slightly larger peak at mass 15. The two mass spectra appear closely analogous to that of ethyl 2-butyl diimide (16), and it seems reasonable to suppose that the one with shorter retention time and larger mass 15 peak is propyl 2-methyl-3-pentyl diimide, and that the other one is propyl 3-hexyl diimide. This tentative identification is supported by the fact that the first product is produced in increasing amounts as temperature and isopropyl concentration increase, while the second product is produced throughout the temperature range of the study. The possibility of these products being *cis–trans* isomers of propanal dipropylhydrazone can be dismissed, since dialkyl hydrazones are known not to display *cis–trans* isomerism (16, 17), and the mass spectrum is not analogous to that of ethanal diethyl hydrazone.

The mechanism adapted for the kinetic treatment is summarized below

$$\text{Azo-}n\text{-propane} \xrightarrow{h\nu} 2n\text{-Pr} + N_2$$

[1] $$n\text{-Pr} + C_3H_8 \rightarrow C_3H_8 + i\text{-Pr}$$

[1*a*] $$i\text{-Pr} + C_3H_8 \rightarrow C_3H_8 + n\text{-Pr}$$

[2*a*] $$n\text{-Pr} + i\text{-Pr} \rightarrow \text{2-Methylpentane}$$

[2*b*] $$n\text{-Pr} + i\text{-Pr} \rightarrow C_3H_8 + C_3H_6$$

[3*a*] $$2n\text{-Pr} \rightarrow n\text{-Hexane}$$

[3*b*] $$2n\text{-Pr} \rightarrow C_3H_8 + C_3H_6$$

[4*a*] $$2i\text{-Pr} \rightarrow \text{2,3-Dimethylbutane}$$

[4*b*] $$2i\text{-Pr} \rightarrow C_3H_8 + C_3H_6$$

[5] $$n\text{-Pr} + \text{double bond} \rightarrow \text{Other products or radical}$$

[6] $$i\text{-Pr} + \text{double bond} \rightarrow \text{Other products or radical}$$

The following assumption is made

$$k_{2a} + k_{2b} = 2(k_{3a} + k_{3b}) = 2(k_{4a} + k_{4b})$$

Terry and Futrell (18) have shown that

$$\frac{k_{2b}}{k_{2a}} = 0.41$$

$$\frac{k_{3b}}{k_{3a}} = 0.15$$

$$\frac{k_{4b}}{k_{4a}} = 0.69$$

from which

$$\frac{R_{2a}}{R_{3a}} = 1.63\,\frac{[i\text{-Pr}]}{[n\text{-Pr}]}$$

and

$$r = \frac{[i\text{-Pr}]}{[n\text{-Pr}]} = 0.61\,\frac{R_{2a}}{R_{3a}}$$

The rates of reactions [5] and [6] may be expressed in terms of mass balance

$$R_0 = R_{N_2} - (R_{2a} + R_{2b} + R_{4a} + R_{4b} + R_{3a} + R_{3b})$$

Using the known values of k_d/k_r

$$R_0 = R_{N_2} - 1.41R_{2a} - 1.69R_{4a} - 1.15R_{3a}$$

Since R_0 represents the mass balance defect in terms of radical pairs, while R_5 and R_6 account for the disappearance of single radicals

$$R_5 + R_6 = 2R_0$$

Now k_5 and k_6 will not, in general, be equal. They will be related at a given temperature by

$$q = \frac{k_5}{k_6}$$

Thus

$$\frac{R_6}{R_5} = \frac{k_6[i\text{-Pr}][X]}{qk_6[n\text{-Pr}][X]} = \frac{1}{q}\cdot\frac{[i\text{-Pr}]}{[n\text{-Pr}]} = \frac{r}{q}$$

where [X] represents the collective concentration of double bonds and radicals other than propyl radicals. Steady state assumption for [*i*-Pr] gives

$$\frac{d[i\text{-Pr}]}{dt} = 0 = R_1 - R_{1a} - R_{2a} - R_{2b} - 2R_{4a} - 2R_{4b} - R_6$$

k_1 and k_{1a} are related thermodynamically and from the known entropies and heats of formation of the isopropyl and *n*-propyl radicals (19)

[I] $$k_{1a} = k_1 \exp(0.6 - 3.6/RT)$$

This further leads to the expression

[II] $$\frac{k_1}{k_{3a}^{1/2}} = \frac{1.41R_{2a} + 3.38R_{4a} + \dfrac{2rR_0}{r+q}}{R_{3a}^{1/2}[C_3H_8](1 - r\exp(0.6 - 3.6/RT))}$$

All the unknown quantities in eq. [II] can be evaluated from photolysis of azo-*n*-propane in the presence of propane with the exception of q. At higher temperatures, reactions of radicals with the azo compound and perhaps with propylene formed in the system are evidently of substantial importance, and, in order to evaluate [II], the value of q must be known.

The value of q was determined from the photolysis of *n*-propane-azo-*iso*-propane (under a large pressure of C_3F_8) at several different temperatures. Nitrogen was pumped off at −196 °C and measured. Propane, propylene, and C_3F_8 were removed at −131 °C, and the heavy fraction was analyzed for hexanes as described previously. The ratio of *n*-propyl/isopropyl radicals consumed in

TABLE I

Photolysis of *n*-propane–azo-*iso*-propane with added C_3F_8

T (°C)	Azo (Torr)	C_3F_8 (Torr)	S_{N_2}* (μmole)	S_{2a}* (μmole)	S_{3a}* (μmole)	S_{4a}* (μmole)	Mass balance†	q‡
28	2.8	0	5.11	1.86	1.09	0.78	1.02	—
62	1.2	0	3.20	1.19	0.70	0.52	1.05	—
90	2.6	0	5.94	2.22	1.33	0.94	1.05	—
126	1.7	0	4.36	1.56	0.89	0.67	1.00	—
123	6.4	48.2	9.13	2.15	1.03	1.01	0.65	1.77
120	5.4	102.4	11.02	2.33	1.06	1.18	0.59	1.88
119	4.5	206.2	3.59	0.74	0.37	0.37	0.58	1.60
90	6.5	50.4	7.78	2.19	1.15	0.99	0.78	1.76
91	6.3	203.4	12.82	3.05	1.33	1.54	0.66	2.30
60	8.7	101.5	7.70	2.18	1.07	0.99	0.78	2.12
60	8.8	201.5	8.04	1.96	0.98	0.94	0.68	1.76

*S_i is the quantity of product formed in reaction [*i*].
†Mass balance is given by $(1.41S_{2a} + 1.15S_{3a} + 1.69S_{4a})/S_{N_2}$
‡q is determined from eq. [III].

Can. J. Chem. Downloaded from www.nrcresearchpress.com by 210.87.254.40 on 09/05/12
For personal use only.

TABLE II

Temperature study of the reaction of *n*-propyl radicals with propane

Series*	$\frac{10^3}{T}$ (T in °K)	Time (h)	Rates × 10^{14} (cc mole^{-1} s^{-1}) R_{N_2}	R_{2a}	R_{3a}	R_{4a}	R_0	$[C_3H_8] \times 10^5$ (mole cc^{-1})	r	q	$\frac{k_1}{k_{3a}^{1/2}} \times 10^4$ (cc mole^{-1} s^{-1})$^{1/2}$
1	3.30	36	24.4	1.13	16.5	—	3.81	4.93	0.042	2.13	8.70
2	3.30	36	18.8	0.96	14.5	—	0.75	4.38	0.040	2.13	8.27
1	2.75	36	22.3	3.86	6.63	0.52	8.36	4.93	0.355	1.87	78.4
1	2.79	36	25.5	3.54	7.68	0.40	11.0	4.93	0.281	1.89	67.6
1	2.75	36	26.7	3.94	7.60	0.48	11.6	4.93	0.316	1.87	78.0
1	2.75	36	24.9	3.94	7.64	0.48	9.74	4.93	0.315	1.87	73.5
2	2.75	36	24.2	3.78	7.84	0.44	9.10	4.38	0.294	1.87	76.2
2	2.75	36	22.1	3.22	5.95	0.44	9.97	4.38	0.330	1.87	85.1
2	2.75	36	16.8	3.01	5.39	0.40	5.68	4.38	0.341	1.87	72.7
1	2.56	36	23.1	3.30	3.22	0.84	13.3	4.93	0.625	1.79	166
2	2.53	36	20.5	3.01	2.73	0.84	11.7	4.38	0.673	1.78	193
2	2.38	36	21.0	2.57	1.57	1.04	13.8	4.38	0.999	1.72	331
1	2.36	36	27.2	3.58	2.29	1.45	17.1	4.93	0.954	1.71	316
1	2.22	36	33.0	5.63	2.97	2.61	17.2	4.93	1.156	1.65	397
2	2.21	36	37.5	7.23	3.82	3.46	17.1	4.38	1.155	1.65	461
1	3.00	36	27.2	2.57	12.9	0.08	8.64	4.93	0.122	1.99	27.7
2	3.06	36	24.6	1.77	15.8	0.04	3.83	4.38	0.068	2.01	16.6
3	3.34	24	33.3	0.42	17.1	—	13.0	3.04	0.015	2.15	6.11
3	3.08	24	16.7	0.45	5.26	—	10.0	3.04	0.052	2.02	16.2
3	2.89	24	23.0	0.57	4.22	0.03	17.3	3.04	0.082	1.94	36.6
3	2.59	20	18.1	0.68	1.66	0.10	15.1	3.04	0.250	1.80	128.6
3	1.98	12	189.0	17.8	10.2	11.1	133.5	3.04	1.065	1.56	1990
4	3.33	36	0.5	nil	nil	nil	—	0.00	—		
4	2.18	36	0.5	0.28	0.03	nil	—	4.93	—		

*Series 1 and 2: cell 238 cm^3, illuminated volume 192 cm^3, 1 lamp; series 3: cell 418 cm^3, illuminated volume 409 cm^3, 2 lamps; series 4: blank runs.

reactions other than combination and disproportionation with each other can be obtained from the mass balance ratio

$$\frac{R_5}{R_6} = \frac{R_{N_2} - (1.41R_{2a} + 2.3R_{3a})}{R_{N_2} - (1.41R_{2a} + 3.38R_{4a})} = M$$

Since $q = r\,R_5/R_6$, one obtains

$$[III] \qquad q = 0.61\frac{R_{2a}}{R_{3a}}M$$

The results are tabulated in Table I. An Arrhenius plot of the data gives a straight line relation corresponding to the equation

$$\log q = -0.011 + 103/T$$

Data obtained from reaction of *n*-propyl radicals with propane are summarized in Table II and the Arrhenius plot is shown in Fig. 1. Least squares treatment gives

$$\log \frac{k_1}{k_{3a}^{1/2}} = 2.60 \pm 0.24 - \frac{7.91 \pm 0.40}{2.3RT} \quad \text{(cc mole}^{-1}\text{ s}^{-1}\text{)}$$

for a 95% confidence limit.

Discussion

In order to derive a value for k_1 one would need to know the value of k_{3a}. The measured value of k_{3a}, reported in the literature (20, 21), exp 15.8 (cc mole^{-1} s^{-1}), however, appears to be too high and cannot be considered reliable. Probably the best one can do is to assume that *n*-propyl radicals recombine with the same rate as ethyl radicals and accept the value for the latter reported by Shepp and Kutschke (22)

$$\log k = 14.2 - (2.0 \pm 1.0)/2.3RT$$

This would lead to a value

$$\log k_1 = 9.7 - 8.9/2.3RT \quad \text{(cc mole}^{-1}\text{ s}^{-1}\text{)}$$

Comparison with the known rate constants of the analogous reactions of the methyl and ethyl radicals; Me + C_3H_8, Me + *n*-C_4H_{10}, and Et + *n*-C_4H_{10}, E_a = 10.2, 9.6, and 11.4 kcal, and log A = 11.87, 11.92, 11.43 (cc mole^{-1} s^{-1}), respectively (1), seems to indicate that our activation energy and A-factor are low with an amount compensating to give approximately the correct rate constant value. Even if allowance is made for the fact that reaction [1] registers the attack of

Can. J. Chem. Downloaded from www.nrcresearchpress.com by 210.87.254.40 on 09/05/12
For personal use only.

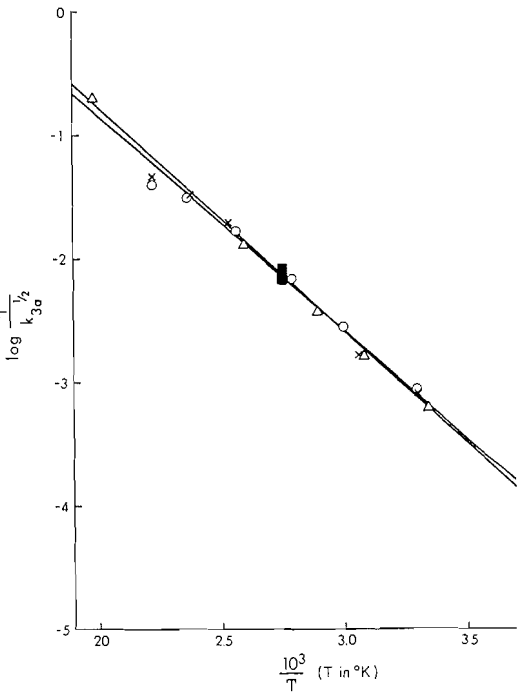

FIG. 1. Arrhenius plot for reaction of *n*-propyl with propane. ○, series 1; ×, series 2; △, series 3. The rectangle represents the mean value of three runs from series 1 and three runs from series 2.

n-propyl radicals only on the secondary hydrogens of propane, the measured activation energy is still about 1 kcal lower than the estimated value of the methyl radical reaction.

As a check on our experimental technique, we have determined the Arrhenius parameters for the hydrogen atom abstraction from azo-*iso*-propane by *i*-propyl radicals. Eight experiments in the temperature range of 27–160 °C gave

$$\log (k_{\text{abstr}}/k_{\text{comb}}^{\frac{1}{2}}) = 4.03 \pm 0.37 - (7.08 \pm 0.61)/2.3RT$$

for a 95% confidence level, which agrees quite well with the literature values of

$$\log (A_{\text{abstr}}/A_{\text{comb}}^{\frac{1}{2}}) = 3.4 \text{ and } 3.5$$

and (5, 13)

$$E_{\text{abstr}} - \tfrac{1}{2}E_{\text{comb}} = 6.5 \text{ and } 6.7 \text{ kcal}$$

A similar study of the abstraction of *n*-propyl from azo-*n*-propane was attempted. However, the temperature range within which reliable data could be obtained for this reaction in our static system was quite narrow due to the low vapor pressure of azo-*n*-propane, and consequently there was a great deal of scatter in the low temperature points. Using six points from the region where the data appeared most reliable, we obtained

$$\log k_{\text{abstr}}/k_{\text{comb}}^{\frac{1}{2}} = 4.8 - 8.0/2.3RT$$

which is consistent with

$$\log (A_{\text{abstr}}/A_{\text{comb}}^{\frac{1}{2}}) = 4.6$$

and

$$E_{\text{abstr}} - \tfrac{1}{2}E_{\text{comb}} = 7.9$$

obtained by Calvert and Kerr (4) in a circulating system.

The most obvious sources of uncertainty in our measurement of k_1 are the processes treated collectively under reactions [5] and [6] which are not directly monitored. These processes include addition and abstraction reactions with propylene and azo-*n*-propane and combination with the resulting radicals. The concentration of propylene should always be very small in the system, and although small quantities of C_9H_{20} hydrocarbons could be detected among the products it is doubtful if radical reactions with propylene are significant. On the other hand, alkyl radicals are known to react very readily with azo-alkanes under the conditions used in this study, and this is undoubtedly the dominant cause of their "disappearance" from the system.

There are two plausible reactions involving the resonance stabilized azo-alkyl radical formed in the abstraction reaction

[7] $n\text{-Pr} + C_3H_7N{=}NC_3H_7 \rightarrow C_3H_8 + CH_3CH_2CH{\cdots}N{\cdots}NC_3H_7$

which are not included in the kinetic treatment; the thermal decomposition and the abstractive attack on propane.

Analogous studies on the reactions of ethyl radicals with azoethane (16) suggest that decomposition of these radicals below 300 °C is unimportant. Also, from a recent study of the pyrolysis of azo-*n*-propane and azo-*iso*-propane, Geiseler and Hoffman (23) have concluded that though reaction [7] is important, the radicals formed in it do not act as chain carriers at temperatures <400 °C.

The abstraction reactions

[8*a*] $CH_3CH_2CH{\cdots}N{\cdots}NC_3H_7 + C_3H_8 \rightarrow$ azo-*n*-propane + *i*-Pr

[8*b*] $\rightarrow$ azo-*n*-propane + *n*-Pr

should have considerable activation energies and the importance of [8*b*] relative to [8*a*] should

Can. J. Chem. Downloaded from www.nrcresearchpress.com by 210.87.254.40 on 09/05/12
For personal use only.

Can. J. Chem. Downloaded from www.nrcresearchpress.com by 210.87.254.40 on 09/05/12
For personal use only.

increase with temperature. Some support for this type of reaction comes from the observation of propanal propylhydrazone among the reaction products. Much of this material may have formed in a heterogeneous reaction, some should have formed through the disproportionation of the azo-alkyl radicals with radicals present in the system, and a small fraction could have arisen by the abstraction reactions

[9a] $CH_3CH_2CH{\cdots}N{=}N{\cdots}C_3H_7 + C_3H_8 \rightarrow CH_3CH_2CH{=}N{-}NHC_3H_7 + i\text{-Pr}$

[9b] $\rightarrow CH_3CH_2CH{=}N{-}NHC_3H_7 + n\text{-Pr}$

The interference by these reactions will tend to be most important under conditions which favor a high rate of abstraction compared to combination. Hence these reactions will be most important in runs with a high value of r, the steady state concentration ratio of isopropyl to n-propyl radicals. We have recalculated the Arrhenius parameters of reaction [1] eliminating the two runs with the highest values of r. Thus, for r less than 1.1, we obtain

$$\log \frac{k_1}{k_{3a}^{1/2}} = 2.83 \pm 0.18 - \frac{(8.25 \pm 0.30)}{2.3RT}$$

for a 95% confidence limit, from which

$$\log k_1 = 9.9 - 9.3/2.3RT \quad (\text{cc mole}^{-1}\ \text{s}^{-1})$$

The activation energy is still 0.6 kcal lower than for the reaction of methyl radicals (1).

Combining the rate parameters with eq. [7] the Arrhenius parameters of the reverse reaction are given by

$$\log k_{1a} = 10.5 - 12.9/2.3RT \quad (\text{cc mole}^{-1}\ \text{s}^{-1})$$

The activation energy for this reaction is 1.3 kcal larger than that measured for methyl radicals.

Acknowledgments

The authors thank the National Research Council of Canada for financial support and Dr. A. M. Hogg for his assistance in the mass spectrometric analyses.

Appendix

Derivation of Expression [II]

$$R_1 = k_1[n\text{-Pr}]\,[C_3H_8] = R_{1a} + R_{2a} + R_{2b} + 2R_{4a} + 2R_{4b} + R_6$$

$$R_{2a} + R_{2b} = 1.41\,R_{2a}$$

$$2(R_{4a} + R_{4b}) = 3.38R_{4a}$$

and

$$k_{1a} = k_1 \exp(0.6 - 3.6/RT)$$

Therefore

$$k_1[n\text{-Pr}]\,[C_3H_8] = k_1 \exp(0.6 - 3.6/RT) \cdot [i\text{-Pr}]\,[C_3H_8] + 1.41R_{2a} + 3.38R_{4a} + R_6$$

Since

$$r = \frac{[i\text{-Pr}]}{[n\text{-Pr}]}$$

$$k_1 = \frac{1.41R_{2a} + 3.38R_{4a} + R_6}{[C_3H_8](1 - r\exp(0.6 - 3.6/RT)[n\text{-Pr}]}$$

R_6 can be expressed in terms of r, R_0, and q, since

$$R_5 + R_6 = 2R_0$$

and

$$R_5 = \frac{q}{r}R_6$$

$$R_6 = \frac{2rR_0}{r+q}$$

Expressing the value of $k_{3a}^{\frac{1}{2}}$ as $R_{3a}^{\frac{1}{2}}/[n\text{-Pr}]$, we obtain for the ratio $k_1/k_{3a}^{\frac{1}{2}}$

$$\frac{1.41R_{2a} + 3.38R_{4a} + \dfrac{2rR_0}{r+q}}{R_{3a}^{1/2}[C_3H_8](1 - r\exp(0.6 - 3.6/RT))} \equiv [II]$$

1. A. F. Trotman-Dickenson. Advan. Free Radical Chem. **1**, 1 (1965).
2. M. H. Jones and E. W. R. Steacie. J. Chem. Phys. **21**, 1018 (1953).
3. H. Cerfontain and K. O. Kutschke. Can. J. Chem. **36**, 344 (1958).
4. J. A. Kerr and J. G. Calvert. J. Amer. Chem. Soc. **83**, 3391 (1961).
5. R. W. Durham and E. W. R. Steacie. Can. J. Chem. **31**, 377 (1953).
6. W. E. Morganroth and J. G. Calvert. J. Amer. Chem. Soc. **88**, 5387 (1966).
7. D. H. Slater, S. S. Collier, and J. G. Calvert. J. Amer. Chem. Soc. **90**, 268 (1968).
8. P. Ausloos and E. W. R. Steacie. Can. J. Chem. **32**, 593 (1954).
9. S. Toby and K. O. Kutschke. Can. J. Chem. **37**, 672 (1959).
10. S. Toby. J. Amer. Chem. Soc. **82**, 3822 (1960).
11. P. Ausloos and E. W. R. Steacie. Bull. Soc. Chim. Belg. **63**, 87 (1954).
12. D. P. Dingledy and J. G. Calvert. J. Amer. Chem. Soc. **85**, 856 (1963).
13. R. H. Riem and K. O. Kutschke. Can. J. Chem. **38**, 2332 (1960).

14. S. S. THOMAS and J. G. CALVERT. J. Amer. Chem. Soc. **84**, 4207 (1962).
15. L. SPIALTER, D. H. O'BRIEN, G. L. UNTEREINER, and W. A. RUSH. J. Org. Chem. **30**, 3278 (1965).
16. O. P. STRAUSZ, R. E. BERKLEY, and H. E. GUNNING. Can. J. Chem. This issue.
17. V. S. STOPSKII, V. B. LEBEDEV, B. V. IOFFE, and A. A. PETROV. Dokl. Akad. Nauk SSSR, **166**, 399 (1966).
18. J. O. TERRY and J. H. FUTRELL. Can. J. Chem. **45**, 2327 (1967).
19. J. G. CALVERT and J. N. PITTS. Photochemistry. John Wiley and Sons, Inc., New York. 1965. Appendix A-3.
20. J. A. KERR and A. F. TROTMAN-DICKENSON. Progr. Reac. Kinet. **1**, 107 (1961).
21. S. G. WHITEWAY and C. R. MASSON. J. Chem. Phys. **25**, 233 (1956).
22. A. SHEPP and K. O. KUTSCHKE. J. Chem. Phys. **26**, 1020 (1957).
23. G. GEISELER and J. HOFFMAN. Z. Phys. Chem. Frankfurt, **57**, 318 (1968).

Can. J. Chem. Downloaded from www.nrcresearchpress.com by 210.87.254.40 on 09/05/12
For personal use only.

Can. J. Chem. Downloaded from www.nrcresearchpress.com by 210.87.254.42 on 09/05/12
For personal use only.

Nuclear magnetic resonance spectral parameters of α,α,α-trifluorotoluene

R. J. KOSTELNIK, M. P. WILLIAMSON, D. E. WISNOSKY, AND S. M. CASTELLANO
Mellon Institute, Carnegie-Mellon University, Pittsburgh, Pennsylvania 15213

Received March 31, 1969

The 60 and 100 MHz proton spectra of α,α,α-trifluorotoluene have been recorded and analyzed in terms of chemical shifts and coupling constants. The results of the analyses are compared and the values of the spectral parameters discussed. The nuclear magnetic resonance spectral data of 2-chloro-5-nitro-α,α,α-trifluorotoluene are also reported.

Canadian Journal of Chemistry, **47**, 3313 (1969)

Introduction

According to standard nomenclature, the nuclear magnetic resonance (n.m.r.) spectrum of α,α,α-trifluorotoluene (benzotrifluoride), **1**, be-

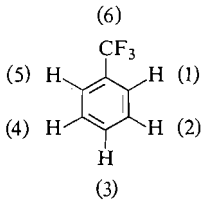

1

longs to the $AA'BB'CX_3$ type, where the labels A, B, and C refer to the *ortho*, *meta*, and *para* protons, and the label X designates a fluorine nucleus. The problems encountered in the iterative analyses of spectra of this type have already been described in a previous study of the n.m.r. spectrum of toluene (1), where a multi-step procedure for the analysis was also proposed and successfully used. We refer to that paper for any more detailed information on the subject and report here the results obtained by the application of the same procedure to the analysis of the proton spectrum of **1**.

Analysis of the Spectra

The complete analysis of the spectrum of benzotrifluoride involved three successive steps

(*a*) First, 60 MHz, CF_3-decoupled spectra of **1** were recorded and readily analyzed using the LAOCN3 computer program (2). The results of the analyses of these spectra of the AA'BB'C type are reported in entries 1 and 7 of Table I for both the neat liquid and a 10% (wt./wt.) solution in CCl_4. The experimental and calculated CF_3-decoupled spectrum of the neat liquid is shown in Fig. 1.

(*b*) In the second step the proton spectrum of 2-chloro-5-nitro-α,α,α-trifluorotoluene[1], **2**, which

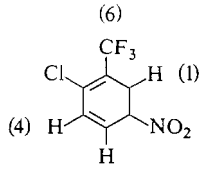

2

belongs to the $ABCX_3$ type, was recorded and analyzed. The resulting spectral parameters are reported in entry 8 of Table I. The analysis of the spectrum of **2** was necessary, since at the time this work was initiated, no reliable values of the long-range CF_3-proton coupling constants had been reported in the literature.

(*c*) The information gathered in (*a*) and (*b*) was then used to initiate the iterative fit of the normal proton spectra of benzotrifluoride. With the aid of the trial calculations, it was possible to dissect the spectrum into two subspectra of the AA'BB'CX type corresponding to the two quantum states ($\pm 1/2$; $\pm 3/2$) of the *z*-component of the total angular momentum of the trifluoromethyl group (1). Each subspectrum was then analyzed independently using the iterative routine of the LAOCN3 program. The results of the complete analyses of the spectra of the neat liquid recorded at 60 and at 100 MHz are reported in entries 2–5 of Table I. For the sake of comparison, the values of the chemical shifts of the 100 MHz spectrum converted to 60 MHz are also presented (in parentheses). The experimental and calculated

[1]The numbering of the magnetic nuclei of **2** corresponds to that used for benzotrifluoride throughout this work and differs from the standard chemical nomenclature.

Can. J. Chem. Downloaded from www.nrcresearchpress.com by 210.87.254.42 on 09/05/12
For personal use only.

TABLE I

Nuclear magnetic resonance spectral parameters of α,α,α-trifluorotoluene and 2-chloro-5-nitrobenzotrifluoride*

Entry number	Remarks	Coupling constant								
		$J(1,2) = J(4,5)$	$J(1,3) = J(3,5)$	$J(1,4) = J(2,5)$	$J(1,5)$	$J(1,6) = J(5,6)$	$J(2,3) = J(3,4)$	$J(2,4)$	$J(2,6) = J(4,6)$	$J(3,6)$
1†	60 MHz, decoupled (neat)	7.935	1.263	0.610	1.977		7.608	1.301		
2†	60 MHz, normal spectrum (neat), spin = 1/2	7.872	1.240	0.645	1.979	−0.710	7.583	1.309	0.808	−0.625
3†	60 MHz, normal spectrum (neat), spin = 3/2	7.939	1.234	0.609	1.991	−0.751	7.573	1.311	0.832	−0.630
4‡	100 MHz, normal spectrum (neat), spin = 1/2	7.907	1.236	0.622	1.972	−0.751	7.589	1.299	0.819	−0.649
5‡	100 MHz, normal spectrum (neat), spin = 3/2	7.900	1.226	0.622	1.984	−0.739	7.573	1.295	0.817	−0.638
6	Mean (neat)	7.911(0.027)	1.240(0.014)	0.622(0.015)	1.985(0.007)	−0.738(0.019)	7.586(0.014)	1.303(0.007)	0.819(0.010)	−0.636(0.010)
7†	60 MHz, decoupled (10% wt./wt.)	7.931	1.239	0.599	1.961		7.551	1.291		
8†	60 MHz, 2-chloro-5-nitrobenzotrifluoride		2.664	0.465		−0.557	8.722		0.657	−0.530

Entry number	Remarks	Chemical shifts*			Root mean square error	Total number of assigned lines	Largest error
		$\nu_1 = \nu_5$	$\nu_2 = \nu_4$	ν_3			
1†	60 MHz, decoupled (neat)	447.107	431.581	435.645	0.029	55	0.086
2†	60 MHz, normal spectrum (neat), spin = 1/2	447.127	431.536	435.639	0.034	120	0.079
3†	60 MHz, normal spectrum (neat), spin = 3/2	447.086	431.555	435.653	0.037	92	0.085
4‡	100 MHz, normal spectrum (neat), spin = 1/2	744.862 (446.917)	718.916 (431.350)	725.717 (435.430)	0.028	130	0.080
5‡	100 MHz normal spectrum (neat), spin = 3/2	744.843 (446.906)	718.935 (431.361)	725.698 (435.419)	0.039	86	0.094
6	Mean (neat)	447.107 (0.020)§ (446.912)(0.006)¶	431.557 (0.022)§ (431.355)(0.005)¶	435.557 (0.007)§ (435.425)(0.006)¶			
7†	60 MHz, decoupled (10% wt./wt.)	453.438	442.705	446.325	0.038	50	0.077
8†	60 MHz, 2-chloro-5-nitrobenzotrifluoride	513.002	464.084	500.933	0.023	36	0.064

*All data in Hz; chemical shifts are referred to TMS as an internal standard.
†Probe temperature of A-60 spectrometer, 36 °C.
‡Probe temperature of HA-100 spectrometer, 32 °C.
§Mean value of the 60 MHz data, entries 1–3.
¶Mean value of the 100 MHz data, entries 4 and 5.

Can. J. Chem. Downloaded from www.nrcresearchpress.com by 210.87.254.42 on 09/05/12
For personal use only.

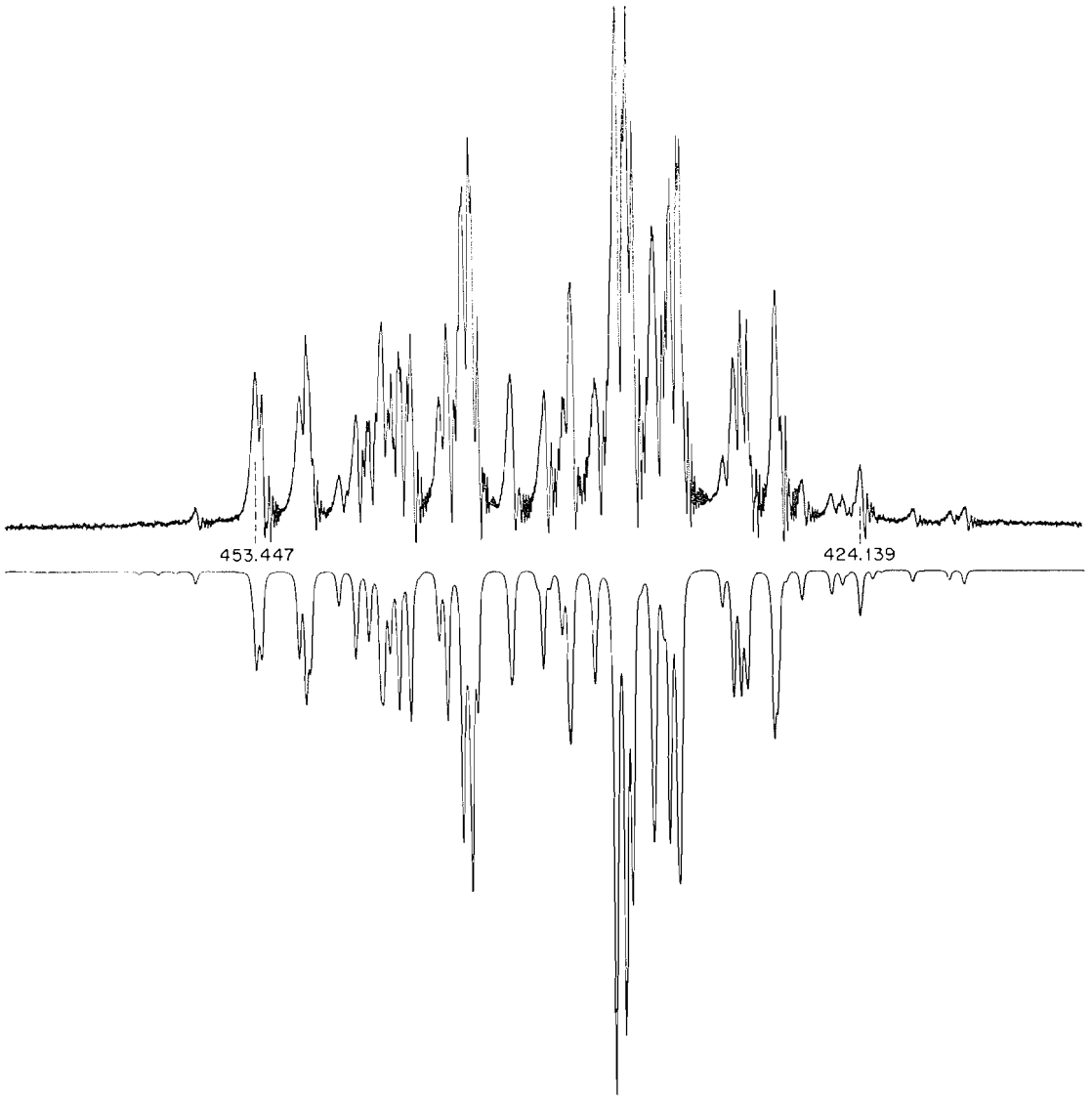

FIG. 1. Experimental and calculated ^{19}F decoupled spectrum of α,α,α-trifluorotoluene at 60 MHz. Frequencies are in Hz from internal TMS.

100 MHz spectrum of benzotrifluoride are shown in Fig. 2.

In Table I all data are reported with three significant decimal digits as obtained directly from the output of the computer. To avoid overcrowding the table, we have not presented the calculated probable errors of the parameters resulting from the fit of each spectrum (2) (or subspectrum) and which, on the average, were always $\leqslant 0.010$ Hz. This value, however, furnishes only a measure of the precision of the experimental determinations but not necessarily their accuracy. The latter can be estimated, in fact, only by comparison of the results of repeated independent measurements. The data in entries 1–5 of Table I are well suited for such a comparison. Their averaged values and standard deviations are reported in entry 6 of Table I. For the coupling constants, the average value (0.013 Hz) of the standard deviations, which were calculated

Can. J. Chem. Downloaded from www.nrcresearchpress.com by 210.87.254.42 on 09/05/12
For personal use only.

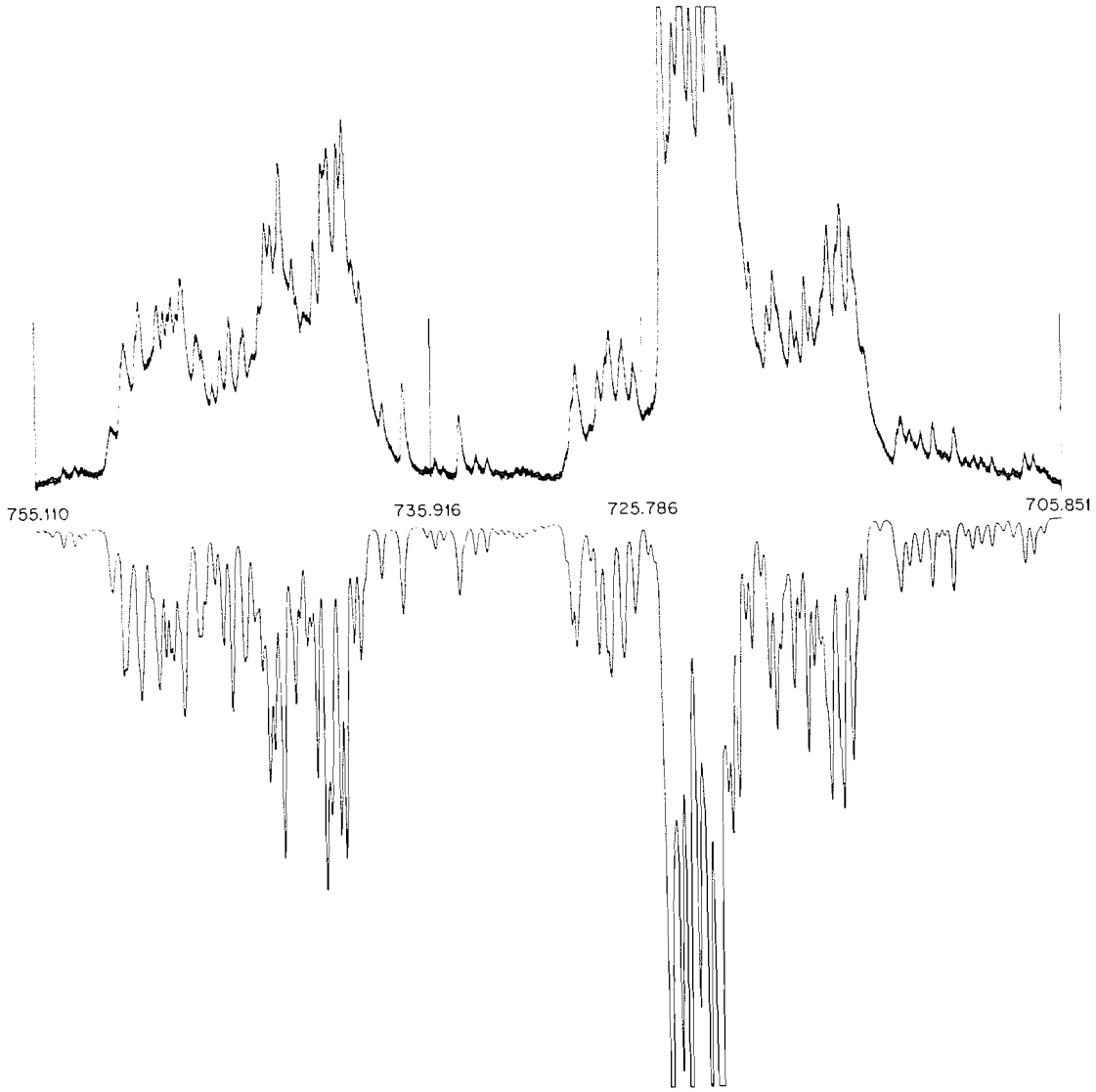

FIG. 2. Experimental and calculated normal spectrum of α,α,α-trifluorotoluene at 100 MHz. Frequencies are in Hz from internal TMS.

using all the data of entries 1–5, indicates that the accuracy of the reported values of the parameters is almost equal to the precision of the fit of the experimental spectra. The same is true for the chemical shifts if the standard deviations of the 60 and 100 MHz results are analyzed independently. A comparison, however, between the averaged values of corresponding parameters of entries 1–3 and of entries 4–5, shows that a systematic deviation of ca. 0.2 Hz is introduced in the measurements by the use of different spectrometers. Since the probe temperatures of the two instruments are sensibly different (see footnotes in Table I), it is most likely that these consistent shifts are entirely due to a temperature effect. We cannot exclude, however, that the observed differences may have, at least in part, some other instrumental origin and, given a choice, we would be inclined to believe that the 60 MHz data are the more reliable.

Can. J. Chem. Downloaded from www.nrcresearchpress.com by 210.87.254.42 on 09/05/12
For personal use only.

Discussion

The values of the coupling constants between the aromatic protons of benzotrifluoride are in agreement with the prediction based on the general trends observed for the variations of these parameters with the electronegativity of the substituents (3), i.e., the values of $J(1,2)$ and $J(1,5)$ are larger, and those of $J(1,3)$ and $J(1,4)$ are slightly smaller than the values of the corresponding parameters of benzene; $J(2,3)$ and $J(2,4)$ remain almost unaffected by the presence of the trifluoromethyl group. Qualitatively these variations are similar to those observed in toluene.

TABLE II

Values (Hz) of J_{cis}, $J(1,2)$, and $J(1,5)$ in some monosubstituted ethylenes and benzenes

Entry	Substituent	J_{cis}	$J(1,2)$	$J(1,5)$
1	—C≡N	11.75*	7.80†	1.78†
2	—CF_3	11.13	7.91	1.96
3	—$C(CH_3)_3$	10.71	7.96‡	2.18‡
4	—CCl_3	10.07	8.11†	2.40†
5	—CH_3	10.02	7.64§	1.86§
6	—H	11.50	7.54‡	1.38‡

*All values of J_{cis} taken from ref. 4.
†Reference 5.
‡Reference 6.
§Reference 1.

Perhaps more significant, however, is the comparison of the data (4–6) reported in Table II which shows the effect of some selected substituents on J_{cis} of monosubstituted ethylenes and on $J(1,2)$ and $J(1,5)$ of the corresponding monosubstituted benzenes. The consistent monotonic trend of the variations of the coupling constants in both series of compounds for the substituents of the first four entries of the table is very remarkable. If this trend is interpreted in terms of the general correlations of the coupling constants with the electronegativity of the substituents, it would appear that the cyano and the trifluoromethyl groups behave as if they were less electronegative than the *t*-butyl and the trichloromethyl groups. This surprising result can be rationalized perhaps by reemphasizing once again the primary role of the hyperconjugative mechanism in determining the overall inductive effect of a substituent (7). Most distressing, however, is the lack of any consistent correlation between the data of the last two entries and those relative to the first four substituents. This is an example of the many inconsistencies found within the framework of the general (but always broadly scattered) correlations between the values of the coupling constants and the electronegativity of the substituents and constitutes a warning against overextended generalizations, particularly if based on a limited number of experimental data.

The signs and values of the long-range coupling constants between the trifluoromethyl group and the aromatic protons are also of some interest. In the trial calculations of the spectrum of **2** the signs of $J(1,6)$ and $J(4,6)$ were chosen equal to those of the corresponding parameters of benzoyl fluoride and the sign of $J(3,6)$ was then directly obtained from the complete analysis of the spectrum. The same sign sequence has been obtained by Blears, Danyluk, and Schaefer (8) from "tickling" experiments on the proton spectrum of 2-amino-5-bromobenzotrifluoride, and it is identical to that found in toluene (1). For the sake of comparison, the values of the long-range coupling constants of benzaldehyde, toluene, benzoyl fluoride, and benzotrifluoride have been summarized in Table III. Since the coupling between the methyl (or the trifluoromethyl) group and the *ortho* and *para* aromatic protons is thought to occur primarily through a $\sigma-\pi$ spin delocalization (and/or polarization) mechanism (8), the near identity of the values of $J(1,6)$ and $J(3,6)$ found in toluene and in benzotrifluoride seems to suggest that the hyperconjugation of the CF_3 group with the aromatic ring is, if not equal, at least comparable to that of the CH_3 group[2]. However, the value of $J(2,6)$ in **1** is more than twice as large as the value of the corresponding parameter in toluene. This observation has already been reported by Blears *et al.* (8), who rationalized the experimental results by postulating for **1** larger (as compared with the corresponding ones in toluene) positive σ contributions to $J(2,6)$ and possibly to $J(1,6)$ also. It is, however, not clear from the text why a σ contribution to $J(1,6)$ should be invoked at all. On the basis of the data in Table III, it would appear that the above

[2]It should be pointed out, however, that the CH_3 and CF_3 groups belong to different substituent classes (7): $+I^+$ and $-I^-$, respectively. The shifts (relative to benzene) of the resonances of all the aromatic protons toward higher fields in toluene (1) and toward lower fields in benzotrifluoride indicate, in fact, that the π-electron charge redistributions induced in the phenyl ring by the two groups are almost complementary and in satisfactory qualitative agreement with those expected for substituents of the above classes (7).

TABLE III

Values (Hz) of the long-range coupling constants of benzaldehyde, toluene, benzoyl fluoride, and α,α,α-trifluorotoluene*

Compound	J values		
	$J(1,6) = J(5,6)$	$J(2,6) = J(4,6)$	$J(3,6)$
$C_6H_5\overset{O}{\overset{\|}{C}}H$†	−0.10	0.38	(−0.03?)
$C_6H_5CH_3$‡	−0.75	0.36	−0.62
$C_6H_5\overset{O}{\overset{\|}{C}}F$†	−0.60	1.33	(−0.02?)
$C_6H_5CF_3$	−0.74	0.82	−0.64

*The label 6 designates the nuclei in italics.
†Reference 5.
‡Reference 1.

assumptions are only partially correct. To the extent, in fact, to which the values of $J(1,6)$, $J(2,6)$, and $J(3,6)$ of benzaldehyde and benzoyl fluoride are indicative of the σ contribution to the long-range coupling, and the almost zero value of $J(3,6)$ in both compounds strongly supports this preposition, it would appear that the latter is indeed larger for the fluorinated compound but that it is positive in the case of $J(2,6)$ and negative in the case of $J(1,6)$. Furthermore, if it is assumed (8) that the σ–π contribution to the long-range coupling is of the same order of magnitude for both $J(1,6)$ and $J(3,6)$, it follows that by the loss of the coplanar conformation characteristic of the carbonyl compounds, the σ contribution to $J(1,6)$ is almost completely removed while that to $J(2,6)$ remains appreciably larger in benzotrifluoride than in toluene. Finally, it is worth reporting that using the additivity relationships of the substituent effects (6) and the values of the spectral parameters of nitrobenzene (9), chlorobenzene (10), and α,α,α-trifluorotoluene, the following values of the proton–proton coupling constants of **2** are obtained: $J(1,3) = 2.580$, $J(1,4) = 0.405$, and $J(2,3) = 7.899$. The agreement between the calculated and experimental values is somewhat less satisfactory than that obtained in other cases (1). Also, the values of the long-range coupling constants of **2** are sensibly different than those of the corresponding parameters of **1**. Both of these results may be indicative of steric (6) and/or mesomeric interactions between the substituents of **2**.

Experimental

All chemicals were of commercial origin (Eastman Organic Chemicals and Aldrich Chemical Co.). The samples of benzotrifluoride and of 2-chloro-5-nitrobenzotrifluoride were distilled, degassed on a vacuum line, and sealed in standard 5 mm NMR tubes after the addition of 3% tetramethylsilane (TMS).

The 100 MHz spectra were recorded on a Varian HA-100 spectrometer which was frequency swept in the HA mode. Two 50 Hz sweep width spectra were recorded for each sweep direction of the magnetic field at a sweep rate of 0.02 Hz/s. Because of the slight nonlinearity of the recorder, the spectra were calibrated by drawing markers approximately every 10 Hz and counting separately the frequencies of the locking oscillator and of the sweep oscillator.

The 60 MHz spectra were obtained on a Varian A-60 spectrometer. Also in this case two 50 Hz sweep width spectra were recorded for each sweep direction, the sweep rate being 0.10 Hz/s. The spectra were calibrated by the standard sideband technique using a Hewlett-Packard 261-A pushbutton oscillator monitored by an Anadex CF-200R counter-timer. The CF_3-decoupled spectra were obtained using an NMR Specialties heteronuclear decoupler (SD-60B).

Experimental line frequencies used in the analysis were the average of four measurements with average standard deviations ≤ 0.025 Hz.

Acknowledgment

This work was performed using, in part, the NMR Facility for Biomedical Studies supported by Grant FR 00292 from the National Institutes of Health.

1. M. P. Williamson, R. J. Kostelnik, and S. M. Castellano. J. Chem. Phys. **49**, 2218 (1968).
2. S. Castellano and A. A. Bothner-By. J. Chem. Phys. **41**, 3863 (1964); LAOCN3, Mellon Institute, Pittsburgh, Pa., 1966.
3. S. Castellano and C. Sun. J. Amer. Chem. Soc. **88**, 4741 (1966).
4. A. A. Bothner-By. Advan. Magn. Resonance, **1**, 195 (1965), and references therein.
5. S. Castellano and R. Kostelnik. Unpublished results.
6. S. Castellano and R. Kostelnik. Tetrahedron Lett. **51**, 5211 (1967).
7. J. A. Pople and M. Gordon. J. Amer. Chem. Soc. **89**, 4253 (1967).
8. D. J. Blears, S. S. Danyluk, and T. Schaefer. Can. J. Chem. **46**, 652 (1968), and references therein.
9. S. Castellano, C. Sun, and R. Kostelnik. Tetrahedron Lett. **51**, 5205 (1967).
10. S. Castellano, R. Kostelnik, and C. Sun. Tetrahedron Lett. **46**, 4635 (1967).

Can. J. Chem. Downloaded from www.nrcresearchpress.com by 210.87.254.42 on 09/05/12
For personal use only.

Can. J. Chem. Downloaded from www.nrcresearchpress.com by 210.87.254.40 on 09/05/12
For personal use only.

Etude des bandes fondamentale ν_1 et première harmonique $2\nu_1$ des haloformes CHF_3, $CHCl_3$ et $CHBr_3$ à l'état gazeux

INGA ROSSI, MM. NGUYEN-VAN-THANH ET CLAUDE HAEUSLER[1]

Laboratoire d'Infrarouge, Chimie Physique, Faculté des Sciences de Paris, Bâtiment 350.(91)-*Orsay, France*

Reçu le 2 avril 1969

Certaines constantes de vibration–rotation des bandes ν_1(CH) et $2\nu_1$(CH) des molécules CHF_3, $CHCl_3$ et $CHBr_3$ à l'état gazeux ont été déterminées. Les mesures d'intensité de ces bandes ont été effectuées et des anomalies observées dans certaines de ces bandes.

Some rotational and vibrational constants in the ν_1(CH) and $2\nu_1$(CH) bands of gaseous CHF_3, $CHCl_3$, and $CHBr_3$ have been determined. Intensity measurements of these bands are obtained and perturbations in some bands of haloforms are pointed out.

Canadian Journal of Chemistry, 47, 3319 (1969)

Introduction

Dans le cadre général de travaux consacrés à l'étude des interactions moléculaires entre soluté et solvant, nous avons été conduits à analyser le spectre d'absorption infrarouge (i.r.) de molécules de soluté, d'une part à l'état gazeux et d'autre part à l'état dissous. En effet, les théories relatives aux effets de solvant relient les intensités intégrées $\mathscr{A}_{gaz}$ et $\mathscr{A}_{solution}$ et les centres de bandes ν^0_{gaz} et $\nu^0_{solution}$.

Plus précisément dans le présent travail, nous nous proposons d'analyser les bandes fondamentales ν_1 et première harmonique $2\nu_1$ des haloformes CHF_3, $CHCl_3$ et $CHBr_3$ à l'état gazeux, en utilisant les spectromètres de type Pfund et Czerny dont les performances et le système d'étalonnage ont été décrits antérieurement (1, 2).

La bande $2\nu_1$ des molécules CHF_3 et $CHCl_3$ a été analysée en 1953 par Wiggins et coll. (3). Anttila (4) a récemment étudié plusieurs bandes d'absorption i.r. de la molécule $CHCl_3$.

Par ailleurs, les mesures d'intensité des bandes ν_1 et $2\nu_1$ des haloformes ont été effectuées à l'aide de la méthode de Wilson et Wells par Robinson et coll. (5).

L'analyse des bandes ν_1 et $2\nu_1$ des haloformes à l'état dissous fera l'objet d'une publication ultérieure.

Rappels Théoriques

Analyse vibrationnelle et rotationnelle des bandes ν_1 et $2\nu_1$

Nous rappelons que la vibration $\nu_1(A_1)$ totalement symétrique correspond essentiellement à la vibration C—H de valence située vers 3.3 μ (6). Ce qui signifie que pratiquement toute l'énergie de vibration est localisée dans la vibration de la liaison C—H.

L'énergie totale de vibration–rotation d'un rotateur symétrique, pour un niveau vibrationnel non dégénéré, s'écrit

$$E_t = E_v + E_r$$

où l'énergie de vibration E_v et celle de rotation E_r sont données par

$$[1] \quad \frac{E_v}{hc} = \sum_{s=1}^{6} \omega_s\left(v_s + \frac{g_s}{2}\right) + \sum_{\substack{s,s'=1 \\ (s'\geq s)}}^{6} x_{ss'}\left(v_s + \frac{g_s}{2}\right)\left(v_{s'} + \frac{g_{s'}}{2}\right)$$

et

$$[2] \quad \frac{E_r}{hc} = B_v[J(J+1) - K^2] + A_vK^2 - D_JJ^2(J+1)^2 - D_{JK}J(J+1)K^2 - D_KK^4$$

Les nombres d'onde des raies $\nu_{m,K}^{P,R}$ des branches P et R d'une bande parallèle peuvent se mettre sous la forme suivante

$$[3] \quad \nu_{m,K}^{P,R} = a_0 + a_1m + a_2m^2 + a_3m^3$$

avec

$m = -J$ pour la branche P

$(\Delta|K| = 0, \Delta J = -1)$

$m = J + 1$ pour la branche R

$(\Delta|K| = 0, \Delta J = +1)$

et

$$a_0 = \nu^0 + (A' - B') - (A'' - B'')$$

$$a_1 = B' + B'' - D_{JK}K^2$$

[1]L'adresse présente: Laboratoire de Chimie Physique Moléculaire, Faculté des Sciences de Rennes.

$$a_2 = B' - B''$$
$$a_3 = -4D_J$$

Ces dernières expressions sont obtenues en supposant que les constantes de distorsion centrifuge D_J, D_{JK} et D_K sont les mêmes pour les niveaux vibrationnels d'arrivée (′) et de départ (″) de la transition considérée.

Les constantes A_v et B_v sont reliées à celles relatives à l'équilibre A_e et B_e, par les relations

$$[4] \qquad B_v = B_e - \sum_{s=1}^{6} \beta_s\left(v_s + \frac{g_s}{2}\right)$$

$$[5] \qquad A_v = A_e - \sum_{s=1}^{6} \alpha_s\left(v_s + \frac{g_s}{2}\right)$$

Les constantes β_1, ${\omega_1}^0$ et x_{11} s'obtiennent à partir des relations [1] et [4]

$$2\beta_1 = -(B' - B'')$$

$$[6] \qquad {\omega_1}^0 = \frac{4({\nu_1}^0) - (2{\nu_1}^0)}{2}$$

$$x_{11} = \frac{(2{\nu_1}^0) - 2({\nu_1}^0)}{2}$$

où les centres de bandes $({\nu_1}^0)$ et $(2{\nu_1}^0)$ sont définis par

$${\nu_1}^0 = {\omega_1}^0 + x_{11}$$

et

$$2{\nu_1}^0 = 2{\omega_1}^0 + 4x_{11}$$

avec

$${\omega_1}^0 = \omega_1 + x_{11}$$

Mesure d'intensité des bandes

D'après la loi de Lambert, l'intensité lumineuse transmise par un échantillon gazeux $I_t(\nu)$ s'exprime en fonction de l'intensité incidente $I_0(\nu)$ par

$$[7] \qquad I_t(\nu) = I_0(\nu) \exp\,[-k(\nu)l]$$

La variation du coefficient d'absorption $k(\nu)$ s'écrit sous la forme bien connue de Lorentz quand les causes d'élargissement des raies sont dues aux collisions moléculaires. La largeur à mi-hauteur de cette courbe est désignée par 2γ.

Nous définirons la transmission $\eta(\nu)$ par la relation

$$[8] \qquad \eta(\nu) = \frac{I_t(\nu)}{I_0(\nu)} = \exp\,[-k(\nu)l]$$

et le coefficient d'absorption intégré $\mathscr{C}$ d'une raie par l'expression

$$[9] \qquad \mathscr{C} = \int_{\nu_1}^{\nu_2} k(\nu)\,d\nu = \frac{1}{l}\int_{\nu_1}^{\nu_2} \ln \frac{I_0(\nu)}{I_t(\nu)}\,d\nu$$

Dans nos conditions expérimentales $\mathscr{C}$ est proportionnel à la pression $\mathscr{P}$ de sorte que nous pouvons écrire

$$\mathscr{C} = \mathscr{A}.\mathscr{P}$$

ce qui n'est pas nécessairement valable pour les pressions très élevées. La grandeur $\mathscr{A}$, intensité intégrée, (c'est-à-dire le coefficient d'absorption intégré rapporté à l'unité de pression) que nous nous proposons d'évaluer, s'écrit donc

$$[10] \qquad \mathscr{A} = \frac{1}{\mathscr{P}l}\int_{\nu_1}^{\nu_2} \ln \frac{I_0(\nu)}{I_t(\nu)}\,d\nu$$

ν_1 et ν_2 désignent les nombres d'onde qui délimitent l'étendue de la raie d'absorption. L'expression précédente suppose en particulier que la diffusion de la lumière par le gaz est négligeable.

L'intensité transmise observée $I_t'(\nu)$ est différente de $I_t(\nu)$ du fait des déformations qu'introduit le spectromètre; $I_t'(\nu)$ est donnée par

$$[11] \qquad I_t'(\nu_i) = \int_{\nu_i-\Delta\nu}^{\nu_i+\Delta\nu} D(\nu - \nu_i) I_t(\nu)\,d\nu$$

où $D(\nu - \nu_i)$ est la fonction d'appareil de largeur à la base $2\Delta\nu$ et ν_i désigne le nombre d'onde qui correspond au maximum de la fonction D. (Dans le cas d'une fonction d'appareil gaussienne, $2\Delta\nu$ devient infini, et dans le cas d'une fonction d'appareil triangulaire, $2\Delta\nu$ vaut le double de la largeur à mi-hauteur.)

L'expérience nous permet d'atteindre la valeur de la transmission apparente

$$\eta'(\nu_i) = \frac{I_t'(\nu_i)}{I_0'(\nu_i)} = \frac{\displaystyle\int_{\nu_i-\Delta\nu}^{\nu_i+\Delta\nu} D(\nu - \nu_i) I_t(\nu)\,d\nu}{\displaystyle\int_{\nu_i-\Delta\nu}^{\nu_i+\Delta\nu} D(\nu - \nu_i) I_0(\nu)\,d\nu}$$

Considérons maintenant la transmission apparente $\eta'(\nu)$. Si l'intensité de la lumière incidente $I_0(\nu)$ est constante dans l'intervalle spectral $2\Delta\nu$, l'intégrale s'écrit

$$\eta'(\nu_i) = \frac{\displaystyle\int_{\nu_i-\Delta\nu}^{\nu_i+\Delta\nu} D(\nu - \nu_i) \exp\,[-k(\nu)l]\,d\nu}{\displaystyle\int_{\nu_i-\Delta\nu}^{\nu_i+\Delta\nu} D(\nu - \nu_i)\,d\nu}$$

Can. J. Chem. Downloaded from www.nrcresearchpress.com by 210.87.254.40 on 09/05/12
For personal use only.

Can. J. Chem. Downloaded from www.nrcresearchpress.com by 210.87.254.40 on 09/05/12
For personal use only.

Kostkowski et Bass (7) ont évalué numériquement cette intégrale pour une fonction d'appareil de Gauss, et Montigny (8) l'a réalisé dans le cas d'une fonction d'appareil triangle.

Afin d'obtenir le coefficient d'absorption intégré $\mathscr{C}$, des courbes facilement utilisables expriment la correction qu'il faut apporter à la valeur de $\mathscr{C}'$, mesuré directement sur l'enregistrement d'une raie, en fonction des rapports $I_t(\nu)/I_0(\nu)$ et $\delta\nu/2\gamma$. Dans ce dernier rapport, $\delta\nu$ représente la largeur à mi-hauteur de la fonction d'appareil.

Précisons que la quantité $\mathscr{C}'$ est obtenue en déterminant directement sur l'enregistrement d'une raie la transmission $\eta'(\nu)$, qui permet ensuite d'atteindre la valeur du coefficient d'absorption apparente $k'(\nu)$ et par conséquent celle de

$$\mathscr{C}' = \int_{\nu_1}^{\nu_2} k'(\nu)\, d\nu$$

Dans le présent travail, nous nous proposons de déterminer la quantité $\mathscr{A}_i = \mathscr{C}_i/\mathscr{P}$ des raies d'absorption relatives aux bandes ν_1 et $2\nu_1$ des haloformes à l'état gazeux. Nous connaissons avec suffisamment de précision la fonction d'appareil D des spectromètres utilisés.

Pour le spectromètre du type Czerny utilisé à 1.7 μ, la fonction D est gaussienne. La largeur à mi-hauteur $\delta\nu$ (déterminée en enregistrant une raie d'absorption de largeur très faible) est de 0.15 cm^{-1}, ce qui fournit pour les haloformes un rapport $\delta\nu/2\gamma$ de l'ordre de 0.5, si nous adoptons 0.1 à 0.2 cm^{-1} par atmosphère pour ordre de grandeur de la demi-largeur à mi-hauteur collisionnelle des raies. Par conséquent, pour une raie la correction que l'on doit apporter à $\mathscr{C}_i'$ (donc à $\mathscr{A}_i'$) mesuré directement, est alors selon Kostkowski et Bass de 5% par défaut. Or l'imprécision des mesures due au seul choix de la ligne de base peut atteindre facilement cet ordre de grandeur.

Par ailleurs, on admet que lorsqu'un spectre d'absorption de vibration–rotation, se présente comme un ensemble de raies bien séparées, l'évaluation de $\mathscr{A}$ pour une bande entière s'obtient en faisant la somme des valeurs de $\mathscr{A}_i$ relatives à chaque raie. A la limite pour des raies rapprochées, explorées pour des pressions de gaz suffisamment élevées, le contour d'une bande ne manifeste plus la présence d'une structure de raies. La valeur de $\mathscr{A}$ pour la bande entière peut alors se mesurer directement sur l'enregistrement.

La fonction d'appareil d'un spectromètre résolutif, même si elle est relativement large par rapport à une raie isolée, peut alors être considérée comme étroite par rapport au contour global de la bande dans laquelle la structure rotationnelle a disparu. De sorte que, valablement on peut espérer obtenir par mesure directe une erreur relative de mesure plus faible sur cette bande totale que celle obtenue lors d'une mesure sur une raie isolée en ne considérant que l'effet de déformation $d\hat{u}$ à la fonction d'appareil. On retrouve alors un problème semblable à celui concernant la mesure de l'intensité d'une bande d'absorption d'un liquide avec un spectromètre résolutif (1). Dans les conditions de nos mesures, effectuées sur les bandes ν_1 et $2\nu_1$ des haloformes, nous nous approchons de ce cas limite.

Afin d'évaluer par l'expérience, l'influence de la largeur $\delta\nu$ sur la valeur de $\mathscr{A}$ mesurée directement sur le spectre, nous avons effectué deux mesures d'intensité de la bande $2\nu_1$ du fluoroforme gazeux en utilisant deux spectromètres ayant des fonctions d'appareil de largeur très différente. Dans un cas favorable à la mesure de $\mathscr{A}$, nous avons utilisé le spectromètre du type Czerny, où $\delta\nu$ est égal à 0.15 cm^{-1} à 1.7 μ (la fonction d'appareil D étant gaussienne). Dans un autre cas, défavorable, nous avons utilisé le spectromètre du type Pfund, pour lequel $\delta\nu$ est égal à 1.5 cm^{-1} à 1.7 μ (D étant une fonction triangle). Les deux mesures directes de $\mathscr{A}$ ne diffèrent que de quelques %. L'influence de la valeur de $\delta\nu$ sur celle de $\mathscr{A}$ est donc faible dans les conditions particulières de cette mesure (pression du gaz 760 Torr).

En adoptant des conditions expérimentales (essentiellement pression suffisamment élevée) favorables, nous pouvons appliquer la méthode directe pour la mesure de l'intensité $\mathscr{A}$ des bandes (CH) des molécules CHF_3, $CHCl_3$ et $CHBr_3$.

Nous estimons l'imprécision de mesure sur $\mathscr{A}$ de l'ordre de 8%. Nous exprimons les valeurs de $\mathscr{A}$ en (cm^{-2} atm^{-1}).

Résultats Expérimentaux

Constantes de vibration–rotation des haloformes

Les Figs. 1–3 représentent les spectres de vibration–rotation de la bande $2\nu_1$ des haloformes CHF_3, $CHCl_3$ et $CHBr_3$, obtenus à l'aide du spectromètre du type Czerny vers 1.7 μ.

Considérons la Fig. 1 relative à la molécule CHF_3. Dans les branches P et R de la bande $2\nu_1$ une structure fine en J a pu être observée, mais les raies ne sont pas

Can. J. Chem. Downloaded from www.nrcresearchpress.com by 210.87.254.40 on 09/05/12
For personal use only.

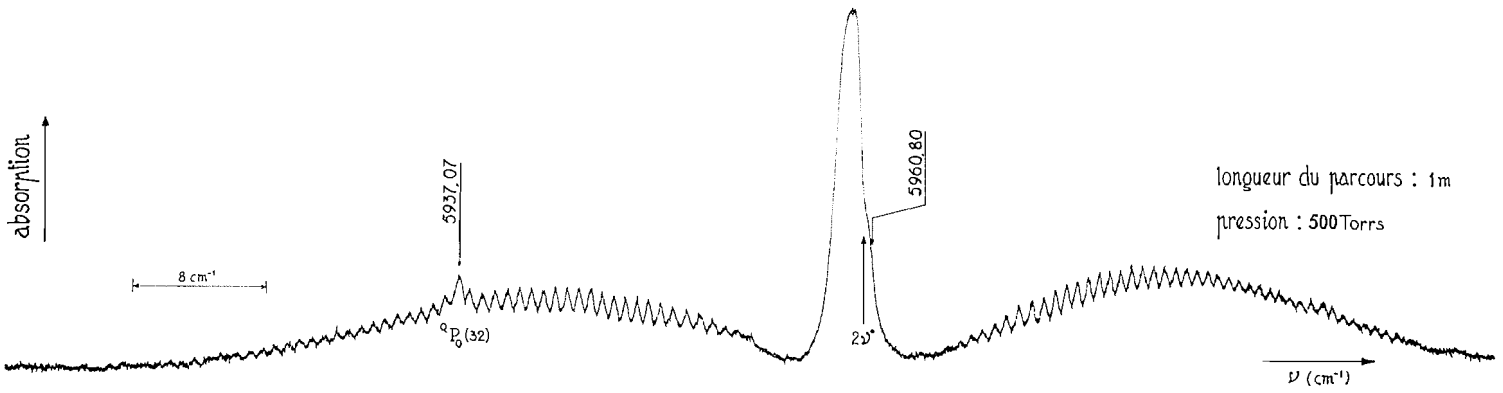

FIG. 1. Spectre de vibration–rotation de la bande $2\nu_1$ de CHF_3 à 1.7 μ.

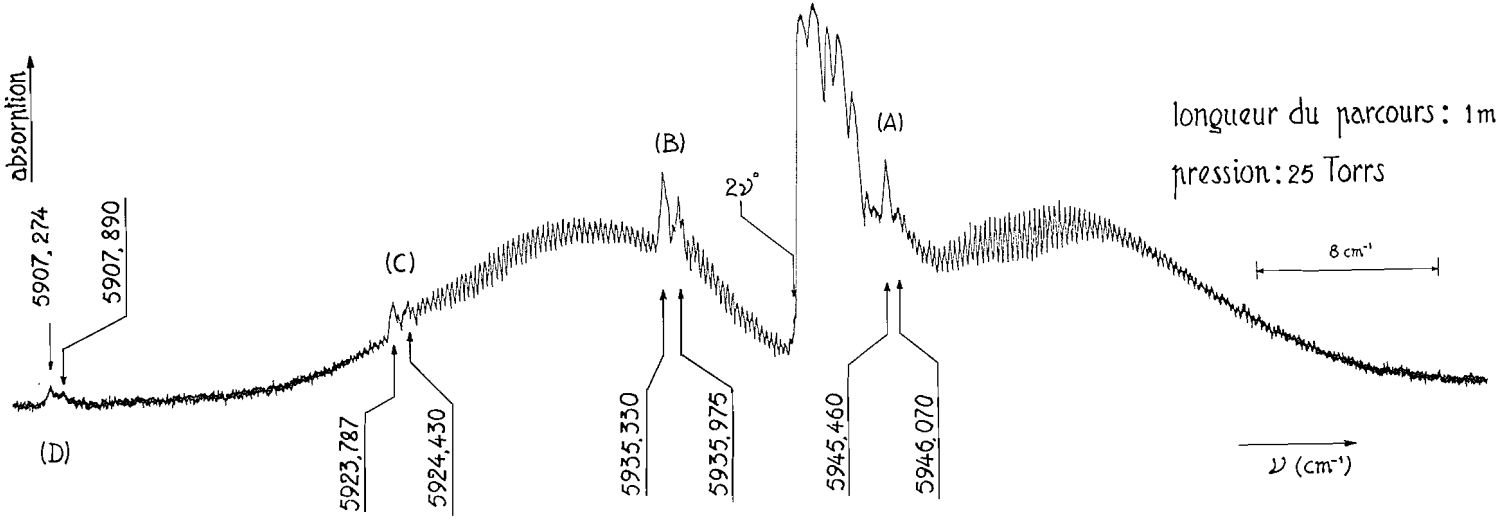

FIG. 2. Spectre de vibration–rotation de la bande $2\nu_1$ de $CHCl_3$ à 1.7 μ.

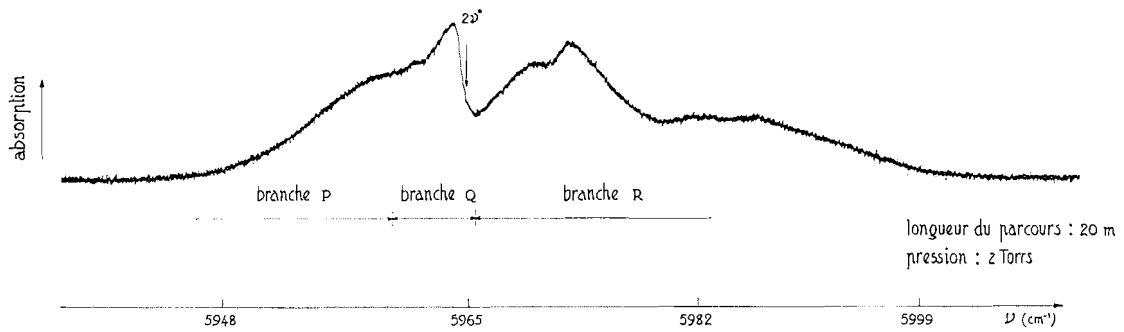

FIG. 3. Spectre de vibration–rotation de la bande $2\nu_1$ de $CHBr_3$ à 1.7 μ.

résolues en K. Les sous-bandes $K = 0$ et $K = 3q$ (q étant un entier) sont théoriquement les plus intenses. En première approximation, nous avons attribué, à la sous-bande $K = 0$, les maximums principaux de la structure observée. On introduit ainsi dans la détermination du nombre d'onde une erreur systématique qui est de l'ordre de l'erreur due au pointé (0.01 cm^{-1}).

La numérotation des branches P et R n'est pas évidente. Nous avons pointé séparément les deux branches. D'après l'aspect de la branche Q (sur un enregistrement à vitesse très lente) dont seule l'enveloppe est observable, on peut prévoir que, (*a*) le centre de bande $2\nu_1^0$ est situé au pied de la branche Q, du côté des nombres d'onde croissants, (*b*) le terme $(A' - B') - (A'' - B'')$ est négatif.

En tenant compte de ces remarques, une numérotation cohérente des branches P et R a été choisie pour définir les nombres d'onde des raies

$$\nu_m^{P,R} = 5959.483 + 0.6905m - 367 \times 10^{-6}m^2 - 16 \times 10^{-7}m^3$$

avec $m = -J$ (branche P), et $m = J + 1$ (branche R). Pour des valeurs de J inférieures à 13, aucune structure fine n'a pu être mise en évidence.

L'existence des bandes étrangères à la bande $2\nu_1$ du fluoroforme se traduit dans le spectre par une anomalie des intensités des raies dans les branches P et Q à $\nu = 5937.07\ cm^{-1}$ (raie P_{32} anormalement large et intense), $\nu = 5960.80\ cm^{-1}$ (raie dans la branche Q).

Les nombres d'onde mesurés, rapportés au vide, sont rassemblés dans le Tableau I. Une méthode des moindres carrés appliqués à la relation [6] donne les valeurs des constantes $2\nu_1^0$, $(B' + B'')$, $(B' - B'')$ et D_J.

La valeur obtenue pour la constante de distorsion D_J est probablement trop élevée, étant donné les simplifications effectuées dans l'expression des nombres d'onde $\nu_m^{P,R}$.

Les valeurs des constantes β_1, ω_1^0, x_{11}, B', B'' et D_J sont relatées dans le Tableau III.

La valeur du centre de bande ν_1^0 est égale à (3034.8 ± 0.2) cm^{-1}, d'après l'enregistrement obtenu à l'aide du spectromètre du type Pfund. La Fig. 4 représente la courbe $k'(\nu)l$ en fonction de ν, déterminée à partir de l'enregistrement.

Considérons maintenant la Fig. 2 relative à la molécule $CHCl_3$. Comme dans le cas du fluoroforme, les branches P et R de la bande $2\nu_1$ du chloroforme présentent une structure fine résolue en J et non en K. En adoptant la numérotation en J de Wiggins et coll. (3), on observe un recouvrement des raies $^QR_K(J)$ par la branche Q pour des valeurs du nombre quantique J inférieures à 20.

Dans la branche Q, sept raies ont été observées (cf. Tableau II). On remarque que, (*a*) l'alternance ternaire

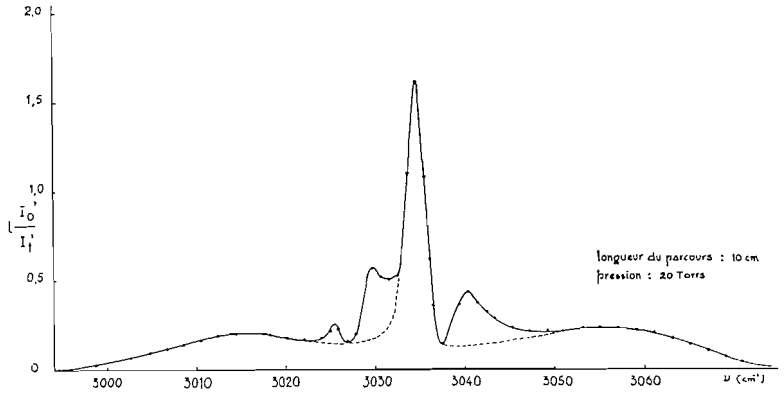

FIG. 4. Bande ν_1 de CHF_3; courbe $k(\nu)l = f(\nu)$.

Can. J. Chem. Downloaded from www.nrcresearchpress.com by 210.87.254.40 on 09/05/12
For personal use only.

Can. J. Chem. Downloaded from www.nrcresearchpress.com by 210.87.254.40 on 09/05/12
For personal use only.

TABLEAU I

Bande $2\nu_1$ de CHF_3 à 1.7 μ*

m	ν_{obs}	ν_{calc}†	$\Delta\nu = \nu_{calc} - \nu_{obs}$
−36	5934.240	5934.224	−0.016
−35	34.919	34.935	+0.016
−34	35.642	35.645	+0.003
−32	37.068	37.064	−0.004
−31	37.767	37.773	+0.006
−30	38.478	38.481	+0.003
−29	39.202	39.189	−0.013
−28	39.894	39.897	+0.003
−27	40.610	40.604	−0.006
−26	41.310	41.311	+0.001
−25	42.021	42.017	−0.004
−24	42.728	42.723	−0.005
−23	43.417	43.428	+0.011
−22	44.116	44.132	+0.016
−21	44.840	44.836	−0.004
−20	45.529	45.540	+0.011
−19	46.256	46.243	−0.013
−18	46.942	46.945	+0.003
−17	47.657	47.647	−0.010
−16	48.337	48.349	+0.012
−15	49.054	49.049	−0.005
−13	50.453	50.449	−0.004
+13	68.413	68.394	−0.019
+14	69.075	69.074	−0.001
+15	69.744	69.752	+0.008
+16	70.438	70.430	−0.008
+17	71.101	71.107	+0.006
+18	71.780	71.784	+0.004
+19	72.465	72.459	−0.006
+20	73.123	73.133	+0.010
+21	73.801	73.807	+0.006
+22	74.478	74.479	+0.001
+23	75.162	75.151	−0.011
+24	75.825	75.821	−0.004
+25	76.479	76.491	+0.012
+26	77.144	77.160	+0.016
+27	77.815	77.828	+0.013
+28	78.507	78.494	−0.013
+29	79.161	79.160	−0.001
+30	79.838	79.825	−0.013
+32	81.165	81.151	−0.014
+33	81.812	81.813	+0.001
+34	82.462	82.473	+0.011
+35	83.124	83.133	+0.009
+36	83.801	83.792	−0.009

*Les nombres d'onde sont rapportés au vide et exprimés en cm^{-1}.
†$\nu_{calc} = 5959.483 + 0.6905\,m - 367 \times 10^{-6}\,m^2 - 16 \times 10^{-7}\,m^3$.

des intensités des raies n'est pas respectée, (*b*) les écarts $\Delta\nu = {}^{Q}Q_K(J) - {}^{Q}Q_{K-1}(J)$ ne suivent pas une loi linéaire en K et (*c*) le terme $(A' - B') - (A'' - B'')$ est positif.

Ceci rend difficile une numérotation cohérente en K des raies ${}^{Q}Q_K(J)$. (La branche Q de la bande fondamentale ν_1 obtenue à l'aide d'un spectromètre S.I.S.A.M.[1] vers 3033 cm^{-1} montre aussi une structure complexe en K et le terme $(A' - B') - (A'' - B'')$ correspondant est positif.)

Dans les branches P et R un dédoublement des "bandes

[1]Nous tenons à remercier Mme M. Morillon, Maître-Assistant et M. G. Graner, Maître de Recherches au CNRS, pour la réalisation de cet enregistrement.

TABLEAU II

Bande $2\nu_1$ de $CHCl_3$ à 1.7 μ

Branches		Nombre d'onde ν (cm^{-1})	Ecarts $\Delta\nu$ (cm^{-1})
Dédoublement des bandes étrangères dans les branches P et R	P	5907.274	0.616
		5907.890	
		5923.787	0.643
		5924.430	
		5935.330	0.645
		5935.975	
	R	5945.460	0.610
		5946.070	
Structure de la branche Q	Q	5941.493	0.662
		5942.155	0.642
		5942.797	0.484
		5943.281	0.618
		5943.899	0.679
		5944.578	0.357
		5944.935	

étrangères" a été observé (cf. Tableau II). Les nombres d'onde relatifs à la bande $2\nu_1$ ne sont pas explicités, nos valeurs étant en bon accord avec celles de Anttila (4) à 0.01 cm^{-1} près.

Les valeurs obtenues pour les constantes β_1, $\omega_1{}^0$ et x_{11} sont réunies dans le Tableau III.

La valeur du centre de bande $\nu_1{}^0$ a été obtenue d'après la courbe $k'(\nu)l = f(\nu)$ (spectromètre de type Pfund (Fig. 5)), égale à $(3032.9 \pm 0.2)\ cm^{-1}$.

Considérons enfin la Fig. 3 relative à la molécule $CHBr_3$. On n'observe que l'enveloppe des branches P, Q et R de la brande $2\nu_1$. Le centre de bande $2\nu_1{}^0$ est égal à $(5964.9 \pm 0.1)\ cm^{-1}$. Dans la branche R, on observe une bande étrangère à la bande $2\nu_1$. En prenant pour centre de bande $\nu_1{}^0$, la valeur $(3048.3 \pm 0.2)\ cm^{-1}$, (Fig. 6), nous obtenons les valeurs des constantes $\omega_1{}^0$ et x_{11} (cf. Tableau III).

Intensité des bandes $2\nu_1$ et ν_1 des haloformes

Les Figs. 4–6 représentent les courbes exprimant $\ln(I'_0(\nu)/I'_t(\nu))$ en fonction de ν relatives à la bande ν_1 des haloformes étudiés. Par application de la méthode directe précédemment décrite, les mesures d'intensité intégrée $\mathscr{A}$ des bandes $2\nu_1$ et ν_1 ont été effectuées. Comme nous l'avons dit auparavant, la valeur de la argeur à mi-hauteur $\delta\nu$ de la fonction d'appareil D

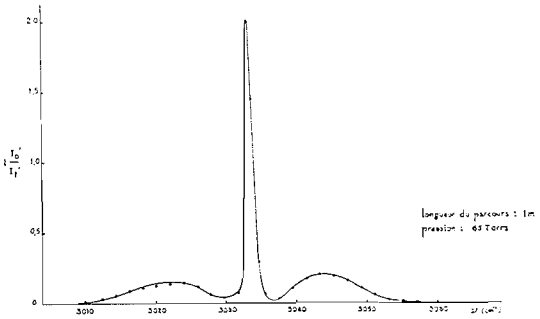

FIG. 5. Bande ν_1 de $CHCl_3$; courbe $k(\nu)l = f(\nu)$.

TABLEAU III

Constantes de vibration–rotation des bandes ν_1, et $2\nu_1$, des molécules CHF_3, $CHCl_3$ et $CHBr_3$

Molécule	Constantes (cm^{-1})			
	$\nu_1{}^0$	$2\nu_1{}^0$	$\omega_1{}^0$	x_{11}
CHF_3	3034.8 ± 0.2	5959.483 ± 0.005 5959.460 (3)	3089.9 ± 0.2	-55.1 ± 0.2
$CHCl_3$	3032.9 ± 0.2	5941.443 (4)	3095.1 ± 0.2	-62.2 ± 0.2
$CHBr_3$	3048.3 ± 0.2	5964.9 ± 0.1	3114.2 ± 0.2	-65.9 ± 0.2

Molécule	Constantes (cm^{-1})			
	B_0	$B_{v_1=2}$	D_J	$2\beta_1$
CHF_3	$(3454.1 \pm 0.8) \times 10^{-4}$	$(3450.5 \pm 0.8) \times 10^{-4}$	$(3.9 \pm 0.5) \times 10^{-7}$	$+(36.7 \pm 0.4) \times 10^{-5}$
$CHCl_3$	1101.5×10^{-4}	1101.8×10^{-4} (4)	5.5×10^{-8} (4)	$-(3.1 \pm 0.2) \times 10^{-5}$
$CHBr_3$	—	—	—	—

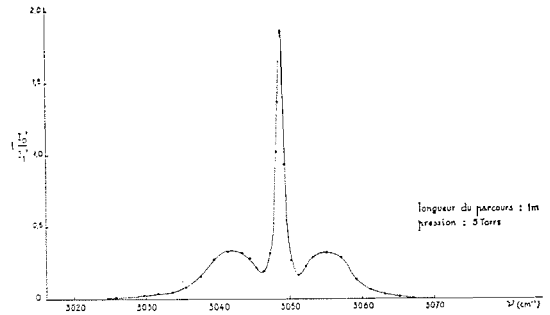

FIG. 6. Bande ν_1 de $CHBr_3$; courbe $k(\nu)l = f(\nu)$.

TABLEAU IV

Intensités intègrées des bandes ν_1 et $2\nu_1$ des molécules CHF_3, $CHCl_3$ et $CHBr_3$

Molécule	$\mathscr{A}_{1\leftarrow 0}$ ($atm^{-1}\,cm^{-2}$)	$\mathscr{A}_{2\leftarrow 0}$ ($atm^{-1}\,cm^{-2}$)	$\rho = \frac{\mathscr{A}_{1\leftarrow 0}}{\mathscr{A}_{2\leftarrow 0}}$
CHF_3	107.4 (5)	0.36 (5)	
	64.1*	0.23	279*
	57.7†		251†
$CHCl_3$	1.34 (5)	7.16 (5)	
	0.71	4.59	0.155
$CHBr_3$	13.43 (5)	3.133 (5)	
	13.53	2.78	4.87

*On considère la bande totale.
†On élimine les bandes dites "étrangères."

influe peu sur la valeur de l'intensité $\mathscr{A}$ dans nos conditions expérimentales. La valeur de $\delta\nu$ était de 0.15 cm^{-1} à 1.7 μ (spectromètre du type Czerny utilisé pour l'étude de la bande $2\nu_1$) et de 0.50 cm^{-1} à 3.3 μ (spectromètre du type Pfund, pour l'étude de la bande ν_1). Les valeurs des intensités obtenues sont relatées dans le Tableau IV.

L'estimation de $\mathscr{A}$ pour la bande ν_1 des haloformes étudiés ne présente pas de difficultés sauf pour la molécule CHF_3 dont le spectre présente des bandes étrangères à la bande ν_1 (Fig. 4). Nous avons dû en tenir compte pour la mesure d'intensité (cf. Tableau IV).

La bande $2\nu_1$ de ces haloformes présente des bandes étrangères. Nous avons déterminé $\mathscr{A}$ d'après le contour global du spectre, ce qui entache ces mesures d'une certaine erreur par excès. Nous n'avons pas pu valablement déterminer cette erreur et nous l'avons estimée inférieure à 10% dans le cas du bromoforme par exemple.

Nous notons que nos valeurs de $\mathscr{A}$ pour les molécules CHF_3 et $CHCl_3$ sont systématiquement inférieures à celles obtenues par la méthode d'extrapolation de Wilson et Wells (5). Par contre, pour la molécule $CHBr_3$, nos résultats sont en assez bon accord avec ceux de Robinson.

A 1.7 μ les bandes étrangères à la bande $2\nu_1$ des molécules CHF_3, $CHCl_3$ et $CHBr_3$ et à 3.3 μ les bandes étrangères à la bande ν_1 de la molécule CHF_3 peuvent être des "bandes chaudes" de la forme $(2\nu_1 + n\nu_6 - n\nu_6)$ et $(\nu_1 + n\nu_6 - n\nu_6)$, n étant égal à 1, 2, ... En effet, les fréquences de vibration les plus basses des haloformes CHX_3 correspondent aux vibrations dégénérées ν_6 de déformation CX_3 (X étant un atome de l'halogène). Par ailleurs, il résulte du calcul de la population relative des niveaux d'énergie ($\nu_6 = n$), que la présence de "bandes chaudes" dans le spectre est probable. Ainsi notamment les bandes A, B, C et D du spectre de $CHCl_3$ à 1.7 μ (Fig. 2) pourraient être du type $(2\nu_1 + n\nu_6 - n\nu_6)$, où n prend les valeurs 1–4.

En outre, un dédoublement (écart $\Delta \simeq 0.6\ cm^{-1}$) de ces mêmes bandes, dans le cas particulier du chloroforme, pourrait s'expliquer par un effet isotopique dans la vibration dégénérée ν_6 de déformation du groupement CCl_3 (9). La molécule $CHCl_3$ est en effet composée essentiellement de deux variétés isotopiques $CH^{35}Cl_3$ et $CH^{35}Cl_2{}^{37}Cl$.

Une bande située normalement hors du domaine spectral étudié pourrait à la suite d'une résonance recouvrir partiellement ou totalement la bande $2\nu_1$ considérée. Nous avons déterminé les niveaux susceptibles de perturber le niveau $\nu_1 = 2$, pour les deux types de résonances accidentelles: résonances vibrationnelles de Fermi et résonances rotationnelles de Coriolis.

Can. J. Chem. Downloaded from www.nrcresearchpress.com by 210.87.254.40 on 09/05/12
For personal use only.

Celles-ci n'ayant lieu qu'avec des niveaux de combinaison quaternaire, paraissent d'un ordre trop élevé pour donner lieu à un effet observable.

En considérant la corrélation entre les intensités $\mathscr{A}$ des bandes ν_1 et $2\nu_1$ des haloformes CHX_3, et l'électronégativité du groupe CX_3 (X = F, Cl, Br), on constate que les grandeurs $\mathscr{A}_{1\leftarrow 0}$ et $\mathscr{A}_{2\leftarrow 0}$ présentent respectivement un minimum et un maximum pour la molécule $CHCl_3$.

Le rapport $\rho = \mathscr{A}_{1\leftarrow 0}/\mathscr{A}_{2\leftarrow 0}$ dont la valeur excède en général l'unité, n'est que de l'ordre de 0.2 pour le chloroforme. Cette anomalie ne semble pas pouvoir s'expliquer uniquement par la présence des bandes étrangères à la bande $2\nu_1$ de la molécule $CHCl_3$. Une anharmonicité électrique importante comme celle déjà observée pour la molécule HI (10) pourrait éventuellement en tenir compte.

1. I. Rossi, A. Levy et C. Haeusler. Can. J. Chem. **46**, 2103 (1968).
2. C. Haeusler, Y. Cornet et P. Barchewitz. J. Phys. Radium, **21**, 808 (1960).
3. T. A. Wiggins, E. R. Shull et D. H. Rank. J. Chem. Phys. **21**, 1368 (1953).
4. R. Anttila. Ann. Acad. Sci. Fenn. Ser. A, **254**, 7 (1967).
5. C. C. Robinson, S. A. Tare et H. W. Thompson. Proc. Roy. Soc. London, Ser. A, **269**, 492 (1962).
6. A. Lecuyer. Thèse Doctorat 3ème Cycle, Paris. 1961.
7. H. J. Kostkowski et A. Bass. J. Opt. Soc. Amer. **46**, 1060 (1956).
8. P. Montigny. Spectrochim. Acta, **20**, 1373 (1964).
9. S. T. King. J. Chem. Phys. **49**, 1321 (1968).
10. C. Meyer, C. Haeusler et P. Barchewitz. J. Phys. **26**, 305 (1965).

Can. J. Chem. Downloaded from www.nrcresearchpress.com by 210.87.254.40 on 09/05/12
For personal use only.

Can. J. Chem. Downloaded from www.nrcresearchpress.com by 210.87.254.6 on 09/05/12
For personal use only.

A study of potential cyclopropyl – silver ion complex formation

B. C. MENON AND RICHARD E. PINCOCK
Department of Chemistry, University of British Columbia, Vancouver 8, British Columbia

Received April 16, 1969

The relative abilities of some cyclopropyl derivatives of norbornene and of norbornadiene to form water soluble complexes with 1 *M* silver nitrate at 25° were determined. Equilibrium constants, K_{eq}, for the reaction

$$\text{compound}_{(\text{pentane})} + \text{Ag}^{+}{}_{(H_2O)} \rightleftarrows \text{complex}_{(H_2O)}$$

were in the order

norbornadiene > norbornene > *exo*-tricyclo[3.2.1.$0^{2,4}$]oct-6-ene > *endo*-tricyclo [3.2.1.$0^{2,4}$]oct-6-ene
≫ di-*exo*-tetracyclo[3.3.1.$0^{2,4}0^{6,8}$]nonane or 5,5-dimethyl-2-norbornene

Quadricyclene (tetracyclo[3.2.0.$0^{2,7}0^{4,6}$]heptane) is rapidly isomerized to norbornadiene in the presence of silver ion under the equilibration conditions. The relative K_{eq} values are interpretable in terms of steric and inductive effects of cyclopropyl groups on olefin – silver ion complex formation and they give no evidence of a stabilizing cyclopropyl – silver ion interaction.

Canadian Journal of Chemistry, 47, 3327 (1969)

There are many chemical and physical properties which illustrate the close relationships between olefinic double bonds and cyclopropyl bonds. The properties held in common by these compounds arise from their basic similarity in bonding (cf. ref. 1). Just as π electrons of olefins are subject to electrophilic attack, π-like cyclopropyl orbitals (formed from overlap of two sp^5 hybrid bonds) (2) are acted upon by many electrophilic reagents (3). For example, cyclopropyl compounds react readily with acids in a manner similar to that of olefins; an edge protonated cyclopropane intermediate (see structure **1**), where the electrophile adds to the in-plane π-like orbital, has been supported both theoretically (4) and experimentally (5).

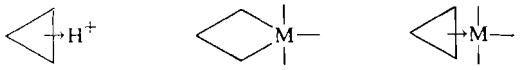

1 **2** **3**

However, one chemical property of a carbon–carbon double bond that has not been found in a cyclopropyl bond is the ability to form relatively weak, but stable complexes with metallic ions. Compounds produced from reaction of cyclopropanes with chloroplatinic acid have been formulated as having two platinum–carbon σ bonds (**2**) (6), while another recent suggestion for these compounds is structure **3** (7). Here the cyclopropyl group retains its ring bonding but donates electrons to the metal in an edgewise manner similar to structure **1**.

The well known existence of olefin – silver ion complexes, the structural similarities of olefin and cyclopropyl groups, and the more recent examples of the ability of cyclopropyl compounds to bond to electrophiles (e.g. ref. 8) all suggest that analogous cyclopropyl – silver ion complexes may exist in aqueous solutions. Following the classical method (9) used to determine the ability of olefins to complex with silver ion, we have studied the relative ability of some cyclopropyl compounds and cyclopropyl olefins to form water soluble complexes in aqueous 1 *M* silver nitrate. The possibility that one of the dicyclopropyl compounds **4** and **5** might have a pair of cyclopropyl orbitals favorably oriented to organometallic bonding was investigated.

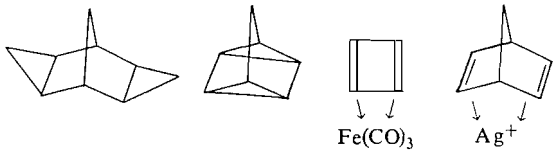

4 **5** **6** **7**

Also by further analogy to the proposed bonding in cyclobutadiene – iron tricarbonyl complex **6** (10) or in the norbornadiene – silver nitrate complex **7** (11), the relative complexing abilities of *exo*- and *endo*-bicyclo[3.2.1.$0^{2,4}$]oct-2-enes (**8** and **9**) were studied. It is known that silver nitrate forms a solid complex with *exo* compound **8** but not with the *endo* isomer **9** (12).

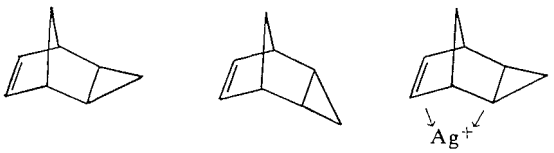

8 **9** **10**

This suggested an accentuation, by the *exo* cyclopropyl group, of the ability of the strained double bond in **8** to form a complex; i.e., a structure and interaction shown in **10.** Of related interest is the possibility of isomerization reactions of compounds **4** and **5** (and of **8** and **9**) by silver ion catalysis similar to that recently reported for some rhodium catalysts (13).

Results and Discussion

The method used to determine relative complex formation was similar to that of Winstein and Lucas (9) and Traynham and Sehnert (14). The cyclopropyl or olefinic compound in pentane was equilibrated at 25° with a 1 *M* aqueous $AgNO_3$ solution and the compound remaining in the organic phase was analyzed by vapor phase chromatography. Equilibrium constants, K_{eq}, for the reaction

$$\text{olefin}_{(\text{pentane})} + \text{Ag}^{+}{}_{(\text{H}_2\text{O})} \rightleftarrows \text{complex}_{(\text{H}_2\text{O})}$$

were then calculated from the change in concentration in the pentane phase before and after equilibration and from the known aqueous silver nitrate concentration. For compounds (like the hydrocarbons used) which are essentially insoluble in water or in 1 *M* potassium nitrate, the equilibrium constants obtained are independent of the solubilities of uncomplexed hydrocarbons in water (9). They are therefore the best measures of relative ability to form complexes with silver ion. The results obtained are shown in Table I.

Not surprisingly, the relative equilibrium constants

norbornadiene > norbornene > cyclohexene

for equilibration with pentane solutions (Table I) follow the order previously obtained (15) for equilibrations using carbon tetrachloride as the organic phase. These compounds then provide standards of comparisons for the others in Table I. The data show that the presence of the cyclopropyl groups in either *exo* or *endo* configurations (**8** and **9**) gives compounds with much less ability than norbornadiene to complex with silver ion. Also, the *exo* cyclopropyl compound **8** forms a more stable complex than the *endo* isomer, but neither of these cyclopropyl derivatives of norbornene has as great a tendency to complex with silver ion as norbornene itself. Easy crystallization of the *exo*-silver nitrate complex of

TABLE I

Equilibrium constants for complex formation in aqueous 1.0 *M* silver nitrate at 25°

Compound	K_{eq}[a]	Compound	K_{eq}
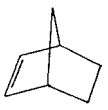	0.39±0.03	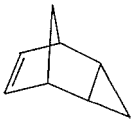	0.087
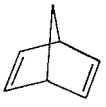	1.6	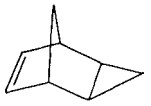	0.21
	0.014	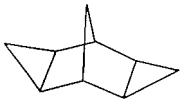	<0.005[b]
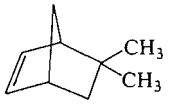	<0.005[b]	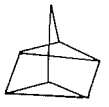	Rearrangement, deposition of silver

[a] $K_{eq} = [\text{complex}_{(\text{H}_2\text{O})}]/\{[\text{Ag}^{+}{}_{(\text{H}_2\text{O})}]\ [\text{olefin}_{(\text{pentane})}]\}$.
[b] No noticeable complex formation under conditions used.

Can. J. Chem. Downloaded from www.nrcresearchpress.com by 210.87.254.6 on 09/05/12
For personal use only.

Can. J. Chem. Downloaded from www.nrcresearchpress.com by 210.87.254.6 on 09/05/12
For personal use only.

compound **8**, which allows its convenient separation from *endo* isomer **9**, then appears to be due only to its low aqueous solubility rather than to any especially great tendency of the *exo* isomer to interact with silver ion.

It may be expected that both norbornene and the *exo* cyclopropyl derivative of norbornene (**8**) would have virtually the same steric properties for complex formation from above or below the olefinic bond. Relative to norbornene, the decrease in equilibrium constant brought about by the presence of the *exo* cyclopropyl group in **8** is probably due to the inductive electron withdrawing properties of cyclopropyl groups (e.g. see ref. 16). The further decrease obtained with the *endo* cyclopropyl isomer is possibly due to steric hindrance for complex formation on the "underside" (i.e., *endo* side) of the norbornene structure. Sensitivity to steric effects was shown by the inability of 5,5-dimethyl-2-norbornene to form a measurable amount of complex under the standard conditions used. If *exo* interaction of olefinic bond and silver ion predominated, this dimethyl substituted norbornene derivative would be expected to form a complex to an equal or possibly greater extent than norbornene itself. The absence of complex formation with this compound is taken as evidence that silver ion complex formation in aqueous solution occurs predominantly on the *endo* side of norbornene and of norbornadiene. In the solid state an example of *exo* configuration has been established (17) while *endo* configurations have been favored in other cases (11, 18).

For the cyclopropyl olefins in Table I, the relative equilibrium constant data can therefore be explained in terms of inductive and steric effects of the cyclopropyl group acting on olefin – silver ion complex formation. Potential cyclopropyl – silver ion interaction, which may still account for the greater complex formation from *exo* compound **8** over *endo* isomer **9**, is not required by the data obtained. But a structural study of the solid *exo* complex, which analyzes as a 1:1 complex of $AgNO_3$ with **8**, would be necessary to finally show the position (and indicate the type of bonding) of silver with respect to the π-bonds of olefin and cyclopropyl groups.

With regard to cyclopropyl groups by themselves, it is known that liquid cyclopropane does not form a complex with solid silver nitrate at room temperature (19). Also as reported in Table I, the *exo* cyclopropyl groups in compound **4** do not act to form measurable amounts of complex with aqueous silver nitrate. However, when cyclopropyl groups are suitably arranged (as in the compound quadricyclene **5**), cyclopropyl–metal interaction occurs and a symmetry allowed (13*a*) isomerization to norbornadiene occurs.

When shaken in pentane with aqueous silver nitrate at room temperature under conditions of the equilibrium experiments, quadricyclene is largely rearranged to norbornadiene. Some oxidation was apparent when metallic silver was also deposited. This rapid reaction prevented the determination of an equilibrium constant for quadricyclene – silver ion interaction. Isomerization of quadricyclene catalyzed by rhodium, palladium, or platinum compounds (13*a*), rearrangement of hexamethylprismane by a rhodium catalyst (13*b*) and oxidation and rearrangement of phenylcyclopropane brought about by palladium chloride (20) are recent examples of similar metal cyclopropyl reactions.

A parallel (as in hexamethylprismane) or almost parallel (as in quadricyclene) arrangement of two cyclopropyl rings gives a π orbital system similar to that in cyclobutadiene. Although no stable complexes of silver ion with cyclopropyl groups were found, the isomerization of **5** (but not of **4**) makes it probable that the π-like electrons in two parallel cyclopropyl rings may interact with silver ion in a manner analogous to that in olefin – metal ion complexes like **6** and **7**.

Except for this rather special interaction followed by rearrangement, the general inability (compared to carbon–carbon double bonds) of cyclopropyl groups to complex reversibly with metals is likely due to increased steric effects as well as decreased availability of π-electrons. In olefins the π-electrons are sterically relatively free above the plane of the atoms attached to the double bond, while in cyclopropyl compounds the π electrons in the edge of the ring are closer to atoms attached to the ring carbons. This steric factor, together with smaller p-character of cyclopropyl ring orbitals seems to prevent noticeable complex formation in aqueous solution.

Experimental

The method used was essentially that of Traynham and Sehnert (14), except that the olefinic concentration was

Can. J. Chem. Downloaded from www.nrcresearchpress.com by 210.87.254.6 on 09/05/12
For personal use only.

determined by gas–liquid chromatographic (g.l.c.) analysis of the organic phase. Pentane was used because it allowed g.l.c. separation of all the olefins used. Analyses were carried out using a 20% Carbowax 20-M on 60–80 Chromsorb W (acid washed) column at 100° in an Aerograph model 90-P3 chromatograph. A series of solutions of olefin of varying concentrations in pentane was prepared. These solutions were then analyzed by g.l.c. and a calibration curve of concentration vs. peak area for the olefin obtained. The equilibration was carried out in a two-necked 250 ml flask fitted with a condenser and a mechanical stirrer. Thirty ml of olefin solution (0.1–1.0 *M*) were buretted into the flask, followed by 100 ml of 1.0 *M* $AgNO_3$ solution. The two phases at 25.2 ± 0.1° were rapidly stirred. At the end of 1 h the organic layer was analyzed for olefin by g.l.c. under the same condition employed for the calibration runs. That the equilibration was complete was shown by the fact that the olefin concentration in the pentane phase remained unchanged from 1 to 2 h. The amount of olefin dissolved but not complexed in the water layer was determined by shaking a mixture of 30 ml of olefin solution and 400 ml of 1.0 *M* KNO_3 for 1 h and then analyzing the organic phase. The amount of olefin lost from the organic phase was noticeable but negligible in every case. The equilibrium constants (K_{eq}) for the reaction

$$\text{olefin}_{(\text{pentane})} + Ag^{+}{}_{(H_2O)} \rightleftarrows \text{complex}_{(H_2O)}$$

were calculated from the data given in Table II by the method given in the footnotes. Mixtures of known ratios of *exo* and *endo* isomers (**8** and **9**) were used and the K_{eq} for *exo* compound calculated from the data, and from the K_{eq} obtained from use of pure *endo* isomer.

*Tricyclo[3.2.1.0^{2,4}]oct-6-enes (exo-**8** and endo-**9**) and Tetracyclo[3.3.1.0^{2,4}0^{6,8}]nonane (**4**)*

These compounds were prepared by treating freshly distilled norbornadiene with diazomethane over anhydrous cuprous chloride in ether. (The general method used is given in ref. 21.) The relative proportion of tricyclooctenes and the tetracyclononane was controlled by the time of passage of CH_2N_2 through the ether solution. The *exo* and *endo* monoadducts were not separable by g.l.c.; the mixture showed the properties reported for these compounds prepared by the CH_2I_2–Zn–Cu reaction with norbornadiene (12). The ratio of *exo* to *endo* was determined by the nuclear magnetic resonance (n.m.r.) peaks at 3.55 (for *exo*) and 4.25 τ (for *endo*). The diadduct (4) was separated by g.l.c.; n.m.r. 7.75 (bridgehead), 8.50–9.45 τ. The n.m.r. spectrum and the method of preparation indicated a di-*exo* configuration for this compound (see also ref. 13*c*).

Anal. Calcd. for C_9H_{12}: C, 90.00; H, 10.00. Found: C, 89.52; H, 10.36.

endo-Tricyclo[3.2.1.0^{2,4}]oct-6-ene (**9**) was prepared by the method of Closs and Krantz (22). Quadricyclene (**5**) was prepared by photolysis of norbornadiene (23). 5,5-Dimethyl-2-norborn-2-ene was kindly supplied by McGreer (24). These compounds were purified for use by g.l.c. collections.

The silver nitrate complex of *exo*-tricyclo[3.2.1.0^{2,4}]-oct-6-ene (**8**) was prepared by adding 0.23 g of a mixture of **8** and **9** to 1 ml of 2.5 *M* $AgNO_3$ solution. A white

TABLE II

Data for equilibration of compounds in pentane with 1.0 *M* aqueous silver nitrate at 25°

Compound	A^a	B^b	$K_{eq}{}^c$
Norbornene	0.612	0.275	0.408
	0.730	0.358	0.350
	0.230	0.098	0.420
Norbornadiene	0.800	0.150	1.61
	0.963	0.185	1.64
	0.204	0.018	3.27[d]
endo-**9**	0.235	0.183	0.087
endo-**9** with *exo*-**8**	0.143[e]	0.093	
	0.275[f]	0.144	
exo-**8**			(0.191[e])[g]
			(0.236[f])[g]
Cyclohexene	0.620	0.592	0.0143
Dicyclopropyl compound (**4**)	0.189[h]		
5,5-Dimethylnorbornene-2	0.136[h]		
Quadricyclene (**5**)	0.188[i]		

[a]Conditions, unless otherwise indicated, are 30 ml of olefin in pentane shaken with 100 ml of 1.0 *M* $AgNO_3$ solution. *A* = initial concentration of olefin in pentane solution.
[b]*B* = final equilibrated concentration of olefin in pentane solution.
[c]Final equilibrium concentration of Ag^+ – olefin complex in aqueous phase = *C* = 0.3 (A − B − D), where *D* = equilibrated concentration of olefin in 1.0 *M* KNO_3. The value of *D* was less than 0.001 *M* in every case and was therefore negligible. The equilibrium constants were then calculated according to $K_{eq} = C/[(1.0 - C)(B)]$.
[d]Increase in K_{eq} apparently due to formation of a two to one complex of silver ion with norbornadiene (not observed in ref. 15 but the solid 2:1 complex has been isolated (11)).
[e]Mixture of *exo* and *endo* isomers used; ratio 3 to 1.
[f]Mixture of *exo* and *endo* isomers used; ratio 5 to 1, and 20 ml of pentane solution shaken with 100 ml of 0.959 *M* $AgNO_3$.
[g]Calculated from data, the known value for K_{eq} of *endo* isomer and the ratio of *endo* to *exo* in mixture used.
[h]No noticeable loss of compound on equilibration with 1 *M* $AgNO_3$.
[i]Rapid isomerization to norbornadiene in presence of $AgNO_3$ at 25°.

precipitate formed on cooling and was filtered and recrystallized from 95% ethanol. The complex was dried in vacuum while shielded from light. It decomposed without melting at ca. 100°.

Anal. Calcd. for $C_8H_{10}AgNO_3$: C, 35.16; H, 3.62. Found, C, 34.71; H, 3.74.

Its n.m.r. spectrum in D_2O showed a singlet at 3.23 (olefinic hydrogen), a broad singlet at 7.02 (bridgehead hydrogens), and multiplets centered at 8.2, 8.86, and 9.35 τ. In deuteroacetone the olefinic hydrogens appeared at 3.98 τ, shifted downfield from the 4.24 τ value for uncomplexed *exo* isomer **8** in this solvent.

Acknowledgments

We gratefully acknowledge support from the donors to the American Chemical Society Petroleum Research Fund, from the National Research Council of Canada, and from the U.S. Air Force Office of Scientific Research (Grant No. 1102-66). The work was aided by an Alfred P. Sloan Foundation Fellowship to R.E.P. (1967–1969).

1. W. A. BERNETT. J. Chem. Educ. **44**, 17 (1967).
2. F. J. WEIGERT and J. D. ROBERTS. J. Amer. Chem. Soc. **89**, 5962 (1967).
3. R. J. OUELLETTE, R. D. ROBINS, and A. SOUTH, JR. J. Amer. Chem. Soc. **90**, 1619 (1968).
4. J. D. PETKE and J. L. WHITTEN. J. Amer. Chem. Soc. **90**, 3338 (1968).
5. C. C. LEE and J. E. KRUKER. Tetrahedron, **23**, 2539 (1967). H. HART and R. H. SCHLOSBERG. J. Amer. Chem. Soc. **90**, 5189 (1968). N. C. DENO, O. LAVIETES, J. MOCKUS, and P. C. SCHOLL. J. Amer. Chem. Soc. **90**, 6457 (1968), and references therein.
6. N. A. BAILEY, R. D. GILLARD, M. KEETON, and D. R. RUSSELL. Chem. Commun. 396 (1966). D. M. ADAMS, J. CHATT, R. G. GUY, and N. SHEPPARD. J. Chem. Soc. 738 (1961).
7. W. J. IRWIN and F. J. MCQUILLIN. Tetrahedron Lett. 1937 (1968).
8. L. JORIS, P. V. R. SCHLEYER, and R. GLEITER. J. Amer. Chem. Soc. **90**, 327 (1968).
9. S. WINSTEIN and H. J. LUCAS. J. Amer. Chem. Soc. **60**, 836 (1938).
10. G. F. EMERSON, L. WATTS, and R. PETTIT. J. Amer. Chem. Soc. **87**, 131 (1965).
11. J. G. TRAYHAM. J. Org. Chem. **26**, 4694 (1961). R. A. ALEXANDER, N. C. BAENZIGER, C. CARPENTER, and J. R. DOYLE. J. Amer. Chem. Soc. **82**, 535 (1960).
12. H. E. SIMMONS, E. P. BLANCHARD, and R. D. SMITH. J. Amer. Chem. Soc. **86**, 1347 (1964).
13. (*a*) H. HOGEVEEN and H. C. VOLGER. J. Amer. Chem. Soc. **89**, 2486 (1967). (*b*) H. HOGEVEEN and H. C. VOLGER. Chem. Commun. 1133 (1967). (*c*) H. C. VOLGER, H. HOGEVEEN, and M. M. P. GAASBEEK. J. Amer. Chem. Soc. **91**, 218 (1969).
14. J. G. TRAYNHAM and M. F. SEHNERT. J. Amer. Chem. Soc. **78**, 4024 (1956).
15. J. G. TRAYNHAM and J. R. OLECHOWSKI. J. Amer. Chem. Soc. **81**, 571 (1959).
16. M. J. S. DEWAR and J. M. HARRIS. J. Amer. Chem. Soc. **90**, 4468 (1968).
17. N. C. BAENZIGER, H. L. HAIGHT, and J. R. DOYLE. Inorg. Chem. **3**, 1535 (1964).
18. R. PETTIT. J. Amer. Chem. Soc. **81**, 1266 (1959).
19. C. F. H. TIPPER. J. Chem. Soc. 2045 (1955).
20. R. J. OUELLETTE and C. LEVIN. J. Amer. Chem. Soc. **90**, 6889 (1968).
21. R. E. PINCOCK and J. I. WELLS. J. Org. Chem. **29**, 965 (1964).
22. G. L. CLOSS and K. D. KRANTZ. J. Org. Chem. **31**, 638 (1966).
23. W. G. DAUBEN and R. L. CARGILL. Tetrahedron, **15**, 197 (1961).
24. D. E. MCGREER. Can. J. Chem. **40**, 1554 (1962).

Can. J. Chem. Downloaded from www.nrcresearchpress.com by 210.87.254.6 on 09/05/12
For personal use only.

Can. J. Chem. Downloaded from www.nrcresearchpress.com by 210.87.254.105 on 09/05/12
For personal use only.

Etude polarographique des méthoxyhydroperoxydes[1]

JEAN RENARD ET SÁNDOR FLISZÁR
Département de Chimie, Université de Montréal, Montréal, Québec

Reçu le 18 mars 1969

La réduction polarographique d'une série de α-méthoxyhydroperoxydes, produits par l'ozonation d'oléfines dans le méthanol, a été étudiée. Un mécanisme est proposé pour le processus d'électrode. L'application analytique pour le dosage de ces méthoxyhydroperoxydes et pour l'étude du mécanisme d'ozonolyse des oléfines dissymétriques est exposée.

The polarographic behavior of selected α-methoxyhydroperoxides, produced by ozonization of olefins in methanol, has been studied. A mechanism is proposed for the electrode process. An analytical application for the quantitative determination of these methoxyhydroperoxides and for the study of the mechanism of ozonolysis of unsymmetrical olefins is described.

Canadian Journal of Chemistry, 47, 3333 (1969)

Le comportement polarographique des produits peroxydiques en relation avec l'étude des produits d'oxydation des corps gras, des caoutchoucs, des polymères et des essences, a fait l'objet de nombreuses publications et de plusieures revues (1–3). Kůta et Quackenbush (4) ont signalé les possibilités d'application des techniques polarographiques à l'étude des produits de la réaction d'ozonation, et Slagel (5) a montré l'intérêt de la polarographie pour l'élucidation de la structure d'un produit issu de l'ozonation du 1,2,3,4,7,7-hexachloro-bicyclo-[2,2,1]hepta-2,5 diène. Cependant, aucune étude systématique du comportement polarographique des produits d'ozonation n'a été publiée.

L'ozonation des oléfines en milieu inerte (CCl_4 ou pentane, par exemple) conduit, en général, à la formation de produits carbonylés et de zwitterions (6), selon un mécanisme proposé par Criegee.

Les proportions des 2 voies de clivage (*a* et *b*), qui dépendent de la nature des oléfines soumises à l'ozonation, ont fait l'objet d'études récentes (7), ainsi que la participation possible de zwitterions *syn* et *anti* dans le mécanisme de formation d'ozonides *cis* et *trans* (8).

En présence de méthanol, les zwitterions sont généralement transformés en α-méthoxyhydroperoxydes $R(R')C(OCH_3)$—OOH (6). Dans de nombreux cas il a été vérifié (7) que l'ozonation en présence de méthanol d'une mole d'oléfine conduit à la formation d'une mole du mélange de composés carbonylés prévus par le mécanisme de Criegee, et d'une mole de méthoxyhydroperoxydes. Il a aussi été établi que ces derniers ne réagissent pas avec les produits carbonylés engendrés lors des ozonations si les mélanges réactionels sont conservés pendant 1–2 h à la température de la pièce.

Le but du présent travail est l'étude du mécanisme de la réduction polarographique d'une série de méthoxyhydroperoxydes $RCH(OCH_3)$—OOH, avec R = H, CH_3, C_2H_5, *n*-C_3H_7, *i*-C_3H_7, *t*-C_4H_9, et phényle (Ph). Une méthode de dosage de ces hydroperoxydes a été élaborée à partir des résultats de cette étude.

Partie expérimentale

Technique polarographique

Les courbes intensité–potentiel ont été enregistrées à l'aide d'un polarographe Metrohm E-261-R offrant la double possibilité d'une analyse par voltage continu croissant linéairement ou d'une analyse à l'aide d'une tension alternative de faible amplitude, superposée au voltage continu d'analyse (polarographie C.A.) (9, 10). Dans la présente étude, la fréquence de la tension alternative utilisée a été de 60 Mc/s et son amplitude de 50 mV. L'électrode a goutte de mercure était constituée par un capillaire, dont le mouvement commandé par un électroaimant assure un temps de goutte de 1/6 s pour un flux de mercure de 0.9 mg/s. L'électrode de référence était une électrode Ag/AgCl commerciale et l'électrode auxiliaire, une électrode de tungstène.

Les oscillo-polarogrammes $i = f(E)$ ont été obtenus à l'aide d'un oscillo-polarographe Chemtrix SSP-2 utilisant un balayage simple par une tension triangulaire. Les électrodes utilisées étaient les mêmes que celles décrites précédemment. Le temps de goutte avait été ramené à 3 s.

Les électrolyses à potentiel contrôlé ont été effectuées dans une cellule d'électrolyse à 3 compartiments, séparés

[1]Travail présenté en partie au Congrès annuel de l'Association Canadienne-Française pour l'Avancement des Sciences, Ottawa, Novembre 1968, extrait de la thèse de Doctorat de M.J.R.

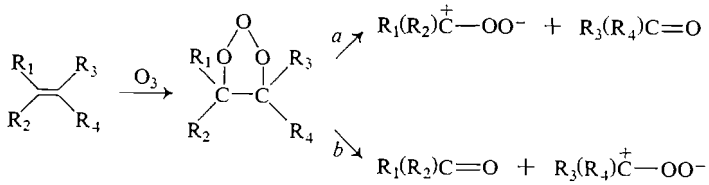

par des verres frittés. L'électrode de travail était constituée d'une nappe de mercure agitée à l'aide d'un agitateur magnétique. L'électrode de contrôle était une électrode Ag/AgCl, l'électrode auxiliaire un fil de cuivre plongeant dans la solution. Les électrolyses ont été effectuées sur des volumes de 75 ml de solution 10^{-2} *M* de méthoxyhydroperoxydes pendant des durées variant de 1 à 5 h. La tension était appliquée à l'aide d'un potentiostat Tacussel PRT 500 LC. Le courant d'électrolyse était enregistré à l'aide d'un enregistreur potentiométrique Tacussel EPL-1. Les quantités de courant ont été déterminées par des mesures planimétriques des courbes $i = i(t)$ ainsi obtenues. La concentration en dépolariseur a été suivie par polarographie.

Préparation des méthoxyhydroperoxydes

Les méthoxyhydroperoxydes $RCH(OCH_3)—OOH$ (R = C_2H_5, *n*-C_3H_7, *i*-C_3H_7, *t*-C_4H_9, et Ph) ont été préparés par l'ozonation à 0 °C des oléfines symmétriques correspondantes R—CH=CH—R dans le méthanol. Après l'ozonation, le solvant a été évaporé et le résidu a été extrait successivement par l'hexane, l'eau, puis l'éther, en suivant la procédure décrite par Keaveney *et al.* (11). Pour obtenir une plus grande pureté (notamment en vue de l'élimination de restes d'aldéhyde), les échantillons ont été chromatographiés sur une colonne de silica gel Baker (200 g/1 g) en utilisant, comme éluants, le CCl_4 et, ensuite, l'acétone. Lors de la purification du méthoxyhydroperoxyde avec R = Ph, un mélange (1:1) de benzène–hexane a été intercalé entre les éluants précédents.

Les méthoxyhydroperoxydes avec R = H et R = CH_3 ont été préparés par l'ozonation dans le méthanol à 0 °C du 1,1-diphényléthylène et du *trans* β-méthylstyrène, respectivement. Dans ces conditions, 1 mole de 1,1-diphényléthylène engendre 0.33 ± 0.01 mole de $CH_2(OCH_3)—OOH$ et le rendement en $CH_3—CH(OCH_3)—OOH$ est de 0.82 ± 0.02 mole par mole de β-méthylstyrène ozonée (*7a*). Les extractions et purifications par chromatographie sur colonne ont été effectuées selon la procédure exposée ci-haut. Lors du traitement avec l'eau, le méthoxyhydroperoxyde $Ph_2C(OCH_3)—OOH$ obtenu lors de l'ozonation du 1,1-diphényléthylène se décompose très rapidement en engendrant de la benzophénone. Par contre, la décomposition du méthoxyhydroperoxyde R = Ph obtenu lors de l'ozonation du β-méthylstyrène et du stilbène est assez lente pour en permettre la préparation. Cependant, ce même hydroperoxyde est entièrement décomposé dans l'eau, en engendrant de l'aldéhyde benzoïque, après un repos de 1 nuit à la température ambiante, ce qui permet la préparation du méthoxyhydroperoxyde aliphatique à partir du β-méthylstyrène.

Les méthoxyhydroperoxydes avec R = H, CH_3, et Ph ainsi préparés sont en tous points conformes à ceux décrits par Keaveney *et al.* (11). L'identification et les contrôles de pureté ont été effectués à l'aide des spectres de résonance magnétique nucléaire (r.m.n.), enregistrés au moyen d'un spectromètre Jeolco 60 H, des spectres d'absorption infrarouge (i.r.) (Perkin–Elmer 221), et par des dosages iodométriques selon une méthode proche de celle décrite par Lohaus (12). Les méthoxyhydroperoxydes avec R = C_2H_5, *n*-C_3H_7, *i*-C_3H_7, et *t*-C_4H_9 se présentent sous forme d'huiles presque incolores. Leurs spectres r.m.n. sont rapportés dans le Tableau I. Leur pureté est estimée ⩾ 98%.

Procédure polarographique

Le méthanol utilisé a été préalablement chauffé à reflux sur du magnésium pendant 2 h et purifié par distillation. L'acétate d'éthyle employé avait été distillé soigneusement au moyen d'une colonne Ilas de type Todd, garnie d'anneaux de Fenske.

Le pH des solutions tampons a été mesuré à l'aide d'un potentiographe Metrohm E336A, équipé d'une électrode de verre combinée à une électrode de référence Ag/AgCl.

Pour les mesures polarographiques, 1 ml de la solution de méthoxyhydroperoxyde dans le méthanol ou 1 ml de la solution ozonée dans l'acétate d'éthyle – méthanol (1 *M*) a été transféré dans 25 ml de la solution tampon. Les concentrations des solutions de méthoxyhydroperoxydes utilisées étaient comprises entre 0.01 et 0.1 *M*. Lors de l'examen des solutions effectuées dans l'acétate d'éthyle – méthanol, une agitation magnétique rapide est nécessaire pour assurer la miscibilité des deux phases. Le polarogramme est enregistré à 25°, après un dégazage de la solution par un courant d'azote pendant 10 min.

Résultats et Discussion

Stabilité des α-méthoxyhydroperoxydes

Comme l'avaient signalé Subluskey *et al.* (13), ainsi que Keaveney *et al.* (11), les alkylohydroperoxydes R—$CH(OCH_3)$—OOH sont très stables en solution aqueuse jusqu'à pH = 10. En accord avec ces auteurs nous avons également constaté la moindre stabilité du phényl-méthoxyhydroperoxyde Ph—$CH(OCH_3)$—OOH et la décomposition très rapide des dialkyl-méthoxyhydroperoxydes $R(R')C(OCH_3)—OOH$ en solution aqueuse. Par conséquent notre étude a été limitée à 7 méthoxyhydroperoxydes dont la stabilité est suffisante pour permettre un dosage polarographique, et dont les caractéristiques spectroscopiques et polarographiques sont données au Tableau I. Il a été vérifié, pour chacun des

Can. J. Chem. Downloaded from www.nrcresearchpress.com by 210.87.254.105 on 09/05/12
For personal use only.

TABLEAU I

Potentiels de demi-vague et spectres de résonance magnétique nucléaire des α-méthoxyhydroperoxydes R—CH(OCH_3)—OOH

R	Spectres r.m.n. (δ)	Intégrat. relative	$E_{1/2}$ (V) Méthanol LiCl (*M*)	Mc Ilvaine, pH 7, méthanol	Mc Ilvaine, pH 7, CH_3OH $CH_3COOC_2H_5$
H	7.7 (b)	—	−1.216	−0.838	−1.04
	4.80 (s)	2			
	3.35 (s)	3			
CH_3	7.8 (b)	—	−1.184	−0.678	−0.98
	4.8 (q) *J*-10 c.p.s.	1			
	3.42 (s)	3			
	1.30 (d) *J*-9 c.p.s.	3			
C_2H_5	7.9 (b)	—	−1.104	−0.256	−0.18
	4.56 (t)	1			
	3.45 (s)	3			
	1.60 (q-d)	2			
	0.92 (t) *J*-11 c.p.s.	3			
n-C_3H_7	8 (b)	—	−1.04	−0.208	−0.16
	4.65 (t) *J*-10 c.p.s.	1			
	3.48 (s)	3			
	1.52 (m)	4			
	0.96 (t)	3			
i-C_3H_7	8 (b)	—	−1.08	−0.208	−0.16
	4.38 (d) *J*-11 c.p.s.	1			
	3.48 (s)	3			
	1.90 (m)	1			
	0.92 (d) *J*-11 c.p.s.	6			
t-C_4H_9	8 (b)	—	−1.06	−0.200	−0.16
	4.35 (s)	1			
	3.68 (s)	3			
	0.90 (s)	9			
C_6H_5	9.70 (b)	—	−0.86	0.0	0.0 (b)
	7.30 (m)	5			
	5.62 (s)	1			
	3.48 (s)	3			

NOTE: (s) singulet, (d) doublet, (t) triplet, (q) quadruplet, (m) multiplet, (b) signal de forme mal définie, (q-d) quadruplet dédoublé, J_1-10 et J_2-2 c.p.s.

méthoxyhydroperoxydes étudiés, que l'intensité maximum du pic polarographique était constante pendant une période d'au moins 1 h, sauf dans le cas du phényl-méthoxyhydroperoxyde qui, cependant, n'accuse pas une décomposition excédant 5% après 1 h.

Irréversibilité des processus d'électrode

Quelque soit la vitesse de balayage, les oscillopolarogrammes $i = f(E)$ ont montré, pour tous les méthoxyhydroperoxydes étudiés, une complète irréversibilité du processus d'électrode (Fig. 1). Ce résultat est corroboré par l'analyse logarithmique des courbes intensité–potentiel d'après l'équation

$$E = E_{1/2} - (RT/\alpha nF) \ln [I/(I_e - I)]$$

Le coefficient de transfert α qui a été calculé à partir des valeurs des pentes des droites obtenues est, compte tenu des 2 électrons mis en jeu, de 0.2–0.3 pour les méthoxyhydroperoxydes avec R = C_2H_5, *n*-C_3H_7, *i*-C_3H_7, *t*-C_4H_9 et de 0.06–0.07 pour R = H et CH_3.

Nombre d'électrons mis en jeu dans le processus d'électrode

L'électrolyse à potentiel contrôlé du *n*-propyl-méthoxyhydroperoxyde 10^{-2} *M* conduit à une valeur moyenne de $n = 1.9$ électrons (4 déterminations avec *n* compris entre 1.8 et 2.05). Ce résultat est, par ailleurs, confirmé par l'étude des courbes $i = i(t)$ selon la méthode de Gilbert et Rideal (14).

$$\log \bar{i}_{l_0} - \log \bar{i}_I = \bar{i}_{l_0} t/2.3nFC_{t=0}V$$

$\log \bar{i}_I$ est une fonction linéaire de *t*. La pente de la

Can. J. Chem. Downloaded from www.nrcresearchpress.com by 210.87.254.105 on 09/05/12
For personal use only.

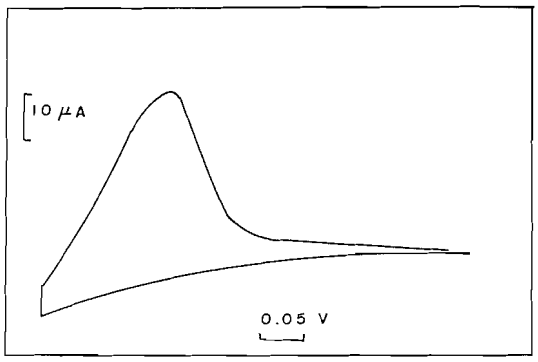

FIG. 1. Oscillo-polarogramme d'une solution 2×10^{-4} *M* de *i*-C_3H_7—$CH(OCH_3)$—OOH dans les tampon Mc Ilvaine, pH = 7; voltage de départ, 0.0 V; domaine de voltage, −0.5 V; vitesse de balayage, 0.5 V s^{-1}.

droite obtenue à partir des valeurs expérimentales $i = i(t)$ conduit au résultat, $n = 1.8$. Ces valeurs trouvées pour n, proches de 2 électrons, sont en bon accord avec la valeur $n = 2$ électrons qui a été déterminée par Skoog et Lauwzecha (15) pour la réduction des alkyl-hydroperoxydes. Contrairement au *n*-propyl-méthoxyhydroperoxyde, le phényl-méthoxyhydroperoxyde subit une décomposition relativement rapide en présence d'une nappe de mercure. On observe, en effet, près de 50% de décomposition en 2 h lorsqu'une solution 10^{-2} *M* de ce méthoxyhydroperoxyde dans l'eau est laissée au contact d'une nappe de mercure. La complexité de cette réaction parallèle à la réaction d'électrolyse rendait difficile toute correction précise des résultats polarographiques. L'ordre de grandeur $n = 2$ a néanmoins pu être vérifié de manière grossière.

Identification des produits d'électrolyse

L'électrolyse de 75 ml d'une solution 10^{-2} *M* de phényl-méthoxyhydroperoxyde dans l'eau a été effectuée à 25°, avec une tension appliquée de −0.4 V par rapport à l'électrode Ag/AgCl. Après 2 h de réaction, le méthoxyhydroperoxyde a réagi dans une proportion estimée à environ 95%, ce qui a été attesté par l'examen polarographique de la solution électrolysée et par le dosage iodométrique de l'oxygène actif. La solution électrolysée a été soumise à une extraction par l'éther, et ce dernier a été ensuite évaporé. Le résidu a été dissous dans 10 ml de CCl_4. L'analyse de cette solution par chromatographie analytique en phase gazeuse, à l'aide d'un appareillage F and M 5750, pourvu d'une colonne "silicone rubber", a permis d'identifier l'aldéhyde benzoïque. Son dosage indique un rendement de production de benzaldéhyde correspondant à 90% par rapport au méthoxyhydroperoxyde initialement mis en jeu.

L'électrolyse de 75 ml d'une solution aqueuse 10^{-2} *M* du méthoxyhydroperoxyde $H_2C(OCH_3)$—OOH, avec une tension appliquée de −1.2 V (par rapport à l'électrode Ag/AgCl), a été effectuée pendant 5 h, c'est-à-dire jusqu'à consommation complète du méthoxyhydroperoxyde. Cette consommation est attestée par l'absence de pic dans le polarogramme de la solution électrolysée. Ce polarogramme ne révèle cependant pas de pic correspondant au formol, qui est le produit attendu de l'électrolyse. Dans le but de mettre le formol engendré en évidence, la solution électrolysée a été additionnée de chlorhydrate de semicarbazide jusqu'à l'obtention d'une concentration 1 *M* de ce réactif, selon une procédure voisine de celle décrite par Souchay et Craizon (16) et Coulson (17). Le polarogramme de cette solution, enregistré après un repos de 30 min, révèle 2 pics à −0.8 V et à −1.05 V qui sont identiques à ceux obtenus à partir d'une solution aqueuse de formol traitée de même manière. D'après les mesures effectuées sur le pic à −0.8 V, le rendement en formol obtenu par électrolyse s'élève à environ 80% par rapport à la quantité de méthoxyhydroperoxyde initialement mise en jeu. En tenant compte de la possibilité de pertes en produits au cours de l'électrolyse, dues, notamment, au courant d'azote employé, il est raisonable de conclure que lors de l'électrolyse de ce méthoxyhydroperoxyde le composé carbonylé est libéré à l'électrode en majeure partie, sinon entièrement, sous forme de son hémiacétal non réductible. Des observations similaires ont déjà été rapportées dans la littérature (18).

Ces expériences confirment ainsi que le produit de l'électrolyse des méthoxyhydroperoxydes est le composé carbonylé correspondant, soit sous forme libre, soit sous forme de son hémiacétal méthanolique, selon la stabilité de l'hémiacétal à l'hydrolyse.

Influence du pH

L'influence du pH sur les potentiels de demi-vague et les courants limités a été étudiée sur des solutions de pH compris entre 3 et 8, réalisées à l'aide d'un tampon universel Mc Ilvaine. Pour les deux premiers termes de la série des méthoxy-

Can. J. Chem. Downloaded from www.nrcresearchpress.com by 210.87.254.105 on 09/05/12
For personal use only.

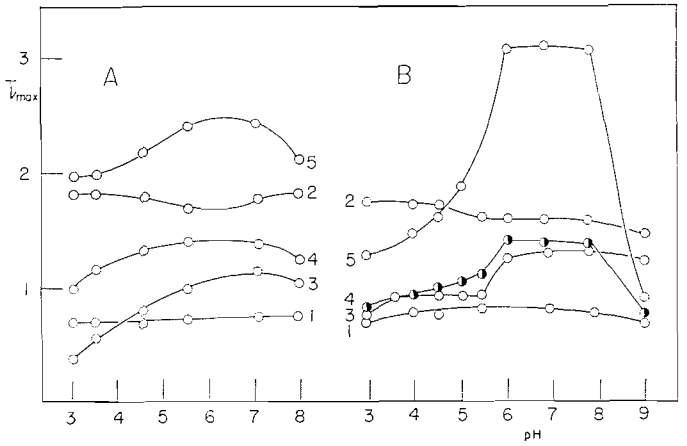

FIG. 2. Variation du courant limite i_{max} (μA) en fonction du pH. A, tampon Mc Ilvaine; B, tampon Clark et Lubs. R = H (1), CH_3 (2), i-C_3H_7 (3), t-C_4H_9 (4), et C_6H_5 (5).

hydroperoxydes étudiés, c'est-à-dire avec R = H et R = CH_3, les potentiels de demi-vague et les courants limites sont indépendants du pH dans le domaine de pH 3 à 8 (Figs. 2 et 3). Les termes supérieurs (R = C_2H_5, et les suivants) montrent un léger déplacement du potentiel de demi-vague vers les potentiels plus positifs lorsque le pH croît, alors que le courant limite passe par un maximum au voisinage de pH = 7. L'étude de l'influence des pH supérieurs, 8.5 et 9, réalisés à l'aide d'un tampon différent (Borax et HCl), indique un déplacement des potentiels de demi-vague vers les potentiels plus négatifs, accompagné d'une diminution des courants limites.

Influence de la composition du tampon

Le domaine de pH compris entre 6 et 8 a été étudié à l'aide (*i*) du tampon Mc Ilvaine et (*ii*) d'un tampon NaH_2PO_4 et NaOH. La comparaison des résultats obtenus à l'aide de ces deux tampons n'indique qu'une faible différence des potentiels de demi-vague, de l'ordre de 50 mV, alors que les courants limites restent du même ordre de grandeur, avec un écart maximum de ±2%, et se comportent de manière similaire lorsque le pH est changé.

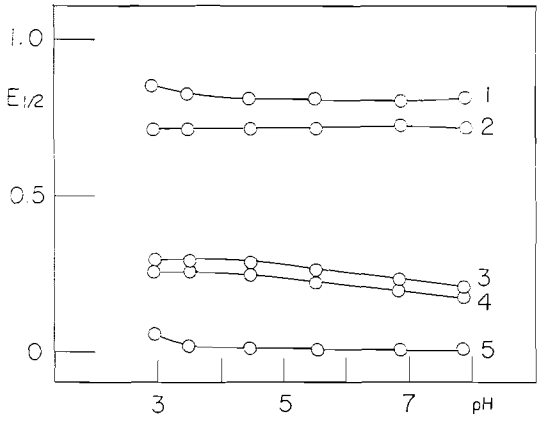

FIG. 3. Variation du potentiel de demi-vague $E_{1/2}$ (V) en fonction du pH (tampon Mc Ilvaine). R = H (1), CH_3 (2), i-C_3H_7 (3), t-C_4H_9 (4), et C_6H_5 (5).

Par contre, le tampon réalisé à base de phtalate acide de potassium, additionné de HCl ou de NaOH, se distingue par son influence des deux tampons précités. Ceci est indiqué par les résultats d'une comparaison entre les tampons phtalate et Mc Ilvaine dans le domaine de pH 3–6. Pour tous les méthoxyhydroperoxydes éxaminés on observe, avec le tampon phtalate, un glissement régulier des potentiels de demi-vague vers les potentiels plus positifs lorsque le pH croît (Fig. 4). Pour les méthoxyhydroperoxydes avec R = H et CH_3, les potentiels de demi-vague observés avec le tampon phtalate diminuent régulièrement et rejoignent, vers pH = 6, les valeurs des potentiels de demi-vague observés avec les tampons NaH_2PO_4 – NaOH et Mc Ilvaine. Avec les autres méthoxyhydroperoxydes (R = C_2H_5 et les suivants), la courbe de décroissance des potentiels de demi-vague (avec les pH croissants) observée en tampon phtalate est pratiquement parallèle aux courbes observées avec R = H et R = CH_3 dans la même région. ($\Delta E_{1/2} \approx 100$ mV entre pH 3 et 5.5.) Contrairement au comportement de ces deux premiers termes, pour R = C_2H_5 (et les termes suivants) le passage à pH = 6

Can. J. Chem. Downloaded from www.nrcresearchpress.com by 210.87.254.105 on 09/05/12
For personal use only.

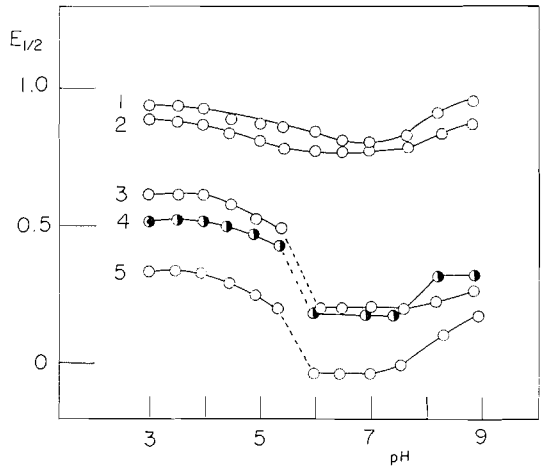

FIG. 4. Variation du potentiel de demi-vague $E_{1/2}$ (V) en fonction du pH (tampon Clark et Lubs). R = H (1), CH_3 (2), i-C_3H_7 (3), t-C_4H_9 (4), et C_6H_5 (5).

en tampon phosphate crée un glissement supplémentaire de 200–250 mV vers les potentiels plus positifs. Les potentiels de demi-vague sont alors à 50 mV près les mêmes qu'en tampon Mc Ilvaine au même pH.

Influence de la vitesse de balayage

Les courants maximum des oscillo-polarogrammes $i = f(E)$ qui ont été observés pour des vitesses de balayage de 0.5 à 20 V/s ont été étudiés en fonction de la racine carrée de la vitesse de balayage. Une relation linéaire est obtenue pour tous les méthoxyhydroperoxydes examinés (Fig. 5). D'après Delahay (19) et Matsuda et Ayabe (20) un tel comportement est caractéristique pour un courant de diffusion d'un processus irréversible

$$i_{max} = k_2 qn(\alpha n_a)^{1/2} CD^{1/2} v^{1/2} \quad (A)$$

Influence de la température

La dépendance de la température du courant maximum obtenu en polarographie en courant alternatif a été étudiée dans le domaine de 10 à 30 °C. Pour les méthoxyhydroperoxydes avec R = H et CH_3, les courants maximum sont pratiquement indépendants de la température. Pour les autres méthoxyhydroperoxydes examinés on observe un coefficient de température moyen de 1.8% par degré, valeur en accord avec celle donnée par Zuman (21) pour un courant contrôlé par diffusion.

Polarographie dans le méthanol–LiCl (M)

Dans ce milieu, l'électrode de référence utilisée

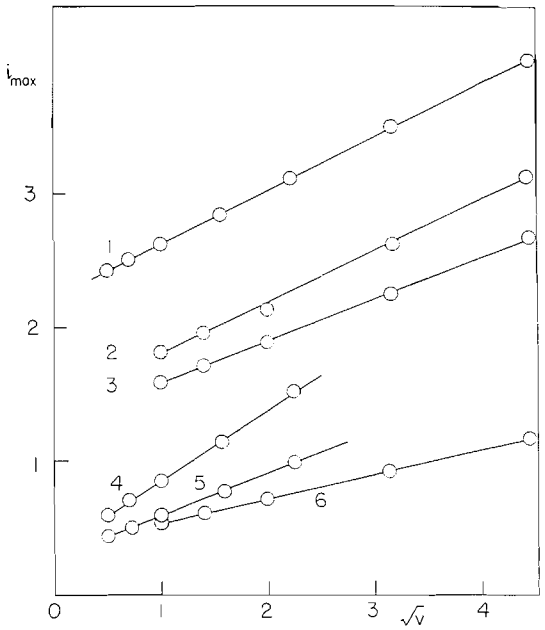

FIG. 5. Variation du courant maximum i_{max} (μA) en fonction de la racine carrée de la vitesse de balayage $(V\ s^{-1})^{1/2}$. R = C_2H_5 (1), H (2), CH_3 (3), n-C_3H_7 (4), i-C_3H_7 (5), et C_6H_5 (6). Les droites 2 et 3 ont été déplacées de 1 μA vers le haut, la droite 1 de 2 μA.

consistait en un fil d'argent plongé dans une solution d'électrolyte saturée en AgCl, séparée de la solution à analyser par un verre fritté fin. On observe, dans ces conditions, un potentiel de demi-vague de −1.54 V pour l'aldéhyde benzoïque; cette valeur est comparable à celle de −1.56 V (vs. calomel saturé) observée par Willits *et al.* (22) dans une solution 0.3 *M* de LiCl dans le benzène–méthanol (1:1). Les potentiels de demi-vague observés sont indiqués au Tableau I. On remarque leur confinement dans le domaine relativement restreint de −1.2 à −0.8 V, c'est-à-dire aux environs du potentiel obtenu dans l'eau pour les deux premiers termes (R = H et CH_3) de la série des méthoxyhydroperoxydes. Ces valeurs sont du même ordre que celles rapportée dans la littérature (4, 22) pour les hydroperoxydes. Ces observations semblent indiquer que la réduction des méthoxyhydroperoxydes avec R = H et R = CH_3 s'effectue dans l'eau selon un mécanisme proche de celui ayant lieu dans le méthanol, ou du mécanisme rapporté pour les hydroperoxydes dans l'eau et dans le méthanol. Les méthoxyhydroperoxydes supérieurs (R = C_2H_5, et les suivants) subiraient, par contre, des phénomènes additionnels dans l'eau, qui auraient

Can. J. Chem. Downloaded from www.nrcresearchpress.com by 210.87.254.105 on 09/05/12
For personal use only.

pour effet de déplacer les potentiels de demi-vague d'environ 600 mV vers les potentiels plus positifs.

Mécanisme proposé

L'ensemble des observations expérimentales exposées suggère le mécanisme de réaction suivant

Mécanisme A

$$R{-}CH(OCH_3){-}OOH + H^{\oplus} \rightleftharpoons R{-}CH(OOH){-}\overset{\oplus}{O}CH_3 \overset{2e^{\ominus}}{\longrightarrow} CH_3OH + R{-}CHO + OH^{\ominus}$$

Mécanisme B

[1] $$R{-}CH(OCH_3){-}OOH + 2e^{\ominus} \xrightarrow{k_e} R{-}CH(OCH_3){-}O^{\ominus} + HO^{\ominus}$$

[2] $$R{-}CH(OCH_3){-}O^{\ominus} + H^{\oplus} \longrightarrow R{-}CH(OCH_3){-}OH$$

[3] $$R{-}\overset{\overset{OCH_3}{|}}{CH}{-}O^{\ominus} \longrightarrow R{-}CHO + CH_3O^{\ominus}$$

[4] $$\overset{\overset{OCH_3}{|}}{R{-}CH{-}OH} + H^{\oplus} \longrightarrow \left[\overset{\overset{\oplus}{H}\overset{\oplus}{O}CH_3}{\underset{|}{R{-}CH}}{-}OH\right] \longrightarrow R{-}CHO + CH_3OH + H^{\oplus}$$

Le mécanisme A qui considère un transfert de proton précédant le transfert d'électron (ou des transferts simultanés) permet une explication de la dépendance des potentiels de demi-vague en fonction du pH, mais implique la formation de composé carbonylé à l'électrode. L'électrolyse à potentiel controllé a montré de façon certaine que pour R = H le composé carbonylé n'est pas libéré sous forme de H—CHO mais sous forme de son hémiacétal. L'ensemble des résultats, qui démontre la similarité de comportement des composés avec R = H et R = CH_3, paraît indiquer que la formation d'hémiacétal à l'électrode doive être envisagée également avec R = CH_3. Donc, pour R = H et R = CH_3, la réduction semble s'effectuer par les réactions [1] et [2] du mécanisme B. Ceci semble être corroboré par le fait que les potentiels de demi-vague et les courants limites sont indépendants du pH, dans la région de pH 3 à 8.

Les termes supérieurs (R = C_2H_5, *n*-C_3H_7, *i*-C_3H_7, *t*-C_4H_9, et Ph), par contre, conduisent à la formation d'aldéhyde soit à la suite d'un processus d'électrode (A), soit en raison d'une hydrolyse très rapide des hémiacétals. Les mécanismes A et B (réactions [1] et [3] ou [1], [2], et [4]) doivent donc être envisagés. Il convient de souligner que l'irréversibilité des réactions étudiées (démontrée dans le présent travail) concerne le phénomène *global* de la réduction polarographique. Les données expérimentales ne permettent, cependant, pas de conclure à l'irreversibilité complète du processus d'électrode lui-même. Dans l'éventualité d'une quasi-réversibilité de la réaction d'électrode, les réactions subséquentes pourraient influencer les valeurs des $E_{1/2}$. Ainsi, pour ces méthoxyhydroperoxydes, le glissement de 600 mV vers des valeurs plus positives pourrait être attribué en partie à une hydrolyse de l'hémiacétal.

Les résultats précédemment exposés, qui concernent (dans le cas des méthoxyhydroperoxydes supérieurs) la dépendance des courants maximum exprimée en fonction de la température et de la vitesse de balayage, ont permis d'établir clairement l'intervention d'un courant contrôlé par diffusion. Cette observation est en accord avec la théorie des réactions de desactivation de l'espèce réduite consécutives au processus d'électrode (23).

L'effet particulier observé en tampon phtalate peut être expliqué soit par un effet de double couche, soit par une interaction phtalate–hydroperoxyde dans la solution. En l'absence d'autres exemples d'effet de double-couche créé par l'ion phtalate, la deuxième hypothèse semble devoir être retenue de préférence et pourrait être formulée comme suit, d'après une suggestion du Professeur Perrin[2].

Le déplacement des potentiels de demi-vague

[2]Nous tenons à remercier M. le Professeur C. L. Perrin pour cette suggestion, ainsi que pour ses suggestions et commentaires concernant le mécanisme proposé.

Can. J. Chem. Downloaded from www.nrcresearchpress.com by 210.87.254.105 on 09/05/12
For personal use only.

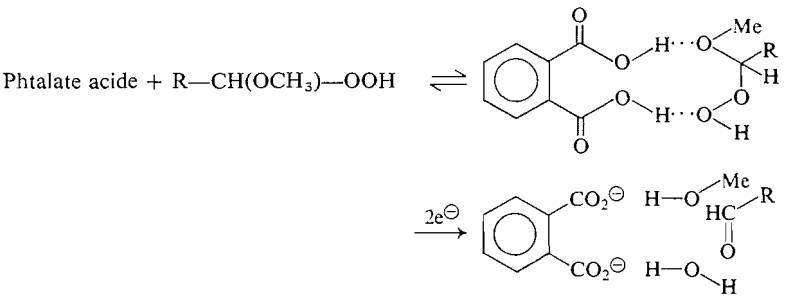

vers des valeurs plus négatives et la diminution de courant observés en milieu basique (tampon Borax–HCl) peuvent être interprétés en termes de réactions précédents le processus d'électrode, soit

$$R—CH(OCH_3)—OOH + HO^{\ominus} \rightleftharpoons R—CH(OCH_3)—OO^{\ominus} + H_2O$$

ainsi qu'il a été suggéré par Perrin (24), ou être dus à la décomposition baso-catalysée des méthoxyhydroperoxydes (25)

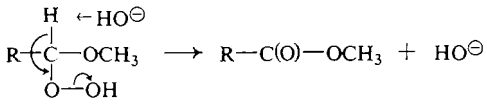

Application analytique

L'étude de l'influence des différents facteurs (pH, tampon, température) sur la position, la forme et l'intensité des pics polarographiques a déterminé le choix du tampon Mc Ilvaine pH = 7 comme électrolyte de support pour les applications analytiques du processus d'électrode étudié. L'étude de la réaction d'ozonolyse dans un solvant participant (CH_3OH) devant être le champ d'application de cette méthode, les conditions opératoires polarographiques devaient être adaptées aux conditions opératoires propres à l'étude de la réaction d'ozonolyse.

L'ozonation des oléfines dissymétriques en présence d'un solvant participant, dans le but de "trapper" les zwitterions de Criegee sous forme d'hydroperoxydes, est fréquemment effectuée dans le méthanol pur (11) ou dans un solvant inerte tel que le CCl_4 contenant une concentration adéquate de méthanol. En général, une concentration 1 *M* de méthanol suffit pour "trapper" quantitativement les zwitterions en les transformant en méthoxyhydroperoxydes (7). Cependant des études récentes (26) tendent à montrer que pour l'étude de certains zwitterions (notamment les zwitterions $R—\overset{+}{C}H—OO^-$ avec R = *i*-C_3H_7 ou *t*-C_4H_9) une concentration supérieure de méthanol (3 *M*) est préférable pour assurer la transformation quantitative des zwitterions en leur méthoxyhydroperoxydes correspondants, à 25 °C.

Il a été vérifié (*7a*) que les méthoxyhydroperoxydes engendrés lors des ozonolyses en présence de méthanol ne réagissent pas, à la température ambiante, avec les produits carbonylés également engendrés lors de l'ozonation. Des bilans d'ozonation ont permis de vérifier que l'ozonolyse, en présence de méthanol, d'une mole d'oléfine engendre 1 mole du mélange de méthoxyhydroperoxydes et 1 mole du mélange de produits carbonylés. Dès lors, l'analyse de ces derniers (notamment par spectroscopie i.r. et chromatographie en phase gazeuse (c.p.g.)) permets de déterminer (*7a*, *7c*) dans quelles proportions les 2 voies de clivage (*a* et *b*) sont suivies. L'analyse des produits carbonylés s'avérant parfois difficile, c'est par l'analyse polarographique des méthoxyhydroperoxydes que ces proportions de clivage (*a* et *b*) pourront être déterminées.

En raison de leur inmiscibilité avec l'eau, les solvants chlorés tels que le chloroforme ou le tétrachlorure de carbone ne peuvent être utilisés. L'acétate d'éthyle, décrit par Greenwood (27) comme étant un bon solvant d'ozonation et qui est miscible à l'eau dans la proportion de 1 ml

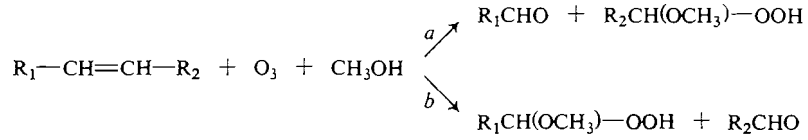

Can. J. Chem. Downloaded from www.nrcresearchpress.com by 210.87.254.105 on 09/05/12
For personal use only.

Can. J. Chem. Downloaded from www.nrcresearchpress.com by 210.87.254.105 on 09/05/12
For personal use only.

dans 25 ml d'eau, a été choisi en raison de ces propriétés.

Deux conditions opératoires ont été éxaminées: (*i*) pour des méthoxyhydroperoxydes en solution dans le méthanol et (*ii*) pour des solutions dans l'acétate d'éthyle – méthanol (3 *M*). Les concentrations en méthoxyhydroperoxydes étaient comprises entre 5×10^{-3} et 5×10^{-2} *M*. Ces concentrations sont obtenues par l'ozonation de solutions 0.1 *M* d'oléfine, à des degrés d'ozonation n'excédant pas 50%. Ces faibles degrés d'ozonation permettent de prévenir l'oxydation du solvant, ainsi que l'autoxydation accélérée par l'ozone des produits carbonylés engendrés par l'ozonolyse. En effet, le méthanol ozoné montre un pic polarographique à −1.14 V pouvant affecter la précision de la détermination des méthoxyhydroperoxydes avec R = H et R = CH_3.

En vue de l'analyse polarographique des solutions méthanoliques de méthoxyhydroperoxydes, 1 ml de solution est transféré dans 25 ml de tampon Mc Ilvaine pH = 7. Pour tous les méthoxyhydroperoxydes étudiés, le courant maximum observé est une fonction linéaire de la concentration en méthoxyhydroperoxyde, à 25° C (Fig. 6). La reproductibilité des mesures est alors excellente ($\Delta i_{max} \leqslant 1\%$). La largeur des pics est cependant assez importante. De ce fait la détermination simultanée de deux méthoxyhydroperoxydes des deux groupes, soit (*i*) avec R = H ou CH_3 et (*ii*) avec R = C_2H_5, *n*-C_3H_7, ou *t*-C_4H_9, est difficile (avec précision), voire même parfois impossible, selon les proportions relatives des deux méthoxyhydroperoxydes.

Pour l'analyse des solutions de méthoxyhydroperoxydes dans l'acétate d'éthyle – méthanol (3 *M*), 1 ml de solution est ajouté à 25 ml de tampon Mc Ilvaine pH = 7. Le courant maximum observé est directement proportionel à la concentration en dépolariseur (Fig. 7). La présence d'acétate d'éthyle apporte une modification intéressante aux phénomènes observés. Les potentiels de demi-vague sont déplacés vers des potentiels plus négatifs pour R = H, CH_3 et vers des potentiels lègérement plus positifs pour R = C_2H_5, *n*-C_3H_7, *i*-C_3H_7, et *t*-C_4H_9 (Tableau I). De plus, la largeur des pics est diminuée, de sorte que la détermination simultanée de deux

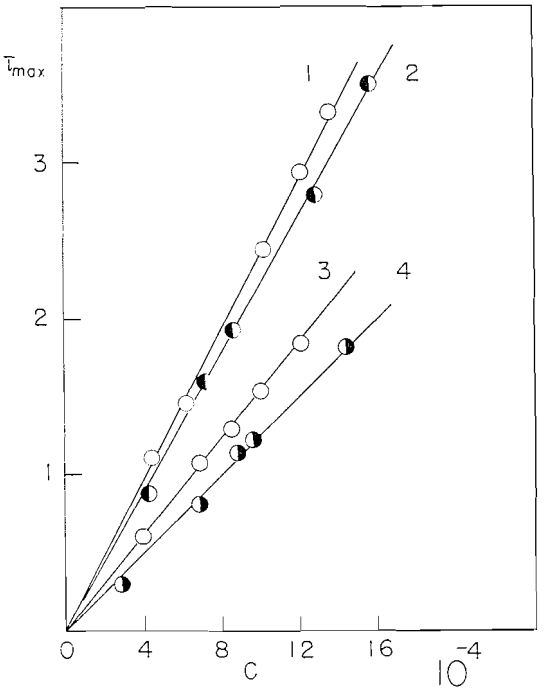

FIG. 6. Intensité des pics polarographiques (μA) vs. concentration *c* (*M*), dans le méthanol, des méthoxyhydroperoxydes. Tampon Mc Ilvaine, pH = 7; température, 25 ± 0.1 °C; R = C_2H_5 (1), *i*-C_3H_7 (2), H (3), et CH_3 (4).

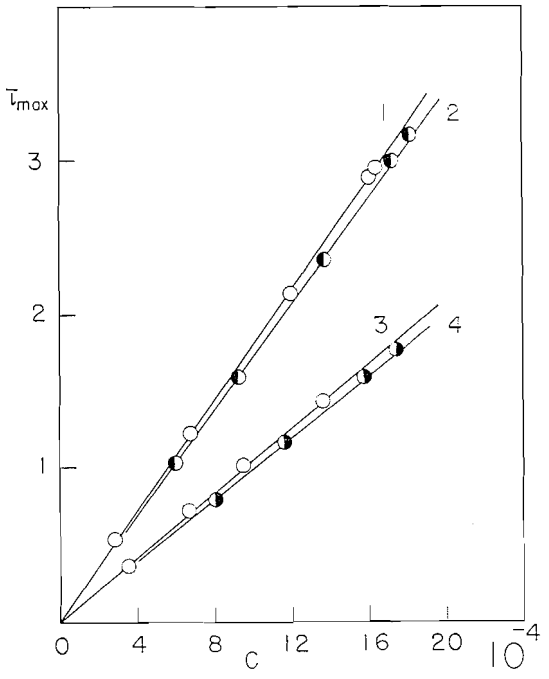

FIG. 7. Intensité des pics polarographiques (μA) vs. concentration *c* (*M*) dans l'acétate d'éthyle – méthanol (3 *M*) des méthoxyhydroperoxydes. Tampon Mc Ilvaine, pH = 7; température, 25.0 ± 0.1 °C. R = *i*-C_3H_7 (1), *t*-C_4H_9 (2), H (3), et CH_3 (4).

TABLEAU II

Ozonolyse de 1 mmole de *trans* 4-méthylpentène-2, en solution (0.1 *M*) dans l'acétate d'éthyle – méthanol (3 *M*), à 25 °C

O actif mAtome	CH_3—$CH(OCH_3)OOH$ mmole	*i*-C_3H_7—$CH(OCH_3)OOH$ mmole	Hydroperox. total, mmole	% Clivage voie *a*		% Clivage voie *b*
				Méthode 1	Méthode 2	
0.250	0.172	0.074	0.246	69.0	70.0	29.6
0.335	0.240	0.086	0.326	71.6	73.6	26.0
0.420	0.300	0.126	0.426	71.4	70.4	30.0
0.430	0.310	0.120	0.430	72.0	72.1	28.0
0.495	0.350	0.138	0.488	70.8	71.7	28.0

méthoxyhydroperoxydes de chaque groupe devient possible. Dans ces conditions la reproductibilité des mesures est, cependant, plus difficile à atteindre que lors des expériences effectuées en absence d'acétate d'éthyle. Toutes les conditions expérimentales doivent être soigneusement contrôlées, notamment la température, la pureté des solvants (acétate d'éthyle et méthanol), le temps d'agitation (pour la solubilisation), ainsi que le temps de dégazage. Une reproductibilité satisfaisante ($\Delta i_{max} \leqslant 3\%$) peut être atteinte.

L'analyse polarographique des méthoxyhydroperoxydes a été appliquée à la détermination des proportions de clivage selon les deux voies possibles (*a* et *b*) dans le cas d'oléfines pour lesquelles les proportions de clivage avaient été déterminées d'après des dosages des composés carbonylés, effectués par c.p.g. et spectroscopie i.r. (*7a*, *7c*). Le Tableau II rapporte les résultats obtenus lors de l'ozonation du *trans* 4-méthylpentène-2 dans l'acétate d'éthyle – méthanol (3 *M*). On note, qu'aux erreurs expérimentales près, le nombre total de mmoles de méthoxyhydroperoxydes trouvés par voie polarographique correspond bien au dosage iodométrique de l'oxygène actif selon Lohaus (12), qui est une mesure de la quantité totale des hydroperoxydes.

La proportion de clivage selon la voie *a*, qui aboutit à la formation de CH_3—$CH(OCH_3)$—OOH et *i*-C_3H_7—CHO, a été calculée en rapportant la quantité de ce méthoxyhydroperoxyde formé à l'oxygène actif mesuré iodométriquement (méthode 1) et en rapportant la quantité de ce même méthoxyhydroperoxyde à la quantité totale des méthoxyhydroperoxydes formés, d'après leurs dosages polarographiques (méthode 2). Le pourcentage de clivage selon la voie *b*, conduisant à la formation de *i*-C_3H_7—$CH(OCH_3)$—OOH et CH_3CHO, a été calculé d'après le dosage polarographique de ce méthoxyhydroperoxyde, rapporté au dosage de l'oxygène actif. Ces résultats expérimentaux montrent bien que les voies *a* et *b* sont complémentaires. La valeur moyenne déterminée par voie polarographique pour la proportion de clivage selon la voie *a* ($71 \pm 1\%$) se compare bien avec la valeur de $73 \pm 4\%$ trouvée d'après des analyses spectroscopiques et par c.p.g.

Le Tableau III permet, pour quelques oléfines dissymétriques, la comparaison des résultats obtenus pour les proportions de clivage selon les deux voies possibles, ainsi qu'ils ont été obtenus par polarographie et par c.p.g., associée à la spectroscopie i.r.

TABLEAU III

Sens de clivage de quelques oléfines dissymétriques

Oléfine	Zwitterion considéré	% de clivage engendrant ce zwitterion		Référence
		Dosage polarographique	Autres méthodes	
p-Chlorostyrène	$^{+}CH_2$—OO^{-}	57.7 ± 1	57 ± 1	*7c*
Anéthole	CH_3—$\overset{+}{C}H$—OO^{-}	67.5 ± 1	68 ± 1	*7a*
1,1-Diphényléthylène	$^{+}CH_2$—OO^{-}	31 ± 1	33 ± 1	
trans-4-Méthylpentène-2	CH_3—$\overset{+}{C}H$—OO^{-}	71 ± 1	73 ± 4	

Can. J. Chem. Downloaded from www.nrcresearchpress.com by 210.87.254.105 on 09/05/12
For personal use only.

La polarographie s'avère donc être une méthode satisfaisante pour le dosage des méthoxyhydroperoxydes et, en particulier, pour l'étude de la réaction d'ozonolyse en solvant participant.

Remerciements

Nous tenons à remercier MM. les Professeurs R. L. Benoît et M. Abraham pour toutes les facilités accordées lors de cette étude, ainsi que MM. M. Gauthier et P. Pichet pour leurs conseils. Nous remercions également le Conseil National de Recherches du Canada pour un octroi qui a permis la présente recherche.

1. L. S. SILBERT. J. Amer. Oil Chem. Soc. **39**, 480 (1962).
2. A. H. M. COSIJN. Chem. Weekblad, **60**, 585 (1964).
3. M. BERNARD. Parfums, Cosmet. Savons, **1**, 467 (1958).
4. E. J. KŮTA et F. W. QUACKENBUSH. Anal. Chem. **32**, 1069 (1960).
5. R. C. SLAGEL. J. Org. Chem. **31**, 593 (1966).
6. R. CRIEGEE et G. WENNER. Ann. Chem. **564**, 9 (1949). R. CRIEGEE. Ann. Chem. **583**, 1 (1953). R. CRIEGEE. Record Chem. Progr. Kresge-Hooker Sci. Lib. **18**, 111 (1957). P. S. BAILEY. Chem. Rev. **58**, 926 (1958).
7. (*a*) S. FLISZÁR et M. GRANGER. J. Amer. Chem. Soc. **91**, 3330 (1969) (*b*) P. S. BAILEY, S. B. MAINTHIA, et C. J. ABSHIRE. J. Amer. Chem. Soc. **82**, 6136 (1960). (*c*) S. FLISZÁR et J. RENARD. Can. J. Chem. **45**, 533 (1967).
8. N. L. BAULD, J. A. THOMPSON, C. E. HUDSON, et P. S. BAILEY. J. Amer. Chem. Soc. **90**, 1822 (1968). S. FLISZÁR et J. CARLES. J. Amer. Chem. Soc. **91**, 2637 (1969). S. FLISZÁR et J. CARLES. Symp. Oxidation of Hydrocarbons, ACS meeting, Minneapolis, April 1969. Preprints of papers. p. A59. S. FLISZÁR et J. CARLES. Can. J. Chem. Sous presse.
9. B. BREYER, F. GUTMANN, et S. HACOBIAN. Aust. J. Sci. Res. Ser. A, **3**, 558 (1950).
10. B. BREYER, F. GUTMANN, et H. H. BAUER. Oesterr. Chem.-Ztg. **57**, 67 (1956).
11. W. P. KEAVENEY, M. G. BERGER, et J. J. PAPPAS. J. Org. Chem. **32**, 1537 (1967).
12. G. LOHAUS. Ann. Chem. **583**, 4 (1953).
13. L. A. SUBLUSKEY, G. C. HARRIS, A. MAGGIOLO, et A. L. TUMOLO. Advan. Chem. Ser. **21**, 149 (1959).
14. (*a*) G. A. GILBERT et E. K. RIDEAL. Trans. Faraday Soc. **47**, 396 (1951). (*b*) J. HEYROVSKÝ et J. KŮTA. Principles of polarography. Academic Press, Inc., New York. 1966. p. 277.
15. D. A. SKOOG et A. B. H. LAUWZECHA. Anal. Chem. **28**, 825 (1956).
16. P. SOUCHAY et M. CRAIZON. Chim. Anal. **36**, 85 (1954).
17. D. M. COULSON. Anal. Chim. Acta, **19**, 284 (1958).
18. P. ZUMAN. Organic polarographic analysis. The Pergamon Press, Ltd., Oxford. 1964. p. 12–13.
19. P. DELAHAY. J. Amer. Chem. Soc. **75**, 1190 (1953).
20. (*a*) H. MATSUDA et Y. AYABE. Z. Elektrochem. **59**, 494 (1955). (*b*) J. HEYROVSKÝ et J. KŮTA. Principles of polarography. Academic Press, Inc., New York. 1966. p. 505.
21. P. ZUMAN. *Dans* Progress in physical organic chemistry. Vol. 5. Interscience Publishers, Inc., New York. 1967. p. 134.
22. C. O. WILLITS, C. RICCIUTI, H. B. KNIGHT, et D. SWERN. Anal. Chem. **24**, 785 (1952).
23. J. HEYROVSKÝ et J. KŮTA. Principles of polarography. Academic Press, Inc., New York. 1966. p. 394–395
24. C. L. PERRIN. *Dans* Progress in physical organic chemistry. Vol. 3. Interscience Publishers, Inc., New York. 1965. p. 278.
25. D. B. SHARP et T. M. PATRICK, JR. J. Org. Chem. **26**, 1389 (1961).
26. G. KLUTSCH, J. GRIGNON, J. RENARD, et S. FLISZÁR. A paraître.
27. F. L. GREENWOOD. J. Org. Chem. **10**, 414 (1945).

Can. J. Chem. Downloaded from www.nrcresearchpress.com by 210.87.254.105 on 09/05/12
For personal use only.

Can. J. Chem. Downloaded from www.nrcresearchpress.com by 210.87.254.105 on 09/05/12
For personal use only.

Collisional deactivation of singlet methylene in the photolysis of ketene[1]

R. A. Cox[2] and K. F. Preston
Division of Applied Chemistry, National Research Council of Canada, Ottawa, Canada

Received March 7, 1969

An investigation has been made into the effect of inert gas additions on product quantum yields for the photolysis at 2800 and 2490 Å of mixtures of ketene and oxygen and for the photolysis at 2800 Å of mixtures of ketene and carbon monoxide. Concentration ratios of O_2 (or CO) to CH_2CO were chosen so that the reaction of $CH_2(^3\Sigma_g^-)$ with CH_2CO could be ignored and C_2H_4 formation could be attributed entirely to the reaction

$$CH_2(^1A_1) + CH_2CO \rightarrow C_2H_4 + CO\ (k_1)$$

Quenching of the C_2H_4 quantum yield by inert gases was interpreted in terms of collisional deactivation of $CH_2(^1A_1)$ to the ground state

$$CH_2(^1A_1) + M \rightarrow CH_2(^3\Sigma_g^-) + M\ (k_2)$$

and rate constant ratios k_2/k_1 have been determined for a number of gases: He (0.018), Ar (0.014), Kr (0.033), Xe (0.074), N_2 (0.052), N_2O (0.10), CF_4 (0.047), C_2F_6 (0.11), and SF_6 (0.045). It has been assumed that collision-induced intersystem crossover in excited singlet ketene makes an insignificant contribution to the observed quenching effects, but it has not been possible to verify this assumption experimentally. The mechanism of collision-induced electronic relaxation of singlet methylene is discussed in the light of the results.

Canadian Journal of Chemistry, 47, 3345 (1969)

Introduction

It is established (1–7) that the photolysis of ketene in the wavelength region 2500–3800 Å yields methylene both in the ground triplet state ($^3CH_2$) and in an electronically excited singlet state ($^1CH_2$). These states are believed to correspond to the $^3\Sigma_g^-$ and $^1A_1$ (in C_{2v}) methylene species observed spectroscopically by Herzberg and co-workers (8, 9) during the flash photolysis of diazomethane. It is generally held (1, 7, 10, 11) that the methylenes result from predissociation of excited singlet and triplet ketene molecules, the latter arising by way of intersystem crossover from the excited singlet. The proportion of singlet species in the methylene is determined by the competition between unimolecular dissociation and spin inversion of the excited singlet ketene, and would be expected to increase with increasing energy of excitation of the ketene molecule. This is in accord with the experimental finding (1–3, 5, 7) that the methylene is predominantly (although not entirely) singlet at short wavelengths of photolysis, but mainly triplet at long wavelengths. Since dissociation to methylene and carbon monoxide occurs via an excited molecule of finite lifetime, bimolecular reactions of the excited molecule are a possible complicating feature of studies of methylene reactions based on ketene photolysis as a source. However, the quantum yield of CO formation at short wavelengths shows little or no dependence (2, 12) on pressure or temperature, suggesting that bimolecular reactions of excited ketene molecules may be ignored for $\lambda < 2900$ Å. This is also suggested by the lack of effect (2, 7, 13) of pressure on the estimated relative yields of singlet and triplet methylene. Thus, photolysis of ketene at $\lambda < 2900$ Å approximates a "clean" source of methylene radicals which may be used to investigate the reactivity of singlet methylene when the ground state species is selectively removed by a triplet scavenger.

Two reagents, O_2 (14) and CO (2, 15), appear to be effective triplet methylene scavengers, O_2 being the less discriminating of the two on account of its high reactivity towards radicals and excited molecules in general. Very small additions of oxygen are sufficient to reduce the quantum yield of ethylene formation from the photolysis of ketene at $\lambda < 2900$ Å to a limiting value, approximately 0.65–0.70 which is unaffected by further addition of oxygen (2, 12), and which is close to some estimates (2, 13) of the quantum yield of singlet methylene production at short

[1]NRCC No. 10 720.
[2]NRCC Postdoctorate Fellow 1966–1968. Present address: Health Physics and Medical Division, Atomic Energy Research Establishment, Harwell, Berkshire, England.

Can. J. Chem. Downloaded from www.nrcresearchpress.com by 210.87.254.105 on 09/05/12
For personal use only.

wavelengths. A plausible explanation of these facts and of the results of recent experiments (14) on the photolysis of mixtures of isotopically labeled ketene, olefins, and oxygen is that $^3CH_2$ reacts very much more rapidly with O_2 than with CH_2CO, but the reverse is true of $^1CH_2$. Since it is most unlikely that the products (14) of the reaction of triplet methylene with O_2 will react further with ketene to generate ethylene, the rate of ethylene production from the photolysis of ketene containing oxygen may be used as a measure of the stationary concentration of singlet methylene.

Recently it has been found (2, 15) that $^3CH_2$ reacts more rapidly with CO than with ketene or butene, whereas the reverse is true of $^1CH_2$. When CO is added in sufficient excess, the reactions of $^3CH_2$ in the photolysis of CH_2CO or CH_2CO/butene mixtures may be quenched so that essentially all the products are formed from the reactions of $^1CH_2$. This method of scavenging $^3CH_2$ is perhaps less disputable than the method using O_2, since CO, unlike O_2 (16), is probably inert towards excited ketene molecules.

An essential preliminary to the study of reactions of an electronically excited species which is metastable with respect to the transition to the ground state is the determination of the efficiencies with which molecules effect collisional relaxation of the electronic energy of excitation. Since Herzberg's (8) observation of collisional relaxation of the $^1A_1$ state of methylene to the $^3\Sigma_g^-$ state, several workers (17, 18) have employed inert gases as coolants to ensure the conversion of photolytically generated methylene to the ground state. Their observations of decreasing stereospecificity of addition of methylene to the C=C bond with increasing ratio of inert gas pressure to olefin pressure are consistent with collisional quenching of $^1CH_2$ to $^3CH_2$ by inert gases. However, the quantitative aspects of quenching of $^1CH_2$ have so far been ignored, largely because of uncertainties regarding the contributions of additional quenching processes (e.g. of excited ketene, excited product molecules) to the observed overall effect of added gases on reactions involving methylene. We believe that the photolysis of ketene at $\lambda < 2900$ Å is free of such complications and that in the presence of sufficient oxygen or carbon monoxide the quantum yield of ethylene may be equated with the yield of $^1CH_2$. Accordingly we have undertaken a study of the effects of inert gas additions upon the quantum yield of C_2H_4 formation from the photolysis of mixtures of CH_2CO and O_2 or CO in order to obtain quantitative rate data for the electronic relaxation of $^1CH_2$.

Experimental

Materials

Ketene was prepared and purified by well established techniques (1) and then stored at −196 °C. It contained CO_2 (< 0.01%) as the only detectable impurity. Gases condensable at −196 °C (Xe, SF_6, N_2O, CF_4, C_2F_6; all from Matheson of Canada, Ltd.) were thoroughly degassed at that temperature and distilled through a trap at −78 °C before use. The O_2 contents of cylinder CO (Matheson) and N_2 (Linde) were substantially reduced by passing the gases over hot copper turnings at ~400 °C; after this treatment the N_2 contained < 2 p.p.m. O_2 and the CO contained ~20 p.p.m. O_2. At this O_2 content the contribution of scavenging of $^3CH_2$ by O_2 in experiments using CO as a scavenger could be ignored for the conversions employed. The coincidence of results obtained using extremely pure CO (O_2 content 4 p.p.m.) with the results for the less pure CO confirmed this assumption. Research Grade Kr (Airco) and O_2 (Matheson) were used as such; He (Airco) and Ar (Linde) were taken from cylinders via drying tubes containing molecular sieve 13X.

Apparatus and Procedure

Photolyses were carried out at 27 ± 2 °C in a cylindrical quartz cell of 15 cm length and 306 cc volume, having plane end windows. The cell was connected by a stopcock to a conventional high vacuum apparatus for the preparation and handling of gas mixtures. The light source was an Osram HB200 super pressure Hg lamp coupled to a Bausch and Lomb high intensity monochromator which served to isolate spectral regions centered at 2490 and 2800 Å with a half bandwidth of 50 Å. An RCA 935 phototube was used to monitor the light beam after it had passed through the reaction cell and contents. The voltage drop resulting from passage of the photocurrent through a 10 KΩ resistor was fed directly to a millivolt pen recorder of high input impedance tolerance.

Before each run the reaction cell was evacuated to better than 10^{-4} mm Hg and ketene introduced to the required pressure. After condensing the ketene in a cold finger, O_2 was measured into the cell with the aid of a calibrated Pirani gauge. The mixture of ketene and oxygen was allowed to warm up and inert gas then added to a measured total pressure by expansion from a large storage bulb. A 20 min period proved quite adequate for thorough mixing at the highest total pressure used. The mixtures were normally irradiated for 60 min at 2490 Å and 15 – 30 min at 2800 Å resulting in ~0.2% and ~0.5% decomposition respectively. (Increasing the extent of decomposition to ~1% was without effect on the product quantum yields.) Light transmitted through the reaction cell was recorded continuously throughout each experiment. After irradiation the contents of the cell were allowed to mix for ~10 min. Samples for

Can. J. Chem. Downloaded from www.nrcresearchpress.com by 210.87.254.105 on 09/05/12
For personal use only.

analysis were then taken by direct expansion from the reaction cell into the gas chromatography injection volume.

A thermistor detector and a flame ionization detector were used in conjunction for quantitative analysis of reaction products. Separation of C_2H_4 from other products and reactants was achieved with either a 12 ft column of Porapak Q or a 12 ft column of alumina deactivated with 2% squalane. C_2H_2 was satisfactorily separated from C_2H_4 on the latter column only. Analysis for CO on these columns was possible in the absence of O_2 and other permanent gases; in their presence an 8 ft column of molecular sieve 13X was used to separate CO. Analyses for each run were normally duplicated. The detectors were calibrated frequently with standard mixtures of CO in He, and C_2H_4 in He which were introduced to the sample volume in precisely the same manner as reaction mixtures. The flame ionization detector responses of C_2H_2, C_2H_4, and C_2H_6 were assumed to be identical.

Product quantum yields were based on the time-integrated value of light transmitted I_{trans} through a path length l of ketene at P_k mm Hg. The product $I_{trans} P_k$ was taken as the value of I_{abs} in arbitrary units since the relationship

$$I_{abs} = I_{trans}\, \varepsilon\, l\, P_k$$

held to a good approximation at the wavelengths and pressures used. Conversion of I_{abs} to absolute units was based on the assumption that $\Phi_{CO} = 2.0$ for the photolysis of pure ketene. In a few experiments a second quartz cell was placed in the path of light emerging from the main reaction vessel. Both cells were filled with an identical pressure of ketene, but additives were introduced to the main cell only. The second cell served as a chemical actinometer, CO yields being used to monitor I_{trans}. The overall uncertainty in the measured quantum yields of C_2H_4 and CO was estimated to be of the order of ±7%.

Results

(a) Photolysis of Ketene–Oxygen Mixtures at 2800 Å

Ketene containing a few per cent of oxygen and mixed with varying amounts of inert gas was irradiated at 2800 Å for 15–30 min and the product yields determined. Table I gives the quantum yields of ethylene $\Phi_{C_2H_4}$ and of other products (where measured) calculated from the integrated photometer readings for each run and an assumed value of $\Phi_{CO} = 2.0$ for the photolysis of ketene alone.

The photolysis of pure ketene was frequently carried out as a check on the photometer calibration. It was found that $\Phi_{C_2H_4}$ was consistently close to 0.94 (relative to $\Phi_{CO} = 2.0$) and that this quantum yield was independent of CH_2CO pressure in the range 10–30 mm Hg. Furthermore, the yield of CO per unit light absorbed (absolute

TABLE I

Product quantum yields from the photolysis of CH_2CO–O_2 mixtures at 2800 Å and 27 °C

Reactant pressures (mm Hg)			Quantum yields‡				
CH_2CO	O_2	M	C_2H_4	CO	CH_4	C_2H_6	Other
10.2	—	—	0.928	2.0*	tr	0.022	0.017 (C_2H_2)
10.6	—	—	0.933	2.0*	nm	nm	
11.8	—	—	0.940	2.0*	tr	0.025	
26.4	—	—	0.940	2.0*	tr	0.026	
10.8	1.2	—	0.578	3.6	—	—	0.5 (CO_2)
26.6	1.2	—	0.636	nm	tr	tr	0.5 (CO_2)
25.2	1.0	407.2 (N_2)	0.340	nm	—	tr	
26.8	1.0	241.2 (N_2)	0.444	nm	—	tr	
10.8	1.2	136.4 (N_2)	0.395	nm	—	tr	
10.8	2.4	99.8 (N_2)	0.443	nm	—	tr	
26.8	1.0	162.4 (C_2F_6)	0.462	nm	—	tr	
10.6	1.2	104.0 (C_2F_6)	0.396	3.0	—	tr	
10.0	1.2	190.8 (Xe)	0.273	2.4	—	tr	
10.2	1.4	104.8 (Xe)	0.389	2.1	—	tr	
11.4	1.0	270.2 (Ar)	0.456	nm	nm	nm	
10.8	1.4	207.8 (Ar)	0.466	nm	nm	nm	
11.6	1.2	98.0 (Ar)	0.541	nm	nm	nm	
10.6	1.4	104.6 (SF_6)	0.363	3.1	—	—	
10.0†	1.6	—	0.650				
10.0†	1.8	621.2 (N_2)	0.144				
10.2†	1.8	551.0 (N_2)	0.164				
10.6†	1.4	342.2 (N_2)	0.236				

*Assumed value used in calculating other quantum yields.
†Light intensity obtained from reference cell containing pure ketene.
‡nm = not measured; tr = trace present, not determined quantitatively.

Can. J. Chem. Downloaded from www.nrcresearchpress.com by 210.87.254.105 on 09/05/12
For personal use only.

Φ_{CO} values were not determined) did not change appreciably, indicating that the primary dissociation yield from CH_2CO is essentially constant over that range of CH_2CO pressures. Minor products from the photolysis of pure ketene included C_2H_6 ($\Phi_{C_2H_6} \simeq 0.022$) and C_2H_2 ($\Phi_{C_2H_2} \simeq 0.017$) and traces of CH_4, C_3H_8, and C_3H_6.

Addition of oxygen to ketene caused a reduction (Table I) in $\Phi_{C_2H_4}$ from the photolysis to approximately 0.60 and an increase in Φ_{CO} to $\sim$ 3.0. The yields of C_2H_6 and C_2H_2 were reduced to trace amounts. CO_2, which was not formed in the absence of O_2, appeared among the products and its quantum yield was estimated at $\sim$ 0.5. Inert gas additions caused further reductions in $\Phi_{C_2H_4}$. These observations are in agreement with the results of earlier investigations (12, 14).

The final section of Table I shows the results obtained when a reference cell containing ketene only was used as an actinometer. Quantum yields obtained by this method were consistent with the values obtained when using the photometer.

(b) Photolysis of Ketene–Oxygen Mixtures at 2490 Å

The influence of inert gas additions on the quantum yield of C_2H_4 from the photolysis of CH_2CO–O_2 mixtures at 2490 Å was determined. Mixtures of CH_2CO ($\sim$ 25 mm Hg), O_2 ($\sim$ 1 mm Hg), and varying amounts of inert gas were irradiated for 60 min and the C_2H_4 yield measured. Quantum yields of C_2H_4 formation, $\Phi_{C_2H_4}$, were expressed in terms of arbitrary units of light flux. The results are summarized in Fig. 1 in the form of plots of $\Phi_{C_2H_4}{}^0 (\Phi_{C_2H_4})^{-1} - 1$ vs. the concentration ratio [M]/[ketene], where $\Phi_{C_2H_4}{}^0$ is the quantum yield of C_2H_4 formation in arbitrary units for [M] = 0. Frequent checks were made on the value of $\Phi_{C_2H_4}{}^0$ since the photometer arrangement was altered several times during the course of these experiments. It was shown (Table II) that $\Phi_{C_2H_4}{}^0$ was independent of oxygen pressure in the range 0.1–8 mm Hg.

With N_2O as an additive, extremely small amounts of N_2 were produced, but they were not measured quantitatively. For the other additives no additional products were detected with the analytical system used, and it is probable that, except for N_2O, no chemical reaction with the added gases occurred.

TABLE II

Quantum yields (arbitrary units) of C_2H_4 from the photolysis of $CH_2CO - O_2$ mixtures at 2490 Å and 27 °C

Reactant pressure (mm Hg)		
CH_2CO	O_2	Quantum yield, $\Phi_{C_2H_4}{}^0$
25.2	0.15	6.82
26.4	1.4	6.88
25.6	8.6	6.20

(c) Photolysis of Ketene – Carbon Monoxide Mixtures at 2800 Å

Table III gives the quantum yields of C_2H_4 and C_2H_6 formation from the photolysis at 2800 Å of various mixtures of ketene, carbon monoxide, and inert gases. Calculations of the quantum yields were based on the assumption that $\Phi_{CO} = 2.0$ for the photolysis of ketene alone. The reaction of $^3CH_2$ with CO is very slow (2) compared to reaction with O_2, necessitating the use of large [CO]/[CH_2CO] ratios to ensure the complete scavenging of $^3CH_2$. DeGraff and Kistiakowsky's results (2) suggest that a ratio of

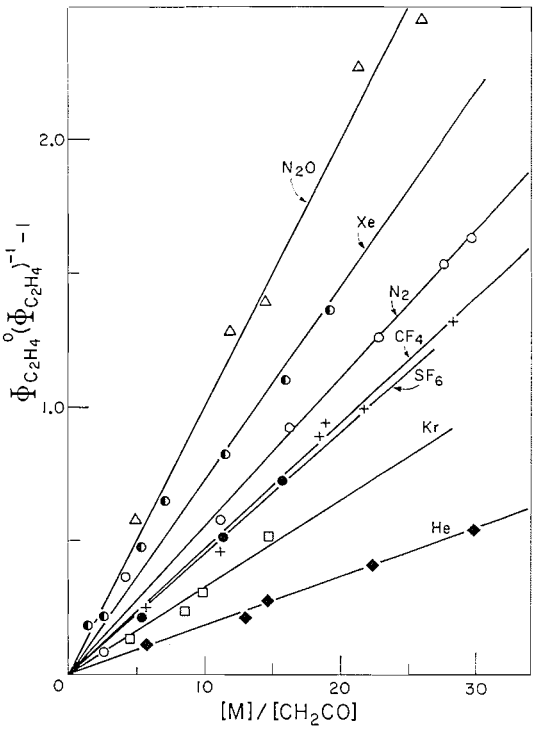

FIG. 1. Plot of $\Phi_{C_2H_4}{}^0 (\Phi_{C_2H_4})^{-1} - 1$ against concentration ratio [M]/[CH_2CO] for the 2490 Å photolysis of mixtures of CH_2CO, O_2, and various added gases, M.

TABLE III

Product quantum yields from the photolysis of CH_2CO–CO mixtures at 2800 Å and 27 °C

Reactant pressures (mm Hg)			Quantum yields*	
CH_2CO	CO	M	C_2H_4	C_2H_6
10.6	40.2	—	0.408	~0.002
10.4	51.0	—	0.375	~0.0005
11.0	70.6	—	0.337	tr
10.0	123.2	—	0.239	"
10.8	50.8	129.6 (N_2)	0.275	"
10.2	50.6	213.0 (N_2)	0.244	"
†10.6	50.4	248.2 (N_2)	0.228	"
10.8	50.6	352.1 (N_2)	0.193	"
10.8	50.2	385.6 (N_2)	0.184	"
10.6	50.8	63.6 (C_2F_6)	0.258	"
11.2	51.0	103.6 (C_2F_6)	0.226	"
11.4	54.0	160.4 (C_2F_6)	0.198	"
10.4	50.4	118.4 (Xe)	0.251	"
10.0	52.0	167.8 (Xe)	0.199	"
11.0	51.0	387.0 (He)	0.275	"
10.2	50.6	166.6 (N_2O)	0.137	"

*Based on $\Phi_{CO} = 2.0$ for photolysis of CH_2CO alone; tr = trace present, not determined quantitatively.
†1.0 mm Hg O_2 added.

at least 4 is necessary to reduce the $^3CH_2$ contribution towards C_2H_4 formation to a negligible level in the photolysis of CH_2CO at 3130 Å. We have used a ratio of approximately 5 (CO = 50 mm Hg, CH_2CO = 10 mm Hg)[3] in examining the effect of inert gas additions on the photolysis at 2800 Å. The quantum yield of C_2H_6 formation (Table III, first section) for that ratio in the absence of additives indicates (2) almost complete removal of $^3CH_2$. Further confirmation of the complete suppression of the reaction of $^3CH_2$ with CH_2CO was provided by the observed lack of effect of O_2 on the value of $\Phi_{C_2H_4}$ for the photolysis of a $CH_2CO/CO/N_2$ mixture (Table III).

At the ratios of $[CO]/[CH_2CO]$ employed some reaction of $^1CH_2$ with CO was unavoidable. The decrease in $\Phi_{C_2H_4}$ with increasing $[CO]/[CH_2CO]$ ratio is a result of this reaction (Table III, first section).

(d) Photolysis of Ketene – Inert Gas Mixtures at 2800 Å

We have examined the effect of inert gas additions on Φ_{CO} and $\Phi_{C_2H_4}$ for the photolysis of CH_2CO at 2800 Å in the absence of $^3CH_2$ scavengers in order to ascertain the importance of the quenching by additives of the primary dissociation yield of CH_2CO. Other workers (2, 10) have shown that at 3130 and 2900 Å large inert gas additions cause only slight reductions in the dissociation yield. Our quantum yield measurements (Table IV) confirm these findings for 2800 Å. Similar results are to be expected for 2490 Å, where the lifetime of the excited ketene molecules is probably even shorter.

TABLE IV

Product quantum yields* for the photolysis of ketene at 2800 Å in the absence of $^3CH_2$ scavengers

Reactant pressures (mm Hg)		Quantum yields	
CH_2CO	M	C_2H_4	CO
11.0	97.0 (N_2)	0.923	nm
26.6	448.0 (N_2)	0.818	nm
11.0	94.8 (Xe)	0.890	1.99
10.6	193.0 (Xe)	0.850	1.93
25.4	112.6 (C_2F_6)	0.878	1.93
11.2	88.0 (")	0.850	1.80
10.6	96.2 (")	0.856	1.89
10.4	195.2 (")	0.857	1.90
10.8	253.2 (")	0.890	1.91

*Based on $\Phi_{CO} = 2.0$ for photolysis of CH_2CO alone, nm = not measured.

Discussion

The results presented above are readily interpreted in terms of the following simplified

[3]50 mm Hg CO in the reaction cell contained ~.03 μmole O_2; since conversions were such that the C_2H_4 yield was from 0.2–0.4 μmole, the observed quenching effects cannot be ascribed to O_2 in the CO.

Can. J. Chem. Downloaded from www.nrcresearchpress.com by 210.87.254.105 on 09/05/12
For personal use only.

Can. J. Chem. Downloaded from www.nrcresearchpress.com by 210.87.254.105 on 09/05/12
For personal use only.

reaction scheme for the photolysis of ketene at short wavelengths

$$CH_2CO + h\nu \rightarrow {}^1CH_2 + CO \qquad \phi_s I_a$$

$$\rightarrow {}^3CH_2 + CO \qquad \phi_t I_a$$

[1] $${}^1CH_2 + CH_2CO \rightarrow C_2H_4 + CO \qquad k_1$$

[2] $${}^1CH_2 + M \rightarrow {}^3CH_2 + M \qquad k_2$$

[3] $${}^3CH_2 + CH_2CO \rightarrow CO + C_2H_4, C_2H_6, C_2H_2, \text{etc.} \qquad k_3$$

where M is an inert additive, and ϕ_s and ϕ_t are the primary quantum yields of singlet and triplet methylene, respectively. We have chosen to ignore possible bimolecular reactions of excited ketene molecules, feeling, in view of the results outlined in (*d*) above, that excited molecules generated in the primary process are too short-lived to play a kinetically significant role in the photolysis. Corrections for the slight extent of the quenching of excited ketene that was observed will be considered later. We have also assumed, following other workers (2, 7, 10), that intersystem crossing in excited ketene, which leads to ${}^3CH_2$ formation, is a first order process and is not collision-induced. These two assumptions are equivalent to the postulate that ϕ_s and ϕ_t are pressure independent.

Under conditions where ${}^3CH_2$ is entirely scavenged by the reaction with O_2 (14)

$${}^3CH_2 + O_2 \rightarrow CO, CO_2, H_2, \text{etc.}$$

which we assume does not generate C_2H_4, the quantum yield of C_2H_4 formation for a steady state in the above elementary reactions is given by

$$[i] \qquad \Phi_{C_2H_4}{}^{-1} = \phi_s{}^{-1}\left(1 + \frac{k_2[M]}{k_1[CH_2CO]}\right)$$

This relation may be alternatively expressed in terms of $\Phi_{C_2H_4}{}^0$, the ethylene quantum yield in the absence of inert additives, and relative quantum yield data may be used to test the resulting expression

$$[ii] \qquad \Phi_{C_2H_4}{}^0(\Phi_{C_2H_4})^{-1} - 1 = k_2[M]/k_1[CH_2CO]$$

Figure 1 shows that [*ii*] is obeyed by the quantum yield data (arbitrary units) obtained for the photolysis of CH_2CO–O_2 mixtures at 2490 Å. Reciprocal quantum yields of ethylene formation taken from Table I have been plotted against [M]/[CH_2CO] (Fig. 2) and the resulting plots are linear, in accordance with [*i*]. Values of ϕ_s and k_2/k_1 derived from the slopes and intercepts in Fig. 2 and values of k_2/k_1 obtained from the slopes in Fig. 1 are summarized in Table V.

To account for the influence of CO on ketene photolysis we incorporate the reactions

[4] $${}^1CH_2 + CO \rightarrow CH_2CO \qquad k_4$$

[5] $${}^3CH_2 + CO \rightarrow CH_2CO \qquad k_5$$

into the scheme given above. Total pressures used

TABLE V

Summary of rate constant ratios k_2/k_1 and ${}^1CH_2$ quantum yields, ϕ_s

Quencher	λ Å	${}^3CH_2$ scavanger	ϕ_s	$k_2/k_1 \times 10^2$
He	2490	O_2		1.83±0.04
	2800	CO		1.73±0.46
Ar	2800	O_2	0.60±0.02	1.4 ±0.2
Kr	2490	O_2		3.3 ±0.2
CF_4	2490	O_2		4.7 ±0.1
N_2	2490	O_2		5.6 ±0.1
	2800	O_2	0.68±0.02	5.96±0.2
	2800	CO		4.6 ±0.1
SF_6	2490	O_2		4.53±0.03
Xe	2490	O_2		7.3 ±0.3
	2800	O_2	0.77±0.24	9.6 ±4.0
	2800	CO		7.8 ±0.5
C_2F_6	2800	O_2	0.64±0.24	6.3 ±4.6
	2800	CO		11.0 ±1.0
N_2O	2490	O_2		10.0 ±0.3
	2800	CO		17 ±2
				$k_4/k_1 \times 10^2$
CO	2800	CO	0.60±0.02	12.1 ±0.5

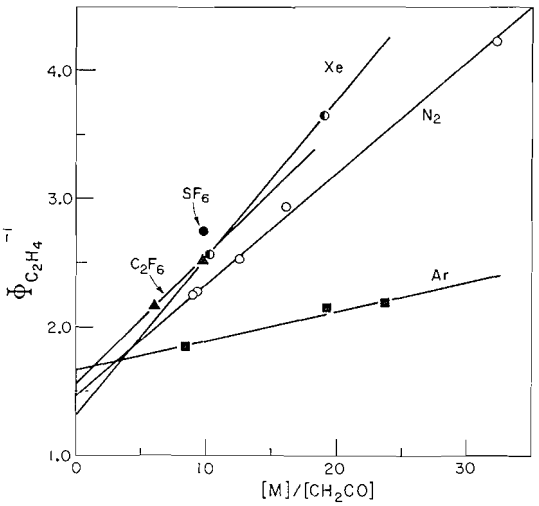

FIG. 2. Plot of reciprocal quantum yield of ethylene from the 2800 Å photolysis of mixtures of CH_2CO, O_2, and additive M against concentration ratio [M]/[CH_2CO].

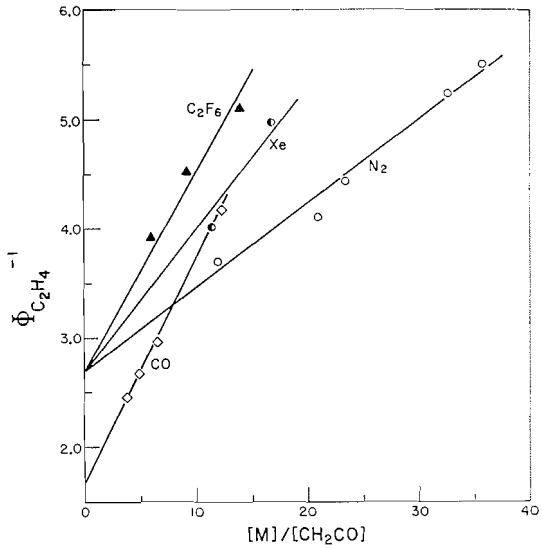

FIG. 3. Dependence of inverse quantum yield of ethylene from the 2800 Å photolysis of mixtures of CH_2CO and CO on the concentration ratios [CO]/[CH_2CO] and [M]/[CH_2CO], where M is an inert additive.

in our experiments were sufficiently high (2) to ensure complete stabilization of the ketene formed in these association reactions. Application of the steady state approximation to the scheme [1]–[5], under conditions where CO is in sufficient excess to eliminate C_2H_4 formation from $^3CH_2$, leads to the following expression

$$[iii] \quad \Phi_{C_2H_4}{}^{-1} = \phi_s{}^{-1}\left\{1 + \frac{k_4[CO]}{k_1[CH_2CO]} + \frac{k_2[M]}{k_1[CH_2CO]}\right\}$$

where k_4 includes a possible contribution from quenching of $^1CH_2$ to $^3CH_2$ by CO. Figure 3 shows that the data of Table III fit the expression [*iii*] satisfactorily. A plot of $\Phi_{C_2H_4}{}^{-1}$ against [CO]/[CH_2CO] at [M] = 0 is linear and from the slope and intercept we obtain $\phi_s = 0.60 \pm 0.02$, $k_4/k_1 = 0.121 \pm 0.005$, in excellent agreement with DeGraff and Kistiakowsky's values (2) for 2900 Å of 0.60 ± 0.03 and 0.12 ± 0.01. Plots of $\Phi_{C_2H_4}{}^{-1}$ against [M]/[CH_2CO] at a fixed [CO]/[CH_2CO] ratio of 5.0 are also linear; values of k_2/k_1 derived from the least squares slopes of the lines and the value $\phi_s = 0.60$ are given in Table V.

The slight reductions in Φ_{CO} and $\Phi_{C_2H_4}$ values (Table IV) caused by inert gas additions to ketene containing no $^3CH_2$ scavenger are suggestive of a small extent of quenching of excited ketene molecules. Assuming (10) that this quenching process does not affect the ratio of singlet to triplet methylene production, the quantum yield $\phi_s{}^M$ of $^1CH_2$ in the presence of additive M is related to the quantum yield ϕ_s in the absence of M by

$$[iv] \quad \phi_s{}^M = \phi_s(\Phi_{CO}{}^M/\Phi_{CO}), \text{ with } \Phi_{CO} = 2.0$$

$\phi_s{}^M$ replaces ϕ_s in expressions [*i*]–[*iii*] above and $\Phi_{CO}{}^M/\Phi_{CO}$ becomes a correction factor to be applied to the $\Phi_{C_2H_4}$ values obtained for photolyses of ketene containing a scavenger of $^3CH_2$. However, the results of Table IV show that even at large pressures of C_2F_6 and Xe the departure of Φ_{CO} from 2.0 is barely significant; at the outside the correction would result in a 10% reduction in the k_2/k_1 values given in Table V. For N_2 additions, analytical difficulties prevented the measurement of CO yields; $\Phi_{C_2H_4}$ values (Table IV) were measured, but these give unreliable indications of variations in the dissociation yield since quenching of $^1CH_2$ to $^3CH_2$ by the additive, even in the absence of a $^3CH_2$ scavenger, contributes to a reduction in the yield of C_2H_4.

Although we favor deactivation of $^1CH_2$ rather than a collision-induced intersystem crossover in excited singlet ketene

$$[6] \quad M + {}^1CH_2CO \rightarrow M + {}^3CH_2CO \rightarrow {}^3CH_2 + CO$$

as the explanation of quenching of ethylene

Can. J. Chem. Downloaded from www.nrcresearchpress.com by 210.87.254.105 on 09/05/12
For personal use only.

Can. J. Chem. Downloaded from www.nrcresearchpress.com by 210.87.254.105 on 09/05/12
For personal use only.

quantum yields by inert additives, we cannot exclude the latter possibility on the basis of our results alone. Our preference was dictated by the findings and suggestions of other workers (2, 7, 10, 13). If [6] were responsible for quenching, the observed linear dependence of $\Phi_{C_2H_4}^{-1}$ on $[M]/[CH_2CO]$ rather than on $[M]$ would require the introduction into the scheme of a reaction of excited ketene with ground state ketene

[7] $$^1CH_2CO + CH_2CO \rightarrow C_2H_4 + 2CO$$

We have adopted the extreme viewpoint that deactivation of excited ketene molecules makes no contribution to the observed quenching effects of inert gases. While this hypothesis is in keeping with existing experimental evidence, we should stress that it is by no means proved. Strictly, our k_2/k_1 comprises unresolved contributions from reactions of both $^1CH_2$ and $^1CH_2CO$.

Relaxation of the $^1A_1$ state of CH_2 to the ground $^3\Sigma_g^-$ state involves a considerable alteration in electronic structure and presumably occurs efficiently only in the neighborhood of points of intersection or near intersection of singlet and triplet potential energy curves. Theoretical curves for the potential energies of the $^1A_1$ and $^3\Sigma_g^-$ states as functions of the $H\hat{C}H$ bond angle exhibit such a crossing point (19). Since the carbon atom Hamiltonian contains a finite spin–orbit interaction term, the possibility arises of a finite relaxation rate of $^1CH_2$ even in the absence of perturbing collisions.

On the basis of Jordan and Longuet-Higgins' (19) theoretical computations, Bader and Generosa (18) estimate that the crossing point is in the region of the $n = 1$ level of the bending mode of vibration of CH_2 ($^1A_1$), and that for this level the first-order rate constant for electronic crossover is as high as 10^{11} s^{-1}. Since this rate constant will decrease with increasing energy content in the bending mode, they suggest that inert gases promote intersystem crossover through vibrational relaxation of $^1CH_2$ which is vibrationally "hot" when generated photochemically. As evidence for this they offer the order of deactivation efficiencies,

$$CF_4 > N_2, Xe$$

for quenching of $^1CH_2$, deduced by them from experiments on the effect of additives on product yields for the reaction of $^1CH_2$ with *cis*-butene-2. Although we feel that the estimate of Bader and Generosa for the first-order rate constant for crossover is probably much too large[4], we cannot entirely dismiss their explanation of quenching of $^1CH_2$ by added gases on the basis of our results. Certainly we find (Table V) that the polyatomics CF_4, C_2F_6, and SF_6, which should effect rapid vibrational relaxation, all quench efficiently. However, the order of deactivation efficiencies for the monatomic gases (Table V) is the inverse of what one would expect for a simple interchange of vibrational and translational energy. In fact, according to our results, Xe is somewhat more effective in relaxing $^1CH_2$ than CF_4 or SF_6. This indicates that spin inversion may occur via a complex between CH_2 and the inert gas molecule in which the latter contributes to the spin–orbit perturbation necessary for mixing of singlet and triplet states. Large spin–orbit forces present in the collision partner are not the only requisite for rapid electronic relaxation in this case; a large attractive interaction between excited species and quenching molecule is also essential. This is clearly seen from the relative rate data (20) for quenching of O ($^1D_2$) to the ground state, a relaxation process which is believed to proceed through complex formation and potential curve crossing; N_2 and CO_2 deactivate O ($^1D_2$) much more rapidly than Kr in spite of the large spin–orbit coupling constant of the latter. The difference is presumably due to the ability of CO_2 and N_2 to form strongly bound complexes, CO_3 and N_2O, with the excited oxygen atom. The surprisingly large efficiencies of CF_4, C_2F_6, and SF_6 for quenching $^1CH_2$ may then simply reflect a tendency for methylene to complex with the peripheral fluorine atoms in these molecules, a tendency which is in fact not shown by the O ($^1D_2$) atom.

Experiments with N_2O as an additive were undertaken in the hope that N_2 formation could be used to monitor $^1CH_2$ concentrations. The N_2 yield was in fact found to be a very small fraction of the total loss of $^1CH_2$ in reaction with and deactivation by N_2O. Nevertheless, trends

[4]A referee of this paper, Professor G. B. Kistiakowsky, has drawn our attention to the incompleteness of Bader's original argument: fast, first-order crossing processes, being *reversible*, would result in the rapid establishment of an approximately 1:3 equilibrium ratio of singlet:triplet methylene. If such were the case, the observed rates of electronic relaxation would be largely determined by the relative rates of vibrational quenching of singlet and triplet methylene *below* the energy of the crossing point.

in N_2 quantum yields observed[5] for the photolysis of mixtures of CH_2CO, N_2O, and inert additive were completely consistent with the deactivation rate data of Table V.

Our rate constant ratios k_2/k_1 agree reasonably well with the few values which have previously been determined (2) and with values which may be estimated from data in the literature (21, 22). Voisey, in a recent study (23) of the reaction of methylene with methyl ethyl ether, has estimated that the efficiencies of C_3F_8, N_2, and Ar for quenching $^1CH_2$ are in the ratio 1.00:0.42:0.29. This order of deactivation efficiencies is consistent with our data, although we find an appreciably higher efficiency for N_2 relative to Ar.

Acknowledgment

We are deeply indebted to Dr. R. J. Cvetanović for his advice, encouragement, and participation in stimulating discussion.

1. S-Y. Ho and W. A. Noyes. J. Amer. Chem. Soc. **89**, 5091 (1967).
2. B. A. DeGraff and G. B. Kistiakowsky. J. Phys. Chem. **71**, 1553 (1967); **71**, 3984 (1967).
3. D. E. Thornton and A. N. Strachan. J. Phys. Chem. **71**, 4583 (1967).
4. J. W. Simons and B. S. Rabinovitch. J. Phys. Chem. **68**, 1322 (1964).
5. S-Y. Ho, I. Unger, and W. A. Noyes. J. Am. Chem. Soc. **87**, 2297 (1965).
6. F. H. Dorer and B. S. Rabinovitch. J. Phys. Chem. **69**, 1964 (1965).
7. R. W. Carr and G. B. Kistiakowsky. J. Phys. Chem. **70**, 118 (1966).
8. G. Herzberg. Proc. Roy. Soc. London, Ser. A, **262**, 291 (1961).
9. G. Herzberg and J. W. C. Johns. Proc. Roy. Soc. London, Ser. A, **295**, 107 (1966).
10. A. N. Strachan and D. E. Thornton. Can. J. Chem. **46**, 2353 (1968).
11. R. N. Dixon and G. H. Kirby. Trans. Faraday Soc. **62**, 1406 (1966).
12. (*a*) A. N. Strachan and W. A. Noyes. J. Amer. Chem. Soc. **76**, 3258 (1954). (*b*) R. A. Holroyd and W. A. Noyes. J. Amer. Chem. Soc. **78**, 4831 (1956).
13. (*a*) C. McKnight, E. K. C. Lee, and F. S. Rowland. J. Amer. Chem. Soc. **89**, 469 (1967). (*b*) F. S. Rowland, C. McKnight, and E. K. C. Lee. Ber. Bunsenges Phys. Chem. **72**, 236 (1968).
14. R. L. Russell and F. S. Rowland. J. Amer. Chem. Soc. **90**, 1671 (1968), and references cited therein.
15. R. A. Cox and R. J. Cvetanović. J. Phys. Chem. **72**, 2236 (1968).
16. G. B. Porter. J. Amer. Chem. Soc. **79**, 1878 (1957).
17. H. M. Frey. Progr. React. Kinet. **2**, 131 (1964).
18. R. F. W. Bader and J. I. Generosa. Can. J. Chem. **43**, 1631 (1965).
19. P. C. H. Jordan and H. C. Longuet-Higgins. Mol. Phys. **5**, 121 (1962).
20. K. F. Preston and R. J. Cvetanović. J. Chem. Phys. **45**, 2888 (1966).
21. H. M. Frey. J. Amer. Chem. Soc. **82**, 5947 (1960).
22. C. H. Bamford, J. E. Casson, and A. N. Hughes. Proc. Roy. Soc. London, Ser. A, **306**, 135 (1968).
23. M. A. Voisey. Trans. Faraday Soc. **64**, 3058 (1968).

[5]R. A. Cox, unpublished work.

Can. J. Chem. Downloaded from www.nrcresearchpress.com by 210.87.254.105 on 09/05/12
For personal use only.

Can. J. Chem. Downloaded from www.nrcresearchpress.com by 210.87.254.42 on 09/05/12
For personal use only.

Oxidation of formaldehyde by copper(II) in aqueous solution

J. J. Byerley and W. K. Teo
Department of Chemical Engineering, University of Waterloo, Waterloo, Ontario
Received August 26, 1968

Copper(II) was found to oxidize formaldehyde in aqueous solutions according to the following reaction

$$2Cu(II) + HCHO + H_2O \rightarrow 2Cu(I) + HCOOH + 2H^+$$

Rates were determined at temperatures between 130 and 166.5 °C. The rate law was found to be of the form

$$\frac{-\,dCu(II)}{dt} = k_1[Cu(II)][HCHO] + k_2\frac{[Cu(II)][HCHO]}{[H^+]}$$

where $k_1 = 1.9 \times 10^{-4}\ M^{-1}\ s^{-1}$ and $k_2 = 2.05 \times 10^{-8}\ s^{-1}$ in 0.125 M acetate solutions at 160 °C. The apparent activation energy is 33 600 cal/mole. The reaction mechanism suggested includes the formation of two bridged intermediates

$$\left(\begin{array}{c} H \\ | \\ Cu—O—CH_2OH \end{array}\right)^{2+} \text{ and } (Cu—O—CH_2OH)^+$$

which account for the acid-dependent and acid-independent reaction paths.

Canadian Journal of Chemistry, 47, 3355 (1969)

Introduction

Aliphatic as well as aromatic aldehydes are readily oxidized in aqueous solution by metal ions and complex metal ions. Among the many reactions of this type which have been reported, the oxidation of formaldehyde by metal ions has received considerable attention. In aqueous solution, formaldehyde under controlled conditions may be converted to formic acid. Under more energetic conditions the oxidation may proceed to completion yielding carbon dioxide. In many cases the final oxidation states of the metal ions involved in the processes are rather unpredictable.

Kinetic and mechanistic data have been reported for the oxidation of formaldehyde by chromium(VI) (1, 2), cerium(IV) (3), vanadium(V) (2), and cobalt(III) (4, 5) in acid solutions. In all cases the reactions were found to be first-order with respect to metal ion and formaldehyde concentrations. On the other hand the acid dependence for these reactions showed little similarity; for example, oxidation by chromium(VI) was second-order with respect to hydrogen ion concentration whereas an inverse dependence was reported for oxidation by cobalt(III).

In general, formaldehyde is more reactive in alkaline solutions, a conclusion that is easily verified by comparing the oxidation potentials for the half cell reaction in alkaline solutions with that in acid media (6). In basic solutions a number of metals including silver, bismuth, copper, mercury, nickel, and gold (7) may be precipitated when subjected to formaldehyde although no detailed kinetic information is available for these reactions.

It is significant that in acid solutions very few examples of oxidation accompanied by metal precipitation have been reported. Generally the reactions result in metal ions of intermediate oxidation states, examples of which have been cited earlier. Gold and platinum apparently are precipitated from their chlorides even in strong acid solutions (8). Copper sulfate is reported (9) not to oxidize formaldehyde even on prolonged heating at 100 °C. In contrast, cupric ions (10) and cuprous oxide (11) are reported to oxidize formaldehyde in alkaline solutions with the evolution of hydrogen.

[1] $2Cu(II) + 2HCHO(aq) + 4OH^- \rightarrow 2Cu^0 + H_2 + 2H_2O + 2HCO_2^-$

[2] $2Cu_2O + 2HCHO(aq) + 2OH^- \rightarrow 2Cu^0 + H_2 + 2HCOO^- + H_2O$

The present paper describes a kinetic and mechanistic investigation of the oxidation of formaldehyde by copper(II) in acetate solutions above 100 °C where reactivity is observed.

Can. J. Chem. Downloaded from www.nrcresearchpress.com by 210.87.254.42 on 09/05/12
For personal use only.

Experimental

Materials

All chemicals were reagent grade and used without further purification. Cupric perchlorate stock solutions were prepared by dissolving cupric oxide in perchloric acid and standardizing using EDTA with murexide as indicator. Stock solutions of formaldehyde were prepared by dissolving in water gaseous formaldehyde obtained by heating paraformaldehyde. Concentrations of formaldehyde were established using the sodium sulfite and chromotropic acid methods.

Kinetic Measurements

The kinetic data for the oxidation of formaldehyde by copper(II) were obtained by continuously recording the decrease in optical density of copper(II)–formaldehyde solutions as the cupric ion (absorption peak approximately 7500 Å) was reduced to the colorless cuprous species. Since measurable rates could only be obtained well above 100 °C, a titanium vessel equipped for pressurization was required. This vessel fitted directly into the sample compartment of a Bausch and Lomb Spectronic 505 recording spectrophotometer. The cell used quartz windows and was capable of continuous operation up to 200 °C.

Experimental Procedure

The spectrophotometer was first balanced at zero absorbance with the reaction and reference compartments filled with distilled water. The water in the sample compartment was then replaced by the solution to be studied. Both compartments were closed and pressurized with nitrogen. The vessel was then inserted into a preheated aluminum block and the entire assembly placed in the spectrophotometer. The desired reaction temperature (generally 160 °C) and temperature control (±0.3 °C) were achieved within 7 min. The interval of 7 min during which a record of the reaction progress could not be observed introduced little error into the kinetic data because the reaction is a relatively slow process. Any errors in establishing initial absorbance were overcome by eliminating the formaldehyde from the system and measuring the absorbance of the blank at the reaction temperature.

Experimental Results

Measurable rates of oxidation of formaldehyde by copper(II) were obtained above 160 °C at pH ranging from 4.2 to 5.0. At lower pH the reaction rates were very slow while at pH above 5.0 the reaction was complicated by hydrolysis of cupric acetate with the formation of blue basic cupric salts. These solids interfered with the spectrophotometric analysis.

Under experimental conditions the oxidation product of formaldehyde was identified as formic acid[1], the blue cupric ions being reduced to colorless cuprous species. In the absence of any strong stabilizing ligand in the system, such as in the formation of a cuprous carbonyl (12), the cuprous ion may undergo further reduction to metallic copper or hydrolyze to cuprous oxide. Disproportionation of the cuprous ion was not observed.

The oxidation of formaldehyde in acid media given by Latimer (6) in terms of a half-cell reaction suggests the following stoichiometry for the oxidation of formaldehyde by cupric ion.

$$[3]\quad 2Cu(II) + HCHO + H_2O \rightarrow 2Cu(I) + HCOOH + 2H^+$$

An effort was made to verify reaction [3] by measuring the ratio of cupric ion consumed to the amount of formic acid generated. Data taken from an experiment of this type[2] are given in Table I. As noted in table, a sample taken very early in the reaction period results in the ratio of cupric ion consumed to formic acid generated being approximately 2:1. Samples taken later in the reaction exhibited a tendency for the formic acid concentration to be progressively in excess of the apparent stoichiometric quantity. This behavior was observed repeatedly over a wide range of experimental conditions. The presence of excess formic acid over that required by a stoichiometry described by reaction [3] was attributed to another formic acid generating reaction, the further reduction of cuprous ion to metallic copper

$$[4]\quad 2Cu(I) + HCHO + H_2O \rightarrow 2Cu^0 + HCOOH + 2H^+$$

Although no attempt was made to examine reaction [4], a reddish precipitate was always found on the walls of the vessel after completion of an experiment. This precipitate was identified as a mixture of metallic copper and cuprous oxide.

The reactivity of formic acid towards cupric ion was tested and was found to be equivalent to formaldehyde. Since all kinetic measurements were carried out in excess formaldehyde (the formaldehyde concentration was always at least 60 times greater than the formic acid concentration) any contribution from formic acid oxidation was negligible.

The possibility of formation of carbon dioxide

[1]Formic acid was determined by the mercuric chloride and chromatographic methods.

[2]Stoichiometry measurements were carried out in a 100 ml shaking autoclave.

TABLE I

Oxidation* stoichiometry

Time (min)	[Cu(II)] × 10^3M consumed	[HCOOH] × 10^3M generated	[HCOOH] × 10^3M, reaction [3]	Excess [HCOOH] %
10	1.29	0.78	0.65	20
60	5.49	4.19	2.97	41
120	8.13	6.58	4.17	58

*Conditions: 0.0092 *M* Cu(II), 0.3 *M* HCHO, 0.25 *M* NaOAc, 0.125 *M* HOAc, temperature, 160 °C.

as the final oxidation product was investigated. This reaction, which is the sum of the oxidation reactions of formaldehyde and formic acid, may be expressed as

[5] $4Cu(II) + HCHO + H_2O \rightarrow 4Cu(I) + CO_2 + 4H^+$

Under this condition formic acid would appear only as an intermediate product. Results using a pressure sensitive autoclave system (13) indicated no gas evolution during the reaction nor did chromatographic analysis detect any gaseous products.

Kinetic data were obtained under a variety of initial conditions ranging from 0.01 to 0.001 *M* cupric ion, 0.1 to 0.8 *M* formaldehyde, pH 4.2 to 5.0, and temperature 130 to 166.5 °C. The dependence of the oxidation rate on copper(II) concentration is shown in Fig. 1. These standard logarithmic plots are diagnostic of a first-order reaction with respect to copper(II) i.e.

$$[6] \qquad \frac{-d[Cu(II)]}{dt} = k'[Cu(II)]$$

The effect of formaldehyde concentration is also shown in Fig. 1. When the rate constant k' is determined for each formaldehyde level and plotted vs. the corresponding formaldehyde

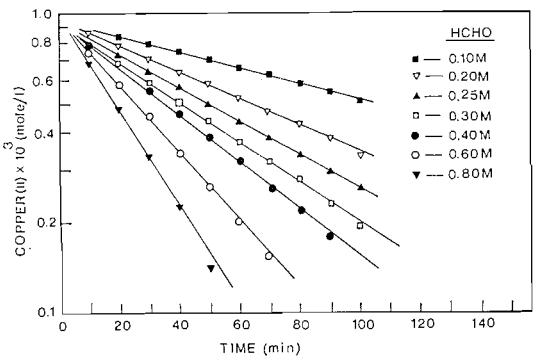

FIG. 1. First-order rate plots at different formaldehyde concentrations: 0.0092 *M* Cu(II), 0.125 *M* NaOAc, 0.25 *M* HOAc; temperature, 160 °C.

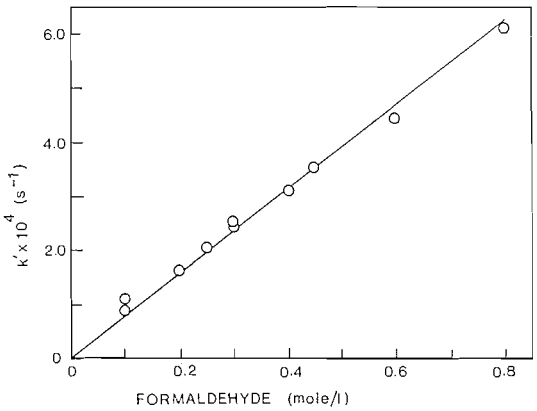

FIG. 2. Effect of formaldehyde concentration on k': 0.0092 *M* Cu(II), 0.125 *M* NaOAc, 0.25 *M* HOAc; temperature, 160 °C.

concentration, the linear relationship shown in Fig. 2 is obtained. The reaction is therefore first-order with respect to formaldehyde concentration with k' being defined in terms of a new rate constant k, given by

$$[7] \qquad k' = k[HCHO]$$

The effect of pH was examined using various acetic acid concentrations while maintaining the sodium acetate level constant. Plots of k vs. the reciprocal of acetic acid at 3 concentrations of sodium acetate are shown[3] in Fig. 3. The result is a set of straight lines with a non-zero intercept. This non zero intercept indicates an acid-independent contribution to the overall reaction rate which may be expressed by a new set of rate constants

$$[8] \qquad k = k_1 + k_2'/[HOAc]$$

[3]The rather sparse and compressed data especially at high pH are the result of the limited pH range available before the onset of complicating reactions such as the hydrolysis of cupric acetate and precipitation of basic cupric salts when heated to the reaction temperature.

Can. J. Chem. Downloaded from www.nrcresearchpress.com by 210.87.254.42 on 09/05/12
For personal use only.

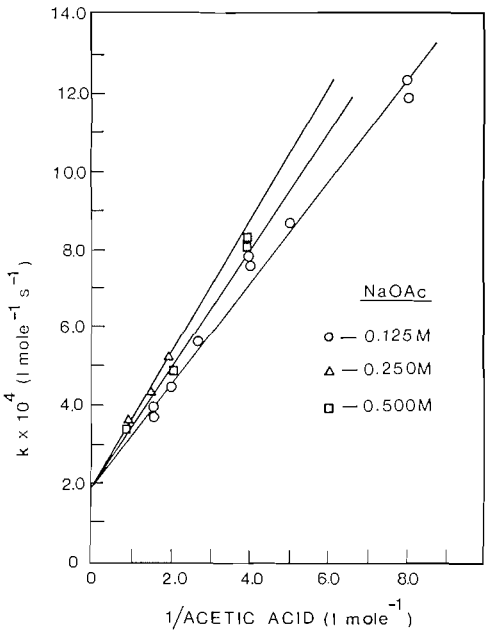

FIG. 3. Dependence of k on 1/[HOAc]: 0.0092 M Cu(II), 0.3 M HCHO; temperature, 160 °C.

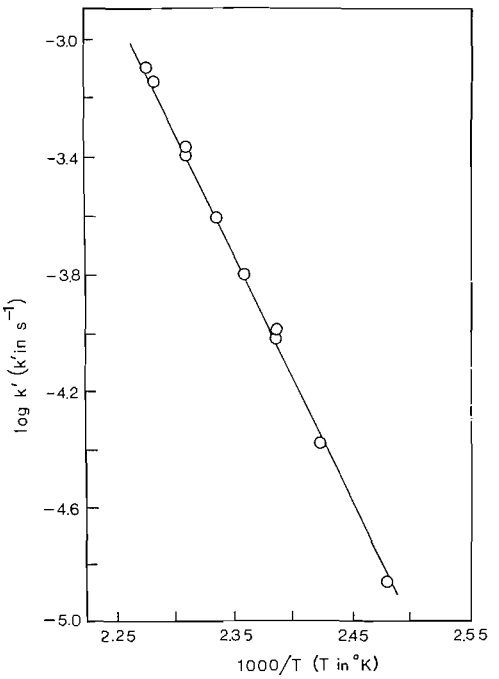

FIG. 4. Arrhenius plot for the oxidation of formaldehyde by copper(II): 0.0092 M Cu(II), 0.125 M NaOAc, 0.25 M HOAc, 0.6 M HCHO.

The hydrogen ion concentration is directly proportional to the acetic acid concentration given by

$$[9] \qquad [H^+] = K_i[HOAc]/[OAc^-]$$

where K_i is the ionization constant of acetic acid and $[OAc^-]$ is assumed to be the total acetate concentration. Using the relationship given in eq. [9] the rate law may be rewritten to include the acid-independent component and the ionization constant K_i

$$[10] \qquad \frac{-d[Cu(II)]}{dt} = k_1[Cu(II)][HCHO] + k_2\frac{[Cu(II)][HCHO]}{[H^+]}$$

where k_2 includes the ionization constant K_i (taking K_i as 1.75×10^{-5}), $k_1 = 1.9 \times 10^{-4}$ $M^{-1}s^{-1} \pm 10\%$, $k_2 = 2.05 \times 10^{-8} M^{-1} \pm 15\%$; conditions: 0.125 M NaOAc, 160 °C.

Although it is clear that the effect of sodium acetate concentration on the reaction rate is directly related to the hydrogen ion concentration through the buffer system, there still remains the question of complexing. Figure 4 may be used to illustrate the inhibiting effect of increasing acetate complexing which has been observed earlier (12, 13) by selecting a point on each line of equivalent [NaOAc]/[HOAc] ratio. Under these conditions the pH is nearly constant and the rate constant is seen to decrease with increasing acetate ligand. No attempt was made to study the effect further and therefore the complexing variable is contained in k_1 and k_2.

Experiments to investigate the effect of temperature on reaction rate produced limited information due to the lack of high temperature equilibrium constant data. Although both k_1 and k_2 were evaluated as functions of temperature the data was not acceptable since the temperature dependence of K_i could not be included in the rate constant calculations. An overall activation energy was obtained using the rate constant k' as defined by eq. [6]. From the Arrhenius plot shown in Fig. 4 an experimental activation energy of 33.6 ± 3.0 kcal/mole was estimated.

Reaction Mechanism

A reaction mechanism which is consistent with the experimental rate law given by eq. [9] may be postulated. This mechanism defines two parallel

Can. J. Chem. Downloaded from www.nrcresearchpress.com by 210.87.254.42 on 09/05/12
For personal use only.

Can. J. Chem. Downloaded from www.nrcresearchpress.com by 210.87.254.42 on 09/05/12
For personal use only.

reaction paths for the oxidation of formaldehyde by copper(II). The reaction sequence may be represented as follows (reaction [11])

(*i*) *Path A*

$$[11a]\quad Cu(II) + HCHO + H_2O \underset{}{\overset{K_a}{\rightleftarrows}} [Cu{-}O{-}CH_2OH]^+ + H^+$$

$$[11b]\quad [Cu{-}O{-}CH_2OH]^+ \overset{k_a}{\rightarrow} Cu(I) + \cdot OCH_2OH$$

$$[11c]\quad Cu(II) + \cdot OCH_2OH \overset{\text{fast}}{\rightarrow} Cu(I) + HCOOH + H^+$$

(*ii*) *Path B*

$$[11d]\quad Cu(II) + HCHO + H_2O \overset{K_b}{\rightleftarrows} \left(\begin{matrix} H \\ | \\ Cu{-}O{-}CH_2OH \end{matrix}\right)^{2+}$$

$$[11e]\quad \left(\begin{matrix} H \\ | \\ Cu{-}O{-}CH_2OH \end{matrix}\right)^{2+} \overset{k_b}{\rightarrow} Cu(I) + H^+\dot{O}CH_2OH$$

$$[11f]\quad H^+\dot{O}CH_2OH \overset{\text{fast}}{\rightarrow} \cdot OCH_2OH + H^+$$

$$[11g]\quad Cu(II) + \cdot OCH_2OH \overset{\text{fast}}{\rightarrow} Cu(I) + HCOOH + H^+$$

The rate law derived from this reaction mechanism corresponds to

$$[12]\quad \frac{-d[Cu(II)]}{dt} = k_bK_b[Cu(II)][HCHO] + k_aK_a\frac{[Cu(II)][HCHO]}{[H^+]}$$

Equation [12] is identical to eq. [10] if

$$k_aK_a = k_2 \quad \text{and} \quad k_bK_b = k_1$$

The proposed mechanism is based on the formation of two bridged complexes as reaction intermediates

$$(Cu{-}O{-}CH_2OH)^+ \quad \text{and} \quad \left(\begin{matrix} H \\ | \\ Cu{-}O{-}CH_2OH \end{matrix}\right)^{2+}$$

The former gives rise to a pH-dependent reaction path while the latter results in a pH-independent reaction path. The second term of the rate equation accounts for more than 70% of the overall reaction rate. This would indicate that

$$(Cu{-}O{-}CH_2OH)^+$$

is more reactive than

$$\left(\begin{matrix} H \\ | \\ Cu{-}O{-}CH_2OH \end{matrix}\right)^{2+}$$

a not unexpected result in view of the difference in charge on the two species.

There are many examples of bridged complexes proposed as intermediate in reaction mechanisms describing metal ion oxidation of aldehydes. In the case of the oxidation of benzaldehyde by chromic acid (14) an ester formation mechanism has been suggested

$$[13]\quad \begin{matrix} H \\ | \\ R{-}C{=}O \end{matrix} + H_2CrO_4 \rightleftarrows \begin{matrix} OH \\ | \\ R{-}C{-}OCrO_3H \\ | \\ H \end{matrix}$$

A similar bridged intermediate

$$\begin{matrix} OH \\ | \\ C_6H_5{-}C{-}OMnO_3 \\ | \\ H \end{matrix}$$

has been postulated for the oxidation of aromatic aldehydes by permanganate ions in acid and neutral solutions (15). The oxidation of formaldehyde by cobaltic ion is said to proceed through the formation of two bridged intermediates (4, 5, 16)

$$(Co{-}O{-}CH_2OH)^+ \quad \text{and} \quad \left(\begin{matrix} H \\ | \\ Co{-}O{-}CH_2OH \end{matrix}\right)^{2+}$$

These species which are analogous to those presented in this work account for the observed pH-dependent and pH-independent portions of the reaction.

An interesting parallel may be drawn between the oxidation of carbon monoxide by copper(II) and the present reaction. Both reactions exhibit acid dependence and acid independent components. In the case of carbon monoxide oxidation by copper(II), this observation is accounted for by 2 insertion complexes

$$\left(\begin{matrix} O \\ | \\ Cu{-}C{-}OH \end{matrix}\right)^+ \quad \text{and} \quad \left(\begin{matrix} OH \\ \vdots \\ Cu{-}C{\equiv}OH \end{matrix}\right)^{2+}$$

which form in pre-equilibrium steps. The rate limiting steps are the subsequent decomposition of these intermediates by cupric ions.

In the oxidation of formaldehyde by copper(II) the rate limiting steps are also preceded by pre-equilibria in which 2 bridged intermediates are formed. The spontaneous decomposition of these intermediates is the rate limiting step. It appears that the copper–oxygen bonds are broken, yielding cuprous ions and free radicals. The removal of a hydrogen ion from $H^+\dot{O}CH_2OH$

should be fast in order to satisfy the condition of acid dependence. Final reaction of the $\cdot OCH_2OH$ with cupric ion is regarded as a fast process.

Acknowledgment

The authors gratefully acknowledge the financial support from the National Research Council of Canada.

1. A. C. CHATTERJU and S. K. MUKERJEE. J. Amer. Chem. Soc. **80**, 3600 (1958).
2. T. J. KEMP and W. A. WALTERS. Proc. Roy. Soc. London, Ser. A, **274**, 480 (1963).
3. G. HARGRAVES and L. H. SUTCLIFFE. Trans. Faraday Soc. **51**, 1105 (1955).
4. G. HARGRAVES and L. H. SUTCLIFFE. Trans. Faraday Soc. **51**, 785 (1955).
5. C. H. E. BAWN and A. G. WHITE. J. Chem. Soc. 339 (1951).
6. W. M. LATIMER. The oxidation states of the elements and their potentials in aqueous solutions. 2nd ed. Prentice-Hall, Inc., Englewood Cliffs, New Jersey. 1952.
7. J. F. WALKER. Formaldehyde. 2nd ed. Reinhold Publishing Corp., New York. 1953.
8. N. AVERKIEFF. Z. Anorg. Allg. Chem. **35**, 329 (1903).
9. J. U. NEW. Ann. **335**, 274 (1904).
10. R. M. LUKES. Plating, **11**, 1066 (1964).
11. A. HARDEN. Proc. Chem. Soc. **15**, 158 (1899).
12. J. J. BYERLEY and E. PETERS. Can. J. Chem. **47**, 313 (1969).
13. J. J. BYERLEY and J. Y. H. LEE. Can. J. Chem. **45**, 3025 (1967).
14. K. B. WIBERG and R. STEWART. J. Amer. Chem. Soc. **77**, 1786 (1955).
15. F. C. TOMKINS. Trans. Faraday Soc. **39**, 280 (1943).
16. J. ROCĖK. The chemistry of the carbonyl group. Interscience Publishers, Inc., New York. 1966. Chap. 10.

Can. J. Chem. Downloaded from www.nrcresearchpress.com by 210.87.254.42 on 09/05/12
For personal use only.

Can. J. Chem. Downloaded from www.nrcresearchpress.com by 210.87.254.5 on 09/05/12
For personal use only.

Coordination complexes of acetylene diphosphines. Part III. Silver(I) and mercury(II) complexes

W. A. ANDERSON, A. J. CARTY, AND A. EFRATY
Department of Chemistry, University of Waterloo, Waterloo, Ontario

Received March 27, 1969

Complexes of bis(diphenylphosphino)acetylene with silver(I) and mercury(II) are described. Infrared and Raman spectra together with chemical evidence suggest that the compounds AgX(DPPA) (X = Cl, Br, I, SCN, NO_3; DPPA = bis(diphenylphosphino)acetylene), $[AgX]_2(DPPA)_3$ (X = Cl), $AgX(DPPA)_2$ (X = BF_4, PF_6), and $HgX_2(DPPA)$ (X = Cl, Br, I) have polymeric structures with bridging bis(diphenylphosphino)acetylene groups.

Les complèxes de bis(diphénylphosphino)acétylène avec l'argent(I) et le mercure(II) sont decrits. Les spectres Raman, infrarouge et l'évidence chimique suggèrent que les composés AgX(DPPA) (X = Cl, Br, I, SCN, NO_3; DPPA = bis(diphénylphosphino)acétylène, $[AgX]_2(DPPA)_3$ (X = Cl), $AgX(DPPA)_2$ (X = BF_4, PF_6) et $HgX_2(DPPA)$ (X = Cl, Br, I) ont des structures polymèriques dans lesquelles les groupes bis(diphénylphosphino)acétylène forment les ponts entre les atomes des métaux.

Canadian Journal of Chemistry. 47, 3361 (1969)

Introduction

Tertiary phosphines form 1:1, 2:1, 3:1, and 4:1 complexes with silver(I) salts (1–7) as well as a variety of mononuclear or halogen bridged polynuclear complexes with mercury(II) halides (2, 8). Whereas silver(I) is normally 3 or 4 coordinate in these compounds (2, 3, 6), mercury(II) prefers tetrahedral coordination (8). Few diphosphine or diarsine complexes have been described (9–11).

There has been considerable recent interest in coordination compounds of unsaturated phosphines and arsines (12–16), particularly with a view to preparing complexes having coordinated olefinic bonds. In other papers in this series (17, 18) we have shown that the acetylenic diphosphine bis(diphenylphosphino)acetylene **1** (DPPA) forms stable binuclear diphosphine bridged complexes with copper(I), gold(I), palladium(II), and platinum(II), and we have now extended these studies to include silver(I) and mercury(II).

Experimental

The diphosphine $Ph_2PC{\equiv}CPPh_2$ was prepared as previously described (17). Silver and mercury salts were Fisher reagent grade materials and were used without further purification.

Microanalyses were carried out by A. B. Gygli, Toronto and A. Bernhardt, Elbach uber Engelskirchen, Germany. Infrared (i.r.) spectra were recorded on Beckman IR 9 and IR 12 spectrometers. Solid state Raman measurements were made using a Spex Helium–Neon laser equipped instrument. Calibrations were made with the carbon tetrachloride line of shift $\Delta\nu = 459\ cm^{-1}$ and frequencies are accurate to $\pm 2\ cm^{-1}$.

Mercury Compounds

Dichloro[bis(diphenylphosphino)acetylene]mercury(II)

Mercuric chloride (0.2 g) dissolved in ethanol (5 ml) was added dropwise to a warm solution of **1** (0.5 g) in

$$Ph_2PC{\equiv}CPPh_2$$

1

ethanol (70 ml). The white crystalline precipitate was filtered off, washed carefully with ethanol, boiling benzene, and dichloromethane, then dried in vacuo, m.p. 192–194° (decomp.).

Anal. Calcd. for $HgCl_2$(DPPA): C, 46.90; H, 3.0; Cl, 10.64. Found: C, 46.66; H, 3.15; Cl, 10.50.

Dibromo[bis(diphenylphosphino)acetylene]mercury(II)

Prepared as above using mercuric bromide, this had m.p. 191–193° (decomp.).

Anal. Calcd. for $HgBr_2$(DPPA): C, 41.37; H, 2.67; Br, 21.16. Found: C, 41.73; H, 2.31; Br, 21.09.

Diiodo[bis(diphenylphosphino)acetylene]mercury(II)

Mercuric iodide (0.45 g) was dissolved in ethanol (50 ml) in the presence of potassium iodide (0.2 g). This solution was added dropwise to a solution of the ligand (0.4 g) in ethanol (50 ml). The precipitated pale yellow product was purified as described above, m.p. 174–176° (decomp.).

Anal Calcd. for HgI_2(DPPA): C, 36.80; H, 2.37; I, 29.97. Found: C, 36.83; H, 2.56; I, 29.65.

Attempts to prepare zinc and cadmium halide complexes by the same techniques were unsuccessful.

Silver Compounds

Nitrato[bis(diphenylphosphino)acetylene]silver(I)

Reaction of **1** (2.0 g) in ethanol (150 ml) with a saturated solution of silver nitrate (0.9 g) in the same solvent gave a white precipitate which was recrystallized from a large volume of ethanol. The compound explodes at 165–175°.

Anal. Calcd. for $Ag(NO_3)$(DPPA): C, 55.35; H, 3.57; P, 10.96; N, 2.48. Found: C, 55.12; H, 3.63; P. 8.77; N, 2.42.

Can. J. Chem. Downloaded from www.nrcresearchpress.com by 210.87.254.5 on 09/05/12
For personal use only.

Thiocyanato[bis(diphenylphosphino)acetylene]silver(I)
Method A

$Ag(NO_3)$(DPPA) (0.3 g) was dissolved in dichloromethane to give a saturated solution. Excess of a warm saturated solution of potassium thiocyanate in ethanol was added and the reaction mixture was left to stir at 50° until all the solvent had evaporated. The resulting white product was washed carefully with water and ethanol and dried at 50°, m.p. 255–257° (decomp.).

Anal. Calcd. for Ag(NCS)(DPPA): C, 57.88; H, 3.60 N, 2.50. Found: C, 57.92; H, 3.76; N, 2.69.

Method B

$Ag(NO_3)$(DPPA) (0.5 g) was suspended in a small volume of ethanol and the solvent heated to boiling. Solid **1** was added gradually to the boiling suspension until all the nitrate had dissolved. Excess of a saturated ethanolic solution of potassium thiocyanate was added and the reaction mixture stirred at room temperature for 5 h. The precipitate was washed thoroughly with acetone and water, then dried in vacuo, m.p. 256–257° (decomp.). Found: C, 58.11; H, 3.77.

Iodo[bis(diphenylphosphino)acetylene]silver(I)
Method A

A similar procedure to *method A* above using potassium iodide gave a white product, m.p. 209–210° (decomp.).

Anal. Calcd. for AgI(DPPA): C, 49.64; H, 3.20. Found: C, 49.33; H, 3.17.

Method B

The same product was obtained using *method B* above.

Anal. Calcd. for $(AgCl)_2(DPPA)_3$: C, 63.74; H, 4.11.

Di[bis(diphenylphosphino)acetylene]silver(I) hexafluorophosphate

$Ag(NO_3)$(DPPA) (0.25 g) was suspended in ethanol (20 ml) and **1** added slowly to the refluxing solvent until a clear solution was obtained. The solution was cooled to room temperature, filtered, and 20 ml of a saturated solution of potassium hexafluorophosphate added. The reaction mixture was left to stir for 2–3 h, and the white precipitate filtered off and washed with small quantities of ethanol, m.p. 168–178°.

Anal. Calcd. for $Ag(PF_6)(DPPA)_2$ (mol. wt. monomer, 1042): C, 59.94; H, 3.87; P. 14.87. Found (mol. wt. (CH_3NO_2) 704): C, 60.45; H, 3.84; P, 13.35.

Di[bis(diphenylphosphino) acetylene] silver(I) tetrafluoroborate

Prepared similarly to the hexafluorophosphate this had m.p. 230–240° (decomp.).

Anal. Calcd: C, 63.48; H, 4.10. Found: C, 63.16; H, 4.29.

Extensive washing of the product with acetone was necessary for purification, m.p. 206–209° (decomp.). Found: C, 48.93; H, 3.43.

Bromo[bis(diphenylphosphino)acetylene]silver(I)

Using *method A*, with potassium bromide replacing potassium thiocyanate gave the pure product in small yield, m.p. 226–228° (decomp.).

Anal. Calcd. for AgBr(DPPA): C, 53.65; H, 3.46; Br, 13.73. Found: C, 52.77; H, 3.45; Br, 13.42.

Treatment of a suspension of $Ag(NO_3)$(DPPA) in ethanol with a large excess of potassium bromide for 48 h followed by boiling of the precipitate in water and ethanol to remove excess KBr and $Ag(NO_3)$(DPPA) gave a similar product. Found: C, 52.68; H, 3.48.

Chloro[bis(diphenylphosphino)acetylene]silver(I)

This compound can be prepared in small yield by *method A* using $Ag(NO_3)$(DPPA) and a saturated ethanolic solution of sodium chloride, m.p. ~200° (decomp.). The compound is very light sensitive. Poor microanalyses were obtained unless reactions were carried out completely in the dark. Halogenated solvents catalyze the decomposition.

Anal. Calcd. for AgCl(DPPA): C, 58.08; H, 3.75; Cl, 6.59. Found: C, 56.26; H, 3.84; Cl, 6.22.

A different compound was obtained by dissolving $Ag(NO_3)$(DPPA) in an ethanolic or methanolic solution of **1** followed by addition of a solution of sodium chloride or aluminum chloride in the same solvent. Decomposition of this compound also occurred on standing in light. Analyses of products gave the following.

$$Ag(NO_3)(DPPA) + DPPA \xrightarrow{\text{ethanol} + NaCl} \text{C, 62.90; H, 4.23}$$

$$Ag(NO_3)(DPPA) + DPPA \xrightarrow{\text{methanol} + NaCl} \text{C, 62.84; H, 4.57}$$

$$Ag(NO_3)(DPPA) + DPPA \xrightarrow{\text{ethanol} + AlCl_3} \text{C, 62.82; H, 4.40}$$

Results and Discussion

Silver Complexes

Silver nitrate reacts with **1** in alcoholic solution to give a colorless, crystalline, diamagnetic complex of empirical formula $Ag(NO_3)$(DPPA). The complex is only slightly soluble in ethanol and dichloromethane, insufficient for molecular weight measurements. The i.r. spectrum (Table I) confirms that the nitrate group is coordinated. $\nu_3(E')$ for $NO_3^-(D_{3h})$ in $AgNO_3$ is at 1378 cm^{-1}. For mono- or bi-dentate nitrate, the degeneracy of ν_3 is removed and the band splits into 2 components, one at higher frequency and the other lower. The magnitude of the band splittings has often been used together with other information as a means of tentatively assigning mono- or bidentate coordination (19). For $Ag(NO_3)$ (DPPA)

TABLE I

Infrared spectra (2200–650 cm^{-1}) of silver(I) and mercury(II) complexes of DPPA

Complex	Spectrum (cm^{-1})*
DPPA	1580w 1478m 1433s 1304w 1275vw 1179w 1154w 1090m 1067w 1023w 998w 967vw 913vw 827s 752vs 742vs 695vs
$HgCl_2$(DPPA)	1580w 1570w 1477w 1435s 1326w 1312w 1270w 1182w 1154w 1097s 1024w 997m 915w 844vs 755s 745s 712m 697sh 688s
$HgBr_2$(DPPA)	1578vw 1565vw 1475m 1432s 1329vw 1309w 1282vw 1266vw 1182w 1156w 1094s 1024w 993m 912w 838vw 751s 742vs 712m 695sh 686vs
HgI_2(DPPA)	1579w 1569w 1477m 1433s 1330w 1308w 1280w 1182w 1160w 1096s 1068w 1025m 999m 970w 928w 916w 848vs 747sh 740vs 709m 690vs
$AgNO_3$(DPPA)	2110vw 1583w 1575w 1478m 1437s 1412s 1297vs 1174w 1160w 1096m 1070w 1034m 1027w 1000m 972vw 842s 835s 759s 740s 725sh 691s
AgCl(DPPA)	1584w 1573w 1476m 1434s 1328vw 1309w 1178v 1160w 1094m 1026w 1000w 973w 830s 742s 725sh 692s
AgBr(DPPA)	1582w 1575w 1478m 1435s 1312vw 1270vw 1183w 1155w 1094m 1070w 1026w 1000w 971vw 830vs 748sh 743vs 693vs
AgI(DPPA)	1585w 1575vw 1475m 1433s 1330w 1308vw 1281w 1182w 1158w 1094m 1070w 1028w 1000w 971vw 920vw 851s 822s 750s 740s 692vs
Ag(NCS)(DPPA)	2084vw 1583w 1574w 1478m 1434s 1305w 1277vw 1180w 1155w 1094m 1070w 1030w 1000m 970w 928vw 912vw 834s 823s 750sh 744vs 702sh 694vs
$(AgCl)_2(DPPA)_3$	1584w 1571w 1478m 1434s 1330vw 1310vw 1178w 1160w 1096m 1030w 1000w 972w 842vs 745vs 712sh 690vs 696vs
$Ag(BF_4)(DPPA)_2$	1582w 1570w 1475m 1435s 1308w 1281w 1183w 1160w 1095m 1060sbr 1040sh 1027sh 1000m 840sh 830s 755s 741s 694s
Ag(PF)(DPPA)	1583w 1568w 1477m 1435s 1328w 1184w 1160w 1095s 1070w 1027w 1000m 970w 920w 876w 824vsbr 754sh 743vs 696s

*w = weak, m = medium, s = strong, sh = shoulder, br = broad, v = very.

the 2 components arising from ν_3 of NO_3^- are at 1412 and 1297 cm^{-1}. The absence of any nitrate absorption above 1412 cm^{-1} argues against a strongly coordinated bidentate or bridging nitrate. Other bands in the spectrum due to coordinated nitrate are at 1034 and 822 cm^{-1}; components arising from a lifting of the degeneracy of the $\nu_4(E')$ bending mode of NO_3^- are, however, obscured by strong ligand absorption in the 700 cm^{-1} region.

$\nu(C{\equiv}C)$ appears at 2097 cm^{-1} (17, 20) in a Raman spectrum of **1** but is i.r. inactive both in **1** and in complexes where the diphosphine is symmetrically bonded to 2 metal atoms via the phosphorus atoms only (20, 21). Conversely, in acetylene complexes of symmetrical disubstituted acetylenes, $\nu(C{\equiv}C)$ appears weakly in the i.r. 200–400 cm^{-1} lower than in the free ligand (22). We were unable to obtain a frequency for $\nu(C{\equiv}C)$ from the Raman spectrum of $AgNO_3$(DPPA) due to decomposition to silver metal in the laser beam. However, a very weak absorption at ca. 2110 cm^{-1} in the i.r. of a strong mull probably arises from $\nu(C{\equiv}C)$. Thus only the phosphorus atoms of the ligand are coordinated (17). Interestingly, no cleavage of the $P{-}C_{sp}$ bond was apparent when **1** reacted with alcoholic $AgNO_3$. This contrasts with the behavior of other non-metal acetylene compounds where the $M{-}C_{sp}$ bond is readily cleaved by this reagent (23). It is likely that $AgNO_3$(DPPA) has a polymeric structure **2** in which bridging DPPA molecules and a monodentate nitrate contribute to a planar geometry around each silver ion. An alternative structure **3**

Can. J. Chem. Downloaded from www.nrcresearchpress.com by 210.87.254.5 on 09/05/12
For personal use only.

Can. J. Chem. Downloaded from www.nrcresearchpress.com by 210.87.254.5 on 09/05/12
For personal use only.

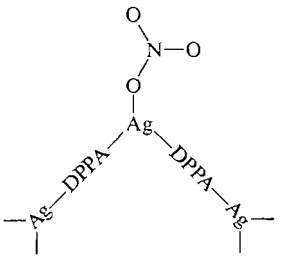

2

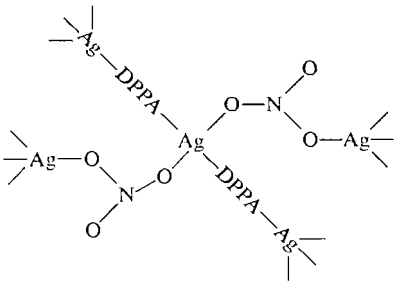

3

with tetrahedral silver receives some support from the known crystal structures of (cyclooctatetraene)$AgNO_3$ (24) and (norbornadiene)$2AgNO_3$ (25) where bridging nitrate groups are present.

$Ag(NO_3)(DPPA)$ is a useful starting material for the preparation of other silver(I) complexes. The reactions are summarized in Scheme 1.

The halide complexes AgX(DPPA) (X = Cl, Br) are obtained in small quantities from these reactions and are difficult to purify due to their insolubility in suitable solvents. Attempts to prepare larger quantities by *method B* (see Experimental) resulted in products having high C and H analyses. In the case of the chloride, analytical figures for products prepared in 3 different ways using solutions of $AgNO_3$(DPPA) and excess ligand in ethanol, agreed consistently with the formulation $(AgCl)_2(DPPA)_3$. Attempts to purify and characterize both series of compounds by physical techniques were hindered by insolubility in suitable solvents. Solid state i.r. spectra confirmed the bidentate behavior of DPPA (Table I), however, and showed that $\nu(C{\equiv}N)$ of Ag(DPPA)SCN occurred as a strong sharp band at 2084 cm^{-1} suggesting the presence of N bonded thiocyanate (24). Silver complexes of stoichiometry $AgX(L_2)$ (L_2 = chelating diphosphine or diarsine; X = Cl, Br, I) are usually formulated as $[Ag(L_2)_2][AgX_2]$ on the basis of conductivity

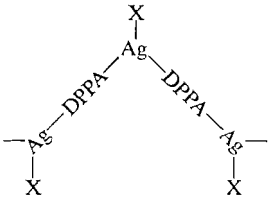

4

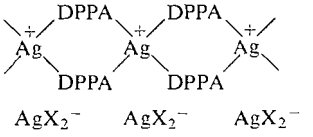

5

measurements (10, 11). Similar structures are unlikely for AgX(DPPA) since the diphosphine is incapable of chelation (20). Moreover, the insolubility in nitromethane, nitrobenzene, and acetonitrile argues against a simple ionic formulation.

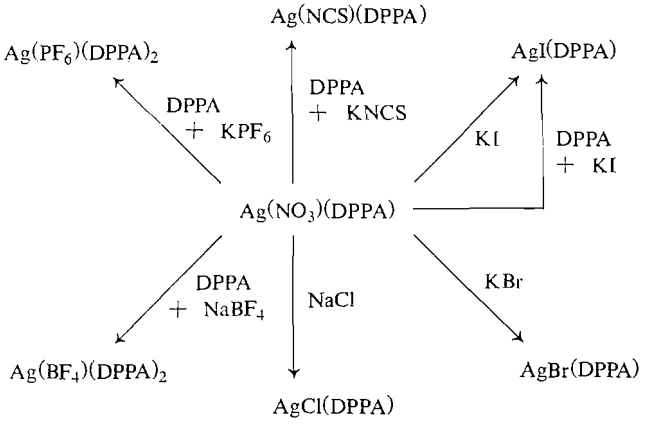

SCHEME 1

Can. J. Chem. Downloaded from www.nrcresearchpress.com by 210.87.254.5 on 09/05/12
For personal use only.

Two structures consistent with the bridging properties of **1**, the i.r. data, and the insolubility of the products are **4** and **5**. A meaningful distinction between these structures cannot be made on the basis of the evidence available. For $(AgCl)_2(DPPA)_3$ a tetrahedral diphosphine bridged structure analogous to that of $(CuX)_2(DPPA)_3$ (X = Cl, Br, I, NCS, BH_4, NO_3) (20) is probable. The compounds $AgX(DPPA)_2$ (X = PF_6, BF_4) contain ionic PF_6^- and BF_4^- respectively, $\nu_3(T_{1u})$ of PF_6^- occurring as a symmetrical absorption at 842 cm^{-1} and $\nu_3(T_2)$ of BF_4^- at 1060 cm^{-1} (Table I). No splitting of these bands as a result of a lowering of symmetry of the ions from O_h or T_d on coordination, was apparent. Both compounds are only sparingly soluble in nitromethane but dissolve in nitrobenzene to give colloidal, conducting solutions. This is in contrast to the analogous gold complexes $AuX(DPPA)_2$ (17) which readily dissolve without decomposition in halogenated solvents as well as nitromethane. Lewis, Nyholm, and Phillips (10) reported similar observations on silver(I) diarsine compounds. Lack of physical evidence again precludes a definite structural assignment. A polymeric structure **6** in which all diphosphine molecules are bridging and silver(I) has its usual tetrahedral coordination agrees with all the available i.r. evidence and is tentatively suggested.

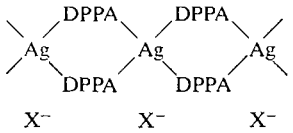

6

The work confirms that silver(I) phosphine complexes are less stable and more difficult to prepare and characterize than the corresponding copper(I) and gold(I) derivatives. This is particularly evident with DPPA, a ligand with apparently higher π acceptor but poorer σ donor properties than alkylene diphosphines (26). The lower effective electronegativity of silver compared with copper and gold (10) implies the necessity of a strongly basic ligand in order to produce a strong Ag—P bond.

Mercury Complexes

Mercuric halides form monomeric tetrahedral $(R_3P)_2HgX_2$, halogen bridged dimeric $(R_3P)_2(HgX_2)_2$, and halogen bridged polymeric $(R_3P)_2(HgX_2)_3$ complexes with tertiary phosphines (8). 1,2-Bis(diphenylphosphino)ethane (diphos) reacts with mercuric bromide to give the expected compound $HgBr_2$(diphos) but gives $(HgCl_2)_2$(diphos) with mercuric chloride (27). Reaction of **1** with mercuric halides in alcohol produces colorless complexes of empirical formula $HgX_2(DPPA)$ which are virtually insoluble in polar and non-polar organic solvents. The compounds are stable in air but decompose on melting. The i.r. spectra (Table I) are virtually identical and changes in the spectrum of the ligand on complexing parallel those reported previously (18). The absence of any i.r. absorption assignable to $\nu(C{\equiv}C)$ of the ligand indicates non-coordination of the triple bond and a symmetrical bidentate ligand. This is confirmed by Raman measurements on the solid complexes. $\nu(C{\equiv}C)$ occurs as an intense absorption at 2123, 2118, and 2115 cm^{-1} for $HgCl_2(DPPA)$, $HgBr_2(DPPA)$, and $HgI_2(DPPA)$, respectively. In the far infrared $HgCl_2(DPPA)$ has a very strong ν(Hg—Cl) absorption at 247 cm^{-1} with a weaker ν(Hg—Cl) mode at 234 cm^{-1}. These values are close to the values reported for ν(Hg—Cl) in the tetrahedral triphenylphosphine complex $(Ph_3P)_2HgCl_2$ (28) and strongly suggest a tetrahedral C_{2v} local symmetry around mercury for which two ν(Hg—X) modes (A_1 + B_1) are expected. The evidence thus points to structure **7** for the mercury complexes in which mercury has its usual tetrahedral configuration and all diphosphine molecules are bridging.

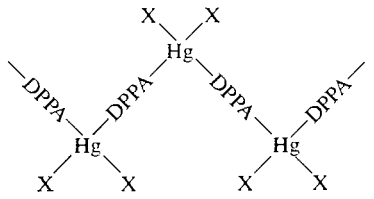

7

All attempts to prepare cadmium and zinc complexes of **1** resulted in failure. Although many cadmium and zinc halide–phosphine adducts are known (28), they are generally less stable than the corresponding mercury compounds. The failure of zinc and cadmium halides to complex with **1** can therefore be attributed to the "*a*" class character of these metals (29) and the weaker σ donor

properties **1** compared with other tertiary alkyl and aryl phosphines.

Acknowledgment

We acknowledge the financial support of the National Research Council of Canada.

1. A. TURCO, C. PANATTONI, and E. FRASSON. Ric. Sci. Suppl. **29**, 544 (1959); Chem. Abstr. **54**, 148 (1960).
2. R. C. CASS, G. E. COATES, and R. G. HAYTER. J. Chem. Soc. 4007 (1955).
3. F. A. COTTON and D. M. L. GOODGAME. J. Chem. Soc. 5257 (1960).
4. C. A. STREULI. Proc. Symp. Titrimetric Methods. Cornwall, Ontario. 1961. p. 97; Chem. Abstr. **57**, 6865 (1962).
5. F. G. MANN, A. F. WELLS, and D. PURDIE. J. Chem. Soc. 1503 (1936).
6. F. G. MANN, A. F. WELLS, and D. PURDIE. J. Chem. Soc. 1828 (1937).
7. F. CARIATI and L. NALDINI. Gazz. Chim. Ital. **95**, 201 (1965).
8. R. C. EVANS, F. G. MANN, H. S. PEISER, and D. PURDIE. J. Chem. Soc. 1209 (1940).
9. W. COCHRAN, F. A. HART, and F. G. MANN. J. Chem. Soc. 2816 (1957).
10. J. LEWIS, R. S. NYHOLM, and D. J. PHILLIPS. J. Chem. Soc. 2177 (1962).
11. C. E. WYMORE and J. C. BAILAR, JR. J. Inorg. Nucl. Chem. **14**, 42 (1960).
12. C. WU and F. J. WELCH. J. Org. Chem. **30**, 1229 (1965).
13. M. A. BENNETT, W. R. KNEEN, and R. S. NYHOLM. Inorg. Chem. **7**, 552 (1968), and references therein.
14. R. B. KING and K. H. PANNELL. Inorg. Chem. **7**, 273 (1968).
15. W. R. CULLEN, P. S. DHALIWAL, and C. J. STEWART. Inorg. Chem. **6**, 2256 (1967).
16. R. D. FELTHAM, H. G. METZGER, and W. SILVERTHORN. Inorg. Chem. **7**, 2003 (1968).
17. A. J. CARTY and A. EFRATY. Inorg. Chem. **8**, 543 1969.
18. A. J. CARTY and A. EFRATY. To be published.
19. N. F. CURTIS and Y. M. CURTIS. Inorg. Chem. **4**, 805 (1965).
20. A. J. CARTY and A. EFRATY. Can. J. Chem. **46**, 1598 (1968).
21. A. J. CARTY and A. EFRATY. J. Inorg. Nucl. Chem. Lett. **4**, 487 (1968).
22. J. CHATT, R. G. GUY, and L. A. DUNCANSON. J. Chem. Soc. 827 (1961).
23. J. E. POIST and C. S. KRAIHANZEL. Chem. Commun. 607 (1968), and references therein.
24. F. S. MATHEWS and W. N. LIPSCOMB. J. Phys. Chem. **63**, 845 (1959).
25. N. C. BAENZIGER, H. L. HAIGHT, R. ALEXANDER, and J. R. DOYLE. Inorg. Chem. **5**, 1399 (1966).
26. A. J. CARTY, A. EFRATY, and T. W. NG. Can. J. Chem. **47**, 1429 (1969).
27. G. E. COATES and D. RIDLEY. J. Chem. Soc. 166 (1964).
28. G. B. DEACON, J. H. S. GREEN, and D. J. HARRISON. Spectrochim. Acta, **24A**, 1921 (1968).
29. S. AHRLAND, J. CHATT, and N. R. DAVIES. Quart. Rev. London, **12**, 265 (1958).

Can. J. Chem. Downloaded from www.nrcresearchpress.com by 210.87.254.5 on 09/05/12
For personal use only.

Can. J. Chem. Downloaded from www.nrcresearchpress.com by 210.87.254.40 on 09/05/12
For personal use only.

Methyl "radicals" on doped silica gel surfaces[1]

E. J. Casey, C. W. M. Grant[2], and C. L. Gardner
Defence Research Establishment Ottawa, Defence Research Board, Ottawa, Canada

Received January 8, 1969

Methyl radicals adsorbed on silica gels containing dopings of the semiconductor ZnO were investigated by electron spin resonance at 77 °K. In addition to the normal 4-line "*a*"-spectrum, with hyperfine splitting of 23.3 ± 0.2 G, a second broader 4-line spectrum "*b*" with splitting 18.8 ± 0.6 G appears. Variations in line intensity with extent of doping were measured. Disappearance of the *b*-spectrum when the doped gels were dried under hot oxygen was observed. Partial delocalization of the radical's free electron and mixing into the *doped* surface were clearly indicated.

Satellites ("*c*") to the *a*-spectrum were observed and are discussed.

Canadian Journal of Chemistry, 47, 3367 (1969)

In the present paper we report on an investigation of the effect of the doping of silica gel, with the semiconductor zinc oxide, on the electron spin resonance (e.s.r.) spectrum of adsorbed methyl radicals. Although ion radicals such as O_2^- have been formed (1) by adsorption of O_2 on irradiated semiconductor materials such as ZnO and MgO, and although NO has been detected (2*a*) on MgO, and the spectrum analyzed (2*b*), it is only very recently that adsorbed, e.s.r.-detectable, neutral free-radicals have been directly observed (3–7), in spite of the fact that they are often postulated as intermediates in kinetic schemes. We imagined that this may be due to the electron of the radical being transferred more or less into the semiconductor or conductor material, forming either an undetectable ion or a charge-transfer complex rather than a detectable stabilized free radical. Information about the distribution of the electronic charge of the adsorbed radical is important, for example, in predicting what intermediates may reasonably be expected in catalytic electro-oxidation reactions such as the electro-oxidation of hydrocarbons.

In these experiments we have attempted to change the adsorbent material from an insulating state (pure silica gel) gradually towards a more semiconducting state, by doping the silica gel with increasing amounts of ZnO, and then to examine the nature of the bonding with CH_3 as the doping is increased.

Preparation and Measurements

Since preparation affects the results, details are given as follows. To a 50 ml 1 *M* sodium silicate solution was added 50 ml of water in a beaker. The solution was constantly stirred and concentrated HCl was added simultaneously from a second buret at such a rate as to keep the pH below 3. At this stage varying amounts of 1 *M* $ZnCl_2$ were added, followed by titration of the solution with 1 *N* NaOH to pH 7, at which point gelling occurred rapidly. The gels were dried at room temperature and washed thoroughly with boiling water. The resulting gel was transparent and colorless. In this way gels with up to 11.7% ZnO by weight were prepared, the zinc content having been determined by analysis after the drying step. Several precautions must be taken in preparing the gels this way. (*a*) The neutral region must be approached from the acid side if premature gelling of the SiO_2 is to be avoided. (*b*) If too much $ZnCl_2$ is added, premature gelling of ZnO occurs and a non-homogeneous mixture results. This fact limits the maximum doping to less than 12%. (*c*) Since ZnO and SiO_2 do not gel at precisely the same time or rate, the percentage of doping is not exactly reproducible. Any unattached ZnO formed is washed away in the washing procedure.

X-Ray diffraction by a gel sample known by chemical analysis to be doped with 6.7% Zn showed the sample to be amorphous, indicating that the ZnO was well dispersed in the gel lattice, and not agglomerated as crystalline islands of ZnO.

The samples for use in the e.s.r. measurements were prepared as follows. The doped gels were degassed at less than 10^{-4} mm Hg for approximately 9 h at 300 °C. Some were dried under 1 atm O_2. Methyl iodide (Brickman and Co., reagent grade) was then allowed to adsorb onto the gel at a pressure of ~10 mm Hg. The sample tube was sealed, cooled to 77 °K, and irradiated with an unfiltered GE-UA2 mercury lamp. Electron spin resonance spectra were taken on a Varian V-4500 spectrometer at this temperature.

The a-Spectrum

The 4-line spectrum of methyl radicals adsorbed on pure silica gel is now well known (3–5) and is shown for reference in Fig. 1*a*. (The line S, absorption by a center in irradiated silica gel, usually appears in addition to the 4 lines (a_1 to a_4) of adsorbed CH_3.) The hyperfine splitting constant is 23.3 ± 0.2 G. Little anisotropy is indicated by the line shapes. In our previous work the variation of linewidth of the *a*-spectrum with nuclear spin

[1]D.R.E.O. Technical Note No. 69-13.
[2]Present address: Chemistry Department, University of British Columbia, Vancouver 8, British Columbia.

Can. J. Chem. Downloaded from www.nrcresearchpress.com by 210.87.254.40 on 09/05/12
For personal use only.

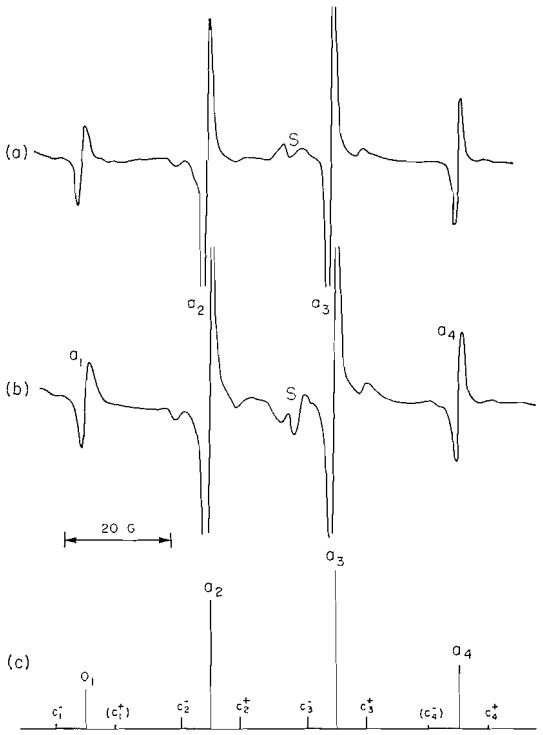

FIG. 1. Electron spin resonance spectra of methyl radicals at 77 °K. (*a*) Undoped silica gel, (*b*) doped silica gel, dried under oxygen, and (*c*) stick spectrum.

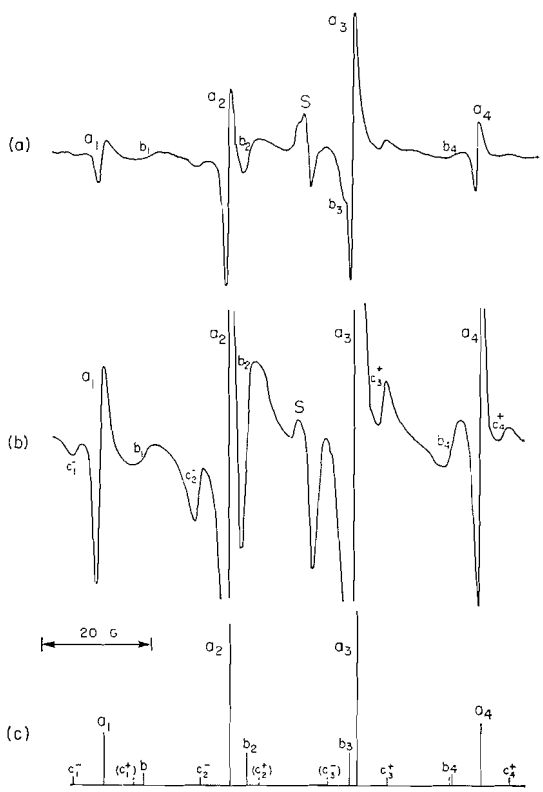

FIG. 2. Electron spin resonance spectra of methyl radicals on ZnO-doped (11.7%) silica gel at 77 °K. (*a*) Low sensitivity, (*b*) high sensitivity, and (*c*) stick spectrum.

quantum number from the predicted 1:3:3:1 was quantitatively interpreted as being due to hindered rotation of the radicals on the surface, and the tumbling frequency was evaluated (6).

By contrast with the pure gel, the e.s.r. spectra observed with the doped gels, Fig. 2 (CH_3 on silica gel with 11.7% ZnO), are more complicated. Furthermore, the intensity of the extra lines depends on the extent of doping. The most intense lines (a_1 to a_4) in the more complex spectra are the same as those of CH_3 on the undoped gels, and although the hyperfine splittings of the *a*-spectrum (23.10, 22.90, 23.18, 22.75, 22.80) observed for 5 doped gels (1 to 11.7%) may be slightly smaller than the splitting we have observed for CH_3 on undoped gels, the difference is very close to the limits of error and is probably not significant.

The b-Spectrum

A second methyl radical spectrum, less intense, and with broader lines and greatly reduced hyperfine splitting (18.8 ± 0.6 G) clearly appears in the doped samples (lines b_1 to b_4). The lines b_1, b_2, and b_4 appear clearly in windows of the *a*-spectrum, and b_3 appears as a shoulder on and a distortion of line a_3, in Fig. 2*a*. Positions of the *a*- and *b*-lines are indicated in the stick spectrum, Fig. 2*c*.

The intensity of the *b*-spectrum relative to the *a*-spectrum increases with amount of ZnO in the gel. Thus the ratio of peak heights for b_1 and a_1 increased with doping as follows: 0.114, 0.136, 0.221, and 0.284 for gels with ZnO present in 4 increasing amounts of about 2, 5, 8, and 11.7%, respectively. We suggest that the *b*-spectrum corresponds to CH_3's adsorbed on "ZnO-sites". These may be faces of silica tetrahedra which have dopant nearby, or real, amorphous ZnO (anhydrous or hydrated?) islands in the substrate. It is obvious that at the molecular level the doping may not be completely homogeneous.

Since the hyperfine splitting shown in the *b*-spectrum is markedly lower than that in the *a*-spectrum, considerably more delocalization of the radical's electron has taken place on the ZnO-sites, approximately 19% more being mixed with the ZnO-site than with the pure silica site.

The marked line-broadening which appeared in these *b*-spectra suggested that considerable variation must exist in the doped sites, possibly in the intensity of the electric field at the adsorbed radical, and possibly due to variation in composition of the ZnO from stoichiometric 1:1. We recall that it is well known (8) that the rate of the homomolecular oxygen reaction varies with ZnO composition. In the present case, the supported ZnO (11.7%), having been dried under vacuum, was probably oxygen-deficient. Therefore, for comparison, a special preparation of the same doped substrate intended to contain oxygen-excess ZnO was made, in which the last stage of drying was done

Can. J. Chem. Downloaded from www.nrcresearchpress.com by 210.87.254.40 on 09/05/12
For personal use only.

under an atmosphere of oxygen at 300 °C. After drying, the sample was cooled under O_2 and then outgassed at 25 °C under vacuum before admission of the CH_3I. All other steps were the same. Although the resulting spectrum still showed strong *a*-lines, it had no trace of *b*-lines (Fig. 1*b*).

This behavior could occur for several reasons: more complete mixing of the radical's electron with the excess O of an n-type semiconductor, or with a distorted silica tetrahedron nearby, so that it is essentially an ion adsorbed on the O-excess doped sites; partial coverage of the doped sites by chemisorbed oxygen and hence no adsorption at all; rearrangement of adsorbed radicals to (adsorbed) methyl ether; and probably others. In summary, we see that the surface composition can markedly affect the nature of adsorption, and that evidence of partial (Fig. 2*a*), as well as possibly complete (Fig. 1*b*), electron-transfer into the surface during adsorption has been obtained.

The c-Spectrum

On the ZnO-doped silica gel, in addition to the "*a*" and "*b*" sets of spectral lines for adsorbed CH_3 radicals, 4 weak lines (called "*c*") are also evident in Fig. 2. c_1^- is very weak and in about 20 samples was found to lie between 4.0 and 5.5 G downfield from a_1. Likewise c_4^+ lies between 4.0 and 5.5 G upfield from a_4. However, c_2^- and c_3^+ in all samples lie 5.4 ± 0.1 G from a_2 and a_3, respectively. Peak heights of the *c*'s are small, 3–5% of the corresponding *a*'s. The observed 4 may be members of a group of 8 (the others being hidden under the *b*'s) arising from interaction of the radical with the ^{29}Si nucleus, which has a nuclear spin quantum number of 1/2 and a 4.7% natural abundance in the gel. Thus, if we assume that the electron is donated into the sp^3 orbital of silicon, the value (9) of the hyperfine splitting constant of 1160 G for an electron in the 3s orbital of ^{29}Si permits the estimate that only about 4% delocalization is needed to account for the observed splitting of *a*'s. The fact that the ratio of peak heights of the clean c_2^- line to the clean a_2 line shows no systematic variation with doping, from 0 (pure gel) to 11.7% ZnO-doped, seems to strengthen this assignment. The main weakness of this view is that only 4 of the supposed 8 lines consistently appear, although in Fig. 1*b* as many as 7 may be imagined.

Other possibilities exist which cannot be unequivocally eliminated. One is that the gel has not become completely freed of —OH groups by the drying procedure, and that the 4 observed *c*'s are due to proton-splitting. It seems improbable, however, that the *c*/*a* ratio would remain constant throughout the study, including the experiment in which the doped gel was kept under oxygen before and during cooling, if the intensity of the *c*-lines depended upon —OH groups at the adsorption sites. Another possibility is that OCH_2, as well as CH_3, is formed at doped sites. Thus, one could consider c_2^- and c_3^+ to be the outside lines of the 3-line spectrum of partly-delocalized, adsorbed OCH_2 radicals, with the center line obscured by the S lines, normally present in irradiated silica gels. The observed splitting would then be 16.5 G (Fig. 2*b*), which is lower than the reported value of 20.5 for $SiOCH_2$ (10), and about 25% delocalization would thus be required. However, there is no evidence whatsoever for *undelocalized* $SiOCH_2$, at 20.5 G, even on the oxygenated, doped gel; nor would the c_1^- and c_4^+ lines be accounted for in this interpretation. Therefore, we favor the ^{29}Si interpretation over proton-splitting, and consider delocalized oxyradicals only a remote possibility in the present investigation.

Conclusion

The experiments have indicated that increased delocalization of the methyl radical's unpaired electron can occur as silica gel is doped with a semiconductor material such as ZnO. The degree of delocalization in the SiO_2–ZnO system seems to be a *site* property rather than a *bulk* property of the material. Adsorbed free-radicals, some undelocalized and some with at least partial delocalization, and possibly even ions, can form from adsorption of CH_3 on different sites on the same surface. One infers that the phenomenon should be observable by e.s.r. techniques whenever the catalytic surface is only partially semiconducting.

Acknowledgment

We wish to thank Dr. M. Fujimoto for a helpful discussion early in this work.

1. J. H. Lunsford and J. P. Jayne. J. Chem. Phys. **44** 1487 (1966); **44**, 1492 (1966).
2. (*a*) J. H. Lunsford. J. Chem. Phys. **46**, 4347 (1967). (*b*) J. H. Lunsford. J. Phys. Chem. **72**, 2141 (1968).
3. G. B. Pariiskii, G. M. Zhidomirov, and V. B. Kazanskii. Zh. Strukt. Khim. **4**, 364 (1963). V. B. Kazanskii and G. B. Pariiskii. Proc. 3rd International Congress on Catalysis. Amsterdam, 1964. Vol. 1. p. 367.
4. J. Turkevich and Y. Fujita. Science. **152**, 1619 (1966).
5. M. Fujimoto, H. D. Gesser, B. Garbutt, and A. Cohen. Science, **154**, 381 (1966). M. Fujimoto, H. D. Gesser. B. Garbutt, and M. Shimizu. Science, **156**, 1105 (1967). G. B. Garbutt, H. D. Gesser, and M. Fujimoto. J. Chem. Phys. **48**, 4605 (1968).
6. C. L. Gardner and E. J. Casey. Can. J. Chem. **46**, 207 (1968).
7. D. R. Smith and A. J. Tench. Can. J. Chem. **47**, 1381 (1969).
8. E. R. S. Winter. Advan. Catal. **10**, 196 (1958). G. K. Boreskov. Discuss. Faraday Soc. **41**, 263 (1966).
9. J. R. Morton. Chem. Rev. **64**, 453 (1964).
10. A. P. Bobrovskii and V. E. Kolmogorov. Teor. i Eksp. Khim. **3**, 112 (1967).

Can. J. Chem. Downloaded from www.nrcresearchpress.com by 210.87.254.6 on 09/05/12
For personal use only.

Reactions of diphos and diars with iron carbonyls: a reinvestigation

W. R. CULLEN AND D. A. HARBOURNE
Chemistry Department, University of British Columbia, Vancouver, British Columbia

Received March 27, 1969

The bidentate ligands diars (**1**) and diphos (**2**) react with iron carbonyls to give the previously known diarsFe(CO)$_3$, diphosFe(CO)$_3$, diphosFe$_2$(CO)$_8$, and the new complex diarsFe$_2$(CO)$_8$. The reactions of diars also yield compounds in which the ligand has been modified. DiarsFe(CO)$_3$ reacts readily with chloroform to give a new paramagnetic iron carbonyl complex.

Canadian Journal of Chemistry, 47, 3371 (1969)

Introduction

The two chelating ligands 1,2-bis(dimethylarsino)benzene, diars (**1**), and 1,2-bis(diphenylphosphino)ethane, diphos (**2**), are well known for their ability to displace carbon monoxide from metal carbonyl compounds (e.g. 1–3).

During the course of our investigation of the complexing abilities of related fluorocarbon-bridged ditertiary phosphines (and arsines) (4–8), it became necessary to reinvestigate the reaction of (**1**) and (**2**) with iron carbonyls. The purpose of this paper is to report these new results which involve (*a*) improved reaction workup procedures which allow a fuller investigation of the products of the reactions, (*b*) improved syntheses of diphosFe(CO)$_3$, diphosFe$_2$(CO)$_8$, and diarsFe(CO)$_3$, (*c*) the characterization of diarsFe$_2$(CO)$_8$, and (*d*) the synthesis of a new paramagnetic iron carbonyl. The structures of most of these compounds have been recently discussed (7) in a paper which describes their infrared (i.r.) spectra in the carbonyl region and their Mössbauer spectra.

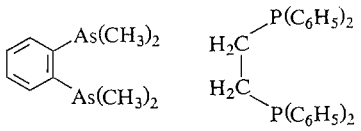

1 2

Experimental

The results of some representative experiments are summarized in Table I. All reaction mixtures were treated in a similar manner which consisted of removal of volatiles and solvents followed by chromatography on Florisil *under nitrogen*. Eluants (which may vary a little depending on column conditions etc.) are indicated for each product in Table I. The eluants used in each experiment were in order, petroleum ether (b.p. 30–60°), petroleum ether/benzene mixtures, benzene, petroleum ether/ether mixtures, ether, and acetone. A product given as eluting with 1:1 petroleum ether/benzene was eluted *after* the column had been cleared of earlier bands by the solvents mentioned above. In some cases recrystallization of a chromatographic band was necessary to obtain a pure product.

The spectrometers used in this investigation have been described previously (6). Microanalyses were done by Mr. Peter Borda of this department.

Results and Discussion

Our study of the reactions of fluorocarbon-bridged ditertiary phosphines (and arsines) with the various iron carbonyls (5–8) has shown the products formed to be critically dependent upon the carbonyl and conditions used. A good number of di- and tri-iron derivatives have been isolated. Our reinvestigation of the reactions of diphos and diars with the iron carbonyls has shown a remarkable *independence* of conditions and carbonyl used (Table I) and a lack of any stable products containing iron–iron bonds, apart from this possibility in trace products (less than 1%).

In all reactions of diphos investigated, the major products are invariably diphosFe$_2$(CO)$_8$ and diphosFe(CO)$_3$. This latter compound does not elute significantly from a Florisil column unless nitrogen saturated conditions are used. This is probably the reason that it was not obtained by Manuel (2). Further products were not separated in above trace (below 1%) quantities apart from one pale yellow powdery material which was isolated in small amounts from reactions [1], [2], and [3] (Table I). It was eluted from Florisil, apparently as a single yellow band, with 1:1 benzene/petroleum ether and its carbonyl i.r. spectrum shows bands at 2057s, 1982s, 1947vs, 1940vs(sh), 1895s, and 1885s(sh) cm^{-1}. The first 4 bands are in the same position and have the same relative intensities as those of diphosFe$_2$(CO)$_8$ (Table II, ref. 7). Recrystallization from benzene/heptane or ether/petroleum

Can. J. Chem. Downloaded from www.nrcresearchpress.com by 210.87.254.6 on 09/05/12
For personal use only.

TABLE I

Reactions of diphos and diars with iron carbonyls

Reaction number	Carbonyl Formula	Carbonyl Amount in g	Carbonyl Amount in mmoles	Ligand Formula	Ligand Amount in g	Ligand Amount in mmoles	Conditions Medium	Conditions Method	Conditions Time (in h)	Products* Formula	Products* Amount (in %)
[1]	$Fe_3(CO)_{12}$	5.30	10.5	Diphos	2.65	6.7	Benzene	Reflux	2 or 6	DiphosFe(CO)$_3$†	28
										DiphosFe$_2$(CO)$_8$‡	33
[2]	$Fe_3(CO)_{12}$	1.90	3.8	Diphos	1.00	2.5	Acetone solution	u.v. irradiation	65	DiphosFe(CO)$_3$†	26
										DiphosFe$_2$(CO)$_8$‡	40
[3]	$Fe_2(CO)_9$	2.00	5.5	Diphos	1.00	2.5	Benzene	Reflux	6	DiphosFe(CO)$_3$†	30
										DiphosFe$_2$(CO)$_8$‡	34
[4]	$Fe(CO)_5$	4.50	23.0	Diphos	0.70	1.8	Acetone solution	u.v. irradiation	65	DiphosFe(CO)$_3$†	11
										DiphosFe$_2$(CO)$_8$‡	63
[5]	$Fe_3(CO)_{12}$	6.00	11.9	Diars	1.6	5.6	Acetone solution	u.v. irradiation	137	DiarsFe(CO)$_3$§	27
										DiarsFe$_2$(CO)$_8$†	~2
										$C_6H_4(AsCH_3)_2CH_2Fe_2(CO)_8$‡	~1
[6]	$Fe(CO)_5$	6.00	30.6	Diars	1.6	5.6	Acetone solution	u.v. irradiation	137	DiarsFe(CO)$_3$§	52
										DiarsFe$_2$(CO)$_8$†	7
										$C_6H_4(AsCH_3)_2CH_2Fe_2(CO)_8$‡	~1
[7]	$Fe(CO)_5$	1.5	7.7	Diars	2.5 (1 g recovered)	8.7	Sealed tube	Heat to 132°	4	DiarsFe(CO)$_3$§	31
										DiarsFe$_2$(CO)$_8$†	Less than 1
										$C_6H_4(AsCH_3)_2CH_2Fe_2(CO)_8$‡	Not isolated

*Only identified products are given here (see text for others).
†Eluted with 50% benzene, 50% petroleum ether.
‡Eluted with 25% benzene, 75% petroleum ether (30–60°).
§Eluted with 7% diethyl ether, 93% petroleum ether.

TABLE II
Infrared bands of complexes*

Complex	Medium	Band positions			
DiphosFe(CO)$_3$†	CCl_4	1482 w	1435 s	1410 w	1308 w
		1182 w (br)	1112 w (sh)	1097 m	1070 w (sh)
		1028 w	880 w	693 s	678 m (sh)
		652 w	627 s	592 s	
DiphosFe$_2$(CO)$_8$†	CCl_4	1484 w	1435 s	1421 w	1334 w
		1310 w	1178 m	1098 s	1072 vw
		1029 w	1000 w	692 s	622 s
DiarsFe(CO)$_3$†	CS_2	1277 m	1260 m	1105 m	910 s
		872 s	756 s	645 s	633 s
		602 s			
DiarsFe$_2$(CO)$_8$†	CCl_4	1417 w	1386 vw	909 w	871 m
		622 s			
$C_6H_4(AsCH_3)_2CH_2Fe_2(CO)_8$†	CCl_4	1447 w	1435 w	1412 w	1373 w
		1270 w	1263 w	1216 m	1107 m
		1087 w	875 s	650 w (sh)	620 vs
(Carbonyl bands	C_6H_{12}	2054 s	1984 s	1950 vs)	
$C_{15}H_{23}Cl_3As_3OFe$‡	§	3050 w (sh)	2997 m	2920 m	1926 s (CO)
		1449 m (sh)	1412 s	1280 m (sh)	1260 m
		1164 w	1105 m	1036 w	913 s
		868 s	780 m (sh)	756 s	615 m
		590 s	440 s	380 s	365 s

*Perkin–Elmer 457 instrument; w = weak, m = medium, s = strong, v = very, sh = shoulder, br = broad.
†Below 1700 cm^{-1}.
‡Full spectrum.
§KBr disc.

ether did not appear to affect the relative intensities of these bands, although chromatography on alumina (under N_2) suggested the material to be a mixture despite eluting as a single band. Carbon and hydrogen analyses are close to those required for a 1:1 mixture of diphosFe$_2$(CO)$_8$ and diphosFe(CO)$_3$ or a compound (diphos)$_2$Fe$_3$(CO)$_{11}$, possibly **3**.

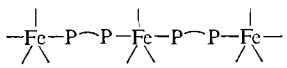

3

Although mass spectral, Mössbauer, and nuclear magnetic resonance (n.m.r.) data tend to suggest the presence of diphosFe$_2$(CO)$_8$ in the material, none was ever separated as such. However, a compound (diphos)$_2$Fe$_3$(CO)$_{11}$ could possibly give similar spectroscopic results. In addition, in order to satisfy the i.r. spectrum, the diphosFe(CO)$_3$ in a 1:1 mixture would need to be the polymeric *trans*-disubstituted derivative described by Manuel (2) (though not observed in our reaction mixtures) as red–brown, which does not correlate well with the observed pale yellow color of our material. It is not inconceivable that this material does contain some (diphos)$_2$Fe$_3$(CO)$_{11}$.

Another compound formed in these diphos reactions is an unstable and somewhat intractable deep-red material which eluted with 1:1 petroleum ether/acetone (reactions [1] and [2] only). Its Mössbauer spectrum possibly indicates that 3 iron atoms are involved but the compound could not be characterized. Materials similar to this have been noted in reactions of the fluorocarbon-bridged ditertiary phosphine ffos (8).

Mass spectral data of diphosFe(CO)$_3$ and diphosFe$_2$(CO)$_8$ are given in Table III. Their formulation is shown to be correct, although some ambiguity is involved in the cracking pattern as, in low resolution, C_2H_4 has the same *m/e* value as CO and loss of C_2H_4 appears to be an important process.

The reactions of diars (**1**) with iron carbonyls afford one main product, diarsFe(CO)$_3$, although they are not as clean as previously reported (1). Our experience with diarsFe(CO)$_3$ is that the complex is very air sensitive, especially in solution, and that it undergoes an extremely interesting and facile reaction with air-free spectroscopic chloroform, despite the fact that this has been mentioned (3) as a solvent for i.r. studies on this complex. Reaction appears to start almost immediately and deep yellow crystals (only slightly

Can. J. Chem. Downloaded from www.nrcresearchpress.com by 210.87.254.6 on 09/05/12
For personal use only.

Can. J. Chem. Downloaded from www.nrcresearchpress.com by 210.87.254.6 on 09/05/12
For personal use only.

TABLE III

Mass spectral data*

Parent	*m/e* of daughter ion	Parent	*m/e* of daughter ion	Identification of daughter ion
$DiarsFe_2(CO)_8$	622	$DiarsFe(CO)_3$	622†	$(LFe_2(CO)_8)^+ \equiv P_1^+$
	594		594†	$(P_1-CO)^+$
	566		566†	$(P_1-2CO)^+$
	538		538†	$(P_1-3CO)^+$
	510		510†	$(P_1-4CO)^+$
	490			
	482		482†	$(P_1-5CO)^+$
	466			$(P_1-5CO-CH_4)^+$
	462			
	454		454†	$(P_1-6CO)^+$, $(P_1-Fe(CO)_4)^+$
	438			$(P_1-6CO-CH_4)^+$, $(P_1-Fe(CO)_4-CH_4)^+$
	434			
	426		426†	$(P_1-7CO)^+$, $(P_1-Fe(CO)_5)^+$, $LFe(CO)_3^+ \equiv P_2^+$
	410		410	$(P_2-CH_4)^+$
	406			
	398		398	$(P_2-CO)^+$
	382		382	$(P_2-CO-CH_4)^+$
	378			
	370		370	$(P_2-2CO)^+$
	354		354	$(P_2-2CO-CH_4)^+$
	350			
	342		342	$(P_2-3CO)^+ \equiv (LFe)^+$
	326		326	$(P_2-3CO-CH_4)^+$
	322			
			~310	$(P_2-3CO-2CH_4)^+$?
	300			
	296		~296	
	286		286	$(P_2-3CO-Fe)^+ \equiv L^+$
	271			
	270		~270	$(L-CH_4)^+$
	262			
	256			
	255		255	$(L-CH_4-CH_3)^+$
			240	$(L-CH_4-C_2H_6)^+$
	239			
	227			
			226	
			225	$(L-CH_4-C_3H_9)^+$
			205	
	182			
	181		181	$(L-As(CH_3)_2)^+$
	167		166	$(L-As(CH_3)_2-CH_3)$
	165		164	
	151		151	$(L-As(CH_3)_2-C_2H_6)$
	141			
	105		105	$(As(CH_3)_2)^+$

Can. J. Chem. Downloaded from www.nrcresearchpress.com by 210.87.254.6 on 09/05/12
For personal use only.

TABLE III *(continued)*

Parent	*m/e* of daughter ion	Identification of daughter ion
$C_6H_4(AsCH_3)_2CH_2Fe_2(CO)_8$	606	$P^+ \equiv (LFe_2(CO)_8)^+$
	578	$(P-CO)^+$
	550	$(P-2CO)^+$
	525	
	522	$(P-3CO)^+$
	494	$(P-4CO)^+$
	466	$(P-5CO)^+$
	438	$(P-6CO)^+$, $(P-Fe(CO)_4)^+$
	410	$(P-7CO)^+$, $(P-Fe(CO)_4-CO)^+$
	382	$(P-8CO)^+$, $(P-Fe(CO)_4-2CO)^+$
	367	$(P-8CO-CH_3)^+$, $(P-Fe(CO)_4-2CO-CH_3)^+$
	354	$(P-Fe(CO)_4-3CO)^+$
	338	$(P-Fe(CO)_4-3CO-CH_4)^+$
	326	$(P-Fe(CO)_4-4CO)^+$
	297	
	283	
	270	$(P-2Fe(CO)_4)^+ \equiv L^+ \equiv (C_6H_4(AsCH_3)_2CH_2)^+$
	255	$(L-CH_3)^+$
	239	$(L-CH_3-CH_4)^+$
	227	$(L-C_3H_7)^+$
	177	
	165	$(L-As-2CH_3)^+ \equiv (C_6H_4AsCH_2)^+$
	151	$(C_6H_4As)^+$
	139	
	125	
	113	
	105	$(As(CH_3)_2)^+$

Can. J. Chem. Downloaded from www.nrcresearchpress.com by 210.87.254.6 on 09/05/12
For personal use only.

TABLE III *(Concluded)*

Parent	*m/e* of daughter ion	Parent	*m/e* of daughter ion	Identification of daughter ion
$DiphosFe_2(CO)_8$	734‡	$DiphosFe(CO)_3$		$(LFe_2(CO)_8)^+ \equiv P_1^+$
	706‡			$(P_1-CO)^+$, $(P_1-C_2H_4)^+$
	678‡			$(P_1-2CO)^+$, $(P_1-C_2H_4-CO)^+$
	650			$(P_1-3CO)^+$, $(P_1-C_2H_4-2CO)^+$
	622			$(P_1-4CO)^+$, $(P_1-C_2H_4-3CO)^+$
	594			$(P_1-5CO)^+$, $(P-C_2H_4-4CO)^+$
	566			$(P_1-6CO)^+$, $(P_1-Fe(CO)_4{}^{++}$, $(P-C_2H_4-5CO)^+$
	538		538	$(P_1-7CO)^+$, $(P_1-Fe(CO)_5)^+ \equiv (LFe(CO)_3)^+ \equiv P_2^+$, $(P_1-C_2H_4-6CO)^+$, $(P_1-C_2H_4-Fe(CO)_4)^+$
	510		510	$(P_2-CO)^+$, $(P_2-C_2H_4)^+$, $(P_1-8CO)^+$, $(P_1-7CO-C_2H_4)^+$
	482		482	$(P_2-2CO)^+$, $(P_2-C_2H_4-CO)^+$, $(P_1-8CO-C_2H_4)^+$
	454		454	$(P_2-3CO)^+$, $(P_2-C_2H_4-2CO)^+$
	426		426	$(P_2-C_2H_4-3CO)^+$
	398		398	$L^+ \equiv (P_2-Fe-3CO)^+$ $(P_2-Fe-2CO-C_2H_4)^+$
	370		370	$(L-C_2H_4)^+$
	348		348	
	328			
			321	$(L-C_6H_5)^+$
	289		289	
	286		286	
	272			
			270	
	262		262	
			242	
			239	
	218		218	
			212	
	210		210	
	203		203	
	183		183	$(P(C_6H_5)_2-2H)^+$

*Major or assignable peaks above *m/e* 104 ± 1 up to *m/e* ≃ 286 ± 3 for higher *m/e*.
†Weak peaks.
‡Intensity of these peaks dies very rapidly.

TABLE IV
Physical properties of complexes

Complex*	Melting point, °C (in vacuo, uncorrected)	Analysis	
		Calculated	Found
		Element %	Element %
$DiphosFe(CO)_3$	143–144	C 64.68 H 4.46	C 65.19 H 4.69
$DiphosFe_2(CO)_8$	186–187	C 55.61 H 3.27	C 55.91 H 3.25
$DiarsFe(CO)_3$	130–132	—	—
$DiarsFe_2(CO)_8$	175–177 Decomp.	C 34.73 H 2.57	C 35.01 H 2.53
$C_6H_4(AsCH_3)_2CH_2Fe_2(CO)_8$	130–131	—	—
$C_{15}H_{23}FeOAs_3Cl_3$	Darkens 240, 260–265 (decomp.)	C 29.70 H 3.79 Cl 17.58 As 37.10 O 2.64 Fe 9.24	C 30.15 H 3.73 Cl 18.00 As 38.71 O 3.02 Fe 9.31

*All yellow solids.

soluble in chloroform) are produced within 1 day at room temperature. The crystals appear to be air stable and a complete analysis establishes the empirical formula $C_{15}H_{23}Cl_3As_3OFe$. One carbonyl stretching band at 1926 cm^{-1} is observed (KBr disc). The Mössbauer spectrum shows a doublet with a quadrupole splitting ($\Delta = 0.57$ mm/s) much less than that shown by normal 5 coordinate iron complexes. The size of this splitting is consistent with a distorted octahedral environment while the isomer shift value of $\delta = 0.42$ mm/s relative to sodium nitroprusside could indicate an oxidation state of +4 for the iron (9). The complex is also paramagnetic with a gram susceptibility of $7.20 (\pm 0.28) \times 10^{-6}$ c.g.s.e.m.u. Using the above formula and applying the appropriate diamagnetic corrections the estimated $\mu_{eff} = 3.31$ B.M. This value also indicates a high oxidation number for the iron, the iron(IV) compound $[Fe(diars)_2Cl_2][ClO_4]_2$ having a μ_{eff} of 2.98 B.M. (10). It is difficult to reconcile the high oxidation state of the iron and paramagnetism with the observation that the compound contains a carbonyl group. Although single crystals of this complex can be obtained, they have so far proved to be unsuitable for the necessary X-ray investigation.

A second product, $diarsFe_2(CO)_8$, may also be separated with difficulty and in low yield from reactions between diars and iron carbonyls (Table I). As with $diarsFe(CO)_3$, the mass spectrum (Table III), confirms its formulation. It is worth noting that in all of the reactions studied a large proportion of the diars is converted into a viscous yellow oil (e.g. 1.0 g in reaction [7], Table I). This oil chromatographs on Florisil to give what appear to be fairly distinct yellow bands eluting with petroleum ether/benzene mixtures. Their carbonyl i.r. spectra indicate that they are all $LFe(CO)_4$ or $LFe_2(CO)_8$ derivatives. However, n.m.r. studies showed the chromatographic bands to be mixtures. Using an alumina column the tail of the second band eluting with 2% diethyl ether/98% petroleum ether gave a yellow solid. The proton n.m.r. (CS_2 solution, internal TMS) of this material shows ostensibly singlet resonances at 1.84 p.p.m. (area 3), 2.61 p.p.m. (area 1), and 7.68 p.p.m. (area 2). The i.r. carbonyl stretching bands at 2054s, 1984s, 1950vs (C_6H_{12} solution), are characteristic of an $LFe(CO)_4$ or $LFe_2(CO)_8$ derivative. The mass spectrum of the complex indicates it to be an $LFe_2(CO)_8$ complex with *m/e* for the ligand at 270. The above facts are consistent (apart from the n.m.r. *singlet* at 7.68 p.p.m. possibly) with a structure **4**.

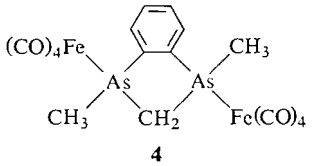

4

Can. J. Chem. Downloaded from www.nrcresearchpress.com by 210.87.254.6 on 09/05/12
For personal use only.

A *trans*-derivative is shown as this is compatible with a singlet CH_2 resonance.

It would thus appear that the yellow oil obtained in the diars reactions consists of $Fe(CO)_4$ and/or $Fe_2(CO)_8$ complexes of ligands formed by fragmentation of diars. Diars$Fe(CO)_4$ itself was not isolated but may well exist in the mixture although it is expected to be unstable.

A recent paper describes how a compound originally reported by Nyholm to be $[(diars)_3Ni][ClO_4]_2$ is in fact $[(diars)(triars)Ni][ClO_4]_2$ (11) where rearrangement of the diars has occurred. The related fluorocarbon bridged ligand, ffars (**5**), gives the compound ffars$Fe_3(CO)_9$ in which an As—C bond in the ligand has been broken and an Fe—C bond formed (8, 12). Thus modification of ligands in complex forming reactions may well be more common than generally thought.

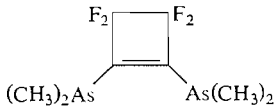

5

Acknowledgments

We wish to thank the National Research Council of Canada for financial support, Dr. J. R. Sams for assistance in obtaining and interpreting the Mössbauer spectra, and Dr. R. C. Thompson for the magnetic susceptibility measurement.

1. H. NIGAM, R. S. NYHOLM, and D. V. RAMANA RAO. J. Chem. Soc. 1397 (1959).
2. T. A. MANUEL. Inorg. Chem. **2**, 854 (1963).
3. J. LEWIS, R. S. NYHOLM, S. S. SANDHU, and M. H. B. STIDDARD. J. Chem. Soc. 2825 (1964).
4. W. R. CULLEN, C. J. STEWART, and P. S. DHALIWAL. Inorg. Chem. 2256 (1967).
5. W. R. CULLEN, D. A. HARBOURNE, B. V. LIENGME, and J. R. SAMS. J. Amer. Chem. Soc. **90**, 3293 (1968).
6. W. R. CULLEN, D. A. HARBOURNE, B. V. LIENGME, and J. R. SAMS. Inorg. Chem. **8**, 95 (1969).
7. W. R. CULLEN, D. A. HARBOURNE, B. V. LIENGME, and J. R. SAMS. Inorg. Chem. In press.
8. W. R. CULLEN and D. A. HARBOURNE. Unpublished results.
9. N. N. GREENWOOD. Chem. Brit. **3**, 56 (1967).
10. R. S. NYHOLM and R. PARISH. Chem. Ind. London, 470 (1956).
11. B. BOSNICH, R. S. NYHOLM, P. J. PAULING, and M. L. TOBE. J. Amer. Chem. Soc. **90**, 4741 (1968).
12. F. W. B. EINSTEIN. Private communication.

Can. J. Chem. Downloaded from www.nrcresearchpress.com by 210.87.254.6 on 09/05/12
For personal use only.

Can. J. Chem. Downloaded from www.nrcresearchpress.com by 210.87.254.6 on 09/05/12
For personal use only.

Préparation et caractérisation de polymères-modèle à structure en étoile, par copolymérisation séquencée anionique

DENIS J. WORSFOLD[1], JEAN-GEORGES ZILLIOX ET PAUL REMPP
Centre de Recherches sur les Macromolécules (CNRS), 67-Strasbourg, France

Reçu le 20 mars 1969

Des polymères à structure "en étoile" ont été préparés par copolymérisation séquencée anionique de styrène et de divinylbenzène (DVB), la proportion de ce dernier monomère étant de l'ordre de quelques molécules par extrémité vivante. Toutes les opérations ont été effectuées sous vide poussé, et le benzène a été choisi comme solvant. Les échantillons obtenus ont été trouvés quasiment exempts de polystyrène linéaire et leur polydispersité est très faible. Le nombre de branches des étoiles dépend de la concentration globale, de la proportion de DVB mise en jeu et de la masse moléculaire du précurseur linéaire. Les résultats obtenus avec des isomères para et méta du DVB ne diffèrent pas de façon significative, pour ce qui est de la structure des produits obtenus. L'étude spectroscopique de la réaction fait apparaître cependant des différences notables, dues au fait que les 2 doubles liaisons de l'isomère para diffèrent par leurs réactivités, ce qui n'est pas le cas de l'isomère méta.

Star-shaped polystyrene samples have been synthesized by anionic block-copolymerization of styrene and divinylbenzene (DVB), the proportion of the latter monomer being of the order of a few molecules per living end. Vacuum technique was used and benzene was chosen as solvent. The samples were found almost free of linear polystyrene, and of very low polydispersity. The number of branches was found to be a function of the overall concentration, of the amount of DVB, and of the molecular weight of the linear precursor. The results obtained with the meta and the para isomers did not differ significantly, as far as the products themselves are concerned. However, spectroscopic investigations carried out during reaction showed that the reactivity of the 2 double bonds of the para isomer differ significantly, whereas this is not the case with the meta isomer.

Canadian Journal of Chemistry, 47, 3379 (1969)

Introduction

Nous avons décrit récemment (1, 2) le principe d'une méthode originale de préparation de polystyrènes à structure "en étoile", par voie anionique. Rappelons que cette méthode consiste à préparer un polystyrène mono-carbanionique et à en utiliser, dans une seconde phase, les extrémités carbanioniques comme promoteurs pour la polymérisation de divinylbenzène (DVB). Ce dernier monomère se polymérise en donnant naissance à un nodule réticulé, lié simultanément à n chaînes linéaires de polystyrène: on obtient donc un polymère "en étoile", tout au moins lorsqu'on prend soin de limiter la proportion de DVB à une valeur aussi faible que possible.

La plupart des préparations de polystyrènes "en étoile" qui ont été relatées jusqu'ici (1, 2) ont été effectuées sous atmosphère d'argon, essentiellement en solution dans le tétrahydrofuranne (THF), à basse température, avec le cumylpotassium comme promoteur, et avec du DVB commercial. Les produits obtenus étaient fortement polydispersés, et souillés de polystyrène linéaire (3, 4).

Aussi, devant les difficultés que nous avons rencontrées, avons-nous effectué une nouvelle série de préparations dans des appareils scellés, sous vide poussé, en utilisant la technique des joints fragiles et des distillations sur parois froides (5). Il nous a en effet paru indispensable d'étudier les facteurs qui influencent le déroulement de la réaction afin d'en déterminer le mécanisme. Ce sont les résultats de cette étude qui font l'objet du présent mémoire.

Choix des Conditions Expérimentales

Solvant

La presque totalité de nos expériences a été effectuée en solution dans le benzène. L'intérêt de ce solvant pour ce type d'expérience réside dans sa faible polarité qui implique une vitesse de polymérisation assez peu élevée pour le styrène et ses homologues. De ce fait lors de l'addition du DVB, un mélange homogène peut être réalisé par agitation, ce dont on ne peut être assuré en milieu THF.

Promoteur

Le souci d'obtenir une vitesse d'amorçage aussi élevée que possible nous a conduit à choisir le sec-butyl-lithium comme promoteur. En effet si l'amorçage était lent par rapport à la vitesse de propagation, la

[1]Adresse permanente: Department of Applied Chemistry, National Research Council of Canada, Ottawa, Canada.

Can. J. Chem. Downloaded from www.nrcresearchpress.com by 210.87.254.6 on 09/05/12
For personal use only.

polydispersité du polystyrène qui sert de "précurseur" s'en trouverait accrue (6). Il a été montré (7) que le butyl-lithium secondaire est plus actif que l'isomère normal, c'est ce qui a déterminé notre choix. Les valeurs obtenues du rapport de polydispersité M_w/M_n pour le polystyrène "primaire" sont voisines de l'unité (< 1.1), de sorte qu'en première approximation l'on peut considérer les branches des étoiles comme identiques entre elles.

Divinylbenzène

Toutes les expériences relatées ici ont été effectuées avec les isomères para ou méta purs du DVB. Le *m*-DVB (99%) nous a été aimablement fourni par la Société Pétrofina; quant au *p*-DVB, nous l'avons obtenu à partir du mélange commercial par la méthode au chlorure cuivreux décrite par Rubinstein et Snyder (8). Deux purifications successives suivies d'une cristallisation du produit obtenu, avec élimination de la phase liquide, conduisent à une substance dont la pureté dépasse 99%.

Température

Les expériences ont été réalisées à température ambiante, et se sont prolongées durant plusieurs heures, car à cette température les polymérisations sont lentes en milieu benzénique.

Caractérisation des Polymères "en Etoile" Obtenus

La masse moléculaire du polystyrène utilisé comme "précurseur" est déterminée sur un prélèvement désactivé au méthanol, par diffusion de la lumière, en solution benzénique.

La masse moléculaire du polystyrène "en étoile" est également mesurée par diffusion de la lumière. La présence éventuelle d'homologue linéaire (précurseur) dans l'échantillon est détectée par chromatographie liquide (g.p.c.) et l'on peut ainsi, le cas échéant, corriger la valeur de M_w pour en tenir compte.

Le rapport de la masse moléculaire du polystyrène en étoile à celle de son "précurseur" linéaire conduit au nombre moyen n de branches de l'étoile. Nous avons calculé n à partir des moyennes en poids (et non à partir des M_n) ce qui conduirait à des valeurs trop élevées si les échantillons étaient fortement polydispersés. L'erreur est en fait peu importante: les résultats des fractionnements montrent en effet que la polydispersité de nos échantillons est très peu marquée.

Discussion des Résultats

Les résultats que nous avons obtenus sont présentés schématiquement au Tableau I.

TABLEAU I

Préparation de polystyrènes en étoile*

Expérience	Numéro	M_{DDL} Précurseur	Concentration globale	DVB/PS$^-$	M_{DDL}	% $PS_{lin\acute{e}.}$	$M_{corr.}$	n
1	M 1	57 500	5	3.7	403 000	0		7
	P 1	57 500	5	3.7	348 000	0		6
2	M 2A	191 000	10	1.8	2 050 000	§		10.7
	M 2B	"	"	3.8	2 300 000	§		12.1
	M 2C	"	"	7.3	2 500 000	§		13.1
	M 2D	"	"	9.5	2 700 000	§		14.2
	M 2E	"	"	21	2 950 000	§		15.5
	P 2C	"	"	7.3	2 300 000	§		12.1
3	M 3	89 000‖	9	7.7	1 364 000	§		15‖
	P 3	71 000‖	10.4	5.1	828 000	§		11.6‖
4	M 4A	109 000	1	1.9	735 000	5	767 000	7
	M 4B	"	2.6	"	880 000	5	903 000	8.3
	M 4C	"	6.2	"	1 005 000	6	1 063 000	9.7
	M 4D	"	12.4	"	1 320 000	8	1 423 000	13
5	M 5A	7 000	10	1.8	95 000	0		13.5
	M 5B	16 000	"	"	223 000	0		13.9
	M 5C	62 000	"	"	651 000	§		10.5
	M 5E	573 000	"	"	4 750 000	5	4 970 000	8.6
6	M 6†	67 000	10	5.8	660 000	8	716 000	10.7
	M 6‡	"	"	"	391 000	25	498 000	7.4
7	M 7A	38 700	11	0.55	180 000	39	270 000	6.9
	M 7B	"	"	0.8	234 000	26	302 000	7.8
	M 7C	"	"	1	298 000	12	333 000	8.6
	M 7D	"	"	1.8	434 000	4	450 000	11.6

*Les lettres M et P désignent les polymères obtenus à l'aide de méta et de para DVB, respectivement.
†Benzène.
‡Tétrahydrofuranne.
§Teneur en PS linéaire (g.p.c.) inférieure à 3%.
‖Masse moléculaire du précurseur déterminée spectroscopiquement: M_n.

Can. J. Chem. Downloaded from www.nrcresearchpress.com by 210.87.254.6 on 09/05/12
For personal use only.

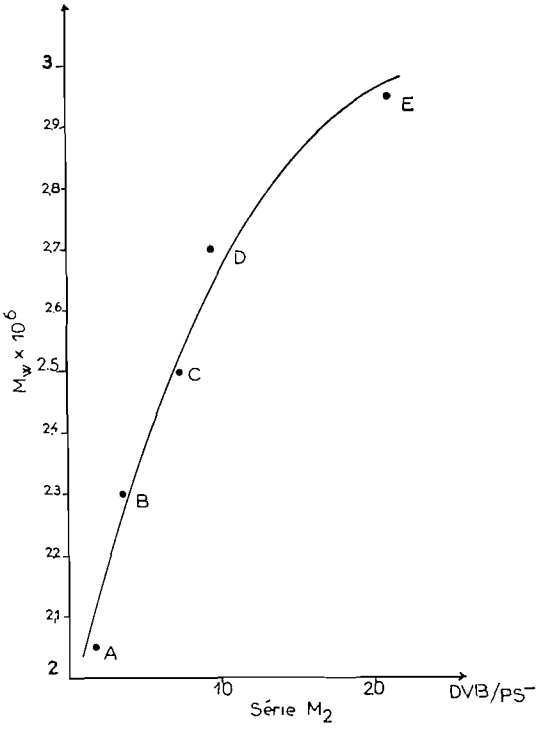

FIG. 1. Variation de la masse moléculaire du polymère en étoile en fonction du rapport DVB/PS⁻.

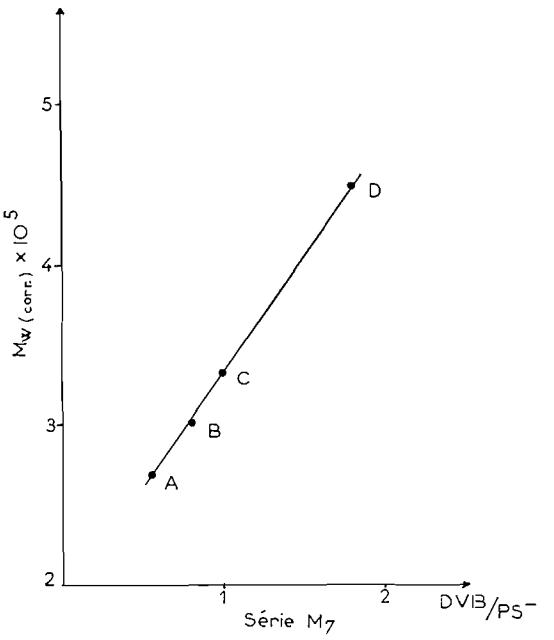

FIG. 2. Variation de la masse moléculaire du polymère en étoile en fonction du rapport DVB/PS⁻.

On peut constater, tout d'abord, que dans la plupart des expériences la proportion de précurseur linéaire dans les échantillons bruts est faible, parfois même indécelable par g.p.c.

L'influence des divers facteurs que nous avons fait varier appelle les commentaires suivants:

(1) Proportion de DVB

Le nombre de branches n des molécules en étoile formées dépend, entre autres, de la proportion de DVB mise en jeu, la concentration globale et la masse moléculaire du précurseur demeurant constantes (exp. 2). La masse moléculaire du produit formé (donc le nombre n de branches) augmente lorsque le rapport du nombre de molécules de DVB au nombre d'extrémités vivantes (DVB/PS⁻) croît de 1.8 à 21 (Fig. 1). La proportion de précurseur linéaire dans les échantillons bruts est très faible.

Lorsque la proportion de DVB est plus faible encore (exp. 7: DVB/PS⁻ variant de 0.55 à 1.8), la masse moléculaire du précurseur et la concentration globale demeurant constantes, la proportion d'homopolymère linéaire dans les échantillons devient plus importante et elle augmente en raison inverse du rapport DVB/PS⁻.

En revanche, la masse moléculaire, et par suite le nombre de branches du polymère en étoile augmente avec la proportion de DVB mise en jeu (Fig. 2). La présence d'un produit de simple couplage du précurseur n'a pu être mise en évidence; ce résultat contredit l'observation effectuée par Baer (9), selon laquelle le produit de couplage constitue l'essentiel de l'échantillon lorsque le rapport DVB/PS⁻ est voisin de 0.5.

(2) Masse Moléculaire du Précurseur

A concentration globale et proportion de DVB constantes, lorsque la masse moléculaire du précurseur linéaire augmente, le nombre de branches décroît, mais cet effet est assez faible (Fig. 3).

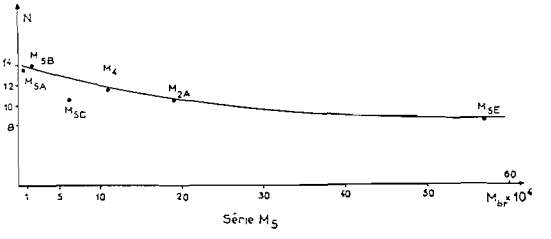

FIG. 3. Variation du nombre de branches du polymère en étoile en fonction de la masse moléculaire de la branche.

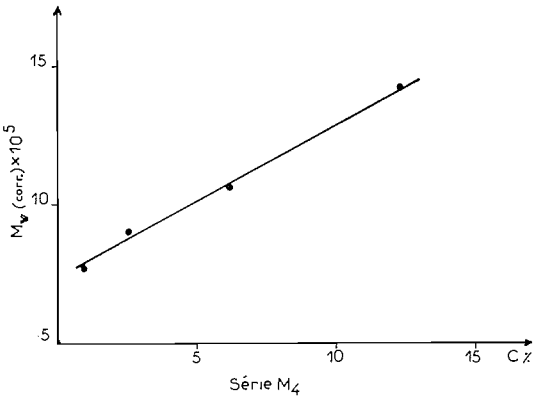

FIG. 4. Variation de la masse moléculaire du polymère en étoile en fonction de la concentration globale.

(3) Concentration Globale

Lorsque la masse moléculaire du précurseur et le rapport DVB/PS$^-$ demeurent constants, la masse moléculaire du polymère en étoile augmente avec la concentration globale du milieu réactionnel, dans le domaine de concentration considéré (exp. 4): Alors que la concentration croît de 1 à 12% la masse moléculaire du produit en étoile double (Fig. 4).

(4) Nature du Solvant

L'expérience 6 ne permet pas de conclure de façon ferme quant au rôle du solvant dans la réaction de formation des étoiles. En milieu THF, les vitesses de polymérisation sont si élevées que l'homogénéité de concentration dans le milieu réactionnel ne peut être assurée de façon satisfaisante, lors de l'addition du DVB. Toutefois la présence de 25% de PS linéaire dans le produit brut M 6 THF peut s'expliquer par des réactions accidentelles de désactivation et/ou d'isomérisation (10) qui se seraient produites pendant l'évaporation du benzène ou lors du processus de redissolution dans le THF. Il n'y en a que 8% dans le produit préparé en milieu benzénique, le précurseur étant le même, la proportion de DVB constante et les concentrations identiques.

(5) Nature de l'Isomère du DVB

La nature de l'isomère utilisé, *p*-DVB ou *m*-DVB n'affecte pas sensiblement la masse moléculaire des polystyrènes "en étoile". Dans des conditions expérimentales identiques, la masse moléculaire du produit obtenu avec le *m*-DVB est légèrement supérieure (exp. 1 et 2). Par contre les 2 isomères se distinguent par la réactivité de leurs doubles liaisons vinyliques, ainsi que le fait apparaître l'étude spectrophotométrique que nous relatons plus loin.

Fractionnement des Produits Obtenus

Nous avons déjà signalé que la présence de polystyrène linéaire dans nos échantillons est le plus souvent indécelable. Mais on peut se demander, d'autre part, si les échantillons de polystyrène "en étoile" obtenus ici sont homogènes en masse et en structure.

Nous avons soumis le produit M 2 B à une précipitation fractionnée (solvant: benzène, précipitant: méthanol) dont les résultats sont rassemblés au Tableau II. Trois fractions, recueillies dans un intervalle de γ très faible, présentent des masses moléculaires presque identiques et constituent la totalité de l'échantillon. Examinées séparément par chromatographie liquide, elles présentent des temps de rétention très voisins. Seule la 3e. fraction contient environ 25% de précurseur linéaire, ce qui correspond à 1% de l'ensemble de l'échantillon. La polydispersité de ce polystyrène "en étoile" est donc suffisamment faible pour que le fractionnement par précipitation s'avère inefficace.

Il est en général admis, que le pouvoir séparateur d'un fractionnement par élution est supérieur à celui d'une précipitation fractionnée. Aussi avons-nous soumis ce même produit (M 2 B) à un fractionnement par élution sur une colonne du type Baker-Williams à cycle de température programmé, réalisée par Koessler *et al.* (11). Le système d'élution utilisé était le mélange benzène–méthanol. Les 8 fractions recueillies ont été précipitées par le méthanol, filtrées et séchées, et elles ont été étudiées par diffusion de la lumière. Ici encore, mis à part la première fraction constituée du précurseur linéaire (3% de l'échantillon) toutes les fractions ont, à peu de chose près, la même masse moléculaire. Ce résultat, confirmé par g.p.c. des fractions, met en évidence la remarquable homogénéité en masse et en structure du polystyrène "en étoile" obtenu ici.

Etude Spectrophotométrique de la Copolymérisation Styrène–DVB

Nous avons vu, dans ce qui précède, que les polymères "en étoile" obtenus avec l'isomère

Can. J. Chem. Downloaded from www.nrcresearchpress.com by 210.87.254.6 on 09/05/12
For personal use only.

TABLEAU II

Fractionnement du produit M 2 B*

(*1*) Précipitation fractionnée (benzène–méthanol)

Fraction	Poids	%	M_w	% $PS_{linéaire}$	$M_{w\ (corr.)}$
1	5.300	67.4	2 350 000		
2	2.240	28.5	2 300 000		
3	0.320	4.1	1 270 000	25	1 500 000

Rendement du fractionnement: 98%

(*2*) Fractionnement par élution sur colonne

Fraction	Poids	%	M_w
1			
2	0.079	3	190 000
3	0.055	2.1	
4	0.347	13.2	2 020 000
5	0.276	10.4	2 390 000
6	0.538	20.2	2 380 000
7	0.532	20.0	2 390 000
8	0.308	11.6	2 370 000
9	0.471	17.7	2 230 000

*M_{br} = 190 000, M_X = 2 300 000, $PS_{linéaire}$ = 2–3%.

para du divinylbenzène et ceux préparés à l'aide de l'isomère méta diffèrent peu du point de vue de leur masse moléculaire. Il est cependant nécessaire, pour connaître le mécanisme de la réaction, de suivre par voie spectroscopique, dans l'un et l'autre cas, l'évolution de l'absorption au cours du temps, en tachant d'identifier les bandes d'absorption pour les attribuer à tel ou tel des intermédiaires de la réaction.

En solution benzénique le polystyryl-lithium présente une bande d'absorption à 334 mμ. Les isomères para et méta du DVB absorbent respectivement à 314 et 305 mμ.

(1) Réaction du PS "Vivant" avec le p-DVB

Lorsqu'on ajoute du *p*-DVB à une solution de polystyryl-lithium, en milieu benzénique, on observe la formation instantanée d'une bande d'absorption à 380 mμ. La bande à 314 mμ, correspondant au DVB monomère disparaît complètement en 20 min environ. L'absorption à 380 mμ décroît en intensité au cours du temps pour faire place à une bande située à 345 mμ, cependant qu'une autre absorption importante se situe à 297 mμ. L'assignation probable de ces diverses bandes d'absorption est présentée schématiquement au Tableau III. Il semble donc que le *p*-DVB réagisse séparément par ses 2 doubles liaisons. Cela ressort de l'existence de doubles liaisons pendantes dans le nodule de polydivinyl benzène (297 mμ). L'absorption à 380 mμ, qui concerne le carbanion en résonance avec la double liaison, confirme également ce fait.

(2) Réaction du PS "Vivant" avec le m-DVB

Si l'on effectue la même réaction, dans les mêmes conditions, avec l'isomère méta, on constate la formation immédiate de 2 bandes d'absorption, à 316 et 347 mμ imputables respectivement aux sites carbanioniques *m*-vinyliques et aux sites carbanioniques alkylés en méta, c'est-à-dire aux molécules de DVB dont les 2 groupes vinyle ont participé à la réaction. L'absorption du *m*-DVB, à 305 mμ, de même que celle à 316 mμ, disparaissent peu à peu mais une faible absorption à 297 mμ (doubles liaisons pendantes) subsiste indéfiniment.

A ces commentaires il convient d'ajouter les 2 remarques suivantes:

(*1*) Les bandes d'absorption relatives aux carbanions issus des 2 isomères se différencient nettement: 316 et 380 mμ pour le méta et le para respectivement. Cela traduit les possibilités de résonance qui n'existent que pour l'isomère para:

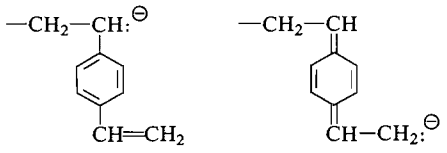

(*2*) En raison même de cette possibilité de

Can. J. Chem. Downloaded from www.nrcresearchpress.com by 210.87.254.6 on 09/05/12
For personal use only.

TABLEAU III

Assignation des bandes d'absorption des espèces chimiques présentes

Espèce chimique	Assignation (mμ)	Espèce chimique	Assignation (mμ)
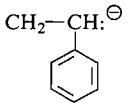	334		
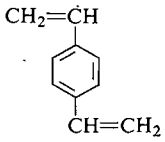	314	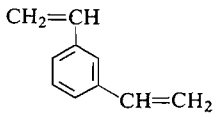	305
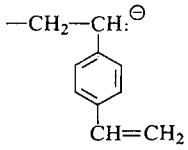	380	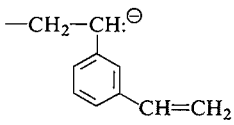	316
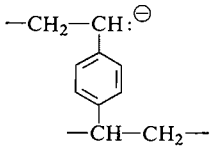	345	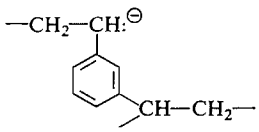	347
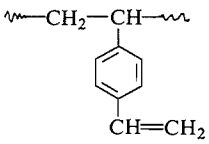	297 (doubles liaisons pendantes)	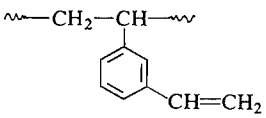	297

mésomérie, la réactivité des 2 groupes vinyle est plus nettement différenciée dans le cas de l'isomère para qu'elle ne l'est pour l'isomère méta. Cependant ce résultat n'est que qualitatif et ne résulte pas de l'examen de la cinétique de la réaction, au demeurant difficile à étudier dans le cas présent. Il reste que le nombre de doubles liaisons pendantes, donc inutilisées, est plus élevé pour le *p*-DVB que pour l'isomère méta.

Conclusions

Le choix de techniques expérimentales appropriées—travail sous vide poussé, utilisation du benzène comme solvant—nous a permis de faire progresser sensiblement l'étude de la préparation de polystyrènes en étoile par copolymérisation séquencée anionique de styrène avec le divinylbenzène, la proportion de ce dernier monomère étant limitée à quelques molécules par extrémité carbanionique.

Nous avons ainsi pu préparer de façon reproductible des échantillons de polystyrène en étoile exempts de "précurseur" linéaire et dont l'homogénéité moléculaire est remarquable. Le nombre moyen de branches de ces polymères en étoile dépend de la concentration globale du milieu réactionnel, de la proportion de DVB mise en jeu, par rapport au nombre de sites carbanioniques, et de la masse moléculaire du "précurseur" linéaire. Les masses moléculaires des produits obtenus avec l'un et l'autre isomère du DVB ne diffèrent guère. L'influence du solvant ne se manifeste sur la réaction que dans la mesure où l'homogénéité en concentration du milieu réactionnel ne peut plus être assurée; c'est le cas du THF, mais non celui du benzène, et

Can. J. Chem. Downloaded from www.nrcresearchpress.com by 210.87.254.6 on 09/05/12
For personal use only.

c'est ce qui nous a fait préférer ce dernier solvant.

L'étude spectrophotométrique de la polymérisation du DVB, amorcée par les sites carbanioniques du polystyrène "vivant" a fait apparaître des différences importantes entre le comportement des isomères méta et para du DVB. La réactivité des 2 doubles liaisons diffère sensiblement dans le cas du *p*-DVB et la proportion de doubles liaisons pendantes est, semble-t-il, bien plus élevée dans les nodules de poly-*p*-DVB que dans ceux constitués d'isomère méta.

Remerciements

Nous tenons à remercier Mme Z. Gallot, MM. A. Kohler, J. Gueguen et E. Schuster pour l'aide qu'ils nous ont apportée.

1. D. DECKER et P. REMPP. C. R. **261**, 1977 (1965).
2. J. G. ZILLIOX, P. REMPP et J. PARROD. J. Polym. Sci. C, **22**, 145 (1968).
3. J. G. ZILLIOX, D. DECKER et P. REMPP. C. R. **262**, 726 (1966).
4. H. BENOIT, Z. GRUBISIC, P. REMPP, D. DECKER et J. G. ZILLIOX. J. Chim. Phys. **63**, 1507 (1966).
5. S. BYWATER et D. J. WORSFOLD. J. Phys. Chem. **70**, 162 (1966).
6. L. GOLD. J. Chem. Phys. **28**, 91 (1958).
7. H. L. HSIEH. J. Polym. Sci. A, **3**, 163 (1965).
8. D. RUBINSTEIN et J. R. SNYDER. U.S. 3 217 051 (Cl. 260–669).
9. M. BAER. Brevet U.S. 1 447 176 (1966).
10. M. LEVY, M. SZWARC, S. BYWATER et D. J. WORSFOLD. Polym. **1**, 516 (1960). G. SPACH, M. LEVY et M. SZWARC. J. Chem. Soc. 355 (1962).
11. J. POLACEK, L. SCHULZ et I. KOESSLER. J. Polym. Sci. C, **16**, 1327 (1967).

Can. J. Chem. Downloaded from www.nrcresearchpress.com by 210.87.254.6 on 09/05/12
For personal use only.

Can. J. Chem. Downloaded from www.nrcresearchpress.com by 210.87.254.6 on 09/05/12
For personal use only.

Electrochemical studies of lanthanum and lanthanum–zinc alloys in fused LiCl–KCl eutectic[1]

JEAN-BAPTISTE P. F. LESOURD AND JAMES A. PLAMBECK
Department of Chemistry, University of Alberta, Edmonton, Alberta

Received April 14, 1969

The electromotive force of cells of the type La(s)/LiCl–KCl (eutectic) + $LaCl_3$/(La + Zn, saturated liquid alloy) has been measured over the temperature range 450–600 °C. Thermodynamic functions for the limiting lanthanum–zinc solid intermetallic compound existing in this range are: ΔG_f^0, −58.8 kcal/mole, ΔS_f^0, −53 cal/deg mole, and ΔH_f^0, −97 kcal/mole at 450 °C. The standard potential (mole fraction scale) of the La(III)/La(0) electrode is −2.883 V with respect to the Pt(II)/Pt reference electrode at 450 °C. The significance of these measurements for the electrochemical separation of lanthanum and uranium is discussed.

Canadian Journal of Chemistry, 47, 3387 (1969)

Introduction

In some methods of processing spent nuclear reactor fuel, the metallic fuel is first dissolved in liquid zinc or bismuth. The separation of fission products from uranium by oxidation–reduction reactions using these solutions has been studied (1–4, and references therein). Studies of dilute solutions of uranium in zinc have been made (4, 5) using electromotive force (e.m.f.) methods, and solubility data for metals in liquid zinc have been compiled (6).

The fission of ^{235}U gives primarily one fragment of 90–100 atomic mass units (a.m.u.) and another of 130–150 a.m.u. (7). In the latter group there are seven isotopes of lanthanum, of which one is stable, and isotopes of many other rare earth metals. Lanthanum can be considered a typical rare-earth fission product impurity, and a study of liquid–metal solutions of it is therefore desirable. A study of the lanthanum–bismuth system by e.m.f. methods has been published (8), and cerium and erbium have been studied in several liquid metals (9) including zinc. The phase diagram of the lanthanum–zinc system has been established by Vogel, Rolla, Iandelli, and Canneri (10). Pascal (11) and Hansen and Anderko (12) point out that there is disagreement on the stoichiometry of the solid compound in equilibrium with the solution in the zinc-rich part of the diagram. According to Vogel *et al.* (10), this would be $LaZn_{13}$, whereas Schramm (13) gives the formula $LaZn_{11}$. Veleckis *et al.* (14) report the existence of both these compounds. For the purpose of this paper, the formula $LaZn_{11}$ will be assumed; the results are essentially unchanged, as will be shown later, as long as the formula includes one lanthanum atom. The aim of this investigation was to study the saturated lanthanum–zinc solution in the zinc-rich portion of the diagram, between 430 and 600 °C, by measuring the e.m.f. of the cell

(−)La(s)/$LaCl_3$–LiCl–KCl/La–Zn (saturated liquid alloy)(+)

Experiments were also made to establish the standard potential of the La(III)/La(0) electrode in the fused LiCl–KCl eutectic at 450 °C.

Experimental

Apparatus

The glassware apparatus used was Pyrex and similar to that used in previous electrode potential studies in molten salts (15–17) and alloy studies by e.m.f. methods involving molten salts (4, 5). The crucible containing the molten salt was a flat-bottomed glass tube. It was contained in an envelope which consisted of a round-bottomed glass cylinder on the wall of which was blown a vacuum-cup stopcock (Corning 7544) connected to a vacuum line. This envelope was closed to the atmosphere by means of a Pyrex cap connected to it with a 75 mm O-ring joint. On this cap were blown five 14/20 female ground-glass joints which were used to insert the thermocouple well, the gas inlet, gas outlet, and the electrodes in the cell. All these were constructed such that the inside of the envelope could be isolated from the outer atmosphere or maintained under vacuum when they had been introduced. This vacuum, of 10^{-2} to 10^{-4} Torr, was maintained inside the envelope by a mercury diffusion pump in series with a mechanical pump.

The thermocouple well consisted of 5 mm glass tubing closed at its lower end, which was below the melt surface, and connected at its upper end to a 14/20 male ground-glass joint. The gas inlet consisted of 5 mm glass tubing

[1]Taken from the thesis of J.-B. P. F. Lesourd, submitted to the Faculty of Graduate Studies, University of Alberta, Edmonton, Alberta, in partial fulfillment of the requirements for the M.Sc. degree.

Can. J. Chem. Downloaded from www.nrcresearchpress.com by 210.87.254.6 on 09/05/12
For personal use only.

connected to a 14/20 male ground-glass joint, sealed at its top, on the side of which was blown a vacuum-cup stopcock. Its lower end was above the melt. The gas outlet was a male 14/20 ground-glass joint on the side of which was blown a vacuum-cup stopcock; its upper end was connected to a 14/20 female ground-glass joint into which the inlet was inserted.

Electrodes

In the lanthanum electrode potential measurements, three electrodes were used: (*a*) a lanthanum electrode, which was a $\frac{1}{8}$ in. diameter and 5 in. length 99.9% lanthanum rod (A. D. Mackay, Inc., New York, N.Y.) to which a copper lead was attached well above the melt level, (*b*) a platinum reference electrode, and (*c*) a counter-electrode, each of which consisted of a large platinum flag (platinum wire and sheet from Engelhard Industries of Canada, Ltd., Toronto) welded to a copper lead and sealed to a 5 mm glass insulation tube below the lower end of the lead. These three electrodes were introduced in compartments made of a 12 mm glass tube closed with a fritted glass disc of porosity D or E (Ace Glass, Inc., Vineland, New Jersey). The bulk of the melt acted as a salt bridge. In the lanthanum–zinc alloy studies, two electrodes were used: a lanthanum electrode, as described above, and a zinc pool electrode. The liquid zinc was contained in a tantalum crucible on the bottom of the cell tube. Contact to it was made with a tungsten wire (0.020 in. diameter; A. D. Mackay, Inc., New York, N.Y.) dipped in the liquid zinc at its lower end and welded to a copper lead at its upper end; this wire and the lead were insulated with 5 mm glass tubing, the lower end of which, made of uranyl glass, was sealed to the tungsten wire about 1 cm above its lower end. At their upper end, the copper leads were sealed through a Kovar seal to a 10/30 male feedthrough which was inserted in a joint on the cap using a reducer.

To avoid thermocouple effects, connections between different metals were all made in the hot central region of the furnace.

Instruments

Potentials were measured with a Hewlett–Packard Model 3400A digital voltmeter. A Model IV coulometric current source (E. H. Sargent and Co., Chicago, Illinois) was used for electrodepositions and anodizations. The bottom part of the cell envelope was inserted in a Lindberg Hevi-Duty Type 54381A furnace with a Type 59344 temperature control unit. A constant temperature could be maintained in the cell within 1 °C. Temperatures were measured with a chromel–alumel thermocouple calibrated at the zinc melting point. The thermocouple e.m.f. was measured with the digital voltmeter.

Preparation of Molten Salt

A modification of the method of Maricle and Hume (18) was used. The anhydrous, crystalline, reagent grade lithium and potassium chlorides (The McArthur Chemical Co., Ltd., Montreal) were mixed thoroughly in eutectic portions. About 1 mole % anhydrous lanthanum trichloride (A. D. Mackay, Inc., New York, N.Y.) was added in the case of the lanthanum–zinc alloy experiments. The mixture was progressively heated under vacuum (10^{-3} to 10^{-4} Torr) to 450 °C and maintained under these conditions for 12 h in the crucible and envelope previously described. Then argon was introduced in this envelope and the crucible transferred to a Hevi-Duty Model 80 furnace under the fume hood where chlorine was bubbled through the melt for 1 h. Argon was bubbled through for 4–6 h to remove the chlorine. The melt was then poured into glass tubes that were sealed under argon for storage of the frozen melt.

Preparation of La–Zn Alloys

About 20 g of reagent grade zinc shot (May and Baker Ltd., Dagenham, Essex, England) were melted in a small glass tube under zinc chloride. The zinc piece obtained was carefully washed, dried, and polished in order to eliminate surface zinc oxide and chloride. It was then cut into smaller pieces and introduced in a 1 in. outside diameter × $\frac{7}{16}$ in. deep tantalum crucible (A. D. Mackay Inc., New York, N.Y.) together with several previously polished small pieces of lanthanum, weighing from 0.3 to 1.0 g. The crucible was then set on the bottom of the glass envelope described above, under a flow of purified argon at 500 °C, for 15–20 h. The piece of alloy was easily removed from the crucible after cooling down, owing to its contraction, and was then carefully polished and stored until use.

Procedure

A tube of purified melt was opened. The salt was introduced in the cell under argon and maintained under vacuum (10^{-3} to 10^{-4} Torr) at 400 °C for 12 h. The argon (purified by successive passage over hot copper, magnesium perchlorate, titanium sponge at 900 °C, and magnesium perchlorate) was introduced while the electrode system was set up. The cell was put under vacuum again. In the La(III)/La(0) electrode potential measurements, the platinum reference electrode was first anodized until a mole fraction of 5×10^{-4} to 10^{-3} in Pt(II) was reached in the corresponding compartment. Similarly, mole fractions of La(III) from 10^{-4} to 3×10^{-3} were obtained in successive generations in the lanthanum compartment. After each generation, the lanthanum electrode was rotated in order to obtain a homogeneous concentration of La(III) in the compartment rapidly. Its potential against the platinum reference and the temperature were then taken as a function of time. The mole fractions of ions in the compartments were calculated from the total number of equivalents generated and the total number of equivalents of chloride in these compartments, obtained by Mohr titration as previously described (19).

In the lanthanum–zinc alloy experiments, the potential of the zinc pool against the lanthanum electrode and the temperature were measured as a function of time. Then the temperature was changed and another point taken. No more than two points could be taken in a given experiment, even in evacuated apparatus which behaved better than that held under a positive pressure of purified argon. However, similar difficulties have been encountered previously and might be ascribed to corrosion tending to remove the lanthanum from the alloy (20). Lanthanum metal is such a strong reducing agent that any reducible impurities reaching the pool will react with it preferentially.

All calculations were carried out on the University of Alberta IBM 360 computer. The programs used are available in the thesis of the junior author (J.-B. P. F. L.). Error limits given are the 95% confidence limits.

Can. J. Chem. Downloaded from www.nrcresearchpress.com by 210.87.254.6 on 09/05/12
For personal use only.

Results and Discussion

Standard Potential of La(III)/La(0)

After elimination of questionable points, usually at the lower concentrations, 36 data points obtained in 6 different experiments were used. Potentials were measured as a function of La(III) concentration at a constant temperature. The time necessary to reach equilibrium varied from 5–30 min, the potential at equilibrium being constant with random variations of less than 2 mV/15 min, due to temperature fluctuations. Potentials at equilibrium were averaged over these small variations. Temperatures at equilibrium were also averaged for small fluctuations, usually of the order of 1 °C. For all experiments the mean e.m.f. values were corrected to correspond to a standard electrode of unit mole fraction Pt(II) (standard mole fraction platinum electrode, s.m.f.p.e.) as a reference (23) using the mean temperatures for each e.m.f.–concentration point. Plots of these e.m.f. values against the logarithm of the mole fraction of La(III) in the lanthanum compartment were linear (Fig. 1), showing that the lanthanum electrode is Nernstian in this solvent. For each run, the slope and the intercept of the straight lines representing the variation of the corrected e.m.f. with the logarithm of the mole fraction of La(III) were calculated by least-square analysis. The mean number of electrons involved in the lanthanum electrode process as calculated from the Nernst slopes was 3.0 ± 0.7, in agreement with the expected value of 3. One experiment gave only a single point, for which the intercept was calculated using the theoretical slope of the line for a trivalent lanthanum electrode process. These intercepts give a set of values of the standard mole fraction potentials of the lanthanum electrode against the s.m.f.p.e. at various temperatures. Linear interpolation (fitting by least-square analysis the best straight line through the experimental temperature–e.m.f. points) gave a standard potential of the La(III)/La(0) couple at 450 °C of −2.883 ± 0.007 V, on the mole fraction scale. The values obtained for this potential on the molarity and molality scales at 450 °C were −2.848 and −2.853 V, respectively, with the same precision. The temperature coefficient obtained was 4.4×10^{-4} V/°C with a standard error of 2×10^{-4} V/°C. Using the data of Laitinen and Pankey (15) for the chlorine electrode against Pt(II)/Pt(0) and the data of Yang and Hudson (21) for the lanthanum electrode against Cl_2/Cl^-, Plambeck (22) calculated a standard potential for this lanthanum electrode against Pt(II)/Pt(0) of −2.912 ± 0.005 V on the mole fraction scale. A temperature coefficient of 6.4×10^{-4} V/°C can also be calculated from these data. The potential value obtained from the present study is 28 mV more positive than that value. The problems involved in the calculation of potential values at 450 °C from the data of Yang and Hudson (21) have been discussed by Plambeck (17, 22). Plambeck (22) also points out that only a few experimental points are given for each couple (10 for La(III)/La(0)). In a study of the very similar Y(III)/Y(0) couple, Hoshino and Plambeck (23) also find electrode potentials about 30 mV higher than those calculated from the data of Yang and Hudson.

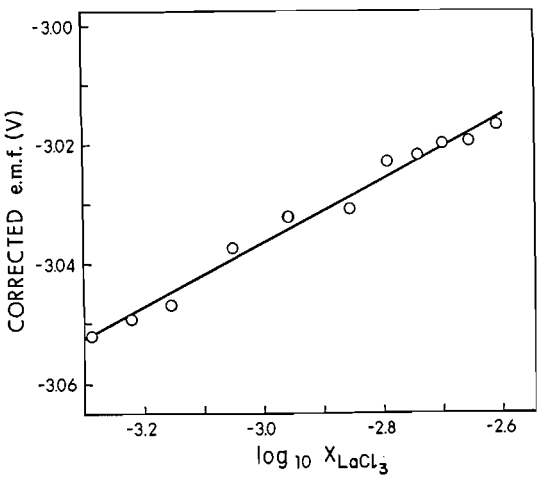

FIG. 1. Nernst plot of typical run, showing e.m.f. of La(III)/La(0) electrode, corrected to s.m.f.p.e., as a function of the mole fraction of $LaCl_3$; temperature 450 °C.

In this work, the temperature coefficient is not known accurately. It agrees satisfactorily with the value calculated from previous work in that this value falls in the range of the rather large experimental error.

Liquid La–Zn Alloy

The equation given by Johnson and Dillon (6) for the solubility of lanthanum in liquid zinc (in g/kg)

$$\log X = 9.573 - 8718/T$$

where T is the absolute temperature, gives a very low solubility of lanthanum in zinc in the range 430–600 °C (0.02 g/kg at 500 °C). It was not possible to prepare unsaturated solutions for

Can. J. Chem. Downloaded from www.nrcresearchpress.com by 210.87.254.6 on 09/05/12
For personal use only.

study due to the extremely small quantities of lanthanum required for saturation. Attempts to prepare the saturated solutions by electrodeposition of lanthanum or by using a quantity of lanthanum slightly in excess of the literature saturation level failed; higher and less stable cell potentials were observed, possibly corresponding to unsaturated solutions. It was found necessary to take a large excess of lanthanum (1 to 5% by weight). When this was done, the potentials were independent of further addition of lanthanum (by electrodeposition on the zinc pool). This shows that saturation had been reached, with the excess lanthanum forming an intermetallic compound assumed here to be $LaZn_{11}$. Therefore at each temperature point, the e.m.f. obtained was that of the cell

$$(-)\text{La(s)/LiCl–KCl–LaCl}_3\text{/La–Zn(saturated)}(+)$$

The activity of lanthanum in this saturated solution is determined by the activity of lanthanum in the solid $LaZn_{11}$ in equilibrium with it, so that the cell can equally well be written as

$$(-)\text{La(s)/LiCl–KCl–LaCl}_3\text{/LaZn}_{11}\text{(s)}$$

A time varying from 1–6 h was found necessary to reach equilibrium, the potential at equilibrium being constant with variations of less than 0.5 mV/30 min in most cases. Potentials at equilibrium were averaged for these small variations. Temperatures were constant within 1 °C as in the La(III)/La(0) potential experiments and were similarly averaged. Thus a set of mean temperature–e.m.f. values was obtained (Table I). The best straight line through these points (Fig. 2) was fitted by least-square analysis, its equation being

$$E = 1.4085 - 7.71 \times 10^{-4}T$$

where E is the e.m.f. (V) and T the temperature

TABLE I

Electromotive force of the cell
$(-)\text{La/LaCl}_3\text{–LiCl–KCl/La–Zn(saturated)}(+)$
as a function of temperature

Mean temperature, °C	Mean e.m.f. (V)
445.5	0.8584
450.4	0.8474
477.8	0.8368
495.5	0.8052
503.9	0.8014
511.1	0.8103
523.1	0.7947
585.5	0.7479

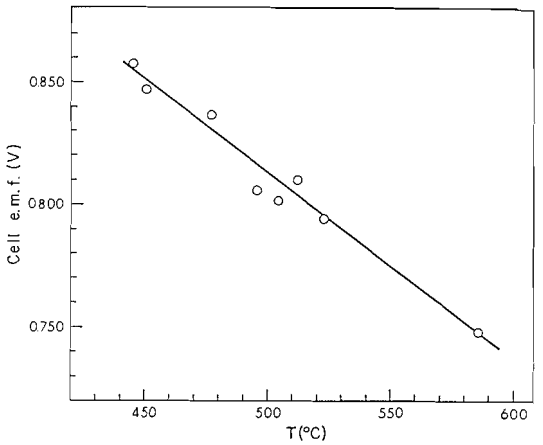

FIG. 2. Behavior of e.m.f. of La(s)/LiCl–KCl–$LaCl_3$/$LaZn_{11}$(s) cell as a function of temperature. Line is least-squares best fit.

(°K). This equation is valid over the range 430–600 °C and gives, at 450 °C, $E = 0.8506 \pm 0.005$ V. The overall process occurring in the cell amounts to the formation of the pure (solid) compound $LaZn_{11}$ from pure (solid) lanthanum and (liquid) zinc saturated with lanthanum. If ΔG is the change in free energy involved, and ΔG_f^0,$LaZn_{11}$ the free energy of formation of $LaZn_{11}$ from pure lanthanum and pure zinc, and a_{Zn} the activity of the zinc in the saturated solution, then

$$\Delta G_f^0,\text{LaZn}_{11}\text{(s)} = \Delta G + 11RT \ln a_{Zn}$$

If one assumes ideal behavior of the zinc, since the solution of lanthanum is very dilute

$$a_{Zn} = 1 - X_{La}$$

where X_{La} is the mole fraction of lanthanum. Then, since X_{La} is very small

$$\Delta G_f^0,\text{LaZn}_{11}\text{(s)} = \Delta G - 11RTX_{La}$$

TABLE II

ΔG_f^0,$LaZn_{11}$
as a function of temperature

Temperature (°C)	ΔG_f^0,$LaZn_{11}$ (kcal/mole)
430	−59.9
450	−58.8
500	−56.2
550	−53.5
600	−50.8

The term $-11RTX_{La}$ is a negligible 0.18 cal/mole at 500 °C. Thus

$$\Delta G_f^0,LaZn_{11}(s) = \Delta G = -nFE$$

where n is the number of electrons involved in the electrode reaction (three). In the same manner, the entropy of formation, $\Delta S_f^0,LaZn_{11}(s)$, is $nF(dE/dT)$, and the enthalpy of formation, $\Delta H_f^0,LaZn_{11}(s)$, can be calculated by extrapolating the free energy to 0 °K. At 450 °C for the free energy and over the temperature range 430–600 °C for the other quantities

$$\Delta G_f^0,LaZn_{11}(s) = -58.8 \pm 0.6 \text{ kcal/mole}$$

$$\Delta S_f^0,LaZn_{11}(s) = -53.4 \pm 8.0 \text{ cal/deg mole}$$

$$\Delta H_f^0,LaZn_{11}(s) = -97.4 \pm 6.0 \text{ kcal/mole}$$

In addition, $\Delta G_f^0,LaZn_{11}(s)$ was calculated at temperatures ranging from 430 to 600 °C (Table II), from the equation

$$\Delta G_f^0,LaZn_{11} = -97.415 + 5.335 \times 10^{-2}T$$

where T is in °K. It appears that these e.m.f. values differ from those obtained in a similar experiment by Johnson (24) by at most 2%. The discrepancies are somewhat greater for the entropy and the enthalpy.

Conclusion

The results of this study show that the compound $LaZn_{11}$ is of much greater stability than $UZn_{8.5}$, the standard free energies of formation at 450 °C being −58.8 and −26.1 kcal/mole, respectively. The standard potentials of pure uranium and pure lanthanum (any scale) differ by 0.630 V, making electrochemical separation of these metals appear quite feasible. Using the free energies given above, however, the difference in standard potentials of uranium (saturated solution of $UZn_{8.5}$ in Zn) and lanthanum (saturated solution of $LaZn_{11}$ in Zn) is only 0.156 V. The effect of alloying with zinc is thus to reduce the feasibility of separating these elements electrochemically by a significant factor.

Acknowledgment

The authors are indebted to the National Research Council of Canada for support of this work through an Operating Grant (to J.A.P.).

1. W. C. Robinson and P. Chiotti. J. Less-Common Metals, **4**, 315 (1962).
2. W. C. Robinson and P. Chiotti. J. Less-Common Metals, **10**, 190 (1966).
3. P. Chiotti, W. C. Robinson, and M. Kanno. J. Less-Common Metals, **10**, 273 (1966).
4. Y. Hoshino and J. A. Plambeck. Can. J. Chem. **47**, 965 (1969).
5. W. C. Robinson and P. Chiotti. U.S. Atomic Energy Commission *IS-1061* (1964).
6. I. Johnson and I. G. Dillon. U.S. At. Energy Comm. *ANL-7023* (1965).
7. Plutonium project. J. Amer. Chem. Soc. **68**, 2411 (1946); Rev. Mod. Phys. **18**, 513 (1946).
8. V. I. Kober, V. A. Lebedev, I. F. Nichkov, and S. P. Raspopin. Russ. J. Phys. Chem. **42**, 360 (1968).
9. A. P. Bayanov and V. V. Serebrennikov. Russ. J. Phys. Chem. **39**, 375 (1965).
10. R. Vogel, L. Rolla, A. Iandelli, and G. Canneri. Ric. Sci. **12**, 1216 (1941).
11. P. Pascal. Nouveau traité de chimie minérale, Vol. XX-2. Masson et Cie, Paris. 1963. p. 2803.
12. M. Hansen and K. Anderko. Constitution of binary alloys. 2nd ed. McGraw-Hill Book Co., Inc., New York. p. 895.
13. J. Schramm. Z. Metallk. **33**, 358 (1941).
14. E. Veleckis, R. V. Shablaske, I. Johnson, and H. M. Feder. Trans. A.I.M.E. **239**, 58 (1967).
15. H. A. Laitinen and J. W. Pankey. J. Amer. Chem. Soc. **81**, 1053 (1959).
16. H. A. Laitinen and J. A. Plambeck. J. Amer. Chem. Soc. **87**, 1202 (1965).
17. J. A. Plambeck. Can. J. Chem. **46**, 929 (1968).
18. D. L. Maricle and D. N. Hume. J. Electrochem. Soc. **107**, 354 (1960).
19. H. A. Laitinen and C. H. Liu. J. Amer. Chem. Soc. **80**, 1015 (1958).
20. V. A. Lebedev, I. F. Nichkov, and S. P. Raspopin. Sov. Electrochem. **2**, 148 (1966).
21. L. Yang and R. G. Hudson. Trans. A.I.M.E. **215**, 289 (1959).
22. J. A. Plambeck. J. Chem. Eng. Data, **12**, 77 (1967).
23. Y. Hoshino and J. A. Plambeck. Unpublished data.
24. I. Johnson. Private communication.

Can. J. Chem. Downloaded from www.nrcresearchpress.com by 210.87.254.6 on 09/05/12
For personal use only.

Electron spin resonance spectra of triple ions: anisotropic effects in the hyperfine splitting patterns of ^{23}Na counter-ions

T. E. GOUGH[1] AND P. R. HINDLE
Department of Chemistry, University of Waterloo, Waterloo, Ontario
Received May 15, 1969

The formation, in tetrahydrofuran, of triple ions of the formula Na_2Q^+ (Q = *p*-benzosemiquinone, 2,3-, 2,5-, 2,6-dimethyl-*p*-benzosemiquinone, durosemiquinone) has been detected by electron spin resonance spectroscopy. The spectra show asymmetric broadening within the ^{23}Na hyperfine multiplets. From the direction of this broadening, it is deduced that the sodium ions lie in the plane of the semiquinone anion, one sodium ion associating with each oxygen.

Canadian Journal of Chemistry, 47, 3393 (1969)

Can. J. Chem. Downloaded from www.nrcresearchpress.com by 210.87.254.105 on 09/05/12
For personal use only.

Introduction

The one-electron alkali metal reduction of duroquinone (D) in ethereal solution forms durosemiquinone (D^-); the electron spin resonance (e.s.r.) spectra of the reaction products indicate extensive ionic association in such media (1–3) though, especially at low temperatures, an equilibrium exists between $M^+ D^-$ and its constituent ions. The reactions which constitute the equilibrium are sufficiently slow that well resolved spectra for $M^+ D^-$ and for D^- are obtained. When the reduction is performed in the presence of an equimolar quantity of sodium tetraphenylboride, the e.s.r. spectra indicate the presence of Na_2D^+, provided that the polarity of the solvent is sufficiently low (4). At higher polarities, e.g. in 1,2-dimethoxyethane, the spectra indicate the presence of intermolecular cation exchange reactions, though a complete interpretation of these spectra has not been achieved.

The polarity of the solvent is not the only factor controlling the formation of triple ions. Listed below are several systems in which strong ionic association occurs, yet triple ions are not observable. All of the following systems contain a semiquinone anion and excess sodium cations dissolved in a solvent of low polarity: 9,10-anthrasemiquinone and sodium iodide in 1,2-dimethoxyethane (5), 9,10-anthrasemiquinone and sodium tetraphenylboride in tetrahydrofuran (6), 2,5-di-*t*-butyl-*p*-benzosemiquinone and sodium iodide in tetrahydrofuran (5), durosemiquinone (7) and 2,6-dimethyl-*p*-benzosemiquinone (8), and sodium *t*-pentoxide in *t*-pentanol.

As part of an experimental survey on the factors governing the formation of triple ions, we report the results of experiments with *p*-benzosemiquinone and its methylated derivatives. The results show that duroquinone is not unique in its ability to form triple ions, and more importantly, provide interesting information concerning the hyperfine splitting of the ^{23}Na nucleus in the triple ions.

Experimental

The experimental techniques for the reduction of quinones and for the recording of their e.s.r. spectra have already been described (3). Addition of sodium tetraphenylboride (Fisher) was performed in two ways; simple addition of equimolar amounts of the salt and the appropriate quinone to the reduction apparatus before sealing was found to be satisfactory. In some cases, a subsidiary vessel containing the salt was joined to the reduction vessel via a high vacuum Teflon needle-valve. The solvent was distilled into this vessel and controlled amounts of the solution of sodium tetraphenylboride added to the system either before or after reduction of the quinone.

Results

When *p*-benzoquinone, 2,3-, 2,5-, and 2,6-dimethyl-*p*-benzoquinone, and duroquinone were reduced by sodium in the presence of sodium tetraphenylboride, the e.s.r. spectra of the reduced solutions indicated the presence of triple ions. In all cases the solubility of the semiquinones was markedly increased by triple ion formation; experiments to prepare sodium–semiquinone ion pairs in tetrahydrofuran were unsuccessful for all but durosemiquinone, because of the low solubility of the ion pairs. However, addition of sodium tetraphenylboride to the sample prior to reduction gave a solution which could be rapidly reduced to give intense e.s.r. spectra of the triple ion.

[1]To whom all correspondence should be addressed.

Can. J. Chem. Downloaded from www.nrcresearchpress.com by 210.87.254.105 on 09/05/12
For personal use only.

When controlled amounts of sodium tetraphenylboride were added, after the reduction, to a solution of the ion-pair sodium–durosemiquinone in tetrahydrofuran, well resolved spectra of both the ion pair and the triple ion were observed. The center of the spectrum of the triple ion was 0.28 G higher than that of the ion pair. Increasing the temperature of the sample favored the triple ion at the expense of the ion pair.

The proton hyperfine splitting constants of the triple ion are given in Table I, together with the literature values for the free ions for comparison. For all the triple ions studied, the proton hyperfine splitting constants were insensitive to changes in the temperature of the sample.

For all the triple ions examined, except that of 2,6-dimethyl-*p*-benzosemiquinone, hyperfine interaction with two equivalent ^{23}Na nuclei split each line of the spectrum into a septet. Within this group of the triple ions, that of durosemiquinone is exceptional since it has a positive value of $d|a_{Na}|/dT$, whereas the triple ions of *p*-benzosemiquinone and of 2,3- and 2,5-dimethyl-*p*-benzosemiquinone have negative values of $d|a_{Na}|/dT$. These data are readily accommodated by postulating that the ^{23}Na hyperfine splitting constant of the durosemiquinone triple ion has the opposite sign to that of the other triple ions. With this assumption, all the triple ions were found to have similar values of da_{Na}/dT.

Hyperfine interactions with the cations of the triple ion [2,6-dimethyl-*p*-benzosemiquinone-Na_2]$^+$ generated more complicated splitting of the spectra; depending on the sample temperature, 4, 5, 6, and 7 line patterns were obtained. These patterns were analyzed by assuming the presence of hyperfine interactions with 2 nonequivalent sodium nuclei. Computer simulations of the expected patterns for two $I = 3/2$ nuclei having hyperfine splitting constants of x and $(1 - x)$ units were performed for values of x from 0.00 to 0.50 in steps of 0.01. Each experimental spectrum was matched with the optimum calculated spectrum, and the numerical values of the 2 splitting constants found by normalization with respect to the total spread of the pattern. By analogy with the results for the other triple ions studied, signs were given to these splitting constants so that all values of da_{Na}/dT are similar. The ^{23}Na hyperfine splitting constants of the triple ions are shown diagrammatically as functions of temperature in Fig. 1. The signs of these splitting constants are discussed further below.

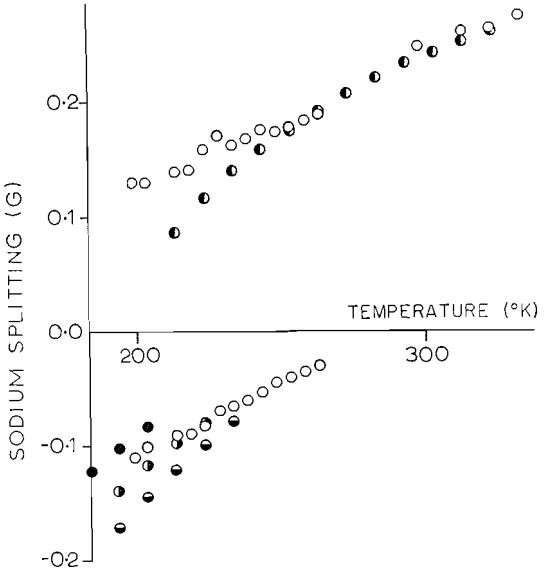

FIG. 1. Experimental ^{23}Na hyperfine splitting constants of the triple ions Na_2Q^+ in tetrahydrofuran plotted as a function of temperature. Q equals: ●, *p*-benzoquinone, ◒, 2,3-dimethyl-*p*-benzoquinone; ◑, 2,5-dimethyl-*p*-benzoquinone; ○, 2,6-dimethyl-*p*-benzoquinone; and ◐, duroquinone.

TABLE I

Proton hyperfine splitting constants of semiquinone anions, Q^-, and of their triple ions with sodium, Na_2Q^+*

	Q^-			Na_2Q^+		
Quinone	Solvent	a_H (G)	a_{Me} (G)	Solvent	a_H (G)	a_{Me} (G)
p-Benzoquinone	1,2-Dimethoxyethane†	2.40	—	Tetrahydrofuran	2.43	—
2,3-Dimethyl-*p*-benzoquinone	1,2-Dimethoxyethane‡	2.74	1.71	Tetrahydrofuran	2.72	1.68
2,5-Dimethyl-*p*-benzoquinone	Ethanol/water§	1.84	2.25	Tetrahydrofuran	1.98	2.20
2,6-Dimethyl-*p*-benzoquinone	Tetrahydrofuran†	2.20	1.90	Tetrahydrofuran	2.40	1.72
Duroquinone	1,2-Dimethoxyethane‡	—	1.95	Tetrahydrofuran	—	1.94

*Correct to ± 0.02 G.
†Reference 9.
‡Reference 3.
§Reference 10.

Can. J. Chem. Downloaded from www.nrcresearchpress.com by 210.87.254.105 on 09/05/12
For personal use only.

At reduced temperatures, asymmetric broadening of the ^{23}Na septets was observed. For the triple ion of durosemiquinone, the septets broadened to low field, while for the triple ions of *p*-benzosemiquinone, and of 2,3- and 2,5-dimethyl-*p*-benzosemiquinone, the septets broadened to high field (see Fig. 2). The direction of this broadening for the species [2,6-dimethyl-*p*-benzosemiquinone-Na_2]$^+$ was obscured by overlap of the lines generated by the two nonequivalent sodium nuclei.

Discussion

The e.s.r. spectra of solutions in tetrahydrofuran of *p*-benzoquinone, 2,3-, 2,5-, 2,6-dimethyl-*p*-benzosemiquinone, and duroquinone reduced by sodium in the presence of sodium tetraphenylboride, all indicate the formation of triple ions. With the exception of 2,6-dimethyl-*p*-benzosemiquinone, there is close agreement between the proton hyperfine splitting constants of an unassociated semiquinone anion and of the corresponding triple ion (see Table I), illustrating the symmetrical nature of the latter species. Because of its inherent asymmetry, the proton hyperfine splitting constants of the 2,6-dimethyl-*p*-benzosemiquinone anion are medium dependent, being affected in a complex manner by the polarity and by the molar volume of the solvent (9). Hence, agreement between the proton hyperfine splitting constants of 2,6-dimethyl-*p*-benzosemiquinone and of its triple ion is not to be expected.

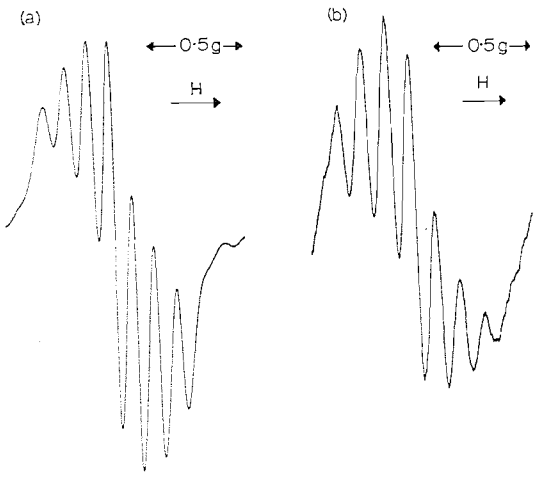

FIG. 2. ^{23}Na hyperfine multiplets of the triple ions (*a*) durosemiquinone-Na_2^+ and (*b*) 2,3-dimethyl-*p*-benzosemiquinone-Na_2^+, showing the asymmetric broadening of the alkali metal splitting.

In Fig. 1, assumptions have been made as to the signs of the sodium hyperfine splitting constants[2]; by analogy with previous studies (11–13), the signs were chosen so as to yield positive values of da_{Na}/dT for the various systems. Experimental support for this positive sign has been provided by measurements of the contact shifts of sodium and rubidium nuclei in alkali metal – aromatic anion ion-pairs (14). In the present cases, there is a correspondence between the signs of the ^{23}Na hyperfine splitting constants and the direction of the asymmetric broadening of the septet pattern, giving further support to the postulate that the spin density at the sodium nucleus may be positive or negative.

Carrington and Longuet-Higgins (15) have shown that for a radical with axial symmetry, provided nuclear relaxation may be neglected, the asymmetric line-width trends within the hyperfine splitting pattern of a nucleus are determined by the sign of the spin density at the nucleus, and by the sign of the product $(g_{\parallel} - g_{\perp})\, t_{\parallel}$ where $t_{\parallel}$ is the principal component of the anisotropic hyperfine interaction in the parallel direction. For *p*-benzosemiquinone the **g** tensor has been shown to be almost axially symmetric (16); assuming that *g* perpendicular to the plane of the ring equals the free spin value of 2.0023, it was shown that *g* along the line joining the oxygens is 2.0091, while the remaining in-plane value is 2.0024. These numerical values probably have little absolute significance, but their general form agrees with the predictions of a more theoretical study (17), and indicates the importance of the nonbonding orbitals on the oxygens in determining the **g**-tensor of a semiquinone.

For the present systems, therefore, the principal direction lies along the line joining the oxygens, and $(g_{\parallel} - g_{\perp})$ is positive: since a positive value of a_{Na} is associated with low-field broadening of the sodium septet (durosemiquinone Fig. 2*a*), and a negative value of a_{Na} with high-field broadening (e.g. 2,3-dimethyl-*p*-benzosemiquinone Fig. 2*b*), following ref. 15, $t_{\parallel}$ must be positive. Thus, the dipole–dipole interaction between the sodium nucleus and the unpaired electron is positive when the polarizing magnetic field is applied along the oxygen–oxygen axis.

[2]These assumptions may be tested by measurements of sodium contact shifts, but the required facilities are not available to the authors.

Can. J. Chem. Downloaded from www.nrcresearchpress.com by 210.87.254.105 on 09/05/12
For personal use only.

A positive value for $t_{\parallel}$ places constraints on the possible location of the sodium ions within the triple ion. Electrostatically, the most stable position for the cations is above the plane of the anion, somewhere between the carbon and oxygen of the C—O bond; however, in this position $t_{\parallel}$ would be negative. If the sodium ions lie in the plane of the ring, the major contribution to $t_{\parallel}$ will be from the unpaired spin on oxygen. Following Slater (18) we may calculate the most probable oxygen-electron distance and then determine that $t_{\parallel}$ will be positive provided that the oxygen–sodium distance is greater than about 0.6 Å. Thus the asymmetric line-width trends observed within the ^{23}Na hyperfine splitting patterns are consistent with a structure for the triple ion in which the sodium ions lie within the plane of the aromatic ring.

To our knowledge, these triple ions are the only species in which asymmetric line-broadening of alkali-metal multiplets has been observed. A combination of factors is probably responsible for the occurrence of the phenomenon for these triple ions; the **g** tensor is, for an aromatic anion, very anisotropic. The presence of 2 sodium nuclei makes the effective nuclear spin high ($I = 3$), while the size of the linear $[NaQ\ Na]^+$ unit, because the sodium ions must retain their solvation shells, is large, causing tumbling to be slow. There is, however, no obvious difference between the extent of asymmetric broadening of the methyl hyperfine multiplets of durosemiquinone-Na and durosemiquinone-Na_2^+, although such comparisons are difficult to make because of the different spin density distributions.

If the sodium nuclei lie completely in the plane of the aromatic ring, overlap between their s orbitals and the π-orbital containing the unpaired electron will be zero, and hence the ^{23}Na hyperfine interaction will be dominated by a negative contribution from excitation of the lone pair electrons on oxygen into the 4s orbital of sodium (11, 19). On increasing the temperature, thermal motion will cause the sodium ions to spend more of their time out of the plane of the aromatic ring thereby increasing the importance of the positive interaction generated by direct overlap between the π-orbital of the unpaired electron and the s orbitals of sodium. Thus the linear model for the triple ions predicts that a_{Na} should be negative and da_{Na}/dT should be positive.

These predictions agree very well with the experimental observations (see Fig. 1) except for the triple ion of durosemiquinone and for one of the sodium ions of the triple ion of 2,6-dimethyl-*p*-benzosemiquinone; it is clear that this sodium must be the one associated with oxygen atom 7, and flanked by 2 methyl groups. Evidently, the steric effects of these flanking methyls are such as to force the sodium ions to spend more of their time away from the plane of the ring, thereby giving a net positive value for a_{Na}.

The agreement between the expected and the observed signs of a_{Na} and da_{Na}/dT may, therefore, be taken as supporting evidence for the assumptions made concerning signs when plotting Fig. 1.

Conclusion

In tetrahydrofuran, triple ions of the formula Na_2Q^+ may be formed for Q^- equal to *p*-benzosemiquinone, 2,3-, 2,5-, 2,6-dimethyl-*p*-benzosemiquinone, and durosemiquinone. One sodium ion associates with each oxygen, and lies in the plane of the aromatic ring unless flanked by two methyl groups in the ortho positions.

Acknowledgment

This work received financial support from the National Research Council of Canada.

1. M. P. KHAKHAR, B. S. PRABHANANDA, and M. R. DAS. J. Amer. Chem. Soc. **89**, 3100 (1967).
2. P. S. GILL and T. E. GOUGH. Can. J. Chem. **45**, 2112 (1967).
3. P. S. GILL and T. E. GOUGH. Trans. Faraday Soc. **64**, 1997 (1968).
4. T. E. GOUGH and P. R. HINDLE. Can. J. Chem. **47**, 1698 (1969).
5. A. W. RUTTER and E. WARHURST. Trans. Faraday Soc. **64**, 2338 (1968).
6. P. R. HINDLE. Unpublished results.
7. T. E. GOUGH and M. C. R. SYMONS. Trans. Faraday Soc. **62**, 269 (1966).
8. T. A. CLAXTON, J. OAKES, and M. C. R. SYMONS. Trans. Faraday Soc. **63**, 2125 (1967).
9. J. OAKES and M. C. R. SYMONS. Trans. Faraday Soc. **64**, 2579 (1968).
10. B. VENKATARAMAN, B. G. SEGAL, and G. K. FRAENKEL. J. Chem. Phys. **30**, 1006 (1959).
11. E. DEBOER. Rec. Trav. Chim. **84**, 609 (1965).
12. N. HIROTA. J. Amer. Chem. Soc. **89**, 32 (1967).
13. N. HIROTA. J. Phys. Chem. **71**, 127 (1967).
14. G. W. CANTERS, E. DEBOER, B. M. P. HENDRICKS, and H. VAN WILLIGEN. Chem. Phys. Lett. **1**, 627 (1968).
15. A. CARRINGTON and H. C. LONGUET-HIGGINS. Mol. Phys. **5**, 447 (1962).
16. J. W. H. SCHREURS and G. K. FRAENKEL. J. Chem. Phys. **34**, 756 (1961).
17. A. J. STONE. Mol. Phys. **6**, 509 (1963).
18. J. C. SLATER. Phys. Rev. **36**, 57 (1930).
19. N. M. ATHERTON. Trans. Faraday Soc. **62**, 1707 (1966).

Kinetic solvent isotope effect, solvent reorganization, and the S_N1–S_N2 mechanism[1]

L. TREINDL[2], R. E. ROBERTSON, AND S. E. SUGAMORI
Division of Pure Chemistry, National Research Council of Canada, Ottawa, Canada

Received March 24, 1969

The temperature dependence of the rates of solvolysis have been determined in D_2O for *t*-butyl chloride, 2,2-dibromopropane, 2-bromo-2-chloropropane, and 2-chloro-2-methyl propyl methyl ether, and corresponding values of $\Delta H^{\neq}$, $\Delta S^{\neq}$, and $\Delta C_p^{\neq}$ are derived. Values of $\Delta H^{\neq}$ and $\Delta S^{\neq}$ from the solvolysis of seven other halides and two benzenesulfonates have been estimated from rate determinations at two temperatures in D_2O.

A comparison of these values with terms from corresponding experiments in H_2O provides values of $\delta_I\Delta G^{\neq}$, $\delta_I\Delta H^{\neq}$, and $\delta_I\Delta S^{\neq}$ characterizing the kinetic solvent isotope effect.

While $\delta_I\Delta G^{\neq}$ appears to have about the same value for a wide range of halides of different structure irrespective of the probable mechanism of reaction, systematic differences in $\delta_I\Delta H^{\neq}$ and $\delta_I\Delta S^{\neq}$ differentiate those reacting by an S_N2 mechanism from those reacting by an S_N1 mechanism. This difference is in the direction suggesting a loosening of solvent structure in the activation process in agreement with indications obtained from the corresponding values of the heat capacity of activation.

Canadian Journal of Chemistry, 47, 3397 (1969)

Can. J. Chem. Downloaded from www.nrcresearchpress.com by 210.87.254.5 on 09/05/12
For personal use only.

One of the surprising facts observed in connection with the kinetic solvent isotope effect (k_{H_2O}/k_{D_2O}, k.s.i.e.) for the hydrolysis of alkyl halides was that those compounds hydrolyzing by an S_N2 mechanism gave no indication of a significant primary isotope effect (1, 2). Equally surprising was the observation that the k.s.i.e. for a series of halides was essentially independent of the size of the displaced ion although there was a clear indication of such a correlation for the transfer energy of the ion from H_2O to D_2O (Table I). Further, it was remarkable, if not frequently remarked on, that the values of k.s.i.e. for hydrolysis by the S_N1 mechanism were just about the same as the corresponding values for the S_N2 mechanism, though all would probably agree that the degree of solvent disruption accompanying the former mechanism was much more extensive than for the latter (3). Few would disagree that primary halides hydrolyze in water by an S_N2 mechanism, or alternatively, tertiary halides hydrolyze by an S_N1 mechanism, the important structural difference in the latter being that charge distribution and steric hindrance preclude nucleophilic interaction. Further, it is reasonable to assume (4) that there will be solute structures which have intermediate requirements with respect to both nucleophilic interaction and solvent reorganization. The secondary halides appear to fall in this grouping for solvolysis in water, the entropy and heat capacity of activation having values which normally lie between those for the primary and for the tertiary halides. If significant differences in the disruption or reorganization of H_2O and D_2O attend the activation process for solvolysis of a series of halides, then these differences should be apparent in the derived terms $\delta_I\Delta H^{\neq}$ and $\delta_I\Delta S^{\neq}$, even though absent in $\delta_I\Delta F^{\neq}$.

There can be little doubt that the k.s.i.e. associated with the solvolysis of alkyl halides in H_2O and D_2O is related in some way to the difference in the structural properties of the solvents. This statement holds whether one favors an explanation based on differences in ion–water interaction at the transition state (5, 6) or alternatively attributes the rate disparity largely to the effect of differences in the work required to disrupt initial state solvent shells of differing sizes and structural stability (7).

In this paper evidence is provided, based on studies of the temperature dependence of the kinetic solvent isotope effect, which supplies a partial answer to some of the questions raised by such observations without pretending to offer final explanations.

Experimental

t-Butyl chloride, 2-chloro-2-methyl-propyl methyl ether, 2,2-dibromopropane, and 2-chloro-2-bromopropane were purified samples which had been used in a previous study (8–10) and kept at low temperatures shielded from the light for the interim. They were redistilled and passed through Al_2O_3 (Fisher, Adsorption) prior to use. All gave strictly first order kinetics. Similar considerations apply to those solutes for which an estimate of $\delta_I\Delta G^{\neq}$, $\delta_I\Delta H^{\neq}$, and $\delta_I\Delta S^{\neq}$ was made from triplicate rate determinations at two temperatures only, i.e.

---

[1]NRCC No. 10 824. Presented in part at the Fall Meeting, American Chemical Society, Atlantic City, September 1965.

[2]NRCC Postdoctorate Fellow, 1965–1966.

Can. J. Chem. Downloaded from www.nrcresearchpress.com by 210.87.254.5 on 09/05/12
For personal use only.

benzyl chloride, cyclobutyl chloride, methyl and cyclopentyl bromide, and methyl, ethyl, and isopropyl iodide; the purity was checked by vapor-phase chromatography, as well as kinetics where the compound was not purified by the former method.

D_2O was 99.8% pure as obtained from Merck, Sharpe and Dohme, Montreal, and was redistilled through a still of the Stuart–Wormwell design to remove extraneous impurities (11).

Rate determinations were made by a conductance method which has been described in previous work (12). Care was taken to minimize the effect of adsorption of ions at the walls and to avoid supersaturation, these being the major sources of trouble.

Calculations

The extraction of information from a series of rate data determined over a range of temperatures involves a number of assumptions and procedures. The fact that these may be arbitrary or in some measure speculative is of little consequence so long as the results provide a better insight into the nature of the process being investigated and the values are not regarded as ends in themselves.

Recently it has been brought to our attention that an equation of the form we have previously used to express the temperature dependence of the rate of hydrolysis viz.

$$[1] \qquad \log_{10} K = A/T + B \log_{10} T + C$$

is ill conditioned where $T = 0$ °K. This difficulty can be avoided if a simple transformation is made as described by Clarke and Glew (13).

The problem would appear to arise, at least in part because of the limited word length available in machine computation.

Clarke and Glew point out that it is not permissible to avoid this objection by dropping lower terms in T in favor of higher powers, if an attempt is to be made to give physical interpretation to the derived constants. Rather they show that the difficulty can be avoided by an expansion based on the familiar equilibrium relation

$$R \ln K = \frac{\Delta G_T^0}{T} = \Delta S^0 - (\Delta H_T^0)/T$$

if a simple transformation of T is adopted. Restated in terms of the kinetic rate constant, k', the basic assumption of their derivation is that k_T' is a "well behaved function of T which is regular as regards continuity and derivability, so that the changes in the standard thermodynamic functions $\Delta G_T^{\ddagger}$, $\Delta H_T^{\ddagger}$, and $\Delta C_p^{\ddagger}$, which are defined by k_T and its temperature derivatives at T, are similarly well behaved functions of T". This is no more than the implicit assumption of [1]. The gain in their approach comes from the use of the mid-temperature, θ, as the reference temperature for the calculation. By expressing the effect of changing T on the value of H_0 at θ in a Taylor series and combining this with similar derivations of $\Delta S_0^{\ddagger}$ and $\Delta C_{p0}^{\ddagger}$, the Clarke and Glew expression for the temperature dependence of k' can be expressed in the form

$$[2] \qquad R \ln k' = -\frac{\Delta G_0^{\ddagger}}{\theta} + \Delta H^{\ddagger}\left[\frac{1}{\theta} - \frac{1}{T}\right] + \Delta C_{p0}^{\ddagger}\left[\frac{\theta}{T} - 1 + \ln\frac{T}{\theta}\right] + \frac{\theta}{2}\left(\frac{d\Delta C_{p\theta}^{\ddagger}}{dT}\right)_0\left[\frac{T}{\theta} - \frac{\theta}{T} - 2\ln\left(\frac{T}{\theta}\right)\right] \ldots \text{etc.}$$

which will be seen to be equivalent to the equation

$$R \ln k' = A + B/T + C \ln T + DT + \ldots .$$

θ is in the mid-range of the experimental data and $k' = k_{obs}/(kT/h)$, a substitution, in accord with transition state theory, made at this point for computational convenience, where $k = 1.38034 \times 10^{-16}$ ergs/°K, $h = 6.256 \times 10^{-27}$ ergs/s.

For the case where $d\Delta C_p^{\ddagger}/dT = 0$, and for any temperature T

$$RA' = -\Delta G_T^{\ddagger}/T + \Delta H_T^{\ddagger}/T - \Delta C_{pT}^{\ddagger}(1 + \ln T)$$

$$RB' = -\Delta H_T^{\ddagger} + \Delta C_{p\theta}^{\ddagger} T$$

$$RC' = \Delta C_p^{\ddagger}$$

The fourth term expresses the temperature dependence of $\Delta C_p^{\ddagger}$ and requires more accurate data than are presently available to us, hence in our work this term was set equal to zero.

The original paper (13) should be consulted for the details of the method of calculating the derived constants and corresponding errors.

Results and Discussion

The rate data for the solvolysis of 2,2-dibromopropane in D_2O are given in Table I. These are typical of the series[3].

Values of $\Delta H^{\ddagger}$, $\Delta S^{\ddagger}$, and $\Delta C_p^{\ddagger}$ (with corre-

[3]Values of rates included in this study but not reported here have been filed with the Depository of Unpublished Data, from which photocopies may be obtained free of charge, on request, from the National Science Library, National Research Council of Canada, Ottawa, Canada.

TABLE I
Rate data for the hydrolysis of 2,2-dibromopropane in D_2O

T (°C)	k_1 ($s^{-1} \times 10^{-5}$)	T (°C)	k_1 ($s^{-1} \times 10^{-5}$)
22.387	2.156	40.025	31.05
	2.152		31.05
	2.162		31.03
27.487	4.928	42.539	43.75
	4.919		43.51
	4.937		43.78
	4.925	45.060	61.43
29.959	7.244		61.41
	7.262	47.402	82.88
	7.241		83.05
	7.253		82.85
32.489	10.53		82.67
	10.54	50.054	115.1
	10.52		115.4
	10.57		
34.958	15.21		
	15.21		
	15.19		
	15.26		

sponding errors) calculated by the method outlined by Clarke and Glew (13) are given in Table II, for several temperatures covering the mid-range of the experiments. Empirical constants corresponding to eq. [2] for the interpolative calculation of k_T are given in Table III.

Data for an assemblage of other alkyl halides at two temperatures are given in Table IV. The aim in these cases was to get a wider indication of the values of $\delta_1\Delta H^{\ddagger}$ and $\delta_1\Delta S^{\ddagger}$ with attempting to define these terms as carefully as was done in Table II.

The Kinetic Solvent Isotope Effect

The fact that the values of the k.s.i.e. for the hydrolysis of the majority of alkyl halides whether reacting by an S_N1 or an S_N2 mechanism lie in the range 1.20–1.30 is well established (2, 12, 14). In many cases small differences can be readily attributed to differences in the experimental temperature or to modification of the initial state

TABLE II
Derived parameters*

Compound	Medium	Temperature (°C)	$\Delta S^{\ddagger}$ (cal $mole^{-1}$ deg^{-1})	$\Delta G^{\ddagger}$ (cal $mole^{-1}$)	$\Delta H^{\ddagger}$ (cal $mole^{-1}$)	$\Delta C_p^{\ddagger}$ (cal $mole^{-1}$ deg^{-1})	Reference
2-Cl-2-Me-propane	H_2O	10	14.41±0.04	19 712±0.3	23 794±12	—83.0±4.5	8
		15	12.96±0.08	19 644±0.3	23 379±24		8
		25	10.13±0.23	19 528±1.5	22 549±67		8
	D_2O	10	16.65±0.43	19 898.6±1	24 612±123	−113±23	
		15	14.67±0.15	19 820.3±1	24 047±43		
		25	10.81±0.82	19 693.0±4	22 196±241		
2-Cl-2-Me-propyl methyl ether	H_2O	15	10.50±0.08	23 015±0.5	26 039±24	−62±2	10
		25	8.38±0.04	22 920±0.5	25 420±11		10
		40	5.34±0.13	22 817.7±0.9	24 491±39		10
	D_2O	15	12.8±0.8	23 199±5	26 880±251	−83±17	
		25	9.92±0.3	23 085±2	26 044±91		
		40	5.82±0.6	22 968±2	24 792±177		
2,2-Dibromo-propane	H_2O	25	12.10±0.15	23 360±0.7	26 967±44	−83±5	10
		35	9.34±0.08	23 253±0.7	26 132±24		10
		50	5.38±0.3	23 143±2	24 880±99		10
	D_2O	25	14.49±0.25	23 556±1	27 877±75	−111±6	*
		35	10.81±0.08	23 430±1	26 761±25		*
		50	5.50±0.3	23 308±2	25 086±91		*
2-Chloro-2-bromopropane	H_2O	15	14.52±0.05	22 688±0.2	26 872±16	−94±2	10
		25	11.32±0.02	22 599±0.3	25 933±8		10
		50	3.75±0.17	22 372±2	23 585±53		10
	D_2O	15	16.44±0.3	22 908±1	27 645±82	−103±7	*
		25	12.90±0.1	22 761±1	26 609±29		*
		50	4.56±0.53	22 545±6	24 016±165		*
2-Bromopropane	H_2O	40	0.44±0.09	24 808±1	24 948±27	−59±2	14
		50	−1.42±0.05	24 813±1	24 355±16		14
		60	−3.22±0.09	24 836±1	23 761±31		14
	D_2O	40	1.06±0.09	24 980±0.7	25 311±28	−66±2	14
		50	−1.03±0.05	24 980±0.6	24 647±14		14
		60	−3.06±0.03	25 000±0.7	23 982±11		14

*The values of $\Delta C_p^{\ddagger}$ correspond to the assumption that $dC_p^{\ddagger}/dT = 0$. Where this assumption is not justified, the value of $\Delta C_p^{\ddagger}$ given will correspond to the correct value for the mid-temperature of the experimental range.

Can. J. Chem. Downloaded from www.nrcresearchpress.com by 210.87.254.5 on 09/05/12
For personal use only.

TABLE III

Empirical constants for rate–temperature relation

$$\log_{10} k = \frac{A}{T} + B \log_{10} T + C$$

Compound	Medium	A	B	C	Reference
2-Cl-2-Me-propane	H_2O	−10 340.7211	−40.7885	134.0848	8
	D_2O	−12 383.5755	−55.9457	178.3218	This work
2-Cl-2-Me-propyl methyl ether	H_2O	−9 594.2444	−30.1755	102.8330	9
	D_2O	−11 138.1808	−41.0448	134.7853	This work
2,2-Dibromopropane	H_2O	−11 335.0952	−41.0083	135.1541	10
	D_2O	−13 370.6831	−55.1926	176.9361	This work
2-Cl-2-Br-propane	H_2O	−11 791.7536	−46.2801	150.3181	10
	D_2O	−12 574.8366	−51.1880	164.9406	This work
2-Bromopropane	H_2O	−9 519.4109	−28.8902	97.9964	14
	D_2O	−10 084.6677	−32.4632	108.5990	14

TABLE IV

Rate data for solvolysis of alkyl halides

Compound	Solvent	Temperature (°C)	k_1 ($s^{-1} \times 10^{-5}$)
Benzyl Cl	D_2O	49.963	17.28±0.005
		32.520	2.512±0.005
Cyclobutyl Cl	D_2O	39.998	30.36±0.008
			10.33±0.001
Methyl Br	D_2O	89.947	54.8±0.11
		70.498	8.55±0.1
Cyclopentyl Br	D_2O	39.998	30.36±0.005
		30.004	8.271±0.009
$MeO(CH_2)_4Br$	D_2O	50.004	36.98±0.03
		40.003	11.39±0.01
Methyl I	D_2O	92.746	26.96±0.015
		70.041	27.94±0.02
Ethyl I	H_2O	77.768	11.18±0.04
		91.354	42.32±0.05
	D_2O	77.751	8.91±0.04
		91.365	33.5±0.1
Allyl I	D_2O	55.016	12.01±0.06
		39.557	1.952±0.2
Isopropyl I	D_2O	50.981	7.53±0.02
		65.900	43.9±0.1

solvation shell—a source of difference most evident where corresponding halides and sulfonates are compared (12). The new results reported here merely confirm these generalizations, the values of $\delta_I\Delta G^{\ddagger}$, Table VI, being remarkably similar for all halides.

We cannot disregard the possibility that some of the differences in $\delta_I\Delta G^{\ddagger}$ are caused by initial state differences as was shown to exist for the methyl halides by Thornton and Swain (16, also 21). In so far as these differences arise from size, some compensation is to be expected between initial and transition state solvation.

Clearly, the values of $\delta_I\Delta G^{\ddagger}$ are not dependent in a systematic way on the size of the displaced halide ion, no trend through the series Cl^-, Br^-, I^- being found, such as is evident in ΔG for the free energy of transfer from D_2O to H_2O for the corresponding sodium salts (15), see Table V.

Reference has already been made to the absence of any apparent contribution to the k.s.i.e. in the solvolysis of these halides where some degree of nucleophilic interaction may be assumed. This is not true for all solvolytic displacements.

Thus we know (17) from parallel studies on benzenesulfonyl chloride that when a larger degree of nucleophilic interaction is required at the transition state (as indicated by the high $k_{OH^-}/k_{H_2O} = 10^5$ ratio for the hydrolysis of benzenesulfonyl chloride (18–20)) an indication of a small primary isotope effect is apparent in the k.s.i.e. ($k_{H_2O}/k_{D_2O} = 1.56$). The implication from the $\delta_I\Delta G^{\ddagger}$ values in Table VI is that in the alkyl halide series, where nucleophilic interaction is required, the latter must be small and consequently the k.s.i.e. in the latter cases reflects solvent reorganization only.

$\delta_I\Delta H^{\ddagger}$ *and* $\delta_I\Delta S^{\ddagger}$

Aside from the absence of any notable changes in $\delta_I\Delta G^{\ddagger}$ with a change in mechanism from S_N1 to S_N2 or of any systematic dependence on the size of the displaced ion through the series Cl^-, Br^-, I^-, the large fact apparent in Table VI is that the $\delta_I\Delta H^{\ddagger}$ values for those molecules reacting by an S_N1 mechanism are larger than the corresponding values for those halides which solvolyze by an S_N2 mechanism.

Before examining the mechanistic implications of this apparent grouping of $\delta_I\Delta H^{\ddagger}$ values in

Can. J. Chem. Downloaded from www.nrcresearchpress.com by 210.87.254.5 on 09/05/12
For personal use only.

TABLE V

Free energy, heat, and entropy of transfer of sodium halides from D_2O to H_2O

Halide	ΔG (cal mole^{-1})	ΔH (cal mole^{-1})	ΔS (cal deg^{-1} mole^{-1})	Equivalent k.s.i.e.* (col. 2)
NaF	-28 ± 92	10	0.13 ± 0.30	0.95
NaCl	110 ± 12	510	1.34 ± 0.04	1.20
NaBr	170 ± 12	650	1.61 ± 0.04	1.33
NaI	230 ± 12	810	1.95 ± 0.04	1.48

*Value of k_{H_2O}/k_{D_2O} corresponding to ΔG col. 2.

terms of S_N1/S_N2 characteristics, it is important to note that in every case $\Delta H^{\neq}$ is *greater* for solvolysis in D_2O than in H_2O and there is a corresponding *increase* in $\Delta S^{\neq}$. If we bear in mind that D_2O gives evidence of greater structural stability than H_2O (21) both of these facts are consistent with the idea that in all cases the activation process involves the break-down of water structure, the greater degree of structure in D_2O providing a ready explanation for the sign of the difference terms (7).

We note that while $\delta_I\Delta S^{\neq}$ tends to cancel out a part of $\delta_I\Delta H^{\neq}$ for those halides which are considered to hydrolyze by an S_N2 mechanism, there is almost a total compensation for the increase in $\delta_I\Delta H^{\neq}$ which characterizes those halides reacting by an S_N1 mechanism. This would seem to suggest that the solvent reorganization about the developing cation is in some respects different from that which occurs about the developing anion. There will be significant differences in charge density at the surface of the anion and cation and, as Samoilov has shown, these differences can result in positive or negative hydration effects (22). However, the phenomena revealed in the above experiments would seem to be closer to a kind of "melting" of the solvation shell about the cation, with a negligible change in free energy. This effect seems inconsistent with the concept of advanced exothermic solvation of the developing cation at the transition state, however widely this hypothesis has been adopted in theoretical speculations (3, 23, 24).

The possibility that these differences arise as a consequence of initial state differences cannot be excluded on the basis of present information but seems very unlikely in view of the known characteristic of aqueous solutions (25–28).

These results are consistent with the well established observation that the S_N1 mechanism appears to involve a more extensive reorganization of solvent than the S_N2 mechanism, and these differences would appear to provide a quantitative basis for mechanistic distinction, if comparisons are made at the same temperature. The latter requirement will be evident if two related hypotheses are considered. The source of the solvent isotope effect depends on the difference in structural stability of H_2O and D_2O at a given temperature (7). The heat capacity of activation $\Delta C_p^{\neq}$ which characterizes such reactions is attributed to the decrease in the structural stability of the initial state solvation shell with increasing temperature (12). Thus, as the average experimental temperature range from which $\delta_I\Delta H^{\neq}$ is derived increases, the apparent structural stability of the initial state solvation shell decreases both absolutely and differentially as between H_2O and D_2O. The latter decrease may be illustrated[4] by the change in the relative viscosity of H_2O and D_2O with temperature: $k_{D_2O}/k_{H_2O} = 1.305$ at 5°, 1.245 at 20°, 1.202 at 40°, 1.164 at 80° (29). Similar results can be found for the related times of dielectric relaxation (30). Hence the requirement is that comparisons of $\delta_I\Delta H^{\neq}$ refer to the same temperature range, or that some allowance be made for decreasing structure with increasing temperature if this is not practical. Similarly the temperature dependence of $\Delta H^{\neq}$ ($\Delta C_p^{\neq}$) due to the temperature dependence of the structure of water will be greatest at low temperatures and will decrease as the temperature increases, regardless of mechanism. These considerations introduce limitations but do not wipe out the inherent utility of $\Delta C_p^{\neq}$ or, in the present instance, of $\delta_I\Delta H^{\neq}$ as useful indicators of solvent reorganization accompanying ionogenic processes in water. These quantitative indicators are all the more useful at this stage because, as yet, $\Delta S^{\neq}$ has proved to be of little value for this purpose.

Data supporting the above consideration for

[4]Anett and McElvey find a similar evidence of enhancement of structure at lower temperatures (37).

Can. J. Chem. Downloaded from www.nrcresearchpress.com by 210.87.254.5 on 09/05/12
For personal use only.

Can. J. Chem. Downloaded from www.nrcresearchpress.com by 210.87.254.5 on 09/05/12
For personal use only.

$\delta_I\Delta H^{\neq}$ are given in Table VI. In each example where $\delta_I\Delta H^{\neq}$ values are given at two temperatures for compounds **1**, **2**, and **3**, there is a sharp decrease between values at 20 and 40°, though part of this decrease may be more apparent than real, due to the increase in error at the extremes of the experimental range. When comparisons are made at 40 °C, we note that the values of $\delta_I\Delta H^{\neq}$ for 2-bromopropane, **5**, and for benzyl chloride, **13**, are significantly lower than those for the tertiary halides, **2**, **3**, and **6** which react by an S_N1 mechanism. Cyclopentyl bromide, **7**, in this comparison and also with respect to the corresponding value of $\Delta C_p^{\neq}$ (12), appears to have an intermediate value.

Initially the large difference in the values of $\delta_I\Delta H^{\neq}$ and of $\delta_I\Delta S^{\neq}$ for the hydrolysis of tertiary halides (e.g. **1**, **2**, and **3**) and the primary halides (e.g. **8**, **9**, **10**, and **11**) prompted the hope that a mechanistic distinction could be based on isotopic solvation differences[5]. The accumulation of the data given in Table VI showed that while significant differences do exist in $\delta_I\Delta H^{\neq}$ and $\delta_I\Delta S^{\neq}$ for tertiary and primary halides where the question of mechanistic distinction hardly exists, no such distinction was apparent in the results for the secondary halides where an additional basis for mechanistic distinction was desirable. A hypothesis to account for the intermediate values of $\delta\Delta H^{\neq}$ and $\delta_I\Delta S^{\neq}$ for secondary halides can be found in the consideration that there is less opportunity for charge dispersal in the quasi-cation in the case of secondary than tertiary halides. This hypothesis would also account for the difference in $\delta_I\Delta H^{\neq}$ and $\delta_I\Delta S^{\neq}$ (Table VI) and in $\Delta C_p^{\neq}$ (12) between 2-bromopropane, **5**, cyclopentyl bromide, **7**, and cyclobutyl chloride, **6**. The values of $\Delta C_p^{\neq}$ determined for the hydrolysis of 2-bromopropane and 2-iodopropane are somewhat more negative than those which characterize the hydrolysis of primary halides (12). This is indicative of a more extensive solvent reorganization in the activation process. The same conclusion can be drawn from the value of $\delta_I\Delta H^{\neq}$ for **5** but not for the corresponding value of **12**. We have no explanation for the latter difference. Values of $\Delta C_p^{\neq}$ calculated for allyl iodide, **11**, and benzyl chloride, **13**, are -47 and -39 cal deg^{-1} mole^{-1} while the corresponding values of $\delta_I\Delta H^{\neq}$ are about the same. Benzyl chloride may react by "mixed kinetics". While $\Delta C_p^{\neq}$ would be sensitive to such a mechanistic change, $\delta_I\Delta H^{\neq}$ would not. This lack of sensitivity of $\delta_I\Delta H^{\neq}$ to mechanistic differences for displacement from primary and secondary carbon is further illustrated by the sulfonates, **14** and **15**. Here $\delta_I\Delta H^{\neq}$ and $\delta_I\Delta S^{\neq}$ are both reduced as would be anticipated from earlier discussions (2) and there is no indication of a mechanistic difference.

Rate data for the primary halides **8**, **9**, **10**, and **11** were obtained at higher average temperatures and reflect, in part, a decrease in $\delta_I\Delta H^{\neq}$ due to this fact as well as to the reduced requirement for solvent reorganization in the S_N2 compared to the S_N1 mechanism.

From the above kinetic evidence we must conclude that while large differences in solvent reorganization are found, as between tertiary and primary halides, there is no corresponding differentiation between primary and secondary halides whether the latter react by an S_N1, S_N2, or "mixed" mechanism.

Finally we draw attention to the similarity between the values of $\delta_I\Delta H^{\neq}$ and $\delta_I\Delta S^{\neq}$ for the activated process of liquid flow, **16**, in water and D_2O (36), and the corresponding values determined for the S_N2 process which may be taken as further support that the transition state corresponds to a state of disruption of solvent structure (14).

$\delta_I\Delta C_p^{\neq}$

The change in heat capacity ($\delta_I\Delta C_p^{\neq}$) in a qualitative way is consistent with the idea that structural stability is greater in D_2O than in H_2O and hence will show a greater (negative) temperature dependency. Unfortunately the errors associated with this term in this study are so large as to prevent any useful deductions other than to note that all are more negative than the corresponding term for hydrolysis in H_2O and much larger than the previous value, $\delta_I\Delta C_p^{\neq} = 5$ (Table II) for 2-bromopropane, **5**, or from the ionization of acetic acid $\delta_I\Delta C_p = 3$ cal mole^{-1} deg^{-1} (32), the ionization of phosphoric acid (K_2) (33), ($\delta_I\Delta C_p =$ 4.3 cal mole^{-1} deg^{-1}) and for the autoprotolysis of water, $\delta_I\Delta C_p = 8$ cal mole^{-1} deg^{-1} (34). The differences in our kinetic measurements do not appear to be random since they are all in the same direction, nor have we been able to find any trivial experimental reason which would account for them.

[5]As presented at the 151st meeting of the American Chemical Society, Pittsburgh, Penn. March 22–31, 1966.

TABLE VI

Thermodynamic differences for hydrolysis of a series of halides*

Compound number	Halide	Mechanism	Temperature (°C)	$\delta_t\Delta G^{\ddagger}$	$\delta_t\Delta H^{\ddagger}$ (cal mole^{-1})	$\delta_t\Delta S^{\ddagger}$ (cal deg^{-1} mole^{-1})	$\delta_t\Delta C_p^{\ddagger}$ (cal deg^{-1} mole^{-1})
1	*t*-BuCl	S_N1	10	187±3	818±134	2.24±0.47	30±28
			20	169±2	518±170	1.2 ±0.5	30±28
2	2,2-Dibromo-propane	S_N1	20	209±3	1050±170	2.9 ±0.5	28±11
			40	170±1.5	488±150	1.0 ±0.2	28±11
3	2-Cl-2-Br-propane	S_N1	20	210±1.2	724±59	1.7 ±0.2	10±7
			40	186±1.4	513±125	1.1 ±0.2	10±7
4	2-Cl-2-Me-propyl methyl ether	S_N1	20	174±2.5	732±184	1.9 ±0.6	22±18
5	2-Bromopropane	S_N2	40	172±2	363±53	0.61±0.1	7±4
6	Cyclobutyl Cl	S_N1	45	169	500	1.05	
7	Cyclopentyl Br	S_N1	35	166	434	0.84	
8	Methyl Br	S_N2	70	147	170	0.07	
9	Methyl I	S_N2	70	165	271	0.3	
10	Ethyl I	S_N2	84	166	277	0.3	
11	Allyl I	S_N2/S_N1	47	204	321	0.3	
12	2-Iodopropane	S_N1	60	220	142	−0.25	
13	Benzyl Cl	S_N2/S_N1	40	154	300	0.46	
14	Methyl benzene-sulfonate	S_N2	25	59	111	0.17	
15	2-Propyl benzene-sulfonate	S_N1	25	44	87	0.14	
16	Fluidity of H_2O	—	35	120	300	0.6	0± ?
17	$MeO(CH_2)_4Br$	S_N2	45	115	268	0.5	

*Where the rate data for solvolysis in water have been taken from earlier work, the compound and its reference are as follows: 1, (8); 2, (10); 3, (10); 4, (9); 5, (14); 6, (35); 7, (12); 8, (12); 11, (31); 12, (12); 13, (31); 14, (12); 15, (12); 16, (36); 17, (38).

In conclusion we may summarize the above results by the observations that while this study of the temperature dependence of the solvent isotope effect does not require any new hypothesis, it does provide substantial supplementary support for those hypotheses already proposed to account for the nature of solvent reorganization accompanying hydrolysis of alkyl halides in water.

1. C. G. SWAIN, R. CARDINAUD, and A. D. KETLEY. J. Amer. Chem. Soc. **77**, 934 (1955).
2. P. M. LAUGHTON and R. E. ROBERTSON. Can. J. Chem. **34**, 1714 (1956).
3. C. K. INGOLD. Structure and mechanism in organic chemistry. Cornell Univ. Press, Ithaca, New York. 1953. Chap. 7, 24a.
4. S. WINSTEIN and A. FAINBERG. J. Amer. Chem. Soc. **79**, 5937 (1957).
5. R. E. ROBERTSON, R. L. HEPPOLETTE, and J. M. W. SCOTT. Can. J. Chem. **37**, 803 (1959).
6. C. G. SWAIN and E. R. THORNTON. J. Amer. Chem. Soc. **84**, 822 (1962).
7. R. E. ROBERTSON and P. M. LAUGHTON. Can. J. Chem. **43**, 154 (1965).
8. E. A. MOELWYN-HUGHES, R. E. ROBERTSON, and S. E. SUGAMORI. J. Chem. Soc. 1965 (1965).
9. K. T. LEFFEK, R. E. ROBERTSON, and S. E. SUGAMORI. J. Amer. Chem. Soc. **87**, 2097 (1965).
10. A. QUEEN and R. E. ROBERTSON. J. Amer. Chem. Soc. **88**, 1363 (1966).
11. J. M. STUART and F. M. WORMWELL. J. Chem. Soc. **85** (1930).
12. R. E. ROBERTSON. Progress in physical organic chemistry. John Wiley and Sons, Inc., New York. 1967. p. 213.
13. E. C. W. CLARKE and D. N. GLEW. Trans. Faraday. Soc. **62**, 539 (1966).
14. R. L. HEPPOLETTE and R. E. ROBERTSON. J. Amer. Chem. Soc. **83**, 1834 (1961).
15. J. GREYSON. J. Phys. Chem. **71**, 2210 (1967).
16. C. G. SWAIN and E. R. THORNTON. J. Amer. Chem. Soc. **84**, 822 (1962).
17. R. E. ROBERTSON and P. M. LAUGHTON. Can. J. Chem. **37**, 1319 (1957).
18. G. C. KRESHECK, H. SCHNEIDER, and H. A. SCHERAGA. J. Phys. Chem. **69**, 3132 (1965).
19. R. V. VISGERT and E. K. SAVCHUCK. J. Gen. Chem. USSR, **26** 2268 (1956).
20. C. G. SWAIN and C. B. SCOTT. J. Amer. Chem. Soc. **75**, 246 (1953).
21. G. NEMETHY and H. A. SCHERAGA. J. Chem. Phys. **41**, 680 (1964).
22. O. YA. SAMOILOV. Structure of aqueous electrolyte solutions and the hydration of ions. *Translated by* D. J. G. Ives Consultants Bureau, New York. 1965. Chap. 3.

Can. J. Chem. Downloaded from www.nrcresearchpress.com by 210.87.254.5 on 09/05/12
For personal use only.

23. J. L FRANKLIN. Trans. Faraday Soc. **48**, 443 (1952).
24. R. A. OGG and M. POLANYI. Trans. Faraday Soc. **31**, 604 (1935).
25. J. L. KAVANAU. Water and solute–water interaction. Holden-Day, San Francisco. 1964.
26. H. S. FRANK and A. S. QUIST. J. Chem. Phys. **34**, 604 (1961).
27. E. WICKE. Angew. Chem. Intern. Ed. **5**, 106 (1966).
28. A. BEN-NAIM. J. Phys. Chem. **69**, 3240 (1965).
29. R. C. HARDY and R. L. COTTINGTON. J. Res. Natl. Bur. Std. **42**, 573 (1949).
30. C. H. COLLIE, J. B. HASTED, and D. M. RITSON. Proc. Phys. Soc. **60**, 145 (1948).
31. J. M. W. SCOTT and R. E. ROBERTSON. J. Chem. Soc. 1596 (1961).
32. R. GARY, R. G. BATES, and R. A. ROBINSON. J. Phys. Chem. **69**, 2750 (1965).
33. R. GARY, R. G. BATES, and R. A. ROBINSON. J. Phys. Chem. **68**, 3806 (1964).
34. A. K. COVINGTON, R. A. ROBINSON, and R. G. BATES. J. Phys. Chem. **70**, 3820 (1966).
35. C. Y. WU and R. E. ROBERTSON. J. Amer. Chem. Soc. **88**, 2666 (1966).
36. B. E. CONWAY. Can. J. Chem. **37**, 613 (1959).
37. E. M. ANETT and D. R. MCELVEY. J. Amer. Chem. Soc. **88**, 5031 (1966).
38. M. J. BLANDANER, H. F. GOLINKIN, and R. E. ROBERTSON. J. Amer. Chem. Soc. **91**, 2678 (1969).

Can. J. Chem. Downloaded from www.nrcresearchpress.com by 210.87.254.5 on 09/05/12
For personal use only.

Can. J. Chem. Downloaded from www.nrcresearchpress.com by 210.87.254.105 on 09/05/12
For personal use only.

Phosphinohydrazines. Part III. Coordination compounds of N,N-dimethyl,N′-diphenylphosphinohydrazine and N,N-dimethyl,N′-diphenylthiophosphinatohydrazine

E. W. AINSCOUGH, L. K. PETERSON[1], K. I. THÉ, AND G. L. WILSON
Department of Chemistry, Simon Fraser University, Burnaby 2, British Columbia

Received May 6, 1969

Reactions between N,N-dimethyl,N′-diphenylphosphinohydrazine, $Me_2NNHP(C_6H_5)_2$, (DPH), or N,N-dimethyl,N′-diphenylthiophosphinatohydrazine, $Me_2NNHP(S)(C_6H_5)_2$, (DPS), and appropriate metal salts have yielded the new coordination complexes $Pd(DPH)Cl_2$, $Pd(DPH)_2Cl_2$, $Pd(DPH)_2Cl(ClO_4)$, $Pt(DPH)_2Cl_2$, $Pt(DPH)Cl_4$, $Hg(DPH)Cl_2$, $Pd(DPS)Cl_2$, $Pt(DPS)Cl_4$, $Ag(DPS)NO_3$, $Zn(DPS)Cl_2$, $Cd(DPS)Cl_2$, and $Hg(DPS)Cl_2$. Notably, complexes of 1:1 ligand: metal stoichiometry predominate, the only exceptions being $Pd(DPH)_2Cl_2$ and $Pt(DPH)_2Cl_2$. In reactions between DPH and Zn(II) or Cd(II) salts, ready cleavage of the P—N bond was observed; the metal complexes of dimethylhydrazine were isolated in both instances. With the ligand DPS, however, the P—N bond was consistently stable against cleavage. Many reactions involving Co(II), Ni(II), Ag(I), Au(III), In(III), and Sn(II) resulted in the formation of intractable oils, or in reduction to the metallic state.

Canadian Journal of Chemistry. 47, 3405 (1969)

In previous communications we reported the synthesis and characterization of a series of perfluoroalkyl-phosphino- and arsino-substituted hydrazines, describing these systems as potential polyfunctional Lewis bases with lone pairs of electrons located on each atom of the P—N—N or As—N—N skeleton (1). One would expect different base character at each site, determined by the electronic, steric, and structural environment of the sites in the free and in the complexed molecule. Thus, whereas the N atoms may only exhibit σ donor character, the P or As atoms may function as π acceptors as well as σ donors, particularly when the substituent on P is the electronegative CF_3 group (2). The location of the most basic site in these systems is a problem of some interest to us. Bidentate functionality should lead to the formation of either chelate or polynuclear complexes. The "mixed" nature of the donor sites on the ligand and the presence of an atom other than carbon linking these sites provide additional features of interest in these systems. The functionality of hydrazine, N_2H_4, may be inferred from published reports (3–5). Several interesting examples of chelation by tetramethylhydrazine with alanes have been reported (6*a*, 6*b*), the complexes involving a three membered Al chelate ring, and five-coordinate aluminum. The symmetrical 1,2-bis(diphenylphosphino)-1,2-dimethylhydrazine, $(C_6H_5)_2PN(CH_3)N(CH_3)P(C_6H_5)_2$, however, reacts with 2 moles of trialkyl aluminum, giving complexes for which tetracoordinate aluminum atoms have been proposed, with each phosphorus serving as the donor site (6*c*). The basicity of hydrazines is diminished by alkyl substitution (7), contrary to the trend observed among alkylamines (8). Various adducts of hydrazines are unstable with respect to condensation reaction, leading to the formation of hydrazino-metallanes, such as the reported derivatives of boranes (9), alanes (6*a*, 6*b*, 10), silanes (11), phosphines (12), and arsines (1*a*). While hydrazine forms complexes with most of the elements of the first transition series (13), structural studies, indicating a variety of modes of coordination, have been performed only with $Co(N_2H_4)_6Cl_2$ (14), $Ni(N_2H_4)_3Cl_2$ (15), $Zn(N_2H_4)_2Cl_2$, $Cd(N_2H_4)_2Cl_2$, and $Mn(N_2H_4)_2Cl_2$ (16), and with $Hg(N_2H_4)Cl_2$ and $Hg(N_2H_4)_2Cl_2$ (17). Hydrazine causes reduction of Ti(IV) halides (18), but reasonably stable complexes are formed with Ti(IV) alkoxides (19), and with UCl_4 (20). Substituted hydrazines effect solvolysis of Ti(IV) halides, without reduction. Octahedral structures are proposed for $M(MeNHNH_2)Cl_2$ and $M(MeNHNH_2)_6Cl_2$, M = Co(II) (14), Ni(II) (17); the type $M(MeNHNH_2)_3Cl_2$ is not formed, perhaps because of the greater basicity of the nitrogen atom bearing the methyl group. This paper describes the synthesis of a series of complexes with phosphinohydrazine ligands, as part of a study of the factors determining the functionality of such systems.

[1]Author to whom correspondence should be addressed.

Can. J. Chem. Downloaded from www.nrcresearchpress.com by 210.87.254.105 on 09/05/12
For personal use only.

Preliminary work with $Me_2NNHP(CF_3)_2$ gave rise to dark brown products, indicative of instability or undesirable side reactions. The diphenylphosphine derivative, $Me_2NNHP(C_6H_5)_2$, however, is more stable, and can be handled quickly in air without serious oxidation (12*d*). In addition, Nielsen *et al.* (21) have already demonstrated that the phosphorus is more basic than either of the nitrogen atoms. Thus with chloramine or methyl iodide, electrophilic attachment occurs on the phosphorus atom. Furthermore, the phosphorylhydrazine $Me_2NNHP(O)(C_6H_5)_2$, DPO, fails to react (at an N center) with methyl iodide or chloramine, indicating a deactivation of both of the nitrogen atoms toward electron acceptor species. The DPO and DPS ligands may provide four- and five-membered chelate ring systems utilizing O (or S) and central N or terminal N coordination. The preferred structure should reflect the combined influence of relative ring strains, steric hindrances, and donor atom basicities, for the various structures.

DPH and $Na_2PdCl_4.H_2O$ react readily in acetone solution, in 1:1 and 2:1 molar ratios, to yield $Pd(DPH)Cl_2$ or $Pd(DPH)_2Cl_2$, respectively. The latter compound was converted into $Pd(DPH)_2Cl(ClO_4)$ by reaction with sodium perchlorate. In similar reactions using DPS, only 1 mole of ligand is taken up, giving $Pd(DPS)Cl_2$. A study of the structural possibilities of mononuclear systems, using molecular models, indicates that a complex containing 2 moles of ligand, i.e. $Pd(DPS)_2Cl_2$, may be constructed with DPS as a monodentate ligand, and with S or N as the donor atom; but if DPS favors chelation, some steric hindrance is indicated for complexes of this type. The complex of platinum, $Pt(DPH)_2Cl_2$, is obtained in the same way as its palladium analogue. It is likely that other members, corresponding to the various palladium compounds, could be synthesized. In its higher oxidation state, Pt(IV) forms both DPH and DPS complexes, without evidence of redox reactions.

Equimolar proportions of mercuric chloride and DPH or DPS yield $Hg(DPH)Cl_2$, a complex which decomposes slowly with liberation of mercury, and stable $Hg(DPS)Cl_2$. Attempts to prepare the complexes containing 2 ligand moieties, using appropriate proportions of reagents, failed in both cases; DPH causes the reduction of $HgCl_2$ to mercury, while DPS yields only $Hg(DPS)Cl_2$, analogous to the DPS–Pd(II) studies. Silver(I) is rapidly reduced by DPH, but it reacts with DPS to form $Ag(DPS)NO_3$. The latter, however, is photosensitive.

For reasons of solubility, methanol was used as the solvent in reactions involving $ZnCl_2$ or $CdCl_2$. Attempts to prepare a series of complexes of DPH yielded derivatives of dimethylhydrazine, DMH, viz., $Zn(DMH)_2Cl_2$ and $Cd(DMH)Cl_2$, indicating solvolysis of the P—N bond. Similar reactions with DPS yielded 1:1 complexes only, $Zn(DPS)Cl_2$ and $Cd(DPS)Cl_2$, the P—N bond remaining intact.

It is evident that phosphinohydrazine systems are effective as ligands with a variety of acceptor species. With DPH, strongly oxidizing conditions must be avoided, since the P(III) atom and the hydrazine moiety are both sensitive to oxidation. DPS, however, is more difficult to oxidize, and may therefore complex with metals in high oxidation states, without the onset of reduction. While the P—N bond in P(III) systems is sensitive to solvolysis, in P(V) systems it is more resistant to cleavage. A study of the physico-chemical properties of the above complexes is in progress.

Experimental

The ligands N,N-dimethyl,N′-diphenylphosphinohydrazine (DPH), and N,N-dimethyl,N′-diphenylthiophosphinatohydrazine (DPS), were prepared by the methods of Nielsen and Sisler (12*d*). The new complexes prepared are given in Table I, together with analytical data[2].

Dichloro(N,N-dimethyl,N′-diphenylphosphinohydrazine) palladium(II), Pd(DPH)Cl₂

Acetone solutions (about 10 ml of each) of DPH (0.122 g) and $Na_2PdCl_4.H_2O$ (0.156 g) were mixed and gently heated on a steam bath until a yellow precipitate was formed. This was collected and recrystallized twice from warm CH_2Cl_2 to remove sodium chloride (yield, 0.12 g, 60%). The compound was soluble in warm acetone, chloroform, and nitrobenzene. The same product was obtained with methanol as solvent.

Dichlorobis(N,N-dimethyl,N′-diphenylphosphinohydrazine)palladium(II), Pd(DPH)₂Cl₂

Acetone solutions of DPH (0.24 g) and $Na_2PdCl_4.H_2O$ (0.156 g, 15 ml) were mixed, causing precipitation of sodium chloride at room temperature. The mixture was filtered and solvent was removed from the filtrate by vacuum distillation, leaving behind an oily residue, which was dissolved in dry CH_2Cl_2 and filtered. A difficult recrystallization was achieved by treating this solution with ether, cooling in an ice bath, and scratching, to yield

[2]Analyses were performed by Pascher, Mikroanalytisches Laboratorium, 53 Bonn, Buschstrasse 54, Germany.

TABLE I

Analytical data for complexes of DPH, DPS, and DMH

Compound*	Color	Analyses					
		Observed			Calculated		
		C	H	N	C	H	N
$Pd(DPH)Cl_2$	Yellow	40.0	4.09	6.62	39.9	4.05	6.6
$Pd(DPH)_2Cl_2$	Yellow	49.9	5.15	8.0	50.5	5.14	8.41
$Pt(DPH)_2Cl_2$	Pale yellow	44.7	4.62	7.42	44.5	4.53	7.40
$Pd(DPH)_2Cl(ClO_4)$	Pale yellow	46.0	4.48	7.57	46.1	4.68	7.67
$Hg(DPH)Cl_2$	White	32.4	3.30	5.39	32.6	3.30	5.40
$Pt(DPH)Cl_4$	Pale yellow	30.1	3.44	5.10	28.9	2.94	4.82
$Zn(DMH)_2Cl_2$	White	18.7	6.00	21.20	18.7	6.24	21.80
$Cd(DMH)Cl_2$	White	9.5	3.04	10.70	9.8	3.28	11.5
$Pd(DPS)Cl_2$	Orange	36.9	3.81	6.18	37.1	3.77	6.17
$Pt(DPS)Cl_4$	Pale yellow	29.1	2.85	4.70	27.4	2.79	4.56
$Ag(DPS)NO_3$	White	37.5	3.80	9.34	37.7	3.80	9.41
$Zn(DPS)Cl_2$	White	41.0	4.03	6.90	40.8	4.14	6.79
$Cd(DPS)Cl_2$	White	35.5	3.7	5.80	36.6	3.72	6.09
$Hg(DPS)Cl_2$	White	30.7	3.18	5.06	30.7	3.12	5.11

*DPH = N,N-dimethyl,N′-diphenylphosphinohydrazine, DPS = N,N-dimethyl,N′-diphenylthiophosphinatohydrazine, and DMH = N,N-dimethylhydrazine.

a pale yellow product (0.210 g, 65%). This substance was slightly soluble in most common solvents.

The corresponding platinum complex, $Pt(DPH)_2Cl_2$, was prepared in a similar way.

Chlorobis(N,N-dimethyl,N′-diphenylphosphinohydrazine) palladium(II)perchlorate, $Pd(DPH)_2Cl(ClO_4)$

Warm acetone solutions of $Pd(DPH)_2Cl_2$ (0.160 g) and excess sodium perchlorate (0.180 g, 15 ml) were mixed and heated until a small volume of solution remained; upon filtering, the filtrate was treated with ether and was cooled at 0 °C to induce precipitation. The pale yellow product was recrystallized twice from CH_2Cl_2 (0.10 g, 60%). It was soluble in several common solvents.

Attempts to replace both chloro groups on $Pd(DPH)_2Cl_2$ by this method were unsuccessful.

Dichloro(N,N-dimethyl,N′-diphenylphosphinohydrazine) mercury(II), $Hg(DPH)Cl_2$

Acetone solutions of DPH (0.24 g, 8 ml) and $HgCl_2$ (0.27 g, 10 ml) were mixed and heated until a small volume of solvent remained. On cooling, a white precipitate was obtained which did not require further purification (0.35 g, 70%). It was sparingly soluble in chloroform, and slowly decomposed on standing, liberating free mercury.

Tetrachloro(N,N-dimethyl,N′-diphenylphosphinohydrazine)platinum(IV), $Pt(DPH)Cl_4$

Acetone solutions of DPH (0.057 g) and Na_2PtCl_6 (0.094 g) were mixed together and heated, resulting in precipitation of sodium chloride. The solution was filtered, most of the solvent was removed, and ether was added to effect precipitation of the product. It was recrystallized from acetone (0.08 g, 70%; color, pale yellow).

The corresponding complex with DPS, $Pt(DPS)Cl_4$, was prepared in a similar way.

Reaction of DPH with $ZnCl_2$ and $CdCl_2 2.5H_2O$

For reasons of solubility, methanol was used as the solvent for the reaction between DPH (0.24 g) and $ZnCl_2$ (0.136 g). The solution was heated to remove most of the solvent, then cooled and diluted with ether to precipitate a white substance with analytical data indicative of bis(N,N-dimethylhydrazine)zinc dichloride, $Zn(DMH)_2Cl_2$ (0.13 g, 50%; DMH = N,N-dimethylhydrazine). This compound was sparingly soluble in acetone and insoluble in chloroform. The same substance was obtained during the attempted synthesis of a bis(DPH) complex of zinc chloride. These results indicate solvolysis of the DPH ligand at the P—N bond, to yield free dimethylhydrazine.

The reaction with cadmium chloride was similar, in that solvolysis of the DPH ligand took place and N,N-dimethylhydrazinecadmium dichloride, $Cd(DMH)Cl_2$, was obtained in 50% yield. This substance was practically insoluble in most solvents.

Dichloro(N,N-dimethyl,N′-diphenylthiophosphinatohydrazine)palladium(II), $Pd(DPS)Cl_2$

Acetone solutions of DPS (0.184 g) and $Na_2PdCl_4H_2O$ (0.209 g) were mixed at room temperature, yielding immediately an orange precipitate which was recrystallized twice from CH_2Cl_2 to remove sodium chloride (0.20 g, 70%).

Attempts to prepare $Pd(DPS)_2Cl_2$ were unsuccessful; the complex described above was obtained in each case.

Nitrato(N,N-dimethyl,N′-diphenylthiophosphinatohydrazine)silver(I), $Ag(DPS)NO_3$

Acetone solutions of DPS (0.069 g) and $AgNO_3$ (0.042 g) were mixed to form a white precipitate which was insoluble in many common solvents (0.08 g, 90%). Attempts to effect dissolution by heating led to decomposition of the complex. This compound turned grey on exposure to light.

Can. J. Chem. Downloaded from www.nrcresearchpress.com by 210.87.254.105 on 09/05/12
For personal use only.

The corresponding DPH complex could not be isolated —a reduction reaction resulted in the formation of metallic silver.

Dichloro(N,N-dimethyl,N'-diphenylthiophosphinato-hydrazine)zinc(II), Zn(DPS)Cl_2

Using methanol as solvent, solutions of DPS (0.212 g) and $ZnCl_2$ (0.092 g) were mixed and briefly heated. Upon cooling, a white precipitate was obtained (0.22 g, 70%). This compound was insoluble in common solvents.

Attempts to prepare $Zn(DPS)_2Cl_2$ were unsuccessful.

Dichloro(N,N-dimethyl,N'-diphenylthiophosphinato-hydrazine)cadmium(II), Cd(DPS)Cl_2

Methanol solutions of DPS (0.138 g) and $CdCl_2$-$2.5H_2O$ (0.114 g), corresponding to a 2:1 molar ratio of reactants, were mixed and boiled until only a small volume of solvent remained. On cooling and adding ether, a white precipitate was obtained (0.16 g, 70%). This compound was insoluble in common solvents.

Dichloro(N,N-dimethyl,N'-diphenylthiophosphinato-hydrazine)mercury(II), Hg(DPS)Cl_2

This compound was prepared in the same way as $Zn(DPS)Cl_2$, using DPS (0.184 g) and $HgCl_2$ (0.181 g) in methanol solution (yield, 0.27 g, 75%). It was soluble in acetone and chloroform. Attempts to prepare $Hg(DPS)_2Cl_2$ failed.

Acknowledgment

The authors gratefully acknowledge financial support from the National Research Council of Canada.

1. (*a*) L. K. Peterson and K. I. Thé. Chem. Commun. 1056 (1967). (*b*) L. K. Peterson and G. L. Wilson. Can. J. Chem. **46**, 685 (1968). (*c*) L. K. Peterson and K. I. Thé. Can. J. Chem. **47**, 339 (1969). (*d*) L. K. Peterson, G. L. Wilson, and K. I. Thé. Can. J. Chem. **47**, 1025 (1969).
2. A. B. Burg and J. Heners. J. Amer. Chem. Soc. **87**, 3092 (1965).
3. R. G. Snyder and J. C. Decius. Spectrochim. Acta, **13**, 280 (1959).
4. (*a*) H. J. Emeléus and F. G. A. Stone. J. Chem. Soc. 840 (1951). (*b*) M. J. Steindler and H. I. Schlesinger. J. Amer. Chem. Soc. **75**, 756 (1953).
5. W. G. Paterson and M. Onyszchuk. Can. J. Chem. **39**, 986 (1961).
6. (*a*) N. R. Fetter, B. Bartocha, F. E. Brinckman, Jr., and D. W. Moore. Can. J. Chem. **41**, 1359 (1963). (*b*) D. F. Clemens, W. S. Brey, Jr., and H. H. Sisler. Inorg. Chem. **2**, 1251 (1963). (*c*) S. F. Spangenberg and H. H. Sisler. Inorg. Chem. **8**, 1004 (1969).
7. R. L. Hinman. J. Org. Chem. **23**, 1587 (1959).
8. H. C. Brown, H. Bartholomay, and M. D. Taylor. J. Amer. Chem. Soc. **66**, 435 (1944).
9. (*a*) H. Nöth. Z. Naturforsch. **16b**, 471 (1961). (*b*) M. S. Bains. Can. J. Chem. **44**, 534 (1966).
10. (*a*) N. R. Fetter and B. Bartocha. Can. J. Chem. **39**, 2001 (1961). (*b*) R. P. Nielsen and H. H. Sisler. J. Chem. Soc. 3818 (1962).
11. (*a*) B. J. Aylett. J. Inorg. Nucl. Chem. **2**, 325 (1956). (*b*) U. Wannagat and F. Höfler. Monatsh. Chem. **97**, 976 (1966). (*c*) G. Gibson, K. Schug, and J. R. Crook. Inorg. Chem. **2**, 876 (1963).
12. (*a*) H. H. Sisler and J. Weiss. Inorg. Chem. **4**, 1514 (1965). (*b*) H. Bock and G. Rudolph. Chem. Ber. **98**, 2273 (1965). (*c*) M. Becke-Goehring and W. Weber. Z. Anorg. Allg. Chem. **333**, 128 (1964). (*d*) R. P. Nielsen and H. H. Sisler. Inorg. Chem. **2**, 753 (1963).
13. L. F. Audrieth and B. A. Ogg. The chemistry of hydrazine. John Wiley and Sons, Inc. New York. 1951.
14. D. Nicholls, M. Rowley, and R. Swindells. J. Chem. Soc. A, 950 (1966).
15. D. Nicholls and R. Swindells. J. Inorg. Nucl. Chem. **30**, 2211 (1968).
16. A. Ferrari, A. Braibanti, and G. Bigliardi. Acta Cryst. **16**, 498 (1963).
17. K. Brodersen. Z. Anorg. Allg. Chem. **290**, 24 (1957).
18. D. Nicholls and R. Swindells. J. Chem. Soc. 4204 (1964).
19. M. S. Bains and D. C. Bradley. Can. J. Chem. **40**, 1350 (1962).
20. I. Kalnins and G. Gibson. J. Inorg. Nucl. Chem. **7**, 55 (1958).
21. R. P. Nielsen, J. F. Vincent, and H. H. Sisler. Inorg. Chem. **2**, 760 (1963).

Can. J. Chem. Downloaded from www.nrcresearchpress.com by 210.87.254.105 on 09/05/12
For personal use only.

Crystal structure of $Cd_2P_2O_7$[1]

C. CALVO AND P. K. L. AU[2]

Department of Chemistry and Institute for Materials Research, McMaster University, Hamilton, Ontario

Received April 17, 1969

Cadmium pyrophosphate forms crystals having triclinic symmetry with the unit cell parameters $a = 6.672(8)$ Å, $b = 6.623(8)$ Å, $c = 6.858(7)$ Å, $\alpha = 95.80(10)°$, $\beta = 115.38(8)°$, and $\gamma = 82.38(8)°$. The space group is $P\bar{1}$ and there are two molecules per unit cell. The structure was refined by least squares methods using 1326 reflections. The pyrophosphate anion, $P_2O_7^{4-}$, has a bent P—O—P bond with a bond angle of 132° and with average inner and outer PO bond lengths of 1.62 and 1.51 Å, respectively. The cations are coordinated to five and six oxygen atoms with average cadmium–oxygen atom bond lengths of 2.33 and 2.31 Å, respectively. This pyrophosphate structure differs from that adopted by other divalent metal ions of small radius in that the ends of the anion are in a nearly eclipsed orientation but shows some similarity to those $A_2B_2O_7$ compounds, where A has a large radius and B a small one.

Canadian Journal of Chemistry, 47, 3409 (1969)

Can. J. Chem. Downloaded from www.nrcresearchpress.com by 210.87.254.40 on 09/05/12
For personal use only.

Introduction

The divalent metal ion pyrophosphates investigated to date fall into two series. The first, characterized by cations of small radii, have closely related structures in all their polymorphs. Included in this group are the pyrophosphates of Mn (1), Cu (2), Mg (3), Co (4), Ni (5), and Zn (6). The second class are those pyrophosphates of the alkaline-earth metals which show four polymorphs, but not all of these occur for each compound. A limited number of structures in this series have been determined. These are: $\alpha Ca_2P_2O_7$ (7), $\beta Ca_2P_2O_7$ (8), and $\alpha Sr_2P_2O_7$ (9). To date no close relationship among those polymorphs of a given compound in this series has been apparent although the structures $\alpha Ca_2P_2O_7$ and $\alpha Sr_2P_2O_7$ are closely related.

The compounds in the first class form structures closely related to that of the mineral thortveitite (10). This structure consists of sheets containing cations octahedrally surrounded by oxygen atoms and each octahedron shares three edges with three neighboring octahedra. The P—O—P part of the anion is accommodated between these sheets, lying opposite empty octahedral sites in the sheets. This structure would be expected to become unstable as the ratio of the cation to anion size diverged from some optimum range. The alkaline earth pyrophosphates seem to have cations too large to be accommodated in this structure. Since $Cd_2V_2O_7$ (11) is known to have the thortveitite structure, it was considered germane to see whether $Cd_2P_2O_7$ formed the upper limit of the thortveitite-like series or the lower limit of the alkaline-earth series.

Experiments

Crystals of $Cd_2P_2O_7$ were prepared by heating stoichiometric amounts of $CdCO_3$ and $(NH_4)_2HPO_4$ until ammonia and carbon dioxide ceased to evolve. The temperature was then raised to beyond 1120 °C, the mixture was melted, slowly cooled across the melting point, and then quenched to room temperature. Clear, colorless parallelopipeds were obtained.

Accurate parameters were obtained from films calibrated with reflections from a crystal of TiO_2 whose lattice parameters were taken as $a = 4.5929(5)$ Å and $c = 2.9591(3)$ Å (12). The values obtained are compiled in Table I along with other crystal data. The density of 4.90 g/cm^3 was measured with a pycnometer.

Intensity photographs of the [100] zone and reflections of the type *hnl* with $n = 0$, 1, and 2 were obtained with MoKα radiation using the Weissenberg camera. The [100], [010], and [101] zones were recorded with the same radiation but taken on a precession camera. The intensities of the reflections were estimated visually, and corrected for absorption, Lorentz, and polarization effects. The former corrections were deemed advisable since the crystals had dimensions of the order of $0.1 \times 0.15 \times 0.2$ mm^3. Thus errors of the order of 20%

TABLE I

$Cd_2P_2O_7$ crystal data

Constant	Value	Units
a	6.672(8)	Å
b	6.623(8)	Å
c	6.858(7)	Å
d	95.8(1)	Degrees
β	115.38(8)	Degrees
γ	82.38(8)	Degrees
ρ_{obs}	4.90	g/cm^3
ρ_{calcd}	5.04	g/cm^3
μ	86.1	cm^{-1}

[1]Research supported by a grant from the Defence Research Board, Number 95 10-44.

[2]Present Address: Department of Chemistry, University of Western Ontario, London, Ontario.

Can. J. Chem. Downloaded from www.nrcresearchpress.com by 210.87.254.40 on 09/05/12
For personal use only.

could result if this effect were ignored. The crystal was assumed to be spherically shaped for this purpose. Data taken from the same zone but with different cameras were averaged.

The positions of the cations were determined from the Patterson functions calculated from the data taken for the [100], [010], and [001] zones. The Patterson functions indicated that at least the cations were related by a center of symmetry. Further, electron paramagnetic resonance (e.p.r.) experiments on crystals doped with either Cu^{2+} or Mn^{2+} (13) showed, in each case, preferred solubility in one of the cation sites but with no indication of a symmetry lower than $P\bar{1}$, Therefore this space group was selected. As it turned out, the Cd–P interactions were sufficiently distinct in the Patterson functions to permit the determination of the phosphorus coordinates although they were, in fact, obtained from subsequent electron density maps. The structure was refined in stages using difference maps to determine the positions of the oxygen atoms. The final refinement was performed with weights chosen as $\omega = [3 + 0.10\,F_o + 0.009\,F_o^2]^{-1}$ using a full matrix least-squares program written for the IBM 7040 by Stephens. This choice of weights resulted in $||F_o| - |F_c||^2\omega$ being independent of $|F_o|$ (14).

The atomic scattering curves for Cd^{2+}, P, and O^- were taken from the International tables for X-ray crystallography (15) and corrected for dispersion. In the refinement those reflections whose calculated structure factor was less than the local minimum observable value were given zero weight. Individual isotropic temperature factors were used until a minimum value of the residual was obtained and then the anisotropic components of the temperature factors of Cd^{2+} were allowed to vary. Each layer of data was scaled independently. Since the value of the residual, $R_2 = \{(\Sigma\omega||F_o| - |F_c||^2)/(\Sigma\omega|F_o|^2)\}^{1/2}$ changed from 0.18 to 0.12, these changes were regarded to be significant. The final values for $R(= \Sigma||F_o| - |F_c||/\Sigma|F_o|)$ and R_2 are 0.093 and 0.113, respectively. A small number (eight) of intense reflections lying at low angle seemed to suffer from extinction and were left out of the refinement. The final atomic parameters are shown in Table II. The 1326 calculated and observed structure factors are listed in Table III. Of this total 916 had intensities strong enough to be measured.

Description of the Structure

The cations are coordinated to five and six oxygen atoms for site (1) and site (2) respectively. In the former case there are two additional cation–oxygen atom distances at 2.88 and 2.69 Å, but these are beyond the primary coordination sphere. The five oxygen atoms about the first site range in distance from 2.27 to 2.41 Å with a mean of 2.33 Å. The average cation–ligand bond length about site (2) is 2.31 Å with the somewhat smaller range extending from 2.25 to 2.34 Å. Since the estimated standard deviations on these lengths are about 0.02 Å, the difference in these means is not significant. The geometric configuration of the ligands about site (1) is that of a highly distorted trigonal bipyramid with O(4) and O(5) as the apex ligands and O($\bar{4}$), O($\bar{3}$), and O($\bar{6}$) as the equatorial ligands. The average equatorial bond

TABLE II

a. Atomic parameters for $Cd_2P_2O_7$*

Atom	Parameters			
	x	*y*	*z*	*U* (Å)
Cd(1)	0.2756(2)	0.3605(2)	0.3380(2)	
Cd(2)	0.1168(2)	0.1604(2)	0.7482(1)	
P(1)	0.3612(6)	0.8664(8)	0.1893(5)	0.02(4)
P(2)	0.2359(6)	0.6598(8)	0.7536(6)	0.13(4)
O(1)	0.4033(19)	0.7447(22)	0.9868(17)	0.52(14)
O(2)	0.0692(18)	0.8337(23)	0.6284(17)	0.48(14)
O(3)	0.6016(22)	0.8690(27)	0.3725(21)	1.15(20)
O(4)	0.3919(16)	0.5591(22)	0.6493(15)	0.31(13)
O(5)	0.2544(19)	0.0764(24)	0.1098(18)	0.57(15)
O(6)	0.1040(20)	0.5099(25)	0.7818(19)	0.80(17)
O(7)	0.2111(22)	0.7492(26)	0.2230(21)	1.04(18)

b. Anisotropic thermal parameters for Cd†

Atom	Parameters × 10^4 (Å^2)					
	U_{11}	U_{22}	U_{33}	U_{12}	U_{13}	U_{23}
Cd(1)	72(4)	45(45)	101(4)	−27(5)	48(3)	−46(4)
Cd(2)	59(4)	11(4)	62(4)	13(47)	35(3)	− 6(3)

*Estimated standard deviations in parentheses.
†Calculated from $\beta_{ij} = 2\pi^2 b_i b_j U_{ij}$ where the β_{ij}'s appear as a thermal effect through exp $[-(\beta_{11}h^2 + 2\beta_{12}hk + \cdots)]$ in the structure factor expression and b_i are reciprocal lattice vectors.

Can. J. Chem. Downloaded from www.nrcresearchpress.com by 210.87.254.40 on 09/05/12
For personal use only.

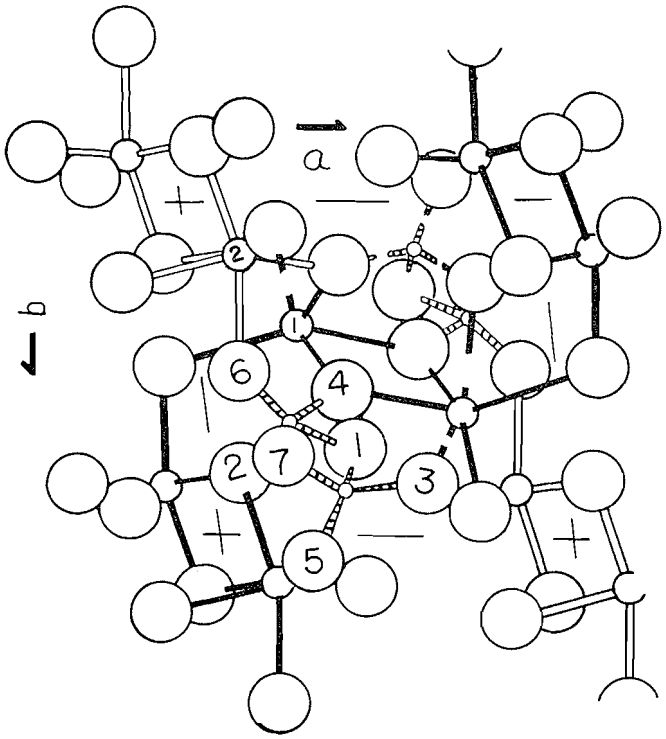

FIG. 1. The structure of $Cd_2P_2O_7$ projected down the *c* axis. The phosphorus atoms, cations, and oxygen atoms are shown as circles of progressively increasing size. The strong bonds between the cations and the oxygen atoms are shown as filled or open bonds. The bonding within the anion is shown cross-hatched.

lengths are larger (2.36 Å) than the average of the axial ones (2.29 Å). Site (2) has an irregular octahedral environment of oxygen atoms. The pertinent bond distances and angles for $Cd_2P_2O_7$ are shown in Table IV.

Cation (1) has two additional oxygen atoms, $O(\bar{2})$ and O(7), lying within 3.0 Å. $O(\bar{2})$ lies on the triangular face formed by $O(\bar{3})$, $O(\bar{5})$, and $O(\bar{6})$ while O(7) lies on the triangular face formed by O(4), O(6), and $O(\bar{4})$. Since these oxygen atoms lie about 0.5 Å beyond the first coordination sphere, they will be regarded as essentially unbonded to cation (1).

Each cation shares a pair of oxygen atoms across a center of symmetry forming groups conveniently called dimers. The O(2)–$O(\bar{2})$ edge is shared by cations of type 2, across the inversion center at 001/2 while the O(4)–$O(\bar{4})$ edge is shared by cations of type 1, across the inversion center at $\frac{1}{2}\ \frac{1}{2}\ \frac{1}{2}$. These dimeric groups are joined by sharing O(6) to form chains running parallel to the $(1\bar{1}0)$ face diagonal of the unit cell. The atoms in the chain are joined with filled bonds in Fig. 1. Parallel chains are bonded by corner sharing $O(\bar{3})$, O(3), $O(\bar{5})$, and O(5). The cations in this structure can be considered to form sheets involving M—O polyhedra with O(6) shared between sheets. These sheets, shown in Fig. 2, parallel the $\bar{1}10$ plane.

The anion, shown with cross-hatched bonds in Fig. 1, consists of two PO_4^{3-} tetrahedra sharing the oxygen atom, O(1). The two tetrahedra on a given anion deviate by 11° from an eclipsed orientation with the central oxygen atom as viewed along the P—P vector. O(3) and O(4) are the oxygen atoms most nearly coplanar with the P—O—P group. The P—O(—P) bond lengths are 1.65 and 1.60 Å on sides 1 and 2 of the anion, respectively. Since the estimated standard deviations for these bond lengths are of the order of 0.02 Å, one must regard these differences as not being significant. On the other hand, the difference between the inner and outer P—O bond lengths is significant. The average values are 1.51 Å on side 1 and 1.52 Å on side 2. One particular P—O short bond, 1.45 Å, involving O(7),

Can. J. Chem. Downloaded from www.nrcresearchpress.com by 210.87.254.40 on 09/05/12
For personal use only.

TABLE III

Observed and calculated structure factors of $Cd_2P_2O_7$

UNOBSERVED REFLECTIONS ARE MARKED WITH AN ASTERISK (*), AND UNRELLABLE REFLECTIONS WITH THE SYMBOL (@).

H	K	L = 0 FOBS	FCALC
0	1*	6	-3
0	2	57	-64
0	3	35	-36
0	4@	88	-112
0	5	14	14
0	6	84	84
0	7*	6	-2
0	8	31	29
0	9	24	-24
0	10	77	-65
0	11	20	18
0	12	24	21
0	13*	17	-9
0	14	18	19
1	9	66	-56
1	8	28	-25
1	7*	12	5
1	6*	12	0
1	5	84	86
1	4*	8	-0
1	3*	83	-106
1	2	13	-12
1	1	26	-28
1	0	28	27
-1	1	72	82
-1	2	22	-20
-1	3	13	-9
-1	4	17	-15
-1	5	47	-52
-1	6	75	80
-1	7	24	27
-1	8*	8	-8
-2	9	19	-23
-2	8	77	-76
-2	7	32	30
-2	6	13	14
-2	5	23	26
-2	4@	99	115
-2	3	84	-91
-2	2	68	-66
-2	1*	5	-1
-2	0	79	-92
-2	1	100	97
-2	2	88	99
-2	3	68	-76
-2	4*	10	-2
-2	5	37	-37
-2	6	58	-54
-2	7	73	72
-2	8	28	27
-3	8	17	-16
-3	7	49	-53
-3	6	15	17
-3	5	11	7
-3	4	15	12
-3	3	75	72
-3	2	61	-65
-3	1	17	-20
-3	0	7	-5
-3	1	30	-29
-3	2	93	87
-3	3	13	10
-3	4	47	-49
-3	5	49	-52
-3	6	47	-44
-3	7	16	14
-3	8	54	56
-4	8	27	27
-4	7	77	-80
-4	6	46	-44
-4	5	27	24
-4	4	21	-18
-4	3@	99	119
-4	2	47	50
-4	1	94	-104

H	K	L = 0 FOBS	FCALC
1	-6	35	-38
-1	8*	62	52
-1	6*	24	-8
1	-9	24	-23
1	12*	17	-3
1	10*	17	4
1	14*	16	-8
1	5	15	-14
2	14*	16	-7
2	13	25	26
2	12*	17	-0
2	11	39	-42
2	10	28	22
2	9	31	30
2	8	48	-47
2	7*	9	-3
2	6	30	33
2	5*	7	-0
2	4	6	-4
2	3	81	-96
2	2	29	-29
2	1	160	175
-2	1@	151	-177
-2	2	86	97
-2	3	55	61
-2	4	60	-62
-2	5	17	-16
-2	6*	9	-6
-2	7*	9	6
-2	8*	7	-0
-2	9	34	-32
-2	10*	21	7
-2	11*	15	12
-2	12*	17	-2
-2	13*	17	4
-2	14*	17	-3
-3	1	54	-52
-3	1	14	10
-3	2	19	17
-3	3	59	56
-3	4	31	-29
-3	5	49	-50
-3	6	38	48
-3	7*	9	-5
-3	8	36	-43
4	13*	17	-4
4	11*	25	21
4	11	19	18
4	10	24	24
4	9	40	-38
4	8*	9	-1
4	7	62	51
4	6*	9	-7
4	5*	22	-21
4	4	9	-6
4	3	101	113
-4	2	75	78
-4	3	88	-89
-4	4	11	11
-4	5	51	44
-4	6	9	-8
-4	7*	8	-6
5	11*	17	-8
5	14*	15	-5
5	13*	16	-6
5	12*	17	2

H	K	L = 0 FOBS	FCALC
10	-6*	17	0
10	-7*	17	-15
11	6	24	22
11	5	46	-45
11	4*	17	-9
11	3	67	60
11	2*	17	-11
11	1	26	-29
11	-1*	16	1
11	-2*	16	1
11	-3*	17	-0
11	-4*	17	-13
11	-5*	17	13
11	-6*	17	2
12	5*	17	8
12	4	19	20
12	3*	17	8
12	2*	17	-3
12	1	30	-29
12	-1	35	38
12	-2	35	-35
12	-3*	17	15
12	-4	35	38
12	-5*	17	-1
13	5*	17	-7
13	4	30	38
13	3*	17	-13
13	2	24	-32
13	1	21	21
13	-1*	17	-13
13	-2*	17	3
13	-3*	17	2
13	-4*	17	-1
13	-5*	17	-3
14	2*	17	-7
14	1*	17	10
14	-4*	17	-7

H	L	K = 0 FOBS	FCALC
1	-14	28	-23
1	-13*	14	-0
1	-12	20	19
1	-11*	14	3
1	-10*	17	-7
1	-9	39	-39
1	-8*	12	1
-1	-7	19	76
-1	6	44	-51
-1	5	113	-103
-1	4	94	87
-1	3	43	42
-1	-2	79	-87
-1	1*	5	-1
1	2	29	-33
1	3	64	-69
1	4	17	22
1	5	74	78
1	6	49	-54
1	7	56	-57
1	8	63	57
1	9	21	25
1	10	27	-29
1	11*	15	-12
1	12*	14	1
1	13*	13	10
1	14*	11	-4
2	-14	15	16
2	-13*	14	-10
2	-12	21	-25
2	-11	31	33
2	-10	19	22
2	-9	53	-53
2	-8	13	13
2	-7	60	54
2	-6	30	-35
2	-5	18	-19
2	-4	28	30

H	L	K = 0 FOBS	FCALC
6	-5	80	85
6	-4	46	-50
6	-3*	90	-100
6	-2	81	84
6	-1	26	30
6	1*	10	-2
6	2	16	-13
6	3	12	12
6	4	24	25
6	5	38	-36
6	6*	14	3
6	7	30	29
6	8	26	-28
6	9	15	-11
6	10	19	21
6	11*	11	1
6	12	13	-9
7	-17	11	14
7	-16*	13	-8
7	-15*	14	-4
7	-14*	14	3
7	-13*	15	7
7	-12	17	23
7	-11	29	-29
7	-10	43	-35
7	-9	69	64
7	-8	19	21
7	-7	64	-59
7	-6	25	24
7	-5	30	32
7	-4	23	-22
7	-3*	10	-1
7	-2*	10	-6
7	-1	17	16
7	1	56	-49
7	2	12	-12
7	3	38	69
7	4*	12	0
7	5	49	-51
7	6*	14	3
7	7	21	22
7	8*	14	0
7	9*	13	-8
7	10	12	-8
8	-17*	15	-2
8	-16	15	18
8	-15*	14	2
8	-14*	16	-33
8	-13*	13	6
8	-12	24	28
8	-11	28	-30
8	-10	14	-11
8	-9	37	33
8	-8*	12	0
8	-7	14	-13
8	-6	31	-29
8	-5*	11	-5
8	-4	60	67
8	-3	16	-15
8	-2	89	-83
8	-1	42	39
8	1	33	-32
8	2	18	-17
8	3	15	12
8	4*	14	3
8	5*	14	1
8	6*	14	-10
8	7*	14	1
8	8	21	20
8	9*	14	-6
9	-15*	13	-4
9	-14	24	-23
9	-13*	14	5
9	-12	21	18
9	-11	17	19
9	-10	17	-14
9	-9	46	-42
9	-8	37	31

H	L	K = 0 FOBS	FCALC
7	1	26	-24
7	2	56	53
9	1	21	23
9	-2*	17	8
8	-2*	16	10
7	-2	55	-56
6	-2	87	-85
5	-2	40	45
4	-2	70	85
3	-2	9	7
-2	-2	53	46
1	-2	45	-46
2	-2	12	-12
3	-2	115	104
4	-2	72	63
5	-2	48	-40
6	-2	62	-58
7	-2*	7	0
8	-2*	18	-3
9	-2	34	-39
9	-3	27	31
8	-3*	16	-9
7	-3*	14	-3
6	-3*	10	1
5	-3	54	-61
4	-3	105	-108
3	-3	13	12
2	-3*	100	111
1	-3	23	20
1	3	74	-76
2	3	18	22
3	3	10	9
4	3*	11	4
5	3	51	43
6	3	50	46
7	3*	18	-3
8	3	34	-35
9	3*	20	-6
9	-4	33	-31
8	-4	43	44
6	-4	30	29
5	-4*	10	-5
4	-4	41	-43
3	-4	37	-41
2	-4	111	-108
1	-4	30	-25
1	4	88	77
2	4	42	-38
3	4	106	-96
4	4	17	-18
5	4	20	21
6	4*	12	14
7	4*	19	10
8	4*	20	21
9	4*	20	16
8	-5*	16	3
7	-5	50	-48
6	-5	21	26
5	-5	120	119
4	-5	41	40
3	-5	31	-32
2	-5	20	-23
1	-5*	9	1
1	5	36	35
2	5*	11	-9
3	5	50	42
4	5*	16	-15
5	5	73	-65
6	5*	18	-9
7	5*	19	11
8	5*	20	3
8	-6	69	-61
7	-6	49	-46
6	-6*	14	8
5	-6	43	-44
4	-6*	13	1
3	-6	112	98
2	-6	56	55

H	L	K = 0 FOBS	FCALC
-8	3	21	-22
-9	3	17	18
-9	-4*	10	-4
-8	-4*	20	6
-7	-4*	19	8
-6	-4	38	-38
-5	-4	62	-58
-4	-4	17	15
-3	-4	65	63
-2	-4*	9	9
-1	-4	12	14
-1	4	30	-28
-2	4	117	112
-3	4	63	65
-4	4	58	-52
-5	4	67	-79
-6	4*	13	-5
-7	-4*	16	15
-8	-4	24	-27
-9	-4*	17	15
-7	-5*	21	-22
-6	-5*	18	10
-5	-5*	17	13
-4	-5*	16	-0
-3	-5	67	64
-2	-5*	35	37
-1	-5*	88	-85
-1	5*	9	3
-2	5	41	-44
-3	5	47	-43
-4	5	17	-17
-5	5	29	-29
-6	5	18	-20
-7	5	70	60
-8	5	56	46
-9	5	22	-22
-7	-6*	20	-2
-6	-6*	20	-6
-5	-6	59	57
-4	-6*	17	10
-3	-6	64	-65
-2	-6*	15	-12
-1	-6*	11	2
-1	6*	11	-10
-2	6	26	-21
-3	6	74	-65
-4	6*	17	2
-5	6	115	95
-6	6	45	44
-7	6	37	-35
-8	6*	17	4
-9	6*	18	12
-7	-7*	38	33
-6	-7*	20	-5
-5	-7*	19	-18
-4	-7*	19	-11
-3	-7	33	-34
-2	-7	18	-18
-1	-7	16	16
-1	7	43	-37
-2	7	17	20
-3	7	22	20
-4	7	95	87
-4	7*	41	23
-5	7	18	-21
-6	7	19	23
-7	7	27	-27
-8	7	71	-59
-8*	20	-3	
-5	-8	28	-31
-4	-8	20	-18
-3	-8	25	25
-2	-8	39	39
-1	-8	17	16
-1	8	42	39
-2	8*	16	-7
-3	8	19	12

H	L	K = 0 FOBS	FCALC
-2	3	16	-14
-1	3	102	-113
1	3	9	-4
2	3	45	36
3	3	18	-22
4	3	56	54
5	3	92	88
6	3	23	-25
7	3	23	-24
8	3	22	-5
9	3*	8	-18
10	3*	23	-6
-9	-3*	32	36
-8	-3*	21	2
-7	-3*	21	-12
-6	-3*	19	10
-5	-3	61	-60
-4	-3	50	-54
-3	-3	38	31
-2	-3*	13	3
-1	-3	10	13
1	-3	101	87
2	-3	14	-13
3	-3*	119	-125
4	-3	10	-8
5	-3	50	-54
6	-3	52	-41
7	-3*	16	-6
8	-3	94	79
9	-3	30	29
10	-3	33	-35
11	-3*	22	-18
-11	4	60	38
-10	4	21	21
-9	4	27	-26
-8	4*	33	-32
-7	4*	17	-6
-6	4	63	-65
-5	4	33	-28
-4	4	93	87
-3	4	30	39
-2	4	45	37
-1	4	61	69
1	4	68	73
2	4	77	79
3	4	13	11
4	4	22	25
5	4	24	27
6	4	22	23
7	4	52	54
8	4*	22	-4
9	4*	22	-31
10	4*	23	-6
-8	-4*	23	-11
-7	-4*	49	-52
-6	-4*	16	-13
-5	-4	23	27
-4	-4*	17	8
-3	-4*	18	6
-2	-4	78	73
-1	-4	54	55
1	-4	70	-79
2	-4	9	-9
3	-4	14	19
4	-4	64	-59
5	-4	111	13
6	-4	111	101
7	-4*	16	0
8	-4	24	-24
9	-4*	19	-6
10	-4	22	-22
11	-4*	22	-17
-9	5*	60	63
-8	5	40	44
-7	5	47	-42
-6	5	43	-37
-5	5*	12	-7
-4	5	57	-55

H	L	K = 0 FOBS	FCALC
-1	-7	76	74
1	-7*	14	-9
1	7*	14	0
3	-7	33	-33
4	-7	56	-58
5	-7	25	-22
6	-7	31	32
7	-7	20	22
8	-7*	17	7
10	-8	22	-21
9	-8	21	-21
8	-8	63	70
6	-8	12	11
7	-8	62	57
6	-8*	12	13
5	-8*	12	7
4	-8	27	29
3	-8	19	18
2	-8	54	43
1	-8	64	60
-1	-8*	13	15
-2	-8*	13	18
-3	-8	56	54
-4	-8	53	48
-5	-8*	15	-8
-6	-8*	15	-19
-7	-8*	15	-10
-8	-8	15	-7
-9	-8	64	57
-8	-9	45	43
-7	-9	19	9
-6	-9	19	-1
-5	-9	19	15
-4	-9	19	-10
-3	-9	19	-7
-2	-9	19	-26
-1	-9	14	-9
1	-9	60	-51
2	-9	13	-10
3	-9	32	15
4	-9	13	14
5	-9	13	14
6	-9	20	28
7	-9	13	12
8	-9	43	-40
-1	-9*	14	9
-2	-9*	14	-2
-3	-9*	15	-7
-4	-9*	15	-6
-5	-9*	15	16
-6	-9*	20	14
-7	-9*	20	8
-8	-9*	31	-30
-7	-9*	23	-32
-6	-9*	23	-24
-5	-9*	29	-34
-4	-10	21	22
-3	-10	22	21
-2	-10	21	19
-1	-10*	22	-6
1	-10*	23	-8
2	-10	23	-49
3	-10	43	-39
4	10	26	24

Can. J. Chem. Downloaded from www.nrcresearchpress.com by 210.87.254.40 on 09/05/12
For personal use only.

TABLE III (*concluded*)

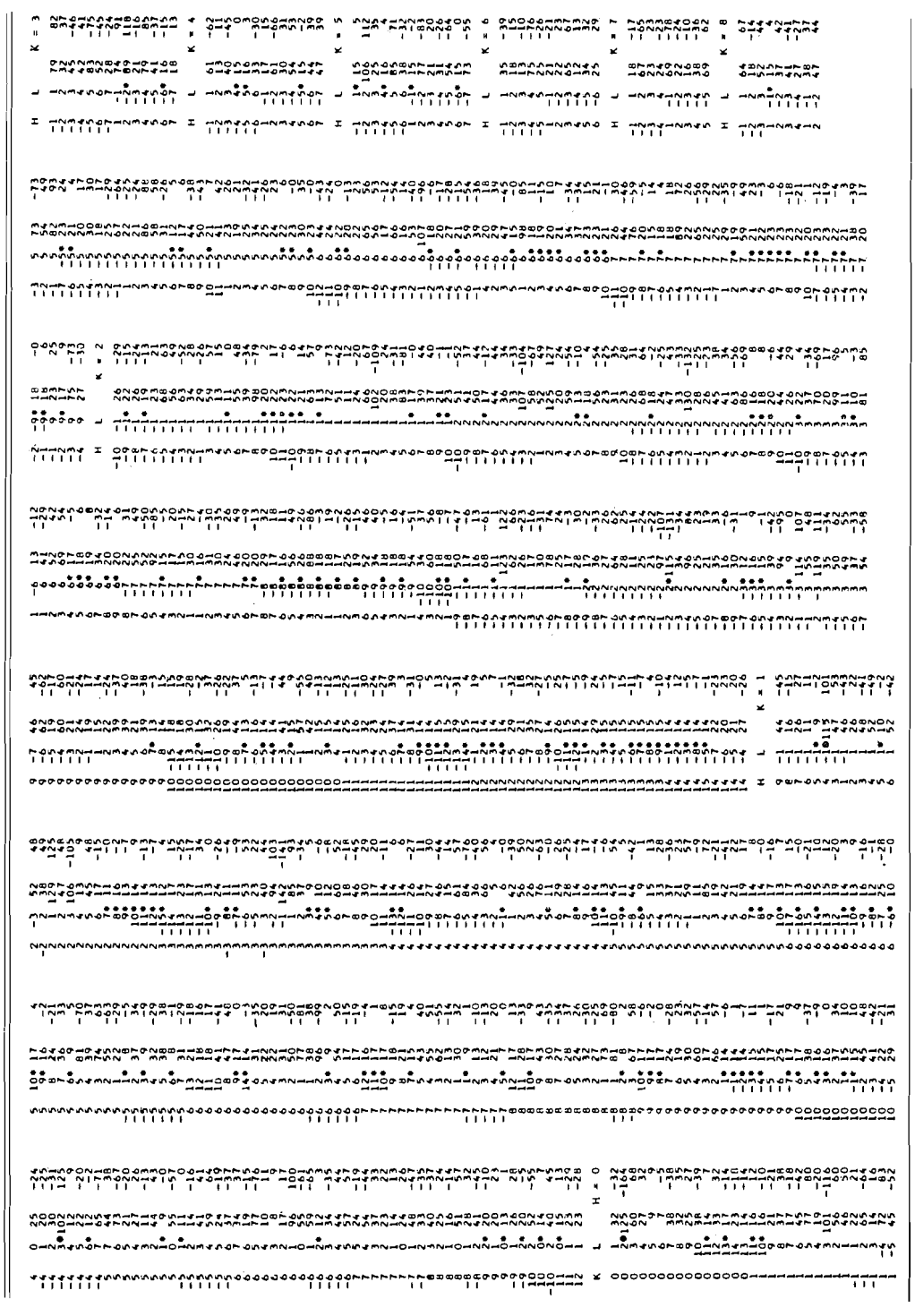

TABLE IV

Bond distances and angles for $Cd_2P_2O_7$*

a. Cd environment

Bond	Distance (Å)	Bonds	Angle (degrees)	Bonds	Angle (degrees)
Cd(1)—O(5)	2.301(15)	O(5)—Cd(1)—O(4)	158.8(3)	O(4)—Cd(1)—O($\bar{4}$)	80.6(4)
—O(4)	2.275(11)	—O($\bar{4}$)	94.5(5)	—O(6)	94.6(4)
—O($\bar{4}$)	2.313(12)	—O($\bar{3}$)	87.2(5)	O($\bar{4}$)—Cd(1)—O(6)	140.8(5)
—O($\bar{3}$)	2.410(16)	—O($\bar{6}$)	101.9(4)	O(7)—Cd(1)—O(5)	125.1(5)
—O($\bar{6}$)	2.368(12)	O($\bar{3}$)—Cd(1)—O(4)	74.0(5)	—O($\bar{3}$)	147.2(5)
—O($\bar{2}$)	2.881(15)	—O($\bar{4}$)	102.6(5)	—O(4)	73.3(5)
—O(7)	2.694(18)	—O(6)	113.4(5)	—O($\bar{4}$)	72.6(5)
		O(2)—Cd(1)—O(5)	78.7(5)	—O(6)	68.8(6)
		—O(3)	64.2(4)	—O(2)	122.0(5)
		—O(4)	100.9(4)	O(2)—Cd(1)—O(6)	53.9(4)
		—O($\bar{4}$)	165.2(3)		

Bond	Distance (Å)	Bonds	Angle (degrees)	Bonds	Angle (degrees)
Cd(2)—O(2)	2.339(10)	O(5)—Cd(2)—O($\bar{3}$)	112.0(5)	O($\bar{3}$)—Cd(2)—O(7)	162.3(5)
—O(5)	2.344(12)	—O(7)	84.7(5)	—O(2)	86.5(6)
—O(6)	2.297(17)	—O(2)	92.3(5)	—O($\bar{2}$)	74.8(5)
—O(7)	2.277(16)	—O($\bar{2}$)	164.7(8)	—O(6)	92.6(6)
—O($\bar{2}$)	2.248(15)	—O(6)	101.5(5)	O(7)—Cd(2)—O(2)	99.1(6)
—O($\bar{3}$)	2.336(17)	O(2)—Cd(2)—O($\bar{2}$)	74.2(5)	—O($\bar{2}$)	90.5(5)
		—O(6)	165.5(5)	—O(6)	77.8(6)
		O($\bar{2}$)—Cd(2)—O(6)	91.6(5)		

b. P_2O_7 group

Bond	Distance (Å)	Bonds	Angle (degrees)	Bonds	Angle (degrees)
P(1)—P(2)	2.972(5)	P(1)—O(1)—P(2)	132.3(7)		
P(1)—O(1)	1.645(14)	O(1)—P(1)—O(3)	102.9(7)	O(3)—P(1)—O(5)	113.1(9)
—O(3)	1.558(12)	—O(5)	105.0(7)	—O(7)	116.8(9)
—O(5)	1.516(16)	—O(7)	104.9(8)	O(5)—P(1)—O(7)	112.6(9)
—O(7)	1.449(19)				
O(1)—O(3)	2.505(16)				
—O(5)	2.508(20)				
—O(7)	2.456(23)				
O(3)—O(5)	2.564(17)				
—O(7)	2.562(21)				
O(5)—O(7)	2.466(25)				
P(2)—O(1)	1.605(11)	O(1)—P(2)—O(2)	110.1(7)	O(2)—P(2)—O(4)	114.6(8)
—O(2)	1.530(14)	—O(4)	104.0(6)	—O(6)	106.8(8)
—O(4)	1.548(13)	—O(6)	109.2(7)	O(4)—P(2)—O(6)	112.1(8)
—O(6)	1.488(18)				
O(1)—O(2)	2.570(13)				
—O(4)	2.484(17)				
—O(6)	2.522(19)				
O(2)—O(4)	2.591(18)				
—O(6)	2.424(23)				
O(4)—O(6)	2.519(21)				
O(2)—O(5)	3.312(17)				
O(3)—O(4)	3.668(20)				
O(6)—O(7)	3.107(19)				

*Estimated standard deviations in parentheses; atom O($\bar{n}$) is derived from O(n) by an inversion through a center of symmetry.

Can. J. Chem. Downloaded from www.nrcresearchpress.com by 210.87.254.40 on 09/05/12
For personal use only.

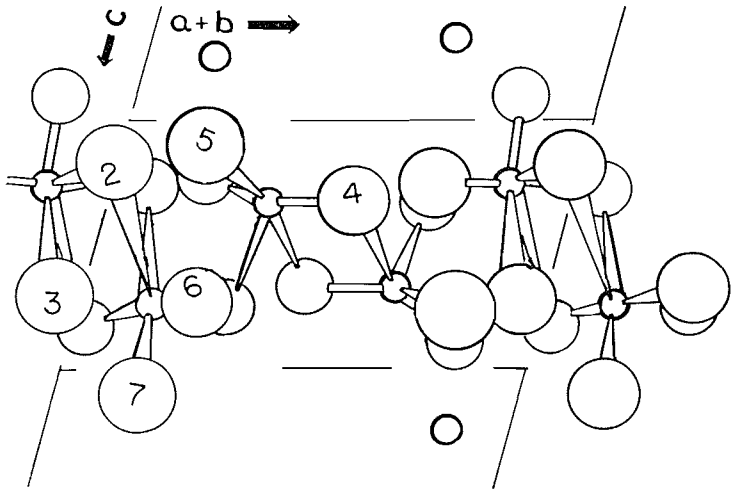

FIG. 2. The bonding near the cation–oxygen atom sheets is shown. The cations are shown as small circles and the anions as large ones. The bonding parallel to the sheet is shown.

involves the terminal oxygen atom ligated to only one cation.

The anion shares O(2) and O(6) from one end of the anion and O(5) and O(7) from the other end with one sheet of cations and O(6), O(4), and O(3) with the adjacent cation sheet. The O(2)—O(5) edge spanning across the two tetrahedra of the anion is shared with one of the cations of type 2. Otherwise, each oxygen atom ligated to a given cation arises from a different anion.

Discussion

The structure of $Cd_2P_2O_7$ differs substantially from that found for other divalent metal ion pyrophosphates although it bears some relationship, in terms of packing, to the $\beta Ca_2P_2O_7$ structure. The cation coordination numbers are the same as in $\alpha Mg_2P_2O_7$ (16) but there the anion has essentially a staggered configuration while in $Cd_2P_2O_7$ it is nearest to an eclipsed configuration. In all the $A_2B_2O_7$ compounds, where the B_2O_7 anion is formed by corner sharing of a pair of tetrahedra, the eclipsed anion configuration appears to be stabilized by having one of the cations sharing oxygen atoms across the anion. In $Cd_2P_2O_7$ this cation is Cd(2) while Cd(1) resides in interstices formed by the terminal oxygen atoms from five anions. It is therefore not unexpected that the solubility of other divalent ions into the two cation sites will differ markedly. In the electron paramagnetic resonance study of Mn^{2+} in $\alpha Sr_2P_2O_7$ (17) it appears that the ion with the larger radius prefers the site bonding across the anion. The occupancy of this site seems to be necessary in order to stabilize the eclipsed anion configuration since point charge calculation suggests about a 5 to 10% greater instability in an anion with the $\alpha Ca_2P_2O_7$ or $Cd_2P_2O_7$ structure over that found for $\alpha Cu_2P_2O_7$, $\alpha Mg_2P_2O_7$, or $\alpha Zn_2P_2O_7$.

The relationship between the $Cd_2P_2O_7$ and $\beta Ca_2P_2O_7$ structures and those of the alkali metal dichromates has been discussed (18). The basic structural unit consists of a pair of anions centrosymmetrically related in contact at the appropriate van der Waals distances. These anions, all in nearly eclipsed orientation, have their B—B vector inclined at about 60° to a plane consisting of these anions pairs at the corners of a pseudosquare. The various members of this series differ primarily in the nature of the packing of adjacent planes. The structure of $Cd_2P_2O_7$ is the simplest of the series and had been predicted by Brown (19) on the basis of his studies of the dichromate series.

The average Cd—O bond lengths found here, 2.33 and 2.31 Å, differ insignificantly from the 2.31 Å found in $Cd_2V_2O_7$ where all cations are octahedrally coordinated and the structure is analogous to thortveitite. The range of bond lengths in the latter case was from 2.24 to 2.39 Å as compared to 2.25 to 2.41 Å in $Cd_2P_2O_7$. The Cd—O bond in the second coordination sphere about cation site 1 in $Cd_2P_2O_7$ are reminiscent

Can. J. Chem. Downloaded from www.nrcresearchpress.com by 210.87.254.40 on 09/05/12
For personal use only.

of those found in $Cd_3(PO_4)$ (20). Here the nine independent cations all show five-fold coordination in the primary coordination sphere, but all cations save one have one additional oxygen atom lying between 2.5 and 3.0 Å. The five strong bonds have average values at each cation lying between 2.25 and 2.30 Å.

The errors on the P—O bonds are too high to make independent conclusions on the basis of this structure. However, in the low temperature phases of the pyrophosphates of Zn (21), Mg (2), and Cu (3), the phosphorus atom is displaced from the center of its tetrahedron toward the terminal oxygen atoms. In addition, when unrestricted by symmetry consideration, the anion becomes dissymmetric in the sense that the bridging PO bonds differ, with the larger bond length on that end of the anion having the shorter PO bond length. This short bond length is invariably related to that oxygen atom strongly bonded to only one cation. All these features also hold in $Cd_2P_2O_7$. In addition, one finds also that the tetrahedron involving the shorter bridging PO bond is the most regular. These results of course imply that the cations are significantly perturbing the π bonding system in the anion. Further, these pyrophosphate anions showing eclipsed configuration have smaller P—O—P bond angles, ranging from 130 to 138°, than are found for anions in the staggered configuration. In the latter case the range is 130 to 157°.

Acknowledgments

We express our gratitude to Dr. C. V. Stager for providing the results of his e.p.r. studies and we are grateful for the financial support of the Defence Research Board.

1. K. Lukaszewicz and R. Smajiewicz. Rocz. Chem. **35**, 741 (1961).
2. B. E. Robertson and C. Calvo. Acta Cryst. **22**, 665 (1967).
3. C. Calvo. Acta Cryst. **23**, 289 (1967).
4. C. Fowlis. Ph.D. Thesis, McMaster University, Hamilton, Ontario. 1969.
5. K. Lukaszewicz. Bull. Acad. Pol. Sci. Ser. Sci. Chim. **15**, 47 (1967).
6. B. E. Robertson. Ph.D. Thesis, McMaster University, Hamilton, Ontario. 1967.
7. C. Calvo. Inorg. Chem. **7**, 1345 (1968).
8. N. C. Webb. Acta Cryst. **21**, 942 (1966).
9. L. Hagman, I. Jansson, and C. Magnéli. Acta Chem. Scand. **22**, 1419 (1968).
10. D. W. J. Cruickshank, H. Lynton, and G. A. Barclay. Acta Cryst. **15**, 491 (1962).
11. P. K. L. Au and C. Calvo. Can. J. Chem. **45**, 2297 (1967).
12. D. J. Cromer and K. Herrington. J. Amer. Chem. Soc. **77**, 4708 (1955).
13. C. V. Stager. Private communication.
14. D. W. J. Cruickshank, D. E. Pelling, A. Bujosa, F. M. Louell, and M. R. Truter. *In* Computing methods and the phase problem in X-ray crystal analysis. *Edited by* R. Pepinsky, J. B. Robertson, and J. C. Speakman. The Pergamon Press, Ltd., New York. 1961.
15. International tables for X-ray crystallography. Vol. II. The Kynoch Press, Birmingham, England. 1951.
16. C. Calvo. Can. J. Chem. **43**, 1139 (1965).
17. C. Calvo, K. Y. Leung, and C. V. Stager. J. Chem. Phys. **49**, 3653 (1968).
18. I. D. Brown and C. Calvo. J. Solid State Chem. To be published.
19. I. D. Brown. Private communication.
20. J. S. Stephens. Ph.D. Thesis, McMaster University, Hamilton, Ontario. 1967.
21. B. E. Robertson and C. Calvo. J. Solid State Chem. In press.

Can. J. Chem. Downloaded from www.nrcresearchpress.com by 210.87.254.40 on 09/05/12
For personal use only.

Constitution of magnesium–indium alloys containing 23–100 atomic % indium[1]

K. M. PICKWICK[2], W. A. ALEXANDER, AND R. H. GAMBLE
Division of Applied Chemistry, National Research Council of Canada, Ottawa, Canada

Received February 3, 1969

A constitutional diagram for magnesium–indium alloys containing between 23.2 and 100 atomic % indium has been established using differential thermal analysis, electrical resistivity, and metallographic methods.

An intermediate solid solution, β, with a wide range of homogeneity, is formed peritectically from the liquid and α, the magnesium primary solid solution. It extends between 23 atomic % indium at 485.3 °C and 86 atomic % indium at 160.2 °C, where it is in equilibrium with γ, the indium primary solid solution. Magnesium has a limited solid solubility in indium of about 6 atomic %.

For alloys containing up to 50 atomic % indium, the derived constitutional diagram is in good agreement with that of a previous investigation (2). Two exceptions are noted: first, there is no evidence of a long period superlattice, β''' of the CuAu II type, and second, a reaction is observed involving a transition between the two ordered phases β′ and β″. For the indium-rich alloys no intermediate or ordered phase formation is observed.

The results have been discussed in terms of the existing phase diagrams.

Canadian Journal of Chemistry, 47, 3417 (1969)

Introduction

Phase relationships in the magnesium–indium system have been the subject of several investigations (1–6). Despite this attention there is disagreement in the literature concerning the form of the equilibrium diagram, especially for alloys containing more than 25% indium[3]. The constitutional diagram of Fig. 1 is derived from the thermal, metallographic, and X-ray diffraction studies of Raynor and co-authors (1–3). At relatively high temperatures alloys which contained more than 23.5% indium consisted of β, a homogeneous face-centered cubic solid solution. Initially the field was thought to extend across the diagram with a gradual transition, though without phase discontinuity, to γ, the face-centered tetragonal indium primary solid solution. A limit of homogeneity was established at 53.5% indium, and the γ solid solution was considered to be formed peritectically from β and the liquid at 333.5 °C (3). However, more recent work has shown single phase alloys beyond this limit (6).

Investigations of intermediate phase formation in the solid solution have revealed similar inconsistencies. Haucke (4) suggested that the system was analogous to that of magnesium–gallium, and contained four intermediate phases Mg_5In_2, Mg_2In, MgIn, and $MgIn_2$ or $MgIn_3$. Subsequently, Raynor (2) showed that the β phase transformed to give two complex phases which were designated β_1 and β_2. The β_1 phase was stable up to 335 °C in a composition range 23.5–25% indium, and the β_2 phase up to 298 °C within a very narrow homogeneity range at an approximate composition of 34.3% indium. The X-ray diffraction study of Schubert *et al.* (5) has since confirmed the existence of the orthorhombic Mg_5In_2 phase, and both β_1 and β_2 were indexed on the basis of a hexagonal unit cell, with compositions corresponding to Mg_3In and Mg_2In, respectively. They also reported two additional phases, Mg_2In_5 and $MgIn_5$, a result at variance with previous work, which had shown extensive solid solubility of magnesium in indium and no indication of intermediate phase formation (3).

Ordering of the β solid solution has been reported over a wide composition range (2, 3, 5, 6). Raynor (2) showed that in alloys containing up to 50% indium, the reactions were analogous to those occurring in the copper–gold system. Alloys containing less than about 35% indium formed β′, a cubic superlattice ($L1_2$ Cu_3Au Type) and β″, an ordered tetragonal structure ($L1_0$ CuAu Type I) for compositions up to 50% indium (8). Between the boundaries of the disordered β and the tetragonal β″, a phase of orthorhombic structure, β''' (CuAu Type II), was observed. Ino *et al.* (6) have questioned the

[1]NRCC No. 10 833.
[2]NRCC Postdoctorate Fellow 1964–1966. Present address: Physical Metallurgy Division, Department of Energy, Mines and Resources, Ottawa, Canada.
[3]Compositions are expressed in atomic % unless otherwise stated.

Can. J. Chem. Downloaded from www.nrcresearchpress.com by 210.87.254.5 on 09/05/12
For personal use only.

Can. J. Chem. Downloaded from www.nrcresearchpress.com by 210.87.254.5 on 09/05/12
For personal use only.

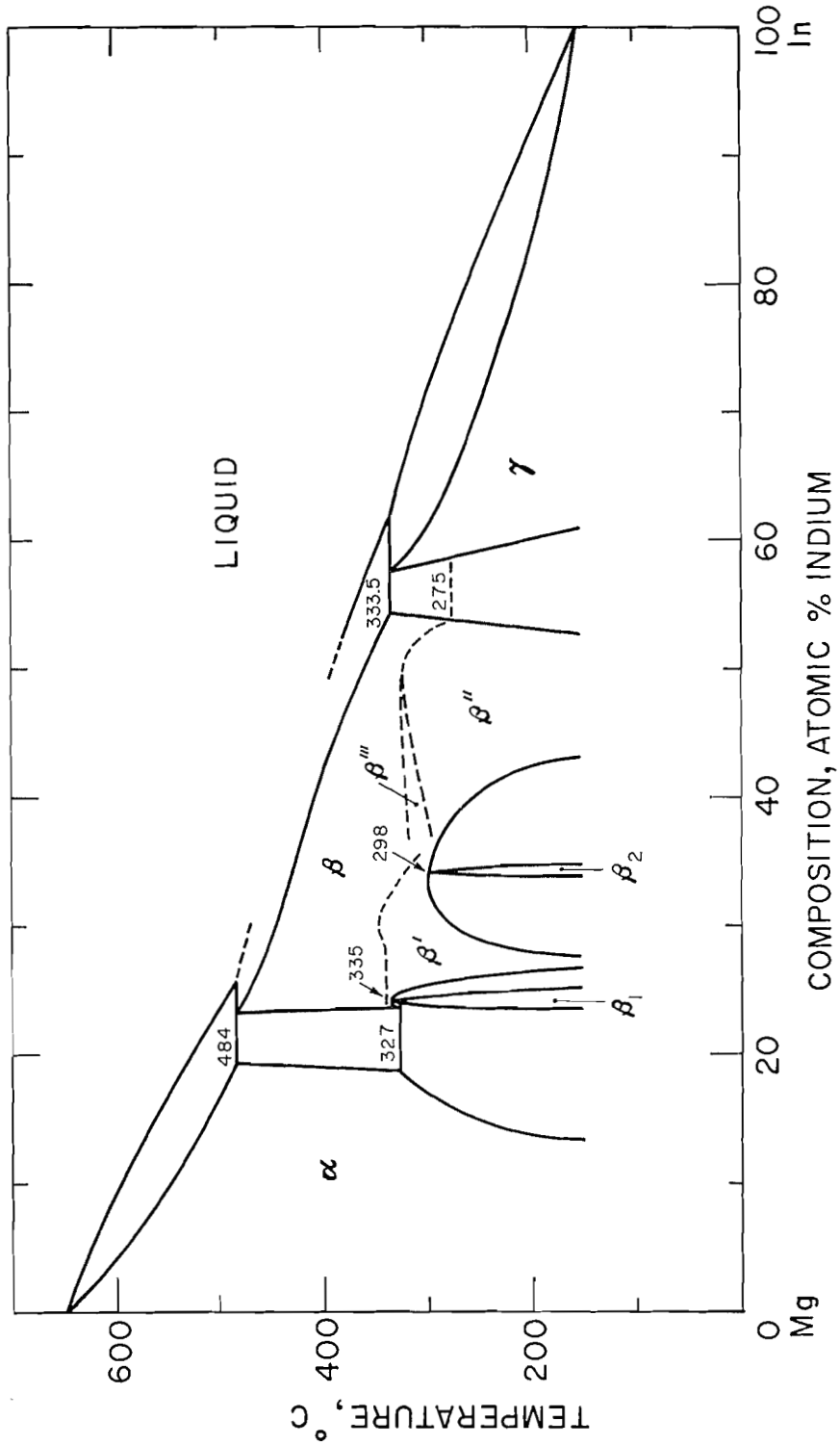

FIG. 1. Phase diagram of the Mg–In system according to (1, 2, 3).

Can. J. Chem. Downloaded from www.nrcresearchpress.com by 210.87.254.5 on 09/05/12
For personal use only.

existence of the β‴ phase in a study which came to the attention of the authors after completion of the present work. Schubert *et al.* (5) detected ordering of the Cu_3Au type near the composition Mg_2In_5 with partial ordering in alloys containing up to 86% indium.

In view of these contradictions, a further investigation of the constitution of magnesium–indium alloys containing more than 25% indium was considered worthwhile. The phase relationships have been studied using thermal, resistometric, and metallographic methods but excluded any X-ray examination of the alloys. Most phase designations used in the text follow those of Raynor (2).

Experimental Procedure

(a) Thermal Analysis

Heating and cooling curves for the 28 compositions investigated were obtained by a standard differential thermal analysis (d.t.a.) technique.

The magnesium used was a high purity distilled sample. Spectrographic analysis indicated copper as the major impurity at a level of less than 50 p.p.m. Other metals checked were: Ca, Al, Mn, Ni, Pb, Si, Sn, and Zn; all were less than 10 p.p.m. The indium used was the "Standard Grade" supplied by the Consolidated Mining and Smelting Co., with their typical analysis of major impurities: Cd, 40; Pb, 30; Sn, 20; Ni, 2; Cu, 1; and Tl, 1 p.p.m. and a claimed minimum purity of 99.97% In.

The alloys were formed from the constituent metals in a stainless steel vessel (7), which was mounted symmetrically with an inert reference specimen within a large cast iron block. The enclosure was initially evacuated, then filled with argon and maintained slightly above 1 atm. Alloy, reference, and differential temperatures were recorded at 2 s intervals by a Hartmann-Braun six-point recorder, at automatically controlled heating and cooling rates. The maximum sensitivity of the differential curve was ±0.02 °C, while that of the direct temperature was ±0.15 °C.

The liquidus/solidus temperatures were taken from the discontinuities in the differential temperature curves. Reliability was based on the reproducibility of the transition temperatures from at least 4 heating and cooling cycles, with rates between 0.5 and 1.0 °C per min. Calibration corrections were carried out for the measuring thermocouple Pt:Pt–13% Rh, during experimentation by comparison with a Cambridge vernier potentiometer and between experiments by standardization against the melting temperatures of pure lead, zinc, and tin.

The liquidus and peritectic arrest temperatures were reproducible to within ±0.1 °C. The absolute accuracy of the arrests is more difficult to estimate, though in consideration of the normal calibration corrections and the interpretation of the differential curves, errors of less than ±0.5 °C are probable. In the case of the solidus and ordering temperatures, the arrests are less distinct than for the liquidus, and additional errors result from their interpretation; thus they are considered correct to within ±1.0 °C.

After each series, the alloy was heated 50–100 °C above the liquidus temperature, and chill cast into a mould contained in a side arm of the vessel. Sections were taken from the top and bottom of the ingot, and analyzed for indium. The compositions of the ingots are listed in Table I*a*.

(b) Electrical Resistivity

Five alloys, R 2, 4, 5, 6, and 7, (Table I*b*), were prepared by melting high purity magnesium and indium in a stainless steel crucible under an atmosphere of purified argon. The magnesium used was the same material mentioned above, but purified by an additional fractional distillation step. The indium used was from the same

TABLE I

a Chemical composition of the thermal analysis alloys

Alloy number	Ingot analysis (wt. % In) Top	Bottom	Average composition (atomic % In)
TA 1	58.84	58.78	23.2
TA 2	60.40	60.18	24.3
TA 3	60.94	60.92	24.8
TA 4	61.75	61.65	25.5
TA 5	63.67	63.93	27.1
TA 6	67.07	67.10	30.2
TA 7	67.66	67.73	30.7
TA 8	68.28	68.14	31.3
TA 9	72.24	72.11	35.5
TA 10	72.64	72.94	36.2
TA 11	75.56	75.42	39.5
TA 12	76.97	77.05	41.5
TA 13	78.40	78.53	43.5
TA 14	80.18	80.13	46.1
TA 15	83.33	83.22	51.4
TA 16	83.58	84.08	52.3
TA 17	84.87	85.04	54.4
TA 18	86.97	86.99	58.6
TA 19	87.35	87.63	59.9
TA 20	88.82	88.87	62.7
TA 21	89.26	88.83	63.2
TA 22	91.41	91.46	69.3
TA 23	93.36	92.90	74.4
TA 24	94.87	95.06	80.1
TA 25	95.99	96.42	84.3
TA 26	97.41	97.43	88.9
TA 27	99.00	99.06	95.6
TA 28	Pure indium		

b Chemical composition of the electrical resistivity specimens

Alloy number	Ingot analysis (wt. % In) Top	Bottom	Average composition (atomic % In)
R 1	60.94	60.92	24.8
R 2	64.71	64.46	27.9
R 3	72.24	72.11	35.5
R 4	73.60	73.60	37.1
R 5	75.90	75.79	40.0
R 6	81.53	81.59	48.7
R 7	83.94	84.15	52.8

Can. J. Chem. Downloaded from www.nrcresearchpress.com by 210.87.254.5 on 09/05/12
For personal use only.

supplier as above, but of the "59 Grade", claimed to be at least 99.999% pure. The impurities listed by the supplier are: Pb 2.0, Cd 1.0, Tl 1.0, Cu 1.0, and Sn 1.0 p.p.m. In addition, two specimens, R 1 and 3, of critical composition, were taken from the chill castings of the thermal analysis work. Alloy R 3 was used primarily to study the precipitation of the β_2 phase. The alloys were sealed in evacuated Pyrex tubes, homogenized for 14 days at a temperature between 325–375 °C depending on composition, and then hot extruded in a modified laboratory press to wire of 0.056 in. diameter. An attempt was made at all stages of processing to minimize atmospheric corrosion, which was particularly severe in the alloys of higher indium content. Specimens were stored in evacuated glass tubes and heat treated either under argon or dynamic vacuum ($< 10^{-3}$ Torr).

The resistance was measured using a standard d.c. potential difference comparison method with both temperature and resistance being recorded continuously during the following heat treatments:

(*i*) Slow heating and cooling through the temperature range of the order–disorder transformation.

(*ii*) Annealing to reach equilibrium conditions at various temperatures over a similar temperature range. The specimens were initially homogenized in the disordered condition at 50 °C above T_c, the critical ordering temperatures, determined in (*i*) above. Starting with the disordered specimen, measurements of resistivity were taken by establishing equilibrium at successively lower temperatures, and then similarly for increasing temperatures. The increment between readings was varied from 2 °C close to T_c up to 20 °C for the less critical points on the curve.

(*iii*) Isothermal annealing at temperatures below T_c in specimens quenched from the disordered region.

Chromel–alumel thermocouples were spot welded to the specimens, and over the length between the potential probes (about 10 cm) the temperature variation was less than ±0.25 °C. Errors in the resistivity values were estimated to be less than ±0.03% due to current instability, ±0.25% in the measurement of specimen dimensions, ±0.5% due to temperature measurement, and ±0.5% due to furnace temperature control. The values are reported with errors of less than 3.0%, but may be considered as apparent resistivities, since no correction has been made for thermal expansion of the wires during testing.

(c) Metallography

Metallographic examination of selected alloys was carried out to confirm the phase transformations and locate the intermediate phase boundaries. Following the heat treatments shown in Table III, sections were mounted and polished using conventional techniques. The microstructures were readily revealed by etching with either alcoholic nitric or picric acids, although considerable difficulty was encountered in preserving the surfaces for photomicrography. Conclusive results could not be obtained for alloys containing more than about 60% indium due to this rapid surface deterioration both during and after polishing.

Results and Discussion

The constitutional diagram derived from the heating and cooling curves of the 28 alloys of the thermal analysis study is shown in Fig. 2. Included in the diagram and indicated according to the symbols of the key are confirmatory points from the resistometric and metallographic investigations. The derived diagram does not conform to any one of the previous investigations (2–6). Up to 50% indium, the results are in general agreement with those of Raynor (2), but compare more favorably with the work of Schubert *et al.* (5) beyond this point. For convenience the system can be discussed in terms of three distinct regions, namely, the liquidus/solidus, the ordering reactions, and the intermediate phase formation.

Liquidus/Solidus Region

The β solid solution forms peritectically from the liquid and α, the magnesium primary solid solution. A peritectic horizontal was located from the cooling curves of alloys TA 1 (23.2% In) and TA 2 (24.3% In) at a temperature of about 485.3 °C (Table II). This compares favorably with the previous determination of 484 °C (2), though there are certain differences in the compositional limits of the reaction. Alloy TA 3 (24.8% In) shows only a liquidus arrest at 484.8 °C on cooling and a solidus arrest on heating. The indium-rich limit of the peritectic lies in the region of 24.8% indium compared with Raynor's (2) value of 25.7%. The position of the invariant point at which β decomposes to form α and liquid was determined by extrapolation of the solidus to the peritectic horizontal, and lies in the vicinity of 23% indium.

The alloy compositions for the diagram were taken as the mean of the chemical analyses of the ingot sections following chill casting. There was excellent agreement between the two samples (Table I*a* and *b*) with a maximum variation of 0.5 wt. % (0.8 atm. %) at the composition of TA 16 (52.3%).

The β phase was found to extend beyond the homogeneity limits of Graham and Raynor (3). In alloys containing more than 24.8% indium, single liquidus and solidus arrests were observed up to 84.3% indium. Subsequent microstructural examination of quenched β phase alloys confirmed that the solid solution was continuous at least up to the composition of alloy TA 19 (59.9% In). The β-phase alloys showed the equiaxed grain structure of a normal solid solution, but without the twinning characteristic

Can. J. Chem. Downloaded from www.nrcresearchpress.com by 210.87.254.5 on 09/05/12
For personal use only.

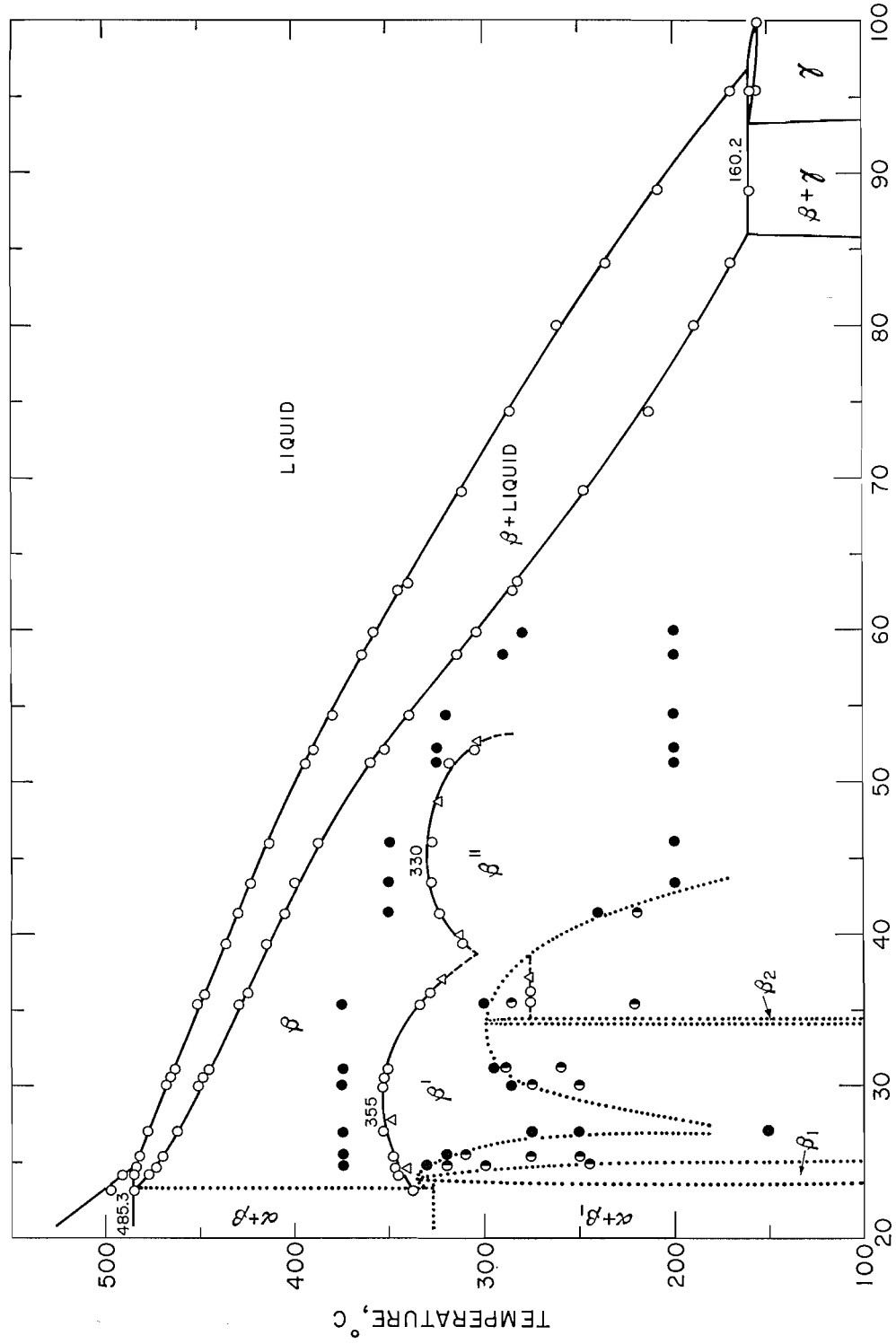

FIG. 2. Derived phase diagram of the Mg–In system. The dotted phase boundaries for the β_1, $\beta_1 + \beta'$, $\beta' + \beta_2$, β_2 and $\beta_2 + \beta''$ phase fields are taken from the diagram of ref. 2; ○, arrests on d.t.a. heating and cooling curves; ●, homogeneous single phase alloys by metallography; ◑, two-phase alloys by metallography; △, transitions on resistivity curves.

TABLE II

Transformation temperatures from the thermal analysis curves

Alloy	Composition (Atomic % In)	Liquidus	Peritectic	Solidus	T_c ordering
1	23.2	497.4	485.3		338.1
2	24.3	491.8	485.3	477.2	346.4
3	24.8	484.8		473.9	347.9
4	25.5	482.8		470.1	348.3
5	27.1	477.9		462.5	354.0
6	30.2	468.1		450.8	353.7
7	30.7	465.4		448.7	353.0
8	31.3	464.0		444.8	350.9
9	35.5	451.4		429.9	334.8
10	36.2	447.4		425.1	329.0
11	39.5	436.7		414.7	312.2
12	41.5	430.5		405.5	323.3
13	43.5	423.4		400.2	328.1
14	46.1	413.4		387.9	327.2
15	51.4	394.4		359.8	318.7
16	52.3	390.0		353.1	305.5
17	54.4	380.2		340.2	
18	58.6	364.3		314.9	
19	59.9	358.6		305.0	
20	62.7	345.9		285.1	
21	63.2	340.1		282.6	
22	69.3	312.1		247.4	
23	74.4	286.8		213.5	
24	80.1	261.8		189.5	
25	84.3	236.5		170.5	
26	88.9	208.8	160.0		
27	95.6	170.1	160.4	158.0	
28	pure indium	156.3 — single arrest			

of the β′ and β″ ordered solutions. Some difficulty was experienced in observing the microstructures beyond this point and the extension of the β phase field across the composition range of alloys TA 20–25 (62.7–84.3% In) could be shown only from the thermal analysis curves. Therefore, smooth curves are drawn to represent the liquidus between 24.8% indium at 485.3 °C and about 97% indium at 160.2 °C, and the solidus between 23% indium at 485.3 °C and about 86% indium at 160.2 °C (Table II, Fig. 2). In view of the wide temperature range of crystallization for the indium-rich alloys, particular care was taken to ensure alloy homogeneity prior to determining the liquidus and solidus arrests. For the former, the melt was stirred continuously until the arrest was well established, and for the latter, observations were made on heating following a homogenization anneal just below the solidus temperatures. In most cases the discontinuities in the differential temperature curves could be easily interpreted, although special care was required with the solidus arrests for the more indium-rich compositions. The results, however, were reproducible throughout the heating and cooling cycles. Oxidation was considered negligible and both the appearance of the ingot and subsequent micro-examination confirmed this conclusion.

The results for the indium-rich alloys suggest that the β phase comes into equilibrium with the γ indium primary solid solution in the region of 86% indium. Alloy TA 26 (88.9% In) showed a liquidus arrest at 208.8 °C on cooling, followed by a distinct constant temperature evolution of heat at 160.0 °C; no solidus arrest was observed on reheating. At 95.6% indium a liquidus and a constant temperature arrest were observed at 180.0 and 160.4 °C, respectively, and a solidus arrest on heating at 158.0 °C. The peritectic horizontal and solidus arrests were small in both magnitude and duration, but were completely reproducible. Thus, despite the limited number of alloys investigated for this concentration range, the thermal analysis curves are consistent with the peritectic formation of the indium primary solid solution from the β solid solution and the liquid. A two phase region, β + γ, which must therefore be present between about 86 and 94% indium, could not be definitely confirmed from the metallographic studies. This indication of a

Can. J. Chem. Downloaded from www.nrcresearchpress.com by 210.87.254.5 on 09/05/12
For personal use only.

Can. J. Chem. Downloaded from www.nrcresearchpress.com by 210.87.254.5 on 09/05/12
For personal use only.

limited solubility of magnesium in indium is in general agreement with the results of Schubert *et al.* (5), and similarly with respect to the two-phase field limits.

The liquidus and solidus curves are clearly inconsistent with either the formation of a Mg_5In_2 phase (4) or a peritectic reaction in the vicinity of 53.5–63% indium (3). Regarding the former, the present results show that a phase Mg_5In_2 cannot be formed from the melt as for Mg_5Ga_2, and it must be assumed that if a phase of this composition does exist it must form as a result of a lower temperature transformation. For the latter, the curves run smoothly across that particular composition range. Furthermore, metallographic examination of alloys TA 17 (54.4% In), 18 (58.6% In), and 19 (59.9% In) revealed single phase microstructures, which, in agreement with the thermal analysis, suggests that the β phase is continuous between the points at which it enters into equilibrium with α and with γ, the respective primary solid solutions.

Ordering Reactions

The transformation curve for ordering of the β solid solution is shown in Fig. 2, the critical ordering temperatures (T_c) being taken from both the resistivity/temperature curves of Fig. 3 (*a*, *b*, and *c*) and the thermal analysis heating curves. The results from each technique are fully consistent, with the exception of the T_c values for R 1 and R 2, which are somewhat low. Identical values of T_c were obtained from both the equilibrium and non-equilibrium (slow heating or cooling) resistivity curves. In contrast to Raynor's X-ray diffraction studies, only two ordered phases were detected, namely, β′ for alloys containing up to about 39% indium and β″ for those richer in indium. The transition between the β′ and β″ phases is discussed below. In the region of the β″ reaction, nonequilibrium thermal and resistometric curves showed only a single discontinuity due to the $\beta \rightarrow \beta''$ transformation. Extensive annealing of alloys at subcritical temperatures failed to reveal the $\beta''' \rightarrow \beta''$ orthorhombic/tetragonal transition suggested by Raynor (2), though it is reasonable to assume that such a transition would, from consideration of the crystallographic change, involve a distinct resistivity and specific heat anomaly. Ino *et al.* (6) also failed to find any evidence of the existence of a β‴ phase. Above about 125 °C, the cooling curves of the thermal analysis study show no indication of an ordered phase at the composition Mg_2In_5.

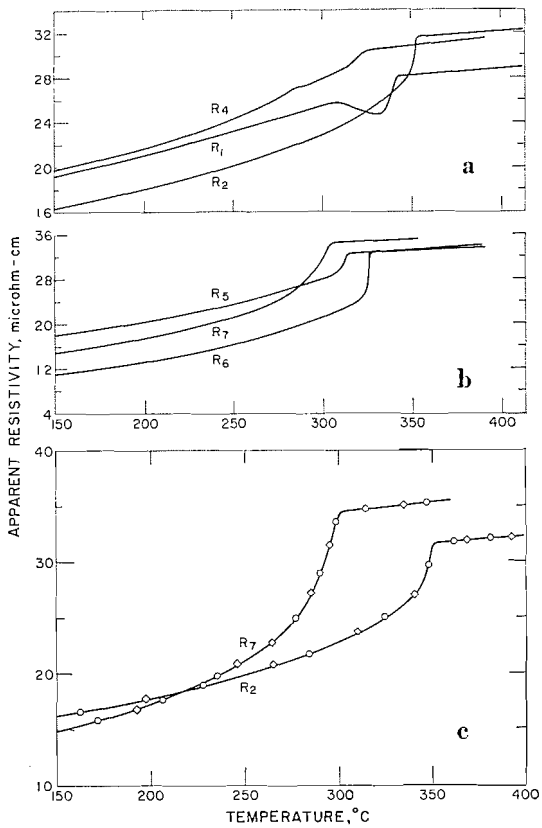

FIG. 3. The variation of apparent resistivity of the specimens with temperature under conditions of continuous heating: (*a*) alloys R 1 (24.8% In), R 2 (27.9% In), and R 4 (37.1% In); (*b*) alloys R 5 (40.0% In), R 6 (48.7% In), and R 7 (52.8% In); and under equilibrium conditions, (*c*) alloys R 2 (27.9% In) and R 7 52.8% In): ○, heating; ◇, cooling.

Simple theoretical calculations usually indicate that there should be a maximum in the ordering transformation curve at or near the stoichiometric composition. For the β′ ordering reaction there is an ill-defined maximum in the region of 29% indium and similarly for β″ near the equiatomic composition. In the latter case the available T_c values favor location of the maximum at a nonstoichiometric composition in the region of 47% indium. Alloys at the compositions of these maxima also exhibited maximum values of electrical conductivity measured at the ambient temperature and maximum heats of transformation (peak area) in the d.t.a. curves. Nonstoichiometric maxima for T_c have been observed

Can. J. Chem. Downloaded from www.nrcresearchpress.com by 210.87.254.5 on 09/05/12
For personal use only.

by Raynor (2) for Mg_3In in the present system and in others such as CuPd, Cu_3Pd, CuPt (8), and Pt_2Mo (9). Hirabayashi *et al.* (10) also found from specific heat measurements that the maximum transformation temperature for MgIn was 328 °C at somewhat less than 50% In. It has also been confirmed by the present work that the T_c maximum coincides with a range of composition where the β′ phase is stable at relatively low temperatures (11).

Some contradictory evidence was found concerning the order of reaction for the formation of β′ and β″ and consequently concerning their representation in the constitutional diagram. Empirically, it appears that ordering changes involving a transformation of the close packed lattice, such as $A1$ (β) → $L1_2$ (β′) and $L1_0$ (β″) (2, 5, 6), occur by a first order reaction, and are second order for all others (13). The former predicts a discontinuous change of order: isothermally at the point of univariant equilibrium and over a range of temperature for bivariant conditions. At compositions close to the β′ and β″ maxima, the major part of the ordering or disordering process was in fact completed within a very small temperature range, approxi-

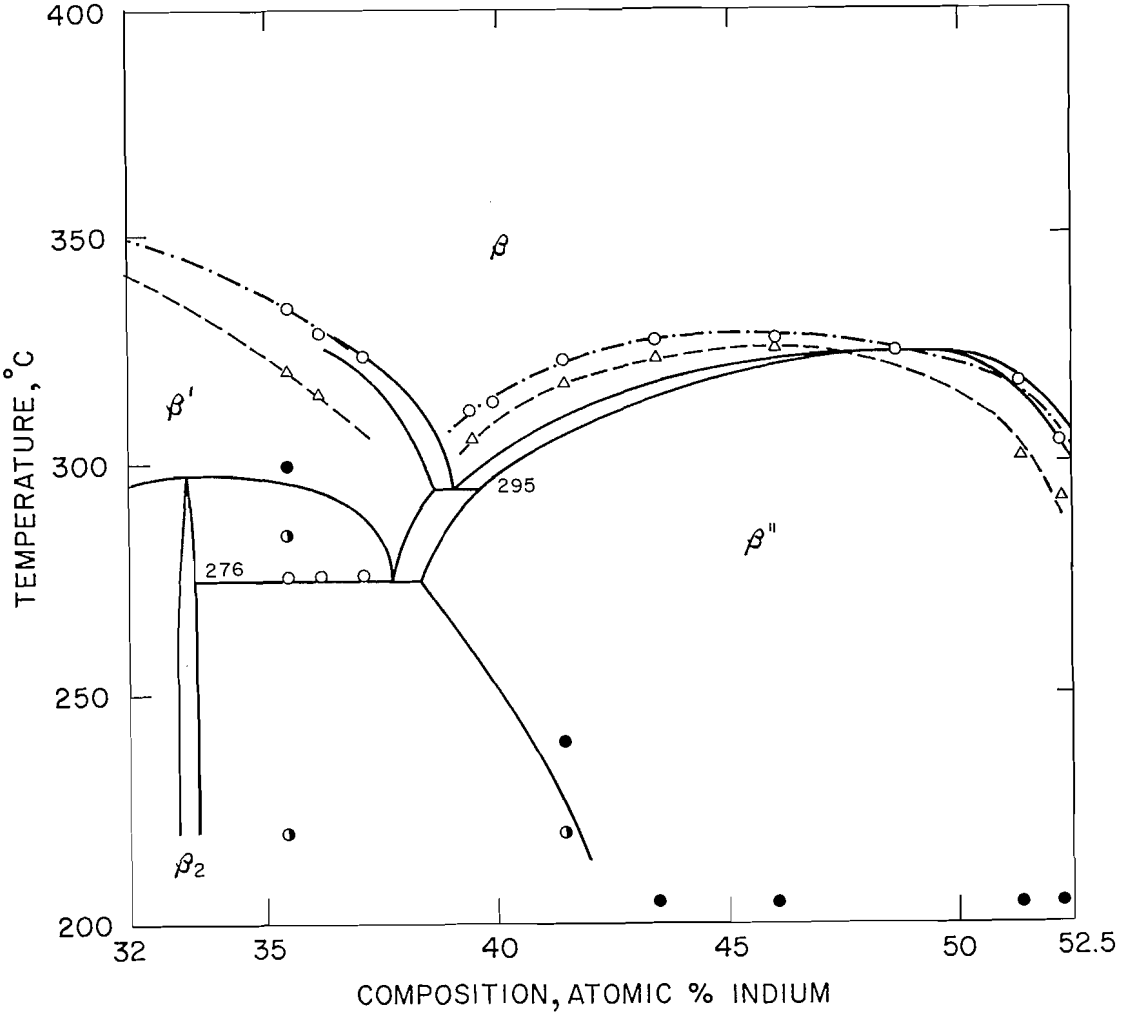

FIG. 4. A comparison of present results with the partial phase diagram proposed by Ino *et al.* (6), which is represented by the solid lines; ○, critical ordering temperatures; △, temperature of disordering from d.t.a. heating curves; ●, homogeneous single-phase alloys by metallography; and ◑, two-phase alloys by metallography.

Can. J. Chem. Downloaded from www.nrcresearchpress.com by 210.87.254.5 on 09/05/12
For personal use only.

mately 2 °C, but over a considerably wider range on either side of the maxima. This has been shown in Fig. 4 for the $\beta \rightarrow \beta''$ transformation only, where the lower broken line corresponds to points on the d.t.a. heating curves at which significant disordering was detected. Similarly, in the resistivity curves the alloys closest to the T_c maxima, namely R 2 and R 6, (Fig. 3*a* and *b*) show a large and almost discontinuous change of resistivity compared with the more continuous variation of the others. These effects are not due to any variation in reaction rate[4], since both β' and β'' order very rapidly in the composition range of R 1–7. A similar widening of the transformation zone about the composition of the T_c maximum was observed by Ino *et al.* (6) and by Hirabayashi *et al.* (10) for β'' alloys, and was explained in terms of the coexistence of ordered and disordered phases. This conforms with accepted first order reaction characteristics (12–14). However, the equilibrium resistivity curves of alloys R 2 and 7 in Fig. 3*c*, which have compositions in the range of the indicated $\beta + \beta'$ and $\beta + \beta''$ phase regions, respectively, show no sharp discontinuities below T_c due to such two-phase boundaries. Clearly, if ordered and disordered phases are in equilibrium, the range must extend over a very small temperature interval and considerably less than that indicated by the peak widths of the d.t.a. curves. In the absence of unequivocal evidence, the ordering reactions have been represented in Fig. 2 by a single line, showing only the variation of T_c with composition.

Intermediate Phases

Intermediate phase formation was investigated with respect to the system of Fig. 1 and the phase boundaries located by the metallographic examination of several critical alloys. The results shown in Figs. 2 and 4 are clearly in agreement with the boundaries and relationships determined by Raynor (2), with the exception of the β_2 + ordered β phase field on the high indium side. We find a series of arrests at 276 °C in this region which Raynor does not show. Resistivity and thermal measurements could not be used due to the prohibitively long times for the precipitation of the β_1 or β_2 phases from the ordered solid solution at temperatures close to those of the equilibrium phase boundaries. Following the heat treatments of Table III, the microstructures were easily developed using the alcoholic nitric or picric acid etchants. In contrast to the β_1 and β_2 phases, both β' and β'' exhibited characteristic twinning (2), although the main identifying feature was the selective etching of the constituent phases. In the two-phase alloys $\beta_1 + \beta'$ and $\beta' + \beta_2$, the second phase was essentially grain boundary nucleated and formed in proportions approximating to the existing diagram. Between the $\beta'/\beta_1 + \beta'$ and $\beta'/\beta' + \beta_2$ boundaries, in the region of alloy TA 5 (27.1% In) the β' phase was stable at temperatures below 200 °C. The microstructure was unchanged following annealing for times up to 21 days at 150 °C. It is interesting to note that this composition range coincides with Schubert's Mg_5In_2 phase. In addition to the metallographic evidence, resistivity curves of a both slowly cooled and equilibrated alloy, R 2 (27.9% In), Fig. 3*c*, gave no indication of a phase transformation. Thus we have found no evidence for the existence of the Mg_5In_2 phase. The exact composition of β_2 was not determined, although it has been located within a very narrow homogeneity range at Mg_2In (5, 6), which is a slightly lower indium content than the results of Raynor at 34.3% In in Fig. 2. For the β_2 + ordered β phase alloys, discontinuities at 276 °C were observed in the d.t.a. heating curves and also in the resistivity curve of R 4 (37.1% In), Fig. 3*a*. The arrest at 276 °C was essentially independent of composition between 35.5–37.1% indium, and corresponds to the eutectoid horizontal of Ino's diagram (Fig. 4). Subsequent examination of the microstructure of alloy TA 9 (35.5% In) quenched from 320 °C and annealed at 220 °C showed that β_2 precipitation had occurred by a cellular or discontinuous growth. Above 276 °C, the temperature of the arrest, the intermediate phase was precipitated preferentially in the grain boundaries as in the $\beta_1 + \beta'$ and $\beta' + \beta_2$ phase fields. Alloys containing between 32 and 52.5% indium have been investigated by Ino *et al.* (6) and our results agree with their diagram (Fig. 4). The two-phase regions $\beta + \beta'$, $\beta + \beta''$, and $\beta' + \beta''$ in their diagram were based on nonequilibrium thermal curves, and were inferred from the variation of specific heat peak width with composition. A similar effect was shown in the d.t.a.

[4]K. M. Pickwick and W. A. Alexander. J. Less-Common Metals. In press.

TABLE III

Heat treatments to locate the intermediate phase boundaries

Alloy	Composition (Atomic % In)	Homogenization treatment		Annealing treatment		Microstructure
TA 3	24.8	14 days	375 °C	9 days	330 °C	β′
				9 days	320 °C	β′+some β_1
				7 days	300 °C	β′+β_1
				7 days	245 °C	β_1+some β′
TA 4	25.5	14 days	375 °C	9 days	320 °C	β′
				9 days	310 °C	β′+some β_1
				7 days	275 °C	β′+β_1
				7 days	250 °C	β_1+some β′
TA 5	27.1	14 days	375 °C	7 days	275 °C	β′
				7 days	250 °C	β′
				21 days	150 °C	β′
TA 6	30.2	14 days	375 °C	8 days	285 °C	β′
				8 days	275 °C	β′+some β_2
				8 days	250 °C	β′+β_2
TA 8	31.3	14 days	375 °C	10 days	295 °C	β′
				10 days	290 °C	β′+some β_2
				8 days	260 °C	β′+β_2
TA 9	35.5	14 days	375 °C	12 days	300 °C	β′
				12 days	285 °C	β′+some β_2
				7 days	220 °C	β_2+some β″
TA 12	41.5	14 days	350 °C	12 days	240 °C	β″
				12 days	220 °C	β″+some β_2
TA 13	43.5	14 days	350 °C	21 days	200 °C	β″
TA 14	46.1	14 days	350 °C	21 days	200 °C	β″
TA 15	51.4	14 days	325 °C	21 days	200 °C	β″
TA 16	52.3	14 days	325 °C	21 days	200 °C	β″
TA 17	54.4	14 days	320 °C	21 days	200 °C	β″
TA 18	58.6	14 days	290 °C	21 days	200 °C	β
TA 19	59.9	14 days	280 °C	21 days	200 °C	β

curves of the present work, although it could not be definitely associated with the coexistence of the ordered and disordered phases. Of the two eutectoidal reactions, the $\beta'' + \beta' \rightleftarrows \beta$ could not be confirmed experimentally, but the cellular nature of the decomposition products in alloys TA 9 (35.5% In) and TA 10 (36.2% In) was most probably due to that of $\beta'' + \beta_2 \rightleftarrows \beta'$, at 276 °C. Provided that the two phase regions between β, β′, and β″ do exist, then Fig. 4 represents a probable form of the constitutional diagram.

Addendum

Since the above work was completed and prepared for publication, a paper by Hiraga, Koiwa, and Hirabayashi (15) has come to our attention, in which an investigation of the indium-rich part of the system is reported. Their results approximately confirm our data beyond about 85% In, although the peritectic formation of the indium primary solid solution involves an intermediate solid solution, γ, not β. In this respect they appear to have equated Graham and Raynor's γ phase, which was in fact the face-centered tetragonal indium primary solid solution in the reaction β + liquid $\rightleftharpoons$ γ (3), with their face-centered cubic intermediate solid solution, also designated γ. No experimental evidence is presented to justify the inclusion of this peritectic reaction. The nature of our apparatus made extension of the cooling curves below about 125 °C prohibitive, hence we did not investigate the ordered γ′ range of Hiraga's work.

Acknowledgments

The authors wish to acknowledge the assistance of Mr. J. A. Perry of the Mines Branch, Department of Energy, Mines and Resources, Ottawa, in the design of the extrusion facility, and of Messrs. D. S. Russell and J. A. H. Desaulniers, of the Analytical Section, for the Chemical analyses.

1. W. Hume-Rothery and G. V. Raynor. J. Inst. Metals, **63**, 203 (1938).
2. G. V. Raynor. Trans. Faraday Soc. **44**, 15 (1948).
3. J. Graham and G. V. Raynor. Phil. Mag. **2**, 1354 (1957).
4. W. Haucke. Naturwiss. **26**, 577 (1938).

Can. J. Chem. Downloaded from www.nrcresearchpress.com by 210.87.254.5 on 09/05/12
For personal use only.

5. K. SCHUBERT, F. GAUZZI, and K. FRANK. Z. Metallk. **54**, 422 (1963).
6. N. INO, M. HIRABAYASHI, and S. OGAWA. Trans. Japan. Inst. Metals, **6**, 172 (1965).
7. W. A. ALEXANDER, L. D. CALVERT, A. DESAULNIERS, H. S. DUNSMORE, and D. F. SARGENT. Can. J. Chem. **47**, 611 (1969).
8. M. HANSEN and K. ANDERKO. Constitution of binary alloys. McGraw-Hill Book Co., Inc., New York. 1958.
9. M. A. SHTREMEL. Phys. Metals Metallog. USSR, Engl. Transl. **20**, No. 6, 28 (1965).
10. M. HIRABAYASHI, M. KOIWA, and N. INO. Sci. Rep. Res. Inst. Tohoku Univ. **A18** suppl. 337 (1966).
11. G. V. RAYNOR. The physical metallurgy of magnesium and its alloys. The Pergamon Press Ltd., London. 1959. p. 356.
12. F. N. RHINES and J. B. NEWKIRK. Trans. Amer. Soc. Metals, **45**, 1029 (1953).
13. J. W. CHRISTIAN. The theory of transformations in metals and alloys. The Pergamon Press Ltd., London. 1965.
14. F. P. BURNS and S. L. QUIMBY. Phys. Rev. **97**, 1567 (1955).
15. K. HIRAGA, M. KOIWA, and M. HIRABAYASHI. J. Less-Common Metals, **15**, 109 (1968).

Can. J. Chem. Downloaded from www.nrcresearchpress.com by 210.87.254.5 on 09/05/12
For personal use only.

Can. J. Chem. Downloaded from www.nrcresearchpress.com by 210.87.254.40 on 09/05/12
For personal use only.

Initial damage centers in γ-irradiated α-aminoisobutyric acid[1]

DAVID G. CADENA, JR., ROBERT E. LINDER, AND JOHN R. ROWLANDS
Department of Physical and Biological Sciences, Southwest Research Institute, San Antonio, Texas 78228

Received March 4, 1969

Electron spin resonance measurements of single crystals of α-aminoisobutyric acid, which are both irradiated and measured at 77 °K, give rise to a strong central absorption line at the center of two weak "satellite" peaks. The species largely responsible for the intensity of the central absorption line has been discussed previously and is considered to be the doubly ionized radical anion. In this paper, evidence is presented which shows that some of the intensity of this central line is contributed by the species giving rise to the satellite lines. Furthermore, this evidence, which is based upon saturation studies, variable temperature measurements, deuteration studies, and complete neglect of differential overlap–self consistent field molecular orbital calculations, suggests that the species giving rise to the satellite spectra is a planar conformation of the radical $(CH_3)_2\dot{C}CO_2H$.

Canadian Journal of Chemistry, 47, 3429 (1969)

I. Introduction

There has been considerable attention focused in recent years upon the identification by electron spin resonance (e.s.r.) of the initial damage centers created by ionizing radiation in organic and biologically important molecules. Recently, there have been two papers published discussing the nature of the initial damage centers formed in α-aminoisobutyric acid by both X- and γ-irradiation. Box and Freund (1) first reported that the e.s.r. spectra of the initial damage centers in single crystals of α-aminoisobutyric acid consisted of a strong central line (considered to arise from the radical $(CH_3)_2C(NH_2^+)CO_2^{2-}$ (1) at the center of two weak satellites, while Fujimoto *et al.* (2) in a more recent publication, report the presence at certain orientations of hyperfine structure on both the central intense line and the satellite peaks. Fujimoto *et al.* assigned the species that gives rise to the satellite lines as one formed by loss of a hydrogen atom from the interacting amino and carboxyl groups, i.e., the radical

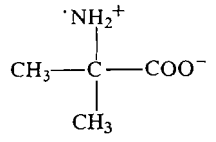

1

They indicate that the observed hyperfine pattern arises from the interaction of the unpaired electron with the nitrogen nucleus and two hydrogen nuclei. In view of the anisotropic behavior of the spectra obtained in a study of the radical $\cdot\overset{+}{N}H_2SO_3^-$ (3), which is formed by γ-irradiation of sulfamic acid, it is difficult to rationalize the observed isotropic behavior of the satellite absorption (see section III) with radical **1**. The principal values of the nitrogen and hydrogen hyperfine coupling tensors in the radical $\cdot\overset{+}{N}H_2SO_3^-$ were found to be nitrogen (103, 17, 33, iso: 51 Mc/s) and hydrogen (−65, −83, −44, iso: −64 Mc/s) respectively. Both the nitrogen and hydrogen hyperfine interaction tensors would be expected to be similar in magnitude for radical **1**. Neither the observed single crystal spectra nor the spectrum of the polycrystalline sample are consistent with such anisotropic hyperfine coupling.

Furthermore, crystals grown from D_2O containing in excess of 85% $(CH_3)_2C(ND_3)^+CO_2^-$ were observed in our studies to give rise to identical e.s.r. spectra. Since hydrogen deuterium exchange reactions are known to take place in radiation processes (4), some caution has to be exercised in drawing conclusions from deuteration studies. However, consideration of the deuteration studies, together with the known anisotropic behavior of the $\cdot\overset{+}{N}H_2—SO_3^-$ radical, is strong evidence for considering that radical **1** is not the species that gives rise to the satellite spectra.

The possibility that the satellite spectrum arises

[1]This research was supported in part by a grant from the Research Grants Section, National Center for Radiological Health, U.S. Public Health Service, No. RH GM 00384-01, and in part by Southwest Research Institute Internal Project No. 05-9015-01.

from a radical produced by loss of a hydrogen from a CH_3 group to give rise to the species

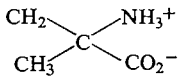

2

was also considered. Hyperfine coupling to a rapidly rotating $\dot{C}H_2R$ group has been observed in the radical $\dot{C}H_2OC(NH_2)_2{}^+Cl^-$ produced in γ-irradiated O-methylisourea (5). This species gave rise to two exactly equivalent hydrogen couplings at all orientations of the crystal with respect to the magnetic field. The e.s.r. spectra were anisotropic, giving rise to principal values of the hyperfine coupling constants of the indistinguishable hydrogens of −24.5, −67.0, and −73.0. Such anisotropy is not compatible with the e.s.r. spectra of the "satellite" species.

The observed spectra are consistent with an isotropic total splitting of the satellite lines. The extra hyperfine structure, which is resolved on all three lines at certain orientations, may be explained in terms of an anisotropic linewidth combined with some anisotropy in the hyperfine coupling of the nuclei, giving rise to the extra structure. Similar behavior has previously been reported in γ-irradiated DL-methionine (6). The e.s.r. spectra of the room temperature species $CH_3S\dot{C}HCH_2CHNH_3{}^+CO^-$, at most orientations, are the typical eight-line pattern of three interacting protons. At certain orientations, each line is observed to further split into a 1:3:3:1 pattern of the weakly coupling methyl group.

II. Results and Discussion

A. Radical Assignment

An alternative assignment for the observed satellite spectra may be made if one assumes that the appearance and disappearance of the hyperfine structure is due to an anisotropic linewidth variation of the hyperfine components rather than anisotropic variation of the magnitudes of the hyperfine interactions. From a close look at Fig. 1*a* and comparison with a computed spectrum (7) shown in Fig. 1*d*, it may be seen that each of the satellite lines splits into a quintet of approximate intensity distribution 1:4:6:4:1. Such an intensity distribution can arise from the interaction of the unpaired electron with four equivalent hydrogens. This intensity distribution can

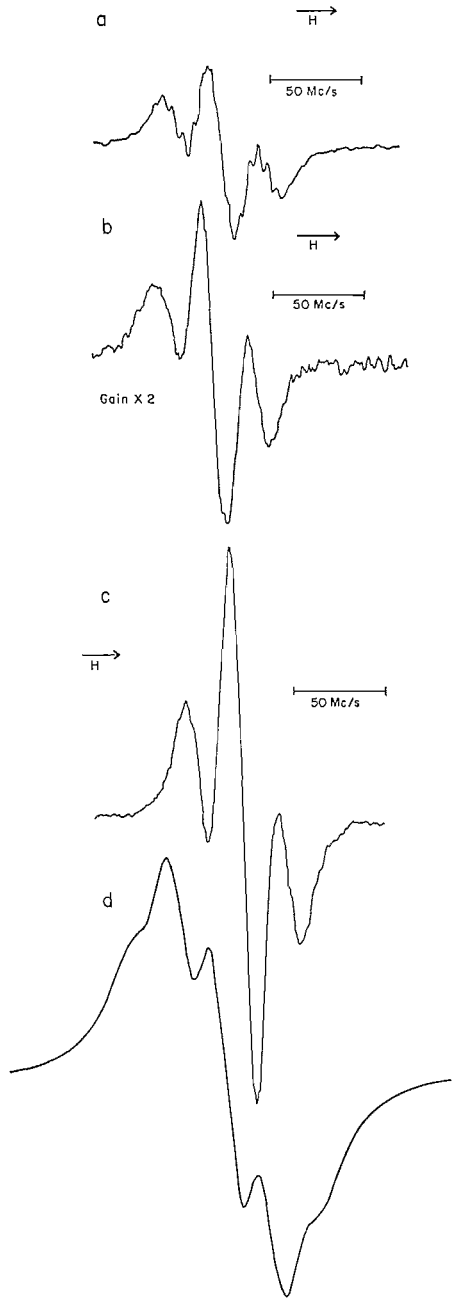

FIG. 1. Electron spin resonance spectra of single crystal α-aminoisobutyric acid (1*a* and 1*b* are different orientations in the *ac* plane), of polycrystalline α-aminoisobutyric acid (1*c*), and of a calculated 1:4:6:4:1 spectrum with a 0.96 linewidth: hyperfine splitting ratio (1*d*).

Can. J. Chem. Downloaded from www.nrcresearchpress.com by 210.87.254.40 on 09/05/12
For personal use only.

Can. J. Chem. Downloaded from www.nrcresearchpress.com by 210.87.254.40 on 09/05/12
For personal use only.

be obtained if one assumes that the species giving rise to the satellite spectrum is yet another conformation of the room temperature stable radical $(CH_3)_2\dot{C}CO_2^-$, in which both the CH_3 groups are frozen into equivalent configurations in which each gives rise to one large and two small hydrogen hyperfine interactions[2].

Hyperfine coupling constants based upon this analysis are tabulated in Table IV. Exact equivalence of the two methyl groups with respect to the carbon 2pπ orbital containing the unpaired electron was assumed, although small deviations from equivalence would not be detected. This assignment requires that the satellite spectrum consist of a major 1:2:1 isotropic hyperfine pattern, in which the line of intensity 2 is hidden by the strong single line signal of the $(CH_3)_2C(NH_3^+)CO_2^{2-}$ radical.

B. Evidence for Radical Assignment

As already reported by Box and Freund and by Fujimoto *et al.* the e.s.r. spectra of radicals trapped in X-irradiated α-aminoisobutyric acid consist of a strong central line at the center of two weak satellites. In agreement with the latter authors, at certain orientations of the crystals with respect to the applied magnetic field, extra hyperfine splitting is observed on all three lines. Spectra obtained at two crystal orientations, together with the spectrum of a polycrystalline sample, are included in Fig. 1.

1. Saturation Studies

It was also observed in our studies that the relative amplitudes of the satellite lines with respect to the amplitude of the central line were sensitive to the microwave power.

In view of the observed differences in saturation behavior of the satellite lines to the central line, detailed saturation studies were conducted in an effort to determine the contribution of the satellite hyperfine pattern to the central line intensity. The results of saturation experiments were analyzed on the basis of two distinct radicals whose spectra were superimposed at the strong central line. Plots of center line amplitude, satellite line amplitude, center line amplitude minus twice the satellite amplitude, coal standard amplitude, all vs. microwave power, are illustrated in Fig. 2.

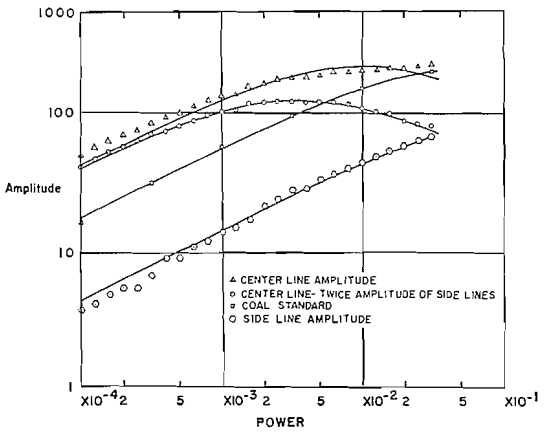

FIG. 2. Power saturation data and the nonlinear least squares fits to the data for the indicated samples.

In the figure, the ordinate gives the peak amplitudes in arbitrary units, while the abscissa gives the microwave power relative to the unattenuated power of 1.0. Also shown in the figure are the calculated least squares best fit of the experimental data.

The saturation behavior was analyzed by assuming that the e.s.r. experiment is described by the steady state Bloch equations (9), with the amplitude at $\Delta\omega$ from resonance being given by

$$[1] \quad \text{Amp.} = \frac{\gamma_e H_1 \tau_2 M_0}{1 + \gamma_e^2 H_1^2 \tau_1 \tau_2 + (\tau_2 \Delta\omega)^2}$$

At resonance ($\Delta\omega = 0$), we have

$$[2] \quad \text{Amp.} = \frac{\gamma_e H_1 \tau_2 M_0}{1 + \gamma_e^2 H_1^2 \tau_1 \tau_2}$$

This curve can be more simply represented by

$$[3] \quad \text{Amp.} = \frac{k_1 H_1}{1 + k_2 H_1^2}$$

taking into account the relative nature of the data. Since the power is proportional to the square of the field amplitude, we finally arrive at

$$[4] \quad \text{Amp.} = \frac{k_1' \sqrt{P}}{1 + k_2' P}$$

where P is the relative power given in Fig. 2.

The amplitude of the absorption peak (Amp.

[2]It should perhaps be noted that the room temperature stable radical has, at 40 °K, a configuration in which one proton has a large hyperfine splitting and the other two are smaller (8). The overall splitting is, however, larger than in the initial damage spectrum.

Can. J. Chem. Downloaded from www.nrcresearchpress.com by 210.87.254.40 on 09/05/12
For personal use only.

in eq. [4]) is taken to be the peak-to-peak amplitude of the experimental derivative curve, since the linewidth was found to be constant to within the experimental error.

The fitting procedure was a nonlinear least squares technique based on Levenberg's (10) method. The calculations were performed on a CDC 3600 computer using a program by McKay (11), and the results of the various fits are given in Table I and Fig. 2.

As an indication of the precision of the data and of the applicability of the method, the saturation curve of a coal sample was measured and the best values for k_1 and k_2 were determined. The overall fit and data spread can be judged by observing the average percent error (last column in Table I), and the validity of the values obtained for the constants can be estimated from the t and Δk values. The t values are the normal statistical t's and are given by the value of the number referred to over its standard error. The Δk values give the range for the k with a 95% probability. For coal, which is seen to be only slightly saturated at the maximum power levels used (Fig. 2), the overall fit and k_1 are good, with k_2 being less reliable. These results are taken to mean that the method is a valid procedure, especially in view of the fact that only seven points were used for the coal data.

The results of the saturation experiments are tabulated in Table I. The center peak data were taken from the spectra as the peak-to-peak amplitude of the center line, with no weighting of points. The first analysis of the side peak data (*3a*) was performed with a weighting on the higher power points, while the second (*3b*) was done with no weighting. The data for the triplet analysis (*4*) were obtained by subtracting from the center peak amplitude the amplitude of the side peak for each power level with no weighting. This corresponds to the assumption of a 1:1:1 pattern superimposed on a singlet. The data for the 1:2:1 pattern were obtained in the same way, but subtracting twice the side peak amplitude at each power level.

The sets *1* and *3* show the accuracy of the method for a strong signal (coal), indicating precision in the power measurements, and for a weak signal (side peak), showing the precision of the amplitude measurements, with the weighting showing up errors at low power levels. The sets *2*, *4*, and *5* may be compared directly, with the conclusion being that a much better fit is obtained when a 1:2:1 distribution is assumed for the superimposed pattern. This is shown in the t values, with a consistent improvement being shown as we go from 1:0:1 to 1:1:1 to 1:2:1 and in the average % error. A 1:3:1 distribution gave negative center peak amplitudes at the highest power levels.

2. Variable Temperature Studies

Variable temperature studies were also conducted in an effort to obtain further evidence for the assignment of the satellite spectrum. Polycrystalline samples were used in this phase of the investigation. Spectra were recorded at 77 °K, using a Varian liquid nitrogen Dewar, and variable temperature measurements were made at temperatures between 101 and 133 °K, using the Varian variable temperature accessory.

With constant microwave power, at temperatures between 77 and 120 °K, an increase in the

TABLE I

Saturation data

Set number	Data fitted	$k_1 \pm \Delta k$ (95% confidence)	t for k_1	$k_2 \pm \Delta k$ (95% confidence)	t for k_2	Average % error
1	Coal (raw data, 7 points)	1800±40	116	19.3±1.5	33.3	2.94
2	Center peak (raw data, 26 points)	3240±370	17.9	42.2±9.3	9.34	15.8
3	(*a*) Side peak (raw data, 28 points)	498±16	64.5	11.4±0.7	32.1	4.68
	(*b*) Side peak (raw data, 26 points)	481±11	86.5	7.51±1.47	10.5	7.23
4	Data from *2* — Data from *3* (triplet)	4120±234	36.1	152±18	17.7	6.35
5	Data from *2* — 2 × data from *3* (1:2:1)	4130±92	91.9	273±12	48.7	2.32

Can. J. Chem. Downloaded from www.nrcresearchpress.com by 210.87.254.40 on 09/05/12
For personal use only.

ratio of the central absorption line relative to the satellite lines caused by a decrease in amplitude and broadening of the satellite peaks was observed. At temperatures above 123 °K, the satellite peaks were observed to move in toward the center and their amplitude began to increase. At temperatures up to 133 °K, these observed spectral changes were shown to be completely reversible. These observations are fully consistent with the type of behavior that one would expect for the temperature dependence of a radical which exhibits hyperfine interactions to two equivalent methyl groups (12). At 77 °K, the rotation of each methyl group is largely restricted ($< 10^7$ c.p.s.), whereas at the higher temperatures, the broadening of the spectra reflects the onset of rotation. Unfortunately, it is not possible to extend these measurements to temperatures greater than 133 °K because of the irreversible changes that take place.

3. CNDO-II Calculations

Hyperfine coupling constants measured from orientations of the single crystal spectra in which the extra hyperfine structure was observed, based upon our assignment, are given in Table II. The analysis is based upon the assumption that the two methyl groups are frozen into equivalent conformations in which the projection of one hydrogen from each methyl is perpendicular to the radical plane. For this analysis to be acceptable, it is further necessary for the radical geometry to be such as to allow extensive delocalization of the unpaired electron. The observed isotropic hyperfine coupling of 63 Mc/s for the strongly coupling protons is approximately one-half of that typically found for β hydrogens frozen into this configuration.

The unpaired electron spin density distribution calculated by the CNDO SCF molecular orbital method is presented in Table IV. Details of the CNDO approximation are given in the original papers of Pople, Segal, and Santry (13, 14). The method is a semi-empirical one with parameters chosen so as to best reproduce the results of a full LCAO-SCF treatment. The program is available in Fortran IV language and was used here as it was received from the Quantum Chemistry Program Exchange, including the semi-empirical parameters.

TABLE II

Experimental hyperfine coupling constants

Atom	Coupling Mc/s
$H_1 = H_4$	63.0
$H_5 = H_6 = H_7 = H_8$	13.0

TABLE III

Radical geometry for

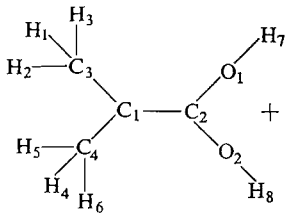

Bond	Bond length (Å)	Bond angle	Degrees
C—H	1.1	CH_3—C—CH_3	120
C—CH_3	1.535	CH_3—C—C	120
C—C	1.4	C—C—O	117.5
C—O	1.4	OH—C—OH	125
O—H	1.1		

TABLE IV

Spin densities

Atom	A.O.	ρ_π	ρ_β	ρ	ΔH(Mc/s)
C_1	$2p_z$	0.6161	0.1714	0.4447	
C_2	$2p_z$	0.4791	0.3371	0.1420	
C_3	$2p_z$	0.4991	0.5019	−0.0028	
C_4	$2p_z$	0.4991	0.5019	−0.0028	
O_1	$2p_z$	0.9585	0.8181	0.1404	
O_2	$2p_z$	0.9585	0.8181	0.1404	
H_1	1s	0.4815	0.4279	0.0536	75.0
H_2, H_3	1s	0.4738	0.4605	0.0133	19.0
H_4	1s	0.4815	0.4279	0.0536	75.0
H_5, H_6	1s	0.4738	0.4605	0.0133	19.0
H_7, H_8	1s	0.3230	0.3230	0.0	0.0

Can. J. Chem. Downloaded from www.nrcresearchpress.com by 210.87.254.40 on 09/05/12
For personal use only.

Since the CNDO method utilizes as a basis set all the valence orbitals, and also uses different molecular orbitals for α and β spins, the unpaired electron spin density distribution is obtained by subtracting the β density from the α density, i.e.

$$[5] \quad \rho_i = \sum_j \underset{\text{(occupied orbitals)}}{C_{ij}^2(\alpha)} - \sum_j \underset{\text{(occupied orbitals)}}{C_{ij}^2(\beta)}$$

or

$$[6] \quad \rho_i = \rho_i(\alpha) - \rho_i(\beta)$$

The radical geometry that was used in the calculations is listed in Table III. No effort was made to optimize this geometry. The choice of both the presence and position of the OH protons represents an attempt to compensate for the effects of proton exchange and hydrogen bonding between nearest neighbors. The methyl hydrogen spin densities were insensitive to the position of these protons. In making the calculations, it was assumed that atoms C_1, C_2, C_3, C_4, O_1, and O_2 are coplanar to ensure maximum delocalization of the unpaired electron and that methyl protons are each frozen into a configuration in which the projections of C_3H_1 and C_4H_4 are perpendicular to the radical plane. The calculated hyperfine coupling constants obtained by multiplying the calculated methyl proton spin densities by the atomic splitting parameters are listed in the last column of Table IV. In view of the many uncertainties involved in such calculations, the agreement between the calculated hyperfine coupling constants to those obtained from an analysis of the spectra must be considered as strong evidence for the correct assignment of the radical as a planar conformation of the room temperature radical $(CH_3)_2\dot{C}CO_2H$.

III. Experimental

Crystals of α-aminoisobutyric acid were grown from saturated aqueous solutions by slow evaporation. Deuterated crystals of α-aminoisobutyric were grown from D_2O solution after three exchanges. The crystals grown in this fashion were shown by infrared analysis to contain in excess of 85% $(CH_3)_2CND_3{}^+CO_2{}^-$. The crystals are of monoclinic symmetry with space group $C2/c$ and contain eight molecules per unit cell (15). In each set of measurements, three separate crystals were chosen and mounted on plastic rods, one on each of the orthogonal a, b, and c^* axes. The crystals were irradiated at 77 °K with 220 kV X-rays. The e.s.r. spectra were recorded every 10° by rotating the crystals about the three orthogonal axes in turn, using a Varian V4500 X-band spectrometer with 100 kc/s magnetic field modulation. Spectra recorded at 77 °K were made using a Varian liquid nitrogen accessory, while variable temperature studies were made using a Varian V4537 variable temperature accessory to control the sample temperature between 101 and 133 °K, with the sample temperature being continuously monitored using a thermocouple and a Hewlett–Packard digital voltmeter.

Saturation experiments were conducted at 77 °K on polycrystalline samples. The spectrometer was used in a low power configuration so that an attenuation of 40 db ($\times 10^{-4}$) could be obtained. Because the Q of the cavity and other factors enter into the calculation of the absolute power at the sample, the power level shown in Fig. 2 is a relative number. (The unloaded Q is 7000, and the klystron power is 0.350 W; however, the loaded Q with the liquid nitrogen accessory is not known.)

IV. Summary

The observed isotropic behavior of the satellite lines has led to a rejection of radicals 1 and 2 as possible species. An alternative assignment has been given which explains the isotropic behavior and which further agrees with the saturation data and with the CNDO-II calculation.

1. H. C. Box and H. G. Freund. J. Chem. Phys. **44**, 2345 (1966).
2. M. Fujimoto, W. A. Seddon, and D. R. Smith. J. Chem. Phys. **48**, 3345 (1968).
3. J. R. Rowlands and D. H. Whiffen. Nature, **193**, 61 (1962).
4. I. Mujagawa and K. Itoh. J. Chem. Phys. **40**, 3328 (1964).
5. D. G. Cadena, Jr. and J. R. Rowlands. J. Chem. Soc. B, 485 (1968).
6. D. G. Cadena, Jr. and J. R. Rowlands. J. Chem. Soc. B, 488 (1968).
7. Ya. S. Lebedev, D. M. Chernikova, N. N. Tikhomirova, and V. V. Voevodskii. Atlas of electron spin resonance spectra. Consultants Bureau, New York. 1963. p. 187.
8. J. R. Morton. J. Chem. Phys. **41**, 2956 (1964).
9. A. Abraham. Principles of nuclear magnetism. Oxford University Press, London. 1961.
10. K. Levenberg. Quart. J. Appl. Math. **2**, 164 (1944).
11. M. D. McKay. Private communication.
12. J. R. Morton. Chem. Rev. **64**, 453 (1964).
13. J. A. Pople, D. P. Santry, and G. A. Segal. J. Chem. Phys. **43**, 5129 (1965).
14. J. A. Pople and G. A. Segal. J. Chem. Phys. **44**, 3289 (1966).
15. S. Hirokawa, S. Kuribayashi, and I. Nitta. Bull. Chem. Soc. Jap. **25**, 192 (1952).

Surface area of cesium perchlorate

P. VENKATARAMANA AND V. R. KRISHNAN[1]
Sri Venkateswara University Chemical Laboratories, Tirupati, India
Received February 4, 1969

Specific surface area of cesium perchlorate has been determined by isotopic surface exchange, air-permeability, and microscopic methods. There is agreement between the values of specific surface area evaluated by air-permeability and microscopic methods. The results obtained by the isotopic surface exchange method are reproducible but are significantly greater than those obtained by the other methods, and the difference is attributed to the fact that while air-permeability and microscopic methods measure the external surface area, the surface exchange method measures the total surface area (external as well as internal) of solids.

Canadian Journal of Chemistry, 47, 3435 (1969)

Can. J. Chem. Downloaded from www.nrcresearchpress.com by 210.87.254.42 on 09/05/12
For personal use only.

Determination of the surface area of solids is important for all quantitative investigations of heterogeneous processes. The measurement is complicated due to the geometrical irregularities with which the solids are always associated. For such estimations numerous methods have been devised, of which the most widely used ones are as follows. (*a*) The gas adsorption method (1), which consists essentially of determining the quantity of gas required to cover the surface of a given weight of powder completely with a monomolecular layer of the gas, with suitable adaptations in cases of multimolecular layer adsorption. (*b*) Air-permeability method (2), which depends upon measurement of the rate of flow of air through a bed of particles, the rate being proportional to factors such as porosity, pressure drop across the bed, area of the bed, thickness of the bed, and the specific surface area of the powder. (*c*) Isotopic surface exchange method (3), which in principle is as follows. When a saturated solution is tagged with an isotopic tracer, a kinetic exchange between the tracer ions in solution and the inactive ions at the solid–solution interface occurs, and if self-diffusion and recrystallization processes are negligible, a pseudo equilibrium is established which enables the evaluation of surface area from the fractions of labelled atoms exchanged. (*d*) The microscopic method (4), which consists essentially of the measurement of the dimensions of the individual particles under a microscope.

One or more of the above procedures has been used to measure the surface areas of anhydrous salts such as $PbSO_4$ (5), $PbCrO_4$ (6), AgBr (7), $CaCO_3$ (8), $BaSO_4$ (9), etc.

In the present investigation, surface exchange, air-permeability, and microscopic methods were employed to measure the surface area of cesium perchlorate.

Experimental

Preparation of Cesium Perchlorate Sample

Cesium perchlorate was precipitated from 1 *M* cesium chloride (thrice recrystallized), by adding slowly 30% perchloric acid. The precipitate was filtered, washed free from chloride ion, and finally dried by drawing dry air through for 48 h. This sample was used in all surface area measurements.

Determination of Solubility

A saturated solution of cesium perchlorate was prepared in 95% alcohol at 30 ± 0.01 °C. An aliquot of the suspension was centrifuged. A known volume of the supernatant liquid was pipetted out into a centrifuge tube and evaporated till it was free from alcohol. The amount of cesium in the remaining aqueous solution was estimated using a Hilger UVISPEK spectrophotometer, with 12-molybdo phosphoric acid (10), at a wave length of 226 mμ.

Determination of Density

The density of cesium perchlorate at 30 ± 0.01 °C was determined by a pycnometric method as described by Weissberger (11). A double stem pycnometer of the type described by Naidu and Krishnan (12) was employed for the purpose. *p*-Xylene was chosen as the displacement fluid.

Determination of Mean Pore Size

The mean pore volume was determined by the method described by Emmett (13), and assuming the pores to be cylindrical, the mean pore radius $\bar{r}$, was calculated using the relation

$$[1] \qquad \bar{r} = \frac{2V}{S_w}$$

where V is the average pore volume and S_w the total surface area per gram of the solid, determined as follows.

[1]Present address: Sri Venkateswara University, Postgraduate Centre, Anantapur, India.

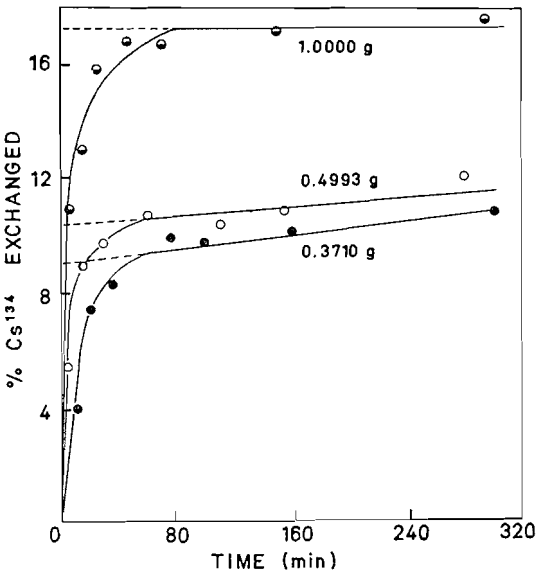

FIG. 1. Plot of % ^{134}Cs exchanged vs. time of shaking in minutes.

Determination of Surface Area

(1) Isotopic Surface Exchange Method

250 ml of a saturated solution of cesium perchlorate was prepared in 95% alcohol and an aliquot of ^{134}CsCl solution was added. This solution was equilibrated for 2 weeks at 30 ± 0.5 °C. (100 λ of this solution gave about 2000 counts per min with a Geiger Müller (G.M.) counter.) 25 ml of the above solution was added to a 100 ml narrow mouthed bottle with a ground-glass stopper, into which a known amount of cesium perchlorate was already weighed. The contents were agitated by an electrical shaker in a thermostat at 30 °C. At desired time intervals, 2 ml of the suspension was centrifuged and 100 λ of the centrifugate was transferred to a stainless steel planchet, by means of a micro-pipette, dried under an infrared lamp, and its beta activity measured with a G.M. counter.

Activity was plotted vs. time of shaking (Fig. 1). This plot was employed to obtain the percentage of ^{134}Cs exchanged at equilibrium, after correcting for recrystallization and self-diffusion by extrapolation to zero time of shaking.

The equilibrium may be represented as

$$[2] \qquad \frac{N_s^+}{N_s} = \frac{N_1^+}{N_1}$$

where N_s^+ and N_1^+ are the number of tracer ions in the solid and solution phases respectively, and N_s and N_1 are the total number of active and inactive species in the corresponding phases.

N_s is readily calculated from the experimentally determined values of solubility (N_1), and N_s^+ and N_1^+. If l^2 is the effective area of the tagged species, the surface area S is given by

$$[3] \qquad S = N_s l^2$$

where

$$[4] \qquad l^2 = \left[\frac{M}{\rho N a}\right]^{2/3}$$

where M is the molecular weight, ρ the density of the powder, a the number of gram ions of the tagged species of ions per mole of the solid, and N, the Avogadro number.

The results are presented in Table I.

(2) Air-Permeability Method

The air-permeability apparatus used was after Lee and Nurse (2) (Fig. 2). The permeability cell had a cross-sectional area of 5.07 sq. cm. A capillary flow-meter 277 cm long with an internal diameter of 0.904 mm was used.

A weight of cesium perchlorate, calculated to give the desired porosity for a predetermined bed thickness, was weighed into the permeability cell and tapped gently to consolidate. A plunger was introduced and the powder was compressed carefully to a bed of known thickness, the knurled flanges having been adjusted to give the desired height. The powder was always compressed to give the same height and the mass of powder in each run was varied to get different porosities. The plunger was twisted clockwise to compress and finally anticlockwise by a half turn so that a uniform surface was obtained. The plunger was finally removed carefully by a twisting action. Air from an air compressor, dried and free from carbon dioxide (by passing through columns of anhydrous calcium chloride and soda lime) was passed through the bed, with the pressure regulated to 60 lb/sq. in. by the two control valves attached to the outlet in the air compressor.

TABLE I

Isotopic surface exchange method

Sample number	Weight of sample (g)	% Exchange of ^{134}Cs	Specific surface area (cm^2/g)
1	0.3710	9.0	9.32×10^3
2	0.4993	10.4	8.21×10^3
3	1.0000	17.2	7.34×10^3
			Mean 8.29×10^3

Solubility of $CsClO_4$ at 30 °C = 0.02273 g/100 ml, density of $CsClO_4$ at 30 °C = 3.286 g/cc.

Can. J. Chem. Downloaded from www.nrcresearchpress.com by 210.87.254.42 on 09/05/12
For personal use only.

Can. J. Chem. Downloaded from www.nrcresearchpress.com by 210.87.254.42 on 09/05/12
For personal use only.

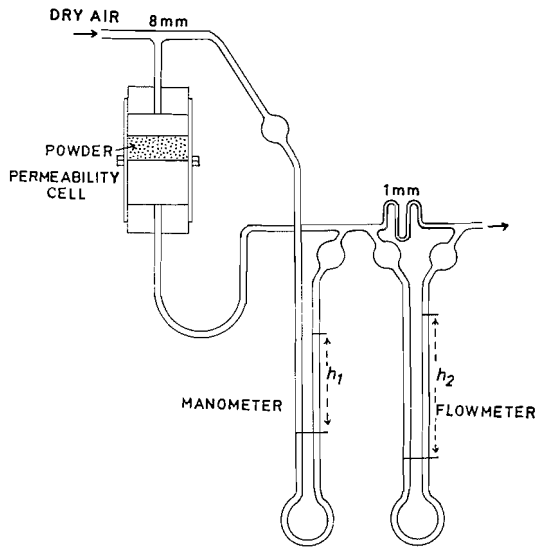

FIG. 2. Permeability apparatus.

For various rates of flow of air, the heights in the manometers across the powder bed (h_1) and the flowmeter (h_2) were recorded. The ratios of the heights in the manometers (h_1/h_2) were then computed and a frequency distribution was made by processing the data to obtain the most probable value.

The most probable value could be considered as the center of gravity of the frequencies (weights) f_1 and f_2 acting at the ends of the modal class i.e. the class of maximum frequency, so that the most probable value is given by the relation

$$[5] \quad \text{Most probable value} = L_1 + \frac{cf_2}{f_1 + f_2}$$

where L_1 is the lower limit of the modal class, f_1 and f_2 are the frequencies of the classes immediately before and immediately after the modal class, and c is the class interval.

The calculations of surface area are based on an equation which was derived by Kozeny and was first applied to surface determinations by Carman (14, 15). The equation is often used in the following form

$$[6] \quad \mu = \frac{\varepsilon^3}{(1-\varepsilon)^2} \frac{g\Delta P}{k\eta L S_w^2 \rho^2}$$

where μ = linear velocity of the fluid, ε = porosity, g = acceleration due to gravity, ΔP = pressure difference across the bed, η = viscosity of fluid, L = thickness of the bed, k = a constant, and ρ = density of powder. Carman found that over a wide range of experimental conditions, $k = 5.0 \pm 0.5$ and this value is almost always used.

The rate of flow of air, Q, through the flow-meter is given by the equation

$$[7] \quad Q = \frac{Ch_2 d}{\eta}$$

where C is a constant for a given capillary, h_2 the difference in the levels in the flowmeter manometer, and d the density of liquid in the manometer. From eq. [7]

$$[8] \quad Q = \mu A = \frac{\varepsilon^3}{(1-\varepsilon)^2} \frac{g\Delta P A}{k\eta L S_w^2 \rho^2}$$

Using the values of $k = 5$ and $g = 980$ cm/s^2, one gets

$$[9] \quad S_w = \frac{14}{\rho(1-\varepsilon)} \left(\frac{\varepsilon^3 A h_1}{C L h_2} \right)^{1/2}$$

where A is the cross-sectional area of the permeability cell and h_1 the difference in the levels of the manometer across the powder bed.

When a gas is used as the permeating fluid, eq. [9] should be modified in order to correct for the "slip" at the walls of the channel where theoretically the gas should be stationary. However, since the pressures used across the powder beds were small, the correction worked out to be negligible.

From the measured values of the area of the bed A, thickness of bed L, porosity of the bed ε, and the density of the powder ρ, the specific surface area was calculated with the use of relation [9].

The flow meter constant C was evaluated by means of the eq. [7]. A calibrated gas-meter was employed to determine Q. The most probable value of C was calculated from over 100 values of flow rates. The value of C obtained was 5.91×10^{-6} c.g.s. units. These results are presented in Table II.

(3) Microscopic Method

Cesium perchlorate powder (of the same sample as above) was mounted and spread out on a perfectly clean and dry object-glass (1 in. × 3 in.) using a fine needle, in such a way that the grains exhibited their outline without aggregation. The glass slide was fixed to an integrating stage with facility for both longitudinal and transverse movement of the slide. In order to determine the grain dimensions, an ordinary eye-piece micrometer, which was calibrated with the help of a stage micrometer, was used. The stage was then mounted on a Leitz polarizing microscope and the maximum length and maximum breadth of each grain were measured and recorded individually. Measurements were carried out for 300 particles at a magnification of 300 times.

The particles were assumed to be parallelepipeds, and the surface area was calculated. The specific surface area was obtained by dividing the area of 300 particles by the mass of the same, obtained in turn by the product of their volume and density. In the above calculations, the thickness and breadth of the particles were assumed to be equal (5). These values are presented in Table III.

Results and Discussion

The values of specific surface area of cesium perchlorate obtained by the three methods are reproducible for each method and satisfactory. The results of specific surface area evaluated in terms of air-permeability agree well with those obtained on the basis of microscopic method. The divergency noticed is within the limitations of the

TABLE II

Air-permeability method

Sample number	Weight of sample (g)	Porosity (void volume/unit volume)	h_1/h_2	Specific surface area (cm^2/g)
1	14.9512	0.5513	0.097	7.93×10^2
2	15.2500	0.5425	0.107	7.97×10^2
3	15.5259	0.5346	0.110	7.77×10^2
4	15.8922	0.5228	0.131	7.97×10^2
5	16.2370	0.5129	0.140	7.87×10^2
6	16.4675	0.5059	0.151	7.90×10^2
7	16.9948	0.4903	0.176	7.88×10^2
8	17.2072	0.4843	0.165	7.41×10^2
9	17.5795	0.4724	0.184	7.36×10^2
10	17.9651	0.4602	0.215	7.49×10^2
11	18.3114	0.4507	0.233	7.42×10^2
			Mean	7.72×10^2

Area of the bed = 5.07 cm^2, thickness of the bed = 2 cm.

TABLE III

Microscopic method

Size of particle		Specific surface area (cm^2/g)
Length (μ)	Breadth (μ)	
30.0*	20.0*	8.12×10^2
30.3†	18.3†	8.66×10^2

*Obtained from the corresponding histograms.
†Obtained by calculating the most probable values from the frequency distributions.

experimental procedures. In the air permeability method, specific surface areas for porosity range 0.55–0.49 are constant. (The small decrease in the surface area in the range 0.49–0.45 may be attributed to a decrease in free permeation of air as a result of closer packing.) However, the specific surface area obtained on the basis of isotopic surface exchange procedure is significantly greater than the results of the other methods. This is understandable when we distinguish the internal surface due to the cracks and fissures in the crystals from the external surface (16). It is obvious that the microscopic method would measure only the external surface leaving out the submicroscopic fissures. The air flow method too would not include the internal surface, as air filling in the cracks and fissures would be relatively stagnant. Isotopic surface exchange would measure the total surface (both internal and external) and may well be expected to give specific surface area values of a higher order. The pore radius measured is of the order 1.3 μ, showing that the contribution to the specific surface area estimated by isotopic surface exchange method includes the internal surface due to the porous nature of cesium perchlorate. The surface porosity may be attributed to the method of preparation and also the inherent porous character of cesium perchlorate.

Conclusions

It is concluded from the present work on the specific surface area of cesium perchlorate, that the air-permeability and microscopic methods yield results in agreement with each other and probably measure the external surfaces of solids. The surface exchange method, on the other hand, gives a measure of the total surface, internal and external, of solids. Independent methods for evaluation of internal surface alone are not available at present. The order of difference observed, between the external surface area and the total surface area as measured by these methods, is comparable to the difference recorded in like situations concerning other solids studied (17–20).

Acknowledgment

One of the authors (P.V.R.) is grateful to the Ministry of Education, Government of India, New Delhi, for financial assistance in carrying out this work.

1. S. Brunauer, P. H. Emmett, and N. Teller. J. Amer. Chem. Soc. **60**, 309 (1938).
2. F. M. Lee and R. W. Nurse. J. Soc. Chem. Ind. (London), **58**, 277 (1939).
3. F. A. Paneth and W. Vorwerk. Z. Phys. Chem. 445 (1922).
4. R. D. Cadle. Particle size determination. Interscience Publishers, Inc., New York. 1955. p. 105.
5. I. M. Kolthoff and C. Rosenblum. J. Amer. Chem. Soc. **55**, 2656 (1933).

Can. J. Chem. Downloaded from www.nrcresearchpress.com by 210.87.254.42 on 09/05/12
For personal use only.

6. I. M. KOLTHOFF and F. T. EGGERTSEN. J. Amer. Chem. Soc. **62**, 2125 (1940).
7. I. M. KOLTHOFF and R. C. BOWERS. J. Amer. Chem. Soc. **76**, 1503 (1954).
8. C. G. INKS and R. B. HAHN. Anal. Chem. **39**, 625 (1967).
9. P. H. EMMETT and T. DEWITT. Ind. Eng. Chem. Anal. Ed. **13**, 28 (1941).
10. F. HUEY and L. G. HARGIS. Anal. Chem. **39**, 125 (1967).
11. A. WEISSBERGER. Technique of organic chemistry. Vol. I. Part I. Interscience Publishers, Inc., New York. 1949. p. 286.
12. P. R. NAIDU and V. R. KRISHNAN. Trans. Faraday Soc. **61**, 1347 (1965).
13. P. H. EMMETT. Catalysis. Vol. II. Part 2. Reinhold Publishing Corp., New York. 1955 p. 108.
14. P. C. CARMAN. J. Soc. Chem. Ind. London, **57**, 225 (1938).
15. P. C. CARMAN. Shape and surface of fine powders by the permeability method. *In* Symposium on new methods for particle size determination in subsieve range. Amer. Soc. for Testing Materials, Philadelphia. 1941.
16. S. J. GREGG and K. W. SING. Adsorption, surface area, and porosity. Academic Press, Inc., London. 1966. p. 5.
17. L. IMRE. Kolloid-Z. **99**, 147 (1942).
18. P. H. EMMETT. Catalysis, Vol. I. Part I. Reinhold Publishing Corp., New York. 1954. p. 32.
19. A. M. SMIRNOVA, N. G. ZAITSEVA, and P. A. REBINDER. Kolloid Z. **18**, 93 (1956).
20. F. CARBONA. Ind. Chim. Paris, **43**, 41 (1956).

Can. J. Chem. Downloaded from www.nrcresearchpress.com by 210.87.254.42 on 09/05/12
For personal use only.

Can. J. Chem. Downloaded from www.nrcresearchpress.com by 210.87.254.6 on 09/05/12
For personal use only.

Stability of fused rings in metal chelates. VI[1]. Structures and stability constants of the copper(II) chelates of dipeptides containing glycine and/or β-alanine

OSAMU YAMAUCHI, YUMI HIRANO, YASUO NAKAO, AND AKITSUGU NAKAHARA
Institute of Chemistry, College of General Education, Osaka University, Toyonaka, Osaka, Japan

Received March 10, 1969

The reactions of the dipeptides containing glycine and/or β-alanine with an equimolar amount of copper(II) nitrate in acid solution were investigated potentiometrically, and the stability constants for the copper(II) chelates formed in acid solution were determined at 25 °C by the method of Datta and Rabin. The chelates with the composition [Cu·peptide(OH_2)] were isolated in the pure state. The dipeptides exhibited analogous reactivities, and the stability constants, log K_1, for the charged chelates, $CuHL^+$, were found to be between 5.5–5.7. Comparison of the values for glycylglycine and β-alanylglycine with those for glycine and β-alanine suggests that these dipeptides act as terdentate ligands forming fused-ring chelates, where the coordinating sites are probably the amino nitrogen, amide nitrogen, and carboxyl oxygen, although the complexing ability of the amide NH group may be weak. The constants, K_c, for the dissociation of the amide hydrogen from the charged chelates to form the deprotonated chelates, CuL, with the rigid 5-5-, 5-6-, or 6-6-membered ring system decrease in the order glycylglycine > β-alanylglycine > glycyl-β-alanine > β-alanyl-β-alanine. The log K_1K_c values indicate that the tendency of forming the deprotonated chelates also decreases in this order.

Canadian Journal of Chemistry, 47, 3441 (1969)

Introduction

The studies on the relative stabilities of the chelates of multidentate ligands are of great importance in finding clues to the subjects relating to the structures and reactions of metal complexes. From this point of view, the relative stabilities of the copper(II)–Schiff base complexes with 5-5-, 5-6-, 6-5-6-, and 5-5-6-membered fused-ring systems[2] were disclosed in the previous investigations on the basis of the numerical results obtained by various physicochemical measurements (1, 2). In order to shed light on the structures and relative stabilities of fused-ring chelates as an extension of the previous studies, investigations have recently been made on the stability constants of the copper(II) chelates formed by the reactions of the dipeptides composed of glycine and/or β-alanine with an equimolar amount of copper(II) nitrate in acid solution, and on the contribution of the peptide bond to the coordination around copper. Although glycylglycine and related peptides were already reported to exhibit quite interesting formation reactions of chelates with copper(II) (3–10), there have been no comparative studies on the structures and stabilities of the copper(II) chelates of glycylglycine (Gly-Gly), glycyl-β-alanine (Gly-β-Ala), β-alanylglycine (β-Ala-Gly), and β-alanyl-β-alanine (β-Ala-β-Ala), which are expected to behave as terdentate ligands forming 5-5-, 5-6-, or 6-6-membered fused-ring chelates with copper(II).

The present paper deals with the determination of the stability constants of the 1:1 copper chelates of the above mentioned dipeptides formed in the pH range 4–7 and discusses their structures and relative stabilities in aqueous solution. These findings may also have a potential significance in the biological field.

Experimental

Reagents

Ligands. Gly-Gly was prepared by the diketopiperazine method. Gly-β-Ala, β-Ala-Gly, and β-Ala-β-Ala were prepared by the carbobenzoxy method. Their purity was checked by the melting points and elemental analyses.

0.01 M $Cu(NO_3)_2$. This was prepared by dissolving copper(II) nitrate in water and was standardized by 0.01 *M* EDTA which had been standardized against standard zinc (99.99% pure).

0.1 N KOH. This was prepared by the method of Armstrong (11) and standardized against potassium hydrogen phthalate.

All the reagents used were of reagent grade, and deionized water was used throughout.

Apparatus

A Yanagimoto Model 66A pH meter with a Horiba 1026-05T glass electrode and a Horiba 2630-05T calomel electrode was used.

pH Titration

Exactly equimolar amounts of a ligand and Cu(II) were mixed in 45 ml of water and to this was added 5 ml

[1]For Part V of this series, see ref. 18.

[2]This type of notation will be used hereafter for the expression of the individual ring size of a fused ring. For example, "5-5-membered" indicates that the fused ring is composed of two 5-membered rings.

Can. J. Chem. Downloaded from www.nrcresearchpress.com by 210.87.254.6 on 09/05/12
For personal use only.

of 1 M KNO_3 to make the concentration 0.004–0.005 M. The mixture was titrated with 0.1 N KOH at 25 °C under a nitrogen atmosphere, and the pH values were measured. The ligands were titrated in the absence of Cu(II) under the same conditions to determine their acid dissociation constants. Conversion of pH to $-\log [H^+]$ and determination of the apparent ion product of water, pK_w', were made by titrating 0.01 N HNO_3 with 0.1 N KOH under the same conditions. Thus, $[H^+] = 10^{-pH}/0.92$; $pK_w' = 13.88$.

Preparation of the Cu(II) Chelates

[*Cu·Gly-β-Ala(OH₂)*]. This was prepared by the method of Manyak *et al.* (4) from Gly-β-Ala (0.005 mole) and a slight excess of freshly prepared $Cu(OH)_2$. After evaporation of the reaction mixture in vacuo, acetone was added, and the mixture was cooled, when a blue crystalline powder, m.p. 193–196 °C (decomp.), separated.

Anal. Calcd. for $C_5H_{10}N_2O_4Cu$: C, 26.62; H, 4.47; N, 12.42. Found: C, 26.33; H, 4.44; N, 12.27.

[*Cu·β-Ala-Gly(OH₂)*]. This was obtained in a similar manner from β-Ala-Gly and $Cu(OH)_2$ as blue prisms, m.p. 205–210 °C (decomp.).

Anal. Calcd. for $C_5H_{10}N_2O_4Cu$: C, 26.62; H, 4.47; N, 12.42. Found: C, 26.44; H, 4.40; N, 12.50.

Results and Discussion

The pH titration curves of the ligands in the absence and presence of Cu(II) are shown in Fig. 1. The dipeptides investigated have analogous titration curves except that precipitation occurred during the titration of the β-Ala-β-Ala-Cu(II) system (curve 5). When Gly-Gly is caused to react with an equimolar amount of Cu(II), the following two reactions have been shown to occur in acid solution (3–7)

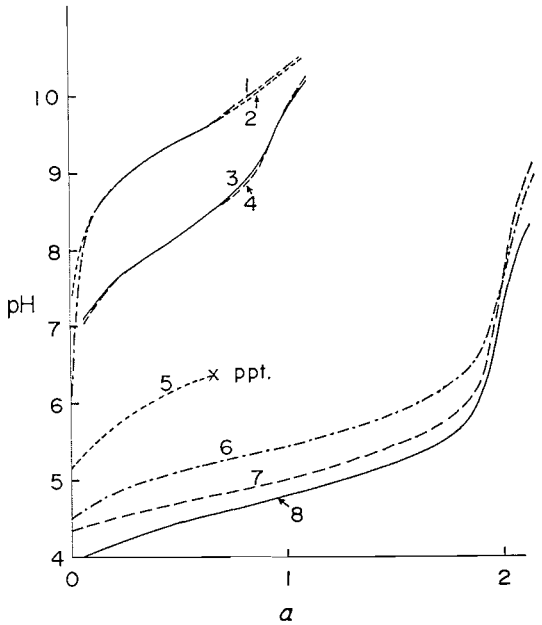

FIG. 1. pH titration curves for the dipeptides at 25 °C (μ = 0.1(KNO_3)): ——— Gly-Gly, – – – Gly-β-Ala, - - - - - - β-Ala-Gly, - - - - - β-Ala-β-Ala; ligands alone (curves 1–4); ligand:Cu(II) = 1:1 (curves 5–8). The term a is the number of moles of KOH added per mole of ligand.

$$[1] \qquad Cu^{2+} + HL^- \overset{K_1}{\rightleftharpoons} CuHL^+$$

$$[2] \qquad CuHL^+ \overset{K_c}{\rightleftharpoons} CuL + H^+$$

where HL^-, $CuHL^+$, and CuL denote respectively the free ligand, the positive chelate **1**, whose structure will be discussed below, and the neutral chelate **2** formed upon the dissociation of the peptide NH of **1**.

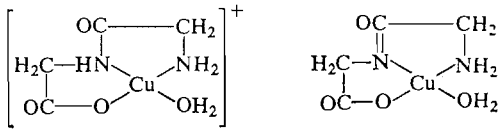

$CuHL^+$ **1**

CuL **2**

The equilibrium constants K_1 and K_c are defined as follows

$$[3] \qquad K_1 = \frac{[CuHL^+]}{[Cu^{2+}][HL^-]}$$

$$[4] \qquad K_c = \frac{[H^+][CuL]}{[CuHL^+]}$$

As is apparent from the curves, two acid dissociations were observed to occur in the acid region before the pH jump, and we may assume the reactions [1] and [2] reported for Gly-Gly also in the reactions of Gly-β-Ala and β-Ala-Gly. Following the method of Datta and Rabin (5), we first obtained graphically the approximate value of K_1 with the aid of eq. [5] by assuming $\beta = 1$ and then inserted it into eq. [5] to calculate the corresponding K_c value at each pH and its average value, $\overline{K_c}$

$$[5] \qquad \frac{1}{K_1} = -\frac{K_{a_2}}{[H^+]}\left(\frac{\beta(2C_L + A) - C_L}{A\alpha - \gamma}\right) \times \left(C_L - \frac{A\alpha - \gamma}{\alpha/\beta - 3\alpha + 1}\right)$$

where $A = -[K^+] - [H^+]$, $\alpha = 1 + [H^+]/K_{a_1}$, $\beta = 1 + K_c/[H^+]$, and $\gamma = C_L[H^+]/K_{a_1}$; K_{a_1} and

Can. J. Chem. Downloaded from www.nrcresearchpress.com by 210.87.254.6 on 09/05/12
For personal use only.

K_{a_2} are the acid dissociation constants of the carboxyl and amino groups of the dipeptides, and $[K^+]$ and C_L are the amount of KOH added and the total concentration of ligand, respectively. Then, the initial log K_1 value was increased or decreased by 0.05 log unit, and K_c was calculated again. The best set of K_1 and $\overline{K_c}$ corresponded to the minimum point in the plot of the variances of $-\log K_c$ (pK_c) against log K_1. Usually, 20–30 sets of $[K^+]$ and $[H^+]$ were used for the calculations of the pK_a values, and 40–60 sets were used for K_1 and K_c. The constants for β-Ala-β-Ala, whose reactions are assumed to be the same as those of Gly-Gly, may be less accurate because sufficient data were not obtained owing to the precipitation of copper(II) hydroxide. The standard deviations of the log K_1 and pK_c values were within 0.03. The validity of the results was checked by duplicate runs, where the differences in the corresponding constants were less than 0.1 log unit. The amounts of alkali at various pH values were calculated from eq. [5] by using the determined constants and were found to correspond well with the experimental results. Hence, this confirms the assumption that under the conditions employed, the reactions [1] and [2] occur. All the computations were made with the use of a NEAC-2200/500 computer of the Osaka University Computation Center. The pK_a values and the stability constants are listed in Table I along with the constants for the chelates of glycine and β-alanine calculated by the method of Irving and Rossotti (12).

The pK_a values of the glycine residue of the dipeptides are lower than the corresponding values of the β-alanine residue, and this fact can be ascribed to the lower pK_a values of glycine as compared with those of β-alanine. The stability constants for Gly-Gly determined by the present investigation are in good agreement with those reported by Dobbie and Kermack (log K_1 = 5.88; pK_c = 4.25) (3), Datta and Rabin (log K_1 = 5.82; pK_c = 4.25) (5), and Bryce *et al.* (log K_1 = 5.50; pK_c = 4.30) (10). With respect to the charged chelates of the peptides, $CuHL^+$, the log K_1 values for Gly-Gly, Gly-β-Ala, and β-Ala-Gly are between 5.6 and 5.7, the differences being almost negligible, but the value for β-Ala-β-Ala is somewhat lower. On the other hand, the log K_1 for the 5-membered glycine–copper(II) chelate is considerably higher than that for the 6-membered β-alanine–copper(II) chelate. Considering that there is practically no difference between the log K_1 for Gly-Gly and β-Ala-Gly in spite of the large difference in the pK_a values of the two NH_2 groups, there seems to be no distinct correlation between the stability constants and the pK_a values of the coordinating groups. Therefore, we may safely infer that steric effects play an important role in the chelate formations by the peptides.

There have been some ambiguities about the coordination sites of the peptides in acid solution. Freeman *et al.* (13) disclosed by X-ray analysis that, in the solid state, the protonated complex of triglycine, $[CuH_2L]^+Cl^-$, has a polymeric structure with the carboxyl group of a ligand molecule coordinating to the neighboring copper atom which is coordinated by the amino nitrogen and peptide oxygen atoms of another ligand molecule. In dilute aqueous solution, however, we can hardly assume the same structure, because we must take into account the solvation by water molecules and the stabilization due to the so-called "chelate effect." As for Gly-Gly, Rabin (14) and Martell (15), by referring to the stability constants and infrared spectra, preferred the coordination through the amino nitrogen and the amide oxygen, regarding the dipeptides as bidentate ligands. If this is the case and the chelates of the type **3** are formed, the log K_1 values for the glycine and β-alanine chelates would predict on

TABLE I

Acid dissociation constants and stability constants in water at 25 °C*

Ligand	pK_{a_1}	pK_{a_2}	log K_1	pK_c	log K_1K_c
Gly-Gly	3.16	8.15	5.68±0.01	4.18±0.01	1.50
Gly-β-Ala†	3.98	8.16	5.70±0.03	4.64±0.02	1.06
β-Ala-Gly	3.25	9.41	5.61±0.02	4.29±0.02	1.32
β-Ala-β-Ala	4.02	9.37	5.5	6.8	−1.3
Glycine	2.41	9.63	8.20	—	—
β-Alanine	3.55	10.15	6.99	—	—

*μ = 0.1 (KNO_3); variances are expressed in standard deviations.
†The values log K_1 = 6.11 and pK_c = 4.69 were reported by Salakhutdinov *et al.* (19).

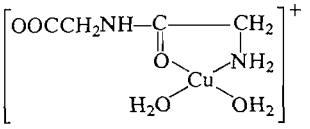

3

stereochemical grounds that the differences between the values for Gly-Gly and β-Ala-Gly, and for Gly-β-Ala and β-Ala-β-Ala would also be as large as the difference between glycine and β-alanine. On the contrary, the fact is that the differences are very small. On the basis of these observations, we are more in line with the view that the dipeptides, when present in dilute solution, react with copper(II) as terdentate ligands, forming fused-ring chelates of the type **1** with the strain of the individual chelate rings dispersed over the chelate as a whole. Although no positive information has been reported as yet about the contribution of the amide NH group without loss of the hydrogen (16), we may reasonably presume that the coordination is through the amide NH of the peptides when they act as terdentate ligands, because participation of the amide oxygen is sterically almost impossible. Whether or not the hydrogen atom is found on the amide nitrogen is not to be clarified at the present stage. The complexing ability of the amide NH group may be so weak that its contribution to the binding with copper would be feasible only through the coordination of the terminal amino and carboxyl groups. Therefore, the amide oxygen will be the preferred coordination site when the participation of the amide nitrogen is sterically difficult[3].

With the increase of the pH of the solution, dissociation of the amide hydrogen of the chelates occurs to an increasing extent, resulting in the formation of the neutral chelates of the type **2**, where the binding between nitrogen and copper is considered to be much stronger. The structure **2** was proposed for Gly-Gly in solution and has been confirmed also in the crystalline state by X-ray analysis (17). The neutral chelates may be regarded as intrinsic fused-ring chelates belonging to the 5-5-, 5-6-, and 6-6-membered ring systems. The relative stabilities among these chelates can be inferred from the following relationship obtained by combining eqs. [4] and [5]

$$[6] \qquad \frac{[CuL]}{[Cu^{2+}][HL^{-}]} = \frac{K_1 K_c}{[H^{+}]}$$

It is apparent from eq. [6] that the relative degrees of formation of the neutral chelates and their relative stabilities at a constant pH are given by the K_1K_c values. Table I shows that these values decrease in the order Gly-Gly > β-Ala-Gly > Gly-β-Ala > β-Ala-β-Ala with the differences somewhat larger than those observed about the log K_1 values (Scheme 1).

The observed stability sequence is also in agreement with the observations about the isolation of the chelates and their absorption spectra in the visible region. The stable copper(II) chelates of Gly-Gly, β-Ala-Gly, and Gly-β-Ala could be isolated as pure crystals in contrast with the unstable chelate of β-Ala-β-Ala which could not be isolated under the same conditions. As shown in Table II, the absorption maxima of the former chelates are found in the range 632–643 mμ at pH 6.6–7.2, whereas the maximum of the latter is found at 708 mμ at this pH and shifts to 650 mμ only at pH above 8. Such a spectral behavior corresponds to the higher pK_c value of the copper(II) chelate of β-Ala-β-Ala as compared with the corresponding values of the other chelates. The low stability of this chelate is explained as due to the greater steric strain of the fused-ring system. This strain affects the formation of the deprotonated complex, resulting in the extremely high pK_c value, because the strain supposedly becomes more prominent in the rigid neutral complex than in the protonated complex.

The present findings about the relative stabilities might seem to be incompatible with the conclusion which we made about the copper(II) chelate of the Schiff base derived from pyruvic

TABLE II

Spectral data for the copper(II) chelates

Chelate	pH	λ_{max} (mμ)	log ε
[Cu·Gly-Gly(OH$_2$)]	6.7	643	1.92
[Cu·Gly-β-Ala(OH$_2$)]	6.6	633	1.87
[Cu·β-Ala-Gly(OH$_2$)]	7.2	632	1.72
[Cu·β-Ala-β-Ala(OH$_2$)]	6.5	708	*
	8.7†	655	*

*Not measured.
†Precipitation occurred.

[3]As Rabin (14) pointed out, the coordination sites of glycylsarcosine are most probably the amino nitrogen and the amide oxygen because the amide nitrogen has a methyl group which sterically impedes the binding of the nitrogen with copper.

Can. J. Chem. Downloaded from www.nrcresearchpress.com by 210.87.254.6 on 09/05/12
For personal use only.

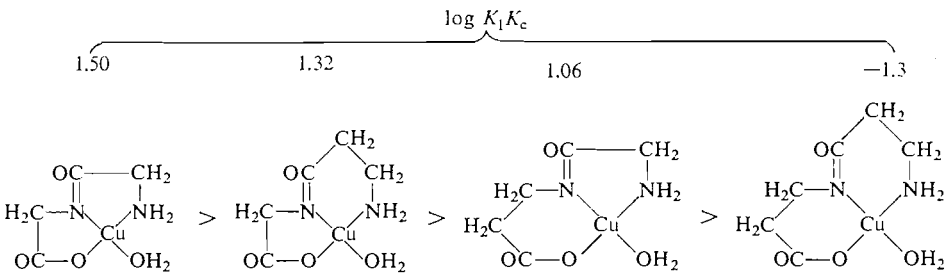

SCHEME 1. Comparison of the stabilities of the neutral copper(II) chelates of the type CuL.

acid and glycine, [Cu·Pyrv=Gly(OH_2)] (5-5-membered), and that from pyruvic acid and β-alanine, [Cu·Pyrv=β-Ala(OH_2)] (5-6-membered), of which the latter was concluded to be the more stable (Scheme 2) (1). In these cases, the

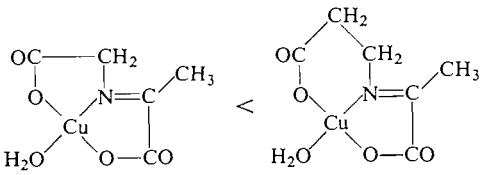

[Cu·Pyrv=Gly(OH_2)] [Cu·Pyrv=β-Ala(OH_2)]

SCHEME 2. Relative stability of the copper(II) chelates of the Schiff bases derived from pyruvic acid and amino acids.

coordinating atoms are an azomethine nitrogen and two carboxyl oxygens as compared with an amino nitrogen, an amide nitrogen, and a carboxyl oxygen in the dipeptide chelates. Accordingly, the steric requirements around the copper atom and hence the ring strain therein would also be different in the two series.

It should be emphasized that the comparison of the stabilities of fused-ring chelates is possible only when the systems being investigated are structurally comparable and consist of coordinating groups of the comparable nature.

The above mentioned relative stabilities of the fused-ring chelates may suggest an explanation of the specificity or selectivity of the enzymic reactions where metal ions are indispensable.

Acknowledgments

We wish to thank Mr. Hiroyuki Ishibashi for measurement of some of the constants and Mr. Toshihiko Kohno for preparation of the copper chelates. We are also indebted to Miss Yoshiko Komuro for the elemental analyses and to the members of the Osaka University Computation Center for computations.

1. A. NAKAHARA, H. YAMAMOTO, and H. MATSUMOTO. Bull. Chem. Soc. Jap. **37**, 1137 (1964).
2. Y. NAKAO, K. SAKURAI, and A. NAKAHARA. Bull. Chem. Soc. Jap. **39**, 1471 (1966).
3. H. DOBBIE and W. O. KERMACK. Biochem. J. **59**, 246 (1955).
4. A. R. MANYAK, C. B. MURPHY, and A. E. MARTELL. Arch. Biochem. Biophys. **59**, 373 (1955).
5. S. P. DATTA and B. R. RABIN. Trans. Faraday Soc. **52**, 1123 (1956).
6. C. B. MURPHY and A. E. MARTELL. J. Biol. Chem. **226**, 37 (1957).
7. W. L. KOLTUN, M. FRIED, and F. R. N. GURD. J. Amer. Chem. Soc. **82**, 233 (1960).
8. W. L. KOLTUN, R. H. ROTH, and F. R. N. GURD. J. Biol. Chem. **238**, 124 (1963).
9. M. K. KIM and A. E. MARTELL. Biochem. **3**, 1169 (1964).
10. G. F. BRYCE, J. M. H. PINKERTON, L. K. STEINRAUF, and F. R. N. GURD. J. Biol. Chem. **240**, 3829 (1965).
11. A. ALBERT and E. P. SERJEANT. Ionization constants of acids and bases. Methuen and Co., Ltd., London. 1962.
12. H. IRVING and H. S. ROSSOTTI. J. Chem. Soc. 3397 (1953).
13. H. C. FREEMAN, G. ROBINSON, and J. C. SCHOONE. Acta Cryst. **17**, 719 (1964).
14. B. R. RABIN. Trans. Faraday Soc. **52**, 1130 (1956).
15. A. E. MARTELL. *In* Proceedings of the Pre-Conference Kyushu Meeting on Coordination Chemistry. Kagaku no Ryoiki Series, No. 84. Nankodo, Tokyo. 1968.
16. H. C. FREEMAN. *In* The biochemistry of copper. *Edited by* J. Peisach, P. Aisen, and W. E. Blumberg. Academic Press, Inc., New York. 1966. p. 77.
17. B. STRANDBERG, I. LINDQVIST, and R. ROSENSTEIN. Z. Krist. **116**, 266 (1961).
18. A. NAKAHARA, I. MIYACHI, and T. KOHNO. Bull. Chem. Soc. Jap. **42**, 573 (1969).
19. U. I. SALAKHUTDINOV, A. P. BORISOVA, Y. V. GRANOVSKII, I. A. SAVICH, and V. I. SPITSYN. Dokl. Akad. Nauk SSSR, **177**, 365 (1967).

Can. J. Chem. Downloaded from www.nrcresearchpress.com by 210.87.254.6 on 09/05/12
For personal use only.

Studies on microcapsules. IV. Preparation and some properties of sulfonated polyphthalamide microcapsules

MASUMI KOISHI, NAOKO FUKUHARA, AND TAMOTSU KONDO

Faculty of Pharmaceutical Sciences, Science University of Toyko, Funagawara-machi, Shinjuku, Tokyo, Japan

Received February 3, 1969

Sulfonated polyphthalamide microcapsules were prepared by making use of the interfacial polycondensation reaction between *p*-phthaloyl dichloride and a mixture of diethylenediamine and 4,4′-diaminostilbene-2,2′-disulfonic acid. These microcapsules were found to be fluorescent as well as negatively charged owing to the presence of sulfonated stilbene skeletons chemically bound in the membranes. The electrophoretic mobility measurements in the presence of inorganic electrolytes revealed a strong resemblance between the microcapsules and hydrophobic colloid particles.

Canadian Journal of Chemistry, 47, 3447 (1969)

Can. J. Chem. Downloaded from www.nrcresearchpress.com by 210.87.254.6 on 09/05/12
For personal use only.

Introduction

A previous paper of this series (1) has dealt with the preparation of polyphthalamide microcapsules, based on the interfacial polycondensation reactions between diamines and phthaloyl dichlorides, under various conditions. However, the microcapsules thus obtained had a tendency to form aggregates in water on prolonged storage unless a considerable amount of dispersing agent, such as Tween 20, was present because they were not electrically charged. This has often made the treatment of microcapsules troublesome in later stages.

An attempt has been made, therefore, to prepare the microcapsules stabilized in water by having strongly ionizable groups in their membranes. The microcapsules of this kind could be obtained, as suggested by Chang (2), by using a mixture of sulfonated and unsulfonated diamines. This paper describes the preparation and some physicochemical properties of the charged polyphthalamide microcapsules.

Experimental

Preparation of Microcapsules

(A) Preparation of Sulfonated Polyphthalamide Microcapsules

The preparation of sulfonated polyphthalamide microcapsules was made by utilizing the interfacial polycondensation reaction between diamines and *p*-phthaloyl dichloride. Thus, the procedure consisted of the following 3 steps.

1. To 7.5 ml of aqueous 1% (wt./wt.) polyethylene glycol (polymerization degree: 4000) solution in a 1 l round bottom flask surrounded by ice, was added an equal volume of a 0.4 *M* solution of a mixture of diethylenediamine (DEDA) and 4,4′-diaminostilbene-2,2′-disulfonic acid (DASSA) in varying ratio, in aqueous 0.45 *M* sodium carbonate solution, containing 1% (wt./wt.) polyethylene glycol. To this solution was added 75 ml of mixed solvent (chloroform–cyclohexane 1:3, v/v, containing 5 or 10% (v/v) Span 85 as an emulsifying agent). The mixed solution was then mechanically emulsified with a Model B-100 Chemistirrer (Tokyo Rika Kikai Co.) at 620 r.p.m. for 5 min to yield a water-in-oil emulsion. The alkali served to neutralize hydrogen chloride formed during the polymerization reaction.

2. Without stopping the stirring, 75 ml of *p*-phthaloyl dichloride solution was quickly added to the emulsion, and the stirring was continued for another 3 min. The *p*-phthaloyl dichloride solution was prepared immediately before use by adding 0.6 g of pure *p*-phthaloyl dichloride to 75 ml of the mixed solvent.

3. To this dispersion was added 75 ml of the mixed solvent, and the dispersion was centrifuged at 350–2000 g to separate the newly formed charged microcapsules. To remove the residual organic solvent, the unreacted reagents, and the salt formed during polymerization, the microcapsules separated from the organic phase were washed twice with 80 ml of aqueous 20% (v/v) Tween 20 solution on the centrifuge. The microcapsules were finally suspended in 80 ml of each of aqueous potassium nitrate, barium nitrate, and lanthanum nitrate solutions containing 4% (v/v) Tween 20, the ionic strengths of which were 1×10^{-2}, 1×10^{-3}, and 1×10^{-4}. Tween 20 was added to prevent the aggregation of microcapsules by the electrolytes.

(B) Partition of Diamines between Aqueous and Organic Phases

The competitive transfer of the diamines into the mixed organic solvent from aqueous solution must first be examined to see the tendency of sulfonate groups to be incorporated in the microcapsule membranes. For this purpose the determination was made of the diamine partitions between the aqueous and the organic phase under the same conditions as those in the preparation of microcapsules.

Thus, the partition coefficients were determined by the following method. To 30 ml of a 0.4 *M* solution of DEDA or DASSA in aqueous 0.45 *M* sodium carbonate solution containing 1% (wt./wt.) polyethylene glycol in a 100 ml Erlenmyer flask surrounded by ice, was added an equal volume of the mixed solvent. The mixed liquid was then mechanically agitated with the Chemistirrer at 620 r.p.m. for 5 min. In each case an emulsion was formed, which

Can. J. Chem. Downloaded from www.nrcresearchpress.com by 210.87.254.6 on 09/05/12
For personal use only.

was centrifuged to completely separate it into two liquid layers. The concentration of DEDA plus sodium carbonate remaining in the aqueous phase was determined by titration with hydrochloric acid using a piston burette and BCG–BTB mixed indicator. The initial concentrations of the diamine plus sodium carbonate and sodium carbonate alone were also determined by the same procedure. In the case of DASSA, the concentration in the aqueous phase was determined fluorophotometrically by a Hitachi model MPF-2A fluorescence spectrophotometer.

Finally, the transferred amounts of the diamines were calculated from their initial and final concentrations in the aqueous phase, and then the partition coefficients between the aqueous and the organic phase were calculated.

Fluorescence of Sulfonated Microcapsules

The sulfonated polyphthalamide microcapsules were remarkably fluorescent under ultraviolet (u.v.) light, very probably due to DASSA chemically incorporated in the membranes. The fluorescence spectra of DASSA in the microcapsule membranes dispersed in aqueous phase were recorded on the Hitachi model MPF-2A fluorescence spectrophotometer using the light of a wavelength of 360 mμ for exciting the sample.

The microcapsules used for the measurements were washed twice with aqueous 20% (v/v) Tween 20 solution after preparation and then suspended in the same medium.

An Olympus model HLS-II photomicroscope was employed for photographing the fluorescent microcapsules. This instrument was equipped with a high-pressure mercury vapor lamp as the source of u.v. light. A blue filter, BG-370, was also used to delimit the wavelength of radiation reaching the specimen from the light source.

Determination of Size and Size Distribution of Sulfonated Microcapsules

Several samples from each batch of the sulfonated microcapsules were photographed under an ordinary microscope. Calculations were made of the length mean diameter, size distribution, standard deviation, mean surface diameter, and mean volume diameter by using an IBM 1620 computer as described in the previous paper (1).

Electrophoretic Mobilities of Sulfonated Microcapsules

Electrophoretic mobilities of the sulfonated microcapsules were measured in a quartz flat electrophoresis cell of rectangular cross section under a microscope. Necessary precautions were taken so that the measurements could be made at the stationary layer of the cell. For each measurement, 40 microcapsules were timed in each direction to eliminate the polarization effect of the electrodes. The dispersion media were aqueous solutions of potassium, barium, and lanthanum nitrates of various ionic strengths containing 4% (v/v) Tween 20.

Zeta potentials of the microcapsules, ζ, were calculated by the Henry equation (3)

$$\zeta = f\pi\eta u/D$$

where u is the mobility of the microcapsules, D and η are respectively the dielectric constant and viscosity of dispersion medium, and f is the numerical factor depending on the value of the product of the reciprocal of double layer thickness around the microcapsules, κ, and their radius, a. The value of 4 was used for f when κa was larger than 300. In other cases, the values of f were calculated according to Overbeek (4).

The surface conductance effect was found to be negligible because preliminary experiments showed that the product of the specific conductance of dispersion medium and the microcapsule radius was much larger than the surface conductance at the interface of the dispersion medium and the microcapsule. Thus, for example, the surface conductance at the interface of the microcapsule and 1×10^{-4} potassium nitrate solution containing 4% (v/v) Tween 20 was 2.64×10^{-10}, while the product of the specific conductance of the same dispersion medium and the microcapsule radius was evaluated to be 1.06×10^{-8}. This satisfies the condition of particles to be insulating (5).

The relaxation correction was made by Booth's method (6), when the zeta potentials were not very low and κa was less than 100.

Results and Discussion

Formation of Sulfonated Microcapsules

The formation of sulfonated microcapsules was practically not affected by the molar mixing ratio of the diamines. Thus, the quantity of microcapsules obtained was nearly constant over the range from 0 to 85 mole % of DASSA in the diamine mixtures. No polymer particles were formed in the organic phases under the experimental conditions used in this work.

The sulfonated polyphthalamide microcapsules were generally more resistant to centrifugation than the unsulfonated ones, presumably owing to the presence of strongly ionizable groups in the membranes, which are able to prevent the microcapsules from aggregating in water by electrostatic repulsive forces.

The shape of the microcapsules was invariably spherical in all cases studied, probably due to the osmotic pressure exerted by the polyethylene glycol solution encapsulated within the semipermeable polymer membranes. The microcapsules were also quite stable and no appreciable aggregates were found to form even on storage for over a month in distilled water.

Partition of Diamines between Aqueous and Organic Phases

The partition coefficients of the diamines varied with the concentration of Span 85. Thus, the values of the partition coefficients determined at 620 r.p.m. decreased with increasing concentration of Span 85 as given in Table I.

A comparison of the partition of DEDA with

TABLE I

Partition coefficients of the diamines in the presence of Span 85

Diamine	[Span 85], % (v/v)	Partition coefficient, $K(C_{aq}/C_{org})$
DEDA	5	26.00
	10	18.83
DASSA	5	2.93
	10	2.33

that of DASSA clearly indicates an easier transfer to the organic phase of the latter compared to the former. This will ensure that the sulfonated microcapsules can be prepared favorably using the diamine mixture of any ratio lying in the range described before in the presence of either 5 or 10% (v/v) of Span 85.

Fluorescence of Sulfonated Microcapsules

Figures 1 and 2 are typical photomicrographs of the sulfonated microcapsules taken under u.v. light, showing a beautiful blue fluorescence.

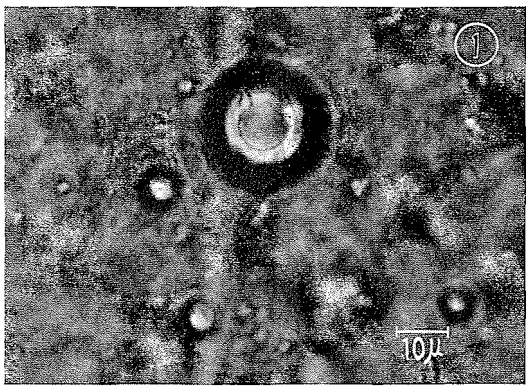

FIG. 1. Photomicrograph of sulfonated polyphthalamide microcapsules taken under ultraviolet light.

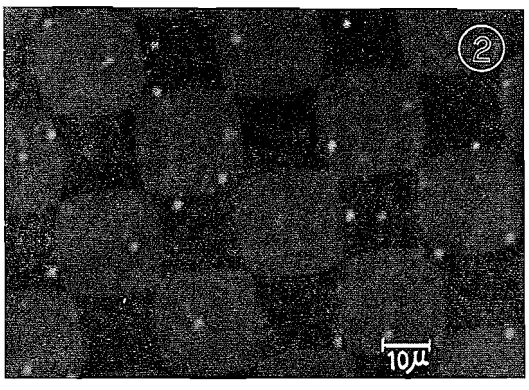

FIG. 2. Photomicrograph of sulfonated polyphthalamide microcapsules taken under ultraviolet light using a yellow filter, FY-4, inserted between the specimen and eyepiece, in addition to the blue one described in text.

The large microcapsules shown in Fig. 1 were specially made by adding sodium methyl sulfate, which is a very effective size controlling agent for microcapsules[1], to the aqueous polyethylene glycol solution to be encapsulated.

The fluorescence spectra of DASSA incorporated in the microcapsule membranes are shown in Fig. 3.

The peak of the spectra appears at about 440 mμ irrespective of the mole percent of DASSA. The fluorescence at this wavelength may arise from the stilbene skeletons of DASSA since some derivatives of DASSA are known to have maximum fluorescence intensity at the same position due to their stilbene skeletons (7, 8).

Size and Size Distribution of Sulfonated Microcapsules

In Fig. 4 is given the size distribution of sulfonated microcapsules in aqueous dispersions in the presence of 10% (v/v) of Span 85. No significant effect is found of varying mole percent of DASSA used on the size distribution curve. This means that the size of the sulfonated microcapsules is mainly determined in the emulsification step of the preparation as in the case of the unsulfonated microcapsules (1).

Table II summarizes the results on the calculations of the length mean diameter, standard deviation, mean surface diameter, and mean volume diameter of the sulfonated microcapsules.

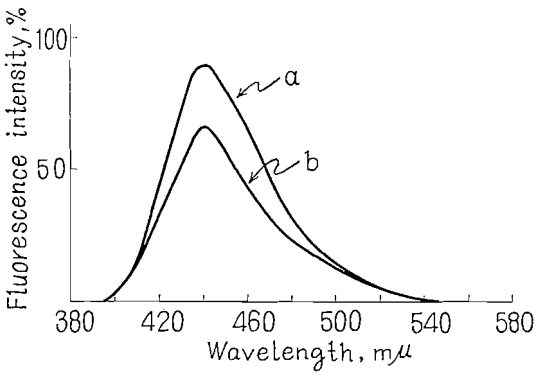

FIG. 3. Fluorescence spectra of DASSA incorporated in the microcapsule membranes prepared at (*a*) 28.6 and (*b*) 23.1 mole % respectively.

[1]Y. Shigeri, M. Koishi, and T. Kondo. Unpublished data.

Can. J. Chem. Downloaded from www.nrcresearchpress.com by 210.87.254.6 on 09/05/12
For personal use only.

Can. J. Chem. Downloaded from www.nrcresearchpress.com by 210.87.254.6 on 09/05/12
For personal use only.

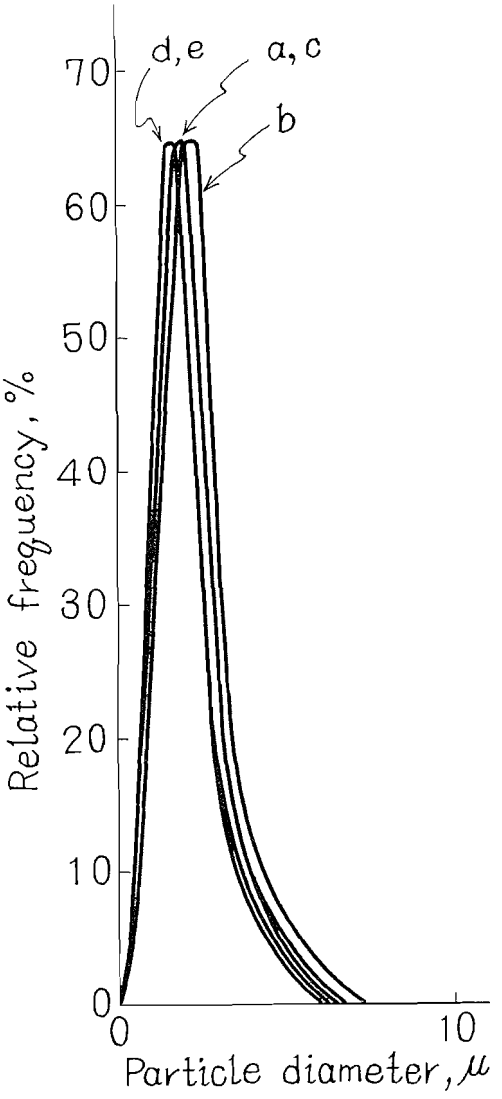

FIG. 4. Size distribution of the sulfonated microcapsules prepared from the mixture of DEDA and DASSA in varying ratio and *p*-phthaloyl dichloride. Mole percent of DASSA: (*a*) 0, (*b*) 28.6, (*c*) 55.6, (*d*) 66.7, and (*e*) 83.3.

TABLE II

Length mean diameter (d_1), standard deviation (δ), mean surface diameter (d_2), and mean volume diameter (d_3) of the sulfonated microcapsules

Mole % of DASSA	d_1(μ)	d_2(μ)	d_3(μ)	δ
0	2.00	2.12	2.25	0.70
28.6	2.32	2.59	2.86	1.15
55.6	2.02	2.26	2.56	1.01
66.7	1.91	2.09	2.33	0.83
83.3	1.89	2.22	2.59	1.17

Electrophoretic Mobilities of Sulfonated Microcapsules

The sulfonated microcapsules always moved toward the anode with a measurable mobility in aqueous potassium nitrate solutions of various ionic strengths, while the unsulfonated microcapsules suspended in the same media had no surface charge detectable by electrophoresis. The presence of Tween 20 did not affect appreciably the values of the zeta potential. The zeta potentials of the microcapsules are plotted in Fig. 5 against the mole % of DASSA in the diamine mixtures used in the preparation.

The absolute value of the zeta potential decreases first as the mole % of DASSA increases and then begins to rise after passing through a minimum at all ionic strengths studied, although the position of the minimum depends slightly on the ionic strength of the medium. The appearance of a minimum was confirmed by separate measurements on several samples of different preparations. This will be interpreted as showing that the increase in the content of sulfonate groups in the membranes facilitates the fixation of counter ions on the left half of the figure, thereby lowering the zeta potentials of the microcapsules, but, on the right half, it tends to exceed the neutralizing effect of counter ions, resulting in an increase of net negative charge of the microcapsules.

Figure 6 shows the effect of counter ion valency

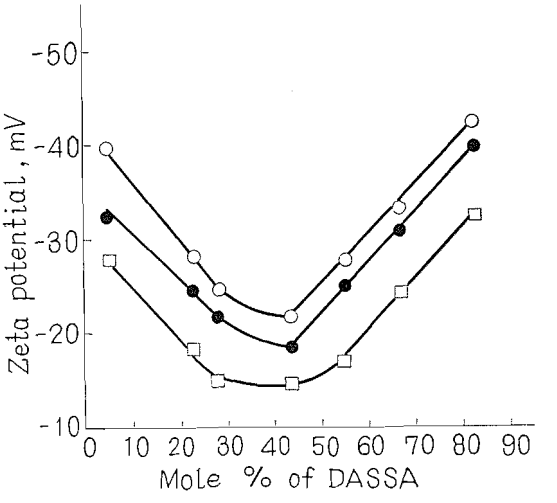

FIG. 5. Zeta potentials of the sulfonated microcapsules in KNO_3 solution as a function of mole % of DASSA. Ionic strength: 1×10^{-2} (□), 1×10^{-3} (●), and 1×10^{-4} (○).

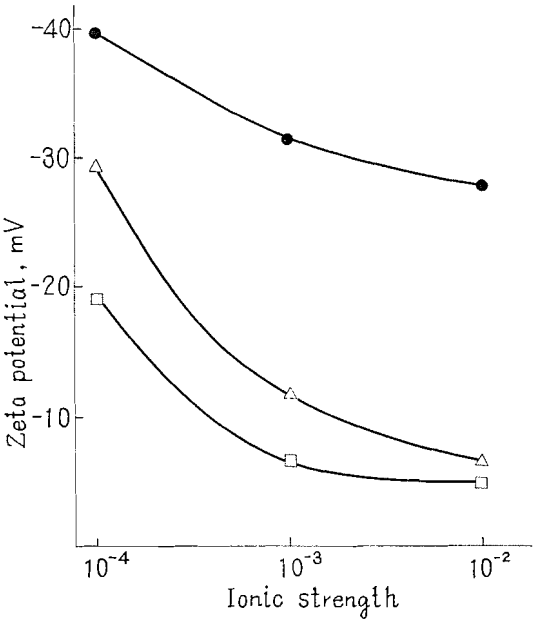

FIG. 6. Effect of potassium, barium, and lanthanum ions on the zeta potentials of sulfonated microcapsules prepared at 4.8 mole % of DASSA. KNO_3 (●), $Ba(NO_3)_2$ (△), and $La(NO_3)_3$ (□).

on the zeta potentials of sulfonated microcapsules. An increasing order, $La^{3+} > Ba^{2+} > K^+$, is evident in the lowering effect of these cations on the zeta potentials. The situation is quite similar to that found in the flocculation of negatively charged hydrophobic colloids by cations of various inorganic electrolytes (9). This will be suggestive in applying the microcapsules to various fields of science and technology.

Acknowledgments

The authors wish to thank the Lion Fat and Oil Company Ltd., Tokyo, for its financial aid and Dr. Stanley G. Mason of McGill University, Montreal, Quebec, for his encouragement and continuing interest in this work.

1. M. KOISHI, N. FUKUHARA, and T. KONDO. Chem. Pharm. Bull. Tokyo. **17**, 804 (1969).
2. T. M. C. CHANG, F. C. MACINTOSH, and S. G. MASON. Can. J. Physiol. Pharmacol. **44**, 115 (1966).
3. D. C. HENRY. Proc. Roy. Soc. London. Ser. A, **183**, 106 (1933).
4. J. TH. G. OVERBEEK. Advances in colloid science. Vol. III. Interscience Publishers, Inc., New York. 1950. p. 116.
5. H. R. KRUYT. Colloid science. Vol. I. Elsevier Publ. Co., Inc., Amsterdam. 1952. p. 208.
6. F. BOOTH. Proc. Roy. Soc. London, Ser. A, **203**, 514 (1950).
7. T. KONDO, A. OKAGAWA, and M. NAGAYAMA. J. Chem. Soc. Japan, Ind. Chem. Sec. **68**, 2125 (1965).
8. T. KONDO and M. NAGAYAMA. Proc. Vth Intern. Congr. Surface Active Substances. In press.
9. H. R. KRUYT. Colloid science. Vol. I. Elsevier Publ. Co., Inc., Amsterdam. 1952. p. 306.

Can. J. Chem. Downloaded from www.nrcresearchpress.com by 210.87.254.6 on 09/05/12
For personal use only.

Can. J. Chem. Downloaded from www.nrcresearchpress.com by 210.87.254.40 on 09/05/12
For personal use only.

Microwave spectrum of morpholine

J. J. SLOAN[1] AND R. KEWLEY
Department of Chemistry, Queen's University, Kingston, Ontario

Received May 21, 1969

The microwave spectra of morpholine and N-deuteromorpholine have been investigated within the 8 to 40 GHz region. For both the normal and the deuterated species, strong *a*-type spectra which are due to the chair conformer with an equatorial imino group were recorded. The ground vibrational state rotational constants and quadrupole coupling constants are (in MHz), for normal morpholine, $A = 4924.88 \pm 0.05$, $B = 4625.15 \pm 0.05$, $C = 2684.25 \pm 0.05$, $\chi_{aa} = 2.22 \pm 0.02$, $\chi_{bb} = 2.51 \pm 0.04$, $\chi_{cc} = -4.73 \pm 0.02$, and for N-deuteromorpholine, $A = 4925.39 \pm 0.05$, $B = 4399.67 \pm 0.05$, $C = 2607.09 \pm 0.05$, $\chi_{aa} = 1.92 \pm 0.02$, $\chi_{bb} = 2.59 \pm 0.04$, $\chi_{cc} = -4.51 \pm 0.02$. The r_s coordinates of the imino hydrogen are (in Å) $a_H = 2.373 \pm 0.005$ and $c_H = 0.10 \pm 0.03$. For the normal species the dipole moment components are (in D) $\mu_a = 1.68 \pm 0.01$, $\mu_c = 0.30 \pm 0.01$, $\mu = 1.71 \pm 0.02$. The value of a_H and the direction of μ with respect to the *a* and *c* principal axes confirm that the observed spectrum is that of the chair equatorial conformer of morpholine.

Canadian Journal of Chemistry, 47, 3453 (1969)

Introduction

Morpholine is a member of a class of compounds which have six-membered heterocyclic aliphatic rings. Its formula may be expressed as

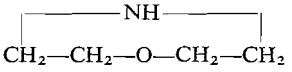

Other compounds of this type for which rotational spectra are known are the oblate symmetric top *sym*-trioxane (1), piperidine (2), and tetrahydropyran (3). All three molecules have been shown to have chair form structures.

Such molecules do not easily lend themselves to complete r_s structure determinations because of the low natural abundances of the atoms ^{13}C, ^{18}O, ^{15}N, and D, and the exorbitant cost of most isotopic syntheses involving these rings. Nevertheless interesting information may be derived from their spectra because of the possibilities of both boat–chair and axial–equatorial isomerism, and also of inversion of the whole molecule by chair–chair interconversion. Also in molecules like piperidine and morpholine the r_s method may still be applied in a limited way to gain a knowledge of the position of the imino hydrogen. This assists in assigning a spectrum to either the axial or the equatorial NH conformer.

The present investigation was undertaken in order to extend knowledge concerning this type of ring system, particularly to discover whether or not the boat form is present in an observable amount and to ascertain, if possible, the relative quantities of axial NH and equatorial NH conformers of the expected chair form of the molecule.

Experimental

The spectrum was observed using a 100 kHz Stark modulation spectrometer which has been described previously (3). Recorder traces were taken by driving the klystron mechanical tuning knob with Bristol synchronous motors having speeds of $\frac{1}{3}$, 1, and $3\frac{1}{3}$ r.p.h. so as to obtain sweep rates of about 10 MHz per min. The charts so produced were valuable for surveying ranges of the spectrum from 50–500 MHz but were not used for accurate frequency measurement, which was achieved as described in ref. 3. The recorder used was a Honeywell Electronik 18, modified to allow the display of both lines and Stark lobes when using phase-sensitive detection.

A sample of the normal morpholine was obtained from the Aldrich Chemical Company Inc. and used without further purification. The index of refraction of this sample was determined as $\eta_{20/D} = 1.4547$ which compares well with the tabulated value of $\eta_{20/D} = 1.4545$ (4). The N-deuteromorpholine sample was prepared by the following procedure. A mixture containing equal volumes of normal morpholine and a solution consisting of 10% sodium deuteroxide in deuterium oxide was stirred vigorously under a dry nitrogen atmosphere for 2 days. The morpholine layer was removed and mixed, again in equal volumes, with a fresh sample of the $NaOD/D_2O$ mixture. This was again stirred under dry nitrogen for a 2 day period. At the end of this time the morpholine layer was removed and added to Linde molecular sieve, type 4A, which had previously been treated with D_2O. On account of the hygroscopic nature of morpholine further drying was required. This was carried out using the type 4A molecular sieve in vacuo. The morpholine/molecular sieve mixture was placed on the vacuum system and degassed. After remaining on the molecular sieve for about 4 h, the morpholine was transferred to a second tube containing freshly degassed molecular sieve. The original molecular sieve was then degassed at 400 °C and all material thus

[1]Present address: Department of Chemistry, Massachusetts Institute of Technology, Cambridge, Massachusetts 02139.

Can. J. Chem. Downloaded from www.nrcresearchpress.com by 210.87.254.40 on 09/05/12
For personal use only.

driven off was discarded. The morpholine was then pumped onto the regenerated sieve. After this procedure had been repeated four times, microwave lines were obtained from the N-deuteromorpholine which were of acceptable intensity and width. Even though some of the stronger lines of the normal morpholine spectrum were still visible at this stage and also some lines of HDO, the pressure broadening due to foreign gases was not considered to contribute significantly to the line width in the N-deuteromorpholine spectrum. The completeness of deuteration was also checked by nuclear magnetic resonance (n.m.r.) using 10% solutions of normal and N-deuteromorpholine in $CHCl_3$ and $CDCl_3$, respectively. From the size of the peak at 200 c.p.s. due to the imino hydrogen, it was concluded that over 95% deuteration was achieved.

Sample pressures ranging from about 10–100 μ were used when observing the spectra. All such observations were made at room temperature on account of the small vapor pressure of morpholine at temperatures below its melting point of −4.9 °C.

Rotational Spectrum

General Features

In order that the assignment of the observed rotational spectrum be achieved more easily, preliminary computations were carried out of the spectra expected from the 4 geometrically possible conformers of morpholine.

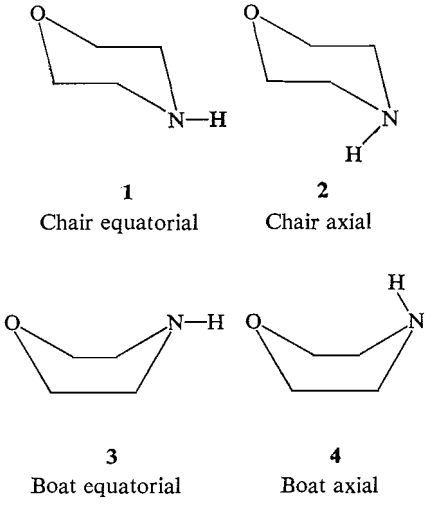

1 Chair equatorial — **2** Chair axial

3 Boat equatorial — **4** Boat axial

This was done with the aid of an IBM FORTRAN IV program which calculates the atomic cartesian coordinates and spectroscopic parameters by means of Euler's angles transformations applied to the assumed bond lengths and angles input data. The program then calculates the estimated dipole moment components using the atomic coordinates and the Pauling electronegativities of the atoms, which are also supplied as input data. The parameters defining the assumed structures were ∠OCC = ∠CCN = ∠OCH = ∠CCH = 109°28′; ∠COC = ∠CNC = 110°; bond lengths C—O, C—C, C—N, C—H, and N—H of 1.43, 1.54, 1.47, 1.11, and 1.01 Å, respectively. The results of these computations for the conformers **1**–**4** are shown in Table I.

TABLE I

Predicted rotational constants and dipole moment components for conformers of normal morpholine

Parameter	Value in conformer 1	2	3	4
A (MHz)	4927.9	4849.5	4759.9	4847.6
B "	4553.1	4642.4	4730.8	4678.6
C "	2667.9	2722.4	2782.5	2851.6
κ	0.67	0.80	0.97	0.83
μ_a (D)	1.12	0.34	1.35	0.00
μ_c (D)	0.21	1.38	2.85	2.00
μ_{total} (D)	1.14	1.42	3.14	2.00

It may be seen that for all 4 conformers, the resulting rotational constants are those for asymmetric tops having $0 < \kappa < 1$. The dominant feature of the microwave spectrum of this type of oblate slightly asymmetric top is the form of the two strong a-type Q-branches ${}^aQ_{0,-1}$ and ${}^aQ_{2,-1}$, which appear as doublet progressions with frequency spacing between members of a doublet, spacing between successive doublets and line intensities all decreasing as each doublet series approaches its branch head. For a molecule such as conformer **3**, having $\kappa = 0.97$ and large μ_a, the Q-branch heads would be very dense and over 20 strong absorption lines would fall within about 30 MHz of a typical branch head. Such a feature would be unmistakeable. From the μ_a values of Table I it can be seen that conformer **1** is the only other form for which a strong a-type spectrum would be expected.

The observed spectra of normal and N-deuteromorpholine do contain many intense Q-branch lines. However, these lines had to be identified initially by their appearance at fairly low Stark voltages, about 40 V cm^{-1}, and by the large number of rapidly moving Stark components associated with each line. The frequency separations and doublet splittings were much larger than the ones predicted on the basis of the conformer **3** structure. This is illustrated in Fig. 1, a portion of the spectrum of undeuterated

Can. J. Chem. Downloaded from www.nrcresearchpress.com by 210.87.254.40 on 09/05/12
For personal use only.

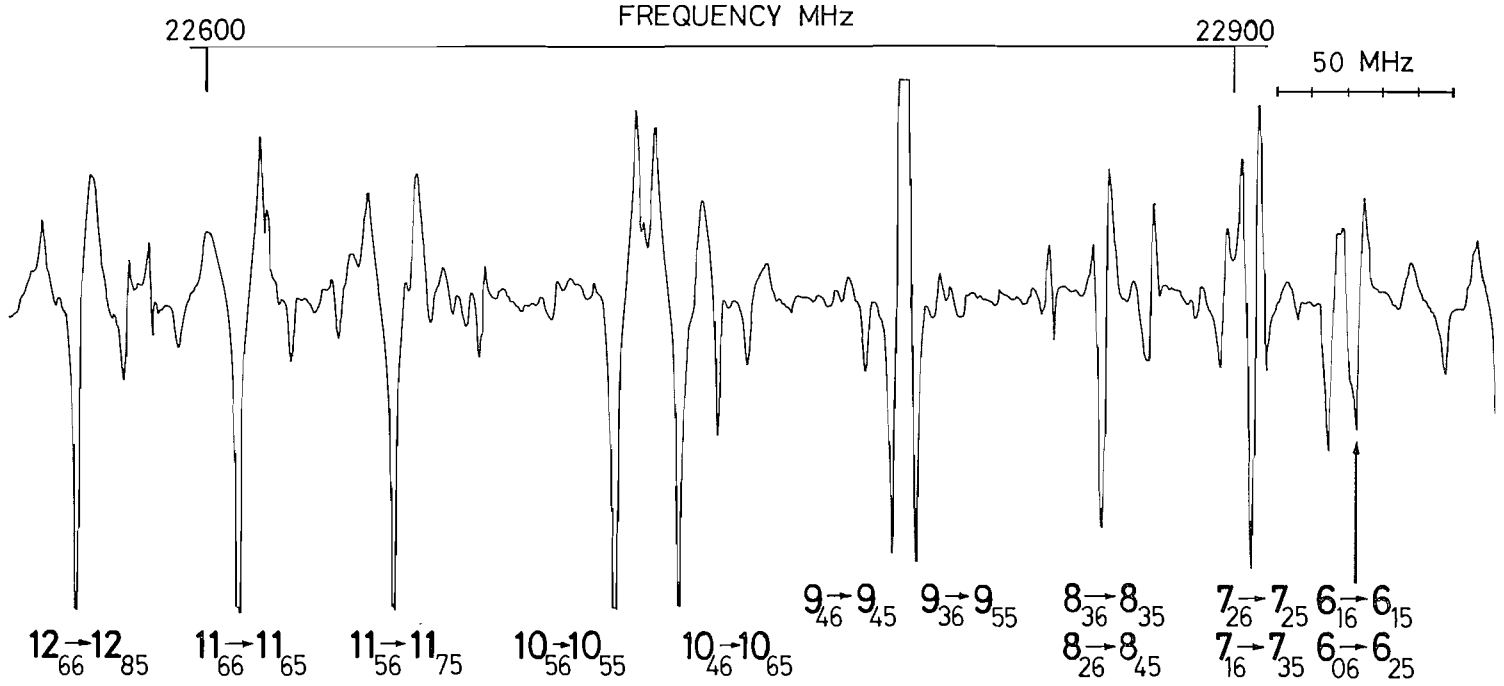

FIG. 1. Recorder trace of the Q-branch doublet series $K_{+1} = 6 \rightarrow 5$ for the ground vibrational state of undeuterated morpholine. For conformers **2** and **4** such a series would not be sufficiently intense to be detectable. For conformer **3** the first 20 lines of the series are predicted to fall within 30 MHz of the $J = 6 \rightarrow 6$ branch head.

Can. J. Chem. Downloaded from www.nrcresearchpress.com by 210.87.254.40 on 09/05/12
For personal use only.

morpholine. Such Q-branch series heads are observed to occur at intervals of slightly more than 4000 MHz for both of the isotopic forms studied. A number of weaker low J a-type R-branch lines were also observed and identified by means of their characteristic Stark patterns. The assignable lines of both isotopic forms in the region studied are therefore to be attributed to the chair equatorial form, conformer **1**. No c-type transitions could be found. This was expected because of the low μ_c estimated for conformer **1**.

None of the lines in any observed region could be positively assigned to the chair axial form. This does not necessarily show that this form is absent, however. As may be seen from the μ_a and μ_c components of conformer **2** in Table I, this form of the molecule is predicted to give rise to a strong c-type spectrum but only a very weak a-type spectrum. A c-type spectrum prediction for J values between 1 and 12 using the computed rotational constants of conformer **2** shows that only 8 R-branch and 5 weak Q-branch lines are expected within the entire attainable frequency range. Because of the extremely rich character of the observed chair equatorial spectrum, it is likely that the 13 lines of the chair axial spectrum are present but cannot be picked out from amongst the many hundreds of strong a-type lines of the chair equatorial form. As indicated above, no spectra due to the much more symmetric boat forms were found.

The observed spectra have many features in common with the spectrum of tetrahydropyran which facilitated the assignment and analysis. An important extra effect in the morpholine spectrum is the hyperfine structure arising from quadrupole coupling of the ^{14}N nucleus. Almost all the assigned lines appear as doublets under high resolution with measurable hyperfine splittings in the range 0.500 to 2.000 MHz. Before precise values of the rotational constants could be evaluated, it was therefore necessary to analyze the small quadrupole splittings and hence calculate the unperturbed line frequencies.

Analysis of ^{14}N Quadrupole Hyperfine Interaction

The effect of quadrupole splitting due to the ^{14}N nucleus was more noticeable for Q-branch than R-branch lines. All Q-branch lines with J less than 8 had measurable splittings, whereas splittings were resolvable only for the $J = 1$–2 and some of the $J = 2$–3 R-branch transitions.

Because of the small values of the ^{14}N quadrupole coupling constants, in no case could more than 2 hyperfine peaks be resolved even though 3 strong hyperfine lines with $\Delta F = \Delta J$ are predicted for a nucleus with spin quantum

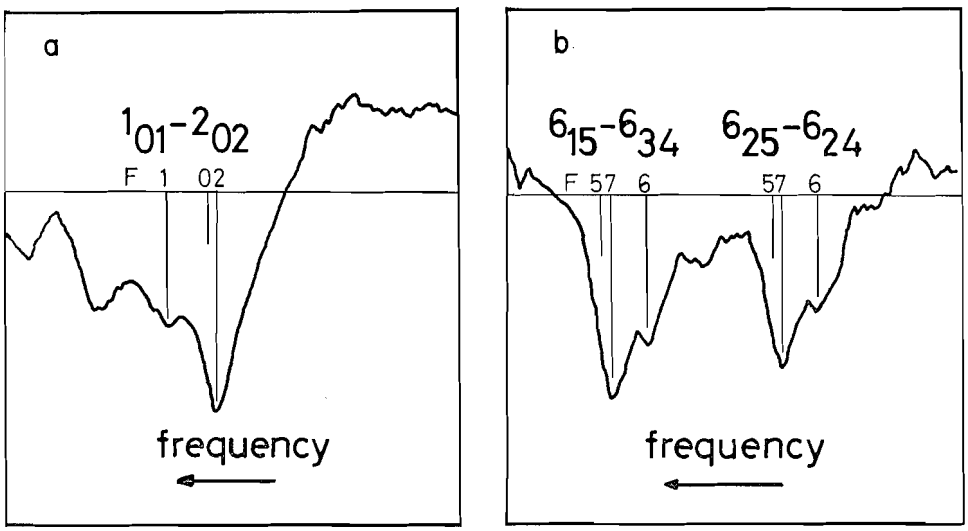

FIG. 2. Oscilloscope photographs showing typical quadrupole hyperfine patterns for a-type R and Q branch transitions. (a) The R-branch transition $1_{01} — 2_{02}$, observed splitting 0.767 MHz. (b) The Q-branch transitions $6_{15} — 6_{34}$ and $6_{25} — 6_{24}$, observed splittings 1.043 and 1.127 MHz, respectively.

Can. J. Chem. Downloaded from www.nrcresearchpress.com by 210.87.254.40 on 09/05/12
For personal use only.

number $I = 1$. For a Q-branch line the component for which $F = J \rightarrow J$ appears as a separately observable peak, whereas the components with $F = J - 1 \rightarrow J - 1$ and $F = J + 1 \rightarrow J + 1$ are contained in the second peak. In such a case the top of the larger resolved peak is taken to correspond to the frequency of the more intense $F = J + 1 \rightarrow J + 1$ hyperfine component. Similarly for a low J R-branch transition the $F = J \rightarrow J + 1$ component is usually separately resolved but the components with $F = J - 1 \rightarrow J$ and $F = J + 1 \rightarrow J + 2$ are coalesced. This is illustrated in Fig. 2.

The elements χ_{aa}, χ_{bb}, and χ_{cc} of the ^{14}N quadrupole tensor, referred to the principal rotation axes of the molecule, were calculated for each of the normal and N-deutero species by the following procedure. The quadrupole energy E_Q may be written as a function of the asymmetry parameter κ and the quantum numbers F and J as

$$[1] \quad E_Q(\kappa, F, J) = \{(\chi_{aa} + \chi_{cc})f_1(\kappa, J) + (\chi_{aa} - \chi_{cc})f_2(\kappa)\} \frac{Y(F)}{J(J+1)}$$

where $Y(F)$ is Casimir's function and

$$f_1(\kappa, J) = J(J+1) - 3\frac{\partial}{\partial \kappa} E(\kappa)$$

$$f_2(\kappa) = E(\kappa) - \kappa \frac{\partial}{\partial \kappa} E(\kappa)$$

The splitting $\Delta\nu$ on a transition between two quadrupole components for which $F_1 \rightarrow F_1'$ and $F_2 \rightarrow F_2'$ can be expressed as a linear equation of the form

$$[2] \quad \Delta\nu = (\chi_{aa} + \chi_{cc})g_1 + (\chi_{aa} - \chi_{cc})g_2$$

where g_1 and g_2 are functions of J, κ, F_1, F_1', F_2, and F_2', which can be evaluated if the asymmetry and the appropriate quantum numbers are known.

The splittings between observed components for 19 transitions in the spectrum of normal morpholine and for 20 transitions in the spectrum of N-deuteromorpholine were measured. The corresponding functions g_1 and g_2 were evaluated for each $\Delta\nu$ and the data were subjected to least squares type fits to obtain $(\chi_{aa} + \chi_{cc})$ and $(\chi_{aa} - \chi_{cc})$ for each species. The calculated and observed splittings are shown in Tables II and III. The variance of least squares residuals was 0.003 MHz in each case.

The values of χ_{bb} were found from the Laplace relation $\Sigma\chi_{mm} = 0$, $m = a, b, c$. The values of χ_{bb} for both isotopic forms of the molecule should be equal on account of the molecular symmetry. From Table IV this may be seen to be the case within experimental error. It would

TABLE II

Quadrupole hyperfine splittings for normal morpholine, chair equatorial conformer

Transition	$\Delta\nu_{obs}$ (MHz)	$\Delta\nu_{obs} - \Delta\nu_{calcd}$ (MHz)
$1_{01} - 2_{02}$	0.767	−0.068
$2_{11} - 3_{12}$	0.822	0.062
$3_{12} - 4_{13}$	0.569	−0.022
$4_{04} - 4_{23}$	1.719	0.018
$5_{24} - 5_{23}$	1.257	0.092
$6_{25} - 6_{24}$	1.127	0.054
$7_{35} - 7_{34}$	0.731	−0.085
$6_{24} - 6_{43}$	0.829	0.000
$7_{34} - 7_{53}$	0.573	−0.050
$8_{44} - 8_{63}$	0.441	−0.031
$6_{15} - 6_{34}$	1.043	−0.029
$7_{25} - 7_{44}$	0.790	−0.023
$8_{35} - 8_{54}$	0.571	−0.066
$6_{34} - 6_{33}$	0.913	0.056
$7_{44} - 7_{43}$	0.681	0.011
$6_{06} - 6_{25}$	1.294	−0.011
$7_{16} - 7_{35}$	1.005	0.015
$8_{26} - 8_{45}$	0.808	0.031
$9_{36} - 9_{55}$	0.559	−0.068

TABLE III

Quadrupole hyperfine splittings for N-deuteromorpholine, chair equatorial conformer

Transition	$\Delta\nu_{obs}$ (MHz)	$\Delta\nu_{obs} - \Delta\nu_{calcd}$ (MHz)
$1_{01} - 2_{02}$	0.896	0.083
$1_{01} - 2_{20}$	1.977	0.011
$2_{11} - 3_{12}$	0.635	−0.056
$3_{03} - 3_{22}$	1.920	0.064
$4_{13} - 4_{32}$	1.030	−0.040
$5_{15} - 5_{14}$	1.438	0.002
$7_{35} - 7_{34}$	0.805	−0.015
$8_{45} - 8_{44}$	0.572	−0.109
$5_{05} - 5_{24}$	1.450	0.017
$6_{15} - 6_{34}$	1.094	0.055
$7_{25} - 7_{44}$	0.750	−0.036
$8_{35} - 8_{54}$	0.498	−0.108
$6_{34} - 6_{33}$	0.912	−0.057
$6_{24} - 6_{43}$	0.738	−0.060
$7_{34} - 7_{53}$	0.504	−0.024
$7_{16} - 7_{35}$	0.952	−0.036
$8_{26} - 8_{45}$	0.732	−0.025
$7_{26} - 7_{25}$	0.990	0.027
$8_{36} - 8_{35}$	0.748	−0.015
$7_{17} - 7_{16}$	1.150	0.050

Can. J. Chem. Downloaded from www.nrcresearchpress.com by 210.87.254.40 on 09/05/12
For personal use only.

TABLE IV

Diagonal elements of the ^{14}N quadrupole coupling tensor in the principal molecular axis system

Element	Value	
	Normal morpholine	N-deuteromorpholine
χ_{aa} (MHz)	2.22±0.02	1.92±0.02
χ_{bb} (MHz)	2.51±0.05	2.59±0.05
χ_{cc} (MHz)	−4.73±0.02	−4.51±0.02

be desirable to obtain also the values of χ_{xx}, χ_{yy}, χ_{zz}, the elements of the ^{14}N quadrupole tensor in the quadrupole axis system. However, this requires a precise knowledge of the angle of principal axes rotation on H → D substitution which is not available in the present case because of the very small c coordinate of the imino hydrogen and the very small value of the angle.

The value of χ_{bb}, however, remains unchanged during the transformation of axes becoming equal to χ_{yy}, where y is perpendicular to the single molecular symmetry plane. The average value of 2.55 ± 0.05 MHz observed for the constant is comparable to the value of the coupling constant for the corresponding direction for each of the related molecules: trimethylamine, 2.74 MHz (5); dimethylamine, 3.04 MHz (6); methylamine, 2.12 MHz (7); and ammonia, 2.04 MHz (8).

Rotational Constants and Imino Hydrogen Coordinates

Using the determined values of χ_{aa} and χ_{cc} the unperturbed line frequencies were calculated using eq. [1]. Because only the a-type spectrum was observed, and because the derived value of the rotational constant A is relatively insensitive to small changes in the frequencies of the a-type lines, the following method was adopted for the determination of A, B, and C. For each isotopic species the unperturbed frequencies of 12 a-type R-branch lines were calculated from the observed frequencies of Tables VI and VII. The resulting frequencies were then subjected to least squares fitting to give the final values of B and C. For these calculations the resulting variances were 0.044 MHz for normal morpholine and 0.024 MHz for N-deuteromorpholine. The exact value of A for each species was then obtained by the well known graphical method in which $\frac{1}{2}(A - C)$ is plotted against the asymmetry parameter κ for a series of Q-branch lines. The resulting rotational constants are given in Table V and the calculated and observed frequencies in Tables VI and VII.

TABLE V

Rotational constants (MHz) and principal moments of inertia* (u Å²) of morpholine, ground vibrational state, chair equatorial conformer

Parameters	Value	
	Normal morpholine	N-deuteromorpholine
A ±0.05	4924.88	4925.39
B ±0.05	4625.15	4399.67
C ±0.05	2684.25	2607.09
κ ±0.00011	0.73246	0.54646
I_a	102.617	102.606
I_b	109.267	114.867
I_c	188.275	193.847

*Conversion factor 5.05377 MHz u Å².

TABLE VI

a-Type transitions of normal morpholine, chair equatorial conformer

Transition	$F \rightarrow F'$	ν_{obs}	$\nu_{obs} - \nu_{calcd}$
R-branch			
$1_{01} - 2_{02}$	2 — 3	12 945.43	0.14
	1 — 2	12 946.19	0.06
$1_{11} - 2_{12}$	2 — 3	12 677.75	0.08
	1 — 2	12 678.36	−0.08
$1_{10} - 2_{11}$	2 — 3	16 559.99	0.34
	0 — 1	16 561.80	0.36
$1_{01} - 2_{20}$	2 — 3	21 373.47	0.22
$2_{02} - 3_{03}$	3 — 4	18 207.15	0.22
$2_{12} - 3_{13}$	3 — 4	18 177.85	0.85
$2_{11} - 3_{12}$	3 — 4	22 669.24	0.17
	2 — 3	22 670.06	0.23
$2_{21} - 3_{22}$	3 — 4	21 928.64	0.60
	1 — 2	21 927.92	0.26
$2_{20} - 3_{21}$	3 — 4	25 648.95	−0.33
$3_{03} - 4_{04}$	4 — 5	23 560.81	0.09
$3_{13} - 4_{14}$	4 — 5	23 558.97	0.29
$3_{12} - 4_{13}$	4 — 5	27 812.00	0.10
	3 — 4	27 812.57	−0.07
Q-branch			
$4_{04} - 4_{23}$	5 — 5	14 583.98	0.28
	4 — 4	14 582.26	0.26
$5_{14} - 5_{33}$	6 — 6	14 566.56	0.21
	5 — 5	14 565.29	0.09
$6_{24} - 6_{43}$	7 — 7	14 555.88	0.01
	6 — 6	14 555.05	0.01
$7_{34} - 7_{53}$	8 — 8	14 573.99	0.35
	7 — 7	14 573.42	0.40
$8_{44} - 8_{63}$	9 — 9	14 655.26	−0.07
	8 — 8	14 654.81	−0.05
$9_{54} - 9_{73}$	10 — 10	14 853.94	0.18
	9 — 9	14 853.62	0.39
$4_{14} - 4_{13}$	5 — 5	14 568.66	0.12
	4 — 4	14 569.39	0.56
$5_{24} - 5_{23}$	6 — 6	14 505.85	0.00
	5 — 5	14 504.59	−0.10
$6_{34} - 6_{33}$	7 — 7	14 376.01	−0.32
	6 — 6	14 375.10	−0.37

TABLE VI *(Concluded)*

Transition	$F \rightarrow F'$	ν_{obs}	$\nu_{obs} - \nu_{calcd}$
$7_{44} - 7_{43}$	8 — 8	14 134.23	−0.84
	7 — 7	14 133.54	−0.86
$6_{15} - 6_{34}$	7 — 7	18 724.13	0.03
	6 — 6	18 723.09	0.06
$7_{25} - 7_{44}$	8 — 8	18 684.11	−0.20
	7 — 7	18 683.32	−0.18
$8_{35} - 8_{54}$	9 — 9	18 632.13	−0.52
	8 — 8	18 631.56	−0.45
$9_{45} - 9_{64}$	10 — 10	18 574.01	−0.81
	9 — 9	18 573.52	−0.79
$10_{55} - 10_{74}$	11 — 11	18 523.33	−1.04
	10 — 10	18 522.78	−1.17
$11_{65} - 11_{84}$	12 — 12	18 504.73	−1.06
$12_{75} - 12_{94}$	13 — 13	18 557.56	−0.64
$5_{15} - 5_{14}$	6 — 6	18 749.46	−0.75
$6_{25} - 6_{24}$	7 — 7	18 718.72	0.06
	6 — 6	18 717.59	0.00
$7_{35} - 7_{34}$	8 — 8	18 664.06	−0.38
	7 — 7	18 663.33	−0.29
$8_{45} - 8_{44}$	9 — 9	18 573.86	0.27
	8 — 8	18 572.99	0.04
$9_{55} - 9_{54}$	10 — 10	18 422.58	−1.20
	9 — 9	18 422.03	−1.22
$10_{65} - 10_{64}$	11 — 11	18 179.22	−1.93
	10 — 10	18 178.74	−1.96
$6_{06} - 6_{25}$	7 — 7	22 923.66	0.22
	6 — 6	22 922.37	0.23
$7_{16} - 7_{35}$	8 — 8	22 899.06	−0.23
	7 — 7	22 898.06	−0.22
$8_{26} - 8_{45}$	9 — 9	22 863.02	−0.47
	8 — 8	22 862.21	−0.50
$9_{36} - 9_{55}$	10 — 10	22 812.52	−0.85
	9 — 9	22 811.96	−0.78
$10_{46} - 10_{65}$	11 — 11	22 745.60	−1.20
	10 — 11	22 745.11	−1.17
$11_{56} - 11_{75}$	12 — 12	22 661.08	−2.03
$12_{66} - 12_{85}$	13 — 13	22 563.06	−2.15
$6_{16} - 6_{15}$	7 — 7	22 923.66	0.28
$7_{26} - 7_{25}$	8 — 8	22 899.06	0.19
	7 — 7	22 898.05	0.17
$8_{36} - 8_{35}$	9 — 9	22 861.40	−0.35
	8 — 8	22 860.55	−0.24
$9_{46} - 9_{45}$	10 — 10	22 806.34	−0.96
	9 — 9	22 805.86	−0.82
$10_{56} - 10_{55}$	11 — 11	22 727.36	−1.41
	10 — 10	22 726.91	−1.34
$11_{66} - 11_{65}$	12 — 12	22 613.42	−2.26
$12_{76} - 12_{75}$	13 — 13	22 449.69	−2.63

The effects of centrifugal distortion were neglected throughout this treatment. The values of $\nu_{obs} - \nu_{calcd}$ for some of the Q-branch transitions indicate, however, that centrifugal stretching becomes noticeable for $J > 8$.

The r_s coordinates of the imino hydrogen were calculated from the observed moments of inertia of Table V using Kraitchman's equations for an asymmetric rotor (9). Because of the symmetry of morpholine the b coordinate is set at zero, the imino group lying in the ac plane. The magnitudes of the a and c coordinates, see Table VIII, confirm that the spectrum is that of the chair equatorial conformer. The large error in the c coordinate is to be expected since the substituted atom lies very close to the c axis of normal morpholine. The angle through which the principal a and c axes rotate on H → D substitution is very small, being estimated at 0.2°.

Dipole Moment

The Stark effect was studied for 3 a-type R-branch transitions in the normal morpholine spectrum. At field strengths above 25 V cm^{-1} some non-quadratic Stark effects were noticed for the $M = 1$ component of the $1_{11} - 2_{12}$ transition. This effect is expected for a near oblate rotor with appreciable a component of the dipole moment and has also been observed in the spectrum of the molecule CH_3CHF_2 (10). This non-quadratic behavior is caused by perturbations between the energy levels 2_{02} and 2_{12}, which are nearly degenerate with a separation of 32 MHz. The $1_{10} - 2_{11}$ transition has a normal Stark behavior. The quadratic behavior at low field strengths was employed in the dipole moment determination. The dipole moment components μ_a and μ_c were obtained by least squares fitting to the observed coefficients $\Delta\nu/E^2$, see Table IX. The value of $\mu_{ocs} = 0.7124 \pm 0.0002$ D (11) was used in calibrating the Stark cell.

An interesting comparison can be made among the dipole moments of tetrahydropyran and the equatorial forms of piperidine and morpholine, see Table X. It may be seen that the a components of the CNC moment and the NH bond moment largely cancel in piperidine to give a small μ_a, so that the larger μ_a in morpholine can be attributed to the COC moment, which is also responsible for the large μ_a of tetrahydropyran. The μ_a values also indicate that in morpholine the NH bond moment is more than the CNC moment. The very small observed value of μ_c for morpholine, which was also predicted for conformer **1**, see Table I, confirms the expectation that the c-type spectrum would most likely be unobservable. The observed angle between the total dipole vector and the principal a axis of normal morpholine is 10°, as shown in Fig. 3, which agrees very closely with that calculated as 10.5° from the estimated dipole moment components of Table I.

Can. J. Chem. Downloaded from www.nrcresearchpress.com by 210.87.254.40 on 09/05/12
For personal use only.

Can. J. Chem. Downloaded from www.nrcresearchpress.com by 210.87.254.40 on 09/05/12
For personal use only.

TABLE VII

a-Type transitions of N-deuteromorpholine, chair equatorial conformer

Transition	$F \rightarrow F'$	ν_{obs}	$\nu_{obs} - \nu_{calcd}$
R-branch			
$1_{01} - 2_{02}$	2 — 3	12 646.50	−0.29
	1 — 2	12 647.38	−0.23
$1_{11} - 2_{12}$	2 — 3	12 220.98	0.26
$1_{10} - 2_{11}$	2 — 3	15 806.03	−0.02
	1 — 2	15 806.51	−0.06
$1_{01} - 2_{20}$	2 — 3	21 069.24	0.77
	1 — 2	21 067.26	0.76
$2_{02} - 3_{03}$	3 — 4	17 728.29	1.24
$2_{12} - 3_{13}$	3 — 4	17 640.87	0.58
$2_{11} - 3_{12}$	3 — 4	22 120.97	0.30
	2 — 3	22 121.60	0.24
$2_{21} - 3_{22}$	3 — 4	21 020.14	0.01
$2_{20} - 3_{21}$	3 — 4	24 312.21	−0.11
$3_{03} - 4_{04}$	4 — 5	22 902.36	0.34
$3_{13} - 4_{14}$	4 — 5	22 891.41	0.24
$3_{12} - 4_{13}$	4 — 5	27 191.53	0.29
$3_{22} - 4_{23}$	4 — 5	26 797.43	0.12
$4_{04} - 5_{05}$	5 — 6	28 110.70	0.09
Q-branch			
$3_{03} - 3_{22}$	4 — 4	10 347.56	0.49
	3 — 3	10 345.64	0.42
$4_{13} - 4_{32}$	5 — 5	10 664.33	0.42
	4 — 4	10 663.30	0.46
$6_{33} - 6_{52}$	7 — 7	12 633.91	1.53
$3_{13} - 3_{12}$	4 — 4	9 858.79	0.35
$4_{23} - 4_{22}$	5 — 5	9 270.22	−0.02
	4 — 4	9 268.81	−0.12
$4_{04} - 4_{23}$	5 — 5	14 242.98	0.61
	4 — 4	14 241.47	0.74
$5_{14} - 5_{33}$	6 — 6	14 237.62	0.50
	5 — 5	14 236.14	0.12
$6_{24} - 6_{43}$	7 — 7	14 325.02	0.34
	6 — 6	14 324.29	0.41
$7_{34} - 7_{53}$	8 — 8	14 626.41	0.00
	7 — 7	14 626.01	0.03
$9_{54} - 9_{73}$	10 — 10	16 639.64	2.19
$4_{14} - 4_{13}$	5 — 5	14 158.85	0.33
	4 — 4	14 156.96	0.11
$5_{24} - 5_{23}$	6 — 6	13 910.12	0.17
	5 — 5	13 908.69	−0.09
$6_{34} - 6_{33}$	7 — 7	13 394.33	−0.45
	6 — 6	13 393.42	−0.40
$5_{05} - 5_{24}$	6 — 6	18 295.86	0.41
	5 — 5	18 294.41	0.37
$6_{15} - 6_{34}$	7 — 7	18 223.20	−0.01
	6 — 6	18 222.11	−0.06
$7_{25} - 7_{44}$	8 — 8	18 139.12	0.17
	7 — 7	18 138.37	0.21
$8_{35} - 8_{54}$	9 — 9	18 079.82	−0.13
	8 — 8	18 079.36	0.02
$9_{45} - 9_{64}$	10 — 10	18 122.22	0.03
$10_{55} - 10_{74}$	11 — 11	18 393.68	−0.07
$11_{65} - 11_{84}$	12 — 12	19 081.21	1.06
$12_{75} - 12_{94}$	13 — 13	20 415.62	2.85
$5_{15} - 5_{14}$	6 — 6	18 284.58	−0.08
	5 — 5	18 283.14	−0.07
$6_{25} - 6_{24}$	7 — 7	18 170.02	0.24
	6 — 6	18 168.83	0.10
$7_{35} - 7_{34}$	8 — 8	17 947.99	−0.10
	7 — 7	17 947.13	−0.14
$8_{45} - 8_{44}$	9 — 9	17 532.87	−0.74
	8 — 8	17 532.30	−0.63
$6_{06} - 6_{25}$	7 — 7	22 373.31	−0.59

TABLE VII *(Concluded)*

Transition	$F \rightarrow F'$	ν_{obs}	$\nu_{obs} - \nu_{calcd}$
$7_{16} - 7_{35}$	8 — 8	22 300.39	0.48
	7 — 7	22 299.44	0.52
$8_{26} - 8_{45}$	9 — 9	22 194.76	0.01
	8 — 8	22 194.03	0.04
$6_{16} - 6_{15}$	7 — 7	22 373.35	0.65
$7_{26} - 7_{25}$	8 — 8	22 293.11	0.32
	7 — 7	22 292.12	0.29
$8_{36} - 8_{35}$	9 — 9	22 164.40	−0.02
	8 — 8	22 163.65	0.00
$9_{46} - 9_{45}$	10 — 10	21 956.41	−0.44
$10_{56} - 10_{55}$	11 — 11	21 614.62	−1.27
$7_{07} - 7_{26}$	8 — 8	26 454.55	0.49
	7 — 7	26 453.40	0.47
$8_{17} - 8_{36}$	9 — 9	26 386.58	−0.03
$9_{27} - 9_{46}$	10 — 10	26 290.83	−0.36
$10_{37} - 10_{56}$	11 — 11	26 161.28	−0.61
$12_{57} - 12_{76}$	13 — 13	25 596.58	−1.67
$7_{17} - 7_{16}$	8 — 8	26 454.55	0.62
	7 — 7	26 453.40	0.57
$8_{27} - 8_{26}$	9 — 9	26 386.58	0.80
$9_{37} - 9_{36}$	10 — 10	26 287.37	0.30
$10_{47} - 10_{46}$	11 — 11	26 145.01	−0.72

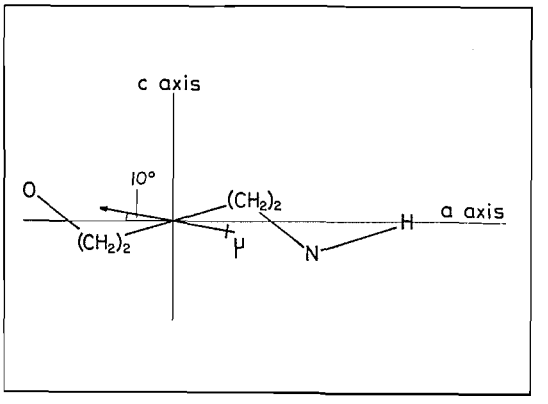

FIG. 3. The conformation, principal rotation axes, and dipole moment direction for the chair equatorial conformer of morpholine. The *b* axis is perpendicular to the plane of the figure.

TABLE VIII

Imino hydrogen r_s coordinates

	Value	
r_s coordinates	H → D substitution	D → H substitution
$\|a\|$ (Å) (±0.005)	2.373	2.343
b (Å)	(0)	(0)
$\|c\|$ (Å) (±0.03)	0.10	0.09

Can. J. Chem. Downloaded from www.nrcresearchpress.com by 210.87.254.40 on 09/05/12
For personal use only.

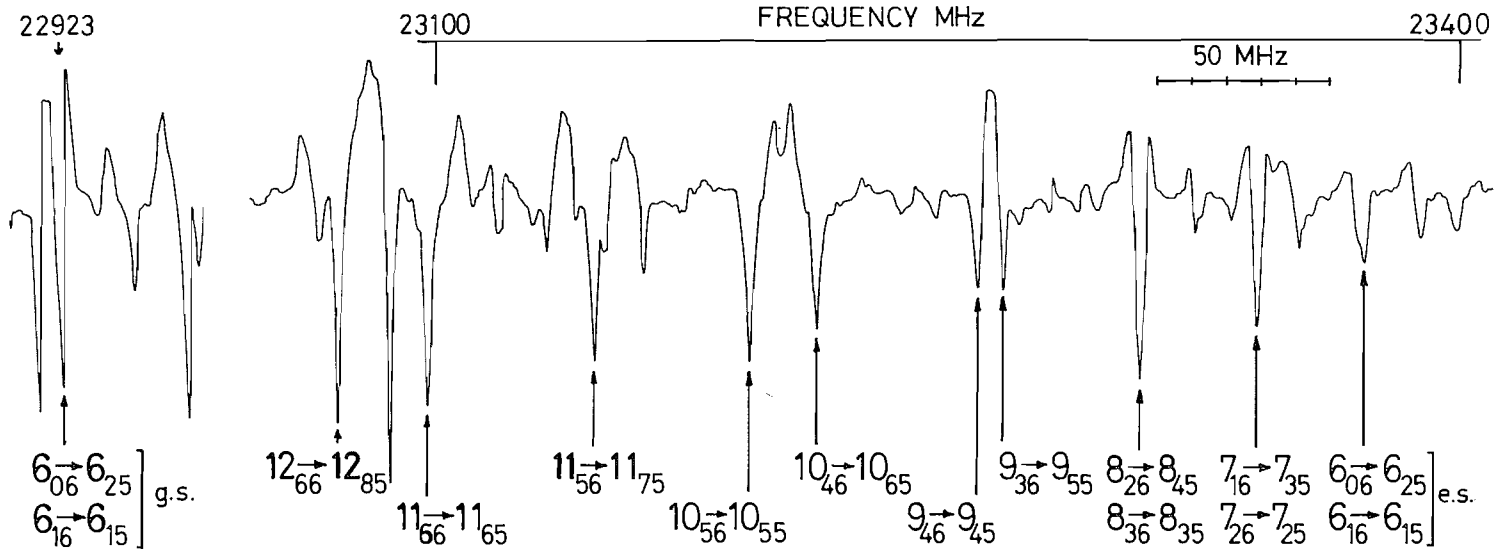

FIG. 4. Recorder trace of the Q-branch doublet series $K_{+1} = 6 \rightarrow 5$ for an excited state (e.s.) of chair equatorial morpholine. The first peak of the corresponding series for the ground state (g.s.) is shown for comparison on the left side of the figure. Because of the relative intensities the vibration is considered to be the lowest energy ring deformation mode.

Can. J. Chem. Downloaded from www.nrcresearchpress.com by 210.87.254.40 on 09/05/12
For personal use only.

TABLE IX

Stark effect coefficients and dipole moment components of normal morpholine, chair equatorial conformer

Transition	M	$10^3 \times \Delta\nu/E^2$ (MHz cm^2 V^{-2}) Observed	Calculated
$1_{11} - 2_{12}$	1	0.6277	0.6244
$1_{11} - 2_{12}$	0	0.0519	0.0550
$1_{10} - 2_{11}$	1	−0.3483	−0.3251
$2_{12} - 3_{22}$	2	0.5805	0.5952
$2_{12} - 3_{22}$	1	0.1582	0.1622
$2_{12} - 3_{22}$	0	0.0174	0.0178

Dipole moment	Value (D)
μ_a	1.68 ± 0.01
μ_c	0.30 ± 0.01
μ	1.71 ± 0.02

TABLE X

Dipole moments of tetrahydropyran, piperidine, and morpholine

Dipole moment (D)	Value Piperidine (ref. 2)	Tetrahydropyran (ref. 3)	Morpholine
μ_a	0.195	1.53	1.68
μ_c	0.781	0.82	0.30
μ	0.80	1.74	1.71

Excited Vibrational States

In addition to the ground state spectrum discussed above, a spectrum from a vibrationally excited form of normal morpholine was observed. Satellites of the two Q-branches having $K_{+1} = 6 \rightarrow 5$ were observed with a branch head $6_{06} - 6_{25}$ and $6_{16} - 6_{15}$ 450 MHz above the corresponding ground state lines, see Fig. 4. From the intensity ratios of the excited state to ground state lines the vibrational state was estimated to lie 200 ± 50 cm^{-1} above the ground state. The infrared and Raman spectra of morpholine have not yet been investigated in this region. However, the energy difference is similar to those for the lowest excited states of piperidine, 246 cm^{-1} (12), and tetrahydropyran, 256 cm^{-1} (13); this vibration is therefore most likely the lowest frequency ring deformation mode of morpholine.

Conclusion

The observed rotational spectra are due to the chair equatorial conformers of morpholine and N-deuteromorpholine. The lack of a *c*-type spectrum for either isotopic form can be ascribed to the small value of μ_c. Although the spectrum of the chair–axial conformer has been observed for the similar molecule piperidine, with this conformer being in about 40% abundance, no analogous spectrum was found for morpholine. This is because of the small number of widely distributed *c*-type lines in the expected spectrum of chair–axial morpholine and because of the extreme difficulty of separating these lines from those in the dense spectrum of the chair equatorial form. No spectra due to boat forms were found, which is not unexpected as the boat conformer for molecules of this type lies typically 7 kcal per mole above the chair form in energy.

Acknowledgments

The authors should like to express their gratitude to Dr. R. F. Curl for his assistance in computing the dipole moment of morpholine and to Dr. D. B. McLay for helpful advice and discussions. They would also like to acknowledge the support of the work by the National Research Council of Canada through operating grants and the award of a Studentship.

1. T. Oka, K. Tsuchiya, S. Iwata, and Y. Morino. Bull. Chem. Soc. Jap. **37**, 4 (1964).
2. P. J. Buckley, C. C. Costain, and J. E. Parkin. Chem. Commun. 668 (1968).
3. V. M. Rao and R. Kewley. Can. J. Chem. **47**, 1289 (1969).
4. R. C. Weast (*Editor*). Handbook of chemistry and physics. 47th ed. The Chemical Rubber Company. 1966.
5. D. R. Lide, Jr. and D. E. Mann. J. Chem. Phys. **28**, 572 (1958).
6. J. E. Wollrab and V. W. Laurie. J. Chem. Phys. **48**, 5058 (1968).
7. D. R. Lide, Jr. J. Chem. Phys. **27**, 343 (1957).
8. G. R. Gunther-Mohr, R. L. White, A. L. Schawlow, W. E. Good, and D. K. Coles. Phys. Rev. **94**, 1184 (1954).
9. J. Kraitchman. Amer. J. Phys. **21**, 17 (1953).
10. G. H. Kwei and D. R. Herschbach. J. Chem. Phys. **32**, 1270 (1960).
11. S. A. Marshall and J. Weber. Phys. Rev. **105**, 1502 (1957).
12. G. A. Crowder and D. W. Scott. U.S. Department of the Interior (Bureau of Mines) Technical Report. 1965. p. 6630.
13. P. A. Akishin, N. G. Rambidi, I. K. Korobitsyna, G. Ya. Kondrat'eva, and Yu. K. Yur'ev. Vestn. Mosk. Univ. **10**, (12) Ser. Fiz. Mat. i Estestv. Nauk. No. 8, 103 (1955). See also Chem. Abstr. **50**, 8330*d* (1956).

Can. J. Chem. Downloaded from www.nrcresearchpress.com by 210.87.254.40 on 09/05/12
For personal use only.

An infrared transmission cell for ultra-thin liquid films[1]

R. P. YOUNG[2] AND R. N. JONES
Division of Pure Chemistry, National Research Council of Canada, Ottawa, Canada

Received May 8, 1969

This note describes the design and use of an ultra-thin cell for the quantitative measurement of infrared absorption bands of strongly absorbing liquids or solutions by transmission. From these measurements the optical constants of the absorbing material can be evaluated. The technique is demonstrated by a comparison with the optical constant data reported in the literature for the 1527 cm^{-1} band of hexafluorobenzene as measured by attenuated total reflection.

Canadian Journal of Chemistry, 47, 3463 (1969)

Introduction

The conventional transmission methods of absorption spectrophotometry are unsuitable for strongly absorbing liquids or concentrated solutions because of the low intensity of the transmitted radiation and the lack of adequate means to correct for reflection losses.

The absolute intensity of the band is most meaningfully described in terms of[3] the *absorption coefficient* k, which is defined as the imaginary component of the complex refractive index ($\hat{n} = n - ik$). The relation between k and the more commonly employed decadic absorbance A is given by

$$[1] \qquad k = \frac{2.30258}{4\pi\nu l} \cdot \log (I_0/I)$$

where ν is the wavenumber, l is the path length (cm), and $\log (I_0/I)$ is the decadic absorbance.

Where k_{max} exceeds 0.1 the film thickness must be reduced to below 10 μ to obtain sufficient transmission for efficient measurement, and the absorption spectrum is then superimposed on an underlying fringe pattern. Within the region of absorption the fringes perturb the true band contour. Beyond the wings of the band the fringe pattern can be used to determine the cell thickness, although this is more usually obtained from the fringe pattern generated by the empty cell (1). If k_{max} exceeds 1.0 a film thickness of 1 μ or less is required to allow the transmission of sufficient radiant energy for accurate measurement. Serious problems are then encountered in constructing cells of conventional design, in measuring the thickness of the film, and in controlling its dimensional uniformity. In recent studies of the absolute absorption intensities of strongly absorbing materials these difficulties have been circumvented by the use of techniques based on dispersion (2, 3), reflection (4, 5), or attenuated total reflection (a.t.r.) measurements (6, 7). These methods give an absorption curve only indirectly after considerable computation and, in the case of the reflection and a.t.r. measurements, extensive modification must be made to the spectrophotometer. It is therefore of interest to develop a technique that will permit the absorption coefficient to be obtained directly from transmission measurements through thin films.

These considerations motivated the design of the ultra-thin liquid film cell described here and also the development of a computational technique to correct the observed absorption spectrum for reflection losses, which will be discussed in a later publication. This cell has been used to produce films of accurately controlled thickness of the order of 1 μ. Since the spacing

---

[1]Issued as NRCC No. 10 841.
[2]NRCC Postdoctorate Fellow 1967–1969.
[3]In the "Manual of symbols and terminology for physicochemical quantities and units" approved by I.U.P.A.C. at the XXVth Conference (Cortina d'Ampezzo, June 30 – July 8, 1969), the expression "absorption coefficient" is used to designate the quantity $\log_{10}(I_0/I)$. This will necessitate a new name for k. Temporarily we shall continue to use the older nomenclature pending the clarification of anomalies of this kind. A joint committee of I.U.P.A.C. Commissions I.1 (Physicochemical Symbols, Terminology, and Units) and Commission I.5 (Molecular structure and spectroscopy) has been established to recommend uniform practice in those areas of symbolism and nomenclature not covered by the Manual. The recommendations of this committee will be published as appendices to the Manual.

of the interference fringe pattern for a cell having an air gap of 1 μ is about 5000 cm^{-1}, the fringes are so extended that no significant fluctuation is induced in the baseline intensity of all but the broadest absorption bands. The elimination of the interference effect in this manner necessitates the use of a different method of measuring the film thickness.

Experimental

The structural details of the cell are shown in Fig. 1. Two potassium bromide plates (40 × 40 mm) are each machined to a uniform thickness of 6 mm ± 20 μ, drilled as shown in (*a*) and (*b*), and polished to an optical flatness of about half a fringe per cm for visible light. A uniform film of aluminum is deposited to the required thickness by evaporation on the inner face of plate (*a*) leaving a rectangular space which is to form the cavity for the liquid. The two plates are mounted together, as shown in (*c*), in a holder designed for use with a Perkin–Elmer Model 521 spectrophotometer.

Before assembly, the thickness of the deposited film is determined interferometrically with an estimated accuracy of ±2% in the range 0.1–5.0 μ. On the basis of the optical flatness of the plates and the evenness of the controlled deposition of the evaporated metal film, it is assumed that the gap thickness of the assembled cell will be the same as the measured thickness of the deposited film. Experimental evidence to support this is given below.

The liquid is introduced into the reservoir cavity R by means of a syringe, with the tube T open. After several minutes the sample space will become filled by capillary action and Teflon stoppers are then inserted at R and T. After the measurements have been made, the liquid is withdrawn from the reservoir and the film space emptied in 10 to 15 min by placing the cell in a vacuum desiccator attached to a rotary oil pump. Cells of this type are unsuited for use with solutions of non-volatile solutes that could deposit the solute in the cell cavity; however, no difficulties have been encountered in maintaining the cells in a clean condition when they are used with volatile solutes, solvents, and pure liquids. The rubber gasket (Fig. 1(*c*)) does not come in contact with the sample liquid and can cause no contamination of the inner cell surfaces. If regular dismantling of the cell is contemplated the surface of the metal film can be protected by an

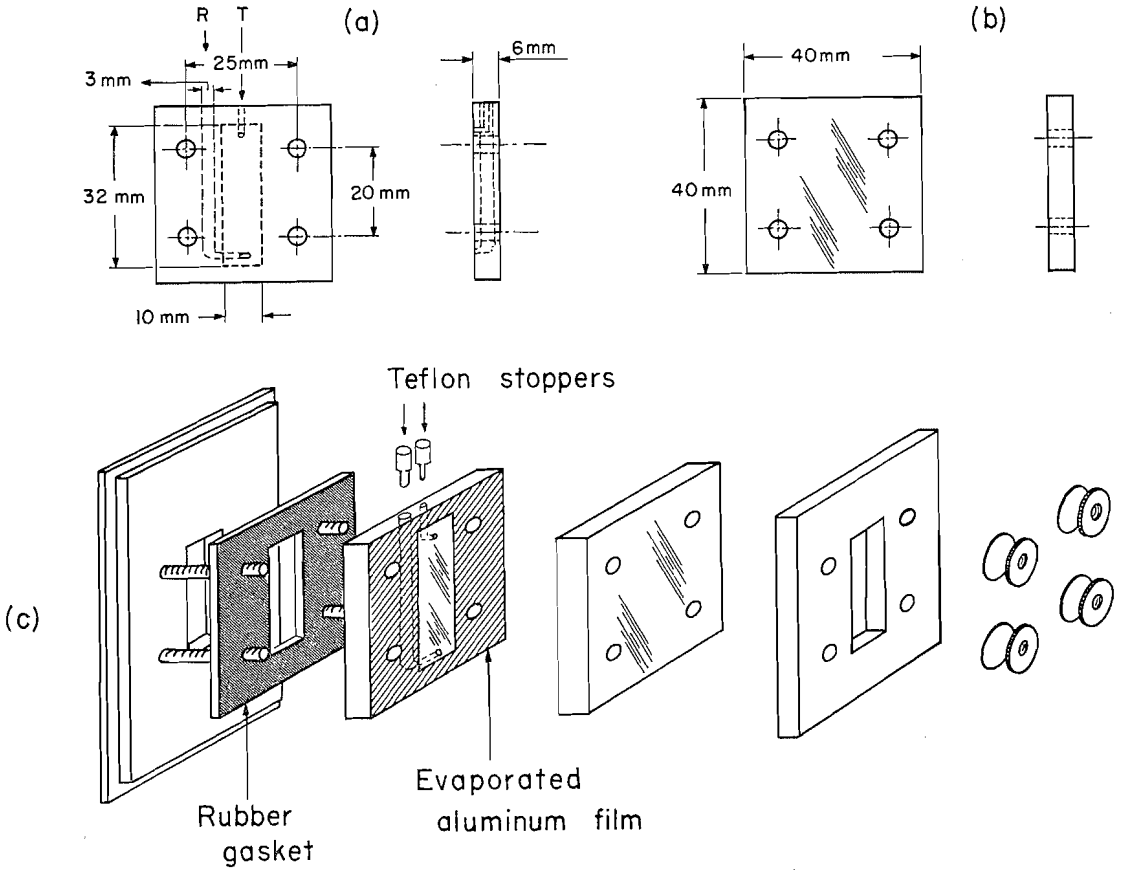

FIG. 1. The two KBr plates (*a*) and (*b*) were drilled as shown before evaporation of the aluminum film on to the inner surface of (*a*). The final assembly is shown in (*c*).

Can. J. Chem. Downloaded from www.nrcresearchpress.com by 210.87.254.40 on 09/05/12
For personal use only.

Can. J. Chem. Downloaded from www.nrcresearchpress.com by 210.87.254.40 on 09/05/12
For personal use only.

overlay of silica about 0.1 μ thick. In such cases the thickness of the combined metal–silica film would be measured.

The spectra have been recorded on a Perkin–Elmer Model 521 spectrophotometer with digital encoding at 1.0 cm^{-1} intervals on punched paper tape; in regions of atmospheric absorption the instrument is flushed with dry nitrogen. The wavenumber scale is calibrated after each set of measurements against accepted standards; liquid indene, or NH_3, H_2O, or HCN vapor have been used for this purpose (8). High speed rotating sector photometers are used to calibrate the transmission scale of the recording system (9, 10). Computation is performed by an IBM 360(50) computer.

Results

It is well known that the transmission spectra of strongly absorbing materials are distorted by reflection loss effects in regions where the refractive index changes rapidly and it is necessary to correct the observed "apparent" absorption curve for this effect (11, 12). A theoretical analysis of these effects has been made and we have developed a corrective procedure. These corrections have been applied to a number of representative absorption bands and details of the method of computation will be discussed in a separate publication. The practicality of the cell is illustrated by measurements on the band at 1527 cm^{-1} in the spectrum of hexafluorobenzene shown in Figs. 2 and 3. The transmission of an empty cell with a gap thickness of 0.62 μ is shown in Fig. 2(*a*). This curve was obtained without any compensation in the control beam of the spectrophotometer and shows the total radiation loss caused by reflection at the front window surface together with the multiple internal reflections within the two windows as modulated by the interference effects of the air gap, i.e. the cell is functioning as a Fabry–Perot etalon. The absolute transmission in the 1600–1450 cm^{-1} region of the same cell when filled with liquid hexafluorobenzene is shown in Fig. 2(*b*). The dotted curve is the directly measured spectrum

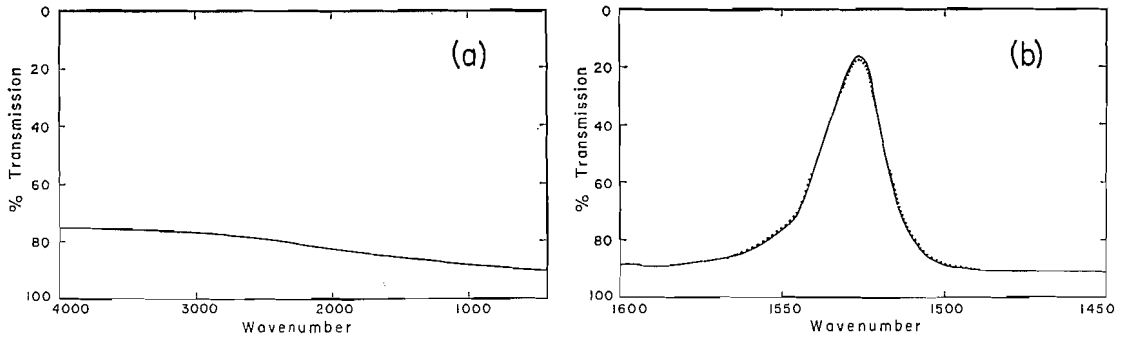

FIG. 2. Absolute transmission spectra after wavenumber and intensity calibration. (*a*) Transmission of the empty cell (0.62 μ air gap between KBr plates). (*b*) Transmission of the cell filled with liquid hexafluorobenzene: ·····, as recorded; and ———, after correction for slit distortion by pseudo-deconvolution.

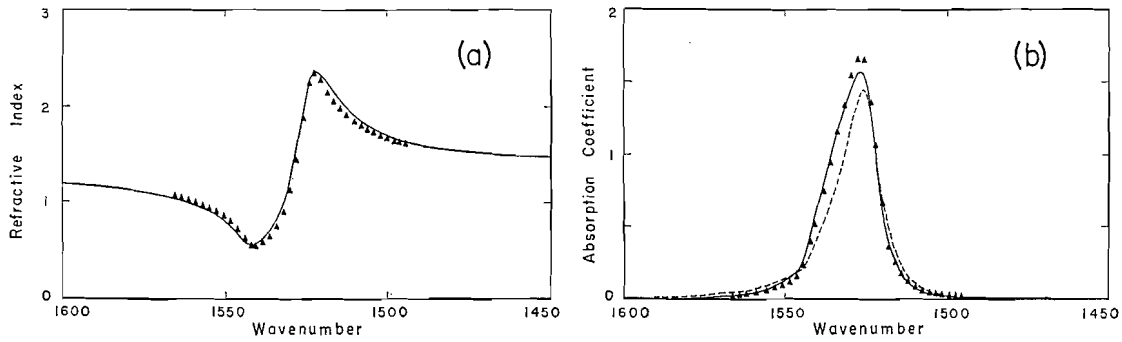

FIG. 3. (*a*) Refractive index curves: ———, calculated from the transmission data after reflection loss correction of the pseudo-deconvoluted spectrum; and ▲, values obtained by the a.t.r. method. (*b*) Absorption coefficient curves; ———, calculated from the transmission data after reflection loss correction of the pseudo-deconvoluted spectrum: ---, experimentally observed pseudo-deconvoluted transmission spectrum without correction for reflection losses; and ▲, values obtained by the a.t.r. method.

and the solid line illustrates the small but significant difference which results from correction for slit distortion by pseudo-deconvolution with a triangular slit function of 3.0 cm^{-1} half width (13). The "apparent" absorption coefficients (k_a) calculated by eq. [1] from the pseudo-deconvoluted spectrum are shown by the dashed line in Fig. 3(*b*). The optical constants (*n* and *k*), obtained from this curve after correcting for the effects of reflection losses, are shown as the solid lines in Fig. 3, together with the values computed from the a.t.r. data by Fujiyama and Crawford (14).

TABLE I

Intensity of the 1525 cm^{-1} band of liquid hexafluorobenzene

	Integrated intensity	
Absorption coefficient	$cm^{-1}\ s^{-1}$ molecule $^{-1}$	$cm^2\ mole^{-1}$
k_a (as measured)	31.58×10^{-4}	41 440
k_a (pseudo-deconvoluted)	31.18×10^{-4}	40 910
k (transmission)	34.08×10^{-4}	44 730
k (a.t.r.)*	34.51×10^{-4}	45 290

*From ref. 14.

In Table I are listed the integrated intensity values calculated both in IUPAC Absolute Units ($cm^{-1}\ s^{-1}$ molecule^{-1}) and in the "absorption cross-section" units (cm^2 mole^{-1}) used by Fujiyama and Crawford. The agreement between the intensity values derived from a.t.r. and transmission data for the absorption coefficient curve (k) is within 2%. The discrepancy of nearly 10% in the "apparent" absorption curve (k_a) results from the reflection distortion losses; it will normally be lower for bands that are less intense. For a series of bands of progressively lower intensity the magnitude of the reflection distortion steadily diminishes so that when k_{max} is less than about 0.1 the discrepancy between the integrated areas of the apparent and reflection-corrected absorption curves is usually between 2 and 5%. However, for very weak bands, where such differences become almost negligible, the film thickness must be increased to obtain accurate transmission data, and care must then be taken to eliminate the interference fringe effects that increasingly perturb the baseline.

Conclusion

The good agreement with the a.t.r. results shown here is well substantiated by measurements on other bands and indicates that the liquid film thickness values derived from the measured thickness of the metal deposit are acceptable. The gap thickness has remained unchanged over many weeks during which the cells have been used extensively, but not dismantled and reassembled. Should frequent dismantling cause the thickness to change, a new value could be readily obtained once some standard bands of known intensity have been established for calibration purposes. The maintenance of the optical flatness of the inner surface of the cavity is readily checked by visual inspection of the empty cell for which the fringe pattern is clearly seen in the natural reflected light of the laboratory.

Acknowledgments

We wish to thank Mr. J. N. Cairns for his invaluable advice and assistance in the construction of these cells in the Optical Shop of the Applied Physics Division of the National Research Council of Canada. We are also grateful to Dr. K. H. Hart of the Optical Physics Section of the same Division for making the interferometric film thickness measurements for us. Finally, we would like to thank Professor B. L. Crawford and Dr. T. Fujiyama of the University of Minnesota, Minneapolis for stimulating discussions on the problem of distortion in infrared transmission spectra.

1. G. B. B. M. Sutherland and H. A. Willis. Trans. Faraday Soc. **41**, 181 (1945).
2. P. N. Schatz. J. Chem. Phys. **32**, 894 (1960).
3. L. Nemes and W. J. Orville-Thomas. Trans. Faraday Soc. **61**, 1839 (1965).
4. P. N. Schatz, S. Maeda, J. L. Hollenberg, and D. A. Dows. J. Chem. Phys. **34**, 175 (1961).
5. D. W. Barnes and P. N. Schatz. J. Chem. Phys. **38**, 2662 (1963).
6. J. Fahrenfort and W. M. Visser. Spectrochim. Acta, **18**, 1103 (1962).
7. A. C. Gilby, J. Burr, W. Krueger, and B. Crawford, Jr. J. Phys. Chem. **70**, 1525 (1966).
8. Tables of wavenumbers for the calibration of infrared spectrometers. Pure and Appl. Chem. **1**, 537 (1961). Republished by Butterworths, London. 1961.
9. R. N. Jones. J. Jap. Chem. **21**, 609 (1967).
10. R. N. Jones. Pure Appl. Chem. In press.
11. S. Maeda and P. N. Schatz. J. Chem. Phys. **35**, 1617 (1961).
12. S. Maeda. Bull. Tokyo Inst. Tech. **59**, 17 (1964).
13. R. N. Jones, R. Venkataraghavan, and J. W. Hopkins. Spectrochim. Acta, **23A**, 925 (1967).
14. T. Fujiyama and B. Crawford, Jr. J. Phys. Chem. **72**, 2174 (1968).

Can. J. Chem. Downloaded from www.nrcresearchpress.com by 210.87.254.40 on 09/05/12
For personal use only.

Equisorptic compositions in reverse osmosis[1]

J. KOPEČEK[2] AND S. SOURIRAJAN
Division of Applied Chemistry, National Research Council of Canada, Ottawa, Canada

Received April 9, 1969

The existence of equisorptic solution compositions in reverse osmosis systems is illustrated.

Canadian Journal of Chemistry, 47, 3467 (1969)

Can. J. Chem. Downloaded from www.nrcresearchpress.com by 210.87.254.5 on 09/05/12
For personal use only.

The reverse osmosis membrane separation process is a general and widely applicable technique for the separation, concentration, or fractionation of substances in fluid solutions. The technique consists of letting the fluid mixture flow, under pressure, through an appropriate porous membrane, and withdrawing the membrane permeated product generally at atmospheric pressure and surrounding temperature. The product is enriched in one or more constituents of the mixture, leaving a concentrated solution on the upstream side of the membrane. No heating of the membrane and no phase change in product recovery are involved in this separation process.

On the basis of the preferential sorption–capillary flow mechanism an appropriate chemical nature of the film surface in contact with the solution, together with the existence of pores of appropriate size on the area of the porous film at the interface, is an indispensable twin requirement for the success of this separation technique (1). Following this approach, the applicability of the reverse osmosis technique for the separation of a number of organic binary liquid mixtures, including azeotropic and isomeric mixtures, has been illustrated (2, 3).

There are two circumstances under which little or no separation will be obtained in the reverse osmosis process, even when the chemical nature of the membrane surface is such that it has some degree of sorption for each of the components of a binary mixture. When the size of the pores on the membrane surface is too big compared to the thickness of the preferentially sorbed layer, separation will obviously be negligible under the reverse osmosis conditions. Further, preferential sorption is a function of the composition of the solution for any given membrane material. If, at a particular composition of the solution, the membrane material has equal sorption for either component in a binary mixture, then under that condition, preferential sorption is zero, and consequently there can be no separation in reverse osmosis whatever the porous structure of the membrane surface. This note illustrates that such equisorptic compositions exist for membrane material – solution systems in reverse osmosis.

Asymmetric porous cellulose acetate membranes (designated here as CA-NRC-18 type films) made in the laboratory by the method of Sourirajan and Govindan (4) were used in this work with isopropyl alcohol – benzene, and isobutyl alcohol – toluene mixtures as the feed solutions. The reverse osmosis experiments were carried out in a stainless steel static cell as described earlier (2, 3). The separation and membrane permeated product rate data reported below represent steady state values for the particular membrane–solution system under study at the laboratory temperature. Figures 1–3 give the experimental separation and product rate data obtained with membranes of different porosities using different compositions of feed solution. The numbers by the side of the product rate data refer to the order in which the experiments were carried out.

The separation data for both the feed solution systems illustrate the existence of equisorptic compositions in reverse osmosis. On one side of the equisorptic composition, the membrane material has a preferential sorption for the alcohol, and on the other side, it has a preferential sorption for the hydrocarbon. With respect to the particular cellulose acetate membrane material and feed solutions studied, the equisorptic compositions (mole ratios) are 26/74 for

---

[1]NRCC No. 10 845.
[2]Present address: Institute of Macromolecular Chemistry, Prague, Czechoslovakia.

Can. J. Chem. Downloaded from www.nrcresearchpress.com by 210.87.254.5 on 09/05/12
For personal use only.

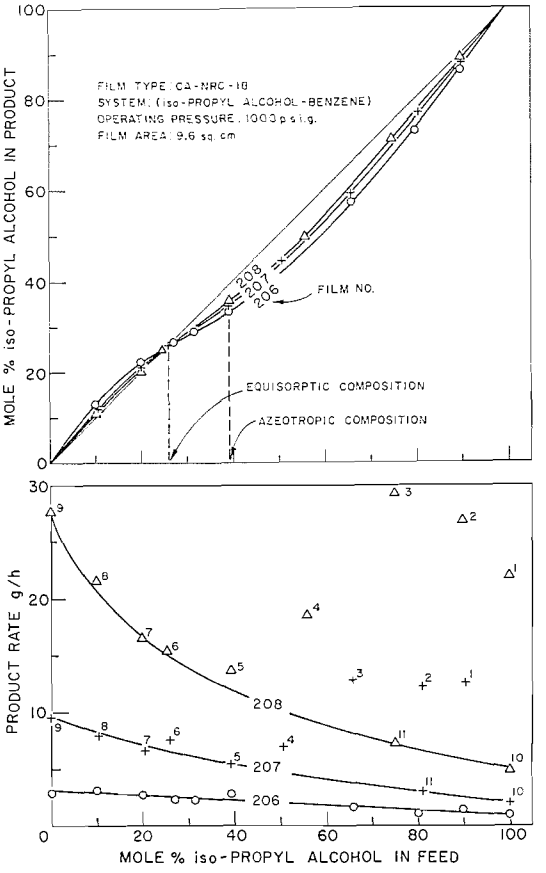

FIG. 1. Separation and product rate data for the system isopropyl alcohol – benzene using porous cellulose acetate membranes.

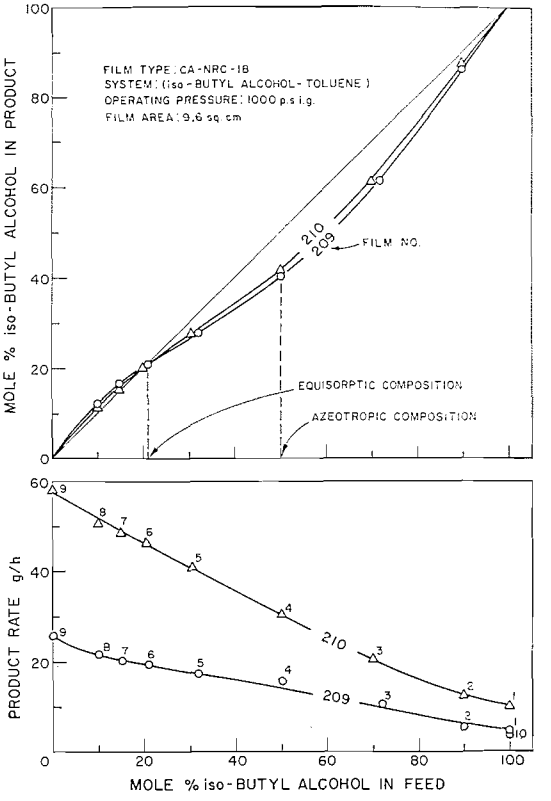

FIG. 2. Separation and product rate data for the system isobutyl alcohol – toluene using porous cellulose acetate membranes.

isopropyl alcohol/benzene, and 21/79 for isobutyl alcohol/toluene systems; for comparison, the azeotropic compositions of the mixtures are 39.3/60.7 and 50/50, respectively. The experimental separation data obtained with different films (Figs. 1 and 2) further show that the equisorptic composition is the same whatever the porous structure of the membrane surface, and, at least for the system isobutyl alcohol – toluene, it is also independent of the operating pressure up to 1000 p.s.i.g. (Fig. 3).

The product rate data for the system isopropyl alcohol – benzene (Fig. 1) illustrate the partial and irreversible collapse of the porous structure of the membrane by feed solutions containing more than about 25 mole % benzene. Such collapse of porous structure did not affect separation data significantly, indicating thereby

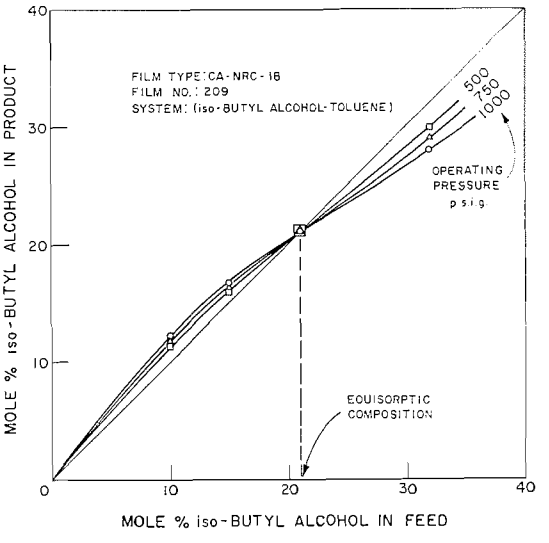

FIG. 3. Effect of operating pressure on equisorptic composition for the system isobutyl alcohol – toluene.

that the porous structure of the dense surface layer of the membrane remained essentially unaffected during the process. The product rate data for the system isobutyl alcohol – toluene (Fig. 2) do not show any indication of irreversible changes in the porous structure of the membrane as a result of changes in the composition of the feed solution. In any case, it is evident that the changes in the porous structure of the membrane brought about by changes in the composition of the feed, do not affect the equisorptic compositions.

At a given operating pressure and temperature, the equisorptic compositions are obviously functions of the chemical nature of the membrane material and that of the feed solution. They are hence significant physical constants in reverse osmosis, analogous to azeotropic compositions in distillation. Their existence adds a new factor in the science and engineering of reverse osmosis.

Acknowledgments

We thank A. G. Baxter and Lucien Pageau for their assistance in this work, and one of us (J. K.) also thanks the National Research Council of Canada for the award of a postdoctoral fellowship.

1. S. Sourirajan. Ind. Eng. Chem. Fundam. **2**, 51 (1963).
2. S. Sourirajan. Nature, **203**, 1348 (1964).
3. J. Kopeček and S. Sourirajan. Ind. Eng. Chem. Process. Des. Develop. MS. 8–386 (1968).
4. S. Sourirajan and T. S. Govindan. 1st Intern. Symp. Water Desalination, Washington, D.C. October 1965. Office of Saline Water, U.S. Dept. Interior. Vol. 1. pp. 251–274.

Thermodynamic properties of ruthenate and molybdate ions

Loren G. Hepler
Department of Chemistry, University of Lethbridge, Lethbridge, Alberta

Received April 3, 1969

Thermodynamic data that have been obtained subsequent to compilations by the U.S. National Bureau of Standards and Latimer now permit calculation of ΔG_f^0, ΔH_f^0, and $\bar{S}_2^0$ values for RuO_4^{2-} (aq) and MoO_4^{2-} (aq). Use of these quantities is illustrated by calculation of thermodynamic properties of Ag_2MoO_4 (c).

Canadian Journal of Chemistry, 47, 3469 (1969)

Data that are now available permit new calculations of the entropy of ruthenate ion and both entropy and free energy of molybdate ion. Both ion entropies are of interest in connection with estimation of entropies of other MO_4^{2-} (aq) ions, and the ΔG_f^0 of molybdate permits direct calculation of some other free energies.

Recent calorimetric measurements by Mercer and Farrar (1) have led them to report $\Delta H_f^0 = -109.4$ kcal/mole for RuO_4^{2-} (aq). Earlier equilibrium investigations (2) have led to $\Delta G_f^0 = -72$ kcal/mole for this ion. These two values now lead to the desired $\bar{S}_2^0 = 11 \pm 3$ cal deg^{-1} mole^{-1} for RuO_4^{2-} (aq).

Calorimetric measurements by Graham and Hepler (3) led to $\Delta H_f^0 = -238.2$ kcal/mole for MoO_4^{2-} (aq). Other calorimetric measurements by Barany (4) led to $\Delta H_f^0 = -369.5$ kcal/mole for $CaMoO_4$ (c) that had been heated at 480–690 °C for 21 days. Earlier calorimetric determination (5) of the heat of precipitation of $CaMoO_4$ (not in a well defined crystalline state) led to $\Delta H_f^0 = -367.3$ kcal/mole. Since the ΔH_f^0 for calcium molybdate in a well defined stable crystalline state is expected to be more exothermic than for the precipitated material, the ΔH_f^0 from Barany (4) is adopted and combined with the third law $S_{298}^0 = 29.3$ cal deg^{-1} mole^{-1} value from Weller and King (6) to obtain $\Delta G_f^0 = -344.0$ kcal/mole for $CaMoO_4$ (c).

The solubility of calcium molybdate (3) led to $K_{sp} = 1 \times 10^{-8}$ and thence to $\Delta G^0 = 10.9$ kcal/mole for solution of $CaMoO_4$ (c). Further combination of this ΔG^0 with the ΔG_f^0 of $CaMoO_4$ (c) given above and the ΔG_f^0 of Ca^{2+} (aq) from Latimer (7) gives us $\Delta G_f^0 = -200.9$ kcal/mole for MoO_4^{2-} (aq). The ΔH_f^0 and ΔG_f^0 values

Can. J. Chem. Downloaded from www.nrcresearchpress.com by 210.87.254.5 on 09/05/12
For personal use only.

that the porous structure of the dense surface layer of the membrane remained essentially unaffected during the process. The product rate data for the system isobutyl alcohol – toluene (Fig. 2) do not show any indication of irreversible changes in the porous structure of the membrane as a result of changes in the composition of the feed solution. In any case, it is evident that the changes in the porous structure of the membrane brought about by changes in the composition of the feed, do not affect the equisorptic compositions.

At a given operating pressure and temperature, the equisorptic compositions are obviously functions of the chemical nature of the membrane material and that of the feed solution. They are hence significant physical constants in reverse osmosis, analogous to azeotropic compositions in distillation. Their existence adds a new factor in the science and engineering of reverse osmosis.

Acknowledgments

We thank A. G. Baxter and Lucien Pageau for their assistance in this work, and one of us (J. K.) also thanks the National Research Council of Canada for the award of a postdoctoral fellowship.

1. S. Sourirajan. Ind. Eng. Chem. Fundam. **2**, 51 (1963).
2. S. Sourirajan. Nature, **203**, 1348 (1964).
3. J. Kopeček and S. Sourirajan. Ind. Eng. Chem. Process. Des. Develop. MS. 8–386 (1968).
4. S. Sourirajan and T. S. Govindan. 1st Intern. Symp. Water Desalination, Washington, D.C. October 1965. Office of Saline Water, U.S. Dept. Interior. Vol. 1. pp. 251–274.

Can. J. Chem. Downloaded from www.nrcresearchpress.com by 210.87.254.6 on 09/05/12
For personal use only.

Thermodynamic properties of ruthenate and molybdate ions

Loren G. Hepler
Department of Chemistry, University of Lethbridge, Lethbridge, Alberta

Received April 3, 1969

Thermodynamic data that have been obtained subsequent to compilations by the U.S. National Bureau of Standards and Latimer now permit calculation of ΔG_f^0, ΔH_f^0, and $\bar{S}_2^0$ values for RuO_4^{2-} (aq) and MoO_4^{2-} (aq). Use of these quantities is illustrated by calculation of thermodynamic properties of Ag_2MoO_4 (c).

Canadian Journal of Chemistry, 47, 3469 (1969)

Data that are now available permit new calculations of the entropy of ruthenate ion and both entropy and free energy of molybdate ion. Both ion entropies are of interest in connection with estimation of entropies of other MO_4^{2-} (aq) ions, and the ΔG_f^0 of molybdate permits direct calculation of some other free energies.

Recent calorimetric measurements by Mercer and Farrar (1) have led them to report $\Delta H_f^0 = -109.4$ kcal/mole for RuO_4^{2-} (aq). Earlier equilibrium investigations (2) have led to $\Delta G_f^0 = -72$ kcal/mole for this ion. These two values now lead to the desired $\bar{S}_2^0 = 11 \pm 3$ cal deg^{-1} mole^{-1} for RuO_4^{2-} (aq).

Calorimetric measurements by Graham and Hepler (3) led to $\Delta H_f^0 = -238.2$ kcal/mole for MoO_4^{2-} (aq). Other calorimetric measurements by Barany (4) led to $\Delta H_f^0 = -369.5$ kcal/mole for $CaMoO_4$ (c) that had been heated at 480–690 °C for 21 days. Earlier calorimetric determination (5) of the heat of precipitation of $CaMoO_4$ (not in a well defined crystalline state) led to $\Delta H_f^0 = -367.3$ kcal/mole. Since the ΔH_f^0 for calcium molybdate in a well defined stable crystalline state is expected to be more exothermic than for the precipitated material, the ΔH_f^0 from Barany (4) is adopted and combined with the third law $S_{298}^0 = 29.3$ cal deg^{-1} mole^{-1} value from Weller and King (6) to obtain $\Delta G_f^0 = -344.0$ kcal/mole for $CaMoO_4$ (c).

The solubility of calcium molybdate (3) led to $K_{sp} = 1 \times 10^{-8}$ and thence to $\Delta G^0 = 10.9$ kcal/mole for solution of $CaMoO_4$ (c). Further combination of this ΔG^0 with the ΔG_f^0 of $CaMoO_4$ (c) given above and the ΔG_f^0 of Ca^{2+} (aq) from Latimer (7) gives us $\Delta G_f^0 = -200.9$ kcal/mole for MoO_4^{2-} (aq). The ΔH_f^0 and ΔG_f^0 values

now lead to $\bar{S}_2^0 = 11 \pm 2$ cal deg^{-1} mole^{-1} for MoO_4^{2-} (aq).

Several earlier thermodynamic calculations for MoO_4^{2-} (aq) and solid molybdates have been based on Latimer's (7) estimated $\bar{S}_2^0 \cong 14$ cal deg^{-1} mole^{-1} rather than experiment-based quantities calculated above.

Combination of the ΔG^0 of solution of Ag_2MoO_4 (c) derived from the solubility product (5) with ΔG_f^0 values for Ag^+ (aq) and MoO_4^{2-} (aq) now leads to $\Delta G_f^0 = -179.5$ kcal/mole for Ag_2MoO_4 (c). Solubility, electrochemical, and calorimetric data gave (5) a "best" $\Delta H_f^0 = -200.4$ kcal/mole for Ag_2MoO_4 (c), which is now used with the ΔG_f^0 above in calculating $S_{298}^0 = 55$ cal deg^{-1} mole^{-1} for Ag_2MoO_4 (c). This value is subject to direct verification by way of heat capacity data and the third law. Similar calculations can be made for other molybdates.

1. E. E. Mercer and D. T. Farrar. Can. J. Chem. **47**, 581 (1969).
2. R. N. Goldberg and L. G. Hepler. Chem. Rev. **68**, 229 (1968).
3. R. L. Graham and L. G. Hepler. J. Amer. Chem. Soc. **78**, 4846 (1956).
4. R. Barany. Bureau of Mines Report of Investigations No. 6143. U.S. Government Printing Office, Washington, D.C. 1962.
5. C. N. Muldrow and L. G. Hepler. J. Phys. Chem. **62**, 982 (1958).
6. W. W. Weller and E. G. King. Bureau of Mines Report of Investigations No. 6147. U.S. Government Printing Office, Washington, D.C. 1963.
7. W. M. Latimer. Oxidation potentials. 2nd ed. Prentice-Hall Inc., Englewood Cliffs, N.J. 1952.

Can. J. Chem. Downloaded from www.nrcresearchpress.com by 210.87.254.6 on 09/05/12
For personal use only.

Secondary reactions in the photolysis and pyrolysis of azoethane

O. P. Strausz, R. E. Berkley, and H. E. Gunning
Department of Chemistry, University of Alberta, Edmonton, Alberta

Received March 19, 1969

A brief study has been made of the secondary reactions occurring in the thermolysis and photolysis of azoethane. In thermolysis the important secondary products found are ethyl 2-butyl diimide and ethanal diethylhydrazone. In photolysis tetraethyl hydrazine has also been detected in substantial yields.

The possible role of secondary reactions in the thermolysis and photolysis of azo compounds is discussed.

Canadian Journal of Chemistry, 47, 3470 (1969)

Azoalkanes are often used as sources of alkyl free radicals for kinetic studies. However, relatively little has been directly observed of their chemistry in photolysis or pyrolysis systems apart from the primary steps. There have been a number of observations which indicate that secondary reactions between azoalkanes and radicals are of potential importance in kinetic systems, and, in a few cases, products from secondary reactions have been tentatively identified (1–5).

We have observed the formation of secondary reaction products in the decomposition of a number of azoalkanes (6). While secondary reactions of the azoalkane molecule are practically negligible at low pressure and room temperature, they become quite important if either the pressure or temperature is increased. Consequently, it is desirable to understand the nature of the more important secondary processes involving azoalkane molecules before they can be used with assurance as sources of alkyl free radicals for radical–molecule reactions. In order to gain an understanding of these processes, we have studied the decomposition of azoethane in both photolysis and pyrolysis systems and have identified the products of the major secondary reactions.

In preliminary experiments, the isomerization of azoethane to ethanal ethylhydrazone in Pyrex vessels at 150 °C was observed. The rate of isomerization was rapid at first, and then, as surfaces became conditioned, the rate decreased until it became quite small. A temperature study of the equilibrium constant for this reaction was carried out, using a KOH lined pyrolysis cell to establish equilibrium rapidly. The results are summarized in Fig. 1. A least-squares treatment of the data indicates $\Delta H = +0.19 \pm 0.08$ kcal/mole and $\Delta S = +2.72 \pm 0.22$ cal/deg mole for a 90% confidence level.

now lead to $\bar{S}_2^0 = 11 \pm 2$ cal deg^{-1} mole^{-1} for MoO_4^{2-} (aq).

Several earlier thermodynamic calculations for MoO_4^{2-} (aq) and solid molybdates have been based on Latimer's (7) estimated $\bar{S}_2^0 \cong 14$ cal deg^{-1} mole^{-1} rather than experiment-based quantities calculated above.

Combination of the ΔG^0 of solution of Ag_2MoO_4 (c) derived from the solubility product (5) with ΔG_f^0 values for Ag^+ (aq) and MoO_4^{2-} (aq) now leads to $\Delta G_f^0 = -179.5$ kcal/mole for Ag_2MoO_4 (c). Solubility, electrochemical, and calorimetric data gave (5) a "best" $\Delta H_f^0 = -200.4$ kcal/mole for Ag_2MoO_4 (c), which is now used with the ΔG_f^0 above in calculating $S_{298}^0 = 55$ cal deg^{-1} mole^{-1} for Ag_2MoO_4 (c). This value is subject to direct verification by way of heat capacity data and the third law. Similar calculations can be made for other molybdates.

1. E. E. Mercer and D. T. Farrar. Can. J. Chem. **47**, 581 (1969).
2. R. N. Goldberg and L. G. Hepler. Chem. Rev. **68**, 229 (1968).
3. R. L. Graham and L. G. Hepler. J. Amer. Chem. Soc. **78**, 4846 (1956).
4. R. Barany. Bureau of Mines Report of Investigations No. 6143. U.S. Government Printing Office, Washington, D.C. 1962.
5. C. N. Muldrow and L. G. Hepler. J. Phys. Chem. **62**, 982 (1958).
6. W. W. Weller and E. G. King. Bureau of Mines Report of Investigations No. 6147. U.S. Government Printing Office, Washington, D.C. 1963.
7. W. M. Latimer. Oxidation potentials. 2nd ed. Prentice-Hall Inc., Englewood Cliffs, N.J. 1952.

Secondary reactions in the photolysis and pyrolysis of azoethane

O. P. Strausz, R. E. Berkley, and H. E. Gunning
Department of Chemistry, University of Alberta, Edmonton, Alberta

Received March 19, 1969

A brief study has been made of the secondary reactions occurring in the thermolysis and photolysis of azoethane. In thermolysis the important secondary products found are ethyl 2-butyl diimide and ethanal diethylhydrazone. In photolysis tetraethyl hydrazine has also been detected in substantial yields.

The possible role of secondary reactions in the thermolysis and photolysis of azo compounds is discussed.

Canadian Journal of Chemistry, 47, 3470 (1969)

Azoalkanes are often used as sources of alkyl free radicals for kinetic studies. However, relatively little has been directly observed of their chemistry in photolysis or pyrolysis systems apart from the primary steps. There have been a number of observations which indicate that secondary reactions between azoalkanes and radicals are of potential importance in kinetic systems, and, in a few cases, products from secondary reactions have been tentatively identified (1–5).

We have observed the formation of secondary reaction products in the decomposition of a number of azoalkanes (6). While secondary reactions of the azoalkane molecule are practically negligible at low pressure and room temperature, they become quite important if either the pressure or temperature is increased. Consequently, it is desirable to understand the nature of the more important secondary processes involving azoalkane molecules before they can be used with assurance as sources of alkyl free radicals for radical–molecule reactions. In order to gain an understanding of these processes, we have studied the decomposition of azoethane in both photolysis and pyrolysis systems and have identified the products of the major secondary reactions.

In preliminary experiments, the isomerization of azoethane to ethanal ethylhydrazone in Pyrex vessels at 150 °C was observed. The rate of isomerization was rapid at first, and then, as surfaces became conditioned, the rate decreased until it became quite small. A temperature study of the equilibrium constant for this reaction was carried out, using a KOH lined pyrolysis cell to establish equilibrium rapidly. The results are summarized in Fig. 1. A least-squares treatment of the data indicates $\Delta H = +0.19 \pm 0.08$ kcal/mole and $\Delta S = +2.72 \pm 0.22$ cal/deg mole for a 90% confidence level.

Can. J. Chem. Downloaded from www.nrcresearchpress.com by 210.87.254.105 on 09/05/12
For personal use only.

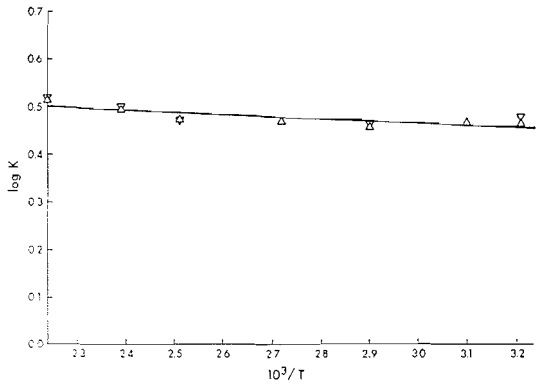

FIG. 1. Plot of log of equilibrium constant vs. $10^3/T$, T in °K; △, runs starting with azoethane; ▽, runs starting with ethanal ethylhydrazone.

Photolysis of azoethane at 100 °C and 5–50 Torr total pressure with 3660 Å light resulted in the formation of 3 major secondary reaction products (see Table I). These were tetraethyl hydrazine, ethanal diethylhydrazone, and ethyl 2-butyl diimide. Some other products also appeared in very small yields. When photolysis was carried out with ~250 Torr added propane, ethanal ethylhydrazone was also formed in low yield. Addition of nitric oxide to the system as a radical scavenger resulted in the complete suppression of heavy products except ethanal ethylhydrazone, a small quantity of which was still formed, probably on the walls.

Pyrolysis of azoethane in the temperature range 240–300 °C yielded, in addition to the expected primary products, more than a dozen secondary products. Most of these were produced in quantities too small to permit identification, and, since their peaks ran together in some regions of the chromatogram, they could not even be accurately counted. These products clearly accounted for a very significant fraction of the azoethane consumed. The 2 major secondary products were ethyl 2-butyl diimide and ethanal diethylhydrazone (see Table II). They were clearly being decomposed as well as formed in the system. When pyrolysis was carried out at 240 °C, where decomposition is fairly slow, with a pressure of about 500 Torr propane, ethanal ethylhydrazone was formed in low yield.

Relative retention times of major products are given in Table III. Molecular structures were determined by mass spectrometry and nuclear magnetic resonance (n.m.r.) spectroscopy. Mass spectral data on the products identified are summarized in Table IV, and n.m.r. spectra are summarized in Table V. Spin decoupling was used to check the apparent positions of the protons. The n.m.r. spectrum of ethanal diethylhydrazone shows no evidence of *cis–trans* isomerism, which is consistent with the results of Stopskii and co-workers (7). A sample of the ethyl 2-butyl diimide produced was irradiated with 3660 Å light. The resulting decomposition

TABLE I

Results of photolysis of 34 Torr azoethane at 97 °C*

Compound	Amount (μmoles)	Compound†	Amount (μmoles)
Azoethane (unreacted)	522		
N_2	20.5	Tetraethyl hydrazine	2.5
$C_2H_4 + C_2H_6$	3.4	Ethyl 2-butyl diimide	1.7
C_4H_{10}	12.9	Ethanal diethylhydrazone	1.5

*0.7 μmoles of ethyl are unaccounted for.
†Assuming the gas chromatography detector response is equal to that of azoethane.

TABLE II

Results of pyrolysis of 29 Torr azoethane at 293 °C*

Compound	Amount (μmoles)	Compound†	Amount (μmoles)
Azoethane (unreacted)	130.5		
N_2	44.5	Ethyl 2-butyl diimide	5.5
$C_2H_4 + C_2H_6$	22.2	Ethanal diethylhydrazone	3.4
C_4H_{10}	14.5		

*9.8 μmoles of ethyl are unaccounted for.
†Assuming the gas chromatography detector response is equal to that of azoethane.

Can. J. Chem. Downloaded from www.nrcresearchpress.com by 210.87.254.105 on 09/05/12
For personal use only.

of the molecule yielded the expected hydrocarbon products. Ethanal ethylhydrazone was synthesized by condensation of ethyl hydrazine and acetaldehyde, and the n.m.r. and mass spectra proved identical to those of the compound obtained from isomerization of azoethane. The n.m.r. spectrum is quite similar to that reported by Lemal and co-workers (8).

The detection of ethanal ethylhydrazone produced in photolysis and pyrolysis of azoethane was complicated by the fact that it had the same retention time as ethyl 2-butyl diimide. The peaks at *m/e* 71 and 86 are quite small in the mass spectrum of ethyl 2-butyl diimide produced in low pressure runs. In runs with high pressures of propane and low decomposition rate (which favored abstraction reactions), there was some increase in the *m/e* 71 and 86 peaks relative to the spectrum of ethyl 2-butyl diimide, and this was presumed to be due to formation of ethanal ethylhydrazone.

TABLE III

Relative retention times* for principal secondary reaction products

Products	Relative retention times
Azoethane	1
Ethanal ethylhydrazone	1.9
Ethyl 2-butyl diimide	1.9
Ethanal diethylhydrazone	3.1
Tetraethyl hydrazine	5.1

*20% SE-30 silicone gum rubber on chromosorb W.A.W. packed in 1/4 in. × 20 ft column operated at 100 °C with 70 cm^3/min helium carrier.

TABLE IV

Summary of mass spectral data

Peak	*m/e*	Intensity	Peak	*m/e*	Intensity
Azoethane			Ethanal ethylhydrazone, $C_4H_{10}N_2$*		
Parent	86		Parent	86	
1	29	100	1	71	100
2	27	26	2	30	85
3	28	17	3	86	74
4	57	14	4	42	49
5	15	6	5	27	23
6	30	6	6	15	21
7	42	5	7	18	16
8	43	5	8	29	16
9	86	5	9	41	16
10	41	4	10	44	16
Ethanal diethylhydrazone			Ethyl 2-butyl diimide, $C_6H_{14}N_2$*		
Parent	114		Parent	114	
1	99	100	1	29	100
2	29	67	2	41	50
3	28	59	3	57	45
4	30	51	4	27	13
5	42	43	5	56	10
6	56	38	6	114	8
7	114	37	7	42	7
8	44	34	8	39	5
9	71	32	9	85	5
10	27	32	10	55	4
Tetraethyl hydrazine, $C_8H_{20}N_2$*					
Parent	144				
1	115	100			
2	144	60			
3	29	39			
4	87	24			
5	28	23			
6	18	20			
7	72	18			
8	42	17			
9	58	15			
10	56	14			

*Molecular formulae, where given, have been established by exact high resolution mass determination on the parent peak.

Can. J. Chem. Downloaded from www.nrcresearchpress.com by 210.87.254.105 on 09/05/12
For personal use only.

TABLE V

Summary of nuclear magnetic resonance spectra

Compound	Structure	τ	Splitting	J
Azoethane	CH_3	8.75	4	7
	$—CH_2—N$	6.28	3	7
Ethanal ethylhydrazone	$CH_3—$ (*trans*)	8.21	2	5
	$CH_3—$ (*cis*)	8.39	2	5
	—CH=N (*trans*)	3.23	4	5
	—CH=N (*cis*)	3.64	4	5
	N—NH—C	~5.7	Broad	—
	$N—CH_2—$	6.95	6	7
	$—CH_3$	8.91	3	7
Ethanal diethylhydrazone	$CH_3—$	8.15	2	5
	—CH=N	3.34	4	5
	$N—CH_2—$	7.03	4	7
	$—CH_3$	8.97	3	7
Ethyl 2-butyl diimide	$CH_3—$	8.75	3	7
	$—CH_2—N$	6.30	4	7
	N—C—H	6.79	Complex	—
	$N—C—CH_3$	8.83	3	7
	$N—C—CH_2—$	8.31	Complex	—
	$N—C—C—CH_3$	9.17	3	7
Tetraethyl hydrazine	$CH_3—$	9.02	3	7
	$—CH_2—N$	7.61	4	7

The products found suggest the following reaction scheme

[1] $EtN{=}NEt \xrightarrow{h\nu \text{ or } \Delta} 2Et + N_2$

[2] $2Et \longrightarrow C_4H_{10}$

[3] $2Et \longrightarrow C_2H_4 + C_2H_6$

[4] $Et + EtN{=}NEt \longrightarrow C_2H_6 + CH_3\dot{C}H{-}N{=}NEt$

[5] $Et + CH_3\dot{C}H{-}N{=}NEt \longrightarrow CH_3CHEtN{=}NEt$

[6] $Et + CH_3\dot{C}H{-}N{=}NEt \longrightarrow CH_3CH{=}N{-}N(Et)_2$

[7] $RH + CH_3\dot{C}H{-}N{=}NEt \longrightarrow R + CH_3CH{=}N{-}NHEt$

[7*a*] $EtN{=}NEt \xrightarrow{\text{wall}} CH_3CH{=}N{-}NHEt$

[8] $RH + CH_3\dot{C}H{-}N{=}NEt \longrightarrow R + EtN{=}NEt$

[9] $Et + EtN{=}NEt \longrightarrow (Et)_2N{-}\dot{N}Et$

[10] $Et + (Et)_2N{-}\dot{N}Et \longrightarrow (Et)_2N{-}N(Et)_2$

Reaction [7*a*] would only be of importance in systems where the walls have not been conditioned. Ethanal ethylhydrazone could possibly be formed by disproportionation as well as by reactions [7] and [7*a*]. The fact that tetraethylhydrazine is not a prominent product in pyrolysis suggests that either the $Et_2N—\dot{N}Et$ radical or the tetraethylhydrazine molecule decomposes rapidly at high temperatures. In either case, formation of ethyl amines would be a possible result. Although no ethyl amines were found in this study, they could well have been present in small amounts as reported by Sandhu (5).

The possibility of a rapid decomposition of the $CH_3CHN_2C_2H_5$ radical has been considered by some authors (4, 5). Our observation of formation of ethyl 2-butyl diimide and ethanal diethylhydrazone in both photolysis and pyrolysis even at 300 °C, however, implies a relatively high stability for this radical.

Gray and Thynne (1) found tetramethyl hydrazine and methyl ethyl diimide in the photolysis of azomethane, but it is notable that they found neither formal methyl hydrazone nor formal dimethylhydrazone. This may mean that the resonance structure $CH_2{=}N{-}N{-}CH_3$ is of less significance in the $CH_2N_2CH_3$ radical than the analogous structure in the $CH_3CHN_2C_2H_5$ radical.

Wacks (2) observed the formation of methyl amine in high temperature pyrolysis of azomethane and suggested that heterogeneous isomerization of azomethane to formal methylhydrazone followed by decomposition of the hydrazone to HCN and methyl amine may occur.

Can. J. Chem. Downloaded from www.nrcresearchpress.com by 210.87.254.105 on 09/05/12
For personal use only.

Cohen and Zand (3) reported spectroscopic evidence for the formation of acetone isopropylhydrazone in the pyrolysis of azo-*iso*-propane, but it must be considered that the ultraviolet absorptions of hydrazones are very intense, and very small yields of hydrazones could have been detected. We find that the analogous isomerization of azoethane is not significant in a conditioned reactor unless circumstances extremely favorable to hydrogen atom abstraction by the $CH_3CHN_2C_2H_5$ radical exist.

The reaction scheme indicated in this work differs from that suggested by Cerfontain and Kutschke (4) only in that formation of ethanal diethylhydrazone occurs parallel to formation of ethyl 2-butyl diimide. This could not seriously affect the activation energy values they calculated for the abstraction of hydrogen from azoethane (8 kcal/mole) and the addition of ethyl radicals to the double bond of azoethane (6 kcal/mole).

Sandhu (5) has proposed a general reaction scheme for pyrolysis of azoethane which is similar to the sequence of reactions proposed here. His scheme, however, includes decomposition of the $CH_3CHN_2C_2H_5$ radical, which does not appear to be significant in this work, and he does not include formation of ethanal diethylhydrazone (reaction [6]). It seems likely that much of the complexity of the azoethane pyrolysis system may stem from decomposition of this molecule.

Acknowledgment

We thank the National Research Council of Canada for financial support and Dr. Thap DoMinh for advice on the synthesis of ethanal ethylhydrazone.

1. P. Gray and J. C. J. Thynne. Trans. Faraday Soc. **59**, 2275 (1963).
2. M. E. Wacks. J. Phys. Chem. **68**, 2725 (1964).
3. S. G. Cohen and R. Zand. J. Amer. Chem. Soc. **84**, 586 (1962).
4. H. Cerfontain and K. O. Kutschke. Can. J. Chem. **36**, 344 (1958).
5. H. S. Sandhu. J. Phys. Chem. **72**, 1857 (1968).
6. R. E. Berkley, G. N. C. Woodall, O. P. Strausz, and H. E. Gunning. To be published.
7. V. S. Stopskii, V. B. Lebedev, B. V. Ioffe, and A. A. Petrov. Dokl. Akad. Nauk SSSR, **166**, 399 (1966).
8. D. M. Lemal, F. Menger, and E. Coats. J. Amer. Chem. Soc. **86**, 2395 (1964).

Quantum yield of Hg $6(^3P_1)$ sensitization of hydrogen

T. L. Pollock, E. Jakubowski, H. E. Gunning, and O. P. Strausz
Department of Chemistry, University of Alberta, Edmonton, Alberta

Received March 31, 1969

The quantum yield for the mercury photosensitized decomposition of hydrogen has been measured using the ethylene scavenging technique and has been found to be equal to unity.

Canadian Journal of Chemistry, 47, 3474 (1969)

The classical experiment of Cario and Franck (1) in 1922 on the mercury photosensitized decomposition of the hydrogen molecule was the first demonstration of the intermolecular conversion of electronic excitation energy into chemical energy. Several studies of this reaction have been reported in the intervening years, but the mechanism and quantum efficiency of the reaction is still a matter of controversy.

Thomas and Gwinn (2) have attempted to measure the quantum yield for the dissociation of hydrogen using copper oxide as a scavenger. By the improbable assumption that the efficiency of the scavenging reaction is unity, the quantum yield of the dissociation reaction was found to be ~ 0.22. Subsequently, Callear and Robb (3) used ethylene as scavenger of hydrogen atoms and obtained a quantum efficiency of unity. From a study of the H + NO reaction Strausz and Gunning (4) also concluded that the primary quantum yield of the dissociation reaction is unity.

More recently Goldschmidt *et al.* (5), employing techniques similar to those of Thomas and Gwinn, have shown that removal of hydrogen atoms from the gas phase by solid molybdenum

Can. J. Chem. Downloaded from www.nrcresearchpress.com by 210.87.254.105 on 09/05/12
For personal use only.

Cohen and Zand (3) reported spectroscopic evidence for the formation of acetone isopropylhydrazone in the pyrolysis of azo-*iso*-propane, but it must be considered that the ultraviolet absorptions of hydrazones are very intense, and very small yields of hydrazones could have been detected. We find that the analogous isomerization of azoethane is not significant in a conditioned reactor unless circumstances extremely favorable to hydrogen atom abstraction by the $CH_3CHN_2C_2H_5$ radical exist.

The reaction scheme indicated in this work differs from that suggested by Cerfontain and Kutschke (4) only in that formation of ethanal diethylhydrazone occurs parallel to formation of ethyl 2-butyl diimide. This could not seriously affect the activation energy values they calculated for the abstraction of hydrogen from azoethane (8 kcal/mole) and the addition of ethyl radicals to the double bond of azoethane (6 kcal/mole).

Sandhu (5) has proposed a general reaction scheme for pyrolysis of azoethane which is similar to the sequence of reactions proposed here. His scheme, however, includes decomposition of the $CH_3CHN_2C_2H_5$ radical, which does not appear to be significant in this work, and he does not include formation of ethanal diethylhydrazone (reaction [6]). It seems likely that much of the complexity of the azoethane pyrolysis system may stem from decomposition of this molecule.

Acknowledgment

We thank the National Research Council of Canada for financial support and Dr. Thap DoMinh for advice on the synthesis of ethanal ethylhydrazone.

1. P. Gray and J. C. J. Thynne. Trans. Faraday Soc. **59**, 2275 (1963).
2. M. E. Wacks. J. Phys. Chem. **68**, 2725 (1964).
3. S. G. Cohen and R. Zand. J. Amer. Chem. Soc. **84**, 586 (1962).
4. H. Cerfontain and K. O. Kutschke. Can. J. Chem. **36**, 344 (1958).
5. H. S. Sandhu. J. Phys. Chem. **72**, 1857 (1968).
6. R. E. Berkley, G. N. C. Woodall, O. P. Strausz, and H. E. Gunning. To be published.
7. V. S. Stopskii, V. B. Lebedev, B. V. Ioffe, and A. A. Petrov. Dokl. Akad. Nauk SSSR, **166**, 399 (1966).
8. D. M. Lemal, F. Menger, and E. Coats. J. Amer. Chem. Soc. **86**, 2395 (1964).

Quantum yield of Hg $6(^3P_1)$ sensitization of hydrogen

T. L. Pollock, E. Jakubowski, H. E. Gunning, and O. P. Strausz
Department of Chemistry, University of Alberta, Edmonton, Alberta

Received March 31, 1969

The quantum yield for the mercury photosensitized decomposition of hydrogen has been measured using the ethylene scavenging technique and has been found to be equal to unity.

Canadian Journal of Chemistry, 47, 3474 (1969)

The classical experiment of Cario and Franck (1) in 1922 on the mercury photosensitized decomposition of the hydrogen molecule was the first demonstration of the intermolecular conversion of electronic excitation energy into chemical energy. Several studies of this reaction have been reported in the intervening years, but the mechanism and quantum efficiency of the reaction is still a matter of controversy.

Thomas and Gwinn (2) have attempted to measure the quantum yield for the dissociation of hydrogen using copper oxide as a scavenger. By the improbable assumption that the efficiency of the scavenging reaction is unity, the quantum yield of the dissociation reaction was found to be ~ 0.22. Subsequently, Callear and Robb (3) used ethylene as scavenger of hydrogen atoms and obtained a quantum efficiency of unity. From a study of the H + NO reaction Strausz and Gunning (4) also concluded that the primary quantum yield of the dissociation reaction is unity.

More recently Goldschmidt *et al.* (5), employing techniques similar to those of Thomas and Gwinn, have shown that removal of hydrogen atoms from the gas phase by solid molybdenum

Can. J. Chem. Downloaded from www.nrcresearchpress.com by 210.87.254.6 on 09/05/12
For personal use only.

Can. J. Chem. Downloaded from www.nrcresearchpress.com by 210.87.254.6 on 09/05/12
For personal use only.

oxide is far from being an efficient process and that the quantum yield of dissociation is close to unity.

At this point Yang and co-workers (6) published a theoretical study, based on phase space theory, of the quenching of $Hg(^3P_1)$ atoms by H_2 molecules and concluded that the quantum yields for H atoms, HgH, and undissociated vibrationally excited hydrogen molecules are 0.52, 0.16, and 0.58, respectively. The claim was also made that in mercury-sensitized decompositions, these vibrationally hot H_2 molecules could undergo reactions which were, in the past, attributed solely to H-atom reactions. Since formation of such vibrationally excited H_2 molecules appeared to be an unusual phenomenon, contradicting most experimental results, we have decided to reexamine the quantum yield of hydrogen atom formation in this system, using ethylene as scavenger.

The ratio of the rate of formation of ethane to butane in the mercury photosensitized hydrogenation of ethylene is known to be dependent upon the experimental conditions (3) and is greater than the accepted value of k_d/k_r for ethyl radicals (7). However, under suitable conditions, high H_2-to-ethylene pressure and low light intensities, the deviation is minimal.

LeRoy and co-workers (8, 9) suggested that the excess ethane is formed by recombination of hydrogen atoms with ethyl radicals, while Callear and Pereira (10) proposed an alternative mechanism wherein ethane would be produced via reactions of ethyl radicals with HgH. The intermediacy of HgH has lately been verified by flash mercury photosensitization (11). Neither of these processes would have any effect on the quantum yield determination as measured by the rate of production of ethane plus butane, were it not for the exothermicity of the ethyl radical and hydrogen atom combination reaction. This reaction produces vibrationally excited ethanes which may subsequently dissociate into methyl radicals. These methyl radicals then appear in the products as propane by recombining with ethyl radicals.

[1] $C_2H_5 + H \rightarrow C_2H_6^*$

[2] $C_2H_6^* \rightarrow 2CH_3$

[3] $C_2H_5 + CH_3 \rightarrow C_3H_8$

Further reactions contributing to ethyl loss are the addition of ethyl to ethylene and the combination of the resulting butyl radicals with ethyl to give hexane

[4] $C_2H_5 + C_2H_4 \rightarrow C_4H_9$

[5] $C_2H_5 + C_4H_9 \rightarrow C_6H_{14}$

Experimental

Three cylindrical quartz cells were used as reaction vessels. Their dimensions were 6, 10, and 19 cm in length with a common diameter of 5 cm. Hanovia low-pressure Hg-arcs equipped with Vycor 7910 filters were used as radiation sources. Prior to each experiment a warm-up time of at least 2 h was allowed. All experiments were done at room temperature allowing a minimum of 2 h for mixing of the gases before irradiation.

Light intensities were determined by nitrous oxide actinometry (12).

After irradiation, the noncondensables were pumped off through two traps at −196 °C in series with one at −210 °C. The whole of the condensable products were then admitted to the sample port of a thermal conductivity gas chromatographic unit. A medium activity silica gel column and an alumina column deactivated with 2.5% silicone oil 550 were used to analyze the C_2–C_4 fraction. The presence of hexane was checked using a silicone oil DC200 column.

Ethylene (Phillips Research Grade) was purified by distillation at −160 °C and degassing at −196 °C while the hydrogen (Airco Assayed Reagent) was used without further purification. The butene-1 (Phillips Research Grade) was distilled at −112 °C and degassed at −130°C. Nitrous oxide (Matheson) was purified by distillation at −130 °C and degassing at −160 °C.

Results and Discussion

From the data, summarized in Table I, the combined quantum yield of ethane and butane formation is unity when the ethylene pressure is near 1 Torr. The mean value of the product ratios C_2H_6/C_4H_{10} is 0.166, only slightly higher than the disproportionation to recombination ratio of ethyl radicals, 0.135. If vibrationally excited H_2^* molecules were participating in the reaction, their two conceivable reactions would be

[6] $H_2^* + C_2H_4 \xrightarrow{M} C_2H_6$

[7] $H_2^* + C_2H_4 \longrightarrow C_2H_5 + H$

Reaction [6] can be dismissed on the ground that the ethane in excess of that due to disproportionation of ethyl radicals is negligible, about 2–3% of the total ethyls.

Reaction [7] would require excess energy in H_2^* of at least 65.8 kcal, the endothermicity of the reaction. Since, however, hydrogen atom addition to ethylene has an activation energy of a few kcal, and H_2 addition should have an even

TABLE I

Hg $6(^3P_1)$ photosensitized decomposition of hydrogen*

$P_{C_2H_4}$ (Torr)	P_{H_2} (Torr)	L_{cell} (mm)	I_0($\times 10^{10}$ einsteins cm^{-2} s^{-1})	$\Phi_{C_2H_6+C_4H_{10}}$	C_2H_6/C_4H_{10}
0.73	640	100	1.60	1.00	0.18
1.01	880	100	1.94	1.03	0.15
1.93	735	100	1.94	0.90	0.16
2.41	760	60	2.06	0.90	0.17
2.62	650	60	2.01	0.94	0.17
2.68	760	60	2.06	0.81	0.17
2.94	595	100	2.02	0.82	0.16
3.07	760	60	2.11	0.87	0.17
3.48	750	190	2.12	0.87	0.16
3.88	770	190	3.44	0.87	0.17
4.30	855	60	2.46	0.85	0.16
4.73	760	60	2.06	0.88	0.17

*T = 25 °C.

higher activation energy requirement[1], the minimal excess energy necessary could not be less than about 70 kcal. Now the concentration ratio of H_2 to C_2H_4 in our system was about 880 and the gas kinetic collision ratio $Z(H_2^*\text{–}H_2)/Z(H_2^*\text{–}C_2H_4) \sim 3300$. Unfortunately, vibrational relaxation data for the H_2 molecule are scant. The $Z_{1,0}$ values (ref. 13, p. 202) at 2280 and 2600 °K are 2500 and 3800. Assuming that $Z_{1,0}$ does not increase with decreasing temperature, it can be estimated from the relation $p_{i,i-1} = ip_{1,0}$ (ref. 13, p. 170) that the number of collisions with H_2 necessary to deplete the excess energy of H_2^* below the critical estimate of 70 kcal, which requires the removal of 7 quanta, $v = 15 \rightarrow v = 8$ (14) is not more than about 1500. Thus the fraction of H_2^* which would be relaxed prior to collision with C_2H_4 is

$$\frac{\frac{3300}{1500}}{\frac{3300}{1500}+1} \sim \frac{2}{3}$$

The steric factor of reaction [7] cannot be higher than that of the abstraction reaction by ethyl radicals from H_2, 10^{-2} (9) and therefore practically all H_2^* would be relaxed by collision with H_2 before reaction with ethylene could take place. Consequently, under the prevailing experimental conditions the possibility of reaction [7] can be dismissed.

[1]Reaction [7] can also be compared to the abstraction reaction by ethyl radicals from hydrogen. The Arrhenius parameters of this latter reaction are: $\log A = 9.6$ (l mole^{-1} s^{-1}) and $E_a = 13.7$ kcal (9).

Thus the only conceivable set of elementary steps which can account for the results is

[8] $Hg + h\nu\,(2537\text{ Å}) \rightarrow Hg^*\,6(^3P_1)$

[9a] $Hg^* + H_2 \rightarrow 2H + Hg$

[9b] $Hg^* + H_2 \rightarrow H + HgH \rightarrow Hg + H$

[10] $H + C_2H_4 \xrightarrow{M} C_2H_5$

[11] $HgH + C_2H_4 \rightarrow C_2H_5 + Hg$

[12] $2C_2H_5 \rightarrow C_4H_{10}$

[13] $\rightarrow C_2H_4 + C_2H_6$

with $\Phi([9a] + [9b]) = 1.0$.

The decrease in the overall quantum yield with increasing ethylene pressure is due to polymerization

[14] $C_4H_9 + nC_2H_4 \rightarrow C_{2n+4}H_{4n+9}$

[15] $C_{2n+4}H_{4n+9} + C_2H_5 \rightarrow C_{2n+4}H_{4n+8} + C_2H_6$

Small quantities of polymer formation could be observed in these experiments and at higher ethylene pressures noticeable quantities of *n*-hexane ($\ll 1\%$) were also detected. Reaction [15] could also account for the slight excess of ethane formation.

At low pressures of ethylene, where scavenging of H-atoms by ethylene was incomplete, in agreement with a previous publication (10), small amounts of propane ($\ll 1\%$) were observed which arose from reactions [2] and [3]. Apparently even 800 Torr hydrogen is not sufficient to completely quench the atomic cracking of the hot ethane molecule.

In conclusion, the spin forbidden reaction

$$Hg(^3P_1) + H_2(X^1\Sigma) \rightarrow Hg(^1S_0) + H_2^*(X^1\Sigma)$$

Can. J. Chem. Downloaded from www.nrcresearchpress.com by 210.87.254.6 on 09/05/12
For personal use only.

postulated on the basis of phase space theory does not occur in reality.

Acknowledgment

The authors thank the National Research Council of Canada for financial support.

1. G. Cario and J. Franck. Z. Phys. Chem. **11**, 161 (1922).
2. L. B. Thomas and W. D. Gwinn. J. Amer. Chem. Soc. **70**, 2643 (1948).
3. A. B. Callear and J. C. Robb. Trans. Faraday Soc. **51**, 638 (1955).
4. O. P. Strausz and H. E. Gunning. Trans. Faraday Soc. **60**, 347 (1964).
5. D. Goldschmidt, J. Villermaux, and R. Gibert. J. Chim. Phys. **63**, 262 (1966).
6. K. Yang, J. D. Paden, and C. L. Hassell. J. Chem. Phys. **47**, 3824 (1967).
7. J. O. Terry and J. H. Futrell. Can. J. Chem. **45**, 2327 (1967).
8. M. J. Smith, P. M. Beatty, J. A. Pinder, and D. J. LeRoy. Can. J. Chem. **33**, 821 (1955).
9. L. E. Reid and D. J. LeRoy. Can. J. Chem. **46**, 3275 (1968).
10. A. B. Callear and W. P. D. Pereira. Trans. Faraday Soc. **59**, 2758 (1962).
11. A. B. Callear and R. E. M. Hedges. Nature, **218**, 163 (1968).
12. R. J. Cvetanovic, W. E. Falconer, and K. R. Jennings. J. Chem. Phys. **35**, 1225 (1961).
13. B. Stevens. Collisional activation in gases. The Pergamon Press Ltd., London. 1967.
14. A. G. Gaydon. Dissociation energies. Chapman and Hall, Ltd., London. 1968. p. 88.

The formation of alkanes in the pyrolysis of *n*-hexadecane: effect of an inert gas on the decomposition of alkyl radicals

François Doue and Georges Guiochon

Laboratoire Professeur L. Jacque, Ecole Polytechnique, 17 rue Descartes, Paris 5°, France

Received June 25, 1968

The rate of formation of alkanes in the pyrolysis of *n*-hexadecane is shown to be drastically reduced in the presence of an inert gas.

The experimental results are in good quantitative agreement with the predictions of a theoretical model, which assumes that the decomposition of alkyl radicals is not monomolecular, because the Maxwell–Boltzmann activation process would be perturbed by a bimolecular reaction having a lower activation energy.

Canadian Journal of Chemistry, 47, 3477 (1969)

In a previous work (1), we have shown that the kinetics of *n*-hexadecane pyrolysis, in the initial stage of the reaction, offered support for the following free radical mechanism

$$C_{16}H_{34} \rightarrow R_i + R_j \qquad \text{Initiation}$$

$$[1]\quad R_1 + C_{16}H_{34} \xrightarrow{k_1} R_1H + \left.\vphantom{\xrightarrow{k_1}}\right\}$$

$$[2]\quad R_2 + C_{16}H_{34} \xrightarrow{k_2} R_2H + \left.\vphantom{\xrightarrow{k_2}}\right\} \quad C_{16}H_{33} \text{ (primary or secondary radicals)}$$

$$[3]\quad R_3 + C_{16}H_{34} \xrightarrow{k_3} R_3H + \left.\vphantom{\xrightarrow{k_3}}\right\}$$

$$[4]\quad R_2 \text{ or } R_3 \xrightarrow{k_4} C_2H_4 + R_i$$

$$[5]\quad R' \xrightarrow{k_5} \text{Alkene} + R_i \quad (R_i \text{ primary radical})$$

$$[6]\quad R_3 \overset{K}{\rightleftharpoons} R' \qquad \text{Isomerization}$$

$$[7]\quad R_i + R_j \rightarrow \text{Products}$$

where $R_1 = CH_3$ or C_2H_5

$R_2 = n\text{-}C_3H_7$ or $n\text{-}C_4H_9$

$R_3 = C_nH_{2n+1}$ $n > 4$ (primary radical)

$R' = C_nH_{2n+1}$ $n > 4$ (secondary radical)

Similar radical mechanisms have been shown by several authors (2–4) to be very useful to account for the kinetics of decomposition of light alkanes.

The reaction was found to be homogeneous, in the following range of experimental conditions: temperature from 380 to 520 °C, pressure from 0.1 to 100 bars, pyrolysis ratio below 5%. The decomposition was performed in small glass tubes, sealed under vacuum (1).

The values derived from this mechanism for the

Can. J. Chem. Downloaded from www.nrcresearchpress.com by 210.87.254.6 on 09/05/12
For personal use only.

postulated on the basis of phase space theory does not occur in reality.

Acknowledgment

The authors thank the National Research Council of Canada for financial support.

1. G. Cario and J. Franck. Z. Phys. Chem. **11**, 161 (1922).
2. L. B. Thomas and W. D. Gwinn. J. Amer. Chem. Soc. **70**, 2643 (1948).
3. A. B. Callear and J. C. Robb. Trans. Faraday Soc. **51**, 638 (1955).
4. O. P. Strausz and H. E. Gunning. Trans. Faraday Soc. **60**, 347 (1964).
5. D. Goldschmidt, J. Villermaux, and R. Gibert. J. Chim. Phys. **63**, 262 (1966).
6. K. Yang, J. D. Paden, and C. L. Hassell. J. Chem. Phys. **47**, 3824 (1967).
7. J. O. Terry and J. H. Futrell. Can. J. Chem. **45**, 2327 (1967).
8. M. J. Smith, P. M. Beatty, J. A. Pinder, and D. J. LeRoy. Can. J. Chem. **33**, 821 (1955).
9. L. E. Reid and D. J. LeRoy. Can. J. Chem. **46**, 3275 (1968).
10. A. B. Callear and W. P. D. Pereira. Trans. Faraday Soc. **59**, 2758 (1962).
11. A. B. Callear and R. E. M. Hedges. Nature, **218**, 163 (1968).
12. R. J. Cvetanovic, W. E. Falconer, and K. R. Jennings. J. Chem. Phys. **35**, 1225 (1961).
13. B. Stevens. Collisional activation in gases. The Pergamon Press Ltd., London. 1967.
14. A. G. Gaydon. Dissociation energies. Chapman and Hall, Ltd., London. 1968. p. 88.

The formation of alkanes in the pyrolysis of *n*-hexadecane: effect of an inert gas on the decomposition of alkyl radicals

François Doue and Georges Guiochon

Laboratoire Professeur L. Jacque, Ecole Polytechnique, 17 rue Descartes, Paris 5°, France

Received June 25, 1968

The rate of formation of alkanes in the pyrolysis of *n*-hexadecane is shown to be drastically reduced in the presence of an inert gas.

The experimental results are in good quantitative agreement with the predictions of a theoretical model, which assumes that the decomposition of alkyl radicals is not monomolecular, because the Maxwell–Boltzmann activation process would be perturbed by a bimolecular reaction having a lower activation energy.

Canadian Journal of Chemistry, 47, 3477 (1969)

In a previous work (1), we have shown that the kinetics of *n*-hexadecane pyrolysis, in the initial stage of the reaction, offered support for the following free radical mechanism

$$C_{16}H_{34} \rightarrow R_i + R_j \qquad \text{Initiation}$$

$$[1]\quad R_1 + C_{16}H_{34} \xrightarrow{k_1} R_1H + \left.\vphantom{\xrightarrow{k_1}}\right\}$$

$$[2]\quad R_2 + C_{16}H_{34} \xrightarrow{k_2} R_2H + \left.\vphantom{\xrightarrow{k_2}}\right\} \quad C_{16}H_{33} \text{ (primary or secondary radicals)}$$

$$[3]\quad R_3 + C_{16}H_{34} \xrightarrow{k_3} R_3H + \left.\vphantom{\xrightarrow{k_3}}\right\}$$

$$[4]\quad R_2 \text{ or } R_3 \xrightarrow{k_4} C_2H_4 + R_i$$

$$[5]\quad R' \xrightarrow{k_5} \text{Alkene} + R_i \quad (R_i \text{ primary radical})$$

$$[6]\quad R_3 \overset{K}{\rightleftharpoons} R' \qquad \text{Isomerization}$$

$$[7]\quad R_i + R_j \rightarrow \text{Products}$$

where $R_1 = CH_3$ or C_2H_5

$R_2 = n\text{-}C_3H_7$ or $n\text{-}C_4H_9$

$R_3 = C_nH_{2n+1}$ $n > 4$ (primary radical)

$R' = C_nH_{2n+1}$ $n > 4$ (secondary radical)

Similar radical mechanisms have been shown by several authors (2–4) to be very useful to account for the kinetics of decomposition of light alkanes.

The reaction was found to be homogeneous, in the following range of experimental conditions: temperature from 380 to 520 °C, pressure from 0.1 to 100 bars, pyrolysis ratio below 5%. The decomposition was performed in small glass tubes, sealed under vacuum (1).

The values derived from this mechanism for the

Can. J. Chem. Downloaded from www.nrcresearchpress.com by 210.87.254.6 on 09/05/12
For personal use only.

Can. J. Chem. Downloaded from www.nrcresearchpress.com by 210.87.254.6 on 09/05/12
For personal use only.

kinetic parameters and for the composition of the pyrolysis products agree very well with the experimental data (1).

The isomerization reaction via internal transfers of hydrogen atoms was shown to be very fast (1), so that primary and secondary radicals are in thermodynamical equilibrium. K is the average equilibrium constant between C_nH_{2n+1} primary and secondary radicals, where $4 < n \leqslant 16$.

Formation of Alkanes

The amount of alkanes was expressed (1) by the ratio $\theta = y/x$ of the number, y, of alkane molecules with 5 to 15 carbon atoms, to the number, x, of alkene molecules with 3 to 15 carbon atoms which result from the decomposition of ρn_0 molecules of n-hexadecane, where n_0 is the initial number of molecules and ρ is the pyrolysis ratio.

In the initial stage of the pyrolysis, the rate of the reaction is supposed to remain constant. Using a theoretical calculation of the different rate constants and an interpretation of the composition of the pyrolysis products, we have shown (1) that the rate of combination and disproportionation of radicals was comparatively very slow. Then

$$\theta \simeq \frac{k_3}{k_5} \cdot \frac{[R_3]}{[R']} \cdot [C_{16}H_{34}] = \frac{k_3}{k_5 K} p$$

where p is the partial pressure of hexadecane at the beginning of the reaction. From the results already published (1) it can be seen that θ is proportional to p in the pressure range 0.5 to 100 bars (Fig. 1).

Effect of an Inert Gas

In the presence of an inert gas (argon or water), θ is also proportional to the pressure of n-hexadecane in the whole pressure range investigated, but the proportionality coefficient is much lower than in the pyrolysis of pure hexadecane.

Figure 2 shows the results obtained at 420 °C in the presence of water vapor. The partial pressure of water in these experiments was always larger than 2 bars and at least 10 times larger than the pressure of n-hexadecane.

Under these conditions, $\theta \simeq 0.2\theta_0$, where θ_0 is the value of θ observed for pure n-hexadecane; this result does not depend on the partial pressure of water. The same result is observed with argon as the inert gas between 400 and 500 °C.

Interpretation of the Results with the Aid of an Activation–Deactivation Mechanism

At high pressure, the Maxwell–Boltzmann energy distribution is known to be valid for mole-

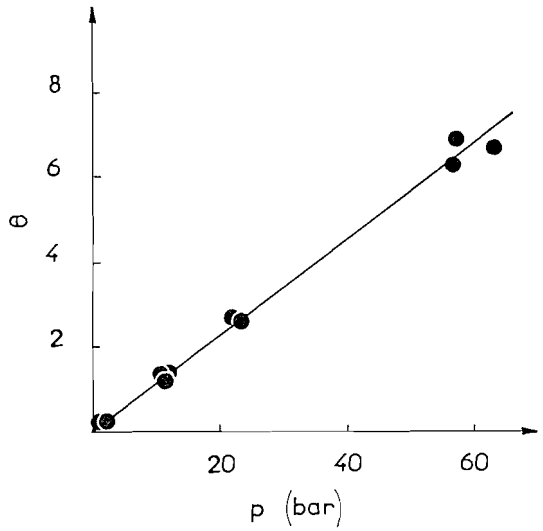

FIG. 1. Variations of the ratio θ of the paraffins to olefines amounts in the pyrolysis products of n-hexadecane with the initial pressure. Temperature, 420 °C; pyrolysis time, 120 s.

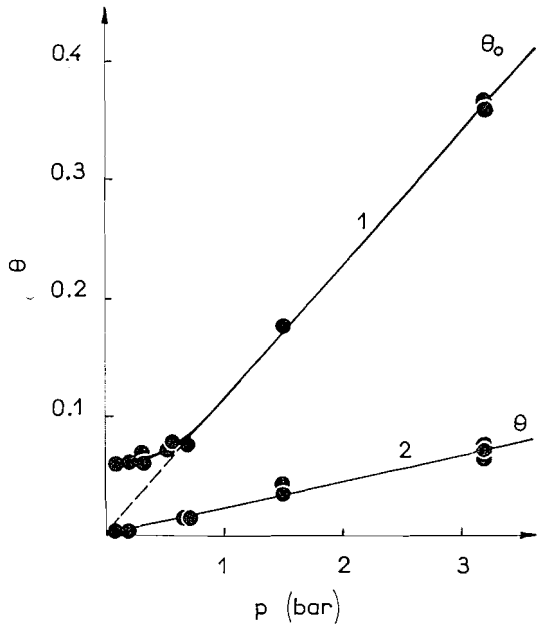

FIG. 2. Variations of the ratio of the paraffins to olefines amounts in the pyrolysis products of n-hexadecane with the initial partial pressure of n-hexadecane. 1, pure n-hexadecane (θ_0); 2, n-hexadecane diluted in argon or water vapor (θ). Experimental conditions as for Fig. 1.

Can. J. Chem. Downloaded from www.nrcresearchpress.com by 210.87.254.6 on 09/05/12
For personal use only.

cules. This might not be true for radicals at all energy levels, and especially at energies higher than the activation energy of a bimolecular reaction.

The rate constants of steps [3] and [4] are k_3 and k_4, with activation energies $E_3 \simeq 10.5$ and $E_4 \simeq 24$ kcal/mole (1, 2, 5), respectively. Those R_3 radicals with an energy $E(E_3 > E > E_4)$, and called hereafter $R_3{}^*$, can get more energy only via collisions with alkane molecules. Such collisions can also produce the saturation of $R_3{}^*$ via reaction [3]. Then, if the number of collisions necessary for $R_3{}^*$ to reach an energy level greater than E_4 is larger than the reciprocal of the steric factor of reaction [4], this reaction may be supposed to disturb the energy distribution of $R_3{}^*$ radicals.

In the presence of an inert gas A, the mechanism can be written as follows

(*a*) Alkane formation

$$[9] \qquad R_3{}^* + C_{16}H_{34} \xrightarrow{k = aZ} RH + \cdots$$

$$[10] \qquad R_3{}^{\ddagger} + C_{16}H_{34} \xrightarrow{k = a'Z} RH + \cdots$$

where $R_3{}^{\ddagger}$ denotes the R_3 radicals with an energy $E \geqslant E_4$.

(*b*) Radical decomposition

$$[11] \qquad R_3{}^{\ddagger} \xrightarrow{k = \nu} C_2H_4 + \cdots$$

(*c*) Activation–deactivation via two types of collision

1. With alkane molecules

$$[12] \qquad R_3{}^* + C_{16}H_{34} \underset{cZ}{\overset{bZ}{\rightleftharpoons}} R_3{}^{\ddagger} + C_{16}H_{34}$$

2. With molecules of an inert gas A

$$[13] \qquad R_3{}^* + A \underset{c'Z}{\overset{b'Z}{\rightleftharpoons}} R_3{}^{\ddagger} + A$$

where Z is the collision frequency per unit concentration of $R_3{}^*$, $R_3{}^{\ddagger}$, $C_{16}H_{34}$, or A; ν is the frequency factor of the decomposition of $R_3{}^{\ddagger}$ radicals; and a, a', b, b', c, c' are efficiency or steric factors. A is assumed to have roughly the same kinetic properties as $C_{16}H_{34}$ in order to keep the same value for Z in reactions [9], [10], [12], and [13].

With this mechanism, it is possible to calculate the ratio $\alpha = d[R_3H]/d[C_2H_4]$, where α is proportional to θ at a given pressure. As long as the rate of equilibrium between radicals R_3 and R′ is supposed to be very fast, any variation of $[R_3]$ acts on [R′], and so the R_3 and R′ rates of decomposition remain proportional. Thus

$$\alpha = [C_{16}H_{34}] \cdot \frac{Z}{\nu} \cdot \frac{a[R_3{}^*] + a'[R_3{}^{\ddagger}]}{[R_3{}^{\ddagger}]}$$

$$\simeq \frac{ap}{s} \cdot \frac{[R_3{}^*]}{[R_3{}^{\ddagger}]} \quad \text{since } [R_3{}^{\ddagger}] \ll [R_3{}^*]$$

where $s = \nu Z^{-1}$ and $p = [C_{16}H_{34}]$.

The stationary state hypothesis applied to the radicals $R_3{}^{\ddagger}$ allows the ratio $[R_3{}^*]/[R_3{}^{\ddagger}]$ to be calculated. Let $n' = 1/b'$ be the number of collisions of $R_3{}^*$ with the inert molecules A necessary for $R_3{}^*$ to obtain energy E_4. Because of reaction [9] the number $n = 1/b$ of collisions with $C_{16}H_{34}$ molecules necessary to obtain the same energy will be greater than n'. After the $R_3{}^*$ radicals have experienced on the average n' collisions, only a fraction $(1 - a)^{n'}$ of these radicals remain unreacted; the necessary number of collisions to transfer an energy ΔE to the radicals $R_3{}^*$ becomes $n = n'(1 - a)^{-n'}$. If we suppose that a is very small (this will be shown later)

$$[14] \qquad n \simeq n'(1 + n'a) \quad \text{or} \quad b'/b \simeq 1 + a/b'$$

It can be found in the same way that

$$[15] \qquad c'/c \simeq 1 + a'/c'$$

Consequently

$$\alpha = \frac{a}{s} \cdot p \cdot \frac{c'p_A - (c + a')p + s}{bp + b'p_A}$$

with $p_A = [A]$; $p = [C_{16}H_{34}]$.

Semiquantitative Interpretation of the Results

At 400 °C several collisions are most probably necessary to transfer an amount of energy $E_4 - E_3 \simeq 13.5$ kcal/mole. For two collisions we should have $c' = 0.5$ and $b' = c'\exp((E_3 - E_4)/RT) \sim 10^{-4}$. The steric factor, for hydrogen atom abstraction is about 10^{-3} (5, 6) for methyl radicals, and a little lower for larger alkyl radicals. Thus a is about 5×10^{-4} (1) and $a \gg b'$. Equation [14] gives $b' \gg b$.

Therefore the Maxwell–Boltzmann activation process is actually disturbed by reaction [3]. On the other hand, a' cannot be much larger than a. Then $a' \ll c'$ and eq. [15] gives $c \simeq c'$. Since θ is proportional to α at any concentration of

hexadecane, θ/θ_0 can be expressed with the rate constant b' and c' only.

$$\frac{\theta}{\theta_0} = \frac{c'(p_A + p) + s}{p + \left(1 + \frac{a}{b'}\right)p_A} \cdot \frac{p}{c'p + s}$$

For our experimental conditions ($p_A > 2$ bars and $p_A > 10p$)

$$s \ll c'pZ \text{ or } c'p_AZ$$

then

$$\frac{\theta}{\theta_0} \simeq \frac{p_A + p}{p + \left(1 + \frac{a}{b'}\right)p_A}$$

and if $p_A \gg p$

$$\frac{\theta}{\theta_0} \simeq \frac{b'}{a + b'}$$

Consequently, this model shows that (a), θ/θ_0 is independent of the initial concentrations of the alkane and the inert gas as long as they are not too low, and provided that $p_A \gg p$ (b), θ is independent of the nature of the inert gas, and (c), θ is smaller than $\theta_0/5$.

These results are in excellent agreement with the experimental data. This model could be useful to account for other types of reactions where the collisions necessary to activate chemical species can also produce a bimolecular reaction.

1. F. Doue and G. Guiochon. J. Chim. Phys. **65**, 395 (1968).
2. J. H. Purnell and C. P. Quinn. Can. J. Chem. **43**, 721 (1965).
3. J. H. Purnell and C. P. Quinn. Proc. Roy. Soc. London, Ser. A, **270**, 267 (1962).
4. S. W. Benson. The foundations of chemical kinetics. McGraw Hill Book Co., Inc., New York. 1960.
5. N. N. Semenov. Some problems in chemical kinetics and reactivity. Princeton Univ. Press, Princeton. 1958.
6. N. H. Sagert and K. J. Laidler. Can. J. Chem. **41**, 848 (1963).

Can. J. Chem. Downloaded from www.nrcresearchpress.com by 210.87.254.6 on 09/05/12
For personal use only.

On the use of a polyelectrolyte in a thermocell[1]

W. G. Breck and E. King[2]
Department of Chemistry, Queen's University, Kingston, Ontario

Received March 7, 1969

Canadian Journal of Chemistry, 47, 3480 (1969)

Agar's thermocell equations (1) have been applied to experiments involving acid–base (2) and redox (3, 4) electrodes. It is the purpose here to consider applying these relations to a polyelectrolyte such as a polystyrene sulfonic acid or a quaternary ammonium salt. For practical reasons as well as for theoretical simplicity, hydrogen gas electrodes are attractive; with them Lin (5) has obtained satisfactory results using a thermocell for initial values but not for the Soret steady state which is also considered in what follows.

For the use of hydrogen gas with an aqueous solution of a strong electrolyte, HA, the electrode reaction is simply

$$[1] \qquad H^+ - \tfrac{1}{2}H_2 + e = 0$$

Substitution of the coefficients of the terms in reaction [1] into Agar's thermocell equations produces relations for the Soret steady state and the initial state (before any concentration changes have occurred owing to thermal diffusion), respectively, as

$$[2] \qquad F\varepsilon_\infty = -\bar{\bar{S}}_{H^+} + \tfrac{1}{2}S_{H_2} - \bar{\bar{S}}_e$$

$$[3] \qquad F\varepsilon_0 = F\varepsilon_\infty + (1 - t_{H^+})S_{H^+}{}^* + t_{A^-}S_{A^-}{}^* = F\varepsilon_\infty + t_{A^-}S_{HA}{}^*$$

Here F is the faraday; $\varepsilon_\infty = dE_\infty/dT$ is the thermoelectric power or temperature coefficient of electromotive force (e.m.f.) at the Soret steady state; $\varepsilon_0 = dE_0/dT$, the analogous property at the initial condition; t is the Hittorf transport number; $\bar{\bar{S}}$ for a constituent is the transported entropy, being the sum of the usual partial molar entropy, S, and the entropy of transport, S^*; $\bar{\bar{S}}_e$ is thus the

[1]From part of the Ph.D. work of E.K., supported by a grant from the National Research Council of Canada.
[2]Holder of a Province of Ontario Graduate Fellowship.

hexadecane, θ/θ_0 can be expressed with the rate constant b' and c' only.

$$\frac{\theta}{\theta_0} = \frac{c'(p_A + p) + s}{p + \left(1 + \frac{a}{b'}\right)p_A} \cdot \frac{p}{c'p + s}$$

For our experimental conditions ($p_A > 2$ bars and $p_A > 10p$)

$$s \ll c'pZ \text{ or } c'p_AZ$$

then

$$\frac{\theta}{\theta_0} \simeq \frac{p_A + p}{p + \left(1 + \frac{a}{b'}\right)p_A}$$

and if $p_A \gg p$

$$\frac{\theta}{\theta_0} \simeq \frac{b'}{a + b'}$$

Consequently, this model shows that (a), θ/θ_0 is independent of the initial concentrations of the alkane and the inert gas as long as they are not too low, and provided that $p_A \gg p$ (b), θ is independent of the nature of the inert gas, and (c), θ is smaller than $\theta_0/5$.

These results are in excellent agreement with the experimental data. This model could be useful to account for other types of reactions where the collisions necessary to activate chemical species can also produce a bimolecular reaction.

1. F. Doue and G. Guiochon. J. Chim. Phys. **65**, 395 (1968).
2. J. H. Purnell and C. P. Quinn. Can. J. Chem. **43**, 721 (1965).
3. J. H. Purnell and C. P. Quinn. Proc. Roy. Soc. London, Ser. A, **270**, 267 (1962).
4. S. W. Benson. The foundations of chemical kinetics. McGraw Hill Book Co., Inc., New York. 1960.
5. N. N. Semenov. Some problems in chemical kinetics and reactivity. Princeton Univ. Press, Princeton. 1958.
6. N. H. Sagert and K. J. Laidler. Can. J. Chem. **41**, 848 (1963).

Can. J. Chem. Downloaded from www.nrcresearchpress.com by 210.87.254.40 on 09/05/12
For personal use only.

On the use of a polyelectrolyte in a thermocell[1]

W. G. Breck and E. King[2]
Department of Chemistry, Queen's University, Kingston, Ontario

Received March 7, 1969

Canadian Journal of Chemistry, 47, 3480 (1969)

Agar's thermocell equations (1) have been applied to experiments involving acid–base (2) and redox (3, 4) electrodes. It is the purpose here to consider applying these relations to a polyelectrolyte such as a polystyrene sulfonic acid or a quaternary ammonium salt. For practical reasons as well as for theoretical simplicity, hydrogen gas electrodes are attractive; with them Lin (5) has obtained satisfactory results using a thermocell for initial values but not for the Soret steady state which is also considered in what follows.

For the use of hydrogen gas with an aqueous solution of a strong electrolyte, HA, the electrode reaction is simply

$$[1] \qquad H^+ - \tfrac{1}{2}H_2 + e = 0$$

Substitution of the coefficients of the terms in reaction [1] into Agar's thermocell equations produces relations for the Soret steady state and the initial state (before any concentration changes have occurred owing to thermal diffusion), respectively, as

$$[2] \qquad F\varepsilon_\infty = -\bar{\bar{S}}_{H^+} + \tfrac{1}{2}S_{H_2} - \bar{\bar{S}}_e$$

$$[3] \qquad F\varepsilon_0 = F\varepsilon_\infty + (1 - t_{H^+})S_{H^+}{}^* + t_{A^-}S_{A^-}{}^* = F\varepsilon_\infty + t_{A^-}S_{HA}{}^*$$

Here F is the faraday; $\varepsilon_\infty = dE_\infty/dT$ is the thermoelectric power or temperature coefficient of electromotive force (e.m.f.) at the Soret steady state; $\varepsilon_0 = dE_0/dT$, the analogous property at the initial condition; t is the Hittorf transport number; $\bar{\bar{S}}$ for a constituent is the transported entropy, being the sum of the usual partial molar entropy, S, and the entropy of transport, S^*; $\bar{\bar{S}}_e$ is thus the

[1]From part of the Ph.D. work of E.K., supported by a grant from the National Research Council of Canada.
[2]Holder of a Province of Ontario Graduate Fellowship.

Can. J. Chem. Downloaded from www.nrcresearchpress.com by 210.87.254.40 on 09/05/12
For personal use only.

transported entropy of a mole of electrons in the metal leads which are not isothermal.

If some other strong electrolyte, HB (with H^+ in common), is added, eq. [2] is unchanged except in so far as the value of $\bar{\bar{S}}_{H^+}$ changes with possible change in concentration of H^+ or interionic effect. On the other hand, for the initial state

$$[4] \quad F\dot{\varepsilon}_0 = F\varepsilon_\infty + (1 - \dot{t}_{H^+})S_{H^+}{}^* + \dot{t}_{A^-}S_{A^-}{}^* + \dot{t}_{B^-}S_{B^-}{}^* = F\varepsilon_\infty + \dot{t}_{A^-}S_{HA}{}^* + \dot{t}_{B^-}S_{HB}{}^*$$

The subscribed dots indicate values of quantities *in the mixture* of electrolytes (e.g., values of transport numbers will be different in the mixtures of HA and HB from values for HA alone).

If the strong electrolyte, KA (with A^- in common), is added to the solution of HA

$$[5] \quad F\dot{\varepsilon}_0 = F\varepsilon_\infty + (1 - \dot{t}_{H^+})S_{H^+}{}^* - \dot{t}_{K^+}S_{K^+}{}^* + \dot{t}_{A^-}S_{A^-}{}^* = F\varepsilon_\infty + (1 - \dot{t}_{H^+})S_{HA}{}^* - \dot{t}_{K^+}S_{KA}{}^*$$

It is now our purpose to indicate what use can be made of the thermoelectric eqs. [2], [3], [4], and [5] as a basis for experimental work.

(*a*) By measurement of the e.m.f. of a suitable thermocell at the Soret steady state the quantity $F\varepsilon_\infty$ can be evaluated; however, the experimental difficulties are great and only a few such experiments have been carried out successfully. The main troubles are to maintain an invariant temperature gradient over a long period of time and to avoid convection at all times. Also electrode behavior must be highly reproducible. In eq. [2] the value of S_{H_2} is well known (31.21 e.u.) as is also the small value of $\bar{\bar{S}}_e$ for copper leads (−0.045 e.u.). It is apparent then that $\bar{\bar{S}}_{H^+}$ can be evaluated by such experiments at various concentrations. By a suitable extrapolation against a function of ionic strength $\bar{\bar{S}}_{H^+}{}^0$ has been evaluated as 5.1 e.u. with the use of quinhydrone electrodes in a thermocell (2). Here it would be difficult to employ electrodes with hydrogen gas bubbling to follow the thermal diffusion to the steady state because of mechanical disturbance in the cell.

(*b*) If, for an electrolyte such as HA, $F\varepsilon_0$ is also evaluated by measurement of ε_0 it can be seen from eq. [3] that the difference of $F\varepsilon_\infty$ from $F\varepsilon_0$ gives the quantity $t_{A^-}S_{HA}{}^*$. If t_{A^-} is known or measured, $S_{HA}{}^*$ can be found and translated into Soret data.

(*c*) It is interesting to speculate on the significance of making HA a strong polyelectrolyte preferably with water solubility. One of the few available as such (as its Na salt) is polystyrene sulfonic acid which is said to ionize completely (6). Its solubility in water is considerable but presumably decreases with increased molecular weight and degree of cross linkage. As judged by the behavior of other polyelectrolytes it is likely that the transport number of the anion is close to zero. A more physical view of this is that the polyanion framework is a stationary matrix to which the hydrogen ions are held electrostatically. Even for ordinary acid solutions (e.g. HCl) the transport number of the anion is lower than 0.2. The important point is that if t_{A^-} is close enough to zero in eq. [3], then $F\varepsilon_\infty$ is given by $F\varepsilon_0$. This means that in this case lengthy and delicate runs need no longer be done to get $F\varepsilon_\infty$. Furthermore, with convection, no threat electrodes with hydrogen gas bubbling become practicable.

For the polyanion, $S_{A^-}{}^*$ need not be zero nor is it likely so. Measurements on benzene sulfonic acid indicate that its S^* value is comparable to values for other monobasic strong acids. In eq. [3] in writing $t_{A^-}S_{A^-}{}^*$ we have been considering a monovalent anion, A^-. However, with a polyelectrolyte, H_nP, which ionizes according to $H_nP = z^-H^+ + P^{z^-}$, there will be $1/z^-$ mole of P^{z^-} for each mole of H^+. If ionization is complete $n = z^-$ and we write $H_{z^-}P = z^-H^+ + P^{z^-}$. Per equivalent, the entropy of transport of the polyanion is $S_{P^{z^-}}{}^*/z^-$ and

$$[6] \quad F\varepsilon_0 = F\varepsilon_\infty + (1 - t_{H^+})S_{H^+}{}^* + t_{P^{z^-}}S_{P^{z^-}}{}^*/|z^-| = F\varepsilon_\infty + t_{P^{z^-}}S_{H_{z^-}P}{}^*/|z^-|$$

For a mole of polyanion the entropy of transport would be z^- times as large, yielding a large value for a large amount of material.

(*d*) Equations [4] and [5] show that ε_0 can be altered by the addition of other electrolytes (e.g. HB, KA) to give an infinite variety of values of ε_0. Thus thermoelectric powers can be controlled by the selection of added electrolyte(s); this situation can resemble that in polarography where the added electrolyte can flood out the function of the key electrolyte in the bulk of the solution but not at the electrode.

(*e*) Provided that the concentration of H^+ is not changed too much, the addition of another electrolyte allows its Soret data to be evaluated by use of eq. [4] (or eq. [5] as appropriate). Thus the initial condition (and final since these are the same) for the strong polyelectrolyte can be used as a framework on which to base the determination of entropies of transport of added electrolytes without having to do measurements at other than the initial condition.

1. J. N. AGAR. The structure of electrolytic solutions. John Wiley and Sons, Inc., New York. 1959. p. 220.
2. W. BRECK, G. CADENHEAD, and M. HAMMERLI. Trans. Faraday Soc. **61**, 37 (1965).
3. W. G. BRECK and J. LIN. Trans. Faraday Soc. **61**, 744 (1965).
4. W. G. BRECK and J. LIN. Trans. Faraday Soc. **61**, 1511 (1965).
5. J. LIN. Private communication.
6. A. KATCHALSKY, A. ALEXANDROWICZ, and O. KEDEM. Chemical physics of ionic solutions. John Wiley and Sons, Inc., New York. 1966. pp. 296, 312.

Can. J. Chem. Downloaded from www.nrcresearchpress.com by 210.87.254.40 on 09/05/12
For personal use only.

Can. J. Chem. Downloaded from www.nrcresearchpress.com by 210.87.254.6 on 09/05/12
For personal use only.

Canadian Journal of Chemistry

Published by THE NATIONAL RESEARCH COUNCIL OF CANADA

VOLUME 47 OCTOBER 1, 1969 NUMBER 19

A new method of synthesis of aldosuloses

D. J. WALTON

Department of Biochemistry, Queen's University, Kingston, Ontario

Received April 16, 1969

As a new approach to the synthesis of aldosuloses (osones), epimeric pairs of the allylic alcohols, **1** and **2**, and **4** and **5**, were oxidized to the corresponding vinyl ketones, **3** and **6**, respectively. Degradation of the latter by reductive ozonolysis and hydrolysis gave D-*glycero*-tetrosulose and D-*arabino*-hexosulose (D-glucosone), respectively.

Canadian Journal of Chemistry, 47, 3483 (1969)

There has recently been renewed biological interest in the aldosuloses, or osones, as 3-deoxy-D-*arabino*-hexosulose is formed when mammalian liver is treated with arsenious oxide (1), and there is probably a connection between mammalian tissue α-keto-aldehyde concentrations and rates of cell division (2). In commencing a study of aldosuloses it was apparent that there are few satisfactory general methods available for their synthesis. Methods of synthesis were reviewed by Bayne and Fewster (3), who mentioned the low yields associated with the oxidation of reducing aldoses, and the deficiencies of the osazone-cleavage method. Subsequent work has included the oxidation of acetone-protected methyl glycosides at C-2, using chromium trioxide (4) or ruthenium tetroxide (5), and the conversion of diazomethyl ketone acetates into the acetates of aldosulose hydrazones (6–8), or into the acetates of aldosulose dithioacetals (9). Most of the derivatives formed in these reactions are not convertible into free aldosuloses, but the aldosulose dithioacetal acetates are exceptional, as they can be successively deacetylated and demercaptalated (9). Hence the diazomethyl ketone → thioacetal route provides a general method of aldosulose synthesis, although little information is available concerning its efficiency.

A new route to the aldosuloses has been devised in this laboratory, and is based on the following sequence of reactions (where R·CHO is an *O*-isopropylidene derivative of an *aldehydo* sugar)

$$\text{R·CHO} \rightarrow \text{R·CHOH·CH=CH}_2 \rightarrow \text{R·CO·CH=CH}_2 \rightarrow \text{R·CO·CHO} \rightarrow \text{aldosulose}$$

A hydroxyl-protected *aldehydo* sugar is vinylated to give a pair of epimeric allylic alcohols as described in previous reports (10, 11). Oxidation of the mixed epimeric alcohols with activated manganese dioxide gives a single vinyl ketone, which is successively ozonolyzed and hydrolyzed to form an aldosulose. The vinyl group, which serves as a potential aldehydo function, makes it possible to obtain the keto group by allylic oxidation, thereby eliminating the need for steps involving aldehyde group protection. Acetal or ketal protecting groups fulfil all the requirements for hydroxyl protection, as they are unaffected by Grignard reagents, manganese dioxide or ozone, but can be removed from a protected aldosulose with acetic acid (12).

The procedure has been used to synthesize D-*glycero*-tetrosulose (see Scheme 1), which cannot be prepared by hydrolysis of D-erythrose phenylosazone (13) and, to the author's knowledge, has not been synthesized previously. The mixed epimeric pentenetriols **1** and **2** were oxidized in 41% yield to 4,5-isopropylidenedioxy-D-*glycero*-1-penten-3-one (**3**). Confirmation of the structure of **3** was obtained from the infrared (i.r.) spectrum, which showed absorption bands

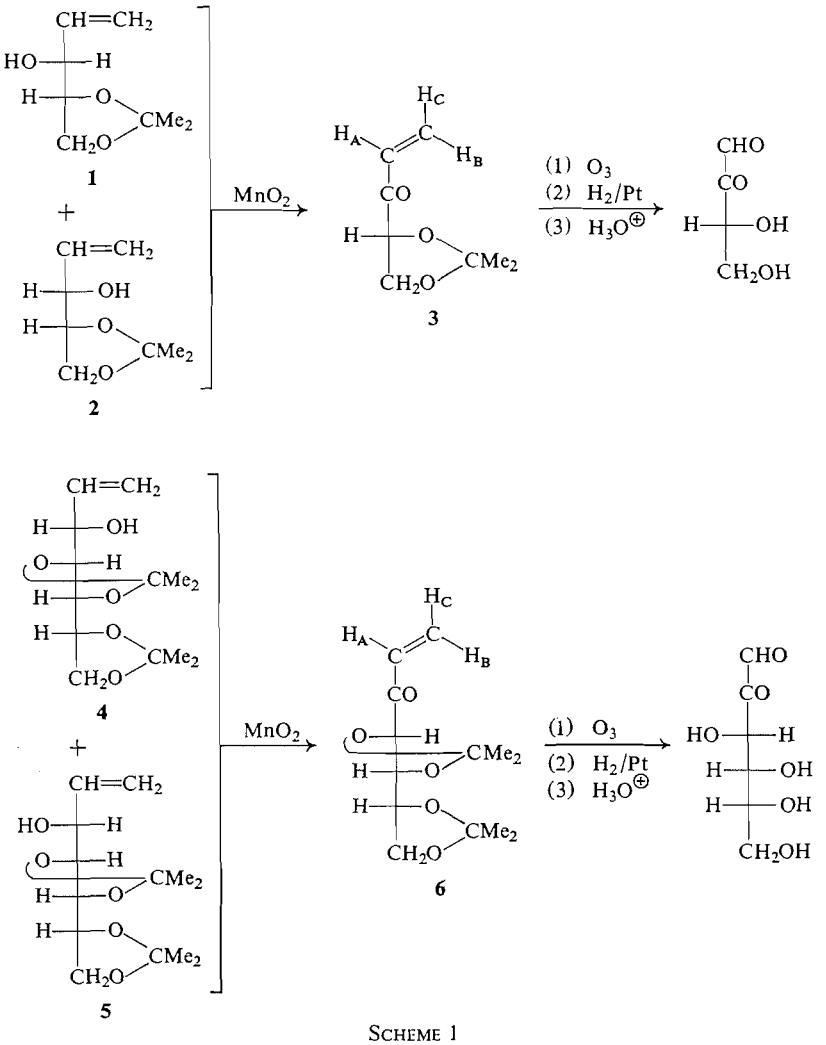

SCHEME 1

due to the conjugated carbonyl group and double bond. The low-field ABX system of the nuclear magnetic resonance (n.m.r.) spectrum was attributed to the vinylic protons. The values of the coupling constants were similar to those reported for vinyl ketones (14, 15; see Table I), and proton H_A resonated at low field as a result of deshielding by the carbonyl group.

Reductive ozonolysis and deketalization of **3** gave a product from which the main component was isolated chromatographically. This substance, a syrup obtained in 18% yield from **3**, was shown by the following methods to be D-*glycero*-tetrosulose. On paper chromatograms it migrated faster than glucose, as a single spot which gave an instant red color with alkaline triphenyltetrazolium chloride, a reagent which is known to react faster with aldosuloses than with aldoses (3). Treatment of the syrup with phenylhydrazine – acetic acid in the cold, or with 2,5-dichlorophenylhydrazine in hot 1-propanol[1] (conditions which preclude conversion of aldoses into osazones) gave D-*glycero*-tetrosulose bis-phenylhydrazone (16) and bis-2,5-dichlorophenylhydrazone (17), respectively. Formation of these derivatives, previously prepared from

[1]Conversion of D-erythrose into D-*glycero*-tetrosulose bis-2,5-dichlorophenylhydrazone requires the inclusion of acetic acid in the reaction mixture (17).

Can. J. Chem. Downloaded from www.nrcresearchpress.com by 210.87.254.6 on 09/05/12
For personal use only.

TABLE I

Nuclear magnetic resonance parameters for vinyl groups of vinyl ketones*

Compound	Observed lines (τ)			Chemical shifts (τ)†			Coupling constants (Hz)†		
	H_A	H_B	H_C	H_A	H_B	H_C	J_{AB}	J_{AC}	J_{BC}
3	2.97, 3.12, 3.26, 3.41	3.50, 3.55, 3.79, 3.84	4.15, 4.20, 4.31, 4.36	3.24	3.62	4.25	17.5	10.3	1.8
6	2.95, 3.11, 3.23, 3.38	3.45, 3.52, 3.73, 3.78	4.07, 4.12, 4.22, 4.27	3.23	3.57	4.16	16.8	10.3	1.8
Methyl vinyl ketone (15)‡				3.73	3.82	4.12	17.6	11.0	1.1
Phenyl vinyl ketone (14)‡							18.4	10.8	2.1

*Line assignments were based on the assumption that $J_{trans} > J_{cis} > J_{gem}$.
†Values obtained by second-order analysis. A check of relative line intensities by computer showed that J_{AC} and J_{BC} have the same sign.
‡Values quoted from the literature. Only *relative* shifts are available for phenyl vinyl ketone. Protons H_A, H_B, and H_C resonate at successively higher magnetic fields, the chemical shift differences being Δ_{AB} 0.75, and Δ_{AC} 1.48 p.p.m.

D-erythrose under more drastic conditions, can only be explained by assuming that the hydrazines had condensed with D-*glycero*-tetrosulose.

Borohydride reduction of D-*glycero*-tetrosulose should proceed nonstereoselectively, to give a 1:1 mixture of erythritol and D-threitol. Accordingly, a portion of the syrup was treated with sodium borohydride, followed by acetic anhydride, using the conditions described by Sjöström *et al.* (18). Gas–liquid partition chromatography (g.l.p.c.) of the product revealed the presence of equal weights of two compounds with retention times of erythritol tetraacetate and D-threitol tetraacetate, thus giving further evidence for the tetrosulose structure.

Application of the procedure to the mixed heptenetetrol epimers, **4** and **5**, gave, in 55% yield, vinyl ketone **6**, whose i.r. and n.m.r. spectra had similar characteristics to those of compound **3**. Degradation of **6** afforded chromatographically pure D-*arabino*-hexosulose (D-glucosone) in 37% yield. The identity of the latter was checked by co-chromatography with a reference sample, and by the preparation of two osazones, using the reaction conditions already described for the tetrosulose.

These examples show that allylic oxidation is an effective way of forming the 2-keto group of an aldosulose, in a synthetical route which should be of general applicability.

Experimental

Thin-layer plates, coated with silica gel, were developed with benzene – ethyl acetate 4:1, and sprayed with the alkaline permanganate reagent (19). Paper chromatograms were developed with 1-butanol – acetic acid – water 4:1:5 (solvent system *a*), or phenol – water 4:1 (solvent system *b*), or ethyl acetate – acetic acid – formic acid – water 18:3:1:4 (solvent system *c*). Rates of movement are quoted relative to that of D-glucose (R_G = 1.0). Compounds were visualized with ammoniacal silver nitrate (20) or with alkaline triphenyltetrazolium chloride (21).

Gas–liquid partition chromatography of *C*-vinyl compounds was performed with a column (152 × 0.155 cm) of 10% carbowax 20 *M* terephthalic acid on 70–80 mesh chromosorb W, with a nitrogen flow of 45 ml per min. The oven temperature was 112° at the time of injection, rising to 187° over 11.1 min. Retention times which are shown in Table II are quoted relative to that of 1,2:5,6-di-*O*-isopropylidene-α-D-glucofuranose (T = 1.0; retention time 10.6 min). The system used for preparative g.l.p.c. was similar to that described in the last report (11), except that the stationary phase was carbowax 20 *M* terephthalic acid.

Nuclear magnetic resonance spectra of deuterochloroform solutions were obtained at 60 MHz, using tetramethylsilane as the internal standard.

Activated manganese dioxide was obtained from Winthrop Laboratories, New York, and behaved similarly to a sample prepared according to Attenburrow *et al.* (22). Tetrahydrofuran was distilled before use. Epimeric mixtures of **1** and **2**, and of **4** and **5**, were prepared as described previously (10, 11). The ratio of **1** to **2** was 1.0:1.5, and of **4** to **5** was 1.3:1.0. The phenylhydrazine reagent (13) was prepared thus: a solution composed of equal volumes of phenylhydrazine and 50% aqueous acetic acid was diluted with two volumes of water.

TABLE II

Chromatographic data for *C*-vinyl compounds

Compound	**1**	**2**	**3**	**4**	**5**	**6**
R_F*	0.27	0.27	0.54	0.33	0.33	0.55
T†	0.18	0.19	0.11	0.49	0.57	0.45

*Silica gel t.l.c. (for conditions see Experimental).
†Gas–liquid partition chromatography (for definitions see Experimental).

Can. J. Chem. Downloaded from www.nrcresearchpress.com by 210.87.254.6 on 09/05/12
For personal use only.

Can. J. Chem. Downloaded from www.nrcresearchpress.com by 210.87.254.6 on 09/05/12
For personal use only.

4,5-Isopropylidenedioxy-D-*glycero*-*1*-*penten*-*3*-*one* (*3*)[2]

A solution of 1,2-*O*-isopropylidene-D-*threo* (and L-*erythro*)-4-pentene-1,2,3-triol (**1** and **2**, 4.0 g) in tetrahydrofuran (200 ml) was stirred with manganese dioxide (40 g) for 1 h at room temperature. The mixture was filtered on a sintered funnel (M), which resulted in evaporation of ca. 80 ml of solvent. The manganese dioxide filter cake was washed with tetrahydrofuran until the volume of the combined filtrate and washings was restored to 200 ml. The resulting solution was treated with two further batches (40 g each) of manganese dioxide. Each addition was followed by stirring and filtration as before. Analysis of the final solution by g.l.p.c. showed that the proportions of **1**, **2**, and **3** were 2:3:95, respectively. (In separate experiments it was established that these proportions were not altered significantly by further manganese dioxide treatment.) Water[3], which had been adsorbed from the atmosphere during the filtrations, was removed with Na_2SO_4, and the solution was concentrated[4] at 35° and 15 cm to give the product (2.1 g) contaminated with **1** and **2**. Purification was effected by silica gel column chromatography. Elution with benzene – ethyl acetate (94:6) gave the pure product (1.6 g, 41%), a colorless, mobile liquid $[\alpha]_D^{21}$ + 68° (*c*, 2.1 in chloroform). Infrared spectrum (film): 1685 (conjugated CO), 1605 (conjugated C=C), 1395 (vinyl CH in-plane deformation), 1365 and 1375 cm^{-1} (CMe_2 doublet); n.m.r. data: τ 2.97–4.36 (ABX system shown in Table I, vinyl group), τ 5.37–6.13 (3-proton multiplet, H-4, 5, and 5′), τ 8.60 and 8.64 (3-proton singlets, CMe_2). A sample for elemental analysis was obtained by preparative g.l.p.c. at 130°.

Anal. Calcd. for $C_8H_{12}O_3$: C, 61.52; H, 7.74. Found: C, 61.71; H, 7.69.

Samples of compound **3** were stable for several weeks in the refrigerator, but polymerized over a period of several days at room temperature. Distillation of **3** was unsatisfactory as it resulted in formation of impurities, detectable by g.l.p.c.

D-*glycero*-*Tetrosulose*

A solution of **3** (1.5 g) in methanol was held at −40° while a stream of ozonized oxygen (400 ml per min; 0.55 mmoles O_3 per min) was bubbled through for 25 min. Nitrogen was bubbled through the solution while its temperature was brought to 0°, and the flow was continued for a further 10 min. The solution, at 0°, was stirred under hydrogen (atmospheric pressure) in the presence of platinum oxide (50 mg). When gas absorption had ceased the solution was filtered and concentrated to dryness. The residue was heated with 85% aqueous acetic acid (20 ml) for 18 h at 50°. The resulting solution was concentrated, and residual acetic acid was removed by co-distillation with ethanol. The residue, dissolved in water, was passed quickly through Rexyn 203 (OH) resin, and concentrated to a syrup which, after drying over phosphorus pentoxide, weighed 0.39 g. Paper chromatography (solvent *a*) revealed a main component, R_G 2.0, which gave an immediate, permanent, red color with the triphenyltetrazolium spray. Minor impurities, R_G 1.4–2.0, and R_G 3.0, were detectable by silver nitrate. A portion (0.25 g) of the syrup was purified by preparative paper chromatography on Whatman 3MM paper, using solvent *a*. The final product was a syrup (0.13 g, 18%), $[\alpha]_D^{21}$ + 5° (*c*, 4.1 in water), which migrated as a single spot in both system *a* (R_G 2.0) and system *c* (R_G 2.2). In system *b* it moved as a single spot, R_F 0.51, tailing to R_F 0.25.

D-*glycero*-*Tetrosulose Bis*-*phenylhydrazone*

Hydrazine derivatives were prepared from D-*glycero*-tetrosulose which had not been purified by chromatography. To a solution of crude D-tetrosulose (8 mg) in water (1.5 ml) was added 1 ml of phenylhydrazine reagent. After 10 min the osazone (15 mg) was precipitated by addition of water, and had m.p. 164–165°, undepressed when mixed with a sample prepared from D-erythrose; lit. m.p. 164–165° (16).

D-*glycero*-*Tetrosulose Bis*-*2,5*-*dichlorophenylhydrazone*

A solution of crude D-tetrosulose (34 mg) in 95% aqueous 1-propanol (10 ml) was heated on a boiling water-bath for 30 min with 2,5-dichlorophenylhydrazine (200 mg). The solvents were removed and the residue was dissolved in acetic acid (3 ml). Precipitation with water gave the title compound (76 mg), m.p. 208–213°, and m.p. 217–219° after recrystallization from benzene – ethyl acetate (1:1). The m.p. was undepressed on mixing with a sample prepared from D-erythrose; lit. m.p. 219–220° (17).

Tetritol Tetraacetates from D-*glycero*-*Tetrosulose*

Chromatographically pure D-*glycero*-tetrosulose (40 mg) was subjected to the borohydride reduction – acetylation procedure of Sjöström *et al.* (18). Analysis of the final solution by g.l.p.c., using columns 1 and 2 of the previous paper (11) in this series, gave two peaks in a 1:1 ratio, with retention times corresponding to those of erythritol tetraacetate and D-threitol tetraacetate.

4,5:*6,7*-*Bis*(*isopropylidenedioxy*)-D-*arabino*-*1*-*hepten*-*3*-*one* (*6*)[2]

A mixture of 1,2:3,4-di-*O*-isopropylidene-L-*gulo* (and D-*manno*)-6-heptene-1,2,3,4,5-pentol (**4** and **5**, 4.0 g) was oxidized by the method[4] used for compounds **1** and **2**, to give a liquid (2.8 g) which contained compounds **4**, **5**, **6**, and a by-product (*T* 0.41) in the proportions 2:2:90:6, respectively. The pure ketone (2.2 g, 55%) was obtained by column chromatography, and had $[\alpha]_D^{22}$ + 2° (*c*, 5.1 in chloroform). Infrared spectrum (film): 1680 (conjugated CO), 1610 (conjugated C=C), 1395 (vinyl CH in-plane deformation), 1365 and 1375 cm^{-1} (CMe_2 doublet); n.m.r. data: τ 2.95–4.27 (ABX system shown in Table I, vinyl group), τ 5.40–6.12 (5-proton multiplet, H-4,5,6,7, and 7′), τ 8.53, 8.59 (3-proton singlets, CMe_2), and τ 8.64 (6-proton singlet, CMe_2). The analytical sample was obtained by preparative g.l.p.c. at 170°.

Anal. Calcd. for $C_{13}H_{20}O_5$: C, 60.92; H, 7.87. Found: C, 61.13; H, 7.90.

Samples of **6** were stored in the cold. Distillation was unsatisfactory, for the reason given for compound **3**.

[2]Prepared by Miss Margaret Michael.

[3]Traces of water did not affect the efficiency of oxidation.

[4]Smaller pressures resulted in the evaporation of **3**. Solutions of **6** could be concentrated at 1.5–2.0 cm without loss of the product.

Can. J. Chem. Downloaded from www.nrcresearchpress.com by 210.87.254.6 on 09/05/12
For personal use only.

D-*arabino-Hexosulose*

Ketone **6** (1.5 g) was subjected to ozonolysis and hydrolysis, as described for compound **3**, but with the omission of any chromatographic purification of the product. The final product, a syrup (0.39 g, 37%), $[\alpha]_D$ − 2° (*c*, 4.4 in water), was chromatographically identical to an authentic sample of D-*arabino*-hexosulose. Chromatograms developed with solvent *a* showed spots at R_G 0.64 and R_G 0.77–1.19, with streaking at R_G 0.41–1.46, as described by Petuely (23). In solvent *b* the product moved as a single spot, R_F 0.25. All the above spots gave the immediate red coloration with triphenyltetrazolium chloride.

D-*arabino-Hexosulose Bis-phenylhydrazone*

The phenylhydrazine reagent (0.5 ml) was added to a solution of D-*arabino*-hexosulose (50 mg) in water (3 ml). The precipitated osazone (90 mg, 89%) was collected after 10 min, and, after recrystallization from aqueous pyridine, had m.p. 206–208°, $[\alpha]_D^{22}$ − 75 → −41° (*c*, 0.7 in pyridine – ethanol 2:3) (2 days); lit. (24) m.p. 208–209°, $[\alpha]_D$ − 40° (equilibrium value, in pyridine – ethanol 2:3).

D-*arabino-Hexosulose Bis-2,5-dichlorophenylhydrazone*

2,5-Dichlorophenylhydrazine (250 mg) was added to a solution of D-*arabino*-hexosulose (50 mg) in 95% aqueous 1-propanol. The mixture was heated for 30 min on a boiling water-bath. The product (78 mg, 56%), m.p. 241–242°, crystallized on cooling, and was washed successively with 50% aqueous acetic acid and water; lit. m.p. 242° (25).

Acknowledgments

The financial support of the Medical Research Council of Canada is gratefully acknowledged. The author wishes to thank Dr. Saul Wolfe for some useful advice.

1. N. Baker and L. G. Együd. Biochim. Biophys. Acta, **165**, 293 (1968).
2. L. G. Együd. Proc. Natl. Acad. Sci. U.S. **54**, 200 (1965).
3. S. Bayne and J. A. Fewster. Adv. Carbohydrate Chem. **11**, 44 (1956).
4. J. S. Burton, W. G. Overend, and N. R. Williams. J. Chem. Soc. 3433 (1965).
5. P. J. Beynon, P. M. Collins, P. T. Doganges, and W. G. Overend. J. Chem. Soc. C, 1131 (1966).
6. M. L. Wolfrom and J. B. Miller. J. Amer. Chem. Soc. **80**, 1678 (1958).
7. E. Fahr and F. Scheckenbach. Ann. Chem. **655**, 86 (1962).
8. H. J. Bestmann, H. Buckschewski, and L. Leube. Chem. Ber. **92**, 1345 (1959).
9. F. Weygand, E. Klieger, and H. J. Bestmann. Chem. Ber. **90**, 645 (1957).
10. D. J. Walton. Can. J. Chem. **45**, 2921 (1967).
11. D. J. Walton. Can. J. Chem. **46**, 3679 (1968).
12. S. Bayne, G. A. Collie, and J. A. Fewster. J. Chem. Soc. 2766 (1952).
13. E. Fischer. Chem. Ber. **22**, 87 (1889).
14. H. S. Gutowsky, M. Karplus, and D. M. Grant. J. Chem. Phys. **31**, 1278 (1959).
15. S. Castellano and J. S. Waugh. J. Chem. Phys. **37**, 1951 (1962).
16. R. C. Hockett. J. Amer. Chem. Soc. **57**, 2260 (1935).
17. A. S. Perlin and C. Brice. Can. J. Chem. **33**, 1216 (1955).
18. E. Sjöström, P. Haglund, and J. Janson. Svensk Papperstidn. **69**, 381 (1966).
19. D. R. Briggs, E. F. Garner, and F. Smith. Nature, **178**, 154 (1956).
20. W. E. Trevelyan, D. P. Procter, and J. S. Harrison. Nature, **166**, 444 (1950).
21. R. B. Burton, A. Zaffaroni, and E. H. Keutmann. J. Biol. Chem. **188**, 763 (1951).
22. J. Attenburrow, A. F. B. Cameron, J. H. Chapman, R. M. Evans, B. A. Hems, A. B. A. Jansen, and T. Walker. J. Chem. Soc. 1094 (1952).
23. F. Petuely. Monatsh. Chem. **83**, 765 (1952).
24. N. K. Richtmeyer. *In* Methods in carbohydrate chemistry. Vol. II. *Edited by* R. L. Whistler and M. L. Wolfrom. Academic Press, Inc., New York. 1963, p. 127.
25. H. H. Stroh and H. Lamprecht. Chem. Ber. **96**, 651 (1963).

Deamination of two steroidal α-aminoketones[1,2]

O. E. EDWARDS AND T. SANO[3]
Biochemistry Laboratory, National Research Council of Canada, Ottawa, Canada
Received May 14, 1969

The two aminoketones 12α-amino-3α,20β-diacetoxy-11-keto-5β-pregnane and 9α-amino-3β,20β-diacetoxy-11-keto-5α-pregnane were prepared. Deamination of the former could be controlled to give either 12-methyl-18-norpregnane derivatives or *C*-nor-*D*-homo (12,14-cyclo-13,14-secopregnane) derivatives. Deamination of the 9α-aminoketone gave a series of 9β-methyl-19-norsteroids.

Canadian Journal of Chemistry, 47, 3489 (1969)

Can. J. Chem. Downloaded from www.nrcresearchpress.com by 210.87.254.5 on 09/05/12
For personal use only.

The nitrous acid deamination of α-aminoketones (1) and the protonation of an α-diazoketone (2) led to unexpected products including cyclopropyl ketones (1) and a cyclobutanone (2*a*). This seems to be a consequence of carbon–carbon bond participation in the C—N bond cleavage, thus by-passing the high energy α-keto carbonium ion (1). By analogy the deamination of 9-amino and 12-amino-11-keto steroids appeared to provide possible routes to 9,11-cyclosteroids (e.g. buxus alkaloids (3)), 9-methyl-19-nor-11-keto steroids (e.g. cucurbitacins (4)), 12-methyl-18-norsteroids, and *C*-nor-*D*-homo 11-keto-steroids (jervine, veratramine (5)).

We had hoped to prepare both 12α- and 12β-amino-11-ketopregnane derivatives.[4] However, the 12β isomer eluded us. Products derived from the corresponding diazonium ion were only formed by protonation of the diazoketone which was a transient intermediate under some deamination conditions.

12α-Amino-3α,20β-diacetoxy-11-keto-5β-pregnane (**3**) was prepared from the known (6) 12α-bromo-3α,20β-diacetoxy-11-keto-5β-pregnane (**1**) by way of the 12α-azido derivative **2**.[5] The reduction of the azide group was accomplished using stannous chloride in ethanol. The ultraviolet (u.v.) absorption of **1** (λ_{max} 317 mμ, ε 145), **2** (λ_{max} 321 mμ, ε 145), and **3** (R = H) (λ_{max} 310 mμ, ε 190) was consistent with the axial 12α orientation in each case (7), as was subsequent reaction of the amino ketone. Most probably the 12α-bromoketone was in equilibrium with the 12β-bromoketone under the reaction conditions. A much more rapid displacement of the β-bromo group relative to the α-bromo would be expected on steric grounds, thus accounting for the formation of the 12α-azide.[6] Lithium aluminum hydride reduction of **2** followed by acetylation in pyridine led to an acetamido alcohol (**4**, R = H). The small coupling constant (2.5 Hz) for the 12-hydrogen in the corresponding fully acetylated compound was consistent with it being 12α-acetamido-3α,11β,20β-triacetoxy-5β-pregnane (**4**, R = Ac). Reduction of **3** by lithium aluminum hydride followed by acetylation also gave **4** (R = H), confirming that the amino and azido groups had the same configuration.

The synthesis of 9α-amino-3β,20β-diacetoxy-11-keto-5α-pregnane (**10**) proceeded from the known 3β,20β-diacetoxy-5α-pregn-9(11)-ene (**5**) (8). The olefin was converted to the rather unstable 9α-bromo-11β-hydroxy derivative **6**, and thence to the β-oxide **7**. The oxide was opened by heating with lithium azide in dry dimethylformamide. The oxidation of the azido alcohol **8** to the keto azide **9** was accomplished efficiently by the use of acetic anhydride and *p*-toluenesulfonic acid in dimethyl sulfoxide (9). In this series the azido ketone could be reduced in good yield to the aminoketone **10** by hydrogen over palladium on charcoal.

Deamination of 3

The aminoketone hydrochloride in aqueous acetic acid was treated with excess sodium nitrite. The major product was a non-conjugated

---

[1]Issued as NRCC No. 10856.
[2]Presented in part at the Symposium on The Chemistry and Biochemistry of Plant Products, Trent University, March 20, 1969.
[3]NRCC Postdoctoral Fellow, 1966–1968.
[4]We are grateful to Dr. N. F. Elmore and Dr. J. W. ApSimon for exploring a number of other possible routes to these amino ketones.
[5]This azido ketone was first prepared by Dr. N. F. Elmore, whom we warmly thank.
[6]Attempts to epimerize the azido ketone **2** and the *N*-acetyl ketone (**3**, R = Ac) were unsuccessful (see Experimental).

Can. J. Chem. Downloaded from www.nrcresearchpress.com by 210.87.254.5 on 09/05/12
For personal use only.

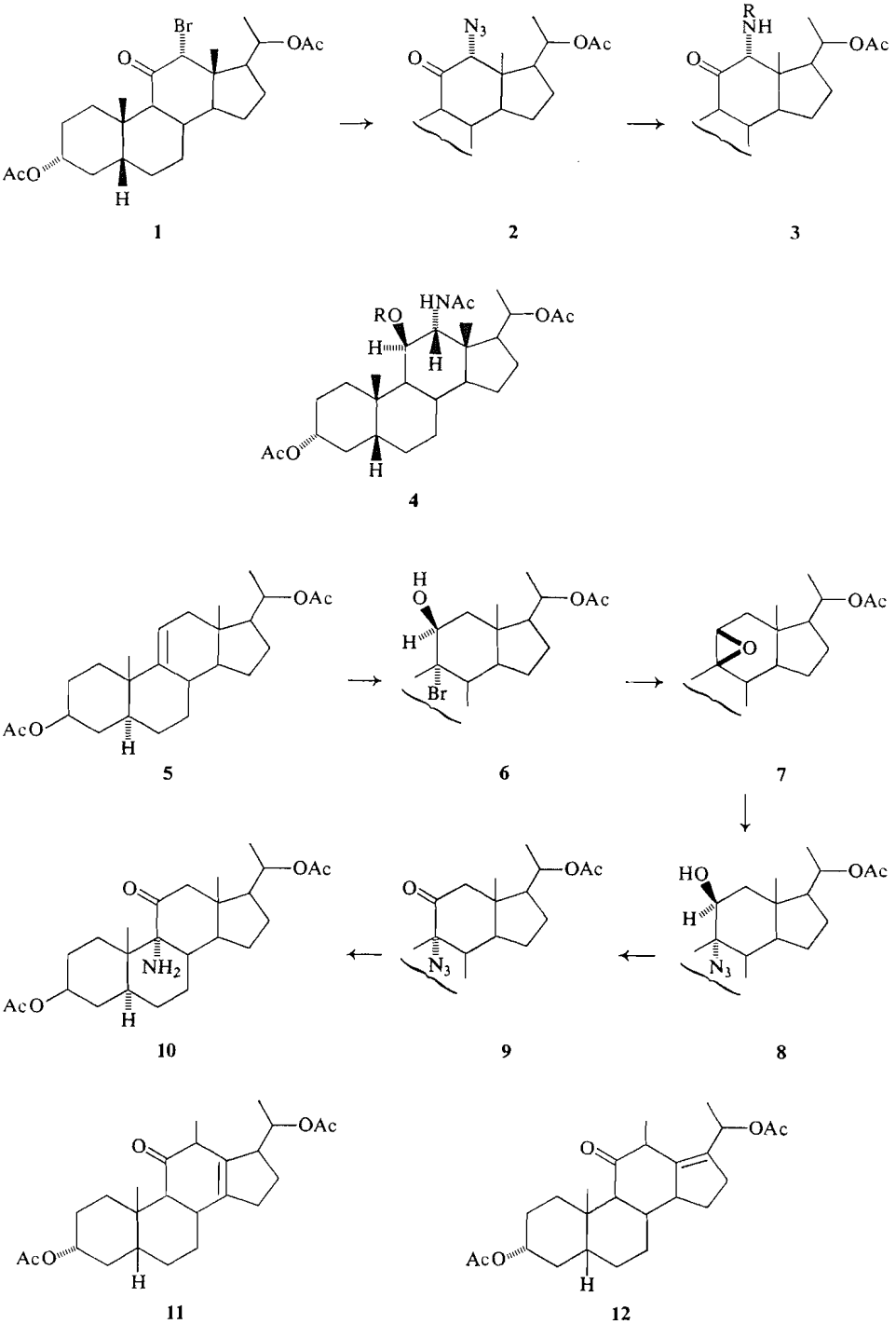

1 2 3

4

5 6 7

10 9 8

11 12

unsaturated ketone, whose properties corresponded to the 12-methyl-18-nor compounds **11** or **12.**

Attempts to purify the product on alumina led to a complex mixture from which a 22% yield of a crystalline mixture of the conjugated ketones **13**

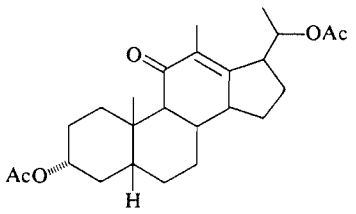

13

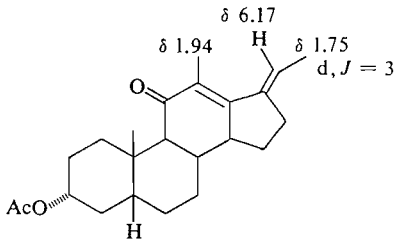

14

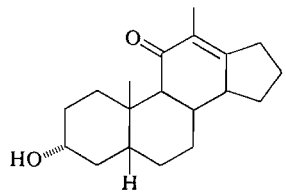

15

(3α,20β-diacetoxy-11-keto-12-methyl-19-nor-5β-pregn-12-ene) and **16** (ratio 4:1 respectively) was obtained. A third product was the dienone **14** (3α-acetoxy-11-keto-12-methyl-19-nor-5β-pregna-12,17(20)-diene). Pure **13** was isolated from the reaction of the hydrochloride of **3** with isoamyl nitrite in chloroform. Its absorption spectra (λ_{max} 250 mμ, ν_{max} 1738, 1665, and 1650 cm^{-1}), and its nuclear magnetic resonance (n.m.r.) spectrum (see formula) were consistent with the structure assigned. Hydrogenation converted it to a dihydro compound with ν_{max} 1730 and 1710 cm^{-1} (shoulder) confirming the ring size of the ketone. The action of hydroxide ion on **13** produced a retroaldol reaction. A 37% yield of **15** (3α-hydroxy-11-keto-12-methyl-19-nor-5β-androst-12-ene) was obtained. This had λ_{max} 248 mμ and ν_{max} 1650 and 1630 cm^{-1}.

The structure of the dienone **14** followed from its λ_{max} at 292 mμ and its n.m.r. spectrum (see formula).

An attempt to form the 12,13-epoxide from **13** using alkaline hydrogen peroxide failed. When a benzene solution of the mixture of non-conjugated ketones from the deamination in protic solvents and dichlorodicyanoquinone was refluxed for 20 h, no aromatization of ring C was observed.

No 12,18- or 12,14-cyclosteroids were detected among the products of deamination of **3** in protic solvents. Since the "aprotic" deamination conditions of Bayless *et al.* (10) generally gave higher yields of cyclopropanes from carbonium ions than aqueous deamination, we submitted **3** to the action of amyl nitrite in benzene. Again no cyclosteroids were detected. Instead the least polar product was now a *C*-nor-*D*-homosteroid. This was characterized as 3α,20β-diacetoxy-11-keto-12,14-cyclo-13,14-seco-5β-pregn-12-ene (**16**) by its absorption spectra (λ_{max} 252 mμ, ν_{max} 1740, 1710, and 1636 cm^{-1}) and its n.m.r. spectrum (see formula). When it was hydrogenated and hydrolyzed, the carbonyl frequency became 1724 cm^{-1}, confirming that the carbonyl was on a five-membered ring.

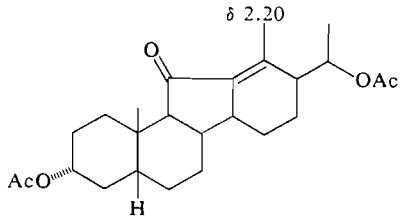

16

The table summarizes the results from deamination of **3** under various conditions. The other products produced were more strongly adsorbed on alumina, and appeared to be ketols and nitrite esters. These were not further characterized.

Deamination of ***10***

In this case, only methyl migration occurred. Three major products were characterized, 3β,20β-diacetoxy-11-keto-9β-methyl-19-norpregn-1(10)-ene (**17**), its $\Delta^{5(10)}$ isomer (**18**), and 3β,20β-diacetoxy-10α-hydroxy-11-keto-9β-methyl-19-norpregnane (**19**). Deamination in aqueous acetic gave 75% of **18** and 5% of **19**.

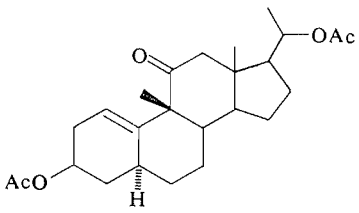

17

Amyl nitrite in benzene and acetic acid gave 42% of **17**, 31% of **18**, and 11% of **19**, while amyl nitrite in benzene gave an equimolar mixture of **17** and **18**. The structures of **17** and **19** follow

Can. J. Chem. Downloaded from www.nrcresearchpress.com by 210.87.254.5 on 09/05/12
For personal use only.

TABLE I
Deamination of 3

Substrate	Solvent	Reagent	% Yield 12-Methyl	% Yield *C*-nor-*D*-homo-
B·HCl	CH_3OH–HCl	$NaNO_2$		(22,ratio 4:1)*
B·HCl	50% HOAc	$NaNO_2$		(25,ratio 4:1)*
B·HCl	HOAc	iso-$C_5H_{11}ONO$	14†	—
B·HCl	$CHCl_3$	iso-$C_5H_{11}ONO$	57†	—
B·HCl	C_6H_6	iso-$C_5H_{11}ONO$		(82,ratio 1:1)‡
B·HOAc	C_6H_6	iso-$C_5H_{11}ONO$	—	50§
Base	C_6H_6	iso-$C_5H_{11}ONO$	—	64§
Base	C_6H_6‖	iso-$C_5H_{11}ONO$	—	45§

*Only non-conjugated products produced. The yields are of a crystalline mixture of conjugated ketones after attempted separation on alumina.
†Yield of **13**.
‡Crystalline mixture of **13** and **16**.
§Yield of **16**.
‖$CaCO_3$ powder added.

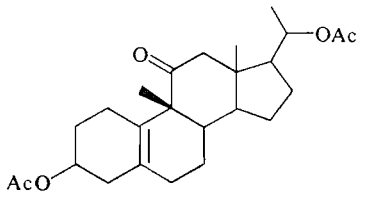

18

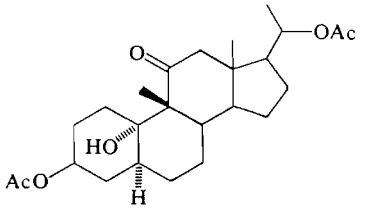

19

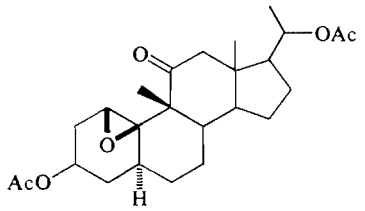

20

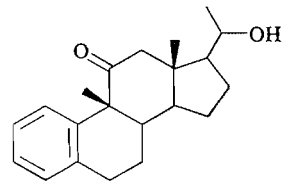

22

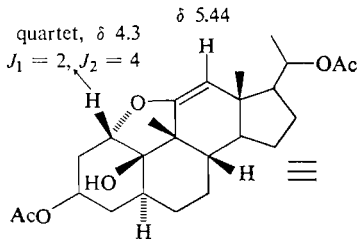

21

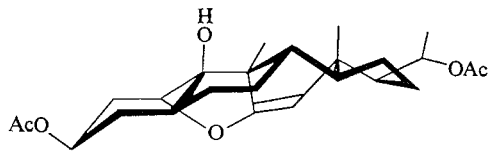

from their n.m.r. spectra and reactions. Thionyl chloride in pyridine dehydrated **19** cleanly to **17**. This is only consistent with an α-orientation of the 10-hydroxyl since it is then *cis* to the 5α-hydrogen. Treatment of **17** with *m*-chloroperbenzoic acid gave a mixture of epoxides. When this was warmed with acetic acid, one oxide was converted to a hydroxy enol ether. On the assumption of favored *trans* diaxial opening of the oxide by the 11-oxygen, we consider that the β-oxide **20** reacted, and that the structure and stereochemistry of the enol ether are correctly represented by **21**. When the enol ether was treated with hydrogen chloride in ethanol, ring A was aromatized, giving 20β-hydroxy-11-keto-9β-methyl-19-nor-5α-pregna-1,3,5-triene (**22**). As

Can. J. Chem. Downloaded from www.nrcresearchpress.com by 210.87.254.5 on 09/05/12
For personal use only.

Can. J. Chem. Downloaded from www.nrcresearchpress.com by 210.87.254.5 on 09/05/12
For personal use only.

required for this structure it had four aromatic hydrogens in its n.m.r. spectrum.

m-Chlorobenzoic acid converted **18** to a single monoxide, probably the α-oxide **23**. This too was aromatized by hydrogen chloride in ethanol. The product was identical with that obtained from **21**.

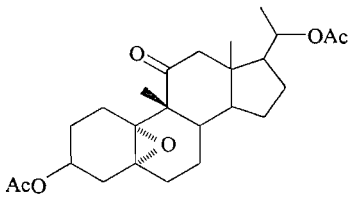

23

Discussion

The *C*-nor-*D*-homo steroid skeleton has been prepared previously in several ways from the normal steroids. The action of base on the 12-tosylhydrazones **24** (11) and **25** (12) gave the corresponding *C*-nor-*D*-homo derivatives.

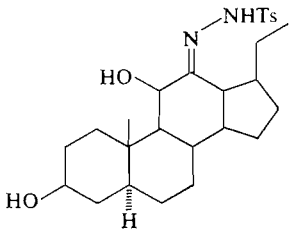

24

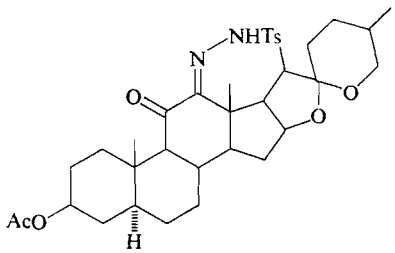

25

Surprisingly, both the 12α and 12β tosylates **26** gave mainly *C*-nor-*D*-homo olefins under solvolytic conditions (13), (presumably largely S_N1 reaction).

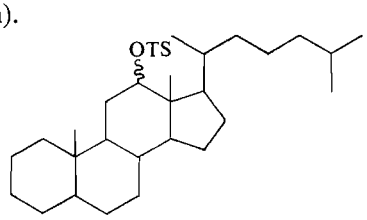

26

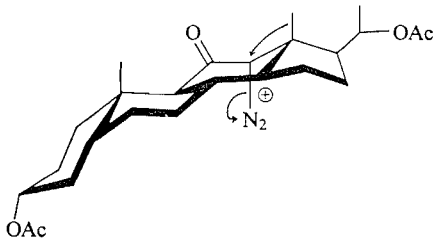

27

A number of cases of migration of C-18 onto C-12 have been reported, initiated by action of hydrogen fluoride on a 9α,11α-oxide (14) dehydration of a 12-hydroxy-7,9(11)-diene (15) and dehydrobromination of a 7,11-dibromo-8-ene on alumina (16).

The deamination of the 12α-aminoketone **3** in protic solvents led predominantly to methyl migration. This is consistent with a concerted migration and nitrogen elimination (see **27** and comments in the introduction). If the cation **28** had been an intermediate, the conjugated olefin should have been a major product, whereas none was formed under essentially neutral conditions.

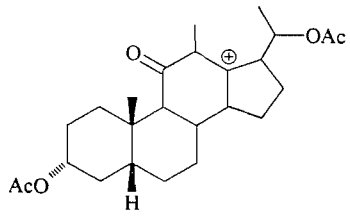

28

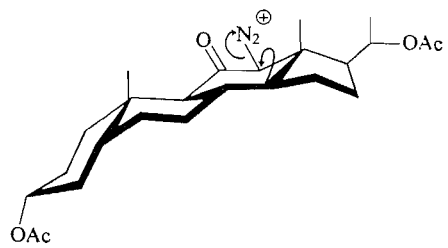

29

The axial nature of the developing electron deficiency on C-12, the methyl group, and the hydrogens on C-14 and C-17 all contribute to the synchronous processes leading to **11** and/or **12**.

On the other hand, the products from aprotic deamination of **3** correspond to formation of the

Can. J. Chem. Downloaded from www.nrcresearchpress.com by 210.87.254.5 on 09/05/12
For personal use only.

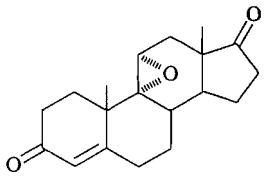

30

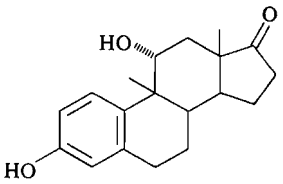

31

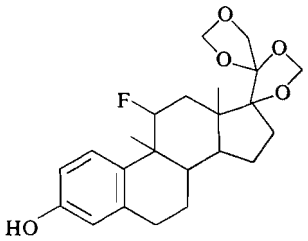

32

diazoketone, followed by axial protonation[7] to give the 12β-diazonium ion **29**. In support of this interpretation, diazoketone (ν_{max} 2090 cm^{-1}) was detected as a transient product of these deaminations.

The Lewis acid-catalyzed rearrangement of the 9α,11α-oxide **30** to give **31** (17), the formation of the fluoro compound **32** (18), and the acid-catalyzed rearrangement of 3,16 diketo-17a,17a-dimethyl-18-nor-D-homoandrost-13-ene(19) seem to be the only previously recorded cases of formation of 19-nor-9β-methyl steroids.

In the deamination of **10** the migration of the 10-methyl group is probably synchronous with the loss of the 9α-diazonium group. An initial methyl bridged ion **33** or protonated cyclopropane could then be stabilized by loss of the 1α-hydrogen to give **17**, of the 5α-hydrogen to give **18**, or by reaction with water to give **19**. A compelling argument for the methyl participation in the deamination is the absence of any $\Delta^{8,9}$ olefin among the products.

Much to our disappointment, a fourth possibility, the loss of a proton from **33** to give the 9,19-cyclo compound **34**, was a minor event if it happened at all under our deamination conditions. It appears likely that the *in vivo* formation of 9,19-cyclosteroids involves a strategically placed basic site on an enzyme, which aids

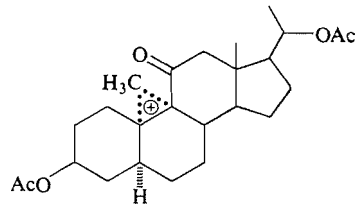

33

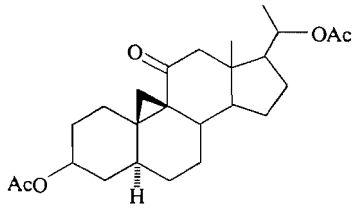

34

removal of a proton from the methyl-bridged ion.

Attempts are underway to duplicate the 10-methyl migration in the lanostane series.

Experimental

Infrared spectra were determined using a Perkin–Elmer model 257 grating spectrometer and n.m.r. spectra using a Varian A-60-A spectrometer. Rotations were measured on solutions in 95% ethanol. Thin layer chromatograms (t.l.c.) were done on silica gel plates and column chromatography on Woelm neutral alumina, with activities according to Brockmann and Schodder (20).

12α-Bromo-3α,20β-diacetoxy-5β-pregnan-11-one (1)

This was prepared as described by Jones and Wenka (6). It had λ_{max} 317 mμ (ε 145) and n.m.r. signals at δ 0.73 (s, 3H) (C-18); 1.12 (s, 3H) (C-19); 1.19 (d, 3H) (C-21); 2.02 (s, 6H) (OAc); 4.03 (s, 1H) (12 βH); and 4.70 (2H) (CHOAc).

12α-Azido-3α,20β-diacetoxy-5β-pregnan-11-one (2)

A solution of 6.37 g of bromoketone (**1**) and 3.58 g of lithium azide (18) in ml of dry dimethylformamide was maintained at 125–130° under nitrogen for 4 h. After cooling the solution was poured into ice water then extracted with *n*-hexane. The hexane solution was washed with water, dried, and distilled, giving 6.27 g of

[7]The protonation of 3-diazonorbornan-2-one appears to be equally stereospecific, leading to the *endo*-diazo compound (*a*), and thence to the cyclobutanone (*b*) (2*a*).

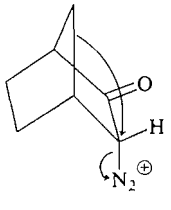

(*a*)

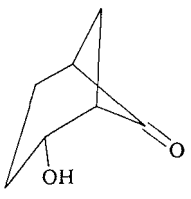

(*b*)

Can. J. Chem. Downloaded from www.nrcresearchpress.com by 210.87.254.5 on 09/05/12
For personal use only.

crystalline solid. This was recrystallized from methanol, to give 3.1 g of **2** as needles, m.p. 162–165°. It had $[\alpha]_D$ +167.5 (*c*, 0.67); λ_{max} 321 mμ (ε 145); ν_{max} 2115 (—N_3), 1730, and 1250 cm^{-1}; and n.m.r. signals at δ 0.63(C-18); 1.17(C-19); 1.22(d, J = 7)(C-21); 2.02; 2.03(two OAc); 3.66(s, 1H)(CH—N_3); and 4.75(multiplet, 2H) (CHOAc). The signal for the 12-hydrogen shifted downfield by 2.5 c.p.s. in benzene solution.

Anal. Calcd. for $C_{25}H_{37}N_3O_5$: C, 65.33; H, 8.12; N, 9.14. Found: C, 65.15; H, 8.30; N, 9.30.

A solution of 12α-azido ketone **2** (146 mg) in 4 ml of methanol and 1 ml of water containing 300 mg of potassium hydroxide was heated briefly, then left at room temperature for 64 h. The amorphous neutral product (ν_{max} 3610, 3410, 2120, and 1710 cm^{-1}) was reacetylated, giving 136 mg of crystalline product. Its n.m.r. spectrum indicated the presence of 70% 12α-azido ketone (>CHN$_3$ at δ 3.63) and 30% of 12β-azido ketone (>CHN$_3$ at δ 3.37). More drastic treatment (potassium *t*-butoxide in *t*-butyl alcohol at reflux under nitrogen) destroyed the azido group of **2**.

12α-Amino-3α,20β-diacetoxy-5β-pregnan-11-one (3, R = H)

A mixture of 2.29 g of azidoketone **2**, 2.3 g of stannous chloride monohydrate in 150 ml of absolute ethanol was refluxed for 2 h. It was then taken to small volume *in vacuo*. The residue was taken up in water and the product extracted into ethyl acetate using a continuous extractor. The 2.17 g of product was adsorbed from benzene onto 30 g of alumina, activity IV. The fraction eluted with benzene gave 450 mg of **3**(R = H). The mother liquors gave 594 mg of the hydrochloride of **3**(R = H) when treated with ethyl ether saturated with hydrogen chloride. The base had m.p. 189–192°, $[\alpha]_D$ +81° (*c*, 0.71); λ_{max} 310 mμ (ε 190); and ν_{max} 1730, 1260(OAc), 1710(C=O) (shoulder). Its n.m.r. spectrum had signals at δ 0.62(3H); 1.12(3H, d, J = 6.5 c.p.s.); 1.17(s,3H); 1.85 (s, 2H) (NH); 1.97(s, 3H); 2.00(s, 3H); 2.10(s, 2–3H); 3.90(s, 1H) (12βH); and 4.70(m,2H). The 12-hydrogen signal was displaced to δ 3.88 in benzene (5 c.p.s. downfield).

Anal. Calcd. for $C_{25}H_{39}NO_5$: C, 69.25; H, 9.07; N, 3.23. Found: C, 69.44; H, 9.15; N, 3.13. The hydrochloride of **3** had m.p. 203–206°, $[\alpha]_D$ +78° (*c*, 0.57); and ν_{max} (Nujol) 3510, 1735, 1716, and 1240 cm^{-1}.

Anal. Calcd. for $C_{25}H_{40}ClNO_5 \cdot H_2O$: C, 61.50; H, 8.62; N, 2.88. Found: C, 61.78; H, 9.01; N, 3.09.

12α-Acetamide-3α,20β-diacetoxy-5β-pregnan-11-one (3, R = Ac)

The aminoketone 3(R = H) was heated at 100° in 1:1 pyridine – acetic anhydride mixture for 2 h. The mixture was poured into water and the amide collected. After recrystallization from acetone – hexane it formed needles with m.p. 238–242°; $[\alpha]_D$ +135° (*c*, 0.76); λ_{max} 312 mμ (ε 147); and ν_{max} 3450, 1720, and 1680 cm^{-1}. Its n.m.r. spectrum had peaks at δ 0.70(s,3H); 1.18(d, J = 6.5 c.p.s., 3H); 1.23(s,3H); 2.04 (s,6H); 2.10(s,3H); 4.00(d, J = 7 c.p.s., 1H); 4.70(m,2H); and 5.92(broad, 1H).

Anal. Calcd. for $C_{27}H_{41}NO_6$: C, 68.18; H, 8.69; N, 2.95. Found: C, 67.94; H, 8.77; N, 2.87.

The *N*-acetyl ketone **3** (R = Ac) was recovered unchanged after 45 h in acetic acid containing boron trifluoride etherate. Hydrolysis of **3** (R = Ac) using 8% potassium hydroxide in refluxing 80% methanol – water gave a dihydroxy keto azide which crystallized as needles from chloroform, m.p. 240–243°. That this was 12α-acetamido-11-keto-5β-pregna-3α-20β-diol was shown by reacetylation to **3** (R = Ac). Hence the 12α configuration seems to be the stable one.

12α-Acetamido-3α,20β-diacetoxy-11β-hydroxy-5β-pregnane (4, R = H)

(*a*) A solution of 100 mg of azido ketone **2** and 200 mg of lithium aluminum hydride in 30 ml of ether was refluxed for 5 h. The product was acetylated at room temperature in 1:1 acetic anhydride – pyridine during 16 h. The mixture was poured into water and the product collected. It was purified by chromatography on a 20 fold ratio of neutral alumina of activity II. The fraction eluted with chloroform formed prisms (41 mg) from ether – hexane with m.p. 254–258°. This had $[\alpha]_D$ +137° (*c*, 0.75); and ν_{max} 3450, 1720, 1678, and 1720 cm^{-1}. Its n.m.r. spectrum had signals at δ 1.00(s,3H); 1.13(3H, d, J = 7.5 c.p.s.); 1.17(s,3H), 2.01(s,3H); 2.05(s,6H); 2.56(s,2H, disappearing when D_2O added); 3.91; 4.00(2H, collapsing to a signal at δ 3.91 when D_2O added); and 4.75 (multiplet, 2H).

Anal. Calcd. for $C_{27}H_{43}NO_6$: C, 67.89; H, 9.07; N, 2.93. Found: C, 67.99; H, 9.19; N, 3.07.

(*b*) A solution of 245 mg of aminoketone **3**(R = H) and 204 mg of lithium aluminum hydride in 30 ml of ether was refluxed for 3 h. The product was acetylated at room temperature in 1:1 acetic anhydride – pyridine (2 ml) during 16 h. The acetate was recrystallized from ether to give 185 mg of prisms m.p. 254–258°. This proved identical to the product from (*a*).

12α-Acetamido-3α,11β,20β-triacetoxy-5β-pregnane (4, R = Ac)

The hydroxyamide **4**(R = H) (62 mg) was fully acetylated by treatment with acetic anhydride (1 ml) containing 15 mg of *p*-toluenesulfonic acid monohydrate for 16 h at room temperature. The crude product was adsorbed from hexane on 1 g of neutral alumina (activity I–II). Benzene eluted 51 mg of a colorless gum which was homogeneous according to t.l.c. and its n.m.r. spectrum. It had $[\alpha]_D$ +105° (*c*, 0.66); and ν_{max} 3450, 1720, and 1680 cm^{-1}. Its n.m.r. spectrum had peaks at δ 0.90 (s,3H); 0.96(s,3H); 1.12(d, J = 6.5 c.p.s., 3H); 2.04(s,6H); 2.07(s,6H); 4.12(q, J_1 = 9 c.p.s., J_2 = 2.5 c.p.s. which collapsed to a doublet with J = 2.5 c.p.s. when D_2O and *p*-toluenesulfonic acid were added); 4.75(multiplet, 2H); 5.04 (multiplet, 1H, $w_{\frac{1}{2}}$ 6 c.p.s.); and 5.65 (broad doublet, J = 9 c.p.s., which disappeared when D_2O and *p*-toluenesulfonic acid were added). A sample was distilled at 180°, 1 × 10^{-3} mm.

Anal. Calcd. for $C_{29}H_{45}NO_7$: C, 67.02; H, 8.73. Found: C, 66.80; H, 8.56.

Deamination of 3(R = H)

1. Protic Solvents

(*a*) Sodium nitrite (1.43 g) was added to a solution of the hydrochloride of **3** (R = H) (566 mg) in 50 ml of 3% hydrogen chloride in methanol at 5 °C. After 1.5 h stirring at 5°, the mixture was diluted with water and the

Can. J. Chem. Downloaded from www.nrcresearchpress.com by 210.87.254.5 on 09/05/12
For personal use only.

product (426 mg) extracted into chloroform and the organic layer washed with sodium carbonate solution. Its u.v. and i.r. spectra showed the absence of conjugated ketone. The n.m.r. spectrum had no signals above δ 0.9. The product was adsorbed onto 15 g of alumina (activity III) from hexane. Hexane eluted 15 mg of dienone **14** (λ_{max} 290 mμ, ν_{max} 1660 and 1650 cm^{-1}) and 39 mg of a mixture of **14** and enones **13** and **16**. More hexane and 10–50% benzene in hexane eluted 165 mg of a mixture of enones **13** and **16**. Benzene eluted 150 mg of hydroxylic products (ν_{max} 3470, 1740, 1720 (shoulder), 1670, and 1555 cm^{-1}) and chloroform eluted 57 mg of similar material. The enone mixture had $\nu_{max}(CCl_4)$ 1740 (OAc), 1710, 1668, 1650, and 1635 cm^{-1}. The ratio of **13** to **16** was estimated from this spectrum to be 3–4:1. Extensive chromatography of this mixture on alumina failed to separate these.

(*b*) A solution of 597 mg of sodium nitrite in 5 ml of water was added to a solution of 180 mg of the hydrochloride of **3**(R = H) in 15 ml of 30% water in acetic acid at 0°. The mixture was stirred at 0° for 1 h, then diluted with water, and extracted with methylene chloride. The organic layer was washed with sodium carbonate solution and water, dried, and distilled, giving 163 mg of product. No conjugated ketone was present (i.r. and u.v. spectra) and its n.m.r. spectrum had no signal above δ 0.9. Chromatography on alumina as for (*a*) separated a 25% yield of the mixed enones **13** and **16**.

2. In Aprotic Solvents

(*a*) Isoamyl nitrite (0.5 ml) was added to a solution of 250 mg of the hydrochloride of **3**(R = H) in 10 ml of chloroform. After 30 min the solvent was removed under reduced pressure. The residue had ν_{max} 1665 and 1650 cm^{-1} corresponding to a cyclohexenone. This was adsorbed on 5 g alumina, activity IV. Hexane – benzene (1:1) eluted 175 mg of crystalline solid. When recrystallized from acetone – hexane this gave 128 mg of needles, m.p. 160–163° identified as **13**. Benzene eluted nothing, while chloroform eluted 45 mg of a complex mixture.

(*b*) One ml of amyl nitrite was added to a solution of 210 mg of **3**(R = H) in 10 ml of benzene containing 0.1 ml of acetic acid. After 30 min at room temperature the solvent was removed *in vacuo*. The residue had absorption characteristic of a cyclopentenone (ν_{max} (CCl_4) 1710 and 1636 cm^{-1}). Chromatography on 4 g of florisil (60–100 mesh) and elution with benzene gave 140 mg of a crystalline compound. Recrystallization from acetone – hexane gave 102 mg of needles m.p. 166–168°, which was characterized as **16**.

(*c*) A solution of **3**(R = H) (66 mg) in 5 ml of benzene to which was added 0.5 ml of isoamyl nitrite was left at room temperature for 10 min. The i.r. spectrum of the mixture showed the pressure of diazo ketone (ν_{max} 2090 cm^{-1}). After 1 h this band had disappeared. Chromatography as for (*b*) gave 41 mg of the conjugated enone **16**.

(*d*) To a solution of 70 mg of **3**(R = H) in 5 ml of benzene containing 150 mg of powdered calcium carbonate was added 0.5 ml of isoamyl nitrite. Nitrogen evolution appeared slow, hence the mixture was left overnight. Evaporation of the solvent and adsorption on 7 g of florisil (60–100 mesh) and elution with benzene gave 51 mg of crystalline solid. On recrystallization from acetone – hexane, this gave 30 mg of **16**.

(*e*) Isoamyl nitrite (1.5 ml) was added to a suspension of 415 mg of the hydrochloride of **3**(R = H) in 30 ml of benzene. After 3 h stirring the solution became clear. The solvent was evaporated under reduced pressure, then the residue adsorbed on 5 g of neutral alumina (grade IV). A 1:1 mixture of hexane – benzene eluted 345 mg of crystalline solid which by its i.r. spectrum appeared to be an approximately 1:1 mixture of **13** and **16**. This could only partially be separated by chromatography on alumina.

3α,20β-Diacetoxy-12-methyl-18-nor-5β-pregn-12-en-11-one (13)

This crystallized from acetone – hexane as needles with m.p. 160–163°, $[\alpha]_D$ −42° (*c*, 0.56); λ_{max} 250 mμ (ε 11 200); and ν_{max} (CCl_4) 1738, 1665, 1650, and 1245 cm^{-1}. Its n.m.r. spectrum had signals at δ 1.00(3H singlet); 1.13(3H doublet, $J = 7$); 1.85(3H, broad singlet); 2.02(6H, singlet); 4.75(1H, multiplet); and 5.26(1H, multiplet).

Anal. Calcd. for $C_{25}H_{36}O_5$: C, 72.08; H, 8.71. Found: C, 72.25; H, 8.89.

The compound was only hydrolyzed by hydrogen peroxide and potassium hydroxide in methanol.

3α,20β-Diacetoxy-12-methyl-18-nor-5β-pregnan-11-one

A solution of 55 mg of **13** in 5 ml of acetic acid was hydrogenated over platinum from 31 mg of Adam's catalyst at one atm during 3 h. A benzene solution of the product was filtered through 1 g of alumina. Evaporation of the benzene left 40 mg of colorless gum with $[\alpha]_D$ +3° *c*, 0.55); and ν_{max} 1730 and 1710 (shoulder) cm^{-1}. It gave n.m.r. signals at δ 0.98(3H, singlet); 1.17(3H, doublet, $J = 7$); 1.21(3H, doublet, $J = 7$); 2.00(3H, singlet); 2.01(3H, singlet); and 4.75(2H, multiplet).

Anal. Calcd. for $C_{25}H_{38}O_5$: C, 71.74; H, 9.15. Found: C, 71.55; H, 9.01.

3α,20β-Diacetoxy-13,14-seco-12,14-cyclo-5β-pregn-12-en-11-one (16)

This crystallized from acetone – hexane as needles with m.p. 166–168°, $[\alpha]_D$ −25° (*c*, 1.21); λ_{max} 252 mμ (ε 14 500); and ν_{max} (CCl_4) 1740, 1710, 1636, and 1245 cm^{-1}. It gave n.m.r. signals at δ 0.97(3H, singlet); 1.10(3H, doublet, $J = 7$); 2.00(3H, singlet); 2.03(3H, singlet); 2.20(3H, broad singlet); 4.75(1H, multiplet); and 5.26(1H, multiplet).

Anal. Calcd. for $C_{25}H_{36}O_5$: C, 72.08; H, 8.71. Found: C, 72.00; H, 8.81.

3α,20β-Diacetoxy-13,14-seco-12,14-cyclo-5β-pregnan-11-one

A solution of 22 mg of **16** in 5 ml of acetic acid was hydrogenated over platinum from 21 mg of Adam's catalyst under 1 atm for 3 h. The residue after filtration and removal of the solvent was dissolved in benzene. The solution was passed through a short column of alumina. The product crystallized from acetone – hexane as needles with m.p. 175–177°, $[\alpha]_D$ +17° (*c*, 0.70); and ν_{max} (CCl_4) 1745 and 1735 cm^{-1}. It gave n.m.r. signals at δ 0.70(3H, doublet, $J = 7$); 0.98(3H, singlet); 1.21(3H, doublet, $J = 7$); 2.00(6H, singlet); and 4.75(2H, multiplet).

Anal. Calcd. for $C_{25}H_{38}O_5$: C, 71.74; H, 9.15. Found: C, 71.64; H, 9.32.

Can. J. Chem. Downloaded from www.nrcresearchpress.com by 210.87.254.5 on 09/05/12
For personal use only.

Hydrolysis of the diacetate with potassium hydroxide in methanol gave the corresponding diol. It separated from acetone – hexane as needles with m.p. 216–217°, ν_{max}($CHCl_3$) 3600 and 1724 cm^{-1} and $[\alpha]_D$ −14° (*c*, 0.23).

Anal. Calcd. for $C_{21}H_{34}O_3$: C, 75.40; H, 10.25. Found: C, 75.36; H, 10.37.

*3α-Acetoxy-12-methyl-19-nor-5β-pregna-12,17(20)-dien-11-one (**14**)*

This was not obtained crystalline (see deamination 1*a*). It had λ_{max} 290 mμ and ν_{max}($CHCl_3$) 1660 and 1650 cm^{-1}. Its n.m.r. spectrum had signals at δ 1.03(3H, singlet); 1.77(3H, broad singlet); 2.03(3H, broad singlet); 4.75(1H, multiplet); and 6.17(1H, multiplet).

*3α-Hydroxy-12-methyl-18-nor-5β-androst-12-en-11-one (**15**)*

A solution of 115 mg of **13** in 20 ml of 10% potassium hydroxide in methanol was refluxed overnight. The methanol was evaporated then the residue taken up in water and chloroform. The chloroform extracted 105 mg of gum which was adsorbed from benzene onto 3 g of alumina, activity IV. Benzene eluted 50 mg of semi-crystalline product. When recrystallized from hexane this gave 27 mg of needles m.p. 75–79°. It had λ_{max} 248 mμ (ε 12 000); and ν_{max} 1650 and 1630 cm^{-1}. Its n.m.r. spectrum had signals at δ 1.01(3H, singlet); 1.65 (3H, broad singlet); and 3.60(1H, broad multiplet).

Anal. Calcd. for $C_{19}H_{28}O_2$: C, 79.12; H, 9.79. Found: C, 78.79; H, 9.56.

Attempted Aromatization of Ring C

Crude non-conjugated ketone (210 mg) from deamination of **3**(R = H) in 50% acetic acid using nitrous acid, and 110 mg of dichlorodicyanobenzoquinone in 20 ml of benzene was refluxed for 20 h. No reaction took place according to t.l.c. and the i.r. spectrum of the recovered steroid.

3β,20β-Diacetoxy-9β,11β-oxido-5α-pregnane (7)

N-Bromosuccinimide (516 mg) was added over 10 min to an ice-cold solution of 3β,20β-diacetoxy-5α-pregn-9(11)-ene (**5**) (976 mg) in 7 ml of dioxane and 2 ml of 0.2 *M* perchloric acid. The mixture was stirred for a further 30 min at 5 °C. Saturated sodium hydrogen sulfite (0.5 ml) was added, then the product extracted into ether. After washing with water, then drying over magnesium sulfate the ether was evaporated leaving a pale yellow gum. This was dissolved in 30 ml of acetone, 2 g of fused potassium acetate added, and the mixture refluxed for 17 h. The solvent was removed, the residue suspended in water, and the product extracted into ether. The gum recovered from the ether was adsorbed from hexane onto 15 g of alumina, activity III. Hexane (600 ml) eluted the β-oxide which crystallized as needles from acetone – hexane. Yield 532 mg, m.p. 150–152°, $[\alpha]_D$ +37° (*c*, 0.53); ν_{max}(CCl_4) 1740 and 1250 cm^{-1}. It gave n.m.r. signals at δ 0.83(3H, singlet); 1.00(3H, singlet); 1.13(3H, doublet); 2.00(3H, singlet); 2.02(3H, singlet); 3.38(1H, $w_{\frac{1}{2}}$ 5 c.p.s.); and 4.75(2H, multiplet).

Anal. Calcd. for $C_{25}H_{38}O_5$: C, 71.74; H, 9.15. Found: C, 71.59; H, 9.02.

9α-Azido-3β,20β-diacetoxy-11β-hydroxy-5α-pregnane (8)

A solution of 22 g of the β-oxide **7** and 23 g of lithium azide in 400 ml of dry dimethylformamide was heated at 155° for 25 h under nitrogen. The cooled mixture was diluted with water and extracted with ether. The ether solution was washed with water, dried, and distilled. The oily residue was acetylated using 400 ml of pyridine and 50 ml of acetic anhydride for 15 h at room temperature. The product crystallized from *n*-hexane giving 11 g of azido alcohol m.p. 180–185°. The mother liquor was adsorbed from hexane onto 250 g of alumina, activity IV. Hexane eluted 1.9 g of unchanged β-oxide. The benzene eluate (500 ml) crystallized from hexane giving 5.2 g of azido alcohol.

The azido alcohol was recrystallized from hexane to give needles, m.p. 183–186° with $[\alpha]_D$ +103° (*c*, 0.82); and ν_{max}($CHCl_3$) 3600, 2100, 1725, and 1250 cm^{-1}. It gave n.m.r. signals at δ 0.90(3H, singlet); 1.17(3H, doublet, J = 7 c.p.s.); 1.21(3H, singlet); 2.01, 2.05(3H, singlets); 4.33(1H, multiplet $w_{\frac{1}{2}}$ 7 c.p.s.); and 4.75(2H, multiplet).

Anal. Calcd. for $C_{25}H_{39}N_3O_5$: C, 65.05; H, 8.52; N, 9.10. Found: C, 64.92; H, 8.70; N, 9.31.

*9α-Azido-3β,20β-diacetoxy-5α-pregnan-11-one (**9**)*

(*a*) To a solution of 2.06 g of azido alcohol **8** in 25 ml of acetone at 5 °C was added 2.5 ml of Jones' reagent (21). After 2.5 h at this temperature the excess reagent was destroyed using ethanol. The product was isolated by dilution with water and extraction into ether. It was adsorbed from hexane onto 15 g of alumina, activity IV. Hexane eluted 382 mg of the desired keto azide. The products eluted with the benzene had no azide absorption in their i.r. spectra.

(*b*) Azido alcohol **8** (4.71 g) in 31 ml of dry dimethyl sulfoxide and 20 ml of acetic anhydride were maintained at 90° for 72 h. The mixture was poured into ice water and the product extracted into ether. The ether solution was washed with 5% sodium bicarbonate solution then with water, dried, and distilled. By crystallization from hexane, and chromatography of the mother liquors on alumina (activity IV) this was separated into 1.49 g of azido ketone **9** and 2.7 g of azido alcohol.

(*c*) In a comparable experiment to (*b*), but run at room temperature for 3 weeks, 5.02 g of azido alcohol gave 2.01 g of azido ketone **9** and 2.45 g of unchanged azido alcohol.

The azido ketone crystallized as prisms from hexane; m.p. 197–199°; $[\alpha]_D$ +123° (*c*, 0.73); ν_{max}($CHCl_3$) 2095 and 1725 cm^{-1}. It gave n.m.r. signals δ 0.65(3H, singlet); 1.10 (3H, singlet); 1.17(3H, doublet); 2.02; 2.07(3H, singlets); 2.54(2H, singlet); and 5.20(2H, multiplet).

Anal. Calcd. for $C_{25}H_{37}O_5N_3$: C, 65.33; H, 8.12; N, 9.14. Found: C, 65.21: H, 8.30; N, 9.32.

*9α-Amino-3β,20β-diacetoxy-5α-pregnan-11-one (**10**)*

A solution of 1.42 g of azido ketone **9** in 100 ml of 95% ethanol was hydrogenated using 886 mg of 5% palladium on charcoal during 3 h. The filtered solution was evaporated to dryness, and the residue adsorbed from benzene – hexane onto 5 g of alumina (activity IV). Benzene eluted the desired product, which after recrystallization from acetone – hexane gave 787 mg of needles m.p.

Can. J. Chem. Downloaded from www.nrcresearchpress.com by 210.87.254.5 on 09/05/12
For personal use only.

197–199°, $[\alpha]_D$ +120° (*c*, 0.58); ν_{max}($CHCl_3$) 3450, 1725, 1700 (shoulder), and 1250 cm^{-1}. It gave n.m.r. signals at δ 0.62; 1.07 (3H, singlets); 1.15(3H, doublet); 1.30(2H, singlet which disappeared when D_2O added); 2.00 (6H, singlet); and 4.66(6H, multiplet).

Anal. Calcd. for $C_{25}H_{39}NO_5$: C, 69.25; H, 9.07; N, 3.23. Found: C, 69.41; H, 9.24; N, 3.41.

The base gave a hydrochloride which crystallized from acetone – ether as prisms m.p. 163–165°, recrystallizing as needles and remelting at 197–198°. It had $[\alpha]_D$ +62° (*c*, 0.84).

Anal. Calcd. for $C_{25}H_{40}ClNO_5$: C, 63.89; H, 8.52; N, 2.98. Found: C, 64.02; H, 8.69; N, 3.13.

Deamination of ***10***

(*a*) To a solution of 733 mg of **10** in 40 ml of acetic acid and 20 ml of water was added a solution of 4.42 g of sodium nitrite in 20 ml of water—all at 0 °C. The solution was stirred at 0° for 3 h, then poured into ice water, and extracted with ether. The ether solution was washed with aqueous bicarbonate solution then water, dried, and distilled. The 698 mg of gummy residue was adsorbed from benzene onto 11 g of alumina (activity II). Elution with benzene (100 ml) gave 530 mg of crude crystalline olefin **18**. Methylene chloride and methylene chloride – methanol (20:1) eluted 116 mg of crude alcohol **19**.

(*b*) Isoamyl nitrite (358 mg) in 5 ml of benzene was added to a solution of 440 mg of **10** in 20 ml of benzene containing 60 mg of acetic acid. The mixture was maintained at 60–65° for 30 min. A further 0.13 g of isoamyl nitrite was added and the heating continued for 2.5 h. The solvent was evaporated *in vacuo*. The crystalline residue was recrystallized from hexane to give 48 mg of pure olefin **17**. Chromatography of the mother liquors on 5 g of alumina (activity IV) and elution with 1:1 hexane – benzene gave 263 mg of a 1:1 mixture of **17** and **18** which could be separated in part by careful chromatography on a 200 fold ratio of alumina (activity IV). Benzene and methylene chloride eluted 48 mg of crude alcohol **19**.

(*c*) Isoamyl nitrite (323 mg) was added to a solution of 157 mg of **10** in 10 ml of benzene. The mixture was maintained at 60° for 30 min. Evaporation of the solvent left a crystalline residue which was shown by its n.m.r. spectrum to be a 1:1 mixture of olefins **17** and **18**.

*3β,20β-Diacetoxy-9β-methyl-19-norpregn-1(10)-en-11-one (**17**)*

This crystallized from hexane as plates, m.p. 183–186°, $[\alpha]_D$ +150° (*c*, 1.10); ν_{max}(Nujol) 1738, 1700, and 1255 cm^{-1}. It gave n.m.r. signals at δ 0.55(3H, singlet); 1.17(3H, doublet, J = 6); 1.25(3H, singlet); 2.05(6H, singlet); 4.83(2H, multiplet); and 5.25(1H, multiplet).

Anal. Calcd. for $C_{25}H_{36}O_5$ (mol. wt. 416): C, 72.08; H, 8.71. Found (mol. wt. (mass spectrum) 416): C, 71.81; H, 8.83.

*3β,20β-Diacetoxy-9β-methyl-19-norpregn-5(10)-en-11-one (**18**)*

This crystallized from acetone – hexane as prisms, m.p. 174–176°, $[\alpha]_D$ 138° (*c*, 1.15); ν_{max}($CHCl_3$) 1725, 1700, and 1250 cm^{-1}. It gave n.m.r. signals at δ 0.58(3H, singlet); 1.15 (3H, doublet); 1.32(3H, singlet); 2.03(6H, singlet); and 4.83 (2H, multiplet).

When **18** (105 mg) was heated for 2 h at 60° in 10 ml of 2.5% hydrochloric acid in ethanol under nitrogen, then the product reacetylated using 1:1 acetic anhydride – pyridine, unchanged **18** was recovered.

3β,20β-Dihydroxy-9β-methyl-19-norpregn-5(10)-en-11-one

A solution of diacetoxy olefin **18** (320 mg) in 20 ml of 2.5% potassium hydroxide in methanol was refluxed for 2 h. After removal of most of the solvent under reduced pressure and dilution with water, the product was extracted into chloroform. It crystallized from acetone – hexane as prisms (251 mg), m.p. 201–202°, $[\alpha]_D$ +119° (*c*, 0.58).

Anal. Calcd. for $C_{21}H_{32}O_5$: C, 75.86; H, 9.70. Found: C, 75.68; H, 9.90.

On reacetylation using 1:1 acetic anhydride – pyridine pure **18**, m.p. 175–177° was recovered.

*3β,20β-Diacetoxy-10α-hydroxy-9β-methyl-19-norpregnan-11-one (**19**)*

This crystallized from acetone – hexane as needles, m.p. 173–175°, $[\alpha]_D$ +91° (*c*, 0.94); ν_{max}($CHCl_3$) 3590, 1725, 1690, and 1250 cm^{-1}. It gave n.m.r. signal at 0.60(3H, singlet); 1.18(3H, doublet, J = 6 c.p.s.); 1.20 (3H, singlet); 2.07(6H, singlet); and 4.83(2H, multiplet).

Anal. Calcd. for $C_{25}H_{38}O_6$: C, 69.09; H, 8.81. Found: C, 69.07; H, 8.84.

Dehydration of ***19***

Thionyl chloride (0.1 ml) was added to a solution of 30 mg of **19** in 2 ml of pyridine. After standing at room temperature overnight the mixture was diluted with water and the product extracted into methylene chloride. The residue from evaporation of the solvent was adsorbed from benzene onto 1 g of alumina (activity IV). Benzene eluted 20 mg of quite pure crystalline solid. This was recrystallized from acetone – hexane to give needles m.p. 174–175°. It did not depress the m.p. of **17**, and their i.r. spectra in chloroform were identical.

*3β,20β-Diacetoxy-10β-hydroxy-9β-methyl-1α,11-oxido-19-nor-5α-pregn-11-ene (**21**)*

A solution of 108 mg of olefin **17** and 300 mg of *m*-chloroperbenzoic acid (74% peracid) in methylene chloride was left at 5° for 4 days. The acids were removed by a bicarbonate wash. The dried solvent was distilled leaving a gummy product. This was adsorbed from benzene onto 2 g of alumina (activity IV). Benzene eluted 80 mg of crystalline solid, m.p. 139–155°. This gave only one spot of t.l.c., but its n.m.r. spectrum was consistent with it being a nearly equimolar mixture of two epoxides.

The epoxide mixture (120 mg) in 5 ml of acetic acid was heated at 100° for 30 min. After removal of the acetic acid *in vacuo*, t.l.c. showed the presence of at least one major and two minor products. Preparative t.l.c. on silica gel plates and development by acetone – hexane (2:1) gave the major component (middle band) as a gum (63 mg). This crystallized from acetone – hexane as prisms, m.p. 132–135°, and analyzed low in carbon (water solvate ?); hence was sublimed for analysis and spectra. It had ν_{max}($CHCl_3$) 3600, 1740, 1670, and 1250 cm^{-1}, $[\alpha]_D$ +20° (*c*, 1.31); and n.m.r. signals at δ 0.80(3H, singlet); 1.17(3H, doublet, J = 6 c.p.s.); 1.28; 2.01 and

2.05(3H, singlets); 4.30(1H, quartet, $J_1 = 4$ and $J_2 = 2$ c.p.s.); 4.87(2H, multiplet); and 5.43(1H, singlet).

Anal. Calcd. for $C_{25}H_{36}O_6$: C, 69.42; H, 8.39. Found: C, 69.20; H, 8.22.

*20β-Hydroxy-9β-methyl-19-norpregna-1,3,5(10)-trien-11-one (**22**)*

(*a*) A solution of 90 mg of olefin **18** and 210 mg of *m*-chloroperbenzoic acid (74% peracid) in 5 ml of chloroform was left in the dark for 16 h. The mixture was diluted with methylene chloride, and the acids extracted into 10% sodium bicarbonate solution. The organic layer was washed with water, dried, and distilled. The residue (92 mg) was dissolved in 5% hydrogen chloride in ethanol, then stirred for 2 days at room temperature. The solvent was then removed *in vacuo* and the residue chromatographed on 1 g of alumina (activity IV). Benzene eluted 39 mg of crystalline solid. This crystallized from acetone – hexane as prisms, m.p. 201–203°, $[\alpha]_D$ 121° (*c*, 0.91); λ_{max} 260 (ε 428), 267 (ε 526), and 274 mμ (ε 494); $\nu_{max}(CHCl_3)$ 3600 and 1696 cm^{-1}. Its n.m.r. spectrum had peaks at 0.78(3H, singlet); 1.10(3H, doublet); 1.38(3H, singlet); 3.68(1H, multiplet); and 6.75–7.20(4H, multiplet).

Anal. Calcd. for $C_{21}H_{28}O_2$: C, 80.73; H, 9.03. Found: C, 80.64; H, 9.11.

(*b*) Hydroxy enol ether **21** (48 mg) and 3 ml of concentrated hydrochloric acid in 10 ml of ethanol was stirred at room temperature for 3 days. The solvents were evaporated *in vacuo*, and the residue adsorbed from benzene onto 1 g of alumina (activity IV). Benzene eluted 23 mg of crystalline solid, proven by t.l.c., mixed m.p., and i.r. spectrum to be **22**.

Acknowledgment

We wish to thank Mr. H. Seguin for the microanalyses, and Mr. A Knoll and Miss F. Johnston for technical assistance.

1. O. E. Edwards and M. Lesage. Can. J. Chem. **41**, 1592 (1963).
2. (*a*) P. Yates and R. J. Crawford. J. Amer. Chem. Soc. **88**, 1561 (1966). (*b*) M. Hanack and J. Dolde. Tetrahedron Lett. 321 (1966).
3. S. M. Kupchan, R. M. Kennedy, W. R. Scheigh, and G. Ohta. Tetrahedron, **23**, 4563 (1967). D. Herlem-Gaulier, F. Khuong-Huu-Laine, R. Goutarel, and M. J. Magdaleine. Bull. Soc. Chim. France, 763 (1968). W. Doepke, B. Mueller, and P. W. Jeffs. Pharmazie, **23**, 37 (1968).
4. G. Ourisson, P. Crabbe, and O. Rodig. Tetracyclic triterpenes. Holden-Day Inc., San Francisco. 1964. p. 173–176.
5. C. R. Narayanan. *In* Progress in the chemistry of natural products. L. Zechmeister (*Editor*). Springer-Verlag, Vienna. 1962. p. 300–371.
6. E. R. H. Jones and D. J. Wenka. J. Chem. Soc. 907 (1959).
7. R. C. Cookson. J. Chem. Soc. 282 (1954).
8. G. Amiard, R. Heymes, T. Van Thuang, and J. Mathieu. Bull. Soc. Chim. Fr. 232 (1965).
9. J. D. Albright and L. Goldman. J. Org. Chem. **30**, 1107 (1965); J. Am. Chem. Soc. **87**, 4214 (1965).
10. J. H. Bayless, F. D. Mendicino, and L. Friedman. J. Amer. Chem. Soc. **87**, 5790 (1965). A. T. Jurewicz and L. Friedman. J. Amer. Chem. Soc. **89**, 149 (1967). J. H. Bayless, A. T. Jurewicz, and L. Friedman. J. Amer. Chem. Soc. **90**, 4468 (1968).
11. H. Mitsuhashi and Y. Shimizu. Tetrahedron, **19**, 1027 (1963).
12. C. F. Hiskey, R. Hirschmann, and N. C. Wendler. J. Amer. Chem. Soc. **75**, 5135 (1953).
13. F. C. Chang and R. C. Ebersole. Tetrahedron Lett. 1985 (1968).
14. J. Fried. U. S. Pat. No. 2891076. Chem. Abstr. **54**, 1616 (1960).
15. D. Levy and R. Stevenson. Tetrahedron Lett. 3063 (1966).
16. C. T. Hammer, D. S. Savage, J. B. Thomson, and R. Stevenson. Tetrahedron, **20**, 929 (1964).
17. J. W. ApSimon and R. R. King. Chem. Commun. 1214 (1967).
18. D. H. R. Barton, L. J. Danks, A. K. Ganguly, R. H. Hesse, G. Tarzia and M. M. Pechet. Chem. Commun. 227 (1969).
19. M-M. Janot, C. Monneret, Q. Khuong-Huu, and R. Goutarel. C. R. (C) 1468, (1967).
20. H. Brockmann and H. Schodder. Chem. Ber. **74**, 73 (1941).
21. K. Bowden, I. M. Heilbron, E. R. H. Jones, and B. C. L. Weedon. J. Chem. Soc. 39 (1946).

Can. J. Chem. Downloaded from www.nrcresearchpress.com by 210.87.254.5 on 09/05/12
For personal use only.

Can. J. Chem. Downloaded from www.nrcresearchpress.com by 210.87.254.6 on 09/05/12
For personal use only.

Steroids and steroidases. VIII.[1] Further data on the preferred conformations of the cycloheptane rings of A-homosteroidketones

J. Bryan Jones and J. Malcolm Zander
Lash Miller Chemical Laboratories, Department of Chemistry, University of Toronto, Toronto 5, Ontario

Received April 28, 1969

The data presented substantiate the conclusions reported previously (1) regarding the applicability of the Hendrickson (2, 3) cycloheptane-based conformational analytical procedure to A-homosteroidketones of the 5α- and 5β- androstane and estrane series. For such cycloheptan*one* derivatives (with no bulky substituents at C-1 to C-5 of ring A) the twist chair conformations with the carbonyl group in the axis or adjacent position appear to be 1–2 kcal mole^{-1} lower in strain energy than predicted from the direct Hendrickson analysis and of these two favored conformers, the former may well be marginally preferred in many cases.

Canadian Journal of Chemistry, 47, 3501 (1969)

Introduction

Previous conformational analyses of the cycloheptane rings of A-homosteroid-3- and 4-ketones showed that, for compounds such as **1**(*a–c*)–**4**(*a–c*), an equilibrium mixture of ring A conformers exists at room temperature and that the main contributors are the twist chairs[2] TC_3, TC_4, and possibly TC_{10} (1). Conformations TC_3 and TC_4 represent those twist chairs in which the carbonyl group is at the axis carbon, or adjacent to it, and of these two carbonyl locations, the previous data indicated that the axis carbon position might be very marginally favored. However, the evidence was not unequivocal, and furthermore, it did not enable the relative importance of TC_{10} to be estimated with any degree of certainty. The investigations described in this paper are an extension of the earlier study (1) and were undertaken in an attempt to define more accurately the conformational preference of the carbonyl group and to clarify the contribution made by TC_{10} to the room temperature equilibrium mixture.

The results reported previously (1) were obtained by application of the conformational analytical procedure described by Hendrickson (2) in 1963 for cycloheptanes. Subsequently Hendrickson has refined the values of the parameters to be used (3)[3] and our current work is based on the revised figures. However, the improved parameters now available do not require any revision of the earlier conclusions (1) and do not remove any of the uncertainties inherent in the application of a substituted cycloheptane-derived analytical procedure[4] to fused ring cycloheptan*one* systems.

As observed previously (1–3) it is difficult to make any quantitative prediction regarding the total effect of inserting a carbonyl group into the seven-membered ring although it is fairly clear that its introduction results in a lowering of the total strain energy. The major factors contributing to this reduction are: (*a*) a reduced torsional barrier for methylene groups adjacent to the carbonyl group (5) and (*b*) the elimination of certain R ↔ H and H ↔ H non-bonded interactions (*cf.* the 3-alkylketone effect (6)). The increased bond angle of the sp^2 carbon is not considered to have a serious effect since it is readily accommodated by an opening of the other bond angles at little energetic expense (2). Nevertheless this effect will distort the geometry of ring A to an unknown extent and accordingly the desirability of applying appropriate physical methods, such as optical rotatory dispersion (o.r.d.) and dipole moment determinations, to check the validity of the conformational predictions made remains unchanged (1).

In order to show how the revised parameters modify the previously calculated energy–pseudorotation functions a comparison of the two curves for the cycloheptane rings of the A-homoandrostanes **1**(*a, c*)–**4**(*a, c*) is reproduced in Fig. 1. This

[1]For Part VII, see ref. 11. Presented in part at the 50th Canadian Chemical Conference, Toronto, June 1967.

[2]The conformational analytical terms and notations used are as defined previously (1, 2).

[3]At about the same time Bixon and Lifson (4) also reported the results of their carefully designed calculations on cycloheptane. Although the energy differences quoted (3, 4) for the cycloheptane conformers are not identical, the deviations are not serious enough to affect the conclusions drawn in this paper.

[4]Discussions regarding the validity of applying this analytical procedure to such complicated systems are summarized in refs. 1–3.

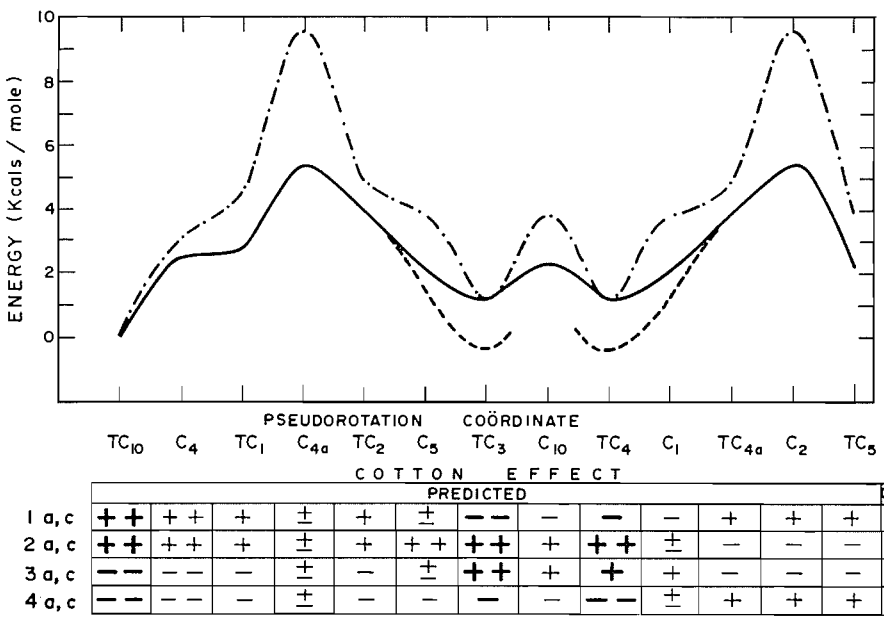

FIG. 1. A comparison of the energy functions calculated for the pseudorotation sequences of the cycloheptanone rings of **1**(*a–c*)–**4**(*a–c*) using the original (2) (—·—·—) and revised (3) parameters (———). These functions were obtained by considering **1**(*a–c*)–**4**(*a–c*) to be substituted cycloheptane derivatives. Previous data (1) have indicated that the introduction of a carbonyl group into the seven-membered ring causes TC_3 and TC_4 (the twist chairs with the carbonyl group at the axis and adjacent carbon respectively) to be reduced in energy by 1.4–2 kcal $mole^{-1}$ as indicated by the broken lines (— — — —). The predicted signs and relative magnitudes of the Cotton effects for each conformation of **1***a*, *c*–**4***a*, *c* were estimated from models (1). The predicted Cotton effects accentuated by heavy lines are those of the preferred conformations.

shows that although the old function exaggerated the energy differences by a factor of ~ 2, the preferred conformations predicted are identical using either set of parameters.

Results and Discussion

A-Homoandrostan-3-one and -4-one Derivatives

Previous attempts (1), including low temperature proton magnetic resonance (p.m.r.) spectroscopic analysis, to determine which of the three ring A conformations, TC_3, TC_4, and TC_{10}, of the series of compounds **1**(*a–c*)–**4**(*a–c*) was most preferred had shown that the energy differences involved were small and indicated that twist chairs with an axis carbonyl ($TC_{axis\ CO}$) to be marginally preferred over twist chairs with the carbonyl group adjacent to the axis carbon ($TC_{adj.\ CO}$). However, owing to the closely similar strain energies involved, the minimum temperature (−55°) attainable (due to solubility and instrumental limitations) with the p.m.r. method did not provide sufficient magnification of the conformational energy differences to enable a decision to be made with respect to TC_{10}. Attention was therefore turned to low temperature circular dichroism (l.t.c.d.) in an attempt to overcome the limitations of the p.m.r. technique.[5]

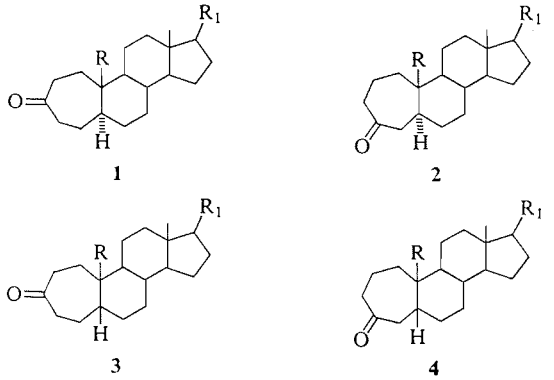

a R = CH_3, R_1 = OH
b R = CH_3, R_1 = =O
c R = CH_3, R_1 = H
d R = H, R_1 = OH
e R = H, R_1 = =O

DIAGRAM 1

[5]For A-homo-B-nor- and A-nor-B-homosteroids the p.m.r. method appears to allow less equivocal conclusions to be drawn (7).

Can. J. Chem. Downloaded from www.nrcresearchpress.com by 210.87.254.6 on 09/05/12
For personal use only.

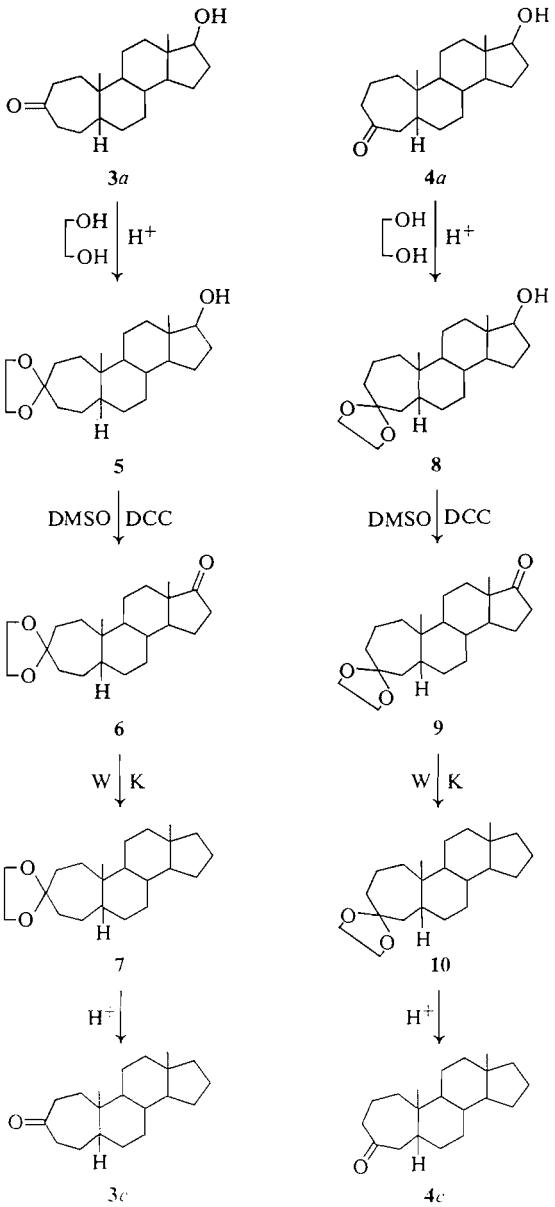

CHART 1

As the temperature of an A-homoketone solution is lowered, the sign and magnitude of its Cotton effect should become increasingly controlled by that of the most preferred conformer. Examination of the predicted and observed signs and relative magnitudes of the Cotton effect for TC_3, TC_4, and TC_{10} (see Fig. 1) showed that if the latter conformer was in fact the most preferred, then the observed Cotton effect should change from − to + for **1**(*a*, *c*) and from + to − for **3**(*a*, *c*) as it came to dominate the mixture. In contrast, if TC_3 and/or TC_4 were more preferred, none of the signs of the Cotton effects would be altered although their magnitude might well vary. The l.t.c.d. method was thus an attractive one since it was felt that the low temperatures (−190°) should ensure a dominant population of the most preferred conformer.

The C-17 oxygenated A-homoandrostanones employed in most of the previous work (1) proved too insoluble to permit satisfactory circular dichroism measurements at the low temperatures required. Accordingly the C-17 desoxy derivatives **1***c*–**4***c* were prepared as outlined for the 5β-series in Chart 1.

The l.t.c.d. spectra obtained are reproduced in Fig. 2 and as the curves show, in no case does the sign of the Cotton effect change in the temperature range +20 to −187° thereby indicating that TC_{10} is not selectively preferred. Closer examination of the spectral changes involved (see Table I) reveals that for **2***c*, **3***c*, and **4***c* the amplitude shifts observed are in a direction compatible with dominance by the conformer previously predicted (1) to be marginally preferred *viz.* the $TC_{axis\ CO}$ species. Unfortunately, for A-homo-5α-androstan-3-one (**1***c*) the positive shift observed is not consistent with the above rationale since the preference for the $TC_{axis\ CO}$ species (TC_3) should have manifested itself in a marked decrease in amplitude at low temperature. The only twist chair conformation compatible with the positive shift actually observed for **1***c* is TC_{10} but in view of the small magnitude of the changes[6] observed for this compound, and for **4***c* also, we would hesitate to place too heavy a weighting on the relevance of the l.t.c.d. amplitude shifts for these two compounds. Overall, however, the l.t.c.d. data do support the conclusion that for A-homoketones such as **1**(*a*–*c*)–**4**(*a*–*c*) the room

[6]Little effort has been put into developing a rationale for the anomalous shift observed for **1***c* since interpretations based on small changes in l.t.c.d. spectra are open to criticism for several reasons. For example, it is well known that differential solvation can cause marked amplitude changes (8) even in conformationally rigid systems. However, it is considered that the data reported in Table I are not due to changes in asymmetric solvation alone since similar results were obtained in two very different solvents, *viz.* methylcycloheptane–isopentane (1:3) (MI) and ether – isopentane – ethanol (5:5:2) (EPA). Furthermore the changes observed are significantly greater than those between the corresponding spectra of analogous six-membered ring A steroids in the same solvent systems (9; G. Snatzke, J. B. Jones, and J. M. Zander. Unpublished observations).

Can. J. Chem. Downloaded from www.nrcresearchpress.com by 210.87.254.6 on 09/05/12
For personal use only.

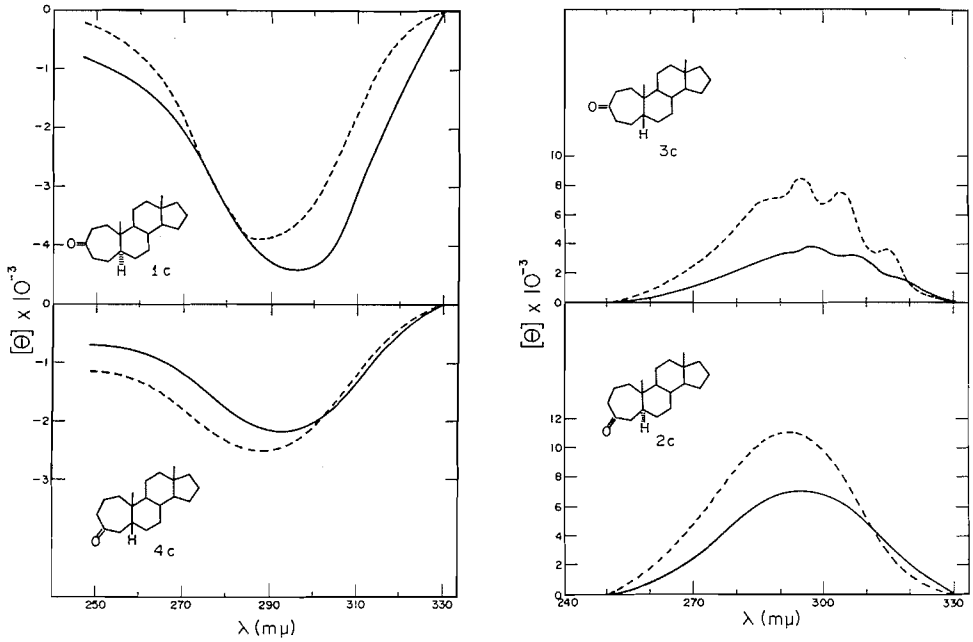

FIG. 2. Circular dichroism spectra at 20° (——) and −187° (— — — —) for solutions of **1***c*–**4***c* in methylcyclohexane–isopentane (1:3).

TABLE I

Correlation of the directions and magnitudes of circular dichroism amplitude shifts observed (Fig. 2) for **1***c*–**4***c* with the preferred twist chair conformations most compatible with the data

Compound	Temperature (°C)	$\Theta \times 10^{-3}$	$\Delta(\Theta_{-187} - \Theta_{+20})$	Most positive rotatory conformation	Most negative rotatory conformation
A-Homo-5α-androstan-3-one (**1***c*)	+20	−4.33	+0.5	TC_{10}	
	−187	−3.86			
A-Homo-5α-androstan-4-one (**2***c*)	+20	+7.03	+4.1	TC_4	
	−187	+11.12			
A-Homo-5β-androstan-3-one (**3***c*)	+20	+3.80	+4.8	TC_3	
	−187	+8.58			
A-Homo-5β-androstan-4-one (**4***c*)	+20	+2.18	−0.4		TC_4
	−187	+2.57			

temperature equilibrium mixtures are dominated by those twist chair conformations with the carbonyl at the axis or adjacent position, with the former probably marginally preferred.

The investigation was then extended to the A-homoestranones **1**(*d*, *e*)–**4**(*d*, *e*). The Hendrickson-derived energy-pseudorotation function for these compounds is reproduced in Fig. 3, and, as a comparison with the curve of Fig. 1 shows, the changes resulting from the absence of a C-10 methyl group are significant. Seven twist chairs are predicted to be equally preferred but in view of the previous evidence (1) that the carbonyl group at the axis or adjacent position reduces the strain energy by 1.4–2 kcal mole^{-1}, one or both of TC_3 and TC_4 should dominate the equilibrium

Can. J. Chem. Downloaded from www.nrcresearchpress.com by 210.87.254.6 on 09/05/12
For personal use only.

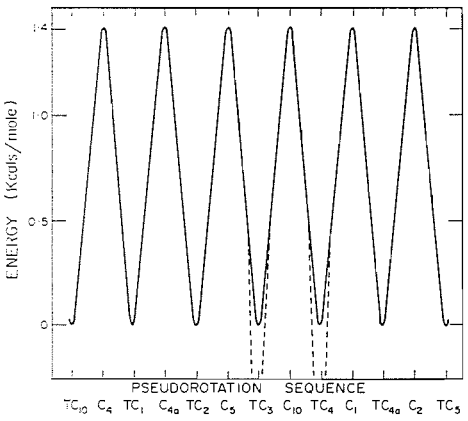

	COTTON EFFECT PREDICTED										OBSERVED
1 d	+		±		±		∓	−		±	+	− −
2 d	±		±		+		+	+	−		−	+ +
3 d	−		±		+		+	+		±	−	+
4 d	−		±		−		−	∓		+	+	− −

FIG. 3. Energy function for the A-homoestrane-3- and -4-ketones together with the signs and relative magnitudes of the Cotton effects predicted for each preferred conformation of the pseudorotation sequence of **1***d*–**4***d*. The dashed (— — — —) lines indicate the reduction in energy of 1–2 kcal mole^{-1} considered applicable to the most preferred $TC_{axis\ CO}$ and $TC_{adj.CO}$ conformations.

to the extent of > 90% (10). A comparison of the signs and magnitudes of the predicted and observed Cotton effects for each of the compounds **1**(*d*, *e*)–**4**(*d*, *e*) bears this out (see Fig. 3) since only for TC_3 and TC_4 are the data consistently in accord. In fact, when the octant rule projections are examined more closely, the agreements between prediction and observation are seen to be remarkably good and indicate that very small proportions of other conformers are present.

The relevant projections are shown in Fig. 4. For the 5α-A-homoestranes, **1**(*d*, *e*) and **2**(*d*, *e*) the $TC_{axis\ CO}$ and $TC_{adj.\ CO}$ contributors bear an almost perfect mirror image relationship to one another and the o.r.d. spectra of **1***d* and **2***d* reflect this dramatically (Fig. 5*a*).

For the 5β-compounds **3**(*d*, *e*) and **4**(*d*, *e*) the corresponding twist chairs have a similar, albeit somewhat distorted, mirror image relationship and again the o.r.d. curves of **3***d* and **4***d* (Fig. 5*b*) provide support for almost total dominance of the conformational mixture by these two species. However, in view of the difficulties involved in making such quantitative o.r.d. predictions (*cf.* footnote 18 of ref. 1) the excellence of agreement between the predicted and observed spectra may well be, in part, fortuitous.

The data on the A-homoandrostanes had indicated $TC_{axis\ CO}$ conformers to be somewhat more

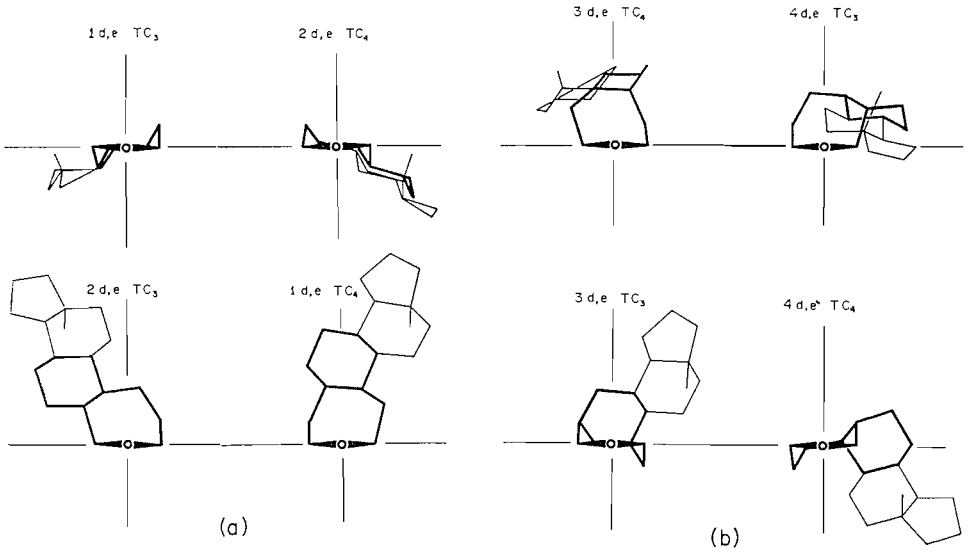

FIG. 4. Comparison of octant-rule projections for the TC_3 and TC_4 conformers of (*a*) A-homo-5α-estran-3- and -4-ones and (*b*) A-homo-5β-estran-3- and -4-ones. Rings A and B, whose atoms and substituents largely control the Cotton effect, are shown in heavy lines; C-17 substituents have been omitted.

Can. J. Chem. Downloaded from www.nrcresearchpress.com by 210.87.254.6 on 09/05/12
For personal use only.

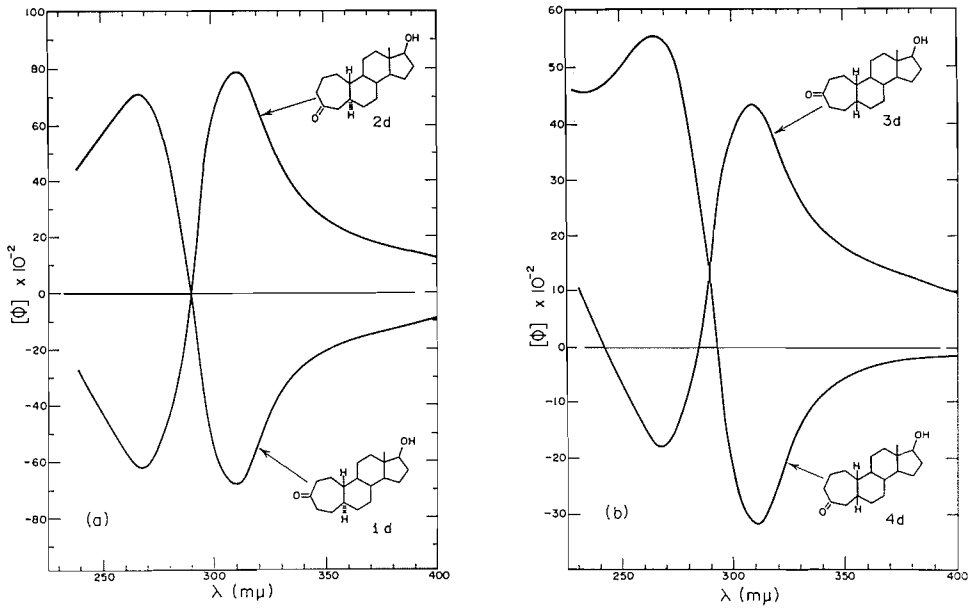

FIG. 5. Optical rotatory dispersion curves obtained in methanol solution for the A-homoestranones **1***d*–**4***d*.

preferred than $TC_{adj.\ CO}$ but the A-homoestrane o.r.d. curves did not give any indication as to which, if either, of the two was favored. In an attempt to clarify the situation the dipole moments of the A-homoestrane diketones **1***e*–**4***e* were determined and the experimental values compared with those predicted for the corresponding $TC_{axis\ CO}$ and $TC_{adj.\ CO}$ conformers.[7]

The data obtained are summarized in Table II and represented graphically in Fig. 6. Although the results are again not unequivocal, they do support the conclusion that $TC_{adj.\ CO}$ and $TC_{axis\ CO}$ are very close in energy and that the latter may well be somewhat favored. Furthermore a comparison of the current dipole moment results with the previous data for the A-homoandrostanes **1***b*–**4***b* (see Fig. 6) indicates that removal of the C-19 methyl group causes the $TC_{axis\ CO}$ conformer to become a slightly more important contributor as evidenced by the observed dipole moment differences between **1***b* and **1***e*, **3***b* and **3***e*, and **4***b* and **4***e*, respectively. Again there is one pair *viz.* **2***b* and **2***e* which does not fit in with this rationale. However, in this case neither of the observed dipole moments is large and it is conceivable that the experimental errors are significantly greater than they were estimated to be (1).

Thus although the l.t.c.d. and dipole moment results each contain one anomaly,[8] the total data now available indicate strongly that the Hendrickson (3) cycloheptane-based conformational analytical procedure is applicable to cycloheptan*one* derivatives provided that it is recognized that a 1–2 kcal mole^{-1} reduction in overall strain energy may well obtain for those twist chair conformations in which the carbonyl group is at the axis or adjacent position.

The original driving force which prompted our interest in this problem arose from the need for information on the preferred conformations of rings A of A-homosteroids as a prerequisite to their evaluation as substrates and inhibitors of a steroid C-1,2-dehydrogenase. In this regard the only conclusion which now seems pertinent is that the energy barriers between the various preferred conformers of the flexible cycloheptanone ring are so low that factors controlling the interaction of the molecule with the enzyme's active center will undoubtedly override many of the conformational analytical criteria developed

[7]The methods used to calculate the dipole moments of the various conformers were as described previously (1).

[8]Unfortunately the anomalies are not of the same series in both cases and it has not proved possible to provide one rationale to account for both deviations.

Can. J. Chem. Downloaded from www.nrcresearchpress.com by 210.87.254.6 on 09/05/12
For personal use only.

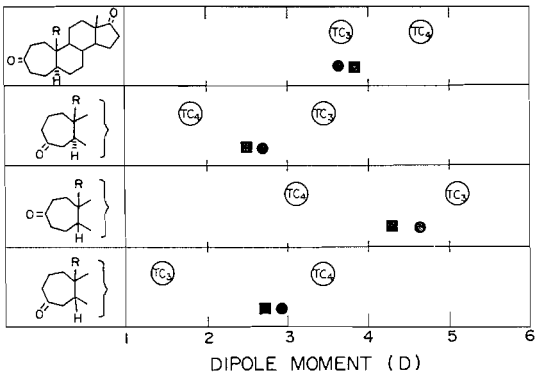

FIG. 6. Comparison of the dipole moments observed ■ (R = CH_3), ● (R = H) for the A-homodiketones **1***b*–**4***b* and **1***e*–**4***e*, respectively with the values calculated for the preferred $TC_{axis\ CO}$ and $TC_{adj.CO}$ conformations.

above and there appears to be little hope that such criteria would be of value in helping to predict the shape of ring A of the A-homosteroids in any enzyme–substrate or enzyme–inhibitor complexes.

Biological testing of a selection of the A-homosteroids prepared in this and previous investigations (1, 11) is in progress.

Experimental

The criteria of purity applied to the A-homosteroids, the analytical instrumentation used, the specifications of the chromatographic supplies, solvents, evaporation methods etc. were as described previously (11). The low temperature circular dichroism data reported in Fig. 2 and Table I were obtained on a Roussel-Jouan Dichrograph.

Compounds

Unless described below the A-homosteroids used in this investigation were prepared as reported in refs. 11 and 12.

*A-Homo-5β-androstan-3-one (**3***c*)*

A solution of 17β-hydroxy-A-homo-5β-androstan-3-one (1.39 g), toluene-*p*-sulfonic acid monohydrate (125 mg), and ethane-1,2-diol (3.0 g) in benzene (110 ml) was refluxed, with magnetic stirring, in a Dean–Stark apparatus for 4 h with periodical withdrawal of the benzene in the side arm. The cooled benzene solution was then washed successively with 10% aqueous sodium carbonate (50 ml) and water (50 ml) and was then dried ($MgSO_4$) and evaporated. The residue (1.6 g) was chromatographed on Florisil (70 g, column packed in *n*-hexane). Elution with ether–*n*-hexane (1:15) gave *3,3-ethylenedioxy-A-homo-5β-androstan-17β-ol* (**5**), which was then obtained as prisms (1.41 g) from *n*-hexane, m.p. 150–151°; infrared (i.r.) ($CHCl_3$): ν_{max} 3600, 1105, and 945 cm^{-1}; p.m.r. ($CDCl_3$): δ 0.72 (3H, s), 0.94 (3H, s), 1.97 (1H, s), and 3.90 (4H, s) p.p.m.; $[\alpha]_D^{23.5}$ +32° (*c*, 1.2 in $CHCl_3$).

A solution of the ketal **5** (1 g), pyridinium trifluoroacetate (316 mg) and dicyclohexylcarbodiimide (2.02 g) in dimethyl sulfoxide (16 ml) (13) was stirred at 55° for 2 h and was then poured into ether (100 ml). The ethereal solution was filtered, washed with water (50 ml), and then dried ($MgSO_4$) and evaporated, and the residue was digested with boiling *n*-hexane (50 ml) for 15 min. The hexane solution was then filtered, concentrated, and applied to a chromatographic column of Florisil (50 g, prepared in *n*-hexane). Elution with *n*-hexane removed the excess dicyclohexylcarbodiimide and further elution with ether–*n*-hexane (1:13) afforded *3,3-ethylene-dioxy-A-homo-5β-androstan-17-one* (**6**), which was then obtained as prismatic needles (833 mg) from *n*-hexane, m.p. 173.5–175°; i.r. ($CHCl_3$): ν_{max} 1725, 1105, and 945 cm^{-1}; p.m.r. ($CDCl_3$): δ 0.87 (3H, s), 0.98 (3H, s), and 3.92 (4H, s) p.p.m.; o.r.d. (*c*, 0.004 in iso-octane): $[\phi]_{326}$ +8700°, $[\phi]_{282}$ −7000° (*a* = +157).

Anal. Calcd. for $C_{22}H_{34}O_3$: C, 76.26; H, 9.89. Found: C, 76.13; H, 10.05.

The above oxo-ketal **6** (700 mg), potassium hydroxide (1.4 g), and 99% hydrazine hydrate (3.4 ml) were dissolved in diethylene glycol (14 ml) and the solution was refluxed under a nitrogen atmosphere for 3 h. The condenser was then removed and the bath temperature raised gradually to 195° and maintained at this level for 5 h. The mixture was then poured into water (150 ml) and the precipitate filtered and washed with water until the washings were neutral. The dried crude product (637 mg, m.p. 123–123.5°) was dissolved in ether – methanol – 2*N* hydrochloric acid (65 ml, 2:10:1) and the solution was stirred at 25° for 30 min, following which it was poured into water (600 ml), and the mixture extracted with ether (6 × 50 ml). The combined ether extracts were washed with water (50 ml), dried ($MgSO_4$), and evaporated. The oil obtained was chromatographed on Florisil (25 g, prepared in *n*-hexane); ether–*n*-hexane (1:13) elution yielded *A-homo-5β-androstan-3-one* (**3***c*) which was purified by recrystallization from petroleum ether (b.p. 40–60°) followed by sublimation at 100°/0.2 Torr. The pure product (600 mg) had m.p. 51.5–52°; i.r. ($CHCl_3$): ν_{max} 1690 cm^{-1}; p.m.r. ($CDCl_3$): δ 0.70 (3H, s) and 1.03 (3H, s) p.p.m.; o.r.d. (*c*, 0.004 in iso-octane): $[\phi]_{322}$ +3200°, $[\phi]_{310}$ +3300°, $[\phi]_{273}$ −1800° (*a* = +52); (*c*, 0.004 in methanol): $[\phi]_{303}$ +4200°, $[\phi]_{268}$ −2700° (*a* = +69).

Anal. Calcd. for $C_{20}H_{32}O$: C, 83.28; H, 11.18. Found: C, 83.55; H, 11.10.

*A-Homo-5β-androstan-4-one (**4***c*)*

This compound was prepared from 17β-hydroxy-A-homo-5β-androstan-4-one (**4***a*) by a route exactly similar in all details to that described above for **3***c*.

17β-Hydroxy-A-homo-5β-androstan-4-one (680 mg) yielded *4,4-ethylenedioxy-A-homo-5β-androstan-17β-ol* (**8**), as prisms (613 mg) from *n*-hexane, m.p. 134.5–135°; i.r. ($CHCl_3$): ν_{max} 3600, 1100, and 945 cm^{-1}; p.m.r. ($CDCl_3$): δ 0.72 (3H, s), 0.92 (3H, s), 1.91 (1H, s), and 3.90 (4H, s) p.p.m.

Anal. Calcd. for $C_{22}H_{36}O_3$: C, 75.82; H, 10.41. Found: C, 75.47; H, 10.28.

On oxidation with dicyclohexylcarbodiimide – dimethyl sulfoxide – pyridinium trifluoracetate, the above ketal **8** (500 mg) afforded *4,4-ethylenedioxy-A-homo-5β-androstan-17-one* (**9**) which was obtained as prismatic needles

Can. J. Chem. Downloaded from www.nrcresearchpress.com by 210.87.254.6 on 09/05/12
For personal use only.

TABLE II

Dipole moment data* for diketones **1***e*–**4***e*

Compound	α	ε	d	β	M_R	P_t	μ (D)
A-Homo-5α-estrane-3,17-dione (**1***e*)	5.20	2.2745	0.87377	0.270	81.84	358.23	3.65±0.02
A-Homo-5α-estrane-4,17-dione (**2***e*)	2.85	2.2745	0.87377	0.271	81.84	229.68	2.67±0.02
A-Homo-5β-estrane-3,17-dione (**3***e*)	7.96	2.2743	0.87377	0.259	81.84	530.16	4.65±0.02
A-Homo-5β-estrane-4,17-dione (**4***e*)	2.89	2.2743	0.87377	0.260	81.84	256.10	2.90±0.02

*Obtained for benzene solutions at 25° (1).

(410 mg) from *n*-hexane, m.p. 153–153.5°; i.r. ($CHCl_3$): ν_{max} 1725, 1105, and 945 cm^{-1}; p.m.r. ($CDCl_3$): δ 0.85 (3H, s), 0.95 (3H, s), and 3.93 (4H, s), p.p.m.; o.r.d. (*c*, 0.004 in iso-octane): $[\phi]_{326}$ +8600°, $[\phi]_{282}$ −5700° (*a* = +143).

Anal. Calcd. for $C_{22}H_{34}O_3$: C, 76.26; H, 9.89. Found: C, 76.42; H, 10.05.

Subsequent Wolff–Kishner reduction of the 17-oxo-ketal **9** (300 mg) gave *4,4-ethylenedioxy-A-homo-5β-androstane* (**10**) (273 mg) which on treatment with acid, followed by chromatography, yielded *A-homo-5β-androstan-4-one* (**4***c*) (215 mg). Further purification was effected by recrystallization from petroleum ether (b.p. 40–60°) and sublimation at 70°/0.005 Torr. The fully purified material had m.p. 60.5–61°; i.r. ($CHCl_3$): ν_{max} 1690 cm^{-1}; p.m.r. ($CDCl_3$): δ 0.72 (3H, s) and 1.00 (3H, s) p.p.m.; o.r.d. (*c*, 0.004 in iso-octane): $[\phi]_{303}$ −1300°, $[\phi]_{257}$ +2400° (*a* = −37); (*c*, 0.004 in methanol): $[\phi]_{311}$ −2400°, $[\phi]_{262}$ +4100° (*a* = −65).

Anal. Calcd. for $C_{20}H_{32}O$: C, 83.28; H, 11.18. Found: C, 83.20; H, 10.97.

*A-Homo-5α-and 5β-estranediones (**1***e*–**4***e*)*

These compounds were prepared by standard Jones' oxidation (14, *cf.* ref. 12) of the corresponding 17β-hydroxyestranes prepared as described previously (11). The yields and physical characteristics of the diones obtained were:

A-Homo-5α-estran-3,17-dione (**1***e*) (87%), was obtained as prisms from petroleum ether (b.p. 60–70°), m.p. 122–122.5°; $[\alpha]_D^{19}$ +16° (*c*, 1.5 in $CHCl_3$); p.m.r. ($CDCl_3$): δ 0.87 (3H, s) p.p.m.

Anal. Calcd. for $C_{19}H_{28}O_2$: C, 79.12; H, 9.79. Found: C, 79.29; H, 9.81.

A-Homo-5α-estran-4,17-dione (**2***e*) (87%), was obtained as rhombs from petroleum ether (b.p. 60–70°), m.p. 140°; $[\alpha]_D^{19}$ +255° (*c*, 1 in $CHCl_3$); i.r. ($CHCl_3$): ν_{max} 1730 and 1695 cm^{-1}; p.m.r. ($CDCl_3$): δ 0.87 (3H, s) p.p.m.

Anal. Calcd. for $C_{19}H_{28}O_2$: C, 79.12; H, 9.79. Found: C, 79.33; H, 9.91.

A-Homo-5β-estran-3,17-dione (**3***e*) (80%), was obtained as prisms from petroleum ether (b.p. 40–60°) m.p. 111–111.5°; $[\alpha]_D^{23}$ +465°; (*c*, 1.5 in $CHCl_3$); i.r. ($CHCl_3$): ν_{max} 1730 and 1695 cm^{-1}.

Anal. Calcd. for $C_{19}H_{28}O_2$: C, 79.12; H, 9.79. Found: C, 79.25; H, 9.91.

A-Homo-5β-estran-4,17-dione (**4***e*) (75%), was obtained as needles from petroleum ether (b.p. 40–60°), m.p. 135–136°, $[\alpha]_D^{23}$ +111° (*c*, 1.1 in $CHCl_3$); i.r. ($CHCl_3$): ν_{max} 1730 and 1695 cm^{-1}.

Anal. Calcd. for $C_{19}H_{28}O_2$: C, 79.12; H, 9.79. Found: C, 79.27; H, 9.91.

Dipole moments of the diketones **1***e*–**4***e* were obtained by the procedure outlined in ref. 1 and the relevant data are summarized in Table II and Fig. 6.

Acknowledgments

Financial support by the National Research Council of Canada and the award (to J.M.Z.) of a University of Toronto Open Fellowship are gratefully acknowledged. We also express our appreciation to Dr. G. F Wright and Mr. H. Huber for providing the dipole moment measurement facilities and to Dr. G. Snatzke for the low temperature circular dichroism data and for helpful discussion.

1. J. B. Jones, J. M. Zander, and P. Price. J. Am. Chem. Soc. **89**, 94 (1967).
2. J. B. Hendrickson. J. Am. Chem. Soc. **83**, 4537 (1961); Tetrahedron, **19**, 1387 (1963).
3. J. B. Hendrickson. J. Am. Chem. Soc. **89**, 7036, 7043 (1967).
4. M. Bixon and S. Lifson. Tetrahedron, **23**, 769 (1967).
5. N. L. Allinger. J. Am. Chem. Soc. **88**, 2999 (1966).
6. E. L. Eliel. Stereochemistry of carbon compounds. McGraw-Hill Book Co., Inc., New York. 1962. p. 240.
7. M. Nussim and Y. Mazur. Tetrahedron, **24**, 5337 (1968).
8. P. Crabbé. Optical rotatory dispersion and circular dichroism in organic chemistry. Holden-Day Inc., San Francisco, California. 1965. pp. 79–83.
9. K. M. Wellman, R. Records, E. Bunnenberg, and C. Djerassi. J. Am. Chem. Soc. **86**, 492 (1964).
10. E. L. Eliel, N. L. Allinger, S. J. Angyal, and G. A. Morrison. Conformational analysis. Interscience Publishers, Inc., New York. 1965. p. 11.
11. J. B. Jones and J. M. Zander. Can. J. Chem. **46**, 1913 (1968).
12. J. B. Jones and P. Price. Can. J. Chem. **44**, 999 (1966).
13. K. E. Pfitzner and J. G. Moffatt. J. Am. Chem. Soc. **85**, 3027 (1963); **87**, 5661, 5670 (1965).
14. K. Bowden, I. M. Heilbron, E. R. H. Jones, and B. C. L. Weedon. J. Chem. Soc. **39** (1946).

Can. J. Chem. Downloaded from www.nrcresearchpress.com by 210.87.254.6 on 09/05/12
For personal use only.

Can. J. Chem. Downloaded from www.nrcresearchpress.com by 210.87.254.40 on 09/05/12
For personal use only.

Sur quelques réactions acide-base dans les solvants fortement basiques anhydres. II. Les amino-2 éthylamidures de sodium et de potassium

W. R. HEUMANN, A. BOUCHARD, ET L. ŠAFAŘÍK
Département de chimie, Université de Montréal, Montréal, Québec

Reçu le 13 mai, 1969

Des solutions d'amino-2 éthylamidure de sodium dans l'éthylènediamine anhydre ont été préparées par dissolution d'amidure de sodium ammoniacal $NaNH_2$ dans l'éthylènediamine anhydre et élimination de l'ammoniac formé par le vide. Lorsque ces solutions sont préparées et gardées sous atmosphère d'azote ne contenant pas plus que 5 p.p.m. d'oxygène et 1 p.p.m. d'humidité environ, elles sont incolores et stables. L'amidure pur se sépare de la solution par addition de benzène sous forme d'une poudre blanche grisâtre également stable sous azote pur. L'amino-2 éthylamidure de potassium, qui a été préparé de la même façon en faisant réagir l'hydrure de potassium sur l'éthylènediamine, ressemble à celui de sodium. Le produit pur cristallin est stable, mais ses solutions dans l'éthylènediamine sont peu stables et se colorent assez rapidement en brun foncé à cause d'une polymérisation. Les forces basiques de ces deux amino-2 éthylamidures ont été comparées avec celle de l'amino-2 éthylamidure de lithium, en suivant potentiométriquement la neutralisation de l'acide chlorhydrique, du *p*-méthoxyphénol, de l'eau, et de l'éthanolamine par les trois amidures dans l'éthylènediamine anhydre. Selon les amplitudes des chutes de potentiel aux points d'équivalence, la force basique des trois amidures augmente avec le cation dans l'ordre Na < Li < K.

Solutions of sodium 2-aminoethylamide in anhydrous ethylenediamine were prepared by dissolving ammoniacal sodium amide $NaNH_2$ in ethylenediamine and removing the ammonia formed in vacuum. When these solutions were prepared and kept under nitrogen containing not more than about 5 p.p.m. of oxygen and 1 p.p.m. of moisture, they remained colorless and stable. Upon addition of benzene to these solutions, the pure amide precipitated as fine greyish-white crystals, which were also stable under pure nitrogen. The potassium 2-aminoethylamide was prepared in a similar way from ethylenediamine and potassium hydride. Its solid product resembles that of the corresponding sodium amide, but its solutions in ethylenediamine are less stable, rapidly turning dark brown because of polymerization. The basic strengths of these two 2-aminoethylamides were compared with the corresponding lithium amide by following potentiometrically the neutralization of ethylenediamine solutions of hydrochloric acid, *p*-methoxyphenol, water, and ethanolamine respectively. According to the heights of the potential jumps at the equivalence points the basic strength of the amides was found to increase in the order Na < Li < K.

Canadian Journal of Chemistry, 47, 3509 (1969)

Introduction

Plusieurs auteurs ont déjà tenter de préparer des solutions d'amino-2 éthylamidure de sodium (que nous appellerons dans la suite du texte "amidure de sodium") dans l'éthylènediamine anhydre (EDA). Ces tentatives n'ont réussi que partiellement ou même échoué. Reggel et ses collaborateurs (1) ont chauffé pendant 9 h un mélange de EDA avec une quantité de sodium suffisante pour donner une solution de l'amidure environ 3 *M* et ils ont obtenu une solution visqueuse colorée brun foncé. Bruckenstein et Mukherjee (2) ont tenté d'obtenir l'amidure de sodium par action sur l'EDA du sodium métallique, ou de l'hydrure de sodium ou de l'amidure ammoniacal $NaNH_2$, mais ils finissaient toujours par obtenir des résidus goudronneux noirs. Heumann et ses collaborateurs (3) ont essayé d'appliquer l'échange ionique en faisant passer une solution d'amino-2 éthylamidure de lithium dans l'EDA à travers une colonne échangeuse de cations à sodium en milieu anhydre d'EDA. Cependant, seulement une petite fraction des cations s'échangeait et les concentrations en amidure de sodium atteintes ne dépassaient pas quelques centièmes de mole par litre. Dans des essais analogues avec échangeur à potassium, les solutions obtenues ne contenaient même pas de potassium du tout. Il semble qu'aucune autre tentative de préparation d'amino-2 éthylamidure de potassium ("amidure de potassium" dans la suite du texte) n'ait été décrite dans la littérature.

La présente étude avait pour but la préparation des amidures de sodium et de potassium, ainsi que la comparaison de leurs propriétés basiques avec celles de l'amidure de lithium correspondant, qui avaient été le sujet d'une étude antérieure (4).

Réaction de l'éthylènediamine avec le sodium et le potassium

Nous avons d'abord étudié *l'action du sodium métallique sur l'EDA.* Placé sous forme de petits morceaux dans l'EDA à la température ambiante

Can. J. Chem. Downloaded from www.nrcresearchpress.com by 210.87.254.40 on 09/05/12
For personal use only.

sous une atmosphère d'azote sec ne contenant pas plus qu'environ 5 p.p.m. d'oxygène, le sodium ne réagit pas de façon perceptible. Seulement aux températures supérieures à 35 °C, la surface du métal se colore légèrement en bleu, mais la solution reste incolore et limpide. Avec du lithium, l'EDA chaude se colore immédiatement en bleu foncé, formant la solution bien connue d'électrons solvatés, qui redevient bientôt incolore par formation de l'amidure de lithium (5). L'EDA a été chauffée à 110 °C avec une quantité de sodium suffisante pour former une solution d'amidure 0.2 *M*, sans que le métal, qui est maintenant liquide, réagisse plus vivement. Après 10 h à cette température, la solution, restée toujours incolore, est refroidie, décantée et titrée avec une solution étalonnée d'acide benzoïque par la méthode décrite ailleurs (4,5). Sa concentration en base n'était que 0.017 *N*, ce qui veut dire qu'environ 8% du sodium avait réagi. Cette basicité a pu être attribuée à l'amidure de sodium et ne pouvait pas être due à une contamination par de l'hydroxyde de sodium, parce que ce dernier est insoluble dans l'EDA. Cette insolubilité a été établie par la constatation, qu'après plusieurs heures d'ébullition en contact avec de l'hydroxyde de sodium solide anhydre, l'EDA ne révélait aucune trace de basicité par titrage avec l'acide benzoïque.

Le *potassium métallique* réagit également peu avec l'EDA. Seulement à des températures légèrement supérieures à celle du point de fusion du métal (62.3 °C), la solution se colorait en bleu foncé. Seulement une fraction de la quantité de potassium suffisante pour former une solution 0.2 *M* d'amidure réagissait à l'état fondu pendant 24 h. Lorsque la réaction se faisait dans une atmosphère ne contenant pas plus qu'environ 5 p.p.m. d'oxygène, la solution chaude de l'amidure, qui était incolore au début, commençait bientôt à se colorer graduellement en brun. Sous une atmosphère plus riche en oxygène cependant, une réaction spontanée, accompagnée d'une effervescence très vive, se déclanchait peu après que la température avait dépassé 60 °C et la solution se transformait rapidement en un liquide visqueux brun foncé. Il est intéressant à noter, qu'un alliage à 78% de potassium et 22% de sodium, liquide à la température ambiante, réagit beaucoup plus facilement avec l'EDA en formant à la température ambiante une solution colorée bleu foncé, qui est stable pendant au moins plusieurs heures. Nous utilisons cette réaction dans la purification de l'EDA pour éliminer des traces d'eau (3).

Contrairement au lithium, le sodium et le potassium ne réagissent donc que peu avec l'EDA. Cependant, l'amidure de sodium se forme facilement par action de l'amidure ammoniacal $NaNH_2$ sur l'EDA et l'amidure de potassium a été préparé par réaction de l'hydrure de potassium avec l'EDA. Les procédés de préparation des deux amidures sont décrits dans la partie expérimentale, tandis que la discussion de leurs propriétés fait partie du chapitre Résultats et discussion.

Nous avons comparé les deux amidures de sodium et de potassium avec celui de lithium, que nous avons déjà étudié dans un travail antérieur (4), en suivant potentiométriquement la neutralisation de plusieurs acides de différentes forces par les trois amidures en solution dans l'EDA.

Partie expérimentale

La préparation de *l'EDA anhydre* a été décrite dans un travail antérieur (3) de même que la préparation de la solution de l'amino-2 éthylamidure de lithium dans l'EDA (5). En opérant soigneusement, nous avons pu maintenir la teneur en eau de l'EDA au-dessous de 5 p.p.m.

Amino-2 éthylamidures de sodium et de potassium

Toute l'opération se fait dans une boîte à gants sous azote pur. Un ballon rond à 3 tubulures est muni de connections pour l'entrée de l'azote, le vide et la vidange par un syphon à pression de gaz. Les joints rodés des cols sont garnis de manchons coniques en Teflon. Pas plus de la moitié du ballon est remplie d'EDA, à laquelle on ajoute une quantité de $NaNH_2$ commercial pur, suffisante pour donner une solution environ 1.5 *M* (par exemple un ballon de 500 ml, 250 ml d'EDA et 15 g de $NaNH_2$). En agitant avec une barre magnétique recouverte de verre ou de polyéthylène, on réduit graduellement la pression jusqu'à environ 100 mm de mercure pour déclencher l'ébullition. Au fur et à mesure que cette dernière diminue, la pression est baissée graduellement jusqu'à environ 1 à 2 mm. Sitôt que tout l'amidure s'est dissout et que l'ébullition a cessé, la pression normale est rétablie avec de l'azote pur. Etant donné qu'une certaine partie du solvant s'est évaporée avec l'ammoniac formé par la réaction, la concentration de la solution aura atteint presque la solubilité de l'amidure de 1.95 à 2 *M*. La solution est syphonnée par pression d'azote dans un autre ballon deux fois plus grand que le premier à l'aide d'un tube descendant au fond du premier ballon. Le bout de ce tube est muni d'un petit filtre en verre fritté de porosité moyenne, lequel retient la petite quantité de NaOH qui a précipité ainsi que l'oxyde ferrique dont l'amidure ammoniacal du commerce est contaminé habituellement. La solution filtrée est additionnée

Can. J. Chem. Downloaded from www.nrcresearchpress.com by 210.87.254.40 on 09/05/12
For personal use only.

lentement de deux à trois fois son volume de benzène pur anhydre et le mélange est agité continuellement par une barre magnétique. L'amidure de sodium $NaHNC_2H_4NH_2$ précipite rapidement en cristaux fins, qui sont séparés par filtration avec suction modérée sur un filtre en verre fritté de porosité moyenne. Le dépôt sur le filtre est lavé plusieurs fois avec du benzène et séché par un courant d'azote. On obtient ainsi une poudre cristalline blanche grisâtre, qui doit être gardée sous azote pur.

L'amidure de potassium est préparé de la même façon que celui de sodium, mais au lieu de l'amidure $NaNH_2$ l'hydrure de potassium KH sous forme d'une suspension poudreuse à 50% dans de l'huile (Metal Hydrides Inc., Beverly, Massachusetts) est ajouté à l'EDA à l'aide d'une pipette.

Solutions des amidures de sodium et de potassium 0.2 M

Ces solutions peuvent être préparées soit comme décrit plus haut, mais sans précipitation par le benzène, ou par dissolution du produit solide qui a été préparé suivant la description du chapitre précédant. Les solutions sont étalonnées potentiométriquement par l'acide benzoïque.

Acides

L'acide chlorhydrique sous forme de chlorure d'éthylènediammonium a été recristallisé à partir de sa solution aqueuse. L'acide benzoïque de qualité "primary standard" a été utilisé tel quel après séchage. Le *p*-méthoxyphénol pur commercial a été recristallisé à partir de sa solution dans le tétrachlorure de carbone et l'éthanolamine pure commerciale a été déshydratée par distillation fractionnée.

Appareil

L'appareil utilisé pour effectuer et suivre potentiométriquement les réactions de neutralisation, était le titreur clos aux électrodes de platine décrit dans un autre mémoire (5). Ce dernier donne aussi la description de la boîte à gants, dans laquelle le titreur était placé et où s'effectuaient aussi les autres manipulations.

Les traces d'humidité dans l'atmosphère de la boîte se déterminaient à l'aide d'un appareil pour la détermination du point de rosé, qui faisait partie du système de purification par recirculation de l'atmosphère. Les traces d'oxygène se déterminaient par chromatographie en phase vapeur sur une colonne de 14 pieds sur 1/4 de pouce contenant des tamis moléculaires (Linde Molecular Sieves 5A). Pour obtenir la séparation entre l'oxygène et l'argon, il fallait maintenir la colonne à une température ne dépassant pas 0 °C.

Mode opératoire

De même que dans notre étude antérieure sur l'amino-2 éthylamidure de lithium (4), nous avons toujours neutralisé 25 ml de solution d'acide 0.065 à 0.066 *N* par une solution étalonnée 0.195 à 0.200 *N* de l'amidure, de sorte qu'aux points d'équivalence les solutions étaient toujours 0.05 *N*.

Résultats et discussion

Les amino-2 éthylamidures de sodium et de potassium

L'amidure de sodium se forme par l'action de l'amidure ammoniacal $NaNH_2$ sur l'EDA lorsqu'on opère sous vide pour enlever l'ammoniac formé par la réaction. A la température ambiante et à la pression normale, $NaNH_2$ se dissout dans l'EDA à raison d'environ 0.2 mole par litre. Aux pressions inférieures à 100 mm de mercure, il y a dégagement de vapeurs d'ammoniac et des quantités beaucoup plus grandes de $NaNH_2$ se dissolvent. L'addition de benzène à une solution débarassée de NH_3 par le vide, entraîne une précipitation d'amidure de sodium sous forme d'une poudre cristalline blanche grisâtre, qui se décompose violemment au contact de l'eau. Le poids moléculaire de l'amino-2 éthylamidure de sodium est 82.1, tandis que celui de l'amidure ammoniacal est 39. Il était donc facile à identifier ce produit par titrage potentiométrique d'une solution dans l'EDA avec une solution étalonnée d'acide benzoïque selon la méthode décrite ailleurs (4,5). De plus, le poids moléculaire a été déterminé par titrage potentiométrique d'une part et conductimétrique d'autre par d'une solution aqueuse obtenue en décomposant le produit par l'eau. Les courbes de neutralisation par l'acide chlorhydrique obtenues par ces deux méthodes sont illustrées dans la Fig. 1. On voit qu'il s'agit d'un mélange de trois bases, c'est-à-dire de l'hydroxyde de sodium et des deux fonctions basiques de l'EDA. Le poids moléculaire trouvé

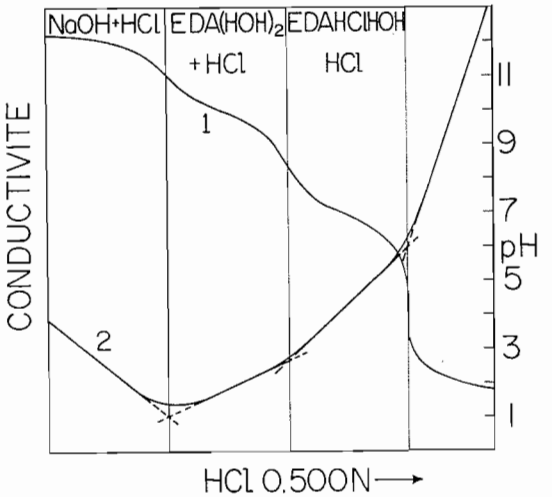

FIG. 1. Titrage de l'amino-2 éthylamidure de sodium. Environ 200 mg (2.5 m.équiv.) d'amidure dans 100 ml d'eau. (1) courbe potentiométrique; (2) courbe conductimétrique.

Can. J. Chem. Downloaded from www.nrcresearchpress.com by 210.87.254.40 on 09/05/12
For personal use only.

ainsi dans plusieurs expériences variait entre 80 et 80.6, ce qui confirmait la présence de l'amino-2 éthylamidure de sodium. Pour déterminer sa solubilité dans l'EDA, on a préparé une solution saturée en agitant l'EDA avec un excès de l'amidure en poudre pendant 20 h. Après filtration et dilution de la solution à dix fois son volume avec de l'EDA, on l'a titrée potentiométriquement avec l'acide benzoïque suivant la méthode déjà mentionnée. La solubilité trouvée ainsi était de 1.95 à 2.0 moles ou environ 160 g par litre, ce qui est bien plus que ce qui laissaient prévoir les résultats obtenus par échange ionique (3). Aucune explication de cette divergence ne peut être proposée, mais la valeur présente paraît digne de confiance par la simplicité de sa détermination.

L'amino-2 éthylamidure de potassium a été préparé et identifié de la même façon que celui de sodium, mais on a fait réagir avec l'EDA l'hydrure de potassium au lieu de son amidure KNH_2, parce que celui-ci est difficile à préparer et le produit commercial est rare est très dispendieux. L'amidure de potassium ressemble aux amidures de lithium et de sodium tant par son apparence de poudre cristalline blanche grisâtre stable sous atmosphère inerte que par sa réaction violente avec l'eau.

Quant aux *solutions des amidures* dans l'EDA, il est à noter que contrairement aux résultats des autres auteurs mentionnés au début, les solutions d'amidure de sodium que nous avons préparées, n'étaient pas colorées et il n'y avait pas formation de résidus goudronneux noirs lors de la préparation des solutions. Ces produits foncés se forment sans doute par polymérisation de l'EDA qui probablement n'a lieu qu'en présence d'oxygène moléculaire. Nous avons pu démontrer (5), que la solution pure de l'amidure de lithium dans l'EDA est incolore et stable et que des traces d'oxygène atmosphérique suffissent à provoquer ces colorations allant du rose au bleu–violet et finalement au brun foncé, qui ont été observées dans d'autres travaux (4,6). Les mêmes observations ont été faites avec les solutions incolores de l'amidure de sodium. De plus, il suffit de faire barboter de l'air dans une solution incolore d'un des amidures dans l'EDA, pour provoquer une précipitation immédiate d'un produit brun. Un échantillon d'une solution d'amidure de sodium incolore et limpide, qui avait été gardé dans un tube de verre scellé, ne manifestait aucun changement perceptible pendant un an. Sitôt que le tube fut ouvert et le contenu exposé à l'atmosphère ambiante, la solution se colora immédiatement en bleu pour devenir brun noirâtre peu après. Tenant compte de ces faits ainsi que du comportement du potassium métallique dans l'EDA chaude décrit plus haut, on peut conclure, que l'oxygène est la cause des polymérisations. Les solutions d'amidure de potassium sont particulièrement sensibles. Même sous une atmosphère d'azote ne contenant que quelques parties par million d'oxygène et moins d'une partie par million d'eau, ces solutions se colorent graduellement en brun foncé au cours de quelques heures. Après 2 ou 3 jours un précipité goudronneux commence à se former. Dans les mêmes conditions, les solutions des deux autres amidures sont stables et restent incolores au moins pendant plusieurs semaines.

Nos expériences démontrent, que les amino-2 éthylamidures des métaux alcalins pures et stables peuvent être préparés sous forme solide ou en solutions incolores à conditions qu'on opère en milieux parfaitement inerte, c'est-à-dire un milieu qui contient au maximum quelques p.p.m. d'oxygène, d'eau et de dioxyde de carbone. Les différentes colorations des solutions qui ont été observées, ainsi que la formation de résidus goudronneux qui ont empêché d'autres auteurs de préparer l'amidure de sodium, ne sont pas dues à une instabilité inhérente de ces amidures, mais à des réactions de décomposition avec des petites quantités d'impuretés. Il est donc indispensable d'opérer dans des conditions rigoureusement contrôlées, dont on peut s'assurer seulement par un contrôle analytique assez fréquent de l'atmosphère de la boîte à gants et du solvant. Trop souvent, des expérimentateurs travaillent dans des conditions extrèmes et difficiles à maintenir, comme par exemple un milieu en même temps hygroscopique et anhydre, sans vérifier analytiquement, si la condition qu'ils supposent être réalisée, existe effectivement. Et tout aussi souvent un tel travail produit des résultats expérimentaux faux conduisant à des conclusions erronées.

Forces basiques des amino-2 éthylamidures

La Fig. 2. donne les courbes de neutralisation de l'acide chlorhydrique, du *p*-méthoxyphénol, de l'eau et de l'éthanolamine par les amidures de lithium, de sodium et de potassium. Ces quatres

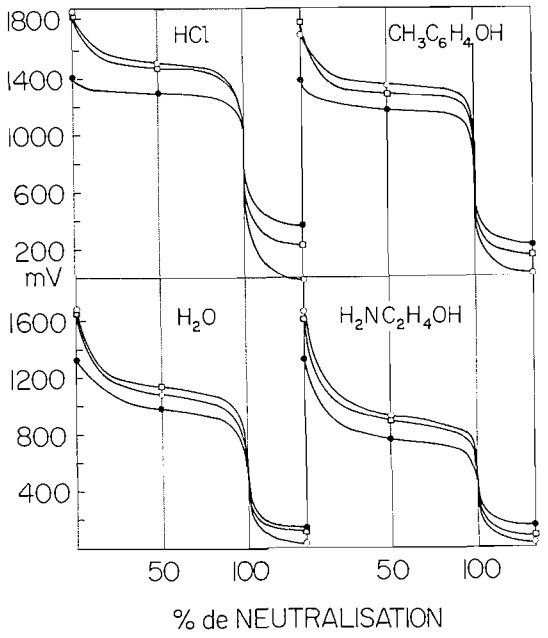

FIG. 2. Courbes potentiométriques de neutralisation de quatre acides par les amino-2 éthylamidures de: ○ potassium; ● sodium; □ lithium.

acides ont été choisis, parce que leurs forces acides sont très différentes et couvrent la majeure partie de la gamme des acidités possibles dans l'EDA.

Les courbes des amidures de lithium et de sodium sont de vraies courbes expérimentales en ce sens que les points de mesures se placent effectivement sur la courbe continue. La reproductibilité des mesures est bonne, les forces électromotrices (f.e.m.) aux points de demi-neutralisation ayant des déviations standards de 10 à 15 mV et aux points d'équivalence entre 5 et 10 mV. Les courbes obtenues avec l'amidure de potassium, cependant, étaient sensiblement moins faciles à reproduire à cause de l'instabilité des solutions de cet amidure. Les solutions fraîchement préparées ne donnaient des mesures potentiométriques exploitables que pendant environ deux jours et les déviations standards des mesures étaient plusieurs fois plus grandes que celles relatives aux deux autres amidures. Les courbes expérimentales étaient donc moins régulières que les courbes "idéalisées" de la Fig. 2., qui représentent les moyennes de trois à quatre essais pour chaque acide.

Notre système potentiométrique à deux électrodes de platine ne donne que des valeurs de repère d'une utilité limitée. Nous avons déjà souligné (4) que les conditions expérimentales de la présente série d'études rendent trop difficile l'usage de l'électrode à hydrogène, mais que ces mesures de repère permettent néanmoins certaines conclusions. Cette étude antérieure a démontré que l'amplitude des chutes de potentiel des courbes de neutralisation par l'amidure de lithium variait directement avec la force des acides. Les courbes de la Fig. 2. permettent par un raisonnement analogue de conclure que les forces basiques des trois amidures doivent être proportionelles à l'amplitude des chutes de potentiel et que par conséquent la force basique augmente avec les cations dans l'ordre Na < Li < K.

Remerciements

Nous remercions sincèrement le Conseil National de Recherches du Canada de l'aide financière sous forme d'octrois de recherches (W.R.H.), qui a rendu possible ce travail.

1. L. REGGEL, S. FRIEDMAN, et I. WENDER. J. Org. Chem. **23**, 1136 (1958).
2. S. BRUCKENSTEIN et L. M. MUKHERJEE. J. Phys. Chem. **66**, 2228 (1962).
3. W. R. HEUMANN, O. DIONNE, et G. TREMBLAY. Can. J. Chem. **43**, 1096 (1965).
4. W. R. HEUMANN, A. BOUCHARD, et G. TREMBLAY. Can. J. Chem. **45**, 3129 (1967).
5. W. R. HEUMANN, A. BOUCHARD, et F. D. ROCHON. Anal. Chem. **40**, 1529 (1968).
6. C. VERMESSE-JACQUINOT. J. Chim. Phys. **62**, 366 (1965).

Can. J. Chem. Downloaded from www.nrcresearchpress.com by 210.87.254.40 on 09/05/12
For personal use only.

Can. J. Chem. Downloaded from www.nrcresearchpress.com by 210.87.254.40 on 09/05/12
For personal use only.

Nuclear magnetic resonance studies. XVIII.[1] The proton parameters of some bicyclo[2·2·2]octane derivatives

GURUDATA[2] AND J. B. STOTHERS
Department of Chemistry, University of Western Ontario, London, Ontario

Received May 2, 1969

The high resolution proton spectra of ten substituted bicyclo[2·2·2]octenes and octanes have been analyzed. The proton shieldings and coupling constants are discussed with particular emphasis on the stereochemical dependence of these parameters. Evidence bearing on the anisotropic effect of carbonyl bonds is presented to substantiate other recent findings on these shielding effects. Certain long-range couplings permit stereochemical assignments.

Canadian Journal of Chemistry, 47, 3515 (1969)

Introduction

In the course of an earlier study of maleopimaric acid derivatives by proton spectroscopy (1), certain features of the parameters for the protons associated with the bicyclo[2·2·2]octene moiety were noted. Since the ^1H–^1H spin couplings in this system differ appreciably from those found for the more popular bicyclo[2·2·1]-heptane system it seemed desirable to investigate in more detail the proton spectra of some simpler model compounds having the bicyclo[2·2·2]-octane skeleton. A comparison of the effects of molecular geometry and strain on the vicinal couplings for the two cases appeared worthwhile. A convenient model system was available via the Diels–Alder reaction and consequently a number of 7,8-disubstituted derivatives of 1,3,5,5-tetramethylbicyclo[2·2·2]oct-2-ene (**1**)

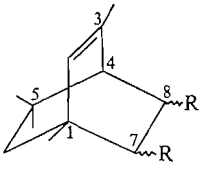

1

was prepared by the reaction of maleic anhydride and dimethylfumarate with "1,3,5,5-tetramethylcyclohexa-1,3-diene" **2** as summarized in Scheme 1. The corresponding bicyclooctanes were obtained by catalytic hydrogenation.

Although the stereochemistry of these products follows directly from the geometry of the starting materials, the well-known angular dependence of vicinal proton–proton couplings (2) permits one to distinguish readily between isomers having *cis* and *trans* carbonyl functions. The assignment of the relative orientation of the substituents follows from (*a*) the relative yields of the adducts, (*b*) a consideration of the geometry of the adduct, and (*c*) an analysis of the effect of the olefinic bond on the C-7 and C-8 proton shieldings (3, 4). Further confirmation is provided by the magnitude of the long-range couplings observed for these protons, a subject that has been reviewed recently (5, 6).

In all cases the C-7 and C-8 substituents are carbomethoxyl or carbonyl groups. Thus the proton spectra of the olefins are particularly simple and are readily analyzed, in fact the signals for each proton type appear separately. For the bicyclooctanes, however, a complete analysis is not readily accomplished and only the signals which are unequivocally assignable were analyzed. These data, therefore, may be useful as reference values for protons in related, but more complicated, systems.

Experimental

Spectra

Most of the proton parameters were determined from spectra obtained on a Varian A-60 spectrometer. The chart calibration was checked regularly using audio-frequency sidebands of tetramethylsilane. The decoupling experiments were performed on a Varian A-60A spectrometer using a Varian decoupling accessory.[3] A few double irradiation experiments were carried out using a Varian DP-60 spectrometer in conjunction with either a unit similar to the Varian V3521 integrator or a single sideband homonuclear decoupler Model HD-60 (NMR

[1]For Part XVII of this series, see ref. 30.

[2]Petroleum Research Fund Predoctoral Fellow, 1964–1965; Ontario Graduate Fellowship 1966–1967. Present address, Department of Chemistry, University of Ottawa, Ottawa, Canada.

[3]We thank Dr. A. Stoessl and Dr. E. Y. Spencer, London Research Institute, Department of Agriculture for time on this instrument.

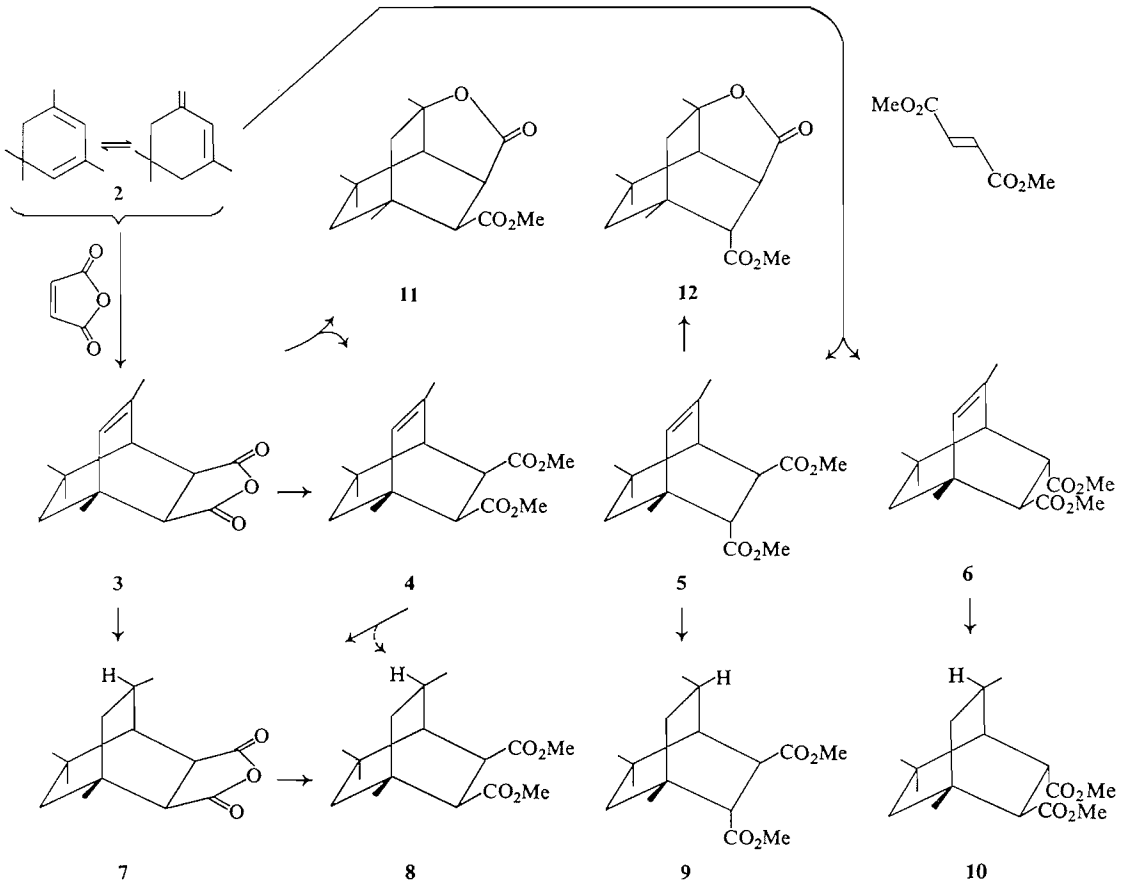

SCHEME 1

Specialties, Inc.). The chemical shifts and coupling constants are judged to have a precision of ±0.01 p.p.m. and ±0.2 Hz, respectively. A few spectra were obtained with Varian HA-60 or HA-100 instruments to check the earlier data and to carry out some nuclear Overhauser experiments. Infrared spectra were recorded on a Beckman IR5A or IR10 spectrophotometer.

Materials

"1,3,5,5-Tetramethylcyclohexa-1,3-diene" (2)

The diene was obtained by a slight modification of the method described by Kharasch (7).

Methyl magnesium iodide, prepared from methyl iodide (114 g) and magnesium turnings (20 g) in 360 ml of ether, was cooled in an ice-bath and a solution of isophorone (96.7 g) in ether (135 ml) was added slowly over 1.75 h. The reaction mixture was allowed to stand for 4 h, refluxed for 1 h, and then allowed to stand overnight. The resulting mixture was poured over 400 g of crushed ice and 46.5 ml of glacial acetic acid was added with stirring. The product was isolated by ether extraction. After evaporation of the solvent, the residual liquid was fractionated on a spinning band column to yield 65 g of **2**, b.p. 45.5–48.0/12 mm [lit. b.p. 151–155/760 mm (7)]; ν_{max} ($CHCl_3$) 1667, 1647, 1616, 900 cm^{-1}; λ_{max} (EtOH) 238, 261 nm.

Maleic Anhydride Adduct of 2 (3)

To 13.6 g of **2** was added a solution of maleic anhydride (9.8 g) in benzene (15 ml). The reaction mixture was warmed until a deep yellow coloration developed at which point heating was discontinued until the reaction slowed considerably. Refluxing the reaction mixture for 1 h resulted in the complete disappearance of the yellow color. Removal of the solvent left a white solid which was recrystallized from a 50/50 mixture of petroleum ether (35–60°) and benzene, to yield 13.1 g of **3**, m.p. 99.5–100.5° [lit. m.p. 98–99° (7)]; ν_{max} ($CHCl_3$) 1855, 1780, 1650 cm^{-1}.

Hydrogenation of 3 (7)

To a solution of **3** (1 g) in 25 ml of glacial acetic acid was added 250 mg of PtO_2 (Engelhard). Three drops of perchloric acid were added and the mixture shaken for ca. 84 h with hydrogen at 50 p.s.i. After removal of the catalyst and solvent, the residue was dissolved in diethyl ether and the solution washed four times with water. After filtration through anhydrous magnesium sulfate, the ether was removed leaving 1.25 g of a syrupy liquid.

Can. J. Chem. Downloaded from www.nrcresearchpress.com by 210.87.254.40 on 09/05/12
For personal use only.

Can. J. Chem. Downloaded from www.nrcresearchpress.com by 210.87.254.40 on 09/05/12
For personal use only.

Crystallization from methanol yielded 600 mg of a white solid, melting at 72–76°. Recrystallization from chloroform gave **7**, m.p. 76–77°; ν_{max} ($CHCl_3$) 1885, 1775 cm^{-1}.

Anal. Calcd. for $C_{14}H_{20}O_3$: C, 71.16; H, 8.53. Found: C, 70.72; H, 8.65.

Esterification of 3 (4)

Adduct **3** (4 g) was dissolved in 100 ml of methanol and 2.4 g of concentrated H_2SO_4 added. The mixture was refluxed overnight.

After removal of most of the excess alcohol, *in vacuo*, the reaction mixture was extracted with diethyl ether. The usual work-up yielded 3.6 g of a colorless viscous liquid, which was chromatographed on silica gel (150 g) with anhydrous ether as eluent. A yield of 3.2 g of **4** was obtained, n_D^{25} 1.4802; ν_{max} ($CHCl_3$) 1740 cm^{-1}.

Anal. Calcd. for $C_{16}H_{24}O_4$: C, 68.54; H, 8.63. Found: C, 68.04; H, 8.77.

Later fractions of the chromatogram crystallized on standing. This material, after recrystallization from anhydrous ether, was identified as the lactone ester **11**, m.p. 87.5–88.5°; ν_{max} ($CHCl_3$) 1780, 1745 cm^{-1}.

Anal. Calcd. for $C_{15}H_{22}O_4$: C, 67.64; H, 8.33. Found: C, 67.97; H, 8.19.

Esterification of **3** with diazomethane, as described for the preparation of **8** below, yielded only **4**.

Esterification of 7 (8)

The saturated anhydride **7** (1.2 g) was dissolved in methanol (30 ml) and an ethereal solution of diazomethane added to the cooled solution. After several hours standing the solvent was removed, leaving a viscous, pale-yellow liquid. To remove traces of unsaturated material which were present in the starting material, the product was dissolved in acetic acid and a few drops of bromine added.

This mixture was allowed to stand for 1 h and then diluted with water and the product isolated by ether extraction. On cooling the residue after removal of most of the ether, a white crystalline solid (216 mg) precipitated. The crystals were separated and the volatile portion of the filtrate evaporated leaving a viscous yellow liquid (0.67 g) whose n.m.r. spectrum showed the absence of unsaturated material. The product was further purified by column chromatography followed by bulb-to-bulb distillation, n_D^{25} 1.4812; ν_{max} ($CHCl_3$) 1730 cm^{-1}.

Anal. Calcd. for $C_{16}H_{26}O_4$: C, 68.05; H, 9.28. Found: C, 67.72; H, 9.09.

Reaction of 2 with Dimethyl Fumarate

Preparation of Dimethyl Fumarate

Dimethyl fumarate was prepared by a method analogous to that described by Vogel (8) for diethyl fumarate.

A mixture of fumaric acid (50 g), methanol (100 ml), benzene (200 ml), and concentrated H_2SO_4 (8 ml) was refluxed for ca. 20 h. On cooling, white crystals precipitated. Recrystallization from chloroform gave 61 g of product, m.p. 101–102° [lit. m.p. 101.2–101.4° (9)].

Diels–Alder Reaction

A mixture of 18.5 g of **2** and 14.5 g of dimethyl fumarate was refluxed for 11 h. The excess diene was removed *in vacuo* (20 mm) and the residue fractionated at 1 mm pressure. The product (20.2 g) distilling between 105–120° was collected.

Isolation of Compound 5

On addition of a small amount of petroleum ether (35–60°) to the distillate, a white crystalline solid precipitated. After several recrystallizations from petroleum ether, the product, **5**, melted at 71–72°; ν_{max} ($CHCl_3$) 1725, 1650 cm^{-1}.

Anal. Calcd. for $C_{16}H_{24}O_4$: C, 68.54; H, 8.63. Found: C, 68.61; H, 8.76.

Conversion of 5 to 12

To glacial acetic acid (50 ml) was added **5** (1 g) and the solution refluxed for 1 h. After cooling and isolation by ether extraction, a white crystalline material **12** was obtained (0.7 g) melting at 100.5–101.0° (from petroleum ether), ν_{max} ($CHCl_3$) 1770, 1735 cm^{-1}.

Anal. Calcd. for $C_{15}H_{22}O_4$: C, 67.64; H, 8.33. Found: C, 67.58; H, 8.06.

Isolation of Compound 6

After the crystallization of **5**, 6.05 g of mother liquor remained. Separation of the components of this mixture was effected by chromatography on alumina (Woelm Neutral, Activity 1). Traces of **5** were eluted with petroleum ether (35–60°), before a new compound, **6**, appeared upon elution with benzene – petroleum ether mixtures. This material was crystallized by cooling to about 10 °C and then adding a small amount of methanol. Recrystallization from petroleum ether gave **6**, m.p. 50–51°, ν_{max} ($CHCl_3$) 1658 cm^{-1}.

Anal. Calcd. for $C_{16}H_{24}O_4$: C, 68.54; H, 8.63. Found: C, 68.00; H, 8.67.

Hydrogenation of Compound 5 (9)

Compound **5** (0.9 g in 25 ml of glacial acetic acid) was hydrogenated over a platinum catalyst (150 mg). A Parr low pressure hydrogenation apparatus was used at a hydrogen pressure of 48 p.s.i. for 36 h. Work-up in the usual way afforded a colorless liquid which was crystallized by cooling to below 0 °C and then adding a small amount of methanol. Recrystallization from petroleum ether (35–60°) gave **9**, m.p. 44.0–45.5°; ν_{max} ($CHCl_3$) 1720 cm^{-1}.

Anal. Calcd. for $C_{16}H_{26}O_4$: C, 68.05; H, 9.28. Found: C, 68.44; H, 9.47.

Hydrogenation of Compound 6 (10)

The diester **6** (450 mg) was dissolved in glacial acetic acid (15 ml) and hydrogenated over a platinum catalyst in the presence of two drops of perchloric acid. A Parr low pressure hydrogenation apparatus was used and the reaction mixture shaken for 72 h at a hydrogen pressure of 58 p.s.i. Work-up yielded 0.45 g of product (**10**).

The saturated diester (**10**) was further purified by column chromatography on silica gel. A sample for analysis was prepared by bulb-to-bulb distillation under reduced pressure, n_D^{25} 1.4742; ν_{max} ($CHCl_3$) 1720 cm^{-1}.

Anal. Calcd. for $C_{16}H_{26}O_4$: C, 68.05; H, 9.28. Found: C, 68.68; H, 8.93.

Results and Discussion

The parent diene was obtained following the method of Kharasch and Tawney from isophorone and methyl magnesium iodide with the subsequent elimination of water from the tertiary alcohol. Although the homoannular diene structure was assigned to **2** by the earlier

Can. J. Chem. Downloaded from www.nrcresearchpress.com by 210.87.254.40 on 09/05/12
For personal use only.

workers, gas–liquid chromatography indicates the presence of two dienes. The infrared spectrum exhibits three maxima in the C=C stretching region as well as a peak at 900 cm^{-1} suggesting the presence of an *exo*-methylene group. Estimations based on the Woodward rules predict ultraviolet absorption maxima at 236 and 263 nm for the two dienes while the product exhibits maxima at 238 and 261 nm in good agreement with these predictions. The conclusion that the diene **2** is actually a mixture of approximately equal amounts of the two dienes, shown in Scheme 1, is borne out by its proton spectrum, the low-field region of which has four multiplets at 4.62, 4.98, 5.43, and 5.85 p.p.m. (from TMS) in the ratio 2.3 : 1.2 : 1.2 : 1.1. Since the diene mixture **2** was found to undergo the Diels–Alder reaction with maleic anhydride quantitatively, no attempts were made to separate the two dienes, although later it was found that an essentially pure sample of the homoannular diene can be obtained by careful fractional distillation.

Before a detailed discussion of the proton spectra of the bicyclooctane derivatives, their preparation, separation and the elucidation of their gross structures is described.

Since the Diels–Alder reaction of **2** with maleic anhydride proceeds virtually quantitatively to **3** it was assumed initially that the *cis–endo*[4] structure is formed on the basis of the Alder rule (10). It was found that methylation of **3** with methanol in sulfuric acid gave both the expected diester **4** as well as compound **11** which contains a γ-lactone (ν_{max} 1780 cm^{-1}), an ester (ν_{max} 1745 cm^{-1}), no olefinic protons and each methyl proton signal is a singlet. The carboxyl functions are *cis* since $J_{7,8}$ = 9.7 Hz. Presumably the lactone is formed by protonation of the double bond followed by reaction with the C-8 carboxyl function. In addition **3** forms a bromo-γ-lactone quantitatively upon reaction with bromine (11) further confirming the *endo* orientation of the anhydrido function. Each of the unsaturated compounds **3–6** was treated with bromine but since it was found that each reaction follows a different preferred course, a full description of these experiments is deferred for a later report. All attempts to isolate another maleic anhydride adduct or to isomerize **3** to the *cis–exo* form (12) have proved unsuccessful and we are confident that **3** has the *cis–endo* stereochemistry.

Adduct formation of **2** with dimethyl fumarate occurs much less readily but two diesters, **5** and **6**, are obtained in a ratio of ~10:1. Because of the steric hinderance due to the *exo*-methyl group at C-5 it was assumed initially that the major product **5** has an *endo* carbomethoxyl group at C-8. Long-range coupling of the C-7 proton provides additional evidence to support this assignment. Confirmation was obtained by the ready formation of **12**, upon heating in acetic acid, having a γ-lactone (ν_{max} 1770 cm^{-1}), an ester (ν_{max} 1735 cm^{-1}), no olefinic protons and singlet methyl proton signals. Structure **6** is assigned to the second, minor diester since there is no evidence that the bicyclo[2·2·2]octene skeleton has been altered.

The saturated derivatives **7–10** were obtained by catalytic hydrogenation using platinum oxide. The up-take of hydrogen was slow even with the addition of a few drops of perchloric acid in the the case of **3** and **6**, and it was found that hydrogenation of **4** leads preferentially to **7**. Consequently **8** was more readily obtained by methylation of **7** using diazomethane. The orientation of the C-3 methyl group in **7–9** was assigned on the basis of the n.m.r. data and this feature is discussed in a later section.

Proton Spectra

General Comments

To show their relative simplicity, the 60 MHz spectra in $CDCl_3$ solution of the bicyclooctenes are presented in Fig. 1. In the main, the assignment of bands to specific protons is straightforward. For example, the spectrum of the maleic anhydride adduct **3** (Fig. 1*a*) contains a low-field olefinic signal at δ 5.57 coupled to the C-3 methyl (1.80 p.p.m.) J = 1.8 Hz and the C-4 bridgehead proton (2.51 p.p.m.) J = 1.5 Hz. The couplings were confirmed by double irradiation. The larger splitting in the latter signal, 3.5 Hz, represents the coupling to the *exo*-methine proton at C-8 (3.51 p.p.m.) which is also coupled to the C-7 *exo*-proton with J = 8.5 Hz. The C-7 proton at 2.72 p.p.m. gives rise to a simple doublet with no further coupling > 0.3 Hz. The three methyl singlets at 1.37, 1.08, and 0.89 p.p.m. are assigned to the C-1, the *exo* C-5 and *endo* C-5 groups, respectively. Evidence of

[4]The *exo* and *endo* orientations are given relative to the C-2,3 bond.

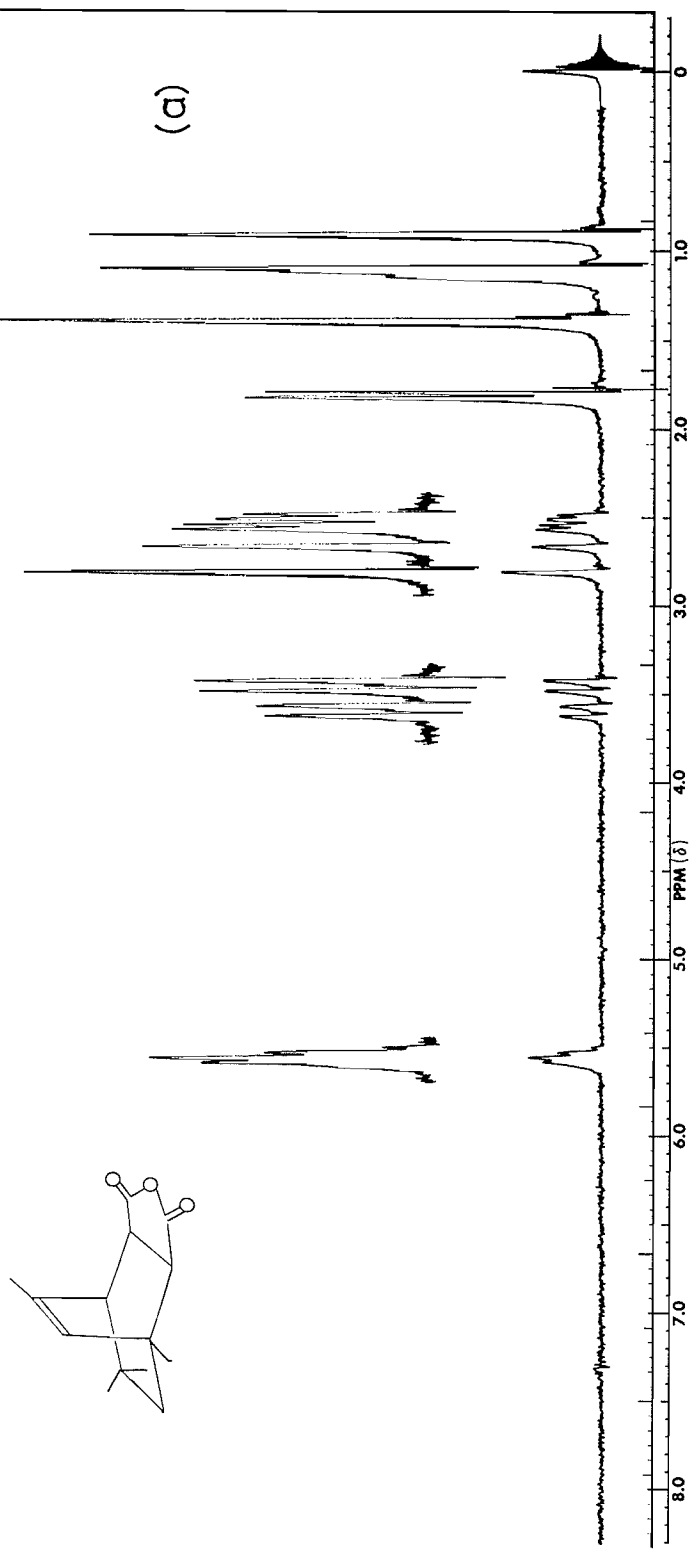

FIG. 1*a*. The 60 MHz spectra (5 mole % in $CDCl_3$) of compound **3** (sweep width 500 Hz).

Can. J. Chem. Downloaded from www.nrcresearchpress.com by 210.87.254.40 on 09/05/12
For personal use only.

Can. J. Chem. Downloaded from www.nrcresearchpress.com by 210.87.254.40 on 09/05/12
For personal use only.

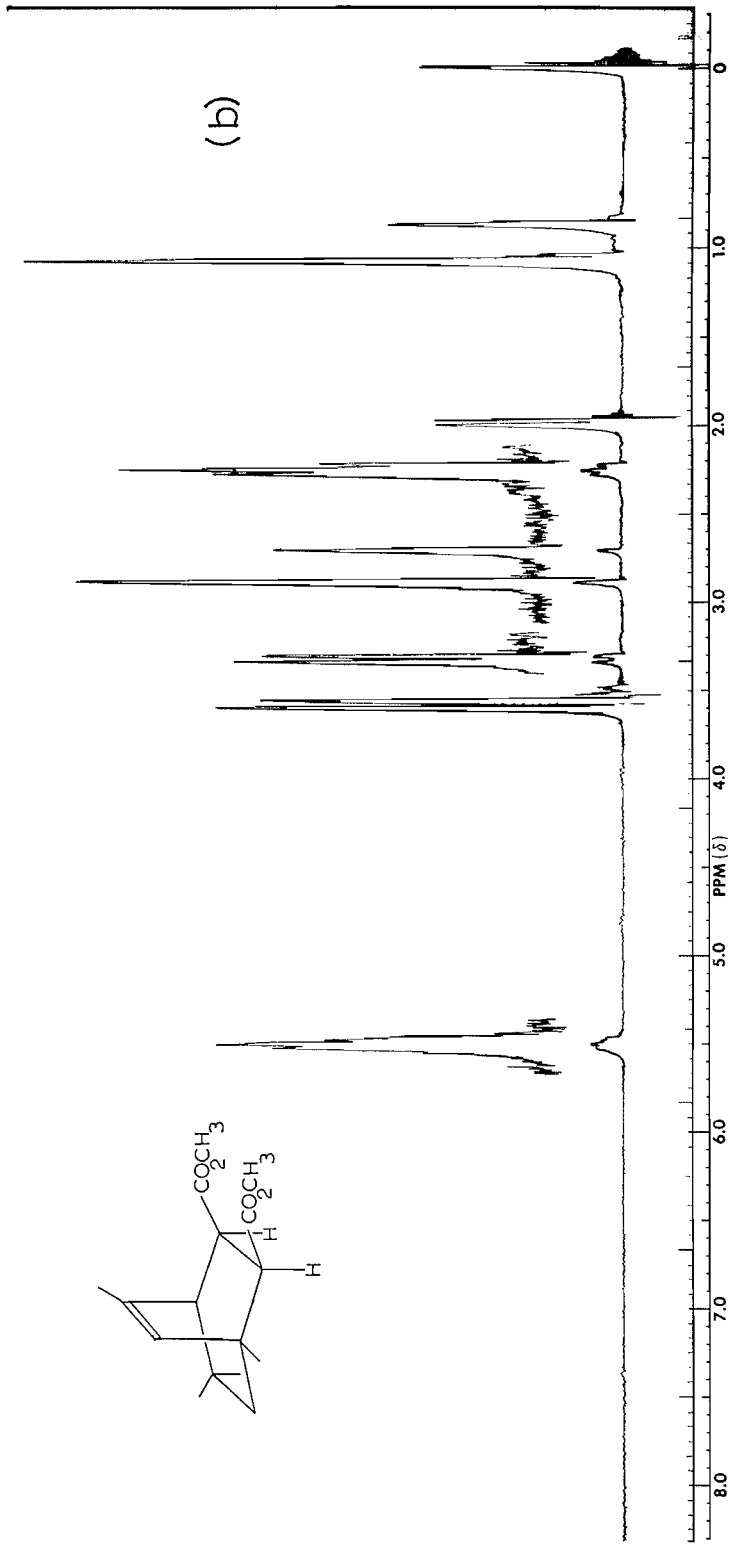

FIG. 1*b*. The 60 MHz spectra (5 mole % in $CDCl_3$) of compound **4** (sweep width 500 Hz).

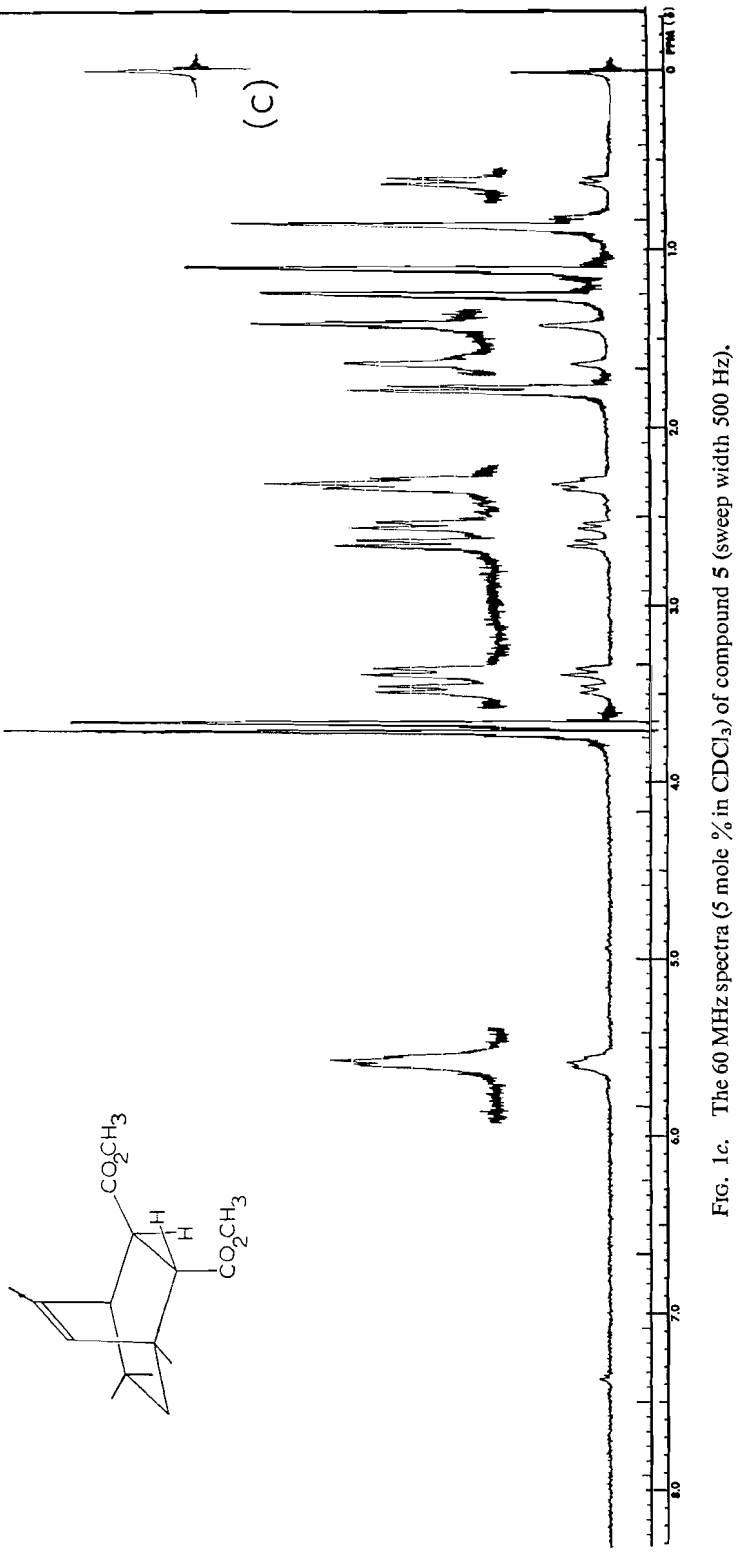

FIG. 1*c*. The 60 MHz spectra (5 mole % in $CDCl_3$) of compound **5** (sweep width 500 Hz).

Can. J. Chem. Downloaded from www.nrcresearchpress.com by 210.87.254.40 on 09/05/12
For personal use only.

Can. J. Chem. Downloaded from www.nrcresearchpress.com by 210.87.254.40 on 09/05/12
For personal use only.

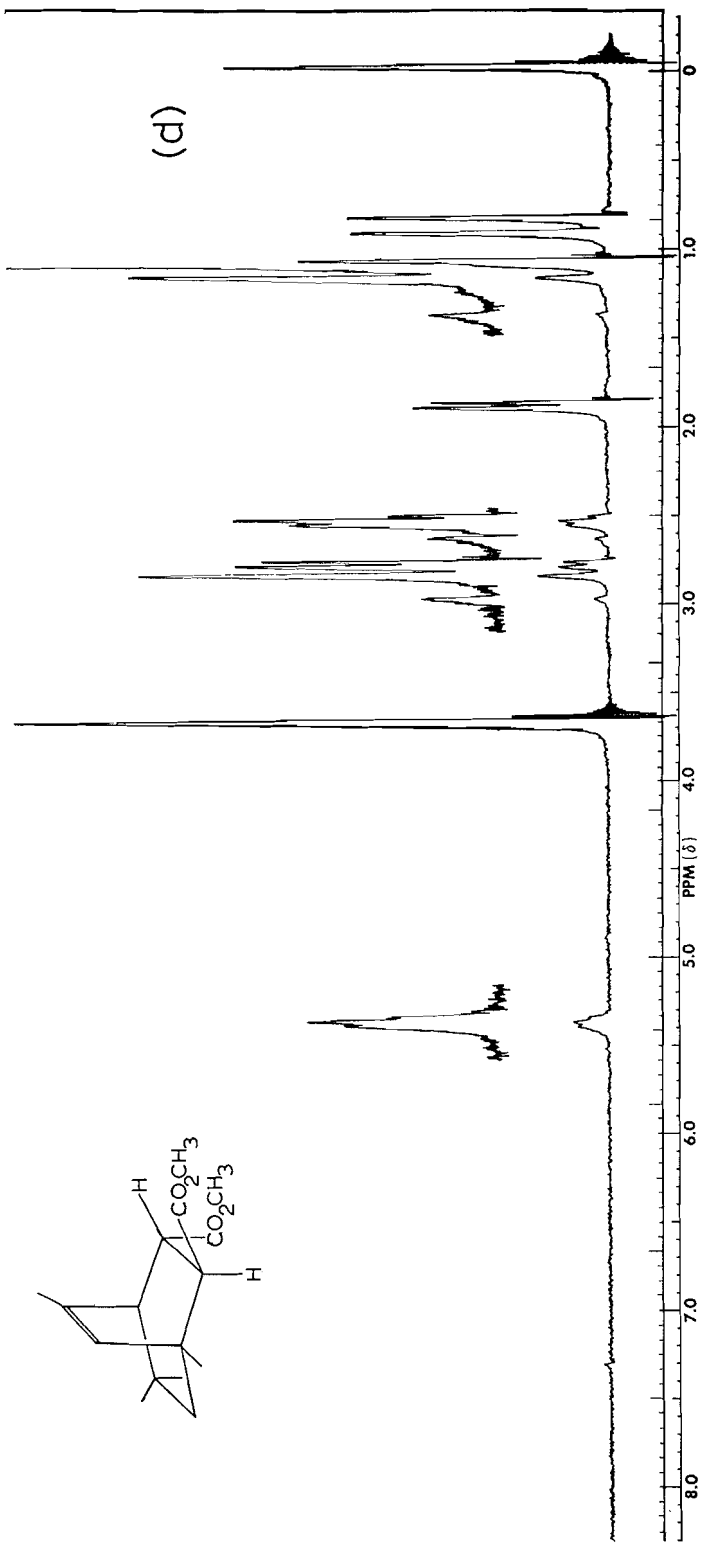

FIG. 1*d*. The 60 MHz spectra (5 mole % in $CDCl_3$) of compound **6** (sweep width 500 Hz).

Can. J. Chem. Downloaded from www.nrcresearchpress.com by 210.87.254.40 on 09/05/12
For personal use only.

long-range coupling between the C-5 methyl protons is provided by the fact that their signals are somewhat broader than that for the C-1 group. Proof that the latter is correctly assigned was obtained by a nuclear Overhauser experiment (13) in which the intensity of the 5.57 p.p.m. signal increases by ca. 14 ± 3% upon saturation of the 1.37 p.p.m. signal.[5] In each case one of these three methyl signals is sharper than the others, which allows a ready assignment for the C-1 methyl group. Recent literature provides ample support for the observation of coupling between geminal methyl groups (14, 15). The assignment of the C-5 methyls follows from the assumption that the olefinic bond will tend to shield the *endo*-methyl preferentially (3, 4). Although this is not unequivocal, these assignments do not affect the arguments presented for the other protons. For **3** the signals due to the C-6 methylene protons remain. In Fig. 1*a*, the inner two lines of the AB pattern are discernible on the low-field side of the 1.08 p.p.m. signal. At 100 MHz, three of the four lines of this pattern appear separately and the analysis is straightforward.

The spectral interpretation for the corresponding dimethyl ester **4** (Fig. 1*b*) follows directly from that just described. Apart from the additional signals at 3.57 and 3.54 p.p.m. for the carbomethoxyl protons, the order of the signals is as expected with some change in the relative shifts and small changes in some of the coupling constants. In Fig. 1*b* only the outer pair of lines of the C-6 methylene AB pattern are visible but an expanded sweep reveals one of the inner lines on the high-field side of the 1.08 p.p.m. signal. The bridgehead methyl protons (on C-1) are at significantly higher field in **4** and coincide with, presumably, the *exo* C-5 methyl band.

Diester **5** exhibits a readily interpretable pattern (Fig. 1*c*) which has one additional coupling, namely, that between one of the C-6 protons (*endo*, 0.73 p.p.m.) and the C-7 proton (*endo*, 2.60 p.p.m.). The remaining C-6 proton appears as a slightly broadened doublet at 1.51 p.p.m., J = 12.9 Hz. For **6**, the proton spectrum (Fig. 1*d*) differs slightly in that the positions of the C-7 and C-8 protons are reversed and the C-4 proton absorbs very close to these nuclei. A three-spin analysis, allowing for the long range coupling to the olefinic proton, however, was readily accomplished.

The complete set of chemical shift data for compounds **3–6** is collected in Table I while the coupling constants are listed in Table III.

The data for the saturated compounds **7–12** were extracted from the spectra in a similar fashion and the results are collected in Tables II (chemical shifts) and III (coupling constants). Since a number of comparisons failed to show significant solvent effects on the coupling constants only a single set of data is listed for each compound.

Chemical Shifts

Since all compounds were studied in $CDCl_3$ solutions these data are considered first. The olefinic proton (C-2) appears to be deshielded by an *endo* C-8 carbomethoxyl group and shielded by an *endo* C-7 carbomethoxyl group, both effects being ca. 0.1 p.p.m. Presumably this is mainly due to the relative orientation of the > C=O bond with respect to the C-2 proton. The fact that the bridgehead proton at C-4 is different in **4** and **5** suggests that the rotation of the —COOMe moiety is affected by a *cis* vicinal carbomethoxyl. A comparison for this proton in **5** and **6** suggests that the *exo* carbomethoxyl group deshields the bridgehead proton by ca. 0.2 p.p.m., while the same comparison for **9** and **10** yields a smaller difference, 0.12 p.p.m. It seems clear that the orientation of the carbonyl bond in the anhydrides is such that its effect at the bridgehead position is small, 0.1 and 0.2 p.p.m. for the olefins and saturated derivatives, respectively. In the γ-lactones, however, the C-4 proton is deshielded by ca. 0.4 p.p.m. presumably by the carbonyl bond, cf. **11** vs. **8** and **12** vs. **9**. On the other hand, the same comparison indicates that the α-proton on C-8 is *shielded* by the carbonyl bond in the lactones. These observations lend support to the recent proposal of Karabatsos (16) that a model for the anisotropic effect of a carbonyl group such as I serves to explain the observed shifts for neighboring protons more

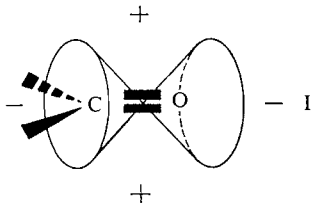

[5]This experiment was done with a degassed, chloroform solution at ambient temperature.

Can. J. Chem. Downloaded from www.nrcresearchpress.com by 210.87.254.40 on 09/05/12
For personal use only.

TABLE I

Proton shifts in some 7,8-disubstituted 1,3,5,5-tetramethylbicyclo[2·2·2]oct-2-enes (p.p.m. from TMS; 5 mole % solutions)

				C-6		C-7		C-8				C-5Me		
Compound	Solvent	C-2	C-4	*exo*	*endo*	*exo*	*endo*	*exo*	*endo*	C-1Me	C-3Me	*exo*	*endo*	OMe
	$CDCl_3$	5.57	2.51	1.24	1.15	2.72	—	3.51	—	1.37	1.80	1.08	0.89	—
3	CCl_4	5.51	2.46	*	*	2.63	—	3.42	—	1.35	1.79	1.09	0.89	—
	C_6H_6	5.14	2.21	*	*	1.98	—	2.79	—	1.22	1.59	0.67	0.57	—
	$CDCl_3$	5.47	2.23	1.12	0.98	2.80	—	3.38	—	1.08	1.97	1.08	0.87	{3.54 3.57
4	CCl_4	5.37	2.18	1.08	0.97	2.69	—	3.26	—	1.03	1.93	1.07	0.85	{3.48 3.51
	C_6H_6	5.48	2.21	*	*	2.76	—	3.28	—	1.05	2.03	0.87	0.78	{3.39 3.43
	$CDCl_3$	5.57	2.31	1.51	0.73	—	2.60	3.42	—	1.11	1.77	1.24	0.86	{3.65 3.70
5	CCl_4	5.49	2.24	1.48	0.67	—	2.46	3.29	—	1.07	1.74	1.23	0.84	{3.59 3.66
	C_6H_6	5.43	2.37	1.66	0.69	—	2.85	3.62	—	1.10	1.79	1.32	0.81	{3.30 3.36
	$CDCl_3$	5.38	2.54	1.24	1.05	2.90	—	—	2.75	1.08	1.89	0.93	0.84	3.68(2)
6	CCl_4	5.30	2.47	1.21	0.98	2.77	—	—	2.64	1.05	1.90	0.90	0.83	{3.61 3.64
	C_6H_6	5.31	2.55	1.13	0.93	3.00	—	—	2.93	1.07	1.77	0.92	0.76	{3.39 3.42

*Obscured by C—Me absorption.

Can. J. Chem. Downloaded from www.nrcresearchpress.com by 210.87.254.40 on 09/05/12
For personal use only.

TABLE II

Proton shifts in some 7,8-disubstituted 1,3,5,5-tetramethylbicyclo[2·2·2]octanes (p.p.m. from TMS; 5 mole % solutions)

Compound	Solvent	C-4	C-6*		C-7*		C-8*		C-1Me	C-3Me	C-5Me		OMe
			exo	*endo*	*exo*	*endo*	*exo*	*endo*			*exo*	*endo*	
7	$CDCl_3$	1.72	1.15	1.26	2.74	—	3.44	—	1.12	0.97	1.07	1.07	—
	CCl_4	1.68	1.13	1.24	2.69	—	3.38	—	1.11	0.98	1.11	1.11	—
8	$CDCl_3$	1.70	†	†	2.56	—	3.24	—	0.87	1.03	1.07	1.07	3.63, 3.67
	CCl_4	1.64	†	†	2.44	—	3.20	—	0.84	0.98	1.08	1.08	3.59(2)
	C_6H_6	1.69	†	†	2.54	—	3.17	—	0.84	1.19	0.91	0.91	3.39, 3.57
9	$CDCl_3$	1.56	†	†	—	2.71	3.32	—	0.84	n.a.‡	n.a.‡	n.a.‡	3.72(2)
	CCl_4	1.55	1.12	0.82	—	2.61	3.19	—	0.83	n.a.‡	n.a.‡	n.a.‡	3.64(2)
10	$CDCl_3$	1.68	†	†	2.81	—	—	3.22	0.80	1.09	1.05	1.05	3.66, 3.70
	CCl_4	1.62	†	†	2.70	—	—	3.10	0.76	1.16	1.01	0.84	3.62, 3.64
	C_6H_6	1.77	†	†	3.01	—	—	3.48	0.81	1.12	0.96	0.98	3.34, 3.44
11	$CDCl_3$	2.07	1.33	1.21	2.64	—	2.92	—	0.93	1.57	1.11	1.08	3.67
	C_6H_6	1.49	†	†	2.72	—	2.45	—	0.80	1.27	0.69	0.64	3.49
12	$CDCl_3$	1.97	†	†	—	2.44	3.01	—	1.02	1.56	1.18	1.10	3.72
	CCl_4	1.89	†	†	—	2.32	2.90	—	0.99	1.52	1.16	1.08	3.69
	C_6H_6	1.42	†	†	—	2.37	3.07	—	0.77	1.24	1.02	0.68	3.26

*_exo_ and _endo_ refer to the orientation with respect to the C-2,3 bond for convenience.
†Obscured by C—Me absorption.
‡n.a. = not assigned.

TABLE III

^1H–^1H Coupling constants for some 7,8-disubstituted derivatives of 1,3,5,5-tetramethylbicyclo[2·2·2]octanes (in Hz)

Compound	Geminal*	Vicinal*							Long-range*					
									Allylic					
	J_{66}	$J_{3,4}$	$J_{Me\text{-}3}$	$J_{4,8x}$	$J_{4,8n}$	$J_{7x,8x}$	$J_{7x,8n}$	$J_{7n,8x}$	$J_{2,4}$	$J_{Me\text{-}2}$	$J_{2,7x}$	$J_{3,8x}$	$J_{6n,7n}$	$J_{2,6x}$
3	13.0	—	—	3.5	—	8.5	—	—	1.5	1.8	—	—	—	—
4	13.7	—	—	2.0	—	10.9	—	—	1.7	1.6	—	—	—	—
5	12.9	—	—	2.0	—	—	—	5.9	1.7	1.6	—	—	2.0	—
6	13.0	—	—	—	1.9	—	8.5	—	1.5	1.8	—	—	—	—
7	†	2.0	7.5	3.5	—	10.8	—	—	—	—	2.3	1.2	—	†
8	†	2.2	7.2	2.3	—	11.9	—	—	—	—	2.2	1.8	—	†
9	13.5	—	6.8	1.2	—	—	—	8.3	—	—	—	—	1.6	†
10	†	1.5	6.7	—	1.5	—	9.9	—	—	—	1.8	—	—	†
11	†	—	—	4.4	—	9.7	—	—	—	—	1.5	—	—	1.6
12	13.7	—	—	4.3	—	—	—	2.1	—	—	—	—	2.0	†

*Subscripts refer to the numbering of the skeleton as set out in **1**.
†Obscured by methyl absorption.

Can. J. Chem. Downloaded from www.nrcresearchpress.com by 210.87.254.40 on 09/05/12
For personal use only.

successfully than that originally suggested (17). According to this model the relatively high-field position of the *endo* C-7 proton in **12** relative to that in **9** must be due in large part to the fixed carbonyl bond in the γ-lactone.

The remaining feature of the data in Tables I and II concerns the effect of solvent on these proton shieldings. It is interesting that there is a general tendency for the proton on or near the olefinic bond or the carbomethoxyl groups to move to higher field in CCl_4 solutions relative to their position in $CDCl_3$ solutions, while the C—Me protons are little affected. In addition, the solvent shifts in benzene are not particularly striking except for those cases having a rigidly fixed carbonyl bond, e.g., the anhydride, **3**, and the γ-lactones, **11** and **12**. This behavior is typical of solutes which tend to associate with aromatic solvents, a subject that has received wide-spread attention and has recently been reviewed (18). In the present system the solvent shifts, $\delta_H^{CDCl_3} - \delta_H^{C_6H_6}$, for these three cases suggest a preferred orientation of the benzene solvent molecules such that certain protons are strongly shielded while others are less affected. For example, in the case of **3**, the protons on C-7 and C-8 are shifted ca. 0.7 p.p.m. to higher field while the others move from +0.15 to +0.43 p.p.m. It is interesting that the C-8 proton shifts +0.47 p.p.m. in **11** but −0.06 p.p.m. in **12** while the C-4 proton is the most shielded, +0.58 and +0.45 p.p.m., respectively. Thus it appears that the solvent molecules are oriented about the carbonyl bond in different ways.

Coupling Constants

(a) Geminal Interactions

Throughout this series the only geminal interaction in common is that for the C-6 methylene protons which is found to be 13.3 ± 0.4 Hz. These values, presumably negative, indicate that there is little strain in the ring system since these differ only slightly from those for methane and other unstrained sp^3-carbons (20). Comparable values, 13.7 ± 0.1 Hz have been reported for similar systems (19).

(b) Vicinal Interactions

A variety of vicinal interactions occurs in the present series and those readily and reliably measured are set out in Table III. These may be considered on the basis of the well-known results of the Karplus treatment (21) for vicinal couplings. While one expects a dependency upon molecular geometry it is well-established that ring-strain and substituent electronegativity also contribute to the magnitude of these couplings (22, 23). Evidence of the effect of ring strain is provided by a comparison of the $J_{7,8}$ values for **3** vs. **4** and **7** vs. **8**. For each, J increases by ca. 1 Hz on opening the anhydride ring. A similar increase is found upon hydrogenation of the double bond, **4** vs. **8**. These changes are comparable to those reported by Tori *et al.* (19) and Roll and Huitric (24) for related systems and to those found for norbornyl systems (22). Presumably these are due to a redistribution of ring strain, assuming that the substituent effect of the anhydrido group is comparable to that of the COOMe. Thus it appears that $J_{7,8} \sim 12$ Hz for a dihedral angle of 0° in this system. The marked decrease in $J_{7,8}$ to 9.7 Hz for the lactone ester **11** must be due in part to the enforced departure from a dihedral angle near 0° because of the formation of the γ-lactone, although part of the decrease may arise from strain.

A dihedral angle of ca. 120° for $J_{7,8}$ is to be expected for **5**, **6**, **9**, **10** but inspection of Table III reveals a range of 4 Hz from 5.9–9.9 Hz. Of the four cases, however, **5** seems the most likely to have a dihedral angle of 120° since in each of the others the C-8 carbomethoxyl group has a "1,3-diaxial" interaction with either a hydrogen atom at C-3 (**9**) or the *exo*-methyl at C-5 (**6** and **10**) while **9** has a similar interaction between the C-3 and -5 methyls as well. Presumably these steric interactions can be reduced by a slight twist of the skeleton. If in a counter-clockwise sense for **9** (as viewed along the C-7,8 bond, Fig. 2) the dihedral angle between the C-7 and C-8 protons will increase from 120° and the dihedral angle between the C-4 and -8 protons will also increase. A comparison of $J_{7,8}$ and $J_{4,8}$ for **5** and **9** shows differences consistent with this rationalization. On the other hand, a clockwise twist of the skeleton for **6** and **10** leads to comparable changes in these dihedral angles. Other evidence to suggest that the *trans* coupling is ca. 6 Hz for the undistorted structure is given by the values for the less cluttered system **13** (1) and **14** (19), both of which have J = 6.0 Hz. Finally, the coupling of 2.1 Hz found for $J_{7,8}$ in **12** is in good agreement with the preceding interpretation since the formation of the γ-lactone between the C-8 carboxyl and C-3 must reduce the dihedral angle

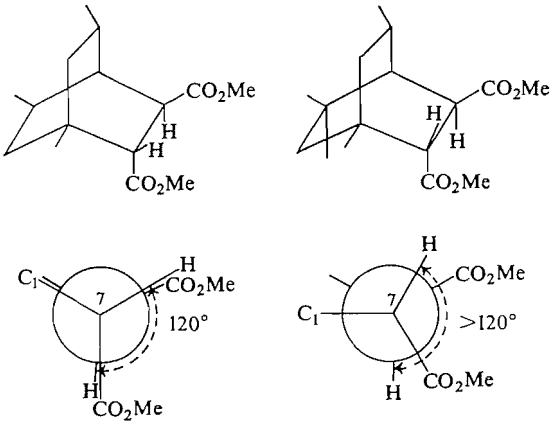

FIG. 2. Diagrammatic representation of the effect of twisting the bicyclo[2·2·2]octane skeleton to reduce non-bonded interactions between neighboring substituents in compound **9**.

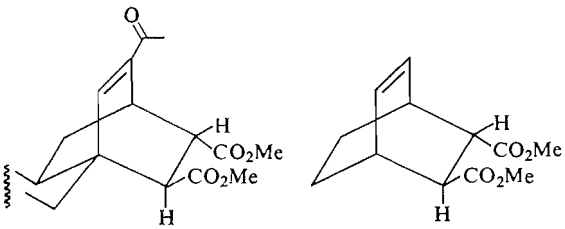

13 **14**

between the C-7 and C-8 protons. As in **11**, however, part of the decrease in the coupling constant may be due to strain.

Dihedral angles near 60° must obtain for the $J_{3,4}$ and $J_{4,8}$ interactions even though these values range from 1.2–4.4 Hz. The larger of these, $J_{4,8}$ for the γ-lactones, are readily rationalized since the formation of the γ-lactone serves to reduce the dihedral angle between the C-4 and *exo* C-8 protons and an inspection of models indicate that it may be as small as 45°. Although models do not reveal an appreciable angle change upon formation of the anhydride the observed $J_{4,8}$ of 3.5 Hz indicates a decrease from 60°. As already noted, the twist illustrated in Fig. 2 tends to increase the dihedral angle between a C-4 proton and an *endo* C-8 proton as in **10** which has $J_{4,8} = 1.5$ Hz. Thus it appears that, for a dihedral angle of 60°, the coupling is ca. 2 Hz in the bicyclooctanes which agrees well with the values found for a number of cases in monocyclic unstrained systems (23). It should be noted that the larger values for $J_{4,8}$ exhibited by the anhydrides and γ-lactones may be reduced somewhat due to a contribution by the strain factor and so it seems unwise to use these couplings to estimate the dihedral angles in these systems.

(c) Long-range Coupling Constants

In the present series two types of long-range interactions are resolved. The first of these is the allylic coupling, H—C—C=C—H, between the C-2 and C-4 protons and between the C-3 methyl protons and the C-2 H. The latter appear to be ca. 0.1 Hz larger. This interaction has attracted many workers and the overall situation was surveyed in 1964 (25). More recently Newsoroff and Sternhell have proposed certain modifications of the current notions on the steric dependence of these couplings (26). The present $J_{2,4}$ values represent examples in which the interacting protons lie in a common plane in a *transoid* configuration. The observed J values of 1.6 ± 0.1 Hz suggest, on the basis of their recent proposal, that the predicted values for this configuration are too low, assuming that the present values are positive, since their curves predict a value of ca. 1 Hz. The present data are in good agreement with those reported by Tori *et al.* (19).

Long-range proton–proton couplings across four single bonds have been recognized for some time and it is well-known that the maximum coupling occurs through a "W" arrangement (5, 6) such that in cyclohexanes 1,3-diequatorial protons are more strongly coupled than either of the corresponding diaxial or axial-equatorial protons. It follows for the bicyclo[2·2·2]octane system that the largest couplings can be expected for an interaction such as that between the 6-*endo* and 7-*endo* protons. The cases in which these 4-bond couplings have been identified are listed in the last four columns of Table III. As mentioned earlier, certain of these permit the assignment of substituent orientation in these derivatives. For example, only one of the bicyclooctenes exhibited a long-range coupling of this type, **5**. This allows an easy distinction between the two *trans* diesters since only the C-7 proton can assume the appropriate orientation. Following a similar argument the fact that the C-8 proton in **7** has a long-range coupling of 1.2 Hz indicates that hydrogenation occurs on the side of the olefinic bond *away* from the *endo*-anhydride grouping. Also the absence of this coupling in **9** indicates that hydrogenation of **5** occurs *anti* to the *endo* C-5 methyl. It seems reasonable to suggest that the

Can. J. Chem. Downloaded from www.nrcresearchpress.com by 210.87.254.40 on 09/05/12
For personal use only.

markedly smaller value for $J_{3,8}$ in **7** is a consequence of the strain imparted by the anhydride grouping. Unfortunately the lack of a long-range coupling for the C-8 proton in **10** does not aid the assignment of stereochemistry for the C-3 methyl group. The orientation of the C-3 methyl group for **10** has been assigned on the basis of the pronounced shift for the *endo* C-8 proton upon hydrogenation of **6** relative to that exhibited by the *endo*-C-7 proton for the change **5** → **9**, a difference of > 0.3 p.p.m.

Conclusion

On the basis of the foregoing results, it seems clear that proton spectroscopy can facilitate the elucidation of stereochemistry in the bicyclo-[2·2·2]octane system, but a certain degree of caution is necessary to avoid misinterpretations as the authors of recent reports on the spectra of the bicyclo[2·2·1]heptenes have emphasized (27–29).

Acknowledgments

We wish to thank the National Research Council of Canada and the donors of the Petroleum Research Fund, administered by the American Chemical Society, for financial support of this investigation. We are also indebted to Mrs. Mary Warren for some preliminary experiments and to Dr. G. W. Buchanan for his efforts, albeit unsuccessful, to isomerize adduct **3** to its *cis–exo* form.

1. W. A. AYER, C. E. MCDONALD, and J. B. STOTHERS. Can. J. Chem. **41**, 1113 (1963).
2. M. KARPLUS. J. Am. Chem. Soc. **85**, 2870 (1963).
3. R. R. FRASER. Can. J. Chem. **40**, 78 (1962).
4. S. YAMAGUCHI, S. OKUDA, and N. NAKAGAWA. Bull. Pharm. Chem. (Tokyo), **11**, 1465 (1963).
5. S. STERNHELL. Rev. Pure Appl. Chem. **14**, 15 (1964).
6. W. A. THOMAS. Ann. Rev. NMR Spectroscopy. *Edited by* E. F. Mooney. Academic Press, London. 1968. pp. 78–82.
7. M. S. KHARASCH and P. O. TAWNEY. J. Am. Chem. Soc. **63**, 2308 (1941).
8. A. I. VOGEL. A textbook of practical organic chemistry. 3rd ed. Longmans, Green and Co., Ltd., London. 1961.
9. P. PINO and A. MIGLIERINA. J. Am. Chem. Soc. **74**, 5551 (1952).
10. K. ALDER and G. STEIN. Angew. Chem. **50**, 510 (1937).
11. GURUDATA. Unpublished observations.
12. G. W. BUCHANAN. Unpublished observations.
13. F. A. L. ANET and A. J. R. BOURN. J. Am. Chem. Soc. **87**, 5250 (1965).
14. VON PASCUAL and W. SIMON. Helv. Chim. Acta. **50**, 94 (1967).
15. W. J. NIJS. Rec. Trav. Chim. **86**, 220 (1967).
16. G. J. KARABATSOS, G. C. SONNICHSEN, N. HSI, and D. J. FENOGLIO. J. Am. Chem. Soc. **89**, 5067 (1967).
17. L. M. JACKMAN. Applications of nuclear magnetic resonance spectroscopy in organic chemistry. Pergamon Press, London. 1959. p. 124.
18. P. LASZLO. Progress in NMR spectroscopy. Vol. 3. *Edited by* J. W. Emsley, J. Feeney, and L. Sutcliffe. Pergamon Press, London. 1967. Chap. 6, p. 348 ff.
19. K. TORI, Y. TAKANO, and K. KITAHONOKI. Ber. **97**, 2798 (1964).
20. R. C. COOKSON, T. A. CRABB, J. J. FRANKEL, and J. HUDEC. Tetrahedron Supp. No. 7, 355 (1966).
21. M. KARPLUS. J. Chem. Phys. **30**, 11 (1959).
22. P. LASZLO and P. VON R. SCHLEYER. J. Am. Chem. Soc. **86**, 1171 (1964).
23. A. A. BOTHNER-BY. Advances in magnetic resonance. Vol. 1. *Edited by* J. S. Waugh. Academic Press, New York. 1965. p. 228 ff.
24. D. B. ROLL and A. C. HUITRIC. J. Pharm. Sci., **54**, 1110 (1965).
25. E. W. GARBISCH. J. Am. Chem. Soc. **86**, 5561 (1964).
26. G. P. NEWSOROFF and S. STERNHELL. Tetrahedron Letters, 6117 (1968).
27. F. A. L. ANET, H. H. LEE, and J. L. SUDMEIER. J. Am. Chem. Soc. **89**, 4431 (1967).
28. B. FRANZUS, W. C. BAIRD, JR., H. F. CHAMBERLAIN, T. HINES, and E. I. SNYDER. J. Am. Chem. Soc. **90**, 3721 (1968).
29. A. P. MARCHAND and J. E. ROSE. J. Am. Chem. Soc. **90**, 3724 (1968).
30. S. H. GROVER and J. B. STOTHERS. J. Am. Chem. Soc. **91**, 4331 (1969).

Can. J. Chem. Downloaded from www.nrcresearchpress.com by 210.87.254.40 on 09/05/12
For personal use only.

Can. J. Chem. Downloaded from www.nrcresearchpress.com by 210.87.254.6 on 09/05/12
For personal use only.

Signs of spin–spin coupling constants between aldehydic and ring protons in 2,6-dinitrobenzaldehyde. Evidence for a hyperconjugative contribution to $J_p^{H,CHO}$

C. L. BELL[1,2], S. S. DANYLUK, AND T. SCHAEFER[1,3]
Argonne National Laboratory, Argonne, Illinois 60439

Received May 12, 1969

The spin–spin coupling constant between the aldehydic proton and the proton in the para position, $J_p^{H,HCO}$ is negative in 2,6-dinitrobenzaldehyde. $J_p^{H,CHO}$ is also very likely negative in 2,6-dichlorobenzaldehyde. It is suggested that steric interaction with the ortho substituents forces the aldehyde group out of a coplanar conformation and leads to an interaction of the aldehydic C–H bond with the π system of the ring. Tentative values of θ, a measure of the deviation from coplanarity, are given.

Canadian Journal of Chemistry, 47, 3529 (1969)

Introduction

The negative spin–spin coupling constants, J_o^{H,CH_3} and J_p^{H,CH_3}, between methyl protons and ring protons in the ortho and para positions of toluene (1) and its derivatives (2–4) are apparently dominated by a π electron mechanism (5, 6) and involve hyperconjugation in the ground state of the molecule (7). On the other hand, the positive couplings over five bonds, $J_m^{H,CHO}$, $J_m^{H,OH}$, $J_m^{H,NHX}$, $J_m^{H,CHCl_2}$ in the derivatives of benzaldehyde, phenol, *N*-substituted aniline, and α,α-dichlorotoluene are thought to occur by a different mechanism (8–11). The evidence for this conclusion involves the "CH_3 replacement" technique (12), the fact that the couplings are the largest when the intervening bonds take up a coplanar "zig-zag" arrangement (13, 14), and the surmise that $J_p^{H,CHO}$ is positive in some benzaldehyde derivatives (15).

In benzaldehyde itself $J_p^{H,CHO} = -0.04$ Hz (16). In α,α,2,6-tetrachlorotoluene $J_p^{H,CHCl_2}$ is zero to within experimental error (11). Rate studies by nuclear magnetic resonance (n.m.r.) (11, 17) suggest that in both molecules at room temperature, the C–H bonds of the sidechain flip rapidly between two equivalent conformations in which they lie coplanar with the aromatic ring. Since the π electron mechanism for this coupling predicts that $J_p^{H,XH} \propto \cos^2\theta$, where θ is the angle between the H—X—C_1 plane and the pπ orbital on the C-1 carbon atom of the aromatic ring, the occurrence of small or zero couplings $J_p^{H,CHO}$, $J_p^{H,OH}$, and $J_p^{H,NHX}$ could therefore be a consequence of the preponderance of the coplanar conformations of these groups when bonded to the benzene ring. Coupling of hydroxyl or amino protons to ring protons is observed only when the hydroxyl or amino protons are held in a coplanar conformation by intramolecular hydrogen bonds (10, 18). Otherwise intermolecular proton exchange makes such couplings unobservable in a slow passage experiment.

The aldehydic proton is less easily exchanged and the presence of sufficiently large ortho substituents may well result in a time-averaged nonplanar conformation of the carbonyl groups. Hyperconjugation between the C–H bond of the carbonyl group and the aromatic π system might then lead to a measurable, *negative* value of $J_p^{H,CHO}$.

In this paper the signs of $J_m^{H,CHO}$ and $J_p^{H,CHO}$ relative to J_o^{HH} in 2,6-dinitrobenzaldehyde are determined by double resonance techniques. The results are discussed in terms of the coupling mechanisms indicated above.

Experimental

Sufficient acetone was added to benzene-d_6 to ensure complete solubility of an approximately 20 mole % solution of 2,6-dinitrobenzaldehyde. Proton double resonance experiments (19, 20) on this solution could be interpreted unequivocally because the proton single resonance spectrum was a loosely coupled A_2BX system. A solution of 2,6-dinitrobenzaldehyde in acetone only was also examined in order to determine solvent effects, if any, on the long-range coupling constants. Single proton resonance spectra were also measured on solutions of 2,6-dichlorobenzaldehyde and of 3,5-dichlorobenzaldehyde in benzene-d_6 and in carbon disulfide, respectively.

---

[1]Visiting summer scientist, 1968.
[2]Permanent address: University of Illinois, Medical Center, Chicago.
[3]Permanent address: University of Manitoba, Winnipeg, Manitoba.

Can. J. Chem. Downloaded from www.nrcresearchpress.com by 210.87.254.6 on 09/05/12
For personal use only.

Tetramethylsilane (TMS) served as an internal reference and as a lock signal in the frequency-sweep mode of a DA-60I Varian spectrometer. Solutions were degassed by the freeze–pump–thaw technique. The benzaldehyde derivatives were obtained from Aldrich Chemical Company.

Results

Signs and Magnitudes of the Long-range Couplings

The proton resonance of 2,6-dinitrobenzaldehyde at 60 MHz is a loosely coupled A_2BX spectrum. For the present purpose the ring proton single resonance spectrum is best displayed schematically, as in Fig. 1. Each of the eight peaks in the A_2B spectrum is split into a doublet by coupling to the aldehydic proton. The 16 transitions in Fig. 1 are labelled with plus or minus signs to indicate the spin states of the other nuclei. A low-field transition of a given nucleus, when labelled with a plus sign for the spin state of another nucleus, corresponds to a positive coupling between these two nuclei.

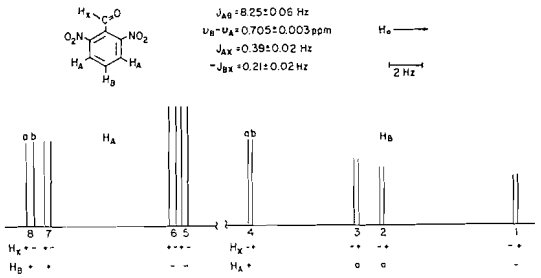

FIG. 1. A stick diagram of the ring proton magnetic resonance spectrum at 60 MHz of 2,6-dinitrobenzaldehyde in a benzene – acetone solvent. The spin states of the coupled protons are indicated by plus and minus signs with the convention that a plus sign under a low-field peak indicates a positive coupling constant to the proton in question.

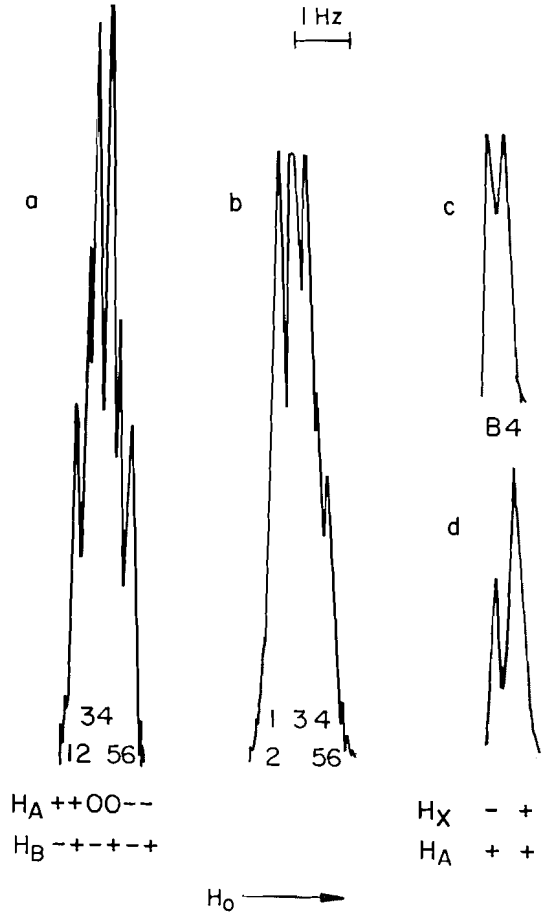

FIG. 2. In *a*) is shown the proton magnetic resonance spectrum of the aldehydic proton of 2,6-dinitrobenzaldehyde under the conditions of Fig. 1. In *b*) the transitions 4*a* and 4*b* of H_B in Fig. 1 are being irradiated leading to collapse of peaks 1 and 2 of the aldehydic proton resonance. In *c*) the single resonance spectrum of transitions 4*a* and 4*b* of H_B is displayed. In *d*) transition 4*a* decreases in intensity when 8*b* of Fig. 1 is weakly irradiated.

In Fig. 2*a*, the single proton resonance spectrum of the aldehydic proton is shown. The triplet of doublets expected for the X part of a loosely coupled A_2BX spectrum is clearly resolved. Simultaneous irradiation of transitions 4*a* and 4*b* in Fig. 1 collapses transitions 1 and 2 of the aldehydic proton resonance as displayed in Fig. 2*b*. This partial decoupling experiment demonstrates that $J_{AB}/J_{AX} > 0$.

In Figs. 2*c* and 2*d* there is shown the result of a generalized Overhauser experiment of the type described by Kaiser (20). This experiment determines the connected transitions in a spin system in a way closely related to the "tickling" experiment originated by Freeman and Anderson (19). In the Overhauser experiment the amplitude of the second radiofrequency field is smaller than in the tickling experiment. As a consequence, the connected transitions change in intensity instead of splitting into doublets. In the present work the Overhauser experiment is more easily performed because γH_2 can be kept small enough so as not to perturb noticeably a transition while its neighbour a few tenths of a Hz away is being irradiated. In Fig. 2*c* the single resonance of transitions 4*a* and 4*b* of H_B is shown while in Fig. 2*d*, the intensity of transition 4*a* of H_B decreases when transi-

FOR ERRATA SEE
V. 48 NO. 17 1970 P 3284

Can. J. Chem. Downloaded from www.nrcresearchpress.com by 210.87.254.6 on 09/05/12
For personal use only.

tion 8*b* of H_A in Fig. 1 is weakly irradiated. No change is noted in the signal intensity of 4*b*. Irradiation of 8*a* of H_A on the other hand, causes a decrease in intensity of transition 4*b* of H_B, while 4*a* is unchanged. Hence $J_{AX}/J_{BX} < 0$.

Finally, the A_2BX spectrum was analyzed by the method of effective Larmor frequencies and gave the parameters shown below.[4]

$$\nu_A = 7.958 \pm 0.005 \text{ p.p.m.}$$
$$\nu_B = 7.253 \pm 0.005 \text{ p.p.m.}$$
$$\nu_X = 10.318 \pm 0.005 \text{ p.p.m.}$$
$$J_{AB} = J_o^{HH} = 8.25 \pm 0.06 \text{ Hz}$$
$$J_{AX} = J_m^{H,CHO} = 0.39 \pm 0.02 \text{ Hz}$$
$$J_{BX} = J_p^{H,CHO} = -0.21 \pm 0.02 \text{ Hz}$$

The proton coupling constants of 2,6-dinitrobenzaldehyde are the same within experimental error in the two solvents, benzene and acetone.

2,6-Dichlorobenzaldehyde

In dilute benzene-d_6 solution the proton resonance spectrum is that of a rather tightly coupled A_2BX system with $J_{AB}/(\nu_B - \nu_A) = 0.653$. In this situation the relevant peak spacings are too small to allow for a reliable sign determination by double resonance techniques. However, in a tightly coupled A_2BX spectrum, any asymmetry in the X part of the spectrum indicates that the three coupling constants are not of the same sign (21). The aldehydic proton resonance was not symmetric about its midpoint. Because $J_m^{H,CHO}$ values in 2,6-dichlorobenzaldehyde; 2,6-dinitrobenzaldehyde; 2,4,6-trinitrobenzaldehyde[5]; and in benzaldehyde itself (16) are equal within experimental error, the negative sign is assigned to $J_p^{H,CHO}$ in 2,6-dichlorobenzaldehyde. A normal A_2BX analysis results in the following parameters for 2,6-dichlorobenzaldehyde

$$\nu_A = 6.595 \pm 0.005 \text{ p.p.m.}$$
$$\nu_B = 6.378 \pm 0.005 \text{ p.p.m.}$$
$$\nu_X = 10.130 \pm 0.003 \text{ p.p.m.}$$
$$J_{AB} = J_o^{HH} = 8.46 \pm 0.06 \text{ Hz}$$
$$J_{AX} = J_m^{H,CHO} = 0.40 \pm 0.03 \text{ Hz}$$
$$J_{BX} = J_p^{H,CHO} = -0.15 \pm 0.02 \text{ Hz}$$

3,5-Dichlorobenzaldehyde

A 15 mole % solution in carbon disulfide gives an A_2BX spectrum in which the aldehydic proton resonates as a single peak of line width at half height of 0.21 ± 0.01 Hz. Similarly, the antisymmetric transition of the para proton shows a single peak whose width at half height is equal to 0.20 ± 0.01 Hz. Any observed splitting of this peak is precisely equal to $J_p^{H,CHO}$ (21). From the width of this peak and from its intensity relative to the other resonance peaks of the para proton, an estimate of $|J_p^{H,CHO}| < 0.07$ Hz is obtained.[6] The parameters are then as follows

$$\nu_A = 7.660 \pm 0.005 \text{ p.p.m.}$$
$$\nu_B = 7.489 \pm 0.005 \text{ p.p.m.}$$
$$\nu_X = 9.883 \pm 0.003 \text{ p.p.m.}$$
$$J_{AB} = 1.93 \pm 0.06 \text{ Hz}$$
$$|J_{AX}| = J_o^{H,CHO} \lesssim 0.10 \text{ Hz}$$
$$|J_{BX}| = J_p^{H,CHO} < 0.07 \text{ Hz}$$

Discussion

$J_p^{H,CHO}$ and Hyperconjugation

The sizeable magnitude and negative sign of $J_p^{H,CHO}$ in the 2,6-disubstituted benzaldehyde is in agreement with a hyperconjugative mechanism similar to that proposed for J_p^{H,CH_3} in toluene derivatives (1, 4, 7). It is here suggested that one may write

$$[1] \qquad J_p^{H,CHO} \propto Q_{CH}Q_{CCHO}$$

where $Q_{CH} < 0$ is the hyperfine interaction constant for a C–H bond and $Q_{CCHO} > 0$ is proportional to $\cos^2\theta$ in a manner similar to Q_{CCH} in toluene derivatives (4). The maximum magnitude of Q_{CCHO} (when $\cos^2\theta = 1$) is not known but the value of $J_p^{H,CHO} = -0.04$ Hz in benzaldehyde implies $Q_{CCHO} \approx 0$ when $\theta = \pi/2$ (the lifetime of the CHO group in the planar conformation is some orders of magnitude larger than for nonplanar conformations (17, 22)).

If it is now assumed that Q_{CCHO} is of similar magnitude to Q_{CCH}, an estimate of the mean value of θ in 2,6-dichloro- and 2,6-dinitrobenzaldehyde can be made. In effect we use an equation of the type

$$[2] \qquad \cos^2\theta = (J(\pi/2) - J)/(J(\pi/2) - J(o))$$

where $J(\pi/2)$ and $J(o)$ are the respective J values for coplanar and orthogonal conformations of the formyl group relative to the plane of the aromatic ring. The methyl group in toluene rotates rapidly (23) and hence $\langle\cos^2\theta\rangle = 1/2$.

[4]The shift parameters are those in the mixed solvent of benzene – acetone.

[5]Unpublished work in this laboratory.

[6]In spectra whose linewidths are no smaller than here, a splitting of 0.10 Hz has been easily observed in this laboratory.

Can. J. Chem. Downloaded from www.nrcresearchpress.com by 210.87.254.6 on 09/05/12
For personal use only.

But $J_p^{H,CH_3} = -0.62$ Hz in toluene (1) and therefore $J_p^{H,CH_3} = -1.2$ Hz for $\theta = 0$. If a similar value of $J_p^{H,CHO}$ for $\theta = 0$ is assumed, i.e., $Q_{CCHO} \approx Q_{CCH}$, then it follows that $\theta = 65°$ and 70° in the nitro and chloro compounds, respectively.

Steric hindrance by the ortho substituents would therefore cause a deviation of 20–25° from a planar conformation of the aldehyde groups. The similar magnitude of θ in the two compounds is reasonable because the larger nitro groups can relieve steric strain by twisting out of plane. The present tentative values of θ are in disagreement with a previous assumption, $\theta = 0$, in the dichloro compound (24).

Dipole moment data (25) suggest that while two ortho methyl groups do not hinder the mesomerism of the CHO group, it is almost completely repressed by two ortho bromine substituents. The effective steric sizes of bromine and methyl are here evidently quite different even though their van der Waals radii are considered to be nearly equal (26). The value of $\theta = 70°$ in 2,6-dimethylbenzaldehyde deduced from the electronic spectrum (27) conflicts with the dipole moment data. Consequently, these results cannot be used to confirm or reject the assumptions underlying our values of θ.

On the other hand, ^{13}C chemical shifts of the carbonyl group yield $\theta = 72$–82° in 2,6-dichloroacetophenone and $\theta = 74$–78° in 2-chloroacetophenone (28). On steric grounds smaller values of θ are expected in 2,6-dichlorobenzaldehyde. In that event the θ value obtained by us is presumably a maximum value.

The techniques mentioned above all use equations of the type [2]. Measurements of electrical birefringence do not depend on eq. [2]. These measurements demonstrate that in 9-formylanthracene (29) a value of $\theta = 73°$ is reasonable. The steric interaction here is with the peri hydrogens.

It would clearly be of interest to measure $J_p^{H,CHO}$ and ^{13}C shifts in more strongly hindered benzaldehydes. Kerr effect studies should also prove informative, as would studies of the electron spin resonance spectra of the appropriate ion radicals.

Finally, the implicit assumption that $J_p^{H,CHO}$ is independent of other than steric properties of the substituent is in agreement with the unobservably small values of $J_p^{H,CHO}$ in 3,5-dichlorobenzaldehyde above, in 3,5-dimethoxylbenzaldehyde[7], and in 3,5-dichlorosalicylaldehyde (18), where the CHO group is clearly in a planar conformation for times approaching seconds (18). Also, J_p^{H,CH_3} is independent of substituents in a large number of toluene derivatives.[7]

$J_m^{H,CHO}$ and the Coupling Mechanism

The present results are in accord with earlier multiple resonance (8) measurements which showed that $J_m^{H,CHO}$ is positive. Replacement of the hydrogen atom by a methyl group in CHO leads to a nonobservable value of $J_m^{H,COCH_3}$ and strongly indicates the absence of a π electron contribution to $J_m^{H,CHO}$ (12). Furthermore, $J_m^{H,CHO}$ is stereospecific. Thus, it couples to H_A but not to H_B in **1** where the intramolecular hydrogen bond

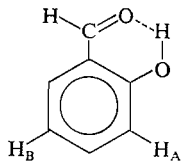

1

holds the CHO group in a coplanar conformation. A σ electron mechanism is again indicated. Contributions by σ electrons to proton–proton couplings over five bonds are predicted theoretically (30).

A π contribution to $J_m^{H,CHO}$ cannot be ruled out completely, however, for nonplanar conformations of the CHO group and could account for the similarity of the couplings in benzaldehyde (0.37 Hz), 2,6-dinitrobenzaldehyde (0.39 Hz), 2,6-dichlorobenzaldehyde (0.40 Hz), and 2,4,6-trinitrobenzaldehyde (0.39 Hz).[5] An additional influence upon $J_m^{H,CHO}$ may result from substituent effects (31) acting primarily via the σ electron system. Clearly, the magnitude of $J_m^{H,CHO}$ is affected by a number of factors whose elucidation requires additional studies currently underway.

1. M. P. Williamson, R. J. Kostelnik, and S. M. Castellano. J. Chem. Phys. **49**, 2218 (1968).
2. G. Kotowycz and T. Schaefer. Can. J. Chem. **44**, 2743 (1966).
3. D. Gagnaire and Trinh-Huu-Ich. Bull. Chem. Soc. Fr. 3763 (1966).
4. D. J. Blears, S. S. Danyluk, and T. Schaefer. J. Chem. Phys. **47**, 5037 (1967).
5. H. M. McConnell. J. Chem. Phys. **30**, 126 (1959).
6. H. M. McConnell. J. Mol. Spectrosc. **1**, 11 (1957).

[7]Unpublished work in one of our laboratories (T.S.).

7. M. J. S. DEWAR and R. C. FAHEY. J. Amer. Chem. Soc. **85**, 2704 (1963).
8. S. FORSÈN, T. ALM, B. GESTBLOM, S. RODMAR, and R. A. HOFFMAN. J. Mol. Spectrosc. **17**, 13 (1965).
9. S. FORSÈN and R. A. HOFFMAN. J. Mol. Spectrosc. **20**, 168 (1966).
10. J. A. WEIL, A. BLUM, A. H. WEISS, and J. K. KINNAIRD. J. Chem. Phys. **46**, 3132 (1967).
11. T. SCHAEFER, R. SCHWENK, C. J. MACDONALD, and W. F. REYNOLDS. Can. J. Chem. **46**, 2187 (1968).
12. R. A. HOFFMAN and S. GRONOWITZ. Ark. Kemi. **16**, 471 (1960).
13. S. STERNHELL. Rev. Pure Appl. Chem. **14**, 15 (1964).
14. G. P. NEWSEROFF and S. STERNHELL. Australian J. Chem. **21**, 747 (1968).
15. D. G. DE KOWALEWSKI and V. J. KOWALEWSKI. Mol. Phys. **9**, 331 (1965).
16. S. CASTELLANO in W. Brügel. Nuclear magnetic resonance spectra and chemical structure. Vol. 1. Academic Press, Inc., New York. 1967.
17. F. A. L. ANET and M. AHMAD. J. Amer. Chem. Soc. **86**, 119, (1964).
18. T. SCHAEFER and G. KOTOWYCZ. Can. J. Chem. **46**, 2865 (1968).
19. R. FREEMAN and W. A. ANDERSON. J. Chem. Phys. **37**, 2053 (1962).
20. R. KAISER. J. Chem. Phys. **39**, 2435 (1963).
21. P. DIEHL and J. A. POPLE. Mol. Phys. **3**, 557 (1960).
22. A. H. MAKI and D. H. GESKE. J. Amer. Chem. Soc. **83**, 1852 (1961).
23. H. RUDOLPH, H. DREIZLER, A. JOESCHKE, and P. WENDLING. Z. Naturforsch. **22***a*, 940 (1967).
24. G. KARABATSOS and F. M. VANE. J. Amer. Chem. Soc. **85**, 3886 (1963).
25. J. W. SMITH. *In* Steric effects in conjugated systems. *Edited by* G. W. Gray. Academic Press, Inc., New York. 1958.
26. L. PAULING. Nature of the chemical bond. 3rd ed. Cornell Univ. Press, Ithaca, N.Y. 1960.
27. E. A. BRAUDE and F. SONDHEIMER. J. Chem. Soc. 3754 (1955).
28. K. S. DHAMI and J. B. STOTHERS. Can. J. Chem. **43**, 479 (1965).
29. R. J. W. LEFÈVRE, L. RADOM, and G. L. D. RITCHIE. J. Chem. Soc. **B**, 775 (1968).
30. H. FRISCHLEDER and G. BÄR. Mol. Phys. **11**, 359 (1966).
31. S. CASTELLANO and R. KOSTELNIK. J. Amer. Chem. Soc. **90**, 141 (1968).

Can. J. Chem. Downloaded from www.nrcresearchpress.com by 210.87.254.6 on 09/05/12
For personal use only.

Calculation of "Dewar" resonance energies in conjugated organic molecules

N. C. BAIRD
Department of Chemistry, University of Western Ontario, London, Ontario.
Received February 3, 1969

Dewar's recent definition of resonance energy (1) for hydrocarbons is extended to molecules containing oxygen, and resonance energy values are calculated from experimental heats of formation for a variety of conjugated organic compounds. A simple additivity scheme is proposed whereby resonance energies and heats of formation can be accurately estimated for benzenoid systems.

Canadian Journal of Chemistry, 47. 3535 (1969)

Can. J. Chem. Downloaded from www.nrcresearchpress.com by 210.87.254.105 on 09/05/12
For personal use only.

Introduction

On the basis of semiempirical molecular orbital calculations, Dewar and co-workers (1) have established that the *effective* energies of the "double" and "single" bonds in acyclic conjugated polyenes are independent of the chain length and chain branching. Consequently, Dewar has proposed that these effective bond energies be used in calculating the "expected" bonding energies for the classical structures of cyclic, conjugated hydrocarbons (1). The *Dewar Resonance Energy* (DRE) for a ring system then represents the extent to which conjugation occurs in *excess* of that operative in a corresponding open-chain polyene. If cyclic systems with zero DRE are defined as non-aromatic, then a positive DRE value for a molecule indicates that it is aromatic, and a negative DRE indicates that it is anti-aromatic.

The purpose of this note is to extend Dewar's definition to conjugated molecules containing oxygen, and to indicate that DRE values can be accurately calculated for polycyclic systems by a completely empirical additivity scheme. The additivity scheme should be useful in calculating heats of formation of molecules belonging to homologous series for which insufficient thermochemical data is available to provide an accurate extrapolation.

Calculation of Dewar Resonance Energies

The bonding energies, E, at 25°C of compounds $C_mH_nO_p$ are evaluated using the heats of formation (ΔH_f) of gaseous carbon, hydrogen, and oxygen atoms, and the ΔH_f of the compound:

$$E = m\,\Delta H_f(C^{\cdot}) + n\,\Delta H_f(H^{\cdot}) + p\,\Delta H_f(O^{\cdot}) - \Delta H_f(C_mH_nO_p)$$

Use of the recent JANAF ΔH_f values for atoms (2) leads to the equation (for E in kcal/mole)

$$E = 170.89\,m + 52.10\,n + 59.56\,p - \Delta H_f(C_mH_nO_p)$$

The resonance energies are computed from E by subtracting the sum of the "effective" C=C, C—C, C=O, C—O, C—H, and O—H bond energies evaluated from model acyclic systems (Table I). The C(sp^2)—H and O—H energies in Table I are calculated from the ΔH_f values of +34.1 and −57.8 kcal/mole for the methyl radical (3) and the water molecule (2) respectively. The C=C and C=O energies are then deduced from the ΔH_f's of ethylene of +12.50 kcal/mole (4) and of formaldehyde of −27.7 kcal/mole (5). Finally, the *effective* C(sp^2)—C(sp^2) and C(sp^2)—O single bond energies are computed from the bond energies above and the ΔH_f's for *trans*-butadiene of +26.33 kcal/mole (4) and for divinylether of −3.03 kcal/mole (6). The C=C and C—C bond energies in Table I differ significantly from those determined by Dewar (1*a*), since we consider the methyl radical to belong to the general series of unsaturated hydrocarbons, and hence we derive E(C—H) from its thermochemistry rather than by recourse to a "best fit" procedure.

TABLE I

Effective bond energies (kcal/mole)

Bond	Energy
C(sp^2)—H	97.7
O—H	110.8
C=C	146.9
C—C (polyene)	89.9
C=O	167.0
C—O	89.4

TABLE II

Dewar resonance energies (kcal/mole)

Compound	ΔH_f	Source	Dewar resonance energy: From ΔH_f	Dewar resonance energy: From additivity
Hydrocarbons				
benzene	+19.82	4	+21.5	+21
fulvene	+47.5	12‡	−0.2*	(0)
styrene	+35.22	4	+19.9	+21
stilbene	+54.8	1*b*	+43.0	+42
biphenyl	+43.52	13	+40.5	+42
1,3,5-triphenylbenzene	+82.9	14	+86.4	+84
naphthalene	+35.99	13	+34.2	+33.5
anthracene	+55.17	13	+43.9	+46
phenanthrene	+49.46	13	+49.6	+50
pyrene	+52.5	1*b*	+61.6	+58
naphthacene	+67.41	15	+60.5	+58.5
3,4-benzophenanthrene	+69.35	15	+58.6	+62.5
1,2-benzanthracene	+66.69	15	+61.2	+62.5
chrysene	+62.58	15	+65.3	+62.5
triphenylene	+61.26	15	+66.7	+63
perylene	+75.6	1*b*	+67.4	+67
9,9′-bianthryl	+112.99	15	+86.4	+92
9,10-diphenylanthracene	+105.41	15	+78.9	+88
9,9′-biphenanthryl	+86.68	15	+112.7	+100
acenaphthylene	+61.7	16	+29.6*	(+33.5)
fluoranthene	+70.4	16	+49.7*	(+55)
azulene	+71.1	17	+11.1*	—
cyclooctatetraene	+69.5	18	−14.4†	—
[18]-annulene	+67	19	+57.0†	—
heptafulvene	~+57	12,15,20§	~+4*	(0)
Oxygen compounds				
furan	−8.293	5	+12.5*	+12.5
phenol	−23.05	5	+21.4	+21
diphenylether	+11.9	21	+42.7	+42
dibenzofuran	+18.2	21	+43.7*	+42
benzaldehyde	−6.0	5	+20.9	+21
p-benzoquinone	−29.4	14,20	+4.1	0
benzophenone	+12.2	14,20	+45.3	+42
formic acid	−90.49	5	+19.8	+21
benzoic acid	−72	14	+44.0	+42
tropolone	−39.8	14	+11.8	(0)

*A strain correction of 6 kcal/mole for each five- or seven-membered ring is used in calculation of this value (see text).

†A ring-strain correction may be necessary here, but none is applied (see text).

‡Estimated from the ΔH_f for dimethylfulvene quoted by C. T. Mortimer (12) and corrected for the methyl groups by comparing the ΔH_f of isobutene with that of ethylene.

§Estimated from the heat of hydrogenation for heptafulvene quoted by Mortimer (12), and a heat of formation of methylcycloheptane calculated from the ΔH_f for cycloheptane (15), and the group equivalent values given in (20).

The calculated DRE values in Table II include results for both hydrocarbons and oxygen-containing molecules. The latter series can be included since we have shown elsewhere (7) that C═O and C—O bonds in polyenones and conjugated alcohols and ethers are "localised" according to Dewar's definition (1*a*). Note that the DRE values for molecules containing five- and seven-membered rings are for the "strainless" molecule, since a strain energy correction of 6 kcal/mole (8) per ring has been added to the experimental bonding energies. Small strain energy corrections should probably also be applied to the DRE values for cyclooctatetraene and for [18]-annulene, but have not been applied due to the uncertainty of the magnitude of these effects. Finally, no corrections for steric strain have been attempted.

Results and Discussion

The DRE for the benzenoid hydrocarbons (Table II) parallel their conventional resonance energy values (8) but are significantly smaller. For example, the DRE value for benzene is approxi-

Can. J. Chem. Downloaded from www.nrcresearchpress.com by 210.87.254.105 on 09/05/12
For personal use only.

Can. J. Chem. Downloaded from www.nrcresearchpress.com by 210.87.254.105 on 09/05/12
For personal use only.

mately 60% of the 36 kcal/mole usually quoted for its resonance energy. As expected from Dewar's arguments (1), the DRE values for benzenoid ring systems are not increased by the presence of side chains or rings linked by "localized" bonds. For example, the DRE's of styrene, phenol, and benzaldehyde are virtually identical to the value for benzene, and those for stilbene, biphenyl, diphenylether, and benzophenone are all close to twice that of benzene. The DRE for formic acid is substantial, in agreement with the existence of relatively short C—O "single" bonds in such molecules (9). Since the DRE in benzoic acid is close to the sum of that for formic acid and that for benzene (Table II), the conjugation between the ring and the carboxyl group here is very similar to that across the "single" bonds in polyolefins.

Of the cyclic, nonbenzenoid molecules listed in Table II, large, positive DRE's are found only for rings containing $4N + 2\pi$ electrons, or for several rings bonded together containing a total of $4N + 2\pi$ electrons (e.g. azulene). The value for [18]-annulene (i.e. $N = 4$) is quite large, in agreement with the fact that the bonds in this molecule are of aromatic length (10). The value for cyclooctatetraene, a $4N\pi$ electron hydrocarbon, is *negative* due to a loss of conjugation across the single bonds in this nonplanar molecule, angular strain in the eight-membered ring, and the slight anti-aromatic nature of the system.

Additivity of Dewar Resonance Energies

An analysis of the DRE listed in Table II for benzenoid systems indicates that this quantity is *additive* for these molecules in the sense that it can be accurately estimated from their classical structures by the use of a few, simple empirical rules. For neutral, *closed-shell* molecules of this type, the following additive contributions have been derived:

(*i*) Zero from chains containing an even number of conjugated atoms, and similarly for "one-membered" chains.

(*ii*) For rings which contribute 6π electrons and in which the double bonds are conjugated 1,3 (or 1,3,5) to each other, a given double bond contributes to the DRE in *only one ring*, even if it is formally shared between rings in the classical structure. The total DRE of a polycyclic benzenoid compound can be calculated by writing the classical structure with the double bonds "within" one ring or the other, and summing the following contributions:

Benzene ring with 3 double bonds written within it = 21 kcal/mole.

Benzene or furan ring with 2 double bonds written within it = 12.5 kcal/mole.

Benzene or furan ring with 1 double bond written within it = 8 kcal/mole.

Benzene or furan ring with 0 double bond written within it = 0 kcal/mole.

(*iii*) The carboxyl group 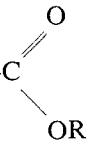 contributes 21 kcal/mole.

The DRE values calculated from these group contributions are compared with the experimental values in Table II. In those cases for which more than one nonequivalent classical structure can be written, that giving to the largest DRE is used. For example, the resonance energy for

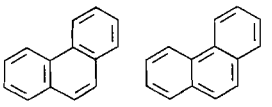

1*a* **1***b*

phenanthrene structure **1***b* of 12.5 + 21 + 12.5 = 46 kcal/mole is less than that of 21 + 8 + 21 = 50 kcal/mole for structure **1***a*, and consequently the latter value is used.

In almost all the cases listed in Table II, the agreement between the experimental DRE values and those derived from additivity rules is very good. The root mean square (r.m.s.) deviation between these values is only ± 2.2 kcal/mole, which compares very favorably with the r.m.s. error of ± 4.0 kcal/mole[1] by the most accurate molecular orbital theories (1).

Given the DRE contributions for chains and benzene rings, the contributions to the total DRE of a molecule made by rings with $4N + 1$ and $4N + 3\pi$ electrons can be assessed. Such contributions are listed in Table III, and were evaluated by subtracting the additive benzenoid contribution to the DRE (values in brackets in

[1]In computing the r.m.s. values, only benzenoid compounds which are both included in Table II and have been calculated by Dewar and co-workers (1) are included.

TABLE III

DRE contributions from odd-membered rings

Compound	Contribution (kcal/mole)	Double bonds within ring
5-Membered rings		
fulvene	−0.2	2
acenaphthylene	−3.9	1
fluoranthene	−5.3	0
7-Membered rings		
heptafulvene	∼+4	3
tropolone	+11.8	3
5+7-Membered ring		
azulene	+11.1	5

Table II) from the experimental DRE's. Substantial positive contributions are found only in azulene (which has a $4N + 2\pi$ electron perimeter) and in tropolone.[2] Otherwise, five-membered rings make a small *negative* contribution to the overall DRE in molecules, and that for the remaining seven-membered ring is positive but small. These results are in agreement with the nonaromatic behavior of such ring components.

Applications

Using the empirical additivity rules, it is possible to derive accurate values for the DRE, and consequently the ΔH_f value, of various series of benzenoid hydrocarbons. For example, the DRE of linear polyacenes containing N fused benzene rings is equal to $12.5N + 8.5$ kcal/mole, compared to $12.5N + 12.5$ for the corresponding phenanthrene-type isomers, and $12.5N + 13$ for the triphenylene series. In the latter type, the classical structure which yields the largest DRE value is that with no double bonds written within the central triphenylene ring, in agreement with Clar's "hole" hypothesis (11) that such component rings make no contribution to the overall aromaticity of the system.

[2]See page 400 of reference 1*a* for a discussion of the aromaticity of such systems.

Acknowledgments

The author thanks Prof. M. J. S. Dewar for supplying preprints of several papers, and the National Research Council of Canada for financial support of this research.

1. (*a*) M. J. S. DEWAR. The molecular orbital theory of organic chemistry. McGraw-Hill Book Co., Inc., New York. 1969. Chapt. 5. (*b*) M. J. S. DEWAR and C. DE LLANO. J. Amer. Chem. Soc. **91**, 789 (1969). (*c*) M. J. S. DEWAR and G. J. GLEICHER. *ibid* **87**, 692 (1965).
2. JANAF thermochemical tables. Dow Chemical Co., Midland, Michigan. 1965.
3. D. M. GOLDEN, R. WALSH, and S. W. BENSON. J. Amer. Chem. Soc. **87**, 4053 (1965).
4. Selected values of physical and thermodynamic properties of hydrocarbons and related compounds. American Petroleum Institute Research Project 44. Carnegie Press, Pittsburgh, Penn. 1953.
5. L. H. S. GREEN. Quart. Rev. **15**, 125 (1961).
6. G. PILCHER, H. A. SKINNER, A. S. PELL, and A. E. POPE. Trans. Faraday Soc. **59**, 316 (1963).
7. N. C. BAIRD. Mol. Phys. In press.
8. A. STREITWIESER, JR. Molecular orbital theory for organic chemists. John Wiley and Sons, Inc., New York. 1961.
9. L. E. SUTTON, ed. Tables of interatomic distances and configurations in molecules and ions. Special Publications Nos. 11 and 18, The Chemical Society, London. 1958 and 1965.
10. J. BERGMAN, F. L. HIRSHFELD, D. RABINOVITCH, and G. M. J. SCHMIDT. Acta Cryst. **19**, 227 (1965).
11. (*a*) E. CLAR and M. ZANDER. J. Chem. Soc. 1861 (1958). (*b*) E. CLAR. Tetrahedron **6**, 355 (1959).
12. C. T. MORTIMER. Reaction heats and bond strengths. Pergamon Press, New York. 1962.
13. D. J. COLEMAN and G. PILCHER. Trans. Faraday Soc. **62**, 821 (1966).
14. G. W. WHELAND. Resonance in organic chemistry. John Wiley and Sons, Inc., New York. 1955.
15. H. A. SKINNER and G. PILCHER. Quart. Rev. **17**, 264 (1963).
16. R. H. BOYD, R. L. CHRISTENSEN, and R. PUA. J. Amer. Chem. Soc. **87**, 3554 (1965).
17. B. D. KYBETT, S. CARROLL, P. NATALIS, D. W. BONNELL, J. L. MARGRAVE, and J. L. FRANKLIN. J. Amer. Chem. Soc. **88**, 626 (1966).
18. H. D. SPRINGALL, T. R. WHITE, and R. C. CASS. Trans. Faraday Soc. **50**, 815 (1954).
19. A. E. BEEZER, C. T. MORTIMER, H. D. SPRINGALL, F. SONDHEIMER, and R. WOLOVSKY. J. Chem. Soc. 216 (1965).
20. H. E. O'NEAL and S. W. BENSON. J. Phys. Chem. **72**, 1866 (1968).
21. R. C. CASS, G. E. FLETCHER, C. T. MORTIMER, H. D. SPRINGALL, and T. R. WHITE. J. Chem. Soc. 1406 (1958).

Can. J. Chem. Downloaded from www.nrcresearchpress.com by 210.87.254.105 on 09/05/12
For personal use only.

Can. J. Chem. Downloaded from www.nrcresearchpress.com by 210.87.254.40 on 09/05/12
For personal use only.

Cinétique d'oxydation de la cyclohexanedione-1,2 par l'ion thallique[1]

R. Favier et M. Zador
Département de Chimie, Université de Montréal, Montréal, Québec

Reçu le 24 mars 1969

The kinetics of thallic ion oxidation of 1,2-cyclohexanedione in aqueous perchloric acid solutions lead to the rate expression

$$V = [\text{Enol}](k_{Tl}[Tl^{3+}] + k_{TlOH}[TlOH^{2+}] + k_{TlCl}[TlCl^{2+}])$$

The importance of traces of chloride ions has been shown. Rate constants and activation parameters has been determined and are discussed.

L'étude cinétique de l'oxydation de la cyclohexanedione-1,2 par le Tl(III) en solution aqueuse d'acide perchlorique a conduit à l'équation de vitesse

$$V = [\text{Enol}](k_{Tl}[Tl^{3+}] + k_{TlOH}[TlOH^{2+}] + k_{TlCl}[TlCl^{2+}])$$

L'importance de traces d'ions chlorure a été mise en évidence. Les constantes de vitesse et les paramètres d'activation sont déterminés et interprétés.

Canadian Journal of Chemistry, 47, 3539 (1969)

Introduction

L'oxydation des divers produits organiques par l'ion thallique a été réalisée au cours des dernières années (1).

Du point de vue cinétique, il est à noter le travail de Henry concernant l'oxydation des oléfines en milieu aqueux (2–4). Des essais effectués sur l'oxydation de la cyclohexanone par un excès d'ion thallique en milieu perchlorique nous ont montré qu'en fait, nous avions une série de réactions. Nous avons identifié comme une étape de cette série l'oxydation de la cyclohexanedione-1,2.

Des études cinétiques sur l'équilibre céto-énol de la cyclohexanedione-1,2 ont été effectuées (5); il s'avère de plus qu'à l'état solide la forme énolique est prépondérante. Dans ces conditions la vitesse mesurée est celle de l'oxydation et non pas celle de formation de l'énol comme dans le cas de l'oxydation de la cyclohexanone (6); on peut ainsi étudier le mécanisme de cette réaction.

L'ion thallique se trouve en solution sous forme partiellement hydrolysée et peut également former des complexes avec l'ion Cl^-: les différentes constantes de stabilité sont données dans la littérature (7).

Partie expérimentale

Réactifs

Le solvant est l'eau distillée. La solution thallique a été obtenue par dissolution de l'oxyde thallique (Fairmount Chemical Co. Inc.) dans l'acide perchlorique. Les titres des solutions, environ 0.1 *M*, ont été déterminés par iodométrie. Les solutions de cyclohexanedione-1,2 (J. T. Baker Chemical Co.) ont été fraîchement préparées pour chaque série d'expériences par dissolution du réactif solide dans l'eau distillée; les solutions ont été dosées par spectrophotométrie u.v. à $\lambda = 265$ mμ (5) et par le brome, montrant l'existence de la forme énolique à 95%. Les études infrarouge et r.m.n. des solutions de dione dans le tétrachlorure de carbone confirment la prédominance de la forme énolique.

Stoechiométrie

La stoechiométrie de la réaction a été étudiée en dosant d'une part par spectrophotométrie u.v. l'excès d'énol restant et d'autre part par dosage iodométrique de l'excès d'ions thallique. Dans les deux cas, on observe une stoechiométrie 1:1.

Identification des produits

Pour isoler le produit de la réaction on a procédé comme suit: à 500 ml de solution 0.1 *M* en Tl (III) en milieu acide perchlorique 3 *M*, on ajoute la quantité équivalente de cyclohexanedione-1,2 en gardant toutefois un très léger excès de l'oxydant pour être certain de consommer la totalité de la dione.

A cette concentration et à température d'environ 25 °C la réaction est presque instantanée et le perchlorate thalleux précipite. La solution est ensuite extraite en continu à l'éther ou chloroforme. Etant donné la très grande solubilité du produit dans l'eau même après une semaine on n'a pu extraire la totalité du produit. Les essais de concentration de la solution par distillation de l'eau n'ont pas donné de bons résultats probablement à cause de l'instabilité du produit.

La phase organique à finalement donné une phase liquide brune huileuse et une phase solide blanche dont la quantité variait entre 40–50% suivant le cas.

La phase solide blanche est très instable à l'air, plus stable lorsqu'on la conserve sous atmosphère d'azote.

[1]Présenté au 36ème Congrès annuel de l'Association Canadienne-Française pour l'Avancement des Sciences, Ottawa, Ontario, novembre 1968.

Can. J. Chem. Downloaded from www.nrcresearchpress.com by 210.87.254.40 on 09/05/12
For personal use only.

Compte tenu de son fort degré hydroscopique et de l'impossibilité de le sécher efficacement à cause de son instabilité, l'analyse élémentaire nous fournit des résultats trop grossiers. Après séchage sur plaque poreuse pendant quelques heures, le tout sous atmosphère d'azote, nous avons pu faire immédiatement les études spectrales. Nous l'avons identifié comme l'hydroxy-3, cyclohexanedione-1,2:

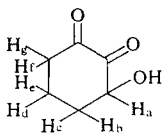

Le spectre de masse montre le poids moléculaire à $m/e = 128$ puis le départ du groupement CO nous donne $m/e = 100$ et suite au réarrangement de Mac Lafferty, le pic à $m/e = 55$, (8–10).

Le r.m.n., dans l'acétone deutérée montre un proton hydroxylique (pic aigu) à $\delta = 5.5$ qui disparaît dans D_2O. Puis le proton carbinolique H_a apparaît à $\delta = 2.3$. Les quatre protons H_b, H_c, H_f, H_g apparaissent dans un massif compris entre $\delta = 2.3$ et $\delta = 2$; enfin les protons H_e, H_d apparaissent à $\delta = 1.8$.

L'infra-rouge montre un OH large compris entre 3.200 cm^{-1} et 2.700 cm^{-1}. Les bandes C=O apparaissent à 1710 cm^{-1}, ainsi qu'une bande large à 1.100 cm^{-1} caractéristique de COH.

L'ultraviolet montre une bande d'absorption après quelques jours dans $HClO_4$ à 255 mμ, qui correspondrait à une forme énolique de l'hydroxy-3, cyclohexanedione-1,2.

Nous avons synthétisé un isomère possible du produit de la réaction le dihydroxy-2,3 cyclohexène-2 one-1 (ou dihydropyrogallol) d'après une méthode décrite auparavant (11). La comparaison des spectres de masse, i.r., u.v. et r.m.n. montre que cet isomère n'est pas le produit de la réaction (12). D'autres isomères 1,2,3 ainsi que l'hydroxy-3, cyclohexanedione-1,2 n'ont pas pu être synthétisés dû au manque de données dans la littérature. La phase brune huileuse de poids moléculaire 256 déterminé par osmométrie (301 Vapor Pressure Osmometer Hewlett–Packard, Mechrolab) représente, pensons-nous, le dimère de l'hydroxy-3, cyclohexanedione-1,2; cette tendance à la dimérisation semble être une caractéristique des cyclohexanediones (5). Les méthodes spectroscopiques n'ont pas pu nous conduire à la détermination de sa structure.

Méthodes cinétiques

La réaction a été suivie par enregistrement de l'augmentation de la transmission à la longueur d'onde $\lambda = 265$ mμ. La quantité x d'énol qui a réagi est donnée par l'expression $x = a(D_o - D)/D_o - D_\infty$ ou "a" est la concentration initiale d'énol "D_o", "D" et "D_∞" respectivement les densités optiques aux temps initial, "t" et infini. Les constantes de vitesses et les vitesses initiales ont pu être reproduites à 5% près.

La température a été maintenue constante à ± 0.1 °C et mesurée dans la cellule réactionnelle à l'aide d'un thermocouple.

La vitesse de transformation énol-cétone est négligeable dans nos conditions expérimentales.

L'oxygène de l'air, l'ion Tl (I) n'ont aucune influence sur la réaction.

Les forces ioniques ont été maintenues constantes par $LiClO_4$ (Alfa Organic, Inc.). Compte tenu de l'influence importante des traces d'ions chlorure sur notre réaction, celui-ci a été dosé par la méthode au thiocyanate mercurique (13). Dans nos conditions expérimentales, les solutions de $LiClO_4$ contenaient 1.5×10^{-5} M d'ions chlorure alors que les solutions de perchlorate de sodium (G. Frederick Smith Chemical, Co.) en contenaient 2.10^{-4} M.

Resultats

Equation de vitesse

Notre étude cinétique a permis d'obtenir l'équation de vitesse:

$$[1] \qquad V = k_{exp}[Tl(III)][E]$$

où $[E]$ est l'énol, [Tl(III)] la concentration du thallium à l'état d'oxydation (III). Le graphe de l'équation intégrée est présenté dans la Fig. 1 à plusieurs concentrations en ion thallique et en énol et l'ordre deux global est vérifié. Toutefois, la constante de vitesse d'ordre 2 diminue légèrement avec des concentrations croissantes en ion thallique ce qui nous a amené à penser que cette perturbation était due aux traces d'ions étrangers dans nos solutions. L'étude de l'influence de l'ion Cl^- sur la vitesse de réaction a permis de constater l'effet catalytique mesurable de celui-ci à partir d'une concentration de 10^{-5} M.

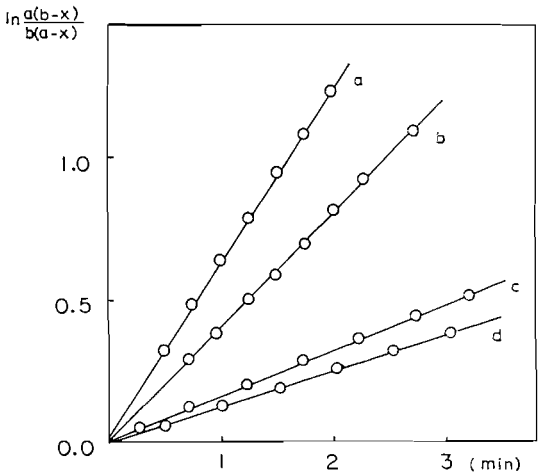

FIG. 1. Equation intégrée d'ordre deux: $T = 25$ °C; $[H^+] = 0.50$ M; force ionique $\mu = 1.0$; a) [Tl(III)] = 7.5×10^{-4} M; [Enol] = 1.0×10^{-4} M; $k_{exp} = 1.0 \times 10^3$ mol^{-1} 1 min^{-1}; b) [Tl(III)] = 5×10^{-4} M; [Enol] = 1.0×10^{-4} M; $k_{exp} = 1.1 \times 10^3$ mol^{-1} 1 min^{-1}; c) [Tl(III)] = 2.5×10^{-4} M; [Enol] = 1.0×10^{-4} M; $k_{exp} = 1.2 \times 10^3$ $mole^{-1}$ 1 min^{-1}; d) [Tl(III)] = 2.5×10^{-4} M; [Enol] = 1.5×10^{-4} M; $k_{exp} = 1.3 \times 10^3$ $mole^{-1}$ 1 min^{-1}.

TABLEAU I

Détermination des constantes de vitesse k_0 et k_{TlCl}*

T = 11.4 °C				T = 25 °C			
$[H^+]$ mole l^{-1}	[Tl(III)] mole l^{-1}	$[Cl^-]$ mole l^{-1}	Vi/[E] min^{-1}	$[H^+]$ mole l^{-1}	[Tl(III)] mole l^{-1}	$[Cl^-]$ mole l^{-1}	Vi/[E] min^{-1}
0.1	$1.0\ 10^{-4}$		0.14	0.1	$1.0\ 10^{-4}$		0.25
	$2.5\ 10^{-4}$		0.28		$2.5\ 10^{-4}$		0.48
	$5.0\ 10^{-4}$		0.44		$5.0\ 10^{-4}$		1.00
	$2.5\ 10^{-4}$	$2.0\ 10^{-5}$	0.32		$2.5\ 10^{-4}$	$2.0\ 10^{-5}$	0.52
	$2.5\ 10^{-4}$	$5.0\ 10^{-5}$	0.37		$2.5\ 10^{-4}$	$5.0\ 10^{-5}$	0.62
	$2.5\ 10^{-4}$	$1.0\ 10^{-4}$	0.45		$2.5\ 10^{-4}$	$1.0\ 10^{-4}$	0.76
0.5	$1.0\ 10^{-4}$		0.08	0.5	$1.0\ 10^{-4}$		0.12
	$6.0\ 10^{-4}$		0.20		$5.0\ 10^{-4}$		0.41
	$1.0\ 10^{-3}$		0.30		$7.5\ 10^{-4}$		0.62
	$6.0\ 10^{-4}$	$1.0\ 10^{-5}$	0.21		$2.5\ 10^{-4}$	$1.0\ 10^{-5}$	0.30
	$6.0\ 10^{-4}$	$5.0\ 10^{-5}$	0.28		$2.5\ 10^{-4}$	$2.0\ 10^{-5}$	0.40
	$6.0\ 10^{-4}$	$1.0\ 10^{-4}$	0.40		$2.5\ 10^{-4}$	$5.0\ 10^{-5}$	0.46
	$6.0\ 10^{-4}$	$2.0\ 10^{-4}$	0.62		$2.5\ 10^{-4}$	$7.0\ 10^{-5}$	0.60
					$2.5\ 10^{-4}$	$1.0\ 10^{-4}$	0.65

T = 11.4 °C			T = 25 °C		
$[H^+]$ mole l^{-1}	k_0 $mole^{-1}\ l\ min^{-1}$	k_{TlCl} $mole^{-1}\ min^{-1}$	$[H^+]$ mole l^{-1}	k_0 $mole^{-1}\ l\ min^{-1}$	k_{TlCl} $mole^{-1}\ l\ min^{-1}$
0.1	800±80	2500±250	0.1	1800±200	4800±500
0.5	250±25	2350±250	0.5	770± 80	4700±500

*[Enol] = 1.0×10^{-4} M; force ionique μ = 1.0.

L'analyse des mélanges réactionnels réalisée dans nos conditions expérimentales a permis d'estimer la concentration en ions Cl^- à 1.5×10^{-5} M.

Ce fait permet d'expliquer la variation de la constante de vitesse. Par la suite, toutes nos solutions ont été analysées quant à leur contenu en ions Cl^-.

Influence de l'ion Cl^-

L'influence de l'ion chlorure est montrée dans la Fig. 2 où on a porté la vitesse initiale, V_i, en fonction de la concentration en ions chlorure.

i) Cas où l'ion thallique est en excès par rapport au chlorure

Dans ce cas d'après les valeurs des constantes de stabilité (7) seul le complexe $TlCl^{2+}$ existe en concentration appréciable et environ 95% de Cl^- se trouve sous cette forme. Dans ce cas, on obtient l'expression de vitesse:

$$[2] \quad V = [E]\{k_0[Tl_0] + k_{TlCl}[TlCl^{2+}]\}$$

où k_{TlCl} et k_0 représentent respectivement les constantes de vitesse de $TlCl^{2+}$ et des espèces sans chlorure, de concentration $[Tl_0]$.

Pour déterminer k_0 on étudie la variation de la vitesse en fonction de la concentration en ion thallique (Tableau I). Dans ce cas, la concentration en $TlCl^{2+}$ demeure constante et à peu près

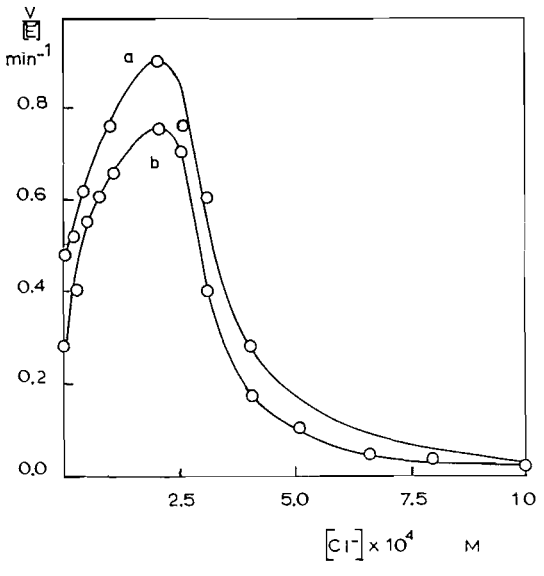

FIG. 2. Influence de l'ion chlorure: T = 25 °C; [Tl(III)] = 2.5×10^{-4} M; [Enol] = 1.0×10^{-4} M; force ionique μ = 1.0 a) $[H^+]$ = 0.1 M; b) $[H^+]$ = 0.5 M.

Can. J. Chem. Downloaded from www.nrcresearchpress.com by 210.87.254.40 on 09/05/12
For personal use only.

TABLEAU II

Influence de l'acidite et détermination de k_{Tl} et k_{TlOH}*

	$T = 25$ °C			$T = 16$ °C			$T = 6.4$ °C		
$[H^+]$ mole l^{-1}	$k_{exp} \times 10^{-3}$ mole^{-1} l min^{-1}	$k_0 \times 10^{-3}$ mole^{-1} l min^{-1}	k_0(calc) $\times 10^{-3}$ mole^{-1} l min^{-1}	$k_{exp} \times 10^{-3}$ mole^{-1} l min^{-1}	$k_0 \times 10^{-3}$ mole^{-1} l min^{-1}	k_0(calc) $\times 10^{-3}$ mole^{-1} l min^{-1}	$k_{exp} \times 10^{-3}$ mole^{-1} l min^{-1}	$k_0 \times 10^{-3}$ mole^{-1} l min^{-1}	k_0(calc) $\times 10^{-3}$ mole^{-1} l min^{-1}
2	0.93	0.81	0.93	0.36	0.27	0.32	0.17	0.12	0.13
1.5	1.02	0.90	0.99	0.45	0.37	0.37	0.23	0.18	0.16
1	1.3	1.19	1.11	0.51	0.43	0.45	0.33	0.28	0.21
0.5	1.5	1.40	1.40	0.81	0.74	0.69	0.39	0.34	0.34
0.25	2.13	2.05	1.88	1	0.93	1.05	0.57	0.53	0.54
0.15	—	—	—	1.61	1.56	1.38	0.73	0.69	0.74
0.1	2.6	2.53	2.53	—	—	—	—	—	—
0.08	—	—	—	1.74	1.70	1.71	0.95	0.92	0.94
0.04	3.05	3.00	2.56	2.2	2.17	1.73	1.41	1.39	0.97
0.02	—	—	—	3	3	1.41	—	—	—

T °C	k_{Tl} mole^{-1} l min^{-1}	k_{TlOH} mole^{-1} l min^{-1}	K_1 mole l^{-1}	K_2 mole^2 l^{-2}
25	750 ± 80	5625 ± 560	0.080	0.0027
16	180 ± 20	4150 ± 420	0.074	0.0027
6.4	50 ± 5	2470 ± 250	0.068	0.0027

*$[Tl^{3+}] = 2.5 \times 10^{-4}$ M; $[Enol] = 1.0 \times 10^{-4}$ M; force ionique $\mu = 2.0$.

égale aux traces d'ions Cl^- du mélange réactionnel.

La détermination de k_{TlCl} est faite à concentration en ion thallique constante et en étudiant la variation de la vitesse avec la concentration en ion $TlCl^{2+}$. L'équation [2] devient dans ce cas:

$$[3] \quad V = [E]\{k_0[Tl_0] + (k_{TlCl} - k_0)[TlCl^{2+}]\}$$
où $[TlCl^{2+}] \sim [Cl^-]$.

L'interprétation graphique des courbes de Vi = f(Cl^-) en utilisant l'équation [3] permet de déduire $(k_{TlCl} - k_0)$.

Les valeurs des constantes obtenues sont données dans le tableau I.

On remarque que la valeur de k_0 dépend de l'acidité tandis que k_{TlCl} n'en dépend pas.

D'autre part, la valeur de la concentration des traces d'ions Cl^- dans le mélange réactionnel calculée à partir de l'équation [3] est de 1.5×10^{-5} M aux deux températures en accord avec notre analyse.

ii) Cas où l'ion chlorure est en excès par rapport à l'ion thallique

Lorsque le chlorure est pris en excès par rapport à l'ion thallique, on constate une diminution de la vitesse de réaction (Fig. 2); ceci laisse supposer que les complexes supérieurs Tl (III)-Cl sont relativement inertes. En utilisant les diverses valeurs publiées des constantes de stabilité (7) pour ce système ainsi que nos constantes de vitesse du tableau I, il ne nous a pas été possible d'obtenir un accord parfait entre vitesses calculées et expérimentales et l'étude approfondie se poursuit avec l'étude de l'influence d'autres anions.

L'influence de l'acidité

Contrairement à ce qui a été observé dans l'oxydation de l'éthylène (2), l'acidité a une influence marquée sur la vitesse de réaction.

Les résultats obtenus dans diverses conditions sont présentés au tableau II où k_{exp} est la constante de vitesse définie par l'éq. [1], k_0 est la constante k_{exp} corrigée d'après l'éq. [3] afin de tenir compte de traces de Cl^- et k_0(calc) a été obtenue en tenant compte de l'oxydation par les ions Tl^{3+} et $TlOH^{2+}$ et de l'influence de l'acidité sur leurs concentrations, c'est-à-dire d'après l'expression:

$$[4] \quad k_0 = \frac{k_{Tl} + k_{TlOH} \cdot \dfrac{K_1}{[H^+]}}{1 + \dfrac{K_1}{[H^+]} + \dfrac{K_2}{[H^+]^2}}$$

où k_{Tl} est la constante de vitesse d'oxydation par l'ion Tl^{3+}, k_{TlOH} est celle de $TlOH^{2+}$, K_1 et K_2 sont définies par:

$$K_n = \frac{[Tl(OH)_n^{3-n}][H^+]^n}{[Tl^{3+}]}$$

Can. J. Chem. Downloaded from www.nrcresearchpress.com by 210.87.254.40 on 09/05/12
For personal use only.

Can. J. Chem. Downloaded from www.nrcresearchpress.com by 210.87.254.40 on 09/05/12
For personal use only.

leurs valeurs ayant été calculées pour nos conditions expérimentales d'après (7).

Les valeurs des constantes de l'éq. [4] sont données dans le Tableau II.

L'accord entre les résultats expérimentaux et calculés est bon sauf à très faibles acidités ou $Tl(OH)^{2+}$ prédomine et où l'erreur due à l'incertitude sur K_2 est très importante.

Discussion

L'ensemble de nos résultats peut être interprété par un mécanisme semblable à celui proposé par Henry pour l'oxydation de l'éthylène (2) (14).

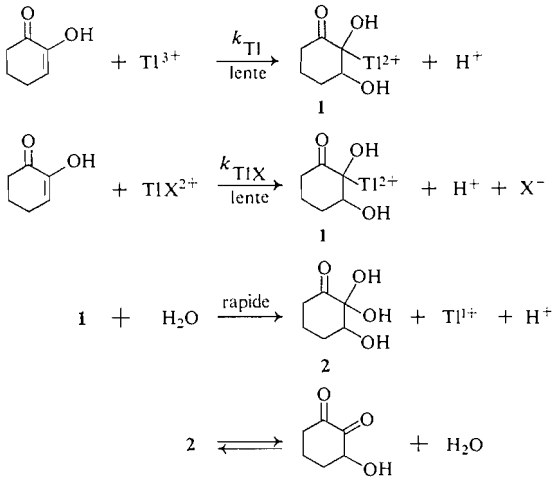

où $X^- = Cl^-$ ou OH^-

Les équations [3] et [4] conduisent à l'expression de vitesse globale

$$V = (k_{Tl}[Tl^3] + k_{TlOH}[TlOH^{2+}] + k_{TlCl}[TlCl^{2+}])[E]$$

Il est évident que l'étude cinétique et l'analyse du produit de la réaction ne permettent pas de déterminer sur quel carbone de la double liaison énolique l'ion thallique se fixe initialement; dans les deux cas, le produit final étant identique. Une alternative à ce mécanisme serait la formation lente d'un chélate entre l'ion thallique et les deux groupes fonctionnels du réactif, suivie de l'attaque du carbone 3 par l'eau ce qui donne un mécanisme cinétiquement impossible à distinguer du premier.

Si on compare les résultats obtenus à ceux concernant la réaction d'échange Tl(III)–Tl(I) on constate que l'influence de l'ion Cl^- est contraire à celle que nous avons obtenue. En effet, on a observé la diminution de la vitesse d'échange à faible concentration en ions Cl^-; l'interprétation des résultats a conduit à une constante de vitesse d'échange plus petite pour $TlCl^{2+}$ que pour Tl^{3+} (15, 16). A haute concentration en Cl^- la vitesse d'échange augmente ce qui est dû à l'intervention de complexes supérieurs tandis que dans notre cas la vitesse diminue ce qui tend à éliminer l'oxydation par ceux-là (Fig. 2).

Nos résultats ne sont pas en désaccord avec ceux de Grinstead (1) obtenus dans l'oxydation de l'éthylène: il a rapporté que $TlCl_3$ n'était pas réactionnel. En effet, en utilisant $TlCl_3$, on se trouve à prendre automatiquement un excès de chlorure et donc on favorise les complexes supérieurs en diminuant la concentration des formes réactionnelles Tl^{3+}, $TlOH^{2+}$ et $TlCl^{2+}$.

Henry a rapporté (2) que l'augmentation de la force ionique du milieu avait comme effet l'augmentation de la vitesse de l'oxydation de l'éthylène par l'ion thallique en milieu $HClO_4$–$NaClO_4$. Il a interprété ces résultats en termes de changement d'activité et de changement d'hydratation. Etant donné que nous avons montré l'influence importante de traces d'ions Cl^-, une variation éventuelle de la vitesse avec la force ionique ne peut pas être interprétée d'une manière univoque car elle peut être due à l'augmentation de la concentration en ions Cl^-. Pour cette raison nous n'avons pas envisagé l'étude de l'influence de la force ionique.

TABLEAU III

Paramètres d'activation

Constantes de vitesse	$\Delta H^{\ddagger}_{25°C}$ Kcal/mole	$\Delta S^{\ddagger}_{25°C}$ u.e.
k_{Tl}	24.0 ± 2.5	27 ± 7
k_{TlOH}	7.0 ± 1	-26 ± 4
k_{TlCl}	7.5 ± 1	-24 ± 4

Dans le but d'éclaircir l'influence catalytique des ions OH^- et Cl^- nous avons déterminé les paramètres d'activation des différentes constantes de vitesse. Bien que les résultats du Tableau III soient entachés d'erreurs assez grandes dues à la détermination simultanée des constantes ainsi que des erreurs sur les constantes d'équilibre que nous ne sommes pas en mesure d'évaluer et qui n'ont pas été incluses, ils permettent néanmoins de tirer des conclusions. L'influence catalytique des ions OH^- et Cl^- est reliée à une diminution importante de l'enthalpie d'activation; la valeur élevée du $\Delta H^{\ddagger}$ pour Tl^{3+} montrerait que l'ion

thallique forme un édifice particulièrement stable avec les molécules d'eau de sa sphère de coordination qui serait partiellement détruit lors de la formation du complexe activé, alors que dans le cas de $TlCl^{2+}$ et $TlOH^{2+}$ ce phénomène se produit lors de la formation des complexes avec les anions. Ce genre d'interprétation serait en accord avec les différences notables dans les $\Delta S^{\neq}$. En effet la libération des molécules d'eau lors de l'attaque par l'ion thallique correspondrait à une augmentation d'entropie tandis que, étant donnée la coordination moins importante de $TlOH^{2+}$ et $TlCl^{2+}$ on obtiendrait des valeurs de $\Delta S^{\neq}$ beaucoup plus faibles. Cette interprétation est basée sur la différence significative des résultats plutôt que sur les valeurs individuelles qui incluent d'autres phénomènes.

Remerciements

Nous remercions le Conseil National de Recherches du Canada pour l'octroi grâce auquel ce travail a pu être réalisé ainsi que Monsieur Veschambre Henri pour ses suggestions concernant l'identification des produits.

1. R. R. GRINSTEAD. J. Org. Chem. **26**, 238 (1961). J. B. LEE and M. J. PRICE. Tetrahedron Letters, 1155, 1962; H. J. KABBE. Ann. **656**, 204 (1962); C. B. ANDERSON and S. WINSTEIN. J. Org. Chem; **28**, 605 (1963); S. UEMURA, R. KITO, and K. ICHIKAWA. Nippon Kagaku Zasshi (Japan) **87** (9) 986 (1966); K. WIBERG and W. KOCH. Tetrahedron letters, No. 16, 1179 (1966); S. UEMURA, T. NAKAND, and K. ICHAKAWA. Nippon Kagaku Zasshi (Japan) **88** (10) 1967, p. 1111; S. UEMURA, T. NAKAND and K. ICHAKAWA. Nippon Kagaku Zasshi (Japan) **89** (2) 203, 1968; M. KUEHNE and T. J. GIACOBBE. J. Org. Chem. **33** (9), 3359 (1968).
2. P. M. HENRY. J. Am. Chem. Soc. **87**, 990 (1965).
3. P. M. HENRY. J. Am. Chem. Soc. **87**, 4423 (1965).
4. P. M. HENRY. J. Am. Chem. Soc. **88**, 1597 (1966).
5. R. BAKULE and F. A. LONG. J. Am. Chem. Soc. **85**, 2309 (1963).
6. J. S. LITTLER. J. Chem. Soc. 827 (1962).
7. R. BENOIT. Bull. Soc. Chim. France, 518 (1949); D. PESCHANSKI and S. VALLADAS-DUBOIS. Bull. Soc. Chim. France, 1170 (1956); G. BIEDERMANN. Rec. Trav. Chim. **75**, 716 (1956); T. E. ROGERS and G. M. WAIND. Trans. Faraday Soc. 1360 (1961); S. AHRLAND, I. GRENTHE, L. JOHANSSON, and B. NOREN. Acta Chem. Scand. **17**, (6), 1567 (1963); J. M. WOODS, O. P. PATRICK, K. CALLAGHER, Z. Z. HUGUS, JR., and E. L. KING. J. Am. Chem. Soc. **3** (9) p. 1313 (1964); F. YAKUL'BA, YU. B. YAKOVLEV, and V. E. MIRONOV. Russ. J. Inorg. Chem. (Engl. Ed.) **9**, 1390 (1964); I. LEDEN and T. RYHL. Acta Chem. Scand. **18**, 1196 (1964); S. AHRLAND and L. JOHANSSON. Acta Chem. Scand. **18**, 2125 (1964); F. YAKUL'BA, YU. B. YAKOVLEV and V. E. MIRONOV. Russ. J. Inorg. Chem. **45**, 618 (1967).
8. N. SCHAMP and M. VANDEWALLE. Bull. Soc. Chim. Belges, **75**, 539 (1966).
9. F. W. MCLAFFERTY. Analyt. Chem. **31**, 82 (1959). Appl. Spectroscopy **11**, 148 (1957).
10. J. H. BOWIE, R. G. COOKS, G. E. GREAM, and M. H. LAFFER. Aust. J. Chem. 1968, **21** 1247.
11. B. PECHERER, L. M. JAMPOLSKY, and H. M. WUEST. J. Am. Chem. Soc. **70**, 2587 (1948).
12. G. HESSE and G. KREHBIEL. Ann. **593**, 42 (1955).
13. D. M. ZALL, D. FISHER, and M. O. GARNER. Anal. Chem. **28**, (11) 1665 (1956).
14. P. M. HENRY. Advan. Chem. Ser. No. **70**, 126 (1968).
15. G. HARBOTTLE and R. W. DODSON. J. Am. Chem. Soc. **73**, 2442 (1951).
16. S. GILKS, T. E. ROGERS and G. M. WAIND. Trans. Faraday Soc. **57**, 1371 (1961).

Can. J. Chem. Downloaded from www.nrcresearchpress.com by 210.87.254.40 on 09/05/12
For personal use only.

Reactions of dimethyl acetylenedicarboxylate. III.[1] Reactions with diamines and anthranilic acid

SUSHIL K. KHETAN AND M. V. GEORGE[2]
Department of Chemistry, Indian Institute of Technology, Kanpur, India

Received February 5, 1969

Dimethyl acetylenedicarboxylate reacts with *m*-phenylenediamine, *p*-phenylenediamine and 2,2′-diaminobiphenyl, giving rise to the corresponding bisenamines, having the furmarate geometry. These bisenamines are thermally cyclized to 4(1*H*)-quinolone derivatives and a selective mode of cyclization is observed. Anthranilic acid reacts with dimethyl acetylenedicarboxylate to give an enamine adduct which when heated in diphenyl ether undergoes cyclization to methyl 7-carboxy-3-oxo-2-indolinylidene-carboxylate. Further heating of this product results in the formation of methyl 3-oxo-2-indolinylidene-carboxylate.

Canadian Journal of Chemistry, 47, 3545 (1969)

Can. J. Chem. Downloaded from www.nrcresearchpress.com by 210.87.254.6 on 09/05/12
For personal use only.

The reaction of dimethyl acetylenedicarboxylate with amines has been investigated by several groups of workers. In general, primary amines give rise preferentially to enamines having a fumarate geometry, whereas secondary amines yield either the maleates or a mixture of both maleates and fumarates. Several factors affecting these additions have been studied in detail (1).

The enamine adducts obtained from the reaction of aromatic amines with dimethyl acetylenedicarboxylate, have been shown to undergo thermal cyclization, yielding 4(1*H*)-quinoline derivatives (2). Thus, when dimethyl anilinofumarate, formed from the reaction of aniline with dimethyl acetylenedicarboxylate, is refluxed in diphenly ether, it undergoes cyclization to give 2-carbomethoxy-4(1*H*)-quinolone (1*a*, 3). The object of the present investigation was to examine the reaction of dimethyl acetylenedicarboxylate with few aromatic diamines and to employ the enamine adducts formed from these reactions for the synthesis of quinoline derivatives.

The reactions of few aromatic diamines are reported in the literature. *o*-Phenylenediamine, for example, reacts with dimethyl acetylenedicarboxylate to give a cyclic product, namely, 2-oxo-3-carbomethoxymethylene-1,2,3,4-tetrahydroquinoxaline (**1**) (4). It is evident that in this reaction, the initially formed intermediate is undergoing cyclization through the attack of the second amino group, present in the starting nucleophile (Scheme I). The reaction of 2,3-diaminonaphthalene with dimethyl acetylenedicarboxylate is analogous to that of *o*-phenylenediamine (5). On the other hand, 1,8-diaminonapthalene reacts with dimethyl acetylenedicarboxylate giving rise to a mixture of products, 2-oxo-3-carbomethoxymethylene-1,2,-3,4-tetrahydronaphtho-[1,8-*ef*]-[1,4]-diazepine (**2**) and 2,3-dicarbomethoxy-1,2,3,4-tetrahydronaphtho-[1,8-*ef*]-[1,4]-diazepine (**3**) (5) (Scheme II).

In the present investigation, we have examined the reactions of *m*-phenylenediamine, *p*-phenylenediamine and 2,2′-diaminobiphenyl with dimethyl acetylenedicarboxylate. *m*-Phenylenediamine reacts with dimethyl acetylenedicarboxylate in methanol medium at room temperature to give a 69% yield of tetramethyl *m*-phenylenediaminobisfumarate (**4**). The nuclear magnetic resonance (n.m.r.) spectrum of **4** showed a sharp singlet at 4.58 τ (2H) due to the two vinylic protons. The observed position of the vinylic proton in **4** is in agreement with the reported values for anilinofumarates (1*a*). Similarly, the reaction of *p*-phenylenediamine with dimethyl acetylenedicarboxylate gave a 62% yield of tetramethyl *p*-phenylenediaminobisfumarate (**7**). Under identical conditions, the reaction of 2,2′-diaminobiphenyl gave a 96% yield of tetramethyl 2,2′-diaminobiphenylbisfumarate (**10**). The n.m.r. spectra of **7** and **10** showed the vinylic proton signals at 4.60 τ and 4.64 τ, respectively, and supports the assigned structures for these enamine adducts.

The infrared spectra of the adducts **4**, **7**, and **10** showed the presence of a hydrogen-bonded N—H, absorbing around 3280 cm^{-1}. The chelated ester carbonyl group absorption in these compounds was found to be around 1670 cm^{-1},

[1]For Part II in this series see ref. 10.
[2]To whom enquiries should be addressed.

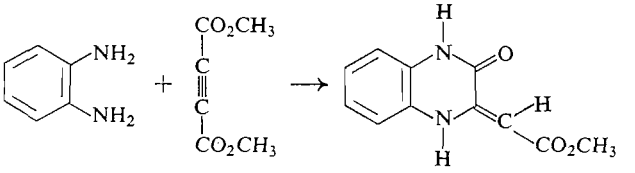

1

SCHEME I

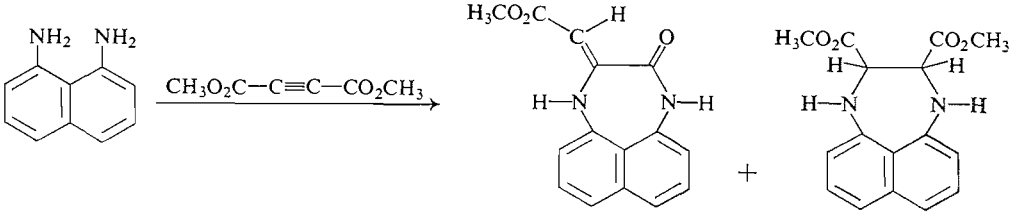

2 3

SCHEME II

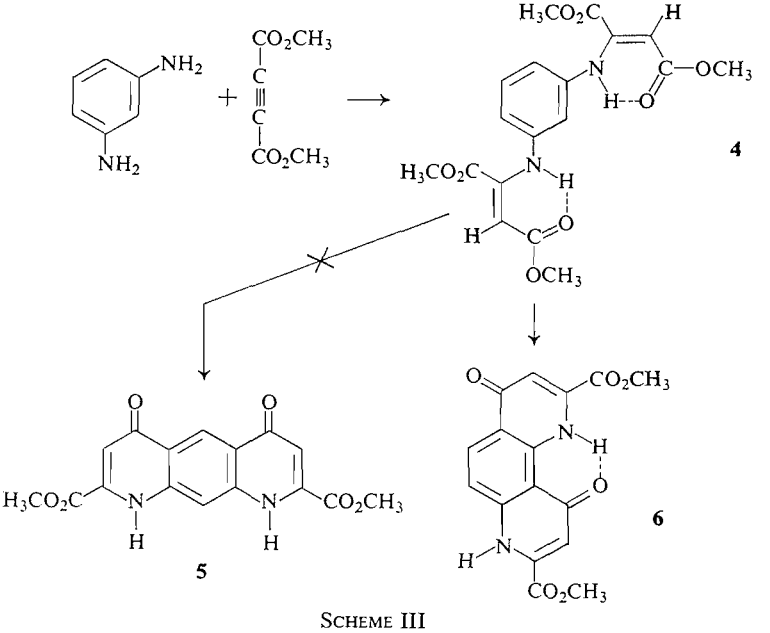

4 5 6

SCHEME III

whereas, the second ester carbonyl group appeared around 1730 cm^{-1}.

A bisenamine adduct like tetramethyl *m*-phenylenediaminobisfumarate (**4**) can undergo cyclization by two different routes giving rise to a linearly fused ring compound, 2,8-dicarbomethoxypyrido-[3,2-*g*]-quinolin-[1*H*, 9*H*]-4,6-dione (**5**) and an angularly fused ring compound, 2,8-dicarbomethoxy-1,7-[1*H*, 7*H*]-phenanthrolin-4,10-dione (**6**) (Scheme III). When the cyclization of **2** was carried out by refluxing it in diphenyl ether for 30 min, a 95% of a single product, melting at 273.5° was isolated. The structure of this product was assigned as **6**, on

Can. J. Chem. Downloaded from www.nrcresearchpress.com by 210.87.254.6 on 09/05/12
For personal use only.

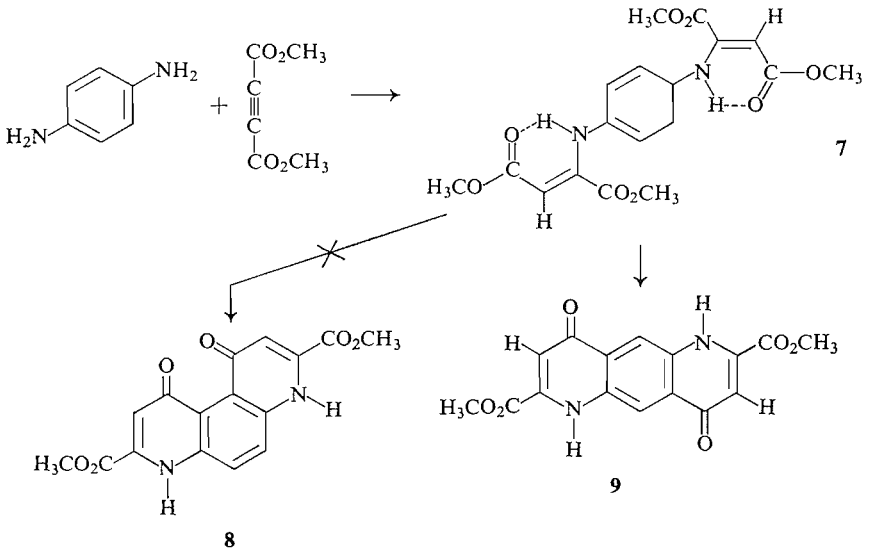

SCHEME IV

the basis of elemental analysis, molecular weight (mass spectral), and spectral evidences. The infrared spectrum of **6** showed two distinctive absorption bands at 3440 cm^{-1} and 3245 cm^{-1}, corresponding to a free and associated NH, respectively. The n.m.r. spectrum of **6**, in trifluoroacetic acid showed signals at 5.79 τ (3H) and 5.94 τ (3H), respectively, due to the ester methyl protons. In addition, the spectrum showed a symmetrical quartet centered around 1.65 τ (2H) of the AB type, with a coupling constant of 9.4 c.p.s. The appearance of this quartet is compatible only with structure **6**, in which there are two ortho protons. A coupling constant of 8–10 c.p.s. is normally observed between the two ortho protons in an aromatic ring (6). The two other olefinic protons present in the pyridone rings of **6**, appeared as two separate singlets at 1.97 τ (1H) and 3.0 τ (1H), respectively. The exact reason for the preferential formation of **6** in the cyclization of the bisenamine adduct **4**, is still not very clear.

Thermal cyclization of tetramethyl *p*-phenylenediaminobisfumarate (**7**), similarly, can give rise to two products **8** and **9**, as shown in Scheme IV. Refluxing a solution of **7** in diphenyl ether resulted in the exclusive formation (97%) of one isomer, namely, 2,7-dicarbomethoxypyrido-[2,3 *g*]-quinolin-[1*H*, 6*H*]-4,9-dione (**9**). The n.m.r. spectrum of **9** showed one singlet at 5.78 τ (6H) due to the ester methyl protons and two separate, sharp singlets at 1.56 τ (2H) and 2.57 τ (2H), respectively, due to the aromatic protons. The spectral data are in full agreement with the assigned structure **9**, for the product. If this compound were to be represented by structure **8**, one would expect the two aromatic ortho protons to appear as a quartet as in the case of **6**. Similarly, the cyclization of tetramethyl 2,2′-diaminobiphenylbisfumarate (**10**), by refluxing in diphenyl ether gave a 95% yield of 8-(2′-carbomethoxy-4′(1′*H*)-quinolonyl)-2-carbomethoxy-4(1*H*)-quinolone (**11**) (Scheme V). Confirmation of the structure **11** was derived from analytical data and spectral evidences. The n.m.r. spectrum of **11** showed a singlet at 5.90 τ (6H), assigned to the carbomethoxyl protons. In addition, the spectrum showed a complex multiplet centered around 1.67 τ (8H), due to the aromatic protons.

In an earlier paper (3), we have reported that ethyl anthranilate reacts with dimethyl acetylenedicarboxylate to give an aminofumarate which on heating undergoes cyclization to give 8-carboethoxy-2-carbomethoxy-4-(1*H*)-quinolone. In the present investigation, we have examined the reaction of anthranilic acid with dimethyl acetylenedicarboxylate with a view to studying the nature of the addition product and also of the mode of cyclization of the enamine

Can. J. Chem. Downloaded from www.nrcresearchpress.com by 210.87.254.6 on 09/05/12
For personal use only.

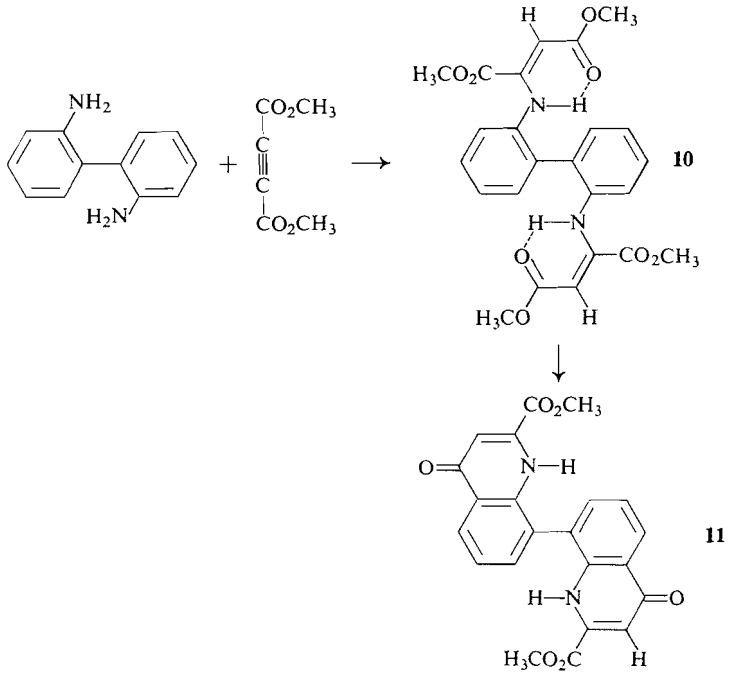

SCHEME V

adduct formed in this reaction. Treatment of anthranilic acid with dimethyl acetylenedicarboxylate in methanol gave a 78% yield of dimethyl 2-carboxyanilinofumarate (**12**). The infrared spectrum of **12** showed an absorption band at 3247 cm^{-1}, characteristic of the NH group. The two ester carbonyl group absorptions were observed at 1692 cm^{-1} and 1742 cm^{-1} respectively and the C=O absorption of the acid group was observed at 1681 cm^{-1}. The stereochemistry of **12** was inferred to be as that of a fumarate, on the basis of the vinyl proton position at 3.94 τ in its n.m.r spectrum.

When the enamine adduct **12** was heated in refluxing diphenyl ether, it gave rise to a 62% yield of a cyclized product, m.p. 264–265° (decomp.), which has been tentatively assigned the structure **13**, on the basis of analytical results and also of the following evidences. The infrared spectrum of **13** showed an ester C=O band at 1742 cm^{-1}. In addition, the spectrum showed an absorption band at 2500 cm^{-1}, characteristic of an NH_2^+ group and a second absorption band at 1620 cm^{-1}, which could be assigned to a CO_2^- group (7). The mass spectrum of **13** showed a correct molecular ion peak at 247. A second peak was observed at 229, corresponding to the loss of a water molecule from the parent compound. A similar loss of water molecule has been observed when indole-7-carboxylic acid was subjected to electron impact (8). A peak at 187, in the mass spectrum of **13**, could be assigned to the loss of a CO_2CH_3 group from the parent molecule. Other prominent peaks at mass units 171, 170, 143, 115, 114, 103, 75, 63, 39, and 28, were also observed in the spectrum of **13**.

Dry distillation of **13** (230° at 2 mm pressure) resulted in the formation of a small quantity (8.5%) of a product, melting at 137° and identified as methyl 3-oxo-2-indolinylidenecarboxylate (**14**). The yield of **15** could be improved to about 30%, by the direct dry distillation of **12**. The infrared spectrum of **14** showed a carbonyl absorption band at 1689 cm^{-1}, characteristic of a five-membered ring C=O in an indogenide system (9). In addition, the spectrum showed a second C=O absorption at 1709 cm^{-1} and an NH absorption band at 3215 cm^{-1}. The n.m.r. spectrum of **14** showed a broad signal at -1.32 τ (1H), due to the NH proton, a multiplet centered around 2.08 τ (4H) due to the aromatic protons and a sharp singlet at 6.07 τ (3H) due to the

Can. J. Chem. Downloaded from www.nrcresearchpress.com by 210.87.254.6 on 09/05/12
For personal use only.

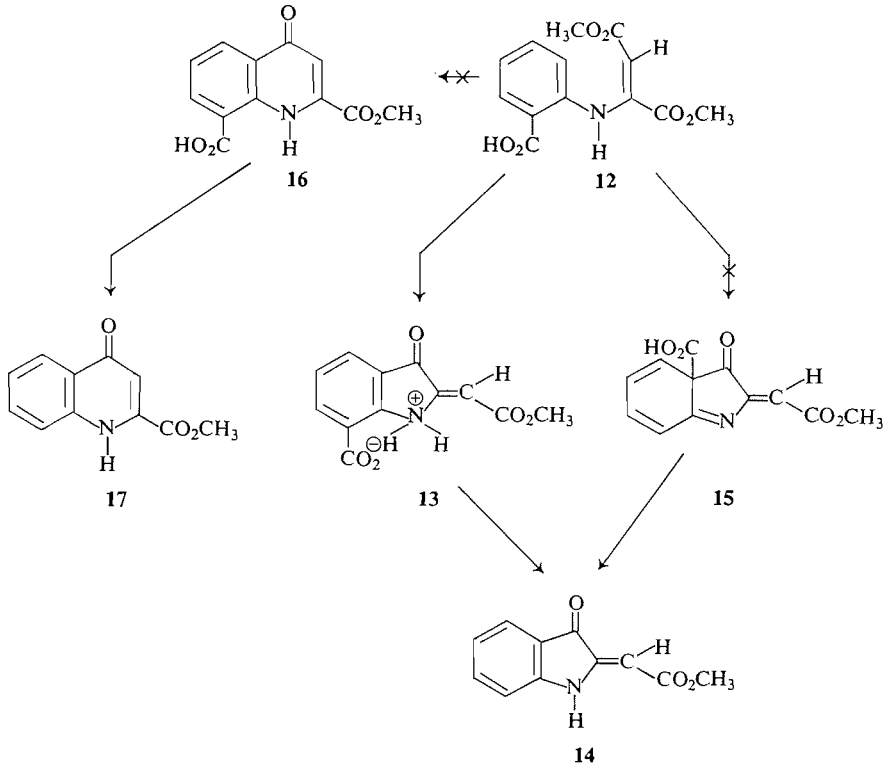

SCHEME VI

carbomethoxy protons. In addition, the spectrum showed a doublet at 3.78 τ (1H) due to the vinylic proton, which was split by the NH proton.

Two other possible structures for the cyclized product obtained from **12** are **15** and **16** shown in Scheme VI. The infrared (i.r.) spectrum of the product which shows the presence of a broad absorption band at 2500 cm^{-1} due to the NH_2^+ group will not favor structure **15**. If structure **16**, on the other hand, correctly represents the product obtained from **12**, then we would expect this product on decarboxylation to give 2-carbomethoxy-4(1*H*)-quinolone (**17**), a known product obtained from the thermal cyclization of dimethyl anilinofumarate (1*a*). The fact that the decarboxylated product (**14**) was not identical with **17**, rules out the possibility of structure **16** for the intermediate, cyclized product.

Experimental

All melting points are uncorrected and were determined in a Thomas–Hoover melting point apparatus. Infrared (i.r.) spectra were determined in a Perkin–Elmer model 137 infrared spectrometer and ultraviolet spectra on a Cary 14-R spectrometer. Nuclear magnetic resonance traces were taken on a Varian HR-100 spectrometer, using TMS as an internal standard.

Reaction of Dimethyl Acetylenedicarboxylate with m-Phenylenediamine

A solution of *m*-phenylenediamine (1.8 g, 0.017 mole) in 10 ml of methanol was treated with a methanolic solution of dimethyl acetylenedicarboxylate (4.9 g, 0.035 mole, in 5 ml). Removal of the solvent under vacuum gave a product which on recrystallization from methanol gave 4.50 g (69%) of tetramethyl *m*-phenylenediaminobisfumarate (**4**), m.p. 146–147°.

Anal. Calcd. for $C_{18}H_{20}N_2O_8$: C, 55.10; H, 5.14; N, 7.14. Found: C, 55.34; H, 5.20; N, 7.51.

Infrared spectrum of **4** (KBr) ν_{max}: 3279 (chelated NH); 3086, 2941 (C—H); 1736 (ester C=O); 1667 (α,β-unsaturated ester C=O); 1603 (C=C), 1435, 1379 (CH_3); 1300, 1264 (C—O—C).

Ultraviolet spectrum of **4** (CH_3OH) λ_{max}: 326 mμ (ε 31 000), 243 (ε 13 800), and 225 (ε 18 200).

Nuclear magnetic resonance spectrum of **4** ($CDCl_3$): 1.07 τ (NH, 2H), 3.54 τ (phenyl, 4H); 4.56 τ (vinylic, 2H) and 6.27 τ (carbomethoxy, 12H).

2,8-Dicarbomethoxy-1,7-[1H, 7H]-phenanthrolin-4,10-dione (6)

Tetramethyl *m*-phenylenediaminobisfumarate (**4**) (1.0 g, 0.003 mole), dissolved in diphenyl ether (10 ml) was

Can. J. Chem. Downloaded from www.nrcresearchpress.com by 210.87.254.6 on 09/05/12
For personal use only.

Can. J. Chem. Downloaded from www.nrcresearchpress.com by 210.87.254.6 on 09/05/12
For personal use only.

heated in an oil bath around 250° for 30 min. Removal of the solvent and treatment of the residue with petroleum ether (60–80°) gave a product, which was recrystallized from glacial acetic acid to give 0.80 g (95%) of 2,8-dicarbomethoxy-1,7-[1*H*,7*H*]-phenanthrolin-4,10-dione (**6**), m.p. 273.5°.

Anal. Calcd. for $C_{16}H_{12}N_2O_6$: C, 58.54; H, 3.68; N, 8.53. Found: C, 58.37; H, 4.0; N, 8.69.

Infrared spectrum of **6** (KBr) ν_{max}: 3106, 2967 (CH); 1745 (ester, C=O); 1639 (ring, C=O); 1570 (C=C); 1435, 1397 (CH_3); 1271 and 1239 cm^{-1} (C—O—C).

Nuclear magnetic resonance spectrum of **6** (CH_3CO_2H): 1.86 τ (aromatic, 4H), 5.79 and 5.84 τ (carbomethoxy, 6H).

Reaction of Dimethyl Acetylenedicarboxylate with p-Phenylenediamine

A solution of *p*-phenylenediamine (1.62 g, 0.015 mole) dissolved in 10 ml of methanol was treated with a methanolic solution of dimethyl acetylenedicarboxylate (4.26 g, 0.03 mole in 5 ml). Removal of the solvent under vacuum gave a product, which on recrystallization from methanol gave 3.60 g (62%) of tetramethyl *p*-phenylenediaminobisfumarate (**7**), m.p. 129.5–130.5°.

Anal. Calcd. for $C_{18}H_{20}N_2O_8$: C, 55.10; H, 5.14; N, 7.14. Found: C, 55.14; H, 5.20; N, 7.04.

Infrared spectrum of **7** (KBr) ν_{max}: 3311 (NH); 2941 (CH); 1733 (ester, C=O); 1675 (α,β-unsaturated ester C=O); 1605 (C=C); 1433, 1383 (CH_3) and 1294, 1266 (C—O—C).

Ultraviolet spectrum of **7** (CH_3OH) λ_{max}: 348 mμ (ε 25 400) and 250 (ε 11 700).

Nuclear magnetic resonance spectrum of **7** ($CDCl_3$): 1.09 τ (NH, 2H); 3.14 τ (phenyl, 4H); 4.60 τ (vinylic, 2H); 6.27 and 6.32 τ (carbomethoxy, 12H).

2,7-Dicarbomethoxypyrido-[2,3 g]-quinolin-[1H, 6H]-4,9-dione (9)

A mixture of 1.0 g (0.003 mole) of tetramethyl *p*-phenylenediaminobisfumarate (**7**) and diphenyl ether (10 ml) was heated in an oil bath around 240–250° for 1 h. The product which separated out was filtered and treated with petroleum ether (60–80°) to give 0.83 g (97%) of impure 2,7-dicarbomethoxypyrido-[2,3 *g*]-quinolin-[1*H*,6*H*]-4,9-dione (**9**). Recrystallization of **9** from glacial acetic acid gave a pure sample, m.p. 262–263° decomp.

Anal. Calcd. for $C_{16}H_{12}N_2O_6$: C, 58.54; H, 3.68; N, 8.53. Found: C, 57.97; H, 3.80; N, 8.10.

Infrared spectrum of **9** (KBr) ν_{max}: 3344 (NH); 3106 (CH); 1712 (ester C=O); 1633 (ring C=O); 1608, 1567 (C=C); 1437, 1370 (CH_3); 1307 and 1271 cm^{-1} (C—O—C).

Nuclear magnetic resonance spectrum of **9** (CF_3CO_2H): 1.50 τ (phenyl, 2H); 2.47 τ (phenyl, 2H) and 5.78 τ (carbomethoxy, 6H).

Reaction of Dimethyl Acetylenedicarboxylate with 2,2′-Diaminobiphenyl

A mixture of 2,2′-diaminobiphenyl (1.0 g, 0.009 mole) in 10 ml of methanol was treated with a methanolic solution of dimethyl acetylenedicarboxylate (2.64 g, 0.0186 mole in 10 ml). The solvent was removed under vacuum to give 3.50 g (96%) of impure tetramethyl 2,2′-diaminobiphenylbisfumarate (**10**), which when recrystallized from a mixture (1:1) of methanol and benzene gave a pure product, m.p. 105°.

Anal. Calcd. for $C_{24}H_{24}N_2O_8$: C, 61.53; H, 5.16; N, 5.98. Found: C, 61.48; H, 5.50; N, 5.87.

Infrared spectrum of **10** (KBr) ν_{max}: 3333 (NH); 2985 (C—H); 1739 (ester C=O); 1680 (α,β-unsaturated ester C=O); 1605 (C=C), 1435, 1387 (CH_3); and 1285, 1275 (C—O—C).

Ultraviolet spectrum of **10** (CH_3OH) λ_{max}: 331 mμ (ε 26 800) and 238 (ε 23 200).

Nuclear magnetic resonance spectrum of **10** ($CDCl_3$): 1.53 τ (NH, 1H); 2.74 τ (phenyl, 8H); 4.63 τ (vinylic, 2H) and 6.40 τ (carbomethoxy, 12H).

8-(2′-Carbomethoxy-4′(1′H)-quinolonyl)-2-carbomethoxy-4(1H)-quinolone

A mixture of tetramethyl 2,2′-diaminobiphenylbisfumarate (**10**) (1.0 g, 0.0026 mole) and diphenyl ether (10 ml) was heated in an oil bath around 250° for 30 min. Removal of the solvent and treatment of the residue with petroleum ether (60–80°) gave a product, which was recrystallized from glacial acetic acid to give 0.80 g (95%) of 8-(2′-carbomethoxy-4′(1′*H*)-quinolonyl)-2-carbomethoxy-4(1*H*)-quinolone, m.p. 225–226°.

Anal. Calcd. for $C_{22}H_{16}N_2O_6$: C, 65.35; H, 3.99; N, 6.93. Found: C, 65.48; H, 4.00; N, 6.52.

Infrared spectrum of **11** (KBr) ν_{max}: 3322 (NH); 2967 (CH); 1730 (ester C=O); 1618 (ring C=O); 1575 (C=C); 1427, 1366 (CH_3); 1261 and 1227 (C—O—C).

Nuclear magnetic resonance spectrum of **11** (CF_3CO_2H): 2.52 τ (aromatic, 8H) and 5.95 τ (carbomethoxy, 6H).

Reaction of Dimethyl Acetylenedicarboxylate with Anthranilic Acid

A mixture of anthranilic acid (13.7 g, 0.1 mole) and dimethyl acetylenedicarboxylate (14.2 g, 0.1 mole) in 50 ml of methanol was stirred for 1 h. The solvent was removed under vacuum to give 21.7 g (78%) of impure dimethyl 2-carboxyanilinofumarate (**12**), which on recrystallization from methanol melted at 138°.

Anal. Calcd. for $C_{13}H_{13}NO_6$ (mol. wt., 279): C, 55.92; H, 4.69; N, 5.02. Found (mol. wt. (vapor pressure osmometry), 275): C, 55.91; H, 4.60; N, 4.97.

Infrared spectrum of **12** (KBr) ν_{max}: 3247 (NH), 1742, 1692 (ester C=O), 1681 (acid C=O), 1577 and 1499 (C=C), 1285, 1249 (O—C—O).

Ultraviolet spectrum of **13** (CH_3OH) λ_{max}: 339 mμ (ε 16 200), 238 (ε 12 800), and 218 (ε 17 900).

Nuclear magnetic resonance spectrum of **12** ($CDCl_3$): −1.11 τ (NH, 1H); 2.07, 2.66, 3.18 τ (aromatic, 4H); 4.32 τ (*trans*-vinylic, 1H); 6.17 τ and 6.22 τ (carbomethoxy, 6H).

Treatment of 2-Carboxyanilinofumarate in Diphenyl Ether at 240°

A mixture of dimethyl 2-carboxyanilinofumarate (2.0 g, 0.007 mole) and diphenyl ether (10 ml) was heated at 240° for 15 min. Removal of the solvent under vacuum and treatment of the residue with petroleum ether (60–80°) gave 1.10 g (62%) of methyl 7-carboxy-3-oxo-2-indolinylidenecarboxylate (**13**), m.p. 264–265° decomp.

Anal. Calcd. for $C_{12}H_9NO_5$ (mol. wt., 247): C, 58.30; H, 3.67; N, 5.67. Found (mol. wt. (mass spectrum), 247): C, 58.72; H, 3.78; N, 5.80.

Infrared spectrum of **12** (KBr) ν_{max}: 3125 (CH); 2500 (NH_2^+); 1742 (ester C=O); 1689 (ring C=O); 1620 (CO_2^-); 1555; 1513 (C=C); 1284, 1212 (C—O—C).

Ultraviolet spectrum of **13** (CH_3OH) λ_{max}: 242 mμ (ε 17 300), 354 (ε 10 000), 373 (ε 11 600), and 219 (ε 24 200).

*Decarboxylation of Methyl 7-Carboxy-3-oxo-2-indolinylidenecarboxylate (**13**)*

Methyl 7-carboxy-3-oxo-2-indolinylidenecarboxylate (**13**) (1.0 g, 0.004 mole) was heated under reduced pressure (2 mm). A compound distilled out around 230° (2 mm), which on purification by chromatography gave 70 mg (8.5%) of methyl 3-oxo-2-indolinylidenecarboxylate (**14**), m.p. 137°.

Anal. Calcd. for $C_{11}H_9NO_3$ (mol. wt., 203): C, 65.02; H, 4.46; N, 6.89. Found (mol. wt. (vapor pressure osmometer), 203): C, 64.83; H, 4.20; N, 6.85.

Infrared spectrum of **14** (KBr) ν_{max}: 3215 (NH-associated); 1709 (ester C=O, associated); 1689 (ring C=O); 1621, 1560, and 1495 (C=C); 1274 and 1110 cm^{-1} (O—C—O).

Ultraviolet spectrum of **14** (CH_3OH) λ_{max}: 352 mμ (ε 10 200), 290 (ε 900), 278 (ε 1 200), and 243 (ε 16 000).

Nuclear magnetic resonance spectrum of **14** (CH_3CN): −1.32 τ (NH, 1H); 1.52, 2.12, and 2.59 τ (phenyl, 4H); 3.78 τ (exo-methylene, 1H) and 6.07 τ (carbomethoxy, 3H).

In a second experiment (4.2 g, 0.001 mole) dimethyl 2-carboxyanilinofumarate (**12**) was directly distilled under reduced pressure (230° at 2 mm) to give 0.90 g (30%) of **14**, m.p. 137° (mixture m.p.).

Acknowledgments

The authors thank Mr. A. H. Siddiqui for his help in Microanalysis. One of the authors (SKK) is thankful to the authorities of the Indian Institute of Technology, Kanpur for the award of a Research Assistantship.

1. (*a*) R. Huisgen, K. Herbig, A. Siegl, and H. Huber. Ber. **99**, 2526 (1966); (*b*) K. Herbig, R. Huisgen, and H. Huber. Ber. **99**, 2546 (1966); (*c*) J. E. Dolfini. J. Org. Chem. **30**, 1298 (1965); (*d*) W. E. Truce and D. G. Brady. J. Org. Chem. **31**, 3543 (1966); (*e*) E. Winterfeldt and H. Preuss. Ber. **99**, 450 (1966); (*f*) T. Y. Chen, H. Kato, and M. Ohta. Bull. Chem. Soc. (Japan), **39**, 1618 (1966); Chem. Abstr. **65**, 13633 (1966); (*g*) R. Huisgen, B. Giese, and H. Huber. Tetrahedron Letters, 1883 (1967).
2. (*a*) N. D. Heindel, T. A. Brodof, and J. E. Kogelschatz. J. Heterocyclic Chem. **3**, 222 (1966); (*b*) N. D. Heindel, I. S. Bechara, and T. F. Lemke. J. Org. Chem. **32**, 4155 (1967); (*c*) E. C. Taylor and N. D. Heindel. J. Org. Chem. **32**, 1666, 3339 (1967); (*d*) J. Reisch. Pharmazie, **22**, 420 (1967).
3. S. K. Khetan, J. G. Hiriyakkanavar, and M. V. George. Tetrahedron, **24**, 1567 (1968).
4. Y. Iwanami. Nippon Kagaku Zasshi, **82**, 778 (1961); Chem. Abstr. **58**, 11354 (1962), see, also (*a*) D. D. Chapman. J. Chem. Soc. (C), 806 (1966); (*b*) M. D. Nair and S. R. Mehta. Indian J. Chem. **6**, 490 (1968).
5. Y. Iwanami. Nippon Kagaku Zasshi, **83**, 597 (1962); Chem. Abstr. **59**, 3919 (1963).
6. L. M. Jackman. Applications of nuclear magnetic resonance in organic chemistry. Pergamon Press, London, 1959, p. 85.
7. K. Nakanishi. Infrared absorption spectroscopy, Holden-Day, Inc., San Francisco, 1962, p. 39.
8. J. C. Powers. J. Org. Chem. **33**, 2044 (1968).
9. (*a*) E. D. Hannah, G. R. Proctor, and M. A. Rehman. J. Chem. Soc. (B), 256 (1967); (*b*) D. Auld and H. G.Heller. J. Chem. Soc. (C), 680, 682 (1967).
10. S. K. Khetan and M. V. George. Tetrahedron, **25**, 527 (1969).

Can. J. Chem. Downloaded from www.nrcresearchpress.com by 210.87.254.6 on 09/05/12
For personal use only.

Reaction of ethanesulfenyl chloride with 2-methoxy-5,6-dihydro-2*H*-pyran[1]

M. J. BALDWIN[2] AND R. K. BROWN
Department of Chemistry, University of Alberta, Edmonton, Alberta

Received April 28, 1969

The reaction of ethanesulfenyl chloride with 2-methoxy-5,6-dihydro-2*H*-pyran gives only 4β-chloro-3α-ethylthio-2β-methoxytetrahydropyran. A rationale is presented to explain the observed highly selective reaction.

Canadian Journal of Chemistry, 47, 3553 (1969)

Can. J. Chem. Downloaded from www.nrcresearchpress.com by 210.87.254.40 on 09/05/12
For personal use only.

Introduction

Two recent reports from this laboratory (1,2) have described the reaction of alkane (or aralkane) sulfenyl chlorides with 3,4-dihydro-2*H*-pyran to produce *trans*-2-chloro-3-alkyl (or aralkyl) thiotetrahydropyran which, in the presence of sodium methoxide in methanol, gave *trans*-3-alkyl (or aralkyl)-2-methoxytetrahydropyrans. A rationale was presented to explain the observed highly selective course of the reaction.

The present communication describes the results obtained from the reaction of ethanesulfenyl chloride with 2-methoxy-5,6-dihydro-2*H*-pyran.

Results and Discussion

Addition of an equimolar quantity of ethanesulfenyl chloride to 2-methoxy-5,6-dihydro-2*H*-pyran (**1**) at $-25°$ to $-30°$ gave in good yield a product which was assigned the *trans,trans* structure, 4β-chloro-3α-ethylthio-2β-methoxytetrahydropyran (**2**) (Scheme 1). This assignment was based on the following information. (*i*) All ionic additions of sulfenyl halides to olefins which have been reported to date have led to products in which the alkylthio group and the halogen are *trans* to each other (1–8). (*ii*) The 60 MHz nuclear magnetic resonance (n.m.r.) spectrum in $CDCl_3$ shows a doublet at τ 5.80 ($J_{2,3}$ = 6.5 Hz) which can be assigned to the anomeric proton H-2. The observed chemical shift is very close to that (τ 5.85) found for the C-2 proton of *trans*-3-ethylthio-2-methoxytetrahydropyran (1) and is the same as that (τ 5.80) for the C-2 proton of *trans*-2-methoxy-3-methylthiotetrahydropyran (1), but it is at higher field than that (τ 5.57) for the C-2 proton of *trans*-3-chloro-2-methoxytetrahydropyran. This indicates that the ethylthio group and not the chlorine atom is the substituent at C-3. The relatively large coupling ($J_{2,3}$ = 6.5 Hz) for the anomeric proton also supports the view that the two relevant protons, H-2 and H-3, are *trans* diaxial.

These assignments were corroborated by the 100 MHz n.m.r. spectrum (Fig. 1) and spin decoupling experiments. Irradiation of the nucleus of the proton whose signal is at τ 5.72 (H-2) converted the quartet at τ 7.32 (H-3) to a doublet, $J_{3,4}$ = 7.5 Hz. The magnitude of this coupling clearly shows that H-3 and H-4 are *trans* diaxially disposed. Irradiation at τ 7.32 (H-3) changed the signal at τ 5.72 (H-2) to a "singlet" and simplified the signals in the region τ 6.10–6.40 where the proton (H-4) attached to a carbon bearing a chlorine atom is expected to absorb (9).

The preferred conformation is clearly that of the chair form in which all three groups are equatorially disposed. Although the anomeric effect (10) would tend to favor the alternate chair form, the serious 1,3-diaxial interactions which are present in this alternate conformer would outweigh the stabilizing influence of the anomeric effect.

The exclusive formation of **2** requires comment. It has been suggested (11) that the anomeric effect (10) would favor to the extent of 80–85% that conformer of **1** in which the C-2 methoxy group is *quasi* axial. Also, it has been suggested by Mueller and Butler (7,8) that the first step of the reaction of olefins with ethanesulfenyl chloride is the formation of the episulfonium ion. On the basis of these two observations, in the present case, electrophilic attack of ethanesulfenyl chloride on **1** should occur preferentially from the least hindered side of the molecule, *trans* to the C-2 methoxyl group and result in the formation

[1]Taken from the thesis of M. J. Baldwin, submitted to the Faculty of Graduate Studies as part of the requirements for the degree of Doctor of Philosophy.

[2]Present address: The Dow Chemical Company, Midland, Michigan. 48640. U.S.A.

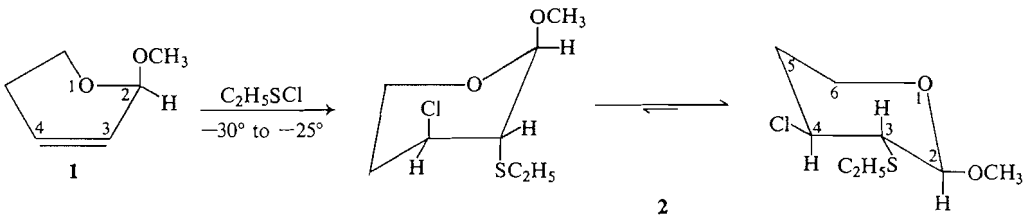

SCHEME 1

of the episulfonium ion intermediate, **3** (Scheme 2). Subsequent attack by the chloride ion could now occur at either C-3 or C-4 with simultaneous opening of the episulfonium ring. Various factors which determine the direction of bond cleavage in such three membered rings have already been discussed (11–13). Keeping these in mind, the course of reaction of the chloride ion with the episulfonium ion **3** can be rationalized. The bulk steric effect of the *quasi* axial methoxy group on C-2, as well as its polar repulsion for the chloride ion, would strongly inhibit attack by the chloride ion at C-3. Both the steric and polar repulsion are minimal or absent when the chloride ion approaches C-4. Furthermore, the preference for a course of reaction in which the negatively charged incoming and "leaving" groups are *trans* diaxial and the six-membered ring assumes the favored chair form (14) will dictate that reaction by the chloride ion occurs at C-4 rather than at C-3.

Another factor which has been considered important in determining the direction of 3-membered bromonium ion ring opening is the inductive effect of the geminal dioxy group at C-2 which would destabilize an incipient positive charge at C-4 less than at C-3, when such a charge is developed by partial C—Br bond breaking (11,15,16). This would favor successful reaction of the chloride ion at C-4 rather than at C-3.

Experimental

All melting points and boiling points are uncorrected. Elemental analyses were made by Mrs. Darlene Mahlow of the Microanalytical laboratory in this Department.

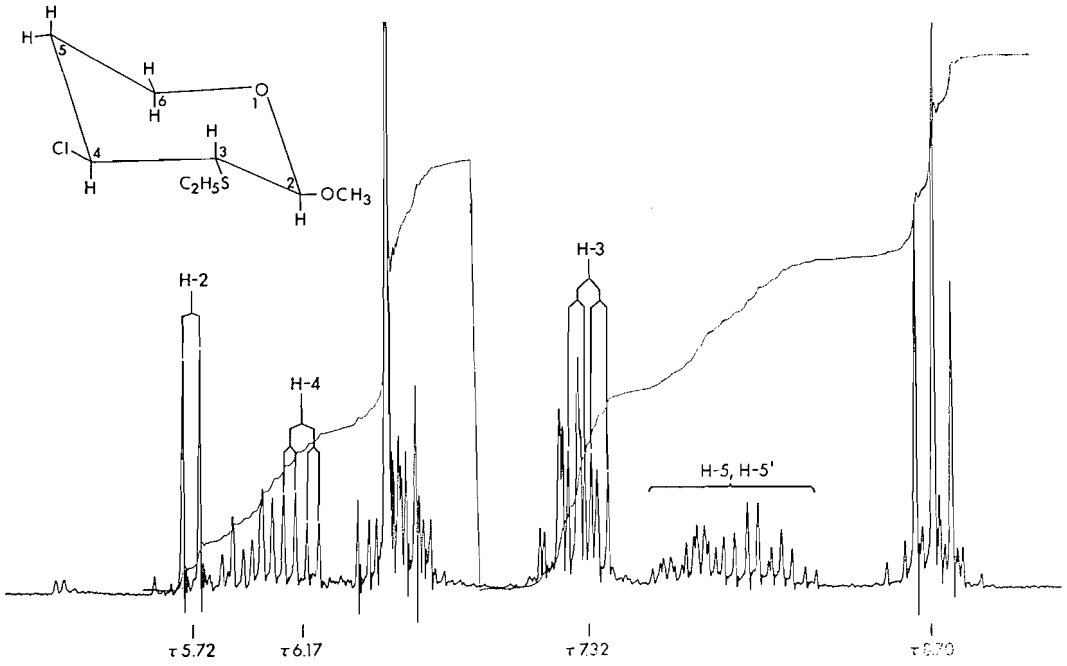

FIG. 1. 100 MHz n.m.r. spectrum in $CDCl_3$ of 4β-chloro-3α-ethylthio-2β-methoxytetrahydropyran.

Can. J. Chem. Downloaded from www.nrcresearchpress.com by 210.87.254.40 on 09/05/12
For personal use only.

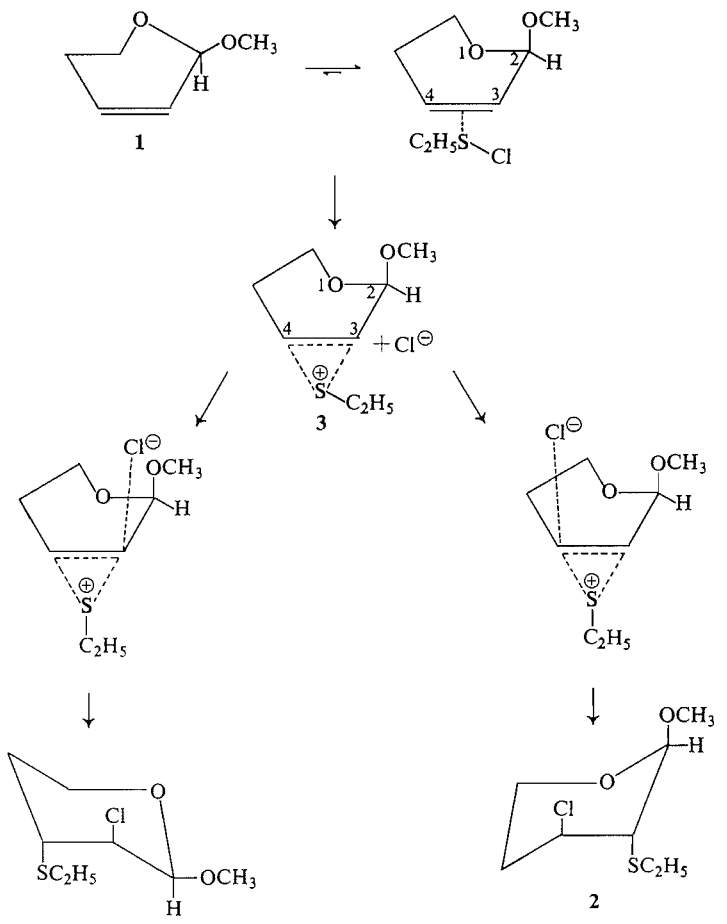

SCHEME 2

The 60 MHz n.m.r. spectra were obtained by Mr. Robert Swindlehurst with a Varian Associates A-60 spectrometer. The 100 MHz n.m.r. spectra and decoupling experiments were made by Mr. Glen Bigham using a Varian Associates HR–100 instrument. The solvent used was $CDCl_3$. The reference material was tetramethylsilane.

Solvents were generally removed by rotary evaporator under vacuum unless otherwise stated.

2-Methoxy-5,6-dihydro-2H-pyran was prepared by a modification (16) of the procedure of Woods and Sanders (17).

Ethanesulfenyl chloride was prepared by the following procedure, based on the general method of Brintzinger *et al.* (18). In an efficient fume hood ethyl disulfide (60 g, 0.4 mole) in a 1 l flask protected with a calcium chloride tube, was cooled to −70° in a dry ice–acetone bath. To this was added sulfuryl chloride (55 g, 0.4 mole) dropwise, with stirring. The solution became orange immediately. During the addition, the solution was allowed to warm slowly to room temperature to prevent precipitation. When the addition was completed, the reaction mixture was heated on a water bath at 45° for 20 min to aid in removal of sulfur dioxide. The mixture was then fractionally distilled under reduced pressure, yielding 51g (66%) of an orange liquid boiling at 40° at 60 mm (lit. b.p. 39° at 58 mm (19)). Ethanesulfenyl chloride was used immediately after its preparation since on standing at room temperature it became dark red within a few hours. Even storage in a freezing compartment failed to prevent its extensive decomposition.

3-Chloro-2-methoxytetrahydropyran was prepared by the method of Riobe (20).

4-Chloro-3-ethylthio-2-methoxytetrahydropyran. To a cold (−30°) stirred solution of ethanesulfenyl chloride (9.6 g, 0.1 mole) in 25 ml of anhydrous methylene chloride was added dropwise 2-methoxy-5,6-dihydro-2*H*-pyran (11.4 g, 0.1 mole). During the course of addition, the yellow color of the sulfenyl chloride slowly disappeared. When the addition was complete, a solution of sodium methoxide (5.4 g, 0.1 mole) in 25 ml of dry methanol was added and the reaction mixture allowed to warm to room

Can. J. Chem. Downloaded from www.nrcresearchpress.com by 210.87.254.40 on 09/05/12
For personal use only.

temperature. Removal of the solvents left a sludge which was dissolved in ether. This caused precipitation of dissolved solids. The ether solution was filtered, washed with water, dried ($MgSO_4$) and freed from solvent. Distillation of the residual pale-yellow oil afforded 14 g (67%) of *trans,trans*-4-chloro-3-ethylthio-2-methoxytetrahydropyran; b.p., 77–79° at 0.05 mm; η_D^{26}-, 1.5001.

Anal. Calcd. for $C_8H_{15}ClO_2S$ (mol. wt.: 210): C, 45.61; H, 7.18; Cl, 16.83. Found (208 (by osmometry)): C, 45.70; H, 7.31; Cl, 16.83. The 100 MHz n.m.r. spectrum is shown in Fig. 1 and the significant details are described in the Discussion.

Acknowledgment

The authors whish to thank the National Research Council of Canada for financial support during the course of this work.

1. M. J. BALDWIN and R. K. BROWN. Can. J. Chem. **45**, 1195 (1967).
2. M. J. BALDWIN and R. K. BROWN. Can. J. Chem. **46**, 1093 (1968).
3. N. KHARASCH and C. M. BUESS. J. Am. Chem. Soc. **71**, 2724 (1949).
4. N. KHARASCH and A. J. HAVLIK. J. Am. Chem. Soc. **75**, 3734 (1953).
5. A. J. HAVLIK and N. KHARASCH. J. Am. Chem. Soc. **78**, 1207 (1956).
6. H. KWART and R. K. MILLER. J. Am. Chem. Soc. **78**, 5678 (1956).
7. W. H. MUELLER and P. E. BUTLER. J. Am. Chem. Soc. **88**, 2866 (1966).
8. W. H. MUELLER and P. E. BUTLER. J. Am. Chem. Soc. **90**, 2075 (1968).
9. G. VAN DYKE TIERS. Characteristic nuclear magnetic resonance shielding values for hydrogen in organic structures. Minnesota Mining and Manufacturing Co., Organic Section, St. Paul, Minnesota. Project 737 602. March 28, 1958. pp. 12–14, Table II.
10. E. L. ELIEL, N. L. ALLINGER, S. J. ANGYAL, and G. A. MORRISON. Conformational analysis. John Wiley and Sons, Inc., New York, N.Y. 1965. pp. 375–377.
11. R. M. SRIVASTAVA, F. SWEET, and R. K. BROWN. Unpublished results.
12. E. J. LANGSTAFF, E. HAMANAKA, G. A. NEVILLE, and R. Y. MOIR. Can. J. Chem. **45**, 1907 (1967).
13. R. A. B. BANNARD, A. A. CASSELMAN, and L. R. HAWKINS. Can. J. Chem. **43**, 2398 (1965).
14. S. J. ANGYAL. Chem. Ind. (London), 1230 (1954).
15. F. SWEET and R. K. BROWN. Can. J. Chem. **46**, 707 (1968).
16. M. J. BALDWIN and R. K. BROWN. Can. J. Chem. **47**, 3099 (1969).
17. G. F. WOODS and H. SANDERS. J. Am. Chem. Soc. **68**, 2484 (1946).
18. H. BRINTZINGER, M. LANGHECK, and H. ELLWANGER . Ber. **87**, 320 (1954).
19. H. BRINTZINGER and M. LANGHECK. Ber. **86**, 557 (1953).
20. O. RIOBE. Bull. Soc. Chim. 829 (1951).

Can. J. Chem. Downloaded from www.nrcresearchpress.com by 210.87.254.40 on 09/05/12
For personal use only.

Can. J. Chem. Downloaded from www.nrcresearchpress.com by 210.87.254.105 on 09/05/12
For personal use only.

Reaction of 3-aroylaziridines with aryl isothiocyanates

J. W. LOWN, G. DALLAS,[1] AND T. W. MALONEY

Department of Chemistry, University of Alberta, Edmonton, Alberta

Received March 10, 1969

3-Aroylaziridines react with a variety of aryl isothiocyanates in refluxing benzene to give either (*a*) 4-aroyl-5-arylamino-4-thiazolines by a [2 + 3] cycloaddition and/or (*b*) 2-arylamino-4-aroyl-4-thiazolines. When the *N*-substituent of the aziridine is cyclohexyl or isopropyl the product type (*a*) is isolated in greater quantity, but when the *N*-substituent is methyl, product type (*b*) is isolated in greater quantity. The reactions provide convenient one-step syntheses of new 4-aroyl-4-thiazolines.

Canadian Journal of Chemistry, 47, 3557 (1969)

Recently, interest has been shown in the addition reactions of substituted aziridines involving cleavage of the 2–3 bond to an azomethine ylid and subsequent [2 + 3] cycloaddition to the acetylenic bond and to activated alkenes (1–14). We have reported the analogous addition of 3-aroylaziridines to the polarized carbonyl bond of diphenylcyclopropenone with the formation of novel 4-oxazolines (15, 16). In a continuing study of these addition reactions of 3-aroylaziridines to heteromultiple bonds we now report their addition to aryl isothiocyanates.

Treatment of 1-cyclohexyl-2-phenyl-3-*p*-toluoylaziridine with an equimolar quantity of *p*-nitrophenyl isothiocyanate in refluxing benzene, followed by chromatographic separation on alumina, afforded 3-cyclohexyl-5-*p*-nitrophenylamino-2-phenyl-4-*p*-toluoyl-4-thiazoline **3** (Table I) in 54% yield as orange-red crystals, m.p. 206–207°. The analytical and spectral data on this and similar 4-thiazolines is summarized in Tables I and II and are clearly consistent with structure **3**. In particular the strong hydrogen bonding in a favorable six-membered ring is confirmed by the infrared (i.r.) data, 3050 (broad, bonded NH), 1605(s) (aryl ketone strongly shifted hydrogen bonding), 1589(s) (C=N stretch), and the observation of the low field exchangeable hydrogen bonded NH proton at 13.4 δ in the nuclear magnetic resonance (n.m.r.), spectrum.

This reaction is mechanistically rationalized as involving thermal cleavage of the aroylaziridine to an azomethine ylid and concerted [2 + 3] cycloaddition of this species to the C=S bond of the aryl isothiocyanate and tautomerisation of the product to **3**. It has been observed that the C=S bond of an isothiocyanate will undergo [2 + 3] cycloaddition with diazocompounds, ketocarbenes, alkylene oxides and thioketocarbenes to form five-membered ring heterocycles (17), and that the C=S bond in general displays unusually great activity as a dipolarophile (18).

Huisgen has pointed out that the orientation of 1,3 dipolar additions may not be safely predicted on pragmatic grounds of the assignment of nucleophilic and electrophilic centers in

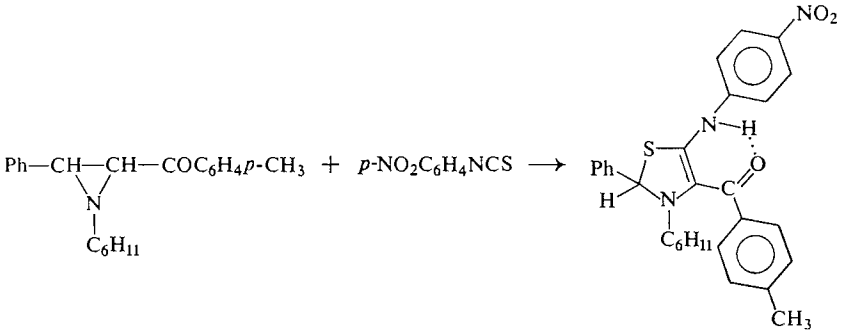

3

[1]NRCC Studentship holder 1967–1969.

Can. J. Chem. Downloaded from www.nrcresearchpress.com by 210.87.254.105 on 09/05/12
For personal use only.

TABLE I

4-Aroyl-5-arylamino-4-thiazolines*

No.	R_3	R_4	R_5	Melting point	Yield (%)	Observed C	H	N	S	Mol. ion (Mass spec.)	Calculated C	H	N	S	Mol. ion
1.	C_6H_{11}	$pCH_3C_6H_4$	C_6H_5	170–171°	59	76.35	6.90	5.93	6.74	454.2081	76.61	6.65	6.16	7.05	454.2079
2.	$(CH_3)_2CH$	C_6H_5	C_6H_5	158°	31	75.10	5.98	6.92	8.15	400.1608	74.96	6.04	7.00	8.00	400.1610
3.	C_6H_{11}	$pCH_3C_6H_4$	$pNO_2C_6H_4$	206–207°	54	69.44	5.80	8.38	6.48	499.1931	69.71	5.85	8.41	6.42	499.1930
4.	C_6H_{11}	$pCH_3C_6H_4$	$mNO_2C_6H_4$	122°	48	69.84	6.31	—	6.37	499.1931	69.71	5.85	—	6.42	499.1930
5.	$(CH_3)_2CH$	C_6H_5	$mNO_2C_6H_4$	97°	20.5	67.35	5.06	9.45	7.36	445.1458	67.39	5.20	9.43	7.20	445.1460
6.	C_6H_{11}	$pCH_3C_6H_4$	1-naphthyl $C_{10}H_8$	204°	32	78.65	6.32	5.53	6.36	504.2235	78.53	6.39	5.55	6.35	504.2236
7.	C_6H_{11}	$pNO_2C_6H_4$	$pNO_2C_6H_4$	160°	49	63.22	5.11	10.51	6.16	530.1628	63.38	4.94	10.56	6.04	530.1624
8.	C_6H_{11}	$pNO_2C_6H_4$	$mNO_2C_6H_4$	167°	20	63.29	4.69	10.38	6.07	530.1620	63.38	4.94	10.56	6.04	530.1624
9.	C_6H_{11}	$pNO_2C_6H_4$	1-naphthyl $C_{10}H_8$	204°	5	71.94	5.41	7.95	6.00	535.1927	71.75	5.45	7.85	5.99	535.1930
10.	C_6H_{11}	$pNO_2C_6H_4$	$pC_6H_5—C_6H_4$	200°	49	72.86	5.40	7.56	5.87	561.2084	72.70	5.56	7.48	5.71	561.2086
11.	C_6H_5	C_6H_{11}	C_6H_5	156°	20	75.99	6.42	6.38	7.47	440.1927	76.33	6.40	6.36	7.28	440.1923

*Compounds of structure 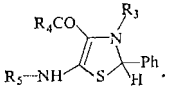

.

Can. J. Chem. Downloaded from www.nrcresearchpress.com by 210.87.254.105 on 09/05/12
For personal use only.

TABLE II

Spectroscopic properties of 4-aroyl-5-arylamino-4-thiazolines

	Infrared spectrum ($CHCl_3$)			Nuclear magnetic resonance ($CDCl_3$)δ						Absorption spectrum (CH_3CN)	
No.	N—H bonded	C=O	C=N	Aryl protons	2-proton	$(CH_3)_2CH$	*N*-Alkyl groups	Aryl methyl	Chelated N—H	λ_{max}	Log ε
1.	3050 br	1610(s)	1595(s)	8.16–6.92 (14H)m	5.90 (1H)s	—	1.96–0.75 (11H)m C_6H_{11}	2.33 (3H)s	13.14 (1H)s	260 350 420	4.16 3.97 4.09
2.	3050 br	1610(s)	1592(s)	8.25–7.0 (14H)m	5.87 (1H)s	3.17(1H) m $J = 7Hz$	1.05–1.09 (3H)d (3H) $J = 7Hz$	—	13.20 (1H)s	250 350 415	4.22 3.10 4.09
3.	3050(m) br	1605(s)	1589(s)	8.4–7.1 (13H)m	6.02 (1H)s	—	2.15–0.75 (11H)m C_6H_{11}	2.32 (3H)s	13.23 (1H)s	255 280 365 440	4.16 4.16 4.09 4.11
4.	3050(m) br	1602(s)	1590(s)	8.31–7.12 (13H)m	6.09 (1H)s	—	2.17–0.77 (11H)m C_6H_{11}	2.36 (3H)s	13.26 (1H)s	233 350 430	3.93 4.05 4.15
5.	3050(m) br	1610(s)	1600(s)	8.36–7.24 (14H)m	6.00 (1H)s	3.18(1H) m $J = 6.5Hz$	1.12 d (6H) $J = 6.5Hz$	—	13.19 (1H)s	252 355 424	4.36 3.98 4.10
6.	2990 br	1600(s)	1592(s)	8.56–6.82 (16H)m	5.97 (1H)s	—	3.31–0.82 (11H)m C_6H_{11}	2.37 (3H)s	13.02 (1H)s	260 350 420	4.31 3.94 4.17
7.	3100 br	1600(s)	1588	8.52–7.10 (13H)m	6.08 (1H)s	—	3.0–0.77 (11H)m C_6H_{11}	—	13.16 (1H)s	250 290 375 460	4.32 4.26 4.09 4.17
8.	3090 br	1590(s)	1580(s)	8.58–7.20 (13H)m	6.10 (1H)s	—	3.10–0.83 (11H)m C_6H_{11}	—	13.07 (1H)s	265 455	4.40 4.14
9.	3050 br	1590(s)	1585(sh)	8.60–6.80 (16H)s	6.01 (1H)s	—	3.25–0.26 (11H)m C_6H_{11}	—	12.96 (1H)s	272 457	4.36 4.16
10.	3050 br	1610(s)	1595(s)	8.54–7.16 (18H)m	6.08 (1H)s	—	3.0–0.68 (11H)m C_6H_{11}	—	13.30 (1H)s	260 340 420	4.71 3.74 3.82
11.	3080 br	1610(s)	1590(s)	8.30–6.90 (15H)m	5.95 (1H)s	—	3.0–0.6 (11H)m C_6H_{11}	—	13.20 (1H)s	250 320 416	4.20 3.98 4.03

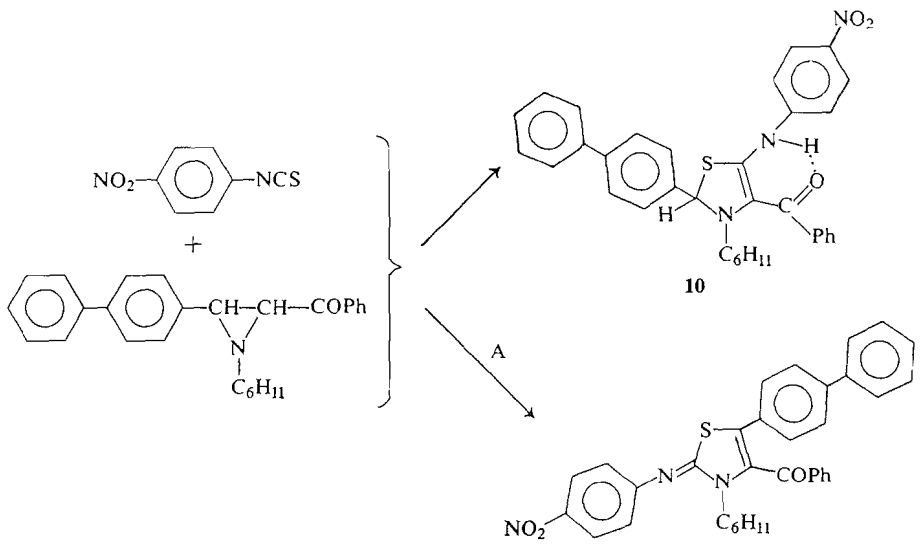

the 1,3 dipole (18). However, in the present reaction, hydrogen bonding of the N—H bond to the carbonyl group uniquely confirms the mode of addition. This reaction therefore provides a useful and facile route to 4-aroylthiazolines and its scope was now explored by examining the reactions of a series of aroylaziridines with a variety of aryl isothiocyanate.

It was anticipated that the above [2 + 3] cycloaddition would in many cases have to compete with nucleophilic attack by the isothiocyanate grouping at the 2-position of the aziridine ring, which Cromwell has pointed out is electrophilic (19).

In the reaction of 3-benzoyl-1-cyclohexyl-2-*p*-biphenylylaziridine with *p*-nitrophenyl isothiocyanate for example products **10** (Tables I and II) and **15** (Tables III and IV) were isolated corresponding respectively to [2 + 3] cycloaddition via the azomethine ylid and to aziridine ring opening at the 2 position and subsequent cyclisation to a 2-arylimino-4-aroyl-4-thiazoline. One of the referees has suggested that compound **15** could also be formed by a [2 + 3] polar cycloaddition.

Gabriel has reported that reaction of aziridine with potassium thiocyanate gives 2-iminothiazolidine (20, 21).

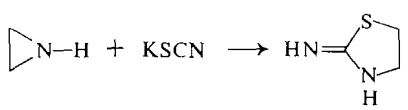

Therefore the initial product of reaction (A) might be expected to be the thiazolidine, and in fact in one example such a thiazolidine was isolated, but in general, the initially formed thiazolidine is dehydrogenated, either during the reaction or in the work-up to the iminothiazoline such as **15**. The iminothiazoline **15** and similar compounds are readily characterized by the observation in the i.r. spectrum of strong C=N stretch and strongly conjugated aryl ketone absorption and the absence of a hydrogen bonded proton characteristic of **10** and similar compounds. In contrast alkyl and aryl isothiocyanates react with aziridines having a free N—H, and gives thioureas (22, 23).

The course of the present reaction of aroylaziridines with aryl isothiocyanates often leads to complex mixtures of oils from which major solid products can be isolated by column chromatography. The data summarized in Table V is given as a preparative guide only, of the dependence of the course of the reaction principally on the nature of the *N*-substituent of the aziridine. While no quantitative conclusions may be drawn from the above observations it is evident in a qualitative sense that when the *N*-substituent of the aziridine is cyclohexyl or isopropyl the [2 + 3] cycloaddition mode is favored in reaction with phenyl isothiocyanate, *p*-nitrophenyl isothiocyanate, *m*-nitrophenyl isothiocyanate, and 1-naphthyl isothiocyanate.

However when the *N*-substituent of the

Can. J. Chem. Downloaded from www.nrcresearchpress.com by 210.87.254.105 on 09/05/12
For personal use only.

Can. J. Chem. Downloaded from www.nrcresearchpress.com by 210.87.254.105 on 09/05/12
For personal use only.

TABLE III

2-Arylimino-4-aroyl-4-thiazolines*

No.	$\frac{R_2}{R_3}$	$\frac{R_4}{R_5}$	Melting point	Yield (%)	Observed C	H	N	S	Mol. ion (Mass spec.)	Calculated C	H	N	S	Mol. ion
12	$\frac{C_6H_5}{CH_3}$	$\frac{C_6H_5}{C_6H_5}$	219–221°	31	74.40	4.69	7.44	8.31	370.1140	74.57	4.90	7.56	8.65	370.1140
13	$\frac{\text{1-naphthyl } C_{10}H_8}{CH_3}$	$\frac{C_6H_5}{C_6H_5}$	275°	20	76.85	4.97	6.37	7.83	420.1301	76.75	5.25	6.63	7.59	420.1297
14	$\frac{C_6H_5}{CH_3}$	$\frac{pCH_3C_6H_4}{C_6H_5}$	248°	20	74.64	5.40	7.25	8.40	(M^+-1)† 383.1220	74.97	5.24	7.29	8.34	(M^+-1) 383.1219
15	$\frac{pNO_2C_6H_4}{C_6H_{11}}$	$\frac{C_6H_5}{pC_6H_5C_6H_4}$	183°	25	72.68	5.38	7.43	5.74	559.1935	72.96	5.22	7.51	7.53	559.1930

*Compounds of structure 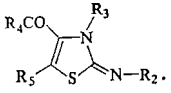

†Parent peak too small to measure.

Can. J. Chem. Downloaded from www.nrcresearchpress.com by 210.87.254.105 on 09/05/12
For personal use only.

TABLE IV

Spectroscopic properties of 2-arylimino-4-aroyl-4-thiazolines*

No.	$\frac{R_2}{R_3}$	$\frac{R_4}{R_5}$	Infrared spectrum ($CHCl_3$) C=O	Infrared spectrum ($CHCl_3$) C=N	Nuclear magnetic resonance $\delta(CDCl_3)$ Aryl protons	Nuclear magnetic resonance $\delta(CDCl_3)$ Alkyl Protons	Absorption spectrum (CH_3CN) λ_{max}	Log ε	λ_{max}	Log ε	λ_{max}	Log ε
12	$\frac{C_6H_5}{CH_3}$	$\frac{C_6H_5}{C_6H_5}$	1615(s)	1597(s)	8.40–7.13 (15H)m	3.78 (3H)s *N*–CH_3	418	3.85	336	3.76	250	4.54
13	$\frac{\text{1-naphthyl } C_{10}H_9}{CH_3}$	$\frac{C_6H_5}{C_6H_5}$	1605(s)	1595(s)	8.35–6.90 (17H)m	3.97 (3H)s *N*–CH_3	420	4.86	320	3.81	250	4.47
14	$\frac{C_6H_5}{CH_3}$	$\frac{pCH_3C_6H_4}{C_6H_5}$	1615(s)	1600(s)	8.30–7.0 (14H)m	2.39(3H)s aryl Me 3.81 (3H)s *N*–Me	420	3.82	340	3.75	255	4.45
15	$\frac{pNO_2C_6H_4}{C_6H_{11}}$	$\frac{C_6H_5}{pC_6H_5C_6H_4}$	1605(s)	1586(s)	8.30–7.15 (18H)m	2.3–0.8 (11H)m C_6H_{11}	420	3.82	340	3.74	260	4.71

*Compounds of structure 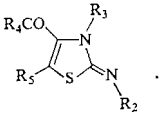 .

TABLE V

Substituent dependence of the reaction course in the reaction of 3-aroylaziridines with arylisothiocyanates

3-Aroylaziridine and number of examples	Product type and % yield range	
	5-Arylamino-4-thiazoline	2-Arylimino-4-thiazoline
Ph-CH—CH-COAr (8) N C_6H_{11}	(59–21)	—
Ph-CH—CH-COAr (2) N $CH(CH_3)_2$	(31–21)	—
Ph-CH—CH-COAr (3) N CH_3	—	(43–20)
pC_6H_5-C_6H_4-CH—CH-COPh (1) N C_6H_{11}	49	25

aziridine is methyl, nucleophilic attack at the 2-position of the aziridine is favored leading to the 2-arylimino-4-thiazoline. The yields in Table V represent isolated and purified products after chromatography and no attempt has been made to optimize the yields. *N*-Benzyl substituted 3-aroylaziridines are found to be unsatisfactory in attempted [2 + 3] cycloadditions in this and in other studies (1, 24) where the superior migratory aptitude of the benzyl group favors a Stevens rearrangement of the intermediate azomethine ylid. The thermolysis of 2,3-diphenylaziridine results in a similar rearrangement (5). 3-Benzoyl-1-cyclohexyl-2-phenylaziridine is exceptional in that upon reaction with phenyl isothiocyanate [2 + 3] cycloaddition affords **11** (Table I) and nucleophilic ring opening and subsequent ring closure given the iminothiazolidine **16** (see Experimental) and not the dehydrogenation product.

Compound **16** isomeric with **11** shows an AB quartet due to the 4,5 protons of the thiazolidine ring, the coupling constant of which, 3Hz, corresponds to a *trans* arrangement (8) of these protons in a five-membered ring and confirms, as predicted, that the original 2–3 bond of the aroylaziridine is still intact. Normally dehydrogenation of the initially formed 2-iminothiazolidine to the 2-iminothiazoline occurs during the reaction but **16** proved to be unusually resistant to dehydrogenation, presumably accounting for its isolation in this reaction.

The dehydrogenation of structurally related thiazolines by quinones has been investigated by Kenner and co-workers (25) who found that 9,10-phenanthrenequinone was often satisfactory whereas higher potential quinones such as 2,3-dichloro-5,6-dicyano-1,4-benzoquinone led to more extensive decomposition. Reaction of **16** with 9,10-phenanthrenequinone in acetic acid

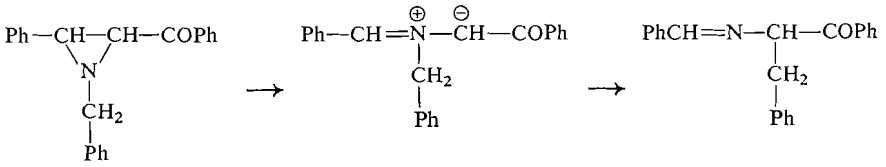

Can. J. Chem. Downloaded from www.nrcresearchpress.com by 210.87.254.105 on 09/05/12
For personal use only.

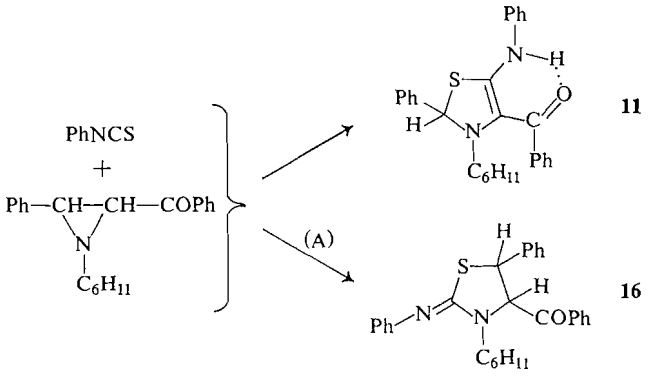

resulted in dehydrogenative elimination of benzaldehyde to form **17.**

Compound **17** gives correct analytical figures, mass spectral parent peak, the i.r. confirms the absence of an aryl ketone band and the 4-vinyl proton is prominent in the n.m.r. spectrum. The above reaction is analogous to decarboxylative dehydrogenation (26). The abnormal resistance to dehydrogenations of this type has been noted in certain other five-membered ring heterocycles (6).

Treatment of **16** with the higher potential quinone tetrachloro-1,2-benzoquinone in benzene afforded the 2-arylaminothiazole **18.** The [2 + 3] cycloaddition of other reactive hetero-multiple bonds to aroylaziridines is currently under investigation.

Experimental

Melting points were determined on a Fisher–Johns apparatus and are uncorrected. Infrared spectra were recorded on a Perkin–Elmer model 421 spectrophotometer, and only the principal, sharply defined peaks are reported. Nuclear magnetic resonance spectra were recorded on Varian A-60 and A-100 analytical spectrometers. The spectra were measured on approximately 10–15% (w/v) solutions in $CDCl_3$, with tetramethylsilane as a standard. Line positions are reported in parts per million (p.p.m.) from the reference. Absorption spectra were recorded in 'spectrograde' solvents on a Beckman DB recording spectrophotometer. Mass spectra were determined on an Associated Electrical Industries MS–9 double focusing high resolution mass spectrometer. The ionisation energy, in general, was 70 eV. Peak measurements were made by comparison with perfluorotributylamine at a resolving power of 15 000. Kieselgel DF-5 (Camag, Switzerland) and Eastman Kodak precoated sheets were used for thin-layer chromatography. Microanalyses were carried out by Dr. C. Daesslé, Organic Microanalysis Ltd., Montreal, Quebec and by Mrs. D. Mahlow of this department.

General Preparation of 3-Aroylaziridines

These compounds were prepared by established methods involving aldol type condensations to form the chalcones, then addition of bromine to form the dibromochalcone and treatment of the latter with primary amines to provide the aroylaziridines. Several new aroylaziridines have been prepared by this method exemplified as follows.

Preparation of 3-Benzoyl-1-isopropyl-2-phenylaziridine

Isopropylamine 24 g, (0.407 mole) was added dropwise to a stirred solution of 50 g (0.136 mole) of 2,3-

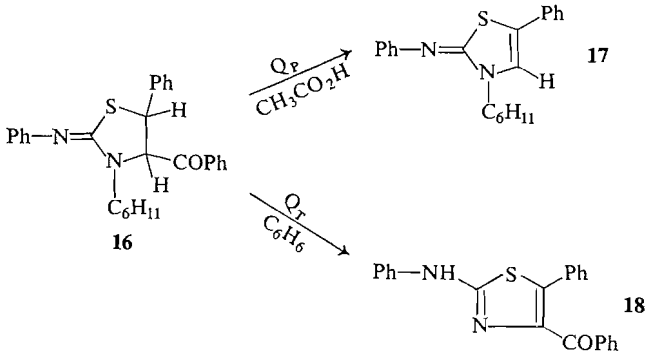

Q_P = 9,10-phenanthrenequinone
Q_T = tetrachloro-1,2-benzoquinone

Can. J. Chem. Downloaded from www.nrcresearchpress.com by 210.87.254.105 on 09/05/12
For personal use only.

Can. J. Chem. Downloaded from www.nrcresearchpress.com by 210.87.254.105 on 09/05/12
For personal use only.

dibromo-3-phenylpropiophenone (Eastman Kodak Co.) in 700 ml of dry benzene at 0°, then the solution was stirred for 1 h at 0° and set aside for 24 h at room temperature. The precipitated isopropylamine hydrobromide was collected (34 g; theoretical yield 34 g) and the yellow filtrate washed with water to remove excess amine, dried ($MgSO_4$), and the solvent removed *in vacuo*. The residual oil consisted of an approximately 1:1 mixture of *cis* and *trans* 3-benzoyl-1-isopropyl-2-phenylaziridines (36 g) 100% yield which crystallized partly on chilling. For reaction with the arylisothiocyanates the mixture of isomeric aroylaziridines was used as in previous work (13) but a small quantity was separated into isomers for analytical purposes by preparative thin-layer chromatography on silica with (3:1) benzene:heptane which afforded the pure *cis* isomer and slightly impure *trans*. The latter could be obtained isomerically pure by further chromatography on Fisher alumina in heptane. The stereochemistry was readily assigned by reference to the n.m.r. spectrum (27).

cis-Isomer, pale-yellow crystals m.p. 90–91° (heptane).

Anal. Calcd. for $C_{18}H_{19}NO$ (mol. wt., 265.1467): C, 81.51; H, 7.17; N, 5.28. Found (mol. wt. (mass spectrum) 265.1468): C, 81.32; H, 7.20; N, 5.34.

Infrared spectrum: ν_{max} ($CHCl_3$); 1683 cm^{-1} (aryl C=O). Nuclear magnetic resonance spectrum ($CDCl_3$): 1.22 (doublet, 6H; J = 5.7Hz; $(CH_3)_2CH$—); 1.86 (septet, 1H, $(CH_3)_2$ C*H*), 3.18 (singlet 2H, aziridine ring protons), 7.00–7.50 and 7.80–8.01 (multiplet 10H, aryl protons).

trans-Isomer, low-melting yellow solid, m.p. <25°.

Anal. Calcd. for $C_{18}H_{19}NO$ (mol. wt., 265): C, 81.51; H, 7.17; N, 5.28. Found (mol. wt. (mass spectrum) 265): C, 81.50; H, 7.39; N, 5.05.

Infrared spectrum: ν_{max} ($CHCl_3$) 1662 cm^{-1} (aryl C=O). Nuclear magnetic resonance spectrum ($CDCl_3$): 0.91 (doublet, 3H; J = 6Hz; 1.18, doublet 3H, J = 6Hz; $(CH_3)_2CH$—), 2.19 (multiplet, 1H, $(CH_3)_2CH$—), 3.46–3.66 (AB quartet, 2H, aziridine ring protons); 7.16–7.58 and 7.96–8.16 (multiplets, 10H, aryl protons).

2,3-Dibromo-3-phenyl-p-nitropropiophenone

Styryl-*p*-nitrophenylketone was prepared in 74% yield m.p. 145–147° (lit. m.p. 149–150°) (28) then brominated to give 2,3-dibromo-3-phenyl-*p*-nitropropiophenone in 85% yield, m.p. 210° by the method of Weygand (29).

1-Cyclohexyl-3-p-nitrobenzoyl-2-phenylaziridine

This aziridine was prepared from 2,3-dibromo-3-phenyl-*p*-nitropropiophenone and cyclohexylamine by the standard procedure in 76% yield as an orange solid m.p. 112–113° (hexane).

Anal. Calcd. for $C_{21}H_{22}N_2O_3$ (mol. wt., 350.1630): C, 72.00; H, 6.29; N, 8.00. Found (mol. wt. (mass spectrum) 350.1634): C, 72.10; H, 6.32; N, 7.94.

Infrared spectrum ($CHCl_3$): ν_{max}: 1681, (C=O *cis* aziridine) 1656 cm^{-1} (C=O *trans* aziridine). Nuclear magnetic resonance spectrum ($CDCl_3$): 0.83–2.00 (multiplet, 10H, cyclohexyl CH_2), 2.33–2.76 (multiplet, 1H, cyclohexyl C*H*), 3.22 (singlet, 2H, *cis* aziridine ring protons) (25), 3.57 (singlet, 2H, *trans* aziridine ring protons), 7.18–8.35 (multiplet, 9H, aryl protons).

3-(p-Biphenylyl)-2,3-dibromo-1-phenyl-1-propanone

A solution of 12.6 g (0.0775 mole) of bromine in 50 ml of chloroform was added dropwise to a stirred solution of 22 g (0.0775 mole) of 4-(*p*-phenyl)-styrylphenyl ketone (32) in 100 ml of chloroform during 30 min. The solution was stirred for 15 min, then the solvent removed *in vacuo* to give the dibromo compound as a yellow solid m.p. 180–181°, 34.4 g, (quantitative yield). The product was purified by recrystallization from benzene: hexane as a white solid m.p. 185.5–186°.

Anal. Calcd. for $C_{21}H_{16}Br_2O$: C, 56.75; H, 3.63; Br, 35.99. Found: C, 56.66; H, 3.56; Br, 36.22.

Infrared spectrum ν_{max} ($CHCl_3$): 1690 cm^{-1} (aryl C=O). Nuclear magnetic resonance spectrum ($CDCl_3$): AB quartet centered at 5.76 and 5.92 (2H, J = 11Hz, 2,3 protons); 7.25–8.3 (multiplet, aryl protons).

3-Benzoyl-2-(p-biphenylyl)-1-cyclohexylaziridine

This aziridine was prepared as a *cis–trans* mixture from 22.2 g (0.05 mole) of 2-(*p*-biphenylyl)-2,3-dibromo-1-phenyl-1-propanone and 54.5 g (0.55 mole) of cyclohexylamine by the standard procedure in approximately quantitative yield as a white solid m.p. 127° (MeOH).

Anal. Calcd. for $C_{27}H_{27}NO$: C, 85.00; H, 7.14; N, 3.67. Found: C, 84.90; H, 7.23; N, 3.64.

Infrared spectrum ($CHCl_3$) ν_{max}: 1680 cm^{-1} (C=O). Nuclear magnetic resonance spectrum ($CDCl_3$): 1.0–3.0 (multiplet, 11H, cyclohexyl protons), 3.23 (singlet, 2H, *cis* aziridine ring protons) (27), 3.53 (singlet, 2H, *trans* aziridine ring protons), 7.2–8.3 (multiplet, 14H, aryl protons).

3-Benzoyl-1-methyl-2-phenylaziridine

This aziridine was prepared as a *cis–trans* mixture m.p. 88–89° by the method of Cromwell and co-workers (30).

3-Benzoyl-1-cyclohexyl-2-phenylaziridine

This aziridine was prepared by the method of Cromwell (31) *cis* isomer m.p. 107–109°; *trans* isomer m.p. 99–101°.

1-Methyl-2-phenyl-3-p-toluoylaziridine

This aziridine was also prepared by the above procedure (31) as a *cis–trans* mixture m.p. 76–78°.

1-Cyclohexyl-2-phenyl-3-p-toluoylaziridine

This aziridine was also prepared by the method of Cromwell (31) *cis* isomer m.p. 111–112°; and the *trans* isomer 89–90°.

Reaction of 3-Aroylaziridines with Aryl Isothiocyanates

General Method

The reaction method is exemplified by one reaction of each type in which [2 + 3] cycloaddition and nucleophilic ring opening predominated.

Reaction of 1-Cyclohexyl-2-phenyl-3-p-toluoylaziridine with p-Nitrophenyl Isothiocyanate

A solution of 2.16 g (0.0068 mole) of 1-cyclohexyl-2-phenyl-3-*p*-toluoyl-aziridine and 1.22 g (0.0068 mole) of *p*-nitrophenyl isothiocyanate in 30 ml of dry benzene was heated under reflux for 17 h when a deep orange color developed. The solution was concentrated *in vacuo* to ca. 12 ml and passed down a column of Grade 1 alumina (120 g). Elution with benzene afforded one main fraction which upon evaporation afforded 3-cyclohexyl-5-*p*-nitrophenylamino-2-phenyl-4-*p*-toluoyl-4-thiazoline as deep orange-red crystals 2.1 g (54% yield) m.p. 206–207° from ethyl acetate.

Can. J. Chem. Downloaded from www.nrcresearchpress.com by 210.87.254.105 on 09/05/12
For personal use only.

Anal. Calcd. for $C_{29}H_{29}N_3O_3S$ (mol. wt., 499.1930): C, 69.71; H, 5.85; N, 8.41; S, 6.42. Found (mol. wt. (mass spectrum) 499.1931): C, 69.44; H, 5.80; N, 8.38; S, 6.48.

Infrared spectrum: ν_{max} ($CHCl_3$), 1605(s) (C=O), 1589(s) (C=N), 1492(m) 3050 cm^{-1}(m) (broad, chelated hydrogen). Nuclear magnetic resonance spectrum ($CDCl_3$): 0.75–2.15 (11H, multiplet cyclohexyl protons), 2.32 (3H, singlet, aryl methyl), 6.02 (1H, singlet, 4-thiazoline proton), 7.10–8.4 (13H, multiplet, aryl protons), 13.23 (1H, singlet, exchangeable with D_2O, chelated NH proton).

Reaction of 3-Benzoyl-1-methyl-2-phenylaziridine with Phenyl Isothiocyanate

A solution of 1.39 g (0.0059 mole) of 3-benzoyl-1-methyl-2-phenylaziridine and 0.8 g (0.0059 mole) of phenyl isothiocyanate in 20 ml of dry benzene was heated under reflux for 12 h when a deep red-brown color developed. The cooled solution was subjected to chromatography on 70 g of Grade 1 alumina. Elution with benzene afforded one main fraction which upon evaporation of the solvent afforded an orange oil which crystallized upon trituration with ethyl acetate as golden-yellow plates of 4-benzoyl-3-methyl-2-phenylimino-5-phenyl-4-thiazoline, 0.68 g, (31% yield) m.p. 220–221° (from ethyl acetate).

Anal. Calcd. for $C_{23}H_{18}N_2OS$ (mol. wt., 370.1140): C, 74.57; H, 4.90; N, 7.56; S, 8.65. Found (mol. wt. (mass spectrum) 370.1140): C, 74.40; H, 4.69; N, 7.44; S, 8.31.

Infrared spectrum: ν_{max} ($CHCl_3$): 1615(s) (C=O), 1597(s) (C=N), 1497 cm^{-1}. Nuclear magnetic resonance spectrum ($CDCl_3$): 3.78 (3H, singlet N—CH_3 group), 7.13–8.40 (15H, multiplet, aryl protons).

Reaction of 3-Benzoyl-1-cyclohexyl-2-phenylaziridine with phenyl isothiocyanate

A solution of 6.35 g (0.0208 mole) of 3-benzoyl-1-cyclohexyl-2-phenylaziridine and 2.8 g (0.0208 mole) of phenyl isothiocyanate in 65 ml of dry benzene was heated under reflux for 7 h when a yellow-orange color developed. The cooled solution was concentrated to ca. 15 ml *in vacuo* and passed down a column of 200 g of Grade 1 alumina. Elution with benzene gave a yellow fraction which upon evaporation of the solvent gave a yellow solid, 1.74 g containing two products. Extraction with hot heptane allowed separation of the products:

(*a*) Insoluble in hexane was 4-benzoyl-3-cyclohexyl-2-phenylimino-5-phenylthiazolidine purified by recrystallization from benzene as pale-yellow crystals, 0.5 g, m.p. 204°.

Anal. Calcd. for $C_{28}H_{28}N_2SO$ (mol. wt., 440.1923): C, 76.33; H, 6.41; N, 6.36; S, 7.28. Found (mol. wt. (mass spectrum) 440.1927): C, 76.57; H, 6.78; N, 6.31; S, 7.34.

Infrared spectrum: ν_{max} ($CHCl_3$): 1673(s) (C=O); 1592(s) (C=N) 1490(m) cm^{-1}. Nuclear magnetic resonance spectrum ($CDCl_3$): 0.4–3.35 (11H, multiplet, cyclohexyl protons); AB quartet centered at 6.23 and 6.46 δ (J = 3Hz) (2H, 4,5 thiazolidine protons with *trans* geometry); 6.70–8.50 (15H, multiplet, aryl protons).

(*b*) Soluble in hexane was 4-benzoyl-3-cyclohexyl-2-phenyl-5-phenylamino-4-thiazoline 1.2 g, (20% yield) m.p. 156° (from benzene/hexane). Full details on this compound as well as the physical properties, analytical data and spectroscopic properties of the other 4-thiazolines synthesised may be found in Tables I to IV.

Reaction of 4-Benzoyl-3-cyclohexyl-2-phenylimino-5-phenyl-thiazolidine with 9,10-Phenanthrenequinone

A solution of 0.250 g (0.00057 mole) of the thiazolidine and 0.165 g (0.0008 mole) of 9,10-phenanthrenequinone in 3 ml of acetic acid was heated under reflux for 30 min, allowed to cool and diluted with 15 ml of ether and 15 ml of benzene and allowed to stand over 2.98 g of sodium carbonate overnight. The filtered solution was evaporated to dryness and the residual yellow solid taken up in 5 ml of benzene and subjected to chromatography on 15 g of Grade 1 alumina. Elution with benzene afforded two fractions:

(*a*) a white crystalline solid of 3-cyclohexyl-2-phenylimino-5-phenyl-1,3-thiazoline, 0.175 g (92% yield) m.p. 205° (from 1:1 benzene: petroleum ether).

Anal. Calcd. for $C_{21}H_{22}N_2S$ (mol. wt., 334.1504): C, 75.41; H, 6.63; N, 8.38; S, 9.59. Found (mol. wt. (mass spectrum) 334.1509): C, 75.57; H, 6.62; N, 8.41; S, 9.53.

Infrared spectrum: ν_{max} ($CHCl_3$): 1590(s) cm^{-1} (C=N). Nuclear magnetic resonance spectrum ($CDCl_3$): 0.83–2.48 (10H, multiplet, cyclohexyl protons), 4.57–5.19 (1H, broad multiplet, 1-cyclohexyl proton), 6.90 (1H, singlet, 4-proton) 6.8–7.50 (10H, multiplet, aryl protons).

Fraction (*b*) consisted of 9,10-phenanthrenequinone, 0.125 g m.p. 207°, mixture m.p. 207° with authentic material.

Reaction of 4-Benzoyl-3-cyclohexyl-2-phenylimino-5-phenyl-1,3-thiazolidine with Tetrachloro-1,2-benzoquinone

A solution of 0.421 g of the thiazolidine and 0.236 g of tetrachloro-1,2-benzoquinone in 20 ml of dry benzene was heated under reflux for 12 h during which time the red colour of the quinone was discharged. The cooled solution was passed down a column of 25 g of Grade 1 alumina and elution with benzene, affording one bright yellow fraction of 4-benzoyl-2-phenylamino-5-phenylthiazole 0.108 g (31% yield) m.p. 135° (from cyclohexane).

Anal. Calcd. for $C_{22}H_{16}N_2SO$ (mol. wt., 356.0984): C, 74.13; H, 4.52; N, 7.86; S, 9.00. Found (mol. wt. (mass spectrum) 356.0983): C, 73.95; H, 4.52; N, 7.87; S, 9.20.

Infrared spectrum: ν_{max} ($CHCl_3$): 1595 (C=O), 3150 (broad, NH). Nuclear magnetic resonance spectrum ($CDCl_3$): 6.91–8.52 (15H, multiplet, aryl protons), 11.92 (1H, exchangeable with D_2O, NH).

Acknowledgments

This research was supported by a National Research Council of Canada grant to J. W. Lown. We thank Mr. J. P. Moser for technical assistance and Mr. R. Swindlehurst and Dr. A. Hogg for the nuclear magnetic resonance and mass spectra, respectively.

1. P. B. Woller and N. H. Cromwell. J. Heterocyclic Chem. **5**, 579 (1968).

2. H. W. HEINE and R. PEAVY. Tetrahedron Letters, 3123 (1965).
3. B. K. CAMPBELL and K. N. CAMPBELL. J. Org. Chem. **9**, 178 (1944).
4. R. HUISGEN, W. SCHEER, G. SZEIMIES, and H. HUBER. Tetrahedron Letters, 397 (1966).
5. G. H. COLEMAN and G. P. WAUGH. Proc. Iowa Acad. Sci. **40**, 115 (1933); **49**, 286 (1942).
6. A. PADWA and L. HAMILTON. Tetrahedron Letters, 4363 (1963).
7. VON R. V. CAPELLER, R. GRIOT, M. HARING, and T. WAGNER-JAUREGG. Helv. Chim. Acta, **40**, 1652 (1957).
8. H. W. HEINE, R. E. PEAVY, and A. J. DURBETAKI. J. Org. Chem. **31**, 3924 (1966).
9. H. W. HEINE, A. B. SMITH, and J. D. BOWER. J. Org. Chem. **33**, 1097 (1968).
10. A. PADWA and L. HAMILTON. J. Heterocyclic Chem. **4**, 118 (1967).
11. A. PADWA and W. EISENHARDT. Chem. Commun. **7**, 380 (1968).
12. R. HUISGEN, W. SCHEER, and H. HUBER. J. Am. Chem. Soc. **89**, 1753 (1967).
13. S. OIDA and E. OHKI. Chem. Pharm. Bull. (Tokyo), **16**, 764 (1968).
14. H. W. HEINE and R. HENZEL. J. Org. Chem. **34**, 171 (1969).
15. J. W. LOWN, R. K. SMALLEY, and G. DALLAS. Chem. Commun. 1543 (1968).
16. J. W. LOWN and R. K. SMALLEY. Tetrahedron Letters, 169 (1969).
17. H. ULRICH. Organic chemistry. Vol. 9. Cycloadditon reactions of heterocumulenes. Academic Press, Inc., New York. 1967. p. 240.
18. R. HUISGEN. Angew. Chem. Intern. Ed. Eng. **2**, 572 (1963).
19. N. H. CROMWELL. Record Chem. Prog. Kresge-Hooker Sc. Li. **19**, 215 (1958).
20. S. GABRIEL and J. COLMAN. Ber. **47**, 1866 (1914).
21. J. E. EARLEY, C. E. O'ROURKE, L. B. CLAPP, J. O. EDWARDS, and B. C. LAWES. J. Am. Chem. Soc. **80**, 3458 (1958).
22. A. S. DEUTSCH and P. E. FANTA. J. Org. Chem. **21**, 892 (1956).
23. S. GABRIEL and R. STELZNER. Ber. **28**, 2929 (1895).
24. J. W. LOWN and R. K. SMALLEY. Unpublished results.
25. M. A. BARTON, G. W. KENNER, and R. C. SHEPPARD. J. Chem. Soc., C, 1061 (1966).
26. L. M. JACKMAN. *In* Advances in organic chemistry. Vol. II. Interscience Publishers, Inc., New York. 1960. p. 344.
27. A. E. POHLAND, R. C. BADGER, and N. H. CROMWELL. Tetrahedron Letters, 4369 (1965).
28. F. J. POND, O. P. MAXWELL, and G. M. NORMAN. J. Am. Chem. Soc. **21**, 966 (1899).
29. C. WEYGAND. Ann. **459**, 115 (1928).
30. N. H. CROMWELL and J. A. CAUGHLAN. J. Am. Chem. Soc. **67**, 2235 (1945).
31. N. H. CROMWELL, N. G. BARKER, R. A. WANKEL, P. J. VANDERHORST, F. W. OLSON, and J. H. ANGLIN. J. Am. Chem. Soc. **73**, 1044 (1951).
32. R. H. WILEY, C. H. JARBOE, F. N. HAYES, E. HANSBURY, J. T. NIELSEN, P. X. CALLAHAN, and M. C. SELLERS. J. Org. Chem. **23**, 732 (1958).

Can. J. Chem. Downloaded from www.nrcresearchpress.com by 210.87.254.105 on 09/05/12
For personal use only.

Can. J. Chem. Downloaded from www.nrcresearchpress.com by 210.87.254.40 on 09/05/12
For personal use only.

Comparison of proton magnetic resonance spectra of cell-wall mannans and galactomannans of selected yeasts with their chemical structures[1]

P. A. J. Gorin, J. F. T. Spencer, and R. J. Magus
Prairie Regional Laboratory, National Research Council of Canada, Saskatoon, Saskatchewan

Received March 3, 1969

Yeasts can often be identified with the aid of the distinctive proton magnetic resonance (p.m.r.) spectra of their cell-wall mannans or galactomannans. Some of the polysaccharides, such as the galactomannan of *Torulopsis gropengiesseri* and the mannan of *Saccharomyces rouxii* give p.m.r. spectra with only slight differences and have closely related chemical structures in terms of main chains and side chains. Other spectrally similar polysaccharides with related chemical structures have also been found. These are firstly the galactomannans of *Trichosporon fermentans* and *Candida lipolytica* and secondly the mannose-containing polysaccharides of *Torulopsis bombi* (*Torulopsis* species PRL 319-67), *Torulopsis magnoliae* and *Torulopsis apicola* (Hajsig strain). The mannans of *Candida catenulata* and *Endomycopsis fibuliger* give p.m.r. spectra with a lesser degree of similarity, but have markedly different chemical structures. These results show that polysaccharides with similar p.m.r. spectra have related chemical structures and may therefore arise from phylogenetically related yeasts.

Canadian Journal of Chemistry, 47, 3569 (1969)

Recently we have isolated mannose-containing polysaccharides from yeast cell-walls by extraction with hot aqueous alkali followed by purification via their insoluble copper complexes. The H-1 portions of proton magnetic resonance (p.m.r.) spectra of the polysaccharides have proved to be of considerable aid in classification and identification of the yeasts from which they originate (1–6). Many spectra can be grouped if they are identical or bear marked similarities to each other and if these similarities reflected resemblances in polysaccharide structure it is then likely that the originant yeasts are related. We therefore determined the chemical structures of three groups of mannose-containing polysaccharides which give similar spectra. These polymers arose from *a*) *Torulopsis gropengiesseri* and *Saccharomyces rouxii*, *b*) *Candida catenulata* and *Endomycopsis fibuliger*, and *c*) *Trichosporon fermentans* and *Candida lipolytica* (Fig. 1). Also the mannan from a glycolipid-producing *Torulopsis* species PRL 319-67 was compared with a spectrally similar galactomannan from *Torulopsis magnoliae*, the mannose-containing polysaccharides of *Torulopsis apicola* (Hajsig strain) and *Torulopsis gropengiesseri*, species which may be related on the basis of biochemical tests.

(i) Mannose-containing Polysaccharides of Torulopsis spp.

Methylation–fragmentation analysis revealed differences between the mannose-containing polysaccharides of PRL 319-67, *T. magnoliae*, *T. apicola* and *T. gropengiesseri*. In particular *T. magnoliae* and *T. gropengiesseri* galactomannans contained galactopyranosyl non-reducing end-units (Table I).

Some dissimilarities between the polysaccharides were found on determination of specific rotations, galactose content, and periodate oxidation characteristics (Table II). On ultracentrifugation *T. magnoliae* galactomannan gave two peaks whereas one peak was obtained from the other polysaccharides.

Significance can be attached to the unit-size distributions of the free oligosaccharides formed following cleavage by partial acetolysis of the α-(1 → 6)-linkages in the polysaccharides. These fragments arise from side-chains of different length. Large fragments of 2–8 hexose units were obtained from the mannan of PRL 319-67, similar to those of *T. magnoliae* galactomannan (2–10 units) and *T. apicola* (Hajsig) mannan (2–6 units) (Table III). Only short fragments of 2 and 3 units were obtained from *T. gropengiesseri* galactomannan. The above fragments were identified as α-(1 → 2)-linked D-mannopyranose oligosaccharides by p.m.r. spectroscopy (2) and their specific rotations (ca. +55°). Each oligosaccharide fraction from *T. magnoliae* galactomannan, although giving a similar type of p.m.r. spectrum gave a trace of galactose on hydrolysis and had slightly higher specific rotations than its mannose-containing counterpart.

It can be seen that the polysaccharides giving closely related p.m.r. spectra have closely related

[1]NRCC No. 10799.

Can. J. Chem. Downloaded from www.nrcresearchpress.com by 210.87.254.40 on 09/05/12
For personal use only.

TABLE I

Gas–liquid chromatographic identification and estimation* of partially methylated glycosides formed on methylation–fragmentation of yeast mannans and galactomannans

Source of mannan or galactomannan	Methyl 2,3,4,6-tetra-*O*-methyl-galactoside	Methyl 2,3,4,6-tetra-*O*-methyl-mannoside	Methyl 2,3,4-tri-*O*-methyl-mannoside	Methyl 3,4,6-tri-*O*-methyl-mannoside	Methyl 2,4,6-tri-*O*-methyl-mannoside	Methyl 3,4-di-*O*-methyl-mannoside	Methyl 2,4-di-*O*-methyl-mannoside
1. *Torulopsis bombi* (PRL 319-67)	—	10	7.2	28.8	—	+	—
2. *Torulopsis apicola* (Hajsig strain) CBS 2868	—	10	11.1	15.4	4.1	+	+
3. *Torulopsis magnoliae* CBS 166	7.7	2.3	3.4	5.2	—	+	—
4. *Torulopsis gropengiesseri* NRRL Y1445	7.7	2.3	2.6	2.1	—	+	—
5. *Saccharomyces rouxii* (14, 15) PRL 411-64	—	10	—	9.4	2.1†	+	—
6. *Trichosporon fermentans* (1) PRL 2263	8.2	1.8	3.5	3.9	—	+	—
7. *Candida lipolytica* CBS 599	8.3	1.7	6.7	5.8	—	+	—
8. *Candida catenulata* PRL 1S20	—	10	—	8.1	8.2	—	+
9. *Endomycopsis fibuliger* NCYC 13	—	10	—	1.7	1.7	+	—
10. *Torulopsis lactis-condensi* CBS 52	9.3	0.7	7.8		—	+	—
11. *Hansenula subpelliculosa* NRRL Y1683	—	10	6.4		1.8	+	+
12. *Schizosaccharomyces octosporus* (13) PRL F2	8.6	1.4	9.8‡	—	—	+	—

*The proportions are based on peak areas.
†Shown to arise from undermethylation since a Smith degradation gave glycerol, but no mannose.
‡7.3 parts of methyl 2,4,6-tri-*O*-methylgalactoside were also detected.

TABLE II

Yields, specific rotations, periodate oxidation data, and sugar ratios of yeast mannans and galactomannans

Source of mannose-containing polysaccharides	% Yield based on dry cells	Specific rotation in degrees	Periodate oxidation: Consumption of oxidant (mole/mole of anhydrohexose unit)	Periodate oxidation: Acid production (mole/mole of anhydrohexose unit)	Galactose to mannose ratio in galactomannan
1. *Torulopsis bombi* (PRL 319-67)	3	+70	1.39	0.39	—*
2. *Torulopsis apicola* (Hajsig strain)	3	+75	1.34	0.43	—*
3. *Torulopsis magnoliae*	5	+42	1.50	0.53	24:76
4. *Torulopsis gropengiesseri*	4	+46	1.38	0.47	21:69
5. *Saccharomyces rouxii* (14, 15)	7	+76	1.35	0.35	—*
6. *Trichosporon fermentans* (1)	6	+115	1.30	0.33	35:65
7. *Candida lipolytica*	4	+88	1.29	0.38	27:73
8. *Candida catenulata*	3	+110	0.89	0.29	—*
9. *Endomycopsis fibuliger*	8	+73	1.37	0.41	—*
10. *Torulopsis lactis-condensi*	6	+14			34:66
11. *Hansenula subpelliculosa*	8	+71	1.19	0.36	—*
12. *Schizosaccharomyces octosporus* (13)	1	+110	1.52	0.51	38:62

*Contains no galactose.

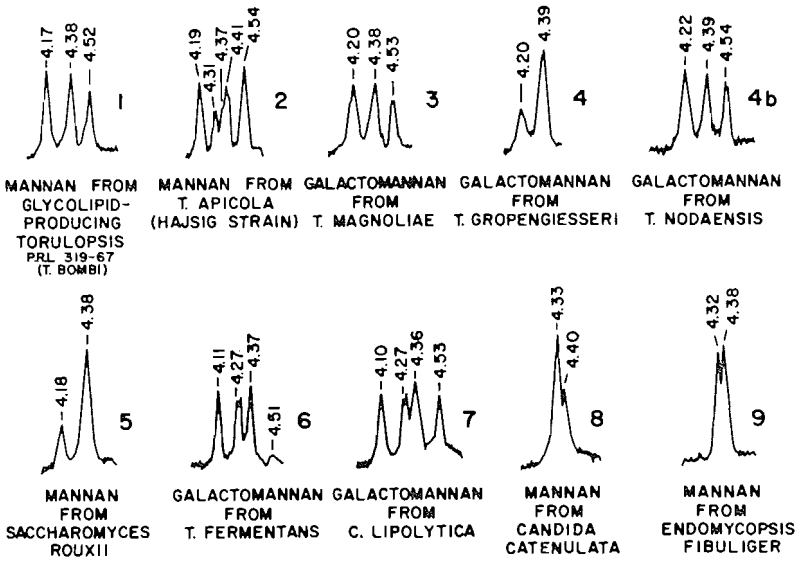

FIG. 1. H-1 Signals of proton magnetic resonance spectra (70°) of mannose-containing yeast polysaccharides (chemical shifts in τ).

TABLE III

Yields of (1 → 2)-linked α-D-mannopyranose oligosaccharides formed following partial acetolysis of mannans and galactomannans of four *Torulopsis* species

Source of mannan or galactomannan	Number of mannose units in oligosaccharide								
	2	3	4	5	6	7	8	9	10
	Percentage yields								
1. *Torulopsis bombi* (PRL 319-67)	7	9	8	9	6	3	1	—	—
2. *Torulopsis apicola* (Hajsig strain)	5	9	17	8	2	—	—	—	—
3. *Torulopsis magnoliae*	9	8	5	4	4	3	2	2	2
4. *Torulopsis gropengiesseri*	23	9	—	—	—	—	—	—	—

chemical structures in terms of main-chains and side-chains.[2] The p.m.r. spectrum (Spectrum 1, Fig. 1) and chemical structure of the mannan of *Torulopsis* sp. PRL 319-67 are close to, but not identical to those of the galactomannan of *T. magnoliae* (Spectrum 3, Fig. 1; Tables I, II, III, IV) and the mannan of *T. apicola* (Spectrum 2, Fig. 1; Tables I, II, III, IV). (There is similarity between the p.m.r. spectrum of the galactomannan of *Torulopsis nodaensis* (Spectrum 4*b*, Fig. 1) and that of PRL 319-67, but the former yeast has differences in its sugar assimilation reactions and does not produce glycolipid.) The p.m.r. spectrum and chemical structure of PRL 319-67 mannan bears little resemblance to those of *T. gropengiesseri* galactomannan (Spectrum 4, Fig. 1; Tables I, II, III, IV).

The p.m.r. and chemical results are relevant since they have a bearing on the identity of a yeast *Torulopsis* species PRL 319-67. In 1954 Spencer isolated it from bumblebee nests and the nectar of sow thistle, clover, and dandelions, growing in the area of Saskatoon and in 1960 it was reisolated and reinvestigated since the yeast produces a glycolipid. This metabolite is of interest since it may be useful as a perfume base or a food additive. Its structure has been investigated (7–10). Since the isolation of this yeast a number of suggestions as to its identity

[2]Each of the polysaccharides contain an α-(1 → 6)-linked D-mannopyranose main-chain (16).

Can. J. Chem. Downloaded from www.nrcresearchpress.com by 210.87.254.40 on 09/05/12
For personal use only.

TABLE IV

Oligosaccharide fragments formed following partial acetolysis of mannose-containing polysaccharides

Source of mannose-containing polysaccharide	Oligosaccharides formed on partial acetolysis of polysaccharide (Yields in parentheses)
1. *Torulopsis bombi* (PRL 319-67)	(α-(1 → 2)-D-Manp)$_{2-8}$
2. *Torulopsis apicola* (Hajsig strain)	(α-(1 → 2)-D-Manp)$_{2-6}$
3. *Torulopsis magnoliae*	(α-(1 → 2)-D-Manp)$_{2-10}$
4. *Torulopsis gropengiesseri*	(α-(1 → 2)-D-Manp)$_{2-3}$
5. *Saccharomyces rouxii* (14, 15)	(α-(1 → 2)-D-Manp)$_{2-3}$, 7% and 17%, respectively
6. *Trichosporon fermentans* (1)	D-Manp$^{1,2\alpha}$D-Man (4%), D-Galp$^{1,2\alpha}$D-Manp$^{1,2\alpha}$D-Man (25%)
7. *Candida lipolytica*	D-Manp$^{1,2\alpha}$D-Man (12%), D-Galp$^{1,2\alpha}$D-Manp$^{1,2\alpha}$D-Man (36%)
8. *Candida catenulata*	D-Manp$^{1,2\alpha}$D-Man (5%), unidentified 2-*O*- and 3-*O*-linked tri- and tetramannoside fractions (5% and 6%, respectively)
9. *Endomycopsis fibuliger*	D-Manp$^{1,2\alpha}$D-Man (57%), D-Manp$^{1,3\alpha}$D-Manp$^{1,2\alpha}$D-Man (8%)
10. *Torulopsis lactis-condensi*	D-Manp$^{1,2\alpha}$D-Man (11%), D-Galp$^{1,6\alpha}$D-Manp$^{1,2\alpha}$D-Man (3%)
11. *Hansenula subpelliculosa*	D-Manp$^{1,3\alpha}$D-Man (7%), (α-(1 → 2)-D-Manp)$_{2-4}$, (7%, 6%, 9%, respectively), D-Manp$^{1,3\alpha}$D-Manp$^{1,2\alpha}$D-Manp$^{1,2\alpha}$D-Manp$^{1,2\alpha}$D-Man (6%)
12. *Schizosaccharomyces octosporus*	D-Galp$^{1,2\alpha}$D-Man (27%)

have been made. Wickerham in 1961 suggested that its morphology and carbon and nitrogen assimilation reactions correspond to a strain related to *Torulopsis magnoliae* that does not assimilate nitrate. Phaff in 1963 and Scheda in 1964 investigated cultures of the yeast and noted that its characteristics were similar to those of *Torulopsis apicola* (Hajsig strain). A culture was supplied later (1965) to the Pharmaceutical Division, Imperial Chemical Industries (I.C.I.), Cheshire, England, who relayed it to the Brewing Industry Research Foundation, Surrey, England. Based on a limited number of assimilation tests the yeast was thought to be *Torulopsis gropengiesseri*, which prompted D. F. Jones of the I.C.I. (11) to carry out further structural studies on the glycolipid. (However, since then the I.C.I. culture has been returned to us and the p.m.r. spectrum of its cell-wall mannan was found to be identical to that of PRL 319-67.) Since the new yeast has the ability to produce a unique glycolipid, has a regular habitat and has a cell-wall mannan component different from other known yeasts it is suggested that it is a new species, which could be called *Torulopsis bombi* from its association with bumblebees.

(ii) Galactomannans of Trichosporon fermentans and Candida lipolytica

The p.m.r. spectrum of *Trichosporon fermentans* galactomannan (Spectrum 6, Fig. 1) is similar to that of *Candida lipolytica* galactomannan (Spectrum 7) except that the latter contains a much larger signal at τ 4.53.

Partial acetolysis of the *C. lipolytica* galactomannan gave an acetylated mixture, which was deacetylated and *O*-α-D-galactopyranosyl-(1 → 2)-*O*-α-D-mannopyranosyl-(1 → 2)-D-mannose isolated. It had a specific rotation and p.m.r. spectrum (Spectrum 13, Fig. 2) identical to authentic material (1) and on methylation followed by methanolysis methyl 2,3,4,6-tetra-*O*-methylgalactoside and methyl 3,4,6-tri-*O*-methylmannoside were detected by g.l.c. in a ratio of 1:1.9. A methylation–fragmentation analysis carried out on the parent galactomannan gave methyl glycosides of 2,3,4,6-tetra-*O*-methylgalactose and 3,4,6-tri-*O*-, 2,3,4-tri-*O*-, and 3,4-di-*O*-methylmannoses (for ratio see example 7, Table I). The 6-*O*-substituted α-D-mannopyranosyl units, on the basis of this evidence, can be either in the main-chain or the side-chains, but the former structure is more common, since it is analogous to those of other yeast mannans and galactomannans (1, 12, 13; see also *Endomycopsis fibuliger* mannan described below). This type of mannopyranosyl unit is likely responsible for the H-1 signal at τ 4.53 (Spectrum 7, Fig. 1) since partial hydrolysis of a galactomannan from *Schizosaccharomyces octosporus* gives a mannan with α-(1 → 6)-D-mannopyranose units with H-1 signals with a similar chemical shift (13).

Can. J. Chem. Downloaded from www.nrcresearchpress.com by 210.87.254.40 on 09/05/12
For personal use only.

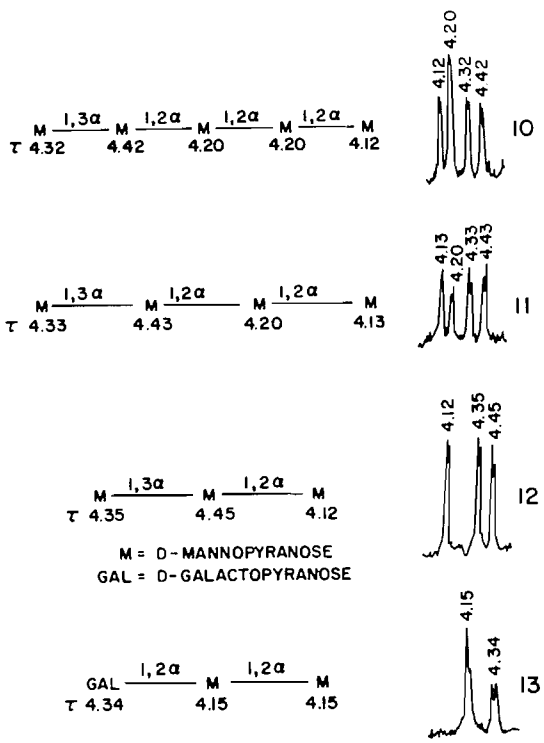

FIG. 2. Proton magnetic resonance spectra of related oligosaccharides from yeast mannans and galactomannan (chemical shifts in τ).

The structural studies, therefore, show that *C. lipolytica* galactomannan contains an α-D-(1 → 6)-D-mannopyranose main-chain which is partially substituted in the 2-positions with *O*-α-D-galactopyranosyl-(1 → 2)-*O*-α-D-mannopyranosyl side-chains (**1**; Fig. 3). The *T. fermentans* galactomannan, on the other hand, contains a similar main-chain and side-chain, except that a higher proportion of main-chain units is substituted with side-chains ((1) **2**; Fig. 3).

(iii) Torulopsis gropengiesseri Galactomannan and Saccharomyces rouxii Mannan

Torulopsis gropengiesseri and *Saccharomyces rouxii* give rise to a galactomannan and a mannan respectively, which provide almost identical p.m.r. spectra (Spectra 4 and 5, Fig. 1, respectively), except for a somewhat broader peak at τ 4.20 in the former spectrum. The two polysaccharides each gave, on acetolysis, α-(1 → 2)-linked D-mannopyranose oligosaccharides of 2–3 units in size (see publication on *S. rouxii* mannan (14, 15), and Table IV). The methylation–fragmentation patterns (Table I), the acetolysis fragments, and enzymolysis data, which show that each polysaccharide contains an α-(1 → 6)-linked D-mannopyranose main-chain (16), show that the galactomannan and mannan are structurally related. Whereas the *T. gropengiesseri* galactomannan has its main-chain substituted in the 2-positions by *O*-galactopyranosyl-*O*-D-mannopyranosyl-(1 → 2)-α-D-mannopyranosyl side-chains, the side-chains in *S. rouxii* mannan are 2-*O*-α-D-mannopyranosyl-D-mannopyranosyl units. (Identical p.m.r. spectra to that of *S. rouxii* mannan have been obtained from those of *Saccharomyces tellustris* CBS 2685, *Saccharomyces elegans* NRRL Y-2228, *Saccharomyces montanus* NRRL 1559, *Saccharomyces mellis* NRRL Y-58, *Saccharomyces pastorianus* NCYC 392, *Saccharomyces acidifaciens* NRRL Y-1011, *Saccharomyces italicus* var. *melibiosi* CBS 2909, *Saccharomyces norbensis* CBS 5378, *Saccharomyces oleaginosus* CBS 3081, and *Saccharomyces oleaceus* CBS 3093 mannans.)

(iv) Mannans from Candida catenulata and Endomycopsis fibuliger

The p.m.r. spectra of mannans from *Candida catenulata* (Spectrum 8, Fig. 1) and *Endomycopsis fibuliger* (Spectrum 9) contain signals with similar chemical shifts, but their proportions are markedly different.

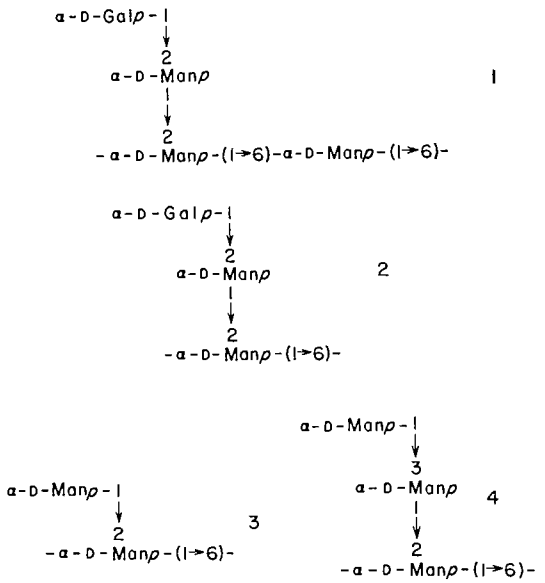

FIG. 3. Structures in some of the yeast polysaccharides.

Can. J. Chem. Downloaded from www.nrcresearchpress.com by 210.87.254.40 on 09/05/12
For personal use only.

Can. J. Chem. Downloaded from www.nrcresearchpress.com by 210.87.254.40 on 09/05/12
For personal use only.

E. fibuliger mannan, following partial acetolysis, gave 2-*O*-α-D-mannopyranosyl-D-mannose (57% yield) and *O*-α-D-mannopyranosyl-(1 → 3)-*O*-α-D-mannopyranosyl-(1 → 2)-D-mannose (8% yield). This structure for the trisaccharide is based on the following evidence. It gave the methyl glycosides of 2,3,4,6-tetra-*O*-, 2,4,6-tri-*O*-, and 3,4,6-tri-*O*-methylmannose (1.1:1:1 ratio by g.l.c.) on methylation–fragmentation and was resistant to lead tetraacetate oxidation, consistent with a (1 → 2)-linked reducing end. Its specific rotation, +72°, is indicative of α-D-linkages. Methylation–fragmentation analysis of *E. fibuliger* mannan gave a high proportion of methyl 2,3,4,6-tetra-*O*-methylmannose compared with the methyl glycosides of 2,4,6- and 3,4,6-tri-*O*-methylmannose (Table I). Methyl 3,4-di-*O*-methylmannose was also formed. These data coupled with its specific rotation of +73°, consistent with predominant α-D-linkages, show that the mannan consists of an α-(1 → 6)-D-mannopyranosyl backbone mainly substituted in the 2-positions by single-unit D-mannopyranosyl side-chains (**3**; Fig. 3) and a small proportion of 3-*O*-α-D-mannopyranosyl-D-mannopyranosyl side-chains (**4**; Fig. 3).[3] In accord with this structure only low molecular weight fragments were obtained in partial Smith degradation (compare below). (The mannans from *Endomycopsis capsularis* PRL R_2a and *Endomycopsis selenospora* CBS 2562 give p.m.r. spectra identical with that of *E. fibuliger*.)

Candida catenulata mannan has a specific rotation of +110°, considerably higher than that of *E. fibuliger* mannan. The methyl tri-*O*-methyl and methyl tetra-*O*-methylmannoside fragments obtained on methylation–fragmentation analysis are the same as those from *E. fibuliger* mannan, but the proportion of non-reducing end-units, represented by methyl 2,3,4,6-tetra-*O*-methylmannoside is much lower. Also detected was methyl 2,4-di-*O*-methylmannoside representing structurally different branch points (Table I). Differences were also reflected in the oligosaccharides obtained on partial acetolysis. *C. catenulata* mannan gave rise to 2-*O*-α-D-mannopyranosyl-D-mannose (5% yield) and uncharacterized straight-chain tri- (4%) and tetrasaccharide (6%) fractions, each fraction containing 2-*O*- and 3-*O*-substituted D-mannopyranose units. The fragments obtained by Smith degradations (17) of *C. catenulata* mannan (incorporating mild hydrolytic conditions) were also difficult to characterize. One Smith degradation gave a mannan ($[\alpha]_D$ +55°) which was analyzed by the methylation–fragmentation technique. Gas–liquid chromatography examination of the product indicated the presence of methyl glycosides of 2,3,4,6-tetra-*O*-methylmannose (1 part), 2,3,4-tri-*O*-methylmannose (3.8 parts) and 2,4,6-tri-*O*-methylmannose (6.3 parts) (18). A further Smith degradation on the partially degraded mannan gave a non-reducing fraction with a paper chromatographic mobility close to that of a hexosyl glycerol. Proton magnetic resonance spectroscopy showed that it was a mixture, and hydrolysis gave spots on a paper chromatogram with mobilities equal to mannose and glycerol.

The mannans from *C. catenulata* and *E. fibuliger*, therefore, have widely different chemical structures, but although their spectra (Spectra 8 and 9, respectively; Fig. 1) contain signals with similar chemical shifts, their proportions are different.

(v) Miscellaneous Mannose-containing Polysaccharides from Yeast Cell-walls

A number of mannans and galactomannans, not described in the above presentation, have also been investigated. Since their structures may be of some interest their methylation–fragmentation characteristics, periodate oxidation figures, fragments formed on partial acetolysis, galactose to mannose ratios, and specific rotations are compiled (Tables I, II, and IV).

General Conclusion

In most of the cases examined above, resemblances in p.m.r. spectra of mannose-containing polysaccharides reflect similarities in chemical structure. It seems likely that if two structurally similar polysaccharides are obtained from different species of yeast, then the yeasts possibly have evolved from a common ancestor. Close resemblances in p.m.r. spectra of mannose-containing polysaccharides might therefore suggest a relationship between the parent yeasts.

[3]This type of side-chain is related to that present in baker's yeast mannan, which contains one more (1 → 2)-linked α-D-mannopyranosyl unit (12). Partial acetolysis of *Hansenula subpelliculosa* mannan gives rise to D-Manp^{1,3a}D-Manp^{1,2a}D-Manp^{1,2a}D-Manp^{1,2a}D-Man (Experimental), which arises from a side-chain with two additional (1 → 2)-linked units.

Can. J. Chem. Downloaded from www.nrcresearchpress.com by 210.87.254.40 on 09/05/12
For personal use only.

Experimental

The proton magnetic resonance spectra of the mannans and galactomannans were obtained (see Fig. 1) from 20% solutions in D_2O at 70° using a 100 MHz Varian nuclear magnetic resonance spectrometer. Chemical shifts are in τ, based on an external tetramethylsilane standard.

Cultural methods for production of yeast cells and isolation of purified galactomannan or mannan are as previously described (1). Yields of polysaccharide are given in Table II. The polysaccharides were shown to be homogeneous by ultracentrifugation of 0.45% aqueous solutions in 0.1 *M* sodium chloride at 59 000 r.p.m. All of the polysaccharides gave a single peak except those from *T. magnoliae* which gave two peaks.

D-Mannose was isolated from mannans by hydrolysis with *N* H_2SO_4 at 100° for 18 h and characterized by its melting point, mixture melting point, and specific rotation. D-Galactose and D-mannose, similarly obtained from galactomannans, were fractionated by cellulose column chromatography using *n*-butanol–water (9:1 v/v) as eluant, and also characterized by melting point, mixture melting points, and specific rotations. The ratios of galactose to mannose were obtained by the gas–liquid chromatography (g.l.c.) method described previously (1) and are given in Table II.

Methylation of mannose-containing polysaccharides, followed by fragmentation to partially methylated methyl glycosides, was carried out as previously described (1). Gas–liquid chromatographic identification and estimation of the fragments (Table I) are by the method of Bhattacharjee and Gorin (18) following fractionation to tetra-*O*-, tri-*O*-, and di-*O*-methyl derivatives of methyl-mannoside (13).

Partial acetolyses were mostly carried out for 5 days on 2 g samples with the reagent proportions used by Lee and Ballou (12). Following deacetylation in methanolic sodium methoxide the oligosaccharide mixtures were fractionated by cellulose column (40 cm × 4.5 cm diameter) chromatography. Three liters of each of the following acetone–water (v/v) mixtures were used to elute each saccharide fraction. Mono- (10:1), di- (7:1), tri- (4:1), tetra- (7:2), penta- (3:1), hexa- (7:3), hepta- (13:7), octa- (5:3), nona- (3:2), deca- (3:2). Yields are presented in Tables III and IV. Paper chromatography of di- up to pentasaccharide was carried out in *n*-butanol – ethanol – water (2:1:1 v/v/v) using the ammoniacal silver nitrate spray. A 1:1:1 ratio was used for fragments with more than five mannose units.

Characterization of Partial Acetolysis Fragments

2-*O*-α-Linked D-mannopyranoside oligosaccharides gave typical H-1 signals, with τ 4.08 (reducing end), τ 4.40 (non-reducing end) and τ 4.20 (internal units) (2). The proportion of the τ 4.40 signal to other signals showed the unit-size of the fragment. The specific rotations of tri- up to octasaccharide varied from +53° to +57°. The physical constants of various other fragments are given below.

i) Schizosaccharomyces octosporus Galactomannan

2-*O*-α-D-Galactopyranosyl-D-mannose monohydrate (from MeOH–EtOH) had m.p. 105–108° and $[\alpha]_D$ +76° (*c*, 0.6 H_2O).

Anal. Calcd. for $C_{12}H_{22}O_{11}\cdot H_2O$: C, 41.86; H, 7.03. Found: C, 42.0; H, 7.0.

Its resistance to lead tetraacetate oxidation indicated 2-*O*-substitution (19). Hydrolysis gave galactose and mannose and hydrolysis of the sodium borohydride – reduced alcohol gave galactose and mannitol.

ii) Torulopsis magnoliae Galactomannan

The fragments had proton magnetic resonance spectra corresponding to 2-*O*-linked D-mannopyranose oligosaccharides. However, each fraction up to decasaccharide gave on hydrolysis a trace of galactose in addition to mannose. Their specific rotations are higher than expected and are as follows: tri- (+59°), tetra- (+63°), penta- (+52°), hexa- (+65°), hepta- (+72°), octa- (+65°), nona- (+61°), and decasaccharide (+57°) Methylation–fragmentation analysis of the decasaccharide gave mainly methyl 3,4,6-tri-*O*-methylmannoside and a trace of methyl 2,3,4,6-tetra-*O*-methylmannoside as shown by gas–liquid chromatography.

iii) Hansenula subpelliculosa and Endomycopsis fibuliger Mannans

The pentasaccharide from *Hansenula subpelliculosa* had $[\alpha]_D$ +78° (*c*, 1.0 H_2O) and its H-1 p.m.r. spectrum (Spectrum 10, Fig. 2) was similar to that of the D-Manp$^{1,3\alpha}$D-Manp$^{1,2\alpha}$D-Manp$^{1,2\alpha}$D-Man tetrasaccharide (Spectrum 11) except that the signal at τ 4.20 was equivalent to 2 protons rather than 1 proton. This, by analogy with the τ 4.20 signal of (1 → 2)-linked D-mannose oligosaccharides (2) indicates that the pentasaccharide has a D-Manp$^{1,3\alpha}$D-Manp$^{1,2\alpha}$D-Manp$^{1,2\alpha}$D-Manp$^{1,2\alpha}$D-Man structure. The signal at τ 4.32 is due to H-1 of the non-reducing end since it is moved downfield 10 Hz on addition of borate (2).

The trisaccharide from *Endomycopsis fibuliger* ($[\alpha]_D$ +72° (*c*, 0.5 H_2O)) appeared to be D-Manp$^{1,2\alpha}$D-Manp$^{1,3\alpha}$D-Man from its H-1 p.m.r. spectrum (Spectrum 12, Fig. 2). It was methylated and then fragmented to give the methyl glycosides of 3,4,6-tri-*O*-, 2,4,6-tri-*O*-, and 2,3,4,6-tetra-*O*-methylmannose (1:1:1.1 g.l.c. peak ratio). The (1 → 2)-linkage is attached to the reducing end since the trisaccharide is inert to lead tetraacetate oxidation.

iv) Candida catenulata Mannan

The acetolysis fragments consisted of 2-*O*-α-D-mannopyranosyl-D-mannose and tri- and tetrasaccharide fractions. The two latter fractions were each straight chain and contained 2-*O*- and 3-*O*- linked mannopyranose units, as shown by methylation–fragmentation gas–liquid chromatography.

v) Torulopsis lactis-condensi Galactomannan

The hydrated trisaccharide (from MeOH) had m.p. 150–153° and $[\alpha]_D$ +99° (*c*, 0.3 H_2O).

Anal. Calcd. for 2 $C_{18}H_{32}O_{16}\cdot 3H_2O$: C, 40.68; H, 6.64. Found: C, 40.6; H, 6.7.

Methylation – fragmentation – gas–liquid chromatography showed the presence of the methyl glycosides of 2,3,4,6-tetra-*O*-methylgalactose, 2,3,4-, and 3,4,6-tri-*O*-methylmannose (approximately 1:1:1 ratio). The latter fragment arises from the reducing end since the trisaccharide is resistant to lead tetraacetate oxidation and a D-Galp$^{1,6\alpha}$D-Manp$^{1,2\alpha}$D-Man structure is indicated.

vi) Candida lipolytica Galactomannan

The trisaccharide fraction had $[\alpha]_D$ +95° (*c*, 1.0 H_2O)

and an H-1 proton magnetic resonance spectrum (Spectrum 13, Fig. 2) identical to that of D-Galp$^{1,2\alpha}$D-Manp$^{1,2\alpha}$D-Man from *Trichosporon fermentans* (1). Methylation – fragmentation – gas–liquid chromatography gave the methyl glycosides of 2,3,4,6-tetra-*O*-methylgalactose and 3,4,6-tri-*O*-methylmannose (1:1.9 ratio), thus confirming the structure.

Smith Degradations of Candida catenulata Mannan

This procedure first described in a communication by Smith and co-workers (17) has been modified slightly (20). The mannan $[\alpha]_D$ +55° (*c*, 1.0 H_2O) obtained on one Smith degradation using mild hydrolytic conditions was analyzed by the methylation–fragmentation technique. The methyl glycosides of 2,3,4-tri-*O*-, 2,4,6-tri-*O*-, 2,3,4,6-tetra-*O*-methylmannose were identified by gas–liquid chromatography. A further Smith degradation gave a hexosyl glycerol, $[\alpha]_D$ +76° (*c*, 0.3 H_2O), with an R_f equal to mannose on a paper chromatogram (solvent: *n*-butanol – ethanol – water, 40:11:19 v/v/v; spray, ammoniacal silver nitrate). Its p.m.r. spectrum contained several H-1 proton signals which indicates a mixture. Hydrolysis of the material gave hexose and glycerol (paper chromatogram).

Acknowledgments

The authors thank Mr. N. R. Gardner for technical assistance. We also thank Mr. M. Mazurek for preparation of proton magnetic resonance spectra and Mr. W. C. Haid for determination of microanalyses.

1. P. A. J. Gorin and J. F. T. Spencer. Can. J. Chem. **46**, 2299 (1968).
2. P. A. J. Gorin, M. Mazurek, and J. F. T. Spencer. Can. J. Chem. **46**, 2305 (1968).
3. J. F. T. Spencer and P. A. J. Gorin. J. Bacteriol. **96**, 180 (1968).
4. J. F. T. Spencer and P. A. J. Gorin. Antonie van Leeuwenhoek, **35**, 33 (1969).
5. J. F. T. Spencer and P. A. J. Gorin. Can. J. Microbiol. **15**, 375 (1969).
6. J. F. T. Spencer and P. A. J. Gorin. Antonie van Leeuwenhoek. To be published.
7. P. A. J. Gorin, J. F. T. Spencer, and A. P. Tulloch. Can. J. Chem. **39**, 846 (1961).
8. A. P. Tulloch, J. F. T. Spencer, and P. A. J. Gorin. Can. J. Chem. **40**, 1326 (1962).
9. J. F. T. Spencer, A. P. Tulloch, and P. A. J. Gorin. Biotechnology and Bioengineering, **4**, 271 (1962).
10. J. F. T. Spencer, A. P. Tulloch, and P. A. J. Gorin. U.S. Patents 3 205 150 and 3 312 684.
11. D. F. Jones. J. Chem. Soc. C, 479 (1967).
12. Y.-C. Lee and C. E. Ballou. Biochemistry, **4**, 257 (1965).
13. P. A. J. Gorin, J. F. T. Spencer, and S. S. Bhattacharjee. Can. J. Chem. **47**, 1499 (1969).
14. P. A. J. Gorin and A. S. Perlin. Can. J. Chem. **34**, 1796 (1956).
15. P. A. J. Gorin and A. S. Perlin. Can. J. Chem. **35**, 262 (1957).
16. P. A. J. Gorin, J. F. T. Spencer, and D. E. Eveleigh. Carbohyd. Res. To be published.
17. I. J. Goldstein, G. W. Hay, B. A. Lewis, and F. Smith. 135th Meeting, American Chemical Society, Boston. 1959. Abstr. Pap. p. 3D.
18. S. S. Bhattacharjee and P. A. J. Gorin. Can. J. Chem. **47**, 1207 (1969).
19. A. J. Charlson and A. S. Perlin. Can. J. Chem. **34**, 1200 (1956).
20. P. A. J. Gorin and J. F. T. Spencer. Can. J. Chem. **46**, 3407 (1968).

Can. J. Chem. Downloaded from www.nrcresearchpress.com by 210.87.254.40 on 09/05/12
For personal use only.

Characterization of plant coumarins by combined gas chromatography, ultraviolet absorption spectroscopy, and nuclear magnetic resonance analysis[1]

WARREN STECK AND B. K. BAILEY
National Research Council of Canada, Prairie Regional Laboratory, Saskatoon, Saskatchewan

Received May 26. 1969

A method for the characterization of sub-milligram quantities of plant coumarins has been devised. Each compound was purified by gas–liquid chromatography, and the collected material analyzed by a combination of ultraviolet absorption and nuclear magnetic resonance spectroscopy. The procedures developed were tested successfully on several plant extracts. Limettin and bergapten were identified in lime peel; angelicin, psoralen, and xanthotoxin in parsnips; and angelicin, xanthotoxin, and bergapten in *Angelica* leaves. Isopimpinellin was found in all three plant materials.

Canadian Journal of Chemistry, 47, 3577 (1969)

Can. J. Chem. Downloaded from www.nrcresearchpress.com by 210.87.254.5 on 09/05/12
For personal use only.

Introduction

The plant coumarins, though widely distributed, seldom occur in high concentrations within plant tissues, so that their isolation and characterization usually require large quantities of starting material. Moreover, since neutral coumarins in particular usually occur as mixtures, lengthy chromatographic procedures may have to be employed to obtain pure components. Today, identification of these constituents usually relies heavily on spectroscopic techniques, particularly nuclear magnetic resonance (n.m.r.).

The use of gas–liquid chromatography (g.l.c.) for separation of coumarins, first reported by Brown and Shyluk in 1962 (1), offered a great simplification of isolation procedures; a number of phenolic (as acetates) and neutral coumarins were successfully eluted and characterized by paper chromatography. Gas–liquid chromatographic separations of coumarin mixtures from lavender, *Angelica archangelica* root, and *Heracleum sibiricum* seeds were demonstrated. These analytical methods were extended somewhat by Furuya and Kojima in 1967 (2) by their work with different columns and additional coumarins. They also stressed the quantitative aspects of the method. Subsequent use of the technique has been limited (3,4), probably because the amounts of pure materials which can be collected conveniently from gas chromatographs have not been considered adequate for structural studies in the absence of matching reference standards. We wish to describe here some of the methods we have used for the characterization of g.l.c. purified coumarins, in particular the application of n.m.r. and ultraviolet (u.v.) absorption analysis to sub-milligram amounts of materials.

Results and Discussion

A number of natural coumarins, along with some other coumarins of structural interest, were chromatographed on several columns under varied conditions. Silicone columns (SE-30), operated near 200°, gave the best separations and offered conveniently short retention times. For most work, a 3 m long column was used, but when compounds of high retention were studied a $1\frac{1}{2}$ m column was preferred. Separations achieved on the longer column are summarized in Table I (the structures of the coumarins are given in Fig. 1). We chose angelicin (**12**) as a standard for measurement of relative retention times (RRT) because it was readily available and because in plant screenings it is frequently the first coumarin of a mixture to elute from the gas chromatograph. It was noted that the phenolic coumarins, umbelliferone (**2**) and scopoletin (**7**) were eluted without difficulty, although 6,7-, 7,8-, and 5,7-dihydroxycoumarin were not recovered from the column. All the simple furanocoumarins (**12–19**, Fig. 1) chromatographed well. The behaviour of prenyl (3,3-dimethylallyl) and related ethers was not consistent; imperatorin (**26**) gave no peaks, undoubtedly because of thermal rearrangement to allo-imperatorin (1), whereas phellopterin (**20**), in which the requisite *ortho–para* positions are blocked, emerged unchanged. More surprisingly, *O*-prenylumbelliferone (**4**) also chromatographed without rearrangement, so that some prenyl ethers can be detected by this method.

[1]Issued as NRCC No. 10860.

TABLE I

Retention and relative retention times of coumarins. Angelicin has been arbitrarily assigned RRT = 1.00

Retention time (min)	RRT	Compound*
2.1	0.35	Coumarin (**1**)
6.0	1.00	Angelicin (**12**)
6.5	1.08	Herniarin (**3**)
6.9	1.15	Psoralen (**16**)
10.2	1.70	6,7-Dimethoxycoumarin (**8**)
10.2	1.70	Umbelliferone (**2**)
10.5	1.75	Limettin (**9**)
11.1	1.85	Scopoletin (**7**)
11.7	1.95	Isobergapten (**13**)
12.0	2.00	Xanthotoxin (**18**)
12.6	2.10	Sphondin (**14**)
13.2	2.20	O-Prenylumbelliferone (**4**)
13.8	2.30	Bergapten (**17**)
15.9	2.65	Pimpinellin (**15**)
15.9	2.65	Osthol (**10**)
16.2	2.70	(**29**)
20.4	3.40	Columbianetin (**28**)
21.6	3.65	Isopimpinellin (**19**)
23.1	3.85	Phellopterin (**20**)
23.1	3.85	Peucedanin (**27**)
26.	4.4	Coumurrayin (**11**)
48. (double peak)	8.0	Oxypeucedanin (**21**)

*Esculetin (5), daphnetin (6), oxypeucedanin hydrate (22), ostruthol (23), ostruthin (24), xanthotoxol (25), and imperatorin (26) did not pass through the column. Chromatographic conditions are given in the experimental section.

Oxypeucedanin (**21**) gave a double peak near RRT 8 which was incompletely resolved. Each portion had the u.v. spectrum of the initial compound. The related diol (**22**) could not be eluted, and neither could ostruthol (**23**), which was surprising since earlier workers had distilled this coumarin (5). The alcohol columbianetin (**28**) behaved normally, and it might be inferred that marmesin and nodakenetin, the linear analogs, would be equally amenable to this type of analysis; this has been confirmed for marmesin (6). The successful chromatography of the synthetic pyronocoumarin **29** similarly implies that this type of natural compound (7, 8) can be detected by g.l.c.

Thus a wide variety of structures may be encountered in practice, and characterization procedures must take this into account. We collected many of the eluted coumarins in small pyrex tubes inserted into the exit port of the chromatograph. The material collected in this way was usually crystalline, but with the exception of coumarin and the sharply-peaking derivatives herniarin (**3**), psoralen (**16**), and angelicin, the melting points were not sufficiently sharp to confirm the identity of the compound. A few micrograms were dissolved in alcohol and the u.v. spectrum measured, while the remainder of the material (about 0.1–1.0 mg) was dissolved in deuterochloroform or deuterodimethylsulphoxide for measurement of the n.m.r. spectrum.

Nuclear magnetic resonance spectra are customarily measured on 10–20 mg pure material, but we soon found that for coumarins in which only a few protons are present satisfactory results (all protons clearly visible) could be obtained with only 1 mg of sample. In favorable cases even half this quantity gave a complete qualitative spectrum. Where multiple signals are involved, as with aromatic methoxyl or aliphatic or vinyl methyl groups, some characterization can be achieved with only 0.1 mg pure sample by noting and comparing the field strengths of these signals. Below 0.5 mg, however, n.m.r. evidence becomes supporting rather than definitive, and in the absence of a reference standard, positive identification of an unknown cannot be made.

Use of a preliminary liquid partition column fractionation (4) has been found to be successful in simplifying mixtures and concentrating minor constituents for gas chromatography, but the procedure is time-consuming and necessitates multiple g.l.c. analyses (of the fractions). We therefore prefer to screen plant materials by g.l.c. initially to see if any coumarins are present, to characterize these on a sub-milligram scale, and then (if interest warrants) to consider the use of a suitable liquid column for the resolution of larger quantities of the coumarin mixtures. In our experience it is usually both quicker and more convenient to collect several g.l.c. passes to obtain sufficient material for n.m.r. analysis than to set up a liquid partition or adsorption column system.

Other methods of extending the range of n.m.r. analysis also seem practicable. For example, if a multiple scanning system were used, a complete spectrum probably could be obtained on about 0.1 mg compound, and the lower limit of analysis would be similarly extended. We did not have such a system at our disposal.

It will be seen at once that a tabulation of n.m.r. signals for the more common coumarins is needed for full exploitation of this micro-method. Data for many derivatives are available in the literature but as these are scattered and incomplete, we had spectra taken of all our chromatographable

Can. J. Chem. Downloaded from www.nrcresearchpress.com by 210.87.254.5 on 09/05/12
For personal use only.

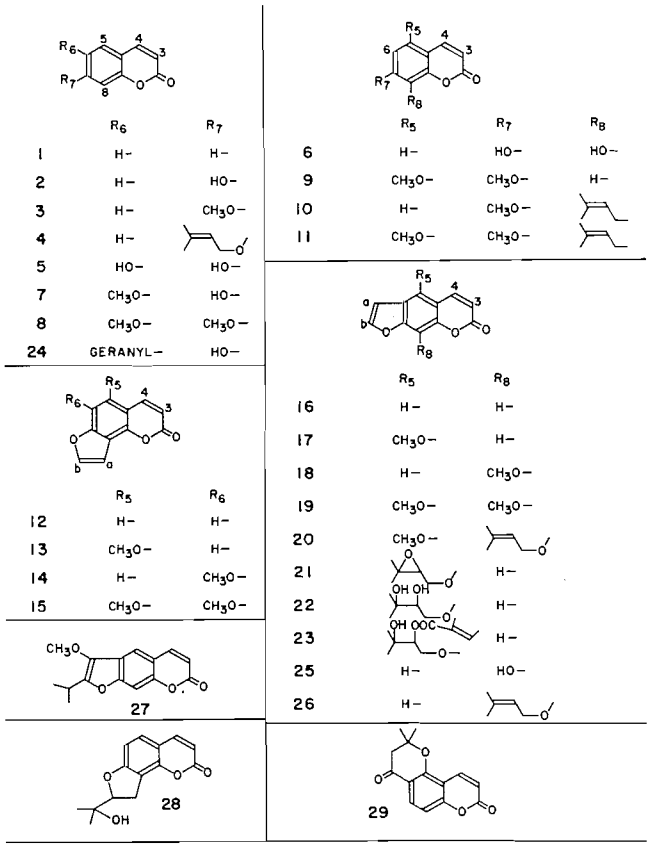

FIG. 1. Structures of some coumarins mentioned in the text. **1** Coumarin; **2** umbelliferone; **3** herniarin; **4** *O*-prenylumbelliferone; **5** esculetin; **6** daphnetin; **7** scopoletin; **8** 6,7-dimethoxycoumarin; **9** limettin; **10** osthol; **11** coumurrayin; **12** angelicin; **13** isobergapten; **14** sphondin; **15** pimpinellin; **16** psoralen; **17** bergapten; **18** xanthotoxin; **19** isopimpinellin; **20** phellopterin; **21** oxypeucedanin; **22** oxypeucedanin hydrate; **23** ostruthol; **24** ostruthin; **25** xanthotoxol; **26** imperatorin; **27** peucedanin; **28** columbianetin.

materials. Table II presents most of these in summary, without comments. The O-methyl and C-methyl signal positions in particular have proved valuable not only for the direct matching of minimal quantities of unknowns with standards, but also for the detection of methyl-bearing sidechains in such unknowns, a feature which u.v. analysis does not show up well.

The u.v. absorption patterns of coumarins are better known, and those of phenolic and neutral derivatives have been discussed elsewhere (e.g. 9,10). In general, 7- and 5,7-hydroxycoumarin derivatives have their strongest absorbance at 320–330 nm, while 6,7- derivatives peak at 340–350 nm; furanocoumarins absorb at 290–310 nm and also in the region of 240–270 nm. The furano compounds possess in general, but not always, a dull yellowish fluorescence under u.v. light, most other coumarins fluorescing violet or blue. Blue fluorescing psoralen and angelicin are notable exceptions.

We tested our methods on several plant materials already reported to contain mixtures of neutral coumarins and obtained good results. Three examples are the analyses of lime peel (*Citrus aurantifolia* Swingle), parsnip root (*Pastinaca sativa* L.) and angelica leaf (*Angelica archangelica* L.). In the first case the peel of one lime was processed to give a lactone fraction (11) and part of this was chromatographed (see Fig. 2*a*). Only one pass was collected. The three major peak fractions, having relative retention times of 1.75, 2.30, and 3.62, were collected and scanned in the n.m.r. machine, then in the u.v. spectrophotometer. The fluorescence of each material was also noted in alcohol in the quartz u.v.

Can. J. Chem. Downloaded from www.nrcresearchpress.com by 210.87.254.5 on 09/05/12
For personal use only.

Can. J. Chem. Downloaded from www.nrcresearchpress.com by 210.87.254.5 on 09/05/12
For personal use only.

TABLE II

Nuclear magnetic resonance signals of some natural coumarins (in deuterochloroform).*

Compound	H_3‡	H_4‡	H_5	H_6	H_8	H_a	H_b	Other protons
Coumarin	6.39	7.68	7.50m	7.26m	7.26m	—	—	7.42m (H_7)
Umbelliferone†	6.11	7.83	7.42d[9]	6.69m	6.64s	—	—	10.2 broad s (OH)
Herniarin	6.17	7.58	7.32m	6.78m	6.77s	—	—	3.82s (OCH_3)
Esculetin†	6.14	7.84	6.96s	—	6.73s	—	—	10.17s (7-OH); 8.86s (6-OH)
Daphnetin†	6.16	7.98	6.99d[9]	6.77d[9]	—	—	—	10.05s (7-OH); 9.30s (8-OH)
Scopoletin†	6.18	7.87	7.18s	—	6.75s	—	—	10.23s (OH); 3.80s (OCH_3)
6,7-Dimethoxycoumarin	6.25	7.58	7.24s	—	6.82s	—	—	3.89s and 3.92s (OCH_3's)
Limettin	6.11	7.93	—	6.37d[2]	6.26d[2]	—	—	3.83s and 3.88s (OCH_3's)
Osthol	6.19	7.59	7.28d[9]	6.82d[9]	—	—	—	3.90s (OCH_3); 3.52d (CH_2); 5.23t (CH); 1.67s and 1.83s (CH_3's)
Angelicin	6.36	7.78	7.40m	7.38m	—	7.12m	7.67d[2]	—
Isobergapten	6.27	8.11	—	6.85s	—	6.99m	7.54d[2]	3.95s (OCH_3)
Sphondin	6.38	7.75	6.78s	—	—	7.12d[2]	7.70d[2]	4.04s (OCH_3)
Pimpinellin	6.36	8.07	—	—	—	7.08d[2]	7.65d[2]	4.04s and 4.14s (OCH_3's)
Psoralen	6.33	7.75	7.64s	—	7.41s	6.79m	7.66d[2]	—
Bergapten	6.25	8.14	—	—	7.12m	7.02m	7.59d[2]	4.25s (OCH_3)
Xanthotoxin	6.32	7.72	7.31s	—	—	6.78d[2]	7.65d[2]	4.25s (OCH_3)
Isopimpinellin	6.25	8.08	—	—	—	6.96d[2]	7.59d[2]	4.14s (OCH_3's)
Phellopterin	6.22	8.06	—	—	—	6.96d[2]	7.59d[2]	4.15s (OCH_3); 4.81d (CH_2); 5.58t (CH); 1.69s and 1.72s (CH_3's)
Oxypeucedanin	6.24	8.15	—	—	7.11m	6.92m	7.57d[2]	4.49m (CH_2); 3.20m (CH); 1.32s and 1.40s (CH_3's)
Peucedanin	6.32	7.75	7.54s	—	7.26s	—	—	3.92s (OCH_3); 3.22m (CH); 1.30s and 1.38s (CH_3's)

*δ values: s = singlet; d[x] = doublet, J = x c.p.s.; t = triplet; m = multiplet.
†Solvent d_6–DMSO.
‡In all cases d[9–10].

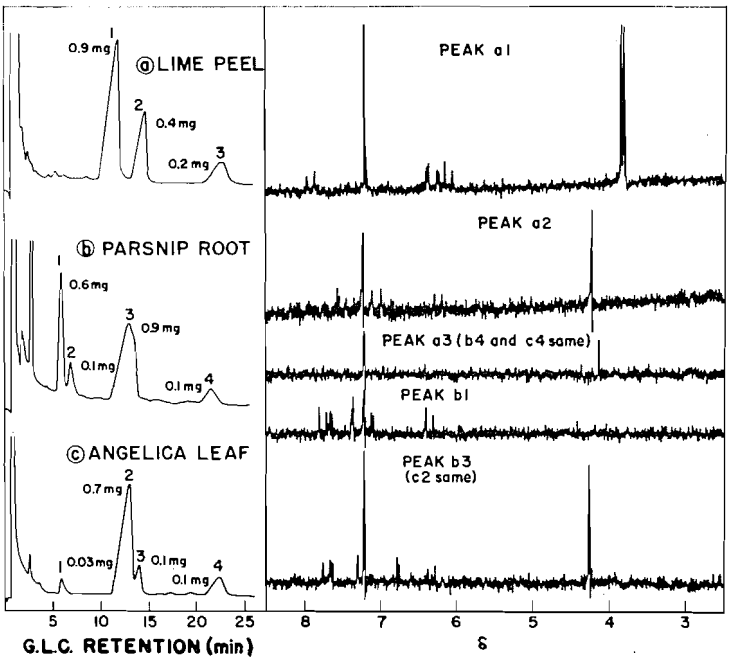

FIG. 2. Gas–liquid chromatography separation and n.m.r. characterization of coumarins from three plant sources. The n.m.r. signals near δ 7.21 are those of chloroform.
(*a*) Lime Peel: Peak 1 = limettin (RRT = 1.75); peak 2 = bergapten (2.30); peak 3 = isopimpinellin (3.62).
(*b*) Parsnip root: Peak 1 = angelicin (RRT = 1.00); peak 2 = psoralen (1.15); peak 3 = xanthotoxin (2.00); peak 4 = isopimpinellin (3.65).
(*c*) Angelica leaf: Peak 1 = angelicin (RRT = 1.00); peak 2 = xanthotoxin (2.00); peak 3 = bergapten (2.26); peak 4 = isopimpinellin (3.68).

cuvettes. The first component's u.v. spectrum suggested an umbelliferone ether (λ_{max} 324 nm, no shift with alkali); the fluorescence was distinctly blue rather than violet, so that a 5-oxygen function seemed likely. The n.m.r. revealed proton signals from two aromatic methoxyl groups and from four other protons, all corresponding to the signals from limettin (**9**). The g.l.c. retention was in agreement. The second component possessed the characteristic u.v. spectrum of bergapten (**17**) (10), and fluoresced dull yellow in u.v. light. The n.m.r. showed a methoxyl signal at δ 4.25 along with five weak aromatic proton signals, all in accord with bergapten. Again the g.l.c. retention was in agreement. The last component had the highly characteristic u.v. spectrum of isopimpinellin (**19**) (10), and this identity was supported by the fluorescence and retention time of the material. The n.m.r. spectrum showed only one sharp signal at δ 4.14, the field strength of the methoxyl six-proton signal of isopimpinellin. Limettin and isopimpinellin are both reported in lime oil (12) and some bergaptol derivatives also (10), but bergapten itself has not been mentioned as an important coumarin of this material.

By similar procedures angelicin (**12**), xanthotoxin (**18**), and isopimpinellin were identified in the lactone fraction of parsnip root (Fig. 2*b*). The minor component, relative retention time 1.15, was not plentiful enough for n.m.r. analysis, but had the u.v. absorption spectrum, violet fluorescence, and typical odour of psoralen (**16**). This identity was confirmed by n.m.r. on combined material from several collections. Bergapten, xanthotoxin, isopimpinellin and the non-chromatographable imperatorin are all reported (13,14) in parsnips but the presence of angelicin and psoralen does not appear to have been appreciated. Chromatography of angelica leaf lactone fraction (Fig. 2*c*), prepared from only a few g of fresh leaves, showed one major peak along with several secondary peaks. Nuclear magnetic resonance showed the main peak was due to

Can. J. Chem. Downloaded from www.nrcresearchpress.com by 210.87.254.5 on 09/05/12
For personal use only.

Can. J. Chem. Downloaded from www.nrcresearchpress.com by 210.87.254.5 on 09/05/12
For personal use only.

xanthotoxin and the latest peak to isopimpinellin. The u.v. absorption and fluorescence of the lesser peaks indicated they were angelicin and bergapten. All these components have been reported from this source (3).

Gas chromatography can thus be used for the direct purification of many natural coumarins, and the collected materials, although minute in amount, can be characterized rather fully. The applications of these methods to the screening of unfamiliar plant materials and to the identification of new coumarins are now under study.

Experimental

Chromosorb W-DMCS, acid-washed, 70–80 mesh, impregnated with 5% SE-30 silicone, was packed into a 4.7 mm i.d. × 3.0 m copper column. An Aerograph model A-700 chromatograph with thermal conductivity detection was used. The column temperature was 205°; injector, 252°; detector, 264°; and helium flow 60 ml/min. Materials were injected in chloroform solutions except for phenolic materials, which were dissolved in alcohol. Collected material was dissolved in deuterochloroform for measurement of the n.m.r. spectrum; a Varian model HA-100 machine was used. Tetramethylsilane was the reference standard. Ultraviolet spectra were taken in alcohol with a Bausch and Lomb model 505 recording spectrophotometer.

Materials

Most of the coumarins tested were available in this laboratory. *O*-Prenylumbelliferone (**4**) was prepared from equimolar amounts of umbelliferone, prenyl bromide and anhydrous potassium carbonate in dry acetone by refluxing for 3 h. The filtered acetone solution was evaporated and the solid residue crystallized from aqueous alcohol and from methanol to give white platelets, m.p. 76–77°, in 70–90% yield.

Anal. Calcd. for $C_{14}H_{14}O_3$: C, 73.0; H, 6.1. Found: C, 72.8; H, 6.2.

The n.m.r. spectrum ($CDCl_3$) showed pyrone ring proton signals at δ 6.28 (H_3) and 7.57 (H_4), both doublets (J = 9.5 c.p.s.); benzene ring proton signals at 7.31 (doublet, J = 9.5 c.p.s.) (H_5), 6.80 (multiplet) (H_6), and 6.76 (singlet) (H_8); and prenyl group signals at 5.43 (triplet) (methyne H), 4.54 (doublet) (2 methylene H's), 1.80, and 1.76 (singlets) (6 vinyl methyl H's).

Compound **29**, 3,4-dihydro-2,2-dimethyl-2*H*,8*H*-benzo[1,2-b:3,4-b′]dipyran-4,8-dione, was prepared by heating 0.45 g 3,3-dimethylacrylic acid and 0.60 g resorcinol in 7 ml polyphosphoric acid for 1 h at 75°. The orange–red solution was poured into excess ice and water; the precipitate was broken up, filtered and washed well with cold water. The crude yellow–orange, 2,2-dimethyl-7-hydroxychromanone (0.85 g, 100%) melted at 160–169°; this was raised to 170–171.5° [lit. 172° (15)] by recrystallization from aqueous alcohol. Pechmann reaction of this phenol with malic acid in hot concentrated H_2SO_4 (5–10 min) gave, after workup similar to that for the chromanone, a 45% yield of crystals, m.p. 210–215°. Sublimation gave white needles whose melting point (215–218°) could not be raised or sharpened further.

Anal. Calcd. for $C_{14}H_{12}O_4$: C, 68.8; H, 4.9. Found: C, 68.8; H, 5.0.

The n.m.r. spectrum of this compound ($CDCl_3$) confirmed it was the angular coumarin possible by this Pechmann reaction, and not the known linear isomer (7): α-pyrone ring proton signals at δ 6.33 and 8.01 (doublets, J = 9.5 c.p.s.); benzene ring proton signals at 6.87 and 7.96 (doublets, J = 9.0 c.p.s.); two γ-pyrone ring methylene protons at 2.74 (singlet); and six *gem*-methyl protons at 1.52 (singlet).

*Identification of Limettin (**9**) and Bergapten (**17**) from Lime Peel*

Limettin

The g.l.c. peak fraction emerging at RRT 1.75 was dissolved in deuterochloroform. The n.m.r. spectrum of the solution showed doublets (J = 9–10 c.p.s.) at δ 6.11 and 7.93 (pyrone ring protons H_3 and H_4 respectively); doublets (J = 2–3 c.p.s.) at 6.26 and 6.37 (H_8 and H_6); and three-proton singlets at 3.83 and 3.88. Authentic 5,7-dimethoxycoumarin gave the same spectrum; the u.v. spectra of the isolated compound and authentic limettin also matched.

Bergapten

The second peak fraction (RRT 2.30) gave doublets (J = 9–10 c.p.s.) at δ 6.25 (H_3) and 8.14 (H_4), the latter indistinct; furan ring doublets (J = 2–3 c.p.s.) at 7.0 and 7.6, a singlet at 7.1, and a three proton singlet at 4.25 (aromatic OCH_3). Authentic bergapten gave the same n.m.r. and u.v. spectra (3).

*Identification of Angelicin (**12**) and Psoralen (**16**) from Parsnip Roots*

Angelicin

The g.l.c. peak fraction emerging at RRT 1.00 was crystalline and melted at 136–138° (lit. 138–139° for angelicin). The n.m.r. spectrum of the deuterochloroform solution of these crystals showed aromatic proton signals at δ 6.36 (doublet, J = 9–10 c.p.s.) (H_3); 7.78 (doublet, J = 9–10 c.p.s.) (H_4); 7.4 (singlets?) (H_5 and H_6); 7.12 (doublet, J = 2–3 c.p.s.) (H_a) and 7.67 (doublet, J = 2–3 c.p.s.) (H_b). Authentic angelicin gave the same spectrum, with signals for two protons unresolved at δ 7.38 and 7.40.

The u.v. of the recovered crystals exhibited absorption maxima (ethanol) at 217, 247, and 297 nm; angelicin afforded an identical spectrum.

Psoralen

Crystals from the g.l.c. peak (RRT 1.15) following angelicin showed u.v. absorption (ethanol) at 240 (shoulder), 245, 289, and 327 nm, the absorption maxima of psoralen. The n.m.r. spectrum ($CDCl_3$) on combined material from six passes showed doublets (J = 9–10 c.p.s.) at δ 6.33 (H_3) and 7.75 (H_4) along with a singlet at 7.41 (H_8), a multiplet at 6.8 (H_a), and an unresolved two-proton signal at 7.65 (H_5 and H_b). Authentic psoralen gave the same spectrum.

Acknowledgments

We wish to thank Prof. T. O. Soine for his generous gift of columbianetin and osthol, Prof.

B. A. Bohm for peucedanin and pimpinellin, and Dr. D. L. Dreyer for phellopterin, oxypeucedanin, and oxypeucedanin hydrate. Special thanks are extended to Mr. M. Mazurek, who measured the n.m.r. spectra.

1. S. A. BROWN and J. P. SHYLUK. Anal. Chem. **34,** 1058 (1962).
2. T. FURUYA and H. KOJIMA. J. Chromatogr. **29**, 382 (1967).
3. W. STECK and B. K. BAILEY. Can. J. Chem. **47**, 2425 (1969).
4. J. KARLSEN, P. VON HAGEN, and A. BAERHEIM-SVENDSEN. Medd. Norsk Farm. Selskap **29**, 153 (1967).
5. E. SPÄTH and A. VON CHRISTIANI. Ber. **66**, 1150 (1933).
6. S. A. BROWN. Private communication.
7. R. J. APLIN and C. B. PAGE. J. Chem. Soc. **C**, 2593 (1967).
8. B. S. JOSHI, V. N. KAMAT, and A. K. SAKSENA. Tetrahedron 4785 (1967).
9. R. H. GOODWIN and B. M. POLLOCK. Arch. Biochem. Biophys. **49**, 1 (1954).
10. W. L. STANLEY and S. H. VANNIER. Phytochem. **6**, 585 (1967).
11. E. SPÄTH. Ber. **70A**, 83 (1937).
12. A. G. CALDWELL and E. R. H. JONES. J. Chem. Soc. 540 (1945).
13. T. O. SOINE, H. ABU-SHADY, and F. E. DIGANGI. J. Amer. Pharm. Ass. **45**, 426 (1956).
14. N. P. MAKSYUTINA and D. G. KOLESNIKOV. Zh. Org. Khim. **29**, 3836 (1959).
15. H. A. OFFE and W. BARKOW. Chem. Ber. **80**, 458 (1947).

Can. J. Chem. Downloaded from www.nrcresearchpress.com by 210.87.254.5 on 09/05/12
For personal use only.

Can. J. Chem. Downloaded from www.nrcresearchpress.com by 210.87.254.40 on 09/05/12
For personal use only.

Structure of sibiricine, an alkaloid of *Corydalis sibirica*

R. H. F. MANSKE AND R. RODRIGO
Department of Chemistry, University of Waterloo, Waterloo, Ontario

AND

D. B. MACLEAN, D. E. F. GRACEY, AND J. K. SAUNDERS
Department of Chemistry, McMaster University, Hamilton, Ontario

Received April 28, 1969

Structure **1** is proposed for sibiricine, a minor alkaloid of *C. sibirica*. The structural assignment rests on an interpretation of its mass spectrum and its proton magnetic resonance (p.m.r.) spectrum.

Canadian Journal of Chemistry, 47, 3585 (1969)

In 1936 Manske (1) examined *C. sibirica* (L.) Pers. for its alkaloidal content. He found two alkaloids each of the protopine, protoberberine, and phthalide isoquinoline groups. Besides these alkaloids whose constitution was known at that time, he also isolated ochotensine (2), and ochrobirine (3) whose structures have recently been resolved, and two bases, F-15 and F-16, which have not yet been subjected to structural study. Another minor alkaloid has been isolated in the interim from the same species. We designate it sibiricine, and assign to it the molecular formula $C_{20}H_{17}NO_6$. Here we present evidence that sibiricine has structure **1**.

The occurrence of sibiricine in conjunction with ochrobirine **2** and ochotensine **3** suggested that it might be structurally related to these two alkaloids. This relationship was apparent on examination of the 100 MHz p.m.r. spectrum of sibiricine (reproduced in Fig. 1) and comparison of this spectrum with that of the synthetic ketone **4** (4) and the alkaloid fumariline **5** (5–7).

In the p.m.r. spectrum of sibiricine the two signals of area 2 at 5.84 and 6.18 δ are assigned to methylenedioxy groups and that of area 3 at

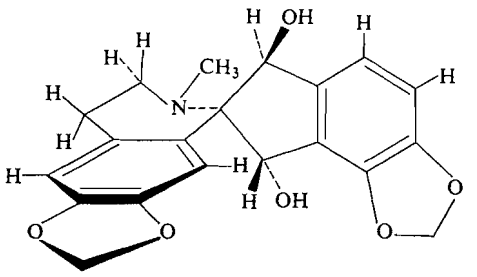

2 Ochrobirine

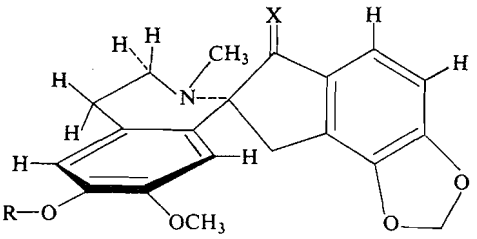

3 Ochotensine R = H; X = CH_2
4 R = CH_3; X = O

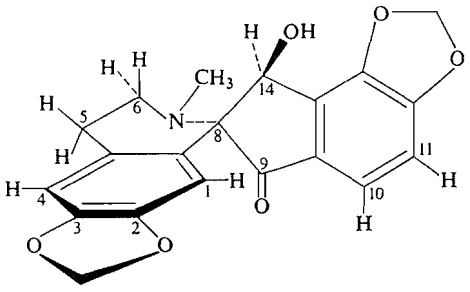

1 Sibiricine

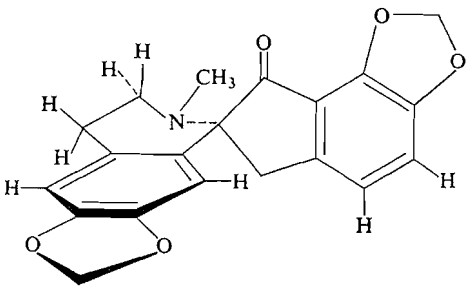

5 Fumariline

Can. J. Chem. Downloaded from www.nrcresearchpress.com by 210.87.254.40 on 09/05/12
For personal use only.

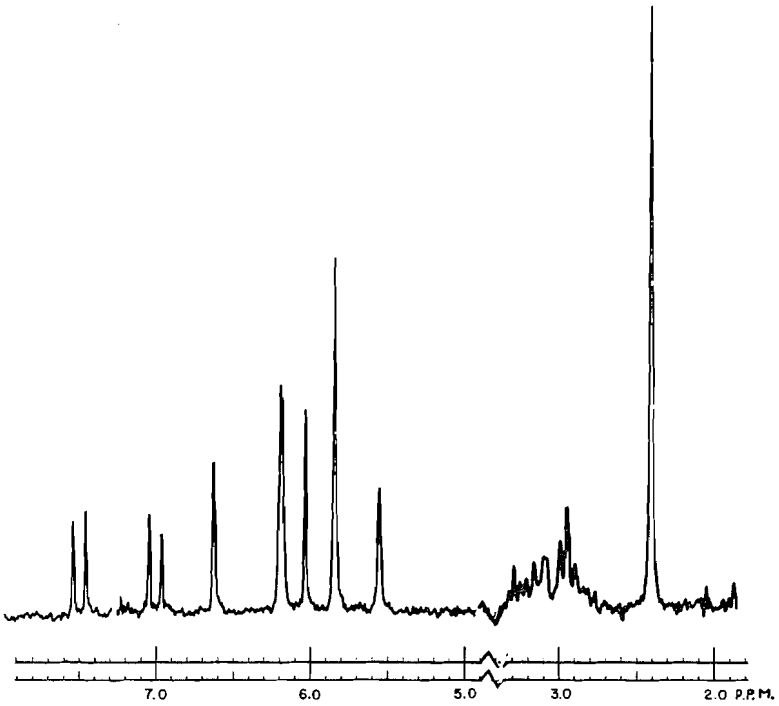

FIG. 1. The 100 MHz p.m.r. spectrum of sibiricine.

2.43 δ to an N—CH_3 group. In the aromatic region of the spectrum there is an AB quartet assigned to the signals at H-10 and H-11, (δ 7.51 (H-10), 7.01 (H-11); $J_{H_{10},H_{11}}$ = 8.0 Hz). The chemical shifts between these two protons and the corresponding protons in the synthetic ketone **4** are very similar and demonstrate that the carbonyl group of **1** must be adjacent to the proton at H-10. (Compare the spectrum of fumariline where the >C=O is not adjacent to the AB quartet.) The two singlets at 6.04 and 6.54 are assigned to aromatic protons at C-1 and C-4, respectively. The positions of these singlets are virtually identical with those of the corresponding protons in the alkaloid fumariline, **5**. (Spectra of **4** and **5** have been published (6).) There is a broad signal of area 1 at 5.57 δ which becomes a sharp singlet on addition of D_2O. This signal is assigned to a proton geminal to the hydroxyl group at C-14. Analogous behavior has been encountered in the case of ochrobirine (3) and fumaricine (5). The hydroxyl proton has been located as a broad singlet centered near 2.55 δ which disappears on addition of D_2O. The remaining protons yield a complex pattern in the region 2.5–4.0 δ of area 4 and are assigned to the aliphatic protons at C-5 and C-6.

The similarities in the p.m.r. spectrum of this alkaloid to the spectra of the synthetic ketone **4**, to fumariline **5**, and to ochrobirine **3**, leave little doubt that it has the same skeletal structure as these alkaloids and the substitution pattern shown in **1**. The relative configuration of the OH group in **1** is apparent from the large Nuclear Overhauser effect (N.O.E.) (8) of 25% observed at C-14 when the signal at 2.43 δ (N—CH_3) is irradiated. This effect is possible only with the configuration shown.

In the infrared (i.r.) spectrum of **1** there is a band at 1710 cm^{-1} which appears at virtually the same frequency as the carbonyl band of **4** and **5**. The ultraviolet (u.v.) spectrum of **1** is also similar to that of **4**.

The molecular formula of sibiricine was established by high resolution mass spectrometry. The peak of highest mass appeared at *m/e* 367. Accurate mass measurement by the peak matching technique gave a value of 367.1071; calculated

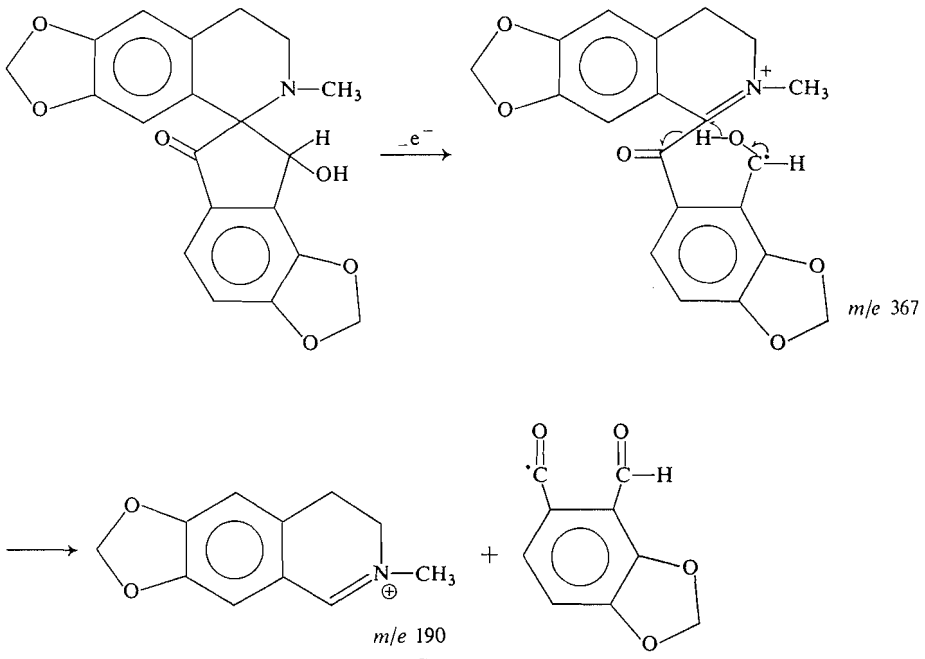

SCHEME 1

for $C_{20}H_{17}NO_6$, 367.1055. Other mass measurements carried out on fragment ion peaks were compatible with this constitutional assignment and the proposed structure. A detailed account of the mass spectrometric work on this and on related alkaloids will be discussed in a subsequent communication. Of particular importance to this investigation, however, is the presence of a fragment ion of *m/e* 190, of composition $C_{11}H_{12}NO_2$ (calculated for $C_{11}H_{12}NO_2$, 190.0868; observed, 190.0864). The formation of this fragment ion is characteristic of alkaloids of this structural type (5) whenever an OH group is present at C-9 or C-14. Its formation may be rationalized as shown in Scheme 1.

Experimental

Methods

The mass spectrum was recorded on a CEC 21-110B double-focussing mass spectrometer. Accurate mass measurements (9) were made by reference to appropriate peaks in the spectrum of perfluorokerosene (10).

The p.m.r. spectrum was recorded using the frequency sweep mode of a Varian HA-100 spectrometer. Samples were dissolved in $CDCl_3$ using added TMS as the internal locking signal. Chemical shifts were measured relative to TMS using a V 4315 frequency counter incorporated in the instrument. Double irradiation was achieved by employing a Hewlett–Packard 201C audiogenerator at the desired frequency. For N.O.E. measurements degassed solutions were used and a procedure similar to that of Anet and Bourn (8) was employed. A Beckmann IR10 spectrometer was used to record i.r. spectra and a Cary 14 spectrometer was used for the u.v. spectrum.

Isolation of Sibiricine

The mother liquor from the separation of protopine and ochrobirine from the extract of *C. sibirica* (1) was acidified with oxalic acid, exhausted with ether, basified, and then extracted several times with ether again. The residue from the latter extract yielded a small crop of ochrobirine and the mother liquor from this, in the course of several days, deposited a crop of stout prisms which were, however, contaminated with some ochrobirine. The mixture was extracted with several portions of hot methanol and the residue recrystallized from chloroform – methanol, m.p. 225°. Another batch of plant material also yielded the same base.

Anal. Calcd. for $C_{20}H_{17}NO_6$: C, 65.39; H, 4.66; N, 3.81. Found: C, 65.85; H, 4.98; N, 3.62.

Infrared spectrum: $\nu_{OH}(CHCl_3)$ 3560 cm^{-1}; $\nu_{C=O}$ ($CHCl_3$) 1710 cm^{-1}; $\nu_{C=O}$(KBr) 1700 cm^{-1}.

Ultraviolet spectrum: λ_{max} 205, 240, 291, and 313 (sh) mμ; log ε 4.80, 3.94, 3.91, and 3.99.

Acknowledgment

We thank the National Research Council of Canada for support of this work.

1. R. H. F. MANSKE. Can. J. Res. **14 B**, 354 (1936).
2. S. MCLEAN, M.-S. LIN, and R. H. F. MANSKE. Can. J. Chem. **44**, 2449 (1966).

Can. J. Chem. Downloaded from www.nrcresearchpress.com by 210.87.254.40 on 09/05/12
For personal use only.

3. D. B. MACLEAN, D. E. F. GRACEY, J. K. SAUNDERS, R. H. F. MANSKE, and R. RODRIGO. This issue.
4. S. MCLEAN, M.-S. LIN, and J. WHELAN. Tetrahedron Letters, 2425 (1968).
5. D. B. MACLEAN, R. A. BELL, J. K. SAUNDERS, C.-Y. CHEN, and R. H. F. MANSKE. This issue.
6. J. K. SAUNDERS, R. A. BELL, C.-Y. CHEN, D. B. MACLEAN, and R. H. F. MANSKE. Can. J. Chem. **46**, 2873 (1968).
7. J. K. SAUNDERS, R. A. BELL, C.-Y. CHEN, D. B. MACLEAN, and R. H. F. MANSKE. Can. J. Chem. **46**, 2876 (1968).
8. F. A. L. ANET and A. J. R. BOURN. J. Amer. Chem. Soc. **87**, 5250 (1965).
9. K. S. QUISENBERRY, T. T. SCOTMAN, and A. O. NIER. Phys. Rev. **102**, 1071 (1956).
10. F. W. MCLAFFERTY. Anal. Chem. **28**, 306 (1956).

Can. J. Chem. Downloaded from www.nrcresearchpress.com by 210.87.254.40 on 09/05/12
For personal use only.

The structure of ochrobirine

R. H. F. MANSKE AND R. G. A. RODRIGO
Department of Chemistry, University of Waterloo, Waterloo, Ontario

AND

D. B. MACLEAN, D. E. F. GRACEY, AND J. K. SAUNDERS
Department of Chemistry, McMaster University, Hamilton, Ontario

Received April 28, 1969

Structure **1** is proposed for ochrobirine from an analysis of the proton magnetic resonance spectra of ochrobirine and its di-*O*-acetate.

Canadian Journal of Chemistry, **47**, 3589 (1969)

Can. J. Chem. Downloaded from www.nrcresearchpress.com by 210.87.254.5 on 09/05/12
For personal use only.

Ochrobirine, $C_{20}H_{19}NO_6$, was first isolated in 1936 from *Corydalis sibirica* (L.) Pers. by Manske (1). It has since been reported in other species of Corydalis (2, 3) but there have been no structural investigations of this alkaloid. Here, we present evidence that ochrobirine has structure **1**.

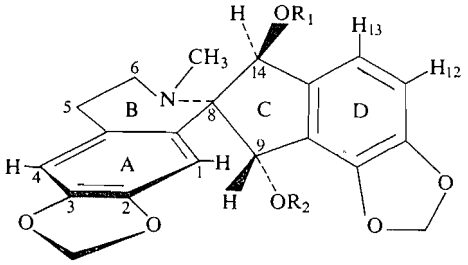

1 $R_1 = R_2 = H$; Ochrobirine
7 $R_1 = R_2 = CH_3CO$; Diacetylochrobirine

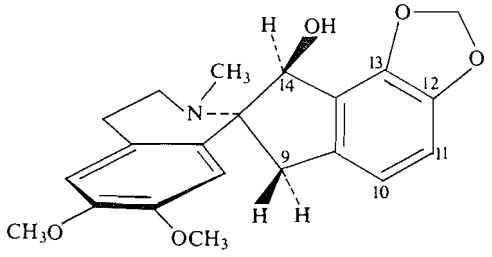

2 Fumaricine

Recently, structures **2** and **3** were proposed for the alkaloids fumaricine and fumariline, respectively (4–6). The structural assignment was based on a comparison of the properties of **2** and **3** with that of the synthetic ketone **4** of established structure (7). Through high resolution proton magnetic resonance (p.m.r.) studies and Nuclear Overhauser effect (N.O.E.) studies (8) the orientation of the substituents of **2** and **3** in rings A and D was established. Sizeable N.O.E.'s were observed between the benzylic protons of rings C and neighboring protons including the adjacent aromatic protons in ring D, the aromatic proton at C-1 in ring A, and the *N*-methyl group. Moreover, there was also a large N.O.E. between the protons at C-5 and the aromatic proton at C-4. An analogous study (9) has been carried out on ochotensimine **5** in which the interactions which were observed in **2**, **3**, and **4** are also present. Thus the N.O.E.'s which have been observed would appear to be characteristic of this ring system.

Ochrobirine occurs in the same plant as ochotensine **6** (10) and its molecular formula led

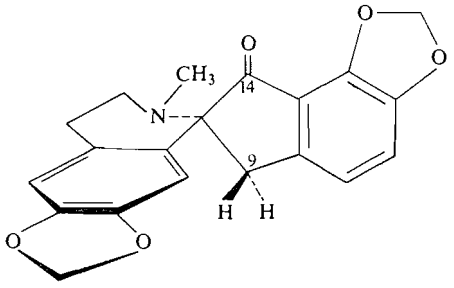

3 Fumariline

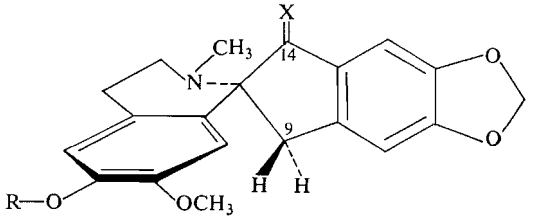

4 X = O; R = CH_3
5 X = CH_2; R = CH_3; Ochotensimine
6 X = CH_2; R = H; Ochotensine

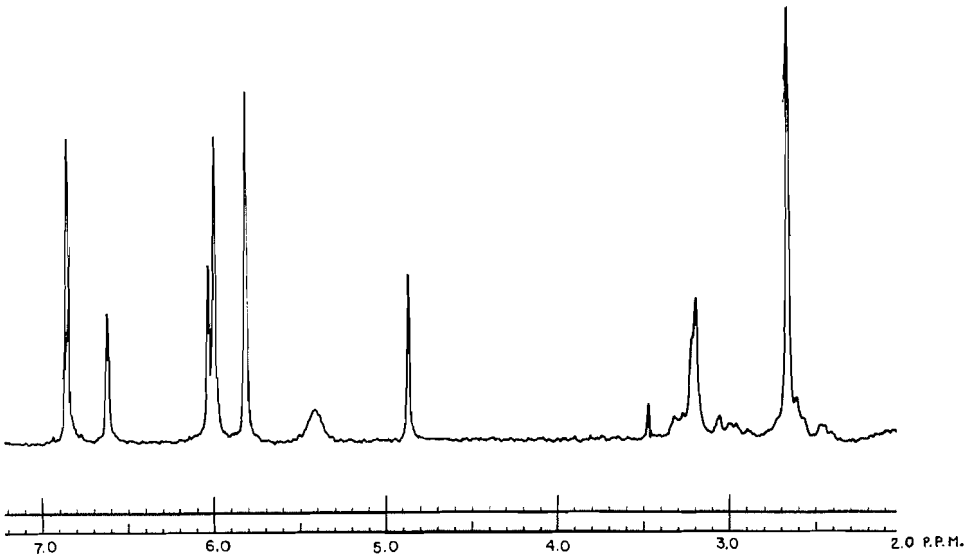

FIG. 1. The p.m.r. spectrum of ochrobirine.

Can. J. Chem. Downloaded from www.nrcresearchpress.com by 210.87.254.5 on 09/05/12
For personal use only.

us to suspect that it might be structurally related to the latter in a manner analogous to **2** and **3**. Accordingly, we examined the 100 MHz p.m.r. spectrum of ochrobirine and its di-*O*-acetate (**7**) and applied N.O.E. studies to ochrobirine. When the results obtained with **1** and **7** were compared with the earlier studies, it was apparent that the ring system of ochrobirine was the same as **2** and **3** and that the position of the substituents and the relative configuration of the alkaloid conforms to that shown in **1**.

The 100 MHz p.m.r. spectrum of ochrobirine (Fig. 1) has singlets of area 1 at 6.04 and 6.62 δ, uncoupled to adjacent aromatic protons, attributed to the protons at C-1 and C-4, respectively. The singlet at 6.62 is broader than that at 6.04 and is long-range coupled to the aliphatic protons at C-5. Two other aromatic protons appear as a signal of area 2 at 6.85 δ. A singlet of area 3 at 2.67 δ is assigned to the *N*-CH_3 group while signals of area 2 at 5.81 and 6.00 δ are attributed to two methylenedioxy groups. There are two signals of area 1 at 4.88 and 5.42 δ which are assigned to aliphatic protons geminal to hydroxyl groups. The higher field peak is a sharp peak while that at lower field is diffuse but sharpens on addition of D_2O. The four remaining protons are spread throughout the region 2.5–3.5 δ and are assigned to the aliphatic protons at C-5 and C-6.

The spectrum of **7**, di-*O*-acetylochrobirine (Fig. 2), lends support to the assignments above. In the high field region there are now three singlets of area 3 at 2.37, 2.12, and 1.89 δ which are attributed to the *N*-CH_3 and to the two acetoxy methyl groups, respectively. One of the latter signals is at higher field than normally expected of an acetoxy methyl group and is apparently shielded by one of the aromatic rings. The four aliphatic protons at C-5 and C-6 appear in an AA′ BB′ pattern centered at 3.00 and 2.72 δ. This is the first instance in this series of alkaloids where a recognizable pattern has been observed for the protons at C-5 and C-6. Its presence may be ascribed to the proximity of one of the two methylene groups at C-5 or C-6 to one or other of the acetoxy groups.

The signal of area 2 at 6.85 δ in **1** is now split into an AB quartet (δ H_{12}, 6.86; δ H_{13}, 6.73; $J_{H_{12},H_{13}}$ = 8.0 Hz) showing that the two aromatic protons are adjacent. The two methylenedioxy signals which appeared as singlets in **1** are shifted slightly downfield and appear as quartets. The protons geminal to the two hydroxy groups of **1** have shifted into the aromatic region where, besides the AB quartet, there are now three signals, one of area 2 at 6.55 δ and two of area 1 at 6.52 and 6.36 δ. Through decoupling experiments it was possible to assign these signals. Irradiation at 2.70 δ sharpened the signal at 6.52 δ and thus this signal is assigned to H-4 (Inset 1, Fig. 2). Irradiation at the $\diagdown\!\!\diagup N—CH_3$

Can. J. Chem. Downloaded from www.nrcresearchpress.com by 210.87.254.5 on 09/05/12
For personal use only.

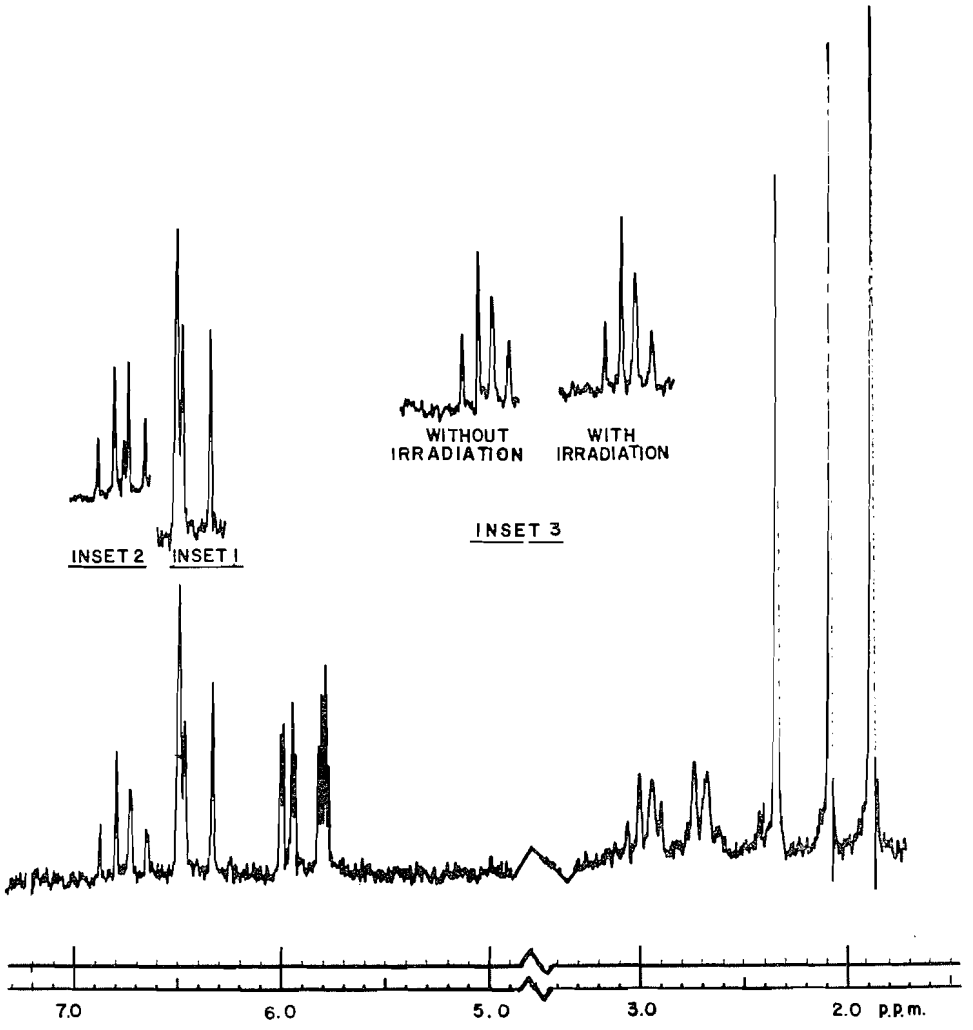

FIG. 2. The p.m.r. spectrum of ochrobirine di-*O*-acetate.

signal increased the area of the signal at 6.55 δ and, therefore, one or both of the protons geminal to the acetoxy groups is present there. Irradiation at 6.55 δ decoupled the higher field proton of the AB quartet but had a negligible effect on that at lower field as expected for ortho and meta benzylic coupling (11) (Inset 2, Fig. 2). We conclude, therefore, that one of the two protons at 6.55 δ is at H-14. Irradiation at 6.36 δ causes the low field doublet of the AB quartet to sharpen relative to the higher field doublet. This is illustrated in Inset 3, Fig. 2 where one can perceive a distinct difference in height of the signals with and without irradiation at 6.36 δ.[1] This behavior would be expected for para and meta benzylic coupling (11) respectively, and, therefore, we assign the signal at 6.36 δ to H-9. By a process of elimination the signal of H-1 is present at 6.55 δ along with that of H-14.

Through N.O.E. studies we were able to confirm the substitution pattern in rings A and D deduced from the decoupling experiments and to arrive at the relative configuration of the molecule. Irradiation of the signal at 2.67 δ in ochrobirine, attributed to the N-CH_3, increased the area of the signal at 5.42 δ by 24% but did not affect the signal at 4.88 δ. Irradiation of the signal at 5.42 δ increased the area of the signal at 6.85 δ by 4% but had no effect on the area of the two aromatic singlets. Accordingly, we assign the proton at 5.42 δ to C-14 and conclude that it is adjacent

[1]The irradiation was carried out several times and in each case the height of the low field doublet relative to that at higher field increased by at least 10%.

Can. J. Chem. Downloaded from www.nrcresearchpress.com by 210.87.254.5 on 09/05/12
For personal use only.

to the pair of ortho aromatic protons. Irradiation at 4.88 δ results in an increase in area of the aromatic singlet at 6.04 δ of 13% but does not affect the other aromatic protons. Accordingly we place the irradiated proton at C-9 and the observed proton at C-1. It follows therefore that the OH groups must be *trans* to one another in the five-membered ring. The OH at C-9 is probably internally hydrogen bonded to the nitrogen which may account for the relatively smaller N.O.E. observed between H-14 and H-13 in this system when compared with the earlier systems which were studied.

Attempts to corroborate this structural assignment by chemical degradation were only partially successful. A small yield of noncrystalline ketonic material was obtained by oxidation of ochrobirine with CrO_3 in pyridine but the product would not crystallize. Oxidation of ochrobirine gave 4,5-methylenedioxyphthalic acid identified as its *N*-ethylimide, thus substantiating the assignment of substituents in ring A. The isomeric 3,4-methylenedioxy acid was not, however, found as an oxidation product.

The molecular formula of ochrobirine was confirmed by accurate mass measurement: calcd. for $C_{20}H_{19}NO_6$, 369.1212; found, 369.1204. As expected the ultraviolet (u.v.) spectrum of ochrobirine was similar to that of fumaricine (**2**), (4).

Experimental

Methods

Mass spectra were recorded on a CEC 21–110B double-focusing mass spectrometer. Accurate mass measurements (12) were made by reference to appropriate peaks in the spectrum of perfluorokerosene (13).

The p.m.r. spectrum was recorded using the frequency sweep mode of a Varian HA-100 spectrometer. Samples were dissolved in $CDCl_3$ using added TMS as the internal locking signal. Chemical shifts were measured relative to TMS using a V4315 frequency counter incorporated in the instrument. Double irradiation was achieved by employing a Hewlett-Packard 201C audiogenerator at the desired frequency. For N.O.E. measurements degassed solutions were used and a procedure similar to that of Anet and Bourn (8) was employed. A Beckmann IR 10 spectrometer was used to record infrared (i.r.) spectra and a Cary 14 spectrometer was used for the u.v. spectrum.

Ochrobirine

The isolation of ochrobirine has been described elsewhere (1–3). Its u.v. spectrum had λ_{max} (MeOH) 205, 240, and 291 mμ; log ε_{max} 4.80, 3.94, and 3.91, respectively. The i.r. spectrum showed two bands in the OH region at 3585 cm^{-1} (sharp) and 3300 cm^{-1} (broad) in CCl_4 solution.

Ochrobirine Di-O-acetate

Ochrobirine (0.1 g) and acetic anhydride (0.6 ml) were heated on a steam bath for 1 h and the cooled solution poured into a dilute solution of sodium carbonate. The crystalline solid which separated was washed thoroughly with water and crystallized twice from methanol after which it melted at 179°. The yield of recrystallized material was 40 mg. The mass spectrum showed a molecular ion at 453.1419; calcd. for $C_{24}H_{23}NO_8$, 453.1423. The diacetate yielded ochrobirine on alkaline hydrolysis showing that the skeletal structure was unaltered during acetylation. This compound is identical with ochrobirine acetate previously reported (2).

Oxidation of Ochrobirine

Ochrobirine (0.2 g) and dilute nitric acid (10 ml) (ca. 15%) were heated for 15 min on a steam bath. The cooled solution was neutralized with sodium hydroxide and extracted with a large volume of ether. The extract was oxidized with potassium permanganate. From the oxidation mixture, after acidification, an acid was extracted which was converted to its *N*-ethylimide. The few mg of imide which were obtained were sublimed and crystallized twice from ether and melted at 129°, either alone, or in a mixture with 4,5-methylenedioxy-*N*-ethylphthalimide.

Acknowledgment

We wish to thank the National Research Council of Canada for financial support of this work.

1. R. H. F. Manske. Can. J. Res. **14 B**, 354 (1936).
2. R. H. F. Manske. Can. J. Res. **17 B**, 89 (1939).
3. R. H. F. Manske. Can. J. Res. **17 B**, 95 (1939).
4. J. K. Saunders, R. A. Bell, C.-Y. Chen, D. B. MacLean, and R. H. F. Manske. Can. J. Chem. **46**, 2873 (1968).
5. J. K. Saunders, R. A. Bell, C.-Y. Chen, D. B. MacLean, and R. H. F. Manske. Can. J. Chem. **46**, 2876 (1968).
6. D. B. MacLean, R. A. Bell, J. K. Saunders, C.-Y. Chen, and R. H. F. Manske. Can. J. Chem. This issue.
7. S. McLean, M.-S. Lin, and J. Whelan. Tetrahedron Letters, 2425 (1968).
8. F. A. L. Anet and A. J. R. Bourn. J. Amer. Chem. Soc. **87**, 5250 (1965).
9. J. K. Saunders and R. A. Bell. Can. J. Chem. **46**, 3421 (1968).
10. S. McLean, M.-S. Lin, and R. H. F. Manske. Can. J. Chem. **44**, 2449 (1966).
11. D. T. Wittiak, D. B. Patel, and Y. Lin. J. Amer. Chem. Soc. **89**, 1908 (1967).
12. K. S. Quisenberry, T. T. Scotman, and A. O. Nier. Phys. Rev. **102**, 1071 (1956).
13. F. W. McLafferty. Anal. Chem. **28**, 306 (1956).

Structures of three minor alkaloids of *Fumaria officinalis* L.

D. B. MACLEAN, R. A. BELL, J. K. SAUNDERS, AND C.-Y. CHEN
Department of Chemistry, McMaster University, Hamilton, Ontario

AND

R. H. F. MANSKE
Research Laboratories, UniRoyal Limited, Guelph, Ontario

Received April 28, 1969

The structures of fumaricine, fumaritine, and fumariline, minor alkaloids of *F. officinalis*, have been deduced by spectroscopic methods and by comparison with model systems. Nuclear Overhauser effects observed in these systems aided in the solution of the structural problem. The three alkaloids have a common ring system and are structurally related to ochotensimine.

Canadian Journal of Chemistry, 47, 3593 (1969)

Can. J. Chem. Downloaded from www.nrcresearchpress.com by 210.87.254.42 on 09/05/12
For personal use only.

In 1938 Manske (1) examined *Fumaria officinalis* L. for its alkaloid content. He isolated and identified several isoquinoline alkaloids, namely protopine, cryptopine, ± stylopine, + and ± scoulerine, and sinactine. Besides these alkaloids of established structure he reported the presence of two new alkaloids, F-37 ($C_{21}H_{23}NO_5$) (**1**) and F-38 ($C_{20}H_{19}NO_6$). In the interim Manske (2) has isolated two other minor alkaloids from this source corresponding in composition to $C_{20}H_{21}NO_5$ (**2**) and to $C_{20}H_{17}NO_5$ (**3**). Compound **2** is a lower homologue of **1** since it yields **1** upon methylation with diazomethane. The names, fumaricine, fumaritine, and fumariline have been assigned to **1**, **2**, and **3** respectively.

In two earlier short communications (3, 4) we described briefly the studies which led to the assignment of structures to **1** and **3**. Here we give a full account of our work and provide evidence for the assignment of the hydroxyl and methoxyl groups in **2**.

We were unable to carry out meaningful chemical degradations of these alkaloids and were forced to rely on physical methods for our structural assignments. The infrared (i.r.) spectrum of **3** showed a band at ν_{max} ($CHCl_3$) 1709 cm^{-1} suggesting the presence of a carbonyl group. Its presence was confirmed by reduction of **3** to an alcohol **4** ($C_{20}H_{19}NO_5$) with sodium borohydride or with lithium aluminium hydride. The i.r. spectrum of **4** lacked a band in the carbonyl region but had a band in the hydroxyl region. The ultraviolet (u.v.) spectrum of **4** was virtually superimposable on that of **1** λ_{max} (EtOH) 207, 235, and 288 mμ, (log ε 4.74, 3.94, and 3.74) but distinctly different from that of **3** λ_{max} (EtOH) 203, 237, 263, 294, and 355 mμ, (log ε 4.60, 4.31, 4.05, 3.66, and 3.51). The change in the u.v. spectrum resulting from the reduction suggested that the carbonyl group of **3** was conjugated, probably to an aromatic system. The i.r. spectrum of **1** had no bands in the carbonyl region but had a band in the hydroxyl region, ν_{max} (CS_2) 3560 cm^{-1}, which did not shift upon dilution suggesting that the hydroxyl group was internally hydrogen bonded.

The proton magnetic resonance (p.m.r.) spectra of **1** and **3** showed that both compounds had one *N*-CH_3 group and four aromatic protons, that **1** had two methoxyl groups and one methylenedioxy group, and that **3** had two methylenedioxy groups. The substituents on **2** and **4** follow from their relationship to **1** and **3**, respectively.

From an examination of their mass spectra (Fig. 1) it is apparent that **1**, **2**, and **4** have a common fragmentation pattern. The major fragment ion in each spectrum shows the shift in mass expected for the different substituents in each of them. (That the spectrum of **3** is very different is a consequence of the difference in its functionality from the other alkaloids.) It seems likely, therefore, that **1** and **3** have a common ring system but differ in their substituents and in their oxidation state. The mass spectra, aside from indicating a common ring system for the alkaloids, did not provide much structural information. The spectra were, however, sufficiently different from the spectra of known isoquinoline systems to suggest that the alkaloids belonged to a hitherto unreported structural group. Compound **4** is isomeric with chelidonine (5) but a comparison of its spectrum (Fig. 1*e*) with that of **4** showed that the two compounds must have different ring systems.

Can. J. Chem. Downloaded from www.nrcresearchpress.com by 210.87.254.42 on 09/05/12
For personal use only.

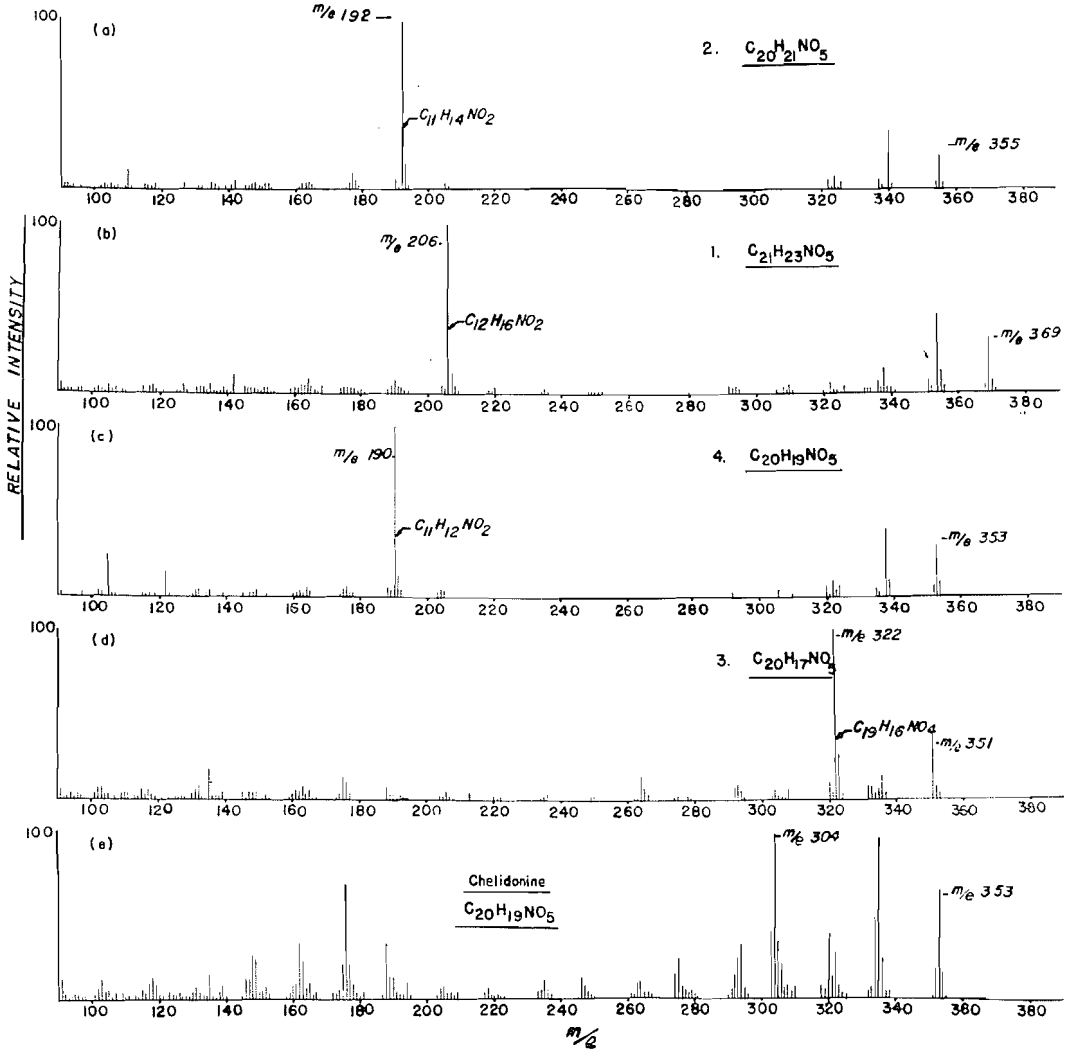

FIG. 1. Mass spectra of (a) fumaritine, (b) fumaricine, (c) dihydrofumariline, (d) fumariline, and (e) chelidonine.

It was through an examination of the 100 MHz p.m.r. spectra of **1**, **2**, **3**, and **4** and an examination of the nuclear Overhauser effects (N.O.E.) (6) in these systems that we were able to arrive at structures for the alkaloids. The salient features of the spectra of **3** and **4** which are discussed first are summarized in Table I. Each spectrum shows four aromatic protons, two ortho and coupled to each other (H-10 and H-11) and two singlets (H-1 and H-4) which are uncoupled. Each has two methylenedioxy groups and one $\diagdown N\text{—}CH_3$. Both show an AB quartet in the region expected of benzylic protons (H-9A, H-9B) which have a large coupling constant but which are uncoupled to neighboring aliphatic protons. In the spectrum of **4** there is a singlet (H-14) attributed to the hydrogen geminal to the hydroxyl group which is absent, as expected, in the spectrum of **3**. This proton is also uncoupled to neighboring aliphatic protons. In each spectrum there are signals corresponding in area to four additional aliphatic protons which lie in the region 2.6–3.6 δ and which are not readily analyzed.

Decoupling experiments carried out on **3** show that H-10 and H-11 are long-range coupled to

TABLE I

The p.m.r. signals of **1**, **2**, **3**, and **4** in p.p.m. (δ)

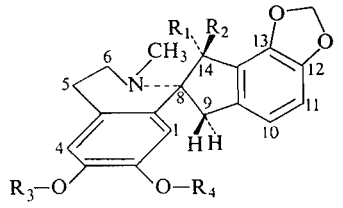

	1 $R_3 = R_4 = CH_3$ $R_1 = H, R_2 = OH$	**2** $R_3 = CH_3, R_4 = H$ $R_1 = H, R_2 = OH$	**3** $R_3 + R_4 = CH_2$ $R_1 + R_2 = O$	**4** $R_3 + R_4 = CH_2$ $R_1 = H, R_2 = OH$
H-1	6.39	6.47	6.16	6.38
H-4	6.57	6.59	6.54	6.56
H-10*	6.68	6.68	6.86	6.68
H-11*	6.73	6.74	7.07	6.75
H-9†	3.29	3.29	3.50	3.23
			3.32	3.31
H-14	5.44	5.42	—	5.42
2-OMe	3.49	—	—	—
3-OMe	3.81	3.85	—	—
2,3 —O, —O, CH_2	—	—	5.80	5.80
12,13 —O, —O, CH_2	5.91	5.95	6.12	5.90
>N—CH_3	2.40	2.41	2.36	2.38

*$J_{H_{10}H_{11}}$ = 8.0 Hz for **1**, **2**, **3**, and **4**.
†J = 18 Hz for **3** and **4**.

the protons of the benzylic AB quartet centered at 3.41 but that the coupling to H-10 is stronger and that H-4 is long-range coupled to an aliphatic proton centered near 3.0 but that H-1 is not coupled or only weakly so.

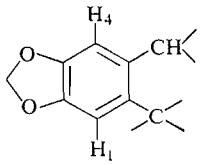

3a

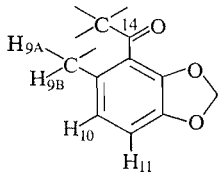

3b

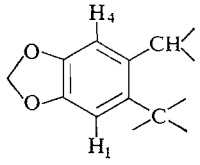

4a

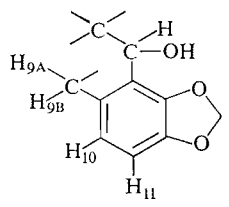

4b

The spectral data suggest the following structural units, *a* and *b*, in **3** and **4**. The carbonyl group is placed in conjugation with the ring carrying H-10 and H-11 since both of these protons undergo an appreciable upfield shift on conversion of ketone **3** to alcohol **4** as does one of the methylenedioxy groups. The carbonyl group is placed adjacent to the methylenedioxy group in **3***b* for the following reasons. The chemical shift difference between H-10 and H-11 is expected of aromatic protons *meta* and *para* to a carbonyl group (7), but is smaller than expected for protons *ortho* and *meta* to a carbonyl group which would be the case if the carbonyl and methylene groups were interchanged in **3***b*. More definitive, however, was the appreciable n.O.e. observed at H-10 in **3** when the protons at C-9 were irradiated (*vide infra*).

The observation that the hydrogen geminal to the OH group of **4***b* at C-4 is uncoupled to neighboring aliphatic protons suggests that a quaternary carbon is adjacent to the >CHOH group

Can. J. Chem. Downloaded from www.nrcresearchpress.com by 210.87.254.42 on 09/05/12
For personal use only.

Can. J. Chem. Downloaded from www.nrcresearchpress.com by 210.87.254.42 on 09/05/12
For personal use only.

of **4** and to the >=O group of **3**. This conclusion is supported by the fact that **3** did not exchange hydrogen for deuterium in basic or in acidic media. The benzylic methylene protons of **3** and **4** are uncoupled to neighboring aliphatic protons and must, therefore, be adjacent to a quaternary carbon or to nitrogen. There are two

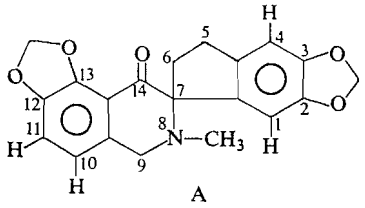

A

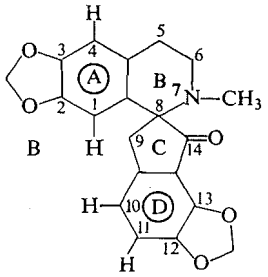

B

structures, A and B, into which these structural units can be incorporated and which appear to meet the requirements of the spectral data discussed thus far. Ring system A has not to our knowledge been encountered in nature although this skeleton has been reported as a transformation product of cryptopine (8). Ring system B is related to that found in ochotensimine, **5**, (9).

Structure A contains a substituted 2,3-dihydro-4 (1*H*) isoquinolone system. Derivatives of this system have recently been synthesized by Grethe *et al.* (10, 11). In these compounds the carbonyl absorption for the most part fell in the range 1680–1700 cm^{-1} which is at lower frequency than the carbonyl absorption observed in **3**. In the p.m.r. spectrum (11) of 2-benzyl-2,3-dihydro-7-methoxy-4 (1*H*) isoquinolone, the two sets of benzylic methylene protons absorb at δ 3.75 and 3.85, both of which are at lower field than in our compound **3**. In other isoquinoline alkaloids, for example, chelidonine (12) and the protoberberines (13), the methylene protons lying between nitrogen and phenyl are observed at lower field than we observe in **3**. Thus, the examination of the model systems casts doubt on the validity of structure A.

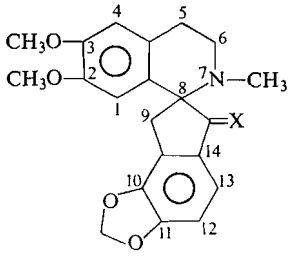

5. ochotensimine X = CH_2
6. X = O

While this work was in progress the synthesis of ochotensimine, **5**, was reported by McLean *et al.* (14). An intermediate in this synthesis is compound **6** which served as an ideal model of structure B. The carbonyl absorption of **6**, ν_{max} ($CHCl_3$) 1711 cm^{-1}, appears at virtually the same frequency as that of **3**. The 100 MHz p.m.r. spectrum of **6** shows a marked similarity to that of **3**. The spectra were reproduced in our earlier communication and need not be repeated here. The major difference in the two spectra, aside from the differences arising from the substituents, lies in the chemical shift of the low-field proton of the aromatic AB quartet. In **6** this proton is centered at 7.46 δ, in **3** at 7.07 δ. In **6** the low-field proton is *ortho* to the carbonyl group. It appears, therefore, that in **3** the low-field proton is *para* to the carbonyl group and such a difference is expected (7). The proton *meta* to the carbonyl has approximately the same chemical shift in each, at 6.86 and 6.91 in **3** and **6**, respectively, as do the aromatic protons at C-1 and C-4 which appear at 6.16 and 6.54 in **3** and at 6.11 and 6.57 in **6**. Similarly, we found the same chemical shift for the protons of the benzylic AB quartet in each of **3** and **6**. The remarkable similarity in the spectral properties of the two compounds leads us to the conclusion that B and not A is the proper formulation of **3**.

In order to substantiate our conclusions regarding the structure of **3**, and at the same time to ascertain the substitution pattern of **1**, we examined **1**, **3**, and **6** for N.O.E. The potential of N.O.E. in structural and stereochemical studies was pointed out by Anet and Bourn (6) who were the first to use the method in this sense. It has since been applied successfully in the examination of other systems (15). Examination of a model of **6** showed that there were a number of uncoupled

Can. J. Chem. Downloaded from www.nrcresearchpress.com by 210.87.254.42 on 09/05/12
For personal use only.

protons lying within 3.0 Å of one another for which N.O.E. should be observed. (There is no ambiguity with respect to the structure of **6** since it has been converted in a single step to ± ochotensimine; the structure of natural ochotensimine was established by X-ray analysis (9).) We, therefore, measured N.O.E. in **6** and wherever possible, measured the same interactions in **1** and **3**.

Model studies on **6** showed that irradiation of the protons at C-9 or the methoxyl protons at C-2 should increase the area of the proton at C-1. Similarly, irradiation at the C-3 methoxyl or at the C-5 protons should affect the proton at C-4, and irradiation of the N-CH_3 should affect one of the protons at C-9. In all cases these predictions were borne out experimentally and the results were reported previously (4). It is important to note that irradiation at C-9 should not and did not affect either of the protons of the aromatic AB quartet. Similar effects have also been observed in ochotensimine (16).

With these results at hand for **6** we looked for similar effects in **3**. We found all that were possible in the light of the altered substitution pattern and, in addition, we observed a sizeable effect (4) at the aromatic proton C-10 when the protons of C-9 were irradiated, thereby confirming the assignment of the substituents in ring D which we had drawn from chemical shift data.

Turning now to fumaricine, we stated earlier that its i.r., u.v., and mass spectra suggested that it has the same ring system as **4**. Its p.m.r. spectrum is compared in Table I with that of **4** and the two spectra are also remarkably similar. Nuclear Overhauser effects measured on **1** were similar to those in **6** except that irradiation at C-9 resulted in an increase in area of the signal attributed to H-10. This finding led us to assign the same substitution pattern to **1** as to **3** and **4**. In our original paper we concluded that the —OH group of **1** was internally hydrogen-bonded to the nitrogen, on the basis of its i.r. spectrum and coupling constant to the hydroxyl proton. We have since found that there is an observable N.O.E. (14%) for the proton at C-14 when the signal due to the N-CH_3 group is irradiated. We must, therefore, revise our original assignment and place the OH group *trans* to the N-CH_3 group. Apparently the hydroxyl group of **1** is π-bonded to the aromatic ring (17) and not to nitrogen as we originally suspected. Since the signal of the proton at C-14 of **4** has the same chemical shift as that of **1** and shows the same behavior, namely, a broad signal which sharpens on addition of D_2O, it seems probable that the configuration of **4** at C-14 is identical with **1**.

Since **2** is converted to **1** by treatment with diazomethane there is only one structural feature of **2** which remains to be resolved, namely the assignment of the OCH_3 group to C-2 or C-3. This assignment was readily made by ascertaining which of the protons, at C-1 or C-4, exhibits an increase in area when the —OCH_3 group of **2** is irradiated. The resonances of the protons of **2** are recorded in Table I. The lower-field and broader signal observed at 6.59 δ has been assigned to C-4 by analogy with the spectra of **1**, **3**, **4**, and **6** and it is this signal which increases in area by 24% when the —OCH_3 group is irradiated. We, therefore, assign the —OCH_3 to C-3 and the OH group to C-2 in **2**.

In the mass spectra of **1**, **2**, and **4** there is only one intense fragment ion, designated *a*, which is found at *m/e* 206 in **1**, at *m/e* 192 in **2**, and at *m/e* 190 in **4**. Exact mass measurements have confirmed the composition of this ion in **1**. A mechanism for the formation of ion *a* is shown in Scheme 1. Compound **4**, deuterated at C-14, was prepared by the reduction of **3** with sodium borodeuteride and its spectrum examined. It was found that *a* still appeared at *m/e* 190 although the molecular ion was at *m/e* 354. When, however, the hydroxyl hydrogen of **4** was exchanged with deuterium it was found that ion *a* was partially shifted to *m/e* 191 in the spectrum of the deuterated compound. These deuteration studies lend support to the mechanism proposed in Scheme 1.

The spectrum of **3** is distinctly different from **1**, **2**, and **4** in that it does not show an intense ion in the low mass region. The major fragment ion appears at *m/e* 322. High resolution mass spectrometry has shown that this peak is a singlet and that it corresponds in composition to $C_{19}H_{16}NO_4$. It is apparently formed by loss of CO followed or preceded by loss of H. The OH function in the five-membered ring appears to be a necessary structural feature for fragmentation leading to ions of type *a*. Their presence in **1**, **2**, and **4** lends further support to that already given for a tetrahydroisoquinoline system in these alkaloids.

Ions of type *a* are also characteristic of the benzylisoquinoline (18) and phthalide isoquinoline alkaloids (19). In these systems the molecular ion is of very low intensity and thus they are

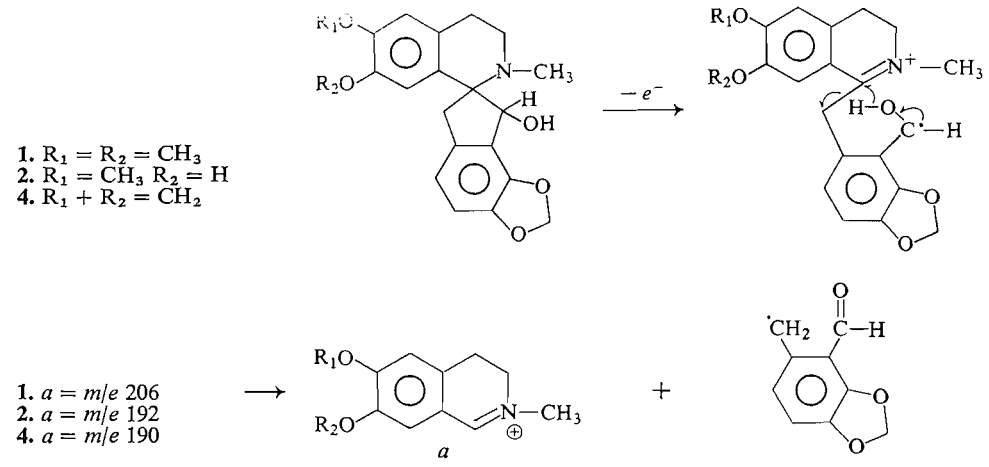

SCHEME 1

readily differentiated from fumaricine and its analogues.

The spectrum of chelidonine is worthy of comment. The major fragment ions appear at *m/e* 335, 320, and 304. That at *m/e* 335 is formed through loss of H_2O, that at 320 through loss of CH_3 from *m/e* 335, and surprisingly that at *m/e* 304 through loss of CH_3NH_2 from *m/e* 335. The composition of these ions has been confirmed by exact mass measurement.

Experimental

Materials and Methods

The isolation and properties of the alkaloids used in this investigation have been described elsewhere (1, 2).

The mass spectra were recorded on a Hitachi Perkin–Elmer RMU-6A mass spectrometer. Samples were introduced through the direct inlet system. Accurate mass measurements (20) were carried out on a CEC-21-110B double-focussing mass spectrometer. The measurements were made by reference to appropriate peaks in the spectrum of perfluorokerosene (21). Observed values agreed with calculated values within ± 0.005 mass units. Exchange of the OH group of **4** was carried out using CH_3OD.

The p.m.r. spectra were recorded using the frequency sweep mode of a Varian HA-100 spectrometer. Samples were dissolved in $CDCl_3$ using added TMS as the internal locking signal. Chemical shifts were measured relative to TMS using a V4315 frequency counter incorporated in the instrument. Double irradiation was achieved by employing a Hewlett–Packard 201C audio generator at the desired frequency. For N.O.E. measurements degassed solutions were used and a procedure similar to that of Anet and Bourn (6) was employed. A Perkin–Elmer 521 spectrometer was used to record i.r. spectra and a Cary 14 spectrometer was used for u.v. spectra.

Reduction of 3 with Lithium Aluminium Hydride

Compound **3** (58 mg) was dissolved in dry ether and added to an excess of $LiAlH_4$ in dry ether and the mixture heated under reflux for 20 min. Excess hydride was destroyed with water, the ether layer separated, and the aqueous layer extracted several times with fresh ether. The combined ether extract was evaporated to dryness yielding a residue which was recrystallized from ether, m.p. 129–133° (45 mg). The i.r. spectrum showed the presence of hydroxyl absorption but there was no band in the carbonyl region. The mass spectrum showed a molecular ion at *m/e* 353.1248; calcd. for $C_{20}H_{19}NO_5$, 353.1263. The compound showed a single spot on thin-layer chromatography.

Reduction of 3 with Sodium Borohydride

Compound **3**, dissolved in methanol, was added to a solution of sodium borohydride in methanol and the mixture allowed to stand at room temperature for several hours. The solution was evaporated to dryness, water was added to the residue, and the aqueous suspension extracted into chloroform. Evaporation of the chloroform extract gave a residue which had spectroscopic properties identical with the product of $LiAlH_4$ reduction of **3**.

Reduction with sodium borodeuteride was carried out in an analogous manner.

Acknowledgment

We wish to thank Professor Stewart McLean for providing us with a generous sample of compound **6**. We thank the National Research Council of Canada for financial support of this work and McMaster University for the award of a University Fellowship to C.-Y. Chen.

1. R. H. F. MANSKE. Can. J. Research, **16B**, 438 (1938).
2. R. H. F. MANSKE. Can. J. Chem. **47**, 1103 (1969).

Can. J. Chem. Downloaded from www.nrcresearchpress.com by 210.87.254.42 on 09/05/12
For personal use only.

3. J. K. SAUNDERS, R. A. BELL, C.-Y. CHEN, D. B. MACLEAN, and R. H. F. MANSKE. Can. J. Chem. **46**, 2873 (1968).
4. J. K. SAUNDERS, R. A. BELL, C.-Y. CHEN, D. B. MACLEAN, and R. H. F. Manske. Can. J. Chem. **46**, 2876 (1968).
5. R. H. F. MANSKE. The alkaloids. Vol. IV. Academic Press, Inc., New York. 1954. p. 253.
6. F. A. L. ANET and A. J. R. BOURN. J. Amer. Chem. Soc. **87**, 5250 (1965).
7. J. W. EMSLEY, J. FEENEY, and L. H. SUTCLIFFE. High resolution nuclear magnetic resonance spectroscopy. Vol. II. The Pergamon Press Ltd., Oxford. 1966. p. 750.
8. D. W. BROWN and S. F. DYKE. Tetrahedron Letters, 3975 (1966).
9. S. MCLEAN, M.-S. LIN, A. C. MACDONALD, and J. TROTTER. Tetrahedron Letters, 3819 (1964). S. MCLEAN, M.-S. LIN, and R. H. F. MANSKE. Can. J. Chem. **44**, 2249 (1966).
10. G. GRETHE, H. L. LEE, M. USKOKOVIĆ, AND A. BROSSI. J. Org. Chem. **33**, 491 (1968).
11. G. GRETHE, H. L. LEE, M. USKOKOVIĆ, AND A. BROSSI. J. Org. Chem. **33**, 495 (1968).
12. C.-Y. CHEN and D. B. MACLEAN. Can. J. Chem. **45**, 3001 (1967).
13. C.-Y. CHEN and D. B. MACLEAN. Can. J. Chem. **46**, 2501 (1968).
14. S. MCLEAN, M.-S. LIN, and J. WHELAN. Tetrahedron Letters, 2425 (1968).
15. R. H. MARTIN and J. C. NOULS. Tetrahedron Letters, 2727 (1968), and references cited therein.
16. J. K. SAUNDERS and R. A. BELL. Can. J. Chem. **46**, 3421 (1968).
17. K. NAKANISHI. Infrared absorption spectroscopy. Holden-Day Inc., San Francisco. 1962. p. 30.
18. H. BUDZIKIEWICZ, C. DJERASSI, and D. H. WILLIAMS. Structure elucidation by mass spectrometry. Vol. I. Holden-Day Inc., San Francisco. 1954. p. 174.
19. A. L. BURLINGAME. Ph.D. Thesis, Massachusetts Institute of Technology. 1963.
20. K. S. QUISENBERRY, T. T. SCOTMAN, and A. O. NIER. Phys. Rev. **102**, 1071 (1956).
21. F. W. MCLAFFERTY. Anal. Chem. **28**, 306 (1956).

Can. J. Chem. Downloaded from www.nrcresearchpress.com by 210.87.254.42 on 09/05/12
For personal use only.

Can. J. Chem. Downloaded from www.nrcresearchpress.com by 210.87.254.40 on 09/05/12
For personal use only.

^{13}C Nuclear magnetic resonance studies. XIII. ^{13}C Carbonyl carbon shieldings of some β,γ-unsaturated ketones[1]

GURUDATA[2] AND J. B. STOTHERS
Department of Chemistry, University of Western Ontario, London, Ontario

Received April 16, 1969

The 15.1 MHz ^{13}C nuclear magnetic resonance spectra of 13 aliphatic and alicyclic ketones having an olefinic bond in the β,γ position with respect to the carbonyl group have been recorded and the carbonyl shieldings measured. The major aim of this study was to investigate the possibility of detecting homoconjugative interactions between the π-systems by comparing the carbonyl shieldings with those for the corresponding saturated and α,β-unsaturated systems. Some evidence of homoconjugation is presented on the basis of our previous interpretation of the factors governing carbonyl shieldings. A qualitative assessment of the observed geometrical dependence of the effect is offered.

Canadian Journal of Chemistry. 47, 3601 (1969)

Introduction

From our earlier studies of aliphatic and alicyclic ketones (1, 2) it was found that the ^{13}C nuclear shieldings of carbonyl carbons are not nearly so sensitive to alkyl substitution as the saturated carbons in hydrocarbons (3). For the latter it is established that the replacement of an α- or β-hydrogen by a methyl group deshields the carbon nucleus by −9 p.p.m. (i.e., —CH—* CH → —CMe—* CH— or —CH—* C—Me). With the carbonyl compounds, this effect is attenuated to ca. −5 p.p.m. for the α-substitution, e.g. RCHO → $RCOCH_3$, and the changes for more remote substitutions are much smaller (1). A significant shielding effect, however, is found for conjugated systems in which either an olefinic bond (2) or an aryl ring (4) is in the α,β-position. This change is typically 10–12 p.p.m. by comparison with the corresponding saturated system. A rationalization of this trend follows from the consideration of the principal contributing resonance forms in each case. For the saturated systems, forms I and II dominate such that polarization of the π-cloud toward oxygen diminishes the electron density at carbon and accounts for the low field position of these nuclei relative

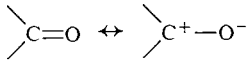

I II

to other sp^2-hybridized carbons. In conjugated systems, the electron withdrawing effect of oxygen at the carbonyl carbon is partially offset by contributions from forms such as IV and it follows, therefore, that the carbonyl carbon shielding will increase relative to that of a saturated system. Factors which interfere with this conjugative interaction would be expected to reduce the carbonyl shielding and several examples have been presented (2, 4). Support for the present interpretation which assumes a predominant electron density contribution is given by the current theoretical notions of carbon shieldings as well as the data for a variety of systems (5).

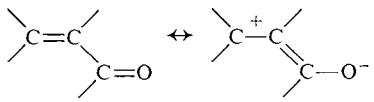

III IV

The total shielding constant, σ, for a carbon nucleus can be viewed as a summation of three major factors,

$$[1] \qquad \sigma = \sigma_d + \sigma_p + \sigma'$$

which include a diamagnetic term, σ_d, a paramagnetic contribution σ_p and a neighbor-atom, or group, factor, σ′. The latter includes effects due to neighboring anisotropic atoms or bonds whose small effects are operative through space and which, as a first approximation, can be neglected. The diamagnetic term depends directly on electron density and has an estimated maximum value of ca. 14 p.p.m. (6) for the addition of a 2p electron. Since the total range of carbon shieldings is more than 300 p.p.m., it is generally

[1]For Part X, see ref. 14; Part XI, see ref. 15; Part XII, see ref. 16.

[2]Petroleum Research Fund Predoctoral Fellow 1964–1965, Ontario Graduate Fellowship 1966–1967. Present address: Department of Chemistry, University of Ottawa, Ottawa, Canada.

TABLE I

^{13}C Carbonyl shieldings of some aliphatic and monocyclic β,γ-unsaturated ketones (p.p.m. from CS_2)

	Compound	δ_c	$\Delta\delta_c$ (β)	$\Delta\delta_c$ (α)
1	4-Penten-2-one	−11.9	+1.9	+10.1
2	5-Hexen-3-one	−13.9	+1.9	+ 9.6
3	3-Methyl-4-penten-2-one	−13.9	+2.5	+11.6
4	4-Hexen-2-one	−11.4	+2.9	+11.5
5	3,3,5-Trimethyl-4-hexen-2-one	−16.9	+1.3	—
6	1-Cyclohexenylacetone	−11.6	+0.8	—
7	3-Cyclopentenone	−23.1	+1.3	+ 9.1
8	3-Cyclohexenone	−15.1	+1.0	+11.8
9	3,5,5-Trimethyl-3-cyclohexene	−14.1	+1.1	+11.4

recognized that the paramagnetic term, σ_p, dominates. Karplus and Pople (6) and Pople (7) have developed an expression having the form,

$$[2] \quad \sigma_p = -\frac{k}{\Delta E}\langle r^{-3}\rangle_{2p}\{Q_{AA} + \Sigma Q_{AB}\}$$

where ΔE represents the excitation energies for transitions between the ground and excited states, which is usually replaced with a mean value for particular classes of compounds. The Q terms contain the elements of the charge density and bond order matrix of the unperturbed molecule and $\langle r^{-3}\rangle_{2p}$ is the mean inverse cube radius of the carbon 2p orbitals. The local electron density on the carbon atom of interest is manifested in the latter term and in the atomic term in Q_{AA}. As the total charge on A increases, the orbitals expand, $\langle r^{-3}\rangle_{2p}$ decreases and σ_p becomes less negative. For carbon no large changes are expected for Q_{AA} (7). Maciel has discussed this theoretical approach with respect to the carbonyl group and has shown that the shieldings correlate with the C=O π-bond polarity (8). Thus, our earlier interpretation of the effect of conjugation is consistent with current theory.

In view of the pronounced effect of an adjacent conjugated π-bond on carbonyl carbon shieldings it seems reasonable to expect that any factor tending to increase its local electron density could be expected to shift the carbonyl absorption to higher field. One such factor is a homoconjugative interaction between a carbonyl group and a more remote olefinic bond which can adopt a geometry to permit overlap of the π-systems. The extent of interaction should be reflected in the observed carbonyl ^{13}C shielding. We would predict, therefore, that the position of the carbonyl absorption should vary with the stereochemistry of β,γ-unsaturated ketones and should lie between that of the corresponding saturated and α,β-unsaturated analogues of the system of interest. To test this proposal we have measured the carbonyl carbon shieldings of a series of thirteen β,γ-unsaturated ketones. In this paper we compare these values with those for the corresponding α,β-unsaturated isomers and the saturated analogues.

Experimental

^{13}C Spectra

The carbonyl carbon absorptions were detected using rapid-passage techniques at 15.1 MHz and their positions measured by interpolation using the audio side-bands of the reference signals which were in most cases those of external, enriched methyl iodide. Most of the data were obtained on the neat liquids, while solids were run as concentrated solutions in carbon disulfide. The data are judged to have a precision of ca. ±0.3 p.p.m. and no bulk susceptibility corrections were made. The results are reported relative to CS_2 (δ_c = 0 p.p.m.).

Materials

With the exception of 1-cyclohexenylacetone, obtained from K & K Laboratories, the β,γ-unsaturated ketones were prepared for this work. All of the materials have been described previously in the literature and samples were obtained having essentially the same physical constants. In addition, proton and infrared spectra were determined for each compound to ensure its identity. For the few α,β-unsaturated ketones which were not included in our earlier work (3) samples were prepared by standard methods. The saturated ketones for the most part are commercially available and the remaining examples were prepared by catalytic hydrogenation of the unsaturated analogue.

Results and Discussion

The carbonyl carbon shieldings for the β,γ-unsaturated ketones examined in this study are

Can. J. Chem. Downloaded from www.nrcresearchpress.com by 210.87.254.40 on 09/05/12
For personal use only.

TABLE II

^{13}C Carbonyl shieldings of some bicyclic β,γ-unsaturated ketones (p.p.m. from CS_2)

	Compound	δ_c	$\Delta\delta_c(\beta)$
10	Bicyclo[2·2·2]oct-5-en-2-one	−20.2	− 0.2
11	Bicyclo[2·2·1]hept-5-en-2-one	−20.4	+ 1.4
12	Bicyclo[3·2·1]oct-2-en-8-one	−22.0	+ 4.0
13	Bicyclo[2·2·1]hept-2-en-7-one	−10.5	+10.6

given in Tables I (aliphatic and monocyclic examples) and II (bicyclic systems) and the differences relative to the corresponding saturated ketones are listed as $\Delta\delta(\beta)$. In addition the differences in the carbonyl shieldings between the saturated and α,β-unsaturated isomers, $\Delta\delta(\alpha)$, are given in Table I for most of the aliphatic and monocyclic skeletons. It is evident that the β,γ-ketones exhibit carbonyl absorption at somewhat higher fields than their saturated derivatives with the observed differences ranging from 0.8 to 10.6 p.p.m. with one exception, compound **10**. It follows that the effect of the β,γ-double bond is not primarily operative through the bonding network but, instead, through space and therefore depends on molecular geometry.

It is known that π-electron systems situated beta to a developing carbonium ion center can significantly influence the course and the rate of reaction at that center. This anchimeric acceleration of rate has been ascribed to delocalization of the neighboring π-electron cloud in the rate-determining step. Simonetta and Winstein (9) employed a semi-empirical M.O. approach to calculate stabilization energies of such systems and found values which follow the same trend as the rate-enhancing effects in solvolysis. For a variety of systems undergoing solvolysis, anchimeric assistance factors have been estimated (10) to compare the relative extent of overlap between the neighboring π-bonds and the cationic centers. These factors, expressed as the logarithm of the rate difference (observed–calculated), for acetolysis of the tosylates are 12.9, for the *anti*-7-norbornenyl, 6.0, for *anti*-8-bicyclo[3·2·1]oct-2-enyl and 3.8, for *exo*-2-norbornenyl systems which may be compared with the $\Delta\delta(\beta)$ values of 10.6, 4.0 and 1.4, for the corresponding ketones, respectively.

For α,β-conjugated systems, a maximum interaction is expected if the nodal planes of the two π-bonds are coplanar so that 2pπ overlap is at a maximum. For β,γ-unsaturation, however, a different relationship is to be expected and can be considered in terms of simple models for the overlap between the 2p-orbitals (11).

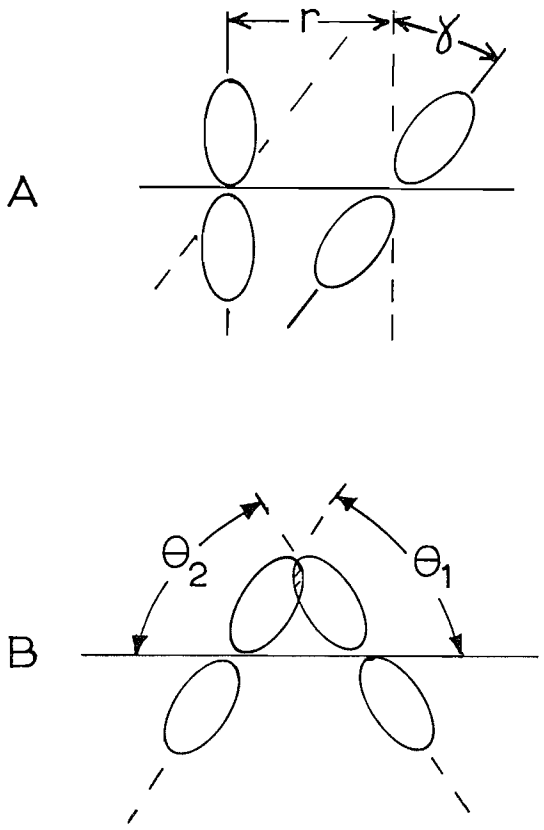

FIG. 1. Modes of overlap for p-orbitals of neighboring atoms.

If the axes of the 2p-orbitals lie in parallel planes at a distance r the overlap integral S_{ij} is given by

$$[3] \qquad S_{ij} = S_{\pi\pi} \cos\gamma$$

where γ is the angle between the axes (Fig. 1*a*). If the axes of the p-orbitals lie in a plane ($\gamma = 0$)

Can. J. Chem. Downloaded from www.nrcresearchpress.com by 210.87.254.40 on 09/05/12
For personal use only.

Can. J. Chem. Downloaded from www.nrcresearchpress.com by 210.87.254.40 on 09/05/12
For personal use only.

but are tilted towards one another at angles Θ_1 and Θ_2, relative to the internuclear axis (Fig. 1*b*), the overlap can be resolved into $\sigma\sigma$ and $\pi\pi$ contributions, for which

$$[4] \quad S_{ij} = S_{\sigma\sigma} \cos \Theta_1 \cos \Theta_2 + S_{\pi\pi} \sin \Theta_1 \sin \Theta_2$$

If, in addition, γ is non-zero the second term will include a cos γ factor. For the case of two directly bonded sp^2-hybridized carbons, Θ_1 and Θ_2 are 90° and the overlap integral is simply eq. [3] from which it is clear that as γ increases from zero S_{12} decreases. This is the basis for our interpretation of the effects of steric hindrance on carbonyl shieldings in α,β-unsaturated systems (4) and we have previously correlated the δ_c values with the angle γ, which was termed the "angle of twist, Θ".

For the case of two sp^2-carbons separated by one sp^3-carbon, however, it is apparent that little π overlap is possible in a planar arrangement. In non-planar conformation with the p-axes aligned (i.e. $\gamma = 0$) the overlap integral S_{13} is given by eq. [4]. For β,γ-unsaturated ketones in which the 1,3 internuclear distance is ca. 2.5 Å, and Θ_1 and Θ_2 are ca. 55° it can be seen that $S_{\sigma\sigma}$ exceeds $S_{\pi\pi}$ by a factor of ca. 3. Thus, $S_{\sigma\sigma}$ can be expected to make a significant contribution to S_{13}.

On the basis of the foregoing arguments it is expected that interactions between the non-conjugated π systems will be maximal in non-planar configurations (or conformations) and that the effect at the carbonyl carbon will be in the direction of increased shielding. These expectations appear to be supported by the present data. The largest effect, 10.6 p.p.m., found for **13** may be compared, for example, with that for 3-cyclopentenone, **7**, 1.3 p.p.m. which can be taken as representative of the nearly, if not exactly, coplanar cases while the former is restrained to a geometry which yields a substantial value for $S_{\sigma\sigma}$. The geometric parameters, $\Theta_1 = 58°55'$, $\Theta_2 = 68°10'$, $\gamma = 17°29'$, $r = 2.296$ Å yield $S_{ij} = 0.08$, $S_{\sigma\sigma} \approx 0.2$ and $S_{\pi\pi} < 0.06$ (11).

While it is clear that this simple approach is qualitative it does account for the stereochemical dependence and gives a basis for the difference between the geometrical dependence in the β,γ- and α,β-unsaturated systems.

Ketone **13** was included in an earlier study of carbonyl shieldings by Savitsky *et al.* (12), who attributed the difference in carbonyl shielding for **13** and 7-ketonorbornane to the difference in λ_{max} values for the $n \rightarrow \pi^*$ transition. These authors assumed (*a*) that the ΔE term in eq. [2] plays a dominant role in the carbonyl shieldings and (*b*) that the $n \rightarrow \pi^*$ transition energies are proportional to ΔE. For the compounds included in their study, an approximately linear relation was found for $\delta^{C=O}$ vs $\lambda_{max}^{n\rightarrow\pi^*}$. The inclusion of other ketones, however, has clearly shown that a good linear correlation of these parameters does not exist (2*b*). We have recently found that, although the carbonyl oxygen-17 shieldings are grossly correlated with their $n \rightarrow \pi^*$ transition frequencies, within a series of closely related ketones the correlation does not hold (13) but the observed trends correlate nicely with variations in the local electron density. At the present time it appears that the available ^{13}C results are readily interpreted in a similar fashion in terms of variation in the local electron density which are manifest in both the σ_d and σ_p contributions to the total shielding constant.

Acknowledgments

We wish to thank the donors of the Petroleum Research Fund, administered by the American Chemical Society, and the National Research Council of Canada for financial support of this investigation.

1. J. B. Stothers and P. C. Lauterbur. Can. J. Chem. **42**, 1563 (1964).
2. D. H. Marr and J. B. Stothers. Can. J. Chem. (*a*) **43**, 596 (1965); (*b*) **45**, 225 (1967).
3. D. M. Grant and E. G. Paul. J. Am. Chem. Soc. **86**, 2984 (1964).
4. K. S. Dhami and J. B. Stothers. Tetrahedron Letters, 631 (1964); Can. J. Chem. **43**, 479, 498 (1965).
5. J. B. Stothers. Quart. Rev. **19**, 144 (1965).
6. M. Karplus and J. A. Pople. J. Chem. Phys. **38**, 2903 (1963).
7. J. A. Pople. Mol. Phys. **7**, 301 (1964).
8. G. E. Maciel. J. Chem. Phys. **42**, 2746 (1965).
9. M. Simonetta and S. Winstein. J. Am. Chem. Soc. **76**, 18 (1954).
10. P. R. Schleyer. J. Am. Chem. Soc. **86**, 1856 (1964).
11. W. G. Woods, R. A. Carboni, and J. D. Roberts. J. Am. Chem. Soc. **78**, 5653 (1956); J. D. Roberts. Molecular orbital calculations. W. A. Benjamin, Inc., New York. 1961. p. 83ff.
12. G. B. Savitsky, K. Namikawa, and G. Zweifel. J. Phys. Chem. **69**, 3105 (1965).
13. D. J. Sardella and J. B. Stothers. Can. J. Chem. **47**, 3089 (1969).
14. K. S. Dhami and J. B. Stothers. Can. J. Chem. **45**, 233 (1967).
15. G. W. Buchanan and J. B. Stothers. Chem. Commun. 1250 (1967).
16. G. W. Buchanan, J. B. Stothers, and S. Wu. Can. J. Chem. **47**, 3113 (1969).

Can. J. Chem. Downloaded from www.nrcresearchpress.com by 210.87.254.6 on 09/05/12
For personal use only.

^{13}C Nuclear magnetic resonance studies. XIV.[1] Conformational effects on carbinyl carbon shieldings in cyclohexanols and derivatives

G. W. BUCHANAN[2] AND J. B. STOTHERS
Department of Chemistry, University of Western Ontario, London, Canada

Received May 20, 1969

The ^{13}C shieldings of the alicyclic carbons bearing oxygen in several cyclohexanols, their acetates and methyl ethers depend on the orientation of the oxygen functions. The compounds examined include the *cis*- and *trans*-4-alkyl derivatives in which the alkyl groups are *t*-butyl, *i*-propyl, ethyl and methyl, as well as the 3-*t*-butyl isomers. The results for the parent compounds are employed for the estimation of the conformational free energies of the hydroxyl, acetoxyl, and methoxyl groups, and serve to establish that ^{13}C magnetic resonance (c.m.r.) spectroscopy offers a new approach to conformational analysis. The data were obtained using the decoupling technique and materials containing ^{13}C in natural abundance.

Canadian Journal of Chemistry, 47, 3605 (1969)

Introduction

Over the past few years sufficient evidence has been accumulated to establish that carbon shieldings depend, at least in part, on molecular geometry and conformation (1–6). From our investigations of certain alicyclic systems (7, 8) by carbon magnetic resonance (c.m.r.) spectroscopy we were led to an examination of the alicyclic alcohols in which were included the *cis*- and *trans*-4-*t*-butylcyclohexanols. The shieldings of the carbinyl carbons in these isomers were found to differ by *ca.* 5 p.p.m. (3) indicating that c.m.r. techniques have promise as an additional tool for conformational analysis. In fact, the method constitutes a new approach to this aspect of stereochemical studies because the pronounced differences observed are a function of substituent orientation entirely since the position of the carbon nucleus of interest is unchanged relative to the other atoms in the molecule for both epimers. Since the difference is relatively large, its measurement with refined techniques may be superior to other nuclear magnetic resonance (n.m.r.) methods.

To determine the utility of the approach for conformational analysis and to confirm that the shielding differences are primarily due to conformational effects we examined the 4-alkyl series including the isopropyl, ethyl, and methyl derivatives as well as the 3-*t*-butyl isomers. The acetates and methyl ethers were also measured to assess the importance of hydrogen bonding contributions to these shieldings. We describe these results in the present paper to amplify the data presented in our preliminary communication (3). All of the earlier results have been redetermined using the more precise "proton-decoupling" technique originally described by Paul and Grant (9).

Experimental

Spectra

The natural abundance ^{13}C spectra were obtained at 15.1 MHz on a Varian DP-60 system which included a NMR Specialties SD-60 Spin-decoupler operating at a nominal frequency of 60 MHz. The proton-decoupling technique (9) was used throughout for the ^{13}C measurements, which are given relative to CS_2 as described previously (6). A H–P 5245L counter was employed for all frequency measurements.

The proton spectra were obtained with a Varian A60 spectrometer using the usual audio side-band technique to determine peak positions to better than 0.5 Hz.

For the most part the compounds were examined as the neat liquids, while solids were run in carbon disulfide and dimethylsulfoxide solutions.

Materials

The alcohols are known compounds and were obtained from commercial sources or by standard methods. Treatment of these alcohols with acetic anhydride and sodium acetate gave the desired acetates. Physical constants and analytical data for the new compounds are given in Table I. The methyl ethers were prepared by either of two methods: (A) treatment of the corresponding sodium alkoxide with methyl iodide or (B) treatment of an ethereal solution of the alcohol and $BF_3 \cdot Et_2O$ with diazomethane at 0°. Data for the new ethers are collected in Table I. The purity of all materials was checked by infrared (i.r.) and proton spectroscopy. Liquid samples for ^{13}C spectra were obtained by fractional distillation through a spinning-band column.

Results and Discussion

The shielding data are collected in Tables II–V, in which the results for the alkylcyclohexanols,

[1]Part XIII in this series, Gurudata and J. B. Stothers, Can. J. Chem. This issue, preceding paper.

[2]Holder of NRCC studentships, 1966–1968. Present address: Department of Chemistry, University of California at Los Angeles, Los Angeles, Calif., U.S.A.

TABLE I

Physical constants and analytical data for new derivatives

Compound	Method of preparation*	Boiling point (mm)	$n_D(T\,°C)$	Elemental analyses calcd. C	calcd. H	found C	found H
cis-4-ethylcyclohexyl acetate		60–61 (2.6)	1.4410 (20)	70.54	10.66	70.75	10.79
trans-4-ethylcyclohexyl acetate		50–52 (1.8)	1.4405 (20)			70.70	10.65
methyl *cis*-4-ethylcyclohexyl ether	B	68–69 (18)	1.4378 (20)	75.99	12.76	75.70	12.63
methyl *trans*-4-ethylcyclohexyl ether	A	70–72 (20)	1.4370 (25)			75.76	12.27
methyl *cis*-4-isopropylcyclohexyl ether	B	84–85 (20)	1.4485 (20)	76.86	12.90	76.60	13.24
methyl *trans*-4-isopropylcyclohexyl ether	A	86–87 (20)	1.4445 (20)			76.83	12.75
methyl *cis*-3-*t*-butylcyclohexyl ether	A	96–97 (20)	1.4518 (25)	77.58	13.02	77.02	12.71
methyl *trans*-3-*t*-butylcyclohexyl ether	B	92–94 (18)	1.4525 (25)			77.07	12.88

*See experimental section.

TABLE II

Carbinyl ^{13}C and ^{1}H shieldings of some alkylcyclohexanols (in p.p.m., δ_C from CS_2, δ_H from TMS)

Substituent	Solvent	*cis*-Isomer δ_C	*cis*-Isomer δ_H	*trans*-Isomer δ_C	*trans*-Isomer δ_H
4-*i*-propyl	nil	125.33 ± 0.11	3.88	121.35 ± 0.09	3.33
4-ethyl	nil	125.23 ± 0.15	3.88	121.33 ± 0.11	3.33
4-methyl	nil	125.14 ± 0.10	3.87	121.36 ± 0.07	3.33
4-*t*-butyl	CS_2*	126.54 ± 0.19	3.88	121.61 ± 0.15	3.32
	DMSO*	126.44 ± 0.09	3.83	121.79 ± 0.13	3.32
3-*t*-butyl	CS_2*	121.94 ± 0.10	3.38	126.31 ± 0.10	4.09

*3 *M* Solutions.

the corresponding methyl ethers and acetates, and the parent systems are separately presented.

As a starting point for discussion it seems reasonable to consider the 4-*t*-butyl substituted systems as the base cases. With the assumption that this alkyl group exerts a negligible effect on the C-1 shielding we can designate the carbinyl shieldings for the *cis*- and *trans*-isomers as the "true" shieldings for carbons bearing these axial and equatorial oxygen functions, respectively. The original basis for this assumption is the fact that alkyl substitution in hydrocarbons has little effect (i.e. < 0.3 p.p.m.) on the shieldings of carbons separated by more than three σ-bonds from the substituent (1). Experimental proof of this is provided by the data for the series of *trans*-4-alkyl derivatives listed in the Tables. For example, the carbinyl shieldings for the series of methyl ethers (Table III) exhibits a total range of 0.21 p.p.m. while the corresponding acetates (Table IV) have a spread of only 0.08 p.p.m. Unfortunately the 4-*t*-butylcyclohexanols are solids and must be examined in solution. Consequently the somewhat larger difference between their carbinyl shieldings and those of the 4-methyl, -ethyl, and isopropyl derivatives may be due in part to a solvent effect. The fact that the shielding differences in CS_2 and DMSO solutions are dissimilar for the

Can. J. Chem. Downloaded from www.nrcresearchpress.com by 210.87.254.6 on 09/05/12
For personal use only.

TABLE III

Carbinyl ^{13}C and ^{1}H shieldings of some methyl cyclohexyl ethers (in p.p.m., δ_C from CS_2, δ_H from TMS)

	cis-Isomer		*trans*-Isomer	
Substituent	δ_C	δ_H	δ_C	δ_H
4-*t*-butyl	117.62 ± 0.10	3.36	112.72 ± 0.13	3.00
4-*i*-propyl	116.82 ± 0.15	3.33	112.73 ± 0.10	3.00
4-ethyl	116.79 ± 0.09	3.31	112.93 ± 0.18	3.00
4-methyl	116.62 ± 0.10	3.30	112.83 ± 0.10	3.00
3-*t*-butyl	112.95 ± 0.15	3.03	116.98 ± 0.09	3.50

TABLE IV

Carbinyl ^{13}C and ^{1}H shieldings of some cyclohexyl acetates (in p.p.m., δ_C from CS_2, δ_H from TMS)

	cis-Isomer		*trans*-Isomer	
Substituent	δ_C	δ_H	δ_C	δ_H
4-*t*-butyl	123.32 ± 0.10	4.96	119.47 ± 0.10	4.53
4-*i*-propyl	122.44 ± 0.11	4.95	119.54 ± 0.09	4.53
4-ethyl	122.41 ± 0.09	4.94	119.46 ± 0.15	4.54
4-methyl	122.26 ± 0.10	4.92	119.51 ± 0.13	4.54
3-*t*-butyl	119.61 ± 0.10	4.62	123.13 ± 0.07	5.11

cis- and *trans*-4-*t*-butyl isomers offers supporting evidence for this. In any event, the solvent effects are small and, as a first approximation, may be neglected. Since the differences, $\delta_C^{cis} - \delta_C^{trans}$, for the 4-*t*-butylcyclohexanols and their methyl ethers are virtually the same, hydrogen-bonding of the hydroxyl grouping has a negligible effect on the carbinyl carbon shieldings. It is interesting that the difference of *ca.* −9 p.p.m. between the alcohols and their methyl ethers is almost identical to the effect found for replacement of a β-hydrogen by methyl in a hydrocarbon chain, viz. −9.1 p.p.m. (1). This "β-effect" has so far eluded attempts to account for its origin (10). Nevertheless, the change is invariably found in ^{13}C spectra. On the other hand, acetylation of the hydroxyl group results in a very much smaller change in the carbinyl carbon shielding, namely *ca.* −2.5 p.p.m. Thus it is clear that the "β-effect" for a carbonyl carbon is very different from that for methyl or methylene carbons.

In the *cis*-4-alkyl isomers, the oxygen function is primarily in the axial orientation and it is apparent that the carbinyl carbon shieldings move to progressively lower field as the alkyl group decreases in size. This is readily explained in terms of the conformational equilibrium **1** ⇄ **2** in which the relative contribution of the equatorial form **2** increases with decreasing bulk of the substituent alkyl group. For the *cis*-4-*t*-butyl derivative one can assume that the equilibrium is almost entirely on the left while **2** would

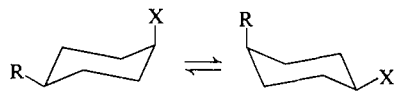

1 **2**

be expected to make an appreciable contribution for the equilibrium of the *cis*-4-methyl derivative. For the simplest related case, methylcyclohexane, **1** (R=Me, X=H), a recent estimate of the conformational free energy of the methyl group (11) indicates that **2** constitutes *ca.* 8% of the mixture. In the present series with X = OR′ the proportion of **2** will be larger since $-\Delta G_{OR'}$ values are *ca.* 0.7 kcal/mole (see below). While there is evidence that the relative spatial orientation of alkyl carbons is an important factor governing carbon shieldings *if those carbons are within three bonds* of each other, the so-called γ-effect (1,10), no appreciable effects have been observed for

Can. J. Chem. Downloaded from www.nrcresearchpress.com by 210.87.254.6 on 09/05/12
For personal use only.

TABLE V

Carbinyl ^{13}C and ^{1}H shieldings of cyclohexanol, cyclohexyl acetate, and cyclohexyl methyl ether (in p.p.m., δ_C from CS_2, δ_H from TMS)

Compound	Solvent	Shieldings	
		δ_C	δ_H
Cyclohexanol	nil	122.70 ± 0.10	3.47
	CS_2*	122.84 ± 0.13	3.48
	DMSO*	122.90 ± 0.15	3.47
Cyclohexyl acetate	nil	120.49 ± 0.10	4.73
Cyclohexyl methyl ether	nil	114.18 ± 0.10	3.08

*3 *M* Solutions.

carbons further separated. Thus it follows that the sequential replacement of hydrogen atoms on the δ-carbon will exert no appreciable shielding influence on the carbinyl carbon. This corresponds to the 4-alkyl series, methyl, ethyl, isopropyl, *t*-butyl.

A similar argument applies for the *cis*-3-*t*-butyl derivatives for which the carbinyl shieldings of the ether and acetate are within experimental error of those for the *trans*-4-alkyl cases. The difference between the value for the *cis*-3-*t*-butyl and *trans*-4-*t*-butyl isomers may be due in part to solvent effects. It is interesting that the carbinyl carbon shieldings for the *trans*-3- and *cis*-4-*t*-butyl alcohols and acetates are the same within our limits of measurement, lending support to the notion that the orientation of the oxygen function is the major factor governing the carbinyl carbon shieldings in these compounds.

In contrast the equatorial carbinyl proton on the carbinyl carbon absorbs at consistently lower field (*ca.* 0.15 p.p.m.) in the *trans*-3-*t*-butyl derivatives relative to the *cis*-4-*t*-butyl isomers, whereas the axial protons have similar shifts in both series of alcohols and ethers. Apparently the proton shieldings are more sensitive to small changes in ring geometry. Differences in the deformations of 3- and 4- alkylcyclohexanols have been discussed recently and a tentative explanation presented (12). It was proposed that the tendency of an axial oxygen to reduce its *syn*-diaxial interactions leads to an uneven flattening of the ring such that the flattening is more severe about the C-1, -2, and -6 centres than at C-3, -4, and -5 and eclipsing interactions between C-3 substituents and C-2 hydrogens will affect the extent to which the *syn*-diaxial interactions can be relieved (i.e. the former will reduce the twisting about the C_1—C_2 and C_1—C_6 bonds). If this is valid, it follows that the equatorial C-1 proton may be in a different magnetic environment than the corresponding proton in the 4-alkyl isomer and, therefore, the shieldings may differ. Although a comparable difference may also obtain for the carbinyl carbon shieldings the present experimental method lacks the precision required for its detection. In any event it is clear that the proton shieldings for the 3-*t*-butyl series cannot be employed for conformational energy estimations in the way that has become popular for the 4-*t*-butylcyclohexyl derivatives.

In the axial orientation the oxygen atom will experience non-bonded interactions with the *syn*-axial protons on C-3 and C-5. It seems reasonable to suggest that the carbinyl carbon shielding is affected by steric perturbation of its local electron distribution because of these non-bonded interactions. Evidence of this effect has been presented for a variety of hydrocarbons (2,5,10,13) and other oxygenated cyclohexane derivatives (6). Preliminary results on a quantitative interpretation of the steric perturbation of carbon shieldings in these and related oxygenated compounds have been presented (14). A similar examination of these functional groups in bicyclic systems of known geometry is in progress with the intention of developing a generalized relation between non-bonded interactions and carbon nuclear shieldings.

With the present results, however, it is possible to examine their use for estimating conformational free energies, $-\Delta G°$, for the hydroxyl, methoxyl, and acetoxyl groupings. Two of these have been the subject of several investigations and a large body of data exists (15). Thus, these groups provide a reasonable test of the validity of the ^{13}C approach for conformational analysis. To this end the carbinyl carbon shieldings of

Can. J. Chem. Downloaded from www.nrcresearchpress.com by 210.87.254.6 on 09/05/12
For personal use only.

TABLE VI

Conformational free energies for OR groups in cyclohexyl systems (kcal/mole)

Group	Solvent	Method of Estimation			
		^{13}C	Other*	"Best" value†	
OH	CS_2	0.65 ± 0.15	0.3–1.0	0.52 ± 0.1*	0.6‡
	DMSO	0.72 ± 0.15			
OAc	nil	0.64 ± 0.13	0.36–1.6	0.60 ± 0.1*	0.7‡
OMe	nil	0.60 ± 0.15	0.4–0.74	0.60 ± 0.1*	0.7‡

*See reference 15.
†See text.
‡See reference 16.

cyclohexanol, cyclohexyl methyl ether, and cyclohexyl acetate were determined and the data are collected in Table V.

Comparison of the results in the Tables reveals that for each case the shielding of the carbinyl carbon for the simple cyclohexyl derivatives lies between those of the *cis*- and *trans*-4-*t*-butyl analogs. Since it appears that the orientation of the oxygen function is the major factor governing these shieldings, it follows that the data can be used to estimate equilibrium constants for the conformational equilibria, **1** ⇄ **2** (R=H, X= OH, OMe, OAc), according to the expression,

$$K = \frac{\delta_{ax} - \delta}{\delta - \delta_{eq}} \qquad [1]$$

where δ_{ax} and δ_{eq} are the shieldings for the "fixed" axial and equatorial forms (taken as the *cis*- and *trans*-4-*t*-butyl derivatives) and δ is the value for the equilibrating system. With these data, the conformational free energy is calculated directly from, $\Delta G^\circ = RT\ln K$. The results are collected in Table VI which also lists the range of $-\Delta G^\circ$ values previously reported as well as the "best" values according to Hirsch (15) and Eliel (16). It is evident that the ^{13}C results agree very well with the currently accepted values although the experimental error is rather large. As noted above, the 3-*t*-butyl group does not appear to affect the carbinyl carbon shieldings and, therefore, it is of interest to compare the $-\Delta G^\circ_{OR}$ values obtained from these data. These are 0.74, 0.58, and 0.68 kcal/mole, for the OH, OMe, and OAc groupings, respectively, which are the same as those listed in Table VI from the 4-*t*-butyl models. In principle, the data for the *cis*-4-methyl, -ethyl, and isopropyl derivatives could be employed to compute the conformational energies of these alkyl groups, assuming additivity of $-\Delta G^\circ$ values for the individual substituents. While this assumption is apparently valid (12), the equilibria favor conformer **1** so heavily that the uncertainty in the calculated $-\Delta G^\circ_R$ values is too high (± 0.7 kcal/mole) to be useful. In fact, calculations lead to averages of 1.34, 1.45, and 1.53 kcal/mole, for methyl, ethyl, and isopropyl groups, respectively, compared to the recently reported values of 1.56, 1.67, and 1.90 kcal/mole (11). Although the order is retained, the ^{13}C results are 0.2–0.4 kcal/mole lower, but the discrepancy may be due entirely to the relatively low precision of the measurements. With the newer instrumentation (17) much higher precision is attainable and the ^{13}C method promises to be valuable. In addition, the enhanced sensitivity provided by "field-locked" spectrometers will permit measurements at high dilution so that solvent effects can be examined in detail.

Recent studies by Jensen, Bushweller, and Beck (18) on the validity of the assumption that the 4-*t*-butylcyclohexyl derivatives are good models for the axial and equatorial conformers require comment. Their results show that the popular method of estimating $-\Delta G^\circ$ values from proton data in a manner analogous to that used here, can lead to erroneous results. These workers have proposed an alternate method which is based on the proton chemical shift measurements but allows for the temperature dependence of these shifts. Of the groups included in the present study only the acetoxyl function was examined by Jensen *et al.* Their value of 0.71 ± 0.05 kcal/mole is further evidence that our ^{13}C result is satisfactory. The trideuteriomethoxyl function was also studied by the Jensen group (18) who found $-\Delta G^\circ_{OCD_3} = 0.547 \pm 0.019$ kcal/mole, which seems to be slightly lower than the value assigned

Can. J. Chem. Downloaded from www.nrcresearchpress.com by 210.87.254.6 on 09/05/12
For personal use only.

by Eliel (16) for OCH_3. Since the precision of the published data, apart from that of Jensen (18), is *ca.* $\pm$ 0.1 kcal/mole it is not possible to decide whether or not there is an isotope effect on the $-\Delta G^\circ_{OMe}$ value but it would be interesting to check this point since the relatively high precision of the Jensen, Bushweller, and Beck method may be sufficient to reveal it. In view of these findings for the proton results, however, it is essential that the ^{13}C method be checked in a similar manner. We hope to be able to report on this aspect of the problem in the near future.

In any event it is clear that ^{13}C n.m.r. spectroscopy offers a new approach to the evaluation of conformational energies and, since the shieldings of the carbon nuclei bearing substituents depend on the orientation of those substituents, the ^{13}C method should provide a means of examining a variety of groupings which are difficult to study by the other more established methods.

Acknowledgments

We are grateful for the financial support of the National Research Council of Canada and the Petroleum Research Fund, administered by the American Chemical Society.

1. D. M. GRANT and E. G. PAUL. J. Amer. Chem. Soc. **86**, 2984 (1964).
2. W. R. WOOLFENDEN and D. M. GRANT. J. Amer. Chem. Soc. **88**, 1496 (1966).
3. G. W. BUCHANAN, D. A. ROSS, and J. B. STOTHERS. J. Amer. Chem. Soc. **88**, 4301 (1966).
4. G. W. BUCHANAN and J. B. STOTHERS. Chem. Commun. 1250 (1967).
5. D. K. DALLING and D. M. GRANT. J. Amer. Chem. Soc. **89**, 6612 (1967).
6. G. W. BUCHANAN, J. B. STOTHERS, and S-T WU. Can. J. Chem. **47**, 3113 (1969).
7. J. B. STOTHERS and P. C. LAUTERBUR. Can. J. Chem. **42**, 1563 (1964).
8. D. H. MARR and J. B. STOTHERS. Can. J. Chem. **45**, 225 (1967).
9. E. G. PAUL and D. M. GRANT. J. Amer. Chem. Soc. **86**, 2977 (1964).
10. B. V. CHENEY and D. M. GRANT. J. Amer. Chem. Soc. **89**, 5319 (1967).
11. E. L. ELIEL and T. J. BRETT. J. Amer. Chem. Soc. **87**, 5039 (1965).
12. E. L. ELIEL, S. H. SCHROETER, T. J. BRETT, F. J. BIROS, and J-C RICHER. J. Amer. Chem. Soc. **88**, 3327 (1966).
13. D. M. GRANT and B. V. CHENEY. J. Amer. Chem. Soc. **89**, 5315 (1967).
14. G. W. BUCHANAN and J. B. STOTHERS. Paper presented at 51st C.I.C. Conference, Vancouver, B.C. June 1968.
15. J. A. HIRSCH. Table of conformational energies – 1967, *in* Topics in Stereochemistry. *Edited by* N. L. Allinger and E. L. Eliel. John Wiley and Sons, Inc. – Interscience, New York. 1967. Vol. 1.
16. E. L. ELIEL. Angew. Chem. Intern. Ed. **4**, 764 (1965).
17. D. M. GRANT. J. Amer. Chem. Soc. **89**, 2228 (1967); F. J. WEIGERT and J. D. ROBERTS. J. Amer. Chem. Soc. **89**, 2967 (1967).
18. F. R. JENSEN and B. H. BECK. J. Amer. Chem. Soc. **90**, 3251 (1968); F. R. JENSEN, C. H. BUSHWELLER, and B. H. BECK. J. Amer. Chem. Soc. **91**, 344 (1969).

Can. J. Chem. Downloaded from www.nrcresearchpress.com by 210.87.254.6 on 09/05/12
For personal use only.

Mass spectra and fragmentation mechanisms of some nitrophenylhydrazines and nitrophenylhydrazones

F. BENOIT AND J. L. HOLMES
Chemistry Department, University of Ottawa, Ottawa 2, Canada
Received April 30, 1969

The mass spectra and fragmentation mechanism of 2- and 4-nitro and 2,4-dinitrophenylhydrazines and their *N,N'* trideutero analogues are discussed with respect to the operation of an "ortho effect". The mass spectra of nitrophenylhydrazones of cyclohexanone, methyl cycolhexanones, and their deuterated analogues are discussed with reference to the fragmentation of the ketone portion of the molecule.

Canadian Journal of Chemistry, 47, 3611 (1969)

Can. J. Chem. Downloaded from www.nrcresearchpress.com by 210.87.254.6 on 09/05/12
For personal use only.

The mass spectra of aldehyde and ketone derivatives of 2,4-dinitrophenylhydrazine (1–5) and *N,N*-dimethylhydrazine (4) have been reported previously. The results were mainly interpreted with respect to McLafferty rearrangements (4) and the sequential losses of water and a hydroxyl radical from the molecular ions (6*a*). Little attention has been given to the fragmentation of the aldehyde or ketone moiety of the molecule. Seibl and Völlmin (1) and Seibl (5) noted that the migration of a hydroxyl radical from the ortho–nitro position produced a fragment ion corresponding to the protonated form of the aldehyde. The operation of an "ortho effect" in aromatic nitro compounds has been considered by Harley–Mason *et al.* (7). We report here on the fragmentation mechanism of 2- and 4-nitro- and 2,4-dinitrophenylhydrazines and also on cyclohexanone and methylcyclohexanone nitrophenylhydrazones. The fragmentations of the ketone moiety of the molecules are discussed with respect to the possible use of the mass spectra of these derivatives in identifying structural features in new keto compounds.

Transitions that are supported by a metastable peak are indicated by an asterisk. Where the deuterated compound has also been investigated, the masses of the deuterated fragment ions are shown in parentheses beside the appropriate species in the fragmentation schemes of the undeuterated compound. It should be emphasized that many of the ion structures presented in the fragmentation schemes are necessarily hypothetical.

Results and Discussion

2,4-Dinitrophenylhydrazine

The mass spectrum of 2,4-dinitrophenylhydrazine **1** (Fig. 1*a*) may be interpreted by invoking an "ortho effect".

The mass spectrum of the *N,N'* trideutero analogue was obtained (Fig. 1*b*) and results therefrom used to support the fragmentation mechanism shown as Schemes I and II.

In Scheme I, two H atoms are shown as migrating from the hydrazine function to the *o*-nitro group and the subsequent loss of water produces fragment ion *a*, *m/e* 180 which further dissociates *via* the successive losses of N_2, NO, and NO to produce fragment ions *b*, *c*, and *d*. The fragment ion *d*, *m/e* 92 then dissociates further to produce the peaks *m/e* 64 and 63 by loss of CO or ·CHO, as is found in the case of aryl oxygen compounds (6*b*). A fragment ion of some interest in the above sequence is *b*, *m/e* 152. Upon deuteration of the hydrazine function (Fig. 1*b*), *m/e* 152 is shifted to *m/e* 153 (2% b.p.) and *m/e* 155, *e*, (1% b.p.) (Scheme II), the former arising by loss of D_2ON_2 (either as D_2O and N_2 successively or as $[D_2ON_2]$) from the molecular ion while the latter arises by loss of NO_2 from the molecular ion. The nitro group lost is believed to be from the ortho position because *e* does not show the loss of D_2O or ·OD that could be expected from interaction of an ortho–nitro group with the hydrazine function. Fragment ion *e* then successively loses ND_2 and NO to yield fragment ions *f* and *g* (corresponding to *f'* and *g'* in Scheme I). Fragment *g'* can then undergo the loss of HCN, CO, or HCO· to produce fragments of *m/e* 79, 78, and 77 respectively. It should be noted that *m/e* 79 is not shifted upon deuteration while *m/e* 78 is shifted to *m/e* 79. Thus the intensity of the latter peak is increased sufficiently for it to become base peak while in the undeuterated compound, *m/e* 51 is base peak.

para- and ortho-Nitrophenylhydrazine

The mass spectra of **1** and *p*-nitrophenylhydrazine **2** are superficially similar, except that in the

Can. J. Chem. Downloaded from www.nrcresearchpress.com by 210.87.254.6 on 09/05/12
For personal use only.

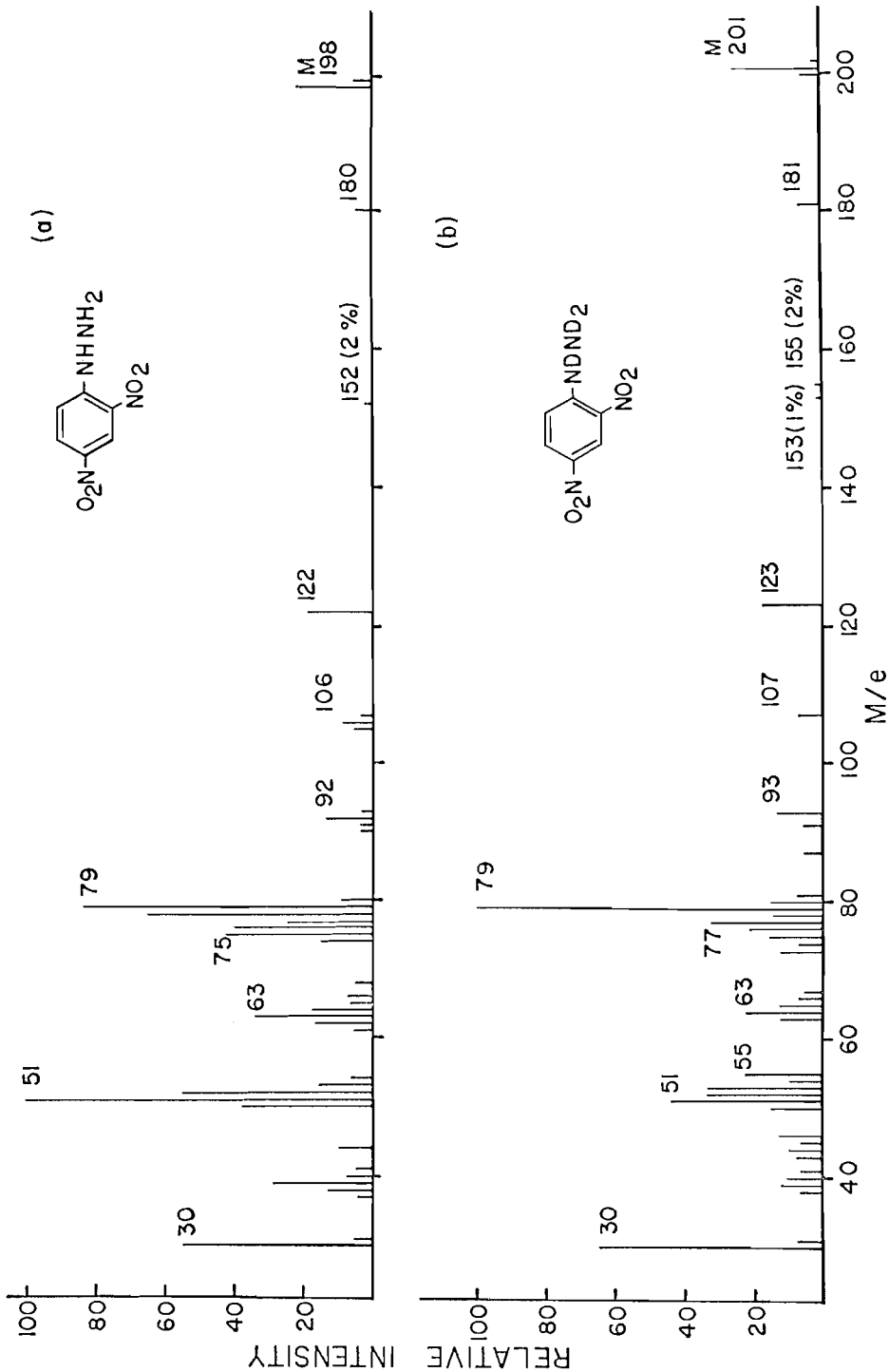

FIG. 1. Mass spectra of (*a*) 2,4-dinitrophenylhydrazine and (*b*) its *N,N'-d*$_3$-analogue.

Can. J. Chem. Downloaded from www.nrcresearchpress.com by 210.87.254.6 on 09/05/12
For personal use only.

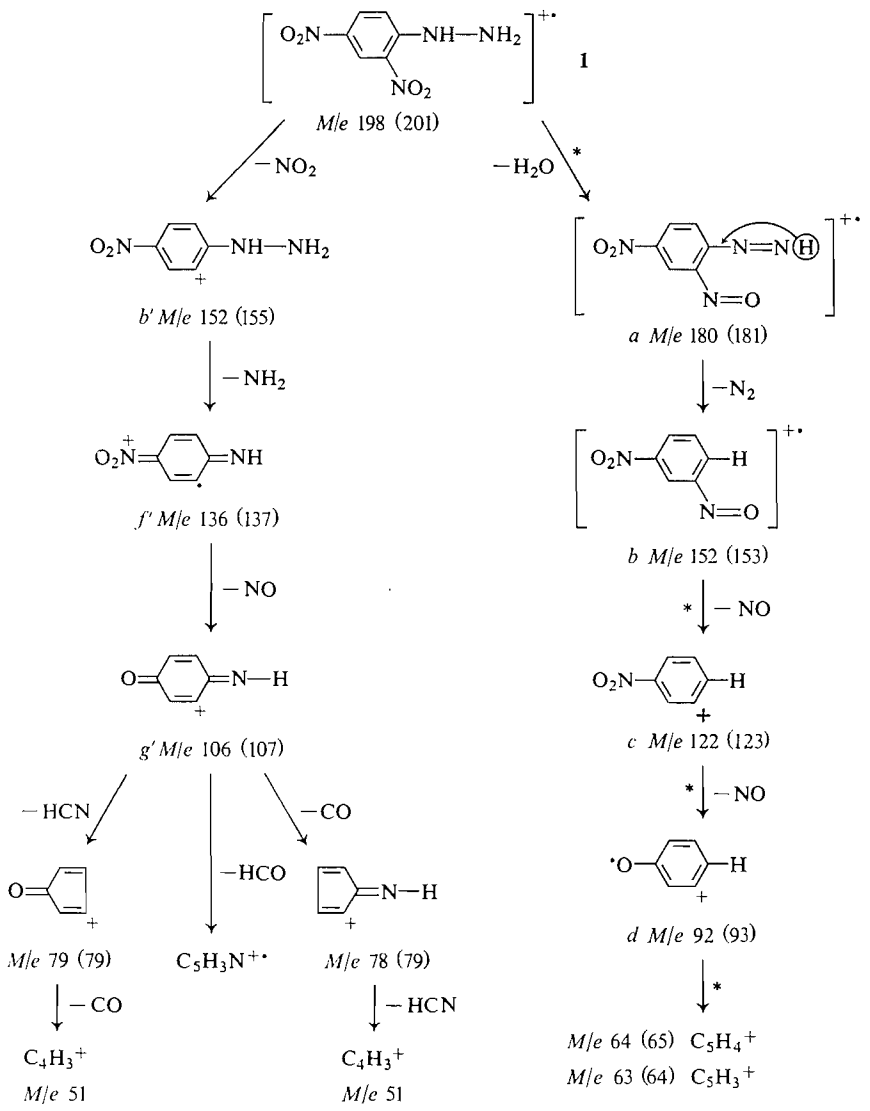

SCHEME I

Fragmentation mechanism of 2,4-dinitrophenylhydrazine.

latter many fragment ions appear at one mass unit higher. For example, peaks at *m/e* 152, 122, 106, and 79 in **1** are observed at *m/e* 153, 123, 107, and 80 in the mass spectrum of **2** which is shown as Fig. 2*a*. One peak prominent in Fig. 2*a* which does not appear strongly in the mass spectrum of **1** is that at *m/e* 90. In the *N,N'*-trideuterated analogue of **2**, the peaks at *m/e* 107 and 90 are shifted to *m/e* 110 and 91 respectively. These can be explained if the loss of NO_2 from the molecular ion is followed by ring opening together with migration of NH_2· to the ortho position, yielding the fragment ions *h* and *h'* shown in Scheme III. The linear structure *h'* would be better able to carry two positive charges than the cyclic form and indeed a small peak (0.1%) is found at *m/e* 53.5. Fragment *h'* can lose either HCN or NH_3 to give ions *m/e* 80 and 90 respectively; the latter pair can undergo conjugate losses as shown, to produce the ion *m/e* 63. It is noteworthy that the ion *m/e* 107 is *not* the analogue of *m/e* 106, *g'* (which contained oxygen) in the mass spectrum

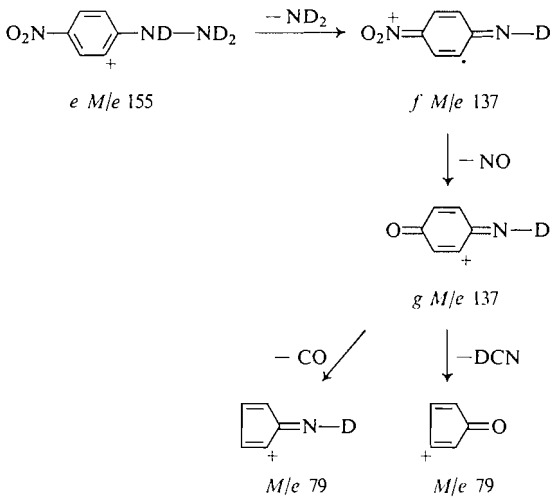

SCHEME II

Fragmentation mechanism of fragment *e* formed in the mass spectrum of *N,N'-d*$_3$-2,4-dinitrophenylhydrazine.

of **1**. This explains the lower intensities of peaks at *m/e* 78 and 79 in **2**; these were found to arise by loss of HCO· or CO from *g'* in **1**.

The mass spectrum of *o*-nitrophenylhydrazine **3** (Fig. 2*b*) is appreciably different from that of the para isomer. This is due to the "ortho-effect" described in the fragmentation of **1**. The ortho isomer sequentially loses H_2O and NO from the molecular ion to give fragment ion *k* as shown in Scheme IV. The loss of N_2 or NH· from *k* to produce ions *m/e* 77 and 90 respectively could occur readily from a cyclic entity. To explain the loss of HCN or CN· from *k* we again propose ring opening following migration of NH· to the ortho position to produce *k'*. The latter can sequentially lose CN· and HCN (or *vice versa*) yielding *m/e* 79, 78, and 52. Thus the ortho isomer, whose mass spectrum is superficially different from that of **2**, fragments by a closely similar mechanism.

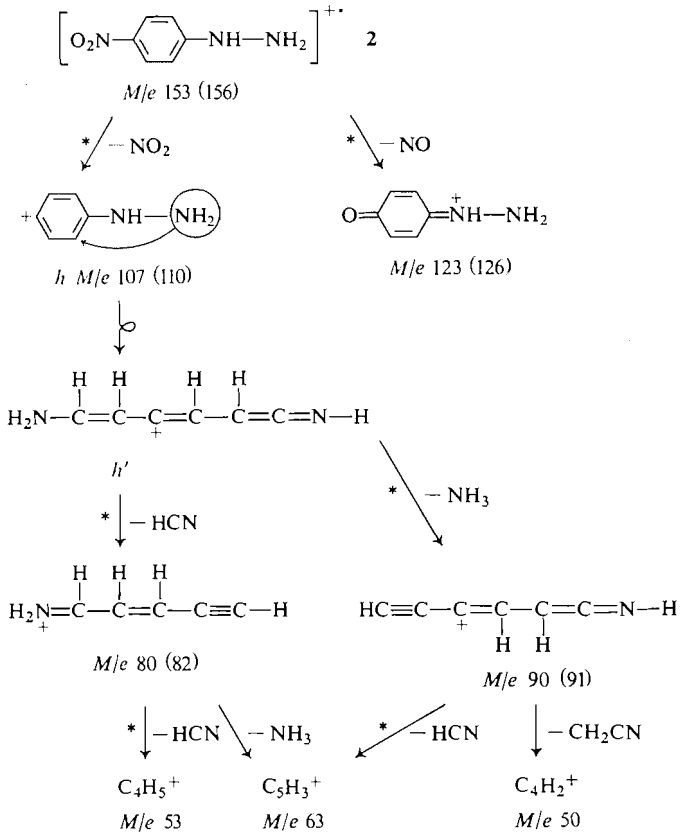

SCHEME III

Fragmentation mechanism of *p*-nitrophenylhydrazine.

Can. J. Chem. Downloaded from www.nrcresearchpress.com by 210.87.254.6 on 09/05/12
For personal use only.

Can. J. Chem. Downloaded from www.nrcresearchpress.com by 210.87.254.6 on 09/05/12
For personal use only.

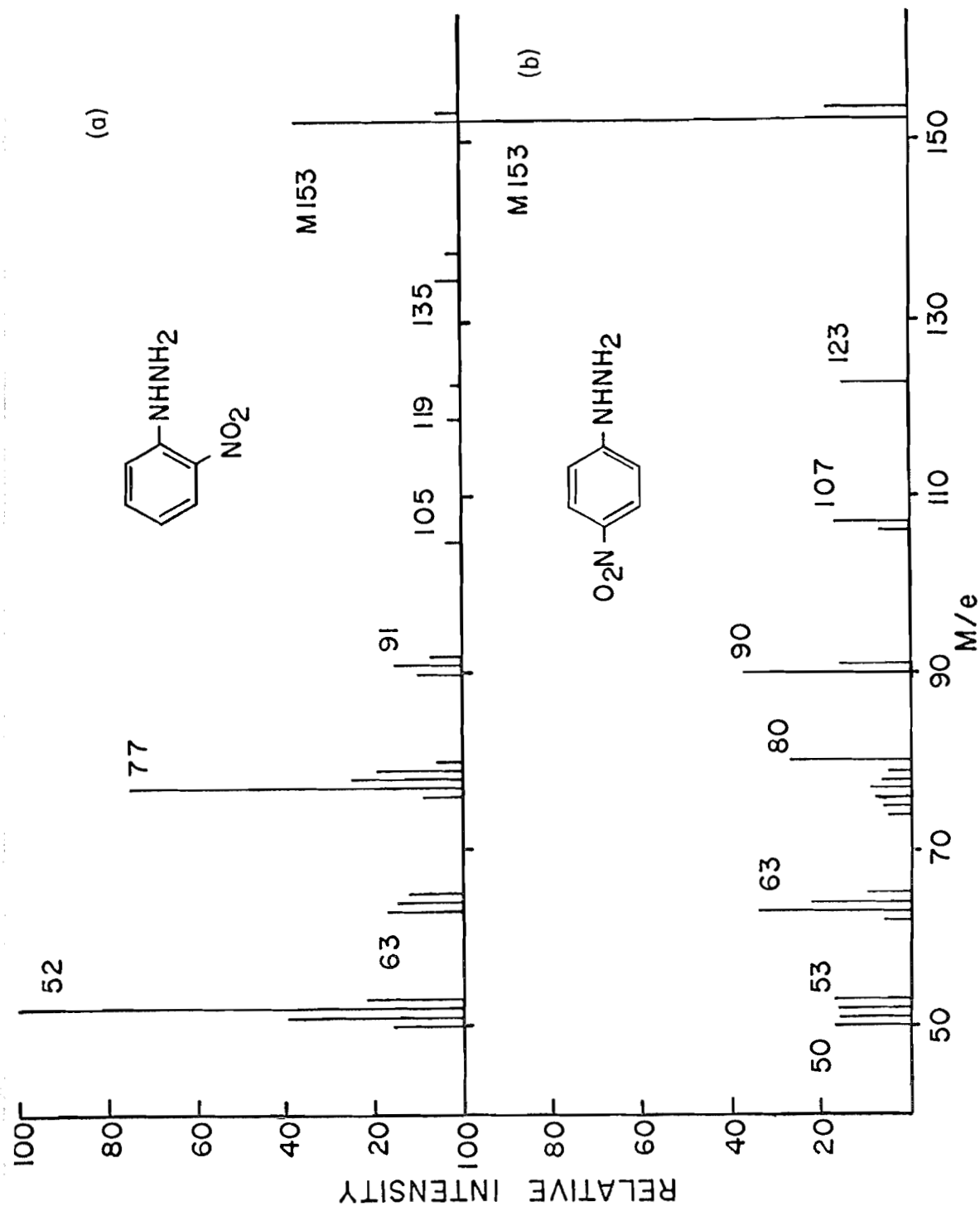

FIG. 2. Mass spectra of (*a*) *o*- and (*b*) *p*-nitrophenylhydrazine.

Can. J. Chem. Downloaded from www.nrcresearchpress.com by 210.87.254.6 on 09/05/12
For personal use only.

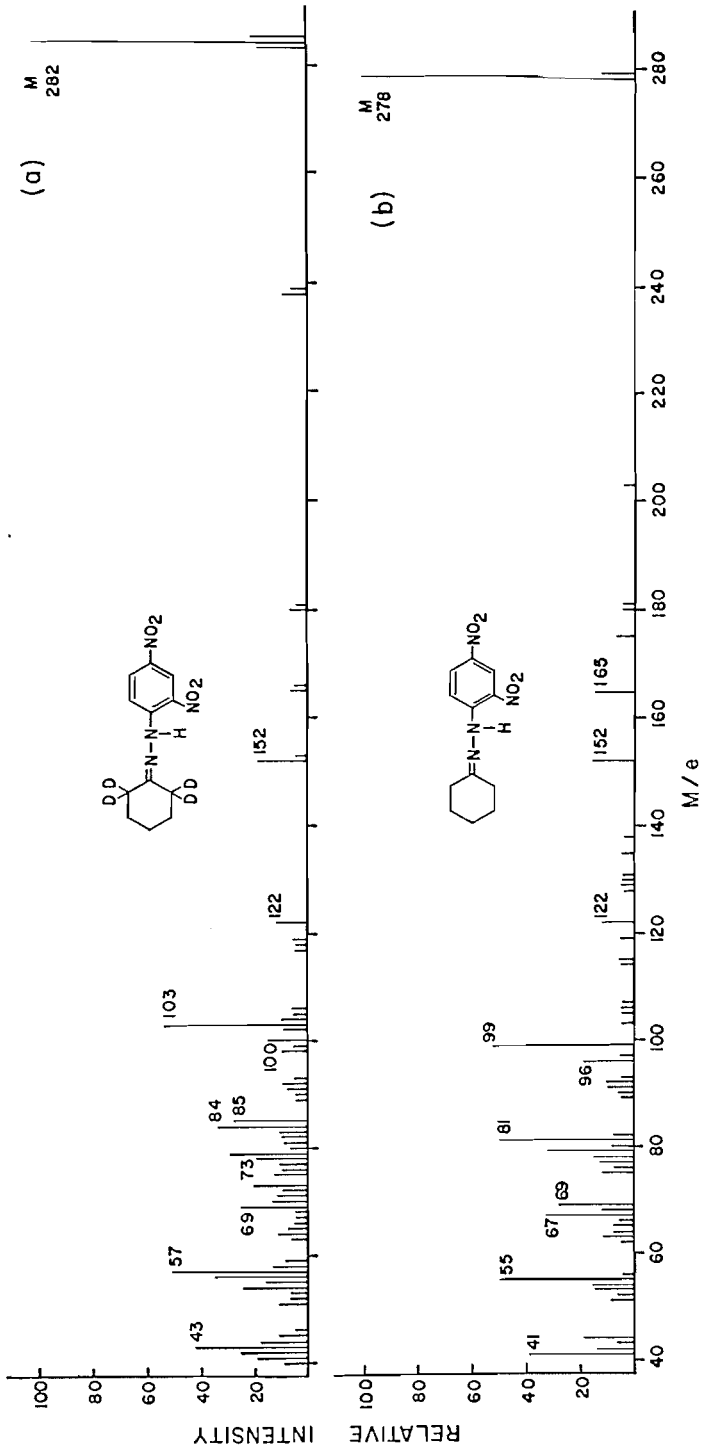

FIG. 3. Mass spectra of (*a*) cyclohexanone-2,4-dinitrophenylhydrazone and (*b*) its α-d_4-analogue.

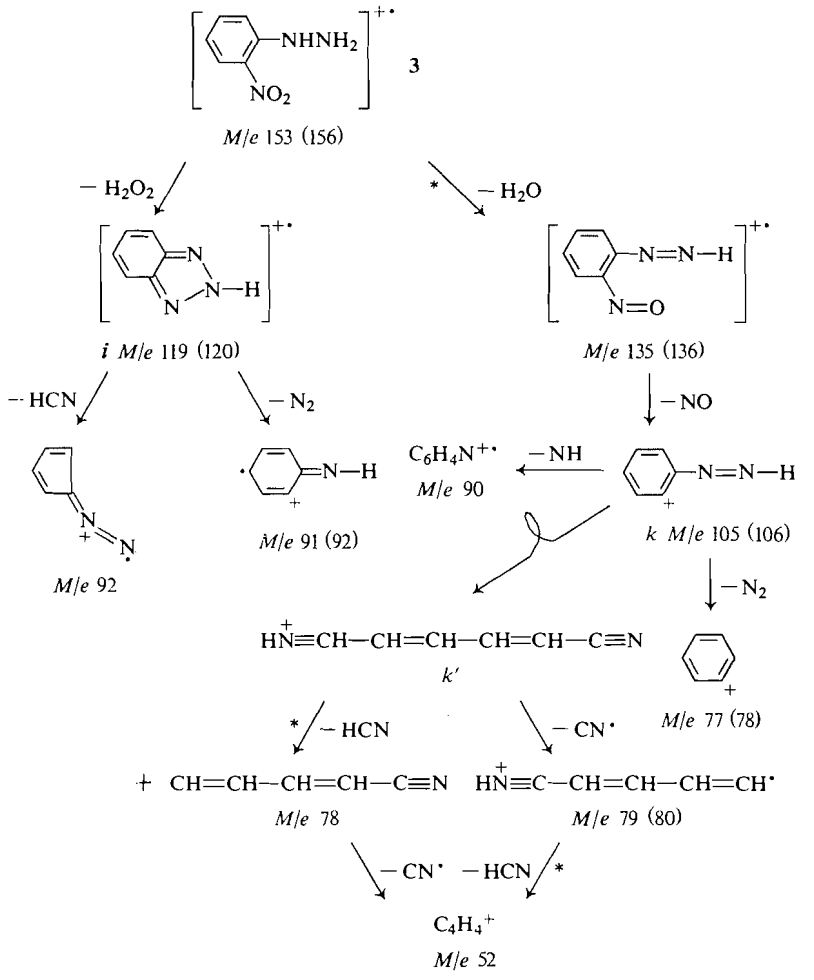

SCHEME IV

Fragmentation mechanism of *o*-nitrophenylhydrazine.

The loss of H_2O_2 from the molecular ion is not widely encountered and deserves mention; the transfer of two H atoms to different oxygen atoms on the nitro group with subsequent loss of H_2O_2 could yield the stable entity **1**, which can further lose either N_2 or HCN to produce *m/e* 91 and 92 respectively as shown in Scheme IV.

Cyclohexanone 2,4-DNP

The mass spectra of ketone 2,4-DNP's show peaks similar to those found in the mass spectrum of 2,4-dinitrophenylhydrazine. Since these fragment ions give little or no information as to the structure of the ketone moiety they will not be discussed further.

A prominent feature in the mass spectrum of cyclohexanone 2,4-DNP (**4**) (Fig. 3*a*) is the intense peak at *m/e* 99 (fragment-*m*). This peak arises from migration of a hydroxyl group from the ortho–nitro group to the ketone moiety to yield the protonated ketone (Scheme V)[1]. This is supported by the observation that the *m/e* 99 peak is shifted to *m/e* 100 in the *N*-deuterated analogue and to *m/e* 103 in the α-d_4 compound (Fig. 3*b*). The structure of *m* is a matter for conjecture but incorporation of the oxygen into a ring (*m'*) is feasible (as shown in Scheme V). Fragment *m'* is then seen to lose water, yielding *m/e* 81; the latter remains in the spectrum of the *N*-deuterated

[1]This migration has been independently suggested by Seibl and Völlmin (1) and Seibl (5).

Can. J. Chem. Downloaded from www.nrcresearchpress.com by 210.87.254.6 on 09/05/12
For personal use only.

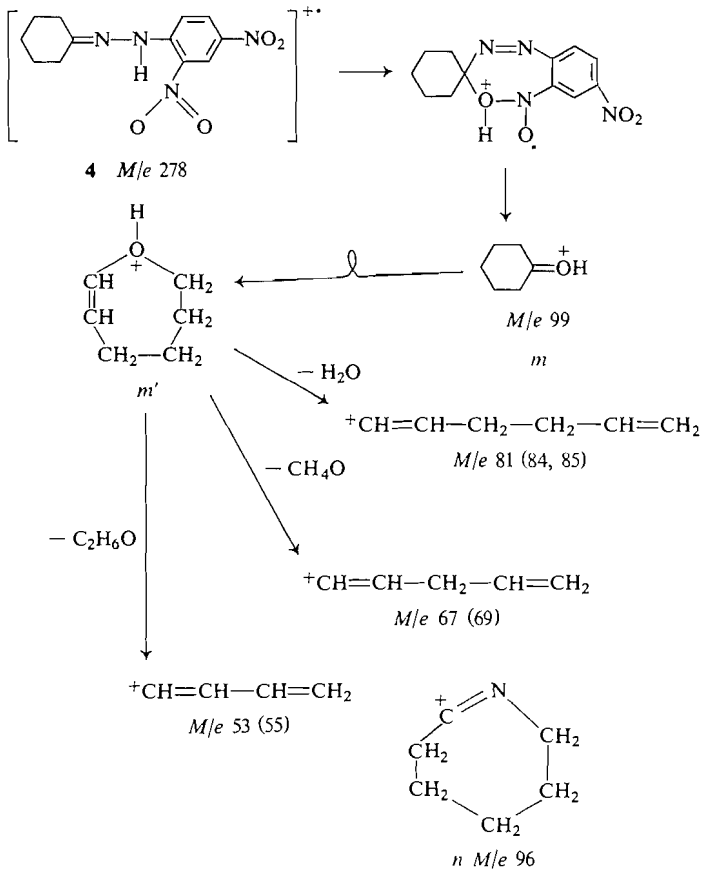

SCHEME V

Fragmentation mechanism of cyclohexanone-2,4-dinitrophenylhydrazone.

species while being shifted to *m/e* 84 and 85 in the α-d_4 compound. This indicates that water loss from *m'* occurs equally by a 1,2 and 1,3 and/or 1,4 elimination. Fragment *m* corresponds to either "protonated cyclohexanone" or the "(M-1) ion of cyclohexanol" and could be expected to show cleavages similar to those observed in the mass spectra of cyclohexanone and cyclohexanol. In cyclohexanol the H atom involved in the loss of water was found to come from either the 3 or the 4 carbon position (6*c*). H_2O loss in cyclohexanone involved H atoms from the 2 or 3 carbon positions (6*d*). The suggested mechanism for the loss of water is shown in Scheme V. Fragment *m'* also loses CH_4O and C_2H_6O. These neutral fragments, corresponding to CH_3OH and C_2H_5OH are believed to be lost by the mechanism shown in Scheme V. The determining factor seems to be the carbon position from which the H atom is transferred. Thus migration of a H atom from the 3 position induces loss of H_2O, from the 4 position loss of CH_4O and from the 5 position loss of C_2H_6O. The fragmentation of the deuterated species supports this dissociation mechanism. Migration of a H atom from the 2 position also gives rise to loss of H_2O and is observed as the loss of HDO from the α-d_4 analogue of *m*.

Even though migration of a H atom from the 4 and 5 positions induces loss of CH_4O and C_2H_6O respectively, water loss may also occur. All the features described above are present in the mass spectrum of cyclohexanone *o*-nitrophenylhydrazone (Fig. 4*a*), but are absent in the *p*-nitro analogue (Fig. 4*b*). The latter fragments differently, *via* cleavage of the central *N-N* bond to produce fragment ion *n*. This species has also been observed in cyclohexanone-*N*,*N*-dimethylhydrazone (4).

Can. J. Chem. Downloaded from www.nrcresearchpress.com by 210.87.254.6 on 09/05/12
For personal use only.

Can. J. Chem. Downloaded from www.nrcresearchpress.com by 210.87.254.6 on 09/05/12
For personal use only.

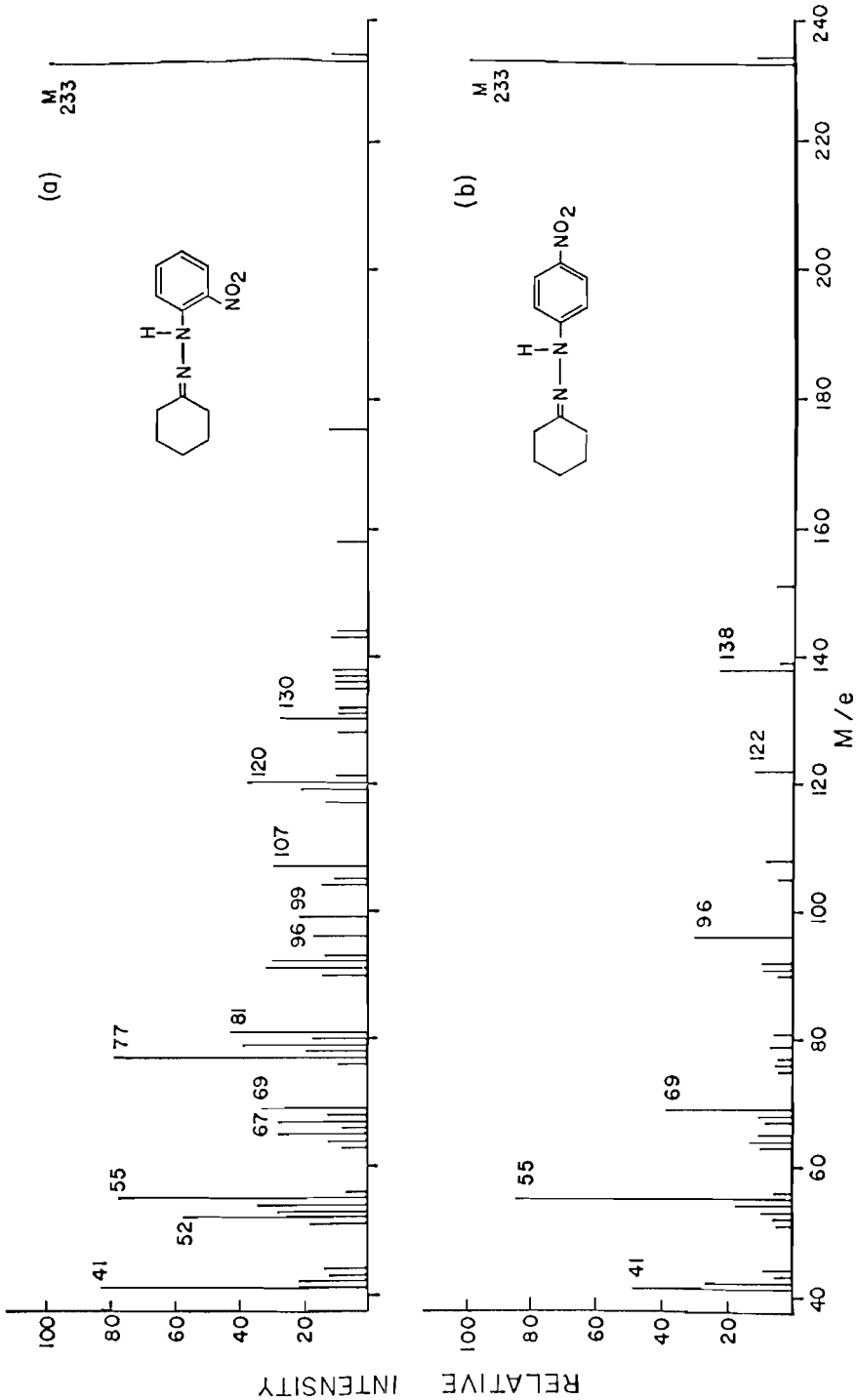

FIG. 4. Mass spectra of (*a*) cyclohexanone-*o*-nitrophenylhydrazone and (*b*) cyclohexanone-*p*-nitrophenylhydrazone.

Can. J. Chem. Downloaded from www.nrcresearchpress.com by 210.87.254.6 on 09/05/12
For personal use only.

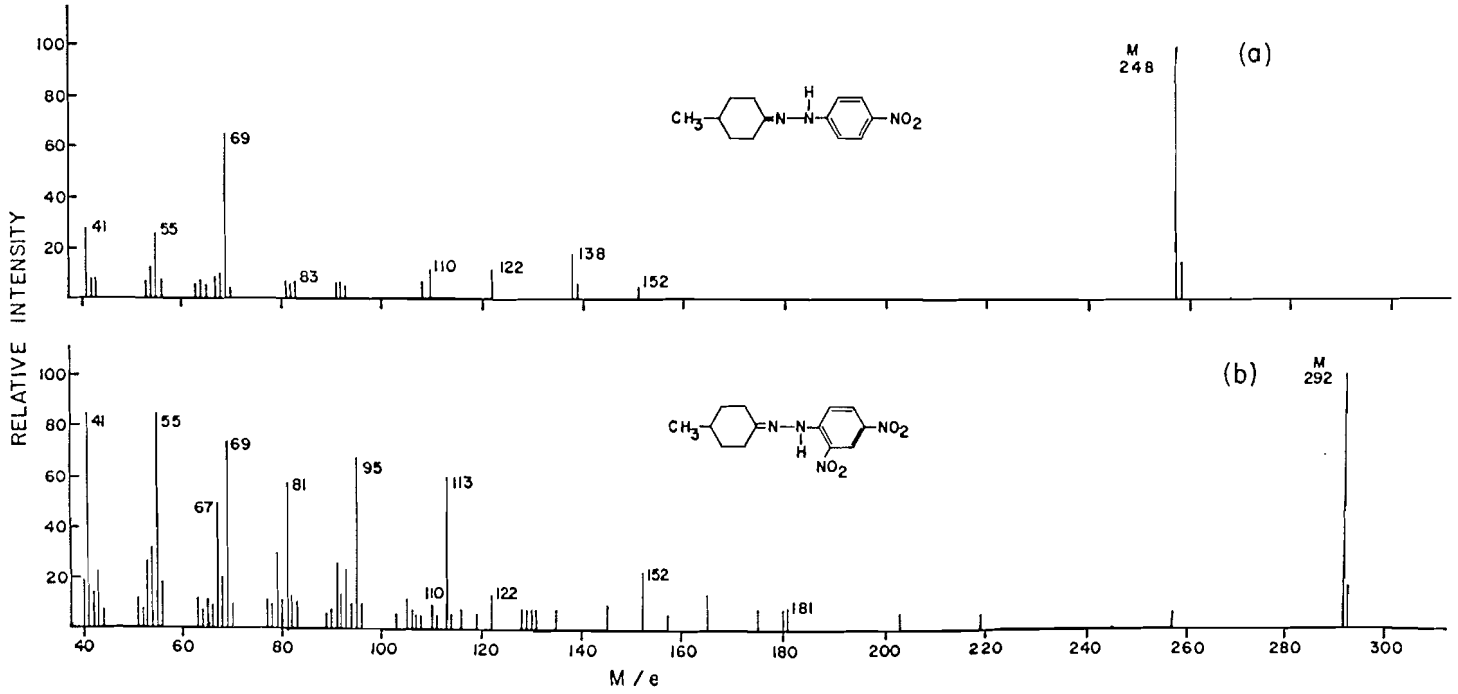

FIG. 5. Mass spectra of (*a*) 4-methylcyclohexanone-*p*-nitrophenylhydrazone and (*b*) 4-methylcyclohexanone-2,4-dinitrophenylhydrazone.

Can. J. Chem. Downloaded from www.nrcresearchpress.com by 210.87.254.6 on 09/05/12
For personal use only.

Fragment ion *n* may be represented by many structures; one of these is shown in Scheme V, i.e. with the nitrogen atom incorporated into a ring. Fragment *n* behaves similarly to fragment *m*; H atom migrations from the various ring positions are associated with losses of HCN, CH_3CN, and C_2H_5CN to yield the species *m/e* 69, 55, and 41. High resolution measurements on *m/e* 69 and 55 showed that these are $C_5H_9^+$ and $C_4H_7^+$ respectively. The charge appears to remain with the aliphatic fragments rather than with the cyanide entity. That H atom migration from the 2 position is associated with the loss of HCN is shown by the loss of DCN in the α-d_4 species.

The mass spectrum of cyclopentanone 2,4-DNP showed peaks corresponding to fragmentations analogous to those described above for cyclohexanone 2,4-DNP and thus a similar mechanism presumably operates.

Methylcyclohexanone Nitrophenylhydrazones

The mass spectra of the three isomeric methylcyclohexanone-2,4-DNP's were found to be very similar. The only differences observed lay in the relative intensities of the major peaks. The presence and position of the methyl substituent does not appear to exert any significant influence on the fragmentation of the ketone moiety of the molecule which behaves similarly to cyclohexanone-2,4-DNP. The similarity is not surprising since the three isomeric methylcyclohexanones (6*e*) and the methylcyclohexanols (6*f*) are not readily distinguishable by means of their mass spectra. The mass spectra of 4-methylcyclohexanone-2,4-DNP and its *p*-nitrophenylhydrazone are shown in Figs. 5*a* and 5*b*. The substituent position in molecules known to be isomeric could be determined (with some uncertainty) from relative intensities of fragment ions in their mass spectra but these alone would be of little aid in structural determinations of unknown molecules.

Experimental

All mass spectra were measured on a Hitachi–Perkin Elmer RMU-6D mass spectrometer using the direct sample inlet system. The 2,4-DNP's were run at an inlet temperature of 250 °C while *o*- and *p*-nitrophenylhydrazine were run at room temperature. The spectra were measured at electron energy 70 eV.

The nitrophenylhydrazones were prepared by reaction of the appropriate nitrophenylhydrazine and the ketone in acid medium with 95% ethanol as solvent. Deuteration of the hydrazine function was carried out by recrystallization of the sample from a mixture of D_2O and dioxane.

1. J. SEIBL and J. VÖLLMIN. Org. Mass Spec. **1**, 713 (1968).
2. R. J. C. KLEIPOOL and J. I. HEINS. Nature, **203**, 1280 (1964).
3. C. DJERASSI and J. D. SAMPLE. Nature, **298**, 1314 (1965).
4. D. GOLDSMITH and C. DJERASSI. J. Org. Chem. **31**, 3661 (1966).
5. J. SEIBL. Helv. Chim. Acta, **50**, 263 (1967).
6. H. BUDZIKIEWICZ, C. DJERASSI, and D. H. WILLIAMS. Mass spectrometry of organic compounds. Holden-Day, Inc., San Francisco, 1967. pp. (*a*) 402, (*b*) 116, (*c*) 111, (*d*) 145, (*e*) 149, (*f*) 109.
7. J. HARLEY-MASON, T. P. TOUBE, and D. H. WILLIAMS. J. Chem. Soc. (B), 396 (1966).

Can. J. Chem. Downloaded from www.nrcresearchpress.com by 210.87.254.5 on 09/05/12
For personal use only.

Conformational studies of some 5,9-dimethyl-6,7-benzomorphan diastereoisomers and related compounds

A. F. Casy and A. P. Parulkar
Faculty of Pharmacy and Pharmaceutical Sciences, University of Alberta, Edmonton, Alberta

Received January 10, 1969

The proton magnetic resonance characteristics of some α/β diastereoisomeric 5,9-dimethyl-6,7-benzomorphans are reported for free base, hydrohalide, and methiodide forms, and differences between α- and β-signals are interpreted in terms of the piperidine ring fragment of the β-salts adopting skew-boat conformations. The steric course of quaternization of benzomorphan isomers is discussed from results of alkylations using trideuteriomethyl iodide and other experiments. A possible correlation between conformational and potency differences in analgesically active benzomorphan diastereoisomers and related compounds is discussed.

Canadian Journal of Chemistry, 47, 3623 (1969)

This paper reports a comparative conformational study of some 6,7-benzomorphan derivatives **1** that are diastereoisomeric with respect to the C-5 and C-9 alkyl substituents. The relative

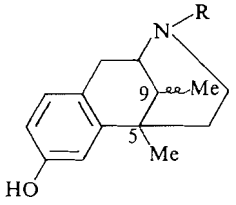

1

5,9-dialkyl configurations of several pairs of benzomorphan isomers are known (α-*cis* and β-*trans* with reference to the hydroaromatic ring) from rates of quaternization and proton magnetic resonance (p.m.r.) data (1), and a recent X-ray analysis of the α-*N*-allyl derivative **1** (R = CH_2-$CH{=}CH_2$) supports these assignments (2). Stereochemical data upon these compounds are of interest in view of the marked analgesic properties found in this class and because of the influence of the 5,9-dialkyl geometry upon analgesic potency (3) (β-diastereoisomers are generally more active than the α-forms).

Evidence of conformation, as in related work upon other classes of analgesic (4*a–c*), has been derived from p.m.r. data, characteristics of two α/β benzomorphan pairs (**1**, R = H and Me) in free base, hydrohalide, and quaternary salt forms being compared. Most of the data refer to solutions in DMSO-d_6 because this was the only convenient solvent which dissolved all forms, and chemical shift values (recorded at 60 MHz) are given in Hz from TMS. Stereochemical information of most value derives from the 5,9-dimethyl and *N*-methyl p.m.r. signals; this information is given in Table I. Differences between α- and β-signals are initially interpreted in terms of the piperidine-chair forms **2** and **3** respectively.

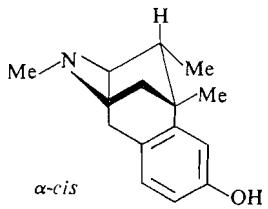

2

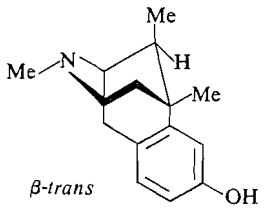

3

Bases

The chemical shifts of the α- and β-5-methyl signals are similar and their low field values (near 70 Hz) compared with the usual *t*-methyl positions near 54 Hz (5) are consistent with both groups lying near the plane of, and fairly close to, the 6,7-fused benzene ring (as in **2** and **3**), a position in which they are subject to aromatic deshielding (6). In the case of the 9-methyl signals, however, α-signals are higher field by over 20 Hz, β-signals being near-coincident with the 5-methyl resonance position. May's group (1*a*) obtained similar results for the *N*-methyl pair in $CDCl_3$ and interpreted differences in terms of differential aromatic shielding (α-9-methyl is shielded because it lies within the diamagnetic screening zone, whereas the β-group is too far removed to be affected by phenyl). The proximity of the nitrogen lone-pair to the

TABLE I

Proton magnetic resonance characteristics of some 5,9-dimethyl-6,7-benzomorphans **1**

R	Isomer*	Form	Solvent	Chemical shift†			Difference (salt–base)¶	
				N-Me—‡	5-Me—§	9-Me—‖	5-Me	9-Me
H	α	Base	DMSO-d_6	—	71	40	5.5	5
		HCl	DMSO-d_6	—	76.5	45		
H	β	Base	DMSO-d_6	—	69	65.5	6	7.5
		HCl	DMSO-d_6	—	75	73		
Me	α	Base	$CDCl_3$	145	78	48		
		Base	DMSO-d_6	131	71	42	7	5.5
		HCl	DMSO-d_6	163	78	47.5		
		HCl	D_2O	172	81	49.5		
		MeI	DMSO-d_6	202 194.5	83	50	12	8
		CD_3I	DMSO-d_6	192	82	49	11	7
CD_3	α	CD_3I	DMSO-d_6	—	81	49	10	7
Me	β	Base	$CDCl_3$	141	78	74.5		
		Base	DMSO-d_6	128	67.5	64.5		
		HCl	DMSO-d_6	161	72.5	75.5	5	11
		HBr	D_2O	173	81	77.5		
		MeI	DMSO-d_6	188 170	77	75.5	9.5	11
		CD_3I	DMSO-d_6	186.5	78.5	81	11	16.5
CD_3	β	CD_3I	DMSO-d_6	—	77	74.5	9.5	10

*α-*cis*- and β-*trans*-5,9-di-Me with respect to the hydroaromatic ring.
†In Hz from TMS (internal with $CDCl_3$ and DMSO-d_6, external with D_2O as solvent) spectra being measured at a frequency of 60 MHz.
‡Singlet except in some salts where spin–spin coupling with $\overset{+}{N}H$ proton occurs to give a doublet ($J \simeq 5$ Hz).
§Singlet.
‖Doublet ($J = 6.5$–7 Hz).
¶DMSO-d_6 solvent data.

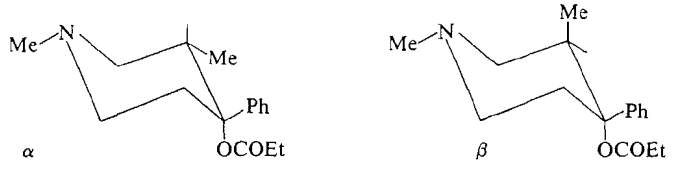

4

β-9-methyl group in benzomorphan bases is probably also of significance in regard to the α/β 9-Me chemical shift difference in view of demonstration of the greater deshielding influence of the lone-pair orbital upon axial than upon equatorial 3-methyl substituents in *trans* quinolizidines (7).

Hydrohalides

Both α- and β-5-methyl signals move downfield by about 6 Hz when basic centers are protonated. Lower field positions (relative to free base signals) also occur for α- and β-9-methyl signals in the protonated bases, the β-shift (7–11 Hz) being a few cycles larger than the α-value (5–5.5 Hz) in DMSO-d_6. 9-Methyl signals of α- and β-hydrohalide salts in D_2O show little difference from corresponding base resonance positions in $CDCl_3$.

9-Methyl-nitrogen geometry in α/β benzomorphans is analogous to that of 3-methyl-nitrogen in α- and β-prodine, (α- and β-**4**) respectively. In these and related compounds, the α-3-methyl signal suffers only a small change when the base is protonated (2–3 Hz downfield shift) while pronounced shifts (14–18 Hz) are observed for the β-signals *in the feebly polar solvent* $CDCl_3$. These differences have provided some of the evidence for the preferred chair conformations of both α- and β-prodine etc. in $CDCl_3$, 3-methyl being close to the deshielding $\overset{+}{N}H$ function in protonated β-**4** but further removed in α-**4** (4*a*). Hence the differences between the α- and β-

Can. J. Chem. Downloaded from www.nrcresearchpress.com by 210.87.254.5 on 09/05/12
For personal use only.

Can. J. Chem. Downloaded from www.nrcresearchpress.com by 210.87.254.5 on 09/05/12
For personal use only.

downfield shifts of the 9-methyl groups of the benzomorphans (induced on protonation) are smaller than those expected on the basis of the chair conformations **2** and **3**. The energy of the β-chair **3** will be raised when the base accepts a proton in a polar solvent through 1,3-diaxial non-bonded interactions between the solvated charged nitrogen and the 9-methyl group (axial with respect to the piperidine chair).[1] This interaction may be relieved in flexible conformations such as the skew-boat **5** and an increase in the population of such forms would explain the reduced influence of $\overset{+}{N}H$ upon the 9-methyl chemical shift since these two functions are further removed in **5** than in the chair **3**. There is similar evidence that skew-boat conformers

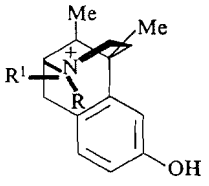

5

are preferred for hydrochlorides of β-prodine (and related esters) and its parent alcohol (β-prodinol) when dissolved in D_2O (4*b*) or DMSO-d_6.[2] In these cases solubility properties of the salts allowed measurements to be made in the feebly polar solvent $CDCl_3$ when clear evidence for chair conformations was obtained (4*a*, *b*). It is probable that greater 9-methyl salt–base chemical shift differences might have been observed in the β-benzomorphans if $CDCl_3$, rather than DMSO-d_6, could have been used as solvent. A further assessment of conformational, solvent, and anion influences upon the chemical shifts of methyl substituents in these piperidine and benzomorphan salts will be given elsewhere.

Further evidence for skew-boat conformations in β-benzomorphans has been obtained by a study of $\overset{+}{N}H$ and $\overset{+}{N}$—Me p.m.r. signals in hydrochloride and quaternary salts. If skew-boat populations are significant in the β-secondary base **1** (R = H) hydrochloride, the difference between the chemical shifts of the two $\overset{+}{N}$—H protons would be expected to be greater than that between the α-$\overset{+}{N}H_2$ pair since one of the β-$\overset{+}{N}H$ protons (R = H in **5**) falls close to and above the plane of the aromatic ring in the skew-boat **5** (R = R′ = H). A shielding factor difference of about 0.8 p.p.m. (48 Hz at 60 Hz) between pseudo-*a* and *e*-$\overset{+}{N}H$ (or $\overset{+}{N}$Me) groups in **5** (R = R′ = H or Me) is anticipated on the basis of Johnson and Bovey's table of aromatic shielding values (6).[3] In fact, while the α-$\overset{+}{N}H_2$ signal formed a two proton multiplet centered at 570 Hz, the β-salt showed two distinct $\overset{+}{N}H$ signals, at 571 and 525 Hz, the latter, higher field value, being consistent with the aromatic screening of one of the protons, as anticipated for **5** (R = R′ = H). The broad nature of these signals (α-w_H 14, β, 24 and 26 Hz) differentiated them from the sharper phenolic OH signals. The latter fell within the aromatic multiplet in bases and hydrohalide salts as confirmed by comparing spectra of salts of α-**1** (R = H) and the corresponding *O*-methyl ether but were moved downfield in methiodides (forming isolated singlets) possibly as a result of hydrogen bonding of OH to iodide. $\overset{+}{N}H$ signals in the α/β *N*-methyl salts (**1**, R = Me) could not be clearly resolved.

Quaternary Salts

Non-chair conformations of the piperidine ring in methiodides of β-benzomorphans **1** (R = alkyl) are even more probable than in corresponding hydrohalide salts because of the axial 1,3-dimethyl interactions which must arise in the chair forms. This expectation is given point by the case of the 4-phenylpiperidine methiodides **6***a* and *b* where separation of the *N*-Me p.m.r. signals in $CDCl_3$ is reduced from 12 (**6***a*) to 3.5 Hz (**6***b*) when an axial 3-methyl substituent is present.[4] This result demonstrates the smaller environmental difference between

[1]Although no previous studies have been reported in DMSO-d_6, there is evidence that the effective size of $\overset{+}{N}H$ protons is increased by the presence of tightly held water molecules of hydration (8).

[2]Chemical shift differences (salt–base) for the prodinols in DMSO-d_6 are 7 Hz for the α- and 11 Hz for the β-isomer (unpublished results).

[3]$\overset{+}{N}H_2$ chemical shifts are unlikely to be averaged through proton exchange because the rate of this process is slow in hydrogen bonding solvents such as DMSO-d_6 (9).

[4]A. F. Casy and A. P. Parulkar. Unpublished results.

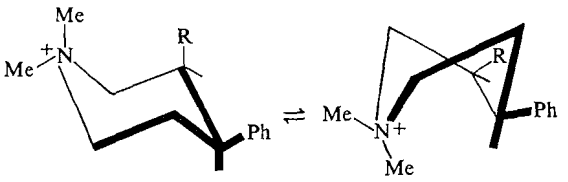

R = (*a*) H; (*b*) Me

6 7

the *N*-Me groups in the 3-methyl derivative as would result from comparable populations of the *e*-Ph chair **6***b* and skew-boat **7***b* (the population of the inverted chair form of **6***b* is likely to be low because of the large $-\Delta G_x^0$ value of phenyl) (10).

Methyl iodide rapidly methylated the α-benzomorphan **1** (R = Me), but a much longer reaction period was required to quaternize completely the corresponding β-isomer, as expected from reported reaction rates (1). The p.m.r. spectrum of the α-methiodide displayed distinct *N*-methyl signals at 202 and 194.5 Hz, whereas that of the β-isomer showed *N*-methyl bands at 188 and 170 Hz (Fig. 1A and D). The greater separation of the β-signals (18 compared with 7.5 Hz for α-) and the unusually high field position of one of the signals is consistent with the β-methiodide having the skew-boat conformation **5** (R = R′ = Me) in DMSO-d_6 with one *N*-methyl group falling well within the aromatic shielding zone. The deshielding influence of charged nitrogen upon the β-9-methyl signal is only a little greater than upon the α-9-methyl resonance ($\nu_{methiodide} - \nu_{base}$: α, 8 Hz; β, 11 Hz), again a result expected for a favored skew-boat rather than piperidine chair β-conformation (cf. argument relating to the conformation of the β-hydrochloride salts).

Quaternization of the α- and β-bases **1** (R = Me) was also carried out using trideuteriomethyl iodide to aid spectral analysis and provide evidence of reaction stereochemistry. In the α-series, the lower field *N*-methyl signal was absent in the mono-*N*-CD_3 iodide, while ring proton signals, hidden in the *N*,*N*-dimethyl form, were revealed in the *N*,*N*-di-CD_3 derivative (Fig. 1, B and C). Identification of the *N*,*N*-dimethyl signals of the β-methiodide itself is equivocal because more than two signals fall in the *N*—Me resonance region (Fig. 1D). One must be the unusually broad 170 Hz band because of its complete absence in the mono-*N*-CD_3 compound, while the other is the 188 Hz signal, as both this and the 170 Hz signal are missing from the spectrum of the *N*,*N*-di-CD_3 derivative (Fig. 1, E and F). Signals near 192 Hz which remain in the last spectrum must be due to ring protons.

There is good evidence that axial rather than equatorial approach is the preferred reaction pathway for the quaternization of cyclic nitrogen compounds, provided the group already attached to nitrogen is not markedly smaller than the incoming group (11, 12). Hence the *N*-methyl signal in the α-*N*-Me,*N*-CD_3 salt is probably due to an equatorial group. This is the higher field member of the *N*,*N*-dimethyl quaternary salt (Fig. 1, A and B), thus the lower field signal (202 Hz) is assigned to axial *N*-methyl. In monocyclic *N*,*N*-dimethyl piperidine salts, the axial *N*-methyl group generally has the *higher* field position (11, 12), and anisotropic effects of the fused hydroaromatic system (influencing *e*- rather than *a*-*N*-methyl) are most probably responsible for the reversal noted in the α-benzomorphan case. In the β-series the lower field methyl signal of the *N*,*N*-dimethyl salt remains in the *N*-Me,*N*-CD_3 salt.[5] This result further supports a radical conformational difference between the methiodide of α- and β-**1** (R = Me) since, if the β-chair **9** were favored, the *higher* field *N*-methyl signal should persist in the mono-*N*-CD_3 compound (as it does in the corresponding α-isomer).

Taking the skew-boat **5** (R′ = R = Me) as the favored β-methiodide conformation, two reaction pathways for quaternization of the β-base **1** (R = Me) with CD_3I may be formulated:

1) axial approach of CD_3I upon the chair conformation **8** and subsequent conformational change of the quaternary chair **9** to the skew-boat **10**;

2) pseudo-axial approach of CD_3I upon the

[5]Hence, assuming the skew-boat conformation **5** (R = R′ = Me), relative positions of pseudo-axial and pseudo-equatorial *N*-methyl chemical shifts are as seen in monocyclic piperidines. The pseudo-equatorial group still falls under the influence of the fused aromatic system (it has a chemical shift close to *e*-*N*-methyl in the α-salt) but the pseudo-axial group is even more subject to the same screening influence.

Can. J. Chem. Downloaded from www.nrcresearchpress.com by 210.87.254.5 on 09/05/12
For personal use only.

Can. J. Chem. Downloaded from www.nrcresearchpress.com by 210.87.254.5 on 09/05/12
For personal use only.

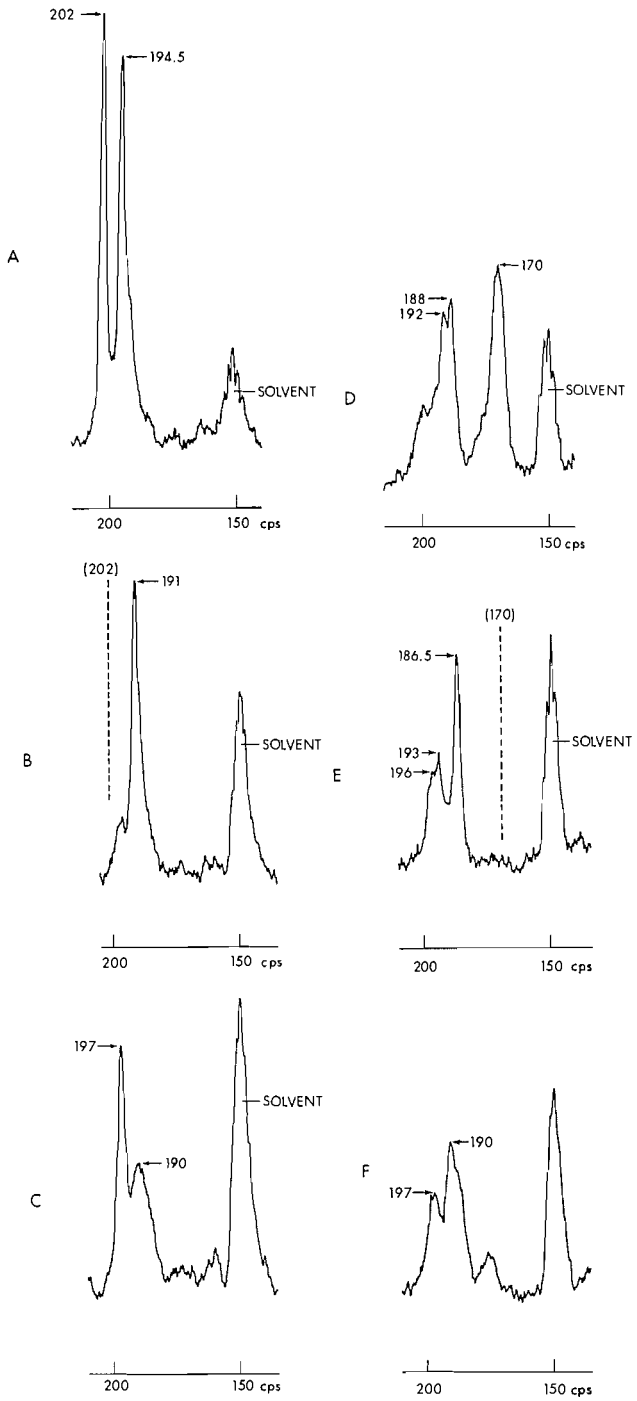

FIG. 1. Part of the proton magnetic resonance spectra of A, *N*,*N*-di-Me; B, *N*-Me,*N*-CD_3; C, *N*,*N*-di-CD_3 iodide salts of α-5,9-dimethyl-2′-hydroxy-6,7-benzomorphan in DMSO-d_6. D, E, and F are spectra of the corresponding salts of the β-isomer. Spectral amplitudes are 12.5 (A), 25 (D), 32 (B and E), and 80 (C and F). Relative signal intensities may be gauged by comparison with solvent signals near 150 Hz. Chemical shifts are in Hz from TMS at a 60 MHz frequency.

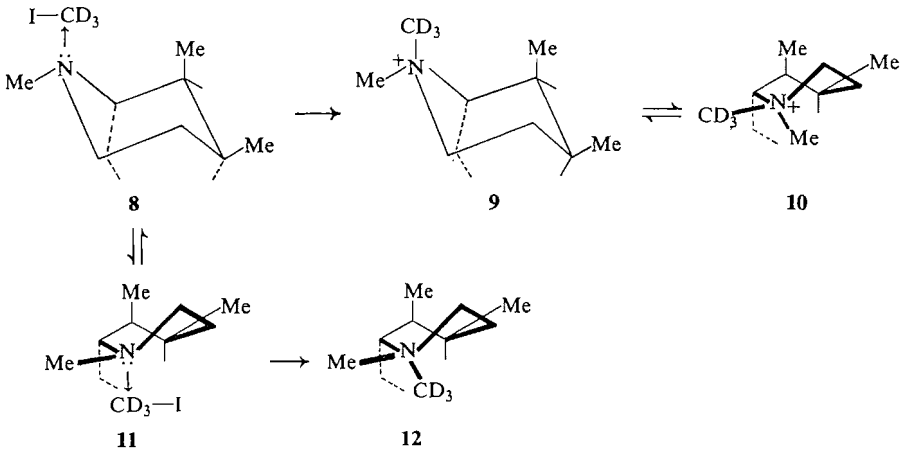

skew-boat conformation **11** of the β-base with direct formation of the favored quaternary salt conformer **12.**

In the former case, the *higher* field *N*-Me signal will remain whereas in the latter, the *lower* field signal; results obtained thus support pathway *2*.

Further evidence for axial *N*-methyl having a lower field chemical shift than equatorial *N*-methyl in α-benzomorphan methohalides was obtained from the results of the methylation of α-**1** (R = Et) (reaction A), and the ethylation of α-**1** (R = Me) (reaction B). Two isomers may result in each case; viz.,

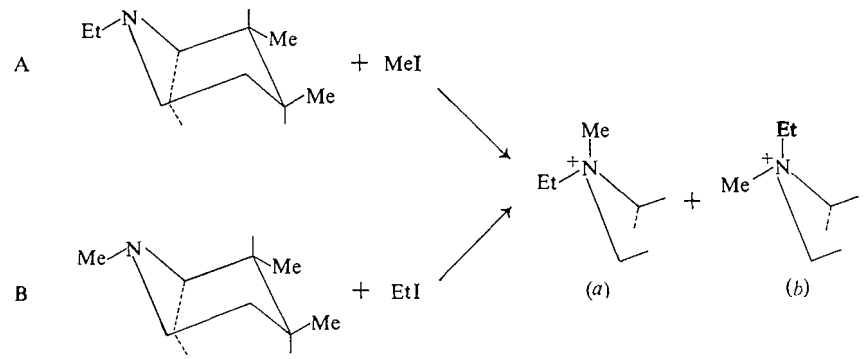

Only one *N*-Me signal (201 Hz) was resolvable in the total product of reaction A and the minor *N*-Me signal (185 Hz) was identified in the spectra of recrystallized samples. The same *N*-Me signals were found for the total product of reaction B but major and minor values were reversed. Hence assuming axial approach of quaternizing reagent (11, 12), the major product of reaction A is the axial *N*-methyl isomer (*a*) (lower field) while that of reaction B is the equatorial isomer (*b*) (higher field).

Ethylation of the β-*N*-methylbenzomorphan **1** (R = Me) (complete only after a 14 day reflux period) gave a total product showing sharp *N*-Me signals at 203 and 184 Hz (a broad band at 195 Hz situated between these signals is provisionally assigned to ring protons) of separation comparable with that found for the *N*-Me signals of the β-**1** (R = Me) methiodide.

The morphinan **13***a* and isomorphinan **13***b* derivatives are close analogues of the α- and β-benzomorphans **1** (R = Me) and similar evidence for favored skew-boat conformations in **13***b* methiodide (in the chair conformation, the 8-methylene group bears a 1,3-diaxial relationship to an *N*-methyl group) derives from

Can. J. Chem. Downloaded from www.nrcresearchpress.com by 210.87.254.5 on 09/05/12
For personal use only.

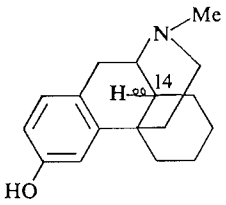

13*a* 14-H *cis* to nitrogen bridge
13*b* 14-H *trans* to nitrogen bridge

N–Me p.m.r. signals. In the methiodide of 3-hydroxy-*N*-methylmorphinan **13***a* (no 8-methylene – *N*-Me interaction), *N*-Me signal separation (8 Hz) approximates to that found in the α-benzomorphan **1** (R = Me) methiodide, whereas a separation of 13.5 Hz (closer to that of the β-benzomorphan analogue) is obtained for the isomorphinan derivative. However, the NMe_2 chemical shift separation of the isomorphinan is not as large as that of the β-benzomorphan methiodide and the higher field member is not moved upfield so markedly; these facts indicate skew-boat conformers to be less favored in **13***b* methiodide than in the corresponding β-benzomorphan salt.

It is attractive to speculate upon a possible correlation between α/β benzomorphan conformational differences and variations in isomeric analgesic potencies, which may arise as a result of the influence of conformation upon drug–receptor interactions and/or processes governing the transport and distribution of isomeric pairs. In the α-derivatives, 9-alkyl groups enhance activity in the 5-methyl series but reduce it in 5-ethyl and 5-propyl analogues (1). In β-derivatives, 9-Me, Et, and Pr substituents yield analgesics of high potency in all examples studied (1, 13). From the present evidence, skew-boat populations are probably high in all the β-derivatives when protonated in aqueous media and it is possible that conformers of this type allow a more effective drug–receptor association than do the chair forms of the α-benzomorphans or are subject more readily to processes governing the transport and distribution of isomeric pairs. These considerations may also be important in regard to the higher potency of isomorphinan over morphinan derivatives (14) and to the remarkably high potency of certain 14-acyloxycodeinones (15).

Experimental

The p.m.r. spectra were recorded on a Varian A-60 spectrometer operating at the normal running temperature with TMS as standard (internal with $CDCl_3$ and DMSO-d_6 and external with D_2O as solvent). Supply of the following chemicals is gratefully acknowledged: α- and β-**1** (R = Me) (Dr. E. L. May, National Institutes of Health); α- and β-**1** (R = H) and the *O*-methyl ether hydrochloride of α-**1** (R = H) (Dr. N. F. Albertson, Sterling Winthrop Research Institute, Rensselaer, New York); dextrorphan (Roche Laboratories, Welwyn Garden City, Herts); (−)-3-hydroxy-*N*-methylisomorphinan (Dr. M. Gates, University of Rochester, Rochester, New York).

The α- and β-benzomorphans **1** (R = H) gave hydrochlorides, m.p. 292–295° decomp. (lit. (16) 290–294° decomp.) and 312–314° decomp., respectively.

Anal. Calcd. for $C_{14}H_{20}ClNO$: C, 66.25; H, 7.9. Found: C, 66.15; H, 7.6.

*Isomeric 2,5,9-Trimethylbenzomorphans **1** (R = Me) and Derivatives*

A mixture of α-**1** (R = H) (3.27 g), 40% formaldehyde solution (2.25 ml), 5% palladized charcoal (0.6 g), and EtOH (20 ml) was shaken with hydrogen (atmospheric pressure and room temperature) until gas absorption ceased. The product was filtered and the filtrate concentrated to give α-**1** (R = Me), m.p. 231–233° from EtOH, lit. 228–233° (17). Reductive methylation of β-**1** (R = H) gave β-**1** (R = Me), m.p. 220–221.5°, lit. 215–217.5° (17), hydrochloride, m.p. 313–315°, lit. 269–272° (17).

Anal. Calcd. for $C_{15}H_{22}ClNO$: C, 67.3; H, 8.3; N, 5.2. Found: C, 67.0; H, 7.9; N, 5.3.

Methiodides

A mixture of α-**1** (R = Me) (0.2 g), MeI (1 ml), and $CHCl_3$ (300 ml) was stirred at 38° (±2°) under reflux for 5 days (solid separated after 8–9 h), then concentrated to 25 ml, and diluted with ether. The solid which separated was recrystallized from EtOH–ether to give α-**1** (R = Me) *methiodide*, m.p. 268–268.5°.

Anal. Calcd. for $C_{16}H_{24}INO$: C, 51.5; H, 6.5; N, 3.75. Found: C, 51.2; H, 6.3; N, 3.5.

β-**1** (R = Me) *methiodide* (it separated from the reaction mixture after 2–3 days) had m.p. 279–281°. Found: C, 51.3; H, 6.4; N,3.7.

N-Trideuteriomethyl Derivatives

A mixture of α-**1** (R = Me) (0.15 g), CD_3I (0.11 g), and $CHCl_3$ (100 ml) was stirred at 33° (±2°) under reflux for 4 days. The methiodide of α-**1** (R = CD_3) which separated had m.p. 250–254°. Similar treatment of β-**1** (R = Me) gave the methiodide of β-**1** (R = CD_3), m.p. 118°. Treatment of α-**1** (R = H) (0.11 g) with CD_3I (0.2 g) gave the trideuteriomethiodide of **1** (R = CD_3), m.p. 254–258° decomp. after a 7 day reaction period. The β-*N*,*N*-di-CD_3 analogue had m.p. 287–288° from EtOH. The p.m.r. spectra of these products closely resembled those of the corresponding *N*,*N*-dimethyl derivatives in all respects save those of the *N*-Me resonance region (Fig. 1).

*N-Ethyl-N-methyl Quaternary Salts of **1** (R = H)*

A mixture of α-**1** (R = Me) (0.4 g), EtI (2 ml), and $CHCl_3$ (250 ml) was heated under reflux for 4 days. The solvent was evaporated and the residue recrystallized

Can. J. Chem. Downloaded from www.nrcresearchpress.com by 210.87.254.5 on 09/05/12
For personal use only.

from EtOH–ether to give an isomeric mixture of *N*-ethyl-*N*-methyl **1** (R = H) iodides, m.p. 265–266.5° decomp.

Anal. Calcd. for $C_{17}H_{26}INO$: C, 52.7; H, 6.8; N, 3.5. Found: C, 52.4; H, 6.5; N, 3.6.

Reductive ethylation of α-**1** (R = Me) using MeCHO instead of formaldehyde gave **1** (R = Et), m.p. 155–157° from $CHCl_3$–ether, lit. m.p. 158–160° (18). The *hydrochloride*, m.p. 166–168° displayed duplicate *N*-CH_2Me (quartets centered on 212 and 217 Hz from TMS, $J = 7$ Hz) and *N*-CH_2Me (triplets centered on 65.5 and 67 Hz, $J = 7$ Hz) p.m.r. signals in DMSO-d_6, indicative of similar populations of $\overset{+}{N}$—H epimers (unfavorable 1,3-diaxial interactions of an *a*-*N*-Et group must be balanced by interactions between *e*-*N*-Et and one of the C-8 methylene protons).

Anal. Calcd. for $C_{16}H_{24}ClNO \cdot H_2O$: C, 64.1; H, 8.7; N, 4.7. Found: C, 64.3; H, 8.4; N, 4.3.

The α-base **1** (R = Et) with MeI gave a quaternary salt mixture, m.p. 165° whose p.m.r. spectrum closely resembled that of the mixture obtained from **1** (R = Me) in all respects save the *N*-Me resonance region (see text). *N*-Ethylation of β-**1** (R = Me) (complete after a 14 day reflux period) gave an *N*-ethyl-*N*-methyl quaternary mixture, m.p. 241–242° from EtOH–ether. Found: C, 52.8; H, 6.9; N, 3.6.

Morphinan and Isomorphinan Methiodides

Dextrorphan (**13***a*) (0.1 g), MeI (2 ml), ether (200 ml), and EtOH (15 ml) were stirred under reflux at 35° (±2°) for 4 days. The solid which separated was recrystallized from $CHCl_3$–EtOH to give *dextrorphan methiodide*, m.p. 285–286°.

Anal. Calcd. for $C_{18}H_{26}INO$: C, 54.1; H, 6.6; N, 3.5. Found: C, 53.75; H, 6.6; N, 3.7.

The analogue derived from (−)-3-hydroxy-*N*-methylisomorphinan (**13***b*) had m.p. 248–250°. Found: C, 53.9; H, 6.6; N, 3.2. *N*-Methyl p.m.r. characteristics in DMSO-d_6 of **13***a* methiodide: singlets at 195.5 and 187.5 Hz from TMS; and **13***b* methiodide: singlets at 184 and 197.5 Hz.

1. (*a*) S. E. Fullerton, E. L. May, and E. D. Becker. J. Org. Chem. **27**, 2144 (1962). (*b*) J. H. Ager, S. E. Fullerton, and E. L. May. J. Medicin. Chem. **6**, 322 (1963).
2. W. Fedeli, G. Giacomello, S. Cerrini, and A. Vaciago. Chem. Commun. 608 (1966).
3. N. B. Eddy and E. L. May. Synthetic analgesics. Part IIB. 6,7-Benzomorphans. The Pergamon Press, Ltd., Oxford. 1966.
4. (*a*) A. F. Casy. Tetrahedron, **22**, 2711 (1966). (*b*) A. F. Casy. J. Medicin. Chem. **11**, 188 (1968). (*c*) A. F. Casy. J. Chem. Soc. B, 1157 (1966).
5. R. H. Bible. Interpretation of NMR spectra. Plenum Press, New York. 1965. p. 16.
6. C. E. Johnson and F. A. Bovey. J. Chem. Phys. **29**, 1012 (1958); Nuclear shielding values table. Minnesota Mining and Manufacturing Company, St. Paul, Minnesota. 1958.
7. T. M. Moynehan, K. Schofield, R. A. Y. Jones, and A. R. Katritzky. J. Chem. Soc. 2637 (1962).
8. J. L. Sudmeier and G. Occupati. J. Am. Chem. Soc. **90**, 154 (1968); E. L. Eliel, E. W. Della, and T. H. Williams. Tetrahedron Letters, 831 (1963).
9. O. L. Chapman and R. W. King. J. Am. Chem. Soc. **86**, 1256 (1964).
10. E. L. Eliel, N. L. Allinger, S. J. Angyal, and G. A. Morrison. Conformational analysis. John Wiley and Sons, Inc., New York. 1965. p. 44.
11. D. R. Brown, R. Lygo, J. McKenna, J. M. McKenna, and B. G. Hutley. J. Chem. Soc. B, 1184 (1967).
12. A. F. Casy, A. H. Beckett, and M. A. Iorio. Tetrahedron, **22**, 2751 (1966).
13. C. F. Chignell, J. H. Ager, and E. L. May. J. Medicin. Chem. **8**, 235 (1965).
14. M. Gates and W. G. Webb. J. Am. Chem. Soc. **78**, 1186 (1958).
15. W. R. Buckett. J. Pharm. Pharmacol. **16**, Suppl. 68T (1964).
16. E. M. Fry and E. L. May. J. Org. Chem. **24**, 116 (1959).
17. E. L. May and J. H. Ager. J. Org. Chem. **24**, 1432 (1959).
18. J. H. Ager and E. L. May. J. Org. Chem. **25**, 984 (1960).

Can. J. Chem. Downloaded from www.nrcresearchpress.com by 210.87.254.5 on 09/05/12
For personal use only.

Can. J. Chem. Downloaded from www.nrcresearchpress.com by 210.87.254.105 on 09/05/12
For personal use only.

Diprotonation equilibria involving 4-hydroxyazobenzene and 4-hydroxyazobenzene-4′-sulfonic acid[1]

W. M. J. Strachan, A. Dolenko, and E. Buncel
Department of Chemistry, Queen's University, Kingston, Ontario

Received April 14, 1969

4-Hydroxyazobenzene and 4-hydroxyazobenzene-4′-sulfonic acid, which are known to be protonated in dilute acid on the azo function, are shown through spectroscopic studies to undergo a second equilibrium protonation in the 100% H_2SO_4 region. The pK_a[2] values are −10.2 and −11.1 respectively. The spectral evidence suggests that with both substrates the second protonation occurs on the phenolic oxygen site, rather than on carbon.

Canadian Journal of Chemistry, 47, 3631 (1969)

The present work was undertaken as a preliminary to the study of the Wallach rearrangement of azoxybenzene in the 100% H_2SO_4 region. Extension of the kinetic and spectral studies (1,2) beyond 96% H_2SO_4 was desirable for a number of reasons, one being the possibility that the postulated dicationic intermediate (3) might be stabilized in anhydrous acid. However, prior to such a kinetic–spectral study with azoxybenzene, it was required to have full understanding of the spectral behavior in such media of 4-hydroxyazobenzene, the normal product of rearrangement (4). The results recorded here reveal a rather complex pattern of spectral changes, which can be dissected into a second equilibrium protonation of 4-hydroxyazobenzene, a fairly rapid sulfonation process to give 4-hydroxyazobenzene-4′-sulfonic acid, as well as a second equilibrium protonation and the much slower sulfonation of this sulfonic acid derivative.

Results

4-Hydroxyazobenzene

The protonation behavior of 4-hydroxyazobenzene in dilute acid has been examined previously (5,6). In aqueous sulfuric acid a pK_a of −0.93 was reported by Klotz *et al.* (5)[2] for ionization of the conjugate acid, corresponding to 50% protonation in about 20% H_2SO_4. In aqueous sulfuric acid containing 20% ethanol a pK_a of −1.02 was found by Yeh and Jaffé (6)[3]. These data were confirmed in the present work using the medium[4] 5% dioxane–95% aqueous H_2SO_4. For the neutral form λ_{max} was found to be 348 mμ ($\varepsilon = 2.18 \times 10^4$), while for the protonated form λ_{max} was 460 mμ ($\varepsilon = 3.96 \times 10^4$), with pK_a −0.99 in this medium. Beyond 45% H_2SO_4 (corresponding to about 99% protonation) no changes were observed in either λ_{max} or in ε_{max} until about 90% H_2SO_4[4], and the spectral absorption was also time invariant.

4-Hydroxyazobenzene in 90–100% H_2SO_4 has been observed to undergo further spectral changes which are time-dependent. In the region 90–96% H_2SO_4 the initial λ_{max} is unchanged at 460 mμ, but with time this absorption grows in intensity and simultaneously shifts to 465 mμ. In the 96–100% H_2SO_4 region, the initial absorption shifts gradually to shorter wavelengths until it reaches 426 mμ. In these acidities the growth in peak height is more rapid: the product spectra exhibit a concurrent gradual shift to 450 mμ. The above time-dependent spectral changes are shown to be the result of the conversion of 4-hydroxyazobenzene to the 4′-sulfonic acid and are dealt with in detail subsequently (see Experimental and reference 11). The immediate (zero time) spectral shifts are due to a protolytic equilibrium which was characterized as follows.

Initial 4-hydroxyazobenzene spectra were obtained for the 90–100% H_2SO_4 region by extrapolation over 400–480 mμ; some of the

[1]Part VI in series on the Wallach rearrangement (Part V: Can. J. Chem. **47**, 911 (1969)).

[2]These authors used the acidity scale of Michaelis and Granick (7) and strictly a minor correction to the pK_a should be applied on conversion to the Hammett acidity scale (8,9).

[3]For the 20% ethanol–80% aqueous H_2SO_4 medium the appropriate acidity function (6) was used.

[4]The appropriate acidity function for this medium (10) was used. Beyond 70% H_2SO_4, where the solubility of 4-hydroxyazobenzene becomes appreciable, a purely aqueous medium was used. The change in medium had no measurable effect on the absorption being monitored. While use of different media by different workers is disadvantageous from the point of view of inter-comparison, it is generally dictated by various practical considerations.

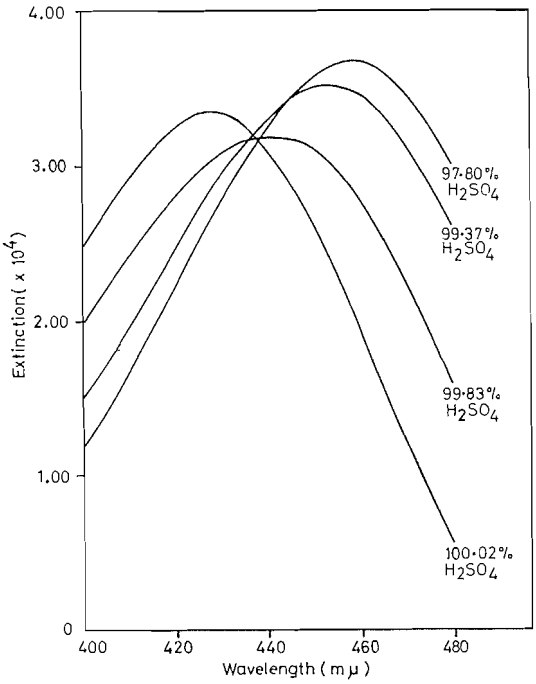

FIG. 1. Spectra of 4-hydroxyazobenzene (reconstituted to zero time) near 100% H_2SO_4 showing mono- and diprotonation.

reconstituted zero-time spectra for the upper acid region are shown in Fig. 1. These have the general character that results from a protonation process, in which medium effects (in addition to errors in extrapolation) may be responsible for the poorly defined isosbestic point (9,12). The 426 mμ absorption is ascribed to diprotonated 4-hydroxyazobenzene.

In order to obtain a pK_a value corresponding to this second equilibrium protonation, the absorbances at 460 mμ were extrapolated to zero time over 90–100% H_2SO_4. The absorbance data are given in Table I. These data when plotted against H_0 (9)[5] give a typical sigmoid curve. From the inflexion point, the pK_a^2 value of −10.1 is obtained as a first approximation.[6] Application of the convergence method of Arnett and Wu (15) to these data yields a pK_a^2 of −10.19, ε_{BH^+} (460 mμ) 3.95×10^4, and $\varepsilon_{BH_2^{++}}$ (460 mμ) 1.05×10^4.

TABLE I

Molar extinction data of 4-hydroxyazobenzene for pK_a^2 determination

Weight % H_2SO_4	H_0	$\varepsilon^{460} \times 10^4$
91.66	−8.50	3.75
95.99	−9.00	3.72
97.80	−9.33	3.60
98.92	−9.68	3.30
99.37	−9.94	3.00
99.59	−10.10	2.75
99.83	−10.42	2.00
99.94	−10.82	1.57
99.99	−11.06	1.53
100.22	−11.45	1.50

4-Hydroxyazobenzene-4′-sulfonic Acid.

The protonation behavior of 4-hydroxyazobenzene-4′-sulfonic acid in the dilute acid region has been examined by Reeves (16). The pK_a for protonation of the azo function is reported as −1.45, λ_B is 350 mμ ($\varepsilon = 2.54 \times 10^4$) and λ_{BH^+} is 464 mμ ($\varepsilon = 5.08 \times 10^4$), in aqueous medium. In the present work spectral examination of this compound was extended to the 90–100% H_2SO_4 region. The spectra were stable except in the highest acid concentrations, where slow changes were observed which can be ascribed to a second sulfonation process. This is described in detail subsequently (11). Initial, zero-time, spectra could hence be obtained with good precision with this substrate. Some of the resulting spectra are reproduced in Fig. 2 and are seen to exhibit reasonably good isosbestic point behavior (442 mμ). The 420 mμ absorption at the highest acid concentration is ascribed to the diprotonated species.

For determination of the pK_a^2, absorbance data were measured at 465 mμ and at 420 mμ as a function of acid concentration. These data are

[5]Since the equilibrium measured here is between a monoprotonated and a diprotonated species, the H_+ acidity function should, strictly, be used. H_+ data in the 100% H_2SO_4 region are apparently not available but indicator measurements in 30–55% and 75–95% H_2SO_4 (13*a*) indicate that the two acidity functions are parallel over these acid regions (see also reference 13*b*). However other work (14) suggests that there may be no unique H_+ function applicable to the protonation of all monocationic substrate types. In the present study a test for Hammett base behavior was made by means of log [ionization ratio (I)] vs. H_0 plots. (I values were calculated using extinction coefficients ε_{BH^+} and $\varepsilon_{BH_2^{++}}$ given by the Arnett–Wu (15) procedure; the log I vs. H_0 plots excluded points falling outside the limits log $I = \pm 1$). For 4-hydroxyazobenzene the slope of the log I vs. H_0 plot was 1.3. In the case of 4-hydroxyazobenzene-4′-sulfonic acid the corresponding slope was 1.2. The deviation of these slopes from unity suggests that these substrates may not be ideal Hammett bases (see also reference 16).

Can. J. Chem. Downloaded from www.nrcresearchpress.com by 210.87.254.105 on 09/05/12
For personal use only.

Can. J. Chem. Downloaded from www.nrcresearchpress.com by 210.87.254.105 on 09/05/12
For personal use only.

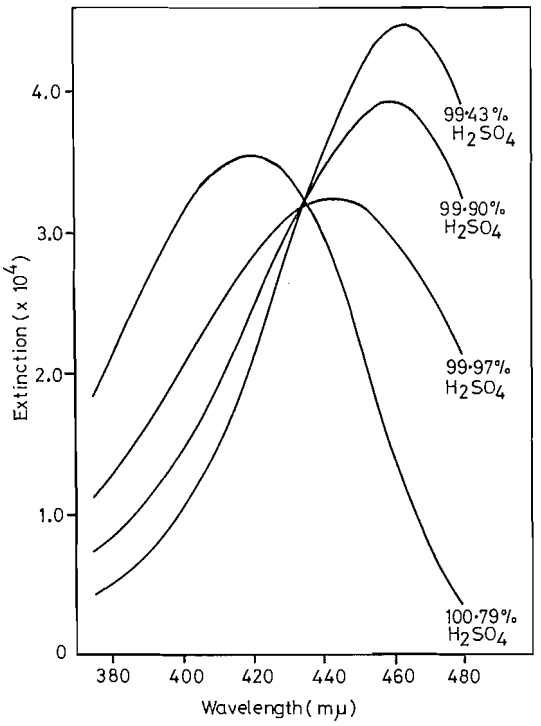

FIG. 2. Spectra of 4-hydroxyazobenzene-4′-sulfonic acid near 100% H_2SO_4 showing mono- and diprotonation.

given in Table II. The plot of the extinctions as a function of H_0[5] gives rise to typical sigmoid curves, from which a visual value of pK_a^2 −11.0 is obtained.[6] Application of the Arnett–Wu method (15) to the 420 mμ data gave pK_a^2 −11.11, ε_{BH^+} 2.10 × 10^4 and $\varepsilon_{BH_2^{++}}$ 3.87 × 10^4.

Discussion

The basic centre in the first protonation of 4-hydroxyazobenzene and related compounds is generally (5,17,18) taken to be the β-nitrogen, in accord with resonance stabilization of charge at that position:

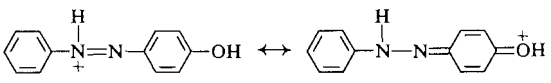

The second equilibrium protonation which is observed in concentrated acid media may occur

[6]The figure showing molar extinction as a function of H_0 is deposited with the Depository of Unpublished Data, National Science Library, National Research Council, Ottawa, Canada. Photocopies may be obtained upon request.

TABLE II

Molar extinction data of 4-hydroxyazobenzene-4′-sulfonic acid for pK_a^2 determination

Weight % H_2SO_4	H_0	$\varepsilon^{465} \times 10^4$	$\varepsilon^{420} \times 10^4$
54.20	−3.83	4.65*	2.20*
89.30	−8.19	4.63	2.12
97.80	−9.32	4.66*	2.15*
99.43	−9.98	4.43	2.07
99.83	−10.42	4.37	2.31
99.90	−10.59	3.88	2.41
99.94	−10.82	3.62	2.72
99.97	−10.99	2.83	2.81
100.03	−11.17	1.61	3.05
100.18	−11.41	1.16	3.46
100.79	−11.76	1.13	3.53

*With these exceptions, all determinations were done from the same stock solution as described in Experimental. (The exceptions noted were determined on individually prepared substrate solutions.)

on aromatic carbon, to give a delocalized structure such as **1**, or on the phenolic oxygen in which case the localized structure **2** results.

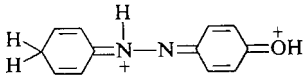

1

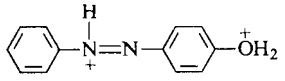

2

Aromatic ring protonation of alkyl benzenes such as mesitylene in HF—BF_3 (19) or HSO_3F (20) is well established. Carbon protonation is also observed with phloroglucinol (and its alkyl ethers) in fluorosulfonic acid or aqueous perchloric acid (21,22):

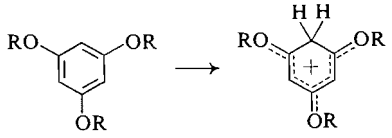

The site of protonation in these instances is given by nuclear magnetic resonance (n.m.r.) evidence. These processes are also characterized by the appearance in the ultraviolet (u.v.) spectrum of a new absorption at ca. 350 mμ. For phenol, anisole, and the dialkoxy analogues the protonation process in aqueous acid is less clear and both O- and C- protonation have been suggested to occur by different workers (14,21,23,24).

If the second protonation of 4-hydroxyazobenzene had occurred on carbon to give (**1**) then

TABLE III

Spectral relationships for first and second protonation equilibria*

Substrate	λ_B mμ	pK_a^1	λ_{BH^+} mμ	pK_a^2	$\lambda_{BH_2^{++}}$ mμ
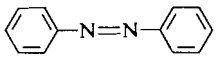	317	−2.48	424	—	—
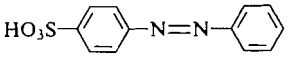	322	−3.13	418	—	—
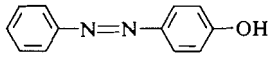	348	−0.93	460	−10.19	426
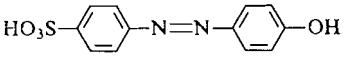	350	−1.45	465	−11.11	420

*The origin of the pK_a^1 data in this Table has been given in the main text. The λ values corresponding to these pK_a^1 data are from the same references or were redetermined in the present work.

the π-electron distribution should have been perturbed considerably and one would have expected a spectral shift in the u.v.–visible region to longer wavelength, by analogy with the other aromatic compounds discussed above. On the other hand protonation of the phenolic oxygen, by removing the p-electrons of oxygen from the aromatic resonance system, should result in a dicationic species (**2**) which is iso-π-electronic with the protonated azobenzene cation. The absorption of the latter (424 mμ) is in fact very close to the absorption of the observed diprotonated species (426 mμ). This is taken as evidence that the second conjugate acid of 4-hydroxyazobenzene has structure **2**.[7]

[7]The possibility that the second protonation occurs on the azo group, to give structure **3**, may also be considered. However in that case, structure **4** should be an important contributor, by analogy with monoprotonated 4-hydroxyazobenzene. Consequently one would expect

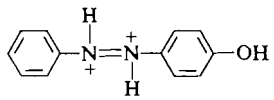

3

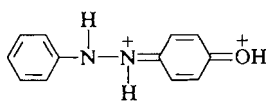

4

diprotonated 4-hydroxyazobenzene to have its absorption maximum largely unchanged from the monoprotonated form, which is not the case. A noteworthy point is that azobenzene itself apparently does not undergo a second protonation even in 100 % H_2SO_4, which suggests that protonation of both nitrogens of the azo function is relatively unfavorable.

The introduction of a sulfonic acid group into an aromatic nucleus generally affects only slightly the longer wavelength absorption of the parent compound (16,25). This is borne out in the present series by the absorptions of azobenzene and its para sulfonic acid derivative, both in the neutral and in the protonated states (Table III). Consequently, the spectral behavior of 4-hydroxyazobenzene and of 4-hydroxyazobenzene-4′-sulfonic acid on protonation is also expected to be similar. The data of Table III show that there is in fact such similarity in the absorptions of the corresponding neutral, the monoprotonated, and the diprotonated species. In view of the previous discussion and by analogy with the iso-π-electronic system of monoprotonated azobenzene, the site of the second protonation in 4-hydroxyazobenzene-4′-sulfonic acid is also indicated to be the phenolic oxygen.

The magnitude of the various pK values, as well as the differences therein, may be commented on briefly. The relevant data are given in Table III. Comparison of azobenzene with its para sulfonic acid derivative shows that introduction of the sulfonic acid group leads to a decrease in the pK_a ($\Delta pK_a^1 = 0.65$). For the 4-hydroxy analogues there is a similar decrease in the first protonation equilibria ($\Delta pK_a^1 = 0.52$), but a slightly larger decrease in the second protonation equilibria ($\Delta pK_a^2 = 0.92$). The larger difference in the pK_a^2 values is presumably the result of the lower overall electron densities corresponding to the second protonation. Perhaps the most striking result of the present data is that in order to effect a second protonation of these substrates the acidity of the medium must be increased, over

Can. J. Chem. Downloaded from www.nrcresearchpress.com by 210.87.254.105 on 09/05/12
For personal use only.

Can. J. Chem. Downloaded from www.nrcresearchpress.com by 210.87.254.105 on 09/05/12
For personal use only.

that required for the first protonation, by some 9–10 H_0 units (see also references 14,26).

Experimental

Materials

4-Hydroxyazobenzene (Eastman) was recrystallized from 40 % ethanol, m.p. 154.5–155.5°, lit. (6) 155–156°. The spectrum in 95 % ethanol showed: ε (348 mμ) = 2.50×10^4; ε (236 mμ) = 1.23×10^4. 4-Hydroxyazobenzene-4′-sulfonic acid (Eastman) was recrystallized from 75 % ethanol and dried over P_2O_5 at 120°/0.1 mm for 24 h, m.p. above 200° (decomp.)

Anal. Calc. for $C_{12}H_{10}N_2O_4S$: C, 51.80; H, 3.60; S, 11.51. Found: C, 51.92; H, 3.90; S, 11.50.

The aqueous spectrum showed: ε_{max} (350 mμ) = 2.40×10^4; lit. (15), ε_{max} (350 mμ) = 2.54×10^4.

Analytical Method

Sulfuric acid solutions less concentrated than 96% were obtained by dilution of 96% Fisher Reagent Grade acid. More concentrated acid solutions were prepared by addition of Fisher 30% SO_3 fuming acid to the 96% H_2SO_4. Concentrations in the 90–100% region were determined by the conductivity method described by Gillespie (27) and Lichty (28), at 25.00 ± 0.02°. The solutions were stored and transferred under nitrogen. Acids of concentration less than 90% were standardized volumetrically. Acid concentrations were expressed as per cent by weight.

pK_a Determinations

The spectral measurements were made on a Unicam SP800B or on a Bausch and Lomb Spectronic 600 spectrophotometer. The latter instrument was used mainly for absorbance measurements at constant wavelength, as recorded on a Sargent SRL Recorder. Absorbance measurements for pK determinations were taken in thermostated cells at 25°.

For determination of the first equilibrium protonation of 4-hydroxyazobenzene, solutions were prepared by addition of 1.25 ml aliquots of a 1.80×10^{-3} M solution of 4-hydroxyazobenzene in dioxane into 25 ml volumetric flasks followed by dilution with acid solutions of appropriate strengths. Absorbance data at 348 mμ and at 460 mμ were taken over the range 0.53–53.2% H_2SO_4 and plotted against H_0 to give the pK_a. The Table of data and resulting plots are deposited and available on request.[6]

Study of the second equilibrium protonation of 4-hydroxyazobenzene was complicated by the concurrent sulfonation which occurs in the 90–100% H_2SO_4 region. The extent to which this rate process interferes is seen by the following times for one half-life of reaction: 38 h in 91.66% H_2SO_4; 160 min in 97.80% H_2SO_4; 4.5 min in 100.02% H_2SO_4. Solutions were generally prepared by addition of 0.1–1.0 mg samples of substrate, weighed on a Cahn M-10 Electrobalance, to 25–100 ml of sulfuric acid. For the reconstituted curves (Fig. 1) spectral sweeps between 400 and 480 mμ were extrapolated at 10 mμ intervals to zero time. For the pK_a determination the absorbance at 460 mμ was followed with time in the various acid media and extrapolated to zero time.

Determination of the second equilibrium protonation of 4-hydroxyazobenzene-4′-sulfonic acid was not appreciably affected by sulfonation, since the highest rate of this process in 100.79% H_2SO_4 corresponded to a half-life of 200 min. While some of the measurements with this substrate were made on individually weighed samples as previously, the general method was as follows. Standard solutions of this substrate were obtained by evaporation to dryness of 1.00 ml samples of a 1.78×10^{-3} M ethanolic solution in 50 ml volumetric flasks followed by addition of acid. The spectra of the various acid solutions were recorded within 5 min over the region 375–480 mμ (Fig. 2) and treated in the manner indicated.

The reversibility of the second equilibrium protonations was tested as follows. A 0.10 ml portion of a 9.52×10^{-3} M solution of 4-hydroxyazobenzene in ethanol was placed in a 25 ml volumetric flask and evaporated to dryness. The residue was dissolved in 25 ml of 100.02% H_2SO_4 at 25°, the resulting solution quickly transferred to a 10 mm cell and the spectrum recorded (1.25 min after the initial mixing): λ_{max} = 424 mμ, $\varepsilon_{max} = 3.08 \times 10^4$. Simultaneously (2.5 min after the initial mixing), 3 ml of the solution of 4-hydroxyazobenzene in 100.02% H_2SO_4 was added with a pipette to 3 ml of 78.5% H_2SO_4 contained in a 20 mm cell and the spectrum taken: λ_{max} = 461 mμ, $\varepsilon_{max} = 3.85 \times 10^4$. Noting that 4-hydroxyazobenzene undergoes a sulfonation reaction in the 100.02% H_2SO_4 medium with a half-life of 4.5 min, one can estimate thatabo ut 15% reaction has occurred by the time the first spectrum was run and about 30% reaction by the time the dilution was made. Allowing for these extents of reaction, the λ_{max} and ε_{max} values obtained agree satisfactorily with those expected on the basis of about 90% diprotonation of 4-hydroxyazobenzene in the 100.02% H_2SO_4 solution and less than 10% diprotonation in the 90% H_2SO_4 solution obtained on dilution (Fig. 1, Table I).

The reversibility test with 4-hydroxyazobenzene-4′-sulfonic acid was performed similarly but was not complicated by a sulfonation process, which is relatively much slower with this substrate. The dilution was performed on a solution of the substrate in 100.71% H_2SO_4 (λ_{max} = 419 mμ, $\varepsilon = 3.32 \times 10^4$ in 10 mm cell), using 89.3% H_2SO_4 as the diluent (1:1). The resulting solution (run in 20 mm cell) had its absorption shifted to 464 mμ ($\varepsilon = 4.59 \times 10^4$), in accord with a shift in equilibrium on dilution to the monoprotonated form (Fig. 2, Table II).

Acknowledgments

We thank the National Research Council of Canada for financial support of this research. Discussions with Dr. R. J. Gillespie are also acknowledged. W.M.J.S. and A.D. are the recipients of Ontario Graduate Fellowships.

1. E. Buncel and B. T. Lawton. Chem. Ind. London, 1835 (1963).
2. E. Buncel and B. T. Lawton. Can. J. Chem. **43**, 862 (1965).
3. E. Buncel, A. Dolenko, I. G. Csizmadia, J. Pin-

COCK, and K. YATES. Tetrahedron, **24**, 6671 (1968); P. H. GORE. Chem. Ind. (London), 191 (1959).
4. E. BUNCEL. Mechanisms of molecular migrations. *Edited by* B. S. Thyagarajan. John Wiley and Sons, Inc., New York. 1968.
5. I. M. KLOTZ, H. A. FIESS, Y. Y. CHEN HO, and M. MELLODY. J. Amer. Chem. Soc. **76**, 5136 (1954).
6. S.-J. YEH and H. H. JAFFÉ. J. Amer. Chem. Soc. **81**, 3274 (1959).
7. L. MICHAELIS and S. GRANICK. J. Amer. Chem. Soc. **64**, 1861 (1942).
8. L. P. HAMMETT and A. J. DEYRUP. J. Amer. Chem. Soc. **54**, 2721 (1932).
9. M. A. PAUL and F. A. LONG. Chem. Rev. **57**, 1 (1957).
10. D. S. NOYCE and M. J. JORGENSON. J. Amer. Chem. Soc. **83**, 2525 (1961).
11. W. M. J. STRACHAN and E. BUNCEL. Can. J. Chem. In press.
12. C. T. DAVIS and T. A. GEISSMAN. J. Amer. Chem. Soc. **76**, 3507 (1954).
13. (*a*) T. G. BONNER and J. C. LOCKHART. J. Chem. Soc. 364 (1957); (*b*) P. VETESNIK, J. BIELAVSKY, and M. VECERA. Collect. Czech. Chem. Commun. **33**, 1687 (1968).
14. P. J. BRIGNELL, C. D. JOHNSON, A. R. KATRITZKY N. SHAKIR, H. O. TARHAN, and G. R. WALKER J. Chem. Soc. B, 1233 (1967).
15. E. M. ARNETT and C. Y. WU. J. Amer. Chem. Soc. **82**, 5660 (1960).
16. R. L. REEVES. J. Amer. Chem. Soc. **88**, 2240 (1966).
17. E. SAWICKI. J. Org. Chem. **22**, 365 (1957).
18. F. GERSON and E. HEIBRONNER. Helv. Chim. Acta, **45**, 51 (1962).
19. C. MACLEAN and E. L. MACKOR. Discuss. Faraday Soc. **34**, 165 (1962) and previous papers in series.
20. T. BIRCHALL and R. J. GILLESPIE. Can. J. Chem. **42**, 502 (1964).
21. T. BIRCHALL, A. N. BOURNS, R. J. GILLESPIE, and P. J. SMITH. Can. J. Chem. **42**, 1433 (1964).
22. A. J. KRESGE, G. W. BARRY, K. R. CHARLES, and Y. CHIANG. J. Amer. Chem. Soc. **84**, 4343 (1962).
23. K. YATES and H. WAI. Can. J. Chem. **43**, 2131 (1965).
24. A. J. KRESGE and L. E. HAKKA. J. Amer. Chem. Soc. **88**, 3868 (1966).
25. V. GOLD and F. L. TYE. J. Chem. Soc. 2172 (1952).
26. T. G. BONNER and J. C. LOCKHART. J. Chem. Soc. 3852 (1958).
27. R. J. GILLESPIE and S. WASIF. J. Chem. Soc. 204 (1953); R. J. GILLESPIE, J. V. OUBRIDGE, and C. SOLOMONS. J. Chem. Soc. 1804 (1957).
28. D. M. LICHTY. J. Amer. Chem. Soc. **30**, 1834 (1908).

Can. J. Chem. Downloaded from www.nrcresearchpress.com by 210.87.254.105 on 09/05/12
For personal use only.

Alkylation of solid sodium and lithium 2,6-dimethylphenoxide with methyl halide vapor[1]

DAVID Y. CURTIN AND ALLAN R. STEIN[2,3]

Department of Chemistry and Chemical Engineering, University of Illinois, Urbana, Illinois, 61801

Received May 20, 1969

The generally accepted hypothesis that the alkylation of metal phenoxides is forced to occur at the *ortho*-carbon in heterogeneous reactions was investigated. Methyl iodide and bromide vapor reacts with crystalline sodium and lithium 2,6-dimethylphenoxides to give *ortho*-carbon/oxygen alkylation ratios not unlike those obtained in sealed tube reactions with an excess of methyl iodide or with added toluene as solvent. However, an unprecedented amount of *para*-methylation also occurred. The implications of these and related observations in other systems are discussed.

Canadian Journal of Chemistry, 47, 3637 (1969)

Can. J. Chem. Downloaded from www.nrcresearchpress.com by 210.87.254.5 on 09/05/12
For personal use only.

The reaction of alkyl halides with the sodium or lithium salt of 2,6-dimethylphenol (**1**) has been found to provide a practical single-step synthesis of certain cyclohexadienones (1, 2). The reaction has the disadvantage that the dienone formed by C-alkylation is accompanied by large amounts of the alkyl aryl ether formed by O-alkylation. Kornblum and Lurie (3) explained alkylation on carbon by postulation of a reaction of alkyl or benzyl chloride at the surface of solid sodium or potassium *p-t*-octylphenoxide.[4] Alkylation of dissolved or dissociated phenoxide would be exclusively at oxygen. This postulate has been accepted by other authors (4) without further experimental verification.

This explanation for carbon versus oxygen alkylation suggests that synthetically useful control of reaction products might result if the reaction could be carried out under conditions that would favor reaction at crystal surfaces to the greatest possible extent. Thus, we were led to examine the reaction of methyl iodide vapor with the solid lithium and sodium salts of 2,6-dimethylphenol, in the hope that, under these extreme conditions, there would be a "pure" heterogeneous reaction giving exclusively or predominately 2,6,6-trimethylcyclo-2,6-hexadienone (**2**). Such a study might also, we felt, shed light upon the validity and applicability of the explanation (3).

Experimental

Lithium and sodium 2,6-dimethylphenoxides (**1**) were prepared by reacting the appropriate metal with the phenol in stirred toluene at reflux (2). After removal of the toluene at 100° (18 mm pressure), the salt was ground in an agate mortar (in a dry box with a nitrogen atmosphere) and the resulting fluffy white solid stored in the dry box in a flask wrapped in aluminum foil to exclude light.

In order to favor heterogeneous reaction to the greatest possible extent, methyl iodide vapor had to be brought into contact with the phenol salt **1** under conditions in which the alkylation products would be vaporized, that is with a temperature greater than about 100° at 15 mm pressure. This was accomplished with an 8" heated column which was packed in a dry box with the phenol salt dispersed either among 12–14 small wads of oven dried glass wool or glass helices.

The column, which had been loosely packed to permit passage of vapor, was equilibrated at the desired temperature in a nitrogen atmosphere and then was attached at one end to a flask containing the methyl iodide or bromide cooled in dry ice–isopropyl alcohol and at the other to an empty flask.

After evacuation the system was sealed and the cooling bath moved to the empty flask. The methyl halide then evaporated, passed through the heated column of phenol salt and condensed again in the cold flask. In addition alkylation products passed from the heated zone and accumulated in the cold flask. This process could be repeated indefinitely by changing the cooling bath from one flask to the other. At the temperature of the column, the vapor pressure of methyl iodide was about 10^4–10^5 times the measured pressure in the system.

Reaction mixtures were analyzed by evaporation of the methyl iodide or bromide from the alkylation products and analysis by vapor phase chromatography (v.p.c.) employing an Aerograph model A–350–B dual column instrument with a 10 ft column packed with Apiezon 1 (distributed by Shell Oil Co.) on silanized Chromosorb

---

[1]Taken from the Ph.D. Thesis of Allan R. Stein, University of Illinois, Urbana, Illinois. 1964.

[2]Firestone Tire and Rubber Co. Fellow, 1961–1962.

[3]To whom correspondence should be addressed. Current Address: Department of Chemistry, Memorial University of Newfoundland, St. John's, Newfoundland.

[4]A heterogeneous reaction in the usual sense need not be involved. Sub-visible ion aggregates, or possibly even simple ion pairs, would suffice as the "heterogeneous" phase.

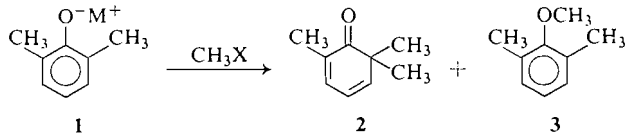

1 2 3

TABLE I

Vapor-solid methylation of alkali metal 2,6-dimethylphenoxide

Metal ion	Temperature °C	Equivalents of CH_3I	Number of passes	Percent* reaction	C/O† ratio
Na^+	208 ± 5	11	2	76	0.04
Na^+	195 ± 5	33	6	82	0.08(0.00)
Na^+	183 ± 5	20	2	51	0.05
Na^+	100 ± 3	17	1	0.0	—
Li^+	250 ± 8	25	1	10.2	0.78(>0.75)‡
Li^+	226 ± 7	31	12	2.5	0.74(2.0)
Li^+	175 ± 5	30	12	0.4	0.43(0.23)
Li^+	150 ± 4	19	1	0.0	—
Li^+	186 ± 5	28§	25	1.5	0.18

*Based upon analysis of the residue from the methyl iodide flasks (see Experimental).
†*Ortho*-Carbon/Oxygen alkylation ratio. (Where determined, the *para*-C/O ratio appears in brackets).
‡This is the minimum *para*-C/O ratio based upon the amount of 2,4,6-trimethylphenol in the residue from the methyl iodide. Because of the reaction sequence shown in Scheme 1, much of the *para*-methylated product would remain in the column. Since considerable charring and decomposition had occurred at this high temperature, no attempt was made to recover the phenols from the column. An upper limit on the *para*-C/O ratio of 6.5 can be calculated on the assumption that no moisture entered the system so that any 2,6-dimethylphenol in the methyl iodide residue would have arisen from the above phenoxide exchange.
§Methyl bromide replaced methyl iodide.

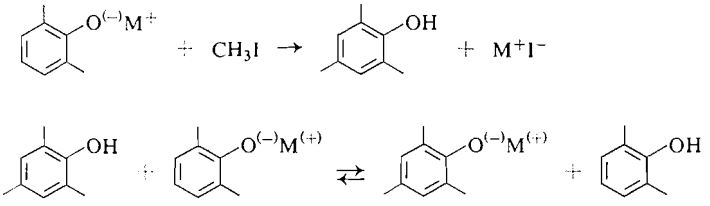

SCHEME 1

W (distributed by Johns Manville Co. Ltd.) at 173° and with a helium flow rate of 60 cm^3/min. Quantitative estimates were made by comparison of peak areas and retention times with those of authentic samples of the products.[5]

In a number of cases, the residual phenoxide salt was removed from the column materials by washes of aqueous base, and the phenolics recovered by ethereal extraction after acidification. The concentrated extracts were analyzed in the same way as the residue from the methyl iodide or bromide.

Description of the sealed-tube reactions in which excess methyl iodide, either neat or diluted with toluene, was reacted with metal phenoxides was given in previous papers (1,2).

Some data are reported in Table I.

[5]Additional details are reported in the Thesis of Dr. A. R. Stein[1] available on microfilm from University Microfilms, Ann Arbor, Michigan.

Results and Discussion

At temperatures above 150°, the sodium salt of 2,6-dimethylphenol reacted quite readily to give an *ortho*-carbon/oxygen methylation ratio of 0.06 ± 0.02. Even at 250°, the lithium salt reacted more slowly than the sodium salt did at 180° and at this high temperature considerable charring of the salt occurred. For the lithium salt the *ortho*-C/O ratio changed from 0.43 at 175° to 0.78 at 250°.

For the sodium salt, the *ortho*-C/O values of 0.06 ± 0.02 over a hundred degree temperature range are equivalent to the 0.04–0.1 values obtained in the sealed-tube reactions of excess methyl iodide with solid sodium 2,6-dimethylphenoxide (**1**), despite the change in medium and of "concentration" of methyl iodide.

Can. J. Chem. Downloaded from www.nrcresearchpress.com by 210.87.254.5 on 09/05/12
For personal use only.

Can. J. Chem. Downloaded from www.nrcresearchpress.com by 210.87.254.5 on 09/05/12
For personal use only.

Sealed-tube methylations of the lithium salt gave the following *ortho*-C/O ratios at the temperatures indicated (1): 130°, 0.50; 180°, 0.39; 200°, 0.15.[6] These values are not radically different from those we report for the vapor–solid reaction: 175°, 0.43; 190°, 0.50; 226°, 0.74; 250°, 0.78. Synthetically, then the vapor–solid alkylation of phenoxides has little advantage over the much more convenient sealed-tube reaction for the preparation of dienones.

In the methylation of the lithium salt, the unexpected (1–3) *para*-alkylation is a major competing reaction. While with the sodium salt at 195°, no 2,4,6-trimethylphenol was detected, even at 175°, the lithium salt gives a *para*-C/O ratio of 0.23 (vs the *ortho*-C/O ratio of 0.43). Also the *para*-C/O ratio increases much more rapidly with temperature than does the *ortho*-C/O ratio so that its value is more than two and one half times the *ortho*-value at 226°. In the earlier sealed-tube studies, no *para*-alkylation had been detected but in most cases no attempt was made to detect such products. For comparison purposes we repeated the sealed-tube reaction of excess methyl iodide with lithium 2,6-dimethylphenoxide at 200 ± 5° for 25 h. The *ortho*-C/O was 0.126[6], the *para*, 0.30, so that in the sealed-tube liquid–solid phase reactions as well as in the vapor–solid phase reactions reported here, *para*-methylation is a major reaction at higher temperatures.

We have no direct evidence that the reaction was, in fact, heterogeneous and cannot exclude the possibility that it occurred in microscopic pockets of a condensed phase. Similarly it is not clear how much, if any, of the alkylations carried out with suspensions of phenol salts in non-polar solvents proceeds by a heterogeneous path.[4]

The conclusion which seems inescapable however, is that either reaction at the crystal surface is so slow that it is not able to compete with reaction in the condensed phase or else it leads to product ratios which are not dramatically different from the ratios obtained from the reaction of simplet ion aggregates such as ion pairs.

The study by Labes and Blakeslee (5) of the isomer distribution formed in the halogenation of solid sodium phenoxide with gaseous chlorine and bromine is of interest. They found that, as in our study, the isomer distribution was not significantly different from that obtained in solution. Again it could not be ascertained whether the reaction occurred in a liquid phase existing at the surface or whether a solid–gas reaction occurred and gave the same ratio as that in solution. Another interesting attempt to find evidence for control of the direction of a reaction by carrying it out at a crystal surface of the reaction of asymmetric crystals of methanesulfinic acid with diazomethane (6). The desired asymmetric induction which might have been found if methylation had occurred in the asymmetric environment of the crystal surface was not obtained.[7]

These accumulated examples of the difficulty of diverting the course of a reaction by inducing it to occur at a crystal surface suggest that the postulation of such an effect (3) in the alkylation of phenol salts in a heterogeneous medium should be treated with caution. This conclusion is reinforced by the demonstration by Smith and Milligan (7) that results of product studies in the alkylation of oxime salts which had previously been attributed to heterogeneous reaction (8) could quite satisfactorily be accommodated by homogeneous reaction involving no aggregates larger than ion pairs.

1. D. Y. Curtin and R. R. Fraser. J. Amer. Chem. Soc. **80**, 6016 (1958); R. R. Fraser. Ph.D. Thesis, University of Illinois, Urbana, Illinois. 1958.
2. D. Y. Curtin and A. R. Stein. *In* Organic syntheses. *Edited by* E. J. Corey. John Wiley and Sons, Inc., New York. 1966, **46**. p. 115 ff.
3. N. Kornblum and A. P. Lurie. J. Amer. Chem. Soc. **81**, 2705 (1959). See A. R. Stein. Can. J. Chem. **43**, 1493 (1965); **43**, 1508 (1965) for more recent references.
4. See for example R. Gompper. Angew. Chem. Intern. Ed. Engl. **3**, 560 (1964).
5. M. M. Labes and H. W. Blakeslee. J. Org. Chem. **32**, 1277 (1967).
6. F. Wudl, D. A. Lightner, and D. J. Cram. J. Amer. Chem. Soc. **89**, 4099 (1967).
7. S. G. Smith and D. V. Milligan. J. Amer. Chem. Soc. **90**, 2393 (1968).
8. P. A. S. Smith and J. E. Robertson. J. Amer. Chem. Soc. **84**, 1197 (1962).

[6]The *ortho*-C/O methylation ratio reported is a minimum value for the sealed-tube reactions, because, especially at the higher temperatures, considerable resinification occurred. The dienone (**2**) would be expected to be the least thermally stable of the major reactants and products present. Such resinification probably explains the lower *ortho*-C/O ratio for the sealed-tube reactions since here, the dienone would be held at the reaction temperature for the duration of the reaction and not removed as it formed. The dienone losses in resinification, are, of course, more significant at higher temperatures and account for the apparently decreasing C/O ratio as the temperature increases.

[7]We have had a similar lack of success in attempts to obtain optically active products from the reaction of an asymmetric crystal of benzil with lithium reagents or metal hydrides (P. E. Bender, unpublished work).

Can. J. Chem. Downloaded from www.nrcresearchpress.com by 210.87.254.42 on 09/05/12
For personal use only.

Condensation de la poly-L-lysine et de la poly-L-ornithine avec des dérivés de bases puriques et de sulfamides[1]

LOUIS BERLINGUET ET JACKY GAUTIER
Département de Biochimie, Faculté de Médecine, Université Laval, Québec, Québec

Reçu le 24 février 1969

Free ε-amino groups of poly-L-lysine and poly-L-ornithine were alkylated in aqueous solution with 6-chloropurine and 6-chloropurine-riboside, were acylated with 4-acetylamino benzene sulfonyl chloride, and were condensed with *N*-(4-acetylamino benzene sulfonyl)-glycine using carbodiimide method. Approximately 50% of the free amino groups of the basic polypeptides were substituted. The same method was used to prepare poly-α-amino acids bearing radioactive substituants.

Les groupements ε-aminés des chaînes latérales de la poly-L-lysine et de la poly-L-ornithine ont été: alkylés en milieu aqueux par la 6-chloropurine et la 6-chloropurine riboside; acylés par le chlorure de l'acide 4-acétylamino benzène sulfonique; et condensés avec la *N*-(4-acétylamino benzène sulfonyl)-glycine par la méthode du carbodiimide. Ces analyses subséquentes montrèrent que la substitution s'opérait sur environ 50% des ε-NH_2 des polymères basiques. Nos méthodes ont été adaptées à des micro quantités pour la préparation de ces mêmes poly-α-amino acides porteurs de substituants radioactifs.

Canadian Journal of Chemistry, 47, 3641 (1969)

Introduction

La polymérisation des anhydrides de Leuch (1) dans des conditions variées (2) permet d'obtenir des acides poly-α-aminés possédant des propriétés biologiques remarquables (3). Nous avons pensé fixer sur ces macromolécules des composés doués d'activités pharmacologiques; aussi, avons-nous retenu des polymères formés à partir d'acides aminés basiques (lysine et ornithine), puisque les groupements ε-NH_2 de leurs chaînes latérales peuvent être facilement alkylés ou acylés par des dérivés halogénés de purines ou par des dérivés de sulfamidés. La synthèse de telles macromolécules ainsi modifiées présente un grand intérêt théorique, car, en plus de leur action pharmacologique propre, nous pouvons espérer que la coupure progressive des liens peptidiques puisse libérer, de façon lente, des courts peptides et des molécules possédant des propriétés biologiques différentes de celles des composés de départ.

Résultats et discussion

Condensation de la L-lysine et de la L-ornithine avec les dérivés halogénés de bases puriques

Carter (4) avait déjà préparé la ε,*N*-(6-purinyl)-L-lysine par condensation directe de la L-lysine avec la 6-chloropurine dans un tampon carbonate; il avait montré que la substitution portait surtout sur le groupement ε-NH_2 de l'acide aminé, cependant un fort pourcentage de L-lysine restait inchangé. Lettré (5) reprit cette synthèse en protégeant au préalable les groupements α-aminés par formation du dérivé dicétopipérazine de la L-lysine et de la L-ornithine, suivant la méthode de Fisher (6).

Afin d'avoir des produits de référence en vue de l'identification par chromatographie sur papier des produits d'hydrolyse de nos polymères, nous avons synthétisé la ε,*N*-(6-purinyl) et la ε,*N*-(6-purinylriboside) dérivant de la L-lysine et de la L-ornithine suivant une méthode inspirée de Ward *et al.* (7). Nous avons de plus fait cette synthèse en utilisant soit les chélates cuivriques des acides aminés (8, 9), soit les dérivés α,*N*-carbobenzoxy, dont l'obtention est plus facile que celle des dérivés dicétopipéraziniques. Ces synthèses nous ont permis d'obtenir de très bons rendements, bien qu'il subsistât toujours dans nos préparations, des traces d'acide aminé non substitué; une purification subséquente par passage sur colonne Dowex-2-X-8 est nécessaire pour obtenir les dérivés purs (7).

La condensation des poly-α-aminoacides basiques avec des dérivés halogénés de purines présente peu de difficultés. En effet, seuls les groupements ε-aminés des monomères sont libres et peuvent être substitués. En procédant en milieu aqueux à pH 9, dans le tampon carbonate, nous avons réussit à condenser la 6-chloropurine et la

[1]Une partie de ce travail a été présentée sous forme de note préliminaire dans réf. 16.

Can. J. Chem. Downloaded from www.nrcresearchpress.com by 210.87.254.42 on 09/05/12
For personal use only.

6-chloropurineriboside avec la poly-L-lysine et la poly-L-ornithine. Par dialyse, on récupère la totalité du polymère, mais il se pose cependant un problème théorique quant à l'homogénéité des produits obtenus.

A la limite, on pourrait obtenir un mélange de deux polymères, l'un étant le produit de départ, l'autre le polymère totalement substitué. L'analyse d'un tel mélange donnerait des valeurs de pourcentage d'azote identiques à celles obtenues pour un polymère dont 50% des ε-NH_2 seraient substitués. L'analyse chimique, par la seule détermination du pourcentage d'azote, n'apporte donc pas la mesure de l'homogénéité des polymères résultants de la condensation de la poly-L-lysine ou de la poly-L-ornithine avec des dérivés halogénés de bases puriques. Deux mesures, cependant, nous apportent la certitude que les produits d'alkylation ne sont pas des mélanges mais bien des composés incomplètement substitués:

a) L'électrophorèse sur papier, permet de montrer que le comportement électrophorétique de nos produits est très différent des polymères de départ, et on ne décèle pas la moindre trace de ceux-ci.

b) Une preuve, plus sensible, nous est fournie par des essais biologiques. Il a en effet été démontré (3) que les poly-α-aminoacides de départ s'avèrent très toxiques chez les souris. Nos produits alkylés ont une toxicité beaucoup plus faible, environ cinq fois inférieure à celle des polymères de départ.

Condensation de la L-*lysine et de la* L-*ornithine avec des dérivés de sulfamides*

En protégeant les α-NH_2 de la L-ornithine et de la L-lysine par formation des chélates cuivriques (8, 9), nous avons opéré la condensation directe en milieu aqueux des groupements ε-NH_2 libres avec le chlorure de l'acide 4-acétylaminobenzène sulfonique, suivant une méthode inspirée de Normand (10). Le rendement obtenu pour cette condensation a été faible, environ 60% de la L-lysine restant sous sa forme initiale.

Nous avons effectué la condensation, en milieu aqueux (10), des acides poly-α-aminés avec le chlorure de l'acide 4-acétylaminobenzène sulfonique. Cette condensation s'effectue avec de bons rendements, et si l'on base les calculs sur la quantité de polymère modifié obtenue, environ 45% des groupements ε-NH_2 ont été acylés. Cette méthode a été adaptée pour la condensation du dérivé sulfamidé marqué au ^{14}C sur le noyau benzènique.

Nous avons aussi condensé la poly-L-lysine et la poly-L-ornithine avec la *N*-(4-acétylaminobenzène sulfonyl) glycine par la méthode du *N*,*N*′-dicyclohexylcarbodiimide (11). Ici encore, environ 55% des ε-NH_2 du polymère de départ ont été condensés avec le dérivé sulfamidé de la glycine. La même méthode a été employée pour la condensation avec la *N*-(4-acétylaminobenzène sulfonyl) glycine marqué au ^{14}C sur le noyau benzènique.

Lors des hydrolyses effectuées en vue d'identifier les produits de dégradation des polymères substitués, nous avons constaté une fois de plus, la grande résistance aux ions H^+ du lien sulfanilamide (—SO_2—NH—). C'est ainsi que l'hydrolysat acide de la poly-ε,*N*-(4-acétylaminobenzène sulfonyl)-L-lysine contient un mélange de L-lysine et du chlorhydrate de la ε,*N*-(4-aminobenzène sulfonyl)-L-lysine. Ce dernier composé ne peut être hydrolysé qu'en présence d'acide phosphorique pur à 100 °C. Avec la poly-ε,*N*-(4-acétylaminobenzène sulfonyl-*N*-glycyl)-L-lysine, l'hydrolyse par HCl 6 *N* fournit de la L-lysine et le chlorhydrate de la *N*-(4-aminobenzène sulfonyl)-glycine, mais on ne peut déceler la présence de glycine.

Essais biologiques des polymères substitués

Les études biologiques de ces poly-α-aminoacides basiques substitués sur les bactéries, les tumeurs (Sarcoma 180 et Erhlich) ainsi que leur hydrolyse par divers systèmes enzymatiques seront rapportés dans une publication ultérieure.

Partie expérimentale

Produits de départ

Le bromhydrate de la poly-L-lysine a été synthétisé dans nos laboratoires par polymérisation de l'anhydride de la ε,*N*-carbobenzoxy-α-*N*-carboxy-L-lysine suivant la méthode de Katchalski (12). Avant la condensation, le bromhydrate a été neutralisé et dialysé pendant 3 jours contre H_2O avant d'être lyophilisé. Le poids moléculaire moyen de la poly-L-lysine (2), déterminé par viscosimétrie, est d'environ 12 000.

La poly-L-ornithine a été synthétisée dans nos laboratoires par polymérisation de l'anhydride de la δ,*N*-trifluoroacétyl-*N*-carboxy-L-ornithine suivant la méthode de Ariély *et al.* (13). Le poids moléculaire moyen a été calculé à environ 17 500 (viscosimétrie).

Anal. calc. pour $(C_5H_{10}N_2O)_n$: N, 24.5. Trouvé: N, 24.3.

La 6-chloropurine et la 6-chloropurine riboside ont été obtenues de K and K Laboratories.

Le chlorure de l'acide *N*-acétyl sulfonique a été obtenu de Matheson, Coleman and Bell Laboratories.

Can. J. Chem. Downloaded from www.nrcresearchpress.com by 210.87.254.42 on 09/05/12
For personal use only.

La *N*-(4-acétylaminobenzène sulfonyl)-glycine a été synthétisée dans nos laboratoires suivant la méthode de Boganz (14).

L'aniline ^{14}C (u.m.) a été obtenue de New England Nuclear Corporation (act. spé. 4 mC/mmole).

Chromatographie

Dans toutes ces expériences, l'analyse des produits d'hydrolyse a été faite par chromatographie descendante sur papier Whatman No. 4 dans le solvant butanol – acide acétique – H_2O (2:1:1).

Synthèse

Condensation de la L-*lysine avec la 6-chloropurine*

À 267 mg de α,*N*-Cbz-L-lysine (10^{-3} mole) dissous dans 30 ml d'eau ajusté à pH 5 par addition de KOH on ajoute 500 mg (0.004 mole) de carbonate de sodium et 232 mg (1.5×10^{-3}) mole de 6-chloropurine (**3**). Le mélange réactionnel est ensuite chauffé à reflux pendant 3 h. Après refroidissement, le pH de la solution est ajusté à 2 par addition d'acide formique et le produit est recueilli par filtration.

On dissout ensuite le produit sec dans 50 ml d'acide acétique glacial et l'on fait barboter HBr sec pendant 5 min à 40 °C et on laisse à température ambiante pendant 6 h. Le produit est précipité par addition d'éther anhydre, filtré et repris dans un minimum d'eau puis reprécipité dans l'alcool.

Une purification subséquente par passage sur colonne Dowex-2-X-8 est nécessaire pour obtenir le dérivé pur (**7**): rendement 104, 7 mg (42%) λ_{max} 273-274 mμ.

Anal. calc. pour $C_{11}H_{16}N_5O_2$: N, 35.59. Trouvé: N, 35.42.

*Chlorure de l'acide 4-acétylaminobenzène sulfonique marqué au ^{14}C sur le noyau benzènique (**9**)*

L'aniline ^{14}C (13 mg, 0.5 mC) est dissout dans 0.4 ml d'eau contenant 0.02 ml de HCl concentré; on y ajoute 0.05 ml d'anhydride acétique et 20 mg d'acétate de sodium anhydre préalablement dissous dans 0.1 ml d'eau, en agitant vigoureusement pendant 15 min dans un bain de glace. Au mélange ainsi obtenu, on ajoute 97 mg d'aniline non radioactive fraîchement distillée et dissoute dans 6 ml d'eau contenant 0.09 ml de HCl concentré et l'on répète les opérations précédentes. L'addition de 20 ml d'eau contenant 2 ml d'alcool précipite l'acétanilide: rendement 104 mg (72%) p.f. 113–114°.

La chlorosulfonation s'opére dans un erlenmeyer de 5 ml suivant Fieser (15). A 100 mg d'acétanilide ^{14}C, on ajoute 0.25 ml d'acide chlorosulfonique et on laisse la réaction s'opérer à température ambiante pendant 10 min, puis, le mélange réactionnel est chauffé dans un bain-marie à 100° pendant 10 min. Après refroidissement, on ajoute 5 ml d'eau glacée en agitant vigoureusement. Le produit est recueilli par filtration sur büchner: rendement 127.4 mg (68%); act. spé. 3.93 mC/mmole. Le produit obtenu ne donne par chromatographie qu'un seul spot radioactif qui absorbe dans l'ultraviolet.

*Poly-ε,N-(6-purinyl)-*L-*lysine (**7**)*

Après avoir dissous 128 mg de poly-L-lysine (10^{-3} mole équivalent de lysine), dans 30 ml d'eau ajustée à pH 9.5 par addition de KOH, on ajoute 500 mg (0.004 mole) de carbonate de sodium et 232 mg (1.5×10^{-3} mole) de 6-chloropurine (**3**). Le mélange réactionnel est ensuite chauffé à reflux pendant 3 h. Après refroidissement le pH de la solution est ajusté à 2 par addition d'acide formique. Le mélange est ensuite dialysé pendant 3 jours contre l'eau pure et lyophilysé: rendement 148 mg (79%), λ_{max} 203–204; 268–269 mμ.

Anal. calc. pour $(C_{11}H_{14}N_6O)_n$: N, 34.14. Trouvé: N, 28.03.

Anal. calc. pour $(C_6H_{12}N_2O)_n$(poly-L-lysine initiale): N, 21.88. Trouvé: N, 21.77.

L'hydrolyse par HCl 6 *N* pendant 5 h donne un mélange de L-lysine, R_f 0.20 et de ε,*N*-(6-purinyl)-L-lysine, R_f 0.57. Un aliquot de l'hydrolysat a été analysé par chromatographie sur un analyseur d'acides aminés "Technicon". Le dosage quantitatif de la lysine résiduelle montra qu'environ 50% des ε-NH_2 avait été substitués; le calcul fait à partir des pourcentages d'azote nous indiquait une substitution de 55%.

Homogénéité des polymères obtenus

Afin de prouver que les produits obtenus sont homogènes et ne contiennent pas de poly-α-aminoacides initiaux, nous avons utilisés l'électrophorèse sur papier et des essais biologiques.

L'électrophorèse dans le tampon B_2 (pH 8.2) sous une intensité de 10 mA pendant 2 h 30 min (figure 1) nous montre que les polymères obtenus après alkylation ont un comportement électrophorétique très différent des polymères basiques de départ. L'électrophorèse de nos produits nous a permis d'obtenir des bandes révélables aussi bien à la nihydrine qu'á l'ultraviolet (u.v.) et qui restent très près de l'origine, indiquant ainsi que la substitution diminue fortement le caractère basique de la poly-L-lysine ou de la poly-L-ornithine. A aucun moment, nous n'avons pu déceler la présence des deux produits de départ sur les électrophorégrammes des polymères substitués. L'étroitesse des bandes obtenues nous permet de croire à la grande homogénéité de nos produits.

Nous avons aussi déterminé, chez la souris, les LD_{25} de nos produits (tableau I). La poly-L-lysine et la poly-L-ornithine s'avèrent entièrement toxiques chez l'animal, ceci étant plus particulièrement du à la présence des charges résiduelles de ces poly-α-aminoacides. Nous avons vérifié que les réactions d'alkylation qui diminuent le nombre de charges positives des polymères de départ, diminuent fortement la toxicité.

L'électrophorèse et les essais de toxicité réalisés avec nos polymères de condensation confirment ce que l'analyse chimique laissait entrevoir. Les réactions d'alkylation portent sur environ 50% des εNH_2 des poly-α-aminoacides de départ et dans nos préparations il ne subsiste pas de poly-L-lysine ou de poly-L-ornithine inchangées.

*Poly-ε,N-(6-purinyl)-*L-*ornithine (**5**)*

En procédant de la même façon avec 114.16 mg de poly-L-ornithine (10^{-3} mole-équivalent ornithine) on obtient 131 mg de poly-ε,*N*-(6-purinyl)-L-ornithine (76%); λ_{max} 205–206; 272–273 mμ.

Anal. calc. pour $(C_{10}H_{12}N_6O)_n$: N, 36.20. Trouvé: N, 30.72.

Anal. calc. pour $(C_5H_{10}N_2O)_n$(poly-L-ornithine initiale): N, 24.5. Trouvé: N, 24.3.

Par hydrolyse acide, le polymère donne la L-ornithine, R_f 0.22 et la ε,*N*-(6-purinyl)-L-ornithine, R_f 0.62.

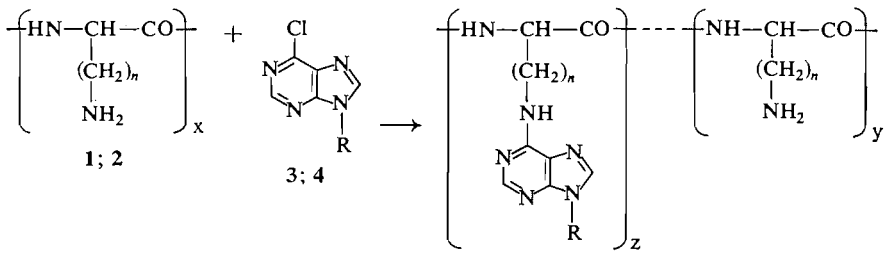

1; **2** **3**; **4** **5**; **6**; **7**; **8**

$\Sigma (y + z) = x$

1; $n = 3$
2; $n = 4$
3; R = H
4; R =

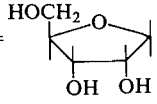

5; $n = 3$; R = H
6; $n = 3$; R =

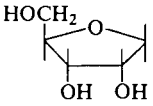

7; $n = 4$; R = H
8; $n = 4$; R =

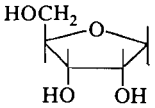

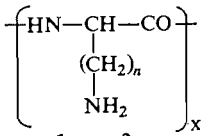

1; $n = 3$
2; $n = 4$

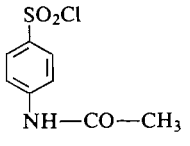

9

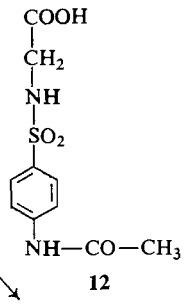

12

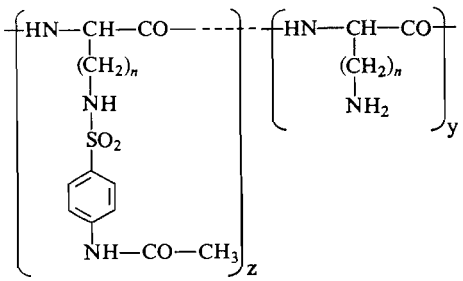

10; $n = 3$
11; $n = 4$

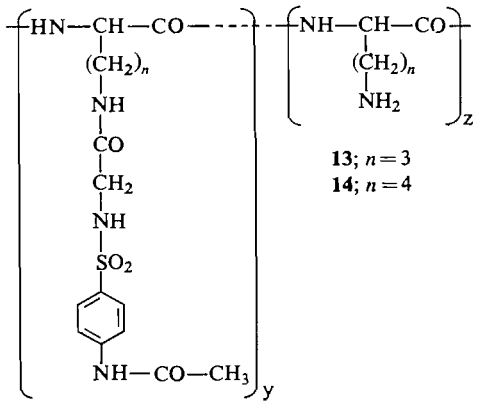

13; $n = 3$
14; $n = 4$

$\Sigma (y + z) = x$

Can. J. Chem. Downloaded from www.nrcresearchpress.com by 210.87.254.42 on 09/05/12
For personal use only.

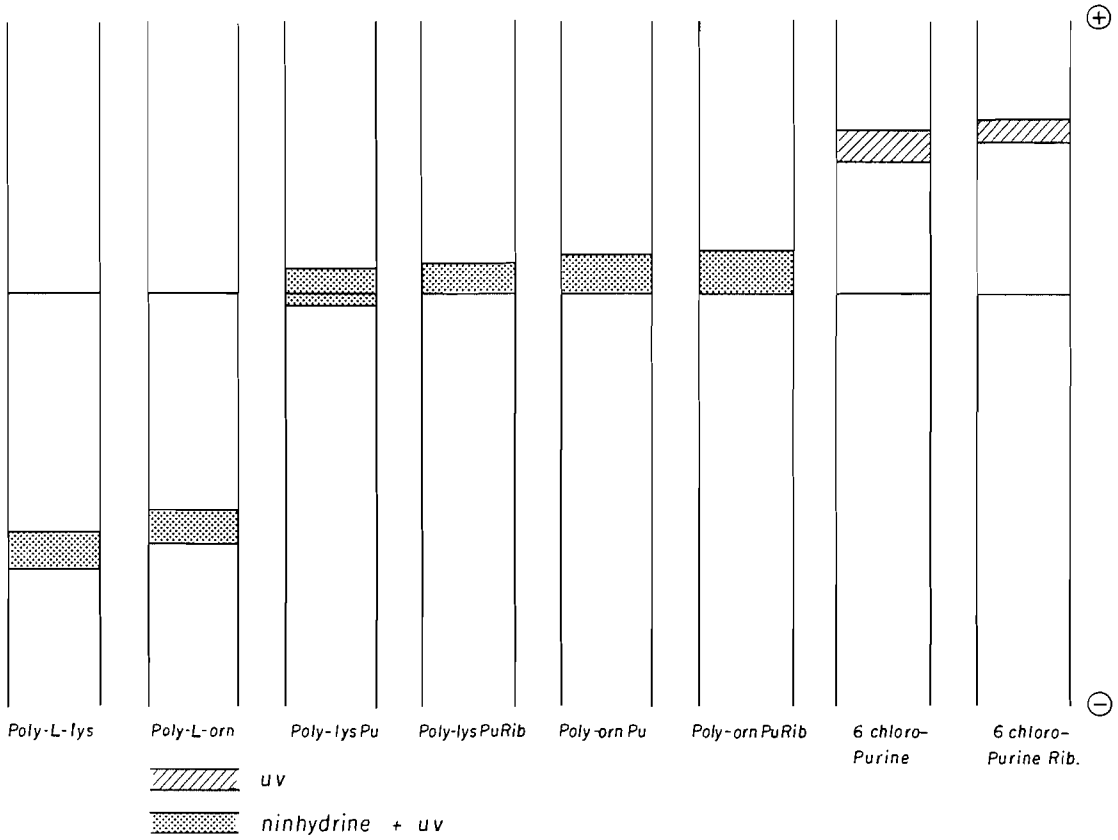

FIG. 1. La migration éléctrophorique des polymères.

L'analyse quantitative d'un aliquot de l'hydrolysat montre qu'environ 55% des ε-NH_2 ont été substitués; le calcul d'après l'analyse en azote donne 53% de substitution.

Poly-ε,N-(6-purinyl riboside)-L-lysine (8)

Avec le même protocole que pour la poly-ε,*N*-(6-purinyl)-L-lysine, mais en ajoutant 582 mg (0.0015 mole) de 6-chloropurine riboside au lieu de la 6-chloropurine, on obtient 177 mg (70%) de poly-ε,*N*-(6-purinyl riboside)-L-lysine; λ_{max} 205–206; 264–265 mμ.

Anal. calc. pour $(C_{16}H_{22}N_5O_5)_n$: N, 19.23. Trouvé: N, 21.42.

Anal. calc. pour $(C_6H_{12}N_2O)_n$(poly-L-lysine initiale): N, 21.8. Trouvé: N, 21.77.

La chromatographie de l'hydrolysat donne deux spots se révélant à la ninhydrine, l'un correspondant à la L-lysine, R_f 0.20, l'autre à la ε,*N*-(6-purinyl riboside)-L-lysine, R_f 0.55. La présence de ribose dans le polymère obtenu fut mis en évidence par la réaction avec l'α-naphtol dans H_2SO_4 concentré. L'analyse quantitative d'un aliquot de l'hydrolysat montre qu'environ 57% des ε-NH_2 ont été substitués; le calcul d'après le pourcentage d'azote trouvé indique une substitution à 54%.

Poly-ε,N-(6-purinyl riboside)-L-ornithine (6)

En employant 114.16 mg de poly-L-ornithine (0.001 mole résidus ornithine) et 582 mg (0.0015 mole) de 6-chloropurine riboside, par le même protocole que celui utilisé pour la synthèse de la poly-ε,*N*-(6-purinyl)-L-lysine, on obtient 163 mg (68%) de poly-ε,*N*-(6-purinyl riboside)-L-ornithine; λ_{max} 204–205; 267–268 mμ. La réaction du polymère avec une solution alcaline d'α-naphtol à 0.3% dans H_2SO_4 concentré donne un anneau violet caractéristique de la présence de ribose.

Anal. calc. pour $(C_{15}H_{20}N_5O_5)_n$: N, 20. Trouvé: N, 21.98.

Anal. calc. pour $(C_5H_{10}N_2O)_n$(poly-L-ornithine initiale) N, 24.5. Trouvé: N, 24.3.

La chromatographie de l'hydrolysat dans HCl 6 *N* donne 2 spots se révélant à la ninhydrine, l'un correspondant à la L-ornithine R_f 0.22, l'autre à la ε,*N*-(6-purinyl riboside)-L-ornithine, R_f 0.54. L'analyse quantitative des produits d'hydrolyse montre une substitution des ε-NH_2 de la poly-L-ornithine d'environ 54% alors que le calcul d'après les pourcentages d'azote indique 56% de substitution.

Poly-ε,N-(4-acétylaminobenzène sulfonyl)-L-lysine (11)

A 50 mg de poly-L-lysine (P.M. 11 000) dissous dans 5 ml d'eau, on ajoute lentement, mais simultanément 100 mg de 4-acétylaminobenzène sulfonyl chloride et 2.5 ml de NaOH 0.2 *N* en gardant une agitation constante. Après 5 h de réaction à température ambiante, on porte le mélange réactionnel à pH 7 par addition de HCl

Can. J. Chem. Downloaded from www.nrcresearchpress.com by 210.87.254.42 on 09/05/12
For personal use only.

TABLEAU I

Toxicité des polymères

Injection par voie I. P.		LD_{25}* mg/kg
Poly-L-lysine (n = 83)		46
		64†
Substitution des ε-$NH_2 \simeq 50\%$	Poly-ε,*N*-(6-purinyl)-L-lysine	200
	Poly-ε,*N*-(6-purinyl riboside)-L-lysine	220
	Poly-ε,*N*-(*N* acétyl sulfanilyl-glycyl)-L-lysine	265
Poly-L-ornithine (n = 76)		93†
Substitution des ε-$NH_2 \simeq 50\%$	Poly-ε,*N*-(6-purinyl)-L-ornithine	> 200
	Poly-ε,*N*-(6-purinyl riboside)-L-ornithine	> 220
	Poly-ε,*N*-(*N* acétyl sulfanilyl-glycyl)-L-ornithine	> 265

*Chaque détermination fut opérée sur des lots de 8 animaux.
†LD_{50}.

dilué et l'on dialyse pendant 3 jours contre l'eau pure; rendement: 74.18 mg (60%).

Anal. calc.: N, 12.84. Trouvé: N, 17.87.

Anal. calc. pour $(C_6H_{12}N_2O)_n$(poly-L-lysine initiale): N, 21.88. Trouvé: N, 21.77.

La chromatographie de l'hydrolysat par HCl 6 *N* révèle 2 spots se colorant à la ninhydrine, l'un correspondant à la L-lysine de R_f 0.20, l'autre au chlorhydrate de la ε,*N*-(4-aminobenzène sulfonyl)-L-lysine de R_f 0.30. Une analyse quantitative des produits d'hydrolyse au "Technicon" montre qu'environ 42% des ε-NH_2 ont été acylés; le calcul basé sur les pourcentages d'azote indique 44% d'acylation.

*Poly-ε,N-(4-acétylaminobenzène ^{14}C sulfonyl)-L-lysine (**11**)*

Le même protocole est employé pour l'acylation de la poly-L-lysine par le chlorure de l'acide 4-acétylaminobenzène sulfonique marqué au ^{14}C sur le noyau benzènique (act. spé. 3.93 mC/mmole). On obtient ainsi 79.68 mg de poly-ε,*N*-(4-acétylaminobenzène ^{14}C sulfonyl)-L-lysine (act. spé. 0.00827 mC/mg); ce qui indique qu'environ 43% des ε-NH_2 de la poly-L-lysine ont été acylés. La chromatographie et l'électrophorèse dans le tampon pH 8.6 (Spinco), sous une intensité de 10 mA, ne révèlent qu'un seul spot radioactif se colorant à la ninhydrine et dont les R_f correspondent à ceux du polymère froid de référence (**11**).

*Poly-ε,N-(4-acétylaminosulfonyl-N, glycyl)-L-lysine (**14**)*

A 128 mg de poly-L-lysine (0.001 mole équivalent lysine) suspendus dans 10 ml de tétrahydrofuranne, on ajoute 309.5 mg (0.0015 mole) de *N,N'*-dicyclohexylcarbodiimide et 400 mg (0.0015 mole) de *N*-(4-acétylaminobenzène sulfonyl) glycine (**12**). Après 5 h d'agitation vigoureuse à température ambiante, on ajoute 3 ml d'acide acétique pour décomposer le réactif en excès, et l'on dialyse pendant 3 jours contre H_2O contenant 20% d'alcool; rendement: 229 mg (57.97%).

Anal. calc. pour $(C_{16}H_{22}N_4O_5S)_n$: N, 14.66. Trouvé: N, 18.82.

Ceci indique qu'environ 42% des ε-NH_2 de la poly-L-lysine ont été acylés.

La chromatographie d'un hydrolysat par HCl 6 *N* indique la présence de L-lysine de R_f 0.20 (coloration à la ninhydrine) et du chlorhydrate de la *N*-(4-aminobenzène sulfonyl)-glycine de R_f 0.41 (absorption dans l'u.v. et coloration jaune pâle à la ninhydrine). L'analyse quantitative des acides aminés au "Technicon" montre qu'environ 40% des ε-NH_2 ont été acylés.

*Poly-ε,N-(4-acétylaminobenzène sulfonyl-N, glycyl)-L-ornithine (**13**)*

Suivant un protocole semblable au précédent, **13** fut obtenu avec un rendement de 60% et un pourcentage d'acylation, calculé par les pourcentages d'azote ainsi que par l'analyse quantiative des produits d'hydrolyse, d'environ 47%.

Remerciements

Les auteurs remercient l'Institut National du Cancer et le Conseil de la Recherche Médicale pour leur aide financière. Ils remercient de plus le Conseil de la Recherche Médicale et les Ententes France–Québec pour la bourse accordée à l'un d'eux (J.G.).

1. H. LEUCH. Ber. **39**, 857 (1906).
2. E. KATCHALSKI et M. SELA. Advan. Protein Chem. **13**, 243 (1958).
3. H. I. SILMAN. *Dans* Poly-α-amino acids. Biological macromolecules series. Vol. I, G. D. Fasman (*éditeur*) (1967).
4. C. CARTER. J. Biol. Chem. 223, 139 (1956).
5. H. LETTRE. Ann. Chem. 633, 171 (1960).
6. E. FISHER. Ber. **38**, 4173 (1905).
7. D. N. WARD, J. WADE, E. WALBORG, et T. S. OSDENE. J. Org. Chem. **26**, 5000 (1961).
8. E. ABDERHALDEN. Ber. **33**, 2383 (1900).
9. L. HOLLANDER. J. Biol. Chem. **94**, 243 (1931–1932).
10. A. NORMAND. Thèse de doctorat, Université Laval. Québec, Québec. 1968.
11. J. C. SHEENAN. J. Am. Chem. Soc. **77**, 1067 (1955).
12. E. KATCHALSKI. J. Am. Chem. Soc. **70**, 2094 (1948).
13. S. ARIELY, M. WILCHEK, et A. PATCHORNIK. Biopolymers, **4**, 91 (1966).
14. H. BOGANZ et H. BOGANZ. Arch. Pharm. 290, 567 (1957).
15. F. FIESER. *Dans* Experiments in organic chemistry. 3ième. ed. D. C. Heath (*éditeur*) (Boston).
16. L. BERLINGUET et J. GAUTIER. Proceedings of the IXth European Symposium on Peptides. Paris, 1968. North Holland Publishing Co., Amsterdam. 1968. p. 272.

Can. J. Chem. Downloaded from www.nrcresearchpress.com by 210.87.254.42 on 09/05/12
For personal use only.

Can. J. Chem. Downloaded from www.nrcresearchpress.com by 210.87.254.105 on 09/05/12
For personal use only.

Derivatives of 2,3-benzo-1-azabicyclo[2·2·1]hept-2-ene

STEWART MCLEAN, A. L. FALLAS, U. O. TROTZ, AND W. F. REYNOLDS
Department of Chemistry, University of Toronto, Toronto 5, Ontario

Received April 9, 1969

2,3-Benzo-1-azabicyclo[2·2·1]hept-2-ene derivatives have been prepared by the introduction of a two-carbon bridge between positions-1 and -3 of the indole ring in 2,3-dimethylindole and tetrahydrocarbazole. In the former case both C-7 epimers were isolated and identified, and their nuclear magnetic resonance spectra were analyzed in detail. In the tetrahydrocarbazole series only one product was obtained and some ambiguity remains concerning the stereochemistry of this material. The physical properties of these compounds are of interest because the lone pair electrons on nitrogen are not able to overlap with the aromatic π system; the chemical properties are characterized by a facile cleavage of the tertiary amine under acylating conditions.

Canadian Journal of Chemistry, 47, 3647 (1969)

In the course of our studies directed towards the synthesis of naturally occurring indole derivatives we have synthesized several compounds which are 2,3-benzo-1-azabicyclo[2·2·1]hept-2-enes. The parent 1-azabicyclo[2·2·1]heptane and some of its derivatives have been described previously (1*a*, *b*, *c*), and the benzo derivative has also been described recently (1*d*). Our synthetic route does not, however, appear to have been used previously and some of the chemistry we have uncovered in this investigation is worth recording at this stage.

Our first synthetic goal was the development of a general method for preparing indolenines substituted as in **2**, where X is a replaceable substituent such as Br, by the introduction of the CH_2CH_2X unit into the disubstituted indole precursor (**1**). The alkylation of indolyl Grignard derivatives has been studied previously (2) and we elected to attempt to apply this method to effect the reaction of the model precursors 2,3-dimethylindole (**1***a*) and tetrahydrocarbazole (**1***b*) with a bifunctional molecule XCH_2CH_2Y. Rather surprisingly, we found conditions under which we could use 1,2-dibromoethane in this reaction and convert the model indoles into the indolenines (**2**; X = Br) in yields in excess of 50%. In agreement with previous workers, we found that the outcome of the reaction was extremely dependent on the precise conditions used; success required the use of reagents and solvents that were very pure and dry, the exclusion of air and moisture during the reaction, care to ensure that the heterocyclic Grignard derivative had completely formed (all unreacted ethyl bromide having been removed before the introduction of the indole into the reaction vessel), and the rapid isolation of the air-sensitive indolenines. Some product in which alkylation had taken place at the nitrogen was also obtained, but in amounts considerably less than that of the 3-substituted indolenine and separation was readily achieved on the basis of the higher base strength of the indolenine.

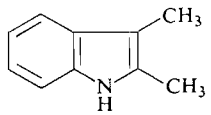

1*a*

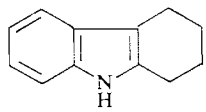

1*b*

a R = Me
b R+R = $(CH_2)_4$

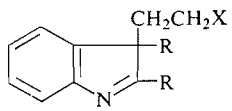

2

The indolenines **2***a* and **2***b* (X = Br) showed absorption near 6.32 μ in the infrared, a position we have found to be characteristic of the N=C stretching vibration in this class of compounds although a somewhat shorter wavelength has been associated with it previously (3). In their nuclear magnetic resonance (n.m.r.) spectra no signals appeared in the region normally associated with CH_2Br, and although the spectra were not analyzed in detail, it was clear that these signals were at higher field than anticipated and were part of the complex pattern above τ 7. This high-field shift, which appears to be associated with the shielding of the Ar—N=C grouping, was confirmed when the corresponding 3-ethylindolenines (**2***a*, *b*; X = H) were also prepared; the

TABLE I
Ultraviolet spectra

	Carbocyclic*	1-Aza derivative
	λ_{max} (mμ) (ε)	λ_{max} (mμ) (ε)
Benzobicyclo[2·2·1]heptene vs. **3***a*	258.5 (662) 264.5 (989) 271.3 (1120)	257 (590) 263 (790) 270 (780)
Benzobicyclo[2·2·2]octene vs. benzoquinuclidine†	254.7 (361) 261.2 (542) 268.0 (748)	255 (308) 261 (423) 267 (419)

*Reference 5.
†Reference 4.

corresponding methyl signal in **2***a* (X = H) was at τ 9.65 and in **2***b* (X = H) it was at τ 9.69.

Reduction of the indolenines **2***a* and **2***b* (X = Br) either by sodium borohydride or by catalytic hydrogenation over a platinum catalyst in methanol (and subsequent basification), led to bromine-free products which, on the basis of their mode of formation, their composition, and their physical properties, were considered to have arisen by spontaneous ring closure leading to 1-azabicyclo[2·2·1]heptane derivatives (**3**, **4**). The products were relatively strong bases (pK_a ca. 7.5), the ultraviolet spectra of which showed only a group of three fairly low intensity bands (ε, 300–800) in the 255–270 mμ region. These properties are very similar to those of 2,3-benzo-1-azabicyclo[2·2·2]octane (pK_a 7.79 (4)) and the rather close correspondence between the ultraviolet spectra of these heterocyclic compounds and their carbocyclic analogues is shown in Table I. In both series the benzenoid chromophore (^1L_b) is slightly more intense and at slightly longer wavelength in the benzobicycloheptene than in the benzobicyclo-octene; in the carbocyclic series this has been associated with the effect of strain on the chromophore (5) and it seems reasonable and sufficient to attribute the difference in the heterocyclic series to the same cause, although some of the difference in the latter case may arise because the lone pair orbital on nitrogen in the benzoazabicycloheptene is not completely orthogonal to the π system as it is in the benzoazabicyclooctene. It is not clear why the extinction coefficients are lower in the heterocyclic compounds than in their carbocyclic analogues.

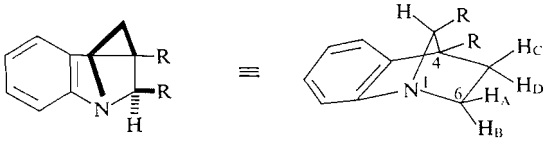

3

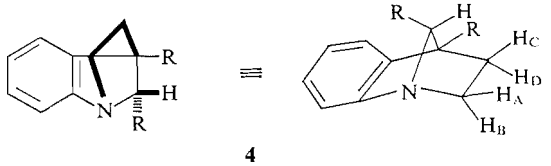

4

When the reduction product of the indolenine **2***a* was examined more closely it became apparent that it consisted of a mixture of isomers, presumably **3***a* and **4***a*. Vapor-phase chromatography showed that the oil initially obtained either by borohydride reduction or catalytic hydrogenation was a mixture of two components in the ratio 19:1. It was possible to induce the major component to separate from pentane as white crystals, m.p. 50–51°, but it was necessary to use vapor-phase chromatography of the material recovered from the mother liquors in order to isolate the minor component. Because it is to be expected that hydrogenation would take place from the less hindered side of the indolenine, the more abundant isomer produced should be **3***a*, and this assignment was supported by a detailed examination of the n.m.r. spectra of the two isomers (*vide infra*).

In the tetrahydrocarbazole series, the product of reduction of **2***b* was an oil which could not be induced to crystallize. No evidence was obtained for the presence of a mixture of isomers and, indeed, the n.m.r. spectrum, although more complex than those just described because of the presence of the methylene protons on the cyclohexane ring, was compatible with the presence of

Can. J. Chem. Downloaded from www.nrcresearchpress.com by 210.87.254.105 on 09/05/12
For personal use only.

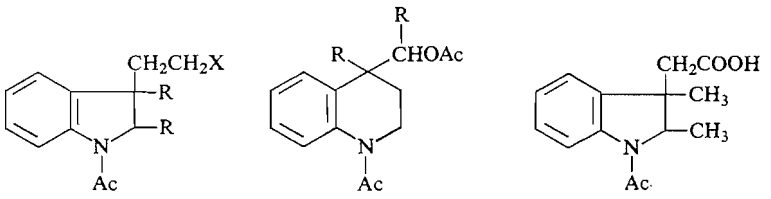

5 6 7

only one isomer, the stereochemistry of which will be discussed below.

The benzoazabicycloheptenes in both series reacted with acetic anhydride under the conditions normally employed to acetylate amines and were converted in good yield to products carrying both *N*-acetyl and *O*-acetyl groups. It was clear that the products arose from a reaction in which the *N*-acetylammonium intermediate, formed by reaction of the tertiary amine with acetic anhydride, underwent nucleophilic attack by an acetate ion and concomitant ring opening. There are two sites adjacent to nitrogen where this attack could take place, C-6 and C-7; the first would lead to the opening of the bridge originally closed in the formation of the bicyclic system and result n a dihydroindole (**5**; X = OAc) as the product, and the second would lead to the opening of the one-carbon bridge and the formation of a tetrahydroquinoline (**6**). The products formed appeared to be those arising from the first process, but since some ambiguity remained about this we have established more rigorously that the products are **5***a* (X = OAc) in the dimethylindole series, and **5***b* (X = OAc) in the tetrahydrocarbazole series. In the first case, **5***a* (X = OAc) was selectively hydrolyzed to the alcohol **5***a* (X = OH) which was then oxidized to a carboxylic acid, the composition and spectroscopic characteristics of which were in accord with structure **7**, thus ruling out **6** as a possible structure for the acetate. It was of particular significance and interest that the CH_2 protons α to the carboxylic acid group in **7** were coupled only to each other (J = 17.5 Hz); they were significantly magnetically non-equivalent, one appearing at τ 7.01 and the other at τ 7.19. In the second case, **5***b* (X = OAc) was converted after selective hydrolysis to the tosylate **5***b* (X = OTs) which was then converted to **5***b* (X = Br) by displacement of tosylate with bromide; this product was identical with that obtained when the original tetrahydrocarbazolenine **2***b* (X = Br) was hydrogenated in acetic anhydride. It follows that in both series the ring opening occurs predominantly if not exclusively in the direction resulting from attack of the acetate ion at C-6, and most probably has the characteristics of an S_N2 process, the unusual facility of the process being a result of the ring strain in the *N*-acylammonium intermediate.

The Nuclear Magnetic Resonance Spectra and Stereochemistry of Isomers 3a and 4a

Both isomeric azabicycloheptanes in the dimethylindole series produced remarkably clean, well resolved nuclear magnetic resonance spectra which in gross appearance were very similar but in detail were characterized by several critical differences in chemical shifts and coupling constants which allowed us to assign with complete confidence formula **3***a* to the major component of the original mixture and **4***a* to its isomer.

The chemical shift evidence concerns the substituents at C-7 (the one-carbon bridge): in **3***a* the methyl group appears as a doublet at τ 9.026 while in **4***a* it is more highly shielded and appears at τ 9.319; the reverse holds true for the C-7 hydrogens, that in **3***a* being at higher field, τ 7.381, than that in **4***a* which appears at τ 7.221. These chemical shift differences, which are almost certainly due to the anisotropic diamagnetic susceptibility of the benzene ring, are compatible with the stereochemical assignments made to **3***a* and **4***a*.

Furthermore, the C-7 hydrogen in **4***a* produces a simple quartet (by coupling to the C-7 methyl) but the corresponding quartet in **3***a* is broadened and spin decoupling experiments have established that this arises from long range coupling to protons B and D on the two-carbon bridge (to be discussed presently). It has generally been found in σ-bonded systems coupling through four bonds is appreciable only when the bonds form a W shape (6). Consequently, the fact that long range

Can. J. Chem. Downloaded from www.nrcresearchpress.com by 210.87.254.105 on 09/05/12
For personal use only.

TABLE II

Nuclear magnetic resonance spectra of **3***a* and **4***a*

Isomer	Chemical shifts (τ)		Coupling constants (Hz)	
3*a*	C-7 H	7.381	$J_{7\text{-H},7\text{-Me}}$	6.73
	C-7 CH_3	9.026		
	C-4 CH_3	8.593		
	Aromatic protons	3.03 (narrow multiplet)		
	H_A	6.741	J_{AB}	−12.07
	H_B	7.709	J_{AC}	+ 8.99
	H_C	8.296	J_{AD}	+ 4.37
	H_D	8.849	J_{BC}	+ 4.44
			J_{BD}	+ 8.35
			J_{CD}	−11.29
			$\lvert J_{B,7\text{-H}}\rvert$	~ 1.1
			$\lvert J_{D,7\text{-H}}\rvert$	~ 1.1
4*a*	C-7 H	7.221	$J_{7\text{-H},7\text{-Me}}$	6.44
	C-7 CH_3	9.319		
	C-4 CH_3	8.595		
	Aromatic protons	3.00 (narrow multiplet)		
	H_A	6.749	J_{AB}	−11.63
	H_B	7.655	J_{AC}	+ 9.30
	H_C	8.182	J_{AD}	+ 4.61
	H_D	8.667	J_{BC}	+ 4.51
			J_{BD}	+ 8.42
			J_{CD}	−10.88

coupling is observable in **3***a* but not **4***a* confirms the stereochemical assignments based on chemical shift data.

The four non-equivalent protons on the two-carbon bridge in each isomer gave rise to a simple or slightly perturbed ABCD spectrum; in **3***a*, the protons designated B and D (see Table II for listing) were split further by the long range coupling already referred to. In each case the ABCD spectrum was analyzed by Bothner-By and Castellano's iterative computer program LAOCN3 (we are very grateful to Professor Bothner-By for letting us have the listing of this program); the rest of the spectrum was analyzed in each case by first order procedures, and the complete analysis is shown in Table II. The labelling (ABCD in order of increasing field) was based on chemical shifts and was supported by the magnitude of the coupling constants associated with each proton; protons that are structurally equivalent received the same label in both isomers. It was assumed that the two low-field protons, A and B, were those adjacent to nitrogen, and, of this pair, the assignment of B was made on the grounds that it should experience some shielding because of the anisotropic diamagnetic susceptibility of the benzene ring. Protons C and D were assigned on the same basis. The assignment is supported by the observation of long range coupling to protons B and D.

The magnitudes of the computed coupling constants fall into the expected range if it is assumed that the methylene groups are eclipsed or nearly eclipsed. The magnitudes of J_{AB} and J_{CD} (see Table II) are consistent with their being geminal coupling constants; the coupling constants assigned to pairs of vicinal protons agree well with values predicted from the modified Karplus equation (7) and have magnitudes similar to those found in a number of model compounds (8). The signs chosen here are also consistent with those obtained in a great number of similar systems (8); other solutions can be obtained with different combinations of signs of coupling constants but their absolute values are only slightly altered. The magnitude of the long range coupling is unexceptional but its sign is undetermined.

Stereochemistry in the Tetrahydrocarbazole Series

Because we have isolated only one azabicycloheptene in the tetrahydrocarbazole series, we have had more difficulty in deciding which stereoisomer it is. A rationale based on its mode of formation would suggest, as with the dimethylindole

Can. J. Chem. Downloaded from www.nrcresearchpress.com by 210.87.254.105 on 09/05/12
For personal use only.

Can. J. Chem. Downloaded from www.nrcresearchpress.com by 210.87.254.105 on 09/05/12
For personal use only.

product, that **3***b* should be the stereoisomer isolated, but the spectroscopic results, while not yet conclusive, favor **4***b*.

The appearance of the n.m.r. spectrum of the product indicates that the material is essentially homogeneous. The protons on the two-carbon bridge again give rise to a distinctive pattern. The proton (H_A) at lowest field appears as a very clean octet centered at τ 6.73; the next octet (from H_B) near τ 7.6 is confused to some extent because it overlaps another multiplet, presumably that arising from the C-7 hydrogen, but it is clear on careful examination that none of the peaks of the octet is split by long range coupling. The signals from H_C and H_D are part of a complex pattern at higher field which includes the cyclohexane ring protons and the octets cannot be described with confidence although it is probable that parts of each one can be recognized. In the absence of the second isomer, no weight can be put on assignments based on chemical shifts (i.e. by comparisons with **3***a* and **4***a*) and the absence of long range coupling is the firmest piece of evidence available here; this indicates that the isomer is **4***b*, but we recognize that the distortion introduced into the molecule by the extra six-membered ring could be sufficient to remove the long range coupling, and the assignment is not rigorous.

When the bridge has been opened by acetylation, the C-2 proton of **5***b* appears in the n.m.r. as a multiplet near τ 5.9, the appearance of which has a strong temperature dependence. Below 0° four peaks are resolved and these appear to be the X part of an ABX system with $|J_{AX} + J_{BX}| \sim 16$ Hz indicating that the C-2 proton is axially oriented and coupled with one adjacent axial proton and one adjacent equatorial proton. This would be compatible with a *trans*-fused ring system or with a *cis*-fused system which exists predominantly in the conformation with the C-2 hydrogen axial. At low temperature an additional smaller signal near τ 5.6 becomes apparent which may be indicative of the presence of a second conformational isomer; as the temperature rises both signals broaden and the smaller signal eventually can no longer be seen. Most significantly, the appearance and temperature dependence of this part of the spectrum is remarkably similar to that of the *N*-acetyl derivative of *cis*-hexahydrocarbazole, if the extra equatorial–axial coupling in the latter case is allowed for. The spectra can, therefore, be explained in terms of a conformationally mobile *cis*-fused system in **5***b*, derived therefore from **4***b*, but the situation is complicated by the conformational mobility of the *N*-acetyl group which also has a temperature-dependent influence on the C-2 proton (9). Further work, which we are presently undertaking, will be required to remove this uncertainty.

Experimental

Melting points were determined on a Thomas–Kofler micro hot stage. Spectrometers used were: Beckman IR8 and Perkin–Elmer model 257 Infracord for infrared (i.r.) spectra, Bausch and Lomb Spectronic 505 for ultraviolet (u.v.) spectra, Varian A60 and Varian HA100 for nuclear magnetic resonance (n.m.r.) spectra; for detailed spectral analysis of **3***a* and **4***a*, n.m.r. spectra were recorded at a sweep rate of 0.05 Hz/s on the HA100 operated in frequency sweep mode at a probe temperature of 30° and each peak position was determined from the average of at least four measurements.

3-(2′-Bromoethyl)-2,3-dimethylindolenine (2a; X = Br)

Magnesium turnings (4.8 g; 0.2 mole) were placed in a one-1 flask equipped with a mercury-sealed stirrer, a dropping funnel, a condenser and an inlet system for maintaining a nitrogen atmosphere. A small amount of ethyl bromide was allowed to fall on the magnesium, and when the reaction began, a solution of ethyl bromide (22 g; 0.2 mole) in 50 ml ether was added at a rate suitable to maintain a steady reaction. When addition was complete, 250 ml anisole were added and the solution warmed and stirred vigorously. Further ethyl bromide was added at this point if necessary to consume any unreacted magnesium. Further anisole (150 ml) was added and any excess ethyl bromide was removed by distillation. The solution was cooled to 0°, stirred, and a solution of 2,3-dimethylindole (29 g; 0.2 mole) in 50 ml anisole was added over a period of 30 min. The solution was allowed to come to room temperature, excess 1,2-dibromoethane (113 g; 0.6 mole) was added, and the reaction mixture was stirred at 90° for 18 h. The flask was then cooled in an ice-bath, 15 ml saturated aqueous ammonium chloride were added dropwise, and any solid material was removed by filtration. The filtrate was extracted five times with 100 ml portions of 2 *N* hydrochloric acid, and the aqueous extract was washed with 100 ml ether and made basic with 4 *N* sodium hydroxide solution, whereupon a yellow oil began to separate. This mixture was thoroughly extracted with ether, and the ether extracts, after they had been washed with water and dried over potassium carbonate, afforded a dark oil (18–27 g; 35–55% yield). This material, which was extremely sensitive to air, could be purified by rapid chromatography on neutral alumina (British Drug Houses) with elution by 50:50 benzene–ether, when it was obtained as a pale oil which darkened rapidly in air; i.r. λ_{max}(film) 6.22 (w), 6.33 (s) μ; u.v. λ_{max}(MeOH) 260 mμ (ε, 4600); n.m.r. (τ, CCl_4) 2.4–3.2 (4 H; complex), 7.3–7.8 (4 H; complex), 7.85 (3 H; singlet); 8.80 (3 H; singlet). Alternatively, the product could be converted to a picrate (from which the base could be recovered by treatment

Can. J. Chem. Downloaded from www.nrcresearchpress.com by 210.87.254.105 on 09/05/12
For personal use only.

with aqueous lithium hydroxide) which, on recrystallization from methanol, afforded yellow–orange needles, m.p. 170–172.5°.

Anal. Calcd. for $C_{18}H_{17}N_4O_7Br$: C, 44.92; H, 3.56; N, 11.64; Br, 16.61. Found: C, 45.25; H, 3.50; N, 11.96; Br, 16.65.

The anisole solution from which the indolenine had been removed by extraction into acid, was reduced to dryness by distillation at reduced pressure. 2,3-Dimethylindole was recovered from the residue by chromatography on neutral alumina (British Drug Houses) by elution with benzene; up to 40% of starting material could be recovered in this way.

2,3-Dimethyl-3-ethylindolenine (2a; X = H)

The Grignard complex prepared as described above was allowed to react with ethyl bromide in place of dibromoethane. The crude base (28% yield) was isolated in the manner described above and purified as its picrate, m.p. 149–151° (lit. (12) 153°).

The free base was regenerated by treatment of the picrate with saturated aqueous lithium hydroxide and isolated as an unstable pale-yellow oil; i.r. λ_{max}(film) 6.20 (w), 6.32 (s) μ; u.v. λ_{max}(MeOH) 255 mμ (ε, 6600); n.m.r. (τ, CCl_4) 2.4–3.0 (4 H; complex), 7.88 (3 H; singlet), 8.22 (quartet J = 7.2 Hz with further fine structure), 8.79 (3 H; singlet), 9.65 (3 H; triplet, J = 7.2 Hz).

4a-(2′-Bromoethyl)-1,2,3,4-tetrahydrocarbazolenine (2b; X = Br)

Replacement of 2,3-dimethylindole by tetrahydrocarbazole in the above preparation led to the isolation of the tetrahydrocarbazolenine as an oil in about 45% yield. After chromatography (1:3 ether–hexane on neutral alumina) the product (33% yield from tetrahydrocarbazole) was obtained as colorless crystals, m.p. 80–81°; (picrate, m.p. 158–160°).

Anal. Calcd. for $C_{14}H_{16}NBr$: C, 60.45; H, 5.78; N, 5.04; Br, 28.73. Found: C, 60.48; H, 5.48; N, 5.10; Br, 28.83.

Infrared λ_{max}($CHCl_3$) 3.10 (w), 6.32 (s) μ; u.v. λ_{max} (MeOH) 257 mμ (ε, 8000); n.m.r. (τ, CCl_4) 2.4–3.1 (4 H; complex); 7.0–9.2 (12 H; complex).

The anisole solution afforded *9-(2′-bromoethyl)-1,2,3,4-tetrahydrocarbazole* in 8% yield. From hexane it formed white prisms, m.p. 71–72°; (picrate, m.p. 94–95°).

Anal. Calcd. for $C_{14}H_{16}NBr$: C, 60.45; H, 5.78; N, 5.04. Found: C, 60.90; H, 5.66; N, 5.20.

Infrared λ_{max}($CHCl_3$) 6.24 (m) μ; u.v. λ_{max}(MeOH) 230 mμ (ε, 25 800), 286 mμ (ε, 6700), 293 mμ (inflect.); n.m.r. (τ, $CDCl_3$) 2.4–3.1 (4 H; complex), 5.82 (2 H; triplet, J = 7.0 Hz), 6.67 (2 H; triplet, J = 7.0 Hz), 7.15–7.65 (4 H; unresolved peak), 7.95–8.45 (4 H; unresolved peak).

4a-Ethyl-1,2,3,4-tetrahydrocarbazolenine (2b; X = H)

The Grignard complex of tetrahydrocarbazole was allowed to react with ethyl bromide (in place of dibromoethane) and the crude base (55% yield) was isolated in the manner described above. The picrate was prepared and obtained, after recrystallization from ethanol, as yellow needles, m.p. 153–155° (lit. (3*a*) 148–150°).

Anal. Calcd. for $C_{20}H_{20}N_4O_7$: C, 56.07; H, 4.71; N, 13.08. Found: C, 55.97; H, 4.61; N, 12.90.

Treatment of the picrate with saturated aqueous lithium hydroxide afforded the free base as a very pale yellow sweet-smelling oil; i.r. λ_{max}(film) 6.20 (w), 6.32 (s) μ-u.v. λ_{max}(MeOH) 256 mμ (ε, 6400), shifted by hydrochloric acid to λ_{max} 231 mμ (ε, 6600), 276 mμ (ε, 5500); n.m.r. (τ, CCl_4) 2.3–3.0 (4 H; complex), 7.0–9.1 (10 H; complex), 9.69 (3 H; 1:2:1 triplet, J = 7.5 Hz).

4,7-Dimethyl-2,3-benzo-1-azabicyclo[2·2·1]hept-2-enes (3a; 4a)

Preparation A

A solution of the indolenine (**2***a*; X = Br) (13.4 g; 52 mmole) in 250 ml methanol was stirred for 2 h with excess sodium borohydride (20 g) dissolved in 100 ml *N* sodium hydroxide. The solution was cooled on ice and acidified with 2 *N* hydrochloric acid. Most of the methanol was removed by distillation under reduced pressure, and the aqueous solution that remained was made basic with 4 *N* sodium hydroxide and then thoroughly extracted with ether. The extract afforded a yellow sweet-smelling oil (9.62 g), which was distilled under reduced pressure (b.p. ca 50°/0.05 mm). A colorless oil (6.2 g; 36 mmole) was obtained, which was a mixture of two components in the ratio 19:1 as determined by analytical v.p.c. on a Versamid column. A solution of the oil in pentane deposited white crystals which, on repeated fractional crystallization from the same solvent, afforded a homogeneous sample of the major component (**3***a*) m.p. 50–51°; (picrate, m.p. 171–172°).

Anal. Calcd. for $C_{12}H_{15}N$: C, 83.22; H, 8.73; N, 8.01. Found: C, 83.10; H, 8.63; N, 8.00.

The pK_a by potentiometric titration in water with 0.01 *N* hydrochloric acid was determined as 7.47. Spectroscopic data: i.r. λ_{max}(CCl_4) 6.32 μ(w); u.v. λ_{max}(MeOH) 257 mμ (ε, 590), 263 mμ (ε, 790), 270 mμ (ε, 780) and on addition of hydrochloric acid λ_{max} 253 mμ (ε, 320), 259 mμ (ε, 360), 265 mμ (ε, 350); for n.m.r. see text.

The mother liquors afforded material in which the proportion of the minor component had increased, but it was not possible to isolate this isomer by further fractional crystallization. Material enriched in the minor component was subjected to vapor-phase chromatography on a 20 ft × 1/4 in. column of 2% Versamid on 60/80 mesh Chromosorb G at 160°; the minor component had retention time 9 min, the major component 10.8 min. The minor component **4***a* was obtained as a colorless oil which eventually formed crystals, m.p. 48.5–50°.

Anal. Calcd. for $C_{12}H_{15}N$: C, 83.22; H, 8.73; N, 8.01. Found: C, 83.21; H, 8.65; N, 8.19.

Preparation B

A solution of the indolenine (5.24 g; 21 mmole) in 50 ml ethanol was hydrogenated at room temperature and atmospheric pressure in the presence of pre-reduced platinum oxide. After 14 h, 20 mmole hydrogen had been consumed and no further reaction was observed. The brown oil obtained by filtration and evaporation of the solvent was dissolved in chloroform and shaken with excess *N* sodium hydroxide. The chloroform solution afforded a yellow oil (3.17 g; 18 mmole) that had, by v.p.c. analysis, the same composition as the product in Preparation A above.

1,2,3,4,4a,9a-Hexahydro-4a-9-ethanocarbazole

Preparation A

A solution of 4a-(2′-bromoethyl)-1,2,3,4-tetrahydrocarbazolenine (7.85 g; 28 mmole) was reduced with sodium borohydride in the manner described above. The

Can. J. Chem. Downloaded from www.nrcresearchpress.com by 210.87.254.105 on 09/05/12
For personal use only.

crude product, a yellow, sweet-smelling oil (5.49 g) was treated with a slight excess of picric acid in hot ethanol. The picrate which precipitated was recrystallized from methanol and obtained as bright yellow crystals (8.13 g; 19 mmole), m.p. 198–200°.

Anal. Calcd. for $C_{20}H_{20}N_4O_7$: C, 56.07; H, 4.67; N, 13.08; O, 26.17. Found: C, 55.94; H, 4.66; N, 13.35; O, 26.64.

A solution of the picrate in carbon tetrachloride was treated with saturated aqueous lithium hydroxide to liberate the free base which was obtained as a pale-yellow oil (3.46 g; 18 mmole); this was purified by distillation under reduced pressure (ca. 85° at 0.05 mm) and isolated as a colorless oil.

Anal. Calcd. for $C_{14}H_{17}N$: C, 84.37; H, 8.60; N, 7.03. Found: C, 84.79; H, 8.41; N, 7.10.

The pK_a by potentiometric titration in water with 0.01 *N* hydrochloric acid was determined as 7.55.

Infrared $\lambda_{max}(CCl_4)$ 6.22 μ (w); u.v. λ_{max}(MeOH) 257 mμ (ε, 500), 266 mμ (ε, 560), 273 mμ (ε, 560) which, when hydrochloric acid was added, gave λ_{max} 256 mμ (ε, 200), 261 mμ (ε, 220), 268 mμ (ε, 210); n.m.r. (τ, $CDCl_3$) 2.9–3.2 (4 H; complex), 6.73 (1 H; octet), 7.4–7.8 (2 H; complex), 8.2–9.2 (10 H; complex); also see text.

Preparation B

The tetrahydrocarbazolenine (1 g; 3.6 mmole) was catalytically hydrogenated in the manner described for indolenine. The product, a yellow oil (0.61 g; 3.1 mmole) afforded after distillation a material, apparently identical with that described in Preparation A, which formed a picrate, m.p. 198–200° alone or on admixture with the picrate described above.

*1-Acetyl-3-(2′-acetoxyethyl)-2,3-dimethylindoline (**5a**; X = OAc)*

A solution of **3***a* (385 mg; 2.2 mmole) in 10 ml acetic anhydride containing a little pyridine was refluxed for 9 h and the mixture was then left at room temperature for a further 18 h. The acetic anhydride was removed by distillation under reduced pressure and the residue was shaken with water and ether. The ether extract afforded a brown oil which was dissolved in benzene and chromatographed on neutral alumina (British Drug Houses); elution was carried out with a benzene–ether mixture in which the proportion of ether was gradually increased and fractions that showed essentially identical i.r. spectra were pooled. A pale yellow oil (543 mg; 2.0 mmole) was obtained and recrystallized from pentane; **5***a* (X = OAc) was obtained as colorless crystals, m.p. 72.5–73.5°.

Anal. Calcd. for $C_{16}H_{21}O_3N$: C, 69.79; H, 7.69; N, 5.09. Found: C, 69.74; H, 8.03; N, 5.08.

Infrared $\lambda_{max}(CCl_4)$ 5.74 (s), 6.01 (s) μ; u.v. λ_{max}(MeOH) 250 mμ (ε, 12 300), 280 mμ (shoulder), 286 mμ (ε, 6500); n.m.r. (τ, CCl_4) 2.3 (1 H; broad), 2.7–3.1 (3 H; complex), 5.76 (3 H; complex), 7.77 (3 H; singlet), 7.98 (3 H; singlet), 7.8–8.1 (2 H; complex), 8.81 (6 H; probably 3 H singlet and 3 H doublet, J = 7 Hz).

*9-Acetyl-4a-(2′-acetoxyethyl)-1,2,3,4,4a,9a-hexahydrocarbazole (**5b**; X = OAc)*

The ethanocarbazole was acetylated in a manner corresponding to that described above with the difference that the reaction was carried out by heating the acetic anhydride solution on a steambath for 3 h. The product was a colorless oil which distilled at 140–150° at 10^{-3} mm.

Anal. Calcd. for $C_{18}H_{23}NO_3$: C, 71.73; H, 7.69; N, 4.65. Found: C, 71.82; H, 7.62; N, 4.73.

Infrared $\lambda_{max}(CCl_4)$ 5.75 (s), 6.03 (s) μ; u.v. λ_{max}(MeOH) 252 mμ (ε, 12 000), 285 mμ (ε, 2450); n.m.r. (τ, $CDCl_3$) 2.0 (1 H; ca. 20 Hz wide), 2.7–3.1 (3 H; complex), 5.95–6.3 (2 H; 7 lines resolved), 7.79 (3 H; singlet), 8.16 (3 H; singlet), 7.8–9.2 (12 H; complex).

*1-Acetyl-3-carboxymethyl-2,3-dimethylindoline (**7**)*

Selective Hydrolysis

A solution of **5***a* (X = OAc) (290 mg; 1.05 mmole) in 15 ml methanol was stirred overnight at room temperature with 3 ml 10% aqueous sodium hydroxide. This solution afforded a pale-brown oil after the usual work-up. Purification was effected by chromatography on silica gel and the major component (**5***a*, X = OH) was eluted with 2:1 chloroform–methanol. This was a colorless oil (140 mg), which showed i.r. $\lambda_{max}(CCl_4)$ 2.71 (m), 2.87 (m), 6.02 (s) μ; u.v. λ_{max}(MeOH) 252 mμ (ε, 7400), 286 mμ (infl.), 276 mμ (infl.); n.m.r. (τ, $CDCl_3$) 2.2 (1 H; broad), 2.85 (3 H; complex), 5.75–6.10 (3 H; complex), 6.54 (1 H; exchanged in D_2O), 7.60 (3 H; singlet), 7.90 (2 H; complex), 8.75 (6 H; probably doublet superimposed on singlet).

Oxidation

To a stirred solution of **5***a* (X = OH) (116 mg; 0.5 mmole) in 5 ml acetone, 0.1 ml Jones reagent (10) was added slowly through a microsyringe. The mixture was stirred for a further 15 min and then diluted with 20 ml water and extracted with methylene chloride. The extract afforded a brown oil (127 mg) which was partitioned between chloroform and aqueous sodium bicarbonate; acidification of the bicarbonate solution and extraction with chloroform yielded, by the standard work-up, white crystals (91 mg; 0.37 mmole), m.p. 84–86°, which had to be sublimed in order to obtain an analytical sample of 7, m.p. 154–155°.

Anal. Calcd. for $C_{14}H_{17}NO_3$: C, 68.01; H, 6.88; N, 5.67. Found: C, 68.23; H, 6.99; N, 5.65.

Infrared $\lambda_{max}(CCl_4)$ 2.75–3.2, 5.82, 6.1 μ; u.v. λ_{max} (MeOH) 251 mμ (ε, 14 700), 278 mμ (shoulder) 286 mμ (ε, 5000); n.m.r. (100 MHz; τ, $CDCl_3$) 1.2 (1 H; broad), 1.8 (1 H; broad) 2.7–2.9 (3 H; complex), 5.5 (1 H; broad), 7.10 (2 H; AB quartet; J = 17.5 Hz; int. chem. shift 0.18 p.p.m.), 7.62 (3 H; singlet) 8.66 (3 H; singlet), 8.77 (3 H; doublet; J = 6.5 Hz).

*9-Acetyl-4a-(2′-bromoethyl)-1,2,3,4,4a,9a-hexahydrocarbazole (**5b**; X = Br)*

Preparation A

Selective hydrolysis of **5***b* (X = OAc) (5.32 g; 17.7 mmole) in the manner described above for **5***a* (X = OAc) converted it to a pale-yellow oil (4.02 g; 15.5 mmole) which could be crystallized from hexane and **5***b* (X = OH) was obtained as a white solid, m.p. 94.5–95.5°.

Anal. Calcd. for $C_{16}H_{21}NO_2$: C, 74.10; H, 8.16; N, 5.40. Found: C, 74.22; H, 7.91; N, 5.65.

Infrared $\lambda_{max}(CCl_4)$ 2.74, 2.80, 6.03 μ; u.v. λ_{max}(MeOH) 254 mμ (ε, 14 750), 280 mμ (ε, 4200), 288 mμ (ε, 3400); n.m.r. (τ, $CDCl_3$) 1.90 (1 H), 2.8–3.0 (3 H; complex), 5.8 (1 H), 6.3–6.6 (2 H; multiplet), 7.10 (1 H; singlet; exchangeable in D_2O), 7.78 (3 H; singlet), 7.8–9.0 (10 H; complex).

The *p*-toluenesulfonate (**5***b*, X = OTs) was prepared

by treatment of the alcohol (1.24 g; 4.8 mmole) in 25 ml pyridine at 0° with *p*-toluenesulfonyl chloride (2.29 g; 11.5 mmole); the reaction was allowed to proceed at 0° for 36 h, the reaction mixture was poured over ice, and the product was extracted into ether. The ether extract afforded a gummy material (3.8 g) which was crystallized with some difficulty from light petroleum ether. The white crystals obtained rapidly became gummy in air at room temperature.

The bromide was prepared by stirring together the tosylate (2.1 g; 5.1 mmole) with sodium bromide (1.0 g; 10 mmole) in 16 ml dimethyl sulfoxide at room temperature for 84 h. The reaction mixture was extracted with ether, the ether extract was washed with dilute sulfuric acid and then water, and the product, obtained in the usual manner, was a white solid (0.44 g; 1.4 mmole) which was recrystallized from hexane. This product, m.p. 95–96°, was identical in every way with the bromide obtained in the following way.

Preparation B

4a-(2′-Bromoethyl)-1,2,3,4-tetrahydrocarbazolenine (**2***b*, X = Br) (2.33 g; 8.38 mmole) in 15 ml acetic anhydride was hydrogenated in the presence of prereduced platinum oxide at room temperature and atmospheric pressure. Reaction ceased after 6 h when 8.17 mmole hydrogen had been consumed. The solution was diluted with water, made basic with sodium carbonate, and extracted with chloroform. The chloroform extract afforded a pale-brown oil (2.6 g) which was purified by chromatography on neutral alumina. The fraction (1.93 g; 6.2 mmole) eluted by 1:1 hexane–ether was solid and, when recrystallized from a mixture of iso-octane and benzene, formed colorless crystals, m.p. 95–96°.

Anal. Calcd. for $C_{16}H_{20}NOBr$: C, 59.64; H, 6.26; N, 4.35; Br, 24.79. Found: C, 59.75; H, 6.15; N, 4.75; Br, 24.91.

Infrared $\lambda_{max}(CHCl_3)$ 6.26 (m) μ; u.v. λ_{max}(MeOH) 252 mμ (ε, 13 100), 286 mμ (ε, 2700); n.m.r. (τ, CCl_4) 1.8–2.3 (1 H; broad), 2.5–3.1 (3 H; complex), 5.8–6.3 (1 H; unresolved), 6.90 (2 H; triplet J = 8.3 Hz, but showing signs of further complexity), 7.79–9.0 (10 H; complex).

Acknowledgments

We are grateful to the National Research Council of Canada for financial support of this research and to the Canadian Commonwealth Scholarship and Fellowship Committee for a Fellowship awarded to one of us (U.O.T.).

1. (*a*) G. R. Clemo and T. P. Metcalfe. J. Chem. Soc. 1523 (1937.) (*b*) G. R. Clemo and V. Prelog. J. Chem. Soc. 400 (1938). (*c*) P. G. Gassmann and R. L. Cryberg. J. Am. Chem. Soc. **90**, 1355 (1968). (*d*) G. Kohl and H. Pracejus. Ann. **694**, 128 (1966).
2. A. H. Jackson and P. Smith. J. Chem. Soc. (C) 1667 (1968). C. R. Ganellin, D. R. Hollyman, and H. F. Ridley. J. Chem. Soc. (C) 2220 (1967). M. Nakazaki. Bull. Chem. Japan, **32**, 838 (1959); **34**, 334 (1961). M. Nakazaki and S. Isoe. Nippon kagaku Zasshi **76**, 1159 (1955); Chem. Abstr. **51**, 17877 (1957). M. S. Kharasch and O. Reinmuth. Grignard reactions of non-metallic substances. Prentice-Hall, Inc., New York. 1954, Chap. 2.
3. (*a*) B. Witkop and J. B. Patrick. J. Am. Chem. Soc. **73**, 1558 (1951). (*b*) B. Witkop and J. B. Patrick. J. Am. Chem. Soc. **73**, 2188 (1951).
4. B. M. Wepster. Rec. Trav. Chim. **71**, 1159 (1952).
5. H. Tanida and R. Muneyuki. J. Am. Chem. Soc. **87**, 4794 (1965). G. D. Abrams. Ph.D. Thesis, University of Toronto, Toronto, Ontario. 1968.
6. S. Sternhell. Rev. Pure Appl. Chem. **14**, 15 (1964).
7. K. L. Williamson and W. S. Johnson. J. Am. Chem. Soc. **83**, 4623 (1961).
8. A. A. Bothner-By. Geminal and vicinal proton–proton coupling constants in organic compounds. *In* Advances in magnetic resonance, Vol. 1. *Edited by* J. S. Waugh. Academic Press, Inc., New York. 1965.
9. S. McLean. Can. J. Chem. **42**, 191 (1964). K. Nagarajan, M. D. Nair, and P. M. Pillai. Tetrahedron, **23**, 1683 (1967). K. Nagarajan and M. D. Nair. Tetrahedron, **23**, 4493 (1967).
10. A. Bowers, T. G. Halsall, E. R. H. Jones, and A. J. Lemin. J. Chem. Soc. 2548 (1953).

Can. J. Chem. Downloaded from www.nrcresearchpress.com by 210.87.254.105 on 09/05/12
For personal use only.

Can. J. Chem. Downloaded from www.nrcresearchpress.com by 210.87.254.6 on 09/05/12
For personal use only.

A nuclear magnetic resonance study of hydrogen bonding of δ-valerolactam

J. M. PURCELL, H. SUSI, AND J. R. CAVANAUGH

Eastern Utilization Research and Development Division, Agricultural Research Service, U.S. Department of Agriculture, Philadelphia, Pennsylvania 19118

Received February 19, 1969

The association of amide groups of δ-valerolactam through hydrogen bonding has been investigated by means of high resolution nuclear magnetic resonance spectroscopy in CCl_4 and $CDCl_3$ solutions. Chemical shifts of the NH proton signal were measured over a wide range of temperatures and concentrations. Thermodynamic properties associated with the N—H·····O=C hydrogen bond formation were evaluated from a least squares analysis by a direct search procedure with a digital computer. The obtained enthalpy values for hydrogen bond formation are in general agreement with results obtained by other methods.

Canadian Journal of Chemistry, 47, 3655 (1969)

Introduction

The application of nuclear magnetic resonance (n.m.r.) spectroscopy to the study of hydrogen bonding equilibria has been extensive and relatively successful (1–4). Our own interest in interamide interactions (5, 6) has prompted us to investigate the utility of n.m.r. for systems involving N—H·····O=C hydrogen bonding. Many systems involving amide-to-amide hydrogen bonding have been previously investigated by infrared (i.r.) spectroscopy (5–10). The purpose of the present study was to examine a model system which has been thoroughly studied by another technique and thus to obtain some information regarding the applicability of n.m.r. spectroscopy to problems involving amide-to-amide hydrogen bonding.

Accordingly, we have investigated the dimerization of δ-valerolactam through hydrogen bonding in CCl_4 and $CDCl_3$ at various temperatures. *cis* Amides, such as lactams, are conformationally not as closely related to polypeptide chains as *trans* amides, such as *N*-methylacetamide. However, the *cis* amides do offer some distinct advantages. It has been shown that polymers higher than dimers are not formed in appreciable amounts (5, 8, 9). This simplifies considerably the interpretation of spectroscopic data and facilitates thermodynamic computations. Furthermore, there are indications that thermodynamic parameters, particularly bond-enthalpies, are quite similar for hydrogen bonds between *cis* amides and between *trans* amides, as evidenced by a comparison of work on *N*-methylacetamide (9) and the latest results on lactams (6).

Experimental

δ-Valerolactam, obtained from the Aldrich Chemical Company,[1] was purified by vacuum distillation. It was stored under nitrogen in the dark at less than 10°. Sample preparation was performed in a nitrogen atmosphere. Carbon tetrachloride, Baker-Analyzed, obtained from the J. T. Baker Company, was dried over Linde type 4A molecular sieve. No differences were observed between the NH chemical shifts of lactam in specially dried CCl_4 and in CCl_4 used without further purification. Chloroform-*d*, obtained from NMR Specialties Company, was also dried over Linde type 4A molecular sieve. It was stored in a nitrogen atmosphere in the dark over molecular sieve. Prior to the preparation of each sample the purity and dryness of the chloroform-*d* were determined by careful observation of the near infrared region where OH groups absorb. Samples were prepared gravimetrically.

The n.m.r. spectra of solutions of δ-valerolactam in CCl_4 and $CDCl_3$ were obtained with a Varian DP-60 and a DA-60 IL spectrometer, respectively. Tetramethylsilane, obtained from NMR Specialties Company, was used as an internal reference. The Varian V-4340 variable temperature apparatus was used with the DP-60. Temperature measurements were made by means of a copper–constantan thermocouple situated just inside the Dewar probe insert in the incoming gas stream. Calibration was performed using a similar thermocouple placed directly in a sample tube at the receiver coil. The Varian V-4343 variable temperature apparatus was used with the DA-60 IL. The Varian charts for the temperature variation of the OH proton resonance of ethylene glycol and of methanol were used to calibrate the apparatus. Accuracy of the temperature measurements was ±1°.

Each solution of δ-valerolactam in CCl_4 and in $CDCl_3$ displayed only one proton resonance which could be assigned to the NH proton. The midpoint of the broad NH line was considered as the chemical shift, δ, of the NH resonance. Line positions, observed with

[1]Mention of commercial items is for your convenience and does not constitute an endorsement by the U. S. Department of Agriculture over others of a similar nature.

Can. J. Chem. Downloaded from www.nrcresearchpress.com by 210.87.254.6 on 09/05/12
For personal use only.

TABLE I

Observed NH chemical shifts for δ-valerolactam in CCl_4 at 33°

Concentration of lactam, (mf)	δ (Hz from TMS)
0.008	475.5
0.009	479.1
0.011	485.1
0.015	487.1
0.018	488.7
0.020	488.9
0.025	491.3
0.030	493.4
0.035	494.5
0.040	495.8
0.045	497.0
0.050	497.7
0.055	497.9
0.060	498.9
0.070	498.7
0.080	499.0
0.090*	498.5
0.100	497.8
0.193	495.0
0.352	491.3
0.478	490.8
0.597	489.5
0.700	489.2
0.798	488.9

*Points at this and higher concentrations were not used in the thermodynamic calculations.

TABLE II

Observed NH chemical shifts for δ-valerolactam in CCl_4

Concentration of lactam, (mf)	δ (Hz from TMS) Temperature 5°	Temperature −10°	Temperature −20°
0.002	485.4	506.5	518.7
0.004	499.1	515.3	523.5
0.006	503.5	517.8	527.5
0.008	509.5	523.0	528.9
0.010	511.4	523.4	530.2
0.020	515.0	525.5	531.0
0.030	515.8	525.5	531.6
0.040	517.3	526.0*	531.1*
0.050	517.9	525.6	530.6
0.070	518.1*	525.3	530.0
0.085	516.5	525.3	529.3
0.100	515.8	523.1	527.0
0.150	514.0	521.4	526.3
0.200	512.0	519.0	522.9

*Points at this and higher concentrations were not used in the thermodynamic calculations.

the DP-60, were determined by interpolation between calibration side bands. Line positions, observed with the DA-60 IL, were determined by interpolation between two values of the frequency difference of the fixed and swept oscillators. All chemical shifts in Hz downfield from tetramethylsilane are the averages of at least four measurements made with the DA-60 IL with alternate up and downfield sweeps. At least fourteen measurements were made with the DP-60 due to its lesser stability. The least accurate values are precise to within 3 Hz on the basis of 2σ (twice the standard deviation) values. Such error is largely the consequence of the uncertainty of locating the midpoint of the broad NH line, especially for the more dilute solutions. The observed NH chemical shifts are given in Tables I, II, and III.

TABLE III

Observed NH chemical shifts for δ-valerolactam in $CDCl_3$

Concentration of lactam, (mf)	δ (Hz from TMS) Temperature 33°	Temperature 5°	Temperature −10°	Temperature −20°
0.010	382.0		412.7	
0.020	408.8	439.1	454.0	464.5
0.030	420.7	446.6	464.6	474.7
0.041	426.2	453.0	466.9	477.9
0.052	442.7	467.4	484.4	494.6
0.061	451.0	476.3	492.5	501.1
0.073	444.8	474.6	488.7	497.3
0.083	453.3	480.5	493.2	502.0
0.091	459.5	483.0	495.9	503.3
0.097	458.4		488.3	
0.150	469.6	492.4	504.9	513.1
0.203	476.9	499.5	511.0	517.2
0.255	484.6	505.0	514.9	521.8
0.300	484.7	507.0	517.7	523.3
0.359	488.3	506.0	516.0	522.0
0.408	491.7	509.0	518.8	525.4
0.449	491.9	509.8	518.9	525.1
0.490	494.3	511.5	519.9	525.5

Treatment of Data

Previous careful studies strongly indicate that δ-valerolactam forms only cyclic dimers with two N—H·····O=C hydrogen bonds per dimer (6, 8, 9). If we assume that in dilute solution only hydrogen bonding occurs among lactam molecules to form cyclic dimers and that the solvent does not compete with the solute in the formation of hydrogen bonds, then dimerization can be represented by the simple equilibrium:

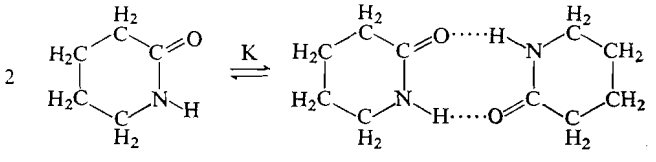

Can. J. Chem. Downloaded from www.nrcresearchpress.com by 210.87.254.6 on 09/05/12
For personal use only.

The dimerization equilibrium constant in reciprocal mole fraction (mf^{-1}) units is

$$[1] \quad K = \frac{[D]}{[M]^2} = \frac{\frac{XS}{(1-X)S}}{\left[\frac{S(C-2X)}{S(1-X)}\right]^2} = \frac{X(1-X)}{(C-2X)^2}$$

where C = initial mole fraction of δ-valerolactam in terms of monomer, S = total number of moles in the system in terms of lactam monomer and of solvent, and X = equilibrium number of moles of the dimer divided by S. At equilibrium the total number of moles equals the sum of the moles of lactam monomer, lactam dimer, and solvent.

$$[2] \quad (C-2X)S + SX + (1-C)S = S(1-X)$$

The observed chemical shift, δ, for the NH resonance is expressed as the weighted average of the contributions of the two NH-containing species

$$[3] \quad \delta = \left(\frac{C-2X}{C}\right)\delta_M + \left(\frac{2X}{C}\right)\delta_D$$

where δ_M = chemical shift of the NH resonance of the lactam monomer and δ_D = chemical shift of the NH resonance of the lactam dimer. The factor 2 results from the presence of two hydrogen bonds in the cyclic dimer. Solving eq. [1] for X, the physically meaningful root is

$$[4] \quad X = \frac{1}{2}\left\{\frac{(4KC+1) - (-4KC^2 + 8KC + 1)^{\frac{1}{2}}}{4K+1}\right\}$$

As shown in Fig. 1, the variation of the NH chemical shift with concentration of lactam in CCl_4 does not increase monotonically but passes through a maximum at approximately 0.04–0.08 mf. Apparently the dimerization equilibrium given above is insufficient to explain all the data. Perhaps at higher concentrations in CCl_4 a different kind of interaction also occurs which influences the NH chemical shift.[2] It is conceivable that models including other equilibria (e.g., stacking of the lactam rings or hydrogen bonding among higher polymers of lactam) could be devised that would fit the experimental data over a wider range of concentration. However, in view of the increase in the number of adjustable parameters, the results of such treatments admit a variety of interpretations. The important aspect regarding dimerization through hydrogen bonding interaction is the variation of the NH chemical shift with concentration in dilute solution. (The dimerization in CCl_4 is virtually complete at the maxima of the experimental curves, e.g., approximately at 0.07 mf at 33° (6, 7).)

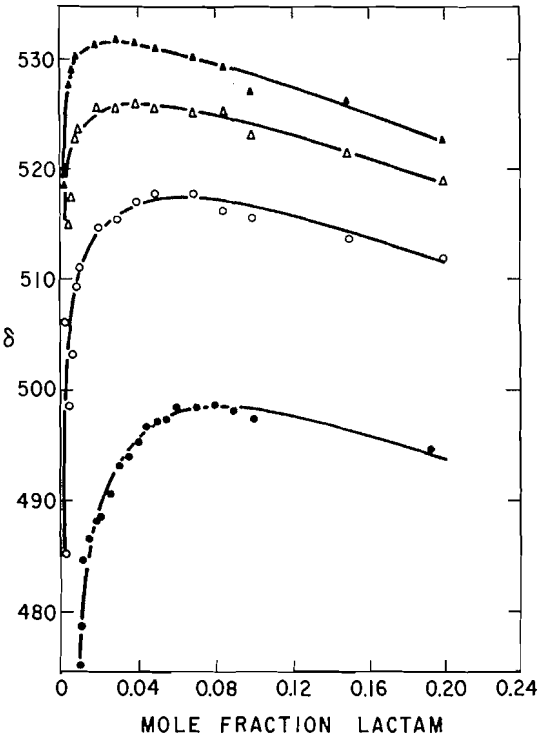

FIG. 1. Variation of δ with concentration in CCl_4 at various temperatures: ▲, −20°; △, −10°; ○, 5°; ●, 33°.

The experimental curves obtained for $CDCl_3$ solution are given in Fig. 2. Slight solvent–solvent hydrogen bonding is possible, but there is reason to believe that hydrogen bonded solvent aggregates are present in very low concentration (12–14). However, in chloroform solution, solvent to solute hydrogen bonding involving the lactam carbonyl group is appreciable. It has been shown (6, 7, 10) that such a system can be treated on the

[2]Yonezawa and Morishima compared the *cis* *N*-methyl proton chemical shifts of neat *N,N'*-dimethylformamide, *N*-methyl-γ-butyrolactam, and *N,N'*-dimethylacetamide with those of 0.1 mf CCl_4 solutions. In each case they observed an upfield shift for the neat liquid relative to the 0.1 mf CCl_4 solution. This observation has been explained in terms of an intermolecular dipolar interaction (association) between the nitrogen and the oxygen (N·····O) of different molecules (11).

TABLE IV

Calculated dimerization equilibrium constants of δ-valerolactam in CCl_4

	Temperature 33°		Temperature 5°		Temperature −10°		Temperature −20°	
δ_M* (Hz)	δ_D† (Hz)	K (mf^{-1})	δ_D (Hz)	K (mf^{-1})	δ_D (Hz)	K (mf^{-1})	δ_D (Hz)	K (mf^{-1})
400	513.0	447	529.0	1704	535.2	4769	537.6	11983
300	511.6	2032	528.1	6493	534.7	16288	537.5	38498
250	511.3	3252	527.9	10046	534.6	24619	537.4	57389
200	511.2	4757	527.8	14370	534.6	34662	537.4	80051
150	511.1	6547	527.7	19466	534.5	46419	537.4	106461
100	511.0	8622	527.6	25334	534.5	59898	537.3	136649

*Preset values of the monomer shift.
†All δ_D values are calculated values of the dimer shift.

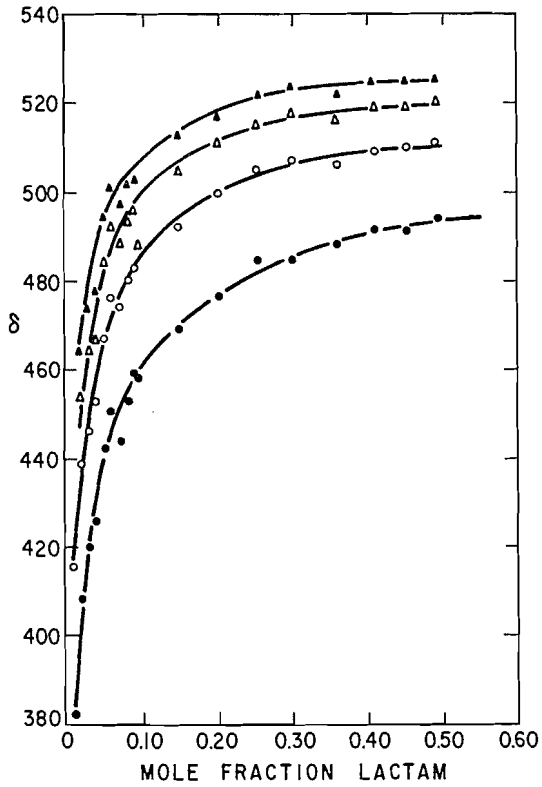

FIG. 2. Variation of δ with concentration in $CDCl_3$ at various temperatures, ▲, −20°; △, −10°; ○, 5°; ●, 33°.

assumption that essentially all lactam monomers are specifically solvated. The equilibrium constant and the ΔH value then pertain to the formation of dimers from solvated monomers. The interaction of $CDCl_3$ with lactam monomer will, in fact, be reflected in the differences in the calculated equilibrium constants and enthalpy values for the two systems, as described by Klemperer *et al.* (10) and others (6, 7).

Methods of Calculation

The relationship between the NH chemical shift and lactam concentration is a function of three parameters: the chemical shifts of lactam monomer, δ_M, and lactam dimer, δ_D, and the dimerization equilibrium constant, K. If the monomer and dimer shifts are known, then either the observed NH chemical shift at any given concentration or the slope of the NH chemical shift – concentration curve at any given point is sufficient to determine K. The dimer shift can be estimated from the maximum of the curve. If the limiting slope at low concentration is known, δ_M can be determined by extrapolation. As shown in Figs. 1 and 2, the slope of the experimental curves continuously increases as the concentration approaches zero. Consequently, no graphical extrapolation can be attempted with a reasonable degree of accuracy.

In order to carry out a more thorough analysis of the experimental data, a numerical method was used. Arbitrary values of δ_M were chosen, and values of K and δ_D were determined from a least squares analysis by a direct search procedure (15).[3] The search procedure involves the independent variation of arbitrary initial values of δ_D and K until the root mean square (r.m.s.) error between the calculated and observed curves reaches a minimum for a given value of δ_M. For the $CDCl_3$ system all the experimental data points (Table III) were used in the calculation. For the CCl_4 system only those data points

[3]The computations were carried out on an IBM-1130 computer.

Can. J. Chem. Downloaded from www.nrcresearchpress.com by 210.87.254.6 on 09/05/12
For personal use only.

TABLE V
Calculated dimerization equilibrium constants of δ-valerolactam in $CDCl_3$

	Temperature 33°		Temperature 5°		Temperature −10°		Temperature −20°	
δ_M* (Hz)	δ_D† (Hz)	K (mf^{-1})	δ_D (Hz)	K (mf^{-1})	δ_D (Hz)	K (mf^{-1})	δ_D (Hz)	K (mf^{-1})
350	531.0	18	537.6	41	546.6	52	545.8	86
300	521.9	45	534.6	81	534.5	100	544.5	154
250	517.2	85	533.0	134	541.7	166	543.6	242
200	514.5	139	531.9	201	540.5	249	543.1	350
150	512.8	207	531.3	281	539.7	348	542.7	478

*Preset values of the monomer shift.
†All δ_D values are calculated values of the dimer shift.

(see Tables I and II, the Experimental section, and footnote 2) pertinent to the dimerization equilibrium were used. The results are shown in Tables IV and V.

Results and Discussion

All the calculated curves based on preset values of δ_M fit the observed data with a relatively small degree of error (r.m.s. error of 1–2 Hz for CCl_4 and 3–5 Hz for $CDCl_3$ which are of the same order of magnitude as experimental error). For the lactam–CCl_4 system, only the low concentration portion of the experimental curves was considered, as discussed in previous sections. The observed and some of the calculated curves for the lactam–$CDCl_3$ system are given in Fig. 3. The calculated dimer shift is nearly independent of the preset monomer shift used in the calculation. The calculated equilibrium constant increases as the preset monomer shift decreases. On this basis, no one value of the monomer shift and the corresponding equilibrium constant can be taken as more realistic than any other.

In general, the information that can be obtained from the chemical shift – concentration curves depends primarily on the value of the equilibrium constant. We have examined the theoretical curves obtained from the treatment given above on the basis of a unit chemical shift difference between the monomer and dimer species. Several values of the equilibrium constant over a wide range were included in the calculations. On this basis certain limitations of the n.m.r. method seem to be indicated. If K is large, the slope at low concentrations is sufficiently steep that no meaningful extrapolation to infinite dilution is possible. On the other hand, if K is very small, the curve is nearly linear; only two of the necessary three parameters can be determined. If K lies in an intermediate range close to unity, the system is amenable to complete analysis. In the lactam systems studied, K lies to the high side of this range.

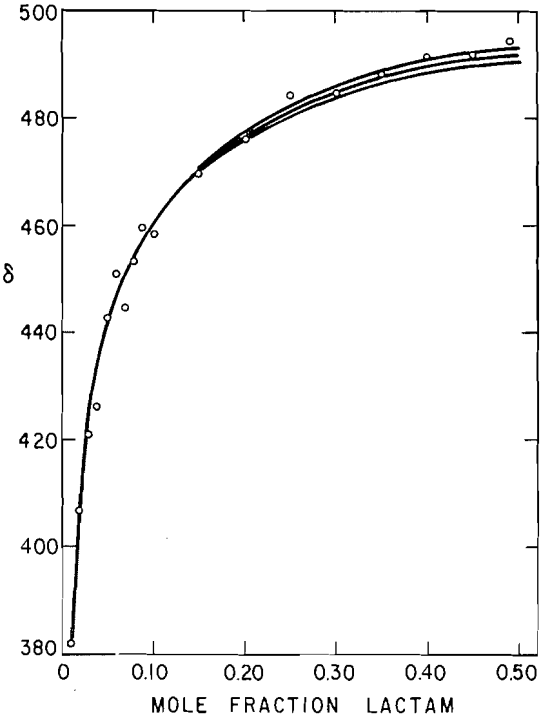

FIG. 3. Comparison of observed and calculated data for lactam in $CDCl_3$ at 33°. Solid lines are calculated curves for various values of δ_M. Upper curve, δ_M = 300 Hz; middle curve, δ_M = 250 Hz; lower curve, δ_M = 200 Hz.

Even though accurate extrapolation cannot be made, one can set limits to the possible choices of δ_M. The downfield limit is given by the lowest

Can. J. Chem. Downloaded from www.nrcresearchpress.com by 210.87.254.6 on 09/05/12
For personal use only.

TABLE VI

Calculated ΔH for the hydrogen bonding dimerization of δ-valerolactam

In CCl_4		In $CDCl_3$	
δ_M* (Hz)	ΔH† (kcal/mole)	δ_M* (Hz)	ΔH† (kcal/mole)
400	−9.43	350	−4.35
300	−8.41	300	−3.43
250	−8.20	250	−2.90
200	−8.06	200	−2.56
150	−7.96	150	−2.22
100	−7.89		

*Preset values of the monomer shift.
†Calculated.

value of the observed shift. The upfield shift can be set by the chemical shift of a nonhydrogen-bonded N—H proton, e.g., that of piperidine monomer (16, 17) at approximately $\tau = 8.9$. This range, in fact, guided the choices for δ_M used in the calculations described above.

Despite the inability to fix precisely the value for K, ΔH can be more closely estimated. With the assumption that δ_M and δ_D are temperature independent, ΔH can be calculated for a given δ_M using the van't Hoff equation with the calculated values for K as given in Tables IV and V. The results are shown in Table VI. Regardless of the appreciable variation of K corresponding to possible choices of δ_M, the calculated values for ΔH fall in a relatively narrow range. Therefore, a reasonable estimate of ΔH can be obtained even though a full analysis of the experimental data cannot be made. The results obtained for ΔH are in essential agreement with those from i.r. measurements as shown in Table VII. Note that the difference in ΔH between the CCl_4 and $CDCl_3$ systems is ~5 kcal/mole. This difference reflects the specific solvation of lactam monomer and amounts to a ΔH of solvation of ~ -2.5 kcal/mole of monomer, close to the value of −2 kcal/mole estimated for $CDCl_3$–amide interactions by Klemperer *et al.* (10).

TABLE VII

Infrared results for δ-valerolactam*

Temperature (°C)	K (CCl_4) (mf^{-1})	K ($CHCl_3$) (mf^{-1})
25	1182	28.0
40	517	20.9
55	273	16.8
	$\Delta H = -7.1$ kcal/mole	$\Delta H = -3.1$ kcal/mole

*Reference 6.

Conclusion

Dimerization equilibria described by equilibrium constants on the order of unity are ideally suited to n.m.r. investigation. For such systems, the chemical shift of both monomer and dimer can be precisely obtained and a value of K readily calculated. For the hydrogen bonding of δ-valerolactam, K is large. Nevertheless, even in this system for which the monomer shift cannot be reasonably estimated, a value for ΔH may still be obtained because of its slow variation with assumed values of the monomer shift.

1. G. C. Pimentel and A. L. McClellan. The hydrogen bond. Reinhold Publishing Corp. New York. 1960.
2. J. A. Pople, W. G. Schneider, and H. J. Bernstein. High-resolution nuclear magnetic resonance. McGraw-Hill Book Co., Inc., New York. 1959. Chap. 15.
3. D. Hadzi. (*Editor*). Hydrogen bonding. The Pergamon Press Ltd., New York. 1960.
4. J. W. Emsley, J. Feeny, and L. H. Sutcliffe. High-resolution nuclear magnetic resonance spectroscopy. Vol. 1. The Pergamon Press Ltd., New York. 1966. Chap. 9.
5. H. Susi, S. N. Timasheff, and J. S. Ard. J. Biol. Chem. **239**, 3052 (1964).
6. H. Susi and J. S. Ard. Arch. Biochem. Biophys. **117**, 147 (1966).
7. M. Tsuboi. J. Chem. Soc. Japan, Pure Chem. Sect. **76**, 376 (1955).
8. R. C. Lord and T. J. Porro. Z. Electrochem. **64**, 672 (1960).
9. M. Tsuboi. Bull. Chem. Soc. Japan, **24**, 75 (1951).
10. W. Klemperer, M. W. Cronyn, A. H. Maki, and G. C. Pimentel. J. Am. Chem. Soc. **76**, 5846 (1954).
11. T. Yonezawa and I. Morishima. Bull. Chem. Soc. Japan, **39**, 2346 (1966).
12. E. D. Becker. Spectrochim. Acta, **14**, 743 (1959).
13. B. B. Howard, C. F. Jumper, and M. T. Emerson. J. Mol. Spectry. **10**, 117 (1963).
14. J. Lascombe, J. Devaure, and M-L. Josies. J. Chim. Phys. **61**, 1271 (1964).
15. R. Hooke and J. A. Jeeves. J. Assoc. Computing Mach. **8**, 212 (1961).
16. V. F. Bystrov and V. P. Lezina. Optics Spectry. **16**, 430 (1964).
17. R. A. Murphy and J. C. Davis. J. Phys. Chem. **72**, 3111 (1968).

Can. J. Chem. Downloaded from www.nrcresearchpress.com by 210.87.254.6 on 09/05/12
For personal use only.

Can. J. Chem. Downloaded from www.nrcresearchpress.com by 210.87.254.40 on 09/05/12
For personal use only.

Dehydrobromination of methyl 11α-bromo-12-oxopodocarpan-19-oate

R. A. Bell and M. B. Gravestock
Department of Chemistry, McMaster University, Hamilton, Ontario
Received May 5, 1969

The configuration and stereochemistry of methyl 11α-bromo-12-oxopodocarpan-19-oate **1** have been determined by application of the nuclear Overhauser effect. The dehydrobromination of **1** with dimethylacetamide – calcium carbonate results in a predominant 1,4-elimination process which for short reaction periods yields the non-conjugated ketone **8** and for long reaction periods yields the conjugated ketone **2**. The 1,2-elimination of hydrogen bromide is a minor process and takes place to the extent of 20–22%. The ketone **8** has been oxidatively cleaved to the keto-acid **11**, a valuable intermediate for the synthesis of bicyclic diterpenoids.

Canadian Journal of Chemistry, **47**, 3661 (1969)

Dehydrohalogenation by high-boiling, aprotic solvents was first introduced in 1953 by Holysz (1). Since that time the reaction has proved to be remarkably useful in organic synthesis (2). The particular dehydrobromination of the bromo-ketone **1** by refluxing dimethylformamide in the presence of lithium chloride – lithium carbonate has been reported (3) to furnish the unsaturated ketone **2** as the sole isolable product. Since this compound is of interest as a potential intermediate in the synthesis of bicyclic diterpenes, we undertook a careful scrutiny of the stereochemistry of the bromo-ketone **1** and a detailed analysis of its dehydrobromination products.

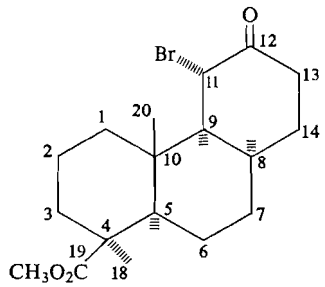

1

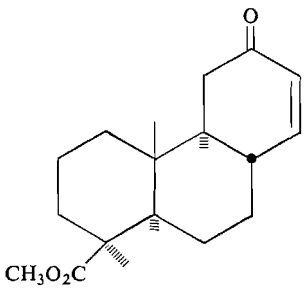

2

The bromo-ketone was prepared by a modification of the procedure adopted by Bible and Burtner (3). Experimental conditions were devised which resulted in a greatly improved overall yield of **1** (see Scheme 1). The saturation of the aromatic ring of podocarpic acid **3***a* by hydrogenation over platinum in acetic acid was noted by Bible and Burtner (3) to produce a high % of 12-deoxy material resulting from the hydrogenolysis of the 12-hydroxyl group. In the present study, hydrogenation of **3***a* with a rhodium-on-alumina catalyst (4) proceeded rapidly and resulted in no observable loss of the 12-hydroxyl group. The proton magnetic resonance (p.m.r.) spectrum of the crude rhodium catalyzed hydrogenation product showed that, although the 12β-hydroxy-B/C-*cis* compound **4***a* was the principal product (55%), there was also 30% of the 12α-hydroxy-B/C-*cis* compound **4***b* and 15% of the 12α- and 12β-hydroxy-B/C-*trans* derivatives **5** present. The product composition was further confirmed by p.m.r. analysis of the mixture of the acetates derived from the crude hydrogenation product and also by p.m.r. analysis of the mixture of the ester-ketones, **6** and **7**, obtained by direct oxidation and methylation of the crude hydrogenation product. The predominance of the B/C-*cis* ring juncture is expected on simple steric grounds, the α-face of the molecule being less sterically congested than the β-face. The minor formation of the B/C-*trans* ring juncture during hydrogenation is explicable if it is assumed that part or whole of the hydrogenation of the aromatic ring is a stepwise process and that the most difficult bond to saturate is the Δ-8(9)-double bond. A number of other Δ-8(9)-olefinic diterpenoids have been noted to yield B/C-*trans*

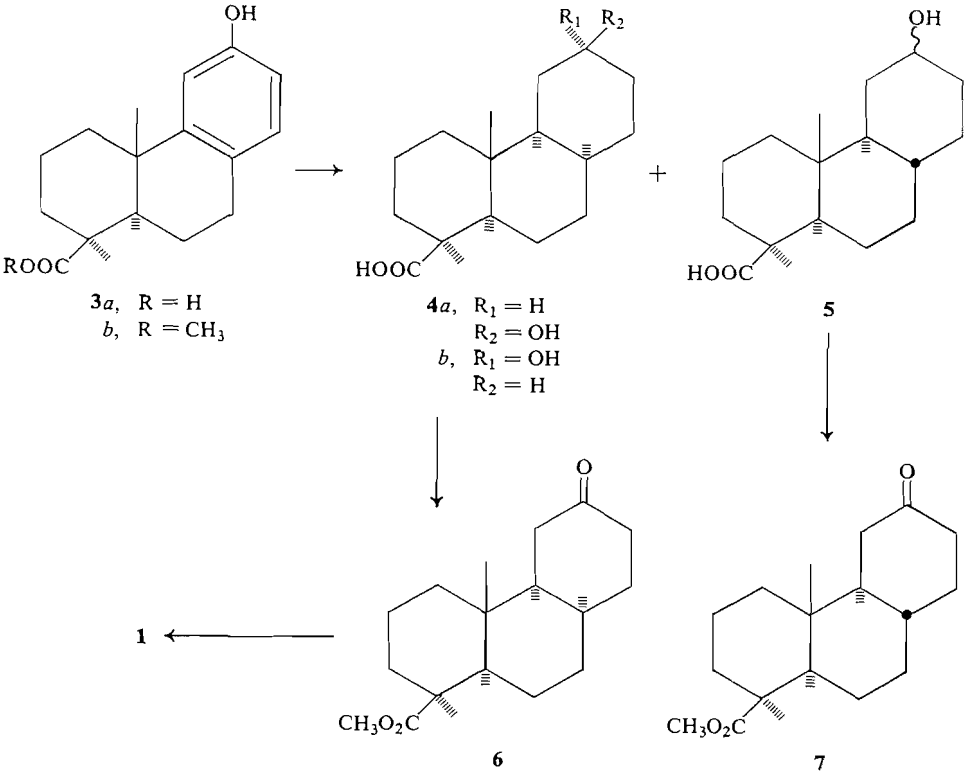

SCHEME 1

products either predominantly (5) or exclusively on catalytic hydrogenation (6).

In practice, isolation of the pure *cis*-keto-ester **6** was best accomplished by methylation of the crude hydrogenated podocarpic acid with diazomethane, oxidation with Jones' reagent (7) and separation of the mixture of **6** and **7** by fractional crystallization from ethyl acetate – hexane. In this manner **6** could be obtained in 70% overall yield from podocarpic acid **3***a*.

The *cis*-bromo-ketone **1** was obtained in 60% yield (isolated) by bromination of **6** with *N*-bromosuccinimide in dilute solution in carbon tetrachloride. Examination of the p.m.r. spectrum of the crude bromination products indicated that the principal component comprised *ca.* 90% of the product. The 11α-configuration assigned (3) to the bromine atom in this bromo-ketone was based on the long wavelength absorption at 310 mμ (ε 130) in the ultraviolet (u.v.) spectrum, which is indicative of an axial bromine (8), and the strong positive Cotton effect observed in the optical rotatory dispersion curve. However, the inspection of a molecular model and application

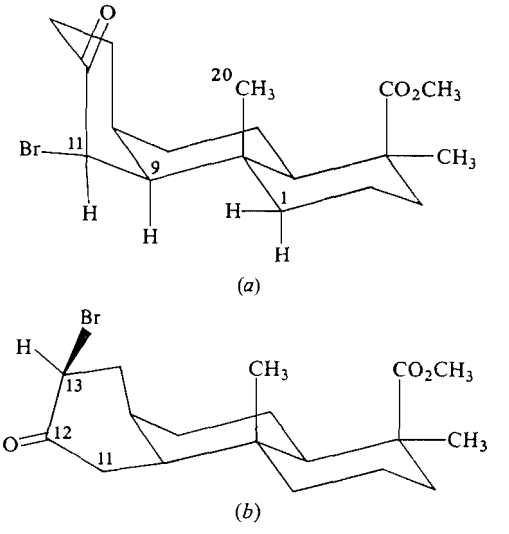

FIG. 1. Possible configurations of **1** showing positive Cotton effect.

of the Octant Rule (9) (see Fig. 1) shows that these spectroscopic properties can be satisfied by an 11α-bromine substituent with ring C in a chair

Can. J. Chem. Downloaded from www.nrcresearchpress.com by 210.87.254.40 on 09/05/12
For personal use only.

Can. J. Chem. Downloaded from www.nrcresearchpress.com by 210.87.254.40 on 09/05/12
For personal use only.

TABLE I
Nuclear Overhauser effects in **1**

Protons saturated	δ p.p.m.	Proton observed	δ p.p.m.	% Area increase
C-20 CH_3	0.675	H-11	4.37	7
H-1, a	1.12	H-11		7
H-1, e	2.17	H-11		17
H-9	2.27	H-11		18
H-1, e*	2.17	H-11		
H-9*	2.27	H-11		37

*Triple irradiation.

conformation (*a*), or by a 13β-bromine with ring C in a twist conformation (*b*). To clearly distinguish between these two possibilities the nuclear Overhauser effect (N.O.E.) (10) properties of the proton adjacent to the bromine atom and carbonyl group (signal at 4.37 p.p.m.) were examined (see Table I). The basis for the intramolecular N.O.E. lies in the contributions which neighboring protons make to the longitudinal relaxation time T_1 of the proton of interest. As a general, qualitative rule (11), if the nearest neighboring protons are within 3.0 Å of the proton of interest, then saturation of any (or all) of these protons with a second *rf* field will result in an area increase for this proton.

The 11-proton of the bromo-ketone showed a 7% area increase[1] when the C-20 methyl group[2] was saturated. This clearly implies that the 11-proton and the C-20 methyl protons must be within 3.0 Å of one another. Measurement of this distance with the aid of a molecular model (Fig. 1) for an 11α-bromine substituent showed a separation of 2.8 Å, whilst measurement of the equivalent distance for a 13β-bromine substituent, placed the 13α-proton and the C-20 methyl 3.6 Å apart. It must, therefore, be concluded that the bromo-ketone possesses the 11α-configuration as in **1** and the original assignment of Bible and Burtner is correct.

On the basis of the structure **1** for the bromo-ketone, the chemical shifts for the other neighboring protons of the 11β-proton can be assigned from the N.O.E. data. It is possible to distinguish between the H-1 and H-9 protons by virtue of the coupling ($J_{9,11}$ = 1 Hz) which exists between H-9 and H-11. Thus an *rf* field which was sufficient to saturate H-9 was also sufficient to decouple (12) H-9 from H-11, and the signal from H-11 not only increased in area but also decreased in line width (13). The coupling constant, $J_{11,13}$ = 1.0 Hz, was now also clearly visible by the splitting of the H-11 signal into a doublet. The numerical values for the N.O.E.'s observed for the axial and equatorial protons at C-1 are subject to some doubt since the strong coupling between these 2 protons means that saturation of one of them will result in significant saturation of the transitions of the other (14). However, it is possible to assign their chemical shifts accurately.

Dehydrobromination of 1

The unequivocal establishment of the stereochemistry of **1** meant that the formation of the products from the dehydrobromination experiments could be rationalized on a firm basis. Dehydrobromination of **1** for 30 min (Table II)

TABLE II
Dehydrobromination of **1** in DMA/$CaCO_3$

Reaction time	Products	% Yield
10 min	Δ-13(14)-ketone **2**	14
	Δ-8(14)-ketone **8**	60
	Δ-9(11)-ketone **9**	16
	Δ-8(9)-ketone **10**	6
	Methyl podocarpate *3b*	4
30 min	Δ-13(14)-ketone **2**	60
	Δ-8(14)-ketone **8**	14
	Δ-9(11)-ketone **9**	16
	Δ-8(9)-ketone **10**	3
	Methyl podocarpate *3b*	7

gave as the principal product the α,β-unsaturated ketone **2** (Scheme 2) which resulted from the elimination of hydrogen bromide in a 1,4-manner. Whilst such 1,4-eliminations have ample precedent (15) in the dehydrobromination of many bromo-ketones there are relatively few examples where the 1,4-elimination product is the principal product[3] (16). The predominance of a 1,4-elimination over the normal 1,2-elimination pathway is usually a simple consequence of the 1,2-elimination being a high energy process because of steric or stereoelectronic reasons. In this respect the bromo-ketone **1** is no exception, for

[1]We have found area increases down to as low as 3% to be quite reproducible with current instrumentation. Many of these small area increases have been noted in compounds of unequivocal structure (11) giving increased confidence in the application of the method in the present study.

[2]The numbering system employed is that proposed by the Committee on Diterpene Nomenclature (IUPAC), July 1968.

[3]Except of course in situations where 1,2-elimination is rendered impossible by complete substitution of the β-carbon. See ref. 17.

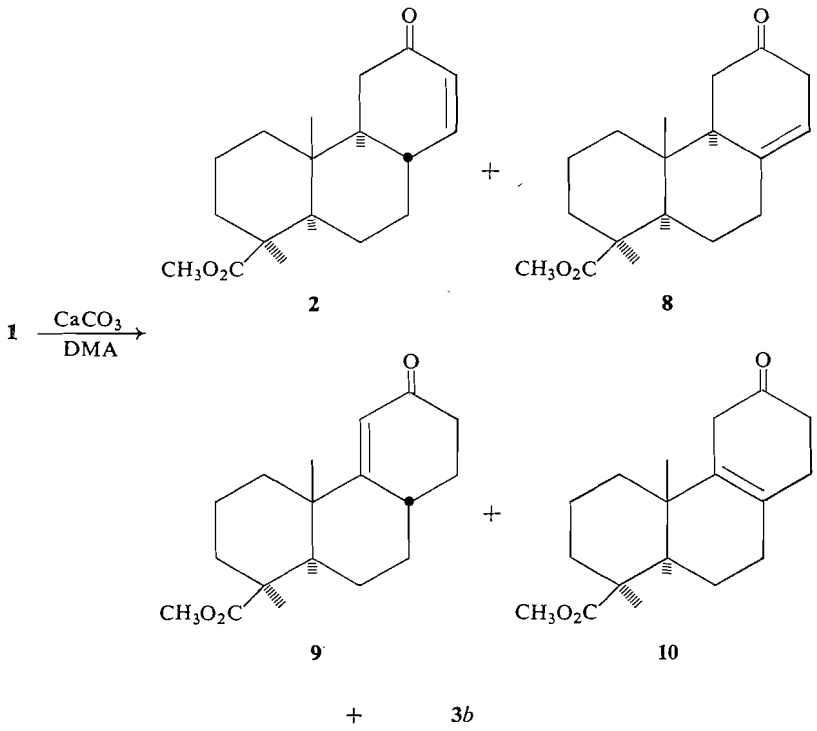

SCHEME 2

the inspection of a molecular model (see Fig. 1 (*a*)) shows that the dihedral angle between the C-9 H bond and the C-11 Br bond is approximately 60–90° and ring C cannot achieve coplanarity of these 2 bonds without undergoing severe distortion. Thus, the activation barrier for a 1,2-elimination will be high (18) and the alternative 1,4-elimination will be open to the molecule. An analogous situation is to be found in Reichstein's (19) work on 11α- and 11β-bromo-12-keto steroids. Dehydrobromination of 11β-bromo-ketones (a *trans* elimination with the C-9 α-proton) was dramatically more facile than dehydrobromination of the 11α-bromo-ketones. In these examples only 1,2-elimination is possible.

Since the unsaturated ketone **2** possesses a *trans* B/C ring juncture, **2** cannot be the primary product of a 1,4-elimination process. In an attempt to find the B/C *cis*-fused ketone **14**, (Scheme 3), which would be the presumed initial product, **1** was exposed to refluxing dimethylacetamide (DMA)/$CaCO_3$ for increasingly shorter periods of time. The appearance of a highly shielded C-20 methyl group at 0.33 p.p.m. in the p.m.r. spectra of the products was observed as the reaction period was decreased. This compound was the predominant product (60%, see Table II) after a reaction period of 10 min. Shorter reaction times down to a period of 5 min resulted in the recovery of unreacted bromo-ketone and no distinguishable change in the composition of the dehydrobromination products. When the principal product from the 10 min reaction was isolated via silica gel or Florisil chromatography and its spectral properties examined, it was clear that it was not the *cis*-fused ketone **14** but the non-conjugated ketone **8**. Thus **8** showed only one vinylic proton at 5.44 p.p.m. in its p.m.r. spectrum, a carbonyl absorption at 1712 cm^{-1} in its infrared (i.r.) spectrum, and only a weak absorption at 282 mμ (ε 100) in its u.v. spectrum. Moreover, on treatment with alumina or dilute acid, **8** was transformed into a mixture consisting of 95% of **2** and 5% of **8**. This equilibrium composition indicates that **2** is thermodynamically more stable than **8**.[4] To firmly secure the structure

[4]The equilibrium composition of 4-alkylcyclohexenones, however, favors the β,γ-form as the size of the alkyl substituent increases (20).

Can. J. Chem. Downloaded from www.nrcresearchpress.com by 210.87.254.40 on 09/05/12
For personal use only.

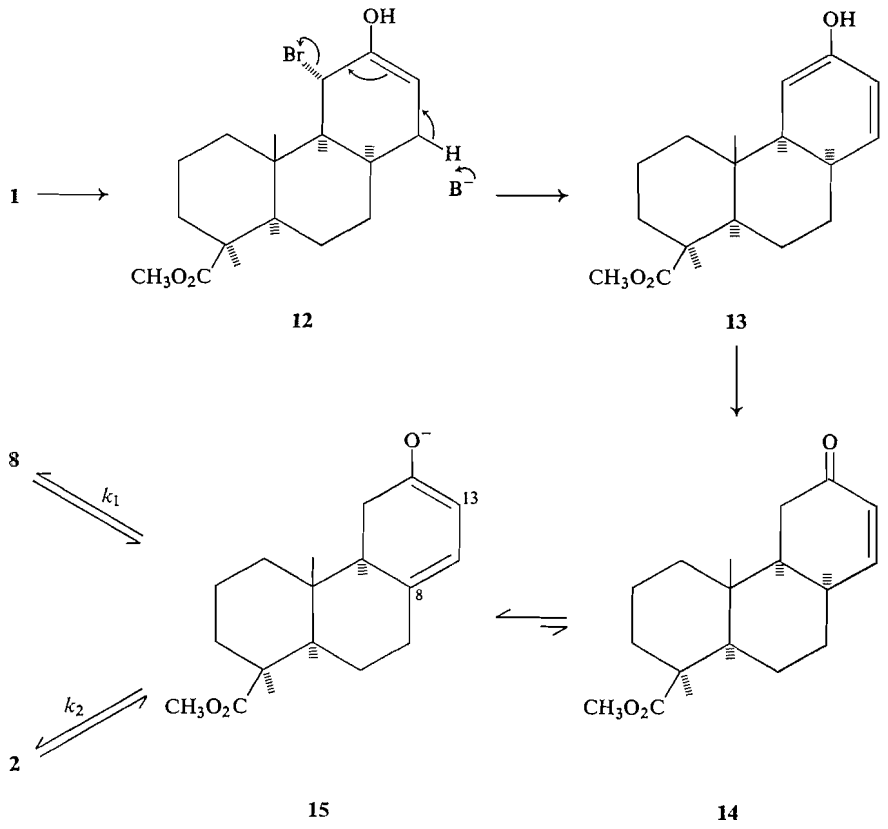

SCHEME 3

assigned to **8**, the compound was oxidized in excellent yield with either potassium permanganate – sodium periodate or ozone to the known keto-acid **11**. This ketone possessed properties and derivatives which were completely consistent with the keto-acid reported by Erdtman *et al.* (21). It is notable that **11** is potentially an exceptionally useful intermediate in the synthesis of bicyclic diterpenoids (22).

A mechanism for the formation of **2** and **8** is shown in Scheme 3. Although a number of mechanisms may be written for the initial steps of the 1,4-elimination (16*c*), the most straightforward is shown since this dehydrobromination offers no new information on this aspect of the process. The enol **12** can, therefore, be considered to furnish the unsaturated enol **13** by 1,4-elimination. Proton transfer to C-11 of **13** via the enolate then leads to the elusive B/C *cis*-ketone **14**. However, the severe steric interaction between the C-20 methyl group and the C-14 carbon provides a strong driving force for base abstraction of the C-8 proton to give the conjugated enolate **15** where this steric interaction is completely removed. In addition the C-8 hydrogen of **14** is pseudo-axial with respect to ring C and therefore its removal by base should be further facilitated for stereoelectronic reasons (23). Because of these two factors, the C-8 hydrogen appears to be more acidic than normal and even a weak base (24) such as DMA can rapidly abstract it although of course it is not necessary that DMA should be the only basic species involved in this proton removal. In

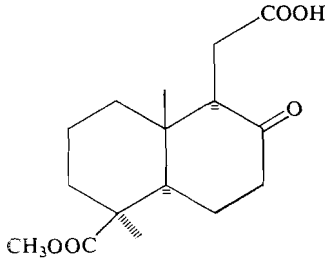

11

Can. J. Chem. Downloaded from www.nrcresearchpress.com by 210.87.254.40 on 09/05/12
For personal use only.

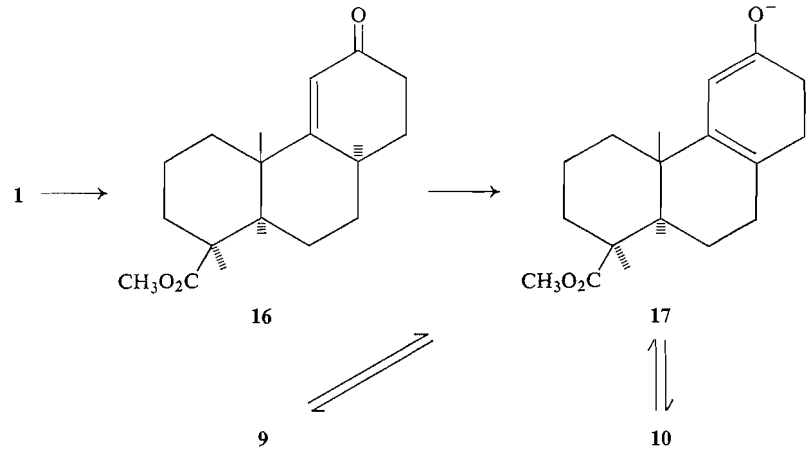

SCHEME 4

other decalin systems, where excessive steric interactions are absent, the removal of a γ-hydrogen by DMA or other bases present appears to be a comparatively slow process and little or no isomerization of the ring junction is observed (25).

The enolate **15** can undergo protonation at either C-13 or C-8. Under conditions of kinetic control, protonation will take place preferentially at the site of highest electron density (26), that is at C-13 (with the second order rate constant $k_1 > k_2$) and the non-conjugated ketone **8** will be formed. Under conditions of thermodynamic control, that is if there is an equilibrium between **8** and **2** the more stable ketone **2** will be formed. The predominant formation of **8** during the short reaction period shows that the reaction is largely kinetically controlled over this period. The longer, 30 min reaction period results in principally thermodynamic control. Since the product ratio of **2** and **8** did not change appreciably for more extended reaction periods the observed ratio of 60:14 for **2**:**8** probably represents the ratio of their stabilities in refluxing DMA.

Although the rate of the 1,2-elimination process is slow, as is noted above, it still occurs to the extent of 20% and, as in the case of 1,4-elimination, the intermediate 8α-conjugated ketone **16** (Scheme 4) possesses only a fleeting existence and is rapidly transformed by enolization and protonation into the 8β-conjugated ketone **9** and the non-conjugated ketone **10**. The ratio of **9** to **10** showed only a slight change with increasing reaction period (see Table II) and this is indicative of a situation which is approaching thermodynamic control very quickly. To achieve this, either the ketones **9** and **10** must be in equilibrium or the rate of protonation at C-11, must be comparable with the rate of protonation at C-8. The latter is considered more reasonable here for, despite the high electron density at C-11, the 11-position suffers steric interactions from both the C-20 methyl group and the C-1 hydrogens, whilst the 8-position suffers only an interaction from the C-20 methyl. It is interesting to note that in contrast to the ratio of about 5:1 for **9**:**10** in refluxing DMA, the equilibrium in either acidic or basic media at room temperature is overwhelmingly in favor of **9** (3).

The only other product aside from the ketones **2**, **8**, **9**, and **10**, obtainable from the dehydrobromination of **1** was methyl podocarpate **3***b*. It appeared to have its origin in the air-oxidation of the unsaturated ketones, since experiments performed with the reaction mixture open to the air resulted in greatly increased yields of **3***b* as well as polymeric materials. A consistent 4–7% yield of **3***b* appeared to be a lower limit and is probably a consequence of the experimental technique employed (see Experimental).

Summary

Improved experimental conditions have been developed for the preparation of the bromoketone **1** and its configuration and stereochemistry have been unequivocally determined by application of the N.O.E. The dehydrobromination of **1** with DMA/calcium carbonate results in a predominant 1,4-elimination process which

Can. J. Chem. Downloaded from www.nrcresearchpress.com by 210.87.254.40 on 09/05/12
For personal use only.

Can. J. Chem. Downloaded from www.nrcresearchpress.com by 210.87.254.40 on 09/05/12
For personal use only.

for a short reaction period takes place under conditions of kinetic control and furnishes the non-conjugated ketone **8** in 60% yield. Reaction periods of 30 min or longer give the conjugated ketone **2** as the principal 1,4-elimination product in 60% yield. The 1,2-elimination of hydrogen bromide from **1** is a minor process and takes place to the extent of 20–22%. It yields a mixture of the unsaturated ketones **9** and **10** which appear to be the products of a thermodynamically controlled process. The non-conjugated ketone **8** is a useful precursor to the keto-acid **11** which is a potential intermediate for the synthesis of a variety of diterpenoids.

Experimental

Melting points were determined on a Kofler hot stage apparatus and are uncorrected. Infrared spectra were obtained in chloroform solution unless otherwise noted and u.v. spectra obtained in methanol. Proton magnetic resonance spectra were recorded using Varian Associates HA-100 and A-60 spectrometers in deuteriochloroform solution with tetramethylsilane as internal reference. Mass spectra were recorded with an Hitachi Perkin–Elmer RMU-6A spectrometer at 80 eV.

12β-Hydroxy-8α-podocarpan-19-oic Acid (4a)

The general procedure of Meyers *et al.* (4) was used. Fifty grams (0.182 mole) of podocarpic acid (recrystallized from 10% aqueous methanol and dried *in vacuo* at 80° for 24 h to remove methanol of crystallization) was added to a mixture of 12.5 g of 5% rhodium-on-alumina (Engelhard Industries Inc.) and 200 ml of 95% ethanol containing 1% acetic acid, and the mixture shaken under hydrogen (40–50 p.s.i.) at room temperature in a Parr apparatus. Uptake of hydrogen effectively ceased after 48 h. The reaction mixture was filtered under reduced pressure, the filter pad being washed well with methanol, and the filtrate evaporated to dryness *in vacuo* to give 50.5 g of crude hydroxy-acid as a colorless solid. Two recrystallizations from ethyl acetate gave 25.0 g (50%) of the *cis*-hydroxy-acid **4a**, m.p. 230–234° (lit. (3), m.p. 234.5–236°); p.m.r. (pyridine/CS_2): δ 0.97 (s, 3H, C-20 CH_3), 1.26 (s, 3H, C-18 CH_3), 3.68 p.p.m. (s, broad, 2H, COOH and OH).

Analysis of the Crude Hydrogenation Product

(*i*) Methylation with diazomethane followed by oxidation with Jones' reagent (see below) gave a mixture of keto-esters which by p.m.r. analysis proved to be a mixture of 85% *cis*, and 15% *trans* B/C ring juncture isomers.

(*ii*) Acetylation. The crude hydroxy-acid mixture was methylated and acetylated in pyridine yielding the *cis*-12α- and *cis*-12β-acetates in an approximate ratio of 3:5, respectively. These acetates were identified by their p.m.r. spectra from an independent synthesis (27).

Methyl 12-Oxo-8α-podocarpan-19-oate (6)

A slurry of 50.5 g of the crude hydroxy-acid **4a** in methanol–ether was treated with portions of ethereal diazomethane at room temperature until the yellow color of excess reagent had been present for 15 min. The solvent was then removed *in vacuo* to give 53.0 g of the crude hydroxy-ester as a pale yellow gum. The gum was dissolved in 500 ml of acetone and Jones' reagent added dropwise to the well stirred solution maintained at 10–25° with an ice-bath. When excess of reagent was visible as a permanent orange coloration, the reaction was arrested by the addition of isopropanol and the bulk of the acetone removed *in vacuo* at 30–40°. The residue was diluted with 500 ml water and extracted with ether (2 × 200 ml) and benzene (1 × 100 ml). The combined organic extracts were washed with water and brine, filtered through sodium sulfate and evaporated *in vacuo* to give 52.0 g (98%) of the mixture of B/C *cis* and *trans* keto-esters **6** and **7** as pale yellow-green crystals. Washing through 300 g of alumina in benzene removed the majority of the color and any non-oxidized material giving 50 g (95%) of the crystalline mixture of **6** and **7**. Integration of the areas of the absorptions at 3.63 and 3.66 p.p.m. ($COOCH_3$) showed that this mixture consisted of 85% **6** and 15% **7**.

Separation of the Ketone Isomers

The above mixture of keto-esters (50 g) was dissolved in 200 ml of boiling ethyl acetate – hexane (1:3) and the solution seeded with pure *cis*-keto-ester and cooled slowly to room temperature. After standing for 48 h at room temperature, 33 g (62% from podocarpic acid) of the *cis*-keto-ester **6** was obtained as colorless crystals, m.p. 120–122° (lit. (3), m.p. 120–121.5°); p.m.r.: δ 0.65 (s, 3H, C-20 CH_3), 1.16 (s, 3H, C-18 CH_3), 3.63 p.p.m. (s, 3H, $COOCH_3$). The mother liquors, after evaporation and dissolution in 50 ml ether – 5 ml ethyl acetate – 15 ml hexane at the boiling point and seeding and standing at room temperature, yielded a further 4.2 g of the *cis*-keto-ester **6** (8% from podocarpic acid), m.p. 118–120° (purity 95% by p.m.r.).

The mother liquors from the above crystallizations contained approximately 60% of the *trans*-ketone **7**. In one experiment, careful seeding with a sample of pure **7** obtained from the hydrogenation of **2** (3) gave **7** as colorless crystals, m.p. 110–115° (>90% pure by p.m.r. spectroscopy) (lit. (3), m.p. 116–121.5°); p.m.r.: δ 0.68 (s, 3H, C-20 CH_3), 1.15 (s, 3H, C-18 CH_3), 3.66 (s, 3H, $COOCH_3$).

Separation by selective reaction with Girard's "T" reagent gave variable results and was of no use as a practical method of separating large quantities of the mixed keto-esters.

12-Oxo-8α-podocarpan-19-oic Acid

Twenty-five grams of the hydroxy-acids **4a**, **4b**, and **5**, obtained from the hydrogenation of podocarpic acid as described above were dissolved in 1.2 l of acetone at 10° and oxidized by the dropwise addition of Jones' reagent (7) until a permanent yellow coloration remained. Excess reagent was then destroyed with isopropanol and the bulk of the acetone removed *in vacuo*. The keto-acid was isolated via ether extraction and on crystallization from ether–hexane yielded 18.3 g (73%) of 12-oxo-8α-podocarpan-19-oic acid as colorless crystals, m.p. 165–170° (lit. (3), m.p. 168–174°); p.m.r.: δ 0.79 (s, 3H, C-20 CH_3), 1.25 (s, 3H, C-18 CH_3), 10–11 p.p.m. (s, 1H, COOH).

Can. J. Chem. Downloaded from www.nrcresearchpress.com by 210.87.254.40 on 09/05/12
For personal use only.

Methyl 11α-Bromo-12-oxo-8α-podocarpan-19-oate (1)

The method of Bible and Burtner (3) was used with some modification.

To a solution of 39.3 g (0.135 mole) of methyl 12-oxo-8α-podocarpan-19-oate, m.p. 120–124°, in 1500 ml of dry carbon tetrachloride (molecular sieves) was added 25.5 g (0.140 mole) of *N*-bromosuccinimide and one drop of 48% hydrobromic acid. An immediate red coloration developed which vanished after 30 s. The reaction was over in 2–4 h as evidenced by the supernatant succinimide present and the absence of any *N*-bromosuccinimide. The solution was washed free of succinimide and hydrogen bromide by shaking with water (3 × 300 ml), filtered through anhydrous sodium sulfate, and evaporated *in vacuo* at 40°. Drying at 0.5 mm overnight gave *ca.* 50 g (100%) of crude bromo-ketone. The p.m.r. spectrum of the crude reaction product showed the presence of 85–90% of the desired compound together with 5% unreacted starting material and 5–10% other stereoisomeric bromo-ketones. Crystallization from hexane–ether at 0° yielded 35.0 g (70%) of **1** as colorless prisms, m.p. 145–150°. A second crystallization gave 30 g of **1**, m.p. 151–152° (lit. (3), m.p. 152–153°); p.m.r.: δ 0.68 (s, 3H, C-20 CH_3), 1.17 (s, 3H, C-18 CH_3), 3.1 (m, 1H, C-13 axial H (28)), 3.57 (s, 3H, $COOCH_3$), 4.37 (s, broad, $W_{h/2}$ = 4 Hz, 1H, C-11 equatorial H). The concentrated mother liquors afforded additional quantities of crystalline **1**, but of poor purity. No attempts were made in this study to isolate the small quantities of other stereoisomeric bromo-ketones which were present.

The N.O.E. measurements were obtained on a carefully degassed 0.16 *M* solution of **1** in deuterioacetone. The experiments were performed at 100 MHz in frequency-sweep mode. The second saturating *rf* field applied was of the order of 0.75–1.0 mG (29) and area integrations were repeated at least 25 times for each signal. The mean area increases observed (see Table I) were reproducible to within 1%.

Dehydrobromination of 1

The general procedure of Green and Long (2) was used throughout. To determine the change in product composition with the time of reaction, a number of small scale runs were carried out. Two grams of methyl 11α-bromo-12-oxo-8α-podocarpan-19-oate, m.p. 151–152°, were added portionwise over 2 min to 40 ml of refluxing dimethylacetamide (dried over calcium hydride) containing 4 g of precipitated calcium carbonate. The boiling solution was protected from atmospheric oxygen by a positive pressure of dry nitrogen. Further reflux was continued for 3, 8, 18, 28, and 48 min in 5 successive runs. Each run was quenched by cooling rapidly in an ice-bath, filtering under pressure with the filter-pad being well washed with ether, the filtrate diluted with twice its volume of water, and the whole extracted with ether. The dried and evaporated extracts yielded pale yellow oily or crystalline products which were examined by p.m.r. spectroscopy. The components were identified by the chemical shifts of their C-20 methyl absorptions which were assigned from the p.m.r. spectra of authentic samples of each compound and which are recorded in Table III. The individual compounds were either prepared by reported methods or, as in the case of the Δ-8(14)-ketone, obtained by direct isolation from the reaction products. The differences between the chemical shifts of the C-20 methyls were sufficient to permit the determination of the product composition either by direct integration or by simple triangulation. The presence of the bromo-ketone itself was readily determined from the signal for the C-11 proton at 4.37 p.p.m. The product composition results were found to be reproducible to within ±3% and are shown in Table IV.

TABLE III

Chemical shifts of C-20 methyl resonances

	δ* p.p.m.
Bromo-ketone **1**	0.68
Δ-13(14)-ketone **2**	0.71†
Δ-8(14)-ketone **8**	0.55
Δ-9(11)-ketone **9**	0.94†
Δ-8(9)-ketone **10**	0.77‡
Methyl podocarpate *3b*	0.97

*Tetramethylsilane as internal standard. Deuteriochloroform solution.
†Proton magnetic resonance spectrum of an authentic sample from Dr. O. E. Edwards, National Research Council of Canada.
‡Sample from Dr. Goldsmidt, Emory University.

TABLE IV

Dehydrobromination of **1** in DMA/$CaCO_3$ for differing times

	Reaction time (min)				
Product (%)	5	10	20	30	50
Bromo-ketone **1**	60	1	0	0	0
Δ-13(14)-ketone **2**	1	14	40	60	60
Δ-8(14)-ketone **8**	30	60	33	14	14
Δ-9(11)-ketone **9**	7	16	16	16	14
Δ-8(9)-ketone **10**	2	6	5	3	2
Methyl podocarpate *3b*	0	4	6	7	10

Methyl 12-Oxopodocarp-8(14)-en-19-oate 8

Ten grams (27.0 mmoles) of the bromo-ketone **1**, m.p. 147–152°, were added portionwise over a period of 2 min to a mixture of 200 ml of dry, refluxing DMA and 20 g of precipitated calcium carbonate, and the whole refluxed for a further 8 min. The products were isolated via ether extraction as described above and upon evaporation of the solvents yielded 7.72 g (99%) of a pale yellow oil, the composition of which is recorded in Table II (10 min reaction). The material was transferred onto 400 g of silica gel (11-200 mesh, Davidson Chemical Co.) in 1:1 benzene – petroleum ether (30–60°). The chromatogram was developed with 500 ml of the same solvent and 1000 ml of benzene. Elution with 1% ethyl acetate in benzene afforded 50 mg of unreacted bromo-ketone and elution with 2% ethyl acetate yielded 4.6 g (60%) of the Δ-8(14)-ketone **8** as a colorless crystalline solid (purity > 90%). Two recrystallizations from 10% ethyl acetate in hexane gave an analytical sample of **8** as colorless prisms, m.p. 99–100°; i.r. ν_{max}: 2940, 2850 (C—H), 1712 cm^{-1} ($COOCH_3$ and saturated CO); u.v. λ_{max}: 282 mμ (ε 100);

Can. J. Chem. Downloaded from www.nrcresearchpress.com by 210.87.254.40 on 09/05/12
For personal use only.

p.m.r. (60 MHz): δ 0.55 (s, 3H, C-20 CH_3), 1.14 (s, 3H, C-18 CH_3), 2.32 (m, $W_{h/2}$ = 4 Hz, 2H, C-11 CH_2), 2.70 (m, $W_{h/2}$ = 7 Hz, 2H, C-13 CH_2), 3.56 (s, 3H, C-19 $COOCH_3$), 5.44 p.p.m. (t, 1H, $J_{apparent}$ = 7 Hz, C-14 H).

Anal. Calcd. for $C_{18}H_{26}O_3$: C, 74.44; H, 9.03. Found: C, 74.42; H, 8.99.

Methyl 12-Oxopodocarp-13-en-19-oate (2)

The crude dehydrobromination product obtained by refluxing 10.0 g of **1** in a mixture of 200 ml of DMA and 20 g of calcium carbonate for 30 min and isolated in the same manner as described above was dissolved in 250 ml of acetone containing 25 ml of 3*N* hydrochloric acid and refluxed under nitrogen for 2 h. The majority of the acetone was removed *in vacuo*, the residue extracted with ether and the washed and dried extracts (anhydrous sodium sulfate) were evaporated in vacuo to give 7.7 g of a pale yellow crystalline solid, containing 70% **2**, 6% **8**, 15% **9**, 2% **10**, and 7% methyl podocarpate **3***b*. Chromatography on silica gel in 1:1 benzene – petroleum ether (30–60°) and elution with 2% ethyl acetate in benzene gave the majority of **8**, **10**, and some of **3***b*. Further elution with 5% ethyl acetate in benzene gave crystalline **2**, 4.5 g (58%), m.p. 120–123°. Recrystallization from methanol gave the conjugated ketone as glistening plates, m.p. 127–130.5° (lit. (3), m.p. 126.5–129°); u.v. λ_{max}: 230 mμ (ε 10 500) (lit. (3), λ_{max} 230 mμ (ε 8 710)); p.m.r.: δ 0.715 (s, 3H, C-20 CH_3), 1.15 (s, 3H, C-18 CH_3), 3.64 (s, 3H, $COOCH_3$), 5.85 (quartet, 1H, $J_{13,14}$ = 10 Hz, $J_{14,15}$ = 2.6 Hz, C-13 H), and 6.65 p.p.m. (quartet, 1H, $J_{13,14}$ = 10 Hz, $J_{11,13}$ = 1.6 Hz, C-14 H).

Oxidative Degradation of Methyl 12-Oxopodocarp-8(14)-en-19-oate (8)

Two methods, ozonolysis and potassium permanganate – sodium periodate oxidation, were employed to degrade **8** to the keto-acid **11**. Both methods gave yields of **11** of the same order of magnitude but the permanganate periodate reagent gave inconsistent results whereas ozone gave reasonably reproducible yields.

A solution of 1.60 g of Δ-8(14)-ketone **8**, m.p. 95–98°, in 80 ml of dry methanol (molecular sieves) was treated with ozone (Welsbach T-408 ozonizer) at −65–75° until the solution assumed a pale blue color. Nitrogen was bubbled through to remove excess ozone and the solution transferred to a 500 ml flask in a total volume of 200 ml methanol. This solution was then refluxed with 20 ml of 30% hydrogen peroxide and 50 ml of 10% sodium hydroxide for 30 min under nitrogen. The majority of the methanol was then removed *in vacuo* and the residue diluted with 300 ml of water and ether extracted. The ethereal extracts were counter-washed once with water and the combined aqueous phases acidified to pH 1 with 2*N* sulfuric acid. The liberated acidic product was extracted with a benzene – ether mixture (3 × 100 ml), the extracts washed with water, saturated brine, and filtered through anhydrous sodium sulfate to yield, on evaporation *in vacuo*, 1.40 g of **11** as an oil which crystallized on standing. The p.m.r. spectrum of this crude product indicated that the desired keto-acid was present in approximately 80% yield. Recrystallization from 10% ethyl acetate – hexane gave 0.84 g (52%) of *8-oxo-(13 → 17)-pentanorlabdan-12,19-dioic acid 19-methyl ester* **11** as colorless needles, m.p. 168–170° (lit. (21), m.p. 170–172°); p.m.r.: δ 0.55 (s, 3H, C-20 CH_3), 1.25 (s, 3H, C-18 CH_3), 3.70 (s, 3H, C-19, $COOCH_3$), 10.6 p.p.m. (s, 1H, broad $W_{h/2}$ = 15 Hz, C-12 COOH).

In another experiment 1.60 g of **8** was ozonized and the crude product directly esterified with diazomethane. Chromatography on 50 g of Florisil in 1:1 benzene – petroleum ether and elution with benzene yielded 1.25 g (73%) of the methyl ester of **11** which was crystallized from 5% ethyl acetate – hexane to give 0.95 g (56%) of the *diester* as colorless prisms, m.p. 96–97° (lit. (21), compound reported only as an oil); p.m.r.: δ 0.54 (s, 3H, C-20 CH_3), 1.27 (s, 3H, C-18 CH_3), 3.60 (s, 6H, $W_{h/2}$ = 1.0 Hz, two $COOCH_3$); mol. wt. 310, mass spectrum. The 2,4-dinitrophenylhydrazone of the diester crystallized from aqueous ethanol as yellow needles, m.p. 161–163° (lit. (21), m.p. 161–163°).

Acknowledgments

The authors wish to thank the National Research Council of Canada for financial assistance and for the award of a Scholarship to M. B. Gravestock. We thank Mr. J. K. Saunders for performing the nuclear Overhauser effect measurements.

1. R. P. Holysz. J. Amer. Chem. Soc. **75**, 4432 (1953).
2. (*a*) G. F. H. Green and A. G. Long. J. Chem. Soc. 2532 (1961). (*b*) J. A. Marshall and D. J. Schaeffer. J. Org. Chem. **30**, 3642 (1965). (*c*) J. A. Marshall, W. I. Fanta, and H. Roebke. J. Org. Chem. **31**, 1016 (1966). (*d*) T. A. Spencer, R. M. Villarica, D. L. Storm, T. D. Weaver, R. J. Friary, J. Posler, and P. R. Shafer. J. Amer. Chem. Soc. **89**, 5497 (1967). (*e*) C. Berger, M. Franck-Neumann, and G. Ourisson. Tetrahedron Lett. 3451 (1968).
3. R. H. Bible and R. R. Burtner. J. Org. Chem. **26**, 1174 (1961).
4. A. I. Meyers, W. Beverung, and G. A. Garcia-Munoz. J. Org. Chem. **29**, 3427 (1964). I. A. Kaye and R. S. Matthews. J. Org. Chem. **28**, 325 (1963).
5. O. E. Edwards. Private communication.
6. J. W. ApSimon, P. V. Demarco, and J. Lemke. Can. J. Chem. **43**, 2793 (1965).
7. K. Bowden, I. M. Heilbron, E. R. H. Jones, and B. C. L. Weedon. J. Chem. Soc. 39 (1946).
8. R. C. Cookson. J. Chem. Soc. 282 (1954).
9. W. Moffitt, R. B. Woodward, A. Moscowitz, W. Klyne, and C. Djerassi. J. Amer. Chem. Soc. **83**, 4013 (1961).
10. F. A. L. Anet and A. R. J. Bourn. J. Amer. Chem. Soc. **87**, 5250 (1965). For other examples of the application of this method see: J. K. Saunders, R. A. Bell, C.-Y. Chen, D. B. MacLean, and R. H. F. Manske. Can. J. Chem. **46**, 2876 (1968). R. A. Bell, and E. N. C. Osakwe. Chem. Commun. 1093 (1968). M. C. Woods, H.-C. Chiang, Y. Nakadaira, and K. Nakanishi. J. Amer. Chem. Soc. **90**, 522 (1968). R. H. Martin and J. C. Nouls. Tetrahedron Lett. 2727 (1968). P. A. Hart and J. P. Davis. J. Amer. Chem. Soc. **91**, 512 (1969).
11. R. A. Bell and J. K. Saunders. In preparation.
12. J. D. Baldeschweiler and E. W. Randall. Chem. Rev. 81 (1963).
13. M. C. Woods, I. Miura, Y. Nakadaira, A. Terahara, M. Maruyama, and K. Nakanishi. Tetrahedron Lett. 321 (1967).

14. B. M. FUNG. J. Amer. Chem. Soc. **90**, 219 (1968).
15. J. J. BEEREBOOM and C. DJERASSI. J. Org. Chem. **19**, 1196 (1954). C. DJERASSI and D. MARSHALL. J. Amer. Chem. Soc. **80**, 3986 (1958). M. E. KUEHNE. J. Amer. Chem. Soc. **83**, 1492 (1961).
16. (*a*) B. J. MAGERLEIN. J. Org. Chem. **24**, 1564 (1959). (*b*) M. YANAGITA and K. YAMAKAWA. J. Org. Chem. **22**, 291 (1957). (*c*) F. G. BORDWELL and K. M. WELLMAN. J. Org. Chem. **28**, 2544 (1963).
17. W. A. AYER, J. A. BEREJOWSKY, and D. A. LAW. Can. J. Chem. **41**, 649 (1963).
18. C. H. DEPUY, R. D. THURN, and G. F. MORRIS. J. Amer. Chem. Soc. **84**, 1314 (1962). J. HINE. J. Amer. Chem. Soc. **88**, 5525 (1966).
19. E. SEEBECK and T. REICHSTEIN. Helv. Chim. Acta, **26**, 536 (1943).
20. K. G. LEWIS and G. J. WILLIAMS. Tetrahedron Lett. 4573 (1965).
21. V. P. ARYA, H. ERDTMAN, and T. KUBOTA. Tetrahedron, **16**, 255 (1961).
22. A. OGISO and S. W. PELLETIER. Chem. Commun. 94 (1967). S. W. PELLETIER, L. B. HAWLEY, JR., and K. W. GOPINATH. Chem. Commun. 96 (1967).
23. H. E. ZIMMERMAN. *In* Molecular rearrangements. Vol. 1. *Edited by* P. deMayo. Interscience Publishers, Inc., New York, N.Y. 1963. pp. 345–372.
24. E. M. ARNETT. Progr. Phys. Org. Chem. **1**, 223 (1963).
25. J. A. MARSHALL and N. H. ANDERSEN. J. Org. Chem. **31**, 667 (1966).
26. S. K. MALHOTRA and H. J. RINGOLD. J. Amer. Chem. Soc. **86**, 1997 (1964). C. K. INGOLD. Structure and mechanism in organic chemistry. Cornell University Press. Ithaca, N.Y. 1953. p. 565. J. WARKENTIN and L. K. M. LAM. Can. J. Chem. **42**, 1676 (1964).
27. R. A. BELL and J. W. EASTON. Unpublished results.
28. G. J. KARABATSOS, G. C. SONNISCHSEN, N. HSI, and D. J. FENOGLIO. J. Amer. Chem. Soc. **89**, 5067 (1967).
29. W. A. ANDERSON. Phys. Rev. **102**, 151 (1956).

Can. J. Chem. Downloaded from www.nrcresearchpress.com by 210.87.254.40 on 09/05/12
For personal use only.

Can. J. Chem. Downloaded from www.nrcresearchpress.com by 210.87.254.40 on 09/05/12
For personal use only.

Ring openings of γ- and δ-lactones to form γ- and δ-hydroxyamides. Cyclodehydration. Mass spectra of δ-hydroxyamides[1]

EARL M. LEVI, CHUNG-LING MAO, AND CHARLES R. HAUSER
Department of Chemistry, Duke University, Durham, North Carolina 27706

Received April 25, 1969

Ring openings of γ- and δ-lactones were effected with potassium amide or hydrazine to form γ- and δ-hydroxyamides, which were cyclodehydrated with sulfuric acid to give γ- and δ-lactams, respectively. These products are, respectively, phthalimidines and 3,4-dihydroisocarbostyrils having no substituent on nitrogen or having the N—NH_2 group. The possible linear dehydration of the δ-hydroxyamides was not observed. The δ-hydroxyamides exhibited, on mass spectrometry, a type of carbon–carbon cleavage that has apparently not been reported for ordinary alcohols. An example of the "*ortho* effect" in mass spectra of *o*-disubstituted benzene derivatives is also discussed.

Canadian Journal of Chemistry, 47, 3671 (1969)

Dilithiations of *N*-methylbenzamide (1) and *N*-methyl-*o*-toluamide (2) have previously been accomplished with *n*-butyllithium to form dilithioamides **1** and **4**, which were condensed with ketones or aldehydes to give γ- and δ-hydroxyamides **2** and **5**, respectively. These compounds have been cyclodehydrated with sulfuric acid to afford γ- and δ-lactams **3** and **6**, respectively (3).

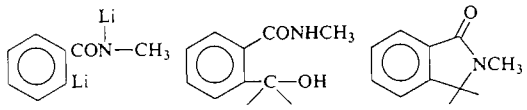

1 **2** **3**

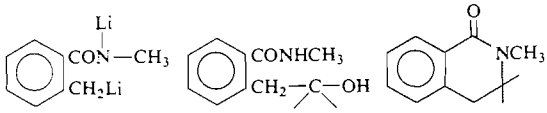

4 **5** **6**

However, similar dilithiations of benzamide (1) and *o*-toluamide[2] have failed. Thus, the above method has not been applicable to preparations of γ- and δ-hydroxyamides and γ- and δ-lactams having no substituent on the nitrogen atom.

We have now prepared such compounds by ring opening of γ- and δ-lactones with potassium amide, followed by ring closure with acid; similarly, hydroxyamides and lactams having the N—NH_2 group were synthesized employing hydrazine. The γ- and δ-lactones were readily obtained by thermal cyclodeamination of γ- and δ-hydroxyamides of types **2** and **5**, respectively (1, 2).

Results with γ-Lactones

γ-Lactone **7** underwent ring opening with potassium amide in tetrahydrofuran (THF) and with hydrazine (neat) to form γ-hydroxyamide **8** and hydrazide **9**, which underwent cyclodehydrations with cold, concentrated sulfuric acid to give γ-lactams **10***a* and **10***b*, respectively.

Crude hydroxyamide **8** and hydrazide **9** were employed in these reactions, since attempted purification of them resulted in reconversion to lactone **7**. The overall yields of **10***a* and **10***b* from lactone **7** were 25 and 20%, respectively.

Similarly, treatment of γ-lactone **11** with hydrazine afforded γ-lactam **12** in 4% yield; this yield might be improved since most of lactone **11** was recovered. The intermediate hydrazide was not isolated. γ-Lactone **11** has previously been

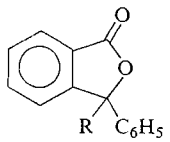

7, R = C_6H_5
11, R = H

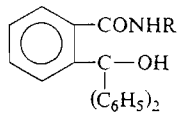

8, R = H
9, R = NH_2

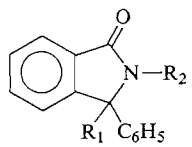

10*a*, R_1 = C_6H_5, R_2 = H
10*b*, R_1 = C_6H_5, R_2 = NH_2
12, R_1 = H, R_2 = NH_2

[1]Supported by Public Health Service Grant No. CA-04455 from the National Cancer Institute and by the National Science Foundation.

[2]Unpublished observation of R. E. Ludt in this laboratory.

Can. J. Chem. Downloaded from www.nrcresearchpress.com by 210.87.254.40 on 09/05/12
For personal use only.

shown to undergo ionization of its benzhydrylic hydrogen atom with potassium amide to form a carbanion which can be alkylated (4).

Attempts to prepare γ-hydroxyamides by the action of potassium amide on the γ-lactones obtained from dilithioamide **1** and cyclohexanone or fluorenone were unsatisfactory. Apparently these lactones underwent ring opening but were again regenerated on work-up.

Results with δ-Lactones

δ-Lactone **13** underwent ring opening with potassium amide in THF and with hydrazine (neat) to form δ-hydroxyamide **14** and the corresponding δ-hydroxyhydrazide (isolated as its acetone derivative **15**) in yields of 69 and 45%, respectively. These compounds were cyclodehydrated with cold, concentrated sulfuric acid to give the 3,4-dihydroisocarbostyrils **16***a* and **16***b* in yields of 89 and 53%, respectively. Interestingly, the possible linear dehydration was not observed.

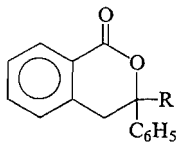

13, R = C_6H_5
22, R = H

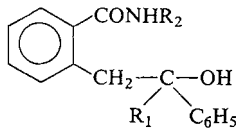

14, $R_1 = C_6H_5$, R_2 = H
15, $R_1 = C_6H_5$, $R_2 = N{=}C(CH_3)_2$
23, $R_1 = R_2$ = H

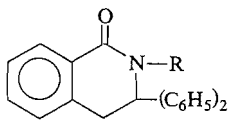

16*a*, R = H
16*b*, R = $N{=}C(CH_3)_2$

Similarly, δ-lactone **17** underwent ring opening with potassium amide to form δ-hydroxyamide **18** in 82% yield. This compound may have undergone cyclodehydration with cold, concentrated sulfuric acid to give δ-lactam **19** but, surprisingly, olefin-amide **20** was obtained on attempted distillation. That the olefinic product was **20**, and not the possible **21**, was supported by the nuclear magnetic resonance (n.m.r.) spectrum with the vinyl proton absorption at δ 5.28 p.p.m.[3] Had the product been **21**, this absorption should have appeared at lower field. In addition, this n.m.r. spectrum shows benzylic methylene protons at δ 3.47 p.p.m. The infrared (i.r.) spectrum is characteristic of a benzamide and the mass spectrum resembles that of the unsubstituted δ-hydroxyamides in that the most abundant fragment ion appears at *m/e* 135 (see below). The base peak in this spectrum is the molecular ion (*m/e* 215). One might expect to observe the formation of **21** as well as **20**; however, none was isolated.

Likewise, δ-lactone **22** underwent ring opening with potassium amide to form δ-hydroxyamide **23** in 78% yield. Such ring openings appear to be quite general and, in contrast to corresponding γ-lactones, uncomplicated by ring closure during work-up.

It should be mentioned that δ-lactone **13** also underwent ring opening with lithium methylamide in THF to form the corresponding δ-hydroxyamide of type **5**. However, this compound can be prepared more conveniently from dilithioamide **4** and benzophenone (2).

The present method of synthesis of 3,4-dihydroisocarbostyrils having no substituent on nitrogen appears more convenient than earlier ones, which have involved cyclizations of urethanes with polyphosphoric acid (6) and of isocyanates with aluminum chloride (7).

Mass Spectra of δ-Hydroxyamides

These hydroxyamides exhibited, on mass spectrometry, a type of cleavage that appears not to have been observed previously (Schemes 1 and 2). Thus, compounds **14**, **18**, and **23** underwent not only a normal alcohol cleavage (course *a*), but also an abnormal one (course *b*) that involves migration of hydrogen from oxygen to nitrogen accompanied by carbon–carbon bond cleavage. The latter cleavage gave the base peak at *m/e* 135, the molecular ion of a toluamide, common to the three spectra (see Scheme 1). A minor fragmentation observed in all 3 spectra is the loss of 17 mass units from the molecular ion. This fragmentation, in the case of **23**, was shown by high resolution to be due to the loss of *ammonia*,[4] and not to loss of *hydroxyl radical*. This is due to either

[3]The positions reported for vinyl protons of similar type lie between δ 5.36–5.43 p.p.m. (5).

[4]Anal. Calcd. for $C_{15}H_{12}O_2$: C, 224.0838. Found: C, 224.0837.

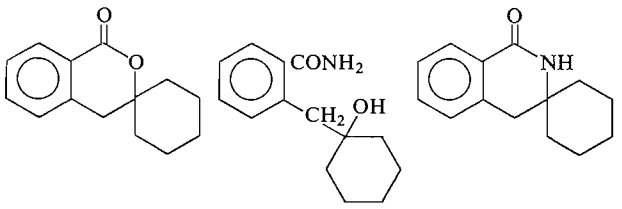

17 18 19

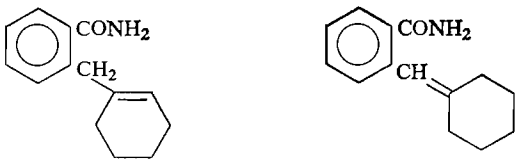

20 21

cyclodeamination before ion impact, loss of ammonia from ion **24** (Scheme 1), or a combination of these effects. The fragmentation from the base peak ion is interesting in that it is another example of the "*ortho* effect" in *o*-disubstituted benzene derivatives. This effect has been observed in the mass spectra of *o*-ethoxybenzamide (8) and *o*-methylbenzoates (9) when compared to the spectra of the *meta* and *para* isomers. The "normal" fragmentation of a toluamide would be expected to follow the pathway *m/e* 135 to *m/e* 119 to *m/e* 91; i.e. loss of an amine radical, followed by loss of carbon monoxide (10). In the mass spectra of the δ-hydroxyamides, part of the fragmentation occurs *via* the pathway *m/e* 135 to *m/e* 118 to *m/e* 90; i.e. loss of ammonia followed by loss of carbon monoxide, as well as following the "normal" pathway.

These rationalizations of the fragmentation pathways are supported by the mass spectra of the *N*-methyl and *N*-phenyl substituted derivatives **25** and **26** (Scheme 2). In these spectra, as in the spectrum of **14**, the major fragmentation follows the abnormal course described above and

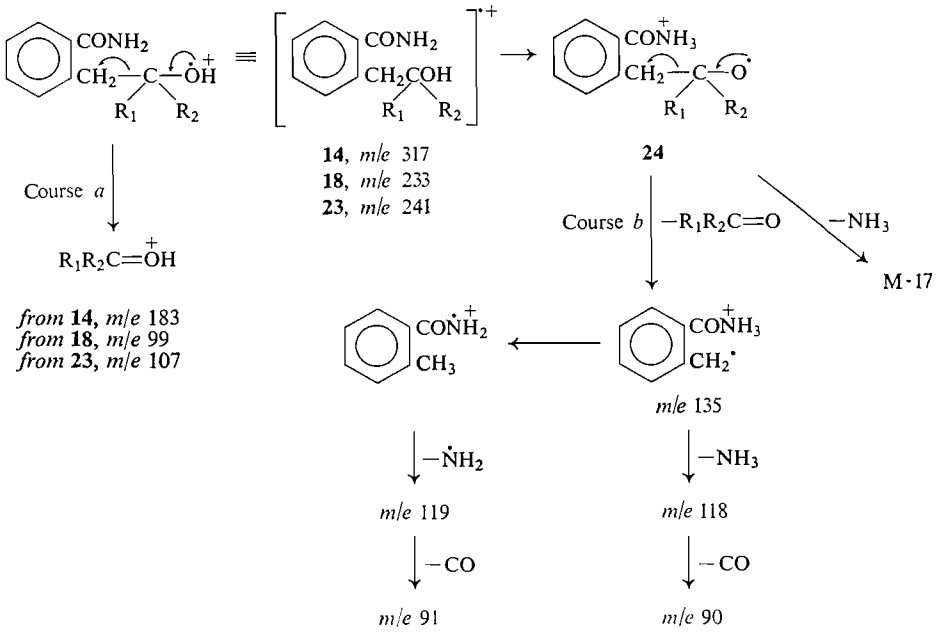

SCHEME 1

Can. J. Chem. Downloaded from www.nrcresearchpress.com by 210.87.254.40 on 09/05/12
For personal use only.

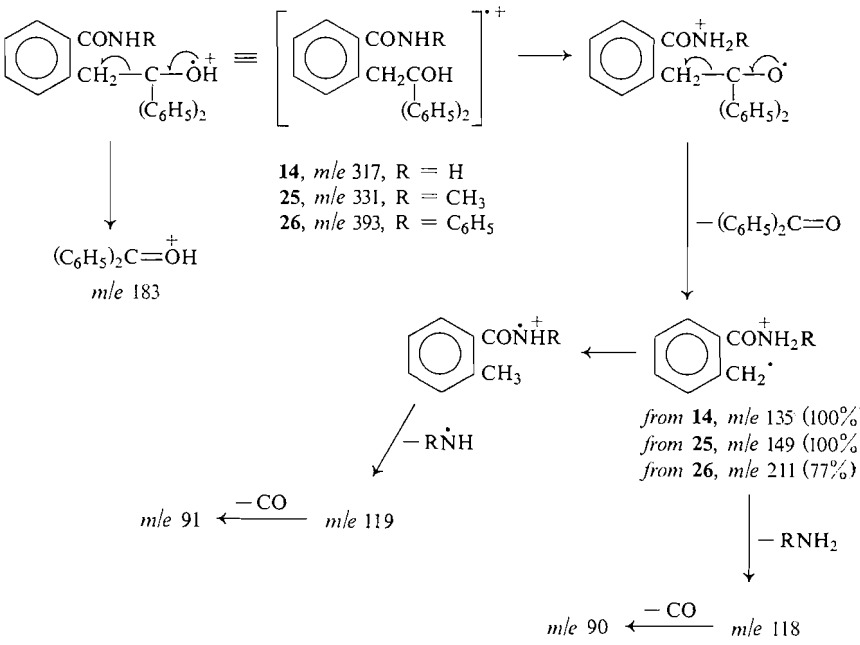

SCHEME 2

is confirmed by shifting of the toluamide peak to *m/e* 149 and *m/e* 211, respectively. The normal elimination of the protonated benzophenone ion is also observed, but to a much lesser extent. The fragmentation from the toluamide ions again follows both the "normal" and the "*ortho* effect" routes. These latter 2 pathways are roughly comparable in terms of ion current carried for all of the 5 spectra examined. The supporting metastable peaks for all of the fragmentations were observed (see Experimental), although not all were observed in each spectrum.

Experimental

Melting points are uncorrected. Infrared spectra were recorded on a Perkin–Elmer Model 137 Infracord and were calibrated against the 6.24 μ band of polystyrene. Nuclear magnetic resonance spectra were taken on a Varian A-60 instrument, operating at 60 MHz, and are reported as downfield shifts in p.p.m. for tetramethylsilane employed as an internal standard.[5] Mass spectra were obtained on an Associated Electrical Industries MS-902 at 70 eV.[6] Tetrahydrofuran (THF) was dried at reflux temperature over lithium aluminum hydride and was freshly distilled before use. Analyses were performed by M-H-W Laboratories, Garden City, Michigan.

2-[(Diphenylhydroxy)methyl]benzamide (8)

A solution of 14.3 g (0.05 mole) of 3,3-diphenylphthalide (**7**) (1) in dry THF (50 ml), was slowly added to a solution of potassium amide prepared from 7.8 g (0.2 g-atom) of potassium in *ca.* 250 ml of liquid ammonia. The reaction mixture was stirred at the b.p. of ammonia for 3 h, 150 ml of dry THF was added, and the ammonia was removed under a slow stream of nitrogen. After stirring for an additional 18 h at room temperature, the reaction mixture was poured into iced hydrochloric acid. The resulting mixture was filtered, and the solid washed well with water, then with acetonitrile to remove lactone **7**. The crude hydroxyamide (10.0 g, 65%), m.p. 170–162° decomp., was recrystallized twice from acetonitrile to give, apparently, pure **8**, m.p. 168–170° decomp.; λ_{max} ($CHCl_3$): 2.90, 3.00, and 6.02 μ.

The analytical data for this compound were unsatisfactory because of the ease with which it decomposed. On standing for about 1 week at room temperature, it was quantitatively reconverted to lactone **7**.

3,3-Diphenylphthalimidine (10a)

Freshly prepared, crude hydroxyamide **8** (10 g) was slowly added to 50 ml of cold (0°), concentrated sulfuric acid (50 ml), giving a dark red solution which was stirred at 0° for 3 h. The reaction mixture was poured onto ice. The resulting mixture was filtered and the solid washed well with water, then with ether to remove lactone **7**. The remaining crude hydrogen sulfate salt of lactam **10***a* was stirred with 20% aqueous sodium

[5]In n.m.r. descriptions: s = singlet, d = doublet, m = multiplet, and b = broad.

[6]We thank Dr. David Rosenthal for the mass spectral determinations, which were done at the Research Triangle Mass Spectrometry Center Supported by Special Facility Grant No. FR-00330-01, National Institutes of Health.

Can. J. Chem. Downloaded from www.nrcresearchpress.com by 210.87.254.40 on 09/05/12
For personal use only.

Can. J. Chem. Downloaded from www.nrcresearchpress.com by 210.87.254.40 on 09/05/12
For personal use only.

hydroxide for 2 h. The resulting precipitate was collected and treated with aqueous hydrochloric acid to give 4.05 g (38%) of the hydrogen chloride salt of lactam **10***a* which, after washing with ether to remove traces of lactone 7 still present, was stirred with aqueous sodium hydroxide solution for 1 h. The precipitate was collected to give lactam **10***a*, m.p. 105–109°. Two recrystallizations from acetonitrile afforded pure **10***a*, m.p. 125–126°; λ_{max} ($CHCl_3$): 3.03 (NH) and 5.97 μ (C=O); n.m.r. ($CDCl_3$): δ 6.82 (b, 1H, NH), 7.30–7.75 (m, 13H), and 7.75–7.95 p.p.m. (m, 1H).

Anal. Calcd. for $C_{20}H_{15}NO$: C, 84.18; H, 5.30; N, 4.91. Found: C, 84.02; H, 5.26; N, 4.93.

*2-Amino-3,3-diphenylphthalimidine (**10b**)*

A solution of γ-lactone **7** (2.0 g) and hydrazine (95%, 10 ml) was refluxed for 5 days. Hydrazide **9**, m.p. 105–107°, separated on cooling. On standing for 24 h at room temperature, the product had m.p. 115–117°. The odor of hydrazine was detected emanating from the sample and the i.r. spectrum was that of lactone **7**. Attempted crystallization of crude hydrazide **9** also led to lactone **7**. Compound **9** was therefore used immediately upon isolation without further purification.

Freshly-prepared crude hydrazide **9** (from 2 g lactone **7**) was stirred with concentrated sulfuric acid to 0° for 6 h. The solution was poured onto ice, and the crude aminolactam **10***b* was recrystallized twice from ethanol to give 0.42 g (20%) of pure **10***b*, m.p. 174.5–176° decomp.; λ_{max} ($CHCl_3$): 2.90, 3.00 (NH_2), and 5.95 μ (C=O); n.m.r. ($CDCl_3$): δ 3.95 (b, 2H, NH_2), 7.0–7.3 (m, 13H), and 7.7–8.0 p.p.m. (m, 1H); mass spectrum, *m/e* (relative intensity): 300 (67), 223 (100), 130 (11).

Anal. Calcd. for $C_{20}H_{16}N_2O$: C, 79.98; H, 5.37; N, 9.33. Found: C, 79.97; H, 5.07; N, 9.27.

*2-Amino-3-phenylphthalimidine (**12**)*

A solution of 10 g of 3-phenylphthalide (4) (**11**) in hydrazine (95%, 20 ml) was refluxed for 4 days. The reaction mixture was cooled overnight to give 0.5 g of white needles, m.p. 150–155°. Two recrystallizations from ethanol gave 0.4 g (4%) of pure **12**, m.p. 155–156°; λ_{max} ($CHCl_3$): 2.90, 3.00 (NH_2), and 5.94 μ (C=O); n.m.r. ($CDCl_3$): δ 3.83 (b, 2H, NH_2), 5.47 (s, 1H, ArCH), and 7.0–8.0 p.p.m. (m, 9H).

Anal. Calcd. for $C_{14}H_{12}N_2O$: C, 74.99; H, 5.38; N, 12.49. Found: C, 75.05; H, 5.10; N, 12.65.

The original reaction mixture was evaporated to an oil. The i.r. spectrum of the residue was indistinguishable from that of lactone **7**.

Reactions of 3,4-Dihydroisocoumarins with Potassium Amide

These δ-lactones (2) were converted to δ-hydroxyamides in the following manner. A solution of the lactone (1 equivalent) in dry THF was added to a solution of potassium amide (4 equivalents) prepared from potassium (4 equivalents) in liquid ammonia (200–300 ml) under dry nitrogen. The ammonia was removed under dry nitrogen, additional dry THF was then added, and the resulting mixture was stirred overnight. The reaction mixture was poured into iced concentrated hydrochloric acid. The product was collected by filtration and recrystallized.

*A. 2-(β,β-Diphenyl-β-hydroxy)ethylbenzamide (**14**)*

This compound was prepared from 4.5 g (0.015 mole) of δ-lactone **13** and 0.06 mole of potassium amide in 250 ml (total volume) of dry THF. The crude product was recrystallized from benzene–heptane to give 3.27 g (69%) of hydroxyamide **14**, m.p. 132–135° decomp. Two additional crystallizations from benzene–heptane gave the analytical sample of **14**, m.p. 134–135° decomp.; λ_{max} ($CHCl_3$): 2.87 (sh), 2.96 (sh), 3.03 (NH_2 and OH), and 6.06 μ (amide C=O); n.m.r. ($CDCl_3$): δ 3.72 (s, 2H, $ArCH_2$), 6.1–6.4 (b, 2H, NH_2), 6.72 (b, 1H, OH), 7.0–7.6 (m, 14H); mass spectrum, *m/e* (relative intensity): 317 (7), 300 (2), 223 (2), 183 (28), 135 (100), 119 (21), 118 (22), 91 (6), 90 (4), 77 (4), metastable peaks, m* (parent, daughter), 283.9 (317, 300), 105.6 (317, 183), 103.1 (135, 118), 69.6 (119, 91), 68.6 (118, 90), 57.5 (317, 135).

Anal. Calcd. for $C_{21}H_{19}NO_2$: C, 79.47; H, 6.03; N, 4.41. Found: C, 79.55; H, 5.97; N, 4.24.

*B. 2-(1-Hydroxycyclohexyl)methylbenzamide (**18**)*

This compound was prepared from 10.80 g (0.05 mole) of lactone **17** and 0.20 mole of potassium amide in 250 ml (total volume) of dry THF. Crude hydroxyamide **18** (10.05 g, 82%), m.p. 182–183° decomp., was recrystallized twice from acetonitrile to give the analytical sample, m.p. 184–185° decomp.; λ_{max} ($CHCl_3$): 2.89 (sh), 2.96 (sh), 3.04 (NH_2 and OH), and 6.05 μ (amide C=O); mass spectrum, *m/e* (relative intensity): 233 (2), 216 (8), 173 (7), 160 (8), 135 (100), 119 (35), 118 (35), 99 (2), 91 (10), 90 (5), 81 (4), 77 (3), metastable peaks, m* (parent, daughter), 200.2 (233, 216), 118.5 (216, 160), 104.9 (135, 119), 103.1 (135, 118), 78.2 (233, 135), 69.6 (119, 91), 68.6 (118, 90).

Anal. Calcd. for $C_{14}H_{19}NO_2$ (mol. wt. 233.1416): C, 72.07; H, 8.21; N, 6.00. Found (mol. wt. 233.1415, mass spectrum): C, 72.44; H, 8.14; N, 5.91.

*C. 2-(β-Hydroxy-β-phenyl)ethylbenzamide (**23**)*

This compound was prepared from 2.24 (0.01 mole) of lactone **22** and 0.04 mole of potassium amide in 150 ml (total volume) of dry THF. Crude hydroxyamide **23** (1.85 g, 78%), m.p. 145–147° decomp., was recrystallized 3 times from acetonitrile to give the analytical sample of **23**, m.p. 149–150° decomp.; λ_{max} ($CHCl_3$): 2.84 (sh), 2.97 (sh), 3.03 (NH_2 and OH), and 6.06 μ (amide C=O); mass spectrum, *m/e*, (relative intensity): 241 (1), 224 (2), 178 (2), 146 (1), 135 (100), 119 (34), 118 (31), 107 (4), 105 (3), 91 (10), 90 (6), 77 (8), 51 (6), metastable peaks, m* (parent, daughter), 208.2 (241, 224), 104.9 (135, 119), 103.1 (135, 118), 75.6 (241, 135), 69.6 (119, 91), 68.6 (118, 90).

Mol. Wt. Calcd. for $C_{15}H_{15}NO_2$: 241.1103. Found: 241.1104.

*N-[2-(β,β-Diphenyl-β-hydroxy)ethyl]benzoyl Acetone Hydrazone (**15**)*

A solution of 5 g of lactone **13** in 20 ml of hydrazine (95%) was refluxed for 3 days. The reaction mixture was evaporated at reduced pressure to leave an oil. Acetone (50 ml) was added to precipitate 2.8 g (45%) of the crude acetone derivative **15**, which was collected by filtration. This compound, m.p. 232–234° decomp., was washed well with benzene and acetonitrile, and a sample recrystallized from chloroform to give the analytical sample

Can. J. Chem. Downloaded from www.nrcresearchpress.com by 210.87.254.40 on 09/05/12
For personal use only.

of **15**, m.p. 242–244° decomp., λ_{max} ($CHCl_3$): 3.16 (NH) and 6.15 μ (C=O).

Anal. Calcd. for $C_{24}H_{24}N_2O_2$: C, 77.39; H, 6.50; N, 7.21. Found: C, 76.94; H, 6.58; N, 7.17.

Cyclodehydration of δ-Hydroxyamides

The compound was dissolved in 25 ml of concentrated sulfuric acid that had been cooled to 0°. The solution was stirred for 3 h at 0° and then poured onto ice. The product was isolated as described below.

A. 3,3-Diphenyl-3,4-dihydroisocarbostyril (16a)

Crude δ-lactam **16***a*, prepared from 2.38 g (0.075 mole) of δ-hydroxyamide **14**, was collected by filtration and recrystallized from acetonitrile to give 1.98 g (89%) of pure **16***a*, m.p. 243–245°; λ_{max} ($CHCl_3$): 2.98 (NH) and 6.05 μ (C=O); n.m.r. ($CDCl_3$): δ 3.28 (s, 2H, ArCH), 6.5–6.7 (b, 1H, NH), 7.3–7.5 (m, 13H), and 7.9–8.1 p.p.m. (m, 1H); mass spectrum, *m/e* (relative intensity): 299 (34), 271 (4), 270 (14), 223 (17), 222 (100), 204 (6), 203 (10), 195 (3), 194 (6), 179 (4), 178 (5), 165 (4), 119 (13), 118 (81), 104 (6), 90 (27), 89 (8), 77 (8), 57 (7), 55 (5), metastable peaks, m*, (parent, daughter), 269.0 (271, 270), 245.6 (299, 271), 187.5 (222, 204), 177.0 (179, 178), 171.2 (222, 195), 164.8 (299, 222), 144.3 (222, 179), 68.6 (118, 90), 57.0 (104, 77).

Anal. Calcd. for $C_{21}H_{17}NO$: C, 84.25; H, 5.72; N, 4.68. Found: C, 84.24; H, 5.71; N, 4.78.

B. 2-(2-Propylideneamino)-3,3-diphenyl-3,4-dihydroisocoumarin (16b)

Crude δ-lactam **16***b*, prepared from 1.75 g of δ-hydroxyhydrazide **15**, was collected by filtration and recrystallized 3 times from acetonitrile to give 0.90 g (53%) of analytically pure **16***b*, m.p. 197–199°; λ_{max} ($CHCl_3$): 6.06 μ (C=O); n.m.r. ($CDCl_3$): δ 1.82, 1.85 (2s, 6H, $2CH_3$), 3.77 (s, 2H, $ArCH_2$), 7.0–7.5 (m, 13H), and 7.7–8.1 p.p.m. (m, 1H).

Anal. Calcd. for $C_{24}H_{22}N_2O$: C, 81.32; H, 6.26; N, 7.90. Found: C, 81.38; H, 6.56; N, 7.90.

C. 2-(1-Cyclohexenyl)methylbenzamide (20)

δ-Lactam **19**, prepared from 9.1 g of δ-hydroxyamide **18** was apparently present as its hydrogen sulfate salt in the aqueous acidic solution. Extraction of the acidic solution with ether gave 0.95 g of a mixture of lactone **17** and δ-hydroxyamide **18**. The aqueous acidic solution was made basic with solid sodium hydroxide, and the resulting mixture was extracted with ether, dried, and evaporated. The residual oil (6.35 g, 75%) had λ_{max} (CCl_4): 3.06 (NH) and 6.14 μ. Attempted purification by distillation (>200°) gave the olefinic product **20**, which did not distil and solidified on cooling. Crystallization from carbon tetrachloride gave 5.25 g (70%) of pure **20**, m.p. 130–131°; λ_{max} ($CHCl_3$): 2.87, 2.97 (NH_2), and 6.02 μ; n.m.r. ($CDCl_3$): δ 1.4–2.2 (m, 8H, cyclohexyl protons), 3.47 (s, 2H, $ArCH_2C{=}C$), 5.28 (b, 1H, $CH_2C{=}CH{-}CH_2$), and 7.0–7.7 p.p.m. (m, 4H); mass spectrum, *m/e* (relative intensity): 215 (100), 198 (57), 172 (35), 170 (15), 135 (75), 119 (27), 118 (24), 91 (14), 81 (21), metastable peaks, m* (parent, daughter), 197.0 (199, 198), 182.3 (215, 198), 170.0 (172, 171), 169.0 (171, 170), 137.6 (215, 172), 104.9 (135, 119), 103.1 (135, 118).

Anal. Calcd. for $C_{14}H_{17}NO$: C, 78.10; H, 7.96; N, 6.51. Found: C, 78.38; H, 7.85; N, 6.39.

Reaction of δ-Lactone 13 with Lithium Methylamide

n-Butyllithium (34 ml of 2.35 *M*, 0.08 mole) in hexane[7] was slowly added to a solution of methylamine (*ca.* 40 ml) in dry THF (100 ml) under nitrogen and the excess amine was then removed under nitrogen. A solution of 6.0 g (0.02 mole) of lactone **13** in dry THF (100 ml) was added and the resulting mixture was stirred at reflux overnight. The crude mixture was cooled and poured onto iced concentrated hydrochloric acid. The precipitate was collected and recrystallized from 95% ethanol to give 4.5 g (66%) of δ-hydroxyamide **25**, m.p. and mixture m.p. 190–191° (lit. (2), m.p. 190–191°); mass spectrum, *m/e* (relative intensity): 331 (1), 283 (1), 183 (7), 182 (1), 149 (100), 148 (13), 134 (4), 119 (37), 118 (13), 105 (15), 91 (9), 90 (2), 77 (12), metastable peaks, m* (parent, daughter), 147.0 (149, 148), 120.5 (149, 134), 93.4 (149, 118), 60.5 (182, 105), 69.6 (119, 91).

N-Phenyl-2-(β,β-diphenyl-β-hydroxy)ethylbenzamide (26)

The mass spectrum of δ-hydroxyamide **26** was obtained on a sample prepared from *N*-phenyl-*o*-toluamide by a method similar to that previously described (2); mass spectrum, *m/e* (relative intensity): 393 (1), 300 (13), 283 (8), 223 (3), 211 (77), 194 (13), 183 (12), 119 (85), 118 (100), 105 (23), 93 (37), 91 (11), 90 (17), 77 (20), metastable peaks, m* (parent, daughter), 113.5 (393, 211), 66.0 (211, 118), 69.6 (119, 91), 68.6 (118, 90), 67.1 (211, 119).

1. W. H. Puterbaugh and C. R. Hauser. J. Org. Chem. **29**, 853 (1964).
2. R. L. Vaulx, W. H. Puterbaugh, and C. R. Hauser. J. Org. Chem. **29**, 3514 (1964).
3. I. T. Barnish, C.-L. Mao, R. L. Gay, and C. R. Hauser. Chem. Commun. 564 (1968).
4. C. R. Hauser, M. T. Tetenbaum, and D. S. Hoffenberg. J. Org. Chem. **23**, 861 (1958).
5. N. S. Bhacca, D. P. Hollis, L. F. Johnson, and E. A. Pier. NMR spectra catalog, Vol. II. Varian Associates, Palo Alto, California. 1963. Spectrum 545. N. S. Bhacca, L. F. Johnson, and J. N. Shoolery. NMR spectra catalog, Vol. I. Varian Associates, Palo Alto, California. 1962. Spectra 359 and 363.
6. E. F. M. Stephenson. J. Chem. Soc. 2557 (1956). S. Karady. J. Org. Chem. **27**, 3720 (1962).
7. T. C. Aschner. U. S. Patent 2,647,902; Chem. Abstr. **48**, 13730d (1954).
8. G. Spiteller. Monatsh. Chem. **92**, 1147 (1961).
9. F. W. McLafferty and R. S. Gohlke. Anal. Chem. **31**, 2076 (1959).
10. H. Budzikiewicz, C. Djerassi, and D. H. Williams. Mass Spectrometry of Organic Compounds. Holden-Day Inc., San Francisco, California. 1967. p. 351.

[7]Obtained from Alfa Inorganic Inc., Beverly, Massachusetts.

Can. J. Chem. Downloaded from www.nrcresearchpress.com by 210.87.254.5 on 09/05/12
For personal use only.

Amination of tetrazoles with hydroxylamine-*O*-sulfonic acid: 1- and 2-aminotetrazoles

R. RAAP
R and L Molecular Research Ltd., 8045 Argyll Road, Edmonton 82, Alberta

Received March 17, 1969

1-Aminotetrazoles and 2-aminotetrazoles can be prepared by reacting tetrazoles with hydroxylamine-*O*-sulfonic acid in weakly alkaline aqueous solutions. The nuclear magnetic resonance spectra and some of the properties of these aminotetrazoles are described.

Canadian Journal of Chemistry, 47, 3677 (1969)

Of the aminotetrazoles, the 5-aminotetrazoles have received by far the most attention in the literature. The synthesis of 5-aminotetrazole itself was described as early as 1892 by Thiele (1). Only a few reports have been published on 1-aminotetrazoles. Stollé and co-workers (2) have prepared some 1-amino-5-aryltetrazoles and the hydrochlorides of 1,5-diaminotetrazole and 1-amino-5-hydrazinotetrazole. Recently Hagedorn and Winkelmann (3) described a synthesis of 1-aminotetrazole itself. As hydroxylamine-*O*-sulfonic acid had been successfully employed as a reagent for the amination of several substances, such as amines (4), alkylboranes (5), benzotriazoles (6), and benzoxazolin-2-one (7), we investigated its reaction with tetrazoles as a possible route to 1-aminotetrazoles and the (thus far) unknown 2-aminotetrazoles.

When a mixture of tetrazole and sodium carbonate in water was treated with hydroxylamine-*O*-sulfonic acid a 2:1 mixture of 1-aminotetrazole (**1***a*) and 2-aminotetrazole (**2***b*) could be isolated in a total yield of 38%. In the same manner were also prepared the compounds **2**–**5**. The isomers were separated by fractional distillation, fractional crystallization, or by elution chromatography on alumina or silica gel. The yields, some physical constants, and nuclear magnetic resonance (n.m.r.) data of the thus prepared *N*-aminotetrazoles are given in Table I.

The identity of **1***a* was confirmed by comparison with an authentic sample prepared by the procedure of Hagedorn and Winkelmann (3). The other isomer assignments are based on the difference in physical behavior and n.m.r. spectra of the isomer pairs. It has been shown that 2-substituted tetrazoles have lower boiling points and better solubilities in organic solvents than the corresponding 1-isomers (8–13) and with a few exceptions (10, 11, 13), the 2-isomers are also the lower melting ones. There have been several reports in the literature on the use of n.m.r. spectroscopy in assigning structural isomers (12–17, 23), and it has been clearly established that a *N*-substituent is more deshielded in the 2-isomer than in the corresponding 1-isomer. As Table I

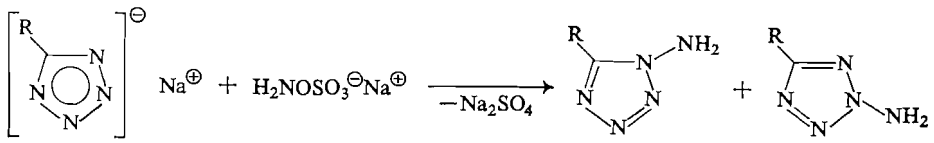

a *b*

1 R = H
2 R = *n*-C_3H_7
3 R = C_6H_5
4 R =

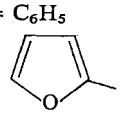

5 R = NH_2

Can. J. Chem. Downloaded from www.nrcresearchpress.com by 210.87.254.5 on 09/05/12
For personal use only.

TABLE I

N-Aminotetrazoles

Compound	% Yield*	Melting point (recrystallizing solvent) or boiling point (mm Hg), (°C)	Nuclear magnetic resonance chemical shifts (τ)†		Formula	Analyses‡					
						% calculated			% found		
			N—NH_2	C^5—R		C	H	N	C	H	N
1-Aminotetrazole (1*a*)	25	137–142(0.7)§	2.90	0.88	CH_3N_5						
2-Aminotetrazole (1*b*)	13	89–91(0.3)	2.03	1.28	CH_3N_5						
1-Amino-5-*n*-propyltetrazole (2*a*)	35	134–139(0.1)	3.73		$C_4H_9N_5$						
2-Amino-5-*n*-propyltetrazole (2*b*)	26	98–100(0.1)	2.93		$C_4H_9N_5$	37.78	7.14	55.09	38.03	7.39	54.70
1-Amino-5-phenyltetrazole (3*a*)	15	156–158(EtOAc)‖	2.70		$C_7H_7N_5$	52.15	4.38	43.46	51.93	4.20	43.82
2-Amino-5-phenyltetrazole (3*b*)	32	109–111(C_6H_6-*n*-C_6H_{14})	1.73		$C_7H_7N_5$	52.15	4.38	43.46	52.14	4.38	43.02
1-Amino-5-(2′-furyl)tetrazole (4*a*)	28	165–167(MeOH)	2.70¶		$C_5H_5N_5O$	39.73	3.33	46.35	39.98	3.20	46.15
2-Amino-5-(2′-furyl)tetrazole (4*b*)	21	116–117(EtOAc-*n*-C_6H_{14})	1.75¶		$C_5H_5N_5O$	39.73	3.33	46.35	39.95	3.34	46.70
1,5-Diaminotetrazole (5*a*)	8.5	187–188 (decomp.)**(H_2O)	3.63	3.63	CH_4N_6	12.00	4.03	83.97	12.37	3.73	83.81
2,5-Diaminotetrazole (5*b*)	4.5	125–127 (decomp.)††(EtOAc)	2.62	4.21	CH_4N_6	12.00	4.03	83.97	12.49	4.31	83.28

*All the yields given refer to the actual isolated amount of pure isomer. The yields for compounds **2**, **3**, and **4** are based on unrecovered starting material (respectively 61, 67, and 71% of the starting materials were recovered). In the case of compounds **1** and **5** no attempt was made to recover starting material.

†The spectra were taken in DMSO-d_6, except for compounds 3*a* and 3*b* where $CDCl_3$ was used as solvent.

‡Some of the aminotetrazoles were analyzed in the form of a more stable derivative (Table II).

§Reported b.p. 118–120 (0.01 mm) (3).

‖Reported m.p. 155° (2*a*).

¶The furyl protons in 4*a* appeared as doublets at τ 1.92 (J = 2 c.p.s.) and 2.44 (J = 3.5 c.p.s.) and a quartet at τ 3.16; in 4*b* these τ values were 2.03, 2.81, and 3.25 respectively.

**The HCl salt decomposed at 175–176°; reported decomposition point 176° (2*b*).

††The HCl salt decomposed at 120°.

Can. J. Chem. Downloaded from www.nrcresearchpress.com by 210.87.254.5 on 09/05/12
For personal use only.

TABLE II

Some derivatives of *N*-aminotetrazoles with aldehydes

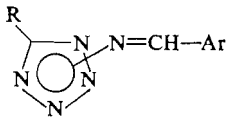

R	Ar	Melting point, (°C)	Recrystallizing solvent	Formula	Analyses					
					% calculated			% found		
					C	H	N	C	H	N
1-Isomers										
H	5-Nitro-2-furyl	158–159 (decomp.)	THF	$C_6H_4N_6O_3$	34.62	1.94	40.37	34.90	1.62	39.95
n-C_3H_7	p-$OCH_3C_6H_4$	91–93	C_6H_6 – n-C_6H_{14}	$C_{12}H_{15}N_5O$	58.75	6.16	28.55	58.87	6.42	29.00
n-C_3H_7	5-Nitro-2-furyl	115–117	EtOAc	$C_9H_{10}N_6O_3$	43.20	4.03	33.59	43.08	4.02	33.34
NH_2	C_6H_5	225–226 (decomp.)*	MeOH	$C_8H_8N_6$	51.05	4.29	44.66	50.46	4.18	44.50
NH_2	p-$OCH_3C_6H_4$	227–228 (decomp.)	DMF	$C_9H_{10}N_6O$	49.53	4.62	38.51	49.34	4.63	38.82
NH_2	5-Nitro-2-furyl	229 (decomp.)	DMF-EtOEt	$C_6H_5N_7O_3$	32.29	2.26	43.93	32.25	2.08	43.78
2-Isomers										
H	p-$OCH_3C_6H_4$	100–102	C_6H_6 – n-C_6H_{14}	$C_9H_9N_5O$	53.20	4.47	34.48	53.42	4.43	34.92
H	p-$O_2NC_6H_4$	161–162 (decomp.)	THF	$C_8H_6N_6O_2$	44.03	2.77		44.19	2.78	
H	5-Nitro-2-furyl	146–147 (decomp.)	THF	$C_6H_4N_6O_3$	34.62	1.94	40.37	34.84	2.21	40.08
n-C_3H_7	p-$OCH_3C_6H_4$	74–75	C_6H_6 – n-C_6H_{14}	$C_{12}H_{15}N_5O$	58.75	6.16	28.55	58.37	6.44	28.65
n-C_3H_7	5-Nitro-2-furyl	135–136 (decomp.)	C_6H_6	$C_9H_{10}N_6O_3$	43.20	4.03	33.59	43.34	4.06	33.78
C_6H_5	p-$O_2NC_6H_4$	169–170 (decomp.)	THF	$C_{14}H_{10}N_6O_2$	57.14	3.43	28.56	57.43	3.70	28.18
NH_2	C_6H_5	159–160 (decomp.)	MeOH	$C_8H_8N_6$	51.05	4.29	44.66	50.48	4.50	45.01
NH_2	p-$OCH_3C_6H_4$	176–177 (decomp.)	EtOH	$C_9H_{10}N_6O$	49.53	4.62	38.51	49.20	4.62	38.85
NH_2	5-Nitro-2-furyl	159 (decomp.)	THF	$C_6H_5N_7O_3$	32.29	2.26	43.93	32.82	2.19	43.45

*Reported m.p. 210° (decomp.) (2*b*).

Can. J. Chem. Downloaded from www.nrcresearchpress.com by 210.87.254.5 on 09/05/12
For personal use only.

shows, there is indeed a substantial difference in chemical shift of the *N*-amino group between isomer pairs ($\Delta\tau$ 0.8–1.0). Compounds **1** and **5** also show the expected difference in chemical shift of the 5-hydrogen and the 5-amino group between two isomers (13, 14, 16).

Whereas heating 1-aminotetrazole with acetic anhydride results in ring opening and the formation of 2-acetylamino-1,3,4-oxadiazole (3), 1-amino-5-phenyltetrazole under these conditions gives 1-diacetylamino-5-phenyltetrazole (2*c*). 1,5-Diaminotetrazole upon heating with acetic anhydride gave a triacetyl derivative, believed to be 5-acetylamino-1-diacetylaminotetrazole as 5-amino-tetrazoles are reported to give only the monoacetylated derivatives under these conditions (17–19). Both the 1- and 2-aminotetrazoles could readily be condensed with aromatic aldehydes. The derivatives thus prepared are listed in Table II. In the case of the diaminotetrazoles the question arose which of the two amino groups reacted; from the position of the amino signals in the n.m.r. spectra (Table III) it could be concluded, however, that the 1- and 2-amino groups underwent reaction in preference to the 5-amino group.[1]

The explosive character of 1-aminotetrazole has already been mentioned (3). The 2-aminotetrazoles appear to be distinctively more explosive than their corresponding 1-isomers, and 2-aminotetrazole and 2,5-diaminotetrazole especially were able to produce devastating explosions.[2] Great care should therefore be exercised in handling the lower members of the *N*-aminotetrazoles. Aryl substitution, and to a lesser extent also alkyl substitution, appears to stabilize the *N*-aminotetrazoles considerably.

[1]Another indication of the higher reactivity of the 1-amino group over the 5-amino group was obtained when an equimolar mixture of 1-amino-5-*n*-propyltetrazole and 5-amino-1-*n*-propyltetrazole was allowed to react with only 0.5 equivalent of anisaldehyde (THF, room temperature). The only product isolated was 1-*p*-methoxybenzylideneamino-5-*n*-propyltetrazole (67% yield) whereas 76% of the 5-amino-1-*n*-propyltetrazole was recovered.

[2]Even a 4 mg sample of 2-aminotetrazole produced a very loud explosion when rapidly heated to 250–300°. 2,5-Diaminotetrazole not only detonated upon impact but when a small sample in a capillary tube was rapidly heated in a pre-heated Gallenkamp melting point apparatus, it detonated already at 210°, with sufficient force to break the bulb of the thermometer. With 1,5-diaminotetrazole on the other hand, no detonation could be affected.

TABLE III

Nuclear magnetic resonance spectra of diaminotetrazole derivatives*

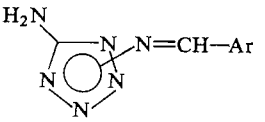

Ar		Chemical shifts (τ) NH_2	—N = CH—
C_6H_5	1-Isomer	2.76	0.80
	2-Isomer	3.43	0.90
O_2N	1-Isomer	2.64	0.86
	2-Isomer	3.27	0.96

*In DMSO-d_6.

Experimental

All melting points and boiling points are uncorrected. The n.m.r. spectra were measured using a Varian Associates model A-60 spectrometer with tetramethylsilane as a reference. Microanalyses were performed by Dr. G. Weiler and Dr. F. B. Strauss, Microanalytical Laboratory, Oxford, England.

Tetrazoles

The tetrazoles were prepared by literature procedures. Tetrazole itself was obtained by a reductive deamination of 5-aminotetrazole (9, 20) which in turn was obtained from dicyandiamide (21). 5-*n*-Propyltetrazole and 5-phenyltetrazole were prepared by the procedure of Finnegan *et al.* (22) from propionitrile and benzonitrile respectively. In the same manner 5-(2′-furyl)tetrazole, m.p. 198–200° (decomp.), could be prepared from 2-furylcyanide (92% yield).

Anal. Calcd. for $C_5H_4N_4O$: C, 44.12; H, 2.96; N, 41.16. Found: C, 44.26; H, 3.11; N, 40.98.

N-Aminotetrazoles

These were all prepared by essentially the same procedure, the only difference being in the work-up. The procedure is illustrated by the preparation of 1-aminotetrazole (**1***a*) and 2-aminotetrazole (**1***b*) as follows. Tetrazole (28.0 g, 0.40 mole) and sodium carbonate (46.4 g, 0.44 mole) were dissolved in 300 ml of water and the resulting mixture was heated to 75°. A solution of hydroxylamine-*O*-sulfonic acid (54.4 g, 0.48 mole) in 240 ml of water was added dropwise, with stirring, over a period of 20 min, the temperature of the reaction mixture being kept at 70–75°. Throughout the reaction a pH of 7–8 was maintained by the periodic addition of a saturated aqueous sodium bicarbonate solution. When the addition was completed the reaction mixture was heated under reflux for 20–30 min. After cooling the mixture was adjusted to pH 8 and then continuously extracted with ethyl acetate for 16 h. The ethyl acetate extract was dried and concentrated. The colorless residual oil was distilled *in vacuo* to give 4.3 g (13%) of 2-amino-

Can. J. Chem. Downloaded from www.nrcresearchpress.com by 210.87.254.5 on 09/05/12
For personal use only.

tetrazole, b.p. 89–91° (0.3 mm). The distillation residue consisted of only 1-aminotetrazole (8.4 g, 25%) which could be distilled only in small quantities without appreciable decomposition, b.p. 137–142° (0.7 mm); reported b.p. 118–120° (0.01 mm) (3). The infrared and n.m.r. spectra of 1-aminotetrazole were superimposable with the corresponding spectra of an authentic sample (3).

The *N*-amino-5-*n*-propyltetrazoles **2***a* and **2***b* were prepared in the same manner. When after continuous extraction of the products with ethyl acetate the solution was acidified and again continuously extracted with ethyl acetate, 61% of 5-*n*-propyltetrazole being recovered. In the preparation of **3** and **4**, the products were extracted with 3–6 portions of ethyl acetate, then the reaction mixture was acidified to give respectively 67 and 71% of unreacted starting material. Isomers **3***a* and **3***b* were separated by elution chromatography on alumina; **3***b* was eluted with a 1:1 benzene – ether mixture, **3***a* was eluted with ether. Isomers **4***a* and **4***b* were separated by recrystallization of the crude mixture from ethyl acetate, which provided pure **4***a*; the residue obtained from the filtrate was then chromatographed on alumina and **4***b* eluted with a 1:1 ether – ethyl acetate mixture. The diaminotetrazoles **5***a* and **5***b* were isolated by continuous extraction with ethyl acetate. The extract was dried, concentrated, and cooled. The precipitated 1,5-diaminotetrazole was then recrystallized from water. The residue obtained from the filtrate was chromatographed on silica gel and 2,5-diaminotetrazole eluted with ethyl acetate. The yields, physical constants, n.m.r. spectra, and analytical data are listed in Table I.

1-Diacetylamino-5-phenyltetrazole

A mixture of 1-amino-5-phenyltetrazole (0.35 g, 2.17 mmole) and acetic anhydride (5 ml) was heated under reflux for 4 h. Removal of the excess acetic anhydride and recrystallization of the residue from methanol gave 0.42 g (79%) of product, m.p. 88–89°; reported m.p. 90° (2*c*). The n.m.r. spectrum ($CDCl_3$) contained a multiplet at τ 2.0–2.4 and a sharp singlet at τ 7.62 with an integrated area ratio of 5:6.

Anal. Calcd. for $C_{11}H_{11}N_5O_2$: C, 53.87; H, 4.52; N, 28.56. Found: C, 53.95; H, 4.53; N, 28.80.

5-Acetylamino-1-diacetylaminotetrazole

A mixture of 1,5-diaminotetrazole (0.40 g, 4.0 mmole) and acetic anhydride (6 ml) was heated under reflux for 2 h. The mixture was cooled and the white crystalline product, m.p. 186–188° (decomp.), collected by filtration. Yield, 0.48 g (53%). The n.m.r. spectrum (DMSO-d_6) contained singlets at τ 7.65 and 7.78 with an integrated area ratio of 2:1.

Anal. Calcd. for $C_7H_{10}N_6O_3$: C, 37.16; H, 4.46; N, 37.15. Found: C, 37.18; H, 4.36; N, 36.91.

Reaction of N-Aminotetrazoles with Aldehydes

Equimolar amounts of the aminotetrazole and the aldehyde were dissolved in benzene, tetrahydrofuran, or dimethylformamide, depending on the solubility of the aminotetrazole. A trace of *p*-toluenesulfonic acid was added and the reaction mixture was left at room temperature overnight. The product was isolated by removal of the solvent and recrystallization of the residue or by the addition of ether to the tetrahydrofuran or dimethylformamide solutions. In many instances the product crystallized from the reaction mixture. The yields amounted to 50–90%. The derivatives prepared are listed in Table II.

Acknowledgments

The author is grateful to Mr. V. R. Baker and Mr. P. K. Wolfert for their capable technical assistance and to Professor R. U. Lemieux for his advice and interest in this work.

1. J. Thiele. Ann. **270**, 54 (1892).
2. (*a*) R. Stollé and Fr. Helwerth. Chem. Ber. **47**, 1132 (1914). (*b*) R. Stollé and E. Gaertner. J. Prakt. Chem. **132**, 209 (1931). (*c*) R. Stollé, H. Netz, O. Kramer, S. Rothschild, E. Erbe, and O. Schick. J. Prakt. Chem. **138**, 1 (1933).
3. I. Hagedorn and H. D. Winkelmann. Chem. Ber. **99**, 850 (1966).
4. (*a*) R. Gösl and A. Meuwsen. Chem. Ber. **92**, 2521 (1959); (*b*) R. Gösl and A. Meuwsen. Org. Syn. **43**, 1 (1963).
5. (*a*) H. C. Brown, W. R. Heydkamp, E. Breuer, and W. S. Murphy. J. Am. Chem. Soc. **86**, 3565 (1964). (*b*) M. W. Rathke, N. Inoue, K. R. Varna, and H. C. Brown. J. Am. Chem. Soc. **88**, 2870 (1966).
6. C. D. Campbell and C. W. Rees. Chem. Commun. 192 (1965).
7. R. S. Atkinson and C. W. Rees. Chem. Commun. 1230 (1967).
8. F. R. Benson. Chem. Rev. **41**, 1 (1947).
9. W. G. Finnegan and R. A. Henry. J. Org. Chem. **24**, 1565 (1959).
10. R. A. Henry and W. C. Finnegan. J. Am. Chem. Soc. **76**, 923 (1954).
11. W. P. Norris. J. Org. Chem. **27**, 3248 (1962).
12. R. N. Butler and F. L. Scott. J. Org. Chem. **31**, 3182 (1966); **32**, 1224 (1967).
13. R. Raap and J. Howard. Can. J. Chem. **47**, 813 (1969).
14. D. W. Moore and A. G. Whittaker. J. Am. Chem. Soc. **82**, 5007 (1960).
15. J. H. Markgraf, W. T. Bachmann, and D. P. Hollis. J. Org. Chem. **30**, 3472 (1965).
16. G. B. Barlin and T. J. Batterham. J. Chem. Soc. B, 516 (1967).
17. F. L. Scott and R. N. Butler. J. Chem. Soc. B, 919 (1967).
18. R. M. Herbst and J. E. Klingbeil. J. Org. Chem. **23**, 1912 (1958).
19. F. Einberg. J. Org. Chem. **32**, 3687 (1967).
20. R. A. Henry and W. G. Finnegan. J. Am. Chem. Soc. **76**, 290 (1954).
21. J. S. Mihina and R. M. Herbst. J. Org. Chem. **15**, 1082 (1950).
22. W. G. Finnegan, R. A. Henry, and R. Lofquist. J. Am. Chem. Soc. **80**, 3908 (1958).
23. R. R. Fraser and K. E. Haque. Can. J. Chem. **46**, 2855 (1968).

Permanganate–periodate oxidation. Part VIII. The oxidation of some cyclic mono-olefins and monoterpenes[1]

T. SUGA[2] AND E. VON RUDLOFF
Prairie Regional Laboratory, National Research Council of Canada, Saskatoon, Saskatchewan

Received November 5, 1968

The reaction of cyclic mono-olefins with the permanganate–periodate reagent was investigated. 4-Terpinenol and its acetate, and to a lesser degree α-terpineol and camphene gave in addition to the expected products, several neutral and acidic products. In contrast, α-pinene, β-pinene, sabinene, pulegone, and several cyclo-olefins which can be considered as simple analogues of these monoterpenes, afforded the predicted products in high yield. Cyclo-hexanone and menthone, though saturated, were oxidized extensively, enolization offering a plausible pathway for this result. Saturated terpene alcohols reacted only very slowly indicating that attack at a tertiary hydrogen is not a significant part of the permanganate–periodate reaction.

Canadian Journal of Chemistry, 47, 3682 (1969)

Can. J. Chem. Downloaded from www.nrcresearchpress.com by 210.87.254.5 on 09/05/12
For personal use only.

Introduction

Recently we have shown that the common acyclic monoterpenes may be oxidized by the permanganate–periodate reagent in high yield to predicted end products (1). In a preliminary experiment it was found that α-terpineol did not give a high yield of the expected product, homoterpenyl methyl ketone. In view of this, and of the different behavior of some dienes as reported recently by Klein and Rojahn (2), Apsimon *et al.* (3), and von Rudloff (4), the oxidation of some cyclic monoterpenes and related cyclo-olefins was studied with the specific purpose of determining whether or not the cyclic mono-olefins, and in particular monoterpenes, would react as predicted with the permanganate–periodate reagent.

Daly and co-workers (5) have employed the reagent in a preparative oxidation of sabinene to yield sabina ketone. We reported briefly (6) on the excellent yields of sabina ketone and nopinone which may be obtained from sabinene and β-pinene respectively, and that the oxidation proceeds at a satisfactory rate in aqueous suspension. Our previous studies (1, 7–12) have shown that the oxidation of an olefinic double bond proceeds in a predictable manner, involving hydroxylation of the double bond by a permanganate ion (via a π complex and hypomanganate ester (13) (see also Wiberg and Geer (14)), followed by periodate cleavage of the diol or ketols thus formed, and subsequent slower oxidation of the resulting aldehydes. Ketones and esters were found to be stable towards the reagent (at pH 7 to 8), whereas alcohols reacted slowly (12). With water-insoluble olefins good results were obtained when the reaction was carried out in aqueous *tert* butyl alcohol solutions (10–50%) (1, 11, 12).

In a few instances, the reaction with mono-olefins did not proceed to the predicted end products. Thus Lin and Cheng (15) reported that 1-cyclopentene-, 1-cyclohexene-, and 1-cycloheptene-carboxylic acids were oxidized to the next lower dicarboxylic acid rather than the expected keto-dicarboxylic acids. We found that carboxylic acids, including pyruvic acid, are not oxidized, although malonic acid was degraded slowly (12). In the same study we found that tetrahydrofurfurol was oxidized to succinic acid rather than to tetrahydro-2-furoic acid. Thus, in certain instances at least, over-oxidation of the type reported by Lin and Cheng must be considered as a possible side reaction.

Experimental

All compounds investigated were of commercial origin (Aldrich Chemical Co., unless otherwise stated). Sabinene was isolated from the oil of Savin (16). If the purity was satisfactory (see Tables I and II) these compounds were used as such. Impure ones were purified as described.

The purity of the starting materials was determined by gas–liquid chromatography (g.l.c.), employing temperature-programming or isothermal conditions and a flame ionization detector. Stainless steel columns, 0.3 cm outer diameter and 2–3 m long, and helium flow rates of 25–40 ml per min were employed. Of the many liquid phases and solid supports tested, polyethyleneglycol (Carbowax 20 *M*, 2%) on Porasil D, 100–150 mesh (17) was found to give the highest degree of separation of cyclo-olefins. For the oxygenated terpenes a standard 5% polyethylene

[1]Issued as N.R.C. No. 10 817. For Part VII, see ref. 1.
[2]National Research Council Postdoctorate Fellow, 1967–1968. Present address: Department of Chemistry, Hiroshima University, Hiroshima, Japan.

Can. J. Chem. Downloaded from www.nrcresearchpress.com by 210.87.254.5 on 09/05/12
For personal use only.

glycol column on Aeropak 30, 70–80 mesh (1, 18) was employed. The quantitative area measurements were obtained with a model 471 Varian Aerograph digital integrater. No correction factors were applied. The standard run was from 55° to 200° at 4° per min (18), but for the lower boiling olefins, a lower starting temperature (40°–50°) and lower rate of heating (2° per min) or isothermal conditions were employed.

Melting points were recorded on a Leitz hotstage microscope and these are uncorrected. Infrared (i.r.) spectra were obtained as films between sodium chloride plates or as potassium bromide disks, using a Perkin–Elmer model 21 double beam spectrophotometer. Nuclear magnetic resonance (n.m.r.) spectra were obtained in carbon–tetrachloride solution with tetramethylsilane as internal standard, using a Varian model HA-100 MHz spectrometer.

The quantitative and preparative oxidation procedures were described in detail previously (1, 7, 12). Tables I and II list the purity of the starting materials as determined by g.l.c., the amount of *tert* butyl alcohol used, the results obtained after 1, 6, 24, 144, and 196 h reaction time (the data obtained after 0.5, 2, 3, 48, 72, 96, and 120 h are not included), as well as the products obtained in the preparative oxidations. Neutral products were recovered by extracting the oxidation mixture with ether and removing the solvents as far as possible by fractional distillation. The weakly alkaline aqueous residue was evaporated to a small volume, the distillate being used for formaldehyde determination by the chromotropic acid method (8). The residual aqueous concentrate was acidified and extracted continuously (1–5 days) with ether to recover the acidic oxidation products. A small aliquot was methylated by the addition of freshly distilled diazomethane (best results were obtained by passing the vapors into a concentrated solution of the acidic product) and the resulting methyl esters were analyzed by g.l.c. (5% SE-30). The balance of the acidic product was used for recrystallization or the preparation of suitable crystalline derivatives. The experimental data for those compounds which gave the expected products in high yield have been placed into the Depository of Unpublished Data.[3]

Allyl Cyclohexane

The commercial sample was found to have a purity of 99.9% by g.l.c. (see, however, below). Preparative oxidation (248 mg, 2 mmoles; 20% *tert* butyl alcohol, 24 h) gave formaldehyde and a liquid acidic product (222 mg, 78%, ν_{max} (liquid) 1703, 1293, and 929 cm^{-1}), the methyl ester of which showed only a single peak with the retention time of the methyl ester of cyclohexane acetic acid. The identity was confirmed by conversion to the amide, m.p. 169–170° (lit (19) m.p. 169–171°). In a repeat experiment the neutral fraction (mainly *tert* butyl alcohol) was analyzed by g.l.c. and a peak with the retention time of allyl cyclohexane was recorded. Fractional distillation gave a small amount of a saturated hydro-carbon which had an i.r. spectrum that differed from that of allyl cyclohexane, but *tert* butyl alcohol was an impurity.

(±)-Camphene

The commercial sample (Lights and Co., England) was purified by preparative g.l.c. to give 98.0% pure camphene. Preparative oxidation (544 mg, 4 mmoles, 5–10% *tert* butyl alcohol, 24 h) afforded a neutral (530 mg) and an acidic (12 mg) product. Analysis by g.l.c of the neutral product showed the presence of *tert* butyl alcohol, unchanged camphene, and a major peak with the retention time of camphenilone. The identity of camphenilone was confirmed by conversion to the crystalline semicarbazone, m.p. and mixed m.p. 221.5–223° (lit. (20) m.p. 224°).

Anal. Calcd. for $C_{10}H_{17}N_3O$: C, 61.51; H, 8.78; N, 21.52. Found: C, 61.52; H, 8.77; N, 22.0.

When the reaction was carried out in 30% *tert* butyl alcohol solution, virtually all the camphene reacted but in addition to camphenilone, a neutral compound of much higher retention time (not the same as the derived diol or ketol) and a larger amount of acidic products were obtained.

α-Terpineol

The commercial sample (Eastman Organic Chemical) was found to be 98.6% pure; m.p. 33.5–34.5°. In the preparative oxidation (310 mg, 2 mmoles; 10% *tert* butyl alcohol, 48 h) the neutral product (247 mg, 67%) was extracted with chloroform instead of with ether. Although the i.r. spectrum, ν_{max} (liquid) 1760 cm^{-1} (γ-lactone) and 1708 cm^{-1} (carbonyl), was in good agreement with that of homoterpenyl methyl ketone, g.l.c. analysis showed that at least 3 major and 3 minor impurities as well as some unchanged α-terpineol were present. The retention times of the major impurities (5% SE-30 at 120°; 8.7, 10.5, and 11.5 min) were higher than that of α-terpineol (3.5 min) but lower than that of homoterpenyl methyl ketone (18.0 min). Homoterpenyl methyl ketone semicarbazone, m.p. and mixed m.p. 204.5–205.5°, was obtained in fairly good yield from the crude product. A small amount of an acidic product (74.2 mg) was also isolated. The chromatogram of the derived methyl esters showed 4 major and 12 minor peaks.

α-Terpinyl Acetate

Commercial α-terpineol was acetylated by heating under reflux with a 6-fold amount of acetic anhydride, an equal amount of sodium acetate, and a 15-fold amount of xylene for 12 h. Crude α-terpinyl acetate was purified by fractional distillation, b.p. 78–78.5° (1 mm), n_D^{25} 1.4621, 95% (g.l.c.).

Preparative oxidation (400 mg, 2.04 mmole; 10% *tert* butyl alcohol, 72 h) gave a small amount of neutral product (24 mg) and a liquid acidic product (489 mg, 98.5% based on the assumption of it being the expected acidic product). The neutral product showed at least 8 peaks in g.l.c. analysis, one of which corresponded to α-terpinyl acetate. Analysis by g.l.c. of the derived methyl esters of the acidic product showed one major peak (95%) and a broad tail (3–5%), indicating an impurity or decomposition. The acidic product was hydrolyzed with sodium ethoxide in excess ethanol. On acidification a neutral product was obtained which had an i.r. spectrum that was superimposable with that of homoterpenyl

[3]Photocopies may be obtained upon request to: The Depository of Unpublished Data, National Science Library, National Research Council of Canada, Ottawa, Canada.

Can. J. Chem. Downloaded from www.nrcresearchpress.com by 210.87.254.5 on 09/05/12
For personal use only.

TABLE I

Permanganate–periodate oxidation of some cyclo-olefins

Compound	Purity* %	Oxidant consumed (atoms oxygen/mole) 1 h	6 h	24 h	144 h	196 h	Calcd.	% *tert* Butyl alcohol	Oxidation product (% yield) and remarks
Cyclopentene	98.5	3.54	3.92	3.97	4.10	—	4	20	Glutaric acid (99)
Cyclohexene	99.2	3.64	3.75	3.79	3.98	—	4	20	Adipic acid (98)
1-Methyl cyclopentene	99.7	2.59	2.71	2.72	3.19	—	3	20	5-Ketohexanoic acid (92)
1-Methyl cyclohexene	100.0	2.35	2.73	2.82	3.09	—	3	20	6-Ketoheptanoic acid (94)
3-Methyl cyclohexene	99.4	3.64	3.91	3.92	4.09	—	4	20	2-Methyl adipic acid (96)
4-Methyl cyclohexene	94.8	3.58	3.74	3.79	4.04	—	4	20	3-Methyl adipic acid (94)
Methylene cyclohexane	99.8	2.99	3.21	3.37	—	4.11	4	20	Cyclohexanone (95) + CH_2O
Vinyl cyclohexane	100.0	3.80	4.05	4.15	—	4.56	5	10	Cyclohexane carboxylic acid (91) + CH_2O
Allyl cyclohexane	99.9†	3.69	3.90	3.99	4.29	—	5	20	Cyclohexane acetic acid (78) + CH_2O
1-Methyl cycloheptene	99.5	2.61	2.96	3.01	3.10	—	3	20	7-Keto octanoic acid (95)
4-Vinyl cyclohexene	97.4	5.04	5.34	5.58	—	6.05	9	20	Butane-1,2,4-tricarboxylic acid (58)
Cyclohexanol	100.0	0.08	0.10	0.17	—	1.39	1	0	—
Cyclohexane-methanol	100.0	0.06	0.13	0.16	—	0.58	2	0	—
2-Cyclohexen-1-ol	98.1	4.65	5.38	5.85	—	—	6	10	Glutaric acid (98)
Cyclohexene oxide	99.5	0.00	0.08	0.20	1.00	—	0	10	—
3-Cyclohexene-1-carboxylic acid	98.2	3.40	3.85	3.97	4.12	—	4	0	Butane-1,2,4-tricarboxylic acid (58)
Cyclohexanone	100.0								Adipic acid
a)		0.02	0.18	0.78	2.21	—	(3)	0	0.5 times K_2CO_3
b)		0.05	0.20	1.09	2.60	—		0	1.0 times K_2CO_3
c)		0.05	0.46	1.13	2.59	—		0	2.0 times K_2CO_3

*As determined by g.l.c.
†See text.

methyl ketone. The melting point of the derived semicarbazone, m.p. 202.5–204.5° was undepressed in admixture with the authentic specimen. This confirmed that the oxidation product from α-terpinyl acetate was the acetate of homoterpenyl methyl ketone.

4-Terpinenol

The commercial sample (Lights and Co., England) was found to be 98.5% pure. Preparative oxidation (616 mg, 4 mmoles; 10% *tert* butyl alcohol, 6 h) gave a neutral (62.8 mg) and an acidic (426.7 mg) product. The neutral product showed 5 peaks with higher retention times than 4-terpinenol, and the derived methyl esters of the acidic product 1 major and 10 minor peaks. The spectrum of the crude acidic product ν_{max} (liquid) 1718, 1285, 1205, and 918 cm^{-1} (COOH), confirmed that the major product was a keto acid but no crystalline semicarbazone or 2,4-dinitrophenyl hydrazone could be obtained.

4-Terpinenyl Acetate

This acetate was prepared from 4-terpinenol in the same manner as α-terpinyl acetate (see above); b.p. 71–73° (1.3 mm), n_D^{25} 1.4623; 95% (g.l.c.). Preparative oxidation (785 mg, 4 mmoles; 10% *tert* butyl alcohol, 6 h) afforded a small amount of a neutral product (27.3 mg) and a liquid acidic product (416 mg); g.l.c. analysis of the derived methyl esters showed it to be composed of 3 major and 4 minor components. The i.r. spectrum of the sodium salts, ν_{max} (KBr) 1735 ($OCOCH_3$), 1707 (CO), 1566 and 1398 cm^{-1} ($COO^{\ominus}$) confirmed that the acetate of a keto acid was present, but no crystalline derivatives were obtained.

Results and Discussion

The amounts of oxidant consumed by the cyclic olefins at different reaction times are shown in Table I. Cyclopentene, cyclohexene, the methyl substituted derivatives, and 1-methyl cycloheptene, as well as the cyclohexanes with exocyclic double bonds all reacted in the expected manner and the predicted end products were isolated in high yield. The 1-methyl cyclo-olefins reacted more slowly than the other cyclo-alkenes. Allyl cyclohexane consumed less than the calculated 5 atoms of oxygen per mole and cyclohexane acetic acid was obtained in only about 78% yield. A saturated impurity having the same retention time on the PEG-Porasil column as allyl cyclohexane was found to be present and this can account for the low results obtained. Similarly, 4-vinyl cyclohexene afforded only a 58% yield of the expected butane-1,2,4-tricarboxylic acid.

Several oxygenated cyclohexane derivatives were also oxidized (see Table I). As expected (7, 12) cyclohexanol, cyclohexane–methanol and cyclohexene oxide consumed oxidant only at a very slow rate. Cyclohexanone consumed very little oxidant during the first 6 h, but thereafter a steady increase was measured, which reached the equivalent of 2.60 atoms of oxygen per mole of cyclohexanone after 7 days. Hence, it appeared that cyclohexanone enolized under conditions which did not produce any oxidation with aliphatic ketones (12). Once a double bond is formed, one would expect hydroxylation, cleavage, and further oxidation to proceed in the normal manner. It was confirmed that enolization is involved by employing one-half and twice the normal concentration of potassium carbonate, when a corresponding decrease and increase in the rates of oxidation was obtained (see Table I). 2-Cyclohexen-1-ol consumed the calculated amount of oxidant in about 3 days and the predicted end product, glutaric acid, was obtained in 98% yield. Similarly, the oxidation of 3-cyclohexene-1-carboxylic acid proceeded as expected. This is in contrast to the results reported by Lin and Cheng for the oxidation of 1-carboxyl cyclo-olefins (15), but the latter must be considered a special case because of the conjugated nature for the double bond.

The results obtained in the oxidation of some cyclic monoterpenes are shown in Table II. (−)-α-Pinene was oxidized smoothly to (−)-pinonic acid. The almost quantitative oxidation of β-pinene and sabinene to nopinone and sabina ketone respectively employing the aqueous reagent (6) was confirmed. It is noteworthy that the retentions of nopinone and sabina ketone differ considerably on most g.l.c. columns, whereas β-pinene and sabinene are not easily separated. The facile oxidation of the latter to the corresponding ketones offers a convenient method for detecting one terpene in the other.

Camphene did not react appreciably with the aqueous reagent, presumably because this terpene is a solid at room temperature. The reaction proceeded only at a satisfactory rate when 30% *tert* butyl alcohol was added. The expected product, camphenilone, was obtained in only about 50% yield. In addition to this, a mixture of acidic products and at least one higher boiling neutral compound was formed. Upon reducing the *tert* butyl alcohol content of the reaction mixture, the relative yield of camphenilone increased but the amount of camphene which reacted was reduced. Hence it appears that the presence of *tert* butyl alcohol tends to increase side-reaction and undesirable by-products.

α-Terpineol was oxidized to the predicted homoterpenyl methyl ketone, but g.l.c. analysis of the neutral fraction showed the presence of 3

Can. J. Chem. Downloaded from www.nrcresearchpress.com by 210.87.254.5 on 09/05/12
For personal use only.

Can. J. Chem. Downloaded from www.nrcresearchpress.com by 210.87.254.5 on 09/05/12
For personal use only.

TABLE II

Permanganate-periodate oxidation of some cyclic monoterpenes

Compound	Purity* %	Oxidant consumed (atoms oxygen/mole) 1 h	6 h	24 h	144 h	Calcd.	% *tert* Butyl alcohol	Oxidation products (% yield) and remarks
(−)-α-Pinene	98.9	2.79	3.06	3.18	3.48	3	20	(−)-Pinonic acid (84)
(−)-β-Pinene	96.5	2.30	2.98	3.50	4.02	4	20†	(−)-Nopinone (95)
(+)-Sabinene	97.3	2.46	2.79	3.23	3.84	4	20†	(−)-Sabina ketone (96)
(±)-Camphene	98.0	0.72	2.60	2.93	3.88	4	30†	(±)-Camphenilone (~50)
α-Terpineol	98.6	2.15	2.31	2.39	3.22	3	10	Homoterpenyl methyl ketone (~50)
α-Terpinyl acetate	95.0	2.60	2.68	2.83	3.34	3	10	Homoterpenyl methyl ketone acetate (94)
4-Terpinenol	98.5	2.35	2.85	3.30	4.09	3	10	Complex mixture of products
4-Terpinenyl acetate	95.0	2.85	3.07	3.33	4.53	3	10	
(+)-Pulegone	94.0	2.93	3.15	3.28	—	3	10	3-Methyl adipic acid (75)
Dihydro-α-terpineol	98.3	—	0.30	0.30	0.72	0	10	—
(−)-Menthol	99.8	0.00	0.05	0.05	0.10	0	10	—
(±)-Borneol	99.5	0.00	0.05	0.05	0.15	0	10	—
(±)-Isoborneol	100.0	0.00	0.10	0.10	0.15	0	10	—
(−)-Menthone	99.5							
a)		0.00	0.25	0.74	1.65	(3–4)	10	0.5 times K_2CO_3
b)		0.00	0.25	0.80	1.75		10	1.0 times K_2CO_3
c)		0.05	0.40	0.82	1.83		10	2.0 times K_2CO_3

*As determined by g.l.c.
†Preparative oxidation also carried out in aqueous suspensions.

Can. J. Chem. Downloaded from www.nrcresearchpress.com by 210.87.254.5 on 09/05/12
For personal use only.

major and 3 minor compounds. The formation of additional neutral products cannot be explained by over-oxidation, as the amount of oxidant consumed did not exceed the theoretical to any appreciable extent (see Table II). Hence, the possibility of the introduction of hydroxyl groups at tertiary hydrogen atoms by reaction with permanganate as reported by Eastman and Quinn (21) was investigated. Dihydro-α-terpineol, menthol, borneol, and isoborneol were oxidized under the same conditions. These saturated alcohols consumed oxidant at a very low rate (see Table II). Hence, any oxidation of a tertiary hydrogen with the permanganate–periodate reagent proceeds at such a slow rate, if at all, that it cannot account for the formation of the additional neutral products in the reaction with α-terpineol. When α-terpinyl acetate was oxidized, both the rate of oxidation (Table II) and the high yield of a single acidic product, which gave homoterpenyl methyl ketone on hydrolysis and acidification, indicated that the typical route of permanganate–periodate oxidation was followed. It appears likely that the side reactions encountered with α-terpineol are not of a general nature, but rather arise from some specific property of this terpene alcohol. This concept was strengthened by the results obtained in the oxidation of 4-terpinenol and its acetate. Not only did both mono-olefins consume more than the calculated amount of oxidant (Table II, 4.1 and 4.5 respectively instead of 3.0 atoms of oxygen per mole), but both gave a rather large number of neutral and acidic products. With these two terpenes it is possible that a reactive methylene group is produced which is oxidized further and may thus lead to a variety of products. Also, one cannot rule out the formation of oxides, as found by Klein and Rojahn (2) in the permanganate oxidation of 1,5-dienes, by Apsimon *et al.* (3) in the oxidation of methyl pimarate, and by us (4) in the oxidation of occidentalol.

When the oxidation of menthone was carried out with different amounts of potassium carbonate, similar results (Table II) as those with cyclohexanone were obtained (see Table I). Hence, enolization may play a considerable role with saturated cyclic ketones unless the pH is kept below 7.5. The reaction with pulegone proceeded in the typical manner and a high yield of the predicted product, 3-methyl adipic acid, was obtained. Therefore, the hydroxylation of the double bond and subsequent cleavage of the diols and ketols produced proceeds rapidly and without any significant side reaction with a conjugated ketone.

It may be concluded that most cyclic mono-olefins react with the permanganate–periodate reagent as predicted to give high yields of the expected products. However, the side-reactions encountered with 4-terpinenol and its acetate, and to a lesser extent with α-terpineol and camphene, indicate that with certain monoterpenes random degradation may take place to such a large degree that the reagent cannot be used for analytical purposes. The facile enolization of the saturated cyclic ketones is a factor which must also be considered when the reagent is applied in terpene analysis.

1. E. VON RUDLOFF. Can. J. Chem. **43**, 2660 (1965).
2. E. KLEIN and W. ROJAHN. Tetrahedron, **21**, 2353 (1965).
3. J. W. APSIMON, A. S. Y. CHAU, W. G. CRAIG, and H. KREHM. Can. J. Chem. **45**, 1439 (1967).
4. E. VON RUDLOFF. Tetrahedron Letters, No. 10, 993 (1966).
5. J. W. DALY, F. C. GREEN, and R. H. EASTMAN. J. Amer. Chem. Soc. **80**, 6330 (1958).
6. E. VON RUDLOFF. 47th Annu. Meet. Chem. Inst. Canada, Kingston, Ontario. June 1–4. 1961.
7. R. U. LEMIEUX and E. VON RUDLOFF. Can. J. Chem. **33**, 1701 (1955).
8. R. U. LEMIEUX and E. VON RUDLOFF. Can. J. Chem. **33**, 1710 (1955).
9. E. VON RUDLOFF. Can. J. Chem. **33**, 1714 (1955).
10. E. VON RUDLOFF. J. Amer. Oil Chemists' Soc. **33**, 126 (1956).
11. E. VON RUDLOFF. Can. J. Chem. **34**, 1413 (1956).
12. E. VON RUDLOFF. Can. J. Chem. **43**, 1784 (1965).
13. S. WOLFE. Ph.D. Dissertation, University of Ottawa, Ottawa, 1957.
14. K. B. WIBERG and R. D. GEER. J. Amer. Chem. Soc. **88**, 5827 (1966).
15. Y. T. LIN and Y. S. CHENG. J. Chin. Chem. Soc. (Taiwan), **7**, 58 (1960).
16. E. VON RUDLOFF. Can. J. Chem. **41**, 2876 (1963).
17. PECHINEY. Saint-Gobain, France. Distributed by Water Associates, Inc., Framingham, Mass. U.S.A.
18. A. R. VINUTHA and E. VON RUDLOFF. Can. J. Chem. **46**, 3743 (1968).
19. K. HOFMANN, S. F. OROCHENA, S. M. SAX, and G. A. JEFFREY. J. Amer. Chem. Soc. **81**, 992 (1959).
20. J. L. SIMONSEN and L. N. OWEN. *In* The terpenes. Vol. II. University Press, Cambridge. 1949. p. 369.
21. R. H. EASTMAN and R. A. QUINN. J. Amer. Chem. Soc. **82**, 4249 (1960).

Conformational dependence of long-range spin-spin coupling constants in 2,6-dichlorobenzylfluoride

T. SCHAEFER, C. M. WONG, AND K. C. TAM
Department of Chemistry, University of Manitoba, Winnipeg, Manitoba

Received April 17, 1969

Double resonance experiments on the proton magnetic resonance spectrum of 2,6-dichlorobenzylfluoride yield the signs of the long-range coupling constants between the ring protons and the fluorine nuclei and protons in the fluoromethyl group. The signs and magnitudes of the long-range couplings are discussed in terms of their dependence on the conformation of the fluoromethyl group.

Canadian Journal of Chemistry, 47, 3688 (1969)

Can. J. Chem. Downloaded from www.nrcresearchpress.com by 210.87.254.40 on 09/05/12
For personal use only.

Spectral Parameters of 2,6-Dichlorobenzylfluoride

At 60 MHz the proton magnetic resonance spectrum of an approximately 10 mole % solution of 2,6-dichlorobenzylfluoride, **1**, in benzene-d_6 is the AB_2X_2 part of an AB_2X_2R spectrum in which rapid rotation of the fluoromethyl group

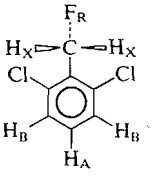

1

ensures the observation of equal coupling from the X_2 protons to the B_2 and A protons, respectively. The properties of such a spectrum are well known (1). However, the AB_2 part is not coupled tightly enough to allow the determination of the relative signs of the long-range couplings from any observed asymmetry in the X_2 resonance peaks (1). Consequently, a series of double resonance experiments under conditions of weak irradiation (2, 3) were performed. In conjunction with the usual analytical procedure (1), these experiments gave the following spectral parameters, where the shifts are quoted in p.p.m. relative to internal tetramethylsilane and coupling constants are measured in Hz.

$$\nu_A = -6.690 \pm 0.003$$

$$\nu_B = -6.927 \pm 0.003$$

$$\nu_X = -5.392 \pm 0.003$$

$$J_{AB} \equiv J_o^{HH} = 8.14 \pm 0.05$$

$$J_{BX} \equiv J_m^{H,CH_2(F)} = 0.34 \pm 0.04$$

$$J_{AX} \equiv J_p^{H,CH_2(F)} = -0.16 \pm 0.02$$

$$J_{XR} \equiv J_g^{CH_2,F} = 47.5 \pm 0.10$$

$$J_{BR} \equiv J_m^{H,C(H_2)F} = 1.25 \pm 0.04$$

$$J_{AR} \equiv J_p^{H,C(H_2)F} = -2.43 \pm 0.02$$

The signs of the proton–proton coupling constants were determined relative to $J_{AB} \equiv J_o^{HH}$ and the signs of the proton–fluorine coupling constants were determined relative to $J_{XR} \equiv J_g^{CH_2,F}$. But J_o^{HH} and $J_g^{H,F}$ are both known to be positive (4, 5).

Conformational Dependence of the Long-range Couplings

Conformation of the Difluoromethyl Group

In the ensuing discussion it will be assumed that the most stable conformation of the fluoromethyl is as depicted in **1**, i.e., with the C—F bond directed perpendicular to the aromatic ring on an average. In this conformation steric interactions between the C—F and C—Cl bonds are at a minimum. From a study (6) of the barriers to rotation in α,α,2,6-tetrachlorotoluene it is known that a conformation in which a sidechain C—Cl bond eclipses the aromatic C—Cl bond is at least 12 kcal/mole less stable than a conformation in which these bonds are staggered. It is a reasonable assumption, therefore, that **1** is favored by at least 3 kcal/mole over a conformation in which the C—F bond eclipses a C—Cl bond. In that case the average population of **1** at room temperature is about 150 times as abundant as the eclipsed conformations. Naturally, near room temperature such a barrier will allow oscillations of substantial magnitude about the relevant C—C bond. However, calculations by Stone and Maki (7) suggest that for barriers as high as 3 kcal/mole the following discussion of coupling constants in terms of the rigid conformation **1** is valid to a very good approximation (7).

The Long-range Proton–Proton Couplings

$J_{BX} \equiv J_m^{H,CH} = 0.34$ Hz has the same magnitude within experimental error as the corresponding coupling in toluene (8), 2,6-dichlorotoluene[1] and benzaldehyde (9). From studies on α,α,2,6-tetrachloro- and α,α,2,6-pentachlorotoluene (6, 10) it is known that this five-bond coupling is conformation dependent. Thus in **2**, $J_m^{H_X,H_A} \approx 0.5$ Hz whereas $J_m^{H_B,H_X} < 0.10$ Hz, indicating a preponderant σ electron contribution to J_m^{H,CHX_2}.

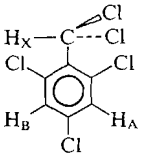

2

However, there may also be a finite π contribution to this coupling when the C—H bond takes on a nonplanar conformation which allows hyperconjugation between the C—H bond and the π system of the ring. Therefore, although the σ contribution appears to decrease from a maximum at $\theta = 0°$ to a minimum at $\theta = 180°$ (θ is here the angle between the aromatic plane and the C—C—H plane), the functional form of this θ dependence is unknown. The magnitude of the π contribution for $0° < \theta < 180°$ to this coupling is also unknown. The two contributions can conceivably compensate in such a way as to lead to the same magnitude of $J_m^{H,CH}$ in the above compounds. Further discussion at this time seems inappropriate, particularly in view of the unknown effect of the fluorine substituent on this coupling.

If a negligible σ electron contribution to $J_p^{H,CH}$ is assumed and if the π electron contribution (11–13) is taken as proportional to $\cos^2 \psi$, where $\psi = 0$ corresponds to a conformation in which the C—H bond lies perpendicular to the aromatic plane and therefore to maximum overlap between the C—H bond and the π system (hyperconjugation); the observed $J_p^{H,CH} = -0.62$ Hz in toluene (8) leads to a predicted $J_p^{H,CH} = -1.2$ Hz when $\psi = 0$ (the methyl group rotates rapidly and $\langle \cos^2 \psi \rangle = 0.5$). In the conformation **1**, $\psi = 60°$ so that in **1**, $J_p^{H,CH} = -1.2 \times 1/4 = -0.3$ Hz; approximately twice the observed value of −0.16 Hz. When fluorine in the sidechain is replaced by larger groups of lower electronegativity, e.g. chlorine or methyl,[1] $J_p^{H,CH}$ approaches −0.3 Hz. This observation suggests that the electronegative fluorine atom polarizes the C—H bond, decreases electron density near the proton, and in terms of the simplest group molecular orbitals used to interpret hyperconjugative effects, leads to a less efficient transfer of electron spin polarization information from the π system to the region of the protons in the sidechain.

The Long-range Proton–Fluorine Couplings

$J_{BR} \equiv J_m^{H,CF} = 1.25$ Hz may be compared with the corresponding values of 1.33 Hz in benzoylfluoride and 0.82 Hz in benzotrifluoride (9). If benzoyl fluoride is planar similar remarks apply here as were made above for $J_m^{H,CH}$. Further discussion appears inappropriate.

$J_{AR} \equiv J_p^{H,CF} = -2.43$ Hz compares with the corresponding values of −0.02 Hz in benzoyl fluoride and −0.64 Hz in benzotriflouride (9). If a planar conformation is assumed for benzoyl fluoride and conformation **1** is assumed for 2,6-dichlorobenzylfluoride, arguments similar to those presented for $J_p^{H,CH}$ predict that $J_p^{H,CF} = -2.4 \times 1/2 = -1.2$ Hz in benzotrifluoride; twice the observed magnitude (the barrier to rotation in benzotrifluoride is so small (14) that $\langle \cos^2 \psi \rangle = 0.5$ can be assumed). Again, substitution of two more fluorine atoms may reduce the net hyperconjugation of the C—F bonds with the π system.

There is a need for coupling constant data on benzylfluoride itself and for 2,6-dichlorobenzalfluoride. The spectral analysis of the former is not a simple problem, whereas the synthesis of the latter compound is still being attempted in this laboratory.

Experimental

Preparation of 2,6-Dichlorobenzylfluoride

α-Bromo-2,6-dichlorotoluene (10 g), triethylamine (5 g), and absolute ethanol (5 ml) were mixed and stirred overnight at 50 °C in an oil bath under anhydrous conditions. The mixture was allowed to cool and then anhydrous ether (100 ml) was added to break up the cake formed. The supernatant was decanted through a filtering crucible and the precipitate was stirred with more anhydrous ether (2 × 50 ml). The precipitate was then dissolved in water (50 ml). The solution was stirred with a suspension of powdered silver oxide (10 g) for 1 h and then filtered. This process was repeated twice more. The final filtrate was neutralized with 20% hydrofluoric acid (approximately 4 ml) and concentrated on a steam bath to half of its original volume. The resulting solution was distilled under a water-pump vacuum (20 mm) from a

[1] T. Schaefer. Unpublished work.

Can. J. Chem. Downloaded from www.nrcresearchpress.com by 210.87.254.40 on 09/05/12
For personal use only.

flask, equipped with a heating mantle, through a condenser into a flask cooled below 0 °C (ice–salt mixture). α-Fluoro-2,6-dichlorotoluene and other impurities were collected as a white solid. The distillate was then exhaustively extracted with ether (5 × 40 ml). The ether extracts were combined, dried (sodium sulfate), and concentrated into a foam (2.2 g). Chromatography (silica gel) of the residue gave a mixture of α-bromo-2,6-dichlorotoluene and α-fluoro-2,6-dichlorotoluene (1.2 g). Rechromatography (silica gel) separated out α-fluoro-2,6-dichlorotoluene as white needles (700 mg), melting point: 58–59 °C.

Proton Magnetic Resonance Spectra

An approximately 10 mole % solution in benzene-d_6 containing internal tetramethylsilane was degassed by the freeze–pump–thaw technique. Spectra were taken on a DA-60I spectrometer in the frequency sweep mode and were calibrated by reading reciprocal frequencies of the sweep and manual oscillators. Weak irradiations under double resonance conditions were performed in the normal way (2, 3).

Acknowledgments

We are grateful to Dr. S. Castellano for sending us his results prior to publication and to the National Research Council of Canada for financial support.

1. P. Diehl and J. A. Pople. Mol. Phys. **3**, 557 (1960).
2. R. Freeman and W. A. Anderson. J. Chem. Phys. **37**, 2053 (1962).
3. R. Kaiser. J. Chem. Phys. **39**, 2435 (1963).
4. A. Saupe. Z. Naturforsch. **19***a*, 161 (1964); **20***a*, 572 (1965).
5. R. A. Bernheim, D. J. Hoy, T. R. Krugh, and B. J. Lavery. J. Chem. Phys. **50**, 1350 (1969).
6. T. Schaefer, R. Schwenk, C. J. Macdonald, and W. F. Reynolds. Can. J. Chem. **46**, 2187 (1968).
7. E. W. Stone and A. H. Maki. J. Chem. Phys. **37**, 1326 (1962).
8. M. P. Williamson, R. J. Kostelnik, and S. M. Castellano. J. Chem. Phys. **49**, 2218 (1968).
9. R. J. Kostelnik, M. P. Williamson, D. E. Wisnosky, and S. M. Castellano. Can. J. Chem. To be published.
10. B. Fuhr, B. Goodwin, H. M. Hutton, and T. Schaefer. To be published.
11. H. M. McConnell. J. Chem. Phys. **30**, 126 (1959).
12. H. M. McConnell. J. Chem. Phys. **1**, 11 (1957).
13. M. J. S. Dewar and R. C. Fahey. J. Am. Chem. Soc. **85**, 2704 (1963).
14. D. W. Scott, D. R. Dauslin, J. F. Messerly, S. S. Todd, I. A. Hossenlopp, T. C. Kincheloe, and J. P. McCullough. J. Am. Chem. Soc. **81**, 1015 (1959).

A new synthesis of poly-γ-D- and L-glutamic acid

J. Kovacs, G. N. Schmit, and B. J. Johnson

Department of Chemistry, St. John's University, Jamaica, New York 11432

Received May 12, 1969

A new synthesis of native polyglutamic acid is described through the polycondensation of γ-glutamylglutamic acid-α,α′-di-*t*-butyl-γ-pentachlorophenyl ester. This route eliminates the possibility of transpeptidation.

Canadian Journal of Chemistry, 47, 3690 (1969)

Degradation (1) of native polyglutamic acids, produced by *B. anthracis* and *B. subtilis*, indicated that they are identical with poly-γ-glutamic acids. The anthrax-polypeptide consists exclusively (2) of D-glutamic acid residues, while the subtilis-polypeptide usually is a mixture (3) of poly-γ-D- and poly-γ-L-glutamic acid.

The synthesis (4) of these polypeptides was achieved by polycondensation of γ-glutamylglutamic acid-α,α′-dimethyl ester through activation of the γ-carboxyl group by various methods used in peptide synthesis. The free poly-γ-glutamic acid was obtained by saponification of the corresponding poly-γ-glutamic acid polymethyl ester. However, under basic conditions transpeptidation (4*a*, 5) could not be completely avoided.

We wish to report a new synthesis of these polypeptides by polymerization of γ-glutamylglutamic acid-α,α′-di-*t*-butyl-γ-pentachlorophenyl ester.[1] Here, the *t*-butyl ester groups can be removed with mild acid treatment of the *C*-protected polypeptide, thus eliminating the possibility of transpeptidation (6). In addition, polymerization through the pentachlorophenyl active ester results in a good yield of high molecular weight polymer (6, 7).

[1]M. Kajtar has applied the method reported here for the synthesis of γ-polyglutamic acids, unpublished work, reported to the authors in a private communication.

Can. J. Chem. Downloaded from www.nrcresearchpress.com by 210.87.254.40 on 09/05/12
For personal use only.

flask, equipped with a heating mantle, through a condenser into a flask cooled below 0 °C (ice–salt mixture). α-Fluoro-2,6-dichlorotoluene and other impurities were collected as a white solid. The distillate was then exhaustively extracted with ether (5 × 40 ml). The ether extracts were combined, dried (sodium sulfate), and concentrated into a foam (2.2 g). Chromatography (silica gel) of the residue gave a mixture of α-bromo-2,6-dichlorotoluene and α-fluoro-2,6-dichlorotoluene (1.2 g). Rechromatography (silica gel) separated out α-fluoro-2,6-dichlorotoluene as white needles (700 mg), melting point: 58–59 °C.

Proton Magnetic Resonance Spectra

An approximately 10 mole % solution in benzene-d_6 containing internal tetramethylsilane was degassed by the freeze–pump–thaw technique. Spectra were taken on a DA-60I spectrometer in the frequency sweep mode and were calibrated by reading reciprocal frequencies of the sweep and manual oscillators. Weak irradiations under double resonance conditions were performed in the normal way (2, 3).

Acknowledgments

We are grateful to Dr. S. Castellano for sending us his results prior to publication and to the National Research Council of Canada for financial support.

1. P. Diehl and J. A. Pople. Mol. Phys. **3**, 557 (1960).
2. R. Freeman and W. A. Anderson. J. Chem. Phys. **37**, 2053 (1962).
3. R. Kaiser. J. Chem. Phys. **39**, 2435 (1963).
4. A. Saupe. Z. Naturforsch. **19***a*, 161 (1964); **20***a*, 572 (1965).
5. R. A. Bernheim, D. J. Hoy, T. R. Krugh, and B. J. Lavery. J. Chem. Phys. **50**, 1350 (1969).
6. T. Schaefer, R. Schwenk, C. J. Macdonald, and W. F. Reynolds. Can. J. Chem. **46**, 2187 (1968).
7. E. W. Stone and A. H. Maki. J. Chem. Phys. **37**, 1326 (1962).
8. M. P. Williamson, R. J. Kostelnik, and S. M. Castellano. J. Chem. Phys. **49**, 2218 (1968).
9. R. J. Kostelnik, M. P. Williamson, D. E. Wisnosky, and S. M. Castellano. Can. J. Chem. To be published.
10. B. Fuhr, B. Goodwin, H. M. Hutton, and T. Schaefer. To be published.
11. H. M. McConnell. J. Chem. Phys. **30**, 126 (1959).
12. H. M. McConnell. J. Chem. Phys. **1**, 11 (1957).
13. M. J. S. Dewar and R. C. Fahey. J. Am. Chem. Soc. **85**, 2704 (1963).
14. D. W. Scott, D. R. Dauslin, J. F. Messerly, S. S. Todd, I. A. Hossenlopp, T. C. Kincheloe, and J. P. McCullough. J. Am. Chem. Soc. **81**, 1015 (1959).

A new synthesis of poly-γ-D- and L-glutamic acid

J. Kovacs, G. N. Schmit, and B. J. Johnson

Department of Chemistry, St. John's University, Jamaica, New York 11432

Received May 12, 1969

A new synthesis of native polyglutamic acid is described through the polycondensation of γ-glutamylglutamic acid-α,α′-di-*t*-butyl-γ-pentachlorophenyl ester. This route eliminates the possibility of transpeptidation.

Canadian Journal of Chemistry, 47, 3690 (1969)

Degradation (1) of native polyglutamic acids, produced by *B. anthracis* and *B. subtilis*, indicated that they are identical with poly-γ-glutamic acids. The anthrax-polypeptide consists exclusively (2) of D-glutamic acid residues, while the subtilis-polypeptide usually is a mixture (3) of poly-γ-D- and poly-γ-L-glutamic acid.

The synthesis (4) of these polypeptides was achieved by polycondensation of γ-glutamylglutamic acid-α,α′-dimethyl ester through activation of the γ-carboxyl group by various methods used in peptide synthesis. The free poly-γ-glutamic acid was obtained by saponification of the corresponding poly-γ-glutamic acid polymethyl ester. However, under basic conditions transpeptidation (4*a*, 5) could not be completely avoided.

We wish to report a new synthesis of these polypeptides by polymerization of γ-glutamylglutamic acid-α,α′-di-*t*-butyl-γ-pentachlorophenyl ester.[1] Here, the *t*-butyl ester groups can be removed with mild acid treatment of the *C*-protected polypeptide, thus eliminating the possibility of transpeptidation (6). In addition, polymerization through the pentachlorophenyl active ester results in a good yield of high molecular weight polymer (6, 7).

[1]M. Kajtar has applied the method reported here for the synthesis of γ-polyglutamic acids, unpublished work, reported to the authors in a private communication.

Can. J. Chem. Downloaded from www.nrcresearchpress.com by 210.87.254.6 on 09/05/12
For personal use only.

Can. J. Chem. Downloaded from www.nrcresearchpress.com by 210.87.254.6 on 09/05/12
For personal use only.

α-*t*-Butyl-D-glutamic acid methyl ester hydrochloride (**1**), prepared by catalytic hydrogenation of *N*-carbobenzoxy-α-*t*-butyl-D-glutamic acid methyl ester (8), was coupled with *N*-carbobenzoxy-α-*t*-butyl-D-glutamic acid pentachlorophenyl ester (8) to give the dipeptide methyl ester **2**. Saponification of the methyl ester gave the free acid **3**, which was converted directly to the dipeptide active ester **4**. Catalytic hydrogenation of **4** in the presence of HCl yielded α-*t*-butyl-D-glutamyl-α-*t*-butyl-D-glutamic acid pentachlorophenyl ester hydrochloride **5**, which was polymerized (8) in dimethylformamide in the presence of 2.5 equivalents of triethylamine. The resulting polypeptide ester **6** was then treated with trifluoroacetic acid, yielding the desired poly-γ-D-glutamic acid **7** with a mol. wt. 8000 as determined by sedimentation equilibrium (9).

A similar series of reactions, starting with *N*-carbobenzoxy-α-*t*-butyl-L-glutamic acid pentachlorophenyl ester and α-*t*-butyl-L-glutamic acid methyl ester hydrochloride gave poly-γ-L-glutamic acid with a mol. wt. 9000 as determined by sedimentation equilibrium.

Experimental

All melting points are uncorrected. The microanalyses were carried out either by Drs. G. Weiler and F. B. Strauss, Oxford, England, or by Schwarzkopf Microanalytical Laboratory, Woodside, N.Y. Infrared (i.r.) spectra were made in potassium bromide pellets on a Perkin–Elmer model 137 spectrophotometer.

α-t-Butyl-γ-methyl-D-glutamic Acid Hydrochloride (1)

A suspension of 0.8 g of 10% palladium on charcoal in 1 ml of glacial acetic acid and 20 ml of methanol was prehydrogenated for 10 min. A solution of 4.46 ml of 3.5 *N* solution of hydrogen chloride in methanol was added, followed by a solution of 5.27 g (15 mmoles) of *N*-carbobenzoxy-α-*t*-butyl-γ-methyl-D-glutamic acid in 25 ml of methanol. Hydrogenation was continued for 7 min. During this time approximately 200 ml of hydrogen was absorbed. The reaction mixture was filtered and the filtrate was concentrated *in vacuo*. The oily residue was triturated with ether and the crystalline material filtered; yield 85–90%, m.p. 133–134°. A portion of the product was purified by dissolving in water, neutralizing with sodium bicarbonate, and extracting with ether. The ether phase was dried over sodium sulfate and the hydrochloride precipitated by bubbling in hydrogen chloride. This procedure raised the m.p. to 134–135°; $[\alpha]_D^{23}$ −21.7° (*c*, 0.96, ethanol); lit. (10) m.p. 135–135.5°; $[\alpha]_D^{20}$ 21.7° (*c*, 2, ethanol) for the L-isomer.

Anal. Calcd. for $C_{10}H_{20}NO_4Cl$: C, 47.34; H, 7.95; N, 5.52; Cl, 13.97. Found: C, 47.54; H, 8.13; N, 5.70; Cl, 14.20.

N-Carbobenzoxy-α-t-butyl-D-glutamyl-α-t-butyl-D-glutamic Acid Methyl Ester (2)

A mixture of 20.0 g (35 mmole) of *N*-carbobenzoxy-α-*t*-butyl-D-glutamic acid pentachlorophenyl ester, 9 g (35 mmole) of α-*t*-butyl-γ-methyl-D-glutamic acid hydrochloride (**1**), 130 ml of methylene chloride, 3.6 g (35 mmole) of triethylamine, and 3.3 g (35 mmole) of 2-hydroxypyridine was stirred at room temperature for 24 h, then concentrated *in vacuo*. The solid residue was dissolved in ethyl acetate and washed quickly with cold dilute hydrochloric acid, water, 5% sodium bicarbonate, and then water until neutral. The organic phase was dried over magnesium sulfate and the solvent was removed *in vacuo*. The resulting oil was placed on a silica gel column and the pentachlorophenol was eluted with benzene. The desired dipeptide derivative was then eluted with ethyl acetate. The ethyl acetate was removed *in vacuo* and the oily residue was recrystallized from ether – petroleum ether (b.p. 40–60°). The yield was 12 g (58%); m.p. 72–73°, $[\alpha]_D^{24}$ −9.8° (*c*, 1.45, methylene chloride). The i.r. spectrum showed peaks at 5.72, 5.86, 6.03, and 6.46 μ.

Anal. Calcd. for $C_{27}H_{40}N_2O_9$: C, 60.43; H, 7.51; N, 5.22. Found: C, 60.58; H, 7.61; N, 5.02.

N-Carbobenzoxy-α-t-butyl-L-glutamyl-α-t-butyl-L-glutamic Acid Methyl Ester

It was prepared similarly in 58% yield. Two recrystallizations from ether – petroleum ether (b.p. 40–60°) gave m.p. 71–72°, $[\alpha]_D^{24}$ 9.9° (*c*, 1.40, methylene chloride). The i.r. spectrum was superimposable on that of the D-isomer.

Anal. Calcd. for $C_{27}H_{40}N_2O_9$: C, 60.43; H, 7.51; N, 5.22. Found: C, 60.34; H, 7.60; N, 5.34.

N-Carbobenzoxy-α-t-butyl-D-glutamyl-α-t-butyl-D-glutamic Acid (3)

A solution of 3.8 g (7 mmole) of *N*-carbobenzoxy-α-*t*-butyl-D-glutamyl-α-*t*-butyl-D-glutamic acid methyl ester (**2**) in 100 ml of methanol and 7 ml of 1 *N* sodium hy-

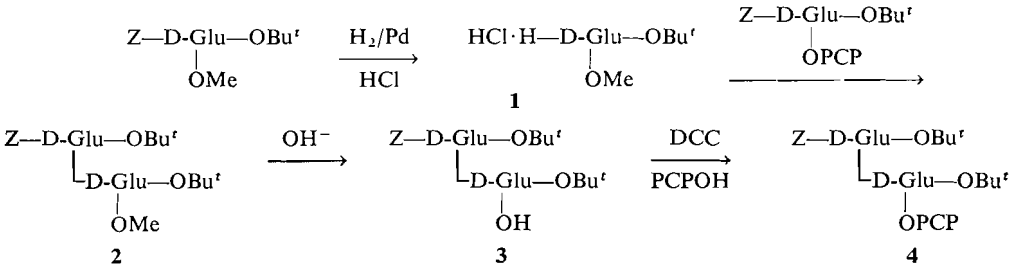

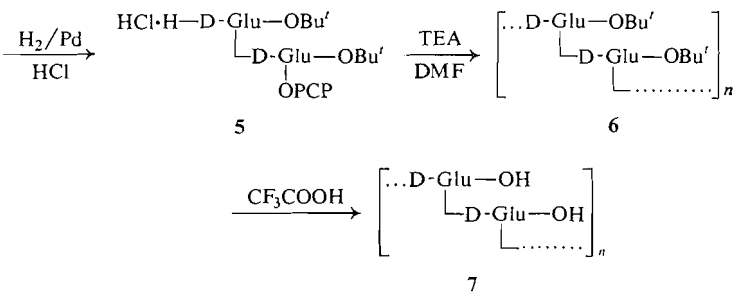

droxide was kept at room temperature for 30 min and then concentrated *in vacuo*. The residue was diluted with 100 ml of water and extracted with ethyl acetate. The aqueous phase was acidified to pH 3 with dilute hydrochloric acid and extracted twice with 50 ml portions of ethyl acetate. The ethyl acetate phase was dried over sodium sulfate and the solvent removed *in vacuo* to yield 3.5 g (94%) of an oil which was used without further purification.

N-Carbobenzoxy-α-t-butyl-L-glutamyl-α-t-butyl-L-glutamic Acid

It was prepared similarly in 95% yield.

N-Carbobenzoxy-α-t-butyl-D-glutamyl-α-t-butyl-D-glutamic Acid Pentachlorophenyl Ester (4)

To a solution of 3.5 g (6.6 mmole) of free acid **3** in 30 ml of methylene chloride, 1.4 g (6.8 mmole) of dicyclohexylcarbodiimide was added, followed after 20 min by a suspension of 1.8 g (6.8 mmole) of pentachlorophenol in 20 ml of methylene chloride. The reaction mixture was stirred at room temperature for 24 h and then concentrated *in vacuo*. The oily residue was dissolved in ethyl acetate and the solution was washed with 5% sodium bicarbonate and with water, dried over magnesium sulfate, and the solvent removed *in vacuo*. The resulting oil was chromatographed on silica gel, eluted with benzene:petroleum ether (b.p. 40–60°) (1:1), benzene, and finally ethyl acetate. The ethyl acetate eluate was concentrated *in vacuo* and the residue was crystallized from ether – petroleum ether (b.p. 40–60°). The yield was 4.1 g (80%); m.p. 77–78°, $[\alpha]_D^{24}$ −11.7° (*c*, 0.29, methylene chloride). The i.r. spectrum showed peaks at 5.60, 5.79, 6.05, and 6.52 μ.

Anal. Calcd. for $C_{32}H_{37}N_2O_9Cl_5$: C, 49.84; H, 4.84; N, 3.64. Found: C, 49.76; H, 4.83; N, 3.49.

N-Carbobenzoxy-α-t-butyl-L-glutamyl-α-t-butyl-L-glutamic Acid Pentachlorophenyl Ester

It was prepared similarly in an 83% yield, m.p. 77–78°, $[\alpha]_D^{24}$ 11.8° (*c*, 1.51, methylene chloride). The i.r. spectrum was superimposable on that of the D-isomer.

Anal. Calcd. for $C_{32}H_{37}N_2O_9Cl_5$: C, 49.84; H, 4.84; N, 3.64. Found: C, 49.93; H, 4.78; N, 3.89.

α-t-Butyl-D-glutamyl-α-t-butyl-D-glutamic Acid Pentachlorophenyl Ester Hydrochloride (5)

A suspension of 500 mg of 10% palladium on charcoal in 20 ml of methanol and 5 ml of glacial acetic acid was prehydrogenated until no further uptake of hydrogen occurred. A solution of 80 mg (2.11 mmole) of hydrogen chloride in 0.6 ml of methanol was added, followed by a solution of 1.59 g (2.1 mmole) of *N*-carbobenzoxy-α-*t*-butyl-D-glutamyl-α-*t*-butyl-D-glutamic acid pentachlorophenyl ester (**4**) in 20 ml of methanol. Hydrogenation was continued for 2 min until 46.5 ml of H_2 had been absorbed. The mixture was filtered, the filtrate concentrated *in vacuo*, and the residue diluted with ether. The resulting precipitate was filtered and washed with ether. The yield was 1.6 g (81%); m.p. 145° decomp. Recrystallization from methanol – ether raised the m.p. to 152–153° decomp., $[\alpha]_D^{24}$ 18.8° (*c*, 0.82, methanol). The i.r. spectrum showed peaks at 5.59, 5.75, 6.05, and 6.54 μ.

Anal. Calcd. for $C_{24}H_{32}N_2O_7Cl_6$: C, 42.82; H, 4.79; N, 4.16. Found: C, 42.72; H, 4.59; N, 4.01.

α-t-Butyl-L-glutamyl-α-t-butyl-L-glutamic Acid Pentachlorophenyl Ester Hydrochloride

It was prepared similarly in a 76% yield, m.p. 152–153° decomp., $[\alpha]_D^{24}$ −18.4° (*c*, 0.58, methanol). The i.r. spectrum was superimposable on that of the D-isomer.

Anal. Calcd. for $C_{24}H_{31}N_2O_7Cl_5 \cdot HCl$: C, 42.82; H, 4.79; N, 4.16; Cl^-, 5.43. Found: C, 42.57; H, 5.14; N, 4.23; Cl^-, 5.38.

Poly-γ-D-glutamic Acid t-Butyl Ester (6)

The dimethylformamide for this reaction was dried over sodium sulfate; any primary and secondary amines were removed by stirring with *N*-carbobenzoxyglycine *p*-nitrophenyl ester; the solution was filtered and distilled at 33° (0.6 mm). The triethylamine was treated similarly and distilled at 89–90°.

A mixture of 119 mg (0.18 mmole) of α-*t*-butyl-D-glutamyl-α-*t*-butyl-D-glutamic acid pentachlorophenyl ester hydrochloride (**5**), 0.12 ml of dimethylformamide, and 0.06 ml (0.45 mmole) of triethylamine was shaken at room temperature for 3 days. The solid reaction mixture was washed with ether, water, and ether, being centrifuged and decanted after each washing. The polymer **6** was dried overnight *in vacuo* over phosphorus pentoxide; yield 35 mg (51%). The i.r. spectrum showed characteristic peaks at 5.77, 6.03, 6.50, and 11.76 μ.

Anal. Calcd. for $(C_9H_{15}NO_3)_\infty$: C, 58.36; H, 8.16; N, 7.56. Calcd. for $(C_9H_{15}NO_3 \cdot 1/4H_2O)_\infty$: C, 56.97; H, 8.23; N, 7.38. Found: C, 56.77; H, 8.39; N, 7.16.

Poly-γ-L-glutamic Acid t-Butyl Ester

It was prepared similarly in a 57% yield. The i.r. spectrum showed characteristic peaks at 5.73, 6.00, 6.49, and 11.73 μ.

Anal. Found: C, 57.92; H, 7.81; N, 7.39.

Poly-γ-D-glutamic Acid (7)

A solution of 25 mg of polymer *6* in 0.5 ml of 90% trifluoroacetic acid was kept at room temperature for 50 min, then diluted with 10 ml of ether, centrifuged, and

Can. J. Chem. Downloaded from www.nrcresearchpress.com by 210.87.254.6 on 09/05/12
For personal use only.

the resulting precipitate washed twice with 10 ml portions of ether and dried overnight *in vacuo* over phosphorus pentoxide. Yield 16 mg (89%), $[\alpha]_D^{23}$ 23.6° (*c*, 0.50, water), mol. wt. 8000, determined by sedimentation equilibrium. The i.r. spectrum showed characteristic peaks at 6.06 and 6.45 μ.

Anal. Calcd. for $(C_5H_7NO_3 \cdot 1/4H_2O)_\infty$: C, 44.94; H, 5.66; N, 10.48. Found: C, 44.69; H, 5.56; N, 10.25.

Optical Purity of Poly-γ-D-glutamic Acid

It was determined by hydrolyzing 40.0 mg of a polymer sample, $[\alpha]_D^{22}$ 23.4° (*c*, 0.70, water), for 24 h under reflux in 1 ml of 6 *N* hydrochloric acid and 1 ml of glacial acetic acid. The hydrolysate was diluted to 3 ml with glacial acetic acid, giving $\alpha_D^{23} - 0.441 \pm 0.01°$. A control sample consisting of 44.0 mg of D-glutamic acid of 100% optical purity, $[\alpha]_D^{23}$ −32.0° (*c*, 1.84, 6 *N* hydrochloric acid), was treated under the same conditions, giving α_D^{23} $-0.441 \pm 0.01°$. This would indicate that the polymer is optically pure.

Poly-γ-L-glutamic Acid

It was prepared similarly in an 89% yield, $[\alpha]_D^{23}$ −23.3° (*c*, 0.58, water) mol. wt. 9000 as determined by sedimentation equilibrium. The i.r. spectrum showed characteristic peaks at 6.06 and 6.44 μ.

Anal. Found: C, 44.59; H, 5.20.

Weight average molecular weights were determined in a Spinco Model E analytical ultracentrifuge by the sedimentation equilibrium method in 0.1 *M* aqueous KCl. The calculations used were those given by Schachman. Measurements were made on concentrations in the range of 0.2–0.5% at 25–30°, using a rotor speed of 25 980 r.p.m. and a schlieren angle of 80°. The charge effect, which can lead to low mol. wt. values in water, was assumed to be minimized by using 0.1 *M* aqueous KCl as the solvent.

Acknowledgments

This work was supported by grants from the National Institutes of Health, Public Health Service (GM 06579 and 08795). We wish to thank Professor H. Horan for the infrared spectra. We wish to thank Mr. J. Mongiello for the improvement of the preparation of α-*t*-butyl-γ-methyl glutamic acid hydrochloride reported in this paper.

1. *a*) J. KOVACS, V. BRUCKNER, and K. KOVACS. J. Chem. Soc. 145 (1953). *b*) V. BRUCKNER, J. KOVACS, and H. NAGY. J. Chem. Soc. 148 (1953).
2. *a*) G. IVANOVICS and V. BRUCKNER. Naturwiss. **25**, 250 (1937). *b*) W. E. HANBY and H. N. RYDON. Biochem. J. **40**, 297 (1946).
3. C. B. THORNE and C. GOMEZ LEONARD. J. Biol. Chem. **233**, 1109 (1958).
4. *a*) V. BRUCKNER, M. KAJTAR, J. KOVACS, H. NAGY, and J. WEIN. Tetrahedron, **2**, 211 (1958). *b*) M. KAJTAR, V. BRUCKNER, and ZS. RIHMER. Acta Chim. Hung., **43**, 161 (1965).
5. J. KOVACS. Polyamino acids, polypeptides, and proteins. Proc. Intern. Symp. at the University of Wisconsin, 1961. *Edited by* M. A. Stahmann. Univ. of Wis. Press, Madison, Wis. 1962. pp. 37–47.
6. J. KOVACS, R. GIANNOTTI, and A. KAPOOR. J. Amer. Chem. Soc. **88**, 2282 (1966).
7. J. KOVACS and A. KAPOOR. J. Amer. Chem. Soc. **87**, 118 (1965).
8. J. KOVACS, G. N. SCHMIT, and U. R. GHATAK. Biopolym. **6**, 817 (1968).
9. H. K. SCHACHMAN. Ultracentrifugation in biochemistry. Academic Press, Inc., New York. 1959.
10. E. TASCHNER, A. CHIMIAK, B. BATOR, and T. SOKOLOWSKA. Ann. Chem. **646**, 134 (1961).

A steroidal 14β-hydroperoxide

ADRIANO AFONSO

Natural Products Research Department, Schering Corporation, Bloomfield, New Jersey

Received February 26, 1969

Air oxidation of Δ^{14}-androsten-3β-ol-17-one acetate (**1**) was found to afford stereospecifically 14β-hydroperoxy-Δ^{15}-androsten-3β-ol-17-one 3-acetate (**2***a*).

Canadian Journal of Chemistry, 47, 3693 (1969)

A common structural feature of most of the naturally-occurring cardiac-active steroidal lactones is the presence of a 14β-hydroxy substituent (1). The stereospecific introduction of a 14β-hydroxy group into the steroidal nucleus is therefore of interest in synthetic and biosynthetic studies of this class of compounds. A few methods for 14β-hydroxylation of steroids have been described in the literature (2), and in this note we report a new method which makes use of the susceptibility of β,γ-unsaturated ketone systems to undergo oxygenation at the γ-position with simultaneous reconjugation (3).

The oxygenation substrate used in our work was Δ^{14}-androsten-3β-ol-17-one acetate (**1**) (2*b*, 4, 5). This compound has been prepared in less than 5% yield by the dehydrobromination of 16-bromo epiandrosterone acetate with collidine (5);

Can. J. Chem. Downloaded from www.nrcresearchpress.com by 210.87.254.6 on 09/05/12
For personal use only.

the resulting precipitate washed twice with 10 ml portions of ether and dried overnight *in vacuo* over phosphorus pentoxide. Yield 16 mg (89%), $[\alpha]_D^{23}$ 23.6° (*c*, 0.50, water), mol. wt. 8000, determined by sedimentation equilibrium. The i.r. spectrum showed characteristic peaks at 6.06 and 6.45 μ.

Anal. Calcd. for $(C_5H_7NO_3 \cdot 1/4H_2O)_\infty$: C, 44.94; H, 5.66; N, 10.48. Found: C, 44.69; H, 5.56; N, 10.25.

Optical Purity of Poly-γ-D-glutamic Acid

It was determined by hydrolyzing 40.0 mg of a polymer sample, $[\alpha]_D^{22}$ 23.4° (*c*, 0.70, water), for 24 h under reflux in 1 ml of 6 *N* hydrochloric acid and 1 ml of glacial acetic acid. The hydrolysate was diluted to 3 ml with glacial acetic acid, giving $\alpha_D^{23} - 0.441 \pm 0.01°$. A control sample consisting of 44.0 mg of D-glutamic acid of 100% optical purity, $[\alpha]_D^{23}$ −32.0° (*c*, 1.84, 6 *N* hydrochloric acid), was treated under the same conditions, giving α_D^{23} $-0.441 \pm 0.01°$. This would indicate that the polymer is optically pure.

Poly-γ-L-glutamic Acid

It was prepared similarly in an 89% yield, $[\alpha]_D^{23}$ −23.3° (*c*, 0.58, water) mol. wt. 9000 as determined by sedimentation equilibrium. The i.r. spectrum showed characteristic peaks at 6.06 and 6.44 μ.

Anal. Found: C, 44.59; H, 5.20.

Weight average molecular weights were determined in a Spinco Model E analytical ultracentrifuge by the sedimentation equilibrium method in 0.1 *M* aqueous KCl. The calculations used were those given by Schachman. Measurements were made on concentrations in the range of 0.2–0.5% at 25–30°, using a rotor speed of 25 980 r.p.m. and a schlieren angle of 80°. The charge effect, which can lead to low mol. wt. values in water, was assumed to be minimized by using 0.1 *M* aqueous KCl as the solvent.

Acknowledgments

This work was supported by grants from the National Institutes of Health, Public Health Service (GM 06579 and 08795). We wish to thank Professor H. Horan for the infrared spectra. We wish to thank Mr. J. Mongiello for the improvement of the preparation of α-*t*-butyl-γ-methyl glutamic acid hydrochloride reported in this paper.

1. *a*) J. KOVACS, V. BRUCKNER, and K. KOVACS. J. Chem. Soc. 145 (1953). *b*) V. BRUCKNER, J. KOVACS, and H. NAGY. J. Chem. Soc. 148 (1953).
2. *a*) G. IVANOVICS and V. BRUCKNER. Naturwiss. **25**, 250 (1937). *b*) W. E. HANBY and H. N. RYDON. Biochem. J. **40**, 297 (1946).
3. C. B. THORNE and C. GOMEZ LEONARD. J. Biol. Chem. **233**, 1109 (1958).
4. *a*) V. BRUCKNER, M. KAJTAR, J. KOVACS, H. NAGY, and J. WEIN. Tetrahedron, **2**, 211 (1958). *b*) M. KAJTAR, V. BRUCKNER, and ZS. RIHMER. Acta Chim. Hung., **43**, 161 (1965).
5. J. KOVACS. Polyamino acids, polypeptides, and proteins. Proc. Intern. Symp. at the University of Wisconsin, 1961. *Edited by* M. A. Stahmann. Univ. of Wis. Press, Madison, Wis. 1962. pp. 37–47.
6. J. KOVACS, R. GIANNOTTI, and A. KAPOOR. J. Amer. Chem. Soc. **88**, 2282 (1966).
7. J. KOVACS and A. KAPOOR. J. Amer. Chem. Soc. **87**, 118 (1965).
8. J. KOVACS, G. N. SCHMIT, and U. R. GHATAK. Biopolym. **6**, 817 (1968).
9. H. K. SCHACHMAN. Ultracentrifugation in biochemistry. Academic Press, Inc., New York. 1959.
10. E. TASCHNER, A. CHIMIAK, B. BATOR, and T. SOKOLOWSKA. Ann. Chem. **646**, 134 (1961).

A steroidal 14β-hydroperoxide

ADRIANO AFONSO

Natural Products Research Department, Schering Corporation, Bloomfield, New Jersey

Received February 26, 1969

Air oxidation of Δ^{14}-androsten-3β-ol-17-one acetate (**1**) was found to afford stereospecifically 14β-hydroperoxy-Δ^{15}-androsten-3β-ol-17-one 3-acetate (**2***a*).

Canadian Journal of Chemistry, 47, 3693 (1969)

A common structural feature of most of the naturally-occurring cardiac-active steroidal lactones is the presence of a 14β-hydroxy substituent (1). The stereospecific introduction of a 14β-hydroxy group into the steroidal nucleus is therefore of interest in synthetic and biosynthetic studies of this class of compounds. A few methods for 14β-hydroxylation of steroids have been described in the literature (2), and in this note we report a new method which makes use of the susceptibility of β,γ-unsaturated ketone systems to undergo oxygenation at the γ-position with simultaneous reconjugation (3).

The oxygenation substrate used in our work was Δ^{14}-androsten-3β-ol-17-one acetate (**1**) (2*b*, 4, 5). This compound has been prepared in less than 5% yield by the dehydrobromination of 16-bromo epiandrosterone acetate with collidine (5);

Can. J. Chem. Downloaded from www.nrcresearchpress.com by 210.87.254.40 on 09/05/12
For personal use only.

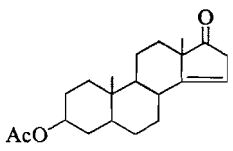

1

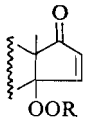

2*a*, R = H
b, R = OAc

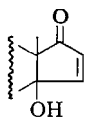

3

we obtained higher yields of **1** (42%) by carrying out the dehydrobromination of the same compound with lithium bromide – lithium carbonate in dimethylformamide (6). Exposure of **1** to oxygen led to the formation of a polar product in 82% yield, λ_{max} 212 mμ, which was characterized as 14β-hydroperoxy-Δ^{15}-androsten-3β-ol-17-one 3-acetate (**2***a*). Its acetylation product **2***b* exhibits the acetoxyperoxide absorption at 5.60 μ (3*b*). Reduction of **2***a* with triethylphosphite in pyridine (8) afforded a product which was identical in all respects with Δ^{15}-androsten-3β,14β-diol-17-one 3-acetate (**3**) prepared by the published procedure (2*b*).[1]

In view of the mild conditions under which **1** undergoes stereospecific oxygenation at C-14, a biogenetic origin for the 14β-hydroxy group of cardenolides and bufadienolides may be suggested. Recently it has been demonstrated that C_{21}-steroids are involved in the biogenesis of cardiac active glycosides (9). However, in the alternative C_{19}–C_4 hypothesis (10), the C_{19}-steroidal fragment could be envisioned to acquire the 14β-hydroxy group in a manner analogous to the one described herein.

Experimental

Melting points are uncorrected. Specific rotations were determined on 0.3% solutions in dioxane. Nuclear magnetic resonance spectra in $CDCl_3$ using TMS as the internal standard were determined on a Varian A-60A spectrometer. The author thanks Mr. M. Yudis and his staff for these physical measurements.

Δ^{14}-Androstene-3β-ol-17-one Acetate (1)

A mixture of 16-bromo epiandrosterone acetate (9.9 g) (5), lithium bromide (10 g), and lithium carbonate (10 g) in dimethylformamide (100 ml) was stirred and heated at 180° under argon for 3 h. The reaction mixture was cooled to room temperature, diluted with ice-water, acidified with dilute hydrochloric acid and extracted with ethyl acetate. The organic extracts were washed with water, dried, and evaporated under reduced pressure. The residue was crystallized twice from ether–hexane to afford colorless needles of **1** (3.3 g, 42%), m.p. 152–155°; $[\alpha]_D$ +110° (chloroform) [reported (2*b*): m.p. 154–156°; $[\alpha]_D$ +112°].

14β-Hydroperoxy-Δ^{15}-androstene-3β-ol-17-one 3-Monoacetate (2a)

A solution of Δ^{14}-androstene-3β-ol-17-one acetate (**1**, 1 g) in the minimum amount of chloroform was distributed as a film on the inside walls of a 4-l conical flask which was then filled with oxygen and allowed to stand at room temperature. The disappearance of **1** was followed by thin-layer chromatography and after 5 days the reaction was complete. During this reaction period additional amounts of chloroform were added as required in order to prevent **1** from crystallizing out. The product was transferred to a smaller flask and triturated with ether to afford **2***a* (502 mg). The filtrate was evaporated and the residue was applied on a 20 × 20 × 0.1 cm silica gel plate which was then developed in 10% ethyl acetate–chloroform. The material from the band corresponding to **2***a* was isolated and crystallized from ether (393 mg, 82% total yield). Recrystallization from ethyl acetate–ether afforded **2***a* as colorless needles, m.p. 175–180° (decomp.); λ_{max}(Nujol) 3.08, 5.79, 5.86 μ; λ_{max} (MeOH) 212 mμ (ε 8800); $[\alpha]_D^{26}$ +43.2°; n.m.r. ($CDCl_3$, 60 Mc.p.s.), δ 0.82, 1.22, 2.01 (singlets, 3H each, 19-CH_3, 18-CH_3 and C_3-OCCH_3), δ 6.39, 7.34 (doublets, 1H each, J = 6.5 c.p.s., C-16 and C_{15}-*H*), δ 7.84 (singlet, 1H, 14-OO*H*, exchangeable with D_2O); positive starch iodide test.

Anal. Calcd. for $C_{21}H_{30}O_5$: C, 69.58; H, 8.34. Found: C, 69.62; H, 8.42.

14β-Hydroperoxy-Δ^{15}-androstene-3β-ol-17-one 3,14-Diacetate (2b)

Acetic anhydride (0.7 ml) was added to a cold (0°) solution of **1** (0.34 g) in pyridine (1.5 ml). After 1 h at 0° the solution was allowed to stand at room temperature for 15 min and then diluted with ice-water. The insoluble product was filtered out, washed with water, and dried. The product was crystallized from hexane as colorless needles (**2***c*, 0.232 g), m.p. 125–131° (decomp.); λ_{max}(Nujol) 5.59, 5.79, 5.82 μ; λ_{max}(EtOH) 212 mμ (ε 8300); $[\alpha]_D^{26}$ −98.1°; n.m.r., δ 0.83, 1.20, 1.90, 2.01 (singlets, 3H each, 19-CH_3, 18-CH_3, C_{14}-OOCCH_3 and C_3-OCCH_3), δ 6.33, 7.40 (doublets, 1H each, J = 6.5 c.p.s., C-16 and C_{15}-*H*).

Anal. Calcd. for $C_{23}H_{32}O_6$: C, 68.29; H, 7.97. Found: C, 68.58; H, 7.85.

Δ^{15}-Androstene-3β,14β-diol-17-one 3-Monoacetate (3)

a) From Δ^{14}-Androsten-3β-ol-17-one Acetate (1)

The procedure described in the literature (2*b*) was followed. The product was crystallized from acetone–hexane as colorless plates, m.p. 162–163°; λ_{max}(Nujol) 2.90, 5.78, 5.82 μ; λ_{max}(MeOH) 212 mμ (ε 8000); $[\alpha]_D^{26}$ +103.6°; optical rotatory dispersion in dioxane[2] (*c*, 0.07):

[1]The physical constants reported (2*b*) for **3** are not in complete agreement with those found by us on chromatographically pure **3**. Low values, like ours, for extinction coefficients have been observed in other 14β-hydroxy-Δ^{15}-17-ketones (7). The identity of our **3** was confirmed from its optical rotatory dispersion curve which shows a positive cotton effect and is identical in shape with the published (2*b*) curve.

[2]The author thanks Dr. M. Tanabe of Stanford Research Institute for determining the optical rotatory dispersion curve.

Can. J. Chem. Downloaded from www.nrcresearchpress.com by 210.87.254.40 on 09/05/12
For personal use only.

$[\alpha]_{700}$ +77°; $[\alpha]_{589}$ +103°; $[\alpha]_{375}$ +1048°; $[\alpha]_{365}$ +976°; $[\alpha]_{330}$ −827°; $[\alpha]_{300}$ −1254° [reported (2*b*): m.p. 153–155°; λ_{max}(KBr) 2.90, 5.78, 5.85 μ; λ_{max}(EtOH) 213 mμ (ε 13 000); o.r.d.: $[\alpha]_{700}$ +37°; $[\alpha]_{589}$ +69°; $[\alpha]_{375}$ +1100°; $[\alpha]_{365}$ +1000°; $[\alpha]_{330}$ −948°; $[\alpha]_{300}$ −1545°].

b) From 14β-Hydroperoxy-Δ¹⁵-androstene-3β-ol-17-one 3-Monoacetate (2a)

A solution of **2***a* (100 mg) in pyridine (1.0 ml) containing triethylphosphite (0.5 ml) was heated on the steam bath for 15 mins and then evaporated under an air draft. The residue was crystallized twice from acetone–hexane as colorless plates, m.p. 162–163°; undepressed on admixture with **3** described under (*a*); λ_{max}(EtOH) 212 mμ (ε 8000); $[\alpha]_D^{26}$ +104.2°. The mobility on thin-layer chromatography and the infrared spectrum of the product were identical with that of **3** prepared by the literature procedure (2*b*).

Acknowledgment

The author is indebted to Professor D. H. R. Barton for helpful discussions.

1. L. F. Fieser and M. Fieser. Steroids, Reinhold Publ. Corp., New York, N. Y. 1959. Chap. 20.
2*a*. P. A. Plattner, L. Ruzicka, H. Heusser, J. Pataki, and K. Meier. Helv. Chim. Acta, **29**, 942 (1946); **30**, 385, 1342 (1947). *b*. F. Sondheimer, S. Burstein, and R. Mechoulam. J. Am. Chem. Soc. **82**, 3209 (1960). *c*. C. R. Engel and G. Bach. Steroids, **3**, 593 (1964).
3*a*. L. F. Fieser, T. W. Greene, F. Bischoff, G. Lopez, and J. J. Rupp. J. Amer. Chem. Soc. **77**, 3928 (1955). *b*. E. L. Shapiro, T. Legatt, and E. P. Oliveto. Tetrahedron Letters, No. **12**, 663 (1964).
4. A. F. St. Andre, H. B. MacPhillamy, J. A. Nelson, A. C. Shabica, and C. R. Scholz. J. Am. Chem. Soc. **74**, 5505 (1952).
5. R. Pappo, B. M. Bloom, and W. S. Johnson. J. Am. Chem. Soc. **78**, 6347 (1956).
6. A. Afonso. J. Am. Chem. Soc. **90**, 7375 (1968).
7. P. J. Sykes and R. W. Kelly. J. Chem. Soc. (C), 2346 (1968).
8. M. S. Kharasch, R. A. Mosher, and I. S. Bengelsdorf. J. Org. Chem. **25**, 1000 (1960).
9*a*. R. Tschesche and G. Lilienweiss. Z. Naturforsch. **19(B)**, 265 (1964); *b*. R. Tschesche, H. Hulpke, and H. Scholten. Z. Naturforsch **22(B)**, 677 (1967).
10. R. Tschesche. *In* Progress in the chemistry of organic natural products. Vol. 12. Springer, Vienna, Austria. 1955. p. 131.

Reductions with sulfurated borohydrides. III. Borohydrides incorporating selenium and tellurium

J. M. Lalancette and M. Arnac
Department of Chemistry, University of Sherbrooke, Sherbrooke, Quebec

Received March 20, 1969

The reactions of selenium and tellurium with lithium, sodium, potassium, and tetramethylammonium borohydrides have been examined, using the hydrogen evolution as a measurement of the replacement of hydrogen by the chalcogen on the borohydride anion. Of all the possible reactions, only the combination of sodium borohydride with tellurium led to a stable compound, easily isolated and of definite stoichiometry. This new borohydride, $NaBH_2Te_3$ offers interesting possibilities as a reducer.

Canadian Journal of Chemistry, **47**, 3695 (1969)

We have reported the sulfuration of sodium borohydride by elemental sulfur, in the presence of organic solvents (1). This reaction gave a new reducer (2, 3), incorporating sulfur, according to eq. [1].

$$[1] \qquad NaBH_4 + 3S \xrightarrow[25°]{THF} H_2 + NaBH_2S_3$$

We had noted from qualitative tests that similar reactions could be obtained with selenium and tellurium. This paper describes the reaction of lower chalcogens with various borohydrides.

Experimental

The reactions were performed with hydrides (British Drug Houses Reagent grade) without purification. Diglyme was used as solvent, after overnight reflux and distillation over sodium. Selenium and tellurium (Fisher Reagent grade) were used in the form of a fine powder, dried in a dessicator under vacuum in the presence of sulfuric acid.

In a typical experiment, a mixture of 0.10 mole (3.78g) of $NaBH_4$ and 0.30 mole (38.4g) of tellurium was placed in a 500 ml, three-neck flask bearing a condenser and an adding funnel. The flask was kept at 40° in a water bath and after flushing with dry nitrogen, 100 ml of dry diglyme was added to the mixture of solids, with stirring. The hydrogen evolved from the system was collected on top of the condenser and measured over water previously saturated with that gas. A drying tube between the gas-collection apparatus and the reacting flask prevented diffusion of water vapors into the reacting vessel.

The infrared (i.r.) spectrum of the borohydride incorporating tellurium was measured in Nujol suspen-

Can. J. Chem. Downloaded from www.nrcresearchpress.com by 210.87.254.40 on 09/05/12
For personal use only.

$[\alpha]_{700}$ +77°; $[\alpha]_{589}$ +103°; $[\alpha]_{375}$ +1048°; $[\alpha]_{365}$ +976°; $[\alpha]_{330}$ −827°; $[\alpha]_{300}$ −1254° [reported (2*b*): m.p. 153–155°; λ_{max}(KBr) 2.90, 5.78, 5.85 μ; λ_{max}(EtOH) 213 mμ (ε 13 000); o.r.d.: $[\alpha]_{700}$ +37°; $[\alpha]_{589}$ +69°; $[\alpha]_{375}$ +1100°; $[\alpha]_{365}$ +1000°; $[\alpha]_{330}$ −948°; $[\alpha]_{300}$ −1545°].

b) From 14β-Hydroperoxy-Δ¹⁵-androstene-3β-ol-17-one 3-Monoacetate (2a)

A solution of **2***a* (100 mg) in pyridine (1.0 ml) containing triethylphosphite (0.5 ml) was heated on the steam bath for 15 mins and then evaporated under an air draft. The residue was crystallized twice from acetone–hexane as colorless plates, m.p. 162–163°; undepressed on admixture with **3** described under (*a*); λ_{max}(EtOH) 212 mμ (ε 8000); $[\alpha]_D^{26}$ +104.2°. The mobility on thin-layer chromatography and the infrared spectrum of the product were identical with that of **3** prepared by the literature procedure (*2b*).

Acknowledgment

The author is indebted to Professor D. H. R. Barton for helpful discussions.

1. L. F. Fieser and M. Fieser. Steroids, Reinhold Publ. Corp., New York, N. Y. 1959. Chap. 20.
2*a*. P. A. Plattner, L. Ruzicka, H. Heusser, J. Pataki, and K. Meier. Helv. Chim. Acta, **29**, 942 (1946); **30**, 385, 1342 (1947). *b*. F. Sondheimer, S. Burstein, and R. Mechoulam. J. Am. Chem. Soc. **82**, 3209 (1960). *c*. C. R. Engel and G. Bach. Steroids, **3**, 593 (1964).
3*a*. L. F. Fieser, T. W. Greene, F. Bischoff, G. Lopez, and J. J. Rupp. J. Amer. Chem. Soc. **77**, 3928 (1955). *b*. E. L. Shapiro, T. Legatt, and E. P. Oliveto. Tetrahedron Letters, No. **12**, 663 (1964).
4. A. F. St. Andre, H. B. MacPhillamy, J. A. Nelson, A. C. Shabica, and C. R. Scholz. J. Am. Chem. Soc. **74**, 5505 (1952).
5. R. Pappo, B. M. Bloom, and W. S. Johnson. J. Am. Chem. Soc. **78**, 6347 (1956).
6. A. Afonso. J. Am. Chem. Soc. **90**, 7375 (1968).
7. P. J. Sykes and R. W. Kelly. J. Chem. Soc. (C), 2346 (1968).
8. M. S. Kharasch, R. A. Mosher, and I. S. Bengelsdorf. J. Org. Chem. **25**, 1000 (1960).
9*a*. R. Tschesche and G. Lilienweiss. Z. Naturforsch. **19(B)**, 265 (1964); *b*. R. Tschesche, H. Hulpke, and H. Scholten. Z. Naturforsch **22(B)**, 677 (1967).
10. R. Tschesche. *In* Progress in the chemistry of organic natural products. Vol. 12. Springer, Vienna, Austria. 1955. p. 131.

Reductions with sulfurated borohydrides. III. Borohydrides incorporating selenium and tellurium

J. M. Lalancette and M. Arnac
Department of Chemistry, University of Sherbrooke, Sherbrooke, Quebec

Received March 20, 1969

The reactions of selenium and tellurium with lithium, sodium, potassium, and tetramethylammonium borohydrides have been examined, using the hydrogen evolution as a measurement of the replacement of hydrogen by the chalcogen on the borohydride anion. Of all the possible reactions, only the combination of sodium borohydride with tellurium led to a stable compound, easily isolated and of definite stoichiometry. This new borohydride, $NaBH_2Te_3$ offers interesting possibilities as a reducer.

Canadian Journal of Chemistry, **47**, 3695 (1969)

We have reported the sulfuration of sodium borohydride by elemental sulfur, in the presence of organic solvents (1). This reaction gave a new reducer (2, 3), incorporating sulfur, according to eq. [1].

$$[1] \qquad NaBH_4 + 3S \xrightarrow[25°]{THF} H_2 + NaBH_2S_3$$

We had noted from qualitative tests that similar reactions could be obtained with selenium and tellurium. This paper describes the reaction of lower chalcogens with various borohydrides.

Experimental

The reactions were performed with hydrides (British Drug Houses Reagent grade) without purification. Diglyme was used as solvent, after overnight reflux and distillation over sodium. Selenium and tellurium (Fisher Reagent grade) were used in the form of a fine powder, dried in a dessicator under vacuum in the presence of sulfuric acid.

In a typical experiment, a mixture of 0.10 mole (3.78g) of $NaBH_4$ and 0.30 mole (38.4g) of tellurium was placed in a 500 ml, three-neck flask bearing a condenser and an adding funnel. The flask was kept at 40° in a water bath and after flushing with dry nitrogen, 100 ml of dry diglyme was added to the mixture of solids, with stirring. The hydrogen evolved from the system was collected on top of the condenser and measured over water previously saturated with that gas. A drying tube between the gas-collection apparatus and the reacting flask prevented diffusion of water vapors into the reacting vessel.

The infrared (i.r.) spectrum of the borohydride incorporating tellurium was measured in Nujol suspen-

Can. J. Chem. Downloaded from www.nrcresearchpress.com by 210.87.254.105 on 09/05/12
For personal use only.

Can. J. Chem. Downloaded from www.nrcresearchpress.com by 210.87.254.105 on 09/05/12
For personal use only.

sion and bands were observed at 1170 (weak), 1080 (weak), and 930cm^{-1} (medium). The very strong bands given by $NaBH_4$ at 2300 (very strong) and 1120 cm^{-1} (very strong) were absent from the spectrum.

When the gas evolution was completed, the reaction mixture was filtered and washed with petroleum ether (b.p. 50–60°) in order to remove diglyme. After drying under vacuum, the black solid was analyzed for Na, B, Te, and H. Determination of boron and sodium was made by flame photometry.

Anal. Calcd.: Na, 5.48; B, 2.63. Found: Na, 5.58; B, 2.68. Sodium borate (analytical) was used as standard. Tellurium was determined by dissolution of a sample in *aqua regia* and subsequent precipitation of tellurium by reduction with SO_2 (4).

Anal. Calcd.: Te, 91.4. Found: Te, 91.1. The hydrogen content of the hydride was obtained by hydrolysis and measurement of the hydrogen evolved. Two hydrogens molecules per mole of hydride were liberated (observed yield of 101%) according to eq. [2]

[2] $$NaBH_2Te_3 + 4H_2O \rightarrow 2H_2 + H_3BO_3 + NaOH + 3Te$$

Selenium and tellurium were allowed to react with lithium, sodium, potassium, and tetramethylammonium borohydrides, using a similar technique to that described above. The kinetics of these reactions and the degree of hydrogen replacement by the chalcogens were ascertained by following the hydrogen evolution. The results of these experiments are reported in Figs. 1, 2, 3, and 4.

Results and Discussion

Selenium

Selenium reacts with all four borohydrides used in our series of experiments. With lithium borohydride, the reaction was extremely brisk with a $Se/LiBH_4$ ratio greater than three and the hydrogen evolution levelled at a $H_2/NaBH_4$ ratio of 1. However, if the $Se/LiBH_4$ ratio was lowered below three, the four hydrogens of the borohydride were evolved. The reaction was somewhat milder with $NaBH_4$, the hydrogen evolution levelling off at a $H_2/NaBH_4$ ratio slightly higher than 1. With potassium borohydride, the reaction was slower and did not level off as the Se/BH_4^- ratio increased. This can be understood either as a decomposition of the seleniated borohydride or a complete replacement of the hydrogen atom of the hydride, at a slower rate, when two hydrogens have been lost. In the case of tetramethylammonium borohydride, the reaction was much slower and did not reach the molar H_2/BH_4^- ratio observed with the other cations.

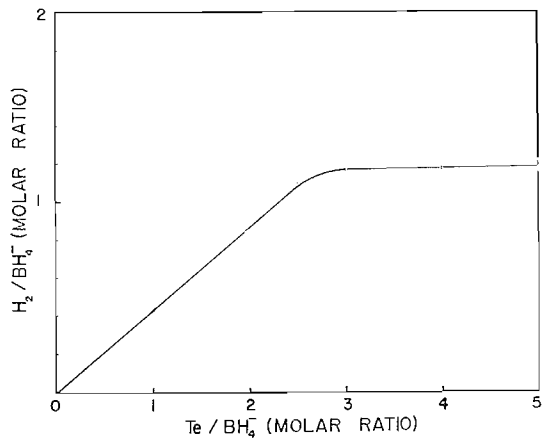

FIG. 1. Variations of the H_2/BH_4^- molar ratio against variations of Te/BH_4^- ratio. Reactions using $NaBH_4$.

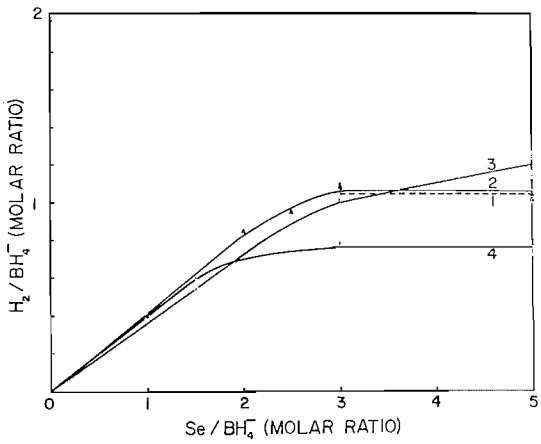

FIG. 2. Variations of the H_2/BH_4^- molar ratio against variations of Se/BH_4^- ratio. Reactions with $LiBH_4$(*1*), $NaBH_4$(*2*), KBH_4(*3*), and $(CH_3)_4NBH_4$(*4*).

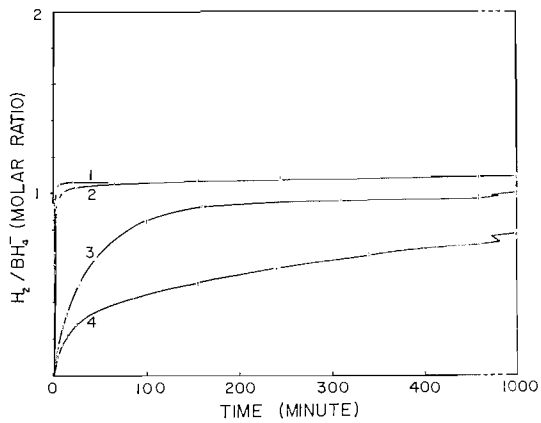

FIG. 3. Corrected volume of hydrogen evolved from a mixture of BH_4^- (0.033 mole) and Se (0.10 mole) in the presence of diglyme, at 25°. Reactions with $LiBH_4$(*1*), $NaBH_4$(*2*), KBH_4(*3*), and $(CH_3)_4BH_4$(*4*).

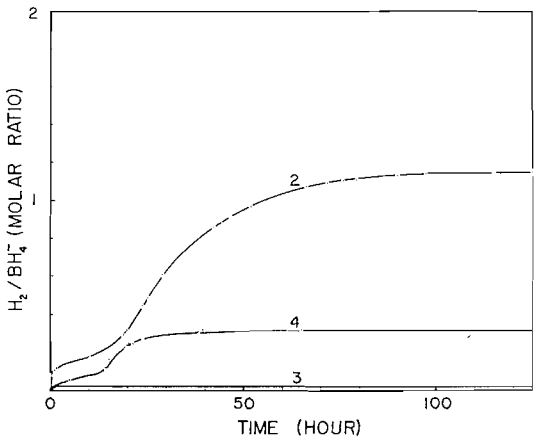

FIG. 4. Corrected volume of hydrogen evolved from a mixture of BH_4^- (0.10 mole) and Te (0.30 mole) in the presence of diglyme, at 56°. Reactions with $NaBH_4$(*2*), KBH_4(*3*), and $(CH_3)_4BH_4$(*4*).

Tellurium

As with selenium, tellurium gave a very fast and even explosive reaction with lithium borohydride in the presence of diglyme. With sodium borohydride, the reaction was very slow but stopped when two hydrogens of the borohydride were replaced by tellurium. Tetramethylammonium borohydride reacted only slightly and potassium borohydride gave no evolution of hydrogen.

These experiments indicate that of the possible combinations of hydrides and chalcogens, only the reaction of sodium borohydride with selenium and tellurium led to relatively stable compounds having the stoichiometry $NaBH_2M_3$ (M = Se, Te). In all other cases, the reaction was either too fast, too slow, or did not stop at a definite level in the course of replacement of the hydrogens by the chalcogens. In the case of $NaBH_2Se_3$, although the hydrogen evolution and subsequent hydrolysis indicated the above formulation, it has not been possible to remove this compound from its solvent, the reddish, rubber like substance retaining important portions of diglyme, even after repeated washings with petroleum ether. This difficulty prevented the elementary analysis as obtained for $NaBH_2Te_3$. The sodium borohydride incorporating tellurium was easily obtained as a black powder, free from diglyme, and showing relative stability for some hours. It is hygroscopic and sensitive to light.

The sodium borohydride incorporating tellurium still retains two hydrogens showing reducing capacity towards organic substrates. Since the anion $BH_2Te_3^-$ is even bulkier than $BH_2S_3^-$, the stereospecificity already observed with the sulfurated borohydride should be enhanced with $BH_2Te_3^-$.

Acknowledgments

We thank the National Research Council of Canada and the Defence Research Board of Canada (grant no. 9530–30) for financial assistance.

1. J. M. LALANCETTE, A. FRÊCHE, and R. MONTEUX. Can. J. Chem. **46**, 2754 (1968).
2. J. M. LALANCETTE and A. FRÊCHE. Can. J. Chem. **47**, 739 (1969).
3. J. M. LALANCETTE and A. LACHANCE. Can. J. Chem. **47**, 859 (1969).
4. H. GOTO and Y. KAKITA. Chem. Abstr. **47**, 2635 (1953).

Electrolysis in liquid ammonia solution in peptide chemistry

D. A. J. IVES
Connaught Medical Research Laboratories, University of Toronto, Toronto, Canada
Received February 10, 1969

An adaptation of an electrolytic method is suggested for the removal of protecting groups in peptide chemistry. Some initial experiments are reported indicating the scope and possible limitations of the method.

Canadian Journal of Chemistry, 47, 3697 (1969)

Introduction

The benzyl group ($C_6H_5CH_2$—) has had a wide use in peptide chemistry, since its introduction by du Vigneaud *et al.* (1) as a protective function. When it is used to protect the thiol group of cysteine the normal method of removal has been, until recently, reduction by sodium and liquid ammonia (Na/NH_3) (2). In 1965, Sakakibara and Shimonishi (3) found that the benzyl group in *S*-benzyl cysteine peptides could be

Can. J. Chem. Downloaded from www.nrcresearchpress.com by 210.87.254.105 on 09/05/12
For personal use only.

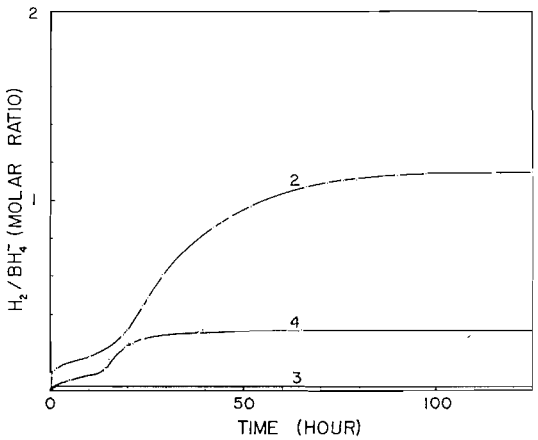

FIG. 4. Corrected volume of hydrogen evolved from a mixture of BH_4^- (0.10 mole) and Te (0.30 mole) in the presence of diglyme, at 56°. Reactions with $NaBH_4$(*2*), KBH_4(*3*), and $(CH_3)_4BH_4$(*4*).

Tellurium

As with selenium, tellurium gave a very fast and even explosive reaction with lithium borohydride in the presence of diglyme. With sodium borohydride, the reaction was very slow but stopped when two hydrogens of the borohydride were replaced by tellurium. Tetramethylammonium borohydride reacted only slightly and potassium borohydride gave no evolution of hydrogen.

These experiments indicate that of the possible combinations of hydrides and chalcogens, only the reaction of sodium borohydride with selenium and tellurium led to relatively stable compounds having the stoichiometry $NaBH_2M_3$ (M = Se, Te). In all other cases, the reaction was either too fast, too slow, or did not stop at a definite level in the course of replacement of the hydrogens by the chalcogens. In the case of $NaBH_2Se_3$, although the hydrogen evolution and subsequent hydrolysis indicated the above formulation, it has not been possible to remove this compound from its solvent, the reddish, rubber like substance retaining important portions of diglyme, even after repeated washings with petroleum ether. This difficulty prevented the elementary analysis as obtained for $NaBH_2Te_3$. The sodium borohydride incorporating tellurium was easily obtained as a black powder, free from diglyme, and showing relative stability for some hours. It is hygroscopic and sensitive to light.

The sodium borohydride incorporating tellurium still retains two hydrogens showing reducing capacity towards organic substrates. Since the anion $BH_2Te_3^-$ is even bulkier than $BH_2S_3^-$, the stereospecificity already observed with the sulfurated borohydride should be enhanced with $BH_2Te_3^-$.

Acknowledgments

We thank the National Research Council of Canada and the Defence Research Board of Canada (grant no. 9530–30) for financial assistance.

1. J. M. LALANCETTE, A. FRÊCHE, and R. MONTEUX. Can. J. Chem. **46**, 2754 (1968).
2. J. M. LALANCETTE and A. FRÊCHE. Can. J. Chem. **47**, 739 (1969).
3. J. M. LALANCETTE and A. LACHANCE. Can. J. Chem. **47**, 859 (1969).
4. H. GOTO and Y. KAKITA. Chem. Abstr. **47**, 2635 (1953).

Electrolysis in liquid ammonia solution in peptide chemistry

D. A. J. IVES
Connaught Medical Research Laboratories, University of Toronto, Toronto, Canada
Received February 10, 1969

An adaptation of an electrolytic method is suggested for the removal of protecting groups in peptide chemistry. Some initial experiments are reported indicating the scope and possible limitations of the method.

Canadian Journal of Chemistry, 47, 3697 (1969)

Introduction

The benzyl group ($C_6H_5CH_2$—) has had a wide use in peptide chemistry, since its introduction by du Vigneaud *et al.* (1) as a protective function. When it is used to protect the thiol group of cysteine the normal method of removal has been, until recently, reduction by sodium and liquid ammonia (Na/NH_3) (2). In 1965, Sakakibara and Shimonishi (3) found that the benzyl group in *S*-benzyl cysteine peptides could be

removed by the use of anhydrous HF. This reagent also removes other groups such as the *N*-carbobenzoxy, *t*-butyloxycarbonyl, benzyl esters, and benzyl ethers used as protective groups in peptide synthesis (4, 5). Unfortunately anhydrous HF does not remove the benzyl group from im.-benzyl histidine, and where benzyl protected cysteine and histidine occur in the same peptide, Na/NH_3 reduction still has to be used.

Du Vigneaud *et al.* (6) showed that in the removal of *S*-benzyl groups by Na/NH_3 reduction of a protected nonapeptide, high yields of physiologically active oxytocin could be obtained. However, Zahn *et al.* (7) and Katsoyannis (8) have indicated that when Na/NH_3 reduction is used on larger peptides, such as the A and B chains of insulin, low yields of the required products are obtained. To avoid the use of Na/NH_3 reduction many other protecting groups for —SH have been suggested in the literature (4, 5), but the benzyl group still seems the most popular.

The blue color obtained on dissolving alkali metals in liquid ammonia or low molecular weight amines has been suggested (9) as being due to the solvated electron. This species is also credited with being the reducing agent in these solutions. The color can also be obtained by electrochemical methods using these solvents (10). Electrolytic reduction of aromatic hydrocarbons in methylamine solution in the presence of LiCl was observed by Benkeser (10) and a similar reduction of estrone was observed by Fentiman and Poirier (11).

Since it was felt that this alternate method of electrolytically generating the active species in ammonia might find use in the field of peptide chemistry, several experiments were carried out to investigate the usefulness of this method for the removal of the benzyl group usually used to block cysteine peptides. Experimental conditions similar to those in the Na/NH_3 reduction procedure were employed in order that comparison of the results from experiments where both procedures were used could be made.

Experimental

The reductions were conducted in a 250 ml three-necked flask, the two side arms being fitted with coiled platinum wire electrodes and the centre neck being fitted with a soda lime drying tube. Liquid ammonia was collected in the flask by condensation of the gas from a tank, one of the electrodes being removed to allow for the inlet. All the materials used dissolved readily in the ammonia and during the electrolysis the solutions were stirred using a teflon coated magnetic stirring bar. The solutions were kept at acetone/dry ice temperature throughout the period of electrolysis, which was normally 90 min. The reduction could be followed by the decrease in resistance of the solution as evidenced by the increase in current flow at constant voltage. This decrease was complete within the 90 min period.

The materials used were synthesized by established methods and the constants agreed with published figures. The protected nonapeptide was synthesized by the stepwise active ester method (12) and the tetrapeptide by a combination of mixed anhydride and active ester techniques (12). The products of the reactions were usually analyzed by hydrolysis followed by chromatography using a Beckman-Spinco Amino acid analyzer, Model 120C. It was established that under the hydrolysis conditions used there were only trace amounts of cysteine produced from the *S*-benzyl cysteine.

The power source was a Heathkit constant voltage supply unit with a maximum of 400 V D.C. at 100 mA.

Electrolytic Reduction of a Protected Nonapeptide to Oxytocin

The protected nonapeptide Z-*S*-bzl-cys-tyr-ileu-gln-asn-*S*-bzl-cys-pro-leu-gly NH_2 (200 mg) was dissolved in liquid ammonia (125 ml) and electrolyzed for 90 min. The initial current was 20 mA at 400 V D.C. After the 90 min period the current had risen to 75 mA at the same voltage and was constant. The ammonia was allowed to evaporate and the last 10 ml removed under vacuum. The resulting solid was dissolved in water (50 ml) and the pH adjusted to 7.0 with dilute acetic acid. A sample (5 ml) was withdrawn, the solvent removed under vacuum and the product hydrolyzed in 6 *N* HCl (1 ml) for 16 h at 110 °C under vacuum. Analysis of the solution showed cysteine present in the correct ratio, no *S*-benzyl cysteine was observed.

Air was bubbled through the remaining solution (45 ml) for 2 1/2 h and, after the pH had been adjusted to 4.0 with dilute acetic acid, it was filtered. Assay of the solution using the isolated rat uterus method gave 390 IU/ml of oxytocic activity or an adjusted total of 21 400 International oxytocic units from 200 mg of protected nonapeptide.

When the experiment was repeated with the addition of NH_4Cl (1 g) to the liquid ammonia solution the observed current was 100 mA at 40 V D.C. This remained constant for 90 min. No oxytocic activity was found in the product and hydrolysis in 6 *N* HCl and analysis showed that all the cysteine was present as the *S*-benzyl derivative.

In a comparable experiment where the reduction was performed using Na/NH_3 instead of electrolysis, the yield was 20 500 oxytocic units from 200 mg of protected nonapeptide. There was no *S*-benzyl cysteine in an hydrolysate of the product.

Electrolytic Reduction of Protected Tetrapeptide

The protected tetrapeptide, Z-*S*-bzl-cys-pro-leu-gly NH_2 (200 mg) was subjected to the electrolytic reduction detailed above. The current was initially 20 mA at 400 V and rose to 90 mA during the 90 min reaction period. A small amount of the product, which would not

crystallize, was hydrolyzed in 6 *N* HCl and analyzed for amino acid composition. Both cysteine and *S*-benzyl cysteine were present in the ratio of about 7:3. Repetition of the experiment gave the same result. The product of the reaction also gave a positive ninhydrin reaction indicating the removal of the *N*-carbobenzoxy group.

Attempted Reduction of Z-S-Bzl-cysteine

No reduction was observed when Z-*S*-bzl-cysteine was used in the described method. The product obtained after removal of the ammonia could be crystallized from ethyl acetate/petroleum ether and was shown by m.p., mixed m.p., and rotation to be starting material. Hydrolysis and analysis showed only the presence of *S*-benzyl cysteine. The current started at 100 mA at 100 V D.C. and stayed at this level throughout the 90 min period of reaction. Na/NH_3 reduction and hydrolysis of the product showed no *S*-benzyl cysteine.

Attempted Reduction of Z-S-Bzl-cysteine Methyl Ester

When Z-*S*-bzl-cysteine methyl ester was used in the electrolytic method and the product hydrolyzed after removal of the ammonia, all the cysteine was found as *S*-benzyl cysteine. The current started at 20 mA at 400 V and dropped slowly to 10 mA at the end of 90 min. Again Na/NH_3 reduction and hydrolysis gave a product with no *S*-benzyl cysteine.

Discussion

It is apparent from the experimental results, that, with the conditions used, there is electrolytic reduction taking place.

When the protected nonapeptide was used, both the *S*-benzyl and *N*-carbobenzoxy groups were removed, since the product had the same biological activity as that obtained from a Na/NH_3 reduction of the same starting material. With the protected tetrapeptide only partial reduction occurred as evidenced by the presence of some *S*-benzyl cysteine in the hydrolysate, whereas no reduction was found with any of the cysteine derivatives used. The mechanism of the reduction would appear to be different from the Na/NH_3 reduction, since the simpler derivatives of cysteine are untouched by the electrolytic method, but are completely reduced by Na/NH_3. When a protected nonapeptide, obtained by the solid phase synthetic method, was substituted, on one occasion, for the regular nonapeptide, no reduction was observed. The peptide from this method of synthesis differed in having *O*-benzyl tyrosine rather than the free tyrosine as in the regular nonapeptide. This would imply that a partially ionizable group was necessary for reduction to occur. At no time was any blue color observed in the reaction vessel to indicate the presence of solvated electrons, although this does not preclude the reduction proceeding through a very short lived species. The particular electrolytic reduction observed in the above experiments would also appear to have a different mechanism from that observed by Benkeser *et al.* (10), since an introduction of a species designed to increase current flow (NH_4Cl) actually inhibited the reduction.

Future work is planned to widen the scope of the reaction, i.e. the removal of other protecting groups used in peptide chemistry, such as *O*-benzyl, *N*-tosyl, and the nitro group used in arginine. Further information is also required to determine the mechanism of the reaction and whether trace amounts of ions are required.

Acknowledgments

The author would like to thank Dr. A. L. Tosoni for his interest and encouragement and the Quality Control Department of the Connaught Laboratories for the biological testing.

1. V. DU VIGNEAUD, L. F. ANDRIETH, and H. S. LORING. J. Amer. Chem. Soc. **52**, 4500 (1930).
2. V. DU VIGNEAUD and R. H. SIFFERD. J. Biol. Chem. **108**, 753 (1935).
3. S. SAKAKIBARA and Y. SHIMONISHI. Bull. Chem. Soc. Japan, **38**, 1412 (1965).
4. E. SCHRÖDER and K. LUBKE. The Peptides. Academic Press, Inc., New York. 1966.
5. M. BODANSZKY and M. A. ONDETTI. Peptide Synthesis. Interscience Publishers, Inc., New York. 1966.
6. V. DU VIGNEAUD, C. RESSLER, J. M. SWAN, C. W. ROBERTS, and P. G. KATSOYANNIS. J. Amer. Chem. Soc. **76**, 3115 (1954).
7. H. ZAHN, T. OKUDA, and Y. SHIMONISHI. Angew. Chem. **79**, 424 (1967).
8. P. G. KATSOYANNIS. Amer. J. Med. **40**, 652 (1966).
9. C. A. KRAUS. J. Amer. Chem. Soc. **30**, 1323 (1908).
10. R. A. BENKESER, E. M. KAISER, and R. F. LAMBERT. J. Amer. Chem. Soc. **86**, 5272 (1964).
11. A. F. FENTIMAN and R. H. POIRIER. Chem. and Ind. 813 (1966).
12. V. DU VIGNEAUD and M. BODANSZKY. J. Amer. Chem. Soc. **81**, 5688 (1959).

Addendum: Cryptosporiopsin, an amended structure

G. M. STRUNZ, A. S. COURT, J. KOMLOSSY, AND M. A. STILLWELL
Forest Research Laboratory, Canada Department of Forestry and Rural Development, Fredericton, New Brunswick

Received May 26, 1969

The structure **1** (R_1 = OH, R_2 = Cl), previously proposed for cryptosporiopsin, has been amended on the basis of new evidence to **1** (R_1 = Cl, R_2 = OH).

Canadian Journal of Chemistry, 47, 3700 (1969)

Can. J. Chem. Downloaded from www.nrcresearchpress.com by 210.87.254.105 on 09/05/12
For personal use only.

The structure **1** (R_1 = OH, R_2 = Cl) was recently advanced for cryptosporiopsin (1), an antifungal metabolite produced by a species of *Cryptosporiopsis*. The latter is an imperfect fungus isolated from yellow birch, *Betula alleghaniensis* Britt. (2).

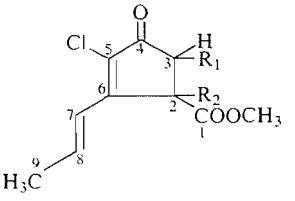

1

The skeletal structure and chromophoric system of cryptosporiopsin were established by spectrometric and chemical studies. The secondary nature of the hydroxyl group and its consequent location were inferred principally on the basis of its ready acetylation and the resulting downfield shift of the nuclear magnetic resonance (n.m.r.) signal for the putative geminal proton on carbon 3.

Recent X-ray studies by McGahren *et al.* (3) on a metabolite produced by the coprophilous fungus *Sporormia affinis* Sacc., Bomm and Rouss have shown this compound to have the structure and absolute configuration **1** (R_1 = β-Cl, R_2 = α-OH). The apparent similarity of the *Cryptosporiopsis* and *Sporormia* metabolites has prompted us to re-examine the chemistry of cryptosporiopsin.

In a search for further chemical evidence relating to the environment of the hydroxyl and chlorine substituents of cryptosporiopsin, we have turned our attention to products derived from reductive removal of the labile chlorine atom. We have previously demonstrated that such a reduction can be effected by treatment of cryptosporiopsin with zinc in refluxing ethanol (ester interchange with ethanol also occurring under these conditions) (1). Whereas the n.m.r. spectrum of the zinc–ethanol product was not particularly revealing with respect to the environment of the newly introduced hydrogen, reduction of cryptosporiopsin with zinc in refluxing methanol yielded a product $C_{10}H_{11}O_4Cl$, whose n.m.r. characteristics are in accord with the structure **1** (R_1 = H, R_2 = OH). In particular an AB quartet can be discerned at 7.19 τ in which $|J_{AB}|$ (18–19 c.p.s.) is of the appropriate magnitude for the *geminal* protons on position 3 (4). Thus the zinc-labile chlorine must have been located on carbon 3, and it follows that the structure of cryptosporiopsin is **1** (R_1 = Cl, R_2 = OH). It may be noted that the downfield shift of the signal for the C-3 proton, on acetylation of the hydroxyl of cryptosporiopsin, implies that these groups occupy a *cis* relationship with respect to each other.

Finally, the melting point of cryptosporiopsin was undepressed on admixture with a sample of the *Sporormia* product[1], confirming the identity of the two metabolites.

Experimental

See ref. (1) for general description of instrumentation, etc.

Zinc–Methanol Reduction of Cryptosporiopsin

To cryptosporiopsin (800 mg) in absolute methanol (64 ml) was added zinc dust (1.040 g). The mixture was set aside with stirring at 25° for 15 h and was then refluxed for 2 h. Filtration removed the solid material, which was washed thoroughly with methylene chloride. The filtrates were evaporated to dryness under reduced pressure and the residue was redissolved in methylene chloride. After washing with 2% sulfuric acid followed by water, the solution was dried over magnesium sulfate, and the removal of solvent *in vacuo* yielded 610 mg of pale yellow oil, which crystallized on standing. Recrystallization from cyclohexane afforded pure **1** (R_1 = H, R_2 = OH), melting at 110–112.5°.

[1]Kindly provided through the courtesy of Dr. E. L. Patterson, Lederle Laboratories, New York.

Mass spectrum: M^+, 230 ($M^+ + 2$, 34% of M^+). Infrared ν_{max} (CCl_4) 3515, 1732, and 1642 cm^{-1}; ν_{max} (KBr disk) 1747, 1717, and 1640 cm^{-1}. Ultraviolet λ_{max} (EtOH) 284 mμ (ε 22 000); n.m.r. 2.93–3.84 τ (m, 2H), 5.93 τ (s, 1H), 6.20 τ (s, 3H), 7.19 τ (q, $|J|$ = 18–19 c.p.s., 2H), 8.07 τ (d, J = 5 c.p.s., 3H).

Anal. Calcd. for $C_{10}H_{11}O_4Cl$: C, 52.07; H, 4.81; Cl, 15.37. Found: C, 52.04; H, 4.80; Cl, 15.39.

Acknowledgments

The authors thank Mrs. H. Moore and Mrs. G. Aarts of the University of New Brunswick for the n.m.r. and mass spectrum determinations respectively.

1. G. M. Strunz, A. S. Court, J. Komlossy, and M. A. Stillwell. Can. J. Chem. **47**, 2087 (1969).
2. M. A. Stillwell. Can. J. Bot. **44**, 259 (1966).
3. W. J. McGahren, J. H. Van den Hende, and L. A. Mitscher. J. Amer. Chem. Soc. **91**, 157 (1969).
4. N. S. Bhacca and D. H. Williams. Applications of n.m.r. spectroscopy in organic chemistry. Holden-Day, Inc., San Francisco. (1964).

Structure of didehydrochelidonine

M. H. Benn and R. E. Mitchell
Department of Chemistry, The University, Calgary 44, Alberta

Received June 2, 1969

Gadamer's didehydrochelidonine is the internal carbinolamine ether **2***c*. The formation of this compound, as also its reduction back to the parent alkaloid, provides chemical proof that the relative stereochemistry of chelidonine is, as previously deduced from spectroscopic studies, that given in **1**.

Canadian Journal of Chemistry, 47, 3701 (1969)

Whilst studying the chemistry of chelidonine J. G. Gadamer observed that mercuric acetate oxidation of this alkaloid yielded a new compound which he named didehydrochelidonine (1).[1,2] Later he and his co-workers discovered that the same compound was obtained in superior yield when the oxidation was performed on chelidonine acetate (3), and that it was also a product of the permanganate oxidation of chelidonine (4).

Didehydrochelidonine was described as a colorless, noncrystalline, basic compound which yielded a number of crystalline derivatives, including a yellow hydrobromide and a colorless pseudocyanide (1, 3). Reduction of didehydrochelidonine, or its hydrobromide salt, with zinc and sulfuric acid was reported to yield unracemized chelidonine (1, 3), and it was also observed that the free base underwent ready dehydration to yield dihydrosanguinarine (**4**) (3).

Gadamer believed that didehydrochelidonine was a carbinolamine (1, 3): in terms of the structure (**1**) subsequently established for chelidonine (without stereochemistry) (5), this would now be formulated as **2***a*(X = OH), and it is in fact commonly so described (6); although others have chosen to represent it as **2***b* (7), presumably to rationalize the dehydration. The salts of didehydrochelidonine have normally been written as **3**, and the pseudocyanide as **2***a*(X = CN) (6*a*).

We anticipated on the basis of experience in the diterpenoid alkaloid field (9) that, *if* the stereochemistry of chelidonine was, as deduced from infrared (8*a*) and proton magnetic resonance (8*b*, *c*) spectroscopic studies, that represented in **1**, didehydrochelidonine would in fact be the internal carbinolamine ether **2***c*. We further anticipated that protic acids would convert **2***c* to acyclic salts (**3**), from which **2***c* would be recovered on basification, except in certain cases, exemplified by basification with cyanide salts, where capture of nucleophile could produce a stable acyclic product (**2***a*) (e.g. X = CN).

Of the other reactions of didehydrochelidonine, the facile reduction to yield chelidonine is in keeping with the known case of reduction of strained carbinolamine ethers (10) and immonium salts, and we visualized the dehydration to

[1]This is one of several historically interesting examples of Gadamer's early use of mercuric acetate oxidations in the structure–determination of alkaloids (2).

[2]In modern terminology the name dehydrochelidonine is to be preferred.

Can. J. Chem. Downloaded from www.nrcresearchpress.com by 210.87.254.105 on 09/05/12
For personal use only.

Mass spectrum: M^+, 230 ($M^+ + 2$, 34% of M^+). Infrared ν_{max} (CCl_4) 3515, 1732, and 1642 cm^{-1}; ν_{max} (KBr disk) 1747, 1717, and 1640 cm^{-1}. Ultraviolet λ_{max} (EtOH) 284 mμ (ε 22 000); n.m.r. 2.93–3.84 τ (m, 2H), 5.93 τ (s, 1H), 6.20 τ (s, 3H), 7.19 τ (q, $|J|$ = 18–19 c.p.s., 2H), 8.07 τ (d, J = 5 c.p.s., 3H).

Anal. Calcd. for $C_{10}H_{11}O_4Cl$: C, 52.07; H, 4.81; Cl, 15.37. Found: C, 52.04; H, 4.80; Cl, 15.39.

Acknowledgments

The authors thank Mrs. H. Moore and Mrs. G. Aarts of the University of New Brunswick for the n.m.r. and mass spectrum determinations respectively.

1. G. M. Strunz, A. S. Court, J. Komlossy, and M. A. Stillwell. Can. J. Chem. **47**, 2087 (1969).
2. M. A. Stillwell. Can. J. Bot. **44**, 259 (1966).
3. W. J. McGahren, J. H. Van den Hende, and L. A. Mitscher. J. Amer. Chem. Soc. **91**, 157 (1969).
4. N. S. Bhacca and D. H. Williams. Applications of n.m.r. spectroscopy in organic chemistry. Holden-Day, Inc., San Francisco. (1964).

Structure of didehydrochelidonine

M. H. Benn and R. E. Mitchell
Department of Chemistry, The University, Calgary 44, Alberta

Received June 2, 1969

Gadamer's didehydrochelidonine is the internal carbinolamine ether **2***c*. The formation of this compound, as also its reduction back to the parent alkaloid, provides chemical proof that the relative stereochemistry of chelidonine is, as previously deduced from spectroscopic studies, that given in **1**.

Canadian Journal of Chemistry, 47, 3701 (1969)

Whilst studying the chemistry of chelidonine J. G. Gadamer observed that mercuric acetate oxidation of this alkaloid yielded a new compound which he named didehydrochelidonine (1).[1,2] Later he and his co-workers discovered that the same compound was obtained in superior yield when the oxidation was performed on chelidonine acetate (3), and that it was also a product of the permanganate oxidation of chelidonine (4).

Didehydrochelidonine was described as a colorless, noncrystalline, basic compound which yielded a number of crystalline derivatives, including a yellow hydrobromide and a colorless pseudocyanide (1, 3). Reduction of didehydrochelidonine, or its hydrobromide salt, with zinc and sulfuric acid was reported to yield unracemized chelidonine (1, 3), and it was also observed that the free base underwent ready dehydration to yield dihydrosanguinarine (**4**) (3).

Gadamer believed that didehydrochelidonine was a carbinolamine (1, 3): in terms of the structure (**1**) subsequently established for chelidonine (without stereochemistry) (5), this would now be formulated as **2***a*(X = OH), and it is in fact commonly so described (6); although others have chosen to represent it as **2***b* (7), presumably to rationalize the dehydration. The salts of didehydrochelidonine have normally been written as **3**, and the pseudocyanide as **2***a*(X = CN) (6*a*).

We anticipated on the basis of experience in the diterpenoid alkaloid field (9) that, *if* the stereochemistry of chelidonine was, as deduced from infrared (8*a*) and proton magnetic resonance (8*b*, *c*) spectroscopic studies, that represented in **1**, didehydrochelidonine would in fact be the internal carbinolamine ether **2***c*. We further anticipated that protic acids would convert **2***c* to acyclic salts (**3**), from which **2***c* would be recovered on basification, except in certain cases, exemplified by basification with cyanide salts, where capture of nucleophile could produce a stable acyclic product (**2***a*) (e.g. X = CN).

Of the other reactions of didehydrochelidonine, the facile reduction to yield chelidonine is in keeping with the known case of reduction of strained carbinolamine ethers (10) and immonium salts, and we visualized the dehydration to

[1]This is one of several historically interesting examples of Gadamer's early use of mercuric acetate oxidations in the structure–determination of alkaloids (2).

[2]In modern terminology the name dehydrochelidonine is to be preferred.

Can. J. Chem. Downloaded from www.nrcresearchpress.com by 210.87.254.5 on 09/05/12
For personal use only.

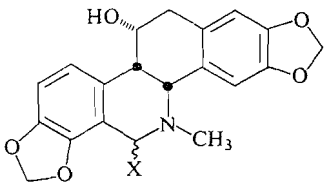

2*a*

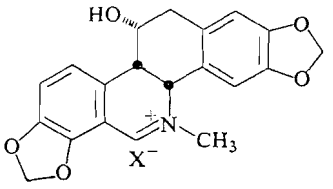

3

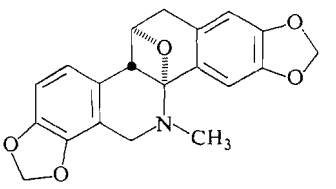

2*d*

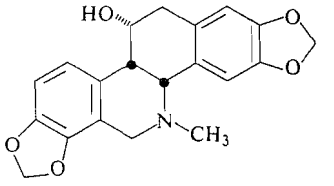

1

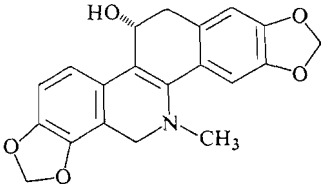

2*b*

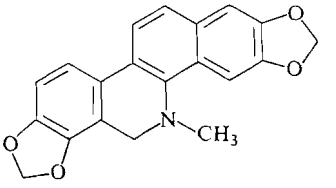

4

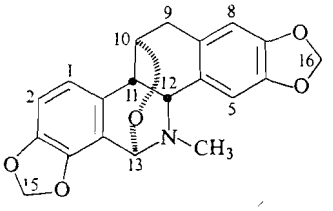

2*c*

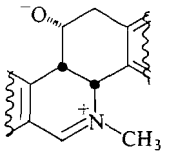

2*e*

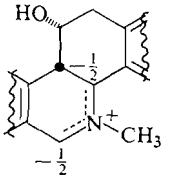

2*f*

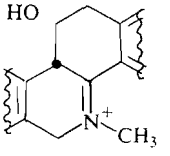

2*g*

dihydrosanguinarine as proceeding through the sequence **2***c* ⇌ **2***e* ⇌ **2***f* ⇌ **2***g* ⇌ **2***b* → **4**.[3]

We obtained didehydrochelidonine, from the products of the permanganate oxidation of chelidonine, and characterized it as the crystalline hydrobromide and pseudocyanide; like other workers we were unable to persuade the free base to crystallize. Sodium borohydride reduced the free base back to chelidonine.

Prompted by a recent report which describes a permanganate oxidation product of corynoline (**5**) as **6** (12), we record here the evidence which established that **2***c* is indeed the correct structure for didehydrochelidonine.

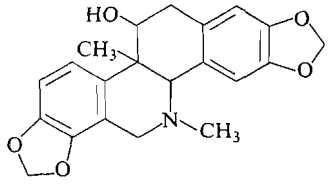

5

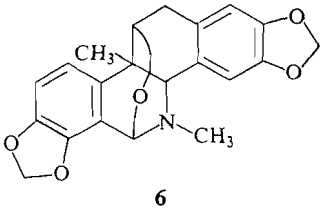

6

The mass spectrum of didehydrochelidonine free base had an apparent M^+ species at *m/e* 351, as required for **2***c*.

Significantly, as judged by the absence of absorption in the 4000–3050 cm^{-1} region of its infrared spectrum, didehydrochelidonine free base did not contain an OH function. (In contrast, the infrared spectrum of didehydrochelidonine hydrobromide had strong absorption at 3300 cm^{-1}.)[4]

[3]The mechanism for the conversion **2***c* ⇌ **2***g* is similar to that proposed for the isomerization of the oxazolidine system in some diterpenoid alkaloids (11).

[4]The infrared spectrum of the hydrobromide also had absorption at 1655 cm^{-1} absent in the spectrum of the free base, which may be ascribed to the C=N$^+$ function. Other evidence which supports **3** (X = Br) as the structure for the hydrobromide includes the ultraviolet light absorption at 397 mμ (ε ~ 7000) consistent with the 3,4-dihydro-2-methyl-6,7-methylenedioxyisoquinolinium chromophone, absent in the spectrum of the parent free base.

Can. J. Chem. Downloaded from www.nrcresearchpress.com by 210.87.254.5 on 09/05/12
For personal use only.

Can. J. Chem. Downloaded from www.nrcresearchpress.com by 210.87.254.5 on 09/05/12
For personal use only.

The proton magnetic resonance spectrum of didehydrochelidonine free base was most informative. Based on the N—CH_3 signal, the spectrum integrated for 17 protons, a result again in accord with **2***c*, but not with **2***a*(X = OH). An analysis of the spectrum is provided in the Experimental, and we comment here only that it was completely consistent with that required for **2***c*, and excludes structures **2***b* and **2***d*.

We conclude that the structure of didehydrochelidonine is **2***c*, and note that the formation of this compound from chelidonine (as well as its reduction back to chelidonine) constitutes *chemical* proof that the relative stereochemistry of chelidonine is as depicted in **1**.

Experimental

Melting points were determined in capillaries, and are uncorrected. Infrared and ultraviolet spectra were recorded on Perkin–Elmer 337 and 202 spectrophotometers, respectively. Proton magnetic resonance spectra were recorded on Varian HA-100 and A-60 spectrometers, with tetramethylsilane as an internal standard. Optical rotations were measured using a Durrum-JASCO U.V.-O.R.D./5 spectrometer. The mass spectrum was recorded on an AEI-MS9 spectrometer, at the University of Alberta, Edmonton, and we report only ions whose abundance was over 20% of the base peak.

Didehydrochelidonine (2c)

Finely powdered potassium permanganate (360 mg, 2.28 mmoles) was added over the course of 1 h to a stirred solution of chelidonine (500 mg, 1.42 mmoles) in acetone (20 ml). After having been stirred at room temperature for a further hour, the reaction mixture was filtered (Celite) and, after washing the filter-cake with acetone, the yellow filtrate and washings were evaporated to dryness under reduced pressure. The residue was taken up in benzene and chromatographed on a column of Florisil (25 g, 1.8 × 20 cm) packed in benzene. Chelidonine was eluted with benzene–ether (9:1, v/v) followed, as the concentration of ether was increased, by didehydrochelidonine.[5]

The yield of didehydrochelidonine, obtained as an almost colorless glass, contaminated with a very faint trace (t.l.c.) of chelidonine, was 195 mg, and a further 185 mg of material containing slightly more chelidonine was also isolated. The total yield of didehydrochelidonine was 76%: λ_{max} (EtOH) 235 (sh) (ε 8720) and 293 mμ (ε 6000), λ_{min} 257 mμ (ε 1100); on addition of one drop of ca. 1% EtOH–HCl, λ_{max} 241, 302 and 394 mμ, λ_{min} 225 and 253 mμ; ν_{max} (KBr or $CHCl_3$) 1610 cm^{-1} (weak), and nothing in the region 4000–3050 cm^{-1}; τ($CDCl_3$) 3.22 (s) (2H), 3.32 (s) (1H) and 3.37 (s) (1H) (4 aromatic protons, probably those at C-1 and -2, C-5 (or -8), and C-8 (or -5), respectively), 4.02 (s) (2H), 4.07 (d) and 4.11 (d) (AB quartet J = 2 c.p.s.) (2H) (4 methylenedioxy protons, probably those at C-16, and C-15, respectively), 4.69 (s) (1H) (H at C-13), 6.08 (broad multiplet) (a complex quintuplet, possibly made up of overlapping quartets, J = 2 c.p.s.) (1H) (H at C-10), 6.85–7.03 (broad, unresolved, complex multiplet) (4H) (H at C-9, C-11 and C-12), and 7.84 (s) (3H) (protons of *N*-CH_3); *m/e* (rel. intensity) 351 (46), 333 (41), 332 (35), 188 (100), and 43 (32).[6]

Didehydrochelidonine hydrobromide was obtained as yellow needles, from 2-propanol, with no distinct m.p. (sinters and decomposes > 210°); λ_{max} (EtOH) 233 (ε 11 000), 298 (ε 9740) and 397 mμ (ε 1690); ν_{max} (KBr) 3300 (strong), and 1655 cm^{-1} (strong); $[\alpha]_D^{27}$ +390 (±5)° (*c* 0.1, EtOH). Literature (3) $[\alpha]_D$ +412° (*c* 1, EtOH).

Didehydrochelidonine pseudocyanide was obtained as colorless prisms, from ethanol, m.p. 194–196°. Literature (3) m.p. 194–195°.

Sodium Borohydride Reduction of Didehydrochelidonine

Sodium borohydride (2.2 mg, 0.057 mmole) was added to a stirred solution of didehydrochelidonine (40 mg, 0.114 mmole) in ethanol (1 ml). After 30 min the solution was acidified and allowed to stand for a few minutes. The solution was then basified (Na_2CO_3) and extracted with chloroform. The chloroform extracts were dried ($MgSO_4$) and evaporated. The residue, which gave a single spot on t.l.c. identical in R_f to chelidonine, was recrystallized from ethanol, and gave off-white crystals, m.p. 120–130° (30 mg, 75%), undepressed on admixture with authentic chelidonine (which also had m.p. 120–130°); the infrared spectrum of the reduction product was also superimposable on that of chelidonine.

Acknowledgments

We are grateful to the National Research Council of Canada for the Grant A-4547 which contributed to the support of this work, and also for the Postgraduate Scholarship awarded to R. E. Mitchell.

1. J. GADAMER. Arch. Pharm. **257**, 298 (1919).
2. J. GADAMER. Arch. Pharm. **253**, 274 (1915); Chem. Abstr. **10**, 1033 (1915).
3. J. GADAMER and K. WINTERFELD. Arch. Pharm. **262**, 452 (1924).
4. J. GADAMER and M. THEISSEN. Arch. Pharm. **262**, 578 (1924).
5. F. VON BRUCHHAUSEN and H. W. BERSCH. Ber. **63**, 2520 (1930); F. VON BRUCHHAUSEN and H. W. BERSCH. Ber. **64**, 947 (1931); E. SPATH and F. KUFFNER. Ber. **64**, 370 (1931).
6. See for example: (*a*) R. H. F. MANSKE. *In* The alkaloids. Vol. 4 *Edited by* R. H. F. Manske and

[5]The chromatogram was monitored by thin-layer chromatography on silica gel-G, with Dragendorf reagent for location of the products: the R_f values for chelidonine and didehydrochelidonine were respectively 0.57 and 0.44 in methanol–benzene (5:95, v/v), and 0.48 and 0.60 in diethylamine-ether (2:98, v/v).

[6]Of the prominent ions in the mass spectrum, other than M^+ at *m/e* 351, we attribute that at *m/e* 333 to the radical–cation of 4, that at *m/e* 332 to the sanguinarine cation, and that at *m/e* 188 to the 2-methyl-6,7-methylenedioxyisoquinolinium cation.

FOR ERRATA SEE
N. 4843.1970 p 511

H. L. Holmes. Academic Press, New York. 1954. p. 259; (*b*) K. W. BENTLEY. The isoquinoline alkaloids. Pergamon Press, Oxford. 1965. p. 212.
7. E. DOMAGALINA and J. OCHÝNSKA. Chem. Anal. (Warsaw) **12**, 267 (1967).
8. (*a*) F. SANTÁVY, M. HORÁK, M. MATUROVA, and J. BRABENA. Coll. Czech. Chem. Comm. **25**, 1344 (1960); (*b*) E. SEONE. Anales real soc. espan. fis. y quim., (Madrid) **61B**, 755 (1965); (*c*) C.-Y. CHEN and D. B. MCLEAN. Can. J. Chem. **45**, 3001 (1967).
9. (*a*) R. ANET, D. W. CLAYTON, and L. MARION. Can. J. Chem. **35**, 397 (1957); (*b*) K. WIESNER, S. ITO, and Z. VALENTA. Experientia, **14**, 167 (1958); T. SUGASAWA. Chem. Pharm. Bull. (Japan) **9**, 897 (1961). See also: N. J. LEONARD and W. K. MUSKER. J. Am. Chem. Soc. **82**, 5148 (1960).
10. D. DVORNIK and O. E. EDWARDS. Tetrahedron, **14**, 54 (1961); S. W. PELLETIER. Tetrahedron, **14**, 76 (1961), and references therein.
11. (*a*) S. NARUTO, S. ARAKAWA, and H. KANEKO. Tetrahedron Letters, 1705 (1968); (*b*) N. TAKEO. Chem. Pharm. Bull. (Japan), **11**, 1306, 1312 (1963).
12. (*a*) C. DJERASSI, C. R. SMITH, A. E. LIPMANN, S. K. FIGDOR, and J. HERRAN. J. Am. Chem. Soc. **77**, 4801 (1955); (*b*) K. WIESNER and Z. VALENTA. Fortschr. Chem. org. Naturstoffe, **16**, 26 (1958).

Central nervous system depressants. XVI. Some newer hydantoins and thiohydantoins

SATISH CHANDRA AND P. C. DANDIYA
Department of Pharmacology, S.M.S. Medical College, Jaipur, India

Received February 4, 1969

The synthesis of hydantoin and thiohydantoin derivatives is described.

Canadian Journal of Chemistry, 47, 3704 (1969)

Can. J. Chem. Downloaded from www.nrcresearchpress.com by 210.87.254.5 on 09/05/12
For personal use only.

5,5-Disubstituted hydantoins are known to possess hypnotic, anticonvulsant, and hypoglycemic properties (1–5). The introduction of methoxy groups has been reported to increase the anticonvulsant activity (6). Oldfield and Cashin (7) synthesized a number of substituted cycloalkanespiro-5-hydantoins which were reported to potentiate hexobarbital-induced hypnosis. Shaffer *et al.* (8) synthesized *N*-3-propionic acid, its ethyl ester, and *N*-3-(2-cyanoethyl) derivatives of 5,5-disubstituted hydantoin and reported that spontaneous motor activity was depressed by these compounds. Further, Dandiya and coworkers (9) have shown that unsaturation in the side chain is one of the most important factors causing central nervous system depressant effect. This led us to the synthesis of hydantoin and thiohydantoin derivatives possessing the methoxy groups and having unsaturation in the side chain.

Experimental

The thiohydantoin and hydantoin derivatives (Table I) were prepared by the following methods.

2-Thio-5-(2,4,5-trimethoxybenzylidene) Hydantoin (Th-1)

A mixture of 2,4,5-trimethoxybenzaldehyde (2.0 g; 0.01 mole), 3-benzoyl-2-thiohydantoin (2.0 g; 0.01 mole),

TABLE I

Analytical data of some trimethoxybenzylidene hydantoins and thiohydantoins.

Compound	Molecular formula	Melting point °C	% yield	% calculated C	% calculated H	% calculated N	% found C	% found H	% found N
2-Thio-5-(2,4,5-trimethoxybenzylidene) hydantoin(**Th-1**)	$C_{13}H_{14}N_2O_4S$	227–228	37	53.06	4.76	9.53	53.45	5.03	9.34
2-Thio-5-(3,4,5-trimethoxybenzylidene) hydantoin(**Th-2**)	$C_{13}H_{14}N_2O_4S$	216–217	33	53.06	4.76	9.53	52.96	4.99	9.45
2-Thio-5-(2,3,4-trimethoxybenzylidene) hydantoin(**Th-3**)	$C_{13}H_{14}N_2O_4S$	186	33	53.06	4.76	9.53	52.97	4.99	9.47
5-(2,4,5-Trimethoxybenzylidene) hydantoin (**H-1**) (10)	$C_{13}H_{14}N_2O_5$	>250	40	56.12	5.03	10.07	56.44	5.15	9.77
5-(3,4,5-Trimethoxybenzylidene) hydantoin (**H-2**) (11)	$C_{13}H_{14}N_2O_5$	>250	36	56.12	5.03	10.07	55.97	5.21	9.92

NOTE. The compounds listed gave infrared spectra that were in accord with the proposed structures.

H. L. Holmes. Academic Press, New York. 1954. p. 259; (*b*) K. W. BENTLEY. The isoquinoline alkaloids. Pergamon Press, Oxford. 1965. p. 212.
7. E. DOMAGALINA and J. OCHÝNSKA. Chem. Anal. (Warsaw) **12**, 267 (1967).
8. (*a*) F. SANTÁVY, M. HORÁK, M. MATUROVA, and J. BRABENA. Coll. Czech. Chem. Comm. **25**, 1344 (1960); (*b*) E. SEONE. Anales real soc. espan. fis. y quim., (Madrid) **61B**, 755 (1965); (*c*) C.-Y. CHEN and D. B. MCLEAN. Can. J. Chem. **45**, 3001 (1967).
9. (*a*) R. ANET, D. W. CLAYTON, and L. MARION. Can. J. Chem. **35**, 397 (1957); (*b*) K. WIESNER, S. ITO, and Z. VALENTA. Experientia, **14**, 167 (1958); T. SUGASAWA. Chem. Pharm. Bull. (Japan) **9**, 897 (1961). See also: N. J. LEONARD and W. K. MUSKER. J. Am. Chem. Soc. **82**, 5148 (1960).
10. D. DVORNIK and O. E. EDWARDS. Tetrahedron, **14**, 54 (1961); S. W. PELLETIER. Tetrahedron, **14**, 76 (1961), and references therein.
11. (*a*) S. NARUTO, S. ARAKAWA, and H. KANEKO. Tetrahedron Letters, 1705 (1968); (*b*) N. TAKEO. Chem. Pharm. Bull. (Japan), **11**, 1306, 1312 (1963).
12. (*a*) C. DJERASSI, C. R. SMITH, A. E. LIPMANN, S. K. FIGDOR, and J. HERRAN. J. Am. Chem. Soc. **77**, 4801 (1955); (*b*) K. WIESNER and Z. VALENTA. Fortschr. Chem. org. Naturstoffe, **16**, 26 (1958).

Central nervous system depressants. XVI. Some newer hydantoins and thiohydantoins

SATISH CHANDRA AND P. C. DANDIYA
Department of Pharmacology, S.M.S. Medical College, Jaipur, India

Received February 4, 1969

The synthesis of hydantoin and thiohydantoin derivatives is described.

Canadian Journal of Chemistry, 47, 3704 (1969)

Can. J. Chem. Downloaded from www.nrcresearchpress.com by 210.87.254.42 on 09/05/12
For personal use only.

5,5-Disubstituted hydantoins are known to possess hypnotic, anticonvulsant, and hypoglycemic properties (1–5). The introduction of methoxy groups has been reported to increase the anticonvulsant activity (6). Oldfield and Cashin (7) synthesized a number of substituted cycloalkanespiro-5-hydantoins which were reported to potentiate hexobarbital-induced hypnosis. Shaffer *et al.* (8) synthesized *N*-3-propionic acid, its ethyl ester, and *N*-3-(2-cyanoethyl) derivatives of 5,5-disubstituted hydantoin and reported that spontaneous motor activity was depressed by these compounds. Further, Dandiya and coworkers (9) have shown that unsaturation in the side chain is one of the most important factors causing central nervous system depressant effect. This led us to the synthesis of hydantoin and thiohydantoin derivatives possessing the methoxy groups and having unsaturation in the side chain.

Experimental

The thiohydantoin and hydantoin derivatives (Table I) were prepared by the following methods.

2-Thio-5-(2,4,5-trimethoxybenzylidene) Hydantoin (Th-1)

A mixture of 2,4,5-trimethoxybenzaldehyde (2.0 g; 0.01 mole), 3-benzoyl-2-thiohydantoin (2.0 g; 0.01 mole),

TABLE I

Analytical data of some trimethoxybenzylidene hydantoins and thiohydantoins.

Compound	Molecular formula	Melting point °C	% yield	% calculated C	% calculated H	% calculated N	% found C	% found H	% found N
2-Thio-5-(2,4,5-trimethoxybenzylidene) hydantoin(**Th-1**)	$C_{13}H_{14}N_2O_4S$	227–228	37	53.06	4.76	9.53	53.45	5.03	9.34
2-Thio-5-(3,4,5-trimethoxybenzylidene) hydantoin(**Th-2**)	$C_{13}H_{14}N_2O_4S$	216–217	33	53.06	4.76	9.53	52.96	4.99	9.45
2-Thio-5-(2,3,4-trimethoxybenzylidene) hydantoin(**Th-3**)	$C_{13}H_{14}N_2O_4S$	186	33	53.06	4.76	9.53	52.97	4.99	9.47
5-(2,4,5-Trimethoxybenzylidene) hydantoin (**H-1**) (10)	$C_{13}H_{14}N_2O_5$	>250	40	56.12	5.03	10.07	56.44	5.15	9.77
5-(3,4,5-Trimethoxybenzylidene) hydantoin (**H-2**) (11)	$C_{13}H_{14}N_2O_5$	>250	36	56.12	5.03	10.07	55.97	5.21	9.92

NOTE. The compounds listed gave infrared spectra that were in accord with the proposed structures.

fused sodium acetate (1.0 g), and glacial acetic acid (10 ml) was heated in a flask on a hot plate, until the mixture was completely liquidified; the heating was then continued for 2 to 3 h on a steam bath. The reaction mixture was cooled and diluted with cold water. The crystals were collected, filtered, and washed with hot water, and then recrystallized from alcohol, m.p. 227–228 °C, yield 1.2 g.

The other compounds listed in Table I were prepared by the same procedure, using 0.01 molar quantities of the appropriate trimethoxybenzaldehyde and 3-benzoyl-2-thio-hydantoin or hydantoin.

Conversion of Thiohydantoin to Hydantoin

A mixture of 2-thio-5-(trimethoxybenzylidene) hydantoin (2.0 g) and monochloroacetic acid (1.0 g in 10 ml of water) was boiled for 4 h. The mixture was then diluted with alcohol and finally evaporated at 100 °C. The crystals obtained by this process were first washed with cold water and then with boiling water. These were recrystallized from alcohol/or acetic acid.

The hydantoins prepared by both different methods gave exactly the same infrared spectra.

Pharmacological Screening

On pharmacological screening of these compounds, it was observed that the thiohydantoin derivatives protected rats markedly against electroshock-induced seizures. All of the three compounds reduced the duration of the tonic phase of convulsion significantly, but no appreciable effect on clonic convulsion was seen. The compound 2-thio-5-(2,4,5-trimethoxybenzylidene) hydantoin also reduced the duration of the post convulsion coma significantly ($P < 0.05$). Hydantoin derivatives failed to offer any protection against electroshock-induced seizures. These compounds decreased motor activity in mice and blocked conditioned avoidance response in trained rats non-specifically.

Acknowledgments

The authors gratefully acknowledge financial support from the Council of Scientific and Industrial Research, New Delhi, India and the Sadtler Research Laboratories, Philadelphia, U.S.A., for carrying out the infrared spectral studies.

1. R. H. Herbst and F. B. Johnson. J. Am. Chem. Soc. **54**, 2463 (1932).
2. V. S. Palkar and P. F. Smith. J. Med. Chem. **8**, 883 (1965).
3. V. S. Palkar and P. F. Smith. J. Org. Chem. **20**, 125 (1965).
4. H. H. Merrit and F. J. Putnam. Epilepsia, **3**, 51 (1945).
5. J. G. Lombardino and C. F. Gerber. J. Med. Chem. **7**, 97 (1964).
6. A. Novelli and A. M. Desantis. J. Med. Chem. **11**, 176 (1968).
7. W. Oldfield and C. H. Cashin. J. Med. Chem. **8**, 239 (1965).
8. J. W. Shaffer, E. Steinberg, V. Krimsley, and M. B. Winstead. J. Med. Chem. **11**, 462 (1968).
9. P. C. Dandiya, P. K. Sharma, and M. K. Menon. Indian J. Med. Res. **50**, 750 (1962).
10. M. Jansen. Rec. Trav. Chim. **50**, 291 (1931).
11. Fr. Schaaf and A. Labouchere. Helv. Chim. Acta, **7**, 357 (1924).

Hydrogen transfer reactions. I. Reduction of carbonyl compounds by alcohols catalyzed by alumina

D. V. Ramana and C. N. Pillai[1]

Department of Chemistry, Indian Institute of Technology, Madras-36, India

Received February 25, 1969

Alumina containing about 2.2% by weight of Na^+ has been found to be an effective catalyst for the vapor phase reduction of carbonyl compounds by alcohols and for the reverse reaction, the oxidation of the alcohols by carbonyl compounds. The reduction of a number of aliphatic and aromatic aldehydes and ketones by isopropyl alcohol and the oxidation of a number of primary and secondary alcohols by ketones like acetone and cyclohexanone are reported.

Canadian Journal of Chemistry, 47, 3705 (1969)

Mekhtiev and Narimanbekov (1) have reported the reduction of a number of aliphatic aldehydes and ketones in the vapor phase at 400 °C, catalyzed by magnesium oxide. The use of alumina as a catalyst for the liquid phase reduction of benzaldehydes by methanol at room temperature has also been reported (2). The present communication reports results which demonstrate the use of alumina impregnated with 2.2% by weight of Na^+ as an effective catalyst for the vapor phase reduction of carbonyl compounds by alcohols and for the reverse reaction.

The alumina was prepared by the hydrolysis of

[1]Author to whom communications regarding this paper should be addressed.

Can. J. Chem. Downloaded from www.nrcresearchpress.com by 210.87.254.42 on 09/05/12
For personal use only.

fused sodium acetate (1.0 g), and glacial acetic acid (10 ml) was heated in a flask on a hot plate, until the mixture was completely liquidified; the heating was then continued for 2 to 3 h on a steam bath. The reaction mixture was cooled and diluted with cold water. The crystals were collected, filtered, and washed with hot water, and then recrystallized from alcohol, m.p. 227–228 °C, yield 1.2 g.

The other compounds listed in Table I were prepared by the same procedure, using 0.01 molar quantities of the appropriate trimethoxybenzaldehyde and 3-benzoyl-2-thio-hydantoin or hydantoin.

Conversion of Thiohydantoin to Hydantoin

A mixture of 2-thio-5-(trimethoxybenzylidene) hydantoin (2.0 g) and monochloroacetic acid (1.0 g in 10 ml of water) was boiled for 4 h. The mixture was then diluted with alcohol and finally evaporated at 100 °C. The crystals obtained by this process were first washed with cold water and then with boiling water. These were recrystallized from alcohol/or acetic acid.

The hydantoins prepared by both different methods gave exactly the same infrared spectra.

Pharmacological Screening

On pharmacological screening of these compounds, it was observed that the thiohydantoin derivatives protected rats markedly against electroshock-induced seizures. All of the three compounds reduced the duration of the tonic phase of convulsion significantly, but no appreciable effect on clonic convulsion was seen. The compound 2-thio-5-(2,4,5-trimethoxybenzylidene) hydantoin also reduced the duration of the post convulsion coma significantly ($P < 0.05$). Hydantoin derivatives failed to offer any protection against electroshock-induced seizures. These compounds decreased motor activity in mice and blocked conditioned avoidance response in trained rats non-specifically.

Acknowledgments

The authors gratefully acknowledge financial support from the Council of Scientific and Industrial Research, New Delhi, India and the Sadtler Research Laboratories, Philadelphia, U.S.A., for carrying out the infrared spectral studies.

1. R. H. Herbst and F. B. Johnson. J. Am. Chem. Soc. **54**, 2463 (1932).
2. V. S. Palkar and P. F. Smith. J. Med. Chem. **8**, 883 (1965).
3. V. S. Palkar and P. F. Smith. J. Org. Chem. **20**, 125 (1965).
4. H. H. Merrit and F. J. Putnam. Epilepsia, **3**, 51 (1945).
5. J. G. Lombardino and C. F. Gerber. J. Med. Chem. **7**, 97 (1964).
6. A. Novelli and A. M. Desantis. J. Med. Chem. **11**, 176 (1968).
7. W. Oldfield and C. H. Cashin. J. Med. Chem. **8**, 239 (1965).
8. J. W. Shaffer, E. Steinberg, V. Krimsley, and M. B. Winstead. J. Med. Chem. **11**, 462 (1968).
9. P. C. Dandiya, P. K. Sharma, and M. K. Menon. Indian J. Med. Res. **50**, 750 (1962).
10. M. Jansen. Rec. Trav. Chim. **50**, 291 (1931).
11. Fr. Schaaf and A. Labouchere. Helv. Chim. Acta, **7**, 357 (1924).

Hydrogen transfer reactions. I. Reduction of carbonyl compounds by alcohols catalyzed by alumina

D. V. Ramana and C. N. Pillai[1]

Department of Chemistry, Indian Institute of Technology, Madras-36, India

Received February 25, 1969

Alumina containing about 2.2% by weight of Na^+ has been found to be an effective catalyst for the vapor phase reduction of carbonyl compounds by alcohols and for the reverse reaction, the oxidation of the alcohols by carbonyl compounds. The reduction of a number of aliphatic and aromatic aldehydes and ketones by isopropyl alcohol and the oxidation of a number of primary and secondary alcohols by ketones like acetone and cyclohexanone are reported.

Canadian Journal of Chemistry, 47, 3705 (1969)

Mekhtiev and Narimanbekov (1) have reported the reduction of a number of aliphatic aldehydes and ketones in the vapor phase at 400 °C, catalyzed by magnesium oxide. The use of alumina as a catalyst for the liquid phase reduction of benzaldehydes by methanol at room temperature has also been reported (2). The present communication reports results which demonstrate the use of alumina impregnated with 2.2% by weight of Na^+ as an effective catalyst for the vapor phase reduction of carbonyl compounds by alcohols and for the reverse reaction.

The alumina was prepared by the hydrolysis of

[1]Author to whom communications regarding this paper should be addressed.

Can. J. Chem. Downloaded from www.nrcresearchpress.com by 210.87.254.40 on 09/05/12
For personal use only.

Can. J. Chem. Downloaded from www.nrcresearchpress.com by 210.87.254.40 on 09/05/12
For personal use only.

TABLE I

Reduction of carbonyl compounds and olefins by isopropyl alcohol

Series No.	Carbonyl compound or olefin	Feed composition*	Product†	Conversion‡
1	Butyraldehyde	1:3	Butanol-1	79
2	Cyclohexanone	1:1	Cyclohexanol	67
3	Cyclohexanone	1:3	Cyclohexanol	90
4	Butanone-2	1:3	Butanol-2	60
5	3,3-Dimethylbutanone-2	1:3	3,3-Dimethylbutanol-2	63
6	Menthone	1:3	Menthol (32) Neomenthol (68)	68
7	Benzophenone	1:10	Benzhydrol	70
8	Acetophenone	1:3	1-Phenylethanol	72
9	Methyl isobutyl ketone	1:3	Methyl isobutyl carbinol	65
10	Hydrocinnamaldehyde	1:3	Hydrocinnamyl alcohol	56
11	Cinnamaldehyde	1:3	Cinnamyl alcohol (26) Hydrocinnamyl alcohol (66) Hydrocinnamaldehyde (8)	68
12	Crotonaldehyde	1:3	Crotyl alcohol (60) Butanol-1 (40)	45
13	Mesityl oxide	1:3	Methyl isobutyl ketone (80) Methyl isobutyl carbinol (20) Methyl isobutenyl carbinol (traces)	66
14	Cinnamyl alcohol	1:3	Hydrocinnamyl alcohol	44
15	Allyl alcohol	1:3	Propanol	1
16	Cinnamyl alcohol	§	Hydrocinnamyl alcohol (50) Cinnamaldehyde (50)	20
17	*o*-Chlorobenzaldehyde	1:1	*o*-Chlorobenzyl alcohol	65
18	*p*-Chlorobenzaldehyde	1:1	*p*-Chlorobenzyl alcohol	57
19	Benzaldehyde	1:1	Benzyl alcohol	51
20	*m*-Tolualdehyde	1:1	*m*-Methylbenzyl alcohol	46
21	*p*-Tolualdehyde	1:1	*p*-Methylbenzyl alcohol	38
22	*m*-Methoxybenzaldehyde	1:1	*m*-Methoxybenzyl alcohol	34
23	*p*-Methoxybenzaldehyde	1:1	*p*-Methoxybenzyl alcohol	28
24	*p*-Methoxybenzaldehyde	1:3	*p*-Methoxybenzyl alcohol	50

NOTE: Catalyst: Al_2O_3 containing 2.2 wt% Na^+ (6g). Temperature: 300 °C. Flow rate: 15 ml/h.
*Mole ratio, carbonyl compound or olefin : isopropyl alcohol.
†Numbers in parentheses indicate the percent composition of the product mixture when more than one product are formed.
‡Conversion, percentages based on the carbonyl compound or olefin.
§Cinnamyl alcohol alone was passed over the catalyst without the addition of any isopropyl alcohol.

TABLE II

Oxidation of alcohols

Series No.	Alcohol	Oxidizing agent	Feed composition*	Product	Conversion†
1	Butanol-1	Cyclohexanone	1:3	Butyraldehyde	37
2	Propanol-1	Cyclohexanone	1:3	Propionaldehyde	43
3	Isobutyl alcohol	Cyclohexanone	1:3	Isobutyraldehyde	37
4	Cinnamyl alcohol	Cyclohexanone	1:3	Cinnamaldehyde‡	40
5	Benzyl alcohol	Cyclohexanone	1:3	Benzaldehyde	31
6	Hydrocinnamyl alcohol	Cyclohexanone	1:3	Hydrocinnamaldehyde	32
7	Amyl alcohol	Cyclohexanone	1:3	Valeraldehyde	37
8	Butanol-2	Cyclohexanone	1:3	Butanone-2	81
9	Isobutyl methyl carbinol	Cyclohexanone	1:3	Isobutyl methyl ketone	81
10	Menthol	Cyclohexanone	1:10	Menthone	32
11	Cyclohexanol	Acetone	1:1	Cyclohexanone	34
12	Benzyl alcohol	Acetone	1:1	Benzaldehyde	34
13	Menthol	Acetone	1:10	Menthone	40
14	Neomenthol	Acetone	1:10	Menthone	73

NOTE: Catalyst: Al_2O_3 containing 2.2 wt % Na^+ (6g). Temperature: 300 °C. Flow rate: 15 ml/h.
*Mole ratio, alcohol: oxidizing agent.
†Conversion, percentages based on alcohol.
‡Traces of hydrocinnamyl alcohol and hydrocinnamaldehyde were also formed.

aluminium isopropoxide and after conversion to 1/8 in. pellets, was calcined at 600 °C in a stream of nitrogen for 6 h. The pellets were then impregnated with a solution of sodium carbonate of sufficient strength to obtain the required catalyst containing 2.2% by weight of sodium ions. This catalyst was calcined at 500 °C for 6 h in a stream of nitrogen and the reactions were carried out in a flow reactor at 300 °C. At higher temperatures, side reactions, especially condensation reactions of the carbonyl compounds became apparent. On alumina catalysts containing lesser amounts of sodium, considerable dehydration of alcohols took place. Some of the typical results are listed in Tables I and II. The products were analyzed by gas–liquid chromatography and were isolated in most cases by distillation.

The reaction is formally similar to the Meerwein–Pondorff reduction and the Oppenauer oxidation and a hydride transfer from the alcohol to the carbonyl group seems to be involved here also. The following surface reaction mechanism can be tentatively proposed for the oxidation reduction process:

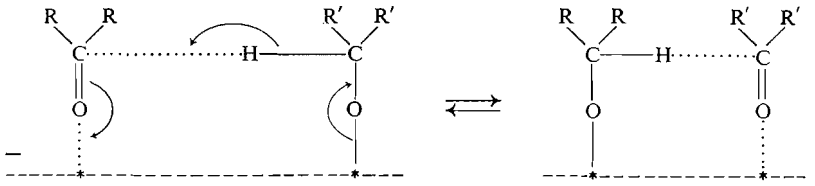

Acknowledgments

Grateful acknowledgment is made to the donors of the Petroleum Research Fund administered by the American Chemical Society for the financial support of this research. The authors also wish to express their thanks to Professor M. V. C. Sastri and Dr. J. C. Kuriacose for their interest and encouragement.

1. S. D. Mekhtiev and O. A. Narimanbekov. Dokl. Akad. Nauk Azerb. SSR, **20(4)**, 33 (1964); Chem. Abstr. **61**, 10579 (1964).
2. V. J. Hruby. Proc. N. Dak. Acad. Sci., **16**, 12 (1962); Chem. Abstr. **62**, 1589 (1965).

Can. J. Chem. Downloaded from www.nrcresearchpress.com by 210.87.254.40 on 09/05/12
For personal use only.

Proton magnetic resonance spectrum of 2,6-dichlorobenzaldoxime. Signs and magnitudes of long-range spin–spin couplings. Degree of nonplanarity

T. Schaefer and R. Wasylishen
Chemistry Department, University of Manitoba, Winnipeg, Manitoba

Received May 7, 1969

From the sign and magnitude of the coupling constant between the C—H proton in the sidechain and the para ring proton in 2,6-dichlorobenzaldoxime it is estimated that the deviation from coplanarity of the sidechain is at least 40°. The hydroxyl proton shift in dimethylsulfoxide solution of −11.7 p.p.m., relative to internal tetramethylsilane, indicates a *cis* arrangement of the hydroxyl and aromatic groups.

Canadian Journal of Chemistry, 47, 3707 (1969)

Spectral Analysis

At 60 MHz the proton magnetic resonance of a 4 mole % solution of 2,6-dichlorobenzaldoxime, **1**, in acetone consists of a tightly coupled AB_2X spectrum (the hydroxyl proton is involved in exchange-averaged hydrogen-bonding equilibria with solvent and solute molecules and is not observed to couple to other protons). Because of

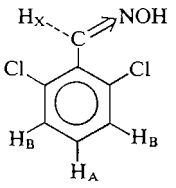

1

aluminium isopropoxide and after conversion to 1/8 in. pellets, was calcined at 600 °C in a stream of nitrogen for 6 h. The pellets were then impregnated with a solution of sodium carbonate of sufficient strength to obtain the required catalyst containing 2.2% by weight of sodium ions. This catalyst was calcined at 500 °C for 6 h in a stream of nitrogen and the reactions were carried out in a flow reactor at 300 °C. At higher temperatures, side reactions, especially condensation reactions of the carbonyl compounds became apparent. On alumina catalysts containing lesser amounts of sodium, considerable dehydration of alcohols took place. Some of the typical results are listed in Tables I and II. The products were analyzed by gas–liquid chromatography and were isolated in most cases by distillation.

The reaction is formally similar to the Meerwein–Pondorff reduction and the Oppenauer oxidation and a hydride transfer from the alcohol to the carbonyl group seems to be involved here also. The following surface reaction mechanism can be tentatively proposed for the oxidation reduction process:

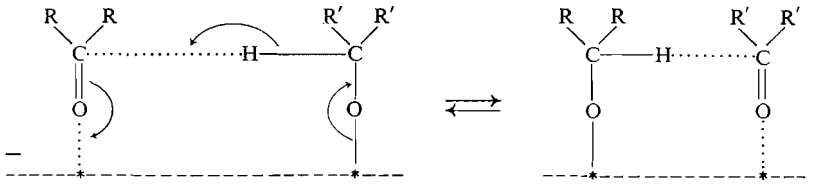

Acknowledgments

Grateful acknowledgment is made to the donors of the Petroleum Research Fund administered by the American Chemical Society for the financial support of this research. The authors also wish to express their thanks to Professor M. V. C. Sastri and Dr. J. C. Kuriacose for their interest and encouragement.

1. S. D. Mekhtiev and O. A. Narimanbekov. Dokl. Akad. Nauk Azerb. SSR, **20(4)**, 33 (1964); Chem. Abstr. **61**, 10579 (1964).
2. V. J. Hruby. Proc. N. Dak. Acad. Sci., **16**, 12 (1962); Chem. Abstr. **62**, 1589 (1965).

Can. J. Chem. Downloaded from www.nrcresearchpress.com by 210.87.254.40 on 09/05/12
For personal use only.

Proton magnetic resonance spectrum of 2,6-dichlorobenzaldoxime. Signs and magnitudes of long-range spin–spin couplings. Degree of nonplanarity

T. Schaefer and R. Wasylishen
Chemistry Department, University of Manitoba, Winnipeg, Manitoba

Received May 7, 1969

From the sign and magnitude of the coupling constant between the C—H proton in the sidechain and the para ring proton in 2,6-dichlorobenzaldoxime it is estimated that the deviation from coplanarity of the sidechain is at least 40°. The hydroxyl proton shift in dimethylsulfoxide solution of −11.7 p.p.m., relative to internal tetramethylsilane, indicates a *cis* arrangement of the hydroxyl and aromatic groups.

Canadian Journal of Chemistry, 47, 3707 (1969)

Spectral Analysis

At 60 MHz the proton magnetic resonance of a 4 mole % solution of 2,6-dichlorobenzaldoxime, **1**, in acetone consists of a tightly coupled AB_2X spectrum (the hydroxyl proton is involved in exchange-averaged hydrogen-bonding equilibria with solvent and solute molecules and is not observed to couple to other protons). Because of

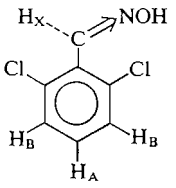

1

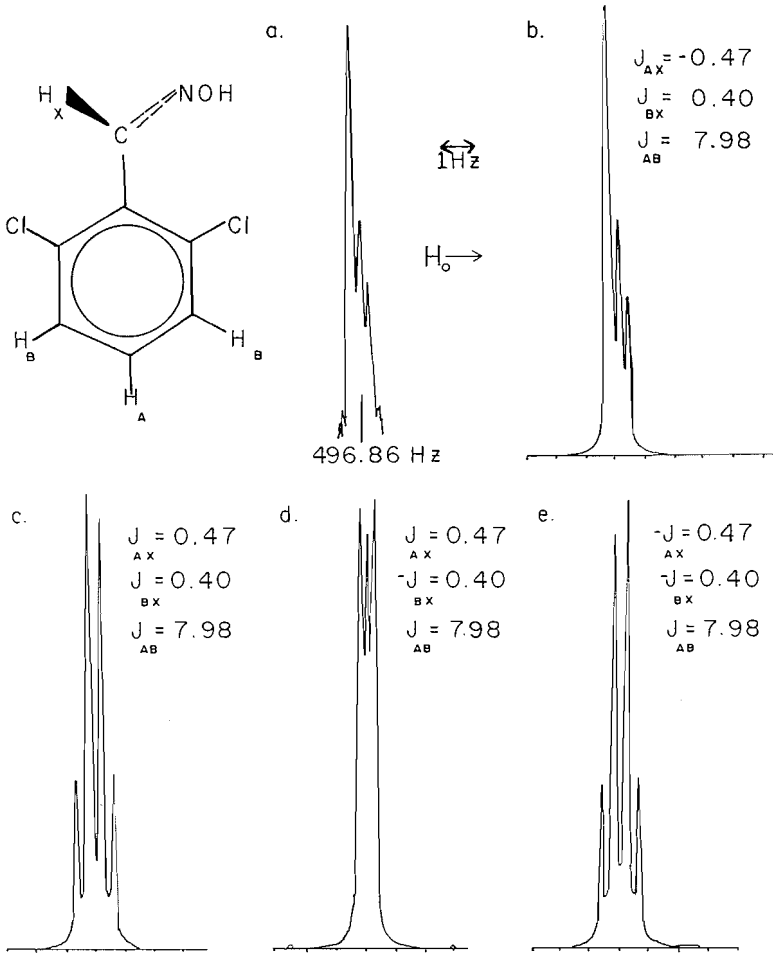

FIG. 1. In *a*, the proton magnetic resonance spectrum of the C—H proton in the sidechain of 2,6-dichlorobenzaldoxime is shown. In *b*, *c*, *d*, and *e*, the computed spectra are shown for various sign combinations J_{AB}, J_{AX}, and J_{BX}. The magnitudes of J_{AB}, J_{AX}, and J_{BX} are in Hz.

the tight coupling between H_A and H_B any asymmetry in the resonance of H_X depends on the relative signs of J_{AB} to J_{AX} and J_{BX} (1,2). In Fig. 1 the observed resonance of H_X is compared with the computed spectra for various combinations of relative signs of the above coupling constants. It is clear that $J_{AX}/J_{AB} < 0$ while $J_{BX}/J_{AB} > 0$. $J_{AB} \equiv J_o^{HH}$ is known to be positive and normal analysis procedures yield the following parameters, where chemical shifts are given relative to internal tetramethylsilane.

$$\nu_A = -7.366 \pm 0.003 \text{ p.p.m.}$$
$$\nu_B = -7.450 \pm 0.003 \text{ p.p.m.}$$
$$\nu_X = -8.283 \pm 0.003 \text{ p.p.m.}$$
$$\nu_{OH} = -10.83 \pm 0.01 \text{ p.p.m.}$$

$$J_{AB} \equiv J_o^{HH} = 7.98 \pm 0.03 \text{ Hz}$$
$$J_{BX} \equiv J_m^{H,CH} = 0.40 \pm 0.02 \text{ Hz}$$
$$J_{AX} \equiv J_p^{H,CH} = -0.47 \pm 0.01 \text{ Hz}$$

Long-range Coupling Constants

At room temperature benzaldehyde flips rapidly between planar conformations (3,4) and $J_p^{H,CHO} = -0.03$ Hz (5), consistent with a σ-π polarization mechanism (6,7) for this coupling. In some ortho disubstituted benzaldehydes the average conformation is nonplanar (8) and leads to larger magnitudes of this negative coupling.

In 2,6-dichlorobenzaldoxime there must also be substantial steric interactions hindering a coplanar conformation of the sidechain and the aromatic ring. An estimate of the deviation from

Can. J. Chem. Downloaded from www.nrcresearchpress.com by 210.87.254.40 on 09/05/12
For personal use only.

Can. J. Chem. Downloaded from www.nrcresearchpress.com by 210.87.254.40 on 09/05/12
For personal use only.

coplanarity can be made on the unproved assumption that $J_p^{H,CH} = -1.2$ Hz when the C—H bond lies perpendicular to the aromatic ring. The value of -1.2 Hz is derived from $J_p^{H,CH_3} = -0.62$ Hz in toluene (9) where $\langle\cos^2\theta\rangle = 0.5$. The angle θ measures the deviation of the C—H bond from a perpendicular conformation and because the barrier to rotation in toluene is only 0.014 kcal/mole (10), $\cos^2\theta$ may be averaged over the rotation in this simple way. On this assumption a value of $\theta = 50°$ is derived for 2,6-dichlorobenzaldoxime. It may be that in this compound the maximum value of $J_p^{H,CH}$ is less than in toluene, in which case the derived value of θ represents an upper limit. At any rate, it is consistent with a value of $\theta = 70°$ derived by a similar assumption for 2,6-dichlorobenzaldehyde (8), where smaller steric interactions are expected, as well as with a value of $\theta = 71°$ found for the *anti* isomer (aromatic ring and hydroxyl groups in a *cis* arrangement) of *p*-chlorobenzaldoxime in the solid state (11).

Because both σ and π electron contributions to $J_m^{H,CH}$ may exist (12) and because for nonplanar conformations the π contribution possibly compensates for a decreased σ contribution, it is not justified to use the value of $J_m^{H,CH}$ as a check on the degree of nonplanarity derived from the magnitude of $J_p^{H,CH}$. The relative constancy of $J_m^{H,CH}$ which lies between 0.35 and 0.40 Hz in 2,6-dichlorobenzaldoxime, 2,6-dichloro- , and 2,6-dinitrobenzaldehydes (8), benzaldehyde (5), toluene (9), and in 2,6-dichlorobenzylfluoride (13) suggests the presence of a compensatory effect.

Hydroxyl Proton Shift in Dimethylsulfoxide

In a 4 mole % solution in dimethylsulfoxide $\nu_{OH} = -11.71$ p.p.m. This is close to the value of -11.58 p.p.m. found for the *anti* isomer of benzaldoxime (14) and suggests that the present compound has the aromatic ring and the hydroxyl group placed *cis* to one another (the *syn* isomer of benzaldoxime has $\nu_{OH} = -11.2$ p.p.m.). In the same solvent, $\nu_{OH} - \nu_{CH} = -3.04$ and -3.82 p.p.m. for the *syn* and *anti* isomers of benzaldoxime, respectively. For the present compound, $\nu_{OH} - \nu_{CH} = -3.54$ p.p.m. close to the average of these two values. However, strong mean square electric fields arising from the proximate chlorine substituents may well cause a downfield shift of the C—H protons in 2,6-dichlorobenzaldoxime. Hence the value of -3.54 p.p.m. is considered to be consistent with a *cis* arrangement of the hydroxyl group and the ring.

Experimental

2,6-Dichlorobenzaldoxime from the Aldrich Chemical Co., m.p. 149 °C, was studied as 4 mole % solutions in acetone and in dimethylsulfoxide. Lines were considerably narrower in acetone, probably because of differing viscosities, and therefore spectral analysis were carried out on the acetone solution. Samples were degassed by the freeze-pump-thaw technique and proton magnetic resonance spectra were taken in the frequency sweep made on a DA-60I spectrometer. Spectra were calibrated by reading reciprocals of the sweep and manual oscillator frequencies. Computations were performed by hand and checked using the LAOCN3 program (15) on an IBM 360/65 computer. Computed spectral curves were obtained on a Calcomp plotter attached to an IBM 1620 computer.

Acknowledgments

We are grateful to the authors for a listing of LAOCN3 and to the National Research Council of Canada for financial support.

1. P. Diehl and J. A. Pople. Mol. Phys. **3**, 557 (1960).
2. R. C. Hirst, D. M. Grant, and E. G. Paul. J. Chem. Phys. **44**, 4305 (1966).
3. S. Forsén and P. N. Skancke. *In* Selected topics in structure chemistry. *Edited by* P. Anderson, O. Bastiansen, and S. Furberg. Universitetsforlaget, Oslo, Norway. 1967.
4. F. A. L. Anet and N. Ahmad. J. Amer. Chem. Soc. **86**, 119 (1964).
5. R. J. Kostelnik, M. P. Williamson, D. E. Wisnosky, and S. M. Castellano. Can. J. Chem. In press.
6. H. M. McConnell. J. Chem. Phys. **30**, 126 (1959).
7. D. J. Blears, S. S. Danyluk, and T. Schaefer. J. Chem. Phys. **47**, 5037 (1967).
8. C. L. Bell, S. S. Danyluk, and T. Schaefer. Can. J. Chem. This issue.
9. M. P. Williamson, R. J. Kostelnik, and S. M. Castellano. J. Chem. Phys. **49**, 2218 (1968).
10. H. Rudolph, H. Dreizler, A. Jaeschke, and P. Wendling. Z. Naturforsch. **22a**, 940 (1967).
11. B. Jerslev. Nature, **180**, 1410 (1958).
12. H. Frischleder and G. Bär. Mol. Phys. **11**, 359 (1966).
13. T. Schaefer, C. M. Wong, and K. C. Tam. Can. J. Chem. This issue.
14. G. G. Kleinspehn, J. A. Jung, and S. A. Studniarz. J. Org. Chem. **32**, 460 (1967).
15. S. Castellano and A. A. Bothner-By. J. Chem. Phys. **41**, 3863 (1964).

Substituent effects in the reaction of aromatic amines and peroxydisulfate

N. VENKATASUBRAMANIAN[1] AND A. SABESAN
Department of Chemistry, Vivekananda College, Madras 4, India

Received April 10, 1969

The kinetics of the reaction between aromatic amines and the peroxydisulfate ion in aqueous basic conditions have been investigated. The effect of substituents has been studied by employing about 25 ortho-, meta-, and para-substituted anilines. The reaction is accelerated by electron-releasing substituents and is retarded by electron-withdrawing substituents, pointing to an electrophilic attack by the $S_2O_8^{2-}$ ion. A better correlation between rate and the Hammett constants is obtained for an electrophilic attack at the nitrogen atom of the amine rather than at the carbon atom of the amine. A good correlation also exists between the log k_2 values and the pK_b of the corresponding amines.

Canadian Journal of Chemistry, 47, 3710 (1969)

Can. J. Chem. Downloaded from www.nrcresearchpress.com by 210.87.254.105 on 09/05/12
For personal use only.

The kinetics of the reaction between aromatic amines and peroxydisulfate in aqueous base, called the Boyland–Sims oxidation (1–4), were recently investigated by Behrman (5) who has proposed a mechanism involving a nucleophilic displacement by the amine nitrogen on the peroxide oxygen to yield the corresponding aryl hydroxylamine *O*-sulfonate (route *A*). This intermediate is then assumed to rearrange to the *o*-amino aryl sulfate.

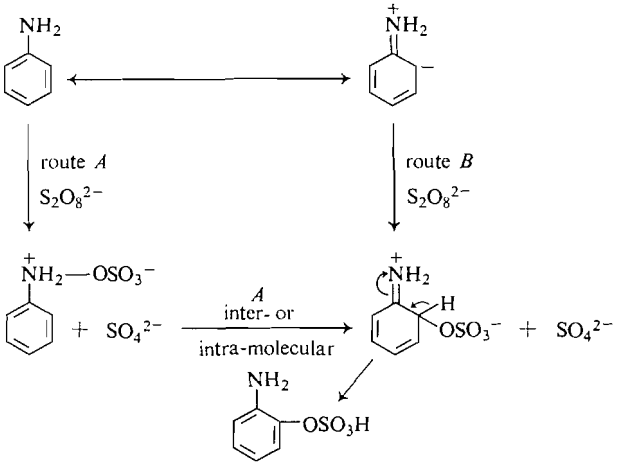

The alternative possibility of a direct rate-limiting attack at the ortho-carbon (route *B*) was ruled out by a comparison of the rates of oxidation of 2,3- and 2,4-disubstituted anilines. We present in this communication the results of our investigation on this reaction for a series of monosubstituted anilines in order that more extensive substituent effects may be used to test the proposed mechanism (5).

The kinetic studies were carried out in 20% aqueous ethanol[2] (v/v) with a phosphate buffer (pH = 7) under pseudo first order conditions with an amine:peroxydisulfate ratio of 10:1. All the liquid organic compounds were of the extra

TABLE I

Order with respect to aniline
Solvent: 0.05 *M* phosphate buffer, pH = 7.0 in 20% EtOH, temperature 30 °C

[Aniline] (*M*)	$[S_2O_8^{2-}]$ (*M*)	$k_1 \times 10^4$ (s^{-1})	$k_2 \times 10^2$ ($l\,mole^{-1}\,s^{-1}$)
0.0127	0.00128	1.45	1.15
0.0289	0.00234	3.44	1.19
0.0423	0.00403	4.87	1.21
0.0516	0.00474	6.49	1.26
0.102	0.00883	12.0	1.18

[1]Author to whom all correspondence should be addressed.

[2]The oxidation of the 20% aqueous ethanol (v/v) by $S_2O_8^{2-}$ is negligible under our experimental conditions. See also ref. 6.

Can. J. Chem. Downloaded from www.nrcresearchpress.com by 210.87.254.105 on 09/05/12
For personal use only.

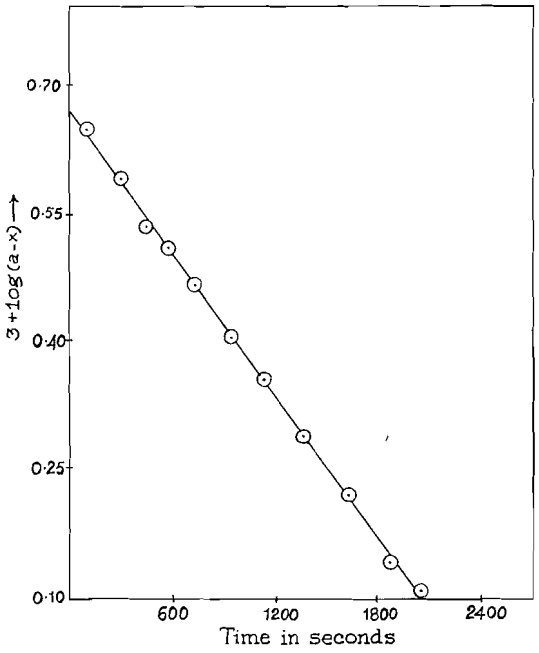

FIG. 1. First order plot for the oxidation of aniline by $S_2O_8^{2-}$. [Aniline] = 0.0516 *M*, $[S_2O_8^{2-}]$ = 0.00474 *M*, temperature 30 °C. Solvent: 0.05 *M* phosphate buffer, pH = 7.0 in 20% EtOH.

pure variety (Fluka AG/Koch-Light/Arapahoe) and were distilled from an all-glass apparatus. Large head and tail fractions were rejected and middle fractions were collected and used. The solid aromatic amines of the extra pure variety (Fluka AG/Koch-Light/Arapahoe) were used without further purification. The reaction was followed by estimating the unreacted peroxydisulfate by the iodometric procedure of Kolthoff and Carr (7). The reaction is of the first order in peroxydisulfate for over 60% of the reaction and also in the neutral amine (Tables I and II; Fig. 1). Allyl acetate, a radical inhibitor has no effect on the rate of consumption of the peroxydisulfate in the present investigations also. The second order rate constants for the oxidation of a number of ortho-, meta-, and para-substituted anilines are presented in Table III. It is evident that electron-releasing substituents on the aniline accelerate the reaction much more when these are para to the $—NH_2$ group than when they are ortho or para to the carbon center where the sulfate group is found ultimately. This, we feel, points to a rate-limiting attack at nitrogen rather than at carbon.

TABLE II

Order with respect to substituted anilines*
Solvent: 0.05 *M* phosphate buffer,
pH = 7.0 in 20% EtOH,
temperature 30 °C

Amine	[Amine] (*M*)	$k_1 \times 10^4$ (s^{-1})	$k_2 \times 10^2$ ($l\ mole^{-1}\ s^{-1}$)
p-Toluidine	0.0503	15.4	3.06
	0.0259	8.07	3.17
m-Toluidine	0.0508	9.21	1.81
	0.0262	4.73	1.80
o-Toluidine	0.0258	6.65	2.58
	0.0132	3.53	2.68
p-Bromo aniline	0.0482	6.46	1.34
	0.0254	3.62	1.42
o-Chloro aniline	0.0504	1.73	0.343
	0.0262	0.973	0.366
m-Chloro aniline	0.0513	2.48	0.484
	0.0247	1.24	0.504
p-Chloro aniline	0.0126	1.91	1.52
	0.0402	5.90	1.47
	0.0497	7.64	1.54
p-Amino acetophenone	0.050	1.31	0.262
	0.0253	0.679	0.268

*In all oxidations the [amine]:$[S_2O_8^{2-}]$ is 10:1.

TABLE III

The effect of substituents on the rate of oxidation of aniline
Solvent: 0.05 *M* phosphate buffer,
pH = 7.0 in 20% EtOH,
temperature 30 °C

Amine	$k_2 \times 10^3$ ($l\ mole^{-1}\ s^{-1}$)
Aniline	12.0
p-Toluidine	31.7
m-Toluidine	18.1
o-Toluidine	26.8
p-Anisidine	165
m-Anisidine	16.7
o-Anisidine	56.2
p-Fluoro-aniline	17.4
m-Fluoro-aniline	4.63
o-Fluoro-aniline	4.15
p-Chloro-aniline	15.4
m-Chloro-aniline	4.84
o-Chloro-aniline	3.43
p-Bromo-aniline	14.2
m-Bromo-aniline	4.51
o-Bromo-aniline	3.66
p-Iodo-aniline	15.7
p-Amino-acetophenone	2.62
p-Amino-benzoic acid	4.39
m-Amino-benzoic acid	3.45
o-Amino-benzoic acid	2.67
p-Nitro-aniline	0.28
m-Nitro-aniline	1.17
o-Nitro-aniline	0.15
m-Phenetidine	17.9
o-Phenetidine	50.7

Can. J. Chem. Downloaded from www.nrcresearchpress.com by 210.87.254.105 on 09/05/12
For personal use only.

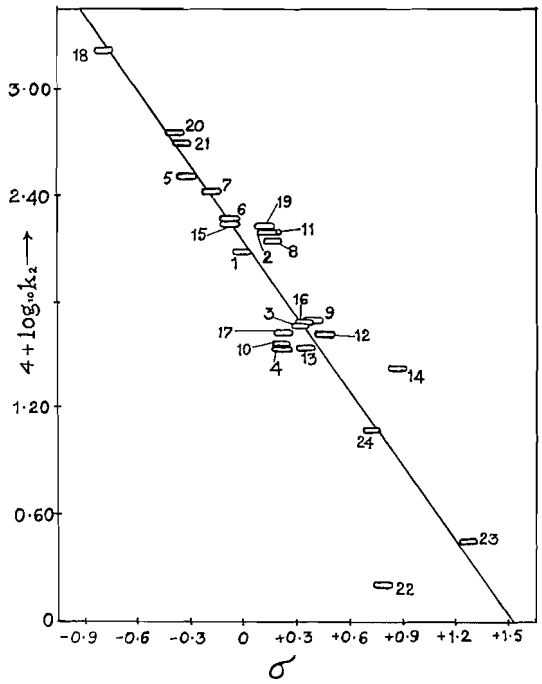

FIG. 2. σ_{p+} values (9) have been used for para substituted anilines, σ_m values for the meta substituted anilines, and σ^* values (14) for the ortho substituted anilines. (*1*) H— (*2*) *p*-Cl (*3*) *m*-Cl (*4*) *o*-Cl (*5*) *p*-CH_3— (*6*) *m*-CH_3— (*7*) *o*-CH_3— (*8*) *p*-Br— (*9*) *m*-Br— (*10*) *o*-Br— (*11*) *p*-I— (*12*) *p*-COOH (*13*) *m*-COOH (*14*) *p*-CH_3CO— (*15*) *p*-F (*16*) *m*-F (*17*) *o*-F (*18*) *p*-CH_3O— (*19*) *m*-CH_3O— (*20*) *o*-CH_3O— (*21*) *o*-C_2H_5O— (*22*) *o*-NO_2— (*23*) *p*-NO_2— (*24*) *m*-NO_2—.

The correlation of these data with the Hammett σ constants (8, 9) is shown in Figs. 2 and 3. The data are plotted in two ways. Figure 2 assumes rate-limiting attack at nitrogen while Fig. 3 assumes a rate-limiting attack at carbon. One might expect that for the meta-substituted anilines, rate-limiting attack at nitrogen should correlate with σ_m while rate-limiting attack at the carbon para to the meta-substituent would give a good correlation of log k_2 for these anilines with σ_{p+} for these substituents. It is already known that the ortho-carbon atom between the NH_2-group and the meta-substituent is not attacked, as steric considerations weigh against this (2) Similarly for *p*-substituted anilines, attack at the nitrogen would be expected to correlate better with σ_{p+} while attack at the carbon should give a correlation with the meta-substitution constants. Further, for the ortho-substituted anilines, nitrogen attack should show a correlation between the logarithm of the rate constants and σ_o while for carbon attack, the same rate constants should be correlated with σ_m for the same substituents. The data displayed in Figs. 2 and 3 show that a good over-all correlation exists only for the plot that assumes attack at the nitrogen rather than at the carbon ortho to the nitrogen. In fact, the points for the second plot for an assumed carbon attack show a random scatter and one cannot discern any linear relationship here. The linear plot in Fig. 2 has a correlation coefficient of 0.9707 (for 22 points excluding the points for *p*-CH_3CO— and *o*-NO_2) which is a fairly satisfactory fit. The Hammett rho for this reaction is −1.41, a value which is nearly the same as was computed by Behrman (5) for the case of the three amines: aniline, *p*-nitro-aniline, and *p*-toluidine (ρ = −1.3). This value compares quite well with the value of −1.86 reported for the reaction of aromatic amines by peroxy acetic acid (10), and of −1.58 for the reaction of nitro-

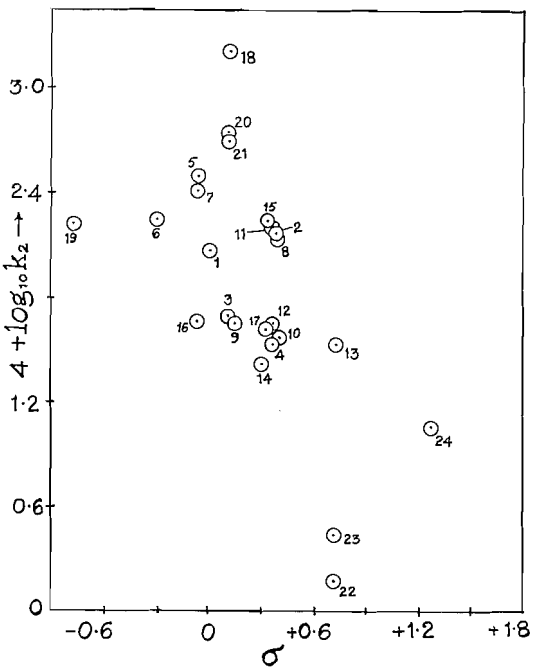

FIG. 3. σ_m values have been used for ortho- and para-substituted anilines and σ_{p+} values for the meta substituted anilines. (*1*) H— (*2*) *p*-Cl (*3*) *m*-Cl (*4*) *o*-Cl (*5*) *p*-CH_3— (*6*) *m*-CH_3— (*7*) *o*-CH_3— (*8*) *p*-Br— (*9*) *m*-Br— (*10*) *o*-Br— (*11*) *p*-I— (*12*) *p*-COOH (*13*) *m*-COOH (*14*) *p*-CH_3CO— (*15*) *p*-F (*16*) *m*-F (*17*) *o*-F (*18*) *p*-CH_3O— (*19*) *m*-CH_3O— (*20*) *o*-CH_3O— (*21*) *o*-C_2H_5O— (*22*) *o*-NO_2— (*23*) *p*-NO_2— (*24*) *m*-NO_2—.

sobenzenes with peroxy acetic acid (11). A good correlation can also be made between log k_2 and the pK_b values of the anilines.

The evidence thus confirms rate-limiting electrophilic attack by the peroxydisulfate ion on the nitrogen of the neutral amine followed by rearrangement to the *o*-amino aryl sulfate. Boyland and Nery (12) have reported that phenyl hydroxylamine *O*-sulfonate rearranges to *o*-amino phenyl sulfate and Behrman (5) has also considered it as a probable intermediate in the reaction between aromatic amines and peroxydisulfate ions.

Initial attack at nitrogen also provides the rationale for the preferential ortho orientation in the Boyland–Sims oxidation as against the preferential para-orientation in the peroxydisulfate oxidation of phenols in alkaline medium (Elbs peroxydisulfate oxidation). The Elbs peroxydisulfate oxidation of phenols further differs from the present work by the fact that in the former case, the use of Hammett correlations as a means of distinguishing the site of attack was indecisive (13).

Acknowledgment

We thank one of the referees for his helpful comments.

1. E. Boyland, D. Manson, and P. Sims. J. Chem. Soc. 3623 (1953).
2. E. Boyland and P. Sims. J. Chem. Soc. 980 (1954).
3. P. Sims. J. Chem. Soc. 44 (1958).
4. E. Boyland and P. Sims. J. Chem. Soc. 4198 (1958).
5. E. J. Behrman. J. Amer. Chem. Soc. **89**, 2424 (1967).
6. L. R. Subbaraman and M. Santappa. Proc. Ind. Acad. Sci. **64**, 345 (1966).
7. I. M. Kolthoff and E. M. Carr. Anal. Chem. **25**, 298 (1953).
8. H. C. Brown. Steric effects in conjugated systems *Edited by* G. W. Gray. Butterworth, London. 1958.
9. L. M. Stock and H. C. Brown. Advan. Phys. Org. Chem. **1**, 35 (1963).
10. K. M. Ibne-Rasa and J. O. Edwards. J. Amer. Chem. Soc. **84**, 763 (1962).
11. K. M. Ibne-Rasa, C. G. Lauro, and J. O. Edwards. J. Amer. Chem. Soc. **85**, 1165 (1963).
12. E. Boyland and R. Nery. J. Chem. Soc. 5217 (1962).
13. E. J. Behrman. J. Amer. Chem. Soc. **85**, 3478 (1963).
14. J. Hine. Physical organic chemistry. McGraw-Hill Book Co., New York. 1962. p. 98.

Can. J. Chem. Downloaded from www.nrcresearchpress.com by 210.87.254.105 on 09/05/12
For personal use only.

Can. J. Chem. Downloaded from www.nrcresearchpress.com by 210.87.254.42 on 09/05/12
For personal use only.

Adamantanethione and its reduction to 2-adamantanethiol

J. W. GREIDANUS[1] AND W. J. SCHWALM
Department of Chemistry, University of Calgary, Calgary, Alberta

Received July 17, 1969

Reaction of adamantanone with phosphorus pentasulfide affords the corresponding thioketone. This new, comparatively very stable alicyclic thione was also obtained by an indirect route from 2-ethoxy-2-adamantanethiol. Reduction of the thioketone with sodium borohydride yields 2-adamantanethiol.

Canadian Journal of Chemistry, 47, 3715 (1969)

An interest in the properties of non-aromatic thioketones as well as in the chemistry of adamantane has prompted us to prepare adamantanethione (**2**). We expected that this non-enolizable thioketone would be comparatively stable and this was found to be the case.

Few stable non-aromatic thioketones are known and as a result the chemistry of these compounds has not been well investigated. Suitably substituted adamantanethiones might be of considerable interest for optical rotatory dispersion studies of the thiocarbonyl group.

Our initial attempts to obtain the thione from adamantanone (**1**) and H_2S at low temperature (1) gave very unsatisfactory results and we decided to treat the ketone with phosphorus pentasulfide. In the few instances where the latter method has been used by others for the preparation of unsubstituted aliphatic or alicyclic thioketones, either no details for the preparation were given or the results have been considered very doubtful by others, it seems. Several reviews on this topic exist (2).

When a solution of 40 mmoles of adamantanone (**1**) and 14 mmoles of P_4S_{10} in dry pyridine was stirred for 96 h at 25° and subsequently added to petroleum ether, adamantanethione (**2**) could be isolated by evaporation of the washed (H_2O) and dried pink–orange supernatant, in 40–55% yield, as a red–orange crystalline[2] solid that could be sublimed readily at 85° and 15 mm, m.p. 173–174°. Its ultraviolet spectrum (*n*-hexane) shows a maximum at 240 mμ (ε with 12 700) a shoulder at 223 mμ; in the visible region (*n*-hexane) it has maxima at 488 mμ (ε 11.3) and 554 mμ (ε 2.7). The band at 488 mμ shows some fine structure as has been observed in the case of other thiones (3). The n.m.r. spectrum of the compound (in CCl_4) shows a broad singlet at τ 6.60 (2H) and a singlet at τ 7.96 (12H). The two bridgehead hydrogens adjacent to the thiocarbonyl group are more strongly deshielded than the corresponding hydrogens in adamantanone, which absorb under identical conditions at τ 7.58. This is another example of the larger anisotropy effect of the thiocarbonyl group as compared to the carbonyl group (4).

Very recently we discovered a new method for the preparation of adamantanethione from the ketone (**1**) via 2-ethoxy-2-adamantanethiol (**3**). The latter compound was prepared according to a reported method (5) and obtained as a colorless solid in a yield of 57%, m.p. 30.5–31.5°. Its infrared (i.r.) spectrum (neat) shows a weak absorption at 2560 cm^{-1} (attributed to the thiol group), its n.m.r. spectrum (in CCl_4) a quartet at τ 6.41 (2H, J = 7 Hz), a triplet at τ 8.84 (3H, J = 7 Hz), a singlet at τ 8.68 (1H) and a complex multiplet between τ 7.5 and 8.6 (14H). When 2-ethoxy-2-adamantanethiol (**3**) was heated for 60 min at 100–130° at 15–100 mm, the colorless liquid turned gradually into a red–orange solid. The product was almost pure adamantanethione (**2**), obtained in yields as high as 93%. The smooth preparation of a thioketone by elimination of an alcohol from a geminal alkoxythiol has not yet been reported to our knowledge.

As it seemed that reduction of the thione might

[1]To whom correspondence should be addressed.

[2]Satisfactory elemental analyses were obtained for all new compounds. Melting points were taken in sealed capillary tubes (liquid bath) and are uncorrected. The nuclear magnetic resonance (n.m.r.) spectra were run at 60 or 100 MHz in the solvent indicated, with tetramethylsilane as an internal standard.

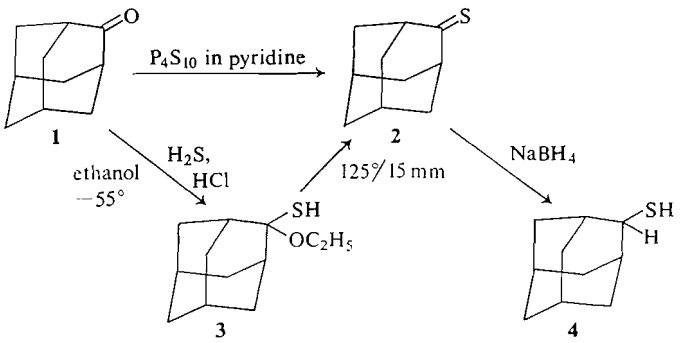

be a convenient route to 2-adamantanethiol (**4**), adamantanethione was treated with an equimolar quantity of sodium borohydride in 1,2-dimethoxyethane. The orange color of the solution disappeared rapidly and 2-adamantanethiol (**4**) was obtained in a yield of 79%. Sublimation in a vacuum (15 mm) at 85° was a convenient method of purification, giving a product with m.p. 160–161°. Its n.m.r. spectrum (CCl_4) shows between τ 7.5 and 8.7 a broad multiplet (14H) with a pattern typical for a 2-substituted adamantane (6), and two doublets at τ 8.53 and 6.68 for the spin-coupled ($J = 7$ Hz) proton of the thiol group and the hydrogen at C-2, respectively. For further characterization of the thiol, 2-adamantyl 3,5-dinitrothiolbenzoate, m.p. 171–172°, and 2-(methylsulfonyl)adamantane, m.p. 113–114°, were prepared. The thiolester shows in the i.r. spectrum (KBr disk) a strong absorption at 1660 cm^{-1} (C=O).

With the methods described a new, comparatively very stable alicylic thioketone and 2-adamantanethiol have become accessible. Further studies of the properties of these and related compounds are in progress.

Acknowledgment

Financial assistance of the National Research Council of Canada and of the University of Calgary for this work is gratefully acknowledged.

1. S. Bleisch and R. Mayer. Chem. Ber. **100**, 93 (1967).
2. (*a*) E. Campaigne. *In* The chemistry of the carbonyl group. 1st ed. *Edited by* S. Patai. Interscience Publishers, New York, N.Y. 1966. Chapter 17; (*b*) R. Mayer, J. Morgenstern, and J. Fabian. Angew. Chem. Intern. Ed. Engl. **3**, 277 (1964); (*c*) A. Schönberg. *In* Methoden der organischen chemie. Vol. IX, 4th ed. *Edited by* E. Müller. G. Thieme Verlag, Stuttgart. 1955. p. 704.
3. J. Fabian and R. Mayer. Spectrochim. Acta, **20**, 299 (1964).
4. (*a*) A. Ohno, T. Koizumi, and G. Tsuchihashi. Tetrahedron Letters, 2083 (1968); (*b*) S. Searles and D. L. Sinclair. 157th National Meeting of the American Chemical Society, Minneapolis, Minn., April 1969, Abstr. No. ORGN 128.
5. M. Demuynck and J. Vialle. Bull. Soc. Chim. France, 1213 (1967).
6. F. W. van Deursen and P. K. Korver. Tetrahedron Letters, 3923 (1967).

Can. J. Chem. Downloaded from www.nrcresearchpress.com by 210.87.254.42 on 09/05/12
For personal use only.

Can. J. Chem. Downloaded from www.nrcresearchpress.com by 210.87.254.6 on 09/05/12
For personal use only.

Canadian Journal of Chemistry

Published by THE NATIONAL RESEARCH COUNCIL OF CANADA

VOLUME 47 OCTOBER 15, 1969 NUMBER 20

An estimation of the magnitudes of the contributions from spin polarization and from hyperconjugation to the hyperfine splitting constant of an hydroxylic proton

T. E. GOUGH[1] AND G. A. TAYLOR

Department of Chemistry, University of Waterloo, Waterloo, Ontario

Received April 21, 1969

Proton hyperfine splitting constants of monoprotonated *p*-benzosemiquinone are presented for a range of solvents and sample-temperatures. The dependences of these splittings upon temperature, together with the assumption that the hydroxyl group can be described as a torsional harmonic oscillator, are used to evaluate an equation linking a_{OH}, the hyperfine splitting constant of the hydroxylic proton, in gauss, with ρ_O and ρ_C, the spin densities on the hydroxyl oxygen and on the adjacent carbon atoms, and θ, the dihedral angle between the O—H bond and the plane of the aromatic ring.

$$a_{OH} = -19\rho_O + 30\rho_C \langle \sin^2 \theta \rangle$$

Experimental evidence of a positive contribution to a_{OH} is obtained from the spectra of monoprotonated durosemiquinone in tri-*n*-butylphosphate at elevated temperatures.

Canadian Journal of Chemistry, 47, 3717 (1969)

Introduction

Ultraviolet irradiation of neutral solutions of quinones results in the formation of monoprotonated semiquinone radicals, of the general

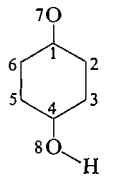

FIG. 1. Structural formula of monoprotonated *p*-benzosemiquinone and the numbering system employed in the present text.

formula shown in Fig. 1, which have been characterized by their electronic (1, 2) and electron spin resonance (3–5) spectra. The latter show that protonation of the semiquinone causes a major redistribution in unpaired electron density; positions ortho to the hydroxyl group carry a small negative spin density (of the order of -0.02) while the meta positions carry an appreciable positive spin density (of the order of $+0.2$). When the medium is sufficiently viscous, the hyperfine splitting pattern of the hydroxylic proton is broadened to high field (see e.g. Fig. 2 of ref. 6), indicating a negative splitting constant for this proton (7).

It is clear (4, 8) that two opposing contributions determine the magnitude and sign of the hyperfine splitting constant of the proton of a hydroxyl group substituted into an aromatic system containing an unpaired electron. Conjugation between the oxygen and aromatic π-systems will place unpaired electron density on the oxygen. This unpaired electron density, ρ_O, will spin-polarize the electrons of the O—H bond, in a manner analogous to that postulated by McConnell for an aromatic CH fragment (9), thereby generating a negative proton hyperfine interaction proportional to ρ_O.

Following the derivation of McConnell and Strathdee (10), Derbyshire calculated a proportionality constant for this interaction of -14 G (11); these calculations involved the assumption that the OH bond has 40% ionic character. However, whenever rotation about the C—O bond places the hydroxylic proton out of the nodal plane of the aromatic π-system, direct

[1]To whom all correspondence should be addressed.

Can. J. Chem. Downloaded from www.nrcresearchpress.com by 210.87.254.6 on 09/05/12
For personal use only.

overlap between this system and the proton will result in a positive hyperfine interaction. The size of this interaction will be determined by ρ_C, the unpaired spin density at the substituted carbon, and also by θ, the dihedral angle between the plane of the aromatic ring and the direction of the O—H bond. Quantitatively, for the radical $HO.CH.CO_2^-$ trapped in anhydrous lithium glycollate, $\theta = 56°$, while in lithium glycollate monohydrate, $\theta = 0°$, the corresponding splittings being $+14$ and -2.5 G (12). Taking ρ_C as 0.78 and neglecting spin-polarization in the O—H bond, Whiffen proposed (12) a hyperconjugative interaction of the form

$$[1] \qquad a_{OH} = (-3.2 + 31 \sin^2 \theta)\rho_C \quad \text{G}$$

The small negative term probably reflects the presence of a significant contribution to a_{OH} from a spin-polarization mechanism.

For the experimental determination of these proportionality constants for a radical in solution, it is necessary to allow for torsional oscillations of the OH group which will cause the time averaged value of $|\theta|$ to be non-zero. The effects of torsional oscillations on the ^{14}N and ^1H hyperfine splitting constants of the amino group of the 4-amino-2,6-di-*t*-butylphenoxy radical have been invoked (13) to interpret the temperature dependence (14) of these splitting constants. In this work we apply similar arguments to the hydroxyl group of monoprotonated-*p*-benzosemiquinone, thereby assuming that the equilibrium configuration of the radical is planar, and that the hydroxyl group may be described as a torsional harmonic oscillator, populating all its vibrational states according to Boltzmann statistics.

With these assumptions, it may be shown (13) that

$$[2] \qquad \langle\theta^2\rangle = \frac{h\nu}{2\kappa} \coth\left(\frac{h\nu}{2kT}\right)$$

where ν is the fundamental frequency of the vibration and κ is the associated force constant. Measurement of the temperature dependence of the hyperfine splitting constant of a hydroxyl group, together with calculations of θ, ρ_C, and ρ_O, will therefore allow an evaluation of the magnitudes of the hyperconjugative and spin-polarization mechanisms contributing to this splitting.

Experimental

The apparatus used for the production of semiquinone radicals, and for the observation of their electron spin resonance spectra, has been described previously (6). Solutions were prepared "in vacuo" because the presence of small amounts of water was found to have some effect on the measured hyperfine splitting constants, and on their variations with changes in temperature. *p*-Benzoquinone-$^{13}C_1$ (52% isotopic purity) was purchased from Merck, Sharp, and Dohme.

Results

The general structural formula of the radicals under investigation, and the numbering system used are given in Fig. 1.

Electron spin resonance spectra of monoprotonated *p*-benzosemiquinone, dissolved in a number of solvents, were recorded over as wide a range of temperatures as possible. The maximum attainable temperature was determined by boiling the solvent; lack of resolution of the components of the spectrum at reduced temperatures determined the lower limit at which observations were made.

The experimentally determined hyperfine splitting constants are given in Table I, where numerical subscripts are used to relate splitting constants to the numbering system of Fig. 1. Thus, a_i is the measured hyperfine splitting constant of the hydrogen bonded to atom i of the molecule. In every spectrum a_3 was found to equal a_5; however, at reduced temperatures, when rotation of the hydroxyl group was slow, a_2 and a_6 were found to differ by approximately 0.35 G (6). In all cases, the value reported in Table I for a_2 is the mean meta splitting constant; at high temperatures rotation of the hydroxyl group effected the averaging, while at low temperatures the averaging was performed numerically. The signs given to the hyperfine splitting constants are those determined in a previous investigation of monoprotonated *p*-benzosemiquinone (4).

Experiments using benzoquinone labelled with 52% ^{13}C at position 1 of the parent quinone (26% labelling at either C_1 or C_4 of the radical) were undertaken to obtain further data with which to evaluate the spin density distribution of the radical. However, such experiments were not in general successful; anisotropic effects, as might be expected, were particularly severe for the ^{13}C splittings, yet it was only in viscous solvents that relatively large stationary-state concentrations of radicals were obtained. Table II contains the experimentally determined hyperfine splitting constants; the signs of the splitting constants, and their assignments to position 1 or 4, were determined from the direction of the

TABLE I

Experimental proton hyperfine splitting constants in gauss, of monoprotonated *p*-benzosemiquinone*

Solvent	Temperature (°K)	Splitting constant (G) a_8	a_2	a_3
Methanol	337	−1.731	0.325	−5.170
	325	−1.775	0.316	−5.170
	316	−1.819	0.294	−5.120
	306	−1.875	0.287	−5.100
	295	−1.895	0.251	−5.100
	287	−1.875	0.250	−5.075
	277	−1.930	0.225	−5.070
	267	−1.950	0.210	−5.010
	259	−1.987	0.200	−5.000
	248	−2.013	0.181	−5.000
	238	−2.060	0.164	−5.000
	228	−2.138	0.148	−4.980
	215	−2.130	0.138	−4.980
	207	−2.138	0.125	−4.980
Ethanol	337	−1.725	0.350	−5.150
	320	−1.725	0.325	−5.125
	307	−1.831	0.312	−5.150
	292	−1.870	0.275	−5.110
	281	−1.925	0.250	−5.090
	271	−1.925	0.240	−5.070
	264	−1.948	0.224	−5.030
	253	−1.981	0.231	−5.070
	243	−1.980	0.200	−5.050
	234	−2.045	0.175	−5.020
	222	−2.050	0.188	−5.050
	209	−2.090	0.175	−4.950
	205	−2.120	0.169	−5.020
Isopropanol	371	−1.538	0.456	−5.300
	359	−1.619	0.444	−5.250
	346	−1.650	0.413	−5.275
	337	−1.719	0.381	−5.220
	325	−1.719	0.350	−5.200
	312	−1.863	0.325	−5.150
	297	−1.875	0.288	−5.163
	286	−1.925	0.275	−5.075
	276	−1.925	0.263	−5.138
	263	−1.988	0.238	−5.075
	252	−1.963	0.255	−5.100
	242	−1.994	0.206	−5.060
Tetrahydrofuran	327	−1.450	0.838	−5.725
	315	−1.494	0.813	−5.688
	305	−1.550	0.763	−5.700
	294	−1.563	0.769	−5.675
	285	−1.600	0.738	−5.675
	275	−1.600	0.750	−5.638
	263	−1.763	0.713	−5.612
	253	−1.763	0.675	−5.612
	243	−1.783	0.688	−5.725
	233	−1.806	0.720	−5.610
	225	−1.793	0.663	−5.625
	213	−1.851	0.683	−5.560
	201	−1.856	0.644	−5.570
	189	−1.888	0.663	−5.550
2-Methyltetrahydrofuran	298	−1.540	0.819	−5.750
	287	−1.575	0.813	−5.760
	284	−1.588	0.794	−5.713
	272	−1.613	0.825	−5.713
	256	−1.663	0.775	−5.750
	239	−1.719	0.738	−5.675
	236	−1.756	0.713	−5.660
	230	−1.738	0.726	−5.650

Can. J. Chem. Downloaded from www.nrcresearchpress.com by 210.87.254.6 on 09/05/12
For personal use only.

Can. J. Chem. Downloaded from www.nrcresearchpress.com by 210.87.254.6 on 09/05/12
For personal use only.

TABLE I (*Concluded*)

Solvent	Temperature (°K)	Splitting constant (G) a_8	a_2	a_3
	220	−1.813	0.700	−5.678
	213	−1.819	0.694	−5.675
	202	−1.893	0.663	−5.663
	191	−1.938	0.650	−5.650
	179	−1.956	0.663	−5.613
Tri-*n*-butylphosphate	374	−1.425	0.750	−5.613
	363	−1.450	0.750	−5.625
	354	−1.500	0.750	−5.625
	342	−1.525	0.750	−5.575
	328	−1.563	0.731	−5.638
	319	−1.588	0.738	−5.570
	307	−1.613	0.700	−5.625
	298	−1.668	0.706	−5.570
	291	−1.681	0.688	−5.590
	279	−1.750	0.688	−5.625
	271	−1.713	0.669	−5.560

*Error in measurements between ± 0.01 G at high temperatures and ± 0.05 G at low temperatures.

TABLE II

Experimental and calculated ^{13}C hyperfine splitting constants of monoprotonated *p*-benzosemiquinone

Solvent	Temperature (°K)	Position*	Splitting constant (G) Experimental	Calculated† $\nu = 300\,cm^{-1}$	$\nu = 320\,cm^{-1}$
Tri-*n*-butylphosphate	330	1	−4.8	−3.6	−3.0
Tri-*n*-butylphosphate	330	4	+4.4	—	—
i-Propanol	300	1	−3.5	−2.3	−2.1
i-Propanol	300	4	+4.1	—	—

*Carbon atoms numbered as in Fig. 1.
†For details of calculations, see text.

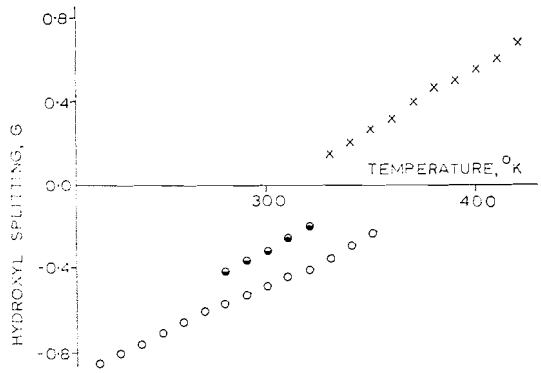

FIG. 2. Experimentally determined hyperfine splitting constants of the hydroxylic proton of monoprotonated durosemiquinone plotted as a function of temperature; solvent equals: ×, tri-*n*-butylphosphate; ◒, *i*-propanol; ○, tetrahydrofuran.

anisotropic broadening, in conjunction with the known (3) gross features of the spin density distribution.

Measurements were also made of a_8 for monoprotonated durosemiquinone in *i*-propanol, tetrahydrofuran, and tri-*n*-butylphosphate at various temperatures. The results are given diagramatically in Fig. 2; the signs used for a_8 in these systems are discussed below.

Discussion

Since both spin-polarization and hyperconjugative mechanisms contribute to the hyperfine splitting of the hydroxylic proton of monoprotonated *p*-benzosemiquinone, we may write

$$[3] \qquad a_8 = Q_\pi \rho_8 + Q_\sigma \rho_4 \langle \sin^2 \theta \rangle$$

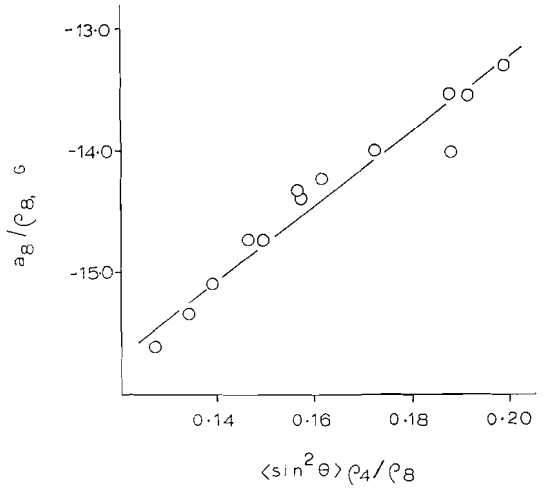

FIG. 3. The plot of a_8/ρ_8 vs. $\langle \sin^2\theta \rangle \rho_4/\rho_8$ for monoprotonated *p*-benzosemiquinone in 2-methyltetrahydrofuran. In generating these points the torsional frequency of the hydroxyl group was taken as 300 cm^{-1}.

or rearranging

$$[4] \qquad a_8/\rho_8 = Q_\pi + Q_\sigma \langle \sin^2\theta \rangle \rho_4/\rho_8$$

where Q_π and Q_σ are the proportionality constants governing the two interactions. Thus a plot of a_8/ρ_8 against $\langle \sin^2\theta \rangle \rho_4/\rho_8$ should be a straight line of slope Q_σ and intercept Q_π. Evaluation of Q_σ and Q_π, therefore, requires knowledge of θ, ρ_4, and ρ_8; evaluation of θ, in turn, requires knowledge of ν and κ (see eq. [2]). The fundamental torsional frequency of the hydroxyl group of phenol has been quoted as occurring at 300 (15), 310 (16), and 320 cm^{-1} (17). We have performed calculations using both extreme values of ν; the corresponding values of κ are 2400 and 2730 cm^{-1} radian^{-2}. In applying these values to the present system, we have assumed that the extra π-electon of the radical does not cause too drastic an increase in ν. Parenthetically, it may be noted that the corresponding value of ν for methanol is 270 cm^{-1} (18).

Calculations of ρ_4 and ρ_8 were performed for each sample, at each temperature, using McLachlan's self-consistent field theory (19). Parameters for the inclusion of the heteroatoms O_7 and O_8 were chosen using methods similar to those already found satisfactory for semiquinone anions (20) and radicals (6). The following parameters, using conventional notation (21), were employed: $\lambda = 1.20$, $h_0 = 1.42$ and 1.17 in protic and aprotic solvents, respectively (22), $k_{C_1O_7} = 1.46 + \Delta$, $k_{C_4O_8} = (1.46 - \Delta)\cos\theta$, where Δ is an adjustable parameter, θ is as defined above, and the value of 1.46 is the optimum value of k_{CO} for symmetrical *p*-benzosemiquinone (22). Thus protonation at O_8 was simulated by increasing the bond order of C_1O_7 and decreasing the bond order of C_4O_8 in keeping with the various valence-bond structures which may be drawn to place high spin density at C_2 and C_6, but not at C_3 and C_5. The factor $\cos\theta$ was applied to $k_{C_4O_8}$ to simulate the decrease in overlap brought about by out-of-plane bending of the hydroxyl group; $\cos\theta$ was evaluated at each temperature, but was assumed independent of solvent.

Once the above numerical constants were fixed, there remained one arbitrary parameter, Δ, with which to describe the effects of solvation upon the spin density distribution (cf. ref. 3). For example, at each temperature Δ was varied, in steps of 0.01, to obtain the optimum agreement between the calculated ratio ρ_2/ρ_3 and the experimental ratio a_2/a_3. In such calculations, a value for $Q_{CH}{}^H$ need not be assigned; however, in all cases the calculated ratio a_2/ρ_2 was found to be close to -24 G, indicating that reasonable spin density distributions were obtained.

From the appropriate calculated and experimental data, numerical values of a_8/ρ_8 and $\langle \sin^2\theta \rangle \rho_4/\rho_8$ were determined and fitted, by the method of least squares, to the straight line represented by eq. [4]. Results for Q_π, Q_σ, and the root-mean-square error (of a_8/ρ_8) are given in Table III. The plot for the results obtained in the solvent 2-methyltetrahydrofuran is given in Fig. 3 ($\nu = 300$ cm^{-1}).

The results for both Q_σ and Q_π fall into two groups, protic and aprotic. It is felt that this difference is to be attributed to the choice of h_0 used for the protic solutions; the value of $h_0 = 1.42$ was derived as the optimum parameter for *p*-benzosemiquinone in a 30–70% water–ethanol mixture (22), a medium of considerably greater solvating power than the three protic solvents used in the current work. Therefore, the value of h_0 used is too high; a value of $h_0 \sim 1.30$ gives good agreement between the results for protic and aprotic solvents. Thus a value of -19 G would seem to be a suitable value for the proportionality constant of the spin-polariza-

Can. J. Chem. Downloaded from www.nrcresearchpress.com by 210.87.254.6 on 09/05/12
For personal use only.

Can. J. Chem. Downloaded from www.nrcresearchpress.com by 210.87.254.6 on 09/05/12
For personal use only.

TABLE III

Calculated values of Q_σ and Q_π for the hydroxylic proton of monoprotonated *p*-benzosemiquinone

Solvent	Q_σ (G)		Q_π (G)		Root-mean-square* error (G)	
	$\nu = 300\,cm^{-1}$	$\nu = 320\,cm^{-1}$	$\nu = 300\,cm^{-1}$	$\nu = 320\,cm^{-1}$	$\nu = 300\,cm^{-1}$	$\nu = 320\,cm^{-1}$
Methanol	27.8	38.4	−23.5	24.3	0.19	0.31
Ethanol	26.0	33.7	−23.1	23.4	0.22	0.24
i-Propanol	26.3	33.0	−23.4	23.5	0.27	0.27
Tetrahydrofuran	32.6	41.1	−19.5	−19.7	0.28	0.28
2-Methyltetrahydrofuran	30.4	38.6	−19.3	−19.5	0.18	0.12
Tri-*n*-butylphosphate	29.3	40.1	−18.8	−19.5	0.37	0.28

*Root-mean-square error in fitting data to straight line represented by eq. [4].

Can. J. Chem. Downloaded from www.nrcresearchpress.com by 210.87.254.6 on 09/05/12
For personal use only.

tional contribution to the hyperfine splitting constant of a hydroxylic proton. This value is in satisfactory agreement with the calculated value of -14 G put forward by Derbyshire (11). The value of Q_π is not a function of ν (within the error involved in fitting the data) since it is obtained by extrapolation to the point where $\theta = 0$.

The value of Q_σ depends on the choice of ν; however, it would seem that a value of Q_σ between 30 and 40 G would be appropriate. The value suggested by Whiffen is 31 G, an agreement which is noteworthy, since much poorer agreement was obtained for the C—N—H fragment (suggested values of Q_σ: for γ-irradiated glycine 38 G (12); for the 4-amino-2,6-di-*t*-butylphenoxy radical 143 G (13)). Although some of this discrepancy may be due to the difference in charge density between the two systems, it would seem that the assumption of a planar equilibrium configuration for the amino group of the aminophenoxy radical (13) is unjustified, and that, as in aniline (23), the nitrogen is pyramidal. Similarly, the agreement between the presently obtained value and that of Whiffen support the assumption that monoprotonated *p*-benzosemiquinone is planar in its equilibrium configuration.

If the hydroxyl proton of a monoprotonated semiquinone is placed sufficiently far out of the plane of the aromatic ring, then the hyperconjugative mechanism will predominate, and a positive value for a_8 will be observed. Previous experiments (3) have shown that for monoprotonated durosemiquinone the ratio a_8/ρ_8 is extremely sensitive to the solvent employed. The results are consistent with the hypothesis (4) that larger solvent molecules, by reinforcing the steric effects of the *ortho* methyl groups, cause the hydroxyl group to be further from the plane of the aromatic ring. Accordingly, we have examined spectra of monoprotonated durosemiquinone, at high temperatures, in tri-*n*-butylphosphate, which has the largest molar volume of the solvents suitable for the present experiments. As may be seen from Fig. 2, the temperature dependence of $|a_8|$ is the reverse of that observed for all other systems, suggesting that under these extreme conditions a_8 is positive. Confirmation of the postulated positive sign is provided by the fact that, unlike the other systems, the components of the OH doublet broaden to low rather than high field.

The results for Q_σ and Q_π are dependent upon calculations of spin densities, and hence upon the choice of input parameters. A detailed study of the ^{13}C hyperfine splitting constants of positions 1 and 4, over a range of temperatures and solvents, would have allowed us to eliminate our arbitrary assignments of h_0 and k_{CO}, and to replace them by values chosen to give the best fit between calculated and observed hyperfine splitting constants. However, we were unable to obtain a sufficiently comprehensive set of data for this purpose. It is of interest, nevertheless, to calculate, from the spin density distributions used to evaluate Q_σ and Q_π, the expected ^{13}C hyperfine splitting constants, and to compare them with the experimental values. Using standard notation (24)

$$[5]\quad a_1^C = (S^C + 2Q_{CC'}^C + Q_{CO}^C)\rho_1 + Q_{C'C}^C(\rho_2 + \rho_6) + Q_{OC}^C\rho_7$$

a similar equation holding for a_4^C. We take $S^C = -12.7$ G, $Q_{CC'}^C = 14.4$ G, and $Q_{C'C}^C = -13.9$ G (25). The values of Q_{CO}^C and Q_{OC}^C have been shown to be dependent upon the chemical identity of the CO bond; for the *p*-benzosemiquinone anion, values of Q_{CO}^C and Q_{OC}^C of 17.7 and -27.1 G, respectively, have been given (24), while for the phenoxy radical the corresponding values are 8.9 and 16.4 G (26).

The monoprotonated *p*-benzosemiquinone radical may be regarded as the 4-hydroxyphenoxy radical, so that a_1^C may be calculated using $Q_{CO}^C = 8.9$ G, $Q_{OC}^C = 16.4$ G. Unfortunately, similar parameters to allow the evaluation of a_4^C, a more crucial calculation in the present context, are not available.

Calculated and experimental ^{13}C hyperfine splitting constants are given in Table II. The agreement between calculation and experiment is as good as might be expected since the calculation involves the summation of larger terms of opposite signs. Furthermore, the extreme sensitivity to chemical environment of Q_{CO}^C and Q_{OC}^C introduces some uncertainty as to the values to be used for these parameters. Thus the limited data so far available for ^{13}C hyperfine splitting constants indicate that the calculated spin density distributions satisfactorily approximate the actual distributions.

The calculations using $\nu = 300\ cm^{-1}$ more closely approximate the observed ^{13}C hyperfine

splitting constants, indicating that a value of $Q_\sigma = 30$ G (cf. 31 G, ref. 12) is to be preferred. Thus the hyperfine splitting constant of a hydroxylic proton in gauss may be described by eq. [6]

$$[6] \qquad a_{OH} = -19\rho_O + 30\rho_C\langle \sin^2 \theta \rangle$$

Acknowledgments

This work received financial support from the Ontario Department of University affairs and from the National Research Council of Canada.

1. N. K. Bridge and G. Porter. Proc. Roy. Soc. London, Ser. A, **244**, 259 (1958).
2. N. K. Bridge and G. Porter. Proc. Roy. Soc. London, Ser. A, **244**, 276 (1958).
3. T. A. Claxton, T. E. Gough, and M. C. R. Symons. Trans. Faraday Soc. **62**, 279 (1966).
4. T. E. Gough. Trans. Faraday Soc. **62**, 2321 (1966).
5. T. A. Claxton, J. Oakes, and M. C. R. Symons. Trans. Faraday Soc. **63**, 2125 (1967).
6. T. E. Gough. Can. J. Chem. **47**, 331 (1969).
7. A. Carrington and H. C. Longuet-Higgins. Mol. Phys. **5**, 224 (1962).
8. A. B. Barabas, W. F. Forbes, and P. D. Sullivan. Can. J. Chem. **45**, 267 (1967).
9. H. M. McConnell. J. Chem. Phys. **24**, 764 (1956).
10. H. M. McConnell and J. Strathdee. Mol. Phys. **2**, 129 (1959).
11. W. Derbyshire. Mol. Phys. **5**, 225 (1962).
12. D. A. Whiffen. Structure hyperfine magnetique des atomes et des molécules. Conseil National de Recherches Scientifiques, 167 (1967).
13. A. J. Stone and A. Carrington. Trans. Faraday Soc. **61**, 2593 (1965).
14. K. Scheffler and H. B. Stegman. Tetrahedron Lett. 3035 (1964).
15. J. C. Evans. Spectrochim. Acta, **16**, 1382 (1960).
16. S. Pinchas, D. Sadeh, and D. Samuel. J. Phys. Chem. **69**, 2259 (1965).
17. H. D. Bist, J. C. D. Brand, and D. R. Williams. J. Mol. Spectrosc. **21**, 76 (1966).
18. J. S. Koehler and D. M. Dennison. Phys. Rev. **57**, 1006 (1940).
19. A. D. McLachlan. Mol. Phys. **3**, 233 (1960).
20. P. S. Gill and T. E. Gough. Trans. Faraday Soc. **64**, 1997 (1968).
21. A. Streitweiser. Molecular orbital theory for organic chemists. John Wiley and Sons, Inc., New York. 1961. Chap. 5.
22. M. Broze, Z. Luz, and B. L. Silver. J. Chem. Phys. **46**, 4891 (1967).
23. D. G. Lister and J. K. Tyler. Chem. Commun. 152 (1966).
24. M. R. Das and G. K. Fraenkel. J. Chem. Phys. **42**, 1350 (1965).
25. M. Karplus and G. K. Fraenkel. J. Chem. Phys. **35**, 1312 (1961).
26. L. Gilbert and R. Kreilick. J. Chem. Phys. **48**, 3377 (1968).

Can. J. Chem. Downloaded from www.nrcresearchpress.com by 210.87.254.6 on 09/05/12
For personal use only.

Can. J. Chem. Downloaded from www.nrcresearchpress.com by 210.87.254.40 on 09/05/12
For personal use only.

Studies on the decomposition of tetra-alkylammonium salts in solution. Part II. Dependence of the activation parameters on the structure of the substrate[1]

J. T. BURNS AND K. T. LEFFEK
Department of Chemistry, Dalhousie University, Halifax, Nova Scotia

Received April 24, 1969

The enthalpy and entropy of activation for the decomposition reaction of seven tetra-alkylammonium iodides in chloroform solution have been measured. All the salts contained the benzyl group attached to the nitrogen atom and decomposed to yield benzyl iodide and a tertiary amine as the only products.

A Hammett free energy correlation is made and used to deduce the nature of the transition state, and a rationalization of the variation of the enthalpy and entropy of activation with the structure of the substrate is given.

Canadian Journal of Chemistry, 47, 3725 (1969)

Introduction

In the first paper of this series (1) the mechanism of the thermal decomposition of phenylbenzylallylmethylammonium iodide in chloroform solution was shown to be a unimolecular decomposition of the ammonium ion, very probably associated with another molecule of the ammonium iodide in the form of a triple ion. The reaction was found to have a high enthalpy of activation and a positive entropy of activation. The present work reports the activation parameters of seven other tetra-alkylammonium iodides, all of which contain the benzyl group and decompose in chloroform to form benzyl iodide, a tertiary amine, and no other product.

Results and Discussion

The products of the decomposition of each iodide were analyzed by vapor phase chromatography (v.p.c.). In each reaction only 2 product peaks were obtained which were identified as benzyl iodide and the aniline, by matching the retention times with those of pure samples under the same chromatographic conditions.

The specific reaction rates were measured conductometrically (1), in duplicate, at 5 different temperatures over a 15–20° range for each compound. Good straight line Guggenheim plots (2) were obtained in all cases, from which first order rate constants were obtained by a least squares analysis.

The first order rate constants are collated in Table I and the activation parameters derived from them, by least squares calculations using the transition state theory equation, are given in Table II.

Hammett Correlation

For the substituted phenyl compounds, a plot of $\log k$ vs. σ yields a ρ value of $+1.4$ for this reaction, confirming that the nitrogen atom has a reduced positive charge in the transition state, but not very much so. Values of ρ, calculated by Jaffé (3) from data by Laidler (4), for the quaternization of N,N-dimethylaniline with methyl iodide in nitrobenzene solution, range from -2.7 to -3.1 for various temperatures. Jaffé also calculated similar negative values from other work for the same reaction in different solvents (5, 6) and further examples were reported by Rossell (7).

In these reactions the movement of electrons is in a direction away from the benzene ring so that electron withdrawing substituents on the ring hinder the reaction. Since such substituents have positive σ values, ρ for these reactions is negative. The magnitude of ρ is similar to that obtained from the equilibrium constants for the protonation of dimethylanilines (8) and therefore indicates that the Menschutkin reaction has a product-like transition state with a large amount of charge development on the nitrogen atom, a conclusion which had been reached earlier (9) by a comparison of the entropy of reaction and the entropy of activation, although Rossell (7) has suggested that the similarity of the two entropies is not a general result. Now for the

[1]Presented at the autumn meeting of the Chemical Society, London, at Durham, England, September 1967.

TABLE I

Specific first order rate constants for the decomposition of tetra-alkylammonium iodides in chloroform solution

Alkylammonium iodide	T (°C)	$10^5 \times k$ (s^{-1})	Alkylammonium iodide	T (°C)	$10^5 \times k$ (s^{-1})
Phenylbenzyldimethyl	25.0	4.41	Phenylbenzylmethylethyl	25.0	4.93
	30.0	8.69		30.0	9.69
	35.0	16.7_6		35.0	19.1_9
	40.0	31.8_1		40.0	37.5_5
	45.0	62.1		45.0	71.2
Phenylbenzylmethyl-*n*-propyl	25.0	7.58	Phenylbenzylmethylallyl*	20.0	2.64
	30.0	15.1_9		25.0	5.53
	35.0	31.2_0		30.1	11.5_8
	40.0	59.8_9		35.0	23.8
	45.0	$118._3$		40.0	47.7
				45.1	93.3
p-Methylphenylbenzyldimethyl	35.0	11.36	*p*-Methoxyphenylbenzyldimethyl	35.0	9.47
	40.0	21.2_3		40.0	17.1
	43.0	30.7_7		45.0	29.5
	45.0	38.4_3		48.0	41.7
	48.0	54.5		50.0	51.7
	50.0	68.2			
	52.0	86.7			
p-chlorophenylbenzyldimethyl	30.0	20.7	*p*-Bromophenylbenzyldimethyl	25.0	20.0
	35.0	39.1		30.0	56.5
	40.0	82.9		35.0	86.0
	43.0	$120._5$		40.0	116.2
	45.0	$158._3$		45.0	$173._1$

*Reference 1.

TABLE II

Activation parameters for the decomposition of tetra-alkylammonium iodides in chloroform solution

Alkylammonium iodide	$\Delta H^{\ddagger}$(kcal $mole^{-1}$)†	$\Delta S^{\ddagger}$(cal $mole^{-1}$ deg^{-1})†	$\Delta G^{\ddagger}$(kcal $mole^{-1}$)§
Phenylbenzyldimethyl	24.0±0.2	2.1±0.7	23.4
Phenylbenzylmethylethyl	24.7±0.1	4.6±0.3	23.3
Phenylbenzylmethyl-*n*-propyl	25.2±0.2	7.5±0.5	23.0
Phenylbenzylmethylallyl*	25.9±0.1	8.9±0.2	23.2
p-Methoxyphenylbenzyldimethyl	21.7±0.1	−6.7±0.1	23.7
p-Methylphenylbenzyldimethyl	23.1±0.1	−1.8±0.2	23.6
Phenylbenzyldimethyl	24.0±0.2	2.1±0.7	23.4
p-Chlorophenylbenzyldimethyl	25.6±0.2	9.1±0.6	22.9
p-Bromophenylbenzyldimethyl	26.8±0.3	13.1±0.9	22.8

*Reference 1.
†Numbers after ± signs are for standard deviation.
§Calculated at 35 °C. Standard deviations would be very similar to those quoted for $\Delta H^{\ddagger}$.

reverse Menschutkin reaction, according to the principle of microscopic reversibility, the transition state would be expected to be reactant-like, that is, it should occur before the electrons bonding the benzyl group to the nitrogen have been transferred to the nitrogen to any large extent. Thus the magnitude of ρ should be small and, since the movement of electrons is in the reverse direction to that in the Menschutkin reaction, i.e., towards the phenyl ring, the sign of ρ should be positive. The value of +1.4 obtained for this reaction is in accord with such a transition state.

Activation Parameters

The compounds listed in Table II fall into 2 series, the first with various alkyl groups replacing one of the methyl groups on the nitrogen atom and the second with para-substituted phenyl groups.

In the first series the free energies of activation, which may be assumed to have the same

Can. J. Chem. Downloaded from www.nrcresearchpress.com by 210.87.254.40 on 09/05/12
For personal use only.

Can. J. Chem. Downloaded from www.nrcresearchpress.com by 210.87.254.40 on 09/05/12
For personal use only.

standard deviations as the corresponding enthalpies of activation, are constant within the experimental error. The enthalpies and entropies of activation do appear to change with the alkyl group attached to the nitrogen atom, but the changes are not large compared to twice the standard deviations so that the interpretation must be cautious. On the other hand, the second para-substituted phenyl series shows definite changes in $\Delta H^{\ddagger}$ and $\Delta S^{\ddagger}$ which do not cancel exactly and hence the free energies of activation show a slight change with substrate structure.

Since the free energies of activation for all eight compounds are within a range of 0.9 kcal/mole there is a good correlation between $\Delta H^{\ddagger}$ and $\Delta S^{\ddagger}$, but the significance of these correlations is by no means established (10–12). It has been suggested (11) that a relation between $\Delta H^{\ddagger}$ and $\Delta S^{\ddagger}$ can be established by plotting the activation energy against the logarithm of the rate constant. Such a graph can be plotted of $\Delta H^{\ddagger}$ (from Table II) against log k, at 35° (from Table I). A reasonable correlation exists, although the points are, of course, more scattered than those for a $\Delta H^{\ddagger}$ vs. $\Delta S^{\ddagger}$ plot. However, little can be concluded from this, other than the reactions of this series all proceed by the same mechanism, which serves only as a confirmation of what has already been assumed implicitly. Therefore, it seems more reasonable to try to interpret the activation parameters directly, in qualitative terms of what factors may be assumed to contribute to their magnitude. Several groups of workers have discussed the Menschutkin reaction in terms of factors arising from within the substrate molecule and those from solvation effects, especially with respect to changes in rate with pressure. These have been summarized recently by Weale (13) who concluded that "bonding" and "solvation" effects were of roughly equal importance for a Menschutkin reaction, but that solvation effects were dominant for the reverse Menschutkin reaction. This may also be inferred simply from the extent of the solubility of these ammonium salts and the ease with which the decomposition reactions proceed in chloroform.

Thus the enthalpy and entropy of activation will be considered to arise from contributions from within the substrate molecule ($\Delta H^{\ddagger}_{\text{int.}}$ and $\Delta S^{\ddagger}_{\text{int.}}$) and from solvent reorganization ($\Delta H^{\ddagger}_{\text{solv.}}$ and $\Delta S^{\ddagger}_{\text{solv.}}$).

With increasing electron release by substituent groups towards the nitrogen atom $\Delta H^{\ddagger}_{\text{int.}}$ should increase, since the electrons from the benzyl carbon atom will be less easily transferred to the nitrogen. $\Delta S^{\ddagger}_{\text{int.}}$ will always be a positive entropy contribution in this unimolecular reaction, but its change in magnitude with substituent group will depend upon the relative extent of bond breaking which cannot be estimated beyond the conclusion reached from the value of ρ.

The contribution $\Delta H^{\ddagger}_{\text{solv.}}$ should decrease with increasing electron release towards the nitrogen atom because greater charge delocalization would yield a weaker solvation shell in the initial state which would require less energy to reorganize it during the activation process. $\Delta S^{\ddagger}_{\text{solv.}}$ may give a negative or positive contribution depending upon whether the positive charge is more or less concentrated in the transition state relative to the initial state. It is possible to imagine that with a strong electron releasing substituent group, the positive charge is extensively delocalized in the initial state and becomes more localized (on the benzyl carbon atom) during activation.

The experimental results may be rationalized to some extent in these terms as it is seen that electron releasing groups in the para position of the phenyl group give low $\Delta H^{\ddagger}$ and negative $\Delta S^{\ddagger}$ values while electron attracting groups give higher $\Delta H^{\ddagger}$ and positive $\Delta S^{\ddagger}$ values, consistent with the postulate that solvation changes are important in these reactions. For the compounds with various alkyl groups substituted on the nitrogen atom, the inductive charge delocalizations would be much less than for the para-substituted series and would change less with change of alkyl group. Thus for these reactions the solvation changes are of lesser importance giving positive $\Delta S^{\ddagger}$ values and generally activation parameters which do not change very much from one compound to the next.

Such a rationalization provides a clearer picture than the various correlations which can be made, and predicts that the relative activation parameters of the para-substituted series should be dependent upon the solvent, which dependence it is hoped to investigate in the immediate future.

In making a rationalization of this sort, attention is focused on one of several contributions

TABLE III

Preparation and physical data for tetra-alkylammonium iodides

Ammonium iodide	Solvent	Yield (%)	Melting point (°C)	Purity (%)
$C_6H_5 \cdot C_7H_7 \cdot (CH_3)_2N^+$	None	43	163–164	100.0
$C_6H_5 \cdot C_7H_7 \cdot CH_3 \cdot C_2H_5N^+$	None	45	139–140	99.9_5
$C_6H_5 \cdot C_7H_7 \cdot CH_3 \cdot C_3H_7 \cdot N^+$	None	42	147	99.9
$p\text{-}CH_3OC_6H_4 \cdot C_7H_7 \cdot (CH_3)_2N^+$	Acetone	75	140–141	99.8
$p\text{-}CH_3C_6H_4 \cdot C_7H_7 \cdot (CH_3)_2N^+$	None	54	156–157	99.9_5
$p\text{-}ClC_6H_4 \cdot C_7H_7 \cdot (CH_3)_2N^+$	Acetone	72	142–143	99.8
$p\text{-}BrC_6H_4 \cdot C_7H_7 \cdot (CH_3)_2N^+$	Benzene	53	137–138	99.9

to the activation parameters in the hope that the one, in this case "solvation effects", dominates the others. Although this approach is far from ideal, it is the only practical method of developing theories in kinetic studies.

Experimental

Materials

The quaternary ammonium iodides were prepared by reacting benzyl iodide, which had been purified by distillation at reduced pressure, with the appropriate tertiary amine in equimolar proportions, either with or without a solvent. The reaction mixture was usually allowed to stand several hours at room temperature before the solid product was separated by filtration, washed, dried, and recrystallized from ethanol or a mixture of ethanol and diethyl ether. Table III shows for each salt the yield, melting point, and % purity determined by potentiometric titration of the iodide ion against standard silver nitrate solution. Some of the melting points are a few degrees higher than those in the literature (14–16). N,N-dimethylaniline, N-methyl-N-ethylaniline, *p*-bromo-N,N-dimethylaniline, and *p*-methyl-N,N-dimethylaniline were commercial products purified by distillation.

N-methyl-N-propylaniline was prepared by the method of Claus and Hirzel (17). An equimolar mixture of N-methylaniline and *n*-propyl bromide was heated on a water bath for 5 h and the hard mass which resulted was dissolved in water. The unreacted starting materials were removed by extraction with diethyl ether. After treatment with concentrated NaOH solution the product was distilled twice (boiling range 216–218 °C). The yield was 69%.

p-Methoxy-N,N-dimethylaniline was prepared according to the method of Thomas *et al.* (18). An equimolar mixture of purified *p*-anisidine and trimethyl phosphate was refluxed for 2 h after the initial reaction had subsided. The mixture was then hydrolyzed for $1\frac{1}{2}$ h with NaOH solution, diluted with water, and the amine was isolated by extraction with diethyl ether. After drying and removal of the ether, the amine was twice distilled (239–240 °C) at atmospheric pressure. The yield was 42% and the melting point was 38–39 °C (ref. 18, 37–38.5 °C).

p-Chloro-N,N-dimethylaniline was prepared by the same method in a yield of 55%. The product had a boiling range 240–241 °C at atmospheric pressure and a melting point of 32–33 °C (ref. 18, 32–33.5 °C).

The chloroform solvent was Matheson, Coleman and Bell chromatoquality reagent 99.8%. Analysis by v.p.c. showed that this contained traces of hydrocarbon stabilizer and chlorinated hydrocarbons.

The kinetic measurements were made with 0.05 *M* solutions by the procedure described previously (1) and the duplicate kinetic runs in all cases fitted the Guggenheim equation as well as the run quoted in that paper (1).

Acknowledgment

The authors are grateful for financial support by the National Research Council of Canada.

1. K. T. Leffek and F. H-C. Tsao. Can. J. Chem. **46**, 1215 (1968).
2. E. A. Guggenheim. Phil. Mag. **2**, 538 (1936).
3. H. H. Jaffé. Chem. Rev. **53**, 191 (1953).
4. K. J. Laidler. J. Chem. Soc. 1786 (1938).
5. W. C. Davies and W. P. G. Lewis. J. Chem. Soc. 1599 (1934).
6. D. P. Evans, H. B. Watson, and R. Williams. J. Chem. Soc. 1345 (1939).
7. J. B. Rossell. J. Chem. Soc. 5183 (1963).
8. K. B. Wiberg. Physical organic chemistry. J. Wiley and Sons, Inc., New York. 1964. pp. 404–406.
9. S. Glasstone, K. J. Laidler, and H. Eyring. Theory of rate processes. McGraw-Hill Book Co. Inc., New York. 1941. p. 418.
10. R. C. Petersen, J. H. Markgraf, and S. D. Ross. J. Amer. Chem. Soc. **83**, 3819 (1961).
11. O. Exner. Coll. Czech. Chem. Commun. **29**, 1094 (1964).
12. O. Exner. Nature, **201**, 488 (1964).
13. K. E. Weale. Chemical reactions at high pressures. Spon Ltd., London. 1967, p. 145.
14. H. O. Jones. Proc. Cambridge Phil. Soc. **11**, 113 (1901).
15. H. O. Jones. J. Chem. Soc. **85**, 223 (1904).
16. E. Wedekind and E. Frolich. Ber. **38**, 3438 (1905).
17. A. Claus and H. Hirzel. Ber. **19**, 2785 (1886).
18. D. G. Thomas, J. H. Billman, and C. E. Davis. J. Amer. Chem. Soc. **68**, 895 (1946).

Can. J. Chem. Downloaded from www.nrcresearchpress.com by 210.87.254.40 on 09/05/12
For personal use only.

Can. J. Chem. Downloaded from www.nrcresearchpress.com by 210.87.254.6 on 09/05/12
For personal use only.

Oxidations involving silver. V. The oxidation of primary aliphatic amines

N. A. HAMPSON, J. B. LEE[1], J. R. MORLEY, AND B. SCANLON
Department of Chemistry, University of Technology, Loughborough, Leicestershire, England

Received March 24, 1969

Primary aliphatic amines are rapidly oxidized using a silver electrode at potentials more positive than 0.6 V normal hydrogen electrode (n.h.e.) in aqueous alkali. Primary aliphatic amines with a mono-substituted α-carbon atom give the corresponding nitrile and aldehyde, α,α-disubstituted ones give the corresponding ketone, and α,α,α-trisubstituted ones give the corresponding alcohol, nitro-compound, and unsaturated hydrocarbons. Some evidence for the reaction pathway is presented. The effect of amine on the kinetic parameters for Ag_2O formation is reported.

Canadian Journal of Chemistry, 47, 3729 (1969)

Introduction

In previous papers in the series, studies on the electrochemical oxidation of silver in aqueous alkali using galvanostatic (1) and potentiodynamic techniques (2) have been reported. We now report the results of experiments on the oxidation of primary amines at a silver electrode and the effect of added amine on the potentiodynamic current curves and kinetic parameters.

Barnes and Mann (3) have studied the oxidation of primary amines at platinum electrodes and found the predominant pathway involved breaking the carbon–nitrogen bond. Using different conditions Benkesser *et al.* (4) isolated trimethylhexahydro-*s*-triazine and formamide from the oxidation of methylamine at platinum. The chemical oxidation of primary amines with AgO has been reported (5). The oxidation of aliphatic amines at platinum (6) and carbon (7) has been investigated using cyclic voltammetry.

Experimental

Apparatus

Electrochemical cells made from borosilicate glass were of two types. The cell in which the potential sweep data were obtained has been described (2). Preparative oxidations were carried out in the cell shown in Fig. 1. This consisted of a working compartment (~ 35 ml capacity) which was separated from the counter electrode compartment by a glass frit (porosity 1). The reference electrode (a wick type standard calomel electrode) was contained in the third compartment connected to the working compartment by a horizontal Luggin capillary. Provision was made for N_2 purging of the working electrode compartment.

The working electrodes were made from silver (99.999%, Johnson–Matthey Limited) rod or sheet. The micro-electrodes used in potential sweep experiments have been described (2). Electrodes for preparative oxidations (~ 2.0 cm^2) were made from silver sheet sealed into polythene. The required area was achieved by trimming the polythene support. The counter electrode was silver gauze (~ 2 × 4 cm).

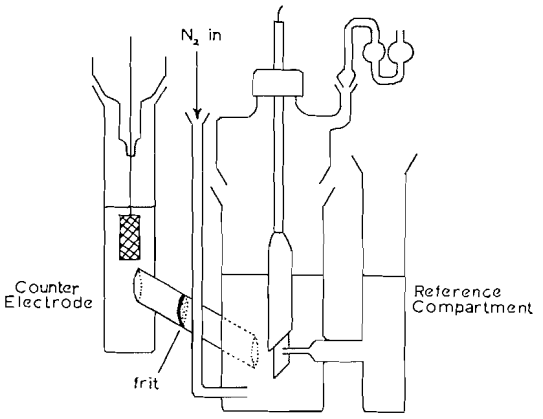

FIG. 1. Electrochemical cell used for preparative oxidations. Vertical plane electrode (2 cm^2) and horizontal Luggin capillary also shown.

The supporting electrolyte was aqueous sodium hydroxide solution prepared from A.R. sodium hydroxide (Fisons Chemicals Limited) and conductivity water.

The amines used were obtained commercially (B.D.H.) and were distilled and analyzed for impurities by gas–liquid chromatography (g.l.c.) immediately before use.

All the preparative experiments were carried out under potentiostatic conditions. Kinetic data were obtained using a fast response potentiostat coupled with either a pulse generator or a linear sweep generator (Chemical Electronics Ltd.). Preparative work was carried out using a potentiostat of higher output (~ 3 A) (Chemical Electronics Ltd.).

Experimental Methods

Potential Sweep Experiments

The general experimental technique has already been described (2). A fixed anodic potential sweep rate of

[1]To whom all correspondence should be addressed.

Can. J. Chem. Downloaded from www.nrcresearchpress.com by 210.87.254.6 on 09/05/12
For personal use only.

5.84×10^{-4} V s^{-1} was used over a potential range of 0.7 V starting at the reversible potential $Ag_2O/Ag/OH^-$ (1*M*). The resultant current–time curve was plotted on a chart recorder (Leeds and Northrup Ltd.).

Preparative Studies

Two main techniques were used. The first involved oxidation at a fixed potential. The effect of OH^- concentration, amine concentration, and electrode potential on the aldehyde/nitrile ratio was examined. The second technique involved the use of a repetitive sequence of square potential pulses (Fig. 2). The effect of pulse frequency, duty ratio, and starting potential on the aldehyde/nitrile ratio was determined.

The products were isolated by extraction of the electrolyte with diethyl ether. The ethereal solution was reduced in volume by distillation, dried over anhydrous sodium sulfate, and examined by g.l.c. (Pye 104) at high and low temperatures. Then the electrolyte was acidified and the analysis repeated. Components were identified by comparison with authentic samples on at least two stationary phases (from dinonylphthalate, silicone oil, carbowax 1500, and polyethylene glycol adipate). Internal standards were used for quantitative determinations.

Galvanostatic Experiments

The technique, cell, and electrodes have been described (1). Additions of amines were made to the electrolyte (1 *M* sodium hydroxide) which was not circulated through charcoal.

Results

At potentials, below that required for the formation of AgO, primary amines are only oxidized very slowly. This reflects the results of chemical oxidations of amines with Ag_2O in alkali which are also very slowly oxidized. Primary amines form a soluble complex with Ag_2O and this leads to the dissolution of the electrode.

The relative oxidation rates for primary amines at platinum and silver electrodes are illustrated by the potential sweeps shown in Fig. 3.

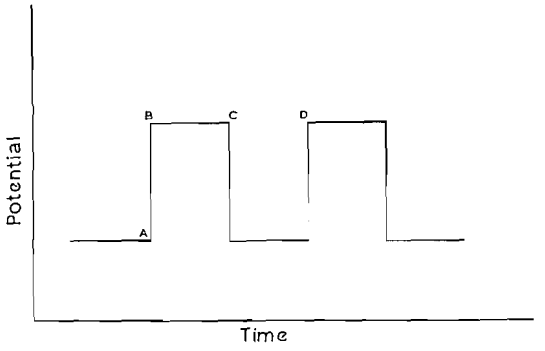

FIG. 2. Potential waveform used in repetitive potential pulse experiments; step height = AB, frequency = 1/BD, duty ratio = BC/BD.

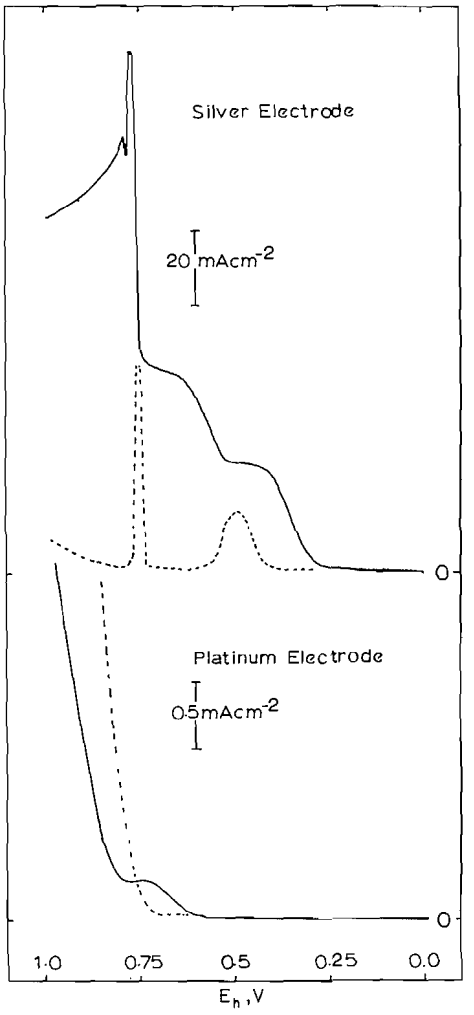

FIG. 3. Effect of electrode material on potentiodynamic current curve for *n*-butylamine in 1 *M* NaOH. Conditions: 4×10^{-1} *M* amine; 23 °C; 5.84×10^{-4} V s^{-1}.

At a silver electrode in aqueous alkali at potentials above 0.6 V n.h.e., primary amines having a mono-substituted α-carbon atom are oxidized to the corresponding nitrile and aldehyde; those having a di-substituted α-carbon atom, to the ketone; and the tri-substituted ones, to alkene, alcohol, and nitro-compounds (Table I). For *n*-butylamine, under conditions where essentially only nitrile is formed, coulombic yields (based on the proposed mechanism) of better than 90% were achieved.

TABLE I

Oxidation of primary amines and oximes in 1 *M* NaOH, (*a*) at silver electrodes at 0.74 V vs. n.h.e., (*b*) with AgO

Amine	Product (relative amounts)	
	Electrochemical oxidation	Chemical oxidation
n-Propylamine	*n*-Propionitrile	
iso-Propylamine	Acetone	
n-Butylamine	*n*-Butyronitrile, *n*-butyraldehyde	*n*-Butyronitrile (8), *n*-butyric acid (1), *n*-butyraldehyde (trace)
iso-Butylamine	iso-Butyronitrile, iso-butyraldehyde	iso-Butyronitrile (10), iso-butyric acid (1), iso-butyraldehyde (trace)
sec-Butylamine	Ethyl methyl ketone	Ethyl methyl ketone
t-Butylamine	*t*-Butanol (15), nitro-*t*-butane (10), 2-methylprop-1-ene (25)	*t*-Butanol(10), nitro-*t*-butane (20), 2-methylprop-1-ene (40)
Benzylamine	Benzonitrile	
n-Butyraldehyde oxime	*n*-Butyronitrile (12), nitro-*n*-butane (3), 2-ethylhex-2-en-al (2), *n*-butyraldehyde (trace)	Butyronitrile, butyraldehyde
Ethyl methyl ketone oxime	Ethyl methyl ketone	

Potential Sweep Experiments

The addition of amine causes the peak due to the formation of Ag_2O to become a wave and to shift to a less positive potential (Fig. 4). Depending on the substitution pattern at the α-carbon, further peaks appear at potentials more positive than that at which the formation of AgO takes place (Fig. 5). The wave height (as measured at the first flat portion of the wave) associated with Ag_2O formation varies with concentration of amine as shown in Fig. 6.

In the case of *n*-butylamine the complex was examined a little further. In a series of experiments different amounts of *n*-butylamine were added to a series of suspensions of Ag_2O (in excess) in normal aqueous alkali. After allowing to equilibriate (12 h) the silver ion in solution was determined by Volhard's method. A graph of "soluble" silver concentration against added amine concentration gave a straight line passing through the origin. The slope $d[amine]/d[Ag^+]$ is 4, indicating that each silver ion is complexed with 4 amine molecules. Attempts to confirm that silver was showing a coordination number of 4 by potentiometric and high frequency titrations were inconclusive.

At potentials more positive than that required for AgO formation, the oxidation of *n*-butylamine gave butyraldehyde and butyronitrile in a ratio dependent on OH^- concentration (Table II), amine concentration (Table III), and electrode potential (Table III). Some results of chemical oxidation using AgO are included for comparison.

TABLE II

Dependence of aldehyde/nitrile ratio on $[OH^-]$

$[OH^-]$, *M*	[*n*-Butyraldehyde]/[*n*-butyronitrile]		
	*a**	*b*†	*c*‡
0.5	0.01	0.01	
1.0	0.02	0.02	0.01
2.0	0.55	0.01	0.01
3.0	1.4	0.01	
4.0	8.0	0.02	0.04
5.0	8.9	0.10	0.12

*E = 0.64 V n.h.e.; amine concentration = 0.02 *M*/l.
†E = 0.74 V n.h.e.; amine concentration = 0.02 *M*/l.
‡Chemical AgO; amine concentration = 1 *M*/l.

TABLE III

Oxidation of *n*-butylamine: effect of amine concentration and electrode potential on product ratio in 1 *M* NaOH, at 23 °C

Amine concentration $\times 10^{-1}$, *M*	Potential vs. n.h.e., V	[*n*-Butyraldehyde]/[*n*-butyronitrile]
2	0.494	Only aldehyde produced, very low yield
2	0.644	0.10
2	0.744	0.05
4	0.744	0.02
8	0.744	0.01

Can. J. Chem. Downloaded from www.nrcresearchpress.com by 210.87.254.6 on 09/05/12
For personal use only.

Can. J. Chem. Downloaded from www.nrcresearchpress.com by 210.87.254.6 on 09/05/12
For personal use only.

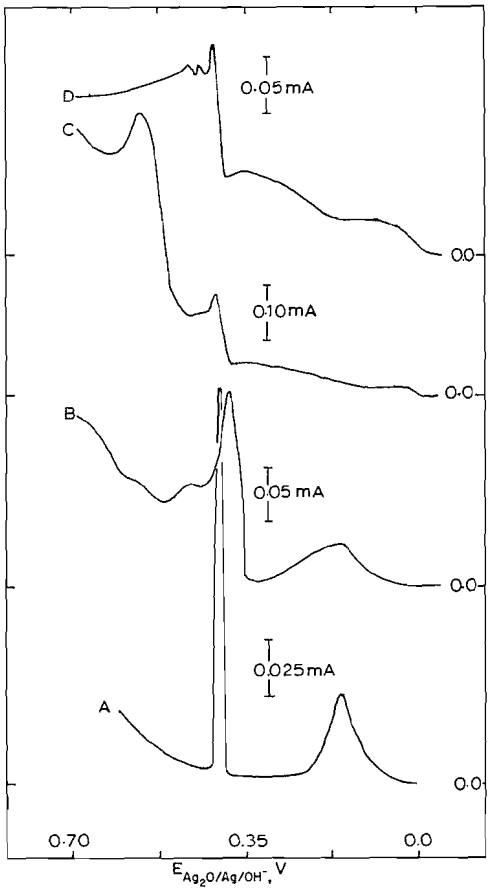

FIG. 4. Effect of amine concentration on the potentiodynamic current curves for *n*-butylamine. Conditions: 1 *M* NaOH; 23 °C; 5.84×10^{-4} V s^{-1}; electrode area, 4.45×10^{-2} cm^2. $A = 0.0$, $B = 3.3 \times 10^{-2}$, $C = 1.3 \times 10^{-1}$, and $D = 2.0 \times 10^{-1}$ *M*.

TABLE IV

Oxidation of *n*-butylamine: effect of pulse frequency on product ratio*

Frequency	[*n*-PrCHO]/[*n*-PrCN]
0.125	2.0
0.25	3.6
0.6	2.0
3.0	0.2
8.0	0.1
22.0	0.05

*$E = 0.60$ V vs. n.h.e.; pulse height = 150 mV; [NaOH] = 1 *M*; [amine] = 4×10^{-1} *M*; $T = 23$ °C; 50% duty ratio.

Pulsed Potential Oxidations

The effect of the pulse parameters (Fig. 2) on the product ratio for *n*-butylamine is shown in Tables IV and V and in Fig. 7.

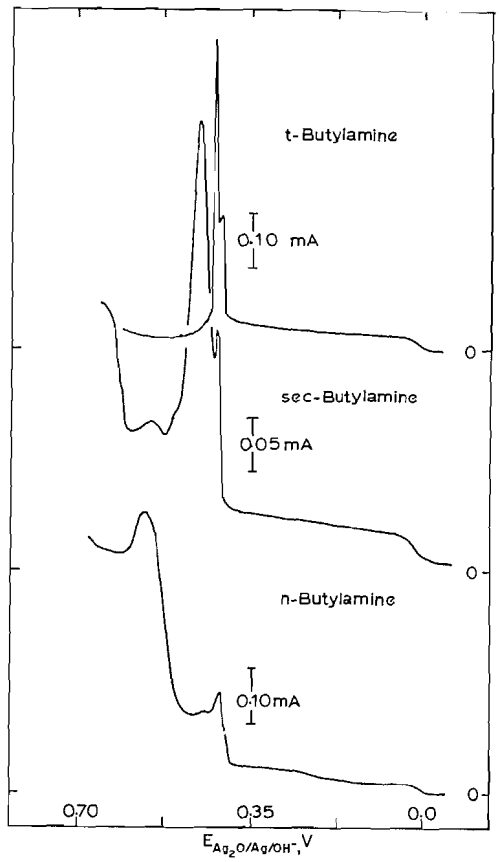

FIG. 5. Potentiodynamic current curves for amines with different substitutions at the α-carbon atom. Conditions: 1 *M* NaOH; 0.13 *M* amine; 23 °C; 5.84×10^{-4} V s^{-1}; electrode area = 4.45×10^{-2} cm^2.

TABLE V

Oxidation of *n*-butylamine: effect of duty ratio on product ratio*

Duty ratio, %	[*n*-Butyraldehyde]/[*n*-butyronitrile]
50	0.2
10	0.3
5	0.9

*Using potential pulses; $E = 0.60$ V vs. n.h.e.; pulse height = 150 mV; [NaOH] = 1 *M*; [amine] = 4×10^{-1} *M*; $T = 23$ °C.

Tafel Plots: Galvanostatic Experiments

The addition of primary amines to the electrolyte has the effect of lowering the apparent activation overpotential (η_D), at a given current density, for the formation of Ag_2O. The addition of primary amine increases the exchange current (i_0), calculated from the intercept of $\eta_D - \log i$,

Can. J. Chem. Downloaded from www.nrcresearchpress.com by 210.87.254.6 on 09/05/12
For personal use only.

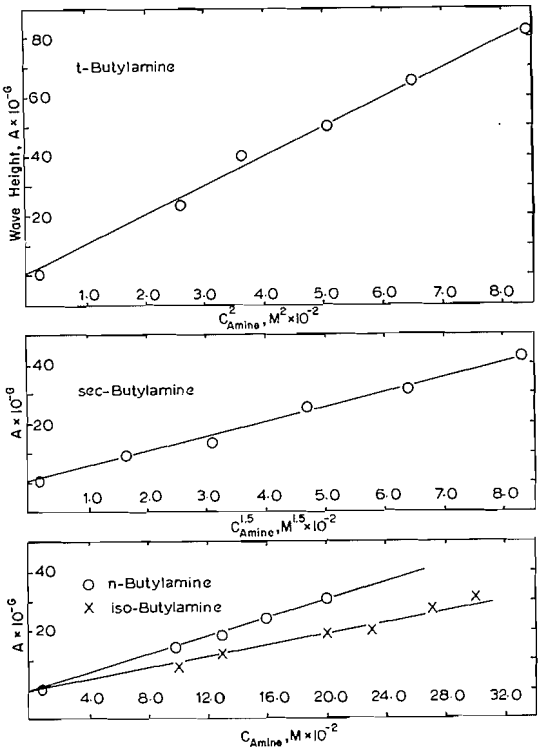

FIG. 6. Effect of concentration of amine on the height of the low potential region wave. Conditions: 1 *M* NaOH; 23 °C; 5.84×10^{-4} V s^{-1}; electrode area = 4.45×10^{-2} cm^2.

while the charge transfer coefficient (α) remains almost constant (Fig. 8).

Discussion

Potential sweep experiments show that at the potential required for Ag_2O formation, the potentiodynamic current curve changes from a peak to a wave (Fig. 4) with increasing amine concentration. At low concentrations of amine the wave height is considerably less than the

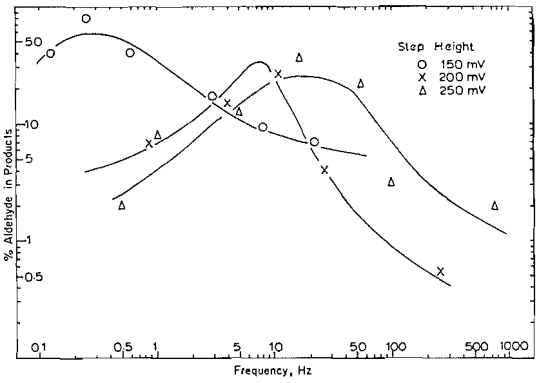

FIG. 7. The effect of pulse frequency and potential step height on the aldehyde:nitrile ratio in the oxidation of *n*-butylamine by repetitive potential pulses. Conditions: 1 *M* NaOH; 4×10^{-1} *M* amine; 23 °C; starting potential 0.600 V (vs. n.h.e.).

Ag_2O peak. This may be the result of the competitive adsorption between amine and hydroxyl ion or a change in mechanism.

The wave results from the formation of a soluble complex between primary amines and Ag_2O. Under alkaline conditions a silver electrode is oxidized to Ag_2O to a depth of about 100 monolayers (2, 9) and then the reaction becomes very slow. In the presence of amine the surface layers of Ag_2O are being continuously removed thus allowing the oxidation to proceed, as the electrode is not oxidized in depth.

The rate of the reaction, as measured by the wave height, is related to the amine concentration. For *n*-butylamine the rate is proportional to $[RNH_2]$; for *sec*-butylamine, to $[RNH_2]^{1.5}$; and for *t*-butylamine, to $[RNH_2]^2$. In each case increasing the agitation of the electrolyte increases the rate of the reaction, indicating that the reactions are, at least in part, controlled by mass transport in solution. The rate is dependent on the slowest step in the reaction sequence below.

$$2Ag + 2OH^- \xrightarrow{-2e} Ag_2O$$

$$RNH_2 \xrightarrow[\text{to electrode}]{\text{diffusion}} n\text{-}RNH_2 + Ag_2O \underset{k'}{\overset{k}{\rightleftharpoons}} [Ag_2O(RNH_2)_n] \xrightarrow[\text{of complex from electrode}]{\text{diffusion}}$$

For *n*-butylamine the reaction rate appears to be controlled by the transport of the amine to the electrode. For *sec*- and *t*-butylamine the reaction rate must be dependent on at least two of the steps in the sequence. The activation energy associated with this reaction for both *n*-butylamine and *t*-butylamine is ~ 1 kcal/mole (as determined from the temperature dependence of

the wave height). Such a low activation energy is characteristic of a diffusion controlled reaction.

The straight line relationship between added amine and the complex formed in the presence of excess Ag_2O indicates that the stability constant of the amine–silver complex is high. Silver is apparently showing a coordination number of 4 instead of 2 which is normally found for amine–silver complexes (8).

The galvanostatic results for Ag_2O formation (Fig. 8) show that the exchange current (i_0) increases with increasing amine concentration. That the rate of Ag_2O formation increases with amine concentration is borne out by the potentiodynamic results. Although the half-wave potential is difficult to measure precisely (the wave is not symmetrical), it can be seen (Fig. 6) that the wave moves to lower potentials on increasing the amine concentration.

At potentials more positive than that for AgO formation primary amines are oxidized rapidly. The products, which are dependent on the degree of substitution at the α-carbon atom, can be explained by the following reaction scheme.

For compounds of the type RCH_2NH_2

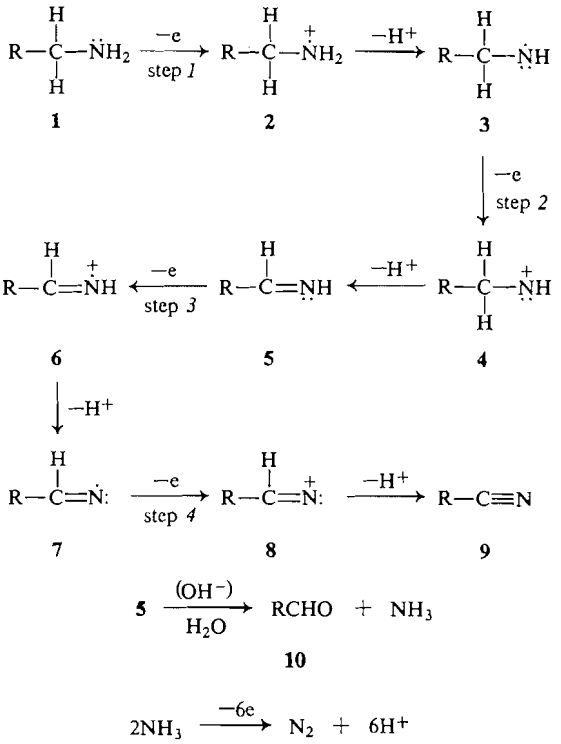

For compounds of the type $RR'CHNH_2$

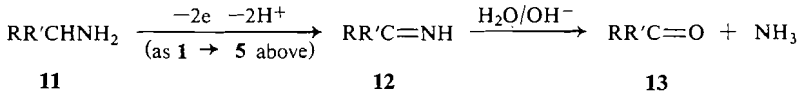

For compounds of the type R_3CNH_2

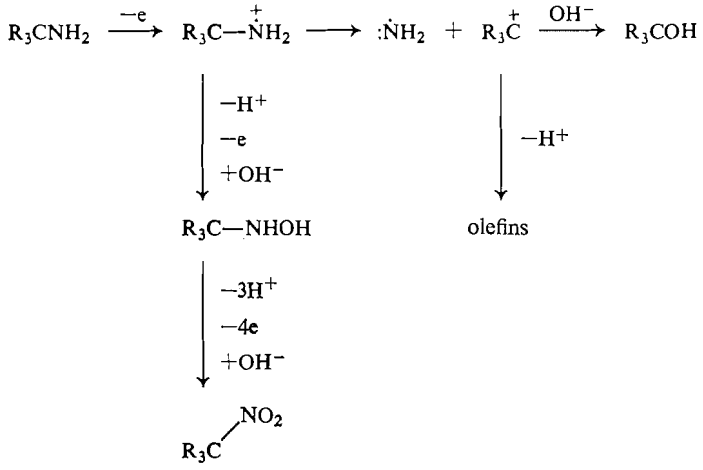

Can. J. Chem. Downloaded from www.nrcresearchpress.com by 210.87.254.6 on 09/05/12
For personal use only.

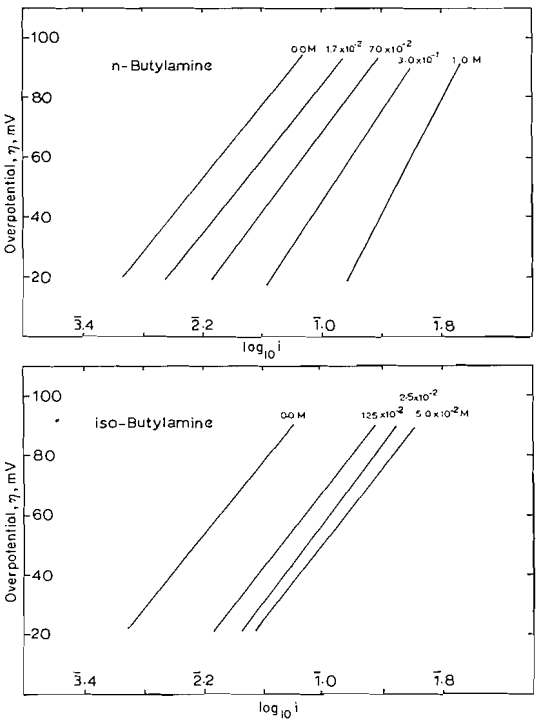

FIG. 8. The effect of added amine on the "Tafel plots" for the formation of Ag_2O. Conditions: 1 *M* NaOH; 23 °C.

Steps *1* and *2* are similar to those proposed by Barnes and Mann (3) for the oxidation of primary amines at a platinum anode. Under the conditions used by these workers (MeCN/$NaClO_3$, Pt at 1.99 V vs. n.h.e.) for saturated primary amines, the major reaction pathway (90–100%) was oxidation step *1* followed by breakdown of the cation radical **2**, to give a carbonium ion and $:\dot{N}H_2$ radical. At a silver electrode at potentials in the range of 0.54–0.74 V, we found no evidence that this pathway was operative. All the evidence indicates that a second oxidation step takes place giving an imine type intermediate.

The oxidation products of the primary amines studied are as predicted by these pathways (Table I).

Typical potential sweeps for the three types of primary amines are shown in Fig. 5. As peaks and not waves are observed above the potential for AgO formation, the reactions are in some way self limiting. In the simplest case, if the oxidation potentials for steps *1–4* increase from left to right, an amine with a mono-substituted α-carbon atom should give four peaks (or waves), a disubstituted one only the first two of these peaks, and a trisubstituted one only the first peak. The potential sweep response for *sec-* and *t*-butylamine approximates to this simple scheme but that for *n*-butylamine is more complex. However, the hydrolysis of the imine is not potential dependent as no charge transfer step is involved, whereas nitrile formation is (see scheme for reactions **5** → **10**, **5** → **9**). Therefore it should be possible to determine the oxidation product by selecting the potential. The direction in which the aldehyde/nitrile ratio changes with the variables discussed below is reproducible. However, individual values of the ratio are more difficult to reproduce as several other variables (such as cell geometry, agitation, and reaction time) affect the result. The oxidation of *n*-butylamine gives a decreasing *n*-butyraldehyde/butyronitrile ratio with increasing potential (Tables II and III). There are two competing reactions for the imine, **5**; it may be oxidized to the nitrile or hydrolyzed to the aldehyde. Increasing the hydroxyl ion concentration at a fixed potential should therefore lead to an increasing aldehyde to nitrile ratio and this is observed (Table II). At a fixed potential and hydroxyl ion concentration the aldehyde/nitrile ratio decreases with increasing amine concentration (Table III). This is explicable if there is competitive adsorption (cf. the competitive adsorption of gases at solids (10)) between amine and hydroxyl ions, and the imine reacts at the surface. Increasing the amine concentration will therefore decrease the hydroxyl ion concentration at the electrode and thus decrease the rate of the hydrolysis reaction **12** → **13**.

The data from the repetitive pulse oxidations for *n*-butylamine show an optimum frequency for the formation of aldehyde. This indicates that the imine concentration is significant. In the long pulses the surface concentration of imine is built up until a "steady state" with respect to imine concentration is achieved. The oxidation then proceeds to give nitrile. In the shorter pulses this "steady state" concentration of imine is not achieved and consequently only a little nitrile is formed. During the rest period the imine is hydrolyzed to give aldehyde. At frequencies higher than the optimum, the reaction cannot

Can. J. Chem. Downloaded from www.nrcresearchpress.com by 210.87.254.6 on 09/05/12
For personal use only.

follow the potential relaxations and the oxidation tends to approximate to one at constant potential. The optimum frequency is higher with higher potential pulses (Fig. 7) because the "steady state" concentration of imine is achieved in a shorter time.

The reaction scheme would be best tested by studying the oxidation of the imines but, as these are very unstable, this is not possible. Oximes are oxidized to the corresponding nitrile under these conditions (Table I). Control experiments showed that the nitrile did not result from base catalyzed dehydration.

From these observations it is clear that the cleavage of the carbon–nitrogen bond is less favorable at a silver anode than at a platinum anode (3). In the case of primary amines, with only one substituent at the α-carbon atom, the reaction pathway is branched and as only one branch involves charge transfer, the product ratio is potential dependent.

1. T. G. CLARKE, N. A. HAMPSON, J. B. LEE, J. R. MORLEY, and B. SCANLON. Can. J. Chem. **46**, 3437 (1968).
2. T. G. CLARKE, N. A. HAMPSON, J. B. LEE, J. R. MORLEY, and B. SCANLON. Ber. Bunsenges. Phys. Chem. In press.
3. K. K. BARNES and C. K. MANN. J. Org. Chem. **32**, 1474 (1967).
4. R. A. BENKESSER, E. M. KAISER, and R. F. LAMBERT. J. Amer. Chem. Soc. **86**, 5272 (1966).
5. T. G. CLARKE, N. A. HAMPSON, J. B. LEE, J. R. MORLEY, and B. SCANLON. Tetrahedron Lett. **54**, 5685 (1968).
6. C. K. MANN. Anal. Chem. **36**, 2424 (1964).
7. M. MASHI, H. SAYO, and Y. TSUDA. J. Chem. Soc. B, 973 (1968).
8. F. A. COTTON and G. WILKINSON. Advanced inorganic chemistry. Interscience Publishers, Inc., London. 1962. p. 963.
9. B. D. CAHAN, J. B. OCKERMAN, R. F. AMLIE, and P. RUETSCHI. J. Electrochem. Soc. **107**, 725 (1960).
10. K. LAIDLER. Chemical kinetics. McGraw-Hill Book Co., Inc., New York. 1950. p. 158.

Can. J. Chem. Downloaded from www.nrcresearchpress.com by 210.87.254.6 on 09/05/12
For personal use only.

Can. J. Chem. Downloaded from www.nrcresearchpress.com by 210.87.254.42 on 09/05/12
For personal use only.

Relative rate constants for reactions of hydroxyl radicals from the reaction of Fe(II) or Ti(III) with H_2O_2[1]

W. A. ARMSTRONG

Defence Research Establishment Ottawa, Defence Research Board, Ottawa 4, Canada

Received March 6, 1969

In an attempt to clarify the reactions of ferrous sulfate and titanous sulfate with hydrogen peroxide, a novel method has been developed to determine the relative rate constants for reactions of the oxidizing species generated in these systems. These species react with hydrogen peroxide to give perhydroxyl radicals which combine with titanium(IV) ions to form the relatively stable $TiOO^{\cdot 3+}$ radical. This radical gives a strong electron spin resonance signal and the competition between hydrogen peroxide and a scavenger for the oxidizing species can be followed by measuring the amplitude of this signal in the presence of various concentrations of scavenger. The relative rate constants calculated in this way for both the Fe(II)–H_2O_2 and Ti(III)–H_2O_2 systems at pH 1.0 agree with those reported for the reactions of hydroxyl radicals in γ-irradiated thymine solutions. This supports the view that hydroxyl radicals are formed in these cases.

Under conditions of acidity favoring the hydrolysis of Fe(II) to $FeOH^+$ ions, hydroxyl radical scavengers do not compete with hydrogen peroxide for the precursors of the $TiOO^{\cdot 3+}$ radical. It is suggested that the $FeOH^+$ ions react with hydrogen peroxide to give a different oxidizing species, possibly the ferryl ion.

Scavengers investigated were thymine, methanol, ethanol, formic acid, acetic acid, chloride ion, and several amino acids.

Canadian Journal of Chemistry, 47, 3737 (1969)

Introduction

There has been much controversy concerning the reaction of hydrogen peroxide with ferrous or titanous ions in acidic aqueous solutions (1–7). It is generally assumed that hydroxyl radicals are formed in both reactions but there is some evidence to suggest that the OH radicals are complexed with titanium in the Ti(III)–H_2O_2 system and that reaction with a scavenger takes place in a $[Ti(H_2O)_4(OH)(scavenger)]^{4+}$ complex (4). Fenton's reagent has been characterized as nucleophilic and Ti(III)–H_2O_2 as electrophilic (2).

The present investigation was designed to measure the relative rate constants for the reactions of a number of solutes with the oxidizing species generated in each of these systems. These constants could then be compared with the reported absolute values obtained by radiolysis experiments (8, 9). Reasonable agreement would indicate that in each case free OH radicals are being scavenged. The method is based on the following reaction scheme

[1] $\text{Fe(II) or Ti(III)} + H_2O_2 \rightarrow \text{Fe(III) or Ti(IV)} + OH^- + \cdot OH$

[2] $\cdot OH + H_2O_2 \rightarrow H_2O + HO_2\cdot$

[3] $\cdot OH + \text{scavenger} \rightarrow X\cdot$

[4] $HO_2\cdot + \text{Ti(IV)} \rightarrow TiOO^{\cdot 3+} + H^+$

The $TiOO^{\cdot 3+}$ radical has a lifetime of several seconds (4) and gives a single electron spin resonance (e.s.r.) line with $g = 2.013$ (5). A second paramagnetic species with $g = 2.012$ is also observed but its identity is in doubt. Fischer (5) suggests it is $TiOOTiOO^{\cdot 5+}$, formed by the reaction of $TiOO^{\cdot 3+}$ with hydrogen peroxide and titanium(IV) ions, but Takakura and Ranby (7) favor the idea of a complex of OH and Ti(IV) ions. However, Arthur and co-workers (10) have observed this species (as well as the $TiOO^{\cdot 3+}$) upon the mixing of a Ce(IV) solution with a solution of H_2O_2 containing Ti(IV) ions and it is unlikely that hydroxyl radicals are produced in this reaction. Under the present experimental conditions the concentration of this second paramagnetic species is small and decreases upon the addition of a scavenger in the same manner as the $TiOO^{\cdot 3+}$ (5). It has, therefore, been ignored. As the lifetimes of most organic radicals are much shorter than the lifetime of the $TiOO^{\cdot 3+}$ radical, the scavenger radicals formed in reaction [3] are not observed.

The e.s.r. spectra observed with the Fe(II)–H_2O_2,Ti(IV) and Ti(III)–H_2O_2,Ti(IV) systems are shown in Fig. 1. For comparison, the spectrum resulting from the illumination of a stream of

[1]Issued as D.R.E.O. Report No. 590.

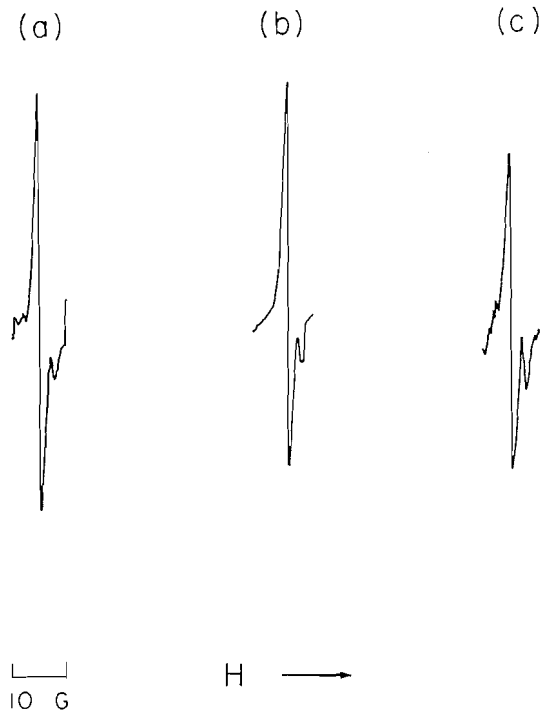

FIG. 1. The e.s.r. spectrum of the $TiOO^{\cdot 3+}$ radical in 0.1 M H_2SO_4. (*a*) 1.0 mM Fe(II) – 80 mM H_2O_2, 30 mM Ti(IV), (*b*) 2.0 mM Ti(III) – 80 mM H_2O_2, 30 mM Ti(IV), (*c*) ultraviolet light, 80 mM H_2O_2, 30 mM Ti(IV).

acidic H_2O_2,Ti(IV) solution with light of 2537 Å (a system which undoubtedly involves the formation of hydroxyl radicals) is included in the same figure. Apparently the same radicals are formed in each system.

If reactions [2] and [3] are the only significant reactions involving OH radicals and all the HO_2 radicals react according to [4], then at a given time of observation and in the absence of a scavenger, $[TiOO^{\cdot 3+}] = [OH]$, the total amount of hydroxyl radicals generated. In the presence of a scavenger

$$[TiOO^{\cdot 3+}] = \frac{k_2[H_2O_2]}{k_2[H_2O_2] + k_3[\text{scavenger}]} \cdot [OH]$$

If A^0 and A are the amplitudes of the $TiOO^{\cdot 3+}$ e.s.r. line in the absence and presence of a scavenger

$$\frac{A^0}{A} = 1 + \frac{k_3}{k_2} \cdot \frac{[\text{scavenger}]}{[H_2O_2]}$$

Thus a plot of A^0/A vs. $[\text{scavenger}]/[H_2O_2]$ should give a straight line with slope $= k_3/k_2$. This approach is similar to that used in the pulse radiolysis experiments where the reaction of OH with I^- or CNS^- was used in the determination of rate constants (11–13).

Experimental

All solutions were prepared immediately before use with triply distilled water which had been saturated with nitrogen. "Low manganese" ferrous sulfate (B and A Laboratories) and "stabilizer-free" 30% hydrogen peroxide (Fisher) were used in the reactant solutions. Both 15% titanous sulfate solution (British Drug Houses, Ltd.) and material prepared in this laboratory by the reduction of titanium basic sulfate in sulfuric acid solution with zinc amalgam (14) were employed. Hydrogen peroxide solutions were standardized by the arsenious oxide method (15). The concentration of titanous sulfate solutions was determined by titration of an aliquot with standardized hydrogen peroxide to a colorless end-point. It was assumed that 1 mole of hydrogen peroxide oxidized 2 moles of titanous sulfate (6). Titanium(IV) sulfate solutions of known concentration were prepared by similar titrations. The acidity of the ferrous and titanous solutions was adjusted with sulfuric acid. The H_2O_2,Ti(IV) solutions for the second stream were prepared by the addition of the desired volume of a 0.4 M titanium(IV) sulfate solution in 2 M sulfuric acid to the aqueous hydrogen peroxide solution. The pH was then adjusted by the addition of either sulfuric acid, sodium monohydrogen phosphate, sodium tetraborate, or sodium hydroxide. At pH > 2.2 titanium hydroxide precipitated.

The e.s.r. spectrometer and flow system have been described elsewhere (16). To permit the accurate adjustment of flow rates, the system was modified to include a flow meter and needle valve in each stream. Normally the flow of each stream was set at 115 ml/min and the radicals were observed about 0.3 s after the mixing of the reactants. Initially, a solution of ferrous or titanous sulfate was mixed with a solution of the same acidity containing the desired amounts of hydrogen peroxide and titanium(IV) sulfate. While these solutions flowed through the mixing chamber and e.s.r. cell, the magnetic field from 5 G below the value for resonance to 5 G above this value was scanned three times. A^0 was the average amplitude of this spectrum. After draining the flow system the process was repeated but with a known amount of scavenger in the Ti(IV)–H_2O_2 solution. Values of A were determined in this way for increasing concentrations of scavenger until $A \approx \frac{1}{3}A^0$. Spectrometer noise prevented the accurate determination of lower values of A. To check the stability of the spectrometer, A^0 was redetermined at the end of each run but for a given set of reaction conditions did not vary significantly over a period of weeks.

Results

The Systems at pH 1.0

In Fig. 2*a* are plotted values of A^0/A vs. $[\text{formic acid}]/[H_2O_2]$ for the reaction of 1.2 mM

Can. J. Chem. Downloaded from www.nrcresearchpress.com by 210.87.254.42 on 09/05/12
For personal use only.

Can. J. Chem. Downloaded from www.nrcresearchpress.com by 210.87.254.42 on 09/05/12
For personal use only.

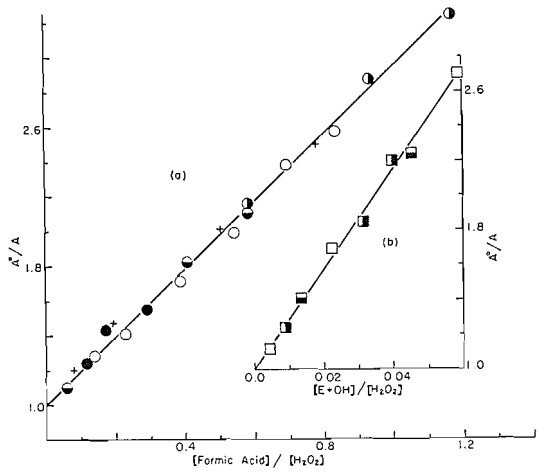

FIG. 2. The effect of reaction conditions on the determination of relative rate constants at pH 1.0. (*a*) 1.2 m*M* Fe(II): ○, 55 m*M* H_2O_2, 33 m*M* Ti(IV); ◑, 71 m*M* H_2O_2, 25 m*M* Ti(IV); ◒, 71 m*M* H_2O_2, 33 m*M* Ti(IV); ●, 71 m*M* H_2O_2, 49 m*M* Ti(IV); +, 107 m*M* H_2O_2, 33 m*M* Ti(IV). (*b*) 1.2 m*M* Fe(II) plus 60 m*M* H_2O_2, 31 m*M* Ti(IV); reaction time: ■, 0.021 s; □, 0.034 s; ▬, 0.065 s.

ferrous sulfate with various concentrations of hydrogen peroxide and titanium(IV) sulfate. All solutions described in this section were 0.1 *M* in sulfuric acid. Changing the concentration of hydrogen peroxide from 55 to 107 m*M* and that of titanium(IV) from 25 to 49 m*M* did not affect the slope of this straight line. The results are independent of flow rate and hence reaction

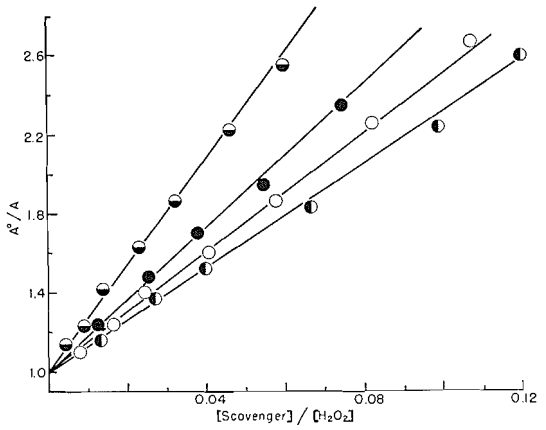

FIG. 3. Competition of scavengers with hydrogen peroxide for OH radicals from Fenton's reagent: 1.2 m*M* Fe(II) plus 60 m*M* H_2O_2, 33 m*M* Ti(IV), scavengers (pH = 1.0): ○, methanol; ◒, acetic acid (multiply abscissa by 100); ◐, l-cystine (multiply abscissa by 0.1); ●, thymine (multiply abscissa by 0.25).

time as shown in Fig. 2*b*. In this instance ethanol was the scavenger and reaction times of 0.021 to 0.065 s were used. Similar linear plots for methanol, acetic acid, cystine, and thymine are given in Fig. 3. Repeated experiments indicated that the measured slope of any plot is accurate to about ±15%.

The slope of each plot should equal k_3/k_2, where k_3 and k_2 are the rate constants for the reactions of hydroxyl radicals with the scavenger and hydrogen peroxide, respectively. However, the literature values of k_2 range from 1.2 to 4.5 $\times 10^7\ M^{-1}\ s^{-1}$ (9). Although less than 2% of the hydrogen peroxide is expended by reaction [1], this does introduce some doubt as to the exact concentration of peroxide which competes for the OH radicals. In view of these factors it was decided to compare all of the results with those obtained with thymine as the scavenger. The rate constant for the reaction of OH with thymine has been determined accurately to be $4.3 \pm 1 \times 10^9\ M^{-1}\ s^{-1}$ and has been used in the determination of the relative reaction rates of OH radicals with many scavengers (8). Assuming this value and employing the measured slope of the thymine plot (72.4), $k_2 = 5.9 \times 10^7$, a value somewhat higher than those quoted above. Results for k_3/k_2 for a variety of scavengers along with rate constants based on the given value for thymine are listed in Table I. For comparison, the rate constants published by Scholes and Willson (8) and derived from studies of the radiolysis of aqueous thymine solutions are also included. Considering the magnitude of the experimental errors, the agreement is good.

A^0/A vs. [scavenger]/[H_2O_2] plots for 1.9 m*M* Ti(III) plus 80 m*M* H_2O_2, 38 m*M* Ti(IV), with formic acid and ethanol as the scavengers are given in Fig. 4. For formic acid, $k_3/k_2 = 1.98$, in excellent agreement with the value obtained with the Fe(II)–H_2O_2 system. Ethanol, however, did not give a straight line plot. As the concentration of the ethanol was increased, the concentration of $TiOO\cdot^{3+}$ decreased to a greater extent than predicted by reactions [2]–[4]. Reaction of the ethanol radicals formed in [3] with the $TiOO\cdot^{3+}$ radicals could explain these results

[5] $\qquad X\cdot + TiOO\cdot^{+3} \rightarrow$ products

The importance of this reaction would depend upon the concentration of $TiOO\cdot^{3+}$ and the reactivity of X·. Under the conditions described

TABLE I

Rate constants for OH radical reaction in solutions of pH 1

Scavenger	Fe(II)–H_2O_2		Ti(III)–H_2O_2		Radiolysis of thymine†
	k_3/k_2	k(OH + scavenger)* M^{-1} s^{-1} × 10^{-9}	k_3/k_2	k(OH + scavenger)* M^{-1} s^{-1} × 10^{-9}	k(OH + scavenger) M^{-1} s^{-1} × 10^{-9}
Thymine	72.4	4.3	71.5	4.3	4.3
Methanol	15.0	0.89	12.8	0.77	0.69
Ethanol	28.9	1.7	24.9	1.5	1.6
Formic acid	1.95	0.12	1.98	0.12	0.14
Acetic acid	0.27	0.016	0.25	0.015	0.019
α-Alanine	0.59	0.035			0.038
1-Cysteine	112	6.6			4.7
1-Cystíne	130	7.6			
DL-Penicillamine	79.2	4.7			
Penicillamine disulfide	110	6.5			
2-Mercaptoethylamine	251	14.9			
2,2′-Dithio,bis(ethylamine)	186	11.0			
Glutathione (reduced)	186	11.0			
Glutathione (oxidized)	143	8.5			

*Based on k(OH + thymine) = 4.3 × 10^9 M^{-1} s^{-1}.
†Taken from Scholes and Willson (8).

above, the initial concentration of $TiOO^{\cdot 3+}$, as determined by the magnitude of A^0, was more than 100 times as great as that observed with Fenton's reagent. When reactant concentrations were reduced to 0.8 mM Ti(III) plus 60 mM H_2O_2, 3.3 mM Ti(IV), A^0 was reduced by a factor of 20 and the addition of ethanol resulted in the straight line shown in Fig. 4. Thymine, methanol, and acetic acid also gave linear plots. The values of k_3/k_2 are listed in Table I. Cystine and cysteine did not give linear plots (Fig. 4), possibly because the CyS· radical (16) reacts more rapidly with $TiOO^{\cdot 3+}$ than do the other scavenger radicals. Attempts to decrease the concentration of $TiOO^{\cdot 3+}$ to the level attained with the Fe(II)–H_2O_2 system were unsuccessful, as hydrolysis of the Ti(III) prevented any further decrease in its concentration.

The results of the addition of chloride ion to both the Fe(II)–H_2O_2 and the Ti(III)–H_2O_2 reagents are shown in Fig. 5. The initial portion of the plot is linear with a slope of 9.5 which corresponds to

$$k(\mathrm{OH} + \mathrm{Cl}^-) = 5.6 \times 10^9\ M^{-1}\ \mathrm{s}^{-1}$$

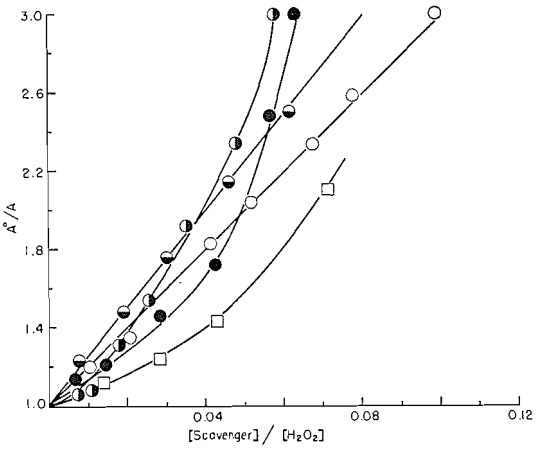

FIG. 4. Competition of scavengers with hydrogen peroxide for OH radicals from Ti(III)–H_2O_2: 1.9 mM Ti(III) plus 80 mM H_2O_2, 38 mM Ti(IV), scavengers (pH = 1.0): ○, formic acid (multiply abscissa by 10); ◑, ethanol. 0.8 mM Ti(III) plus 60 mM H_2O_2, 3.3 mM Ti(IV), scavenger: ◒, ethanol; ●, cystine (multiply abscissa by 0.1); □, cysteine (multiply abscissa by 0.1).

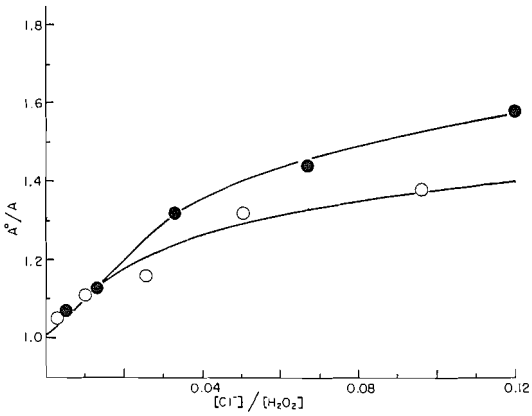

FIG. 5. Effect of chloride ions at pH 1.0: ●, 1.2 mM Fe(II) plus 60 mM H_2O_2, 33 mM Ti(IV); ○, 0.8 mM Ti(III) plus 80 mM H_2O_2, 3.3 mM Ti(IV).

Can. J. Chem. Downloaded from www.nrcresearchpress.com by 210.87.254.42 on 09/05/12
For personal use only.

Can. J. Chem. Downloaded from www.nrcresearchpress.com by 210.87.254.42 on 09/05/12
For personal use only.

The reported values for this constant are 4.0×10^8 at pH 1 and 4.0×10^9 at pH 0 (9). As the chloride concentration was increased the concentration of $TiOO^{\cdot 3+}$ decreased to a lesser extent than predicted by reactions [2]–[4]. The excess chloride ions may complex with the Fe(II) or Ti(III) and be unavailable for reaction with the hydroxyl radicals. An alternative explanation is that the Cl atoms or Cl_2^- radicals formed by the reaction of hydroxyl radicals with chloride ions (17, 18) react with hydrogen peroxide to give perhydroxyl radicals which, by way of [4], form $TiOO^{\cdot 3+}$. The yield of $TiOO^{\cdot 3+}$ would then become independent of the chloride ion concentration. Attempts to observe the e.s.r. spectrum of the Cl_2^- radical were unsuccessful.

The other reactions which might interfere with the proposed mechanism are

[6] Fe(II) or Ti(III) + OH $\rightarrow$ Fe(III) or Ti(IV) + OH^-

[7] $HO_2\cdot$ + scavenger $\rightarrow$ Y·

[8] $TiOO^{\cdot 3+}$ + scavenger $\rightarrow$ Y·

Reaction [6] was minimized by keeping the concentration of H_2O_2 at least 50 times as great as that of the ferrous or titanous ion. To investigate reaction [7], hydroperoxyl radicals were generated in the flow system by the reaction of ceric ammonium sulfate with hydrogen peroxide. Mixing 0.08 m*M* ceric ammonium sulfate in 100 m*M* sulfuric acid with a solution of 16.5 m*M* Ti(IV) and 80 m*M* H_2O_2 in 100 m*M* H_2SO_4 resulted in the formation of an amount of $TiOO^{\cdot 3+}$ comparable with that formed in the Ti(III)–H_2O_2 reagent described above. Addition to the Ti(IV)–H_2O_2 solution of a concentration of scavenger 4 times greater than the maximum amount used in the determination of relative rate constants did not significantly decrease the concentration of $TiOO^{\cdot 3+}$. The first 8 scavengers listed in Table I were investigated and the maximum decrease observed was 3%.

A simple three-stream mixer constructed from 1 mm bore Pyrex tubing was used to investigate reaction [8]. It was arranged so that the third stream entered 0.15 s after the mixing of streams 1 and 2 and, therefore, after the completion of the Ti(III)–H_2O_2 reaction (19). With 3 m*M* Ti(III) – 100 m*M* H_2SO_4 in stream 1, 16.5 m*M* Ti(IV) – 40 m*M* H_2O_2 – 100 m*M* H_2SO_4 in stream 2, and 100 m*M* H_2SO_4 added through stream 3, a concentration of $TiOO^{\cdot 3+}$ radicals 10 times greater than that observed with the Ti(III)–H_2O_2 system was generated. The addition of the same scavengers to the third stream in the same amounts as described in the preceding paragraph did not appreciably affect the concentration of radicals. The maximum decrease observed was <4%. The low reactivity of $TiOO^{\cdot 3+}$ radicals with methanol has been demonstrated previously (19, 20).

Under the present experimental conditions, the most likely path by which the $TiOO^{\cdot 3+}$ radicals disappear is by the relatively slow process of dimerization (19). Increasing the time between the mixing of the reactants and the observation of the radicals from 0.02 to 0.07 s caused a decrease in the measured radical concentration of less than 10%. Only when the concentration of $TiOO^{\cdot 3+}$ was high and the reactivity of the scavenger radical X· great did the addition of a scavenger have any apparent affect on the dimerization reaction.

The Effect of Increasing pH

The results obtained at pH > 1.0 are summarized in Fig. 6. The slope of the plot of A^0/A vs. [ethanol]/[H_2O_2] at pH 1.2 is 30.0 for both

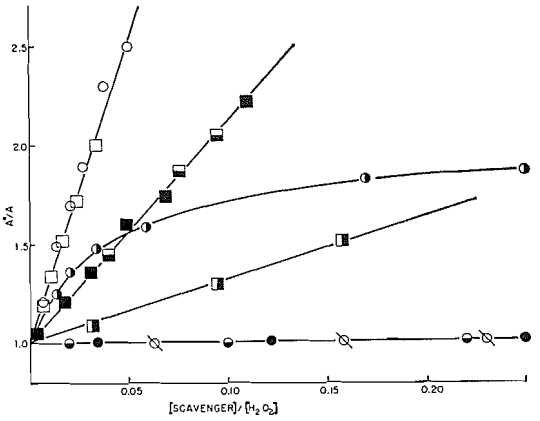

FIG. 6. Competition of scavengers with hydrogen peroxide for oxidizing species at higher pH. (*a*) 0.6 m*M* Fe(II) plus 80 m*M* H_2O_2, Ti(IV), scavenger. (*i*) 8.3 m*M* Ti(IV), ethanol: ○, pH 1.2; ◑, pH 1.6; ●, pH of Fe(II) 3.8, pH of H_2O_2, Ti(IV), EtOH 2.2. (*ii*) 41 m*M* Ti(IV), ethanol: ◒, pH of Fe(II) 3.8, pH of H_2O_2, Ti(IV), EtOH 2.2. (*iii*) 8.3 m*M* Ti(IV), thymine: ⊘, pH of Fe(II) 3.8, pH of H_2O_2, Ti(IV), thymine 2.2 (multiply abscissa by 0.1). (*b*) 0.8 m*M* Ti(III) plus 80 m*M* H_2O_2, 8.3 m*M* Ti(IV), scavenger. (*i*) Ethanol: □, pH 1.2; ■, pH 2.2. (*ii*) Thymine: ◨, pH 2.2 (multiply ordinate by 0.1). (*iii*) 0.3 m*M* Fe(III), ethanol: ⬓ pH 2.2.

Can. J. Chem. Downloaded from www.nrcresearchpress.com by 210.87.254.42 on 09/05/12
For personal use only.

the ferrous and titanous systems, in agreement with the value of 28.9 obtained at pH 1. With the titanous system this slope decreases to 11.3 at pH 2.2. Similarly, when thymine is the scavenger, k_3/k_2 decreases from 71.5 at pH 1.0 to 32.6 at pH 2.2. If the thymine and ethanol results at pH 2.2 are compared and it is assumed that $k(\text{OH} + \text{thymine}) = 4.3 \times 10^9\ M^{-1}\ s^{-1}$, then $k(\text{OH} + \text{ethanol}) = 1.5 \times 10^9\ M^{-1}\ s^{-1}$. This is in agreement with the value measured at pH 1.0. These results may be explained by an increase in k_2 with increasing pH. There is some other evidence suggesting this (9).

The ferrous – hydrogen peroxide system behaves in a different manner. Addition of either thymine or ethanol in concentrations up to 100 times that used at pH 1 to an H_2O_2,Ti(IV) solution of pH 2.2 had no appreciable affect on the amplitude of the $TiOO\cdot^{3+}$ signal observed when this solution was mixed with a ferrous sulfate solution of pH 3.8. The exact pH of the mixture during the reaction is unknown and will be referred to as pH > 2. Under these conditions the scavengers did not compete for the precursors of the $TiOO\cdot^{3+}$ radical.

The mechanism for the reaction of ferrous ions with hydrogen peroxide proposed by Haber and Weiss (21) and modified by Baxendale and co-workers (22) consists of reactions [1], [2], and [6] as well as

[9] $\quad HO_2\cdot + Fe(II) \rightarrow HO_2^- + Fe(III)$

[10] $\quad HO_2\cdot + Fe(III) \rightarrow O_2 + H^+ + Fe(II)$

Baxendale and co-workers (22) examined the change in kinetics of the Fe(II)–H_2O_2 reaction and the evolution of oxygen with changing acidity and found that k_{10}/k_9 increases from 0.14 to 0.70 as the pH is increased from 1.35 to 2.35. To ensure that all the HO_2 reacted according to [4], the concentration of Ti(IV) was raised from 8.3 to 42 mM (as compared with 0.6 mM Fe(II)) with no observable difference in the results. Other evidence that the behavior of the Fe(II)–H_2O_2,Ti(IV) system at pH > 2 is not due to reactions of the Fe(III) species was obtained by the addition of Fe(III) to the H_2O_2,Ti(IV), ethanol solutions. This had no effect on the results when these solutions were mixed with Ti(III) solutions at pH 2.2 (Fig. 6).

The concentration of scavenger radicals formed during the Fe(II)–H_2O_2, scavenger reaction is also dependent on pH. Shiga (1) has shown that the $\cdot CH_2CHOH$ radical is formed by the reaction of Fe(II)–EDTA at pH 7 with H_2O_2 in the presence of ethanol. We have confirmed this and also observed the same radical spectrum when the reaction was carried out at pH 1.2 in the absence of EDTA. However, when a 10 mM $FeSO_4$ solution at pH 3.8 was mixed with a solution 150 mM in H_2O_2 and 400 mM in ethanol, no radicals were detected. Changing reactant concentrations had no effect. When α-alanine was substituted for ethanol, similar results were obtained. The alanine radical was observed in solutions of pH 1.2 but not at pH 3.8. As $k(\text{Fe(II)} + H_2O_2)$ increases with increasing pH (23), it might be expected that the concentration of scavenger radicals available for observation would be greater at the higher pH.

Discussion

The Systems at pH 1.0

From the data obtained at pH 1.0 and presented in Table I it is evident that the relative reaction rates of the oxidizing species from Fe(II)–H_2O_2, Ti(III)–H_2O_2, and the γ-radiolysis of water are identical for a variety of substances. This suggests that the same oxidizing species is produced in each system. A comparison of the Fenton's reagent with the radiolysis of air-saturated aqueous solutions has been made recently by Kraljić (3) .Competition studies with *p*-nitrosodimethylaniline indicated that the OH radical is generated in both systems. The present investigation confirms this conclusion and shows that the Ti(III)–H_2O_2 reaction also produces hydroxyl radicals.

The experimental results fit the mechanism outlined in eqs. [1]–[4]. It is almost identical with that of Fischer (5), the main difference being that reactions [2] and [4] replace

$$OH + Ti(IV)/H_2O_2 \rightarrow TiOO\cdot^{3+} + H_2O + H^+$$

where $Ti(IV)/H_2O_2$ is the titanium – hydrogen peroxide complex and can be written as TiO_2^{2+} (24). Our results indicate that it is the hydrogen peroxide rather than the complex which competes for hydroxyl radicals. Because the Ti(IV) is complexed, it might be more accurate to write eq. [4] as

$$HO_2 + H^+ + TiO_2^{2+} \rightarrow TiOO\cdot^{3+} + H_2O_2$$

Whether the $TiOO\cdot^{3+}$ species is a titanium peroxyl radical or a hydroperoxyl radical com-

Can. J. Chem. Downloaded from www.nrcresearchpress.com by 210.87.254.42 on 09/05/12
For personal use only.

plexed by titanium(IV) ions is not material to the overall reaction scheme. The identity of the second paramagnetic species, present in very low concentrations, is of greater importance. As it can be formed under conditions where hydroxyl radicals are not likely to be present (10), the case for a Ti(IV)–OH complex is not completely convincing. However, the occurrence to a small extent of

[11] $$OH + Ti(IV) \rightarrow Ti(IV)\text{-}OH$$

or the back reaction of OH, [6], would not affect the values of the relative rate constants for the reactions of OH radicals with the various scavengers. It would interfere with the evaluation of k_2. That our value of k_2 is somewhat higher than the figure reported previously (5.9×10^7 vs. $4.5 \times 10^7\ M^{-1}\ s^{-1}$) may be related to interference by either reaction [6] or [11].

The suggestion, made by Turkevich and coworkers (4), that the reaction of the hydroxyl radical with the scavenger takes place during the decomposition of a $[Ti(H_2O)_4(OH)(scavenger)]^{4+}$ complex was based primarily on 2 observations. They found that, during the initial reaction period of about 0.01 s, the scavenger radical concentration decreased while the $TiOO^{\cdot 3+}$ signal increased. Although this behavior shows that the signal is not due to free OH radicals, it has been pointed out by Florin *et al.* (6) that it does not require the postulation of this complex. The second observation concerned an increase in the intensity of the $TiOO^{\cdot 3+}$ signal of more than a factor of 2 when small amounts of methanol were added to the hydrogen peroxide solution before it was mixed with a titanium trichloride solution. With higher methanol concentrations, the signal decreased. We repeated this experiment with titanous sulfate instead of titanium trichloride. In all cases the signal intensity decreased with increasing amounts of methanol. Thus the phenomenon they observed is apparently related to reactions of chloride ions. It is evident that the presence of chloride ions greatly complicates any study of the reaction mechanism.

Although the identity of the scavenger radical or radicals resulting from attack by the oxidizing species of Fenton's reagent is often the same as that observed with the Ti(III)–H_2O_2 system (16), there are some exceptions. As the evidence presented here suggests that the oxidizing species is the same in both cases, the differences in spectra may be due to differences in the reactions of the scavenger radicals with Fe(II), Fe(III), Ti(III), or Ti(IV) ions.

The Effect of Increasing pH

It is obvious that reactions [1] to [4] do not explain the results observed with the ferrous – hydrogen peroxide system at pH > 2. Studies with the Ti(III)–H_2O_2 system at the same pH show that changes in k_3/k_2 with pH are not sufficient to account for the decrease in the scavenging ability of ethanol and thymine, and also indicate that reaction [4] occurs at pH > 2. As the pK for the dissociation of HO_2 is 4.4 (25), only reactions of the unionized form are pertinent to this investigation. The results can best be explained on the assumption that hydroxyl radicals are not formed by the reaction of ferrous ions with hydrogen peroxide in solutions of high pH. A possible mechanism is outlined below

[12] $$Fe(II) + H_2O \rightleftarrows FeOH^+ + H^+$$

[13] $$FeOH^+ + H_2O_2 \rightarrow FeO^{2+} + H_2O + OH^-$$

[14] $$FeO^{2+} + H_2O_2 \rightarrow HO_2 + OH^- + Fe(III)$$

[15] $$FeO^{2+} + \text{scavenger} \rightarrow \text{product}$$

All the iron ions are aquated.

It is known that K_h for reaction [12] is about 4×10^{-4} and that the rate of reaction of ferrous ion with hydrogen peroxide increases at pH > 3 (23). The competition studies described in the present investigation were carried out by mixing a ferrous sulfate solution of pH 3.8 with a Ti(IV)–H_2O_2 solution of the highest allowable pH (2.2). Under these conditions reaction [13] could predominate over [1]. The experimental results reported here show that $k_{15}/k_{14} \ll k_3/k_2$. The formation of the ferryl ion, FeO^{2+}, in the reaction

$$Fe(II) + H_2O_2 \rightarrow FeO^{2+} + H_2O$$

was originally proposed by Bray and Gorin (26). Kolthoff and Medalia (27, 28) have pointed out that it is possible to replace the hydroxyl radical by the ferryl ion throughout the Haber–Weiss reaction scheme without altering the kinetics and that reaction with ethanol may take place according to [15]. It is therefore suggested that, under conditions favoring the presence of $FeOH^+$ ions rather than Fe(II) ions, reaction with hydrogen peroxide produces an oxidizing species

which is not the hydroxyl radical and may be the ferryl ion. If the Fe(II) ions are complexed with EDTA, the formation of $FeOH^+$ is prevented and hydroxyl radicals are generated at higher pH.

In addition to providing information about the reaction mechanisms of ferrous and titanous ions with hydrogen peroxide, the technique described offers a novel method for determining the relative rate constants for reactions of hydroxyl radicals with a wide variety of organic compounds in solutions of pH 1.

Acknowledgment

The author thanks Mr. W. G. Humphreys for valuable technical assistance.

1. T. SHIGA. J. Phys. Chem. **69**, 3805 (1965).
2. T. SHIGA, A. BOUKHORS, and P. DOUZOU. J. Phys. Chem. **71**, 4264 (1967).
3. I. KRALJIĆ. The chemistry of ionization and excitation. Taylor and Francis Ltd., London. 1967. p. 303.
4. Y. S. CHIANG, J. CRADDOCK, D. MICKEWICH, and J. TURKEVICH. J. Phys. Chem. **70**, 3509 (1966).
5. H. FISCHER. Ber. Bunsenges. Phys. Chem. **71**, 685 (1967).
6. R. E. FLORIN, F. SICILIO, and L. A. WALL. J. Phys. Chem. **72**, 3154 (1968).
7. K. TAKAKURA and B. RANBY. J. Phys. Chem. **72**, 164 (1968).
8. G. SCHOLES and R. L. WILLSON. Trans. Faraday Soc. **63**, 2983 (1967).
9. M. ANBAR and P. NETA. Int. J. Appl. Radiat. Isotop. **18**, 493 (1967).
10. M. S. BAINS, J. C. ARTHUR, JR., and O. HINOJOSA. J. Phys. Chem. **72**, 2250 (1968).
11. J. K. THOMAS. Trans. Faraday Soc. **61**, 702 (1965).
12. G. E. ADAMS, J. W. BOAG, J. CURRANT, and B. D. MICHAEL. Pulse radiolysis. Academic Press, Inc., New York and London. 1965. p. 131.
13. J. H. BAXENDALE, P. L. T. BEVAN, and D. A. STOTT. Trans. Faraday Soc. **64**, 2389 (1968).
14. H. WILKINSON and A. G. TYLER. J. Soc. Dyers Colour. **43**, 114 (1927).
15. A. I. VOGEL. A text-book of quantitative inorganic analysis. 3rd ed. Longmans, Green, and Co., London. 1961. p. 379.
16. W. A. ARMSTRONG and W. G. HUMPHREYS. Can. J. Chem. **45**, 2589 (1967).
17. T. J. SWORSKI. Radiat. Res. **2**, 26 (1955).
18. M. ANBAR and J. K. THOMAS. J. Phys. Chem. **68**, 3829 (1964).
19. J. STAUFF and H. J. HUSTER. Z. Phys. Chem. **55**, 39 (1967).
20. C. R. E. JEFCOATE and R. O. C. NORMAN. J. Chem. Soc. B, 48 (1968).
21. F. HABER and J. WEISS. Proc. Roy. Soc. London, Ser. A, **147**, 332 (1934).
22. W. G. BARB, J. H. BAXENDALE, P. GEORGE, and K. R. HARGRAVE. Trans. Faraday Soc. **47**, 462 (1951).
23. C. F. WELLS and M. A. SALAM. J. Chem. Soc. A, 24 (1968).
24. J. A. CONNOR and E. A. V. EBSWORTH. Advan. Inorg. Chem. Radiochem. **6**, 280 (1964).
25. G. CZAPSKI and L. M. DORFMAN. J. Phys. Chem. **68**, 1169 (1964).
26. W. C. BRAY and M. H. GORIN. J. Amer. Chem. Soc. **54**, 2124 (1932).
27. A. I. MEDALIA and I. M. KOLTHOFF. J. Polym. Sci. **4**, 377 (1949).
28. I. M. KOLTHOFF and A. I. MEDALIA. J. Amer. Chem. Soc. **71**, 3777 (1949).

Can. J. Chem. Downloaded from www.nrcresearchpress.com by 210.87.254.42 on 09/05/12
For personal use only.

Can. J. Chem. Downloaded from www.nrcresearchpress.com by 210.87.254.42 on 09/05/12
For personal use only.

Etude spectroscopique des dérives du peroxyde d'hydrogène. II. L'oxalate perhydrate, $Na_2C_2O_4.H_2O_2$

JOSÉ L. ARNAU ET PAUL A. GIGUÈRE
Centre de Recherches sur les Atomes et les Molécules, Université Laval, Québec 10, Québec

Reçu le 21 mai 1969

Dans les spectres de vibration du composé d'addition $Na_2C_2O_4.H_2O_2$, les fondamentales actives en infrarouge (i.r.) sont inactives en Raman et vice versa. Cette caractéristique, vérifiée par l'étude du composé partiellement deutérié, est en accord avec les résultats de la diffraction des rayons X et la résonance magnétique nucléaire (r.m.n.), à savoir que la molécule de peroxyde d'hydrogène est plane et centrosymétrique dans ce cristal. Grâce à cette déformation la molécule de peroxyde peut former des liaisons hydrogène très fortes (9 kcal $mole^{-1}$) avec l'anion oxalate, également plan. La majorité des vibrations de réseau prévues par la théorie des groupes ont pu être répérées. Pour fin de comparaison, les spectres du réseau cristallin de l'oxalate de sodium anhydre ont été mesurés en i.r. et en Raman.

The vibrational spectra of the addition compound $Na_2C_2O_4.H_2O_2$ show mutual exclusion of all the fundamentals in infrared (i.r.) and Raman. This feature is confirmed by a study of the partly deuterated compound. It agrees with the conclusion of a previous X-ray and nuclear magnetic resonance study that the hydrogen peroxide molecule in that crystal is planar and centrosymmetric. The two component molecules are held together by strong (9 kcal $mole^{-1}$) hydrogen bonds. Some 20 lattice modes were detected in i.r. or Raman. For comparison purposes, the lattice spectra of anhydrous sodium oxalate were also investigated.

Canadian Journal of Chemistry, **47**, 3745 (1969)

Introduction

Parmi les composés d'addition du peroxyde d'hydrogène l'oxalate perhydrate de sodium est d'un intérêt exceptionnel. En effet, il a été démontré par Pedersen et Pedersen (1) que dans ce cristal la molécule de peroxyde d'hydrogène existe sous la configuration plane *trans*, alors que normalement elle prend la configuration *gauche* (2). A cause de sa symétrie plus élevée, C_{2h}, la molécule plane doit avoir des spectres de vibration quelque peu différents de ceux de la molécule *gauche* (symétrie C_2). Ainsi les modes symétriques seront actifs en Raman seulement et inversement les modes antisymétriques, seulement en i.r. Dans le cadre de ce programme d'études spectroscopiques (3) il nous a semblé intéressant de vérifier ce point ainsi que l'influence de la forte déformation de la molécule sur ses fréquences fondamentales. En cours de route nous avons pris connaissance de la publication récente de Pedersen (4) sur les spectres i.r. des oxalates des métaux alcalins, leurs hydrates et leurs perhydrates. Nos résultats sur les composés du sodium sont cependant plus complets puisqu'ils s'étendent à l'i.r. lointain, jusqu'à 40 cm^{-1}, aussi bien qu'au Raman.

Partie Expérimentale

Le composé a été préparé suivant la méthode originale (1) soit par cristallisation à température ambiante d'une solution saturée d'oxalate de sodium (Baker's, C.P.) dans du peroxyde d'hydrogène (BECCO) à quelque 30%. Après évaporation lente (~20 h) on obtenait de fines aiguilles transparentes. Peu après avoir été séparées de la solution-mère elles se recouvraient d'un film blanc dû à un début de décomposition. Pour le composé deutérié on a utilisé du peroxyde de deutérium de même concentration produit par dissociation de la vapeur d'eau lourde dans une décharge électrique, tel que décrit antérieurement (5). La composition isotopique n'a pas été déterminée avec précision, mais d'après l'intensité des bandes i.r. la concentration de la molécule hybride HDO_2 semblait à peu près la même que celle de H_2O_2, et celle de D_2O_2, de l'ordre de 10 à 15%. La préparation des échantillons ainsi que les conditions d'enregistrement des divers spectres ont déjà été décrites dans le travail précédent (3). Sauf indication contraire les présents résultats se rapportent à la température de l'azote liquide.

Discussion des Résultats

Bandes du Peroxyde

En comparant les spectres du perhydrate avec ceux de l'oxalate anhydre en i.r. (Fig. 1) et en Raman (Fig. 2) on peut identifier tout de suite les bandes dues au peroxyde d'hydrogène (Tableau I). Ainsi dans la région de 3 μ, où l'ion oxalate n'a pas de fondamentales, la forte bande à 2672 cm^{-1} en Raman ne peut être que la vibration de valence O—H symétrique ν_1 et celle à 2605 cm^{-1} en i.r. (2645 cm^{-1} à température ambiante), la vibration antisymétrique ν_5. Cette dernière valeur est la plus basse de toutes celles trouvées jusqu'ici dans les composés d'addition

Can. J. Chem. Downloaded from www.nrcresearchpress.com by 210.87.254.42 on 09/05/12
For personal use only.

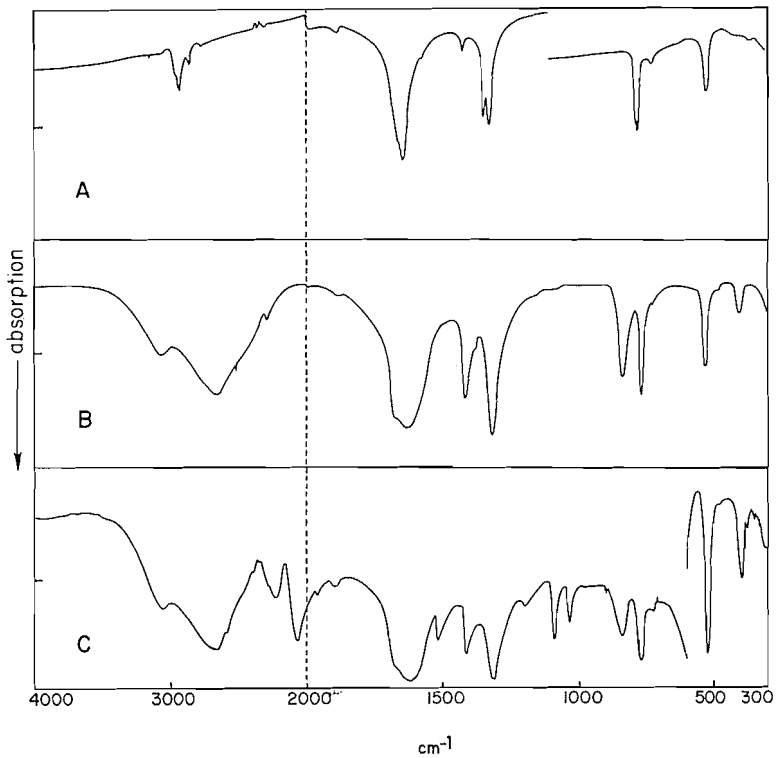

FIG. 1. Spectres d'absorption i.r. à température ambiante: A, $Na_2C_2O_4$ anhydre; B, $Na_2C_2O_4.H_2O_2$; C, $Na_2C_2O_4.(H_2O_2, HDO_2, D_2O_2)$.

TABLEAU I

Vibrations du peroxyde d'hydrogène dans divers cristaux*

Frequences en (cm^{-1})				
$Na_2C_2O_4.H_2O_2$		$Na_2C_2O_4.HDO_2$	H_2O_2 D_2O_2	
Raman	i.r.	i.r.	i.r.	Modes
	3040m	3045m		$(\nu_2 + \nu_6)$?
2864f				$2\nu_2$
2672F			3292	ν_1
	2645F	2650F	3182	ν_5
		2575é		$\nu_{O-H}(HDO_2)$
		2270é		$\nu_2 + \nu_6(D_2O_2)$
		2220m		$2\delta_{OOD}(HDO_2)$?
		2058F	(2400)	$\nu_{O-D}(HDO_2)$
		1956f	(2050)	$\nu_5(D_2O_2)$
	1654é	1654é		$2\nu_4$?
1553m			1410	ν_2
		1508f		$\delta_{OOH}(HDO_2)$
	1407F	1405m	1385	ν_6
		1192f		$2\nu_4(D_2O_2)$
		1086m	(1070)	$\delta_{OOD}(HDO_2)$
		1030m	(1030)	$\nu_6(D_2O_2)$
897F		895ff	880	ν_3
857f			656	ν_{Rx}
	828F	838F	690	ν_4
		602	(511)	$\tau_{OD}(HDO_2)$ et $\nu_4(D_2O_2)$

*m = médium, f = faible, F = forte, é = épaule.

Can. J. Chem. Downloaded from www.nrcresearchpress.com by 210.87.254.42 on 09/05/12
For personal use only.

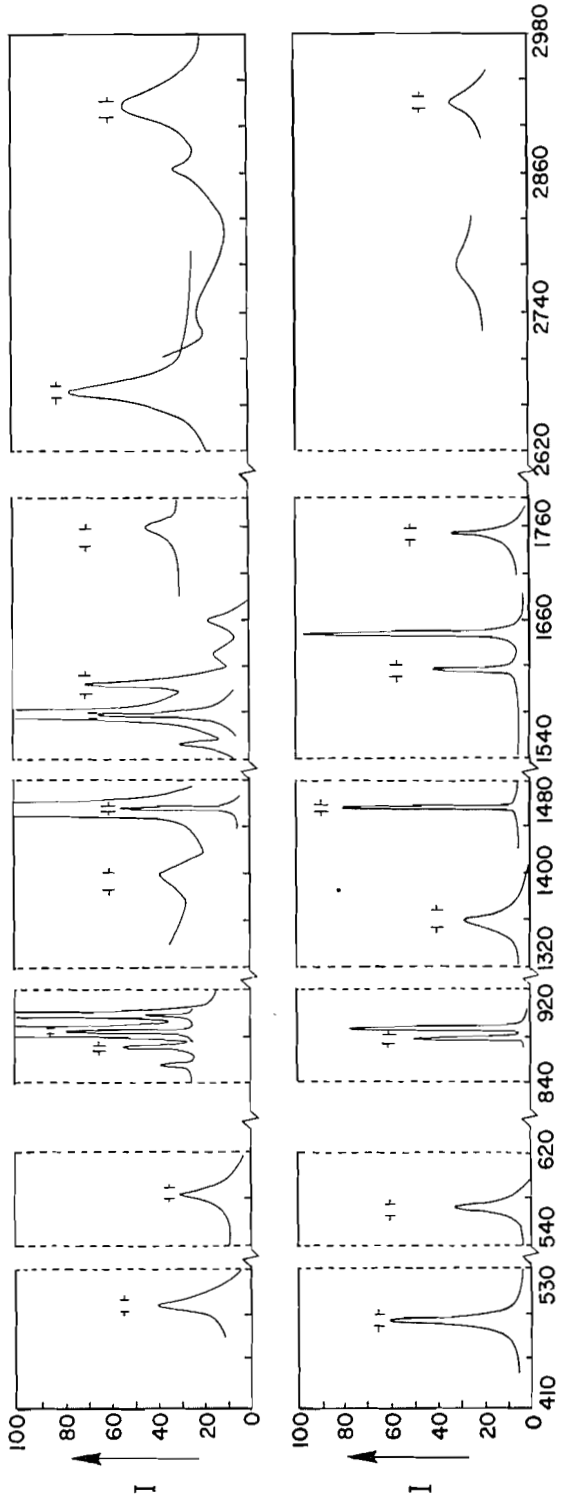

FIG. 2. Spectres Raman de l'oxalate perhydrate de sodium (haut) et de l'oxalate anhydre (bas) à température de l'azote liquide.

Can. J. Chem. Downloaded from www.nrcresearchpress.com by 210.87.254.42 on 09/05/12
For personal use only.

du peroxyde d'hydrogène. Elle confirme l'existence de ponts d'hydrogène très forts déjà indiquée par les distances O—H...O relativement courtes, 2.588 ± 0.06 Å, entre les molécules de peroxyde et les ions oxalate alternant dans des chaines planes infinies (1). En appliquant la relation de Pimentel et Sederholm (6) à la fréquence observée en i.r., 2640 cm^{-1}, Pedersen (4) est arrivé indirectement à une distance O—H...O un peu plus longue, soit 2.62 Å. Cependant il est plus utile ici de se baser sur la distance expérimentale, connue avec précision, pour évaluer par exemple la force des ponts d'hydrogène, ou encore la longueur de la liaison O—H moins bien connue. Ainsi le modèle de Lippincott et Schroeder (7) conduit à des valeurs d'environ 9 kcal $mole^{-1}$ et 1.05 Å, respectivement pour ces deux quantités. Cette dernière est certainement plus près de la réalité que celle de 0.89 ± 0.05 Å basée sur les diagrammes de densité électronique. Par contre elle est en accord avec celle de 1.1 Å tirée de l'analyse de la structure protonique par résonance magnétique nucléaire (r.m.n.) (1).

Les bandes de déformation OH sont décalées, tout comme les bandes de valence, mais en sens inverse naturellement, par rapport au cristal de peroxyde pur ou de son dihydrate (8). Cet effet est particulièrement marqué dans le cas du mode symétrique ν_2. Vraisemblablement c'est là le résultat combiné de la forte association intermoléculaire et de la haute symétrie, non seulement de la molécule de peroxyde mais encore de son site dans la maille cristalline. La bande de déformation antisymétrique ν_6 vers 1400 cm^{-1} coïncide presque exactement avec une bande faible de l'oxalate. C'est seulement aux basses températures que les deux peuvent être séparées. Effectivement notre interprétation se trouve confirmée par les décalages isotopiques dans les échantillons partiellement deutériés. Par ailleurs la bande d'intensité moyenne à 1475 cm^{-1} dans les spectres des oxalates perhydrates de potassium, de rubidium et de cesium (4) doit être attribuée à ν_6 plutôt qu'à ν_2 vu la faible activité des modes symétriques en i.r. Quant à la forte bande à 828 cm^{-1}, elle appartient au mode fondamental ν_4 dit de torsion interne et non à une combinaison de celui-ci avec un mode de libration présumé de fréquence environ 260 cm^{-1}. Il en est de même de la bande vers 940 cm^{-1} dans des spectres des autres oxalates perhydrates alcalins. Tel que mentionné précédemment (9, 10) cette vibration, à cause de sa faible force de rappel (2), dépend dans une large mesure des interactions moléculaires dans les états condensés. Comme on peut le prévoir la fréquence de ν_4 doit être assez voisine de celle du mode de libration autour de l'axe mineur, ν_{R_x}. Dans le cas de la molécule plane les règles de sélection permettent d'attribuer l'une et l'autre sans ambiguité.

Les spectres i.r. des échantillons partiellement deutériés sont particulièrement révélateurs. Ainsi l'apparition d'une faible absorption à 895 cm^{-1} due à la vibration O—O de la molécule hybride HDO_2 confirme la planéité de la molécule de peroxyde puisque cette fréquence est totalement absente du spectre de H_2O_2. En Raman son intensité n'est pas aussi grande qu'on pourrait le prévoir. Il se peut que le voisinage des fortes bandes de valence C—C de l'ion oxalate conduise à une redistribution d'intensité.

Bandes de l'Oxalate

Les vibrations de l'ion oxalate se retrouvent ici à peu près aux mêmes fréquences que dans le solide anhydre, tant en Raman (11) qu'en i.r. (11–16), sauf pour la vibration C—O antisymétrique dont le doublet à 1648/1618 cm^{-1} est décalé de quelque 40 cm^{-1} vers les basses fréquences. (Les deux faibles bandes vers 1660/1630 cm^{-1} toujours présentes dans nos spectres Raman du perhydrate provenaient sans doute d'une légère décomposition en surface lors du broyage des cristaux.) Six bandes apparaissent dédoublées (surtout dans les spectres à basse température) sous l'effet du champ cristallin dans le cristal anhydre, mais non dans celui du perhydrate. Dans ce dernier, l'insertion alternée de molécules de peroxyde doit amoindrir considérablement le couplage entre les ions oxalate. Les attributions présentes (Tableau II) sont en général les mêmes que celles de Murata et Kawai sauf pour le mode de déformation ν_{10} que nous attribuons à la bande i.r. vers 520 cm^{-1}, tel que proposé par Begun et Fletcher, et non pas à celle de 770 cm^{-1} qui doit appartenir au mode de rotation des groupes CO_2, ν_{12}. La valeur de 295 cm^{-1} calculée pour ce dernier par Murata et Kawai est certainement trop basse. L'attribution des deux fondamentales de basses fréquences ν_8 et ν_4 est conforme à celle de Lorenzelli *et al.* (17).

Can. J. Chem. Downloaded from www.nrcresearchpress.com by 210.87.254.42 on 09/05/12
For personal use only.

TABLEAU II

Spectres de vibration de l'oxalate de sodium et de son perhydrate*

Raman		Infrarouge		
Oxalate	Perhydrate	Oxalate	Perhydrate	Modes†
		2930ff	2920ff	$\nu_5 + \nu_9(B_{3u})$
2910f	2920m			$2\nu_1$ ou $\nu_9 + \nu_{11}(B_{1g})$
		2862ff	2850ff	
2780ff	2740ff			
		2275ff		$\nu_6 + \nu_{11}(B_{2u})$
		1886f	1878f	$\nu_6 + \nu_9(B_{3u})$
				$2\nu_2(A_g)$
1755f	1740f			
1648FF }	1605F }			$\nu_5(B_{1g})$
1618F }	1579FF }	1638FF	1615F	$\nu_{11}(B_{3u})$
1458 } F				$\nu_1(A_g)$
1448 }	1459F			
		1418ff	1415f	$\nu_{11}(B_{3u})$
1360m	1400f			$\nu_2 + \nu_3(A_g)$
		1339 } F		
		1321 }	1308F	$\nu_9(B_{2u})$
887FF }	882FF }			
878F }	872F }			$\nu_2(A_g)$
		778 } F		
		773 }	763F	$\nu_{12}(B_{3u})$
577 } m				
571 }	584m			$\nu_6(B_{1g})$
		520F	519F	$\nu_{10}(B_{2u})$
485 } F				
475 }	500F			$\nu_3(A_g)$
308f	313f			$\nu_7(B_{3g})$
		252m	260m	$\nu_8(B_{1u})$
		148m	164m	$\nu_4(A_u)$

*Fréquences en cm^{-1}; m = médium, f = faible, F = forte, é = épaule.

†La présente notation diffère des précédentes (8–13) en ce qu'elle se rapporte aux axes $0y$ et $0x$, définis suivant la même convention que dans les tables internationales de cristallographie. Les vibrations sont ici numérotées par ordre de fréquence décroissante dans chacune des classes de symétrie successivement, soit Ag, Au, B_{1g}, B_{3g}, B_{1u}, B_{2u} et B_{3u}.

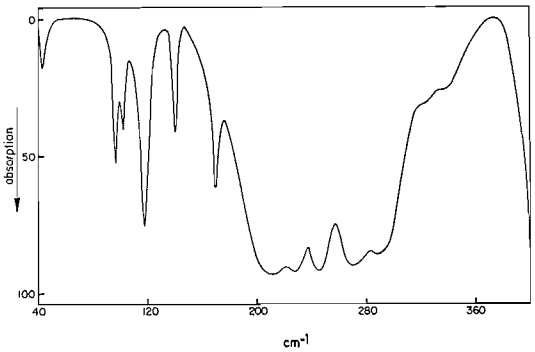

FIG. 3. Spectre d'absorption dans l'i.r. lointain à −190 °C de l'oxalate perhydrate de sodium (suspension dans le Nujol).

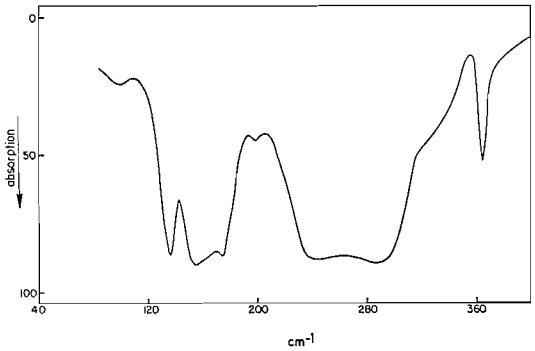

FIG. 4. Spectre i.r. lointain de $Na_2C_2O_4$.

Bandes de Réseau

L'oxalate perhydrate de sodium cristallise dans le système monoclinique (groupe spatial $P2_1/C$) avec deux "molécules" par maille élémentaire. Celle-ci contient donc un total de 8 molécules ou ions individuels: 4 cations Na^+, 2 anions oxalate et 2 molécules de peroxyde, soit un total de 24 degrés de liberté pour les vibrations dans la maille. La représentation réductible pour les translations est donnée par l'expression

$$\Gamma_{réd} = 3A_g + 3B_g + 9A_u + 9B_u$$

Can. J. Chem. Downloaded from www.nrcresearchpress.com by 210.87.254.42 on 09/05/12
For personal use only.

TABLEAU III

Diagrammes des corrélations de symétrie

Molécule ou ion	Modes		Site	Groupe spatial	Activité
H_2O_2		C_{2h}	C_1	C^5_{2h}	
	ν_1, ν_2, ν_3, R_z	A_g	A_g	A_g	Raman
	R_x, R_y	B_g		B_g	Raman
	ν_4, T_z	A_u	A_u	A_u	i.r.
	ν_5, ν_6, T_x, T_y	B_u		B_u	i.r.
$C_2O_4^{2-}$		D_{2h}	C_1	C^5_{2h}	
	ν_1, ν_2, ν_3	A_g		A_g	Raman
	ν_5, ν_6, R_x	B_{1g}	A_g		
	R_y	B_{2g}		B_g	Raman
	ν_7, R_z	B_{3g}			
	ν_4	A_u		A_u	i.r.
	ν_8, T_z	B_{1u}	A_u		
	ν_9, ν_{10}, T_y	B_{2u}		B_u	i.r.
	ν_{11}, ν_{12}, T_x	B_{3u}			
Na^+		$D_{\infty h}$	C_1	C^5_{2h}	
	T_z	Σ_u^+	A_u	A_g	Raman
				B_g	Raman
				A_u	i.r.
	T_x, T_y	Σ_u^-		B_u	i.r.

TABLEAU IV

Spectres de basse fréquence (cm^{-1}) de l'oxalate anhydre et du perhydrate

$Na_2C_2O_4$				$Na_2C_2O_4.H_2O_2$			
Raman		i.r.		Raman		i.r.	
25°	−190°	25°	−190°	25°	−190°	25°	−190°
		58	?			41	43
85	92.5	?	78	82	86		
						94	95
							101
119	123					117	117
128	133.5			124	128.5		
135	141.5	132	136		137.5	135	138
156	166.5			150	166		
167–170	~166 (large)	148	154	170	184.5	164	168
			174		206		
			200			204	212
	~225				217.5	218	228
	~235				243	240	245
	~255	252	240		~262	260	269
			284		~290 ?	280	284
	~288		320*			300	320
	308				313		
					342		339
		363	363		353	395	395
					~383 ?		

*Épaule.

Can. J. Chem. Downloaded from www.nrcresearchpress.com by 210.87.254.42 on 09/05/12
For personal use only.

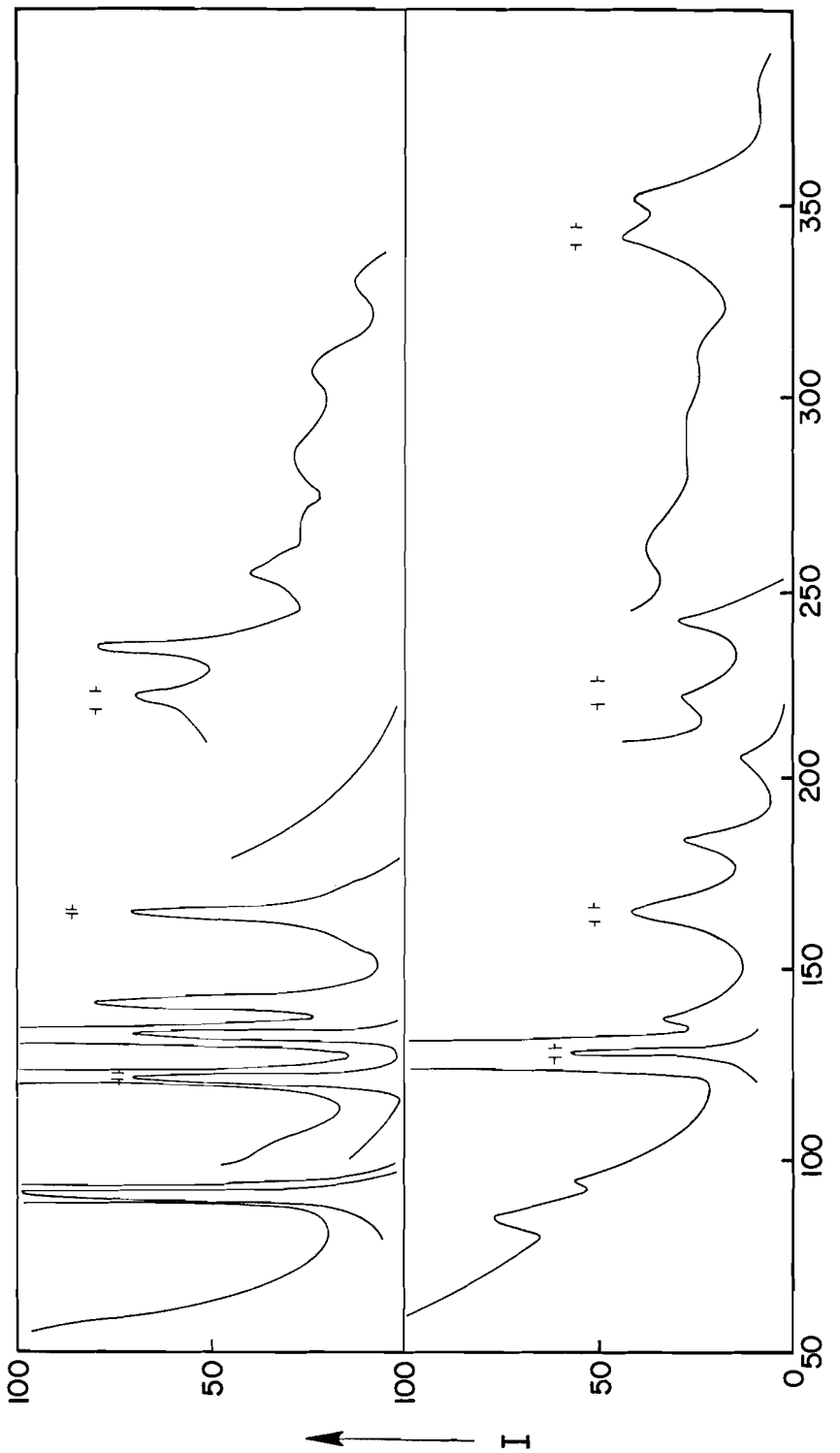

FIG. 5. Spectres Raman de basse fréquence de l'oxalate perhydrate (haut) et de l'oxalate anhydre (bas) à −190 °C.

De ceci il faut soustraire les trois modes $A_u + 2B_u$ appartenant à la branche acoustique; il reste donc un total de 15 modes de translation actifs en i.r. et 6 actifs en Raman (cf. Tableau III).

Quant aux rotations gênées ou librations, les corrélations de symétrie en prévoient 6 chacune pour l'ion oxalate et la molécule de peroxyde, toutes actives en Raman. Les résultats expérimentaux (Tableau IV) concordent assez bien avec ces prévisions puisque l'on trouve 12 bandes dans l'i.r. lointain (Fig. 3) — outre les 2 fondamentales de l'ion oxalate à 260 et 164 cm^{-1} (Fig. 4) — et un nombre égal en Raman des basses fréquences (Fig. 5). A celles-ci il faut ajouter la bande de libration ν_{R_x} à 857 cm^{-1} qui est en fait un mode de réseau. Il serait téméraire de chercher ici une attribution pour chacune de ces bandes de réseau. Notons cependant que celles qui n'ont pas d'équivalent dans les spectres de l'oxalate anhydre (soit à 383, 353 et 342 cm^{-1} en Raman, et à 339 et 228 cm^{-1} en i.r.) doivent être des librations de la molécule H_2O_2. Ces fréquences sont un peu plus hautes que dans le peroxyde cristallin (10) ce qui s'explique par les liaisons hydrogène plus fortes de l'oxalate perhydrate.

Remerciement

Ce travail a été exécuté avec l'aide financière du Conseil National des Recherches du Canada.

1. B. F. PEDERSEN et B. PEDERSEN. Acta Chem. Scand. **18**, 1454 (1964).
2. W. C. SCHUMB, C. N. SATTERFIELD, and R. I. WENTWORTH. Hydrogen Peroxide. Reinhold Publ. Corp., New York (1955).
3. J. L. ARNAU et P. A. GIGUÈRE. J. Mol. Struct. In press.
4. B. F. PEDERSEN. Acta Chem. Scand. **21**, 801 (1967).
5. P. A. GIGUÈRE, E. A. SECCO et R. S. EATON. Discuss. Faraday Soc. **14**, 104 (1953).
6. G. C. PIMENTEL et C. H. SEDERHOLM. J. Chem. Phys. **24**, 639 (1956).
7. E. R. LIPPINCOTT et R. SCHROEDER. J. Chem. Phys. **23**, 1099 (1955).
8. P. A. GIGUÈRE et K. B. HARVEY. J. Mol. Spectrosc. **36**, 3 (1959).
9. Y. AMAKO and P. A. GIGUÈRE. Can. J. Chem. **40**, 765 (1962).
10. P. A. GIGUÈRE et C. CHAPADOS. Spectrochim. Acta, **22**, 1131 (1966).
11. F. DOUVILLÉ, C. DUVAL et J. LECOMTE. C. R. **212**, 697 (1941).
12. K. ITO et H. J. BERNSTEIN. Can. J. Chem. **34**, 170 (1956).
13. H. MURATA et K. KAWAI. J. Chem. Phys. **25**, 589 (1956).
14. M. J. SCHMELZ, T. MIYAZAWA, S. MIZUSHIMA, T. J. LANE et J. V. QUAGLIANO. Spectrochim. Acta, **9**, 51 (1957).
15. G. M. BEGUN et W. H. FLETCHER. Spectrochim. Acta, **19**, 1343 (1963).
16. L. BARDET et G. FLEURY. C. R. **265**, 983 (1967).
17. V. LORENZELLI, F. GESMUNDO et G. RANDI. Rend. Accad. Naz. XL 16–17 (4) 63–87 (1965–66).

Can. J. Chem. Downloaded from www.nrcresearchpress.com by 210.87.254.42 on 09/05/12
For personal use only.

Can. J. Chem. Downloaded from www.nrcresearchpress.com by 210.87.254.42 on 09/05/12
For personal use only.

Reactions of organotin compounds. X. Reactions of tin hydrides with CF_2=$CFRe(CO)_5$, CF_3CF=$CFRe(CO)_5$, and some fluorinated alkenes

M. AKHTAR AND H. C. CLARK
Department of Chemistry, University of Western Ontario, London, Ontario

Received April 21, 1969

Trimethyltin hydride reacts with CF_2=$CFRe(CO)_5$ under ultraviolet irradiation to give new fluorovinyl derivatives of —$Re(CO)_5$. Similar products were obtained using dimethyltin dihydride, but no reaction occurred between trimethyltin hydride and CF_3CF=$CFRe(CO)_5$. The reactions of trifluoroethylene, 1,1-difluoroethylene, and vinyl fluoride with trimethyltin hydride have been studied, thus completing the sequence of such reactions with fluorinated ethylenes. While both possible addition products were obtained with trifluoroethylene, and also from the corresponding reaction with perfluoropropene, 1,1-difluoroethylene gave only $(CH_3)_3SnCH_2CF_2H$, and with vinyl fluoride only trimethyltin fluoride and ethylene were isolated. Possible explanations are proposed and spectroscopic data for the new compounds are presented.

Canadian Journal of Chemistry, 47, 3753 (1969)

Introduction

Our previous studies established that the addition of trimethyltin hydride to the C=C bonds of perfluorovinyl derivatives of silicon, germanium, and tin (1, 2) occurs by a free radical mechanism and that both possible isomers, $R_3MCF[Sn(CH_3)_3]CF_2H$ and $R_3MCFHCF_2Sn(CH_3)_3$ (M = Si, Ge, or Sn), are formed. These reactions differ from the additions of organotin hydrides to acetylenes where both a polar as well as a radical mechanism are probably involved, and particularly from the non-terminal additions with electrophilic acetylenes which are controlled mainly by polar effects (3–6).

In the present work, the reactivity of some perfluorovinyl derivatives of a transition metal towards organotin hydrides has been studied, as well as the related reactions of trimethyltin hydride with some unsymmetrically substituted fluoro-olefins.

Discussion

Trimethyltin hydride did not react with pentacarbonylperfluorovinylrhenium in benzene at 25° over a long period. At 45° for 48 h in butyronitrile, only a limited reaction occurred with the formation of *cis*-CFH=$CFRe(CO)_5$ and CF_2=$CHRe(CO)_5$ in approximately equal amounts. The reaction therefore occurs much less readily under thermal conditions than the comparable additions of trimethyltin hydride to perfluorovinyl-silicon, germanium, and tin derivatives (1, 2).

When trimethyltin hydride and CF_2=$CFRe(CO)_5$ were exposed to ultraviolet (u.v.) irradiation at 35° for 36 h in benzene, a considerable amount of trimethyltin fluoride was deposited, with *trans*-CFH=$CFRe(CO)_5$ being the main volatile product. The *cis* isomer and CF_2=$CHRe(CO)_5$ were formed in smaller but approximately equal amounts. Similarly, extensive reaction also occurred at 50° in benzene in the presence of azobisisobutyronitrile (AIBN). A considerable amount of trimethyltin fluoride was deposited, and *trans*-CFH=$CFRe(CO)_5$, CF_2=$CHRe(CO)_5$, and *cis*-CFH=$CFRe(CO)_5$ were formed in order of decreasing yield. No addition compounds were isolated, but the nature of the reaction products strongly suggests that addition has occurred, followed by the rapid elimination of trimethyltin fluoride, probably by a β-fluorine elimination process.

$$(CO)_5ReCFHCF_2Sn(CH_3)_3 \rightarrow CF_2{=}CHRe(CO)_5 + (CH_3)_3SnF$$

$$(CO)_5ReCF[Sn(CH_3)_3]CF_2H \rightarrow CFH{=}CFRe(CO)_5 + (CH_3)_3SnF$$

Such a process has already been proposed in connection with the products formed in the addition of trimethyltin hydride to other perfluorovinyl compounds (1, 2), and is also consistent with the formation of *cis*- and *trans*-CFH=$CFMn(CO)_5$ and trimethylfluorogermane or trimethyltin fluoride from the reaction of trifluoroethylene with $(CH_3)_3GeMn(CO)_5$ and $(CH_3)_3SnMn(CO)_5$, respectively (7, 8).

In the present case, *trans*-CFH=$CFRe(CO)_5$ was always more abundant than its *cis* isomer, although in cases reported previously (1, 2), the

Can. J. Chem. Downloaded from www.nrcresearchpress.com by 210.87.254.42 on 09/05/12
For personal use only.

cis isomer was in higher yield. Again, however, it was established that isomerization of *cis* to *trans* occurred under u.v. irradiation; after 6 h under such irradiation, 75% of the *cis* isomer had rearranged to the *trans* form. Seyferth and Vaughan (9) have also reported that the *cis* addition product of trimethyltin hydride and propyne did not rearrange thermally or in the presence of either AIBN or benzoyl peroxide, but did so upon u.v. irradiation. It is also known, however, that such *cis* to *trans* conversion proceeds under the influence of a triorganotin radical (10).

Dimethyltin dihydride did not react with $CF_2{=}CFRe(CO)_5$ in benzene at 25°, but considerable reaction occurred at 25° under u.v. irradiation. Dimethyltin difluoride was deposited, the products being, in order of decreasing yield, *trans*-$CFH{=}CFRe(CO)_5$, *cis*-$CFH{=}CFRe(CO)_5$, and $CF_2{=}CHRe(CO)_5$. This is entirely consistent with the results of other similar addition reactions (1, 2, 11) and with both the greater reactivity of dimethyltin dihydride (12) and the high lattice energy of dimethyltin difluoride (13). It thus appears that a perfluorovinyl transition metal derivative does not differ substantially from its Group IVB analogue in its addition reaction with organotin hydrides, other than showing a somewhat increased reluctance to participate in such reactions.

Introduction of a CF_3 group as a substituent about the vinylic C=C bond, greatly reduced the latter's reactivity. Trimethyltin hydride and $CF_3CF{=}CFRe(CO)_5$ did not react at 45° in butyronitrile, nor under u.v. irradiation in benzene at 40°. In the presence of AIBN in benzene at 45°, complete decomposition of the hydride to hexamethylditin occurred.

The free radical additions of organotin hydrides across the C=C bonds of fluoro-olefins, such as tetrafluoroethylene, have been previously described (14). The unsymmetrically substituted olefin, trifluoroethylene, has now also been found to react with trimethyltin hydride under u.v. irradiation at 25° to give in high yield approximately equal amounts of the two possible addition products, $(CH_3)_3SnCF_2CFH_2$ and $(CH_3)_3SnCFHCF_2H$. A similar reaction involving trimethyltin hydride and perfluoropropene gave $(CH_3)_3SnCF_2CFHCF_3$ and $(CH_3)_3SnCF(CF_3)CF_2H$ in approximately equal amounts. However, when trimethyltin hydride and 1,1-difluoroethylene were allowed to react under u.v. light at 25°, quantitative addition occurred to give only one product, $(CH_3)_3SnCH_2CF_2H$. This preferred formation of just one isomer is possibly due to the presence of the 2 fluorine atoms, as a consequence of which ionic forms, e.g. $F^-(FC{=}CH_2)^+$, have been described (15, 16). Similarly, an increase in the polarity of the C=C bond in $CF_2{=}CCl_2$ has been attributed to the strong inductive effect of the halogens (15, 16) so that RO^- ions attack the carbon atom having the fluorine substituents

$$C_2H_5OH + CF_2{=}CCl_2 \rightarrow C_2H_5OCF_2CHCl_2$$

It appears, then, that the reaction of trimethyltin hydride with 1,1-difluoroethylene might be described in terms of attack of hydride (from $(CH_3)_3Sn^{\delta+}{-}H^{\delta-}$) on the carbon atom bearing the fluorine substituents. Alternatively, the exclusive formation of 1,1-difluoro-2-(trimethylstannyl)ethane may be explained in terms of a free radical mechanism

$$R_3Sn\cdot + CF_2{=}CH_2 \rightarrow \cdot CF_2CH_2SnR_3$$
$$\cdot CF_2CH_2SnR_3 \xrightarrow{R_3SnH} HCF_2CH_2SnR_3 + R_3Sn\cdot$$

The formation of $\cdot CF_2CH_2SnR_3$ will be greatly favored over the formation of $\cdot CH_2CF_2SnR_3$, due to the presence of the fluorine atoms, whereas such exclusiveness is neither expected nor observed in the reaction with the more symmetrically substituted trifluoroethylene.

To complete this sequence of reactions of the hydride with a complete series of substituted olefins, the reaction of trimethyltin hydride with vinyl fluoride was finally studied. Since this olefin contains only one fluorine atom, the configuration of the addition product would be of particular interest. Unfortunately, a stable addition product could not be isolated, the formation of trimethyltin fluoride and ethylene being very rapid even at 25°.

The configurations of the fluorovinyl derivatives of pentacarbonylrhenium have been assigned from the values of the H—F coupling constants observed in their proton magnetic resonance (p.m.r.) spectra, together with the observed frequencies of the C=C stretching absorptions, both of which are consistent with values previously reported for fluorovinyl derivatives of silicon, germanium, and tin (1, 2, 11). The complete spectroscopic data for the fluorovinyl

TABLE I

Infrared and p.m.r. assignments for fluorovinyl derivatives of —$Re(CO)_5$ and —$Mn(CO)_5$*

	$\delta_{H\ vinyl}$	J_{12}	J_{23}	J_{13}	$\nu_{C=C}$ (cm^{-1})
$(CO)_5Re$, H, F, F	−5.78	82	—	26	1625
$(CO)_5Re$, F, F, H	−7.57	87	10	—	1675
$(CO)_5Re$, F, H, F	−3.8	—	12	46	1615
$(CO)_5Mn$, H, F, F	−5.7	80	—	25	1630
$(CO)_5Mn$, F, F, H	−8.1	86.5	10.2	—	1670

*Chemical shifts (p.p.m.) with respect to internal TMS and coupling constants in Hz. The data for manganese compounds are taken from ref. 7.

derivatives of pentacarbonylmanganese (7) and pentacarbonylrhenium are given in Table I.

The addition products obtained from the reactions of trimethyltin hydride with fluoro-olefins were characterized by their ^1H and ^{19}F magnetic resonance studies. From the closely coincident values of H—F coupling constants the ^1H and ^{19}F spectra were matched. The complete nuclear magnetic resonance (n.m.r.) data obtained by normal first order analysis are given in Table II for $(CH_3)_3SnCH_2CF_2H$ and in Table III for $(CH_3)_3SnCF_2CFH_2$ and $(CH_3)_3SnCFHCF_2H$. In these compounds the following ranges of coupling constants were observed

$$J_{(H-F)gem} = 47\text{–}62\ Hz$$
$$J_{(H-F)vic} = 8\text{–}24\ Hz$$
$$J_{(F-F)vic} = 10\text{–}23\ Hz$$

These values are in good agreement with coupling constants observed in similar compounds whose spectra have been discussed in considerable detail (1, 2, 17–19). In the molecule $(CH_3)_3SnCFHCF_2H$ there are 3 different substituents on the C atom α to tin which causes the 2 fluorine atoms in the $—CF_2H$ group to be magnetically non-equivalent, thus giving rise to $J_{(F-F)gem} = 294$ Hz. Two non-equivalent H—F coupling constants are also observed, due to the coupling of these 2 fluorine atoms with one geminal proton. Similarly, 2 non-equivalent coupling constants arise from the coupling of these 2 fluorine atoms with one vicinal proton. Such non-equivalent coupling constants between an alkane proton and 2 magnetically non-equivalent vicinal fluorine atoms have also been observed in other compounds (1, 2, 17, 20).

The values of other coupling constants, for example, arising from the satellites due to ^{119}Sn, ^{117}Sn, and ^{13}C, are consistent with the observed data for other fluorocarbon derivatives of tin (1, 2, 17, 18).

The n.m.r. data for the molecule $(CH_3)_3SnCF(CF_3)CF_2H$ are given in Table II. In both

Can. J. Chem. Downloaded from www.nrcresearchpress.com by 210.87.254.42 on 09/05/12
For personal use only.

Can. J. Chem. Downloaded from www.nrcresearchpress.com by 210.87.254.42 on 09/05/12
For personal use only.

TABLE II

Nuclear magnetic resonance data for $(CH_3)_3SnCF(CF_3)CF_2H$ and $(CH_3)_3SnCH_2CF_2H$*

	$(CH_3)_3SnCF^b(CF_3{}^c)CF^aF^{a1}H^a$		$(CH_3)_3SnCH_2{}^bCF_2{}^aH^a$	
Parameter	^1H spectrum	^{19}F spectrum	^1H spectrum	^{19}F spectrum
δ_{CH_3}	−0.25		−0.20	
δ_{H^a}	−5.9		−6.0	
δ_{H^b}			−1.35	
δ_{F^a}		120		97.67
$\delta_{F^{a1}}$		124.5		
δ_{F^b}		213		
δ_{F^c}		72		
$J^{119}_{Sn-CH_3}$	58.5		56	
$J^{117}_{Sn-CH_3}$	56		54	
$J^{13}_{C-CH_3}$	132		127	
$J^{119}_{Sn-H^a}$ }	26		36	
$J^{117}_{Sn-H^a}$ }				
$J^{119}_{Sn-H^b}$			50	
$J^{117}_{Sn-H^b}$			48	
$J^{119}_{Sn-F^a}$ }		Below noise		85
$J^{117}_{Sn-F^a}$ }				
$J^{119}_{Sn-F^b}$ }		224		
$J^{117}_{Sn-F^b}$ }				
$J_{F^a-F^{a1}}$		320		
$J_{F^a-F^b}$		12		
$J_{F^{a1}-F^b}$		15		
$J_{F^a-F^c}$		6.0±0.5		
$J_{F^{a1}-F^c}$		8.55±0.5		
$J_{F^b-F^c}$		14		
$J_{H^a-F^a}$	60	60	61	60.52
$J_{H^a-F^{a1}}$	56	56		
$J_{H^a-F^b}$	8	8		
$J_{H^a-F^c}$	Not resolved	Not resolved		
$J_{H^b-F^a}$			24	23.1
$J_{H^a-H^b}$			4.5	

*Chemical shifts are in p.p.m. with TMS and CCl_3F as internal references. Coupling constants in Hz.

TABLE III

Nuclear magnetic resonance data for $(CH_3)_3SnCF_2CFH_2$ and $(CH_3)_3SnCFHCF_2H$

	$(CH_3)_3SnCF_2{}^bCF^aH_2{}^a$		$(CH_3)_3SnCF^bH^bCF^aF^{a1}H^a$	
Parameter	^1H spectrum	^{19}F spectrum	^1H spectrum	^{19}F spectrum
δ_{CH_3}	−0.29		−0.29	
δ_{H^a}	−4.38		−6.06	
δ_{H^b}			−4.92	
δ_{F^a}		229.32		117.54
$\delta_{F^{a1}}$				124.1
δ_{F^b}		111.48		237.43
$J^{119}_{Sn-CH_3}$	56		56	
$J^{117}_{Sn-CH_3}$	53		53	
$J^{13}_{C-CH_3}$	128		128	
$J^{119}_{Sn-F^b}$ }		267	260	
$J^{117}_{Sn-F^b}$ }				
$J_{H^a-F^a}$	48	47.62	61	61.76
$J_{H^a-F^{a1}}$			57	58.82
$J_{H^a-F^b}$	16.5	17.65	10	9.52
$J_{H^a-H^b}$			3	
$J_{H^b-F^a}$			26	26.41
$J_{H^b-F^{a1}}$			16	15
$J_{H^b-F^b}$			47	46.03
$J_{F^a-F^{a1}}$				294.14
$J_{F^b-F^a}$		10.9		17.61
$J_{F^b-F^{a1}}$				23

*Chemical shifts (p.p.m.) are relative to internal TMS and CCl_3F for ^1H and ^{19}F spectrum, respectively. Coupling constants in Hz.

Can. J. Chem. Downloaded from www.nrcresearchpress.com by 210.87.254.42 on 09/05/12
For personal use only.

molecules $(CH_3)_3SnCF(CF_3)CF_2H$ and $(CH_3)_3SnCF_2CFHCF_3$, magnetic non-equivalence of the 2 fluorine atoms of the CF_2 group arises due to the fact that there are 3 different substituents on the adjacent carbon atoms. The spectrum of $(CH_3)_3SnCF_2CFHCF_3$ has already been discussed in detail by Clark *et al.* (17), hence assignments could readily be made for the other molecule $(CH_3)_3SnCF(CF_3)CF_2H$.

Experimental

All general techniques have been described previously (1, 2). Trimethyltin hydride and dimethyltin dihydride were prepared by the procedure of Finholt *et al.* (21), using *n*-butyl ether as solvent. Pentacarbonylperfluorovinylrhenium and pentacarbonylperfluoropropenylrhenium were prepared by the procedure described by Jolly *et al.* (22). Trifluoroethylene, vinyl fluoride, and 1,1-difluoroethylene were obtained from Matheson of Canada, and perfluoropropene from Columbia Organic Chemicals. Proton magnetic resonance spectra were obtained with a Varian A60 spectrometer, and ^{19}F spectra with a Varian HA100 spectrometer operating at 94.1 Mc.p.s.

Reactions of Organotin Hydrides with Pentacarbonylperfluorovinylrhenium and Pentacarbonylperfluoropropenylrhenium

(*a*) Trimethyltin hydride (0.1 g, 0.6 mmole) and $(CO)_5ReCF{=}CF_2$ (0.234 g, 0.57 mmole) were allowed to react in benzene (4 ml) at 25° for 1 week. There was no visible reaction and vacuum fractionation led to complete recovery of the reactants.

A similar mixture, sealed with azobisisobutyronitrile (50 mg) at 50° for 20 h, gave firstly a small amount of a non-condensable gas, some unreacted trimethyltin hydride, and benzene as volatile products.

The remaining solids were washed with tetrahydrofuran and filtered to give a white residue (0.155 g, *ca.* 70% yield), identified spectroscopically as trimethyltin fluoride. Tetrahydrofuran was removed from the filtrate at 0° to give a yellow solid whose infrared spectrum (Nujol mull) showed three new C=C stretching absorptions (cm^{-1}) at 1675 s, 1625 m, and 1615 m in addition to the ν (C=C) for unreacted $(CO)_5ReCF{=}CF_2$ at 1705 cm^{-1}. This solid mixture was dissolved in acetonitrile and its ^1H n.m.r. spectrum recorded (Table I). This confirmed the presence of *trans*-$CFH{=}CFRe(CO)_5$ (60%), *cis*-$CFH{=}CFRe(CO)_5$ (13%), and $(CO)_5ReCH{=}CF_2$ (27%). Acetonitrile was then removed from this mixture at 0°, under vacuum. The remaining solids were sublimed under reduced pressure at room temperature, over a −78° cold probe. During the first 10 min, $(CO)_5ReCF{=}CF_2$ and *cis*-$CFH{=}CFRe(CO)_5$ were collected. The presence of *cis*-$CFH{=}CFRe(CO)_5$ was confirmed by its p.m.r. spectrum and the corresponding C=C stretching absorption at 1625 cm^{-1}. After the removal of *cis*-$CFH{=}CFRe(CO)_5$ from the mixture, *trans*-$CFH{=}CFRe(CO)_5$ and $(CO)_5ReCF{=}CF_2$ were collected on the cold probe for the next 20 min. The p.m.r. spectrum of this fraction corresponded to *trans*-$CFH{=}CFRe(CO)_5$, the C=C stretching absorption being at 1675 cm^{-1}. The i.r. spectrum of the remaining solid material at the bottom of the sublimation flask showed weak absorptions at 1705 and 1675 cm^{-1} and a strong absorption at 1615 cm^{-1}. The p.m.r. spectrum of this material (Table I) showed the presence of only $(CO)_5ReCH{=}CF_2$. Hence the C=C stretching absorption at 1615 cm^{-1} was assigned to $(CO)_5ReCH{=}CF_2$.

The products *trans*-$CFH{=}CFRe(CO)_5$, *cis*-$CFH{=}CFRe(CO)_5$, and $(CO)_5ReCH{=}CF_2$ could not be separated completely from $(CO)_5ReCF{=}CF_2$. Hence, due to the overlapping of absorptions in the CO and C—F stretching region, individual assignments could not be made for the new reaction products.

In the following experiments (*b–e*) the reaction mixtures were worked up as (*a*) above, and the products were identified by their i.r. and p.m.r. spectra.

(*b*) Trimethyltin hydride (0.1 g, 0.6 mmole) and $(CO)_5ReCF{=}CF_2$ (0.237 g, 0.58 mmole) were exposed to u.v. irradiation at 35° for 36 h in benzene. Examination of the reaction mixture gave some unreacted $(CO)_5ReCF{=}CF_2$ and $(CH_3)_3SnH$, along with *trans*-$CFH{=}CFRe(CO)_5$ as the main product and *cis*-$CFH{=}CFRe(CO)_5$ and $(CO)_5ReCH{=}CF_2$ in about equal amounts. From the reaction tube, trimethyltin fluoride (0.049 g) was recovered, corresponding to 47.6% reaction.

A sample (0.15 g) containing $(CO)_5ReCF{=}CF$ and *cis*-$CFH{=}CFRe(CO)_5$ was exposed to u.v. irradiation at 35° for 8 h in benzene. The i.r. spectrum of this mixture showed a strong band at 1675 cm^{-1} (C=C stretch) characteristic of *trans*-$CFH{=}CFRe(CO)_5$, along with the bands at 1705 and 1625 cm^{-1}, corresponding to the starting materials $(CO)_5ReCF{=}CF_2$ and *cis*-$CFH{=}CFRe(CO)_5$, respectively. The band at 1625 cm^{-1} (C=C stretch), characteristic of *cis*-$CFH{=}CFRe(CO)_5$, was about 25% of its original intensity.

(*c*) Trimethyltin hydride (0.1 g, 0.6 mmole) and $(CO)_5ReCF{=}CF_2$ (0.234 g, 0.57 mmole) were allowed to react at 45° for 48 h in butyronitrile. The i.r. spectrum of the reaction mixture showed 2 weak bands of almost equal intensity at 1625 and 1615 cm^{-1} corresponding to the C=C stretching frequencies of *cis*-$CFH{=}CFRe(CO)_5$ and $(CO)_5ReCH{=}CF_2$, respectively. From the reaction tube, trimethyltin fluoride (0.018 g) was recovered, corresponding to 17% reaction.

(*d*) Dimethyltin dihydride (0.2 g, 0.13 mmole) and $(CO)_5ReCF{=}CF_2$ (0.54 g, 1.3 mmoles) did not react in benzene (4 ml) at 25° after 48 h. Considerable reaction occurred when a similar mixture was exposed to u.v. irradiation at 25° for 6 h. Dimethyltin difluoride (0.035 g, *ca.* 14% yield) was deposited, and in addition to small amounts of the starting materials, the reaction products *trans*-$CFH{=}CFRe(CO_5)$, *cis*-$CFH{=}CFRe(CO)_5$, and $(CO)_5ReCH{=}CF_2$ were identified. However, the amounts of these products were too small to be determined quantitatively even by integration of the p.m.r. spectrum.

(*e*) Trimethyltin hydride (0.29 g, 1.75 mmoles) and $(CO)_5ReCF{=}CFCF_3$ (0.8 g, 1.75 mmoles) were allowed to react at 45° in butyronitrile (4 ml) for 1 week. Examination of the i.r. spectrum of the gas phase mixture showed the presence of a non-condensible gas, presumably a mixture of hydrogen and methane, and some unreacted trimethyltin hydride. The i.r. spectra of the involatile compounds in the reaction tube, confirmed the presence

Can. J. Chem. Downloaded from www.nrcresearchpress.com by 210.87.254.42 on 09/05/12
For personal use only.

of unreacted $(CO)_5ReCF{=}CFCF_3$ and hexamethylditin (22, 23). The p.m.r. spectrum of this mixture did not show the presence of any vinylic proton. From the reaction tube, a mixture (0.024 g) of metallic tin and a trace of trimethyltin fluoride was recovered.

When similar reaction mixtures were exposed to u.v. irradiation at 40° or allowed to react at 45° in the presence of azobisisobutyronitrile, no reaction products could be identified except from the decomposition of the tin hydride to hexamethylditin and hydrogen.

Reactions of Trimethyltin Hydride with Fluoro-olefins

(*a*) Trimethyltin hydride (0.5 g, 3 mmoles) and 1,1-difluoroethylene (0.2 g, 3 mmoles) were exposed to u.v. irradiation at 25° for 4 h. A small amount of trimethyltin fluoride, identified spectroscopically, was deposited. Vacuum fractionation gave, at −78°, a high yield (0.62 g, 90% yield) of a slightly volatile liquid product. This was identified from its n.m.r. spectra (Table II) to be $(CH_3)_3SnCH_2CF_2H$.

This reaction was repeated, but always the only product obtained in quantitative yields was $(CH_3)_3SnCH_2CF_2H$. This compound slowly decomposed to give visible amounts of trimethyltin fluoride after about 8 h at room temperature. Decomposition to $(CH_3)_3SnF$ and $CH_2{=}$ CFH was complete after 48 h at room temperature.

(*b*) Trimethyltin hydride (0.5 g, 3 mmoles) and trifluoroethylene (0.26 g, 3 mmoles) were exposed to u.v. irradiation at 25° for 6 h. A trace of trimethyltin fluoride, identified spectroscopically, was deposited. Vacuum fractionation gave, at −78°, a high yield (0.69 g, 93% yield) of a liquid product with a vapor pressure of about 1 cm at room temperature. This was identified from its n.m.r. spectra (Table III) as a mixture of 2 addition products, $(CH_3)_3SnCF_2CFH_2$ and $(CH_3)_3SnCFHCF_2H$, in approximately equal amounts.

Anal. Calcd. for $SnC_5F_3H_{11}$: H, 4.89; C, 24.37; F, 23.09. Found: H, 4.56; C, 24.64; F, 23.33.

(*c*) Trimethyltin hydride (0.5 g, 3 mmoles) and perfluoropropene (0.45 g, 3 mmoles) were exposed to u.v. irradiation at 25° for 6 h. Vacuum fractionation gave, at −78°, a high yield (0.897 g, 95% yield) of a liquid product with very low (~ 0.5 cm at 25°) vapor pressure. This was identified from its n.m.r. spectra (Table II) as a mixture of 2 addition products $(CH_3)_3SnCF_2CFHCF_3$ and $(CH_3)_3SnCF(CF_3)CF_2H$ in about equal amounts (17).

Anal. Calcd. for $SnC_6F_6H_{10}$: H, 3.20; C, 22.89; F, 36.20. Found: H, 3.47; C, 22.74; F, 36.52.

(*d*) Trimethyltin hydride (0.5 g, 3 mmoles) and vinyl fluoride (0.138 g, 3 mmoles) were exposed to u.v. irradiation at 25°. After ½ h, substantial amounts of trimethyltin fluoride (0.39 g) had been deposited. Ethylene was the only other reaction product identified, in addition to small amounts of the starting materials.

Acknowledgment

The financial support of the National Research Council of Canada is gratefully acknowledged.

1. M. AKHTAR and H. C. CLARK. Can. J. Chem. **46**, 633 (1968).
2. M. AKHTAR and H. C. CLARK. Can. J. Chem. **46**, 2165 (1968).
3. A. J. LEUSINK and J. W. MARSMAN. Rec. Trav. Chim. **84**, 1123 (1965).
4. A. J. LEUSINK, J. W. MARSMAN, and H. A. BUDDING. Rec. Trav. Chim. **84**, 689 (1965).
5. A. J. LEUSINK, H. A. BUDDING and W. DRENTH. J. Organometal. Chem. Amsterdam, **9**, 295 (1967).
6. A. J. LEUSINK and H. A. BUDDING. J. Organometal. Chem. Amsterdam, **11**, 533 (1968).
7. H. C. CLARK and J. H. TSAI. Inorg. Chem. **5**, 1407 (1966).
8. H. C. CLARK, J. D. COTTON, and J. H. TSAI. Inorg. Chem. **5**, 1582 (1966).
9. D. SEYFERTH and L. G. VAUGHAN. J. Organometal. Chem. Amsterdam, **1**, 138 (1963).
10. A. J. LEUSINK, H. A. BUDDING, and W. DRENTH. J. Organometal. Chem. Amsterdam, **11**, 541 (1968).
11. A. D. BEVERIDGE, H. C. CLARK, and J. T. KWON. Can. J. Chem. **44**, 179 (1966).
12. H. G. KUIVILA. *In* Advances in organometallic chemistry. Vol. I. *Edited by* F. G. A. Stone and R. West. Academic Press, Inc., New York. 1964. p. 47.
13. H. C. CLARK and R. G. GOEL. J. Organometal. Chem. Amsterdam, **7**, 263 (1967).
14. H. C. CLARK, S. G. FURNIVAL, and J. T. KWON. Can. J. Chem. **41**, 2889 (1963).
15. L. J. BELLAMY. Spectrochim. Acta, **13**, 60 (1958).
16. M. STACEY, J. C. TATLOW, and A. G. SHARPE (*Editors*). Advances in fluorine chemistry. Vol. 4. Butterworths Scientific Publications, London. 1965. pp. 50, 75.
17. H. C. CLARK, N. CYR, and J. H. TSAI. Can. J. Chem. **45**, 1073 (1967).
18. H. C. CLARK, J. T. KWON, L. W. REEVES, and E. J. WELLS. Can. J. Chem. **41**, 3005 (1963).
19. P. M. TREICHEL, E. PITCHER, and F. G. A. STONE. Inorg. Chem. **1**, 511 (1962).
20. J. A. POPLE, W. G. SCHNEIDER, and J. H. BERNSTEIN. High resolution nuclear magnetic resonance. McGraw-Hill Book Co., Inc., New York. 1959. p. 377.
21. A. E. FINHOLT, A. C. BOND, JR., K. E. WILZBACH, and H. I. SCHLESINGER. J. Amer. Chem. Soc. **69**, 2692 (1947).
22. P. W. JOLLY, M. I. BRUCE, and F. G. A. STONE. J. Chem. Soc. 5830 (1957).
23. T. L. BROWN and G. L. MORGAN. Inorg. Chem. **2**, 736 (1963).

Can. J. Chem. Downloaded from www.nrcresearchpress.com by 210.87.254.42 on 09/05/12
For personal use only.

Reaction of hydrogen atoms with propane: relative Arrhenius parameters for the attack on the 1 and 2 positions

J. M. CAMPBELL, O. P. STRAUSZ, AND H. E. GUNNING
Department of Chemistry, University of Alberta, Edmonton, Alberta

Received May 26, 1969

Arrhenius parameters were measured for the relative rate of attack of hydrogen atom on the primary and secondary C—H bonds of propane. The mercury photosensitization of hydrogen was used as the source of hydrogen atom and the abstraction reactions were monitored by the formation of isomeric hexanes.

Detailed kinetic analysis was applied to assess the importance of secondary reactions.

Canadian Journal of Chemistry, 47, 3759 (1969)

The abstraction reactions of hydrogen atoms with numerous paraffin molecules have been studied and Arrhenius parameters determined (1). In relatively few cases, however, was the site of attack specified. The Arrhenius parameters $\log k = 12.7 - 7400/2.3RT$ cc mole^{-1} s^{-1} reported for the propane reaction, for example (2), refer to the composite sum of the two concurrent reactions

[1] $$H + C_3H_8 \rightarrow i\text{-}C_3H_7 + H_2$$

[2] $$H + C_3H_8 \rightarrow n\text{-}C_3H_7 + H_2.$$

The ratio k_2/k_1 has not been determined directly. An estimate of the ratio can be made if it is assumed that the reactivity of the primary C—H bonds in propane is the same as that of the C—H bonds in ethane. Using the known rate constants, $10^{12.5} \exp(-9000/RT)$ cc mole^{-1} s^{-1} for ethane (2) and $10^{12.7} \exp(-7400/RT)$ cc mole^{-1} s^{-1} for propane (3), one obtains for the ratio

$$k_2/(k_2 + k_1) = 0.63 \exp(-1600/RT)$$

which leads to a value of k_2/k_1 of about 0.8 exp $(-1700/RT)$ between 30 and 200 °C.

In the present article we report an experimental determination of the k_2/k_1 ratio. The triplet mercury photosensitization of hydrogen was used as the source of hydrogen atoms and reactions [1] and [2] were monitored by the rate of formation of the three isomeric hexanes, *n*-hexane, 2,3-dimethylbutane, and 2-methylpentane.

Experimental

The initial experiments were done in a static system. In order to achieve better control of the Hg concentration, further experiments were carried out in a circulating system.

The static system consisted of a 50 mm diameter by 300 mm length cell with a total volume of 524 cc. The valve and cell were enclosed in a close fitting aluminum block furnace with double windows on each end. The furnace temperature was kept constant to within ±0.4 °C. Temperature was read with a calibrated thermocouple.

The circulating system consisted of a 50 mm diameter by 40 mm length quartz cell enclosed in an aluminum block furnace. Heating tape was wrapped for about 6 in. along the tube ahead of the cell to insure that the gas was equilibrated before entering the cell. Both furnace and tape were heated by temperature control units. The gas was circulated by a magnetically operated stirrer which incorporated metal vanes and shaft, teflon bearings, and a glass encased magnet. The gas was passed through a ballast volume, an empty U-trap, and then through one filled with 1/8 in. diameter glass helices before entering the cell. The Hg concentration could then be controlled by the temperature of this trap. The total volume of the system was about 970 cm^3. In reactions done with Hg concentrations corresponding to 0 °C vapor pressure, the gases were circulated for at least 15 min with the trap at −78 °C, then 1 h at 0 °C before each run.

The propane used was Phillips Research Grade and was purified by bubbling it through a 60 cm column of H_3PO_4 in H_2SO_4, then through 120 cm of saturated basic $KMnO_4$ and finally a drierite–ascarite drying column. The propane was then distilled from −130 into −161 °C, saving the middle 2/3 portion. This procedure effectively eliminated all traces of unsaturated compounds (notably propylene) from the propane.

Hydrogen was obtained from a Canadian Liquid Air cylinder. In the initial runs it was first passed through degassed charcoal at −198 °C before pressuring up the reaction system. In later runs, a column of copper turnings heated to about 200 °C to convert the traces of O_2 into H_2O was placed before a molecular sieve column at −198 °C. Both methods seemed adequate to eliminate traces of oxygen and condensable gases.

A Hanovia low pressure mercury lamp #87A-45 was used in all photolyses except the last five where a Hanovia high intensity low pressure quartz spiral mercury lamp was used. This was powered by a 5000 V 120 mA luminous tube transformer and had a 2537 Å line intensity about 30 times greater than that of the low intensity lamp. A Vycor 7910 filter was used to eliminate all wavelengths below 2500 Å.

After irradiation the H_2 was first circulated through the two U-traps at −198 °C to freeze down the condensable

products and then carefully pumped off. The remaining condensable products were distilled at −139 °C. The products not volatile at this temperature (primarily hexanes) were analyzed by gas chromatography on a 20 ft 40% isoquinoline on Chromosorb WAW column at 27 °C. This afforded good separation of all products with the exception of dimethylbutane (DMB) which tailed somewhat into the 2-methylpentane (MP) peak. Since the *n*-hexane (Hx) peak was often too small to measure, it was calculated from the cross-combination ratio (4)

$$\frac{R_{MP}}{(R_{DMB}R_{Hx})^{\frac{1}{2}}} = 2.0$$

The disproportionation to recombination ratios were taken from Terry and Futrell (5) as 0.69 for *i*-Pr + *i*-Pr, 0.408 for *n*-Pr + *i*-Pr, and 0.151 for *n*-Pr + *n*-Pr.

In all experiments the H_2 to C_3H_8 concentration ratio was kept sufficiently high to avoid the mercury sensitized decomposition of propane Quenching of mercury by propane was in the order of 1% or less. The scavenging of H atoms by the propylene product was minimized by limiting the conversion of propane to 0.1% or less.

Results and Discussion

The important reactions taking place subsequent to steps [1] and [2] may be embodied into the following sequence

[3] $n\text{-Pr} + C_3H_8 \rightleftarrows i\text{-Pr} + C_3H_8$

[4] $2\ n\text{-Pr} \rightarrow Hx$

[5] $\rightarrow C_3H_6 + C_3H_8$

[6] $n\text{-Pr} + i\text{-Pr} \rightarrow MP$

[7] $\rightarrow C_3H_6 + C_3H_8$

[8] $2i\text{-Pr} \rightarrow DMB$

[9] $\rightarrow C_3H_6 + C_3H_8$

and the reverse of reactions [1] and [2].

Steady state treatment of this sequence leads to the following expression for the fractional yield of *n*-Pr radicals

$$[10]\quad \frac{R_{(n)}}{R_{(n+i)}} = \frac{k_2[H][C_3H_8]}{(k_1 + k_2)[H][C_3H_8] - \{k_{-2}[n\text{-Pr}] + k_{-1}[i\text{-Pr}]\}[H_2]} - \frac{k_{-2}[H_2][n\text{-Pr}]}{R_{(n+i)}} - \frac{[C_3H_8]\{k_3[n\text{-Pr}] - k_{-3}[i\text{-Pr}]\}}{R_{(n+i)}}$$

$$\equiv Q_1 - Q_2 - Q_3$$

It is now necessary to take into account the fact that the concentration distribution of primary radicals is not homogeneous, but has a more or less steep gradient along the light path in the cell. This is due to the high extinction coefficient of mercury vapor and the consequent attenuation of the light intensity. In this connection Reid and LeRoy (6) have recently developed an explicit correction formula for a light intensity dependence of $-\frac{1}{2}$ power, which has the form

$$\delta = \frac{2(1 - e^{-\varepsilon[Hg]L/2})}{\{\varepsilon[Hg]L(1 - e^{-\varepsilon[Hg]L})\}^{\frac{1}{2}}}$$

where ε is the extinction coefficient of mercury vapor and L is the optical path-length.

In eq. [10] the first term Q_1 is nearly independent of light intensity, while Q_2 and Q_3, which when combined contribute only a few % of that of Q_1, are proportional to the $-\frac{1}{2}$ power of light intensity. Therefore eq. [10] can be written as

$$[11]\quad \frac{R_{(n)}}{R_{(n+i)}} = Q_1 - \delta(Q_2 + Q_3)$$

This can be further rearranged to the form

$$[12]\quad \frac{1}{\dfrac{R_{(n)}}{R_{(n+i)}} + \delta(Q_2 + Q_3)} + \frac{[H_2]\{k_{-2}[n\text{-Pr}] + k_{-1}[i\text{-Pr}]\}\delta}{k_2[H][C_3H_8]} - 1 = \frac{k_1}{k_2}$$

The second term is defined as Q_1'. It will be noted again that the value of k_1/k_2 is determined largely by the ratio $R_{(n)}/R_{(n+i)}$. The other terms having only minor significance can then be evaluated with some approximations.

It will be assumed that Beer's law is obeyed, that

$$k_2[H][C_3H_8] \approx 2I_a \frac{k(H + C_2H_6)}{k(H + C_3H_8)}$$

Can. J. Chem. Downloaded from www.nrcresearchpress.com by 210.87.254.42 on 09/05/12
For personal use only.

TABLE I

Product ratios for the sensitization of H_2 in the presence of propane

Temperature (°C)	H_2 (Torr)	C_3H_8 (Torr)	$R_{(n)}/R_{(n+i)}$	δQ_1	δQ_2	δQ_3	k_2/k_1
45	745	267	0.0505	0.0017	0.00010	0.00006	0.0533
45	745	266	0.0536	0.0020	0.00010	0.00008	0.0568
93	833	307	0.0845	0.0248	0.00180	0.00051	0.0948
144	981	347	0.0920	0.176	0.0163	0.00153	0.1208
167	1028	369	0.0948	0.380	0.0369	0.00222	0.1460
116	921	326	0.0855	0.0595	0.00485	0.00075	0.0996
70	806	388	0.0667	0.0066	0.00041	0.00016	0.0721
116	945	232	0.0934	0.0660	0.00540	0.00061	0.1096
177*	909	152	0.1000	0.1781	0.0193	0.00050	0.1328
86*	907	151	0.0666	0.0055	0.00037	0.00005	0.0718
70*	901	150	0.0591	0.0024	0.00014	—	0.0630
37*	902	151	0.0497	0.0004	—	—	0.0523
140*	902	150	0.0923	0.0387	0.0037	0.00017	0.1060

*High intensity lamp with 40 mm cell and circulating system used.

and that k_{-2} is equal to that of the analogous reaction of ethyl radical, $10^{12.57}$ exp $(-13\ 730/RT)$ cc mole^{-1} s^{-1} (6), and lastly that k_{-1} is equal to $10^{12.57}$ exp $(-17\ 730/RT)$ cc mole^{-1} s^{-1}. Using the recently determined values of k_3 and k_{-3} as $10^{9.9}$ exp $(-9\ 300/RT)$ and $10^{10.5}$ exp $(-12\ 900/RT)$ cc mole^{-1} s^{-1} (7), respectively, and the experimental values of $R_{(n)}$ and $R_{(n+i)}$, the ratio k_1/k_2 can be calculated. The results are given in Table I and plotted against $1/T$ in Fig. 1.

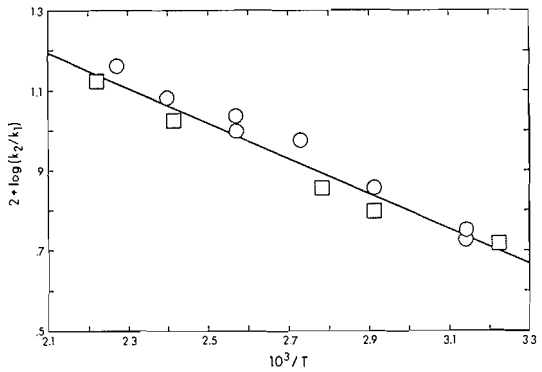

FIG. 1. Arrhenius plot of k_2/k_1: ○, low intensity static system; □, high intensity circulating system.

From least square treatment the Arrhenius parameters are

$$\log (k_2/k_1) = 0.11 \pm 0.11 - \frac{2000 \pm 190}{2.303RT}$$

for 90% confidence limit. Thus

$$k_2/k_1 = 1.29 \exp\left(\frac{-2000}{RT}\right)$$

which is quite close to the value derived from the propane and ethane rate constants (*v.s.*). The normalized A factor ratio A_2/A_1 is 0.43 per C—H bond.

Acknowledgment

We thank the National Research Council of Canada for continuing financial support.

1. A. F. TROTMAN-DICKENSON. Advances in free-radical chemistry. Vol. I. Academic Press, Inc., New York. 1965. p. 6.
2. K. YANG. J. Phys. Chem. **67**, 562 (1963).
3. K. YANG. J. Amer. Chem. Soc. **84**, 719 (1962).
4. J. A. KERR and A. F. TROTMAN-DICKENSON. Progress in reaction kinetics. Vol. I. The Pergamon Press, Ltd., New York. 1961. p. 105.
5. J. O. TERRY and J. H. FUTRELL. Can. J. Chem. **45**, 2327 (1967).
6. L. E. REID and D. J. LEROY. Can. J. Chem. **46**, 3275 (1968).
7. R. E. BERKLEY, G. N. C. WOODALL, O. P. STRAUSZ, and H. E. GUNNING. Can. J. Chem. In press.

Appendix

Derivation of Eq. [10]

The steady state equations for the reactions [1] to [9] are

$$\frac{d[n\text{-Pr}]}{dt} = 0 = k_2[H][C_3H_8] - k_{-2}[H_2][n\text{-Pr}] - [C_3H_8]\{k_3[n\text{-Pr}] - k_{-3}[i\text{-Pr}]\} - 2(k_4 + k_5)[n\text{-Pr}]^2 - (k_6 + k_7)[n\text{-Pr}][i\text{-Pr}]$$

Can. J. Chem. Downloaded from www.nrcresearchpress.com by 210.87.254.42 on 09/05/12
For personal use only.

$$\frac{d[i\text{-Pr}]}{dt} = 0 = k_1[H][C_3H_8] - k_{-1}[H_2][i\text{-Pr}] + [C_3H_8]\{k_3[n\text{-Pr}] - k_{-3}[i\text{-Pr}]\} - (k_6 + k_7)[n\text{-Pr}][i\text{-Pr}] - 2(k_8 + k_9)[i\text{-Pr}]^2$$

If we take the rate of *n*-propyl radicals as observed by the hexane products we have

[A] $$R_{(n)} = 2(1 + k_5/k_4)R_{Hx} + (1 + k_7/k_6)R_{MP}$$
$$= 2(k_4 + k_5)\,[n\text{-Pr}]^2 + (k_6 + k_7)\,[n\text{-Pr}]\,[i\text{-Pr}]$$
$$= k_2\,[H]\,[C_3H_8] - k_{-2}\,[H_2]\,[n\text{-Pr}] - [C_3H_8]\,\{k_3\,[n\text{-Pr}] - k_{-3}\,[i\text{-Pr}]\}$$

Similarly for the sum of the *n*- and isopropyl radicals

[B] $$R_{(n+i)} = 2(1 + k_5/k_4)R_{Hx} + 2(1 + k_7/k_6)R_{MP} + 2(1 + k_9/k_8)R_{DMB}$$
$$= 2(k_4 + k_5)\,[n\text{-Pr}]^2 + 2(k_6 + k_7)\,[n\text{-Pr}]\,[i\text{-Pr}] + 2(k_8 + k_9)\,[i\text{-Pr}]^2$$
$$= (k_1 + k_2)\,[H]\,[C_3H_8] - [H_2]\,\{k_{-2}\,[n\text{-Pr}] + k_{-1}\,[i\text{-Pr}]\}$$

Dividing [A] by [B] gives

$$\frac{R_{(n)}}{R_{(n+i)}} = \frac{k_2[H][C_3H_8] - k_{-2}[H_2][n\text{-Pr}] - [C_3H_8]\{k_3[n\text{-Pr}] - k_{-3}[i\text{-Pr}]\}}{R_{(n+i)}}$$
$$= \frac{k_2[H][C_3H_8]}{(k_1 + k_2)[H][C_3H_8] - [H_2]\{k_{-2}[n\text{-Pr}] + k_{-1}[i\text{-Pr}]\}} - \frac{k_{-2}[H_2][n\text{-Pr}]}{R_{(n+i)}} - \frac{[C_3H_8]\{k_3[n\text{-Pr}] - k_{-3}[i\text{-Pr}]\}}{R_{(n+i)}}$$
$$\equiv Q_1 - Q_2 - Q_3$$

which is eq. [10].

Can. J. Chem. Downloaded from www.nrcresearchpress.com by 210.87.254.42 on 09/05/12
For personal use only.

Effect of temperature on the Hg6($^3P_1$) photosensitized decomposition of propane

J. M. CAMPBELL, H. E. GUNNING, AND O. P. STRAUSZ
Department of Chemistry, University of Alberta, Edmonton, Alberta
Received May 26, 1969

The relative yields of *n*-propyl and isopropyl radicals from the primary step of the Hg6($^3P_1$) photosensitization of propane have been measured as a function of temperature between 0 and 202 °C. The ratio of *n*-propyl to isopropyl yield increases with increasing temperature according to the equation

$$\log \frac{k_n}{k_i} = -0.206 \pm 0.041 - \left(\frac{1072 \pm 62}{2.303RT}\right)$$

The primary yields of the propyl radicals were determined from the measured yields of the hexane and pentane products in ethylene scavenging experiments and from the yields of the isomeric hexane products in pure propane, after making proper allowance in the kinetics for all secondary reactions.

Canadian Journal of Chemistry, 47, 3763 (1969)

Can. J. Chem. Downloaded from www.nrcresearchpress.com by 210.87.254.5 on 09/05/12
For personal use only.

It is well established that the triplet mercury photosensitized decomposition of simple alkanes proceeds exclusively via carbon–hydrogen bond cleavage (1). With propane, both primary and secondary carbon–hydrogen bond cleavage occur. At room temperature, the ratio of the primary to secondary bond cleavage is 0.10 (1–3). This value seems to coincide with that of the relative quenching efficiency of the two different C—H bonds in the propane molecule, indicating that decomposition occurs at the site of quenching (1).

For the elucidation of the mechanism of the energy transfer reaction a knowledge of the temperature dependence of the various modes of possible decomposition of a paraffin molecule would be of primary importance. Takamuku and Back (4) in a semi-quantitative study have observed that the relative amount of quenching by propane and propane-d_2 in propane–ammonia mixtures varied with temperature. On the other hand, Yang (5) could not detect any effect of temperature on the relative quenching efficiency of propane and propane-d_2 in phosphorescence quenching measurements.

The present article describes a detailed quantitative study of the relative quenching efficiency of the two types of C—H bonds in the propane molecule. The quenching ratio can be determined from the observed yields of *n*-propyl and isopropyl radicals provided all other reactions producing propyl radicals in the system are suppressed, or alternately can be taken quantitatively into account, and the only reactions removing propyl radicals from the system are radical–radical recombination and disproportionation. The important steps in the mercury photosensitization of propane at sufficiently high pressure to make H-atom scavenging complete are as follows

[1] $Hg^* + C_3H_8 \rightarrow i\text{-Pr} + H + Hg$

[2] $\rightarrow n\text{-Pr} + H + Hg$

[3] $H + C_3H_8 \rightarrow i\text{-}C_3H_7 + H_2$

[4] $\rightarrow n\text{-}C_3H_7 + H_2$

[5] $n\text{-Pr} + C_3H_8 \rightleftarrows i\text{-Pr} + C_3H_8$

[6] $2n\text{-Pr} \rightarrow n\text{-hexane (Hx)}$

[7] $\rightarrow C_3H_6 + C_3H_8$

[8] $n\text{-Pr} + i\text{-Pr} \rightarrow \text{2-methylpentane (MP)}$

[9] $\rightarrow C_3H_6 + C_3H_8$

[10] $2i\text{-Pr} \rightarrow \text{2,3-dimethylbutane (DMB)}$

[11] $\rightarrow C_3H_6 + C_3H_8$

Arrhenius parameters for reactions [3], [4], [5], and [−5], and reliable disproportionation–recombination ratios for reactions [6] to [11] have recently become available (6–8), and therefore it is possible to derive the ratio k_2/k_1 from the observed yields of the isomeric hexane products.

Alternately it is possible to scavenge the H atoms by addition of small quantities of an olefin to the system and thereby to eliminate steps [3] and [4] from the sequence. A variation of this technique has been successfully exploited

TABLE I

Product yields for the sensitization of propane with added ethylene

Temperature (°C)	$[C_3H_8]$ (Torr)	$\frac{[C_2H_4]}{[C_3H_8]}$	$\frac{R_3 + R_4}{R_3 + R_4 + R_{12}}$	$\frac{k_2}{k_1}$
29	298	0.0155	0.050	0.1011
28	301	0.0281	0.028	0.1007
0	449	0.0103	0.032	0.0867
0	362	0.0069	0.047	0.0861
0	352	0.0197	0.017	0.0924

by Holroyd and Klein (1). Using ethylene, the following sequence prevails

[12] $H + C_2H_4 \rightarrow C_2H_5$

[13] $Et + n\text{-}Pr \rightarrow n\text{-pentane (P)}$

[14] $\rightarrow C_2H_4 + C_3H_8$ or $C_2H_6 + C_3H_6$

[15] $Et + i\text{-}Pr \rightarrow$ isopentane (i-P)

[16] $\rightarrow C_2H_4 + C_3H_8$ or $C_2H_6 + C_3H_6$

[17] $2Et \rightarrow n\text{-butane (B)}$

[18] $\rightarrow C_2H_4 + C_2H_6$

From the measured yields of the pentane and hexane products one can deduce the value of k_2/k_1.

This scavenging technique employing ethylene is particularly useful in room temperature or lower temperature experiments. At elevated temperatures it becomes less practical because of the large concentrations of ethylene required to suppress reactions [3] and [4]. Both techniques were employed in the present study.

Experimental

The circulatory reaction system and photolysis lamps were described in another paper (6). The runs with added ethylene were done in a 50 mm diameter by 99 mm length cell with a total volume of 203 cc.

In the pure propane reactions, the hydrogen was measured volumetrically and analyzed by gas chromatography on a 13X molecular sieve column. Excess propane was distilled off at −139 °C and the condensable fraction, shown to be hexanes and pentanes, was analyzed on 20 ft 40% isoquinoline on Chromosorb WAW.

Results and Discussion

Experiments with added ethylene were done at two temperatures, 0 and 29 °C. In the kinetic treatment it was assumed that all the hydrogen atoms were scavenged by the ethylene, and reactions [5] and [−5] could be neglected. Under these conditions the rates of n-propyl and isopropyl radical formation can be expressed in terms of the hexane and pentane products

$$R_n = 2(1 + k_7/k_6)[\text{Hx}] + (1 + k_9/k_8)[\text{MP}] + (1 + k_{14}/k_{13})[\text{P}]$$

$$R_i = (1 + k_9/k_8)[\text{MP}] + 2(1 + k_{11}/k_{10})[\text{DMB}] + (1 + k_{16}/k_{15})[i\text{-P}]$$

and R_n/R_i is taken as equal to k_2/k_1. The disproportionation to recombination ratios were adopted from the work of Terry and Futrell (8) as $k_7/k_6 = 0.151$, $k_9/k_8 = 0.408$, $k_{11}/k_{10} = 0.69$, $k_{14}/k_{13} = 0.118$, and $k_{16}/k_{15} = 0.306$.

The results are tabulated in Table I. The fractional amount of abstraction from propane by H atom can be estimated from the relation

$$\frac{R_3 + R_4}{R_3 + R_4 + R_{12}} = \frac{1}{1 + \dfrac{k_{12}[C_2H_4]}{(k_3 + k_4)[C_3H_8]}}$$

where $(k_3 + k_4)/k_{12}$ is taken as 1.1 exp $(-4400/RT)$ (9). As seen from the table there is some abstraction occurring, but this has little effect on the deduced value of k_2/k_1. The average of the observed values at room temperature, 0.1009, is in good agreement with that reported by Chesick (3), 0.1010.

The elevated temperature runs were carried out with pure propane. The conversion was always kept small (< 0.04%) to avoid self scavenging of hydrogen atoms by the propylene product. The upper temperature was limited by the thermal decomposition of the n-propyl radical which became noticeable at 220 °C.

Steady state approximation for this system yields the following rate expression

$$[19] \quad \frac{R_{(n)}}{R_{(n+i)}} = \frac{k_2}{2(k_1 + k_2)} + \frac{k_4}{2(k_3 + k_4)} - \frac{R_{\text{DMB}}^{\frac{1}{2}}}{R_{(n+i)}}\left(0.50\frac{R_{\text{MP}}}{R_{\text{DMB}}} - \frac{1}{K_5}\right)\frac{k_5}{k_{10}^{\frac{1}{2}}}[C_3H_8]$$

where $K_5 = k_5/k_{-5} = \exp(3.6/RT - 0.51)$ (7).

Can. J. Chem. Downloaded from www.nrcresearchpress.com by 210.87.254.5 on 09/05/12
For personal use only.

Can. J. Chem. Downloaded from www.nrcresearchpress.com by 210.87.254.5 on 09/05/12
For personal use only.

TABLE II

Product ratios for the Hg6($^3P_1$) sensitization of propane

Temperature (°C)	t (min)	$[C_3H_8]$ (Torr)	$[H_2]$ (μmole)	$R_{(n)}/R_{(n+l)}$	k_2/k_1
164	60	184	2.11	0.1264	0.1820
139	50	178	3.49	0.1205	0.1701
115	40	179	2.16	0.1050	0.1459
96	40	180	1.75	0.1005	0.1430
57	50	184	1.93	0.0816	0.1188
190	40	184	1.58	0.1335	0.1922
37	35	184	1.24	0.0746	0.1130
203	16	101	0.98	0.1379	—
203	20	201	1.40	0.1305	—
201	70	254	2.45	0.1186	—
201	17	95	0.95	0.1407	—
201	180	203	1.12	0.1072	—
202	70	205	1.07	0.1177	—

To minimize the effect of uneven distribution of radicals on the last term of eq. [19] the mercury vapor pressure in the system was kept low, corresponding to the saturation pressure at 0 °C. The final term in eq. [19] can be calculated taking $k_5/k_{10}^{\frac{1}{2}}$ as $10^{2.91}\exp(-8250/RT)$ (cc mole^{-1} s^{-1})$^{\frac{1}{2}}$ (7). As a check, a series of runs was done at 202 °C and $R_{(n)}/R_{(n+i)}$ plotted against

$$R_{DMB}^{\frac{1}{2}}(0.5R_{MP}/R_{DMB} - K_5^{-1})[C_3H_8]/R_{(n+i)}$$

The slope of this line shown in Fig. 1 is -1.26×10^{-1} (cc mole^{-1} s^{-1})$^{\frac{1}{2}}$, in excellent agreement with $k_5/k_{10}^{\frac{1}{2}}$ calculated at 202 °C of -1.30×10^{-1} (cc mole^{-1} s^{-1})$^{\frac{1}{2}}$. Taking this reported value of $k_5/k_{10}^{\frac{1}{2}}$ (7) and k_4/k_3 as $1.29\exp(-2000/RT)$ (6), k_2/k_1 can be calculated at each temperature. The data are summarized in Table II. An Arrhenius plot for k_2/k_1, including the present results and all those reported earlier for the propane reaction, is shown in Fig. 2. A least-mean-square calculation of these points gives

$$\log k_2/k_1 = -0.206 \pm 0.041 \exp\left(-\frac{1072 \pm 62}{2.303RT}\right)$$

for 90% confidence limits.

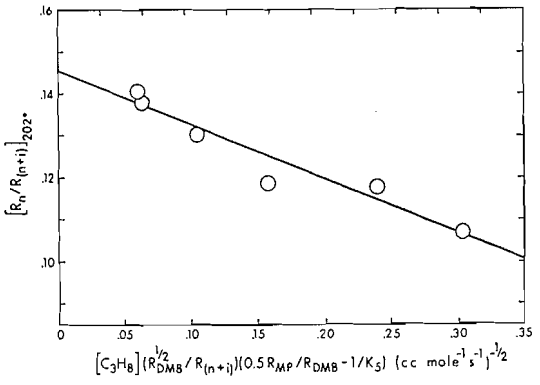

FIG. 1. Plot of $R_{(n)}/R_{(n+l)}$ against $[C_3H_8](R_{DMB}^{\frac{1}{2}}/R_{(n+i)})(0.5\ R_{MP}/R_{DMB} - 1/K_5)$ at 202 °C from Table II.

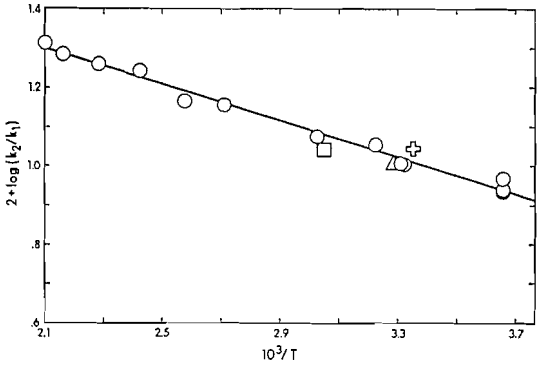

FIG. 2. Arrhenius plot of k_2/k_1: ○, this work; +, Holroyd and Klein (1); △, Chesick (3); and □, Jakubowski *et al.* (2).

This result is significant in that it is the first unambiguous experimental demonstration that the energy transfer reaction from an excited mercury atom to a paraffin molecule possesses an energy barrier. This underlies the analogy between quenching and hydrogen abstraction from paraffins by atoms and radicals. Considering the quenching process as a hydrogen abstraction reaction by an excited mercury atom

$$RH + Hg^* \rightarrow R + HHg$$

a difference in the potential energy of activation, $E_2 - E_1$, of about 1.26 kcal has been calculated recently (10) by the bond-energy–bond-order

method, which is in satisfactory agreement with the experimental value obtained in this work.

Acknowledgment

The financial assistance of the National Research Council of Canada is gratefully acknowledged.

1. R. A. HOLROYD and G. W. KLEIN. J. Amer. Chem. Soc. **84**, 4000 (1962); J. Phys. Chem. **67**, 2273 (1963).
2. E. JAKUBOWSKI, P. KEBARLE, O. P. STRAUSZ, and H. E. GUNNING. Can. J. Chem. **45**, 2287 (1967).
3. J. P. CHESICK. J. Amer. Chem. Soc. **86**, 3597 (1964).
4. S. TAKAMUKU and R. A. BACK. Can. J. Chem. **42**, 1426 (1964).
5. K. YANG. J. Amer. Chem. Soc. **89**, 5344 (1967).
6. J. M. CAMPBELL, O. P. STRAUSZ, and H. E. GUNNING. Can. J. Chem. This issue.
7. R. E. BERKLEY, G. N. C. WOODALL, O. P. STRAUSZ, and H. E. GUNNING. Can. J. Chem. **47**, 3305 (1969).
8. J. O. TERRY and J. H. FUTRELL. Can. J. Chem. **45**, 2327 (1967).
9. K. YANG. J. Amer. Chem. Soc. **84**, 719 (1962).
10. H. S. SANDHU, H. E. GUNNING, and O. P. STRAUSZ. To be published.

Can. J. Chem. Downloaded from www.nrcresearchpress.com by 210.87.254.5 on 09/05/12
For personal use only.

Determination of the dipole moments of some polar liquids dissolved in polar solvents

H. A. Rizk, N. Youssef, and H. Grace
Department of Chemistry, Faculty of Science, University of Cairo, Cairo, Egypt, United Arab Republic

Received March 11, 1969

The application of a modified form of the Onsager equation at the condition of infinite dilution of a polar solute in a polar solvent leads to reasonable dipole moments for water, pyridine, acetone, tert-butyl alcohol, *n*-butyl alcohol, and β-octyl alcohol, except in the case of water in tert-butyl alcohol at 30 and 40 °C and the case of acetone in *n*-butyl alcohol at 30 to 50 °C. The initial decrease of the dielectric constant of solvent by addition of solute in each of these two cases is associated with a reduction in the Kirkwood *g*-factor of solute. In all 12 systems investigated, strong hydrogen bonding occurs between solute and solvent molecules and often between solvent molecules themselves. It is thought that this equation must fail when short-range interactions assume predominant importance, but why it works so well for those cases which are also strongly interacting systems is not clear.

Canadian Journal of Chemistry, 47, 3767 (1969)

Can. J. Chem. Downloaded from www.nrcresearchpress.com by 210.87.254.42 on 09/05/12
For personal use only.

In the course of testing the validity of the method suggested in a previous investigation (1) for the determination of the apparent solution moment of a polar solute dissolved in a polar solvent by the use of a modified form of Onsager's equation, a redetermination of the dipole moments of water, pyridine, acetone, tert-butyl alcohol, *n*-butyl alcohol, and β-octyl alcohol, over the temperature range 30 to 50 °C, seemed worthwhile. Thus in the case of water, the polar solvents chosen were pyridine, acetone, and tert-butyl alcohol, and conversely, in the case of each of the latter three compounds, water was used as the solvent. Each of the liquids *n*-butyl alcohol, β-octyl alcohol, and acetone, was used in turn as solute in, and solvent of, the other two liquids.

Experimental and Results

Bidistilled water was purified by the method of Thiessen and Hermann (2). Pyridine, acetone, tert-butyl alcohol, *n*-butyl alcohol, and β-octyl alcohol were purified according to recommended procedures (3). Measurements were made as previously described (4). Calculations of the apparent solution moments with regard to the condition of infinite dilution, within the temperature range 30 to 50 °C, were made using the following equation, which was derived from Onsager's equation (5) as shown in the previous investigation (1)

$$\mu_2^2 = F\frac{d\varepsilon_{12}}{dC_2}\cdot\frac{1}{A_2} + \frac{(A_1\mu_1^2C_1^0V_2 + B_1C_1^0V_2 - B_2)}{A_2}$$

Here C_2 = the number of gram-molecules of solute per liter of solution,

C_1^0 = the molar concentration of pure solvent,

V_2 = the molar volume (in liters) of pure solute, and

$$A_1 = \frac{4\pi N_a}{9000kT}\cdot\frac{(n_1^2+2)^2\,\varepsilon_{12}(2\varepsilon_{12}+1)}{(2\varepsilon_{12}+n_1^2)^2}$$

$$A_2 = \frac{4\pi N_a}{9000kT}\cdot\frac{(n_2^2+2)^2\,\varepsilon_{12}(2\varepsilon_{12}+1)}{(2\varepsilon_{12}+n_2^2)}$$

$$B_1 = 3V_1\frac{\varepsilon_{12}(n_1^2-1)}{(2\varepsilon_{12}+n_1^2)}$$

$$B_2 = 3V_2\frac{\varepsilon_{12}(n_2^2-1)}{(2\varepsilon_{12}+n_2^2)}$$

$$F = 1 - C_2\mu_2^2A_2\frac{n_2^2+4\varepsilon_{12}n_2^2-2\varepsilon_{12}}{\varepsilon_{12}(2\varepsilon_{12}+1)(2\varepsilon_{12}+n_2^2)} - C_1\mu_1^2A_1\frac{n_1^2+4\varepsilon_{12}n_1^2-2\varepsilon_{12}}{\varepsilon_{12}(2\varepsilon_{12}+1)(2\varepsilon_{12}+n_1^2)} - C_2B_2\frac{n_2^2}{\varepsilon_{12}(2\varepsilon_{12}+n_2^2)} - C_1B_1\frac{n_1^2}{\varepsilon_{12}(2\varepsilon_{12}+n_1^2)}$$

TABLE I

Apparent solution moments of polar solutes in polar solvents

Solute/solvent	T (°C)	n^2_{1-D}	$\mu_1 \times 10^{18}$	C_1^0	lim $(d\varepsilon_{12}/dC_2)_{C_2 \to 0}$	$(F)_{C_2 \to 0}$	$\mu_2 \times 10^{18}$
Water/pyridine	30	2.2635	2.20	12.315	0.3051	0.883	1.88
	40	2.2485	2.20	12.189	0.3022	0.885	1.87
	50	2.2329	2.20	12.058	0.2981	0.888	1.87
Water/acetone	30	1.8339	2.85	13.436	0.2132	0.943	1.88
	40	1.8203	2.85	13.238	0.2071	0.941	1.87
	50	1.8069	2.85	13.035	0.1993	0.940	1.87
Water/*t*-butanol	30	1.9107	1.65	10.489	Negative	0.9491	—
	40	1.8958	1.65	10.347	Negative	0.9405	—
	50	1.8807	1.65	10.204	+0.380	0.9287	1.89
Pyridine/water	30	1.7740	1.84	55.315	−1.189	0.9942	2.25
	40	1.7703	1.84	55.123	−1.166	0.9939	2.25
	50	1.7661	1.84	54.894	−1.145	0.9936	2.23
Acetone/water	30	1.7740	1.84	55.315	−0.745	0.9942	2.89
	40	1.7703	1.84	55.123	−0.745	0.9939	2.90
	50	1.7661	1.84	54.894	−0.744	0.9936	2.90
t-Butanol/water	30	1.7740	1.84	55.315	−2.086	0.9942	1.67
	40	1.7703	1.84	55.123	−2.041	0.9939	1.67
	50	1.7661	1.84	54.894	−2.000	0.9936	1.67
n-Butanol/β-octanol	30	2.0221	1.65	6.244	0.1472	0.921	1.65
	40	2.0107	1.65	6.189	0.1408	0.909	1.65
	50	1.9994	1.65	6.134	0.1345	0.897	1.65
n-Butanol/acetone	30	1.8339	2.85	13.418	−1.036	0.943	1.65
	40	1.8203	2.85	13.220	−0.985	0.942	1.65
	50	1.8069	2.85	13.017	−0.940	0.940	1.65
β-Octanol/*n*-butanol	30	1.9466	1.65	10.820	−0.2722	0.973	1.65
	40	1.9366	1.65	10.718	−0.2611	0.971	1.65
	50	1.9265	1.65	10.617	−0.2505	0.969	1.65
β-Octanol/acetone	30	1.8339	2.85	13.418	−2.062	0.943	1.67
	40	1.8203	2.85	13.220	−1.961	0.942	1.67
	50	1.8069	2.85	13.017	−1.871	0.940	1.67
Acetone/*n*-butanol	30	1.9466	1.65	10.820	−0.5067	0.973	—
	40	1.9366	1.65	10.718	−0.4447	0.971	—
	50	1.9265	1.65	10.617	−0.3829	0.969	—
Acetone/β-octanol	30	2.0221	1.65	6.244	0.950	0.921	2.92
	40	2.0107	1.65	6.189	0.911	0.909	2.92
	50	1.9994	1.65	6.134	0.870	0.897	2.92

The results obtained for the 12 combinations made are summarized in Table I; for ease of comparison, the solution moment values obtained in this way, together with those obtained by previous authors with the aid of usual methods, are given in Table II.

Discussion

It can be seen from Table II that in all cases, except in the case of water dissolved in tert-butyl alcohol at 30 and 40 °C, and also in the case of acetone dissolved in *n*-butyl alcohol at 30, 40, and 50 °C, there exists good agreement between the apparent solution moments obtained by applying the modified form of the Onsager equation at the condition of infinite dilution and those obtained with the aid of the usual Debye equation. Also, the dipole moments obtained this way are in better agreement with the corresponding vapor moments than with the solution values obtained in the usual way.

Surely hydrogen-bonded complexes between solute and solvent molecules and often between solvent molecules exist in all 12 combinations investigated. Since the applicability of the equation to polar solutes in polar solvents appears to be satisfactory in some of these combinations but not in others, one cannot predict a priori the validity of this equation for a given pair of polar substances. It is evidently difficult to understand why water in tert-butyl alcohol at 30 to 40 °C and acetone in *n*-butyl alcohol at 30 to 50 °C give negative dipole moments while correct dipole

Can. J. Chem. Downloaded from www.nrcresearchpress.com by 210.87.254.42 on 09/05/12
For personal use only.

Can. J. Chem. Downloaded from www.nrcresearchpress.com by 210.87.254.42 on 09/05/12
For personal use only.

TABLE II

Comparison of dipole moment values*

Solute	Polar solvent	Solution moment (D) (Onsager's equation) 30 °C	40 °C	50 °C	Vapor moment (D)	Non-polar solvent	Solution moment (D) (Debye's equation)
Water	Pyridine	1.88	1.87	1.87	1.84 (6, 7)		
Water	Acetone	1.88	1.87	1.87		Dioxane	1.9 (8), 1.89 (9), 1.90 (10), 1.86 (11), 1.91 (12), 1.93 (13)
Water	tert-Butyl alcohol	—	—	1.89			
Pyridine	Water	2.25	2.25	2.25		Benzene	2.20 (14, 15), 2.27 (16)
						Dioxane	2.22 (14, 17, 18), 2.33 (16)
Acetone	Water	2.89	2.90	2.90	2.97 (19), 2.84 (20), 2.85 (21), 2.95 (22)	Benzene	2.72 (23), 2.78 (24), 2.74 (25, 26)
						CCl_4	2.70 (27)
tert-Butyl alcohol	Water	1.67	1.67	1.67		Benzene	1.44 (28), 1.66 (29), 1.55 (30), 1.65 (31), 1.70 (32)
						Hexane	1.55 (30)
n-Butyl alcohol	β-Octyl alcohol	1.65	1.65	1.65	1.65 (33, 34), 1.67 (35)	Benzene	1.53 (28), 1.69 (29), 1.73, (36), 1.95 (37)
n-Butyl alcohol	Acetone	1.65	1.65	1.65			
β-Octyl alcohol	*n*-Butyl alcohol	1.65	1.65	1.65	1.65 (38)	Benzene	1.66 (39)
β-Octyl alcohol	Acetone	1.67	1.67	1.67			
Acetone	*n*-Butyl alcohol	—	—	—			
Acetone	β-Octyl alcohol	2.92	2.92	2.92			

*References in parentheses.

Can. J. Chem. Downloaded from www.nrcresearchpress.com by 210.87.254.42 on 09/05/12
For personal use only.

moments are obtained when the roles of solute and solvent are interchanged, though complex formation is present in both situations. Curiously also, when the temperature is raised to 50 °C for water in tert-butyl alcohol and when β-octyl alcohol is used instead of *n*-butyl alcohol as a solvent for acetone, correct dipole moments are obtained.

Based on the assumption that hydrogen-bonded complexes exist at all concentration ratios, the question is, therefore, how do these complexes affect the measurements as a function of the concentration ratio. The failures of our equation, which is based on Onsager's model of a spherical cavity of a homogeneous dielectric, are perhaps more easily explained than the successes.

Since neither water nor tert-butyl alcohol has large molecular moments, the high dielectric constants of these substances in the pure state arise because the short-range association forces favor molecular orientations which lead to cooperative reinforcement of dipole fields. This is expressed by Kirkwood (40) in terms of a correlation parameter, g, which has, in such cases, a value greater than unity. The value of this parameter in the Onsager model is considered by Kirkwood to be equal to unity, since in this model only the effect of electrostatic forces on hindered rotation was taken into account. For normal liquids, devoid of specific, short-range association forces, $g = 1$, and the interaction between a dipole molecule and its surroundings is then similar to that which would exist if the surroundings were replaced by material of the same macroscopic dielectric constant (41). Therefore, one may have the opinion that since the Onsager equation is derived on such a basis for which $g = 1$, or on the assumption that hydrogen bonding is purely electrostatic in nature, which is hardly acceptable (42), the application of our equation of polar solutes in polar solvents to any system for which g exceeds unity would be as inappropriate as the application of Debye's equation to any associated liquid. According to this view, the success of our equation can be regarded as only coincidental in those cases where it affords the correct result.

Our measurements (Table III)[1] and those of others (43) show a tremendous reduction of the dielectric constant of tert-butyl alcohol in the pure state with increase of temperature. Dannhauser and Cole (43) associate this with a rapid fall in g towards 1, arising from a decrease in the mean chain length. That the addition of water to tert-butyl alcohol at 30 and 40 °C should initially cause a reduction of the dielectric constant, i.e.

$$\lim (d\varepsilon_{12}/dC_2)_{C_2 \to 0}$$

is negative (Table I), is reflected in a failure of the modified form of Onsager's equation. Associating this reduction of dielectric constant with a rapid fall in the Kirkwood g-factor of the alcohol, the effect of added water at each of these two temperatures is apparently the same as a shift towards higher temperature in the pure alcohol. The fact that, when water is dissolved in the alcohol at 50 °C, the dielectric constant of the solution increases as expected and

$$\lim (d\varepsilon_{12}/dC_2)_{C_2 \to 0}$$

is sufficiently positive to give the right dipole moment (Table I) may lead one to suggest that perhaps g has become effectively unity between 40 and 50 °C. The fall in the g value of tert-butyl alcohol on the addition of water at 30 and 40 °C may be explained by assuming that the association which occurs between solute and solvent molecules involves complexes long-lived enough to be oriented as polymeric units in response to the low-frequency field, and thus the dielectric constant is reduced. When the temperature is raised to 50 °C the complexes formed are probably very short-lived, so that they cannot contribute directly to the static dielectric constant by orientation as molecular entities and, consequently, the observed increase of the dielectric constant can be accounted for. Also as a consequence of the short-lived complexes in this system at 50 °C, the interactions involved may be regarded as effectively smeared out into spherical symmetry, and then the dipole-in-a-cavity model or the modified form of Onsager's equation for a polar solute in a polar solvent becomes appropriate. This means that the short-range intermolecular forces are perhaps much less important at 50 than at 30 or 40 °C.

On the other hand, the observed decrease of the dielectric constant of *n*-butyl alcohol on the addition of acetone at 30 to 50 °C or the negative value of $\lim (d\varepsilon_{12}/dC_2)_{C_2 \to 0}$ (Table I), which is also reflected in a failure of the equation, may be

[1]Detailed tables of original data have been deposited with the Depository of Unpublished Data, National Science Library, National Research Council, Ottawa, Canada. Photocopies are available free of charge, on request to the Depository.

explained by assuming that acetone probably serves to reduce the high Kirkwood *g*-factor of *n*-butyl alcohol (2.6 at 30 °C) by chain termination.

It may therefore be thought that the modified form of Onsager's equation can usefully define limiting cases, but must fail when short-range interactions assume predominant importance. The fact that this relationship still holds so well for those cases which are also complicated hydrogen-bonded systems is, however, far from clear.

1. H. A. RIZK and I. M. ELANWAR. Can. J. Chem. **46**, 507 (1968).
2. P. THIESSEN and K. HERMANN. Z. Elektrochem. **43**, 66 (1937).
3. A. WEISSBERGER and E. PROSKAUER. Organic solvents, physical constants and methods of purification. The Clarendon Press, Oxford. 1935. pp. 126, 141, 156.
4. A. R. TOURKY, H. A. RIZK, and Y. M. GIRGIS. J. Phys. Chem. **64**, 565 (1960).
5. L. ONSAGER. J. Amer. Chem. Soc. **58**, 1486 (1936).
6. R. SANGER. Phys. Z. **31**, 306 (1930).
7. J. D. STRANATHAN. Phys. Rev. **48**, 538 (1935).
8. J. W. WILLIAMS. J. Amer. Chem. Soc. **52**, 1838 (1930).
9. A. J. WEITH, M. F. HOBBS, and P. M. GROSS. J. Amer. Chem. Soc. **70**, 805 (1948).
10. E. P. LINTON and O. MAASS. Can. J. Res. **7**, 81 (1932).
11. P. ABADIE and G. CHAMPETIER. C. R. Acad. Sci. **200**, 1590 (1935).
12. Y. L. WANG. Z. Phys. Chem. **45B**, 323 (1940).
13. A. R. TOURKY, H. A. RIZK, and Y. M. GIRGIS. J. Phys. Chem. **65**, 40 (1961).
14. D. G. LEIS and B. COLUMBA. J. Amer. Chem. Soc. **67**, 79 (1945).
15. JACQUELINE BARASSIN and M. HENRI LUMBROSO. Bull. Soc. Chim. France, 1947 (1959).
16. W. P. PURCELL and A. JUDITH. J. Phys. Chem. **69**, 4097 (1965).
17. R. S. HOLLAND and C. P. SMYTH. J. Phys. Chem. **59**, 1088 (1955).
18. JACQUELINE BARASSIN and M. HENRI LUMBROSO. Bull. Soc. Chim. France, 492 (1961).
19. K. HÖJENDAHL. Studies of dipole moment. Copenhagen. 1928. Calculated from the experiments of Port. Ann. Phys. **42**, 569 (1913).
20. H. A. STUART. Phys. Z. **31**, 80 (1930).
21. C. T. ZAHN. Phys. Z. **33**, 686 (1932).
22. K. L. RAMASWAMY. Proc. Indian Acad. Sci. Sect. A, **4**, 108 (1936).
23. O. HASSEL and E. NAESHAGEN. Z. Phys. Chem. **B4**, 217 (1929).
24. O. HASSEL and A. H. UHL. Z. Phys. Chem. **B8**, 187 (1930).
25. K. L. WOLF and W. J. GROSS. Z. Phys. Chem. **B14**, 305 (1931).
26. H. FUCHS and H. L. DONLE. Z. Phys. Chem. **B22**, 1 (1933).
27. J. W. WILLIAMS and I. J. KRCHMA. J. Amer. Chem. Soc. **49**, 1676 (1927).
28. B. LAKSHMI NARAYANA. J. Sci. Ind. Res. **B18**, 304 (1959).
29. A. A. MARYOTT. J. Amer. Chem. Soc. **63**, 3079 (1941).
30. C. HENNINGS. Z. Phys. Chem. **B28**, 267 (1935).
31. C. P. SMYTH and R. W. DORNTE. J. Amer. Chem. Soc. **53**, 545 (1931).
32. H. L. DONLE. Z. Phys. Chem. **B28**, 267 (1935).
33. L. LANGE. Z. Phys. **33**, 169 (1925).
34. M. KUBO. Sci. Papers Inst. Phys. Chem. Res. Tokyo, **27**, 65 (1935).
35. J. B. MILES. Phys. Rev. **34**, 964 (1929).
36. C. P. SMYTH and W. N. STEEPS. J. Amer. Chem. Soc. **51**, 3312 (1929).
37. WEI- CHUWAN LIN and FU- TAI TUAN. J. Chin. Chem. Soc. **5**, 33 (1958).
38. MME. R. DALBERT. J. Chim. Phys. **50**, 329 (1953).
39. J. B. M. COPPOCK and F. R. GOSS. J. Chem. Soc. 1789 (1939).
40. J. G. KIRKWOOD. J. Chem. Phys. **7**, 911 (1939); Ann. N. Y. Acad. Sci. **40**, 315 (1940); Trans. Faraday Soc. A, **42**, 7 (1946).
41. F. E. HARRIS and B. J. ALDER. J. Chem. Phys. **21**, 1031 (1953).
42. C. A. COULSON. *In* Hydrogen bonding, *Edited by* Hadzi. The Pergamon Press, Ltd., London. 1959. p. 339.
43. W. DANNHAUSER and R. H. COLE. J. Chem. Phys. **23**, 1762 (1955).

Can. J. Chem. Downloaded from www.nrcresearchpress.com by 210.87.254.42 on 09/05/12
For personal use only.

Kinetics of the anation reaction of nickel(II) and 1,10-phenanthroline in methanol–water mixtures

M. L. SANDUJA AND W. MACF. SMITH
Department of Chemistry, Queen's University, Kingston, Ontario
Received May 22, 1969

The kinetics of formation of the monophenanthroline complex of nickel(II) has been studied spectrophotometrically in water–methanol mixtures of 0 to 97 weight % of methanol, at ionic strength 0.050, at varying acidities at 25 °C. Values for the rate constants for the acid independent and acid dependent reactions together with values for the equilibrium acid ionization quotient of phenanthrolium ion over the range of solvent mixtures have been determined. The values of the acid independent rate constant show little dependence on solvent compositions up to 76% methanol, then decrease and show no correlation with trends in the ionization quotient of phenanthrolium ion. The acid dependent rate constant shows only a modest dependence on solvent composition over most of the range of solvent compositions except in the range of highest methanol content where it is not significantly different from zero.

Canadian Journal of Chemistry, 47, 3773 (1969)

Can. J. Chem. Downloaded from www.nrcresearchpress.com by 210.87.254.6 on 09/05/12
For personal use only.

Introduction

Investigations of anation reactions of metal ions in mixed solvents are understandably sparse. A variety of cationic species with different compositions for the inner solvation sphere are present in mixed solvents and quantitative assessment of data consequently difficult. However, trends in kinetic behavior which could be correlated even semi-quantitatively with trends in solvent properties and the populations of solvated species may point out features which studies in single solvents would miss. With this approach we have examined the reaction of nickel(II) with 1,10-phenanthroline in methanol–water mixtures over a wide range of compositions and over a range of low acidities. To permit interpretation of our primary data we have also obtained values for the equilibrium acid ionization quotient for phenanthrolium ion at ionic strength 0.050 and the same range of solvent compositions involved in the kinetic measurements.

Pearson and Ellgen (1) have examined the reaction of nickel(II) with bipyridine in methanol and in methanol–water mixtures containing up to 25 volume % of water and also the reaction of nickel(II) with 1,10-phenanthroline in 100 % methanol. Their results support the view that the mechanism in methanol is the same as that operative in water, i.e., that the rate controlling step is solvent loss from the inner solvation sphere of nickel ion, which is part of an outer sphere complex involving the metal ion and the potential ligand. On the basis of the "ion-pair interchange" mechanism, if the concentration of outer sphere complexes (ion-pairs) is small compared to the concentrations of the unassociated metal and species L, the expression for the rate of reaction should be

$$[1] \qquad -\frac{d}{dt}[NiL^{2+}] = k_o K_o [Ni^{2+}][L] \doteq k_f [Ni^{2+}][L]$$

where K_o is the association constant for outer sphere complex formation and k_o is the first order rate constant for reorganization of the outer to the inner sphere complex. The data for reactions in water (2) and in methanol (1) support the view that k_o is nearly independent of ligand type and proportional to the rate constant for solvent loss from the solvated Ni(II) species. Pearson and Ellgen found that in solution containing 3 volume % of water the rate constant of the reaction with bipyridine was about 3 times that in pure methanol, and attribute this increase to an increase in the effective value of k_o, which is associated with enhanced values of solvent loss from each of the partly aquated nickel ion species, $Ni(CH_3OH)_{6-x}(H_2O)_x^{2+}$, present.

Our choice of phenanthroline as ligand was determined largely by experimental convenience. The association constant for the monocomplex with nickel(II) is high and reaction proceeds essentially to completion under all conditions of this work. Also, the concentration of free phenanthroline, which is kinetically much more active than phenanthrolium ion, may be held at low values by maintaining moderate values for the hydrogen ion concentration and consequently the rates of reaction can be reduced to the range measurable by conventional techniques. On the

Can. J. Chem. Downloaded from www.nrcresearchpress.com by 210.87.254.6 on 09/05/12
For personal use only.

other hand, there are possible complications in interpretation because of the rather complex dependence of overall rate constant on hydrogen ion concentration (3) and of the bidentate nature of the monocomplex. We have obtained values for the acid independent rate constant by simple extrapolation and have followed Wilkins and co-workers (4) in assuming that the rate determining step in the acid independent reactions is the formation of the monodentate intermediate.

Experimental

All substances used were of reagent grade (G. F. Smith or Fisher). Reagent grade methanol was distilled using a Widmer column and the center cut, along with triply distilled water, used in preparing the solutions. All solutions involving methanol were prepared freshly on the day of the determination.

The kinetic measurements were made spectrophotometrically with stop-watch timing. The concentrations of nickel(II) ranged from 2×10^{-2} to 2×10^{-3} M, that of total phenanthroline from 2×10^{-4} to 2×10^{-5} M. In most runs the concentration of nickel(II) was 2×10^{-3} M, that of phenanthroline 2×10^{-5} M. Solutions of the two reactants, adjusted to the appropriate acidity and ionic strength, were ejected from thermostatted syringes into a 5 cm optical cell thermostatted in a DK–1 spectrophotometer and the variation with time of the absorbance at λ310 mμ recorded. At the wavelength λ310 mμ the essential absorbing species are phenanthroline, phenanthrolium ion, and the monocomplex. The extinction coefficient of the complex is substantially less than that of phenanthrolium ion, which constitutes over 99% of the uncomplexed phenanthroline in all solutions, and a substantial decrease in absorbance occurs as reaction proceeds. The overall change in absorbance for reacting solutions of given initial concentration of nickel and total phenanthroline was independent of acidity in each solvent medium, in accord with the assumption of substantially complete transformation of phenanthroline to the complex. As the nickel(II) concentration was in 100-fold excess over that of phenanthroline, the reaction was pseudo first order and the slope of the plot of log $(D - D_\infty)$ against time is identifiable with

$$[2] \qquad -k_f \frac{[\mathrm{Ni}]_0}{2.303} \frac{Q_a}{Q_a + [\mathrm{H}^+]}$$

where D represents the optical density of the solution, k_f is the value of

$$-\frac{d}{dt}[\mathrm{Niphen}^{2+}]/[\mathrm{Ni}^{2+}][\mathrm{phen}]$$

where [phen] represents the concentration of the free base phenanthroline and Q_a is the equilibrium acid ionization quotient of phenanthrolium ion.

Q_a was determined electrometrically using a radiometer pH meter 4. Solutions containing known concentrations of phenanthroline and phenanthrolium perchlorate adjusted to appropriate ionic strength were assessed for hydrogen ion concentration in cells involving an aqueous calomel and a glass electrode using the techniques developed by Grunwald and co-workers (5). Calibration curves relating E_{cell} with $-\log [H^+]$ were prepared using solutions of perchloric acid adjusted to the same ionic strength as the test solutions. The slopes and associated standard errors of the plots of E_{cell} against $-\log [H^+]$ at 25 °C for solutions containing 45, 54.2, 75.94, 87.0, and 97.0 weight % methanol were, respectively, 0.0589 ± 0.0017, 0.0585 ± 0.0003, 0.0586 ± 0.0003, 0.0590 ± 0.0013, 0.0591 ± 0.0001 V (per pH_c). Extrapolation of these curves by at most 1.4 units of $-\log [H^+]$ was necessary to attain to the values of E_{cell} developed by the phenanthroline solutions. The slopes of the plots of E_{cell} vs. $-\log [H^+]$ in this region were assessed using benzoic acid – sodium benzoate buffers and for solutions with methanol content in the solvent of 54.2 and 75.94 weight % the slopes were 0.0583 ± 0.0005 and 0.0588 ± 0.0004. For the solutions of higher methanol content the ratio [phenanthrolium ion]/[phenanthroline] was assessed spectrophotometrically as well as from "make-up" compositions and the two values agreed to within 1.5%.

The concentration of $[H^+]$ for the kinetic experiments was estimated from "make-up" composition and the values checked with electrometric measurements. Agreement was within ±2%.

Results and Discussion

Values for the rate constant k_f were assessed as indicated above using plots of log $(D_\infty - D)$ against time and relation [1] The results are displayed in Fig. 1. Over the range of acidity investigated, the values of the rate constant k_f increase linearly with the concentration of hydrogen ion.

We consider that the intercept at $[H^+] = 0$ of the line of regression through the points is the value of the rate constant (k_f^0) of the reaction involving phenanthroline as the free base. Our value for k_f^0 for 100% water is 4.2×10^{-3} $\mathrm{mole}^{-1}\,\mathrm{l}\,\mathrm{s}^{-1}$ which compares favorably with the value 3.9×10^{-3} obtained by Wilkins and co-workers (4) by stop-flow methods using solutions near neutrality, where the phenanthroline was present almost entirely as the free base.

Values for the acid independent rate constant k_f^0, for the slopes (S) of the lines of regression, and for the equilibrium acid ionization quotient Q_a for phenanthrolium ion are presented in Table I. The trend in the values of Q_a is notable, the values rising sharply over the range of methanol content 35 to 54 weight % and dropping substantially in the highest range of methanol content.

Over the range where the values of Q_a are rising fairly sharply the slopes (S) are undergoing a sharp decrease. As emphasized below, this de-

Can. J. Chem. Downloaded from www.nrcresearchpress.com by 210.87.254.6 on 09/05/12
For personal use only.

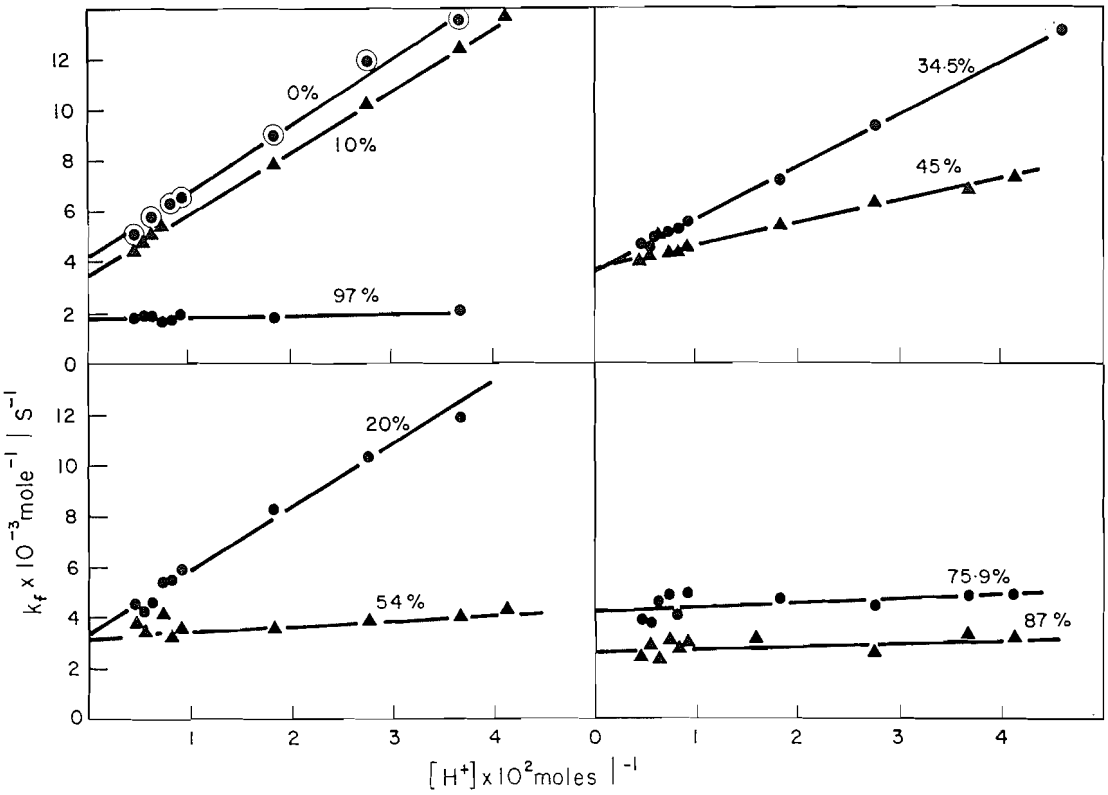

FIG. 1. Plots of overall rate constant k_f against [H$^+$] for various solvent mixtures.

TABLE I

Values for the rate constants k_f^0 and k_f^1 for the formation of Ni (phen)$^{2+}$ and for the equilibrium acid ionization quotient Q_a for phenanthrolium ion in methanol–water mixtures*

Weight % methanol	$k_f^0 \times 10^{-3}$ mole^{-1} l s^{-1}	$S \times 10^{-5}$† mole^{-2} l^2 s^{-1}	$Q_a \times 10^5$ mole l^{-1}	$k_f^1 (= Q_a \times S)$ mole^{-1} l s^{-1}
0.0	4.2±0.40‡	2.6 ±0.16‡	1.18	3.0
10.0	3.5±0.22	2.4 ±0.10	1.47	3.5
20.0	3.4±0.38	2.4 ±0.22	1.92	4.8
34.37 (μ = 0.10)	3.6±0.12	2.1 ±0.06	2.96	6.1
45.0	3.8±0.26	0.8 ±0.12	5.40	4.5
54.2	3.2±0.28	0.24 ±0.12	11.6	3.6
75.94	4.3±0.40	0.15 ±0.18	12.6	1.8
75.94 (μ = 0.10)	3.8±0.72	0.16 ±0.26	12.0	1.9
87	2.6±0.28	0.12 ±0.13	13.1	1.6
97	1.8±0.13	0.053±0.082	2.09	0.10
100 (μ = 0.20)§	0.35	—	—	—

*At 25 °C; ionic strength (μ) is 0.050 *M* except where otherwise indicated.
†S = slope of plot of k_f against [H$^+$].
‡95% confidence limits.
§From ref. 1.

crease in slope may be directly related to the rise in Q_a and need not imply any marked change in kinetic features of the acid dependent path of this reaction. The values k_f^0 deviate only slightly from constancy for solutions of methanol content from 0 up to 76%. For methanol content greater than 76% there is a significant but not marked decrease in the value of k_f^0. Our value of 1.7×10^3 for solutions 97% in methanol (at ionic strength 0.05) is nearly five times greater than the value 0.35×10^3 determined by Pearson and Ellgen (1) for 100% methanol solution and ionic strength 0.20. A corresponding though not so marked increase in rate constant was observed by Pearson and Ellgen for the reaction between nickel(II) and bipyridine.

Our data for a given solvent mixture may be formally systematized in terms of two parallel reaction paths

$$Ni^{2+} + phen \xrightarrow{k_f^0} Ni\,(phen)^{2+}$$

$$Ni^{2+} + Hphen^{+} \xrightarrow{k_f^1} Ni\,(phen)^{2+} + H^{+}$$

with

$$\frac{d}{dt}[Niphen^{2+}] = k_f^0[Ni^{2+}][phen] + k_f^1[Ni^{2+}][Hphen^{+}] = \left(k_f^0 + k_f^1 \frac{[H^+]}{Q_a}\right)[Ni^{2+}][phen]$$

$k_f^0 + k_f^1[H^+]/Q_a$ is identifiable with k_f, so the slope of the plot of k_f against $[H^+]$ is k_f^1/Q_a or $k_f^1 = Q_a \times$ slope.

The values of $Q_a \times$ slope $(= k_f^1)$ are also included in Table I. It may be noted that the change in the values of k_f^1 over the range 34 to 59% methanol, over which Q_a is changing markedly, is small. There does seem to be a significant decrease of k_f^1 for solutions of higher methanol content, although the small magnitude and the wide confidence limits of the slope prevent precise estimates of k_f^1. Indeed for solutions with methanol content 87 and 97%, the slight positive slopes of the lines of regression on the graph are not significant.

The essential features of the kinetic results in the table are: *a*, near independence of k_f^0 on solvent composition over the range 0 to 76% methanol followed by a significant decrease in value as the water content is further decreased, with the effect of the removal of the last few % of water being quite pronounced; *b*, values for k_f^1 which rise to a significant but not pronounced maximum in the region of 35% methanol content and which are substantially less than those of k_f^0 by a factor of about 10^{-3} except in the solvents of highest methanol content where the values drop markedly and are not significantly different from zero.

If the "ion-pair exchange" mechanism applies over the entire range of solvent compositions, the near constancy of k_f^0 over the range 0 to 76 weight % of methanol could be the consequence of the effective values of K_0 and k_0 remaining constant or of compensating change in each. Pearson and Ellgen (1) suggested that with uncharged ligands K_0 should be approximately the same in water and in methanol. The fact that the ratio of the values of k_f^0 for the nickel phenanthroline anation in water and in methanol is about 11/1 (3, 1) and the ratio of the rate constants for solvent exchange from nickel(II) ions in the two solvents is about 30/1 (6, 7) may be taken as at least consistent with this view. K_0 relates to an essentially physical process which should not be sensitively dependent on the exact composition of the solvation sphere, and it may be expected that there would be little change in the values of K_0 in the mixed solvents from the values in the pure solvents. Consequently one may consider the variation in k_f^0 as paralleling the variations in k_0.

On this basis our data imply that the effective rate constant for transformation of the various nickel(II)–phenanthroline outer complexes (various because of the variety of the solvation spheres of nickel(II)) in solvents up to 76% by weight methanol stays very close to that of fully aquated nickel(II) ion in 100% water solvent. On the other hand, our data, along with that of Pearson and Ellgen for behavior in 100% methanol, imply close to a 5-fold drop in k_0 as the water content of the solvent decreases from 3 to 0 %, whereas the decrease in water content from 100 to 3% yields a somewhat smaller relative decrease. Reliable data on the nature of the solvated nickel(II) species in methanol–water are not available but Luz and Meiboom (8) were able to assess the population of various cobalt(II) species in such solvent mixtures at −60 °C. In 97%

Can. J. Chem. Downloaded from www.nrcresearchpress.com by 210.87.254.6 on 09/05/12
For personal use only.

Can. J. Chem. Downloaded from www.nrcresearchpress.com by 210.87.254.6 on 09/05/12
For personal use only.

methanol the predominant species appear to be $[Co(CH_3OH)_5(H_2O)]^{2+}$ and $[Co(CH_3OH)_6]^{2+}$ with the former constituting about 2/3 of the total cobalt(II). At 87% methanol the predominant species are the mono-, bi-, and tri-aquated cobalt(II) ions with the bi-aquated form in the highest concentration. Our data imply that k_f^0 and presumably k_0 for the reaction of nickel(II) with phenanthroline in solvents of methanol content 97 and 87% have values about 2/5 and 2/3 the values in 100% water. In the absence of quantitative information about the distribution of solvated nickel(II) species it is not possible to make worthwhile quantitative interpretations, but if one assumes that the distribution of nickel(II) species very roughly approximates that of cobalt(II) species in methanol–water mixtures at −60 °C, it is apparent that the effective value of k_0 for the mono- plus bi-aquated species would be close to 2/3 the value for the fully aquated ions.

An acceptable mechanism for the acid dependent contribution to the reaction must explain the trends in k_f^1 with solvent composition summarized above and also the decrease in the slope of the plot of k_f against $[H^+]$ at high concentrations of H^+ which, though not implied by our data, does occur (3). A mechanism explaining the fall-off in slope at higher hydrogen concentrations could involve Ni^{2+} and $Hphen^+$ yielding a monodentate intermediate, Ni—$phen^{2+}$, which becomes involved significantly in the reverse reaction with H^+ only at high hydrogen ion concentrations. If the mechanism is of the "interchange" rather than the "dissociative" type (9), the outer sphere ion pairs which collapse to give the intermediate would be collision complexes of short life involving the normally solvated nickel(II) species and $Hphen^+$. The Fuoss relation (10), while admittedly not applicable for precise quantitative calculations, should give approximate indication of the magnitudes of K_0 and of the value of the ratio (K_0 for Ni^{2+} and $Hphen^+$)/(K_0 for Ni^{2+} and phen). This ratio should *decrease* with increase in methanol content of the solvent, and for essentially aqueous solution at ionic strength 0.050 and a distance of closest approach of 5 Å, would be of the order of 1/10 rather than 1/1000 which is the value suggested by the observed ratio of the rate constants and a simple ion-pair interchange mechanism in which the rate controlling step in bidentate complex formation is the formation of the monodentate intermediate. Taken along with the observed increase in the value of k_f^1 with increase in methanol content in the range 0 to 35% methanol, this suggests that a simple ion-pair interchange mechanism in which the overall rate of reaction is effectively that of collapse of the ion-pair with a rate constant approximating that for solvent loss from nickel(II) ions is not applicable to the acid dependent reactions.

It seems possible that the low values of k_f^1 are associated with a mechanism involving a protonated monodentate intermediate which (unlike the unprotonated monodentate intermediate at low acidities) reverts to reactants much more rapidly than it converts via a deprotonated intermediate to the bidentate product, e.g. $k_{-1} \gg k_2$ in the scheme

$$Ni^{2+},phenH^+ \underset{k_{-1}}{\overset{k_1}{\rightleftharpoons}} Ni\text{-}phenH^{3+} \underset{k_{-2}}{\overset{k_2}{\rightleftharpoons}} Ni{-}phen^{2+} + H^+ \rightarrow Ni{<}phen^{2+}$$

where $Ni^{2+},phenH^+$ represents the ion-pair and $Ni{<}phen^{2+}$, the bidentate complex. Steric resistance to the formation of a monodentate intermediate involving the rigid monoprotonated phenanthroline might be expected. However, there appears to be no positive evidence which precludes the formation of such a species which might involve the ligand bent back from the nickel with a strained bond to the one coordinating nitrogen. Moreover, the relatively low values for the acid dissociation rate constants of amines (11) suggest that the assumption that $k_2 \ll k_1$ is reasonable. If the step with rate constant k_2 is the slow step then general base catalysis may be anticipated, but our data are too restricted to allow reliable assessment of this implication.

Perhaps the most pertinent of our findings about the acid dependent reaction is that its contribution to the overall reaction appears to approach insignificance in the most methanolic solvents. This may be taken to imply that the reactivity of phenanthrolium ion with the solvated

nickel(II) species decreases much more sharply than does that of phenanthroline as the water of the solvent becomes the minor component. The decrease in K_0 for the nickel(II)–phenanthrolium ion-pair with increase in methanol content could contribute to such a decrease. The precision of the values for k_f^1 in the highly methanolic solvents is too low to permit judgment as to whether the drop in k_f^1 is too great to be explicable on this basis.

Acknowledgment

We thank the National Research Council of Canada for financial support of this work.

1. R. G. PEARSON and P. ELLGEN. Inorg. Chem. **6**, 1379 (1967).
2. R. G. WILKINS and M. EIGEN. Mechanisms of inorganic reactions. Advan. Chem. Ser. No. 49. Amer. Chem. Soc. Washington, D.C. 1965.
3. D. W. MARGERUM, R. I. BYSTROFF, and C. V. BANKS. J. Amer. Chem. Soc. **78**, 4211 (1956).
4. R. H. HOLYER, C. D. HUBBARD, S. F. A. KETTLE, and R. G. WILKINS. Inorg. Chem. **4**, 929 (1965).
5. A. L. BARCARELLA, E. GRUNWALD, H. P. MARSHALL, and E. L. PURLEE. J. Org. Chem. **20**, 747 (1955); J. Phys. Chem. **62**, 856 (1958).
6. R. E. CONNICK and D. FIAT. J. Chem. Phys. **44**, 4103 (1966).
7. Z. LUZ and S. MEIBOOM. J. Chem. Phys. **40**, 2686 (1964).
8. Z. LUZ and S. MEIBOOM. J. Chem. Phys. **40**, 1058 (1964).
9. C. H. LANGFORD and H. B. GRAY. Ligand substitution processes. W. A. Benjamin, Inc., New York. 1965.
10. R. M. FUOSS. J. Amer. Chem. Soc. **80**, 5059 (1958).
11. E. GRUNWALD and M. COCIVERA. Discuss. Faraday Soc. **39**, 105 (1965).

Can. J. Chem. Downloaded from www.nrcresearchpress.com by 210.87.254.6 on 09/05/12
For personal use only.

Crystal structures of $NaNiIO_6$, $NaMnIO_6$, and $KMnIO_6$

I. D. BROWN

Institute for Materials Research, McMaster University, Hamilton, Ontario

Received May 16, 1969

$NaNiIO_6$ (a = 4.962, c = 5.148 Å, space group $P312$) is shown from X-ray powder patterns to be isostructural with trigonal $KNiIO_6$. Approximate coordinates for the oxygen atoms are given. $NaMnIO_6$ (a = 4.972, c = 5.136 Å) and $KMnIO_6$ (a = 5.009, c = 6.000 Å) are probably also isostructural but the broadening of the X-ray powder lines in these compounds makes a complete analysis impossible. Powder patterns for all three compounds are given.

Canadian Journal of Chemistry, 47, 3779 (1969)

Can. J. Chem. Downloaded from www.nrcresearchpress.com by 210.87.254.105 on 09/05/12
For personal use only.

$KNiIO_6$ and $NaNiIO_6$ were first prepared by Rây and Sarma (1). More recently Reimer and Lister (2) have characterized the manganese analogues and have shown by means of X-ray powder diffraction patterns that they are isomorphous with the corresponding nickel complexes. Also using X-ray powder diffraction, Vannerberg and Blockhammar (3) and Eddy and Vannerberg (4) have shown that $KNiIO_6$ consists of hexagonal sheets of linked NiO_6 and IO_6 octahedra with the potassium atoms lying in the octahedral holes between the sheets.

The samples used in this work were those prepared by Reimer and Lister (2). All four complexes are highly insoluble in water and it was not possible to obtain crystals large enough for a single crystal X-ray diffraction study. Consequently, X-ray powder patterns of each compound were recorded using a Philips horizontal diffractometer equipped with a focusing LiF monochromator. Filtered copper radiation was used throughout. The powder pattern of $KNiIO_6$ agreed with that observed by Vannerberg and Blockhammar (3). The powder patterns of the other three compounds could be indexed by assuming that they were isostructural. The crystal data, which were refined by least squares analysis, are summarized in Table I and the diffraction patterns are given in Tables II and III. Both the nickel complexes gave diffraction patterns which could be indexed out to high angles, but the lines in the manganese complexes were very broad and weak and could not be recorded much beyond a Bragg angle of 30 or 40 degrees. However, enough was visible to confirm that their unit cells were almost identical to the corresponding nickel complexes. The cause of the broadening of the lines was not examined but the fact that the degree of broadening was roughly proportional to the l index suggests that the crystals in the sample were 00.1 plates about 150 Å in thickness.

The diffractometer was used to record integrated intensities from the $NaNiIO_6$ sample in

TABLE I
Crystal data

Molecule	a(Å)	c(Å)	Space group	Remarks
$KNiIO_6$	4.964±0.003* 4.969±0.005†	6.004±0.003* 6.000±0.005†	$P312(D_3^1)$	1 K in 1(a) 1 Ni in 1(d) 1 I in 1(f) 6 O in 6(l)
$KMnIO_4$	5.009±0.004	6.000±0.021	$P312(D_3^1)$(?)	—
$NaNiIO_6$	4.962±0.001	5.148±0.001	$P312(D_3^1)$	1 Na in 1(a) 1 Ni in 1(d) 1 I in 1(f) 6 O in 6(l)
$NaMnIO_6$	4.972±0.002	5.136±0.007	$P312(D_3^1)$(?)	—

*Present work.
†Reference 3.

TABLE II

Crystal spacings, d, and intensities, I, for $NaNiIO_6$ and $NaMnIO_6$; observed and calculated structure factors for $NaNiIO_6$

	$NaNiIO_6$							$NaMnIO_6$		
				Structure factor						
hkl	d_{obsd} (Å)	d_{calcd} (Å)	I	$(\Sigma F_o^2)^{\frac{1}{2}}$	σ	$(\Sigma F_c^2)^{\frac{1}{2}}$	F_c	d_{obsd} (Å)	d_{calcd} (Å)	I
001	5.143	5.148	100	85.1	8.2	81.2		5.155	5.146	86
100	4.291	4.297	39	36.5	3.4	38.2		4.303	4.317	57
101	3.297	3.299	78	48.1	4.3	48.9		3.307	3.307	100
002	2.571	2.574	8	49.0	4.3	45.6		—	2.573	—
110	2.475	2.481	27	54.3	5.8	54.2		2.492	2.492	37
111, 11$\bar{1}$	2.227	2.235	51	83.6	8.2	71.8	22.4, 68.2	2.243	2.243	43
102	2.206	2.208	4	17.8	4.8	25.6		—	2.210	—
200	2.141	2.149	1	13.9	7.7	20.6		—	2.159	—
201	1.981	1.983	13	34.1	1.9	35.8		2.006	1.991	18
112, 11$\bar{2}$	1.787	1.786	48	103.3	11.1	99.6	54.5, 83.3	1.791	1.790	53
003	1.716	1.716	—	17.3	29.8	20.7		—	1.715	—
202	1.649	1.649	4	24.5	3.8	30.2		—	1.654	—
210	1.623	1.624	4	33.2	5.8	26.1		—	1.632	10
103	1.593	1.594	8	33.7	2.9	33.1		—	1.594	—
211, 21$\bar{1}$	1.549	1.549	15	66.2	6.7	51.9	30.0, 42.4	1.561	1.555	16
300	1.4332	1.4324	14	69.2	7.7	66.8		1.4427	1.4390	24
113, 11$\bar{3}$	1.4101	1.4113	14	71.6	7.7	68.1	54.0, 41.4	—	1.4130	—
301	1.3804	1.3800	—	39.4	7.2	43.6				
212, 21$\bar{2}$	1.3711	1.3736	13	43.7	22.6	32.2	19.8, 25.5	1.3894	1.3859, 1.3780	17
203	1.3404	1.3408	5	32.7	4.3	39.0				
004	1.2851	1.2870	2	51.4	18.3	48.3				
302	1.2521	1.2516	5	35.6	4.8	37.8				
220	1.2403	1.2405	4	37.0	18.3	42.3				
104	1.2343	1.2329		18.8	18.8	21.9				
221, 22$\bar{1}$	1.2066	1.2060	5	50.4	7.2	47.9	41.9, 23.4			
310	1.1926	1.1918	2	35.1	10.6	25.8				
213, 21$\bar{3}$	1.1793	1.1796	5	49.9	7.2	41.1	31.0, 27.1			
311, 31$\bar{1}$	1.1616	1.1611	6	55.7	6.7	46.4	39.9, 23.7			
114, 11$\bar{4}$	1.1413	1.1424	6	58.1	6.7	64.0	56.6, 29.7			
222, 22$\bar{2}$	1.1174	1.1175	6	62.9	3.4	64.6	51.9, 38.5			
204	1.1060	1.1041	—	12.5	15.9	20.7				
303	1.0995	1.0996	1	19.2	10.6	20.7				
312, 31$\bar{2}$	1.0827	1.0815	—	13.0	32.2	28.5	22.7, 17.0			
400	1.0753	1.0743	—	13.0	32.2	22.0				
401	1.0525	1.0516	1	19.2	10.6	28.4				

Can. J. Chem. Downloaded from www.nrcresearchpress.com by 210.87.254.105 on 09/05/12
For personal use only.

TABLE II *(concluded)*

	$NaNiIO_6$							$NaMnIO_6$		
				Structure factor						
hkl	d_{obsd} (Å)	d_{calcd} (Å)	*I*	$(\Sigma F_o^2)^{\frac{1}{2}}$	σ	$(\Sigma F_c^2)^{\frac{1}{2}}$	F_c	d_{obsd} (Å)	d_{calcd} (Å)	*I*
005	1.0325	1.0296	2	53.4	24.0	43.9				
214	1.0065	1.0087	8	—	—	29.4	22.9			
$21\bar{4}$							18.4			
233		1.0053		—	—	45.5	28.8			
$23\bar{3}$							35.2			
105		1.0013		—	—	28.0				
402	—	0.9914	—	—	—	19.8				
320	—	0.9858	—	—	—	17.0				
313	0.9783	0.9789	1	29.4	14.4	33.0	21.0			
$31\bar{3}$							25.4			
321	0.9667	0.9683	2	37.0	11.5	35.6	23.5			
$32\bar{1}$							24.9			
304	0.9581	0.9573	6	39.9	5.3	36.8				

TABLE III

Crystal spacings, *d*, and intensities, *I*, for $KNiIO_6$ and $KMnIO_6$

	$KNiIO_6$			$KMnIO_6$		
hkl	d_{obs} (Å)	d_{calcd} (Å)	*I*	d_{obs} (Å)	d_{calcd} (Å)	*I*
001	6.002	6.004	100	5.985	6.000	73
100	4.291	4.299	17	4.311	4.338	27
101	3.480	3.495	75	3.507	3.515	100
002	2.998	3.002	13	—	3.000	2
110	2.479	2.482	23	2.501	2.504	—
102	2.455	2.461			2.467	
111	2.292	2.294	15	2.309	2.311	29
200	2.151	2.149	—	—	2.169	19
201	2.023	2.024	13	2.032	2.040	18
003	1.973	2.001			2.000	
112	1.914	1.913	39	1.918	1.922	56
103	1.815	1.814	9	—	1.816	—
202	1.743	1.748	5	—	1.758	—
210	1.623	1.624	2	1.642	1.640	—
211	1.570	1.568	19	1.580	1.582	26
113	1.561	1.558			1.563	
004	1.501	1.501	2	—	1.500	—
203	1.4658	1.4647	6	—	1.4703	—
300	1.4328	1.4330	10	1.4467	1.4460	12
212	1.4308	1.4290			1.4387	
104	—	1.4171			1.4176	
301	1.3949	1.3938	4	1.4079	1.4057	7
302	1.2960	1.2932	7	—	—	—
114	1.2869	1.2844	7	—	—	—
213	1.2635	1.2614	6	—	—	—
220	1.2425	1.2410	2	—	—	—
204	1.2316	1.2306	1	—	—	—
221	—	1.2153	2	—	—	—
005	—	1.2008	—	—	—	—
310	1.1931	1.1923	1	—	—	—

Can. J. Chem. Downloaded from www.nrcresearchpress.com by 210.87.254.105 on 09/05/12
For personal use only.

Can. J. Chem. Downloaded from www.nrcresearchpress.com by 210.87.254.105 on 09/05/12
For personal use only.

reflection. An estimated standard error (σ) was assigned to each measurement and the data were corrected for the Lorentz effect and the polarization occurring in both the sample and monochromator. The structure of $NaNiIO_6$ was assumed to be the same as that of $KNiIO_6$. Models in which the Ni and I atoms were in turn placed in 1(a) gave considerably worse agreement. Unfortunately, in the space group $P312$, which Vannerberg and Blockhammar (3) found for $KNiIO_6$, only those reflections with either h, k, or l equal to zero can be measured unambiguously. The intensities measured for the remainder were the sum of the intensities of the hkl and $hk\bar{l}$ reflections which are not equivalent. Consequently, the initial refinement involved only the use of the $h0l$ and $hk0$ reflections. The position of the oxygen atom was chosen to give reasonable bond distances (Na—O = 2.4 Å, Ni—O = 2.1 Å, I—O = 1.9 Å), and the scale and individual isotropic temperature factors were varied in a least squares refinement which minimized the sum of the squares of the differences between the observed and calculated structure factors, F_o and F_c, respectively, weighted according to the estimated standard errors. The resulting weighted agreement index (R) was 0.14 and an application of the χ^2 test, using the estimated standard errors as a measure of the expected deviation in individual measurements, led to a probability[1] $P(\chi^2)$ of 5%. The scale, isotropic temperature factors, and the coordinates of the oxygen atom were then refined, at each stage the values of $F_o(hkl)$ and $F_o(hk\bar{l})$ being chosen so that $F_o^2(hkl) + F_o^2(hk\bar{l})$ agreed with the observed intensity and $F_o(hkl)/F_o(hk\bar{l})$ was the same as $F_c(hkl)/F_c(hk\bar{l})$ for the previous round. After several rounds, no further significant changes occurred, R was equal to 0.105 and $P(\chi^2)$ was equal to 76%. The final set of parameters is given in Table IV.

The results of this study are not, unfortunately, as accurate as could be wished. All four compounds appear to be isostructural but the broad lines in the powder patterns of $KMnIO_6$ and $NaMnIO_6$ do not permit refinement of their structures. The refinement of the structure of $NaNiIO_6$ leads to temperature factors which are rather small, two being negative, although not significantly so. The Ni—O and I—O distances, whose errors are estimated to be at least 0.13 Å, do not differ significantly from the values found in $KNiIO_6$ (Table IV) nor does the Na—O distance differ significantly from the value of 2.35 Å expected from the sum of the crystal radii (5). As was observed by Vannerberg and Blockhammar (3), the X-ray diffraction analysis shows no sign of the water which has been found in the chemical analyses of all these complexes. It can be assumed that since the crystallites composing the sample are very small, the water is adsorbed onto the crystal surfaces and is not true water of crystallization.

TABLE IV

Positional and temperature parameters and interatomic distances in $NaNiIO_6$

Parameter*	$NaNiIO_6$ Initial model	$NaNiIO_6$ Final model†	$KNiIO_6$‡
x(O)	0.630	0.608(0.014)	0.671
y(O)	0.040	−0.013(0.019)	0.039
z(O)	0.280	0.312(0.006)	0.312
B(Na, K) (Å^2)	−2.3	−0.3(1.2)	4.4
B(Ni) (Å^2)	−0.2	2.1(0.9)	3.2
B(I) (Å^2)	0.4	0.3(0.4)	1.2
B(O) (Å^2)	−0.4	−0.2(0.8)	1.7
R	0.145	0.105	0.120
$P(\chi^2)$	0.05	0.76	
Ni—O (Å)	2.06	1.78(0.13)	2.10(0.06)
I—O (Å)	1.95	1.87(0.13)	1.85(0.06)
Na, K—O(Å)	2.42	2.35(0.13)	2.56(0.06)

*x(O), y(O), z(O) are the coordinates of the oxygen atom, B is the isotropic temperature factor.
†Standard errors are given in parentheses.
‡From ref. 4.

Acknowledgments

I would like to thank Dr. M. W. Lister for suggesting this problem to me and the National Research Council of Canada for the operating grant which made this research possible.

1. P. RÂY and B. SARMA. J. Indian Chem. Soc. **25**, 205 (1948).
2. I. REIMER and M. W. LISTER. Can. J. Chem. **39**, 2431 (1961).
3. N-G. VANNERBERG and I. BLOCKHAMMAR. Acta Chem. Scand. **19**, 875 (1965).
4. L. P. EDDY and N-G. VANNERBERG. Acta Chem. Scand. **20**, 2886 (1966).
5. L. PAULING. The nature of the chemical bond. 3rd ed. Cornell Univ. Press, Ithaca, New York. 1960. p. 514.

[1] $P(\chi^2)$ measures the probability of finding worse agreement between the observed and calculated structure factors, assuming that the latter are calculated from the correct model.

Can. J. Chem. Downloaded from www.nrcresearchpress.com by 210.87.254.6 on 09/05/12
For personal use only.

Gas phase radiolysis of hydrogen chloride, hydrogen bromide, and nitrous oxide with intense electron pulses[1]

C. WILLIS AND A. W. BOYD
Physical Chemistry Branch, Chalk River Nuclear Laboratories, Atomic Energy of Canada Limited, Chalk River, Ontario

AND

D. A. ARMSTRONG
Department of Chemistry, University of Calgary, Calgary, Alberta

Received June 11, 1969

Hydrogen chloride and hydrogen bromide have been irradiated with single electron pulses at a very high intensity (10^{27} eV g^{-1} s^{-1}) with a Febetron 705. At room temperature the yields of hydrogen from hydrogen chloride and hydrogen bromide, for pressures between 700 and 1200 Torr, are $G(H_2) = 8.1 \pm 0.2$ and $G(H_2) = 9.9 \pm 0.3$, respectively. These are the same as the yields observed at low dose rates. Detailed lifetime calculations, however, show that the mechanism is significantly different at the higher dose rate. Scavenger experiments with chlorine in hydrogen chloride show that the negative ion intermediates form thermal hydrogen atoms.

The value of $G(N_2) = 12.4 \pm 0.2$ from nitrous oxide at a dose rate of 10^{27} eV g^{-1} s^{-1} is confirmed and the use of nitrous oxide as a dosimeter for pulsed electron beams is discussed. The higher nitrogen yield at Febetron dose rates appears to be due to changes in the reactions of electrons.

Canadian Journal of Chemistry, 47, 3783 (1969)

Introduction

The radiation chemistry of gases using pulsed electron beams with dose rates of 10^{26} to 10^{28} eV g^{-1} s^{-1} is a relatively new field. We have previously described the radiolysis of nitrous oxide, ethylene (1), and ammonia (2) and discussed the use of nitrous oxide as a dosimeter at these dose rates (1, 3). The nitrogen yield, $G(N_2) = 12.4$ molecules per 100 eV, was significantly higher than the value of $G(N_2) = 10.0$ accepted for low dose rates (4). The present study was undertaken to examine the radiolysis of hydrogen chloride and hydrogen bromide at high dose rates and to investigate the reason for the difference in nitrogen yields from nitrous oxide. Diatomic gases, such as hydrogen chloride and hydrogen bromide, provide model systems for studying fundamental processes and their radiolytic mechanisms at low dose rates (5, 6) are currently much better understood than that of nitrous oxide.

The average energy of the primary electrons used in the irradiations at 10^{27} eV g^{-1} s^{-1} will not be much larger than that of the electrons traversing a gas in typical γ-ray radiolyses, and differences in linear energy transfer will be negligible. Primary ionization and excitation events will be the same. Differences between normal γ-ray radiolyses and those at very high dose rates, therefore, must arise from the much higher concentrations of reactive intermediates produced. Recombination times of ions and neutral intermediates will be very much shorter and may be reflected by changes in mechanism which can further elucidate the primary processes occurring.

Experimental

Pulsed Electron Accelerator and Dosimetry

The pulsed electron accelerator was a Febetron 705 which gives short pulses of 1.0 to 1.7 MeV electrons with a maximum current of about 5000 A. Details have been given elsewhere (1, 7, 8).

The dosimetry was based on a nitrogen yield of $G(N_2) = 12.4$ for the radiolysis of nitrous oxide at 1 atm. This value was obtained by comparing the yields from nitrous oxide with the dose per pulse measured by adiabatic calorimetry (1). The yield is independent of temperature from 20–200 °C (3). The dose absorbed in hydrogen chloride and hydrogen bromide was calculated from the measured dose in nitrous oxide using the relative stopping power for 1 MeV electrons derived from the Bethe equation (9).

Gas samples were contained in quartz cells (2) with ~0.5 mm quartz electron windows. The actual pulse shape and duration in these cells is somewhat uncertain. However, the voltage range of the transmitted pulse is estimated to be 0.4 to 1.1 MeV with its half-duration as 30 ns. The average energy of the electrons is estimated to be 1 MeV.

Materials and Analytical Procedures

All gases were obtained from Matheson Company.

[1]Issued as A.E.C.L. No. 3399.

Can. J. Chem. Downloaded from www.nrcresearchpress.com by 210.87.254.6 on 09/05/12
For personal use only.

The hydrogen chloride (Technical Grade 99.0%) and hydrogen bromide (99.8%) were purified as previously described (10). Nitrous oxide (98.0%), sulfur hexafluoride (98.0%), and chlorine (High Purity Grade 99.5%) were taken from the cylinders and subjected to freeze–pump–thaw cycles to remove non-condensible impurities.

Analysis of the gaseous products was achieved by immersing the irradiated cell in liquid nitrogen and pumping off the noncondensible gases into a McLeod gauge. After the volume of gas had been measured, its composition was determined by mass spectrometry.

Results

Radiolysis of the Pure Gases

Nitrogen yields from nitrous oxide and hydrogen yields from hydrogen chloride and hydrogen bromide, determined at pressures in the range 600 to 1500 Torr, are given in Table I.

Effect of Chlorine on the Hydrogen Yields from Hydrogen Chloride

Hydrogen yields from the Febetron radiolysis of hydrogen chloride – chlorine mixtures are plotted as a function of $[Cl_2]/[HCl]$ in Fig. 1. They are the same, within experimental error, for hydrogen chloride pressures of 700 and 1200 Torr, but differ significantly from those observed at low dose rates under similar conditions of temperature and pressure. The latter are included in Fig. 1 for comparison.

TABLE I

Product yields in Febetron radiolysis of nitrous oxide, hydrogen chloride, and hydrogen bromide

Gas	Pressure (Torr)		G values
			$G(N_2)$
N_2O	760		12.4*
	790		12.5
	900		12.4
	1367		12.5
	1498		12.4
		Mean =	12.4 ± 0.2
			$G(H_2)$
HCl	609		8.2
	604		7.9
	603		8.6
	610		8.0
	661		8.0
	709		8.2
	732		7.9
	1148		7.8
	1200		8.2
		Mean =	8.1 ± 0.2
			$G(H_2)$
HBr	728		10.8
	734		9.9
	735		9.5
	1129		9.9
	1385		9.6
		Mean =	9.9 ± 0.3

*Standard value taken from ref. 1.

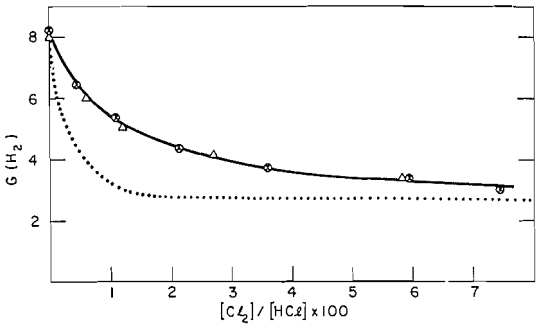

FIG. 1. Effect of chlorine addition on hydrogen yield from HCl at 10^{27} eV g^{-1} s^{-1}: Δ, 700, ⊗, 1200 Torr HCl; dotted line gives yields observed at low dose rates from 19.

Effect of SF_6 on the Hydrogen Yields from Hydrogen Chloride

The values of $G(H_2)$ for the Febetron and X-ray radiolysis (11) of hydrogen chloride at 1200 Torr and varying proportions of SF_6 are compared in Fig. 2. A difference between the two dose rates may be noted.

Effect of SF_6 on the Nitrogen Yields from Nitrous Oxide

Figure 3 shows a plot of $G(N_2)$ vs. $[SF_6]/[N_2O]$

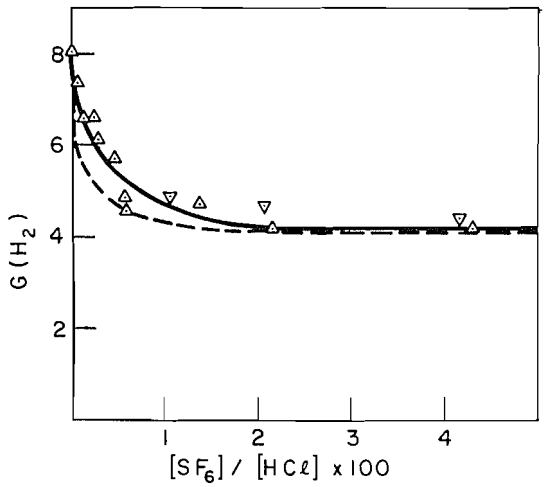

FIG. 2. Effect of sulfur hexafluoride on hydrogen yield from HCl at 10^{27} eV g^{-1} s^{-1}: ▽, 700, Δ, 1200 Torr HCl; dotted line gives yields observed at low dose rates from ref. 11.

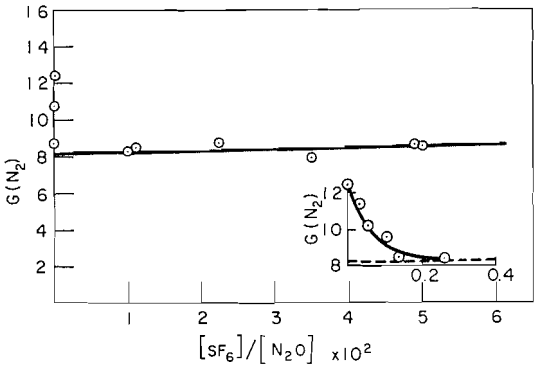

FIG. 3. Effect of sulfur hexafluoride on nitrogen yield from N_2O at 10^{27} eV g^{-1} s^{-1} at 700 Torr N_2O. The inset shows the nitrogen yields in the fall-off region at very low SF_6 concentrations of 0–0.6 mole %.

at a nitrous oxide pressure of 700 Torr. The inset figure shows the nitrogen yield at very low concentrations of SF_6 in the fall-off region.

Discussion

Hydrogen Chloride

The total hydrogen yield from the X-ray and γ-ray radiolysis of hydrogen chloride is $G(H_2) = 8.0 \pm 0.3$ (5). The present investigation shows that the hydrogen yield at 10^{27} eV g^{-1} s^{-1}, at room temperature, is the same; $G(H_2) = 8.1 \pm 0.2$. In accord with the W value of 25.0 ± 0.3 eV per ion pair (10), the yield of HCl^+ ions and electrons, e^-, from primary ionization is 4.0 ± 0.1 per 100 eV.

[1] $$HCl \rightarrow HCl^+ + e^-$$

HCl^+ undergoes the ion molecule reaction

[2] $$HCl^+ + HCl \rightarrow H_2Cl^+ + Cl$$

Experiments with SF_6 in γ-ray and X-ray radiolyses have shown (5) that each electron produces 1 molecule of hydrogen. The reduction of $G(H_2)$ from 8.1 to 4.1 in Fig. 2 indicates that this is also true at Febetron dose rates. The remaining 4 molecules of hydrogen per 100 eV are due mainly to the formation of hydrogen atoms from neutral excited molecules

[3] $$HCl \rightarrow HCl^* \rightarrow H + Cl$$

At low dose rates there is a yield of hydrogen, $G_{H_2} = (G_{H'}) = 2.2 \pm 0.2$ (5), which cannot be scavenged by chlorine or bromine. This means that some of the hot hydrogen atoms formed in reaction [3] undergo reaction [4]

[4] $$H + HCl \rightarrow H_2 + Cl$$

before being moderated to thermal energies. However, there is a thermal hydrogen atom yield, G_γ, of 1.7 per 100 eV. These must come from the collisional moderation of H

[5] $$H + HCl \rightarrow H + HCl$$

and threshold dissociation processes which need not be considered in detail here. The yields of H_2 and H from reactions [4] and [5] will clearly be unaffected by dose rate.

Figure 4 shows a reciprocal plot of the hydrogen yields from the Febetron radiolysis of hydrogen chloride – chlorine mixtures at 700 and 1200 Torr of hydrogen chloride. This is based on the expression

$$\frac{1}{\Delta G(H_2)} = \frac{1}{G_H}\left(1 + \frac{k_{H+HCl}[HCl]}{k_{H+Cl_2}[Cl_2]}\right)$$

which assumes that hydrogen chloride and chlorine are competing for thermal hydrogen atoms in reactions [6] and [7]

[6] $$H + HCl \rightarrow H_2 + Cl$$

[7] $$H + Cl_2 \rightarrow HCl + Cl$$

For simplicity, only the best line for the 700 Torr results is given. It gives $G_H = 5.7$ and $k_6/k_7 = 1.10 \times 10^{-2}$. The best line for the 1200 Torr data gives $G_H = 5.5$ and $k_6/k_7 = 1.03 \times 10^{-2}$. The mean value of k_6/k_7 is 1.07×10^{-2}. The agreement with $1.08 \pm 0.15 \times 10^{-2}$ from photochemical experiments (12) means that at 10^{27} eV g^{-1} s^{-1} chlorine reacts only with thermal hydrogen atoms. Since the yield of these, 5.6 ± 0.2 per 100 eV, is equal to the yield of thermal hydrogen atoms from neutral dissociations ($G_\gamma = 1.7$) plus $G_e = 4.0$, each electron must produce a

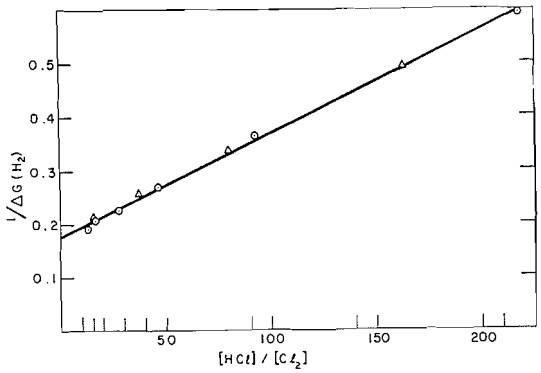

FIG. 4. Reciprocal plot for hydrogen yields in presence of added chlorine: Δ, 700, ○, 1200 Torr HCl.

Can. J. Chem. Downloaded from www.nrcresearchpress.com by 210.87.254.6 on 09/05/12
For personal use only.

Can. J. Chem. Downloaded from www.nrcresearchpress.com by 210.87.254.6 on 09/05/12
For personal use only.

thermal hydrogen atom. Hence combinations of free electrons with H_2Cl^+

[8] $$e + H_2Cl^+ \rightarrow H + HCl$$

and HCl^+

[9] $$e + HCl^+ \rightarrow H + Cl$$

cannot be important, since they are highly exothermic and should produce hot hydrogen atoms. Chlorine cannot scavenge free electrons below 1.6 eV (13) and thus the occurrence of reactions [8] and [9] should enhance $G_{H'}$. The observed value at Febetron dose rates is 2.5 ± 0.2 $(=8.1 - 5.6)$, which agrees within experimental error with 2.2 ± 0.2 at low dose rates.

Experiments reported elsewhere (14) have shown that secondary electrons acquire energy from the transient electric field due to the space charge of the intense electron beam of the Febetron. The effects of this are most serious at pressures below 500 Torr where the electrons gain sufficient energy to give enhanced decomposition through reaction [10]. In the pressure

[10] $$e\ (\text{k.e.} > 6\ \text{eV}) + HCl \rightarrow e^- + HCl^*$$

range 600–1200 Torr the energy gained by an electron per mean free path is much less, and enhanced yields are not observed. However, even at these pressures the electrons would not be expected to be completely thermal. This is shown in Fig. 2 by the fact that larger concentrations of SF_6 are required to reduce the hydrogen yield at Febetron dose rates than at low dose rates. Since

[11] $$e + SF_6 \rightarrow SF_6^-$$

k_{11} decreases sharply as the energy of the electron rises above 0.03 eV (15–17), its effective value in Febetron radiolysis will be significantly less than in an X-ray or γ-ray radiolysis where there is no electric field. The total electron capture cross section for hydrogen chloride apparently does not decrease as markedly with energy (18). This may in part be due to the resonance capture process

[12] $$e + HCl \rightarrow H + Cl^-$$

which sets in at 0.65 eV (18). However, the cross section for this process is small ($\sigma_{\varepsilon_{max}} = 2 \times 10^{-17}$ cm^2). Therefore, most electrons are probably captured in the low energy processes which are observed at normal dose rates.

From a study (5*a*, 19) of the effects of chlorine on the hydrogen yields at low dose rates it was concluded that 1.4 electrons per 100 eV gave hydrogen atoms by reaction [13] (20)

[13] $$e + 3HCl \rightarrow HCl_2^- + HCl + H$$

while the remaining 2.5 per 100 eV formed a negative ion intermediate, HCl^-

[14] $$e^- + 3HCl \rightarrow HCl^- + 2HCl$$

The structure of this species is as yet unknown, but in view of the low electron affinity of hydrogen chloride (< 0.3 eV) (5*a*), it would probably be better represented as the electron dimer complex (Cl—H···e···H—Cl) for which Raff and Pohl (21) have estimated a binding energy of 0.8 eV. At normal dose rates HCl^- reacts with hydrogen chloride to produce hydrogen

[15] $$HCl^- + HCl \rightarrow H + HCl_2^-$$

[6] $$H + HCl \rightarrow H_2 + Cl$$

or, if chlorine is present, it can be scavenged in reaction [16]

[16] $$Cl_2 + HCl^- \rightarrow Cl + HCl_2^- \text{ or } Cl_2^- + HCl$$

Assuming that reaction [16] goes on every collision, the chlorine results (5*a*) give the minimum lifetime of HCl^- in pure hydrogen chloride at room temperature and 1 atm pressure as 200 ns.

The effects of chlorine on hydrogen yields from hydrogen chloride at low dose rates and Febetron dose rates are compared in Fig. 1. The reduction of $G(H_2)$ at much lower chlorine concentrations in the low dose rate experiments is due to the scavenging of HCl^- in reaction [16]. From our analysis of the reciprocal plot in Fig. 4 it is obvious that this does not occur at Febetron dose rates. Hence if HCl^- is formed under these conditions it must be reacting with positive ions

[17] $$HCl^- + H_2Cl^+ \rightarrow H + 2HCl$$

[18] $$HCl^- + HCl^+ \rightarrow H + Cl + HCl$$

too rapidly to be scavenged by chlorine at the concentrations shown in Fig. 1. Furthermore, the above analysis of the experiments with added chlorine requires that these reactions produce thermal hydrogen atoms. To assess their importance relative to reactions [15] and [16] we have calculated the concentrations of products and of atomic and ionic intermediates during and after a Febetron pulse, using a computer program WR16 (22). This was based on all the relevant foregoing reactions, except the resonance capture

process [12], and the following additional ionic and free radical reactions

[19] $HCl_2^- + H_2Cl^+ \rightarrow 3HCl$

[20] $HCl_2^- + HCl^+ \rightarrow Cl + 2HCl$

[21] $H + H + HCl \rightarrow H_2 + HCl$

[22] $H + Cl + HCl \rightarrow HCl + HCl$

[23] $Cl + Cl + HCl \rightarrow Cl_2 + HCl$

Reaction [19] is, of course, the neutralization process and reaction [23], the atom combination process, which occur at low dose rates. The primary yields used in the program were those derived from low dose rate studies: $G_{H'} = 2.2$, $G_\gamma = 1.8$, $G_{HCl^+} = 4.0$, and $G_{Cl} = 6.2$ (from reactions [3] and [4]). The pulse shape was approximated by a step function with 2 ns steps. The calculated concentrations are shown in Fig. 5 for the Febetron radiolysis of hydrogen chloride at 830 Torr in a quartz cell at 25 °C.

Theoretical considerations (23) show that the rate constant for the clustering of HCl^+ ions in hydrogen chloride at high pressures ($\sim$ 1 atm) will be of the order of $3 \times 10^{11}\ M^{-1}\ s^{-1}$ or larger. This is large enough that even at 10^{27} eV $g^{-1}\ s^{-1}$ all ions will have been clustered before neutralization occurs, although the clusters may not have reached equilibrium size as would be the case at low dose rates. A formal distinction between clustering of HCl^+ and the rate of the ion–molecule reaction [2]

[2] $HCl^+ + HCl \rightarrow H_2Cl^+ + Cl$

to give H_2Cl^+ is impossible at high pressures, and we assume k_2 equal to the rate constant for clustering. This and all other relevant rate constants are summarized in Table II.

From the computer calculated concentrations it follows that the mean ion combination lifetime is less than 10 ns, confirming that reactions [15] and [16] will not compete with reaction [17]. Using the peak concentrations of HCl^+, e, HCl^-, and HCl_2^-, reactions [9], [18], and [20] can be shown to be negligible. Similarly, less than 2% of the free electrons should give direct neutralization in reaction [8]. This is consistent with the

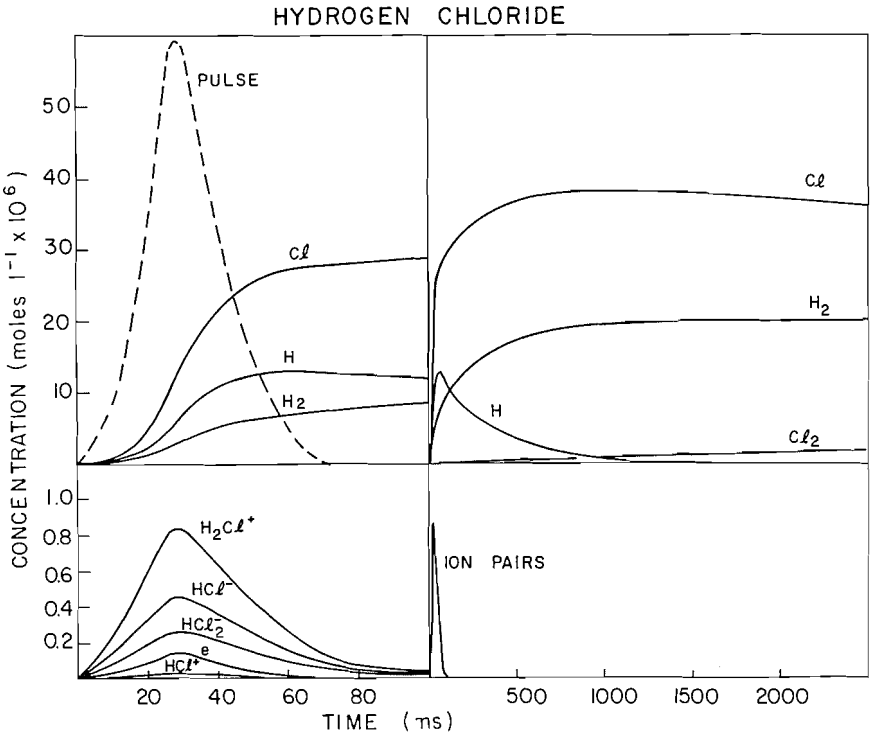

FIG. 5. Calculated ionic and atomic concentrations in hydrogen chloride during and following a Febetron pulse at 25 °C and 830 Torr pressure. Total dose = 1.5×10^{20} eV l^{-1}. The pulse intensities can be taken from the ordinate axis. The units for these are 10^{26} eV $l^{-1}\ s^{-1}$: i.e., the maximum intensity is 5.95×10^{27} eV $l^{-1}\ s^{-1}$.

Can. J. Chem. Downloaded from www.nrcresearchpress.com by 210.87.254.6 on 09/05/12
For personal use only.

TABLE II
Reactions in irradiated hydrogen chloride

	Reaction	Rate constant[a] M^{-1} s^{-1} at 25 °C	Remarks
[2]	$HCl^+ + HCl \rightarrow H_2Cl^+ + Cl$	3×10^{11}	*b*
[6]	$H + HCl \rightarrow H_2 + Cl$	6.7×10^7	*c*
[7]	$H + Cl_2 \rightarrow HCl + Cl$	6.7×10^9	*d*
[8]	$e + H_2Cl^+ \rightarrow H + HCl$	1.2×10^{14}	*e*
[9]	$e + HCl^+ \rightarrow H + Cl$	1.2×10^{14}	*e*
[13]	$e + 3HCl \rightarrow H + HCl_2^- + HCl$	2.2×10^{10}	*f*
[14]	$e + 3HCl \rightarrow HCl^- + 2HCl$	3.8×10^{10}	*f*
[15]	$HCl^- + HCl \rightarrow H + HCl_2^-$	1.0×10^8	*g*
[16]	$Cl_2 + HCl^- \rightarrow Cl_2^- + HCl$	1.0×10^{11}	*g*
[17]	$HCl^- + H_2Cl^+ \rightarrow H + 2HCl$	6.0×10^{14}	*e*
[18]	$HCl^- + HCl^+ \rightarrow H + Cl + HCl$	6.0×10^{14}	*e*
[19]	$H_2Cl^+ + HCl_2^- \rightarrow 3HCl$	6.0×10^{14}	*e*
[20]	$HCl_2^- + HCl^+ \rightarrow 2HCl + Cl$	6.0×10^{14}	*e*
[21]	$H + H + HCl \rightarrow H_2 + HCl$	3.0×10^8	*h*
[22]	$H + Cl + HCl \rightarrow 2HCl$	1.0×10^9	*i*
[23]	$Cl + Cl + HCl \rightarrow Cl_2 + HCl$	6.0×10^8	*j*

[a]All rate constants are given in equivalent two-body rate constants for 830 Torr hydrogen chloride.
[b]This is estimated from the data of ref. 23 to be the minimum rate constant for clustering of HCl^+ at 800 Torr. k_2 is assumed equal to it.
[c]See ref. 24.
[d]$k_7 = 10^2 \times k_6$ from ref. 12.
[e]All negative ion – positive ion combination coefficients are taken to be 6×10^{14} M^{-1} s^{-1} consistent with recent experimental data on ion lifetimes in irradiated hydrogen chloride (30). Free electron – positive ion combination coefficients are assumed to be a factor of 6 slower as usually observed (31).
[f]The sum of k_{13} and k_{14} was calculated from the SF_6 scavenging results at low dose rates (5*a*, 20) using $k_{11} = 1.8 \times 10^{14}$ (15). At 800 Torr hydrogen chloride it is equivalent to a second order rate constant of 6×10^{10} M^{-1} s^{-1}. The ratio of k_{13}/k_{14} is taken from ref. 5*a*.
[g]Reaction [16] is assumed to go on every collision and $k_{15}/k_{16} = 10^{-3}$ from ref. 5*a*.
[h]k_{21} was taken to be $2 \times k_{H+H+Ar}$, taken from ref. 32*c*.
[i]k_{22} was taken to be 1.0×10^9 M^{-1} s^{-1} by analogy with rate constants for related reactions given in ref. 32*a* and *c*.
[j]k_{23} was assumed to be $2 \times k_{Br+Br+Ar}$, taken from ref. 32*b*.

equivalence of $G_{H'}$ at low and high dose rates as discussed above. Even if the difference in $G_{H'}$ of 0.3 is real, this only accounts for 5% of the electrons. The absence of a significant change in $G_{H'}$ under these circumstances lends further support to the formation of the unscavengeable hydrogen in reactions [3] and [4] rather than in ion combination reactions (5*b*).

The above calculations did not explicitly include the resonance capture process (reaction [12]). However, since Cl^- will rapidly cluster to form HCl_2^- it is formally equivalent to reaction [13]. Also its rate constant for 0.8 eV electrons (i.e. at maximum cross section) does not exceed k_{13}. Its only effect, therefore, would be to decrease the proportion of HCl^- relative to HCl_2^-, but this should not invalidate the conclusions drawn above.

The concentration of hydrogen at infinite time corresponds to a predicted $G(H_2) = 7.98$, confirming that reactions [7], [21], and [22] are negligible at 25 °C and 10^{27} eV g^{-1} s^{-1}. The excellent agreement between $G(H_2) = 8.1 \pm 0.3$ observed in the X-ray and γ-ray radiolysis, at similar pressures, was therefore to be expected.

At −80 °C, $k_6 = 2.64 \pm 0.04 \times 10^6$ M^{-1} s^{-1} which is a factor of 30 smaller than the room temperature value (24). Using this value of k_6 in the computer program, the predicted hydrogen yield was $G(H_2) = 5.4$. This is in good agreement with a value we have measured at −80 °C of $G(H_2) = 5.3 \pm 0.3$. The reduction cannot be attributed to reaction [7] because of the very slow rate of formation of chlorine (see Fig. 5), and is due almost entirely to reaction [22]. Our choice of rate constant for reaction [22] is thus supported.

Hydrogen Bromide

The reactions occurring in irradiated hydrogen bromide are very similar to those occurring in hydrogen chloride (6). Those of importance are summarized in Table III. Using these and data from low dose rate radiolyses, the concentrations of products and intermediates for a Febetron irradiation have been calculated and are shown in Fig. 6. The significant differences between hydrogen chloride and hydrogen bromide are due to the much greater rates at which electrons and hydrogen atoms react with hydrogen bromide.

Can. J. Chem. Downloaded from www.nrcresearchpress.com by 210.87.254.6 on 09/05/12
For personal use only.

TABLE III

Reactions in irradiated HBr

	Reaction	Rate constant M^{-1} s^{-1} at 25 °C	Remarks
[24]	$HBr^+ + HBr \rightarrow H_2Br^+ + Br$	3×10^{11}	*a*
[25]	$e + 2HBr \rightarrow H + HBr_2^-$	3.6×10^{11}	*b*
[26]	$H_2Br^+ + HBr_2^- \rightarrow 3HBr$	6×10^{14}	*c*
[27]	$H + HBr \rightarrow H_2 + Br$	3.3×10^{9}	*d*
[28]	$H + Br + HBr \rightarrow 2HBr$	1.0×10^{9}	*e*
[29]	$H + H + HBr \rightarrow H_2 + HBr$	3.0×10^{8}	*f*
[30]	$Br + Br + HBr \rightarrow Br_2 + HBr$	6.0×10^{8}	*g*

[a] See *b* of Table II.
[b] The equivalent second order rate constant is calculated from the data of ref. 6*a*.
[c] See *e* of Table II.
[d] Calculated from the data of ref. 32*d*.
[e] See *i* of Table II.
[f] See *h* of Table II.
[g] See *j* of Table II.

This is illustrated clearly in Fig. 6 by the lower calculated concentrations of the free electron and hydrogen atom. The concentration of the hydrogen atoms follows the pulse and the behavior is very similar to that of ions. As in the case of hydrogen chloride, the computer calculations show that $G(H_2)$ should be the same at Febetron and low dose rates. Excellent agreement is in fact found between $G(H_2) = 9.9 \pm 0.3$ at 10^{27} eV g^{-1} s^{-1} and 9.8 ± 0.2 (6*a*) and 9.7 ± 0.2 (6*b*) for the X-ray and γ-ray radiolysis at low dose rates.

The agreement between the yields from both hydrogen bromide and hydrogen chloride at 10^{27} eV g^{-1} s^{-1} and those observed at low dose

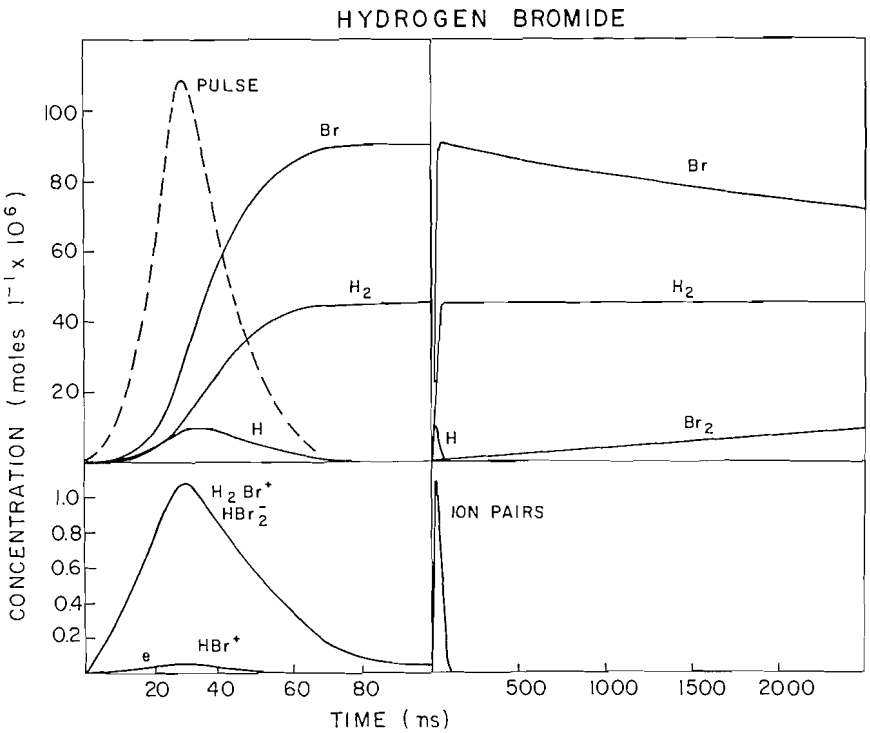

FIG. 6. Calculated ionic and atomic concentration in hydrogen bromide during and following Febetron pulse at 25 °C and 830 Torr pressure. Total dose = 2.76×10^{20} eV l^{-1}. The pulse intensities can be taken from the ordinate axis. The units for these are 10^{26} eV l^{-1} s^{-1}, i.e., the maximum intensity is 1.08×10^{28} eV l^{-1} s^{-1}.

Can. J. Chem. Downloaded from www.nrcresearchpress.com by 210.87.254.6 on 09/05/12
For personal use only.

Can. J. Chem. Downloaded from www.nrcresearchpress.com by 210.87.254.6 on 09/05/12
For personal use only.

rates strongly supports the value of $G(N_2) = 12.4 \pm 0.2$ from nitrous oxide which is used for the dosimetry at the high dose rates.

Nitrous Oxide

The yields reported in Table I and previous work (11, 14) show that the nitrogen yield from the Febetron radiolysis of gaseous nitrous oxide is $G(N_2) = 12.4 \pm 0.2$, independent of pressure from 600 to 3500 Torr. Figure 3 shows the effect of SF_6 on the Febetron radiolysis of nitrous oxide at 700 Torr. The yield of nitrogen extrapolated to zero concentration of SF_6 is $G(N_2) = 8.2 \pm 0.3$. It is in good agreement with $G(N_2) = 8.0 \pm 0.2$ reported for the plateau yield with SF_6 for ^{60}Co γ-ray radiolysis (25). This implies that it is differences in the electron reactions which cause the nitrogen yield at Febetron dose rates to be 12.4 instead of 10.0 molecules per 100 eV as at low dose rates.

It is known that the capture of thermal electrons in N_2O is a three-body process

[31] $$e + 2N_2O \rightarrow \text{Products}$$

with a rate constant of $2.2 \times 10^9\ M^{-2}\ s^{-1}$ (26, 27). At 700 Torr of N_2O the lifetime of electrons with respect to this reaction is therefore 250 ns. Assuming a rate constant of $6 \times 10^{13}\ M^{-1}\ s^{-1}$ for reaction [32]

[32] $$e + N_2O^+ \rightarrow \text{Products}$$

the electron–ion combination time for a typical low dose rate (^{60}Co) radiolysis would be 0.01 s or longer. Therefore at low dose rates all electrons would be consumed in reaction [31]. Unfortunately the situation is complicated by the fact that reaction [31] may produce O_2^- and NO^- as well as N_2O^-. Furthermore, charge transfer and other ionic reactions with the products are likely to occur and the ions of greatest thermodynamic stability will be the ones that recombine. For example, N_2O^+ may react with NO

[33] $$N_2O^+ + NO \rightarrow N_2O + NO^+ \qquad \Delta H = -3.5 \text{ eV}$$

and negative ion reactions are also possible.

Assuming rate constants of the order of $5 \times 10^9\ M^{-1}\ s^{-1}$, these ionic reactions will give mean lifetimes of the order of 10^{-4} s as soon as the product concentrations have reached the typical detection limit of 10 p.p.m. in N_2O at 700 Torr. This lifetime is much shorter than the recombination time, therefore these reactions will occur in N_2O at low dose rates in the same way that ozone must react with O_2^- (or O_4^-) in the radiolysis of

[34] $$O_3 + O_2^- \rightarrow O_3^- + O_2$$

oxygen at low dose rates. The ozonide ion has in fact been observed (28) in the mass analysis of the negative ions in irradiated oxygen.

Reaction [11] has a rate constant of $1.8 \times 10^{14}\ M^{-1}\ s^{-1}$ (15) and at 3×10^{-3} mole % of sulfur hexafluoride, in 700 Torr of N_2O, the lifetime of electrons for this reaction would be about 3 ns, which is $\sim$ 100 times shorter than their lifetime in reaction [31]. The suppression of $G(N_2)$ by SF_6 at low dose rates can therefore be attributed to the replacement of reaction [31] by reaction [11], and will obviously be complete at an SF_6 concentration of 10^{-2} mole %.

From the foregoing discussion, it is apparent that there is at present insufficient information on the ionic reactions in nitrous oxide to permit calculations of the type performed for hydrogen chloride and hydrogen bromide at 10^{27} eV g^{-1} s^{-1}. However, the concentrations of ions will be similar to those shown in Fig. 5 for hydrogen chloride, and, taking $k_{32} = 6 \times 10^{13}\ M^{-1}\ s^{-1}$ as above, the mean electron lifetime with respect to reaction [32] is found to be 3 ns. Hence this reaction would occur to the exclusion of reaction [31]. Also there would be insufficient time for charge transfer from primary ions to products. Thus the greater reduction of $G(N_2)$ by SF_6 at 10^{27} eV g^{-1} s^{-1} can be explained by the fact that the ionic reactions are different from those at low dose rates.

The results in the inset of Fig. 3 show the fall-off in $G(N_2)$ at low concentrations of SF_6. The reduction is halfway to the plateau at 0.1 mole % of SF_6. This is over 10 times the SF_6 concentration calculated above to be equivalent to an electron lifetime of 3 ns. As in the case of HCl, the discrepancy is attributed to the fact that under Febetron conditions the electrons are not thermal and that k_{11} decreases sharply with electron energy. It should also be noted that the resonance capture of electrons by nitrous oxide

[35] $$e^- + N_2O \rightarrow N_2 + O^-$$

occurs at a much lower energy (29) than reaction [12] in hydrogen chloride. Hence, in the presence of electrical fields generated in the Febetron, radiolysis reaction [35] should be a significant electron loss process. The O^- ion will disappear in reaction [36]

[36] $$O^- + N_2O^+ \rightarrow \text{Products}$$

The importance of reactions [35] and [36], relative to reaction [32], will decrease as the mean energy of the electrons is decreased. This will occur as the nitrous oxide pressure is raised. The absence of a pressure dependence of $G(N_2)$ over the range 600 to 3500 Torr implies that the reaction sequence [35]–[36] gives a similar stoichiometry for nitrogen to reaction [32].

An important point relating to the use of N_2O as a dosimeter is that $G(N_2)$ should change from 10.0 to 12.4 in the dose rate range 10^{22} to 10^{25} for 1 atm of nitrous oxide. This arises from the competition between reactions [31] and [32]. Therefore, it will not be practical to use nitrous oxide at these pressures as a dosimeter in this range of dose rates which is typical of many pulsed lineacs and Van de Graaffs.

Acknowledgments

D.A.A. wishes to thank A.E.C.L. for a Visiting Scientist's Appointment and the University of Calgary for sabbatical leave (1968–1969).

1. C. Willis, O. A. Miller, A. E. Rothwell, and A. W. Boyd. Advan. Chem. Ser. **81**, 539 (1968).
2. C. Willis, A. W. Boyd, and O. A. Miller. Can. J. Chem. **47**, 3007 (1969).
3. A. W. Boyd, C. Willis, and O. A. Miller. Can. J. Chem. **47**, 351 (1969).
4. F. T. Jones and T. J. Sworski. J. Phys. Chem. **70**, 1546 (1966).
5. (*a*) R. S. Davidow and D. A. Armstrong. J. Chem. Phys. **48**, 1235 (1968). (*b*) R. S. Davidow, R. A. Lee, and D. A. Armstrong. J. Chem. Phys. **45**, 3364 (1966).
6. (*a*) J. D. Chen and D. A. Armstrong. J. Chem. Phys. **48**, 2310 (1968). (*b*) R. A. Lee and D. A. Armstrong. Int. J. Appl. Radiat. Isotop. **19**, 585 (1968).
7. C. Willis, O. A. Miller, A. E. Rothwell, and A. W. Boyd. Radiat. Res. **35**, 428 (1968).
8. A. W. Boyd, C. Willis, O. A. Miller, and A. E. Rothwell. Advan. Chem. Ser. **82**, 456 (1968).
9. H. E. Johns and J. S. Laughlin. Interaction of radiation with matter. *In* Radiation dosimetry. *Edited by* G. J. Hine and G. L. Brownell. Academic Press, Inc., New York. 1956. Chap. 2.
10. R. S. Davidow and D. A. Armstrong. Radiat. Res. **28**, 142 (1966).
11. J. D. Chen and D. A. Armstrong. To be published.
12. F. S. Klein and M. Wolfsberg. J. Chem. Phys. **34**, 1494 (1961).
13. D. C. Frost and C. A. McDowell. Can. J. Chem. **38**, 407 (1960).
14. A. W. Boyd, D. A. Armstrong, C. Willis, and O. A. Miller. To be published.
15. B. H. Mahan and C. E. Young. J. Chem. Phys. **44**, 2192 (1966).
16. R. N. Compton, L. G. Christophorou, G. S. Hurst, and P. W. Reinhardt. J. Chem. Phys. **45**, 4634 (1966).
17. R. N. Compton, R. H. Huebner, P. W. Reinhardt, and L. G. Christophorou. J. Chem. Phys. **48**, 901 (1968).
18. L. G. Christophorou, R. N. Compton, and H. W. Dickson. J. Chem. Phys. **48**, 1949 (1968).
19. (*a*) R. A. Lee, R. S. Davidow, and D. A. Armstrong. Can. J. Chem. **42**, 1906 (1964). (*b*) R. S. Davidow. Ph.D. Thesis, The University of Calgary, Calgary, Alberta. 1965.
20. G. R. A. Johnson and J. L. Redpath. J. Phys. Chem. **72**, 765 (1968).
21. L. Raff and M. A. Pohl. *In* Solvated electron. Advan. Chem. Ser. No. 50. *Edited by* E. J. Hart. Amer. Chem. Soc. Washington, 1965. p. 172.
22. K. M. Schmidt. U.S.A.E.C. research and development report ANL-7199 (1966).
23. J. V. Dugan and J. L. Magee. J. Chem. Phys. **47**, 3103 (1967).
24. A. A. Westenberg and N. De Haas. J. Chem. Phys. **48**, 4405 (1968).
25. S. Takao, S. Shida, Y. Hatano, and H. Yamagashi. Bull. Chem. Soc. Jap. **41**, 2221 (1968).
26. A. V. Phelps and R. E. Voshall. J. Chem. Phys. **49**, 3246 (1968).
27. J. M. Warman and R. W. Fessenden. J. Chem. Phys. **49**, 4719 (1968).
28. D. C. Conway and L. E. Nesbitt. J. Chem. Phys. **48**, 509 (1968).
29. (*a*) R. K. Curran and R. E. Fox. J. Chem. Phys. **34**, 1590 (1961). (*b*) G. J. Schulz. J. Chem. Phys. **34**, 1778 (1961).
30. (*a*) D. A. Armstrong and R. A. Back. Can. J. Chem. **45**, 3079 (1967). (*b*) D. E. Wilson and D. A. Armstrong. To be published.
31. L. B. Loeb. Basic process of gaseous electronics. Univ. Calif. Press, Berkeley and Los Angeles. 1961.
32. (*a*) G. Porter. Discuss. Faraday Soc. **33**, 198 (1962). (*b*) J. K. K. Ip and G. Burns. Discuss. Faraday Soc. **44**, 241 (1967). (*c*) K. Schofield. Planet. Space Sci. **15**, 643 (1967). (*d*) B. A. Thrush. Progr. React. Kinet. **3**, 65 (1965).

Can. J. Chem. Downloaded from www.nrcresearchpress.com by 210.87.254.6 on 09/05/12
For personal use only.

Absolute rate constants for hydrocarbon autoxidation. XIV. Termination rate constants for tertiary peroxy radicals[1]

J. A. HOWARD, K. ADAMIC[2], AND K. U. INGOLD
Division of Applied Chemistry, National Research Council of Canada, Ottawa, Canada

Received May 23, 1969

Absolute rate constants for chain termination by ten *t*-peroxy radicals have been measured at 30° by the rotating sector technique, the photochemical pre- and after-effect method, and by electron spin resonance. The different methods generally give results in good agreement with one another. The termination rate constants vary from a low of $\sim 4 \times 10^2\ M^{-1}\ s^{-1}$ for *t*-butylperoxy to a high of $\sim 3 \times 10^4\ M^{-1}\ s^{-1}$ for 1,1-diphenylethylperoxy radicals.

Canadian Journal of Chemistry, 47, 3793 (1969)

Can. J. Chem. Downloaded from www.nrcresearchpress.com by 210.87.254.40 on 09/05/12
For personal use only.

Introduction

In the liquid phase the self-reaction of *t*-alkylperoxy radicals occurs by the following reaction sequence (1–8)

$$[1] \quad \mathrm{ROO\cdot} + \mathrm{ROO\cdot} \underset{k_{-1}}{\overset{k_1}{\rightleftharpoons}} \mathrm{ROOOOR} \quad \left(K_1 = \frac{k_{-1}}{k_1}\right)$$

$$[2] \quad \mathrm{ROOOOR} \xrightarrow{k_2} [\mathrm{RO\cdot}\ \ \mathrm{O_2}\ \ \cdot\mathrm{OR}]_{\mathrm{cage}}$$

$$[3] \quad [\mathrm{RO\cdot}\ \ \mathrm{O_2}\ \ \cdot\mathrm{OR}]_{\mathrm{cage}} \xrightarrow{k_3} \mathrm{ROOR} + \mathrm{O_2}$$

$$[4] \quad [\mathrm{RO\cdot}\ \ \mathrm{O_2}\ \ \cdot\mathrm{OR}]_{\mathrm{cage}} \xrightarrow{k_4} \mathrm{RO\cdot} + \mathrm{O_2} + \cdot\mathrm{OR}$$

For most organic substrates, RH, which are oxidized by a chain process involving primarily the attack of tertiary peroxy radicals on RH, the measured rate constant for chain termination corresponds to a rather complex kinetic expression (3, 6). The reason for this is that although the *t*-alkoxy radicals produced in reaction [4] may attack the substrate to regenerate *t*-ROO· radicals, they may also undergo β-scission to give a carbonyl compound and a new radical. This new radical will generally be a primary or secondary radical and, after the addition of oxygen, it may react with RH to continue the chain or with a *t*-ROO· to terminate the chain. The latter process can have a profound influence on the overall rate constant for chain termination because it will generally have a much higher rate constant than termination by the reaction of two *t*-peroxy radicals (6).

We have previously shown that it is possible to trap all the RO· radicals produced in reaction [4] and convert them to ROO· radicals by the addition of a sufficient concentration of the appropriate hydroperoxide (5, 6).

$$[5] \quad \mathrm{RO\cdot} + \mathrm{ROOH} \rightarrow \mathrm{ROH} + \mathrm{ROO\cdot}$$

Under these conditions, the measured rate constant for chain termination, $2k_t$, corresponds to $(2k_2/K_1)(k_3/(k_3 + k_4))$. Our initial measurements of $2k_t$ for a few *t*-peroxy radicals (5) indicated that this composite rate constant was not independent of the nature of the group R. That is, at 30° our measured values of $2k_t$ ranged from $\sim 1 \times 10^3\ M^{-1}\ s^{-1}$ for *t*-butylperoxy, to $\sim 6 \times 10^3\ M^{-1}\ s^{-1}$ for cumylperoxy, to $\sim 6 \times 10^4\ M^{-1}\ s^{-1}$ for 1,1-diphenylethylperoxy radicals. There are three separate factors that might produce this variation in $2k_t$: (*i*) a variation in K_1, the equilibrium constant for tetroxide formation, (*ii*) a variation in k_2, the rate constant for irreversible decomposition of tetroxide, and (*iii*) a variation in the ratio $k_3/(k_3 + k_4)$ which measures the fraction of alkoxy radical pairs which undergo combination in the cage. The present set of three papers describes work leading to the conclusion that differences in k_2 are the prime cause of the differences in $2k_t$. This, the first paper, describes the measurement by three independent methods of $2k_t$ at 30° for ten *t*-peroxy radicals. The second paper describes the radical induced decomposition of some *t*-hydroperoxides from which it is possible in certain cases to derive the ratio $k_3/(k_3 + k_4)$. The final paper is concerned with the measurement of K_1 and k_2 at low temperatures by the electron spin resonance procedure pioneered by Bartlett and Guaraldi (4).

---

[1]NRCC No. 10 896.
[2]NRCC Postdoctorate Fellow 1967–1969.

TABLE I

Rate constants for the oxidation of cumene at 30° in the presence of *t*-hydroperoxides

Hydroperoxide	$\frac{k_p}{(2k_t)^{1/2}} \times 10^3$[a] $M^{-1/2}\,s^{-1/2}$	$2k_t \times 10^{-3}$ ($M^{-1}\,s^{-1}$) r.s.	p.e.	e.s.r.[b]	k_p $M^{-1}s^{-1}$	$2k_t \times 10^{-3}$ $M^{-1}\,s^{-1}$ Best value[c]
t-Butyl	6.1	1.3	0.7[d]	1.0	0.16	0.37
2-Ethyl-2-propyl	3.3	0.26	—	0.45	0.06	1.3
2-Isopropyl-2-propyl	2.7_5	1.5	0.42	1.0	0.06	1.8
2-Benzyl-2-propyl	2.7_5	3.5	—	1.7	0.14	1.8
Cumyl	2.3	6.0	—	8.0	0.18	2.6
1-Methylcyclohexyl	2.2	1.0	—	1.0	0.09	2.8
2-Neopentyl-2-propyl	1.6	3.0[e]	3.0	1.0	0.09	5.3
1-Methylcyclopentyl	1.2	5.7_5	6.0	23	0.09	9.4
2-Phenyl-2-butyl	0.88	33	—	25–100	0.16	18
1,1-Diphenylethyl	0.7_1	64	—	640	0.18	27

[a]Measured in ~7.0 *M* cumene at hydroperoxide concentrations from 0.1 to 1.0 *M*.
[b]0.6 *M* [Hydroperoxide] in CCl_4 initiated with 3.3×10^{-2} *M* [TBH].
[c]Calculated from $k_p/(2k_t)^{1/2}$ and the mean value of $k_p(=0.11_7\ M^{-1}\,s^{-1})$ for all peroxy radicals.
[d]At 35°; ref. 12.
[e]The present value is believed to be more accurate than that originally reported (5).

Experimental

Procedures

Cumene was oxidized in the presence of a sufficient concentration of the appropriate tertiary hydroperoxide to ensure that the *t*-peroxy radicals from the hydroperoxide were the only terminating radicals. The absolute rate constants for the self-reactions of the *t*-peroxy radicals in cumene were measured by the rotating sector (r.s.) technique (9) and by the photochemical pre- and/or after-effect (p.e.) (10). The precautions necessary to obtain reliable rate constants by the r.s. method have been described previously (9, 11). The increase or decrease in the rate of reaction under non-steady state conditions resulting from a sudden increase or decrease in the rate of chain initiation (p.e. method) is particularly useful with *t*-peroxy radicals because of the comparatively small values of the termination rate constants (12).

Tertiary peroxy radicals are also well suited to the measurement of their steady concentration $[ROO\cdot]_s$ by electron spin resonance spectroscopy (the e.s.r. method). At a rate of initiation, R_i, the termination rate constant is defined by the relation

$$R_i = 2k_t[ROO\cdot]_s^2$$

In the e.s.r. experiments, decomposition of the tertiary hydroperoxides was initiated by the thermal decomposition of *t*-butyl hyponitrite (TBH) (13).

All work described in this paper was done at 30 °C.

Materials

Cumene (Phillips Research Grade) was used immediately after passage through activated basic alumina. *t*-Butyl hydroperoxide was purified by crystallization. Cumene hydroperoxide and 2-neopentyl-2-propyl hydroperoxide (Lucidol) were purified via their sodium salts. 2-Phenylbutyl-2-hydroperoxide was prepared by the emulsion oxidation of *sec*-butylbenzene and was purified via its sodium salt (14). 1,1-Diphenylethyl hydroperoxide was prepared from 1,1-diphenylethanol and 30% H_2O_2 (15). The remaining hydroperoxides were synthesized by reaction of the appropriate *t*-alcohols with 100% H_2O_2 and a trace of sulfuric acid (16)[3]. Great care was taken to ensure that the liquid hydroperoxides were free from H_2O_2 by repeated washings with water. The presence of H_2O_2 gave high values for $2k_t$, presumably because hydroperoxy radicals were involved in chain termination.

α,α′-Azo-bis-cyclohexylnitrile (ACHN) and α,α′-azo-bis-isobutyronitrile (AIBN) were the photo-initiators in the p.e. method. ACHN was the photo-initiator in the r.s. method. Rates of chain initiation were measured with 2,6-di-*t*-butyl-4-methoxyphenol.

Results and Discussion

Rate constants for the oxidation of cumene in the presence of ten *t*-hydroperoxides are given in Table I. The oxidizability of cumene, $k_p/(2k_t)^{1/2}$, depends on the added hydroperoxide, decreasing by an order of magnitude between *t*-butyl hydroperoxide and 1,1-diphenylethyl hydroperoxide. The three methods used to measure the termination rate constants give results which are in reasonable agreement with one another except for the 1,1-diphenylethylperoxy radical. The e.s.r. signal due to the 1,1-diphenylethylperoxy radical was rather small and the measured steady state concentration of this peroxy radical could be in serious error. The measurement of $2k_t$ by the e.s.r. method might also be affected by low concentrations of oxygen in the reaction mixture. It is worth noting that the 1,1-diphenylethoxy radical

[3]This reaction should be carried out with extreme caution. Although none of the reaction mixtures described here detonated, an attempted synthesis of 2-*t*-butyl-2-propyl hydroperoxide exploded violently.

Can. J. Chem. Downloaded from www.nrcresearchpress.com by 210.87.254.40 on 09/05/12
For personal use only.

behaves rather differently to other alkoxy radicals (see following paper).

The measured termination rate constants confirm our previous observation (5) that $2k_t$ is not the same for all *t*-peroxy radicals. In most cases the values of k_p given in Table I have been calculated from $k_p/(2k_t)^{1/2}$ and the average values of $2k_t$. The $2k_t$'s determined by the e.s.r. method for 1-methylcyclopentylperoxy, 2-phenyl-2-butylperoxy, and 1,1-diphenylethylperoxy radicals were not included in the averages because they were not considered accurate. Since there is no obvious correlation between k_p and the structure of the peroxy radical, it seems most probable that the variations in $k_p/(2k_t)^{1/2}$ are due entirely (or almost entirely) to changes in $2k_t$. Because the ratio $k_p/(2k_t)^{1/2}$ can be measured a great deal more accurately than its component rate constants, we feel justified in calculating a "best value" for $2k_t$ based on values of $k_p/(2k_t)^{1/2}$ and the average value of k_p for all the peroxy radicals studied ($0.11_7\ M^{-1}\ s^{-1}$). These best values of $2k_t$ increase by almost two orders of magnitude along the series of *t*-peroxy radicals from *t*-butyl to 1,1-diphenylethyl. This change is too large to be wholly attributed to any change in the fraction of the alkoxy radicals which combine in the cage (i.e., in $k_3/(k_3 + k_4)$). However, the importance of alkoxy radical cage combination relative to diffusion from the cage would be expected to increase as the size of the alkoxy radicals increases. It is therefore conceivable that some of the variation in $2k_t$ is due to changes in $k_3/(k_3 + k_4)$. Our measurements of this ratio for a few selected radicals are described in the following paper.

1. P. D. BARTLETT and T. G. TRAYLOR. J. Amer. Chem. Soc. **85**, 2407 (1963).
2. A. FACTOR, C. A. RUSSELL, and T. G. TRAYLOR. J. Amer. Chem. Soc. **87**, 3692 (1965); **87**, 3698 (1965).
3. J. R. THOMAS. J. Amer. Chem. Soc. **87**, 3935 (1965); **89**, 4872 (1967).
4. P. D. BARTLETT and G. GUARALDI. J. Amer. Chem. Soc. **89**, 4799 (1967).
5. J. A. HOWARD and K. U. INGOLD. Can. J. Chem. **46**, 2655 (1968).
6. J. A. HOWARD, W. J. SCHWALM, and K. U. INGOLD. Advan. Chem. Ser. **75**, 6 (1968).
7. J. R. THOMAS and K. U. INGOLD. Advan. Chem. Ser. **75**, 258 (1968).
8. T. MILL and R. S. STRINGHAM. J. Amer. Chem. Soc. **90**, 1062 (1968).
9. G. M. BURNETT and H. W. MELVILLE. Investigation of rates and mechanisms of reactions. *In* Technique of organic chemistry. Vol. VIII. Part II. *Edited by* S. L. Friess, E. S. Lewis, and A. Weissberger. Interscience Publishers, Inc., New York. 1963. Chap. 20.
10. L. BATEMAN and G. GEE. Trans. Faraday Soc. **47**, 155 (1951).
11. J. A. HOWARD and K. U. INGOLD. Can. J. Chem. **43**, 2729 (1965).
12. D. G. HENDRY. J. Amer. Chem. Soc. **89**, 5433 (1967).
13. H. KIEFER and T. G. TRAYLOR. Tetrahedron Lett. 6163 (1966).
14. E. G. E. HAWKINS. J. Chem. Soc. 2076 (1949).
15. D. E. BISSING, C. A. MATUSZAK, and W. E. MCEWEN. J. Amer. Chem. Soc. **86**, 3824 (1964).
16. A. G. DAVIES, R. V. FOSTER, and A. M. WHITE. J. Chem. Soc. 1541 (1953).

Can. J. Chem. Downloaded from www.nrcresearchpress.com by 210.87.254.40 on 09/05/12
For personal use only.

Can. J. Chem. Downloaded from www.nrcresearchpress.com by 210.87.254.6 on 09/05/12
For personal use only.

Absolute rate constants for hydrocarbon autoxidation. XV. The induced decomposition of some *t*-hydroperoxides[1]

J. A. HOWARD AND K. U. INGOLD
Division of Applied Chemistry, National Research Council of Canada, Ottawa, Canada

Received May 23, 1969

The radical induced decomposition of several *t*-hydroperoxides at 30° has been studied. In the self reaction of *t*-alkylperoxy radicals the ratio of the rates of alkoxy radical diffusion from the cage to combination in the cage is essentially independent of the size of the *t*-alkyl group.

The rate constant for abstraction from hydroperoxides of the hydroperoxidic hydrogen by alkoxy radicals is about $4 \times 10^6\ M^{-1}\ s^{-1}$ at 30°. This reaction has a deuterium isotope effect, $k_H/k_D \approx 5$.

The 1,1-diphenylethoxy radical undergoes a 1,2-phenyl shift to yield the 1-phenyl-1-phenoxyethyl radical more rapidly that it undergoes β-scission.

Canadian Journal of Chemistry, 47, 3797 (1969)

Introduction

Previous workers have shown that *t*-butyl hydroperoxide (1–3) and cumene hydroperoxide (4) undergo radical induced chain decompositions in solution with chain lengths of about 5–10 in solvents of normal viscosity at ambient temperatures. The decomposition of *t*-butyl hydroperoxide (in an inert solvent) can be represented by[2]

$$\text{Initiator} \rightarrow \text{ROO}\cdot$$

[1] $$\text{ROO}\cdot + \text{ROO}\cdot \rightleftarrows \text{ROOOOR}$$

[2] $$\text{ROOOOR} \rightarrow [\text{RO}\cdot \quad \text{O}_2 \quad \cdot\text{OR}]_{\text{cage}}$$

[3] $$[\text{RO}\cdot \quad \text{O}_2 \quad \cdot\text{OR}]_{\text{cage}} \rightarrow \text{ROOR} + \text{O}_2$$

[4] $$[\text{RO}\cdot \quad \text{O}_2 \quad \cdot\text{OR}]_{\text{cage}} \rightarrow \text{RO}\cdot + \text{O}_2 + \cdot\text{OR}$$

[5] $$\text{RO}\cdot + \text{ROOH} \rightarrow \text{ROH} + \text{ROO}\cdot$$

The rate of hydroperoxide decomposition and the rate of oxygen evolution, R_{O_2}, are given by eqs. [I] and [II]

$$[\text{I}] \qquad -\frac{d[\text{ROOH}]}{dt} = R_i(1 + k_4/k_3)$$

$$[\text{II}] \qquad R_{O_2} = \frac{R_i}{2}\left(1 + \frac{k_4}{k_3}\right) = -\tfrac{1}{2}\frac{d[\text{ROOH}]}{dt}$$

where R_i is the rate of chain initiation. At a known rate of initiation either of these rates yields the ratio of non-terminating to terminating rate constants for *t*-butylperoxy radicals (k_4/k_3).

The decomposition of certain other *t*-hydroperoxides is more complicated because the *t*-alkoxy radicals formed in reaction [4] can undergo β-scission to give carbonyl compounds and alkyl radicals

[6] $$\text{R}_1\text{R}_2\text{R}_3\text{O}\cdot \rightarrow \text{R}_1\text{R}_2\text{C}{=}\text{O} + \text{R}_3\cdot$$

The stability of the incipient ketone and alkyl radical determines the mode of β-scission. Cumyloxy radicals, for example, give acetophenone and methyl radicals

[6a] $$\text{Ph(CH}_3)_2\text{CO}\cdot \rightarrow \text{PhCOCH}_3 + \text{CH}_3\cdot$$

The methylperoxy radicals formed in the presence of oxygen may react with cumene hydroperoxide (chain transfer)

[7] $$\text{CH}_3\text{OO}\cdot + \text{Ph(CH}_3)_2\text{COOH} \rightarrow \text{CH}_3\text{OOH} + \text{Ph(CH}_3)_2\text{COO}\cdot$$

or with cumylperoxy radicals (chain termination)

[8] $$\text{CH}_3\text{OO}\cdot + \text{Ph(CH}_3)_2\text{COO}\cdot \rightarrow \text{Non-radical products}$$

The kinetics for the decomposition of *t*-hydroperoxides which undergo β-scission are greatly simplified if sufficient hydroperoxide is present to suppress chain termination by reactions such as [8]. The rate of decomposition of the *t*-hydroperoxide is described by eq. [I] but the rate would be difficult to measure because of the accumulation of the alkyl hydroperoxide formed in reaction [7]. The rate of oxygen evolution and ketone formation ($R_{C=O}$) are given by

$$[\text{III}] \qquad R_{O_2} = \frac{R_i}{2}\left(1 + \frac{k_4}{k_3}\right) - R_{C=O}$$

$$[\text{IV}] \qquad R_{C=O} = \frac{R_i k_4 k_6}{k_3 k_5([\text{ROOH}] - k_6/k_5)}$$

[1]NRCC No. 10 897.
[2]The reactions are numbered in the same way as in the preceding paper.

Can. J. Chem. Downloaded from www.nrcresearchpress.com by 210.87.254.6 on 09/05/12
For personal use only.

Under ideal conditions, the measurement of R_{O_2} and $R_{C=O}$ enables both k_4/k_3 and k_6/k_5 to be determined.

The radical induced decompositions of some *t*-hydroperoxides are not described by the above reactions because the *t*-alkoxy radicals undergo various intramolecular rearrangements. Two examples of these more complicated decompositions are described.

Experimental

Materials

The preparation of the hydroperoxides used in this work was described in the preceding paper (5).

1-Phenylethyl phenyl ether was prepared from 1-phenylethyl chloride and phenol (6). It was crystallized and zone refined before use. Only one peak was observed by gas–liquid chromatography (g.l.c.).

1,1-Diphenylethyl peroxide, m.p. 149–151°, was prepared from 1,1-diphenylethyl hydroperoxide by the procedure of Bassey *et al.* (7). This compound has not been previously prepared.

1,1-Diphenylethane was prepared by the catalytic reduction of 1,1-diphenylethylene and its purity was better than 99.5%.

Procedures

The induced decompositions of the *t*-hydroperoxides (0.1–0.5 *M*), at various rates of chain initiation, were studied in carbon tetrachloride in the presence of oxygen at atmospheric pressure. The reactions were initiated by the thermal decomposition of *t*-butylhyponitrite (TBH). The calculated rates of chain initiation ($1.8 \times 2.7 \times 10^{-6}$ [TBH] (8)) were confirmed by measurement of the rates of the TBH initiated oxidations of hydrocarbons with well established values of $k_p/(2k_t)^{1/2}$ (e.g. cumene and tetralin). The rates of oxygen evolution were monitored by a Dynesco pressure transducer (DPT 85–2) and were corrected for nitrogen evolution from the TBH. Rates of ketone formation were followed by infrared analysis (1650–1750 cm^{-1} region) of aliquots.

1,1-Diphenylethane and 1-phenylethyl phenyl ether were oxidized both thermally and photochemically. The products from the oxidation of these compounds and from the decomposition of 1,1-diphenylethyl hydroperoxide and 1,1-diphenylethyl peroxide were identified by thin layer chromatography and g.l.c. All reactions were carried out at 30 °C unless stated otherwise.

Results and Discussion

Ratio of Diffusion (k_4) to Cage Combination (k_3) for t-Alkoxy Radicals

Kinetic data for the induced decomposition of six *t*-hydroperoxides at 0.2 *M* are presented in Table I. Within experimental error the ratio k_4/k_3 for *t*-alkoxy radicals is constant for all the hydroperoxides studied. This implies that most of the variation in the termination rate constants ($2k_t$) between different *t*-peroxy radicals is due to differences in K_1 or k_2 (see preceding paper).

The Alkoxy Radical – Hydroperoxide Reaction

The ratio of the rate constants for *t*-alkoxy radical β-scission (k_6) to abstraction from the parent hydroperoxide (k_5) were calculated from eq. [IV]. Values of k_6/k_5 for five alkoxy radicals are given in Table II and are compared with the ratios of β-scission (k_d) to abstraction from cyclohexane (k_a) for the same alkoxy radicals (9.) Absolute values of k_5 have been calculated from the ratios k_6/k_5 and k_d/k_a since k_5 should equal k_d for each alkoxy radical (10).

The values of k_a have been assumed to be constant and equal to $3 \times 10^4\ M^{-1}\ s^{-1}$, the value for the *t*-butoxy radical (11). The absolute values of k_5 are in the range $1–7 \times 10^6\ M^{-1}\ s^{-1}$ and this variation almost certainly reflects experi-

TABLE I

Kinetic data for the *t*-butyl hyponitrite induced decomposition of some *t*-hydroperoxides (0.2 *M*) in CCl_4 at 30°

Hydroperoxide	R_{O_2}/R_i	$R_{C=O}/R_i$	k_4/k_3*	$2k_t \times 10^{-3}$, $M\ s^{-1}$†
t-Butyl	4.0	0	7.0	0.37
Cumyl	3.55	0.1	6.3	2.6
2-Ethyl-2-propyl	2.68	0.32	5.0	1.3
2-Benzyl-2-propyl‡	2.5	1.2	6.4	1.8
1-Methylcyclohexyl	2.0	0.8	4.6	2.8
2-Phenyl-2-butyl	~0	3.5	6.0	18
Cumyl(H_2O)	3.6	0.1	6.4	2.6
Cumyl(D_2O)	3.2	0.58	6.6	2.6

*Averages calculated from values of R_{O_2}/R_i and $R_{C=O}/R_i$ from at least two hydroperoxide concentrations and two rates of chain initiation.

†Reference 5.

‡R_{O_2} was corrected for oxidation at the benzylic position on the assumption that $k_p = 0.16\ M^{-1}\ s^{-1}$ (i.e., k_p is equivalent to k_p for ethylbenzene) and that $2k_t = 1.8 \times 10^3\ M^{-1}\ s^{-1}$ (the best value of $2k_t$ for 2-benzyl-2-propylperoxy radicals in cumene).

TABLE II

Relative and absolute rate constants for some *t*-alkoxy radicals at 30°

Radical	$\frac{k_6}{k_5} \times 10^2$, M	$\frac{k_d}{k_a}$, M*	$k_d \times 10^{-4}$, s^{-1}	$k_5 \times 10^{-6}$, $M^{-1}\,s^{-1}$
Cumyloxy	0.33	0.36	1.1	3.3
2-Ethyl-2-propoxy	1.6	1.75	5.5	3.4
2-Benzyl-2-propoxy	4.6	1.87†	5.9	1.2
1-Methylcyclohexyloxy	4.0	9.5	30	7.5
2-Phenyl-2-butoxy	7.4	‡	—	—
Cumyloxy(H_2O)	0.33	0.36	1.1	3.3
Cumyloxy(D_2O)	1.75	0.36	1.1	0.63

*Reference 9.
†C. Walling, in a paper presented to the 156th ACS National Meeting (1968), reported that this value of k_d/k_a is probably too low. A value 3–5 times greater would improve the consistency of the k_5 values.
‡C. Walling and A. Padwa (20) did not report a k_d/k_a value for this alkoxy radical. Our work suggests that it undergoes β-scission about twice as readily as the 1-methylcyclohexyloxy radical.

mental errors in the determination of k_6/k_5 and k_d/k_a rather than actual differences in k_5.

The average value of k_5 is $3.7 \times 10^6\ M^{-1}\ s^{-1}$ and is about three orders of magnitude larger than the rate constant (k_9) for abstraction of the hydroperoxidic hydrogen from cumene hydroperoxide (COOH) by the tetralylperoxy radical (TOO·) (12)

[9] $\quad TOO\cdot + COOH \rightarrow TOOH + COO\cdot$

Reaction [9] has a large deuterium isotope effect ($(k_9)_H/(k_9)_D \sim 17$) which was estimated by measurement of k_9 in the presence of light and heavy water (12). The same procedure for the induced decomposition of cumene hydroperoxide gave an isotope effect of about 5 for abstraction of the hydroperoxidic hydrogen from cumene hydroperoxide by the cumyloxy radical (reaction [5]). This value agrees with other isotope effects for similar symmetric H-atom abstraction reactions (12).

1,1-Diphenylethoxy Radical

Because alkoxy radicals produced by the induced decomposition of some *t*-hydroperoxides undergo intramolecular reactions, rate constant ratios, k_4/k_3, could not be measured. The 1,1-diphenylethoxy radical provides an intriguing example of this effect. This radical is of further interest since its termination rate constant is the highest we have measured for a *t*-peroxy radical (5).

Although it was expected that β-scission of the 1,1-diphenylethoxy radical would give mainly benzophenone

[10] $\quad Ph_2(CH_3)CO\cdot \rightarrow Ph_2CO + CH_3\cdot$

none of this ketone was formed during the induced decomposition of the hydroperoxide. Instead, acetophene, phenol, and *p*-benzoquinone (and presumably other oxidation products of phenol) were produced. Similar products have recently been found by Kropf *et al.* in the oxidation of 1,1-diphenylethane at 100 °C and in the copper phthalocyanine catalyzed decomposition of the hydroperoxide (13). We found that the same products were formed during the oxidation of 1,1-diphenylethane (at 30 °C) and also by photolysis (3650 Å) of 1,1-diphenylethyl peroxide in CCl_4 in the presence of oxygen[3].

These results suggest that β-scission might occur by the alternative route

[11] $\quad Ph_2(CH_3)CO\cdot \rightarrow PhCOCH_3 + Ph\cdot$

with the phenyl radical as the source of phenol and quinone. However, this reaction can probably be ruled out because chlorobenzene was not detected when the oxidation of 1,1-diphenylethane or the induced decomposition of 1,1-diphenylethyl hydroperoxide were carried out in

[3]Thermal decomposition of the peroxide at 120° in CCl_4 yielded some benzophenone which implies that reaction [10] can occur at this temperature. The product yields (calculated on the basis of the number of alkoxy groups) in the presence and absence of oxygen were: acetophenone, 10% and 30%; phenol, 30% and 30–50%; benzophenone, 8% and 4%; 1,1-diphenylethylene, 3% and 30%. The last named product may arise by dehydration of 1,1-diphenylethanol (formed by hydrogen abstraction by the ethoxy radical) or perhaps by a concerted decomposition of the peroxide which does not involve free radicals

$$Ph_2(CH_3)COOC(CH_3)Ph_2 \rightarrow PhCOCH_3 + Ph_2C{=}CH_2 + PhOH$$

Traces of chlorobenzene were also formed in these reactions, which suggests that reaction [11] may occur at this temperature.

Can. J. Chem. Downloaded from www.nrcresearchpress.com by 210.87.254.6 on 09/05/12
For personal use only.

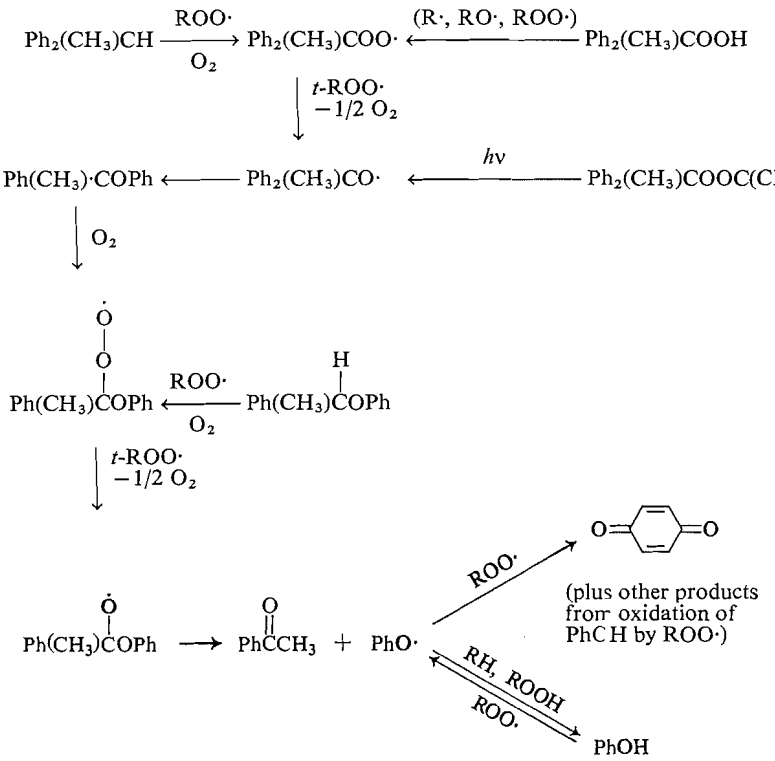

SCHEME I. The formation of acetophenone, phenol, and *p*-quinone.

dilute solution in CCl_4. The attack of phenyl radical on CCl_4, reaction [12]

[12] $\quad Ph\cdot + CCl_4 \rightarrow PhCl + CCl_3\cdot$

is extremely rapid (14) and reaction [11] would lead to the production of chlorobenzene. Our results are consistent with the reactions given in Scheme I. That is, the diphenylethoxy radical isomerizes to the 1-phenyl-1-phenoxyethyl radical more rapidly than it undergoes β-scission. The ethyl radical then adds to oxygen and, by a non-terminating reaction with a second *t*-peroxy radical, is converted to the 1-phenyl-1-phenoxyethoxy radical which then undergoes β-scission to give acetophenone and the resonance stabilized phenoxy radical[4]. Oxidation of the phenoxy radical by a peroxy radical yields *p*-quinone and its reduction by hydrogen abstraction from a suitable donor, such as the hydroperoxide (15), yields phenol.

[4]An alternative reaction sequence involving hydrogen abstraction by the phenoxyethoxy radical followed by direct decomposition to acetophenone and phenol cannot be ruled out by the present data.

The 1,2-phenyl shift of the diphenylethoxy radical is analogous to the rearrangement of triarylmethoxy radicals (16–19), e.g.

[13] $\quad Ph_3CO\cdot \rightarrow Ph_2\dot{C}OPh$

The intermediacy of the phenoxyethyl radical in the above reactions is supported by the formation of acetophenone, phenol, and oxidation products of phenol during the oxidation of 1-phenylethyl phenyl ether.

2-Neopentyl-2-propoxy Radical

Induced decomposition of 0.35 *M* 2-neopentyl-2-propyl hydroperoxide gave $R_{O_2}/R_i = 0.5$, $R_{C=O}/R_i = 0.04$ and the rather low value of 0.08 for k_4/k_3. We believe that these values result from the facile intramolecular hydrogen abstraction of the 2-neopentyl-2-propoxy radical. It has previously been shown that alkoxy radical intramolecular abstractions from the δ-position (i.e., via a 6-membered cyclic transition state) are very fast (20). The hydrogens on the *t*-butyl group of the 2-neopentyl-2-propoxy radical are in this favorable position

Can. J. Chem. Downloaded from www.nrcresearchpress.com by 210.87.254.6 on 09/05/12
For personal use only.

[14] 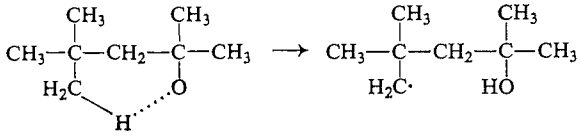

The resultant primary alkyl radical will add to oxygen to give the corresponding hydroperoxide (reaction [9]). The overall result is that this alkoxy radical yields a product which absorbs oxygen without simultaneously forming a ketone. The kinetic analysis used to derive eqs. [III] and [IV] is therefore not valid.

Although no evidence was found for intramolecular abstraction from the γ position of an alkoxy radical (20), the induced decomposition of 2-isopropyl-2-propyl hydroperoxide (at 0.2 M, $R_{O_2}/R_i = 0.13$, $R_{C=O}/R_i = 1.6$, $k_4/k_3 = 2.5$) suggests that the 2-isopropyl-2-propoxy radical may abstract a hydrogen from the γ position. 1-Methylcyclopentyl hydroperoxide also gave a low value for k_4/k_3 (at 0.26 M, $R_{O_2} = 0.44$, $R_{C=O} = 0.45$, $k_4/k_3 = 0.8$). In this case the ketone group produced by β-scission may be partly destroyed by recyclization of the 5-acetylpentyl radical to give a pyran ring system, i.e.

[15] 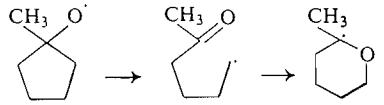

The reactions of alkoxy radicals derived from both these hydroperoxides clearly deserve further investigation.

1. R. HIATT, J. CLIPSHAM, and T. VISSER. Can. J. Chem. **42**, 2754 (1964).
2. A. FACTOR, C. A. RUSSELL, and T. G. TRAYLOR. J. Amer. Chem. Soc. **87**, 3692 (1965).
3. J. R. THOMAS. J. Amer. Chem. Soc. **87**, 3935 (1965).
4. J. R. THOMAS. J. Amer. Chem. Soc. **89**, 4872 (1967).
5. J. A. HOWARD, K. ADAMIC, and K. U. INGOLD. Can. J. Chem. This issue.
6. H. HART and H. S. ELEUTERIO. J. Amer. Chem. Soc. **76**, 516 (1954).
7. M. BASSEY, E. BUNCEL, and A. G. DAVIES. J. Chem. Soc. 2550 (1951).
8. H. KIEFER and T. G. TRAYLOR. Tetrahedron Lett. 6163 (1966); J. Amer. Chem. Soc. **89**, 6667 (1967).
9. C. WALLING and A. PADWA. J. Amer. Chem. Soc. **85**, 1593 (1963).
10. C. WALLING and P. WAGNER. J. Amer. Chem. Soc. **85**, 2333 (1963); **86**, 3368 (1964).
11. D. J. CARLSSON and K. U. INGOLD. J. Amer. Chem. Soc. **89**, 4891 (1967).
12. J. A. HOWARD, W. J. SCHWALM, and K. U. INGOLD. Advan. Chem. Ser. **75**, 6 (1968).
13. H. KROPF, W. GEBERT, and K. FRANKE. Tetrahedron Lett. **24**, 5527 (1968).
14. R. F. BRIDGER and G. A. RUSSELL. J. Amer. Chem. Soc. **85**, 3754 (1963).
15. J. R. THOMAS. J. Amer. Chem. Soc. **85**, 2166 (1963); **86**, 4807 (1964).
16. H. WIELAND. Ber. **44**, 2553 (1911).
17. M. S. KHARASCH, A. FONO, and W. NUDENBERG. J. Org. Chem. **15**, 763 (1950).
18. M. S. KHARASCH, A. C. POSHKUS, A. FONO, and W. NUDENBERG. J. Org. Chem. **16**, 1458 (1951).
19. P. D. BARTLETT and J. COTMAN, JR. J. Amer. Chem. Soc. **72**, 3095 (1950).
20. C. WALLING and A. PADWA. J. Amer. Chem. Soc. **85**, 1597 (1963).

Can. J. Chem. Downloaded from www.nrcresearchpress.com by 210.87.254.6 on 09/05/12
For personal use only.

Can. J. Chem. Downloaded from www.nrcresearchpress.com by 210.87.254.5 on 09/05/12
For personal use only.

Absolute rate constants for hydrocarbon autoxidation. XVI. Reactions of peroxy radicals at low temperatures[1,2]

K. ADAMIC[3], J. A. HOWARD, AND K. U. INGOLD
Division of Applied Chemistry, National Research Council of Canada, Ottawa, Canada

Received May 23, 1969

The equilibrium constants for the formation of some *t*-alkyl tetroxides and the rate constants for irreversible decay of the tetroxides have been measured by electron spin resonance spectroscopy at low temperatures. The equilibrium constant appears to be virtually independent of the nature of the alkyl groups. It is concluded that differences in the rate of constants for chain termination by *t*-peroxy radicals at ambient temperatures are due chiefly to the differences in rate constants for irreversible tetroxide decomposition. The activation parameters for this reaction indicate that it occurs by one bond rather than two bond scission.

Canadian Journal of Chemistry, **47**, 3803 (1969)

Introduction

Bartlett and Guaraldi (1) have shown that di-*t*-butyl tetroxide is stable at temperatures below about $-80°$. The tetroxide was prepared both by the irradiation of di-*t*-butylperoxycarbonate in frozen methylene chloride at $-196°$ and by the oxidation of *t*-butyl hydroperoxide with lead tetraacetate at $-90°$ in the same solvent. The equilibrium constant, $K_1 (= k_{-1}/k_1)$ and the rate constant for tetroxide decomposition k_2, were determined by using electron spin resonance (e.s.r.) spectroscopy to monitor changes in the peroxy radical concentration[4].

$$[1] \qquad \mathrm{ROO\cdot} + \mathrm{ROO\cdot} \underset{k_{-1}}{\overset{k_1}{\rightleftarrows}} \mathrm{ROOOOR}$$

$$[2] \qquad \mathrm{ROOOOR} \xrightarrow{k_2} [\mathrm{RO\cdot}\ \ \mathrm{O_2}\ \ \cdot\mathrm{OR}]_{\mathrm{cage}}$$

$$[3] \qquad [\mathrm{RO\cdot}\ \ \mathrm{O_2}\ \ \cdot\mathrm{OR}]_{\mathrm{cage}} \xrightarrow{k_3} \mathrm{ROOR} + \mathrm{O_2}$$

$$[4] \qquad [\mathrm{RO\cdot}\ \ \mathrm{O_2}\ \ \cdot\mathrm{OR}]_{\mathrm{cage}} \xrightarrow{k_4} \mathrm{RO\cdot} + \mathrm{O_2} + \cdot\mathrm{OR}$$

Di-*t*-butyl tetroxide has also been prepared by the photolysis of azo-isobutane in the presence of oxygen (2) and by the reaction of *t*-butyl hydroperoxide with iodosobenzene and iodosobenzene diacetate (3). The low temperature photolysis of azo-isobutyronitrile (AIBN) and azo-cyclohexylnitrile (ACHN) in the presence of oxygen has also been reported to yield tetroxides (2). At temperatures below about $-30°$, di-*t*-butyl trioxide and dicumyl trioxide are stable (4). They are believed to be formed by the trapping of the RO· radicals formed in reaction [4] by peroxy radicals

$$[16] \qquad \mathrm{RO\cdot} + \mathrm{ROO\cdot} \underset{> -30°}{\rightleftharpoons} \mathrm{ROOOR}$$

Our interest in the self-reactions of peroxy radicals comes from our measurements of the rate constants for chain termination in hydrocarbon oxidation. Part XIV of this series (5) describes the measurement of termination rate constants in the presence of concentrations of tertiary hydroperoxides sufficient to trap all the RO· radicals formed in reaction [4] and convert them to ROO· radicals

$$[5] \qquad \mathrm{RO\cdot} + \mathrm{ROOH} \rightarrow \mathrm{ROH} + \mathrm{ROO\cdot}$$

Under these conditions the termination rate constant, $2k_t$, corresponds to $(2k_2/K_1)(k_3/(k_3 + k_4))$. Values of $2k_t$ at 30° for tertiary peroxy radicals range from $\sim 4 \times 10^2\ M^{-1}\ s^{-1}$ for for *t*-butylperoxy radicals, to $\sim 3 \times 10^3\ M^{-1}\ s^{-1}$ for cumylperoxy, to $\sim 3 \times 10^4\ M^{-1}\ s^{-1}$ for 1,1-diphenylethylperoxy radicals. This range cannot be accounted for by any variation in the ratio of alkoxy radical combination in the cage to diffusion from the cage (6). Bartlett and Guaraldi's experimental approach appeared to provide a simple method for determining whether the variation in $2k_t$ was due primarily to changes in K_1 or k_2. The present paper describes an e.s.r. study of the low temperature reactions of some representative peroxy radicals.

---

[1]NRCC No. 10 898.
[2]A preliminary account of some of this work has appeared in Chem. Commun. 505 (1969).
[3]NRCC Postdoctorate Fellow 1967–1969.
[4]The reactions are numbered as in the two preceding papers.

Can. J. Chem. Downloaded from www.nrcresearchpress.com by 210.87.254.5 on 09/05/12
For personal use only.

Experimental

Radical Formation

Peroxy radicals were prepared by three different methods, all of which, for *t*-butylperoxy at least, gave very similar results in the temperature range in which the equilibrium constant for tetroxide formation was determined. However, at the higher temperatures where the irreversible decomposition of tetroxide was studied, similar results were not obtained by the different methods. In this region, the most satisfactory procedure involved photolysis of 10^{-2} *M* azoalkanes in oxygen saturated CF_2Cl_2 (freon 12, f.p. $-155°$) at liquid nitrogen temperatures (2). With this procedure the rates of peroxy radical decay were very reproducible and were exactly second order. In contrast, the photolysis of hydroperoxides under similar conditions gave rather irreproducible decay rates which were not always second order. These effects are probably due, in part, to the fact that the RO· radicals are scavenged both by reaction [16] (which leads to the loss of an ROO· radical) and by reaction [5] (which leads to the formation of an ROO· radical). The relative importance of these two processes obviously depends on the relative concentrations of ROO· and ROOH and will, therefore, vary during a decay experiment. The ROOH concentration will itself depend on its initial concentration and on the amount photolyzed in the radical generation. It is also possible that the highly reactive ·OH radical produced in the photolysis forms secondary radicals which in some way interfere with the peroxy radical decay.

Peroxy radicals were also prepared by the rapid cooling from 30° of *t*-butyl hyponitrite (2.5×10^{-2} *M*) induced decompositions of 0.1 *M* hydroperoxide solutions in CF_2Cl_2 and in isopentane. Although this method was quite satisfactory for the determination of the equilibrium constant the radical decays were not exactly second order.

Solvents

In most of the present work CF_2Cl_2 was used as the solvent. A few experiments were also done in isopentane. Methylene chloride, the solvent used by Bartlett and Guaraldi (1), was less satisfactory than either CF_2Cl_2 or isopentane, because its freezing point ($-97°$) is in the middle of the temperature range of the experiments. Although there does appear to be some kind of equilibrium between the peroxy radicals and tetroxide in solid methylene chloride (1) in our hands, the measured equilibrium constants were not very reproducible and appeared to depend on the rate at which the methylene chloride was solidified.

Radical Concentrations

The peroxy radicals were monitored in the V-4557 variable temperature accessory of a Varian E-3 e.s.r. spectrometer. The signal at ~2 kG from a single crystal of synthetic ruby was used to correct for variations in cavity Q (7). The radical concentrations were determined at each temperature[5] by double integration of the first derivative e.s.r. signal using a Honeywell G.P.I.-10 general purpose integrator. The calibration of concentration was done over the entire temperature range with 2,2-diphenyl-1-picrylhydrazyl (DPPH) and 2,2,6,6-tetramethylpyridone nitroxide solutions. This is necessary because the second integral for these stable radicals (normalized to the ruby signal) varied with temperature (Fig. 1).

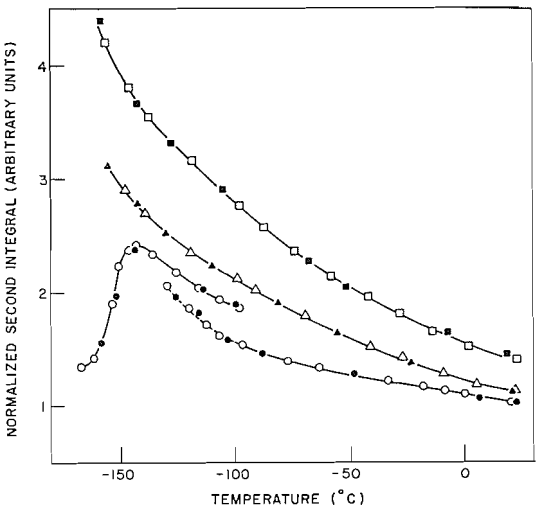

FIG. 1. Calibration curves for the stable radicals in the different solvents; ○, methylene chloride; △, isopentane; □, freon 12 (CF_2Cl_2). Open points refer to nitroxide and solid points to DPPH.

Results

The effect of temperature on the concentration of peroxy radicals is illustrated schematically in Fig. 2. The picture is generally similar to that previously found by Bartlett and Guaraldi (1).

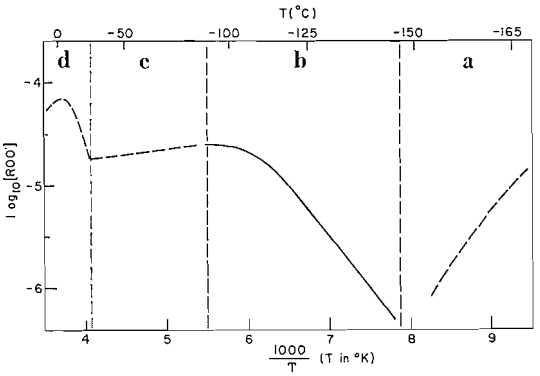

FIG. 2. The temperature dependence of the concentration of *t*-alkylperoxy radicals. The line is dotted in regions *a*, *c*, and *d* because the peroxy radical concentration at a given temperature can vary significantly during the time involved in an experiment.

[5]The line width for peroxy radicals is strongly temperature dependent (8), even at temperatures below $-90°$. For example, the line width for *t*-butylperoxy radicals at $-90°$ (4.2 ± 0.2 G) is twice as great as at $-148°$.

Can. J. Chem. Downloaded from www.nrcresearchpress.com by 210.87.254.5 on 09/05/12
For personal use only.

The region *a* is characteristic of peroxy radicals generated by photolysis at −196°. As the temperature is increased the radical concentration decreases owing to the formation of tetroxide. The disappearance of the radicals in the solid matrix as they are slowly converted to tetroxide occurs even at temperatures as low as −170 to −180°. The ease of this reaction has been commented on previously (9). At these low temperatures the e.s.r. line shape is not symmetrical but the asymmetry is not connected with the presence of a second radical (9). The asymmetry has been previously analyzed in terms of a single radical whose *g* value is anisotropic but has an axis of symmetry (9, 10*c*). The asymmetric line shape depends not only on the radical concentration (10) but also on the temperature. Provided little tetroxide is formed the line shape is reversible with temperature. There is no signal in the region *a* if tetroxide is allowed to form. That is, a sample containing peroxy radicals which is cooled from higher temperatures into region *a* does not give an e.s.r. signal.

For most practical purposes peroxy radicals can be considered to be in equilibrium with the tetroxide in region *b*. There is, in actual fact, a slow disappearance of radicals in this region but it is not until region *c* that radical loss becomes significant on the time scale (and at the concentrations) of the present experiments. In region *b* the concentrations of radicals and tetroxide are related to one another by

$$[\mathrm{ROO}\cdot] + 2[\mathrm{RO_4R}] = [\mathrm{ROO}\cdot]_{max}$$

where $[\mathrm{ROO}\cdot]_{max}$ is the radical concentration at complete dissociation. The equilibrium constant is given by

$$K_1 = \frac{[\mathrm{ROO}\cdot]^2}{[\mathrm{RO_4R}]} = \frac{2[\mathrm{ROO}\cdot]^2}{[\mathrm{ROO}\cdot]_{max} - [\mathrm{ROO}\cdot]}$$

Its variation with temperature can be represented by the van't Hoff relation

$$K_1 = e^{\Delta S_1/R}\, e^{-\Delta H_1/RT}$$

where ΔS_1 is the change in entropy and ΔH_1, the change in enthalpy.

The behavior of *t*-butylperoxy radicals in the temperature range where they are in equilibrium with tetroxide is illustrated in Fig. 3. The data in this figure were obtained in a single experiment. The individual points on each of the three curves were obtained in a completely random manner. After curve I was obtained, about 90% of the radicals were allowed to decay at ~ − 50° and curve II was obtained. The sample was then warmed to about −20° (region *d*) at which temperature trioxide decomposition was sufficiently rapid that the radical concentration *increased* (see Fig. 2). The sample was recooled and curve III was obtained. This general procedure for changing the radical concentration by warming the sample into region *c* (smaller) and *d* (greater) was employed in a majority of the experiments in order to increase the number of individual measurements of ΔS_1 and ΔH_1.

The values found for ΔS_1 and ΔH_1 from curves such as those in Fig. 3 are summarized in Table I. The errors are standard deviations from the average value for several different experiments. With cumene hydroperoxide and 2-phenyl-2-butyl hydroperoxide, ΔS_1 values were not measured because irreversible decomposition of the tetroxide started to occur at a temperature below which it was fully dissociated into peroxy radicals, i.e., $[\mathrm{ROO}\cdot]_{max}$ could not be determined.

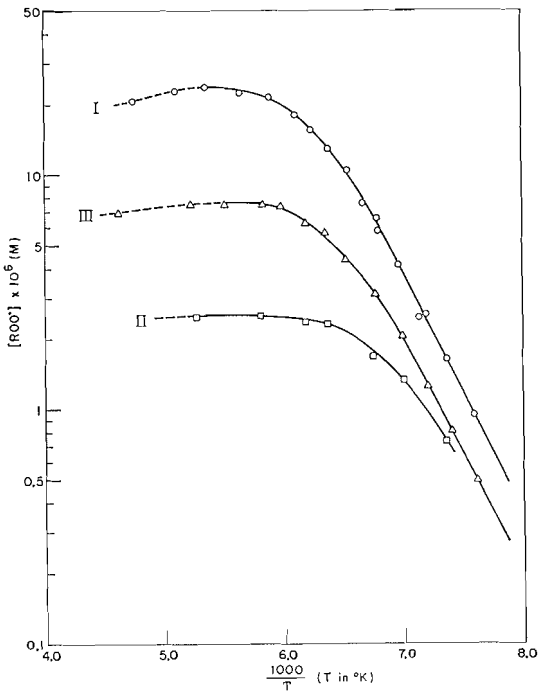

FIG. 3. The *t*-butylperoxy radical – *t*-butyl tetroxide equilibrium. The radicals were prepared by low temperature photolysis of azo-isobutane.

TABLE I

Activation parameters for di-*t*-alkyl tetroxides (RO_4R)

R	K_1		$k_{e.s.r.}$		k_2		
	ΔH_1 (kcal mole^{-1})	ΔS_1 (cal deg^{-1} mole^{-1})	$E_{e.s.r.}$ (kcal mole^{-1})	$\log_{10}A_{e.s.r.}$ (M^{-1} s^{-1})	E_2 (kcal mole^{-1})	$\log_{10}A_2$ (M^{-1} s^{-1})	$\log_{10} 2k_t$[a] (M^{-1} s^{-1})
t-Butyl[b]	8.8±0.4	34±1	8.7±0.3	9.7	17.5	16.6	2.57
t-Butyl[c]	8.0±0.2	31±1	5.1±0.2	5.5			2.57
t-Butyl[d]	8.4±0.4	30					2.57
2-Ethyl-2-propyl[c]	7.5±0.3	29±1	4.7±0.5	5.7			3.11
2-Isopropyl-2-propyl[d]	8.6±0.4	33±1					3.25
Cumyl[b]	9.2±0.4	32±1	7.3±0.3	10.7	16.5	17.1	3.41
Cumyl[c]	10.6±0.8	*e*					3.41
1-Methylcyclohexyl[c]	7.0±0.4	35	6.1±0.5	7.7			3.45
2-Neopentyl-2-propyl[c]	7.8±0.5	31	4.0±0.2	5.7			3.72
1-Methylcyclopentyl[c]	8.0±0.3	30±1	5.7±0.3	7.5			3.97
2-Phenyl-2-butyl[c]	11 ±1	*e*					4.25

[a]"Best values" at 30° (5, 9).
[b]From RNNR in CF_2Cl_2.
[c]From ROOH in CF_2Cl_2.
[d]From ROOH in isopentane.
[e]ΔS_1 was not measured because irreversible decay started to occur at a temperature below that at which the tetroxide was fully dissociated into peroxy radicals.

For some of the more unstable tetroxides, region *c* extends to lower temperatures. The presence of a tetroxide can only be inferred by the fact that a short-lived peroxy radical signal appears when the irradiated samples are warmed rapidly into region *b*. Thus, with 1,1-diphenylethyl hydroperoxide the intensity of the 1,1-diphenylethylperoxy radical signal rose with temperature throughout region *b*. The tetroxide was definitely formed reversibly but its irreversible decomposition was too rapid for ΔH_1 to be determined.

Although Mill and Stringham (2) apparently obtained tetroxides from azo-bis-isobutyronitrile (AIBN) and azo-bis-cyclohexylnitrile (ACHN), we had great difficulty in detecting any peroxy radicals when these compounds were irradiated in CF_2Cl_2. In some experiments a small asymmetric signal, probably due to peroxy radicals, was detected at −165°. This signal disappeared at −130° and reappeared as a symmetric signal at −100°, lasting only for about 200 s at this temperature[6]. These small signals had only about 1% of the intensity of the signals from azo-isobutane and azo-cumene and were not always observed. Instead, a radical signal with three lines of approximately equal intensity and separation was generally obtained from AIBN and ACHN. This triplet appeared on warming the irradiated sample to about −110° and was not reversible with temperature. It was moderately stable up to about −90° but disappeared rapidly at −60° (half life ~200 s). The triplet had splittings of 30.0 ± 0.1 G on the low field side and 30.4 ± 0.1 G on the high field side. The line width was 2.0 ± 0.3 G with 0.5 G modulation. The maximum radical concentration was $\sim 1 \times 10^{-7}$ *M*. This radical has not been identified but it is worth noting that it was not detected when AIBN was irradiated in the absence of oxygen. On warming the samples to 0° a second very weak triplet was observed. The splittings were ~8–9 G suggesting that this radical may be a nitroxide.

The photolysis of 2-cyano-2-propyl hydroperoxide, which should give the same *t*-peroxy radical as the photolysis of AIBN and oxygen, did not give a peroxy radical signal. Preliminary experiments on the oxidation of cumene in the presence of 2-cyano-2-propyl hydroperoxide gave $k_p/(2k_t)^{\frac{1}{2}} \sim 0.33 \times 10^{-3}\ M^{-\frac{1}{2}}\ s^{-\frac{1}{2}}$, $k_p \sim 0.18\ M^{-1}\ s^{-1}$, and $2k_t \sim 3 \times 10^5\ M^{-1}\ s^{-1}$. It is possible that a *t*-peroxy radical with a termination rate constant of about $10^5\ M^{-1}\ s^{-1}$ would not be seen under our experimental conditions.

Cyclohexyl hydroperoxide gave a peroxy radical signal in region *b*. Although short-lived,

[6]The irradiation of AIBN in the e.s.r. cavity at −95° (cf. ref. 2) gave no detectable signal in 900 s. In contrast, a peroxy radical signal was easily detected within 50 s of the irradiation of azo-isobutane under the same conditions.

Can. J. Chem. Downloaded from www.nrcresearchpress.com by 210.87.254.5 on 09/05/12
For personal use only.

Can. J. Chem. Downloaded from www.nrcresearchpress.com by 210.87.254.5 on 09/05/12
For personal use only.

the intensity of the signal did increase with an increase in temperature. However, the radical concentration decreased too rapidly for confirmation of the reversibility of tetroxide formation. Di-*sec*-alkyl tetroxides have not previously been directly detected. Mill and Stringham originally reported (2) and we have confirmed that peroxy radicals cannot be detected in photolyzed azo-isopropane samples. There is no obvious reason for the difference in the low temperature behavior of cyclohexylperoxy radicals and isopropylperoxy radicals because, at 30°, the rate constants for their self-reactions are similar (11).

With azo-bis-1-propanol diacetate, $(CH_3C(O)OCH_2C(CH_3)_2N)_2$, the concentration of peroxy radicals was too low to measure ΔH_1, although a tetroxide was definitely formed reversibly.

In region *c*, where the tetroxide is almost completely dissociated, the radical concentration decreases with time according to a second order rate law (1). As was mentioned in Experimental section, the radical decay is accurately second order for radicals derived from the azoalkanes (see also Fig. 4) but it is rather irreproducible and frequently is not exactly second order for the radicals from hydroperoxides. Now the measured bimolecular rate constant, $k_{e.s.r.}$, will be equal to $2k_2/K_1$ provided the RO· radicals formed in reaction [4] have no effect on the ROO· radical concentration and provided $k_{-1} \gg k_2$. In the experiments in which hydroperoxides were used the RO· radicals can be scavenged by ROO· (reaction [16], $k_{e.s.r.} = (2k_2/K_1)(1 + k_4/(k_3 + k_4))$) and by ROOH (reaction [5], $k_{e.s.r.} = (2k_2/K_1)(k_3/(k_3 + k_4))$). The rather poor reproducibility of $k_{e.s.r.}$ values in the hydroperoxide experiments chiefly reflects variations in the relative contributions of reactions [5] and [16] to RO· scavenging. The excellent reproducibility of the $k_{e.s.r.}$ values in the azoalkane experiments presumably reflects the exclusive scavenging of RO· in reaction [16]. The activation parameters for reaction [2] (see Table I) have therefore been calculated only from the azoalkane data. In these calculations, it was assumed that $k_{e.s.r.} = 4k_2/K_1$ on the basis that k_4/k_3 is about 6–7 at 30° (6 and references cited therein) and that although this ratio decreases slightly with temperature the value of $k_4/(k_3 + k_4)$ will probably still be reasonably close to unity in the temperature range in which $k_{e.s.r.}$ is measured (cf. ref. 4).

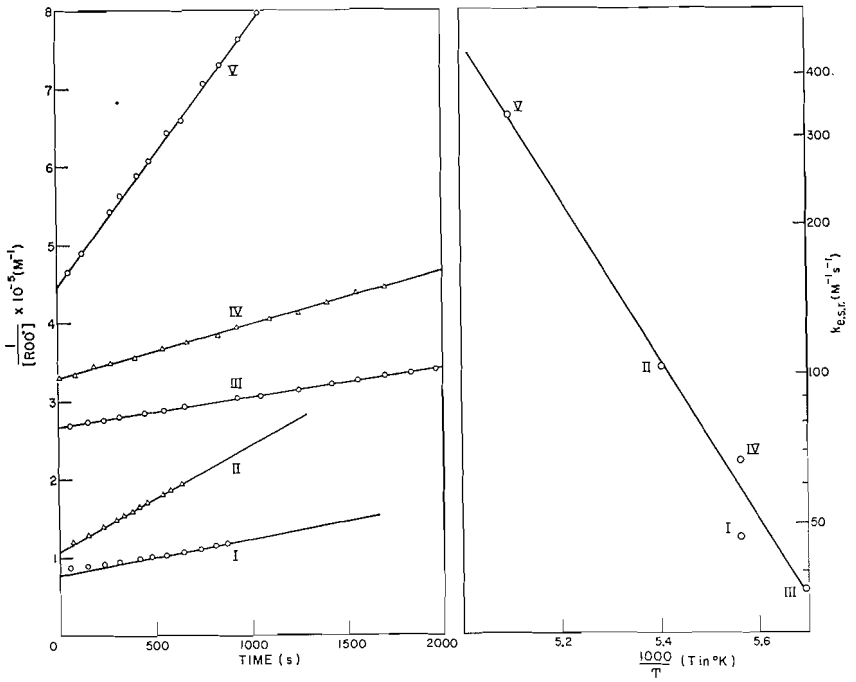

FIG. 4. The irreversible decay of cumyl tetroxide. The cumylperoxy radicals were prepared by low temperature photolysis of azocumene.

Can. J. Chem. Downloaded from www.nrcresearchpress.com by 210.87.254.5 on 09/05/12
For personal use only.

Discussion

The values of ΔS_1 and ΔH_1 for the tetroxides listed in Table I are in excellent agreement with the values obtained by Bennett, Brown, and Mile for a number of other *t*-alkyl tetroxides prepared by the low temperature photolysis of *t*-butyl peroxide in oxygen saturated branched chain hydrocarbons (12). These parameters are also in reasonably good agreement with the original estimate that ΔS_1 should be ~ 25 cal deg^{-1} mole^{-1} and $\Delta H_1 \sim 5$ kcal/mole (13). These estimates were made by Benson on thermochemical grounds before tetroxides had been observed experimentally.

Within our limits of experimental accuracy the values of ΔS_1 and ΔH_1 are identical for the different tetroxides. This implies that differences in behavior of *t*-alkylperoxy radicals in the termination of oxidation chains at 30° ($2k_t$) are due chiefly to differences in the rate constants for irreversible tetroxide decomposition, k_2. Evidence favoring this conclusion is also provided by the fact that both cumyl tetroxide and 1,1-diphenylethyl tetroxide undoubtedly decomposed more rapidly than the *t*-alkyl tetroxides. The activation parameters for *t*-butyl tetroxide and cumyl tetroxide decomposition suggest that rate differences are due to differences in activation energy rather than activation entropy.

The chain termination rate constants for *t*-butylperoxy and cumylperoxy radicals at 30° can be calculated from the relation $2k_t = (2k_2/K_1)(k_3/(k_3 + k_4))$ using the values of K_1 and k_2 found in this work and the values of k_4/k_3 given in the preceding paper (6). Assuming that K_1 is the same for both radicals, the azoalkane photolytic results give $\Delta H_1 = 9.0$ kcal/mole, $\Delta S_1 = 33$ cal deg^{-1} mole^{-1} and $(K_1)_{30°} = 5.2\ M$. For *t*-butylperoxy radicals at 30°, $k_2 = 1 \times 10^4$ s^{-1} (Table I) and $(k_3 + k_4)/k_3 = 8.0$ giving $2k_t = 5 \times 10^2\ M^{-1}$ s^{-1}, in excellent agreement with the "best" value of 4.0×10^2 (5). For cumylperoxy radicals, $k_2 = 1.6 \times 10^5$ and $(k_3 + k_4)/k_3 = 7.3$, giving $2k_t = 8 \times 10^3\ M^{-1}$ s^{-1}, which is in good agreement with the measured values ($6–8 \times 10^3\ M^{-1}$ s^{-1}) but is rather larger than the "best" value of $2.6 \times 10^3\ M^{-1}$ s^{-1}. Considering the temperature range over which K_1 and k_2 have been extrapolated, the agreement between the calculated and measured rate constants is very satisfactory.

The pre-exponential factors in the Arrhenius equation for reaction [2] are such as to indicate that only one bond in the tetroxide is cleaved in the rate determining step.

$$\text{ROOOOR} \xrightarrow{k_2} \text{RO}\cdot + \cdot\text{OOOR} \rightarrow \text{RO}\cdot + \text{O}_2 + \cdot\text{OR}$$

That is, the *A* factors for simple one bond fission are expected (14) to be in the range 10^{15}–10^{17} s^{-1}, while lower values are obtained if two O—O bonds are cleaved at the same time. The pre-exponential factors found in the present work (together with the value of Bennett *et al.*, $10^{17.5}$ s^{-1}, for the tetroxide derived from 2,2,3-trimethylbutane (12)) contrast with earlier values of $10^{9.3}$ (1) and 10^{12} s^{-1} (2), which implied that reaction [2] occurred by concerted cleavage of the 1,2 and 3,4 O—O bonds. The activation energies of reaction [2] are also consistent with Benson's estimate that the 1,2 O—O bond strength is about 20 kcal/mole (13). Further support for single bond fission of the tetroxide comes from Fessenden's recent identification of the $CF_3OOO\cdot$ radical (15). However, we could not detect any peroxy radicals in the photolysis of *t*-butyl hyponitrite, which implies that oxygen is not readily trapped by a *t*-butoxy radical even at liquid nitrogen temperatures.

1. P. D. Bartlett and G. Guaraldi. J. Amer. Chem. Soc. **89**, 4799 (1967).
2. T. Mill and R. S. Stringham. J. Amer. Chem. Soc. **90**, 1062 (1968).
3. N. A. Milas and B. Plesnicar. J. Amer. Chem. Soc. **90**, 4450 (1968).
4. P. D. Bartlett and P. Günther. J. Amer. Chem. Soc. **88**, 3288 (1966).
5. J. A. Howard, K. Adamic and K. U. Ingold. Can. J. Chem. This issue.
6. J. A. Howard and K. U. Ingold. Can. J. Chem. This issue.
7. L. S. Singer. J. Appl. Phys. **30**, 1463 (1959).
8. J. R. Thomas. J. Amer. Chem. Soc. **88**, 2064 (1966).
9. J. E. Bennett, B. Mile, and A. Thomas. 11th Symposium on Combustion. Pittsburgh, Combustion Institute. 1967. p. 853.
10. (*a*) S. J. Wyard and R. C. Smith. Bulletin Ampère fasc. spécial, **9**, 224 (1960). (*b*) J. W. Searle, R. C. Smith, and S. J. Wyard. Bulletin Ampère fasc. spécial, **9**, 236 (1960). (*c*) J. W. Searle, R. C. Smith, and S. J. Wyard. Proc. Phys. Soc. **78**, 1174 (1961).
11. J. A. Howard and K. U. Ingold. J. Amer. Chem. Soc. **90**, 1058 (1968).
12. J. E. Bennett, D. M. Brown, and B. Mile. Chem. Commun. 504 (1969).
13. S. W. Benson. J. Amer. Chem. Soc. **86**, 3922 (1964). S. W. Benson and R. Shaw. Advan. Chem. Ser. **75**, 288 (1968).
14. S. W. Benson. Thermochemical kinetics. John Wiley and Sons, Inc., New York. 1968. Chap. 3.
15. R. W. Fessenden. J. Chem. Phys. **48**, 3725 (1968).

Absolute rate constants for hydrocarbon autoxidation. XVII. The oxidation of some cyclic ethers[1]

J. A. HOWARD AND K. U. INGOLD
Division of Applied Chemistry, National Research Council of Canada, Ottawa, Canada

Received June 30, 1969

The propagation and termination rate constants have been determined for the autoxidation of 1,4-dioxan, tetrahydropyran, tetrahydrofuran, 2,5-dimethyltetrahydrofuran, and phthalan. The rate constants for α-hydrogen atom abstraction from some of the ethers by the tetralylperoxy radical and from tetralin by some ether peroxy radicals have been measured and compared. The chain transfer rate constants have been estimated for the reaction of the cumylperoxy radical with α-hydroperoxytetrahydrofuran, α-hydroperoxytetrahydropyran, and α-ethoxyethyl hydroperoxide.

Canadian Journal of Chemistry, 47, 3809 (1969)

Can. J. Chem. Downloaded from www.nrcresearchpress.com by 210.87.254.6 on 09/05/12
For personal use only.

Introduction

It has been known for some time that ethers react with molecular oxygen at ambient temperatures to form peroxides and hydroperoxides (1–3). The free radical initiated oxidation of tetrahydrofuran (EH) has been shown to yield α-hydroperoxytetrahydrofuran (4) and to obey the kinetic expression (5)

$$[\mathrm{I}] \qquad \text{Rate of oxidation} = -\frac{d[O_2]}{dt} = \frac{k_p[EH]R_i^{1/2}}{(2k_t)^{1/2}}$$

where k_p and $2k_t$ are the propagation and termination rate constants and R_i is the rate of chain initiation. It is, therefore, possible to describe the oxidation of tetrahydrofuran, at oxygen pressures above about 100 mm Hg, by a reaction scheme which is similar to that used to describe the oxidation of many organic substances

$$[1] \qquad I_2 \xrightarrow[O_2 + EH]{k_i} EOO\cdot \qquad (R_i = 2ek_i[I_2])$$

$$[2] \qquad EOO\cdot + EH \xrightarrow{k_p} EOOH + E\cdot$$

$$[3] \qquad E\cdot + O_2 \longrightarrow EOO\cdot$$

$$[4] \qquad EOO\cdot + EOO\cdot \xrightarrow{2k_t} \text{Non-radical products}$$

where E· is the tetrahydrofuranyl radical, EOO· the tetrahydrofuranylperoxy radical, and I_2 is the free radical chain initiator. This scheme can almost certainly be used to describe the autoxidation of many other cyclic ethers.

There are no directly measured absolute rate constants for the oxidation of ethers reported in the literature. However, Gosborne and Seree de Roch (5) have estimated the termination rate constants for *n*-butyl, isopropyl, benzyl, and α-methylbenzyl ethers, tetrahydrofuran, and 2-methyl tetrahydrofuran to be about $10^6\ M^{-1}\ s^{-1}$ by the co-oxidation method (6). These results imply a fundamental difference between hydrocarbon and ether oxidations since the termination rate constants for secondary and tertiary hydrocarbons have been shown to vary considerably (7). In this paper we report our measurements of the absolute propagation and termination rate constants for the oxidation of a number of readily oxidizable cyclic ethers.

Experimental

Tetrahydrofuran, tetrahydropyran, 1,4-dioxan, 2,5-dimethyltetrahydrofuran, tetralin, cumene, *t*-butyl hydroperoxide, and chlorobenzene were commercial materials purified to > 99.5% by standard techniques. Phthalan was prepared by dehydration of phthalyl alcohol (8). The preparation of tetralin hydroperoxide has been described previously (9). α-Hydroperoxytetrahydrofuran and 2-hydroperoxy-2,5-dimethyltetrahydrofuran were prepared by the α,α′-azo-bis-isobutyronitrile initiated oxidation at 30° of tetrahydrofuran and 2,5-dimethyltetrahydrofuran, respectively. α-Hydroperoxytetrahydropyran, α-ethoxyethyl hydroperoxide, and 2-hydroperoxy-2-methyltetrahydrofuran were prepared by the reaction of 50% H_2O_2 with 2,3-dihydropyran, ethyl vinyl ether, and 2-methyl-4,5-dihydrofuran, respectively (10).

The rates of oxidation were determined from the consumption of oxygen as monitored by a Dynisco pressure transducer (DPT 85–2). The reaction cell and the transducer were both thermostatted at 30°. The output from the transducer was displayed on a Sargent recorder (Model SRG). The absolute rate constants were generally measured by the rotating sector technique. The photochemical pre- and after-effect method (11) was used for the determination of the absolute rate constants (i.e.,

[1]NRCC No. 10 906.

Can. J. Chem. Downloaded from www.nrcresearchpress.com by 210.87.254.6 on 09/05/12
For personal use only.

$k_p/2k_t$) for the oxidation of 2,5-dimethyltetrahydrofuran and some oxidations in the presence of 2-hydroperoxy-2,5-dimethyltetrahydrofuran and 2-hydroperoxy-2-methyltetrahydrofuran. The rate constants for attack on an ether by a peroxy radical not derived from the ether have been determined by oxidation of the ether in the presence of the appropriate hydroperoxide (e.g. tetralin hydroperoxide served as a source of tetralylperoxy radicals (9)).

α,α′-Azo-bis-cyclohexyl nitrile was the photoinitiator and α,α′-azo-bis-isobutyronitrile and *t*-butylhyponitrite were the thermal initiators. The rates of chain initiation were measured using 2,6-di-*t*-butyl-4-methoxyphenol as inhibitor. The hydroperoxide yields for the oxidation of the pure ethers were determined by iodometric titration.

The carbonyl compounds formed in many of the oxidations were investigated by infrared analysis (1650–1750 cm^{-1} region).

Results and Discussion

The propagation and termination rate constants for the oxidation of tetrahydrofuran at 30° are given in Table I. α-Hydroperoxytetrahydrofuran (0.38 *M*) has no effect on the rate constants for the oxidation of the parent ether.

The rate constants for the oxidation of tetrahydrofuran in the presence of a number of ether hydroperoxides and hydrocarbon hydroperoxides are given in Table II.

α-Hydroperoxytetrahydropyran, α-ethoxyethylhydroperoxide, and tetralin hydroperoxide have little or no effect on the rate of oxidation of tetrahydrofuran. The termination rate constants for the secondary peroxy radicals derived from the ether hydroperoxides (E′OOH) and from tetralin hydroperoxide (TOOH) are very similar. These peroxy radicals also have a similar reactivity in H-atom abstraction from tetrahydrofuran. The transfer reaction between the added hydroperoxide and tetrahydrofuranylperoxy radicals (EOO·) does indeed take place, since the carbonyl compounds formed in the oxidations in the presence of the hydroperoxides correspond to the carbonyl compounds formed in the free radical induced decomposition of the hydroperoxides, i.e.

$$\text{EOO}\cdot + \text{ROOH (or E′OOH)} \rightarrow \text{EOOH} + \text{ROO}\cdot \text{ (or E′OO}\cdot\text{)}$$

This implies that the majority of the chain terminating radicals in the oxidations are derived from the added hydroperoxide.

For *t*-butyl hydroperoxide concentrations in the range 4–8 *M* the rate of oxidation of tetrahydrofuran is increased by a factor of about 14. This change in rate combined with the fact that the measured termination rate constant is similar

TABLE I

Rate constants for the oxidation of tetrahydrofuran (12.3 *M*) at 30°

$R_i \times 10^8$ ($M\,s^{-1}$)	$R_s \times 10^6$ ($M\,s^{-1}$)	$k_p/(2k_t)^{1/2} \times 10^4$ ($M^{-1/2}\,s^{-1/2}$)	k_p ($M^{-1}\,s^{-1}$)	$2k_t \times 10^{-7}$ ($M^{-1}\,s^{-1}$)
20	4.2	7.8	4.3	3.0
5	2.1	7.8	4.5	3.3
2	1.38	7.8	4.3	3.0
33.7*	5.37	7.8	4.5	3.3
37*	5.6	7.9	4.3	3.0

*In the presence of α-hydroperoxytetrahydrofuran (0.38 *M*).

TABLE II

Rate constants for the oxidation of tetrahydrofuran in the presence of some ether hydroperoxides and hydrocarbon hydroperoxides

Hydroperoxide	$k_p/(2k_t)^{1/2} \times 10^4$ ($M^{-1/2}\,s^{-1/2}$)	k_p ($M^{-1}\,s^{-1}$)	$2k_t \times 10^{-7}$ ($M^{-1}\,s^{-1}$)
None	7.8	4.3	3.1
Tetrahydrofuran	7.9	4.3	3.1
Tetrahydropyran	7.7	4.4	3.2
α-Ethoxyethyl	6.7	4.5	4.6
Tetralin	6.0	3.0	2.5*
t-Butyl	82	0.34	0.00018

*This termination rate constant is slightly higher than the values determined in hydrocarbon media. Thus, $2k_t = 7.6 \times 10^6\ M^{-1}\,s^{-1}$ for pure tetralin (9).

Can. J. Chem. Downloaded from www.nrcresearchpress.com by 210.87.254.6 on 09/05/12
For personal use only.

TABLE III

Rate constants for the oxidation of tetralin in the presence of some ether hydroperoxides

Hydroperoxide	Concentration (M)	$R_i \times 10^7$ ($M\,s^{-1}$)	Chain length	$k_p/(2k_t)^{1/2} \times 10^3$ ($M^{-1/2}\,s^{-1/2}$)	k_p ($M^{-1}s^{-1}$)	$2k_t \times 10^{-7}$ ($M^{-1}\,s^{-1}$)
None		2.3	8	2.3	6.3	0.76
Tetrahydrofuranyl	0.16	3.2	19	1.7	6.0	1.3
Tetrahydrofuranyl	0.31	2.6	22	1.6	6.2	1.5
Tetrahydropyranyl	0.16	0.12	100	1.6	—	—
Tetrahydropyranyl	0.32	0.12	92	1.4	—	—
Tetrahydropyranyl	0.14	3.1	22	1.7	7.0	1.7
Tetrahydropyranyl	0.14	1.6	23	1.3	6.0	2.0
Tetrahydropyranyl	0.27	3.4	17	1.4	5.3	1.5
α-Ethoxyethyl	0.09	2.8	18	1.3	—	—
α-Ethoxyethyl	0.18	4.75	14	1.2	7.1	3.5
α-Ethoxyethyl	0.36	5.5	11	1.2	10	7.0

to the value found previously for *t*-butylperoxy radicals serves to confirm that the chain transfer reaction takes place. The propagation rate constant is a factor of 10 lower than the values found for the secondary peroxy radicals. This result is in agreement with our earlier conclusions that tertiary peroxy radicals are less reactive than secondary peroxy radicals in chain propagation (9, 12).

The propagation and termination rate constants for the oxidation of tetralin in the presence of three secondary ether hydroperoxides (Table III) are similar to one another and to the values found for tetralin alone or in the presence of tetralin hydroperoxide. Infrared analysis of the termination products again demonstrated that the similar rate constants are not due to the absence of the transfer reaction. These results supplement the results in Table II and confirm that secondary peroxy radicals from ethers and hydrocarbons have similar termination rate constants and similar reactivities towards H-atom abstraction.

The rate of oxidation of cumene is reduced by small concentrations of tetrahydrofuranyl, tetrahydropyranyl, and α-ethoxyethyl hydroperoxides (Table IV and Fig. 1). The rate is also reduced by the addition of tetrahydrofuran (Fig. 1). Similar reductions in the rate of oxidation of cumene have been reported for tetralin hydroperoxide (13) and tetralin (14). We have determined "cross" propagation rate constants for the attack of tetralylperoxy radicals (TOO·) on cumene (CH), i.e. k_p^{TC}

$$\mathrm{TOO\cdot + CH \xrightarrow{k_p^{TC}} TOOH + C\cdot}$$

and for the attack of cumylperoxy radicals (COO·) on tetralin (TH), i.e., k_p^{CT}

$$\mathrm{COO\cdot + TH \xrightarrow{k_p^{CT}} COOH + T\cdot}$$

by a study of the co-oxidation of cumene and tetralin and the oxidation of each of these hydrocarbons in the presence of the hydroperoxide of the other hydrocarbon (9). The results of the present work show that tetralylperoxy and tetrahydrofuranylperoxy radicals have similar reactivities towards H-atom abstraction, which means that $k_p^{TC} \approx k_p^{EC}$. Moreover, it can be concluded that the rate constants for the attack of cumylperoxy radicals on tetrahydrofuran and on tetralin are approximately equal (i.e., $k_p^{CT} \approx k_p^{CE}$). Since tetralin and tetrahydrofuran produce comparable retardations of the oxidation of cumene (Fig. 1) it seems likely that the "cross" termination rate constants, $2k_t^{CT}$ and $2k_t^{EC}$, are of similar magnitude[2]

$$\mathrm{TOO\cdot + COO\cdot \xrightarrow{2k_t^{CT}} Non\text{-}radical\ products}$$

$$\mathrm{EOO\cdot + COO\cdot \xrightarrow{2k_t^{EC}} Non\text{-}radical\ products}$$

We have demonstrated (9) that the rate constant for the peroxy radical – hydroperoxide transfer reaction, k_{trans}^{CTOOH}

$$\mathrm{COO\cdot + TOOH \xrightarrow{k_{trans}^{CTOOH}} COOH + TOO\cdot}$$

may be calculated from measurements of the retardation of the oxidation of cumene by low

[2]For small amounts of added tetralin (or tetrahydrofuran) the co-oxidation rate expression (9) reduces to

$$-\frac{d[O_2]}{dt} = \frac{(k_p^{CC}[CH] + 2k_p^{CT}[TH])R_i^{1/2}}{\left(2k_t^{CC} + \frac{4k_t^{CT}k_p^{CT}[TH]}{k_p^{TC}[CH]}\right)^{1/2}}$$

so that if $k_p^{TC} \approx k_p^{EC}$ and $k_p^{CT} \approx k_p^{ET}$, then $2k_t^{CT} \approx 2k_t^{EC}$.

Can. J. Chem. Downloaded from www.nrcresearchpress.com by 210.87.254.6 on 09/05/12
For personal use only.

TABLE IV

Effect of some ether hydroperoxides on the oxidation of cumene

Hydroperoxide	Concentration $\times 10^4$ (M)	Rate $\times 10^6$* ($M\,s^{-1}$)	k_{trans} ($M^{-1}\,s^{-1}$)
None	—	3.87	—
Tetrahydrofuranyl	5.1	3.37	34
Tetrahydrofuranyl	7.7	2.52	44
Tetrahydrofuranyl	24.7	1.77	35
Tetrahydropyranyl	5.0	2.84	42.5
Tetrahydropyranyl	10	2.18	52
α-Ethoxyethyl	10	1.94	66

*$R_i = 1.38 \times 10^{-7}\,M\,s^{-1}$.

concentrations of tetralin hydroperoxide combined with the appropriate absolute rate constants for "uncrossed" and "crossed" propagation (k_p^{CC}, k_p^{TC}) and termination ($2k_t^{CC}$, $2k_t^{CT}$,$2k_t^{TT}$). Since the appropriate rate constants for tetrahydrofuran appear to be very similar to those for tetralin (see above) the weaker retarding effect of tetrahydrofuran hydroperoxide relative to tetralin hydroperoxide (Fig. 1) implies that $k_{trans}^{CEOOH} < k_{trans}^{CTOOH}$. This is not entirely unexpected since the hydroperoxidic hydrogen of the ether hydroperoxide is involved in a stronger intermolecular (and/or intramolecular) hydrogen bond and we have shown that intermolecular hydrogen bonds reduce k_{trans}^{CTOOH} (9). If it is assumed that the appropriate rate constants for tetrahydrofuran and tetralin are exactly equal then $k_{trans}^{CEOOH} = 38\,M^{-1}\,s^{-1}$, compared with $k_{trans}^{CTOOH} = 600\,M^{-1}\,s^{-1}$. The same assumptions for the rate constants for tetrahydropyran and for diethyl ether give transfer constants of 47 and 66 $M^{-1}\,s^{-1}$, respectively, for the attack of cumylperoxy radicals on their α-hydroperoxides.

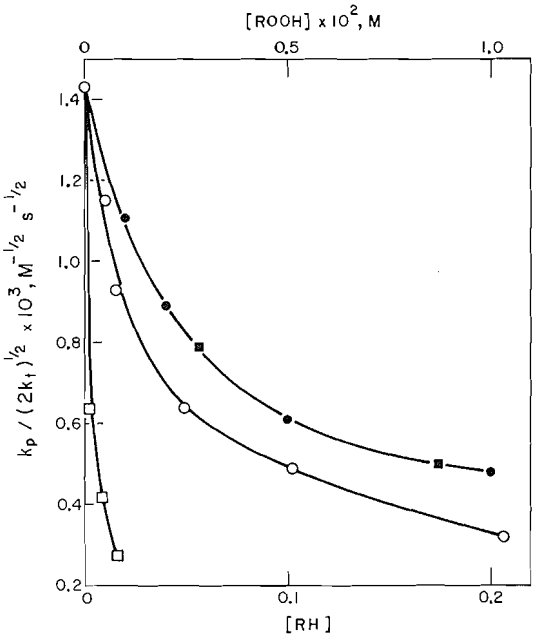

FIG. 1. Variation in the oxidizability of cumene with added tetrahydrofuran, ●; tetralin, ■; α-hydroperoxytetrahydrofuran, ⊙; and tetralin hydroperoxide, □. (N.B. The larger concentration scale refers to tetrahydrofuran and tetralin.)

The rate constants for the oxidation of 1,4-dioxan, tetrahydropyran, and phthalan are given in Table V. These three cyclic ethers give α-hydroperoxides as the primary reaction products in nearly 100% yields and the kinetics for their oxidation obey eq. [I]. The directly measured rate constants for the oxidation of tetrahydropyran are rather inaccurate because of the short chain length involved in the oxidation of this ether. The oxidations of tetrahydrofuran and of tetralin in the presence of α-hydroperoxytetrahydropyran give an average value of 2.1×10^7 $M^{-1}\,s^{-1}$ for the termination rate constant for α-tetrahydropyranylperoxy radicals. This value should be more accurate than the value obtained with neat tetrahydropyran because of the longer chain lengths of the oxidations (Tables II and III). The oxidation of 1,4-dioxan gives $2k_t = 5 \times 10^7$ $M^{-1}\,s^{-1}$ which is close to the values for tetrahydrofuranyl peroxy and tetrahydropyranyl peroxy radicals. The termination rate constant for phthalan ($1.2 \times 10^8\,M^{-1}\,s^{-1}$) is somewhat greater than for the three aliphatic cyclic ethers.

The propagation rate constants for the cyclic ethers increase in the order 1,4-dioxan ~ tetrahydropyran < tetrahydrofuran < phthalan.

TABLE V

The rate constants for the oxidation of 1,4-dioxan, tetrahydropyran, and phthalan

Ether	Concentration (M)	$R_i \times 10^7$ ($M\,s^{-1}$)	$R_s \times 10^7$ ($M\,s^{-1}$)	$k_p/(2k_t)^{1/2} \times 10^4$ ($M^{-1/2}\,s^{-1/2}$)	k_p ($M^{-1}s^{-1}$)	$2k_t \times 10^{-7}$ ($M^{-1}\,s^{-1}$)	Hydroperoxide yield (%)*
Tetrahydropyran	10.3	0.13	1.3	1.2	0.55†	—	98
	10.3	0.35	2.3	1.2	0.55†	~10	—
	10.3	0.86	3.4	1.2	0.55†	—	—
1,4-Dioxan	11.7	0.13	0.84	0.68	0.50	—	99
	11.7	0.86	2.4	0.70	0.50	—	—
	11.7	0.5	1.8	0.70	0.50	5.0	—
Phthalan	0.34‡	0.85	22	220	290	17	94
	0.34‡	0.86	21	220	240	12	—
	8.5	11	3900	430	480	12	—
	8.5	7.7	3160	420	393	9	—

*Based on the concentration of oxygen absorbed.
†These k_p values are based on $2k_t = 2.1 \times 10^7\,M^{-1}\,s^{-1}$, the average of the values measured in tetralin and tetrahydrofuran containing α-hydroperoxytetrahydropyran.
‡In chlorobenzene.

Since this difference is not due to any difference in the reactivity of the peroxy radicals, it must be due to differences in the reactivity of the ethers. Although the propagation rate constants for dioxan and tetrahydropyran are similar, dioxan has twice as many hydrogens α to oxygen. Dioxan has been reported to have a low reactivity towards the *t*-butoxy radical and it was shown that the hydrogens attached to a carbon which is β to oxygen are deactivated relative to the secondary hydrogens in a fully saturated hydrocarbon (15). The low reactivity of dioxan towards oxidation must result from the fact that although all the hydrogens are activated by an α-oxygen they are also deactivated by a β-oxygen.

Tetrahydrofuran is more reactive than tetrahydropyran towards the *t*-butoxy radical (15) and the phenyl radical (16), as well as towards peroxy radicals. The difference in reactivity towards the *t*-butoxy radical has been attributed to the greater availability of electrons (as judged by ether basicity) in the 5-membered ring (15), the rate being enhanced by electron donation because the *t*-butoxy radical is an electrophilic species. However, this explanation cannot apply to phenyl radicals because they are essentially nonpolar (16). It seems possible that the differences in reactivity result from the fact that steric repulsion between the α and β hydrogens will be released to a greater extent by abstraction of hydrogen from the 5-membered ring than from the less strained 6-membered ring.

The high reactivity of phthalan is not unexpected since the reactive C—H bond is weakened both by an α-phenyl group and by an α-alkoxy group.

Under our usual experimental conditions, the chain length for the oxidation of the tertiary aliphatic cyclic ether, 2,5-dimethyltetrahydrofuran, is quite high (~ 700). At low conversion the α-hydroperoxide is formed in approximately 100% yield. There appears to be little or no difference between the rates of oxidation of the racemic mixture and the meso form[3]. The rate constants for the oxidation of this ether are given in Table VI. It is apparent that its facile oxidation is due to the low value of the termination rate constant ($4.6 \times 10^4\,M^{-1}\,s^{-1}$). This rate constant is in the range normally observed for the peroxy radicals involved in the oxidation of tertiary hydrocarbons, i.e., 10^3–$10^5\,M^{-1}\,s^{-1}$ (17). The propagation rate constant per α hydrogen is about twice as high as for tetrahydrofuran. That is, the tertiary hydrogen is more readily abstracted than the secondary hydrogen. Although this is the order usually observed for the abstraction of secondary and tertiary hydrogens from similar molecules by free radicals, exceptions have been noted in hydrocarbon oxidations. For example, the propagation rate constant for the oxidation of cumene is lower than that for the oxidation of ethylbenzene (18).

The rates of oxidation of cumene and many other tertiary hydrocarbons are increased by the addition of their hydroperoxides because there

[3]The racemic mixture and the meso form are resolved by gas–liquid chromatography and appear to be consumed at the same rate.

Can. J. Chem. Downloaded from www.nrcresearchpress.com by 210.87.254.6 on 09/05/12
For personal use only.

TABLE VI

Rate constants for the oxidation of 2,5-dimethyltetrahydrofuran (8.3 M)

$R_i \times 10^8$ (M s^{-1})	$R_s \times 10^6$ (M s^{-1})	$k_p/(2k_t)^{1/2} \times 10^4$ ($M^{-1/2}$ s$^{-1/2}$)	$k_p/2k_t \times 10^{4}$*	k_p (M^{-1} s^{-1})	$2k_t \times 10^{-4}$ (M^{-1} s^{-1})
8.5	53	220	0.89	5.4	6.1
0.53	14	235	1.4	3.9	2.8
8.5	57	234	—	5.1	4.8
2.9	16	225	—	4.8	4.6
0.2†	7.8	210	—	—	—

*Determined by the photochemical pre- and after-effect method.
†Initiated with α,α'-azo-bis-isobutyronitrile.

TABLE VII

Oxidation of 2,5-dimethyltetrahydrofuran in the presence of 2-hydroperoxy-2,5-dimethyltetrahydrofuran and 2-hydroperoxy-2-methyltetrahydrofuran

Hydroperoxide	Concentration (M)	$R_i \times 10^7$ (M s^{-1})	$R_s \times 10^5$ (M s^{-1})	$k_p/(2k_t)^{1/2} \times 10^2$ ($M^{-1/2}$ s$^{-1/2}$)	$k_p/2k_t \times 10^{4}$*	k_p (M^{-1} s^{-1})	$2k_t \times 10^{-4}$ (M^{-1} s^{-1})
None		—	—	2.3	1.2	4.2	3.5
2,5-Dimethyltetrahydrofuranyl	0.3	2.3	2.0	0.53	0.45	0.6	1.4
2,5-Dimethyltetrahydrofuranyl	0.45	0.9	2.1	0.88	—	—	—
2,5-Dimethyltetrahydrofuranyl	0.6	4.0	1.8	0.37	1.1	0.13	0.12
2-Methyltetrahydrofuranyl	0.17	2.1	3.3	0.87	0.8	0.9	1.2
2-Methyltetrahydrofuranyl	0.34	1.7	2.6	0.8	1.2	0.53	0.44
2-Methyltetrahydrofuranyl	0.51	1.8	2.6	0.8	0.27	3.0	8.2

*Determined by the photochemical pre- and after-effect method.

is a decrease in the overall termination rate constant (19). This change in the rate constant results from the suppression of termination processes involving products of the β-scission of the *t*-alkoxy radicals formed in the self-reaction of the main chain carrying *t*-peroxy radicals (9, 20–22). We attempted to investigate this phenomenon for the oxidation of 2,5-dimethyltetrahydrofuran by studying the oxidation of the ether in the presence of its hydroperoxide and in the presence of 2-hydroperoxy-2-methyltetrahydrofuran. Both the hydroperoxides, however, *reduce* the rate of oxidation of the ether at a constant rate of initiation (Table VII). The absolute rate constants for these oxidations could not be measured very accurately because of the thermal instability of the ether hydroperoxides[4]. The measured propagation and termination rate constants are listed in Table VII merely to illustrate the impossibility of interpreting the decrease in $k_p/(2k_t)^{1/2}$ (which can be measured fairly accurately) in terms of a change in k_p or in $2k_t$. 2-Hydroperoxy-2,5-dimethyltetrahydrofuran (DOOH) inhibits the oxidation of cumene (Table VIII) in which it appears to be thermally stable. If it is assumed that the peroxy radical derived from this hydroperoxide has a reactivity similar to that of the cumylperoxy radical[5], then its termination rate constant is about 3×10^6 M^{-1} s^{-1}. Although DOOH is less stable in tetralin than in cumene, it was possible to obtain an approximate value of 3.6×10^6 M^{-1} s^{-1} for DOO· radicals in this hydrocarbon. In this connection, it is worth noting that our samples of DOOH and 2-hydroperoxy-2-methyltetrahydrofuran did not give a peroxy radical signal detect-

[4]For example, the ratio of the dark rate to the photochemical rate is 0.3 for the oxidation of 8.0 M 2,5-dimethyltetrahydrofuran containing 0.4 M 2-hydroperoxy-2,5-dimethyltetrahydrofuran.

[5]That is, assuming $k_p^{DC} = 0.18$ M^{-1} s^{-1}.

Can. J. Chem. Downloaded from www.nrcresearchpress.com by 210.87.254.6 on 09/05/12
For personal use only.

TABLE VIII

Rate constants for the oxidation of cumene and tetralin in the presence of 2-hydroperoxy-2,5-dimethyltetrahydrofuran

Hydrocarbon	Hydroperoxide (M)	$k_p/(2k_t)^{1/2} \times 10^4$ ($M^{-1/2}$ s$^{-1/2}$)	k_p (M^{-1} s^{-1})	$2k_t \times 10^{-6}$ (M^{-1} s^{-1})
Cumene	None	15	0.18	0.015
Cumene	0.15	0.94	—	—
Cumene	0.30	1.15	—	—
Tetralin	None	23	6.3	7.6
Tetralin*	0.25	14.6	2.8	3.6

*The ratio of the dark rate to the photo rate was 0.2 in this experiment.

TABLE IX

Collected rate constants for the oxidation of some cyclic ethers

Ether	$k_p/(2k_t)^{1/2} \times 10^3$ ($M^{-1/2}$ s$^{-1/2}$)	k_p (M^{-1} s^{-1})	$2k_t \times 10^{-7}$ (M^{-1} s^{-1})
1,4-Dioxan	0.069	0.50	5.0
Tetrahydropyran	0.12	0.55	2.1
Tetrahydrofuran	0.78	4.3	3.1
2,5-Dimethyltetrahydrofuran	22.5	4.8	0.0046
Phthalan	42.5	425	10.5

able by electron spin resonance spectroscopy under conditions where tertiary hydroperoxides from hydrocarbons (with $2k_t \approx 3 \times 10^4\ M^{-1}$ s^{-1}) give reasonably large peroxy radical signals (23, 24).

The results with 2-hydroperoxy-2-methyl-, and 2-hydroperoxy-2,5-dimethyl-tetrahydrofuran suggest that these two hydroperoxides may both contain impurities which give peroxy radicals (possibly secondary peroxy radicals) having high termination rate constants. Although such impurities were not detected they need not be present in high concentration, since small amounts of secondary hydroperoxides and secondary ethers or hydrocarbons drastically reduce the rate of oxidation of a tertiary substrate (see above and refs. 13 and 14).

The rate constants for the cyclic ethers oxidized in this work are summarized in Table IX.

1. A. M. CLOVER. J. Amer. Chem. Soc. **44**, 1107 (1922).
2. N. A. MILAS. J. Amer. Chem. Soc. **53**, 221 (1931).
3. A. RIECHE and R. MEISTER. Angew. Chem. **49**, 101 (1936).
4. A. ROBERTSON. Nature, **162**, 153 (1948).
5. P. GOSBORNE and I. SEREE DE ROCH. Bull. Soc. Chim. France, 2260 (1967).
6. G. A. RUSSELL. J. Amer. Chem. Soc. **77**, 4583 (1955).
7. J. A. HOWARD and K. U. INGOLD. Can. J. Chem. **45**, 793 (1967).
8. A. J. WEINHEIMER, S. W. KANTOR, and C. R. HAUSER. J. Org. Chem. **18**, 801 (1953).
9. J. A. HOWARD, W. J. SCHWALM, and K. U. INGOLD. Advan. Chem. Ser. **75**, 6 (1968).
10. N. A. MILAS, R. L. PEELER, and O. L. MAGELI. J. Amer. Chem. Soc. **76**, 2322 (1954).
11. L. BATEMAN and G. GEE. Trans. Faraday Soc. **47**, 155 (1951).
12. J. A. HOWARD, K. U. INGOLD, and M. SYMONDS. Can. J. Chem. **46**, 1017 (1968).
13. J. R. THOMAS and C. A. TOLMAN. J. Amer. Chem. Soc. **84**, 2079 (1962).
14. G. A. RUSSELL. J. Amer. Chem. Soc. **77**, 4583 (1955).
15. C. WALLING and M. J. MINTZ. J. Amer. Chem. Soc. **89**, 1515 (1967).
16. G. A. RUSSELL. Private communication.
17. J. A. HOWARD, K. ADAMIC, and K. U. INGOLD. Can. J. Chem. This issue (Part XIV).
18. J. A. HOWARD and K. U. INGOLD. Can. J. Chem. **45**, 793 (1967).
19. J. A. HOWARD and K. U. INGOLD. Can. J. Chem. **46**, 2655 (1968).
20. J. R. THOMAS. J. Amer. Chem. Soc. **89**, 4872 (1967).
21. T. G. TRAYLOR and C. A. RUSSELL. J. Amer. Chem. Soc. **87**, 3698 (1965).
22. D. G. HENDRY. J. Amer. Chem. Soc. **89**, 5433 (1967).
23. K. ADAMIC, J. A. HOWARD, and K. U. INGOLD. Chem. Commun. 505 (1969).
24. K. ADAMIC, J. A. HOWARD, and K. U. INGOLD. Can. J. Chem. This issue (Part XVI).

Can. J. Chem. Downloaded from www.nrcresearchpress.com by 210.87.254.6 on 09/05/12
For personal use only.

Isomer ratios of ^{90}Y and ^{91}Y in the fission of ^{235}U and ^{238}U by protons of energies 20–85 MeV[1]

A. H. KHAN[2], G. B. SAHA, AND L. YAFFE
Radiochemistry Laboratory, Department of Chemistry, McGill University, Montreal, Quebec
Received June 13, 1969

Isomer ratios of ^{90}Y and ^{91}Y formed in the fission of ^{235}U and ^{238}U induced by protons of energies 20–85 MeV have been determined. For both ^{90}Y and ^{91}Y the isomer ratios are always higher in ^{235}U fission than in ^{238}U fission. Isomer ratios of ^{90}Y in ^{238}U fission and those of ^{91}Y in ^{235}U and ^{238}U fission remain almost constant in the energy range of 20–85 MeV, whereas those of ^{90}Y in ^{235}U fission increase with increasing bombarding energy. A theoretical calculation of these ratios indicates that the primary fragments leading to the formation of these isomers possess 2–3 $\hbar$ units of angular momentum.

Canadian Journal of Chemistry, 47, 3817 (1969)

Can. J. Chem. Downloaded from www.nrcresearchpress.com by 210.87.254.40 on 09/05/12
For personal use only.

Introduction

Huizenga and Vandenbosch (1, 2) have developed a statistical model formalism for the calculation of isomer ratios in nuclear reactions. Several authors (3–5) have used this calculation as a basis for comparison with experimentally-determined isomer ratios in spallation reactions where the angular momentum of the initial nucleus was unique, and in general obtained good agreement.

The theoretical interpretation of isomeric yields in fission in terms of the formalism of Huizenga and Vandenbosch is much more complicated than in simple nuclear reactions, because the initial spin distributions of the primary fragments are not known. However, on the basis of an assumed spin distribution of the primary fragments, one can calculate the isomer ratios in fission. From a comparison between the calculated and the experimental values one can then estimate the average spin of the primary fragment.

Several studies (6–14) have been made of the isomer ratios in the heavy-mass region in fission of different targets at various energies. In many of these studies (6–8, 12, 13), calculations of isomer ratios have been made on the basis of an assumed functional form for the primary spin distribution, and various values for different parameters entering into the calculation. Saha and Yaffe (12) also included in the calculation the competition between fission and neutron emission in medium-energy fission. From all these studies it has been concluded that angular momentum is generated in the fission process and also that a fraction of the initial angular momentum appears as orbital angular momentum and the rest as the intrinsic spin of the primary fragments.

Very few isomer ratio data for the light-mass fission products are known compared to the heavy-mass products. Haller and Andersson (15) measured the isomer ratio of ^{80}Br in the fission of uranium by protons of energies 70–100 MeV and found an increase in the ratios with increasing energy. Hagebo (16) determined the isomer ratios of ^{95}Nb in the fission of lead, bismuth, thorium, and uranium of natural composition by 15–157 MeV protons. These results indicated that the isomer ratios for all targets increase with increasing energy and at a given energy, the isomer ratio is highest for lead targets and lowest for uranium targets. From a calculation based on the statistical model he obtained a very low value of 1–2 $\hbar$ for the primary fragment spin in low-energy fission of uranium.

Rudy *et al.* (17) have recently found that about 12 $\hbar$ of angular momentum are necessary for the primary fragment to explain the observed isomer ratio of ^{95}Nb in ^{235}U fission with 10-MeV protons. This is in contradiction to the value of 1–2 $\hbar$ reported by Hagebo (16), and the discrepancy has been attributed to possible experimental error in the measured ratio found by Hagebo.

No work on isomeric yield ratios of ^{90}Y and ^{91}Y in fission has been reported so far. It was considered interesting to determine these isomer ratios and correlate them with those in the heavy-mass region and also compare them with those

[1]This research received financial assistance from the National Research Council of Canada.
[2]Present Address: Chemistry Division, Atomic Energy Centre, P.O. Box 164, Ramna, Dacca, East Pakistan.

found for ^{95}Nb. We have measured the isomer ratios of ^{90}Y and ^{91}Y in the fission of ^{235}U and ^{238}U by protons of energies 20–85 MeV. A comparison of the ratios for the two targets has been made in an attempt to obtain information about the dependence of the isomer ratios on target spin. A calculation has been performed to estimate the average spin of the primary fragment which has been compared with those in the heavy-mass region.

Experimental

The details of the experimental procedures are given elsewhere (18). Only a brief outline is given below.

The two target materials were natural uranium (99.3% ^{238}U) and ^{235}U (94%). The thickness of target foils varied from 0.001 to 0.003 in. The intensity of the proton beam was monitored with the ^{65}Cu(p,pn)^{64}Cu reaction (19). All bombardments were performed in the internal circulating proton beam of the McGill synchrocyclotron. The duration of irradiation varied from 2 to 20 min.

After irradiation the target was dissolved and the chemical separation of yttrium was made as described (18). The activities of 3.2-h ^{90}Y^{m} (202-keV isomeric transition) and 50-min ^{91}Y^{m} (551-keV isomeric transition) were measured with a 3 × 3 in. NaI(Tl) crystal coupled to a 400-channel pulse-height spectrometer. The beta activities of 64-h ^{90}Y^{g} and 59-day ^{91}Y^{g} were measured by gas-flow end-window proportional counters. While ^{90}Y isomers could be considered shielded because of the long-lived precursor (28-yr ^{90}Sr), the activities of ^{91}Y^{m} and ^{91}Y^{g} had to be corrected for the growth from their precursor, 9.7-h ^{91}Sr (about 40% and 7%, respectively, for a typical irradiation time of 10 min and a separation time of 15 min).

The activities measured were corrected for the chemical yield, branching ratio, and counter efficiencies, and were used to calculate absolute cross sections of both isomers of ^{90}Y and ^{91}Y. The measured cross sections and the isomer ratios are given in Tables I and II. The errors in isomer ratios were estimated from the uncertainties in the activity measurements and the counter efficiencies.

Results and Discussion

From Table I it can be seen that in ^{235}U fission the cross sections of ^{90}Y^{m} increase rather sharply with increasing bombarding energy, compared to those of ^{90}Y^{m+g}, whereas the relative energy dependence of the excitation functions of ^{91}Y^{m} and ^{91}Y^{m+g} is almost the same. The excitation

TABLE I

Experimental cross sections (mb) of ^{90}Y and ^{91}Y isomers and their ratios in the fission of ^{235}U by protons of energies 20–85 MeV

Proton energy (MeV)	^{90}Y			^{91}Y		
	σ_m	$\sigma_m + \sigma_g$	$\sigma_m/(\sigma_m + \sigma_g)$	σ_m	$\sigma_m + \sigma_g$	$\sigma_m/(\sigma_m + \sigma_g)$
20	0.13±0.02	2.41±0.36	0.05±0.01	1.32±0.17	2.98±0.66	0.44±0.11
30	0.22±0.03	3.44±0.48	0.06±0.01	2.14±0.28	4.91±1.08	0.43±0.11
40	0.32±0.05	3.99±0.52	0.08±0.02	3.53±0.53	7.49±1.72	0.47±0.12
50	0.67±0.10	4.60±0.73	0.14±0.03	3.87±0.50	8.97±1.97	0.43±0.11
60	0.79±0.11	4.74±0.76	0.17±0.03	5.49±0.82	11.3 ±2.38	0.48±0.12
70	0.98±0.15	5.77±0.86	0.17±0.03	6.06±0.96	12.2 ±2.93	0.49±0.13
77	1.43±0.21	6.08±0.91	0.23±0.05	5.18±0.67	11.9 ±2.61	0.44±0.11
85	1.33±0.20	6.00±0.90	0.22±0.06	5.01±0.65	11.5 ±2.53	0.44±0.11

TABLE II

Experimental cross sections (mb) of ^{90}Y and ^{91}Y isomers and their ratios in the fission of ^{238}U by protons of energies 20–85 MeV

Proton energy (MeV)	^{90}Y			^{91}Y		
	σ_m	$\sigma_m + \sigma_g$	$\sigma_m/(\sigma_m + \sigma_g)$	σ_m	$\sigma_m + \sigma_g$	$\sigma_m/(\sigma_m + \sigma_g)$
20	0.12±0.02	2.91±0.41	0.04±0.01	0.97±0.13	4.48±0.98	0.22±0.06
30	0.15±0.02	3.03±0.48	0.05±0.01	1.60±0.25	5.56±1.33	0.29±0.08
40	0.19±0.03	3.53±0.53	0.05±0.01	1.80±0.25	5.37±1.23	0.33±0.09
50	0.22±0.03	3.88±0.62	0.06±0.01	1.95±0.29	6.19±1.30	0.32±0.08
60	0.22±0.03	3.47±0.59	0.06±0.01	2.00±0.26	6.41±1.41	0.31±0.08
70	0.28±0.04	4.07±0.57	0.07±0.01	1.80±0.23	6.75±1.49	0.27±0.07
77	0.33±0.05	4.40±0.66	0.08±0.02	1.80±0.23	7.56±1.66	0.24±0.06
85	0.37±0.05	4.36±0.70	0.08±0.02	2.00±0.26	7.71±1.70	0.26±0.07

Can. J. Chem. Downloaded from www.nrcresearchpress.com by 210.87.254.40 on 09/05/12
For personal use only.

functions of both $^{91}Y^{m}$ and $^{91}Y^{m+g}$ in ^{235}U fission show maxima at about 70 MeV. In the case of ^{238}U fission (Table II), the cross sections of $^{90}Y^{m}$ increase more rapidly than those of $^{90}Y^{m+g}$ with increasing bombarding energy. On the other hand, the cross sections of both $^{91}Y^{m}$ and $^{91}Y^{m+g}$ in ^{238}U fission vary with energy almost in similar fashion. The relative formation probabilities of both metastable and ground states and their energy dependence will be discussed in the following sections.

The experimental isomer ratios, $\sigma_m/(\sigma_m + \sigma_g)$, of ^{90}Y have been illustrated in Fig. 1 and those of ^{91}Y in Fig. 2 for both ^{238}U and ^{235}U targets in the energy range of 20–85 MeV. Figure 1 shows that for ^{90}Y isomers, the ratio $\sigma_m/(\sigma_m + \sigma_g)$ increases very slowly with increasing energy in ^{238}U fission, whereas it is highly energy dependent in the case of ^{235}U fission, for example, increasing from a value of 0.05 at 20 MeV to about 0.23 at 85 MeV. On the other hand, in the case of ^{91}Y isomers, as can be seen in Fig. 2, the ratios are almost constant within experimental error in both ^{235}U and ^{238}U fission, although they are higher in the latter

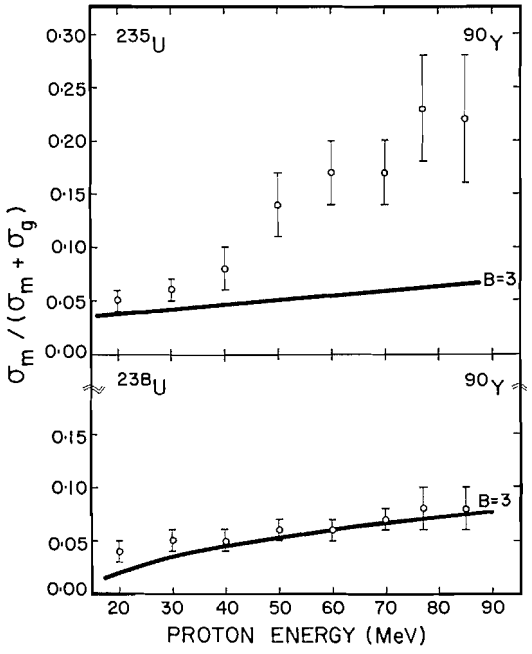

FIG. 1. Experimental and calculated isomer ratios of ^{90}Y in the fission of ^{235}U and ^{238}U: ○, experimental; —, calculated.

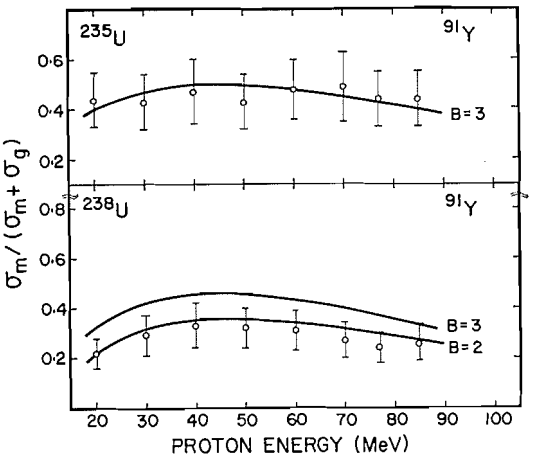

FIG. 2. Experimental and calculated isomer ratios of ^{91}Y in the fission of ^{235}U and ^{238}U: ○, experimental; —, calculated.

than in the former case. It can thus be seen that the observed isomer ratios are somewhat affected by the nature of the target and also the projectile energy. We shall discuss these effects briefly.

(a) Effect of Target

It has been observed by Forster and Yaffe (8) from their study of isomer ratios of ^{133}Xe in various fissioning systems that the spin and type of target do not appreciably affect the isomer ratios. At proton energies up to 115 MeV, Hagebo's (10) measured isomer ratios of ^{117}In were about the same for ^{232}Th ($I = 0$), ^{238}U ($I = 0$), and ^{209}Bi ($I = 9/2$). However, in another work (16) on ^{95}Nb, the isomer ratios were smaller in ^{238}U fission than in ^{232}Th, ^{209}Bi, and ^{208}Pb fission. On the other hand, isomer ratios of ^{134}Cs were almost the same in the fission of ^{233}U (6, 13), ^{235}U (13), ^{238}U (9), ^{232}Th (14), and ^{239}Pu (12), indicating no significant effect of the target on the ratios. From an examination of the calculated results Forster and Yaffe (8) concluded that many factors in the complex fission process overshadow the effect of small changes in target spin.

With all these diversified data it is difficult to correlate the ^{90}Y and ^{91}Y data with those observed in the heavy-mass region. For both ^{90}Y and ^{91}Y isotopes, isomer ratios are always higher in ^{235}U fission than in ^{238}U fission. This follows the same trend as observed by Hagebo (16) for ^{95}Nb isomers. Since fission is considered

Can. J. Chem. Downloaded from www.nrcresearchpress.com by 210.87.254.40 on 09/05/12
For personal use only.

Can. J. Chem. Downloaded from www.nrcresearchpress.com by 210.87.254.40 on 09/05/12
For personal use only.

to be a high angular momentum process, it is surprising to see how a difference of 3.5 units of spin between ^{235}U and ^{238}U can affect the formation of two isomeric states. This difference in isomer ratios might be a reflection of different fission mechanisms in two targets leading to these isomers.

(b) Effect of Projectile Energy

The isomer ratios for ^{90}Y and ^{91}Y, except those of ^{90}Y in ^{235}U fission, remain almost constant in the energy range of 20–85 MeV. While the isomer ratios of ^{134}Cs (9, 12–14) show very little energy dependence, those of ^{117}In (10) and ^{95}Nb (16) vary strongly with energy. On the other hand, the isomer ratios of ^{80}Br (15) were found to increase only slightly with energy.

At higher energies, several factors become important. As the projectile energy is increased, direct interactions become important, with the transfer of less energy and less angular momentum to the target. At higher projectile energies the orbital angular momentum of fragments may increase and consequently the primary fragments may share less spin. Also neutron and gamma cascades of high multiplicity, largely quadrupole radiations would remove a relatively large amount of angular momentum from fragments formed with very high spin. A combination of all these factors may lead to constant isomer ratios of ^{91}Y in both ^{235}U and ^{238}U fission and of ^{90}Y in ^{238}U fission at all energies. However, the energy dependence of ^{90}Y in ^{235}U fission cannot be readily understood from the above arguments. Several authors (6, 7) have, however, maintained that as the spin of the fissioning nucleus increases with increasing bombarding energy, most of it appears as the intrinsic spin of the primary fragments leaving only a little for orbital angular momentum. Thus the isomer ratio is expected to increase with energy until the initial spin of the fissioning nucleus becomes a limiting value due to direct interaction. However, this explanation for the energy dependence of the isomer ratios of ^{90}Y in ^{235}U fission is obviously at variance with the interpretations given above for the ratios of ^{90}Y and ^{91}Y in ^{238}U fission and for those of ^{91}Y in ^{235}U fission.

(c) Theoretical Estimation of the Average Spin of the Primary Fragments

The theoretical calculation of isomer ratios of ^{90}Y and ^{91}Y in ^{235}U and ^{238}U fission has been made according to the prescription of Saha and Yaffe (12). According to this prescription the formation probability of a product is weighted by the mass-yield, the fractional chain yield, and the fissionability of the fissioning nuclei, and also by the evaporation probability of different fragments yielding the product of interest. The details of the calculation have been given elsewhere (12, 13) and only pertinent points will be mentioned here.

Compound nucleus formation was assumed at energies up to 50 MeV and a direct interaction above this energy. The excitation energy of the compound nucleus was calculated from the energetics of the reaction, while at 60–85 MeV, the average excitation energy of the residual nucleus was taken from Metropolis *et al.* (20). A fission–evaporation competition was considered to follow the initial compound nucleus formation or direct interaction. After evaporation of each neutron the excitation energy, U', of the residual nucleus was calculated as $U' = U - B_n - 2T$ where U is the excitation energy of the preceding nucleus, B_n is the binding energy, and $2T$ is the kinetic energy of the emitted neutron. T is the nuclear temperature given by $U = aT^2 - 4T$ where a is the level-density parameter. We assumed the value of a to be 10.5 MeV^{-1} (21). The pairing energy was taken to be 1.1 MeV in order to correct for the odd–even nature of the residual nuclei. The neutron binding energy and the fission barrier were taken from the mass table of Myers and Swiatecki (22). The fission branching ratio, $G = \Gamma_f/(\Gamma_f + \Gamma_n)$, was calculated for each fissioning nucleus using the equations of Huizenga and Vandenbosch (21).

A number of complementary fragment pairs were selected corresponding to the light-mass region of $A = 90$–96 for each fissioning nucleus. The total energy of these fragments was then calculated from mass-excess values of Myers and Swiatecki (22). The average kinetic energy, taken from Milton and Fraser (23), was subtracted from the total energy released in a particular mode of fission, and the excitation energy was assumed to be shared by two complementary fragments in the ratio of their masses.

Neutron evaporation from each of the light-mass primary fragments was considered in the same way as discussed above in the case of the fissioning nuclei. Only those primary fragments which, after neutron evaporation, could lead to ^{90}Y and ^{91}Y were sorted. The evaporation

Can. J. Chem. Downloaded from www.nrcresearchpress.com by 210.87.254.40 on 09/05/12
For personal use only.

probability of these fragments was assumed to be unity. The fractional chain yields of these fragments were calculated on the basis of a Gaussian charge distribution and the mass-yields were assumed to be the same for all masses in this mass region for all fissioning nuclei.

The relative formation probabilities of two isomeric states were calculated from each of the selected fragments with the use of the computer code of Hafner, Huizenga, and Vandenbosch (24). The initial spin distributions of the primary fragments were taken as (6)

$$[1] \quad P(J) = (2J + 1) \exp [-J(J + 1)/B^2]$$

where $P(J)$ is the probability of a fragment having spin J and B is related to the root-mean-square of the spin.

The transmission coefficients for neutron emission from the fragments were calculated using Auerbach's (25) computer code. The number of gamma rays were calculated from the residual energy after neutron emission using the relationship of Vonach *et al.* (4). The isomer-deciding gamma ray was assumed to be emitted when the residual energy was 1 MeV or less. Only dipole radiations were considered.

The spin cut-off parameter σ is given as $\sigma^2 = It/\hbar^2$ (26) where I is the moment of inertia of the nucleus and t is the thermodynamic temperature. At high excitation energy the moment of inertia of a nucleus equals that of a rigid body. In general, neutron emission takes place in the high excitation energy region and gamma-ray emission in the low excitation energy region of the deexcitation process. Therefore, σ_n was calculated from $\sigma_n^2 = I_R t/\hbar^2$ and σ_γ as $\sigma_\gamma^2 = I_{eff} t/\hbar^2$. The values of I_{eff} were taken from Dudey and Sugihara (3).

The spins of $^{90}Y^m$ and $^{90}Y^g$ are 7+ and 2−, respectively, with an intermediate 3− excited state. The penultimate spin distributions of the residual nuclei were, therefore, divided at $J = 5$. Similarly for $^{91}Y^m$ ($\frac{9}{2}+$) and $^{91}Y^g$ ($\frac{1}{2}-$), the spin distribution was divided at $J = 5/2$.

Because of the relatively low values of the experimental isomer ratios, the calculation was performed for values of $B = 2$ and 3. The calculated values are illustrated by solid lines in Figs. 1 and 2. The open circles are the experimental values. It is seen that, except for ^{90}Y in ^{235}U fission, the experimental values are well reproduced with $B = 3$ for ^{90}Y in ^{238}U fission and ^{91}Y in ^{235}U fission, whereas $B = 2$ gives a better fit for ^{91}Y in ^{238}U fission. Obviously a larger value of B is required to account for the increasing isomer ratios of ^{90}Y in ^{235}U fission with increasing bombarding energy. However, for reasons given previously, we have not attempted further to calculate these isomer ratios.

In the study of isomer ratios of the heavy-mass products in photofission (6) and thermal fission (7), the spin of the primary fragment was found to be about 5–7 $\hbar$. At higher energies (20–85 MeV) Saha *et al.* (12, 13) obtained 12–16 $\hbar$ in the study of isomer ratios of ^{134}Cs in ^{239}Pu, ^{235}U, and ^{233}U fission.

Such a low B value of 2–3 $\hbar$ in the mass region of $A = 90$–94 obviously does not agree with the values obtained for heavy fragments and a great deal of ambiguity exists in the light-mass region. For example, as pointed out earlier, Hagebo (16) reported a very low value of 1–2 $\hbar$ for the spin of the primary fragment for ^{95}Nb isomers in 15-MeV proton fission of ^{238}U and Rudy *et al.* (17) obtained a value of 12 $\hbar$ for these isomers in the 10-MeV proton fission of ^{235}U. The latter authors attributed this discrepancy to the large uncertainty in the data of Hagebo (16).

The only systematic error in the present work might be in the decay schemes if they were not correct. Barring this we can conclude that a value of 2–3 $\hbar$ may well be characteristic for the spin of the light-mass primary fragments in ^{235}U and ^{238}U fission at medium energies. If one accepts the Strutinski hypothesis (27) that angular momentum is generated in the fissioning act, these data would indicate an unequal sharing of the angular momentum between the light and heavy fragments in fission.

Hoffman (28) calculated the average angular momentum of fragments on the basis of an electrostatic torque applied to uniformly charged spheroidal fragments at the moment of scission and obtained a value of 5–7 $\hbar$ per fragment in thermal fission. He further predicted that those fragments having relatively low kinetic energy and those close to nuclear shells (where fragment distortion is very small) will have little or no induced angular momentum. The yttrium fragments contributing to ^{90}Y and ^{91}Y should have neutron number $N = 51$–54. This may account in part for the low value of the primary fragment spin.

1. J. R. HUIZENGA and R. VANDENBOSCH. Phys. Rev. **120**, 1305 (1960).

2. R. VANDENBOSCH and J. R. HUIZENGA. Phys. Rev. **120**, 1313 (1960).
3. N. D. DUDEY and T. T. SUGIHARA. Phys. Rev. **139**, 896 (1965).
4. H. K. VONACH, R. VANDENBOSCH, and J. R. HUIZENGA. Nucl. Phys. **60**, 70 (1964).
5. R. VANDENBOSCH, L. HASKIN, and J. C. NORMAN. Phys. Rev. **137**, 1134 (1965).
6. H. WARHANEK and R. VANDENBOSCH. J. Inorg. Nucl. Chem. **26**, 669 (1964).
7. D. G. SARANTITES, G. E. GORDON, and C. D. CORYELL. Phys. Rev. **138**, B353 (1965).
8. J. H. FORSTER and L. YAFFE. Can. J. Chem. **46**, 1763 (1968).
9. J. H. DAVIES and L. YAFFE. Can. J. Chem. **41**, 1836 (1963).
10. E. HAGEBO. J. Inorg. Nucl. Chem. **27**, 927 (1965).
11. E. HAGEBO. J. Inorg. Nucl. Chem. **29**, 2515 (1967).
12. G. B. SAHA and L. YAFFE. J. Inorg. Nucl. Chem. **32**, 1891 (1969).
13. G. B. SAHA, I. TOMITA, and L. YAFFE. J. Inorg. Nucl. Chem. In press.
14. P. P. BENJAMIN, D. A. MARSDEN, N. T. PORILE, and L. YAFFE. Can. J. Chem. **47**, 301 (1969).
15. I. B. HALLER and G. ANDERSSON. J. Inorg. Nucl. Chem. **20**, 12 (1961).
16. E. HAGEBO. J. Inorg. Nucl. Chem. **25**, 1201 (1963).
17. C. RUDY, R. VANDENBOSCH, and C. T. RATCLIFFE. J. Inorg. Nucl. Chem. **30**, 365 (1968).
18. A. H. KHAN. Ph.D. Thesis, McGill University, Montreal, Quebec. 1968.
19. S. MEGHIR. Ph.D. Thesis, McGill University, Montreal, Quebec. 1962.
20. N. METROPOLIS, R. BIVINS, M. STORM, A. TURKEVICH, J. M. MILLER, and G. FRIEDLANDER. Phys. Rev. **110**, 185 (1958).
21. J. R. HUIZENGA and R. VANDENBOSCH. *In* Nuclear reactions. *Edited by* P. M. Endt and P. B. Smith. North Holland Publishing Co., Amsterdam. 1962. p. 42.
22. W. D. MYERS and W. J. SWIATECKI. U.S. At. Energy Comm. Rep. UCRL-11980 (1965). Unpublished.
23. J. C. D. MILTON and J. S. FRASER. Can. J. Phys. **40**, 1626 (1962).
24. W. L. HAFNER, JR., J. R. HUIZENGA, and R. VANDENBOSCH. U.S. At. Energy Comm. Rep. ANL-6662 (1962). Unpublished.
25. E. H. AUERBACH. U.S. At. Energy Comm. Rep. ABACUS-2, BNL-6562 (1960). Unpublished.
26. T. ERICSON. Advan. Phys. **9**, 425 (1960).
27. V. M. STRUTINSKI. J. Exp. Theor. Phys. **10**, 613 (1960).
28. M. M. HOFFMAN. Phys. Rev. **133**, B714 (1964).

Can. J. Chem. Downloaded from www.nrcresearchpress.com by 210.87.254.40 on 09/05/12
For personal use only.

Can. J. Chem. Downloaded from www.nrcresearchpress.com by 210.87.254.5 on 09/05/12
For personal use only.

Reactions of ruthenium(III) ammine complexes. I. Competing acid hydrolysis and redox reactions of pentaammineruthenium(III) ions

T. ELIADES, R. O. HARRIS, AND P. REINSALU
Chemistry Department, Scarborough College, University of Toronto, West Hill, Ontario

Received April 3, 1969

A study of acid hydrolysis of acidopentaammines of ruthenium(III) shows that aquation is not the only reaction taking place. For the halopentaammines, both in the presence and absence of light, reduction occurs with the formation of ruthenium(II) and free halogen. When azide, instead of halide ion, is coordinated to the metal, ruthenium(II) nitrogen complexes can be prepared. The solid state decomposition of $[Ru(trien)(N_3)_2]^+$ ion to $[Ru(trien)N_3N_2]^+$ is described.

Canadian Journal of Chemistry, 47, 3823 (1969)

Introduction

Studies in acid and base hydrolysis reactions for complexes of the type $[M(III)(NH_3)_5X]^{2+}$ are well established for the cobalt group metals but little corresponding work has been done in the iron group. Iron ammine complexes are unstable, losing ammonia in the solid, and the osmium(III) pentaammines have been well characterized only recently (1). For ruthenium, acid and base hydrolysis studies on the chloropentaammineruthenium(III) ion have been reported (2). A similar study on the bromopentaammine ion could not be carried out because of unexplained behavior in its electronic spectrum. The only reported ultraviolet (u.v.) – visible spectrum of the iodopentaammine ion (3) shows changes with time that are difficult to explain in terms of replacement of the iodide by solvent water or by sulfate ion, the spectrum being recorded in 2 *M* sulfuric acid. Finally, the azidopentaammine ion, either in solution or as a salt, has been reported (4) to give the ruthenium(II) complex ion, $[Ru(II)(NH_3)_5N_2]^{2+}$. In view of the diverse nature of their reactivity, it was decided to study these compounds further.

Experimental

Starting material for the preparation of the pentaammines was ruthenium trichloride obtained from Engelhard Industries, Inc., New Jersey. All other chemicals were reagent grade or better.

Hexaammineruthenium(III) Oxalate

The most convenient way into the pentaammine series is by refluxing a hexaammineruthenium(III) salt in hydrochloric acid to give the chloropentaammineruthenium(III) dichloride. The nitrate salt is the most easily prepared hexaammine from commercial ruthenium trichloride by the method of Lever (5) but it has the disadvantage that it often gives dark brown decomposition products when refluxed in acid. The chloride and sulfate salts can be made from the nitrate but since the nitrate is the most insoluble salt of the 3, the yields of the other 2 are always poor. It was found that the addition of a saturated solution of potassium oxalate to a slurry of the nitrate in water caused the solid to dissolve to give a light yellow solution from which precipitated almost immediately the white hexaammineruthenium(III) oxalate. This was filtered from the ice-cooled solution, washed with water, alcohol, and ether, and dried in air; yield 60–70%.

Chloropentaammineruthenium(III) Dichloride

This was prepared from the hexaammine oxalate by the method of Gleu and Rehm (6). Samples used for kinetics were recrystallized twice from dilute hydrochloric acid as orange–yellow crystals, which were washed with water and alcohol until the filtrate showed no trace of chloride ion. The salt was dried under vacuum at 100°; yield 95%.

Anal. Calcd. for $[Ru(NH_3)_5Cl]Cl_2$:total Cl, 36.4; ionized Cl, 24.2; H, 5.17; N, 23.9; Ru, 34.6. Found: total Cl, 36.8; ionized Cl, 24.8; H, 5.24; N, 24.5; Ru, 34.5.

Bromopentaammineruthenium(III) Dibromide

Similar preparations of the bromopentaammine from the hexaammine gave lower yields. The alternative method suggested by Gleu and Rehm (6) was found to give almost quantitative yields; yield 90%.

Anal. Calcd. for $[Ru(NH_3)_5Br]Br_2$: total Br, 56.3; ionized Br, 37.6; H, 3.55; N, 16.4; Ru, 23.7. Found: total Br, 56.1; ionized Br, 37.8; H, 3.53; N, 15.6; Ru, 24.0.

Iodopentaammineruthenium(III) Diiodide

The almost black crystals of the iodopentaammine were prepared in a similar manner to the bromopentaammine dibromide; yield 90%.

Anal. Calcd. for $[Ru(NH_3)_5I]I_2$: total I, 67.2; ionized I, 44.8; H, 2.67; N, 12.4; Ru, 18.1. Found: total I, 67.2; ionized I, 44.8; H, 2.95; N, 11.8; Ru, 17.8.

Aquopentaammineruthenium(III) 2-Naphthalenesulfonate Tetrahydrate

Chloropentaammine dichloride (1.0 g) was dissolved in dilute ammonia solution (10 ml) and the solution warmed for several min. The light red solution was ice-cooled and a saturated solution of 2-naphthalenesulfonic acid was added dropwise to pH 3.0. From the resulting light yellow

Can. J. Chem. Downloaded from www.nrcresearchpress.com by 210.87.254.5 on 09/05/12
For personal use only.

solution, colorless crystals of the aquopentaammine salt precipitated. These were recrystallized from dilute naphthalenesulfonic acid, washed with alcohol and ether, and dried in air; yield 40%.

Anal. Calcd. for $[Ru(NH_3)_5H_2O](C_{10}H_7SO_3)_3 \cdot 4H_2O$: C, 40.1; H, 5.13; N, 7.80; Ru, 11.2. Found: C, 40.7; H, 5.33; N, 8.34; Ru, 10.9.

The aquopentaammine salt is unstable in the solid state with respect to replacement of the complexed water by the outside ion unless this is very bulky. A number of other anions such as perchlorate and methanesulfonate were used as precipitating agents. The absorption spectra of freshly prepared solutions of these salts in 0.01 *M* methanesulfonic acid have an absorption band at 268 mμ with ε_{max} of 770 ± 15 which agrees with previously recorded values (7). Addition of dilute ammonium hydroxide to such solutions yielded the hydroxypentaammineruthenium(III) ion with an absorption band at 295 mμ and ε_{max} of 2.0 × 10^3.

cis-Diazidotriethylenetetramineruthenium(III) Iodide

cis-Dichlorotriethylenetetramineruthenium(III) chloride (0.5 g), prepared by the method of Broomhead and Kane-Maguire (8), was added to 10 ml water containing 1 g of sodium azide. The mixture was stirred at room temperature until all the complex ion had dissolved. At this time, the resulting deep red solution was ice-cooled. Addition of potassium iodide gave a precipitate of a deep red solid which was filtered off but not dried. The moist precipitate was transferred to 25 ml water containing Dowex 1X8–100 resin (chloride form). The precipitate dissolved after a few minutes stirring, when the solution was filtered. Addition of potassium iodide to the filtrate gave the desired deep red product. This was filtered off, washed with water and ethanol, and air dried (yield 0.15 g, 23%). The initial precipitate of iodide salt always contains free azide ion. Dried samples of this tended to explode whereas no such tendency was found in the purified iodide salt.

Anal. Calcd. for $[Ru(C_6H_{18}N_4)(N_3)_2]I$: C, 15.7; H, 3.93; N, 30.6; I, 27.8; Ru, 22.0. Found: C, 16.3; H, 3.99; N, 29.0; I, 27.1; Ru, 22.2.

Analyses for carbon, nitrogen, and hydrogen were by Bernhardt microanalytical laboratories, Max Planck Institute, West Germany. Ruthenium analyses were carried out by heating the complex in a stream of hydrogen and weighing the residue as ruthenium metal. Halide analyses were done potentiometrically.

Instruments used were a Perkin–Elmer 521 infrared spectrophotometer (Nujol mull between KBr plates), a Bausch and Lomb 505 spectrophotometer (1 cm fused silica cells). A Gouy balance supplied by Alpha Scientific Laboratories, Inc., was used for the magnetic susceptibilities.

Absorption spectra were obtained in the range 200 to 800 mμ for the ruthenium(III) complexes $[Ru(NH_3)_5Cl]^{2+}$, $[Ru(NH_3)_5Br]^{2+}$, $[Ru(NH_3)_5I]^{2+}$, $[Ru(NH_3)_5H_2O]^{3+}$ in dilute methanesulfonic acid and for $[Ru(NH_3)_5OH]^{2+}$ in dilute ammonia solutions. The position of absorption maxima and molar extinction coefficients are summarized in Table I. The data for the chloro- and bromo-pentaammineruthenium(III) salts agree with previously reported values (3). That for the iodopentaammineruthenium(III) ion does not agree with the value given by Hartmann and Buschbeck but this was indicated to be doubtful. The hydroxypentaammine ion was not isolated from solution but was formed by the addition of dilute ammonia to solutions of the aquopentaammine ion.

All the pentaammines are very sensitive to base, decomposition with loss of ammonia in sodium hydroxide being rapid. In ammonia, however, they react to form the hydroxypentaammine which is moderately stable even in hot concentrated ammonia. The spectra of the aquo- and hydroxy-ions are sufficiently different for relative amounts of each to be determined in solutions containing both. This was used as a method of finding the pK_a of the aquo-complex. A sample of the aquopentaammine salt was dissolved in a known amount of freshly boiled, doubly distilled water. Varying aliquots of standard methanesulfonic acid were added to known samples of the stock complex solution which were then made up to a fixed volume. The pH of the solutions and their spectra were then recorded (Fig. 1). The absorption curve for $[Ru(NH_3)_5OH]^{2+}$ ion was taken in moderately strong ammonia and it can be seen that this last spectrum does not go through the isosbestic point for the series at 265 mμ. Whether this is due to some slight decomposition or to ionic effects in solution is not known. At 313 mμ the molar extinction coefficient for $[Ru(NH_3)_5OH]^{2+}$ is 1.65 × 10^3 and for $[Ru(NH_3)_5H_2O]^{3+}$ it is 1.14 × 10^2. Since the aquopentaammine has an absorption at this

TABLE I

Position (λ mμ) and intensities (ε_{max}) of absorption bands in the electronic spectra of some ruthenium(III) pentaammines, in dilute methanesulfonic acid (10^{-2} *M*)

Absorbing ion	λ (mμ)	$\varepsilon_{max} \times 10^{-3}$	λ (mμ)	ε_{max}
$[Ru(NH_3)_5Cl]^{2+}$	328	2.00	262	200
$[Ru(NH_3)_5Br]^{2+}$	398	1.95	324	510
$[Ru(NH_3)_5I]^{2+}$	545	1.87	370	220
$[Ru(NH_3)_5H_2O]^{3+}$	268	0.77	328	130
$[Ru(NH_3)_5OH]^{2+}$*	295	2.10	†	†
$[Ru(NH_3)_5N_3]^{2+}$‡	463	—	—	—

*Measured in dilute ammonia solution.
†Not observed.
‡Reference 4.

Can. J. Chem. Downloaded from www.nrcresearchpress.com by 210.87.254.5 on 09/05/12
For personal use only.

wavelength, the ratio A/B in Fig. 1 does not measure directly the ratio $[HX]/[X^-]$, where $HX = [Ru(NH_3)_5H_2O]^{3+}$, $X^- = [Ru(NH_3)_5OH]^{2+}$, but a small correction can be applied knowing the molar extinction coefficient for the aquo ion. It follows from the equation

$$pH = pK_a + \log [HX]/[X^-]$$

neglecting any activity coefficients, that by plotting the ratio of the corrected A/B against the pH of the solution, pK_a can be found. The data are contained in Table II. A value of 3.7 ± 0.1 at 21° was calculated. Other methods using the pH of weighed samples of acid in water, and the values from the half equivalence point in potentiometric titrations against 2×10^{-3} N NaOH give, for several determinations, a result of 3.9 ± 0.1. These figures agree with the value of 4.2 for the pK_a at 25° quoted by Basolo and co-workers (2). It is noteworthy that ruthenium(III) aquopentaammine is a significantly stronger acid than the aquopentaammines of Co(III), Rh(III), and Cr(III).

Kinetic Studies

The acid hydrolysis reactions were carried out in approximately 10^{-2} M methanesulfonic acid solutions, sufficiently acid to suppress completely any loss of protons by the product. Concentrations of complex were of the order of 10^{-4} M. To measure the rate of hydrolysis, sealed 5 ml samples of the solution were removed at noted intervals from a constant temperature bath and the reaction "frozen" in ice. The optical density (o.d.) of the sample was then measured directly at room temperature. The spectra obtained from a typical series of readings for the hydrolysis of the chloropentaammine ion are shown in Fig. 2.

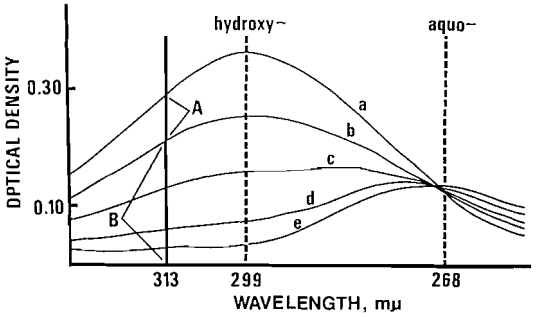

FIG. 1. Spectra of $[Ru(NH_3)_5H_2O]^{3+}$ at various pH. (*a*) 10.0, (*b*) 3.98, (*c*) 3.59, (*d*) 2.73, (*e*) 1.0.

TABLE II

Determination of pK_a at 25° for the reaction $[Ru(NH_3)_5H_2O]^{3+} \rightleftharpoons [Ru(NH_3)_5OH]^{2+} + H^+$

pH of solution	$\frac{[Ru(NH_3)_5H_2O]^{3+}}{[Ru(NH_3)_5OH]^{2+}}$	Ionic strength $\mu \times 10^3$	pK_a
3.98	0.44	0.9	3.64
3.59	1.42	1.1	3.74
2.73	7.33	2.9	3.60

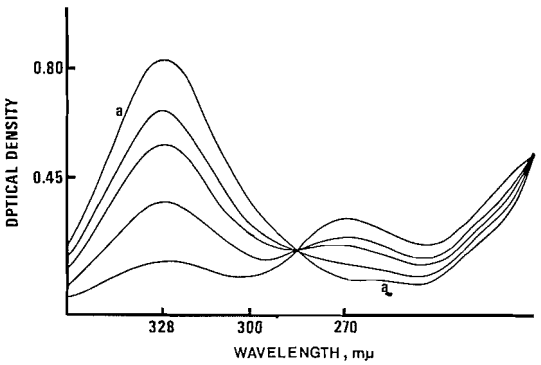

FIG. 2. Absorption spectra changes during aquation of $[Ru(NH_3)_5Cl]^{2+}$ in 7.0×10^{-2} M $MeSO_3H$ at 49.5°. Curve *a* is at $t = 0$. Successive curves are at 4.3, 8.0, 17.0, 52.0 h.

From preliminary runs, it was evident that the reaction

$$[Ru(NH_3)_5Cl]^{2+} + H_2O \rightarrow [Ru(NH_3)_5H_2O]^{3+} + Cl^-$$

does not go to completion but reaches a position of equilibrium, the presence of an isosbestic point at 286 mμ indicating a simple reaction. The position of equilibrium was at approximately 80% reaction for the chloropentaammine and 90% reaction for the corresponding bromopentaammine hydrolysis reactions. In such cases, approach to equilibrium can be considered to a first approximation as a reversible first order process

$$A \underset{k_{-1}}{\overset{k_1}{\rightleftharpoons}} B$$

By plotting $\log (o.d._o - o.d._e)/(o.d._t - o.d._e)$ against time, where $o.d._o$, $o.d._e$, and $o.d._t$ are optical densities at zero time, at equilibrium, and at time t (in s), respectively, k_1 can be determined. Good first order plots were obtained up to 3 half-lives of the reaction. All kinetic runs were carried out in triplicate.

Results

Kinetics

Data for acid hydrolysis of the chloropentaammine ion are listed in Table III. The results show the hydrolysis reaction to be independent of added anion and acid strength but that a slight decrease in rate constant is found with increasing ionic strength. Temperature dependence of the rate constants was plotted in the usual way. An enthalpy of activation of 22.2 kcal and an entropy of activation of -10 e.u. being calculated, in good agreement with the values of 22.6 kcal and -11 e.u. reported by Basolo and co-workers (2).

Acid hydrolysis of bromopentaammineruthenium(III) ion was followed under the same conditions. The spectra for the disappearance of

the bromopentaammine absorption band at 398 mμ with time are not as straightforward as those for the chloropentaammine ion. From Fig. 3 it can be seen that the main differences are that no isosbestic point is observed in the system although there is a region of cross-over in the spectra in the region of 310–280 mμ, and that the aquopentaammine maximum at 268 mμ does not increase regularly with time, corresponding to the disappearance of the bromopentaammine band but first increases, slightly decreases, and finally continually increases. Lastly, as the system approaches equilibrium, a new band with ε_{max} at 247 mμ appears.

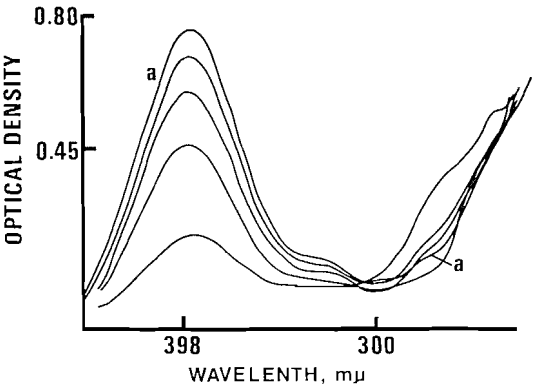

FIG. 3. Absorption spectra changes during reaction of $[Ru(NH_3)_5Br]^{2+}$ in 3.5×10^{-2} *M* $MeSO_3H$ at 49.5°. Curve *a* is at $t = 0$. Successive curves are at 1.75, 4.0, 8.0, 18.0 h.

The rate of disappearance of the bromopentaammine absorption band was studied as before, and the relevant rate constant data are shown in Table IV. Again the rate constant for the disappearance is independent of added anion and acid strength, but is slightly decreased with increasing ionic strength. However, the interpretation of these results is difficult since the lack of isosbestic point in the system indicates that other reactions are taking place. The starting material or the products, bromide ion and aquopentaammine ion, could be involved in these reactions. Solutions of bromide ion over a wide range of concentration in methanesulfonic acid show no spectral changes with time. Aquopentaammine ion can complex with methanesulfonic acid to give methanesulfonatopentaammine ion with an absorption band at 330 mμ and ε_{max} of approximately 2×10^3. Such a product would have been difficult to detect in the chloropentaammine system where the main absorption band of the chloropentaammine ion is at 328 mμ. However,

TABLE III

Observed first order rate constants for the hydrolysis of $[Ru(NH_3)_5Cl]Cl_2$ in methanesulfonic acid

Temperature, °C	$[MeSO_3H] \times 10^2$	Added anion	Ionic strength $\mu \times 10^2$	k_1, $s^{-1} \times 10^6$
49.5	2.63	—	2.8	15.7
49.5	3.48	Cl^-	4.0	15.4
49.5	2.78	Br^-	6.0	15.0
49.5	3.71	$MeSO_3^-$	11.8	14.9
49.5	13.9	—	14.2	14.5
37.3	2.63	—	2.8	3.55
29.2	2.63	—	2.8	1.35

TABLE IV

Observed first order rate constants for the hydrolysis of $[Ru(NH_3)_5Br]Br_2$ in methanesulfonic acid

Temperature, °C,	$[MeSO_3H] \times 10^2$	Added anion	Ionic strength $\mu \times 10^2$	k_1, $s^{-1} \times 10^6$
49.5	3.48	—	3.7	17.4
49.5	3.48	Cl^-	6.5	17.2
49.5	3.48	CNS^-	6.9	17.0
49.5	6.96	—	7.1	17.2
55.0	3.48	—	3.7	28.3
37.3	3.48	—	3.7	4.00
29.2	3.48	—	3.7	1.76
25.0	3.48	—	3.7	0.98

Can. J. Chem. Downloaded from www.nrcresearchpress.com by 210.87.254.5 on 09/05/12
For personal use only.

TABLE V

Observed first order rate constants for the hydrolysis of $[Ru(NH_3)_5Br]^{2+}$ in methanesulfonic acid (3.5×10^{-2} *M*) at 55.0°

Conditions	k_1, $s^{-1} \times 10^5$
—	2.83
5% Allyl alcohol present	2.86
Under nitrogen	2.82
In the dark	2.66
In the dark, under nitrogen, 5% allyl alcohol present	2.56

solutions of aquopentaammineruthenium(III) methanesulfonate in 10^{-2} *M* methanesulfonic acid show no detectable spectral changes with time. The starting material could react in solution with other than the solvent but it was found that the addition of possible nucleophiles (Table IV) produces, if anything, a decrease in the measured rate constant. If, however, bromopentaammine could react by an alternative first order process, this would maintain pseudo first order reactivity overall. Such a system would produce spectra with time that still contain an isosbestic point unless the products of this secondary reaction undergo further reaction.

A possible reaction route is photolytic decomposition. Preliminary kinetic runs using iodopentaammineruthenium(III) diiodide were found to contain large amounts of triiodide ion after a very short period of time, the intense absorption of this ion in the visible region making it difficult to obtain kinetic data from the spectra. A general reaction can be written[1]

$$[M(III)(NH_3)_5X]^{2+} + h\nu \rightarrow [M(II)(NH_3)_5]^{2+} + X\cdot$$

The free radical may react in several ways. With iodopentaamminecobalt(III) ion, iodine is produced (9)

$$[Co(NH_3)_5I]^{2+} \rightarrow Co(II) + 5NH_3 + I\cdot$$

In the corresponding reaction with bromopentaamminecobalt(III) ion, bromine has not been detected. This may be because bromine would oxidize the liberated ammonia. However, for ruthenium, Endicott and Taube have shown (7) that in $[Ru(II)(NH_3)_5H_2O]^{2+}$, the Ru(II)—$NH_3$ bonds remain intact in up to 10^{-2} *M* acidic solution for at least 1 h. It should therefore be possible to detect bromine if it were being formed by this type of reaction.

Kinetic runs with bromopentaammine dibromide were made therefore under various conditions. They were carried out in darkened sample tubes, under nitrogen and with small amounts of allyl alcohol present. Allyl alcohol reacts rapidly and irreversibly with bromine and itself has no absorption down to 200 mμ. Both bromine and tribromide ion have a strong absorption maximum at 264 mμ, very close to the relatively weak absorption maximum of the aquopentaammine ion at 268 mμ. Data from the various conditions are summarized in Table V. Figure 4 shows the spectra obtained with time in the acid hydrolysis reaction with added allyl alcohol, under nitrogen and carried out in darkened sample tubes. This series of spectra was chosen since it shows an initial isosbestic point at 323 mμ which eventually is lost as the new band at 247 mμ begins to appear.

Spectra of cis-[Ru(trien)$(N_3)_2$]I

(i) Electronic Spectra

The visible spectrum of $[Ru(trien)(N_3)_2]^+$ ion (trien = triethylenetetramine) in dilute acid

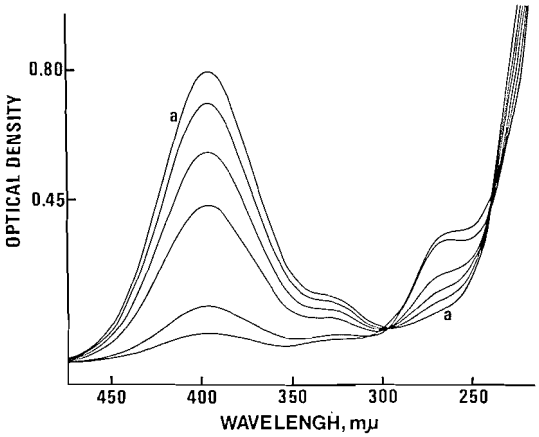

FIG. 4. Absorption spectra changes during reaction of $[Ru(NH_3)_5Br]^{2+}$ in 3.5×10^{-2} *M* $MeSO_3H$ containing 5% allyl alcohol at 49.5°, under nitrogen, in the absence of light. Curve *a* is at $t = 0$. Successive curves are at 1.5, 4.0, 7.5, 23.5, 55.0 h.

[1]The species $[M(II)(NH_3)_5]^{2+}$ would probably be $[M(II)(NH_3)_5H_2O]^{2+}$ in the systems studied.

Can. J. Chem. Downloaded from www.nrcresearchpress.com by 210.87.254.5 on 09/05/12
For personal use only.

Can. J. Chem. Downloaded from www.nrcresearchpress.com by 210.87.254.5 on 09/05/12
For personal use only.

shows two main bands at 485 mμ (ε_{max} 2.4 × 10^3) and 377 mμ (ε_{max} 2.0 × 10^3). Pentaammines, *cis*- and *trans*-tetraammines of ruthenium(III) can be distinguished by their visible spectra. In the pentaammines, one relatively intense absorption band is found (Table I). In the *cis*-tetraammines, this is split into two bands, of roughly the same intensity, one band at higher and the other at lower wavelength to the original pentaammine band (3). In the corresponding *trans*-isomer, only one band is found, roughly twice the intensity of the pentaammine band and at almost exactly the same wavelength (10). On this basis the diazido complex would be considered the *cis*-isomer.

(ii) Infrared Spectrum

Supporting evidence that this is the *cis*-isomer comes from its infrared (i.r.) spectrum. In the 2100–2000 cm^{-1} region, 2 bands are found, at 2046 and 2002 cm^{-1}, both assigned to asymmetric stretches of the coordinated azides. From Table VI, it can be seen that similar diazido complexes show 2 bands in this region if they are *cis*, whereas the more symmetrical *trans*-diazido complexes only show one.

Salts of $[Ru(trien)(N_3)_2]^+$ slowly decompose with time. The deep red compound changes to a grey–white powder, during which time the magnetic moment of 1.87 B.M. drops to zero. The complete change takes place over several weeks at room temperature but can be completed within 24 h if the salt is kept at 75°. The decomposition can be monitored by following changes in the i.r. spectrum. Figure 5 shows the changes with time of the two azido bands in the 2100–2000 cm^{-1} region. The disappearance of the lower azido band at 2002 cm^{-1} is accompanied by the appearance of a new band at 2096 cm^{-1}. It is assumed that the final product is [Ru(II)trien N_2N_3]I. Its slow rate of formation is in direct contrast to the similar rapid formation of $[Ru(II)(NH_3)_5N_2]^{2+}$ from $[Ru(III)(NH_3)_5N_3]^{2+}$ (4).

TABLE VI

Asymmetric stretching frequencies of coordinated azide ion in some trivalent metal complexes

Compound*	Stretching frequency cm^{-1}
trans-$[Co(en)_2(N_3)_2]ClO_4$	2020†
trans-$[Rh(en)_2(N_3)_2]Cl$	2026‡
cis-$[Co(en)_2(N_3)_2]ClO_4$	2075, 2028†
cis-$[Cr(trien)(N_3)_2]Br$	2090, 2055§
cis-$[Ru(trien)(N_3)_2]I$	2046, 2002

*en = ethylenediamine, trien = triethylenetetramine.
†Reference 15.
‡Reference 16.
§Reference 17.

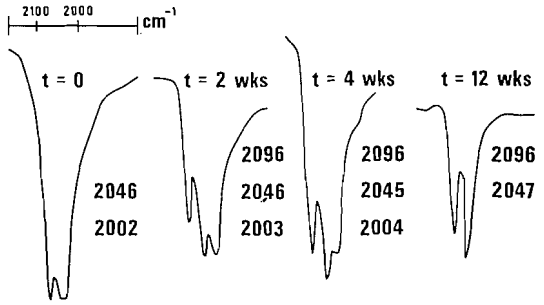

FIG. 5. Infrared spectral changes with time in a solid sample of $[Ru(trien)(N_3)_2]^+$ at room temperature.

Discussion

Kinetics

The only reaction found for the chloropentaammine ion in dilute acid is hydrolysis. However, reaction of the bromopentaammine is complicated by the appearance of redox reactions. From the spectra and rate data obtained, the overall reactions appear best represented by the following scheme

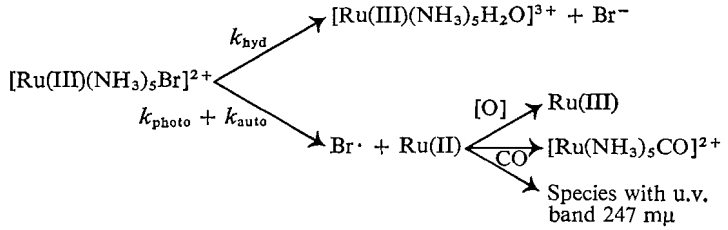

where k_{hyd} is the first order rate constant for the hydrolysis reaction, k_{photo} is the first order rate constant for the light-induced redox reaction, and k_{auto} is the first order rate constant for the self induced redox reaction. The overall observed rate constant for the disappearance of the bromo-

Can. J. Chem. Downloaded from www.nrcresearchpress.com by 210.87.254.5 on 09/05/12
For personal use only.

pentaammine ion is then first order. Both products of the redox reaction react further. Unless precautions are taken to immediately remove these redox products, no isosbestic point will appear in the spectrum as it changes with time. The ruthenium(II) probably reacts immediately with the solvent to give $[Ru(II)(NH_3)_5H_2O]^{2+}$ but this is also reactive. It is, for example, fairly easily air-oxidized. Its presence was confirmed by carrying out a reaction with carbon monoxide bubbling through the solution. Precipitation of the final products with potassium bromide gave a solid whose i.r. spectrum contained a band at 1940 cm^{-1}, indicative of $[Ru(NH_3)_5CO]Br_2$ (11). An identical reaction for $[Ru(III)(NH_3)_5Cl]^{2+}$ with carbon monoxide bubbling through the solution gave only the hydrolysis reaction, showing that the carbon monoxide itself was not reducing the ruthenium(III).

Although several kinetic runs were carried out under nitrogen, which also can attack $[Ru(II)(NH_3)_5H_2O]^{2+}$ (12), no evidence was obtained for the formation of $[Ru(NH_3)_5N_2]^{2+}$. This may be merely an indication of the relative rates of attack of these 2 species on the ruthenium(II) complex. The following observations are relevant to the above scheme.

(*i*) Addition of allyl alcohol to the reaction removes any bromine formed. There is therefore no interference with the absorption of 268 mμ for the hydrolysis product, $[Ru(NH_3)_5H_2O]^{3+}$. This band is found to increase uniformly with time in the presence of allyl alcohol. No isosbestic point is observed although deviation from it is small. Interference is believed to come from reoxidation of Ru(II) since reactions under nitrogen show an isosbestic point (see (*iii*)).

(*ii*) If the reaction is carried out in the dark, the observed rate constant for the disappearance of bromopentaammine ion falls to 2.66×10^{-5} s^{-1} from 2.86×10^{-5} s^{-1} at 55° (Table V), since k_{photo} has been eliminated. However, bromine is still produced in solution.

(*iii*) If the reaction is carried out under nitrogen to eliminate air-oxidation of Ru(II), in the dark to eliminate photoreduction, and in the presence of allyl alcohol to remove the interference of bromine, an isosbestic point is obtained in solution (Fig. 4). The rate constant, 2.56×10^{-5} s^{-1} at 55°, is the sum ($k_{hyd} + k_{auto}$).

(*iv*) The band at 247 mμ appears in all spectra, even in the one where carbon monoxide was bubbled through the solution. The band appeared after the reaction had proceeded for some time and continued to increase after the hydrolysis reaction had come to effective equilibrium. The exact nature of the species is not known but it is thought to be some polymeric ruthenium(II) species formed slowly from the ruthenium(II) produced in the redox reaction.

(*v*) Trace amounts of ruthenium(II) have been reported (12) to catalyze reactions of ruthenium(III). To show that the ruthenium(II) produced had no effect upon the rate of hydrolysis of ruthenium(III) bromopentaammine ion, kinetic runs containing up to 10% ruthenium(II) hexaammine dichloride relative to the ruthenium(III) present were carried out. No appreciable effect upon the rate of reaction was noted[2].

From the results summarized in Table V, it is evident that the redox reactions only occur to a small extent. The photoinduced reaction at 55° is only about 7% of the total reaction. Comparison of spectra, under various conditions, shows that the amount of bromine produced in the autoredox reaction at 55° is somewhat smaller. We therefore estimate that the true hydrolysis rate constant is approximately 10–15% lower than that observed in runs carried out without any precautions.

Spectra

The strong band ($\varepsilon_{max} \sim 2000$) in the visible spectra of the ruthenium halopentaammines has been assigned by Jorgenson (13) to a transfer of a π-electron on the halogen to the unfilled d^5 subshell on the metal. The position of the band should be related to the ease of removal of an electron from the halogen, and the data in Table I support this. The order of ease of removal would be $I^- > Br^- > Cl^-$ and the order found for the wavelength at the band maximum in the halopentaammines is $-I > -Br > -Cl$. From the rate data, decomposition of the intermediate formed, $[Ru(II)(NH_3)_5 \ldots X]^{2+}$ occurs most readily if X is iodine, and least if chlorine. The same type of intermediate is expected to occur with azidopentaammine except that there is now possibility of decomposition within the free radical formed to give a nitrogen molecule in situ before the metal–ligand bond has time to break. Decomposition of $[Ru(III)(NH_3)_5N_3]^{2+}$ in solution does give $[Ru(II)(NH_3)_5N_2]^+$ (4) but the

[2]We would like to thank the referees for this suggestion.

reaction is too fast to follow conveniently. Solid state decomposition at room temperature is slow, but within the beam of the i.r. spectrophotometer it is again too fast to follow conveniently. The corresponding reactions of $[Ru(III)(trien)(N_3)_2]^+$ were found to be slower. From reactions carried out in solution, a ruthenium(II) nitrogen complex could be isolated but analyses for total nitrogen were always low. It is known (11) that the corresponding carbonyl series, $[Ru(II)(NH_3)_4CO\ X]^+$, where X is Cl or Br, is difficult to prepare in aqueous solution, because of the rapid hydrolysis to give $[Ru(II)(NH_3)_4CO\ H_2O]^{2+}$. The evidence suggests that similar behavior can be expected in the $[Ru(II)(NH_3)_4N_2\ X]^+$ series, so that the low analyses for nitrogen are due to hydrolysis of the coordinated azide from $[Ru(II)(NH_3)_4N_2\ N_3]^+$. The experiments were therefore carried out on solid samples to show that only one azide was decomposing.

It is difficult to say exactly why this azide decomposition in $[Ru(III)trien(N_3)_2]^+$ is slower than in $[Ru(III)(NH_3)_5N_3]^{3+}$. From the position of the absorption band, it would seem that the energy required to produce the intermediate is roughly the same. However, small changes in the σ- and π-donation by other ligands to the metal may have a significant role in deciding whether the intermediate once formed will return to its original state, or undergo ligand rearrangement to give a nitrogen-containing complex. Recently, Basolo and co-workers (14) have prepared the similar *cis*-azidonitrogenbisethylenediamineruthenium(III) hexafluorophosphate salt by solid state decomposition of the diazido compound. The rate of decomposition appears to be intermediate between that of the ammonia and triethylenetetramine complexes.

Acknowledgment

Grateful acknowledgment is made to the National Research Council of Canada for support of this research.

1. A. D. ALLEN and J. R. STEVENS. Chem. Commun. 1147 (1967).
2. J. A. BROOMHEAD, F. BASOLO, and R. G. PEARSON. Inorg. Chem. **3**, 826 (1964).
3. H. HARTMANN and C. BUSCHBECK. Z. Phys. Chem. **11**, 192 (1957).
4. A. D. ALLEN, F. BOTTOMLEY, R. O. HARRIS, V. P. REINSALU, and C. V. SENOFF. J. Amer. Chem. Soc. **89**, 5595 (1967).
5. F. M. LEVER. Ph.D. Thesis, London University, London, England. 1955.
6. K. GLEU and K. REHM. Z. Anorg. Allg. Chem. **227**, 237 (1936).
7. J. ENDICOTT and H. TAUBE. J. Amer. Chem. Soc. **84**, 4984 (1962).
8. J. A. BROOMHEAD and L. A. P. KANE-MAGUIRE. J. Chem. Soc. A, 546 (1967).
9. A. HAIM and H. TAUBE. J. Amer. Chem. Soc. **85**, 495 (1963).
10. This laboratory. Unpublished results.
11. A. D. ALLEN, T. I. ELIADES, R. O. HARRIS, and P. REINSALU. Can. J. Chem. **47**, 1605 (1969).
12. I. J. ITZKOVITCH and J. A. PAGE. Can. J. Chem. **46**, 2743 (1968).
13. C. K. JORGENSEN. Orbitals in atoms and molecules. Academic Press, Inc., New York. 1962. p. 109.
14. L. A. P. KANE-MAGUIRE, P. S. SHERIDAN, F. BASOLO, and R. G. PEARSON. J. Amer. Chem. Soc. **90**, 5295 (1968).
15. P. J. STAPLES and M. L. TOBE. J. Chem. Soc. **4**, 4812 (1960).
16. S. A. JOHNSON and F. BASOLO. Inorg. Chem. **14**, 925 (1962).
17. D. A. HOUSE and C. S. GARNET. J. Amer. Chem. Soc. **88**, 2156 (1966).

Can. J. Chem. Downloaded from www.nrcresearchpress.com by 210.87.254.5 on 09/05/12
For personal use only.

Infrared spectroscopic investigations of zeolites and adsorbed molecules. Part V. Carbon dioxide

C. L. ANGELL AND M. V. HOWELL
Union Carbide Research Institute, P.O. Box 278, Tarrytown, N.Y. 10591

Received May 7, 1969

When bivalent cation-exchanged, but not univalent or decationized, Type X or Y zeolites are heated at 500° in the presence of carbon dioxide, two or three bands appear in the 1600 to 1300 cm^{-1} region of the infrared spectrum. These bands are stable even at 700°, and their frequencies are cation-dependent. They are assigned to a unidentate surface carbonate species, which (in the case of CaY) blocks about 20% of the surface cations.

Canadian Journal of Chemistry, 47, 3831 (1969)

Can. J. Chem. Downloaded from www.nrcresearchpress.com by 210.87.254.6 on 09/05/12
For personal use only.

Introduction

The adsorption of carbon dioxide on a number of metal oxides, e.g., beryllium oxide (1), nickel oxide (2), alumina (3), zinc oxide (4), and magnesium oxide (5), has been investigated by means of infrared spectroscopy. In all these cases the formation of carbonate-like species was indicated. Evans and Whateley (5) investigated the spectra of carbon dioxide adsorbed on magnesium oxide in the range of 4000 to 750 cm^{-1} and identified both uni- and bidentate forms of surface carbonate species. The behavior of carbon dioxide adsorbed on zeolites has been investigated by Habgood and co-workers (6, 7). They observed physical adsorption of carbon dioxide on the X zeolites containing bivalent cations and showed that the asymmetric stretching band near 2350 cm^{-1} depended on the cation. Angell (8) extended this to the Y zeolites containing alkaline-earth cations and showed that the shift of the asymmetric stretching band can be correlated with the electrostatic field strength due to the cation. Habgood and co-workers (6, 7) found additional bands in the region 1750 to 1250 cm^{-1} on monovalent cation-containing X zeolites. These were ascribed to carbon dioxide chemisorbed on surface oxygen to give a bent carbonate-like structure. However, no similar species were observed when the alkaline-earth ion exchanged X zeolites were exposed to carbon dioxide at room temperature. Ward and Habgood (7) interpreted this as indicating that the surface bivalent cations are located in Sites S_{II} only, while the surface monovalent cations also occupy the more exposed Sites S_{III}, where it is likely that the reaction of carbon dioxide would result in carbonate-like species.

In the present work we are reporting the strong interaction of carbon dioxide with bivalent cation-containing X and Y zeolites[1] on exposure to carbon dioxide at high temperatures ($\sim$ 500°). The role of the cation in promoting the interaction of the carbon dioxide with the zeolite surface is discussed.

Experimental

The compositions of the zeolite samples used in this work have been given previously (Part I, Table I (9)). The short path length infrared cells, the preparation of the pellets, and the activation techniques have also been described in Part I (9). In air-activation, the pellets were placed at the bottom of the cell, which was left open at the top. The samples were then heated slowly to 500° and kept at this temperature for 2 h. (No special effort was made to improve the air circulation around the pellets.) At the end the cell was evacuated at 500° and cooled in vacuum. Activations at 700° were carried out in cells with bottoms made of quartz. The infrared spectra were obtained on the following spectrophotometers: a Perkin–Elmer Model 21 prism spectrometer, a Beckman Model IR 10 grating spectrometer, and a Perkin–Elmer Model 225 grating spectrometer. The carbon dioxide and the carbon monoxide were obtained from Matheson Company. Carbon dioxide impurity in the carbon monoxide was removed by cooling the cylinder to liquid nitrogen temperature. Quantitative carbon monoxide adsorption data were obtained on a Cahn vacuum microbalance. The technique of simultaneous measurement of infrared spectra and gas adsorption has been described previously (10). The infrared spectrometer used in the experiments with the microbalance was a Perkin–Elmer Model 112 single beam, double pass spectrometer converted to grating operation.

Results

When bivalent cation-exchanged Y zeolites

[1]Throughout this article the Type X and Type Y zeolites are designated NaX and NaY, respectively; see U.S. Patents No. 2 882 244 and 3 130 007. Forms in which sodium has been exchanged with other cations are designated as CaY, etc. The term "decationized Y" will mean NH_4Y which was heat treated to decompose the NH_4 ions; see U.S. Patent No. 3 130 006.

Can. J. Chem. Downloaded from www.nrcresearchpress.com by 210.87.254.6 on 09/05/12
For personal use only.

were activated at 500° in ordinary laboratory air, two or three bands appeared in the 1600 to 1300 cm^{-1} region. These bands did not occur when the same samples were activated at 500° in vacuum. Once these bands have appeared in the spectrum, activation in a vacuum at 500° does not remove them. To establish the cause of these bands, various bivalent cation-exchanged Y zeolites were activated in an atmosphere of pure oxygen or pure nitrogen. In neither case was the formation of these bands observed. However, when samples of the same zeolites, activated under vacuum at 500°, were heated at 500° with 10 Torr carbon dioxide, the same bands appeared that were observed after air activation. In this way the origin of the bands was definitely tied to the presence of carbon dioxide during the heating process. For most of our subsequent experiments these bands were generated by activation in air at 500 °C, since the small amount of carbon dioxide in ordinary air was apparently sufficient to create bands the same size as those obtained from samples heated in an atmosphere of carbon dioxide. Although the possibility of interaction between carbon dioxide and oxygen could not be excluded, the spectra showed no evidence that such did occur. In contrast to the bands observed by Bertsch and Habgood (6) on monovalent cation-containing X zeolites, which appeared at room temperature, our spectra only showed bands due to physically adsorbed carbon dioxide. However, the other bands did appear on heating at 500°. Experiments on CoY, MnY, and MgY exposed to carbon dioxide at 500° indicated that these bands did not diminish at all on heating in vacuum at 700° for a prolonged period.

All the bivalent cation-exchanged zeolites studied gave these bands, except the sample of NiY. Among the monovalent cation-exchanged zeolites, NaY and AgY did not produce any bands in this range when heated with carbon dioxide at 500°. NaX at room temperature showed the same bands as observed by Habgood and Bertsch (6), and after heating at 500° and then cooling, these bands were still present. However, evacuation at 500° immediately removed these bands, indicating a much weaker chemisorption of carbon dioxide. A sample of 90% exchanged ammonium Y which was activated at 500° in vacuum did not produce any bands in the 1600 to 1300 cm^{-1} region when exposed to carbon dioxide at 500°.

The frequencies of the bands observed with bivalent cation-exchanged zeolites are given in Table I. Figure 1 shows the appearance of these bands on air-activated CaY, ZnY, MgY, and CoY.

The interaction of various adsorbed molecules with these carbonate-type bands was studied on CoY zeolite. When water was adsorbed on a CoY sample containing these bands, both the 1575 and the 1380 bands were removed completely. A band appeared at 1620 cm^{-1} and the band at 1450 cm^{-1} became much larger (see Fig. 2). Removal of the water by evacuation at 300° completely restored the original bands. Adsorption of heavy water did not produce the 1620 cm^{-1} band, but did result in the complete removal of the 1575 and 1380 cm^{-1} bands. Evacuation at 300° and removal of the heavy water again resulted in the reappearance of the bands in their original positions. Similar results were obtained on adsorption of ammonia; the 1575 and 1380 cm^{-1} bands were completely removed and a strong band appeared at about 1450 cm^{-1}. On removal of the ammonia at 300° the original bands were restored. Adsorption of benzene on a ZnY sample, air-activated at 500°, did not change the two

TABLE I

Bands on various zeolites caused by high temperature exposure to carbon dioxide

Cation	Bands, cm^{-1}							
	Zeolite Y				Zeolite X			
Mg^{2+}	1589	—	1414	—	1585	—	1400	—
Ca^{2+}	—	1493	1435	—	—	—	—	—
Ba^{2+}	—	1465	1430	—	—	—	—	—
Mn^{2+}	1560	1460	—	1387	—	—	—	—
Co^{2+}	1575	1460	—	1389	1545	1455	—	1385
Zn^{2+}	1575	1480	—	1389	1530	—	—	1375

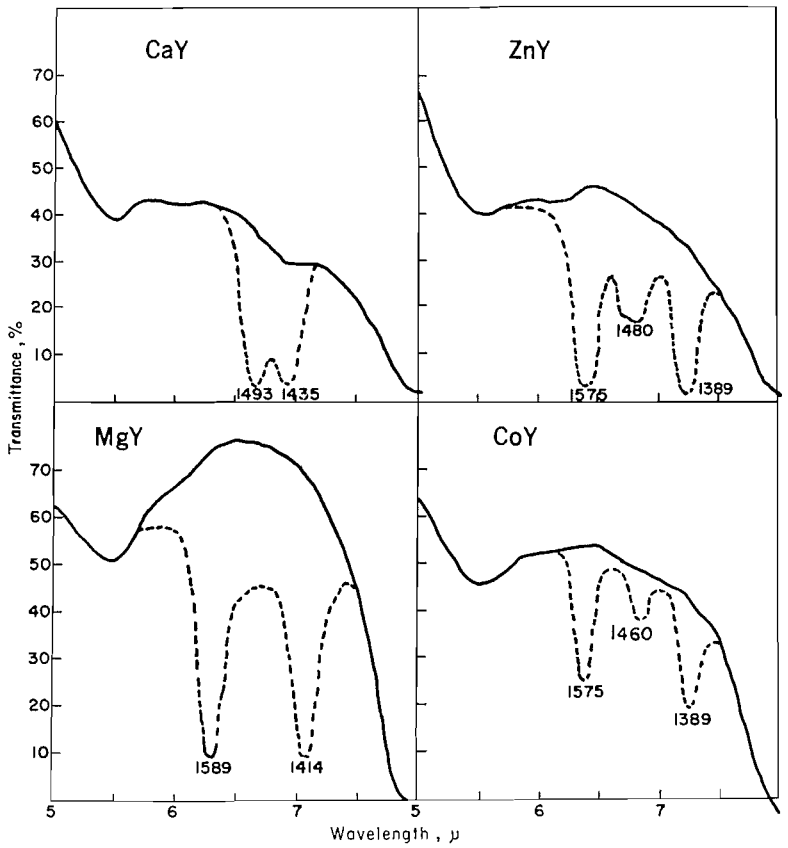

FIG. 1. Bands formed by the high-temperature interaction of carbon dioxide with various zeolites; —, vacuum-activated at 500°; - - -, air-activated at 500°.

outer bands of the carbonate complex, although a very strong band appeared at 1480 cm^{-1}. This band is one of the fundamentals of benzene.

For the quantitative measurement of the number of bivalent cations available on the surface, a calcium Y sample was vacuum-activated in the Cahn microbalance system at 500°. The spectrum of the sample did not show any carbonate-type bands. After this, a carbon dioxide isotherm was measured at room temperature up to about 400 Torr carbon dioxide pressure. The infrared spectrum showed no carbonate-type bands even under the highest pressure of carbon dioxide. The sample was then heated at 500° in 400 Torr carbon dioxide for 4 h. After cooling, the infrared spectrum showed the two characteristic carbonate type bands at 1493 and 1435 cm^{-1}. The sample was then heated in vacuum at 500° till constant weight was reached. The weight increase corresponded to 1.62 cc of carbon dioxide per gram of zeolite. After this, the simultaneous measurements of the gas adsorption isotherm of carbon monoxide and the optical density isotherm for the cation-specific carbon monoxide band were carried out as described previously (10). Comparing these data with the data obtained from the adsorption of carbon monoxide on a sample[2] of the same CaY vacuum activated at 500°, the constants in Table II were obtained by calculations described previously (11).

It can be seen that there has been very little change in the Langmuir combining constant (k_1) or the slope of the linear part of the adsorption curve (C), but the number of adsorption sites has decreased. The high temperature carbon dioxide

[2]Note that this CaY is that given in ref. 9: 77% exchanged, not the 84% exchanged CaY mentioned in ref. 11.

Can. J. Chem. Downloaded from www.nrcresearchpress.com by 210.87.254.6 on 09/05/12
For personal use only.

TABLE II

Adsorption of carbon monoxide on CaY zeolite*

Sample treatment	k_1	C	n_0 cc/g	n_0'	Sites/unit cell
Vacuum-activated	0.285	0.0166	9.35	0.242	5.31
Heated in CO_2	0.280	0.0145	7.23	0.188	4.11

*The effective adsorption is expressed in number of carbon monoxide molecules per gram zeolite, n_0, or as the proportion of total cations reacted with the carbon monoxide, n_0'.

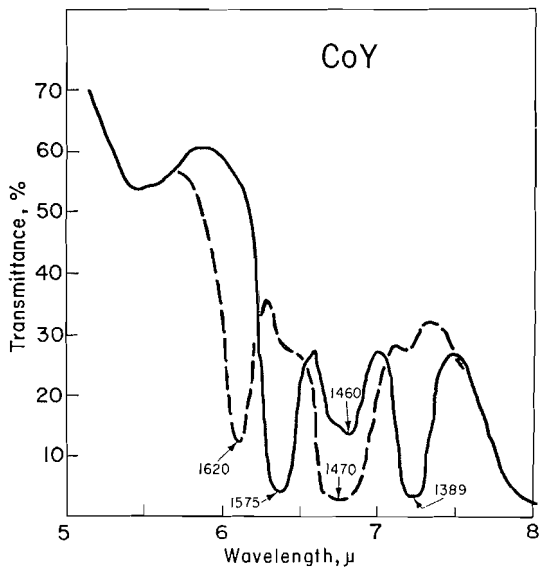

FIG. 2. Interaction of water with the carbonate-type bands on CoY Zeolite; —, sample air-activated at 500°; - - -, same, with small amount of water.

uptake of 1.62 cc/g corresponds to 0.92 CO_2 molecules per unit cell. This is in reasonably good agreement with the decrease of sites (5.31 − 4.11 = 1.20), as indicated by the cation specific CO capacity after exposure to carbon dioxide.

These results indicate that one adsorbed carbon dioxide molecule is responsible for the blocking of approximately one surface site. Since the sites measured by carbon monoxide adsorption are the surface cations (11), the above results also mean that the high temperature adsorption of carbon dioxide in some way blocks the surface cations in an approximate ratio of one CO_2 molecule per surface cation.

Discussion

Evans and Whateley (5) have summarized the characteristic infrared bands of groups that can be formed by the interaction of carbon dioxide with metal oxide surfaces. They list the frequencies of the carbonate ion (CO_3^{2-}), of unidentate carbonate (—O—CO_2), of bidentate carbonate

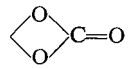

and of the bicarbonate ion, (HO—CO_2^-). Comparison with our results leaves little doubt that the bands observed in the 1600–1300 cm^{-1} region of the spectra of zeolites exposed to carbon dioxide are due to the unidentate carbonate type species. The interaction, therefore, consists of a carbon dioxide molecule chemisorbing in a bent configuration on a surface oxygen to form the unidentate type carbonate species. The appearance of a band at 1460 cm^{-1} in some cases would indicate that in addition some carbonate ion species are also formed.

Our results lead to three important conclusions. First, since even heating at 700° does not remove this group, the unidentate carbonate formed on the zeolite surface is extremely stable, comparable in stability to the zeolite structure itself. Second, it must be the bivalent cations on the surface that cause this chemisorption of carbon dioxide, since the same reaction does not occur on zeolites with monovalent cations. Finally, the chemisorbed carbon dioxide is on the zeolitic surface in proximity to the cations, since the frequencies of the carbonate-type grouping are cation-dependent (see Table I). The quantitative aspect of carbon dioxide adsorption on CaY shows that the adsorbed molecules block some, but not all, of the available surface cations. This indicates that about 20% of the calcium cations may differ in some way from the other surface cations. Distribution of the surface cations between Sites S_{II} and Sites S_{III} is a distinct possibility, since the carbon monoxide adsorption method used for the quantitative measurement of the available surface cations does not differentiate between these two surface positions.

Can. J. Chem. Downloaded from www.nrcresearchpress.com by 210.87.254.6 on 09/05/12
For personal use only.

Can. J. Chem. Downloaded from www.nrcresearchpress.com by 210.87.254.6 on 09/05/12
For personal use only.

Ward and Habgood (7) have suggested that the reason why the monovalent cation exchanged X zeolites do form carbonate-like structures when exposed to carbon dioxide at room temperature, while the alkaline-earth cation exchanged X's do not, is that in the first case the cations can occupy both Sites S_{II} and the more exposed Sites S_{III}, while in the bivalent cation cases the cations most likely occupy only Sites S_{II}. Cations in Sites S_{III} are less shielded than those in Sites S_{II} and have stronger electric fields in their vicinity. It was therefore assumed that only cations in Sites S_{III} interact with carbon dioxide at room temperature.

Although it might be easy for the carbon dioxide to adsorb on any surface cation in the end-on configuration (see refs. 7, 8), it must be more difficult to adsorb parallel-to-the-surface in the configuration necessary for surface carbonate formation, and this apparently happens only on the more exposed Site S_{III} cations. This explains our results on NaY, where no carbonate formation was observed: NaY has very few (8) cations in Sites S_{III}, compared to NaX (38), assuming the normal distribution of cations as 16 in Sites S_I, 32 in Sites S_{II}, and the rest in Sites S_{III}[3]. The above mechanism would also explain why the bivalent cation zeolites require heating to 500° in the presence of carbon dioxide before these bands form: a considerable activation energy would be needed for the carbon dioxide molecules to reach the bivalent cations in Sites S_{II} in a symmetrical coordination, or to make the cations mobile enough to be able to move into Sites S_{III}. On the other hand, it does not explain the lack of formation of high temperature carbon dioxide bands with the monovalent cation zeolites. To explain this difference between mono- and bivalent cations in the formation of the chemisorbed carbonate complex, we have to assume that it is the much stronger electrostatic field of the bivalent cation which is necessary for the reaction. This strong field polarizes the carbon dioxide molecule, presumably adsorbed on the cation, and it is this highly polarized form of the molecule which is then able to react with the neighboring oxygen of the structure to yield the carbonate-type grouping. The final product then is a carbon dioxide molecule very strongly attached to a surface oxygen which is quite close to a cation; so close that it can block the adsorption of other molecules (e.g. carbon monoxide) on the cation and the cation can in turn influence the vibrational frequencies of the carbonate group.

The interaction of adsorbed molecules with the carbonate-type bands can be explained as follows: when water is adsorbed on a CoY (see Fig. 2), it hydrogen-bonds with the surface carbonate species and this shifts both bands to lower frequencies: the 1575 cm^{-1} band to about 1470 cm^{-1} and the 1380 cm^{-1} band to a position where it cannot be detected due to the strong zeolite absorption. The 1620 cm^{-1} band is the bending frequency of the water molecule and of course does not appear when heavy water is adsorbed. When the water is removed, the bands shift back to their original positions. The same hydrogen-bonding effect is responsible for the similar changes in ammonia adsorption. On the other hand, the bands are not affected by benzene, since benzene is not a hydrogen-donor and thus does not form hydrogen bonds. These effects confirm our suggestion that the carbonate-type grouping is on the zeolitic surface.

To assess the practical significance of our findings we have to consider that, although the total chemisorption of carbon dioxide of the type that is stable at high temperature is quite small (1.6 cc of carbon dioxide per gram of zeolite), it is definitely associated with and, to some degree, blocks available surface cations. This fact should be taken into consideration whenever reactions are carried out which are thought to occur through interaction with the surface cations. Exposure to ordinary air in the high temperature activation process makes it possible for the small amounts of carbon dioxide present to interact with the zeolite to form this highly stable, chemisorbed species.

[3]The formation of Na_6^{5+} centers in NaX (11) indicates that there might be even more Na^+ ions in Sites S_{III} than given here.

Acknowledgment

The authors wish to express their thanks to Paul C. Schaffer for some of the experimental results.

1. W. I. STUART and T. L. WHATELEY. Trans. Faraday Soc. **61**, 2763 (1965).
2. R. P. EISCHENS and W. A. PLISKEN. Advan. Catal. **9**, 662 (1957).
3. L. H. LITTLE and C. H. AMBERG. Can. J. Chem. **40**, 1997 (1962).
4. S. MATSUSHITA and T. NAKATA. J. Chem. Phys. **36**, 665 (1962).

5. J. V. EVANS and T. L. WHATELEY. Trans. Faraday Soc. **63**, 2769 (1967).
6. L. BERTSCH and H. W. HABGOOD. J. Phys. Chem. **67**, 1621 (1963).
7. J. W. WARD and H. W. HABGOOD. J. Phys. Chem. **70**, 1178 (1966).
8. C. L. ANGELL. J. Phys. Chem. **70**, 2420 (1966).
9. C. L. ANGELL and P. C. SCHAFFER. J. Phys. Chem. **69**, 3463 (1965).
10. C. L. ANGELL. Vac. Microbalance Tech. **6**, 77 (1967).
11. J. A. RABO, C. L. ANGELL, P. H. KASAI, and VERNER SCHOMAKER. Discuss. Faraday Soc. **41**, 328 (1966).

Can. J. Chem. Downloaded from www.nrcresearchpress.com by 210.87.254.6 on 09/05/12
For personal use only.

Radiolysis of gaseous isobutylene by ^{60}Co γ-rays. II. Irradiation of isotopic mixtures: iso-C_4H_8 + iso-C_4D_8

J. A. HERMAN AND G. COLLIN[1]

Centre de Recherche pour les Atomes et les Molécules et Département de Chimie, Université Laval, Québec

Received May 29, 1969

The radiolysis of the isotopic mixture: iso-C_4H_8 + iso-C_4D_8 shows that, at 48 Torr pressure, about 40% of isobutane is formed in an ion–molecule reaction between isobutyl ion and the monomer. Half of the propene produced in radiolysis is formed in ion–molecule reactions, the H^- transfer reaction to $C_3H_5^+$ ion being the most important process. Small fractions of CH_4, C_2H_2, C_2H_4, allene, and propyne are also formed in ionic processes, but the main part results from unimolecular decomposition processes of the excited isobutylene.

La radiolyse du mélange isotopique iso-C_4H_8 + iso-C_4D_8 indique qu'à 48 Torr, environ 40% d'isobutane est formé dans une réaction ion–molécule qui fait intervenir, selon toute vraisemblance, l'ion isobutyle. Environ la moitié du propène est formé dans des réactions ioniques, dont le transfert de H^- à l'ion $C_3H_5^+$ est le plus important. Le restant du propène apparaît à la suite de décomposition monomoléculaire de la molécule parent. De faibles proportions de CH_4, C_2H_2, C_2H_4, allene et propyne sont aussi formées dans des processus ioniques, mais la majeure partie de ces produits est le résultat de décomposition monomoléculaire de l'isobutylène excité.

Canadian Journal of Chemistry, 47, 3837 (1969)

Can. J. Chem. Downloaded from www.nrcresearchpress.com by 210.87.254.40 on 09/05/12
For personal use only.

Introduction

In a recent paper (1), we reported yields of products formed during the radiolysis of gaseous isobutylene in the presence and absence of additives, and we suggested some mechanisms leading to the formation of isobutane and the C_2 and C_3 products. However, the evidence for these mechanisms was based mainly on mass balance and energetic considerations. The case of isobutane formation is of special interest; at a sample pressure of 40 Torr, the total yield per 100 eV of absorbed energy is 2.1 ± 0.2 molecules, and the addition of nitric oxide as a radical scavenger diminishes the yield by ~60%, thus indicating an important non-radical contribution to the formation of this molecule. This was explained (1) by assuming the following sequence of reactions

[1] $\text{iso-}C_4H_8^+ + \text{iso-}C_4H_8 \rightarrow t\text{-}C_4H_9^+ + C_4H_7$

[2] $t\text{-}C_4H_9^+ + \text{iso-}C_4H_8 \rightarrow C_4H_7^+ + \text{iso-}C_4H_{10}$

According to Lias and Ausloos (2) and Miyazaki and Shida (3), the tertiary butyl ion cannot produce iso-C_4H_{10} by a hydride transfer reaction with neopentane, because of the endothermicity of such a reaction ($\Delta H = 0.55$ eV). In the present case, the endothermicity of reaction [2] is smaller than that of a reaction between t-$C_4H_9^+$ ion and neopentane. However, even if the energy balance is more favorable, it is necessary to assume that the tertiary butyl ion is internally excited, in order to react in process [2]. The necessary excitation energy of the tertiary butyl ion may be provided in reaction [1], which is slightly exothermic as estimated from the available data (4, 5). Recent studies of Volpi and coworkers (6) on the variation of the mass spectrum of isobutylene with pressure showed that the $C_4H_9^+$ ion (which was assumed to have a tertiary structure) reacts with the parent molecule in an ion–molecule chain

[3] $t\text{-}C_4H_9^+ \xrightarrow{M} C_9H_{17}^+ \xrightarrow{M} C_{12}H_{25}^+ \xrightarrow{M} C_{4n}H_{8n+1}^+$

The "polymerization" chain probably propagates via an alkyl carbonium ion of tertiary structure, which is thermodynamically more stable. Another sequence involves the $C_5H_9^+$ ion

[4] $C_5H_9^+ \xrightarrow{M} C_9H_{17}^+ \xrightarrow{M} C_{13}H_{25}^+$

In the region of 10^{-2} Torr pressure, the 2 sequences account for more than 95% of the total ion intensity. With increasing pressure other ions appear of the general formulas $C_nH_{2n-1}^+$ and $C_nH_{2n-3}^+$.

It is clear that the proposed ion–molecule reaction [2], accounting for the formation of isobutane, is in disagreement with the mass-spectrometric investigation of Volpi and co-workers

[1]Present address: National Bureau of Standards, Washington, D.C.

TABLE I

Radiochemical yields of products*

Additive	Yield							
	H_2	CH_4	C_2H_2	C_2H_4	C_3H_6	Propyne	Allene	i-C_4H_{10}
Pressure of iso-C_4H_8 = 48 ± 3 Torr								
—	1.3	0.76	0.54	0.60	0.81	0.99	1.01	2.09
O_2 6%	—	0.35	0.53	0.60	0.75	0.97	—	0.82
O_2 15%	—	—	0.48	—	0.79	0.80	—	0.80
NO 6%	—	0.28	0.54	0.59	0.76	0.98	—	0.39
NO 15%	—	0.28	0.43	0.60	0.79	—	—	0.30
NO 30%	—	—	0.54	0.59	0.75	0.95	—	0.31
NH_3 10%	—	0.78	0.49	0.57	0.69	0.97	—	1.43
NH_3 8% + O_2 4%	—	0.32	0.52	0.58	0.68	0.96	—	0.01
Pressure of iso-C_4H_8 = 95 ± 5 Torr								
—	1.36	0.54	0.40	0.40	0.51	0.74	0.76	1.44
O_2 6%	—	0.28	0.37	0.40	0.47	0.74	—	0.50
NO 6%	—	0.20	0.38	0.39	0.46	0.71	—	0.22
NH_3 6%	1.32	—	—	—	—	—	—	—

*Yields are calculated relative to G(allene) 1.01 ± 0.05 at 48 Torr, and 0.76 ± 0.05 at 95 Torr.

(6). Therefore, in order to elucidate the possible ionic mechanism of isobutane formation, we carried out a set of radiolysis experiments on mixtures of perprotonated and perdeuterated isobutylenes in the presence of a suitable radical scavenger. Another series of radiolyses was conducted in an electric field; from such experiments one can differentiate, to some extent, between ionic and excited neutral decomposition reactions (7).

Experimental

Purification of reagents, the irradiation cell, the dosimetry, and the product analysis were previously described (1), and therefore only experimental details relevant to the present study are outlined below. The principal difference in the present analytical procedure, compared to that of ref. 1, is the systematic use of a gas–liquid chromatograph (g.l.c.) equipped with a flame ionization detector. A 30 ft. squalane chromatographic column was used for the separation of the radiolysis products. Previously (1), we separated the gases in a LeRoy still before injecting them into the g.l.c. equipped with a thermoconductivity detector, and in such a procedure some compounds (i.e. C_2H_2) were partially lost. All G values are calculated relative to the yield of allene in an unscavenged radiolysis experiment, because the formation of this compound is dose and dose-rate independent at a given pressure, and it is also insensitive to radical scavengers.

Ammonia from Matheson Co. was purified by trap-to-trap distillation at −195 °C. Isobutylene-d_8 from Merck, Sharp and Dohme Ltd was purified further by g.l.c. before its use. It contained 5.35% of isobutylene-d_7, as shown by mass spectrometry. In order to compensate for the presence of iso-C_4D_7H, a statistical correction was made to the calculation of yields of all hydrocarbons. The isotopic mixtures were prepared in the following ratio: (iso-C_4H_8:iso-C_4D_8:NO) = (50:50:8) in all experiments where nitric oxide was used as radical scavenger. After irradiation, the products were separated by g.l.c. and trapped at −195°. Immediately after, they were transferred for further analysis to the high resolution mass spectrometer, Hitachi Perkin–Elmer RMU-6.

The experiments involving an electric field were performed in irradiation cells of the same shape and dimensions as those described in (1). They were coated from inside with graphite, the inner electrode being a wire of tungsten.

Results

In Table I are presented the G values at 48 and 95 Torr for isobutane and the major decomposition products of isobutylene. The G values calculated in the present case are comparable to those obtained previously (1). At 48 Torr pressure, $G(CH_4)$ is somewhat higher, but the yields are smaller for C_2H_2 and C_3H_6. The present results show that G(propyne) is always a little smaller than the corresponding value of allene. It is worthwhile to note that, with the present analytical procedure, the $G(C_2H_2)$ does not show the strong pressure dependence as described in Part I.

As noted in Part I, the presence of radical scavengers, oxygen and nitric oxide, have no effect on C_2H_2, C_2H_4, propyne, and allene formation, but have a strong effect on CH_4 and iso-C_4H_{10} and, to a lesser extent, on C_3H_6 formation. The presence of ammonia, which acts as a proton scavenger, also has no effect on the yields of H_2, CH_4, C_2H_2, C_2H_4, and the C_3H_4 isomers, but has an important one on G(iso-C_4H_{10}) and a smaller one on $G(C_3H_6)$. Moreover,

Can. J. Chem. Downloaded from www.nrcresearchpress.com by 210.87.254.40 on 09/05/12
For personal use only.

TABLE II

Relative isotopic composition of products*

Parent compound	Relative isotopic composition										
	$-d_0$	$-d_1$	$-d_2$	$-d_3$	$-d_4$	$-d_5$	$-d_6$	$-d_7$	$-d_8$	$-d_9$	$-d_{10}$
Hydrogen	33.3	13.9	52.8								
Methane	49.9	1.9	—	5.0	43.2						
Acetylene	52.9	1.9	45.2								
Ethylene	49.5	3.1	3.2	2.8	41.4						
Allene	53.0	0.6	0.9	0.1	44.7						
Propyne	52.7	1.0	—	2.2	44.0						
Propene	34.7	11.3	6.4	4.7	6.2	10.6	26.1				
Isobutane	?	?	?	?	?	?	?	~0	155	123	100

*iso-C_4H_8:iso-C_4D_8:NO = 50:50:8; pressure of the mixture = 48 Torr.

the formation of isobutane is almost completely suppressed by the combined action of O_2 and NH_3.

In the presence of an electric field, the yields of C_2H_4 and C_3H_6 are affected little (C_3H_6) or not at all (C_2H_4), whereas the yields of propyne and allene increase very strongly (Fig. 1).

The relative isotopic compositions of products formed during radiolysis of isotopic mixtures at 40 Torr are presented in Table II. In the case of isobutanes, only $-d_{10}$, $-d_9$, and $-d_8$ species could be estimated. Their relative composition was inferred from the abundance of propyl ions in the mass spectrum. The lack of adequate standard mass spectral patterns of partially deuterated butanes made a detailed quantitative analysis of the isobutane fractions only approximate. The isobutane-d_9 was assumed to have only the $(CD_3)_3CH$ structure. In comparison with the abundances of $-d_{10}$, $-d_9$, and $-d_8$ isobutanes, the $-d_7$ fraction seems to be very small.

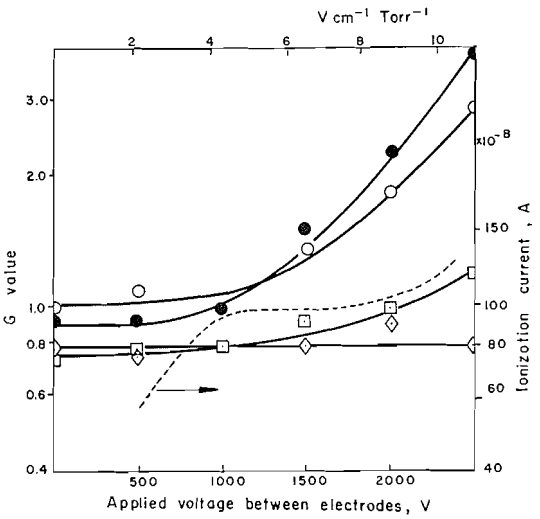

FIG. 1. Radiochemical yields of ethylene (◇), propene (□), propyne (○), and allene (●) as a function of the electric field. The dashed line represents the ionization current in the cell.

In order to check the ionic mechanism for formation of isobutane, we performed radiolyses of mixtures of neopentane and isobutylene. The mixture (neo-C_5H_{12}:iso-C_4D_8:O_2) = (100:5:0.4) has a G(isobutane)$_{total}$ = 0.01 relative to the energy absorbed by neopentane, but a G' (isobutane) = 1.5 ± 0.5 if calculated relative to the energy absorbed by isobutylene-d_8 only. In the case of irradiation of a mixture (neo-C_5D_{12}:iso-C_4H_8:O_2) = (50:50:14), only perprotonated isobutane is formed and its yield, G(iso-C_4H_{10}) = 0.82 is relative to the energy absorbed by the isobutylene.

Discussion

Formation of Isobutane

The action of radical scavengers and of ammonia in the radiolysis of isobutylene indicates that isobutane is formed in part in radical reactions (~60%) and in ion–molecule processes (~40%). The formation of iso-C_4H_{10} in radical reactions proceeds via disproportionation between tertiary butyl radicals (8–11), the t-C_4H_9· being formed efficiently by thermal hydrogen addition to the tertiary carbon in isobutylene. The addition of nitric oxide has a more pronounced effect on the formation of iso-C_4H_{10} than does oxygen (Table I), and that can be attributed to the charge transfer between iso-$C_4H_8^+$ (ionization potential (i.p.) = 9.23 eV) and NO (i.p. = 9.25 eV) (12)

[5] iso-$C_4H_8^+$ + NO → iso-C_4H_8 + NO^+

Can. J. Chem. Downloaded from www.nrcresearchpress.com by 210.87.254.40 on 09/05/12
For personal use only.

Can. J. Chem. Downloaded from www.nrcresearchpress.com by 210.87.254.40 on 09/05/12
For personal use only.

However, reaction [5] is relatively slow (13) and it is therefore possible that, even at 30% NO, not all iso-$C_4H_8^+$ ions have been intercepted. Incidentally, reaction [5] is another proof of the ionic character of the mode of formation of that part of the isobutane which is not scavengable by oxygen.

Recent studies on the photolysis of gaseous isobutylene by 10.0 and 11.6–11.8 eV photons (14) have shown that 3 isobutane molecules are produced for every 10 isobutylene ions, and that this ionic mechanism is the only one which accounts for the nonradical formation of isobutane. If we admit that this ratio also described the situation for oxygen or ammonia scavenged radiolysis experiments, then it is possible to calculate the yield of these iso-$C_4H_8^+$ parent ions which did not decompose before the first reactive collision. At 48 Torr, G(iso-$C_4H_8^+$) = 2.7 or 2.2, depending which of the two effects, oxygen or ammonia, is taken into account. The smaller G value calculated from radiolysis experiments in the presence of ammonia (Table I) results most probably from the fact that the concentration of ammonia is not sufficiently important in order to intercept all iso-$C_4H_8^+$ ions before the formation of isobutane. At 95 Torr, G(iso-$C_4H_8^+$) = 1.7, as calculated from radiolysis experiments done in the presence of oxygen (Table I). However, the increase of pressure from 48 to 95 Torr is not sufficient to change appreciably the yields of parent ions, and it is more probable that the present difference in G(iso-$C_4H_8^+$) is the result of experimental incertitude. Tentatively, we shall admit a G(iso-$C_4H_8^+$) = 2.5 ± 0.3 at 48 Torr.

According to a mass spectrometric investigation (15) in the case of iso-C_4H_8, the proton transfer

[6] $\text{iso-}C_4H_8^+ + \text{iso-}C_4H_8 \rightarrow C_4H_9^+ + C_4H_7$

is essentially the only mode of reaction between the parent ion and iso-C_4H_8. It is well established that the t-$C_4H_9^+$ ions are efficiently intercepted by NH_3 (3, 16), but it is also possible that the iso-$C_4H_8^+$ parent ions are intercepted by ammonia. The effect of NH_3 in the radiolysis of isobutylene is comparable to that of water vapor (17) and of nitric oxide in the radiopolymerization of gaseous iso-C_4H_8 (18). However, if 0.1% of NO inhibits 95% of the polymerization yield (18), 30% of NO inhibits only 85% of the isobutane production. Similar observations are applicable to the ammonia effect in this system. Therefore, if the polymer and the ionic isobutane have the same common precursor, the reaction sequences are different. In order to check the role of the t-$C_4H_9^+$ ions in the formation of iso-C_4H_{10}, we irradiated mixtures of neopentane-d_{12} and isobutylene-d_0 with oxygen as radical scavenger (see Results). Irradiated neopentane is recognized to produce tertiary butyl ions by fragmentation of the parent molecule (19, 20), and if an ion–molecule reaction occurs between t-$C_4D_9^+$ and iso-C_4H_8, the isobutane-d_9 should be formed by H^- transfer. The results of such an experiment show clearly that the afore-mentioned reaction does not take place and that the proposed mechanism, reaction [2], is wrong (1).

Volpi and co-workers (6) reported that reaction [6] is followed by consecutive processes [3] and [4] which lead to the polymer formation in the gas phase. When the pressure increases above 10^{-2} Torr, the intensity of the polymeric ions $(C_nH_{2n+1})^+$ and $(C_nH_{2n-1})^+$ drops rapidly, while a new generation of ions of the general formula $(C_nH_{2n-1})^+$ and $(C_nH_{2n-3})^+$, which could result from an H_2 transfer, simultaneously appear

[7] $(C_nH_{2n+1})^+ + \text{iso-}C_4H_8 \rightarrow (C_nH_{2n-1})^+ + \text{iso-}C_4H_{10}$

Isotopic analysis of the unscavenged isobutane fraction (Table II) shows the presence of C_4D_{10}, C_4D_9H, and $C_4D_8H_2$, and such an isotopic composition is in qualitative agreement with mechanism [7]. The thermodynamic considerations are also favorable; the heat of formation of $(C_nH_{2n+1})^+$ and $(C_nH_{2n-1})^+$ ions do not differ appreciably when n is large ($n > 10$), and reaction [7] is then exothermic by 28 kcal/mole. A similar mechanism was assumed for the formation of propane by an H_2 transfer process in the photoionization of propene (21). However, the $(C_nH_{2n+1})^+$ ions formed in the radiolysis of neo-C_5D_{12}:iso-C_4H_8:O_2 = 50:50:14 mixture might contain at most 9 deuterium atoms if originating from a t-$C_4D_9^+$ ion. Therefore, one can expect that isobutane formed in reaction [7] might contain 1 or 2 deuterium atoms, but this is not the case (see Results).

There is still the possibility that a part of the $C_4H_9^+$ ions produced in reaction [6] retain the isobutyl structure, and that these ions react with the monomer by hydride transfer

[8] $(CH_3)_2CHCH_2^+ + \text{iso-}C_4H_8 \rightarrow \text{iso-}C_4H_{10} + C_4H_7^+$

Can. J. Chem. Downloaded from www.nrcresearchpress.com by 210.87.254.40 on 09/05/12
For personal use only.

Reaction [8] would also be in qualitative agreement with the observed isotopic composition. If reaction [8] contributes to the formation of isobutane, then the iso-C_4D_9H fraction formed in radiolysis of iso-C_4D_8:iso-C_4H_8:NO mixture (Table II) is a mixture of $(CD_3)_3CH$ and $(CD_3)_2CDCHD_2$ structures. The calculation of the mass spectrum of partially deuterated isobutanes is cumbersome, the reason being the lack of adequate standard mass spectral patterns, but if we assume that the isobutanes-d_{10}, -d_9, and -d_8 are a mixture of $[(CD_3)_3CD]:[(CD_3)_3CH]:[(CD_3)_2CDCHD_2]:[(CD_3)_2CDCDH_2] = 1:1:1:1$, the calculated results fit the experimental mass spectrum better than these in which we ignore the third structure. However, the formation of the isobutyl ion from the ground state of the parent ion, iso-$C_4H_8^+$, is slightly endothermic ($\Delta H = 5$ kcal/mole); thus the necessary energy required for such a reaction should be provided by the excited parent ion. This was verified in photolysis by 10.0 eV photons (krypton resonance line) of isobutylene in a great excess of argon with oxygen added as a radical scavenger (14). In these conditions, the production of isobutane decreases very strongly, which means that the ionic precursor of isobutane is deactivated by argon.

This last observation indicates that the isobutyl ions are responsible for the formation of isobutane, whereas the tertiary butyl ions lead to the ionic polymerization as suggested by Volpi and co-workers (6). The length of the kinetic "ionic polymerization" chain is either sufficiently long, or the process is relatively slow, in order that small concentrations of NH_3, H_2O, or NO ($< 10^{-2}\%$) inhibit the formation of the polymer (18). On the other hand, the formation of isobutane by a rapid H^- ion transfer to the isobutyl ion explains the much lower sensitivity of the process [8] to the presence of NO or H_2O.

Propene, Allene, and Propyne

The radiolytical yield of propene formation is about 6 times higher than the corresponding yield in photolysis experiments at 11.6–11.8 eV (14). It follows that formation of C_3H_6 involves either a substantial increase of processes already operating at photon energies of 8.4 to 11.8 eV, or the occurrence of new mechanisms, or both together. The relatively high abundance of -d_0 and -d_6 propenes indicates an elimination of a methylene group from isobutylene

[9] $$(CD_3)_2CCD_2^* \rightarrow CD_2 + C_3D_6$$

The C_3D_5H and C_3H_5D formation might result from the decomposition of the excited isobutyl radical formed in a hot deuterium/hydrogen addition

[10] $$D + (CH_3)_2CCH_2 \rightarrow (CH_3)_2CDCH_2^* \rightarrow CH_3 + CH_3CDCH_2$$

Both mechanisms were postulated as being responsible for the propene production in photolysis at 1460, 1236, and 1067–1048 Å (14). However, the d_2, d_3, and d_4 propenes are not formed in the photolysis, and their production in radiolysis experiments suggests another reaction path for propylene formation. In the photolysis of isobutylene by 1067–1048 Å photons, there is practically no fragmentation of the parent ion (14); therefore, the formation in radiolysis of d_2, d_3, and d_4 propenes must proceed by an ionic mechanism involving fragmentation of the parent ion followed by ion–molecule reaction with isobutylene. The small decrease of the yield of propene in the presence of NH_3 (Table I) is a supplementary indication of such a process.

The total yield of ions formed per 100 eV of absorbed energy is 4.2 (22). If one assumes the correctness of the $G(\text{iso-}C_4H_8^+) = 2.5 \pm 0.3$, it follows that the yield of fragment ions is 1.7 ± 0.3. The most important ion in the isobutylene mass spectrum is the $C_3H_5^+$ species, which accounts for around 31% of all ions produced by 70 eV electrons in the mass-spectrometric source at very low pressure. At 48 Torr, the relative abundance of this ion over all other fragment ions from isobutylene is at least the same or higher, and $G(C_3H_5^+) > 0.5 \pm 0.1$. Abramson and Futrell (15) concluded that about 70% of the $C_3H_5^+$ ions react with isobutylene in a formal H^- transfer process

[11] $$C_3H_5^+ + \text{iso-}C_4D_8 \rightarrow C_3H_nD_{6-n} + C_3D_{2n}H_{5-n}^+$$

but, in fact, reaction [11] proceeds via a strong complex, where many hydrogens are exchanged. At first sight, reaction [11] could explain the formation of all partially deuterated propenes, but a more careful examination of the results shows some discrepancies between the Abramson and Futrell values and ours. In the tandem mass-spectrometry experiments (15) the formation of the $C_3D_3H_3$ is favored, while, in the present case, it is the less important species. Several factors might be responsible for this discrepancy, but the pressure effect is probably the most important. At 40 Torr, the stabilization of a strong (long

Can. J. Chem. Downloaded from www.nrcresearchpress.com by 210.87.254.40 on 09/05/12
For personal use only.

lived) intermediate complex is very likely, and it might undergo further condensation process. Therefore, a process such as [11] will contribute only to a small extent to the propene formation, and its yield can be estimated as 0.12 from the ammonia effect.

If an ion–molecule process similar to [11] takes place in the present system, it will probably result from an encounter between $C_3H_5^+$ and iso-C_4H_8, where only a weak (short lived) intermediate complex is involved and the result is a true H^- transfer reaction

[12] $C_3H_5^+ + \text{iso-}C_4H_8 \rightarrow C_3H_5D + C_4D_7^+$

An estimation of $G[10] + G[12] = 0.35$ can be made, where isotope effects were not taken into consideration (Tables I and II). The photolysis data provide an upper limit of $G[10] \leqslant 0.10$ (14); it follows then, that the yield per 100 eV of hydride transfer reaction [12] is around 0.25. Therefore, the total yield of propene formed in ionic processes (reactions [11] and [12]) is about 0.4, and this value explains in part the important difference of $G(C_3H_6)$ between radiolysis and photolysis experiments.

In the presence of an electric field, $G(C_3H_6)$ increases slightly but seems to follow the increase of the ionization current in the "plateau" region. This increase of $G(C_3H_6)$ results from the enhancement of process [9] as electrons gain more kinetic energy with increasing field strength.

The action of the electric field (Fig. 1) on allene and propyne production and the isotopic analysis (Table II) of these products indicate that they are formed in elimination processes of the excited isobutylene molecule. This is consistent with the previously proposed mechanism (1)

[13] $\text{iso-}C_4H_8^* \begin{cases} \nearrow H_2C{=}C{=}CH_2 + H + CH_3 \text{ (or } CH_4) \\ \searrow HC{\equiv}C{-}CH_3 + H + CH_3 \text{ (or } CH_4) \end{cases}$

The C_3H_4 species can originate by secondary fragmentation either from $C_3H_5^{\cdot}$ or $C_4H_7^{\cdot}$ radicals. This is not unexpected, because the energy requirements to form these radicals from isobutylene are almost equal[1]. However, radiolysis experiments carried out in order to determine the nature of the radical intermediates in isobutylene at −90 °C showed that the major radical species is 2-methylallyl (67%), while the yield of 1-methylvinyl is small (2%) (24). This suggests that the $C_3H_5^{\cdot}$ species undergoes fast secondary fragmentation

[14] $CH_3C{=}CH_2^* \begin{cases} \nearrow H_2C{=}C{=}CH_2 \\ \searrow H_3C{-}C{\equiv}CH \end{cases}$

and does not accumulate within the system, whereas the $C_4H_7^{\cdot}$ is stabilized. However, the last argument might be fallacious, because there is no experimental evidence that process [14] is taking place in the condensed phase.

About 2.5% of allene and propyne are partially deuterated (Table II). Such species are not formed in photolysis experiments (14); therefore, we concluded that ion–molecule processes are responsible for their production. The partially deuterated allene and propyne might originate in the following process involving $C_3H_3^+$ ions (whose relative abundance in the American Petroleum Institute mass spectrum of iso-C_4H_8 is 13.6%)

[15] $C_3H_3^+ + \text{iso-}C_4D_8 \rightarrow C_3H_3D + C_4D_7^+$

As in the case of C_3H_5 ion, process [15] can be a true H^- transfer reaction, or involves a long lived intermediate complex where reshuffling of hydrogens is very likely.

Methane, Acetylene, and Ethylene

The fact that the unscavenged methane in radiolysis of C_4H_8–C_4D_8–NO mixtures (Table II) consists mainly of CH_4 and CD_4 demonstrates that this molecule is nearly exclusively formed in unimolecular processes. Either the primary process

[16] $(CH_3)_2CCH_2^* \rightarrow CH_4 + CH_3CCH$

or a secondary fragmentation such as

[17] $\begin{matrix} H_3C \\ \diagdown \\ \quad C{=}CH_2 \\ \diagup \\ H_2C \end{matrix} \rightarrow CH_4 + CH_2CCH$

could account for the observed results. The small $-d_1$ and $-d_3$ contributions to the methane can be explained by addition of a hot hydrogen atom to isobutylene and subsequent fragmentation of the excited molecule. The decomposition of an excited parent ion is also a process which contributes to the production of "molecular" meth-

[1]Heats of reaction are based on thermodynamic data presented in ref. 23.

Can. J. Chem. Downloaded from www.nrcresearchpress.com by 210.87.254.40 on 09/05/12
For personal use only.

ane. Such a decomposition process occurs in an interval less than 10^{-10} s before a first collision happens; therefore, even an important increase of pressure does not seriously interfere with this process. Nevertheless, the present results do not allow us to calculate the contribution of each of these unimolecular decomposition reactions to the formation of molecular methane.

Acetylene formed in the radiolysis of isotopic mixtures consists of perprotonated and perdeuterated molecules and indicates, therefore, that unimolecular fragmentation process is responsible for its formation. On the other hand, the yield of ethylene, which also consists mainly of $-d_0$ and $-d_4$ species, is close to that of acetylene. In fact, the yields of perprotonated and perdeuterated acetylene and ethylene are equal within experimental error. Moreover, the equal decrease in the yields of C_2H_2 and C_2H_4 with increasing pressure of isobutylene (Table I) give evidence that these products have a common excited precursor with an appreciable lifetime. A mechanism such as

[18] $(CH_3)_2CCH_2^* \rightarrow H_2 +$ 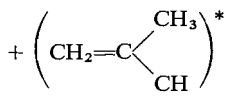

followed by

[19] 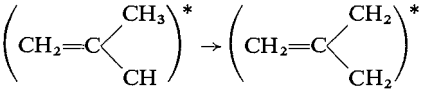

$\rightarrow C_2H_2 + C_2H_4$

is in harmony with established mechanisms (25, 26) for the formation of both perprotonated and perdeuterated acetylene and ethylene. The fact that during radiolysis in the presence of an electric field there is no increase in the C_2H_2 and C_2H_4 yields (Fig. 1) does not necessarily rule the occurrence of processes [18] and [19]. Indeed, electrons accelerated by the electric field do not gain enough energy to excite the isobutylene to such a level where processes [18] and [19] could take place. However, the excitation reached by isobutylene in collision with accelerated electrons is sufficient to detach a methyl group, which requires only 5.83 eV (23).

There are some minor contributions of other processes leading to the production of ethylene and acetylene, as demonstrated by the formation of partially deuterated species. These species are not formed in photolysis experiments at 1067–1048 Å (14); we assume that they originate in ion–molecule reactions in the same manner as partially deuterated propenes, allenes, and propynes. The $C_2H_3^+$ ion is an important fragment in the 70 eV electron mass spectrum of isobutylene ($\sim 6.4\%$). It reacts with isobutylene in the following processes

[20] $C_2H_3^+ + \text{iso-}C_2H_8 \rightarrow C_2H_4 + C_4H_7^+$

[21] $\rightarrow C_2H_2 + C_4H_9^+$

and their cross-sections are relatively important (15). Assuming that "ionic" ethylene is produced in process [20], where the intermediate complex has a sufficient lifetime for reshuffling of hydrogen atoms, the yield of partially deuterated ethylenes is then $G[20] = 0.08$. Another important fragment in the mass spectrum of iso-C_4H_8 is the $C_2H_4^+$ ion ($\sim 6.6\%$). This species reacts quantitatively with isobutylene in a charge transfer process (15) leading to the "molecular" ethylene. Such a process should be insensitive to an increase of the pressure (within the limits of the present study), as it does not require the formation of a strong intermediate complex.

Conclusions

(*a*) The formation of the unscavenged isobutane proceeds via an ion–molecule reaction involving most probably isobutyl ions, whereas the tertiary butyl ions lead to the ionic polymerization.

(*b*) Assuming the same ionic yield for unscavenged isobutane formation in radiolysis as in photolysis at 1067–1048 Å (14), the yield per 100 eV of fragment ions is then 1.7 ± 0.3.

(*c*) About half the production of propene proceeds through an ionic process, $G(C_3H_6, \text{ionic}) \sim 0.4$.

(*d*) All other decomposition products, CH_4, C_2H_2, C_2H_4, allene, and propyne show small ionic contributions to their formation. However, the total ionic contribution of these species, including that of propene, is less than the yield of fragmentions. We conclude, therefore, that a part of these ionic reactions leads to condensation products in similar processes to those described by Volpi and co-workers (6).

Acknowledgments

The authors are indebted to Dr. P. Ausloos for very valuable comments on this paper. The authors wish to thank the National Research Council of Canada for financial support and also

acknowledge the award of a "Conseil des Arts du Canada" studentship to one of them (G.J.C.).

1. G. J. COLLIN and J. A. HERMAN. Can. J. Chem. **45**, 3097 (1967).
2. S. LIAS and P. AUSLOOS. J. Chem. Phys. **43**, 2748 (1965).
3. T. MIYAZAKI and S. SHIDA. Bull. Chem. Soc. Jap. **39**, 2344 (1966).
4. F. FIELD and J. FRANKLIN. Electron impact phenomena. Academic Press, Inc., New York. 1957.
5. F. LOSSING, P. KEBARLE, and J. SOUSA. Advances in mass spectrometry. The Pergamon Press, Ltd., London. 1959. p. 431.
6. V. AQUILANTI, A. GALLI, A. GIARDINI-GUIDONI, and G. VOLPI. Trans. Faraday Soc. **63**, 926 (1967).
7. V. L. TALROSE. Actions chimiques et biologiques des radiations. Vol. 11. *Edited by* Masson. Paris. 1967.
8. H. M. FREY. Proc. Chem. Soc. 385 (1959).
9. R. N. BIRREL and A. F. TROTMAN-DICKENSON. J. Chem. Soc. 4218 (1960).
10. J. A. GARCIA DOMINGUEZ, J. A. KERR, and A. F. TROTMAN-DICKENSON. J. Chem. Soc. 3357 (1962).
11. J. O. TERRY and J. H. FUTRELL. Can. J. Chem. **46**, 664 (1968).
12. K. WATANABE, T. NAKAYAMA, and J. MOTTL. J. Quant. Spectrosc. Radiative Transfer, **2**, 369 (1967).
13. L. W. SIECK and J. H. FUTRELL. J. Chem. Phys. **48**, 1409 (1968).
14. J. HERMAN, K. HERMAN, and P. AUSLOOS. J. Chem. Phys. To be published.
15. F. P. ABRAMSON and J. H. FUTRELL. J. Phys. Chem. **72**, 1994 (1968).
16. T. MIYAZAKI. J. Phys. Chem. **71**, 4282 (1967).
17. FF. WILLIAMS. Fundamental processes in radiation chemistry. John Wiley and Sons, Inc., New York. 1968. p. 554.
18. H. OKAMOTO, K. FUEKI, and Z. KURI. J. Phys. Chem. **71**, 3222 (1967).
19. S. G. LIAS and P. AUSLOOS. J. Chem. Phys. **38**, 36 (1963).
20. G. G. MEISELS. Fundamental processes in radiation chemistry. John Wiley and Sons, Inc., New York. 1968 p. 381.
21. R. GORDON, R. DOEPKER, and P. AUSLOOS. J. Chem. Phys. **44**, 3733 (1966).
22. R. M. LEBLANC and J. A. HERMAN. J. Chim. Phys. **63**, 1055 (1966).
23. S. W. BENSON. Thermodynamic kinetics. John Wiley and Sons, Inc., New York. 1968.
24. R. A. HOLROYD and G. W. KLEIN. J. Phys. Chem. **69**, 194 (1965).
25. E. TSCHUIKOW-ROUX and J. R. NCNESBY. Trans. Faraday Soc. **62**, 2158 (1966).
26. R. K. BRINTON. J. Phys. Chem. **72**, 321 (1968).

Can. J. Chem. Downloaded from www.nrcresearchpress.com by 210.87.254.40 on 09/05/12
For personal use only.

Can. J. Chem. Downloaded from www.nrcresearchpress.com by 210.87.254.40 on 09/05/12
For personal use only.

Pyrolysis of hydrocinnamic acid[1,2]

A. T. C. H. TAN[3] AND A. H. SEHON[4]
Department of Chemistry, McGill University, Montreal, Quebec

Received January 15, 1969

The pyrolysis of hydrocinnamic acid was investigated by the toluene-carrier technique over the temperature range 910–985 °K. The overall decomposition was first-order with respect to hydrocinnamic acid, and could be represented by reactions [1] and [2], respectively,

[1] $$C_6H_5CH_2CH_2COOH \xrightarrow{k_1} C_6H_5CH_2 + \cdot CH_2COOH$$

[2] $$C_6H_5CH_2CH_2COOH \xrightarrow{k_2} C_6H_5CH_2CH_3 + CO_2$$

Both reactions [1] and [2] were found to be homogeneous first-order processes, and the rate constants may be represented by the following expressions

$$k_1 = 1.1 \times 10^{12} \exp(-55\,000/RT) \quad s^{-1}$$

$$k_2 = 1.0 \times 10^{15} \exp(-69\,000/RT) \quad s^{-1}$$

The activation energy of reaction [1] is identified tentatively with $D(C_6H_5CH_2—CH_2COOH)$.

Canadian Journal of Chemistry, 47, 3845 (1969)

Introduction

In a previous study (1) the $\cdot CH_2COOH$ radical was produced by the rupture of the C_6H_5-S—CH_2COOH bond in the pyrolysis of phenylmercaptoacetic acid using the toluene-carrier technique. It was found that the $\cdot CH_2COOH$ radicals either abstracted a hydrogen atom from toluene to form acetic acid or decomposed to give other ill-defined fragments. The pyrolysis of hydrocinnamic acid was studied in the present investigation with a view to producing this radical from another source and in the hope of throwing additional light on the mechanism of the reactions of this radical.

It was anticipated that due to the resonance stabilization of the benzyl radical, the weakest bond in hydrocinnamic acid would be the C_6H_5-CH_2—CH_2COOH bond. Thus, on dissociation of this bond, one benzyl radical would be produced for each $\cdot CH_2COOH$ radical formed. It is a well-known fact that the benzyl radicals tend to dimerize to form dibenzyl. Consequently, if all the $\cdot CH_2COOH$ radicals abstracted hydrogen from toluene, the rate of formation of acetic acid would be equal to the rate of production of dibenzyl and either of these rates would measure the rate of dissociation of the corresponding C—C bond in hydrocinnamic acid. The activation energy of the decomposition reaction could then be identified with the bond dissociation energy, if the assumption is made that the activation energy of the reverse reaction is zero. On the other hand, if not all the $\cdot CH_2COOH$ radicals were removed by abstraction of hydrogen atoms from toluene, this study would provide the opportunity to study the decomposition reaction of this radical.

Experimental

Hydrocinnamic acid was the highest purity product of Eastman Organic Chemicals, Rochester, N.Y. Mass spectrometric analysis revealed that it was contaminated with a substance of molecular weight 198 in a fraction of 1%. It was used without further purification. The toluene was supplied by Gulf Petroleum Company, Pittsburgh, Pa. It was stirred for 20 h with calcium chloride and distilled through an efficient column; the fraction boiling at 110.5 °C was used in this study.

The pyrolysis of hydrocinnamic acid in a stream of toluene was studied over the temperature range 910–985 °K. The apparatus and procedure used were identical with those employed for the pyrolysis of phenylmercaptoacetic acid (1). Toluene was passed through the reaction vessel for 5 min both before and after the reaction to ensure that no pyrolysis of toluene alone occurred under the present experimental conditions.

---

[1]Presented at the 150th National Meeting of the American Chemical Society, Atlantic City, New Jersey, September 1965.

[2]These results were incorporated in the thesis submitted by A. T. C. H. Tan in partial fulfillment of the requirements for the Ph.D. degree, McGill University, 1965.

[3]Present address: Ophthalmology Research, McIntyre Medical Science Centre, McGill University, Montreal, Quebec.

[4]Present address: Department of Immunology, University of Manitoba, Faculty of Medicine, Winnipeg, Manitoba.

Can. J. Chem. Downloaded from www.nrcresearchpress.com by 210.87.254.40 on 09/05/12
For personal use only.

TABLE I

Products and overall rate constants for the pyrolysis of hydrocinnamic acid

Expt. No.*	Temp. (°K)	Toluene pressure (mm Hg)	Acid pressure (mm Hg)	Time of contact (s)	Acid decomp. (mmole)	$[CH_3COOH]$ (mmole)	Substance in liquid air trap (mmole)	$[CO_2]$ (mmole)	$[C_2H_4]$ (mmole)	$(\phi CH_2)_2$ (mmole)	Noncondensable gases (mmole)			k_0 (s^{-1})	k_1 (s^{-1})	k_2 (s^{-1})
											H_2	CO	CH_4			
19	985	16.43	0.52	0.83	0.600	0.171	0.327			0.350	0.050	0.161	0.066	1.40		
34	984	13.07	0.13	0.17	0.271	0.123	0.112	0.102	0.0004	0.229	0.005	0.038	0.026	1.47	0.91	0.56
36	984	8 29	0.16	0.42	0.491	0.173	0.213	0.193	0.0014	0.285	0.023	0.065	0.060	1.38	0.84	0.54
15	983	19.95	0.43	0.77	0.919	0.183	0.605			0.673	0.091	0.196	0.126	1.36		
33	983	6.11	0.09	0.20	0.380	0.099	0.184	0.168	0.0007	0.259	0.007	0.072	0.041	1.30	0.70	0.60
35	983	6.13	0.29	0.20	0.742	0.153	0.365	0.349	0.0016	0.622	0.037	0.115	0.098	1.30	0.75	0.55
48p	979	17.66	0.42	0.67	0.566	0.182	0.294			0.377	0.035	0.136	0.074	1.30		
20	978	15.30	0.59	0.85	0.597	0.176	0.332			0.367	0.040	0.118	0.083	1.15		
32	977	7.29	0.08	0.15	0.271	0.109	0.121	0.112	0.0005	0.188	0.008	0.043	0.037	1.09	0.64	0.45
8	976	15.75	0.35	0.86	0.870	0.192	0.408			0.593	0.050	0.230	0.084	1.20		
17	973	17.00	0.48	0.82	0.709	0.219	0.363			0.455	0.049	0.163	0.088	1.02		
16	971	18.90	0.40	0.75	0.513	0.176	0.271			0.333	0.034	0.107	0.065	0.91		
37	969	8.30	0.26	0.46	0.443	0.126	0.196	0.178	0.0011	0.271	0.016	0.067	0.050	0.80	0.48	0.32
38	969	10.32	0.35	0.35	0.502	0.146	0.213	0.197	0.0013	0.395	0.017	0.070	0.066	0.84	0.51	0.33
14	968	18.37	0.44	0.74	0.598	0.168	0.343			0.417	0.031	0.142	0.071	0.87		
9	967	18.69	0.28	0.72	0.624	0.267	0.270			0.468	0.025	0.144	0.092	0.77		
10	963	19.70	0.38	0.80	0.637	0.203	0.268			0.383	0.031	0.123	0.088	0.77		
11	961	18.15	0.30	0.72	0.514	0.227	0.205			0.336	0.019	0.098	0.096	0.63		
13	961	21.14	0.36	0.71	0.419	0.168	0.185			0.246	0.026	0.074	0.049	0.75		
3	956	20.00	0.28	0.73	0.398	0.172	0.174			0.299	0.015	0.073	0.067	0.56		
25	955	16.21	0.49	0.72	0.560	0.192	0.242	0.220	0.0002	0.402	0.025	0.092	0.072	0.57	0.35	0.22
42	955	16.77	0.36	0.32	0.319	0.150	0.105	0.097	0.0004	0.206	0.011	0.043	0.026	0.55	0.38	0.17
44	955	7.84	0.28	0.41	0.425	0.121	0.188			0.394	0.014	0.076	0.036	0.53		
47p	955	10.55	0.20	0.24	0.350	0.158	0.164	0.144	0.0015	0.248	0.017	0.064	0.033	0.56	0.34	0.22
43	954	7.62	0.36	0.42	0.409	0.121	0.165			0.296	0.013	0.066	0.039	0.51		
30	951	6.75	0.12	0.17	0.120	0.045	0.068			0.111	0.006	0.035	0.015	0.61		
46p	951	9.49	0.16	0.38	0.300	0.107	0.105			0.240	0.009	0.049	0.014	0.51		
2	949	21.13	0.33	0.79	0.347	0.154	0.137			0.214	0.014	0.064	0.042	0.45		
4	945	17.48	0.07	0.77	0.532	0.185	0.274			0.397	0.016	0.099	0.049	0.52		
24	945	16.49	0.49	0.79	0.406	0.150	0.181			0.327	0.014	0.084	0.049	0.39		
12	944	19.49	0.37	0.79	0.446	0.173	0.168			0.319	0.013	0.068	0.066	0.43		
23	944	12.93	0.63	0.85	0.564	0.173	0.310	0.183	0.0008	0.414	0.022	0.118	0.069	0.41	0.28	0.13
7	937	18.38	0.27	0.78	0.309	0.125	0.143			0.221	0.012	0.058	0.025	0.34		
39	936	14.99	0.28	0.30	0.219	0.095	0.089			0.162	0.003	0.024	0.013	0.33		
41	935	7.13	0.35	0.40	0.237	0.058	0.136	0.074	0.0006	0.162	0.008	0.032	0.018	0.27	0.18	0.09
40	934	7.40	0.05	0.43	0.239	0.127	0.086			0.171	0.008	0.039	0.018	0.27		
1	931	19.13	0.39	0.78	0.269	0.093	0.138			0.152	0.015	0.038	0.030	0.33		
6	924	19.91	0.34	0.75	0.232	0.112	0.114			0.116	0.008	0.035	0.016	0.22		
45p	917	8.85	0.33	0.38	0.108	0.040	0.062			0.068	0.001	0.014	0.005	0.22		
27	917	17.66	0.78	0.81	0.211	0.088	0.068			0.157	0.014	0.027	0.027	0.17		
5	910	17.81	0.77	0.91	0.192	0.011	0.092			0.106	0.014	0.029	0.026	0.14		

*The experiments marked p refer to those done in the packed reaction vessel. The packed reaction vessel has a surface/volume ratio 27 times that of the unpacked reaction vessel.

Can. J. Chem. Downloaded from www.nrcresearchpress.com by 210.87.254.40 on 09/05/12
For personal use only.

The set-up and experimental conditions for gas chromatographic analysis were described in a previous paper (1). A column of apiezon L on firebrick operated at 66 °C and a 30% TCP (Tricresylphosphate) on firebrick column operated at 120 °C were used to separate the products condensed at dry ice – acetone and liquid air temperatures, respectively.

The methods of analysis for the products were identical with that described in ref. 1, with the exception that the contents of the dry ice – acetone and liquid air traps from typical experiments in the present investigation were also analyzed by mass spectrometry. The products of the decomposition that were determined quantitatively are shown in Table I. In column 8 of Table I is given the total amount of substances trapped at liquid air temperature, which consisted of carbon dioxide, toluene, ethylene, and trace amounts of ketene.

Gas chromatographic analysis of the materials trapped at −78 °C revealed the presence of acetic acid, ethylbenzene, styrene, and unreacted toluene. In some experiments trace amounts of acetone and benzene were also detected by mass spectrometry.

Infrared analysis of the substances trapped at −188 °C demonstrated that carbon dioxide was the main product. In addition, small amounts of ethylene and ketene were characterized by the two peaks at 950 (2) and 2150 cm^{-1} (3), respectively. Mass spectrometric analysis of the contents in this trap from 12 experiments indicated the presence of more than 90% of carbon dioxide in most experiments, a few % of unreacted toluene which had not been completely trapped out at −78 °C, and less than 1% of ethylene. In some experiments trace amounts of water, C_2 (other than ethylene), and higher hydrocarbons were also detected.

The noncondensable gases consisted of 42–70% of carbon monoxide, the remainder being hydrogen and methane.

The sum of carbon dioxide, acetic acid, and carbon monoxide was almost equal to the amount of hydrocinnamic acid decomposed. The ratio of the two quantities varied from 0.85 to 1.1, except in experiment 41, where this ratio was as low as 0.69. This run was performed at 935 °K, i.e., at the lower end of the whole temperature range used, at which the extent of decomposition was small and consequently the experimental error larger than in other experiments.

The quantity of dibenzyl was equivalent to 55–93% of the acid decomposed, and was approximately 65% in most experiments. The ratio of carbon dioxide to acid decomposed was from 0.30 to 0.47, being about 0.4 in most experiments.

Ethylbenzene and styrene were trapped together in a large excess of toluene. Since the latter two compounds represented about 0.5% of the toluene, it was rather difficult to determine their quantities accurately.

Discussion

Mechanism of Decomposition

The products of the pyrolysis suggest that the thermal decomposition of hydrocinnamic acid might occur primarily by the two simultaneous processes [1] and [2], involving a free radical and a molecular dissociation reaction, respectively.

$$[1]\quad C_6H_5CH_2CH_2COOH \xrightarrow{k_1} C_6H_5CH_2\cdot + \cdot CH_2COOH$$

$$[2]\quad C_6H_5CH_2CH_2COOH \xrightarrow{k_2} C_6H_5CH_2CH_3 + CO_2$$

Thus, reaction [1] would represent the dissociation of the C—C bond resulting in the formation of the benzyl and $\cdot CH_2COOH$ radicals, and reaction [2] would represent the molecular dissociation yielding ethylbenzene and carbon dioxide. From the relative amounts of the products formed, reaction [1] appears to predominate over the temperature range studied.

If each of the $\cdot CH_2COOH$ radicals produced in reaction [1] were to abstract one hydrogen atom from toluene

$$[3]\quad \cdot CH_2COOH + C_6H_5CH_3 \rightarrow C_6H_5CH_2\cdot + CH_3COOH$$

and all the benzyl radicals dimerized to dibenzyl

$$[4]\quad 2C_6H_5CH_2 \rightarrow (C_6H_5CH_2)_2$$

one would expect to have the following stoichiometry

$$[C_6H_5CH_2CH_2COOH \text{ decomposed}] = [CH_3COOH] + [CO_2]$$

$$[C_6H_5CH_2CH_3] = [CO_2]$$

and

$$[(C_6H_5CH_2)_2] = [CH_3COOH]$$

However, the results indicated that

$$[C_6H_5CH_2CH_2COOH \text{ decomposed}] > [CH_3COOH] + [CO_2]$$

$$[(C_6H_5CH_2)_2] > [CH_3COOH]$$

Therefore, it must be concluded that reaction [3] was not sufficiently rapid to remove all the $\cdot CH_2COOH$ radicals. This conclusion is supported by the fact that other products were also formed in this reaction system.

Calculation of $D(C_6H_5CH_2—CH_2COOH)$

If the rate of the overall decomposition were first-order with respect to hydrocinnamic acid, the overall rate constant k_o could be calculated by using the following rate expression

$$k_o = \frac{1}{t} \ln \frac{A}{A - X}$$

where t is the time of contact in s, A the amount of

Can. J. Chem. Downloaded from www.nrcresearchpress.com by 210.87.254.40 on 09/05/12
For personal use only.

hydrocinnamic acid introduced, and $A - X$ represents the amount of hydrocinnamic acid recovered in trap "U" surrounded with ice. Furthermore, if the two modes of decomposition, as represented by reactions [1] and [2], were first-order reactions, and if reactions [3] and [4] were very fast by comparison with reaction [1], one could obtain the rate constants k_1 and k_2 for reactions [1] and [2], respectively, by the following expressions

$$k_1 = \frac{[(C_6H_5CH_2)_2]}{[A]} k_o [1 - \exp(-k_o t)]^{-1}$$

$$k_2 = \frac{[CO_2]}{[A]} k_o [1 - \exp(-k_o t)]^{-1}$$

where $[(C_6H_5CH_2)_2]$ and $[CO_2]$ represent the amounts of dibenzyl and carbon dioxide formed in time t, respectively.

According to the proposed mechanism, the only source for carbon dioxide would be reaction [2]. Therefore, the rate of formation of CO_2 would be a measure of the rate of reaction [2]. The difference between the total amount of hydrocinnamic acid decomposed and the amount of carbon dioxide would thus correspond to the amount of acid decomposed via reaction [1]. The rate constants k_1 and k_2 thus calculated for 12 experiments are shown in Table I.

The rate constant of the overall decomposition of hydrocinnamic acid, k_o, at a given temperature was not affected, within experimental accuracy, by the variation of the partial pressure of acid by a factor of 9, of the toluene pressure by a factor of 2, and of the time of contact by a factor of 5. These results are also shown in Table I. It is also evident from Table I that the increase in surface/volume ratio by a factor of 27 had practically no effect on the rate constant k_o. The effects of the variation of the partial pressures of the acid and toluene, of the time of contact, and of the surface/volume ratio on k_1 and k_2 are shown in Table I. From these results it is deduced that the overall decomposition of hydrocinnamic acid, as well as the two modes of its decomposition, [1] and [2], were homogeneous, first-order reactions. The plots of log k_o vs. $1/T$, log k_1 vs. $1/T$, and log k_2 vs. $1/T$ are shown in Figs. 1, 2, and 3, respectively. The plots are linear over the temperature range studied. From these plots the corresponding parameters in the Arrhenius equation, $k = A \exp(-E/RT)$, were calculated as given below.

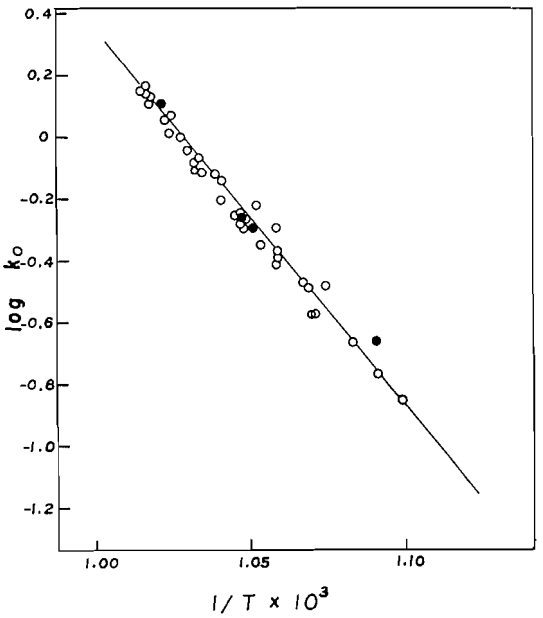

FIG. 1. Plot of log k_o vs. $1/T$. Experiments done in the packed reaction vessel are indicated by the filled circles.

For the overall decomposition

$$E_o = 56 \quad \text{kcal/mole}$$

$$A_o = 3.0 \times 10^{12} \quad \text{s}^{-1}$$

for reaction [1]

$$E_1 = 55 \quad \text{kcal/mole}$$

$$A_1 = 1.1 \times 10^{12} \quad \text{s}^{-1}$$

and for reaction [2]

$$E_2 = 69 \quad \text{kcal/mole}$$

$$A_2 = 1.0 \times 10^{15} \quad \text{s}^{-1}$$

The A factor of 1.1×10^{12} s^{-1} for reaction [1] is within the range of 10^{12}–10^{14} s^{-1} associated with most unimolecular reactions. However, A_1 is only 0.14 and 0.003 of the A factors for the pyrolyses of phenylacetic acid (4) and ethylbenzene (5), respectively. The experimentally estimated activation energy for reaction [1] is of the right order of magnitude when compared with the value of 55 kcal/mole (4) associated with the decomposition of phenylacetic acid, but is considered somewhat low if compared with the value

Can. J. Chem. Downloaded from www.nrcresearchpress.com by 210.87.254.40 on 09/05/12
For personal use only.

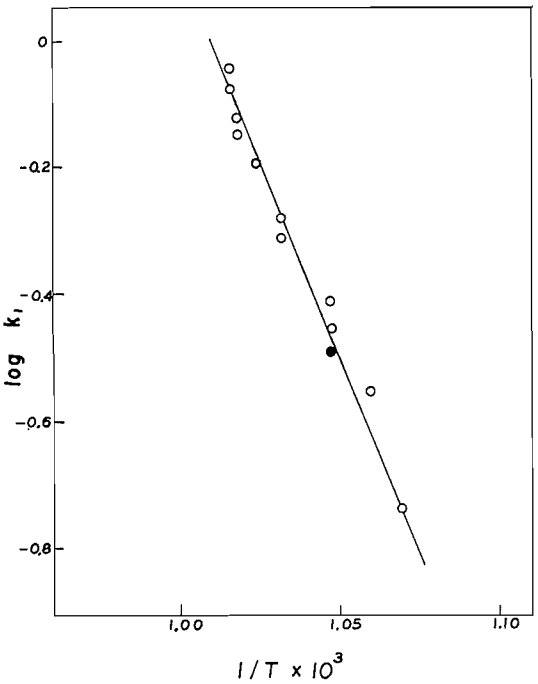

FIG. 2. Plot of log k_1 vs. $1/T$. Experiment done in the packed reaction vessel is indicated by the filled circle.

of 70 kcal/mole (5) assigned to $D(C_6H_5CH_2—CH_3)$. Keeping in mind the complexity of the decomposition of hydrocinnamic acid and the assumptions made in the estimation of k_1, it is possible to visualize that in addition to reaction [2], side reaction or reactions producing carbon dioxide might have occurred to a small extent; the linearity of the Arrhenius plot may not be noticeably affected though the activation energy calculated from it may be erroneous. Owing to this uncertainty, the identification of E_1 with the $D(C_6H_5CH_2—CH_2COOH)$ is only tentative.

The Secondary Reactions

The $\cdot CH_2COOH$ radicals may abstract hydrogen according to reaction [3] stated previously, or may decompose according to reaction [5]

[5] $$\cdot CH_2COOH \rightarrow CH_2CO + \cdot OH$$

The ·OH radicals would be expected to disappear by reaction [6]

[6] $$\cdot OH + C_6H_5CH_3 \rightarrow C_6H_5CH_2\cdot + H_2O$$

Water was detected in the liquid air trap by mass spectrometry. However, its amount was small and it could have been due to extraneous sources rather than to reaction [6] exclusively. Nevertheless, under the experimental conditions used in this investigation, reaction [6] appears to be the most probable reaction of the ·OH radical; this has also been suggested by other workers (4).

The detection of ketene among the products supports reaction [5]. However, the amount of ketene is too small to account for the difference between the amounts of the $\cdot CH_2COOH$ radicals produced, as reflected by the amount of dibenzyl formed, and that of acetic acid. This indicates that some ketene underwent further reaction. On concentration grounds alone, dimerization of ketene is considered unlikely. Failure to detect diketene among the products of the pyrolysis of ketene (6, 7) supports this proposal.

Carbon monoxide has been found to be the major product of the pyrolysis of ketene, both using the static system at 510–590° (6), 396–563° (7), 500–550° (8), and 570° (9) and the flow system at 1120° (10). The ratio of carbon monoxide to methane varied between 2.1 (8) and 6.1 (9), and that of carbon monoxide to ethylene ranged from 2.1 (10) to 18.6 (8) at temperatures larger than 500°. The CO to $(CH_4 + C_2H_4)$ ratio in all reports is about 2 (7–10). The discrepancies in

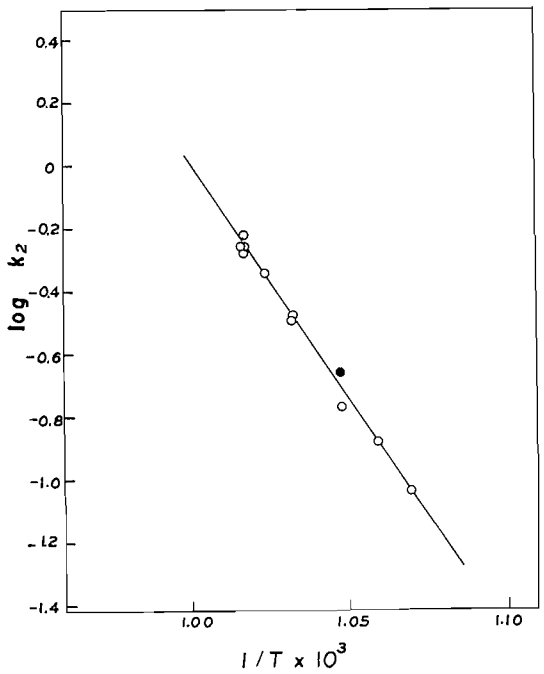

FIG. 3. Plot of log k_2 vs. $1/T$. Experiment done in the packed reaction vessel is indicated by the filled circle.

CO/CH_4 and CO/C_2H_4 may be due to analytical error, as trap-to-trap distillation used in the determination of these compounds may not be perfect, although changes in the mechanism of decomposition under various experimental conditions may also play an important role. The fact that the $CO/(CH_4 + C_2H_4)$ is about 2 in the present investigation suggests that further reaction of ketene produced in reaction [5] is probably responsible for the formation of carbon monoxide, methane, and ethylene. Moreover, the further reaction of ketene might also explain the formation of C_2 and higher hydrocarbons (6, 7, 10).

Carbon dioxide was also detected among the products in the pyrolysis of ketene using a static system by Young (6), Akeroyd (9), and Guenther and Walters (7), but not by Williamson (8), at temperatures lower than 590°. In a flow system at 1120°, carbon dioxide was absent (10). Guenther and Walters (7) studied the temperature dependency of the ketene decomposition products volatile at −78° and found that the mole % of carbon dioxide decreased with increasing temperature from 52.5 at 498° to 20 at 563°, whereas the mole % of carbon monoxide increased from 19.1 at 498° to 48 at 563°. The lowest temperature used in the present study was about 50° higher than the highest temperature used in the decomposition of ketene where carbon dioxide was detected (6, 7, 9). On the basis of the results of the pyrolysis of ketene (7, 8, 10), it appears that the amount of carbon dioxide which might have been produced from ketene decomposition in the present system was probably negligible. This conclusion is supported by the linearity of the Arrhenius plots.

The following reaction would account for the formation of hydrogen and styrene

[7] $$C_6H_5CH_2CH_3 \rightarrow C_6H_5CH{=}CH_2 + H_2$$

Reaction [7] occurred also in the pyrolysis of ethylbenzene using the toluene-carrier technique (11). Further reactions of ketene is also a possible source for hydrogen (6, 7, 9, 10).

The presence of trace quantities of benzene in some experiments may be explained by (*a*) benzene might exist as an impurity in the original toluene that had not been removed completely by the distillation treatment, (*b*) benzene may be formed by the molecular decomposition of ethylbenzene (5), and (*c*) benzene may be formed by the pyrolysis of toluene to a small extent. Under the experimental conditions used in the present investigation, reason (*a*) perhaps is the most probable one.

The source of trace quantities of acetone is not clear. Since acetone was used to clean the removable traps in the system, one would be tempted to suspect it might have originated from the system.

In view of the complex nature of the decomposition of hydrocinnamic acid and the incomplete analysis of the products, it is advisable to postpone further consideration of the mechanism until additional data are available.

Acknowledgments

The authors wish to acknowledge their indebtedness to Mr. S. Meyerson, American Oil Company, Indiana, for the mass spectrometric analysis.

This work was supported in part by the Petroleum Research Fund administered by the American Chemical Society. Grateful acknowledgment is hereby made to the donors of said fund. The authors wish to thank also the National Research Council of Canada for continued financial assistance.

1. A. T. C. H. Tan and A. H. Sehon. Can. J. Chem. **46**, 191 (1968).
2. R. N. Jones and C. Sandorfy. Chemical applications of spectroscopy. Interscience Publishers, Inc., New York. 1956.
3. Infrared spectral data. Curve 699, ketene. American Petroleum Institute Research Project 44, Texas A & M University, College Station, Texas.
4. M. H. Back and A. H. Sehon. Can. J. Chem. **38**, 1261 (1960).
5. G. L. Esteban, J. A. Kerr, and A. F. Trotman-Dickenson. J. Chem. Soc. 3873 (1963).
6. J. R. Young. J. Chem. Soc. 2909 (1958).
7. W. B. Guenther and W. D. Walters. J. Amer. Chem. Soc. **81**, 1310 (1959).
8. A. T. Williamson. J. Amer. Chem. Soc. **56**, 2216 (1934).
9. E. I. Akeroyd. Ph.D. Thesis, Cambridge University, Cambridge, England. 1936.
10. J. A. Muller and E. Peytral. C. R. **196**, 279 (1933).
11. M. Szwarc. J. Chem. Phys. **17**, 431 (1949).

Can. J. Chem. Downloaded from www.nrcresearchpress.com by 210.87.254.40 on 09/05/12
For personal use only.

Can. J. Chem. Downloaded from www.nrcresearchpress.com by 210.87.254.40 on 09/05/12
For personal use only.

Ion exchange and solvent extraction equilibria in mixed electrolytes

S. K. PATIL AND H. D. SHARMA[1]

Radiochemistry Division, Bhabha Atomic Research Centre, Trombay, Bombay

Received November 27, 1968

The distribution coefficients of 2-thenoyl trifluoroacetone (TTA) between the organic and aqueous phase containing mixtures of ClO_4^-, NO_3^-, Cl^-, SCN^-, and SO_4^{2-} ions indicate that the activity coefficients of TTA in the aqueous phase are given by $\ln \gamma = \Sigma ks_i Cs_i$ where ks_i and Cs_i are the salting-out parameter and molar concentration of the ith component, respectively. The salting-out effect on TTA follows the usual pattern for a non-electrolyte, i.e. $SO_4^{2-} > Cl^- > Br^- > ClO_4^- > SCN^-$ for anions and $Li^+ > Na^+ > H^+$. In the solvent extraction equilibria, the extraction behavior of the neutral species $M(TTA)_n$ may not be similar to that of TTA and thus stability constants determined by this method, wherein there are large changes of anion composition in the aqueous phase to maintain the ionic strength constant, may be in error. The ion exchange equilibria have also been investigated by determining distribution coefficients, D, of metal ions in trace concentrations in mixed electrolyte solutions. The large, poorly hydrated ions are salted into the resin phase in the presence of anions like ClO_4^- having the property of breaking the water structure. In mixed electrolytes containing perchlorate, nitrate, and chloride ion mixtures, the D values are difficult to rationalize on the basis of the activity coefficients of ions alone. The stability constants for the formation of $CaCl^+$, $CaNO_3^+$, $BaCl^+$, and $BaNO_3^+$ determined by the ion exchange method at $\mu = 1$ are not in agreement with those obtained by the spectroscopic method.

Canadian Journal of Chemistry, 47, 3851 (1969)

Introduction

Ion exchange and 2-thenoyl trifluoroacetone (TTA) extraction methods have been widely used for the determination of stability constants of complexes in aqueous systems (1–6). During the course of work on the determination of stability constants of the actinide elements, in particular Am(III), it was observed that the values obtained by the TTA method differed from ones obtained by the ion exchange and solubility methods (7, 8). In these methods one of the assumptions is that the activity coefficients of the distributed species in the two phases do not alter when ionic composition in the aqueous phase is changed for maintaining a constant ionic strength. This is generally achieved by taking mixed electrolytes like SO_4^{2-}, NO_3^-, Cl^-, or ClO_4^- in varying composition assuming one of them, usually ClO_4^-, complexes least. While there have been various suggestions to refine the ion exchange method by determining distribution coefficients in different cross-linked resins (9), there exist no studies wherein the distribution coefficients have been determined in mixed electrolytes. It is expected that the distribution coefficient of the metal ion will remain constant if there is no ion association or complexing in the aqueous phase. Similarly, the variation in activity coefficients of TTA in the aqueous phase is not known in the presence of the mixed electrolytes. In this paper are reported the results of the study of the distribution of TTA and metal ions in the organic and the aqueous phases, and also of the metal ions in the ion exchange resin, in the presence of mixed electrolytes, and maintaining constant ionic strength.

Experimental

All sodium salts and acids used were AnalaR grade except sodium perchlorate which was prepared by neutralizing sodium hydroxide (AnalaR) with standard perchloric acid. Lithium salts used were C.P. grade (E. Merck) except lithium sulfate which was AnalaR grade. TTA obtained from Peninsular Chemical Research Inc. was recrystallized from AnalaR benzene. The resin used was air-dried Amberlite IR-120 (52–100 mesh) in acid form. In the experiments with resins of varying cross-linkage, Dowex-50 was used.

The acids were standardized against sodium hydroxide solution. The accuracy of standardization was checked using standard sodium carbonate solution. The pH of the solution was measured by using a glass electrode and Beckman (Model G) pH-meter. Perchloric acid was used to maintain a constant ionic strength of 1. Sodium or lithium perchlorate was used for maintaining a constant ionic strength of 1 with pH = 3.0. The complexing anions were added by replacing perchloric acid by hydrochloric, nitric, or sulfuric acid when the hydrogen ion concentration was 1 M, whereas at pH = 3.0 sodium or lithium perchlorate was replaced by the corresponding chloride, nitrate, or sulfate to maintain constant ionic strength.

Americium-241 was obtained from The Atomic Energy Research Establishment, Harwell, England and

[1]Present address: University of Waterloo, Waterloo, Ontario.

Can. J. Chem. Downloaded from www.nrcresearchpress.com by 210.87.254.40 on 09/05/12
For personal use only.

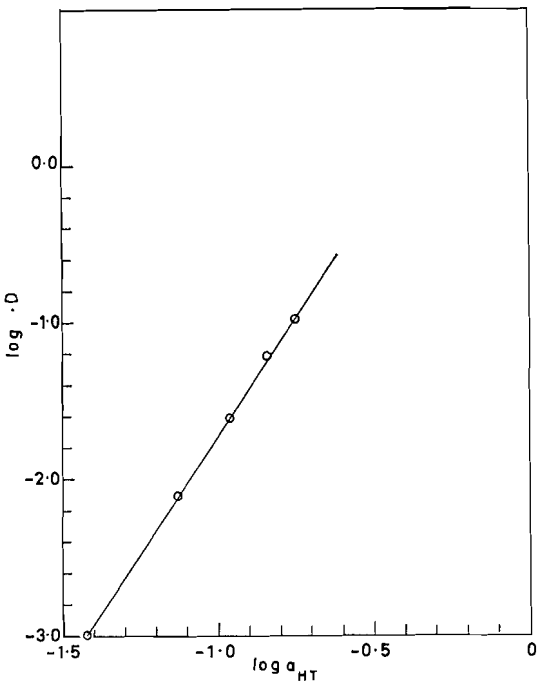

FIG. 1. Distribution coefficients of Am(III) vs. the activity of TTA.

used after purification. ^{24}Na, ^{86}Rb, ^{45}Ca, ^{133}Ba, and ^{181}Hf tracers were produced in the Apsara reactor and ^{137}Cs was separated from the fission product mixture. The radiochemical purity of all these isotopes was checked by γ-ray spectroscopy.

In the TTA extraction experiment with ^{241}Am, 5 ml aqueous solution of ionic strength 1, pH = 3.2, and 1 *M* in chloride ion containing tracer americium(III) was contacted with an equal volume of pre-equilibrated solution of TTA in benzene. The ^{241}Am concentration in both the phases was determined radiometrically using an NaI(Tl) scintillation counter.

Equal volumes of an aqueous phase with constant ionic strength and hydrogen ion concentration, but varying salt composition and 0.2 *M* TTA in benzene, were equilibrated for 1 h, which was found to be the equilibration time. The concentration of TTA in the equilibrated aqueous phase was determined spectrophotometrically by measuring optical density at 292 mμ (ε 292 = 7875). All the experiments were done in duplicate and the results of these duplicates usually agreed within 2% with a maximum difference of ±5%.

Distribution coefficients of Hf^{4+} between 2 *M* $HClO_4$ and 2 *M* HCl and TTA in different solvents, namely toluene, hexane, and carbon tetrachloride, were determined. Each experiment was done 4–6 times and the values given are the average ones.

The experimental details used in ion exchange are described in our earlier paper (7). In the case of ^{24}Na, ^{137}Cs, and ^{86}Rb, the distribution coefficient being quite small, it could be reproduced within only ±10% although in some cases 8 duplicates were done to get reliable values.

Results

The variation of distribution coefficients of Am(III) with the activity of TTA is shown in Fig. 1. The activity coefficients of TTA in benzene were taken from King and Reas (10).

The variation of concentration of TTA in the aqueous phase having constant hydrogen ion concentration and constant ionic strength but varying salt composition is shown in Figs. 2, 3, and 4. The change in solubility of TTA in aqueous phase at pH = 3 and ionic strength of 1 in Cl^-–ClO_4^- mixtures, determined by equilibrating the aqueous solution with solid TTA for 65 h, is shown in Fig. 5. The distribution coefficients, *D*, of Hf^{4+} in 2 *M* $HClO_4$ and 2 *M* HCl solution with TTA in various solvent are given in Table I.

The distribution coefficients, *D*, are presented in Tables II and III for Na^+, Rb^+, Cs^+, Ca^{2+}, and Ba^{2+} in tracer concentrations in ion exchange resin and aqueous solutions having varying Cl^-–ClO_4^-, NO_3^-–ClO_4^- mixtures of constant ionic strength of 1. Table IV gives the values of *D* for Am(III) in Cl^-–ClO_4^- solutions and different cross-linked resins.

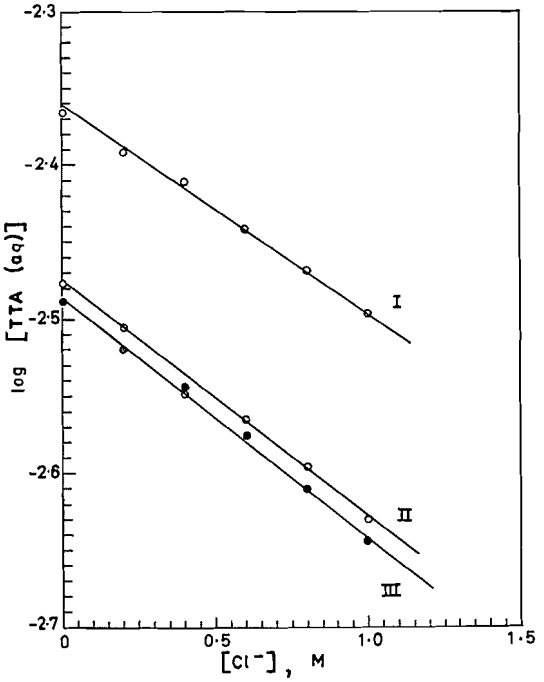

FIG. 2. Concentration of TTA in aqueous phase at μ = 1, 0.2 *M* TTA in benzene. I, HCl + $HClO_4$ solutions; II, NaCl + $NaClO_4$ solutions; III, LiCl + $LiClO_4$ solutions.

Can. J. Chem. Downloaded from www.nrcresearchpress.com by 210.87.254.40 on 09/05/12
For personal use only.

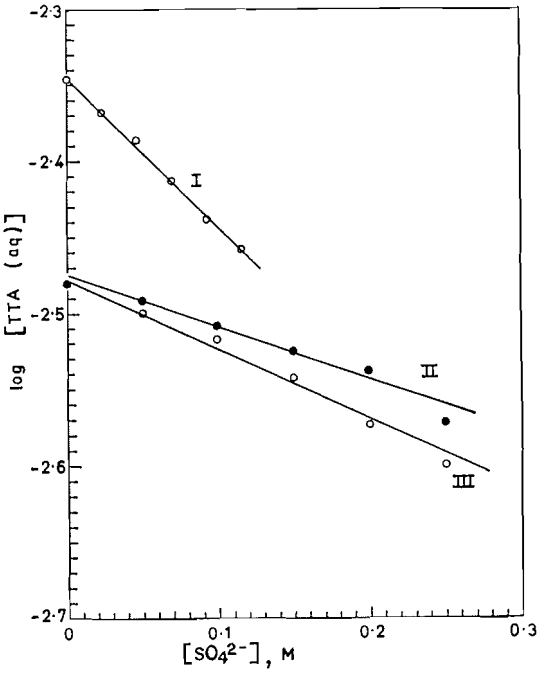

FIG. 3. Concentration of TTA in aqueous phase at $\mu \sim 1$, 0.2 *M* TTA in benzene. I, H_2SO_4 and $HClO_4$ solutions; II, Na_2SO_4 and $NaClO_4$ solutions; III, Li_2SO_4 and $LiClO_4$ solutions.

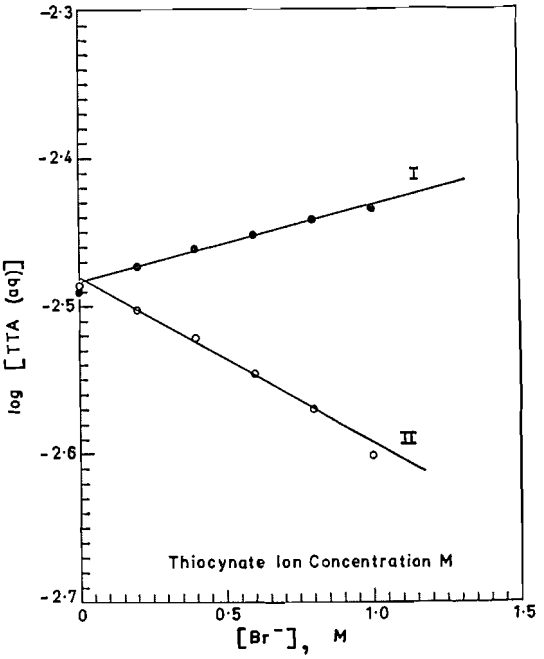

FIG. 4. Concentration of TTA in aqueous phase at $\mu = 1$, 0.2 *M* TTA in benzene. I, NaSCN–$NaClO_4$ solutions; II, NaBr–$NaClO_4$ solutions.

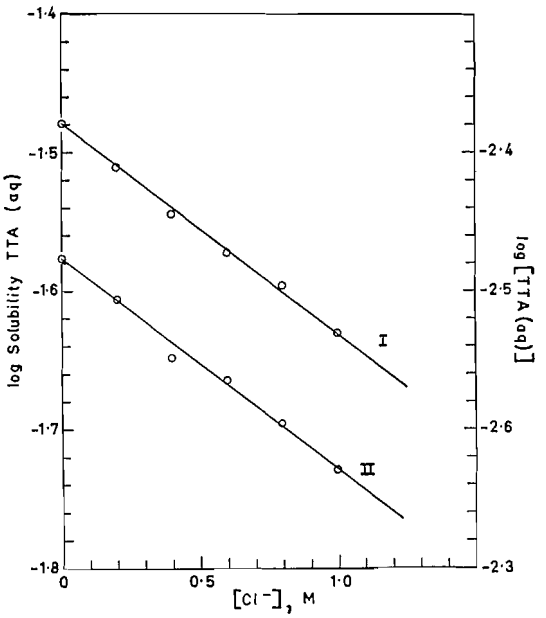

FIG. 5. Solubility of TTA in NaCl–$NaClO_4$ system. I, solubility of TTA; II, distribution data.

Discussion

Solvent Extraction

The extraction of the metal ion, Am^{3+}, from the aqueous phase into the organic phase in the presence of TTA can be depicted by the following equilibria, if it is assumed that AmT_3 is the only species extracted into the organic phase

$$Am^{3+} + nHT \rightleftharpoons AmT_n^{(3-n)+} + nH^+$$

$$AmT_3(aq) \rightleftharpoons AmT_3(org)$$

$$HT(aq) \rightleftharpoons HT(org)$$

and the equilibrium and extraction constants are defined as follows

$$[1] \quad \beta_n = \frac{[AmT_n^{(3-n)+}][H^+]^n \gamma_{AmT_n^{(3-n)+}}}{[Am^{3+}][HT]^n \gamma_{Am^{3+}} \gamma_{HT}^n}$$

$$[2] \quad K' = \frac{[HT(org)]\gamma_{HT(org)}}{[HT(aq)]\gamma_{HT(org)}}$$

$$[3] \quad K'' = \frac{[AmT_3(org)]\gamma_{AmT_3(org)}}{[AmT_3(aq)]\gamma_{AmT_3(aq)}}$$

where γ is the activity coefficient of the species as denoted by the subscript. The terms for organic phase only are further denoted by another subscript (org) hereafter. γ_{H^+} terms have not been included.

TABLE I

Distribution coefficients, D, of Hf^{4+} in TTA in solvents

Solvent	TTA Concentration (M)	D_0 in 2 M $HClO_4$	D_a in 2 M HCl	D_0/D_a
Carbon tetrachloride	0.0278	1.160±0.02	0.265±0.01	4.38±0.1
Hexane	0.0280	1.066±0.02	0.329±0.015	3.24±0.1
Toluene	0.0287	1.323±0.08	0.244±0.010	5.42±0.1

TABLE II

Distribution coefficients, D, of alkali metal ions in ion exchange resin

Anion concentration (M)	Na^+		Rb^+		Cs^+	
	Cl^-	NO_3^-	Cl^-	NO_3^-	Cl^-	NO_3^-
0 0	3.71±0.7	3.71±0.7	4.24±0.2	4.24±0.2	8.51±0.5	8.51±0.5
0.25	4.25±0.5	4.25±0.2	5.61±0.2	6.05±0.2	8.00±0.5	
0.50	3.71±0.3	4.25±0.2	8.35±0.2	5.55±0.2	10.95±0.7	9.3 ±0.9
0.75	4.45±0.5	3.84±0.4	9.71±0.7	6.42±0.2	13.24±0.3	
1.00	5.12±0.3	3.78±0.2	12.54±0.8	11.29±0.5	16.42±0.4	10.4 ±0.9

The distribution coefficient is defined as

$$[4] \qquad D_0 = \frac{[AmT_3(org)]}{\sum_{n=0}^{n} [AmT_n^{(3-n)+}]}$$

The expression for D_0 can be rewritten by substituting terms for $[AmT_n^{(3-n)+}]$ and $[AmT_3(org)]$ from eqs. [2] and [3]

$$[5] \qquad D_0 = \frac{K''\beta_3}{\gamma_{AmT_3(org)} \sum_{n=0}^{3} \beta_n \dfrac{[H^+]^{3-n}}{[HT]^{3-n}\gamma_{AmT_n^{(3-n)+}}\gamma_{HT}^{3-n}}}$$

Similarly, in the presence of complexing anion, X^{-1}, the following equilibria are considered

$$Am^{3+} + jX^{-1} \rightleftharpoons AmX_j^{(3-j)+}$$

$$AmT_n^{(3-n)+} + jX^{-1} \rightleftharpoons AmT_nX_j^{(3-n-j)+}$$

and the equilibrium constants

$$[6] \qquad \beta_j = \frac{[AmX^{(3-j)+}]\gamma_{AmX^{(3-j)+}}}{[Am^{3+}][X^-]^j\gamma_{Am^{3+}}\gamma_X^j}$$

$$[7] \qquad \beta_{nj} = \frac{[AmT_nX_j^{(3-n-j)+}]\gamma_{AmT_nX_j^{(3-n-j)+}}}{[AmT_n^{(3-n)+}][X^-]^j\gamma_{AmT_n^{(3-n)+}}\gamma_X^j}$$

where $\beta_{0j} = \beta_j$, $\beta_n = \beta_{n0}$, and $\beta_0 = \beta_{00} = 1$.

The distribution coefficient, D_a, in the presence of complexing anion is similarly given by the following expression, assuming neutral species like AmT_2X as well, are extracted.

$$[8] \qquad D_a = \frac{K''\beta_3}{\gamma'_{AmT_3(org)} \sum_{n=0}^{3} \sum_{j=0}^{j} \beta_{nj} \dfrac{[H^+]^{3-n} \cdot X^j \cdot \gamma'^j_X}{[HT]^{3-n}\gamma'^{3-n}_{HT} \cdot \gamma'_{AmT_nX_j^{(3-n-j)+}}}} + \frac{K'''\beta_{21}}{\gamma'_{AmT_2X(org)} \sum_n \sum_j \beta_{nj} \dfrac{[H^+]^{2-n}X^{j-1}\gamma'^{j-1}_X}{[HT]^{2-n}\gamma'^{2-n}_{HT}\gamma'^{(3-n-j)+}_{AmT_nX_j}}}$$

Can. J. Chem. Downloaded from www.nrcresearchpress.com by 210.87.254.40 on 09/05/12
For personal use only.

Can. J. Chem. Downloaded from www.nrcresearchpress.com by 210.87.254.40 on 09/05/12
For personal use only.

TABLE III
Distribution coefficients, D, of Ca^{2+} and Ba^{2+}

Anion concentration (M)	Ca^{2+}		Ba^{2+}	
	Cl^-	NO_3^-	Cl^-	NO_3^-
0.0	76.9±1.0	76.9±1.0	174.1	174.1
0.25	64.7±0.3		164.7	133.1
0.50	56.6±0.8	58.9±0.1	159.3	101.7
0.75	50.8±0.2		150.8	81.8
1.00	44.7±0.1	44.6±1.5	146.3	70.3

TABLE IV
Distribution coefficients, D, for Am(III) in ion exchange resin

	Amberlite IR−120 × 8		Dowex 50 × 12		Dowex 50 × 16	
$[Cl^-]$	D	$\left(\frac{D_0}{D_a}-1\right)[Cl^-]^{-1}$	D	$\left(\frac{D_0}{D_a}-1\right)[Cl^-]^{-1}$	D	$\left(\frac{D_0}{D_a}-1\right)[Cl^-]^{-1}$
0.0	1397	—	2307	—	3292	—
0.1	1289	0.84	—	—	—	—
0.2	1156	1.04				
0.25			1964	0.91	2751	0.96
0.3	1083	0.97	—	—	—	—
0.5	968	0.89	1665	0.89	2416	0.83
0.6	887	0.96	—	—	—	—
0.7	827	0.98				
0.75			1394	0.97	1933	1.02
0.8	753	1.07	—	—	—	—
1.0	696	1.01	1223	0.97	1802	0.89

where

$$K''' = \frac{[AmT_2X(org)]\gamma'_{AmT_2X}}{[AmT_2X]\gamma'_{AmT_2X}}$$

and γ' is the activity coefficient in the presence of complexing anion.

Activity Coefficients of TTA (γ_{HT})

The activity coefficients of TTA in the aqueous phase were examined by the solubility and distribution methods (11), so as to enable evaluation of D_0 and D_a. In two experiments, one involving 1 M ClO_4^- and the other involving ClO_4^- and another anion (Cl^-, NO_3^-, SO_4^{2-}, Br^-, or SCN^-) having total ionic strength of 1 in the aqueous phase, the concentration of TTA in the reference phase (benzene) was kept constant, and the following equation applies

$$\gamma_0 C_0 = b\gamma_R C_R = \gamma_i C_i$$

where

γ_0 = the activity coefficient of TTA in ClO_4^- medium in the aqueous phase

γ_i = the activity coefficient of TTA in the mixed solution in the aqueous phase

γ_R = the activity coefficient of TTA in the organic phase

C_0, C_i, and C_R = concentration of TTA in the respective phases

b = constant

$$\frac{C_0}{C_i} = \frac{\gamma_i}{\gamma_0}$$

Similarly, for the solubility of TTA in the aqueous phase in contact with solid TTA, the following relationship holds

$$S_0\gamma_0 = S_i\gamma_i$$

where S_0 = solubility of TTA in 1 M ClO_4^- and S_i = solubility of TTA in the mixed solution.

The results as shown in Figs. 2–5, indicate that

$$\frac{C_0}{C_i} = \frac{S_0}{S_i}$$

Can. J. Chem. Downloaded from www.nrcresearchpress.com by 210.87.254.40 on 09/05/12
For personal use only.

for the same pair of systems. It can also be deduced that

$$\ln \gamma_i = k_s . C_s$$

where k_s is a salting-out parameter and there is no contribution due to self-interaction of the non-electrolyte in the solution. The salting-out effect follows the order

$$SO_4^{2-} > Cl^- > Br^- > ClO_4^- > SCN^-$$

and

$$Li^+ > Na^+ > H^+$$

which is the usual one observed for non-electrolytes (11). The activity of TTA in the aqueous phase can thus be directly related to its activity in the organic phase. The activity coefficients of TTA in benzene have been determined by King and Reas (10) and can be used for further evaluation of eqs. [5] and [8].

The expressions for D_0 and D_a have terms in polynomials of $[H^+]$ and [HT]. The determinations of D_0 and D_a at various [HT(org)] in the presence of mixtures of electrolytes, viz. ClO_4^-, ClO_4^-, and Cl^- showed that both D_0 and D_a varied with $[HT(org)]^3\ \gamma_{HT(org)}{}^3$ when the $[H^+]$ concentration was maintained constant, as shown in a typical plot of log D vs. log $a_{HT(org)}$ (Fig. 1). Similarly, the results of Khopkar and Sharma showed that D_0 and D_a varied with $[H^+]^3$ when [HT] was maintained constant (7*b*). It is thus verified that the terms in eqs. [5] and [8] involving $[H^+]^{3-n-j}$ and $[HT]^{3-n-j}$ for $n \geqslant 1$ do not contribute significantly in the expression for D_0 and D_a. In other words, the concentrations of species like $AmT_n^{(3-n)}$ for $n \geqslant 1$ are small as compared to $AmX_j^{(3-j)+}$ under the experimental conditions. Furthermore, the earlier assumption that AmT_3 is the only species extracted into the organic phase holds good and no mixed species like AmT_nX_{3-n} are extracted. The expression for the ratio D_0/D_a reduces as follows when they are determined at the same $[H^+]$ and [HT]

$$[9] \qquad \frac{D_0}{D_a} = \frac{\gamma'_{AmT_3(org)}}{\gamma_{AmT_3(org)}} \times \sum_{j=0}^{j} \frac{\gamma_{Am^{3+}}}{\gamma'_{AmX_j^{(3-j)+}}} \beta_j X^j \gamma'_X{}^j$$

The determination of ratio D_0/D_a enables evaluation of β_j by the solvent extraction method provided the activity coefficients of the species are assumed to be constant. The metal ion is present in tracer concentration in solution and thus the assumption that $\gamma_{AmT_nX_j^{(3-n-j)+}}$ are constant is often justified. However, $\gamma_{sAmX_j^{(3-j)+}}$ and γ'_X may not be constant when large changes are effected in aqueous phase. The values of β_j are thus reported for specified experimental conditions in the aqueous phase, since it is difficult to determine the activity coefficient of the ionic species in mixed electrolytes. The extraction behavior of neutral species like AmT_3 is also assumed to be ideal according to eq. [3]. In order to verify this, the Hf–TTA system, earlier studied by us (12), was chosen for ease of handling radioactivity. The values for the ratio D_0/D_a were determined in 2 *M* $HClO_4$ and 2 *M* HCl solutions using different inert solvents. In such solvents, the values of D_0 and D_a are likely to vary (13), but according to eq. [9] the ratio D_0/D_a should not alter since the aqueous phase activity coefficients of the ionic species are not affected by the solvents in the organic phase. The activity coefficients of the neutral species present in very low concentration in the organic phase should remain constant. The value of D_0/D_a for the solvents differ significantly (Table I). The reason for the variation is not clearly understood. It can be attributed to the change in the extraction behavior of the neutral species. Nevertheless, the stability constants determined by this method, wherein large changes are effected in the anionic composition in the aqueous phase, may not be correct.

Ion Exchange Equilibria

In ion exchange equilibria, the metal ion is distributed between the aqueous and resin phases and the following equilibrium applies

$$M^{n+} + n\overline{RH} \rightleftharpoons \overline{MR}_n + nH^+$$

and

$$[10] \qquad K_d = \frac{[\overline{MR}_n][H^+]^n \gamma_{\overline{MR}_n}}{[M^{n+}][\overline{RH}]^n \gamma_{M^{n+}} \gamma_{\overline{RH}}{}^n}$$

where $[\overline{MR}_n]$ and $[\overline{RH}]$ are concentrations of metal- and hydrogen-form of resin. (If $[\overline{MR}_n]$ is very small, i.e. metal ion is present in tracer concentration, the ion exchanger is mainly present as $\overline{RH}$.) Here γ again represents the activity coefficient of the species designated by the subscript.

$$D_0 = \frac{[\overline{MR}_n]}{[M^{n+}]}$$

or

Can. J. Chem. Downloaded from www.nrcresearchpress.com by 210.87.254.40 on 09/05/12
For personal use only.

$$[11] \qquad D_0 = \frac{K_d[\overline{RH}]^n \gamma_{M^{n+}} \gamma_{\overline{RH}}^n}{[H^+]^n \gamma_{\overline{MR}_n}}$$

Similarly, in the presence of complexing anions

$$[12] \qquad D_a = \frac{[\overline{MR}_n] + [\overline{MXR}_{n-1}]}{\sum_{j=0}^{j} [MX_j^{n-j}]}$$

Following eq. [6] and

$$MX_j^{(n-j)+} + (n-j)\overline{RH} \rightleftharpoons MXR_{n-j} + (n-j)H^+$$

we have

$$[13] \quad K_{d_j} = \frac{[\overline{MXR}_{n-j}][H^+]^{n-j} \gamma'_{MXR_{n-j}}}{[M^{(n-j)+}][\overline{RH}]^{n-j} \gamma'_{M^{(n-j)+}} \gamma'^{n-j}_{\overline{RH}}}$$

and

$$[14] \quad D_a = \frac{K_d[\overline{RH}]^n \gamma'_{M^{n+}} \gamma'^{n}_{\overline{RH}}}{[H^+]^n \gamma'_{\overline{MR}_n} \sum_{j=0}^{j} \beta_j \frac{X_j^j \gamma_x^j}{\gamma'^{3-j}_{MX}}} + \frac{K_{d_1}[\overline{RH}]^{n-1} \gamma'_{MX^{(n-j)+}}}{[H^+]^{n-1} \gamma'_{\overline{MXR}_n} \sum_{j=0}^{j} \beta_j \cdots}$$

γ' is the activity coefficient in the mixed electrolyte solution.

By examining the variation of D values with respect to $[H^+]$ it can be verified that the second term does not contribute significantly (7). K_{d_1} is much smaller in magnitude as compared to K_d for most of the systems. If constant hydrogen ion concentration is maintained and the D values are determined for constant amount of resin, the expression for D_0/D_a becomes

$$[15] \quad \frac{D_0}{D_a} = \frac{\gamma_{\overline{RH}}^n \gamma'_{\overline{MR}_n}}{\gamma'^{n}_{\overline{RH}} \gamma_{\overline{MR}_n}} \sum_{j=0}^{j} \beta_j \frac{\gamma_{M^{n+}}}{\gamma'_{MX_j^{(n-j)+}}} X^j \gamma_x^j$$

The expression is similar to the one derived for solvent extraction equilibria except for the activity coefficients in the resin phase of the two species in the presence of mixed electrolyte systems. In the absence of any data, they are usually assumed to be constant. This assumption is examined by choosing cations which are not complexed appreciably in the presence of anions like Cl^- and NO_3^-. The alkali metal ions do not form contact ion pairs in ClO_4^- or NO_3^- media in 1 M solutions as indicated by Raman spectra (14–16). At constant ionic strength and $[H^+]$, and the metal ion in tracer concentration, the distribution coefficients should vary according to eq. [15], as the activity coefficients of metal ion in mixed electrolytes change assuming $\beta_1 = 0$. It can be seen from Table II that there are significant but small variations in the D values for Na^+ but very large variations are found for Cs^+ and Rb^+ ions. These large variations can partly be attributed to the changes in the activity coefficients of metal ions in the aqueous phase since they are present in tracer concentration in solution. If they do change to such an extent, the values of β_j obtained by these methods will have large uncertainties. The activity coefficients in the resin phase are perhaps affected by the presence of differing composition of electrolytes in the aqueous phase contrary to the earlier concepts (17–20). Diamond (21) and Diamond and Whitney (22) have discussed the behavior of these ions on the basis of water structure forming or breaking properties of hydrated ions. The structure forming ions are preferentially taken into the resin phase. Na^+ and H_3O^+ ions are considered structure forming ones, whereas ClO_4^- is considered as structure breaking type, and Cl^- and NO_3^- fall in between the two. The large, poorly hydrated ions in the presence of ClO_4^- ions are forced into the resin phase and thus the D values for these ions in 1 M ClO_4^- are large. However, in the mixtures, the behavior cannot be rationalized and at present it can be explained only qualitatively on the above basis. The structure forming ions may not show such behavior.

The D values for Ca^{2+} and Ba^{2+} ions depict a typical behavior indicating considerable ion association or complexing with Cl^- and NO_3^- ions. The stability constants, β_1, for the formation of $CaCl^+$ and of $CaNO_3^+$ are calculated to be 0.6 (Table III) whereas values of β_1 for $BaCl^+$ and $BaNO_3^+$ are 0.2 and 1.4, respectively. The Raman spectra in the Ca^{2+}–NO_3^- system indicate that for the formation of contact ion pairs in the nitrate system, β_1 is 0.16 and 0.12 in high ionic strength. Hester and Plane (14, 15) and Irish and Walrafen (16) do not find evidence for the formation of the complex in 1 M solution, which is not in agreement with the results obtained by the ion exchange method. It appears that this method for the determination of stability constants of weak complexes may not give accurate results when large changes are effected in the aqueous phase.

The stability constants determined for Am(III)

with chloride ions were reinvestigated by using different cross-linked resins. There does not seem to be much change in the value of ~ 1, but in all the resins with 8 determinations for each D value, there are very small deviations from the expected values, which makes us doubt the accuracy of this method. The activity coefficients of species in the resin phase perhaps do not remain constant when large changes in the salt composition are effected in the aqueous phase. The different values of β_j obtained by the two methods can perhaps be attributed to either the extraction behavior of the neutral species or changes in the distribution coefficients D_0 in ion exchange when there are large changes in the aqueous phase composition.

In summary, the experimental methods for the determination of stability constants of weak complexes require large changes in electrolyte composition in aqueous phase. The activity coefficients of the species under such changes may not be constant. The evaluation of stability constants from the experimental data may have large errors if the activity coefficients of the species are assumed to be constant. In the distribution methods, the activity coefficients in the non-aqueous phase may also alter when the salt composition is varied in aqueous phase and thus give rise to additional errors in the values of the stability constants. The disagreement between the values of stability constants obtained by the solvent extraction and ion exchange methods can be attributed to the changes in the activity coefficients of the distributed species in the non-aqueous phases when salt composition in the aqueous phase is altered.

1. S. FRONAEUS. Acta Chem. Scand. **5**, 859 (1951).
2. S. FRONAEUS. Sv. Kem. Tidskr. **64**, 317 (1952).
3. F. J. C. ROSSOTTI and H. S. ROSSOTTI. The determination of stability constants. McGraw-Hill Book Company, Inc., London. 1962
4. R. E. CONNICK and W. H. MCVEY. J. Amer. Chem. Soc. **71**, 3182 (1949).
5. R. A. DAY and S. W. STOUGHTON. J. Amer. Chem. Soc. **72**, 5662 (1950).
6. R. A. DAY, R. N. WHITE, and F. D. HAMILTON. J. Amer. Chem. Soc. **77**, 3180 (1955).
7. (*a*) B. M. L. BANSAL, S. K. PATIL, and H. D. SHARMA. J. Inorg. Nucl. Chem. **26**, 993 (1964). (*b*) P. K. KHOPKAR and H. D. SHARMA. Unpublished results.
8. B. M. K. BANSAL and H. D. SHARMA. J. Inorg. Nucl. Chem. **26**, 799 (1964).
9. H. LOMAN and E. VAN DALEN. J. Inorg. Nucl. Chem. **28**, 2037 (1966).
10. E. L. KING and W. H. REAS. J. Amer. Chem. Soc. **73**, 1806 (1951). U.S. At. Energy Comm. Decl. Rep. AECD—2573.
11. F. A. LONG and W. F. MCDEVIT. Chem. Rev. **51**, 119 (1952).
12. R. G. DESHPANDE, P. K. KHOPKAR, C. L. RAO, and H. D. SHARMA. J. Inorg. Nucl. Chem. **27**, 2171 (1965).
13. T. SEKINE and D. DYRSSEN. J. Inorg. Nucl. Chem. **29**, 1457 (1967).
14. R. E. HESTER and R. A. PLANE. J. Chem. Phys. **40**, 411 (1964).
15. R. E. HESTER and R. A. PLANE. Inorg. Chem. **3**, 769 (1964).
16. D. E. IRISH and G. E. WALRAFEN. J. Chem. Phys. **46**, 378 (1967).
17. A. P. VANSELOW. J. Amer. Chem. Soc. **54**, 1307 (1932).
18. J. SCHUBERT. J. Phys. Colloid Chem. **52**, 340 (1948).
19. J. SCHUBERT. J. Amer. Chem. Soc. **73**, 4488 (1951).
20. R. H. BETTS and A. N. MACKENZIE. Can. J. Chem. **30**, 146 (1952).
21. R. M. DIAMOND. J. Phys. Chem. **67**, 2513 (1963).
22. D. C. WHITNEY and R. M. DIAMOND. Inorg. Chem. **2**, 1284 (1963).

Can. J. Chem. Downloaded from www.nrcresearchpress.com by 210.87.254.40 on 09/05/12
For personal use only.

Crystal and molecular structure of $CuSiF_6 \cdot 4H_2O$

M. J. R. CLARK, J. E. FLEMING[1], AND H. LYNTON
Department of Chemistry, University of New Brunswick, Fredericton, New Brunswick

Received June 12, 1969

The structure of $CuSiF_6 \cdot 4H_2O$ has been shown to consist of chains of $[Cu(H_2O)_4F_2]$ and $[SiF_6]$ octahedra linked through a common fluorine atom. The space group is monoclinic $P2_1/a$, with cell dimensions $a = 7.22 \pm 0.01$ Å, $b = 9.64 \pm 0.01$ Å, $c = 5.36 \pm 0.01$ Å and $\beta = 105.2 \pm 0.3°$. There are 2 molecules in the unit cell and the copper and silicon atoms occupy centers of symmetry. Atomic parameters have been obtained from a block diagonal least squares refinement using anisotropic temperature parameters. The final agreement residual for 574 observed reflections is $R = 0.083$.

Canadian Journal of Chemistry, 47, 3859 (1969)

Can. J. Chem. Downloaded from www.nrcresearchpress.com by 210.87.254.105 on 09/05/12
For personal use only.

Introduction

In a previous paper (1) the authors were able to show that a compound identified in the literature as $CuBF_3O \cdot 5H_2O$ was in fact $CuSiF_6 \cdot 4H_2O$. Details of the preparation and analysis of this compound have been given.

Two general classes of simple fluosilicates are known, the anhydrous compounds such as Na_2SiF_6 and $BaSiF_6$, and the hexahydrates such as $MgSiF_6 \cdot 6H_2O$ and $FeSiF_6 \cdot 6H_2O$. Both the anhydrous and hydrated salts are thought to have discrete $[SiF_6]^{2-}$ octahedra. The metal ions in the hexahydrates are believed to be coordinated octahedrally to the 6 water molecules. $CuSiF_6 \cdot 4H_2O$ would appear to be a hydrated compound intermediate in character.

Crystallographic and Intensity Data

The crystal data are given in Table I. The compound is monoclinic and the systematic absences establish the space group as $P2_1/a$. Unit cell dimensions were measured with a single crystal equi-inclination diffractometer. The density measurements indicate 2 molecules of $CuSiF_6 \cdot 4H_2O$ in the unit cell.

All intensity data were collected from a small needle-shaped crystal mounted on the [101] axis inside a lithium borate capillary tube. Using the multiple film pack technique, equi-inclination Weissenberg photographs were obtained of all layers accessible with Cu Kα radiation. The total number of independent reflections is calculated to be 727, of which 43 are systematically absent. The structure analysis utilized 574 intensities which were above the minimum intensity limit for observation.

TABLE I
Crystal data for $CuSiF_6 \cdot 4H_2O$

System	Monoclinic
Space group	$P2_1/a$
Systematic absences	$h0l: h = 2n + 1$ $0k0: k = 2n + 1$
Molecular weight	277.7
Unit cell dimensions	
a	7.22 ± 0.01 Å
b	9.64 ± 0.01 Å
c	5.36 ± 0.01 Å
β	$105.2 \pm 0.3°$
Volume	360 Å^3
Measured density (by flotation)	2.56 g cm^{-3}
Calculated density (assuming 2 molecules in the unit cell)	2.56 g cm^{-3}

The intensities of all reflections were estimated by visual comparison with a calibrated strip prepared using a suitable reflection from the intensity crystal. Lorentz polarization factors were applied to all intensity data. No corrections were made for absorption.

Structure Analysis

A three dimensional Patterson synthesis established the sites for the copper atoms as special positions $2a$—000 and $\frac{1}{2}\frac{1}{2}0$, and the silicon atoms as special positions $2d$—$\frac{1}{2}0\frac{1}{2}$ and $0\frac{1}{2}\frac{1}{2}$. A three dimensional Fourier synthesis then gave the coordinates of all the fluorine and oxygen atoms.

The refinement was by successive cycles of block diagonal least squares[2], employing only the observed reflections. The quantity minimized was

[1]Present address: St. Paul's School for Girls, London, England.

[2]All computations were done on an I.B.M. 360/50 computer using programs by Ahmed *et al.* (2).

TABLE II

Fractional atomic coordinates and estimated standard deviation*

Atom	Fractional atomic coordinates			Estimated standard deviation		
	x	y	z	$\sigma(x)$	$\sigma(y)$	$\sigma(z)$
Cu	00 000	00 000	00 000			
Si	50 000	00 000	50 000			
F(1)	45 649	10 473	73 028	69	47	92
F(2)	61 222	13 282	39 071	69	47	100
F(3)	29 165	04 841	29 967	67	52	97
O(1)	−12 242	15 956	12 517	81	55	106
O(2)	08 151	12 478	−24 018	89	59	115

*All values have been multiplied by 10^5.

TABLE III

Anisotropic temperature parameters*

Atom	Anisotropic temperature parameters					
	β_{11}	β_{22}	β_{33}	β_{23}	β_{13}	β_{12}
Cu	400	243	1002	30	73	11
Si	273	220	659	−73	−173	−14
F(1)	960	436	1836	−701	810	−190
F(2)	780	382	2579	225	1097	149
F(3)	351	651	1657	393	−309	133
O(1)	932	384	1454	−298	368	188
O(2)	882	461	1998	223	600	−5

*All values have been multiplied by 10^5.
$T = \exp -[h^2\beta_{11} + k^2\beta_{22} + l^2\beta_{33} + kl\beta_{23} + hl\beta_{13} + hk\beta_{12}]$

$\sum\omega(F_o - F_c)^2$. The matrices used were 3 × 3 for the positional parameters and 6 × 6 for the anisotropic thermal parameters of each atom. The weighing scheme $\omega = 1/(a + |F_o| + c|F_o|^2)$ was employed with the following values: $a = 4.00$ and $c = 0.020$. Scattering factor curves used were those given in International tables (3).

No corrections were made for extinction, and in the last cycle, no parameter shift exceeded 0.3 estimated standard deviation (e.s.d.). The final agreement residual, $R = \sum|F_o - F_c|/\sum|F_o|$, for observed reflections was $R = 0.083$.

Results and Discussion

There are 2 molecules of $CuSiF_6 \cdot 4H_2O$ in the unit cell, the copper and silicon atoms being situated on centers of symmetry. The silicon atoms are surrounded octahedrally by 6 fluorine atoms and the copper atoms surrounded octahedrally by 4 water molecules and 2 fluorine atoms. The 2 octahedra form chains along the [101] direction linked by the common fluorine atom F(3), Fig. 1. The angle Cu—F(3)—Si is 152.15 (0.29)°.

The final atomic coordinates are given together with their e.s.d. in Table II. The temperature parameters are given in Table III. Tables IV and V give the intramolecular distances and angles, together with their e.s.d. A final set of structure factors has been placed in the Depository of Unpublished Data[3].

The closest approach distances between non-bonded atoms are O(1)—O(2), 2.762(9) Å, and F(1)—F(3), 2.366(7) Å between atoms in the same chain, and O(1)—F(2), 2.682(8) Å between atoms in adjacent chains. Each water molecule has as nearest non-bonding neighbors 2 other water molecules at 2.762(9) and 2.808(8) Å, and 2 fluorine atoms at 2.682(8) and 2.763(7) Å for O(1), and 2.750(7) and 2.760(8) Å for O(2). These distances are within the range expected for hydrogen bonding. The hydrogen atoms were not located in the structure analysis. Each water molecule has in addition 3 other fluorine atoms

[3]Photocopies may be obtained free of charge, upon request, to: Depository of Unpublished Data, National Science Library, National Research Council of Canada, Ottawa, Canada.

Can. J. Chem. Downloaded from www.nrcresearchpress.com by 210.87.254.105 on 09/05/12
For personal use only.

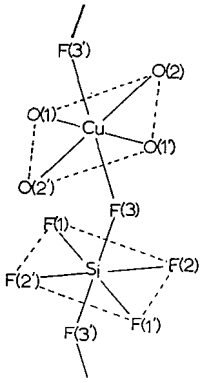

FIG. 1. $[Cu(H_2O)_4F_2]$ and $[SiF_6]$ octahedra linked through F(3).

TABLE IV

Intramolecular distances*

Atoms	Distance (Å)
Cu—O(1)	1.977(6)
Cu—O(2)	1.962(6)
Cu—F(3)	2.336(5)
Si—F(1)	1.687(5)
Si—F(2)	1.699(5)
Si—F(3)	1.669(5)
O(1)—O(2)	2.762(9)
O(1)—O(2′)	2.808(8)
F(1)—F(2)	2.392(7)
F(1)—F(2′)	2.396(7)
O(1)—F(3)	3.081(8)
O(2)—F(3)	2.986(8)
O(1)—F(3′)	3.040(7)
O(2)—F(3′)	3.114(8)
F(1)—F(3)	2.366(7)
F(2)—F(3)	2.380(7)
F(1)—F(3′)	2.380(7)
F(2)—F(3′)	2.384(7)

*Estimated standard deviations in parentheses.

as neighbors located at distances in the range 2.986(8)–3.114(8) Å.

In the copper octahedron, the 4 copper–oxygen bonds are short and the 2 copper–fluorine bonds long by comparison with values found in the recent literature. Short Cu—O bonds are often in the range 1.95–1.98 Å and long bonds in the range 2.2–2.5 Å (4–9). Short Cu—F bonds seem to be of the order 1.90–1.93 Å, long bonds 2.2–2.5 Å (10–13).

In the silicon octahedron, the 6 silicon–fluorine bonds are comparable with those found in a recent

TABLE V

Intramolecular angles*

Atoms	Angle (degrees)
O(1)—Cu—F(3)	90.79(0.20)
O(2)—Cu—F(3)	87.55(0.22)
O(1)—Cu—O(2)	89.05(0.24)
F(1)—Si—F(3)	89.66(0.24)
F(2)—Si—F(3)	89.90(0.24)
F(1)—Si—F(2)	89.91(0.23)
Cu—F(3)—Si	152.15(0.29)

*Estimated standard deviations in parentheses.

structure analysis of Na_2SiF_6 (14), where all bonds are in the range 1.673–1.693 Å. The silicon–fluorine F(3) bridging bond distance seems to be a little shorter than the silicon–fluorine terminal bonds.

All angles in both copper and silicon octahedra are very close to 90°.

Acknowledgment

We wish to acknowledge the financial support of the National Research Council of Canada for this work.

1. M. J. R. CLARK and H. LYNTON. Can. J. Chem. In press.
2. F. R. AHMED, C. P. HUBER, M. E. PIPPY, and S. R. Hall. N.R.C. Crystallographic programs for the I.B.M./360 system. Divisions of Pure Physics and Pure Chemistry, National Research Council of Canada, Ottawa, Canada.
3. International tables for X-ray crystallography. Vol. III. The Kynoch Press, Birmingham, England. 1962. Table 3.3.1.A.
4. G. M. BROWN and R. CHIDAMBARAM. Acta Cryst. **B25**, 676 (1969).
5. M. HANDLOVIČ. Acta Cryst. **B25**, 227 (1969).
6. T. UEKI, T. ASHIDA, Y. SASADA, and M. KAKUDO. Acta Cryst. **B25**, 328 (1969).
7. M. I. KAY, I. ALMODOVAR, and S. F. KAPLAN. Acta Cryst. **B24**, 1312 (1968).
8. T. UEKI, T. ASHIDA, Y. SASADA, and M. KAKUDO. Acta Cryst. **B24**, 1361 (1968).
9. R. F. ZAHROBSKY and W. H. BAUR. Acta Cryst. **B24**, 508 (1968).
10. C. BILLY and H. M. HAENDLER. J. Amer. Chem. Soc. **79**, 1049 (1957).
11. S. C. ABRAHAMS. J. Chem. Phys. **36**, 56 (1962).
12. S. C. ABRAHAMS and E. PRINCE. J. Chem. Phys. **36**, 50 (1962).
13. D. S. BROWN, J. D. LEE, and B. G. A. MELSOM. Acta Cryst. **B24**, 730 (1968).
14. A. ZALKIN, J. D. FORRESTER, and D. H. TEMPLETON. Acta Cryst. **17**, 1408 (1964).

Can. J. Chem. Downloaded from www.nrcresearchpress.com by 210.87.254.105 on 09/05/12
For personal use only.

Kinetics of the pyrolysis of *n*-butane

JOHN TOROK[1] AND SAMUEL SANDLER
Department of Chemical Engineering and Applied Chemistry, University of Toronto, Toronto, Ontario

Received June 19, 1969

The thermal decomposition of *n*-butane was investigated at temperatures ranging from 330 to 420 °C. This extension of the temperature range for such studies was made possible by the use of a highly sensitive analytical system, consisting of a gas–liquid chromatograph equipped with a hydrogen-flame-ionization detector which permitted the determination of the major products of the reaction at reactant conversions as low as 0.0002%. At temperatures below 400 °C the reaction order was both temperature and pressure dependent, a lower order, approaching 0.5, being favored at lower temperatures and higher pressures. The contribution to the reaction mechanism of a chain-termination step consisting of the combination of 2 secondary butyl radicals explains the observed phenomena.

Canadian Journal of Chemistry, 47, 3863 (1969)

Can. J. Chem. Downloaded from www.nrcresearchpress.com by 210.87.254.6 on 09/05/12
For personal use only.

Introduction

Recent investigators of the thermal decomposition of *n*-butane (1, 2) have been concerned with the reaction in the temperature range of 420–590 °C. On the other hand, studies of the sensitized decomposition have generally been conducted at temperatures below 340 °C. Thus, though this reaction has been studied extensively, no thorough investigation at the intermediate temperatures had been made prior to the present one.

Although the pyrolysis of *n*-butane is one of the better understood free-radical chain reactions, it is still necessary to point out, as in a recent publication by the present authors (3), that the main chain-ending step of this reaction at temperatures above 420 °C is still obscure. The present work is mainly concerned with the elucidation of the chain-termination mechanism at temperatures below 420 °C.

Purnell and Quinn (1) have made the most significant contribution of the last 2 decades to the clarification of the mechanism of this reaction. They identified most of the products, including the minor ones, thoroughly investigated the temperature and pressure dependence of the distribution of the major products, and determined that the decomposition of the ethyl radical was in its pressure-dependent region.

Due to the large apparent activation energy for this reaction (about 63 kcal/mole) the reaction rate rapidly decreases with a decrease in reaction temperature. Thus, this extension of the temperature range over which the pyrolysis of *n*-butane could be studied required, and was made possible only as a result of, the development of a highly sensitive analytical system. Gas–liquid chromatography in conjunction with hydrogen-flame-ionization detection was used to determine the major products of the reaction at conversions as low as 0.0002%.

[1]Present address: Norton Research Corporation, Chippawa, Ontario.

Experimental

A conventional static reaction system was used. The reactor and auxiliary glass vessels were connected to a vacuum system capable of maintaining pressures near 10^{-5} Torr.

Phillips Petroleum Co. Research Grade *n*-butane was treated to remove traces of isobutane, propane, and butene impurities. It was first adsorbed at ambient temperature on Linde molecular sieve, Type 5A, and the unadsorbed vapors containing isobutane were pumped off and discarded. The adsorbed *n*-butane and propane were then desorbed at 170 °C, a temperature at which olefins would still be retained, and passed through a bed of Type 4A molecular sieve at ambient temperature to remove propane. The reactant now contained no hydrocarbon impurities detectable by sensitive gas–liquid chromatography.

Traces of oxygen and other fixed gases were carefully removed by prolonged degassing of the condensed reactant at −107 °C. This was followed by repeatedly bubbling the gas through a 100 mm column of aluminum amalgam (4) to further lower the oxygen content to a negligible value.

The reaction bulb was housed and heated in an electronically controlled 3 section oven capable of maintaining a constant temperature along the length of the reactor, within ±0.3 °C. Two 80 ml quartz reaction vessels were used. The bodies of the reactors were cylindrical, 2.5 cm in diameter and 21 cm in length. Each contained a coaxial thermowell terminating at the center of the reactor. One of the reactors was unpacked and had a surface-to-volume ratio (s/v) of 2.1 cm^{-1}. The other

Can. J. Chem. Downloaded from www.nrcresearchpress.com by 210.87.254.6 on 09/05/12
For personal use only.

was packed with enough quartz tubing to yield a value of s/v of 7.7 cm^{-1}. The effect of using reaction times between 15 s and 2 h, and pressures in the range 16 to 600 mm Hg, could be usefully investigated with this apparatus.

At any desired stage of the reaction, the reactor contents were expanded into a previously evacuated bulb. Subsequently, the bulb contents were compressed over mercury and a portion transferred into the 2 ml sample loop of a Varian–Aerograph Model 600-D gas chromatograph equipped with a high sensitivity hydrogen-flame-ionization detector.

The gas–liquid chromatographic analysis was limited to the 4 major hydrocarbon products of the reaction, since it was not possible to obtain quantitatively significant quantities of the minor products at the low conversion conditions of this study. Furthermore, since a hydrogen-flame-ionization detector was needed at its ultimate sensitivity to detect the major products, product hydrogen could not be detected. Three identical column trains were prepared. Each train contained a 25 ft long, 0.25 in. o.d. copper tube column packed with 60–80 mesh Chromosorb P acid-washed fire brick coated with 29% by weight of dimethylsulfolane (DMS). To this was attached a 6 in. column packed with 60–80 mesh Chromosorb W fire brick coated with 15% by weight of Carbowax 20M. The purpose of the latter was to hold back any DMS tending to bleed from the first column.

The 3 column trains were connected to a common carrier-gas source and any one of them could be connected to the inlet of the hydrogen-flame-ionization detector. Following the elution of methane, ethane, ethylene, and propylene, respectively, from one column, another was connected to the detector for the next analysis. This procedure reduced analysis time and eliminated the necessity for burning excessive amounts of the unreacted butane in the detector. Due to the large sample size required to obtain measurable quantities of reaction products, the column had to be overloaded insofar as *n*-butane was concerned. However, this did not affect the reaction product peaks eluted ahead of *n*-butane, and the latter could be purged from the column to air while one of the other columns was being used for the analysis of another sample.

The analysis for *n*-butane itself was neither feasible nor required, so long as the sample size injected was reproducible and the same sample loop was used for calibration. The calibration was performed on samples of known and very low concentrations of the major hydrocarbon reaction products. Since conversions were always extremely low, reaction rates could be calculated directly from a carbon balance based on the product analysis, assuming that all significant carbon containing products had been determined and that the conversion–time relationship was linear in the region investigated.

Results

The poor reproducibility of the results obtained at temperatures below approximately 380 °C was a major problem in this investigation. Various cleaning and coating procedures (5) served only to enhance this problem. Clean reactors, freshly fabricated by the glass blower but otherwise untreated, gave the most reproducible results and were used for all final runs.

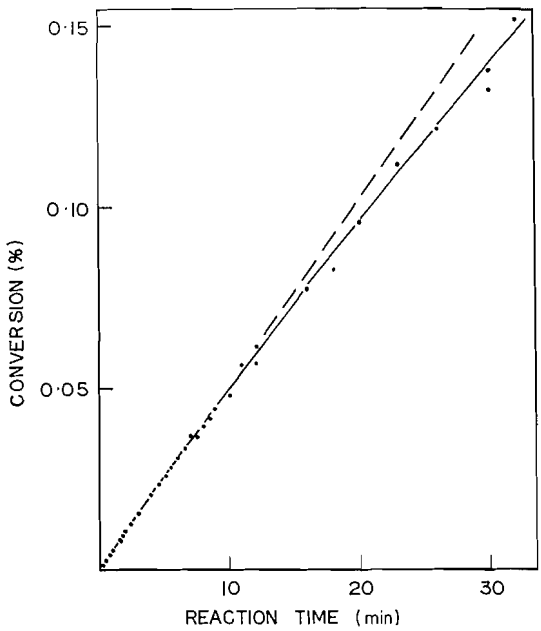

FIG. 1. Reactant conversion as a function of reaction time at 393 °C and 200 mm Hg.

Figure 1 demonstrates the effect of residence time on conversion at 393 °C and 200 mm Hg pressure. The following points may be noted from this figure. (*i*) The reaction has no observable induction period. This coincides with the observation of Purnell and Quinn (1), but is not consistent with the findings of Sagert and Laidler (2), who observed a short induction period. (*ii*) After an initial period of several minutes, corresponding to a conversion of less than 0.05%, the reaction rate decreases slightly with reaction time. The broken line is the extension of the initial linear portion of the curve.

At conversions rising to 0.15% product selectivities (defined as moles of product/100 moles of butane decomposed) were found to be independent of conversion.

Figure 2 demonstrates as well the independence of the product selectivities of the reaction pressure at a temperature of 370 °C. It is also apparent that the selectivities for methane and propylene on the one hand, and ethane and ethylene on the other, are equivalent.

Several runs were conducted at temperatures

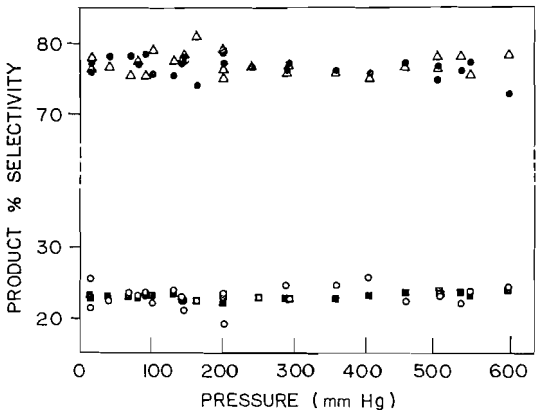

FIG. 2. Product selectivity as a function of reaction pressure at 370 °C. Reaction time range 8–25 min. △, methane; ■, ethane; ○, ethylene; ●, propylene.

above 420 °C to establish some connection with the work of previous investigators. Product selectivities in this temperature range were quite comparable to those obtained by Purnell and Quinn (1). An Arrhenius-type plot of the product selectivities is given in Fig. 3. The slope and position of the line drawn were calculated by the method of least squares and correspond to the equation

$$[\mathrm{I}] \quad \frac{[C_2H_4] + [C_2H_6]}{[CH_4] + [C_3H_6]} = 1.8 \exp\left(-2300/RT\right)$$

This is comparable with the result obtained by Purnell and Quinn as expressed in the equation

$$\frac{[C_2H_4] + [C_2H_6]}{2[CH_4]} = 1.3 \exp\left(-2000/RT\right)$$

Overall Reaction Order

The temperature and pressure dependence of the overall order were thoroughly investigated. At temperatures above 410 °C, the order was found to be both temperature and pressure independent and approximately 1.5.

A log–log plot of the relative rate of pyrolysis at 370 °C against reaction pressure is given in Fig. 4. In this plot the rates are measured relative to the reaction rate at the reference pressure of 194 mm Hg. Every second run was conducted at the reference pressure, while intermediate runs were executed at randomly selected pressures ranging from 16 to 620 mm Hg. The relative rate in Fig. 4. is defined as the rate of reaction at the specified pressure divided by the rate of the succeeding reaction conducted at 194 mm Hg. This treatment of the experimental data was necessary since the results of successive runs at temperatures below 380 °C were much more reproducible than those of runs further separated in time. Points in Fig. 4 were fitted with both linear and curvilinear regressions. A statistical analysis of the 2 regressions indicated that the

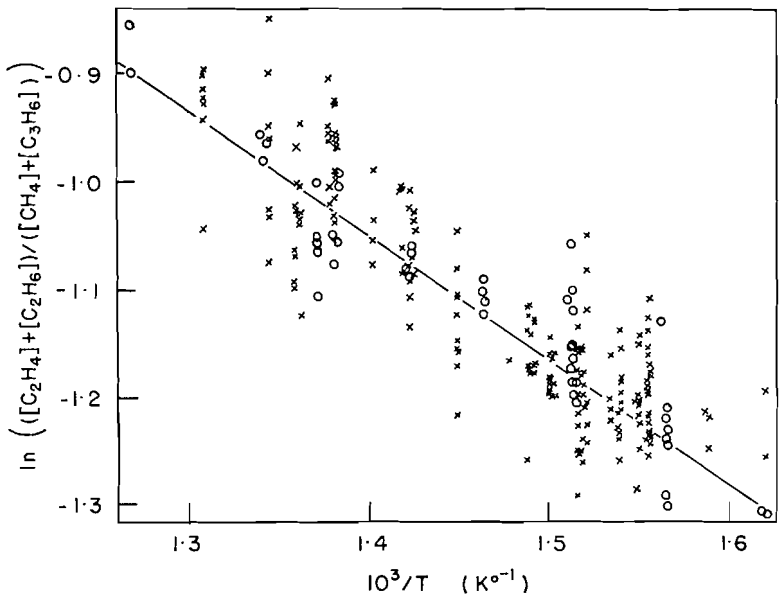

FIG. 3. Arrhenius plot for product selectivities. ○, packed reactor; X, unpacked reactor.

Can. J. Chem. Downloaded from www.nrcresearchpress.com by 210.87.254.6 on 09/05/12
For personal use only.

Can. J. Chem. Downloaded from www.nrcresearchpress.com by 210.87.254.6 on 09/05/12
For personal use only.

departure from the linear regression is significant. The slope of a log (rate) vs. log (pressure) curve (at constant temperature) is equivalent to the overall order of reaction. Thus, at 370 °C, the overall reaction order is in its pressure dependent region, a higher order being favored at lower pressures.

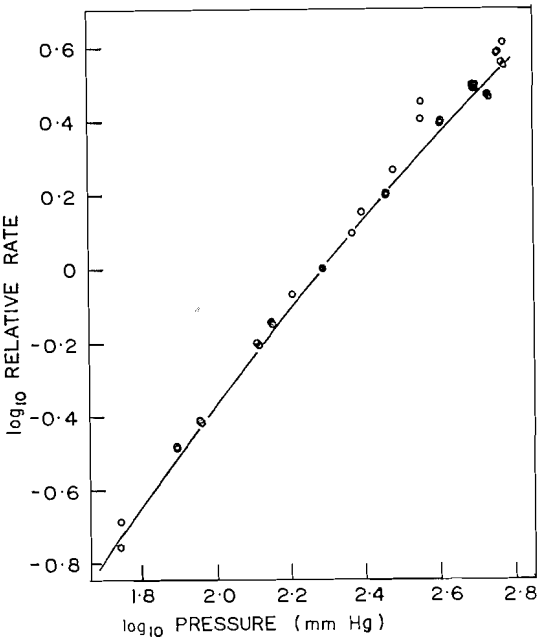

FIG. 4. Logarithm of relative rate as a function of the logarithm of the pressure for the pyrolysis at 370 °C. (Relative rate is defined as the reaction rate at the specified pressure divided by the reaction rate at 194 mm Hg pressure.)

Figure 5 demonstrates the variation of reaction order with temperature. At each temperature, successive runs were conducted at reaction pressures alternating between 94 and 200 mm Hg. From the rates of successive pairs of runs, a reaction order was calculated and plotted against temperature. The differences in the results obtained with packed and unpacked reactors were not significant. The broken line in the figure is a third-degree polynomial least squares fit of all the points. The solid curve is calculated and is described later.

A plot of the natural logarithm of the reaction rate as a function of the reciprocal of the reaction temperature for runs in the unpacked reactor is given in Fig. 6. The upper line is a linear regression for runs at 200 mm Hg, the lower line for runs at 94 mm Hg reaction pressure. The activation energies calculated from the slopes of these regressions are 63.5 and 60.3 kcal/mole, respectively.

Discussion

In a previous publication (3), the authors proposed the following mechanism for this pyrolysis at temperatures above 410 °C.

Initiation

[1] $C_4H_{10} \rightarrow 2C_2H_5\cdot$

Propagation

[2] $p\text{-}C_4H_9\cdot \rightarrow C_2H_4 + C_2H_5\cdot$

[3] $s\text{-}C_4H_9\cdot \rightarrow C_3H_6 + CH_3\cdot$

[4] $C_2H_5\cdot + C_4H_{10} \rightarrow C_2H_6 + s\text{-}$ or $p\text{-}C_4H_9\cdot$

[5] $CH_3\cdot + C_4H_{10} \rightarrow CH_4 + s\text{-}$ or $p\text{-}C_4H_9\cdot$

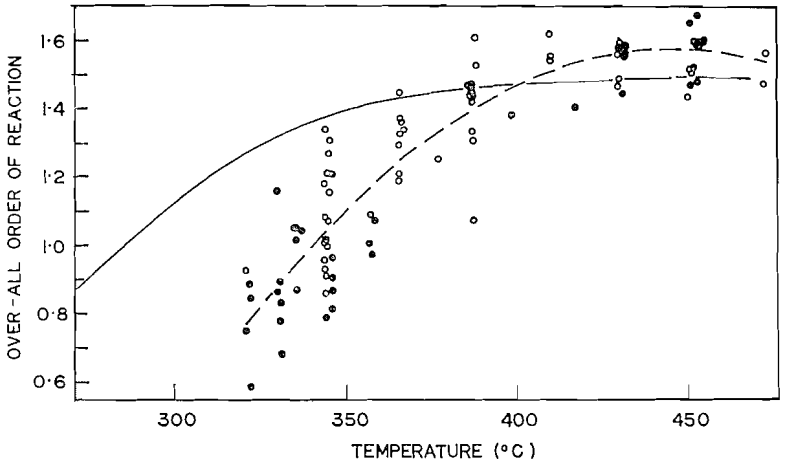

FIG. 5. Variation of overall reaction order with temperature. ———, theoretical curve; - - -, 3rd degree polynomial fit to data; ○, packed reactor; ●, unpacked reactor.

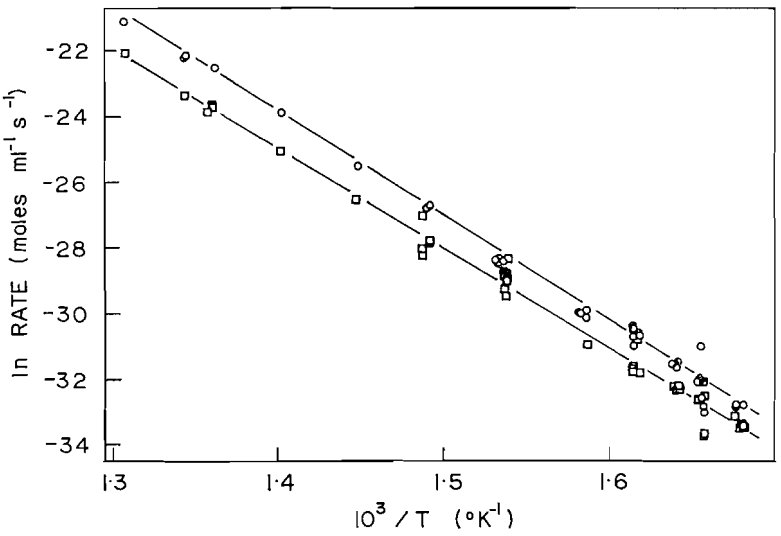

FIG. 6. Natural logarithm of reaction rate as a function of reciprocal temperature for unpacked reactor. Reaction pressure: ○, 200 mm Hg; □, 94 mm Hg.

[6][2] $C_2H_5\cdot + eC_4H_{10} \rightarrow C_2H_4 + H\cdot + eC_4H_{10}$

[7] $H\cdot + C_4H_{10} \rightarrow H_2 + s\text{- or } p\text{-}C_4H_9\cdot$

Termination

For the derivation of an expression for the overall order, all possible combination reactions were considered, including radical combination and cross-combination reactions. Of these the following are the possible radical combination reactions

[8] $2CH_3\cdot \rightarrow C_2H_6$

[9] $2C_2H_5\cdot \rightarrow C_4H_{10}$ (or $C_2H_4 + C_2H_6$)

[10] $2s\text{-}C_4H_9\cdot \rightarrow C_8H_{18}$ (or $C_4H_8 + C_4H_{10}$)

[11] $2p\text{-}C_4H_9\cdot \rightarrow C_8H_{18}$ (or $C_4H_8 + C_4H_{10}$)

[12] $2H\cdot \rightarrow H_2$

Table I lists the kinetic parameter ratios for elementary reactions involved in the above mechanism, with the exception of parameters for reactions [7] and [12].

Since most radical combination reactions have zero or very low activation energies, the values $E_i - \frac{1}{2}E_j$ in Table I are approximately equal to E_i.

In the following discussion it will be assumed that (*i*) the fundamental hypothesis of Bodenstein, that the intermediate products of the reaction are of almost stationary concentration, is valid and (*ii*) the chain lengths involved are large.

Based on the proposed mechanism, a relationship between reaction products and rates may be established

$$([C_2H_4]/[C_2H_6]) - 1 = r_6/r_4$$

where r_i denotes the rate of reaction [*i*]. Above approximately 420 °C, the yield of ethylene is higher than the yield of ethane, thus reaction [6] has an appreciable rate. It is apparent from Fig. 2 that at lower temperatures the yields of ethane and ethylene are practically equivalent, and thus the rate of reaction [6] is negligible relative to the rate of reaction [4]. The temperature dependence of the relative rates of reactions [4] and [6] is mainly due to the difference in their activation energies (approximately 27.6 kcal).

Reactions [3] and [5] and reactions [2] and [4] are consecutive. Either one of these reaction pairs can complete a chain cycle converting a molecule of butane to products. Due to the large chain length, the rates of reactions [3] and [5] are approximately equal. The relative steady-state concentration of methyl and secondary butyl radicals is then dependent on the value of $k_3/k_5[C_4H_{10}]$. Above approximately 400 °C, $k_3 \gg k_5[C_4H_{10}]$ and therefore $[CH_3\cdot] \gg [s\text{-}C_4H_9\cdot]$. Similarly, $k_2 \gg (k_4[C_4H_{10}]$ or $k_6[C_4H_{10}]^e)$ and therefore $[C_2H_5\cdot] \gg [p\text{-}C_4H_9\cdot]$.

The above relative radical concentrations are

[2]The second term is introduced to represent the pressure dependence of this reaction, "*e*" is a stoichiometric coefficient, where $0 < e < 1$.

Can. J. Chem. Downloaded from www.nrcresearchpress.com by 210.87.254.6 on 09/05/12
For personal use only.

TABLE I

Kinetic parameters for the ratios of elementary reactions

Reaction i	Reaction j	Frequency factor* $A_i/A_j^{1/2}$	Activation energy $E_i - \frac{1}{2}E_j$ (kcal/mole)	Reference
2	11	7.94×10^{6}	28.7	Morganroth and Calvert (6)
3	10	1.31×10^{8}	32.6	Lin and Laidler (7)
4	9	2.45×10^{4}	10.4	Boddy and Steacie (8)
5	8	1.56×10^{4}	8.3	Trotman-Dickenson, Birchard, and Steacie (9)
6	9	8.5×10^{6}†	38.0†	Lin and Back (10)

*In units of $cc^{1/2}$ $mole^{-1/2}$ $s^{-1/2}$ or $cc^{-1/2}$ $mole^{1/2}$ $s^{-1/2}$.
†First order region, at high pressures, extrapolated value.

pressure dependent. A higher pressure produces a higher butyl radical concentration relative to that of the methyl or ethyl radicals.

Since $E_3 > E_5$, then, as the temperature is lowered the value of $k_3/k_5[C_4H_{10}]$ decreases, resulting in an increased concentration of secondary butyl radicals relative to the concentration of the methyl radicals. A similar argument applies to the relationship between primary butyl and ethyl radicals. Thus, at lower temperatures and higher pressures butyl radicals become the main chain terminators.

The rates of reactions [4] and [5] are pressure dependent since *n*-butane is one of the reactants. The rates of reactions [2] and [3] are pressure independent. A higher pressure, therefore, produces a higher butyl radical concentration relative to that of the methyl or ethyl radicals.

In the previous recent publication already mentioned (3), an equation was developed to predict the reaction order for the pyrolysis of *n*-butane

$$[II] \quad \text{Order} = \frac{\sum_{m=8}^{m=12}\sum_{n=8}^{n=12}(F_m + F_n)(r_m r_n)^{1/2}}{\sum_{m=8}^{m=12}\sum_{n=8}^{n=12}(r_m r_n)^{1/2}}$$

where values of m, n, F_m, and F_n are as given below.

Radical	m or n	$2(F_{m \text{ or } n})$
Methyl	8	1.5
Ethyl	9	$0.5 + u$
s-Butyl	10	0.5
p-Butyl	11	0.5
Hydrogen	12	$1.5 + u - e$

and

$r_{m \text{ or } n}$ = rate of reaction m or n

$$u = \frac{k_4[C_4H_{10}] + ek_6[C_4H_{10}]^e}{k_4[C_4H_{10}] + k_6[C_4H_{10}]^e}$$

$$0 < e < 1 \text{ and } 0 < u < 1$$

It was also shown that equations such as [II] for the overall order may be expressed in terms of the kinetic parameters of the propagation reactions; in this case, they are the parameters listed in Table I, and eq. [I] represents the product distribution[3].

Such an equation involving the kinetic parameters of the propagation reactions has been used for the prediction of the pressure and temperature dependence of the overall order of the pyrolysis of *n*-butane.

Equation [II] indicates that when reactions [10] or [11] predominate, the overall order is 0.5. When reaction [8] predominates, the overall order is 1.5, and when reaction [9] predominates it is between 0.5 and 1.5 (approximately 1.35 (3)).

The solid curve in Fig. 5 is a calculated one, assuming the predominance of reaction [8] over reaction [9] (at higher temperatures). The apparent difference between the experimental results and the calculated curve is most likely due to the uncertainties in the values of the kinetic parameters used in the calculations. The same equation was also used for the calculation of the log (rate) vs. log (pressure) curve shown in Fig. 4 along with the experimental points.

Lin and Laidler (7) studied the methyl radical initiated decomposition of *n*-butane in the 260–340 °C temperature region. They analyzed for the octanes which would be expected to be formed by the recombination of butyl radicals. Since 3,4-dimethylhexane was identified and *n*-octane was absent, it was indicated that

[10] $\quad 2s\text{-}C_4H_9\cdot \rightarrow C_8H_{18}$

[3]Activation energies and frequency factors involved in the computation of $k_7/k_{12}^{1/2}$ are not listed in Table I and were not used in the calculation of the overall order, since reaction [12] is in its third-order region. The value of $k_7/k_{12}^{1/2}$ enters only into the calculation of r_{12} in eq. [II]. Since the rate of reaction [12] is much smaller than the rate of other chain-termination reactions, the value of r_{12} in eq. [II] may be assumed to be 0.

Can. J. Chem. Downloaded from www.nrcresearchpress.com by 210.87.254.6 on 09/05/12
For personal use only.

Can. J. Chem. Downloaded from www.nrcresearchpress.com by 210.87.254.6 on 09/05/12
For personal use only.

was the major chain-termination reaction. Calculations also indicate that the rate of reaction [10] is expected to be approximately 2 orders of magnitude larger than the rate of reaction [11].

Chain-termination Mechanisms

In the previous publication (3), it was pointed out that the nature of the chain-termination mechanism at temperatures above 400 °C is still subject to considerable controversy. Either reaction [8] or reaction [9] may predominate.

In Fig. 5 it may be observed that at approximately 340 °C and 150 mm Hg the overall order is 1.0. Under these conditions the rate of the radical cross-combination reaction

[13] $$CH_3\cdot + s\text{-}C_4H_9\cdot \rightarrow C_5H_{12}$$

or

[14] $$C_2H_5\cdot + s\text{-}C_4H_9\cdot \rightarrow C_6H_{14}$$

should become as important as the sum of the rates of the recombination reactions of the participating radicals.

The relative concentrations of C_5 and C_6 minor products of the sensitized decomposition of *n*-butane at 340 °C should reveal the relative concentrations of methyl and ethyl radicals, thereby providing useful information about the high temperature chain-termination mechanism.

Based on the results of this investigation, it may be concluded that reaction [10] predominates at temperatures below about 320 °C. At temperatures between 320 and 400 °C, both the high and the low temperature mechanism plus the cross-combination reaction of the 2 radicals involved is operative. Thus, assuming that reaction [8] is dominant at temperatures above 400 °C, the following chain-termination mechanism would apply to the 320–400 °C range

[8] $$2CH_3\cdot \rightarrow C_2H_6$$

[10] $$2s\text{-}C_4H_9\cdot \rightarrow C_8H_{18}$$

[13] $$CH_3\cdot + s\text{-}C_4H_9\cdot \rightarrow C_5H_{12}$$

Conclusions

Organic radical decomposition reactions such as reactions [2], [3], and [6] generally have a higher activation energy than radical exchange reactions like reactions [4] and [5]. At high temperatures, the small radicals are present at the highest concentrations and are thus the predominant chain terminators. As the temperature is lowered and the pressure increased, the larger radicals become more important as chain terminators. In a study of the pyrolysis of propane at 440 °C, Leathard and Purnell (11) observed an order change similar to the one described here. A likely reason for the apparent lack of other evidence is that order changes occur in a yet unexplored temperature region, where the reaction rate is extremely low. Extension of pyrolytic reaction studies to lower temperatures and moderately high pressures may reveal that many other organic, free-radical chain reactions can undergo a change in overall reaction order resulting from a change in the termination mechanism.

Acknowledgments

The authors wish to thank the National Research Council of Canada for financial assistance under Grant No. A1637 and the Spruce Falls Power and Paper Company for a fellowship to one of them (J.T.). They are also grateful to Mr. S. R. Rao for many stimulating discussions.

1. J. H. PURNELL and C. P. QUINN. Proc. Roy. Soc. Ser. A, **270**, 267 (1962).
2. N. H. SAGERT and K. J. LAIDLER. Can. J. Chem. **41**, 838 (1963).
3. J. TOROK and S. SANDLER. Can. J. Chem. **47**, 2707 (1969).
4. E. STEINMETZ, K. W. LANGE, and K. K.-G. SCHMITZ. Chem. Ing. Tech. **36**, 1103 (1964).
5. J. H. PURNELL and C. P. QUINN. J. Chem. Soc. 4128 (1961).
6. W. E. MORGANROTH and J. G. CALVERT. J. Amer. Chem. Soc. **88**, 5387 (1966).
7. M. C. LIN and K. J. LAIDLER. Can. J. Chem. **45**, 1315 (1967).
8. P. J. BODDY and E. W. R. STEACIE. Can. J. Chem. **38**, 1576 (1960).
9. A. F. TROTMAN-DICKENSON, J. R. BIRCHARD, and E. W. R. STEACIE. J. Chem. Phys. **19**, 163 (1951).
10. M. C. LIN and M. H. BACK. Can. J. Chem. **44**, 2357 (1966).
11. D. A. LEATHARD and J. H. PURNELL. Proc. Roy. Soc. Ser. A, **306**, 553 (1968).

Can. J. Chem. Downloaded from www.nrcresearchpress.com by 210.87.254.5 on 09/05/12
For personal use only.

Direct photolysis of tetrafluoroethylene at 1849 Å

J. R. DACEY AND J. G. F. LITTLER[1]

Department of Chemistry and Chemical Engineering, Royal Military College of Canada, Kingston, Ontario

Received February 3, 1969

The photolysis of C_2F_4 at 1849 Å gives the following products, whose quantum yields are strongly dependent on substrate pressure: C_2F_6, C_2F_2, cyclo-C_4F_8, cyclo-C_3F_6, C_3F_6, C_3F_8, and polymer. The primary photochemical reactions are tentatively identified, and involve double bond fission and fluorine molecule and fluorine atom elimination.

Canadian Journal of Chemistry, 47, 3871 (1969)

Introduction

The mercury photosensitized decomposition of tetrafluoroethylene (TFE) has been studied by Atkinson (1) and Cohen and Heicklen (2), and the flash photolysis by Dalby (3).

Cohen and Heicklen, using a filter to eliminate wavelengths shorter than 2200 Å, found only perfluorocyclopropane at room temperature, plus small amounts of (tentatively identified) perfluoropropene at temperatures above 175 °C. However, Atkinson, using silica cells with an unfiltered lamp, found perfluorocyclopropane plus polymer. In view of the present work, it seems probable that some direct photolysis was occurring in Atkinson's work.

The flash photolysis results suggest only the formation of perfluoropropene in the direct photolysis.

The thermal decomposition of TFE has been studied by Atkinson and co-workers (4), Miller (5), and Lacher (6). At low temperatures (300–500 °C), the only product found is perfluorocyclobutane; but at higher temperatures, perfluoropropene and perfluoroisobutene are the major products, and are probably formed (4) via a mechanism involving difluoromethylene radicals in the following sequence

$$2C_2F_4 \rightarrow \text{cyclo-}C_4F_8$$

$$\text{cyclo-}C_4F_8 \rightarrow CF_3{-}CF{=}CF_2 + CF_2$$

$$CF_2 + CF_3{-}CH{=}CF_2 \rightarrow \begin{matrix} CF_3 \\ \diagdown \\ \quad C{=}CF_2 \\ \diagup \\ CF_3 \end{matrix}$$

It does not, however, seem probable that similar steps are involved in the formation of products found in the present work.

[1]To whom correspondence should be addressed at The Chemistry Department, Marshall University, Huntington, W. Va. 25701.

Experimental

Tetrafluoroethylene (TFE) from Peninsular Chemical Research Inc. was used without further purification except for degassing at −196 °C, and contained small amounts (¼%) of C_2F_6 as an impurity.

The photolysis cell was 35 cm by 16 cm in diameter, and contained an axial low pressure mercury lamp based on the design by Dacey and Hodgins (7). The lamp, made of suprasil (Englehard Industries Inc.), was surrounded by a vacuum jacket to reduce the temperature of the surface exposed to the TFE. (The internal temperature of the lamp was 95 °C; the external temperature was thus low enough to prevent appreciable thermal polymerization of the TFE.)

The TFE was circulated through the cell by an all glass pump. Photolyses were carried out at 25 °C, from 1–10% conversion without appreciable affect on the quantum yields.

The lamp output (ca. 5×10^{16} quanta s^{-1}) was measured using ammonia as an actinometer, before and after each TFE photolysis. The quantum yield for ammonia decomposition was taken to be 0.45 (8) at a pressure of 15 cm.

Analysis was carried out, using a Burrell Kromo Tog Model KD vapor phase chromatograph on a 10 foot silica gel column (9), operating between 50 and 275 °C, with thermal conductivity detectors. The instrument was calibrated with known quantities of each of the perfluorocarbons found in the photolysis (apart from difluoroacetylene, which is unstable even at low concentrations (10)).

Mass spectrometry was used to distinguish C_2F_3H and C_3F_8 which were scarcely separated on the silica gel column.

Methane was added to the photolysis system, and the relative retention times for various additional species which might be formed by the attack of difluoromethylene or fluorine atoms on methane were measured.

Photolyses and gas collection were carried out on a newly constructed mercury-free vacuum line, employing oil diffusion pumps, and regularly held at 10^{-5} Torr between runs.

Some polymer and very small amounts of carbon gradually built up on the cell walls which were periodically cleaned. There was also very slight etching of the glass.

The absorption spectrum of TFE at 1.16 Torr, using

TABLE I

Quantum yields vs. TFE pressure

$P_{C_2F_4}^{-1}$ cm^{-1}	Quantum yield of					Column *A* cyclo-C_3F_6 / (C_3F_6 + C_3F_8)	Column *B* ΣC_3 / C_2F_6	Column *C* cyclo-C_4F_8 / (C_2F_6 + ΣC_3)
	C_2F_6	cyclo-C_4F_8	cyclo-C_3F_6	C_3F_6	C_3F_8			
0.5	0.009	0.13	0.210	0.000	0.015	4.0	24.8	0.555
1.0	0.040	0.16	0.170	0.002	0.020	7.72	4.82	0.690
2.0	0.080	0.20	0.123	0.004	0.032	3.42	1.99	0.837
4.0	0.140	0.28	0.073	0.009	0.053	1.18	0.965	1.02
8.0	0.225	0.39	0.029	0.018	0.096	0.25	0.635	1.12
12.0	0.280	0.46	0.015	0.027	0.140	0.09	0.650	0.996
20.0	0.330	0.47	0.013	0.046	0.222	0.05	0.852	0.77*
35.0	0.360	0.48	0.010	0.054	0.290	0.03	0.980	0.67*

*ϕ cyclo-C_4F_8 reaches a maximum value of 0.48 and does not rise with a further diminution in pressure.

a 10 cm path length, was recorded on a Beckman DK-1 spectrophotometer fitted with far ultraviolet optics.

Results

Quantum yields were calculated using the measured lamp output, the extinction coefficient of TFE, and the vapor phase chromatographic analysis results. Inherently this is a poor method for gathering yields, which are probably accurate to $\pm 15\%$. Of course, accuracy also depends upon the value used for the quantum efficiency of the decomposition of ammonia.

Table I gives the quantum yields for the formation of perfluoro-cyclopropane, propene, propane, ethane, and cyclobutane in terms of the number of product molecules formed. Owing to the difficulty in analyzing for difluoroacetylene, no quantum yields are given; however, difluoroacetylene was observed in all photolyses.

Other higher molecular weight compounds were formed but not identified, except to note that of all the possible perfluoro-C_4 compounds, cyclo-C_4F_8 was by far the most important.

In some experiments excess methane was added to the TFE in order to take up any fluorine atoms. The amount of fluorine atom formation was monitored by determining the ethane formed in the following reaction

$$CH_4 + F \rightarrow CH_3 + HF$$

$$2CH_3 \rightarrow C_2H_6$$

The product distribution in the mass spectral analysis indicates that other routes to the formation of CH_3 radicals are of minor importance. In Table II the ratios of various products are listed against methane pressure at a constant TFE pressure, and are discussed below.

Additional experiments in which difluorodiazirine was decomposed in the presence of TFE are summarized in Table III. In view of these results, further experiments were carried out at 2537 Å using various pressures of difluorodiazirine and TFE. The pressure dependence of the degree of isomerization of perfluorocyclopropane to perfluoropropene is presented in Fig. 1.

The absorption spectrum of TFE, Fig. 2, is in agreement with unpublished results previously obtained by Walsh[2].

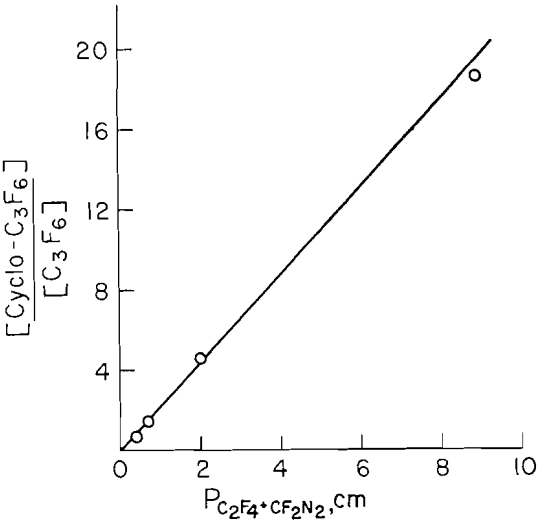

FIG. 1. Pressure dependence of the degree of isomerization of perfluorocyclopropane to perfluoropropene.

[2]In a personal communication, Professor A. D. Walsh suggests that the diffuse bands at 1940 and 1882 Å represent the symmetrical C—C stretching frequency appearing in the allowed lowest energy Rydberg transition, and that the continuous background arises from the allowed $^1(\pi^* \leftarrow n)$ transition.

Can. J. Chem. Downloaded from www.nrcresearchpress.com by 210.87.254.5 on 09/05/12
For personal use only.

TABLE II

Relative product yields in the presence of excess methane*

P_{CH_4} cm	Column *A* $\frac{C_2F_6}{C_2H_6}$	Column *B* $\frac{\text{cyclo-}C_4F_8}{\Sigma C_3 + C_2H_6 + C_2F_6}$
0.5	0	1.50
1.0	0.2	0.85
2.0	0.5	0.48
4.0	3.2	0.07
8.0	8.5	< 0.01
12.0	17	< 0.01
20.0	39	< 0.01
35.0	87	< 0.01

*P_{TFE} = 0.5 cm.

TABLE III

Decomposition of difluorodiazirine in the presence of TFE

Method of decomposing CF_2N_2	Perfluorocyclopropane formed	Perfluoropropene formed
Thermally, 160 °C	Yes	No
Photolytically, 3650 Å	Yes	No
Photolytically, 3130 Å	Yes	No
Photolytically, 2537 Å	Yes	Yes

Discussion

The following reactions should be considered as possible primary processes in the direct photolysis of TFE

[1] $C_2F_4 \rightarrow C_2F_2 + F_2$

[2] $C_2F_4 \rightarrow C_2F_2 + 2F$

[3] $C_2F_4 \rightarrow 2CF_2$

[4] $C_2F_4 \rightarrow C_2F_3 + F$

[5] $C_2F_4 \rightarrow C_2F_4^*$

Reactions [1] and [2] are analogous to the primary processes in the direct photolysis of ethylene at 1849 Å (11), and reaction [3] has been found in the mercury sensitized decomposition of TFE at 2537 Å (1) and in the flash photolysis (3) of TFE. Reaction [5] is postulated to permit the formation of octafluorocyclobutane by collision of either a hot ground state TFE molecule or a collisionally deactivated TFE molecule in the first excited state with the substrate. Finally, process [4] (which does not occur in the direct (11) or mercury-sensitized (12, 13) photolyses of ethylene) is included to account for the formation of C_2F_3H when TFE is photolyzed in the presence of methane.

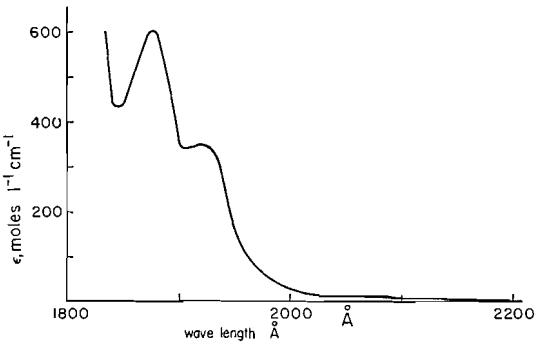

FIG. 2. Absorption spectrum of TFE.

Difluoromethylene Reactions

The heats of formation of TFE and C_3F_6 are −151.7 and −259 kcal/mole, respectively. Assuming that ΔH_f cyclo-C_3F_6 is also approximately −260 kcal/mole, then a reaction in which TFE is converted to cyclo-C_3F_6*, following light absorption at 1849 Å (154.8 kcal/mole), will form the cyclo-C_3F_6* at an energy of 110 kcal/mole above its ground state, providing that no energy is lost by collisions before reaction [6] is complete.

[6] $CF_2^* + C_2F_4 \rightarrow \text{cyclo-}C_3F_6^*$

It seems highly probable then that the hot (ground electronic state) perfluorocyclopropane can isomerize to perfluoropropene to an extent determined by the pressure in the system. Table I shows that the quantum yield for the perfluoropropene rises at low TFE pressures, whereas that for perfluorocyclopropane falls. However, the data in Table I also suggest that much of the perfluorocyclopropane in fact appears not as perfluoropropene, but as perfluoropropane, at low TFE pressures.

It is difficult to justify exclusively a mechanism for the formation of perfluoropropane. Reactions [7] to [9] indicate a probable pathway[3]

[7] $\text{cyclo-}C_3F_6^* \rightarrow C_3F_6^*$

[8] $C_3F_6^* + M \rightarrow C_3F_6$

[9] $C_3F_6^* \rightarrow CF_3 + CF{=}CF_2$

[3]The authors are grateful to a referee for suggesting this mechanism.

Can. J. Chem. Downloaded from www.nrcresearchpress.com by 210.87.254.5 on 09/05/12
For personal use only.

Can. J. Chem. Downloaded from www.nrcresearchpress.com by 210.87.254.5 on 09/05/12
For personal use only.

[10] $C_2F_4 + F \rightarrow C_2F_5$

[11] $C_2F_5 + CF_3 \rightarrow C_3F_8$

It is possible that C_3F_6 could acquire two fluorine atoms consecutively to form C_3F_8. However, since this mechanism does not appear to be followed in the formation of C_2F_6, and in view of the ratio of C_2F_4/C_3F_6 in the system, such a process appears unlikely.

Data concerning the isomerization of perfluorocyclopropane are shown in Table I, Column *A*, where the degree of isomerization displays the expected dependence on TFE pressure. A similar trend is found on the addition of methane, which is, however, far less efficient at quenching the hot perfluorocyclopropane.

Perfluorocyclopropane, made by decomposing difluorodiazirine thermally and photolytically in the presence of TFE, failed to isomerize unless the difluorodiazirine was decomposed at wavelengths shorter than 3130 Å (Table III). Since the heat of formation of difluorodiazirine is not available, it is difficult to use these experiments to bracket the energy required to isomerize perfluorocyclopropane. However, following the decomposition of difluorodiazirine at 2537 Å in the presence of TFE, a considerably higher pressure of TFE, as illustrated in Fig. 1, was required to prevent the isomerization to perfluoropropene than was the case in the direct photolysis of TFE (Table I), implying that the CF_2 fragment formed from CF_2N_2 at 2537 Å is more energetic than that formed from TFE at 1849 Å.

C_2F_6 and cyclo-C_4F_8 Production

Formation of C_2F_6 appears to proceed via the addition of F_2 from process [1] to the substrate. That the alternative pathway in which C_2F_4 successively acquires two fluorine atoms is not dominant is demonstrated by the continued formation of C_2F_6 in the presence of excess methane.

Comparison of Column *C*, Table I, and Column *B*, Table II, shows that excess methane suppresses cyclo-C_4F_8 formation, but rising C_2F_4 pressure augments substrate dimerization. Presumably those excited TFE molecules which do not undergo fission via steps [1]–[4] are collisionally deactivated in the presence of excess methane, whereas they may dimerize with undiluted TFE.

Energetics of the Primary Processes

The energy of the C=C bond in TFE is 77 ± 3 kcal/mole (14). In Table I, Column *B*, the *ratio* of the yields of products consequent upon primary process [3], namely the "C_3" compounds, over the yield of C_2F_6 from process [1] is listed against TFE pressure and shows that process [3] is favored at high pressures. Such behavior is in agreement with the greater energy required to effect process [1] (at least 100 kcal/mole).

According to the data available, primary process [1] is endothermic by 137 ± 15 kcal/mole, and in practice it is difficult to separate the probable products of reactions [2] and [4]. No C_4F_6 compounds were observed; however, C_2F_3H was found, presumably as a result of the following reaction

$$CH_4 + C_2F_3 \rightarrow C_2F_3H + CH_3$$

The fluorine atoms from primary processes [2] and [4] also react with methane to yield methyl radicals, and Table II, Column *A*, indicates that of the processes [1], [2], and [4],

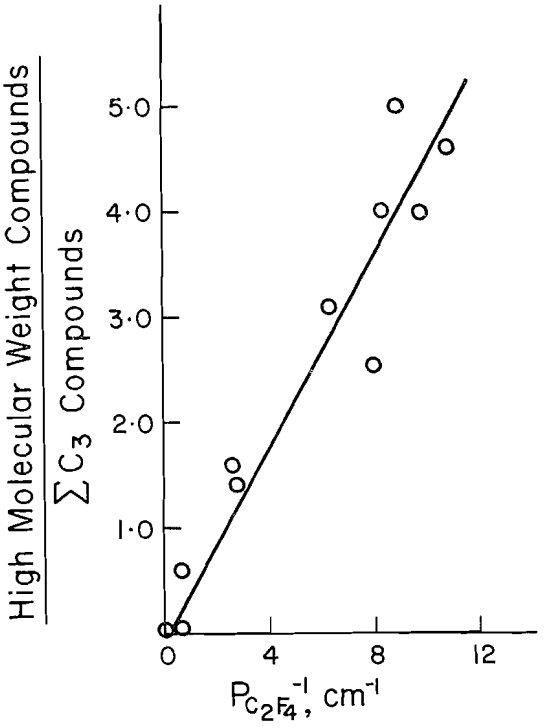

FIG. 3. Formation of higher molecular weight products with respect to TFE pressure.

[1] is the preferred path at high methane pressures, in agreement with the high C—F bond strength in C_2F_4.

Figure 3 shows that the higher molecular weight products formed increase in importance with respect, for instance, to the "C_3" compounds at low TFE pressures, implying that they are formed via a high energy primary step, which may support processes [2] and [4] as important reactions at low TFE pressures. Furthermore, the addition of a large excess of methane completely suppresses the production of these higher molecular weight compounds, but results in the appearance of C_2F_3H and C_2H_6. It seems probable that one important route to such polymers is via chain reactions with the substrate of the type

$$C_2F_3 + C_2F_4 \rightarrow C_4F_7 \xrightarrow{C_2F_4} C_6F_{11} \text{ etc.}$$

Acknowledgments

Thanks are due to G. O. Pritchard and M. Perona of the University of California at Santa Barbara for the mass spectrometric analyses, to W. MacFarland-Smith of Queen's University, Kingston, Ontario, for the use of a far ultraviolet spectrometer, to R. A. Mitsch of the Central Research Laboratories of Minnesota Mining and Manufacturing Co., for a sample of difluorodiazirine, and to the Defence Research Board of Canada for financial support on Grant No. 9530/13.

1. B. ATKINSON. J. Chem. Soc. 2684 (1952); Nature, **163**, 291 (1949).
2. N. COHEN and J. HEICKLEN. J. Chem. Phys. **43**, 871 (1965).
3. F. W. DALBY. J. Chem. Phys. **41**, 2297 (1964).
4. B. ATKINSON and V. A. ATKINSON. J. Chem. Soc. 2086 (1957). B. ATKINSON and A. B. TRENWITH. J. Chem. Soc. 2082 (1953).
5. D. M. MILLER. Preparation and technology of fluorine and organic fluorine compounds. Vol. VII. National Nuclear Energy Series. 1951. Chap. 32.
6. J. R. LACHER, G. W. THOMPKIN and J. D. PARK. J. Amer. Chem. Soc. **74**, 1693 (1952).
7. J. R. DACEY and J. W. HODGINS. Can. J. Res. **28B**, 90 (1950).
8. H. JUCKER and E. K. RIDEAL. J. Chem. Soc. 1058 (1957).
9. S. A. GREENE and F. M. WACHI. Anal. Chem. **35**, 928 (1963).
10. J. HEICKLEN and V. KNIGHT. J. Phys. Chem. **69**, 2484 (1965).
11. H. OKABE and J. R. MCNESBY. J. Chem. Phys. **36**, 601 (1962).
12. R. J. CVETANOVIĆ and A. B. CALLEAR. J. Chem. Phys. **23**, 1182 (1954).
13. N. L. RULAND and R. PERTEL. J. Am. Chem. Soc. **87**, 4213 (1965).
14. K. F. ZMBOV, O. M. UY, and J. L. MARGRAVE. J. Amer. Chem. Soc. **90**, 5090 (1968).

Can. J. Chem. Downloaded from www.nrcresearchpress.com by 210.87.254.5 on 09/05/12
For personal use only.

Can. J. Chem. Downloaded from www.nrcresearchpress.com by 210.87.254.5 on 09/05/12
For personal use only.

Infrared spectra and rotational isomerism of mono-, di-, and tri-ethylene glycol monoalkyl ethers[1]

T. K. K. Srinivasan, C. I. Jose, and A. B. Biswas[2]
National Chemical Laboratory, Poona-8, India

Received April 30, 1968

Infrared spectra have been recorded of the following mono-, di-, and tri-ethylene glycol monoalkyl ethers: $C_nH_{2n+1}OCH_2CH_2OH$ where $n = 17$ and 19; $C_nH_{2n+1}(OCH_2CH_2)_2OH$ where $n = 17$, 18, 19, and 22; and $C_{18}H_{37}(OCH_2CH_2)_3OH$. Spectra of the pure liquids, solutions in CCl_4, and the solids at room and liquid air temperatures have been studied. From a study of the CH_2 rocking modes at 927–934, 889, 900, and 862 cm^{-1} during the liquid–solid transformation and from solution studies, it has been shown that both the OCH_2CH_2O groups in diethylene glycol monoalkyl ethers exist predominantly in the *gauche* conformation in liquid and in solution. However, in the solid, while the end OCH_2CH_2O group takes both *trans* and *gauche* forms, the OCH_2CH_2O group adjacent to the polymethylene chain appears to take a *trans* configuration. The long polymethylene chain is found to pack in a triclinic subcell in the solid state, while in the quenched liquid state an orthorhombic or monoclinic packing is indicated. The present investigation has led to the conclusion that the difference in the conformations of end $CH_2CH_2CH_2OH$ groups found between the odd and even chain *n*-alcohols is removed in mono- and diethylene glycol monoalkyl ethers by the introduction of one or two OCH_2CH_2 groups.

Canadian Journal of Chemistry, 47, 3877 (1969)

Introduction

Previous infrared investigations of a series of long chain alkoxy ethanols ($C_nH_{2n+1}OCH_2CH_2OH$ where $n = 16$, 18, 20, and 22) have shown that the OCH_2CH_2O group in these compounds is present in both *gauche* and *trans* forms in the solid state and largely in the *gauche* form in the liquid or in solution (1). In the present work the study has been extended to compounds where *n* is odd (17 and 19) and compounds containing more than one OCH_2CH_2O group, namely some diethylene glycol monoalkyl ethers $C_nH_{2n+1}(OCH_2CH_2)_2OH$ where $n = 17$, 18, 19, and 22, and one triethylene glycol monoalkyl ether $C_{18}H_{37}(OCH_2CH_2)_3OH$.

The 4 important conformations of OCH_2CH_2O groups in a diethylene glycol monoalkyl ether ($R—OCH_2CH_2OCH_2CH_2OH$) molecule, namely *gauche–trans*, *trans–trans*, *trans–gauche*, and *gauche–gauche* are represented in Fig. 1.

An analysis of the hydroxyl stretching bands of $C_{18}H_{37}(OCH_2CH_2)_2OH$ has been made to obtain information on the association behavior of this compound in CCl_4 solution. The CH_2 group absorptions in compounds containing long polymethylene chains have been found to depend on the nature of chain packing (subcell) (2). In orthorhombic and monoclinic subcell packing, both symmetry considerations and interchain distance favor interaction leading to splitting of certain CH_2 fundamental modes. In the hexagonal subcell on the other hand, both symmetry considerations and interchain distance, which is practically the same as in the liquid, rule out splitting. In the triclinic subcell, there is only a single chain in the unit cell and, therefore, there is only a single component for every fundamental vibration. Using these arguments, an analysis of CH_2 group absorptions has enabled us to deduce the packing of the long polymethylene chains in terms of the possible subcells, for all the compounds studied in both solid and quenched liquid states.

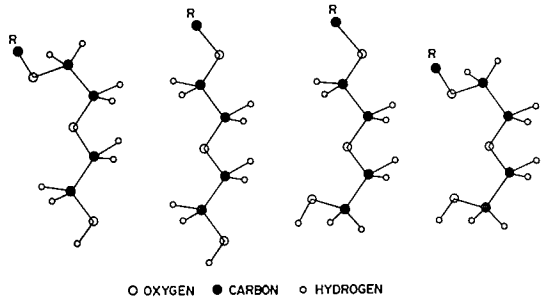

FIG. 1. Conformations of OCH_2CH_2O groups in a diethylene glycol monoalkyl ether: *gauche–trans*, *trans–trans*, *trans–gauche*, and *gauche–gauche*.

[1]Communication No. 2020 from the National Chemical Laboratory, Poona-8, India.

[2]Present address: Department of Chemistry, Indian Institute of Technology, Powai, Bombay-76, India.

Can. J. Chem. Downloaded from www.nrcresearchpress.com by 210.87.254.5 on 09/05/12
For personal use only.

TABLE I

Infrared spectra of solid diethylene glycol monoalkyl ethers at −180 °C*

Infrared frequency (cm^{-1})					
$C_{17}H_{35}(OCH_2CH_2)_2OH$	$C_{18}H_{37}(OCH_2CH_2)_2OH$	$C_{19}H_{39}(OCH_2CH_2)_2OH$	$C_{22}H_{45}(OCH_2CH_2)_2OH$	$C_{18}H_{37}(OCH_2CH_2)_3OH$	Assignment†
3280 s	3290 s	3290 s	3270 s	3300 s	$\nu_{(OH)}$
3165 s,b	3165 s,b	3185 s,b	3185 s,b	3185 s,b	$\nu_{(OH)}$
2925 vs	2925 vs	2915 vs	2915 vs	2925 vs	$\nu_{CH asym.}$
2875 vs	2875 vs	2875 vs	2870 vs	2875 vs	$\nu_{CH sym.}$
1495 s	1495 s	1499 s	1498 sh	1499 s	$B(OC_2H_4)$
1470 vs	1473 vs	1473 vs	1475 vs	1473 vs	B
—	—	—	1464 vs	—	B, $B_{asym.}CH_3$
1452 sh	1456 sh	1453 sh	1451 w	1453 w	$B_{asym.}CH_3$
1425 m	1435 m	1429 m	1420 w	1420 m	$\nu_{C-O}+B_{O-H}$
1406 w	1404 w	1404 w	1404 w	1404 w	$\nu_{C-O}+B_{O-H}$
1385 w	1387 w	1385 w	1385 w	1385 w	$B_{sym.}CH_3$
1368 s	1370 m	1370 s	1376 m	1370 s	W
—	1351 s	—	1351 m	1355 vw	$W(OC_2H_4)$
—	—	1344 vw	—	1342 w	W
—	—	1331 sw	—	—	—
1327 s	1328 s	1325 s	1328 s	1321 s	$W(OC_2H_4)$
—	1316 s	—	316 s	—	W
1309 sh	1302 sh	—	1309 sh	1302 vw	W
—	—	1295	—	—	W
1280 w	1285 vw	1285 vw	1285 vw	1282 w	W
1269 vw	1261 vw	1261 vw	—	1266 vw	W
1252 vw	1248 vw	1245 sw	1243 vw	1248 vw	W
1232 s	1237 s	1233 s	1230 sh	1235 s	$T(OC_2H_4)$
—	1224 m	—	1221 s	1225 sh	$T(OC_2H_4)$
1215 m	1208 m	1215 m	1208 vw	1215 m	$T(OC_2H_4)$
—	1192 sh	—	1199 vw	—	T
1188 vw	1186 sh	—	1182 vw	1188 vw	T
1170 sh	—	1171 w	—	—	T
—	—	—	—	1160 vs	$\nu_{(C-O-C)}$
1145 vs,b	1152 vs,b	1147 vs	1149 vs,b	1152 vs	$\nu_{(C-O-C)}$
—	1139 sh	—	—	—	S
—	1134 sh	—	—	—	S
1127 sh	1114 w	1121 m	1129 sh	1126 sh	$\nu_{(C-O-C)}$, S
1104 w	—	1109 w	1094 w	1092 w	S

Can. J. Chem. Downloaded from www.nrcresearchpress.com by 210.87.254.5 on 09/05/12
For personal use only.

TABLE I (*concluded*)

Infrared frequency (cm^{-1})					
$C_{17}H_{35}(OCH_2CH_2)_2OH$	$C_{18}H_{37}(OCH_2CH_2)_2OH$	$C_{19}H_{39}(OCH_2CH_2)_2OH$	$C_{22}H_{45}(OCH_2CH_2)_2OH$	$C_{18}H_{37}(OCH_2CH_2)_3OH$	Assignment†
1079 s	1080	1082 s	—	1081 sh	$\nu_{(CO)+B(OH)}$, S
1070 s	1065 vs	1071 s	1072 vs	1076 s	
1055 vs	1056 sh	1057 vs	1064 vs	1066 s	
—	—	1053 sh	—	1053 vs	
1048 sh	1048 sh	1047 m	1048 m	—	S
1039 sh	1039 m	1037 m	1045 sh	—	S
1033 m	1033 m	—	1034 w	1021 w	S
1024 m	1016 m	1026 m	1027 m	1013 w	S
1005 m	1008 s	1015 m	1014 m	—	S
—	1004 s	1007 s	—	1003 s	S
998 m	995 s	997 s	997 s	995 s	R, S
986 s	984 s	986 s	981 s	979 s	R, S
—	980 s	—	—	—	R, S
972 s	969 s	972 s	970 s	969 s	$R(OC_2H_4)_t$
900 sh	—	900 sh	—	900 sh	$R(OC_2H_4)_t$
892 s	897 s	892 s	897 s	892 s	$R(OC_2H_4)_g$
864 s	874 s	864 s	874 s	864 s	$R(OC_2H_4)_t$
832 vw	832 w	—	834 vw	—	R
818 w	821 vw	823 w	820 vw	818 w	R
—	804 vw	—	795 vw	—	R
—	791 vw	781 vw	790 vw	—	R
759 vw	—	—	760 vw	—	R
736 w	750 m	745 w	746 w	750 w	R
—	727 sh	—	732 vs	726 w	R
718 vs	720 vs	718 vs	720 vs	719 vs	R
687 vs,b	677 vs,b	689 vs,b	704 vs,b	681 vs,b	$(OH)_{o.p.}$

*s = strong, b = broad, w = weak, sh = shoulder, m = medium, v = very.
†B = CH_2 bending, W = CH_2 wagging, T = CH_2 twisting, R = CH_2 rocking and twisting, S = CC stretching and CCC deformation, o.p. = out of plane, *t* = *trans*, *g* = *gauche*.

Can. J. Chem. Downloaded from www.nrcresearchpress.com by 210.87.254.5 on 09/05/12
For personal use only.

Experimental

Alkoxy ethanols, di- and tri-ethylene glycol monoalkyl ethers were synthesized from the respective alcohols and the corresponding ethylene glycols (3). The odd chain heptadecyl and nonadecyl alcohols were synthesized from cetyl and octadecyl alcohols, respectively. The latter were first converted to heptadecanoic and nonadecanoic acids according to the procedure of Levene and Taylor (4) and the corresponding esters were reduced with lithium aluminum hydride to give the alcohols. All the compounds investigated in this study were at least 99% pure except the C_{17} compounds which are 97% pure as checked by gas–liquid chromatography. The melting points of the compounds reported below are correct to half a degree.

Melting point of the glycols

Compound	Melting point (°C)
$C_{17}H_{35}(OCH_2CH_2)_2OH$	38.8
$C_{18}H_{37}(OCH_2CH_2)_2OH$	44.5
$C_{19}H_{39}(OCH_2CH_2)_2OH$	48.4
$C_{22}H_{45}(OCH_2CH_2)_2OH$	58.8
$C_{18}H_{37}(OCH_2CH_2)_3OH$	42.4
$C_{17}H_{35}OCH_2CH_2OH$	46.6
$C_{19}H_{39}OCH_2CH_2OH$	53.6

Spectral Studies

The spectra were obtained with a Perkin–Elmer model 221 infrared spectrophotometer equipped with a sodium chloride prism and grating interchanges. The instrument was kept in a constant temperature room at 25 °C. The spectral slit widths for the grating and prism interchanges were 5 cm^{-1} (at 3400 cm^{-1}) and 4 cm^{-1} (at 1500 cm^{-1}), respectively. The reported frequencies are accurate within ± 2 cm^{-1}.

The experimental methods were essentially the same as those described in the previous studies (1). A cell similar to that of Wagner and Hornig (5), with additional provision for heating the sample, was used for obtaining the spectra at liquid air temperatures. Association studies were carried out at 25 °C in carbon tetrachloride solution in the concentration range 0.005–0.5 *M*. Carbon tetrachloride (Merck proanalyse) was dried over P_2O_5 and distilled just before making up the solutions. Dilute solutions were made by successive dilution of the concentrated solution.

Results and Discussion

The frequencies of the principal maxima along with proposed assignments for di- and tri-ethylene glycol monoalkyl ethers in the solid state (−180 °C) are presented in Table I. Table II lists the observed frequencies with assignments for $C_{19}H_{39}(OCH_2CH_2)_2OH$ in the various states. The observed frequencies and assignments of the monoethylene glycol monoalkyl ethers (alkoxy ethanols) are presented in Table III. Some typical spectra are shown in Fig. 2.

All the compounds showed two strong bands at 2910 and 2840 cm^{-1} which arise from the CH asymmetric and symmetric stretching modes, respectively. The spectrum of solid $C_{19}H_{39}(OCH_2CH_2)_2OH$, recorded using the grating interchange, showed a series of bands at 2950 (ms), 2930 (sh), 2915 (vs), 2875 (sh), 2870 (w), and 2850 cm^{-1} (vs). A broad shoulder near 2940 cm^{-1} and bands at 2910 (vs) and 2840 cm^{-1} (vs) were observed in the liquid. The strong bands at 2915 and 2850 cm^{-1} are respectively ascribed to the asymmetric and symmetric stretching vibrations of the methylene group of the polymethylene chain, while the shoulders at 2930 and 2875 cm^{-1} are assigned to the stretching modes of the CH_2 groups adjacent to the oxygen. The methyl asymmetric and symmetric stretching modes occur at 2950 and 2870 cm^{-1}.

The methylene group deformation vibrations are classified as bending (scissoring), wagging, twisting, and rocking modes in order of decreasing frequency. In polymethylene chains there is some overlap among the different modes as well as with the skeletal modes. As mentioned in the introduction, splitting of certain fundamental modes occurs due to interaction between adjacent polymethylene chains in certain subcell packings (2). The doublets at 1472 and 1463 cm^{-1} in the spectra of alkoxy ethanols and the singlet at 1472 cm^{-1} in the di- and tri-ethylene glycol monoalkyl ether spectra (except $C_{22}H_{45}(OCH_2CH_2)_2OH$) are assigned to the methylene deformation of the chain in the orthorhombic or monoclinic and triclinic subcells, respectively. These assignments have been made by comparison with similar results reported for orthorhombic *n*-$C_{23}H_{48}$ and triclinic *n*-$C_{24}H_{50}$ (6). The methylene rocking modes also reflect the changes in the packing of the polymethylene chain, the triclinic giving rise to a singlet and the monoclinic or orthorhombic to a doublet near 720 cm^{-1}. However, $C_{22}H_{45}(OCH_2CH_2)_2OH$ shows splitting of the methylene bending and rocking modes indicating a monoclinic or orthorhombic packing, in contrast to the triclinic packing in the other diethylene glycol monoalkyl ethers. In the liquid state (see Fig. 3) all these compounds show a single band at 1466 cm^{-1}. The methyl asymmetric deformation mode in alkoxy ethanols appears to merge with the methylene deformation at 1463 cm^{-1}, while it is present as a weak band at 1453 cm^{-1} in di- and tri-ethylene glycol monoalkyl ethers. Similar assignments have been made for triclinic *n*-C_{24}-

Can. J. Chem. Downloaded from www.nrcresearchpress.com by 210.87.254.5 on 09/05/12
For personal use only.

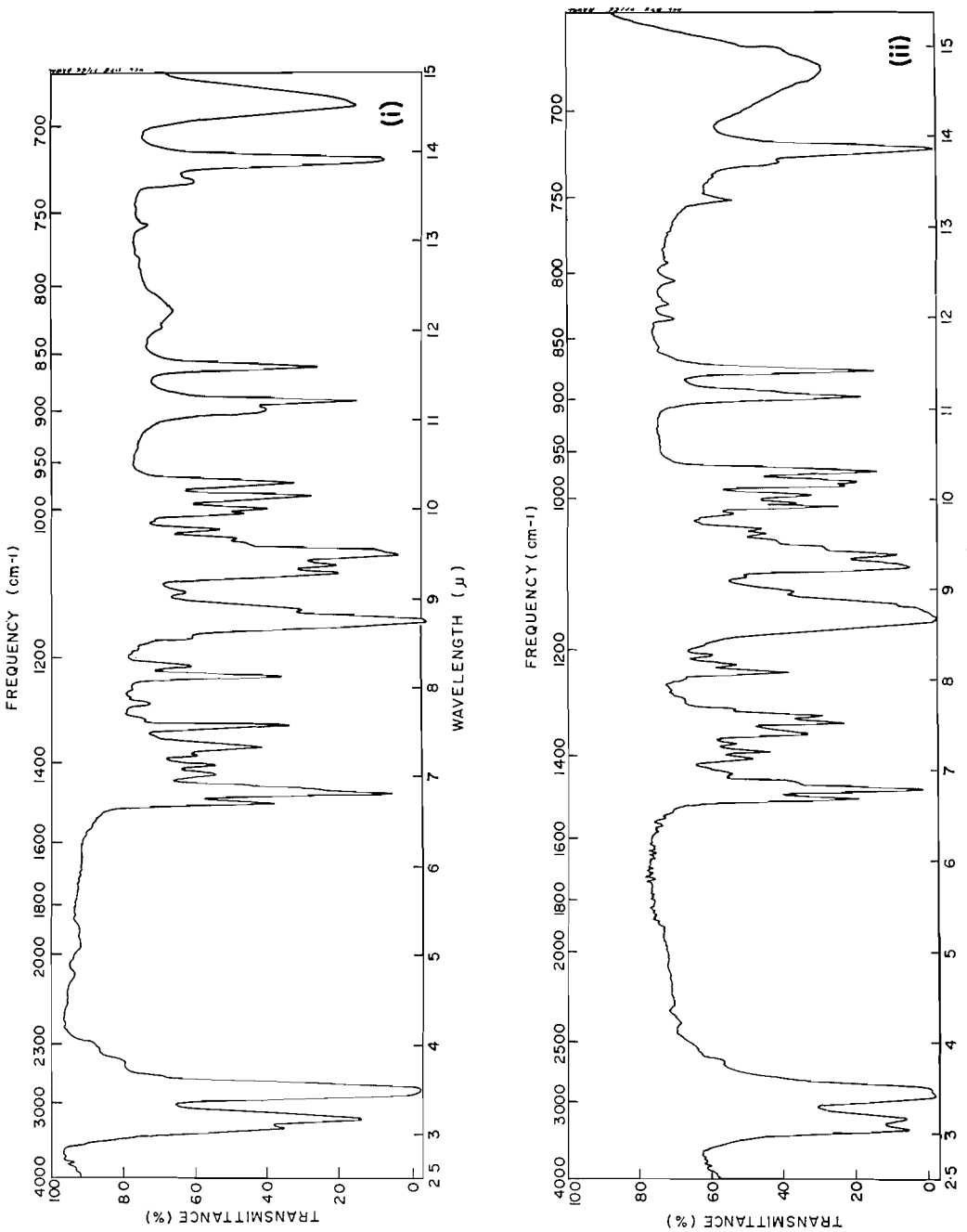

FIG. 2*a*. Infrared spectra of (*i*) $C_{17}H_{35}(OCH_2CH_2)_2OH$ and (*ii*) $C_{18}H_{37}(OCH_2CH_2)_2OH$ at −180 °C.

Can. J. Chem. Downloaded from www.nrcresearchpress.com by 210.87.254.5 on 09/05/12
For personal use only.

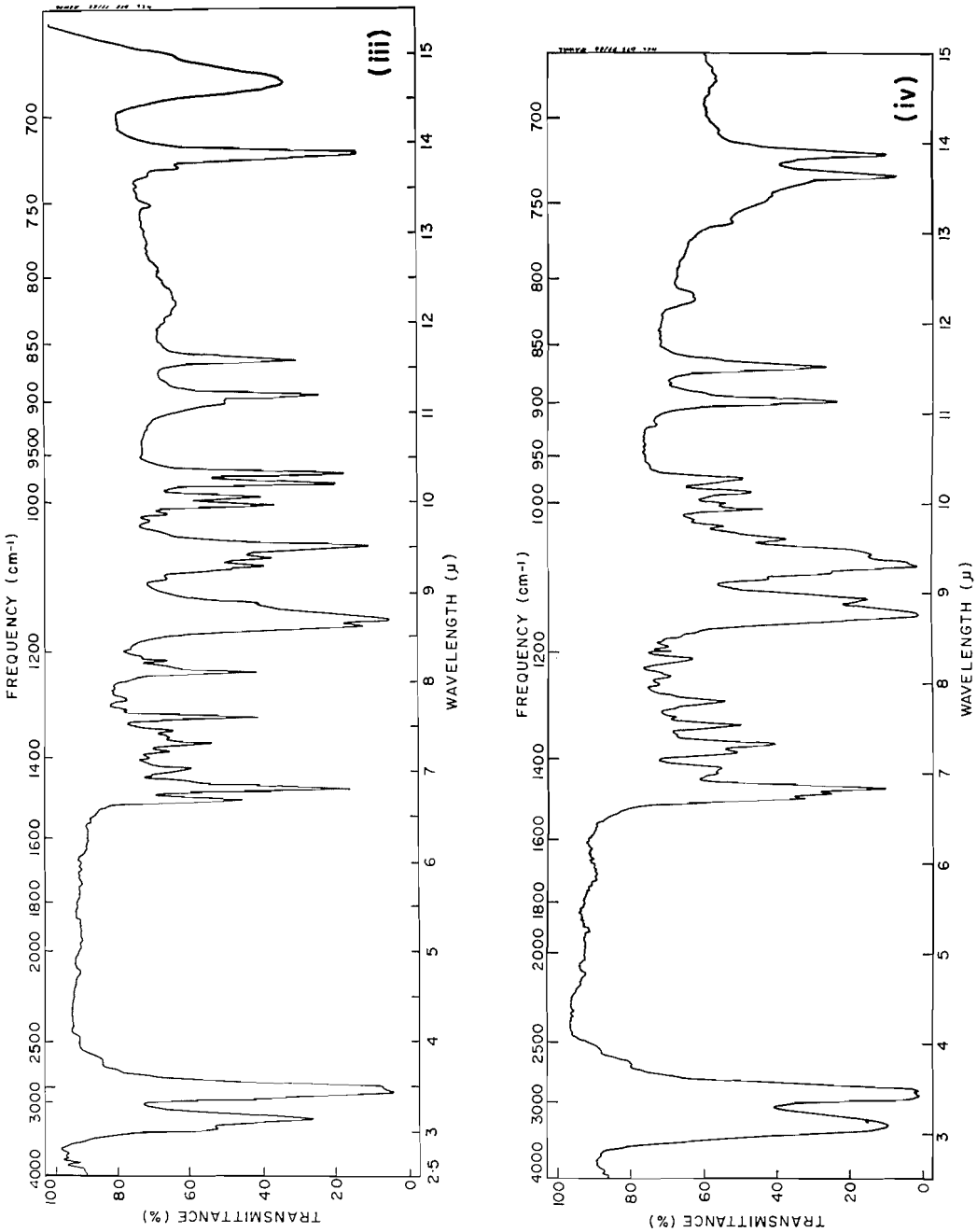

FIG. 2*b*. Infrared spectra of (*iii*) $C_{18}H_{37}(OCH_2CH_2)_3OH$ and (*iv*) $C_{17}H_{35}OCH_2CH_2OH$ at −180 °C.

Can. J. Chem. Downloaded from www.nrcresearchpress.com by 210.87.254.5 on 09/05/12
For personal use only.

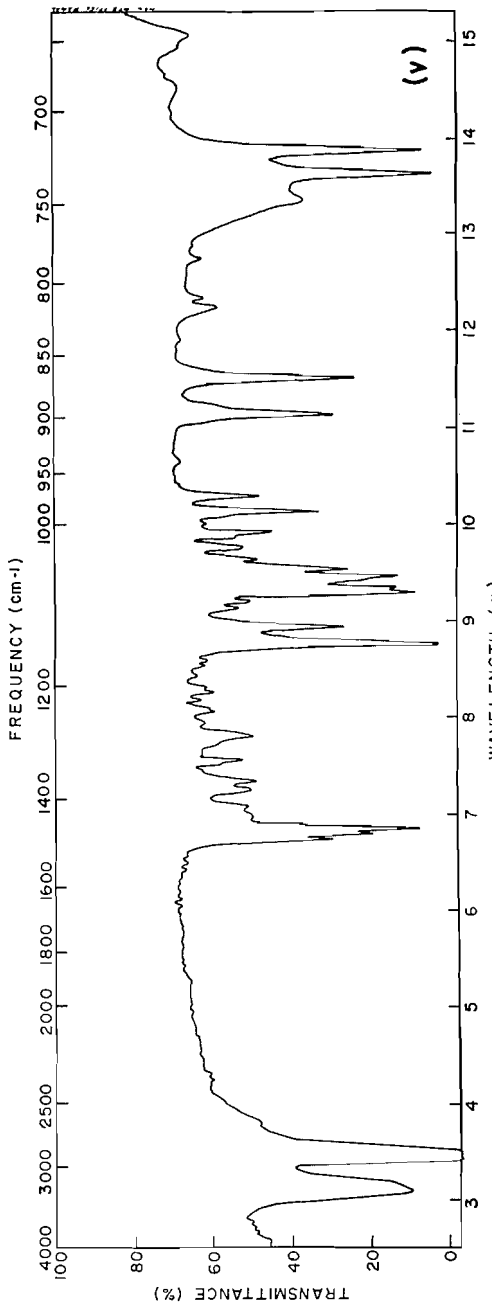

FIG. 2c. Infrared spectrum of (v) $C_{19}H_{39}OCH_2CH_2OH$ at −180 °C.

TABLE II

Infrared spectra of di-ethylene glycol monononadecylether ($C_{19}H_{39}(OCH_2CH_2)_2OH$)*

Infrared frequency (cm^{-1})				
Solid (25 °C)	Solid (−180 °C)	Liquid	Quenched liquid	Assignment†
3333 b	3290 s	3450 s,b	—	$\nu_{(OH)}$
3250 s,b	3185 s,b	—	3250 s,b	$\nu_{(OH)}$
2924 vs	2915 vs	2905 vs	2900 vs	$\nu_{asym.\ CH\ (CH_3,\ CH_2,\ OC_2H_4)}$
2875 vs	2875 vs	2855 vs	2850 vs	$\nu_{sym.\ CH\ (CH_3,\ CH_2,\ OC_2H_4)}$
1497 s	1499 s	—	1497 sh	$B(OC_2H_4)$
1473 vs	1473 vs	—	1473 vs	B
—	—	1466 vs	1460 vs	B, $B_{asym.\ CH_3}$
1453	1453 sh	—	—	$B_{asym.\ CH_3}$
1418 m	1429 m	—	—	$\nu_{C-O+B(OH)\ i.p.}$
1408 m	1404 w	1400 vvw	1401 w	and $W(OC_2H_4O)$
1385 w	1385 w	1379 vw	1377 w	$B_{sym.\ CH_3}$
1372 m	1370 s	1366 vw	—	W
—	—	1351 m	1351 w	$W(OC_2H_4)$
1342 vw	1344 vw	—	—	W
—	1331 sh	—	1332 sh	W
1325 s	1325 s	—	1321 m	$W(OC_2H_4)$
—	1295 vw	1290 m	—	W
1282 vw	1285 vw	—	1282 vw	W
1258 vw	1261 vw	—	—	W
—	1245 sh	1250 m	—	W
1232 s	1233 s	—	1239 vw	$T(OC_2H_4)$
1215 w	1215 m	—	1222 m	$T(OC_2H_4)$
—	1171 w	—	—	T
1145 vs,b	1147 vs	—	1149 vs,b	ν_{C-O-C}
1127 w	1121 m	1124 vs,b	1126 sh	ν_{C-O-C}
1107 vw	1109 w	—	—	S
1080 m	1082 s	—	—	$\nu_{C-O+B(OH)}$, S
1068 m	1071 s	1070 s,b	1075 sh	$\nu_{C-O+B(OH)}$, S
1057 s	1057 vs	—	1062 vs,b	$\nu_{C-O+B(OH)}$, S
—	1053 sh	—	—	$\nu_{C-O+B(OH)}$, S
1047 sh	1047 sh	—	—	S
1036 m	1037 m	—	—	S
1022 w	1026 m	—	1022 sh	S
1012 m	1015 m	—	1012 sh	S
1004 m	1007 s	—	1005 m	S
	997 s	—	—	R, S
984 s	986 s	—	985 s	R, S
968 s	972 s	—	971 s	R, S
—	—	926 w,b	930 w,b	$R(OC_2H_4O)_g$
898 inf	900 sh	—	—	$R(OC_2H_4O)_t$
891 s	892 s	890 m,b	892 m,b	$R(OC_2H_4)_g$
862 s	864 s	—	—	$R(OC_2H_4)_t$
—	823 w	—	—	R
784 vw	781 vw	—	—	R
746 vw	745 w	—	746 vw	R
717 vs	718 vs	719 s,b	733 vs	R
—	—	—	720 vs	R
—	689 vs,b	—	—	$B(OH)_{o.p.}$

*Frequency in cm^{-1}; s = strong, b = broad, w = weak, sh = shoulder, m = medium, v = very.
†B = CH_2 bending, W = CH_2 wagging, T = CH_2 twisting, R = CH_2 rocking and twisting, S = CC stretching and CCC deformation, o.p. = out of plane, i.p. = in plane, *t* = *trans*, *g* = *gauche*.

H_{50} (6), *n*-$C_{18}H_{38}$ (7), and orthorhombic *n*-$C_{23}H_{48}$ (6).

A band at 1495 ± 5 cm^{-1} whose intensity increases with increasing number of OCH_2CH_2 groups is found in the solid state spectra of all compounds, although in the liquid state there is no band in this position. A methylene scissoring mode has not been generally found at such a high frequency. However, Matsuura and Miyazawa (8) have recently reported the presence of a band at 1484 cm^{-1} in the spectrum of diethylene glycol, although no specific assignment was made. A band at 864–871 cm^{-1} found in the spectra of the solid compounds and also absent in the spectra of

Can. J. Chem. Downloaded from www.nrcresearchpress.com by 210.87.254.5 on 09/05/12
For personal use only.

TABLE III
Infrared spectra of alkoxy ethanols*

Infrared frequency (cm^{-1})		
$C_{17}H_{35}OCH_2CH_2OH$	$C_{19}H_{39}OCH_2CH_2OH$	Assignment†
3226 vs,b	3247 vs,b	$\nu_{(OH)}$
2924 vs	2924 vs	$\nu_{asym.CH(CH_3,CH_2,OCH_2CH_2)}$
2865 vs	2865 vs	$\nu_{sym.CH(CH_3,CH_2,OCH_2CH_2)}$
1488 s,sh	1488 m	$B(OC_2H_4)$
1475 s	1476 s	B
1462 s	1464 s	B, $B_{asym.\ CH_3}$
1431 vw	1433 vw	$\nu_{C-O}+B(OH)_{i.p.}$ and $W(OC_2H_4)$
1418 w	1416 vw	
1381 m	1385 m	$B_{sym.CH_3}$
1366 m	1366 m	W, T
1312 vw	—	
1282 m	1287 m	
	1263 vw	
1250 w	1244 w	
	1238 w	
	1227 w	
	1214 w	
1208 w	1206 w	
1190 w	1188 vw	
	1176 vw	
1140 vs,b	1144 vs,b	$\nu_{(C-O-C)}$
1119 m	1121 s	$\nu_{(C-O-C)}$, S
	1099 w	S
	1089 w	S
1072 vs,b	1078 s	$\nu_{(C-O)}+B(OH)$, S
	1075 s	
1058 m	1059 s	
	1051 s	
1038 m	1039 m	S, R
1026 w	1027 m	
	1018 w	
1006 w	1010 m	
1000 w	1000 w	
987 m	988 s	
976 m	974 m	$R(OC_2H_4O)$, S,
898 s	898 s	$R(OC_2H_4)_g$
868 s	868 s	$R(OC_2H_4)$
816 w	817 w	R
810 w	810 w	R
762 vw	784 w	R
746 vw	748 vw	R
732 vs	734 vs	R
721 vs	721 vs	R

*s = strong, b = broad, w = weak, sh = shoulder, m = medium, v = very.
†B = CH_2 bending, W = CH_2 wagging, T = CH_2 twisting, R = CH_2 rocking and twisting, S = CC stretching and CCC deformation, o.p. = out of plane, i.p. = in plane, *t* = *trans*, *g* = *gauche*.

the liquids has been ascribed to the methylene rocking of the OCH_2CH_2O group in the *trans* form (see below). We have therefore assigned the band at 1495 $\pm$ 5 cm^{-1} to a methylene deformation of the *trans* OCH_2CH_2O group.

The quenched liquid alkoxy ethanols produced spectra which were the same as the spectra of the solids. However, di- and tri-ethylene glycol monoalkyl ethers (see Fig. 4) showed a splitting of the band at 1464 cm^{-1} (liquid) into two components at 1463 and 1472 cm^{-1} on quenching, (see Fig. 3). Similar splitting was also observed in the CH_2 rocking mode near 720 cm^{-1}. These splittings as mentioned earlier are characteristic of orthorhombic or monoclinic subcell packing of the polymethylene chain. The spectra of the quenched liquids differ from the solid spectra which show single bands in these regions (near 1460 and 720 cm^{-1}). The latter are characteristic of triclinic packing.

Can. J. Chem. Downloaded from www.nrcresearchpress.com by 210.87.254.5 on 09/05/12
For personal use only.

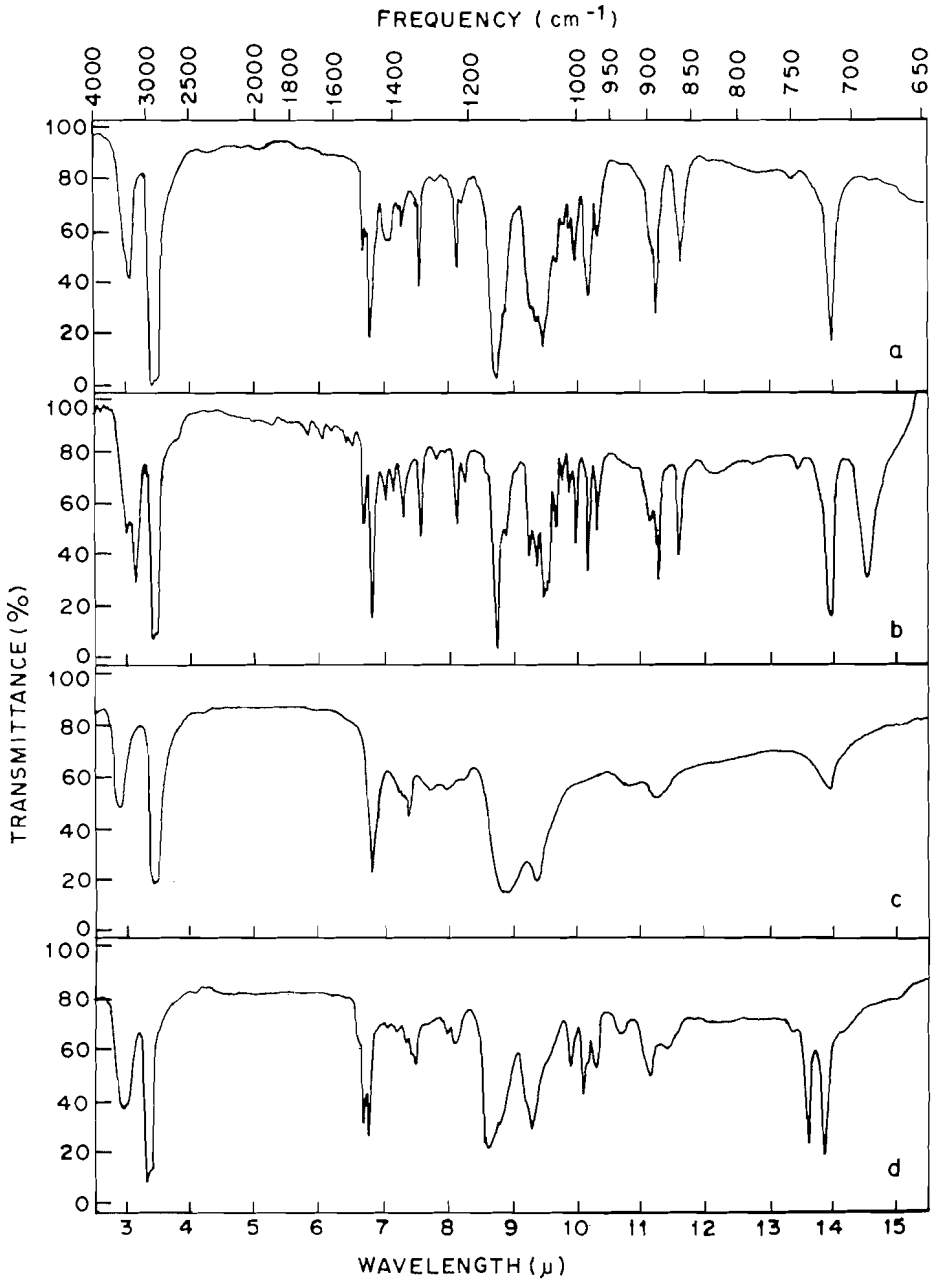

FIG. 3. Infrared spectra of $C_{19}H_{39}(OCH_2CH_2)_2OH$: (*a*) solid at 25 °C, (*b*) solid at −180 °C, (*c*) liquid, and (*d*) quenched liquid at −180 °C.

Liquid $C_{22}H_{45}(OCH_2CH_2)_2OH$ on quenching gives the same packing of the polymethylene chain as the solid, which as mentioned earlier was either orthorhombic or monoclinic. However, the bands at 1495, 862–871, and 964–969 cm^{-1} which are characteristic of the OCH_2CH_2O group in the *trans* form and were found in the spectra of the solids, are absent or very weak in the spectra of the quenched liquids. On warming the quenched liquids, the spectra revert to those

Can. J. Chem. Downloaded from www.nrcresearchpress.com by 210.87.254.5 on 09/05/12
For personal use only.

Can. J. Chem. Downloaded from www.nrcresearchpress.com by 210.87.254.5 on 09/05/12
For personal use only.

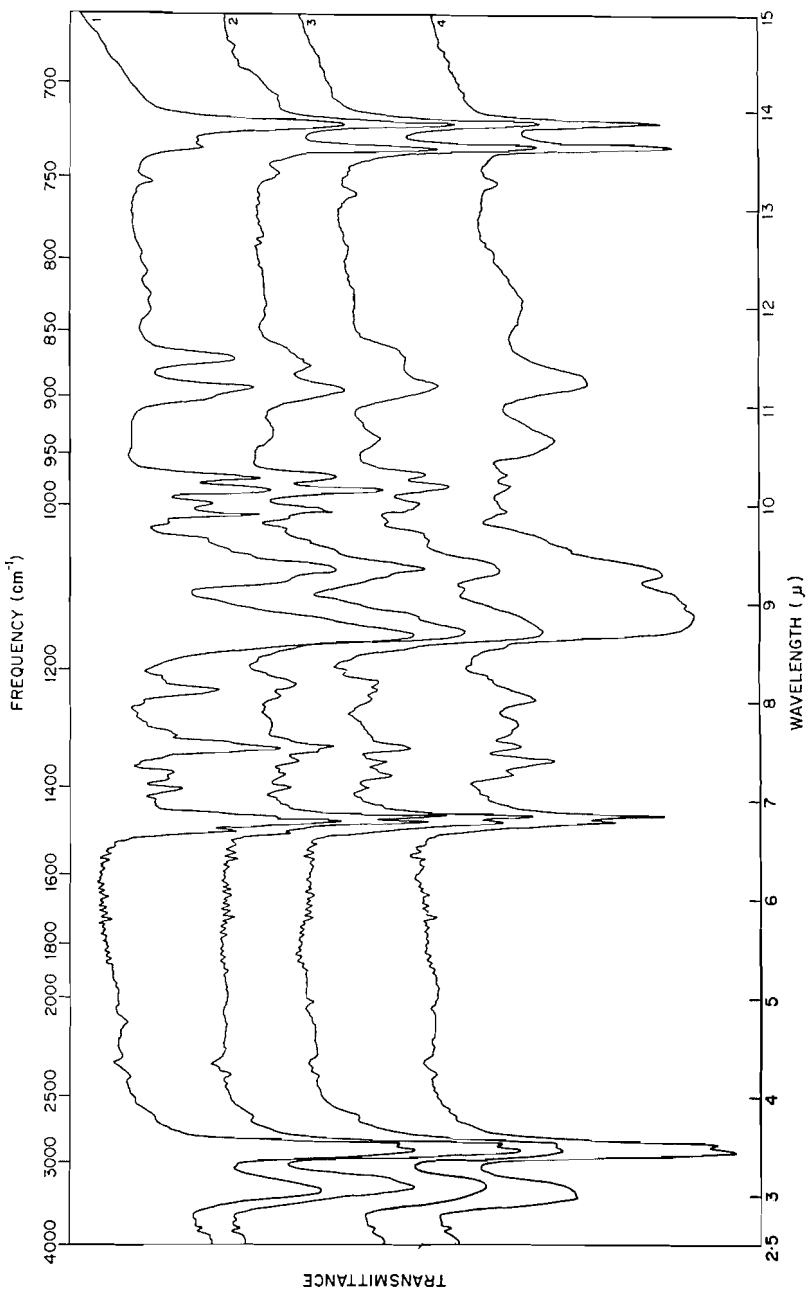

FIG. 4. Infrared spectra of (*1*) $C_{18}H_{37}(OCH_2CH_2)_2OH$, (*2*) $C_{19}H_{39}(OCH_2CH_2)_2OH$, (*3*) $C_{22}H_{45}(OCH_2CH_2)_2OH$, and (*4*) $C_{18}H_{37}(OCH_2CH_2)_3OH$ in the quenched liquid state.

Can. J. Chem. Downloaded from www.nrcresearchpress.com by 210.87.254.5 on 09/05/12
For personal use only.

of the solid in all cases. These results can be explained on the basis that in the quenched state, while the long polymethylene chain packs in the orthorhombic or monoclinic subcell (in contrast to the triclinic subcell in the normal solid), the OCH_2CH_2O groups have been frozen into a disordered structure consisting mainly of the *gauche* conformations. Various polymorphic forms of monostearin obtained by different conditions of crystallization are found to give different packing of the polymethylene chain (9). In view of the transformation to the normal solid state structure on warming, it is unlikely that the OCH_2CH_2O groups are rotating. Rapidly frozen 1,1,2,2-tetrabromoethane has been shown (10) to have a *gauche* conformation, while the solid obtained by slow cooling crystallizes in the *trans* form (11).

The bands in the region 1380–1150 cm^{-1} have their origin in the wagging and twisting vibrations of the methylene groups. The bands at 1370, 1321 $\pm$ 5, 1225 $\pm$ 3, and 1212 $\pm$ 4 cm^{-1} in the spectra of di- and tri-ethylene glycol monoalkyl ethers, are stronger than those observed in the alkoxy ethanols at similar positions, and are ascribed to the CH_2 wagging and twisting modes of the OCH_2CH_2O groups. Miyake (12) and Buckley and Giguère (13) have also assigned bands at similar positions in the spectra of solid ethylene glycol to methylene wagging and twisting modes. However, Matsuura and Miyazawa (14) prefer to assign them to coupled modes of OH deformation and CH_2 wagging.

The bands in the region between 1150 and 1050 cm^{-1} are assigned to the C—O—C antisymmetric stretching vibrations ($\sim$ 1148, $\sim$ 1126 cm^{-1}), to the coupled C—O stretching and O—H deformation ($\sim$ 1080, $\sim$ 1075, $\sim$ 1055 cm^{-1}) (15), and C—C stretching modes (16). The bands between 1050 and 950 cm^{-1} arise from the various skeletal modes.

The spectra of mono-, di-, and tri-ethylene glycol monoalkyl ethers in the region 950–800 cm^{-1} are widely different in the liquid and solid states (see Fig. 3 for $C_{19}H_{39}(OCH_2CH_2)_2OH$ as an example). Changes in the absorption patterns for a typical liquid–solid transformation for the compound $C_{18}H_{37}(OCH_2CH_2)_2OH$ are represented in Fig. 5. In the case of certain alkoxy ethanols these changes have been explained as being due to different rocking modes of the 2 rotational isomeric configurations (RG and RT) of the OCH_2CH_2O group (1). In diethylene glycol monoalkyl ethers, as mentioned in the introduction, there are 4 such configurations for the two OCH_2CH_2O groups (see Fig. 1).

The bands at 889 cm^{-1} in the spectrum of the liquid and 891–897, 862–871, and 964–969 cm^{-1} in the solid spectra of di- and tri-ethylene glycol monoalkyl ethers are similar to those observed for the 2 alkoxy ethanols in the corresponding states studied in this work and earlier (1). They have thus been ascribed to the *gauche* (889–897 cm^{-1}) and *trans* (862–871 and 964–969 cm^{-1}) forms of the end OCH_2CH_2O group. The 927–934 cm^{-1} band in the liquid and 900 cm^{-1} in the solid spectra of di- and tri-ethylene glycol monoalkyl ethers are then ascribed to the *gauche* and *trans* configurations of the OCH_2CH_2O group adjacent to the polymethylene chain.

The band at 927–934 cm^{-1} in the liquid state of di- and tri-ethylene glycol monoalkyl ethers is similar to that found at 936–941 cm^{-1} in di-, tri-, and poly-ethylene glycols (17) and also to that at 934 cm^{-1} in mono alkylated polyethylene glycols (18). This band is not found in alkoxy ethanols. Further, in ethylene glycol dimethyl ether, 2 bands observed at 935 and 928 cm^{-1} are attributed to the *gauche* form by Miyake (17). This is in agreement with our assignment of the band at 927–934 cm^{-1} in the present compounds to the *gauche* OCH_2CH_2O group adjacent to the paraffin chain, which is different from the one containing the hydroxyl group. However, a band at 900 cm^{-1} observed in ethylene glycol ethers (19) and in $O_2NOCH_2CH_2ONO_2$ (20) has been ascribed to the methylene rocking in the *gauche* form. The absence of the 927–934 cm^{-1} band in the spectra of solid di- and tri-ethylene glycol monoalkyl ethers and the presence of a new band at 900 cm^{-1} shows the conversion of the RG- to RT-form during liquid–solid transformation.

The above results thus show that diethylene glycol monoalkyl ethers take the RGG conformation in the liquid and both RTG and RTT configurations in the solid state. The spectra of alkoxy ethanols (C_{17} and C_{19}) studied in the present work are similar to those of the even chain compounds studied earlier and have mainly RG configuration in the liquid and both RG and RT configurations in the solid. The triethylene glycol monoalkyl ether has probably RGGG configuration in the liquid and RTTG and RTTT configurations in the solid. The *trans* configuration of the OCH_2CH_2O group placed adjacent

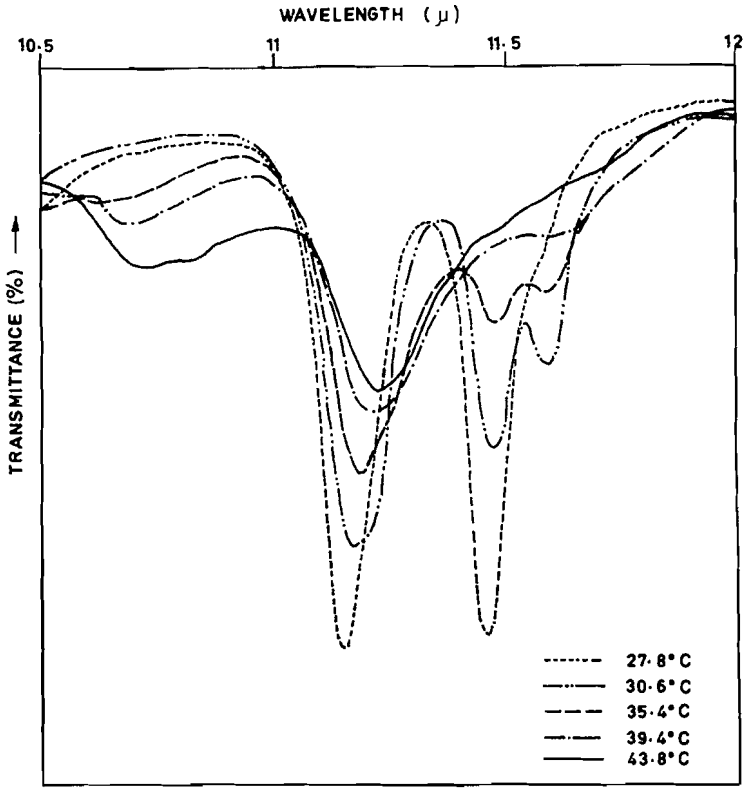

FIG. 5. Variation of intensity of the CH_2 rocking mode with temperature in $C_{18}H_{37}(OCH_2CH_2)_2OH$.

to the long methylene chain in the solid state of mono-, di-, and tri-ethylene glycol monoalkyl ethers is not unexpected in view of the known extended TTT . . . . T configuration (21) of the polymethylene chain itself. However, the occurrence of the end OCH_2CH_2O groups carrying a hydroxyl group in both *gauche* and *trans* configurations in all the present compounds is unexpected, since usually only one rotational isomer exists in the crystalline solid. Recently Tasumi *et al.* (22) have reported the odd (C_{17}–C_{29}) chain alcohols (β-form) to have equal numbers of *gauche* and *trans* configurations for the end $CH_2CH_2CH_2O$ group in the solid. The even (C_{18}–C_{34}) chain alcohols (γ-form) have, on the other hand, only the *trans* configuration for this group. The odd chain (hydrocarbon part) diethylene glycol monoalkyl ethers and even chain alkoxy ethanols may be compared to the odd chain alcohols if the ether oxygen is considered similar to a CH_2 group. However, our results show that even chain alcohols (γ-form), which have only the *trans* configuration for the end $CH_2CH_2CH_2O$ group, have no analogues either in the odd chain alkoxy ethanols or even chain diethylene glycol monoalkyl ethers. This leads to the conclusion that the effect of the number of carbon atoms (odd, even) on the end conformation, i.e. $CH_2CH_2CH_2O$ group found in alcohols, is destroyed by the presence of ether oxygen in the mono-, di-, and tri-ethylene glycol monoalkyl ethers.

Hydroxyl Absorptions

The liquid state spectra of all the di- and triethylene glycol monoalkyl ethers showed a broad band at 3450 ± 25 cm^{-1} attributable to an O—H stretching vibration. Solidification leads to a splitting into two peaks at 3335 ± 15 cm^{-1} and 3255 ± 15 cm^{-1} which occurs at 25 °C (see Fig. 6*a*). These two components are shifted down to 3280 and 3180 cm^{-1}, respectively, at −180 °C. However, the monoethylene glycol monoalkyl ethers showed a single O—H stretching band at

Can. J. Chem. Downloaded from www.nrcresearchpress.com by 210.87.254.5 on 09/05/12
For personal use only.

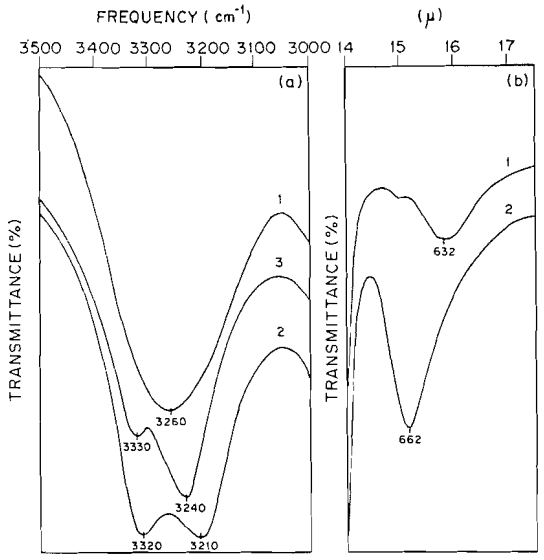

FIG. 6. (*a*) The OH stretching vibration region of the spectra of (*1*) $C_{18}H_{37}OCH_2CH_2OH$, (*2*) $C_{18}H_{37}(OCH_2CH_2)_2OH$, (*3*) $C_{19}H_{39}(OCH_2CH_2)_2OH$. (*b*) CsBr region (in part) of the spectra of (*1*) $C_{18}H_{37}OCH_2CH_2OH$, (*2*) $C_{18}H_{37}(OCH_2CH_2)_2OH$.

3270 cm^{-1} in the solid state. Two bands at 1427 $\pm$ 8 and 1406 $\pm$ 2 cm^{-1} are observed in the spectra of mono-, di-, and tri-ethylene glycol monoalkyl ethers. In previous work on alcohols (23), bands in this region have been assigned to the O—H in-plane deformation coupled with a C—O stretching mode. The O—H in-plane deformation modes in odd and even chain alcohols have been found at 1408 and 1427 cm^{-1}, respectively (20). Bands at 1414 and 1392 cm^{-1} in ethylene glycol have recently been assigned to the coupled vibration of the O—H in-plane deformation and a CH_2 wagging mode (12). A band at 1422 cm^{-1} in the spectrum of liquid di-ethylene glycol (8) which shifts to 1439 cm^{-1} in the solid, has been attributed to an O—H in-plane deformation. The O—H out-of-plane deformation for solid $C_{18}H_{37}(OCH_2CH_2)_2OH$ at 25 °C is observed at 660 cm^{-1}. This is higher than that observed (634 cm^{-1}) in the spectrum of the alkoxy ethanol $C_{18}H_{37}OCH_2CH_2OH$ (see Fig. 6 *b*). These peaks are shifted to higher frequencies at -180 °C. The O—H out-of-plane deformation modes in the odd and even chain alcohols at 25 °C are found at 687 and 612 cm^{-1}, respectively (20).

Hydrogen Bonding

In order to elucidate the association behavior of diethylene glycol monoalkyl ethers, the spectrum of $C_{18}H_{37}(OCH_2CH_2)_2OH$ was studied in detail in the hydroxyl stretching region. In dilute CCl_4 solution (0.005 *M*) 3 bands at 3645, 3615, and 3480 cm^{-1} have been observed. These are similar to those observed by Flett (24) for diethylene glycol monoethyl ether. These absorptions are assigned to a free OH (*trans* or non-bonded *gauche*) and intramolecularly bonded 5 and 8 membered ring monomers, respectively. The assignments have been made by comparison with the spectrum of octadecoxy ethanol, which exhibits the monomer bands at 3640 and 3610 cm^{-1} at this concentration. With increasing concentration up to 0.5 *M* no new band was observed, but the relative intensity of the band near 3480 cm^{-1} increased with respect to that at 3615 cm^{-1}. The intensity of the free OH band at 3640–3645 cm^{-1} of these 2 compounds is small and is estimated to be less than 10% of the band at 3480 cm^{-1} at these concentrations. In octadecoxy ethanol, a band attributable to a dimer was found at 3480 cm^{-1} at concentrations above 0.02 *M*. It is concluded that at higher concentrations, the band near 3480 cm^{-1} observed in the spectrum of $C_{18}H_{37}(OCH_2CH_2)_2OH$ may also include absorption due to the dimer. Since no bands below 3480 cm^{-1} were observed even at the highest concentration (0.5 *M*) and since the pure liquid shows a broad band close to this frequency ($\sim$ 3450 cm^{-1}), it is concluded that the liquid consists largely of dimers. The formation of dimers only by $C_{18}H_{37}(OCH_2CH_2)_2OH$ and $C_{18}H_{37}OCH_2CH_2OH$ in concentrated solutions (0.5 *M*) is in sharp contrast to the higher polymers formed by long chain alcohols under similar conditions.

Conclusions

The present study has shown that the OCH_2CH_2O groups in mono-, di-, and tri-ethylene glycol monoalkyl ethers exist largely in the *gauche* configuration in the liquid (RG, RGG, RGGG) and in both *trans* and *gauche* configurations in the solid state (RG and RT, RTG and RTT, and RTTG and RTTT). The existence of 2 different configurations of the end OCH_2CH_2O group containing the hydroxy group bears similarity to the β-form of long chain alcohols. The conversion of the OCH_2CH_2O group adjacent to the long polymethylene chain from a *gauche* to a *trans* configuration on solidification shows the

Can. J. Chem. Downloaded from www.nrcresearchpress.com by 210.87.254.5 on 09/05/12
For personal use only.

influence of the extended TT . . . T configuration of the polymethylene chain. While the quenching of liquid di- and tri-ethylene glycol monoalkyl ethers brings about a change in the polymethylene chain packing (subcell) as compared to the solid state spectra, quenching of monoethylene glycol monoalkyl ethers produced normal solid state spectra. Further quenching did not bring about any appreciable change in the configuration of the OCH_2CH_2O groups in the case of di- and tri-ethylene glycol monoalkyl ethers. Solution studies on $C_{18}H_{37}OCH_2CH_2OH$ and $C_{18}H_{37}(OCH_2CH_2)_2OH$ have shown that these compounds form largely dimers in concentrated solutions (~ 0.5 M) in contrast to polymers formed by simple alcohols.

Acknowledgment

Thanks are due to the referees for many helpful comments.

1. T. K. K. Srinivasan, C. I. Jose, and A. B. Biswas. Bull. Chem. Soc. Jap. **37**, 1770 (1964).
2. D. Chapman. J. Chem. Soc. 4489 (1957).
3. A. N. Wrigley, A. J. Striton, and E. Howard, Jr. J. Org. Chem. **25**, 439 (1960).
4. P. A. Levene and F. A. Taylor. J. Biol. Chem. **59**, 919 (1924).
5. E. L. Wagner and D. F. Hornig. J. Chem. Phys. **18**, 296 (1950).
6. R. G. Snyder J. Mol. Spectrosc. **7**, 116 (1961).
7. R. F. Holland and J. R. Nielsen. J. Mol. Spectrosc. **8**, 383 (1962).
8. H. Matsuura and T. Miyazawa. Spectrochim. Acta, **23A**, 2433 (1967).
9. D. Chapman. Spectrochim. Acta, 609 (1957).
10. M. Hashimoto, T. Shimanouchi, and S. Mizushima. J. Chem. Phys. **24**, 172 (1956).
11. R. E. Kagarise. J. Chem. Phys. **23**, 207 (1955).
12. A. Miyake. J. Polym. Sci. **38**, 478 (1959).
13. P. Buckley and P. Giguère. Can. J. Chem. **45**, 397 (1967).
14. H. Matsuura and T. Miyazawa. Bull. Chem. Soc. Jap. **40**, 85 (1967).
15. L. J. Bellamy. Infrared spectra of complex molecules. John Wiley and Sons, Inc., New York. 1958.
16. R. G. Snyder and J. H. Schachtschneider. Spectrochim. Acta, **19**, 85 (1963); **19**, 117 (1963).
17. Y. Kuroda and M. Kubo. J. Polym. Sci. **36**, 453 (1959).
18. N. Chakhovsky, R. H. Martin, and R. Van Nechel. Bull. Chem. Soc. Belg. **65**, 453 (1956).
19. A. Miyake. J. Amer. Chem. Soc. **82**, 3040 (1960).
20. T. Urbanski and M. Witanowski. Trans. Faraday Soc. **59**, 1046 (1963).
21. A. Muller. Proc. Roy. Soc. London, Ser. A, **120**, 437 (1928).
22. M. Tasumi, T. Shimanouchi, A. Watanabe, and R. Goto. Spectrochim. Acta, **20**, 629 (1964).
23. A. V. Stuart and G. B. B. M. Sutherland. J. Chem. Phys. **24**, 559 (1956).
24. M. St. C. Flett. Spectrochim. Acta, **10**, 21 (1957).

Can. J. Chem. Downloaded from www.nrcresearchpress.com by 210.87.254.5 on 09/05/12
For personal use only.

The critical constants and orthobaric densities of acetone, chloroform, benzene, and carbon tetrachloride[1]

A. N. CAMPBELL AND R. M. CHATTERJEE
Department of Chemistry, University of Manitoba, Winnipeg, Manitoba

Received April 18, 1969

The specific volumes and pressures in the saturated states of the pure liquids acetone, benzene, chloroform, and carbon tetrachloride have been determined from a temperature of 100 °C and a pressure of about 2 atm up to the highest temperatures and pressures at which liquid and vapor coexist. The critical temperatures have been determined by the method of disappearance of meniscus, critical densities from the law of the rectilinear diameter, and critical pressures by extrapolation of the log P vs. $1/T$ line to the critical temperature.

Canadian Journal of Chemistry, 47, 3893 (1969)

Can. J. Chem. Downloaded from www.nrcresearchpress.com by 210.87.254.40 on 09/05/12
For personal use only.

Introduction

Acetone, chloroform, benzene, and carbon tetrachloride were chosen for study as a preliminary to an investigation of critical phenomena in binary systems containing them. The literature data, even of well known liquids such as those of this research, are surprisingly limited. A survey of critical data, measured in different ways, shows not only a wide variation in the values reported by different investigators for a single liquid, but very frequently a considerable variation in the data of the same investigator.

Campbell, Kartzmark, and Chatterjee (1) have investigated the excess volumes and total and partial pressures of the binary systems acetone–chloroform, benzene–chloroform, acetone–benzene, and of the ternary system acetone–chloroform–benzene. From these data, the excess Gibbs free energies and excess entropies were calculated. Since the publication of this work, Abbott (2) has obtained second virial coefficients from measurements on a vapor density balance. The orthobaric densities and vapor pressures of acetone, chloroform, and benzene have previously been reported by us (3).

Experimental

The methods of purification, experimental technique, and results have already been reported for acetone, chloroform, and benzene (3). It remains only to report the purification of carbon tetrachloride. This was distilled through a vacuum jacketed column with glass helix packing. The temperature of distillation was found to be constant throughout (76.6 °C at 750 mm Hg). The middle third fraction was examined for purity by gas chromatography. A column of 6 ft length, containing dimethylformamide on chromosorb P as supporting material for the liquid stationary phase, was used. The carrier gas was helium. Only one main peak was observed. All liquids were transferred to the vacuum line (for removal of non-condensible gases) in a dry-box.

Experimental Results

The orthobaric densities and vapor pressures of acetone, benzene, and chloroform have been reported previously (3). Table I gives the saturated densities of carbon tetrachloride at approximately 40 temperatures, ranging from near the standard boiling point to the critical point. Critical phenomena were observed, at a constant temperature of 283.15 °C, at the following densities: 0.4953, 0.5095, 0.5424, 0.5578, 0.5829, and 0.6047 g/cc.

The vapor pressures of carbon tetrachloride are shown in Table II. The critical temperatures of all 4 liquids were observed visually with the following results: acetone, 235.0°; benzene, 288.95°; chloroform, 262.9°; carbon tetrachloride, 283.15°.

Discussion

Because of the difficulties discussed by Campbell and Chatterjee (3), we obtained the critical pressure by an extension of the log P vs. $1/T$ line to the critical temperature; the agreement with the latest published data is good. Our results are

Acetone	P_c = 46.96 atm
Benzene	P_c = 48.22 atm
Chloroform	P_c = 52.59 atm
Carbon tetrachloride	P_c = 44.98 atm

[1]An extensive bibliography and complete details of experimental procedure are to be found in the Ph.D. thesis of Chatterjee at University of Manitoba, Winnipeg, Manitoba, 1968.

Can. J. Chem. Downloaded from www.nrcresearchpress.com by 210.87.254.40 on 09/05/12
For personal use only.

TABLE I

Orthobaric densities of carbon tetrachloride (t_c = 283.5°)

Temperature (°C)	Density of liquid (g/cc)		Density of vapor (g/cc), experimental	$(t_c - t)^{1/3}$
	Experimental	Calculated		
101.50	1.4315	1.4332	0.0118	
109.85	1.4131	1.4145	0.0141	
116.35	1.3984	1.3998	0.0162	
120.85	1.3880	1.3895	0.0179	
124.10	1.3808	1.3820	0.0190	
128.35	1.3716	1.3721	0.0202	
132.55	1.3621	1.3623	0.0220	
138.15	1.3486	1.3491	0.0239	
142.50	1.3390	1.3388	0.0259	
145.80	1.3311	1.3308	0.0276	
147.65	1.3263	1.3264	0.0284	
152.35	1.3151	1.3149	0.0316	
159.90	1.2973	1.2962	0.0362	
163.60	1.2880	1.2869	0.0389	
170.85	1.2700	1.2682	0.0447	
174.90	1.2597	1.2576	0.0481	
180.15	1.2458	1.2437	0.0529	
185.70	1.2312	1.2285	0.0579	
190.55	1.2181	1.2150	0.0626	
196.40	1.2009	1.1982	0.0694	
202.60	1.1808	1.1798	0.0778	4.316
208.75	1.1598	1.1607	0.0862	4.206
214.40	1.1412	1.1425	0.0952	4.097
219.95	1.1337	1.1238	0.1042	3.983
225.30	1.1028	1.1048	0.1143	3.867
231.05	1.0810	1.0832	0.1253	3.734
235.25	1.0640	1.0665	0.1340	3.632
240.00	1.0441	1.0464	0.1462	3.507
243.10	1.0269	1.0325	0.1566	3.422
247.55	1.0110	1.0114	0.1670	3.291
251.45	0.9910	0.9915	0.1797	3.164
256.05	0.9641	0.9659	0.1960	3.004
259.60	0.9419	0.9444	0.2122	2.866
264.15	0.9120	0.9139	0.2351	2.668
267.75	0.8838	0.8869	0.2568	2.488
271.35	0.8560	0.8567	0.2792	2.277
274.80	0.8261	0.8241	0.3076	2.029
276.95	0.8059	0.8015	0.3258	1.837
278.10	0.7910	0.7886	0.3386	1.716
280.10	0.7612	—	—	1.450
281.20	—	—	0.3788	1.249
281.55	0.7284	—	—	1.169

*Values were calculated using eq. [1] and the constants given in Table III.

The critical density can only be obtained by extrapolation of results obtained at lower temperatures and it is the most difficult of the 3 constants to measure accurately. The most commonly used method is to extrapolate the mean of the orthobaric liquid and vapor densities to the critical temperature, that is, to employ the law of Cailletet and Mathias, expressed analytically as

$$\tfrac{1}{2}(\rho_l + \rho_v) = \rho_c + b(t_c - t)$$

We restricted the application to a range of 50° below the critical temperature and obtained the following results

Acetone	ρ_c = 0.269 g/cc
Benzene	ρ_c = 0.306 g/cc
Chloroform	ρ_c = 0.491 g/cc
Carbon tetrachloride	ρ_c = 0.557 g/cc

The method of the rectilinear diameter, whatever may be its theoretical basis, or lack of it, does in fact work rather well if the true values of the orthobaric densities are known.

It has been shown repeatedly (4) that the dependence of both orthobaric densities on temperature are represented by a leading term

Can. J. Chem. Downloaded from www.nrcresearchpress.com by 210.87.254.40 on 09/05/12
For personal use only.

TABLE II

Vapor pressure of carbon tetrachloride

Temperature (°C)	Pressure (atm)	
	Experimental*	Calculated†
374.65	2.014	2.008
383.00	2.464	2.473
389.50	2.892	2.891
394.00	3.217	3.210
397.25	3.453	3.457
401.50	3.788	3.801
405.70	4.167	4.167
411.30	4.701	4.695
415.65	5.037	5.129
418.95	5.492	5.493
420.80	5.771	5.707
425.50	6.253	6.253
433.05	7.291	7.233
436.75	7.726	7.739
444.00	8.800	8.824
448.05	9.471	9.482
453.30	10.43	10.40
458.85	11.45	11.41
463.70	12.38	12.36
469.55	13.61	13.58
475.75	14.95	14.98
481.90	16.43	16.45
487.55	17.86	17.91
493.10	19.39	19.43
498.45	21.02	21.01
504.20	22.84	22.80
508.40	24.18	24.16
513.15	25.82	25.79
516.25	26.94	26.90
520.70	28.62	28.56
524.60	30.06	30.04
529.20	31.95	31.92
532.75	33.48	33.42
537.30	35.32	35.37
540.90	37.05	37.05
544.50	38.72	38.75
547.95	40.41	40.43
550.10	41.52	41.54
553.25	43.21	43.19
554.70	44.06	43.99

*Standard deviation = 0.038 atm.
†Values were calculated from eq. [4] using the constants given in Table IV.

proportional to $(T_c - T)^{1/3}$. When and if the $(T_c - T)^{1/3}$ relation is obeyed, the slope of the curve, e.g., of orthobaric density vs. T, will be very slight in the neighborhood of the critical temperature. The question then is, is the slope of the curve near T_c less than that predicted by the $(T_c - T)^{1/3}$ relation? If it is, the existence of a horizontal on the curve, with all this implies, might then be conceded. To settle the point experimentally, one requires materials of the highest purity and a temperature control of great accuracy, e.g., $\pm 0.001°$. Since our control was only good to $\pm 0.03°$, we can draw no conclusion. When our data are plotted in the form of orthobaric density vs. $(T_c - T)^{1/3}$, two straight lines are obtained for each substance, which, presumably, intersect at the critical density for $(T_c - T) = 0$. Since, however, our experimental measurements do not extend quite to the critical temperature, we are really not justified in assuming that the 1/3 power relation extends all the way and, even if it does, the possibility of a truly horizontal top still exists. There is no doubt that the top is "flat" in the ordinary sense of the word, but whether it is truly horizontal in the mathematical sense can never be decided. It is an old observation, recently reaffirmed by Lorentzen (5), that the disappearance of the meniscus in the body of the tube, and not by "moving out" (as Lorentzen calls it), is not confined to the critical volume, but this does not necessarily prove that the nose of the curve of orthobaric densities vs. temperature is horizontal.

In our previous paper (3), we obtained critical densities by extrapolation of ρ_l and ρ_v plots against $(T_c - T)^{1/3}$, with the result that our values for the critical density are much lower than those reported by other workers. The discrepancy is due, however, to the method of extrapolation, and not to experimental inaccuracy. The values for critical density which we now propose, based on the law of rectilinear diameter, agree very well with literature values[2].

Francis (6) has shown that the saturated density of the liquid phase (i.e. ρ_l under its own vapor pressure) as a function of t (temperature on the centigrade scale) can be expressed by the empirical equation

$$[1] \qquad \rho_l = A + Bt + C/(E - t)$$

In this equation, A is a constant, generally about 0.06 higher than the density at 20 °C; B is the slope coefficient, a little lower than the

[2]We are greatly indebted to Dr. D. Ambrose, of the Division of Chemical Standards, National Physical Laboratory, Teddington, England, who has processed our data for benzene. He says in a letter of July 25, 1968, "We have processed your values for benzene by our standard program to obtain the critical density from the law of rectilinear diameters, and to fit equations for the variation in $(\rho_l + \rho_v)$ and $(\rho_l - \rho_v)$ as power series in $(T_c - T)$ and $(T_c - T)^{1/3}$ respectively. From this we find your results give us a critical volume (*sic.* obviously density is intended) of 0.306 g/cc, in very close agreement with the values of Young and of Bender, Furukawa, and Hyndman. In fact, the agreement throughout the whole range of your experiments with those of Young is very good."

Can. J. Chem. Downloaded from www.nrcresearchpress.com by 210.87.254.40 on 09/05/12
For personal use only.

TABLE III

Statistical analysis of the coefficients of eq. [1]*

Compound	Coefficients and standard deviations				Multiple correlation coefficient	Standard error of estimate ($\times 10^2$)
	A	*B*	*C*	*E*		
Acetone†	0.840081 (0.0)	-0.961206×10^{-3} $(0.186739 \times 10^{-4})$	−9.04112 (0.124244)	269.0 (0.0)	0.999894	0.141144
Benzene†	0.934348 (0.0)	-0.102571×10^{-2} $(0.958163 \times 10^{-5})$	−8.52229 (0.0914741)	323.0 (0.0)	0.999920	0.132441
Chloroform†	1.87908 (0.0)	-0.324651×10^{-2} $(0.406807 \times 10^{-4})$	-0.125809×10^{2} (0.337744)	297.0 (0.0)	0.999875	0.374888
Carbon tetrachloride	1.69534 (0.0)	-0.191825×10^{-2} $(0.189715 \times 10^{-4})$	-0.145197×10^{2} (0.169265)	317.0 (0.0)	0.999907	0.267937

*Standard deviations in parentheses.
†Data from ref. 3.

TABLE IV

Statistical analysis of the coefficients of eq. [4]*

Compound	Coefficients and standard deviations				Multiple correlation coefficient	Standard error of estimate
	A	*B*	*C*	*D*		
Acetone†	0.261062×10^{2} (0.0)	-0.269100×10^{4} (0.948664×10^{2})	−7.14004 (0.497585)	1007.0 (0.0)	0.999897	0.427330×10^{-2}
Benzene†	0.131489×10^{2} (0.0)	-0.195618×10^{4} (0.494399×10^{2})	−2.96899 (0.248025)	1200.0 (0.0)	0.999933	0.416288×10^{-2}
Chloroform†	0.220199×10^{2} (0.0)	-0.24567×10^{4} (0.137857×10^{2})	−5.82143 (0.0706142)	1001.0 (0.0)	0.999997	0.756441×10^{-3}
Carbon tetrachloride	0.182145×10^{2} (0.0)	-0.226846×10^{4} (0.794815×10^{2})	−4.61431 (0.397608)	1260.0 (0.0)	0.999842	0.646184×10^{-2}

*Standard deviations in parentheses.
†Data from ref. 3.

Can. J. Chem. Downloaded from www.nrcresearchpress.com by 210.87.254.40 on 09/05/12
For personal use only.

expansion coefficient at ordinary temperature; C is an integer, generally between 6 and 10; and E is a number generally 34° above the critical temperature. We evaluated the 4 constants, for all 4 liquids, with the aid of an IBM 360/65 computer, using a multiple regression method of analysis. The values of the constants, together with the multiple correlation coefficients, and the standard error of estimate, are given in Table III. Using these constants, we calculated the liquid densities for all our experimental points. The agreement is very good; the calculated liquid densities are within 0.0010 g/cc of the experimental values.

Waring (7) has suggested a criterion, which need not be dealt with here, for the suitability of the various vapor–pressure equations. Recently, Ambrose *et al.* (8) have chosen the equations of Cox (9), Cragoe (10), and Frost–Kalkwarf (11) as possibly the best. These are

[2] Cox $\log P = A(1 - (T_b/T))$

[3] Cragoe $\log P = A + BT + CT + DT^2$

[4] Frost–Kalkwarf
$$\log P = A + B/T + C \log T + DP/T^2$$

In addition to these equations, Ambrose *et al.* (8) have used a 7-constant equation to represent their vapor–pressure data, but they find that this equation is only slightly better than the Frost–Kalkwarf equation over the whole temperature range, except for the range $T_R = 0.95$ to 1.00 (T_R = reduced temperature), where the 7-constant equation gave a markedly better fit. We therefore chose to fit our data to the Frost–Kalkwarf equation. In this semi-theoretical equation, the slight reverse curvature in the plot of $\log P$ vs. $1/T$ is explained on the basis of the non-ideal behavior of the vapor, together with the change in the heat of vaporization with temperature. If it is assumed that ΔH is linear in T and that the van der Waals a/V^2 term is a first approximation to the deviation from ideality, the Frost–Kalkwarf equation is obtained by integration of the Clapeyron–Clausius equation. The constant D is related to the van der Waals "a" as follows

$$D = a/(2.303R^2)$$

According to Thodos (12)

$$a = 27R^2T_c^2/64P_c$$

so that

$$D = 27T_c^2/(64 \times 2.303P_c)$$

The remaining constants were obtained by multiple regression analysis. The statistical analysis of the coefficients is given in Table IV, which lists the values of the constants, the standard deviation in their estimation, the values of the multiple correlation coefficient, etc. We have calculated the vapor pressures corresponding to each experimental point. The agreement with the observed values is fairly good for benzene, acetone, and carbon tetrachloride. The chloroform results scatter, especially at high temperatures. This is probably due to decomposition of this compound near the critical temperature and, therefore, we have not attempted to fit the data for chloroform to either the Cox or Cragoe equations.

The constants[3] obtained are shown in Table V. As we stated in our previous communication (3), we used the van der Waals equation to obtain the equilibrium pressure in our air manometer. Thus, at a temperature 0.45° below the critical temperature of benzene, the van der Waals equation gave a pressure of 3636.7 cm Hg. Had we used the Beattie–Bridgman equation we should have obtained a value of 3651.2 cm Hg, while the experimental value of Bender, Furukawa, and Hyndman (14) is 3641.0. The discrepancy is about 0.3% and this is about the same as the discrepancies between the observed vapor pressures and those calculated by the Cox and by the Cragoe equations.

TABLE V

Constants obtained by fitting vapor pressure data for benzene and carbon tetrachloride to the Cox and the Cragoe equations

Constant	Benzene	Carbon tetrachloride
$\log A_c$*	0.6408	0.6475
E*	−0.2445	0.1719
T_b*	346.10	349.71
T_c*	657.60	547.28
A†	+2.217305	+1.062382
B†	−7.035734	−2.033738
C†	+1.005633	−7.418258
D†	−6.508827	+5.463349

*Constant obtained for Cox equation (ref. 9).
†Constant obtained for Cragoe equation (ref. 10).

[3]We are indebted to Dr. J. F. Counsell (13) of the National Physical Laboratory, Teddington, for an analysis of our benzene and carbon tetrachloride data, using the equations of Cox and of Cragoe.

Chebyshev (15) has discussed the use of polynomials of an orthogonal system in the solution of the problem of the best approximation of continuous functions. Thus $T \log P$ can be fitted to an orthogonal series in T and the constants rearranged so that $T \log P$ is expressed as a Chebyshev series. It is then possible to write $T \log P$ as

$$T \log P = 1/2\, a_0 + a_1 c_1(x) + a_2 c_2(x) + \cdots$$

where a_0, a_1, a_2, $\cdots$ are constants and $c_1(x)$, $c_2(x), \cdots$ are Chebyshev polynomials. Truncation may occur wherever desired by the size of the residuals and smoothness of fit[4], and x is defined by

$$x = [2T - (T_{max} - T_{min})]/(T_{max} - T_{min})$$

We think, however, that these extensive tables are of no interest to the general reader; they can always be obtained directly from us. Klaus and Van Ness (16) have recently advocated the use of orthogonal polynomials for representing thermodynamic excess functions and, in view of this, we thought it worthwhile to mention their application to vapor pressure data, as suggested by Counsell, since vapor pressure is a property of pure liquids very often used to give other thermodynamic functions.

[4]Again, we are indebted to Dr. Counsell for carrying out the fits for the 4 compounds.

1. A. N. CAMPBELL, E. M. KARTZMARK, and R. M. CHATTERJEE. Can. J. Chem. **44**, 1183 (1966).
2. M. M. ABBOTT. Ph.D. Thesis, Rensselaer Polytechnic Inst., Troy, New York. 1965.
3. A. N. CAMPBELL and R. M. CHATTERJEE. Can. J. Chem. **46**, 575 (1968).
4. M. A. WEINBERGER and W. G. SCHNEIDER. Can. J. Chem. **30**, 422 (1952); A. N. CAMPBELL and E. M. KARTZMARK. Can. J. Chem. **45**, 2433 (1967); E. A. GUGGENHEIM. J. Chem. Phys. **13**, 253 (1945); D. A. GOLDHAMMER. Z. Phys. Chem. **71**, 577 (1910); H. VON JUPTNER. Z. Phys. Chem. **85**, 1 (1913); H. H. LOWRY and W. R. ERICKSON. J. Amer. Chem. Soc. **49**, 2729 (1927); D. COOK. Trans. Faraday Soc. **49**, 716 (1953).
5. H. L. LORENTZEN. Acta Chem. Scand. 7, 1335 (1953).
6. A. W. FRANCIS. Ind. Eng. Chem. **49**, 1779 (1957).
7. W. WARING. Ind. Eng. Chem. **46**, 762 (1954).
8. D. AMBROSE, B. E. BRODERICK, and R. TOWNSEND. J. Chem. Soc. A 633 (1967).
9. E. R. COX. Ind. Eng. Chem. **28**, 613 (1936).
10. C. S. CRAGOE. International critical tables. Vol. III. McGraw-Hill Book Co., Inc., New York. 1928. p. 228.
11. A. A. FROST and D. R. KALKWARF. J. Chem. Phys. **21**, 264 (1953).
12. G. THODOS. Ind. Eng. Chem. **42**, 1514 (1950).
13. J. F. COUNSELL. Private communication.
14. P. BENDER, G. T. FURUKAWA, and J. R. HYNDMAN. Ind. Eng. Chem. **44**, 387 (1952).
15. L. A. LYUSTERNIK and A. R. YANPOL'SKII. Mathematical analysis. The Pergamon Press, Ltd., New York. 1965.
16. R. L. KLAUS and H. C. VAN NESS. Chem. Eng. Progr. Symp. Ser. 81, **63**, 88 (1967).

Can. J. Chem. Downloaded from www.nrcresearchpress.com by 210.87.254.40 on 09/05/12
For personal use only.

Can. J. Chem. Downloaded from www.nrcresearchpress.com by 210.87.254.105 on 09/05/12
For personal use only.

Semiconduction in charge-transfer complexes[1]

S. N. BHAT AND C. N. R. RAO[2]
Department of Chemistry, Indian Institute of Technology Kanpur, Kanpur, India

Received April 16, 1969

Electrical conductivities, electron spin resonance spectra, electronic spectra, and Seebeck coefficients of solid charge-transfer complexes of benzidine–iodine, *p*-phenylenediamine–iodine, and phenothiazine–iodine as well as two antimony chloride complexes of phenothiazine have been studied. The phenothiazine–I_2 system shows change in sign of the majority charge carriers with the donor–acceptor ratio. The effect of ambient gases on the conductivities of a few donors, acceptors, and their complexes in the solid state have been examined. Seebeck coefficient measurements show that the conduction in TCNQ salts takes place by a hopping mechanism.

Canadian Journal of Chemistry, 47, 3899 (1969)

Solid charge-transfer (c.t.) complexes, particularly those involving appreciable contribution from the dative structures, exhibit high conductivities and interesting magnetic properties (1). We have presently investigated semiconduction in the iodine complexes of *p*-phenylenediamine (PDA), benzidine (BZ), and phenothiazine (PTZ) as well as two antimony chloride complexes of phenothiazine. There is some evidence in the literature for the relatively high conductivities of these amine–iodine complexes (1) and for the formation of ion radicals in the antimony chloride complexes of PTZ (2). We were interested in comparing the activation energies for the conduction process in these complexes with the c.t. energies ($h\nu_{ct}$) from electronic absorption spectra and the spin activation energies (E_s) from temperature-dependent electron spin resonance (e.s.r.) spectra. Further, we were interested in finding whether the sign of the majority charge carriers varied with the donor–acceptor ratio. We have also examined the anisotropic conductivity and the sign of the majority carriers in single crystals of two salts of TCNQ.

Experimental

The organic compounds employed were of high purity and were further purified by crystallization and zone-refining. The conductivities of the complexes were measured as functions of temperature by employing a cell described earlier (3). The E_a ($= E_g/2$) values obtained from the relation

$$\sigma = \sigma_0 \exp(-E_a/kT)$$

were reproducible in the pressed pellets of charge-transfer complexes as well as in the single crystals of the TCNQ salts. The Seebeck coefficients, α, were measured employing a cell fabricated locally. E_s was obtained by measuring the spin concentration (from areas of e.s.r. signals) relative to DPPH at different temperatures. A Varian V-4502 e.s.r. spectrometer with 100 k.c. modulation was used for the purpose. Electronic absorption spectra were recorded employing a Cary 14 spectrophotometer by taking the samples as mulls (in Nujol) between quartz plates. Typical absorption spectra of a solid c.t. complex obtained in this manner are shown in Fig. 1.

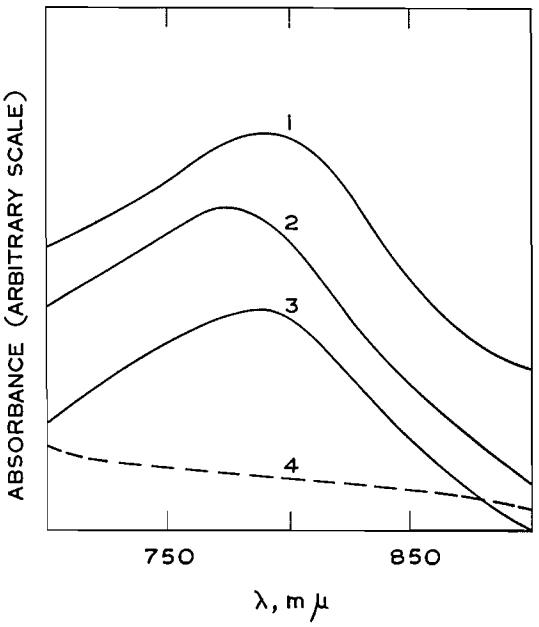

FIG. 1. Long wavelength absorption band of the PTZ–I_2 system in the solid state: curve 1, donor–acceptor ratio, 1.5:1; curve 2, 1:1; curve 3, 3:1; and curve 4, pure donor.

[1]Taken, in part, from the Ph.D. thesis of S. N. Bhat.
[2]To whom all correspondence should be addressed.

TABLE I

Electrical conductivities, spin activation energies, charge-transfer energies, and Seebeck coefficients of solid charge-transfer complexes

System	Composition	$\sigma_{30°C}$* (Ω^{-1} cm^{-1})	E_a (eV)	E_s (eV)	$h\nu_{ct}$ (eV)§	α (μV/deg, 30 °C)
PDA–I_2	0.8:1	2.5×10^{-9}	0.38	0.04	1.72(1.67)	+40
	1:1	2.6×10^{-9}	0.28	0.03	1.65(1.60)	+50
	1.6:1	1.6×10^{-9}	0.58	0.05	1.65(1.59)	+60
BZ–I_2	0.75:1	8.1×10^{-6}	0.28	0.05	0.76(0.75)	+1000
	1:1	6.3×10^{-6}	0.19	0.03	0.73(0.72)	+1200
	1.25:1	5.2×10^{-6}	0.19	0.06	0.82(0.79)	+100
PTZ–I_2	1:3	9.2×10^{-5}†	0.43†	‡	1.60(1.52)	+132
	1:1	2.6×10^{-4}†	0.17†	‡	1.56(1.53)	−150
	3:1	8.8×10^{-5}†	0.26†	‡	1.58(1.53)	+300
PTZ–$SbCl_5$	1:1	2.8×10^{-11}	0.45	‡	1.18(1.13)	—
PTZ–$SbCl_4$	1:1	3.1×10^{-9}	0.45	0.02	1.24(1.20)	—

*Conductivity (d.c.) in a nitrogen atmosphere, temperature range was −80 to +50 °C in all cases except the last two where the range was −160 to +60 °C.
†Conductivity (a.c., 1 k.c.) and E_a values are nearly the same as expected of electronic semiconductors.
‡E_s may be taken as zero.
§These values are for absorption maxima and the values in parenthesis correspond to the absorption edges.

Results and Discussion

All the solid c.t. complexes showed e.s.r. signals. The signal intensities of PDA–I_2 (g = 2.0111), BZ–I_2 (g = 2.0123), and PTZ–$SbCl_4$ (g = 2.0054) increased with increase in temperature. This may be taken to indicate the presence of ground-singlet and excited-triplet states; the E_s values for these complexes are shown in Table I. PTZ–I_2 (g_{ave} = 2.005) and PTZ–$SbCl_5$ (g_{ave} = 2.005), however, showed Curie law behavior typical of two independent doublet states (Fig. 2); the interesting doublet structure (Fig. 2) could arise from g-factor anisotropy. Both these PTZ complexes had very high spin concentrations (of about 85% at 25 °C).

The conductivity data of the complexes are summarized in Table I. The data are in general agreement with some of the literature reports (1). Among the I_2 complexes, the highest conductivity and the lowest E_a values are found in PTZ–I_2, probably because of the formation of the radical cation with large polarizability. The E_a (as well as E_s) is generally lowest when the donor–acceptor ratio is close to 1:1, even though one would expect them to be lowest in the presence of neutral molecules. E_a is higher than E_s in all the systems including PTZ–$SbCl_5$ and PTZ–I_2 where e.s.r. and magnetic measurements (1, 2) show the concentration of the radical ion to be about 85%. This is because E_s reflects only the formation of the charge carriers while E_a mainly depends upon the mode of transport of charge carriers; ($E_a - E_s$) may be taken as the energy required for the separation of the charge carriers (4).

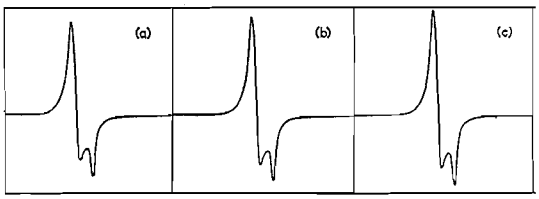

FIG. 2. Electron spin resonance spectra of a powder sample of PTZ–I_2 at different temperatures showing behavior of two independent doublet states: (*a*) 20 °C (*b*) 0 °C, and (*c*) −20 °C.

Thermoelectric power measurements indicate that the majority charge carriers in PDA–I_2 and BZ–I_2 are positive holes, independent of the donor–acceptor ratio. In PTZ–I_2, however, the sign of the majority carriers varies with the donor–acceptor ratio, a phenomenon which has been reported only in one other c.t. system (perylene–$FeCl_3$) hitherto (1). The variation of the sign of the majority carriers can be understood in terms of the proposal of Kearns (as quoted in ref. 1, pp. 470–471) according to which the positive charge moves through the crystal by electron transfer from adjacent neutral donor molecules, while the negative charges become mobile due to electron transfer from negative to neutral acceptors. The hole and electron mobilities calculated from the data on α and σ are in the range 6×10^{-5} to 7×10^{1} cm^2 V^{-1} s^{-1} and the

Can. J. Chem. Downloaded from www.nrcresearchpress.com by 210.87.254.105 on 09/05/12
For personal use only.

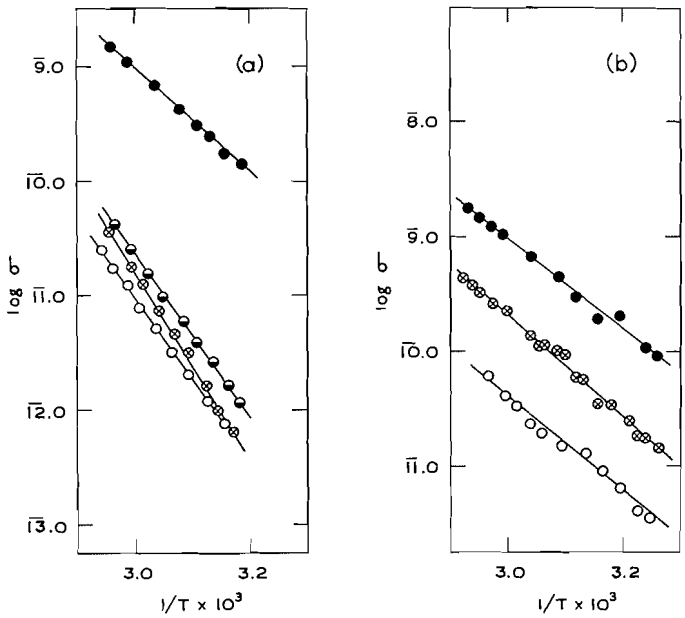

FIG. 3. Effect of ambient gases on the electrical conductivity of solid charge-transfer complexes: (*a*) anthracene–TCNE, (*b*) anthracene – tropylium bromide. Dry oxygen (open circles), moist oxygen, $p_{H_2O} \approx 18$ mm Hg (half-shaded circles), vacuum (crossed circles), ammonia (fully shaded circles).

carrier concentrations are in the range 10^{10} to 10^{18} cm^{-3}.

The energies corresponding to the absorption maxima as well as the edges of the lowest energy bands in the electronic absorption spectra (Table I) are appreciably higher than the E_a values. It appears that E_a for the conduction process is comparable to $h\nu_{ct}$ or E_s only in the case of the weak c.t. complexes (5, 6).

The conductivities of a few c.t. complexes as well as their component donors and acceptors were measured in vacuum and in ambient atmospheres of O_2 and NH_3. Compared to the data in vacuum, the conductivity of the donor, PDA, increases (from 4.0×10^{-13} to 8.7×10^{-13} Ω^{-1} cm^{-1} at 50 °C) in the presence of O_2 which is an acceptor; E_a decreases from 1.21 to 1.15 eV. Similarly, the conductivity of acceptors like tropylium bromide increases (from 4.0×10^{-9} to 9.0×10^{-8} Ω^{-1} cm^{-1} at 50 °C) and E_a decreases (from 1.19 to 1.10 eV) in the presence of NH_3 which acts as a donor. The effect of ambient gases on the conductivities of the c.t. complexes was significant only if the gas was a better donor or an acceptor than the corresponding component in the complex. Thus, the conductivity of anthracene–TCNE (3.0×10^{-12} Ω^{-1} cm^{-1} at 50 °C; E_a, 0.67 eV) or anthracene – tropylium bromide (9.0×10^{-11} Ω^{-1} cm^{-1} at 50 °C; E_a, 0.39 eV) is not affected much in the presence of oxygen, but increases in an atmosphere of NH_3 (3.6×10^{-10} Ω^{-1} cm^{-1} and 3.8×10^{-10} Ω^{-1} cm^{-1}, respectively, for the above systems) as shown in Fig. 3; the E_a values for these two systems were 0.55 and 0.36 eV, respectively, in an ammonia atmosphere.

We have measured the anisotropic conductivities and Seebeck coefficients in single crystals of two salts of TCNQ employing techniques similar to those reported earlier (7, 8). Triethylammonium $(TCNQ)_2$ showed anisotropic conduction with σ values of 3.0, 0.04, and 0.0008 Ω^{-1} cm^{-1} at 25 °C along the *a*, *b*, and *c* axes, respectively; the E_a values along the three axes were 0.15, 0.14, and 0.15 eV, respectively. The absence of anisotropy in the activation energy is indeed surprising, as noted by earlier workers (7). The quinolinium $(TCNQ)_2$ showed σ values of 10^2 and 10^{-2} Ω^{-1} cm^{-1} along two axes with E_a values of 0.02 and 0.04 eV, respectively; it is difficult to consider these observed changes in E_a as due to anisotropy since the

Can. J. Chem. Downloaded from www.nrcresearchpress.com by 210.87.254.105 on 09/05/12
For personal use only.

magnitudes are rather small. The α value of the triethylammonium salt was negative (−250 μv/deg) and remained constant with temperature (from −78 to 50 °C); this may indicate that the transport of charge carriers is by the hopping mechanism (9).

1. F. GUTMANN and L. E. LYONS. Organic semiconductors. John Wiley and Sons, Inc., New York. 1967.
2. Y. SATO, M. KINOSHITA, M. SANO, and M. AKAMATU. Bull. Chem. Soc. Jap. **40**, 2539 (1967).
3. (*a*) S. N. BHAT and C. N. R. RAO. J. Chem. Phys. **47**, 1863 (1967). (*b*) P. N. MEHROTRA, G. V. CHANDRASHEKHAR, E. C. SUBBARAO, and C. N. R. RAO. Trans. Faraday Soc. **62**, 3586 (1966).
4. A. OTTENBERG, C. J. HOFFMAN, and J. OSIECKI. J. Chem. Phys. **38**, 1898 (1963).
5. H. KURODA, K. YOSHIHARA, and H. AKAMATU. Bull. Chem. Soc. Jap. **35**, 1604 (1962).
6. L. S. SINGER and J. KOMMANDEUR. J. Chem. Phys. **34**, 133 (1961).
7. R. G. KEPLER, P. E. BIERSTEDT, and R. E. MERRIFIELD. Phys. Rev. Lett. **5**, 503 (1960).
8. C. N. R. RAO and S. N. BHAT. Inorg. Nucl. Chem. Lett. In press.
9. T. C. HARMAN and J. M. HONIG. Thermoelectric and thermomagnetic effects. McGraw-Hill Book Co., Inc., New York. 1967.

Spectral reflectance studies of some metal chelates in the adsorbed state[1]

R. W. FREI
Department of Chemistry, Dalhousie University, Halifax, Nova Scotia

AND

H. ZEITLIN
Department of Chemistry, University of Hawaii, Honolulu, Hawaii

Received February 5, 1969

Adsorption phenomena of a group of metal chelates of pyridine-2-aldehyde-2-quinolylhydrazone (PAQH) have been investigated. Formulas have been postulated for the chelates on the basis of ultraviolet and visible transmittance and reflectance spectra, ion exchange studies of charges, and chromatographic and temperature behavior. Shifts of spectra with varying adsorbents have been explained on the basis of the electronic polarization theory. Unusual behavior of the chelates has been observed on starch and cellulose and the existence of mixed ligand species due to interaction of adsorbents with the chelates has been suggested.

Canadian Journal of Chemistry, 47, 3902 (1969)

Pyridine - 2 - aldehyde - 2 - quinolylhydrazone (PAQH) has been used successfully for the colorimetric analysis of traces of various transition metals (1–4). PAQH has also shown considerable promise as a spraying reagent for cobalt, nickel, and copper following chromatographic separation of the cations (5, 6). The chromatographic properties of PAQH complexes have been investigated for use in trace metal analysis (7). In this paper, ultraviolet and visible reflectance spectroscopy is used to investigate the adsorption properties of these complexes on a group of important chromatographic adsorbents. Suggestions are made as to the possible composition of the compounds in the adsorbed state. The present study is not intended as an exhaustive structural investigation but it is hoped that it will enhance the applicability of the existing analytical methods which make use of PAQH.

[1]Presented at the 5th Caribbean Chemical Conference, Barbados, January 1969.

Experimental

The stock solutions of the cations (1 g/l) were prepared from reagent grade chemicals. PAQH was prepared as described previously (1) and dissolved in 95% ethanol (0.03% wt./vol). Doubly distilled water was used throughout. Thin layer chromatographic grades of alumina and silica gel (H. Merck) and cellulose (Macherey Nagel) were used. The starch, alkaline earth, and alkaline metal carbonates were reagent grade. Solvents used for chromatographic purification, ion exchange studies, and extraction were reagent grade. Amberlite ion exchange resins type IR–120, IRC–50, IR–45 were used for investigation of complex charges.

Transmittance and reflectance spectra were recorded with Beckman DK-2 and Spectronic 505 recording spectrophotometers equipped with standard reflectance attachments. For ultraviolet reflectance measurements

Can. J. Chem. Downloaded from www.nrcresearchpress.com by 210.87.254.105 on 09/05/12
For personal use only.

magnitudes are rather small. The α value of the triethylammonium salt was negative (−250 μv/deg) and remained constant with temperature (from −78 to 50 °C); this may indicate that the transport of charge carriers is by the hopping mechanism (9).

1. F. GUTMANN and L. E. LYONS. Organic semiconductors. John Wiley and Sons, Inc., New York. 1967.
2. Y. SATO, M. KINOSHITA, M. SANO, and M. AKAMATU. Bull. Chem. Soc. Jap. **40**, 2539 (1967).
3. (*a*) S. N. BHAT and C. N. R. RAO. J. Chem. Phys. **47**, 1863 (1967). (*b*) P. N. MEHROTRA, G. V. CHANDRASHEKHAR, E. C. SUBBARAO, and C. N. R. RAO. Trans. Faraday Soc. **62**, 3586 (1966).
4. A. OTTENBERG, C. J. HOFFMAN, and J. OSIECKI. J. Chem. Phys. **38**, 1898 (1963).
5. H. KURODA, K. YOSHIHARA, and H. AKAMATU. Bull. Chem. Soc. Jap. **35**, 1604 (1962).
6. L. S. SINGER and J. KOMMANDEUR. J. Chem. Phys. **34**, 133 (1961).
7. R. G. KEPLER, P. E. BIERSTEDT, and R. E. MERRIFIELD. Phys. Rev. Lett. **5**, 503 (1960).
8. C. N. R. RAO and S. N. BHAT. Inorg. Nucl. Chem. Lett. In press.
9. T. C. HARMAN and J. M. HONIG. Thermoelectric and thermomagnetic effects. McGraw-Hill Book Co., Inc., New York. 1967.

Spectral reflectance studies of some metal chelates in the adsorbed state[1]

R. W. FREI
Department of Chemistry, Dalhousie University, Halifax, Nova Scotia

AND

H. ZEITLIN
Department of Chemistry, University of Hawaii, Honolulu, Hawaii

Received February 5, 1969

Adsorption phenomena of a group of metal chelates of pyridine-2-aldehyde-2-quinolylhydrazone (PAQH) have been investigated. Formulas have been postulated for the chelates on the basis of ultraviolet and visible transmittance and reflectance spectra, ion exchange studies of charges, and chromatographic and temperature behavior. Shifts of spectra with varying adsorbents have been explained on the basis of the electronic polarization theory. Unusual behavior of the chelates has been observed on starch and cellulose and the existence of mixed ligand species due to interaction of adsorbents with the chelates has been suggested.

Canadian Journal of Chemistry, 47, 3902 (1969)

Pyridine - 2 - aldehyde - 2 - quinolylhydrazone (PAQH) has been used successfully for the colorimetric analysis of traces of various transition metals (1–4). PAQH has also shown considerable promise as a spraying reagent for cobalt, nickel, and copper following chromatographic separation of the cations (5, 6). The chromatographic properties of PAQH complexes have been investigated for use in trace metal analysis (7). In this paper, ultraviolet and visible reflectance spectroscopy is used to investigate the adsorption properties of these complexes on a group of important chromatographic adsorbents. Suggestions are made as to the possible composition of the compounds in the adsorbed state. The present study is not intended as an exhaustive structural investigation but it is hoped that it will enhance the applicability of the existing analytical methods which make use of PAQH.

[1]Presented at the 5th Caribbean Chemical Conference, Barbados, January 1969.

Experimental

The stock solutions of the cations (1 g/l) were prepared from reagent grade chemicals. PAQH was prepared as described previously (1) and dissolved in 95% ethanol (0.03% wt./vol). Doubly distilled water was used throughout. Thin layer chromatographic grades of alumina and silica gel (H. Merck) and cellulose (Macherey Nagel) were used. The starch, alkaline earth, and alkaline metal carbonates were reagent grade. Solvents used for chromatographic purification, ion exchange studies, and extraction were reagent grade. Amberlite ion exchange resins type IR–120, IRC–50, IR–45 were used for investigation of complex charges.

Transmittance and reflectance spectra were recorded with Beckman DK-2 and Spectronic 505 recording spectrophotometers equipped with standard reflectance attachments. For ultraviolet reflectance measurements

Can. J. Chem. Downloaded from www.nrcresearchpress.com by 210.87.254.42 on 09/05/12
For personal use only.

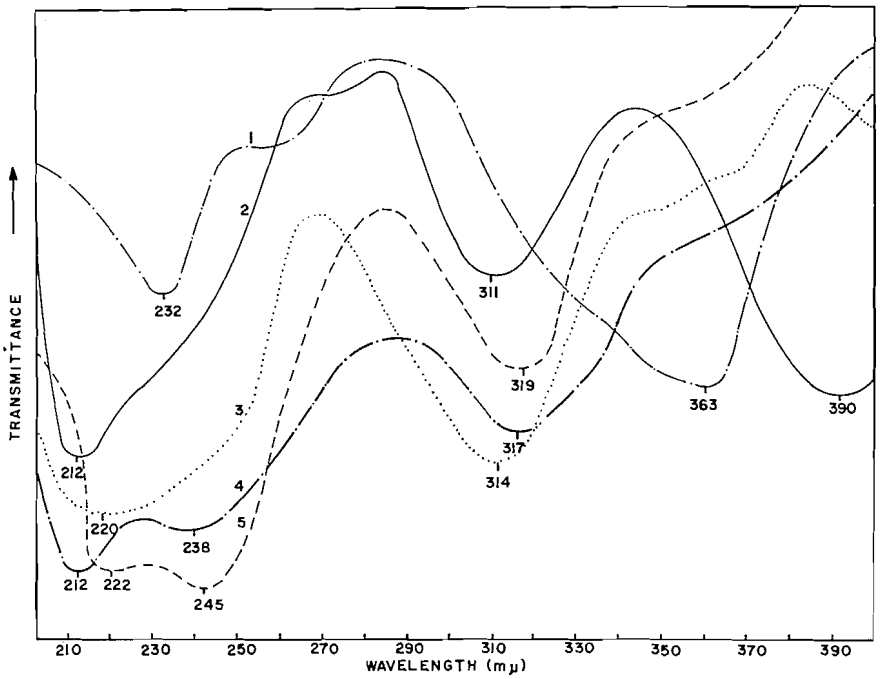

FIG. 1. Ultraviolet transmittance spectra of (1), reagent; (2), Fe chelate; (3), Ni chelate; (4), Cu chelate; (5), Co chelate.

windowless cells (8) and, in the visible region, glass covered cells (9) were employed.

The complexes were prepared and extracted according to a previous communication. Chromatographic purification was carried out on a column packed with Woelm alumina, chromatography grade (neutral), with chloroform as the eluant, or directly on alumina or silica gel thin-plates. Transmittance measurements were made from ethanolic solutions of the metal chelates. The adsorbents were sieved through 200 mesh screens. Drying procedures, after application of samples on the adsorbent with micropipettes, were carried out at 110 °C for controlled time periods (usually 5 min). The samples, ranging from 20 to 60 mg and containing between 1–5 μg of metal ion, were mixed thoroughly in a small agate mortar, equilibriated in an air-conditioned room of controlled humidity and packed in the appropriate cells. For a study of the effect of temperature, the same samples were heated at 110 °C for various periods of time ranging from 5 min to 2 h and the spectra recorded immediately.

Results and Discussion

In an earlier paper (7) it was reported that chromatographic separation of these chelates occurred in the order of R_f-values on alumina layers

$$Co^{3+},0.00 < Fe^{2+},0.05 < Cu^{2+},0.07 < Ni^{2+},0.35 < Fe^{3+},0.82$$

Decomposition of the adsorbed chelates at high temperature follows a similar pattern, with the cobalt chelate showing the highest temperature stability and the iron(III) complex decomposing irreversibly at 180 °C after 1.5 h.

Since the chelates have been separated on regenerated alumina layers with chloroform as a single phase developing system, the separation mechanism is believed to be primarily based on adsorption chromatography. Accordingly, the degree of adsorption would be greatest in the case of the cobalt complex and least for the iron(III) chelate. It is believed that the variation in degree of chelate–adsorbent interaction of the compounds studied, based on current and previous observations on the nature of metal chelates, is a function of charge and relative polarities.

From previous work (10) and the present ion exchange studies, the following structures for the analytically important complexes can be postulated with some certainty: $[(Co(III)\text{-}(PAQH)_2)]^+$ Anion, $Ni(II)(PAQH)_2$, $Cu(II)(PAQH)_2$, and $Fe(II)(PAQH)_2$.

The strong retention and interaction of the cobalt species on the adsorbent (R_f-value of zero)

Can. J. Chem. Downloaded from www.nrcresearchpress.com by 210.87.254.42 on 09/05/12
For personal use only.

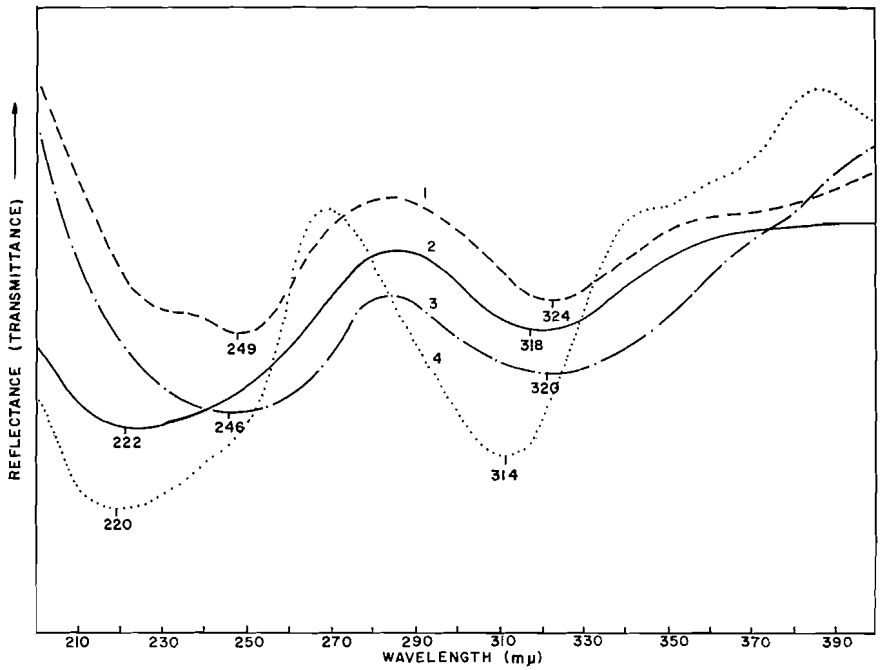

FIG. 2. Ultraviolet reflectance spectra of (1), Co chelate and (3), Ni chelate adsorbed on alumina; (2), Ni chelate adsorbed on silica gel; (4), transmittance spectrum of Ni chelate in ethanol.

in comparison to the other chelates (which were found to be neutral) can, therefore, be explained satisfactorily on the basis of its charge. It may well be possible that the anion for the above complex is provided by an active site on the adsorbent.

Both 1:1 and 2:1 (reagent-to-metal) complexes of nickel and copper were found in solution and adsorbed on silica gel, depending on ligand concentration and pH (5). Only the 2:1 species were investigated. The formation constants of these chelates as determined from Bjerrum plots were reported for copper chelate ($\log K_1 = 11.60$) and for nickel chelate ($\log K_1 = 10.46$) (1). The difference in complex stability may account for the apparent difference in polarity (as determined from chromatographic data) for the two compounds, which otherwise have similar magnetic and structural properties.

The green Fe(III) complex formed in basic solution was also investigated by ion exchange and found to be neutral. It is concluded that there is evidence for at least a 3:1 reagent-to-metal species. On the ultraviolet spectrum (Fig. 1) an absorption maximum can be seen at 390 mμ for the iron(III) chelate (Fig. 1). This is close to the maximum for the free reagent (Fig. 1) at 363 mμ and is unique to the iron complex, suggesting that at least one ligand is only loosely attached to the complex species. The additional maxima at 212 and 311 mμ occur in the vicinity of maxima of the other metal chelates and suggest some bonding between Fe(III) and PAQH to be similar to that with the other metals. The high R_f-value (higher than for the free reagent) and the low decomposition temperature (7), and hence stability, suggest an unusual complex formation.

Upon adsorption of the metal chelates on adsorbents of varying polarity or activity, regular shifts are observed (Fig. 2 and Table I).

The polarizing effects of various adsorbents was further investigated by adsorbing the chelates on several carbonates. Bathochromic shifts in the order

$$BaCO_3 > SrCO_3 > CaCO_3 > MgCO_3$$

and

$$K_2CO_3 > Na_2CO_3 > Li_2CO_3$$

were observed for all four chelates. Similar observations have been made for nitrophenols and nitroanilines adsorbed on alkaline metal carbonates (11, 12) and on alkaline earth oxides and

Can. J. Chem. Downloaded from www.nrcresearchpress.com by 210.87.254.42 on 09/05/12
For personal use only.

TABLE I

Reflectance and transmittance maxima of PAQH complexes in various media

PAQH complex	Wave length (mμ)				
	EtOH	SiO_2	Al_2O_3	Cellulose	Starch
Fe complex	470	475	490	475	475
Ni complex	475	479	494	518	520
Cu complex	478	483	498	509	508
Co complex	494	500	522	530	530

carbonates (13, 14). The shifts can be interpreted partially in terms of the electronic polarization theory. When the alkaline earths or alkaline metals are arranged in the order of increasing cationic size, i.e. Mg to Ba, or Li to K, the effective nuclear charge decreases due to increased screening by additional electron levels. The cation in the crystal lattice of the adsorbent exerts a polarizing action on the chelate, followed by a chemisorptive process similar to a Lewis acid–base type interaction. The polarization on the π-bond system of the chelate should then increase in the order

$$Ba^{2+} < Sr^{2+} < Ca^{2+} < Mg^{2+}$$

or

$$K^{+} < Na^{+} < Li^{+}.$$

Partial freezing or localization of the electron cloud of the chelate would render electronic excitation more difficult and thereby account for the shift of absorption maxima toward the more energetic shorter wavelength.

The resolution in reflectance spectroscopy is poorer, both because larger slitwidths have to be used to get sufficient radiation energy and because of the light scattering effect. As an illustration, the double peak at 224/248 mμ observed in the cobalt chelate transmission spectrum (Fig. 1) is barely noticeable in the reflectance spectrum (Fig. 2).

In accordance with previous studies (5), a reversible bathochromic shift was observed upon heating of the adsorbent–adsorbate system at 110 °C for various periods of time. Partial or complete removal of co-adsorbed water, which competes for the adsorption sites, is believed to be the reason for this phenomenon. When water covers a large portion or all of the first monomolecular layer (zone of chemisorption), the chelate–adsorbent system comes closer to an aqueous solution. The attractive forces exerted on the chelate may consist primarily of van der Waals forces or bonding between the water layer and the complex, similar to conditions in solution. This would explain the shift of maxima to lower wavelengths upon increased saturation of the adsorbent with moist air.

Surprisingly large bathochromic shifts are observed on cellulose and starch (see Table I). At the equilibrium condition with air humidity, these two chromatographic adsorbents would be classified as relatively weak (11) and one would expect maxima to appear near or below those observed on silica gel. Previous studies (5) have shown that the nickel or copper species observed on cellulose are probably identical to the 1:1 chelates. If the brownish bis-chelates are applied to a cellulose or starch layer, their change to the red 1:1 configuration can be observed visually to occur within a few seconds. According to this observation the cellulose– or starch–water complex may be blocking some of the coordination sites of the metal and hence permitting only one PAQH ligand to react. The existance of a mixed ligand complex, for example of the formula

$$[Ni(PAQH)\text{–}Cellulose:(H_2O)_x]$$

with unknown charge is, therefore, suggested as a possibility.

Acknowledgments

This study was supported by grants of the National Research Council of Canada and the Petroleum Research Fund administered by the American Chemical Society. Dr. D. E. Ryan is to be thanked for helpful discussions and suggestions regarding this research.

1. M. L. Heit and D. E. Ryan. Anal. Chim. Acta, 32, 448 (1965).
2. M. L. Heit and D. E. Ryan. Anal. Chim. Acta, 34, 407 (1966).

Can. J. Chem. Downloaded from www.nrcresearchpress.com by 210.87.254.42 on 09/05/12
For personal use only.

3. S. P. SINGHAL and D. E. RYAN. Anal. Chim. Acta, **37**, 91 (1967).
4. B. K. AFGHAN and D. E. RYAN. Anal. Chim. Acta, **41**, 167 (1968).
5. R. W. FREI, R. LIIVA, and D. E. RYAN. Can. J. Chem. **46**, 167 (1968).
6. R. W. FREI. J. Chromatogr. **34**, 563 (1968).
7. R. W. FREI, D. E. RYAN, and C. A. STOCKTON. Anal. Chim. Acta, **42**, 59 (1968).
8. M. M. FRODYMA and V. T. LIEU. Anal. Chem. **39**, 814 (1967).
9. R. W. FREI and M. M. FRODYMA. Anal. Chim. Acta, **32**, 5016 (1965).
10. M. L. HEIT. Ph.D. Thesis, Dalhousie University, Halifax, Nova Scotia. 1965.
11. H. ZEITLIN, N. KONDO, and W. JORDAN. J. Phys. Chem. Solids, **25**, 641 (1964).
12. H. ZEITLIN and V. T. LIEU. J. Catal. **4**, 546 (1965).
13. H. ZEITLIN, R. W. FREI, and M. MCCARTER. J. Catal. **4**, 77 (1965).
14. R. W. FREI, H. ZEITLIN, and G. FUJIE. Can. J. Chem. **44**, 305 (1965).

Can. J. Chem. Downloaded from www.nrcresearchpress.com by 210.87.254.42 on 09/05/12
For personal use only.

Dual interaction of anisole with surface hydroxyls

M. J. D. LOW AND J. A. CUSUMANO
Department of Chemistry, New York University, New York, N.Y. 10453

Received March 31, 1969

Infrared spectra were recorded of anisole adsorbed on porous glass which had been dehydroxylated to various extents, on highly dehydroxylated silica, and on fully fluoridated porous glass. Spectra recorded at various surface coverages showed 2 broad bands near 3600 and 3400 cm^{-1} due to perturbed surface hydroxyls, indicating that the adsorbed anisole was weakly held to the surface in 2 ways. The surface structures and mechanism are discussed.

Canadian Journal of Chemistry, **47**, 3906 (1969)

The adsorption of molecules on hydroxylated surfaces generally leads to an easily observed perturbation of the stretching fundamental of the surface hydroxyl. The effects are small with simple, nonpolar adsorbates and may involve only a small shift to lower wavenumbers and a slight diminution, broadening, and "tailing" of the hydroxyl band. Interaction of the hydroxyls with the π systems of adsorbed aromatics brings about somewhat larger changes, and can cause a broad shoulder or a distinct band approximately 100–160 cm^{-1} below the position of the bank of "free" hydroxyls. The most pronounced changes of the spectrum, including the formation of a broad and frequently intense band approximately 300–500 cm^{-1} below the hydroxyl band, are caused by molecules capable of hydrogen-bonding to the hydroxyls through the lone electron pairs of atoms such as oxygen or nitrogen. The various aspects of such adsorbate–hydroxyl interactions have been extensively reviewed by Little and in supplementary chapters by Kiselev and Lygin (1).

Complex adsorbates have also been of interest. The adsorption of benzene derivatives such as aniline or phenol, which have an atom with a lone electron pair, led to the large changes caused by hydrogen bonding via the lone electron pairs; but the effects produced by nitrobenzene, which does not have a lone electron pair on its nitrogen atom, were smaller than those of the π-OH interaction. In general, the observations made so far indicate that the "strongest" mechanism predominated, so that a substituted benzene would interact with the hydroxyls in one of two ways. Dual binding does not seem to have been considered. We have found, however, that two clearly distinguishable perturbations were produced when anisole was adsorbed on hydroxylated surfaces.

Experimental

The adsorbents used were Cab-O-Sil silica[1], porous glass[2], and fully fluoridated porous glass (2). The porous glass was used for most of the work because of the ease of preparing and handling of the samples. Porous glass specimens were subjected to the following treatment: (*a*) a specimen was alternately degassed at 700° and hydrated, 7 or 8 times, (*b*) heated in 100 Torr oxygen at 600° for 4 h, (*c*) exposed to 4 Torr water vapor at 25° for 45 min, and (*d*) degassed at 250, 500, or 750° for 12 h. Samples hydroxylated to various extents could be prepared reproducibly by means of these steps. C.P. anisole was subjected to freeze–thaw cycles and was distilled in vacuo. Some minor experimental details are given elsewhere (2). Spectra were recorded with a Perkin–Elmer model 621 spectrometer.

[1]Obtained from G. Cabot Co., Boston, Mass.
[2]Corning Code 7930, 1 mm thick sheet.

3. S. P. SINGHAL and D. E. RYAN. Anal. Chim. Acta, **37**, 91 (1967).
4. B. K. AFGHAN and D. E. RYAN. Anal. Chim. Acta, **41**, 167 (1968).
5. R. W. FREI, R. LIIVA, and D. E. RYAN. Can. J. Chem. **46**, 167 (1968).
6. R. W. FREI. J. Chromatogr. **34**, 563 (1968).
7. R. W. FREI, D. E. RYAN, and C. A. STOCKTON. Anal. Chim. Acta, **42**, 59 (1968).
8. M. M. FRODYMA and V. T. LIEU. Anal. Chem. **39**, 814 (1967).
9. R. W. FREI and M. M. FRODYMA. Anal. Chim. Acta, **32**, 5016 (1965).
10. M. L. HEIT. Ph.D. Thesis, Dalhousie University, Halifax, Nova Scotia. 1965.
11. H. ZEITLIN, N. KONDO, and W. JORDAN. J. Phys. Chem. Solids, **25**, 641 (1964).
12. H. ZEITLIN and V. T. LIEU. J. Catal. **4**, 546 (1965).
13. H. ZEITLIN, R. W. FREI, and M. MCCARTER. J. Catal. **4**, 77 (1965).
14. R. W. FREI, H. ZEITLIN, and G. FUJIE. Can. J. Chem. **44**, 305 (1965).

Can. J. Chem. Downloaded from www.nrcresearchpress.com by 210.87.254.6 on 09/05/12
For personal use only.

Dual interaction of anisole with surface hydroxyls

M. J. D. LOW AND J. A. CUSUMANO
Department of Chemistry, New York University, New York, N.Y. 10453

Received March 31, 1969

Infrared spectra were recorded of anisole adsorbed on porous glass which had been dehydroxylated to various extents, on highly dehydroxylated silica, and on fully fluoridated porous glass. Spectra recorded at various surface coverages showed 2 broad bands near 3600 and 3400 cm^{-1} due to perturbed surface hydroxyls, indicating that the adsorbed anisole was weakly held to the surface in 2 ways. The surface structures and mechanism are discussed.

Canadian Journal of Chemistry, **47**, 3906 (1969)

The adsorption of molecules on hydroxylated surfaces generally leads to an easily observed perturbation of the stretching fundamental of the surface hydroxyl. The effects are small with simple, nonpolar adsorbates and may involve only a small shift to lower wavenumbers and a slight diminution, broadening, and "tailing" of the hydroxyl band. Interaction of the hydroxyls with the π systems of adsorbed aromatics brings about somewhat larger changes, and can cause a broad shoulder or a distinct band approximately 100–160 cm^{-1} below the position of the bank of "free" hydroxyls. The most pronounced changes of the spectrum, including the formation of a broad and frequently intense band approximately 300–500 cm^{-1} below the hydroxyl band, are caused by molecules capable of hydrogen-bonding to the hydroxyls through the lone electron pairs of atoms such as oxygen or nitrogen. The various aspects of such adsorbate–hydroxyl interactions have been extensively reviewed by Little and in supplementary chapters by Kiselev and Lygin (1).

Complex adsorbates have also been of interest. The adsorption of benzene derivatives such as aniline or phenol, which have an atom with a lone electron pair, led to the large changes caused by hydrogen bonding via the lone electron pairs; but the effects produced by nitrobenzene, which does not have a lone electron pair on its nitrogen atom, were smaller than those of the π-OH interaction. In general, the observations made so far indicate that the "strongest" mechanism predominated, so that a substituted benzene would interact with the hydroxyls in one of two ways. Dual binding does not seem to have been considered. We have found, however, that two clearly distinguishable perturbations were produced when anisole was adsorbed on hydroxylated surfaces.

Experimental

The adsorbents used were Cab-O-Sil silica[1], porous glass[2], and fully fluoridated porous glass (2). The porous glass was used for most of the work because of the ease of preparing and handling of the samples. Porous glass specimens were subjected to the following treatment: (*a*) a specimen was alternately degassed at 700° and hydrated, 7 or 8 times, (*b*) heated in 100 Torr oxygen at 600° for 4 h, (*c*) exposed to 4 Torr water vapor at 25° for 45 min, and (*d*) degassed at 250, 500, or 750° for 12 h. Samples hydroxylated to various extents could be prepared reproducibly by means of these steps. C.P. anisole was subjected to freeze–thaw cycles and was distilled in vacuo. Some minor experimental details are given elsewhere (2). Spectra were recorded with a Perkin–Elmer model 621 spectrometer.

[1]Obtained from G. Cabot Co., Boston, Mass.
[2]Corning Code 7930, 1 mm thick sheet.

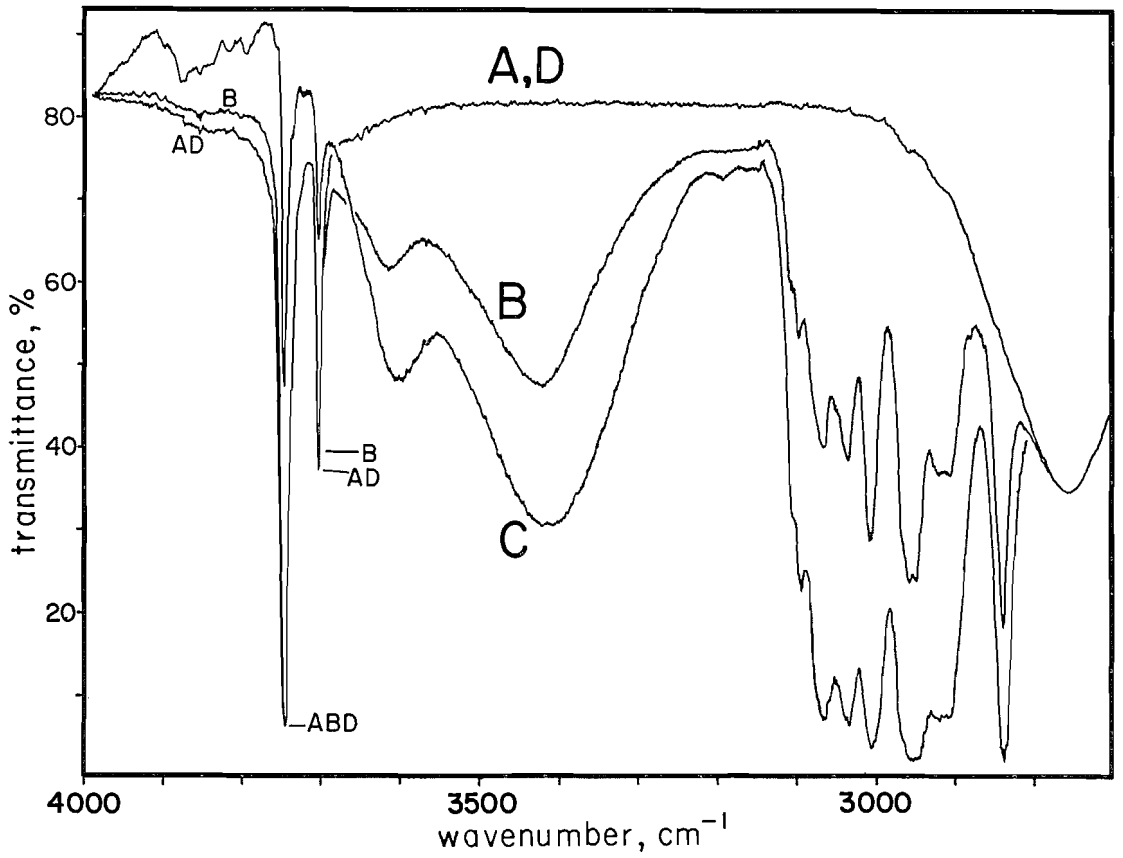

FIG. 1. Infrared spectra of anisole on porous glass. A, clean surface, after 750° degassing; B, 0.5 Torr anisole; C, 2 Torr anisole; D, after 25° degassing.

Results

Porous glass specimens prepared and finally degassed at 250, 500, or 750° were exposed to anisole vapor at 25° at relative pressures, p/p_0, ranging from 0.01 to 0.44. The various results, in part illustrated by Fig. 1, can be summarized as follows.

(*a*) When anisole became adsorbed, a group of 10 absorptions was observed in the C—H region, initially at positions $\sim$ 3 to 5 cm^{-1} higher than the corresponding absorptions of liquid anisole. The absorptions increased in concert with increasing anisole pressure and shifted by 2 to 3 cm^{-1} toward the positions of the bands of the liquid at 3102, 3094, 3063, 3033, 3004, 2957, 2947, 2925, 2907, and 2838 cm^{-1}. Some additional bands were observed near 2912, 2550, 2495, and 2283 cm^{-1} at the highest pressures.

(*b*) The 3747 cm^{-1} Si—OH and 3703 cm^{-1} B—OH bands (3) declined in intensity, retaining their intensity ratio, and shifted to 3746 and 3702 cm^{-1} with increasing anisole coverage.

(*c*) Two broad bands initially observed near 3625 and 3440 cm^{-1} at $p/p_0 \sim 0.01$ shifted to 3612 and 3422 cm^{-1} at $p/p_0 = 0.11$, and then shifted to near 3602 and 3407 cm^{-1} when p/p_0 was increased from 0.32 to 0.44. These will be termed the 3600 and 3400 cm^{-1} bands.

(*d*) Changes in the background transmittance in the O—H region make it difficult to assess precisely the changes in the intensities of all bands. However, measurements of the optical densities and integrated band intensities, I, made it clear that the ratio I_{3600}/I_{3400} of the two broad bands increased with increasing coverage. (I values were estimated using the base-line method, by drawing a tangent to the transmission curve for each band. The area of each segment was then measured with a planimeter.)

(*e*) Increasing the degassing temperature (and

Can. J. Chem. Downloaded from www.nrcresearchpress.com by 210.87.254.6 on 09/05/12
For personal use only.

Can. J. Chem. Downloaded from www.nrcresearchpress.com by 210.87.254.6 on 09/05/12
For personal use only.

consequently increasing the degree of dehydroxylation) caused a decrease in the amount of anisole adsorbed at a particular p/p_0 value, a decline in I_{3600} and I_{3400}, but I_{3600}/I_{3400} was not changed. Conversely, the Si—OH and B—OH band intensities decreased to a greater extent with increasing p/p_0 with highly degassed than with poorly degassed samples. Prior to adsorption, the OH bands of the highly degassed 750° specimens were sharp, e.g., spectrum A of Fig. 1, but those of specimens degassed at lower temperatures exhibited the "tailing" on the low wave number side of the OH bands, which is characteristic of the presence of hydrogen-bonded hydroxyls.

(*f*) The adsorption and the effects produced by it were completely reversible.

A small number of experiments were carried out with Cab-O-Sil, anisole adsorption also causing the 3600 and 3400 cm^{-1} bands to appear. In general, the effects observed with the pure silica were like those found with porous glass except, of course, that the B—OH band was not present. The interaction of anisole with fluoridated glass was only briefly studied because the amounts adsorbed were quite small. In distinct contrast to porous glass, e.g., spectrum B of Fig. 1, exposing a fluoridated porous glass specimen to anisole at 25° at $p/p_0 = 0.11$ caused the transmittance in the C—H region to decrease by only 3–4%.

Discussion

The observations on the small shift of the C—H bands, reversibility, perturbation of free OH bands, and the greatly decreased adsorption in the absence of hydroxyls plainly indicate that anisole was adsorbed in a molecular form and was weakly held to the surfaces by interactions with OH groups. The formation of two "perturbed hydroxyl bands" is of greater interest.

The 3600 and 3400 cm^{-1} bands, respectively shifted by approximately 150 and 350 cm^{-1} from the position of the band of free silanols, were observed with pure silica as well as with porous glass. Possible effects of B—OH groups can therefore be discounted. The behavior of the hydroxyl bands and of each of the broad bands (which are not found in the spectrum of liquid anisole) is like that found in many instances involving adsorbate–OH interactions. Also, the 150 cm^{-1} shift of the 3600 cm^{-1} band falls well within the range of shifts found with benzene and substituted benzenes not having an atom with a lone electron pair. The 350 cm^{-1} shift of the 3400 cm^{-1} band, while differing somewhat from the 450 cm^{-1} shift produced by diethyl ether, falls in the range found for substituted benzenes and other molecules having an atom with a free lone electron pair. In view of such similarities (1, and supplementary chapters), it is reasonable to assign the 3600 cm^{-1} band to hydroxyls perturbed by a π–OH interaction such as the one shown in structure **1**, and the 3400 cm^{-1} band to hydroxyls perturbed by hydrogen bonding as shown in structure **2**.

The larger increase of the 3600 cm^{-1} than the 3400 cm^{-1} band with increasing adsorption then implies the occurrence of a change in the structure of the adsorbed layer, the π–OH interaction becoming less important at higher coverages. Also, as the intensities of the sharp OH bands were diminished to a greater extent at higher degrees of dehydroxylation, it appears that both bonding modes occurred preferentially with OH groups which had already been perturbed by hydrogen bonding.

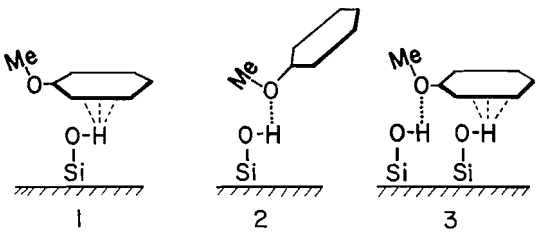

1 2 3

Although both broad bands were always observed even at the lowest coverages, it is not possible to use individual spectra to establish if both types of bonding occurred simultaneously as in structure **3**. However, the observed relations of increasing band shift with increasing differential heat of adsorption (1) indicate that the bonding of **1** would be weaker than that of **2**. The observed change in I_{3600}/I_{3400} indicates an increase in the relative number of structures **2** at higher pressures. If only structures **1** and **2** existed, this would imply an increase in the heat of adsorption with increasing coverage, in contrast to the *decrease* in the heat of adsorption reported for the adsorption of several substituted benzenes on hydroxylated surfaces (supplementary chapter in ref. 1). This apparent discrepancy, which rests on the reasonable assumption that the physical adsorption of anisole and

other similar molecules would show similar energetic trends, is removed by postulating that the doubly bound structure **3** would form preferentially to **1**.

These considerations suggest that the adsorbed layer consisted of a mixture of structures. At the lowest coverages a large fraction of the molecules would be "flat" on the surface; e.g., structure **3**. As the coverage was increased, additional adsorbed molecules would stand "on end", e.g., structure **2**, and some **3** would be converted to **2**.

The mechanism is of interest per se, but the steric and energetic changes implied by it would also be important to theoretical studies attempting to relate various adsorption parameters. Although two distinct bands were observed and the existence of two surface species is reasonably clear in the present case, severe overlapping of bands may not make it possible to recognize such effects with other adsorbates, so that changes in adsorption heats and shifts with increasing coverage should be approached with caution.

Acknowledgment

Support from the National Center for Air Pollution Control is gratefully acknowledged.

1. L. H. LITTLE. Infrared spectra of adsorbed species. Academic Press, Inc., New York. 1966.
2. M. J. D. LOW and N. RAMASUBRAMANIAN. J. Phys. Chem. **70**, 2740 (1966).

Can. J. Chem. Downloaded from www.nrcresearchpress.com by 210.87.254.6 on 09/05/12
For personal use only.

Investigations of copper(II) complexes of bispyridylglycol and 6,6′-dimethyl bispyridylglycol

G. S. MANKU, R. D. GUPTA, A. N. BHAT, AND B. D. JAIN
Department of Chemistry, University of Delhi, Delhi-7, India

Received January 21, 1969

The formation of a greenish blue 1:1 metal:ligand chelate at pH 5–7 and a faint violet 1:1:1 metal:ligand:hydroxyl chelate at pH > 10 has been observed in Cu(II) complexes with bis-2-pyridylglycol and its 6,6′-dimethyl derivative using spectrophotometric, conductometric, and pH-metric methods.

Canadian Journal of Chemistry, **47**, 3909 (1969)

Bis-2-pyridylglycol (**1**) (BPG) has already been used as a gravimetric reagent (1) for aluminum(III), beryllium(II), and uranium(VI) and as a spectrophotometric reagent for iron(III) (2) and cobalt(II) (3). The present note deals with the studies of copper(II) complexes of BPG and its 6,6′-dimethyl derivative (**2**) (DMBPG) using spectrophotometric, conductometric, and pH-metric methods. With both these ligands, the formation of a greenish blue 1:1 metal:ligand complex at pH 5–7 and a faint violet 1:1:1 metal:ligand:hydroxyl complex at pH > 10 is indicated.

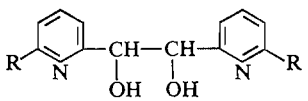

1 R = H
2 R = CH_3

Experimental

Chemicals and Instruments

BPG and DMBPG, obtained from F. Raschig, GmbH, Ludwigschafen, were used in aqueous solutions without further purification. Copper(II) solution, prepared from $CuSO_4 \cdot 5H_2O$ (Analar BDH), was standardized as sulfocyanide. Other chemicals used were of Analyzed Reagent grade. pH of the solutions was adjusted with sulfuric acid and sodium hydroxide. Carbonate-free sodium hydroxide used for pH-metric titrations was standardized with potassium hydrogen phthalate.

A Beckman pH meter Model H-2 with glass electrode, Unicam Spectrophotometer Model SP600 with 1 cm cells, and Leeds and Northrup drum-type conductometer were used for all the pH, absorbance, and conductance measurements, respectively.

Results and Discussion

Absorption Spectra

The absorption spectra of copper(II)–BPG and copper(II)–DMBPG complexes show a single

other similar molecules would show similar energetic trends, is removed by postulating that the doubly bound structure **3** would form preferentially to **1**.

These considerations suggest that the adsorbed layer consisted of a mixture of structures. At the lowest coverages a large fraction of the molecules would be "flat" on the surface; e.g., structure **3**. As the coverage was increased, additional adsorbed molecules would stand "on end", e.g., structure **2**, and some **3** would be converted to **2**.

The mechanism is of interest per se, but the steric and energetic changes implied by it would also be important to theoretical studies attempting to relate various adsorption parameters. Although two distinct bands were observed and the existence of two surface species is reasonably clear in the present case, severe overlapping of bands may not make it possible to recognize such effects with other adsorbates, so that changes in adsorption heats and shifts with increasing coverage should be approached with caution.

Acknowledgment

Support from the National Center for Air Pollution Control is gratefully acknowledged.

1. L. H. LITTLE. Infrared spectra of adsorbed species. Academic Press, Inc., New York. 1966.
2. M. J. D. LOW and N. RAMASUBRAMANIAN. J. Phys. Chem. **70**, 2740 (1966).

Investigations of copper(II) complexes of bispyridylglycol and 6,6′-dimethyl bispyridylglycol

G. S. MANKU, R. D. GUPTA, A. N. BHAT, AND B. D. JAIN
Department of Chemistry, University of Delhi, Delhi-7, India

Received January 21, 1969

The formation of a greenish blue 1:1 metal:ligand chelate at pH 5–7 and a faint violet 1:1:1 metal:ligand:hydroxyl chelate at pH > 10 has been observed in Cu(II) complexes with bis-2-pyridylglycol and its 6,6′-dimethyl derivative using spectrophotometric, conductometric, and pH-metric methods.

Canadian Journal of Chemistry, **47**, 3909 (1969)

Bis-2-pyridylglycol (**1**) (BPG) has already been used as a gravimetric reagent (1) for aluminum(III), beryllium(II), and uranium(VI) and as a spectrophotometric reagent for iron(III) (2) and cobalt(II) (3). The present note deals with the studies of copper(II) complexes of BPG and its 6,6′-dimethyl derivative (**2**) (DMBPG) using spectrophotometric, conductometric, and pH-metric methods. With both these ligands, the formation of a greenish blue 1:1 metal:ligand complex at pH 5–7 and a faint violet 1:1:1 metal:ligand:hydroxyl complex at pH > 10 is indicated.

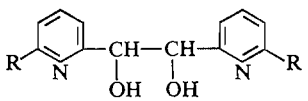

1 R = H
2 R = CH_3

Experimental

Chemicals and Instruments

BPG and DMBPG, obtained from F. Raschig, GmbH, Ludwigschafen, were used in aqueous solutions without further purification. Copper(II) solution, prepared from $CuSO_4 \cdot 5H_2O$ (Analar BDH), was standardized as sulfocyanide. Other chemicals used were of Analyzed Reagent grade. pH of the solutions was adjusted with sulfuric acid and sodium hydroxide. Carbonate-free sodium hydroxide used for pH-metric titrations was standardized with potassium hydrogen phthalate.

A Beckman pH meter Model H-2 with glass electrode, Unicam Spectrophotometer Model SP600 with 1 cm cells, and Leeds and Northrup drum-type conductometer were used for all the pH, absorbance, and conductance measurements, respectively.

Results and Discussion

Absorption Spectra

The absorption spectra of copper(II)–BPG and copper(II)–DMBPG complexes show a single

Can. J. Chem. Downloaded from www.nrcresearchpress.com by 210.87.254.105 on 09/05/12
For personal use only.

TABLE I

The dissociation constants of BPG and DMBPG in aqueous medium at 30 °C in the presence of 0.3 *M* sodium perchlorate as the ionic medium.

Ionization reaction	Ionization constant	p*K* BPG	p*K* DMBPG
$(RH_2(OH)_2)^{2+} \rightleftharpoons RH(OH)_2^+ + H^+$	K_{NH}'	2.6	2.9
$(RH(OH)_2)^+ \rightleftharpoons R(OH)_2 + H^+$	K_{NH}''	4.6	5.4
$R(OH)_2 \rightleftharpoons R(OH)O^- + H^+$	K_{OH}'	10.2*	10.3*
$(R(OH)O)^- \rightleftharpoons RO_2^{2-} + H^+$	K_{OH}''	11.1*	11.1*

*Determined by a method similar to that used for the determination of stability constants of 1:2 metal:ligand complexes.

absorption maximum at 600–620 and at 660–680 mμ, respectively, within the pH range 3.7–12.7. From Fig. 1, it is observed that the absorbance of the solutions containing a copper(II):ligand ratio of 1:5 remains constant in the pH ranges 4.0–6.3 and >9.3 for BPG and in the pH ranges 7.0–7.5 and >10.6 for DMBPG complexes. Furthermore, the color of the solution is greenish blue at lower pH and faint violet at higher pH for both ligands, thus indicating the formation of different complexes at different pH values.

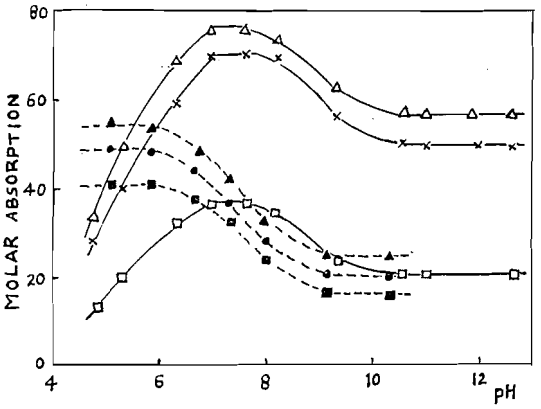

FIG. 1. Effect of pH on the absorbance of copper(II)–BPG (---) and copper(II)–DMBPG (—) complexes containing 2.5 m*M* copper(II) and 12.5 m*M* BPG/DMBPG. Wavelength (in mμ) for △, ▲, 620; ●, 700; ■, 725; ×, 750; and □, 900.

Molar Composition

The metal:ligand ratio in these complexes was determined spectrophotometrically by the modified method of continuous variations (4) as well as by the slope ratio method (5). Between 600–800 mμ, the formation of the 1:1 complex only was observed at pH 7.0 and 11.0 for BPG and 7.2 and 11.2 for DMBPG complexes. The precipitation of copper(II) during these studies was prevented by the addition of tartrate ions, as no mixed-ligand complexes could be detected spectrophotometrically in the ternary system copper(II)–tartrate–BPG or –DMBPG.

The metal:ligand ratio in the greenish blue complex, determined by the conductometric titrations of 20 ml of 2.5 m*M* copper(II) and 2 m*M* ligand solutions against ligand and copper(II), respectively, was also found to be 1:1, thus confirming the above results.

Determination of the Stability Constants

Table I shows the acid and base dissociation constants of these ligands ($R(OH)_2$ being the unionized and unprotonated reagent) which were determined pH-metrically (ref. 6. p. 158); both BPG and DMBPG contain two basic nitrogen atoms and two ionizable hydroxyl groups.

The pH-titration of the reagents against sodium hydroxide, in the absence as well as in the presence of copper(II) ions, showed that when copper (II) ions are present, the pH of the solution is lowered as a result of liberation of two protons per copper(II) ion. Thus chelation with both of the ionized hydroxyl groups of the ligands is indicated, since the metal:ligand ratio in these complexes is 1:1.

The stability constant of the greenish blue chelate (K_{11}) was determined spectrophotometrically using (*i*) Harvey and Manning's method of calculation of degree of complex formation (5), (*ii*) Foley and Anderson's method of preparing solutions having equal absorbance (7) and (*iii*) from Bjerrum's formation curves (8) (Fig. 2) from the intercepts of linear plots of log $[\bar{n}/(1-\bar{n})]$ against log [L] (ref. 6. p. 86) ($\bar{n}$ = average ligand number, [L] = equilibrium concentration of

Can. J. Chem. Downloaded from www.nrcresearchpress.com by 210.87.254.105 on 09/05/12
For personal use only.

TABLE II

The stability constants (K_{11}) of the copper(II) complexes with BPG and DMBPG in aqueous medium at 30 °C.

Method used	log K_{11} Cu–BPG	log K_{11} Cu–DMBPG
Degree of complex formation (5)	12.1±0.1	11.6±0.1
Solutions having equal absorbance (7)	12.0±0.1	11.6±0.1
Formation curves obtained spectrophotometrically (8)	12.0±0.1	11.5±0.1
Formation curves obtained by pH-metric titrations (6)	12.1±0.1	11.5±0.1

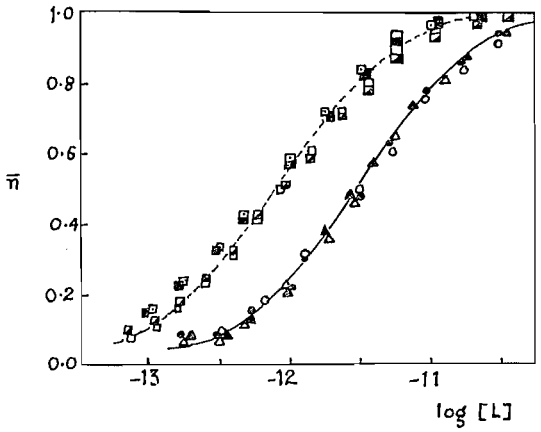

FIG. 2. Bjerrum's formation curves for copper(II)–BPG (---) and copper(II)–DMBPG (—) complexes. Points from spectrophotometric measurements are ⊡ and △ at 640 mμ, and □ and ▲ at 720 mμ (concentration: copper(II), 1.0 mM; reagent, 2 mM). For pH-metric titrations, concentration of reagents = 3 mM; copper, for ◪ and ○, 0.75 mM; for ◙ and ●, 1.5 mM.

ligand present as RO_2^{2-} anion) as well as from the formation curves obtained pH-metrically (9) using Calvin–Wilson's technique (10). The results obtained are given in Table II. The log K_{11} values as determined above were found to be constant (within ± 0.1 units) when copper(II) and the ligand concentrations were varied within 2–20 mM, indicating the absence of polynuclear complexes within the concentration ranges employed.

Since the metal:ligand ratio in the faint violet complex formed at high pH was 1:1, we only considered the formation of polynuclear as well as hydroxy complexes. The degree of formation of the faint violet complex, determined spectrophotometrically at different pH values using copper(II) and reagent of 2–20 mM concentration, was found to be independent of the concentration of ligand or metal at constant pH value, thus indicating the absence of a higher or polynuclear complex, but not excluding possible formation of hydroxy complexes (Fig. 3). Since both BPG as well as DMBPG are tetradentates, formation of only the mono- and the di-hydroxy species was considered. The following methods were used to study their formation.

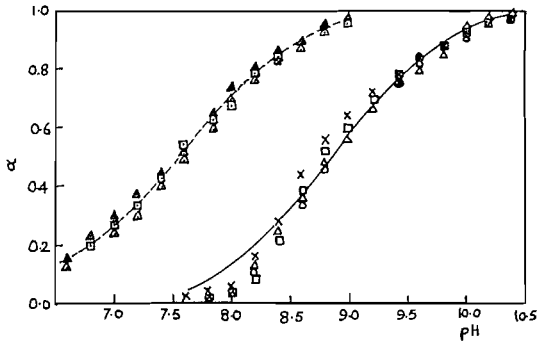

FIG. 3. Plots of degree of formation of the faint violet complexes (α) of BPG (---) and DMBPG (—), with copper(II). Wavelength (in mμ) for □, 640; △, 660; ▲, 680; ×, ⊡, 700; △, 725; and ○, 750.

Method 1

In the absence of any lower complexes, the formation of $CuL(OH)_n^{n-}$ from CuL can be written as

[1] $$CuL + nOH^- \rightarrow CuL(OH)_n^{n-}$$

with the corresponding equilibrium constant

[2] $$K_{11} = [CuL(OH)_n^{-n}]/[CuL][OH^-]^n$$

If, at equilibrium

$$a_0 = [CuL]/\{[CuL] + [CuL(OH)_n^{-n}]\}$$

$$K_w = [H^+][OH^-]$$

Can. J. Chem. Downloaded from www.nrcresearchpress.com by 210.87.254.105 on 09/05/12
For personal use only.

and

$$pH = -\log[H^+]$$

eq. [2] transforms into

$$[3] \quad \log \frac{1 - a_0}{a_0} = (\log K_{11n} + n \log K_w) + npH$$

From spectrophotometric measurements the plot of $\log (1 - a_0)/a_0$ against pH was found to be linear with unit slope, indicating $n = 1$ (Fig. 4); from the intercept of the above plots, K_{111} was found to be $(2.6 \pm 0.2) \times 10^6$ and $(1.0 \pm 0.1) \times 10^5$ for BPG and DMBPG complexes, respectively (at 30 °C).

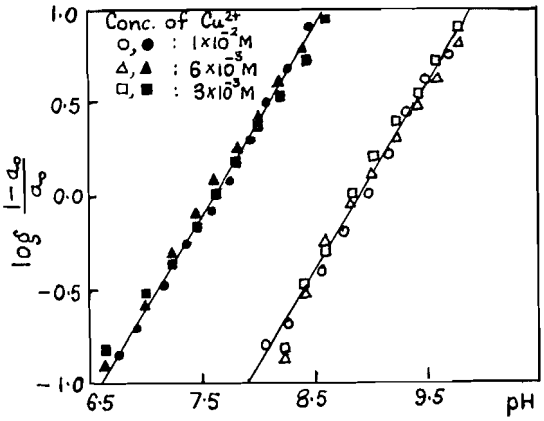

FIG. 4. Plots of $\log (1 - a_0)/a_0$ against pH for the faint violet copper(II) complexes with BPG (●, ▲, ■) and DMBPG (○, △, □).

Method 2

The formation of $CuL(OH)_2^{-2}$ from CuL is similar to the formation of 1:2 metal:ligand complex. The following relation must, therefore, hold between a_0 and $[OH^-]$ (ref. 6. p. 89)

$$[4] \quad \frac{1 - a_0}{a_0}[OH^-]^{-1} = K_{111} + K_{111} \cdot K_{112}[OH^-]$$

where K_{111} and K_{112} are the corresponding step stability constants for these complexes. From the plots of $(1 - a_0)/(a_0[OH^-])$ against $[OH^-]$, which were straight lines parallel to the $[OH^-]$ axis, the value of K_{111} was found to be $(2.65 \pm 0.2) \times 10^6$ and $(1.02 \pm 0.10) \times 10^5$ for BPG and DMBPG complexes, respectively, whereas K_{112} was zero for both these ligands, showing that under the experimental conditions, $CuL(OH)_2^{2-}$ is not formed.

Furthermore, during the pH-titrations, the conversion of the greenish blue chelate into faint violet chelate proceeds with the consumption of one mole of OH^- ions per mole of copper(II), thus confirming the above conclusions.

The anionic nature of the faint violet complexes was confirmed by their complete exchange by Amberlite ion exchanger IRA 400 (OH) as well as by IRA 410 (OH).

1. A. N. BHAT, R. D. GUPTA, and B. D. JAIN. Proc. Indian Acad. Sci. Sect. A, **63**, 356 (1966).
2. A. N. BHAT, R. D. GUPTA, and B. D. JAIN. Indian J. Appl. Chem. **29**, 64 (1966).
3. A. N. BHAT, R. D. GUPTA, and B. D. JAIN. Proc. Indian Acad. Sci. Sect. A. In press.
4. W. C. VOSBURGH and G. R. COOPER. J. Amer. Chem. Soc. **63**, 437 (1941).
5. A. E. HARVEY and D. L. MANNING. J. Amer. Chem. Soc. **72**, 4488 (1950).
6. F. J. C. ROSSOTTI and H. ROSSOTTI. Determination of stability constants. McGraw-Hill Book Co., Inc., New York. 1961.
7. R. T. FOLEY and R. C. ANDERSON. J. Amer. Chem. Soc. **70**, 1195 (1948); **71**, 909 (1949).
8. R. G. ANDERSON and G. NICKLESS. Anal. Chim. Acta, **39**, 469 (1967).
9. H. IRVING and H. S. ROSSOTTI. J. Chem. Soc. 2901 (1954).
10. M. CALVIN and K. W. WILSON. J. Amer. Chem. Soc. **67**, 2003 (1945).

Can. J. Chem. Downloaded from www.nrcresearchpress.com by 210.87.254.105 on 09/05/12
For personal use only.

Absorption of β particles from tritium and rhenium 187 in helium and aluminum

S. N. NALDRETT
The Royal Military College of Canada, Kingston, Ontario
Received June 21, 1968

The absorption of the β particles from tritium and from ^{187}Re was found to obey an exponential law for a range of about 6 or 7 times the half-thicknesses. In helium the half-thicknesses of tritium and of ^{187}Re are found to be $0.046_0 \pm 0.000_7$ and $0.039_3 \pm 0.001_2$ mg/cm^2; in aluminum they are $0.036_7 \pm 0.000_9$ and $0.033_6 \pm 0.001_3$ mg/cm^2, respectively.

Canadian Journal of Chemistry, 47, 3913 (1969)

Can. J. Chem. Downloaded from www.nrcresearchpress.com by 210.87.254.40 on 09/05/12
For personal use only.

Introduction

Naturally occurring ^{187}Re decays by β emission to ^{187}Os. The ratio of rhenium to osmium offers promise as a means of determining ages in geochemistry and cosmology, provided that the rate of decay of rhenium to osmium can be determined with sufficient accuracy. Gas counting is generally the most accurate technique, but unfortunately all of the compounds of rhenium which are sufficiently volatile behave as "counter poisons" and attempts to measure the half-life of ^{187}Re in gas counters have not been very successful (1, 2). An accurate determination of the range of the β particles emitted in the decay is required in order to permit a calculation of the half-life of this isotope from the activity of solid samples. The particles are very feeble, apparently of about the same energy as those from tritium. Moreover, the activity is low, considerably less than 1 d/m per cm^2 of surface, so that measurement of absorption is difficult. It was thought that comparison with absorption of tritium which is available in high specific activity, through the same absorbers would provide the best data since the tritium would in effect be used to calibrate the very thin absorbers involved. Unfortunately it was found that there do not seem to be any data for tritium which are generally accepted or of sufficient precision. For example, Dorfman (3) estimated the half-thicknesses as 31, 61, and 80 μg/cm^2 in hydrogen, helium, and oxygen, respectively. Suttle and Libby (4) and Libby (5) gave an estimate of 50 μg/cm^2 in helium and argon. Rydberg (6) gave the half-thickness in *p*-aminosalicylic acid as 80 μg/cm^2. The data of Beltz (7) give a calculation of half-thickness of 12 μg/cm^2 in very thin samples of thymidine and 116 μg/cm^2 in thick samples. Determinations of the absorption of the β particles from tritium as well as from ^{187}Re in several materials were therefore made.

Experimental

Measurements were made using a screen-wall type counter (cylindrical geometry) with a solid sample area of about 400 cm^2. Details of this instrument and of the preparation of the rhenium samples have already been reported (1). Tritium was counted as tritiated succinic acid or lucite. With the screen-wall counter the distance between the sample and the active counter space was not variable, but the thickness of the gas absorber, helium, argon, etc., could be varied by using different pressures, and in addition, one or more thicknesses of aluminum film could be placed over the screen as additional absorbers.

Another series of measurements was made using a Beckman–Sharp Low Beta Counter with a solid sample area of about 20 cm^2 (sandwich geometry). This is a flow-type counter in which the pressure of the gas (helium 98.5, propane 1.5) is constant. The thickness of the gas absorber could be changed by raising or lowering the surface of the sample a few millimeters by means of spacing discs. It was determined that the count rate was affected by absorber thickness and not by geometry within the limits studied. One or more thicknesses of aluminum foil or other material could be placed directly over the top of the sample to observe the absorbing effects of solid materials.

Background count rates were minimized by mass shielding and by anticoincidence circuitry. Data were collected by automatic print-out of counts collected over intervals of 20 or 50 min so that periods in which irregular behavior occurred could be recognized. Evaluation was made by means of a computer which had been programmed to reject by Chauvenet's criterion, and to make a Pearson's χ^2 assessment. This was advantageous since a large amount of data was needed to reduce the statistical error, and moreover, on several occasions the rejection of data by the computer for non-randomness was the first evidence that an electronic fault was developing. The error estimates in what follows are the statistical standard deviations.

TABLE I

Absorption of β particles

β particle from	In helium		In aluminum	
	$t_{\frac{1}{2}}$, mg/cm^2	μ	$t_{\frac{1}{2}}$, mg/cm	μ
T	$0.046_0 \pm 0.000_7$	15.07 ± 0.22	$0.036_7 \pm 0.000_9$	18.90 ± 0.46
^{187}Re	$0.039_3 \pm 0.001_2$	17.65 ± 0.53	$0.033_6 \pm 0.001_3$	20.66 ± 0.80

Observations

Absorption of β Particles in Helium or Aluminum

No significant differences were observed between cylindrical and sandwich geometry and all data were therefore combined, weighted according to statistical error. The absorption of the β particles from T and from ^{187}Re in helium and in aluminum are shown in Fig. 1. Except towards the end of the range, the absorption of β particles from simple decay processes can be expressed by an equation of the form

$$[1] \qquad \ln \frac{I_0}{I} = \mu t$$

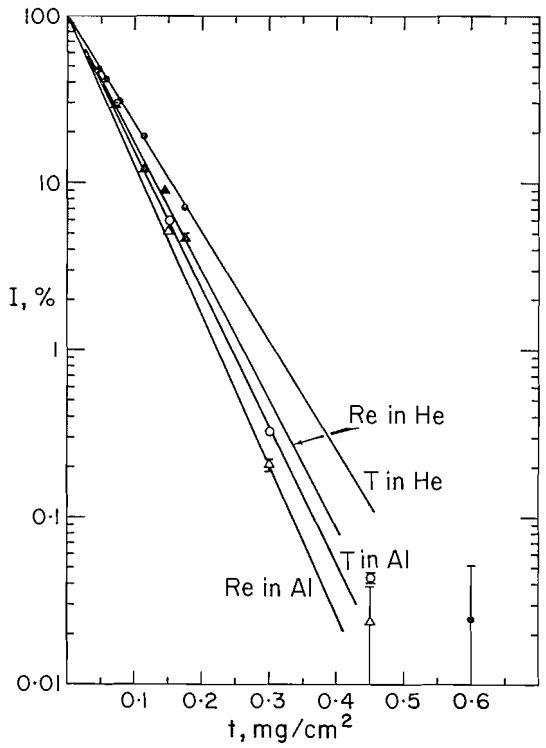

FIG. 1. The absorption of the β particles from T and from ^{187}Re in helium and in aluminum.

where I_0 is the original activity, I is the activity after passing through an absorber of thickness t and absorption coefficient μ. The "maximum range", although frequently quoted, is an arbitrary term since it depends upon the reduction which is significant for the problem in hand or on the sensitivity of the detection methods, and is not given here. For these low energy particles, exponential behavior persists up to about 6 or 7 times the half-thickness. This is a useful approximation of the "maximum range". For example, in Libby's equation, recommended for calculating saturation activities, I_∞,

$$[2] \qquad \frac{I}{I_\infty} = 1 - e^{-5t/t_\infty}$$

from measurements of layers which are less than "infinite thickness", or "maximum range", t_∞, the maximum range is taken as 7.2 times the half-thickness (8). Table I shows the thickness of helium or of aluminum which reduces the initial activity to ½. The absorption coefficients, μ, of eq. [1] are also given, from which one can calculate the thickness of absorber which will produce any other reduction.

In order to determine the disintegration rate of ^{187}Re from the activity of samples of Re_2S_7 it is necessary to know the range of the rhenium β particles in Re_2S_7. Empirical equations relating absorption coefficients of γ-free β particles to the average atomic weight of the absorber have been proposed, for example by Lerch (9). Direct observation of the range of the β particles from tritium in Re_2S_7 have also been made by us. The validity of using these data to estimate the range of rhenium β particles in Re_2S_7, and the disintegration rate of ^{187}Re calculated from these data, will be discussed in another communication.

Acknowledgments

The author owes thanks to Officer Cadets R. S. Dziver, J. E. G. Lalonde, D. F. Smith,

Can. J. Chem. Downloaded from www.nrcresearchpress.com by 210.87.254.40 on 09/05/12
For personal use only.

R. W. Staple, R. A. S. Jackson, J. B. Butler, and K. C. Birch for their help with the experimental observations, computer programming, and calculations.

1. S. N. Naldrett. Ann. N.Y. Acad. Sci. **72**, 215 (1958).
2. C. J. Wolf and W. H. Johnston. Phys. Rev. **125**, 307 (1962).
3. L. M. Dorfman. Phys. Rev. **95**, 393 (1954).
4. A. D. Suttle and W. F. Libby. Anal. Chem. **27**, 921 (1955).
5. W. F. Libby. Phys. Rev. **103**, 1900 (1956).
6. J. Rydberg. Acta Chem. Scand. **12**, 399 (1958).
7. R. E. Beltz. Anal. Biochem. **2**, 303 (1961).
8. W. F. Libby. Anal. Ed. Ind. Eng. Chem. **19**, 2 (1947).
9. P. Lerch. Helv. Phys. Acta, **26**, 663 (1953).

Can. J. Chem. Downloaded from www.nrcresearchpress.com by 210.87.254.40 on 09/05/12
For personal use only.

Studies on metal hydroxy compounds. IX. Kinetics of thermal decomposition of twelve copper halide derivatives

P. Ramamurthy and E. A. Secco
Chemistry Department, St. Francis Xavier University, Antigonish, Nova Scotia

Received May 30, 1969

The kinetics of the thermal decomposition of 12 halide (F, Cl, Br, I) derivatives of copper hydroxide are reported. The kinetic results and their interpretation in terms of activated complex theory are compared with the results and interpretation of the thermal decomposition of zinc and cadmium hydroxyhalides.

Canadian Journal of Chemistry, **47**, 3915 (1969)

Introduction

This report represents the second part of a systematic program of study on the solid-state decomposition kinetics of metal hydroxy compounds dealing with copper hydroxide and its halide (F, Cl, Br, I) derivatives. Details of these decomposition reactions and analyses have already been reported (1, 2).

Experimental

All compounds used in this study were prepared in this laboratory using procedures already described (1).

The decomposition kinetics were determined gravimetrically, i.e. weight loss vs. time, using a duPont TGA-950 plug-in module for the duPont DTA-900 thermal analyzer console, calibrated and programmed as already described in Part VI (3).

The recorded weight loss vs. time trace was translated into decomposition fraction, α, vs. time data. The kinetic data were subsequently computer processed and plotted to obtain the best straight line or linear fit with the known rate expressions. The kinetic data from a continuous recording of the progress of reaction can be evaluated in a more critical manner thus minimizing the inherent risk of fitting the data to a rate expression of questionable validity.

All decomposition experiments were done in nitrogen gas atmosphere as previously described (3).

Results and Discussion

The kinetic results for decomposition according to the written reaction equations are given in Table I. These results represent the best fit between the experimental data and the known rate expressions over the maximum reaction fraction $\alpha \geq 0.8$ and over the temperature ranges studied. In all cases excepting $CuF_2.2H_2O$, the fitting of the data to a particular rate expression was straightforward and clear-cut. In contrast, the $CuF_2.2H_2O$ data are fitted equally well to three rate equations; (*i*) Avrami–Erofeyev (A–E) type with $n = \frac{3}{2}$, (*ii*) the contracting sphere or Roginskii – Todes – Mampel (R–T–M) equation, and (*iii*) modified Prout–Tompkins (P–T) equation, in order of listing in Table I. The general kinetic features contained in the Table, that is, predominance of first order rate and the single instance of second order rate, along with the group of three rate equations for $CuF_2.2H_2O$, bear a striking parallel to the results observed for zinc and cadmium compounds (3).

The decomposition of CuOHF was also studied but the kinetic data could not be fitted to any known rate expression. This failure results

R. W. Staple, R. A. S. Jackson, J. B. Butler, and K. C. Birch for their help with the experimental observations, computer programming, and calculations.

1. S. N. Naldrett. Ann. N.Y. Acad. Sci. **72**, 215 (1958).
2. C. J. Wolf and W. H. Johnston. Phys. Rev. **125**, 307 (1962).
3. L. M. Dorfman. Phys. Rev. **95**, 393 (1954).
4. A. D. Suttle and W. F. Libby. Anal. Chem. **27**, 921 (1955).
5. W. F. Libby. Phys. Rev. **103**, 1900 (1956).
6. J. Rydberg. Acta Chem. Scand. **12**, 399 (1958).
7. R. E. Beltz. Anal. Biochem. **2**, 303 (1961).
8. W. F. Libby. Anal. Ed. Ind. Eng. Chem. **19**, 2 (1947).
9. P. Lerch. Helv. Phys. Acta, **26**, 663 (1953).

Can. J. Chem. Downloaded from www.nrcresearchpress.com by 210.87.254.40 on 09/05/12
For personal use only.

Studies on metal hydroxy compounds. IX. Kinetics of thermal decomposition of twelve copper halide derivatives

P. Ramamurthy and E. A. Secco
Chemistry Department, St. Francis Xavier University, Antigonish, Nova Scotia

Received May 30, 1969

The kinetics of the thermal decomposition of 12 halide (F, Cl, Br, I) derivatives of copper hydroxide are reported. The kinetic results and their interpretation in terms of activated complex theory are compared with the results and interpretation of the thermal decomposition of zinc and cadmium hydroxyhalides.

Canadian Journal of Chemistry, **47**, 3915 (1969)

Introduction

This report represents the second part of a systematic program of study on the solid-state decomposition kinetics of metal hydroxy compounds dealing with copper hydroxide and its halide (F, Cl, Br, I) derivatives. Details of these decomposition reactions and analyses have already been reported (1, 2).

Experimental

All compounds used in this study were prepared in this laboratory using procedures already described (1).

The decomposition kinetics were determined gravimetrically, i.e. weight loss vs. time, using a duPont TGA-950 plug-in module for the duPont DTA-900 thermal analyzer console, calibrated and programmed as already described in Part VI (3).

The recorded weight loss vs. time trace was translated into decomposition fraction, α, vs. time data. The kinetic data were subsequently computer processed and plotted to obtain the best straight line or linear fit with the known rate expressions. The kinetic data from a continuous recording of the progress of reaction can be evaluated in a more critical manner thus minimizing the inherent risk of fitting the data to a rate expression of questionable validity.

All decomposition experiments were done in nitrogen gas atmosphere as previously described (3).

Results and Discussion

The kinetic results for decomposition according to the written reaction equations are given in Table I. These results represent the best fit between the experimental data and the known rate expressions over the maximum reaction fraction $\alpha \geq 0.8$ and over the temperature ranges studied. In all cases excepting $CuF_2.2H_2O$, the fitting of the data to a particular rate expression was straightforward and clear-cut. In contrast, the $CuF_2.2H_2O$ data are fitted equally well to three rate equations; (*i*) Avrami–Erofeyev (A–E) type with $n = \frac{3}{2}$, (*ii*) the contracting sphere or Roginskii – Todes – Mampel (R–T–M) equation, and (*iii*) modified Prout–Tompkins (P–T) equation, in order of listing in Table I. The general kinetic features contained in the Table, that is, predominance of first order rate and the single instance of second order rate, along with the group of three rate equations for $CuF_2.2H_2O$, bear a striking parallel to the results observed for zinc and cadmium compounds (3).

The decomposition of CuOHF was also studied but the kinetic data could not be fitted to any known rate expression. This failure results

Can. J. Chem. Downloaded from www.nrcresearchpress.com by 210.87.254.40 on 09/05/12
For personal use only.

TABLE I

Kinetic results for decomposition

Compound	Reaction equation	Temperature range (°C)	Number of temperatures	Rate expression	Activation energy, E_a (kcal)	log A	Heat of reaction, ΔH (kcal/mole)
$Cu(OH)_2$	$Cu(OH)_2 \rightarrow CuO + H_2O$	140–180	4	First order*	18.2±1.0	7.9	12.30
$CuBr_2$	$CuBr_2 \rightarrow CuBr + \frac{1}{2}Br_2$	180–220	4		21.6±1.3	9.0	8.70
$Cu_2(OH)F_3$	$Cu_2(OH)F_3 \rightarrow CuO + CuF_2 + HF$	350–390	5		39.3±1.5	9.0	28.67
$Cu(OH)Cl$	$2Cu(OH)Cl \rightarrow CuO + CuCl_2 + H_2O$	230–280	5		36.9±1.5	14.1	8.07
δ-$Cu_2(OH)_3Cl$	$2Cu_2(OH)_3Cl \rightarrow 3CuO + CuCl_2 + 3H_2O$	240–270	4		34.7±2.0	13.1	21.98
β-$Cu_2(OH)_3Cl$	,,	260–300	6		38.5±3.5	13.8	22.69
α-$Cu_2(OH)_3Cl$	,,	240–280	4		43.3±2.2	16.4	21.79
γ-$Cu_2(OH)_3Cl$	,,	260–300	4		52.3±3.0	19.1	22.72
$Cu_2(OH)_3Br$	$2Cu_2(OH)_3Br \rightarrow 3CuO + CuBr + 3H_2O + \frac{1}{2}Br_2$	230–280	4		44.8±4.0	17.7	23.61
$Cu_2(OH)_3I$	$2Cu_2(OH)_3I \rightarrow 3CuO + 3H_2O + CuI + \frac{1}{2}I_2$	180–220	4		42.4±2.5	23.0	17.06
$Cu_2(OH)_3F$	$Cu_2(OH)_3F \rightarrow 2CuO + HF + H_2O$	310–360	4	$(1-\alpha)^{-1} = 1 + kt$	35.8±1.5	12.0	28.55
$CuF_2.2H_2O$	$2CuF_2.2H_2O \rightarrow Cu_2(OH)F_3 + HF + 3H_2O$	150–190	4	$\ln(1-\alpha) = -kt^{3/2}$	34.5±1.0	15.6	28.06
				$1-(1-\alpha)^{1/3} = kt$	29.0±0.5	12.8	
				$\log\left(\frac{\alpha}{1-\alpha}\right) = k \log t + C$	21.0±2.0		

*Listed in order of increasing pre-exponential factor A with an effort to retain the 4 structural forms of $Cu_2(OH)_3Cl$ together in one group.

from the interference of, and our inability to separate, two overlapping processes contributing to the weight loss, viz.

[1] $4CuOHF \rightarrow Cu_2(OH)F_3 + HF + H_2O$

and

[2] $Cu_2(OH)F_3 \rightarrow CuO + CuF_2 + HF$

The kinetic behavior of CuOHF is in contrast to $Cu_2(OH)_3Br$ and $Cu_2(OH)_3I$; the latter undergo simultaneous dehydroxylation and disproportionation according to a first order rate law.

In the $CuF_2.2H_2O$ case, the modified P–T rate equation is disregarded since the requirement $E_a \geq \Delta H$ for an endothermic reaction is not fulfilled. From their respective plots of the function of α vs. time for the rate laws

$$-\ln(1 - \alpha) = kt^{\frac{1}{2}}$$

and

$$1 - (1 - \alpha)^{\frac{1}{3}} = kt$$

which were unquestionably linear, we are unable to distinguish between these two rate expressions.

The rate equation

[3] $$-\ln(1 - \alpha) = kt^{\frac{3}{2}}$$

has been routinely disregarded (4) on the basis that this equation has no theoretical significance in solid phase kinetics. A theoretical basis for this equation, however, has been found in precipitation kinetics. Turnbull (5), in a review of the theory of phase change kinetics, has included a kinetic description of precipitation reactions as derived by Wert and Zener. In this derivation Wert and Zener assumed that the particle growth of the β phase was governed by the diffusion of its components in the bulk γ phase rather than processes at the γ–β interface for the simplest case of spherical particles, and showed that the kinetic law of precipitation is given by eq. [3]. This precipitation process can be translated into a decomposition process visualizing the initial decomposition to germinate at the center of the reactant bulk. The growth of the product particle or the extent of decomposition in the bulk is governed by diffusion of the volatile product-species through the reactant matrix. Such a decomposition mechanism parallels the precipitation process envisaged by Wert and Zener and would be expected to obey the rate eq. [3].

No dependence of E_a on ΔH is revealed in Table I nor is there any relationship discernible between the pre-exponential factor A of the Arrhenius equation and E_a. However, the E_a values of all hydroxyhalide compounds, excluding γ-$Cu_2(OH)_3Cl$, are noted to fall within the range 35–45 kcal/mole.

Ball and Coultard (6) have reported activation energies evaluated from the differential weight loss vs. temperature curves. All their activation energy values from thermogravimetric curves are appreciably higher than the E_a values reported herein from isothermal experiments. Their fitting of the CuOHCl thermogram to a "second order" equation also differs from our kinetic results. These discrepancies illustrate the lack of reliability of the present analytical procedures used to extract kinetic data from dynamic methods such as thermogravimetric analysis or differential thermal analysis.

The existence of 4 crystalline structures of $Cu_2(OH)_3Cl$ incorporating a variation in the crystalline lattice with no alteration in the molecular conformation could be a kinetically useful parameter especially if the reaction rate is controlled by the molecularity alone and not by the topochemistry of the solid. The relatively constant ΔH values and the different E_a values of these 4 structures suggest that the pertinent kinetic parameter resides in the activated complex configurations.

From the Arrhenius rate equation, in the form derived from activated complex theory

$$k_r = \left[10^{13} \cdot \frac{Q^*}{Q}\right] e^{-E_a/RT} = A\, e^{-E_a/RT}$$

A values of approximately 10^{13}, as for δ- and β-structures, imply a Q^*/Q ratio of unity with an equal number of active modes of freedom in both the activated complex and reactant configurations. On the other hand, α- and γ-$Cu_2(OH)_3Cl$ with A values of 10^{16}–10^{19} imply a Q^*/Q ratio greater than unity with more modes of freedom in the complex configuration relative to the reactant configuration. Cordes (7) has predicted A values of 10^{16} for a monomolecular reaction and 10^{18} for a bimolecular reaction in terms of an increased number of rotational modes in the complex, and assuming bulk decomposition, i.e. where any molecule is as likely to react as any other. We can assume therefore that α-$Cu_2(OH)_3Cl$ undergoes bulk

Can. J. Chem. Downloaded from www.nrcresearchpress.com by 210.87.254.40 on 09/05/12
For personal use only.

decomposition via a monomolecular process whereas γ-$Cu_2(OH)_3Cl$ occurs via a bimolecular one. These data illustrate that the crystal structure parameter does affect the active modes of freedom in the complex in its decomposition course but the analysis of this parameter in the absence of detailed torsional, rotational, and vibrational data can be at best an exercise in conjecture.

The excellent agreement between the observed A value of 10^{18} for $Cu_2(OH)_3Br$ with the prediction by Cordes lends strong support to the interpretation that $Cu_2(OH)_3Br$, along with γ-$Cu_2(OH)_3Cl$, undergoes bulk decomposition in a bimolecular manner. The exceedingly high A value of 10^{23} for $Cu_2(OH)_3I$ cannot be accommodated by increased rotational modes of freedom and therefore must involve translational modes as was suggested (3) for ZnOHCl and ZnOHF.

For the compounds $Cu(OH)_2$, $CuBr_2$, and $Cu_2(OH)F_3$ the pre-exponential values of 10^8–10^9 can be interpreted in terms of a complex highly restricted in its modes of rotation as discussed by Cordes.

Acknowledgment

The authors acknowledge the financial support of this research program by the National Research Council of Canada.

1. P. RAMAMURTHY and E. A. SECCO. Can. J. Chem. **47**, 2181 (1969).
2. P. RAMAMURTHY and E. A. SECCO. Can. J. Chem. **47**, 2185 (1969).
3. P. RAMAMURTHY and E. A. SECCO. Can. J. Chem. **47**, 2303 (1969).
4. D. A. YOUNG. Decomposition of solids. International encyclopedia of physical chemistry and chemical physics. *Edited by* F. C. Tompkins. Pergamon Press, London. 1966. p. 35.
5. D. TURNBULL. Solid State Phys. **3**, 256 (1956).
6. M. C. BALL and R. F. M. COULTARD. J. Chem. Soc. A, **6**, 1417 (1968).
7. H. F. CORDES. J. Phys. Chem. **72**, 2185 (1968).

Can. J. Chem. Downloaded from www.nrcresearchpress.com by 210.87.254.40 on 09/05/12
For personal use only.

Can. J. Chem. Downloaded from www.nrcresearchpress.com by 210.87.254.40 on 09/05/12
For personal use only.

Preparation of ferrimagnetic barium- and strontium-iron oxides, $BaFe_{12}O_{19}$ and $SrFe_{12}O_{19}$

R. J. Routil and D. Barham

Department of Chemical Engineering and Applied Chemistry, University of Toronto, Toronto 181, Ontario

Received August 21, 1969

Ferrimagnetic $BaFe_{12}O_{19}$ and $SrFe_{12}O_{19}$ were prepared from $BaSO_4$ and from $SrSO_4$ by heating the sulfates in mixtures with Fe_2O_3 and Na_2CO_3 to 900–1400 °C. The highest yields were obtained from mixtures containing 6 moles of Fe_2O_3 and 1 mole of Na_2CO_3 per mole of sulfate. Similar results were observed when Na_2CO_3 was substituted with compounds yielding oxides of sodium, potassium, or calcium but not with analogous lithium compounds.

Canadian Journal of Chemistry. 47, 3919 (1969)

Preparation of $SrFe_{12}O_{19}$ from mixtures of Fe_2O_3 and $SrCO_3$ containing Na_2SO_4 and other impurities, as reported by Cochardt (1) was basis to a hypothesis that $SrFe_{12}O_{19}$ should exist as a stable phase in certain regions of the $SrSO_4$–Fe_2O_3–Na_2O system. This was confirmed by an investigation of the system at high temperatures. Similarly, the occurrence of $BaFe_{12}O_{19}$ in the $BaSO_4$–Fe_2O_3–Na_2O system was anticipated and proved.

High temperature reactions of the $x\ MSO_4 + y\ Fe_2O_3 + z\ Na_2CO_3$ mixtures were studied first by keeping $x:z = 1$ and by changing $x:y$ within the limits which, according to refs. 2 to 5, yielded $MFe_{12}O_{19}$ as the main phase of the MO–Fe_2O_3 systems (M = Ba or Sr). Then the effects of $x:z \neq 1$ were investigated in ranges for which the lowest melting points were reported in refs. 6 to 8.

Ferrimagnetic phases isolated from the reacted mixtures were identified by X-ray diffraction analysis as being of the magnetoplumbite crystal structure. Chemical analyses verified the composition as $MFe_{12}O_{19}$.

The highest yield of $MFe_{12}O_{19}$ was found when $x = z = 1$ and $y = 6$. Omitting intermediate stages the following overall reaction was proposed

$$[1]\quad MSO_4 + 6\ Fe_2O_3 + Na_2CO_3 \rightarrow MFe_{12}O_{19} + Na_2SO_4 + CO_2$$

The reaction proceeded very slowly below 900 °C and, depending on the grain size of starting reagents, it was completed in less than 1 h at 1200 °C. Theoretical yields were approached within experimental errors. Heating above 1400 °C caused partial decomposition of $MFe_{12}O_{19}$ and lower yields.

The lowest melting point (about 1140 °C) was observed when $x = 1$, $y = 12$, and $z = 7$. The main overall reaction was formulated as

$$[2]\quad MSO_4 + 12\ Fe_2O_3 + 7\ NaCO_3 \rightarrow MFe_{12}O_{19} + 12\ NaFeO_2 + Na_2SO_4 + 7\ CO_2$$

The yields of $MFe_{12}O_{19}$ were more than 90% of the theory.

By similar reactions $MFe_{12}O_{19}$ was prepared from mixtures in which Na_2CO_3 was substituted with NaOH, $NaNO_3$, CH_3COONa, K_2CO_3, or with $CaCO_3$. (Initial heating of mixtures containing CH_3COONa had to be slow enough to prevent reduction of Fe_2O_3.)

$MFe_{12}O_{19}$ was not produced when Na_2CO_3 was substituted with Li_2CO_3. Ferrimagnetic phases isolated from these samples were of the spinel type.

Experimental

Reagent grade strontium sulfate from British Drug Houses Ltd. and "Certified" grade reagents from Fisher Scientific Co. were used.

The preparation procedure comprised following steps: (*a*) Mixing $BaSO_4$ or $SrSO_4$ with Fe_2O_3 and with a third component which was either dry Li_2CO_3, Na_2CO_3, K_2CO_3, $CaCO_3$, a solution of NaOH, $NaNO_3$, or CH_2COONa. (*b*) Heating the mixture in a platinum crucible to a temperature between 900 and 1400 °C in air atmosphere. Samples containing visible particles of unreacted $BaSO_4$ or $SrSO_4$ were homogenized by crushing and screening and the heating was repeated at a higher temperature. (*c*) Separation of the ferrimagnetic phase from other components of the reacted mixture. Leaching with water or with diluted nitric acid and

magnetic separation were employed. Samples which did not disintegrate by leaching were crushed to pass 100 mesh and the leaching was repeated.

Example to Reaction [1]

$BaSO_4$, Fe_2O_3, and Na_2CO_3 were mixed in the stoichiometric ratio of reaction [1]. The mixture was fired at 900 °C for 1 h and after cooling, it was ground to pass 100 mesh and then refired at 1200 °C for 1 h. The resulting cake was crushed to pass 100 mesh. The powder was leached with hot water which was changed frequently until the extract remained clear on addition of $BaCl_2$ solution.

Example to Reaction [2]

$SrSO_4$, Fe_2O_3, and Na_2CO_3 were mixed in the stoichiometric ratio of reaction [2] and the mixture was melted by heating to 1150 °C. On cooling the melt divided into a heavy black layer and a lighter white layer. The white layer containing mainly Na_2SO_4 was washed out with water and the remaining black layer was leached with hot 5% nitric acid. Loosening of ferrimagnetic particles from the $NaFeO_2$ matrix was facilitated by magnetic stirring and by occasional mechanical prying. Separated ferrimagnetic particles were washed with water and dried.

1. A. W. COCHARDT. U.S. Pat. 3,113,927. Dec. 10, 1963.
2. P. BATTI. Ann. Chim. Rome, **50**, 1461 (1960).
3. Y. GOTO and T. TAKADA. J. Amer. Ceram. Soc. **43**, 150 (1960).
4. P. BATTI. Ann. Chim. Rome, **52**, 941 (1962).
5. P. BATTI and F. DI TELLA. Ann. Chim. Rome, **57** 64 (1966).
6. G. CALCAGNI. Gazz. Chim. Ital. **42 II**, 655 (1912).
7. R. KNICK and E. J. KOHLEMEYER. Anorg. Allg. Chem. **224**, 77 (1940).
8. R. J. GAMBINO and F. LEONHARD. J. Amer. Ceram. Soc. **44**, 221 (1961).

Can. J. Chem. Downloaded from www.nrcresearchpress.com by 210.87.254.40 on 09/05/12
For personal use only.

Can. J. Chem. Downloaded from www.nrcresearchpress.com by 210.87.254.105 on 09/05/12
For personal use only.

Canadian Journal of Chemistry

Published by THE NATIONAL RESEARCH COUNCIL OF CANADA

VOLUME 47 NOVEMBER 1, 1969 NUMBER 21

Quantitative investigation of the ozonolysis reaction. IX. On the mechanism of ozonide formation

SÁNDOR FLISZÁR AND JACQUES CARLES

Department of Chemistry, University of Montreal, Montreal, Quebec

Received January 14, 1969

The ozonide *cis–trans* ratios, for both normal and cross-ozonides, have been examined, in a number of cases, in pentane and in benzene solutions. In benzene, at 25 °C, almost invariant *cis–trans* ratios are observed, regardless of the geometry and initial concentration of olefin. In pentane, these ratios have been found to depend, both at −78 and 25 °C, on the geometry and the initial concentration of the olefin when 1,2-disubstituted ethylenes with bulky substituents are ozonized. However, the cross-ozonide *cis–trans* ratios obtained from trisubstituted ethylenes do not depend on the initial olefin concentration. A tentative mechanistic proposal is suggested in terms of transitory zwitterion–olefin adducts.

Canadian Journal of Chemistry, 47, 3921 (1969)

The mechanism of ozonolysis proposed by Criegee (1) (Scheme 1) has been the object of recent discussions (2–4), and has received considerable experimental support (5). This support includes (*i*) the reaction of the zwitterion with those solvents which participate in the ozonolysis, forming hydroperoxides, or the reaction with added aldehyde to form an ozonide other than that of the original olefin, and (*ii*) the formation of cross-ozonides from unsymmetrical olefins (3).

The primary ozonides **1** are unstable even at low temperatures, and this instability did not readily permit their detection. However, evidence for their existence has been obtained by Criegee and Schröder (6) for the primary ozonide of *trans*-di-*t*-butylethylene, and by Greenwood (7) for the primary ozonides of some *trans* alkenes. In the ozonolysis of *trans*-di-*t*-butylethylene at −78° in pentane, a crystalline product is formed, which, upon "heating" to −60°, decomposes explosively to give the normal products of ozonolysis (6). The 1,2,3-trioxolane structure **1** for the primary ozonide of *trans*-di-*t*-butylethylene was confirmed by Bailey (8) from low temperature (−110°) nuclear magnetic resonance (n.m.r.) experiments which indicated that both methine protons are equivalent.

The detection of primary ozonides from *cis* olefins has been even more difficult, apparently due to their greater instability at temperatures as low as −110°. Greenwood (9) has reported some evidence for the existence of the *cis* primary ozonides (at −130° in CF_2Cl_2 solutions) of butene-2, pentene-2, and hexene-3. While the

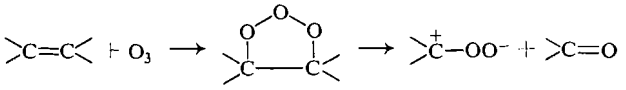

1 **2** **3**

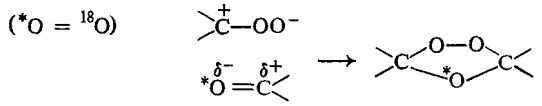

($^*O = {}^{18}O$)

SCHEME 1

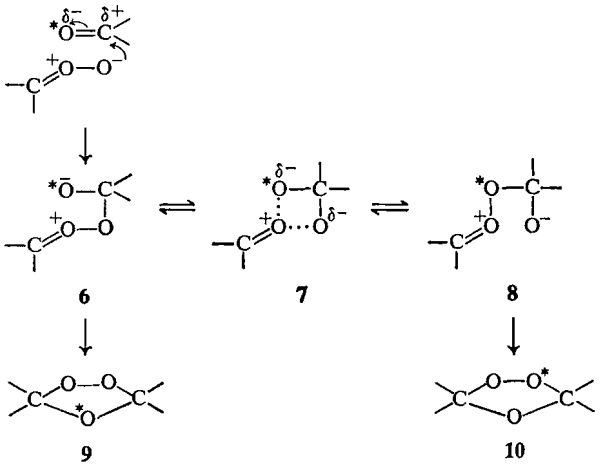

SCHEME 2

evidence for a 1,2,3-trioxolane structure is not unambiguous for the *cis* primary ozonides, an analogous structure to the *trans* primary ozonides is expected.

The participation of zwitterions in the formation of ozonides from phenylethylenes has been clearly established from the ozonolysis of *cis*- and *trans*-stilbene, styrene, β-methyl-styrene, and triphenylethylene in the presence of ^{18}O-labelled benzaldehyde (4, 10). The ^{18}O atoms are incorporated *exclusively* in the ether position of the ozonides formed, as predicted by Criegee's mechanism.

The original Criegee mechanism (Scheme 1) predicts that all the products arising from the ozonolysis of *cis* and *trans* olefins will be formed in the same proportions. It is found, however, that *cis* and *trans* olefins often give different ozonide *cis–trans* ratios (2, 11), both for the normal and the cross-ozonides. This indicates that the Criegee mechanism requires refinement or that an alternative mechanism is in operation. Possible alternative routes to ozonide formation are discussed in this paper.

Bailey (3) has suggested that the dependence of the *cis–trans* ozonide distribution on the geometry of the olefin may be accommodated within the Criegee mechanism if the zwitterions have *syn* and *anti* forms, and has discussed in detail the formation of *syn* and *anti* zwitterions from *cis* and *trans* primary ozonides.[1] These *syn* and *anti* forms, which were originally suggested by Criegee (12), may be considered analogous to the recently observed *syn* and *anti* forms of protonated aldehydes, ketones, and carboxylic acids at low temperature (13).

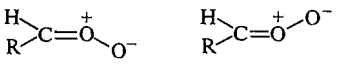

4 *syn* **5** *anti*

A consideration of the zwitterion–^{18}O–aldehyde reaction leads to a novel interpretation of the mechanism which accounts for the formation of ozonides in which the incorporation of the label is in the peroxide or the ether position.

The "oxonium" intermediate **6** can react to give the ozonide **9** (Criegee product). Alternatively, it may be reversibly transformed into the isomeric form **8**, via an intermediate species approaching structure **7**, which would give the ozonide **10**. Thus, the formation of an ozonide of type **10** in the ozonolysis (14) of *trans*-1,2-diisopropylethylene in the presence of acetaldehyde-^{18}O can be rationalized on the basis of the mechanism shown in Scheme 2. However the possible participation of this mechanism requires further investigation. It is justified, at present, by its ability to explain, within the frame of a refined Criegee mechanism, the incorporation of aldehyde-^{18}O in the peroxide position of the ozonide. From a consideration of **6** it would be expected that an electron-releasing group, such as the isopropyl group, would render the original zwitterionic carbo-cation less electrophilic, thus

[1]It results, from Bailey's (3) stereochemical analysis, that aldehydes preferentially interact with *anti* zwitterions so as to orient bulky substituents diequatorially (*cis*) and with *syn* zwitterions to orient bulky substituents into an equatorial, axial (*trans*) conformation.

Can. J. Chem. Downloaded from www.nrcresearchpress.com by 210.87.254.105 on 09/05/12
For personal use only.

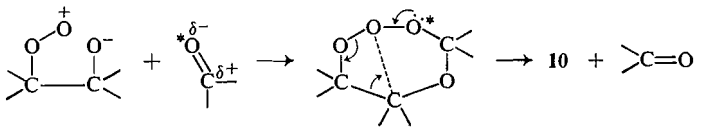

SCHEME 3

retarding the ozonide formation **6** → **9**, and, hence, promoting the equilibrium **6** ⇌ **8**. This would consequently increase the possibility for the formation of the ozonide corresponding to **10**. This is indicated by the ozonolysis (14) of *trans*-1,2-diisopropylethylene in the presence of acetaldehyde-^{18}O which led to a substantial ^{18}O incorporation in the peroxide position.[2] It should be considered, however, that electronic factors may not be solely responsible in directing the reaction paths, but in addition steric factors may influence the proportions of ozonides **9** and **10**.

The formation of an ozonide of type **10** can also be accounted for by the mechanism proposed by Story *et al.* (2), which has been used to explain the stereospecific dependence of the ozonide *cis–trans* distribution on olefin geometry (Scheme 3). It is considered that ^{18}O is perhaps incorporated in the peroxidic position only in the case of the *trans* olefin at a low temperature, where the Murray–Story–Youssefyeh mechanism could play a part due to excess aldehyde and the greater stability of the *trans* initial ozonide in comparison to the *cis* initial ozonide. Of course, this possibility would not be relevant if ^{18}O was incorporated into the peroxidic position in the case of the *cis* olefin. Further studies are in progress to clarify this question.

The incorporation of labelled oxygen in the peroxide position of the ozonide does not, in itself, support one mechanism in preference to the other. Additional parameters affecting the *cis–trans* ozonide distributions must be taken into consideration which would reconcile these data with the stereospecificity observed in ozonide formation from *cis* and *trans* olefins. These include temperature and olefin concentration.

Results and Discussion

It is found that, in general, the ozonide *cis–trans* ratios are affected when the temperature of ozonolysis is changed from −78 to 25° (Table 1). Significant differences are observed for the cross-ozonides from 1,2-disubstituted ethylenes and for the normal *cis–trans* ozonides of *cis*- and *trans*-2,2-dimethylhexene-3. The *cis–trans* ratios observed for the normal ozonides of *trans*-1,2-diisopropylethylene and of *cis*- and *trans*-4-methylpentene-2 appear, however, to be insensitive to the change in temperature of ozonolysis.

An examination of the results given in Table I indicates that the ozonide *cis–trans* ratios depend on the olefin geometry at −78°, more *cis* ozonide being obtained from the *cis* olefin than from the *trans* isomer. This remarkable structural effect, which has been widely observed (2, 11) at −78°, is now found to occur also at 25°. The *cis*- and *trans*-4-methylpentene-2 are, once again, an exceptional case, in that the observed *cis–trans* ratios for the *normal* ozonides do not appear to be related to the *cis* or *trans* configuration of the olefin. Similar exceptional behavior is also observed at −78°. It should be pointed out, however, that for these relatively unhindered

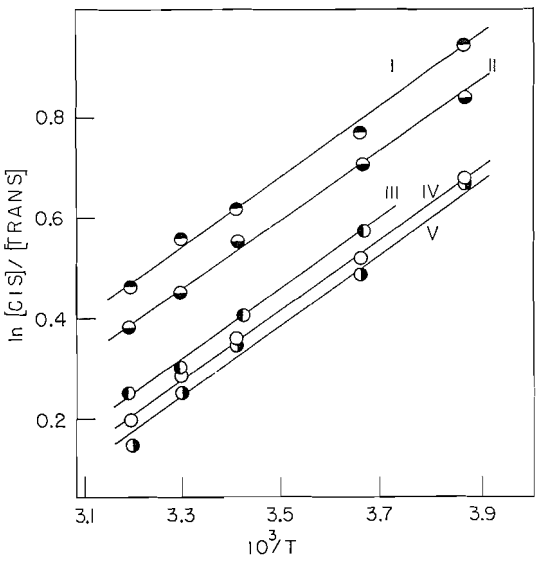

FIG. 1. A plot of ln [*cis*]/[*trans*] (stilbene ozonide) vs. $1/T$ from: I, triphenylethylene; II, *cis*-stilbene; III, *trans*-stilbene; IV, styrene; V, β-methylstyrene.

[2]A calculation (15) from the literature data (14) for the ozonolysis of *trans*-di-isopropylethylene in the presence of acetaldehyde-^{18}O indicates that ~43% of ozonide **10** and, hence, 57% of ozonide **9** are formed. From the reported results (14) of methyllithium reduction of the ozonide, ~39% of ozonide **10** and, hence, 61% of ozonide **9**, can be calculated.

Can. J. Chem. Downloaded from www.nrcresearchpress.com by 210.87.254.105 on 09/05/12
For personal use only.

TABLE I

Ozonide *cis–trans* ratios obtained from selected olefins†

Ozonide formed	Olefin used	Olefin concentration (*M*)	Pentane		Benzene
			−78°	25°	25°
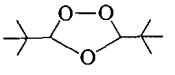	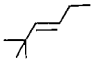	0.1	65/35	59/41	*
		1.0	68/32	63/37	—
		0.1	66/40	63/37	*
		1.0	73/27	68/32	—
		0.1	72/28	59/41	60/40
		1.0	76/24	67/33	61/39
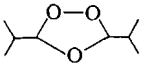		0.1	32/68	45/55	52/48
		1.0	48/52	55/45	52/48
	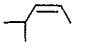	0.1	65/35	55/45	54/46
		1.0	67/33	59/41	54/46
		0.1	47/53	45/55	48/52
		1.0	52/48	51/49	48/52
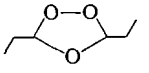		0.1	45/55	43/57	51/49
		1.0	50/50	47/53	51/49
		0.1	38/62	36/64	44/56
		1.0	51/49	43/57	43/57
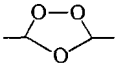		0.1	34/66	37/63	42/58
		1.0	37/63	41/59	43/57
		0.1	46/54	40/60	42/58
		1.0	49/51	45/55	41/59
		0.1	*	41/59	47/53
		1.0	46/54	47/53	47/53
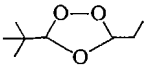		0.1	33/67	35/65	45/55
		1.0	38/62	48/52	48/52
		0.1	55/45	52/48	49/51
		1.0	60/40	56/44	48/52
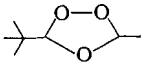		0.1	28/72	35/65	47/53
		1.0	31/69	37/63	47/53
		0.1	44/56	43/57	44/56
		1.0	49/51	45/55	45/55
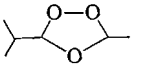		0.1	46/54	48/52	49/51
		1.0	48/52	50/50	49/51
		0.1	45/55	47/53	47/53
		1.0	49/51	49/51	47/53

*Not determined.

†Di-*t*-butylozonide from *trans*-methyl-*t*-butylethylene, diethylozonide from *trans*-ethyl-*t*-butylethylene, and dimethylozonide from *trans*-methyl-*t*-butylethylene were produced, but the isomer ratios could not be obtained.

Can. J. Chem. Downloaded from www.nrcresearchpress.com by 210.87.254.105 on 09/05/12
For personal use only.

TABLE II

Proportions of *cis*-stilbene ozonide obtained from selected phenylethylenes

Olefin	Temperature °C				
	−15	0	20	30	40
Triphenylethylene	72.1±0.8	68.4±0.5	65.0±0.8	63.8±0.4	61.4±1.3
cis-Stilbene	69.9±0.8	67.0±0.7	63.6±0.8	61.1±1.1	59.5±0.6
trans-Stilbene	*	64.0±0.8	59.7±0.4	57.4±0.8	56.2±1.0
Styrene	66.2±1.1	62.6±0.7	58.9±0.5	57.2±0.9	54.9±0.5
β-Methylstyrene	66.1±1.5	61.7±1.0	58.7±0.6	56.3±1.0	53.7±1.0

*Not determined.

olefins the cross-ozonide *cis–trans* ratios exhibit a significant stereochemical dependence on olefin geometry, both at −78 and at 25 °C.

A similar stereochemical dependence of the ozonide *cis–trans* ratio on olefin geometry is also observed in the ozonolysis of phenylethylenes in CCl_4 solution, at temperatures between −15 and 40° (Table II, Fig. 1).

The extreme instability of the primary ozonides (6–9) indicates that a reaction between such intermediates and aldehyde molecules, as depicted in Scheme 3, will be highly improbable at 25°. The results presented here thus favor the explanation for the dependence of the *cis–trans* distribution on the geometry of the olefin given in terms of *syn* and *anti* zwitterions (3), rather than Scheme 3, which is based on a reaction between primary ozonide and aldehyde.

However, it would be expected that, at 25°, the *syn* and *anti* zwitterions will rapidly equilibrate. Such an equilibration would affect the *cis–trans* distributions so that the same distribution would be observed with a *cis* and the corresponding *trans* olefin isomer. This is in variance with the experimental results.

A possible explanation for the non-equilibration of the *syn* and *anti* zwitterions can be drawn from a consideration that the ozonide *cis–trans* ratios are solvent dependent (3, 16). Pertinent examples are the results obtained (11g) in the ozonolysis of *trans*-hexene-3 (0.2 *M* at −30°) in pentane, CH_2Cl_2, and Et_2O, in addition to the normal and cross-ozonide *cis–trans* ratios observed (3) in the ozonolysis of *cis*- and *trans*-4-methylpentene-2 (1.0 *M* at −75°) in pentane, CH_2Cl_2, and AcOEt. Similar observations have also been made with *cis*- and *trans*-1,2-diisopropylethylene, when ozonized in different solvents (16). The results indicated in Table I also show a significant difference between the *cis–trans* ratios measured at 25° in pentane and in benzene. Moreover, in contrast with most of the results obtained in pentane, the *cis–trans* ratios observed in benzene appear to be independent of olefin concentration.

The results given in Table I indicate that, in pentane solution, there is a significant increase in the normal and cross-ozonide *cis–trans* ratios when the initial olefin concentration is changed from 0.1 to 1.0 *M*. This is found to occur both at −78 and at 25°. Similar results have been reported previously (16) for the ozonolysis of *cis*- and *trans*-1,2-diisopropylethylene in pentane at −70°. The present results indicate that the dependence of the ozonide *cis–trans* ratio on the olefin concentration is particularly pronounced in the low concentration region, whereas, at olefin concentrations above 1.0 *M*, the ozonide distribution appears to vary little and to tend to an asymptotic value, independent of olefin concentration. (Fig. 2).

It is also noteworthy that in the early stages of the reaction, the ozonide *cis–trans* ratios are higher than those measured when most of the olefin has reacted with ozone (Figs. 3, 4). This is in agreement with the observed effect of olefin concentration, owing to the fact that the olefin concentrations are higher at the beginning than toward the completion of the ozonolysis.

The observations on the effect of the solvent and of the olefin concentration on the ozonide *cis–trans* ratios may be rationalized by considering that the olefin itself, when dissolved in an inert solvent, such as pentane, may influence the course of the ozonolysis by a "solvent effect".

The effect of the olefin concentration, or of the solvent, cannot be readily interpreted in terms of interactions between olefin, or solvent and the primary ozonide **1**, or the seven membered ring depicted in Scheme 3. The participation of olefin

Can. J. Chem. Downloaded from www.nrcresearchpress.com by 210.87.254.105 on 09/05/12
For personal use only.

Can. J. Chem. Downloaded from www.nrcresearchpress.com by 210.87.254.105 on 09/05/12
For personal use only.

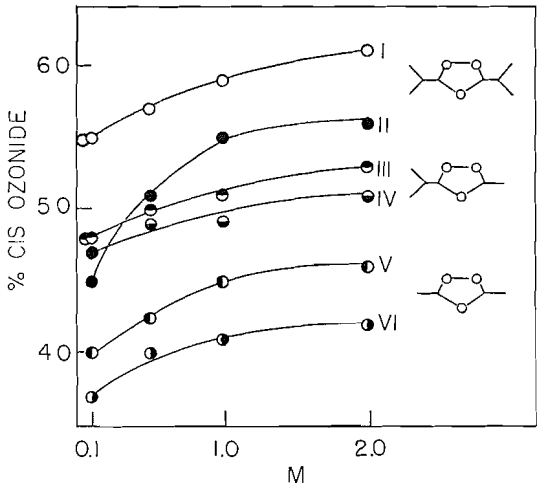

FIG. 2. A plot of % *cis* ozonide formed vs. olefin initial concentration (*M*), in pentane at 25 °C. Curves I, III, and V: from *cis*-4-methylpentene-2. II, IV, and VI: from *trans*-4-methylpentene-2. The ozonides formed are diisopropylethylene ozonide (I and II), 4-methylpentene-2 ozonide (III and IV) and butene ozonide (V and VI).

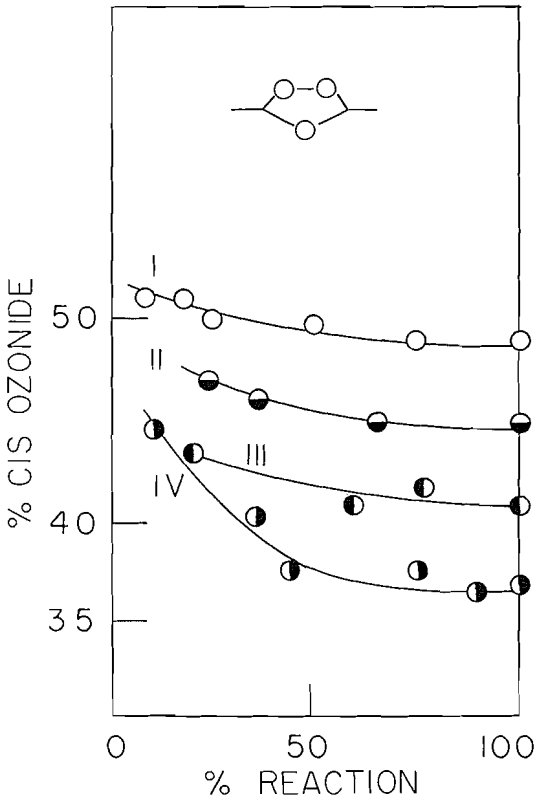

FIG. 3. A plot of % *cis*-butene ozonide formed vs. percentage of 4-methylpentene-2 reacted, in pentane, from *cis* olefin at −78° (I) and 25° (II), and from *trans* olefin at 25° (III) and −78° (IV).

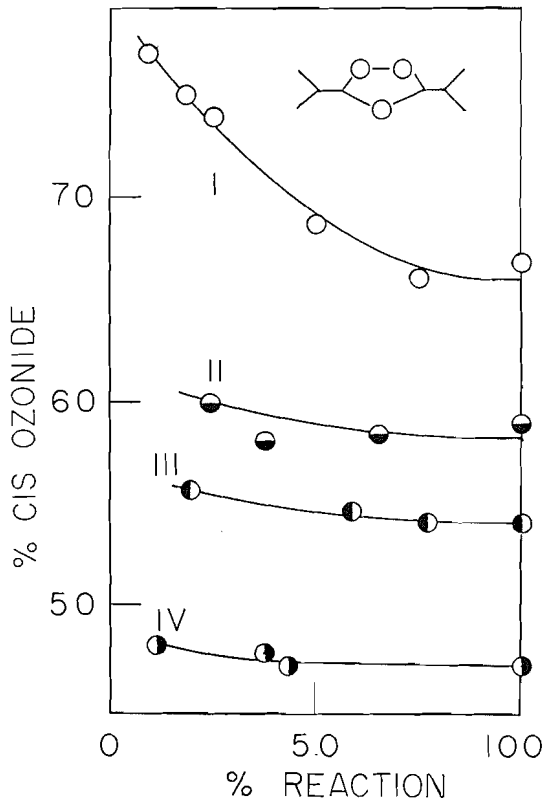

FIG. 4. A plot of % *cis*-diisopropylethylene ozonide formed vs. % of 4-methylpentene-2 reacted in pentane, from *cis* olefin at −78° (I) and 25° (II), and from *trans* olefin at 25° (III) and −78° (IV).

in directing the ozonide *cis–trans* distributions can, however, be interpreted by the postulation of a zwitterion–olefin interaction which could "stabilize" the zwitterion in a *syn* or *anti* configuration. Such transitory zwitterion–olefin adducts could approach the structures indicated in Scheme 4.

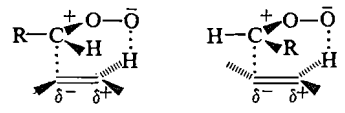

SCHEME 4

The mode of stabilization of the zwitterionic positive charge by the olefin is subject to some reservations owing to the difficulty of localizing the positive charge. It can be considered, however, that the negative charge of the zwitterion may interact with an olefinic hydrogen atom to

Can. J. Chem. Downloaded from www.nrcresearchpress.com by 210.87.254.105 on 09/05/12
For personal use only.

form a hydrogen bond. Unfortunately there appears to be little information on whether the ethylenic hydrogen atoms are sufficiently acidic to cause the hydrogen bonding depicted in Scheme 4. However, self-consistent field (s.c.f.) calculations by Cook *et al.* (17) indicate a low but definite acidity of H atoms attached to sp^2 carbon atoms compared with the H atoms in paraffins. Hence, *in the presence of a strong proton acceptor*, such as the O^- of the zwitterion, the postulated hydrogen bond seems quite plausible. Similar interactions have already been considered by Sidgwick *et al.* (18), and by Dippy *et al.* (19) for the *o*-nitrophenylpropionic and *o*-nitrocinnamic acids. Such a zwitterion–olefin interaction

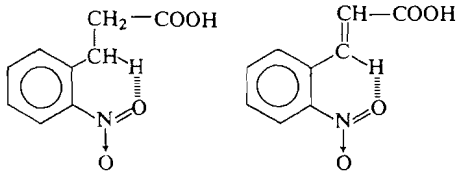

may explain the dependence of the ozonide *cis–trans* distribution on the olefin concentration and also provide a possible explanation for the non-equilibration of the *syn* and *anti* forms, which is observed at 25°. The stereochemical requirements necessary for the formation of zwitterion–olefin adducts may influence the direction of the ozonide *cis–trans* distributions. A consideration of the mutual interactions in such adducts between the substituents of the olefin and of the zwitterion seems to indicate that a *cis* olefin is capable of stabilizing an *anti* zwitterion rather than a *syn* zwitterion, and hence favoring the formation of *cis* ozonide.[1] As indicated by Scheme 4, if the group R of the zwitterion was in the *syn* configuration, strong interactions between this group and the two substituents of the *cis* olefin would occur. The *syn* zwitterion, which is expected to lead predominantly to a *trans* ozonide (3),[1] appears to be better stabilized by *trans* olefin, than by *cis* olefin. The *trans* olefin, however, would also be capable of stabilizing the *anti* zwitterion. It would be expected, therefore, that the increase in olefin concentration, both for the *cis* and the *trans* isomer, would favor the stabilization of *anti* zwitterions. This is, indeed, indicated by the results in Table I which show a definite increase of the ozonide *cis–trans* ratio accompanying the increase in *cis* or *trans* olefin concentration.

It is, however, not clear to what extent the stereoselective decomposition, suggested by Bailey (3), of the *cis* and *trans* primary ozonides to isomeric *syn* and *anti* zwitterions, is responsible for the stereospecificity in ozonide and cross-ozonide formation; and what contribution is due to the stabilization of the *syn* and *anti* forms by the olefin.

The observation that, in benzene solutions, the ozonide *cis–trans* ratios (Table I) are almost independent of olefin geometry and concentration can be interpreted by considering that this solvent, which is in great excess with respect to the olefin, can play a similar role in stabilizing the zwitterions (possibly by formation of π complexes) without favoring any particular zwitterion configuration.

From a consideration of the structures postulated for the zwitterion–olefin adducts, which are dependent upon the formation of a hydrogen bond as indicated in Scheme 4, it would be expected that with olefins which are not capable of forming such a hydrogen bond no such adducts should be formed. Consequently, in the case of the trisubstituted ethylenes, the cross-ozonide *cis–trans* distributions are expected to be independent of the olefin concentration inasmuch as the inductive effect of the substituents does not produce a charge δ^+ on the carbon atom bearing the H atom. This is the case with the substituents considered here. The results given in Table III confirm this prediction.

From an inspection of all the data presented, it is concluded that zwitterions are likely, in pentane solution, to form transitory adducts with 1,2-disubstituted olefins. The formation of such adducts participates in distributing the ozonide *cis–trans* ratios, as indicated by their dependence on olefin concentration. These observations, in addition to the observation that the stereochemical dependence of the ozonide *cis–trans* ratio on olefin geometry is significant at 25°, i.e. at a temperature at which a primary ozonide–aldehyde reaction is unlikely, strongly support a refined zwitterion–aldehyde mechanism for ozonolysis. Although there is no evidence to suggest that, at low temperature, the mechanism of ozonolysis is different in principle from that at room temperature, the possibility of a reaction at *very low temperature* between primary ozonide and aldehyde cannot, from the data presented, be ruled out.

TABLE III

Ozonide *cis–trans* ratios observed in pentane

Ozonide formed	Olefin used	Olefin concentration (*M*)	Temperature °C −78	25
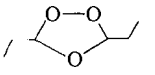		0.1	49/51	48/52
		1.0	47/53	48/52
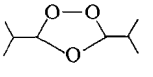		0.1	59/41	59/41
		1.0	60/40	59/41

Experimental

The ozonolyses were carried out using O_2–O_3 mixtures. The ozone output was 0.15–0.20 mmole O_3 per min and the ozonolyses were continued to 90–95% of the theoretical amount of ozone required.

The ozonide *cis–trans* ratios indicated in Tables I and III were measured by an F and M 5750 gas chromatograph, equipped with a 20 ft 10% Nitrilesilicone–Chromosorb P column, operated at temperatures not in excess of 60°. Each of the reported results were obtained from several independent experiments and have a maximum variation of ±1%. Retention times were checked with authentic samples of the ozonides and the reliability of the method used for the ozonide *cis–trans* determinations confirmed with ozonide mixtures of known proportions. In order to further verify the reliability of the gas chromatographic method used for determining the ozonide *cis–trans* ratios, n.m.r. measurements of these ratios were also performed in some cases. The ozonide *cis–trans* ratios, as determined by n.m.r. spectroscopy, were identical to those found by gas chromatographic analytical techniques. For example, the diisopropylethylene ozonide *cis–trans* ratios were determined by ozonizing a 1 *M* solution of *trans*-diisopropylethylene in pentane at −78°. After the ozonolysis was achieved with about 90% of the theoretical amount of ozone, the solvent was evaporated at room temperature and the residue dissolved in CCl_4 containing some tetramethylsilane. The n.m.r. methine proton signals of the *cis* ozonide (τ 5.23) and of the *trans* isomer (τ 5.25) were integrated and were found to correspond to a 52/48 ozonide *cis–trans* ratio, which is the value as determined by gas chromatography. Similarly, the 3-hexene ozonide *cis–trans* ratio, as obtained in the ozonolysis of a 1.0 *M* solution of *trans* 3-hexene in pentane at −78°, was determined by means of integrated n.m.r. spectra recorded on the 100 c.p.s. scale. The measurements were made on the methine proton triplets at τ 5.02 for the *cis* ozonide and at τ 5.04 for the *trans* ozonide. A 50/50 ozonide *cis–trans* ratio was observed, which is in complete agreement with the results obtained by gas chromatography.

The ozonide *cis–trans* ratios indicated in Table II were measured as follows. For each experiment, 5 mmoles of olefin, dissolved in 25 ml of CCl_4, were maintained at the appropriate temperature (±0.1 °C) until temperature equilibration was attained. In the 5–7 runs made for each olefin, the amounts of ozone used were varied between 30 and 80% of the theoretical amount. The stilbene ozonide *cis–trans* distributions were calculated from n.m.r. spectra recorded using a Varian A-60 and a Jeolco C-60 H spectrometer. On the 100 c.p.s. scale, the signals for the *cis* stilbene ozonide (τ 3.79) and the *trans* isomer (τ 3.83) can be integrated separately. Measurements made with known proportions of *cis–trans* mixtures, which were prepared from the pure isomers, confirmed the reliability of the method used. It was found that the *cis–trans* distributions did not depend on the extent of the reaction. The given proportions were calculated from 5–7 independent experiments in each case and they are expressed with a 95% confidence limit.

Acknowledgment

We wish to thank Professor P. S. Bailey for helpful discussions. The financial support given by the National Research Council of Canada is gratefully acknowledged.

1. R. Criegee and G. Wenner. Ann. **564**, 9 (1949); R. Criegee. Ann. **583**, 1 (1953); R. Criegee. Rec. Chem. Progr. Kresge-Hooker Sci. Lib. **18**, 111 (1957).
2. P. R. Story, R. W. Murray, and R. D. Youssefyeh. J. Amer. Chem. Soc. **88**, 3144 (1966); R. W. Murray, R. D. Youssefyeh, and P. R. Story. J. Amer. Chem. Soc. **89**, 2429 (1967).
3. N. L. Bauld, J. A. Thompson, C. E. Hudson, and P. S. Bailey. J. Amer. Chem. Soc. **90**, 1822 (1968).
4. S. Fliszár and J. Carles. J. Amer. Chem. Soc. **91**, 2637 (1969).
5. P. S. Bailey. Chem. Rev. **58**, 926 (1958).
6. R. Criegee and G. Schröder. Chem. Ber. **93**, 689 (1960).
7. F. L. Greenwood. J. Org. Chem. **29**, 1321 (1964).
8. P. S. Bailey, J. A. Thompson, and B. A. Shoulders. J. Amer. Chem. Soc. **88**, 4098 (1966).
9. L. J. Durham and F. L. Greenwood. Chem. Commun. 24, (1968); L. J. Durham and F. L. Greenwood. J. Org. Chem. **33**, 1629 (1968).
10. S. Fliszár, J. Carles, and J. Renard. J. Amer. Chem. Soc. **90**, 1364 (1968); J. Castonguay, M. Bertrand, J. Carles, S. Fliszár, and Y. Rousseau. Can. J. Chem. **47**, 919 (1969).
11. (*a*) R. Criegee, S. S. Bath, and B. von Bornhaupt. Chem. Ber. **93**, 2891 (1960); (*b*) G. Schröder. Chem. Ber. **95**, 733 (1962); (*c*) P. Kolsaker. Acta Chem. Scand. **19**, 223 (1965); (*d*) F. L. Greenwood and B. J. Haske. Tetrahedron Letters, 631 (1965); (*e*) O. Lorenz and C. R. Parks. J. Org. Chem.

Can. J. Chem. Downloaded from www.nrcresearchpress.com by 210.87.254.105 on 09/05/12
For personal use only.

30, 1976 (1965); (*f*) R. W. MURRAY, R. D. YOUSSEFYEH, and P. R. STORY. J. Amer. Chem. Soc. **88**, 3143 (1966); (*g*) F. L. GREENWOOD. J. Amer. Chem. Soc. **88**, 3146 (1966).
12. R. CRIEGEE. *In* Peroxide reaction mechanisms. J. O. Edwards, Ed., Interscience Publishers, Inc., New York, N.Y., 1962, p. 29.
13. M. BROOKHART, G. C. LEVY, and S. WINSTEIN. J. Amer. Chem. Soc. **89**, 1735 (1967).
14. P. R. STORY, C. E. BISHOP, J. R. BURGESS, R. W. MURRAY, and R. D. YOUSSEFYEH. J. Amer. Chem. Soc. **90**, 1907 (1968).
15. J. CARLES and S. FLISZÁR. Can. J. Chem. **47**, 1113 (1969).
16. R. W. MURRAY, R. D. YOUSSEFYEH, G. J. WILLIAMS, and P. R. STORY. Tetrahedron, **24**, 4353 (1968).
17. D. B. COOK, P. C. HOLLIS, and R. MCWEEMY. Mol. Phys. **13**, 553 (1967).
18. N. V. SIDGWICK and R. K. CALLOW. J. Chem. Soc. **125**, 538 (1924).
19. J. F. J. DIPPY and J. E. PAGE. J. Chem. Soc. 357 (1938); J. F. J. DIPPY. Chem. Rev. **25**, 151 (1939).

Can. J. Chem. Downloaded from www.nrcresearchpress.com by 210.87.254.105 on 09/05/12
For personal use only.

Synthesis of L-glucurone. Conversion of D-glucose into L-glucose

WALTER SOWA
Ontario Research Foundation, Sheridan Park, Ontario
Received May 5, 1969

L-Glucurone (**2**) was readily prepared on a small scale by treatment of D-*glycero*-D-*gulo*-heptonolactone (**1**) with a molar equivalent of periodic acid; thin-layer chromatography was used for its isolation. On a larger scale pure crystalline L-glucurone was obtained in over 80% yield from 3,5;6,7-di-*O*-isopropylidene-D-*glycero*-D-*gulo*-heptonolactone (**4**) in two steps consisting of concomitant hydrolysis and oxidation of **4** with periodic acid followed by treatment of the intermediate oxidation product with trifluoroacetic acid. L-Glucose was prepared from L-glucurone by borohydride reduction and hydrolysis of the 1,2-*O*-isopropylidene derivative. Since **1** was derived from D-glucose, the result of this series of reactions was the conversion of D-glucose into its enantiomer L-glucose.

Canadian Journal of Chemistry, 47, 3931 (1969)

Can. J. Chem. Downloaded from www.nrcresearchpress.com by 210.87.254.6 on 09/05/12
For personal use only.

The first chemical synthesis of a uronic acid was carried out in 1890 by Fischer who obtained D-glucuronic acid and its lactone by reduction of D-glucaro-1,4-lactone with sodium amalgam in acid solution (1). Niemann and Link in 1934 used the same procedure for the enantiomer L-glucuronic acid (2). The starting material, L-glucaro-1,4-lactone, was prepared via calcium L-glucarate from nitric acid oxidation of D-gulono-1,4-lactone. The yield of L-glucurone (**2**), the form in which the L-glucuronic acid was isolated, was about 1% based on calcium L-glucarate. L-Glucuronic acid is of interest because it has been reported to occur naturally, along with D-glucuronic acid, as a metabolic product of the action of rat kidney enzymes on inositol (3). Other workers, however, were unable to detect L-glucuronic acid and have found that inositol is converted into D-glucuronic and L-gulonic acids (4). This discrepancy has not been explained.

The biochemical and pharmacological importance of D-glucuronic acid (5) has led to a thorough investigation of methods for its synthesis, especially those based on oxidation of suitably protected D-glucose derivatives (6). Undoubtedly these procedures can be applied to the synthesis of L-glucuronic acid from L-glucose, but this is not attractive because L-glucose is not readily available. The present publication describes a facile synthesis of L-glucurone (**2**) from D-*glycero*-D-*gulo*-heptonolactone (**1**), a starting material easily prepared from ordinary D-glucose by the Kiliani synthesis (7). This work is an example of the application of a simple and general method for the preparation of uronic acids directly as their lactones, namely selective periodate cleavage of the exocyclic glycol system of an aldonolactone. The procedure has been used on two previous occasions. Woods and Neish treated 2-*C*-hydroxymethyl-D-glucono-1,4-lactone with an equimolar amount of periodate and obtained 4-*C*-hydroxymethyl-L-xyluronolactone, which crystallized as the acid (8). Similarly, Hulyalkar and Perry oxidized D-galactono-1,4-lactone to obtain L-lyxuronic acid, isolated as methyl L-lyxuronate (9). Essentially, oxidative removal of the primary alcohol of an aldonolactone results in inversion of the molecule with the penultimate carbon atom of the aldonolactone becoming C-1 of the uronic acid lactone.

Trial experiments followed by paper chromatography indicated that D-*glycero*-D-*gulo*-hepto nolactone (**1**) is oxidized by an equimolar quantity of periodic acid to yield approximately equal amounts of arabinose (**3**), glucurone (**2**), and unreacted starting material. The arabinose and glucurone arise from glycol cleavage of the heptonolactone at C_2—C_3 and C_6—C_7, respectively. Apparently, 2-*O*-glyoxylyl-D-arabinose, the initial product expected from oxidation at C_2—C_3, is unstable under the experimental conditions which were used. The products were identified as D-arabinose and L-glucurone by isolation as the crystalline derivatives D-arabinose diethyl dithioacetal and 2,4,5-tri-*O*-acetyl-L-glucurone diethyl dithioacetal.

Two procedures were developed for the preparation of L-glucurone. Small quantities (ca. 25 mg) were very simply obtained by treatment of D-*glycero*-D-*gulo*-heptonolactone with an equimolar amount of periodic acid followed by thin-layer chromatography (t.l.c.) of the oxidation mixture on cellulose. The L-glucurone was either crystallized directly or converted to the triacetate.

Can. J. Chem. Downloaded from www.nrcresearchpress.com by 210.87.254.6 on 09/05/12
For personal use only.

For larger scale work it was desirable to improve the yield of L-glucurone and avoid chromatographic isolation. It was therefore necessary to prevent cyclic glycol cleavage and ensure that oxidation of the exocyclic triol (C_5—C_6—C_7) was restricted to C_6—C_7. This was accomplished by using a suitably substituted starting material, the 3,5;6,7-di-*O*-isopropylidene derivative (**4**) of D-*glycero*-D-*gulo*-heptonolactone.

Isopropylidene acetals involving primary alcohol groups are often acid-labile as, for example, in the case of exocyclic acetal groups of di-*O*-isopropylidene hexofuranoses (11). A similar sensitivity to acid has been found with the C_6—C_7 isopropylidene group of **4** (12).[1] It was advantageous to effect both hydrolysis and oxidation of **4** in one step with periodic acid. The product, presumably 2,4-*O*-isopropylidene-*aldehydo*-L-glucurone (**5**), gave positive reactions with Fehling's solution and Schiff reagent. According to t.l.c. the oxidation product was a mixture of two compounds both of which gave a distinctive purple color with the *p*-anisidine hydrochloride spray reagent. The two compounds were probably **5** in the form of lactone and acid. Treatment of the syrupy mixture with 90% trifluoroacetic acid for hydrolysis of the isopropylidene group (13) afforded crude crystalline L-glucurone in almost theoretical yield based on **4**. The yield of pure recrystallized L-glucurone was over 80%.

L-Glucose was prepared from L-glucurone by procedures previously developed for the enantiomeric compound. This involved temporary blocking of the reducing group as the 1,2-*O*-isopropylidene acetal (14), followed by reduction of the lactone with sodium borohydride in the presence of boric acid (15). The crude 1,2-*O*-isopropylidene-L-glucose which was obtained was hydrolyzed with trifluoroacetic acid to L-glucose. Since D-glucose was the precursor of D-*glycero*-D-*gulo*-heptonolactone from which the L-glucurone was derived, this overall sequence of reactions constitutes the conversion of D-glucose into L-glucose.

[1]In two publications Brimacombe and co-workers discuss the acetonation of **1** to yield **4** and refer to an analogous case (25) stating "acid-catalyzed acetonation of D-glucurono-δ-lactone diethyl dithioacetal yields a 2,4-*O*-isopropylidene derivative, presumably with contraction in size of the lactone ring" (10), and "D-glucurono-6,2-lactone diethyl dithioacetal, which yields a 2,4-*O*-isopropylidene derivative, presumably with contraction in size of the lactone ring" (12). The assumption of ring contraction is erroneous and has apparently arisen from a typographical error in Gorin's paper in which compounds referred to as δ-lactones were actually γ-lactones. This is indicated by infrared (i.r.) data for the isopropylidene derivative of D-glucurone diethyl dithioacetal (absorption at 1780 cm^{-1}). Moreover the starting material "D-glucurono-δ-lactone diethyl dithioacetal prepared by the method of Zinner and Dassler" was in fact the γ-lactone (26).

Experimental

Melting points were determined on a Fisher–Johns melting point apparatus and are uncorrected. Paper chromatography was carried out by the descending method on Whatman No. 4 paper using ethyl acetate–pyridine–water (10:4:3 v/v) as developing solvent. Thin-layer chromatography was performed on silica gel G with development in ethyl acetate. Spray reagents for detection of compounds were *p*-anisidine hydrochloride (16) and alkaline silver nitrate (17); for t.l.c. 50% sulfuric acid was also used. Chromatograms sprayed with *p*-anisidine hydrochloride or sulfuric acid were heated at 120° for visualization. Solutions were concentrated under reduced pressure using a rotary evaporator and a water bath at a temperature of 50° or less.

L-*Glucurone (2) from Unsubstituted* D-*Glycero*-D-*gulo*-*heptonolactone (1)*

(a) Characterization of Products

In small scale (mmole) experiments followed by paper chromatography, solutions of **1** (7) were treated with an equimolar amount of periodic acid at 5° and at room temperature, and for periods ranging from a few min to 1 h. Under all conditions there appeared to be roughly equal amounts of arabinose (**3**), glucurone (**2**), and unreacted **1**. The products were characterized from an oxidation carried out on a larger scale.

Solutions of periodic acid (4.56 g) and **1** (4.16 g), each in 100 ml of water, were mixed and left for 1 h at room temperature. Barium acetate (2.8 g) in water (25 ml) was added to the mixture, the precipitate was removed by filtration and the filtrate was evaporated. The residue was treated with hydrochloric acid (5 ml) and ethanethiol (5 ml) for 1 h at 10°. Ice and water (15 ml) were added to the reaction and the mixture was extracted with ethyl acetate (5 × 50 ml). The aqueous layer was evaporated to dryness and the residue was crystallized from methanol–water to recover unoxidized heptonolactone (1.5 g, 36%), m.p. 152–154°. The combined ethyl acetate extracts were washed with saturated sodium bicarbonate solution (30 ml) and water (2 × 30 ml) and dried over anhydrous sodium sulfate. The solution was concentrated to about 30 ml and cooled to yield D-arabinose diethyl dithioacetal (0.9 g), m.p. 126–127° and $[\alpha]_D^{23}$ −11.2° (*c*, 3.67 in methanol). The reported values are m.p. 126° and $[\alpha]_D^{24}$ −11.0° (*c*, 3.69 in methanol) (18).

Anal. Calcd. for $C_9H_{20}O_4S_2$: C, 42.16; H, 7.89; S, 25.01. Found: C, 42.54; H, 7.60; S, 25.11.

The mother liquor from the D-arabinose diethyl dithioacetal was evaporated to a syrup which was dried over phosphorus pentoxide in a vacuum desiccator. The residue (2.3 g) was acetylated with acetic anhydride (10 ml) and pyridine (8 ml) for 5 h at 4°. The mixture was poured into ice and water containing sodium bicarbonate and extracted with ether. The combined ether

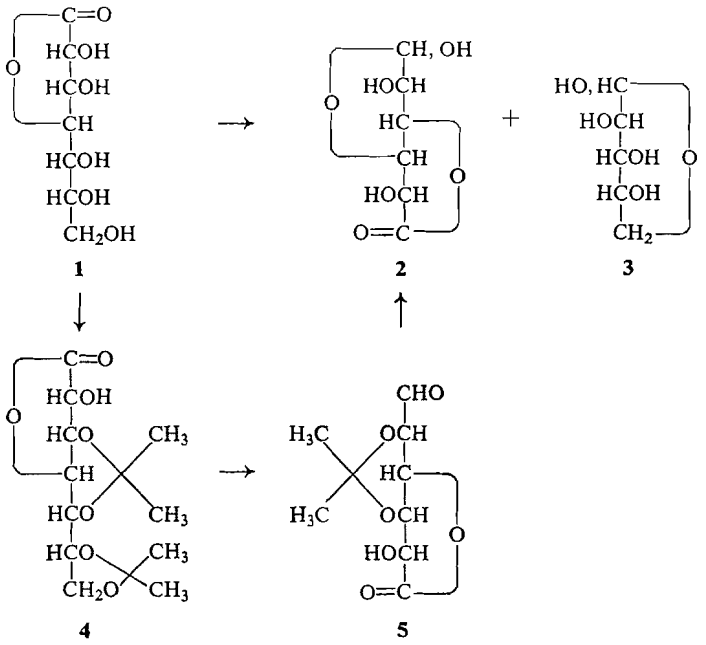

extracts were washed successively with cold dilute sulfuric acid, water, saturated sodium bicarbonate solution and water and then dried over anhydrous sodium sulfate. The ether solution was evaporated to a residue which was redissolved in ether–petroleum ether to crystallize 2,4,5-tri-*O*-acetyl-L-glucurone diethyl dithioacetal (1.0 g from 4 crops); m.p. 113–114° and $[\alpha]_D^{23}$ −53.3° (*c*, 4.30 in chloroform). Literature values for 2,4,5-tri-*O*-acetyl-D-glucurone diethyl dithioacetal are m.p. 113–114° and $[\alpha]_D^{25}$ +58° (*c*, 4.1 in chloroform) (19); and m.p. 110–112° and $[\alpha]_D^{16}$ +53.9° (*c*, 1.61 in methanol) (20).

Anal. Calcd. for $C_{16}H_{24}O_8S_2$: C, 47.04; H, 5.93; S, 15.69. Found: C, 46.83; H, 5.81; S, 15.59.

(b) L-Glucurone

L-Glucurone was conveniently prepared in small amounts directly from **1** by using t.l.c. for its isolation. A solution of periodic acid (H_5IO_6, 228 mg) in water (5 ml) was added to a solution of D-*glycero*-D-*gulo*-heptonolactone (208 mg) in water (5 ml). The reaction mixture was left for 15 min at room temperature and barium acetate (137 mg) was added. The precipitate was removed by filtration and the filtrate was evaporated to a syrup (*ca.* 210–220 mg). Preparative t.l.c. of the mixture on microcrystalline cellulose (21) (0.5 mm layers on 2 plates 20 × 20 cm) using double development in acetone–water (19:1 v/v) gave syrupy L-glucurone. Yields ranged from 40 to 52 mg. For crystallization the syrupy product (42 mg) was first dissolved in hot acetic acid. The solution was then evaporated and the residue was crystallized from methanol–ether to obtain L-glucurone (28 mg, 16% yield from **1**) with m.p. 174–176° and $[\alpha]_D^{23}$ −19° (*c*, 2.07 in water). The reported values for L-glucurone are m.p. 169–172° and $[\alpha]_D^{25}$ −18.5° (*c*, 0.6 in water) (2); for D-glucurone m.p. 180° and $[\alpha]_D^{23}$ +18.55° (*c*, 1.914 in water) (22).

Anal. Calcd. for $C_6H_8O_6$: C, 40.91; H, 4.59. Found: C, 41.22; H, 4.59.

Syrupy L-glucurone (52 mg) isolated by t.l.c. was acetylated by treatment for 1 h with acetic anhydride (0.5 ml) containing boron trifluoride etherate (0.05 ml). The mixture was poured into ice and water and the resulting precipitate was recrystallized from methanol to obtain 1,2,5-tri-*O*-acetyl-β-L-glucurone (53 mg) having m.p. 195–196° and $[\alpha]_D^{21}$ −85.4° (*c*, 2.58 in chloroform). Literature values for 1,2,5-tri-*O*-acetyl-β-D-glucurone are m.p. 193–194° and $[\alpha]_D^{20}$ +89.6° (*c*, 2.21 in chloroform) (23).

Anal. Calcd. for $C_{12}H_{14}O_9$: C, 47.68; H, 4.68. Found: C, 47.69; H, 4.66.

L-Glucurone (2) from 3,5;6,7-di-O-isopropylidene-D-glycero-D-gulo-heptonolactone (4)

A solution of periodic acid (H_5IO_6, 2.28 g) in water (25 ml) was added to **4** (10) (2.88 g) in an equal volume of water and the mixture was shaken for 1 h at room temperature. Barium carbonate (1.5 g) was added and shaking was continued for 15 min. The neutralized mixture was filtered and the filtrate was evaporated to dryness. The residue was extracted with acetone and the extract was concentrated to obtain a hygroscopic syrup (2.10 g) having $[\alpha]_D^{22}$ −83° (*c*, 1.9 in acetone). This product, which gave positive reactions with Fehling's solution and Schiff reagent, was a mixture of two compounds according to t.l.c. Both produced a distinctive purple color with the *p*-anisidine hydrochloride spray reagent. The major compound was mobile with a tendency to streak, while the minor compound remained on the starting line. The mixture (1.00 g) was hydrolyzed with 90% trifluoroacetic acid (13) (10 ml) for 10 min at room temperature. Evaporation of the hydrolyzate gave crude crystalline L-glucurone, m.p. 165–167°, (0.81 g,

Can. J. Chem. Downloaded from www.nrcresearchpress.com by 210.87.254.6 on 09/05/12
For personal use only.

yield 97% from **4**). On recrystallization from acetic acid (10 ml) the product (0.69 g, yield 83% from **4**) had m.p. 180–181° and $[\alpha]_D^{22}$ −18° (*c*, 2.0 in water).

Anal. Calcd. for $C_6H_8O_6$: C, 40.91; H, 4.59. Found: C, 41.06; H, 4.52.

L-Glucose

1,2-*O*-Isopropylidene-L-glucurone, m.p. 122–123° and $[\alpha]_D^{22}$ −68° (*c*, 1.2 in water), was prepared from L-glucurone and acetone using sulfuric acid catalyst according to procedures described for the D-glucurone derivative (14) except that the calculated quantity of ammonium hydroxide instead of barium carbonate or sodium carbonate was used for neutralization of the sulfuric acid. The corresponding constants recorded for 1,2-*O*-isopropylidene-D-glucurone are m.p. 120° and $[\alpha]_D^{18}$ +70° (*c*, 1.0 in water) (14).

Anal. Calcd. for $C_9H_{12}O_6$: C, 49.99; H, 5.60. Found: C, 50.03; H, 5.56.

1,2-*O*-Isopropylidene-L-glucurone was reduced in boric acid solution with sodium borohydride (15). A stirred solution of the sugar (0.54 g) in 0.4 *M* boric acid (15 ml) was cooled in an ice-bath and treated with 0.3 *M* sodium borohydride (25 ml) added over 30 min. The reaction was stored at 4° for 22 h with a further addition of 0.3 *M* sodium borohydride (15 ml) after 4 h. The solution was neutralized with dilute acetic acid, passed through Rexyn 101 (H^+) (Fisher Scientific Co., Ltd.) and evaporated to dryness. Some of the borate was removed from the residue by adding methanol and evaporating to dryness several times. The mixture was then hydrolyzed with 90% trifluoroacetic acid (6 ml) for 15 min at room temperature. The hydrolyzate, after concentration to dryness, was repeatedly treated with methanol until the remaining borate was removed. The syrupy product was crystallized from ethanol–water to obtain 2 crops of L-glucose (390 mg) having m.p. and mixed m.p. 146–147° and $[\alpha]_D^{24}$ −53° (*c*, 3 0 in water). Reported values for α-L-glucose are m.p. 146–147° and $[\alpha]_D^{22}$ −53° (at equilibrium; *c*, 2.6 in water) (24).

Acknowledgments

The author is grateful to Mrs. Brigitte Licht for technical assistance. This work was made possible by funds received from the Province of Ontario through the Department of Trade and Development.

1. E. Fischer. Ber. **23**, 930 (1890); E. Fischer and O. Piloty. Ber. **24**, 521 (1891).
2. C. Niemann and K. P. Link. J. Biol. Chem. **106**, 773 (1934).
3. F. C. Charalampous and C. Lyras. J. Biol. Chem. **228**, 1 (1957).
4. J. J. Burns, N. Trousof, C. Evans, N. Papadopoulos, and B. W. Agranoff. Biochim. Biophys. Acta, **33**, 215 (1959).
5. Geoffrey J. Dutton (*Editor*). Glucuronic Acid, Free and Combined. Academic Press, Inc., New York. 1966.
6. L. Hough, A. C. Richardson, and C. H. Bolton. *In* Rodd's chemistry of carbon compounds. Volume I. Part F. *Edited by* S. Coffey. Elsevier Publ. Co., Inc., Amsterdam. 1967. p. 282–284; C. L. Mehltretter. Advan. in Carbohyd. Chem. **8**, 231 (1953).
7. H. Kiliani. Ber. **19**, 767 (1886); N. K. Richtmyer. *In* Methods in carbohydrate chemistry. Vol. I. Academic Press, Inc., New York. 1962. p. 160.
8. R. J. Woods and A. C. Neish. Can. J. Chem. **32**, 404 (1954).
9. R. K. Hulyalkar and M. B. Perry. Can. J. Chem. **43**, 3241 (1965).
10. J. S. Brimacombe and L. C. N. Tucker. Carbohyd. Res. **2**, 341 (1966).
11. A. N. de Belder. Advan. Carbohyd. Chem. **20**, 219 (1965).
12. J. S. Brimacombe, A. B. Foster, and L. C. N. Tucker. Carbohyd. Res. **3**, 76 (1966).
13. J. E. Christensen and L. Goodman. Carbohyd. Res. **7**, 510 (1968).
14. L. N. Owen, S. Peat, and W. J. G. Jones. J. Chem. Soc. 339 (1941); M. Fieser, L. F. Fieser, E. Toromanoff, Y. Hirata, H. Heymann, M. Tefft, and S. Bhattacharya. J. Amer. Chem. Soc. **78**, 2825 (1956).
15. B. A. Lewis, F. Smith, and A. M. Stephen. *In* Methods in carbohydrate chemistry. Vol. II. Academic Press, Inc., New York. 1963. p. 68.
16. L. Hough, J. K. N. Jones, and W. H. Wadman. J. Chem. Soc. 1702 (1950).
17. W. E. Trevelyan, D. P. Procter, and J. S. Harrison. Nature, **166**, 444 (1950).
18. H. Zinner, H. Brandner, and G. Rembarz. Ber. **89**, 800 (1956).
19. M. L. Wolfrom and K. Onodera. J. Amer. Chem. Soc. **79**, 4737 (1957).
20. H. Zinner, C. Dassler, and G. Rembarz. Ber. **91**, 427 (1958).
21. M. L. Wolfrom, D. L. Patin, and R. M. Lederkremer. J. Chromatogr. **17**, 488 (1965).
22. W. F. Goebel and F. H. Babers. J. Biol. Chem. **100**, 573 (1933).
23. K. Tsou and A. M. Seligman. J. Amer. Chem. Soc. **74**, 5605 (1952).
24. J. C. Sowden. *In* Methods in carbohydrate chemistry. Vol. I. Academic Press, Inc., New York. 1962. p. 132.
25. P. A. J. Gorin. Can. J. Chem. **43**, 2078 (1965).
26. H. Zinner and C. Dassler. Ber. **93**, 1597 (1960).

Can. J. Chem. Downloaded from www.nrcresearchpress.com by 210.87.254.6 on 09/05/12
For personal use only.

Can. J. Chem. Downloaded from www.nrcresearchpress.com by 210.87.254.6 on 09/05/12
For personal use only.

Substitutions électrophiles en série naphtalènique. VI. Sur le diméthoxy-2,6 naphtalène[1]

JEAN-CLAUDE RICHER ET ARMAND ROSSI
Département de Chimie, Université de Montréal, B.P. 6128, Montréal, Québec

Reçu le 29 novembre 1968

Les réactions de chloration, bromation, iodation, et nitration du diméthoxy-2,6 naphtalène et de ses dérivés ont été étudiées. La nature des produits obtenus a été établie grâce à la résonance magnétique nucléaire. Les effets isotopiques qui affectent les réactions de chloration, bromation, iodation, et nitration du diméthoxy-2,6 naphthalène ont aussi été évalués.

Canadian Journal of Chemistry, 47, 3935 (1969)

Introduction

Il a été établi au cours de travaux précédents (1,2) sur les réactions de substitutions électrophiles des naphtalènes (**1***a* et **1***b*) disubstitués en position 2 et 6 que le groupe *tert*-butyle provoque un encombrement stérique tel qu'il modifie considérablement le cours de la réaction. Il s'avérait intéressant d'examiner les facteurs mésomériques sur cette réaction, et pour fins de comparaison, le groupe méthoxy qui est reconnu pour fournir des électrons par résonance a été choisi. Les résultats obtenus au cours de ces études font l'objet de la présente communication.

Resultats

La chloration par SO_2Cl_2, la bromation par le brome dans le chloroforme, l'iodation par ICl, et la nitration par l'acide nitrique du diméthoxy-2,6 naphtalène (**1***c*) conduisent aux dérivés monosubstitués en position 1 (**2***a–d*) et disubstitués en positions 1 et 5 (**3***a–d*). La chloration par SO_2Cl_2 et la bromation par le brome dans l'acide acétique du diméthoxy-2,6 iodo-1 naphtalène (**2***c*) conduit aux dérivés halogénés mixtes correspondants (**3***e* et *f*). La chloration, la bromation, et l'iodation (HIO_3; I_2) du diméthoxy-2,6 nitro-1 naphtalène (**2***d*) fournissent les dérivés nitrohalogénés en positions 1 et 5 (**3***g*, *h*, et *i*). La nitration du dinitro-1,5 diméthoxy-2,6 naphtalène (**3***d*) ou des dérivés nitrohalogénés **3***g* et *h* conduit aux dérivés correspondants **4***a*, *b*, et *c* possédant un groupe nitro supplémentaire; par ailleurs la nitration du diméthoxy-2,6 iodo-1 nitro-5 naphtalène (**3***i*) conduit à une substitution de l'iode par le groupe nitro menant au dinitro-1,5 diméthoxy-2,6 naphtalène (**3***d*). La nitration des dichloro-1,5 (**3***a*) et dibromo-1,5 (**3***b*) diméthoxy-2,6 naphtalène conduit aux dérivés nitrés correspondants **4***d* et *e* alors que la nitration du diiodo-1,5 diméthoxy-2,6 naphtalène (**3***c*) conduit à une substitution des deux iodes par deux groupes nitro et fournit ainsi le dérivé **3***d*.

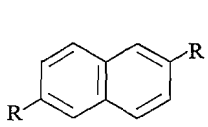

1

(*a*) R = Me
(*b*) R = *tert*-Bu
(*c*) R = OMe

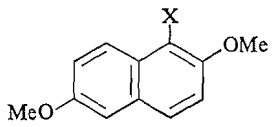

2

(*a*) X = Cl
(*b*) X = Br
(*c*) X = I
(*d*) X = NO_2
(*e*) X = D

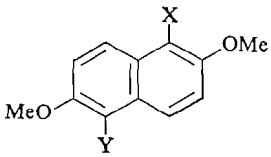

3

(*a*) X = Y = Cl
(*b*) X = Y = Br
(*c*) X = Y = I
(*d*) X = Y = NO_2
(*e*) X = I; Y = Cl
(*f*) X = I; Y = Br
(*g*) X = NO_2; Y = Cl
(*h*) X = NO_2; Y = Br
(*i*) X = NO_2; Y = I

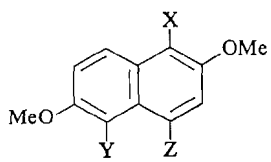

4

(*a*) X = Y = Z = NO_2
(*b*) X = Cl; Y = Z = NO_2
(*c*) X = Br; Y = Z = NO_2
(*d*) X = Y = Cl; Z = NO_2
(*e*) X = Y = Br; Z = NO_2

La nitration des dichloro-1,5 (**4***d*) et dibromo-1,5 (**4***e*) diméthoxy-2,6 nitro-4 naphtalènes mène d'une part à une substitution de l'un des halogènes par le groupe nitro et fournit ainsi les chloro-1

[1]Les résultats rapportés dans cette communication sont extraits en partie du mémoire soumis par M. Armand Rossi à la Faculté des Sciences de l'Université de Montréal, Montréal, P.Q., en vue de l'obtention du grade de Maitre ès Sciences, Août, 1968.

(**4***b*) et bromo-1 (**4***c*) diméthoxy-2,6 dinitro-4,5 naphtalènes et d'autre part aux chloro-5 (**6***b*) et bromo-5 (**6***a*) méthoxy-6 nitro-8 naphtoquinones-1,2 caractérisées sous forme des quinoxalines **7** correspondantes; cette quinone se formerait par l'intermédiaire des produits d'addition **5** dont l'un (**5***a*) a pu être caractérisé. La nitration des quinones **6** dans des conditions plus poussées conduit à des mélanges de dinitro-3,8 et dinitro-4,8 méthoxy-6 halogéno-5 naphtoquinone-1,2 (**8** et **9**)

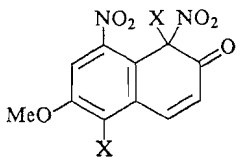

5

(*a*) X = Br
(*b*) X = Cl

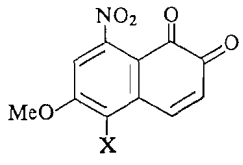

6

(*a*) X = Br
(*b*) X = Cl

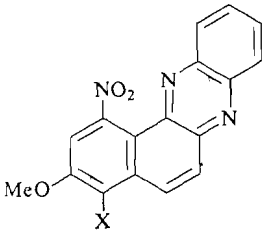

7

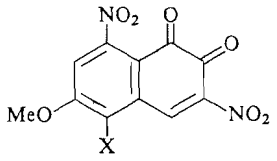

8

(*a*) X = Br
(*b*) X = Cl

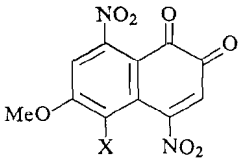

9

Utilisant du diméthoxy-2,6 naphtalène-*d*, (**2***e*) préparé par hydrolyse de l'organomagnésien du diméthoxy-2,6 iodo-1 naphtalène avec un mélange D_2O/DCl, les effets isotopiques des réactions de chloration par SO_2Cl_2, de bromation par le brome dans le chloroforme, de l'iodation par ICl, et de nitration très ménagées ont été évalués. Les résultats obtenus au cours de ces études sont consignées dans le tableau I qui montre que les effets isotopiques moyens varient de 1.07 pour la chloration à 6.2 pour la réaction d'iodation.

Discussion

D'une manière générale, la structure des produits obtenus a été établie en se basant sur les spectres infra-rouges (i.r.) (3), les spectres de masse, et les couplages des bandes dues aux protons aromatiques dans les spectres de résonance magnétiques nucléaire (r.m.n.). Les positions des bandes dûes à des protons sont résumées dans les tableaux II et III. Dans le cas des dérivés nitrés la méthode empirique proposée par Wells et Alcorn (4), et appliquée dans les cas précédents (1,2,5, et 6), a aussi été utilisée. Les positions des bandes déduites par l'application de cette méthode sont mises en regard des valeurs observées dans le tableau II.

L'utilisation d'une méthode semblable à celle utilisée pour les dérivés nitrés a permis d'élucider sans ambiguité la structure des dérivés halogénés dans la série du diméthoxy-2,6 naphtalène (**1***c*). Une observation a été faite concernant la possibilité de prévoir les positions de résonance de différents protons aromatiques des dérivés dihalogénés et nitrohalogénés obtenus. Cette méthode consiste à ajouter aux déplacements chimiques des protons de la molécule monosubstituée des incréments déterminés expérimentalement à partir des spectres de r.m.n. des dérivés halogénés en position 1 (**1***a*, *b*, et *c*) du diméthoxy-2,6 naphtalène. Le tableau III montre les déplacements chimiques dus à un halogène

TABLEAU I

Effets isotopiques de quelques réactions de substitutions électrophiles du diméthoxy-2,6 naphtalène

Réaction	*A**	*A*'†	k_H/k_D	*A**	*A*'†	k_H/k_D	k_H/k_D moyen
Chloration	84.3	43.0	1.04	89.1	46.3	1.09	1.07
Bromation	84.3	45.4	1.20	89.1	48.9	1.25	1.23
Iodation	84.3	64.3	5.4	89.1	72.0	6.9	6.2
Nitration	84.3	45.3	1.19	89.1	48.7	1.24	1.22

*Pourcentage de deutérium dans le naphtalène de départ (1*c*).
†Pourcentage de deutérium dans les naphtalènes substitués (2).

Can. J. Chem. Downloaded from www.nrcresearchpress.com by 210.87.254.6 on 09/05/12
For personal use only.

Can. J. Chem. Downloaded from www.nrcresearchpress.com by 210.87.254.6 on 09/05/12
For personal use only.

TABLEAU II

Spectres de résonance magnétique nucléaire de diméthoxy-2,6 nitronaphtalènes*

Dérivé	Calculé† Trouvé	H_3	H_4	H_7	H_8
dinitro-1,5 (**3***d*)		7.95	7.96	7.95	7.96
		7.95	7.81	7.95	7.81
chloro-1 nitro-5 (**3***g*)		7.77	7.65	7.85	8.47
		7.85	7.60	7.92	8.40
bromo-1 nitro-5 (**3***h*)		7.75	7.70	7.85	8.47
		7.57	7.70	7.80	8.34
iodo-1 nitro-5 (**3***i*)		7.68	7.71	7.85	8.43
		7.70	7.70	7.84	8.42
chloro-1 dinitro-4,5 (**4***b*)		8.51	—	8.13	8.66
		8.42	—	8.10	8.63
bromo-1 dinitro-4,5 (**4***c*)		8.49	—	8.13	8.69
		8.33	—	8.06	8.66
dichloro-1,5 nitro-4 (**4***d*)		8.44	—	7.98	8.40
		8.22	—	7.88	8.32
dibromo-1,5 nitro-4 (**4***e*)		8.39	—	7.93	8.47
		8.06	—	7.79	8.42

*Les spectres ont été déterminés à la température ambiante dans la diméthylacétamide utilisant le TMS comme référence interne.

†Les valeurs calculées ont été évaluées d'après la méthode de Wells et Alcorn (4) utilisant les valeurs suivantes comme déplacements provoqués par un groupe nitro en position 1 adjacent à un substituant en position 2:2, +0.74; 3, +0.57; 4, +0.42; 5, +0.25; 6, +0.28; 7, +0.26; et 8, −0.22. Ces valeurs tiendraient compte du fait que le groupe NO_2 n'est pas dans le plan de la molécule de naphtalène.

TABLEAU III

Déplacements chimiques dus à un halogène en position 1 dans les diméthoxy-2,6 naphtalène

Produits	H_3	H_4	H_5	H_7	H_8
1*c*	7.12	7.76	7.30	7.12	7.76
2*a*	7.51	7.87	7.40	7.28	8.05
$\Delta\delta_{Cl}$	+0.39	+0.11	+0.10	+0.16	+0.29
2*b*	7.49	7.92	7.40	7.28	8.05
$\Delta\delta_{Br}$	+0.37	+0.16	+0.10	+0.16	+0.29
2*c*	7.42	7.93	7.39	7.28	8.01
$\Delta\delta_{I}$	+0.30	+0.17	+0.09	+0.16	+0.25

entrant en position 1 dans le diméthoxy-2,6 naphtalène. L'application des incréments ainsi déterminés à des dérivés de structure non prouvée a été faite; les prédictions ainsi que les valeurs expérimentales observées pour quelques dérivés du diméthoxy-2,6 naphtalène sont résumées dans le tableau IV. La concordance entre les valeurs calculées et les valeurs expérimentales est assez bonne dans tous les cas considérés. Cette méthode ne peut toutefois pas être généralisée aux dérivés halogénés des diméthoxy-2,7 et diméthoxy-1,7 naphtalènes; elle permet cependant d'assigner sans ambiguité aux bandes de résonance des spectres des chloro-1 (**3***e*) et bromo-1 (**3***f*) diméthoxy-2,6 iodo-1 naphtalène et des dérivés nitrohalogénés en positions 1 et 5 (**3***g*, *h*, et *i*) les protons correspondants.

La structure des quinones préparées peut être attribuée elle aussi en se basant sur le couplage des bandes des protons. Les spectres de r.m.n. des naphtoquinones-1,2 (**6***a*, *b*) correspondent à la superposition d'un singulet (H_7) sur les éléments d'un système AB (H_3 et H_4). Il est possible d'attribuer à la paire de doublet (J = 11 c.p.s.) les protons correspondants, H_3 pour le doublet se trouvant vers les champs les plus hauts, et H_4 pour le doublet se trouvant vers les champs les plus bas; l'étude des spectres de r.m.n. des dérivés donnés dans le tableau V confirme cette hypothèse. Il s'avère plus difficile d'attribuer avec certitude les structures aux nitronaphtoquinones **8** et **9**; cependant Fieser et Ames (9) ayant démontré que la nitration d'une naphtoquinone-1,2 conduit principalement au dérivé nitré en position 3, il est possible de suggérer d'après l'intégration des groupes méthoxy ou des protons en position 3 et 4 que la nitronaphtoquinone **8***b* représente 64% du produit de nitration de la quinone **6***b*.

Les résultats obtenus au cours du présent travail montrent l'influence nette des effets mésomériques des groupes méthoxy en position 2 et 6 qui orientent essentiellement toutes les réactions

TABLEAU IV

Spectres de résonance magnétique nucléaire de dérivés diméthoxy-2,6 naphtalènes halogenés

Produits	Calculé Trouvé	H_3	H_4	H_7	H_8
3*a*		7.67	8.16	7.67	8.16
		7.70	8.15	7.70	8.15
3*b*		7.65	8.21	7.65	8.21
		7.65	8.22	7.65	8.22
3*e*		7.67	8.12	7.58	8.22
		7.62	8.11	7.53	8.22
3*g*		7.75	7.65	7.85	8.44
		7.85	7.60	7.92	8.40
3*h*		7.73	7.70	7.85	8.44
		7.57	7.70	7.80	8.34
3*i*		7.66	7.71	7.85	8.40
		7.70	7.70	7.84	8.42

Can. J. Chem. Downloaded from www.nrcresearchpress.com by 210.87.254.6 on 09/05/12
For personal use only.

TABLEAU V

Déplacements chimiques de protons éthylèniques présentant une analogie avec les quinones (*6a* et *b*) préparées

Produits	H_a	H_b
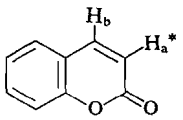	6.42	7.72
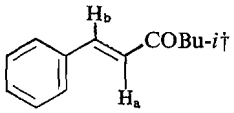	6.62	7.45
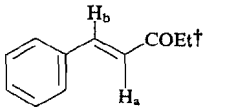	6.69	7.54
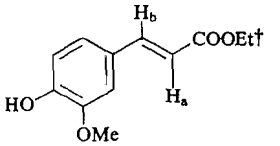	6.12	7.49

*Voir référence 7.
†Voir référence 8.

vers les positions α adjacentes à savoir les positions 1 et 5. Cette influence se manifeste de plus par la facilité avec laquelle des substituants déjà fixés à ces positions sont déplacés au cours de réactions de substitution subséquentes; la formation des quinones **6** par l'intermédiaire des produits d'additions **5** correspondants pourrait aussi être attribuée essentiellement à l'orientation d'une substitution vers une position adjacente à un groupe méthoxy. L'ensemble de ces résultats montre que, contrairement aux résultats obtenus lors des réactions de substitution sur le diméthyl-2,6 (**1***a*) et sur le di-*tert*-butyl-2,6 (**1***b*) naphtalènes, les facteurs influençant l'orientation des réactions de substitution, qui sont dans le cas présent des facteurs de nature électroniques, conduisent toujours à une orientation similaire des réactions de substitutions.

La formation des naphtoquinones-1,2 (**6**) doit être rapprochée du résultat rapporté par Bell (10) lors de la nitration du chloro-1 diméthoxy-2,7 nitro-8 naphtalène qui conduirait à une dinitro-3,8 méthoxy-7 naphtoquinone-1,2. Les conditions expérimentales utilisées étant plus douces que celles utilisées par Bell (température ambiante et acide nitrique densité 1.42) les différentes séquences de la nitration ont pu, dans notre étude, être mises en évidence.

Les réactions de chloration, de bromation, d'iodation, et de nitration de dérivés aromatiques procèdent vraisemblablement par stades multiples; les effets isotopiques mesurés pour ces réactions sont généralement faibles (11,12) ou quelque fois même inversés (11–14). Des effets isotopiques plus grands que l'unité ont toutefois été observés lors de substitutions au cours desquelles des effets stériques pouvaient intervenir (15–20). Les effets isotopiques déterminés pour les réactions de chloration, de bromation, et de nitration du diméthoxy-2,6 naphtalène, sont faibles. Bien que tous ces effets soient plus grands que l'unité, il est difficile considérant les conditions diverses sous lesquelles ces réactions ont été conduites, d'en tirer des conclusions concernant l'étape déterminante de la réaction. La réaction d'iodation de **1***c* qui peut-être rapprochée des résultats obtenus avec l'anisole (20) permet toutefois de préciser que l'étape déterminante de cette réaction est l'enlèvement de l'hydrogène. Ce résultat confirmerait l'importance des effets stériques sur la nature de l'étape déterminante dans les réactions de substitutions électrophiles en série aromatique. Il permettrait aussi d'envisager (voir schéma 1) que la nature des produits formés lors des réactions de substitutions électrophiles sur le di-*tert*-butyl-2,6 naphtalène **1***b* (2) est déterminée par la diminution de la vitesse (k_2) d'élimination de l'hydrogène en position 1 par rapport à la vitesse (k_2') d'élimination de l'hydro-

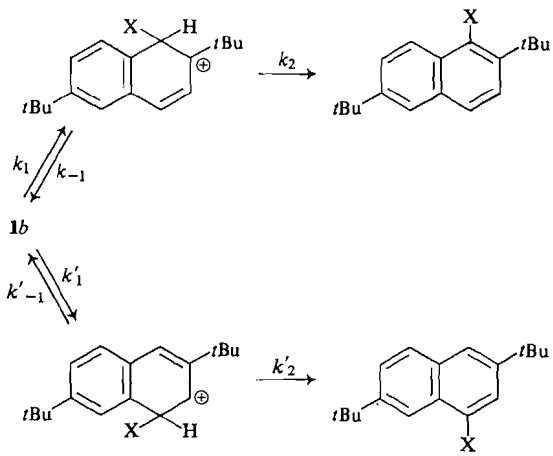

SCHÉMA 1

gène en position 4 au fur et à mesure de l'accroissement de la taille de 10. Un raisonnement semblable pourrait être développé pour expliquer les résultats obtenus lors des substitutions sur le di-*tert*-butyl-2,7 naphtalène (21).

Partie expérimentale

Les techniques expérimentales générales ont été décrites dans une publication précédente (21). Les spectres de masse sous forme de graphiques et la description des spectres ultra-violets (u.v.) et (i.r.) des produits décrits dans cette publication sont rapportés en détail dans le mémoire de Maitrise de M. Armand Rossi dont une copie a été déposée à la bibliothèque du Conseil National de Recherches.

Les caractéristiques des produits obtenus au cours du présent travail sont résumées dans le tableau VI. Les techniques de chloration, bromation, iodation, et nitration sont essentiellement celles qui ont déjà été rapportées.

Préparation de naphtoquinones-1,2 substituées

Bromo-5 méthoxy-6 nitro-8 naphtoquinone-1,2 (6a)

A 3 g (8.7 mmoles) de dibromo-1,5 diméthoxy-2,7 naphtalène (3*b*) dans 30 ml d'acide acétique, 5 ml d'acide nitrique (d = 1.42) sont ajoutés et le mélange agité à la température ambiante durant 1.5 h. Le produit solide (1.21 g) obtenu par filtration et chromatographié sur une colonne de gel de silice conduit à : 1.01 g (30% du rendement théorique) du dibromo-1,5 diméthoxy-2,6 nitro-4 naphtalène (4*e*), p.f. 228–230 °C (benzène/éthanol) et 50 mg (0.5% du rendement théorique) du bromo-1 diméthoxy-2,6 dinitro-4,5 naphtalène (4*c*) p.f. 268–269°. La dilution du filtrat avec 5 fois son volume d'eau conduit à un précipité qui est recueilli, lavé rapidement avec une faible quantité de méthanol puis d'éther de pétrole; on obtient ainsi 657 mg (18% du rendement théorique) de dibromo-1,5 dihydro-1,2 méthoxy-6 dinitro-1,8 oxo-2 naphtalène (5*a*) de p.f. 210° (décomposition).

Par dissolution dans 20 ml de tétrachlorure de carbone bouillant ce composé perd NOBr; après refroidissement de la solution et filtration, 407 mg d'un produit sont obtenus et chromatographiés sur 40 g de gel de silice utilisant comme éluant du benzène mélangé au chloroforme. On obtient ainsi 380 mg de bromo-5 méthoxy-6 nitro-8 naphtoquinone-1,2 (6*a*) de p.f. 235–236° (avec décomposition). Cette quinone est caractérisée sous forme de quinoxaline (7*a*).

Ce dérivé est obtenu en ajoutant une solution contenant 60 mg d'*o*-phénylènediamine dans 2 ml d'acide acétique à 45 mg de naphtoquinone (6*a*) dissoute dans 10 ml d'acide acétique glaciale, et en chauffant le mélange à reflux pendant 30 min. Ce dérivé fond à 293–294° et donne une coloration bleue foncé avec l'acide sulfurique concentré. Son spectre de masse montre un pic à *m/e* 383.

Bromo-5 méthoxy-6 dinitro-3,8 naphtoquinone-1,2 (8a)

A 190 mg de naphtoquinone 6*a* dissoute dans 4 ml d'acide acétique glaciale, 5 ml d'acide nitrique (d = 1.42) sont ajoutés et le mélange est chauffé à reflux pendant 40 min. Le solide obtenu par refroidissement est filtré et conduit à 161 mg d'un produit montrant un pic à 356 unités dans le spectre de masse et dont l'étude du spectre r.m.n. laisse supposer qu'il s'agit d'un mélange de composants qui serait les bromo-5 méthoxy-6 dinitro-3,8 (8*a*, 64%) et bromo-5 méthoxy-6 dinitro-4,8 (9*a*, 36%) naphtoquinone-1,2.

TABLEAU VI

Caractéristiques des produits obtenus

Produit	Point de fusion °C	T_R (min)† A	T_R (min)† B	RF‡	r.m.n. OCH_3 (p.p.m.)	Littérature
2*a**	117–118	3	—	—	3.90–3.99	—
2*b**	126–128	4.5	—	—	3.91–3.99	—
2*c**	123–124	6	—	—	3.92–3.99	—
2*d**	189–190	—	2.5	—	3.93–4.06	189° (22)
3*a**	225–226	5	—	—	4.03	—
3*b*	266–267	8	—	—	4.05	257° (22)
3*c**	293–294	—	—	—	—	—
3*d*	283–284	—	4	—	4.10	265° (22)
3*e**	245–247	10	—	—	4.02–4.04	—
3*f**	276–277	—	—	—	—	—
3*g**	211–212	—	4.8	—	4.12–4.17	—
3*h**	222–223	—	5	—	4.02–4.05	—
3*i**	219–220	—	6.5	—	4.15–4.19	—
4*a**	240–241	—	—	—	4.18–4.25	—
4*b**	243–244	—	—	0.5	4.19–4.22	—
4*c**	268–269	—	—	0.51	4.18–4.21	—
4*d**	200–201	—	—	0.71	4.11–4.17	—
4*e**	228–230	—	—	0.65	4.08–4.12	—

*Les produits nouveaux marqués d'un astériste ont été caractérisés par des méthodes physiques.

†Chromatographie en phase gaseuse: Colonne 4′ × 1/4″ remplie de SE-30 à 5% sur chromport XXX. Conditions A: température de la colonne 200 °C et débit d'hélium 70 ml/min et conditions B: température de la colonne 230 °C et débit d'hélium 60 ml/min.

‡Chromatographie sur couches minces de silica gel GF-254 utilisant le benzène comme éluant.

Can. J. Chem. Downloaded from www.nrcresearchpress.com by 210.87.254.6 on 09/05/12
For personal use only.

Effets isotopiques

Préparation du diméthoxy-2,6 naphtalène-d_1 (2e)

A une solution de 5 g (16 mmoles) de diméthoxy-2,6 iodo-1 naphtalène (**2c**) dans 60 ml de T.H.F. strictement anhydre, 450 mg de magnésium et une trace d'iode sont ajoutés. Le mélange est maintenu sous une atmosphère d'azote avec agitation et chauffé à reflux durant 4 h: après refroidissement, 5 ml de D_2O et 3 ml de DCl (38% dans D_2O) sont ajoutés. Les produits (1.72 g, 71% de rendement après recristallisation dans l'éthanol) sont extraits au chloroforme. Le p.f. de ce naphtalène est le même que celui du diméthoxy-2,6 naphtalène non deutérié.

Evaluation des effets isotopiques

Les effets isotopiques (E.I.) sont évalués à partir des pourcentages (A) de deutérium dans le naphtalène **2e** et (A') de deutérium présent dans les dérivés monosubstitués obtenus et à l'aide de l'équation:

$$\text{E.I.} = AA'/100A + AA' - 200A'.$$

Cette équation est strictement applicable dans les cas où la conversion en dérivé monosubstitué est faible: dans le cas actuel elle représente une approximation correcte de l'effet isotopique. Les pourcentages de deutérium présents sont mesurés par spectrométrie de masse utilisant un appareil Hilachi–Perkin-Elmer, modèle RMU-6D muni d'un mécanisme d'introduction à la source. Les échantillons de dérivés monosubstitués (accompagnés de **2e** qui n'a pas réagi) qui ont ainsi été analysés ont été obtenus en faisant réagir à la température ambiante des méthoxy-2,6 naphtalène-1, avec des quantités déficitaires (approximativement 0.5 mole de réactif/mole de naphtalène) de réactifs. Ces réactions ont été conduites pour des temps courts (15 min) afin de s'assurer que la conversion est faible (évalué à 25%) et que des réactions de disubstitution n'ont pas lieu (il a été établi par chromatographie en phase gaseuse (c.p.g.) que les échantillons analysés ne contenaient pas de produits disubstitués).

Remerciements

Les auteurs remercient vivement le Conseil National de Recherches du Canada et le Service de l'Aide Extérieure du Ministère de l'Education de la Province de Québec pour l'Aide financière apportée sous forme de subventions de recherches et bourse d'études.

L'un de nous (J. C. R.) tient à exprimer sa gratitude au Dr. Pierre Maroni et Mlle. Marthe Benoit de la Faculté des Sciences de Toulouse pour l'acceuil et l'aide apportés au cours de la préparation de ce manuscrit.

1. J.-C. Richer et N. Baskevitch. Can. J. Chem. **46**, 2975 (1968).
2. J.-C. Richer, N. Baskevitch, L. Erichomovitch, et F. L. Chubb. Can. J. Chem. **46**, 3363 (1968).
3. J. G. Hawkins, E. R. Ward, et D. H. Whiffen. Spect. Acta, **10**, 105 (1957).
4. P. R. Wells et P. G. E. Alcorn. Aust. J. Chem. **16**, 1108 (1963).
5. J.-C. Richer et C. Lamarre. Can. J. Chem. **43**, 715 (1965).
6. J.-C. Richer et Y. Pepin. Can. J. Chem. **43**, 3443 (1965).
7. N.M.R. Spectra Catalog. Varian Associates, Spectrum No. 225.
8. The Sadtler Standard Spectra. N.M.R. Spectra Sadtler Research Laboratories. No. 343, 572, et 656.
9. L. F. Fieser et M. A. Ames. J. Amer. Chem. Soc. **49**, 2604 (1927).
10. F. Bell. J. Chem. Soc. 5293 (1961).
11. L. Melander. Isotope effects on reactions rates. The Ronald Press Co., New York. 1960.
12. H. Zollinger. Hydrogen isotope effects in aromatic substitutions reactions. *In* Advances in physical organic chemistry Vol. 2. Academic Press, Inc., New York. 1964.
13. E. Baciocchi, G. Illuminati, et G. Sleiter. Tetrahedron Letters, **23**, 30 (1960).
14. P. B. D. de la Mare et J. S. Lomas. Rec. Trav. Chim. **86**, 1082 (1967).
15. E. Baciocchi, G. Illuminati, G. Sleiter, et F. Stegel. J. Amer. Chem. Soc. **89**, 125 (1967).
16. P. C. Myhre et M. Beug. J. Amer. Chem. Soc. **88**, 1569 (1966).
17. P. C. Myhre. Acta Chem. Scand. **14**, 219 (1960).
18. E. Helgstrand et A. Nilsson. Acta Chem. Scand. **20**, 1463 (1966).
19. E. Helgstrand. Acta Chem. Scand. **19**, 1583 (1965).
20. E. Berliner. Chem. Ind. (London) 177 (1960).
21. L. Erichomovitch, M. Menard, F. L. Chubb, Y. Pepin, et J.-C. Richer. Can. J. Chem. **44**, 2305 (1966).
22. S. N. Chakravarti et V. Pasupati. J. Chem. Soc. 1859 (1937).

Can. J. Chem. Downloaded from www.nrcresearchpress.com by 210.87.254.6 on 09/05/12
For personal use only.

Branched-chain sugar nucleosides.[1] III. 9-(3-Deoxy-3-*C*-methyl-β-D-allofuranosyl and ribofuranosyl)adenine

ALEX ROSENTHAL AND MATEJ SPRINZL
Department of Chemistry, University of British Columbia, Vancouver, B.C.
Received May 20, 1969

Condensation of triphenylphosphinemethylene (Wittig reagent) with 5-*O*-benzyl-1,2-*O*-isopropylidene-α-D-*erythro*-pentafuranos-3-ulose and with 1,2:5,6-di-*O*-isopropylidene-α-D-*ribo*-hexofuranos-3-ulose (**1**) afforded 5-*O*-benzyl-1,2-*O*-isopropylidene-3-deoxy-3-*C*-methylene-α-D-ribofuranose in 36% yield and 1,2:5,6-di-*O*-isopropylidene-3-*C*-methylene-α-D-*ribo*-hexofuranose (**2**) in 55% yield, respectively. A detailed study of the affect of reaction conditions on the yield of the unsaturated sugar is described. Hydrogenation of **2** proceeded stereoselectively to yield **4** which was hydrolyzed selectively to the 1,2-*O*-monoisopropylidene derivative **5**. Benzoylation of the latter gave **6** which was converted by acetolysis to the 1,2-diacetate **7**. Condensation of this compound with 6-benzamidochloromercuripurine in the presence of titanium tetrachloride followed by deblocking with methanolic sodium methoxide, yielded 9-(3-deoxy-3-*C*-methyl-β-D-allofuranosyl)adenine (**10**) in 48% yield based on **7**. Sodium metaperiodate oxidation of **10**, followed by sodium borohydride reduction of the *aldehydo* derivative, afforded 9-(3-deoxy-3-*C*-methyl-β-D-ribofuranosyl)adenine (**11**) in 85% yield.

Canadian Journal of Chemistry, 47, 3941 (1969)

Interest in 3′-deoxyribofuranosyl nucleosides stems partly from the fact that 3′-deoxyadenosine (cordycepin, the first isolated nucleoside antibiotic) inhibits nucleic acid synthesis in Ehrlich ascites cells (1,2). The recent synthesis of 3′-*C*-methyladenosine (3) and the finding that it also exhibits biological activity, has further stimulated a concern in the nucleoside antibotics. Branched-chain sugar nucleosides have recently been prepared from 3-deoxy-3-*C*-hydroxymethyl-D-erythrofuranose (4). Our laboratory has been interested in developing a general method of synthesis of branched-chain sugar nucleosides (5), and in particular, the synthesis of 3′-deoxy and 2′-deoxy branched-chain sugar nucleosides having the ribofuranosyl skeleton in the sugar moiety. In this paper we wish to report the synthesis of several deoxy branched-chain sugar nucleosides and in particular, the synthesis of a structural analogue of cordycepin by application of a Wittig reaction to ketoses.

The readily available 1,2:5,6-di-*O*-isopropylidene-α-D-*ribo*-hexafuranos-3-ulose (**1**) (6,7) is a useful intermediate for the synthesis of 3-deoxy-3-*C*-substituted branched-chain sugars. In a previous communication (8) we described the application of the modified Wittig reaction to **1** to afford a 3-hydroxyethyl substituted branched-chain sugar, and in this paper we report the application of the basic Wittig reaction to the ketose **1**. Condensation of triphenylphosphinemethylene with **1** in the ratio 3:1 using methyl sulfoxide as solvent (9,10) gave 1,2:5,6-di-*O*-isopropylidene-3-*C*-methylene-α-D-*ribo*-hexofuranose (**2**) in 55% yield, and in addition, a by-product **3** of unknown constitution. Compounds **2** and **3** were separated by column chromatography on silica gel. The yield of **2**, as shown in Table I, was dependent on the reaction conditions. In all cases the reaction was monitored by thin layer chromatography (t.l.c.) and stopped when all ketose (except in procedure 5) was consumed. When the temperature was increased from 22° to 60°, the yield of by-product was significantly increased and the yield of **2** decreased to 23%. On the other hand, use of an equimolar ratio of ketose and ylid (see procedure 4) led to a significant decrease in the yields of both products. When 1,2-dimethoxyethane (glyme) was used as a solvent, elevated temperature (60°) was required and the maximum yield of unsaturated sugar was 28%. From the results shown in procedures 2 and 3 it would appear that the yield of **2** is approximately the same when the ketose is added to the ylid as when all the reactants are mixed together at the beginning of the reaction.

Product **3** reacted slowly with bromine in carbon tetrachloride to give an unstable halide. It also reacted with potassium permanganate but absorbed less than 0.2 mole equivalent of hydrogen over palladium. Attempts to purify it by preparative t.l.c. on silica gel led to degradation as evidenced by the fact that **3** was converted into a mixture of three new substances. Compound **3** did not contain any phosphorus or sulfur. Based

[1]For papers I and II see references 20 and 21.

Can. J. Chem. Downloaded from www.nrcresearchpress.com by 210.87.254.105 on 09/05/12
For personal use only.

TABLE I

Wittig reaction of triphenylphosphinemethylene with 1,2:5,6-di-*O*-isopropylidene-α-D-*ribo*-hexofuranose (**1**) to yield unsaturated sugar **2** and by-product **3**

Procedure	Ketose:Ylid ratio	Solvent	Temperature (°C)	Time (h)	Yield **2** %	Products **2** and **3** ratio
1*	1:3	DMSO	60	2	23	2:1
2*	1:3	DMSO	22	5	53	3:1
3†	1:3	DMSO	22	1	55	3:1
4†	1:1	DMSO	22	5	30	10:1
5*	1:3	Glyme	22	12	0	
6*	1:3	Glyme	70	10	28	1:0

*Ketose added directly to the mixture of methyltriphenylphosphonium bromide, sodium hydride, and methyl sulfoxide.
†Methyltriphenylphosphonium bromide converted into the ylid before addition of the ketose.

on the work of Walling and co-worker (11) and the molecular weight of **3** (determined from its mass spectrum), it might be inferred that side products from methyl sulfoxide might have added to the ketose to afford addition products. The great difficulty in isolating sufficient material of sufficient stability to do structural work led us to abandon this phase of the research.

Hydrogenation of **2** using palladium on charcoal proceeded stereoselectively to afford, after high vacuum distillation, compound **4** in 75% yield. The configuration of C-3 of **4** was readily ascertained from its nuclear magnetic resonance (n.m.r.) spectrum. The H-2 signal of **4** appears as a triplet (resolved into two doublets under magnification) showing that H-2 is coupled to H-3 and to H-1. On the other hand, in the glucofuranose series (12) there is no coupling between H-2 and H-3, thus leading to a doublet for H-2. Therefore, the only possible configuration for C-3 is the *allo*-configuration. This was further proved by spin–spin decoupling experiments. Irradiation of H-2 of **4** collapsed H-1 into a singlet and altered H-3. Therefore, **4** is undoubtedly 1,2:5,6-di-*O*-isopropylidene-3-deoxy-3-*C*-methyl-α-D-allofuranose.

Selective hydrolysis of the 5,6-*O*-isopropylidene group of **4** to yield **5** in 81% yield was accomplished using aqueous methanol containing sulfuric acid. Benzoylation of the latter gave the dibenzoate **6** in 94% yield which was purified by column chromatography on silica gel. Acetolysis of **6** with acetic acid, acetic anhydride, and sulfuric acid for 3 days gave mainly the β-anomer **7** in 82% yield. Condensation of the latter with 6-benzamidochloromercuripurine by the titanium tetrachloride method (13) afforded the blocked *allo*-nucleoside **9**. Deacylation of **9** using methanolic sodium methoxide afforded crystalline β-nucleoside **10** in 48% yield based on **7**. The assignment of structure and anomeric configuration to 9-(3-deoxy-3-*C*-methyl-β-D-allofuranosyl)-adenine (**10**) was based on the following: (*1*) ultraviolet (u.v.) absorption data of **10** substantiates the site of glycosylation (14) at N-9, (*2*) the trans rule (15) indicates that **10** has a β-configuration, and (*3*) the *allo*-nucleoside **10** exhibits a negative Cotton effect that is consistent with the proposals advanced (16,17) for assignment of structure to purine nucleosides. The mother liquor from **10** was carefully investigated by paper chromatography and also by column chromatography on Dowex 1 × 2 (OH^-) (18) using gradient elution but the presence of any α-anomer of **10** was not detected.

Sodium metaperiodate oxidation of the *allo*-nucleoside **10** yielded an *aldehydo*-nucleoside that was immediately reduced with sodium borohydride to yield the crystalline *ribo*-nucleoside **11** in 85% yield. Surveillance of the degradation reaction using a starch–iodine test was essential to minimize production of a by-product which was difficult to remove. Based on the fact that the *allo*-nucleoside **10** was degraded to the *ribo*-nucleoside **11** by steps which are known not to alter the configuration of sugars, therefore, **11** can be assigned the structure 9-(3-deoxy-3-*C*-methyl-β-D-ribofuranosyl)adenine. In the latter nucleoside, n.m.r. evidence (H-1′ gave a doublet having $J_{1',2'} = 1.5$ Hz) corroborates the β-anomeric configuration of **11**.

The general applicability of the Wittig reaction for preparing methyl analogues of cordycepin was demonstrated by condensing 5-*O*-benzyl-1,2-*O*-isopropylidene-α-D-*erythro*-pentafuranos-3-ulose (19) with triphenylphosphinemethylene to

Can. J. Chem. Downloaded from www.nrcresearchpress.com by 210.87.254.105 on 09/05/12
For personal use only.

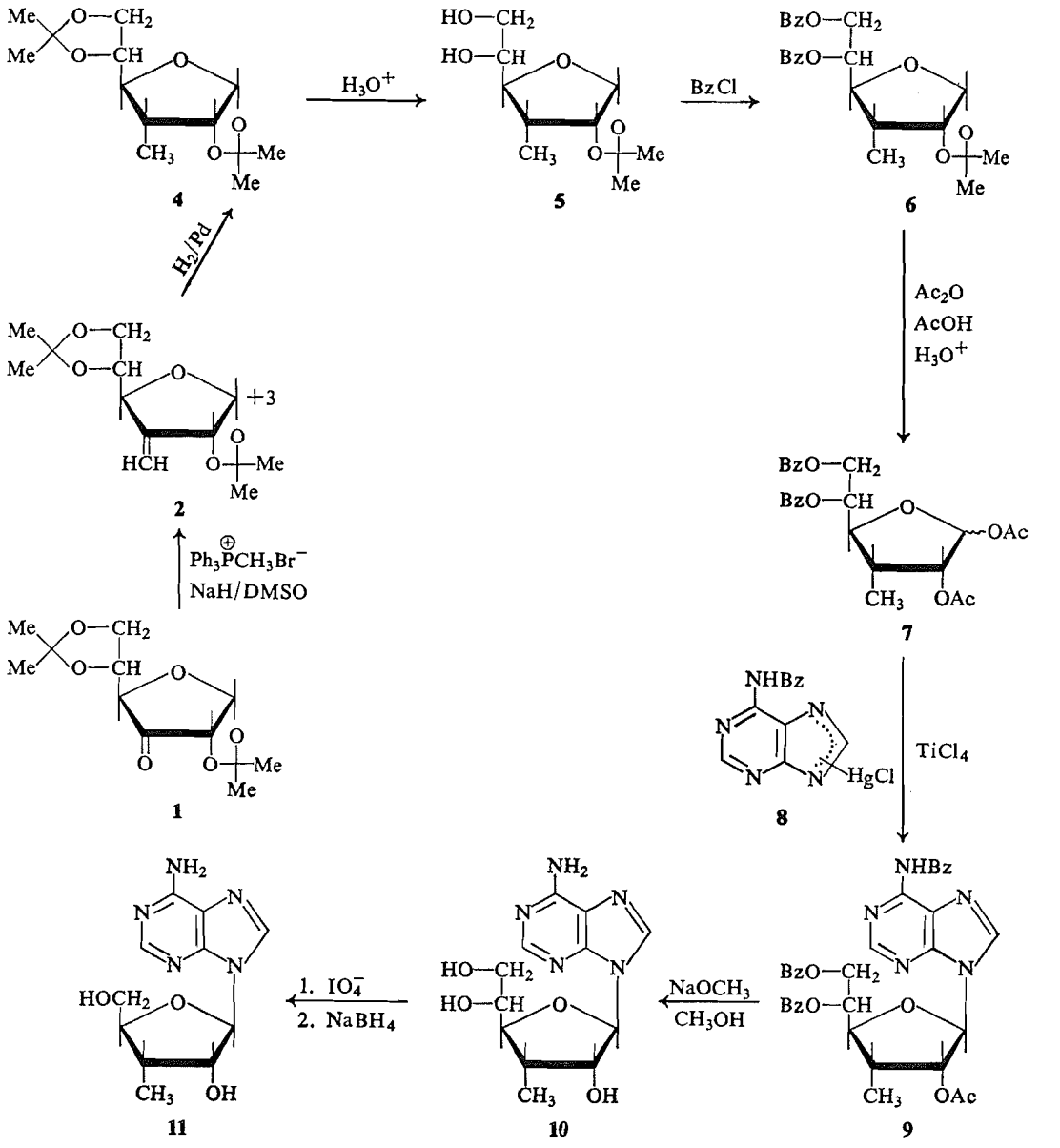

yield, after column chromatography on silica gel, 5-*O*-benzyl-1,2-*O*-isopropylidene-3-deoxy-3-*C*-methylene-α-D-ribofuranose in 36% yield.

Experimental

General Considerations

Nuclear magnetic resonance (n.m.r.) spectra were obtained on deuteriochloroform solution (unless otherwise stated) with tetramethylsilane as the internal standard (set at τ 10) using a Jeolco 60, a Varian A-60, or Varian HA-100 spectrometers. Mass spectroscopy was obtained with an A.E.I. M.S.9 spectrometer. The ultraviolet (u.v.) spectral measurements were performed on a Cary 140 spectrophotometer. The optical rotary dispersion (o.r.d.) measurements were performed on a Jasco Model ORD/UV-5 Spectropolarimeter at room temperature on aqueous solutions. All melting points (micro hot stage) are corrected. Silica gel G was used in the thin layer chromatography (t.l.c.). For column chromatography Silica gel Woelm 100-200 mesh, activity grade II, was used. Elemental analyses were performed by the Microanalytical Laboratory, University of British Columbia.

Can. J. Chem. Downloaded from www.nrcresearchpress.com by 210.87.254.105 on 09/05/12
For personal use only.

Can. J. Chem. Downloaded from www.nrcresearchpress.com by 210.87.254.105 on 09/05/12
For personal use only.

Application of Wittig Reaction to 1,2:5,6-Di-O-isopropylidene-α-D-ribo-hexofuranos-3-ulose (1) to Yield 1,2:5,6-Di-O-isopropylidene-3-C-methylene-α-D-ribo-hexofuranose (2)

Sodium hydride (0.240 g, 0.01 mole) was suspended in 30 ml of anhydrous methyl sulfoxide and the mixture was heated at 75° for 45 min in a dry box in an anhydrous nitrogen atmosphere. After the solution was cooled to 20° methyltriphenylphosphonium bromide (3.95 g, 0.011 mole) was added and the mixture stirred for 30 min. To the resulting mixture was added dropwise with stirring (with external cooling at 20°) a solution of 1,2:5,6-di-*O*-isopropylidene-α-D-*ribo*-hexofuranos-3-ulose (0.84 g, 0.0033 mole) in 10 ml of anhydrous methyl sulfoxide. After the addition, the reaction mixture was stirred for an additional 2 h and then poured into 100 ml water. The aqueous solution was extracted with 5 separate portions of 30 ml ether. The combined ether extracts were washed with water (5 × 30 ml), dried over magnesium sulfate, filtered, and evaporated under reduced pressure to yield a syrup. This syrup was dissolved in petroleum ether (50 ml, b.p. 60–90°) and then left stand overnight at 0°. Triphenylphosphonium oxide was removed by filtration and washed with several small portions of cold petroleum ether. The combined filtrate and washings were evaporated under reduced pressure to yield a syrup (0.760 g). Thin layer chromatography on silica gel G using benzene–ethyl acetate (20:1) as developer and 2% potassium permanganate or sulfuric acid as detector revealed two spots having R_f's of 0.6 and 0.5. The syrup was separated by column chromatography (60 × 1.5 cm diam) on silica gel using 100 ml of benzene followed by 600 ml of benzene–ethyl acetate (9:1) as developer. Aliquots were collected on a fraction collector and analyzed by t.l.c. as described above. Evaporation of the eluents afforded compound **2** (0.458 g, 55% yield) and a second faster moving fraction **3** (0.140 g, 17% yield).

Compound **2** showed no carbonyl in its infrared (i.r.) spectrum. It showed the presence of a methylene group (1660 cm^{-1}); τ ($CDCl_3$), 4.2 (1-H, d, $J_{1,2}$ = 4.5 Hz due to H-1), 4.55 (1-H, m, due to H-3), 5.1 (1-H, d, $J_{2,1}$ = 4.5 Hz, due to H-2), 6.0 (m, due to H-4, H-5, and H-6), 8.5 (12-H, t, due to isopropylidene groups); the compound was homogeneous by vapor phase chromatography (v.p.c.) at 160°; t.l.c. R_f 0.5, $[\alpha]_D^{22}$ + 104° (*c*, 2, chloroform).

Anal. Calcd. for $C_{13}H_{20}O_5$: C, 60.90; H, 7.84. Found: C, 61.13; H, 8.00.

The faster moving component **3** (R_f 0.6) was recrystallized from petroleum ether (b.p. 35–60°), m.p. 35–37°, and sublimed at 50 °C (0.056 mm pressure), $[\alpha]_D^{22}$ −174° (*c*, 2, chloroform). Mass spectroscopy: 304, 289. The n.m.r. spectrum showed τ ($CDCl_3$), 3.7–4.1 (1-H, m), 4.4–4.9 (1-H, m), 5.7–6.0 (m), 8.5 (12-H, due to isopropylidene groups); i.r., 1660 cm^{-1}. The compound was unstable at room temperature or on rechromatography on silica gel G (gave three new compounds). Attempts to hydrogenate this substance were unsuccessful (less than 0.2 mole equivalent of hydrogen was absorbed).

1,2:5,6-Di-O-isopropylidene-3-deoxy-3-C-methyl-α-D-allofuranose (4)

Compound **2** (1.024 g) dissolved in methanol (30 ml), was allowed to react with hydrogen at room temperature and 1 atm pressure using 10% palladium on charcoal (0.2 g) as catalyst until the gas pressure remained constant (86 ml of hydrogen absorbed). Work-up of the product **4** in the usual way followed by distillation under high vacuum (b.p. 77–80° at 0.05 mm) gave an oil, yield 0.765 g (75%), which was homogeneous by v.p.c. (at 160°) and by t.l.c. (benzene–ethyl acetate, 20:1), R_f 0.5. The n.m.r. spectrum showed τ ($CDCl_3$), 4.25 (H-1, d, $J_{1,2}$ = 3.7 Hz), 5.50 (H-2, t, $J_{2,1}$ = 3.7 Hz and $J_{2,3}$ = 3.7 Hz), 5.9–6.4 (m, due to H-4, H-5, and H-6), 8.1 (m, due to H-3), 8.6 (t, due to isopropylidene groups), 8.4 (d, due to H-3′, $J_{3,3'}$ = 7 Hz). Irradiation of H-3 collapsed the doublet at 8.5 p.p.m. to a singlet; $[\alpha]_D^{22}$ +37° (*c*, 1, chloroform).

Anal. Calcd. for $C_{13}H_{22}O_5$: C, 60.40; H, 8.52. Found: C, 60.28; H, 8.52.

5-O-Benzyl-1,2-O-isopropylidene-3-deoxy-3-C-methylene-α-D-ribofuranose

Application of the Wittig reaction to 5-*O*-benzyl-1,2-*O*-isopropylidene-α-D-*erythro*-pentafuranos-3-ulose as described in the first part of the experimental gave after column chromatography of the product 5-*O*-benzyl-1,2-*O*-isopropylidene-3-deoxy-3-*C*-methylene-α-D-ribofuranose in 36% yield, τ ($CDCl_3$), 4.12 (d, H-1, $J_{1,2}$ = 4 Hz), 4.5–4.8 (m), 5.1 (d, due to =CH_2), 5.42 (s, due to O—$CH_2C_6H_5$), 6.04 (m, due to H-5), 8.55 (d, due to isopropylidene group), R_f = 0.55 (benzene–ethyl acetate 10:1), $[\alpha]_D^{22}$ +63° (*c*, 1, chloroform).

Anal. Calcd. for $C_{16}H_{20}O_4$: C, 69.60; H, 7.26. Found: C, 70.02; H, 7.15.

1,2-O-Isopropylidene-3-deoxy-3-C-methyl-α-D-allofuranose (5)

To a solution of 0.520 g of **4** in 4 ml of methanol was added 4 ml of 0.1 *N* sulfuric acid. After the reaction mixture was left standing at room temperature for 3.5 h it was neutralized with barium hydroxide (p*H* kept at 7), boiled, and filtered through Celite. The filtrate was evaporated to dryness and the residue dissolved in 20 ml water. The solution was extracted with 5 ml chloroform to remove a trace of **4**. After the water solution was again evaporated to dryness the residue was extracted with 3 × 20 ml of boiling chloroform. The combined chloroform extracts were dried over magnesium sulfate, filtered, and evaporated to dryness, yield 0.356 g (81%) of a syrup, R_f = 0.45 (benzene–methanol 3:1), $[\alpha]_D^{22}$ + 35° (*c*, 1, chloroform).

5,6-Di-O-benzoyl-1,2-O-isopropylidene-3-deoxy-3-C-methyl-α-D-allofuranose (6)

To a solution of **5** (0.870 g) in pyridine (10 ml) was added dropwise freshly distilled benzoyl chloride (1 ml). After the reaction mixture was kept at room temperature overnight it was poured into water, and the product extracted with chloroform in the usual way, yield 1.48 g (94%). Fractionation of the crude product on silica gel (80 × 2 cm diam) with 20:1 benzene–ethyl acetate gave 1.35 g of product which was dissolved in methanol to yield a glass, R_f = 0.6 (10:1 benzene–ethyl acetate), τ ($CDCl_3$), 1.9–2.5 (10-H due to phenyl), 4.15 (d, H-1, $J_{1,2}$ = 3.5 Hz), 8.0 (m, due to H-3), 8.8 (d, due to H-3′, $J_{3,3'}$ = 7 Hz), $[\alpha]_D^{22}$ +32° (*c*, 1, chloroform).

Can. J. Chem. Downloaded from www.nrcresearchpress.com by 210.87.254.105 on 09/05/12
For personal use only.

Anal. Calcd. for $C_{24}H_{26}O_6$: C, 70.3; H, 6.39. Found: C, 70.5; H, 6.72.

1,2-Di-O-acetyl-5,6-di-O-benzoyl-3-deoxy-3-C-methyl-α(β)-D-allofuranose (7)

To a well-stirred solution (kept at 0°) of **6** (1.230 g) in glacial acetic acid (15 ml) and acetic anhydride (1.5 ml) was added dropwise 0.82 ml of concentrated sulfuric acid. After storage at room temperature for 4 days the solution was poured into 50 ml of vigorously stirred mixture of ice and water. The resulting mixture was extracted with chloroform (2 × 20 ml), the chloroform extracts washed with 20 ml of water, aqueous sodium bicarbonate, water, dried over magnesium sulfate, filtered, and evaporated to dryness *in vacuo* to give 1.12 g (83%) of a syrup **7**; $[\alpha]_D^{22}$ 0° (*c*, 2, chloroform), τ ($CDCl_3$), 3.95 (s, due to H-1), 4.75 (d, H-2, $J_{2,3}$ = 5.2 Hz).

9-(3-Deoxy-3-C-methyl-β-D-allofuranosyl)-adenine (10)

A mixture of 1.35 g (0.003 mole) of sugar **7**, 1.60 g (0.0037 mole) of 6-benzamidochloromercuripurine (**8**), and 1 g of Celite and anhydrous xylene (20 ml) was dried by distilling off the xylene under reduced pressure. To the resulting residue was added 50 ml of anhydrous ethylene dichloride and 15 ml of the solvent was distilled. To the partially cooled mixture was added a solution of 0.338 ml of titanium tetrachloride in 4 ml of ethylene dichloride, and the reaction mixture was heated under reflux for 4 h. The cooled reaction mixture was then poured into 50 ml of saturated sodium bicarbonate and stirred vigorously for 30 min, and then filtered through Celite. The Celite cake was washed with chloroform, and the combined organic extracts washed with 15 ml of 30% aqueous potassium iodide and 15 ml of water. After evaporation of the solvent under reduced pressure the residue was dissolved in 30 ml methanol and the resulting solution decolorized with charcoal, filtered through a Celite column, and then evaporated to dryness under *vacuo* to give 0.98 g (52%) of the blocked nucleoside **9**, R_f = 0.32 using 1:2 benzene–ethyl acetate as developer. Compound **9** was deacylated by refluxing with 15 ml of 0.05 *N* methanolic sodium methoxide for 4 h. The cooled solution was neutralized with glacial acetic acid and left stand overnight at 0°. The unblocked nucleoside **10** was removed by filtration, yield 0.275 g. The mother liquor was evaporated under reduced pressure and the residue dissolved in 20 ml water. The aqueous solution was then extracted with 2 × 10 ml ether. Passage of the aqueous solution through a Dowex 1 × 2 (OH^-) column (15 × 1 cm diam) followed by elution with water (to remove inorganic ions), 30% methanol, and finally 60% methanol (total about 200 ml) afforded 0.090 g of **10** in the last fraction. No observable amount of the α-anomer of **10** was found in any fraction of the eluent. Recrystallization of combined **10** from 80% methanol-water afforded 0.35 g (79%) of crystalline **10**, m.p. 227–228°, $[\alpha]_D^{22}$ −25° (*c*, 1, water), $\lambda_{max}(H_2O)$ (mμ) 261 (ε 18,250), R_f (adenine) 0.96 on Whatman paper No. 1 using water as developer. The o.r.d. spectrum of **10** showed a negative Cotton effect, $[\phi]_{270}$ −780°, $[\phi]_{262}$ 0°, $[\phi]_{247}$ +975° (*c*, 1.0 × 10^{-4} in water), λ (D_2O, at 60°); 4.08 (d, H-1′, $J_{1,2}$ = 2.5 Hz), 7.45 (m, H-3′), 8.85 (d, CH_3, $J_{3,3'}$ = 6 Hz).

Anal. Calcd. for $C_{12}H_{17}O_5N_4$: C, 48.80; H, 5.80; N, 23.72. Found: C, 48.65; H, 5.77; N, 23.88.

*Sodium Metaperiodate Oxidation and Reduction of the Allo-nucleoside **10** to Yield 9-(3-Deoxy-3-C-methyl-β-D-ribofuranosyl)-adenine (11)*

To a solution of the allo nucleoside **10** (0.295 g, 0.001 mole) in 30 ml of water and 15 ml of ethanol was added with stirring a 5% aqueous solution of sodium metaperiodate (0.214 g, 0.001 mole). The progress of the reaction was monitored by the starch–iodine test (compared with a blank). It was essential to avoid use of excess oxidant as this caused a significant decrease in yield of **11**. The solution was kept at neutral p*H* with saturated sodium bicarbonate solution (about 0.5 ml). The reaction mixture was left standing at room temperature in the dark for 2 h. To the resulting solution was added with stirring sodium borohydride (0.300 g) and the mixture stirred for 3 h. Excess of sodium borohydride was decomposed by addition of glacial acetic acid. The reaction mixture was evaporated under reduced pressure and the residue treated with 3 × 5 ml of methanol followed by evaporation. The crystalline residue was dissolved in 2% acetic acid (5 ml) and applied onto a column of Dowex 50 (NH_4^+) resin (15 ml of 1 cm diam column). The inorganic ions were eluted with 300 ml water and the nucleoside was then eluted with 5% ammonium hydroxide. Evaporation of the solvent followed by recrystallization of **11** from 80% methanol–water gave 0.225 g of **11** (85%), m.p. 231–232°, $[\alpha]_D^{22}$ −36° (*c*, 1, water), $\lambda_{max}(H_2O)$ 261 (ε 13,400), $R_{adenine}$ 1.2; τ (deuteriomethylsulfoxide) 1.68 (s, H-2), 1.95 (s, H-8), 2.82 (s, NH_2), 4.15 (d, H-1′, $J_{1',2'}$ = 1.5 Hz), 4.4 (d), 5.0 (m), 5.75 (m), 6.4 (m), 8.4 (m near DMSO peak), 9.1 (d, CH_3, $J_{3,3'}$ = 7 Hz).

Anal. Calcd. for $C_{11}H_{15}O_3N_5$: C, 49.80; H, 5.70; N, 26.40. Found: C, 49.87; H, 5.74; N, 26.57.

Acknowledgment

This work was supported by the National Research Council of Canada.

1. H. KLENOW and S. FREDERIKSEN. Biochim. Biophys. Acta, **87**, 495 (1964).
2. (*a*) S. S. COHEN. Progr. Nucl. Acid Res. Mol. Biol. **5**, 1 (1967) and references cited therein; (*b*) J. J. FOX, K. A. WATANABE, and A. BLOCH. Progr. Nucl. Acid Res. Mol. Biol. **5**, 251 (1967).
3. E. WALTON, S. R. JENKINS, R. F. NUTT, M. ZIMMERMAN, and F. W. HOLLY. J. Amer. Chem. Soc. **88**, 4524 (1966).
4. E. J. REIST, D. F. CALKINS, and L. GOODMAN. J. Amer. Chem. Soc. **90**, 3852 (1968).
5. A. ROSENTHAL. Advan. Carbohyd. Chem. **23**, 59 (1968).
6. P. J. BEYNON, P. M. COLLINS, and W. G. OVEREND. Proc. Chem. Soc. 342 (1964).
7. (*a*) K. ONODERA, S. HIRANO, and N. KASHIMURA. J. Amer. Chem. Soc. **87**, 4651 (1965); (*b*) K. ONODERA, S. HIRANO, and N. KASHIMURA. Carbohyd. Res. **6**, 276 (1968).
8. A. ROSENTHAL and L. NGUYEN. Tetrahedron Letters, 2393 (1967).
9. E. J. COREY and M. CHAYKOVSKY. J. Amer. Chem. Soc. **84**, 866 (1962).
10. R. GREENWALS, M. CHAYKOVSKY, and E. J. COREY. J. Org. Chem. **28**, 1128 (1963).

11. C. WALLING and L. BOLLYKY. J. Org. Chem. **28**, 256 (1963); J. Org. Chem. **29**, 2699 (1969).
12. R. J. ABRAHAM, L. D. HALL, L. HOUGH, and K. A. MCLAUCHLAN. J. Chem. Soc. 3699 (1962).
13. J. PROKOP and D. H. MURRAY. J. Pharm. Sci. **54**, 359 (1965).
14. J. M. GULLAND and E. R. HOLIDAY. J. Chem. Soc. 765 (1936).
15. (*a*) R. S. TIPSON. J. Biol. Chem. **55**, 130 (1939); (*b*) B. R. BAKER. Chemistry and biology of purines. Ciba Foundation Symposium. Little, Brown and Co., Boston, Mass. 1957. p. 157.
16. T. R. EMERSON, R. J. SWAN, and T. L. V. ULBRICHT. Biochem. Biophys. Res. Commun. **22**, 505 (1966).
17. T. MISHIMURA, B. SHIMIZU, and I. IWAI. Biochem. Biophys. Acta, **157**, 221 (1968).
18. A. P. MARTINEZ, W. W. LEE, and L. GOODMAN. J. Org. Chem. **34**, 92 (1969).
19. A. ROSENTHAL and D. A. BAKER. Tetrahedron Letters, 397 (1969).
20. A. ROSENTHAL and L. (BENZING) NGUYEN. J. Org. Chem. **34**, 1029 (1969).
21. A. ROSENTHAL, M. SPRINZL, and H. J. KOCH. Can. J. Chem. **47**, 3263 (1969).

Can. J. Chem. Downloaded from www.nrcresearchpress.com by 210.87.254.105 on 09/05/12
For personal use only.

Carbohydrates in alkaline systems. I. Kinetics of the transformation and degradation of D-glucose, D-fructose, and D-mannose in 1 *M* sodium hydroxide at 22 °C[1]

DONALD J. MACLAURIN[2] AND JOHN W. GREEN[3]
The Institute of Paper Chemistry, Appleton, Wis. 54911

Received November 18, 1968

Rates of isomerization, epimerization, and degradation reactions were measured for D-glucose (**1**), D-fructose (**2**), and D-mannose (**3**) at 0.002 *M* in 1 *M* NaOH under N_2 in the dark at 22 °C. Reaction system resolution was by column chromatography on anion resins in the borate form. Assay for **1**, **2**, and **3** was by continuous automated colorimetry of column effluent using orcinol/sulfuric acid as a reagent. D-Allose and D-altrose were not detected. Reaction rate constants (h^{-1}) found: k_{12} 0.038, k_{13} 0.0005, k_{15} 0.002, k_{21} 0.036, k_{23} 0.006, k_{24} 0.072, k_{31} 0.0005, k_{32} 0.011, k_{36} 0.002, where **4**, **5**, and **6** are products formed from **1**, **2**, or **3**, respectively.

Canadian Journal of Chemistry, 47, 3947 (1969)

Can. J. Chem. Downloaded from www.nrcresearchpress.com by 210.87.254.6 on 09/05/12
For personal use only.

Introduction

The isomerization, epimerization, and degradation of carbohydrates in alkaline systems have been extensively studied and reviewed (1–6). Interest in these reactions continues because of their important theoretical physiological and industrial implications. Previous work (e.g., 7–21) gives much insight into the mechanism of these reactions and provides some semiquantitative kinetic information. However, specific kinetic studies do not appear to be available. Apparently, this is due to the previous lack of facile methods of assay for reaction system components. This study shows that chromatographic separations on anion-exchange resin columns in the borate form, together with continuous automated colorimetry of the column effluent, offers an assay method of apparent potential for studies of these reactions. Kesler (22) has reviewed these assay techniques and has reported methods which were the basis of the procedures used in this work.

For this study, 1 ml (10 mg) of an aqueous solution of a carbohydrate was combined with 25 ml of 1 *M* NaOH in a capped pyrex tube. Solutions and the reaction vessel were essentially freed of oxygen and saturated with nitrogen. Light was excluded by wrapping the tube with aluminum foil. The reaction was quenched to p*H* 1–2 with 25 ml 1 *M* HCl. A 20 ml aliquot of the quenched system was combined with 10 ml of 0.36 *M* H_3BO_3 which had been adjusted to p*H* 9.0 with 12 *M* KOH. Samples (0.250–1.000 ml) from the borated system were applied to a 6 × 700 mm anion resin column (borate form) held at 30 °C. A carefully designed graded eluant (H_3BO_3–$K_2B_4O_7$) was pumped through the column at 500 psig and 3.5 ml/min/cm^2 resin bed cross section area. These conditions freed D-glucose, the slowest moving material of interest, from the column in 8 h and provided for good simultaneous resolution of the monosaccharides of present interest and certain disaccharides of interest in continuing studies. A column effluent sample was monitored continuously with a Technicon Auto-Analyzer using orcinol/sulfuric acid to give a colorimetric assay on a strip chart chromatogram. The chromatogram peaks were calibrated against weights of known material. Thus, concentrations of D-glucose, D-fructose, and D-mannose were measured at selected reaction times. The overall accuracy of individual measurements of these concentrations was about ±2–3%.

Derivation of Reaction Rate Constants

The analytical data showed qualitatively that when a reaction was begun with D-glucose, D-fructose, or D-mannose, the other two of these quickly appeared in the system. This was as expected and was in harmony with the generally accepted theory and observations of the Lobry de Bruyn–Alberda van Ekenstein transformations for these materials. Separate experiments with D-allose and D-altrose established that these

[1]A portion of a thesis submitted by D.J.M. in partial fulfillment of the requirements of The Institute of Paper Chemistry for the degree of Doctor of Philosophy from Lawrence University, Appleton, Wis., Jan., 1969.

[2]Present address: Department of Chemistry, University of Victoria, Victoria, B.C.

[3]Senior Research Associate, The Institute of Paper Chemistry, Appleton, Wis. 54911.

Can. J. Chem. Downloaded from www.nrcresearchpress.com by 210.87.254.6 on 09/05/12
For personal use only.

materials did not appear in detectable amounts (i.e., more than 0.25% of the starting material) in any of the various reaction mixtures that were chromatographed. Plots of the logarithm of the relative concentration of the starting material against time gave quite good straight lines in each case for the early stages of the reaction. From this observation and the experimental design which provided essentially no change in concentration of the base during the disappearance of at least half the starting material, it was concluded that the several reactions involving the starting material were pseudo first order. On the basis of these observations and conclusions, a simplified reaction scheme (Scheme 1) was postulated as a basis for calculation of reaction rate constants. In this scheme, A (**4**), B (**5**), and C (**6**) are reaction products (saccharinic acids, etc., which were not determined) other than fructose, glucose, and mannose, arising from each of these latter, respectively. Possible intermediates are omitted from the triangle; such intermediates will be discussed in more detail later.

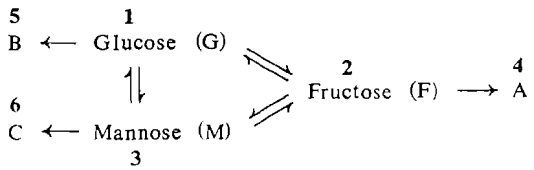

SCHEME 1

For Scheme 1 with first order reactions, the following equations apply.

$$[1]\quad dG/dt = k_{21}F + k_{31}M - (k_{12} + k_{13} + k_{15})G$$

$$[2]\quad dF/dt = k_{12}G + k_{32}M - (k_{21} + k_{23} + k_{24})F$$

$$[3]\quad dM/dt = k_{13}G + k_{23}F - (k_{31} + k_{32} + k_{36})M$$

$$[4]\quad dA/dt = k_{24}F$$

$$[5]\quad dB/dt = k_{15}G$$

$$[6]\quad dC/dt = k_{36}M$$

The data from Table VIII were then substituted into these equations. It soon became apparent that direct calculation of final values of the several rate constants could not be done through algebraic manipulation of the rate equations. A best preliminary set of values of these constants was then obtained from estimation of initial rates and selected use of the rate equations. These preliminary values were then fed into a digital analog-simulator program (PACTOLUS) on a 1620 IBM computer to generate a set of curves preliminary to those of Fig. 1. The values of the various rate constants were then slowly adjusted until the generated curves gave an acceptable fit to the experimental data. The values of the several rate constants thus obtained are given in Table I. The precisions assigned to values in this table are liberal estimates based on observed effects during curve fitting. The computer-derived curves, using these rate constants and eqs. [1], [2], and [3], superimposed on the experimental data points for glucose, fructose, and mannose are given in Fig. 1. Computer plots for eqs. [4], [5], and [6] are given in Fig. 2. The fit between the curves and the experimental points in Fig. 1 for each of the three systems is considered to give support to the validity of the experimental methods, the data obtained, the reaction scheme, and the rate constants derived from the data. A paper on the computer program is planned (23).

Discussion and Results

In this paper the term "transformation" is used to describe, in a collective sense, epimerization and isomerization reactions of the Lobry de Bruyn–Alberda van Ekenstein type; the term "degradation" is used to describe other reactions undergone by carbohydrates in alkaline systems. Actually, the overall rate constants represent not only changes within an alkaline system but also conversion of the intermediates in the system to

TABLE I

Rate constants in the system 0.002 *M* glucose in 1 *M* sodium hydroxide at 22 °C

Reaction pathway	Rate constant	Rate constant value (h^{-1})
G→F	k_{12}	0.036±0.001
G→M	k_{13}	0.0005±0.0002
G→B	k_{15}	0.002±0.0005
F→G	k_{21}	0.038±0.001
F→M	k_{23}	0.006±0.0005
F→A	k_{24}	0.072±0.001
M→G	k_{31}	0.0005±0.0002
M→F	k_{32}	0.011±0.0005
M→C	k_{36}	0.002±0.0005

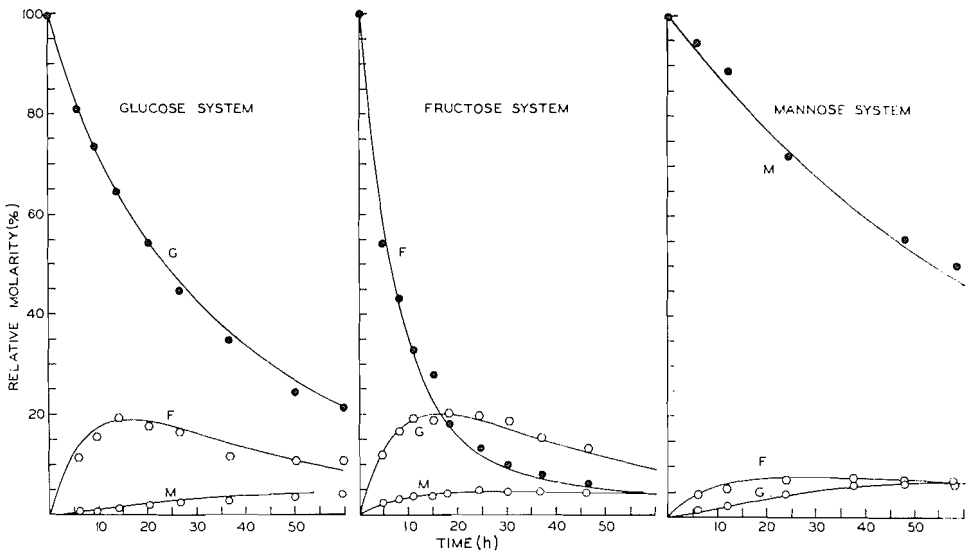

FIG. 1. Monosaccharide systems, carbohydrates, in 1 *M* sodium hydroxide at 22 °C.

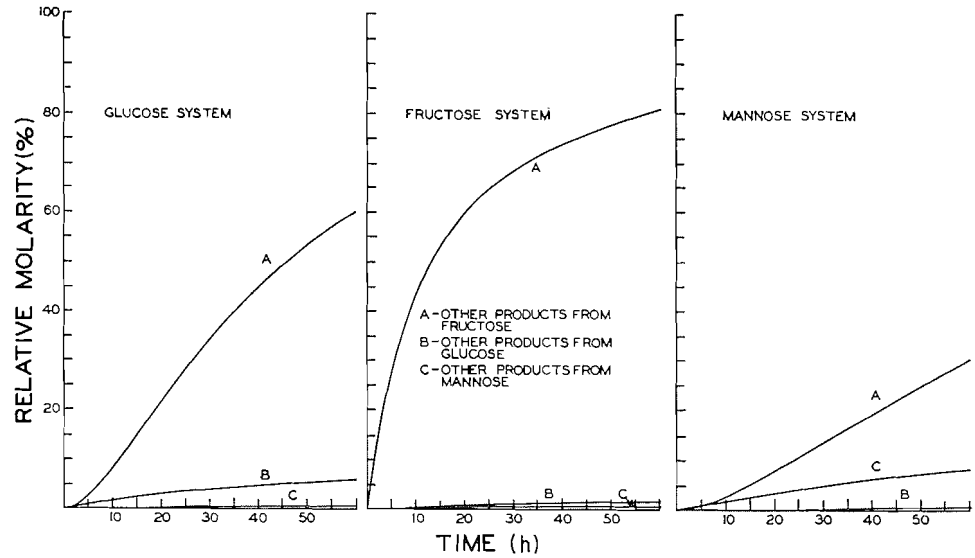

FIG. 2. Monosaccharide systems, calculated plots of other products in 1 *M* sodium hydroxide at 22 °C.

final products by a process of acidification. The various reactions involved are so complex that it is difficult to draw definite conclusions from the kinetic data.

The present work has been confined to an analysis for D-glucose, D-mannose, and D-fructose. No attempt has been made to explore the "triangle" comprising D-altrose, D-allose, and D-psicose (D-*ribo*-hexulose). Control experiments were carried out involving D-allose and D-altrose. It was concluded that these two sugars did not occur in the present systems, at least to any extent greater than about 0.25% of the starting material; this percentage was the limiting sensitivity of the analytical procedures employed.

No attempt was made to look for D-psicose, because of the trace amounts at best, present of D-allose and D-altrose; epimerization at C-3 is

Can. J. Chem. Downloaded from www.nrcresearchpress.com by 210.87.254.6 on 09/05/12
For personal use only.

Can. J. Chem. Downloaded from www.nrcresearchpress.com by 210.87.254.6 on 09/05/12
For personal use only.

considered to be rather remote (2). This ketose has been reported in 0.6% yield from D-glucose (24) after 48 h treatment with 3 *N* ammonium hydroxide at 37 °C; it has also been prepared by the action of lime water on turanose (12), D-altrose (25), and sugar beet juice (26). The action of potassium aconitate at p*H* 8 on D-fructose gave small amounts of DL-*ribo*-hexose (as the phenylosazone), formed presumably by recombination of triose fragments (27).

The rate constants for the three reversible pathways (Table I) are interesting for two reasons: (*a*) the constants for each pathway, for the forward and for the reverse reactions, are almost the same (with the exception of the fructo–manno pathway); (*b*) the magnitude of these constants falls into three levels, a very low level for the gluco–manno system (0.0005), a higher level for the manno–fructo system (0.006 to 0.011), and a much higher value for the gluco–fructo pathway (0.036 to 0.038).

At present all that can be said of the kinetic data is that they show clearly, and for the first time, that the gluco–manno epimerization reaction is energetically very unfavorable compared with the observed isomerization reactions. Presumably there is some higher energy barrier in the formation of possible intermediates and along possible pathways to and from the mannose molecule. A greater amount of non-bonded interactions for the acyclic form of mannose may be a factor here; such interactions of course would be much less prevalent than in the cyclic form.

Isbell and co-worker (28) have recently suggested pseudo-acyclic intermediates, which have conformations similar to the parent sugars; these are converted into *cis*- and *trans*-enediols and various sugars produce different ratios of the two isomers. They have concluded that glucose, mannose, and fructose did not form the same enediol, as the rates of conversion of these several sugars into one another (at 5–7°) were not proportional to the rates of enolization. Hence, the difference in the rates must be attributed to two different types of 1,2-enediols.

They also studied the enolization (uptake of tritium in 0.5 *M* sodium carbonate in water-*t*) at 25° (29). The rate was very low; after 28 h the reaction for glucose was only 1.39% complete. The relative rates of enolization for glucose, mannose, and fructose were found to be 1.0, 0.5, and 10.7. These are in the same order as the relative rates of initial disappearance of glucose, mannose, and fructose in 1 *M* sodium hydroxide determined in the present work.[4] These latter rates are 1.0, 0.3, and 3.0 and are calculated before reverse reactions or indirect pathways become important. So undoubtedly the formation of enediols plays an important role in the transformation of the various sugars.

It should be pointed out that the relative rates of initial disappearance are for the overall disappearance of a given sugar and represent at least three pathways: i.e., the conversion of glucose to mannose, to fructose, and to other products. Similar pathways exist for the other two starting sugars. The enolization rates are, in contrast, measurements of all products containing tritium; they comprise the three pathways mentioned and also one other, the reconversion of the starting sugar, via the enediol, to itself again. This fourth pathway, an "equilibration", may account for the higher relative rate of enolization of fructose (10.7) in contrast to the relative rate of disappearance (3.0) of the same compound from the alkaline system. Part of this higher rate may also be attributed to a possibly easier attack on the two primary hydrogens at C-1, as well as that of the secondary hydrogen at C-3, in contrast to an attack on the single secondary hydrogen at C-2 of an aldose. Thus, the rate constant k_{24}, with a value of 0.072, would involve 2,3-enediols, β-eliminations, the formation of unsaturated sugars and cleavage products, and benzilic acid rearrangements, as well as reactions involving 1,2-enediols. The lower rate constants k_{15} and k_{36} would involve initially only the 1,2-enediols. Many factors are involved in these rate constants and it is difficult to ascribe the rate-determining steps to any particular one.

Isbell *et al.* (29) have also pointed out the higher rate of enolization of 2-deoxy-sugars (90–155 compared to 1.0 for glucose) and ascribed this to the higher proportions of acyclic intermediates. Penta-*O*-methyl-*aldehydo*-D-glucose, containing a free carbonyl group, is extremely reactive to alkali; Anet (30) found that it was readily rapidly converted by 0.02 *N* lime water into an unsaturated derivative. Since these open-chain compounds seem to react so readily, ring-opening could be a definite rate-determining factor in the enolization and subsequent transformations of sugars existing normally in the ring form.

[4]These relative rates were calculated by a comparison of the rate constants for identical concentrations of reactants at 22°; the constants are given in Table I.

Can. J. Chem. Downloaded from www.nrcresearchpress.com by 210.87.254.6 on 09/05/12
For personal use only.

It is interesting to note in connection with the gluco–manno isomerization that the finding in this study of equal values for the rate constants in each direction of this reaction is in harmony with the early work of Wolfrom and Lewis (31) and Greene and Lewis (32) on the observation of an "equilibrium" isomerization between 2,3,4,6-tetra-*O*-methyl-D-glucose and 2,3,4,6-tetra-*O*-methyl-D-mannose. While they used quite different reaction conditions (1 *M* carbohydrate in 0.018 *M* calcium hydroxide and reaction run to exhaustion of the base, compared with the present 0.002 *M* carbohydrate in 1 *M* sodium hydroxide), they reported a 50/50 "equilibrium mixture" of the epimers. This finding is in harmony with the present finding of equal rate constants for each direction of this reversible reaction. However, it is probable that the equal rate constants observed here and the approximate equality observed for the constants of the gluco–fructo pathway are fortuitous.

Work with deuterium labeling on the formation of D-mannose from D-glucose in saturated lime water (33, 34) has shown that the former sugar can be formed both by a direct pathway and indirectly from D-fructose. An examination of the triangle in the present work will show that initially the rate of direct mannose formation will be appreciable, despite the low value of the rate constant ($k_{13} = 0.0005$), because of the high initial concentration of glucose. The rate of indirect formation, via the fructo–manno pathway, will be low, despite the higher rate constant ($k_{23} = 0.006$), as the initial concentration of fructose will be very low. With increasing reaction time the concentration of fructose formed directly from glucose will increase, and the rate of the fructo–manno pathway will also increase. Thus, analysis of deuterated products (specifically D-mannose), formed after appreciable reaction time, will show a combination of both direct and indirect pathways.

Similar reasoning can be applied to a study of pathways when D-fructose or D-mannose are the starting materials. The interpretation will necessarily become blurred as reverse reactions become appreciable; also degradation reactions, especially that for fructose, will be a factor.

Experimental

Materials

Carbohydrates

The carbohydrates were assessed for chromatographic purity and then further purified as necessary and possible. A chromatographically pure material was taken as one which gave a single symmetrical peak when assayed by the chromatographic procedure to be used in subsequent analytical work and by a procedure with a different column elution gradient. The criterion that purity be established by at least two different gradients was imposed to minimize overlooking the unlikely event that more than one material resulted in a single peak for a particular gradient. A carbohydrate producing a minor peak of less than 1% at a point on the chromatogram not occupied by any of the other carbohydrates of interest (or a very minor peak of a carbohydrate of interest) while not chromatographically pure was accepted in some cases.

In assessing the purity, an aqueous solution (boiled, N_2-saturated, distilled water) of the carbohydrate to be chromatographed was prepared so that it was 0.0100–0.01500 ± 0.00005 g/100.0 ml in the carbohydrate, 0.33 *M* in NaCl, and 0.12 *M* in H_3BO_3 at p*H* 7–8. Thus, this solution contained essentially the same concentrations of the several inorganic ions present in a reaction run sample as prepared for chromatography. A volume of this solution containing 500–1500 μg of the carbohydrate was then chromatographed. By these procedures, chromatographic purity can be assessed to within ±0.1%. The carbohydrates used were: D-glucose (Baker AR Dextrose, anhydrous powder, Lot 25814). Found to be ≮99.9% pure and dry as received. Used as received, D-fructose (Pfanstiehl C.P. Special Lot 3155). Found to be ≮99.9% pure. Used after drying over Drierite, D-mannose (Matheson, Coleman and Bell, and Pfanstiehl, Lot 6799-A). Both were found to be about 98% pure as received. MCB material was recrystallized from methanol–isopropanol (35), dried over Drierite, and used.

Nitrogen

This was Matheson Prepurified Grade, of 99.997% purity.

Solutions

H_3BO_3 (0.12 M) pH 8.50

30.00 ± 0.01 g H_3BO_3 (Mallinckrodt AR) dissolved in 4000 ± 1 ml. (72 °F) distilled water and nominal 12 *M* KOH added to p*H* 8.50 ± 0.02 at 72 °F, (about 10 ml KOH solution required). The solution was filtered through a Whatman GF/A, 5.5 cm glass filter paper supported on a Millipore sintered disk-and-funnel unit and stored in a clear glass bottle at 72 °F.

$K_2B_4O_7$ (0.15 M), pH 9.4

184 ± 0.05 g $K_2B_4O_7 \cdot 4H_2O$ (Mallinckrodt AR) was dissolved in 4000 ± 1 ml (72 °F) distilled water and filtered as above. It was stored in a clear glass bottle at 72 °F.

$K_2B_4O_7$ (0.50 M), pH 9.7

611.0 ± 0.5 g $K_2B_4O_7 \cdot 4H_2O$ (Mallinckrodt AR) was dissolved in 4000 ± 1 ml (72 °F) distilled water and filtered as above. It was stored in a clear glass bottle at 72 °F.

Orcinol/70% H_2SO_4

95.5–96.5% sp.gr. 1.84 H_2SO_4, was slowly added with cooling to 600.0 ± 1 ml (72 °F) distilled water in a 2 l volumetric flask. The addition of the final 1–2 ml of H_2SO_4 to the mark is done after the well-mixed H_2SO_4/H_2O solution has stood at least 12 h at 72 °F. The 2 l of

Can. J. Chem. Downloaded from www.nrcresearchpress.com by 210.87.254.6 on 09/05/12
For personal use only.

70% H_2SO_4 is slowly poured onto 3.500 ± 0.001 g of near-white color orcinol monohydrate (K and K Laboratories) in a 2 1/2 l wide-mouth brown glass bottle. The orcinol/H_2SO_4 solution is stirred with a magnetic stirrer for about 1/2 h and then carefully examined, particularly at the scum line, for complete solution of the orcinol. The color of this solution deepens with time, and in this research a solution more than 24 h old was not used for quantitative work. It appears, though, that orcinol solutions even a week old are useful for qualitative work.

1 M NaOH

In a Teflon beaker, 500 g NaOH (Mallinckrodt AR) was dissolved in 500 ml boiled, N_2-saturated, distilled water. This "lye-oil" is let stand under N_2 in a thick-walled, 1 l, tightly capped polypropylene bottle at room temperature for no less than two weeks to allow Na_2CO_3 to settle out. Aliquots of the clear supernate were transferred by pipet to 2 l of boiled, distilled, N_2-saturated water in a polyethylene bottle in which the stock 1 *M* NaOH was stored. The 1 *M* NaOH solution was standardized against $KHC_3H_4O_4$ (Mallinckrodt Primary Standard) to the phenolphthalein end point. The carbonate content of the 1 *M* NaOH was determined by the carbon dioxide evolution method (TAPPI T 624 m-60) and found to be 0.002–0.003 molar.

Apparatus and Procedures

Constant-Temperature Bath

A 40-gallon tank of water was maintained at temperature with a precision of ±0.05 °C and an accuracy of ±0.05 °C.

Resin Column Chromatography and Automated Analytical Equipment

A schematic diagram showing the equipment and its arrangement as used for the chromatographic separation and quantitative analysis of the compounds of interest in reaction mixture samples is shown in Fig. 3. All components and accessories except the Haake Type FJ constant-temperature circulator were supplied by the Technicon Corporation, Research Park, Ardsley, New York 20502.

Reaction Run Chromatography Sample Preparation

A 25.00 ± 0.02 ml (72 °F) volume of about 1 *M* HCl of strength just sufficient to result in a mixture with p*H* 1–2 was delivered by pipet to the 26.0 ml reaction system. The stopping time of the reaction was defined as when the last of the HCl from the pipet entered the reaction system. The mixture was shaken and then cooled in the constant-temperature bath. A 20.00 ± 0.02 ml (72 °F) aliquot of this acidic mixture was combined in a capped 1 oz glass bottle with 10.00 ± 0.01 ml (72 °F) of 0.36 *M* H_3BO_3, p*H* 9.0. This gave a solution, p*H* 7–8, 0.12 *M* in H_3BO_3 and 0.33 *M* in NaCl. The H_3BO_3 concentration was thus the same as at the beginning of the subsequent elution.

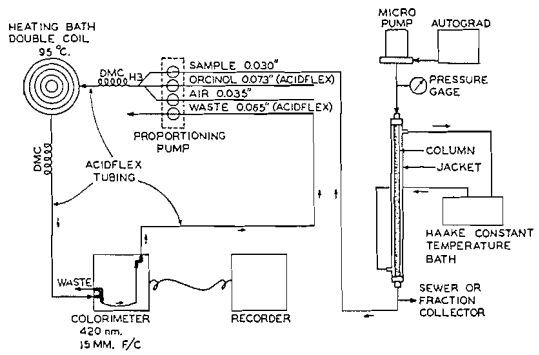

FIG. 3. Schematic diagram for equipment used for chromatographic separation and quantitative analysis.

Chromatography and Auto-Analyzer Conditions

The following conditions were established for column chromatography and Auto-Analyzer operation. Column: 6 mm i.d. × 750 mm water-jacketed glass tube column, resin bed length of 700 mm. Resin: Technicon 3/28/VI; spherical beads. Diameters: 11% > 30 μ, 5% < 10 μ; average diameter = 21 μ. Several resins were used successfully in this study. However, the resin used to obtain the bulk of the data (Technicon 3/28/VI) had a narrower range of particle size at an apparently better average particle diameter and more nearly spherical particles than other resins available. Presumably, these factors contributed significantly to its better performance, compared with say Bio-Rad AG1-X8, 325–400 mesh resin which is Dowex AG1, sized and prepared by the Bio-Rad Corporation of California. It is understood that the Technicon Corporation is actively pursuing the production of resin equivalent to the 3/28/VI resin which at present has an experimental status.

Column Temperature: 30.0 ± 0.1 °C, measured at the jacket outlet. Eluent flow rate: 1.00 ± 0.01 ml/min. This gave a maximum pressure drop of about 500 psig across the column, which occurred during column washing with 0.5 *M* $K_2B_4O_7$. Elution system: in the nine-chambered, rectangular, form Autograd - chambers 1–4, each 100 ml of 0.12 *M* H_3BO_3, p*H* 8.50; chambers 5–8, each 100 ml of 0.15 *M* $K_2B_4O_7$, p*H* 9.30; chamber 9, empty. Proportioning pump tubing: sample from column, color code, black, Tygon, 0.030 in. (i.d.); air supply, color code, orange, Tygon, 0.035 in. (i.d.); orcinol/H_2SO_4 reagent, color code, green, Acidflex, 0.073 in. (i.d.); from colorimeter cell, color code, blue, Acidflex, 0.065 in. (i.d.); Micropipet: Gilmont Micrometer Syringe, 2.0 ml capacity, Cat. No. 7844, Cole-Parmer, Chicago, Ill.

Chromatography Run Procedures

The chromatography and Auto-Analyzer units were operated essentially in accordance with manufacturer's instructions. Upon completion of a run, the column was immediately washed for 1 h with 0.50 *M* $K_2B_4O_7$ and then for 1 h with 0.12 *M* H_3BO_3, p*H* 8.50, by pumping through to the drain with the micro pump.

Experimental Data

Three series of reaction runs were made using in turn D-glucose, D-fructose, and D-mannose as starting material. The reaction conditions and chromatography data for these are given in Table II. A series of column runs was made for calibration purposes using solutions of known concentration of carbohydrates and the same concen-

TABLE II

Reaction runs for the glucose system–chromatography data*

Reaction time (h)	G_0 basis (μg)	Glucose		Mannose		Fructose	
		Absorbance†	Peak time (h:min)	Absorbance†	Peak time (h:min)	Absorbance†	Peak time (h:min)
0.00	82.7	0.520	8:05	0	—	0	—
0.00	82.7	0.533	8:07	0	—	0	—
0.00	68.9	0.454	8:07	0	—	0	—
6.17	68.9	0.378	8:20	0.0018	5:40	0.0098	6:55
10.00	68.9	0.342	7:52	0.0026	5:25	0.0129	6:32
14.53	82.7	0.362	8:05	0.0049	5:25	0.0195	6:43
20.63	68.9	0.253	7:55	0.0058	5:25	0.0145	6:36
27.00	68.9	0.209	8:09	0.0072	5:29	0.0135	6:44
37.00	82.7	0.196	8:10	0.0099	5:29	0.0117	6:47
50.37	68.9	0.114	8:10	0.0106	5:29	0.0088	6:45
60.22	68.9	0.099	7:55	0.0121	5:20	0.0090	6:35
71.00	68.9	0.081	7:56	0.0130	5:27	0.0058	6:37
89.45	68.9	0.037	8:14	0.0076	5:35	0.0027	6.47

NOTE: This is an example of original data; similar data were obtained for the fructose and mannose systems.
*$[G]_0 = 0.00224$; $[OH^-]_0 = 0.9833$; T °C = 22.20 ± 0.02.
†Absorbance measured at 420 nm.

TABLE III

Chromatography calibration data for reaction runs with glucose, fructose, and mannose

Glucose			Fructose			Mannose		
Applied (μg)	Absorbance	Peak time (h:min)	Applied (μg)	Absorbance	Peak time (h:min)	Applied (μg)	Absorbance	Peak time (h:min)
54.3	0.405	8:10	52.9	0.077	6:47	23.1	0.125	5:31
26.5	0.205	8:10	25.9	0.035	6:46	11.1	0.064	5:30
82.7	0.520	8:05	0	—	—	0	—	—
82.7	0.533	8:07	0	—	—	0	—	—
68.9	0.454	8:07	0	—	—	0	—	—
0	—	—	66.6	0.081	6:52	0	—	—
66.3	0.451	8:03	64.1	0.081	6:36	63.4	0.295	5:26
66.3	0.451	7:53	64.1	0.077	6:35	63.4	0.294	5:27
33.2	0.245	7:52	32.1	0.035	6:32	31.7	0.160	5:27
33.2	0.230	7:51	32.1	0.038	6:31	31.7	0.155	5:25
66.3	0.454	7:52	64.1	0.092	6:31	63.4	0.289	5:25
0	—	—	0	—	—	65.5	0.276	5:25
0	—	—	0	—	—	65.5	0.267	5:22
0	—	—	0	—	—	68.2	0.299	5:15

TABLE IV

Absorbance–weight conversion factors between glucose (G), fructose (F), and mannose (M) in chromatography data from reaction runs*

Calibrated absorbance at 50 μg		Glucose	Fructose	Mannose
		0.340	0.061	0.220
$X\rightarrow$				
$Y_0\downarrow$	G_0	1/abs.† G_0	5.574/abs. G_0	1.545 /abs. G_0
	F_0	0.1794/abs. F_0	1/abs. F_0	0.2773/abs. F_0
	M_0	0.6470/abs. M_0	3.606/abs. M_0	1/abs. M_0

*For a given reaction system and on the basis of the same chromatogram sample size for X and Y_0, multiply the absorbance of X by the factors above and by 100 to obtain the quantity of X in a reaction system expressed as the percent relative molarity of Y_0 in that reaction system.
†Abs. = absorbance.

Can. J. Chem. Downloaded from www.nrcresearchpress.com by 210.87.254.6 on 09/05/12
For personal use only.

Can. J. Chem. Downloaded from www.nrcresearchpress.com by 210.87.254.6 on 09/05/12
For personal use only.

trations of inorganic ions as present in column samples prepared from reaction systems. The chromatography data from this series of calibration runs are given in Table III.

The studies of Kesler (22) showed that for absorbance values below about 0.400 there is a straight line relationship between the height of a chromatogram peak and the quantity of that carbohydrate applied to the column. This finding was fully supported by separate experiments in the present study and was used in relating absorbance to weight rather than say area under a chromatogram peak. For a given carbohydrate, the slope of this straight line varies with the operating parameters of both the column and the Auto-Analyzer. In this work, the final choice of operating parameters was directed in part toward those which gave calibration lines of higher slopes, thus increasing the sensitivity of the detection and measurement. Large scale plots (500 × 500 mm) were made of chromatogram peak height *vs* weight of carbohydrate applied to the column from the calibration data of Table III. Visual best-fit straight lines were drawn through these data and the origin. The conversion factors given in Table IV were then derived from these plots. Then the chromatography data of Table II were converted, using these factors, to the relative molar data given in Tables V, VI, and VII. Visual best-fit curves were drawn through large scale plots of these relative molar data.

The slopes of these curves in regions where the data were considered to be the most reliable were then determined by graphical means as follows: 2 250 mm lengths of clear and uniform 10 mm diameter glass rod were tapered snugly together, in parallel arrangement with ends even, using a few wraps of clear Scotch Tape. A sharp, black ink ordinate line was drawn through the curves at the selected times. The pair of glass rods was laid across a curve at a point where the slope was to be measured. The curve line and the black ordinate line were viewed through the pair of glass rods from directly above the point of interest. Then the position of the glass rods was adjusted slowly until simultaneously (*1*) the curve appeared a continuous line, and (*2*) the two wavy, discontinuous segments of the black ordinate line were equidistant from the curve. When the rods were thus positioned, their long axis was parallel with the normal to the tangent to the curve at the point of intersection of the curve and the black

TABLE V

Reaction runs for the glucose system – relative carbohydrate percent molarities*

Reaction time (h)	Glucose (%$M\ G_0$)	Mannose (%$M\ G_0$)	Fructose (%$M\ G_0$)
0.00	100.0	0.0	0.0
6.17	81.2	0.6	11.7
10.00	73.5	0.9	15.5
14.53	64.7	1.4	19.5
20.63	54.3	2.0	17.4
27.00	44.8	2.4	16.2
37.00	34.9	2.7	11.7
50.37	24.4	3.5	10.5
60.22	21.2	4.0	10.8
71.00	17.4	4.3	7.0
89.43	7.9	2.5	3.7

*$[G]_0 = 0.00224$; $[OH^-]_0 = 0.9833$; $T\,°C = 22.20 \pm 0.02$.

TABLE VI

Reaction runs for the fructose system – relative carbohydrate percent molarities*

Reaction time (h)	Fructose (%$M\ F_0$)	Mannose (%$M\ F_0$)	Glucose (%$M\ F_0$)
0.00	100.0	0.0	0.0
4.82	57.4	1.8	11.8
8.13	45.6	2.5	16.4
11.00	34.8	2.9	18.4
14.98	29.3	3.1	18.4
18.12	18.9	3.5	20.2
24.60	13.8	4.0	19.5
30.15	10.0	3.8	18.7
37.00	8.3	3.9	15.4
46.42	6.1	3.8	13.1
71.43	2.7	3.4	7.7

*$[F]_0 = 0.00218$; $[OH^-]_0 = 0.9833$; $T\,°C = 22.20 \pm 0.02$.

TABLE VII

Reaction runs for the mannose system – relative carbohydrate percent molarities*

Reaction time (h)	Mannose (%$M\ M_0$)	Fructose (%$M\ M_0$)	Glucose (%$M\ M_0$)
0.00	100.0	0.0	0.0
5.95	93.0	3.9	1.0
12.03	89.5	5.0	2.0
12.03	—	5.2	2.0
24.00	73.9	5.6	4.3
24.00	—	7.5	4.4
37.20	—	7.9	6.3
48.00	55.5	6.1	7.6
48.00	—	7.5	6.5
58.30	50.6	6.6	7.7
78.00	38.8	6.1	6.7
96.00	27.4	3.4	5.7

*$[M]_0 = 0.00214$; $[OH^-]_0 = 0.9833$; $T\,°C = 22.20 \pm 0.02$.

TABLE VIII

Relative concentration and rate of change of relative concentration of carbohydrates

Starting material	Reaction time (h)	Relative concentration (moles/mole of starting material)			Change of relative concentration (moles/mole of starting material/h)		
		G	*F*	*M*	d*G*/d*t*	d*F*/d*t*	d*M*/d*t*
G	0	1.000	0	0	−0.035	—	—
G	5	0.842	0.101	0.006	−0.02439	+0.01575	+0.0009523
G	9	0.749	0.150	0.010	−0.02041	+0.009756	+0.0009523
G	13	0.673	0.179	0.014	−0.01770	+0.005277	+0.0009523
F	0	0	1.000	0	—	−0.10	—
F	4	0.104	0.666	0.015	+0.01923	−0.06897	+0.002647
F	7	0.150	0.486	0.022	+0.01242	−0.04762	+0.002356
F	12	0.195	0.312	0.031	+0.00493	−0.02532	+0.001339
M	0	0	0	1.000	—	—	−0.012
M	8	0.013	0.041	0.909	+0.001862	+0.003745	−0.01124
M	14	0.025	0.060	0.844	+0.001773	+0.002882	−0.01087
M	21	0.039	0.075	0.771	+0.001745	+0.001475	−0.00976
M	21	0.051	0.078	0.703	+0.001629	0.0000	−0.00901

ordinate. A conveniently placed line was drawn on the squared paper of the plot to be parallel to this tangent, using a pair of large sized set squares to transfer the tangent direction. The data thus obtained are summarized in Table VIII.

Acknowledgments

Financial support for this work from the University of Victoria, Sandwell and Company Limited, and The Institute of Paper Chemistry is gratefully acknowledged by D.J.M.

1. R. L. Whistler and J. N. BeMiller. Advan. Carbohyd. Chem. **13**, 289 (1958).
2. J. C. Speck, Jr. Advan. Carbohyd. Chem. **13**, 63 (1958).
3. J. C. Sowden. Advan. Carbohyd. Chem. **12**, 35 (1957).
4. A. Meller. Holzforschung, **14**, 78, 129 (1960).
5. L. F. McBurney. Degradation of cellulose-kinetics of degradation reactions. *In* E. Ott and H. M. Spurlin's High Polymers. Vol. V. Cellulose, Part I. p. 124. Interscience Publishers, Inc., New York. 1955.
6. G. N. Richards. Alkaline degradation. *In* Methods in carbohydrate chemistry. Vol. III. Cellulose. Academic Press, Inc., New York. 1963. p. 154.
7. J. Kenner and G. N. Richards. J. Chem. Soc. 2240 (1953).
8. W. M. Corbett and J. Kenner. J. Chem. Soc. 2245 (1953).
9. J. Kenner and G. N. Richards. J. Chem. Soc. 278 (1954).
10. J. Kenner and G. N. Richards. J. Chem. Soc. 1784 (1954).
11. W. M. Corbett and J. Kenner. J. Chem. Soc. 1789 (1954).
12. W. M. Corbett and J. Kenner. J. Chem. Soc. 3274 (1954).
13. J. Kenner and G. N. Richards. J. Chem. Soc. 3277 (1954).
14. W. M. Corbett and J. Kenner. J. Chem. Soc. 3281 (1954).
15. W. M. Corbett and J. Kenner. J. Chem. Soc. 1431 (1955).
16. W. M. Corbett, J. Kenner, and G. N. Richards. J. Chem. Soc. 1709 (1955).
17. J. Kenner and G. N. Richards. J. Chem. Soc. 1810 (1955).
18. J. Kenner and G. N. Richards. J. Chem. Soc. 2916 (1956).
19. J. Kenner and G. N. Richards. J. Chem. Soc. 2921 (1956).
20. W. M. Corbett and J. Kenner. J. Chem. Soc. 928 (1957).
21. J. Kenner and G. N. Richards. J. Chem. Soc. 3019 (1957).
22. R. B. Kesler. Anal. Chem. **39** (12), 1416 (1967).
23. R. A. Holm and D. J. MacLaurin. J. Chem. Ed. To be submitted.
24. L. Hough, J. K. N. Jones, and E. L. Richards. J. Chem. Soc. 2005 (1953).
25. F. W. Zerban, L. Sattler, G. Rosenthal, and A. Glaubach. Sugar **47** (2), 33 (1952).
26. A. Carruthers, J. F. T. Oldfield, M. Shore, and A. E. Wooten. Brit. Sugar Corp. 7th Tech. Conf. 1954, 84 pp.; Sugar Ind. Abstr. **16**, 133–134, Chem. Abstr. **50**, 11042d (1956).
27. M. L. Wolfrom and J. N. Schumacher. J. Amer. Chem. Soc. **77**, 3318 (1955).
28. H. S. Isbell and R. A. Verell. Unpublished work, cited in Ref. (29).
29. H. S. Isbell, H. L. Frush, C. W. R. Wade, and C. E. Hunter. Carbohyd. Res. **9**, 163 (1969).
30. E. F. L. J. Anet. Carbohyd. Res. **3**, 251 (1966).
31. M. L. Wolfrom and W. L. Lewis. J. Amer. Chem. Soc. **50**, 837 (1928).
32. R. D. Greene and W. L. Lewis. J. Amer. Chem. Soc. **54**, 1040 (1932).
33. Y. J. Topper and D. Stetten, Jr. J. Biol. Chem. **189**, 191 (1951).
34. J. C. Sowden and R. Schaffer. J. Amer. Chem. Soc. **74**, 505 (1952).
35. J. F. Bates. Polarimetry, saccharimetry, and the sugars. Circular C440, National Bureau of Standards. p. 472. United States Printing Office, Washington, D.C., 1942.

Can. J. Chem. Downloaded from www.nrcresearchpress.com by 210.87.254.6 on 09/05/12
For personal use only.

Carbohydrates in alkaline systems. II. Kinetics of the transformation and degradation reactions of cellobiose, cellobiulose, and 4-*O*-β-D-glucopyranosyl-D-mannose in 1 *M* sodium hydroxide at 22 °C[1]

DONALD J. MACLAURIN[2] AND JOHN W. GREEN[3]
The Institute of Paper Chemistry, Appleton, Wis. 54911

Received November 18, 1968

Rates of isomerization, epimerization, and degradation reactions were measured for cellobiose (**7**), cellobiulose (**8**), and 4-*O*-β-D-glucopyranosyl-D-mannose (**9**) at 0.001 *M* in 1 *M* NaOH under N_2 in the dark at 22 °C. Reaction system resolution was by column chromatography on anion resins in the borate form. Assay for D-glucose (**1**), D-fructose (**2**), D-mannose (**3**), and **7**, **8**, and **9** was by continuous automated colorimetry of column effluent with orcinol–sulfuric acid as reagent. Reaction rate constants (h^{-1}) found: k_{78} 0.078, k_{79} 0.0005, $k_{7,10}$ 0.002, k_{87} 0.022, k_{89} 0.003, k_{81} 0.065, $k_{8,12}$ 0.023, k_{97} 0.002, k_{98} 0.013, $k_{9,11}$ 0.006 where **10**, **11**, and **12** are other products than **1**, **2**, **3**, **7**, **8**, and **9**. Details for preparation of **8** and **9** are given.

Canadian Journal of Chemistry, 47, 3957 (1969)

Can. J. Chem. Downloaded from www.nrcresearchpress.com by 210.87.254.6 on 09/05/12
For personal use only.

Introduction

Previous work (1) on D-glucose, D-fructose, and D-mannose gave rate constants for the various interconversions and degradations in 1 *M* sodium hydroxide at 22 °C. These data were necessary and were utilized in studying the present work with cellobiose, cellobiulose, and 4-*O*-β-D-glucopyranosyl-D-mannose. This permits further investigation of the "peeling" and "stopping" reactions, studied by Kenner and associates (2–4) and reviewed by Whistler and BeMiller (5).

Derivation of Reaction Rate Constants

The analytical data showed qualitatively that when a reaction was begun with cellobiose, cellobiulose, or 4-*O*-β-D-glucopyranosyl-D-mannose, (glucosylmannose), each of the other two disaccharides and the three hexoses (D-glucose, D-fructose, and D-mannose) appeared in the system. On a similar basis as that previously described for the hexoses (1), the reaction scheme shown in Fig. 1 was postulated for calculation of reaction rate constants.

For this reaction scheme with first-order reactions, the following equations apply:

$$[1]\quad dG/dt = k_{81}GF + k_{21}F + k_{31}M - (k_{12} + k_{13} + k_{15})G$$

$$[2]\quad dF/dt = k_{12}G + k_{32}M - (k_{21} + k_{23} + k_{24})F$$

$$[3]\quad dM/dt = k_{13}G + k_{23}F - (k_{31} + k_{32} + k_{36})M$$

$$[4]\quad dA/dt = k_{24}F$$

$$[5]\quad dB/dt = k_{15}G$$

$$[6]\quad dC/dt = k_{36}M$$

$$[7]\quad dGG/dt = k_{87}GF + k_{97}GM - (k_{78} + k_{79} + k_{7,10})GG$$

$$[8]\quad dGF/dt = k_{78}GG + k_{98}GM - (k_{81} + k_{87} + k_{89} + k_{8,12})GF$$

$$[9]\quad dGM/dt = k_{79}GG + k_{89}GF - (k_{97} + k_{98} + k_{9,11})GM$$

$$[10]\quad dD/dt = k_{7,10}GG$$

$$[11]\quad dE/dt = k_{9,11}GM$$

$$[12]\quad dH/dt = k_{8,12}GF$$

where: GG = cellobiose; GF = cellobiulose; GM = glucosylmannose; G = glucose; F = fructose; M = mannose; A, B, C, D, E, H = other products; S = saccharinic acids.

A preliminary set of values for the rate constants of the reactions involving the disaccharides was obtained by estimation from plots of concentrations *vs.* time. These preliminary values and the reaction rate constants previously obtained (1) for the monosaccharide portion of the system were then refined on a computer as before (1). The final values of the rate constants

[1]A portion of a thesis submitted by D. J. M. in partial fulfillment of the requirements of The Institute of Paper Chemistry for the degree of Doctor of Philosophy from Lawrence University, Appleton, Wis., January, 1969.

[2]Present address: Department of Chemistry, University of Victoria, Victoria, B.C.
[3]Senior Research Associate, The Institute of Paper Chemistry, Appleton, Wis. 54911.

obtained are shown in Fig. 1 and listed in Table I. The precisions assigned in the table are liberal estimates based on effects observed during curve fitting. The computer-derived curves, using these rate constants and equations [1], [2], [3], [8], and [9] are shown in Fig. 2 for the cellobiose, cellobiulose, and glucosylmannose systems.

Computer plots for other products (saccharinic acids etc. which were not determined analytically) are shown in Fig. 3. The computer plots for the disaccharides only in each of these systems, superimposed on the experimental data, are shown in Fig. 4, and those for the monosaccharides only in Fig. 5. The fit between the curves and the experimental points in Fig. 4 and 5 is considered to give support to the validity of the experimental methods, the data obtained, the reaction scheme, and the rate constants derived from the data.

TABLE I

Rate constants in the system 0.001 *M* cellobiose in 1 *M* sodium hydroxide at 22 °C

Reaction pathway	Rate constant	Rate constant value (h^{-1})
G→F	k_{12}	0.036 ±0.001
G→M	k_{13}	0.0005±0.0002
G→B	k_{15}	0.002 ±0.0005
F→G	k_{21}	0.038 ±0.001
F→M	k_{23}	0.006 ±0.0005
F→A	k_{24}	0.072 ±0.001
M→G	k_{31}	0.0005±0.0002
M→F	k_{32}	0.011 ±0.0005
M→C	k_{36}	0.002 ±0.0005
GG→GF	k_{78}	0.078 ±0.001
GG→GM	k_{79}	0.0005±0.0002
GG→D	$k_{7,10}$	0.002 ±0.0005
GF→GG	k_{87}	0.022 ±0.0005
GF→GM	k_{89}	0.003 ±0.0005
GF→S+G	k_{81}	0.065 ±0.001
GF→H	$k_{8,12}$	0.023 ±0.001
GM→GG	k_{97}	0.002 ±0.0005
GM→GF	k_{93}	0.013 ±0.001
GM→E	$k_{9,11}$	0.006 ±0.

Discussion of Results

The alkaline peeling reaction has been demon-

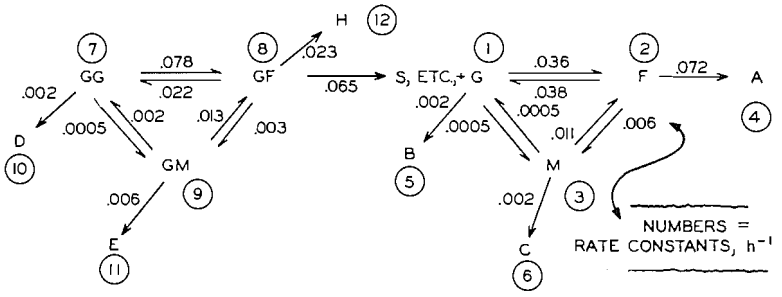

FIG. 1. Reaction scheme in 1 *M* sodium hydroxide at 22 °C. GG = cellobiose; GF = cellobiulose; GM = glucosylmannose; G = glucose; F = fructose; M = mannose; A, B, C, D, E, H = other products; S = saccharinic acid.

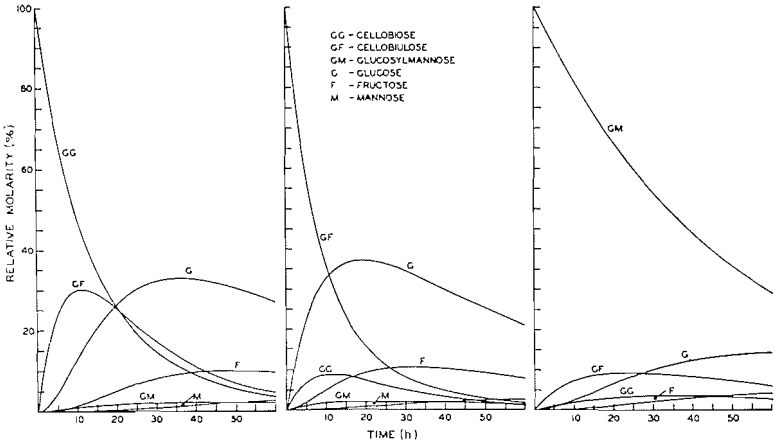

FIG. 2. Carbohydrates present in 1 *M* sodium hydroxide at 22 °C.

Can. J. Chem. Downloaded from www.nrcresearchpress.com by 210.87.254.6 on 09/05/12
For personal use only.

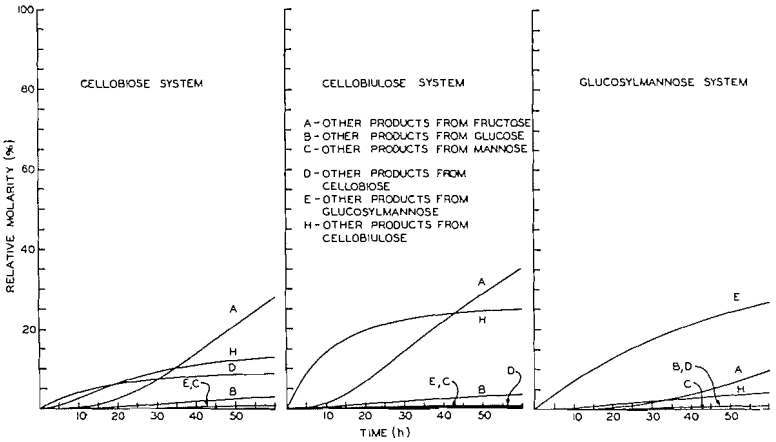

FIG. 3. Calculated plots of other products formed in 1 *M* sodium hydroxide at 22 °C.

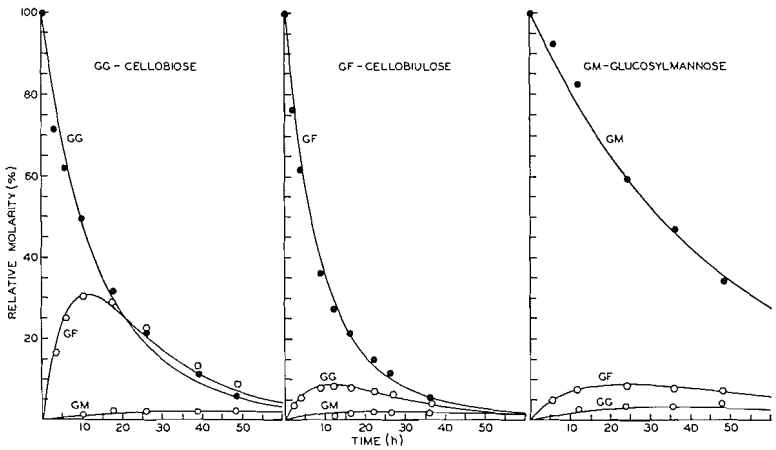

FIG. 4. Disaccharides present in 1 *M* sodium hydroxide at 22 °C.

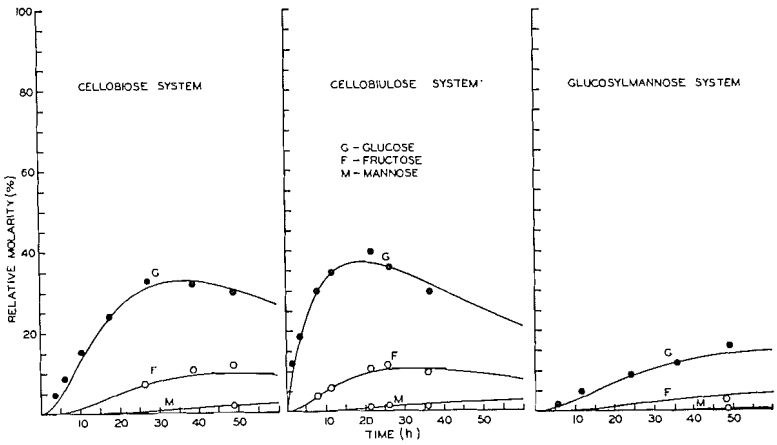

FIG. 5. Disaccharide systems. Monosaccharides formed in 1 *M* sodium hydroxide at 22 °C.

Can. J. Chem. Downloaded from www.nrcresearchpress.com by 210.87.254.6 on 09/05/12
For personal use only.

Can. J. Chem. Downloaded from www.nrcresearchpress.com by 210.87.254.6 on 09/05/12
For personal use only.

strated qualitatively by Corbett and Kenner (6) for cellobiose; the base used was saturated lime water at 25 °C and the reaction was observed over a period of several weeks. These authors also showed qualitatively that cellobiulose was formed initially and that glucose and fructose were formed later in the reaction. The peeling reaction was found to be much faster for cellobiulose than for cellobiose. The quantitative studies were confined to the disappearance of total disaccharides and the appearance of total monosaccharides (7); these data suggested that the aldose is first converted to a ketose before the peeling reaction occurs.

In the present work, carried out in 1 *M* sodium hydroxide at 22 °C, the formation of cellobiulose from cellobiose and its faster conversion during peeling to give D-glucose (and then D-fructose) has been confirmed, and in addition the rates of these individual reactions have been determined quantitatively. Also, the reversible formations of 4-*O*-β-D-glucopyranosyl-D-mannose and of D-mannose have been demonstrated, and rate constants determined. As in the case for the monosaccharides (1), the disappearance of the disaccharides from the several systems seems to be mostly through the ketose, cellobiulose.

Thus, the greater role of the ketose, whether mono- or disaccharides, in alkaline systems, as demonstrated earlier by Kenner, *et al.*, is clearly shown in the present kinetic data.

In addition, it has been demonstrated that, while the interconversion of the several disaccharides is reversible, no equilibrium conditions exist when an excess of alkali is present, because degradation of the disaccharides, either directly or by a peeling reaction, proceeds indefinitely. The main loss of disaccharides seems to occur through cellobiulose as an intermediate, predominantly by peeling, but also by other undetermined pathways.

As in the preceding paper (1) the term "transformation" is used to describe, in a collective sense, reversible epimerization and isomerization reactions of the Lobry de Bruyn–Alberda van Ekenstein type which occur between carbohydrates. The term "degradation" is used to describe other, generally, more drastic irreversible reactions undergone by carbohydrates in alkaline systems. The overall rate constants obtained represent not only changes within the alkaline system but also the conversion of the intermediates in the system to final products by a process of acidification. The various reactions involved here are part of a complex system so that it is difficult to draw definite conclusions from the kinetic data.

In the present system (see Fig. 1) there are two triangles. Each is composed of reversible epimerization and isomerization reactions. Equilibrium conditions do not exist in the overall system, studied with an excess of alkali. The disaccharide triangle is connected to the monosaccharide triangle by an irreversible "peeling" reaction, proceeding through cellobiulose, and characterized by the rate constant k_{81}. Equilibrium conditions are also disturbed by other less specific degradation reactions, characterized by k_{15}, k_{24}, k_{36}, $k_{7,10}$, $k_{8,12}$, and $k_{9,11}$.

As reported for D-glucose, D-fructose, and D-mannose, reversible transformation reactions involving C-1 and C-2 are now reported for the first time between the three parallel disaccharides. Transformation reactions involving C-3, of these disaccharides, did not occur, at least to any greater extent than about 1% of the starting material.

The results obtained in this work clearly confirm the existence of the peeling reaction (5,8,9) and extend the findings of Kenner and associates (2–4,6) by showing that mannose and 4-*O*-β-D-glucopyranosyl-D-mannose appear as intermediate products in the alkaline degradation of cellobiose and cellobiulose under the conditions used. However, it is noted that under these conditions it appears, as shown in Fig. 3, that only about 80% of the starting cellobiose molecules proceed through cellobiulose (either directly or in very small amount via 4-*O*-β-D-glucopyranosyl-D-mannose), and on to the peeling reaction. About 10% of the cellobiose molecules are converted directly (GG to D in Fig. 1) to unknown products. A further 10% are converted on a nonpeeling reaction route via cellobiulose (GF to H in Fig. 1). About 1–2% of the cellobiose molecules are converted on a nonpeeling reaction route via 4-*O*-β-D-glucopyranosyl-D-mannose (GM to E).

In the monosaccharide triangle the constants for the forward and reverse reactions were almost the same. In the disaccharide triangle (Fig. 1) the three sets of rate constants are in ratios of roughly three or four to one instead, but are of the same order of magnitude as the monosaccharide analogs. Thus, the cellobiose to glucosylmannose conversion has the same rate

Can. J. Chem. Downloaded from www.nrcresearchpress.com by 210.87.254.6 on 09/05/12
For personal use only.

constant as that observed for the glucose-to-mannose pathway. However, the reverse pathway is much faster for the disaccharides.

The situation is different for the cellobiulose to glucosylmannose pathway; here the rate constant is only half that observed for the monosaccharide system. In both of the pathways starting with glucosylmannose, however, the "equilibrium" is increasingly unfavorable, in contrast to that observed for mannose.

The "equilibrium" between cellobiose and cellobiulose has also been displaced in favor of the latter, whereas for the monosaccharide analogs the two opposing rate constants were almost equal. This increased rate constant favoring cellobiulose may be a steric effect of the bulky glucosyl group at C-4, which is eased by ketose formation at C-2.

The rate constant for the degradation of cellobiose is similar to that of glucose (0.002) but that for glucosylmannose is larger (0.006) than that for mannose (0.002). Thus, this second disaccharide shows less stability in both transformation and degradation reactions.

Comparison of the degradation reactions for cellobiulose and fructose shows that those for the disaccharide (defined by two rate constants) are much faster than those for the monosaccharide. The constant k_{81} defines the elimination of a glucosyloxy anion from C-4; the corresponding elimination of a hydroxyl group from C-4 of fructose is only one of many reactions involved in the rate constant k_{24}. One would expect the elimination of the glucosyloxy group to be easier than that of the hydroxyl group, based on the more acidic character of the former group. This leaving group tendency has been shown in the alkaline cleavage of methyl β-cellobioside (10), where the interior glycosidic linkage (removal of methyl D-glucoside) is broken more readily than the glycosidic linkage containing the methoxyl group.

Isbell and co-worker (11) have postulated the existence of *cis*- and *trans*-isomers of the 1,2-enediols to explain the transformation of various sugars; thus, the ratio of these two isomers, formed as intermediates, would be different for an aldose and for a ketose. While the principal enolization is between C-1 and C-2, they found that the rates of conversion of glucose, mannose, and fructose into one another were not proportional to the rates of enolization. The existence of the two types of enediols was then suggested, since the same 1,2-enediol cannot be formed from the several starting sugars.

While this work was confined mostly to monosaccharides, they did determine the rate of enolization (uptake of tritium in 0.5 *M* sodium carbonate in water-*t*) at 25° for several disaccharides (12). The relative rate of enolization was 2.6, compared to 1.0 for glucose. The relative rates for the initial disappearance of cellobiose, compared to that for glucose, are 2.2 and 1.0. (These rates were obtained by a comparison of the rate constants in the present work, Table I, for identical concentrations and 22°.)

The relative rates of initial disappearance for cellobiulose and glucosylmannose are 2.9 and 0.6. Isbell, *et al.* do not give any data for these compounds; however, the relative rates of lactose and the corresponding ketose, lactulose, are 2.0 and 37.0. Here again, as was noted for the monosaccharide system (1), the relative rate of enolization of the ketose is much greater than the relative rate of initial appearance of the ketose from the alkaline system. The reconversion of the ketodisaccharide, via an enediol, to the ketodisaccharide (tritiated) again, may be a factor here.

The relative rates of disappearance for the three disaccharides are 2.1, 0.55, and 3.0, whereas those for glucose, mannose, and fructose are 1.0, 0.36, and 2.9. The rates for the two aldodisaccharides are approximately twice those for the corresponding monosaccharides, presumably showing the crowding effect of the 4-glucosyloxy group. However, no such accelerating effect is shown for the ketodisaccharide. The relative rate is surprisingly low, and the relative rate of enolization found by Isbell, *et al.* for lactulose is surprisingly high. In all cases studied the disaccharides showed higher enolization rates than did the monosaccharides; the relative rate of initial disappearance for cellobiulose simply does not follow this trend.

As suggested for the monosaccharides (1), both enolization and ring-opening may be involved in the rate-determining process for the transformations of the several disaccharides. The relatively low rate of initial disappearance for cellobiulose, less than anticipated, suggests that different rate-determining processes may be operative here than for fructose.

No precise quantitative data were obtained in this study with respect to the postulated stopping reaction (elimination of a hydroxyl group at

Can. J. Chem. Downloaded from www.nrcresearchpress.com by 210.87.254.6 on 09/05/12
For personal use only.

C-3). However, some semiquantitative chromatography data indicated the presence of a reaction product (appearing late on the chromatogram and thus suggestive of a molecule containing a carboxyl group) which on hydrolysis gave glucose. The amounts of glucose so produced were in approximate accord with what might arise from the sum of the molecules D and H arising from cellobiose and cellobiulose, respectively. There was an indication that a higher percentage of the starting material appeared as glucose from the spent system, when the starting material was cellobiulose. This indication agrees with the calculated findings and suggests that the route to the stopped molecule, D-glucosylmetasaccharinic acid, is preferentially via cellobiulose. On the basis that molecules D and H and possibly also E are largely stopped biose molecules, then perhaps as much as 10–15% of a given amount of cellobiose proceeds under the conditions used to the glucosylmetasaccharinic acid molecule, as hypothesized for the stopping reaction. This tentative conclusion is in fair agreement with the recent studies of Lindberg, Theander, and Uddegard (13), who report a 3% stopping reaction for cellobiose in 0.02% molar sodium hydroxide at 90 °C and an increase to 4.5% at 60 °C.

Corbett and Kenner (14) observed a time-lag in the decomposition of lactose and ascribed this to the "necessary genesis of the ketose." In the present work this time-lag is shown very plainly in Fig. 5 for the generation of glucose from both cellobiose and from glucosylmannose, where time is needed to build up an appreciable concentration of the intermediate cellobiulose, before the peeling reaction, i.e., elimination of glucose at C-4, can occur in detectable amounts. In the case of cellobiulose (Fig. 5) the formation of glucose is very rapid, with no time-lag observed.

In contrast, the formation of fructose shows a time-lag in the case of all three disaccharides (Fig. 5), demonstrating that this monosaccharide is a secondary product, and must be formed from glucose, the initial product of the peeling reaction. The amounts of mannose formed are too small to show a similar effect.

Experimental

Apparatus and Procedures

All apparatus and procedures used were as previously described (1). The nitrogen was Matheson Prepurified Grade, of 99.997% purity.

Carbohydrates

The carbohydrates used were assessed for chromatographic purity as previously described (1). Cellobiose (Pfanstiehl Lot 7236) was found to contain 1% glucose. It was slowly recrystallized from 2:3 v/v acetone–water (25 g. from 56 ml) to give a fraction containing about 0.15% glucose and no other impurity. This material was dried over Drierite before use. Slow crystallization from a methanol-water system was not successful.

Cellobiulose

This syrupy sugar was prepared from cellobiose by a modification of the method used by Corbett and Kenner (6). Cellobiose (50 g) was treated with 0.015 *M* $Ba(OH)_2$ (500 ml) for 6.5 h at 30 °C and the reaction then quenched with Amberlite IR-120-H resin (200 ml). The filtrate and washings (1000 ml) were concentrated *in vacuo*, and the residue taken up in methanol (250 ml). The precipitate (45 g of 99% cellobiose) was removed. Concentration of the filtrate and washings (400 ml) to 75 ml gave more precipitate (1.5 g 97% cellobiose); further concentration to dryness and treatment of the residue with methanol (75 ml) gave a third precipitate (0.3 g, 90% cellobiose). The final filtrate was concentrated to dryness, and dissolved in water (500 ml); the solution was shown by paper chromatography to contain 1% cellobiulose, 0.2% cellobiose, and 0.2% glucose.

The aldoses in this solution were oxidized by NaOI with the method of Kline and Acree (15). The resultant solution was treated with Amberlite IR-120-H resin to p*H* 1.7. The filtrate and washings were concentrated to 1000 ml and treated with Amberlite IRA-400-OH resin to p*H* 9. The mixture was quickly filtered and IR-120-H resin added to the filtrate to p*H* 6.8. The solution, concentrated to 600 ml, contained a trace of glucose. Repetition of the NaOI and resin treatments, on a suitably reduced scale, gave a cellobiulose solution that was not chromatographically pure; it was concentrated to 5 ml syrup. Treatment with methanol (40 ml) at 75 °C gave a green–yellow solution and a fine dusty precipitate formed on cooling. Addition of methanol (100 ml) and ethyl ether (200 ml) to the cooled solution gave quickly a copious white floc. It was filtered off and washed with acetone and anhydrous ether under dry nitrogen. The 5% yield was amorphous, pure white and very hygroscopic. Found $[\alpha]_D^{20} - 75°$ (*c* 10 [anhydrous basis], H_2O). Reported (6) $[\alpha]_D^{23} - 60.1°$ (*c* 2.40, H_2O).

A chromatogram of the hydrolyzate of this material (1 *M* sulfuric acid for 6 h at 100°) showed only glucose and fructose, and in about equal amounts.

This material was weighed up under dry nitrogen for preparation of kinetic solutions.

4-O-β-D-glucopyranosyl-D-mannose

This disaccharide was prepared from cellobiose octaacetate by a modification of the method of Brauns (16).

A 1000 ml heavy-walled polypropylene screw-cap bottle containing cellobiose octaacetate (70 g) was cooled to −50 °C. By means of a 1/4 in. polyethylene tube anhydrous HF gas (140 g) was slowly bled (3.5 h) from a cylinder and condensed on the carbohydrate material, which went into solution during the first 2 h. The capped bottle was maintained at room temperature for 6.5 h, then recooled, opened, and cold $CHCl_3$ (300 ml) cautiously added. The mixture, with $CHCl_3$ (100 ml) as a rinse, was

TABLE II

Reaction runs for the cellobiose system – chromatography data*

Reaction time (h)	Column run no.	GG_0 Basis (μg)	Cellobiose Absorbance†	Cellobiose Peak time (h:min)	Glucosylmannose Absorbance†	Glucosylmannose Peak time (h:min)	Cellobiulose Absorbance†	Cellobiulose Peak time (h:min)
3.45	195	48.4	0.243	1:17	Trace	4:15	0.0305	4:41
6.00	197	48.4	0.202	1:25	Trace	4:20	0.0463	4:55
10.00	199	69.1	0.232	1:20	0.0036	4:15	0.0767	4:50
10.68	198	53.3	0.184	1:20	0.0031	4:25	0.0659	4:59
17.73	196	69.1	0.147	1:17	0.0058	4:10	0.0771	4:42
26.08	201	96.6	0.140	1:18	0.0075	4:15	0.0840	4:51
38.80	204	110.5	0.084	1:17	0.0081	4:05	0.0558	4:43
48.13	203	96.6	0.037	1:20	0.0080	4:08	0.0350	4:43
71.00	200	96.6	0.019	1:17	0.0071	4:10	0.0153	4:47
			Mannose		Fructose		Glucose	
3.45	195	—	0	—	0	—	0.0085	7:46
6.00	197	—	0	—	0	—	0.0152	8:05
10.00	199	—	0	—	0	—	0.0355	8:00
10.68	198	—	0	—	0	—	0.0311	8:10
17.73	196	—	0	—	0	—	0.0595	7:49
26.08	201	—	Trace	5:23	0.0044	6:40	0.1140	8:06
38.80	204	—	Trace	5:20	0.0076	6:33	0.1250	7:55
48.13	203	—	0.0027	5:14	0.0072	6:29	0.1020	7:50
71.00	200	—	0.0053	5:18	0.0053	6:35	0.0811	7:59

NOTE: This table is given as an example of original data; similar data were obtained for the cellobiulose and glucosylmannose systems.
*$[GG]_0 = 0.00119$; $[OH^-]_0 = 0.9845$; T °C = 22.20 ± 0.02.
†Absorbance measured at 420 nm.

TABLE III

Reaction runs for the cellobiose system – relative carbohydrate percent molarities*

Reaction time (h)	Cellobiose (%M GG_0)	Glucosylmannose (%M GG_0)	Cellobiulose (%M GG_0)	Mannose (%M GG_0)	Fructose (%M GG_0)	Glucose (%M GG_0)
0.00	100.0	0.0	0.0	0.0	0.0	0.0
3.45	71.5	Trace	16.5	0.0	0.0	4.9
6.00	62.0	Trace	25.0	0.0	0.0	8.8
10.00	49.6	1.3	29.0	0.0	0.0	14.4
10.68	49.2	1.5	31.2	0.0	0.0	15.8
17.73	31.5	2.1	29.2	0.0	0.0	24.0
26.08	21.4	2.0	22.6	Trace	7.0	33.0
38.80	11.3	1.9	13.2	Trace	10.8	31.6
48.13	5.7	2.1	9.5	1.2	11.5	29.5
71.00	2.9	1.9	4.1	2.7	8.6	23.4

*$[GG]_0 = 0.00119$; $[OH^-]_0 = 0.9845$; T °C = 22.20 ± 0.02.

TABLE IV

Reaction runs for the cellobiulose system – relative carbohydrate percent molarities*

Reaction time (h)	Cellobiulose (%M GF_0)	Cellobiose (%M GF_0)	Glucosylmannose (%M GF_0)	Mannose (%M GF_0)	Fructose (%M GF_0)	Glucose (%M GF_0)
0.00	100.0	0.0	0.0	0.0	0.0	0.0
2.00	76.6	3.4	0.0	0.0	0.0	12.0
4.00	62.0	5.7	0.0	0.0	0.0	18.4
8.55	36.0	7.7	Trace	0.0	3.0	29.8
12.00	27.4	8.0	1.0	0.0	5.3	34.4
16.13	21.4	7.6	1.9	—	—	—
22.00	15.0	7.2	1.2	1.0	10.5	39.7
26.62	11.3	6.4	1.4	0.8	11.0	35.6
36.28	5.4	4.6	—	1.2	9.7	29.6

*$[GF]_0 = 0.00080$; $[OH^-]_0 = 0.9845$; T °C = 22.20 ± 0.02.

Can. J. Chem. Downloaded from www.nrcresearchpress.com by 210.87.254.6 on 09/05/12
For personal use only.

TABLE V

Reaction runs for the glucosylmannose system – relative carbohydrate percent molarities*

Reaction time (h)	Glucosylmannose (%MGM_0)	Cellobiose (%MGM_0)	Cellobiulose (%MGM_0)	Mannose (%MGM_0)	Fructose (%MGM_0)	Glucose (%MGM_0)
0.00	100.00	0.0	0.0	0.0	0.0	0.0
6.00	92.5	1.6	5.0	0.0	0.0	2.0
12.10	82.8	2.8	7.2	0.0	0.0	5.0
24.83	59.4	3.8	8.5	0.0	0.0	9.3
36.00	47.5	3.3	8.6	Trace	Trace	12.4
48.18	26.5	4.4	7.1	0.6	2.0	16.1

*$[GM]_0 = 0.00110$; $[OH^-]_0 = 0.9845$; $T\,°C = 22.20 \pm 0.02$.

transferred to a polyethylene vessel containing ice and water (800 ml each) and $CHCl_3$ (400 ml), and stirred with a polyethylene rod. After the ice had melted, the clear water layer was decanted and the organic layer repeatedly stirred with water (20 l in all) until neutral washings were obtained. The final water washing was treated with $NaHCO_3$ (25 g) to give p*H* 8. The $CHCl_3$ layer (1500 ml) was dried over Na_2SO_4, and concentrated to about 30 ml syrup.

The syrup was treated with Ac_2O (470 ml), giving a clear solution (green–gold) within 5 min. Perchloric acid (72%, 3 ml) was then added and the mahogany–red solution maintained 1 h at 35–40 °C with occasional shaking. It was then added (with a rinse of 50 ml Ac_2O) to crushed ice and water (1 l each) and the mixture stirred 2.5 h. The brown precipitate was washed with water (20 ml) and dissolved in boiling 97% EtOH (2 l). After 3 h cooling with stirring, the fibrous crystals were filtered on glass filter paper (Whatman GF/A) and washed with 95% EtOH. (No product could be isolated from the mother liquor.) The product was washed by stirring with water (2.5 l) and dried at 43 °C *in vacuo* to 24 g weight; m.p. 204° corrected, compared with literature values of 202–203° for glucosylmannose octaacetate and 229° for cellobiose octaacetate.

The product (24 g) was deacetylated in dry MeOH (250 ml) with NaOMe solution (0.015 g Na in 30 ml MeOH) for 45 min (clear brown solution). IR-120-H Resin (10 ml) was then added (p*H* change from 8 to 6) with stirring, and the solution concentrated to 15 ml syrup. This was dissolved in 98% EtOH (300 ml) and cooled overnight with stirring. The product was washed with 95% EtOH and Me_2CO to give 8.7 g, m.p. 177°. It was dissolved in water (150 ml), decolorized with 5 ml of a 1:1 v/v mixture of Darco G-60/Celite 545 for 5 min with stirring, and the mixture filtered through 3 sheets of GF/A glass paper. The filtrate was concentrated to 10 ml syrup which was dissolved in boiling 95% EtOH (175 ml). Cooling with stirring 12 h, gave 8.3 g product, m.p. 178.5–179.5 °C corrected. Drying 4.5 h at 100 °C *in vacuo* gave a weight loss of 5.6% but no change in m.p. Reported 174–175 °C (8) and 175–176 °C (17,18). $[\alpha]_D^{20}$ 6.3° (*c* 2.2, H_2O) initially, and 6.5° after 60 min; reported (19) 14.6° and 6.2°, respectively. The material had a chromatographic purity of 99.8% with 0.2% cellobiose as impurity. Its chromatographic behavior was identical with that for a known sample (20).

Kinetic runs

Three series of reaction runs were made, using cellobiose, cellobiulose, or 4-*O*-β-D-glucopyranosyl-D-mannose as starting material. The reaction conditions and chromatographic data for these are given in Table II. These chromatographic data were converted to the relative molar data given in Tables III, IV, and V by the same procedures as previously reported (1).

Acknowledgments

Financial support for this work from the University of Victoria, Sandwell and Company Limited, and The Institute of Paper Chemistry is gratefully acknowledged by D. J. M. Acknowledgment is also given to L. R. Schroeder and to N. S. Thompson for samples of sugars.

1. D. J. MacLaurin and J. W. Green. Can. J. Chem. This issue.
2. J. Kenner and G. M. Richards. J. Chem. Soc. 2240(1953); 278, 1784, 3277(1954); 1810, 2916(1955); 3019(1957).
3. W. M. Corbett and J. Kenner. J. Chem. Soc. 2245(1953); 3274, 3281(1954); 927(1957).
4. W. M. Corbett, J. Kenner, and G. M. Richards. J. Chem. Soc. 1709(1955).
5. R. L. Whistler and J. N. BeMiller. Advan. Carbohyd. Chem. **13**, 63(1958).
6. W. M. Corbett and J. Kenner. J. Chem. Soc. 1431(1955).
7. W. M. Corbett. Chem. Ind. (London), 1285(1953).
8. J. U. Nef. Ann. **357**, 294 (1907).
9. H. S. Isbell. J. Res. Nat. Bur. Stand. **32**, 45 (1944).
10. E. V. Best and J. W. Green. In press.
11. H. S. Isbell and R. A. Verell. To be published in Tappi.
12. H. S. Isbell, H. L. Frush, C. W. R. Wade, and C. E. Hunter. Carbohyd. Res. **9**, 163 (1969).
13. B. Lindberg, O. Theander, and J. Uddegard. Sv. Papperstidn. **69**, 360 (1966).
14. W. M. Corbett and J. Kenner. J. Chem. Soc. 1789 (1954).
15. G. M. Kline and S. F. Acree. J. Res. Nat. Bur. Stand. **5**, 1063 (1930); Ind. Eng. Chem., Anal. Ed. **2**, 413 (1930).
16. D. H. Brauns. J. Amer. Chem. Soc. **48**, 2781 (1926).
17. M. Bergmann and H. Schotte. Ber. **54**, 1570 (1921).
18. W. N. Haworth, E. L. Hirst, H. R. L. Streight, H. A. Thomas, and J. Webb. J. Chem. Soc. 2636 (1930).
19. H. S. Isbell. J. Res. Nat. Bur. Stand. **5**, 1179 (1930).
20. N. S. Thompson, J. K. Hamilton, and H. W. Kircher. J. Amer. Chem. Soc. **80**, 4703 (1958).

Can. J. Chem. Downloaded from www.nrcresearchpress.com by 210.87.254.6 on 09/05/12
For personal use only.

Can. J. Chem. Downloaded from www.nrcresearchpress.com by 210.87.254.105 on 09/05/12
For personal use only.

Pyrazolines IX. Chemistry of some 3-cyano-3-carbomethoxy-1-pyrazolines[1]

DONALD E. MCGREER AND Y. Y. WIGFIELD
Department of Chemistry, University of British Columbia, Vancouver, B.C.

Received June 5, 1969

Product and kinetic studies have been made on the pyrolysis of a series of 3-cyano-3-carbomethoxy-1-pyrazolines substituted at C-4 with a methyl and an aryl group (phenyl, *p*-methoxyphenyl, and *p*-nitrophenyl). Evidence is presented supporting a transition state structure in which little progress to bond breaking of the C-5 to N bond has taken place at the transition state. The product distribution is largely dependent on the stereochemistry of the initial pyrazoline and to a lesser degree on the nature of the aryl group at C-4. The *cis* pyrazolines gave products resulting primarily from aryl migration while the *trans* pyrazolines gave products predominantly from methyl migration.

Canadian Journal of Chemistry, 47, 3965 (1969)

As a continuation of our interest in the mechanism of the pyrolysis of pyrazolines we have extended our studies to a series of 3-cyano-3-carbomethoxy-1-pyrazolines (**1**) substituted with a variety of groups at C-4 having a known stereo-

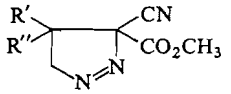

1

chemical relation to the substituents on C-3. As the mechanism for the pyrolysis reaction evolves it becomes apparent that a spectrum of mechanisms may develop based on the nature of substituents attached to the ring carbons. Earlier studies on the kinetics (1) and stereochemistry (2) for the pyrolysis of **1** have indicated a change of mechanism occurs in going from pyrazolines substituted with one electron withdrawing group at C-3 to those with two electron withdrawing groups at C-3. It is our purpose in the present paper to evaluate this change in more detail. Recently Hamelin and Carrie (3–5) have reported results on a closely related series of compounds which differ primarily by the use of a carboethoxy group at C-3 rather than a carbomethoxy group. Because of this overlap we will emphasize that chemistry which we can add to their contributions.

Preparation of Pyrazolines

The pyrazolines for this study were all prepared by the addition of diazomethane to the appropriate methyl α-cyanoacrylate and are shown in Chart 1. Compounds **2–4** are isolated in the *trans*[2] form, from the condensation of benzaldehyde with methyl cyanoacetate. The *trans* form of compounds **8–10** is isolated as the only product from the pyrazolines **5–7** (herein, 6, and 7). The *cis* form of **8** and **10** are derived from *cis–trans* isomeric mixtures obtained by equilibration followed by separation and purification.

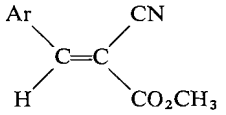

2 Ar = C_6H_5
3 Ar = *p*-$CH_3OC_6H_4$
4 Ar = *p*-$NO_2C_6H_4$

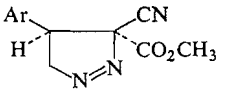

5 Ar = C_6H_5
6 Ar = *p*-$CH_3OC_6H_4$
7 Ar = *p*-$NO_2C_6H_4$

$Ar(CH_3)C{=}C(CN)CO_2CH_3$

cis and *trans* **8** Ar = C_6H_5
trans **9** Ar = *p*-$CH_3OC_6H_4$
cis and *trans* **10** Ar = *p*-$NO_2C_6H_4$

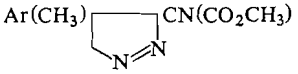

cis and *trans* **11** Ar = C_6H_5
trans **12** Ar = *p*-$CH_3OC_6H_4$
cis and *trans* **13** Ar = *p*-$NO_2C_6H_4$

CHART 1

A complication which continually appears in our work is the ease by which the *cis* and *trans* forms of the α-cyanoacrylates can be equilibrated. The sensitivity of **8** to base and heat can be illustrated by the following. After 2 h at room temperature a solution of 0.5 mmoles of *cis* **8** and 0.5 mmoles of pyridine in 0.6 ml of deuteriochloroform was found to be changed to a mixture of *trans* **8** and *cis* **8** in the ratio of 1:3 respectively.

[1]Taken in part from the Ph.D. Thesis of Y. Y. Wigfield, University of British Columbia, Vancouver, B.C., April, 1969.

[2]*Cis* and *trans* throughout this paper define the relative position of the carbomethoxy group to the aryl or benzyl group on the vicinal carbon.

Can. J. Chem. Downloaded from www.nrcresearchpress.com by 210.87.254.105 on 09/05/12
For personal use only.

After 30 min at 140° *trans* **8** is converted to the equilibrium mixture of *trans* **8** and *cis* **8** of 2:1. It has in fact been pointed out in the literature that similar olefins can be titrated reversibly as monobasic acids (8).

Base catalysis appears responsible for the following observations in the pyrazoline syntheses. Attempts to prepare *cis* **5**, as a mixture with *trans* **5**, from a mixture of *cis* and *trans* **2** gave only *trans* **5**; and examination of the reaction mixture after partial reaction showed that all of the *cis* **2** originally present had been converted to the more stable *trans* **2**. Synthesis of *trans* **13** from pure *trans* **10** gave yields of only 53% although *trans* **13** was easily isolated as it was only slightly soluble in the reaction medium. Examination of the remaining solution showed the presence of *cis* **13**. Reaction of *trans* **10** with less than one molar equivalent of diazomethane provided a reaction mixture containing *cis* and *trans* **10** and *cis* and *trans* **13**.

Our interpretation of these results is that the pyrazolines are sufficiently basic to induce equilibration of the α-cyanoacrylates and this is supported by some observations reported below. The degree to which isomerization occurs will depend on: (*1*) the rate of isomerization reactions, which is dependent on the olefin structure, (*2*) the concentration of the reactants, which is affected by the solubility of the pyrazolines, and (*3*) the time of contact between the pyrazoline and olefin, which is affected by the rate of pyrazoline formation and (see below) the rate of pyrazoline pyrolysis. We have not evaluated these three factors in detail in the present report.

The pyrazolines *trans* **11–13** and *cis* **13** were crystalline and as such were stable enough to be fully characterized. The pyrazolines *cis* **11** and **13** were readily distinguished from *trans* **11** and **13** in that the C-5 hydrogens gave a single broad peak for the *cis* series and an AB quartet for the *trans* series with $J \simeq 17$ Hz and $\Delta \simeq 0.5\,\tau$. Pyrazoline **7** on one occasion crystallized, indicating a definite occurrence of such a species, and gave an apparent m.p. of 45 °C. Recently the spectra of a number of such pyrazolines at low temperatures have been reported (*9*).

Pyrolysis of Pyrazolines

The only product formed in the reaction of **2–4** with diazomethane was the *trans* form of **8–10**. The formation of a single isomer has been noted earlier (6) and the *trans* stereochemistry is consistent with a mechanism involving concerted migration of hydrogen from C-4 to C-5 on the side *trans* to the leaving nitrogen (10,11).

The pyrazolines *cis* **11** and *cis* **13** on pyrolysis gave the olefin **14**, resulting from migration of the aryl group, as the major product (see runs 20–24 in Table I). The stereochemistry of this olefin was predominantly *cis* as predicted by the model reaction. The *trans* **14** is believed to be

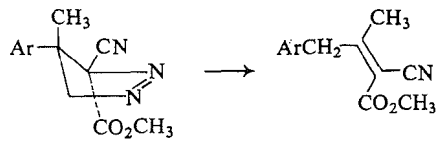

cis **14** chief product

formed by isomerization of the initially formed *cis* **14**.

The reaction products from the *trans* isomers of pyrazolines **11–13** are much more complicated and are presented in runs 1–19 in Table I. In addition to aryl migration there is also methyl migration to give the methyl α-cyano-β-ethylcinnamates (**15**) and the formation of appreciable amounts of methyl 2-methyl-2-aryl-1-cyanocyclopropanecarboxylates (**16**). Not all of the products have been isolated pure due to complications resulting from the ease of *cis–trans* isomerization

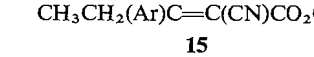

15

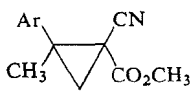

16

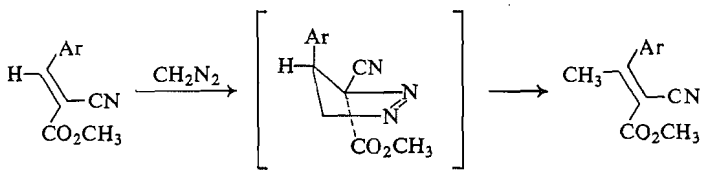

2–4 *trans* **8–10**

TABLE I

Product distribution for the pyrazoline decompositions under a variety of conditions

		Conditions			Products					
					Ar migration		methyl migration		cyclopropanes	
Run	Compound	solvent	time(h)	temperature (°C)	*trans* **14**	*cis* **14**	*trans* **15**	*cis* **15**	*trans* **16**	*cis* **16**
1	*trans* **11**	benzene	0.5	70	29	3	50	2	13	3
2	*trans* **11**	benzene	2.0	70	26	5	52	1	13	3
3	*trans* **11**	benzene	6.5	70	22	9	49	3	14	3
4	*trans* **11**	tetralin	8.0	60	19	13	30	20	9	9
5	*trans* **11**	nitrobenzene	2.0	70	20	13	49	4	5	9
6	*trans* **11**-5,5-d_2	nitrobenzene	2.0	70	20	16	48	4	2	10
7	*trans* **11**	neat	2 mos	room temperature	19	13	50	3	5	10
8	product from *trans* **11** (benzene)	$CDCl_3$(Py)	29.0	room temperature	18	13	50	3	13	3
9	product from *trans* **11** (benzene)	$CDCl_3$(Py)	equilibrium	room temperature	18	13	33	20	13	3
10	product from *trans* **11** (benzene)	neat	2.0	140	17	15	32	20	13	3
11	*trans* **12**	benzene	2.0	70	38	4	47	0	8	3
12	*trans* **12**	tetralin	8.0	60	27	17	39	11	0	6
13	*trans* **12**	nitrobenzene	2.0	70	27	11	52	0	2	8
14	*trans* **12**	neat	2 mos	room temperature	32	9	50	4	3	2
15	*trans* **12**	formamide	10 min	30	19	15	41	7	5	11
16	*trans* **13**	benzene	2.0	70	13	7	53	6	17	4
17	*trans* **13**	nitrobenzene	2.0	70	16	18	37	12	8	9
18	*trans* **13**	tetralin	2.0	70	10	10	25	27	20	7
19	*trans* **13**	formamide	10 min	30	8	8	49	9	4	22
20	*cis* **11**	benzene	2.0	70	5	91	0	0	0	4
21	*cis* **11**	nitrobenzene	2.0	70	36	64	0	0	0	0
22	*cis* **11**	neat	24.0	room temperature	11	86	0	0	0	3
23	*cis* **13**	benzene	4.0	70	7	77	0	0	0	16
24	*cis* **13**	nitrobenzene	20 min	70	8	84	0	0	0	8

in the olefin series. From *trans* **13** we have isolated *trans* **15**, *cis* **16**, *trans* **16**, a mixture of *cis* and *trans* **15**, and a mixture of *cis* and *trans* **14**. Hayashi (12) has reported the nuclear magnetic resonance (n.m.r.) spectra of related olefins and his data assists our stereochemical assignments. The stereochemistry of the cyclopropanes was readily determined since the *trans* **16** ring, when heated to 175° for 30 min, opened to a γ,δ-unsaturated ester (1,13) while *cis* **16** did not. Thus, characteristic n.m.r. peaks for all of the components in the product could be found so that product analysis on the crude mixtures could be made. In addition during the pyrolysis (for the *p*-nitrophenyl series only) some of the pyrazoline was isomerized to a 2-pyrazoline by tautomerization of a C-5 hydrogen.

Figures 1 and 2 show the n.m.r. analysis of runs 2 and 10 and clearly illustrate the presence of the indicated isomers due to changes in relative peak heights. Some of the *trans* cyclopropane **16** has rearranged as evidenced by the reduction of the τ 8.38 peak in Fig. 2. The data in Table I is reproducible to 2%.

Equilibration of the olefin products is achieved by the addition of a trace of pyridine (run 9) and heat (run 10) demonstrating the sensitivity of these compounds to base and heat. The product distribution in tetralin (runs 4, 12, 18) shows both olefins **14** and **15** close to equilibrium while in benzene (runs 2, 11, 16) shows mainly *trans* **14** and **15**. The pyrazolines are only slightly soluble in benzene. The greater solubility in tetralin maintains a higher concentration of pyrazoline to act as a base catalyst for the isomerization of these olefins. Nitrobenzene is intermediate in its effect.

Can. J. Chem. Downloaded from www.nrcresearchpress.com by 210.87.254.105 on 09/05/12
For personal use only.

Can. J. Chem. Downloaded from www.nrcresearchpress.com by 210.87.254.105 on 09/05/12
For personal use only.

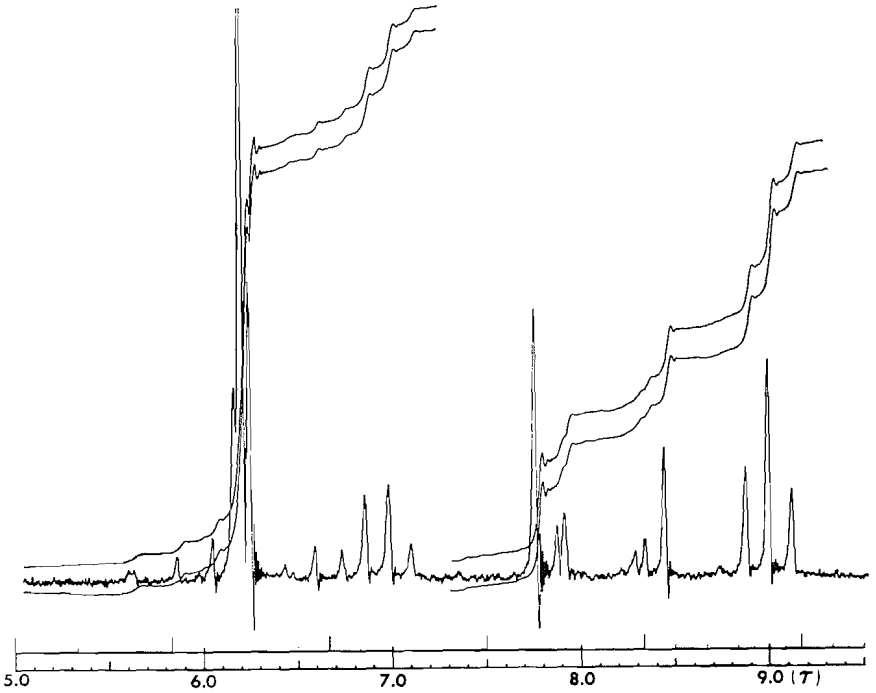

FIG. 1. The nuclear magnetic resonance spectrum of the product from run 2, Table I.

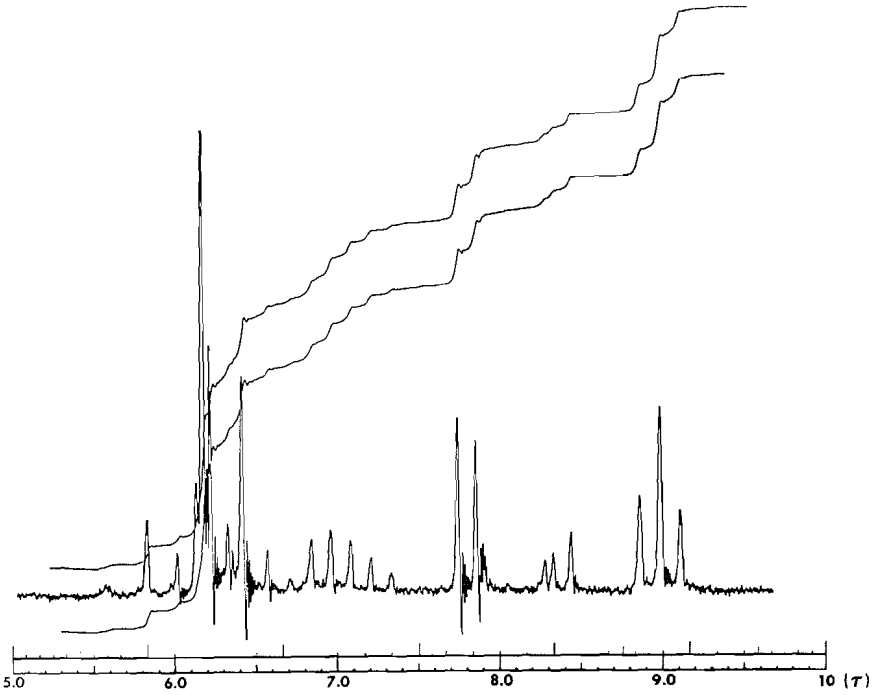

FIG. 2. The nuclear magnetic resonance spectrum of the product from run 10, Table I.

TABLE II

Rate constants and activation parameters for the pyrolysis of 1-pyrazolines

Compound	Solvent	Temperature (°C)	$k \times 10^4$(sec^{-1})	ΔH†(kcal/mole)	ΔS†(e.u.)
trans **11**	nitrobenzene*	44.9	2.06, 2.06		
trans **11**	nitrobenzene*	49.8	3.73±0.04		
trans **11**-5,5-d_2	nitrobenzene	49.8	3.66, 3.76		
trans **11**	nitrobenzene*	54.8	6.41±0.09	22.2	−5.67
trans **11**	tetralin	54.8	2.05, 2.05		
trans **11**	nitrobenzene*	64.9	18.0, 17.8		
trans **12**	nitrobenzene*	35.0	0.86 (calcd.)		
trans **12**	tetralin	35.0	0.024 (calcd.)		
trans **12**	formamide	35.0	88.5, 85.9		
trans **12**	nitrobenzene *	44.9	2.51, 2.52		
trans **12**	nitrobenzene *	49.8	4.22, 4.30		
trans **12**	nitrobenzene *	54.8	7.36±0.09	20.8	−9.58
trans **12**	tetralin	54.8	2.77, 2.79		
trans **12**	nitrobenzene *	64.9	19.5, 18.9		
trans **12**	nitrobenzene	75.2	49.8 (calcd.)		
trans **12**	tetralin	75.2	27.6, 27.5		
trans **12**	decalin	75.2	15.0, 15.1		
trans **13**	nitrobenzene*	44.9	2.09, 2.03		
trans **13**	nitrobenzene*	49.8	3.75, 3.78		
trans **13**	nitrobenzene*	54.8	6.62, 6.53	23.0	−3.19
trans **13**	tetralin	54.8	1.56, 1.56		
cis **13**	nitrobenzene	54.8	9.33, 9.23		
trans **13**	nitrobenzene*	64.9	18.9, 18.9		

*Runs used for the calculation of ΔH† and ΔS†.

Kinetics of the Pyrolysis Reaction

Further to the product studies we have carried out a kinetic study on the pyrolysis reaction for those pyrazolines which were crystalline. The apparatus and procedure for this study is described in a following paper (14). The weighed sample was added to 50 ml of solvent and the nitrogen evolved was measured in a gas burett. Runs were normally carried to over 80% completion. The V_∞ used was the calculated value and was shown to be within 2% of the observed value. A typical run is illustrated in Fig. 3. The results of this study are summarized in Table II. The solvents chosen were limited by the low solubility of the pyrazolines in benzene and hydrocarbon solvents. Standard error calculations showed that the limiting error is due to control of the temperature to ±0.1°.

Discussion

The value of the secondary α-deuterium kinetic isotope effect of $k_H/k_D = 1.01 \pm 0.07$ suggests that at the transition state there is little progress in the bond breaking of the C-5 to N bond. This is a major change in mechanistic detail from that found in 1-pyrazoline-α,α,α′,α′-d_4 ($k_H/k_D = 1.13$ per deuterium (15)), 3-methyl-3-carbomethoxy-5,5-d_2 ($k_H/k_D = 1.11$ per deuterium (14)), and the symmetric azo compound azobis-α-phenylethane-α,α′-d_2 ($k_H/k_D = 1.14$ per deuterium (16)). In the unsymmetric azo compound, α-phenylethylazomethane, with 3-deuteriums on the methyl, $k_H/k_D = 0.99$ per deuterium (16). The absence of an isotope effect in this case was attributed to a stepwise breaking of the two C—N bonds.

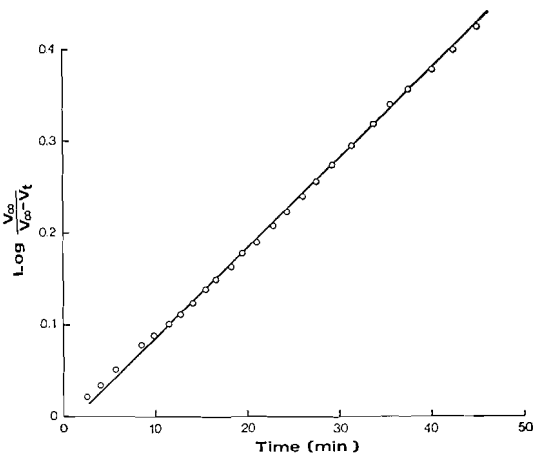

FIG. 3. Rate plot for *trans*-3-carbomethoxy-3-cyano-4-methyl-4-phenyl-1-pyrazoline (*trans* **11**) at 49.8 °C in nitrobenzene.

Can. J. Chem. Downloaded from www.nrcresearchpress.com by 210.87.254.105 on 09/05/12
For personal use only.

Can. J. Chem. Downloaded from www.nrcresearchpress.com by 210.87.254.105 on 09/05/12
For personal use only.

We also see from the kinetic results in Table II that there is negligible effect on the rate in going from *p*-methoxyphenyl to phenyl to *p*-nitrophenyl where the rate constants are 7.36, 6.41, and 6.57 respectively in nitrobenzene at 54.84°. This suggests that migration of the aryl group and the resulting effect of such participation has also progressed to a negligible degree in the transition state. Here again this is a major change from that observed in 3-methyl-3-carbomethoxy-1-pyrazoline-4,4-d_2 which showed an overall isotope effect of k_H/k_D of 1.36 attributable to considerable participation by the C-4 hydrogen in the transition state for that reaction (14).

The product analyses provide further information concerning the reaction mechanism. From this data we would like to be able to clearly determine whether after the transition state there is the opportunity for bond rotation as might be anticipated for an intermediate of the zwitterion type illustrated by **17**. The occurrence of olefin products of mixed stereochemistry suggests that

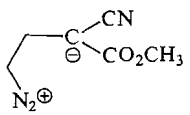

17

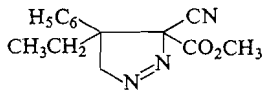

18

such is the case. However, the mixed stereochemistry in the olefin products can also be explained by isomerization after initial product formation. To clearly demonstrate this possibility, we pyrolized a pyrazoline **18** in the presence of a less than equimolar amount of *cis* **14**. Upon completion of the pyrolysis a mixture of *cis* **14** and *trans* **14** could clearly be shown to be present due to their n.m.r. peaks at τ 7.87 and 7.77 in the ratio of 54:46 respectively. It is significant that the benzyl olefins (**14**) are more readily isomerized than the aryl olefins (**15**) (see run 8 Table I) and it is the benzyl olefins in the product mixtures which are closest to equilibrium. The following additional observations also speak against **17** occurring as a distinct intermediate with sufficient lifetime for rotation of the C-3 to C-4 bond. The product distribution is largely controlled by the stereochemistry of the initial pyrazoline (compare runs 1–19 with runs 20–24 in Table I). If **17** were a distinct intermediate, it should be common to pyrazolines of both stereochemistries. Product formation from **17** would be expected to be markedly influenced by the ionic character of **17**. Aryl and particularly *p*-methoxyphenyl migration should be markedly favored over methyl or *p*-nitrophenyl. In fact for the *trans* pyrazolines, methyl migration is preferred to aryl migration by a ratio of 1.2:1.8:3 for *p*-methoxyphenyl, phenyl, and *p*-nitrophenyl respectively in benzene. This suggests that at the time the product is determined there is little positive charge at C-5 and there is still a stereochemical restriction controlling which groups migrate. Occurrence of **17** as an intermediate would imply that the transition state should also have a high degree of ionic character. Ionic character in the transition state can be evaluated by the solvent effect on the kinetics (17). The *p*-methoxyphenylpyrazolene (*trans* **12**) gave relative rate constants in tetralin, nitrobenzene, and formamide of $1:34:3.4 \times 10^3$. The change from tetralin to nitrobenzene is less than expected for a truly ionic transition state. However, the change in going to formamide may certainly be attributed to a normal ionic transition state and may imply that in formamide formation of a structure like **17** is fully realized. The negative value of the entropy is not consistent with earlier studies on the pyrazoline pyrolysis reaction where positive values have previously been found (14,18). The negative values of the entropy are consistent with additional constraint in the degrees of freedom of the transition state compared to the starting material. Such an effect is frequently observed in reactions occurring via ionic transition states, however, here again the magnitude of the effect is not as large as found in fully ionized systems.

Conclusions

The pyrazolines in the present study react by a mechanism for which the transition state can be described by **19** in which bond breaking of the C-3 to N bond is well advanced over bond breaking of the N to C-5 bond. This structure has a

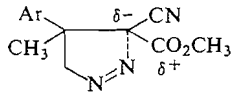

19

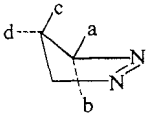

20

polar character greater than the starting pyrazoline but less than expected for the zwitterion **17**. The product distribution is largely determined by the *cis* or *trans* geometry of the reacting pyrazoline presumably due to the steric requirements of the substituent groups and their influence on the conformational preference of the starting material and the transition state. This aspect has been

Can. J. Chem. Downloaded from www.nrcresearchpress.com by 210.87.254.105 on 09/05/12
For personal use only.

discussed elegantly by Hamelin and Carrie (5). It can be concluded that the smaller group (CN) on C-3 preferentially adopts the pseudo equatorial position (a) of structure **20**. This is particularly evident from the product analysis when (c) and (d) are both phenyl (5) but less evident when (c) and (d) are both methyl (1). The larger group on C-4 appears to prefer the pseudo equatorial position (d). This is evident from the reaction of 3,3-dicyano-1-pyrazolines substituted with different alkyl groups at C-4 (19), from the kinetic evidence of Crawford and co-worker on the reaction of 4,4-dimethyl-1-pyrazoline (18), and from the n.m.r. evaluation of the preferred conformation of some 1-pyrazolines with a hydrogen and an alkyl group at C-4 (11,20).

We prefer to attribute the nonstereospecific olefin formation to isomerization after product formation rather than the alternative formation of a zwitterion intermediate capable of bond rotation before product formation. The stereochemistry of the cyclopropane products is solvent dependent and evidence to date has not permitted a rationalization of this part of the reaction.

Experimental

*Methyl trans-α-Cyano-β-methylcinnamate (trans **8**)*

Treatment of methyl *trans*-α-cyanocinnamate (**2**) (21) in benzene with excess diazomethane at 0 °C gave, on evaporation of the solvent at 0 °C, an unstable oil which decomposed to give nitrogen and methyl *trans*-α-cyano-β-methylcinnamate (*trans* **8**), b.p. 122° at 0.2 mm, m.p. 43–44 °C. The absence of *cis* **8** was revealed through a comparison of the n.m.r. spectrum with that recorded in the literature for the *cis–trans* mixture (12).

*Methyl trans-α-Cyano-β-methyl-p-methoxycinnamate (trans **9**)*

Reaction of methyl *trans*-α-cyano-*p*-methoxycinnamate (**3**) (12) by the manner described above gave methyl *trans*-α-cyano-β-methyl-*p*-methoxycinnamate (*trans* **9**), m.p. 90.5–92 °C (lit. (22), m.p. 73–74 °C for the *cis–trans* mixture); n.m.r. ($CDCl_3$) τ 2.48 and 3.02 (doublets with J = 8.8 Hz), 6.08, 6.10, and 7.30.

Anal. Calcd. for $C_{13}H_{13}NO$: C, 67.50; H, 5.67; N, 6.06. Found: C, 67.79; H, 5.81; N, 5.98.

*Methyl trans-α-Cyano-β-methyl-p-nitrocinnamate (trans **10**)*

Addition of diazomethane in ether to methyl *trans*-α-cyano-*p*-nitrocinnamate (**4**), m.p. 177–178 °C (lit. (12), 153–154 °C) in benzene gave after 1 h an unstable solid, m.p. 45° (d), which decomposed to give nitrogen and methyl *trans*-α-cyano-β-methyl-*p*-nitrocinnamate (*trans* **10**), m.p. 119–121 °C (lit. (12), m.p. 153–154 °C); n.m.r. ($CDCl_3$) τ 1.17 and 2.37 (doublets with J = 8.8 Hz), 6.07, and 7.25.

Anal. Calcd. for $C_{12}H_{10}N_2O_4$: C, 58.55; H, 4.09; N, 11.39. Found: C, 58.62; H, 4.29; N, 11.49.

*Methyl cis-α-Cyano-β-methylcinnamate (cis **8**)*

A solution of 8.0 g of distilled methyl *trans*-α-cyano-β-methylcinnamate in 70 ml of ether was irradiated in a silica tube in a Rayonet Photochemical Reactor using 75 W, 250 V, 2537 Å lamps for 2 days. Evaporation of the ether and filtration gave 3.0 g of methyl *cis*-α-cyano-β-methylcinnamate (*cis* **8**), m.p. 75–76 °C; n.m.r. (CCl_4) τ 2.60–3.05 (multiplet), 6.40, and 7.50.

Anal. Calcd. for $C_{12}H_{11}NO_2$: C, 71.64; H, 5.51; N, 6.96. Found: C, 71.78; H, 5.57; N, 7.08.

*Methyl cis-α-Cyano-β-methyl-p-nitrocinnamate (cis **10**)*

Methyl *trans*-α-cyano-β-methyl-*p*-nitrocinnamate (*trans* **10**) was heated at 150° for 2 h, cooled, and slurried with ether (3 × 70 ml). The remaining solid (0.4 g) was crystallized 3 times from methanol to give methyl *cis*-α-cyano-β-methyl-*p*-nitrocinnamate (*cis* **10**), m.p. 158–159 °C; n.m.r. ($CDCl_3$) τ 1.73 ar d 2.67 (doublets with J = 8.5 Hz), 6.30, and 7.43.

Anal. Calcd. for $C_{12}H_{10}N_2O_4$: C, 58.55; H, 4.09; N, 11.39. Found: C, 58.57; H, 4.17; N, 11.53.

*trans-3-Carbomethoxy-3-cyano-4-methyl-4-phenyl-1-pyrazoline (trans **11**)*

Reaction of *trans* **8** with diazomethane in ether gave in quantitative yield after standing overnight white crystals of *trans* **11**, m.p. 93–94 °C (d); n.m.r. ($CDCl_3$) τ 2.68 (multiplet), 4.70, and 5.22 (doublets with J = 18.0 Hz), 6.06, and 8.53.

Anal. Calcd. for $C_{13}H_{13}N_3O_2$: C, 64.16; H, 5.39; N, 17.27. Found: C, 63.95; H, 5.51; N, 17.16.

*trans-3-Carbomethoxy-3-cyano-4-methyl-4-p-methoxyphenyl-1-pyrazoline (trans **12**)*

By a procedure similar to the above *trans* **9** was converted in quantitative yield to *trans* **12**, m.p. 82–83 °C (d); n.m.r. ($CDCl_3$) τ 2.88, and 3.13 (doublets with J = 9.0 Hz), 4.70 and 5.25 (doublets with J = 17.7 Hz), 6.05, 6.20, and 8.52.

Anal. Calcd. for $C_{14}H_{15}N_3O_3$: C, 61.53; H, 5.53; N, 15.37. Found: C, 61.41; H, 5.71; N, 15.21.

*trans-3-Carbomethoxy-3-cyano-4-methyl-4-p-nitrophenyl-1-pyrazoline (trans **13**)*

By a procedure similar to the above *trans* **10** was converted in 50% yield to *trans* **13**, m.p. 101–102 °C (d); n.m.r. ($CDCl_3$) τ 1.80, and 2.63 (doublets with J = 9.0 Hz), 4.65, and 5.06 (doublets with J = 16.4 Hz), 5.95, and 8.46.

Anal. Calcd. for $C_{13}H_{12}N_4O_4$: C, 54.15; H, 4.20; N, 19.43. Found: C, 54.20; H, 4.30; N, 19.20.

The filtrate from the above preparation was evaporated and examined by n.m.r. and found to contain *trans* **13** (5%), *cis* **13** (35%); n.m.r. ($CDCl_3$) τ 1.78 and 2.58 (doublets with J = 8.5 Hz), 4.74, 6.48, and 8.50 and 4-methyl-4-*p*-nitrophenyl-5-carbomethoxy-5-cyano-2-pyrazoline (see below) (60%); n.m.r. ($CDCl_3$) τ 1.73, and 2.40 (doublets with J = 8.8 Hz), 3.19, 3.49, 6.00, and 8.33.

*cis-3-Carbomethoxy-3-cyano-4-methyl-4-phenyl-1-pyrazoline (cis **11**)*

The liquid pyrazoline *cis* **11** was obtained in quantitative yield from the reaction of *cis* **8** with one mole of diazomethane in ether followed by evaporation of the solvent at 0 °C; n.m.r. ($CDCl_3$) τ 2.55–3.0 (multiplet), 4.80, 6.65, and 8.56. No further data could be obtained due to the instability of this compound.

Can. J. Chem. Downloaded from www.nrcresearchpress.com by 210.87.254.105 on 09/05/12
For personal use only.

cis-3-Carbomethoxy-3-cyano-4-methyl-4-p-nitrophenyl-1-pyrazoline (cis **13***)*

Reaction of *cis* **10** with diazomethane gave on evaporation of the solvent at 0° a quantitative yield of *cis* **13**, m.p. 90–91 °C (d); n.m.r. ($CDCl_3$) τ 1.78 and 2.58 (doublets with J = 8.5 Hz), 4.74, 6.48, and 8.50.

Anal. Calcd. for $C_{13}H_{12}N_4O_4$: C, 54.15; H, 4.20; N, 19.43. Found: C, 54.08; H, 4.20; N, 19.41.

Pyrolysis of the Pyrazolines

The conditions for the pyrolyses and the analysis of the product mixtures are given in Table I. When benzene and decalin were used as solvents these solvents were evaporated under reduced pressure after complete pyrolysis and the product analyses were made from the n.m.r. spectrum of the residue in deuteriochloroform. When nitrobenzene and tetralin were used as decomposition solvents the product compositions were measured directly in the same solvents. When formamide was used, the products which were insoluble in these solvents were dissolved in deuteriochloroform to an equivalent volume to the formamide used and n.m.r. spectra were measured in both solvents under identical conditions.

A typical spectrum for the analysis of the product from *trans* **11** is given in Fig. 1. Peak positions characteristic of the individual products for the phenyl, *p*-methoxyphenyl, and *p*-nitrophenyl respectively in $CDCl_3$ in units of τ were: *trans* **14**: 7.77, 7.80, 7.70; *cis* **14**: 5.86, 5.97, 5.72 and 7.87, 7.90, 7.80; *trans* and *cis* **15**: 9.03, 9.00, 8.95 (triplets); *cis* **15**; 6.52, 6.43, 6.32; *trans* **16**: 8.50, 8.50, 8.38; *cis* **16**: 6.67, 6.58, 6.41. In addition the 2-pyrazoline from *trans* **13** was identified by peaks at τ 3.19 and 3.49. The following new compounds were characterized from the product mixtures.

Methyl α-Cyano-β-ethyl-p-nitrocinnamate

The decomposition products from *trans* **13** in benzene were separated by preparative thin layer chromatography (t.l.c.) on silica with carbon tetrachloride and ether (2:1) as solvent. Extraction of the component with R_f = 0.39 with chloroform and crystallization from methanol gave methyl *trans*-α-cyano-β-ethyl-*p*-nitrocinnamate, m.p. 100–101 °C; n.m.r. ($CDCl_3$) τ 1.68 and 2.46 (doublets with J = 8.5 Hz), 6.09, 6.85 (quartet with J = 7.5 Hz), and 8.95 (triplet with J = 7.5 Hz).

Anal. Calcd. for $C_{13}H_{12}N_2O_4$: C, 59.98; H, 4.65; N, 10.76. Found: C, 59.78; H, 4.63; N, 10.88.

A 1:1 mixture of methyl *cis* and *trans*-α-cyano-β-ethyl-*p*-nitrocinnamate was isolated from a thin layer chromatogram on alumina with chloroform. Analysis of the component with R_f = 0.8 provided the following n.m.r. assignments for the *cis* isomer ($CDCl_3$); τ 1.73 and 2.68 (doublets with J = 9.0 Hz), 6.32, 7.09 (quartet with J = 7.5 Hz), and 8.90 (triplet with J = 7.5 Hz).

Methyl trans-2-p-Nitrophenyl-2-methyl-1-cyano-1-cyclopropanecarboxylate

The fraction from the above separation on silica with an R_f of 0.29 was a mixture of the *trans* cyclopropane component and the *cis* and *trans* benzyl olefins (**14**). Recrystallization from methanol gave methyl *trans*-2-*p*-nitrophenyl-2-methyl-1-cyano-1-cyclopropanecarboxylate, m.p. 142–143 °C; n.m.r. ($CDCl_3$) τ 1.75 and 2.48 (doublets with J = 8.8 Hz), 6.10, 7.82, and 8.38.

Anal. Calcd. for $C_{13}H_{12}N_2O_4$: C, 59.98; H, 4.65; N, 10.76. Found: C, 59.70; H, 4.71; N, 10.91.

A sample of this cyclopropane was heated to 175° for 3 h and the residue purified by t.l.c. to give methyl 2-cyano-4-*p*-nitrophenylpent-4-enoate as an oil; n.m.r. ($CDCl_3$) τ 1.79 and 2.45 (doublets with J = 8.5 Hz), 4.41, 4.53, 6.26, 6.44 (quartet with J = 9.0 Hz and 5.8 Hz), 6.71 (quartet with J_{gem} = 14.2 Hz and J = 5.8 Hz), and 6.96 (J_{gem} = 14.2 Hz and J = 9.0 Hz). There was not sufficient sample for microanalysis.

Methyl cis-2-Methyl-2-p-nitrophenyl-1-cyano-1-cyclopropanecarboxylate

Pyrolysis of *cis* **13** in the absence of solvent gave on standing a small amount of crystalline material in addition to the major oily product. Filtration and crystallization from methanol gave the methyl *cis*-2-methyl-2-*p*-nitrophenyl-1-cyano-1-cyclopropanecarboxylate, m.p. 167.5–168.5 °C; n.m.r. ($CDCl_3$) τ 1.78 and 2.54 (doublets with J = 8.8 Hz), 6.41, 7.52, and 8.12 (doublets with J = 5.8 Hz), and 8.19.

Anal. Calcd. for $C_{13}H_{12}N_2O_4$: C, 59.98; H, 4.65; N, 10.76. Found: C, 59.78; H, 4.47; N, 10.67.

This sample was heated at 170° for 2 h with no change.

4-Methyl-4-p-nitrophenyl-5-cyano-5-carbomethoxy-2-pyrazoline

During pyrolysis of *trans* **13** in tetrachloroethylene a precipitate formed which was isolated and crystallized from chloroform to give the 2-pyrazoline (**18**), m.p. 171–172.5 °C; n.m.r. ($CDCl_3$) τ 1.73 and 2.40 (doublets with J = 8.8 Hz), 3.19, 3.49, 6.00, and 8.33. The peak at 3.49 disappeared on the addition of D_2O.

Anal. Calcd. for $C_{13}H_{12}N_4O_4$: C, 54.14; H, 4.20; N, 19.43. Found: C, 54.17; H, 4.35; N, 19.29.

Methyl cis-4-Phenyl-3-methyl-2-cyano-2-butenoate (cis **14***)*

The product from the pyrolysis of *cis* **11** in benzene was distilled to give a liquid which was 91% *cis* **14** in the presence of 5% of *trans* **14** and 4% of *cis* **16**. The n.m.r. spectrum ($CDCl_3$) showed peaks for *cis* **14** at τ 2.79, 5.86, 6.22, and 7.87.

Anal. Calcd. for $C_{13}H_{13}NO_2$: C, 72.54; H, 6.09; N, 6.50. Found: C, 72.74; H, 6.29; N, 6.30.

Equilibration of *cis* **14** with a trace of pyridine gave a ratio of *cis* **14** to *trans* **14** of 42:58 respectively. Peaks in the n.m.r. due to *trans* **14** appeared at τ 2.79, 6.16, 6.22, and 7.77.

trans-3-Carbomethoxy-3-cyano-4-methyl-4-phenyl-5,5-dideuterio-1-pyrazoline

Dideuteriodiazomethane was prepared from diazomethane in ether by exchange with D_2O catalyzed by potassium carbonate. The deuteriodiazomethane was reacted with *trans* **8** to give *trans* **11**-5,5-d_2 which contained 80% deuterium at C-5 as estimated by n.m.r. and mass spectral analysis.

Acknowledgment

The authors gratefully appreciate the support received for this work from the National Re-

search Council of Canada in the form of an operating grant to D.E.M. and a studentship to Y.Y.W.

1. D. E. McGREER, R. S. McDANIEL, and M. G. VINJE. Can. J. Chem. **43**, 1389 (1965).
2. J. HAMELIN and R. CARRIE. C. R. **261**, 5545 (1965).
3. J. HAMELIN and R. CARRIE. Bull. Soc. chim. Fr. 2162 (1968).
4. J. HAMELIN and R. CARRIE. Bull. Soc. chim. Fr. 2513 (1968).
5. J. HAMELIN and R. CARRIE. Bull. Soc. chim. Fr. 2521 (1968).
6. J. HAMELIN and R. CARRIE. C. R. **260**, 3102 (1965).
7. F. D. POPP and A. CATALA. J. Org. Chem. **26**, 2738 (1961).
8. F. WESSELEY and A. EITEL. Angew. Chem. Int. Ed. **3**, 240 (1964).
9. H. KISCH, O. E. POLANSKY, and P. SCHUSTER. Tetrahedron Letters 805 (1969).
10. D. E. McGREER, N. W. K. CHIU, M. G. VINJE, and K. C. K. WONG. Can. J. Chem. **43**, 1407 (1965).
11. D. E. McGREER and W.-S. WU. Can. J. Chem. **45**, 461 (1967).
12. T. HAYASHI. J. Org. Chem. **31**, 5253 (1966).
13. D. E. McGREER and N. W. K. CHIU. Can. J. Chem. **46**, 2217 (1968).
14. D. E. McGREER and I. M. E. MASTERS. Can. J. Chem. This issue.
15. B. H. AL-SADER and R. J. CRAWFORD. Can. J. Chem. **46**, 3301 (1968).
16. S. SELTZER and S. MYLONAKIS. J. Amer. Chem. Soc. **89**, 6584 (1968).
17. R. HUISGEN and P. OTTO. J. Amer. Chem. Soc. **90**, 5342 (1968).
18. R. J. CRAWFORD and A. MISHRA. J. Amer. Chem. Soc. **88**, 3963 (1966).
19. J. BUS, H. STEINBERG, and TH. J. DE BOER. Monatsh. Chem. **98**, 74 (1967).
20. R. J. CRAWFORD, A. MISHRA, and R. J. DUMMEL. J. Amer. Chem. Soc. **88**, 3959 (1966).
21. A. LAPWORTH and W. BAKER. *In* Organic synthesis. *Edited by* H. Gilman and A. H. Blatt. Vol. I. John Wiley and Sons, Inc., New York. 1956. p. 181.
22. H. FIESSELMAN and W. EHMANN. Chem. Ber. **91**, 1706 (1958).

Can. J. Chem. Downloaded from www.nrcresearchpress.com by 210.87.254.105 on 09/05/12
For personal use only.

Can. J. Chem. Downloaded from www.nrcresearchpress.com by 210.87.254.40 on 09/05/12
For personal use only.

Pyrazolines X. Kinetics for the pyrolysis of some deuterated 1-pyrazolines in solution[1]

DONALD E. MCGREER AND IAN M. E. MASTERS
Department of Chemistry, University of British Columbia, Vancouver, British Columbia

Received June 5, 1969

The kinetics and product distribution have been measured for the pyrolysis of 3-methyl-3-carbomethoxy-1-pyrazoline (**1**) and its 4,4-d_2 and 5,5-d_2 analogues in tetralin, *n*-butyl phthalate, nitrobenzene, and formamide. The isotope effect k_H/k_D for **1**-5,5-d_2 of 1.22 and for **1**-4,4-d_2 of 1.36 is consistent with a mechanism involving migration of the C-4 hydrogen concerted with loss of nitrogen.

Canadian Journal of Chemistry, 47, 3975 (1969)

The use of deuterium isotope effects as a probe of mechanisms is well known. As a further evaluation of the mechanism of the pyrolysis of pyrazolines we have investigated the kinetics of this reaction for a series of pyrazolines and their deuterated analogues.

Experimental

Materials

3-Methyl-3-carbomethoxy-1-pyrazoline (**1**) and 3-methyl-3-cyano-1-pyrazoline (**2**) have been prepared previously (1,2). The 3-methyl-3-carbomethoxy-1-pyrazoline-5,5-d_2 was prepared using dideuterated diazomethane (prepared by exchange with D_2O using potassium carbonate) and analysis showed it to contain 80% deuterium at C-5. In a similar way 3-methyl-3-cyano-1-pyrazoline-5,5-d_2 was prepared and contained over 95% deuterium at C-5. Methyl methacrylate-3,3-d_2 was prepared by the Mannich reaction from methyl hydrogen methylmalonate and a 30% solution of formaldehyde-d_2 in water (Merck Sharp and Dohme of Canada, Ltd.). Yields of only 12% were obtained compared to 50% for trial runs in which methyl methacrylate was made from formalin solution. 3-Methyl-3-carbomethoxy-1-pyrazoline-4,4-d_2 was prepared from the methyl methacrylate-3,3-d_2 with diazomethane.

Kinetic Measurements

The rates of decomposition of the pyrazolines studied were determined by volumetric measurement of the rate of formation of nitrogen using an apparatus similar to that described by Peterson and co-workers (3). The reaction flask was heated in an oil bath (Dow Corning silicon fluid DC-550) and the reaction solution was stirred by a magnetic stirrer. The bath temperature was controlled to $\pm 0.05°$ and measured by a thermometer calibrated against an N.B.S. calibrated thermometer. The solvents used were all reagent grade and twice distilled at reduced pressure.

For the kinetic runs standard solutions of the pyrazolines were prepared in a 5 or 10 ml volumetric so that 1 ml of solution contained enough pyrazoline to yield 40–45 ml of nitrogen. Fifty ml of solvent was preheated in the reaction flask and purged with nitrogen for 30 min. The solution was stirred an additional 30 min to allow equilibration of the dissolved nitrogen with the surrounding gas. At this point 1 ml of the standard pyrazoline solution was added and the time recorded as 0 time. For most runs the reaction was followed to over 70% completion and in several to completion (ten half lives), permitting a comparison of the V_∞ observed with that calculated. This proved to be within 1% in *n*-butyl phthalate but greater in the more volatile solvents.

Product Analyses

Samples in solution or neat were heated in sealed ampoules in a constant temperature bath. The products were separated from the solvent or any unreacted pyrazoline by bulb to bulb distillation and analyzed by vapor chromatography. The instrument used was an Aerograph A-90P with thermal conductivity detectors and the peaks were recorded on an Electronic 15 recorder. The peak areas were determined by disc integration. For the data in Table II a 10′ × 1/4″ diisodecyl phthalate column at 100 °C with a helium flow rate of 50 ml/min was used.

Results and Discussion

Table I provides the kinetic results from this investigation. We were particularly concerned

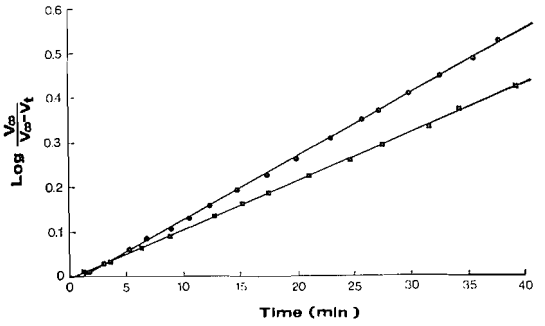

FIG. 1. Rate plots for 3-methyl-3-carbomethoxy-1-pyrazoline (**1**) (●) and its 4,4-dideuterio derivative (■) in *n*-butyl phthalate. (T = 127.0°).

[1]Taken in part from the Ph.D. thesis of I. M. Masters, University of British Columbia, Vancouver, B.C., February, 1969.

TABLE I

Rate constants and activation parameters for the pyrolysis of 1-pyrazolines

Compound	Solvent	Temperature (°C)	10^4k(sec^{-1})	$\Delta H\dagger$ (kcal mole^{-1})	$\Delta S\dagger$(e.u.)
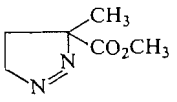 **1**	tetralin	109.4	1.28, 1.28		
		114.0	2.00		
		119.5	3.87		
		123.4	5.10	30.0	1.5
		126.0	6.82, 6.55		
		127.0	7.31 (calcd.)		
		125.9	7.17 (2)		
	n-butyl phthalate	107.3	0.662		
		116.1	1.75	32.4	7.0
		127.0	5.63 ± 0.21		
	nitrobenzene	113.3	0.819, 0.829		
		121.3	2.02, 2.03		
		126.1	3.32, 3.37	33.8	9.7
		131.3	5.99 ± 0.18		
		127.0	3.81 (calcd.)		
	formamide	127.0	2.54 ± 0.12		
1-4,4-d_2	*n*-butyl phthalate	127.0	4.15, 4.14		
1-5,5-d_2	*n*-butyl phthalate	127.0	5.04 ± 0.12 (80% d)		
		127.0	4.62 (calcd. 100% d)		
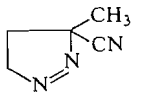 **2**	*n*-butyl phthalate	89.3	0.765		
		99.7	2.58	30.3	6.0
		109.4	7.34 ± 0.18		
2-5,5-d_2	*n*-butyl phthalate	109.4	5.95 ± 0.04		

for the reliability of the kinetics measured in this way using a magnetic stirrer. In view of the reproducibility of our results, the minimum scatter in the points as shown in Fig. 1 and the evidence provided by De Tar on this method (4), we feel the limiting factor is still in the control of the temperature. We estimate the temperatures reported to be reliable to better than ±0.1 °C corresponding to a maximum error of ±3% in the rate constants, ±5% in the enthalpies of activation ($\Delta H\dagger$) and ±3 e.u. in the entropies of activation ($\Delta S\dagger$).

The kinetic isotope effect k_H/k_D of 1.36 for **1**-4,4-*d* compared with **1** is considerably larger than the value of 1.07 found by Crawford and Mishra (5) for 4-methyl-1-pyrazoline-4-*d*, although their product distribution showed a larger isotope effect (1.80). The kinetic isotope effect observed by Crawford and Mishra can be attributed to a secondary effect due to hyperconjugation by the deuterium in a nitrogen free intermediate. We feel our value is too high for this interpretation and suggest that there must be some bond breaking of the C-4 to H bond at the transition state. An attractive approach to interpreting these results is to consider separate paths for the formation of the olefin and cyclopropane products. This possibility has been suggested earlier (6). Isotope effects for both paths can be calculated by making use of the product distributions given in Table II and the following equations.

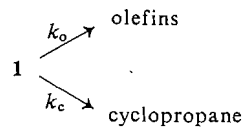

$$k_H/k_D = (k_{oH} + k_{cH})/(k_{oD} + k_{cD}) = 1.36$$

but

$$k_{oH}/k_{cH} = 31.1/68.9 \text{ and } k_{oD}/k_{cD} = 21.8/78.2$$

this gives

$$k_{oH}/k_{oD} = 1.94 \text{ and } k_{cH}/k_{cD} = 1.20$$

Can. J. Chem. Downloaded from www.nrcresearchpress.com by 210.87.254.40 on 09/05/12
For personal use only.

TABLE II

Product compositions for the pyrolysis of **1**, **1**-4,4-d_2, and **1**-5,5-d_2 at 127 °C

Reactant	Conditions	Product			
		Cyclopropane	*cis*-α,β	*trans*-α,β	β,γ
1	neat	66.8±0.9	12.2±0.7	16.4±1.2	4.6±0.4
	n-butylphthalate	68.9±0.8	14.7±0.6	12.3±0.6	4.1±0.5
	formamide	44.5±0.3	15.4±0.3	37.4±0.3	2.7±0.3
	tetralin	72.6	13.3	9.9	4.2
	nitrobenzene	72.5	13.0	10.1	4.4
1-4,4-d_2	neat	77.8±0.6	8.9±0.3	10.5±0.5	2.8±0.2
	n-butylphthalate	78.2±1.2	9.6±0.6	10.2±0.8	2.0±0.3
	formamide	61.0±0.7	11.3±0.8	26.2±0.6	1.5±0.2
1-5,5-d_2	neat	63.8±0.6	14.6±0.5	16.2±0.5	5.4±0.3

The isotope effect k_H/k_D for the olefin forming reaction thus becomes 1.94 and that for the cyclopropane forming reaction becomes 1.20.

We envisage the olefin forming reaction to involve an intermediate such as **3** (6). A primary isotope effect for the hydrogen on C-4 is expected with a magnitude of between 1.41 and 2.36 based

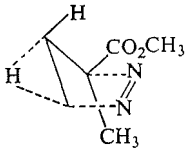

on studies by Rabinovitch and co-workers (7,8) and Blades (9) for the isomerization of cyclopropane to propylene. The isotope effect in the cyclopropane to propylene reaction has been attributed to a primary effect associated with breaking of the C—D bond as migration proceeds.

The isotope effect of 1.20 for the cyclopropane forming reaction is in line with that found by Al-Sader and Crawford (10) for conversion of trimethylene substituted by deuterium at the middle carbon to cyclopropane and amounting to 13% per deuterium. This affect was attributed to a secondary effect related to the hybridization change from sp^3 to sp^2 at that carbon.

The isotope effect of 1.22 and 1.23 for **1**-5,5-d_2 and **2**-5,5-d_2 is in excellent agreement with isotope effects found by Crawford and Cameron (11) for α-deuterated pyrazolines (10–14% per deuterium) and Seltzer and Mylonakis (12) for azobis-α-phenylethane-α,α-d_2 (14% per deuterium). This secondary isotope effect provides evidence for breaking of the C-5 to N bond at the transition state.

The presence of a carbomethoxy group at C-3 in the 1-pyrazoline system influences the reactivity of the pyrazoline to the extent that migration of the hydrogen from C-4 becomes concerted with loss of nitrogen. This is a subtle change in mechanism from that found for alkyl substituted pyrazolines in which loss of nitrogen clearly precedes migration (5,13). Although we might also expect the 3-carbomethoxy-1-pyrazoline to yield a polar transition state due to heterolytic cleavage of the C-3 to N bond this is not borne out by the solvent effects noted in Table I which instead suggest a reduction in the overall polarity of the transition state compared to the initial pyrazoline. The increase in olefin and particularly the *trans*-α,β-olefin in formamide suggests, however, that the olefin reaction is subject to a solvent effect and we attribute this change due to coordination of the solvent around the carbomethoxy group in the transition state resulting in an increased effective bulk of that group and thus an increased relative yield of the *trans* olefin.

Acknowledgments

The authors gratefully appreciate the support received for this work from the National Research Council of Canada and from the Committee on Research of the University of British Columbia. An N.R.C.C. Studentship was received by I.M.E.M. and is hereby acknowledged.

1. D. E. McGREER, W. WAI, and G. CARMICHAEL. Can. J. Chem. **38**, 2410 (1960).
2. H. R. SNYDER. Ph.D. Thesis, Boston University, Boston, Mass. 1958.
3. R. C. PETERSON, J. H. MARKGRAF, and S. D. ROSS. J. Amer. Chem. Soc. **83**, 3819 (1961).
4. D. DE TAR. J. Amer. Chem. Soc. **78**, 3911 (1956).

Can. J. Chem. Downloaded from www.nrcresearchpress.com by 210.87.254.40 on 09/05/12
For personal use only.

5. R. J. CRAWFORD and A. MISHRA. J. Amer. Chem. Soc. **88**, 3963 (1966).
6. D. E. MCGREER and W.-S. WU. Can. J. Chem. **45**, 461 (1967).
7. E. W. SCHLAG and B. S. RABINOVITCH. J. Amer. Chem. Soc. **82**, 5986 (1960).
8. D. W. SETSER and B. S. RABINOVITCH. J. Amer. Chem. Soc. **86**, 564 (1964).
9. A. T. BLADES. Can. J. Chem. **39**, 1401 (1961).
10. B. H. AL-SADER and R. J. CRAWFORD. Can. J. Chem. **46**, 3301 (1968).
11. R. J. CRAWFORD and D. M. CAMERON. Can. J. Chem. **45**, 691 (1967).
12. S. SELTZER and S. MYLONAKIS. J. Amer. Chem. Soc. **89**, 6584 (1968).
13. R. J. CRAWFORD and G. L. ERICKSON. J. Amer. Chem. Soc. **89**, 3907 (1967).

Can. J. Chem. Downloaded from www.nrcresearchpress.com by 210.87.254.40 on 09/05/12
For personal use only.

Can. J. Chem. Downloaded from www.nrcresearchpress.com by 210.87.254.105 on 09/05/12
For personal use only.

Polarography of thioketones[1]

R. M. ELOFSON, F. F. GADALLAH, AND L. A. GADALLAH
Research Council of Alberta, Edmonton, Canada

Received March 26, 1969

Aliphatic and aromatic thiones are reduced at the dropping mercury electrode at potentials well below those of the corresponding ketones. The reductions take place by a mechanism whereby an electron is added to the molecule before protonation. The reducibility of camphorthione adds the isolated C=S group to the list of polarographically reducible functions. The half-wave potentials in acetonitrile correlate linearly with $n \rightarrow \pi^*$ transitions in the electronic spectra.

Canadian Journal of Chemistry, 47, 3979 (1969)

Sartori and Furlani (1) reported the polarographic reduction of a number of substituted thiobenzophenones. They found that the thioketones were reduced at somewhat less negative potentials than are the corresponding ketones. This behavior is indeed to be expected because the thioketones show electronic absorption bands at longer wavelengths than the ketones (2). The present paper presents the polarographic reduction of a wider structural range of thioketones including one aliphatic thioketone. Decidedly different behavior with change of p*H* was noted in this study than in that of Sartori and Furlani. The polarographic behavior in aprotic solvents has also been studied and the results correlated with the longest wavelength electronic absorption band which is an $n \rightarrow \pi^*$ transition (3).

Experimental

Polarograms were run with a Leeds and Northrup Electrochemograph Type E at 25°. With a mercury height of 48 cm the flow rate of mercury was 3.75 mgm/s and the drop rate was 2.55 s. Absorption spectra in isopropyl alcohol were measured with a Beckmann DK2 recording spectrophotometer. Acetonitrile was dried over phosphorus pentoxide and distilled. Buffers were prepared according to Clark and Lubs. No attempt was made to establish the true p*H* of the buffered isopropyl alcohol solutions.

Half-wave potentials have been corrected for small infrared (i.r.) drops. Consumption of electrons was measured by comparison with the well known behavior of 2-methylanthraquinone. No maximum suppression was used or needed at the concentrations used and with the electrode used in this investigation. At higher concentrations maxima did occur which could be partly suppressed with gelatin.

Camphorthione was prepared according to Sen (4). The resulting material contains some unchanged camphor and was further purified by chromatography on Florosil using hexane as eluant. The resulting material was pure as indicated by a single peak on gas–liquid chromatography (g.l.c.) using SE30 on chromosorb as packing. The m.p. was 115–117°.

Five grams of 3,3′-diaminobenzophenone was dissolved in 100 ml anhydrous hydrogen fluoride cooled to −20° and hydrogen sulfide was passed through it for 2 h. The resulting solution was poured into sodium bicarbonate solution and filtered. The mixture of sodium fluoride and 3,3′-diaminobenzothione was extracted with hot chloroform. Crystallization from chloroform produced 3.2 g of 3,3′-diaminobenzothione, m.p. 128°.

Anal. Calcd. for $C_{13}H_{12}N_2S$: S, 14.03. Found (mol. wt. (mass spectrometry) 228): S, 13.92.

Benzothione m.p. 52°, Michler's thione m.p. 209°, *p,p′*-dimethoxybenzothione m.p. 116–118°, and thiofluorenone m.p. 75–76° were prepared according to Elofson *et al.* (5). Xanthione was prepared according to Meyer (6) and had m.p. 158.0–158.5°; reported m.p. 155–156°.

Results

In Table I are presented the polarographic half-wave potentials of four thiones run in 77% isopropyl alcohol as a function of p*H* in buffered solutions. Contrary to Sartori and Furlani no adsorption currents were noted on any of the polarograms. In contrast to the results of Sartori and Furlani (1) little increase in half-wave potentials occurred above p*H* 5 for these thiones. Below p*H* 5 the half-wave potentials were dependent on p*H* as suggested by the former workers with approximate slopes of 0.70, 0.70, and 0.76 mV/p*H* unit for benzothione, xanthione, and Michler's thione respectively. At low p*H*, xanthione shows two one-electron reduction steps, the lower wave of which shows the linear relationship with p*H*. The total height of the waves corresponded to two electrons as measured against 2-methylanthraquinone. For camphorthione, measurements could not be made below p*H* 5 due to interference by hydrogen discharge. At p*H* 5 and above the half-wave potentials were

[1]Contribution No. 452, Research Council of Alberta.

TABLE I

Half-wave potentials of selected thiones in 77% isopropyl alcohol at various p*H*

	V vs. s.c.e.			
p*H*	Camphorthione	Benzothione	Michler's thione	Xanthione
1	—	−0.60	−0.66	−0.62 to −0.83
3	—	−0.70	−0.82	−0.77 to −0.98
5	−1.61	−0.88	−1.03	−0.90 to −1.01
6	−1.61	−0.88	−1.04	−0.89 to −0.97
7	−1.62	−0.95	—	−1.01
8	−1.66	−1.10	−1.18	—
9	−1.67	—	—	—
10	—	−1.08	−1.25	−1.10
13	−1.70	−1.06	−1.37	−1.07 to −1.49

essentially constant. At p*H* 7.0 and 9.0 single two-electron waves were obtained.

At p*H* 10 the wave for camphorthione was shortened and at p*H* 13.0 one-electron waves were obtained for all four compounds. Controlled potential electrolysis at −1.8 V at p*H* 7.0 for camphorthione produced only thioborneol as determined by g.l.c. At p*H* 13 small quantities of thioborneol but over 70% thioborneol disulfide, m.p. 168° (7), was obtained.

Xanthione showed additional reduction at higher potentials in neutral and alkaline media with a definite reduction wave at p*H* 13.0 at −1.49 V with a height corresponding to three electrons. Presumably the product of reduction was xanthene. Controlled potential electrolysis at −1.6 V vs. standard calomel electrode (s.c.e.) at p*H* 9 in an ammonia buffer produced xanthene. No evidence for other than one electron reductions at high p*H* even with quaternary ammonium salts as supporting electrolytes was apparent with the three thiones, camphorthione, benzothione, or Michler's thione. Controlled potential electrolyses produced no evidence of thiopinacols for any of these compounds under any conditions of p*H*. Detailed study of the behavior of the wave height of Michler's thione as a function of p*H* was made in the range of 10–13. For p*H* of 10.1, 10.4, 11.3, 12.2, 12.5, and 12.9 the respective wave heights corresponded to 2, 1.8, 1.7, 1.5, 1.2, and 1.1 electrons respectively.

In contrast to the results in aqueous media, all the thiones showed a more or less distinct pre-wave in anhydrous acetonitrile 0.1 *M* with respect to tetrabutylammonium bromide (Table II and Fig. 1). These pre-waves were shown to be due to adsorption of the reduced form of the thione by the fact that their heights depended directly on the height of the mercury in the reservoir. Addition of 20–40% of water destroyed the adsorption curve and lowered the half-wave potential of the diffusion-controlled wave. The overall reduction in acetonitrile and acetonitrile – water mixtures required two electrons in all cases.

When the energy of the longest wavelength absorption band, as measured, is plotted against the half-wave potential in acetonitrile a straight line, Fig. 2, results. The actual bands of the long-

TABLE II

Half-wave potentials* and absorption spectra† of thiones

	$E_{1/2}$, (V) vs. s.c.e.		
Thione	Adsorption wave	Diffusion wave	Absorption band $n \rightarrow \pi^*$ eV
Benzothione	0.98	1.10	2.10
Xanthione	1.00	1.11	2.16
Dimethoxybenzothione	1.04	1.16	2.13
Michler's thione	1.24	1.42	2.29
3,3′-Diaminobenzothione	1.05	1.19	2.13
Thiofluorenone	0.79	0.92	2.00
Camphorthione	1.74	1.89	2.59

*$E_{1/2}$ in 0.05 *M* tetrabutyl ammonium bromide in acetonitrile 5×10^{-4} *M*.
†Absorption spectra in isopropyl alcohol.

Can. J. Chem. Downloaded from www.nrcresearchpress.com by 210.87.254.105 on 09/05/12
For personal use only.

Can. J. Chem. Downloaded from www.nrcresearchpress.com by 210.87.254.105 on 09/05/12
For personal use only.

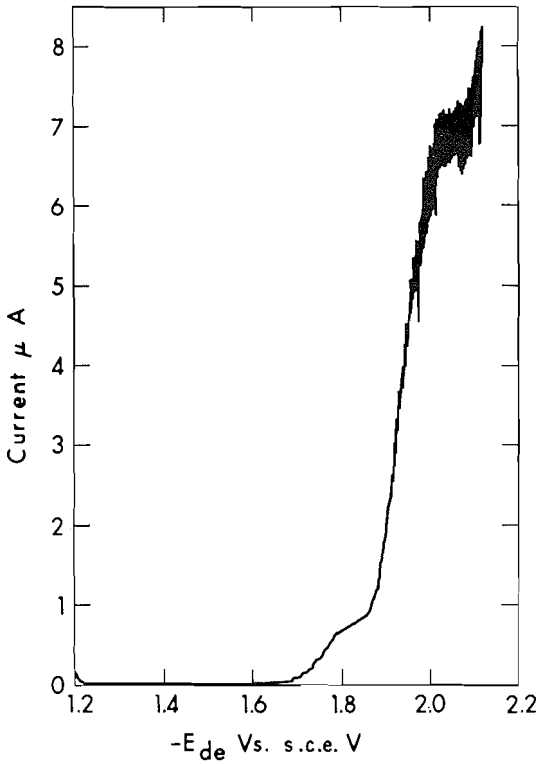

FIG. 1. Polarogram of 5.0×10^{-4} *M* camphorthione dissolved in 0.05 *M* tetrabutylammonium bromide in acetonitrile.

wavelength band frequently had fine structure (8) and the shorter wavelength maxima were chosen for the energy plot. The equation of the best fit line is

$$\bar{\nu} = -(0.592 \pm 0.037)\, E_{1/2} + 1.455 \pm 0.112 \text{ V}$$

Discussion

The two-electron reduction waves of the thiones in acetonitrile must arise from, first, the addition of a single electron followed rapidly by protonation and reduced further at the same potential since it has been shown by Hoijtink *et al.* (9) that the reduction potential of a radical RH must always be less negative than that of the hydrocarbon molecule R from which it is formed. Therefore, if it is assumed that the mechanism of protonation and the availability of protons are the same for all thiones, the half-wave potentials should be related to the energy required to put one electron into the lowest unoccupied molecular orbital. Since the energy of the n → π* absorption band has been shown to be linearly related to the calculated energy requirement of moving an electron from the highest occupied molecular orbital to the lowest empty molecular orbital (3), it seemed worthwhile to try to correlate the half-wave potentials with the absorption spectra. Bergmann (10) has already shown for alternate hydrocarbons that a straight line relationship exists for the plot of the absorption spectra of the π → π* band against the half-wave potentials. The slope of the plot of this transition energy of hydrocarbons vs. half-wave potentials is near the theoretical value of 2 (11). When n → π* transition of thiones vs. the half-wave potentials is plotted the slope is much lower at 0.60.

The reduction in aqueous alcohol solution corresponds to some extent to that observed of aryl alkyl ketones (12). Thus in acid solution the dependency of $E_{1/2}$ on p*H* suggests that reduction occurs simultaneously or following protonation.

$$\text{[1]}\quad \text{R'R''C=S} \xrightarrow{\text{H}^+} \text{R'R''C(H)—S}^+ \xrightarrow{+\,e,\ E_1} \text{RĊSH}^+$$

$$\text{RĊSH} \xrightarrow[+\,e,\ E_2]{-\,\text{H}^+} \text{RR'CSH} \rightarrow \text{RCHSH}$$

For xanthione the first wave is p*H* dependent corresponding to [1] whereas the second wave is p*H* independent so the waves merge above p*H* 6. For the remainder of the thiones $E_1 = E_2$ and the observed p*H* dependence results. The fate of the product of one-electron reduction of xanthione is not known. From the results of controlled potential electrolysis no evidence for thiopinacal formation could be obtained.

At intermediate and higher p*H* direct reduction of the thione occurs prior to protonation

$$\text{[2]}\quad \text{R'R'C=S} \xrightarrow[+\,e,\ E_3]{} \text{RR'C—S}\cdot^- \xrightarrow{\text{H}^+} \text{RR'CHS}\cdot$$

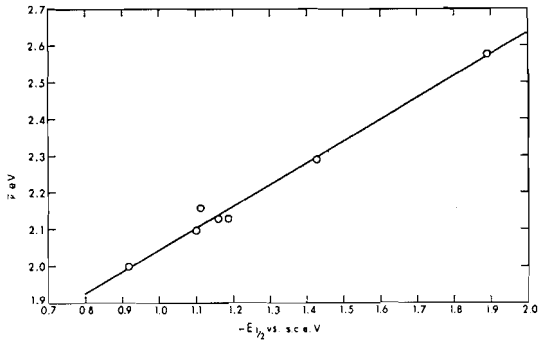

FIG. 2. Plot of absorption spectra of thiones in eV vs. $E_{1/2}$ in acetonitrile.

[3] 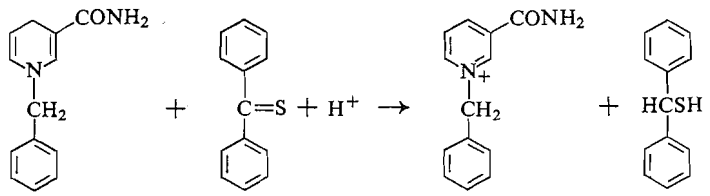

In neutral solution further reduction occurs to produce the mercaptan. In strongly alkaline solution dimerization of the radicals occurs to produce the disulfide with no further reduction occurring except in the case of xanthione wherein reduction to the parent hydrocarbon occurs.

This ready availability of thiones toward direct reduction by electrons at low voltages correlates well with the ability of DPNH analogues to reduce thioketones but not ketones eq. [3] (13, 14).

It is a more satisfactory explanation of this phenomenon than that of Westheimer and coworkers who suggested the greater polarity of thioketones relative to ketones might be the explanation. This is manifestly not so since thioketones elute more quickly on adsorbents such as Florosil than ketones do. Our mechanism is further supported by the failure in this laboratory to isolate thiopinacols by electrolysis even with xanthione at low p*H* and at the potential of the first reduction wave. The independence of reaction [3] to p*H* changes further demonstrates the analogy between this reaction and reducibility at the electrode.

1. C. SARTORI and C. FURLANI. Ann. Chim. (Rome) **44**, 95, 113 (1954).
2. A. E. GILLIAM and E. S. STERN. Electronic absorption spectra. Edward Arnold and Co., London. 1957. p. 49.
3. J. FABIAN and A. MELHORN. Tetrahedron Letters, **22**, 2049 (1967).
4. D. C. SEN. J. Indian Chem. Soc. **12**, 647 (1935).
5. R. M. ELOFSON, L. A. BAKER, F. F. GADALLAH, and R. A. SIKSTROM. J. Org. Chem. **29**, 1355 (1964).
6. R. MEYER. Ber. **33**, 2580 (1900).
7. J. HARBEN and H. DOESCHER. Ber. **39**, 3503 (1906).
8. J. FABIAN and R. MEYER. Spectrochim. Acta **20** (3), 299 (1964).
9. C. J. HOIJTINK, J. VON SCHOOTEN, E. DE BOER, and W. Y. AALBERSBERG. Rec. Trav. Chim. **73**, 355 (1955).
10. I. BERGMANN. Trans. Faraday Soc. **50**, 829 (1954); Trans. Faraday Soc. **52**, 690 (1956).
11. A. T. WATSON and F. A. MATSEN. J. Chem. Phys. **18**, 1305 (1950).
12. P. J. ELVING and J. T. LEONE. J. Amer. Chem. Soc. **80**, 1021 (1958).
13. R. H. ABELES, R. F. HUTTON, and F. H. WESTHEIMER. J. Amer. Chem. Soc. **79**, 712 (1957).
14. J. C. POWERS and F. H. WESTHEIMER. J. Amer. Chem. Soc. **82**, 5431 (1960).

Can. J. Chem. Downloaded from www.nrcresearchpress.com by 210.87.254.105 on 09/05/12
For personal use only.

Oxidation with lead tetraacetate. IV. Cyclization of phenylhydrazones of levulinic acid, levulinanilide, 5-ketohexanoic acid, 4-keto-1-pentanol, and of levulinic acid oxime

GERTFRIED B. GUBELT AND JOHN WARKENTIN
Department of Chemistry, McMaster University, Hamilton, Ontario

Received June 23, 1969

The phenylhydrazones of levulinic acid (**3***a*) and 5-ketohexanoic acid (**4**) are cyclized by lead tetraacetate (LTA) to γ-phenylazo-γ-valerolactone (**9***a*) and δ-phenylazo-δ-caprolactone (**11**), respectively. Oxidation of levulinanilide phenylhydrazone (**3***b*) leads, by analogous oxygen-to-carbon ring closure, to γ-phenylazo-α-phenylimino-γ-valerolactone (**15**) which is hydrolyzed to **9***a*. Similarly, the phenylhydrazone of 4-keto-1-pentanol (**5**) is cyclized to 2-phenylazo-2-methyl tetrahydrofuran (**12**) and the oxime of levulinic acid (**7**) is converted to γ-nitroso-γ-valerolactone which is isolated as the dimer, *trans*-bis[γ-nitroso-γ-valerolactone] (**14**).

Canadian Journal of Chemistry, 47, 3983 (1969)

Can. J. Chem. Downloaded from www.nrcresearchpress.com by 210.87.254.40 on 09/05/12
For personal use only.

Introduction

Among the many organic compounds that have been oxidized with lead tetraacetate (LTA) are carbonyl derivatives such as oximes (1), hydrazones (2), carbohydrazones (3), and semicarbazones (4). Hydrazones and oximes react according to the generalized equation [1], forming azoacetates and nitrosoacetates, respectively (1,2).

[1] 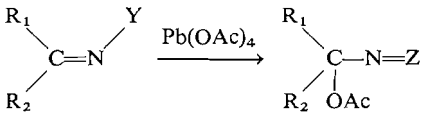

Y = NHR, OH Z = NR, O

Carbohydrazones, on the other hand, are cyclized by LTA and it is now established that the products are oxadiazolines (**1***a*) (3) rather than triazolinones (**1***b*) (5). Semicarbazones are cyclized to analogous oxadiazolines (**2**) (4).

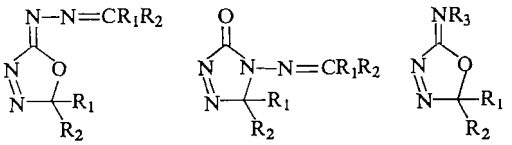

1*a* **1***b* **2**

These cyclizations probably involve organolead intermediates which undergo ring closure to carbonyl oxygen through cationic transition states (6). Such a mechanistic picture led us to look for other heterocyclic systems, arising from attack of a nucleophilic center in R of 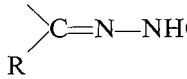

on the erstwhile carbonyl carbon. The present work adds to the variety of heterocyclic compounds now available by oxidative cyclization with LTA.

Results and Discussion

The systems studied include aryl hydrazones of substituted ketones with the substituent so situated that cyclization would produce either a 5-membered or a 6-membered ring, eq.[2]. Cyclization was pitted against azoacetate formation (eqs. [1] and [2]) which is the major reaction in systems lacking the potential for cyclization.

Aryl hydrazones of levulinic acid (**3***a*, **3***d*) gave mainly the corresponding γ-arylazo-γ-valerolactones, **9***a* and **9***b*, with small amounts of the azoacetates, **10***a* and **10***b*.[1] Similarly, **4** and **5** gave mainly **11** and **12**, respectively. The oxime **7** was also smoothly oxidized to form, presumably, γ-nitroso-γ-valerolactone which dimerized to **14**.[2] The dimer is stable for several days at room temperature, in contrast to the ready decomposition of bis-nitrosoacetates and nitrosoacetates (1). At its melting point, **14** decomposes to levulinic acid and other, unidentified products.

[1]The presence of azoacetate in the crude product, after acetic acid had been removed with bicarbonate, (see Experimental) was inferred from the proton magnetic resonance spectrum and from the infrared spectrum. Since our interest was primarily in the cyclic compounds no effort was made, in general, to isolate the azoacetates.

[2]The product does not show typical N=O absorption near 1555 cm^{-1} but absorbs instead at 1200 cm^{-1}. Nitroso dimers (1) are said to absorb in the region 1185–1195 cm^{-1}. The low value (Table II) obtained for the molecular weight (Rast) suggests that the dimer is partly dissociated at higher temperatures. The *trans* configuration is assigned by analogy (1).

[2] 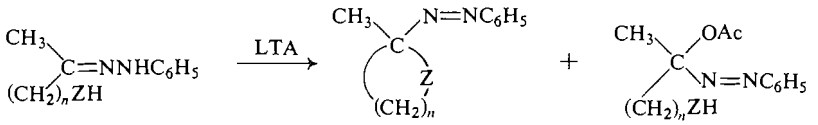

[3] 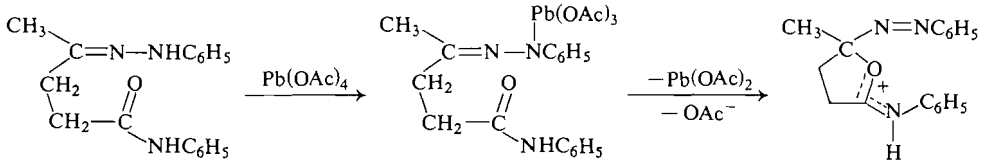

The phenylhydrazone of levulinanilide (**3***b*) was oxidized by LTA to a crude product which absorbed at 1691 cm^{-1} and less strongly at 1750 and 1787 cm^{-1}. The 1787 cm^{-1} band was assigned to **9***a* which, together with aniline, was the product of hydrolysis during workup. An *N*-aryl-5-membered lactam is expected to resist hydrolysis and to show carbonyl absorption near 1715 cm^{-1}, well above the 1691 cm^{-1} band observed. On the basis of the infrared (i.r.), the ease of hydrolysis, and the hydrolysis products, it is likely that a major component of the crude product was the iminolactone **15**.

This preference for closure to oxygen rather than nitrogen in the case of **3***b* is readily rationalized in terms of a likely mechanism (eq. [3]) for the cyclization.[3] The organolead intermediate is formulated as having a nitrogen-to-lead bond (6)

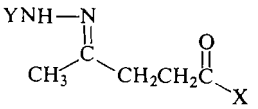

3*a* X = OH; Y = C_6H_5
3*b* X = NHC_6H_5; Y = C_6H_5
3*c* X = OC_2H_5; Y = C_6H_5
3*d* X = OH; Y = $C_6H_3(NO_2)_2$-2,4

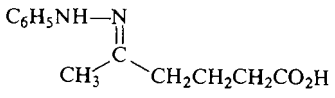

4

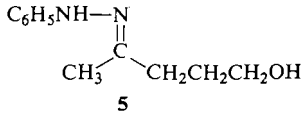

5

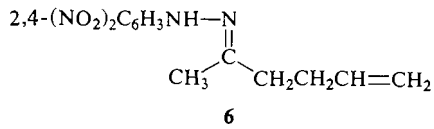

6

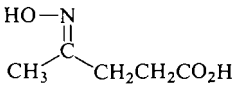

7

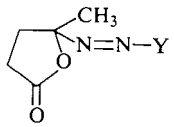

9*a* Y = C_6H_5
9*b* Y = $C_6H_3(NO_2)_2$-2,4

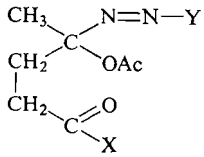

10*a* Y = C_6H_5; X = OH
10*b* Y = $C_6H_3(NO_2)_2$-2,4; X = OH
10*c* Y = C_6H_5; X = OC_2H_5

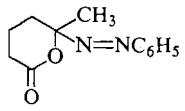

11

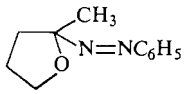

12

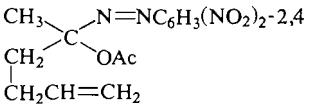

13

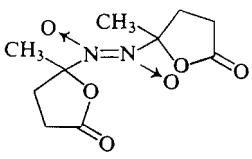

14

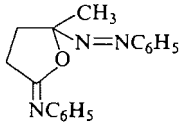

15

[3]The same rationale applies to oxadiazoline formation (3,4). Cyclization to sulfur rather than nitrogen is probably also preferred. The yield of a Δ^3-1,3,4-thiadiazoline prepared from acetone thiocarbohydrazone (3) was not high enough, however, to prove such a preference.

Can. J. Chem. Downloaded from www.nrcresearchpress.com by 210.87.254.40 on 09/05/12
For personal use only.

TABLE I

Spectra of the oxidation products

Compound	i.r. (vC=O, cm^{-1})	Solvent	(p.m.r.) ($CDCl_3$), δ, type (relative area)
9*a*	1797* 1787* 1780*	CCl_4 neat $CHCl_3$	1.73, s (3); 2.44, m (4); 7.55, m (5)
9*b*	1800	KBr	1.86, s (3); 2.60, m (4); 7.50, d (1); 8.62, m (1); 8.93, d (1)
10*c*	1750	neat	1.10, t (3); 1.73, s (3); 2.05, s (3); 2.35, m (4); 4.02, q (2); 7.22–7.85, m (5)
11	1756* 1750* 1737*	CCl_4 neat $CHCl_3$	1.18–2.66, m (6); 1.73, s (3); 7.24–7.91, m (5)
12	1135†	neat	1.17–2.50, m (4); 1.55, s (3); 4.03, m (2); 7.00–8.00, m (5)
14	1800	KBr	1.82, s (3); 1.99, s (3); 2.62, m (8)‡

*Perkin-Elmer 521 instrument.
†Ether chromophore.
‡The nitrosodimer must be a mixture of diastereoisomers and therefore has more than one methyl signal.

although the allylic alternative has been suggested (7) and a π-bonded species is also conceivable. Whatever its structure, ready heterolysis is to be expected and the cationic precursor (eq. [3]) of **15** should be considerably more stable than that resulting from use of the amide nitrogen in cyclization.

Neither **3***c* nor **6** were cyclized by LTA; azoacetates **10***c* and **13** being formed instead.[1] The double bond is probably not sufficiently nucleophilic to allow cyclization to compete with azoacetate formation. Whether the ester (**3***c*) cyclizes in the sense of eq. [3], with subsequent ring opening faster than displacement on the ethyl group, is not known.

The carbonyl stretching frequencies (Table I) of the azo-substituted lactones are increased slightly by the arylazo substituents.[4] Carbonyl stretching frequencies of δ-valerolactone and of γ-lactones in $CHCl_3$ are 1732 and 1775–1777 cm^{-1}, respectively (8).

Experimental

Infrared spectra and proton magnetic resonance (p.m.r.) spectra were obtained with Perkin-Elmer, Model 337 and Varian Associates, A-60 instruments, respectively, unless otherwise indicated. Melting points were determined with a Thomas "Unimelt" capillary-melting-point apparatus. Analyses were by Alfred Bernhardt, Elbach, Germany and by A. B. Gygli, Toronto, Canada.

Chemicals

Methylene chloride was used as supplied by Matheson, Coleman and Bell (MCB). Lead tetraacetate (MCB), wet with acetic acid, was washed with petroleum ether (30–60°) before use. Levulinic acid, 4-keto-1-pentanol, 5-ketobutyric acid, 5-hexene-2-one, phenylhydrazine,2,4-dinitrophenylhydrazine, and aniline were obtained from the Aldrich Chemical Co., Milwaukee. Florisil (60–100 mesh), for column chromatography, was obtained from the Fisher Scientific Co., Toronto.

Levulinic Acid Phenylhydrazone (3a)

Levulinic acid (20 g, 0.17 mole) and phenylhydrazine (18.6 g, 0.19 mole) in 20 ml of ether gave 32 g (91%) of **3***a*, m.p. 108–109° (lit. (9) m.p. 109–110°).

Levulinic Acid-2,4-dinitrophenylhydrazone (3d)

Levulinic acid (11.6 g, 0.1 mole) was refluxed for 6 h in benzene with 2,4-dinitrophenylhydrazine (19.8 g, 0.1 mole). After cooling, the precipitate was filtered off and recrystallized from ethanol to give 21 g (71%) of yellow **3***d*, m.p. 204° (lit. (10) m.p. 206°).

5-Ketohexanoic Acid Phenylhydrazone(4)

5-Ketohexanoic acid (5 g, 0.038 mole) was mixed with phenylhydrazine (4.15 g, 0.038 mole) in 10 ml of ether. A yellow oil was obtained which crystallized after several days to yield 7.2 g (86%) of **4**, m.p. 48–51°; p.m.r. ($CDCl_3$) δ 1.71 (s, 3, CH_3), 1.72–2.55 (m, 6, CH_2),

[4]The direction of the effect is that expected from inductive electron withdrawal by the arylazo function. Its magnitude (ca. 5 cm^{-1}) is appreciable when compared with the effect of equatorial bromine and chlorine *alpha* to carbonyl of cyclohexanones (Δ vCO = 15 and 20 cm^{-1}, respectively).

Can. J. Chem. Downloaded from www.nrcresearchpress.com by 210.87.254.40 on 09/05/12
For personal use only.

TABLE II

Analyses and physical properties

Compound	Yield (%)	Properties (mm Hg), °C	Analysis* C	H	N	Mol.wt.
9*a* from **3***a*	67	b.p. (0.25), 106–108; n_D^{22}, 1.5510	64.69 64.61	5.92 5.39	13.72 13.91	— —
9*b*	40	m.p. 115–117	44.91 44.62	3.43 3.61	19.04 18.84	294.2 295
9*a* from **3***b*	41	b.p. (0.01), 92–93	64.69 64.87	5.92 5.49	13.72 13.92	— —
11	55	b.p. (0.6), 128	66.03 66.07	6.47 6.47	12.84 12.80	218.3 228
12	79	b.p. (0.1), 44	69.44 69.35	7.42 7.42	14.73 14.96	190.2 189
14	56	m.p. 118–119	46.51 46.31	5.47 5.48	10.85 10.69	258.3 236

*Calculated values in the upper rows. Analytical results in the lower rows.

6.59–7.41 (m, 5, C_6H_5), 8.32 (s, 2, *NH* and *OH*); i.r. (neat) 1780 cm^{-1} (C=O).

4-Keto-1-pentanol Phenylhydrazone (5)

Heating phenylhydrazine (10.8 g, 0.1 mole) with 4-keto-1-pentanol (10.2 g, 0.1 mole) for 0.5 h in 6 ml of acetic acid at 100° gave, after addition of NH_4OH and extraction with ether, 15 g (78%) of **5**, m.p. 64–65° (lit. (11) m.p. 60–66°).

Ethyllevulinate Phenylhydrazone (3c)

To a saturated solution of phenylhydrazine hydrochloride (43.2 g, 0.3 mole) in water was added ethyllevulinate (43.2 g, 0.3 mole). The mixture was shaken and after a few h the crystals which had separated were recovered and recrystallized from benzene. The yield of **3***c*, m.p. 108–109° (lit. (12) m.p. 103–104°), was 54 g (77%).

Levulinanilide Phenylhydrazone (3b)

Levulinic anilide (19.1 g, 0.1 mole) and phenylhydrazine (10.8 g, 0.1 mole) gave 22 g (78%) of **3***b*, m.p. 110–111°; p.m.r. ($CDCl_3$) δ 1.71 (s, 3, CH_3), 2.65 (s, 4, CH_2), 6.70–7.60 (m, 10, C_6H_5), 8.42 (s, 2, *NH*); i.r. (KBr) 1670 cm^{-1} (C=O).

5-Hexen-2-one-2,4-dinitrophenylhydrazone (6)

2,4-Dinitrophenylhydrazine (18.2 g, 0.1 mole) was refluxed briefly with 5-hexen-2-one (9.8 g, 0.1 mole) in 100 ml of ethanol. The mixture was cooled, 5 ml of conc. HCl was added, and the resulting mixture was heated again for 2 min. After cooling there was obtained 10.5 g (38%) of **6**, m.p. 104° (lit. (13) m.p. 104°).

Levulinic Acid Oxime (7)

Hydroxylamine hydrochloride (50 g, 0.72 mole) and levulinic acid (8.3 g, 0.07 mole) were dissolved in a little water and a hot, saturated solution of Na_2CO_3 (38 g) in H_2O was added. On cooling 6.7 g (76%) of **7** precipitated, m.p. 95–96° (lit. (14) m.p. 95–96°).

Oxidation of Phenylhydrazones

The general procedure involved gradual addition of 0.03 mole of the hydrazone in methylene chloride solution to a stirring solution of 20 g (0.045 mole) LTA in methylene chloride at 0–5°. The mixture was allowed to warm to room temperature and stirred another h after which time cold water was added. Filtration through a bed of Celite, separation of the organic layer, washing with cold water and with cold bicarbonate solution, drying with Na_2SO_4, and evaporation of the solvent gave the reaction product. Preliminary purification was done by chromatography on Florisil with methylene chloride as eluent. The first small fraction contained mainly azobenzene, the second fraction contained the desired reaction product while the azoacetates remained on the column.[5] Further purification was achieved by recrystallization or distillation. Analyses and physical constants of the oxidation products are in Table II.

Oxidation of Levulinic Acid Oxime

To 33.3 g (0.075 mole) of LTA in 150 ml of methylene chloride was added, gradually and with stirring, 9.82 g (0.075 mole) of the oxime at 0–5 °C. The reaction mixture was kept 2 h at room temperature, water was added, the organic layer was separated, washed with cold water and bicarbonate solution, dried, and the solvent evaporated. After recrystallization from methylene chloride–petroleum ether, 5.4 g (56%) of *trans*-bis[γ-nitroso-γ-valerolactone] (**14**) was obtained, m.p. 118–119 °C.

Acknowledgments

Acknowledgment is made to the donors of the Petroleum Research Fund, administered by the American Chemical Society, for partial support of this research. We are grateful also to the National Research Council of Canada for financial assistance.

[5]Azoacetates **10***c* and **13**, which lack the polar functional groups of the other azoacetates, were eluted.

Can. J. Chem. Downloaded from www.nrcresearchpress.com by 210.87.254.40 on 09/05/12
For personal use only.

1. H. KROPF and R. LAMBECK. Ann. **700**, 1 (1966), and references therein.
2. The literature concerned with LTA oxidation of substituted hydrazones has been reviewed by R. N. Butler. Chem. and Ind. 437 (1968).
3. P. R. WEST and J. WARKENTIN. J. Org. Chem. **33**, 2089 (1968).
4. A. M. CAMERON, P. R. WEST, and J. WARKENTIN. J. Org. Chem. In press.
5. J. WARKENTIN and P. R. WEST. Tetrahedron Letters, 5815 (1966).
6. M. J. HARRISON, R. O. C. NORMAN, and W. A. F. GLADSTONE. J. Chem. Soc. **C**, 735 (1967).
7. P. BOUCHET, J. ELGUERO, and R. JACQUIER. Bull. Soc. Chim. France, 4716 (1967).
8. R. N. JONES, C. L. ANGELL, T. ITO, and R. J. D. SMITH. Can. J. Chem. **37**, 2007 (1959).
9. T. MITSUI. J. Agr. Chem. Soc. Japan, **24**, 465 (1950); Chem. Abstr. **47**, 9302 (1953).
10. H. H. STRAIN. J. Amer. Chem. Soc. **57**, 759 (1935).
11. J. J. GRANDBERG, A. N. KOST, and A. P. TERENTEV. Zh. Obshch. Khim. **27**, 3342 (1957).
12. P. P. T. SAH. J. Amer. Chem. Soc. **52**, 4882 (1930).
13. C. H. F. ALLEN. J. Amer. Chem. Soc. **52**, 2958 (1930).
14. AD. MÜLLER. Ber. Deut. Chem. Ges. **16**, 1618 (1883).

Can. J. Chem. Downloaded from www.nrcresearchpress.com by 210.87.254.40 on 09/05/12
For personal use only.

Can. J. Chem. Downloaded from www.nrcresearchpress.com by 210.87.254.42 on 09/05/12
For personal use only.

1,2:5,6-Di-*O*-isopropylidene-D-hexofuranoses and their 3-keto derivatives

K. N. SLESSOR AND A. S. TRACEY
Department of Chemistry, Simon Fraser University, Burnaby 2, British Columbia

Received May 12, 1969

The synthesis of the only unknown 1,2:5,6-di-*O*-isopropylidene-D-hexose, D-mannose, is reported. Its preparation involved the stereospecific borohydride reduction of the 3-keto intermediate prepared from D-altrose. An improved synthesis of the known D-talose derivative proceeded in an analogous manner from the parent ketone. The four 3-keto derivatives of the diacetone D-hexoses were prepared and their properties compared. In an attempt to explain the differences found in the ease of hydration of these materials, high resolution infrared hydrogen bonding studies were carried out on the eight hexose derivatives and the one hydrated ketone.

Canadian Journal of Chemistry, 47, 3989 (1969)

The synthetic utility of the isopropylidene blocking group has been well recognized for many years in the synthesis of specifically substituted carbohydrates (1, 2). Quite recently the application of oxidative methods to these derivatives has resulted in the facile synthesis of the rare hexoses, D-allose (3) and D-gulose (4). If some of the other isopropylidene hexoses were available, analogous reactions could be used, yielding other more difficultly obtained hexoses.

It should be pointed out that the hydrolysis of the isopropylidene group occurs under mildly acidic conditions probably involving cleavage of the C—O bond of the ketal (5). This is important when dealing with sugars which readily form 1,6-anhydro derivatives under acidic conditions as it allows hydrolysis to the free sugar, rather than a mixture of anhydride and the free sugar that one obtains upon hydrolysis of a glycoside. An example is the quantitative yield of D-gulose from the 1,2:5,6 ketal (4) whereas under more strongly acidic conditions, D-gulose gave 41% of the 1,6-anhydro-β-D-gulopyranose as well as the free sugar (6).

In order to study the conformational properties of the *cis* fused isopropylidene derivatives of furans, the synthesis of all the 1,2:5,6-di-*O*-isopropylidene-D-hexofuranoses was undertaken. Although seven of the eight were known, the synthetic procedures for several of them were poor in terms of yield. As noted below, the 3-keto derivatives are excellent synthetic intermediates as well as derivatives which provide an optically active chromophore for optical rotatory dispersion studies.

Theander's synthesis of D-allose (**2**) from the keto compound (**1**) clearly indicated the stereospecific nature of the hydride reduction of 3-keto-1,2-*O*-isopropylidene compounds (3). The presence of the *endo* methyl group of the isopropylidene acetal completely prevents reduction from this side, giving the alcohol *cis* to the 1,2-ring as in the D-allose derivative. With the appropriate ketones being available the 1,2:5,6-di-*O*-isopropylidene derivatives of D-talose (**4**), D-mannose (**6**), and D-gulose (**8**) are readily prepared.

1,2:5,6-Di-*O*-isopropylidene-β-D-talofuranose (**4**) is known as a side product in the acetonation

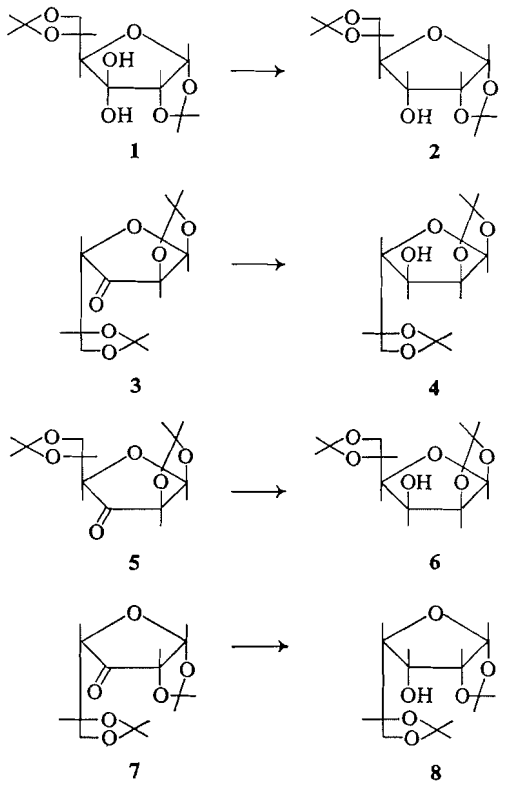

Can. J. Chem. Downloaded from www.nrcresearchpress.com by 210.87.254.42 on 09/05/12
For personal use only.

of D-talose (7). The D-gulose can be readily prepared by the borohydride reduction of 3-*O*-acetyl-1,2:5,6-di-*O*-isopropylidene-α-D-*erythro*hexofuran-3-enose (4) or as described below. The mannofuranose derivative has not previously been prepared as acetonation of D-mannose gives only 2,3:5,6-di-*O*-isopropylidene-D-mannofuranose (8).

1,2:5,6-Di-*O*-isopropylidene-α-D-gulofuranose (**8**) has been synthesized by Meyer zu Reckendorf (4) by conversion of the hydrated 1,2:5,6-di-*O*-isopropylidene-α-D-*ribo*hexofuranos-3-ulose (**1**) into the enol acetate (**9**). Reduction of this material with sodium borohydride yields the diacetone gulose. The reaction is complicated by loss of the 5,6-*O*-isopropylidene acetal and the yield in the borohydride reduction is often low due to this. We have found catalytic hydrogenation of the enol acetate gives an excellent yield of the 3-*O*-acetate (**10**). Catalytic deacetylation with methoxide then gives the gulose derivative (**8**) in very high yield.

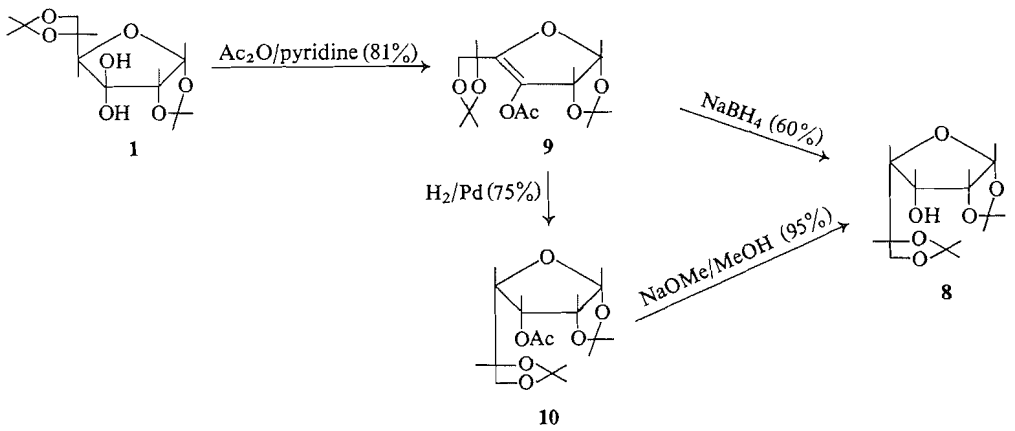

1 **9** **8** **10**

It is worth mentioning that the reduction is not a simple addition of hydrogen across the 3,4-ene but involves a rearrangement which is being investigated and will be reported later.

The preparation of the ketones was carried out in an analogous way to the known route for 3-keto diacetone glucose (**1**) (9). D-Altrose was prepared from methyl 4,6-benzylidene-α-D-glucoside and was converted into the known 1,2:5,6-di-*O*-isopropylidene-β-D-altrofuranose (**11**). Oxidation of this material by the very convenient IO_4^-/RuO_2 method of Parikh and Jones (9*b*) yielded the desired keto sugar as a syrup which crystallized after vacuum distillation. Borohydride reduction allowed isolation of the hitherto unknown 1,2:5,6-di-*O*-isopropylidene-β-D-mannofuranose (**6**). D-Idose was prepared from its penta-acetate (10) and condensed with acetone to give the known 1,2:5,6-acetonate (**12**) (11). Oxidation yielded a crystalline ketone which on borohydride reduction gave the known β-D-talofuranose derivative (**4**) (12). 1,2:5,6-Di-*O*-isopropylidene-α-D-galactofuranose (**13**) was readily prepared by hydroboration of 3-deoxy-1,2:5,6-di-*O*-isopropylidene-α-D-*erythro*hexofuran-3-enose (13).

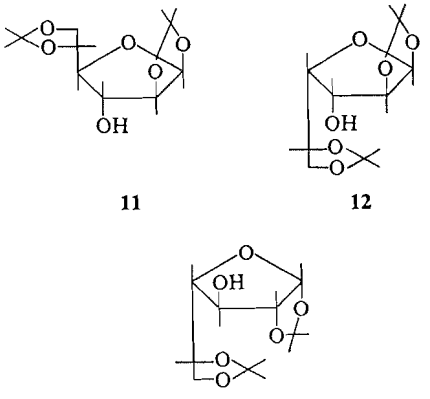

11 **12** **13**

The reduction of the four ketones with borodeuteride gives excellent yields of the 3-deutero-D-allose, -D-talose, -D-mannose, and -D-gulose[1], which are valuable compounds for spectroscopic

[1]Unpublished results.

TABLE I

Proton magnetic resonance chemical shift data*

Sugar	H_1	$J_{1,2}$(Hz)	H_2	H_3	H_4	H_5	H_{6_1}	H_{6_2}	CH_3's
Diacetone mannose (**6**)	4.30	4.1	5.32	5.71	6.15	5.43	5.89	6.04	8.38, 8.62(3)
arabino Ketone (**5**)	3.99	4.3	5.53	5.60 to 6.08					8.48, 8.60(3)
xylo Ketone (**7**)	3.94	4.4	5.49	5.60 to 6.20					8.50, 8.56(3)
lyxo Ketone (**3**)	3.88	4.2	5.51	5.54 to 6.24					8.70, 8.58(3)

*Run on a Varian A 56–60 at room temperature using $CDCl_3$ as solvent and internal TMS as standard (10.0 τ).

analyses of the diacetone hexoses. In an attempt to introduce deuterium at the 4-position, the ketones were treated with pyridine–D_2O (2:1) (14) at temperatures ranging from 20–100° for periods of up to 1 h. No introduction of deuterium was observed at either the 2 or 4 positions nor did any epimerization of the 4 position take place. Under the conditions used the ketones decomposed at varying rates. Deuteration was checked by reisolation of the ketone, purification, and nuclear magnetic resonance (n.m.r.) spectroscopy (see Table I). We believe the resistance to enolization to be due to the hydration of the ketone in aqueous solution. This is born out by the absence of a ketone absorption at 325 mμ in aqueous solutions of all the ketones. The optical rotatory dispersion studies (15) show no anomalous dispersion in aqueous solution but strong Cotton effects when run in non-aqueous media. This phenomenon has already been reported for 3-keto diacetone glucose (4).

Not too surprising is the observation that the ketones hydrate with varying ease as is evident from Table II. On isolation, however, only one of the ketones is isolated as the hydrate, the others all existing in their keto modification as shown by the presence of a strong band at 1770–1780 cm^{-1} indicating C=O, and the absence of a band at 3300–3600 cm^{-1} indicating no OH in the infrared spectra of the samples in KBr discs. Crystalline 1,2:5,6-di-*O*-isopropylidene-α-D-*ribo*hexofuranos-3-ulose (**1**) has been shown to be hydrated and this was substantiated by the strong band at 3400 cm^{-1} and the complete absence of a ketone absorption.

In an attempt to explain the differential hydration of these substances, intramolecular hydrogen bonding studies were carried out by high resolution infrared spectroscopy on dilute carbon tetrachloride solutions. Spedding has reviewed the applicability of this technique to conformational assignments in carbohydrate chemistry (16). Spectra were run at 3 concentrations (0.005, 0.0025, and 0.0012 *M*) in carbon tetrachloride that had been dried over molecular sieve (Linde type 3A). In all nine compounds no observable peak change or shift occurred on changing concentration. The spectra are shown in Fig. 1.

Figures 1*A* and 1*B* represent compounds (*altro* and *galacto*) in which intramolecular hydrogen bonding of the 3-hydroxyl would not be expected because of its distance from any suitable oxygen. The similarity of these spectra and the position of the band at 3630 cm^{-1} indicate a free hydroxyl on a secondary center. Figures 1*C* and 1*D* are compounds (*allo* and *talo*) in which the stereochemistry only allows the hydroxyl to hydrogen bond to the 2-*O* in the 1,2-*O*-isopropylidene ring. This is in agreement with the position of the bands in 1*C* and 1*D* at

TABLE II

Extent of hydration (%) of the 1,2:5,6-di-*O*-isopropylidene-D-hexofuranos-3-uloses*

Ketone	0.5 h	1.5 h	3.5 h	8 h	18 h
Acetonitrile containing 4.25% water					
ribo† (**1***a*)	2	7	14	26	45
arabino (**5**)	1	3	4	6	10
xylo (**7**)	5	14	17	17	17
lyxo (**3**)	2	4	9	17	29
Acetonitrile containing 10% water					
ribo† (**1***a*)	34	69	82	83	84‡
arabino (**5**)	11	26	39	41	43
xylo (**7**)	25	34	38	39	39
lyxo (**3**)	23	46	60	61	61

*Measured on a Unicam SP200 at 320 mμ at a sugar concentration of 0.015–0.017 *M* in 1 cm cells. Beer's law was obeyed for the ketones in acetonitrile over this concentration range giving ε values of (1*a*) 23, (5) 31, (7) 28, (3) 30. All the ketones showed no absorption at 320 mμ after 5 min of being dissolved in water.

†The *ribo* ketone (1*a*) was prepared by vacuum distillation of the hydrated ketone (1*b*) (b.p. 112°/0.04 mm) to give a mobile syrup which crystallized, m.p. 38–39°.

‡After 18 h in acetonitrile containing 10% water the hydrated *ribo* ketone (1*b*) showed 85% hydration, confirming that equilibrium conditions had been reached.

Can. J. Chem. Downloaded from www.nrcresearchpress.com by 210.87.254.42 on 09/05/12
For personal use only.

Can. J. Chem. Downloaded from www.nrcresearchpress.com by 210.87.254.42 on 09/05/12
For personal use only.

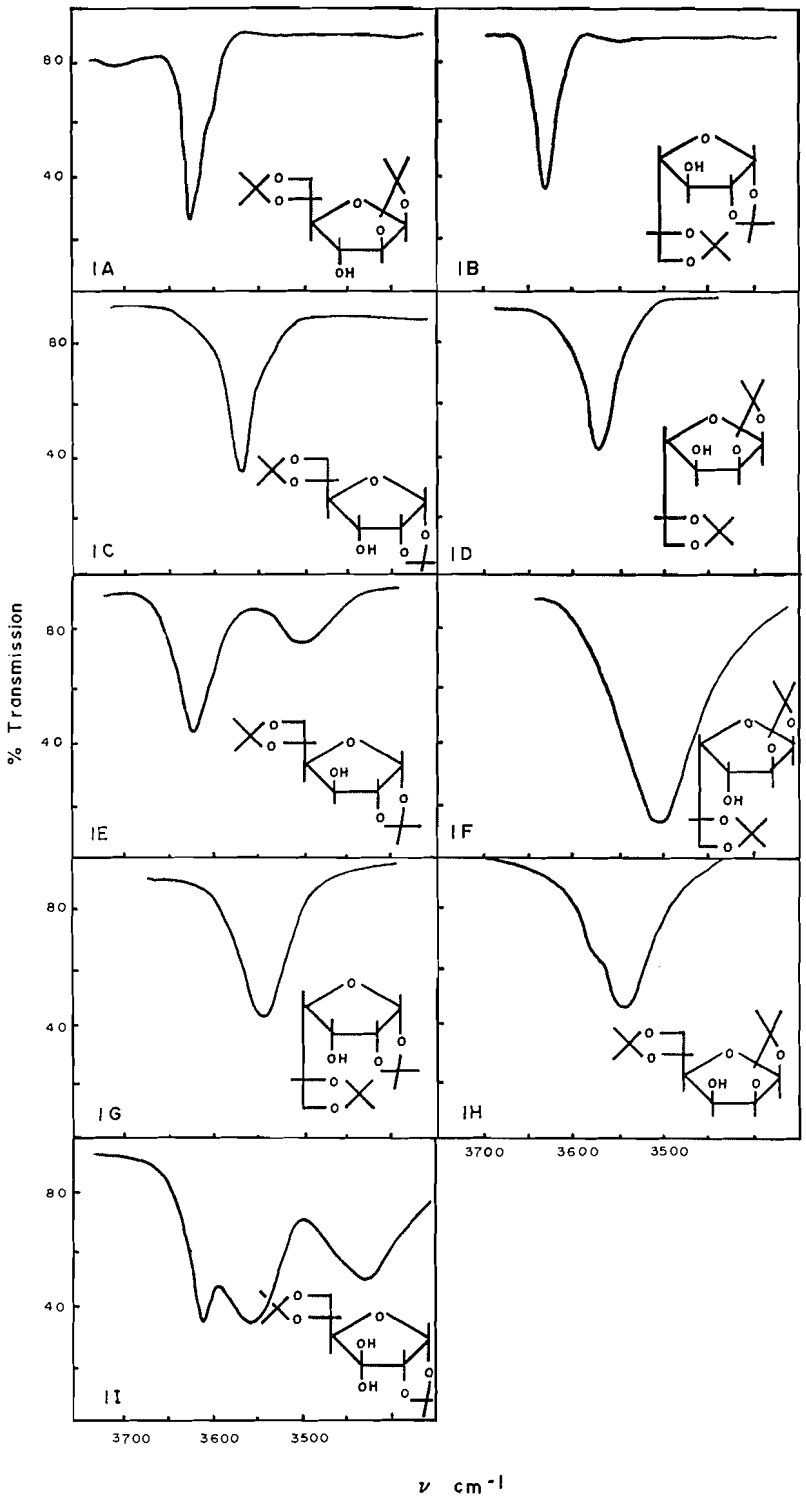

FIG. 1. Infrared spectra of the 1,2:5,6-di-*O*-isopropylidene-D-hexofuranoses and 1,2:5,6-di-*O*-isopropylidene-α-D-*ribo*-hexofuranos-3-ulose in carbon tetrachloride (0.005 *M*).

Can. J. Chem. Downloaded from www.nrcresearchpress.com by 210.87.254.42 on 09/05/12
For personal use only.

3570 cm^{-1} indicating a 5 membered hydrogen bond ring (17).

$$C_2—O_2\cdots H—O_3—C_3$$

The stereochemistry of compounds 1*E* and 1*F* (*gluco* and *ido*) restricts any hydrogen bonding of the 3-OH to the oxygen at C_5 involved in the 5,6-*O*-isopropylidene ring. Surprisingly, the spectra are quite different, the glucose derivative having 2 peaks, one at 3622 cm^{-1} (free OH) and the less intense band at 3485 cm^{-1}. The latter band indicates a larger $\Delta\nu$ as could be expected from the formation of a six membered ring (17)

$$C_3—O—H\cdots O_5—C_5—C_4.$$

Hydrogen bonding of this type will prevent free rotation of the "tail" (C_5—C_6 and their substituents) about the C_4—C_5 bond. At room temperature it is unlikely that free rotation is completely hindered in the glucose derivative, and thus the band at 3622 cm^{-1} can be attributed to that fraction of the 3-OH in which the "tail" is in a rotamer that cannot be hydrogen bonded. The diacetone idose spectrum shows only one band at 3502 cm^{-1} indicating complete hydrogen bonding to the "tail". Careful examination of molecular models indicates that when the "tail" and the 3-OH are *cis*, then in the D-C_5:D-C_3 configuration (D-*gulo* and D-*ido*) rotation about the C_4—C_5 bond is more hindered than for the D-C_5:L-C_3 configuration (D-*gluco* and D-*manno*).

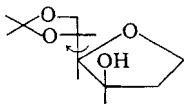

Rotation easier

D-C_5; L-C_3

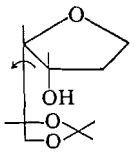

Rotation more difficult

D-C_5; D-C_3

It would seem that the formation of a 3-OH···O_5 hydrogen bond as well as the hindered rotation effectively maintains the "tail" of 1,2:5,6-di-*O*-isopropylidene-β-D-idofuranose in one rotamer.

Figures 1*G* and 1*H* (*gulo* and *manno*) indicate the spectra in which the 3-OH is able to choose whether it bonds with the "tail" or the oxygen at the 2 position. We believe the peaks at 3532 and 3538 cm^{-1} respectively, indicate a preferential formation of the hydrogen bond to the "tail". The shoulder in the *manno* (1H) derivative at 3585 cm^{-1} we feel corroborates the evidence that the D-C_5:L-C_3 system (*gluco* and *manno*) has freer rotation about the C_4—C_5 bond. Such rotation would prevent complete hydrogen bonding to the "tail" and allow the 3-OH to form a hydrogen bond to the 2 oxygen of the 1,2-*O*-isopropylidene unit, thus giving rise to the 3585 cm^{-1} shoulder.

Figure 1*I* shows the spectrum of the hydrated 3-keto diacetone glucose (**1**). Both hydroxyl groups at the 3 position can hydrogen bond. The band at 3550 cm^{-1} we ascribe to the OH group hydrogen bonded to the C_2 oxygen and the bands at 3608 and 3423 cm^{-1} to the other OH. The 3423 cm^{-1} band is attributed to the one hydrogen bonded to the "tail" and the 3608 cm^{-1} band being due to free OH not being able to bond because of the "tail" being in another rotamer. The apparent strengthening (lowering of the frequency) of these bands is readily ascribed to the extra electronegative OH group at C_3.

Two di-*O*-isopropylidene compounds are capable of double hydrogen bonding in their hydrated keto form. The first is the keto glucose (**1**) that we have just discussed, the second the keto idose derivative (**3**).

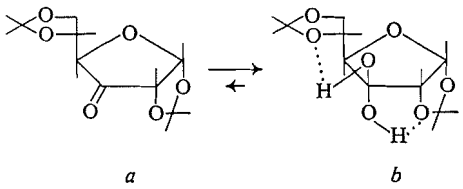

a *b*

1

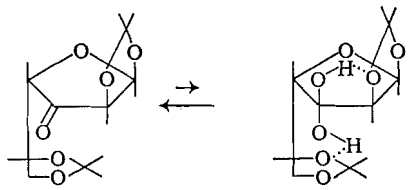

a *b*

3

In its crystalline state, the latter exists in the keto form. That this is not just a property of the crystalline material is obvious from the ease of extraction from aqueous solution and the inability to form an enol acetate under identical conditions to those for the hydrated keto glucose derivative. That is, in spite of the ability of 1,2:5,6-di-*O*-isopropylidene-β-D-idofuranose to form a strong hydrogen bond with its "tail", the hydrated keto

Can. J. Chem. Downloaded from www.nrcresearchpress.com by 210.87.254.42 on 09/05/12
For personal use only.

form of **3***b* is not stabilized by such formation. We believe the reason for this is that in the very rigid conformation that must be adopted to simultaneously form two hydrogen bonds, there is steric interaction of the "tail" with the furan ring. This does not seem to be the situation in the hydrated keto D-glucose derivative (**1***b*).

The hydrogen bonding results must be regarded with care as they pertain only to dilute, non-polar solutions and will not be applicable to aqueous systems. Nevertheless, the information one can derive from such results allows a much better appreciation for the forces acting within the molecule and thus a better understanding of the chemistry of these compounds.

Experimental

Melting points were determined on a Fisher–Johns apparatus and are uncorrected. Evaporations were carried out on Buchi rotary evaporators at bath temperatures not exceeding 45°. Optical rotations were measured on a Perkin Elmer Model P22 spectropolarimeter using thermostatted jacketed cells of varying path lengths at 20°. Hydrogen bonding studies were performed in matched cells of 1 cm path length on a Beckman IR 12. Thin layer chromatography (t.l.c.) was carried out on Silica gel G using 10% sulfuric acid and heat for development.

1,2:5,6-Di-O-isopropylidene-α-D-glucofuranose

It was prepared from D-glucose by the method of Schmidt (18), m.p. 110°, $[\alpha]_D$ −17.5° (*c*, 0.4, water). Lit. (18), m.p. 110–111°, $[\alpha]_D$ −18.5° (*c*, 5, water).

*1,2:5,6-Di-O-isopropylidene-α-D-ribohexofuranos-3-ulose (**1**)*

To 1,2:5,6-di-*O*-isopropylidene-α-D-glucofuranose (5.0 g) in carbon tetrachloride (50ml), sodium bicarbonate (0.4 g) in water (4 ml) was added. Ruthenium dioxide (40 mg) was added and 5% aqueous sodium metaperiodate was added dropwise[2] with stirring until the oxidation was complete, as indicated by t.l.c. The mixture was separated and the aqueous phase extracted twelve times with an equal volume of chloroform. The organic phases were combined, dried over calcium chloride, filtered, and evaporated to give a syrup which crystallized readily. Recrystallization from chloroform – petroleum ether (30–60°) (1:2) gave (**1**) 4.0 g, m.p. 109–111°, $[\alpha]_D$ 37.5° (*c*, 0.4, water). Lit. (3), m.p. 108–110°, $[\alpha]_D$ 40.2 (*c*, 0.5, water).

*1,2:5,6-Di-O-isopropylidene-α-D-allofuranose (**2**)*

It was prepared by the sodium borohydride reduction of (**1**) as described by Theander (3), m.p. 73–74°, $[\alpha]_D$ 34° (*c*, 0.4, water). Lit. (3), m.p. 76–77°, $[\alpha]_D$ 37.7° (*c*, 0.5, water).

[2]Periodate is added only if the black RuO_2 is reformed after each addition of periodate.

*3-O-Acetyl-1,2:5,6-di-O-isopropylidene-α-D-gulofuranose (**10**)*

Catalytic reduction of 3-*O*-acetyl-1,2:5,6-di-O-isopropylidene-α-D-*erythro*hexofuran-3-enose (**9**) (3 g) in ether (60 ml) at room temperature and atmospheric pressure with palladium black for 2 h gave upon filtration and evaporation of the solvent, crystalline 3-*O*-acetyl-1,2:5,6-di-*O*-isopropylidene-α-D-gulofuranose (2.3 g), m.p. 73–74°, recrystallized from ethanol, $[\alpha]_D$ 66.0° (*c*, 0.36, $CHCl_3$).

Anal. Calcd. for $C_{14}H_{22}O_7$: C, 55.62; H, 7.33. Found: C, 55.43; H, 7.16.

*1,2:5,6-Di-O-isopropylidene-α-D-gulofuranose (**8**)*

Deacetylation of the 3-*O*-acetate (1.55 g) with 0.01 *N* sodium methoxide (50 ml) for 2 h followed by neutralization of the base with solid carbon dioxide gave the known gulose derivative (1.25 g) m.p. 103°, $[\alpha]_D$ 10.0° (*c*, 0.4, $CHCl_3$). Lit. (4), m.p. 105–106°, $[\alpha]_D$ 7.5° (*c*, 1, $CHCl_3$).

*1,2:5,6-Di-O-isopropylidene-α-D-xylohexofuranos-3-ulose (**7**)*

1,2:5,6-Di-*O*-isopropylidene-α-D-gulofuranose (1.1 g) was oxidized by the IO_4^-/RuO_2 method described above. Only four extractions with chloroform were necessary to give the product (0.79 g) which crystallized readily. Recrystallization from petroleum ether (65–110°) gave the ketone m.p. 76–77°, $[\alpha]_D$ −58.5° (*c*, 0.4, water).

Anal. Calcd. for $C_{12}H_{18}O_6$: C, 55.80; H, 6.96. Found: C, 55.63; H, 6.89.

*1,2:5,6-Di-O-isopropylidene-α-D-galactofuranose (**13**)*

It was prepared by hydroboration of 3-deoxy-1,2:5,6-di-*O*-isopropylidene-α-D-*erythro*hexofuran-3-enose as described by Paulsen and Behre (13), m.p. 94–95°, $[\alpha]_D$ −20.5° (*c*, 0.4, $CHCl_3$). Lit. (13), m.p. 97.5–98°, $[\alpha]_D$ −35.3° (*c*, 0.8, methanol).

*1,2:5,6-Di-O-isopropylidene-β-D-altrofuranose (**11**)*

Syrupy D-altrose (19) (1.3 g) was dissolved in a mixture of dry acetone (100 ml) that contained zinc chloride (12 g) and 85% phosphoric acid (0.5 ml). The solution was stirred overnight at room temperature and then neutralized by careful addition of 50% aqueous sodium hydroxide. The mixture was then filtered, the precipitate washed thoroughly with acetone, and the filtrate and washings combined and evaporated. The resultant thin syrup was dissolved in chloroform (25 ml) and washed with 1% aqueous sodium bicarbonate (15 ml). The bicarbonate wash water was extracted once with chloroform (15 ml) and the extracts pooled, dried over calcium chloride, filtered, and evaporated. The resultant syrup crystallized readily and could be recrystallized from petroleum ether (65–110°) to yield the diacetone altrose (1.22 g), m.p. 87–88°, $[\alpha]_D$ 28.5° (*c*, 0.4, acetone). Lit. (20), m.p. 87–88°, $[\alpha]_D$ 28.7° (*c*, 1.04, acetone).

*1,2:5,6-Di-O-isopropylidene-β-D-arabinohexofuranos-3-ulose (**5**)*

1,2:5,6-Di-*O*-isopropylidene-β-D-altrofuranose (1.65 g) was oxidized in the same manner as was the glucofuranose. The oxidation yielded a non-crystalline material (1.28 g) after four extractions, which was free of impurities as judged by n.m.r. and t.l.c. (ethyl ether:toluene, 2:1). Vacuum distillation of the syrup (b.p. 87°/0.01 mm) gave a colorless liquid which crystallized spontaneously. Recrystallization from petroleum ether (65–110°) gave

material (1.11 g) melting at 31–32°, $[\alpha]_D$ 25.5° (*c*, 0.49, water).

Anal. Calcd. for $C_{12}H_{18}O_6$: C, 55.80; H, 6.96. Found: C, 55.59; H, 7.09.

1,2:5,6-Di-O-isopropylidene-β-D-mannofuranose (6)

1,2:5,6-Di-*O*-isopropylidene-β-D-arabinohexofuranos-3-ulose (440 mg) was dissolved in ethanol:water (5:1) (50 ml) and sodium borohydride (50 mg) was added. The reduction was carried out at room temperature for 30 min after which time the solution was neutralized with carbon dioxide. Extraction of this solution with chloroform (4 × 50 ml) gave a solution which was dried with calcium chloride, filtered, and evaporated to a syrup. The syrup was dissolved in chloroform (50 ml) and washed with 2% aqueous sodium bicarbonate (25 ml). The bicarbonate wash was extracted once with chloroform (50 ml), the chloroform layers combined, dried, filtered, and evaporated to a syrup which crystallized. Recrystallization from petroleum ether (65–110°) gave material (400 mg) melting at 52–53°, $[\alpha]_D$ 12.5° (*c*, 0.4, water).

Anal. Calcd. for $C_{12}H_{20}O_6$: C, 55.37; H, 7.75. Found: C, 55.27; H, 7.86.

2,3:5,6-Di-O-isopropylidene-D-mannofuranose

1,2:5,6-Di-*O*-isopropylidene-β-D-mannofuranose (**6**) (200 mg) was dissolved in a solution of acetone (12 ml) containing concentrated sulfuric acid (0.2 ml). After 1 h at room temperature, sodium carbonate (1 g) was added and the mixture was stirred for 6 h. The neutral acetone solution was then filtered and the filtrate evaporated. The solid residue was dissolved in a minimum of hot petroleum ether (65–110°) which upon cooling yielded crystalline material (180 mg) melting at 118–119°. Three recrystallizations from petroleum ether (65–110°) gave m.p. 118–119°, mixed melting point with the 2,3:5,6 ketal prepared from D-mannose, 118–119°. Freudenberg and Hixon (21) give the m.p. as 118°. The 2,3:5,6 ketal prepared from the 1,2:5,6 had an identical infrared spectrum to that of the material prepared in the standard way (22).

1,2:5,6-Di-O-isopropylidene-β-D-idofuranose (12)

Amorphous D-idose was prepared by the method of Paulsen *et al.* (10). The D-idose so produced (5 g) was converted into the known di-*O*-isopropylidene derivative using zinc chloride (12 g), 85% phosphoric acid (0.5 ml) in dry acetone (100 ml). On working up the product as described above for 1,2:5,6-di-*O*-isopropylidene-β-D-altrofuranose, a crystalline product was obtained by cooling a petroleum ether (65–110°) solution of the material. The mother liquor contained an isomeric di-*O*-isopropylidene derivative, presumably the 1,2:3,5 furanose derivative. This material could be retreated with the acetal forming reagents to produce further amounts of **12**. Recrystallization from petroleum ether (65–110°) gave 1,2:5,6-di-*O*-isopropylidene-β-D-idofuranose (3.5 g), m.p. 151–152°, $[\alpha]_D$ 33.5° (*c*, 0.4, acetone). Lit. (11), m.p. 151–152.5°, $[\alpha]_D$ 36.0° (acetone).

1,2:5,6-Di-O-isopropylidene-β-D-lyxohexofuranos-3-ulose (3)

1,2:5,6-Di-*O*-isopropylidene-β-D-idofuranose (1.3 g) was oxidized in the same manner as the glucofuranose. The oxidation yielded a crystalline material (1.1 g), m.p. 87.5–88° from petroleum ether (65–110°), $[\alpha]_D$ −21.0° (*c*, 0.4, water).

Anal. Calcd. for $C_{12}H_{18}O_6$: C, 55.80; H, 6.96. Found: C, 55.95; H, 6.79.

1,2:5,6-Di-O-isopropylidene-β-D-talofuranose (4)

Borohydride reduction of 1,2:5,6-di-*O*-isopropylidene-β-D-*lyxo*hexofuranos-3-ulose (400 mg) was carried out in the same way as described for the conversion of the *arabino* ketone (**5**) to the mannofuranose (**6**). The reduced product (350 mg) was recrystallized from petroleum ether (65–110°), m.p. 83–84°, $[\alpha]_D$ −25.0° (*c*, 0.40, $CHCl_3$). Lit. (7), m.p. 85–86°, $[\alpha]_D$ −25° (*c*, 0.47, $CHCl_3$).

Acknowledgments

We are very pleased to acknowledge the financial support of the National Research Council of Canada. We wish to thank Mr. C. R. Haylock for the Optical Rotary Dispersion studies.

1. A. N. DE BELDER. Advan. Carbohyd. Chem. **20**, 220 (1965).
2. S. A. BARKER and E. J. BOURNE. Advan. Carbohyd. Chem. **7**, 137 (1952).
3. O. THEANDER. Acta Chem. Scand. **18**, 2209 (1964).
4. W. MEYER ZU RECKENDORF. Angew. Chem. Int. Ed. **6**, 177 (1967).
5. (*a*) E. H. CORDES. *In* Progress in physical organic chemistry. Vol. 4. A. Streitwieser and R. W. Taft, Eds., Interscience Publishers, Inc., New York. 1967. p. 1. (*b*) P. M. COLLINS. Tetrahedron **21**, 1809 (1965).
6. E. L. ELIEL, N. L. ALLINGER, S. J. ANGYAL, and G. A. MORRISON. Conformational analysis. Interscience Publishers, Inc., New York. 1965. p. 417.
7. W. BOSSHARD. Helv. Chim. Acta, **18**, 482 (1935).
8. O. TH. SCHMIDT. Methods Carbohyd. Chem. **2**, 319 (1963).
9. (*a*) H. NAKATA. Tetrahedron, **19**, 1959 (1963). (*b*) V. M. PARIKH and J. K. N. JONES. Can. J. Chem. **43**, 3452 (1965).
10. H. PAULSEN, W-P. TRAUTWEIN, F. G. ESPINOSA, and K. HEYNS. Chem. Ber. **100**, 2822 (1967).
11. K. IWADARE. Bull. Chem. Soc. Jap. **19**, 27 (1944).
12. J. S. BRIMACOMBE and P. A. GENT. Carbohyd. Res. **9**, 231 (1969).
13. H. PAULSEN and H. BEHRE. Carbohyd. Res. **2**, 80 (1966).
14. G. M. CREE and A. S. PERLIN. Can. J. Biochem. **46**, 765 (1968).
15. C. R. HAYLOCK. Optical Rotary Dispersion of the 1,2:5,6-Di-*O*-isopropylidene-D-hexofuranoses. B.Sc. Thesis, Simon Fraser University, Burnaby, B.C. (1969).
16. H. SPEDDING. Advan. Carbohyd. Chem. **19**, 23 (1964).
17. L. P. KUHN, P. VON R. SCHLEYER, W. F. BATINGER, JR., and L. EBERSON. J. Amer. Chem. Soc. **86**, 650 (1964).
18. O. TH. SCHMIDT. Methods Carbohyd. Chem. **2**, 320 (1963).
19. N. K. RICHTMYER. Methods Carbohyd. Chem. **1**, 107 (1962).
20. F. H. NEWTH and L. F. WIGGINS. J. Chem. Soc. 1734 (1950).
21. K. FREUDENBERG and R. M. HIXON. Ber. Deut. Chem. Ges. **56**, 2119 (1923).
22. K. IWADARE. Bull. Chem. Soc. Jap. **16**, 144 (1941).

Can. J. Chem. Downloaded from www.nrcresearchpress.com by 210.87.254.42 on 09/05/12
For personal use only.

Can. J. Chem. Downloaded from www.nrcresearchpress.com by 210.87.254.40 on 09/05/12
For personal use only.

Aliphatic diazo compounds. IX. The base-induced dimerization of α-diazo ketones[1,2]

PETER YATES, R. G. F. GILES, AND D. G. FARNUM

Department of Chemistry, University of Toronto, Toronto 5, Ontario, and Department of Chemistry, Harvard University, Cambridge, Massachusetts

Received June 2, 1969

Treatment of 2-diazoacetophenone (**1**) with potassium *t*-butoxide in *t*-butyl alcohol gives a colorless dimer, which is shown to be 5-benzoyl-2-phenacyltetrazole (**4**) by its independent synthesis by phenacylation of 5-benzoyltetrazole. The latter reaction also gives 5-benzoyl-1-phenacyltetrazole (**3**), which is distinguished from **4** by its reduction to di(2-hydroxy-2-phenylethyl)amine and by its cyclization on treatment with ammonium acetate. The assignment of the structure of the colorless dimer of **1** permits the postulation of related pathways for its formation and that of the red–brown dimer obtained on treatment of **1** with potassium hydroxide in dimethyl sulfoxide. 2-Phenacyltetrazole (**22**) and benzoic acid are formed in addition to **4** on treatment of **1** with potassium *t*-butoxide in *t*-butyl alcohol; these are considered to arise via cleavage of **4**, since prolonged treatment of **4** and **3** with potassium *t*-butoxide in *t*-butyl alcohol gives **22** and 1-phenacyltetrazole (**24**), respectively. Compounds **22** and **24** have been prepared independently by phenacylation of tetrazole.

Canadian Journal of Chemistry, 47, 3997 (1969)

α-Diazo ketones have been observed to give two types of dimer on reaction with bases. Treatment of 2-diazoacetophenone (**1**) with potassium hydroxide in dimethyl sulfoxide gives a red–brown dimer that has been shown to be 3,6-dibenzoyl-1,2(4)-dihydrotetrazine (**2**) by independent synthesis (3). Treatment of 2-diazoacetophenone with potassium *t*-butoxide in *t*-butyl alcohol gives a colorless dimer that was previously considered to be 5-benzoyl-1-phenacyltetrazole (**3**) (2), but is now shown to be 5-benzoyl-2-phenacyltetrazole (**4**). Both types of dimer have also been obtained from the α-diazo ketones **5** and **6** under various basic conditions (3, 4).

$RCOCHN_2$
1, R = Ph
5, R = 2,4,6-$(CH_3)_3C_6H_2$
6, R = $(CH_3)_3C$

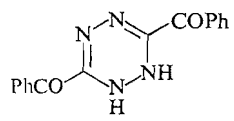

2

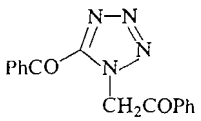

3

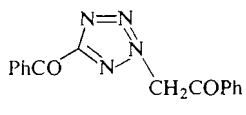

4

The colorless dimer, m.p. 114–114.5°, was obtained in 69% yield by reaction of 2-diazoacetophenone (**1**) with 1.2 molar equivalents of potassium *t*-butoxide in dilute solution in *t*-butyl alcohol at room temperature. Its infrared spectrum, which included bands at 5.85 and 5.95 μ, suggested that it contained two carbonyl groups; the absence of a band in the 2.75–3.2 μ region further indicated that the dimer possessed no N—H bond. These conclusions and the earlier observation of the formation of 5-benzoyltetrazole (**7**) in the reaction of **1** with methanolic sodium methoxide (1) led to the formulation of the dimer as either **3** or **4**. These structures were in accord with its proton magnetic resonance (p.m.r.) spectrum, which showed a two-proton singlet at δ 6.31 and a ten-proton multiplet at δ 7.5–8.5, assignable to the methylene and aromatic protons, respectively. Its formulation as a *C*-benzoyl nitrogen heterocycle was also in accord with the presence of a strong band at 10.82 μ in its infrared spectrum (5).

This structural assignment was confirmed by the independent synthesis of **3** and **4** by treatment of **7** with phenacyl bromide and potassium carbonate in acetone. The major product (65% yield) from this reaction was a compound shown

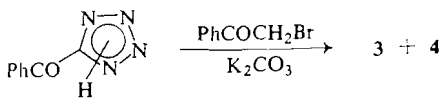

7

to be identical with the colorless dimer of **1**. A second, isomeric product, m.p. 126–127°, was obtained in 14% yield; its infrared spectrum, which included bands at 5.85, 5.97, and 10.80 μ,

[1]For Part VIII, see reference 1.
[2]Part of this work has been reported in a preliminary communication (2).

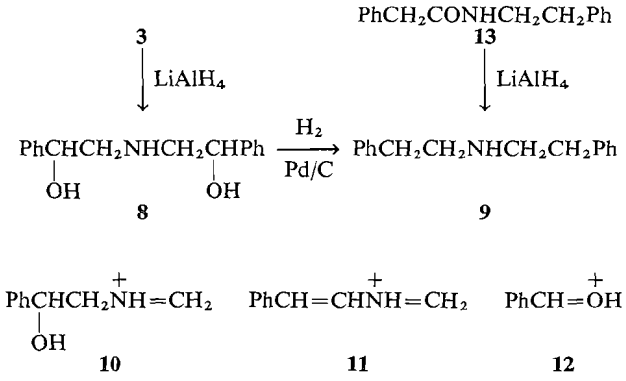

and its p.m.r. spectrum, with signals at δ 6.33 (2H, s) and 7.5–8.6 (10H, m), were very similar to the spectra of the major product. These compounds were clearly the two possible *N*-phenacylation products derivable from **7**; the unusually short wavelength (5.85 μ) of the carbony-stretching band attributable to the phenacyl carbonyl group can be interpreted in terms of the strong electron-withdrawing effect of the tetrazole ring.

It remained to assign individual structures to the two phenacylation products. The isomer, m.p. 126–127°, was shown to have structure **3** in the following way [cf. (6)]. Reduction with lithium aluminium hydride gave a compound, $C_{16}H_{19}NO_2$, which was shown to be di(2-hydroxy-2-phenylethyl)amine (**8**) by its spectral properties and its conversion on catalytic hydrogenolysis to di(2-phenylethyl)amine (**9**). The amine **8** showed bands at 2.77 and 3.0 μ in its infrared spectrum, but no band in the carbonyl-stretching region. Its p.m.r. spectrum showed a two-proton multiplet at δ 4.75 and a ten-proton signal at δ 7.36, assigned to the methine and aromatic protons, respectively. The remaining protons gave rise to a seven-proton multiplet at δ 2.75–3.0 that was replaced by a four-proton doublet (*J* 6 Hz) at δ 2.82, assigned to the methylene protons, after treatment of the sample with deuterium oxide. The mass spectrum of the product showed no molecular ion peak, but exhibited a fragmentation pattern in accord with the structural assignment [cf. (7)], with peaks at *m/e* 150, 132 (base peak), and 107, attributable, respectively, to the ions **10**, **11**, and **12**; a metastable peak at 116.1 corroborated the formation of **11** from **10** (calcd. 116.2). The structure of the hydrogenolysis product **9** was established by direct comparison of it and its hydrochloride with authentic samples prepared via reduction of *N*-(2-phenylethyl)phenylacetamide (**13**) with lithium aluminium hydride.

The formation of **8** on reductive cleavage of the tetrazole, m.p. 126–127°, establishes that this tetrazole has structure **3** rather than **4**, and leads to the assignment of the latter structure to the dimer, m.p. 114–114.5°, of 2-diazoacetophenone. Reduction of **4** with lithium aluminium hydride failed to cleave the tetrazole ring; the product obtained was the diol **14**.[3] This was converted by hydrogenolysis to 2-benzyl-5-(2-phenylethyl)-tetrazole (**15**), which was also obtained directly from **4** by hydrogenolysis under analogous conditions. The tetrazole ring of **15** was also resistant to cleavage by lithium aluminium hydride.

The individual assignments of structure **3** and **4** were confirmed by treatment of **3** with ammonium acetate in boiling acetic acid. There was thus obtained a product, $C_{16}H_{11}N_5$, in 78% yield, that is assigned structure **16**. Its infrared spectrum showed no bands in the N—H or C=O stretching regions, and its p.m.r. spectrum, which was confined to the δ 7.5–9.1 region, included a three-proton signal at δ 8.9–9.1 consisting of a singlet superimposed on a multiplet. Subjection of **4** to similar conditions failed to effect any analogous reaction. The difference between the ultraviolet spectra of **3** and **4** could also be interpreted in terms of these structural assignments. The spectrum of compound **3** showed a maximum at 252 mμ (ε 19 500) with a shoulder at 272 mμ (ε 15 500), while that of **4** showed a simple max-

[3]Although both diastereomers of the diols **14** and **8** are very probably formed during the reduction of **4** and **3**, respectively, the sharp-melting product isolated in each case may well have been a single diastereomer.

Can. J. Chem. Downloaded from www.nrcresearchpress.com by 210.87.254.40 on 09/05/12
For personal use only.

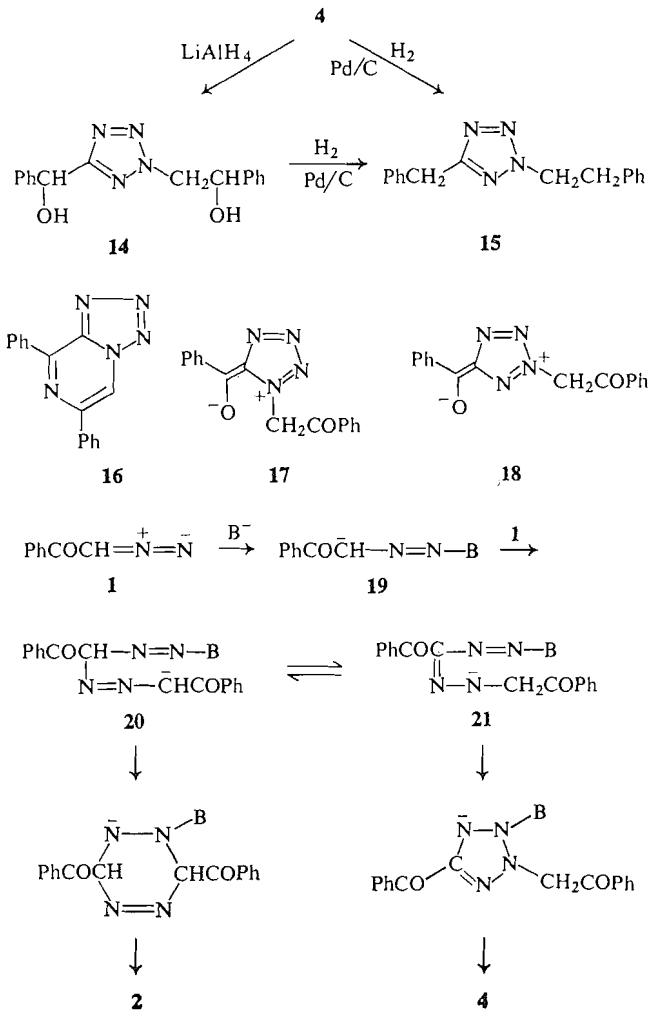

imum at 250 mμ (ε 24 600). These spectra represent the superimposition of bands due to the $C_6H_5COCH_2X$ system [cf. acetophenone, λ_{max}(EtOH) 243 mμ (ε 12 600) (8)] and the *C*–benzoyltetrazole system [cf. 5-benzoyltetrazole, λ_{max}(EtOH) 261 mμ (ε 12 600) (9)]. The presence of the long wavelength shoulder in the case of **3**, but not of **4**, is compatible with the circumstance that the *C*–benzoyltetrazole system of the former is linearly conjugated, while that of the latter is cross-conjugated (cf. reduced charge separation in **17** vs. **18**).[4]

[4]A misinterpretation of the relationship between the ultraviolet spectra of **3** and **4** originally led to erroneous individual structural assignments (2).

The establishment of **4** as the structure of the dimer of 2-diazoacetophenone (**1**) formed on its treatment with potassium *t*-butoxide in *t*-butyl alcohol[5] reveals that it has a close relationship to the dimer **2** formed on treatment with potassium

[5]It is appropriate here to clarify several confusing aspects of the literature. In the paper by Yates and Farnum (2) there is a typographical error on p. 24, where 5-benzoyl-1-phenacylpyrazole(VII) should have read 5-benzoyl-1-phenacyltetrazole(VII). In the paper by Yates, Meresz, and Morrison (3) there is a typographical error in the first sentence, where 5-benzoyl-2-phenacyltetrazole(I) should have read 5-benzoyl-1-phenacyltetrazole(I). In a recent review (10) it is erroneously stated that Yates and Farnum (2) observed the formation of *both* **3** and **4** from **1** on treatment with potassium *t*-butoxide in *t*-butyl alcohol.

Can. J. Chem. Downloaded from www.nrcresearchpress.com by 210.87.254.40 on 09/05/12
For personal use only.

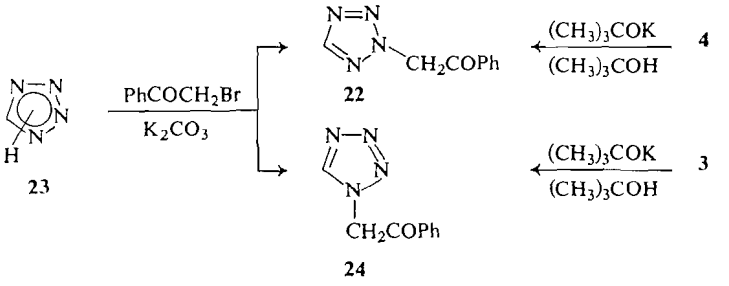

hydroxide in dimethyl sulfoxide. The formation of both can readily be rationalized in terms of the intermediacy of an anion of type **19**, formed via terminal attack (11) of base (B^-) on **1**. Addition of **19** to a second molecule of **1** could give **20** and **21**, which could serve as the source of **2** and **4**, respectively.[6] The manner in which the nature of the basic reagent controls the type of dimer found has not been established.

As previously mentioned, the yield of **4** on treatment of **1** with potassium *t*-butoxide in *t*-butyl alcohol is 69%; the remainder of the starting material is accounted for by two other products, benzoic acid and a compound, $C_9H_8N_4O$. The spectra of the latter suggested that it was 2-phenacyltetrazole (**22**), and this was established by its independent synthesis by phenacylation of tetrazole (**23**) and by cleavage of **4** with potassium *t*-butoxide in *t*-butyl alcohol. The major product in the phenacylation of **23** was 1-phenacyltetrazole (**24**), which was also obtained by the cleavage of **3** with potassium *t*-butoxide in *t*-butyl alcohol.

The cleavage of **4** with base was also carried out by treating it with potassium *t*-butoxide in commercial "anhydrous" ether. The solution momentarily assumed a red coloration, which changed to pale yellow with concomitant formation of a precipitate. Work-up with aqueous ammonium chloride gave **22** and benzoic acid. The possibility that reaction occurred by attack of *t*-butoxide ion at the 5-benzoyl group to give *t*-butyl benzoate and the anion **25**, was excluded by the demonstration that *t*-butyl benzoate was neither a reaction product nor was it converted in major extent to benzoic acid under the conditions of the reaction. It seemed probable that the cleavage of **4** had occurred as a result of the adventitious presence of water, and that the cleavage involved formation of the anion **25** by attack of hydroxide ion at the 5-benzoyl group and was of a type recently investigated by Gassman and co-workers (13). This view was corroborated by the observation that treatment of **4** with potassium *t*-butoxide in ether that had been distilled from lithium aluminium hydride immediately prior to use led to a red coloration that persisted in the anhydrous medium. Work-up

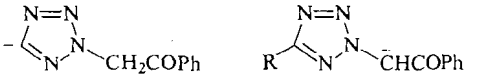

25 **26**, R = PhCO
28, R = D
30, R = H

with deuterium chloride in acetic acid-*d* led to the recovery of **4** with partial deuteration of the methylene group, indicating the formation of the anion **26** in the basic medium; no 2-phenacyltetrazole (**22**) was formed. When the anhydrous ether was treated with deuterium oxide (1.67 moles per mole of **4**) before use, the red coloration again rapidly gave way to a yellow coloration, and after work-up with aqueous ammonium chloride the deuterated cleavage product **27** was obtained. It seems likely that **27** is first formed in the reaction mixture by transfer of deuterium to the anion **25** from benzoic acid-*d* formed simultaneously in the cleavage reaction; subsequent reaction with *t*-butoxide ion could give the anion **28**, from which **27** would be regenerated in the aqueous work-up. Further, when **4** was cleaved with potassium *t*-butoxide in commercial "anhydrous" ether and the solid obtained from the reaction mixture was treated with methyl iodide, only the side-chain methylation product **29** was isolated, suggesting that the anion **25** is converted by reaction with benzoic acid to **22** which then reacts

[6]A related route involving initial proton abstraction (12) rather than terminal attack also leads to an anion that could serve as an intermediate in the formation of both **2** and **4**.

Can. J. Chem. Downloaded from www.nrcresearchpress.com by 210.87.254.40 on 09/05/12
For personal use only.

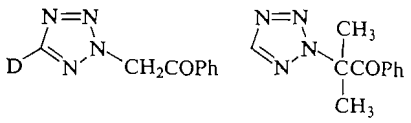

27 29

with *t*-butoxide ion to give the anion **30**. The isolation of the dimethylated product is ascribed to the presence of excess potassium *t*-butoxide in the solid product subjected to methylation.

The demonstration that the presence of water is required for the cleavage of **4** by potassium *t*-butoxide in ether suggests that the cleavage of both **3** and **4** with potassium *t*-butoxide in *t*-butyl alcohol may also have involved the intervention of adventitious water.

Experimental

Melting points, which were determined with a Thomas Hoover "Uni-melt" capillary melting point apparatus, are uncorrected. Solutions in organic solvents were dried over anhydrous magnesium sulfate. Unless otherwise stated, infrared spectra were recorded in solution in dichloromethane, ultraviolet spectra in 95% ethanol, and proton magnetic resonance (p.m.r.) spectra at 100 MHz in deuteriochloroform with tetramethylsilane as internal reference.

Reaction of 2-Diazoacetophenone (1) with Potassium t-Butoxide in t-Butyl Alcohol: Formation of 5-Benzoyl-2-phenacyltetrazole (4) and 2-Phenacyltetrazole (22)

2-Diazoacetophenone (1.00 g) was added to a solution of potassium *t*-butoxide (0.92 g) in *t*-butyl alcohol (55 ml) and the mixture was swirled to dissolve the diazo ketone. The solution immediately became red and after standing for 30 min at room temperature was poured into cold, dilute hydrochloride acid. The mixture was extracted with several portions of dichloromethane, and the extract was dried and stripped of solvent. The resulting solid was dissolved in benzene and chromatographed on a Florisil column (100 g, packed in benzene). Elution with dichloromethane – benzene (1:1) gave 2-phenacyltetrazole (**22**) (0.15 g, 23%), m.p. 104–104.5° after recrystallization from benzene – hexane (*vide infra*).

Elution of the column with 2% methanol – dichloromethane yielded 5-benzoyl-2-phenacyltetrazole (**4**) (0.69 g, 69%), m.p. 114–114.5° after recrystallization from 95% ethanol; λ_{max} 5.85, 5.95, 6.23, 6.30, 10.82 μ; λ_{max} 250 mμ (log ε 4.39); δ 6.31 (2H, s), δ 7.5–8.5 (10H, m).

Anal. Calcd. for $C_{16}H_{12}N_4O_2$: C, 65.75; H, 4.14; N, 19.17. Found: C, 65.58; H, 4.25; N, 18.80.

Elution of the column with 10% methanol – dichloromethane gave benzoic acid (0.17 g).

Phenacylation of 5-Benzoyltetrazole (7): Formation of 5-Benzoyl-1-phenacyltetrazole (3) and 5-Benzoyl-2-phenacyltetrazole (4)

5-Benzoyltetrazole[1] (0.87 g) was dissolved in dry acetone (20 ml) and potassium carbonate (0.35 g) was added. The mixture was swirled and warmed until most of the base had dissolved, and phenacyl bromide (1.00 g) was added. The reaction mixture was boiled gently under reflux for 30 min, diluted to the cloud point with water, and chilled to 0°. The crystalline deposit was recrystallized from 95% ethanol to give **4** (0.70 g, 47%), m.p. 113.5–114°, undepressed on admixture with the 5-benzoyl-2-phenacyltetrazole (**4**) obtained above; the infrared spectra of the two samples were identical.

The original filtrate was combined with the recrystallization mother liquors, diluted with water, and extracted with dichloromethane. The extract was dried and evaporated, and the residue (0.64 g) was chromatographed on a Florisil column packed in benzene. Elution of a pale yellow band with dichloromethane – benzene (1:1) afforded colorless needles of 5-benzoyl-1-phenacyltetrazole (**3**) (0.20 g, 14%), m.p. 126–127° after recrystallization from 95% ethanol; λ_{max} 5.85, 5.97, 6.23, 6.30, 10.80 μ; λ_{max} 252 mμ (log ε 4.29), 272 mμ (sh, log ε 4.19); δ 6.33 (2H, s), 7.5–8.6 (10H, m).

Anal. Calcd. for $C_{16}H_{12}N_4O_2$: C, 65.75; H, 4.14; N, 19.17. Found: C, 65.69; H, 4.23; N, 19.39.

Elution with 5% methanol – dichloromethane gave a further quantity of tetrazole **4** (0.25 g; total yield 65%).

Reduction of 3 with Lithium Aluminium Hydride: Formation of Di(2-hydroxy-2-phenylethyl)amine (8)

A solution of the tetrazole **3** (0.151 g) in tetrahydrofuran (15 ml) was added dropwise to a suspension of lithium aluminium hydride (0.240 g) in boiling tetrahydrofuran (20 ml) under reflux. The solution was boiled under reflux for 18 h, and the excess of the hydride was decomposed by the cautious addition of 0.2 *N* hydrochloric acid. The mixture was added to concentrated aqueous sodium hydroxide and extracted with ether. The extract was dried and stripped of solvent to give crude **8** in quantitative yield. Recrystallization from benzene afforded plates (0.075 g, 54%), m.p. 115–117°; λ_{max} 2.77, 3.0, 6.68 μ; δ 2.75–3.0 (7H, m) [2.82 (4H, d, *J* 6 Hz) after treatment with D_2O], 4.75 (2H, m; t, *J* 6 Hz, after treatment with D_2O), 7.36 (10H, m).

Anal. Calcd. for $C_{16}H_{19}NO_2$: C, 74.68; H, 7.44; N, 5.44. Found: C, 74.77; H, 7.46; N, 5.54.

Hydrogenolysis of 8: Formation of Di(2-phenylethyl)amine (9)

The amine **8** (0.245 g) in acetic acid (10 ml) was added to a stirred suspension of 10% palladium on charcoal (0.065 g) in acetic acid (10 ml) containing a catalytic amount of dilute hydrochloric acid. The solution was maintained at 80° under hydrogen for 12 h. After cooling, the hydrogen uptake was 45 ml at 27° and 753 mm (96% of the volume of hydrogen required for complete hydrogenolysis). The catalyst was removed by filtration, and the filtrate was cautiously added to cold, concentrated aqueous sodium hydroxide. The mixture was extracted with several portions of chloroform. The extract was dried and stripped of solvent to give di(2-phenylethyl)-amine (**9**) (0.170 g, 79%); $\lambda_{max}(CHCl_3)$ 3.13, 6.26, 6.76 μ. This was shown by infrared spectral comparison to be identical with an authentic sample (*vide infra*).

The amine (**9**) was dissolved in ether containing a little chloroform, and hydrogen chloride was bubbled through the solution. The solid deposited was recrystallized from

Can. J. Chem. Downloaded from www.nrcresearchpress.com by 210.87.254.40 on 09/05/12
For personal use only.

Can. J. Chem. Downloaded from www.nrcresearchpress.com by 210.87.254.40 on 09/05/12
For personal use only.

ethanol – ether to give di(2-phenylethyl)amine hydrochloride, m.p. 265–266° [lit. (14) m.p. 267–268°], undepressed on admixture with an authentic sample (*vide infra*); its infrared spectrum was identical with that of the authentic sample.

*Reduction of N-(2-Phenylethyl)phenylacetamide (**13**) with Lithium Aluminium Hydride: Formation of Di(2-phenylethyl)amine (**9**)*

Phenylacetyl chloride (15.4 ml) was added dropwise to a solution of 2-phenylethylamine (24.2 ml) in benzene (40 ml). After standing for 1 h the reaction mixture was partitioned between dichloromethane and water. The organic layer was dried and stripped of solvent to give *N*-(2-phenylethyl)phenylacetamide (**13**) (16.5 g), m.p. 93.5–94° after recrystallization from benzene – ligroin [lit. (15) m.p. 94–95°]; λ_{max} 3.02, 6.04, 6.66 μ; δ 2.72 (2H, t), 3.3–3.7 (4H, s superimposed on m), 5.5 (1H, br s), 7.0–7.5 (10H, m).

A solution of **13** (0.98 g) in 1,2-dimethoxyethane (20 ml) was added dropwise to a suspension of lithium aluminium hydride (0.30 g) in boiling 1,2-dimethoxyethane (25 ml), and the mixture was boiled under reflux for 50 h. The excess of hydride was decomposed by the successive addition of anhydrous magnesium sulfate, Celite, and aqueous 1,2-dimethoxyethane. The solution was filtered, dried, and stripped of solvent to give **9** as an oil. This was converted to its hydrochloride as described above; m.p. 266–267°; λ_{max} 3.70, 3.95, 4.15, 6.3 μ; δ (CF_3CO_3H) 3.05 (4H, t, *J* 7 Hz), 3.3–3.7 (4H, m), 7.1–7.5 (10H, m).

*Reduction of **4** with Lithium Aluminium Hydride: Formation of **14***

A solution of the tetrazole **4** (0.28 g) in anhydrous ether (250 ml) was slowly added to a suspension of lithium aluminium hydride (0.64 g) in ether (30 ml). The mixture was boiled under reflux for 4 h and then cooled to room temperature. Celite and anhydrous magnesium sulfate were added, followed by moist ether. The mixture was filtered, and the filtrate was dried and stripped of solvent to give an oily residue; crystallization at 0° from benzene – ligroin gave **14** (0.16 g, 57%), which was recrystallized from benzene; m.p. 108–109.5°; λ_{max} 2.85, 2.95, 6.23, 6.71 μ; δ 3.50 (1H, br s; absent after D_2O treatment), 3.78 (1H, br s; absent after D_2O treatment), 4.6–4.9 (2H, m), 5.3 (1H, m), 6.14 (1H, d, *J* 4 Hz; s after treatment with D_2O), 7.4 (10H, m).

Anal. Calcd. for $C_{16}H_{16}N_4O_2$: C, 64.85; H, 5.44; N, 18.91. Found: C, 65.04; H, 5.67; N, 18.79.

*Hydrogenolysis of **14**: Formation of 5-Benzyl-2-(2-phenylethyl)-tetrazole (**15**)*

A solution of the diol **14** (0.100 g) in acetic acid (3 ml) was added to a stirred suspension of 10% palladium on charcoal (0.015 g) in acetic acid (10 ml) under hydrogen. The mixture was stirred for 20 h at room temperature, and hydrogen (6.1 ml at 27° and 754 mm, ca. 0.8 molar equiv.) was absorbed; it was then heated to 80–90° and maintained at this temperature for a further 7 h. The total hydrogen consumption was 19.1 ml at 27° and 745 mm (ca. 2.25 molar equiv.). The mixture was filtered, and the solvent was removed from the filtrate by freeze-drying to yield **15** (0.090 g, 100%) as an oil, b.p. 150–152° (0.02 mm); $\lambda_{max}(CCl_4)$ 6.23, 6.73 μ; δ 3.30 (2H, t, *J* 8 Hz), 4.16 (2H, s), 4.82 (2H, t, *J* 8 Hz), 7.0–7.5 (10H, m).

Anal. Calcd. for $C_{16}H_{16}N_4$: C, 72.70; H, 6.10; N, 21.20. Found: C, 72.45; H, 6.38; N, 21.35.

The tetrazole **4** was also converted directly to **15** under analogous conditions.

*Reaction of **3** with Ammonium Acetate in Acetic Acid: Formation of **16***

A solution of **3** (0.145 g) in acetic acid (15 ml) containing ammonium acetate (0.200 g) was boiled under reflux for 19 h. The solvent was removed by freeze-drying, the residue was dissolved in chloroform, and the solution was washed with aqueous sodium bicarbonate. The organic layer was dried and stripped of solvent to give **16**, (0.105 g, 78%), m.p. 160.5–161° after recrystallization from ethanol; λ_{max} 6.24, 6.33, 6.84 μ; δ 7.5–7.8 (6H, m), 8–8.3 (2H, m), 8.9–9.1 (3H, s superimposed on m).

Anal. Calcd. for $C_{16}H_{11}N_5$: C, 70.31; H, 4.06; N, 25.63. Found: C, 70.47; H, 4.35; N, 25.58.

Similar treatment of **4** failed to give an analogous product; thin layer chromatography of the crude reaction product showed that it consisted mainly of starting material.

*Phenacylation of Tetrazole (**23**): Formation of 2-Phenacyltetrazole (**22**) and 1-Phenacyltetrazole (**24**)*

A solution of tetrazole (**23**) (0.35 g) and phenacyl bromide (1.00 g) in hot acetone (50 ml) was treated with potassium carbonate (0.70 g), and the mixture was boiled gently under reflux for 30 min. The reaction mixture was poured into water, and the oil which separated was extracted with dichloromethane. The extract was dried and stripped of solvent to yield an oil, which crystallized from benzene to give 1-phenacyltetrazole (**24**) (0.53 g, 56%) as needles, m.p. 100–104°. Several recrystallizations of the crude product from benzene afforded pure material, m.p. 110.5–111.5°; λ_{max} 5.86, 6.26, 6.34, 8.51, 9.09 μ; δ 6.01 (2H, s), 7.5–8.2 (5H, m), 8.94 (1H, s).

Anal. Calcd. for $C_9H_8N_4O$: C, 57.44; H, 4.29; N, 29.77. Found: C, 57.56; H, 4.33; N, 29.94.

The semi-solid residue obtained upon evaporation of the mother liquors, after several recrystallizations from aqueous methanol with treatment with Norit, afforded faintly yellow needles of 2-phenacyltetrazole (**22**) (0.050 g, 5%), m.p. 104–104.5°, undepressed on admixture with material obtained from the reaction of 2-diazoacetophenone (**1**) and of 5-benzoyl-2-phenacyltetrazole (**4**) with potassium *t*-butoxide in *t*-butyl alcohol; the infrared spectra of these samples were identical.

*Cleavage of **4** with Potassium t-Butoxide in t-Butyl Alcohol: Formation of **22***

A solution of 5-benzoyl-2-phenacyltetrazole (**4**) (0.69 g) in hot *t*-butyl alcohol (5 ml) was poured into a solution of potassium *t*-butoxide prepared from potassium (0.29 g) and *t*-butyl alcohol (25 ml). The reaction mixture, which immediately became red, was stirred at room temperature for 84 h, during which time the intensity of the red color diminished. The resulting orange solution was added to an excess of 10% aqueous sodium bicarbonate, and the mixture was extracted with dichloromethane. The crude product obtained by drying and stripping the extract of solvent was chromatographed on

Can. J. Chem. Downloaded from www.nrcresearchpress.com by 210.87.254.40 on 09/05/12
For personal use only.

a Florisil column (100 g, packed in benzene). 2-Phenacyltetrazole (**22**) (0.29 g, 70% based on unrecovered starting material) was eluted with dichloromethane – benzene (1:1) and after recrystallization from benzene – hexane had m.p. 104–104.5°; λ_{max} 5.85, 6.26, 6.32, 8.37, 8.42, 8.92 μ; δ 6.18 (2H, s), 7.5–8.2 (5H, m), 8.69 (1H, s).

Anal. Calcd. for $C_9H_8N_4O$: C, 57.44; H, 4.29; N, 29.77. Found: C, 57.76; H, 4.41; N, 29.87.

Starting material (**4**) (0.035 g) was isolated on elution of the column with 5% methanol – dichloromethane. Benzoic acid (0.091 g) was isolated from the sodium bicarbonate extract.

*Cleavage of **3** with Potassium t-Butoxide in t-Butyl Alcohol: Formation of **24***

5-Benzoyl-1-phenacyltetrazole (**3**) (0.69 g) was treated with potassium *t*-butoxide as in the case of **4** above, except that the reaction period was reduced to 66 h. Chromatography gave 1-phenacyltetrazole (**24**) (120 mg, 28%), which, after recrystallization from benzene with treatment with Norit, had m.p. 111–111.5°, undepressed on admixture with an authentic sample; its infrared spectrum was identical with that of the authentic sample.

*Reaction of 5-Benzoyl-2-Phenacyltetrazole (**4**) with Potassium t-Butoxide in Ether*

(a) In Commercial "Anhydrous" Ether

The tetrazole **4** (0.73 g) was dissolved in commercial "anhydrous" ether (350 ml) by heating. The solution was cooled to room temperature and poured into a stirred slurry of potassium *t*-butoxide (1.25 g) in ether (25 ml). The solution became red momentarily and then turned pale orange–yellow. It was stirred at room temperature for 10 min and then filtered, giving a whitish–yellow solid whose color deepened on exposure to air. Aqueous ammonium chloride was added to the filtrate, and the organic layer was separated, dried, and evaporated to give 2-phenacyltetrazole (**22**) (0.030 g), m.p. and mixed m.p. 103–104°. Its infrared spectrum was identical with that of authentic material. The whitish–yellow solid from above was added to the aqueous ammonium chloride solution and the mixture was extracted with ether. The extract was dried and stripped of solvent to give additional 2-phenacyltetrazole (0.40 g), identified as before. The total yield of **22** was 0.43 g (91%). Benzoic acid (0.30 g, 99%) was isolated from the aqueous layer after acidification.

(b) In Anhydrous Ether

Commercial "anhydrous" ether was boiled under reflux over lithium aluminium hydride and distilled therefrom immediately prior to use. A solution of **4** (1.00 g) in anhydrous ether (400 ml) was rapidly added to a suspension of potassium *t*-butoxide (1.54 g) in anhydrous ether (30 ml) whereupon the mixture turned red. This color persisted while the reaction mixture was stirred at room temperature for 10 min. The mixture was then added to a solution of deuterium chloride in acetic acid-*d*, prepared by mixture of acetyl chloride (12 ml) and deuterium oxide (4 ml). The ethereal solution became colorless (with concomitant salt precipitation) and was extracted with aqueous sodium bicarbonate. The organic phase was dried and stripped of solvent to give a residue which was recrystallized from ethanol. The infrared, n.m.r., and mass spectra of this product (0.59 g) indicated it to be 5-benzoyl-2-phenacyltetrazole partially deuterated at the methylene group. Its n.m.r. spectrum showed a relative intensity of the methylene to phenyl proton signals of ca. 1.5:10. Its mass spectrum showed a ratio of 1:1 in the abundances of the *m/e* 293 and 292 ions, as compared with a ratio of 1:5 in the spectrum of non-deuterated **4**.

A control experiment showed that in the absence of base no deuterium was incorporated into **4**.

(c) In Anhydrous Ether and Deuterium Oxide

The tetrazole **4** (0.61 g) was dissolved in anhydrous ether (rigorously dried as in (*b*), 300 ml) and deuterium oxide (0.7 ml) was well stirred into the solution. This mixture was then added to potassium *t*-butoxide (0.90 g) in ether (25 ml). A red color developed momentarily, rapidly turning to a pale yellow. The solution was stirred for 10 min and then added to aqueous ammonium chloride, whereupon the color was discharged. The ethereal layer was separated, and the aqueous layer was extracted with dichloromethane. The combined organic layers were dried and stripped of the solvent; the residue was crystallized from benzene – hexane affording 2-phenacyltetrazole-5-*d* (**27**) (0.25 g, 64%), m.p. 101.5–103°; δ 6.18 (2H, s), 7.5–8.2 (5H, m), 8.69 (0.3H, s). Its infrared spectrum differed in minor respects from that of 2-phenacyltetrazole (**22**). Its mass spectrum showed a ratio of 2:1 in the abundances of the *m/e* 189 and 188 ions, as compared with a ratio of 1:7 in the spectrum of **22**.

*2-(1,1-Dimethylphenacyl)tetrazole (**28**)*

A solution of **4** (0.73 g) in commercial "anhydrous" ether (not further dried, 350 ml), was added to a suspension of potassium *t*-butoxide (1.22 g) in ether (25 ml), and the mixture was stirred for 10 min. The precipitate was collected by filtration and rapidly transferred to a flask containing a solution of methyl iodide (10 ml) in dimethylformamide (50 ml) under nitrogen. The contents of the flask were stirred for 54 h under nitrogen at room temperature. The solution was added to aqueous ammonium chloride, and the mixture was extracted with dichloromethane. The extract was dried, and stripped of solvent to give an oily crystalline product which possessed the characteristic odor of methyl benzoate. Recrystallization from cyclohexane and sublimation gave **28** (0.23 g, 53%), m.p. 81.5–82°; λ_{max} 5.96, 6.28, 7.23, 7.33 μ; δ 2.11 (6H, s), 7.2–7.6 (5H, m), 8.56 (1H, s).

Anal. Calcd. for $C_{11}H_{12}N_4O$: C, 61.09; H, 5.59; N, 25.91. Found: C, 60.92; H, 5.68; N, 25.73.

Acknowledgments

We thank the National Research Council for generous support of this work. One of us (D.G.F.) acknowledges fellowship support from the National Institutes of Health, U.S.A.

1. P. YATES and D. G. FARNUM. J. Amer. Chem. Soc. **85**, 2967 (1963).
2. P. YATES and D. G. FARNUM. Tetrahedron Letters, No. 17, 22 (1960).
3. P. YATES, O. MERESZ, and H. MORRISON. Tetrahedron Letters, 77, 1575 (1967).

4. P. YATES, A. L. CROWTHER, and P. A. GILBERT. Unpublished results.
5. D. G. FARNUM and P. YATES. J. Org. Chem. **27**, 2209 (1962).
6. R. A. LAFORGE, C. E. COSGROVE, and A. D'ADAMO. J. Org. Chem. **21**, 988 (1956).
7. H. BUDZIKIEWICZ, C. DJERASSI, and D. H. WILLIAMS. Mass spectrometry of organic compounds. Holden-Day, Inc., San Francisco. 1967. p. 297.
8. A. I. SCOTT. Interpretation of the ultraviolet spectra of natural products. Pergamon Press, Ltd., New York. 1964. p. 104.
9. B. E. FISHER, A. J. THOMSON, and J. P. HORWITZ. J. Org. Chem. **24**, 1650 (1959).
10. F. R. BENSON. *In* Heterocyclic compounds. Vol. 8. *Edited by* R. C. Elderfield. John Wiley and Sons, Inc., New York. 1967. p. 39.
11. P. YATES and B. L. SHAPIRO. J. Amer. Chem. Soc. **81**, 212 (1959).
12. H. A. MORRISON and P. YATES. Chem. Ind. (London), 931 (1962).
13. P. G. GASSMAN, J. T. LUMB, and F. V. ZALAR. J. Amer. Chem. Soc. **89**, 946 (1967); cf. G. A. SWAN. J. Chem. Soc. 1408 (1948).
14. VON K. KINDLER, G. MELAMED, and D. MATTHIES. Ann. **644**, 23 (1961).
15. H. DECKER and W. KROPP. Ber. **42**, 2075 (1909).

Can. J. Chem. Downloaded from www.nrcresearchpress.com by 210.87.254.40 on 09/05/12
For personal use only.

Long-range spin–spin coupling constants between ring protons and aldehydic protons in some *para*-substituted benzaldehydes

S. S. DANYLUK, C. L. BELL[1,2] AND T. SCHAEFER[1,3]

Division of Biological and Medical Research, Argonne National Laboratory, Argonne, Illinois

Received June 16, 1969

The long-range proton–proton coupling constants between the ring protons and the aldehydic proton are reported for a series of *para*-substituted benzaldehyde derivatives. It was found that $J_o^{H,CHO} < 0$ and $J_m^{H,CHO} > 0$. Furthermore, $J_o^{H,CHO}$ increases in magnitude as the electron donating power of the substituent increases. A similar trend is observed for $J_m^{H,CHO}$ but the ratio of the increase to the magnitude of $J_m^{H,CHO}$ is much less than for $J_o^{H,CHO}$. A good correlation is obtained between $J_o^{H,CHO}$ and the substituent parameters of Swain and Lupton.

The coupling constant data are discussed in terms of σ and π coupling mechanisms and it is concluded that σ electron mechanisms are dominant for both $J_o^{H,CHO}$ and $J_m^{H,CHO}$.

Canadian Journal of Chemistry, 47, 4005 (1969)

Can. J. Chem. Downloaded from www.nrcresearchpress.com by 210.87.254.40 on 09/05/12
For personal use only.

Introduction

A number of nuclear magnetic resonance (n.m.r.) parameters correlate with Hammett sigma constants[4] (1). ^{19}F, ^{13}C, and ^{1}H chemical shifts are linearly related to σ_p, the sigma constant of a substituent in the *para* position of a benzene derivative. The linear relationships have been theoretically related to the modification of the π system by the substituent. The substituent contribution to the coupling between fluorine nuclei in *meta* difluorobenzene derivatives also depends on σ_p (2,3), suggesting the importance of π electron contributions to J_m^{FF}. The directly bonded C^{13}—H coupling constants of the methyl group in *para*-substituted toluenes are also related to σ_p of the substituent (4).

No strong correlation of couplings between ring protons and sigma constants has been reported for benzene derivatives. The available evidence indicates that $J_{o,m,p}^{HH}$ are affected via the σ electron system by a substituent and therefore such a correlation does not appear likely (5).

As part of a study of coupling mechanisms between aldehydic protons and ring protons in substituted benzaldehydes we have measured the long-range spin–spin coupling constants between the CHO proton and ring protons in a number of *para*-substituted benzaldehydes. In this communication we report a correlation of $J_o^{H,CHO}$ with the substituent constants of Swain and Lupton (28).

Experimental

The benzaldehyde derivatives were of commercial origin. Whenever solubility allowed, dilute solutions of these compounds were prepared in carbon disulfide together with about 10% tetramethylsilane (TMS) as internal reference. Other solvents were benzene-d_6 and acetone. Solutions were carefully degassed by the freeze-pump–thaw technique.

Proton magnetic resonance (p.m.r.) spectra were recorded on a DA60I spectrometer in the frequency sweep mode. Double resonance experiments were carried out in the usual manner (6). Calibration of peak positions involved the reading of sweep and manual oscillator frequencies together with an interpolation between pen positions on the recorder chart. Care was taken to achieve conditions whereby line broadening by saturation and radiation damping was minimized. In this way splittings of as little as 0.10 Hz were easily observable in the dilute, degassed solutions.

Solvent effects on the long-range couplings were evidently zero within experimental error. For example, solutions of *p*-methoxybenzaldehyde in carbon disulfide and in acetone displayed identical long-range couplings.

Results

Spectral Analysis

In Table I the measured long-range coupling constants are given for a series of benzaldehyde derivatives. Chemical shifts of the aldehyde protons are not included because earlier workers have discussed these at length (7) and because of varying solvent conditions in the present work. For most of the compounds the ring proton spectra were not analyzed completely. The magnitudes of the long-range couplings between the aldehyde proton and the ring protons could be

[1]Visiting summer scientist, 1968.
[2]Medical Center, University of Illinois, Chicago.
[3]University of Manitoba, Winnipeg, Canada.
[4]See ref. 1 for a review of early work in this area of research.

TABLE I

Long-range coupling constants*, $J_{m,o}^{H,CHO}$, and substituent parameters in some *para*-substituted benzaldehydes

Substituent	$J_m^{H,CHO}$	$-J_o^{H,CHO}$	R†	F‡
H§	0.38	0.10	0.000	0.000
$N(CH_3)_2$	0.47±0.02	0.23±0.02	−0.681‖	0.037‖
OCH_3	0.48±0.02	0.19±0.02	−0.500	0.413
F	0.46±0.02	0.14±0.02	−0.336	0.708
Cl	0.45±0.02	0.10±0.02	−0.161	0.690
$CH(CH_3)_2$	0.48±0.02	0.16±0.02	−0.126¶	−0.084¶
CH_3	0.43±0.02	0.15±0.02	−0.141	−0.052
CN	0.38±0.02	< 0.06	0.184	0.847
NO_2	0.41±0.02	< 0.06	0.155	1.109

*In Hz.
†Resonance substituent constant from reference (28).
‡Field substituent constant from reference (28).
§Coupling constants taken from reference (11).
‖Substituent constants for the amino group (8).
¶Substituent constant taken as the mean of the constants of the ethyl and *t*-butyl groups (28).

reliably obtained both from the aldehydic p.m.r. spectrum and from the small splittings in the ring proton spectra. Solvent effects were used in some cases to induce sufficiently large shifts (> 0.25 p.p.m.) between the ring protons to ensure the reliability of this procedure.

As a check of the latter we consider an extreme case where the chemical shift between the ring protons is 12 Hz, $J_o^{H,CHO} = -0.17$ Hz and $J_m^{H,CHO} = 0.43$ Hz. Then direct calculation shows that for an A_2B_2X system there arises an error of 0.02 Hz in $J_o^{H,CHO}$ and $J_m^{H,CHO}$ when these are extracted from the X spectrum by first order rules. None of the coupling constants in Table I were obtained under such extreme conditions.

Experiments in which the aldehydic proton was decoupled identified the splittings in the ring proton spectra caused by the aldehyde proton spin states. Other side-chain protons could also be decoupled from the ring protons.

As an example of the observed proton spectra, Fig. 1 illustrates the aldehydic p.m.r. spectra of *p*-isopropylbenzaldehyde and of *p*-cyanobenzaldehyde. The triplet, of triplets resulting from coupling to the two sets of two ring protons is clearly observable in *p*-isopropylbenzaldehyde. From the linewidths of the three peaks in the aldehyde spectrum of *p*-cyanobenzaldehyde and from its ring proton spectrum it is certain that $|J_o^{H,CHO}| < 0.06$ Hz.

Double Resonance Experiments

Sign of $J_o^{H,CHO}$

In Fig. 2(a) the aldehydic proton single resonance spectrum of *p*-N,N-dimethylaminobenzaldehyde is displayed. For this compound $|J_o^{H,CHO}| = \frac{1}{2}|J_m^{H,CHO}|$. Consequently, a spectrum of seven peaks is observed because two pairs of peaks (3,4 and 6,8) overlap. The net spin states of the *ortho* protons (H_A) are given in Fig. 2(a) with the convention that a positive sign beneath a low-field peak corresponds to positive coupling with the labelled protons. In Fig. 2(b) and (c), weak irradiation of *meta* ring proton (H_B) peaks corresponding to either *net* negative or "zero" spin states of the H_A protons (high field transitions in the H_B spectrum) results in a perturbation of a number of peaks in the aldehyde proton resonance. In (b) the weak irradiating field is of smaller amplitude than in (c). The important point is that 9 at high field is not perturbed under these conditions. Consequently, $J_o^{H,CHO}/J_o^{HH} < 0$. Because $J_o^{HH} > 0$, (8), it follows that $J_o^{H,CHO} < 0$. In Fig. 2(d), low-field peaks in the H_B region corresponding to net negative or "zero" spin states of the H_A protons are being irradiated by a second r.f. (radio frequency) field. Peak 1 is unaffected, confirming the above result. The negative sign of $J_o^{H,CHO}$ has previously been inferred from a computer analysis of the tightly coupled ring proton spectra in 2,4-dimethoxybenzaldehyde, 3-nitro-4-hydroxybenzaldehyde, and 2-chloro-4-*N*,*N*-dimethylaminobenzaldehyde (9).

That $J_m^{H,CHO} > 0$ has been established previously (10) by multiple resonance techniques. In benzaldehyde itself $J_o^{H,CHO} < 0$ and $J_m^{H,CHO} > 0$ (11).

Discussion

Conformation of the Aldehyde Group

The p.m.r. experiments show that the free energy of activation for rotation of the aldehyde

Can. J. Chem. Downloaded from www.nrcresearchpress.com by 210.87.254.40 on 09/05/12
For personal use only.

Can. J. Chem. Downloaded from www.nrcresearchpress.com by 210.87.254.40 on 09/05/12
For personal use only.

On page 4007, right-hand column, Fig. 2 should be shown as below and not as printed.

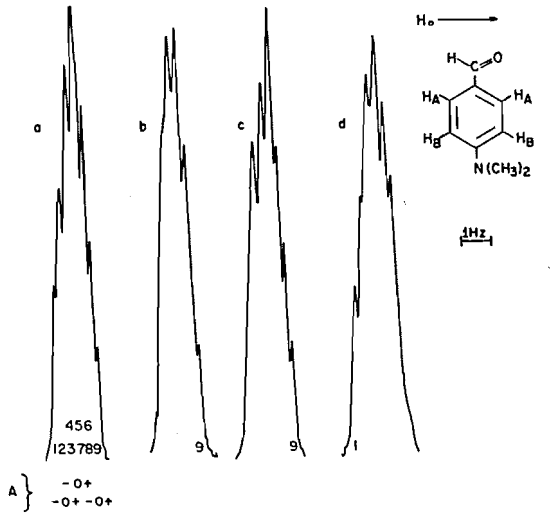

FIG. 2. In (*a*), the single proton resonance spectrum of the aldehydic proton in *p*-dimethylaminobenzaldehyde is shown. In (*b*), (*c*), (*d*), double resonance spectra are recorded under conditions described in the text.

Can. J. Chem. Downloaded from www.nrcresearchpress.com by 210.87.254.40 on 09/05/12
For personal use only.

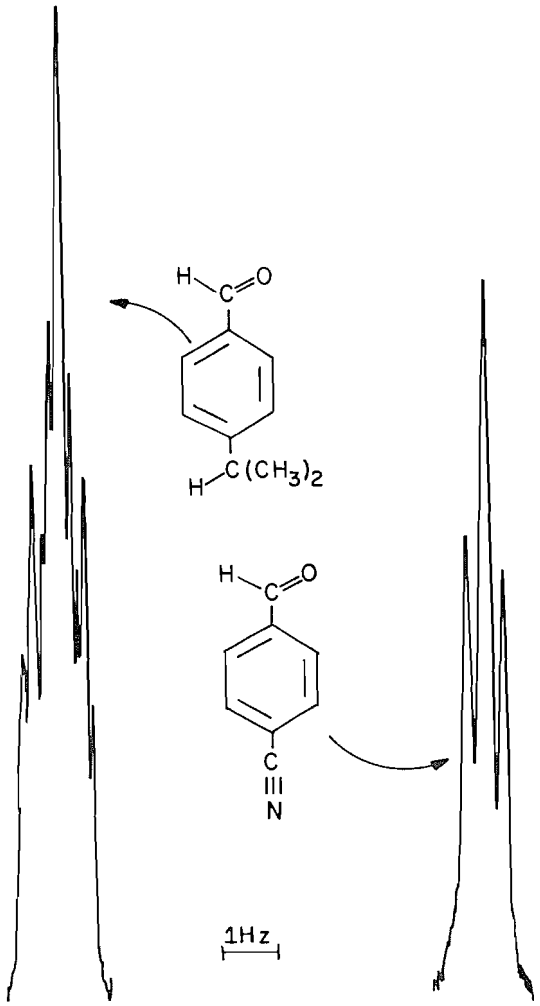

FIG. 1. The proton magnetic resonance spectrum at 60 MHz of the aldehydic group in *p*-isopropyl- and *p*-cyanobenzaldehyde. See text for further details.

group in benzaldehyde is 7.9 kcal/mole at 150 °K but rises to 9.2 kcal/mole in *p*-methoxybenzaldehyde at 172 °K (12). Electron spin resonance (e.s.r.) data on the negative ion radical of *p*-nitrobenzaldehyde place an upper limit of about 10^6 s^{-1} on the rotational frequency of the aldehyde group at room temperature (13). The free energies of activation $\Delta F^{\ddagger}$, at temperature T, are derived from transition state theory via a relation of the type

$$[1] \qquad 1/\tau = h/kT \exp \Delta F^{\ddagger}/RT$$

where h, k, and R are the Planck, Boltzmann, and molar gas constants, respectively. τ is the mean time spent before rotation by the aldehyde group in a site coplanar with the aromatic ring. The n.m.r. and e.s.r. data agree in the conclusion that, even at room temperature, τ is some orders of magnitude larger than the time taken for a reorientation from one planar site to the other equivalent planar site. That is, the time spent by the aldehyde proton in planar conformations, **1** and **2**, is much larger than the time spent in nonplanar conformations. The planar conformation in an unhindered benzaldehyde arises from

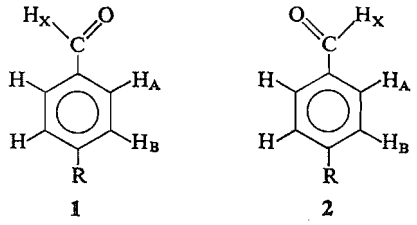

the strong conjugation of the carbonyl group with the aromatic π electrons. This conclusion is supported by extensive molecular orbital calculations which also show that nonbonded interactions between the carbonyl group and neighbouring atoms in benzaldehyde affect the barrier to rotation by only about 1 kcal/mole (14).

A planar conformation of sterically unhindered

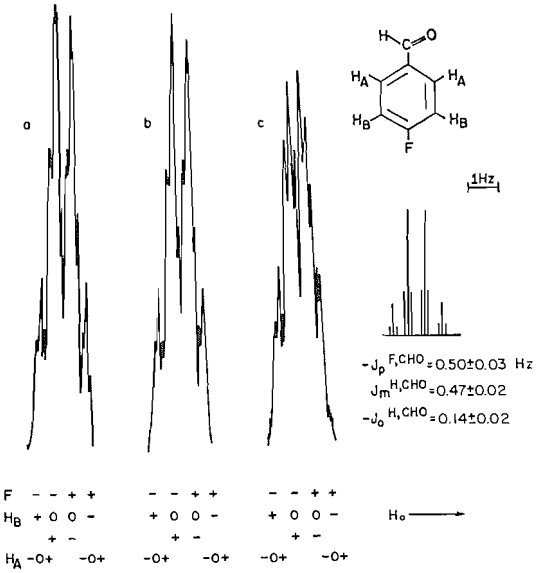

FIG. 2. In (*a*), the single proton resonance spectrum of the aldehydic proton in *p*-dimethylaminobenzaldehyde is shown. In (*b*), (*c*), (*d*), double resonance spectra are recorded under conditions described in the text.

FOR ERRATA SEE
V.49,12,1971 P.3911

Can. J. Chem. Downloaded from www.nrcresearchpress.com by 210.87.254.40 on 09/05/12
For personal use only.

benzaldehydes was assumed in a previous discussion of $J_m^{H,CHO}$ (15).

Sign and Magnitude of $J_o^{H,CHO}$

From the discussion above it follows that in the *para*-substituted benzaldehydes of Table I,

$$[2] \quad J_o^{H,CHO} = (J_1^{H_A,CHO} + J_2^{H_A,CHO})/2$$

It is not known whether $J_1^{H_A,CHO} > J_2^{H_A,CHO}$. The inequality is of interest when attempting to establish whether $J_o^{H,CHO}$ is a result of π or of σ contributions. If a σ–π mechanism is operative then a negative coupling is generally expected for out-of-plane arrangements of the two C—H bonds and a zero coupling for a coplanar arrangement (16–18). On the other hand, $J_4^{\sigma} > +1$ Hz when the H—C—C—C—H fragment takes on a planar zigzag arrangement (19). Nevertheless, in other conformations J_4^{σ} may evidently be small and negative, i.e., near -0.20 Hz (20,21).

The closest analogy to the present molecules is acrolein where the *S-trans* form, **3**, is more stable by 2 kcal/mole (22), than the *S-cis* form, **4**. Near room temperature the ratio of *S-trans* to *S-cis* molecules is therefore about 25 to 1.

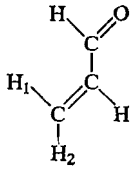

3

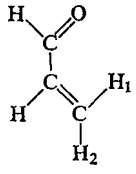

4

In **3**, $J^{H_2,CHO} = -0.3$ Hz while $J^{H_1,CHO} = -0.15$ Hz (23). The latter is analogous to $J^{H_A,CHO}$ in **2** but unfortunately $J^{H_1,CHO}$ in **4**, analogous to $J^{H_A,CHO}$ in **1**, is unknown.

It is known, however, that when H_2 in **3** is replaced by CH_3 $J^{CH_3,CHO} = 0.0$ Hz (24). The "CH_3 replacement" technique (25) therefore suggests that in acrolein the small negative four-bond coupling is dominated by σ electron contributions. Similarly, in a series of acetophenone derivatives no coupling from the acetyl to the ring protons is observed (26,26*a*) again indicating a σ electron mechanism[5] for $J_o^{H,CHO}$.

This partial evidence for a σ electron dominated

[5]Steric hindrance by *ortho* substituents will twist the aldehyde group out of a planar conformation and lead to a measurable π contribution to $J_p^{H,CHO}$ (27).

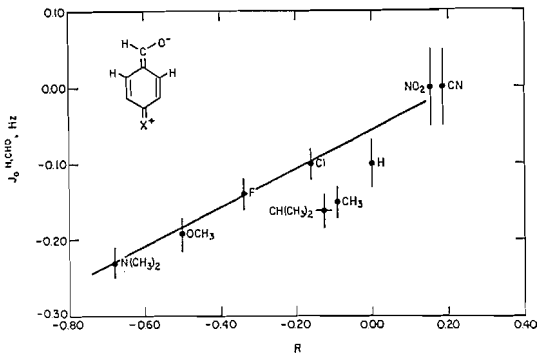

FIG. 3. A plot of $J_o^{H,CHO}$ in Hz versus the resonance substituent constant, R, of the substituent, X, in some *para*-X-benzaldehydes.

$J_o^{H,CHO}$ in planar benzaldehyde derivatives can be augmented in the following way. In Fig. 3 there is shown a plot of $J_o^{H,CHO}$ versus the resonance constant, R, of the *para*-substitutent (28). Note that $J_o^{H,CHO}$ is too small to measure for the cyano and nitro substituents and has been taken as zero. However, the linewidths of the aldehyde p.m.r. peaks in these instances are consistent with $J_o^{H,CHO}$ values falling exactly on the line in Fig. 3. The correlation between R, which is currently the best available measure of conjugation of a substituent with the aromatic ring, and $J_o^{H,CHO}$ is quite reasonable.

A plausible resonance structure illustrated in Fig. 3 can be drawn only for *para*-substituents which donate electrons by resonance, i.e., not for the nitro or cyano groups. For the latter, resonance structures **5** and **7** are intuitively expected to be less important than **6**, but **6** leads to a zero mobile bond order between the aldehyde carbon and the aromatic carbon atoms.

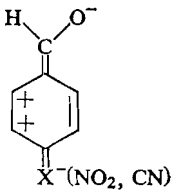

5

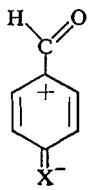

6

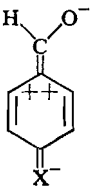

7

At first sight it is tempting to ascribe the observed correlation between $J_o^{H,CHO}$ and R to an increase in a π electron contribution to $J_o^{H,CHO}$. Molecular orbital calculations (29) do indeed substantiate the qualitative valence bond description above. The mobile bond order of the bond in question is 0.476, 0.400, 0.393 for X = NH_2, H,

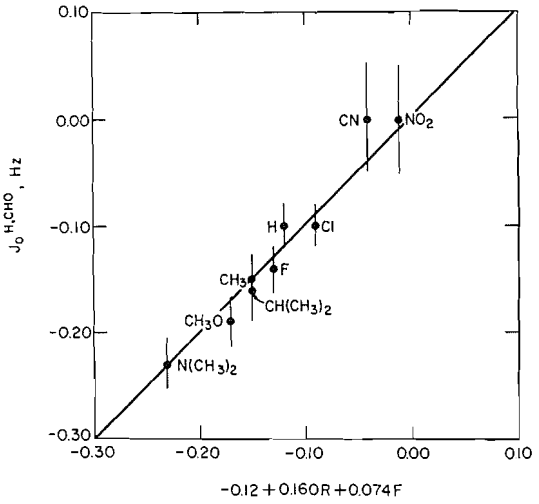

FIG. 4. A plot of $J_o^{H,CHO}$ in Hz versus the quantity $-0.12 + 0.160R + 0.074F$, as discussed in the text. The straight line is of unit slope.

NO_2, respectively. Yet a correlation of a coupling constant with a mobile bond order of an intervening bond does not prove the existence of a π contribution to the coupling (5). A good example is the vicinal proton coupling constant in a series of condensed aromatic molecules (30). In the present example it may well be that an increased mobile bond order shortens the bond, leads to a stronger correlation of the sigma electrons in that bond and therefore to a larger magnitude of the coupling constant.

Support for the latter argument comes from the negative deviation in Fig. 3 of the points for X = CH_3, $CH(CH_3)_2$. These are the only substituents in Fig. 3 which have negative field constants F, as well as negative R constants (28). Hence, both effects cause increased electron density in the distant bond and therefore, as it were, and excess magnitude of $J_o^{H,CHO}$ (the other substituents are all electron withdrawing by inductive effects). The negative inductive effect of the alkyl groups would lead, at the level of sophistication of the model, to an increase in σ electron density in the ring and hence would not increase $|J_o^{H,CHO}|$ if the latter were dominated by a π electron mechanism.[6]

On this basis a correlation of $J_o^{H,CHO}$ with the R and F substituent constants of the form $J = a + b\,R + c\,F$, where $b,c > 0$, should be found. This is indeed the case. Equation 3 reproduces the $J_o^{H,CHO}$ values in Table I with a mean deviation of just over 0.01 Hz, well within

$$[3]\quad J_o^{H,CHO} = -0.12 + 0.160R + 0.074F$$

experimental error. Figure 4 shows a graphical plot of the correlation. The straight line has the required unit slope (note that the coupling values for the nitro and cyano substituents *could* be placed precisely on the straight line).

Thus, although $J_o^{H,CHO} < 0$, a consideration of all the above evidence shows that a σ electron mechanism for $J_o^{H,CHO}$ is more favored than a π electron mechanism.[7]

It might be argued that the above discussion in terms of σ and π contributions is not really satisfactory in that recent molecular orbital formulations (32) do not make a rigid distinction between σ and π electrons. Nevertheless, the present discussion is in the spirit of most experimental papers and with some theoretical work (33) based on the valence bond method.

Magnitude of $J_m^{H,CHO}$

The "CH_3 replacement" technique indicates a dominant σ electron mechanism (26) for this coupling, as does the fact that $J_m^{H_B,CHO}$ is much larger in derivatives of **1** than of **2** (34). Stereospecificity of this kind in $J_m^{H,CHO}$ is difficult to account for by a π mechanism; although there may be a small contribution to $J_m^{H,CHO}$ from the latter.

The maximum magnitude of the increases in $J_m^{H,CHO}$ caused by the substituents in Table I is only 0.10 Hz and the cyano and nitro substituents cause the smallest increase, if any. Although a fair correlation with F and R constants may again be found (eq. [4]) it is preferable to simply note

$$[4]\quad J_m^{H,CHO} = 0.41 - 0.122R + 0.013F$$

that the increase in $J_m^{H,CHO}$ is, in general, largest for those substituents which increase most the electron density in the ring. As a final point, it may be of interest to mention a fairly good correlation of $J_m^{H,CHO}$ in the present compounds with $J_m^{H_2,H_4}$ in the corresponding phenyl compounds (35–37), i.e., the decrease of $J_m^{H_2,H_4}$ in

[6]A referee argues that the observed correlation between $J_o^{H,CHO}$ and R should be accepted as evidence for the π mechanism and suggests that the small deviations of the alkyl groups in Fig. 3 are insignificant. We feel, however, that these deviations are real and, together with the other evidence, that they indicate a σ mechanism.

[7]The apparent, small negative Q value for the aldehyde proton in certain paramagnetic γ-formyl nickel (II) aminotroponeimine derivatives (31) actually suggests a small positive π electron contribution to $J_o^{H,CHO}$.

Can. J. Chem. Downloaded from www.nrcresearchpress.com by 210.87.254.40 on 09/05/12
For personal use only.

the 1-X-benzenes roughly parallels the increase of $J_m^{H,CHO}$ in the *p*-X-benzaldehydes. At present there is no quantitative theory for the substituent effect on these coupling constants.

Acknowledgments

We are grateful to Dr. S. M. Castellano for a copy of a paper prior to publication.

1. T. K. Wu and B. P. Dailey. J. Chem. Phys. **41**, 2796 (1964).
2. R. J. Abraham, D. B. Macdonald, and E. S. Pepper. J. Amer. Chem. Soc. **90**, 147 (1968).
3. M. G. Hogben and W. A. G. Graham. J. Amer. Chem. Soc. **91**, 283 (1969).
4. C. H. Yoder, R. H. Tuck, and R. E. Hess. J. Amer. Chem. Soc. **91**, 539 (1969).
5. S. M. Castellano and R. Kostelnik. J. Amer. Chem. Soc. **90**, 141 (1968).
6. R. Freeman and W. A. Anderson. J. Chem. Phys. **37**, 2053 (1962).
7. R. E. Klinck and J. B. Stothers. Can. J. Chem. **40**, 1071 (1962).
8. A. Saupe. Z. Naturforsch. **19***a*, 161 (1964); **20***a*, 572 (1965).
9. D. G. Kowalewski and V. J. Kowalewski. Mol. Phys. **9**, 331 (1965).
10. S. Forsén and T. Alm. J. Mol. Spectrosc. **17**, 13 (1965).
11. R. J. Kostelnik, M. P. Williamson, D. E. Wisnosky, and S. M. Castellano. Can. J. Chem. **47**, 3313 (1969).
12. F. A. L. Anet and N. Ahmad. J. Amer. Chem. Soc. **86**, 119 (1964).
13. A. H. Maki and D. H. Geske. J. Amer. Chem. Soc. **83**, 1852 (1961).
14. S. Forsén and P. N. Skancke. *In* Selected topics in structure chemistry. *Edited by* P. Andersen, O. Bastiansen, and S. Furberg. Universitetsforlaget, Oslo, Norway. 1967.
15. G. J. Karabatsos and F. M. Vane. J. Amer. Chem. Soc. **85**, 3886 (1963).
16. M. Karplus. J. Chem. Phys. **33**, 1842 (1960).
17. H. M. McConnell. J. Mol. Spectrosc. **1**, 11 (1957).
18. M. J. S. Dewar and R. C. Fahey. J. Amer. Chem. Soc. **85**, 2704 (1963).
19. M. Barfield. J. Chem. Phys. **41**, 3825 (1964).
20. E. W. Garbisch, Jr. J. Amer. Chem. Soc. **86**, 5561 (1964).
21. V. F. Bystrov and A. U. Stepanyants. J. Mol. Spectrosc. **21**, 241 (1966).
22. M. S. DeGroot and J. Lamb. Proc. Roy. Soc. (London) **A242**, 36 (1957).
23. J. E. Davies. J. Mol. Spectrosc. **29**, 499 (1969).
24. A. W. Douglas and J. H. Goldstein. J. Mol. Spectrosc. **16**, 1 (1965).
25. R. Hoffman and S. Gronowitz. Ark. Kim., **16**, 471 (1960).
26. S. Forsén, B. Akermark, and T. Alm. Acta Chem. Scand. **18**, 2313 (1964).
26a. S. M. Castellano. *In* Nuclear magnetic resonance spectra and chemical structure. *Edited by* W. Brugel. Academic Press, Inc., New York. 1967.
27. C. L. Bell, S. S. Danyluk, and T. Schaefer. Can. J. Chem. **47**, 3529 (1969).
28. C. G. Swain and E. G. Lupton, Jr. J. Amer. Chem. Soc. **90**, 4328 (1968).
29. N. F. Phelan and M. Orchin. J. Chem. Educ. **45**, 633 (1968).
30. N. Jonathan, S. Gordon, and B. P. Dailey. J. Chem. Phys. **36**, 2443 (1962).
31. D. R. Eaton, A. D. Josey, and R. E. Brown. J. Amer. Chem. Soc. **89**, 4040 (1967).
32. J. A. Pople and M. Gordon. J. Amer. Chem. Soc. **89**, 4253 (1967).
33. M. Barfield. J. Chem. Phys. **48**, 4463 (1968).
34. S. Forsén and B. Akermark. Acta Chem. Scand. **17**, 1712 (1963).
35. S. M Castellano, R. Kostelnik, and C. Sun. Tetrahedron Letters, **46**, 4635 (1967).
36. S. M. Castellano, C. Sun, and R. Kostelnik. Tetrahedron Letters, **51**, 5205 (1967).
37. M. P. Williamson, R. J. Kostelnik, and S. M. Castellano. J. Chem. Phys. **49**, 2218 (1968).

Can. J. Chem. Downloaded from www.nrcresearchpress.com by 210.87.254.40 on 09/05/12
For personal use only.

Can. J. Chem. Downloaded from www.nrcresearchpress.com by 210.87.254.6 on 09/05/12
For personal use only.

Kinetics of sulfonation of 4-hydroxyazobenzene[1]

W. M. J. STRACHAN AND E. BUNCEL
Department of Chemistry, Queen's University, Kingston, Ontario

Received June 18, 1969

Spectral changes exhibited by 4-hydroxyazobenzene in the 90–100% H_2SO_4 region are shown to be the result of a sulfonation process, superimposed (above 98% H_2SO_4) on a second equilibrium protonation. The reaction product is 4-hydroxyazobenzene-4′-sulfonic acid. The rate of this sulfonation reaction increases by a factor of 500 over 91.7–100.0% H_2SO_4. The increase in rate is more gradual in acid media in which diprotonation of reactant is effective.

In 100% H_2SO_4 and above, a second, much slower, rate process is discerned from the spectral changes in this system and is probably the result of a further sulfonation of 4-hydroxyazobenzene-4′-sulfonic acid. Kinetic data for this reaction are reported for 99.99–100.76% H_2SO_4.

The results are in agreement with previous qualitative reports on the formation of sulfonation products from 4-hydroxyazobenzene or from azoxybenzene, its precursor in the Wallach rearrangement. The mechanism of the consecutive sulfonation reactions is discussed.

Canadian Journal of Chemistry, 47, 4011 (1969)

In early studies of the Wallach rearrangement (1) of azoxybenzene in the 100% H_2SO_4 region, in addition to the formation of 4-hydroxyazobenzene, sulfonic acid derivatives were also noted to be present (2,3). In particular, Wilsing in 1882 (2) obtained mono-, di-, tri-, and even tetrasulfonic acid derivatives of 4-hydroxyazobenzene upon treatment of azoxybenzene with fuming sulfuric acid of unspecified concentration at temperatures in excess of 100°. Of these only the monosulfonic acid was fully identified (3) as 4-hydroxyazobenzene-4′-sulfonic acid, though it was shown (2) that the second and third sulfonic acid groups entered the ring containing the hydroxyl substituent. More recent work, by Gore and Hughes (4) and by Newbold and Akhtar (5), has confirmed the formation of sulfonic acid derivatives in the rearrangement of azoxybenzene and of substituted azoxybenzenes even under less vigorous conditions.

In order to evaluate quantitatively the importance of the sulfonation process in Wallach rearrangement reactions in the 100% H_2SO_4 region, we embarked on a systematic study with 4-hydroxyazobenzene under controlled conditions of temperature and acid concentration. In our previous kinetic study with azoxybenzene in acids up to 96% H_2SO_4, it was noted that in the upper acid region 4-hydroxyazobenzene undergoes a further, relatively slow, reaction whose nature was not identified (6).

[1]Part VII in series on the Wallach rearrangement.

Results

4-Hydroxyazobenzene in Acids Below 100% H_2SO_4

Examination of 4-hydroxyazobenzene in the present work was carried out spectrally (substrate concentration 10^{-5}–10^{-4} *M*), for 90–100% H_2SO_4, at 25°. The spectral changes in the lower acid region are illustrated by the following experiment using 94.73% H_2SO_4 (Fig. 1). The initial

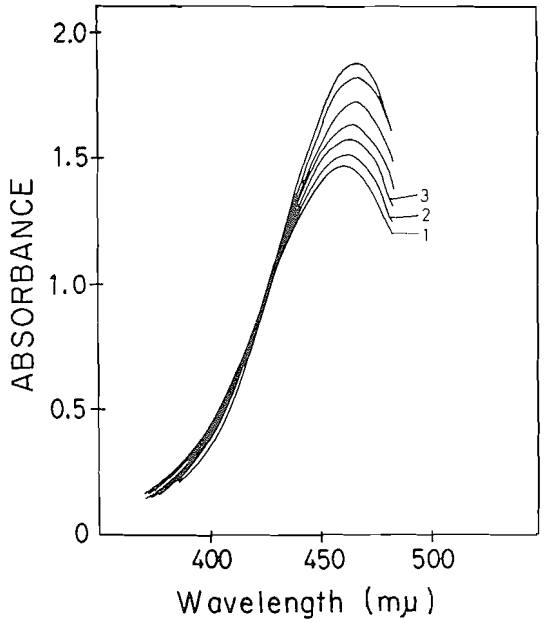

FIG. 1. 4-Hydroxyazobenzene in 94.73% H_2SO_4, 3.92×10^{-5} *M* substrate (25°, 1.00 cm cuvette). Scans noted are 1–0.1 h, 2–4 h, 3–9.5 h, last scan 120 h.

Can. J. Chem. Downloaded from www.nrcresearchpress.com by 210.87.254.6 on 09/05/12
For personal use only.

spectrum of 4-hydroxyazobenzene in this medium shows absorption in the visible region at 460 mμ ($\varepsilon = 3.78 \times 10^4$), which can be ascribed to the azo-protonated substrate (7). This absorption slowly grows in intensity and simultaneously shifts to slightly longer wavelengths. After 10 h the absorbance has increased by about 8% with the peak shifted to 462 mμ, while after 50 h the increase is about 25% (λ_{max} 465 mμ), and beyond 120 h ($\varepsilon_{465} = 4.78 \times 10^4$) there is no further spectral change. The pseudo-first order rate constant for the growth of the absorption, calculated at 465 mμ by the log $(A_\infty - A_t)$ versus t plot where A_∞ is the final absorbance, is 1.16×10^{-5} s^{-1} ($T_{\frac{1}{2}} = 16.6$ h). Using the Guggenheim method and absorbance changes at 460 mμ, a rate constant of 1.18×10^{-5} s^{-1} is obtained. In an analogous manner, examination of 4-hydroxyazobenzene was extended to about 100% H_2SO_4. Over this range of acid concentration there is a gradation in the spectral changes, as illustrated by Figs. 1–3 and discussed below.

It is seen from Figs. 1–3 that the initial spectrum of 4-hydroxyazobenzene shifts to shorter wavelengths as the acid concentration is increased; this has been ascribed to a second equilibrium protonation of the substrate (7). The rate process

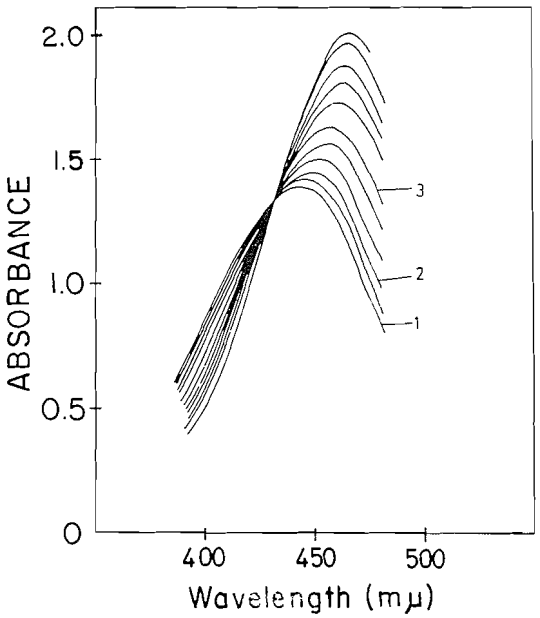

FIG. 2. 4-Hydroxyazobenzene in 99.72% H_2SO_4, 4.01×10^{-5} M substrate (25°, 1.00 cm cuvette). Scans noted are 1–1.5 min, 2–4 min, 3–12 min, last scan 60 min.

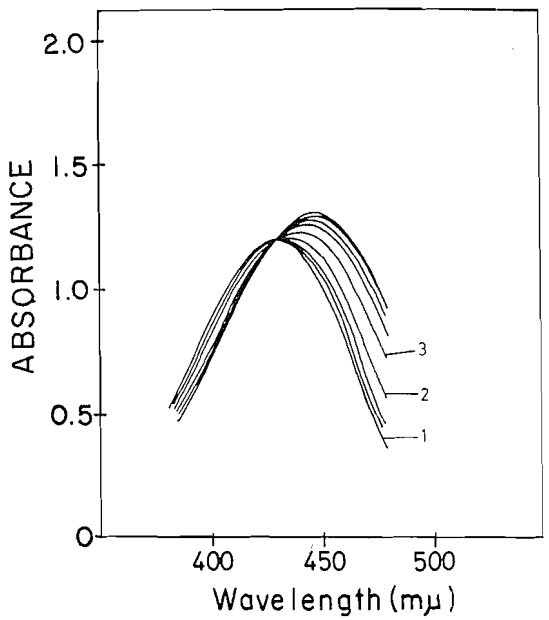

FIG. 3. 4-Hydroxyazobenzene in 99.96% H_2SO_4, 3.88×10^{-5} M substrate (25°, 1.00 cm cuvette). Scans noted are 1–1.5 min, 2–5 min, 3–9 min, last scan 55 min.

corresponding to the growth in absorbance, for which rate constants were obtained as previously (Table I), is characterized in each case by a sharp isosbestic point. The observed reaction is identified as sulfonation, to give 4-hydroxyazobenzene-4′-sulfonic acid; the shifts in λ_{max} of the product absorption with increasing acid concentration are ascribed to a second equilibrium protonation of this sulfonic acid (7).

4-Hydroxyazobenzene-4′-sulfonic acid has spectral absorption in concentrated sulfuric acid solutions which agrees quantitatively with the final "infinity" spectra of 4-hydroxyazobenzene following reaction in 94.5–98.9% H_2SO_4 (see Experimental). Near the 100% H_2SO_4 region, spectral comparison is made more difficult as a result of extensive diprotonation, with accompanying changes in absorption (7), and also due to the advent of a second sulfonation (*vide infra*).

The total rate data for this sulfonation process are given in Table I. The kinetic methods are described in detail in the Experimental section.

4-Hydroxyazobenzene and 4-Hydroxyazobenzene-4′-sulfonic Acid in the 100% H_2SO_4 Region

The spectral behaviour of 4-hydroxyazobenzene takes on distinctly different character close

TABLE I

Kinetic data for sulfonation of 4-hydroxyazobenzene to 4-hydroxyazobenzene-4′-sulfonic acid at 25°

Weight (%) H_2SO_4	H_0	$10^5 k_{obs}$ (s^{-1})	Kinetic method	(λ mμ)
91.66	−8.47	0.51	*	(460)
93.50	−8.68	1.08	*	(460)
94.52	−8.81	1.41	*	(460)
94.73	−8.83	1.18	*	(460)
—	—	1.16	†,*	(465)
94.73	−8.83	1.12	‡	(463)
96.18	−9.03	3.22	‡	(463)
97.33	−9.22	6.15	*	(460)
97.56	−9.28	6.63	*	(460)
97.78	−9.32	6.30	‡	(463)
97.80	−9.32	7.06	*	(460)
—	—	6.66	†,*	(463)
98.92	−9.68	26.0	‡	(460)
99.00	−9.74	28.2	‡	(463)
99.37	−9.93	50.8	*	(460)
99.37	−9.93	50.7	‡	(460)
99.59	−10.10	80.1	‡	(460)
99.59	−10.10	84.1	‡	(463)
99.72	−10.24	102	*	(460)
—	—	111	†,*	(465)
99.72	−10.24	152	‡	(463)
99.83	−10.42	164	‡	(460)
99.83	−10.42	211	‡	(463)
99.94	−10.82	246	‡	(460)
99.96	−10.94	250	*	(460)
99.96	−10.94	290	‡	(463)
99.99	−11.06	252	‡	(460)
99.99	−11.06	253	†,‡	(460)
100.01	−11.12	252	†,*	(480)
100.01	−11.12	265	†,*	(480)
100.02	−11.14	259	†,*	(480)
100.07	−11.25	238	†,*	(480)

*Reaction followed by periodic scanning. Rate constant calculated at wavelength indicated by Guggenheim method.

†Rate constant calculated using $A_\infty - A_t$ plot. Data obtained either as indicated under footnote * or as in footnote ‡. (When a rate constant was recalculated by the $A_\infty - A_t$ plot but using the raw data in a previous run, then the acid concentration is not re-stated in the first column.)

‡Reaction followed at constant wavelength shown. Rate constant calculated by Guggenheim method.

to 100% H_2SO_4 from that described hitherto. Figure 4 shows an illustrative run for 100.01% H_2SO_4. Two rate processes are reflected in Fig. 4, for which the corresponding spectra are drawn in dashed lines and in full lines for clarity. The two sets of curves correspond to different time scales, the former being taken minutes apart and representing an initial fast reaction and the latter taken hours apart and representing a subsequent slow reaction. The two processes were first observed on a scan of absorbance (460 mμ) versus time, as an initial rapid increase ($T_{\frac{1}{2}}$ = 4.5 min by the Guggenheim method) followed by a very slow increase ($T_{\frac{1}{2}}$ = 27.5 h) in absorbance. The fast reaction is identified as the sulfonation process discussed in the preceding section.

A further characteristic which differentiates the 4-hydroxyazobenzene runs near the 100% H_2SO_4 region is isosbestic point behaviour. Figure 4 shows that the initial dashed spectral curves do not pass through an isosbestic point but are nearly tangential on the short wavelength side of λ_{max} (426 mμ).[2] The isosbestic point that is observed (422 mμ) is common to the later full curves. It is shown below that the rate process corresponding to this isosbestic point is a second

[2]The absence of an isosbestic point with respect to the first sulfonation process represented by the dashed curves in Fig. 4 is explained by the very close wavelength maxima of the absorptions due to the largely diprotonated 4-hydroxyazobenzene reactant ($\lambda^{BH_2^{2+}}$ 426 mμ) and the partly diprotonated 4-hydroxyazobenzene-4′-sulfonic acid product ($\lambda^{BH_2^{2+}}$ 420 mμ) in 100.01% H_2SO_4.

Can. J. Chem. Downloaded from www.nrcresearchpress.com by 210.87.254.6 on 09/05/12
For personal use only.

Can. J. Chem. Downloaded from www.nrcresearchpress.com by 210.87.254.6 on 09/05/12
For personal use only.

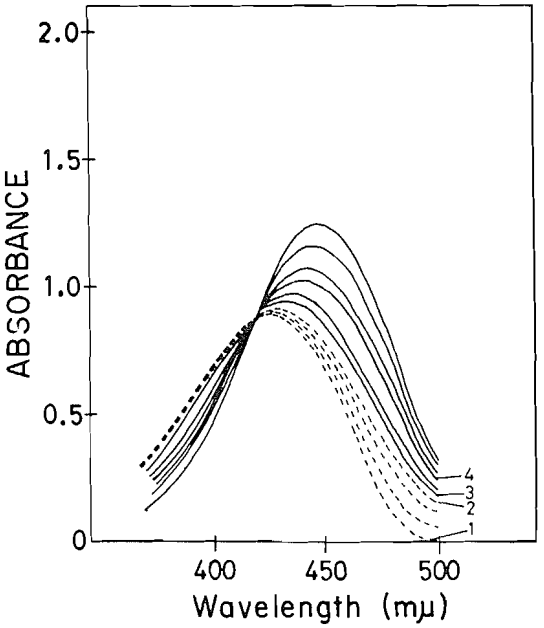

FIG. 4. 4-Hydroxyazobenzene (2.84×10^{-5} *M*) in 100.01% H_2SO_4 (25°, 1.00 cm cuvette). Scans noted are 1–1 min, 2–30 min, 3–4 h, 4–19 h, last scan 141 h.

sulfonation of 4-hydroxyazobenzene-4′-sulfonic acid. The positions of the maxima in Fig. 4 first need commenting on. The initial λ_{max} (426 mμ) corresponds to almost complete diprotonation in this medium of the reactant (pK_a^2 for 4-hydroxyazobenzene = −10.2 (7)). The first sulfonation is about complete with curve 2 (30 min, λ_{max} 429 mμ), which corresponds to about 50% diprotonation of the formed 4-hydroxyazobenzene-4′-sulfonic acid (pK_a^2 = −11.1). The final product spectrum (λ_{max} 449 mμ) is ascribed to a disulfonic acid derivative present essentially in monoprotonated form in this medium (see Experimental for an estimate of pK_a^2).

The reactivity of 4-hydroxyazobenzene-4′-sulfonic acid in the 100% H_2SO_4 region was confirmed by means of a kinetic run carried out with this substrate in 100.07% H_2SO_4, shown in Fig. 6. The spectral changes in Fig. 6 are typical of a rate process (isosbestic point at 422 mμ, $T_{\frac{1}{2}}$ = 15.0 h by the Guggenheim method). A kinetic run carried out with 4-hydroxyazobenzene in the same medium is shown in Fig. 5. The full curves in this 4-hydroxyazobenzene run show all the features (isosbestic point at 422 mμ, $T_{\frac{1}{2}}$ = 15.0 h) which characterized the reaction of 4-hydroxyazobenzene-4′-sulfonic acid (Fig. 6). However in addition Fig. 5 shows that 4-hydroxyazobenzene first undergoes a rapid rate process (dashed curves, $T_{\frac{1}{2}}$ = 4.5 min), which can clearly be ascribed to the first sulfonation reaction.

Rate data for the second reaction, as observed with 4-hydroxyazobenzene reactant, were obtained analogously over the region 99.99–100.76% H_2SO_4 and are given in Table II. Rate data for the first sulfonation process, which were obtained for part of this acid range from the initial fast increase in absorbance at 460/463 mμ, are included in Table I.

The product of the second process is tentatively identified as 4-hydroxyazobenzene-3,4′-disulfonic acid, though conclusive evidence is not available. The identification is made on the basis of the spectral absorptions in 100.79% H_2SO_4, 96% H_2SO_4, 0.2 *N* H_2SO_4, and 0.2 *N* KOH, in which media this product is expected to be present in several different ionization states (see Experimental). Also, this is the expected product on the basis of the directive effects of the substituents in 4-hydroxyazobenzene-4′-sulfonic acid toward electrophilic substitution (*vide infra*).

Independent evidence for the sulfonation pro-

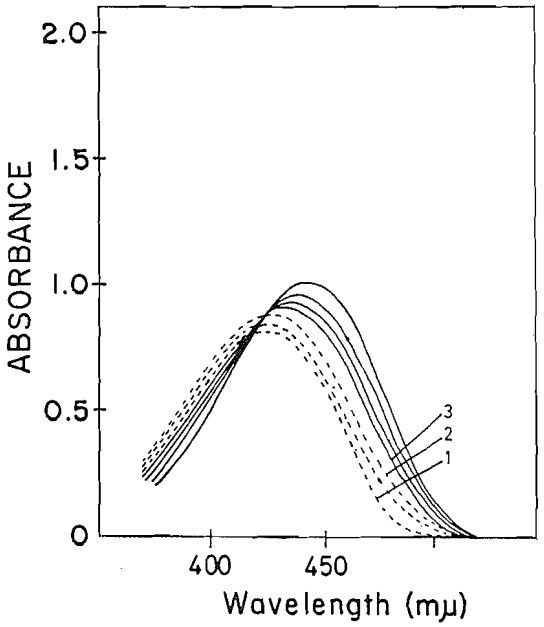

FIG. 5. 4-Hydroxyazobenzene (0.72×10^{-5} *M*) in 100.07% H_2SO_4 (25°, 4.00 cm cuvette). Scans noted are 1–1.5 min, 2–30 min, 3–9 h, last scan 36 h.

TABLE II

Kinetic data for sulfonation of 4-hydroxyazobenzene-4′-sulfonic acid observed with 4-hydroxyazobenzene as substrate

Weight (%) H_2SO_4	H_0	$10^5 k_{obs}$ (s^{-1})	Kinetic method	(λ mμ)
99.99	−11.06	0.568	‡	(460)
100.00	−11.09	0.680	‡	(460)
100.01	−11.12	0.731	‡	(460)
100.01	−11.12	0.703	*	(460)
100.07	−11.25	1.04	*	(460)
—	—	1.32	†,*	(449)
100.07	−11.25	1.42	‡	(463)
100.07	−11.25	1.23§	*	(460)
100.22	−11.45	2.25	‡	(460)
100.76	−11.77	5.57	‡	(463)

*,†,‡Kinetic methods as described for Table I.
§Rate constant using 4-hydroxyazobenzene-4′-sulfonic acid as substrate.

cesses described above derives from cryoscopic and conductivity measurements obtained with 4-hydroxyazobenzene in 100% H_2SO_4 (8).

Discussion

The results of the quantitative study of the sulfonation of 4-hydroxyazobenzene described above are in accord with previous qualitative reports in the literature on the conversion of 4-hydroxyazobenzene (or of azoxybenzene, its precursor in the Wallach rearrangement) to 4-hydroxyazobenzene-4′-sulfonic acid and to higher sulfonation products (2–5).

The acidity dependence of the sulfonation of 4-hydroxyazobenzene is in many ways comparable to that in the sulfonation of benzene (9–11), *p*-nitrotoluene (12,13), benzenesulfonic acid (14*a*), and other aromatic derivatives, in concentrated sulfuric acid–dilute oleum media. Such sulfonation processes are recognized to belong to the class of electrophilic aromatic substitution reactions (15,16). However differences have been expressed concerning the detailed nature of the sulfonation mechanism (9–16), partly as a result of the uncertainty as to the identity of the sulfonating species (17): H_2SO_4, SO_3, $H_2S_2O_7$, S_2O_6, SO_3H^+, $H_3SO_4^+$, and others. The statement (15*a*) "that monomeric sulfur trioxide, or, possibly, a sulfuric acid solvate of it, is the active species contained in sulfonating media of this type" forms the basis of the mechanism proposed for the sulfonation of 4-hydroxyazobenzene:

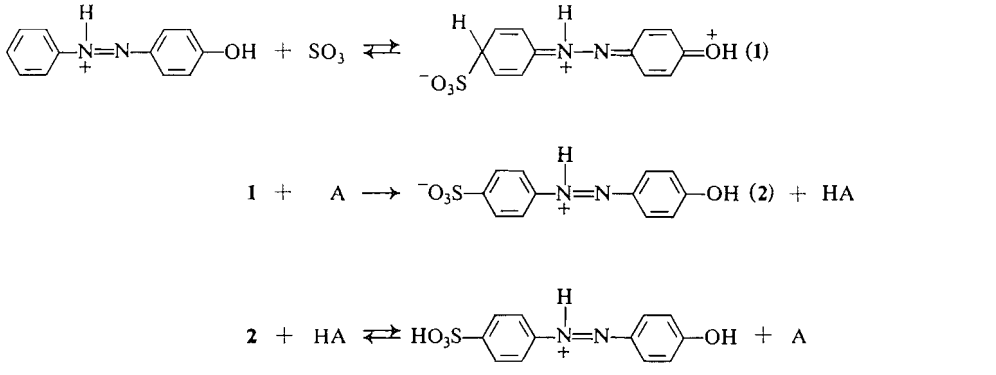

In this mechanism the 4-hydroxyphenylazo group is taken as activating toward electrophilic substitution but its effect should be considerably reduced by the deactivating nature of the protonated azonium function. In accord with this consideration, the reactivity of 4-hydroxyazobenzene is greater than of benzene derivatives containing the trimethylammonio or nitro substituents (12,13), though less than of benzene itself (9–11).

Can. J. Chem. Downloaded from www.nrcresearchpress.com by 210.87.254.6 on 09/05/12
For personal use only.

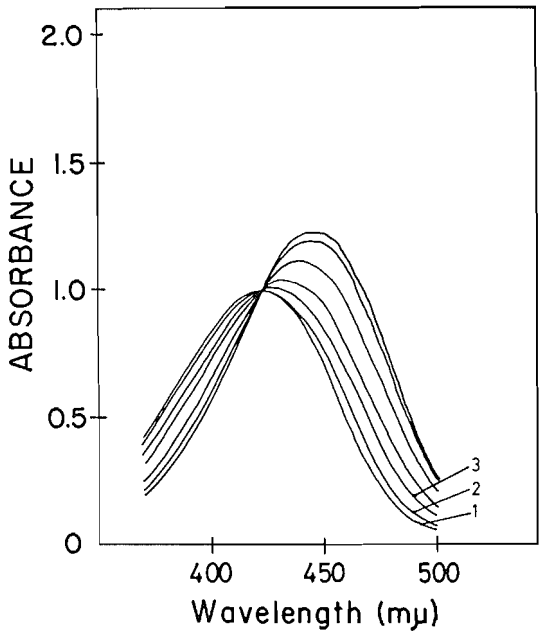

FIG. 6. 4-Hydroxyazobenzene-4′-sulfonic acid (2.97 × 10^{-5} M) in 100.07% H_2SO_4 (25°, 1.00 cm cuvette). Scans noted are 1–2.5 min, 2–2 h, 3–6 h, last scan 37 h.

The above scheme considers monoprotonated 4-hydroxyazobenzene to be the effective reactant on the ground that, with a pK_a^1 of −1.0 (reference 7 and others quoted therein) 4-hydroxyazobenzene is already 99.9% protonated in ca. 55% H_2SO_4. It is only in considerably more acidic media (ca. 90% H_2SO_4) that the sulfonating species reach effective concentration for reaction in this system.

It has been shown that above 98% H_2SO_4 a second equilibrium protonation of 4-hydroxyazobenzene becomes effective ($pK_a^2 = -10.2$ (7)) and that the site of the second protonation is the phenolic oxygen. The resulting diprotonated species should be very much less reactive toward sulfonation since *O*-protonation effectively negates the activating ability of the hydroxyphenylazo moiety. Some support for this view is given by the observation that the linearity range of the log k versus $-H_0$ plot is extended to higher acid concentrations when account is taken of the material present in diprotonated form by plotting log k − log $C_{SH^+}/(C_{SH^+} + C_{SH_2^{++}})^3$ versus H_0 (Fig. 7). The slope of the linear portion of this plot (1.50) is not readily interpretable but non-unit slopes appear to be general for reactions occurring in the concentrated sulfuric acid media (21,22).

The kinetic dependence of the second sulfonation is very similar to the first and requires little comment. The plot of log k − log $C_{SH^+}/(C_{SH^+} + C_{SH_2^{++}})$ versus H_0 is linear, which is analogously interpreted to mean that the reactive species is monoprotonated 4-hydroxyazobenzene-4′-sulfonic acid and that the diprotonated species is unreactive. It was shown previously (7) that for this substrate the second equilibrium protonation ($pK_a^2 = -11.1$) is also on phenolic oxygen. The above mentioned plot has a slope of 2.0

The observed orientation in these sulfonation reactions is of interest. The apparently exclusive first sulfonation in the 4′-position (rather than in the 3-position) is probably due in part to a steric factor, since it has been shown (15*b*) that *ortho* orientation is relatively disfavoured in aromatic sulfonation. However another factor (15*c*) influencing orientation in this system is the

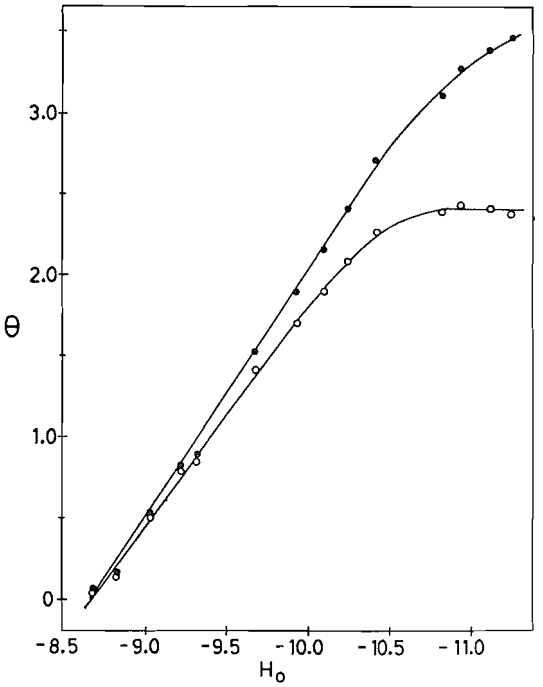

FIG. 7. Acidity function correlations for conversion of 4-hydroxyazobenzene to 4-hydroxyazobenzene-4′-sulfonic acid in sulfuric acid solutions at 25°.
O, Θ = 5 + log k_{obs}; ●, Θ = 5 + log k_{obs} − log $C_{SH^+}/(C_{SH^+} + C_{SH_2^{++}})$

[3]This term was evaluated by means of the expression log $C_{SH_2^{++}}/C_{SH^+} = pK_a^2 - H_0$ using the H_0 values (18) in Table I. The possible application of an H_+ function (19,20) in this system was considered previously (7).

Can. J. Chem. Downloaded from www.nrcresearchpress.com by 210.87.254.6 on 09/05/12
For personal use only.

Can. J. Chem. Downloaded from www.nrcresearchpress.com by 210.87.254.6 on 09/05/12
For personal use only.

increased through-conjugation in the reaction product (and in the reaction intermediates and transition states) which results when sulfonation occurs in the 4-position. The second sulfonation should then be directed in the position *ortho* to the hydroxyl group, which will be more activating than the azo-nitrogen bonded to the second proton-bearing nitrogen.

Experimental

Materials

4-Hydroxyazobenzene and 4-hydroxyazobenzene-4′-sulfonic acid had physical properties as described previously (7). Sulfuric acid solutions were prepared by addition of fuming acid (30% SO_3) to 96% acid and analyzed conductimetrically (23). Acid concentrations are given as weight per cent.

Kinetic Measurements

The bulk of the kinetic data were obtained by following the reactions (10^{-4} to 10^{-5} *M* in substrate) spectrally *in situ* in thermostated cells mounted in a constant temperature holder in the spectrophotometer (the "direct method"). The substrate (0.1–1.0 mg, weighed on a Cahn-M10 Electrobalance in glass boats of tare less than 5 mg) was added to a pre-thermostated, weighed quantity of sulfuric acid (25–100 ml) and transferred to the thermostated 1 cm cells (25.00 ± 0.03°). The spectrophotometers used were either a Unicam SP800B or a Bausch and Lomb Spectronic 600 Spectrophotometer, the latter in conjunction with a Sargent SRL recorder. In kinetic runs carried out on the former instrument spectral sweeps were taken at various times over the region of interest and rate constants calculated from absorbance values read off these sweeps. The latter instrument was generally used for following the reaction at constant wavelength. A small variation (2–4 mμ) in absorption characteristics (peak or isosbestic point wavelengths) was observed between runs, presumably as the result of small differences in acid concentration (particularly in the 100% H_2SO_4 region) and in instrumental settings over a period of time.

The wavelength at which absorbance changes were computed was usually in the region 460–465 mμ, being close to, though not necessarily at λ_{max} for the product of reaction. In acid media over 100% H_2SO_4 the first sulfonation was also followed on occasion at 480 mμ, which gave more optimum changes in absorbance than was afforded at 460–465 mμ (cf. Fig. 4); the rate of the second sulfonation was also computed on occasion for ca. 450 mμ.

Most of the rate constants were calculated by the Guggenheim method since this removed the uncertainty with respect to "infinity" absorbance values current with the small sized substrate samples employed, the slow rates in the lower acid range, and the two consecutive sulfonation processes above the 100.0% H_2SO_4. Where "infinity" absorbance values could be obtained, some of the rate constants were also evaluated by means of log $(A_\infty - A_t)$ versus t plots; in such cases experimental A_∞ values were used, which was deemed more accurate with the small sized samples.

Rate constants were calculated by means of a least square program using an IBM 360/–50 computer, with a Calcomp Digital Plotter 663 to plot the data. A correlation coefficient of 0.994 was taken as prepresentative of acceptable linearity. An illustrative plot is shown in Fig. 8.

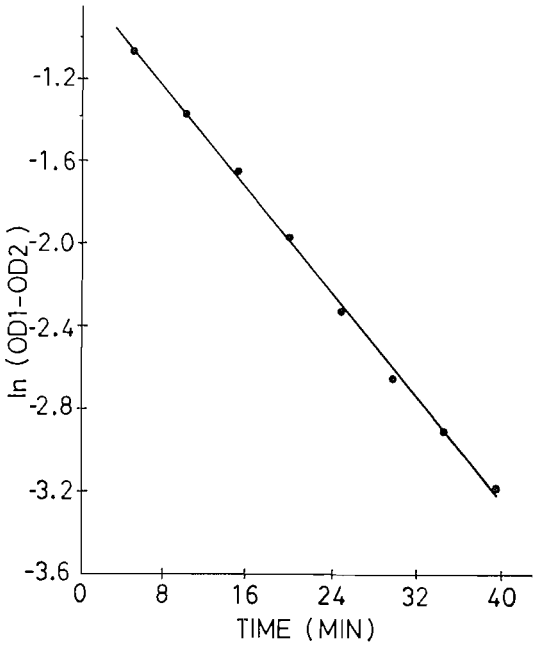

FIG. 8. Kinetic plot for sulfonation of 4-hydroxyazobenzene in 99.72% H_2SO_4. Data correspond to kinetic run illustrated in Fig. 2. Absorbance values at 460 mμ are plotted according to the Guggenheim method with Δt = 15 min and yield $k_{obs} = 102 \times 10^{-5}$ s^{-1}.

One kinetic run in this series was carried out by the base-quenching procedure ("the indirect method" (24)). The reaction solution was prepared by adding 2.49 mg of 4-hydroxyazobenzene in 20 ml (36.6 g) of 97.80% H_2SO_4 in a constant temperature bath (25.00 ± 03°). Aliquots (0.991 ml) were periodically quenched with cold 1 *N* aqueous KOH, diluted to 50 ml at 25°, and the spectra taken in 4.00 cm cells. The rate constant was calculated from the absorbance changes at 440 mμ, being λ_{max} for 4-hydroxyazobenzene-4′-sulfonic acid in basic medium. Using the log $(A_\infty - A_t)$ versus t plot, $k = 6.27 \times 10^{-5}$ s^{-1}.

Identification of Product of First Sulfonation

Spectral characteristics of "infinity" solutions (≥ 97% reaction) of 4-hydroxyazobenzene were compared with the spectrum of 4-hydroxyazobenzene-4′-sulfonic acid. For the range 94.52–98.92% H_2SO_4, the λ_{max} of the "infinity" solutions for 11 kinetic runs varied over 463–467 mμ, with molar extinctions taking the values 4.56×10^4–4.88×10^4. 4-Hydroxyazobenzene-4′-sulfonic acid in 89.3% H_2SO_4 showed λ_{max} 465 mμ ($\varepsilon = 4.61 \times 10^4$) and in 97.80% H_2SO_4, λ_{max} 463 mμ ($\varepsilon = 4.70 \times 10^4$). Below 94.5% H_2SO_4 "infinity" readings were not obtained due to the low reaction rate. Over 99% H_2SO_4, where the second equilibrium protonation of 4-hydroxyazobenzene-4′-sulfonic acid becomes important, the

TABLE III

Spectral characteristics of 4-hydroxyazobenzene and sulfonated derivatives in several states of ionization

	Basic (ArO^-)		Neutral (B)		Monoprotonated (BH^+)		Diprotonated (BH_2^{++})	
	λ(mμ)	$10^{-4}\varepsilon$	λ(mμ)	$10^{-4}\varepsilon$	λ(mμ)	$10^{-4}\varepsilon$	λ(mμ)	$10^{-4}\varepsilon$
4-Hydroxyazobenzene	440 402	2.18 2.16	348	2.50	460	3.81	426‡	3.30‡
4-Hydroxyazobenzene-4′-Sulfonic acid	448*	2.56	350	2.40	465	4.65	420	3.87
4-Hydroxyazobenzene-3,4′(?)-Disulfonic acid	440*	2.66	348	2.51	452	4.46	(436)†	(3.72)†

*The basic spectra have a broad shoulder in the 400–410 mμ region.
†Observed values in 100.79% H_2SO_4.
‡Observed values in 100.02% H_2SO_4.

"infinity" extinctions of the product solutions from the 4-hydroxyazobenzene reaction were found to fit well along the pK_a^2 curve of this sulfonic acid (see reference 7, footnote 6).

Partial Identification of Product of Second Sulfonation

4-Hydroxyazobenzene and 4-hydroxyazobenzene-4′-sulfonic acid were allowed to react in 100.79% at 25° (separate runs, substrate concentrations ca. 3×10^{-4} *M*) for periods of 24 and 65 h (corresponding to 6 and 16 half-lives). The spectra were then examined in that medium as well as in 96% H_2SO_4, 0.2 *N* H_2SO_4, and 0.2 *N* KOH, obtained by dilution (1:50) of the original 100.79% reaction solution with 96% H_2SO_4, 0.6 *N* KOH and 1.0 *N* KOH, respectively. The reaction solutions derived from 4-hydroxyazobenzene and from 4-hydroxyazobenzene-4′-sulfonic acid showed virtually identical absorption, for both reaction times, as expected on the basis of product identity, and average ε values are considered below. The spectrum in 0.2 *N* KOH is identified with the azophenolate anion (ArO^-); the spectrum in 0.2 *N* H_2SO_4 with the neutral species (B) with respect to the azo linkage; in 96% H_2SO_4 with the azo-protonated species (BH^+); and the 100.79% H_2SO_4 spectrum is ascribed to partial diprotonation.

In Table III the λ and ε values for the various ionized forms of 4-hydroxyazobenzene and 4-hydroxyazobenzene-4′-sulfonic acid are compared with corresponding values for this reaction product, tentatively identified as 4-hydroxyazobenzene-3,4′-disulfonic acid. This identification rests largely on the close similarity in these λ,ε data, since it is known that the introduction of a sulfonic acid group in the azobenzene system does not significantly alter the spectral characteristics of the parent compound (7).

The site of the second equilibrium protonation in the disulfonic acid product is probably the phenolic oxygen (7) and a λ_{max} in the region of 420 mμ for this species can be assumed. Since λ_{max} shifts from 452 to 436 mμ between 96% H_2SO_4 and 100.79% H_2SO_4, the extent of this shift would roughly correspond to ~50% diprotonation, with a pK_a^2 of ca. −12.

Acknowledgments

The award of an Ontario Graduate Fellowship to W.M.J.S. is gratefully acknowledged, as is continued financial support from the National Research Council of Canada.

1. E. Buncel. *In* Mechanisms of molecular migrations. B. S. Thyagarajan, Editor. John Wiley and Sons, Inc. – Interscience Publishers, Inc., New York. 1968.
2. H. Wilsing. Ann. **215**, 228 (1882).
3. A. Lachman. J. Amer. Chem. Soc. **24**, 1178 (1902).
4. P. H. Gore and G. R. Hughes. Aust. J. Sci. Res. **A3**, 136 (1950).
5. B. T. Newbold and M. H. Akhtar. Private communication.
6. E. Buncel and B. T. Lawton. Can. J. Chem. **43**, 862 (1965).
7. W. M. J. Strachan, A. Dolenko, and E. Buncel. Can. J. Chem. **47**, 3631 (1969).
8. E. Buncel, W. M. J. Strachan, R. J. Gillespie, and R. Kapoor. Chem. Commun. 765 (1969).
9. V. Gold and D. P. N. Satchell. J. Chem. Soc. 1635 (1956).
10. M. Kilpatrick, M. W. Meyer, and M. L. Kilpatrick. J. Phys. Chem. **64**, 1433 (1960).
11. A. W. Kaandorp, H. Cerfontain, and F. L. J. Sixma. Rec. Trav. Chim. **81**, 969 (1962).
12. W. A. Cowdrey and D. S. Davies. J. Chem. Soc. 1871 (1949).
13. (*a*) J. C. D. Brand. J. Chem. Soc. 1004 (1950). (*b*) J. C. D. Brand, A. W. P. Jarvie, and W. C. Honig. J. Chem. Soc. 3844 (1959).
14. (*a*) H. Cerfontain. Rec. Trav. Chim. **80**, 296 (1961). (*b*) C. W. F. Kort and H. Cerfontain. Rec. Trav. Chim. **87**, 24 (1968).
15. C. K. Ingold. Structure and mechanism in organic chemistry. Bell & Sons, Ltd., London. 1953. (*a*) p. 299. (*b*) p. 259. (*c*) p. 266.
16. (*a*) L. Melander. Isotope effects on reaction rates. The Ronald Press Co., New York. 1960. (*b*) R. O. C. Norman and R. Taylor. Electrophilic substitution in benzenoid compounds. Elsevier Publ. Co., Inc., Amsterdam. 1965. (*c*) H. Cerfontain. Mechanistic aspects in aromatic sulfonation and desulfonation. Interscience Publishers, Inc., New York. 1968.
17. R. J. Gillespie. Rev. Pure Appl. Chem. (Australia) **9**, 1 (1959); R. J. Gillespie and E. A. Robinson. Non-aqueous solvents. *Edited by* T. C. Waddington. Academic Press, Inc., London. 1965.
18. M. A. Paul and F. A. Long. Chem. Rev. **57**, 1 (1957).

Can. J. Chem. Downloaded from www.nrcresearchpress.com by 210.87.254.6 on 09/05/12
For personal use only.

19. T. G. BONNER and J. C. LOCKHART. J. Chem. Soc. 364 (1957); P. VETESNIK, J. BIELAVSKY, and M. VECERA. Coll. Czech. Chem. Commun. **33**, 566 (1968).
20. P. J. BRIGNELL, C. D. JOHNSON, A. R. KATRITZKY, N. SHAKIR, H. O. TARHAN, and G. WALKER. J. Chem. Soc. **B**, 1233 (1967).
21. F. A. LONG and M. A. PAUL. Chem. Rev. **57**, 935 (1957).
22. T. G. BONNER and J. C. LOCKHART. J. Chem. Soc. 3852 (1958); J. C. LOCKHART. J. Chem. Soc. **B**, 1174 (1966).
23. R. J. GILLESPIE and S. WASIF. J. Chem. Soc. 204 (1953); R. J. GILLESPIE, J. V. OUBRIDGE, and C. SOLOMONS. J. Chem. Soc. 1804 (1957); D. M. LICHTY. J. Amer. Chem. Soc. **30**, 1834 (1908).
24. E. BUNCEL and W. M. J. STRACHAN. Can. J. Chem. **47**, 911 (1969).

Can. J. Chem. Downloaded from www.nrcresearchpress.com by 210.87.254.6 on 09/05/12
For personal use only.

Can. J. Chem. Downloaded from www.nrcresearchpress.com by 210.87.254.6 on 09/05/12
For personal use only.

p*H* Effects in trypsin catalysis

H. P. KASSERRA AND K. J. LAIDLER
Department of Chemistry, University of Ottawa, Ottawa, Canada

Received December 12, 1968

A kinetic study has been made of the trypsin-catalyzed hydrolysis of *N*-benzoyl-L-alanine methyl ester, at p*H* values ranging from 6 to 10. The substrate concentrations varied from 1.7×10^{-3} to 4.3×10^{-2} *M*. From the rates were calculated, at each p*H*, values of $\tilde{k}_c$ (corresponding to $[S] \gg K_m$), $\tilde{k}_c/\tilde{K}_m$ (corresponding to $[S] \ll K_m$) and $\tilde{K}_m$. The specific levorotation of trypsin was measured and found to vary with p*H* in the p*H* region 5–11, the change in specific rotation following the ionization of a single group with p*K*(app) of 9.4. At p*H* 11 the specific rotation of trypsin, its zymogen, and its phosphorylated derivative were approximately the same, suggesting similar conformations for all three forms of the protein.

The kinetic results on the acid side were very similar to those obtained by other investigators for chymotrypsin; they imply that there is a group of $pK_b \approx 7$ in the free enzyme, presumably the imidazole function of a histidine residue, and that this group is involved in acylation and deacylation, which can only occur if it is unprotonated. The behavior on the basic side was found to be different from that with chymotrypsin revealing a decrease in $\tilde{k}_c$ at high p*H* corresponding to a value of $pK_a \approx 9.5$, whereas $\tilde{k}_c/\tilde{K}_m$ showed sigmoid p*H*-dependence. An interpretation of these results that is consistent with all available information is that a group of $pK \approx 9.5$ (presumably the $-NH_3^+$ function of the terminal isoleucine) controls the conformation and thereby the activity of the enzyme at different stages of complex formation. In contrast to chymotrypsin, the p*K* of this ionizing group appears to be generally lowered by covalent complex formation between trypsin and its substrates.

Canadian Journal of Chemistry, 47, 4021 (1969)

Introduction

Derivatives of lysine and arginine (1) appear to be the best substrates for bovine pancreatic trypsin (Enzyme Commission (E.C.) No. 3.4.4.4.). In recent years, it has been shown, however, that the enzyme is not absolutely specific with respect to the length (2–5) or type (6–8) of the substrate side-chain. This behavior, particularly that shown towards aromatic substrates, has been clearly established as being due to trypsin (6, 9) and not to contamination by small amounts of chymotrypsin (E.C. 3.4.4.5) which are usually found in commercial trypsin preparations.

Relatively few studies have been made of the influence of p*H* on the trypsin-catalyzed hydrolysis of esters (10–14) and all of these were done at substrate concentrations which are high relative to the apparent Michaelis constant; this constant, for the specific amino acid ester substrates, is of the order of 10^{-5} *M* or less. The kinetics of chymotrypsin action, however, have been investigated over a wider range of substrate concentrations, and have been interpreted in much greater detail (15, 16). On the basis of the striking similarities between trypsin and chymotrypsin (17), it has been generally concluded that in all important mechanistic aspects, catalyses by trypsin and α-chymotrypsin are similar. The present more detailed study of p*H* effects in trypsin kinetics indicates some significant differences between the two enzymes, a matter which is further considered in the following paper.

In the present investigation a study was made of the effect of p*H* on the hydrolysis of *N*-benzoyl-L-alanine methyl ester (BAME) by trypsin. This choice of substrate made it possible to cover low substrate concentrations relative to the apparent Michaelis–Menten constant (≈ 0.1 *M*) and to examine a wide range of p*H*.

Theory

The influence of p*H* on the kinetics of enzyme-catalyzed reactions involving two intermediates has been discussed in detail by Kaplan and Laidler (18). Most hydrolytic enzymes, such as trypsin and chymotrypsin, obey the modified Michaelis–Menten law

$$[1] \qquad v = \frac{\tilde{k}_c[E]_0[S]}{\tilde{K}_m + [S]}$$

where $[E]_0$ and $[S]$ are the total enzyme and substrate concentrations and $\tilde{k}_c$ and $\tilde{K}_m$ are constants at a given p*H*; the symbol $\sim$ indicates that they are usually p*H*-dependent quantities. A general reaction mechanism involving two intermediates and two ionizing groups on the enzyme is shown in Scheme 1.

An approximate steady-state treatment leads to eqs. [2]–[4], expressions for the kinetic parameters.

$$[2]\qquad \tilde{k}_c = \frac{k_2}{\dfrac{1 + \dfrac{K_a'}{[H]} + \dfrac{[H]}{K_b'}}{1 + \dfrac{aK_a'}{[H]} + \dfrac{b[H]}{K_b'}} + \dfrac{k_2}{k_3}\dfrac{1 + \dfrac{K_a''}{[H]} + \dfrac{[H]}{K_b''}}{1 + \dfrac{\alpha K_a''}{[H]} + \dfrac{\beta[H]}{K_b''}}}$$

$$[3]\qquad \tilde{K}_m = \frac{\dfrac{k_{-1} + k_2}{k_1}\dfrac{1 + \dfrac{K_a}{[H]} + \dfrac{[H]}{K_b}}{1 + \dfrac{aK_a'}{[H]} + \dfrac{b[H]}{K_b'}}}{\dfrac{1 + \dfrac{K_a'}{[H]} + \dfrac{[H]}{K_b'}}{1 + \dfrac{aK_a'}{[H]} + \dfrac{b[H]}{K_b'}} + \dfrac{k_2}{k_3}\dfrac{1 + \dfrac{K_a''}{[H]} + \dfrac{[H]}{K_b''}}{1 + \dfrac{\alpha K_a''}{[H]} + \dfrac{\beta[H]}{K_b''}}}$$

$$[4]\qquad \frac{\tilde{k}_c}{\tilde{K}_m} = \frac{k_1 k_2}{k_{-1} + k_2}\frac{1 + \dfrac{aK_a'}{[H]} + \dfrac{b[H]}{K_b'}}{1 + \dfrac{K_a}{[H]} + \dfrac{[H]}{K_b}}$$

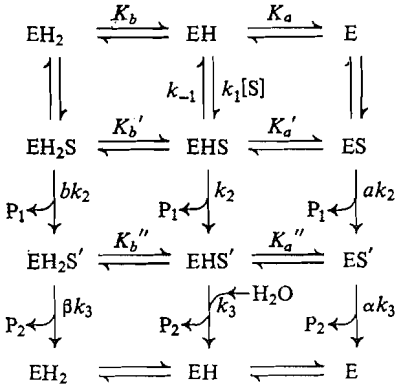

SCHEME 1

A general mechanism for p*H*-dependence. The symbols are defined in the same way as in the paper by Kaplan and Laidler (18).

The ratio $\tilde{k}_c/\tilde{K}_m$ is particularly significant in that it relates to the kinetic behavior at low substrate concentrations. It has been shown (18) that when one obtains K_a and K_b values from studies at low [S], one can conclude that the corresponding groups not only ionize in the free enzyme but are *essential to the subsequent reaction of the enzyme-substrate complex*. They may also be involved at a later stage, e.g. deacylation, but this must be investigated in other ways. Even if one is using a substrate for which deacylation is rate-limiting, one can still determine the ionizing groups involved in acylation by studying the p*H* dependence of $\tilde{k}_c/\tilde{K}_m$.

Experimental

Materials

N-Benzoyl-L-alanine methyl ester was prepared essentially according to the method used by Kaplan and Laidler (16). An improvement in yield and ease of purification was achieved by carrying out the reaction in an ice-water bath which caused the crude product to precipitate as a solid rather than a liquid. The yield after two recrystallizations was 66.4% of BAME, m.p. 57.5–58 °C, $[\alpha]_D^{22}$ +30.1° (*c*, 5 in *sym*-tetrachloroethane). This agrees well with previously reported results (16, 19).

Trypsin (twice crystallized, salt-free, Lot No. TRL 7EC) was obtained from Worthington Biochemical Corporation and used without further purification for most of the kinetic work. Enzyme concentrations, calculated on the basis of a molecular weight of 23 800 (20), ranged from 2 to 4 × 10^{-5} *M*. One gram of trypsin (same lot as above) was treated with L-(1-tosylamido-2-phenyl) ethylchloromethyl ketone (TPCK) according to the method described by Kostka and Carpenter (9). After dialysis and lyophilization, the yield of treated enzyme

Can. J. Chem. Downloaded from www.nrcresearchpress.com by 210.87.254.6 on 09/05/12
For personal use only.

Can. J. Chem. Downloaded from www.nrcresearchpress.com by 210.87.254.6 on 09/05/12
For personal use only.

was 84%. This enzyme in which all chymotrypsin activity is irreversibly inhibited was used as a control for some kinetic runs at pH 8.0. TPCK was purchased from Calbiochem (Lot No. 53227).

All proteins used for optical rotation studies were obtained from Worthington Biochemical Corporation; trypsin (twice crystallized, salt-free, Lot No. TRL 8CA), trypsin treated with diisopropyl fluorophosphate (DIP-trypsin, twice crystallized, Lot No. TDIP 7AA), and typsinogen (crystallized, Lot No. TG 7JH).

Water was doubly distilled, deionized, and free of carbon dioxide. The titrant used for pH-stat work was 0.02 N NaOH (0.05 N at pH 10.0) periodically restandardized with Fisher Certified hydrochloric acid.

Kinetic Procedure

Rates of hydrolysis were determined by the pH-stat method with a Radiometer automatic titrator (Model TTTlc) and titrigraph (Model SBR 2c). The reaction vessel was surrounded by a jacket through which water was circulated at 25.0 ± 0.05 °C. Inserted into the cell were a glass electrode (Radiometer G202B), a saturated calomel reference electrode, a stirrer, and leads for sodium hydroxide solution and nitrogen. The nitrogen was washed with acid and alkali and then with water before being passed in a slow stream over the surface of the reaction mixture. The titrant was delivered by a Radiometer syringe burette (Model SBUla) into the cell containing 15 ml of solution.

Stock solutions of trypsin were made up in 0.033 M $CaCl_2$(I = 0.10) and stored frozen for no longer than 3 days. A stock solution of BAME in water could be maintained indefinitely in the refrigerator. Substrate concentrations ranged from 0.167 to 4.33 × 10^{-2} M. In a typical run, substrate solution, water, and 1 ml of 1.4 M sodium chloride solution were mixed in the cell to make up 14 ml (I = 0.10). The pH was adjusted to the desired value with 1 N sodium hydroxide solution delivered by a micrometer screw gauge. The reaction was then started by the addition of 1.0 ml of enzyme solution and usually followed to 5–10% completion.

Methods of Computation

At higher pH values a correction had to be applied for the alkaline hydrolysis of BAME. The first-order rate constant ($k_{OH} = v/[S]$) was determined at various pH values and plotted against $1/[H^+]$ as in Fig. 1. The correction can then be directly calculated at all other pH values.

Throughout this work the v vs. [S] plots gave a non-zero intercept which (after correction for alkaline hydrolysis of BAME) could only be accounted for by an "enzyme-blank" reaction. This phenomenon has previously been observed and discussed (21, 22) and suitable corrections were made. In this study all experimental data have been analyzed and the kinetic constants computed on the IBM 360/65 computer using a slightly modified version of the program written by Hanson *et al.* (23). The program fits experimental data directly to the Michaelis–Menten equation according to the method described by Bliss and James (24). From an analysis of the standard errors in $\tilde{K}_m$ and $\tilde{k}_c$, the "enzyme-blank" correction could be deduced, assuming that the "enzyme-blank" rate was proportional to the total enzyme concentration. The correction amounts to 3–25% depending on rate, pH, and enzyme concentration.

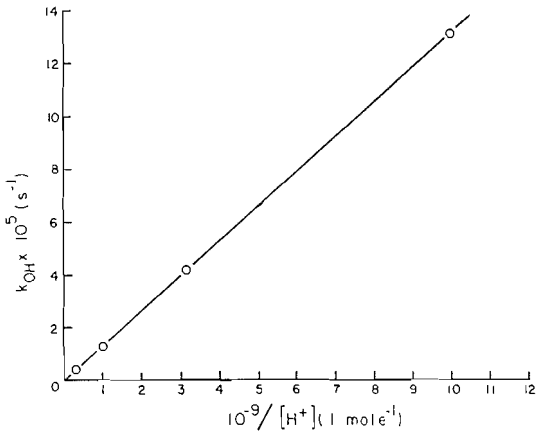

FIG. 1. Plot of first-order rate constant for the alkaline hydrolysis of BAME in water (0.1 M NaCl, 0.033 M $CaCl_2$) at 25.0 °C against the reciprocal of the hydrogen ion concentration.

Optical Rotation Measurements

Protein solutions of 1 mg per ml concentration were made up in 0.033 M $CaCl_2$ (I = 0.10). The solution of trypsinogen was centrifuged at 6000 r.p.m. in a Sorvall Superspeed RC2-B automatic refrigerated centrifuge to remove water-insoluble impurities. Protein concentrations were determined on a Perkin Elmer Model 350 spectrophotometer at 280 mμ with values of extinction $E_{1\,cm}$ (1%) = 14.4 for trypsin and DIP-trypsin and 13.9 for trypsinogen (25). Samples of each solution were adjusted to the desired pH with 1 N NaOH and placed in a 1-dm polarimeter tube with water jacket maintained at 23 °C. A Perkin Elmer Model 141 polarimeter was used to measure optical rotations at 365 and 436 mμ.

Results

pH Dependence of Kinetic Parameters

The values and standard errors of $\tilde{k}_c$, $\tilde{K}_m$, and $\tilde{k}_c/\tilde{K}_m$ for the hydrolysis of BAME by trypsin are given in Table I. The pH dependencies of these parameters are shown in Figs. 2–4.

The kinetic parameters are average values based on computed results from 3 to 5 runs covering the full range of substrate concentration from 0.167 to 4.33 × 10^{-2} M. The condition of low substrate concentration is strictly satisfied at pH 6 and 6.5 where a plot of rate against [S] is a straight line. At higher pH values, the plot becomes slightly curved as the order of the reaction becomes less than unity. Representative curves are shown in Fig. 5. Above pH 7.0 a slight extrapolation has therefore been made to obtain the second-order

TABLE I

Kinetic parameters for the trypsin-catalyzed hydrolysis of BAME at 25.0° and $I = 0.10$

pH	$\tilde{k}_c$ (s^{-1})	$\tilde{K}_m$ (M)	$\tilde{k}_c/\tilde{K}_m$ ($M^{-1}\ s^{-1}$)
6.0	—	—	0.175 ± 0.005
6.5	0.109 ± 0.009	0.243 ± 0.020	0.448 ± 0.009
7.0	0.185 ± 0.010	0.171 ± 0.012	1.08 ± 0.07
7.5	0.232 ± 0.009	0.129 ± 0.006	1.79 ± 0.10
7.8	0.248 ± 0.008	0.112 ± 0.006	2.22 ± 0.11
8.0	0.265 ± 0.006	0.111 ± 0.003	2.40 ± 0.07
8.5	0.248 ± 0.015	0.098 ± 0.003	2.19 ± 0.21
9.0	0.184 ± 0.012	0.078 ± 0.004	2.37 ± 0.16
9.2	0.168 ± 0.008	0.077 ± 0.002	2.19 ± 0.20
9.5	0.122 ± 0.005	0.052 ± 0.003	2.35 ± 0.18
9.7	0.105 ± 0.005	0.047 ± 0.003	2.24 ± 0.17
10.0	0.070 ± 0.011	0.035 ± 0.003	1.98 ± 0.22

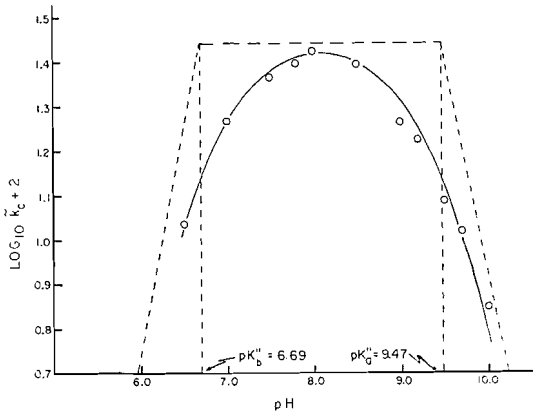

FIG. 2. Variation of $\log_{10} \tilde{k}_c$ with pH for the trypsin-catalyzed hydrolysis of BAME at 25.0 °C and $I = 0.10$ in $CaCl_2$ and NaCl.

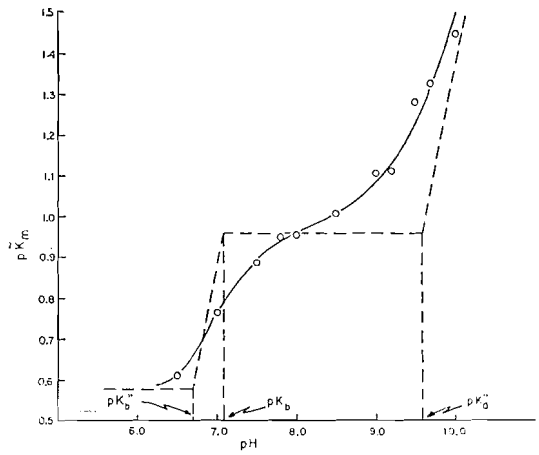

FIG. 3. Variation of $p\tilde{K}_m$ with pH for the trypsin-catalyzed hydrolysis of BAME at 25.0 °C and $I = 0.10$, in $CaCl_2$ and NaCl.

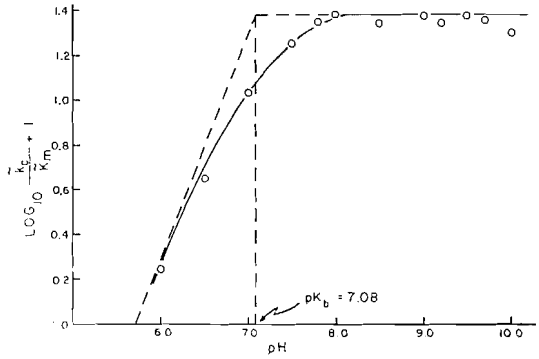

FIG. 4. Variation of $\log_{10} \tilde{k}_c/\tilde{K}_m$ with pH for the trypsin-catalyzed hydrolysis of BAME at 25.0 °C and $I = 0.10$ in $CaCl_2$ and NaCl.

rate constant $\tilde{k}_c/\tilde{K}_m$. The standard errors reported in Table I show that, with a few exceptions, the kinetic parameters can be considered reliable to ±5–10%.

Two control runs at pH 8.0 with TPCK-treated trypsin demonstrated within experimental error that the observed hydrolysis of BAME was indeed due to trypsin and not due to contaminating chymotrypsin. The results are shown in Table II.

The curves in Figs. 2 and 4 are the theoretical curves obtained by a reiterative process[1] which give the closest fit to the experimental points. The theoretical relationship between $p\tilde{K}_m$ and pH (eq. [3]) is too complex to permit such a fit and the curve in Fig. 3 is the best visual fit to the experimental data. The bell-shaped form of the $\log_{10} \tilde{k}_c$

[1]Knowledge of the pH-independent rate constants (see eqs. [2] and [4]) is not necessary. In the process of curve fitting, suitable values for these quantities can be found which give a best fit to the experimental points.

Can. J. Chem. Downloaded from www.nrcresearchpress.com by 210.87.254.6 on 09/05/12
For personal use only.

TABLE II

Comparison of rate constants for the trypsin-catalyzed hydrolysis of BAME by commercial trypsin and TPCK-treated trypsin at pH 8.0, T = 25.0 °C, and I = 0.10

Compound		$\tilde{k}_c$ (s^{-1})	$\tilde{K}_m$ (M)	$\tilde{k}_c/\tilde{K}_m$ (M^{-1} s^{-1})
Commercial trypsin		0.265 ± 0.006	0.111 ± 0.003	2.40 ± 0.07
TPCK-treated trypsin	(*1*)	0.264	0.110	2.40
	(*2*)	0.261	0.114	2.29

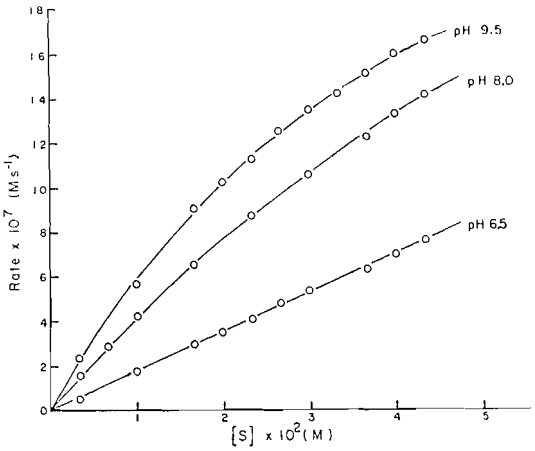

FIG. 5. Plots of rates against [S] for the trypsin-catalyzed hydrolysis of BAME at 25.0 °C and I = 0.10 in $CaCl_2$ and NaCl. The curves have been corrected for alkaline hydrolysis and "enzyme-blank" rate. At pH 8.0, $[E]_0 = 2 \times 10^{-5}$ M, at pH 9.5, $[E]_0 = 3 \times 10^{-5}$ M, and at pH 6.5, $[E]_0 = 4 \times 10^{-5}$ M.

– pH profile in Fig. 2 seems to suggest the participation of two groups in the catalytic reaction of the acylenzyme, $pK_b'' = 6.69$ and $pK_a'' = 9.47$. This implies that for the trypsin-catalyzed hydrolysis of BAME, deacylation is the rate-limiting step. It appears safe to make such an assumption in view of the extensive work done on α-chymotrypsin kinetics (26), as well as two studies on trypsin using *N-trans*-cinnamoyl imidazole (27) and *p*-nitrophenyl acetate (28).

As explained earlier, the pH profile of $\log_{10} \tilde{k}_c/\tilde{K}_m$ reveals the kinetically important groups on the free enzyme. In this case, the sigmoid-shaped curve in Fig. 4 shows that a basic group with $pK_b = 7.08$ is implicated in catalysis. It is believed that this is the first time that the trypsin-catalyzed hydrolysis of an ester has been studied at low substrate concentration over the full range of pH. The $p\tilde{K}_m$—pH profile in Fig. 3 provides an independent check for pK_a'' which is found to agree well with the value of 9.47 obtained from Fig. 2. The theoretical positions of pK_b and pK_b'' have also been indicated on Fig. 3.

The shape of the $\log_{10} \tilde{k}_c$—pH profile in Fig. 2 is essentially the same as that obtained by other investigators (11, 12, 29) for the trypsin-catalyzed hydrolysis of specific ester substrates. Similar bell-shaped behavior of the catalytic rate constant ($\tilde{k}_c$) has been reported by Chevallier and Yon (30) for the hydrolysis of benzoyl-L-arginin-amide at substrate concentrations larger than K_m and 35 °C. Their results qualitatively agree with those of Shukuya and Watanabe (31) and Wang and Carpenter (32). It must be remembered that, for amides, acylation is considered to be the rate-limiting step (33).

Effect of pH on Optical Rotation

The pH dependence of optical rotation at 365 mμ for trypsin, DIP-trypsin, and trypsinogen is shown in Fig. 6. Similar results were obtained for trypsin at 436 mμ involving smaller overall

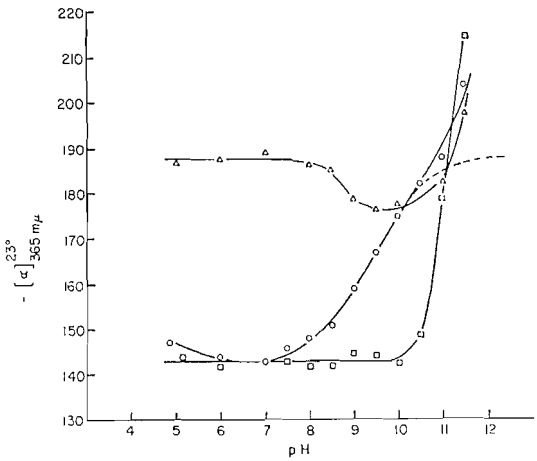

FIG. 6. Plots of specific rotation against pH at 365 mμ and 23 °C. Solutions contained 3.26 to 4.20 × 10^{-5} M protein in 0.033 M $CaCl_2$. Symbols: ○, trypsin; □, DIP-trypsin; △, trypsinogen.

Can. J. Chem. Downloaded from www.nrcresearchpress.com by 210.87.254.6 on 09/05/12
For personal use only.

Can. J. Chem. Downloaded from www.nrcresearchpress.com by 210.87.254.6 on 09/05/12
For personal use only.

changes in optical rotation. Samples at pH 11 were brought back to pH 8 and were found to exhibit complete reversibility in specific rotation within periods up to 20 min. Figure 6 shows that the specific rotation values for DIP-trypsin and trypsinogen are significantly different from each other. The optical rotation of DIP-trypsin is pH-independent between pH 5–10, and approximately 45° higher than that of trypsinogen which exhibits a small change in $[\alpha]$ above pH 8. The curve for trypsin has been extrapolated (dashed line) to a value of specific rotation equal to that of the inactive zymogen at neutral pH. Experimentally this value is not reached, owing to the ionization of titratable tyrosine residues which has been related by D'Albis and Béchet (34) to a decrease in the enzyme's rotary power. The specific levorotation of all three proteins decreases sharply above pH 11, presumably due to irreversible denaturation setting in. Similar results have been obtained by Neurath *et al.* (35) for trypsin and trypsinogen.

Using the same treatment as applied by Oppenheimer *et al.* (36) to acetylated δ-chymotrypsin, the pH-dependent change in specific levorotation of active trypsin can be related to the specific rotation of its precursor and its phosphorylated derivative as shown in Fig. 7. The equation used as basis for this plot is

$$[5] \qquad pH = pK + \log_{10} \frac{[E]}{[EH]}$$

where E and EH represent the different ionization states of the enzyme molecule. If $\Delta[\alpha]_{max}$ is defined as the total change in specific rotation between the value at pH 7 and the limiting value given by the dashed curve in Fig. 6, and $\Delta[\alpha]$ as the change in specific rotation between pH 7 and any pH, eq. [5] becomes

$$[6] \qquad pH = pK + \log_{10} \frac{\Delta[\alpha]}{\Delta[\alpha]_{max} - \Delta[\alpha]}$$

As can be seen from the plot in Fig. 7, eq. [6] is obeyed, indicating that the specific levorotation of trypsin follows the ionization of a single group. The pK(app) of the group controlling the change in specific rotation may be obtained from the abscissa of the plot in Fig. 7 at the point where $\log_{10} \Delta[\alpha](\Delta[\alpha]_{max} - \Delta[\alpha])^{-1} = 0$. A value of p$K$(app) = 9.4 was found.

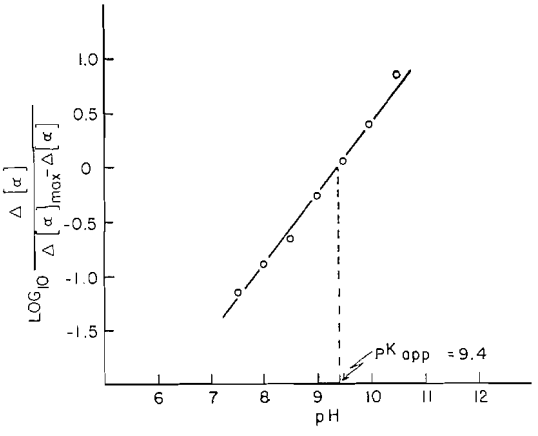

FIG. 7. Plot of $\log_{10} \Delta[\alpha](\Delta[\alpha]_{max} - \Delta[\alpha])^{-1}$ against pH for trypsin at 365 mμ.

Discussion

The pH dependencies shown in Figs. 2–4 at first sight appear to suggest a different mechanism of catalysis by trypsin as opposed to that by chymotrypsin. Much evidence has been accumulated for chymotrypsin (16, 26, 37) which has been incorporated in a reaction mechanism as shown in Scheme 2. We propose that the same mechanism is in fact applicable to trypsin on the basis that the observed kinetic behavior of the enzyme is related to changes in conformation with pH. The relationship between the scheme and the catalytic action of trypsin is best discussed separately for the acid and basic sides.

Ionizations in Acidic Solution

The ionizations on the acid side are the same for trypsin and chymotrypsin, the entire pattern of kinetic behavior on the acid side being very similar. Figure 4, which relates to low substrate concentrations, shows that there is a decrease in rate on the acid side corresponding to a pK_b value of 7.08. This undoubtedly relates to the ionization of the imidazoyl side-chain of histidine-46[2]. The fact that this residue is revealed in the $\log_{10} (\tilde{k}_c/\tilde{K}_m)$ plot indicates not only that the group is free to ionize in the free enzyme, but also that it is involved in the acylation process; in other words, acylation requires the function to be in the unprotonated form and cannot occur if it is protonated. It is for this reason that (as with chy-

[2]Our numbering in trypsin is according to the linear sequence of amino acids in trypsinogen as given in ref. (38).

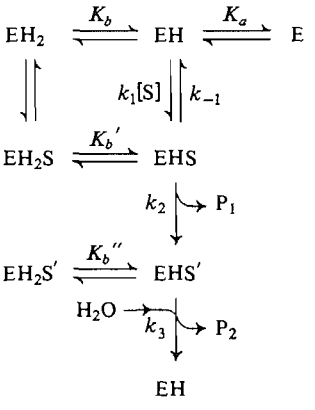

SCHEME 2

Reaction mechanism for trypsin and chymotrypsin catalysis.

motrypsin) the scheme shows no arrow between EH_2S and EH_2S'.

Figure 2, which relates to high substrate concentrations, provides information about the process of deacylation, which for esters is slower than that of acylation. The decrease in rate at low pH values corresponds to a pK_b'' value of 6.69. This undoubtedly can be attributed to the same imidazole group, and the fact that there is a falling-off in rate shows that this group is essential to deacylation, which can only occur if the function is unprotonated. The conclusion that the imidazole residue is essential to deacylation was first proposed by Gutfreund (10), who obtained pK_b'' = 6.25 with benzoyl-L-arginine ethyl ester. Béchet (12), on the other hand, found pK_b'' = 7.35 using tosyl-L-arginine methyl ester. Similar variations in pK values with different substrates are not uncommon.

Ionizations in Basic Solution

The situation on the basic side appears to be very different for trypsin from that with chymotrypsin. It is convenient to consider first the enzymatic behavior at high substrate concentrations, which relates to the rate-determining deacylation process. It is seen from Fig. 2 that (in contrast to chymotrypsin) there is a significant decrease in $\tilde{k}_c$ in basic solution, corresponding to the ionization of a group of pK_a'' equal to 9.47. In the case of chymotrypsin there seems to be no doubt (37) that one of the active residues in that enzyme is the $-NH_3^+$ group of the terminal isoleucine-16, and it is reasonable to suggest that in trypsin the observed pK relates to the corresponding $-NH_3^+$ group of the terminal isoleucine-7. Himoe *et al.* (37) propose, however, that this group is not *catalytically* active in chymotrypsin, but controls an equilibrium between two major conformations of the enzyme and thereby the enzymatic activity.

Similar evidence to ours has been obtained by Béchet (13) with tosyl-L-arginine methyl ester as substrate; he obtained pK_a'' = 10.1. It is significant in this connection that the reaction of nitrous acid with the α-amino group of the terminal isoleucine-7 causes inactivation of trypsin. Scrimger and Hofmann (39) have suggested that this is due to a complete destruction of the active site, and not to a change in the kinetic parameters, since the ability of the enzyme to react with diisopropyl fluorophosphate is lost at the same rate as the catalytic activity towards benzoyl-L-arginine ethyl ester. We suggest therefore on the basis of existing evidence that the observed fall-off in the rate of deacylation by trypsin in alkaline solution is the result of a conformational change in the acylenzyme and does not reflect the participation of an acidic group in the catalytic process. Ionization of the group with pK_a'' equal to 9.47 induces a catalytically inactive conformation of the acylenzyme and thereby controls the rate of deacylation.

Such an interpretation would also explain the observed shifts with pH in the bell-shaped deacylation curves of different trypsin substrates (Fig. 2, refs. 13, 29, 40) if it is assumed that different substrates stabilize the acylenzyme to a different extent and thus affect the pK of the conformation-controlling group. This is in contrast to most forms of acylchymotrypsin which do not exhibit a fall-off in $\tilde{k}_c$ up to pH 10 (16, 26). The specific rotation curve for DIP-trypsin (cf. Fig. 6) shows that even the irreversibly inhibited enzyme undergoes a conformational change at a lower pH (above pH 10) than does acetylated DIP-δ-chymotrypsin (above pH 11) (36). Similar variations in specific rotation relating to conformational stability have been observed by D'Albis and Béchet (34) and in this laboratory[3] for trypsin in the presence of reversible competitive inhibitors.

The work at low substrate concentrations (cf. Fig. 4) shows no significant decrease in the

[3]Unpublished experiments.

Can. J. Chem. Downloaded from www.nrcresearchpress.com by 210.87.254.6 on 09/05/12
For personal use only.

second-order rate constant at high pH values. This result seems to suggest that the ionizing group, observed in deacylation, is free but not involved in complex formation (in contrast to the situation with chymotrypsin) or in the acylation process. We have summarized, in the paper following this one, the evidence leading to the conclusion that the terminal isoleucine residue does in fact play a less prominent role in trypsin than it does in chymotrypsin with regard to substrate binding. The interpretation of the optical rotation studies reported in Fig. 6 is that the conversion of catalytically inactive trypsinogen to active trypsin is accompanied by the appearance of a new ionizing group which controls the conformation of the enzyme. Evidence that a conformational change accompanies the activation of zymogen to enzyme has been previously published (35). We have shown that the specific levorotation of trypsin varies with pH and that the change in specific rotation follows the ionization of a single group with pK(app) of 9.4 (cf. Figs. 6 and 7). It can be seen in Fig. 6 that the specific rotation of trypsin is approximately the same as that of trypsinogen at pH 11 beyond which irreversible denaturation is known to set in.

The experimental results obtained in this work together with some facts presented below are consistent with the hypothesis that both kinetic and optical rotation studies in basic solution reveal the same group in the enzyme, namely the terminal isoleucine-7 residue. These facts are that (*a*) activation of trypsinogen to trypsin results in isoleucine-7 as the new NH_2-terminal residue (41), (*b*) reaction of nitrous acid with the isoleucine group causes inactivation of the enzyme (39), (*c*) acetylation of all lysyl ε-amino groups and exposed tyrosyl groups of trypsin does not cause reduced enzymatic activity (42). In contrast to chymotrypsin, however (16), conformational changes induced by ionization of the NH_2-terminal group do not become apparent in the kinetics of Michaelis complex formation between trypsin and the non-specific ester substrate BAME. The existence of inactive forms of the enzyme in subsequent stages of the catalytic process is revealed by a decrease in the kinetic constant (k_c) for both the amidase and esterase activity of trypsin. It is tempting to suggest that this difference in enzymatic behavior between chymotrypsin and trypsin in alkaline solution is related to their differences in specificity, i.e. to electrostatic interactions between substrate and enzyme which are present in trypsin but not in chymotrypsin. We have attempted in the following paper to elucidate this matter to some extent.

The present study has been carried out with a non-specific substrate, lacking a positive charge on the side chain. There is good reason to believe that the mechanisms are the same for both specific and non-specific substrates in view of the same pH dependence of the deacylation processes for the two classes of compounds (11, 29, 40).

Acknowledgments

H. P. K. is indebted to the National Research Council of Canada for the award of a studentship. The authors wish to thank Mr. J. V. R. Barbour for his technical assistance.

1. M. Dixon and E. C. Webb. Enzymes. Longmans, Green and Co., Ltd., London. 1964. p. 243.
2. N. Izumiya, H. Okazaki, I. Matsumoto, and H. Takiguchi. J. Biochem. (Tokyo), **46**, 1347 (1959).
3. K. Kitagawa and N. Izumiya. J. Biochem. (Tokyo), **46**, 1159 (1959).
4. N. J. Baines, J. B. Baird, and D. T. Elmore. Biochem. J. **90**, 470 (1964).
5. J. B. Baird, E. F. Curragh, and D. T. Elmore. Biochem. J. **96**, 733 (1965).
6. T. Inagami and J. M. Sturtevant. J. Biol. Chem. **235**, 1019 (1960).
7. T. Inagami and H. Mitsuda. J. Biol. Chem. **239**, 1388 (1964).
8. M. Gorecki and Y. Shalitin. Biochem. Biophys. Res. Commun. **29**, 189 (1967).
9. V. Kostka and F. H. Carpenter. J. Biol. Chem. **239**, 1799 (1964).
10. H. Gutfreund. Trans. Faraday Soc. **51**, 441 (1955).
11. G. W. Schwert, H. Neurath, S. Kaufman, and J. E. Snoke. J. Biol. Chem. **172**, 221 (1948).
12. J.-J. Béchet. J. Chim. Phys. **61**, 584 (1964).
13. J.-J. Béchet. J. Chim. Phys. **62**, 1095 (1965).
14. T. Inagami and J. M. Sturtevant. Biochim. Biophys. Acta, **38**, 64 (1960).
15. M. L. Bender, G. E. Clement, F. J. Kézdy, and H. d'A. Heck. J. Amer. Chem. Soc. **86**, 3680 (1964).
16. H. Kaplan and K. J. Laidler. Can. J. Chem. **45**, 547 (1967).
17. L. B. Smillie, A. Furka, N. Nagabhushan, K. J. Stevenson, and C. O. Parkes. Nature, **218**, 343 (1968).
18. H. Kaplan and K. J. Laidler. Can. J. Chem. **45**, 539 (1967).
19. G. E. Hein and C. Niemann. J. Amer. Chem. Soc. **84**, 4487 (1962).
20. L. W. Cunningham, Jr. J. Biol. Chem. **211**, 13 (1954).
21. H. R. Almond, Jr. and C. Niemann. Biochim. Biophys. Acta, **44**, 143 (1960).
22. D. W. Ingles and J. R. Knowles. Biochem. J. **99**, 275 (1966).
23. K. R. Hanson, R. Ling, and E. Havir. Biochem. Biophys. Res. Commun. **29**, 194 (1967).
24. C. I. Bliss and A. T. James. Biom. **22**, 573 (1966).

Can. J. Chem. Downloaded from www.nrcresearchpress.com by 210.87.254.6 on 09/05/12
For personal use only.

25. E. W. DAVIE and H. NEURATH. J. Biol. Chem. **212**, 515 (1955).
26. M. L. BENDER and F. J. KÉZDY. Ann. Rev. Biochem. **34**, 49 (1965).
27. M. L. BENDER and E. T. KAISER. J. Amer. Chem. Soc. **84**, 2556 (1962).
28. J. A. STEWART and L. OUELLET. Can. J. Chem. **37**, 751 (1959).
29. P. BENMOUYAL and C. G. TROWBRIDGE. J. Chim. Phys. **62**, 576 (1965).
30. J. CHEVALLIER and J. YON. Biochim. Biophys. Acta. **112**, 116 (1966).
31. R. SHUKUYA and K. WATANABE. J. Biochem. (Tokyo), **44**, 481 (1957).
32. S.-S. WANG and F. H. CARPENTER. J. Biol. Chem. **243**, 3702 (1968).
33. H. GUTFREUND and J. M. STURTEVANT. Proc. Nat. Acad. Sci. U.S. **42**, 719 (1956).
34. A. D'ALBIS and J.-J. BÉCHET. Biochem. Biophys. Acta, **140**, 435 (1967).
35. H. NEURATH, J. A. RUPLEY, and W. J. DREYER. Arch. Biochem. Biophys. **65**, 243 (1956).
36. H. L. OPPENHEIMER, B. LABOUESSE, and G. P. HESS. J. Biol. Chem. **241**, 2720 (1966).
37. A. HIMOE, P. C. PARKS, and G. P. HESS. J. Biol. Chem. **242**, 919 (1967).
38. O. MIKEŠ, V. TOMÁŠEK, V. HOLEYŠOVSKY, and F. ŠORM. Collect. Czech. Chem. Commun. **32**, 655 (1967).
39. S. T. SCRIMGER and T. HOFMANN. J. Biol. Chem. **242**, 2528 (1967).
40. C. J. MARTIN, J. GULOBOW, and A. E. AXELROD. J. Biol. Chem. **234**, 1718 (1959).
41. H. NEURATH. Advan. Protein Chem. **12**, 391 (1957).
42. J. LABOUESSE and M. GERVAIS. European J. Biochem. **2**, 215 (1967).

Can. J. Chem. Downloaded from www.nrcresearchpress.com by 210.87.254.6 on 09/05/12
For personal use only.

Mechanisms of action of trypsin and chymotrypsin

H. P. KASSERRA AND K. J. LAIDLER
Department of Chemistry, University of Ottawa, Ottawa, Canada
Received December 12, 1968

The mechanistic evidence for reactions catalyzed by chymotrypsin and trypsin is briefly reviewed and is considered with reference to the structure as determined by the X-ray studies. Conclusions are drawn about the detailed nature of the processes of complex formation, acylation, and deacylation. Although there are significant differences between the two enzymes as far as specificity and p*H* effects are concerned, it appears that the mechanisms of their action are very similar.

Canadian Journal of Chemistry, **47**, 4031 (1969)

Can. J. Chem. Downloaded from www.nrcresearchpress.com by 210.87.254.42 on 09/05/12
For personal use only.

The preceding paper has presented evidence on trypsin which shows the kinetic behavior of this enzyme to be slightly different from that of chymotrypsin. The present paper is concerned with comparing and contrasting the two enzymes in some detail, and with drawing conclusions about the mechanisms of their action.

Structural Evidence

The three-dimensional structure of α-chymotrypsin has now been established by X-ray methods (1–4). Figure 1 has been constructed from Fig. 4 of reference 1 and Fig. 2 of reference 3, with the help of a model we have built. It shows in a purely schematic way the groups that appear to exist in the region of the active center, and their relative positions. The histidine-57 and serine-195 groups[1] are known from kinetic and other evidence to be catalytically important, whereas the $-NH_3^+$ group of *N*-terminal isoleucine-16 and the $-COO^-$ groups of aspartic acid-194 and aspartic acid-102[2] are believed to be more indirectly involved in the enzymatic process. Buried more deeply within the molecule are a number of non-polar groups, such as the side chains of isoleucine-16, leucine-163, and isoleucine-212. Some of these groups are probably concerned with forming hydrophobic bonds with the non-polar groups on the substrate.

The detailed X-ray structure of trypsin has not yet been established. However, there is very persuasive evidence that the general conformation of the enzyme is very similar to that of chymotrypsin. There is a very close correspondence between the amino acids along the chains, and there is a particularly strong homology as far as polar and non-polar groups are concerned (5). Further support for the similarity in conformation comes from the demonstration (2) that the two extra disulfide bridges that exist in trypsin can be built into the chymotrypsin model without distortion of the structure.

Figure 2 has been prepared for trypsin on the assumption that its general structure is the same as that of chymotrypsin. It is striking that so many of the groups near the active centers of the two enzymes are the same or very similar. The absence in trypsin of any group equivalent to leucine-13 of chymotrypsin is probably not significant, since this group is probably too far away in chymotrypsin to be actively involved. We are left with the result that the only significant difference between the two enzymes is that the neutral serine-189 in chymotrypsin has become the negatively-charged aspartic acid-177 in trypsin[3]. This strongly suggests that the different specificities of the two enzymes are largely due to the difference between these two groups; in particular, the fact that trypsin favors substrates having a positively-charged group in a suitable position (e.g. derivatives of arginine and lysine) seems to be related to the existence of the $-COO^-$ group at position 177 in trypsin.

Mechanistic Evidence

In Tables I–III we have summarized the most important mechanistic evidence for the two

[1]The present numbering of amino acids in chymotrypsin is the same as that in ref. 1.

[2]This group was originally identified as asparagine-102, but this has now been corrected (3).

[3]Our numbering for trypsin corresponds to consecutive numbering in trypsinogen, the order of amino acids (but not the numbering) being as in ref. 5, except for aspartic acid-177 which in the past has erroneously been reported as being asparagine-177 [B. S. Hartley, to be published; quoted in (4)].

Can. J. Chem. Downloaded from www.nrcresearchpress.com by 210.87.254.42 on 09/05/12
For personal use only.

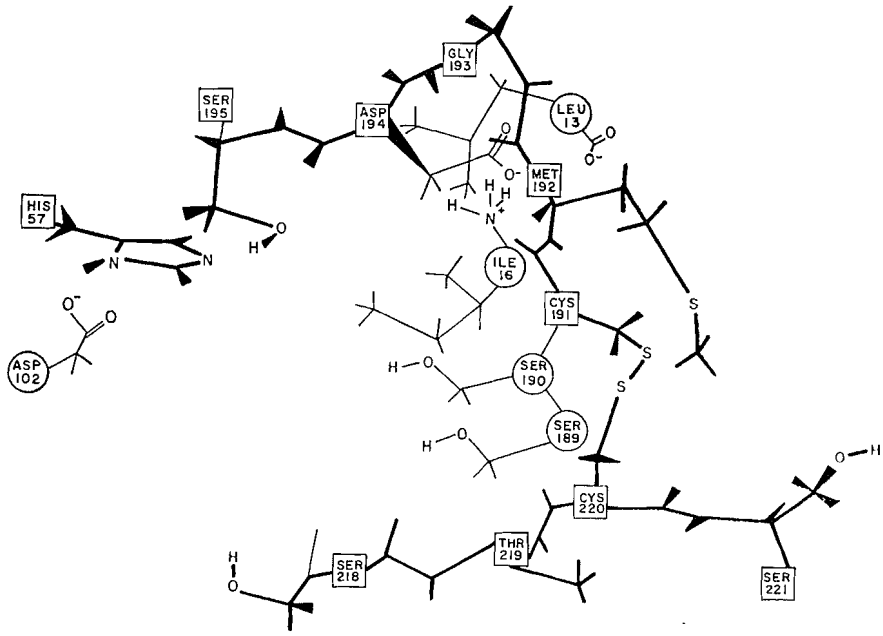

FIG. 1. Schematic diagram for α-chymotrypsin, showing the approximate conformation of the more important residues in the region of the active center.

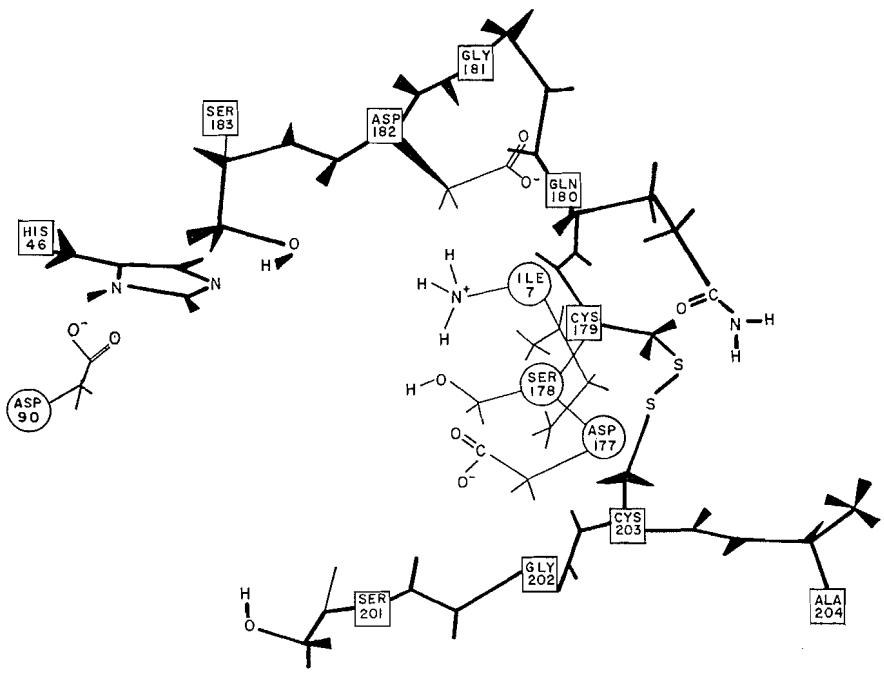

FIG. 2. Schematic diagram for trypsin.

Can. J. Chem. Downloaded from www.nrcresearchpress.com by 210.87.254.42 on 09/05/12
For personal use only.

TABLE I

Evidence relating to complex formation in chymotrypsin and trypsin

Kind of evidence	Chymotrypsin	Trypsin	Reference
p*H* Studies at low substrate concentrations	Bell-shaped curve; p*K* of ~7 and ~9	Sigmoid curve; p*K* of ~7; no falling-off up to p*H* ~10	6, 7
p*H* Studies in mixed solvents	Group of p*K* ~7 is a cationic acid; group of p*K* ~9 is a neutral or ion-pair acid	—	6
p*H* Studies at low p*H*	Carboxyl group (p*K* ~4) present	Carboxyl group (p*K* ~4) present	8, 9
Chemical and kinetic studies	Single histidine residue involved in reaction, but not in complex formation	Single histidine residue involved in reaction, but not in complex formation	6, 7, 10–12
Chemical and kinetic studies	*N*-terminal isoleucine-16 (p*K* ~9) indirectly participates in the binding process	—	13

TABLE II

Evidence relating to acylation of chymotrypsin and trypsin

Kind of evidence	Chymotrypsin	Trypsin	Reference
Chemical and kinetic studies	Acylation involves the hydroxyl group of serine-195	Acylation involves the hydroxyl group of serine-183	18–24
p*H* Studies with amides, for which acylation is rate-limiting	Rate falls off at p*H* < 7.5; no fall-off in alkaline solution up to p*H* 9.5	Rate falls off at p*H* < 7.5; no fall-off in alkaline solution up to p*H* 9.5	13, 16, 25–27
Substituent effects	Proton transfer is involved in acylation	—	28
Deuterium isotope effects	Proton transfer is involved in acylation	—	25
p*H* Studies at low concentrations of esters, for which deacylation is rate-limiting	Both ionizing groups are apparently involved in acylation	Single ionizing group (p*K* ≈ 7) participates in acylation	6, 7

TABLE III

Evidence relating to deacylation of chymotrypsin and trypsin

Kind of evidence	Chymotrypsin	Trypsin	Reference
p*H* Studies with *N*-α substituted esters, for which deacylation is rate limiting	Sigmoid curve; p*K* of ~7; no falling-off up to p*H* ~10	Bell-shaped curve; p*K* of ~7 and ~9.5. *Apparently* both groups involved in deacylation	6, 7, 15, 25, 31–34
p*H* Studies with esters on which the α-amino group is not substituted	Bell-shaped curve; p*H* optimum shifted from p*H* ~ 8 to p*H* ~ 6	Bell-shaped curve; p*H* optimum shifted from p*H* ~ 8 to p*H* ~ 6	35–37
Effect of added nucleophiles	Deacylation is first-order in nucleophile (e.g. methanol)	—	38
Kinetic studies	No intermediate detected in deacylation	—	15
Deuterium isotope effects	Proton transfer is involved in deacylation	Proton transfer is involved in deacylation	25, 39

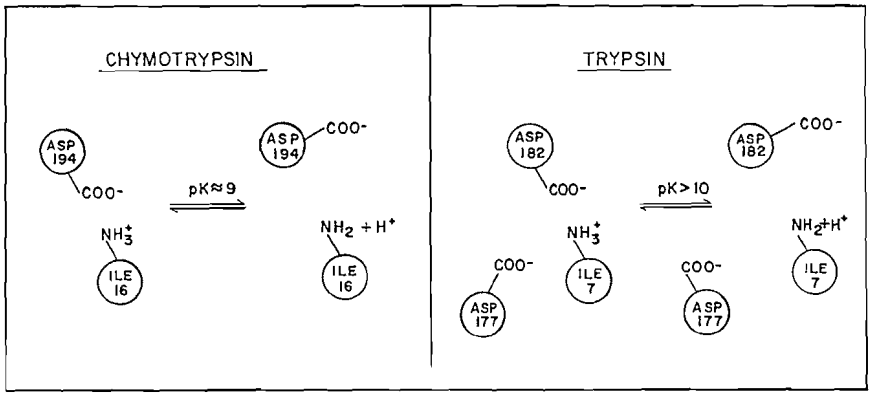

FIG. 3. Ionizations in chymotrypsin and trypsin.

enzymes, classifying it according to its relevance to (*1*) complex formation, (*2*) the acylation process, and (*3*) the deacylation process.

Complex Formation

Table I summarizes the evidence and conclusions regarding the process of complex formation. The main difference between the behavior of the two enzymes lies in their p*H* dependence at low substrate concentrations; with chymotrypsin there is evidence for a group of p$K \sim 9$, while with trypsin there is no falling-off in rate up to p$H \sim 10$.

There is no reason to doubt that the groups ionizing at pH ~ 7 are histidine-57 in the case of chymotrypsin and histidine-46 in the case of trypsin; support for this is provided by the work with chymotrypsin in mixed solvents (6). The mixed-solvent work also supports the conclusion that the group of p$H \sim 9$ in chymotrypsin is the $-NH_3^+$ group of isoleucine-16, existing in the charged state as an ion-pair with the $-COO^-$ group of aspartic acid-194 (1). When this $-NH_3^+$ group loses its proton it is postulated (2) that the $-COO^-$ group of aspartic acid-194 moves to a more polar environment. It appears likely that this causes a shift in the position of the reactive serine-195 residue which, as will be discussed, has an effect on subsequent processes.

A suggestion as to why the pK of the $-NH_3^+$ group in trypsin is higher than that in chymotrypsin is illustrated in Fig. 3. In trypsin the $-NH_3^+$ group is close to two $-COO^-$ groups, and it is therefore more difficult for the proton to leave.

The upper portions of Figs. 4 and 5 present more detailed mechanisms for the ionizations of chymotrypsin and trypsin, and for the way in which Michaelis-complex formation occurs. It is postulated, in agreement with other workers (13–17), that binding in the complexes does not directly involve the ionizing groups, but is primarily due to hydrophobic bonding between non-polar groups on the substrate and enzyme. In addition to this, the anionic site in trypsin (aspartate-177) forms an electrostatic bond with the positively-charged side chain of specific trypsin substrates. The state of ionization of the histidine residues has no effect on complex formation. However, ionization of the $-NH_3^+$ groups of the terminal isoleucines has an indirect effect on binding by bringing about a conformational change in the enzyme molecules; support for this in the case of chymotrypsin is provided by the work of Oppenheimer *et al.* (14), and is later discussed further with reference to trypsin.

Acylation

The evidence and conclusions relating to the acylation steps for the two enzymes are summarized in Table II. It has already been seen from the results relating to complex formation that the forms of the free enzyme in which the isoleucine $-NH_3^+$ group has lost its proton cannot bind substrate; expressed differently, the Michaelis complex cannot lose a proton from the $-NH_3^+$ group as readily as can the free enzyme, and the unprotonated form is of no significance within the range of pH that has been investigated.

The fact that with both enzymes the acylation rates fall off at pH values below about 7.5 implies that the imidazole ring of histidine-57 or histidine-42 must be unprotonated. The function of the unprotonated imidazole ring is no doubt to

Can. J. Chem. Downloaded from www.nrcresearchpress.com by 210.87.254.42 on 09/05/12
For personal use only.

Can. J. Chem. Downloaded from www.nrcresearchpress.com by 210.87.254.42 on 09/05/12
For personal use only.

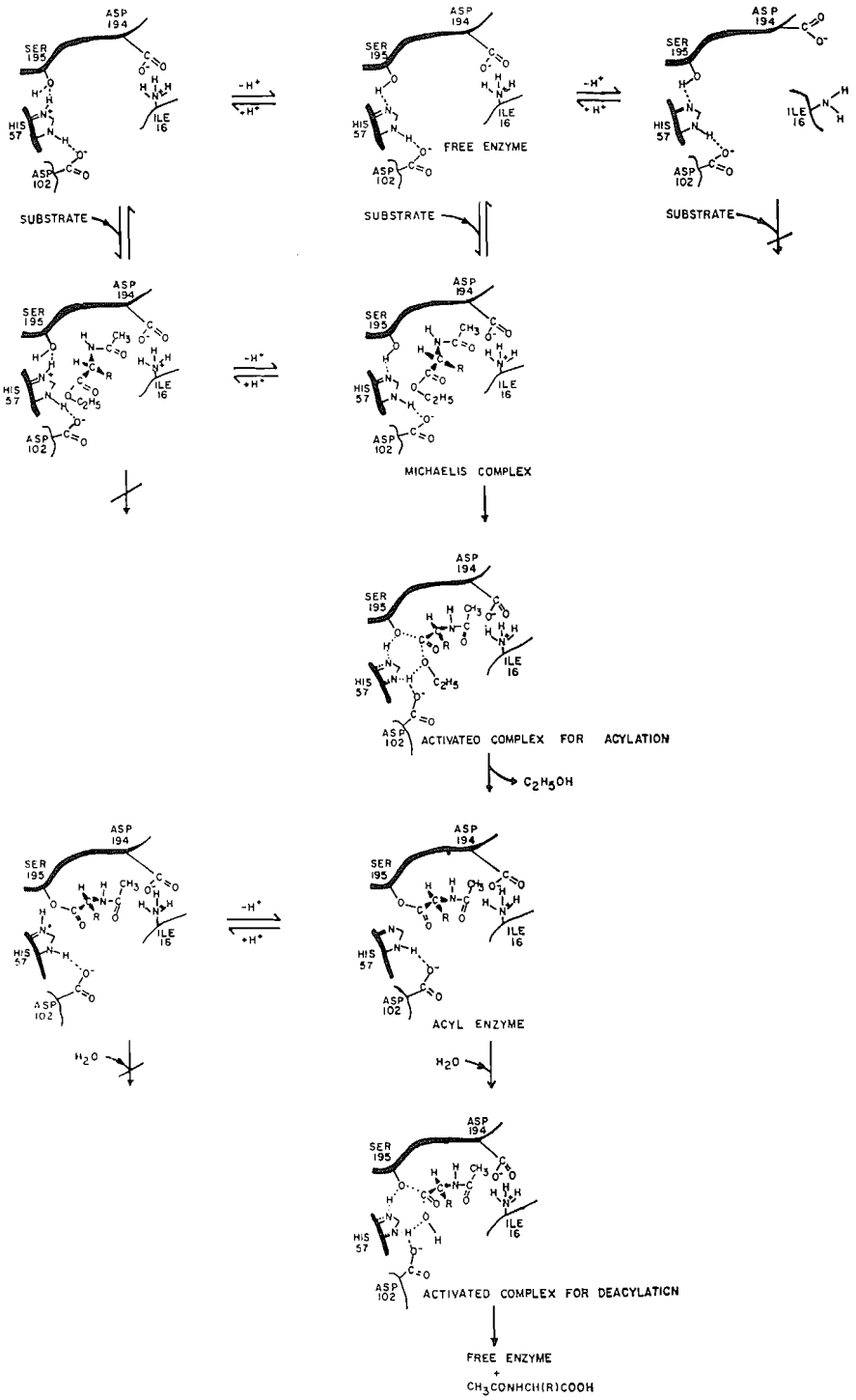

FIG. 4. Reaction mechanism for the α-chymotrypsin-catalyzed hydrolysis of *N*-acetyl-L-tyrosine ethyl ester. The important groups are shown in schematic relationship to one another. Hydrogen bonds are indicated by dashed lines.

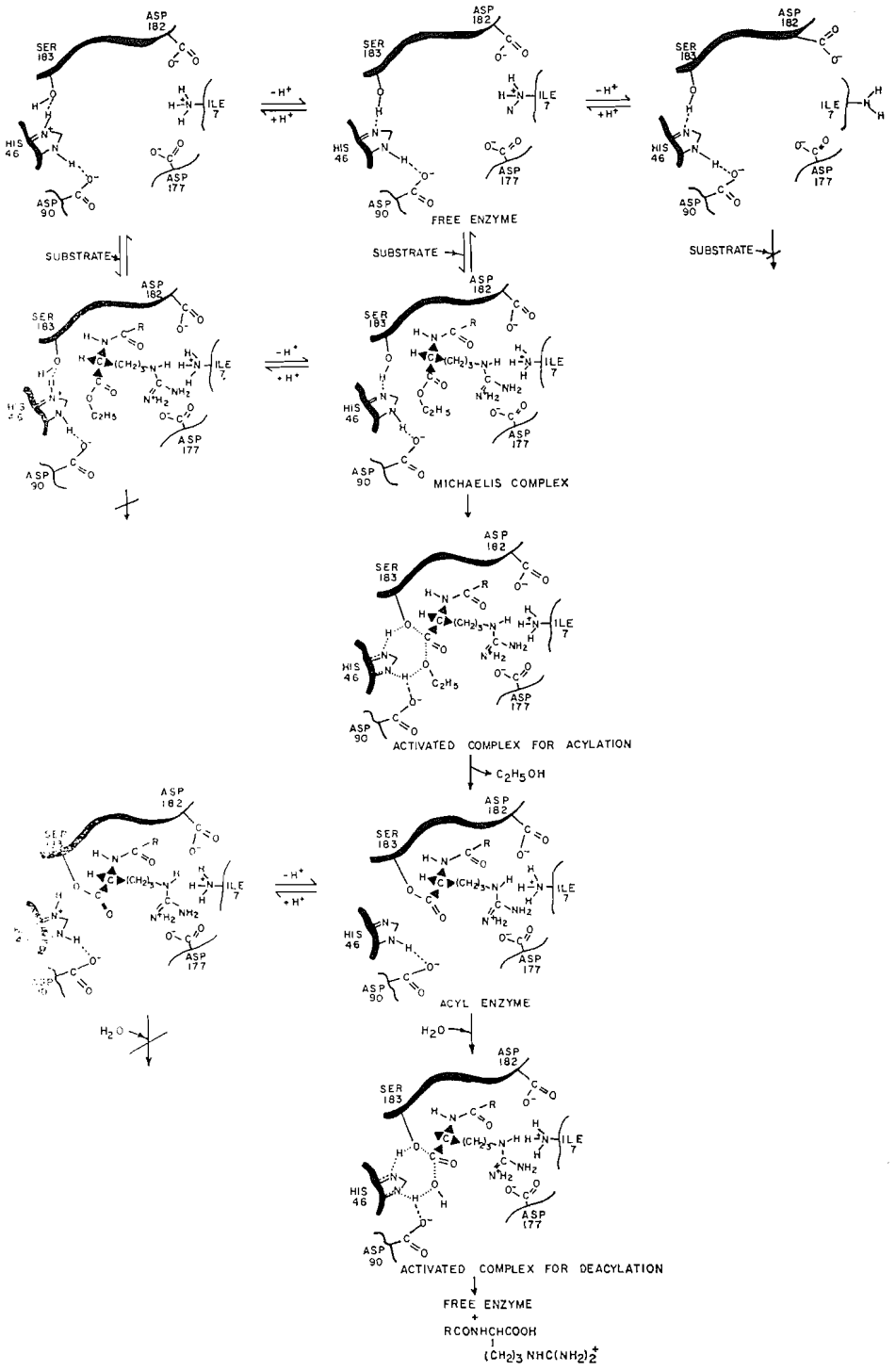

FIG. 5. Reaction mechanism for the trypsin-catalyzed hydrolysis of *N*-benzoyl-L-arginine ethyl ester. Hydrogen bonds are indicated by dashed lines.

Can. J. Chem. Downloaded from www.nrcresearchpress.com by 210.87.254.42 on 09/05/12
For personal use only.

aid in the removal of the proton from the serine hydroxyl group. At the same time a proton must be transferred to the alcoholic oxygen atom of the substrate. A way in which these processes can occur in a single stage is shown in Fig. 6. The

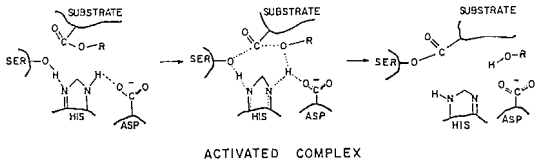

FIG. 6. Proton transfer processes during acylation.

suggested scheme makes use of the remarkable properties of the imidazole group as a proton-transfer agent. Eigen *et al.* (29, 30), who studied this as well as other acid–base catalysts, have shown that the effectiveness of this system is further increased by hydrogen bonds between the donor and acceptor molecules. In addition, the tautomeric character of the unprotonated imidazole ring makes it possible for this group to accept and donate a proton at the same time. These ideas are incorporated into the mechanisms shown in Figs. 4 and 5. As far as the behavior on the basic side is concerned it is suggested that, for both enzymes, the substrate has the effect of locking the enzyme into a conformation in which the $—COO^-$ group of aspartic acid-194 or -182 is held close to the $—NH_3^+$ group of the terminal isoleucine residue. This makes it more difficult for the α-amino group to lose a proton, a fact that explains why there is no decrease in the acylation rates up to high p*H* values. With trypsin this ionization is also difficult in the free enzyme, and we have suggested that this is due to the presence of the second $—COO^-$ group, i.e. aspartate-177. With chymotrypsin, however, the ionization is less difficult in the free enzyme, a p*K* of ~ 9 being observed.

Deacylation

Table III summarizes the evidence and conclusions relating to the deacylation step. It is seen that there is again a difference between the two enzymes in their p*H* dependence; with trypsin there is a falling-off above p*H* ~ 9, whereas with chymotrypsin there is no decrease in rate up to p*H* ~ 10; the results with chymotrypsin are consistent with a p*K* of 10.5 or greater.

In both enzymes the imidazole ring of histidine-57 or -46 must be in its unprotonated form in order for deacylation to occur. The function of the unprotonated imidazole group is to aid in the splitting of a water molecule acting as the nucleophile and to facilitate the transfer of a proton to the serine oxygen atom. This again involves a prototropic change in the imidazole ring, one of the nitrogen atoms accepting a proton from the water molecule and the other donating its proton to the serine oxygen atom. This process is the reverse of that shown in Fig. 6 with R = H. The lower portions of Figs. 4 and 5 show the conclusions arrived at for the deacylation process.

The behavior of trypsin on the alkaline side can be explained along the following lines. The $—NH_3^+$ group of isoleucine-7 splits off its proton with a p*K* of 9.5, and when this occurs there is a movement (probably to a more polar environment) of the $—COO^-$ group of aspartic acid-182; this movement affects the position of the neighboring serine residue and diminishes the ease with which the acyl portion of the substrate can be removed from the serine by the action of the imidazole group. The fact that this ionization occurs at p*H* 9.5, rather than at a higher value as in the free enzyme, is possibly the result of slightly different relative spatial arrangements of the $—NH_3^+$ and the two $—COO^-$ groups in the acyl enzyme compared with the free enzyme; the two $—COO^-$ groups may be a little further away from the $—NH_3^+$ group in the acyl enzyme and so allow the proton to leave more readily.

The different behavior of chymotrypsin is perhaps also to be explained in terms of slight conformational changes during complex formation and acylation. It is suggested that in acyl chymotrypsin the $—COO^-$ group of aspartic acid-194 has been brought a little closer to the $—NH_3^+$ group of isoleucine-16 than in the free enzyme; this could have the effect of raising the p*K* from the value of ~ 9.0 in the free enzyme to a value of 10.5 in the acyl enzyme.

The differences in kinetic behavior on the alkaline side between trypsin and chymotrypsin suggest the possibility that during the catalytic process the trypsin molecule is subjected to a general loosening of its three-dimensional structure, while chymotrypsin undergoes a tightening in conformation. The X-ray results for trypsin should prove to be of great interest.

Can. J. Chem. Downloaded from www.nrcresearchpress.com by 210.87.254.42 on 09/05/12
For personal use only.

Can. J. Chem. Downloaded from www.nrcresearchpress.com by 210.87.254.42 on 09/05/12
For personal use only.

General Discussion

The preceding discussion has led to the conclusion that, in spite of some differences in kinetic behavior, the mechanisms of chymotrypsin and trypsin action appear to be the same. We propose that the substrates fit into the two enzymes in a similar manner, the carbonyl carbon atom of the substrate forming roughly an equilateral triangle with the imidazole nitrogen atom and the alcoholic hydrogen atom of the serine residue. The alcoholic oxygen atom of the substrate also forms roughly an equilateral triangle with these two atoms on the enzyme. Both enzymes exhibit very low specificity as far as the alcoholic function of ester substrates is concerned, and this group almost certainly remains outside the enzyme. For chymotrypsin the X-ray evidence (4) indicates that the aromatic side chain of the substrate fits into a cavity which lies to the lower right of the histidine–serine pair (cf. Fig. 1); it is presumably held there largely by hydrophobic bonding. In trypsin the positively-charged side chain of the substrate, or the corresponding grouping in the case of a non-cationic substrate, is held in a similar position, there being electrostatic attraction to the aspartate-177 residue of the enzyme in the case of the cationic substrates. We suggest that this anionic binding site on trypsin makes an important contribution to the stereospecificity.

For α-chymotrypsin catalysis there have been proposed many mechanisms involving the imidazole and serine hydroxyl groups (10). Some of these mechanisms contained features which were later found to be inconsistent with experimental evidence, notably (*a*) the existence of a large deuterium-isotope effect in the acylation and deacylation steps, (*b*) the absence of an observable intermediate in the deacylation process, (*c*) the presence of a single histidine group in the active center, and (*d*) the conformation-controlling role attributed to the *N*-terminal residue. Specific mechanisms involving aspartic acid or arginine residues in the catalytic process can now be eliminated in view of the additional information derived from the three-dimensional structure of α-chymotrypsin (1–4). Recently Wang and Parker (40) have published a most interesting treatment applicable to the chymotrypsin-catalyzed hydrolysis of peptides, amides, and anilides which involves a pre-transition state protonation of the substrate. Unfortunately this hypothesis does not seem to be valid for substituted anilides or ester substrates. The mechanism of trypsin and chymotrypsin catalysis suggested in this paper is the product of as much kinetic, chemical, and crystallographic information as has been found to date, and can serve as a working hypothesis for the future.

Conformational Changes

A variety of evidence leads to suggestions of conformational changes during the action of these enzymes, and will be referred to briefly. The X-ray studies on chymotrypsin (1) have shown that there is an ion-pair between aspartic acid-194 and isoleucine-16. It has been suggested (2) that, as the latter group ionizes, the former moves away into a more polar environment, and this, we believe, indirectly affects the kinetic behavior. The resultant conformational change probably accounts for the decrease in catalytic properties at alkaline p*H*. In support of this suggestion, Oppenheimer *et al.* (14) find that acetylation of the α-amino group of isoleucine-16 inactivates δ-chymotrypsin, while all other amino groups can be acetylated without loss of activity. Furthermore Karibian *et al.* (41) have recently shown that the change in activity and structure of acetyl-δ-chymotrypsin in the alkaline p*H* range is not correlated with the ionizations of titratable tyrosine residues.

It seems likely that the terminal isoleucine-7 in trypsin performs a similar function to isoleucine-16 in chymotrypsin; this implies the existence of an ion-pair bond between this residue and aspartic acid-182. Support for this is provided by the work of Scrimger and Hofmann (42) who report that the reaction of nitrous acid with the *N*-terminal isoleucine group of trypsin causes inactivation of the enzyme. In the preceding paper (7) it was shown that the p*H*-dependent change in the specific levorotation of trypsin at 365 mμ can be associated with a single group having an apparent p*K* of 9.4. It is reasonable to suggest that this is the p*K* of isoleucine-7; its ionization probably causes a conformational change in the enzyme, but this does not become apparent in the kinetics of complex formation with the non-specific substrate benzoyl-L-alanine methyl ester. In this connection it should be noted that Wang and Carpenter (27) report a p*K* of 10.4 for the free enzyme using benzoyl-L-argininamide; this ionization can probably also be related to the *N*-terminal isoleucine residue.

The p*K* of this group appears to be strongly affected by the degree of conformational stability

Can. J. Chem. Downloaded from www.nrcresearchpress.com by 210.87.254.42 on 09/05/12
For personal use only.

of the enzyme resulting from non-electrostatic, electrostatic, and even steric interactions between the substrate and various portions of the enzyme. Our results with diisopropylphosphoryl trypsin (7), showing that the specific rotation of the enzyme is p*H*-independent up to p*H* 10, are consistent with this suggestion.

The relatively high p*K* value of 9–10 observed for trypsin catalyses in alkaline solution has led previous investigators (32, 43) to suggest that this ionization relates to a tyrosine or lysine ε-amino group. Labouesse and Gervais (44) have recently shown, however, that at alkaline p*H* homogeneous *N*-ε-acetyltrypsin exhibits the same activity as native trypsin towards synthetic substrates. Furthermore, acetylation of the free tyrosines (4–5 out of 10) leads to an enzyme which, below p*H* 9, is even more active as an esterase than is native trypsin. As a result of the X-ray diffraction studies by Matthews *et al.* (1) on chymotrypsin, it is now likely that the existence of an ion-pair bond between isoleucine and aspartic acid contributes to the unusually high p*K* value of the isoleucine α-amino group in trypsin, compared to a p*K* of 8 or less in peptide terminal α-amino groups (45).

Acknowledgments

The authors are indebted to Dr. David M. Blow for his help and suggestions with regard to the structure of α-chymotrypsin. H. P. K. acknowledges the award of a studentship by the National Research Council of Canada.

1. B. W. Matthews, P. B. Sigler, R. Henderson, and D. M. Blow. Nature, **214**, 652 (1967).
2. P. B. Sigler, D. M. Blow, B. W. Matthews, and R. Henderson. J. Mol. Biol. **35**, 143 (1968).
3. D. M. Blow, J. J. Birktoft, and B. S. Hartley. Nature, **221**, 337 (1969).
4. D. M. Blow. Biochem. Conf. Protein Structure and Function. Ste. Marguerite, Quebec. March 2–7, 1969.
5. L. B. Smillie, A. Furka, N. Nagabhushan, K. J. Stevenson, and C. O. Parkes. Nature, **218**, 343 (1968).
6. H. Kaplan and K. J. Laidler. Can. J. Chem. **45**, 547 (1967).
7. H. P. Kasserra and K. J. Laidler. Can. J. Chem. Preceding paper.
8. J. A. Stewart, H. S. Lee, and J. E. Dobson. J. Amer. Chem. Soc. **85**, 1537 (1963).
9. J. A. Stewart and J. E. Dobson. Biochem. **4**, 1086 (1965).
10. L. Cunningham. *In* Comprehensive biochemistry. (*Editors* M. Florkin and E. H. Stotz), Vol. 16. Elsevier, Amsterdam. 1965. p. 85.
11. E. Shaw and S. Springhorn. Biochem. Biophys. Res. Commun. **27**, 391 (1967).
12. J. G. Beeley and H. Neurath. Biochem. **7**, 1239 (1968).
13. A. Himoe, P. C. Parks, and G. P. Hess. J. Biol. Chem. **242**, 919 (1967).
14. H. L. Oppenheimer, B. Labouesse, and G. P. Hess. J. Biol. Chem. **241**, 2720 (1966).
15. M. L. Bender and F. J. Kézdy. Ann. Rev. Biochem. **34**, 49 (1965).
16. M. L. Bender, M. J. Gibian, and D. J. Whelan. Proc. Natl. Acad. Sci. U.S. **56**, 833 (1966).
17. M. Mares-Guia, S. Shaw, and W. Cohen. J. Biol. Chem. **242**, 5777 (1967).
18. A. K. Balls and E. F. Jansen. *In* Advances in enzymology. (*Editor* F. F. Nord). Vol. 13. Interscience Publishers, New York. 1952. p. 32.
19. N. K. Schaffer, S. C. May, and W. H. Summerson. J. Biol. Chem. **206**, 201 (1954).
20. A. K. Balls and H. N. Wood. J. Biol. Chem. **219**, 245 (1956).
21. R. A. Oosterbaan, P. Kunst, J. Van Rotterdam, and J. A. Cohen. Biochim. Biophys. Acta, **27**, 556 (1958).
22. N. K. Schaffer, R. P. Lang, L. Simet, and R. W. Drisko. J. Biol. Chem. **230**, 185 (1958).
23. G. H. Dixon, D. L. Kauffman, and H. Neurath. J. Biol. Chem. **233**, 1373 (1958).
24. W. B. Lawson, M. D. Leafer, Jr., A. Tewes, and G. J. S. Rao. Z. Physiol. Chem. **349**, 251 (1968).
25. M. L. Bender, G. E. Clement, F. J. Kézdy, and H. d'A. Heck. J. Amer. Chem. Soc. **86**, 3680 (1964).
26. J. Chevallier and J. Yon. Biochim. Biophys. Acta, **112**, 116 (1966).
27. S.-S. Wang and F. H. Carpenter. J. Biol. Chem. **243**, 3702, (1968).
28. T. Inagami, S. S. York, and A. Patchornik. J. Amer. Chem. Soc. **87**, 126 (1965).
29. M. Eigen and G. G. Hammes. Advan. Enzymol. **25**, 1 (1963).
30. M. Eigen, G. G. Hammes, and K. J. Kustin. J. Amer. Chem. Soc. **82**, 3482 (1960).
31. C. J. Martin, J. Golubow, and A. E. Axelrod. J. Biol. Chem. **234**, 1718 (1959).
32. J.-J. Béchet. J. Chim. Phys. **61**, 584 (1964).
33. J.-J. Béchet. J. Chim. Phys. **62**, 1095 (1965).
34. P. Benmouyal and C. G. Trowbridge. J. Chim. Phys. **62**, 576 (1965).
35. H. Goldenberg and V. Goldenberg. Arch. Biochem. **29**, 154 (1950).
36. M. Castañeda-Agulló and L. M. del Castillo. J. Gen. Physiol. **44**, 19 (1960).
37. M. Castañeda-Agulló and L. M. del Castillo. Biochim. Biophys. Acta, **139**, 398 (1967).
38. M. L. Bender, G. E. Clement, C. R. Gunter, and F. J. Kézdy. J. Amer. Chem. Soc. **86**, 3697 (1964).
39. R. Mason and C. A. Ghiron. Biochim. Biophys. Acta, **51**, 377 (1961).
40. J. H. Wang and L. Parker. Proc. Natl. Acad. Sci. U.S. **58**, 2451 (1967).
41. D. Karibian, C. Laurent, J. Labouesse, and B. Labouesse. European J. Biochem. **5**, 260 (1968).
42. S. T. Scrimger and T. Hofmann. J. Biol. Chem. **242**, 2528 (1967).
43. Y. Inada, M. Kamata, A. Matsushima, and K. Shibata. Biochim. Biophys. Acta. **81**, 323 (1964).
44. J. Labouesse and M. Gervais. European J. Biochem. **2**, 215 (1967).
45. J. T. Edsall and J. Wyman. Biophysical chemistry. Vol. 1. Academic Press, Inc., New York. 1958. p. 470.

Mechanism of initiation in the thermal polymerization of styrene. Thermal decomposition of *cis*-3,6-diphenyl-3,4,5,6-tetrahydropyridazine[1,2,3]

KARL R. KOPECKY AND SYAMALARAO EVANI
Department of Chemistry, University of Alberta, Edmonton, Alberta

Received June 12, 1969

Thermal decomposition of *cis*-3,6-diphenyl-3,4,5,6-tetrahydropyridazine, **1**, ($k = 5.6 \times 10^{-4}$ s^{-1} at 79.5°) results in the formation of about 60% styrene, 27% *cis*- and 13% *trans*-1,2-diphenylcyclobutane. The relative product yields vary little over the temperature range 64–133°. This indicates that **1** decomposes exclusively to the 1,4-diphenyl-1,4-butadiyl diradical, **2**, and nitrogen. The diradical, **2**, cannot be trapped by styrene and **1** is not an initiator of styrene polymerization. Therefore, **2** is not the radical intermediate responsible for the thermal initiation of styrene polymerization.

Canadian Journal of Chemistry, 47, 4041 (1969)

Can. J. Chem. Downloaded from www.nrcresearchpress.com by 210.87.254.5 on 09/05/12
For personal use only.

The thermal decomposition of 3,6-diphenyl-3,4,5,6-tetrahydropyridazine, **1**, was studied a number of years ago (1). A possible initial decomposition product, the 1,4-diphenyl-1,4-butadiyl diradical, **2**, has a structure identical to the classical Flory diradical whose formation by "tail to tail" dimerization of styrene, eq. [1], had been held to be responsible for the initiation of the

[1] $$2\ \mathrm{CH(C_6H_5)=CH_2} \longrightarrow \mathrm{\dot{C}H(C_6H_5)CH_2CH(C_6H_5)\dot{}}$$

2

thermal polymerization of this monomer (2). The only nitrogen-free decomposition product from **1** which was identified was styrene, as the dibromide, in 7% yield. There was no evidence to indicate whether the diradical, **2**, was actually formed as an intermediate in the decomposition of **1** or whether there occurred a concerted decomposition reaction to give styrene and nitrogen directly. It was found that **1** was a poor initiator of styrene polymerization. Previous reports also indicated that diradicals generated by thermal decomposition of cyclic peroxides (3, 4), by photolysis of a cyclic disulfide (5), and by thermal decomposition of a cyclic azo compound (6) are poor polymerization initiators. These experimental results had been anticipated by kinetic considerations (7, 8).

For these and other (9) reasons it had come to be considered unlikely that the thermal polymerization of styrene is initiated by formation of **2**. However, the report (9–11) that 1,2-diphenylcyclobutane, among other dimers, could be isolated from the thermal polymerization of styrene in dilute solution or in the presence of inhibitors maintained the question of the formation of **2** from dimerization of styrene.

In the present study the decomposition of **1** has been reinvestigated in order to determine the mode and products of the reaction, and to measure more accurately the efficiency of **1** as an initiator of styrene polymerization.

Results

Preparation and Stereochemistry of 1

Attempted preparation of **1** according to the published procedure (1) resulted in the isolation in low yield of material which did evolve gas upon melting but which always melted over a broad temperature range. This material was shown by ultraviolet (u.v.) and nuclear magnetic resonance (n.m.r.) spectroscopy to consist of **1** contaminated with appreciable amounts of the corresponding hydrazone, 3,6-diphenyl-2,3,4,5-tetrahydropyridazine, **9**. In this procedure saponification of *cis*-1,2-dicarbethoxy-3,6-diphenylhexahydropyridazine, **4**, with potassium hydroxide in methanol is followed by dilution of the reaction mixture with water and then ether extraction of the resulting basic solution. Decarboxylation of the dipotassium salt, **5**, was assumed to take place after the aqueous dilution. In the present study it was found the decarboxylation was slow and incomplete even in only slightly alkaline solution. The azo compound, **1**, could be obtained in a high state of purity in 75% yield, based on **4**, if

[1]Presented at the 50th Annual Conference of the Chemical Institute of Canada, Toronto, Ontario, June, 1967. Abstracts, p. 29.

[2]Abstracted from a thesis submitted by S. Evani to the Faculty of Graduate Studies of the University of Alberta in partial fulfillment of the requirements for the Ph.D. Degree, 1967.

[3]The research for this paper was supported in part by the Defense Research Board of Canada, grant number 9530-51.

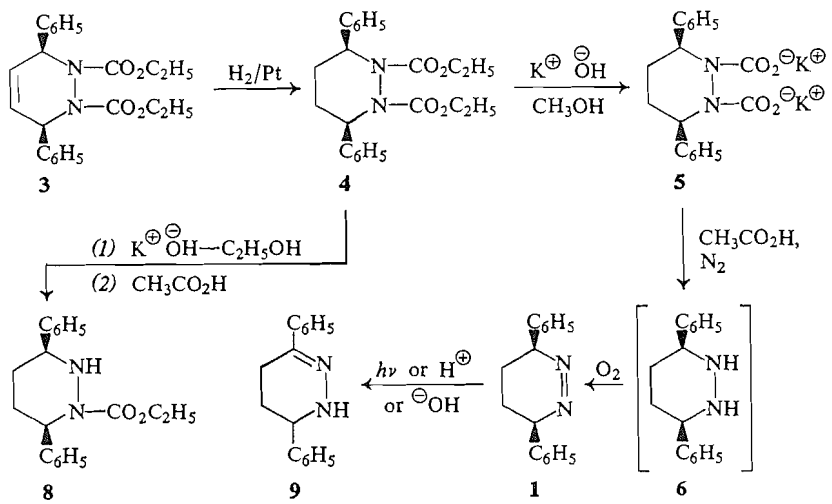

SCHEME 1

decarboxylation of **5** was carried out in acidic solution and all operations involving the hydrazine, *cis*-3,6-diphenylhexahydropyridazine, **6**, and its salts were carried out under nitrogen until **6** was oxidized by atmospheric oxygen in a dried ether solution free of inorganic acid or base (Scheme 1).

When a solution of **4** and potassium hydroxide in ethanol was heated under reflux for several hours, a water-soluble precipitate formed. This was shown to be mainly the half acid salt–half ester, **7**, by its conversion to the mono-ester, *cis*-3,6-diphenyl-1-carbethoxyhexahydropyridazine, **8**, in 53% overall yield upon addition of acid.

The presence of small amounts of acid resulted in the immediate isomerization of **1** to **9**. Attempts to take spectra of **1** even in purified carbon tetrachloride or chloroform resulted only in spectra corresponding to **9**. Stable solutions of **1** could be prepared in purified hydrocarbon solvents and in ether. The n.m.r. spectrum of **1** taken in benzene-d_6 confirms its structure and shows a complex multiplet centered at τ 3.2 for the phenyl protons, a multiplet centered at τ 7.2 for the benzylic protons, and a broad multiplet absorption from τ 8.9 to 9.8 for the methylene protons. The shifts given are relative to tetramethylsilane used as external standard. The stereochemistry of **1** cannot be determined with certainty from its n.m.r. spectrum, but can be deduced from the n.m.r. spectra of its precursors, **3** and **4**. It is now well established that **3** prepared by treatment of 1,4-diphenylbutadiene with diethyl azodicarboxylate has the *cis* configuration (12–17). Hydrogenation of **3** to **4** would not be expected to be accompanied by isomerization. That it was not, is shown by the n.m.r. spectrum of **4** taken in carbon tetrachloride which shows two broad one proton absorptions centered at τ 4.70 and at τ 5.16 for the benzylic protons. Only one signal would have been expected for these protons if **4** were the *trans* isomer. It is also unlikely that any isomerization occurred during saponification of **4** since **4** could be recovered unchanged after prolonged treatment with sodium ethoxide in boiling ethanol. It thus seems quite certain that **1** also has the *cis* configuration.

A number of attempts were made to prepare the corresponding *trans* azo compound, but these were unsuccessful.

Products from 1

The thermal decomposition of **1** was accompanied by only small amounts of isomerization to **9** if carried out in carefully cleaned apparatus and purified hydrocarbon solvents. In preliminary experiments the yield of nitrogen from the decomposition of **1** at 100° under these conditions was 90–100%. At lower temperatures somewhat less nitrogen was evolved. The presence of the hydrazone, **9**, could be detected in these reaction mixtures by u.v. spectroscopy. Control experiments showed that **9** did not rearrange or decompose under the experimental conditions used in this study.

Rates of decomposition of **1** were determined

Can. J. Chem. Downloaded from www.nrcresearchpress.com by 210.87.254.5 on 09/05/12
For personal use only.

Can. J. Chem. Downloaded from www.nrcresearchpress.com by 210.87.254.5 on 09/05/12
For personal use only.

by measuring the volume of nitrogen evolved as a function of time from solutions of **1** in ethylbenzene. The rate of decomposition of **1** at 79.5°, 5.6×10^{-4} s^{-1} (Table I) agrees well with the value of 6×10^{-4} s^{-1} at 80° estimated previously (1), but is about 10^2 as fast as that of the acyclic analogue, 1,1′-diphenylazoethane (18). A discussion of this difference is best deferred until data are available for the decomposition of the *trans* isomer of **1**.

TABLE I

Decomposition of **1** in ethylbenzene

Temperature, °C	$\%N_2$	$k^* \times 10^4$, s^{-1}
64.7	80	1.0
75.0	100	3.0
79.5	96	5.6

*At 79.5°, $\Delta H^* = 26.7$ kcal/mole, $\Delta S^* = 2.4$ eu.

Product analyses were made on a series of runs carried out with degassed solutions of **1** in benzene-d_6 in sealed n.m.r. tubes. The solutions were heated for 10 half-lives of decomposition and analyzed by n.m.r. spectroscopy and by gas chromatography (g.c.). Styrene and *cis*- and *trans*-1,2-diphenylcyclobutane, *cis*- and *trans*-**10**, were the only products detected by both methods. The presence of 10% hydrazone could have been detected in the n.m.r. spectrum. The composition of the products changes but little with temperature over the range 64–133°, Table II. In this range **1** decomposes to give 58–62% styrene, 25–29% *cis*-**10**, and 12–14% *trans*-**10**. The proportions of styrene and *trans*-**10** formed, increase somewhat with increasing temperature at the expense of *cis*-**10**. In each case the n.m.r. spectrum of the solution after decomposition of **1** was essentially superimposable upon that of a benzene-d_6 solution of styrene, *cis*- and *trans*-**10** present in the molar ratio 57.5:28.0:14.5 and in a concentration corresponding to 100% decomposition of **1**. The formation of diphenylcyclobutane in low yield from decomposition of **1** has previously been reported but the stereochemistry of the product was not determined (19).

Authentic samples of *cis*- and *trans*-**10** were prepared from 1,2-diphenylcyclobutene (20). Hydrogenation of this material gave *cis*-**10** which was isomerized to *trans*-**10** by potassium *t*-butoxide in dimethyl sulfoxide. The syntheses of *cis*- and *trans*-**10** by this route have since been reported (21). The properties of these compounds prepared in the present study agree with those reported except for the n.m.r. absorption of the phenyl protons of *cis*-**10**. These were reported to appear as a singlet whereas we find a multiplet similar to that reported for the absorptions of the phenyl protons of *cis*-1,2-diphenylcyclopropane (22).

A careful search was made for the presence of 1-phenyltetralin, **11**, among the products of decomposition of **1** but it could not be detected. Had **11** been formed in 0.1% yield it could have been found.

Attempts to decompose **1** photochemically resulted in the formation of only traces of styrene, *cis*- and *trans*-**10**. Irradiation of a benzene solution of **1** in Pyrex apparatus at 0° with light from a medium pressure mercury lamp gave the hydrazone, **9**, as the major product. Similar photoinduced rearrangements of azo compounds to hydrazones have been observed with 1-phenylazoalkanes (23).

1 as a Polymerization Initiator

The efficiency of **1** as an initiator in the polymerization of styrene was measured by determining the amount of diphenylcyclobutanes formed in the decomposition of **1** in pure styrene and by following the rate of polymerization of styrene containing **1**.

The yields of *cis*- and *trans*-**10** formed from decomposition of **1** at 98° in styrene and in an

TABLE II

Product distribution* from the thermal decomposition of **1** in benzene

				Styrene	*cis*-**10**
Temperature, °C	%Styrene	%*cis*-**10**	%*trans*-**10**	*cis*- + *trans*-**10**	*trans*-**10**
64	60.0, 57.9	28.6, 29.4	11.9, 12.8	1.42	2.35
78	60.4, 58.0	27.2, 28.7	12.4, 13.2	1.46	2.19
98	61.2, 58.9	26.5, 28.0	12.3, 13.1	1.50	2.15
133	62.2, 59.7	24.8, 26.3	13.1, 14.0	1.56	1.89

*Relative yields.

TABLE III

Product yields from decomposition of **1** in benzene and styrene at 98 °C

Solvent	**9**	%*cis*-**10**	%*trans*-**10**	Styrene
Benzene	9.8*	24.2†	12.9†	57.8†
		26.8‡	14.3‡	64.0‡
Styrene	20.3*	20.2†	10.5†	—
		25.4‡	13.2‡	—

*Percent yield as determined by u.v. analysis.
†Percent yield as determined by g.l.c. using chlorobenzene as internal standard.
‡Percent yield based on 1 not isomerized to 9.

TABLE IV

Rates of polymerization of styrene in the presence of **1** and ABN‡ at 70.0 °C

Added compound	Concentration $M \times 10^3$	k_d* $\times 10^4$ s^{-1}	$R_p \times 10^6$ $M^{-1}\ s^{-1}$	Kinetic chain length
None	—	—	4.70†	—
ABN‡	3.79	45.6§	102†	674‖
1	3.79	1.9¶	5.76**	8‖
				1.5††

*k_d = rate constant for decomposition.
†Reference 24.
‡2,2′-Azobis-(2-methylpropionitrile).
§Reference 25.
‖Molecules of styrene polymerized per molecule of initiator decomposed calculated using eq. [2].
¶Calculated from data in Table II.
**Average of two determinations: 5.66×10^{-6} and 5.86×10^{-6}.
††Contribution due to **1** only after correction for thermal rate.

additional run in benzene are shown in Table III. Undetectable amounts of *cis*- and *trans*-**10** were formed when pure styrene was heated at 98° in the absence of **1** for the same length of time. There appears to be an error in the analysis as the total yield of **9**, *cis*-**10**, *trans*-**10**, and styrene formed from decomposition of **1** in benzene in this run is 105.1%. Also, upon correction of the product yields for isomerization of **1** to **9**, the yield of styrene seems to be ca. 4% too high by comparison with the results from the runs given in Table II. The corrected yields of *cis*- and *trans*-**10** are more in line. It appears that the quantitative g.c. analysis for styrene was in error and that the u.v. analysis for **9** was correct. This means that the corrected yields for *cis*- and *trans*-**10** given in Table III must be near the actual values, and the amounts of *cis*- and *trans*-**10** formed in styrene are only slightly smaller than the amounts formed in benzene. Very little, if any, of the diradical, **2**, is trapped under these conditions.

The rate of polymerization of styrene at 70° in the presence of **1** was followed by the dilatometric method. The data in Table IV indicate that the rate of polymerization of styrene in the presence of **1** is about 20% greater than the thermal rate, whereas the 2,2′-azobis-(2-methyl-propionitrile), ABN, initiated rate was 22 times faster. The rate of polymerization in the presence of **1** was slower than that in the presence of ABN at the same concentration in spite of the faster rate of decomposition of **1**. That **1** is a poor initiator is also seen by a comparison of the apparent kinetic chain lengths in the two cases. These were calculated using the relationship in eq. [2] where R_p is the rate of

$$[2] \quad \text{kinetic chain length} = R_p/R_i = R_p/k_d I$$

polymerization, R_i is the rate of initiation, k_d is the rate of decomposition of the initiator, and I is its concentration. The kinetic chain length, **8**, determined in this way for polymerization in the presence of **1** must be corrected for the contribution which the thermal rate makes to the overall rate of polymerization. When this is done it is seen that only 1.5 molecules of styrene are polymerized for each molecule of **1** which decomposes. This shows **1** to be about 0.4% as efficient as ABN in initiating the polymerization of styrene. By either

Can. J. Chem. Downloaded from www.nrcresearchpress.com by 210.87.254.5 on 09/05/12
For personal use only.

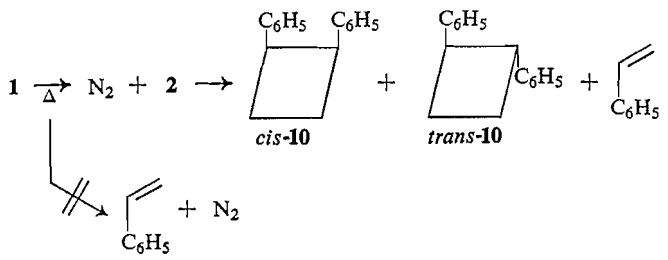

SCHEME 2

method of analysis it is seen that **1** is indeed a very inefficient initiator. This is in agreement with the earlier work (1) in which it was estimated from the increase in weight of polymer isolated from polymerization of styrene containing **1**, that about 8 molecules of styrene were polymerized per molecule of **1** decomposed at 80°.

Discussion

Decomposition of 1

There is good evidence that the thermal decomposition of symmetrical aliphatic azo compounds leads directly in a one step process to a pair of radicals in acyclic systems (18, 26), and to 1,3-diradicals in 5-membered ring systems (27, 28). But it does not follow that the 1,4-diradical, **2**, is formed from the thermal decomposition of **1**, for **1** has available to it a concerted, thermally allowed route (29) which leads directly to styrene and nitrogen. That **1** does not decompose exclusively by such a process is shown by the isolation of the 1,2-diphenylcyclobutanes, *cis*- and *trans*-**10**, in ca. 40% yield from the decomposition of **1**. In fact, although it is difficult to rule it out definitely, the concerted process does not appear to contribute to the thermal decomposition of **1** at all. The concerted route leading directly to styrene and the route leading to **2** would undoubtedly have different stereoelectronic requirements, and, therefore, probably different activation parameters. If both routes were operative this might result in a change in product distribution with temperature. In fact, there is a very small change in product distribution with temperature. This suggests that the products are formed exclusively from a common intermediate, the 1,4-diradical, **2**, via paths requiring small activation energies, Scheme 2.

Other 6-membered ring azo compounds also decompose to diradical intermediates, at least to a large extent, rather than by way of concerted processes (30, 31). These examples do not constitute violations of the Woodward–Hoffmann rules. It has already been pointed out (29) that these are not obligatory rules.

Reactions of the 1,4-Diradical, 2

The cyclization of **2**, obtained from **1**, is stereoselective and results predominantly in the formation of the thermodynamically less stable *cis*-**10** of retained configuration. This cyclization is less stereoselective than are the cyclizations of the diradicals obtained from both the thermal and photochemical decompositions of *meso*- and *dl*-3,6-diethyl-3,6-dimethyl-3,4,5,6-tetrahydropyridazine (31). The cyclobutanes obtained from these compounds are formed with virtual complete retention of configuration. Thus, while cyclization of **2** does compete well with internal rotation about the 1,2- and 3,4-carbon–carbon bonds of **2**, the competition is much less effective than is the case with either of the other diradicals. On the other hand the ratio of cleavage to cyclization of **2**, ca. 60:40, is only slightly greater than it is in the other systems, ca. 53:47. A meaningful evaluation of these differences must await information for the decomposition of the *trans* isomer of **1**.

In order for cyclization of **2** to compete effectively with internal rotation about the carbon–carbon bonds of **2** the rate constant for cyclization must be at least 10^{10} s^{-1} (32). This is equivalent to an intermolecular rate constant for the coupling of two monoradicals of at least 2×10^{10} M^{-1} s^{-1} (8) which corresponds well with the rate constant, 3×10^9, for the coupling of benzylic radicals (33) considering that the radical ends of **2** probably have no diffusive barrier to overcome. Such a rate is far too great for chain transfer with styrene or addition to styrene [for styrene at 60°, $k_{tr} \sim 10^{-2}$ (34) and $k_p \sim 10^2$ (35)] to compete with cyclization of **2**, unless, as has been pointed out (9), **2** is

Can. J. Chem. Downloaded from www.nrcresearchpress.com by 210.87.254.5 on 09/05/12
For personal use only.

Can. J. Chem. Downloaded from www.nrcresearchpress.com by 210.87.254.5 on 09/05/12
For personal use only.

very abnormally reactive compared to a polystyryl radical.

The results obtained from the decomposition of **1** in styrene provide further evidence on this point. Only 1.8 molecules of styrene are consumed for each diradical **2** produced, and little, if any, decrease in yield of *cis*- and *trans*-**10** is observed compared with yields from decompositions carried out in benzene. This indicates that most of the extra styrene consumed as a result of the presence of **1** is converted to high polymer. Assuming a molecular weight of ca. 10^6 for polystyrene produced at low conversions and under the conditions used (36), then only one of each 5000 to 10 000 of **2** produced will cause the formation of a molecule of high polymer. Approximately 40% of the diradicals produced cyclize. On this basis, if the diradical, **2**, were responsible for the initiation in the thermal polymerization of styrene, there should be roughly about 1/4 to 1/2 as much 1,2-diphenylcyclobutane formed, by weight, as of polystyrene in the thermal polymerization of pure styrene. This is not observed (9). The weight of dimers produced is only a small fraction of the weight of polymer formed. If some of the small amount of extra polymer formed in the presence of **1** is due to an impurity in **1** then the fraction of **2** diverted to polymer is even smaller than indicated. The present results provide direct experimental evidence for arguments made long ago (9) that **2** cannot be involved in the initiation of the thermal polymerization of styrene.

A recent report describes the study of the dimerization of styrene under a variety of conditions (37). The stereochemistry of the 1,2-diphenylcyclobutanes produced, varied considerably depending upon the experimental conditions. Thermal dimerization at 110° resulted in the formation of *cis*- and *trans*-**10** in a *cis*/*trans* ratio of 1/2. Thermal decomposition of **1** gives these materials with a *cis*/*trans* ratio of **2**. While the ratios are different the results are still compatible with the formulation in both cases that the 1,2-diphenylcyclobutanes are formed by way of the 1,4-diradical, **2**. Since in **2** cyclization competes with bond rotation, the stereochemistry of the products will be dependent upon the conformation of **2** when it is initially produced. The results suggest that **2** derived from **1** has a very different initial conformation from that of **2** obtained by thermal "tail to tail" dimerization of styrene, and it appears that both of these initial conformations are different from that of **2** formed by the photosenitized dimerization of styrene (37).

Experimental

Melting points and boiling points are uncorrected. Refractive indices were measured on a Bausch and Lomb Abbe-3L refractometer. Infrared spectra were recorded on a Beckman IR-7 recording spectrophotometer. The n.m.r. spectra were recorded on a Varian analytical spectrometer, Model A-60. Unless otherwise specified ca. 10% solutions in carbon tetrachloride containing tetramethylsilane as internal standard were used. Analyses by g.c. were carried out with an Aerograph-202 gas chromatograph using a 9.5 ft × 1.4 in. stainless steel column packed with 20% SF-96 on 60/80 Chromosorb P. Ultraviolet spectra were recorded on a Bausch and Lomb Spectronic 600 spectrophotometer. Elemental analyses were performed by Mrs. Darlene Mahlow.

cis-3,6-Diphenyl-1,2-dicarbethoxy-1,2,3,6-tetrahydropyridazine (3)

This material was prepared according to the method of Alder and Niklas (38) by the addition of diethyl azodicarboxylate to 1,4-diphenylbutadiene and had a m.p. 132–133°. Reported (38) m.p., 132°.

cis-3,6-Diphenyl-1,2-dicarbethoxyhexahydropyridazine (4)

The Diels–Alder adduct, **3**, was hydrogenated in ethanol using platinum oxide at 30 p.s.i. at room temperature. The syrupy liquid remaining after filtering the catalyst and removing the solvent was taken up in the minimum amount of methanol. Water was added until the solution just became turbid. The crystals which were deposited on allowing the solution to stand at 0° overnight were recrystallized in the same manner, m.p. 83–87°. Reported (38) m.p., 87°. Further recrystallization from methanol water did not improve the melting point. The n.m.r. spectrum ($CDCl_3$) showed absorption at τ 2.45–3.18 (multiplet with a strong, sharp absorption at τ 2.98, 9.96H) for the phenyl protons, at τ 4.60 (broad, 1/2 width = 17 c.p.s., 1.0H) and τ 5.03 (broad, 1/2 width = 10 c.p.s., 1.0H) for the benzylic protons, at τ 5.85 and 6.10 (a pair of overlapping quartets, J = 7.0 c.p.s., 4.0H) for the methylene protons of the carbethoxy groups, at τ 7.8–8.5 (broad multiplet, 4.0H) for the methylene protons of the ring and τ 8.76 (a pair of closely overlapping triplets, J = 7.0 c.p.s., 6.0H) for the protons of the methyl groups.

cis-3,6-Diphenyl-1-carbethoxyhexahydropyridazine (8)

A solution of 10 g (0.0254 mole) of **4** and 11.5 g (0.2 mole) of potassium hydroxide in 100 ml absolute ethanol was boiled under nitrogen for 6 h. A fine white precipitate had formed. The solvent was removed under vacuum and the remaining residue stirred in ether. The precipitate was filtered and dried, yield 11.0 g. The precipitate was taken up in water and the resulting solution acidified with acetic acid. There was effervescence and an oil separated which solidified on standing. The solid was taken up in ether, the ether solution dried over magnesium sulfate, and then pentane was added. On cooling 5.0 g (53%) of crystals were deposited, m.p. 59–60°.

Can. J. Chem. Downloaded from www.nrcresearchpress.com by 210.87.254.5 on 09/05/12
For personal use only.

The infrared spectrum (KBr) showed N—H absorption at 3420 cm^{-1} and absorption at 1695 cm^{-1} for the carboethoxy group.

The n.m.r. spectrum showed absorption at τ 2.9 (multiplet, 10.0H) for the phenyl protons, at τ 4.65 (broad, 1.0H) for the benzylic hydrogen at C-6, at τ 5.20 (broad, exchanges with D_2O, 0.95H) for the amine proton, at τ 5.85 (quartet, $J = 7$ c.p.s., 2.0H) for the methylene protons of the carbethoxy group, at τ 6.22 (broad multiplet, 1.0H) for the benzylic proton at C-3, at τ 7.6–8.1 (broad multiplet, 2.0H) and at τ 8.15–8.41 (broad multiplet 2.0H) for the methylene protons of the ring, and τ 8.74 (triplet, $J = 7.0$ c.p.s., 3.0H) for the protons of the methyl group.

Anal. Calcd. for $C_{19}H_{22}O_2N_2$: C, 73.52; H, 7.14; N, 9.03. Found: C, 73.66; H, 6.88; N, 8.98.

*cis-3,6-Diphenyl-3,4,5,6-tetrahydropyridazine (**1**)*

A solution of 3.75 g (0.095 mole) of **4** and 7.5 g (0.13 mole) of potassium hydroxide in 17.5 ml methanol was boiled for 4 h and then cooled. Twenty-five ml of water were added to the reaction mixture and the resulting solution was acidified under nitrogen with acetic acid. There was effervescence and an oil separated. The mixture was stirred for 30 min and was then made alkaline to phenolphthalein with aqueous potassium hydroxide. Potassium carbonate was added to this mixture until the aqueous layer became saturated. The resulting mixture was extracted with ether and the ether layer was dried over potassium carbonate. All these operations were carried out under nitrogen. After drying, the loosely stoppered ether solution was allowed to stand overnight. Long flat crystals were formed. Concentration of the mother liquor yielded further crystals, total yield 1.9 g, m.p. 109–112° with decomposition. Recrystallization from benzene–octane yielded 1.75 g (75%) of plates, m.p. 112–113° with gas evolution. Reported (1) decomp. at 110° with gas evolution.

This material's facile isomerization to the hydrazone, **9**, made characterization difficult. It was stable in redistilled hydrocarbon solvents and methanol when the glassware containing its solutions had been carefully neutralized. The n.m.r. spectrum has been given in the text. The u.v. spectrum showed maximum absorption at 285 mμ, log ε 2.45 and at 385 mμ, log ε 2.56. Reported (1) λ_{max} (cyclohexane) 287 mμ, log ε 3.49 and 387 mμ, log ε 2.89. Material prepared in this way contained less than 2% of the hydrazone, **9**, on the basis of its absorbance at 285 mμ.

*3,6-Diphenyl-2,3,4,5-tetrahydropyirdazine (**9**)*

A small quantity of **1** was dissolved in carbon tetrachloride and in a few minutes, fine, needle-shaped crystals formed, m.p. 157–158°, λ_{max} (methanol) 285 mμ, log ε 4.14. Reported (1) m.p. 157–159°, λ_{max} (chloroform) 292 mμ, log ε 4.19. Solutions of this material in ethylbenzene did not evolve any gas upon prolonged heating at 100°, and it could be recovered quantitatively.

*cis-1,2-Diphenylcyclobutene (*cis*-**10**)*

cis-1,2-Diphenylcyclobutene (20) (250 mg), m.p. 53–54°, reported (20) m.p. 53–54°, was hydrogenated at atmospheric pressure in methanol solution with 5% palladium on charcoal. The hydrogenation was interrupted after one mole had been consumed. The catalyst was filtered and the solvent removed to give an oil which solidified at 0°. This was recrystallized twice from methanol at −20° to yield 180 mg (72%) crystals, m.p. 37–38°. Reported (21) m.p. 38–39°. The n.m.r. spectrum showed absorption at τ 2.8–3.3 (multiplet centered at τ 3.10, 10.0H) for the phenyl protons, at τ 6.06 (broad multiplet, 2.02H) for the benzylic protons, and at τ 7.57 (multiplet, 4.0H) for the methylene protons).

*trans-1,2-Diphenylcyclobutane (*trans*-**10**)*

A solution of 45 mg of *cis*-**10** and 100 mg potassium *t*-butoxide in 5 ml anhydrous dimethyl sulfoxide was heated on a steam bath for 15 min. The reaction mixture was diluted with water and the resulting mixture extracted with 10 ml carbon tetrachloride. The organic layer was dried and the solvent removed. The residue was distilled in a microdistillation apparatus to give 37 mg of an oil. Analysis by g.c. showed that no starting material (*cis*-**10**) or 1,4-diphenylbutane were present in the product. The n.m.r. spectrum showed absorption at τ 2.90 (singlet, 10.0H) for the phenyl proton, at τ 6.51 (multiplet, 1.9H) for the benzylic protons and at τ 7.25 (multiplet, 4.0H) for the methylene protons, in excellent agreement with the reported (21) n.m.r. spectrum.

Product Studies

All operations and reactions involving **1** were carried out using glassware which had been cleaned with a mixture (3:1) of concentrated sulfuric acid and nitric acid, rinsed several times with distilled water, soaked for several hours with dilute ammonium hydroxide solution, and finally dried at 130°.

Benzene-d_6 solutions 0.033 *M* in **1** were placed in n.m.r. sample tubes and degassed with 3 freeze–thaw cycles to 10^{-3} mm. The tubes were sealed and then heated at the appropriate temperature for 10 half-lives of decomposition. The n.m.r. spectra of the solutions were then taken and were found to be superimposable upon the spectrum of a benzene-d_6 solution of styrene, *cis*-**10** and *trans*-**10** present in the molar ratio 57.5:28.0:14.5 and in a concentration corresponding to 100% decomposition of **1**. No absorption attributable to the hydrazone, **9**, could be detected. Quantitative relative product yields were determined by analyzing the contents of the tubes by g.l.c. using temperature programming from 100 to 180° at 4°/min and a helium flow rate of 60 ml/min. The only products detected were styrene, *cis*-**10**, and *trans*-**10**. These were identified by comparison of their relative retention times with authentic samples. No trace of 1-phenyltetralin could be found at the time where authentic material was eluted. The product distributions, corrected using molar response factors, are given in Table II.

Determinations of the absolute product yields from the decomposition of **1** in benzene and in styrene were made on runs carried out as described above. After decomposition was complete a measured amount of chlorobenzene was added to each tube, the contents mixed, and analyzed by g.c. as above. The relative thermal response factors used are chlorobenzene, 100; styrene, 96; *cis*-**10**, 153; *trans*-**10**, 163. Solvent was then completely removed from the samples at reduced pressure and the residue was taken up in methanol. The amount

of hydrazone, **9**, present was estimated by measuring the absorbance of the methanol solutions at 285 mμ. The results are presented in Table III.

Kinetics of Decomposition of ***1***

The rates of nitrogen evolution from solutions of **1**, ca. 0.1 *M* in ethylbenzene, were measured using an apparatus and a procedure similar to that described by Petersen *et al.* (39). At 64.7° insufficient nitrogen was evolved and plots of log $(V_\infty - V_t)$ showed curvature after one half life. Rate constants were determined from the slopes of plots of log $(V_\infty - V_t)$ vs. time. For runs at 64.7° initial slopes and the theoretical values for V_∞ were used. The results are summarized in Table I.

Polymerization of Styrene in the Presence of ***1***

The rate of polymerization of styrene in the presence of **1** was measured by the dilatometric method described in the accompanying paper (24). The results are given in Table IV.

Control Experiments

A sample of *cis*-**10**, together with some diphenylmethane as an internal standard, was heated at 140° in a degassed benzene solution for 18 h. Analysis by g.c. of the solution after heating showed no change had taken place. No trace of styrene or of *trans*-**10** could be detected.

A sample of the hydrazone, **9**, was heated in benzene solution at 98° for 39 min. Analysis by g.c. after heating showed the presence of no materials other than the starting compound. Another sample of **9** was heated at 80° in ethylbenzene solution for 24 h in the apparatus used for measuring nitrogen evolution. No nitrogen was evolved.

1. S. G. COHEN, S. HSIAO, E. SAKLAD, and C. H. WANG. J. Amer. Chem. Soc. **79**, 4400 (1957).
2. P. J. FLORY. J. Amer. Chem. Soc. **59**, 241 (1937).
3. B. BAYSAL. Commun. fac. sci. univ. Ankara. **4*B***, 57 (1953), quoted in B. BAYSAL. J. Polym. Sci. **33**, 381 (1958).
4. (*a*) W. HAHN and A. FISCHER. Makromol. Chem. **16**, 36 (1955). (*b*) W. HAHN and H. LECHTENBÖHMER. Makromol. Chem. **16**, 50 (1955). (*c*) W. HAHN and A. FISCHER. Makromol. Chem. **21**, 106 (1956).
5. K. E. RUSSELL and A. V. TOBOLSKY. J. Amer. Chem. Soc. **76**, 345 (1954).
6. C. G. OVERBERGER and M. LAPKIN. J. Amer. Chem. Soc. **77**, 4651 (1955).
7. R. N. HAWARD. Trans. Faraday Soc. **46**, 204 (1950).
8. B. H. ZIMM and J. K. BRAGG. J. Polym. Sci. **9**, 476 (1952).
9. F. R. MAYO. J. Amer. Chem. Soc. **75**, 6133 (1953).
10. F. R. MAYO. J. Amer. Chem. Soc. **90**, 1289 (1968).
11. I. S. BENGELSDORF. J. Org. Chem. **25**, 1468 (1960).
12. J. C. BRELIERE and J. M. LEHN. Chem. Commun. 426 (1965).
13. B. J. PRICE, R. V. SMALLMAN, and I. O. SUTHERLAND. Chem. Commun. 319 (1966).
14. R. DANIELS and K. A. ROSEMAN. Tetrahedron Lett. 1335 (1966).
15. B. H. KORSCH and N. V. RIGGS. Tetrahedron Lett. 5897 (1966).
16. B. PRICE, I. O. SUTHERLAND, and F. G. WILLIAMSON. Tetrahedron, **22**, 3477 (1966).
17. J. E. ANDERSON and J. M. LEHN. Tetrahedron, **24**, 137 (1968).
18. S. SELTZER. J. Amer. Chem. Soc. **83**, 2625 (1961).
19. R. YA. LEVINA, YU. S. SHABAROV, M. G. KUZ'MIN, N. I. VASIL'EV, and E. G. TRESCHCHOVA. Dokl. Akad. Nauk. SSSR, **121**, 303 (1958); Chem. Abstr. **53**, 13556 (1959).
20. M. A. BATTISTE and M. E. BURNS. Tetrahedron Lett. 523 (1966).
21. R. M. DODSON and A. ZIELSKE. J. Org. Chem. **32**, 28 (1967).
22. D. Y. CURTIN, H. GRUEN, Y. G. HENDRICKSON, and H. E. KNIPMEYER. J. Amer. Chem. Soc. **83**, 4838 (1961).
23. K. R. KOPECKY and T. GILLAN. Can. J. Chem. **47**, 2371 (1961).
24. K. R. KOPECKY and S. EVANI. Can. J. Chem. This issue.
25. M. TALÂT-ERBEN and S. BYWATER. J. Amer. Chem. Soc. **77**, 3712 (1955).
26. S. SELTZER and S. G. MYLONAKIS. J. Amer. Chem. Soc. **89**, 6584 (1967).
27. R. J. CRAWFORD and A. MISHRA. J. Amer. Chem. Soc. **88**, 3963 (1966).
28. R. J. CRAWFORD and G. L. ERICKSON. J. Amer. Chem. Soc. **89**, 3907 (1967).
29. R. HOFFMANN and R. B. WOODWARD. J. Amer. Chem. Soc. **87**, 2046 (1965).
30. W. R. ROTH and M. MARTIN. Tetrahedron Lett. 3865 (1967).
31. P. D. BARTLETT and N. A. PORTER. J. Amer. Chem. Soc. **90**, 5317 (1968).
32. J. E. LEFFLER and E. GRUNWALD. Rates and equilibria of organic reactions. John Wiley and Sons, Inc., New York. 1963. pp. 109–119.
33. R. D. BURKHART. J. Amer. Chem. Soc. **90**, 273 (1968).
34. F. R. MAYO, R. A. GREGG, and M. S. MATHESON. J. Amer. Chem. Soc. **73**, 1691 (1951).
35. M. S. MATHESON, E. E. AUER, E. B. BEVILACQUA, and E. J. HART. J. Amer. Chem. Soc. **73**, 1700 (1951).
36. K. F. MÜLLER. Makromol. Chem. **79**, 128 (1964).
37. W. G. BROWN. J. Amer. Chem. Soc. **90**, 1916 (1968).
38. K. ALDER and H. NIKLAS. Ann. Chem. **585**, 81 (1954).
39. R. C. PETERSEN, J. H. MARKGRAF, and S. D. ROSS. J. Amer. Chem. Soc. **83**, 3819 (1961).

Can. J. Chem. Downloaded from www.nrcresearchpress.com by 210.87.254.5 on 09/05/12
For personal use only.

Can. J. Chem. Downloaded from www.nrcresearchpress.com by 210.87.254.42 on 09/05/12
For personal use only.

Mechanism of initiation in the thermal polymerization of styrene. Kinetic deuterium isotope effects in the initiation step of the thermal polymerization of some deuterated styrenes[1,2,3]

KARL R. KOPECKY AND SYAMALARAO EVANI
Department of Chemistry, University of Alberta, Edmonton, Alberta

Received June 12, 1969

A convenient synthesis of 2,6-dideuteriostyrene starts with *N*,*N*-dimethyl-(1-phenylethyl)-amine which is deuterated in the 2 and 6 positions by a series of exchanges using *n*-butyllithium followed by deuterium oxide. The deuterium isotope effects at 70° on the rates of the thermal polymerization, $\frac{R_{PH}}{R_{PD}}$, of 2,6-dideuterio-, α-deuterio-, and β,β-dideuteriostyrene are 1.29, 1.00, and 0.78, respectively. The deuterium isotope effects at 70° on the 2,2′-azobis-(2-methylpropionitrile) initiated rates of polymerization, $\frac{R'_{PH}}{R'_{PD}}$, are 0.96, 0.86, and 0.81, respectively. From these values the deuterium isotope effects on the rates of initiation of the thermal polymerization, k_{IH}/k_{ID}, are calculated to be 1.80, 1.31, and 0.92, respectively. At 147° the presence of 1.5% potassium *t*-butoxide decreases the rate of the thermal polymerization of neat styrene by a factor of 17, and results in the formation of 1-phenyltetralin as the greatly predominant dimer. The results support the suggestion that the thermal polymerization of styrene is initiated by hydrogen transfer from 1-phenyl-1,2,3,9-tetrahydronaphthalene, formed by a concerted dimerization of two molecules of styrene, to a third molecule of styrene.

Canadian Journal of Chemistry, 47, 4049 (1969)

Introduction

It has been known for a long time that pure styrene undergoes spontaneous polymerization at rates which are highly reproducible (1). This thermal polymerization can be inhibited by radical scavengers (2). An early proposal (3) that the polymerization was initiated by the formation of the 1,4-diphenyl-1,4-butadiyl diradical, eq. [1],

[1] $$2\ \underset{\displaystyle C_6H_5}{\overset{|}{CH}}{=}CH_2 \longrightarrow \dot{C}HCH_2CH_2\underset{\displaystyle C_6H_5}{\overset{|}{\dot{C}H}}$$

followed by the addition of monomer units to the diradical, was shown to be untenable by kinetic arguments (4) from which it was concluded that long chain polymer could result only from monoradical initiation. Also, it was shown (5, 6) that 3,6-diphenyl-3,4,5,6-tetrahydropyridazine, which decomposes thermally to give the 1,4-diphenyl-1,4-butadiyl diradical (6), is a very inefficient initiator of styrene polymerization as are other diradical sources (7). The thermal initiation step must be a reaction which involves only styrene molecules and which produces monoradicals. Several routes for the formation of monoradicals have been proposed. It has been shown that the radical forming reaction is third order in styrene (8, 9). This, coupled with the isolation of 1-phenyltetralin from the thermal polymerization of styrene in the presence of inhibitors (8, 10) led to the suggestion that the polymerization is initiated by monoradicals which are produced as shown in eqs. [2] and [3].

[2] 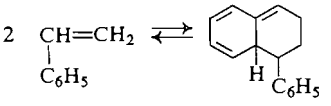

[3] 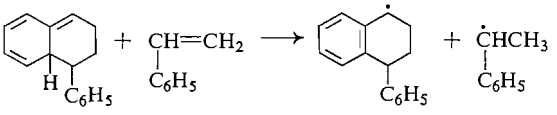

Another route for the formation of monoradicals which appears to be energetically feasible and consistent with the observed third order kinetics, provided that eq. [1] is reversible, is given by eq. [1] followed by eq. [4] (9). The reported lack of an isotope effect in the thermal

[4] $$\dot{C}HCH_2CH_2\underset{\displaystyle C_6H_5}{\overset{|}{\dot{C}H}} + \underset{\displaystyle C_6H_5}{\overset{|}{CH}}{=}CH_2 \rightarrow \dot{C}HCH_2CH{=}\underset{\displaystyle C_6H_5}{\overset{|}{CH}} + \dot{C}H\underset{\displaystyle C_6H_5}{\overset{|}{CH_3}}$$

---

[1]Presented at the 51st Annual Conference of the Chemical Institute of Canada, Vancouver, B.C., June, 1968. Abstracts, p. 97.

[2]Abstracted from a thesis submitted by S. Evani to the Faculty of Graduate Studies of the University of Alberta, Edmonton, Alberta, in partial fulfillment of the requirements for the Ph.D. degree, 1967.

[3]The research for this paper was supported in part by the Defense Research Board of Canada, grant Number 9530-51.

Can. J. Chem. Downloaded from www.nrcresearchpress.com by 210.87.254.42 on 09/05/12
For personal use only.

polymerization of β,β-dideuteriostyrene (11) was taken as evidence against this mode of formation of monoradicals.

A bimolecular process, eq. [5], for the formation of monoradicals has also been proposed (12),

[5] $$2\ \underset{\underset{C_6H_5}{|}}{CH{=}CH_2} \rightarrow \underset{\underset{C_6H_5}{|}}{\dot{C}{=}CH_2} + \underset{\underset{C_6H_5}{|}}{\dot{C}HCH_3}$$

but this proposal was made before the kinetic order of the initiation reaction had become clarified (9).

All three proposals have in common the feature that a carbon–hydrogen bond is broken in the rate-determining step leading to monoradicals. The hydrogen atoms involved in the various proposals are those in the side chain and in the 2 and 6 positions of the ring. Intuitively, it would appear that these are the most likely hydrogen atoms to be involved in transfer processes. The purpose of the present study was to determine whether monoradicals are in fact produced by a process in which a carbon–hydrogen bond is broken in the rate-determining step and, if so, to identify the position(s) from which the transfer occurs. For this purpose β,β-dideuteriostyrene, α-deuteriostyrene, and 2,6-dideuteriostyrene were prepared and the kinetic deuterium isotope effect in the initiation step of the thermal polymerization of each of these monomers was determined.

When the experimental work described in this study had been largely completed two reports appeared describing the rates of the thermal polymerization of several ring deuterated and side chain deuterated styrenes (13). It was shown in one study (13*a*) that deuteration of the 2 and 6 positions of styrene resulted in a significantly decreased rate of thermal polymerization and that deuteration in the side chain slightly increased this rate. Similar results were obtained in the other study (13*b*) in the case of the side chain deuterated styrenes, but in contrast, the rate of the thermal polymerization of ring-d_5-styrene was found to be greater than that of normal styrene. The magnitude of the isotope effect in the initiation step of these polymerizations was not determined.

The Kinetic Method

Assuming a third order initiation step for the thermal polymerization of styrene the overall rate of thermal polymerization, R_P, is given by eq. [6] (3) in which $[M]$ is the monomer concentration

[6] $$R_P = k_p[M]^{5/2}(k_i/k_t)^{1/2}$$

and k_p, k_t, and k_i are the specific rate constants for the propagation, termination, and thermal initiation reactions, respectively. The kinetic deuterium isotope effect for the thermal initiation reaction, k_{iH}/k_{iD}, which is the quantity to be determined in this study, is given by eq. [7]. The

[7] $$k_{iH}/k_{iD} = \left(\frac{R_{PH}}{R_{PD}}\right)^2\left(\frac{k_{pD}k_{tH}^{1/2}}{k_{pH}k_{tD}^{1/2}}\right)^2\left(\frac{[M_D]}{[M_H]}\right)^5$$

kinetic parameters for the normal and deuterated styrenes are indicated by the subscripts H and D, respectively. The value of the middle term in eq. [7] can be determined from the ratio of the rates of the initiated polymerization of the deuterated and normal monomers, R'_{PD}/R'_{PH}, measured with identical initiator concentrations. This ratio, obtained from eq. [8] (14), is given in eq. [9], where

[8] $$R'_P = k_p[M]([I]fk_d/k_t)^{1/2}$$

[9] $$R'_{PD}/R'_{PH} = \left(\frac{k_{pD}k_{tH}^{1/2}}{k_{pH}k_{tD}^{1/2}}\right)\frac{[M_D]}{[M_H]} \times \frac{(k_d f[I])^{1/2}(\text{in deuterated styrene})}{(k_d f[I])^{1/2}(\text{in normal styrene})}$$

k_d is the specific rate constant for the decomposition of initiator, f is the fraction of radicals formed from the initiator which initiate polymer chains, and $[I]$ is the concentration of initiator. Since the rate of decomposition, k_d, of 2,2′-azobis-(2-methylpropionitrile), the initiator used in this study, is independent of solvent in similar solvents (15) the rates of its decomposition in deuterated and normal styrene would surely be equal. The rate of addition of 2-cyano-2-propyl radicals to normal styrene will probably differ from that to deuterated styrene (at least in the cases of the side chain deuterated styrenes). However, at low concentrations of initiator ($\sim 10^{-3}$ M) all radicals formed from the initiator which escape from the solvent cage will eventually add to monomer (16). Thus, under these conditions, the efficiency of initiation, f, will also be the same in deuterated as in normal styrene. If the rates of the initiated polymerizations of normal and deuterated styrene are measured under identical conditions of temperature and initiator concentrations eq. [10] can be obtained from eq. [9]. Equation [11], which results by combining eq. [7] with eq. [10], is an expression for the deuterium isotope effect of the

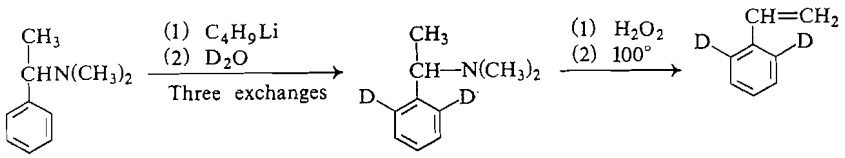

SCHEME 1

$$[10] \qquad \frac{k_{pD}k_{tH}^{1/2}}{k_{pH}k_{tD}^{1/2}} = \frac{[M_H]R'_{PD}}{[M_D]R'_{PH}}$$

$$[11] \qquad k_{iH}/k_{iD} = \left(\frac{R_{PH}R'_{PD}}{R_{PD}R'_{PH}}\right)^2\left(\frac{[M_D]}{[M_H]}\right)^3$$

initiation step of the thermal polymerization of styrene in terms of parameters which can be directly measured.

Deuteration will undoubtedly affect the rate of chain transfer, but this effect should be independent of any effect on the parameters in eq. [11].

Results

Preparation of Deuterated Styrenes

The side chain deuterated styrenes, α-deuteriostyrene and β,β-dideuteriostyrene, were prepared by pyrolysis of 1-deuterio-1-phenylethyl acetate and 1,1-dideuterio-2-phenylethyl acetate, respectively. Reduction of acetophenone and ethylphenylacetate by lithium aluminium deuteride provided the alcohols from which these esters were synthesized.

The preparation of 2,6-dideuteriostyrene, outlined in Scheme 1, is based upon the observation (17) that *N,N*-dimethylbenzylamine and related tertiary benzylic amines are readily metallated by *n*-butyllithium and that metallation occurs exclusively at the 2 position of the benzene ring. *N,N*-Dimethyl-(1-phenylethyl)-amine was treated in dry ether with *n*-butyllithium and deuterium oxide dispersed in benzene was added to the metallated amine. It was necessary to carry out the exchange three times in order to obtain product containing more than 90% dideuterioamine. Mass spectral analysis at low ionizing voltage (11 e.v.) shows that the product from the first exchange contains 5% undeuterated amine, 93% monodeuterio-, and 2% dideuterioamine, the product from the second exchange contains 2% undeuterated amine, 28% monodeuterio-, and 70% dideuterioamine, and the material from the third exchange consists of 0.6% undeuterated amine, 6.0% monodeuterio-, 91.4% dideuterio-, and 1.5% trideuterioamine. The nuclear magnetic resonance (n.m.r.) spectrum of the product of the third exchange shows that this material contains three aromatic protons. This shows, as was shown previously (17*a*), that essentially all the exchange took place in the benzene ring. The deuterium isotope effect for the metallation reaction is shown from these data to be 2.7.

The *N,N*-dimethyl-[1-(2,6-dideuteriophenyl)-ethyl]-amine obtained from the third exchange was converted to 2,6-dideuteriostyrene in 77% overall yield by conversion to and subsequent decomposition of its *N*-oxide (18). The mass spectrum taken at 12.5 e.v. shows that the product consists of 1.5% undeuterated styrene, 5% monodeuterio-, 92.7% dideuterio-, and 0.7% trideuteriostyrene. The n.m.r. spectrum of the product shows that it contains aromatic and vinyl protons in a 1:1 ratio, as required if the deuterium atoms are present in the benzene ring only. The aromatic protons of this material give a sharp singlet absorption peak in the n.m.r. spectrum, in contrast to those of normal and the other styrenes prepared which give a multiplet absorption peak.

Rates of Polymerization

The expression used to calculate the ratio, k_{iH}/k_{iD}, eq. [11], contains two terms of which the square of the product of four measured rates of polymerization will undoubtedly have the larger error. It is therefore necessary to measure these rates very accurately in order to keep the resulting uncertainty in k_{iH}/k_{iD} as small as possible. The rates of polymerization were followed by measuring the rate of decrease in the height of the meniscus of the degassed, pure monomer in a dilatometer of 6.7 ml capacity. This made possible the accurate measurement of rates with relatively small amounts of material per run and allowed recovery of unreacted monomer. In order to minimize errors further, all polymerization rates were measured using the same dilatometer. The rates of thermal polymerization were measured at 70° and were usually followed for about 12 h (ca. 2.5% polymerization). Runs for which plots

Can. J. Chem. Downloaded from www.nrcresearchpress.com by 210.87.254.42 on 09/05/12
For personal use only.

TABLE I

Rate of thermal polymerization of styrene at 70.0°

Styrene	Run	$R_P \times 10^6\ M^{-1}s^{-1}$	Average* $R_P \times 10^6\ M^{-1}s^{-1}$	$\frac{R_{PH}}{R_{PD}}$†	$\frac{k_{iH}}{k_{iD}}$†
Commercial	5	4.67			
	6	4.51			
	7	4.56			
	8	5.25‡			
	9	4.87			
	43	4.62			
	66	4.58	—	—	—
Synthetic§	10	4.79			
	11	4.79			
	12	4.68			
	13	4.53	—	—	—
Synthetic‖	57	4.79			
	59	4.68	—	—	—
Synthetic¶	32	4.62			
	33	4.84			
	49	4.51	4.67±0.10	—	—
α-d**	14	4.57			
	21	4.52			
	23	4.73			
	64	4.90	4.71±0.14	1.00±0.05	1.31±0.22
β,β-d_2††	60	5.97			
	61	5.98	5.98±0.05	0.78±0.04	0.92±0.22
2,6-d_2§§	51	3.63			
	52	3.67			
	53	3.54	3.61±0.05	1.29±0.06	1.80±0.31

*Errors are average errors.
†Errors were obtained by adding % errors of the factors.
‡Not included in the averaged rate.
§Synthetic styrene prepared by the synthetic sequence used for the preparation of α-deuteriostyrene.
‖Synthetic styrene prepared by the synthetic sequence used for the preparation of β,β-dideuteriostyrene.
¶Synthetic styrene prepared by the synthetic sequence used for the preparation of 2,6-dideuteriostyrene.
**This material consisted of 1.2% undeuterated styrene, 98.5% monodeuterio-, and 0.2% dideuteriostyrene.
††This material consisted of 1.1% undeuterated styrene, 1.6% of monodeuterio-, and 97.3% of dideuteriostyrene.
§§This material consisted of 1.6% undeuterated styrene, 5.0% of monodeuterio-, 92.7% of dideuterio-, and 0.7% of trideuteriostyrene.

of the height of the meniscus versus time were not linear throughout were discarded. The initiated polymerizations, using 2,2′-azobis-(2-methylpropionitrile) as initiator, were also carried out at 70°. Details of the apparatus and rate measurements are given in the Experimental section.

The rates of thermal polymerization, Table I, of the synthetic styrenes prepared by the routes used to synthesize the various deuterated styrenes all fall within the range of rates obtained for the thermal polymerization of commercial styrene and show that no extraneous material which affects the rate of polymerization of styrene was formed in the syntheses. These rates of thermal polymerization of synthetic styrene were also used to obtain the overall average rate of the thermal polymerization of normal styrene. The results of Table I also show that reproducibility was maintained throughout the period during which the rate measurements were made since runs 5, 43, and 66, for example, which were carried out near the beginning, near the middle, and near the end of this period, respectively, agree very well. These rates are in reasonable agreement with the rate previously measured at 70° for the thermal polymerization of styrene, $R_P = 5.56 \times 10^{-6}\ M^{-1}\ s^{-1}$ (1*d*).

The rates of the thermal polymerization of the deuterated styrenes are also listed in Table I, together with the deuterium isotope effects on the overall rate of thermal polymerization, $\frac{R_{PH}}{R_{PD}}$, and with the deuterium isotope effects in the initiation step of the thermal polymerization, k_{iH}/k_{iD}. The latter ratio was obtained by combining the rates of the thermal polymerizations with the rates of the initiated polymerizations, Table II, according

Can. J. Chem. Downloaded from www.nrcresearchpress.com by 210.87.254.42 on 09/05/12
For personal use only.

TABLE II

Rate of polymerization of styrene initiated by 3.79×10^{-3} M 2,2′-azobis-(2-methylpropionitrile) at 70.0°

Styrene	Run	$R'_P \times 10^4\ M^{-1}s^{-1}$	Average* $R'_P \times 10^4\ M^{-1}s^{-1}$	$\frac{R'_{PH}}{R'_{PD}}$†
Commercial	17	1.00		
	18	1.01		
	19	0.98		
	26	1.07		
	27	1.02	1.02±0.02	—
α-*d*	20	1.20		
	24	1.17		
	25	1.19		
	65	1.19	1.19±0.01	0.86±0.03
β,β-d_2	62	1.23		
	63	1.29	1.26±0.03	0.81±0.04
2,6-d_2	54	1.07		
	55	1.04	1.06±0.02	0.96±0.04

*Errors are average errors.
†Errors were obtained by adding % errors of the factors.

to eq. [11]. The effects of deuteration on the rate of contraction of the polymerizing solutions are shown in Fig. 1 for the thermal polymerizations and in Fig. 2 for the initiated polymerizations. The results of the present study are compared in Table III with the results of previous studies on the rates of the thermal and initiated polymerizations of several deuterated styrenes.

As was observed previously (13*a*) styrene deuterated in the 2 and 6 positions undergoes thermal polymerization at a significantly slower rate than does normal styrene but the rate of the initiated polymerization is the same as that of normal styrene. On the other hand, deuteration in the β-position of styrene results in an increase in the rates of both the thermal and the initiated polymerizations. Deuteration in the α-position has little effect on the rate of the thermal polymerization but results in an increase in the rate of initiated polymerization. This last observation contrasts somewhat with previous work (13). However, the discrepancies which do exist in the data listed in Table III are very slight. In fact, the agreement between the various studies can be said to be remarkably good.

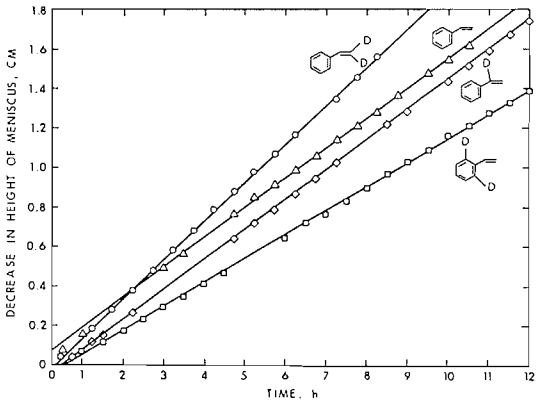

FIG. 1. Rate of contraction in the thermal polymerization of styrene and deuterated styrenes. △, run 9; ○, run 60; ◇, run 14; □, run 51.

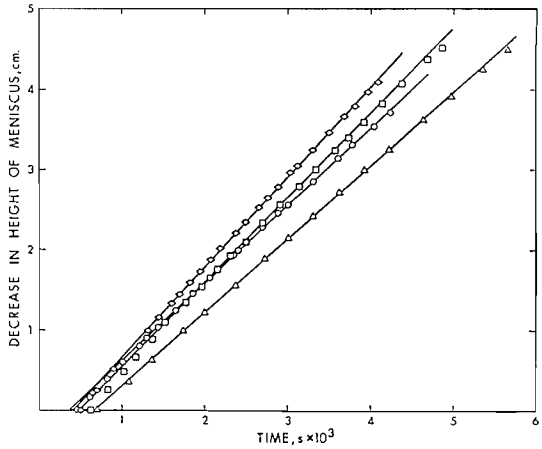

FIG. 2. Rate of contraction in the 2,2′-azobis-(2-methylpropionitrile) initiated polymerization of styrene and deuterated styrenes. □, α-deuteriostyrene, run 25; △, commercial styrene, run 17; ◇, β,β-dideuteriostyrene, run 62; ○, 2,6-dideuteriostyrene, run 54.

Can. J. Chem. Downloaded from www.nrcresearchpress.com by 210.87.254.42 on 09/05/12
For personal use only.

TABLE III

Collection of isotope effects on overall rates of polymerization of deuterated styrenes

Reference	$\frac{R_{PH}}{R_{PD}}$				$\frac{R'_{PH}}{R'_{PD}}$			
Temperature	This work	13*a*	13*b*	11	This work	13*a*	19	11
Styrene	70°	127°	60°	80°	70°	49.3°	60°	80°
α-*d*	1.00±0.05	0.88	0.84	—	0.86±0.03	0.90	0.91	—
β,β-d_2	0.78±0.04	0.88	0.59	1.0	0.81±0.04	0.86	0.88	1.0
2,6-d_2	1.29±0.06	—	—	—	0.96±0.04	—	—	—
2,4,6-d_3	—	1.35	—	—	—	1.0	—	—
4-*d*	—	1.0	—	—	—	1.0	—	—
2,3,4,5,6-d_5	—	—	0.56*	—	—	—	0.82	—

*This value is quite probably in error (W. A. Pryor, private communication).

Discussion

The Radical Forming Step in the Thermal Initiation

Theoretical estimates of the maximum value of the secondary deuterium isotope effect range as high as 1.5 (20) and 1.74 (21). The deuterium isotope effect in the initiation step of the thermal polymerization of 2,6-dideuteriostyrene is calculated to be 1.80 ± 0.31. Taking into account the error this value falls within the realm of the theoretical maximum values for the secondary deuterium isotope effect. However, the maximum values observed experimentally for the secondary deuterium isotope effect (22–24) all lie below 1.3. On this latter basis it seems very improbable that the value of 1.80 ± 0.31 is a secondary deuterium isotope effect, and it is therefore quite likely that in the thermal polymerization of styrene the initiating monoradicals are formed in a process in which the carbon–hydrogen bond at the 2 or at the 6 position is broken in the rate determining step. This gives strong support to the suggestion (8) that the thermal initiation proceeds by way of eq. [2] and [3] where the transfer of the hydrogen atom at C-9 of the trienic styrene dimer, eq. [3], is rate determining. The magnitude of this isotope effect is rather small, although not unusually so (25), and can be accommodated on theoretical grounds (26).

The "true" isotope effect in the hydrogen transfer step, eq. [3], is probably different from that calculated on the basis of eq. [11]. Equation [11] gives a composite isotope effect made up of an isotope effect in the pre-equilibrium step, eq. [2], in addition to the isotope effect in the hydrogen transfer step, eq. [3]. In the case of 2,6-dideuteriostyrene, one would normally expect an inverse secondary deuterium isotope effect in the forward reaction of eq. [2] and a normal secondary deuterium isotope effect in the back reaction of eq. [2] (27). Experimental data which would test these predictions is very scanty. Small inverse secondary deuterium isotope effects of about 6% have been found in Diels–Alder reactions (28) and a small normal secondary deuterium isotope effect of about 7% has been found in a retro-Diels–Alder reaction (29). In each of these cases deuterium atoms were attached to the carbon atoms of the dienes which were undergoing a change of hybridization as is the case in eq. [2]. If secondary deuterium isotope effects of similar magnitude were operating in the reactions of eq. [2] then the "true" isotope effect in the hydrogen transfer step would be about 2.0 ($k_{iH}/k_{iD} \times k_{2D}/k_{2H} \times k_{-2H}/k_{-2D}$, where k_2 and k_{-2} are the specific rate constants for the forward and back reactions, respectively, of eq. [2]). If the magnitude of the secondary deuterium isotope effects in the reactions of eq. [2] were larger, then the "true" isotope effect in the hydrogen transfer step would be greater still.

However, not only is the magnitude of secondary deuterium isotope effects in cycloaddition reactions uncertain, recent evidence even puts into doubt predictions as to whether the effects will be normal or inverse. A relatively large *normal* secondary deuterium isotope effect of 1.23 was observed in the cycloaddition reaction between α-deuteriostyrene and diphenylketene (30). Therefore, a decision as to how much and in which direction the "true" isotope effect in the hydrogen transfer step, eq. [3], will differ from

Can. J. Chem. Downloaded from www.nrcresearchpress.com by 210.87.254.42 on 09/05/12
For personal use only.

Can. J. Chem. Downloaded from www.nrcresearchpress.com by 210.87.254.42 on 09/05/12
For personal use only.

the value of 1.80, calculated on the basis of eq. [11], cannot now be made.

The effect of deuteration in the side chain of styrene on the rate of thermal initiation is also interesting. During the reactions involved in the initiation step, eqs. [2] and [3], the hybridization of the β-C—H bonds changes from sp^2 to sp^3 in all three of the styrene molecules involved. It is surprising that no significant secondary deuterium isotope effect results. A larger inverse secondary deuterium isotope effect might be expected (27, 31). At any rate the results indicate that the β-hydrogens are not involved in the radical forming process. Such a change in hybridization occurs in the α-C—H bond of only one of the three styrene molecules involved in the initiation steps, and a significant normal secondary isotope effect results. As pointed out above, the reactions are complex and it is difficult to rationalize these secondary deuterium isotope effects.

Further Support for the Trienic Intermediate

If the monoradicals which initiate the thermal polymerization of styrene are formed by eqs. [2] and [3], it might be possible to convert the reversibly formed trienic dimer to 1-phenyltetralin with a strong base, such as potassium *t*-butoxide, eq. [12], and thereby reduce the rate of the thermal polymerization. Such an experiment has already been carried out (32). Stabilized styrene containing 1.5% potassium *t*-butoxide was heated under reflux for 24 h. Styrene was recovered in 46% yield and 5.5% of 1-phenyltetralin was isolated. We have repeated this experiment, primarily to determine whether any 1,2-diphenylcyclobutane (6) was present in the dimeric product, using styrene freed from stabilizer. Again, considerable, 55%, styrene was recovered and 1-phenyltetralin was obtained in 5% yield. Only trace amounts, less than 0.01%, of *cis*- and *trans*-1,2-diphenylcyclobutane, in about a 1:3 ratio, were formed.

[12] 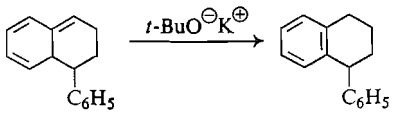

No more than 40% of the styrene polymerized in the presence of base under these conditions. This corresponds to a rate of polymerization of less than 1.7% per hour. At 127° pure styrene polymerizes at a rate of 14% per hour (33), and at the reflux temperature (~ 140°) this rate would be at least 30% per hour (1*c*). The presence of 1.5% potassium *t*-butoxide reduces the thermal rate of polymerization by a factor of at least 17. It is unlikely that *t*-butoxide would terminate a growing polymer radical once it was formed. An attractive mode for the retardation is that *t*-butoxide diverts an intermediate responsible for the formation of radicals, namely, the triene as shown in eq. [12].

Formation of the Triene

It now appears certain that the 1,4-diphenyl-1,4-butadiyl diradical, eq. [1], is not directly involved in the initiation of the thermal polymerization of styrene. It may, however, be indirectly involved, affording a route to the triene, eq. [13] (34). The thermal formation of diphenylcyclobutane from styrene has been reported a number of times (8, 10, 34, 35). This is unlikely to be a concerted reaction (36) and may be taken as evidence for the intermediate formation of the diradical.[4] It has been shown that the diradical, when formed from the corresponding cyclic azo compound, does give diphenylcyclobutane in appreciable yield (6). The conformation which would be required for the diradical in order for it to close to form the triene must be similar to that required in order for it to form the diphenylcyclobutane. This makes it unlikely that the diradical would be formed in a conformation which could form the triene without also forming a considerable amount of diphenylcyclobutane. Since a great majority of the triene molecules, once formed, must revert to styrene (8, 9), it follows that a considerable fraction, at least, of the dimeric material formed during the thermal polymerization of styrene would have to be diphenylcyclobutane if the triene were formed by

[13] [14] 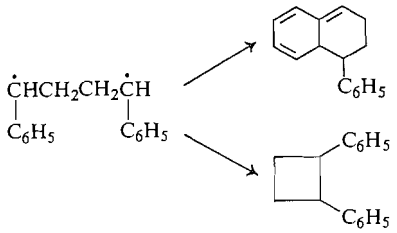

[4]There is good evidence that diradicals are intermediates in a number of other thermal cycloaddition reactions (37).

Can. J. Chem. Downloaded from www.nrcresearchpress.com by 210.87.254.42 on 09/05/12
For personal use only.

way of the diradical, eq. [13]. This is not observed (8, 10, 34, 35). Even in neat styrene, where a minimum amount of the triene would be diverted by extraneous materials (8, 34) to 1-phenyltetralin, resulting in the most favorable diphenylcyclobutane:1-phenyltetralin ratio, this ratio is only about 1:5[5] (35). This supports the original suggestion (8, 10) that the triene and the diphenylcyclobutane are formed by different reactions, eqs. [13] and [14], respectively. A reasonable route to the triene is the thermally allowed Diels–Alder reaction between two styrene molecules.

Experimental

Boiling points and melting points are uncorrected. Refractive indices were measured on a Bausch and Lomb Abbe-3L Refractometer. Infrared spectra (i.r.) were recorded on a Beckman IR-7 Recording Spectrophotometer. The n.m.r. spectra were obtained with a Varian Analytical Spectrophotometer, Model A-60. Ca. 10% v/v solutions in carbon tetrachloride were used. Tetramethylsilane was used as the internal standard. Mass spectra were obtained with an A.E.I. MS-2-H mass spectrometer. Gas chromatography (g.c.) was carried out on an Aerograph-202 Gas Chromatograph. A 5 ft × 1/4 in. column packed with 20% SF-96 on 60/80 Chromosorb P was used.

Materials

Commercial styrene was shaken 3 times with cold 10% sodium hydroxide solution, with saturated aqueous sodium chloride until free from alkali, dried over magnesium sulfate, and then distilled. A middle cut was collected, b.p. 44–45° (20 mm), n_D^{27} 1.5435.

Commercial 2,2′-azobis-(2-methylpropionitrile) was recrystallized twice from acetone–Skelly B and stored in the dark over phosphorous pentoxide, m.p. 101–102° (decomposition).

α-Deuteriostyrene

The alcohol, 1-deuterio-1-phenylethanol, was prepared by the reduction of acetophenone with lithium aluminium deuteride (38) b.p. 63–65° (6 mm), n_D^{29} 1.5230; reported (38) b.p. 79° (23 mm), n_D^{24} 1.5267. This material was acetylated (39) to give 86% of 1-deuterio-1-phenylethyl acetate, b.p. 91–92° (8 mm). This acetate (57 g) was pyrolyzed (40) at 400° to α-deuteriostyrene (27 g, 77%), b.p. 55° (28 mm), n_D^{27} 1.5425; reported (38) b.p. 76° (82 mm), n_D^{24} 1.5435. The n.m.r. spectrum agrees very well with that reported (41) for this material and shows no extraneous peaks. Mass spectral analysis (42) using an ionizing voltage of 11 e.v. shows that the product consists of 1.2% undeuterated styrene, 98.5% monodeuterio-, and 0.2% dideuteriostyrene. It was stored in degassed, sealed ampoules at −20°.

β,β-Dideuteriostyrene

Ethyl phenylacetate (49.2 g) was reduced with a slight excess of lithium aluminium deuteride to 1,1-dideuterio-2-phenylethanol (33.5 g, 90%), b.p. 103° (12 mm), n_D^{29} 1.5279; reported (11) b.p. 91–93° (8 mm), n_D^{25} 1.5269. This product was acetylated (39) in 94% yield to 1,1-dideuterio-2-phenylethyl acetate, b.p. 93° (7 mm), n_D^{29} 1.4962; reported (11) b.p. 122–123° (26 mm). Pyrolysis (40, 11) of this acetate (36 g) gave β,β-dideuteriostyrene (11.3 g, 50%), b.p. 53–54° (30 mm), n_D^{25} 1.5438; reported (11) b.p. 54° (31 mm). Mass spectral analysis (42) using an ionizing voltage of 11.5 e.v. shows that the product consists of 1.1% undeuterated styrene, 1.6% of monodeuterio-, and 97.3% of dideuteriostyrene.

N,N-Dimethyl-[1-(2-deuteriophenyl)-ethyl]-amine

This procedure is a slight modification of that used for the deuteration of *N,N*-dimethylbenzylamine (17*a*).

N,N-Dimethyl-(1-phenylethyl)-amine (43) b.p. 84° (20 mm), n_D^{29} 1.4980; reported (43) b.p. 71° (11 mm), n_D^{25} 1.5000, 44.7 g (0.3 mole) in 40 ml anhydrous ether was treated with a 1.6 *M* solution of *n*-butyllithium in hexane, 360 ml (0.6 mole). The resulting solution was stirred for 36 h and then added to a suspension of 48 ml deuterium oxide in 250 ml dry benzene. The resulting mixture was stirred for 6 h and then allowed to settle. The clear top layer was decanted from the white sludge and the sludge washed 3 times with 50 ml ether. The combined organic solutions were dried over sodium sulfate, concentrated, and the residual oil distilled to give 42.3 g (94%) of a colorless liquid, b.p. 73° (13 mm), n_D^{29} 1.4986. The i.r. spectrum (neat) of the product shows a strong absorption band at 2270 cm^{-1}. The n.m.r. spectrum shows absorption at τ 2.82 (singlet 4.03H) for the phenyl protons, at τ 6.86 (quartet, J = 7 Hz, 1.03H), for the methine proton, at τ 7.87 (singlet, 5.93H) for the protons of the *N*-methyl groups and at τ 8.71 (doublet, J = 7 Hz, 2.9H) for the protons of the 1-methyl group. Mass spectral analysis (42) using an ionizing voltage of 11 e.v. shows that the product consists of 5% undeuterated amine, 93% monodeuterio-, and 2% dideuterioamine.

N,N-Dimethyl-[1-(2,6-dideuteriophenyl)-ethyl]-amine

Repetition of the exchange reaction described above using 40 g of the monodeuterated amine gave 37.5 g (94%) of product. Mass spectral analysis using an ionizing voltage of 11 e.v. indicates that this product consisted of 2% undeuterated amine, 28% monodeuterio-, and 70% dideuterioamine. This material was again subjected to the exchange reactions from which 34 g (92.5%) of product was obtained, b.p. 97° (50 mm), n_D^{29} 1.4975. The n.m.r. spectrum of this product shows absorption in exactly the same places as does that of the monodeuterioamine, above, but the ratio of the areas for these absorptions is now 2.98:1.0:6.0:3.1. Mass spectral analysis (42) using an ionizing voltage of 11 e.v. shows that the product consists of 0.6% undeuterated amine, 6.0% of monodeuterio-, 91.4% of dideuterio-, and 1.5% of trideuterioamine.

2,6-Dideuteriostyrene

The above dideuterioamine (30 g) was converted (18) to the amine oxide which was, in turn, decomposed at 100° (18) to give 16.3 g (76.8%) of the styrene, b.p. 63° (48 mm), n_D^{27} 1.5419. The n.m.r. spectrum shows that the ratio of the aromatic to the vinyl protons is 1.0:1.0.

[5]Diphenylcyclobutane is thermally stable at the temperature used in this experiment (6).

TABLE IV

Density, molarity, and C for some styrenes at 70°

Styrene	D, g/cc	$[M]$, moles/l	$C = \frac{2[M]\,AD\,\mathrm{d}X}{100\,\mathrm{d}D}$
Normal	0.860	8.26	0.728
α-d	0.866	8.23	0.730
β,β-d_2	0.871	8.20	0.732
2,6-d_2	0.872	8.21	0.733

The aromatic protons in this compound appear as a sharp singlet in the n.m.r. spectrum. Mass spectral analysis (42) using an ionizing voltage of 12.5 e.v. shows that the product consists of 1.6% undeuterated styrene, 5.0% monodeuterio-, 92.7% dideuterio-, and 0.7% trideuteriostyrene. The product was stored in degassed, sealed ampoules at −20°.

Polymerization Rate Measurements

The rates of polymerization were determined by measuring the rate of decrease in the height of the meniscus of the monomer in the capillary of a dilatometer. The dilatometer had capillaries 15 cm long made of precision bore tubing 1.0 mm in diameter and was similar in design to one described by Bartlett (44) except that the monomer reservoir was on the same side as the volume cell. The volume of the dilatometer, up to an arbitrary mark in the capillary, was 6.748 ml.

The procedure used for the measurement of the thermal rates of polymerization is as follows. Monomer was introduced into a storage reservoir on a high-vacuum line and degassed to 10^{-4} mm with 4 freeze-thaw cycles. From this reservoir the monomer was distilled into the reservoir of the dilatometer which had been sealed to the vacuum line.[6] The monomer was again degassed to 10^{-4} mm with two more freeze-thaw cycles. The dilatometer was then sealed off and tilted to allow the monomer to flow into the volume cell. The volume cell was filled to a mark chosen such that when the dilatometer was heated to 70° the meniscus would be near the arbitrary mark near the top of the capillary. The dilatometer was then completely immersed in a constant temperature bath which was maintained at 69.96 ± 0.02° throughout with the aid of two high-speed stirrers. The height of the meniscus in the capillary was measured with a precision cathetometer. Readings were taken at about 1/2 h intervals for about 12 h except for the runs using β,β-dideuteriostyrene, which were terminated after 8 h. After 12 h the rates of contraction of the solutions began to decrease noticeably. After completion of a run using a deuterated styrene the unreacted monomer was distilled and stored in degassed, sealed ampoules at −20°. After each run the dilatometer was drained, filled with distilled benzene, and placed in a warm bath for 1/2 h. This was repeated twice more. It was then rinsed 4 times with distilled acetone, several times with distilled water, and dried at 110°. After every second run the dilatometer was, after the above rinsings, filled with a warm 3:1 concentrated sulfuric acid:concentrated nitric acid solution, allowed to stand 1/2 h, drained, rinsed several times with water, and filled with dilute ammonium hydroxide solution. After standing for 2 h the dilatometer was drained, rinsed several times with water, and dried.

The procedure used in the case of the initiated runs was as follows: A weighed amount of the initiator, 2,2′-azobis-(2-methylpropionitrile), was added to a weighed amount of freshly distilled monomer. This solution was transferred into the dilatometer reservoir and degassed to 10^{-4} mm pressure with 4 freeze-thaw cycles. The solution was protected from the light. The remainder of the procedure is the same as that described for the thermal rates except that during the rate runs readings were taken about every 300 s for about 1.5 h.

The rate of polymerization, R_P, was calculated from the expression $R_P = \frac{C\,\mathrm{d}h}{V\,\mathrm{d}t}$ where C is a constant for each monomer and equal to $\frac{2[M]AD\,\mathrm{d}X}{100\,\mathrm{d}D}$. V is the volume of the polymerizing solution, $[M]$ is the monomer concentration, t is the time, h is the height of the meniscus in the capillary, A is the cross-sectional area of the capillary, X is the mole percent of polymer in the solution, and D is the density of the solution. A linear relationship exists between the density and the mole percent polymer for dilute solutions of polystyrene in styrene and $\mathrm{d}X/\mathrm{d}D$ at 70° has the numerical value 682 (1d). The same value of $\mathrm{d}X/\mathrm{d}D$ was used for the deuterated styrenes. The densities of the deuterated styrenes were measured with the dilatometer. The dilatometer, containing a known volume at 70° of the deuterated styrene, was carefully cleaned and weighed after a thermal kinetic run. The seal was broken carefully, the dilatometer drained, cleaned, dried, and weighed together with the broken seal. Table IV lists the values of the density, molarity, and the constant C determined for each of the monomers.

Potassium t-Butoxide Inhibited Polymerization of Styrene

A solution of 7.4 g of the potassium t-butoxide–t-butyl alcohol complex (32) in 208 g styrene was heated under reflux (140°) under an atmosphere of nitrogen for 24 h. The unreacted styrene, which was flash distilled under vacuum, weighed 119 g (55%). The thick residue was dissolved in benzene and the polymer precipitated from the resulting solution with methanol. The clear solvent was drained from the precipitated polymer which was then kneaded with several fresh portions of methanol. The combined solutions were concentrated to an oil which was then diluted with ether. The solid which

[6]Highly erratic rates were obtained if the dilatometer was attached to the vacuum line with a greased ground glass joint.

Can. J. Chem. Downloaded from www.nrcresearchpress.com by 210.87.254.42 on 09/05/12
For personal use only.

precipitated was filtered and the filtrate was concentrated. The residual oil was distilled to give 10.5 g of product, b.p. 154–163° (8 mm). This was shown by g.c. to consist of 96% 1-phenyltetralin, traces (less than 0.1%) of *cis*- and *trans*-1,2-diphenylcyclobutane, in about a 1:3 ratio, and about 4% of several other unidentified materials which were eluted both before and after 1-phenyltetralin. Under the g.c. conditions used, column temperature 220°, gas flow 80 ml/min, the elution times for authentic *cis*- and *trans*-1,2-diphenylcyclobutane (6) and 1-phenyltetralin were 13.4 min, 15.2 min, and 16.6 min, respectively. The i.r. and n.m.r. spectra of the product were superimposable with those of authentic (32) 1-phenyltetralin. The *cis*- and *trans*-1,2-diphenylcyclobutanes were identified solely on the basis of their retention times.

Acknowledgment

We wish to thank Professor W. A. Pyror for some helpful comments.

1. (*a*) H. Dostal and W. Jorde. Z. Phys. Chem. **179**A, 23 (1937); (*b*) H. Suess, K. Pilch, and H. Rudorfer. Z. Phys. Chem. **179**A, 361 (1937); (*c*) G. V. Schulz and E. Huseman. Z. Phys. Chem. **36**B, 184 (1937); (*d*) G. Goldfinger and K. Lauterbach. J. Polym. Sci. **3**, 145 (1948); (*e*) C. Walling, E. R. Briggs, and F. R. Mayo. J. Amer. Chem. Soc. **68**, 1145 (1946).
2. S. G. Foord. J. Chem. Soc. 48 (1940).
3. P. J. Flory. J. Amer. Chem. Soc. **59**, 241 (1937).
4. (*a*) R. N. Haward. Trans. Faraday Soc. **46**, 204 (1950); (*b*) B. H. Zimm and J. K. Bragg. J. Poly. Sci. **9**, 476 (1952).
5. S. G. Cohen, S. Hsiao, E. Saklad, and C. H. Wang. J. Amer. Chem. Soc. **79**, 4400 (1957).
6. K. R. Kopecky and S. Evani. Can. J. Chem. This issue.
7. (*a*) W. Hahn and A. Fischer. Makromol. Chem. **16**, 36 (1955); (*b*) W. Hahn and H. Lechtenbohmer. Makromol. Chem. **16**, 50 (1955); (*c*) W. Hahn and A. Fischer. Makromol. Chem. **21**, 106 (1956); (*d*) K. E. Russell and A. V. Tobolsky. J. Amer. Chem. Soc. **76**, 345 (1950); (*e*) C. G. Overberger and M. Lapkin. J. Amer. Chem. Soc. **77**, 4651 (1955).
8. F. R. Mayo. J. Amer. Chem. Soc. **75**, 6133 (1953).
9. R. R. Hiatt and P. D. Bartlett. J. Amer. Chem. Soc. **81**, 1149 (1959).
10. F. R. Mayo. J. Amer. Chem. Soc. **90**, 1289 (1968).
11. G. S. Hammond and K. R. Kopecky. J. Polym. Sci. **60**, S54 (1962).
12. C. Walling. Free radicals in solution. John Wiley and Sons, Inc., New York. 1967. p. 183.
13. (*a*) R. Kirchner. Makromol. Chem. **96**, 179 (1966); (*b*) W. A. Pryor, R. Henderson, N. Carroll, and E. Ciuffarin. Abstracts of papers presented at the 150th national meeting of the American Chemical Society, Atlantic City, N.J., September, 1965, p. 7S.
14. P. J. Flory. Principles of polymer chemistry. Cornell University Press, Ithaca, New York. 1953. p. 113.
15. (*a*) F. M. Lewis and M. S. Matheson. J. Amer. Chem. Soc. **71**, 749 (1949); (*b*) C. G. Overberger, M. T. O'Shaughnessy, and H. Shalit. J. Amer. Chem. Soc. **71**, 2661 (1949); (*c*) R. C. Petersen, J. H. Markgraf, and S. D. Ross. J. Amer. Chem. Soc. **83**, 3819 (1961).
16. T. Manabe, T. Utsumi, and S. Okamura. J. Polym. Sci. **58**, 121 (1962).
17. (*a*) F. N. Jones and C. R. Hauser. J. Org. Chem. **28**, 663 (1963); (*b*) F. N. Jones and C. R. Hauser. J. Org. Chem. **28**, 3461 (1963); (*c*) R. L. Gay, T. F. Crimmins, and C. R. Hauser. Chem. Ind. 1635 (1966).
18. A. C. Cope, T. T. Foster, and P. H. Towle. J. Amer. Chem. Soc. **71**, 3929 (1949).
19. W. A. Pryor, R. Henderson, R. A. Patsiga, and N. Carroll. J. Amer. Chem. Soc. **88**, 1199 (1966).
20. (*a*) M. Wolfsberg and M. J. Stern. Pure Appl. Chem. **8**, 225 (1964); (*b*) M. Wolfsberg and M. J. Stern. Pure Appl. Chem. **8**, 325 (1964).
21. K. J. Laidler. Chemical kinetics. 2nd ed. McGraw-Hill Book Co. Inc., New York. 1965. p. 98.
22. K. B. Wiberg. Chem. Rev. **55**, 713 (1955).
23. E. A. Halevi. Progress in physical organic chemistry. Interscience Publishers, Inc., New York. 1963. Vol. 1, p. 109.
24. (*a*) S. Seltzer. J. Amer. Chem. Soc. **83**, 2625 (1961); (*b*) S. Seltzer. J. Amer. Chem. Soc. **85**, 14 (1963); (*c*) S. Seltzer and E. J. Hamilton, Jr. J. Amer. Chem. Soc. **88**, 3775 (1966).
25. F. H. Westheimer. Chem. Rev. **61**, 265 (1961).
26. J. Bigeleisen. Pure Appl. Chem. **8**, 217 (1964).
27. A. Streitweiser, R. H. Jagow, R. C. Fahey, and S. Suzuki. J. Amer. Chem. Soc. **80**, 2326 (1958).
28. (*a*) D. E. Van Sickle and J. O. Rodin. J. Amer. Chem. Soc. **86**, 3091 (1961); (*b*) P. Brown and R. C. Cookson. Tetrahedron, **21**, 1993 (1965).
29. S. Seltzer. J. Amer. Chem. Soc. **87**, 1534 (1965).
30. J. E. Baldwin. J. Amer. Chem. Soc. **91**, 3106 (1969).
31. (*a*) D. B. Denny and N. Tunkel. Chem. Ind. 1383 (1959); (*b*) M. Matsuoka and M. Szwarc. J. Amer. Chem. Soc. **83**, 1260 (1961).
32. A. Zwierzak and H. Pines. J. Org. Chem. **28**, 3392 (1963).
33. C. Walling, E. R. Briggs, and F. R. Mayo. J. Amer. Chem. Soc. **68**, 1145 (1946).
34. W. G. Brown. J. Amer. Chem. Soc. **90**, 1916 (1968).
35. K. F. Müller. Makromol. Chem. **79**, 128 (1964).
36. R. Hoffmann and R. B. Woodward. J. Amer. Chem. Soc. **87**, 2046 (1965).
37. (*a*) P. D. Bartlett, L. K. Montgomery, and B. Seidel. J. Amer. Chem. Soc. **86**, 616 (1964); (*b*) L. K. Montgomery, K. Schueller, and P. D. Bartlett. J. Amer. Chem. Soc. **86**, 622 (1964); (*c*) P. D. Bartlett and L. K. Montgomery. J. Amer. Chem. Soc. **86**, 628 (1964).
38. C. G. Overberger and P. A. Jarovitzky. J. Polym. Sci. **C**. Symposia, 37 (1963).
39. T. D. Nevitt and G. S. Hammond. J. Amer. Chem. Soc. **76**, 4124 (1954).
40. C. H. Depuy and R. W. King. Chem. Rev. **60**, 431 (1960).
41. M. Buza and E. J. Snyder. J. Amer. Chem. Soc. **88**, 1161 (1966).
42. K. Biemann. Mass spectrometry: organic chemical application. McGraw-Hill Book Co. Inc., New York. 1962. p. 223.
43. H. T. Clarke, H. B. Gillespie, and S. W. Weishaus. J. Amer. Chem. Soc. **55**, 4571 (1933).
44. P. D. Bartlett and H. Kwart. J. Amer. Chem. Soc. **72**, 1051 (1950).

Can. J. Chem. Downloaded from www.nrcresearchpress.com by 210.87.254.42 on 09/05/12
For personal use only.

Can. J. Chem. Downloaded from www.nrcresearchpress.com by 210.87.254.6 on 09/05/12
For personal use only.

Hydrogenolysis by $LiAlH_4$–$AlCl_3$ of an ether solution of norcamphor isobutylene ketal[1]

P. C. Loewen, W. W. Zajac, Jr.,[2] and R. K. Brown
Department of Chemistry, University of Alberta, Edmonton, Alberta

Received March 14, 1969

An approximately 1:1 mixture of the two isomers (**3** and **4**) of norcamphor isobutylene ketal was hydrogenolyzed by AlH_2Cl in ether at room temperature. The slow reaction (62% complete in 20 h; ~96% complete in 168 h) produced only 1-(2-*endo*-norbornyloxy)-2-methyl-2-propanol (**7**), 2-(2-*exo*-norbornyloxy)-2-methyl-1-propanol (**6**), 2-*exo*-norborneol (**10**), and unchanged **3** and **4** in the proportion 64.5:26.5:4.5:4.5. Recovery of materials was at least 95%.

Compound **10** is believed to arise from slow hydrogenolysis of the product **6**. Since the unreacted ketal was still an approximately 1:1 mixture of the isomers **3** and **4**, and because it is known that in the hydrogenolysis of acetals and ketals, the reduction by hydride donation is much faster than is the isomerization of the ketals, it is inferred that the two isomers (**3** and **4**) of norcamphor isobutylene ketal hydrogenolyze at approximately the same rate.

Arguments are presented to support the view that isomer **4** reacts with *two* molecules of AlH_2Cl, one as the Lewis acid and the other as the hydride donor, to provide product **7** and possibly some of product **6**, while isomer **3** reacts with *one* molecule of AlH_2Cl, which acts as the Lewis acid and the hydride donor, to provide most if not all of product **6** and some of product **7**.

Canadian Journal of Chemistry, 47, 4059 (1969)

Introduction

Recent work from this laboratory (1) has shown that lithium aluminum hydride–aluminum chloride reductive cleavage of norcamphor ethylene ketal (**1**) gave 2-(2-*endo*-norbornyloxy)-ethanol in 98% yield whereas similar reduction of camphor ethylene ketal (**2**) gave both 2-(2-isobornyloxy)ethanol and 2-(2-bornyloxy)-ethanol in 78% and 22% yield respectively (Scheme 1). These products were considered to be the result of steric approach control.

The question concerning the detail of the reductive cleavage, as to whether it took place via route *a* (Scheme 2) involving *both* Lewis acid attack of the reactive reducing species AlH_2Cl (2,3) *and* hydride donation by the same molecule,

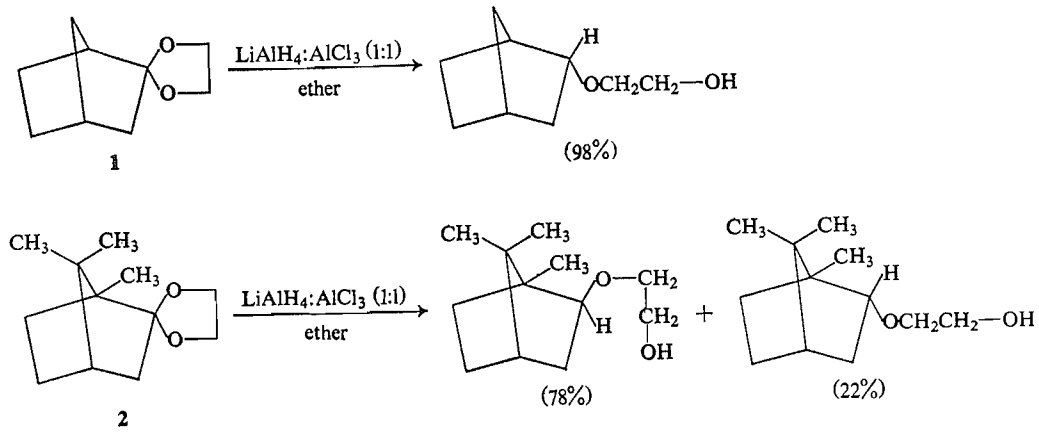

Scheme 1

or via route *b* (Scheme 2) in which one molecule of AlH_2Cl played the part of the Lewis acid while a second molecule donated the hydride ion, could not be answered (1). However, considering the results of the hydrogenolysis of camphor

[1]Taken in part from the thesis of P. C. Loewen submitted to the Faculty of Graduate Studies, University of Alberta, Edmonton, Alberta, as part of the requirements for the degree of Doctor of Philosophy.

[2]On leave during 1965–1966 from Villanova University, Villanova, Pennsylvania, U.S.A.

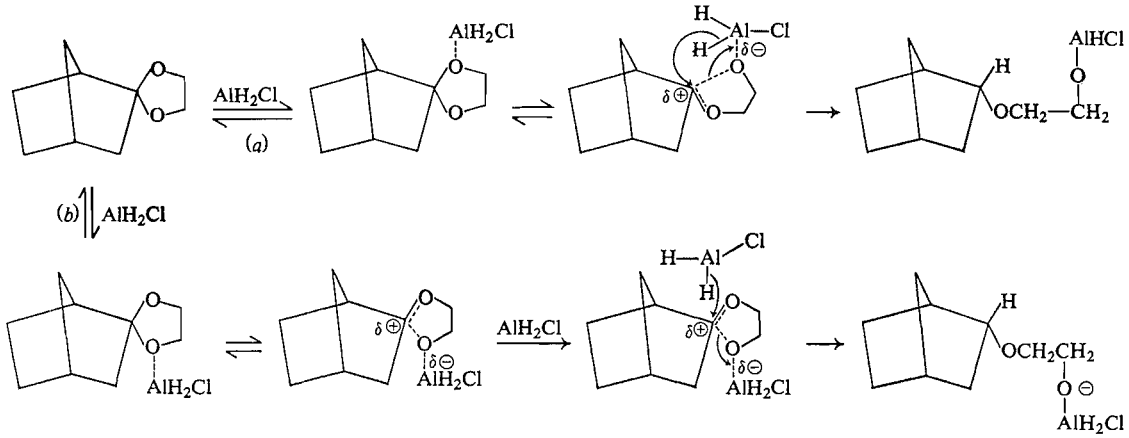

SCHEME 2

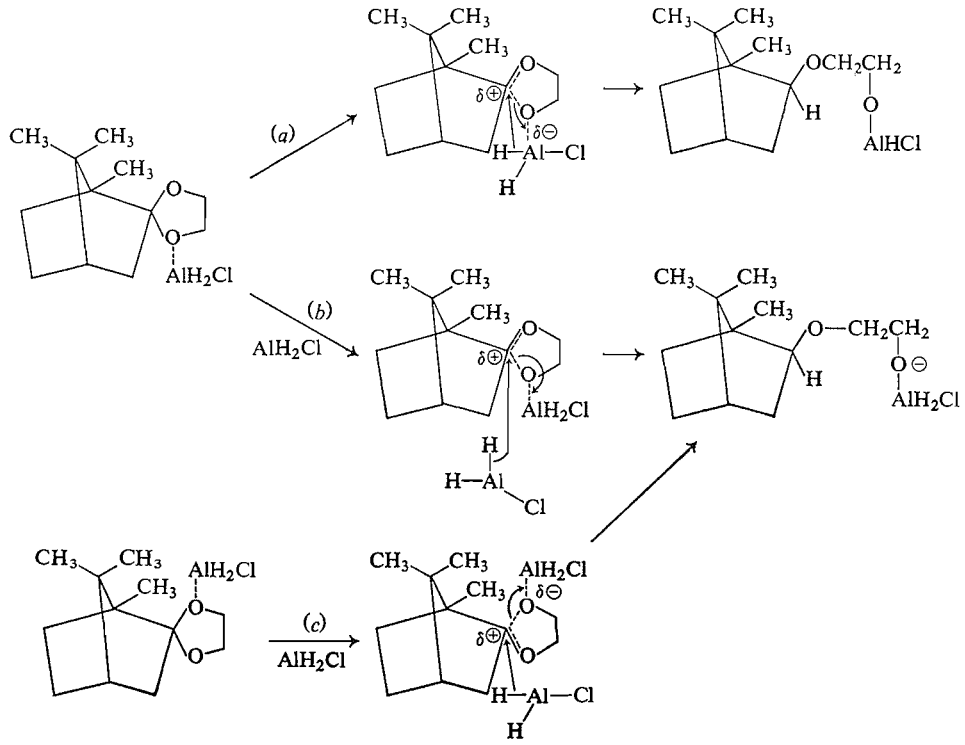

SCHEME 3

ethylene ketal, for the formation of the major product (78% yield), route *a* (Scheme 3) involving the dual function of the same molecule of AlH_2Cl would seem from a steric point of view to be more reasonable than routes *b* and/or *c* which involve two molecules of AlH_2Cl. As yet a suitable system for a kinetic study of this reaction has not been devised.

We have now examined the hydrogenolysis, by AlH_2Cl, of the isomeric norcamphor isobutylene ketals, **3** and **4**, in order to obtain more information concerning this question. The reason

Can. J. Chem. Downloaded from www.nrcresearchpress.com by 210.87.254.6 on 09/05/12
For personal use only.

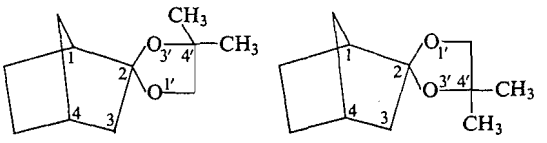

3 4

for the choice of this particular ketal stemmed from some previous work (4) in this laboratory in which it was found that hydrogenolysis of 2,2,4,4-tetramethyl-1,3-dioxolane (**5**) did not cleave the O_1—C_2 bond as expected on the basis of the inductive effects of the C-4 methyl groups (5), but instead gave nearly total cleavage (94%) of the O_3—C_2 bond of the ketal (Scheme 4).[3] This anomalous cleavage was interpreted as being due to a steric repression in the intermediate oxocarbonium ion resulting from O_1—C_2 bond cleavage, such steric repression being minimal or absent in the oxocarbonium ion which arises due to O_3—C_2 cleavage.

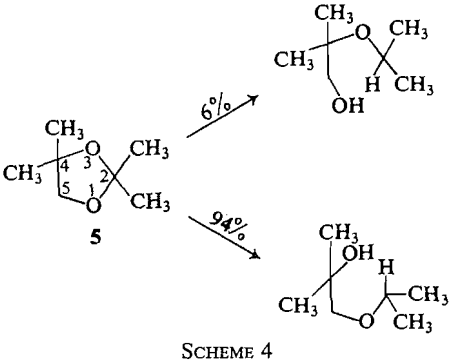

SCHEME 4

It is seen that both **3** and **4** possess the same structural feature as is found in 2,2,4,4-tetramethyl-1,3-dioxolane (Scheme 4). One would then expect, on the basis of the results of the hydrogenolysis of the tetramethyl-1,3-dioxolane, that both **3** and **4** would hydrogenolyze preferentially by cleavage of the C_2—$O_{3'}$ bond. However, the work on the norcamphor ethylene ketal (1) shows that the favored approach of the reducing agent is to the *exo* side. This would result in preferential cleavage of the C_2—$O_{3'}$ bond in **3** and the C_2—$O_{1'}$ bond in **4**, thus forming the *endo*-norbornyloxy compound. It was thus of interest to find out how these two directive systems behaved in the hydrogenolysis of **3** and **4**.

[3]E. L. Eliel *et al.* (14) have also reported that the mixed hydride hydrogenolysis of cyclohexanone isobutylene ketal produces exclusively that product which is the tertiary alcohol.

Results and Discussion

Preparation of Compounds

The norcamphor isobutylene ketals were prepared by the acid catalyzed reaction of norcamphor with isobutylene glycol. The product of this reaction was no doubt an equilibrium mixture of the isomers **3** and **4**. The elemental analysis agreed well with that expected for these isomers. The 60 MHz nuclear magnetic resonance (n.m.r.) spectrum in $CDCl_3$ (Fig. 1) shows the presence of two isomers. It is expected that for each isomer the methylene protons of the 1,3-dioxolane portion of the ketal should provide a simple AB quartet and these signals should appear in the portion of the spectrum, between τ 6.0 and 7.0 where protons attached to carbon atoms which are in turn attached to an ether oxygen are known to absorb. Since the multiplet lying between τ 6.2 and 6.6 is not a simple quartet, it is clear that more than one isomer must be present. From the 100 MHz n.m.r. spectrum, expanded to show these signals more clearly (see inset, Fig. 1), it is seen that the multiplet between τ 6.2 and 6.6 is due to two overlapping quartets. The areas under the two sets of peaks are in the approximate ratio of 45:55 (i.e. nearly 1:1).

The gas liquid chromatogram (g.l.c.) of this mixture of isomers gave a single peak which showed no evidence whatsoever of the presence of two isomers. All attempts to separate these, either by careful fractional distillation with a spinning band column, or by using a variety of g.l.c. columns, among which were those containing butanediol succinate, carbowax, silicone rubber, or Apiezon L on Gas-Chrom W, were quite ineffective. This was a serious handicap, since the solution of this problem would have been greatly facilitated had the two pure isomers been individually available. Accordingly, there was no way of determining which of the two isomers was in the greater abundance.

Of the four possible reduction products of **3** and **4** (Scheme 5), only the tertiary alcohols **7** and **8** were successfully prepared. These were made by the reaction of 2-*exo*- and 2-*endo*-norborneol with ethyl bromoacetate by the method of Leffler and Calkins (6), followed by treatment of the product with methymagnesium bromide. That both of these compounds, **7** and **8**, were

Can. J. Chem. Downloaded from www.nrcresearchpress.com by 210.87.254.6 on 09/05/12
For personal use only.

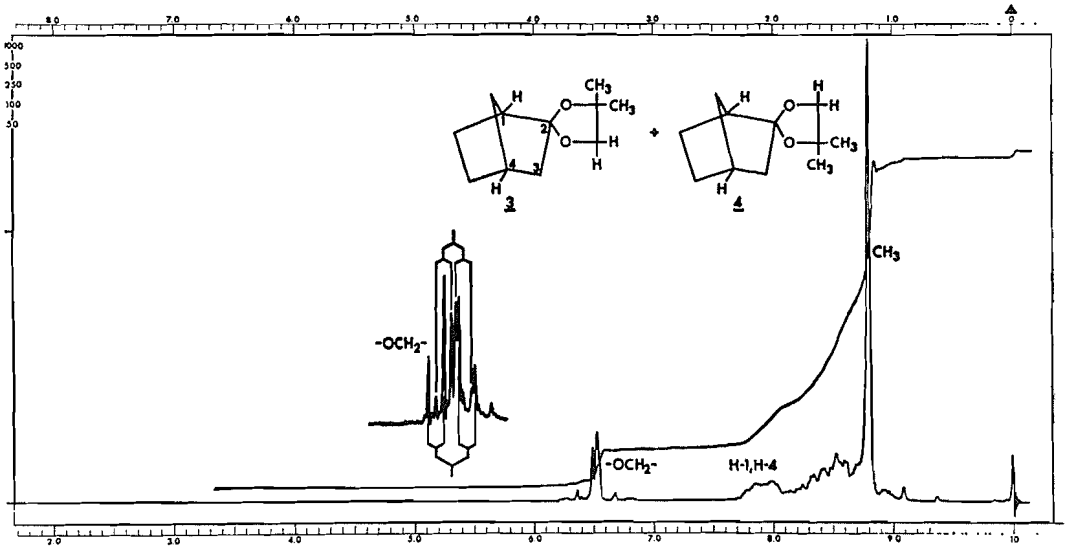

FIG. 1. The 60 MHz n.m.r. spectrum of the equilibrium mixture of the two isomeric norcamphor isobutylene ketals **3** and **4**; reference, tetramethylsilane. The inset is a partial 100 MHz n.m.r. spectrum, showing the two overlapping AB quartets of the two geminal protons of the methylene group in the dioxolane ring.

tertiary alcohols was verified by their infrared (i.r.) spectra, which showed a band for hydroxyl group absorption, and by their n.m.r. spectra in dimethyl sulfoxide-d_6 (DMSO-d_6) which showed the signal for the hydroxyl proton shifted downfield from τ 7.75 (in $CDCl_3$) to 5.85 as a sharp singlet (8). The *exo* and *endo* isomers could be distinguished by a characteristic feature indicated in our previous work (1). The signals for the bridgehead protons (C-1 and C-4) of the *endo* isomer, **7**, appear as *two* unresolved closely spaced multiplets ($W/2 \sim 10$ Hz and $W/2 \sim 12$ Hz) centred at τ 7.65 and 7.85 respectively in the spectrum in DMSO-d_6 (Fig. 2) whereas the spectrum of the *exo* isomer in the same solvent shows only *one* closely spaced unresolved multiplet at τ 7.8 ($W/2 \sim 10$ Hz)(Fig. 3).

All attempts to prepare the primary alcohols, **6** and **9**, met with failure. However, this did not interfere seriously with the identification of the products of hydrogenolysis of **3** and **4**.

Hydrogenolysis of 3 and 4

The hydrogenolysis of the mixture of the two isomers (**3** and **4**) of norcamphor isobutylene ketal was carried out according to published directions (7) using an equimolar mixture of $LiAlH_4$ and $AlCl_3$ in dry diethyl ether. The

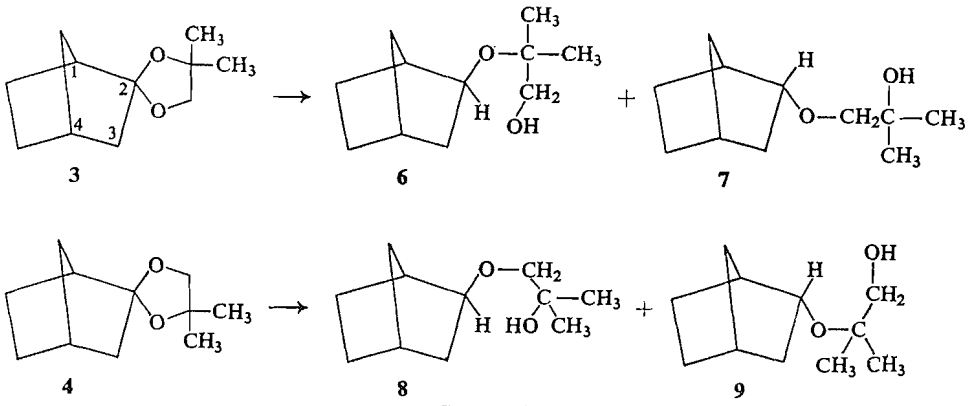

SCHEME 5

Can. J. Chem. Downloaded from www.nrcresearchpress.com by 210.87.254.6 on 09/05/12
For personal use only.

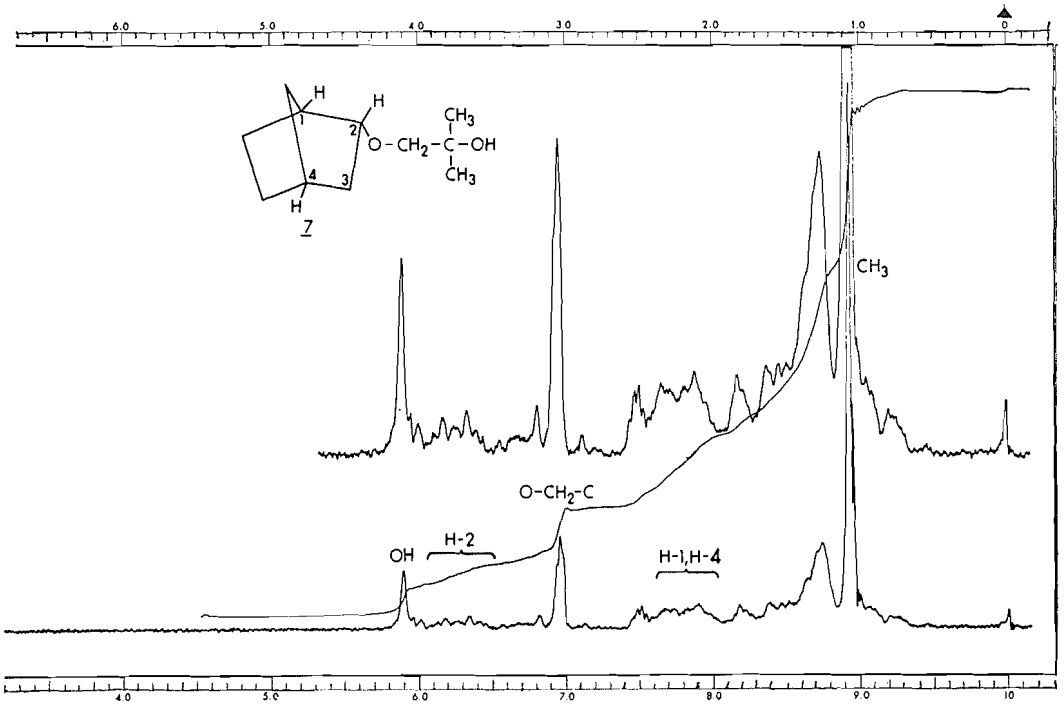

FIG. 2. The 60 MHz spectrum of synthetic 1-(2-*endo*-norbornyloxy)-2-methyl-2-propanol (7) in dimethylsulfoxide-d_6.

TABLE I

Hydrogenolysis of the mixture of the two isomers **3** and **4** of norcamphor isobutylene ketal by a 1:1 mixture of $LiAl_4$ and $AlCl_3$ in ether at room temperature*

Time of reaction (h)	Extent of reduction (%)	Products of the reaction, % of the total product				Total recovery of materials (%)
		10	**7**	**6**	**3**+**4**	
20	62	2.5	42.5	17.0	38	95
168	95.5	4.5	64.5	26.5	4.5	95

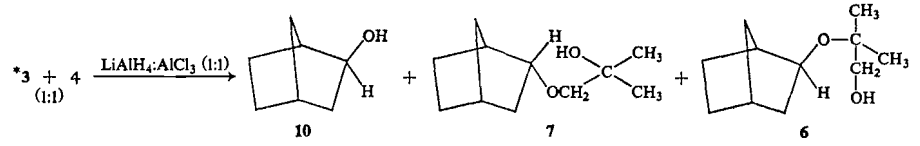

results of the hydrogenolysis are assembled in Table I.

Each of the products of hydrogenolysis was collected by preparative g.l.c. and identified with the aid of elemental analysis, a g.l.c. retention time and n.m.r. spectrum, and by comparison with these characteristics of authentic specimens of compounds **10** and **7**. The structure of the primary alcohol **6** obtained from the hydrogenolysis was determined by its elemental analysis, i.r. spectrum and particularly the n.m.r. spectrum in DMSO-d_6 (Fig. 4). The latter spectrum showed the hydroxyl proton signal shifted downfield from a broad singlet in $CDCl_3$ at τ 7.85 to a triplet (J = 6 Hz) centred at τ 5.6 which is indicative of a primary alcohol (8). The spectrum also showed one closely spaced unresolved multiplet ($W/2 \sim 12$ Hz) centred at

Can. J. Chem. Downloaded from www.nrcresearchpress.com by 210.87.254.6 on 09/05/12
For personal use only.

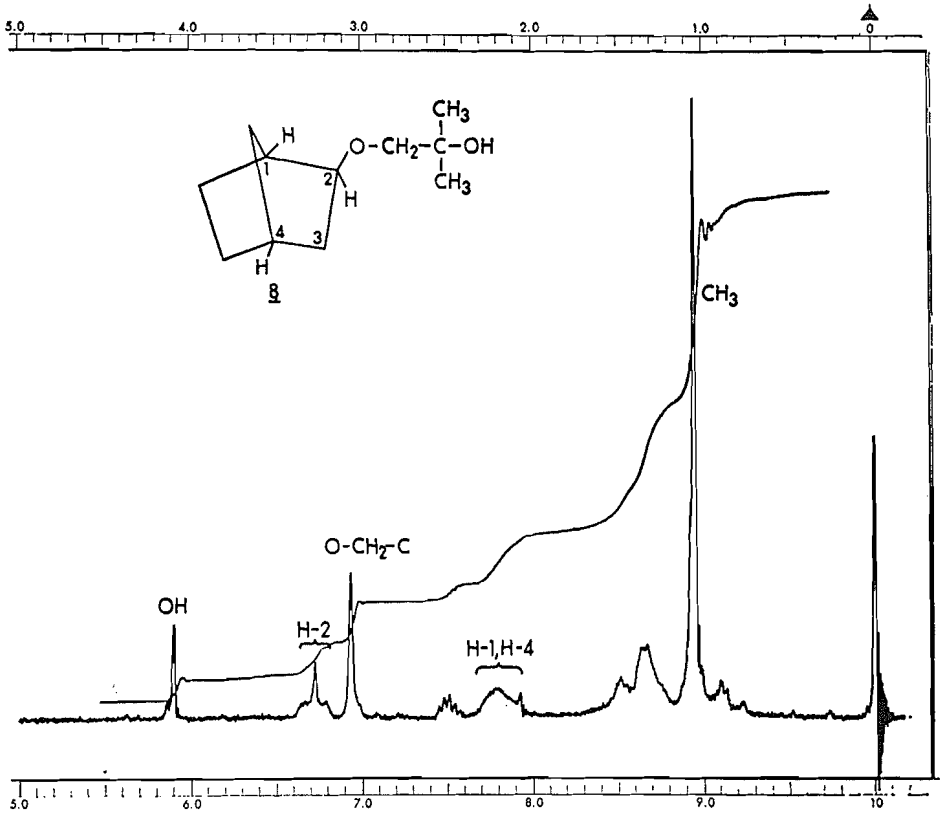

FIG. 3. The 60 MHz spectrum of synthetic 1-(2-*exo*-norbornyloxy)-2-methyl-2-propanol (8) in dimethylsulfoxide-d_6.

τ 7.92 indicative of the signals for the bridgehead protons when an *exo* substituent is present (1).

The n.m.r. spectrum of the recovered unreacted ketal mixture **3** and **4**, obtained after 20 h of reduction, was clearly identical to the n.m.r. spectrum of the starting isomeric mixture. This indicates that *either* the rate of hydrogenolysis of both isomers is practically the same, *or* that one isomer, **3** or **4**, might be reduced more rapidly, but the rate of isomerization of the unreduced material, under the reaction conditions, is sufficiently greater than the rate of reduction that maintenance of an equilibrium mixture of **3** and **4** is ensured. Work recently reported (9) has shown that when both *cis*- and *trans*-2,4-dimethyl-1,3-dioxolane were hydrogenolyzed separately and under identical conditions, but with sufficient $LiAlH_4$–$AlCl_3$ to reduce only half of the dioxolane, no significant isomerization of the unreacted *cis* or *trans* isomers had occurred. This supported the view that the slow, rate-determining step of the reaction was indeed the C_2—O bond breaking, leading to the formation (or incipient formation) of the intermediate oxocarbonium ion, and that subsequent (and nonreversible) reduction by hydride donation to this oxocarbonium ion was very much faster than was isomerization (Scheme 6).

Unfortunately, because we were unable to separate the isomers **3** and **4**, it was not possible to ascertain, by partial hydrogenolysis, whether isomerization of the starting isomer **3** or **4** did or did not occur. However it is not unreasonable to assume that, as in the case of the *cis*- and *trans*-2,4-dimethyl-1,3-dioxolanes, reduction by hydride donation here is also much faster than C—O bond cleavage to form the intermediate oxocarbonium ion. Accordingly, the following discussion is based on the acceptance of this view.

Several points are quite clear. (*i*) If indeed there is no significant isomerization of the unreacted isomers **3** or **4**, then from the knowledge

Can. J. Chem. Downloaded from www.nrcresearchpress.com by 210.87.254.6 on 09/05/12
For personal use only.

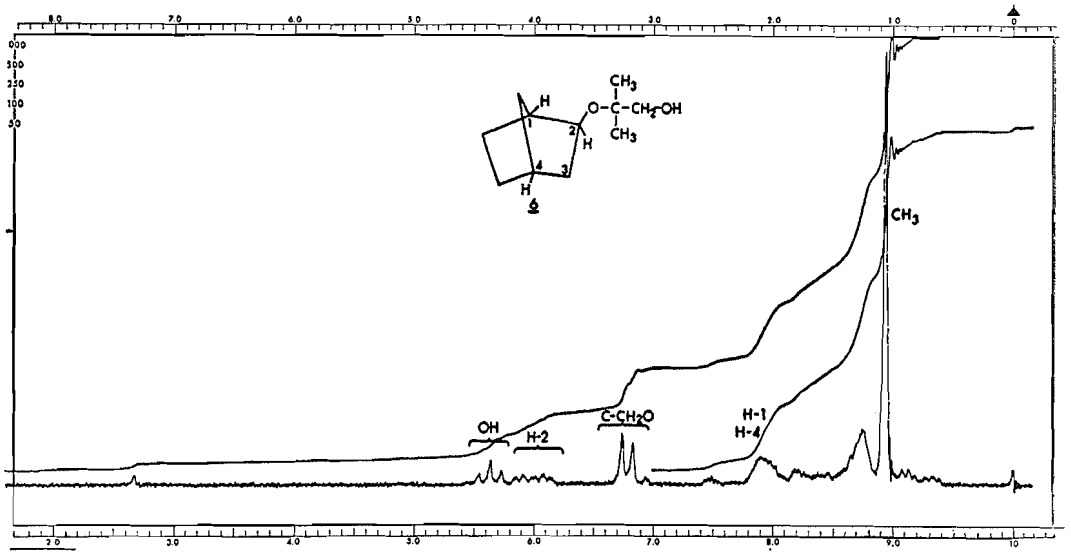

FIG. 4. The 60 MHz n.m.r. spectrum of one of the products from the AlH_2Cl hydrogenolysis of the equilibrium mixture of the two isomeric norcamphor isobutylene ketals **3** and **4**.

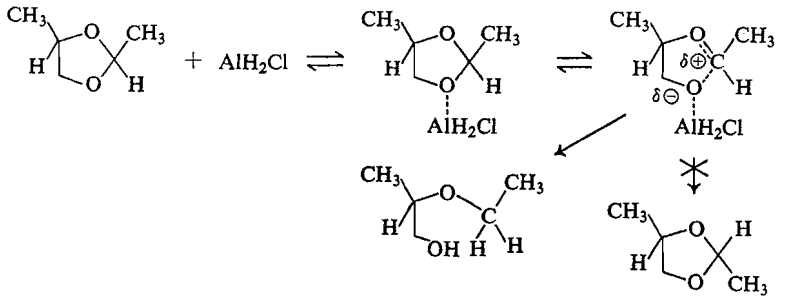

SCHEME 6

that the ratio of the products **7** to **6** is 64.5 to 26.5, it can be inferred that each of the two isomers **3** or **4** does not reduce specifically to one of the products. If this had been so, then the product ratio would also have been 55:45 (or 45:55), the same as that found for the original material. It is however quite possible that one isomer **3** (or **4**) could produce essentially the product **7**, while the other isomer **4** (or **3**) would then provide both **7** and **6**. (*ii*) Since a substantial amount (26.5%) of the product is the primary alcohol **6**, the steric restriction (4) which strongly retarded the C_2—O_1 bond breaking of **5** (Scheme 4) could not have been as important in retarding the C_2—O_1, bond cleavage in **3** and/or **4**. Some factor must then retard the alternate C_2—O_3, bond cleavage sufficiently to allow C_2—O_1, bond cleavage to become competitive to the extent of 26.5% (four times as much as was found for **5**). (*iii*) From the work on norcamphor ethylene ketal (1) it is also clear that approach of the reducing species to C-2 of structures **3** and **4**, from the *exo* side is preferred to approach from the *endo* side. However, if structural features are present which inhibit approach from the *exo* side, then *endo* attack by the reducing agent becomes competitive and important as shown by the hydrogenolysis of camphor ethylene ketal (1). (*iv*) It is also quite certain that for hydrogenolysis of the acetals or ketals to occur at all, the Lewis acid property of the reducing species, AlH_2Cl, must be involved, and the particular C—O bond which is broken is that in which the Lewis acid is associated with the oxygen atom.

Can. J. Chem. Downloaded from www.nrcresearchpress.com by 210.87.254.6 on 09/05/12
For personal use only.

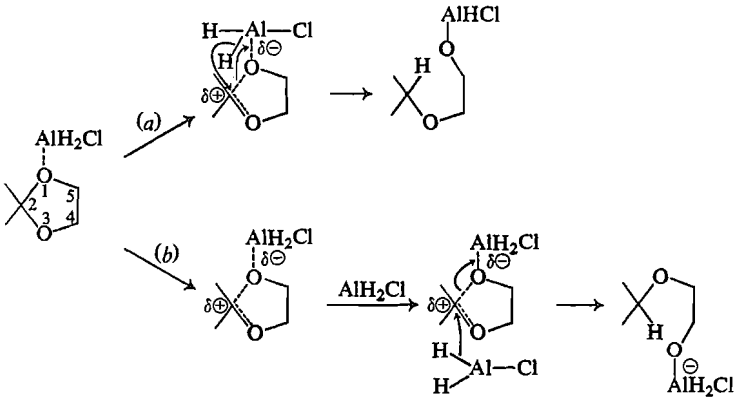

SCHEME 7

A point which has not been determined to date is whether the molecule which acts as the Lewis acid is also the one which donates the hydride ion (route *a*, Scheme 7). If this is so then the hydride ion will enter on the same side of the C-2 carbon atom of the 1,3-dioxolane as that from which the oxygen atom leaves, and thus the stereochemistry of the C-2 carbon is maintained. On the other hand, it is possible that one molecule of AlH_2Cl acts as the Lewis acid while a second molecule provides the hydride ion (route *b*, Scheme 7). If this is so, then the hydride ion will enter on the side of C-2 opposite to that from which the oxygen atom leaves, thus inverting the stereochemistry about the C-2 atom.

There are therefore, for each of the compounds **3** and **4**, two possible products if the stereochemistry about C-2 is maintained (Scheme 8). Compounds **7** and **6**, the products expected by hydrogenolysis of **3** by this route which maintains C-2 stereochemistry, are indeed those which are observed. Compounds **8** and **9**, the products expected from hydrogenolysis of **4** by the same route are *not* found among the products of hydrogenolysis. Hence, hydrogenolysis of **4** by such a route can be eliminated as a possibility.

Of the two courses of hydrogenolysis of compound **3** (Scheme 8), route *b* has two features militating against its easy accomplishment. The first is the cleavage of the C_2—$O_{1'}$ bond to produce an intermediate (or incipient) oxocarbonium ion which possesses the unfavorable steric factor (4) noted for the tetramethyl-1,3-dioxolane (**5**) (Scheme 4). As well, attack by the AlH_2Cl from the *endo* direction is also less favored (1). However, route *a* requires association of the AlH_2Cl with the oxygen atom in the *exo* position, an oxygen atom in a steric environment similar to that found for 2,2,5,5-tetramethyltetrahydrofuran. It is known that a bulky Lewis acid ($SnCl_4$) is associated to a lesser extent with 2,5-dimethyltetrahydrofuran than with 2-methyltetrahydrofuran or with tetrahydrofuran (10). This was considered to be due to steric factors rather than electronic factors. It is thus quite conceivable that such steric factors in compound **3** would retard association of the Lewis acid AlH_2Cl with the *exo* oxygen atom sufficiently so that the alternate route *b* becomes competitive.

Since isomer **4** does hydrogenolyze about as easily as does **3**, then it can do so by the route (route *b* in Scheme 7) involving *two* molecules of AlH_2Cl. This is shown in Scheme 9. It is seen that both of the compounds **6** and **7** actually found as hydrogenolysis products, can be obtained by this method. If one considers these two paths *a* and *b* (Scheme 9) in more detail, it is seen that the hydrogenolysis by route *a* which might provide compound **6** is less likely than the alternate route which provides **7** (route *b*). For route *a* to take place, there must be at least partial C_2—$O_{1'}$, bond breaking with a tendency for the remaining substituents at C-2 to become coplanar about C-2. Attack at C-2 by a second molecule of AlH_2Cl would require its approach via a path perpendicular to the plane in which C-2 lies. Models show that such an approach is strongly inhibited by the three *endo* hydrogen atoms of the norcamphor system. On the other hand, models show that the association of the Lewis acid with the *endo* oxygen atom (route *b*)

Can. J. Chem. Downloaded from www.nrcresearchpress.com by 210.87.254.6 on 09/05/12
For personal use only.

Can. J. Chem. Downloaded from www.nrcresearchpress.com by 210.87.254.6 on 09/05/12
For personal use only.

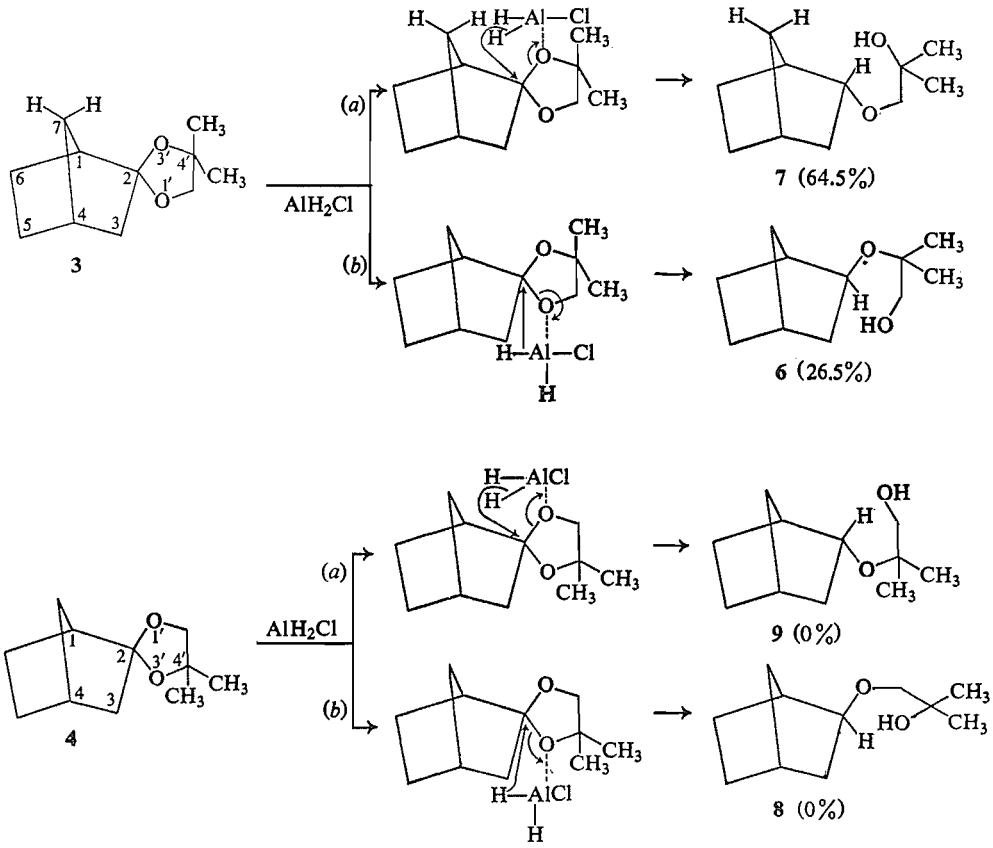

SCHEME 8

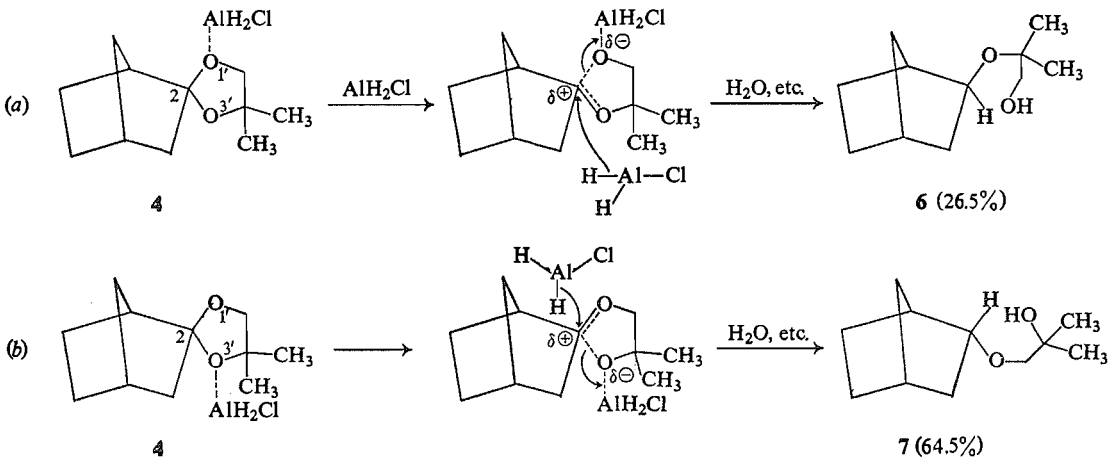

SCHEME 9

Can. J. Chem. Downloaded from www.nrcresearchpress.com by 210.87.254.6 on 09/05/12
For personal use only.

is possible. This would lead to incipient C_2—O_3, bond breaking. Subsequent attack at C-2 by the second molecule of AlH_2Cl is then quite easy (1). From these arguments, it is our view that compound **4** reacts practically completely via route *b* (Scheme 9) to provide the product **7**. We realize that this conclusion can be verified only by direct experimental evidence.

Reaction of compound **3** with two molecules of AlH_2Cl by the same sequence as is shown for compound **4** in Scheme 9, would provide the substances **8** and **9**. Since these were not observed as products of the hydrogenolysis, such a scheme of reaction for compound **3** can be dismissed.

If then practically all of **4** provides product **7**, then one must conclude that compound **3** provides all of the alternate product **6** along with some of **7**. The feasibility of such dual production from compound **3** has already been discussed above. Final proof as to whether this is in fact the case must await isolation or preparation of the individual isomers **3** and **4**. The necessity of this is quite apparent, but as yet this goal has not been realized.

Our view, based upon the above arguments, is that hydrogenolysis by AlH_2Cl can occur by two routes. One involves a single molecule of AlH_2Cl, and the other requires two molecules of AlH_2Cl. The proportion of hydrogenolysis taking place by these two methods depends upon the steric factors involved in the ketal under consideration.

A final point concerns the small amount of the third product, 2-*exo*-norborneol (**10**) isolated from the reduction. The source of this compound might be from Lewis acid catalyzed cleavage of the compound **6**, which is an ether containing an oxygen atom linked to a tertiary carbon. It is known that hydriodic acid cleaves ethers in such a way that the more stable carbonium ion is formed (11).

Experimental

All boiling points are uncorrected.

Infrared spectra were obtained with a Perkin–Elmer Model 337 grating spectrometer.

Nuclear magnetic resonance spectra were obtained with a Varian Associates A-60 instrument by Mr. Robert Swindlehurst, and an HR-100 spectrometer by Mr. Glen Bigham. All spectra were referred to tetramethylsilane.

Gas chromatographic analyses were carried out with either an F and M Model 700 instrument using 1/8″ × 12′ columns or an Aerograph Model A-700 equipped with 1/4″ × 12′ columns. The column packings employed were 20% butanediol succinate on Chromosorb W, 60–80 mesh (the most useful column packing); 25% Carbowax 6000 on Gas Chrom P, 60–80 mesh; 10% silicone rubber on Chromosorb W, 30–60 mesh and 10% Apiezon L on Chromosorb W. Helium was the carrier gas. The g.l.c. instruments were each equipped with an integrator and temperature programming unit. The temperature program was begun at ~50°.

2-Methyl-1,2-propanediol (Isobutylene Glycol)

This compound was prepared in 53% yield by $LiAlH_4$ reduction of methyl α-hydroxyisobutyrate(5).

Norcamphor Isobutylene Ketal (3 and 4)

This compound was prepared in 69% yield from norcamphor and isobutylene glycol according to the method of Salmi (12); b.p., 56–57° at 3.0 mm; η_D^{23}, 1.4603.

Anal. Calcd. for $C_{11}H_{18}O_2$: C, 72.49; H, 9.95. Found: C, 72.33; H, 9.82.

The i.r. spectrum (neat) showed no absorption attributable to hydroxyl or carbonyl groups. Significant features of the 60 MHz n.m.r. spectrum (Fig. 1) in $CDCl_3$ are described in the Discussion.

Ethyl(2-exo-norbornyloxy)acetate

This acetate was prepared in 30% yield by the reaction, in either benzene or 1,2-dimethoxyethane solution, of 2-*exo*-norborneol (Aldrich Chemical Co.) with ethyl bromoacetate in the presence of sodium hydride following the procedure of Leffler and Calkins (6); b.p., 83° at 2.5 mm; η_D^{23}, 1.4668 (lit. (1) b.p., 77° at 1 mm; η_D^{25}, 1.4162).

Ethyl(2-endo-norbornyloxy)acetate

This acetate was prepared in 25% yield by the reaction of 2-*endo*-norborneol (13) with ethyl bromoacetate in benzene or 1,2-dimethoxyethane, in the presence of sodium hydride (6); b.p., 77° at 0.8 mm; η_D^{22}, 1.4680 (lit. (1) b.p., 80° at 0.1 mm; η_D^{25}, 1.4160).

1-(2-exo-norbornyloxy)-2-methyl-2-propanol (8)

To a quantity (2.64 g, 0.11 mole) of magnesium turnings in 100 ml of dry ether kept at 0° to −5° by an ice bath, was added, with stirring, 15.4 g (0.11 mole) of methyl iodide dropwise. When all the methyl iodide had been added, the solution was stirred for 10 min at room temperature and then 10 g (0.05 mole) of ethyl (2-*exo*-norbornyloxy)acetate was added dropwise to the stirred solution at a rate which maintained the ether solution at gentle reflux. When the acetate had been added, the solution was stirred for 2 h at room temperature, whereupon 2 ml of water was cautiously added to decompose the complex. The ether layer was decanted and the residue diluted with sufficient 15% hydrochloric acid to dissolve the solids. An ether extract of this aqueous mixture, combined with the decanted ether, was dried ($MgSO_4$) and the drying agent then removed by filtration. Elimination of the solvent by rotary evaporator under vacuum gave an oil which was fractionally distilled to give 5 g (55%) of the alcohol **8**; b.p., 71° at 2.5 mm; η_D^{24}, 1.4640.

Anal. Calcd. for $C_{11}H_{20}O_2$: C, 71.69; H, 10.94. Found: C, 71.92; H, 10.91.

Can. J. Chem. Downloaded from www.nrcresearchpress.com by 210.87.254.6 on 09/05/12
For personal use only.

The n.m.r. spectrum in CCl_4 (reference, tetramethylsilane) was consistent with the structure of **8** and showed a multiplet between τ 6.6 and 6.8 (1H), a singlet at τ 6.9 (2H), *one* closely spaced unresolved multiplet centred at τ 7.72 (2H, bridgehead protons of the *exo* isomer), a singlet at τ 7.9 (1H), a multiplet between τ 8.1–9.3 overlapping a singlet at τ 8.91 (8H + 6H). In dimethylsulfoxide-d_6 (DMSO-d_6) the spectrum (Fig. 3) had essentially the same features except that the singlet at τ 7.9 (in CCl_4) moved downfield to τ 5.88 and remained a singlet, indicating that this signal was due to the proton of a tertiary hydroxyl group (8).

The i.r. spectrum (neat) showed a strong broad absorption band between 3100 and 3600 cm^{-1} and strong broad absorption in the region 1200 to 1050 cm^{-1} (C—O stretching).

The g.l.c. (butanediol succinate column) showed one sharp symmetrical peak.

1-(2-endo-norbornyloxy)-2-methyl-2-propanol (7)

This compound was prepared according to the method described immediately above for the preparation of the *exo* isomer, **8**. Because of the small quantity of material, it could not be satisfactorily purified by fractional distillation. The g.l.c. of each fraction still showed several small peaks of the contaminants. Final purification was carried out by preparative g.l.c. on a column using butanediol succinate; b.p. (micro), 79–80° at 3.0 mm; η_D^{25}, 1.4642.

Anal. Calcd. for $C_{11}H_{20}O_2$: C, 71.69; H, 10.94. Found: C, 71.44; H, 10.65.

The n.m.r. spectrum in CCl_4 agreed with the structure of **7**. The significant features were *two* narrowly spaced unresolved multiplets for the bridgehead protons centred at τ 7.65 and 7.86 indicative of the *endo* substitution (1) and a singlet at τ 7.57 in the n.m.r. spectrum in CCl_4 which shifted downfield to τ 5.93 and remained as a sharp singlet in the n.m.r. spectrum in DMSO-d_6 (Fig. 2), thus indicating that the proton was that of a tertiary hydroxyl group (8).

The i.r. spectrum (neat) showed strong broad absorption between 3600 and 3100 cm^{-1} (OH) and strong broad absorption between 1200 and 1050 cm^{-1} (C—O stretching).

2-(2-exo-norbornyloxy)-2-methyl-1-propanol (6)

This compound was isolated by g.l.c. on a column of 20% butanediol succinate on Chromosorb W, from the mixture of products obtained from the hydrogenolysis of the mixture of the two isomers of norcamphor isobutylene ketal, **3** and **4**; b.p. (micro), 77–79° at 1.5 mm; η_D^{23}, 1.4734.

Anal. Calcd. for $C_{11}H_{20}O_2$: C, 71.69; H, 10.94. Found: C, 71.35; H, 10.37.

The n.m.r. spectrum in DMSO-d_6 is shown in Fig. 4. The position of the signals and their integrated areas agree with a structure such as **6**. The significant details are described in the Discussion.

Hydrogenolysis of Norcamphor Isobutylene Ketal (3 and 4)

The hydrogenolysis was carried out either as described for the reduction of acetals and ketals (7) or preferably by adding the ketal to a previously prepared solution of equimolar amounts of $LiAlH_4$ and $AlCl_3$ in anhydrous ether. Both procedures gave the same results. The reduction was allowed to proceed at room temperature for the appropriate length of time (20 h or 168 h), whereupon sufficient 15% aqueous KOH was added dropwise to decompose the complex and form a colorless precipitate which was readily removed by filtration. The ether was then removed by rotary evaporator. Recovery of material was 95% (2.8 g from 3.0 g of ketal mixture). The oil was then subjected to g.l.c. and the products obtained were those indicated in Table I along with unreacted starting material.

Acknowledgment

The authors wish to thank the National Research Council of Canada for financial support during the course of this work.

1. W. W. Zajac, Jr., B. Rhee, and R. K. Brown. Can. J. Chem. **44**, 1547 (1966).
2. U. E. Diner, H. A. Davis, and R. K. Brown. Can. J. Chem. **45**, 207 (1967).
3. E. C. Ashby and J. Prather. J. Amer. Chem. Soc. **88**, 729 (1966).
4. B. E. Leggetter and R. K. Brown. Can. J. Chem. **42**, 1005 (1964).
5. B. E. Leggetter and R. K. Brown. Can. J. Chem. **42**, 990 (1964).
6. M. T. Leffler and A. E. Calkins. *In* Organic syntheses. Collective Vol. III. John Wiley and Sons, Inc., New York. 1955. p. 544.
7. B. E. Leggetter and R. K. Brown. Can. J. Chem. **41**, 2671 (1963).
8. O. L. Chapman and R. W. King. J. Amer. Chem. Soc. **86**, 1256 (1964).
9. B. E. Leggetter and R. K. Brown. Can. J. Chem. **43**, 1030 (1965).
10. F. J. Cioffe and S. T. Zenchelsky. J. Phys. Chem. **67**, 357 (1963).
11. D. J. Cram and G. S. Hammond. Organic chemistry. 2nd ed. McGraw-Hill Book Co., Inc., New York. 1964. Pp. 259–260.
12. E. J. Salmi. Ber. **71**, 1803 (1938).
13. G. F. Wilcox, M. Sexton, and M. F. Wilcox. J. Org. Chem. **28**, 1079 (1963).
14. E. L. Eliel, V. G. Badding, and M. N. Rerick. J. Amer. Chem. Soc. **84**, 2371 (1962).

Can. J. Chem. Downloaded from www.nrcresearchpress.com by 210.87.254.105 on 09/05/12
For personal use only.

Pyrolytic rearrangement of norbornene oxide[1]

DAVID L. GARIN
Department of Chemistry, University of Missouri-St. Louis, St. Louis, Mo. 63121

Received May 26, 1969

Norbornene oxide (**4**), stable to pyrolysis at 500°, rearranges at 550° to give Δ^3-cyclohexenylcarboxaldehyde (**8**), norcamphor (**6**), and Δ^2-cyclopentenone (**7**).

Canadian Journal of Chemistry, 47, 4071 (1969)

Introduction

The formation of cycloalkene acetaldehydes (**3**) from the pyrolysis of bridged cyclobutene epoxides (**1**) led to the consideration of a diradical intermediate **2** (1,2) (see Scheme 1). It appeared plausible that the pyrolysis of *exo*-2,3-epoxybicyclo[2.2.1]heptane (**4**, norbornene oxide) might give similar products via the closely related intermediate **5**. To examine this possibility, norbornene oxide was subjected to pyrolysis in a fashion similar to that reported for the pyrolysis of the cyclobutene epoxides (1).

Results

The solid epoxide (**4**) was added in small portions to a vertical pyrolysis column packed with glass helices under slow nitrogen flow. At temperatures up to 500°, the epoxide passed through the heated column unchanged but at 550° it was completely transformed into a large number of compounds. Analysis by vapor phase chromatography (v.p.c.) showed three major peaks whose ratios varied slightly from run to run. Samples of these three products were collected from the gas chromatograph and shown to be (in order of appearance) **7** (5–10%), **8** (62–67%), and **6** (5–10%) by spectral analysis and comparison with authentic samples. Percentage compositions refer to the relative areas observed for the different components in the chromatogram. A comparison of v.p.c. retention times showed that **3** ($n = 1$) was not present in the pyrolysate. These results are similar to those reported by Crandall for the acid catalyzed rearrangement of **4** which gives **6** and **8** (in approximately equal amounts) and nortricyclanol as primary products but no **7** (3). Norcamphor is not an intermediate in this reaction being stable to pyrolysis at 550°.

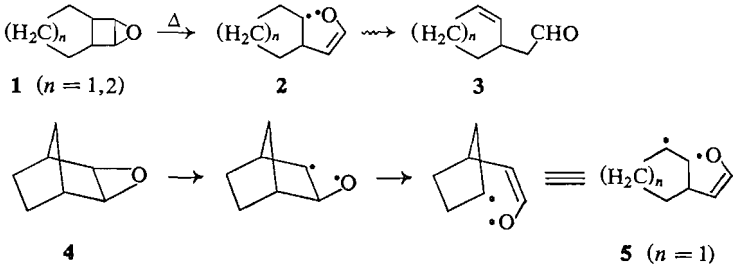

SCHEME 1

Discussion

Schematically, intermediate **9** could account for the observed products (equation A, Scheme 2) but various mechanisms can be considered depicting either homonuclear or heteronuclear

[1]Presented in part at the Midwest Regional American Chemical Society Meeting, Columbia, Missouri, November, 1967.

Portions of this manuscript were abstracted from the Ph.D. Thesis of D. L. Garin, Iowa State University, 1964.

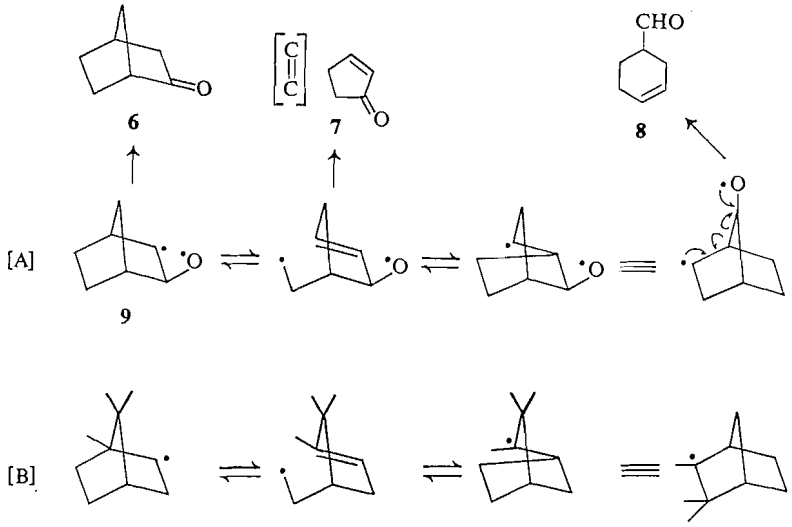

SCHEME 2

cleavage. (A referee has suggested the formation of **7** via a retro Diels–Alder reaction of the enol of norcamphor derived directly from **9**.) This intermediate (**9**) is analogous to that reported (4) for the rearrangement of the camphane radical (equation B, Scheme 2).

Experimental

Melting points and boiling points are uncorrected.

Norbornene Oxide (4)

Following the epoxidation procedure of Korach, Nielsen, and Rideout, norbornene (8.0 g, 0.085 mole) was reacted with 18 g of a 40% peracetic acid solution (FMC Corp., 0.095 mole) over 0.5 h, maintaining the temperature at 20° (5). The crude product was sublimed at atmospheric pressure using an oil bath at 130° to give 7.0 g (75%) of a white crystalline material m.p. 120–122° [lit. m.p. 118–119° (6) and 125–127° (7)]; infrared (i.r.) (CCl_4): 848 cm^{-1}. The peracid preparation of **4** is reported to give an isomeric composition that is 94% *exo* and 6% *endo* (8).

Pyrolysis of 4

Norbornene oxide, in *ca.* 50 mg portions, was manually dropped onto a vertical column of glass helices in a temperature control oven kept under continual nitrogen flow occasionally broken for 2–3 seconds for addition of the epoxide. Products were separated and collected by v.p.c. using a Perkin–Elmer RX column (two meter, 1/4" diameter column utilizing Ucon oil LB-550-X on diatomaceous earth) at 125°. The retention times for the products (in min) were 7.0 (**7**), 10.1 (**8**), and 13.2 (**6**).

Δ^2-Cyclopentenone (7)

The nuclear magnetic resonance (n.m.r.) spectrum of the unsaturated ketone, collected by preparative v.p.c. from the pyrolysis of **4**, was consistent with that reported (9). The 2,4-dinitrophenylhydrazone was deep red and had m.p. 165–166°; lit. m.p. 165–166° (10).

Δ^3-Cyclohexenylcarboxaldehyde (8)

The n.m.r. and i.r. spectra of the aldehyde from the pyrolysis of **4** was identical to that of an authentic sample of Δ^3-cyclohexenylcarboxaldehyde (kindly supplied by Dr. H. E. Hennis, Dow Chemical Co., Midland, Michigan). The 2,4-dinitrophenylhydrazone had m.p. 176–177°; lit. m.p. 176–177° (11).

Norcamphor (6)

The i.r. spectrum of the solid ketone was superimposable with that of an authentic sample (Aldrich Chemical Co., Inc.). The 2,4-dinitrophenylhydrazone had m.p. 131–131.7°; lit. m.p. 130–131.5° (12).

1. D. L. GARIN. J. Org. Chem. **34**, 2355 (1969).
2. D. L. GARIN. Ph.D. Thesis, Iowa State University, Ames, Iowa. 1964.
3. J. K. CRANDALL. J. Org. Chem. **29**, 2830 (1964).
4. J. A. BERSON, C. J. OLSEN, and J. S. WALIA. J. Amer. Chem. Soc. **82**, 5000 (1960).
5. K. M. KORACH, R. D. NIELSEN, and H. W. RIDEOUT. J. Amer. Chem. Soc. **82**, 4328 (1960).
6. H. KWART and W. G. VOSBURGH. J. Amer. Chem. Soc. **76**, 5400 (1954).
7. H. M. WALBORSKY and D. F. LONCRINI. J. Amer. Chem. Soc. **76**, 5396 (1954).
8. H. KWART and T. TAKESHITA. J. Org. Chem. **28**, 670 (1963).
9. C. E. LYONS. Ph.D. Thesis, Iowa State University, Ames, Iowa. 1961.
10. P. PINO and A. MIGLIERINA. J. Amer. Chem. Soc. **74** 5551 (1952).
11. I. N. NAZAROV, L. A. KAZITSYNA, and I. I. ZARETSKAYA. J. Gen. Chem. (U.S.S.R.), **27**, 675 (1957); Chem. Abstr. **51**, 16383 f (1957).
12. J. D. ROBERTS, F. O. JOHNSON, and R. A. CARBONI. J. Amer. Chem. Soc. **76**, 5692 (1954).

Can. J. Chem. Downloaded from www.nrcresearchpress.com by 210.87.254.105 on 09/05/12
For personal use only.

New approach to the synthesis of optically active trityl systems

K. G. RUTHERFORD, J. L. H. BATISTE, AND J. M. PROKIPCAK
Department of Chemistry, University of Windsor, Windsor, Ontario

Received August 13, 1968

A new method for the resolution of potentially optically active trityl alcohols is reported. Three trityl alcohols as pilot compounds were converted to hydracrylic acid derivatives. Esterification with diazomethane was followed by degradation (reverse Michael reaction) to the original alcohols with sodium hydride. The resolution of phenyl-α-naphthyl-*p*-tolylcarbinol was effected conveniently by this route.

Canadian Journal of Chemistry, 47, 4073 (1969)

Can. J. Chem. Downloaded from www.nrcresearchpress.com by 210.87.254.40 on 09/05/12
For personal use only.

The fundamental procedure of preparative optical resolution is conversion of the racemic compound to diastereoisomeric salts of an optically active acid or base obtained from nature. Racemic primary and secondary alcohols are usually esterified with a dicarboxylic acid to provide racemic half esters for neutralization with the chiral base (alkaloid) and the enantiomers are isolated in good yield and with negligible racemization on hydrolysis of the separated salts (1). Racemic tertiary alcohols, however, because of their tendency for alkyl-oxy bond fission, readily lose structural integrity and hence, routes leading to optically active triaryl carbinols have been scarce in the literature since Wallis' first report on the resolution of phenylbiphenyl-α-naphthylcarbinol (2).

In 1962 Thaker and Dave (3) reported the synthesis of optically active phenyl-α-naphthyl-*p*-tolylcarbinol by the classical procedure which involved preparation of the hydrogen phthalate derivative of the alcohol. Resolution of this by brucine followed by hydrolysis of the ester reportedly yielded the optically active *d*-ROH. Several attempts to repeat Thaker's synthesis of the hydrogen phthalate derivative failed including the use of a method previously developed in this laboratory for the preparation of hydrogen phthalate esters of sterically hindered alcohols (4).

In 1963 Murr (5) reported on the resolution of phenylbiphenyl-α-naphthylcarbinol by an elegant procedure which involved conversion of the *dl*-ROH to the *dl*-glycolic acid derivative. Resolution of this with brucine followed by degradation yielded the *d*-ROH (Sequence I). Simultaneously our laboratory using triphenylcarbinol as a pilot system succeeded in degrading the glycolic acid derivative back to the ROH in good yield by the following procedure:

$$\mathrm{ROCH_2COOH} \xrightarrow[(3)\ \mathrm{Mg}\\(4)\ \mathrm{H_3O^+}]{(1)\ \mathrm{LAH}\\(2)\ \mathrm{SOCl_2}} \mathrm{ROH} + \mathrm{CH_2{=}CH_2}$$

Attempts to apply this to the preparation of optically active phenyl-*p*-chlorophenyl-*p*-bromophenyl-carbinol failed at the salt resolution stage, although this does not detract from the potential usefulness of this procedure for other compounds. Recently Murr and Feller (6) succeeded in effecting a spontaneous resolution of phenylbiphenyl-1-(8-methylnaphthyl) carbinol according to the method of Powell (7).

We wish to report the use of hydracrylic acid derivatives as useful intermediates for the resolution of triarylcarbinols. These derivatives can be readily prepared and degraded giving good yields in all steps with triphenylcarbinol and phenyl-α-naphthyl-*p*-tolylcarbinol as pilot compounds

$$\textit{dl}\text{-ROH} \xrightarrow{\mathrm{AcCl}} \textit{dl}\text{-RCl} \xrightarrow[\mathrm{HOCH_2COOCH_3}\\(2)\ \mathrm{KOH}]{(1)\ \text{pyridine, benzene,}} \textit{dl}\text{-}\mathrm{ROCH_2COOH}$$

$$\xrightarrow[(2)\ \mathrm{H_3O^+}]{(1)\ \textit{l}\text{-brucine}} \textit{l}\text{-}\mathrm{ROCH_2COOH} \xrightarrow[(3)\ t\text{-butyl-hypochlorite}\\(4)\ \mathrm{NaOCH_3},\ \text{benzene}]{(1)\ \mathrm{CH_2N_2}\\(2)\ \mathrm{NH_3}} \textit{d}\text{-ROH}$$

SEQUENCE I

$$ROH + CH_2 = CHCOOCH_3$$

SEQUENCE II

(Sequence II). The hydracrylic acid from phenyl-*p*-bromophenyl-*p*-chlorophenylcarbinol could be obtained directly in good yield by reacting the ROH with propiolactone in the presence of *p*-toluenesulfonic acid, thus saving the hydrolysis step. The diazomethane reactions proceeded smoothly and the reverse Michael reactions were carried out most conveniently and in excellent yields using either triphenylmethyl sodium or sodium hydride in anhydrous ether. The latter base is preferred because of its ready availability.

Attempts to completely resolve phenyl-α-naphthyl-*p*-tolylcarbinol (Thaker's alcohol) are still somewhat inconclusive. However, it is felt that a reasonable degree of resolution has been effected and that the low rotations indicated below are not due to some impurity because of the appreciable difference in melting points of the *dl*- and *d*-ROH as well as those of the *dl*- and *d*-RCOOH. The *dl*-ROH (m.p. 110–112°) was converted to methyl β-(phenyl-α-naphthyl-*p*-tolylmethoxy)-propionate by reaction with methyl β-hydroxypropionate in trifluoroacetic acid. Hydrolysis of this methyl ester afforded the *dl*-β-(phenyl-α-naphthyl-*p*-tolylmethoxy)-propionic acid (m.p. 151–152.5°). Conversion of the propionic acid to the optically active brucine salt, $[\alpha]_{436}^{25}$ −23.5° (c = 4.0524) proceeded in low yield (*ca.* 20%). It should be noted that brucine is levorotating in chloroform. The salt was decomposed by aqueous hydrochloric acid to optically active *d*-β-(phenyl-α-naphthyl-*p*-tolylmethoxy)-propionic acid, $[\alpha]_{436}^{25}$ +3.19° (c = 1.0176), m.p. 159–160.5°. The infrared (i.r.) spectrum of this acid was identical to that of the *dl*-acid. The optically active propionic acid was converted with diazomethane to the methyl ester which on subsequent treatment with sodium hydride in anhydrous ether yielded optically active phenyl-α-naphthyl-*p*-tolylcarbinol, $[\alpha]_{436}^{25}$ + 3.12 (c = 1.0092), m.p. 90–93°. The i.r. spectrum was identical to that of the *dl*-alcohol. The overall yield from the *d*-acid was *ca.* 85%. The optical purity of the *d*-acid was not determined. However, the brucine salt of the *d*-acid was crystallized until no significant change could be observed in optical rotation.

It would appear that the hydracrylic acid route to potentially optically active trityl alcohols could be a very useful procedure because of the ease of preparation and degradation which is less involved than the glycolic acid route. Hydracrylic acids should be no more difficult to resolve than corresponding glycolic acids although many variables are involved here.

Experimental

Melting points were determined on a Fisher–Johns apparatus and are uncorrected. Optical rotation measurements were determined in chloroform with a Rudolph Model 80 polarimeter equipped with a mercury vapor lamp (λ 4358 Å). Infrared spectra were recorded in chloroform with a Beckman IR-10 spectrophotometer equipped with potassium bromide cells. Microanalyses were performed by Midwest Microlab, Inc., 6000 East 46th Street, Indianapolis, Indiana, 46226.

Hydracrylic Acid Derivatives

β-*(Triphenylmethoxy)-propionic acid* was prepared by the two procedures outlined.

Procedure 1

A solution of triphenylcarbinol (1.032 g, 3.96 mmole) in 3 ml trifluoroacetic acid was added dropwise to 15 ml (0.159 mole) methyl β-hydroxypropionate which was cooled by means of an ice bath. The reaction mixture was poured onto cracked ice and neutralized with sodium bicarbonate. Methyl β-(triphenylmethoxy)-propionate was removed by filtration and air dried. Yields of 90–95% of quite pure product (m.p. 116–118°) were obtained consistently.

Anal. Calcd. for $C_{23}H_{22}O_3$: C, 79.74; H, 6.40. Found: C, 79.69; H, 6.40.

The ester (1.0 g, 2.89 mmole) was dissolved in 50 ml methanol. To this solution was added 10 ml 20% aqueous sodium hydroxide solution. After the solution was refluxed for 6 h, more water was added and the methanol was removed by distillation. Hydrochloric acid (3 *N*) was added to the cooled solution to p*H* 3. The product was filtered, air dried, and recrystallized from chloroform–petroleum ether (b.p. 30–60°), m.p. 164–166° (literature (8) 164–166°). Yields in this hydrolysis step ranged from 80–85% of recrystallized β-(triphenylmethoxy)-propionic acid.

Procedure 2

Triphenylcarbinol (2.01 g, 7.7 mmole) and 2 ml (0.032

Can. J. Chem. Downloaded from www.nrcresearchpress.com by 210.87.254.40 on 09/05/12
For personal use only.

Can. J. Chem. Downloaded from www.nrcresearchpress.com by 210.87.254.40 on 09/05/12
For personal use only.

mole) propiolactone were dissolved in 6 ml dry benzene. *p*-Toluenesulfonic acid (54 mg) was added and the solution was refluxed for 6 h. Aqueous potassium hydroxide solution (5%, 70 ml) was added and the solution was refluxed an additional 4 h. The addition of 30 ml ether to the cooled reaction mixture gave a good separation of layers. The aqueous layer was heated (50–60°) *in vacuo* to remove last traces of benzene and ether. Hydrochloric acid (6 *N*) was added to p*H* 3. The product was filtered and air dried. Recrystallization from chloroform–petroleum ether (b.p. 30–60°) yielded between 75–80% of pure β-(triphenylmethoxy)-propionic acid.

Methyl β-*(phenyl-α-naphthyl-p-tolylmethoxy)-propionate* was made in 80–85% yield by procedure 1 and was recrystallized from chloroform–heptane, m.p. 96–97°. The i.r. spectrum showed bands at 1735 cm^{-1} (C=O stretch), 1200–1170 cm^{-1} (ester C—O stretch) and 1065 cm^{-1} (R—O—R′ stretch).

Anal. Calcd. for $C_{28}H_{26}O_3$: C, 81.92; H, 6.39. Found: C, 81.74; H, 6.35.

β-*(Phenyl-α-naphthyl-p-tolylmethoxy)-propionic acid* was prepared in 95% yield from the methyl ester by hydrolysis using 5% aqueous sodium hydroxide. Recrystallization from chloroform–heptane gave m.p. 151–152.5°. The i.r. spectrum showed bands at 3600–2500 cm^{-1} (O—H stretch), 1715 cm^{-1} (C=O stretch), 1080–1060 cm^{-1} (R—O—R′ stretch).

Anal. Calcd. for $C_{27}H_{24}O_3$: C, 81.79; H, 6.10. Found: C, 81.66; H, 6.28.

β-*(Phenyl-p-bromophenyl-p-chlorophenyl)-propionic acid* was made from phenyl-*p*-bromophenyl-*p*-chlorophenyl-carbinol (prepared by the method of Stagner (9)) and propiolactone according to Procedure 2 in yields of 75–80%. Recrystallization from chloroform–petroleum ether (30–60°) gave m.p. 138–139°. The i.r. spectrum showed bands at 3600–2400 cm^{-1} (O—H stretch), 1715 cm^{-1} (C=O stretch) and 1090–1070 cm^{-1} (R—O—R′ stretch).

Anal. Calcd. for $C_{22}H_{18}O_3BrCl$: C, 59.30; H, 4.07. Found: C, 59.74; H, 3.84.

N.E. (Neutral Equivalent) Calcd.: 445.7. Found: 444.9.

Reactions of Hydracrylic Acids with Diazomethane

Methyl β-*(triphenylmethoxy)-propionate* was prepared in the following manner.

An ethereal solution of diazomethane (approx. 1.56 g, 0.0372 mole) was prepared by adding a solution of 8.0 g (0.0372 mole) *N*-methyl-*N*-nitroso-*p*-toluenesulfonamide in 37 ml ether to a mixture of 3 ml water, 10 ml ethanol, and 2.0 g (0.0351 mole) potassium hydroxide heated to 65° (10). The liberated diazomethane was carefully distilled directly into a solution of 0.9 g (2.71 mmole) β-(triphenylmethoxy)-propionic acid in 10 ml ether cooled in an ice bath (11). After the reaction had ceased, the excess diazomethane was destroyed with 2.3 ml (*ca.* 0.0372 mole) glacial acetic acid. The ether layer was extracted with saturated sodium bicarbonate solution, dried over anhydrous magnesium sulfate, and evaporated *in vacuo*. The crude product was recrystallized from chloroform–petroleum ether (b.p. 30–60°), m.p. 114–116° (80–85% yield).

Methyl β-*(phenyl-p-bromophenyl-p-chlorophenylmethoxy)-propionate* was not isolated in crystalline form. The i.r. spectrum however showed bands at 1735 cm^{-1} (C=O stretch), 1170 cm^{-1} (ester C—OR stretch) and 1090–1065 cm^{-1} (R—O—R′ stretch). Hydrolysis to the acid proceeded cleanly with potassium hydroxide.

Resolution of β-*(Phenyl-α-naphthyl-p-tolylmethoxy)-propionic Acid*

All rotations were taken in chloroform in a 2 dm cell and deviations in specific rotations were not greater than ± 0.5°. The brucine salt was prepared in acetone by the standard method (1), $[\alpha]_{436}^{25}$ −30.9° (c = 4.0236). Several recrystallizations of this salt from toluene-methylcyclohexane gave a fraction (*ca.* 20% yield) with constant rotation $[\alpha]_{436}^{25}$ −23.5° (c = 4.0524). The salt was decomposed in an ether–water system with an excess of 0.25 *N* hydrochloric acid. The ether layer was dried with anhydrous magnesium sulfate, heptane was added and the *d*-acid slowly recrystallized, m.p. 159–160.5°, $[\alpha]_{436}^{25}$ +3.19° (c = 1.6176). The i.r. spectrum of the *d*-acid was identical to that of the *dl*-acid.

Reverse Michael Reactions

The reaction of methyl β-(triphenylmethoxy)-propionate with sodium hydride is given: sodium hydride (7g of a 50% dispersion in mineral oil, 0.146 mole NaH) was suspended in 75 ml dry ether in a 250 ml 3-necked flask which was equipped with a glass stopper, a pressure-equalizing addition funnel, and a reflux condenser. A solution of the ester (1.8 g, 5.2 mmole) in 100 ml dry ether was added rapidly with stirring to the flask. The mixture was stirred for 24–26 h, cooled to ice bath temperature, and 75 ml water was added slowly. The ether layer was separated from the water layer, dried over anhydrous magnesium sulfate, and evaporated *in vacuo*. The triphenylcarbinol was separated from the mineral oil by filtration and recrystallized from methanol–benzene, m.p. 163–164° (yield *ca.* 90%). Similarly, and with excellent yields, reverse Michael reactions were carried out with methyl β-(phenyl-*p*-bromophenyl-*p*-chlorophenyl-methoxy)-propionate and methyl β-(phenyl-α-naphthyl-*p*-tolylmethoxy)-propionate. The optically active methyl β-(phenyl-α-naphthyl-*p*-tolylmethoxy)-propionate was not isolated from the diazomethane reaction with the corresponding *d*-acid but was subjected directly to the reverse Michael reaction in ether solution. The *d*-alcohol was separated from the mineral oil by filtration and recrystallized several times from ether–heptane, $[\alpha]_{436}^{25}$ +3.12° (c = 1.0092), m.p. 90–93°. The i.r. spectrum of the *d*-alcohol was identical to that of the *dl*-alcohol. The yield of *d*-alcohol was *ca.* 85% from the *d*-acid.

Acknowledgments

The financial support given by the National Research Council of Canada and by the Petroleum Research Fund (Grant No. 1575-A4) administered by the American Chemical Society is gratefully acknowledged.

Both J. L. H. Batiste and J. M. Prokipcak wish to acknowledge gratefully, support from the

National Research Council of Canada in the form of postgraduate studentship.

1. A. W. INGERSOLL. *In* Organic reactions. Vol. II. John Wiley and Sons, Inc., New York, 1944, p. 376.
2. E. S. WALLIS and F. H. ADAMS. J. Amer. Chem. Soc. **55**, 3838 (1933).
3. K. A. THAKER and N. S. DAVE. J. Sci. Ind. Res. **21***B*, 374 (1962).
4. K. G. RUTHERFORD, J. M. PROKIPCAK, and D. P. C. FUNG. J. Org. Chem. **28**, 582 (1963).
5. B. L. MURR. J. Amer. Chem. Soc. **85**, 2866 (1963).
6. B. L. MURR and L. W. FELLER. J. Amer. Chem. Soc. **90**, 2966 (1968).
7. H. M. POWELL. Nature, **170**, 155 (1952).
8. B. F. HELFERISH, L. MOOG, and A. JUNGER. Ber. **58**, 881 (1925).
9. B. A. STAGNER. J. Amer. Chem. Soc. **38**, 2078 (1916).
10. TH J. DE BOER and H. J. BACKER. *In* Organic Synthesis. *Edited by* N. Rabjohn. Coll. Vol. IV. John Wiley and Sons, Inc., New York, 1963. pp. 250, 943.
11. R. B. WAGNER and H. D. ZOOK. Synthetic organic chemistry. John Wiley and Sons, Inc., New York, 1953. p. 485.

Polarographic half-wave potentials and ultraviolet absorption spectra of some conjugated heteroenoid compounds

H. L. HOLMES AND D. J. CURRIE
Chemistry Section, Defence Research Establishment, Suffield, Ralston, Alberta

Received September 9, 1968

The half-wave potentials of phenyl substituted derivatives for each series of conjugated heteroenoid compounds studied follow a Hammett relationship. The effect of change in the functional groups and of increase in length of the conjugated system upon half-wave potentials and ultraviolet absorption maxima is briefly discussed. Terephthalylidene derivatives of active methylene compounds function like the cinnamylidene derivatives.

Canadian Journal of Chemistry, 47, 4076 (1969)

Can. J. Chem. Downloaded from www.nrcresearchpress.com by 210.87.254.40 on 09/05/12
For personal use only.

Equations already developed for calculating the stimulatory activities (1) and the bacterial growth inhibitory activities (2) of a number of conjugated heteroenoid compounds with the generalized formula **1**, required the determination of their polarographic half-wave potentials. This note discusses the effect of phenyl substituents,

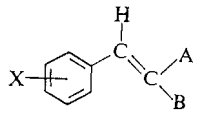

1

(*a*) A = B = $COCH_3$; (*b*) AB = 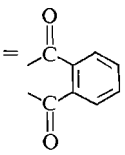 ;

(*c*) A = $COCH_3$, B = $CO_2C_2H_5$; (*d*) A = $COCH_3$, B = COC_6H_5; (*e*) A = $CO_2C_2H_5$, B = COC_6H_5; (*f*) A = COC_6H_5, B = CN; (*g*) A = $CO_2C_2H_5$, B = CN; (*h*) A = B = CN; (*i*) A = $CONH_2$, B = CN; (*j*) A = $CONHC_6H_5$, B = CN; (*k*) A = B = $CONH_2$; (*l*) A = B = $CO_2C_2H_5$; (*m*) A = $CO_2C_2H_5$, B = $CONH_2$.

X, and functional groups, A and B, on the half-wave potentials of these compounds. The mechanism of the polarographic reduction in aqueous and non-aqueous media has been examined by Bargain *et al.* (3–5) and Marciszewski (6) has reduced methyl 1-methylbutylidenecyanoacetate.

In this work, the reduction of these compounds (7,8) was carried out under conditions similar to those used by Silver and Holmes (9). In all but a few cases single waves were obtained (Tables I and II). The second wave in the polarogram for the 2-benzal-1,3-indanediones (**1***b*) appears to be due to the hydrolysis product, 1,3-indanedione ($E_{\frac{1}{2}} = -1.182$ V) but not to the respective aldehyde (Table IV). The polarogram of the α-cyano-*trans*-benzalacetophenones (**1***f*) appears to be similarly complicated by reduction of benzoylacetonitrile. The ranges of diffusion currents for the various classes of compounds are listed in Table III.

For the reduction of these various classes of compounds, the relationship between half-wave potentials and Hammett's σ or Taft's σ* value is linear except for compounds containing strong electron-withdrawing X groups, e.g. NO_2, CN. The ρ values (Table V) fall into three groups: the *gem*-diketones, **1***a*, **1***b*, and **1***d*, all have a ρ value between 0.26 and 0.29; the keto-esters, **1***c* and **1***e*, and the benzalmalonamides, **1***k*, have a ρ value

National Research Council of Canada in the form of postgraduate studentship.

1. A. W. INGERSOLL. *In* Organic reactions. Vol. II. John Wiley and Sons, Inc., New York, 1944, p. 376.
2. E. S. WALLIS and F. H. ADAMS. J. Amer. Chem. Soc. **55**, 3838 (1933).
3. K. A. THAKER and N. S. DAVE. J. Sci. Ind. Res. **21***B*, 374 (1962).
4. K. G. RUTHERFORD, J. M. PROKIPCAK, and D. P. C. FUNG. J. Org. Chem. **28**, 582 (1963).
5. B. L. MURR. J. Amer. Chem. Soc. **85**, 2866 (1963).
6. B. L. MURR and L. W. FELLER. J. Amer. Chem. Soc. **90**, 2966 (1968).
7. H. M. POWELL. Nature, **170**, 155 (1952).
8. B. F. HELFERISH, L. MOOG, and A. JUNGER. Ber. **58**, 881 (1925).
9. B. A. STAGNER. J. Amer. Chem. Soc. **38**, 2078 (1916).
10. TH J. DE BOER and H. J. BACKER. *In* Organic Synthesis. *Edited by* N. Rabjohn. Coll. Vol. IV. John Wiley and Sons, Inc., New York, 1963. pp. 250, 943.
11. R. B. WAGNER and H. D. ZOOK. Synthetic organic chemistry. John Wiley and Sons, Inc., New York, 1953. p. 485.

Polarographic half-wave potentials and ultraviolet absorption spectra of some conjugated heteroenoid compounds

H. L. HOLMES AND D. J. CURRIE
Chemistry Section, Defence Research Establishment, Suffield, Ralston, Alberta

Received September 9, 1968

The half-wave potentials of phenyl substituted derivatives for each series of conjugated heteroenoid compounds studied follow a Hammett relationship. The effect of change in the functional groups and of increase in length of the conjugated system upon half-wave potentials and ultraviolet absorption maxima is briefly discussed. Terephthalylidene derivatives of active methylene compounds function like the cinnamylidene derivatives.

Canadian Journal of Chemistry, 47, 4076 (1969)

Can. J. Chem. Downloaded from www.nrcresearchpress.com by 210.87.254.105 on 09/05/12
For personal use only.

Equations already developed for calculating the stimulatory activities (1) and the bacterial growth inhibitory activities (2) of a number of conjugated heteroenoid compounds with the generalized formula **1**, required the determination of their polarographic half-wave potentials. This note discusses the effect of phenyl substituents,

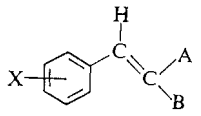

1

(*a*) A = B = $COCH_3$; (*b*) AB = 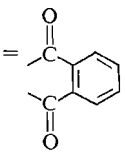 ;

(*c*) A = $COCH_3$, B = $CO_2C_2H_5$; (*d*) A = $COCH_3$, B = COC_6H_5; (*e*) A = $CO_2C_2H_5$, B = COC_6H_5; (*f*) A = COC_6H_5, B = CN; (*g*) A = $CO_2C_2H_5$, B = CN; (*h*) A = B = CN; (*i*) A = $CONH_2$, B = CN; (*j*) A = $CONHC_6H_5$, B = CN; (*k*) A = B = $CONH_2$; (*l*) A = B = $CO_2C_2H_5$; (*m*) A = $CO_2C_2H_5$, B = $CONH_2$.

X, and functional groups, A and B, on the half-wave potentials of these compounds. The mechanism of the polarographic reduction in aqueous and non-aqueous media has been examined by Bargain *et al.* (3–5) and Marciszewski (6) has reduced methyl 1-methylbutylidenecyanoacetate.

In this work, the reduction of these compounds (7,8) was carried out under conditions similar to those used by Silver and Holmes (9). In all but a few cases single waves were obtained (Tables I and II). The second wave in the polarogram for the 2-benzal-1,3-indanediones (**1***b*) appears to be due to the hydrolysis product, 1,3-indanedione ($E_{\frac{1}{2}} = -1.182$ V) but not to the respective aldehyde (Table IV). The polarogram of the α-cyano-*trans*-benzalacetophenones (**1***f*) appears to be similarly complicated by reduction of benzoylacetonitrile. The ranges of diffusion currents for the various classes of compounds are listed in Table III.

For the reduction of these various classes of compounds, the relationship between half-wave potentials and Hammett's σ or Taft's σ* value is linear except for compounds containing strong electron-withdrawing X groups, e.g. NO_2, CN. The ρ values (Table V) fall into three groups: the *gem*-diketones, **1***a*, **1***b*, and **1***d*, all have a ρ value between 0.26 and 0.29; the keto-esters, **1***c* and **1***e*, and the benzalmalonamides, **1***k*, have a ρ value

Can. J. Chem. Downloaded from www.nrcresearchpress.com by 210.87.254.105 on 09/05/12
For personal use only.

Polarographic half-wave potentials, $E_{\frac{1}{2}}$, of some conjugated heteroenoid compounds*

		$E_{\frac{1}{2}}$ (−V)							
X	Y	A = B = $COCH_3$	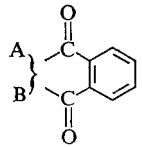	A = $COCH_3$ B = CO_2-C_2H_5	A = CO_2-C_2H_5 B = CN	A = B = CN	A = $CONH_2$ B = CN	A = CO-NHC_6H_5 B = CN	A = B = $CONH_2$
H	H	1.076	0.840†	1.142	1.251	1.175	1.328	1.329	⩾1.4
2-CH_3	H	1.057	0.891	1.140	1.192	1.180	1.343	1.332	⩾1.4
3-CH_3	H	—	—	1.132	—	1.183	—	—	1.372
4-CH_3	H	1.054	0.891	1.113	1.291	1.229	⩾1.4	1.365	⩾1.4
2-C_2H_5	H	—	—	—	—	1.198	—	—	—
2-F	H	—	0.815	—	—	1.073	1.240	—	—
3-F	H	—	—	1.067	1.134	1.069	—	—	—
4-F	H	1.100	—	—	—	1.177	—	—	1.319
2-Cl	H	0.951	0.798	1.032	—	—	1.220	1.198	1.294
3-Cl	H	0.965	—	1.040	1.105	1.017	—	—	1.290
4-Cl	H	1.006	0.775†	1.083	1.182	1.081	1.243	—	1.307
2-Br	H	—	0.788	—	—	—	—	—	—
3-Br	H	—	—	—	—	0.981	—	—	—
4-Br	H	1.020	—	—	—	1.042	—	—	—
2-CH_3O	H	1.081	0.905	1.135	1.298	⩾1.35	1.366	1.351	⩾1.4
3-CH_3O	H	1.034	—	1.107	1.201	1.132	1.312	1.310	1.327
4-CH_3O	H	1.077	0.906†	1.131	1.348	⩾1.35	⩾1.4	1.401	⩾1.4
2-C_2H_5O	H	—	—	—	—	⩾1.35	—	—	—
3-C_2H_5O	H	—	—	1.098	—	1.131	—	—	—
3,*n*-C_3H_7O	H	—	—	1.115	—	—	—	—	—
3,*i*-C_3H_7O	H	—	—	—	—	⩾1.35	—	—	—
3,*n*-C_4H_9O	H	—	—	1.109	1.213	—	—	—	—
3-CHO	H	0.995	—	—	—	—	—	—	—
4-CN	H	—	—	—	0.900	—	—	—	—
4-CO_2CH_3		—	—	—	—	0.867 1.175	—	—	—
3-NO_2		—	—	—	0.597	0.711	—	—	—
4-NO_2	H	—	—	—	—	0.544 0.805	—	—	—
2-Cl	4-Cl	—	—	0.971	1.036	—	—	—	1.248
2-Cl	6-Cl	—	—	1.006	1.189	—	—	—	—
3-Cl	4-Cl	—	—	0.991	—	0.925	—	—	—
2-CH_3O	3-CH_3O	—	—	1.093	—	—	—	—	—
2-CH_3O	4-CH_3O	1.050	—	1.120	⩾1.35	—	—	—	⩾1.4
3-CH_3O	4-CH_3O	—	—	1.145	1.322	1.245	1.367	—	—
		—	—	1.122	—	—	—	1.351	—

*The general structure is 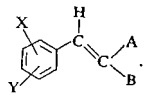

†A second wave begins at about −1.0 V. This is probably due to 1,3-indanedione.

Can. J. Chem. Downloaded from www.nrcresearchpress.com by 210.87.254.105 on 09/05/12
For personal use only.

TABLE II

Polarographic half-wave potentials, $E_{\frac{1}{2}}$, of some α-substituted benzalacetophenones*

X	$E_{\frac{1}{2}}$ (−V) A = $COCH_3$ B = COC_6H_5	A = $CO_2C_2H_5$ B = COC_6H_5	A = COC_6H_5 B = CN
H	1.030	1.060	0.838; 0.990
2-CH_3	1.033	—	—
3-CH_3	—	1.072	—
4-CH_3	1.073	1.092	0.829; 1.045
2-Cl	0.932	0.977	0.783; 1.191
3-Cl	—	0.991	—
4-Cl	0.967	1.004	0.743; 0.923
2-Br	—	0.952	—
2-CH_3O	1.046	1.075	0.875; 0.980
3-CH_3O	—	1.038	0.792; 0.967
4-CH_3O	1.126	1.102	0.816; 1.103
4-CH_3CONH	—	—	0.834; 0.988

*The general structure is 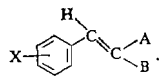 .

TABLE III

Range of diffusion currents, I_D, for the classes of compounds* examined in this work

A	B	I_D (amps × 10^6)
$COCH_3$	$COCH_3$	2.88–6.00
$CH{=}C(COCH_3)_2$	H	2.13
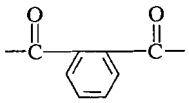		1.58–2.50
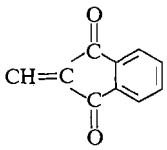	H	1.83
$COCH_3$	COC_6H_5	3.30–3.69
$CO_2C_2H_5$	COC_6H_5	2.64–4.11
COC_6H_5	CN	1.32–3.54; 1.35–3.69
$CH{=}C(CO_2C_2H_5)_2$	H	3.88
$CO_2C_2H_5$	CN	2.08–9.60
CN	CN	1.38–3.48
$CONH_2$	CN	3.44–4.40
$CONHC_6H_5$	CN	4.24–5.76
$CONH_2$	$CONH_2$	4.24–5.76

*The actual compounds are listed in Tables I and II.

TABLE IV

Polarographic half-wave potentials, $E_{\frac{1}{2}}$, and diffusion currents, I_D, of some benzaldehydes, benzalacetone, and benzalacetophenone†

A	X	$E_{\frac{1}{2}}$ (−V)	I_D (amps × 10^6)
CHO*	4-CHO	0.911	2.36
CH=CH—$COCH_3$	H	1.141	2.96
CH=CH—COC_6H_5	H	0.946	2.56
$(CH=CH)_2$—COC_6H_5	H	0.886;1.272	3.08;2.85

*The 2-methyl, 4-methyl, 2-fluoro, 2-chloro, 4-chloro, 4-bromo, 2-methoxy-, 3-methoxy-, and 4-methoxybenzaldehydes have half-wave potentials more negative than −1.3 volts.

†The general structure is 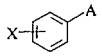

TABLE V

Hammett ρ values* for the polarographic reduction of some series of conjugated heteroenoid compounds substituted at C_3 and C_4†

A	B	ρ
$COCH_3$	$COCH_3$	0.295
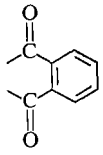		0.265
$COCH_3$	$CO_2C_2H_5$	0.160
$COCH_3$	COC_6H_5	0.267
$CO_2C_2H_5$	COC_6H_5	0.167
COC_6H_5	CN	0.269; 0.363
$CO_2C_2H_5$	CN	0.372
CN	CN	0.391
$CONH_2$	CN	0.370
$CONHC_6H_5$	CN	0.158
$CONH_2$	$CONH_2$	0.185

*For the relationship $E_{\frac{1}{2}XY} = \rho\sigma$ + constant.

†The general structure is 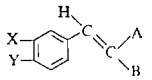

between 0.16 and 0.19; while the cyano-containing compounds, **1***g*, **1***h*, and **1***i*, comprise a third group with ρ values between 0.36 and 0.39.

Half-wave potentials were obtained for the terephthalylidene derivatives of some active methylene compounds, **2** (Table VI). The tetracarbethoxy compound (**2**) has a half-wave

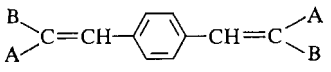

2

A = B = $CO_2C_2H_5$

potential much less negative than that of diethyl benzalmalonate (**1***l*) ($E_{\frac{1}{2}} \geqslant -1.4$ V) (9), and even less than that of diethyl cinnamylidenemalonate (**3**). This is not the case for the related *meta* isomer of **2** ($E_{\frac{1}{2}} \geqslant -1.4$ V). The alternating system of

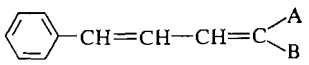

3

A = B = $CO_2C_2H_5$

single and double bonds in these terephthalylidene compounds probably acts as one long conjugated system with reduced transmission of the mesomeric effect through the ring (10). The marked similarity in the long-wavelength absorption maxima and extinction coefficients of **2**

Can. J. Chem. Downloaded from www.nrcresearchpress.com by 210.87.254.105 on 09/05/12
For personal use only.

TABLE VI

Polarographic half-wave potentials, $E_{\frac{1}{2}}$, of some cinnamylidene and terephthalylidene derivatives of some active methylene compounds

A	B	$E_{\frac{1}{2}}$ (−V) 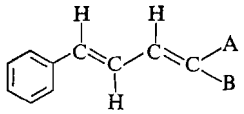	$E_{\frac{1}{2}}$ (−V) 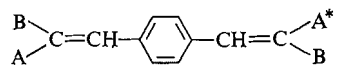
CO_2H	H	—	1.086
$CO_2C_2H_5$	H	⩾1.4	0.873
COC_6H_5	H	0.886; 1.271	⩾1.4
NO_2	H	—	0.526; 0.612
NO_2	CH_3	—	0.552; 0.771
$COCH_3$	$COCH_3$	0.893	0.721
$COCH_3$	$CO_2C_2H_5$	—	0.775
$CO_2C_2H_5$	$CO_2C_2H_5$	~1.263	1.064†
CO_2H	CN	—	1.009
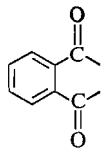		0.732	⩾1.4

*A saturated solution was used in these cases.
†The corresponding *meta* isomer had a half-wave potential more negative than −1.4 V.

compounds with those of the analogous **3** derivatives (Table VII) indicate that this is the case. A method for calculating the long-wavelength absorption maxima of these terephthalylidene derivatives has already been described (11).

The half-wave potentials of diethyl benzalmalonate (**1***l*), ethyl benzalmalonamate (**1***m*), (⩾ −1.3 V), and ethyl benzalcyanoacetate (**1***g*) are all more negative than the analogous 3-substituted coumarins, **4** (Table VIII), indicating that the carbethoxyl group of ethyl benzalmalonamate probably is *trans* to the phenyl group.

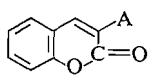

4

A = $CO_2C_2H_5$; $CONH_2$; CN

Experimental

The preparations of the terephthalylidene, isophthalylidene, and cinnamylidene derivatives of some active methylene compounds are summarized in Tables IX and X. The absorption spectra of ethanolic solutions of the compounds were recorded in a model 15 Cary spectrophotometer.

The polarograms were recorded on a Sargent model XV polarograph. Stock solutions of the compounds were made up in ethanol and the determinations were made on 25 ml samples of a 75% v/v aqueous ethanolic solution, 8×10^{-4} *M* in the reducible substance, containing 0.1 *M* acetic acid and 0.1 *M* sodium acetate. The p*H* of the ethanolic buffer solution as measured with a glass electrode was 6.6 and methylene blue thiocyanate (0.01%) was used as a maximum suppressor. The half-wave potential was measured against a saturated calomel electrode. The cell resistance was ~6800 Ω; with no applied voltage and the mercury at a height of 84 cm the drop mass was 2.68 mg/s and the drop time was 3.27 s.

Before the polarogram was recorded at 25 °C the solution was deaerated by bubbling nitrogen through it for 20 min. A second polarogram was recorded on the same solution after a further 10 min sweep with nitrogen. The half-wave potentials recorded are the averages of the values obtained from the two determinations and are accurate to ±0.01 V. The hydrogen wave occurred at −1.4 V and half-wave potentials more negative than this could not be obtained.

Acknowledgments

The determination of the polarographic half-wave potentials by Messrs. F. K. McClusky and R. F. Silver and the recording of the absorption

Can. J. Chem. Downloaded from www.nrcresearchpress.com by 210.87.254.105 on 09/05/12
For personal use only.

TABLE VII

Ultraviolet absorption maxima and extinction coefficients for some cinnamylidene and terephthalylidene derivatives of some active methylene compounds

		Absorption maxima (mμ) and extinction coefficients	
A	B	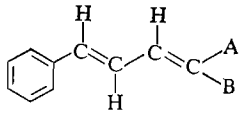	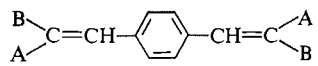
$CO_2C_2H_5$	H	309.5(37 800), ~240(~7400), 233(10 000), ~228(~8200)	331(—), 319(42 500), ~234(—), 228(15 900), 223(15 000), 202(23 000)
COC_6H_5	H	344(37 200), 269–263(8900), 234.5(8400)	354.5(48 000), 275(12 400), 233(13 600)†
NO_2	H	—	345(35 900), 230(10 700), <200(—)
NO_2	CH_3	—	335(25 200), 225.5(11 500)
$COCH_3$	$COCH_3$	326(23 800), ~225(—), 207(20 000)	326(33 800), ~225(—), 207(20 000)
$COCH_3$	$CO_2C_2H_5$	330.5(30 800), 235(8200), ~229(—)	324.5(33 800), 225(12 000), 204.5(20 400)
$CO_2C_2H_5$	$CO_2C_2H_5$	321(34 400), ~241(—), 234.5(8800), ~229(—)	319.5(35 500), 221(13 000), 203(21 900)‡
$CO_2C_2H_5$	CN§	345(—)	~362(—), 346.5(41 600), 227(11 300), 202(14 200)
CO_2CH_3	CN‖	341.3(31 040)	—
CN	CN	350(33 000), 247.5(7400), 241(7400), ~235(—)	~365(—), 349(35 800), ~335(—), 226(9000), ~209(—), 203.5(11 200)
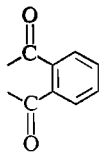		384(44 300), 270(14 900), 253.5(21 600)	~402(—), 392(—), 226(—)*

*Due to the insolubility of the product a saturated solution was used.
†The *meta* isomer had an absorption maximum at 307 mμ (ε = 46 000).
‡The *meta* isomer had an absorption maximum at 277 mμ (ε = 38 000).
§Reported in reference 12.
‖Reported in reference 13.

TABLE VIII

Polarographic half-wave potentials, $E_{\frac{1}{2}}$, and diffusion currents, I_D, of some 3-substituted coumarins*

A	$E_{\frac{1}{2}}$ (−V)	I_D (amps × 10^6)
H	⩾1.4	—
$COCH_3$	0.922	2.08
	1.268	2.44
$CO_2C_2H_5$	1.146	2.72
CN	1.052	2.28
$CONH_2$	1.286	2.72
$CONHC_6H_5$	⩾1.4	—

*The general structure is 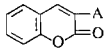

spectra by Mr. C. E. Lough are gratefully acknowledged.

1. H. L. Holmes and D. J. Currie. Unpublished work.
2. H. L. Holmes, J. R. Maltman, and D. J. Currie. Unpublished work.
3. M. M. Bargain. C. R. **254**, 130 (1962).
4. M. M. Bargain. C. R. **255**, 1948 (1962).
5. M. M. Bargain. C. R. **256**, 1990 (1963).
6. H. Marciszewski. Chem. Anal. (Warsaw), **5**, 119 (1960).
7. R. F. Silver, K. Ann Kerr, Peggy D. Frandsen, Sheila J. Kelley, and H. L. Holmes. Can. J. Chem. **45**, 1001 (1967).
8. D. J. Currie and H. L. Holmes. Can. J. Chem. **47**, 863 (1969).
9. R. F. Silver and H. L. Holmes. Can. J. Chem. **44**, 1031 (1966).
10. J. M. Stewart, I. Klundt, and K. Peacock. J. Org. Chem. **25**, 913 (1960).
11. D. J. Currie, C. E. Lough, R. F. Silver, and H. L. Holmes. Can. J. Chem. **45**, 1567 (1967).
12. R. Wizinger and H. Sontag. Helv. Chim. Acta, **38**, 363 (1955).
13. M. Coenen and M. Pestemer. Z. Elektrochem. **57**, 785 (1953).
14. D. E. Worral. J. Amer. Chem. Soc. **62**, 3253 (1940).

Can. J. Chem. Downloaded from www.nrcresearchpress.com by 210.87.254.105 on 09/05/12
For personal use only.

Can. J. Chem. Downloaded from www.nrcresearchpress.com by 210.87.254.105 on 09/05/12
For personal use only.

TABLE IX

Preparation of terephthalylidene and isophthalylidene derivatives of some active methylene compounds*

A	B	Reference for method	Melting point (°C)	Analytical figures: Calculated % C	Calculated % H	Calculated % N	Found % C	Found % H	Found % N
CO_2H	H	17,18	238.0–240.0 (vacuum)	—	—	—	—	—	—
CN	H	17,18	255–256 (uncorrected)	—	—	—	—	—	—
$CO_2C_2H_5$	H	19	97.0–98.0	—	—	—	—	—	—
COC_6H_5	H†	20	192.0–193.0	85.18	5.36	—	84.98	5.49	—
NO_2	H	14,15	234.0–235.0	—	—	—	—	—	—
NO_2	CH_3	15	122.2–123.2	—	—	—	—	—	—
$COCH_3$	$COCH_3$	—	143.2–144.2	72.46	6.08	—	72.31	5.85	—
$COCH_3$	$CO_2C_2H_5$	—	143.0–144.0	67.02	6.18	—	66.81	6.11	—
$CO_2C_2H_5$	$CO_2C_2H_5$‡	15	137.0–138.0	—	—	—	—	—	—
$CO_2C_2H_5$	CN	16,15	202.2–203.2	—	—	—	—	—	—
CN	CN	16	265-266 (uncorrected)	73.03	2.62	24.33	73.04	2.74	24.51
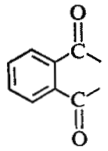		16	> 300 (uncorrected)	—	—	—	—	—	—

*The general structure is 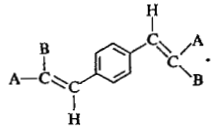

†The *meta* isomer (22) had a melting point of 141.5–142.0 °C.
‡The *meta* isomer (21) had a melting point of 101.0–102.0 °C.

TABLE X

Preparation of cinnamylidene derivatives of some active methylene compounds*

A	B	Reference for method	Melting (boiling) point (°C)
CO_2H	H	26	163.0–165.0
$CO_2C_2H_5$	H	27	25
$COCH_3$	$COCH_3$	23,24	102.0–102.5
$COCH_3$	$CO_2C_2H_5$	25	148–151/0.2 mm
$CO_2C_2H_5$	$CO_2C_2H_5$	28,29	34.0–35.0
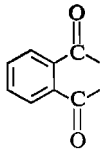		30,31, 32	154.0–155.0

*The general structure is 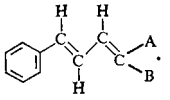

15. V. V. PEREKALIN and O. M. LERNER. Zh. Obshch. Khim. **28**, 1815 (1958).
16. H. KAUFFMANN. Ber. **50**, 525 (1917).
17. K. H. SLOTTA and H. HELLER. Ber. **63**, 3029 (1930).
18. S. MALINOWSKI and S. BENBENEK. Roczniki Chem. **27**, 379 (1953); Chem. Abstr. **49**, 1034 (1955).
19. H. POHL. J. Prakt. Chem. **141**, 44 (1934); Chem. Abstr. **29**, 135 (1935).
20. Z. S. ARIYAN and B. MOONEY. J. Chem. Soc. 1519 (1962).
21. F. RUGGLI and A. STAUB. Helv. Chim. Acta, **20**, 918 (1937); Chem. Abstr. **32**, 562 (1938).
22. D. DAVEY and D. H. MAASS. J. Chem. Soc. 4386 (1963).
23. E. KNOEVENAGEL and A. HERZ. Ber. **37**, 4483 (1904).
24. S. RUHEMANN. J. Chem. Soc. **85**, 1458 (1904).
25. E. KNOEVENAGEL. Ber. **31**, 734 (1898).
26. A. G. ANDERSON and S. Y. WANG. J. Org. Chem. **19**, 277 (1954).
27. V. N. BELOV and E. I. SHEPELENKOVA. Trudy Vsesoyuz. Inst. Sintet. i Natural. Dushistykh Veshchestv. 24, (1955); Ref. Zh. Khim. No. 747 (1956); Chem. Abstr. **51**, 17818 (1957).
28. C. F. H. ALLEN and F. W. SPANGLER. Org. Syn. Coll. Vol. III p. 377.
29. J. THIELE and J. MEISENHEIMER. Ann. **306**, 253 (1898).
30. L. GEITAARD and G. VANAGS. Zh. Obshch. Khim. **27**, 3109 (1951).
31. V. PETROV, J. SAPER, and B. STURGEON. J. Chem. Soc. 2134 (1949).
32. S. KOSTANECKI and L. LACZKOWSKI. Ber. **30**, 2138 (1897).

Proton magnetic resonance and mass spectrometric studies on derivatives of sodium 2-*O*-α-D-mannopyranosyl-D-glycerate and related compounds

J. N. C. WHYTE

Fisheries Research Board of Canada, Vancouver Laboratory, 6640 N.W. Marine Drive, Vancouver 8, B.C.

Received April 11, 1969

The proton magnetic resonance (p.m.r.) and mass spectra of the methyl ester pentaacetate of sodium 2-*O*-α-D-mannopyranosyl-D-glycerate from the red alga *Rhodomela larix* are compared to those of related compounds to affirm the assigned structure.

Canadian Journal of Chemistry, **47**, 4083 (1969)

The observation that the water soluble components of an 80% aqueous methanol extract of *Rhodomela larix* inhibited the growth of *E. coli* (1) prompted an interest in the low molecular weight components of this alga. Extraction of the seaweed with a chloroform–methanol–water mixture yielded sodium 2-*O*-α-D-mannopyranosyl-D-glycerate (**1**) (2) as the major water soluble component. The corresponding free acid provided a poorly resolved p.m.r. spectra, but that of the

Can. J. Chem. Downloaded from www.nrcresearchpress.com by 210.87.254.105 on 09/05/12
For personal use only.

TABLE X

Preparation of cinnamylidene derivatives of some active methylene compounds*

A	B	Reference for method	Melting (boiling) point (°C)
CO_2H	H	26	163.0–165.0
$CO_2C_2H_5$	H	27	25
$COCH_3$	$COCH_3$	23,24	102.0–102.5
$COCH_3$	$CO_2C_2H_5$	25	148–151/0.2 mm
$CO_2C_2H_5$	$CO_2C_2H_5$	28,29	34.0–35.0
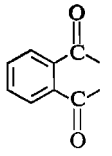		30,31, 32	154.0–155.0

*The general structure is 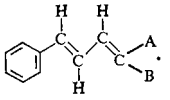

15. V. V. PEREKALIN and O. M. LERNER. Zh. Obshch. Khim. **28**, 1815 (1958).
16. H. KAUFFMANN. Ber. **50**, 525 (1917).
17. K. H. SLOTTA and H. HELLER. Ber. **63**, 3029 (1930).
18. S. MALINOWSKI and S. BENBENEK. Roczniki Chem. **27**, 379 (1953); Chem. Abstr. **49**, 1034 (1955).
19. H. POHL. J. Prakt. Chem. **141**, 44 (1934); Chem. Abstr. **29**, 135 (1935).
20. Z. S. ARIYAN and B. MOONEY. J. Chem. Soc. 1519 (1962).
21. F. RUGGLI and A. STAUB. Helv. Chim. Acta, **20**, 918 (1937); Chem. Abstr. **32**, 562 (1938).
22. D. DAVEY and D. H. MAASS. J. Chem. Soc. 4386 (1963).
23. E. KNOEVENAGEL and A. HERZ. Ber. **37**, 4483 (1904).
24. S. RUHEMANN. J. Chem. Soc. **85**, 1458 (1904).
25. E. KNOEVENAGEL. Ber. **31**, 734 (1898).
26. A. G. ANDERSON and S. Y. WANG. J. Org. Chem. **19**, 277 (1954).
27. V. N. BELOV and E. I. SHEPELENKOVA. Trudy Vsesoyuz. Inst. Sintet. i Natural. Dushistykh Veshchestv. 24, (1955); Ref. Zh. Khim. No. 747 (1956); Chem. Abstr. **51**, 17818 (1957).
28. C. F. H. ALLEN and F. W. SPANGLER. Org. Syn. Coll. Vol. III p. 377.
29. J. THIELE and J. MEISENHEIMER. Ann. **306**, 253 (1898).
30. L. GEITAARD and G. VANAGS. Zh. Obshch. Khim. **27**, 3109 (1951).
31. V. PETROV, J. SAPER, and B. STURGEON. J. Chem. Soc. 2134 (1949).
32. S. KOSTANECKI and L. LACZKOWSKI. Ber. **30**, 2138 (1897).

Proton magnetic resonance and mass spectrometric studies on derivatives of sodium 2-*O*-α-D-mannopyranosyl-D-glycerate and related compounds

J. N. C. WHYTE

Fisheries Research Board of Canada, Vancouver Laboratory, 6640 N.W. Marine Drive, Vancouver 8, B.C.

Received April 11, 1969

The proton magnetic resonance (p.m.r.) and mass spectra of the methyl ester pentaacetate of sodium 2-*O*-α-D-mannopyranosyl-D-glycerate from the red alga *Rhodomela larix* are compared to those of related compounds to affirm the assigned structure.

Canadian Journal of Chemistry, **47**, 4083 (1969)

The observation that the water soluble components of an 80% aqueous methanol extract of *Rhodomela larix* inhibited the growth of *E. coli* (1) prompted an interest in the low molecular weight components of this alga. Extraction of the seaweed with a chloroform–methanol–water mixture yielded sodium 2-*O*-α-D-mannopyranosyl-D-glycerate (**1**) (2) as the major water soluble component. The corresponding free acid provided a poorly resolved p.m.r. spectra, but that of the

Can. J. Chem. Downloaded from www.nrcresearchpress.com by 210.87.254.105 on 09/05/12
For personal use only.

Can. J. Chem. Downloaded from www.nrcresearchpress.com by 210.87.254.105 on 09/05/12
For personal use only.

TABLE I

Chemical shifts of methine, methylene, methoxyl, and acetoxyl protons (τ values)

Compound*	Solvent	H-1	H-2	H-3	H-4	H-6_1†	H-6_2†	H-5	–OMe	–OAc (protons)			
Methyl α-D-mannopyranoside	D_2O	4.73	5.55	———	——5.59——	5.85‡	———	~5.88	6.06	—	—	—	—
Methyl β-D-mannopyranoside	D_2O	4.95	5.52	5.95——	5.85‡	5.79	5.56	6.08	5.96	—	—	—	—
Methyl α-D-mannopyranoside tetraacetate	$CDCl_3$	5.29	——4.58–4.86‡——			5.69	5.91	~6.04	6.59	7.88(3)	7.93(3)	7.98(3)	8.04(3)
Methyl β-D-mannopyranoside tetraacetate	$CDCl_3$	5.41	4.52	4.93	4.71	5.65	5.85	6.30	6.48	7.83(3)	7.91(3)	7.96(3)	8.02(3)
α-D-Mannopyranose pentaacetate	$CDCl_3$	3.92	——4.59–4.81‡——			5.70	5.92	~5.95	—	7.84(6)	7.93(3)	7.96(3)	8.01(3)
β-D-Mannopyranose pentaacetate	$CDCl_3$	4.10	4.50	4.83	4.69	5.67	5.87	6.19	—	7.80(3)	7.91(6)	7.96(3)	8.01(3)
Methyl α-D-mannopyranosyl-glycerate pentaacetate (4) (ring protons)	$CDCl_3$	4.95	(4.59)–4.54–4.86‡			5.70	5.89	~5.91	6.22	7.86(3)	7.91(6)	7.96(3)	8.01(3)
(glycerate protons)		—	5.36–5.71‡(3H)		—	—		—					

NOTE: The sign (~) indicates H-5 overlaps with the high field portion of the H-6_2 quartet.
*The spectrum of D-mannose in D_2O showed H-1 for the α anomer at τ 4.30 and H-1 for the β anomer at τ 4.58.
†H-6_1 and H-6_2 are designated as per Hall *et al.* (9).
‡In the case of complex overlapping resonances, the multiplets are within these limits.

TABLE II

Observed coupling constants of methine and methylene protons

Compound	$J_{1,2}$	$J_{2,3}$	$J_{3,4}$	$J_{4,5}$	$J_{5,6_1}$	$J_{5,6_2}$	$J_{6_1,6_2}$
Methyl α-D-mannopyranoside	1.6	2.9	†	†	†	†	†
Methyl β-D-mannopyranoside	1.0	3.0*	9.5*	9.0*	5.7	2.3	12.1
Methyl α-D-mannopyranoside tetraacetate	1.3	†	†	†	5.0	2.5	12.5
Methyl β-D-mannopyranoside tetraacetate	1.2	3.0	10.0	9.3	5.0	3.0	12.0
α-D-Mannopyranose pentaacetate	1.3	†	†	†	5.0	2.3	12.5
β-D-Mannopyranose pentaacetate	1.2	3.0	9.6	9.0	5.0	2.6	12.1
Methyl α-D-mannopyranosyl-glycerate pentaacetate (**4**) (ring protons)	1.5	†	†	†	5.7	2.0	12.1

*Values taken from the spectrum in pyridine-d_5.
†Overlapping signals.

methyl ester **3** in deuterium oxide displayed a doublet of intensity 1 at τ 4.57, $J_{1',2'} = 1.7$ Hz for the anomeric proton, which on irradiation, collapsed the quartet for H-2′ at τ 5.45 to a doublet, splitting 3.0 Hz. The protons of the glycerate moiety appeared as a simple AB_2 pattern with H-2 appearing as a triplet at τ 5.0 coupled to the doublet with a spacing of 3.8 Hz for the methylene protons (H-3_1 and H-3_2) at τ 5.6.

The corresponding acetate, methyl 3-*O*-acetyl-2-*O*-(2′,3′,4′,6′-tetra-*O*-acetyl-α-D-mannopyranosyl)-D-glycerate (**4**) furnished a p.m.r. spectrum in chloroform-d_1, in which the proton signals were assigned from double irradiation experiments, Tables I and II. The observation that the methine proton of the glycerate moiety resonated to higher field than that in the spectrum of methyl 2,3-di-*O*-acetyl-DL-glycerate (τ 4.71) where it is geminal to a deshielding acetoxyl group, together with the comparable chemical shifts for the methylene protons in both compounds, would substantiate the structure having the glycosidic linkage at C-2 of the glycerate moiety. Although the configuration at C-1 for mannose derivatives cannot be assessed by the spacing of the anomeric signal (3) the coalescence of the H-5′ with the H-6_2′ signal, together with the complex pattern to low field for H-2′, H-3′, and H-4′ signals, was consistent with an α-glycoside of mannopyranose tetraacetate. Of interest from Table I was the observed long range deshielding effect (0.1 p.p.m.) on the protons at C-3 and C-5 by the carbonyl function of the C-1 acetoxyl group in β-D-mannopyranose pentaacetate. The chemical shifts of the acetoxyl groups in the spectrum of **4**, indicate that the mannose ring must exist, predominantly in the C-1 (D) conformation with one acetoxyl group at C-2, axially oriented (4).

The mass spectra of methyl β-D-mannopyranoside and methyl α-D-mannopyranoside tetraacetates and the derivative **4** showed a corresponding increase in the A relative to the C and F series (5) of ion fragments where the percentage of the A_1 (*m/e* 331) to F_2 (*m/e* 115) peaks was 2.9, 8.9, and 80% respectively. This increase in the A series depends on the rate of elimination of the C-1 substituent favored by the α anomeric configuration, presumably a reversed anomeric effect caused by removal of an electron from the ring oxygen in the formation of the molecular ion, and by the anchimeric assistance of the *trans vicinal* acetoxyl group; a factor substantiated by the ratio of the A_1 peaks for the anomers of glucose and mannose pentaacetate (6) and by the relative exclusion of the A series of ions in the spectrum of 2-*O*-methyl-β-D-glucopyranose tetraacetate which are abundant in that of the corresponding 3-*O*-methyl isomer (7). Although the spectrum of **4** lacked a molecular ion, it exhibited peaks of low intensity at *m/e* 433 ($M - CO_2CH_3$) and *m/e* 419 ($M - CH_2OCOCH_3$). Apart from the characteristic base peak at mass 43 the most intense peak in the spectrum at mass 145 was attributed to the stable glycerate fragment formed by cleavage of the glycosidic bond. The contribution to the species at mass 145 by the triacetyloxonium ion was minimal as it is invariably less abundant than the diacetyloxonium ion at mass 103. The sodium salt **1** exhibited no antibacterial activity.

Experimental

Proton magnetic resonance spectra were obtained with

Can. J. Chem. Downloaded from www.nrcresearchpress.com by 210.87.254.105 on 09/05/12
For personal use only.

a Varian HA 100 spectrometer, τ values are relative to tetramethylsilane as an internal or external standard in the solvent specified at 30°. The mass spectra were obtained with a Nuclide spectrometer.

The seaweed, 1750 g fresh weight, was exhaustively extracted with the solvent mixture, chloroform–methanol–water, to afford an aqueous methanol layer which was passed through a column of cation, then anion, exchange resins; the latter of which on elution with 0.2 *N* formic acid gave an eluate, neutralised with sodium bicarbonate and evaporated to a residue subsequently recrystallized from aqueous methanol to give sodium 2-*O*-(α-D-mannopyranosyl)-D-glycerate (**1**) (300 mg) m.p., mixed m.p. 265°, $[\alpha]_D$ + 106° (*c*, 1.4 in H_2O).

The free acid **2** as a syrup $[\alpha]_D$ + 93° (*c*,2.3 in H_2O) gave a p.m.r. spectrum in D_2O displaying a signal at τ 4.65 (1H) multiplets at τ 5.25 and 5.51 (each 1H) and a complex multiplet τ 5.60–6.00 (7H's). Treatment of **2** (150 mg) with diazomethane gave the methyl ester **3** (157 mg), $[\alpha]_D$ + 95° (*c*,2.1 in H_2O) which on acetylation of a portion (125 mg) gave the corresponding pentaacetate **4** (190 mg) recrystallized from ethyl acetate–*n*-pentane, m.p. 91°, $[\alpha]_D$ + 73.1° (*c*,1.2 in methanol).

Anal. Calcd. for $C_{20}H_{28}O_{14}$: C, 48.78; H, 5.73. Found: C, 49.06; H, 5.67.

Methyl 2,3-di-*O*-acetyl-DL-glycerate, b.p. 84° at 0.05 mm, prepared from the parent calcium salt as above, gave a p.m.r. spectrum in $CDCl_3$ showing a quartet signal at τ 4.71 (H-2), two overlapping quartets at τ 5.49 (H-3_1, $J_{2,3_1}$ = 3.7 Hz) and τ 5.71 (H-3_2, $J_{2,3_2}$ = 5.0 Hz) with $J_{3_1,3_2}$ = 11.5 Hz. The compounds cited in Tables I and II were prepared by well established procedures (8).

1. K. SAITO and M. SAMESHIMA. Nippon Nogei-Kagaku Kaishi, **29**, 427 (1955).
2. H. BOUVENG, B. LINDBERG, and B. WICKBERG. Acta Chem. Scand. **9**, 807 (1955); J. GERVAIS. Rev. Gen. Bot. **66**, 395 (1959).
3. R. U. LEMIEUX and J. D. STEVENS. Can. J. Chem. **43**, 2059 (1965).
4. F. W. LICHTENTHALER and P. EMIG. Tetrahedron Lett. 577 (1967).
5. N. K. KOCHETKOV and O. S. CHIZHOV. Advan. Carbohyd. Chem. **21**, 39 (1966).
6. K. BIEMANN, D. C. DE JONGH, and H. K. SCHNOES. J. Amer. Chem. Soc. **85**, 1763 (1963).
7. D. C. DE JONGH and K. BIEMANN. J. Amer. Chem, Soc. **85**, 2289 (1963).
8. J. STANEK, M. CERNY, J. KOCOUREK, and J. PACAK. The monosaccharides. Academic Press, Inc., New York. 1963.
9. L. D. HALL, J. F. MANVILLE, and N. S. BHACCA. Can. J. Chem. **47**, 1 (1969).

Bisglycosidylamines, a new class of amino sugars[1,2]

HANS H. BAER AND FAROUK RAJABALEE

Department of Chemistry, University of Ottawa, Ottawa, Canada

Received May 7, 1969

Nucleophilic addition of methyl 2-amino-4,6-*O*-benzylidene-2,3-dideoxy-3-nitro-α-D-glucopyranoside (**2**) to methyl 4,6-*O*-benzylidene-2,3-dideoxy-3-nitro-α-D-*erythro*-hex-2-enopyranoside (**1**) furnished bis(methyl 4,6-*O*-benzylidene-2,3-dideoxy-3-nitro-α-D-glucopyranosid-2-yl)amine (**3**). The debenzylidenated product (**4**) gave a tetraacetate (**5**) and, on catalytic hydrogenation, it afforded bis(methyl 3-amino-2,3-dideoxy-α-D-glucopyranosid-2-yl)amine which crystallized as a trihydrochloride (**6**). Acetylation of **6** gave a di-*N*-acetyltetra-*O*-acetyl derivative (**7**); the secondary amino group remained free, presumably owing to steric hindrance.

Canadian Journal of Chemistry, **47**, 4086 (1969)

In continuation of our synthetic work on aminonitro sugars (1), branched-chain dinitro sugars (2), and nitro disaccharides (3), which made use of the facile addition of nucleophiles to carbohydrate nitroolefins (4), we wish to report another application of the same principle. Reaction between methyl 4,6-*O*-benzylidene-2,3-dideoxy-3-nitro-α-D-*erythro*-hex-2-enopyranoside (**1**) and methyl 2-amino-4,6-*O*-benzylidene-2,3-dideoxy-3-nitro-α-D-glucopyranoside (**2**) furnished in up to 75% yield a secondary amine representing a new type of carbohydrate structure, namely, a bisglycosidylamine. The product, bis(methyl 4,6-*O*-benzylidene-2,3-dideoxy-3-nitro-α-D-glucopyranosid-2-yl)amine (**3**), was debenzylidenated with trifluoroacetic acid (5) to give bis(methyl 2,3-dideoxy-3-nitro-α-D-glucopyranosid-2-yl)amine (**4**) from which a tetraacetate (**5**) was obtained by boron trifluoride-catalyzed acetylation (6). The dinitroamine **4** was hydrogenated catalytically to the triamine, bis(methyl 3-amino-2,3-dideoxy-α-D-glucopyrano-

[1]Part XIII in a series on the reactions of nitro sugars. For part XII see reference 3.

[2]Abstracted from a Ph.D. thesis submitted by F. R. to the University of Ottawa (1969). Financial assistance by the National Research Council of Canada, through research grant A 1350 and a postgraduate fellowship to F. R., is gratefully acknowledged.

Can. J. Chem. Downloaded from www.nrcresearchpress.com by 210.87.254.105 on 09/05/12
For personal use only.

a Varian HA 100 spectrometer, τ values are relative to tetramethylsilane as an internal or external standard in the solvent specified at 30°. The mass spectra were obtained with a Nuclide spectrometer.

The seaweed, 1750 g fresh weight, was exhaustively extracted with the solvent mixture, chloroform–methanol–water, to afford an aqueous methanol layer which was passed through a column of cation, then anion, exchange resins; the latter of which on elution with 0.2 *N* formic acid gave an eluate, neutralised with sodium bicarbonate and evaporated to a residue subsequently recrystallized from aqueous methanol to give sodium 2-*O*-(α-D-mannopyranosyl)-D-glycerate (**1**) (300 mg) m.p., mixed m.p. 265°, $[\alpha]_D$ + 106° (*c*, 1.4 in H_2O).

The free acid **2** as a syrup $[\alpha]_D$ + 93° (*c*,2.3 in H_2O) gave a p.m.r. spectrum in D_2O displaying a signal at τ 4.65 (1H) multiplets at τ 5.25 and 5.51 (each 1H) and a complex multiplet τ 5.60–6.00 (7H's). Treatment of **2** (150 mg) with diazomethane gave the methyl ester **3** (157 mg), $[\alpha]_D$ + 95° (*c*,2.1 in H_2O) which on acetylation of a portion (125 mg) gave the corresponding pentaacetate **4** (190 mg) recrystallized from ethyl acetate–*n*-pentane, m.p. 91°, $[\alpha]_D$ + 73.1° (*c*,1.2 in methanol).

Anal. Calcd. for $C_{20}H_{28}O_{14}$: C, 48.78; H, 5.73. Found: C, 49.06; H, 5.67.

Methyl 2,3-di-*O*-acetyl-DL-glycerate, b.p. 84° at 0.05 mm, prepared from the parent calcium salt as above, gave a p.m.r. spectrum in $CDCl_3$ showing a quartet signal at τ 4.71 (H-2), two overlapping quartets at τ 5.49 (H-3_1, $J_{2,3_1}$ = 3.7 Hz) and τ 5.71 (H-3_2, $J_{2,3_2}$ = 5.0 Hz) with $J_{3_1,3_2}$ = 11.5 Hz. The compounds cited in Tables I and II were prepared by well established procedures (8).

1. K. SAITO and M. SAMESHIMA. Nippon Nogei-Kagaku Kaishi, **29**, 427 (1955).
2. H. BOUVENG, B. LINDBERG, and B. WICKBERG. Acta Chem. Scand. **9**, 807 (1955); J. GERVAIS. Rev. Gen. Bot. **66**, 395 (1959).
3. R. U. LEMIEUX and J. D. STEVENS. Can. J. Chem. **43**, 2059 (1965).
4. F. W. LICHTENTHALER and P. EMIG. Tetrahedron Lett. 577 (1967).
5. N. K. KOCHETKOV and O. S. CHIZHOV. Advan. Carbohyd. Chem. **21**, 39 (1966).
6. K. BIEMANN, D. C. DE JONGH, and H. K. SCHNOES. J. Amer. Chem. Soc. **85**, 1763 (1963).
7. D. C. DE JONGH and K. BIEMANN. J. Amer. Chem, Soc. **85**, 2289 (1963).
8. J. STANEK, M. CERNY, J. KOCOUREK, and J. PACAK. The monosaccharides. Academic Press, Inc., New York. 1963.
9. L. D. HALL, J. F. MANVILLE, and N. S. BHACCA. Can. J. Chem. **47**, 1 (1969).

Bisglycosidylamines, a new class of amino sugars[1,2]

HANS H. BAER AND FAROUK RAJABALEE
Department of Chemistry, University of Ottawa, Ottawa, Canada

Received May 7, 1969

Nucleophilic addition of methyl 2-amino-4,6-*O*-benzylidene-2,3-dideoxy-3-nitro-α-D-glucopyranoside (**2**) to methyl 4,6-*O*-benzylidene-2,3-dideoxy-3-nitro-α-D-*erythro*-hex-2-enopyranoside (**1**) furnished bis(methyl 4,6-*O*-benzylidene-2,3-dideoxy-3-nitro-α-D-glucopyranosid-2-yl)amine (**3**). The debenzylidenated product (**4**) gave a tetraacetate (**5**) and, on catalytic hydrogenation, it afforded bis(methyl 3-amino-2,3-dideoxy-α-D-glucopyranosid-2-yl)amine which crystallized as a trihydrochloride (**6**). Acetylation of **6** gave a di-*N*-acetyltetra-*O*-acetyl derivative (**7**); the secondary amino group remained free, presumably owing to steric hindrance.

Canadian Journal of Chemistry, **47**, 4086 (1969)

In continuation of our synthetic work on aminonitro sugars (1), branched-chain dinitro sugars (2), and nitro disaccharides (3), which made use of the facile addition of nucleophiles to carbohydrate nitroolefins (4), we wish to report another application of the same principle. Reaction between methyl 4,6-*O*-benzylidene-2,3-dideoxy-3-nitro-α-D-*erythro*-hex-2-enopyranoside (**1**) and methyl 2-amino-4,6-*O*-benzylidene-2,3-dideoxy-3-nitro-α-D-glucopyranoside (**2**) furnished in up to 75% yield a secondary amine representing a new type of carbohydrate structure, namely, a bisglycosidylamine. The product, bis(methyl 4,6-*O*-benzylidene-2,3-dideoxy-3-nitro-α-D-glucopyranosid-2-yl)amine (**3**), was debenzylidenated with trifluoroacetic acid (5) to give bis(methyl 2,3-dideoxy-3-nitro-α-D-glucopyranosid-2-yl)amine (**4**) from which a tetraacetate (**5**) was obtained by boron trifluoride-catalyzed acetylation (6). The dinitroamine **4** was hydrogenated catalytically to the triamine, bis(methyl 3-amino-2,3-dideoxy-α-D-glucopyrano-

[1]Part XIII in a series on the reactions of nitro sugars. For part XII see reference 3.

[2]Abstracted from a Ph.D. thesis submitted by F. R. to the University of Ottawa (1969). Financial assistance by the National Research Council of Canada, through research grant A 1350 and a postgraduate fellowship to F. R., is gratefully acknowledged.

Can. J. Chem. Downloaded from www.nrcresearchpress.com by 210.87.254.42 on 09/05/12
For personal use only.

Can. J. Chem. Downloaded from www.nrcresearchpress.com by 210.87.254.42 on 09/05/12
For personal use only.

sid-2-yl)amine. In this compound the secondary amine nitrogen appears to be severely crowded in by the bulky glycosidyl substituents; for although the compound crystallized as a trihydrochloride (**6**), only two *N*-acetyl groups were introduced by its treatment with acetic anhydride in pyridine, the product being a di-*N*-acetyltetra-*O*-acetyl derivative (**7**).

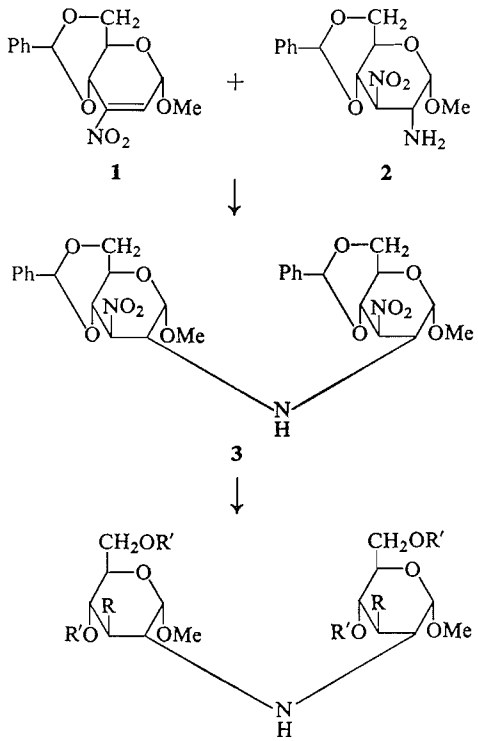

The bis-α-D-*gluco* configuration of the new compounds was ascertained by nuclear magnetic resonance (n.m.r.) spectroscopy. The 100 MHz spectra of **3**, **5**, and **7** clearly indicated that the two glycosidyl moieties in each of the compounds were identical, since each compound gave only one set of substituent resonances. That is to say, one sharp methoxyl signal was given by **3**, **5**, and **7**, and one benzylidenic proton singlet was given by **3**; compound **5** showed two *O*-acetyl signals and compound **7**, one *N*-acetyl signal and two *O*-acetyl signals. Inspection of the ring proton resonances (to the extent that they were resolved well enough) likewise revealed equal chemical shifts and spin couplings of corresponding protons in the two glycosidyl moieties of each compound analyzed, proving the moieties to be identical. This fact alone already suggested the bis-α-D-*gluco* configuration since it was considered highly unlikely that the α-D-*gluco* reaction partner (**2**) should have suffered any stereochemical change during its addition to the α-D-*erythro* component (**1**). Direct proof was obtained most conveniently by a more detailed analysis of the spectrum of **5** (in chloroform-*d*) in which the ring proton signals were resolved best. Two symmetrical triplets, each of 2-proton intensity,[3] occurred at τ 4.66 and 5.37 and were assignable to the protons in the positions 3 and 4, respectively. Their large splittings of ca. 10 Hz not only confirmed the known axial orientation of the protons on C-5 and C-4, but also required axial orientation of those on C-3 and C-2, thus establishing the *gluco* configuration. The anomeric protons gave at τ 5.56 a 2-proton doublet which was split by 3 Hz in accord with 1,2-equatorial–axial interaction. The C-6 methylene groups produced two unsymmetrical quartets with an integrated intensity of four protons in the region τ 5.7–6.0, and the protons in position 5 gave a 2-proton octet (width, 18 Hz) centered at τ 6.18. The methoxyl peak (6H) occurred at τ 6.64. It partially overlapped a 2-proton multiplet which was centered slightly upfield and must belong to the protons on C-2. Despite this overlap a large splitting (by H-3) and a small splitting (by H-1) were recognizable in that signal which showed additional, weak coupling with the vicinal amine hydrogen.[4] The amine hydrogen gave a somewhat broadened signal (apparently a narrow triplet) at τ 8.33, upfield from the two *O*-acetyl singlets (τ 7.92, 7.99). The existence of vicinal coupling between the hydrogen atoms on C-2 and the amine hydrogen indicates a retardation of intermolecular exchange of the latter, and bespeaks the low reactivity at this site.

Experimental

Melting points were determined in capillaries in an electrically heated aluminum block equipped with a

[3]This intensity and all others recorded are relative to the strength of an upfield signal attributable to the secondary amine proton (the only proton not duplicated in the molecule).

[4]Similar multiplets, fortuitously unobscured by the methoxyl absorption, were found in the spectra of **3** and **7**.

Can. J. Chem. Downloaded from www.nrcresearchpress.com by 210.87.254.42 on 09/05/12
For personal use only.

calibrated thermometer. Thin-layer chromatography (t.l.c.) was performed on silica gel G plates with chloroform–ethyl acetate (1:1, v/v). Petroleum ether refers to the fraction of boiling range 30–60°. Infrared (i.r.) spectra were obtained from Nujol mulls on a Beckman IR-8 instrument; only the most characteristic bands are listed. Optical rotations were measured at about 23° in a Perkin-Elmer 141 automatic polarimeter. Nuclear magnetic resonances (n.m.r.) were recorded on a Varian Associates HA-100 instrument.

Bis(methyl 4,6-O-benzylidene-2,3-dideoxy-3-nitro-α-D-glucopyranosid-2-yl)amine (3)

Reagent grade benzene was refluxed for 15 h over sodium wire and distilled before use. The nitroolefin **1** (1*e*,7) (147 mg) and the amine **2** (1*f*) (155 mg) were refluxed in benzene (40 ml) in the presence of a pellet of potassium hydroxide and a few pieces of fresh Drierite. Thin-layer chromatography revealed a gradual appearance, after 2 h, of a product migrating faster than either reactant. In several runs the reaction required 1–3.5 days for completion, with time variations apparently being occasioned by the quality of the solvent and (or) inadvertent access of traces of moisture. The yellow solution was then treated with activated charcoal, filtered, and evaporated to give a white residue. By recrystallization from ethyl acetate–petroleum ether, **3** was obtained as beautiful, colorless needles (204–235 mg, 67–78%): m.p. 284–285° (decomposition); $[\alpha]_D$ +78.5° (*c*, 0.8, dimethylformamide); ν_{max} 3360 (w, NH), 1555 (s, NO_2) with shoulder at 1565 (NH bending?), 765 and 705 cm^{-1} (ms, phenyl); n.m.r. ($CDCl_3$): τ 2.65 (narrow multiplet, C_6H_5), τ 4.50 (singlet, $PhCHO_2$), τ 5.30 (triplet, H-3, $J_{2,3} = J_{3,4} = 10$ Hz), τ 5.56 (doublet, H-1, $J_{1,2} = 3.5$ Hz); τ 5.67–6.45 (overlapping signals ascribable to H-4, H-5, H-6, and H-6′), τ 6.61 (singlet, OCH_3), τ 6.74 (multiplet, H-2, width ca. 18 Hz), τ 8.2 (broad signal, NH).

Anal. Calcd. for $C_{28}H_{33}N_3O_{12}$ (603.6): C, 55.72; H, 5.51; N, 6.96. Found: C, 55.61; H, 5.38; N, 6.95.

Bis(methyl 2,3-dideoxy-3-nitro-α-D-glucopyranosid-2-yl)amine (4)

The benzylidene compound **3** (517 mg) was dissolved in 90% trifluoroacetic acid (6 ml). The slightly exothermic reaction was allowed to proceed at ambient temperature for 10 min. The mixture was then evaporated to give a yellow syrup from which two portions of added water and two portions of ethanol were consecutively evaporated. Trituration of the syrup with ether then produced a first crop (262 mg) of **4** as small colorless prisms which were washed with ether. The ethereal mother liquor was evaporated to dryness and the residue, which was not homogeneous on t.l.c., yielded a second crop (20 mg) of **4** upon repetition of the hydrolysis with trifluoroacetic acid. The combined crops were recrystallized from ethyl acetate–petroleum ether. The crystals thereafter exhibited a medium strong i.r. band at 1740 cm^{-1} which was not present in the initial, crude product and which evidently was due to retained solvent. Drying of the product for 50 h at 100° and 1 mm removed this band, and 218 mg (60%) of pure **4** was obtained: m.p. 212–213° (decomposition, gradual darkening from 205°); $[\alpha]_D$ +161.2° (*c*, 0.7, water); ν_{max} 3500–3100 (broad, OH, NH), 1557 cm^{-1} (NO_2).

Anal. Calcd. for $C_{14}H_{25}N_3O_{12}$ (427.4): C, 39.34; H, 5.89; N, 9.83. Found: C, 39.37; H, 5.75; N, 9.95.

Debenzylidenation of **3** could also be effected with 70% acetic acid (1 h on a steam bath). The recrystallized product was identical with **4** in every respect, but its yield was only 37%.

Bis(methyl 4,6-di-O-acetyl-2,3-dideoxy-3-nitro-α-D-glucopyranosid-2-yl)amine (5)

Compound **4** (100 mg) was suspended in acetic anhydride (3 ml), and 3 drops of boron trifluoride etherate were added. The dissolution of **4** was completed by gentle warming, and the reaction mixture was then allowed to stand at ambient temperature for 40 min and was thereafter poured into excess, cold ethanol. The solution was evaporated, and the residue was co-evaporated five times with added ethanol and then recrystallized from ethyl acetate–petroleum ether. The tetraacetate (**5**) was obtained as colorless, elongated platelets (85 mg, 61%): m.p. 208–209°; $[\alpha]_D$ +118.5° (*c*, 1.1, chloroform); ν_{max} 3440 (w, NH), 1740 with shoulder at 1755 (s, ester CO), 1565 (w, NH bending), 1552 cm^{-1} (s, NO_2). For the n.m.r. data, see the discussion section.

Anal. Calcd. for $C_{22}H_{33}N_3O_{16}$ (595.5): C, 44.36; H, 5.58; N, 7.05. Found: C, 44.35; H, 5.56; N, 7.15.

Bis(methyl 3-amino-2,3-dideoxy-α-D-glucopyranosid-2-yl)amine Trihydrochloride (6)

In some experiments the benzylidene compound **3** was debenzylidenated as described above and the crude, chromatographically inhomogeneous syrup that contained **4** was hydrogenated directly. In a typical run, the syrup obtained from 542 mg of **3** was dissolved in water (40 ml), *N* hydrochloric acid (2.5 ml) and platinum catalyst (200 mg PtO_2, prehydrogenated) were added, and the mixture was hydrogenated for 24 h at ordinary temperature and pressure. The filtered solution was evaporated to give a syrup which was twice co-evaporated with water. The product (**6**) then crystallized from absolute ethanol as white prisms, in a yield of 190 mg (44% based on **3**). It gave a single, ninhydrin-positive spot on paper chromatography, R_{GN} 1.11,[5] and it showed $[\alpha]_D$ +144.7 (*c*, 0.9, water) and decomposed at 245–250° with gradual darkening from 200°. The i.r. spectrum exhibited a sharp band at 3540 and broad absorption in the 3300 cm^{-1} region with ν_{max} 3340, 3300, and 3250 (OH, NH), a band at 3060 and broad absorption in the 2700–2400 region, as well as bands at 1640, 1612, 1598, and 1520 cm^{-1}.

Anal. Calcd. for $C_{14}H_{32}Cl_3N_3O_8$ (476.8): Cl, 22.31; N, 8.81. Found: Cl, 22.5; N, 8.90.

A similarly performed hydrogenation of crystalline **4** (300 mg) gave **6** in higher yield (230 mg, 69%). Inadvertently, an insufficient amount of hydrochloric acid had been added in this experiment; this circumstance precluded an even better yield of crystalline trihydrochloride. The product had R_{GN} 1.11 and $[\alpha]_D$ +142.9° (*c*, 0.7, water), decomposed slowly above 205° and extensively at 240–250°, and its i.r. spectrum was identical with that from a previous preparation.

[5]Speed relative to D-glucosamine hydrochloride in descending chromatography using the system pyridine–ethyl acetate–water–acetic acid (5:5:3:1, v/v) according to Fischer and Dörfel (8).

Bis(methyl 3-acetamido-4,6-di-O-acetyl-2,3-dideoxy-α-D-glucopyranosid-2-yl)amine (7)

The trihydrochloride **6** (121 mg), acetic anhydride (3.5 ml), and pyridine (7 ml) were magnetically stirred for 16 h at room temperature in a stoppered flask. Excess methanol was added and the mixture was evaporated. The residue was evaporated in succession with fresh methanol, several portions of toluene, and again with methanol. A solution of the resulting, brownish syrup in chloroform was washed with water to remove pyridine hydrochloride, dried over sodium sulfate, and evaporated with an ultimate addition of ethanol. Recrystallization of the semi-solid residue from absolute ethanol–petroleum ether gave **7** (68 mg, 40%) as colorless platelets: m.p. 328° (decomposition); $[\alpha]_D$ +123.5° (*c*, 0.8, chloroform); ν_{max} 3310 (NH), 1740 (ester CO), 1658 (amide I), and 1560 cm^{-1} (amide II); n.m.r. ($CDCl_3$): τ 3.27 (broadened doublet, amide NH), τ 5.15 (triplet, J = 9.5 Hz, H-4), τ 5.44 (doublet, J = 3 Hz, H-1), τ 5.6–6.3 (overlapping signals ascribable to H-3, H-5, H-6, and H-6′), τ 6.64 (singlet, OCH_3), τ 7.00 (multiplet, width ca. 18 Hz, H-2), τ 7.92, 7.95 (singlets, *O*-acetyl), τ 8.05 (singlet, *N*-acetyl), τ 8.27 (broadened signal of *sec.*-amine NH).

Anal. Calcd. for $C_{26}H_{41}N_3O_{14}$ (619.6): C, 50.40; H, 6.67; N, 6.78. Found: C, 50.26; H, 6.48; N, 6.79.

1. (*a*) H. H. BAER and T. NEILSON. J. Org. Chem. **32**, 1068 (1967); (*b*) H. H. BAER, T. NEILSON, and W. RANK. Can. J. Chem. **45**, 991 (1967); (*c*) H. H. BAER and K. S. ONG. J. Org. Chem. **34**, 560 (1969); (*d*) H. H. BAER and F. KIENZLE. J. Org. Chem. In press; (*e*) H. H. BAER, F. RAJABALEE, and F. KIENZLE. J. Org. Chem. In press; (*f*) H. H. BAER and F. RAJABALEE. Part XVI in this series. Carbohyd. Res. In press.
2. H. H. BAER and K. S. ONG. Can. J. Chem. **46**, 2511 (1968).
3. H. H. BAER and F. KIENZLE. Can. J. Chem. **47**, 2819 (1969).
4. For a review see H. H. BAER. Advan. Carbohyd. Chem. **24** (1969). In press.
5. J. E. CHRISTENSEN and L. GOODMAN. Carbohyd. Res. **7**, 510 (1968).
6. H. H. BAER, F. KIENZLE, and F. RAJABALEE. Can. J. Chem. **46**, 80 (1968).
7. H. H. BAER and F. KIENZLE. Can. J. Chem. **45**, 983 (1967).
8. F. G. FISCHER and H. DÖRFEL. Z. Physiol. Chem. **301**, 224 (1955).

Absolute configurations of the (−)-*erythro* and (−)-*threo*-2,3-dihydroxybutyric acids

F. W. BACHELOR AND G. A. MIANA[1]

Department of Chemistry, University of Calgary, Calgary 44, Alberta, Canada

Received June 23, 1969

The absolute configurations of (−)-*erythro*-2,3-dihydroxybutyric acid and (−)-*threo*-2,3-dihydroxybutyric acid have been determined by optical rotatory dispersion and found to be 2(R), 3(R) for the *erythro* acid and 2(S), 3(R) for the *threo* acid.

Canadian Journal of Chemistry, **47**, 4089 (1969)

We recently found it necessary to determine the absolute configurations of the active *erythro*-2,3-dihydroxybutyric and *threo*-2,3-dihydroxybutyric acids for use in a stereospecific synthesis. Because of the inquiries which we have received regarding these compounds we felt it expedient to communicate this information prior to the completion of the synthetic problem.

The absolute configuration of (−)-*threo*-2,3-dihydroxybutyric acid has been indirectly determined by its production from L-threonine with nitrous acid (1). Since the stereochemistry of the deaminations of α-amino acids has been established to give unequivocably retention of configuration (2), this establishes the stereochemistry of the (−)-*threo*-dihydroxybutyric acid as being the same as L-threonine.

Erythro-2,3-dihydroxybutyric acid was prepared by hydroxylation of *trans*-crotonic acid with hydrogen peroxide and tungstic acid according to the method of Mugdan and Young (3). This acid was resolved through its quinine salt (4) to give (−)-*erythro*-2,3-dihydroxybutyric acid with a specific rotation of −9.5°.

The *threo*-isomer was prepared by a Milas oxidation of *trans*-crotonic acid with osmium tetroxide and hydrogen peroxide (5) and the dihydroxy acid resolved through its quinidine salt (6) to give (−)-*threo*-2,3-dihydroxybutyric acid with a specific rotation of −17.75°.

Because of the poor recovery of the resolved acids from their salts by previously reported procedures (4,6) the free acids were regenerated by their passage through a weak acid ion exchange column, a method recently communicated by us (7).

[1]Holder of an NRCC Studentship 1965–1966.

Can. J. Chem. Downloaded from www.nrcresearchpress.com by 210.87.254.42 on 09/05/12
For personal use only.

Bis(methyl 3-acetamido-4,6-di-O-acetyl-2,3-dideoxy-α-D-glucopyranosid-2-yl)amine (7)

The trihydrochloride **6** (121 mg), acetic anhydride (3.5 ml), and pyridine (7 ml) were magnetically stirred for 16 h at room temperature in a stoppered flask. Excess methanol was added and the mixture was evaporated. The residue was evaporated in succession with fresh methanol, several portions of toluene, and again with methanol. A solution of the resulting, brownish syrup in chloroform was washed with water to remove pyridine hydrochloride, dried over sodium sulfate, and evaporated with an ultimate addition of ethanol. Recrystallization of the semi-solid residue from absolute ethanol–petroleum ether gave **7** (68 mg, 40%) as colorless platelets: m.p. 328° (decomposition); $[\alpha]_D$ +123.5° (*c*, 0.8, chloroform); ν_{max} 3310 (NH), 1740 (ester CO), 1658 (amide I), and 1560 cm^{-1} (amide II); n.m.r. ($CDCl_3$): τ 3.27 (broadened doublet, amide NH), τ 5.15 (triplet, J = 9.5 Hz, H-4), τ 5.44 (doublet, J = 3 Hz, H-1), τ 5.6–6.3 (overlapping signals ascribable to H-3, H-5, H-6, and H-6′), τ 6.64 (singlet, OCH_3), τ 7.00 (multiplet, width ca. 18 Hz, H-2), τ 7.92, 7.95 (singlets, *O*-acetyl), τ 8.05 (singlet, *N*-acetyl), τ 8.27 (broadened signal of *sec.*-amine NH).

Anal. Calcd. for $C_{26}H_{41}N_3O_{14}$ (619.6): C, 50.40; H, 6.67; N, 6.78. Found: C, 50.26; H, 6.48; N, 6.79.

1. (*a*) H. H. BAER and T. NEILSON. J. Org. Chem. **32**, 1068 (1967); (*b*) H. H. BAER, T. NEILSON, and W. RANK. Can. J. Chem. **45**, 991 (1967); (*c*) H. H. BAER and K. S. ONG. J. Org. Chem. **34**, 560 (1969); (*d*) H. H. BAER and F. KIENZLE. J. Org. Chem. In press; (*e*) H. H. BAER, F. RAJABALEE, and F. KIENZLE. J. Org. Chem. In press; (*f*) H. H. BAER and F. RAJABALEE. Part XVI in this series. Carbohyd. Res. In press.
2. H. H. BAER and K. S. ONG. Can. J. Chem. **46**, 2511 (1968).
3. H. H. BAER and F. KIENZLE. Can. J. Chem. **47**, 2819 (1969).
4. For a review see H. H. BAER. Advan. Carbohyd. Chem. **24** (1969). In press.
5. J. E. CHRISTENSEN and L. GOODMAN. Carbohyd. Res. **7**, 510 (1968).
6. H. H. BAER, F. KIENZLE, and F. RAJABALEE. Can. J. Chem. **46**, 80 (1968).
7. H. H. BAER and F. KIENZLE. Can. J. Chem. **45**, 983 (1967).
8. F. G. FISCHER and H. DÖRFEL. Z. Physiol. Chem. **301**, 224 (1955).

Absolute configurations of the (−)-*erythro* and (−)-*threo*-2,3-dihydroxybutyric acids

F. W. BACHELOR AND G. A. MIANA[1]

Department of Chemistry, University of Calgary, Calgary 44, Alberta, Canada

Received June 23, 1969

The absolute configurations of (−)-*erythro*-2,3-dihydroxybutyric acid and (−)-*threo*-2,3-dihydroxybutyric acid have been determined by optical rotatory dispersion and found to be 2(R), 3(R) for the *erythro* acid and 2(S), 3(R) for the *threo* acid.

Canadian Journal of Chemistry, **47**, 4089 (1969)

We recently found it necessary to determine the absolute configurations of the active *erythro*-2,3-dihydroxybutyric and *threo*-2,3-dihydroxybutyric acids for use in a stereospecific synthesis. Because of the inquiries which we have received regarding these compounds we felt it expedient to communicate this information prior to the completion of the synthetic problem.

The absolute configuration of (−)-*threo*-2,3-dihydroxybutyric acid has been indirectly determined by its production from L-threonine with nitrous acid (1). Since the stereochemistry of the deaminations of α-amino acids has been established to give unequivocably retention of configuration (2), this establishes the stereochemistry of the (−)-*threo*-dihydroxybutyric acid as being the same as L-threonine.

Erythro-2,3-dihydroxybutyric acid was prepared by hydroxylation of *trans*-crotonic acid with hydrogen peroxide and tungstic acid according to the method of Mugdan and Young (3). This acid was resolved through its quinine salt (4) to give (−)-*erythro*-2,3-dihydroxybutyric acid with a specific rotation of −9.5°.

The *threo*-isomer was prepared by a Milas oxidation of *trans*-crotonic acid with osmium tetroxide and hydrogen peroxide (5) and the dihydroxy acid resolved through its quinidine salt (6) to give (−)-*threo*-2,3-dihydroxybutyric acid with a specific rotation of −17.75°.

Because of the poor recovery of the resolved acids from their salts by previously reported procedures (4,6) the free acids were regenerated by their passage through a weak acid ion exchange column, a method recently communicated by us (7).

[1]Holder of an NRCC Studentship 1965–1966.

Can. J. Chem. Downloaded from www.nrcresearchpress.com by 210.87.254.6 on 09/05/12
For personal use only.

Can. J. Chem. Downloaded from www.nrcresearchpress.com by 210.87.254.6 on 09/05/12
For personal use only.

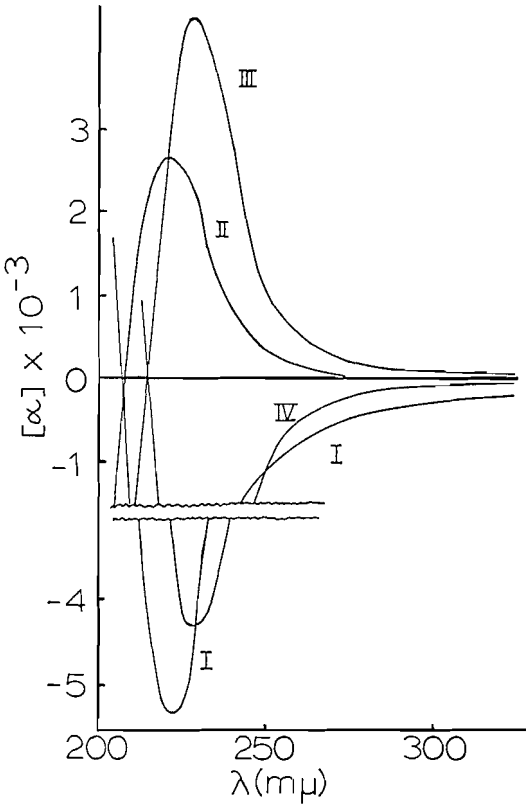

FIG. 1. Optical rotatory dispersion curves of: I, (−)-*erythro*-2,3-dihydroxybutyric acid; II, (−)-*threo*-2,3-dihydroxybutyric acid; III, (S)-(−)-tartaric acid; IV, (R)-(+)-tartaric acid.

Since the observation by Dirkx and Sixma (8) that the 210 mμ absorption band of active α-substituted acids is optically active the Cotton effects of a number of acids of known absolute configuration have been measured (8, 9). These workers have shown that α-hydroxy acids having the S-configuration at the α-carbon atom exhibit a positive Cotton effect in the region 220–235 mμ, depending on the solvent and the p*H*.

We have measured the optical rotatory dispersion curves of our resolved acids and these are shown in Fig. 1. The curves for (R)-(+)- and (L)-(−)-tartaric acids are included for comparison. As can be seen, (−)-*threo*-2,3-dihydroxybutyric acid exhibits a positive Cotton effect with an absorption maximum at 221 mμ and a specific rotation of +2640°. This acid therefore has the S-configuration at the α-carbon atom. On the other hand, (−)-*erythro*-2,3-dihydroxybutyric acid shows a negative Cotton effect with a trough at 221 mμ and a specific rotation of −5380°, and therefore has the R-configuration at the α-carbon atom.

From the stereospecific methods of preparation it then follows that the complete configuration for (−)-*erythro*-2,3-dihydroxybutyric acid (**1**) is 2(R), 3(R) and that for (−)-*threo*-2,3-dihydroxybutyric acid (**2**) is 2(S), 3(R).

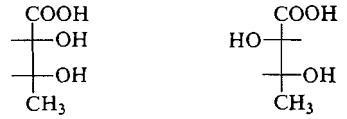

1 **2**

Experimental

All rotations and optical rotatory dispersion (o.r.d.) measurements were taken on a Jasco ORD/UV-5 spectropolarimeter.

(±)-Erythro-2,3-dihydroxybutyric Acid

86 g (1 mole) of *trans*-crotonic acid was dissolved in 500 ml of hot water and the solution stirred vigorously. A 30% hydrogen peroxide solution (106 ml, 0.95 mole) containing 540 mg of tungstic acid was added portionwise in about 10 min. The temperature of the reaction mixture was raised to 70° and maintained for 4 h. The reaction mixture was cooled to room temperature, extracted with chloroform, and the chloroform extract washed with distilled water. The combined aqueous extracts were filtered to remove inorganic material, and the filtrate concentrated *in vacuo* at 50° to give a syrup. The syrup was dissolved in one part of boiling anhydrous ethyl acetate and treated with charcoal. The filtered solution, when cooled to 0°, deposited colorless crystals of (±)-*erythro*-2,3-dihydroxybutyric acid. Yield, 67.2 g (70%); m.p. 80–83° (over P_2O_5).

(±)-Threo-2,3-dihydroxybutyric Acid

50 ml of a 0.5% solution of osmium tetroxide in *tert*-butanol was added slowly and cautiously to a cooled solution of 86.0 g (1 mole) of *trans*-crotonic acid in 125 ml of 30% hydrogen peroxide, made up to a volume of 600 ml. The solution, which becomes very hot after complete addition of the osmium tetroxide solution, was allowed to stand for 2 h at room temperature. The reaction mixture was extracted 3 times with 300 ml of benzene to remove the osmium tetroxide and was further extracted with chloroform. The aqueous layer was evaporated to dryness *in vacuo* to a syrup. The syrup was dissolved in anhydrous ethyl acetate, treated with charcoal and filtered. The filtrate on cooling deposited crystalline (±)-*threo*-2,3-dihydroxybutyric acid. Yield, 74 g (64%); m.p. 73–74° (over P_2O_5).

(−)-Erythro-2,3-dihydroxybutyric Acid (1)

20 g (0.165 mole) of (±)-*erythro*-2,3-dihydroxybutyric acid was dissolved in 250 ml of water. The solution was heated to 50 °C and neutralized with 60 g (0.185 mole) of

quinine. The cooled solution was filtered to remove undissolved quinine and cooled to 0°. After two days the crystals formed were collected and washed with ice water. The crystals (30 g) were recrystallized twice from water and dried *in vacuo* over H_2SO_4. Yield, 29.0 g; m.p. 195°; $[\alpha]_D^{20}$ −115° (*c*, 5.04, H_2O); [lit. (4), $[\alpha]_D^{20}$ −113° (*c*, 5.0, H_2O)].

Concentration of the original filtrate gave a further 6 g of crystalline material.

The free acid was regenerated by passing an aqueous solution of the resolved quinine salt through a Bio-Rex-70 (H^+) resin column (7) yielding (−)-*erythro*-2,3-dihydroxybutyric acid, $[\alpha]_D^{25}$ −9.5° (*c*, 1.0, H_2O); [lit. (4), $[\alpha]_D^{20}$ −9.30° (*c*, 0.5, H_2O)].

Rotatory dispersion (*c*, 0.5, H_2O): $[\alpha]_{589}$ −9.5°, $[\alpha]_{250}$ −1060°, $[\alpha]_{221}$ −5380° (trough), $[\alpha]_{210}$ −1790°.

(−)-Threo-2,3-dihydroxybutyric Acid (2)

To a hot solution of 20 g (0.165 mole) of (±)-*threo*-2,3-dihydroxybutyric acid in 500 ml of water 60 g (0.185 mole) of quinidine was added. The hot solution was filtered and cooled. The crystalline salt (37.3 g) was dried in a vacuum desiccator over H_2SO_4. Concentration of the filtrate gave a further 2.0 g of material. After several recrystallizations from water, a salt with constant rotation was obtained, m.p. 117°; $[\alpha]_D^{20}$ +145.5° (*c*, 3.3, H_2O); [lit. (6), m.p. 114°, $[\alpha]_D^{18}$ +142.2°, (*c*, 3.31, H_2O)].

Regeneration of the free acid was accomplished in the same manner as with the *erythro* acid yielding (−)-*threo*-2,3-dihydroxybutyric acid as a syrup, $[\alpha]_D^{25}$ −17.75° (*c*, 1.0 H_2O); [lit. (6), $[\alpha]_D^{16}$ −13.51° (*c*, 6.0, H_2O)].

Rotatory dispersion (*c*, 0.5, H_2O): $[\alpha]_{589}$ −17.75°, $[\alpha]_{250}$ +360°, $[\alpha]_{221}$ +2640° (peak), $[\alpha]_{210}$ +880°.

Acknowledgments

We wish to thank the National Research Council of Canada and the University of Calgary for financial support.

1. C. E. Meyer and W. C. Rose. J. Biol. Chem. **115**, 721 (1936).
2. P. Brewster, E. D. Hughes, C. K. Ingold, and P. A. D. S. Rao. Nature, **166**, 178 (1950).
3. M. Mugdan and D. P. Young. J. Chem. Soc. 2988 (1949).
4. E. Hoff-Jørgensen. Z. Physiol. Chem. **268**, 194 (1941).
5. N. A. Milas and S. Sussman. J. Amer. Chem. Soc. **58**, 1302 (1936).
6. R. S. Morrell and E. K. Hanson. J. Chem. Soc. **85**, 197 (1904).
7. F. W. Bachelor and G. A. Miana. Can. J. Chem. **45**, 79 (1967).
8. I. P. Dirkx and F. J. L. Sixma. Rec. Trav. Chim. **83**, 522 (1964).
9. J. C. Craig and S. K. Roy. Tetrahedron, **21**, 1847 (1965).

Chromatographic analysis of methyl ethers of 2-amino-2-deoxy-D-glucopyranose[1]

M. B. Perry and Ann C. Webb

The Biochemistry Laboratory, National Research Council of Canada, Ottawa, Canada

Received May 27, 1969

The mono-, di-, and tri-*O*-methyl ether derivatives of 2-amino-2-deoxy-D-glucopyranose have been analyzed by gas–liquid chromatography of their fully acetylated 2-acetamido-2-deoxy-D-glucitol derivatives which were prepared from the glycoses by reduction with sodium borohydride followed by acetylation with acetic anhydride. The methyl ethers of 2-amino-2-deoxy-D-glucopyranose were also characterized by degradation with ninhydrin to the corresponding methyl ether derivatives of D-arabinose which were identified by paper chromatography.

Canadian Journal of Chemistry, 47, 4091 (1969)

The identification of the methyl ether derivatives of 2-amino-2-deoxy-D-glucose from the hydrolyzates of methylated glycans containing 2-amino-2-deoxy-D-glucose units is usually a part of the procedure involved in the structural analysis of the original glycan. The paper chromatographic (1–6) method has been used for the identification of the methyl ethers of 2-amino-2-deoxy-D-glucose. However, in our experience, this method did not provide a satisfactory separation of the individual mono- and di-*O*-methyl derivatives. Gas–liquid chromatography (g.l.c.) has been used to identify some methyl ethers as their methyl 2-acetamido-2-deoxy-D-glucoside derivatives (7–9). A recent thin-layer chromatographic (t.l.c.) method for the separation of the methyl ethers of ethyl 2-deoxy-2-(2,4-dinitroanilino)-α-D-glucopyranoside and of 2-deoxy-2-(2,4-dinitroanilino)-D-glucose (10) offers a practical procedure for the analysis of mixtures of the methyl ethers of 2-amino-2-deoxy-D-glucose. This note records a

[1]Issued as NRCC No. 10 899.

Can. J. Chem. Downloaded from www.nrcresearchpress.com by 210.87.254.6 on 09/05/12
For personal use only.

quinine. The cooled solution was filtered to remove undissolved quinine and cooled to 0°. After two days the crystals formed were collected and washed with ice water. The crystals (30 g) were recrystallized twice from water and dried *in vacuo* over H_2SO_4. Yield, 29.0 g; m.p. 195°; $[\alpha]_D^{20}$ −115° (*c*, 5.04, H_2O); [lit. (4), $[\alpha]_D^{20}$ −113° (*c*, 5.0, H_2O)].

Concentration of the original filtrate gave a further 6 g of crystalline material.

The free acid was regenerated by passing an aqueous solution of the resolved quinine salt through a Bio-Rex-70 (H^+) resin column (7) yielding (−)-*erythro*-2,3-dihydroxybutyric acid, $[\alpha]_D^{25}$ −9.5° (*c*, 1.0, H_2O); [lit. (4), $[\alpha]_D^{20}$ −9.30° (*c*, 0.5, H_2O)].

Rotatory dispersion (*c*, 0.5, H_2O): $[\alpha]_{589}$ −9.5°, $[\alpha]_{250}$ −1060°, $[\alpha]_{221}$ −5380° (trough), $[\alpha]_{210}$ −1790°.

(−)-Threo-2,3-dihydroxybutyric Acid (2)

To a hot solution of 20 g (0.165 mole) of (±)-*threo*-2,3-dihydroxybutyric acid in 500 ml of water 60 g (0.185 mole) of quinidine was added. The hot solution was filtered and cooled. The crystalline salt (37.3 g) was dried in a vacuum desiccator over H_2SO_4. Concentration of the filtrate gave a further 2.0 g of material. After several recrystallizations from water, a salt with constant rotation was obtained, m.p. 117°; $[\alpha]_D^{20}$ +145.5° (*c*, 3.3, H_2O); [lit. (6), m.p. 114°, $[\alpha]_D^{18}$ +142.2°, (*c*, 3.31, H_2O)].

Regeneration of the free acid was accomplished in the same manner as with the *erythro* acid yielding (−)-*threo*-2,3-dihydroxybutyric acid as a syrup, $[\alpha]_D^{25}$ −17.75° (*c*, 1.0 H_2O); [lit. (6), $[\alpha]_D^{16}$ −13.51° (*c*, 6.0, H_2O)].

Rotatory dispersion (*c*, 0.5, H_2O): $[\alpha]_{589}$ −17.75°, $[\alpha]_{250}$ +360°, $[\alpha]_{221}$ +2640° (peak), $[\alpha]_{210}$ +880°.

Acknowledgments

We wish to thank the National Research Council of Canada and the University of Calgary for financial support.

1. C. E. Meyer and W. C. Rose. J. Biol. Chem. **115**, 721 (1936).
2. P. Brewster, E. D. Hughes, C. K. Ingold, and P. A. D. S. Rao. Nature, **166**, 178 (1950).
3. M. Mugdan and D. P. Young. J. Chem. Soc. 2988 (1949).
4. E. Hoff-Jørgensen. Z. Physiol. Chem. **268**, 194 (1941).
5. N. A. Milas and S. Sussman. J. Amer. Chem. Soc. **58**, 1302 (1936).
6. R. S. Morrell and E. K. Hanson. J. Chem. Soc. **85**, 197 (1904).
7. F. W. Bachelor and G. A. Miana. Can. J. Chem. **45**, 79 (1967).
8. I. P. Dirkx and F. J. L. Sixma. Rec. Trav. Chim. **83**, 522 (1964).
9. J. C. Craig and S. K. Roy. Tetrahedron, **21**, 1847 (1965).

Chromatographic analysis of methyl ethers of 2-amino-2-deoxy-D-glucopyranose[1]

M. B. Perry and Ann C. Webb

The Biochemistry Laboratory, National Research Council of Canada, Ottawa, Canada

Received May 27, 1969

The mono-, di-, and tri-*O*-methyl ether derivatives of 2-amino-2-deoxy-D-glucopyranose have been analyzed by gas–liquid chromatography of their fully acetylated 2-acetamido-2-deoxy-D-glucitol derivatives which were prepared from the glycoses by reduction with sodium borohydride followed by acetylation with acetic anhydride. The methyl ethers of 2-amino-2-deoxy-D-glucopyranose were also characterized by degradation with ninhydrin to the corresponding methyl ether derivatives of D-arabinose which were identified by paper chromatography.

Canadian Journal of Chemistry, **47**, 4091 (1969)

The identification of the methyl ether derivatives of 2-amino-2-deoxy-D-glucose from the hydrolyzates of methylated glycans containing 2-amino-2-deoxy-D-glucose units is usually a part of the procedure involved in the structural analysis of the original glycan. The paper chromatographic (1–6) method has been used for the identification of the methyl ethers of 2-amino-2-deoxy-D-glucose. However, in our experience, this method did not provide a satisfactory separation of the individual mono- and di-*O*-methyl derivatives. Gas–liquid chromatography (g.l.c.) has been used to identify some methyl ethers as their methyl 2-acetamido-2-deoxy-D-glucoside derivatives (7–9). A recent thin-layer chromatographic (t.l.c.) method for the separation of the methyl ethers of ethyl 2-deoxy-2-(2,4-dinitroanilino)-α-D-glucopyranoside and of 2-deoxy-2-(2,4-dinitroanilino)-D-glucose (10) offers a practical procedure for the analysis of mixtures of the methyl ethers of 2-amino-2-deoxy-D-glucose. This note records a

[1]Issued as NRCC No. 10 899.

Can. J. Chem. Downloaded from www.nrcresearchpress.com by 210.87.254.40 on 09/05/12
For personal use only.

TABLE I

Retention times of acetylated methyl ether derivatives of 2-amino-2-deoxy-D-glucitol relative to 2-acetamido-1,3,4,5,6-penta-*O*-acetyl-2-deoxy-D-glucitol (= 1.00)

Acetylated methyl ether derivative of 2-amino-2-deoxy-D-glucitol	Relative retention time
2-Acetamido-1,5-di-*O*-acetyl-2-deoxy-3,4,6-tri-*O*-methyl-D-glucitol	0.29
2-Acetamido-1,4,5-tri-*O*-acetyl-2-deoxy-3,6-di-*O*-methyl-D-glucitol	0.33
2-Acetamido-1,3,5-tri-*O*-acetyl-2-deoxy-4,6-di-*O*-methyl-D-glucitol	0.51
2-Acetamido-1,5,6-tri-*O*-acetyl-2-deoxy-3,4-di-*O*-methyl-D-glucitol	0.54
2-Acetamido-1,3,4,5-tetra-*O*-acetyl-2-deoxy-6-*O*-methyl-D-glucitol	0.59
2-Acetamido-1,3,5,6-tetra-*O*-acetyl-2-deoxy-4-*O*-methyl-D-glucitol	0.67
2-Acetamido-1,4,5,6-tetra-*O*-acetyl-2-deoxy-3-*O*-methyl-D-glucitol	0.72
2-Acetamido-1,3,4,5,6-penta-*O*-acetyl-2-deoxy-D-glucitol	1.00

Can. J. Chem. Downloaded from www.nrcresearchpress.com by 210.87.254.40 on 09/05/12
For personal use only.

g.l.c. and a paper chromatographic method for the identification of the methyl ethers of 2-amino-2-deoxy-D-glucopyranose.

Initial attempts to analyze mixtures of *O*-methyl derivatives of 2-amino-2-deoxy-D-glucopyranose by g.l.c. of either their trimethylsilylated 2-acetamido-2-deoxy-D-glucopyranoside or methyl 2-acetamido-2-deoxy-D-glucopyranoside derivatives gave complex chromatograms with peak overlaps. Simplified chromatograms were however achieved on g.l.c. of the fully acetylated methyl ether derivatives of 2-acetamido-2-deoxy-D-glucitol derived from the original methyl ethers of 2-amino-2-deoxy-D-glucopyranose.

Authentic mono-, di-, and tri-*O*-methyl derivatives of 2-acetamido-2-deoxy-D-glucopyranose were reduced to their corresponding D-glucitol derivatives with sodium borohydride and after acidification with acetic acid, the mixtures were concentrated to dryness and the boric acid was removed by repeated distillations with methanol. The residual D-glucitol derivatives and sodium acetate were treated with acetic anhydride and the resulting acetylated products were analyzed directly by g.l.c. The retention times of the derivatives, quoted relative to 1,3,4,5,6-penta-*O*-acetyl-2-acetamido-2-deoxy-D-glucitol, are recorded in Table I.

The use of the polyester liquid phase column gave a good separation of the individual derivatives one from another and since it was found that the derivatives gave equal molar response, determined by measurement of peak areas, the procedure can be extended to the quantitative analysis of the mixed methyl ethers of 2-amino-2-deoxy-D-glucopyranose with an accuracy of $\pm$ 4%.

A further characterization of the methyl ethers of 2-amino-2-deoxy-D-glucopyranose can be made by paper chromatographic analysis of the methyl ethers of D-arabinose produced by degradation of the aminoglycoses with ninhydrin (11) following the experimental procedure of Stoffyn and Jeanloz (12). The chromatographic mobilities of the D-arabinose derivatives are recorded in Table II. Of the possible methyl ether derivatives of D-arabinose derived from methyl ethers of 2-amino-2-deoxy-D-glucopyranose, only 2,5- and 3,5-di-*O*-methyl-D-arabinose (13), derived from 2-amino-2-deoxy-D-glucose 3,6- and 4,6-di-*O*-methyl derivatives respectively, failed to separate on paper chromatography. The identity of the above di-*O*-methyl-D-arabinose derivatives can be established by paper electrophoretic examination of this fraction using sodium borate buffer. The 2,5-di-*O*-methyl-D-arabinose has zero mobility whereas the 3,5-di-*O*-methyl-D-arabinose shows considerable migration (M_G 0.67).

When the above procedures are applied to the identification of 2-amino-2-deoxy-D-glucopyranose derivatives in the hydrolysates of methylated glycans containing neutral glycoses, the basic glycoses are best separated from the neutral compounds before analysis, by using cation-exchange resin (H^+ form) from which they can be subsequently eluted with dilute mineral acid (14,15).

Experimental

The 3-, 4-, 6-mono-*O*-, 3,4-, 3,6-, 4,6-di-*O*-, and 3,4,6-tri-*O*-methyl derivatives of 2-amino-2-deoxy-D-glucose hydrochloride and 2-acetamido-2-deoxy-D-glucose were prepared by the methods of Jeanloz (16) and they had physical and chemical properties in agreement with those recorded in the literature.

Gas-liquid chromatography was done using a Hewlett-Packard model 402 gas chromatograph with a hydrogen

TABLE II

Paper chromatographic mobilities of the methyl ethers of D-arabinose obtained by the degradation of the methyl ethers of 2-amino-2-deoxy-D-glucopyranose with ninhydrin

Methyl ether of 2-amino-2-deoxy-D-glucose	Methyl ether of D-arabinose obtained by ninhydrin degradation	Chromatographic mobility*
2-Amino-2-deoxy-3-*O*-methyl-D-glucose	2-*O*-Methyl-D-arabinose	0.18
2-Amino-2-deoxy-4-*O*-methyl-D-glucose	3-*O*-Methyl-D-arabinose	0.12
2-Amino-2-deoxy-6-*O*-methyl-D-glucose	5-*O*-Methyl-D-arabinose	0.37
2-Amino-2-deoxy-3,4-di-*O*-methyl-D-glucose	2,3-Di-*O*-methyl-D-arabinose	0.55
2-Amino-2-deoxy-3,6-di-*O*-methyl-D-glucose	2,5-Di-*O*-methyl-D-arabinose	0.75
2-Amino-2-deoxy-4,6-di-*O*-methyl-D-glucose	3,5-Di-*O*-methyl-D-arabinose	0.77
2-Amino-2-deoxy-3,4,6-tri-*O*-methyl-D-glucose	2,3,5-Tri-*O*-methyl-D-arabinose	1.00

*Mobilities are quoted relative to 2,3,5-tri-*O*-methyl-D-arabinose (= 1.00). Solvent system: butan-2-one saturated with 3% aqueous ammonium hydroxide (13).

flame detector, and fitted with glass U tubes (5 ft × 6 mm × 3 mm i.d.) packed to each end with 10% (w/w) neopentylglycol sebacate polyester (Chromatographic Specialities, Brockville, Ont.) on 80–100 mesh acid-washed Chromosorb W (Johns-Manville). Development was made with dry helium at a flow rate of 100 ml/min and column temperature of 245 °C, and the flash heating system was not used.

Paper chromatography was performed by the descending method on Whatman No. 1 filter paper using butan-2-one saturated with 3% aqueous ammonium hydroxide as the mobile phase. Paper electrophoresis was done on Whatman No. 1 filter paper in 0.1 *M* sodium tetraborate at 750 V (potential gradient 25V/cm) and 30–40 ma for 2 h. Glycoses were detected using the 3% *p*-anisidine hydrochloride in ethanol spray reagent (17).

Preparation of Acetylated Methyl Ethers of 2-Acetamido-2-deoxy-D-glucitol for Gas-liquid Chromatography

The methyl ethers of 2-acetamido-2-deoxy-D-glucitol (2–5 mg) in water (2 ml) were reduced with sodium borohydride (15 mg) for 40 h. The mixtures were acidified with acetic acid and after concentration to dryness under reduced pressure, the residues were taken down with methanol containing 3% acetic acid (5 × 20 ml). The final residues were treated with acetic anhydride (1.2 ml) and were kept at 130 °C for 3 h. Samples (1 µl) of the reaction mixtures were injected directly onto the gas chromatographic column packing.

Degradation of Methyl Ethers of 2-Amino-2-deoxy-D-glucopyranose with Ninhydrin

Samples of the methyl ethers of 2-amino-2-deoxy-D-glucopyranose hydrochloride (0.1 mg) were dissolved in a 2% (w/v) solution of ninhydrin in water containing 4% (v/v) pyridine (0.2 ml) and the mixtures, contained in sealed tubes, were kept at 100° C for 40 min. The reaction mixtures were dried in an air stream and the residues were mixed with 2 drops of water and the solutions were applied directly to paper chromatograms. In each case a single glycose spot was detected on the developed chromatograms which corresponded in mobility with that of the expected authentic methyl ether derivative of D-arabinose.

In analyses in which a spot corresponding to either 2,5- or 3,5-di-*O*-methyl-D-arabinose was present, a preparative paper chromatogram was made and the excised spot corresponding to the di-*O*-methyl glycose was eluted and examined by paper electrophoresis. 2,5-Di-*O*-methyl-D-arabinose had zero mobility and the 3,5-di-*O*-methyl-D-arabinose had a mobility relative to D-glucose of 0.67 (M_G). This analysis permits the identification of either one or both of the glycoses in the degradation mixture.

Acknowledgment

We thank Mrs. S. C. Williams for supplying us with authentic methyl ethers of arabinose.

1. R. KUHN and H. H. BAER. Chem. Ber. **89**, 504 (1956).
2. R. KUHN, H. H. BAER, and A. GAUHE. Chem. Ber. **91**, 364 (1958).
3. S. HIRANO, P. HOFFMAN, and K. MEYER. J. Org. Chem. **26**, 5064 (1961).
4. R. KUHN and A. GAUHE. Chem. Ber. **95**, 518 (1962).
5. I. DANISHEFSKY, H. B. EIBER, and A. E. WILLIAMS. J. Biol. Chem. **238**, 2895 (1963).
6. S. AKIYA and M. TOMODA. Yakugaku Zasshi, **77**, 697 (1957); Chem. Abstr. **51**, 15338 (1957).
7. R. KUHN and H. EGGE. Chem. Ber. **96**, 3338 (1963).
8. R. KUHN. *In* Gas chromatography. *Edited by* M. van Sway. Butterworths, London, 1962. p. XVIII.
9. K. WALLENFELS, G. BECHTLER, R. KUHN, H. TRISCHMANN, and H. EGGE. Angew. Chem. **75**, 1014 (1963).
10. P. F. LLOYD, B. EVANS, and R. J. FIELDER. Carbohyd. Res. **9**, 471 (1969).
11. S. GARDELL, F. HEIJKENSKJOLD, and A. ROCH-NORLUND. Acta Chem. Scand. **4**, 970 (1950).
12. P. J. STOFFYN and R. W. JEANLOZ. Arch. Biochem. Biophys. **52**, 373 (1954).
13. S. C. WILLIAMS and J. K. N. JONES. Can. J. Chem. **45**, 275 (1967).
14. M. B. PERRY. Can. J. Biochem. **42**, 451 (1964).
15. M. B. PERRY and ANN C. WEBB. Can. J. Biochem. **46**, 1163 (1968).
16. R. W. JEANLOZ. Advan. Carbohyd. Chem. **13**, 189 (1958).
17. L. HOUGH, J. K. N. JONES, and W. H. WADMAN. J. Chem. Soc. 1702 (1950).

Can. J. Chem. Downloaded from www.nrcresearchpress.com by 210.87.254.40 on 09/05/12
For personal use only.

Can. J. Chem. Downloaded from www.nrcresearchpress.com by 210.87.254.42 on 09/05/12
For personal use only.

4,6-*O*-Benzylidene-3-deoxy-3-*C*-(iodomethyl)-D-allal: precursor of a cyclopropylcarbinyl-oxo-carbonium ion

BERT FRASER-REID AND BRUNO RADATUS
Department of Chemistry, University of Waterloo, Waterloo, Ontario

Received May 16, 1969

Treatment of methyl 4,6-*O*-benzylidene-α-D-*erythro*-hex-2-enopyranoside (**5**) with the Simmons–Smith reagents gives 85% of the expected cyclopropane adduct **6** and about 10% of a second product **4**. When the cyclopropane derivative **6** is allowed to react further with the Simmons–Smith reagents, it is 40% converted to **4**. The structure of compound **4** is established to be 4,6-*O*-benzylidene-3-deoxy-3-*C*-(iodomethyl)-D-allal (4,6-*O*-benzylidene-1,2,3-trideoxy-3-*C*-iodomethyl-D-*ribo*-hex-1-enopyranose), and the unusually high solvolytic reactivity observed for it, as well as its formation from **6**, are rationalized as proceeding through the *cyclopropylcarbinyl-oxo-carbonium ion* **3**.

Canadian Journal of Chemistry, 47, 4095 (1969)

The stabilized carbonium ion **1** is frequently invoked as an intermediate in reactions occurring at the anomeric center of carbohydrate molecules (1). Another stabilized ion, **2**, has been demonstrated to be an intermediate in reactions where a cationic center is generated at a homoallylic site (2). Carbonium ion **3** is a combination of **1** and **2**. In this communication we describe a novel

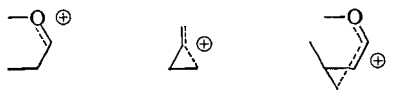

1 **2** **3**

vinyl ether, **4**, whose unusually high solvolytic reactivity appears best rationalized by invoking the intervention of the cyclopropylcarbinyl-oxo-carbonium ion **3**.[1]

Cyclopropanation[2] of olefin **5** (4), as with most additions to this compound (3), proceeds with difficulty[3]; however, a procedure was established whereby **5** could be converted to the cyclopropane derivative **6** in greater than 80% yield based on unrecovered olefin. A minor component (**4**) was produced in about 10% yield and this was isolated in a fairly high state of purity by silica column chromatography.[4]

This component **4** gave: m.p. 130–132 °C; $[\alpha]_D^{23}$ + 129.0° (*c*, 2.8 in $CHCl_3$).

Anal. Calcd. for $C_{14}H_{15}IO_3$: C, 46.92; H, 4.22; I, 35.47. Found: C, 46.87; H, 4.22; I, 34.67.[5]

The nuclear magnetic resonance (n.m.r.) spectrum showed the absence of a methoxyl signal but retention of the benzylidene group. Infrared (i.r.) absorptions at 1645, 1235, and 1081 cm^{-1} suggested a vinyl ether (7), and n.m.r. support for this feature was provided by two quartets at τ 3.66 and 5.00 (ascribable to the α-(H-1) and β-(H-2) hydrogens) with a common coupling constant $J_{1,2}$ of 6.5 Hz, excellent diagnosis of a glycal (8). The iodine was located at a primary carbon since reduction with lithium aluminum hydride afforded a substance whose n.m.r. spectrum contained a methyl group. The latter

[1]The drawing of **3** is not intended to convey anything about the geometry of the species. This aspect of the ion will be discussed when appropriate data have accumulated.

[2]A well stirred mixture of methylene iodide (1.44 ml; 0.0179 mole), zinc–copper couple (5) (1.0 g; 0.0513 mole), and ether (6 ml; 0.0576 mole) was refluxed for 1 h. Olefin **5** (2.0 g; 0.008 mole) was then added along with ether (4 ml; 0.0384 mole) and dimethoxyethane (0.16 ml) (6). After (total) reaction periods of 0.5, 1, 3, and 4 h, further 0.16 ml portions of dimethoxyethane were added. After a total reaction time of 8 h, isolation in the usual way (5) afforded 2.255 g of material, 85% of which was judged (n.m.r.) to be **5** and **6** in ratio 1:2. Physical constants of **6** agree with those reported by Horton and co-workers (3).

[3]After our work had commenced we learned of similar studies in progress at Ohio State University. We are grateful to Professor Horton for informing us of the progress of his work prior to publication (3).

[4]R_f on thin layer chromatography (silica) 0.8 in EtOAc–petroleum ether (1:4).

[5]Horton and co-workers (3) isolated a compound: C, 60.65; H, 5.28; I, 19.60; m.p. 81–83° with "no intense singlet for an OMe group" in the n.m.r.

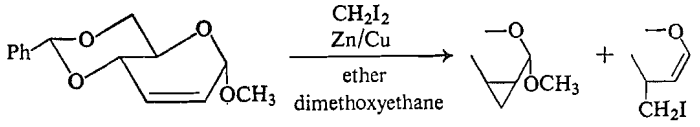

5 6 4

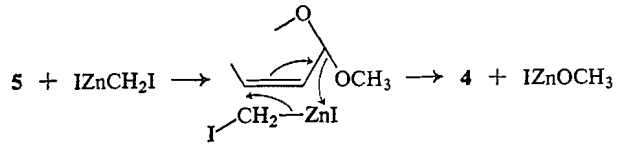

SCHEME 1

appeared as a doublet and was therefore adjacent to a methine proton (*vide infra*). The iodide evidently had structure **4**. The iodomethyl group is judged to be axially oriented since the coupling constant $J_{2,3}$ (6.0 Hz) is closer to that observed in allal and gulal derivatives (8*a*,*b*), in which H-3 is pseudo-equatorial (9), than is observed in glucal (8) and galactal (10) derivatives in which H-3 is pseudo-axial.[6] Detailed description of the n.m.r. spectrum will be presented elsewhere but it may be noted here that the asymmetry at carbon-3 renders the adjoining methylene protons non-equivalent (11). Thus for the moiety

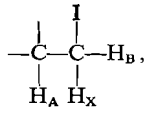

H_B is a quartet at τ 7.00 with $J_{A,B}$ = 8.5 Hz and $J_{B,X}$ = 10.5 Hz, while H_X occurs 0.6 p.p.m. to lower field. H_A (i.e. H-3) whose coupling to H_B, H_X, and H-4 could be demonstrated by double irradiation experiments, is a complex multiplet centered at τ 7.20. In the lithium aluminum hydride-reduced material this signal is shifted to τ 7.43; the latter is simplified on irradiation of a methyl doublet at τ 8.86.

The formal accomplishment in the synthesis of **4** is addition of the iodomethyl anion to carbon-3 of **5** and expulsion of the methoxy substituent. The allylic rearrangement depicted in Scheme 1 is attractive in that it provides for *cis*-relationship between entering and leaving nucleophiles, in accordance with the observed stereochemical course for such rearrangements (12). However, although "forward" allylic rearrangements in which glycals are converted to hex-2-enopyranosides are well known (1*b*,9*a*), the "reverse" rearrangement such as that implied in Scheme 1 has not been reported (1*b*,3,9*a*). An alternative route to **4** (Scheme 2) originates with cleavage of the methoxyl of **6** to give ion **7**,[7] which undoubtedly goes to the more delocalized form represented by **3**, which then suffers iodinolysis at the methylene group to give

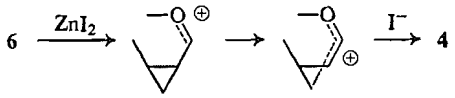

7 3

SCHEME 2

4. Such a route is indeed possible since **6** was 40% converted to **4**,[8] the reaction conditions[2] being maintained for 8 h. This conversion provides independent proof of the configuration assigned to **4**, since under the reaction conditions epimerization at carbon-3 is inconceivable.

Ion **3** would also be expected to intervene and facilitate nucleophilic displacement of the iodine atom of **4**. Indeed, *under conditions where methyl*

[6]The allylic coupling constant ($J_{1,3}$) observed is 1.5 Hz and could be compatible with either axial or equatorial orientation of the iodomethyl group. Data presented in Table I of ref. 8*b* indicate that these long range coupling constants are very sensitive to changes in electronegativity.

[7]Cleavage could conceivably be induced by zinc iodide produced in the Simmons–Smith reaction (6). However, surprisingly, compound **6** has so far not given **4** when treated with zinc iodide in ether!!

[8]This observation does not specifically preclude Scheme 1; it merely demonstrates that under the reaction conditions, **6** is convertible to **4**.

Can. J. Chem. Downloaded from www.nrcresearchpress.com by 210.87.254.42 on 09/05/12
For personal use only.

6-deoxy-6-iodo-α-D-glucopyranoside triacetate (13) required more than 24 h to react appreciably with excess silver nitrate in 50% aqueous dioxan buffered with silver carbonate, the iodide 4 was solvolyzed completely in less than 1 min.

Investigation of the synthetic utility of **4** and of the chemistry of the cyclopropylcarbinyl-oxocarbonium ion **3** is underway and will be reported in due course.

Acknowledgments

The authors are grateful to the National Research Council of Canada and the University of Waterloo for providing generous financial support for this work. We express our deep appreciation to the Chemistry Department of McMaster University and in particular Mr. Brian Sayer, for the 100 MHz n.m.r. determinations.

1. (*a*) R. U. LEMIEUX and B. FRASER-REID. Can. J. Chem. **43**, 1460 (1965); (*b*) R. J. FERRIER. Advan. Carbohyd. Chem. **20**, 101 (1965); (*c*) J. N. BEMILLER. Advan. Carbohyd. Chem. **22**, 25 (1967); (*d*) R. U. LEMIEUX and W. P. SHYLUK. Can. J. Chem. **33**, 120 (1955); (*e*) R. U. LEMIEUX, C. BRICE, and G. HUBER. Can. J. Chem. **33**, 134 (1955); (*f*) E. P. PAINTER. J. Amer. Chem. Soc. **75**, 1137 (1954); (*g*) B. LINDBERG. Acta. Chem. Scand. **3**, 1153 (1949).
2. J. D. ROBERTS and R. H. MAZUR. J. Amer. Chem. Soc. **73**, 2509 (1951); S. WINSTEIN and R. ADAMS. J. Amer. Chem. Soc. **70**, 838 (1948); S. WINSTEIN and A. H. SCHLESSINGER. J. Amer. Chem. Soc. **70**, 3528 (1948).
3. E. L. ALBANO, D. HORTON, and J. H. LAUTERBACH. Carbohyd. Res. **9**, 149 (1969).
4. B. FRASER-REID and B. BOCTOR. Can. J. Chem. **47**, 393 (1969).
5. J. D. ROBERTS (editor). Organic syntheses. Vol. 41. John Wiley and Sons, Inc., New York. 1961. p. 72.
6. H. E. SIMMONS, E. P. BLANCHARD, and R. D. SMITH. J. Amer. Chem. Soc. **86**, 1347 (1964).
7. K. NAKANISHI. Infrared absorption spectroscopy. Holden-Day, Inc., San Francisco. 1964. Figs. 28 and 38.
8. (*a*) R. U. LEMIEUX, E. FRAGA, and K. A. WATANABE. Can. J. Chem. **46**, 61 (1968); (*b*) M. SHARMA and R. K. BROWN. Can. J. Chem. **44**, 2825 (1966); (*c*) L. D. HALL and L. F. JOHNSON. Tetrahedron, **20**, 883 (1964).
9. (*a*) R. J. FERRIER and N. PRASAD. J. Chem. Soc. 570, 575, 581 (1969); (*b*) E. W. GARBISCH. J. Amer. Chem. Soc. **86**, 5561 (1964); E. F. L. J. ANET. Carbohyd. Res. **1**, 348 (1966).
10. B. FRASER-REID. Ph.D. Thesis, University of Alberta, Edmonton, Alberta. 1964.
11. L. M. JACKMAN. Applications of nuclear magnetic resonance spectroscopy in organic chemistry. The Pergamon Press, Ltd., Oxford. 1959. pp. 99–103.
12. G. STORK and W. N. WHITE. J. Amer. Chem. Soc. **78**, 4609 (1956).
13. M. ZIEF and R. C. HOCKETT. J. Amer. Chem. Soc. **67**, 1267 (1945).

Distribution of reaction products (theory). VII. $D^+ + H_2 \rightarrow DH + H^+$ using an *ab initio* potential-energy surface

I. G. CSIZMADIA, J. C. POLANYI, A. C. ROACH,[1] AND W. H. WONG[2]

Department of Chemistry, University of Toronto, Toronto, Ontario

Received September 10, 1969

A three-dimensional classical trajectory calculation has been made of the dynamics of the reaction $D^+ + H_2 \rightarrow DH + H^+$. In contrast to earlier trajectory studies the potential-energy surface was obtained *ab initio*, consequently the results have predictive interest.

Canadian Journal of Chemistry, 47, 4097 (1969)

In this Communication we give a preliminary report of a computer study of the dynamics of the reaction $D^+ + H_2 \rightarrow DH + H^+$. This is, to our knowledge, the first calculation of the dynamics of a chemical reaction using an *ab initio* potential-energy surface.

The variational treatment (for some recent treatments of H_3^+, see ref. 1) took the form of an l.c.a.o.–m.o.–s.c.f. (linear combination of atomic orbitals, molecular orbital, self-consistent field) calculation with configuration interaction (c.i.). A basis-set of 24 Gaussian-type functions (g.t.f.'s) were used (reasons for this choice are in ref. 2); 8 functions centered on each of the 3 nuclei (5 s-type;[3] 3 p-type, i.e. p_x, p_y, p_z).[4] The

[1]Holder of a University of Toronto Postdoctoral Fellowship, 1967–1968. Present address: Department of Chemistry, Manchester University, Manchester, England.

[2]Holder of a National Research Council of Canada Scholarship, 1967–1969. Present address: Department of Chemistry, University of Illinois, Urbana, Illinois.

[3]Exponents were taken from the work of S. Huzinaga, ref. 3.

[4]Exponent = 0.9.

Can. J. Chem. Downloaded from www.nrcresearchpress.com by 210.87.254.42 on 09/05/12
For personal use only.

6-deoxy-6-iodo-α-D-glucopyranoside triacetate (13) required more than 24 h to react appreciably with excess silver nitrate in 50% aqueous dioxan buffered with silver carbonate, the iodide 4 was solvolyzed completely in less than 1 min.

Investigation of the synthetic utility of **4** and of the chemistry of the cyclopropylcarbinyl-oxocarbonium ion **3** is underway and will be reported in due course.

Acknowledgments

The authors are grateful to the National Research Council of Canada and the University of Waterloo for providing generous financial support for this work. We express our deep appreciation to the Chemistry Department of McMaster University and in particular Mr. Brian Sayer, for the 100 MHz n.m.r. determinations.

1. (*a*) R. U. LEMIEUX and B. FRASER-REID. Can. J. Chem. **43**, 1460 (1965); (*b*) R. J. FERRIER. Advan. Carbohyd. Chem. **20**, 101 (1965); (*c*) J. N. BEMILLER. Advan. Carbohyd. Chem. **22**, 25 (1967); (*d*) R. U. LEMIEUX and W. P. SHYLUK. Can. J. Chem. **33**, 120 (1955); (*e*) R. U. LEMIEUX, C. BRICE, and G. HUBER. Can. J. Chem. **33**, 134 (1955); (*f*) E. P. PAINTER. J. Amer. Chem. Soc. **75**, 1137 (1954); (*g*) B. LINDBERG. Acta. Chem. Scand. **3**, 1153 (1949).
2. J. D. ROBERTS and R. H. MAZUR. J. Amer. Chem. Soc. **73**, 2509 (1951); S. WINSTEIN and R. ADAMS. J. Amer. Chem. Soc. **70**, 838 (1948); S. WINSTEIN and A. H. SCHLESSINGER. J. Amer. Chem. Soc. **70**, 3528 (1948).
3. E. L. ALBANO, D. HORTON, and J. H. LAUTERBACH. Carbohyd. Res. **9**, 149 (1969).
4. B. FRASER-REID and B. BOCTOR. Can. J. Chem. **47**, 393 (1969).
5. J. D. ROBERTS (editor). Organic syntheses. Vol. 41. John Wiley and Sons, Inc., New York. 1961. p. 72.
6. H. E. SIMMONS, E. P. BLANCHARD, and R. D. SMITH. J. Amer. Chem. Soc. **86**, 1347 (1964).
7. K. NAKANISHI. Infrared absorption spectroscopy. Holden-Day, Inc., San Francisco. 1964. Figs. 28 and 38.
8. (*a*) R. U. LEMIEUX, E. FRAGA, and K. A. WATANABE. Can. J. Chem. **46**, 61 (1968); (*b*) M. SHARMA and R. K. BROWN. Can. J. Chem. **44**, 2825 (1966); (*c*) L. D. HALL and L. F. JOHNSON. Tetrahedron, **20**, 883 (1964).
9. (*a*) R. J. FERRIER and N. PRASAD. J. Chem. Soc. 570, 575, 581 (1969); (*b*) E. W. GARBISCH. J. Amer. Chem. Soc. **86**, 5561 (1964); E. F. L. J. ANET. Carbohyd. Res. **1**, 348 (1966).
10. B. FRASER-REID. Ph.D. Thesis, University of Alberta, Edmonton, Alberta. 1964.
11. L. M. JACKMAN. Applications of nuclear magnetic resonance spectroscopy in organic chemistry. The Pergamon Press, Ltd., Oxford. 1959. pp. 99–103.
12. G. STORK and W. N. WHITE. J. Amer. Chem. Soc. **78**, 4609 (1956).
13. M. ZIEF and R. C. HOCKETT. J. Amer. Chem. Soc. **67**, 1267 (1945).

Distribution of reaction products (theory). VII. $D^+ + H_2 \rightarrow DH + H^+$ using an *ab initio* potential-energy surface

I. G. CSIZMADIA, J. C. POLANYI, A. C. ROACH,[1] AND W. H. WONG[2]

Department of Chemistry, University of Toronto, Toronto, Ontario

Received September 10, 1969

A three-dimensional classical trajectory calculation has been made of the dynamics of the reaction $D^+ + H_2 \rightarrow DH + H^+$. In contrast to earlier trajectory studies the potential-energy surface was obtained *ab initio*, consequently the results have predictive interest.

Canadian Journal of Chemistry, 47, 4097 (1969)

In this Communication we give a preliminary report of a computer study of the dynamics of the reaction $D^+ + H_2 \rightarrow DH + H^+$. This is, to our knowledge, the first calculation of the dynamics of a chemical reaction using an *ab initio* potential-energy surface.

The variational treatment (for some recent treatments of H_3^+, see ref. 1) took the form of an l.c.a.o.–m.o.–s.c.f. (linear combination of atomic orbitals, molecular orbital, self-consistent field) calculation with configuration interaction (c.i.). A basis-set of 24 Gaussian-type functions (g.t.f.'s) were used (reasons for this choice are in ref. 2); 8 functions centered on each of the 3 nuclei (5 s-type;[3] 3 p-type, i.e. p_x, p_y, p_z).[4] The

[1]Holder of a University of Toronto Postdoctoral Fellowship, 1967–1968. Present address: Department of Chemistry, Manchester University, Manchester, England.

[2]Holder of a National Research Council of Canada Scholarship, 1967–1969. Present address: Department of Chemistry, University of Illinois, Urbana, Illinois.

[3]Exponents were taken from the work of S. Huzinaga, ref. 3.

[4]Exponent = 0.9.

Can. J. Chem. Downloaded from www.nrcresearchpress.com by 210.87.254.40 on 09/05/12
For personal use only.

Can. J. Chem. Downloaded from www.nrcresearchpress.com by 210.87.254.40 on 09/05/12
For personal use only.

c.i. was complete for the lowest 15 s.c.f.–m.o.'s. Approximately 15 min of IBM 7094 computer time were required for each of the 250 nuclear configurations. The calculated energies of the most stable equilateral, collinear, and reactant configurations were respectively 3, 4, and 5 kcal $mole^{-1}$ above the estimated true values, indicating that our surface ran closely parallel to the true one (4).

A potential curve, composed of three superimposed Morse-like functions, was "rotated" about a separated-atom configuration to produce a potential-energy surface for a given $(H—H—H)^+$ angle.[5] The curve parameters varied with both "rotational" and bending angles, yielding an expression for the full hypersurface with a standard deviation of 6.65 kcal $mole^{-1}$ from the *ab initio* points.

Classical trajectories (6) were run in three dimensions[6] for the mass-combination $D^+ + H_2$. Fixed center-of-mass (c.m.) collision energies of 3, 4.5, and (in a smaller sample) 6 eV were used. Other variables (including H_2 rotation and vibration) were chosen by Monte Carlo selection.[7]

The main results can be summarized as follows:

(*i*) As expected for an energy-surface with a very deep potential-well, reaction proceeded by way of a complex. At a collision-energy of 3 eV (i.e. 3 eV in excess of the energy required to dissociate the complex), the complex had a lifetime which was typically $\sim 1 \times 10^{-13}$ s. The great majority (> 90%) of trajectories took from $(0.4–3.0) \times 10^{-13}$ s; the low figure corresponded to approximately one rotation of the complex. The duration of the reactive trajectories increased markedly with increasing impact parameter, b.

(*ii*) Reaction occurred out to maximum impact parameters, b_{max}, significantly in excess of the Gioumousis and Stevenson polarization limit, $b_{max}{}^{p}$ (10). For the present reaction $b_{max} > 2.4$ Å, at both 3 and 4.5 eV,[8] whereas $b_{max}{}^{p}$ is 1.66 Å at 3 eV, and 1.5 Å at 4.5 eV (see eq. [12] of ref. 11). This discrepancy [9] can be explained qualitatively by the effect of the valence forces in the neighborhood of $b_{max}{}^{p}$ in increasing the *attraction* and hence decreasing the height of the rotational barrier on the effective potential. It does not follow that the polarization-model cross-sections will be smaller than the computed ones, since the trajectories led to a reaction probability of 0.2–0.3 for $b \leqslant 2.4$ Å (the polarization theory assumes unit probability).

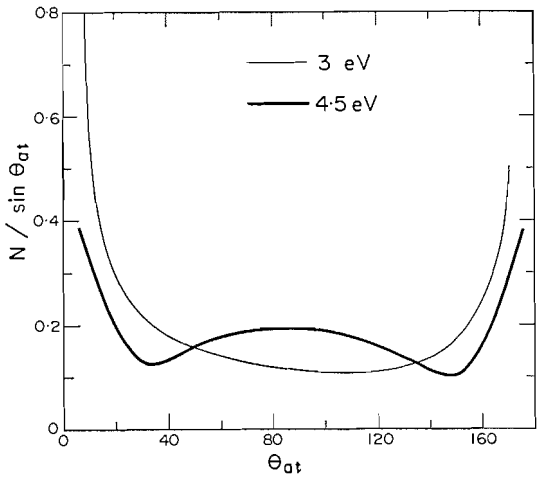

FIG. 1. Center-of-mass differential cross-section for the atomic product of $D^+ + H_2 \rightarrow DH + H^+$ at 3 eV (104 reactive trajectories) and 4.5 eV (83 reactive trajectories).

(*iii*) The c.m. differential cross-section (Fig. 1) showed forward and backward peaked scattering of the molecular product. At 3 eV collision energy the backward peak was slightly more prominent; at 4.5 eV the scattering was symmetrical (giving the appearance of purely statistical behavior).[10] Probably due to the large (positive) slope of the potential-energy surface along the coordinate of separation, the stripping threshold energy is very high (see Fig. 1 of ref. 13) (so high as to be inaccessible, see (*v*) below).

(*iv*) The product vibrational and rotational energy-distributions[10] at 3 eV were characterized

[5]F. T. Wall and R. N. Porter (5) originated this method in a simpler form suitable for collinear reaction.

[6]The coordinate system (see also footnote 7) and method for integrating the equations of motion is described in part V of this series (7).

[7]The Monte Carlo selection procedure is described in refs. 8 and 9.

[8]We do not yet have precise values for b_{max} or for the reactive cross-section, since a number of complex trajectories remain to be computed. The total reactive cross-section is $S_r > 2.7$ Å^2 at 3 eV, and > 2.2 Å^2 at 4.5 eV.

[9]Failure of the polarization theory at collision energies $\gtrsim$ 1 eV has been predicted: see refs. 10 and 12. The valence forces were presumed to be *repulsive*, hence $b_{max} < b_{max}{}^{p}$.

[10]Though the data are incomplete (see footnote 8), the results are unlikely to alter; partial histograms which included only the shorter trajectories closely resembled those for the more complex trajectories.

Can. J. Chem. Downloaded from www.nrcresearchpress.com by 210.87.254.40 on 09/05/12
For personal use only.

by a steadily descending curve of probability from zero energy up to the maximum[11] possible energy of 76 kcal mole^{-1}. The mean vibrational and rotational energies in the products were $\langle E_V' \rangle \simeq \langle E_R' \rangle \simeq 23$ kcal mole^{-1}. At 4.5 eV collision energy the N (E_V') curve, giving the distribution of product over vibrational energies, was double-peaked with a more prominent low-energy peak at 28 kcal mole^{-1} and a smaller high-energy peak at 88 kcal mole^{-1} (available energy 112 kcal mole^{-1}).[11] The N (E_R') curve at 4.5 eV descended steadily from $E_R' = 0$ to $E_R' \simeq$ 70 kcal mole^{-1}, with evidence of a secondary peak centered at approximately 84 kcal mole^{-1}. The tendency for DH to be formed with greatest probability in low states of rotation implied that the outcome of the reaction was not statistical, despite the complexity of the trajectories.[12]

The translational energy-distributions at 3 and 4.5 eV were roughly Boltzmann in shape; mean values were $\langle E_T' \rangle \simeq 30$ kcal mole^{-1} at 3 eV, and $\langle E_T' \rangle \simeq 38$ kcal mole^{-1} at 4.5 eV.

(*v*) Approximately 20% of the reactive trajectories at 4.5 eV led to fragmentation into 3 particles, despite the fact that the collision-energy was only 0.1 eV in excess of the dissociation energy, D_0. At 6 eV it appeared that over 90% of the reactive trajectories gave fragmentation. This very steep rise in percentage of fragmentation immediately above the dissociation energy may be connected with the complexity of the trajectories (arising from the existence of deep potential-well) which partitions the energy among all three atoms.[13]

[11]This figure is the c.m. collision energy, plus 6.3 kcal mole^{-1} of vibration, plus the mean rotational energy (0.6 kcal mole^{-1}).

[12]If the product states were populated in proportion to the available phase-space, there would be increasing population toward higher J levels (14). It is noteworthy that a statistical distribution over angles need not imply a statistical distribution over energy states (see results for 4.5 eV collision energy). The former merely requires that the particles shall have scrambled their momenta to the point that the initial direction of approach of D^+ has been "forgotten". The latter makes the more stringent requirement that there be no preferred paths through phase-space for the dissociation of $DH_2^+ \rightarrow DH + H^+$.

[13]Two studies of *direct* reaction (15) showed a more gradual increase in the proportion of fragmentation.

There is at the present time no experimental information concerning the dynamics of the $D^+ + H_2$ reaction, but beam studies are planned in several laboratories.

Acknowledgments

We are indebted to the National Research Council of Canada, the U.S. Air Force Cambridge Research Laboratories, and the Petroleum Research Fund administered by the American Chemical Society, for financial support. We thank the Institute of Computer Sciences, University of Toronto, for the use of their facilities.

1. (*a*) W. KUTZELNIGG, R. AHLRICHS, I. LABIB-ISKANDER, and W. A. BINGEL. Chem. Phys. Lett. **1**, 447 (1967). (*b*) R. E. CHRISTOFFERSEN. J. Chem. Phys. **41**, 960 (1964). (*c*) W. A. LESTER and M. KRAUSS. J. Chem. Phys. **44**, 207 (1966). (*d*) H. CONROY. J. Chem. Phys. **41**, 1341 (1964). (*e*) M. E. SCHWARTZ and L. J. SCHAAD. J. Chem. Phys. **47**, 5325 (1967).
2. I. G. CSIZMADIA, J. Chem. Phys. **44**, 1849 (1966).
3. S. HUZINAGA. J. Chem. Phys. **42**, 1293 (1965).
4. (*a*) A. C. ROACH, M. A. ROBB, J. C. POLANYI, and I. G. CSIZMADIA. 51st Annual Conference, Chem. Inst. of Canada, Vancouver, 1968. (*b*) I. G. CSIZMADIA, R. E. KARI, J. C. POLANYI, A. C. ROACH, and M. A. ROBB. J. Chem. Phys. To be published.
5. F. T. WALL and R. N. PORTER. J. Chem. Phys. **36**, 3256 (1962).
6. (*a*) F. T. WALL, L. A. HILLER, JR., and J. MAZUR. J. Chem. Phys. **29**, 255 (1958); **35**, 1284 (1961). (*b*) D. L. BUNKER. Theory of elementary gas reaction rates. The Pergamon Press, Ltd., Oxford, England. 1966. (*c*) M. KARPLUS. *In* Structural chemistry and molecular biology. *Edited by* A. Rich and N. Davidson. W. H. Freeman Co., San Francisco, 1968.
7. P. J. KUNTZ, M. H. MOK, and J. C. POLANYI. J. Chem. Phys. **50**, 4623 (1969).
8. J. C. POLANYI and W. H. WONG. J. Chem. Phys. To be published.
9. W. H. WONG. Ph.D. Thesis. University of Toronto, Toronto, Ontario. 1969.
10. G. GIOUMOUSIS and D. P. STEVENSON. J. Chem. Phys. **29**, 294 (1958).
11. F. A. WOLF. J. Chem. Phys. **44**, 1619 (1966).
12. (*a*) N. BOELRIJK and W. H. HAMILL. J. Amer. Chem. Soc. **84**, 730 (1962). (*b*) A. HENGLEIN. *In* Ion molecule reactions in the gas phase. *Edited by* R. F. Gould. Amer. Chem. Soc. Adv. Chem. Series, No. 58, 1966. p. 63.
13. J. C. POLANYI. Discuss. Faraday Soc. **44**, 293 (1967).
14. (*a*) J. C. LIGHT and J. LIN. J. Chem. Phys. **43**, 3209 (1965). (*b*) P. PECHUKAS, J. C. LIGHT, and C. RANKIN. J. Chem. Phys. **44**, 794 (1966).
15. (*a*) M. KARPLUS, R. N. PORTER, and R. D. SHARMA. Chem. Phys. **45**, 3871 (1966). (*b*) P. J. KUNTZ, E. M. NEMETH, J. C. POLANYI, and W. H. WONG. J. Chem. Phys. To be published.

Can. J. Chem. Downloaded from www.nrcresearchpress.com by 210.87.254.5 on 09/05/12
For personal use only.

Canadian Journal of Chemistry

Published by THE NATIONAL RESEARCH COUNCIL OF CANADA

VOLUME 47 NOVEMBER 15, 1969 NUMBER 22

Structural aspects of the hydrolysis products of metal alkoxides and metal trialkylsilyloxides[1]

J. W. LORIMER AND D. E. G. JONES[2]

Department of Chemistry, University of Western Ontario, London, Ontario

Received April 30, 1969

The average degree of polymerization $\bar{n}_n$ depends on the average degree of hydrolysis $\bar{x}_n$ as $1/\bar{n}_n = a + b\bar{x}_n$ over a large range of $\bar{x}_n$ for all metal oxide alkoxides and oxide trialkylsilyloxides that have been formed by hydrolysis and examined in solution. A number of general theoretical models are developed which permit quantitative interpretation of the parameters a and b. Mixtures of linear or branched chains in proportions governed wholly or partly by the degree of polymerization of the unhydrolyzed alkoxide can explain all the data on oxide alkoxides in solution in their corresponding alcohol, and the model leads to a plausible mechanism for disproportionation. Similar models with more complex structure can be involved in the metal oxide trialkylsilyloxides. Heterogeneity in the composition of the repeating units or in the number of metal–oxygen–metal bridges between successive repeating units can also be significant for both oxide alkoxides and oxide trialkylsilyloxides. Models involving cyclic chains are possible, but steric effects make them improbable in many cases. Mixtures of chains with equal average degrees of hydrolysis for each type of chain have been assumed in previous analyses, but are shown to be special cases of the more general model.

Canadian Journal of Chemistry, 47, 4101 (1969)

Introduction

Bradley and co-workers have examined a large number of the polymeric hydrolysis products of metal alkoxides (1–7) and of metal trialkylsilyloxides (8–11). Hydrolysis of metal alkoxides gives metal oxide alkoxides, or polyalkylmetalloxanes, e.g.

$$[1a] \quad n\mathrm{Sn(OPr^i)_4} + nx\mathrm{H_2O} \rightarrow [\mathrm{SnO}_x(\mathrm{OPr^i})_{4-2x}]_n + 2nx\mathrm{Pr^iOH}$$

while hydrolysis of metal trialkylsilyloxides gives metal oxide trialkylsilyloxides, or polytrialkylsiloxanometalloxanes, e.g.

$$[1b] \quad n\mathrm{Ti(OSiMe_3)_4} + nx\mathrm{H_2O} \rightarrow [\mathrm{TiO}_x(\mathrm{OSiMe_3})_{4-2x}]_n + 2nx\mathrm{Me_3SiOH}$$

The number of metal atoms per polymer molecule, n, is called the degree of polymerization or molecular complexity, and the number of water molecules per metal atom, x, is called the degree of hydrolysis. In the case of the oxide alkoxides, the stoichiometry or analysis for the metal gives the value of x. For the oxide trialkylsilyloxides, condensation of trialkylsilanols can produce more water and enhance the degree of hydrolysis, so that analysis for the ratio of silicon to metal is required to find the value of x. In either case, combination of the number average molecular weight (obtained by ebullioscopy or cryoscopy, for example), with the value of x gives the value of n.

For almost all the soluble polymers examined, $1/n$ was a linear function of x over a large range of x, and neither n nor x were integral. This linear dependence has been explained by a general theory of "regular polymer series" (7). By combining this theory with the postulate that the polymers adopt the smallest possible structural unit consistent with attainment of the highest possible coordination number by all metal atoms (12), information about the structure of the polymers has also been derived. Conclusions concerning structure obtained in this

[1]The research for this paper was supported, in part, by the Defence Research Board of Canada, Grant number 7583-04.

[2]Present address: Division of Pure Chemistry, National Research Council of Canada, Ottawa, Canada.

Can. J. Chem. Downloaded from www.nrcresearchpress.com by 210.87.254.5 on 09/05/12
For personal use only.

way have been criticized (13, 14) in the case of the titanium oxide ethoxides. X-Ray analysis of one crystalline hydrolysis product of titanium tetraethoxide (15) confirms the prediction (1) that titanium has a coordination number of 6, although the structures in the solid state and in solution (1) appear to be different. Recent investigations in this laboratory of light scattering, refractivity, specific volume, and viscosity in solutions of titanium oxide trimethylsilyloxide (16) lend support to the structural model proposed on the basis of the theory of regular polymer series (8). However, it became clear that the theory as originally formulated lacked sufficient generality. The object of this paper is to give a correct and complete theory of regular polymer series, to ascertain what information may or may not be obtained from the linear dependence of $1/n$ on x, and to apply the theory systematically to existing experimental data.

General Theory for Homogeneous Polymer Chains

(a) Single Linear or Branched Chains

A "regular polymer series" is defined as a set of hydrolysis products with structures that fulfill the following requirements (7). (*i*) Each member of the series is considered to be derived from an integral number r of repeating units linked together by an integral number q of metal–oxygen–metal bridges formed by condensation. The value of q will be called the "bridge multiplicity". (*ii*) The degree of polymerization p of the repeating units must retain the same integral values throughout the series. (*iii*) The bridge multiplicity must be constant throughout the series. Requirements (*ii*) and (*iii*) define the chains to be homogeneous. This definition of a regular polymer series will be expanded to include polydisperse, mixed, and heterogeneous polymers in subsequent sections.

The degree of polymerization of chain i is

$$[2] \qquad n_i = pr, \quad r = 1, 2, 3, \ldots$$

If there are l water molecules per metal atom in an isolated repeating unit ($r = 1$), the number of water molecules used to form the chain is

$$[3] \qquad n_i x_i = q(r - 1) + plr$$

Elimination of r from eqs. [2] and [3] and rearrangement gives

$$[4] \qquad 1/n_i = (l/q + 1/p) - x_i/q$$

Inspection of eqs. [1*a*] and [1*b*] indicates that the molecular weight of chain i will be of the form

$$[5] \qquad M_i = Ar + B$$

where A and B are constants to be determined from the chemical formula of the structural model. Substitution of eq. [2] in eq. [5] and use of eq. [4] gives

$$[6] \qquad 1/(M_i - B) = (pl/q + 1 - px_i/q)/A$$

Thus, x_i is more simply related to n_i than to M_i.

The equation deduced by Bradley and Holloway (7) is the same as eq. [4] without the term in l/q, which must be included if the repeating units are themselves hydrolysis products. This term has been introduced previously in only one specific case, that of the zirconium oxide trimethylsilyloxides (9). Several features of eq. [4] should be noted. First, a branched chain is always isomeric with a linear chain of the same degree of polymerization. Chain branching cannot, therefore, be detected by use of eq. [4]. Secondly, coordinated bridging oxygens are not included in the definition of q, but may account wholly for the value of p. Thus, eq. [4] offers incomplete evidence, at best, concerning the coordination number of the metal atom. Thirdly, the derivation of the equation implies that the molecular weights are the true values measured at infinite dilution. Hydrolysis experiments carried out at finite concentrations may show effects due to the changing activities of various species, and corrections for these effects may be necessary.

(b) Cyclic Chains

If a homogeneous chain closes upon itself, the term $q(r - 1)$ in eq. [3] becomes qr, and eq. [4] becomes

$$[7] \qquad 0 = l/q + 1/p - x_i/q$$

and x_i is a constant independent of n_i. This corresponds to the case of a non-cyclic chain with infinite degree of polymerization but finite degree of hydrolysis.

(c) Linear or Branched Chains Polydisperse in Number of Metal Atoms

(i) Number Average Quantities

In general, the observed degrees of polymerization and hydrolysis are not integral, and a distribution of these values must occur. If the

Can. J. Chem. Downloaded from www.nrcresearchpress.com by 210.87.254.5 on 09/05/12
For personal use only.

mole fraction of chains with degree of polymerization n_i is N_i, rearrangement of eq. [4], multiplication by N_i, and summation over all species give

$$[8] \qquad 1/\bar{n}_n = (l/q + 1/p) - \bar{x}_n/q$$

where

$$\bar{n}_n = \sum_i N_i n_i$$

is the number average degree of polymerization, and

$$\bar{x}_n = \sum_i N_i x_i n_i/\bar{n}_n$$

is the number average degree of hydrolysis. From eqs. [2] and [5], the number average molecular weight is

$$[9] \qquad \bar{M}_n = \sum_i N_i M_i = A\bar{n}_n/p + B$$

and the average number of repeating units per chain is, from eq. [2]

$$[10] \qquad \bar{r}_n = \sum_i N_i n_i/p = \bar{n}_n/p$$

The values of $\bar{x}_n$ and $\bar{n}_n$ are those determined by ordinary chemical analysis and measurements of the number average molecular weight (by cryoscopy or ebullioscopy, for example). Equation [8] also holds for cyclic chains if the term in $\bar{n}_n$ is set equal to zero.

(ii) Weight Average Quantities

If w_i is the weight fraction of chains with molecular weight M_i, a series of equations analogous to eqs. [8] through [10] may be written, with weight average quantities replacing the number average quantities. The weight average molecular weight can be determined by light scattering measurements (16), but the weight average degree of hydrolysis cannot be obtained by direct experiment. The weight average molecular weight is thus an independent parameter of a particular distribution, unless the distribution happens to be known. The relation between the weight average molecular weight $\bar{M}_w$ and the weight average degree of polymerization $\bar{n}_w$ is readily found to be $p(\bar{M}_w - B) = A\bar{n}_w$.

(d) Mixtures of Homogeneous, Polydisperse Chains

(i) Linear or Branched Chains. Models I, II

Let a mole fraction α of metal atoms be in polymer series A, and a mole fraction $1 - \alpha$ be in series B. The two series are characterized by the parameters p_A, q_A, l_A and p_B, q_B, l_B. The number of molecules in series A and B per total number of metal atoms is $\alpha/\bar{n}_A$ and $(1 - \alpha)/\bar{n}_B$, respectively, where

$$[11] \qquad 1/\bar{n}_j = (l_j/q_j + 1/p_j) - \bar{x}_j/q_j \qquad j = A, B$$

Bradley and Holloway (7) assumed that the number average degree of hydrolysis was identical for each series. Consideration of two single chains with $n_A = n_B$, $p_A = p_B$, $l_A = l_B$, but $q_A \neq q_B$, shows at once that this assumption is not generally true. The observed number average degree of hydrolysis is

$$[12] \qquad \bar{x}_n = \alpha\bar{x}_A + (1 - \alpha)\bar{x}_B$$

and the total number of molecules per total number of metal atoms is

$$[13] \qquad 1/\bar{n}_n = \alpha/\bar{n}_A + (1 - \alpha)/\bar{n}_B$$

Hence

$$[14] \qquad \alpha q_A/\bar{n}_A + (1 - \alpha)q_B/\bar{n}_B = \bar{l} + \overline{(q/p)} - \bar{x}_n$$

where

$$\bar{l} = \alpha l_A + (1 - \alpha)l_B$$

and

$$\overline{(q/p)} = \alpha q_A/p_A + (1 - \alpha)q_B/p_B$$

If β is the mole fraction of A-type molecules, then by definition and eq. [13]

$$[15] \qquad \beta = \alpha\bar{n}_n/\bar{n}_A, \quad 1 - \beta = (1 - \alpha)\bar{n}_n/\bar{n}_B$$

Equation [14] then becomes

$$[16] \qquad 1/n_n = [\bar{l} + \overline{(q/p)}]/\bar{q} - \bar{x}_n/\bar{q} \qquad \text{(Model I)}$$

where

$$\bar{q} = \beta q_A + (1 - \beta)q_B$$

is the average bridge multiplicity. If α and β are constants, eq. [16] has the form observed experimentally. If $\alpha/\beta \gtrless 1$, then eqs. [15] and [16] show that, correspondingly, $\bar{n}_A \gtrless \bar{n}_B$. Equation [16] describes the properties of Model I for a regular polymer series, and includes eq. [8] as a special case.

In many cases, the value of $1/\bar{n}$ for the unhydrolyzed "monomer" in solution is equal to the intercept of the plot of $1/\bar{n}_n$ against $\bar{x}_n$; that is, α and β are the same for the monomer and the polymers, and the intercept must therefore be independent of $\bar{l}$, q_A, and q_B. If $\bar{n}_n$ for the monomer is non-integral, it is customary to assume that the monomer forms ideal self-associated solutions (13, 17–19). For such monomers, if N_A and N_B are the number of molecules of type A($p = p_A$) and type B($p = p_B$), respectively, then

$$\beta = N_A/(N_A + N_B)$$

$$\alpha = N_A p_A/(N_A p_A + N_B p_B)$$

from which

[17] $$(1 - \alpha)p_A/\alpha = (1 - \beta)p_B/\beta$$

Substitution of eq. [17] into the value of $1/\bar{n}_n$ at $\bar{x}_n = \bar{l}$ in eq. [16] gives

$$(\overline{q/p})/\bar{q} = \alpha/\beta p_A = (\overline{1/p})$$

where

$$(\overline{1/p}) = \alpha/p_A + (1 - \alpha)/p_B$$

Equation [16] may then be written as

[18] $$1/\bar{n}_n = (\overline{1/p})[1 - (\bar{x}_n - \bar{l})/(\overline{q/p})] \quad \text{(Model II)}$$

Values of α calculated from the slope and intercept should be the same in this case. Substitution of eq. [15] into eq. [10] and use of eq. [17] give

[19] $$\bar{r}_A/\bar{r}_B = \bar{n}_A p_B/\bar{n}_B p_A = 1$$

or, if the value of $1/\bar{n}$ at $\bar{x}_n = 0$ or $\bar{l}$ is independent of $\bar{q}$, the average degree of polymerization of type A and type B molecules must be equal. Note that eq. [16] and eq. [18] are identical if $1/\bar{n}_n$ at $\bar{x}_n = 0$ or $\bar{l}$ is independent of $\bar{q}$. From eqs. [11] and [19], it is found that

$$(\bar{x}_A - l_A)p_A/q_A = (\bar{x}_B - l_B)p_B/q_B$$

Thus, the average degrees of hydrolysis of chains A and B are simply related.

Model II (as defined by eq. [18]) may be extended to include mixtures containing mole fractions α_A, α_B, $1 - \alpha_A - \alpha_B$ of metal atoms in polymer series A, B, and C, respectively. Equation [18] is again obtained, with averages taken over the 3 series, with

$$\alpha_A/p_A\beta_A = \alpha_B/p_B\beta_B = (1 - \alpha_A - \alpha_B)/p_C(1 - \beta_A - \beta_B)$$

with $(\overline{q/p}) = \bar{q}(\overline{1/p})$ as before, with $\bar{r}_A = \bar{r}_B = \bar{r}_C$, and with

$$(\bar{x}_A - l_A)p_A/q_A = (\bar{x}_B - l_B)p_B/q_B = (\bar{x}_C - l_C)p_C/q_C$$

Values of α_A and α_B can be found from the slope and intercept.

If a plot of $1/\bar{n}_n$ against $\bar{x}_n$ is not linear over the whole range of $\bar{x}_n$, but extrapolates to the value of $(\overline{1/p})$ for the monomer at $\bar{x}_n = \bar{l}$, α and β must be considered to be functions of $\bar{x}_n$. In this case, it is no longer possible to obtain separate values of α and β from eqs. [16] or [18].

If it is assumed that $\bar{x}_A = \bar{x}_B$, eqs. [11] and [13] give

[20] $$1/\bar{n}_n = (\overline{1/p}) + (\overline{l/q}) - (\overline{1/q})\bar{x}_n$$

where

$$(\overline{1/q}) = \alpha/q_A + (1 - \alpha)/q_B$$

$$(\overline{l/q}) = \alpha l_A/q_A + (1 - \alpha)l_B/q_B$$

This equation has been deduced previously by Bradley and Holloway (7), who write $1/\bar{q}$ for $(\overline{1/q})$ and neglect the term $(\overline{l/q})$. In practice, eq. [20] cannot be distinguished from eq. [18]. For example, mixtures of equal proportions of metal atoms in a p_2q_3 series and a p_3q_4 series give a slope of -0.294 from eq. [18] and a slope of -0.292 from eq. [20]. Note that β does not appear in eq. [20], that the intercept is necessarily independent of $\bar{q}$ if $\bar{l} = 0$, and that $\bar{r}_A \neq \bar{r}_B$. This model thus lacks sufficient generality to be useful in all cases, and, in addition, no evidence is available to support the assumption that $\bar{x}_A = \bar{x}_B$. For these reasons, this model is considered to be simply a special case of Model II with $l_A = l_B = 0$ and $p_A/q_A = p_B/q_B$.

(ii). Cyclic Chains and Mixed Types. Model III

It follows readily from eqs. [7], [8], [11], [12], [13], and [16] that a mixture of two cyclic chains is described by

$$\bar{x}_n = \bar{l} + (\overline{q/p})$$

For a mixture of linear or branched chains (mole fraction α of metal atoms) and cyclic chains (mole fraction $1 - \alpha$ of metal atoms), eq. [11] holds for the linear or branched chains A. For the cyclic chains B

[21] $$0 = (q_B/q_A)(l_B/q_B + 1/p_B) - \bar{x}_B/q_A$$

Multiplication of eq. [11] by α and of eq. [21] by $1 - \alpha$ and addition give

[22] $$1/\bar{n}_n = \alpha/\bar{n}_A = \{\bar{l} + (\overline{q/p})\}/q_A - \bar{x}_n/q_A \quad \text{(Model III)}$$

If the value of $1/\bar{n}_n$ at $\bar{x}_n = 0$ or $\bar{l}$ is independent of $\bar{q}$ and equal to $(\overline{1/p})$, then it is found that $q_A = q_B$, with $\bar{x}_A \neq \bar{x}_B$.

General Theory for Heterogeneous Polymer Chains

(a) Single Linear, Branched, or Cyclic Chains

In this and the following sections, the restric-

Can. J. Chem. Downloaded from www.nrcresearchpress.com by 210.87.254.5 on 09/05/12
For personal use only.

Can. J. Chem. Downloaded from www.nrcresearchpress.com by 210.87.254.5 on 09/05/12
For personal use only.

tions of fixed bridge multiplicity (q) and size of repeating unit (p) will be removed, giving rise to heterogeneous chains.

Let the relative numbers of bridges of multiplicity q_A be γ, and that of multiplicity q_B be $1 - \gamma$. Further, let the relative numbers of repeating units with $p = p_A$ be ε, and of repeating units with $p = p_B$ be $1 - \varepsilon$. Equations [2] and [3] become

$$n_i = \{\varepsilon p_A + (1 - \varepsilon)p_B\}r \equiv \bar{\bar{p}}r$$

$$n_i x_i = \{\gamma q_A + (1 - \gamma)q_B\}(r - 1) + \{\varepsilon p_A l_A + (1 - \varepsilon)p_B l_B\}r \equiv \bar{\bar{q}}(r - 1) + \overline{\overline{pl}}r$$

where the double bars indicate averages over a single heterogeneous chain. Thus

$$1/n_i = (\overline{\overline{pl}}/\bar{\bar{q}} + 1)/\bar{\bar{p}} - x_i/\bar{\bar{q}}$$

an equation that holds for heterogeneous cyclic chains, as well, if $1/n_i$ is set equal to zero.

(b) Polydisperse Linear, Branched, or Cyclic Heterogeneous Chains. Model IV

Application of the same procedure that led to eq. [8] gives

$$\sum_{i,\gamma,\varepsilon} \overline{\overline{pq}} N_i = \sum_{i,\gamma,\varepsilon} (\overline{\overline{pl}} + \bar{\bar{q}}) n_i N_i - \sum_{i,\gamma,\varepsilon} \bar{\bar{p}} n_i x_i N_i$$

where $N_i(\gamma, \varepsilon)$ is the mole fraction of chains with degree of polymerization i, distribution of bridge multiplicity γ, and distribution of repeating units ε. The sums are no longer related simply to $\bar{x}_n$ and $\bar{n}_n$ since $\bar{\bar{p}}$ and $\overline{\overline{pl}}$ are functions of ε and q is a function of γ. If it is assumed that each chain has the same distribution of bridge multiplicity and of repeating units, summation may be carried out to give

$$[23] \quad 1/\bar{n}_n = (\overline{\overline{pl}}/\bar{\bar{q}} + 1)/\bar{\bar{p}} - \bar{x}_n/\bar{\bar{q}} \qquad \text{(Model IV)}$$

This is probably a good assumption if the chains are sufficiently long and if the free energies of formation of bridges of different multiplicity and of repeating units of different size are not very different. Again, eq. [23] holds for cyclic chains if $1/\bar{n}_n$ is set equal to zero.

Two special cases of eq. [23] may be considered. If $\varepsilon = 1$, $\bar{\bar{p}} = p_A$, $\overline{\overline{pl}} = p_A l_A$, chains with 3 types of multiplicity, q_A, q_B, q_C, can be then treated. If $\gamma = 1$, analogous conclusions can be drawn. From the nature of the model, it is obvious that the intercept of eq. [23] is independent of q only if $l_A = l_B = 0$ and if $\varepsilon = 1$; i.e., the reciprocal intercept is integral.

(c) Mixtures of Heterogeneous and Homogeneous Polydisperse Chains

Even if constant distributions of bridge multiplicity and of repeating units are assumed, no mixture of this type can be analyzed completely. For example, a mixture of homogeneous chains with parameters α, β, p_A, q_A, $l_A = 0$ with heterogeneous chains with parameters $1 - \alpha$, $1 - \beta$, p_A, q_A, q_B, $l_A = l_B = 0$ gives the value of $\bar{q}$ in eq. [16] as

$$\bar{q} = q_B + (q_A - q_B)(\beta + \gamma - \beta\gamma)$$

a lineo-linear equation in β and γ which possesses no unique solution, but can be consistent with experiment in special cases. If $q_A = 2$, $q_B = 1$, $\bar{q} = 1 + \delta$, where $0 < \delta < 1$, for example, the equation is satisfied if β and γ are both less than δ.

Equations [16], [18], [22], and [23], corresponding to Models I–IV, are basic for the analysis of experimental data.

Discussion of Experimental Data

Table I contains an analysis of all published data on the metal oxide alkoxides (1–7) and the metal oxide trialkylsilyloxides (8–10), with the exception of the titanium oxide triethylsilyloxides (11), which will be discussed elsewhere along with new experimental data (20).

For each product, the simplest formula, initial molality (where reported) and reciprocal degree of polymerization ($y_0 = 1/\bar{n}_n$ at $\bar{x}_n = 0$) are given for the monomer. For the polymers, the range of $\bar{x}_n$ (excluding $\bar{x}_n = 0$) over which a plot of $y = 1/\bar{n}_n$ was observed, by inspection, to be linear in $\bar{x}_n$ and the number of points N in this range are tabulated. The remainder of Table I contains a least-squares analysis of the data, carried out by means of Fortran IV computer programs and standard statistical methods (21, 22).

In general, since the degree of hydrolysis is used to derive values of $\bar{n}_n$, the errors in $\bar{n}_n$ and $\bar{x}_n$ are correlated. However, errors in the molecular weight measurements are much greater than those from the chemical analyses, and unweighted least squares, assuming that only the

Can. J. Chem. Downloaded from www.nrcresearchpress.com by 210.87.254.5 on 09/05/12
For personal use only.

TABLE I

Hydrolysis products of metal alkoxides and trialkylsilyloxides

Entry No.	Monomer	Initial Molality	Range of $\bar{x}_n$	N'	Reciprocal D.P. of Monomer	Intercept a	Intercept σ(a)	Slope b	Slope σ(b)	Ratio a/|b|	Ratio σ(a/b)	Correlation Coefficients ρ(xy)	Correlation Coefficients ρ(ab)	Standard Error	t
1.	$Sn(OPr^i)_4$	0.264	0.10-0.92	6	0.541	0.559	0.012	-0.405	0.022	1.381	0.080	-0.994	-0.848	0.016	0.89
2.	"	0.310	0.20-1.08	4	0.541	0.571	0.019	-0.386	0.026	1.477	0.114	-0.996	-0.890	0.017	1.16
3.	$Ti(OEt)_4$	0.0425	0.10-0.70	9	0.435	0.404	0.007	-0.290	0.017	1.391	0.074	-0.989	-0.870	0.010	-2.56
4.	"	0.185	0.16-1.04	11	0.417	0.404	0.003	-0.298	0.005	1.356	0.028	-0.999	-0.900	0.005	-2.11
5.	"	0.767	0.20-1.02	6	0.344	0.345	0.002	-0.257	0.002	1.339	0.014	-1.000	-0.912	0.002	0.32
6.	$Ti(OPr^n)_4$	0.144	0.53-1.11	4	0.610	0.607	0.044	-0.419	0.051	1.451	0.231	-0.985	-0.949	0.028	-0.05
7.	$Ti(OBu^n)_4$	0.0632	1.00-2.00	3	1.000	0.985	0.030	-0.255	0.019	3.862	0.279	-0.997	-0.965	0.013	-0.46
8.	$Ti(OBu^i)_4$ / $Ti(OBu^s)_4$	0.0462 / 0.0606	0.50-1.00 / 0.50-1.00	3	1.000	1.025	0.025	-0.384	0.029	2.668	0.172	-0.997	-0.962	0.012	0.93
9.	$Zr(OEt)_4$	0.186	0.22-0.92	5	0.476	0.435	0.004	-0.309	0.006	1.408	0.030	-0.999	-0.914	0.003	-8.49
10.	"	0.409	0.15-1.03	6	0.461	0.399	0.003	-0.298	0.005	1.342	0.028	-0.999	-0.875	0.004	-11.70
11.	"	0.723	0.12-0.77	7	0.446	0.383	0.003	-0.277	0.007	1.382	0.035	-0.998	-0.873	0.004	-11.91
12.	$Zr(OPr^n)_4$	0.147	0.16-1.47	5	0.410	0.392	0.005	-0.221	0.005	1.773	0.044	-0.999	-0.852	0.005	-2.54
13.	$Zr(OPr^i)_4$	0.382	0.12-0.46	3	0.524	0.500	0.008	-0.363	0.026	1.378	0.086	-0.997	-0.893	0.006	-2.33
14.	$Zr(OBu^n)_4$	0.0707	0.48-0.95	2	0.565	0.554		-0.306		1.810		-1.000			
15.	$Zr(OBu^i)_4$	0.0766	0.22-1.85	5	0.658	0.674	0.008	-0.199	0.007	3.382	0.105	-0.998	-0.855	0.010	1.21
16.	$Zr(OBu^s)_4$	0.101	0.13-0.83	3	0.516	0.509	0.010	-0.383	0.017	1.329	0.067	-0.999	-0.858	0.009	-0.52
17.	$Ta(OMe)_5$	0.157	0.07-1.15	8	0.568	0.579	0.004	-0.395	0.005	1.464	0.021	-0.999	-0.856	0.005	1.73
18.	"	0.165	0.08-1.13	10	0.568	0.569	0.004	-0.395	0.006	1.442	0.025	-0.999	-0.869	0.006	0.13
19.	$Ta(OEt)_5$	0.064	0.11-1.18	12	0.541	0.549	0.003	-0.359	0.004	1.530	0.019	-0.999	-0.894	0.005	1.52
20.	"	0.132	0.16-1.17	11	0.541	0.545	0.002	-0.341	0.003	1.595	0.015	-1.000	-0.929	0.003	1.03
21.	"	0.153	0.10-1.24	10	0.541	0.550	0.003	-0.330	0.003	1.666	0.018	-1.000	-0.878	0.004	1.93
22.	"	0.246	0.06-1.34	13	0.541	0.551	0.002	-0.335	0.003	1.647	0.014	-1.000	-0.874	0.004	2.49
23.	"		0.27-0.75	7	0.541	0.563	0.010	-0.450	0.022	1.252	0.068	-0.994	-0.931	0.010	1.57
24.	$Ta(OPr^n)_5$	0.0745	0.16-1.26	6	0.629	0.649	0.001	-0.389	0.002	1.668	0.007	-1.000	-0.879	0.001	9.98
25.	"	0.0750	0.16-1.06	5	0.629	0.643	0.003	-0.396	0.004	1.625	0.016	-1.000	-0.895	0.003	3.85
26.	$Ta(OBu^n)_5$	0.0617	0.30-1.46	5	0.735	0.791	0.009	-0.343	0.009	2.305	0.062	-0.999	-0.908	0.009	4.52
27.	"	0.0798	0.14-1.54	7	0.735	0.796	0.014	-0.314	0.016	2.533	0.109	-0.994	-0.838	0.020	2.51
28.	$Ta(OBu^s)_5$	0.0861	0.12-1.48	10	0.935	0.858	0.006	-0.493	0.007	1.742	0.027	-0.999	-0.872	0.009	-6.87
29.	"	0.0982	0.08-1.43	11	0.935	0.873	0.004	-0.509	0.005	1.714	0.018	-1.000	-0.870	0.007	-7.85
30.	$Ce(OPr^i)_4$	0.109	0.11-1.03	5	0.533	0.541	0.004	-0.369	0.007	1.466	0.030	-0.999	-0.852	0.005	1.17
31.	"	0.127	0.11-1.03	5	0.533	0.534	0.002	-0.351	0.003	1.520	0.014	-1.000	-0.844	0.002	0.26
32.	"	0.173	0.13-0.51	3	0.533	0.538	0.006	-0.387	0.017	1.388	0.055	-0.999	-0.894	0.005	0.61
33.	"	0.205	0.09-0.41	3	0.533	0.537	0.003	-0.378	0.013	1.420	0.038	-0.999	-0.873	0.003	0.87
34.	$U(OEt)_5$	0.167	0.07-1.08	9	0.676	0.681	0.006	-0.394	0.008	1.726	0.036	-0.998	-0.880	0.008	0.46
35.	"	0.217	0.09-1.50	10	0.676	0.674	0.001	-0.381	0.002	1.770	0.008	-1.000	-0.855	0.002	-0.73
36.	$Ti(OSiMe_3)_4$		1.51-1.65	18	1.000	1.027	0.036	-0.603	0.023	1.702	0.108	-0.989	-1.000	0.004	0.74
37.	$Zr(OSiMe_3)_4$ *		0.13-0.95	8	0.488	0.486	0.025	-0.389	0.045	1.249	0.170	-0.962	-0.893	0.031	-0.04
38.	" †		1.49-1.61	9	0.488	0.686	0.053	-0.416	0.035	1.648	0.233	-0.976	-1.000	0.004	3.70
39.	$Ta(OSiMe_3)_5$		0.47-1.20	12	0.917	0.818	0.025	-0.588	0.030	1.391	0.094	-0.987	-0.954	0.026	-2.77

* Before thermal disproportionation.

† After thermal disproportionation.

Can. J. Chem. Downloaded from www.nrcresearchpress.com by 210.87.254.5 on 09/05/12
For personal use only.

$y = 1/\bar{n}_n$ were in error, were used to derive estimates of the intercept a and the slope b in the general relation $y = a + bx$, where x is written for $\bar{x}_n$. The large absolute values of the correlation coefficient ρ_{xy} for the variables supports this assumption. The estimated standard deviation of the observed y-values from the calculated values is σ (with $N - 2$ degrees of freedom), the estimated standard deviations of the intercept and slope are given by

$$\sigma(a)^2 = \sigma(b)^2 \sum x^2/N$$

$$\sigma(b)^2 = \sigma^2 N/\{N\sum x^2 - (\sum x)^2\}$$

respectively, and the correlation coefficient for the parameters a and b is

$$\rho_{ab} = -\sum x/(N\sum x^2)^{\frac{1}{2}}$$

The standard error in the ratio $a/|b|$ is then given approximately by

$$\sigma(a/b)^2/(a/b)^2 = \sigma(a)^2/a^2 + \sigma(b)^2/b^2 - 2\rho_{ab}\sigma(a)\sigma(b)/a|b|$$

The value y_0 at $\bar{x}_n = 0$ is not included in these calculations, and its deviation from the intercept a is measured by the statistic

$$t = (a - y_0)/\{\sigma^2 + \sigma(a)^2\}^{\frac{1}{2}}$$

for $N - 2$ degrees of freedom. If t is greater than the theoretical value at a 95% confidence level (23), a and y_0 are considered to differ significantly. For three cases in Table I (entries 3, 22, 27), significant differences are not clearly indicated, and decisions are made to conform with similar cases.

It is convenient to discuss the results in terms of the four general models.

Model I

Table II lists the cases that conform to Model I, eq. [16]. The subscripts in the specification of the structural models refer to the values of the parameters, and α, β refer to the set of parameters listed first. Thus, the titanium oxide trimethylsilyloxides are described by a mixture of series A molecules with $l_A = 3/2$, $p_A = 8$, $q_A = 1$, $\alpha = 0.38$, $\beta = 0.34$ and series B molecules with $l_B = 3/2$, $p_B = 8$, $q_B = 2$, $1 - \alpha = 0.62$, $1 - \beta = 0.66$. The respective standard errors in α and β are

$$\sigma(\alpha) = \sigma(a/b)/(q_A/p_A - q_B/p_B + l_A - l_B)$$

and

$$\sigma(\beta) = \sigma(b)/b^2(q_A - q_B)$$

For all those products with $q_A = q_B$, t-tests for equality between the observed and theoretical values were significant within 95% confidence levels.

All the metal oxide alkoxides in Table II show curvature towards the value $1/\bar{n}_n$ for the monomer for values of $\bar{x}_n$ less than 0.1–0.2, and curvature beyond the maximum value of $\bar{x}_n$ listed in Table I is also apparent. Hence, these products can be considered to conform to Model II, with values of α and β that vary with $\bar{x}_n$ over part of the range of $\bar{x}_n$. Note that in each case the more complex series has the higher average degree of polymerization. The parameters listed agree with those assigned previously (3, 6) except

TABLE II

Hydrolysis products described by Model I

Entry number*	Monomer	Structural parameters	α	$\sigma(\alpha)$	β	$\sigma(\beta)$	t
9	$Zr(OEt)_4$	$p_2q_3+p_3q_4$	0.45	0.18	0.76	0.06	—
10	,,	,,	0.05	0.17	0.64	0.06	—
11	,,	,,	0.29	0.21	0.39	0.08	—
24	$Ta(OPr^n)_5$	$p_1q_2+p_2q_3$	0.34	0.01	0.43	0.01	—
25	,,	,,	0.25	0.03	0.48	0.03	—
26	$Ta(OBu^n)_5$	$p_1q_3+p_2q_3$	0.54	0.04	—	—	1.11
27	,,	,,	0.69	0.07	—	—	1.19
28	$Ta(OBu^s)_5$	$p_1q_2+p_2q_2$	0.74	0.03	—	—	1.00
29	,,	,,	0.71	0.02	—	—	1.80
36	$Ti(OSiMe_3)_4$	$l_{3/2}p_8q_1+l_{3/2}p_8q_2$	0.38	0.86	0.34	0.06	—
38	$Zr(OSiMe_3)_4$	$l_{3/2}p_8q_2+p_2q_3$	0.59	0.93	0.59	0.21	—
		$l_{3/2}p_8q_2+p_3q_4$	0.76	0.56	0.75	0.10	—
		$p_1q_2+p_2q_3$	0.30	0.47	0.59	0.21	—
39	$Ta(OSiMe_3)_5$	$p_1q_1+p_2q_3$	0.22	0.19	0.65	0.04	—

*Entry numbers correspond to those in Table I.

Can. J. Chem. Downloaded from www.nrcresearchpress.com by 210.87.254.5 on 09/05/12
For personal use only.

for the p_2q_2 series. This series may be considered to be a p_2q_3 type with one M—O → M and two M—O—M bridges between dimer units.

For the titanium oxide trimethylsilyloxides, previous analysis (8) did not reveal that the observed intercept is fortuitously close to unity, and is not directly related to the degree of polymerization of the monomer. The estimated value of $\bar{n}_n$ at $\bar{x}_n = \bar{l} = 3/2$ is 8.13, which differs from the theoretical value 8 by 1.6%. For the thermally disproportionated zirconium oxide trimethylsilyloxides, the parameters in Table I do not agree with previous values, because fewer points over a narrower range of $\bar{x}_n$ were used and presumably the assumption that $y_0 = 1$ was made (9). No valid reason could be found for excluding any of the observations, but the range of extrapolation is still large. The parameters for the tantalum oxide trimethylsilyloxides agree with those deduced previously (10).

Model II

Table III lists those cases for which the intercept is equal to the reciprocal degree of polymerization of the monomer, and which thus conform to Model II. The values α_a and α_b calculated from the intercept and slope have the respective standard errors

$$\sigma(\alpha_a) = \sigma(a)/(1/p_A - 1/p_B)$$

and

$$\sigma(\alpha_b) = \sigma(a/b)/(q_A/p_A - q_B/p_B)$$

The $Ti(OBu^s)_4$ and $Ti(OBu^i)_4$ products were evidently similar, and the few available data were combined.

For those cases in which only one series is present, the statistics

$$t_a = |a - 1/p_A|/\sigma_a$$

and

$$t_b = |b - 1/q_A|/\sigma b$$

show that the observed and theoretical parameters are equal within 95% confidence limits. For those cases with $q_A = q_B$, α_a only may be obtained, and appropriate t-tests for equality of the theoretical and experimental slopes are signifi-

TABLE III

Hydrolysis products described by Model II

Entry number*	Monomer	Structural parameters	α_a	$\sigma(\alpha_a)$	α_b	$\sigma(\alpha_b)$	t'	t_a	t_b
1	$Sn(OPr^i)_4$	$p_1q_1+p_2q_3$	0.12	0.02	0.24	0.16	0.71	—	—
2	”	”	0.14	0.04	0.15	0.22	0.42	—	—
3	$Ti(OEt)_4$	$p_2q_3+p_3q_4$	0.42	0.04	0.35	0.44	0.13	—	—
4	”	”	0.42	0.02	0.14	0.17	1.95	—	—
5	”	”	0.17	0.01	0.03	0.08	0.23	—	—
6	$Ti(OPr^n)_4$	$p_1q_3+p_2q_2$	0.21	0.09	0.23	0.12	0.20	—	—
7	$Ti(OBu^n)_4$	p_1q_3	1.00	—	1.00	—	—	0.50	4.10
8	$Ti(OBu^s)_4$, $Ti(OBu^i)_4$	p_1q_3	1.00	—	1.00	—	—	1.00	1.76
12	$Zr(OPr^n)_4$	$p_2q_3+p_3q_4$	variable α				—	—	—
13	$Zr(OPr^i)_4$	p_2q_3	1.00	—	1.00	—	—	0.00	1.15
14	$Zr(OBu^n)_4$	$p_1q_3+p_2q_3$	0.13	—	—	—	—	—	—
15	$Zr(OBu^i)_4$	$p_1q_3+p_2q_3$	variable α				—	—	—
16	$Zr(OBu^s)_4$	p_2q_3	1.00	—	1.00	—	—	0.90	2.94
17	$Ta(OMe)_5$	$p_1q_1+p_2q_3$	0.16	0.01	0.07	0.04	2.98	—	—
18	”	”	0.14	0.01	0.12	0.05	0.63	—	—
19	$Ta(OEt)_5$	$p_1q_2+p_2q_3$	0.10	0.01	0.06	0.04	1.06	—	—
20	”	$p_1q_2+p_1q_3+p_2q_3$	0.04†	0.02	0.05‡	0.02	—	—	—
21	$Ta(OEt)_5$	$p_1q_3+p_2q_3$	0.10	0.01	—	—	—	—	1.00
22	”	”	0.10	0.00	—	—	—	—	1.67
23	”	$p_1q_2+p_2q_2$	0.13	0.02	—	—	—	—	2.27
30	$Ce(OPr^i)_4$	$p_1q_1+p_2q_3$	0.08	0.01	0.07	0.06	0.24	—	—
31	”	”	0.07	0.00	−0.04	0.03	3.78	—	—
32	”	”	0.08	0.01	0.22	0.11	1.06	—	—
33	”	”	0.07	0.01	0.16	0.08	0.81	—	—
34	$U(OEt)_5$	$p_1q_2+p_2q_3$	0.36	0.01	0.45	0.07	1.49	—	—
35	”	$p_1q_2+p_1q_3+p_2q_3$	0.25†	0.10	0.10‡	0.01	—	—	—
37	$Zr(OSiMe_3)_4$	$p_2q_2+p_2q_3$	—	—	0.43	0.30	—	0.56	—

*Entry numbers correspond to those in Table I.
†Value of α_A.
‡Value of α_B.

Can. J. Chem. Downloaded from www.nrcresearchpress.com by 210.87.254.5 on 09/05/12
For personal use only.

cant at the 95% level except for one set of tantalum oxide ethoxides and one set of uranium oxide isopropoxides which require 3 series to account for the data. For the remaining cases, the values of α_a and α_b should be equal, but are highly susceptible to errors in the slope and intercept. Rather than guess at suitable parameters, a better procedure in this case is to equate the values of α_a and α_b to obtain, from eq. [18]

$$[24] \quad q_A(p_B - 1/a) + q_B(1/a - p_A) = (p_B - p_A)/|b|$$

The left side of this equation is denoted by L, and has a relative standard error

$$\sigma(L)/L = [\sigma(a)/a]/[1 + ap_Ap_B(q_A/p_A - q_B/p_B)/(q_B - q_A)]$$

while the right side R has a relative standard error $\sigma(R) = \sigma(b)/|b|$. These errors are roughly equal in magnitude. Equation [24] is a Diophantine equation in the four integral unknowns, p_A, p_B, q_A, and q_B, and may be solved systematically by assigning values of p_A and p_B, then choosing q_A and q_B so that the difference between the two sides of the equation is a minimum. The statistic

$$t' = |1 + R/L|/\{\sigma(L)^2/L^2 + \sigma(R)^2/R^2\}^{\frac{1}{2}}$$

is then a measure of deviations due to random errors between the two sides. The t'-values indicate that in all but two cases the equation is satisfied to within random error at the 95% confidence level, and a very slightly greater standard error would bring cases 17 and 31 into agreement as well.

A second method of testing Model II is to plot theoretical lines for various series along with the least-square lines. If the theoretical lines are suitably chosen, and the same value of α applies throughout, the lines will have a common point of intersection. This method is very sensitive to errors in the slope, and can be used to eliminate certain choices of the parameters and to detect a variable α. The zirconium oxide *n*-propoxides and oxide isobutoxides do not fit any reasonable model with constant α. Plots show that the oxide *n*-propoxides conform roughly to a $p_2q_3 + p_3q_4$ mixture, while the oxide isobutoxides conform roughly to a $p_1q_3 + p_3q_4$ mixture, and eq. [17] shows that the ratio $\beta/\alpha = (1 + p_A)/(\alpha + p_A)$ (for $p_B - p_A = 1$) is not very sensitive to the value of α. Hence, if the ratio β/α remains roughly constant, α can vary, and a reasonably linear relation between $1/\bar{n}_n$ and $\bar{x}_n$ will still be obtained. Significant variations in α with $\bar{x}_n$ can thus be masked by a linear plot. The same structural parameters and variation of α with $\bar{x}_n$ have been proposed previously for these two zirconium oxide alkoxides (3). In general, structural parameters assigned for the other products agree with those assigned by Bradley and co-workers with a few exceptions. For the tantalum oxide ethoxides, no sharp distinction can be drawn between the p_1q_2 and the p_1q_3 series. The mixture $p_1q_1 + p_2q_3$ fits the data on stannic and ceric oxide isopropoxides better than the mixture $p_1q_2 + p_2q_3$ (7). The p_2q_2 series provides a better fit than the p_2q_3 series for the titanium oxide *n*-propoxides (2) and the tantalum oxide ethoxides, entry number 23, which were examined in boiling benzene instead of boiling ethanol (4).

The condition $\bar{r}_A = \bar{r}_B$, under which Model II applies, implies that the free energy of formation from the monomer of chains with different parameters but with the same average number of repeating units must be close to zero. As an example, the formation of p_2q_3 molecules from titanium ethoxide is described by

$$n[Ti(OEt)_4]_2 + 3nH_2O \rightarrow [Ti_2O_3(OEt)_2]_n + 6n\text{EtOH}$$

while the formation of p_3q_4 molecules is described by

$$m[Ti(OEt)_4]_3 + 4mH_2O \rightarrow [Ti_3O_4(OEt)_4]_m + 8m\text{EtOH}$$

Here, $\bar{r}_A = \bar{r}_B$ gives $n = m$, and the free energy changes for these two processes differ by the free energy change for the process

$$n[Ti(OEt)_4]_3 + nH_2O + [Ti_2O_3(OEt)_2]_n \rightarrow n[Ti(OEt)_4]_2 + 2n\text{EtOH} + [Ti_3O_4(OEt)_4]_n$$

If the free energy change for this process is zero, the process must be an equilibrium, and provides a mechanism through which disproportionation processes (1) can occur readily. The general validity of Model II for all the oxide alkoxides examined in solution in their corresponding alcohols is thus seen to be a consequence of equilibria among various species. For products examined in non-polar solvents, variations in the type of model are to be expected, and are found with 3 of the 4 metal oxide trimethylsilyloxides. The initial hydrolysis products of zirconium

Can. J. Chem. Downloaded from www.nrcresearchpress.com by 210.87.254.5 on 09/05/12
For personal use only.

trimethylsilyloxide, however, could be fitted best by a $p_2q_2 + p_2q_3$ mixture, but not by the series suggested previously (9). Another possibility is that the products contain monomers, and a $p_2q_0 + p_2q_3$ mixture gives $\alpha = 0.14$ for the p_2q_0 monomer, an assumption that is consistent with establishment of an equilibrium system on initial hydrolysis.

Model III

For a number of cases, the reciprocal slopes are integral, and a mixture of cyclic and linear (or branched) series can be used to describe the products. These cases include all those entries in Tables II and III for which there is only one series, or for which the two linear series have the same value of q.

The relevant cases in Table II (entries 26–29) can be described by the same parameters given in Table II if either of the two sets of parameters corresponds to a cyclic series, and the other set corresponds to a linear series. The relevant cases in Table III (entries 7, 8, 13–16, 21–23) have a value of $1/\bar{n}_n$ at $\bar{x}_n = 0$ equal to the reciprocal degree of polymerization of the unhydrolyzed alkoxide, and Model III requires that the cyclic and linear series have the same value of q. The parameters are then the same as those listed in Table III, where either of the two sets corresponds to a cyclic series. If the values of p and q are the same for both the cyclic and linear series, no difference can be detected between a single linear series and a mixture of linear and cyclic series (entries 7, 8, 13, 16).

Martin and Winter (13, 24) have given arguments in favor of cyclic polymers in the titanium oxide alkoxides. While we do not wish to revive the polemical discussion on this point (13, 14), it should be noted that, in practice, Model III is of much less general applicability than Model I and, especially, Model II in describing the experimental results. In addition, the only cyclic polymers that arise on application of Model III are of the types p_1q_2, p_1q_3, p_2q_2, and p_2q_3. The models proposed for these types (2, 5) indicate that bridge multiplicities of 2 or 3 would fix the orientation of successive repeating units such that formation of cyclic polymers would be difficult.

Model IV

Table IV lists those products that can be described by Model IV. These fall into two classes: (*i*) $a = y_0$, $\varepsilon = 1$, reciprocal intercept integral; (*ii*) $a \neq y_0$, neither reciprocal slope nor reciprocal intercept integral. For either class, the standard error in γ is

$$\sigma(\gamma) = \sigma(b)/b^2(q_A - q_B)$$

For class (*i*), *t*-tests for the equality of the theoretical and observed intercept are contained

TABLE IV

Hydrolysis products described by Model IV

Entry number*	Monomer	Structural parameters	γ	$\sigma(\gamma)$	ε	$\sigma(\varepsilon)$	t
8	$Ti(OBu^t)_4$, $Ti(OBu^s)_4$	$p_1q_2+p_1q_3$	0.40	0.20	1.00	—	1.76
9	$Zr(OEt)_4$	$p_2q_2+p_3q_3$	0.76	0.06	0.70	0.02	—
10	,,	,,	0.64	0.06	0.49	0.02	—
11	,,	,,	0.39	0.09	0.39	0.02	—
13	$Zr(OPr^i)_4$	$p_2q_2+p_2q_3$	0.25	0.20	1.00	—	0.00
16	$Zr(OBu^s)_4$	$p_2q_2+p_2q_3$	0.39	0.12	1.00	—	0.90
24	$Ta(OPr^n)_5$	$p_1q_1+p_2q_2$	0.43	0.01	0.46	0.00	—
25	,,	,,	0.48	0.03	0.45	0.01	—
26	$Ta(OBu^n)_5$	$p_1q_3+p_2q_3$	1.00	—	0.74	0.01	1.11
27	,,	,,	1.00	—	0.74	0.02	1.19
28	$Ta(OBu^s)_5$	$p_1q_2+p_2q_2$	1.00	—	0.83	0.01	1.40
29	,,	,,	1.00	—	0.86	0.01	1.80
30	$Ce(OPr^i)_4$	$p_1q_2+p_2q_3$	0.15	0.05	0.29	0.01	—
31	,,	,,	0.13	0.02	0.15	0.01	—
32	,,	,,	0.14	0.11	0.42	0.02	—
33	,,	,,	0.14	0.09	0.35	0.01	—
37	$Zr(OSiMe_3)_4$	$p_2q_2+p_2q_3$	0.43	0.30	1.00	—	0.56
38	,,	$l_{3/2}p_8q_1+p_3q_4$	0.53	0.20	0.68	—	—
39	$Ta(OSiMe_3)_5$	$p_1q_1+p_2q_3$	0.65	0.09	0.78	0.04	—

*Entry numbers correspond to those in Table I.

in Table IV, and $\sigma(\varepsilon) = \sigma(a)/a^2$, while for class (*ii*), the standard error in ε is

$$\sigma(\varepsilon) = \sigma(a)/a^2(p_A - p_B)$$

except when $pl \neq 0$, when the expression for the standard error is complicated. The structural parameters listed first are those with fractions ε and γ. Thus, $p_1q_2 + p_2q_3$ signifies heterogeneous chains with fractions ε, $1 - \varepsilon$ of repeating units with $p = 1$, 2, respectively, and with fractions γ, $1 - \gamma$ of bridge multiplicities 2 and 3, respectively.

The titanium oxide *n*-butoxides and the titanium oxide trimethylsilyloxides are the only two cases that fulfil the requirements for class (*i*) but do not give acceptable values of γ. It is not difficult to propose mechanisms by which heterogeneity could arise. By introduction of more parameters (e.g., mixtures of homogeneous and heterogeneous chains), all cases in Table I could be described eventually, and it must be concluded that heterogeneity with respect to bridge multiplicity or size of repeating unit is an ever-present possibility.

The above analysis does not include discussion of departures from linearity beyond the range of $\bar{x}_n$ listed in Table I. Such departures occur for entries 2–6, 8, 13, 14, 16–22, 24–29, and 37. For discussion of these data and for more details about the structural types, reference is made to the original sources (1–11).

Acknowledgments

The authors wish to thank Prof. D. C. Bradley for his helpful criticism of the manuscript, Dr. R. K. Misra and Dr. T. H. Wonnacott for their advice on statistical methods, and the Government of Ontario for a graduate fellowship to D.E.G.J.

1. D. C. Bradley, R. Gaze, and W. Wardlaw. J. Chem. Soc. 721 (1955); 3977 (1955).
2. D. C. Bradley, R. Gaze, and W. Wardlaw. J. Chem. Soc. 469 (1957).
3. D. C. Bradley and D. G. Carter. Can. J. Chem. **39**, 1434 (1961).
4. D. C. Bradley and H. Holloway. Can. J. Chem. **39**, 1818 (1961).
5. D. C. Bradley and D. G. Carter. Can. J. Chem. **40**, 15 (1962).
6. D. C. Bradley and H. Holloway. Can. J. Chem. **40**, 62 (1962).
7. D. C. Bradley and H. Holloway. Can. J. Chem. **40**, 1176 (1962).
8. D. C. Bradley and C. Prevedorou-Demas. Can. J. Chem. **41**, 629 (1963).
9. D. C. Bradley and C. Prevedorou-Demas. J. Chem. Soc. 1580 (1964).
10. D. C. Bradley and C. Prevedorou-Demas. J. Chem. Soc. 1139 (1966).
11. D. C. Bradley and C. Prevedorou-Demas. J. Chem. Soc. A, 43 (1967).
12. D. C. Bradley. Nature, **182**, 1211 (1958).
13. R. L. Martin and G. Winter. Nature, **188**, 313 (1960); **191**, 274 (1961).
14. D. C. Bradley and A. H. Westlake. Nature, **191**, 273 (1961).
15. K. Watenpaugh and C. N. Caughlan. Chem. Commun. 76 (1967).
16. D. E. G. Jones and J. W. Lorimer. Unpublished results.
17. I. Prigogine and R. Defay. Chemical thermodynamics. (*Translated by* D. H. Everett). Longmans, Green and Co., Ltd., London. 1954. pp. 410–414.
18. D. C. Bradley and I. M. Thomas. J. Chem. Soc. 3404 (1959).
19. D. C. Bradley and C. E. Holloway. Inorg. Chem. **3**, 1163 (1964).
20. D. C. Bradley, J. W. Lorimer, and C. Prevedorou-Demas. Can. J. Chem. This issue
21. G. W. Snedecor. Statistical methods. 5th ed. Iowa State College Press, Ames, Iowa. 1956. Sections 6.2–6.8.
22. W. C. Hamilton. Statistics in physical science. Ronald Press, New York. 1964. Sections 4–1, 5–8.
23. E. S. Pearson and H. O. Hartley (*Editors*). Biometrika tables for statisticians. Vol. I. Cambridge Univ. Press, Cambridge, England. 1954.
24. R. L. Martin and G. Winter. J. Chem. Soc. 2947 (1961).

Can. J. Chem. Downloaded from www.nrcresearchpress.com by 210.87.254.5 on 09/05/12
For personal use only.

Can. J. Chem. Downloaded from www.nrcresearchpress.com by 210.87.254.5 on 09/05/12
For personal use only.

Metal oxide trialkylsilyloxide polymers. Part V. Further studies on titanium oxide triethylsilyloxide polymers[1]

D. C. BRADLEY[2], J. W. LORIMER, AND C. PREVEDOROU-DEMAS
Department of Chemistry, The University of Western Ontario, London, Ontario

Received June 4, 1969

Tetrakis(triethylsilyloxy)titanium, $Ti(OSiEt_3)_4$, was hydrolyzed under controlled conditions in dioxane at 60 °C. The soluble initial products $[TiO_x(OSiEt_3)_{4-2x}]_n$, with $x = 0.1$–0.5, underwent disproportionation when heated at 65 °C under high vacuum to give $Ti(OSiEt_3)_4$ and products with values of x in the range 0.4–1.4. Molecular weights were determined by cryoscopy in cyclohexane, and the linear dependence of $1/n$ on x was used as a basis for structural proposals. The results are compared with those obtained previously for the initial products of hydrolysis.

Canadian Journal of Chemistry, 47, 4113 (1969)

Introduction

In Part IV of this series (1), the hydrolysis of tetrakis(triethylsilyloxy)titanium(IV) was described, and some possible structures for the titanium oxide triethylsilyloxides were proposed by considering the variation of the number average degree of polymerization as a function of the number average degree of hydrolysis. Heating of the oxide triethylsilyloxides at 150–180 °C under vacuum caused disproportionation into $Ti(OSiEt_3)_4$ and a slightly soluble residue (1). This paper describes the removal of $Ti(OSiEt_3)_4$ from the initial hydrolysis products at a much lower temperature (65 °C), the examination of the residues, and some tentative structural and compositional parameters which may be obtained by application of the theory of regular polymer series (2, 3) to the experimental data.

Experimental

Tetrakis(triethylsilyloxy)titanium(IV) (titanium triethylsilyloxide, $Ti(OSiEt_3)_4$) was prepared and hydrolyzed for 2 h at 60 °C in dioxane containing h moles of water per mole of $Ti(OSiEt_3)_4$, as described previously (1). The solvent and volatile silanols were removed under vacuum.

The initial hydrolysis products were kept under high vacuum (oil diffusion pump, backing pressure 10^{-4} Torr) in a sublimation apparatus (path length 1 cm) overnight at room temperature to remove the last traces of solvent and silanols. The temperature was then raised to 65 °C, and a sublimate was collected on the water-cooled condensing surface of the sublimation apparatus. Quantitative recovery was difficult. Analysis of the residues and sublimates for Ti and Si (4) gave values of x and the formula weights in $[TiO_x(OSiEt_3)_{4-2x}]_n$, while molecular weight determinations (by cryoscopy in cyclohexane solution (5)) could be combined with the formula weights to obtain values of n. The values of n and x are in general not integral, and are written as number averages $\bar{n}_n$ and $\bar{x}_n$, respectively. No OH groups could be detected in any of the hydrolysis products by infrared spectroscopy in CS_2 solution.

Results and Discussion

Table I gives the percentages by weight of titanium and silicon, the number average molecular weight $\bar{M}_n$, and derived values of $\bar{n}_n$ and $\bar{x}_n$ for the residual hydrolysis products. Values of $\bar{x}_n$ are found from the ratio of silicon to titanium, and can be used in the formula $TiO_x(OSiEt_3)_{4-2x}$ to calculate the percentages of titanium and silicon. The good agreement between the observed and calculated values indicates that the formula is accurate and, for example, the polymers are not contaminated with solvent (6). The sublimates were pure $Ti(OSiEt_3)_4$ and accounted for 60–80% of the total mass of a sample.

Figure 1 shows that a plot of $1/\bar{n}_n$ against $\bar{x}_n$ is linear over the whole range of $\bar{n}_n$ given in Table I. For comparison, the data for the initial hydrolysis products (1) are also plotted in Fig. 1. Table II contains the results of a least squares analysis for the data in Table I and that for the initial hydrolysis products (1), assuming that errors in $\bar{x}_n$ were negligible compared to those in $1/\bar{n}_n$ (3). The slope, a, and intercept, b, in the general relation $y = 1/\bar{n}_n = a + b\bar{x}_n$ are given, together with the ratio $a/|b|$, the corresponding standard errors, the standard error $\sigma(y)$ in $1/\bar{n}_n$ and the correlation coefficients $\rho(xy)$ for the

[1]The research for this paper was supported, in part, by the Defence Research Board of Canada, Grant number 7583-04.

[2]Present address: Queen Mary College, Mile End Road, London E. 1, England.

TABLE I

Hydrolysis products of $[TiO_x(OSiEt_3)_{4-2x}]_n$

Moles water per mole Ti	Wt. % Ti		Wt. % Si		Molecular weight	Degree of hydrolysis	Degree of polymerization
	Obsd.	Calcd.	Obsd.	Calcd.	$\bar{M}_n$	$\bar{x}_n$	$\bar{n}_n$
0.05	9.6	10.0	18.3	19.0	599	0.375	1.25
0.1	10.3	10.3	18.8	18.9	600	0.444	1.29
0.125	11.2	11.1	18.7	18.6	610	0.576	1.42
0.15	11.7	11.4	18.9	18.5	653	0.623	1.56
0.175	12.0	11.8	18.7	18.3	694	0.671	1.70
0.2	12.0	12.6	17.1	18.0	808	0.785	2.13
0.3	12.7	13.2	17.1	17.8	874	0.852	2.41
0.4	13.4	13.6	17.3	17.6	960	0.899	2.73
0.45	14.8	14.7	17.3	17.2	996	1.003	3.06
0.5	15.2	15.5	16.6	16.9	1328	1.069	4.29
0.7	16.5	17.0	15.9	16.3	1950	1.178	6.90
0.75	19.1	19.9	14.7	15.2	Insoluble	1.347	—
0.80	21.0	19.9	16.1	15.2	Insoluble	1.346	—
0.90	21.6	20.8	15.5	14.9	Insoluble	1.388	—
Standard deviation	0.54		0.54				

variables and $\rho(ab)$ for the parameters. These values were computed by methods described elsewhere (3).

The theory of regular polymer series (3) gives rise to 4 general models for the structure of metal oxide trialkylsilyloxide polymers. For Model I, if the repeating units are not themselves hydrolysis products

$$[1] \qquad 1/\bar{n}_n = \overline{(q/p)}/\bar{q} - \bar{x}_n/\bar{q}$$

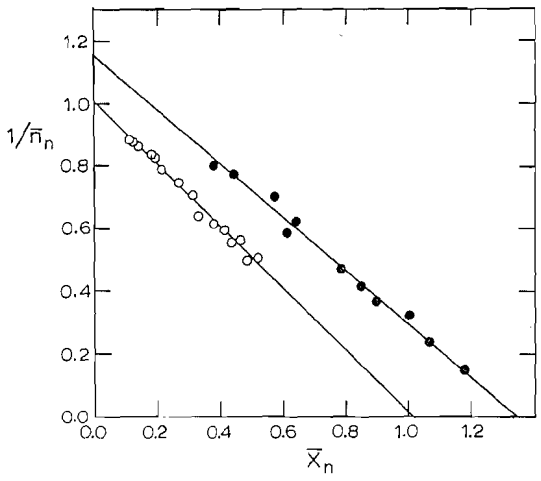

FIG. 1. Dependence of reciprocal degree of polymerization on degree of hydrolysis for titanium oxide triethylsilyloxides: ○, before thermal disproportionation; ●, after thermal disproportionation. The lines are the least-squares equations with parameters given in Table II.

where

$$\overline{(q/p)} = \alpha(q_A/p_A) + (1 - \alpha)(q_B/p_B)$$

$$\bar{q} = \beta q_A + (1 - \beta)q_B$$

describes a mixture of series A polymers containing a mole fraction α of metal atoms and a mole fraction β of molecules, with p_A metal atoms per repeating unit and with q_A metal–oxygen–metal bridges between repeating units, and series B polymers with corresponding parameters $1 - \alpha$, $1 - \beta$, p_B, q_B. The relation between α and β is

$$\alpha/\beta = \bar{n}_A/\bar{n}_n, (1 - \alpha)/(1 - \beta) = \bar{n}_B/\bar{n}_n$$

For Model II, the intercept of the plot of

TABLE II

Hydrolysis products of $Ti(OSiEt_3)_4$

$y = 1/\bar{n}_n = a + b\bar{x}_n$

Parameter	Value	
	Initial products	Final products
Range of $\bar{x}_n$	0.11–0.52	0.37–1.18
No. of points	15	11
Intercept, a	1.004	1.154
$\sigma(a)$	0.012	0.024
Slope, b	−0.999	−0.853
$\sigma(b)$	0.035	0.029
Ratio, $a/\|b\|$	1.005	1.353
$\sigma(a/b)$	0.046	0.062
$\rho(xy)$	−0.992	−0.995
$\rho(ab)$	−0.914	−0.953
$\sigma(y)$	0.018	0.024

Can. J. Chem. Downloaded from www.nrcresearchpress.com by 210.87.254.5 on 09/05/12
For personal use only.

Can. J. Chem. Downloaded from www.nrcresearchpress.com by 210.87.254.5 on 09/05/12
For personal use only.

$1/\bar{n}_n$ against $\bar{x}_n$ is equal to the reciprocal degree of polymerization of the unhydrolyzed trialkylsilyloxide, and

$$1/\bar{n}_n = (\overline{1/p})[1 - \bar{x}_n/(\overline{q/p})]$$

where

$$(\overline{1/p}) = \alpha/p_A + (1 - \alpha)/p_B$$

Clearly, the initial hydrolysis products satisfy Model II, since the unhydrolyzed $Ti(OSiEt_3)_4$ is truly monomeric (4), and since the intercept is unity to well within one standard deviation. Since the slope is also unity to well within one standard deviation, these products can be described as linear molecules with one metal atom per repeating unit and one metal–oxygen–metal bridge between adjacent repeating units; i.e., a p_1q_1 series. Since $q = 1$, there is no possibility for chain branching.

The final products satisfy Model I with $\alpha = 0.65$, $\beta = 0.83$, if $p_A = p_B = 1$, $q_A = 1$, $q_B = 2$. Hence the average degree of polymerization of the B-series molecules is greater than that of the A-series molecules. This mixture of p_1q_1 and p_1q_2 series can arise by thermal disproportionation. The general formula for series A molecules is $Ti_nO_{n-1}(OSiEt_3)_{2n+2}$, while that for series B molecules is $Ti_nO_{2n-2}(OSiEt_3)_4$, with $n = 1,2,\ldots$. The disproportionation reaction may occur by condensation of two series A molecules

$$2Ti_2O(OSiEt_3)_6 \rightarrow Ti_2O_2(OSiEt_3)_4 + 2Ti(OSiEt_3)_4$$

followed by successive end-to-end condensations of type B molecules

$$2Ti_2O_2(OSiEt_3)_4 \rightarrow Ti_3O_4(OSiEt_3)_4 + Ti(OSiEt_3)_4$$

$$2Ti_nO_{2n-2}(OSiEt_3)_4 \rightarrow Ti_{2n-1}O_{4n-4}(OSiEt_3)_4 + Ti(OSiEt_3)_4$$

or

$$Ti_nO_{2n-2}(OSiEt_3)_4 + Ti_{n-1}O_{2n-4}(OSiEt_3)_4 \rightarrow Ti_{2n-2}O_{4n-6}(OSiEt_3)_4 + Ti(OSiEt_3)_4$$

Similar disproportionations have been proposed for the trimethylsilyloxides of titanium (6) and zirconium (7). In solution, the p_1q_1 and p_1q_2 series may be regarded as consisting of 4 coordinate titanium atoms linked through 1 or 2 bridging oxygens. In the solid or in concentrated solutions, coordination between chains could result in an increase of the coordination number of titanium to 6, as observed in the titanium oxide ethoxides (8). The first hydrolyzed members of these series are $Ti_2O(OSiEt_3)_6$ (p_1q_1) and $Ti_2O_2(OSiEt_3)_4$ (p_1q_2). If only these were present, the minimum degree of polymerization would be 2. Since degrees of polymerization as low as 1.25 are observed, and since the monomer is the first member of each series, it must be concluded that the hydrolysis products still contain monomer. Presence of monomer is consistent with the disproportionation reactions postulated above, if these are equilibria. An equilibrium mechanism for disproportionation has been proposed previously (3). This mechanism also accounts readily for the observations that heating in vacuum at higher temperatures produces less soluble products, for removal of monomer will simply shift the equilibrium to favor products of higher degree of polymerization.

The final products can also be described by Model I with $\alpha = 0.53$, $\beta = 0.83$ if $p_A = 1$, $p_B = 8$, $q_A = 1$, $q_B = 2$, $l_B = 3/2$; i.e., by mixtures of p_1q_1 and $l_{3/2}p_8q_2$ chains. The chains with octameric repeating units and $l = 3/2$ molecules of water required to form a repeating unit have been postulated previously to describe the titanium and zirconium oxide trimethylsilyloxides (3, 6, 7). The minimum degree of polymerization for this mixture (even if monomer were present as the first member of the p_1q_1 series) would only be 1.7, and almost half the observed values are less than this value. The $l_{3/2}p_8q_2$ chains cannot be ruled out completely, since their formation at higher degrees of hydrolysis could occur in such proportions that the linearity of the plots of $1/\bar{n}_n$ against $\bar{x}_n$ would not be affected appreciably. It is clear, however, that octameric repeating units are formed with greater difficulty from $Ti(OSiEt_3)_4$ molecules than from $Ti(OSiMe_3)_4$ molecules, and molecular models suggest that this is due simply to steric effects of the bulkier ethyl groups.

Model III consists of a mixture of a linear series A, containing a mole fraction α of metal atoms, and a cyclic series B, containing the remaining fraction $1 - \alpha$ of metal atoms, and gives eq. [1] if $\bar{q}$ is replaced by q_A (3). The nonintegral reciprocal slope makes this model improbable for the final products. For the initial products, a mixture of linear chains with $p_A = q_A = 1$ and cyclic chains with $p_B = q_B = 1$ (general formula $Ti_{n+1}O_{n+1}(OSiEt_3)_{2n+2}$, $n =$

1, 2, ...) would give $1/\bar{n}_n = 1 - \bar{x}_n$, in agreement with experiment. Cyclic chains with $\bar{n}_n = 4$ make up parts of the octameric repeating units postulated for the titanium oxide trimethylsilyloxides (6). Their presence in the initial hydrolysis products of the triethylsilyloxide is thus a possibility that cannot be established with certainty by the present analysis.

Model IV consists of heterogeneous chains with the same distribution of repeating units and number of metal–oxygen–metal bridges in each chain. Heterogeneous chains with single and double bridges can be rejected as unnecessary for the initial products. For the final products, the non-integral reciprocal intercept would require repeating units with both $p = 1$ and 2, which appears to be unreasonable. A mixture of heterogeneous chains with $p = 1$ and 2, $q = 1$ and 2, and homogeneous p_1q_1 or p_1q_2 chains could describe the results, although the relative proportions in the mixture cannot be determined (3). Heterogeneous chains could arise by reaction between series A and series B molecules, for example

$$Ti_2O(OSiEt_3)_6 + Ti_2O_2(OSiEt_3)_4 \rightarrow Ti(OSiEt_3)_4 + (OSiEt_3)_3TiOTi(OSiEt_3)O_2Ti(OSiEt_3)_2$$

For the final products, another possibility which involves cyclic chains is a mixture of the Model I series described above ($p_A = p_B = 1$, $q_A = 1$, $q_B = 2$) with the cyclic molecule $Ti_3O_4(OSiEt_3)_4$. This molecule contains a 6-atom ring, 2 oxygen atoms in single bridges and 2 in double bridges. If η is the mole fraction of atoms in the Model I series, then this model gives the same slope as eq. [1], but an intercept $\eta(2 - \alpha) = 1.353$, from which acceptable values of α and η lie in the range $0 < \alpha \leqslant 0.65$ and $0.68 < \eta \leqslant 1$. The next member of the cyclic series $Ti_{2n-1}O_{4n-4}(OSiEt_3)_4$, $n = 2, 3, \ldots$, would contain a 10-atom ring whose formation would be less probable than a linear chain of the same number of atoms.

The lower solubility of the titanium oxide triethylsilyloxides compared to the titanium oxide trimethylsilyloxides for the same degree of hydrolysis is consistent with the occurrence of $p_1q_1 + p_1q_2$ chains for the former, and chains based on octameric repeating units (6) for the latter. The solubility process can be discussed conveniently in terms of an equivalent thermodynamic process involving melting of the polymer and mixing of the melt with solvent. The free energies of melting and the entropies of mixing are probably comparable for each polymer. However, the more compact octameric repeating units expose more trialkylsilyloxy groups per unit volume than do the extended p_1q_1 and p_2q_2 structures, resulting in a lower energy of mixing and a higher solubility for the oxide trimethylsilyloxides.

1. D. C. Bradley and C. Prevedorou-Demas. J. Chem. Soc. A, 43 (1967).
2. D. C. Bradley and H. Holloway. Can. J. Chem. **40**, 1176 (1962).
3. J. W. Lorimer and D. E. G. Jones. Can. J. Chem. This issue.
4. D. C. Bradley and I. M. Thomas. J. Chem. Soc. 3404 (1959).
5. D. C. Bradley, R. Gaze, and W. Wardlaw. J. Chem. Soc. 721 (1955).
6. D. C. Bradley and C. Prevedorou-Demas. Can. J. Chem. **41**, 629 (1963).
7. D. C. Bradley and C. Prevedorou-Demas. J. Chem. Soc. A, 1580 (1964).
8. K. Watenpaugh and C. N. Caughlan. Chem. Commun. 76 (1967).

Can. J. Chem. Downloaded from www.nrcresearchpress.com by 210.87.254.5 on 09/05/12
For personal use only.

Vibrational spectra of halopentacarbonylmanganese(I) derivatives

I. S. BUTLER AND H. K. SPENDJIAN
Department of Chemistry, McGill University, Montreal, Quebec

Received April 21, 1969

The solid-state infrared (i.r.) and laser Raman spectra of the halopentacarbonylmanganese(I) derivatives, $Mn(CO)_5X$ (X = Cl, Br, and I), have been recorded in the C—O stretching and the low frequency (700–33 cm^{-1}) regions. The i.r. overtone and combination spectra recorded in the regions 2800–2250 and 1350–700 cm^{-1} have been used to help in the assignment of some of the low frequency fundamentals. The solid-state i.r. and laser Raman spectra of the dimeric halotetracarbonylmanganese(I) derivatives, $[Mn(CO)_4X]_2$ (X = Br and I), have been recorded in the C—O stretching and the low frequency regions for comparative purposes and shown to be consistent with the expected D_{2h} symmetry of the molecules.

Canadian Journal of Chemistry, 47, 4117 (1969)

Can. J. Chem. Downloaded from www.nrcresearchpress.com by 210.87.254.42 on 09/05/12
For personal use only.

Introduction

The recent interest in the low frequency infrared (i.r.) (1–5) and Raman (3, 4) spectra of the halopentacarbonylmanganese(I) derivatives, $Mn(CO)_5X$ (X = Cl, Br, and I), prompts us to report our results for the solid-state and carbon disulfide solution i.r. and solid-state laser Raman spectra of these compounds in the region 700–33 cm^{-1}. Our results are substantially in agreement with those published, although in some cases we observed a few additional frequencies and managed to resolve certain bands in the i.r. spectra previously reported as shoulders. In addition, we wish to report overtone and combination spectra in the regions 2800–2250 and 1350–700 cm^{-1} and their use in assigning some of the low frequency fundamentals. With a few exceptions (such as refs. 6–11), the overtones and combinations associated with the low frequency fundamentals of metal carbonyl derivatives have previously been ignored.

Although the solid-state laser Raman spectra of the $Mn(CO)_5X$ derivatives in the C—O stretching region have recently been reported (4, 12), we also wish to present our results for this region because we found that under high resolution certain of the lines reported for $Mn(CO)_5Cl$ and $Mn(CO)_5Br$ could be split into well defined doublets. The $Mn(CO)_5X$ derivatives are known to be readily decomposed thermally to form the dimeric $[Mn(CO)_4X]_2$ derivatives (13). In view of this, it was initially felt that the additional lines observed in the Raman spectra of $Mn(CO)_5Cl$ and $Mn(CO)_5Br$ might well have been the result of the presence of some of the dimers as impurities. These dimers could have been formed by thermal decomposition induced by the laser beam. In order to test this possibility, the solid-state laser Raman spectrum of $[Mn(CO)_4Br]_2$ was recorded and compared with that of $Mn(CO)_5Br$. From this comparison, the chance of any decomposition occurring while the spectrum of $Mn(CO)_5Br$ was being recorded was quickly ruled out. Since definite splittings were also observed in the C—O stretching region of the solid-state i.r. spectra of $Mn(CO)_5Cl$ and $Mn(CO)_5Br$, it appears most likely that the splittings in both the Raman and the i.r. spectra were the result of correlation effects. With this in mind, the solid-state spectra of the $Mn(CO)_5X$ derivatives are discussed here in terms of the recently determined[1] crystal structure of $Mn(CO)_5Cl$.

The solid-state i.r. spectrum of $[Mn(CO)_4Br]_2$ and the solid-state i.r. and Raman spectra of $[Mn(CO)_4I]_2$ were also recorded and the results are presented here. The i.r. and Raman data for these 2 compounds are in accord with the D_{2h} symmetry expected.

Experimental

Materials

The compounds studied, prepared by the methods described in the literature, were $Mn(CO)_5Cl$ and $Mn(CO)_5Br$ (13), $Mn(CO)_5I$ (14), and $[Mn(CO)_4Br]_2$ and $[Mn(CO)_4I]_2$ (13). The purity of the compounds was established by the absence of any impurity bands in their i.r. spectra in the C—O stretching region.

Spectra

All spectra were recorded using freshly prepared samples.

[1]Personal communication from Professor R. F. Bryan, Department of Chemistry, University of Virginia, Charlottesville, Virginia.

Can. J. Chem. Downloaded from www.nrcresearchpress.com by 210.87.254.42 on 09/05/12
For personal use only.

Infrared spectra below 300 cm^{-1} were recorded on a Beckman IR-11 spectrophotometer. In the other regions, spectra were recorded on a Perkin–Elmer Model 521 spectrophotometer. All measurements were carried out at room temperature with the samples in the form of Nujol mulls pressed between plates appropriate for the spectral region under investigation. The solution spectrum of $Mn(CO)_5I$ was studied using spectrograde CS_2 (Fisher Chemical Co.). The frequencies shown in the Tables are accurate to ± 1 cm^{-1}.

Raman spectra of the powdered solids were recorded on either a Spex Ramalog or a Jarrell–Ash Model 25-300 Raman spectrophotometer using helium–neon (6328 Å) excitation. The frequencies shown in the Tables are accurate to ± 1–2 cm^{-1}.

Results and Discussion

The crystal and molecular structure of $Mn(CO)_5Cl$ has recently been determined.[1] The space group is *Pnma* (D_{2h}^{16}) and there are 4 molecules per unit cell. The site symmetry of the molecules is C_s. The molecular symmetry is C_s, but the deviations from C_{4v} are within experimental error. $Mn(CO)_5Br$ is isomorphous[1] with $Mn(CO)_5Cl$, and so, presumably, is $Mn(CO)_5I$.

The vibrational representation for an isolated $Mn(CO)_5X$ molecule of C_{4v} symmetry reduces as follows

$$\Gamma_{vib}^{C_{4v}} = 7a_1 + 4b_1 + 8e + a_2 + 2b_2$$

The correlation between the C_{4v} symmetry of the free molecule, the C_s site symmetry, and the D_{2h}^{16} symmetry of the crystal is shown in Table I, together with the spectroscopic activity. The factor group D_{2h}^{16} is isomorphous with the corresponding point group D_{2h}. It is apparent from the correlation diagram that non-degenerate modes in the free $Mn(CO)_5X$ molecule could be split into 4 components in the crystal and doubly degenerate modes into 8. Furthermore, the irreducible representations for the internal and external optically active vibrational modes of crystalline $Mn(CO)_5X$ are given by

$$\Gamma_{vib}^{D_{2h}} = 19a_g + 19b_{2g} + 19b_{1u} + 19b_{3u} + 11b_{1g} + 11b_{3g} + 11b_{2u}$$

for the internal modes and

$$\Gamma_{vib}^{D_{2h}} = 3a_g + 3b_{2g} + 2b_{1u} + 2b_{3u} + 3b_{1g} + 3b_{3g} + 2b_{2u}$$

for the external modes.

In our treatment of the vibrational spectra of the $Mn(CO)_5X$ molecules, therefore, it is important to know whether or not any correlation splitting occurs in the solid-state spectra, and also whether or not any of the frequencies observed below 150 cm^{-1} result from external rather than internal modes.

The only compound whose i.r. spectrum was measured in CS_2 solution and in the solid-state was $Mn(CO)_5I$. The observed frequencies are given in Table II. There was no difference between the spectrum of the solution and that of the solid, apart from some frequency shifts. (The slight differences in the overtone and combination regions are excluded from this discussion.) The observed frequencies for the solid-state i.r. spectra of $Mn(CO)_5Cl$ and $Mn(CO)_5Br$ are also given in Table II. By comparison with the spectra in CCl_4 solution reported by El-Sayed and Kaesz (15), these solid-state spectra are very complex, owing to splittings in some of the bands. Other research groups have investigated the solution and solid-state i.r. spectra of $Mn(CO)_5Cl$ and $Mn(CO)_5Br$ throughout the various spectral regions and found that differences only occurred in the C—O stretching region (1, 4, 5).

Solution Raman spectra of the $Mn(CO)_5X$ compounds were not measured in the present study. Other workers have experienced considerable difficulty in measuring solution spectra of the compounds in the low frequency region (3, 4), but fortunately solution spectra in the C—O stretching region have proved more readily obtainable (16). Solid-state Raman data for the C—O stretching region have been published recently (4, 12), and we have also studied the solid-state spectra in this region. A comparison of our results with those already published is given in Table III. The spectrum of $Mn(CO)_5Br$ recorded in this work is shown in Fig. 1. For C_{4v} symmetry, four Raman active C—O modes ($2a_1 + b_1 + e$) are expected, and from i.r. studies involving force constant calculations (17, 18), these modes decrease in frequency in the order

$$a_1 \text{ (radial)} > b_1 > e > a_1 \text{ (axial)}$$

Reference to Table IV shows that Cotton *et al.* (16) observed 4 strong Raman lines for $Mn(CO)_5Br$ in CS_2 and in *n*-hexane solution, while Clark and Crosse (4) found 4 strong lines and 1 very weak line in the solid-state spectrum of the same compound. Our solid-state spectrum of $Mn(CO)_5Br$ was recorded under very high resolution (slit width ~ 1 cm^{-1}) and 6 strong

TABLE I

Correlation between the various symmetries associated with $Mn(CO)_5X$ molecules

Molecular group, C_{4v}	Site group, C_s	Factor group, D_{2h}^{16}
a_1 (i.r., Raman)		a_g (Raman)
		b_{2g} (Raman)
b_1 (Raman)	a' (i.r., Raman)	b_{1u} (i.r.)
		b_{3u} (i.r.)
e (i.r., Raman)		
		b_{1g} (Raman)
a_2 (inactive)	a'' (i.r., Raman)	b_{3g} (Raman)
		a_u (inactive)
b_2 (Raman)		b_{2u} (i.r.)

lines and no weak ones were observed. (The very weak line observed by Clark and Crosse suggests the presence of a small amount of some impurity.) It is apparent that, in addition to some fairly large frequency shifts, there are 2 new lines in going from the solution spectrum of $Mn(CO)_5Br$ to that of the solid. These new lines resulted from small splittings in the a_1 (axial) and b_1 modes. The splittings may have been the result of correlation effects; the correlation diagram in Table I indicates that modes of a_1 or b_1 symmetry in the free molecule could be split into 2 Raman components ($a_g + b_{2g}$) in the crystal. The a_1 (axial) mode of $Mn(CO)_5Cl$ was also observed to be split in the solid-state spectrum, but no splittings at all could be detected in the spectrum of $Mn(CO)_5I$. The latter was unique in that only 3 lines were observed. Since the 2 outermost lines were readily assigned as a_1 modes, and the third line was in the region where the b_1 mode was expected, it seems that in this case either the b_1 and e modes were accidentally degenerate or that the e mode was too weak to be observed.

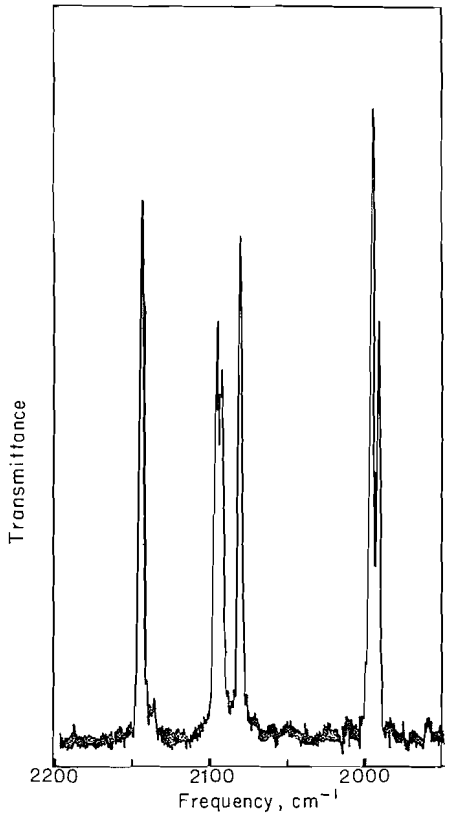

FIG. 1. Raman spectrum of $Mn(CO)_5Br$ in the C—O stretching region (powdered solid).

It was felt that before we could attribute the splittings in the solid-state Raman spectra of $Mn(CO)_5Cl$ and $Mn(CO)_5Br$ to correlation effects, there was one other possibility which should be considered. The $Mn(CO)_5X$ compounds are readily thermally decomposed to form the dimeric $[Mn(CO)_4X]_2$ compounds (13). It was possible that the laser beam could cause such decompositions to take place, resulting in the appearance of additional lines in the Raman spectra. In view of this, the solid-state laser Raman spectra of $[Mn(CO)_4Br]_2$ was recorded in both the C—O stretching and the low frequency regions. The solid-state Raman spectrum of

Can. J. Chem. Downloaded from www.nrcresearchpress.com by 210.87.254.42 on 09/05/12
For personal use only.

Can. J. Chem. Downloaded from www.nrcresearchpress.com by 210.87.254.42 on 09/05/12
For personal use only.

TABLE II

Vibrational spectra of $Mn(CO)_5X$ (X = Cl, Br, or I)

Frequency, cm^{-1} [a]							
X = Cl		X = Br		X = I			
Infrared (solid)[b]	Raman (solid)	Infrared (solid)	Raman (solid)	Infrared (solid)	Infrared (CS_2)	Raman (solid)	Assignment[c]
		50 vw	54 m			45 m,sh	*e* δ(CMnX), ν_{22}
		64 vw					b_1 δ(CMnC), ν_{12} ?
(79 w)		88 w		98 w			*e* δ(CMnC), ν_{20} or ν_{21}
(102 m)		103 m	100 s	107 m			a_1 δ(CMnC), ν_7
(115 w)	112 s						b_2 δ(CMnC), ν_{14} ?
(127 s)	125 s	123 s	117 s	116 m		122 vs	*e* δ(CMnC), ν_{20} or ν_{21}
(143 m)	132 s	133 ms		137 m		133 vs	*e* δ(CMnC), ν_{20} or ν_{21}
(295 s)	291 s	222 s	219 s	188 s		190 vs	a_1 ν(Mn—X), ν_6
	382 vs		385 s	386 vw		389 vs	a_1 ν(Mn—C), (radial)[g], ν_5
409 s	408 w	408 m		406 ms	410 m[h]	413 w	a_1 ν(Mn—C), (axial)[g], ν_4
418 s		415 s, 422 s	415	427 s	431 vs	425 mw	*e* ν(Mn—C), ν_{19}
478 w	477 s	471 w	475 m	467 w	464 w	466 m	a_1 δ(MnCO), ν_3
~535[d]	534 vw	~535[d]		~525[d]	~525[d]		a_2 δ(MnCO), ν_8
550 s	548 vw	547 m	540 ms	544 m	547 w	544 w	*e* δ(MnCO), ν_{18}
					608 w		?
	628 w		630 w	~620[d]			b_2 δ(MnCO), ν_{13} ?
638 vs	640 vw	638 vvs	638 w	638 vs	641 s	633 ms	*e* δ(MnCO), ν_{17}
654 s,sh	649 vw	651 s,sh	650 w	652 s,sh	651 m		*e* δ(MnCO), ν_{16}
					695 vw		$\nu_{17}+(54?)$
					713 vw		$\nu_{17}+(72?)$
					730 vw		$\nu_{17}+(89?)$
				794 w	794 w		$137+\nu_{16}$
785 s		795 s		812 m	813 m		$\nu_5+\nu_{19}$; $\nu_4+\nu_5$
810 m,sh		813 m,sh					$2\nu_4$
		881 m,sh		871 w	876 w		$\nu_3+\nu_4$
900 s		900 s		900 s	897 s		$\nu_3+\nu_{19}$
914 m				920 w			$\nu_5+\nu_8$?
954 m		951 m		945 ms	951 w		$\nu_4+\nu_{18}$; $\nu_8+\nu_{19}$
				966 w	973 w		$\nu_{18}+\nu_{19}$
988 m		986 m		990 m	1000 s		ν_{10}[e] $+\nu_{19}$; ν_{11}[f] $+\nu_{17}$
1003 w,sh		1002 vw		1001 vw			$\nu_5+\nu_{13}$; ν_{11}[f] $+\nu_{16}$
		1018 vw,sh?		1019 vw			$\nu_3+\nu_{18}$
1049 m		1040 m		1035 s	1047 s		$\nu_4+\nu_{17}$
1063 m		1053 m		1050 m			$\nu_4+\nu_{16}$
1079 m		1077 m		1079 m	1087 m		$\nu_{16}+\nu_{19}$

Can. J. Chem. Downloaded from www.nrcresearchpress.com by 210.87.254.42 on 09/05/12
For personal use only.

TABLE II—(*Concluded*)

Frequency, cm^{-1} [a]							
X = Cl		X = Br		X = I			
Infrared (solid)[b]	Raman (solid)	Infrared (solid)	Raman (solid)	Infrared (solid)	Infrared (CS_2)	Raman (solid)	Assignment[c]
		1128 vw		1125 vw	1127 w		$\nu_3+\nu_{16}$
1175 m		1170 m		1169 m			$\nu_8+\nu_{17}$; $\nu_{13}+\nu_{18}$
		1187 m		1184 sh	1181 m		$\nu_{17}+\nu_{18}$
1264 w							$2\nu_{13}$; $\nu_{13}+\nu_{17}$
1281 w		1275 w			1280 w		$2\nu_{17}$
1302 w							$2\nu_{16}$
1988 m	1983 ms,sh	1992 s	1989 ms	2002 m	2005 m	2005 s	a_1 (C—O) (axial), ν_2[j]
2001 m	1985 s	2002 m	1993 s				
2050 s	2076 s	2049 s	2078 s	2043 s	2045 s		e (C—O), ν_{15}
						2070 s	
2073 m	2091 s	2068 m	2090 ms		2080[i]		b_1 (C—O), ν_9[k]
2086 m		2081 m	2093 ms				
2144 w	2141 s	2139 w	2142 s	2132 w	2127 w	2133 s	a_1 (C—O) (radial), ν_1
2435 s		2434 s		2438 s	2444 s		$\nu_5+\nu_{15}$
2474 s		2468 s		2472 s	2476 s		$\nu_2+\nu_3$; $\nu_{15}+\nu_{19}$
2503 s		2501 s		2507 s	2504 s		$\nu_9+\nu_{19}$
		2548 w		2536 w	2535 w		$\nu_2+\nu_{18}$
2554 m		2556 m		2558 m	2558 m		$\nu_1+\nu_{19}$
		2580 w					$\nu_8+\nu_{15}$; $\nu_2+\nu_{10}$[e]
					2590 w		$\nu_{15}+\nu_{18}$
					2644 w		$\nu_2+\nu_{17}$
2726 w		2720 w		2716 w	2710 w		$\nu_9+\nu_{17}$
2780 w		2772 w		2762 m	2767 m		$\nu_1+\nu_{17}$
2798 w		2789 w		2776 w			$\nu_1+\nu_{16}$

[a]Each list of frequencies has been divided into several sections and the intensities given are relative to the most intense peak within each section; s = strong, m = medium, w = weak, sh = shoulder, v = very.
[b]The spectrum was not measured below 300 cm^{-1}; the frequencies shown in parentheses are from ref. 4.
[c]The frequency designations are from ref. 3.
[d]Predicted from combination spectra.
[e]b_1 δ(MnCO) predicted at ~570 (Cl), ~570(Br), and ~565(I) cm^{-1}.
[f]b_1 ν(Mn—C) predicted at ~350 (Cl, Br, and I) cm^{-1}.
[g]The terms radial and axial refer to the Mn—C bonds *trans* to each other and *trans* to X, respectively.
[h]In *n*-hexane solution.
[i]From ref. 16.
[j]The split a_1 modes are assigned as: $(b_{1u}+b_{3u})$, i.r. active; (a_g+b_{2g}), Raman active.
[k]The split b_1 modes are assigned as: $(b_{1u}+b_{3u})$, i.r. active; (a_g+b_{2g}), Raman active.

TABLE III

Raman spectra of the $Mn(CO)_5X$ derivatives in the C—O stretching region

Compound	Mode	Frequency (cm^{-1}) Davison and Faller (12)[a,b]	Cotton *et al.* (16)[a,c]	Clark and Crosse (4)[b]	This work[b]
$Mn(CO)_5Cl$	a_1 (radial)			2143 ms	2141 s
	b_1			2092 s, 2077 ms	2091 s
	e			2046 w	2076 s
	a_1 (axial)			1986 s	1985 s, 1983 ms,sh
$Mn(CO)_5Br$	a_1 (radial)	2137 s	2133	2138 s	2142 s
	b_1	2086 s	2080	2088 s, 2074 ms	2093 ms, 2090 ms
	e	2072 s	2051	2045 vw	2078 s
	a_1 (axial)	1984 s	2000	1989 s	1993 s, 1989 ms
$Mn(CO)_5I$	a_1 (radial)			2130 ms	2133 s
	b_1[d]			2072 s	2070 s
	e				
	a_1 (axial)			2004 ms	2005 s

[a]No assignments proposed in this work.
[b]Solid-state spectra.
[c]CS_2 and *n*-hexane solution spectra, no relative intensities given.
[d]Observed at 2072 cm^{-1} in cyclohexane solution (18).

$[Mn(CO)_4I]_2$ was studied in the same regions for comparative purposes. The spectrum of the dimeric chloro-compound was not investigated. Both $[Mn(CO)_4Br]_2$ and $[Mn(CO)_4I)_2$ proved to be extremely poor scatterers and only a few lines could be clearly discerned above the noise level. The observed frequencies are given in Table IV. A comparison of the C—O stretching frequencies of $Mn(CO)_5Br$ and $[Mn(CO)_4Br]_2$ immediately reveals that no detectable amount of the dimer was being formed while the spectrum of the pentacarbonyl was being recorded. Even without the obvious differences in the C—O frequencies, the vastly different scattering properties of the 2 compounds and the high intensity of all the lines in the $Mn(CO)_5Br$ spectrum would have been enough to rule out the possibility of any dimer formation.

From the above discussion, it appears that there was some correlation splitting in the solid-state spectra of the $Mn(CO)_5X$ derivatives but that it was restricted to the C—O stretching region. Owing to this, the low frequency vibrational spectra of the pentacarbonyls will be discussed in terms of the C_{4v} symmetry of an isolated $Mn(CO)_5X$ molecule.

Low Frequency Vibrations of the $Mn(CO)_5X$ Molecules

On the basis of C_{4v} symmetry, the fundamentals expected for the $Mn(CO)_5X$ molecules in the region below 700 cm^{-1} are: MnCO bending ($a_1 + a_2 + b_1 + b_2 + 3e$), Mn—C stretching ($2a_1 + b_1 + e$), Mn—X stretching ($a_1$), CMnC bending ($a_1 + b_1 + b_2 + 2e$), and CMnX bending ($e$). The a_1 and e modes are the only i.r. active ones, whereas all but the a_2 MnCO bending mode are Raman active. Most of our low frequency assignments shown in Table II are in agreement with those proposed by other research groups (1–5). Consequently, in the following discussion we will only consider those frequencies which have not been reported before and those for which we prefer alternative assignments to those already suggested. It should be mentioned that the assignments proposed for the frequencies below 150 cm^{-1} are particularly suspect, owing to the likelihood of external modes of the solids becoming active in this region. Some of the external modes might be coupled with each other, as well as with some of the very low frequency internal modes, rendering the interpretation of the region below 150 cm^{-1} even more speculative.

There is a weak band at 50 cm^{-1} in the i.r. spectrum of $Mn(CO)_5Br$ and a medium intensity Raman line at 54 cm^{-1}. Neither of these frequencies had been reported before and we have tentatively assigned them both to the CMnBr bending e mode, which is expected to occur below 70 cm^{-1} (4). This mode is almost certainly the lowest fundamental frequency of the

Can. J. Chem. Downloaded from www.nrcresearchpress.com by 210.87.254.42 on 09/05/12
For personal use only.

Can. J. Chem. Downloaded from www.nrcresearchpress.com by 210.87.254.42 on 09/05/12
For personal use only.

TABLE IV

Vibrational spectra of $[Mn(CO)_4X]_2$ (X = Br and I)

Compound	Source	Frequency (cm^{-1})										
		ν(C—O)					δ(MnCO) and ν(Mn—C)					ν(Mn—X)
$[Mn(CO)_4Br]_2$	i.r. (solid)	2103 m, 2020 s 1958 s,sh	2089 w 2012 vs 1951 s	2048 s,br 2001 m,sh	2037 s 1982 s	2030 s	658 s 545 w	632 s 465 vw	610 s 419 s	603 s 410 s,br	565 vw	
	i.r. (CCl_4)*	2099 m	2042 vs	2011 m	1975 s							
	Raman (solid)	2117 s	2015 m	2000 m	1953 s		570 w					202 vvs
$[Mn(CO)_4I]_2$	i.r. (solid)	2100 w 2018 s	2089 s 2012 vs	2065 vw 2007 s	2039 s 2000 m,sh	2027 s	654 s 543 w	631 s 467 vw	612 s 435 s	607 s 410 m	565 vw	
	i.r. (CCl_4)*	2087 w	2033 vs	2009 m	1976 s							
	Raman (solid)	2105 s	2006 m	1994 m	1944 s		600 w	473 s	455 m,sh	391 m		185 vvs

*Data from ref. 15.

Can. J. Chem. Downloaded from www.nrcresearchpress.com by 210.87.254.42 on 09/05/12
For personal use only.

$Mn(CO)_5Br$ molecule and is expected to be extensively mixed with the 2 CMnC bending e modes.

There is a weak band at 64 cm^{-1} in the i.r. spectrum of $Mn(CO)_5Br$ which had previously only been observed by Edgell and Cengel (5). These workers assigned the band to the a_1 CMnC bending mode. We might have provided some support for their assignment if a strong Raman line had appeared at the same frequency, but unfortunately the presence of an intense laser line at 65 cm^{-1} prevented us from making any measurements in this region. The i.r. band can also be explained either by one of the 2 i.r. inactive CMnC bending modes (b_1 or b_2), becoming active because of site symmetry effects, or by one of the 6 i.r. active external modes of the $Mn(CO)_5Br$ lattice. Hyams *et al.* (6) have recently assigned a line at 57 cm^{-1} in the solid-state Raman spectrum of $Re(CO)_5I$ to the CReC bending b_1 mode, but this line, too, may have been derived from an external rather than an internal mode of the lattice.

The 4 Mn—C stretching modes ($2a_1 + b_1 + b_2$) are expected in the region 500–300 cm^{-1}, while the 7 MnCO bending modes ($a_1 + a_2 + b_1 + b_2 + 3e$) should lie in the region 700–450 cm^{-1} (19). Owing to the proximity of the 2 regions, extensive mixing of modes of the same symmetry type is anticipated. Since our assignments in the Mn—C stretching region differ somewhat from those given previously, we will discuss them in some detail.

The strongest i.r. active Mn—C stretching vibration of $Mn(CO)_5Br$ was at approximately 420 cm^{-1}. Under high resolution this band appeared as a doublet. The splitting could have been the result of (*i*), factor group effects on one of the a_1 modes or on the b_1 mode: both of these non-degenerate species would have given rise to 2 i.r. active modes ($b_{1u} + b_{3u}$) in the crystal, or (*ii*), site symmetry effects on the degenerate e mode which would have also led to 2 i.r. active modes ($a' + a''$) in the crystal. By analogy with the C—O stretching region, the most intense band in the Mn—C stretching region would be expected to result from the e mode and, as a consequence, the formation of the doublet is attributed to the second possibility above. The e mode should also be Raman active. A medium intensity line was found at 415 cm^{-1}, but no splitting could be detected in this case. It will be demonstrated later in this paper that the assignment proposed for the e mode can be verified from overtone and combination spectra. The strong i.r. bands at 418 and 427 cm^{-1} for $Mn(CO)_5Cl$ and $Mn(CO)_5I$, respectively, have been similarly designated as Mn—C stretching e modes. Our assignments for the e modes are in agreement with those proposed by other research groups (3–5).

Each pentacarbonyl derivative exhibited a strong Raman line in the neighborhood of 385 cm^{-1}, but only in the case of $Mn(CO)_5I$ was there a corresponding i.r. band, and even then it was extremely weak. These frequencies have been assigned to the a_1 (radial) Mn—C stretching modes, which, by analogy with the a_1 (radial) C—O stretching modes, would be expected to exhibit strong Raman lines and weak i.r. bands, in accord with our experimental observations. The same assignment has been proposed by Adams and Squire (3).

There was a fairly strong band near 410 cm^{-1} in the i.r. spectrum of each compound[2]. These bands have previously been reported as shoulders, but in our spectra they were quite well resolved, especially in the case of $Mn(CO)_5I$. There were weak Raman lines coincident with the i.r. bands. With the exception of the work of Clark and Crosse (4), these frequencies have been completely disregarded in all previous assignments of the Mn—C stretching modes. Clark and Crosse studied the i.r. spectra in tetrachloroethylene solution and indicated that the bands near 410 cm^{-1} most probably arose from a_1 Mn—C stretching modes, but they did not suggest which type. We have assigned the frequencies to the a_1 (axial) modes. If this designation is correct, then the Raman lines should be polarized. Unfortunately, the lines were too weak for polarization measurements. Our proposed assignment of the a_1 (axial) modes is contrary to that of Adams and Squire (3) and Edgell and Cengel (5), who assigned these modes to the frequencies observed near 470 cm^{-1}. However, we feel that the i.r. bands at 470 cm^{-1} were too weak,

[2]In the case of $Mn(CO)_5Cl$, the band at 409 cm^{-1} was in fact the strongest in the Mn—C stretching region. On the basis of its intensity, this band would normally have been assigned to the e mode, but it turned out that the overtone and combination spectra were better explained if it was assigned to the a_1 (axial) mode and the somewhat weaker band at 418 cm^{-1} was assigned to the e mode.

Can. J. Chem. Downloaded from www.nrcresearchpress.com by 210.87.254.42 on 09/05/12
For personal use only.

compared with those at 410 cm^{-1}, to support their assignment. In the present study, the former have been assigned to the a_1 MnCO bending modes. This assignment is in harmony with the solution Raman work of Adams and Squire (3) who found that the lines at 470 cm^{-1} were polarized.

A weak Raman line was observed near 630 cm^{-1} for both $Mn(CO)_5Cl$ and $Mn(CO)_5Br$ but not for $Mn(CO)_5I$. These lines had previously been noted by Edgell and Cengel (5) and by Adams and Squire (3). These research groups assigned the frequencies to the a_1 and one of the e MnCO bending modes, respectively. However, both of these assignments would necessitate the appearance of one i.r. band for each compound in the region of 630 cm^{-1}, and, since these were not observed, we prefer to assign the frequencies to either the b_1 or the b_2 purely Raman active MnCO bending modes.

One unusual feature of the CS_2 solution i.r. spectrum of $Mn(CO)_5I$ was the appearance of a weak band at 608 cm^{-1}, which was *not* observed in the solid-state spectrum. Reference to the literature shows that a similar band appears in tetrachloroethane (4), cyclohexane, and carbon tetrachloride solutions (1*b*). We are unable to offer an explanation for this anomaly.

In conclusion, it should be re-emphasized that because modes of the same symmetry type are known to be extensively mixed in the low frequency region, none of the frequencies in this region will be comprised of the assigned motion alone. This caveat applies particularly to the a_1 and e modes in the Mn—C stretching and MnCO bending regions.

Overtone and Combination Spectra of the $Mn(CO)_5X$ Molecules in the 1350–700 and 2800–2250 cm^{-1} Regions

The selection rules for the binary combinations of the $Mn(CO)_5X$ molecules assuming C_{4v} symmetry are shown in Table V. It is evident that i.r. inactive modes must combine with e modes in order to produce i.r. allowed combinations. This point is important in some of the low frequency assignments to be discussed shortly. All first overtones are allowed, but are expected to be only weakly i.r. active. The frequencies observed in the 1350–700 and 2800–2250 cm^{-1} regions and the proposed assignments are given in Table II. In order to facilitate the interpretation of the assignments, a table containing frequency information for only the fundamentals is provided (Table VI). Typical spectra in the 1350–700 and 2800–2250 cm^{-1} regions are shown in Figs. 2 and 3, respectively.

In the discussion of the low frequency vibrations, the Mn—C stretching e modes were assigned to the frequencies observed near 420 cm^{-1}. The non-appearance of the first overtones, although these modes apparently combine with the other Mn—C stretching fundamentals to produce fairly strong combinations, provides some support for this assignment. A more important observation, however, is that the combination bands at 2500 cm^{-1} can only be satisfactorily explained by the combination of the bands at 420 cm^{-1} with the i.r. inactive

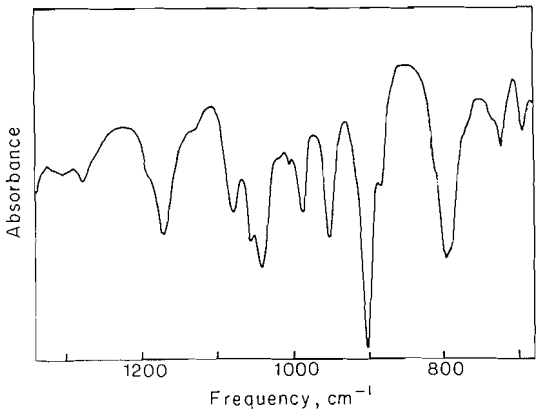

FIG. 2. Overtone and combination spectrum of $Mn(CO)_5Br$ in the 1350–700 cm^{-1} region (Nujol mull).

TABLE V

Selection rules for binary combinations under C_{4v} symmetry

	a_1	a_2	b_1	b_2	e
a_1	A_1	A_2	B_1	B_2	E
a_2		A_1	B_2	B_1	E
b_1			A_1	A_2	E
b_2				A_1	E
e					$A_1+A_2+B_1+B_2$

Can. J. Chem. Downloaded from www.nrcresearchpress.com by 210.87.254.42 on 09/05/12
For personal use only.

TABLE VI

Fundamental modes of the $Mn(CO)_5X$ molecules used in the assignment of the overtone and combination spectra[a]

i in ν_i	Symmetry	Approximate description	Frequency (cm^{-1}) X=Cl	X=Br	X=I[b]
1	a_1	C—O radial stretch	2144	2139	2132 (2127)
2	a_1	C—O axial stretch	1994	1997	2002 (2005)
3	a_1	MnCO bend	478	471	467 (464)
4	a_1	Mn—C axial stretch	409	408	406 (410)[c]
5	a_1	Mn—C radial stretch	382	385	386
8	a_2	MnCO bend	535[d]	533[d]	518[d] (520)[d]
9	b_1	C—O stretch	2080	2075	2070 (2080)[e]
10	b_1	MnCO bend	570[d]	568[d]	563[d] (569)[d]
11	b_1	Mn—C stretch	350[d]	348[d]	352[d] (359)[d]
13	b_2	MnCO bend	628	630	625[d]
15	e	C—O stretch	2050	2049	2043 (2045)
16	e	MnCO bend	654	651	652 (651)
17	e	MnCO bend	638	638	638 (641)
18	e	MnCO bend	550	547	544 (547)
19	e	Mn—C stretch	418	418	427 (431)

[a]Some of the fundamentals in the solid-state spectra were split by correlation effects. Consequently, whenever this occurred, the frequency shown in the Table is the mean of the observed frequencies. For those fundamentals where both i.r. and Raman data were available, the frequencies given in the Table are from the i.r. spectra.
[b]The values shown in parentheses are for the CS_2 solution i.r. spectrum. In those cases where solution data were not available, the frequencies from the solid-state spectrum were used.
[c]In *n*-hexane solution.
[d]Predicted from combination spectra.
[e]From ref. 16.

b_1 C—O stretching modes at approximately 2080 cm^{-1}. It could perhaps be argued that forbidden combination bands may have become active because of solid-state effects, but the intensity of these combination bands, as well as the appearance of a similar band for $Mn(CO)_5I$ in CS_2 solution, make this possibility somewhat remote. Consequently, in order for the combination bands at 2500 cm^{-1} to satisfy the selection rules, the i.r. bands at 420 cm^{-1} must be of *e* symmetry.

It is also possible to verify the assignment of some of the other low frequency *e* modes from studies of the combination spectra in the 2800–2250 cm^{-1} region and knowledge of the b_1 C—O stretching modes from Raman spectra. For example, all 3 compounds exhibit weak intensity combination bands at about 2720 cm^{-1}, which are best explained as arising from combinations of the b_1 C—O stretching modes with the MCO bending modes at about 640 cm^{-1}. The activity of the combination bands suggests the MnCO bending modes must be of *e* symmetry, in accord with the previous assignments (3–5).

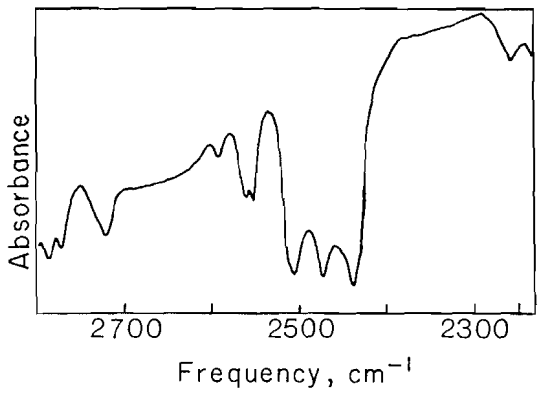

FIG. 3. Combination spectrum of $Mn(CO)_5Br$ in the 2800–2250 cm^{-1} region (Nujol mull).

A few of the bands in the combination spectra can only be explained by the combination of *e* fundamentals with low frequency fundamentals which were not observed in either the i.r. or Raman spectra. The predicted frequencies and suggested assignments for these unobserved fundamentals are given in footnotes *e* and *f* of Table II. The assignments cannot at present be substantiated further.

Vibrational Spectra of $[Mn(CO)_4Br]_2$ and $[Mn(CO)_4I]_2$

It has already been mentioned that, during the course of our studies on the $Mn(CO)_5X$ derivatives, we had occasion to record the solid-state

i.r. and laser Raman spectra of $[Mn(CO)_4Br]_2$ and $[Mn(CO)_4I]_2$ in the C—O stretching and low frequency regions. In this section we wish to comment briefly on the spectra.

The solution i.r. spectra of the three $[Mn(CO)_4X]_2$ derivatives have been thoroughly investigated in the C—O stretching region by El-Sayed and Kaesz (15) and Abel and Butler (20). The former research workers have also reported data for the solid-state i.r. spectrum of the iodo-compound in the region 700–250 cm^{-1}. However apart from these studies there have been the dimers were extremely poor scatterers, 4 sharp lines were easily observable in both cases, in agreement with the group theoretical prediction for D_{2h} symmetry. There were no splittings detected in any of the lines. Although it is not strictly valid to compare frequencies from different physical states, it is apparent that there are no coincidences between the CCl_4 solution i.r. and the solid-state Raman data. The complexity of the solid-state i.r. spectra in the C—O stretching region renders a similar comparison less meaningful However even though fewer Raman

Can. J. Chem. Downloaded from www.nrcresearchpress.com by 210.87.254.42 on 09/05/12
For personal use only.

8. I. J. HYAMS, R. T. BAILEY, and E. R. LIPPINCOTT. Spectrochim. Acta, **23A**, 273 (1967).
9. L. H. JONES. J. Chem. Phys. **36**, 2375 (1962).
10. R. S. MCDOWELL, W. D. HORROCKS, JR., and J. T. YATES. J. Chem. Phys. **34**, 530 (1961).
11. W. F. EDGELL, J. W. FISHER, G. ASATO, and W. M. RISEN, JR. Inorg. Chem. **8**, 1103 (1969).
12. A. DAVISON and J. W. FALLER. Inorg. Chem. **6**, 845 (1967).
13. E. W. ABEL and G. WILKINSON. J. Chem. Soc. 1501 (1959).
14. E. O. BRIMM, M. A. LYNCH, JR., and W. S. SESNY. J. Amer. Chem. Soc. **76**, 3831 (1954).
15. M. A. EL-SAYED and H. D. KAESZ. Inorg. Chem. **2**, 158 (1963).
16. F. A. COTTON, A. MUSCO, and G. YAGUPSKY. Inorg. Chem. **6**, 1357 (1967).
17. B. F. G. JOHNSON, J. LEWIS, J. R. MILLER, B. H. ROBINSON, P. W. ROBINSON, and A. WOJCICKI. J. Chem. Soc. A, 522 (1968).
18. H. D. KAESZ, R. BAU, D. HENDRICKSON, and J. M. SMITH. J. Amer. Chem. Soc. **89**, 2844 (1967).
19. D. M. ADAMS. J. Chem. Soc. 1771 (1964).
20. E. W. ABEL and I. S. BUTLER. Trans. Faraday Soc. **63**, 44 (1967).
21. L. F. DAHL and C.-H. WEI. Acta Cryst. **16**, 611 (1963).

Can. J. Chem. Downloaded from www.nrcresearchpress.com by 210.87.254.42 on 09/05/12
For personal use only.

Can. J. Chem. Downloaded from www.nrcresearchpress.com by 210.87.254.6 on 09/05/12
For personal use only.

Equilibrium constants for σ-complex formation between cyanide ion and 1,3,5-trinitrobenzene in alcoholic solvents

E. Buncel, A. R. Norris, W. Proudlock, and K. E. Russell
Department of Chemistry, Queen's University, Kingston, Ontario

Received June 6, 1969

Equilibrium constants have been determined spectrophotometrically for the reaction of cyanide ion with 1,3,5-trinitrobenzene in methanol, ethanol, *n*- and iso-propanol, and *n*- and *t*-butanol. The equilibrium constants at 25 °C vary from 39 l mole^{-1} for the reaction in methanol to 500 000 l mole^{-1} with *t*-butanol as solvent. Enthalpy changes, determined from equilibrium measurements and by direct calorimetry, vary from 0 to −15.5 kcal mole^{-1} and the calculated entropy changes decrease from 7 to −26 cal deg^{-1} mole^{-1} as the solvent is changed from methanol to *t*-butanol. These results are interpreted on the basis that desolvation of the small cyanide ion is the primary factor influencing enthalpies and entropies of reaction. The equilibrium constant in *t*-butanol is comparable to the values observed for aprotic solvents such as chloroform and acetone.

Canadian Journal of Chemistry, 47, 4129 (1969)

Introduction

The reaction of cyanide ion with 1,3,5-trinitrobenzene in chloroform gives rise to a deep red solution which is fairly stable at low temperatures (1). Proton magnetic resonance (p.m.r.) studies (2, 3) establish the structure of the red product as the σ-complex **1** formed as in reaction [1]

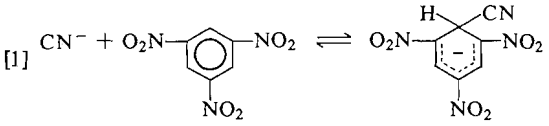

[1]

1

The complex has absorption maxima in chloroform solution at 442 mμ ($\varepsilon = 3.98 \times 10^4$ l mole^{-1} cm^{-1}) and 558 mμ ($\varepsilon = 2.24 \times 10^4$ l mole^{-1} cm^{-1}). Red solutions with similar absorption characteristics are observed in a variety of other solvents and it is considered that the σ-complex **1** is formed in all cases (1, 4). The equilibrium constant in chloroform solution at 25 °C is 3.35×10^5 l mole^{-1} and in acetone solution 1.44×10^5 l mole^{-1} (1). In this study we have investigated the effect of alcoholic solvents on the equilibrium constant and on the enthalpy and entropy changes in reaction [1]. The equilibrium constant for the reaction in *t*-butanol is very large and it is not feasible to estimate the enthalpy change from the variation of equilibrium constant with temperature. Direct calorimetric measurements of enthalpy change have therefore been made, using a solution calorimeter.

Experimental

Materials

1,3,5-Trinitrobenzene was recrystallized twice from ethanol and dried in vacuo.

Tetraphenylarsonium cyanide was prepared by adding a concentrated solution of sodium cyanide to an aqueous solution of tetraphenylarsonium chloride. The resulting tetraphenylarsonium cyanide was recrystallized twice from water in the presence of sodium cyanide, care being taken that the solution temperature did not exceed 60 °C. The compound was dried in vacuo and stored over silica gel.

Methanol and ethanol were dried over Drierite and fractionally distilled in the absence of atmospheric moisture.

n-Propanol, iso-propanol, *n*-butanol, and *t*-butanol were dried over Drierite and passed through a column of neutral alumina. They were fractionally distilled from Linde 4A molecular sieves.

Procedure

Solutions of tetraphenylarsonium cyanide and 1,3,5-trinitrobenzene were made up in an atmosphere of dry nitrogen. All flasks were sealed with silicone rubber serum caps and wrapped in aluminum foil to protect the solutions from light. In a typical experiment, 5 ml of 1,3,5-trinitrobenzene solution was placed in a quartz cell of 2 cm path length and the cell stoppered with teflon stoppers. The solution was allowed to reach the temperature of the thermostated cell compartment in the spectrophotometer and 0.1–0.5 ml solution of tetraphenylarsonium cyanide added by means of a calibrated "Repette" syringe. Spectra were determined using a Unicam SP800 spectrophotometer or occasionally Beckman DKl or DU spectrophotometers. The cell temperature was controlled to better than ±0.5 °C in the temperature range 5–45 °C. Condensation on cell windows at temperatures below 25 °C was prevented by purging with dry air or nitrogen.

Calorimetric measurements were made using a Guild Corporation Solution Calorimeter (Model 400) equipped with a base line compensator. Solvent (215 ml) was placed in the Dewar flask (capacity 250 ml). Normally

Can. J. Chem. Downloaded from www.nrcresearchpress.com by 210.87.254.6 on 09/05/12
For personal use only.

0.1–0.5 g 1,3,5-trinitrobenzene was weighed into a tube whose base consisted of a thin-walled glass bulb, and the tube and breaker inserted through the teflon cover of the Dewar flask so that the glass bulb was immersed in the solvent. After a period of not less than 1 h, 2 electrical calibrations of the heat capacity of the system were made. The glass bulb was then broken and the heat of solution of 1,3,5-trinitrobenzene in the solvent determined. To the resulting solution was added 0.04–0.18 g tetraphenylarsonium cyanide using the same procedure. In some experiments the order of addition was reversed, the heat of solution of tetraphenylarsonium cyanide being determined in the first step. The molar ratio of 1,3,5-trinitrobenzene to tetraphenylarsonium cyanide was always greater than 4:1. The initial temperature of the solvent in the calorimetric studies was close to 25 °C with all solvents except *t*-butanol for which the initial temperature was about 26.5 °C.

Results

Preliminary spectroscopic studies were performed with ethanol as solvent. The concentration of 1,3,5-trinitrobenzene was low (about 10^{-5} *M*) and a large excess of tetraphenylarsonium cyanide was added to give solutions which were 10^{-3} to 10^{-2} *M* in cyanide ion. A red color developed but the color faded rapidly to pale yellow even in the dark and no meaningful absorption spectrum could be obtained.

Addition of a small amount of tetraphenylarsonium cyanide to a large excess of 1,3,5-trinitrobenzene in ethanol solution gave a red solution whose absorbance at 435 mμ reached a maximum after a few minutes. The absorbance did not change significantly over a period of 15–20 min. The visible spectrum showed maxima at 435 and 544 mμ, the absorbance at 435 mμ being nearly twice that at 544 mμ ($\varepsilon_{435}/\varepsilon_{544} = 1.76$ for ethanol). Similar results were obtained with other alcohols; the wavelengths of the absorption maxima are given in Table I. The spectrum in each solvent is almost identical with that of the red substance formed in chloroform or acetone solution which has been shown to be the σ-complex **1** (2, 3). The 1:1 stoichiometry has been confirmed in the case of *n*-propanol as solvent by the method of continuous variations.

TABLE I

Wavelengths of absorption maxima of σ-complex **1** in various alcohols at 25 °C

Solvent	λ_{max} (mμ)	λ_{max} (mμ)
Methanol	428	540
Ethanol	435	544
n-Propanol	435	542
iso-Propanol	436	546
n-Butanol	435	540
t-Butanol	437	549

Equilibrium constants were determined by analysis of absorbance measurements at the short wavelength maximum for solutions which were initially 2–7 × 10^{-5} *M* in tetraphenylarsonium cyanide and 10^{-4}–10^{-2} *M* in 1,3,5-trinitrobenzene (TNB). For the reaction

$$[2] \qquad TNB + CN^- \rightleftharpoons TNB{\cdot}CN^-$$

the equilibrium constant

$$K = \frac{[TNB{\cdot}CN^-]}{[TNB][CN^-]}$$

If the absorbance at equilibrium in the 2 cm cell is given by *A* and the extinction coefficient for this wavelength is ε, it follows that

$$\frac{1}{K} = \frac{A}{2\varepsilon} - [CN^-]_0 - [TNB]_0 + \frac{2[CN^-]_0[TNB]_0}{A}$$

where $[CN^-]_0$, $[TNB]_0$ are the initial concentrations of cyanide ion and 1,3,5-trinitrobenzene. Following the Rose–Drago method of analysis (5), plots were made of $1/K$ vs. assumed values of ε for each set of initial concentrations of cyanide ion and 1,3,5-trinitrobenzene (Fig. 1). Values of *K* and ε were obtained from the points of intersection of the lines and error limits were based on average deviations from the mean of individual estimates of *K* and ε. Equilibrium constants were in some cases also determined from absorbances

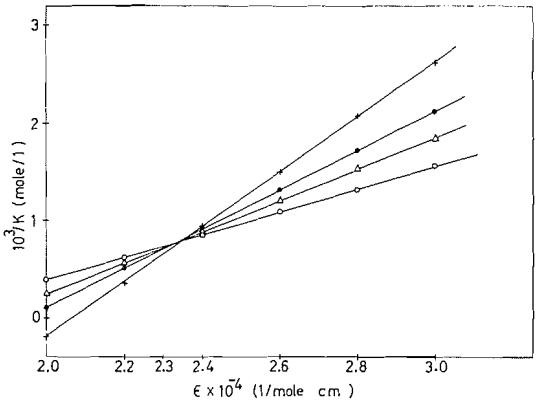

FIG. 1. Rose–Drago plot for the reaction of cyanide ion with 1,3,5-trinitrobenzene in ethanol at 25 °C. K = 1265 ± 20 l mole^{-1}; ε = 23 500 ± 300 l mole^{-1} cm^{-1}.

Can. J. Chem. Downloaded from www.nrcresearchpress.com by 210.87.254.6 on 09/05/12
For personal use only.

at the long wavelength maximum and these agreed within experimental error with values of K obtained at the short wavelength maximum.

The equilibrium constants K of reaction [1] at 25 °C and the extinction coefficients of the σ-complex at the lower wavelength maxima for the solvents methanol, ethanol, *n*-propanol, iso-propanol, *n*-butanol, and *t*-butanol are given in Table II. With methanol as solvent the low equilibrium constant results in a relatively high concentration of free cyanide, with the consequence that at 25 °C the maximum absorbance begins to decrease significantly after a period of only 2 or 3 min. The rate of fading was lower at 6 and 15 °C; maximum absorbance values were constant for over 5 min at these temperatures. Rose–Drago plots at 25 °C gave reproducible values of K, but the value of 39 ± 2 l mole^{-1} is probably less than the true value because of the fade reaction. The maximum absorbances for reactions in ethanol, *n*-propanol, iso-propanol, and *n*-butanol are not subject to significant fading under the chosen experimental conditions and the equilibrium constants are hence assigned narrow limits of error. The equilibrium constant for the reaction in *t*-butanol is very large and its value is probably not known to better than ±20% because complexing occurs to a large extent over the whole range of 1,3,5-trinitrobenzene concentrations employed.

TABLE II

Equilibrium constants K for reaction [1] at 25 °C and extinction coefficients at lower wavelength maximum

Solvent	K (l mole^{-1})	$10^{-4}\,\varepsilon$ (l mole^{-1} cm^{-1})
Methanol	39 ± 2	2.37 ± 0.02
Ethanol	1 265 ± 20	2.35 ± 0.03
n-Propanol	1 470 ± 50	2.43 ± 0.02
iso-Propanol	10 000 ± 300	2.63 ± 0.02
n-Butanol	2 020 ± 50	2.40 ± 0.03
t-Butanol	5 ± 1 × 10^5	2.60 ± 0.03

Enthalpies of reaction have been obtained from the variation of equilibrium constants with temperature over the range 6–25 °C with methanol as solvent, 15–45 °C with ethanol, and 25–45 °C with *n*-propanol and *n*-butanol. The values are recorded as ΔH_{eq}^{0} in Table III. Enthalpies of reaction determined calorimetrically ΔH_{cal} are also given in Table III. The fraction of cyanide ion converted to complex varied from 83 to close to 100% dependent on solvent and reaction conditions and the calorimetric enthalpies of reaction are based on the amount of complex formed calculated from the equilibrium constants of Table II.

The maximum concentration of tetraphenylarsonium cyanide used in the calorimetric measurements was 2×10^{-3} M and the ratio of concentrations of 1,3,5-trinitrobenzene to cyanide ion was always at least 4:1; even so, some difficulties were experienced because of secondary reactions. With ethanol as solvent, for example, the temperature of the reaction system continued to rise slowly after equilibrium should have effectively been reached and the measured heat of reaction was dependent on the concentration of free cyanide ion in the final solution. The ΔH_{cal} for ethanol was obtained by extrapolating the experimental values of ΔH to zero concentration of free cyanide ion. The reproducibility of individual values of ΔH was better than ±2% and the larger limits of error are assigned in Table III because of the difficulties with secondary reactions.

No solubility problems were encountered with the first 5 alcohols listed in Table III. With *t*-butanol as solvent, however, the 1,3,5-trinitrobenzene dissolved slowly and precipitation of the

TABLE III

Thermodynamic data for formation of σ-complex **1** at 25 °C

Solvent	$-\Delta G^0$ (kcal mole^{-1})	$-\Delta H_{eq}^{0}$* (kcal mole^{-1})	$-\Delta H_{cal}$ (kcal mole^{-1})	$-\Delta S^0$ (cal deg^{-1} mole^{-1})
Methanol	2.17	0 ± 1.5	—	−7.2 ± 5
Ethanol	4.23	6.2 ± 0.5	7.8 ± 1.5	8.7 ± 3
n-Propanol	4.32	7.1 ± 0.5	—	10.0 ± 3
iso-Propanol	5.46	—	7.1 ± 0.6	5.5 ± 3
n-Butanol	4.51	7.2 ± 0.5	7.8 ± 0.6	10.4 ± 3
t-Butanol	7.78	—	15.5 ± 1.0	25.0 ± 3

*ΔH_{eq}^{0} in methanol was calculated using equilibrium constants determined at 6, 15, and 25 °C. All other ΔH_{eq}^{0} values were calculated using equilibrium constants determined at 25, 35, and 45 °C. The larger error associated with ΔH_{eq}^{0} in methanol reflects the greater uncertainty in the equilibrium constants in this solvent due to the presence of a slow secondary reaction.

red complex occurred when the initial cyanide concentration was greater than 1.5×10^{-3} M.

Free energy changes, ΔG^0, and entropy changes, ΔS^0, for reaction [1] in the various alcoholic solvents are also given in Table III. The standard state is 1 mole l^{-1}.

Discussion

Since the concentration of tetraphenylarsonium cyanide does not exceed 0.002 M, it is probable that ion pair formation between the bulky tetraphenylarsonium ion and the cyanide ion is small in the alcohols studied. The equilibrium measurements are therefore considered to apply to the reaction between free cyanide ion and 1,3,5-trinitrobenzene. Differences of solvation of reactants and products may vary considerably from one solvent to another. The cyanide ion is small with a relatively localized negative charge and it should be strongly solvated by polar protic solvents such as methanol and ethanol (6). The charge on the σ-complex is dispersed and hydrogen bonding between the complex and polar protic solvents is probably fairly weak. Formation of the σ-complex thus requires desolvation of cyanide ion to occur and this is likely to be a major factor in determining enthalpy and entropy changes for reaction [1] in methanol. At the other extreme, *t*-butanol solvates the cyanide ion only to a limited extent and solvation effects are likely to be of minor importance.

The highest equilibrium constant observed is 5×10^5 l mole^{-1} for reaction [1] in *t*-butanol; there is a large negative enthalpy change and the effect of the enthalpy term on the equilibrium constant is only partially compensated by the large entropy decrease. Differences in solvation of reactants and products are expected to be small with *t*-butanol as solvent. It might therefore be anticipated that the reaction of cyanide ion with 1,3,5-trinitrobenzene to give the σ-complex in a weakly interacting solvent would be characterized by a high equilibrium constant, a large enthalpy of reaction (~ -15 kcal mole^{-1}) and a large negative entropy change (~ -25 cal deg^{-1} mole^{-1}). Values of ΔH and ΔS of this order of magnitude are associated with σ-complex formation in chloroform and acetone[1].

The other alcoholic solvents possess OH groups which are considerably less shielded by methyl groups and solvation by these alcohols has a considerable effect on the equilibrium constant. The equilibrium constant in methanol at 25 °C is some 10 000 times smaller than in *t*-butanol; for the former, the enthalpy change is approximately zero and the entropy change is small and positive. The most important reason for the striking behavior of methanol as solvent is the solvation of the small cyanide ion. Apparently a large positive enthalpy change accompanies the reduction in solvation as the σ-complex is formed. There is a simultaneous decrease in order, and, although methanol has some structure, the overall result is a much more positive entropy change for the reaction in methanol than in *t*-butanol.

The equilibrium constants at 25 °C in ethanol, *n*-propanol, and *n*-butanol are all in the range 1000–2000 l mole^{-1} at 25 °C. The heats of reaction are -7 ± 1.5 kcal mole^{-1} and the entropy changes -9 ± 3 cal deg mole^{-1}. They thus show intermediate behavior between the 2 extremes of methanol and *t*-butanol. Desolvation of the cyanide ion appears to be the main factor causing a decrease in equilibrium constant from the value in *t*-butanol, but the effect is smaller than in methanol and there is a slight trend towards larger equilibrium constants as the size of the alkyl group is increased. As judged by the equilibrium constant, the solvating effect of iso-propanol is significantly weaker than that of the normal alcohols. It was anticipated that the equilibrium constant of 10 000 l mole^{-1} would be associated with a heat of reaction of about -9 kcal mole^{-1}. The lower observed value was reproducible in calorimetric studies but secondary reactions at higher temperatures prevented confirmation of this heat of reaction in equilibrium studies.

The enthalpy and entropy changes recorded here for the reaction of cyanide ion with 1,3,5-trinitrobenzene in ethanol may be compared with an enthalpy change of 0.3 kcal mole^{-1} and an entropy change of 16.3 cal deg^{-1} mole^{-1} for the formation of the σ-complex between ethoxide ion and 1,3,5-trinitrobenzene in ethanol (7). The larger entropy change in the latter case may imply that desolvation of ethoxide ion in the formation of its σ-complex with 1,3,5-trinitrobenzene is greater than with cyanide ion. Ethoxide ion attacks 2,4,6-trinitrotoluene under some conditions to form almost exclusively the trinitro-

[1]A. R. Norris. Unpublished results.

Can. J. Chem. Downloaded from www.nrcresearchpress.com by 210.87.254.6 on 09/05/12
For personal use only.

benzyl anion (8).

[4] 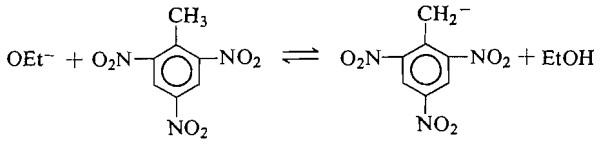

The entropy change in this reaction is 27 cal deg mole^{-1}, and this large value has been interpreted by Caldin as being largely due to desolvation of ethoxide ion (7).

We have attempted to determine whether any relationship exists between the observed solvent effects on reaction [1] and the various empirical solvent polarity parameters (9). Figure 2 shows a plot of $-\Delta G^0$ for reaction [1] at 25 °C against E_T which measures the energy of the intramolecular charge transfer transition in a pyridinium N-phenol betaine (10). It appears that the results for σ-complex formation in the 6 alcohol solvents are correlated well by the parameter E_T. The closeness of the correlation may be in part due to the fact that these solvents are all of the same general type. The significance of such correlations and the extension to other systems are being investigated.

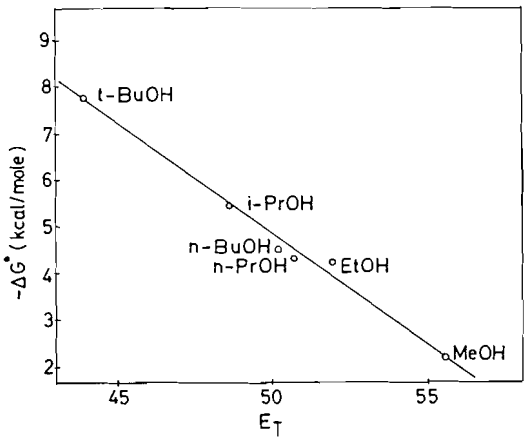

FIG. 2. Plot of $-\Delta G^0$ for reaction of cyanide ion with 1,3,5-trinitrobenzene in various alcohols at 25 °C vs. the solvent parameter E_T.

Acknowledgments

The authors are grateful to the National Research Council of Canada and the Defence Research Board of Canada for financial support of this work. The assistance of Mrs. J. Scouten in some of the calorimetric studies is gratefully acknowledged.

1. A. R. NORRIS. Can. J. Chem. **45**, 2703 (1967).
2. E. BUNCEL, A. R. NORRIS, and W. PROUDLOCK. Can. J. Chem. **46**, 2759 (1968).
3. A. R. NORRIS. Can. J. Chem. **47**, 2895 (1969).
4. E. BUNCEL, A. R. NORRIS, and K. E. RUSSELL. Quart. Rev. London, **22**, 123 (1968).
5. N. J. ROSE and R. S. DRAGO. J. Amer. Chem. Soc. **81**, 6138 (1959).
6. R. A. ALEXANDER, E. C. F. KO, A. J. PARKER, and T. J. BROXTON. J. Amer. Chem. Soc. **90**, 5049 (1968).
7. E. F. CALDIN. J. Chem. Soc. 3345 (1959).
8. E. F. CALDIN and G. LONG. Proc. Roy. Soc. London, Ser. A, **226**, 263 (1955).
9. C. REICHHARDT. Angew. Chem. Intern. Ed. Engl. **4**, 29 (1965).
10. K. DIMROTH and C. REICHHARDT. Palette, No. 11, 28 (1962).

Can. J. Chem. Downloaded from www.nrcresearchpress.com by 210.87.254.6 on 09/05/12
For personal use only.

A study of the complexing of gold(I) with tertiary phosphine, arsine, and stibine

A. D. WESTLAND
Department of Chemistry, University of Ottawa, Ottawa, Canada
Received April 29, 1969

The equilibrium

$$(Ph_3P)AuX + (n - 1)Ph_3P \leftrightarrows (Ph_3P)_nAu^+ + X^-$$

was studied in nitrobenzene solution and evidence for the occurrence of tricoordinate $(Ph_3P)_2AuX$ was obtained. The results indicate that π-bonding of phosphine to gold(I) is much stronger than that of phosphine to silver(I). Attempts to prepare tricoordinate complexes from di(tertiary)phosphine or arsine failed. Chloro- and bromo(triphenylstibine)gold(I) have been prepared. The dipole moments of Ph_3MAuX, where M = P or As, and X = Cl, Br, and I, or M = Sb and X = Br have been determined. Metal–ligand stretching frequencies are compared.

Canadian Journal of Chemistry, 47, 4135 (1969)

Can. J. Chem. Downloaded from www.nrcresearchpress.com by 210.87.254.42 on 09/05/12
For personal use only.

Triphenylphosphine and triphenylarsine form reasonably stable complexes with gold(I) but attempts to isolate a pure triphenylstibine complex have hitherto failed (1). We have now succeeded in preparing crystalline halo(triphenylstibine)gold(I) complexes containing either chlorine or bromine.

With the availability of these complexes, it became possible to examine dipole moments and bond stretching frequencies of the series of complexes containing P, As, and Sb as ligand donor atoms. The complexing ability of the ligands Ph_3P, Ph_3As, and Ph_3Sb falls off with increasing size of the donor atom. It was hoped that one could study the equilibria

$$LAuX + (n - 1)L \leftrightarrows L_nAu^+ + X^-$$

where L is one of the above ligands. However, the equilibria lay so far toward the left hand side of the equation that it was possible to obtain sufficiently accurate results only with triphenylphosphine.

These studies enable us to make some inferences about the nature of the bonding in these complexes, i.e., the relative importance of π-bonding with gold(I).

Experimental

Preparation of Complexes

Chloro(triphenylstibine)gold(I)

Chloroaurous acid trihydrate (3 g) was dissolved in ethanol (50 cc) and triphenylstibine (3.82 g, 1.05 equivalent) was added. The solution was heated on the steam bath until it became colorless. The solution was then allowed to cool and a white precipitate of crude $Ph_3SbAuCl$ was separated by filtration. The product was recrystallized from tetrahydrofuran by addition of petroleum ether (30–60°) and white needles decomposing at 90° were obtained in 28% yield. Colloidal gold appeared slowly in the dark and rapidly when the product was exposed to light. The compound was best preserved at low temperature.

Anal. Calcd. for $C_{18}H_{15}AuClSb$: C, 36.93; H, 2.58; Cl, 6.05. Found: C, 36.92; H, 2.66; Cl, 6.20.

Bromo(triphenylstibine)gold(I)

Crude chloro(triphenylstibine)gold(I) (0.5 g) was dissolved in benzene using no heat. Concentrated hydrobromic acid (1.1 cc) was added immediately[1] whereupon the solution began to turn dark blue. Thin layer chromatography was used to determine when all of the starting material had been converted (about 10 min). The aqueous layer was separated and the benzene solution washed twice with water. The benzene solution was dried with sodium sulfate and evaporated to dryness. The residue was recrystallized from tetrahydrofuran by the addition of petroleum ether. The product (white needles) was much more stable than the chloro compound. A yield of 43.5% was obtained.

Anal. Calcd. for $C_{18}H_{15}AuBrSb$: C, 34.32; H, 2.40; Br, 12.69. Found: C, 34.60; H, 2.17; Br, 12.82.

Halo Complexes of Triphenylphosphine and Triphenylarsine

Halo complexes containing triphenylphosphine and triphenylarsine were prepared by a method of which the following example is typical.

Bromo(triphenylphosphine)gold(I). Chloro(triphenylphosphine)gold(I) (1 g) was dissolved in warm acetone (50 cc) and concentrated hydrobromic acid (2.5 cc) added. Evaporation of the solvent under reduced pressure and cooling gave white crystals (m.p. 250–251°) in 92% yield.

Anal. Calcd. for $C_{18}H_{15}AuBrP$: C, 40.10; H, 2.80; Br, 14.82. Found: C, 40.32; H, 2.82; Br, 14.67.

The melting points and analytical data of the other compounds are as follows.

Ph_3PAuI: m.p. 230–231°. Anal. Calcd. for $C_{18}H_{15}AuIP$: C, 36.88; H, 2.58; I, 21.65. Found: C, 37.21; H, 2.65; I, 22.02.

$Ph_3AsAuCl$: m.p. 219–220°. Anal. Calcd. for $C_{18}H_{15}AsAuCl$: C, 40.14; H, 2.81; Cl, 6.58. Found: C, 41.03; H, 2.70; Cl, 6.66.

[1]Benzene solutions of the chloro complex are very unstable and rapidly turn brown.

Can. J. Chem. Downloaded from www.nrcresearchpress.com by 210.87.254.42 on 09/05/12
For personal use only.

$Ph_3AsAuBr$: m.p. 224–225°. Anal. Calcd. for $C_{18}H_{15}AsAuBr$: C, 37.08; H, 2.59; Br, 13.70. Found: C, 37.25; H, 2.42; Br, 13.56.

Ph_3AsAuI: m.p. 201–202°. Anal. Calcd. for $C_{18}H_{15}AsAuI$: C, 34.31; H, 2.40; I, 20.14. Found: C, 34.51; H, 1.81; I, 20.37.

Bis(triphenylphosphine)gold(I) Fluoroborate

Chloro(triphenylphosphine)gold (0.25 g) was dissolved in acetone (50 cc) and the solution cooled to 0 °C. Crystals of $AgBF_4$ (0.202 g) and Ph_3P(0.132 g) were added and a precipitate of AgCl separated by filtration. Evaporation of the filtrate gave an oil which crystallized upon adding MeOH. Recrystallization gave a white product (m.p. 234–236°) in 66% yield.

Anal. Calcd. for $C_{36}H_{30}AuBF_4P_2$: C, 53.49; H, 3.74. Found: C, 53.44; H, 3.70.

Dichloro-μ-1,2-bis(diphenylphosphino)ethanedigold(I)

Chloroauric acid trihydrate (1 g) in water (8 cc) was diluted with ethanol (50 cc) and the solution warmed on the steam bath. Excess ligand 1,2-bis(diphenylphosphino)-ethane (2 g) was added and the warming continued until the yellow color had disappeared and a white product (m.p. 276–279°) was collected in 83% yield. This was slightly soluble in warm chloroform and in warm acetone.

Anal. Calcd. for $C_{26}H_{24}Au_2Cl_2P_2$: C, 36.17; H, 2.80; Cl, 8.21. Found: C, 36.33; H, 2.94; Cl, 8.05.

Dichloro-μ-1,2-bis(diphenylarsino)ethanedigold(I)

This was prepared in the same way as the preceding compound in 84% yield (m.p. 221–224°) and it had similar properties.

Anal. Calcd. for $C_{26}H_{24}As_2Au_2Cl_2$: C, 32.83; H, 2.54. Found: C, 32.13; H, 2.53.

Dichloro-μ-1,2-bis(diphenylphosphino)acetylenedigold(I)

This was prepared in the same way as the preceding compounds in 95% yield (m.p. 262–265°). The C≡C stretch appeared in the infrared (i.r.) spectrum weakly at 2340 cm^{-1}.

Anal. Calcd. for $C_{26}H_{20}Au_2Cl_2P_2$: C, 36.35; H, 2.35. Found[2]: C, 36.35; H, 2.54.

The molar conductivity of 5×10^{-4} *M* solutions in nitrobenzene of each of the above compounds except $[(Ph_3P)_2Au]BF_4$ was less than 0.5 mho cm^2.

Conductivity Measurements

Measurements were carried out at 25 °C. using an Industrial Instruments, Inc., Model RC18 conductivity bridge. The solvent was redistilled nitrobenzene which had a specific conductivity of less than 0.1×10^{-6} mho. The equilibria were investigated over a range of total gold concentrations from 1×10^{-4} to 2×10^{-3} *M* and excess triphenylphosphine concentrations up to 0.1 *M*. Conductivities were corrected for a small contribution to the conductivity, probably due to an impurity, which was introduced by the triphenylphosphine. Conductivities reached a steady value in the time it took to prepare a sample solution for measurement.

Dipole Moment Measurements

A Wissenschaftlich–Technische Werkstätten Dipolmeter Model DM-01 was used for measuring dielectric constants of solutions at 25 °C. Measurements were made on benzene or dioxane solutions. Benzene was employed wherever possible, but solutions of $Ph_3SbAuBr$ and Ph_3AsAuI in this solvent were unstable. The dipole moments were calculated by the method of Smith (2). Refractive indices were measured at 25 °C with an Abbé refractometer, but the term involving refractive index in the equation for dipole moment was negligible in all cases.

Infrared Spectra

Infrared spectra in the range 600–200 cm^{-1} were carried out using a Beckman Instruments Model IR-12 spectrometer. The complexes were contained in cesium iodide pellets.

Results and Discussion

Examination of Solution Equilibria

The addition of triphenylphosphine to a solution of $(Ph_3P)AuX$ produced an electrolyte, and when the concentration of ligand was raised to about 0.1 *M*, the specific conductivity appeared to be close to reaching a limiting value corresponding, presumably, to the process

$$LAuCl + (n - 1)L \leftrightarrows L_nAu^+ + X^-$$

where $L = Ph_3P$.

The limiting value referred to was obtained for several concentrations of gold by a graphical extrapolation of the quantity κ^{-1} plotted against $\kappa/[L]^2$ which was found empirically to be satisfactory, as the plot was either linear or only slightly curved. The value of κ^{-1} reached its limiting value at $\kappa/[L]^2 = 0$. The values of κ so obtained were used to construct a plot of the molar conductivity of L_nAuX against $\sqrt{c}$ (c =

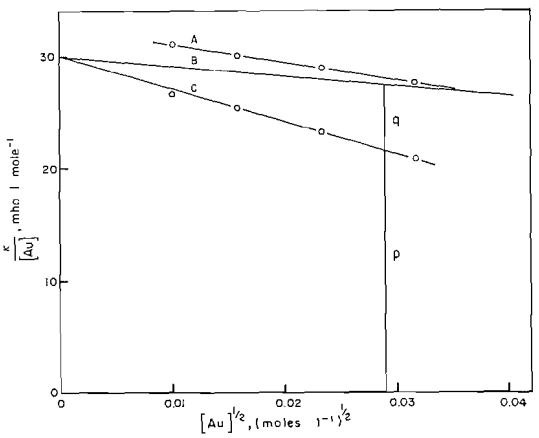

FIG. 1. Plots of molar conductivity against (concentration)$^{\frac{1}{2}}$. *A*, $[(Ph_3)_2Au]BF_4$; *B*, theoretical line (Robinson and Stokes equation); *C*, system: Ph_3PAuCl plus excess Ph_3P.

[2]Microanalyses were performed by the firm of A. Bernhardt, Elbach, West Germany.

Can. J. Chem. Downloaded from www.nrcresearchpress.com by 210.87.254.42 on 09/05/12
For personal use only.

concentration of gold complex). This is shown in Fig. 1 as curve *C*.

It was assumed that the molar conductivity of L_nAuX, if completely ionized, would be given by the limiting law equation as modified by Robinson and Stokes (3). This is shown as curve *B* in Fig. 1. The fraction $p/(p + q)$ is then the degree of dissociation at concentration *c*. Curve *A* shows a plot for $[Ph_3P)_2Au]BF_4$ which is similar to the Robinson–Stokes line. The association may be due to outer sphere ion-pairing. Fuoss' treatment predicts for the chloride an equilibrium constant $K = \alpha^2 c/(1 - \alpha)$ of 0.045 mole l^{-1}. For $c = 5 \times 10^{-4}$ this gives a degree of dissociation, α, of 0.9, which is in good agreement with the observed value of 0.84.

The data shown in Fig. 1 enabled us to relate conductivities of samples to their ion and ion-pair concentrations. The expression

$$K_{n-1} = \frac{[L_nAu^+][X^-]}{\{[Au_t] - [L_nAu^+] - [L_nAuX]\}[L]^{n-1}}$$

may be rearranged to

$$\frac{[L_nAu^+]}{[L]^{n-1}} = K_{n-1}\left\{\frac{[Au_t] - [L_nAuX]}{[L_nAu^+]} - 1\right\}$$

where $[Au_t]$ represents the total gold concentration.

It follows that a plot of $[L_nAu^+]/[L]^{n-1}$ against $1/[L_nAu^+]$ will be very nearly a straight line if *n* is a unique constant and $[L_nAuX]$ is small relative to $[L_nAu^+]$. These conditions are met for the chloro compound when the concentrations of Ph_3P are relatively large and *n* is set equal to 3. A plot of the data is shown in Fig. 2. For small concentrations of excess ligand, *n* tends toward 2.

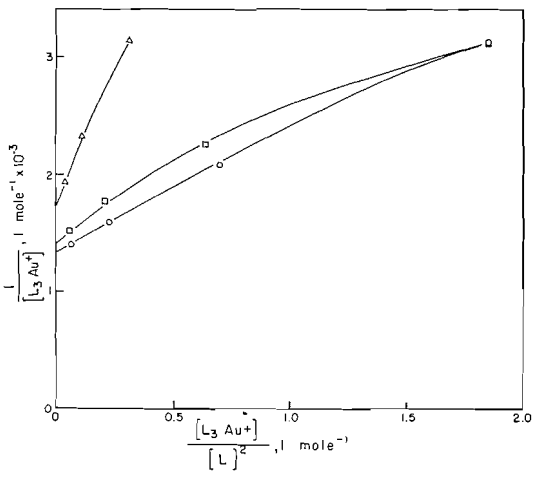

FIG. 2. Plots which illustrate second order dependence upon concentration of excess ligand. Total gold concentrations: 1×10^{-3} *M*. ○, Ph_3PAuCl; □, Ph_3PAuBr; Δ, Ph_3PAuI.

By substituting in the equilibrium expression, approximate values of K_{n-1} for $n = 3$ were obtained. These were not quite constant for the chloro compound and showed large variations for the bromo and iodo compounds. Limiting values were obtained by plots of the approximate *K* values against $[L_nAu^+]/[L]$ and extrapolating to infinite ligand concentration. The results are given in Table I.

TABLE I

Equilibrium constants for the addition of triphenylphosphine to $(Ph_3P)AuX$

Compound	$K_1 \times 10^{-2}$	K_2 (m/l)	$\frac{K_1}{K_2}$	$\frac{K_1^2}{K_2} \times 10^{-4}$
$(Ph_3P)AuCl$	7±1	1.5±0.1	480	33
$(Ph_3P)AuBr$	3.0±0.2	3.7±0.1	83	2.4
$(Ph_3P)AuI$	2.2±0.2	>35	<6.3	<0.14

The variation in apparent values of *K* is evidently due to the intermixing of the equilibrium with $n = 2$, resulting in the formation of some L_2Au^+ ions. Meyer and Allred have commented upon the existence of $[(Ph_3P)_2Au^+]Cl^-$ both in solution and in the crystalline state (4). Compounds in which univalent gold assumes a coordination number of 3 and 4 have been reported (5–10) even though 2 is the usual number. This equilibrium is of decreasing importance as $[L_nAu^+]/[Ph_3P]$ approaches zero.

An attempt was made to estimate K_1, i.e., *K* for $n = 2$. It was assumed that the ionic conductivity of L_2Au^+ was about the same as that of L_3Au^+ and hence the measured values of the concentration of ionic gold were in fact $[L_3Au^+] + [L_2Au^+]$. From the value of K_2, $[L_3Au^+]$ was calculated for each concentration of ligand. The limit of K_1 as $[Ph_3P]$ approached zero was then taken to be the best value. The assumption made is at best an approximation, so the values of K_1 have significance only in relation to one another. Values for the bromo and iodo compounds and a lower limit for the chloro compound appear in Table I.

The quotient K_1/K_2 is the equilibrium constant which refers to the addition of the third mole of

Ph_3P to the ion L_2Au^+ or to L_2AuX, i.e.

$$\frac{K_1}{K_2} = \frac{[L_2Au^+][L]}{[L_3Au^+]}$$

or

$$\frac{K_1}{K_2} = \frac{[L_2AuX][L]}{[L_3Au^+][X^-]}$$

If the first of these two expressions is valid, K_1/K_2 should be independent of the choice of halogen in the starting compound. The values shown in Table I show that this is not the case. We conclude that the undissociated complex, L_2AuCl, is present in appreciable concentrations. The values of K_1 for the bromo and iodo complexes are not greatly different, which indicates that for these systems, very little ionization occurs until the addition of the third molecule of Ph_3P.

Ahrland and Chatt have observed that only three monotertiary phosphine molecules can be added to Ag^+ ion even though it is normal for four monodentate groups to add (11). They attribute this difference to the important role of π-bonding in the phosphine complexes. Their theoretical arguments to support this have been discounted (12), but the empirical evidence that typical π-bonding ligands seem to prefer lower coordination numbers with d^{10} ions appears to be significant. The present stability studies of gold(I) phosphine complexes are of interest in view of the paucity of information available on π-bonding in gold(I) compounds.

For reasons referred to above, Ahrland and Chatt state that the value of the ratio of the equilibrium constants for the successive addition of ligand molecules to Ag^+ ion is an indication of the degree of π-bonding. They obtained a large ratio $K_1/K_2 = 160$ for the first and second additions, respectively.

In our experiments, the addition of the additional ligand molecules is accompanied by the breaking of a gold–halogen bond. For this reason we have defined K_2 for our gold complexes in a different way. Ahrland and Chatt's ratio now becomes $K_1/(K_2/K_1)$ or K_1^2/K_2. These values are given in Table I. They show a variation because of the increasing difficulty of breaking the gold–halogen bond in the order Cl < Br < I. The very large ratios of K_1^2/K_2 indicate that π-bonding is of great importance in bonding triphenylphosphine to gold.

Reaction of $Ph_2PC_2H_4PPh_2$ and the corresponding arsine with $HAuCl_4$ did not lead to tricoordinate complexes of the type (chel)AuCl. Instead, the stoichiometry of the products suggests that the ligand served as a bridge between two Au—Cl units. The properties of the complex formed from $Ph_2PC{\equiv}CPPh_2$, which cannot serve as chelating ligand, were almost identical with those of the more flexible ligands. Thus, gold(I) is asserting its tendency toward 2-coordination in these reactions.

Dipole Moments

Attempts to prepare iodo(triphenylstibine)gold were unsuccessful. Only the bromo complex was stable enough to permit a determination of the dipole moment. The dipole moments are given in Table II. Owing to their instability in benzene solution, some of the complexes had to be examined in dioxane. The solubility in this solvent was very low so that the values are probably not so precise as those obtained with benzene.

TABLE II

Dipole moments of the compounds Ph_3MAuX

Compound	Dipole moments (D) in Benzene	Dipole moments (D) in *p*-Dioxane
Ph_3PAuCl	9.0	
Ph_3PAuBr	8.6	
Ph_3PAuI	8.2	
$Ph_3AsAuCl$	8.9	9.9
$Ph_3AsAuBr$	8.5	9.1
Ph_3AsAuI		8.6
$Ph_3SbAuBr$		8.5

It can be seen that the dipole moment of LAuCl, LAuBr, and LAuI vary in the order Cl > Br > I which is the normal order for halogenated hydrocarbons for example. Jensen's values for *cis* complexes of platinum are: $(Et_3P)_2PtCl_2$, 10.7 D; $(Et_3P)_2PtBr_2$, 11.2 D; and $(Et_3P)_2PtI_2$, 8.2 D (13). For *trans*-$(Et_3P)_2PtRX$, where R is an alkyl group, the order is Cl < Br < I (14). In the series of platinum compounds there is uncertainty about the bond angles and hence about the distribution of charge, but it appears that chlorine is not decidedly more negative than the other halogen atoms. Parshall has suggested that the halogens may be π-donors toward platinum and his results indicate that chlorine should be a stronger donor than bromine (15).

Gold with an oxidation state of only 1 will be a much poorer acceptor of π-electron density and

Can. J. Chem. Downloaded from www.nrcresearchpress.com by 210.87.254.42 on 09/05/12
For personal use only.

Can. J. Chem. Downloaded from www.nrcresearchpress.com by 210.87.254.42 on 09/05/12
For personal use only.

TABLE III

Infrared frequencies of the complexes LAuX in the range 600–200 cm^{-1}

Compound	Band frequencies, cm^{-1}*									
Ph_3PAuCl	619 (w),	548 (vs),	507 (sh),	503 (vs),	448 (w),†	438 (sh),	431 (sh),	330 (sh),‡	320 (sh)	
Ph_3PAuBr	620 (w),	549 (vs),	507 (vs),	449 (s),†	332 (w),	320 (w),	326 (s)‡			
$Ph_3AsAuCl$	481 (s),	470 (vs),	367 (w),†	338 (sh),‡	330 (vs)					
$Ph_3AsAuBr$	545 (w),	500 (w),	472 (sh),	467 (vs),	352 (s),†	332 (vs),	235 (vs)‡			
$Ph_3SbAuCl$	547 (s),	503 (s),	462 (vs),	451 (vs),	444 (sh),	333 (vs),‡	291 (vs),	272 (vs),	232 (w),†	220 (w)
$Ph_3SbAuBr$§	457 (vs),	309 (w),	274 (vs),	250 (sh),	230 (w),†	220 (sh)				

*s = strong, m = medium, w = weak, v = very, sh = shoulder.
†Tentative assignment of the M—Au stretching frequency.
‡Au—X stretching frequency.
§The expected intense Au—Br stretching band was not observed. The very weak shoulder at 250 cm^{-1} may be due to Au—Br stretching.

thus the Au—X bond should be of nearly pure σ-character. The very large values of dipole moment suggest, moreover, that the Au(I)—X bond is much more polar than the Pt(II)—X bond.

The moments of Ph_3PAuBr, $Ph_3AsAuBr$, and $Ph_3SbAuBr$ are interrelated in an almost identical way to those of the corresponding *cis*-platinum compounds. Chatt and Wilkins obtained the following values: $(Et_3P)_2PtCl_2$, 10.9 D; $(Et_3As)_2PtCl_2$, 10.9 D; and $(Et_3Sb)_2PtCl_2$, 10.45 D (16). These values would be expected to get progressively larger in the sequence $P \rightarrow As \rightarrow Sb$ if some counteracting influence were not present. If π-bonding in the M—Pt bond becomes progressively more important in this sequence a near constancy of the dipole moment values might well result. We have previously given independent evidence of such a trend (17). The present results with gold complexes indicate that very similar bonding influences are involved.

Infrared Spectra

The i.r. frequencies observed in the range 600–200 cm^{-1} are listed in Table III. The Au—X stretching frequencies were identified fairly easily by comparison of the corresponding chloro and bromo compounds. In the case of $Ph_3AsAuCl$, however, a band characteristic of triphenylarsine falls in the range expected for Au—Cl stretching. The band for this compound at 330 cm^{-1} with an indication of a shoulder at 338 cm^{-1} is probably therefore a composite band. The Au—X stretching frequencies for Ph_3PAuCl and Ph_3PAuBr have previously been reported (18).

The Au—X stretching frequencies show only a slight dependence on the nature of the other ligand. This is similar to the behavior of *cis*-$(R_3M)_2PtCl_2$ and *cis*-$(R_3M)_2PtBr_2$ (19).

The assignment of the Au—M stretching frequencies is less certain owing to the fact that their intensities are subject to wide variation. We note that these bands are weak for the chloro complexes but moderately strong for the bromo analogues.

Acknowledgments

The author wishes to express his thanks to Miss M. Flett for technical assistance and to the National Research Council of Canada for a grant in aid of research.

1. A. S. KASENALLY, J. LEWIS, A. R. MANNING, J. R. MILLER, R. S. NYHOLM, and M. H. B. STODDARD. J. Chem. Soc. 3407 (1965).
2. J. W. SMITH. Trans. Faraday Soc. **46**, 394 (1950).
3. R. A. ROBINSON and R. H. STOKES. J. Amer. Chem. Soc. **76**, 1991 (1954).
4. J. M. MEYER and A. L. ALLRED. J. Inorg. Nucl. Chem. **30**, 1328 (1968).
5. R. S. NYHOLM. Nature, **168**, 705 (1951).
6. W. COCHRAN, F. A. HART, and F. G. MANN. J. Chem. Soc. 2816 (1957).
7. M. DAVIS and F. G. MANN. J. Chem. Soc. 3791 (1964).
8. L. MALATESTA, L. NALDINI, G. SIMONETTA, and F. CARIATI. Coord. Chem. Rev. **1**, 255 (1966).
9. C. KOWALA and J. M. SWAN. Aust. J. Chem. **19**, 547 (1966).
10. A. J. CARTY and A. EFRATY. Inorg. Chem. **8**, 543 (1969).
11. S. AHRLAND and J. CHATT. Chem. Ind. London, 96 (1955).
12. F. A. COTTON. J. Chem. Soc. 5269 (1960).
13. K. A. JENSEN. Z. Anorg. Allg. Chem. **229**, 250 (1936).
14. J. CHATT and B. L. SHAW. J. Chem. Soc. 4020 (1959).
15. G. W. PARSHALL. J. Amer. Chem. Soc. **86**, 5367 (1964).
16. J. CHATT and R. G. WILKINS. J. Chem. Soc. 4300 (1952).
17. A. D. WESTLAND. J. Chem. Soc. 3060 (1965).
18. G. E. COATES and C. PARKIN. J. Chem. Soc. 421 (1963).
19. D. M. ADAMS, J. CHATT, J. GERRATT, and A. D. WESTLAND. J. Chem. Soc. 734 (1964).

Can. J. Chem. Downloaded from www.nrcresearchpress.com by 210.87.254.42 on 09/05/12
For personal use only.

Can. J. Chem. Downloaded from www.nrcresearchpress.com by 210.87.254.6 on 09/05/12
For personal use only.

Binuclear copper(II) complexes of the tetradentate ligand 1,4-di(2′-pyridyl)aminophthalazine: some novel five-coordinate derivatives

L. K. THOMPSON, V. T. CHACKO, J. A. ELVIDGE[1], A. B. P. LEVER, AND R. V. PARISH[2]
Department of Chemistry, York University, Downsview, Toronto, Ontario

Received May 7, 1969

Reaction of the title ligand (L) with copper salts leads to the formation of three principal series of compounds, $LCu_2X_3(OH)\cdot H_2O$ (X = Cl, Br), $LCu_2(RCO_2)_3$, and $LCu_2(RCO_2)_4$, where RCO_2 represents various aliphatic and aromatic carboxylate species. Magnetic data, electronic spectroscopic data both at room temperature and at −196 °C, infrared spectra, and microanalytical data are correlated to reveal that these complexes contain a binuclear copper–copper system in which the copper atoms are 5-coordinate and square pyramidal. Brief details are presented of an X-ray structural analysis of the chloride complex confirming the structure proposed. The ligand forms complexes both in its neutral form and in an anionic deprotonated form. The ultraviolet spectra of the complexes distinguish these modes of bonding. The electronic spectra are discussed in terms of the 5-coordinate square pyramidal copper chromophore deemed to be present. In the complex L_2Cu, the copper atom has a trigonally distorted 6-coordinate environment with tridentate anionic ligand.

Canadian Journal of Chemistry, **47**, 4141 (1969)

The ring expansion of 1,3-di(2′-pyridyl)-iminoisoindoline with hydrazine hydrate yields the novel ligand 1,4-di(2′-pyridyl)aminophthalazine L (**1**). This ligand has the unusual property

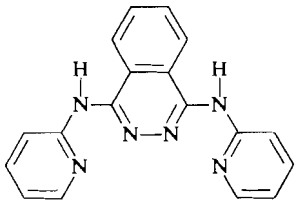

1

of preferentially combining with 2 metal atoms to yield binuclear derivatives of the general formula LM_2X_n, where X is a halogen or carboxylate group, *n* is commonly 3 or 4, and M is Co(II), Ni(II), or Cu(II). Of these the copper(II) complexes were most extensively studied, and form the content of this paper. Very recently a closely related ligand 1,4-di(hydrazinyl)phthalazine has been reported (1) to yield binuclear derivatives of nickel.

Experimental

Magnetic susceptibility measurements were obtained using a Newport Magnetic (Gouy) balance. Mercury tetrathiocyanatocobaltate(II) was used as calibrant. Infrared (i.r.) spectra were obtained with Perkin–Elmer 21, 257, and 125 spectrophotometers and electronic spectra with an "Optika" CF_4 double beam grating instrument and a Cary 14 instrument. Molecular weight data were obtained with a "Mechrolab" series 300 osmometer, and a Gallenkamp model 7665K semimicro-ebulliometer. In the latter case, measurements were made over the concentration range 0.02 to 0.14 *M* and the molecular weight estimated graphically. Conductivity measurements were made using a Cambridge instruments conductivity bridge or a Wayne Kerr B221A bridge. Copper was determined as $CuPy_2(NCS)_2$. C, H, and N analyses were carried out in part by the Microanalytical Laboratory of the University of Manchester Institute of Science and Technology under the direction of Mr. Manohin, and in part by Galbraith Laboratories, Knoxville, Tenn. (see Table I). L is 1,4-di(2′-pyridyl)-aminophthalazine.

Preparation and Characterization of the Ligand L

1,3-di(2′-pyridyl)-iminoisoindoline (2) (4 g) was refluxed in methanol (200 ml) for ½ h, and the solution then filtered from undissolved material. Some crystallization usually occurred and hence the filtrate was refluxed once more until a clear yellow solution was obtained (charcoal if necessary). A solution of hydrazine hydrate (10 ml, 64%) was added to the hot solution and the mixture allowed to stand at room temperature overnight. Yellow crystals, m.p. 205° (4 g, 96%) were obtained. Other solvents were investigated for the hydrazine reaction. Methanol gives the highest yield but ethanol gives a very much larger crystalline form. The product was sublimed at 190°/10^{-6} mm and the sublimate recrystallized from acetone, m.p. 210°.

Anal. Calcd. for $C_{18}H_{14}N_6$ (mol. wt. 314): C, 68.8; H, 4.5; N, 26.7. Found (mol. wt. 306): C, 68.45; H, 4.65; N, 27.1.

Nitrate Salt

The ligand, L, was recrystallized twice from 0.5 *N*

[1]Present address: University of Surrey, Guildford, England.
[2]Present address: University of Manchester Institute of Science and Technology, Manchester, England.

TABLE I

Analyses of complexes

Compound	Source	Analytical data (%) C	H	N	Cu	X
$Cu_2L(CH_3COO)_3$	Found	47.0	3.7	13.9	21.1	
$C_{24}H_{22}Cu_2N_6O_6$	Calcd.	46.8	3.6	13.6	20.6	
$Cu_2L(CH_3CH_2COO)_3$	Found	49.4	4.5	13.2	19.7	
$C_{27}H_{28}Cu_2N_6O_6$	Calcd.	49.2	4.25	12.7	19.3	
$Cu_2L(CH_3CH_2CH_2CH_2COO)_3$	Found	53.0	5.7	11.6	16.95	
$C_{33}H_{40}Cu_2N_6O_6$	Calcd.	53.4	5.25	11.3	17.1	
$Cu_2L((CH_3)_2CHCOO)_3$	Found	51.6	4.9	12.2	18.2	
$C_{30}H_{34}Cu_2N_6O_6$	Calcd.	51.4	4.85	12.0	18.1	
$Cu_2L(CH_2{=}CHCOO)_3$	Found	49.6	3.7	13.1	19.3	
$C_{27}H_{22}Cu_2N_6O_6$	Calcd.	49.6	3.4	12.8	19.5	
$Cu_2L(CH_2{=}CHCH_2COO)_3$	Found	52.0	4.2	12.4	18.05	
$C_{30}H_{28}Cu_2N_6O_6$	Calcd.	51.9	4.0	12.1	18.25	
$Cu_2L(CH_2{=}CHCH_2CH_2COO)_3$	Found	53.5	4.5	11.6	17.3	
$C_{33}H_{34}Cu_2N_6O_6$	Calcd.	53.7	4.6	11.4	17.2	
$Cu_2L((CH_3)_2CH{\cdot}CH_2COO)_3$	Found	53.1	5.5	11.2	17.0	
$C_{33}H_{40}Cu_2N_6O_6$	Calcd.	53.3	5.5	11.3	17.1	
$Cu_2L(C_6H_5COO)_3$	Found	58.2	3.5	10.3	15.6	
$C_{39}H_{28}Cu_2N_6O_6$	Calcd.	58.4	3.6	10.4	15.8	
$Cu_2L(C_6H_5COO)_3OMe{\cdot}MeOH$*	Found	54.1	4.1		14.7	
$C_{41}H_{36}Cu_2N_6O_8$	Calcd.	54.0	4.3	9.7	14.6	
$Cu_2L(m\text{-}Cl{-}C_6H_4COO)_3OMe{\cdot}MeOH$*	Found	50.6	3.5		13.1	
$C_{41}H_{33}Cu_2Cl_3N_6O_8$	Calcd.	50.7	3.4	8.65	13.1	
$Cu_2L(HCOO)_4$*	Found	42.7	3.1	13.7	20.2	
$C_{22}H_{18}Cu_2N_6O_8$	Calcd.	42.6	2.9	13.5	20.5	
$Cu_2L(ClCH_2COO)_4$*	Found	38.7	2.7	10.8	15.7	
$C_{26}H_{22}Cl_4Cu_2N_6O_8$	Calcd.	38.4	2.7	10.6	15.7	
$Cu_2L(Cl_2CH{-}COO)_4$*	Found	32.6	1.9	9.1	13.1	
$C_{26}H_{18}Cl_8Cu_2N_6O_8$	Calcd.	32.8	1.9	8.8	13.3	
$Cu_2L(Cl_3C{-}COO)_4$*	Found	28.8	1.6	7.5	11.4	
$C_{26}H_{14}Cl_{12}Cu_2N_6O_8$	Calcd.	28.6	1.3	7.7	11.6	
$Cu_2L(F_3C{-}COO)_4$*	Found	35.1	1.6	9.2	14.2	
$C_{26}H_{14}Cu_2F_{12}N_6O_8$	Calcd.	35.0	1.6	9.4	14.2	
CuL_2	Found	62.6	3.8		9.2	
$C_{36}H_{26}N_{12}Cu$	Calcd.	62.6	3.8		9.2	
$Cu_2LCl_3(OH)(H_2O)$*	Found	36.9	3.2	13.8		18.7
$C_{18}H_{17}Cl_3Cu_2N_6O_2$	Calcd.	37.1	2.9	14.4	21.8	18.2 (Cl)
$Cu_2LBr_3(OH)(H_2O)$*	Found	30.3	2.35	11.8	17.7	33.4
$C_{18}H_{17}Br_3Cu_2N_6O_2$	Calcd.	30.2	2.4	11.7	17.7	33.5 (Br)
$Cu_2L(IO_3)_3(OH)(H_2O)_3$*	Found	20.7	2.5	8.3	11.7	36.4
$C_{18}H_{21}Cu_2I_3N_6O_{13}$	Calcd.	20.8	2.0	8.1	12.2	36.7 (I)

*Contains neutral ligand $C_{18}H_{14}N_6$. The other complexes contain the anionic ligand $C_{18}H_{13}N_6$.

nitric acid, yielding the dinitrate, (m.p. 187°, decomp.). It was dried at 50°/15 mm.

Anal. Calcd. for $L{\cdot}2HNO_3$: C, 49.1; H, 3.7. Found: C, 48.7; H, 3.5.

Dichromate Salt

The ligand L (48 mg) was dissolved in 2 *N* hydrochloric acid (15 ml), and sodium dichromate solution (50 mg in 5 ml H_2O) added to the solution. A yellow precipitate of $L{\cdot}H_2Cr_2O_7$ (78 mg, 100%) was produced. The product decomposes if recrystallized.

Anal. Calcd. for $C_{18}H_{16}N_6Cr_2O_7$: C, 40.6; H, 3.0; N, 15.8. Found: C, 40.8; H, 3.0; N, 16.0.

The dichromate salt may be used analytically to estimate the quantity of ligand in a metal complex. (N.B. if H_2O_2 was added to the acid solution followed

Can. J. Chem. Downloaded from www.nrcresearchpress.com by 210.87.254.6 on 09/05/12
For personal use only.

Can. J. Chem. Downloaded from www.nrcresearchpress.com by 210.87.254.6 on 09/05/12
For personal use only.

by addition of sodium dichromate, a purple precipitate was produced which could not be purified. This was probably $L \cdot CrO_5$).

Alternative Preparative Route

1,4-Diphenoxyphthalazine (3) (2.0 g) was refluxed under nitrogen in 2-aminopyridine (10 g, b.p. 204°) for 13 h. Phenol was soon observed on the sides of the tube, whilst on cooling, yellow crystals were obtained suspended in the solid 2-aminopyridine. The reaction mixture was crushed and washed with methanol. The 2-aminopyridine dissolved leaving a yellow crystalline mass, m.p. 205°, which was recrystallized from *n*-butanol and shown to be compound L, m.p. 209°, mixed m.p. 210°.

Hydrolysis of Ligand L

The compound (115 mg) was refluxed in concentrated hydrochloric acid (15 ml) for 6 h. The solvent was removed at the pump and the residue shaken with aqueous potassium hydroxide (10 ml). 1-2(2'-pyridyl)-aminophthalaz-4-one (80 mg, 0.98 equivalent), m.p. 305° was obtained as a white precipitate. This was recrystallized twice from dimethylformamide.

Anal. Calcd. for $C_{13}H_{10}N_4O$: C, 65.5; H, 4.2; N, 23.5. Found: C, 65.25; H, 4.2; N, 23.4.

The alkaline filtrate was just acidified (HCl) and excess picric acid was added. A yield of 75 mg, 1.15 moles of 2-aminopyridine picrate, m.p. 216° (lit. 216°) was obtained. (N.B. under similar conditions, 100 mg of 2-aminopyridine yielded 185 mg of picrate).

Preparation of 1-(2'-pyridyl)aminophthalaz-4-one

3-Oxo-1-(2'-pyridyl)iminoisoindoline (1.2 g) was dissolved in methanol (30 ml) and hydrazine hydrate (5 ml, 64%) added to the hot solution. After standing at 0° for 24 h, a white product was obtained, (0.6 g, 47%), m.p. 270°. This was recrystallized from dimethylformamide, m.p. 304°, mixed m.p. with sample from degradation, 305°.

$Cu_2L(acetate)_3$

Cupric acetate (2.8 g) was dissolved in ethanol (140 ml) and the solution filtered. The ligand (2.0 g) was added and the mixture refluxed for 15 min. The resulting khaki-green solution was filtered and placed in a refrigerator. A khaki-green crystalline product was obtained (3.6 g, 91%). This was filtered off, washed with ethanol and ether, and dried in air. The product was recrystallized from methanol and dried in air.

The other carboxylate complexes were prepared in a similar fashion (see Table I). The copper carboxylates, where not available commercially, were prepared by reaction of the appropriate acid with copper carbonate and extracting the product with a suitable solvent.

Acetonitrile was used for recrystallization in some cases, particularly those where a solvated species was obtained from methanol. The complexes were dried at 100°/15 mm prior to analysis and study.

$Cu_2LCl_3.(OH)H_2O$

The ligand (L) (1.4 g) was crushed and refluxed in an aqueous solution of cupric chloride (5 g in 100 ml) for 5 min. After cooling, the green crystalline product (2.1 g, 81%) was filtered and washed with water, methanol, and ether. The product was recrystallized from water and dried at 50°/15 mm. The bromide complex was prepared by a similar procedure.

The X-ray structure of the chloride complex (4) indicates the presence of an additional molecule of lattice water per 2 molecules of complex[3]. Our compounds, after drying under vacuum, gave analyses which suggested that this additional water was no longer present. The difference between the required analytical figures for the two formulations is, however, relatively small.

$Cu_2L(IO_3)_3.(OH)3H_2O$

$Cu_2LCl_3.(OH)H_2O$ (0.2 g) was dissolved in hot water (20 ml) and an aqueous solution of potassium iodate (0.5 g in 10 ml) was added. After maintaining the solution at 0 °C for some time, a green crystalline product was obtained which was recrystallized from water and dried at 100°/15 mm.

The complexes are all green in color; the alkanoate derivatives are very soluble in many organic solvents but almost insoluble in water. The dark green aquo-halide and iodate complexes are insoluble in most organic solvents but slightly soluble in water.

CuL_2

Aqueous ammonium hydroxide was added to an aqueous solution of $Cu_2LCl_3(OH)H_2O$. A precipitate was obtained, which, upon drying, analyzed approximately for $CuL_2(OH)_2$. This was dissolved in chloroform, boiled momentarily, then the solvent was removed at the pump. The residue was recrystallized twice from *n*-butanol to yield large black crystals of the product.

Variable Temperature Range Magnetic Study

The magnetic moment of the iodate complex, $Cu_2L(IO_3)_3OH.3H_2O$ was investigated over the temperature range 108–295 °K using the standard Gouy method. The system was calibrated with nickel chloride solution. The diamagnetic correction of the complex was taken from Pascal's constants to be 190×10^{-6} c.g.s.u. The data obtained are as follows

Variable temperature magnetic data

Temperature (°K)	χ_m^{corr}	μ_{eff} (B.M.)
295	758	1.34
275	731	1.28
243.5	701	1.17
213.5	651	1.06
191	607	0.97
159	523	0.82
136	440	0.69
117.5	370	0.59
108.5	315	0.52

Note: See text for the calculated parameters.

[3]The derivative investigated contained an extra molecule of water per 4 copper atoms, located in the lattice. It would be correctly formulated $2LCu_2(OH)Cl_3.3H_2O$.

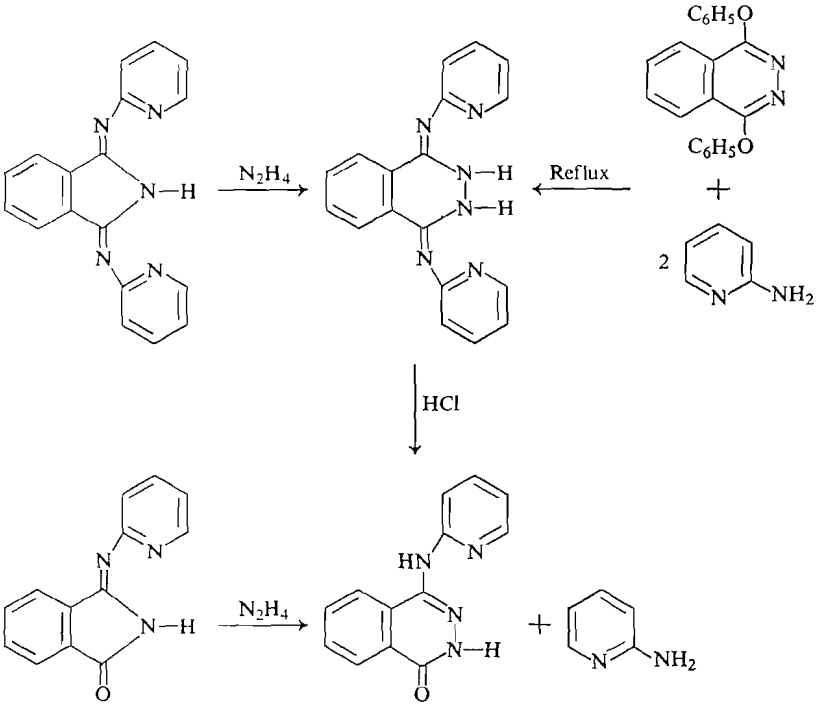

FIG. 1. The synthesis and degradation of 1,4-di(2′-pyridyl)aminophthalazine.

Results and Discussion

Synthesis and Characterization of the Ligand

The phthalazine ligand was prepared by the ring expansion of 1,3-di(2′-pyridyl)-iminoisoindoline (2) with hydrazine hydrate. The structure (**1**) of the new ligand was substantiated by an alternative synthesis and by degradation, as indicated in Fig. 1.

An unequivocal proof of the structure of the ligand was obtained by an X-ray structural investigation of the copper complex $LCu_2Cl_3(OH).H_2O$, full details of which will appear elsewhere (4).

The Complexed Ligand

Reaction of the ligand with copper halides yielded the derivatives $Cu_2LX_3(OH)H_2O$ where X = Cl and Br. Reaction of these complexes with potassium iodate gave $Cu_2L(IO_3)_3(OH).3H_2O$. Reaction with copper carboxylates generated 2 series of complexes, $Cu_2L(RCO_2)_3$ and $Cu_2L(RCO_2)_4$.

The mode of bonding of the ligand in these complexes was investigated by vibrational and electronic spectroscopy. The hydrated halide complexes and the tetracarboxylate series give rise to a rich spectrum in the N—H stretching region. These complexes are assumed to contain the neutral ligand. In the case of the chloride complex alluded to above, the X-ray study confirms that this complex contains the neutral ligand. The complexes $Cu_2L(RCO_2)_3$ would appear, on the basis of stoichiometry, to contain a monoanionic ligand derived from the ligand by loss of 1 hydrogen atom. In agreement with this supposition the N—H stretching region of the i.r. spectra of these derivatives is considerably weaker, relative to the aromatic ν_{CH} vibrations, than is the corresponding region of the tetracarboxylate series.

The ligand may be thought of as a 2-substituted pyridine derivative. In such complexes it is well documented (5–8) that the ring breathing mode of vibration near 990 cm^{-1} is a reliable guide to coordination of the pyridine residue. Upon coordination of the pyridine group this band increases in energy generally to above 1000 cm^{-1}. The ligand (**1**) exhibits a band at 989 cm^{-1} which may safely be assigned to this vibration since 1,4-diaminophthalazine is transparent from 950

Can. J. Chem. Downloaded from www.nrcresearchpress.com by 210.87.254.6 on 09/05/12
For personal use only.

Can. J. Chem. Downloaded from www.nrcresearchpress.com by 210.87.254.6 on 09/05/12
For personal use only.

to 1010 cm^{-1}. None of the complexes has a band in this region but all exhibit an additional band between 1010 and 1022 cm^{-1} which we assign to coordinated pyridine. Thus in all cases *both* pyridine residues of the ligand are coordinated to the metal atoms (6). Whilst there are a number of other pyridine vibrations which have been used in the past (6–8) as a guide to coordination of the pyridine residue to a metal ion, these cannot reliably be picked out from the extremely complex spectra of the phthalazine derivatives.

The X-ray structural determination (4) of the copper chloride derivative reveals that the ligand exists in the tautomeric form (**1**) with both hydrogen atoms on exocyclic nitrogen atoms, and not in the tautomeric forms (**2**) and (**3**). This conclusion is based on the angles at the nitrogen atoms, tetrahedral hybridization of the exocyclic nitrogen atoms being inferred therefrom. Because of the similarity of their N—H stretching frequencies and their ultraviolet (u.v.) spectra (see below) the aquo-halide and tetracarboxylate series of complexes are all believed to contain the neutral ligand in tautomeric form (**1**). The tricarboxylate series, with a monoanionic ligand are believed to involve tautomeric form (**4**) since (*a*) this form will surely be more stable than (**5**) when a metal is coordinated to the phthalazine nitrogen atoms, and (*b*) the N—H stretching frequency of the group —NH—M is likely to be lower (9) than 3280 cm^{-1}.

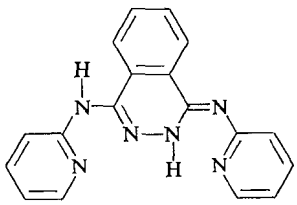

2

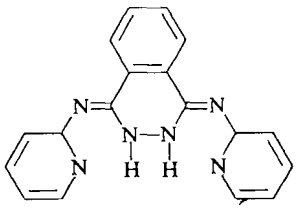

3

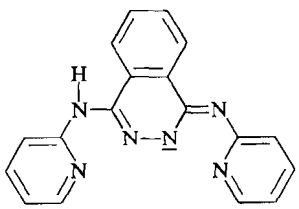

4

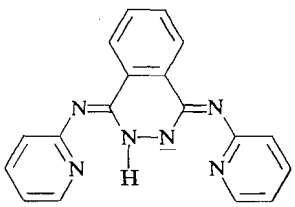

5

There is a clear distinction in the near-u.v. region between the complexes believed to contain a neutral ligand and those believed to contain an anionic ligand.

The lowest energy *peak* in the u.v. spectrum of the neutral ligand species is observed between 27 400 and 29 600 cm^{-1}, whilst in the anionic ligand complexes, the lowest energy peak (not shoulders) occurs between 24 000 and 25 600 cm^{-1} (Table II). This band, which also appears in the uncomplexed ligand (at 26 200 cm^{-1}), is assigned by virtue of its moderate intensity to a π–π^* transition. Its energy would be sensitive to the degree of conjugation in the molecule. Whilst nitrogen atoms are not very effective in extending a conjugated pathway, nevertheless it remains true that the tautomeric form (**4**) involves a longer conjugated pathway (phthalazine and one pyridine ring conjugated) than tautomeric form (**1**) (no conjugation across the exocyclic nitrogen atoms). This is in keeping with the movement of the band in question to lower energies on formation of the anion. The compound L_2Cu which must contain anionic ligand groups also has its first major absorption band in the anionic region at 24 500 cm^{-1}. Having established the nature of the phthalazine ligand bound to the metal atoms in these complexes, it is convenient to discuss the stereochemistry of the copper atoms by dividing the discussion into two parts, halide complexes and carboxylate complexes.

Halide Complexes

These green complexes are slightly soluble in

TABLE II
Electronic spectra

Compound	Conditions*	Spectrum (cm^{-1}, shoulders are in parentheses)
$Cu_2L(CH_3COO)_3$	Mull-rt	17 200, 25 600
	Mull-lt	14 800, 17 400, 25 600
	Soln.	(15 100), 16 850(2.18), 24 800(4.25), (32 400), 33 700(4.29), (35 800), 37 000(4.4), (41 200), 44 600(4.57)†
$Cu_2L(CH_3CH_2COO)_3$	Mull-rt	17 150, 25 000, (38 600)
	Mull-lt	(14 100), 17 100, 25 000
	Soln.	17 700(2.42), 24 800(4.29), (34 000), 37 800(4.42)‡
$Cu_2L(CH_3CH_2CH_2CH_2COO)_3$	Mull-rt	17 300, 25 600, (39 200)
	Mull-lt	(12 800), 14 900, 17 600, 24 700
	Soln.	14 850(2.37)‡, (17 200), 24 200(4.23), (32 000), 35 600(4.40), 39 600(4.40)‡
$Cu_2L((CH_3)_2CHCOO)_3$	Mull-rt	17 700, 24 800, (39 000)
	Mull-lt	(12 900), 17 600, 24 400
	Soln.	(14 900), (17 350), (23 500), 24 000(4.28), (31 600), 35 800(4.42), 39 000(4.41)‡
$Cu_2L((CH_3)_2CHCH_2COO)_3$	Mull-rt	16 650, (23 800), 25 100
	Mull-lt	(14 600), 17 100, 25 000, (27 500)
	Soln.	15 900(2.35), (21 500), 23 200(4.25), (23 800)‡
$Cu_2L(CH_2{=}CHCOO)_3$	Mull-rt	16 400, 24 700, (39 200)
	Mull-lt	(13 400), 16 000, 25 000
	Soln.	17 100(2.17), 25 600(4.16), (34 500), 37 800(4.36), 47 000(4.50)†
$Cu_2L(CH_2{=}CHCH_2COO)_3$	Mull-rt	(14 800), 16 700, 25 600, 40 800
	Mull-lt	(12 700), (14 800), 17 400, 25 000
	Soln.	(15 100), 16 850(2.26), 24 800(4.37), (32 000), (33 400), 35 200(4.48), 44 300(4.63)†
$Cu_2L(CH_2{=}CHCH_2CH_2COO)_3$	Mull-rt	(14 800), 17 000, 25 600, (40 000)
	Mull-lt	(12 750), (14 900), 17 600, 23 600
	Soln.	(14 900), (17 300), 23 400(4.31), 24 300(4.33), (31 600), 36 300(4.47), (38 800)‡
$Cu_2L(C_6H_5COO)_3$	Mull-rt	14 300, 23 800
	Mull-lt	(11 170), 14 800, 24 500, (27 800)
	Soln.	15 750(2.44), (21 150), (23 300), 24 400(4.30)
$Cu_2L(C_6H_5COO)_3OMe{\cdot}MeOH$	Mull-rt	15 100, (23 300), 27 000
	Mull-lt	(11 100), 15 400, (23 550), 27 600
	Soln.	15 750(2.33), (21 150), (23 220), 24 400(4.23)§
$Cu_2L(m\text{-}Cl{-}C_6H_4COO)_3OMe{\cdot}MeOH$	Mull-rt	(11 000), 14 800, (23 550), 27 200
	Mull-lt	(11 100), 15 100, (23 800), 27 050
	Soln.	15 750(2.42), 23 800(4.26), (24 050)§
$Cu_2L(HCOO)_4$	Mull-rt	15 700, (23 550), 27 400
	Mull-lt	(12 900), 16 000, (23 250), 27 400
	Soln.	16 000(2.61), (21 200), (23 150), 24 400(4.24)§
$Cu_2L(ClCH_2{-}COO)_4$	Mull-rt	15 400, 27 900
	Mull-lt	(12 500), 15 400, (23 550), 28 200
	Soln.	15 300(2.45), 26 620(4.34)§
$Cu_2L(Cl_2CH{-}COO)_4$	Mull-rt	16 100, 28 100
	Mull-lt	(14 300), 17 100, (23 250), 28 400
	Soln.	15 300(2.32), (23 600), (25 000), 26 150(4.24)§
$Cu_2L(Cl_3C{-}COO)_4$	Mull-rt	15 100, (23 300), 28 300
	Mull-lt	(11 400), (12 900), 15 400, (23 250), 28 350
	Soln.	13 200(2.30), (26 200), 27 400(4.20)§
$Cu_2L(F_3C{-}COO)_4$	Mull-rt	16 950, 29 000
	Mull-lt	(14 300), 17 400, 28 250, 29 800
	Soln.	15 620(2.20), (26 200), 27 400(4.29)§
$Cu_2LCl_3(OH)(H_2O)$	Mull-rt	15 700, (29 600)
	Mull-lt	16 300, 28 200
	Soln.	15 600(1.23), (25 600), 29 000(4.08), 34 500(4.32)‖

Can. J. Chem. Downloaded from www.nrcresearchpress.com by 210.87.254.6 on 09/05/12
For personal use only.

TABLE II *(Concluded)*

Compound	Conditions*	Spectrum (cm^{-1}, $\log_{10}\varepsilon$, shoulders are in parentheses)
$Cu_2LBr_3(OH)H_2O$	Mull-rt	15 800, (29 400)
	Mull-lt	16 300, 28 200
	Soln.	15 950(1.20), (25 600), 29 000(4.37), 34 500(4.58)‖
$Cu_2L(IO_3)_3(OH)(H_2O)_3$	Mull-rt	16 000, 29 400
	Mull-lt	(13 800), 16 600, 28 200
	Soln.	15 600(1.71), (25 000), 29 400(4.29), 34 500(4.42)‖
L	Mull-rt	(23 800), 26 200
	Soln.	(24 400), 25 800(4.32), (27 050), (34 500), 38 300(4.40)‡

*Mull-rt, mull transmittance at room temperature. Mull-lt, mull transmittance at liquid nitrogen temperature.
†In methanol.
‡In chloroform.
§In pyridine.
‖In water.

TABLE III

Magnetic moments, conductivities, and molecular weights*

Compound	Magnetic moment μ_{eff}* (B.M.)	Conductivity (mhos $mole^{-1}$ cm^{-2})	Molecular weight†
$Cu_2L(CH_3COO)_3$	1.66	[a]96	[c]297 (r.617)
$Cu_2L(CH_3CH_2COO)_3$	1.80	[a]88	—
$Cu_2L(CH_3CH_2CH_2CH_2COO)_3$	1.78	[a]95	[d]748 (r.743)
$Cu_2L((CH_3)_2CHCOO)_3$	1.86	[a]88	[d]693 (r.700)
$Cu_2L((CH_3)_2CH{\cdot}CH_2COO)_3$	1.82	[a]47	—
$Cu_2L(CH_2{=}CHCOO)_3$	1.77	[a]75	—
$Cu_2L(CH_2{=}CHCH_2COO)_3$	1.80	[a]86	[c]312 (r.695)
$Cu_2L(CH_2{=}CHCH_2CH_2COO)_3$	1.76	[a]94	[d]738 (r.737)
$Cu_2L(C_6H_5COO)_3$	1.68	[a]60	—
$Cu_2L(CF_3COO)_4$	1.90	[a]168	—
$Cu_2L(CCl_3COO)_4$	1.74	[a]155	—
$Cu_2L(HCCl_2COO)_4$	1.79	[a]95	—
$Cu_2L(H_2CClCO_2)_4$	1.75	[a]79	—
$Cu_2L(HCOO)_4$	1.39	[a]73	—
$Cu_2L(M{-}Cl{-}C_6H_4COO)_3OMe{\cdot}MeOH$	1.33	[a]55	—
$Cu_2L(C_6H_5CO_2)_3OMe{\cdot}MeOH$	1.42	[a]55	—
$Cu_2LCl_32H_2O$	1.66	[b]384	—
$Cu_2LBr_32H_2O$	1.60	[b]404	—
$Cu_2L(IO_3)_34H_2O$	1.39	[b]275	—
L	—	—	[d]306 (r.314)

*The magnetic moments and conductivities were measured at room temperature. *a* = methanol, *b* = water, *c* = methanol (osmometric), *d* = chloroform (ebullioscopic). Calculated molecular weight in parentheses.

water but are insoluble in common organic solvents. The water molecule is difficult to remove, the complexes being stable in vacuo up to 150°. Aqueous solutions of the halides are conductors (Table III) and react with silver nitrate yielding 3 equivalents of halogen. The aqueous solution spectra of all 3 complexes are essentially identical with each other and with the solid state spectrum of the iodate complex. This latter complex is assumed to contain iodate ions and the cationic species $LCu_2(OH)(H_2O)_3^{3+}$, which is also assumed to be the predominant species in aqueous solution.

The basic structural unit presented in the chloride complex is depicted in Fig. 2. The X-ray study by Lingafelter and Marongiu (4) has shown the presence of two 5-coordinated copper atoms in square pyramidal environments. The square pyramids share a corner (hydroxy bridge) and the apex (bridging chloride). It is not unreasonable to suppose that the bromide complex has a similar structure. The presence of 3 different bridging groups (OH, Cl, —N—N—) is remarkable. It seems likely that the iodate complex and the aqueous solution species have essentially the same structure with the halogen atoms replaced by water molecules. The presence of a water bridge on the apices of the square

Can. J. Chem. Downloaded from www.nrcresearchpress.com by 210.87.254.6 on 09/05/12
For personal use only.

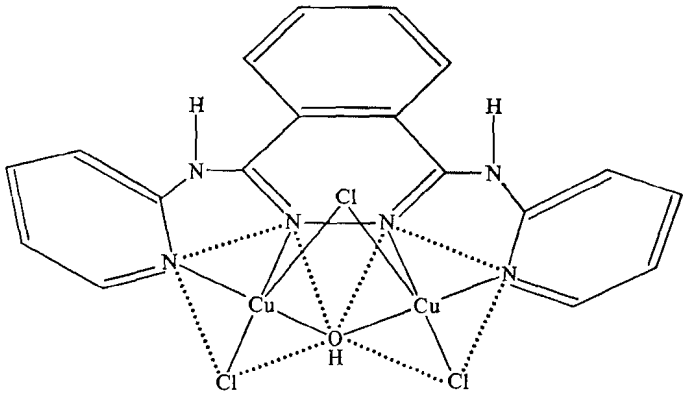

FIG. 2. The structure of $Cu_2LCl_3(OH)\cdot H_2O$ as indicated by X-ray crystallography (4). The water molecule is in the lattice uncoordinated to the copper atoms. The dotted lines indicate the planes of the square pyramids about each copper atom. These planes are canted towards one another. The apical copper–chlorine distance is some 0.3 Å longer than the in-plane copper chlorine distance. Complete details of this structure will be published shortly (4). The $LCu_2(RCO_2)_4$ series are presumed to have a similar structure in which the Cl^- and OH^- groups are replaced by RCO_2^-. Only one intramolecular bridge is presumed to be present in the $LCu_2(RCO_2)_3$ series (replacement of OH^- by RCO_2^-). The apical Cl is replaced by intermolecular bridging (—OCO—) and the ligand is in tautomeric form **4**.

R

pyramids is debatable since water does not readily act as a bridge between 2 metal atoms.

There is a regular increase in the energy of the principal d–d absorption band in the spectra of these complexes as one replaces chloride by bromide by water (Table II). However, the magnetic moment (Table III) of the iodate complex is much lower than those of the halides suggesting that the copper–copper distance has been decreased. A temperature range magnetic study (see Experimental) yields $2J = -335$ cm^{-1}, $g = 1.95$, and $N\alpha = 145 \times 10^{-6}$ c.g.s., using the conventional model for two interacting $S = \frac{1}{2}$ states (10).

Carboxylate Complexes

Reaction of copper carboxylates with the ligand in alcoholic or acetonitrile solution leads to the formation of 2 principal series of complexes, $LCu_2(RCO_2)_3$ and $LCu_2(RCO_2)_4$. The former series comprises those acids whose pK_a is greater than 3.8 whilst the latter series arises when the pK_a value of the acid is less than 3.8. The u.v. spectra of the complexes reveal that the tricarboxylic series contains anionic ligand, whilst the tetracarboxylic series contains neutral ligand. This suggests that the pK_a of the ligand is close to 3.8. In the case of formic acid with a pK_a of 3.75 placing the complex close to the crossover point, solution of the tetracarboxylate complex in the basic solvent pyridine, leads to the formation in solution of the tricarboxylate complex, as indicated by the u.v. spectrum (Table II). The methoxyl derivatives behave in a similar manner. With the exception of the formate complex, the magnetic moments of the complexes range from 1.66 to 1.90 B.M. suggesting little or no copper–copper interaction in either series. The tricarboxylic series shows ready solubility in many organic solvents including chloroform; the tetracarboxylic series, on the other hand, shows rather more limited solubility in organic solvents. Both series are insoluble in water.

$LCu_2(RCO_2)_3$

It is likely that the ligand is acting as a quadridentate donor in the carboxylate derivatives as well as the halides and we may assume that the i.r. absorption of the ligand will be similar in both series of complexes. Comparison of the spectra of the carboxylates with the halides allows us to isolate absorption bands arising from the $—CO_2$ groups. The i.r. spectra of carboxylate complexes have been adequately discussed in the past (11–17). Suffice to say that since the symmetry of the carboxylate group is unchanged upon coordination, no new bands will appear in its spectrum. Structural assignments generally rely on the positions of the symmetric and antisymmetric $—CO_2$ stretching vibrations.

The carboxylate complexes under discussion exhibit multiple symmetric stretching bands

Can. J. Chem. Downloaded from www.nrcresearchpress.com by 210.87.254.6 on 09/05/12
For personal use only.

TABLE IV
Infrared Spectra*

Compound	N—H bands (cm^{-1})†	Carboxylate bands (cm^{-1})	Coordinated pyridine band (cm^{-1})
$Cu_2L(CH_3COO)_3$	[a]3280(m)	[a]1585(m), 1400(m) 1367(s)	1012
$Cu_2L(CH_3CH_2COO)_3$	[a]3265(m) [b]3265(m)	[a]1580(s), 1405(m) 1365(m), [b]1710(w) 1584(s), 1404(m) 1360(s)	1010
$Cu_2L(CH_3CH_2CH_2CH_2COO)_3$	[a]3280(m) [b]3280(ms)	[a]1580(s), 1400(m) 1363(s), [b]1709(ms) 1580(ms), 1398(m) 1360(s)	1010
$Cu_2L((CH_3)_2CHCOO)_3$	[a]3265(m) [b]3265(m)	[a]1581(s), 1404(s) 1361(s), [b]1708(m) 1578(ms), 1400(m), 1360(s)	1010
$Cu_2L(CH_2{=}CHCOO)_3$	[a]3265(m)	[a]1580(s), 1405(msh) 1360(m)	1017
$Cu_2L(CH_2{=}CHCH_2COO)_3$	[a]3278(m)	[a]1588(s), 1406(m) 1366(s), [b]1710(w) 1590(w), 1386(mw), 1360(m)	1015
$Cu_2L(CH_2{=}CHCH_2CH_2COO)_3$	[a]3280(m) [b]3280(m)	[a]1582(ms), 1404(wsh) 1363(s), [b]1710(m) 1584(s), 1400(m) 1360(s)	1013
$Cu_2LCl_3(OH)H_2O$	[c]3590(m), [c]3560(ms) [c]3530(m), [c]3460(m) 3285(s)		1019
$Cu_2LBr_3(OH)H_2O$	[c]3600(ms), [c]3565(m) [c]3500(m), [c](3460) 3300(ms), 3250(s)		1018
$Cu_2L(IO_3)_3(OH)(H_2O)_3$	[c]3600–3300(br) 3300–3100(br)		1022

*a = mull, b = solution in chloroform, c = O—H bands, br = broad, w = weak, m = medium, s = strong, sh = shoulder. Shoulders in parentheses.
†Only the principal NH stretching frequency is reported. In addition to this band the complexes generally show up to 4 additional and weaker bands between 3100 and 3285 cm^{-1}.

indicative of the presence of both bridging and terminal carboxylate groups.

Absorption bands are observed in the following regions in the mull spectra (Table IV): (*i*) 1578–1590 cm^{-1} assigned to the antisymmetric stretching vibration of a bridging carboxyl group, (*ii*) 1390–1410 cm^{-1} assigned to the symmetric stretching vibration in a bridging carboxyl group, and (*iii*) 1360–1370 cm^{-1} assigned to the symmetric stretching vibration in a carboxyl group apparently bound in a terminal manner to the copper atom.

The above assignments may be rationalized as follows. The antisymmetric vibrational frequencies observed in a series of alkanoate complexes (12), known unequivocally to contain carboxylate groups bridging between 2 copper atoms, lie in the range 1560–1603 cm^{-1}. The symmetric stretching vibrations in these same compounds lie between 1410–1430 cm^{-1}. Thus the assignments cited above for the bridging carboxylate groups are fully consistent with the earlier literature.

There is less information available concerning molecules which unequivocally contain terminally bound carboxylate groups. In such complexes (11) the symmetric frequency should be lower than 1400 cm^{-1} since the vibration will

Can. J. Chem. Downloaded from www.nrcresearchpress.com by 210.87.254.6 on 09/05/12
For personal use only.

Can. J. Chem. Downloaded from www.nrcresearchpress.com by 210.87.254.6 on 09/05/12
For personal use only.

have more single bond C—O stretching character. Similarly, the antisymmetric vibration will lie above 1600 cm^{-1}, since it will possess more double bond C=O character than the bridging ligand. In the complexes of picolinic acid N-oxide (12), bands attributable to the antisymmetric vibration of a terminally bound carboxyl group are observed between 1650–1700 cm^{-1}. However, when water is present in the molecule, hydrogen bonding of the "ketonic" oxygen atom can occur leading to a considerable reduction in the antisymmetric frequency.

The carboxylate complexes have a band around 1360 cm^{-1} which is absent in the halide spectra; such a band could be the symmetric frequency of a terminally bound $-CO_2$ group. The highest energy band observed in this region of the spectrum lies at about 1640 cm^{-1}. This band is also present in the free ligand and in the halide complexes and is probably a $\nu_{(C=N)}$ vibration. No evidence was found for the terminal asymmetric frequency in the mull spectra. Accepting the validity of the assignments so far, there are two reasons why the asymmetric frequency might not be observed. The "ketone" residue may be hydrogen bonded, presumably to the NH group on the ligand or it may be coordinated to a copper atom. It would be reduced in frequency and might be obscured by the multiple C=N absorption of the ligand. Hydrogen bonding would necessarily be intermolecular and should be absent in solution. In chloroform solution all the carboxylate complexes (which were sufficiently soluble for investigation) showed a strong band near 1700 cm^{-1} which is absent in the mull spectrum. There can be little doubt that this is the "missing" antisymmetric stretching frequency of the terminally bound carboxyl groups. The other $-CO_2$ bands were observed in the solution spectra at frequencies close to their mull spectra. Moreover, the $\nu_{(NH)}$ band appeared at precisely the same frequency as it does in the mull spectra. This is not consistent with the presence of a hydrogen bond which is broken in solution. It follows that the terminal carboxyl groups must be associated with copper atoms, and it is suggested that in the solid state there is a loose intermolecular association between neighboring binuclear units leading to a reduction in the antisymmetric frequency of the "terminal" carboxyl groups. A 5-coordinate configuration for the copper atoms is then inferred (Fig. 2, caption). The electronic spectra, discussed below in detail, suggest the presence of square pyramidal copper atoms.

In solution this association is destroyed. Molecular weight measurements (Table III) show that these complexes are monomeric (but binuclear) in chloroform solution. Since chloroform is unlikely to coordinate to the copper, the species must be 4-coordinate and square planar. In methanol the complexes behave as 1:1 electrolytes, and yield molecular weights approximately one-half their formula weights. Apparently methanolysis is occurring, probably at the intramolecular carboxylate bridge.

$LCu_2(RCO_2)_4$

The i.r. spectra of the tetracarboxylate series infer quadridentate coordination of the neutral ligand and the presence of 2 types of carboxylate group. Unfortunately, most members of this series are haloacetates where the i.r. criterion for the mode of bonding of the carboxylate group is uncertain (16, 17).

Comparison of the i.r. spectra of the complexes with the spectra of the aquo-halide derivative reveals at least 4 bands in the region 1300–1700 cm^{-1} assignable to the carboxyl group (Table IV). Utilizing some previous work by Kettle and Pioli (17) who studied the complexes (2-picoline)$_x$Cu$(RCO_2)_2$ ($x = 2$ or 4), a band near 1350 cm^{-1} in our complexes may be assigned to the antisymmetric stretching vibration of a terminally bound haloacetate carboxyl group. An additional band occurring between 1400 and 1475 cm^{-1}, which cannot always be positively identified, is assigned to the symmetric stretching frequency of a bridging haloacetate group. The intense absorption between 1650 and 1700 cm^{-1} contains one or more bands assignable to the antisymmetric stretching vibrations of haloacetate carboxyl groups. Absorption in this region does not distinguish bridging from terminal ligands (16).

The low solubility of these complexes in organic solvents precludes molecular weight determination. They are, however, soluble in pyridine in which most or all of them appear to be solvated.

The electronic spectra of these complexes do not differ appreciably from those of the tricarboxylate series, and therefore a 5-coordinate square pyramidal structure with 2 intramolecular

Can. J. Chem. Downloaded from www.nrcresearchpress.com by 210.87.254.6 on 09/05/12
For personal use only.

bridging acetate groups and 2 terminal acetate groups is proposed (Fig. 2, caption). The possibility that there are 2 intermolecular rather than intramolecular bridges cannot be excluded. However, the presence of intramolecular bridges in the halide complexes, and the inferred presence of such a bridge in the tricarboxylate series, leads us to prefer this formulation (**8**). Two tricarboxylate complexes also appear to belong to this neutral ligand series. They are LCu_2(*m*-Cl-benzoate)$_3$-OMe(MeOH) and LCu_2(benzoate)$_3$OMe(MeOH), and are formulated to contain a methoxy group, rather than to be solvated by 2 methanol residues since their principal low energy u.v. absorption implies that they contain the neutral ligand. It seems likely that the methoxyl group acts as a bridge between the 2 copper atoms. Their magnetic moments indicate the presence of an exchange interaction.

Electronic Spectra

Further support for the 5-coordinate square pyramidal model for these complexes stems from a more detailed consideration of the electronic spectra.

Recent studies (18–20) with 5-coordinate square pyramidal copper(II) complexes have revealed that at least 3 transitions may normally be observed. The lowest energy band assigned to the $z^2 \rightarrow x^2 - y^2$ transition (xy molecular plane, z is the four-fold axis) lies in the region 10 000 – 13 000 cm^{-1}. The $xy \rightarrow x^2 - y^2$ (10 Dq) transition lies next in the region 13 000 – 15 000 cm^{-1}, whilst the most intense band is the doubly degenerate transition, $xz,yz \rightarrow x^2 - y^2$ lying at 15 000 – 18 000 cm^{-1}. In symmetry lower than D_{4h} this last transition may split into 2. The actual band energies depend on the ligating atoms. In our case we do not have a regular square pyramid since there are several different ligating atoms. However, it does seem possible to make some tentative assignments based on this model.

The strong absorption band observed in the visible region in the mull transmittance spectra of these derivatives may be resolved at −196 °C. Whilst some of the tricarboxylates show 3 bands at low temperature, the tetracarboxylates in general only show 2, but not always the same 2. In the former series the 3 bands lie in the regions (*i*) 12 700 – 13 400 cm^{-1}, (*ii*) 14 100 – 14 900 cm^{-1}, and (*iii*) 15 900 – 17 100 cm^{-1}. The benzoate is atypical in band (*iii*). In the latter series band (*i*) falls in the range 11 000 – 13 000 cm^{-1}, band (*ii*) 14 300 cm^{-1}, and band (*iii*) 15 400 – 17 400 cm^{-1} (Table II). One of us has recently discussed the spectra of 5-coordinate square pyramidal copper complexes (18) which will therefore not be repeated here. The following band assignments may tentatively be made

$$\text{Band } (i) \qquad z^2 \rightarrow x^2 - y^2$$

$$\text{Band } (ii) \qquad xy \rightarrow x^2 - y^2$$

$$\text{Band } (iii) \quad xz, yz \rightarrow x^2 - y^2$$

Bands (*ii*) and (*iii*) might alternatively be assigned as $xz \rightarrow x^2 - y^2$ and $yz \rightarrow x^2 - y^2$, since the xz and yz levels will not be degenerate in this rather distorted system; however, this assignment is considered unlikely on the basis that the energy of band (*ii*) is almost independent of the complex under discussion. The invariance of band (*ii*) confirms its assignments to the 10 Dq transition since all the complexes have essentially the same in-plane CuN_2O_2 chromophore. It is known (20, 21) that 10 Dq for the CuO_4 chromophore in a square pyramidal CuO_4X system generally lies between 13 000 and 14 000 cm^{-1}. The value observed above, between 14 000 and 15 000 cm^{-1} for the CuO_2N_2 in-plane chromophore, is quite acceptable. Thus the electronic spectroscopic data are in complete agreement with the assignment of square pyramidal structures for these complexes. Unfortunately the spectra of the square pyramidal halide derivatives did not resolve well at low temperature.

In closing it is necessary to ensure that the above spectroscopic interpretation is not consistent with any other stereochemistry about the copper atom. Trigonal bipyramidal (22), octahedral, trigonal 6-coordinate (23), and tetrahedral (24) copper stereochemistries can be definitely eliminated since their absorption maxima for d–d transitions always lie below about 15 000 cm^{-1} for ligand atoms of the type under discussion. Square complexes frequently absorb at fairly high energies since the crystal field splitting for the square stereochemistry is large. Copper acetylacetonate, for example, with a CuO_4 chromophore absorbs (20) at 18 500 cm^{-1} with a lower energy band at 15 000 cm^{-1}. Other acetylacetonates absorb at a similarly high energy. Distortion will tend to decrease these

energies so that our results might be deemed consistent with a distorted square environment. However, we feel that this alternative interpretation can be discarded on the basis that in a square environment in which there is little distortion towards a tetrahedron there should be no low energy band. The $z^2 \rightarrow x^2 - y^2$ transition lies at a high energy since the z^2 orbital is not unduly perturbed by the ligand in a square environment (20). There cannot be appreciable distortion towards a tetrahedron in our case, since this would result in an overall shift of the entire spectrum to lower energies (25). Thus the presence of both low energy (band (*i*)) and high energy bands (band (*iii*)) in the spectrum is in itself an indication of the 5-coordinate square pyramidal environment.

Other Complexes

Reaction of the copper chloride complex with ammonium hydroxide leads to the formation of L_2Cu. The electronic spectrum of this complex in chloroform shows 3 main bands in the region 5 000 – 30 000 cm^{-1} at 8 700 (85), 16 680 (460), and 24 500 (3 050) cm^{-1}, with shoulders at 23 500, 26 000, and 27 200 cm^{-1}. The 24 500 cm^{-1} absorption is indicative of the anionic ligand as would be deduced from the stoichiometry whilst the d–d bands at 8 700 and 16 680 would strongly infer a trigonal 6-coordinate environment for the copper atom (cf. Cu(dipyridyl)$_3^{2+}$ with d–d bands (23) at 6 400 (28) and 14 400 (54)). The bands are assigned to the $^2A_1 \leftarrow {}^2E$ and $^2E \leftarrow {}^2E$ transitions in D_3 symmetry, respectively. The intensities are rather high when compared with the dipyridyl derivative and intensity stealing from the low lying ligand band is probably responsible for this. This structure requires the ligand to be tridentate. Molecular models show that this can be achieved without strain using the 2 pyridine residues and the tetrahedrally disposed phthalazine nitrogen atom of tautomer (**4**). The i.r. spectrum has a strong band at 1007 cm^{-1} (with a very weak absorption peak at 993 cm^{-1}) assigned to the ring breathing mode of the coordinated pyridine residues. The magnetic moment was observed to be 1.79 B.M. at room temperature.

Acknowledgments

We are indebted to the National Research Council of Canada and Department of University Affairs, Ontario, for support of L.K.T. and V.T.C., and to the Science Research Council, London, England for earlier support of L.K.T.

1. J. E. Andrew, P. W. Ball, and A. B. Blake. Chem. Commun. 143 (1969).
2. J. A. Elvidge and R. P. Linstead. J. Chem. Soc. 5000 (1952).
3. J. A. Elvidge and A. P. Redman. J. Chem. Soc. 1710 (1960).
4. E. C. Lingafelter and G. Marongiu. To be published.
5. A. R. Katritzky and A. R. Hands. J. Chem. Soc. 2202 (1958).
6. D. A. Baldwin, A. B. P. Lever, and R. V. Parish. Inorg. Chem. **8**, 107 (1969).
7. S. P. Sinha. Spectrochim. Acta, **20**, 879 (1964).
8. P. E. Figgins and D. H. Busch. J. Phys. Chem. **65**, 2236 (1961).
9. L. G. Warner, N. J. Rose, and D. H. Busch. J. Amer. Chem. Soc. **90**, 6938 (1968). D. P. Madden and S. M. Nelson. J. Chem. Soc. **A**, 2342 (1968). N. F. Curtis. Coord. Chem. Rev. **3**, 3 (1968).
10. B. Bleaney and K. D. Bowers. Proc. Roy. Soc. London, Ser. A, **214**, 451 (1952).
11. K. Nakamoto, Y. Morimoto, and A. E. Martell. J. Amer. Chem. Soc. **83**, 4528 (1961).
12. A. B. P. Lever, J. Lewis, and R. S. Nyholm. J. Chem. Soc. 5262 (1962).
13. K. Nakamoto. Infrared spectra of inorganic and coordination compounds. John Wiley and Sons, Inc., New York. 1963.
14. F. A. Cotton. Modern coordination chemistry. *Edited by* J. Lewis and R. G. Wilkins. Interscience Publishers, Inc., New York. 1960. p. 301.
15. B. J. Edmondson and A. B. P. Lever. Inorg. Chem. **4**, 1608 (1965).
16. A. B. P. Lever and D. Ogden. J. Chem. Soc. A, 2041 (1967).
17. S. F. A. Kettle and A. J. P. Pioli. J. Chem. Soc. A, 1243 (1968).
18. A. B. P. Lever, F. J. C. Rossotti, D. H. Schärer and B. J. Edmonson. In preparation.
19. A. B. P. Lever and L. K. Thompson. Unpublished observations.
20. L. L. Funck and T. R. Ortolano. Inorg. Chem. **7**, 657 (1968).
21. D. E. Billing and B. J. Hathaway. J. Chem. Soc. **A**, 1516 (1968).
22. M. Ciampolini and N. Nardi. Inorg. Chem. **5**, 41 (1966).
23. R. A. Palmer and T. S. Piper. Inorg. Chem. **5**, 864 (1966).
24. D. M. L. Goodgame and F. A. Cotton. J. Chem. Soc. 2298 (1961).
25. L. Sacconi and M. Ciampolini. J. Chem. Soc. 276 (1964).

Can. J. Chem. Downloaded from www.nrcresearchpress.com by 210.87.254.6 on 09/05/12
For personal use only.

Can. J. Chem. Downloaded from www.nrcresearchpress.com by 210.87.254.6 on 09/05/12
For personal use only.

Selenium tetrafluoride adducts. I. Trifluoroselenium fluorosulfate

R. J. GILLESPIE AND W. A. WHITLA
Department of Chemistry, McMaster University, Hamilton, Ontario

Received June 13, 1969

The structure of the adduct between selenium tetrafluoride and sulfur trioxide in the solid state, in the molten state, and in solution has been investigated using infrared, Raman, nuclear magnetic resonance spectroscopy, conductivity measurements in fluorosulfuric acid and nitrobenzene, and cryoscopic measurements in nitrobenzene. The data can be best interpreted in terms of a polymeric bridged fluorosulfate structure for the solid and the melt, which is broken down in solution to form mainly a dimeric species.

Canadian Journal of Chemistry, 47, 4153 (1969)

A large number of adducts of selenium tetrafluoride with acceptor molecules have been prepared. The first of these was made by Peacock (1). He isolated a white solid $SeF_4.SO_3$ which he suggested might have the ionic structure SeF_3^+-SO_3F^-. Bartlett and Robinson (2, 3) prepared adducts with boron trifluoride, arsenic pentafluoride, and antimony pentafluoride. Subsequently a number of other similar adducts have been prepared and it has been suggested that all these adducts contain the SeF_3^+ ion (4). Recently, the X-ray structure of trifluoroselenium(IV)fluorobis[pentafluoroniobate(V)] (5) has given the first direct evidence for the SeF_3^+ ion. Considerable interaction through fluorine bridging with the $Nb_2F_{11}^-$ ion was observed giving the selenium a pseudoseven coordinate environment. Still more recently Evans and Long (6) have interpreted the Raman spectra of the molten adducts $SeF_4.SbF_5$ and $SeF_4.AsF_5$ in terms of the ionic structures $SeF_3^+.SbF_6^-$ and $SeF_3^+.AsF_6^-$.

We have investigated a series of 1:1 adducts of selenium tetrafluoride using infrared, Raman, and nuclear magnetic resonance (n.m.r.) spectroscopy, and conductimetric and cryoscopic measurements. This paper reports the results of our investigation of the adduct with sulfur trioxide, $SeF_4.SO_3$.

Experimental

Selenium tetrafluoride was prepared by the fluorination of selenium (Analar) at 0 °C. The product was stored in liquid air in glass containers with break seals until used. Sulfur trioxide was obtained either by distillation from 65% oleum (Allied Chemicals) or from Sulfan-B (Allied Chemicals).

The adduct $SeF_4.SO_3$ was prepared by direct combination of selenium tetrafluoride and sulfur trioxide using an excess of selenium tetrafluoride as solvent (1). Excess selenium tetrafluoride was removed under vacuum, leaving a fine white powder. The product was used directly or, if it had been stored for some time in a sealed ampoule, was sublimed immediately before use.

Anal. Calcd. for SeF_4SO_3: Se, 33.60; F, 32.34; SO_3, 34.07. Found: Se, 34.1; F, 32.5; SO_3, 33.4.

Infrared spectra were obtained using a Perkin–Elmer model 521 grating infrared spectrometer with extended range interchange. A modified gas cell with silver chloride or polythene windows was used in which the sample was sublimed onto a silver chloride or polythene plate held by a copper cold finger in the center of the cell and cooled by filling the cold finger with liquid air.

A Hilger Watts E612 Raman spectrometer was used in conjunction with a water cooled Toronto-type mercury-arc lamp (7). Spectra of the solid were obtained from 1–2 cm of powder packed in the bottom of a cylindrical sample cell. Generally a fine powder gave better results than a crystalline sample. Spectra of the melt were obtained by passing a stream of heated air around the Raman tube to melt the sample. Temperatures up to 150 °C were readily obtained in this manner.

The ^{19}F n.m.r. spectra were recorded with a Varian DP-60 high resolution n.m.r. spectrometer operating at 56.4 Mc/s. The Varian variable temperature probe was used for both the low and high temperature studies. Referencing was performed by sample exchange with either fluorosulfuric acid or trifluoroacetic acid.

Conductivity measurements were made using methods and conductivity cells described previously (8). The cryoscopic measurements in nitrobenzene were made using the equilibrium technique and a cryoscope identical to that used for sulfuric acid (9). A platinum resistance thermometer was used to record the freezing point. The nitrobenzene was purified by fractional distillation at atmospheric pressure and stored over molecular sieve until used.

Results and Discussion

Vibrational Spectra

The observed vibrational frequencies for the solid adduct in the infrared and for the molten adducts in the Raman are given in Table I and Fig. 1. The Raman spectra of the solid were not satisfactory below 700 cm^{-1} because of an intense background. At higher frequencies sharp lines were obtained which agreed well with those observed for the melt (Table I). The spectrum of

TABLE I

Observed vibrational spectra for $SeF_4 \cdot SO_3$

Frequency* (cm^{-1})				Frequency (cm^{-1})		
	Raman			SO_3F^-		
Infrared	Solid	Melt	Assignment	Infrared†	Raman‡	AsF_3§
		154 vw 178 vw 269 vw	Torsional and bending modes of the polymeric chain			
317 m		321 w	SeF asym. bend. $\nu_4(E)$			274
375 m		381 w	SeF sym. bend. $\nu_2(A_1)$			341
406 w 426 w		416 w	SF wag. $\nu_6(E)$		409	
540 sh 561 m		567	SO sym. bend. $\nu_3(A_1)$	565	566	
597 m		587 w 605 w	SO asym. bend. $\nu_5(E)$	583	592	
699 s	717 m br	709 s br	SeF asym. str. $\nu_3(E)$			644
736 m	753 s	753 s	SeF sym. str. $\nu_1(A_1)$			707
807 m 824 m	819 m	805 w sh 829 m	SF str. $\nu_2(A_1)$	732	786	
1076 s	1081 s	1083 s	SO sym. str. $\nu_1(A_1)$	1073	1082	
1224 s 1238 s 1276 s	1237 m br 1290 m	1235 m br 1250 sh 1290 m	SO asym. str. $\nu_4(E)$	1277 1299	1250	
1422			$\nu_2+\nu_5$?			

*w = weak, m = medium, s = strong, v = very, br = broad, sh = shoulder.
†KSO_3F, see ref. 15.
‡KSO_3F in H_2O, see ref. 16.
§Raman, liquid, see ref. 17.

both the solid and the melt can be reasonably satisfactorily interpreted in terms of the simple ionic formulation $SeF_3^+.SO_3F^-$. The infrared and Raman spectra of the fluorosulfate ion are well known and typical values for the vibrational frequencies are given in Table I. The frequencies for the SeF_3^+ ion would be expected to be close to those for the isoelectronic AsF_3, for which the vibrational frequencies are also listed in Table I. On this basis, appropriate frequencies are readily assigned to SeF_3^+ although we note that they are slightly higher than those for AsF_3. This is consistent with the formal charge on selenium, which would be expected to reduce the polarity of the Se—F bonds compared to the As—F bonds and hence increase their strength. We note that there are splittings of the degenerate vibrations ν_4, ν_5, and ν_6 of the fluorosulfate ion which could be attributed to lowered site symmetry in the crystal. However, as some of these splittings are also observed in the melt, there is presumably some strong specific association between the ions in the liquid state which would also lower the symmetry of the SO_3F^- ion. The splittings of ν_3 and ν_2 and the splitting of $\nu_4(E)$ into a triplet might be factor group splittings in the crystal, although this leaves unexplained the fact that the splittings of ν_2 and ν_4 are also observed in the melt. The frequency of the S—F stretch (ν_2) is rather higher than has been observed previously for an ionic fluorosulfate and, indeed, approaches the values observed for covalent fluorosulfates which lie in the range from 842 cm^{-1} for $SF_5.SO_3F$ (10) to 876 cm^{-1} for $S_3O_8F_2$ (11).

As an ionic structure $SeF_3^+.SO_3F^-$ does not seem completely compatible with the experimental data, and, as the compound SbF_4SO_3F has previously been shown to have a highly polymerized structure involving fluorosulfate bridges in the liquid state (12), it seems reasonable to postulate a similar structure for $SeF_3.SO_3F$ (**1**). If the bridge

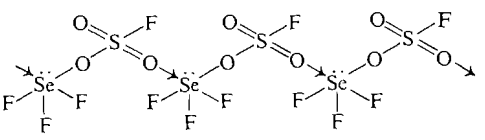

1

Can. J. Chem. Downloaded from www.nrcresearchpress.com by 210.87.254.6 on 09/05/12
For personal use only.

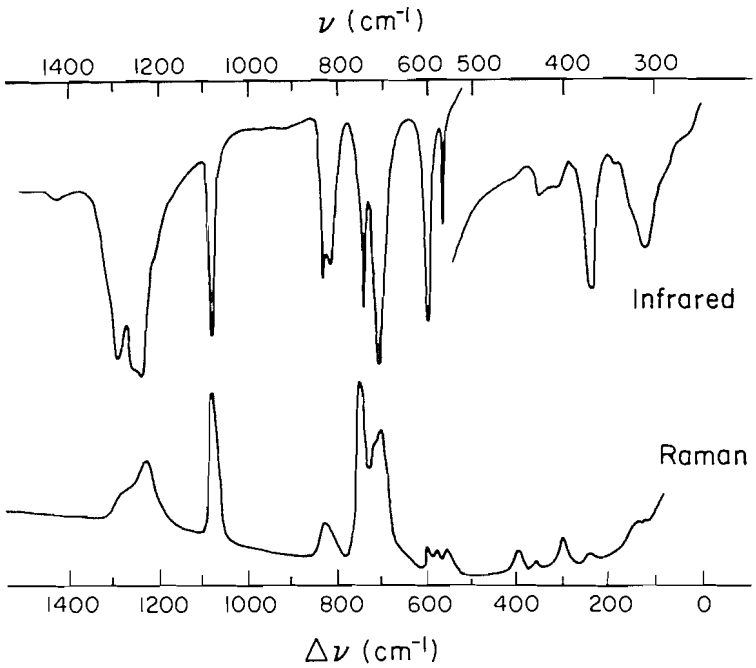

FIG. 1. Vibrational spectra for $SeF_4.SO_3$.

bonds have a certain amount of ionic character then this accounts for the S—F frequency being intermediate between that expected for an ionic and a covalent fluorosulfate. The reduced symmetry of the bridging fluorosulfate group could also account for at least part of the splitting of the S—O asymmetric stretching and bending vibrations ν_4 and ν_5. If the polymeric chains are not very long, the presence of fluorosulfate as both a bridging group and an end group could account for the splitting of ν_2 and the additional splitting of ν_4.

Our assignment for the SeF_3^+ ion agrees with that of Evans and Long except ν_4 to which they assign a frequency of 275 cm^{-1}, which is lower than would be expected on the basis of the relation of the other frequencies to those of AsF_3. This is further discussed in a following paper. The good agreement between the observed frequencies for both the solid and liquid states indicates that the structure of $SeF_3.SO_3F$ is essentially the same in both states.

Conductivity Measurements

The conductivities of solutions of $SeF_3.SO_3F$ in fluorosulfuric acid are shown in Fig. 2. It is clear that ionization is not complete as the conductivities are considerably less than those of a typical strong electrolyte such as KSO_3F. Assuming the simple equilibrium

$$SeF_3.SO_3F \rightleftarrows SeF_3^+ + SO_3F^-$$

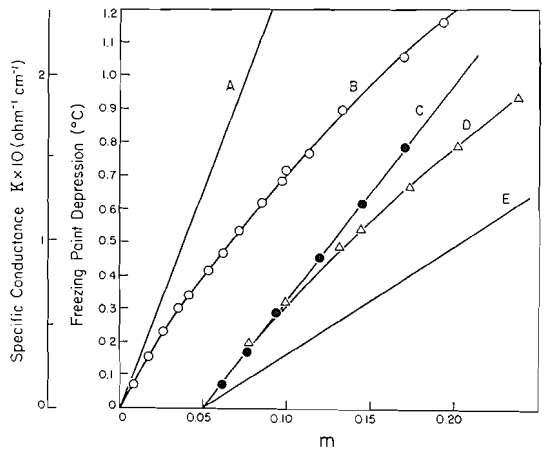

FIG. 2. *A*, conductivity of KSO_3F solution in HSO_3F; *B*, conductivity of $SeF_3.SO_3F$ solution in HSO_3F; *C*, freezing point depression for the non-electrolyte trinitrobenzene in nitrobenzene; *D*, freezing point depression for $SeF_3.SO_3F$ in nitrobenzene; *E*, freezing point depression for a dimeric non-electrolyte.

Can. J. Chem. Downloaded from www.nrcresearchpress.com by 210.87.254.6 on 09/05/12
For personal use only.

Can. J. Chem. Downloaded from www.nrcresearchpress.com by 210.87.254.6 on 09/05/12
For personal use only.

the degree of ionization can be obtained by comparison with the conductivity curve of the strong base KSO_3F. If the concentration of KSO_3F giving the same conductivity as a solution of $SeF_3.SO_3F$ of concentration $m_{SeF_3.SO_3F}$ is m_{KSO_3F}, then the degree of dissociation $\alpha = m_{KSO_3F}/m_{SeF_3.SO_3F}$ and the equilibrium constant for the above ionization is $K_b = \alpha^2/(1 - \alpha)$. Values of K_b calculated in this manner varied markedly with concentration and we conclude, therefore, that $SeF_3.SO_3F$ does not ionize as a simple base. This is perhaps not surprising in view of our previous conclusion that it is probably a polymeric material. If this is the case we might write the ionization in the following manner

$$(SeF_3.SO_3F)_n \rightarrow (SeF_3)_n(SO_3F)_{n-1}^+ + SO_3F^-$$

If it is assumed that this ionization is complete, then, if $[SeF_3.SO_3F]_s$ is the stoichiometric concentration of $SeF_3.SO_3F$, the degree of polymerization n of the cation in solution is given by

$$n = \frac{[SeF_3.SO_3F]_s}{[SO_3F^-]}$$

where the concentration of fluorosulfate ion is determined by comparison with the conductivity of a solution of the strong base KSO_3F. The values of n were found to be constant at about 1.6 at concentrations up to approximately 0.08 m and then to gradually increase to ~ 2.1 at 0.18 m. If there is also incomplete ionization then the results cannot be interpreted quantitatively, but one could say that probably $n \geq 2$, i.e., the dimer is probably the predominant species at low concentrations. If, as seems very likely, the selenium at one end of the chain is solvated with a solvent molecule, the species (**2**) is very similar to the polymeric chain postulated for the solid and molten states

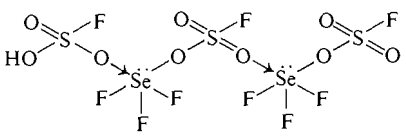

2

Conductivity measurements were also made in nitrobenzene. This solvent was selected because it gave stable solutions and has a relatively high dielectric constant of 34.8 at 30°. Solutions of $SeF_3.SO_3F$ in nitrobenzene were, however, found to have conductivities that are lower than those of solutions of $AlCl_3$ over the same concentration range (13). As $AlCl_3$ appears to be a very weak electrolyte in nitrobenzene, we conclude that $SeF_3.SO_3F$ is only very slightly ionized in this medium.

The molten complex has a low conductivity at 70° of only 6×10^{-4} ohm^{-1} cm^{-1} which, taking any reasonable value for the ionic mobilities, indicates a degree of ionization of only 1% or less. This again provides supporting evidence for our suggestion that the melt consists largely of the polymeric chain **1** and contains very few free ions.

Nuclear Magnetic Resonance

The ^{19}F n.m.r. spectrum of a solution of $SeF_3.SO_3F$ in HSO_3F at room temperature consisted of one line at -86.6 p.p.m. from CF_3CO_2H which may be assigned to fluorine on selenium in addition to the solvent line at -119.4 p.p.m. from CF_3CO_2H. The spectrum remained essentially the same down to $-85°$ except for a slight down-field shift of the higher field peak from -86.6 to -83.8 p.p.m. and also a broadening of this peak. Clearly the SO_3F group is exchanging rapidly with the solvent, as would indeed be expected if it is partially ionized. The single resonance observed for fluorine on selenium is consistent with the presence of the symmetrical SeF_3^+ ion. However, this signal becomes quite broad at low temperatures and was observed to have a width of 48 Hz at $-85°$. This must be attributed presumably to the slowing down of some exchange process between non-equivalent fluorines on selenium and this is consistent with the proposed bridged polymeric structure in which all three fluorines on the pseudo six-coordinated selenium cannot all be equivalent. Signals from non-equivalent fluorines on antimony have been observed for the analogous polymeric compound $SbF_4.SO_3F$ (12). Intramolecular fluorine exchange could occur via breaking and reforming of the fluorosulfate bridge. However, we also found that the expected ^{77}Se—F satellites could only be observed at $-85°$ ($J_{Se-F} = 1088$ Hz) so at higher temperatures there must be some relatively rapid intermolecular exchange involving the breaking of the Se—F bonds. The simplest explanation for this is that there is exchange via a small equilibrium concentration of SeF_4 and SO_3 at temperatures above $-85°$. This observed down-field shift in the F-on-Se resonance

Can. J. Chem. Downloaded from www.nrcresearchpress.com by 210.87.254.6 on 09/05/12
For personal use only.

from -83.8 to -86.8 p.p.m. from CF_3CO_2H on raising the temperature from $-85°$ to room temperature is also consistent with an increasing dissociation into SeF_4 and SO_3, as the chemical shift of SeF_4 is -141 p.p.m. from CF_3CO_2H. The Se—F coupling constant of 1088 Hz is of the same order of magnitude as the value of 837 Hz observed for $SeOF_2$ (14).

Molten $SeF_3.SO_3F$ also gave two resonances: one at -119 p.p.m. which may be attributed to the SO_3F group and one at -84.2 p.p.m. which may be attributed to the SeF_3 group. These resonances had the expected relative areas of 1:3.

Cryoscopy in Nitrobenzene

The freezing point depression of nitrobenzene produced by $SeF_3.SO_3F$ is compared with that produced by the non-electrolyte trinitrobenzene in Fig. 2. It may be seen that at very low concentrations $SeF_3.SO_3F$ apparently behaves like a non-electrolyte, and there cannot be more than a very small amount of ionization. As the concentration is increased, however, the slope of the freezing point curve for $SeF_3.SO_3F$ rapidly decreases until at 0.2 *M* it is scarcely more than half that for trinitrobenzene indicating essentially complete dimerization.

Conclusions

All our observations can be interpreted consistently in terms of a polymeric fluorosulfate bridged structure for the solid and molten states of the adduct $SeF_4.SO_3$. There is evidence that this polymeric structure persists in solution and that in dilute solution in nitrobenzene a dimer is probably the predominant species. This dimer could have the following cyclic structure

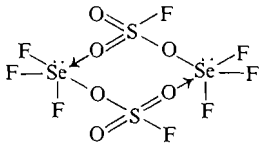

3

but a linear structure is equally probable particularly in a solvating solvent such as HSO_3F when one end of the chain could be stabilized by a solvent molecule (**2**). The spectroscopic evidence, in particular, shows that the bridge bonds in the polymer have appreciable ionic character, but there is no evidence in the solid or the melt for a free SeF_3^+ ion which is apparently a strong enough Lewis acid to form a bond of significant covalent character, even with the very weakly basic SO_3F^- ion. Only in the strongly ionizing fluorosulfuric acid does there appear to be any considerable amount of dissociation to free ions.

Acknowledgments

We thank the National Research Council of Canada for financial support of this work. We also thank the Council and the International Nickel Company for the award of scholarships (to W.A.W.).

1. R. D. Peacock. J. Chem. Soc. 3617 (1953).
2. N. Bartlett and P. L. Robinson. Chem. Ind. 1351 (1956).
3. N. Bartlett and P. L. Robinson. J. Chem. Soc. 3417 (1961).
4. R. D. Peacock. Progr. Inorg. Chem. **2**, 237 (1960).
5. A. J. Edwards and G. R. Jones. Chem. Commun. 346 (1968).
6. J. A. Evans and D. A. Long. J. Chem. Soc. 1688 (1968).
7. R. J. Gillespie and E. A. Robinson. Can. J. Chem. **39**, 2179 (1961).
8. J. Barr, R. J. Gillespie, and R. C. Thompson. Inorg. Chem. **3**, 1149 (1964).
9. R. J. Gillespie, E. D. Hughes, and C. K. Ingold. J. Chem. Soc. 2473 (1950).
10. H. J. Emeleus and K. J. Packer. J. Chem. Soc. 171 (1962).
11. R. J. Gillespie and E. A. Robinson. Can. J. Chem. **39**, 2179 (1961).
12. R. J. Gillespie and R. A. Rothenbury. Can. J. Chem, **42**, 416 (1964).
13. R. E. Van Dyke and H. E. Crawford. J. Amer. Chem. Soc. **73**, 2018 (1951).
14. T. Birchall, R. J. Gillespie, and S. L. Vekris. Can. J. Chem. **43**, 1672 (1965).
15. D. W. A. Sharp. J. Chem. Soc. 3761 (1957).
16. H. Siebert. Z. Anorg. Allg. Chem. **289**, 15 (1957). R. J. Gillespie and E. A. Robinson. Can. J. Chem. **40**, 644 (1962).
17. C. E. Aynsley, R. E. Dodd, and R. Little. Spectrochim. Acta, **18**, 1005 (1962). J. A. Evans and D. A. Long. J. Chem. Soc. 1688 (1968).

Can. J. Chem. Downloaded from www.nrcresearchpress.com by 210.87.254.42 on 09/05/12
For personal use only.

An investigation of the structures of the adducts of SF_4 with BF_3, PF_5, AsF_5, and SbF_5 in the solid state and in solution in HF

M. AZEEM[1], M. BROWNSTEIN, AND R. J. GILLESPIE
Department of Chemistry, McMaster University, Hamilton, Ontario

Received May 22, 1969

The structure of the solid adducts of SF_4 with several fluoride acceptors has been studied by investigations of the ^{18}F exchange between $S^{18}F_4$ and BF_3 and between SF_4 and $B^{18}F_4$, the infrared spectrum of $SF_4.BF_3$, and the Raman spectra of $SF_4.BF_3$, $SF_4.PF_5$, $SF_4.AsF_5$, and $SF_4.SbF_5$. The experimental observations are best accounted for in terms of an ionic structure $SF_3^+.MX_n^-$ in each case, but there is good evidence for relatively strong fluorine bridging between the ions.

In anhydrous hydrogen fluoride solution, SF_4 and the adducts $SF_4.BF_3$ and $SF_4.SbF_5$ were studied conductimetrically and by ^{19}F nuclear magnetic resonance. Both methods indicate complete ionization of the adducts to SF_3^+ and the complex fluoroanion. SF_4 is a weak base in hydrogen fluoride ionizing to SF_3^+ and HF_2^-.

Canadian Journal of Chemistry, 47, 4159 (1969)

Introduction

Bartlett and Robinson (1, 2) first reported that SF_4 forms a series of solid complexes with a number of inorganic fluorides that act as fluoride ion acceptors, e.g. $SF_4.BF_3$, $SF_4.AsF_5$, $SF_4.SbF_5$. These authors first postulated (1) that these compounds are simple donor–acceptor complexes, e.g., $F_4S{:}BF_3$. Since that time, there has been considerable discussion of the structures of these compounds. It has been generally supposed that they are either ionic, e.g., $SF_3^+.BF_4^-$, or fluorine-bridged (2–5), but convincing experimental evidence has been lacking. The great reactivity of the compounds towards moisture and solvents and their insolubility in all solvents except HF has made spectroscopic studies extremely difficult. Cotton and George (3) were unable to obtain an infrared (i.r.) spectrum, but later Seel and Detmer (4) observed a few bands in the i.r. spectrum of the solid. In particular, they found a band at 1050 cm^{-1} which they assigned to BF_4^- and bands at 908 and 940 cm^{-1} which, by comparison with the known spectrum of the isoelectronic PF_3, they assigned to SF_3^+.

We have attempted to obtain further information on the structures of these complexes by (*a*) studying the ^{18}F exchange when they are formed from the 2 components and then decomposed by a suitable donor molecule, (*b*) measuring the i.r. and Raman spectra of the solids, and (*c*) investigating solutions of the complexes in anhydrous hydrogen fluoride by means of electrical conductivity and nuclear magnetic resonance (n.m.r.) measurements. Since our work was completed, Evans and Long (6) have reported the Raman spectrum of the molten complex $SF_4.SbF_5$ at 250 °C and they have interpreted their results in terms of the ionic formulation $SF_3^+.SbF_6^-$.

Results and Discussion

^{18}F Exchange Studies

The adduct $SF_4.BF_3$ was prepared using BF_3 labelled with ^{18}F (7) by condensing equal volumes of the 2 gases into a trap cooled with liquid air. The trap was then allowed to warm up to some higher temperature in the range $-100°$ to room temperature and to remain at this temperature for some period of time between 5 and 60 min in order to allow the formation of the adduct. Any excess reactants were then pumped off and after again cooling the adduct to liquid air temperature, it was decomposed by the addition of tetrahydrofuran or diethyl ether (precooled to $\sim -80°$) and then warmed to $-20°$, or to the temperature at which the adduct had previously been formed if this was lower. The liberated SF_4

$$BF_3.SF_4 + R_2O \rightarrow BF_3.OR_2 + SF_4$$

was collected and its specific activity determined. The exchange was also studied using labelled SF_4. The results are given in Table I. The results obtained at room temperature show that, for reaction times of 20 min or more, the exchange was complete. Shorter reaction times were not

[1]Present Address: College of Engineering, P.O. Box 800, Riyadh, Saudi Arabia.

TABLE I

^{18}F exchange between SF_4 and BF_3

Temperature (°C)	Exchange time (min)	^{18}F transferred (%)	
		From BF_3 to SF_4	From SF_4 to BF_3
25	30	55.8, 55.0, 57.1	43.7, 43.1
−15	30	48.6	
−30	30	44.2, 45.1	
−40	30	33.1, 36.6	34.7
−60	30	27.4	
−80	5	17.5	
	10	15.5	
	20	14.5, 18.2, 17.9, 16.8	
	30	18.7	8.6, 11.1
	60	17.4	
−100	10	18.7	

studied. The average values of 56% transfer of activity from $B^{18}F_3$ to SF_4 and of 43% transfer of activity from $S^{18}F_4$ to BF_3 agree well with the values of 57 and 43%, respectively, expected for complete exchange. At temperatures of −15° and below, exchange was incomplete even after 1 h and the amount of exchange after a fixed reaction time, e.g., 20 min, decreased and appeared to reach a constant limiting value, at −80°, which was independent of time (Table I).

At room temperature, the adduct is in equilibrium with its components in the vapor state and has a vapor pressure of approximately 100 mm. It seems reasonable to suppose, therefore, that rapid and complete exchange occurs by the rapid formation and dissociation of the adduct. If the adduct were a simple donor–acceptor complex, then there would be no obvious mechanism for exchange. However, if the adduct is a fluorine-bridged compound or an ionic compound, $SF_3^+BF_4^-$, then exchange can occur on the formation and dissociation of the adduct.

At low temperatures of −80° and below, a constant minimum amount of exchange occurs even after 5 min reaction time. Because this amount of exchange occurs so rapidly, and because the vapor pressure is extremely small at this temperature, it seems reasonable to suppose that exchange is not occurring via the vapor phase, but directly on the formation and decomposition of the adduct. On the formation of the ionic complex $SF_3^+BF_4^-$ with labelled BF_3, 1 of the 4 fluorines in BF_4^- would be labelled, and hence, on decomposing the adduct with ether or tetrahydrofuran, 25% of the activity would be transferred to the SF_4, assuming that BF_4^- is free to rotate in the solid or during the reaction with the ether. If labelled SF_4 is used to form the adduct, then we expect that 25% of the activity will be transferred to the BF_4^- and then 25% of this activity will be returned to SF_4 when the adduct is decomposed, i.e., we expect an overall transfer of 19% of the activity. In both types of experiment, less activity was transferred at −80° than predicted. We conclude, therefore, that either the adduct does not have a simple ionic structure, or, if it is ionic, the ions have their rotational motion restricted in the solid state and during the reaction with ether.

Hindrance to rotational motion could arise from fluorine bridging between the ions. We therefore now consider the expected results for a fluorine-bridged structure. If the bridging between molecules was relatively weak and unsymmetrical as in **1**, the weak component of the bridge would be expected to break on decomposition, and no fluorine transfer would be observed. However, if both fluorine bridge bonds are identical as in **2**–**4**, giving an essentially ionic compound, then fluorine exchange between SF_4 and BF_3 will be observed on formation and decomposition of the adduct. If BF_3 is labelled, then there is a 33% chance of forming a bridge bond containing ^{18}F, and on decomposition of the adduct, one of the two B—F bridge bonds must break, transferring one of the fluorines to SF_4. Thus, about 17% of the $B^{18}F_3$ activity is expected to be transferred to SF_4. The experimental results at −80 and −100° showed that between 15 and 19% of the activity was transferred. When labelled SF_4 is used to form the adduct, the

Can. J. Chem. Downloaded from www.nrcresearchpress.com by 210.87.254.42 on 09/05/12
For personal use only.

TABLE II

Raman spectrum of $SF_4.SbF_5$

Solid			Melt*	
Relative intensity	Frequency (cm^{-1})	Assignment	Frequency (cm^{-1})	Assignment*
26	288	ν_5 SbF_6^-	291	ν_5 SbF_6^-
5	411	ν_4 SF_3^+	356	ν_4 SF_3^+
11	529	ν_2 SF_3^+		
19	554	ν_2 SbF_6^-	568	ν_2 SbF_6^-
20	582			
100	652	ν_1 SbF_6^-	645	ν_1 SbF_6^-
24	680	ν_3 SbF_6^-	690	ν_2 SF_3^+
sh	928		922	ν_3 SF_3^+
66	943	ν_1, ν_3 SF_3^+	943	ν_1 SF_3^+
sh	955			

*Reference 6.

probability of forming an ^{18}F bridge will be 25%. Hence, when the adduct is decomposed, the fluorine in one of the two bridge bonds to each boron will be transferred to the boron and thus there will be a transfer of approximately 12.5% of the activity. The observed results that approximately 9–11% of the activity was transferred are in reasonable agreement with this prediction.

Thus the results of the fluorine exchange experiments are best interpreted in terms of fluorine-bridged ionic structures such as **2**–**4**. These structures differ only in the position of the fluorine in the bridge. Structure **2** corresponds to fluorine bridges between BF_4^- and SF_3^+, structure **4** to fluorine bridges between BF_2^+ and SF_5^- and structure **3** is intermediate with a symmetrical fluorine bridge.

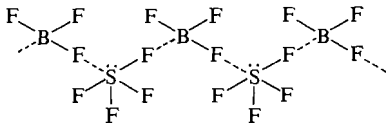

1

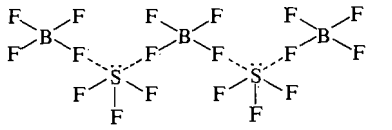

2

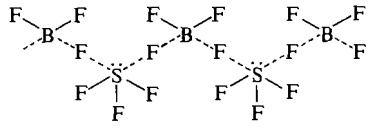

3

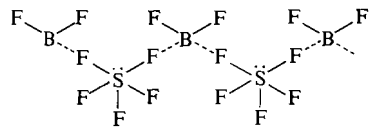

4

Vibrational Spectra

$SF_4.SbF_5$

The Raman spectrum of the molten complex has been reported very recently by Evans and Long (6) and interpreted in terms of the ionic structure $SF_3^+SbF_6^-$. We have obtained the Raman spectrum of the solid. The results are given in Table II.

The hexafluoroantimonate ion belongs to the point group O_h and therefore has 6 normal modes of vibration: $\nu_1(A_{1g})$, $\nu_2(E_g)$, $\nu_3(T_{1u})$, $\nu_4(T_{1u})$, $\nu_5(T_{2g})$, $\nu_6(T_{2u})$; ν_1, ν_2, and ν_5 are Raman active and ν_3 and ν_4 are i.r. active. Previous assignments for SbF_6^- are given in Table III. We can assign the fundamental vibrations of the SbF_6^- ion observed in our spectra of the solid complex by comparison with these earlier assignments. Our assignments for SbF_6^- agree quite well with those of Evans and Long (6), except that we found ν_2 and ν_5 to be doublets, and we attribute the weak line at 680 cm^{-1} to ν_3, which is formally forbidden, instead of to the SF_3^+ ion. We assume that the splitting of ν_2 and ν_5 and the observation of ν_3 in the Raman spectrum arise from some lowering of the symmetry of the SbF_6^- in the crystal, probably as a result of fluorine bridging with SF_3^+.

The bands observed at 928, 943, 529, and 411

Can. J. Chem. Downloaded from www.nrcresearchpress.com by 210.87.254.42 on 09/05/12
For personal use only.

TABLE III

Vibrational frequencies of the SbF_6^- ion, cm^{-1}

Raman					Infrared		
$LiSbF_6$* solid	$KSbF_6$† solid	$KSbF_6$‡ solution in DMF	$SeF_3.SbF_6$‡ molten	$SF_3.SbF_6$‡ molten	$KSbF_6$‡ solid	$LiSbF_6$* solid	Assignment
668	664	645	645	645			$\nu_1(A_{1g})$
558	583	572	550	568			$\nu_2(E_g)$
					660	669	$\nu_3(T_{1u})$
						350	$\nu_4(T_{1u})$
294	298 270	279	290	291			$\nu_5(T_{2g})$

*Reference 8.
†This work.
‡Reference 6.

TABLE IV

Vibrational frequencies for the SF_3^+ ion and PF_3, cm^{-1}

Frequency of PF_3*	Assignment	Frequency of SF_3^+ in			
		$SF_3.BF_4$	$SF_3.PF_6$	$SF_3.AsF_6$	$SF_3.SbF_6$
892	$\nu_1(A_1)$	939	954	945	943
487	$\nu_2(A)$	529	531	530	529
860	$\nu_3(E)$	913	929	926	928
344	$\nu_4(E)$	414	408	411	411

*Reference 9.

cm^{-1} are assigned by comparison with the spectrum of the isoelectronic molecule PF_3 (9) to ν_3, ν_1, ν_2, and ν_4, respectively, of the SF_3^+ ion (Table IV). A shoulder on the ν_3 band is apparent at 955 cm^{-1}. This is consistent with some reduction in symmetry as a consequence of fluorine bridging. This assignment differs from that proposed by Evans and Long (6) on two points: (*a*) We assign the weak band at 529 cm^{-1} rather than the band at 690 cm^{-1} to ν_2; this latter band, which we observed at 680 cm^{-1}, being assigned to ν_3 of SbF_6^-. Although ν_3 should be forbidden, it is reasonable to assume that it is weakly allowed in the melt as well as in the crystal because of fluorine bridging. This assignment is confirmed by the fact that no line at 680 cm^{-1} is found in the spectra of $SF_4.BF_3$ and $SF_4.PF_5$ although both contain the SF_3^+ ion. Evans and Long themselves regarded the assignment of the 690 cm^{-1} band to ν_2 as rather unsatisfactory; (*b*) We find the ν_4 band at 411 cm^{-1} rather than at 356 cm^{-1}. This is confirmed by the observation of bands having frequencies close to this value in all the other SF_3^+ compounds that we have studied (Table IV). Perhaps this difference is a consequence of passing from the liquid to the solid state.

$SF_4.BF_3$

The results of our measurements on the i.r. and Raman spectra of solid $SF_4.BF_3$ are given in Table V. The incomplete i.r. spectrum obtained previously by Seel and Detmer (4) was interpreted by them in terms of the ionic structure $SF_3^+BF_4^-$.

The tetrafluoroborate anion belongs to the point group T_d and therefore has 4 normal modes of vibration, all of which are active in the Raman ($\nu_1(A_1)$, $\nu_2(E)$, $\nu_3(T_2)$, and $\nu_4(T_2)$) and only ν_3 and ν_4 are active in the i.r. An assignment of the observed bands in the i.r. and Raman spectra can be made in terms of the ionic model SF_3^+-BF_4^- using the previous assignments for BF_4^- (Table VI) and PF_3 (Table IV). However, the forbidden i.r. frequencies ν_1 and ν_2 appear with reasonable intensity, and ν_2 appears as a doublet. In addition, ν_3 for SF_3^+ is also split. The occurrence of the forbidden bands and the additional splittings can be attributed to a lowering of the symmetry of both ions in the crystal, probably as a result of fluorine bridging.

Can. J. Chem. Downloaded from www.nrcresearchpress.com by 210.87.254.42 on 09/05/12
For personal use only.

TABLE V

Infrared* and Raman spectra of $SF_4.BF_3$

Raman		Infrared frequency (cm^{-1})			
Relative intensity	Frequency shift (cm^{-1})	This work		Seel and Detmer (4)	Assignment
23	357	357	w		ν_2 BF_4^-
		370	w		
21	414	409	m		ν_4 SF_3^+
6	529	520	vs		ν_2 SF_3^+
7	546	536	vs		ν_4 BF_4^-
43	770	753	m		ν_1 BF_4^-
		773	m		
46	913	910	vs	908	ν_1, ν_3 SF_3^+
sh	921				
100	939	935	vs	940	
		1035–1090	vs,br	1050	ν_3 BF_4^-
		1140	s		

*s = strong, m = medium, w = weak, v = very, br = broad.

TABLE VI

Vibrational frequencies for the BF_4^- ion (cm^{-1})

Raman						
Aqueous $NaBF_4$			Solid KBF_4	Infrared		
Ref. 10	Ref. 11	This work	(This work)	KBF_4 (Ref. 12)	$NaBF_4$ (Ref. 13)	Assignment
369	353	358	358			$\nu_2(E)$
541	524	530	529	525	516	$\nu_4(T_2)$
			536	536	527	
786	769	767	773	773	779	$\nu_1(A_1)$
1100	984			1038	1036	$\nu_3(T_2)$
	1016			1063		
				1078	1078	

TABLE VII

Raman spectrum of $SF_4.PF_5$

			KPF_6*	
Relative intensity	Frequency shift (cm^{-1})	Assignment	Raman frequency shift (cm^{-1})	Infrared frequency (cm^{-1})
13	408	ν_4 SF_3^+		
5	463	ν_5 PF_6^-		
14	479		477	
10	531	ν_2 SF_3^+		
19	558	ν_2 PF_6^- or ν_2, ν_4 PF_6^-		558
8	580		580	
90	748	ν_1 PF_6^-	751	
5	815	ν_3 PF_6^-		830
21	929			
100	954	ν_1, ν_3 SF_3^+		
sh	964			

*Reference 8.

Can. J. Chem. Downloaded from www.nrcresearchpress.com by 210.87.254.42 on 09/05/12
For personal use only.

Can. J. Chem. Downloaded from www.nrcresearchpress.com by 210.87.254.42 on 09/05/12
For personal use only.

$SF_4.PF_5$

The vibrational spectrum of this compound has not been previously studied. The Raman spectrum (Table VII) can again be assigned on the basis of the ionic structure $SF_3^+PF_6^-$ making use of previous assignments for PF_6^- and PF_3. The spectrum of PF_6^- is very similar to that of SbF_6^- and again indicates a lower symmetry than O_h. Thus, we see that ν_5 and ν_2 are split into doublets, and the forbidden ν_3 vibration appears weakly at 815 cm^{-1}. As in all the other compounds studied, ν_3 of SF_3^+ is split into a doublet. These observations are consistent with fluorine bridging between the ions SF_3^+ and PF_6^-.

$SF_4.AsF_5$

The vibrational spectrum of this compound has not been previously studied. As for $SF_3.PF_6$ and $SF_3.SbF_6$, a reasonable assignment can be made in terms of the ionic structure $SF_3^+.AsF_6^-$ (Table VIII). Again we note that ν_2 for AsF_6^- and ν_3 for SF_3^+ are split, indicating probable fluorine bridging. The frequencies assigned to SF_3^+ in all 4 compounds studied have been summarized in Table IV. The good agreement between the observed frequencies gives further confirmation of the correctness of the assignment.

TABLE VIII

The Raman spectrum of $SF_4.AsF_5$

Relative intensity	Frequency shift (cm^{-1})	Assignment	$CsAsF_6$* Frequency shift (cm^{-1})
36	379	ν_5 AsF_6^-	372
11	411	ν_4 SF_3^+	
7	530	ν_2 SF_3^+	
35	563	ν_2 AsF_6^-	
10	587		576
76	686	ν_1 AsF_6^-	685
19	926		
100	945	ν_1, ν_3 SF_3^+	
sh	960		

*Reference 8.

Conductivity Measurements in HF Solution

The two adducts $SF_4.BF_3$ and $SF_4.SbF_5$ give solutions in anhydrous HF which have conductivities that are closely similar to, although slightly lower than, those of KBF_4 and $KSbF_6$ (14) (Table IX and Fig. 1). We conclude, therefore, that the 2 adducts are fully ionized in solution in HF, e.g.

$$SF_4.BF_3 \rightarrow SF_3^+ + BF_4^-$$

TABLE IX

Conductivities of solutions of $SF_4.BF_3$, $SF_4.SbF_5$, and SF_4 in HF

$SF_4.BF_3$		$SF_4.SbF_5$	
Concentration × 10 (*m*)	$\kappa \times 10^2$ (ohm^{-1} cm^{-1})	Concentration × 10 (*m*)	$\kappa \times 10^2$ (ohm^{-1} cm^{-1})
0.522	1.109	0.305	0.714
0.935	1.806	0.546	1.169
1.26	2.455	0.698	1.548
1.38	2.446	0.732	1.457
1.55	2.67	0.945	1.806
1.77	2.97	1.19	2.231
1.92	3.16	1.43	2.507
2.63	4.08	2.20	3.471
5.61	7.21	3.08	4.415
8.39	8.83		
8.40	9.01		
12.38	11.09		

SF_4			
Concentration × 10 (*m*)	$\kappa \times 10^2$ (ohm^{-1} cm^{-1})	Concentration* of KF × 10 (*m*)	$K\dagger \times 10^2$
0.41	0.73	0.20	2
0.72	1.1	0.32	3
1.8	2.3	0.76	6
2.4	2.4	0.80	4
			Mean 4 ± 2

*Molalities of the KF solutions having the same conductivities as the SF_4 solutions, $[KF] = [SF_3^+]$.
†$K = [SF_3^+][HF_2^-]/[SF_4]$.

A solution of SF_4 also has a moderate conductivity, although this is considerably smaller than the fully ionized $SF_4.BF_3$ and $SF_4.SbF_5$. We conclude that SF_4 behaves as a partially ionized weak base in solution in anhydrous HF

$$SF_4 + HF \rightleftarrows SF_3^+ + HF_2^-$$

The results in Fig. 1 show that the mobility of the SF_3^+ ion must be similar to that of the K^+ ion. Hence, by comparing the observed conductivity of SF_4 with that of KF at any given temperature, one can obtain the degree of dissociation and hence the equilibrium constant for its ionization

$$K = [SF_3^+][HF_2^-]/[SF_4] = 4 \pm 2 \times 10^{-2}$$

at 0 °C

Nuclear Magnetic Resonance Spectra

Solutions of $SF_4.BF_3$ in anhydrous HF gave spectra consisting of a single broad line at room temperature which split into 2 lines at low temperatures. Similar behavior was observed for $SF_4.SbF_5$ and $SF_4.AsF_5$ solutions (Table X).

TABLE X

^{19}F chemical shifts (p.p.m. from $CFCl_3$)

Solute	T (°C)	Chemical shift: SF_3^+	Chemical shift: HF	Chemical shift: BF_4^-, SbF_6^-, and $Sb_2F_{11}^-$
$SF_4.BF_3$	25	—	195.3	—
	0	—	195.3	—
	−50	−26.7	194.2	—
	−70	−25.9	193.2	—
	−90	−25.5	191.3	—
$SF_4.BF_3 + KBF_4$	−30	−26.9	194.5	—
	−50	−26.1	194.5	—
$SF_4.BF_3 + KF$	0	—	191.6	153.5
	−30	—	190.0	152.9 (BF_4^-)
	−50	—	189.7	153.5 (BF_4^-)
$SF_4.BF_3 + NH_4F$	−55	—	175.8	151.7
$SF_4.AsF_5$*	25	−30.5	191.7	
$SF_4.2AsF_5$	25	−29.2	181.3	
	−5	−28.4	180.6	
	−30	−27.5	181.5	
	−60	−26.8	178.3	
$SF_4.SbF_5$	−60	−27.1	198	
	−90	−26	195.4	
$SF_4.2SbF_5$	−85	−27.6	191.1	124.3 (SbF_6^-)
				95.2
				120.7 ($Sb_2F_{11}^-$)†
				142.6

*Slight excess of AsF_5.

†The values may be compared with those for $CsSb_2F_{11}$ in SO_2 (89.4, 109.1, and 131.2 (p.p.m. from $CFCl_3$) (16)) and for $Sb_2F_{11}^-$ in HF ((ref. 15 and this work) 93.0, 120.1, and 141.8). We note that there is an appreciable solvent shift in going from HF to SO_2, probably because of some ion-pair formation in SO_2.

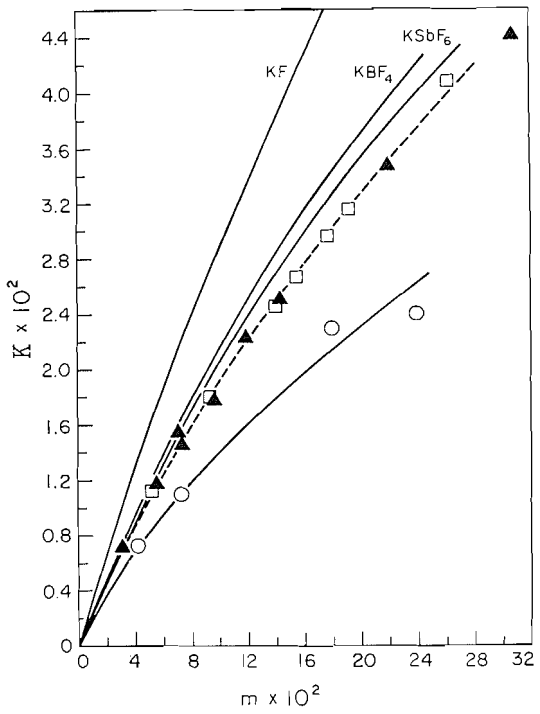

FIG. 1. Conductivities κ (ohm^{-1} cm^{-1}) of solutions in anhydrous HF. □, $SF_4.BF_3$; ▲, $SF_4.SbF_5$; ○, SF_4.

The low field line has very nearly the same chemical shift in each case (−25 to −30 p.p.m. from $CFCl_3$) and is in the fluorine-on-sulfur region of the spectrum. We attribute this peak to the SF_3^+ ion. The high field peak is due to the anion BF_4^-, SbF_6^-, or AsF_6^- exchanging with the solvent. Additions of a small amount of fluoride ion to solutions of $SF_4.BF_3$ resulted in the appearance of a new peak at 153.5 p.p.m. from $CFCl_3$ and the simultaneous disappearance of the peak assigned to SF_3^+, which could not then be observed even at low temperatures. The new peak is due to BF_4^- (cf. the shift of +153.6 p.p.m. observed for a solution of KBF_4 in HF). The addition of fluoride represses the exchange of fluoride between BF_4^- and the solvent

$$BF_4^- + HF \rightleftarrows BF_3 + HF_2^-$$

while at the same time promoting the exchange between SF_3^+ and the solvent

$$SF_3^+ + HF_2^- \rightleftarrows SF_4 + HF$$

Addition of a slight excess of AsF_5 to the $SF_4.AsF_5$ solution gave an SF_3^+ peak which was observable, although rather broad, even at room temperature. Addition of 1 mole of AsF_5 per

Can. J. Chem. Downloaded from www.nrcresearchpress.com by 210.87.254.42 on 09/05/12
For personal use only.

Can. J. Chem. Downloaded from www.nrcresearchpress.com by 210.87.254.42 on 09/05/12
For personal use only.

mole of $SF_4.AsF_5$ gave a sharp SF_3^+ peak even at room temperature. No AsF_6^- peak was observed in any of the spectra, presumably because of exchange of fluoride with the solvent and quadrupole relaxation of the ^{75}As nucleus. For the solutions of $SF_4.SbF_5$, a peak at -27.6 p.p.m. which may be attributed to SF_3^+ was obtained at low temperature in addition to a peak due to the solvent. No peak was observed from SbF_6^-, presumably because of partially relaxed coupling to $^{121}Sb(I = 5/2)$ and ^{127}Sb $(I = 7/2)$ and exchange with the solvent, giving a very broad spectrum which could not be detected above the base line noise. Addition of SbF_5 to this solution, however, gave signals which can be attributed to SbF_6^- and $Sb_2F_{11}^-$ (15, 16). The n.m.r. data thus provides strong support for the conclusion that all 3 adducts are completely ionized to SF_3^+ and the corresponding anion in solution in HF.

A solution of SF_4 in HF gave only a single resonance at all temperatures, showing that exchange occurs. This is consistent with the conductimetric evidence for incomplete ionization of SF_4 in HF.

Experimental

Fluorine Exchange Reactions

The labelled fluorides were prepared and their specific activity determined as described previously (7). The adduct $SF_4.B^{18}F_3$ was prepared by condensing equal volumes of the 2 gases into a trap cooled in liquid air. The trap was then allowed to warm up to some higher temperature in the range $-100°$ to room temperature and allowed to remain at this temperature for some time between 5 and 60 min in order to allow formation of the adduct. Any excess of the reactants was pumped off. After again cooling the adduct to liquid air temperature, it was decomposed by the addition of tetrahydrofuran or diethyl ether, precooled to $-80°$, and then warmed to $-20°$ or to the temperature at which the adduct had previously been formed if this was lower. The liberated SF_4 was collected in a trap cooled in liquid air. Sodium hydroxide solution was then added to the cold trap and the temperature allowed to rise gradually to room temperature to obtain complete hydrolysis of the SF_4. The solution was then made up to a standard volume for determination of the activity, and hence the % activity transferred from the $B^{18}F_3$ was determined. Portions of this solution were taken for the determination of the ^{18}F activity and for analysis. The remaining tetrahydrofuran solution was also analyzed and the ^{18}F activity determined. Sulfur was determined as barium sulfate and boron as boric acid. From the analytical and ^{18}F activity data, the percentage of activity transferred from BF_3 to SF_4 was calculated. The exchange between $S^{18}F_4$ and BF_3 was studied in the same manner.

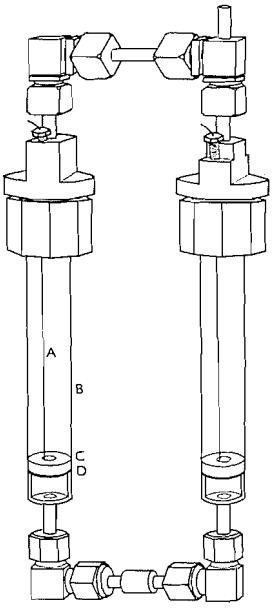

FIG. 2. Conductivity cell: A, platinum lead; B, Kel-F tube; C, teflon washer; D, platinum disk electrode supported on ledge at side of tube.

Conductivity Measurements

These were made as described previously (15). Solutions of the SF_4 adducts appeared to attack the platinum black coating used on the electrodes, which were, therefore, replaced by rhodium electrodes coated with a layer of rhodium black which appeared to be resistant to attack. Some measurements were made with the same type of cell as described previously, while some, particularly on dilute solutions, were made with the type of cell shown in Fig. 2, which was constructed entirely of Kel-F, Teflon and platinum (or rhodium). The larger volume of this cell enabled measurements to be made more easily on dilute solutions.

Nuclear Magnetic Resonance Spectra

Solutions were contained in thin-wall Kel-F tubes which were inserted into precision glass tubes. The reference liquid $CFCl_3$ was contained in the annular space. Spectra were obtained on either a Varian Associates HA-100 or a DA-60 spectrometer.

Raman Spectra

These were obtained using a Spex Industries double monochromator with a phototube detector and electronic amplifier and recorder. Spectra Physics Model 125 helium–neon and Model 145 argon-ion lasers were used as light sources.

Materials

Hydrogen fluoride was purified as previously described (15). Antimony pentafluoride (Ozark-Mahoning Co.) was distilled twice in an all glass apparatus immediately before use. Sulfur tetrafluoride (Matheson) was purified by bubbling through mercury to remove SCl_2 and then

distilled on a vacuum line. Boron trifluoride and phosphorus pentafluoride (Matheson) and arsenic pentafluoride (Ozark-Mahoning Co.) were purified by trap-to-trap distillation on a vacuum line. The purity of the SF_4, PF_5, and AsF_5 was checked by determining their i.r. spectra in a 10 cm Monel gas cell with silver chloride windows.

The adducts $SF_4.BF_3$, $SF_4.PF_5$, and $SF_4.AsF_5$ were prepared by direct combination of the gases in a glass vacuum line. Excess of either component was removed by pumping on the solid adduct. The adduct $SF_4.SbF_5$ was prepared in a similar manner, using an excess of SF_4. To ensure complete reaction, the product was heated to 200 °C under an atmosphere of SF_4 and then pumped, after cooling to room temperature. An X-ray powder photograph gave the space group and cell dimensions previously found by Bartlett and Robinson (3).

Infrared Spectra

The i.r. spectrum of $SF_4.BF_3$ was determined by condensing the adduct onto a window which was held in a brass frame mounted on a glass tube into which liquid air could be poured. The window was thus cooled and the $SF_4.BF_3$ was sublimed onto the cold window until a sufficient thickness was obtained. The spectrum was recorded between 2100 and 500 cm^{-1} using a silver chloride window, and between 600 and 250 cm^{-1} with a polythene window.

Acknowledgments

We thank the Office of Scientific Research of the United States Air Force and the National Research Council of Canada for financial support of this work. One of us (M.B.) also thanks the Council for the award of a scholarship.

1. N. Bartlett and P. L. Robinson. Chem. Ind. London, 1351 (1956).
2. N. Bartlett and P. L. Robinson. J. Chem. Soc. 3417 (1961).
3. F. A. Cotton and J. W. George. J. Inorg. Nucl. Chem. **7**, 397 (1958).
4. F. Seel and O. Detmer. Z. Anorg. Allg. Chem. **301**, 113 (1959).
5. A. L. Oppegard, W. C. Smith, E. L. Muetterties, and V. A. Engelhardt. J. Amer. Chem. Soc. **82**, 3836 (1960).
6. J. A. Evans and D. A. Long. J. Chem. Soc. A, 1688 (1968).
7. R. J. Gillespie and M. Azeem. J. Inorg. Nucl. Chem. **28**, 1791 (1966).
8. G. M. Begun and A. C. Rutenberg. Inorg. Chem. **6**, 2212 (1967).
9. M. K. Wilson and S. R. Polo. J. Chem. Phys. **20**, 1716 (1952).
10. J. O. Edwards, G. C. Morrison, V. F. Ross, and J. W. Schultz. J. Amer. Chem. Soc. 77, 266 (1955).
11. J. Goubeau and W. Bues. Z. Anorg. Allg. Chem. **268**, 221 (1952).
12. N. N. Greenwood. J. Chem. Soc. 3811 (1959).
13. G. L. Cote and H. W. Thompson. Proc. Roy. Soc. London, Ser. A, **210**, 217 (1951).
14. M. Brownstein and R. J. Gillespie. To be published.
15. R. J. Gillespie and K. C. Moss. J. Chem. Soc. 1170 (1966).
16. J. Bacon, P. A. W. Dean, and R. J. Gillespie. Can. J. Chem. **47**, 1655 (1969).

Can. J. Chem. Downloaded from www.nrcresearchpress.com by 210.87.254.42 on 09/05/12
For personal use only.

Can. J. Chem. Downloaded from www.nrcresearchpress.com by 210.87.254.105 on 09/05/12
For personal use only.

The photolyses of acetyl and ethyl isocyanates in the vapor phase: new examples of Type II photodissociation[1]

N. J. FRISWELL[2] AND R. A. BACK
Division of Pure Chemistry, National Research Council of Canada, Ottawa, Canada

Received June 24, 1969

The photolyses of acetyl and ethyl isocyanate vapors have been studied at 25 °C, at pressures between about 2 and 30 Torr, using either monochromatic 2288 Å radiation or light from a medium-pressure mercury arc equipped with a Vycor filter. Molecular photodissociations were of major importance with both compounds, with formation of HNCO + CH_2CO and HNCO + C_2H_4 accounting for about 70 and 60% of the decomposition of the acetyl and ethyl esters, respectively. It is suggested that these products were formed through a 6-membered ring transition state analogous to that involved in the Norrish Type II process observed in other carbonyl compounds.

Minor free-radical processes also occurred with both isocyanates, with evidence for photodissociation of both R—NCO and RN—CO bonds. There was also apparently some collisional deactivation of excited precursors of both the molecular and free-radical photodissociations.

Vapor pressure data for the 2 isocyanates, and molar extinction coefficients between about 2200 and 3000 Å, are also reported.

Canadian Journal of Chemistry, 47, 4169 (1969)

Introduction

The photolysis of isocyanic acid vapor has been studied in some detail recently, in this laboratory (1) and elsewhere (2); the isocyanate esters are of obvious interest for comparison. Their photolyses are also of interest as possible sources of nitrenes or NCO radicals, and for comparison with other types of carbonyl compounds and with azides. Previous studies of isocyanate photolyses are very limited. The photolysis of CH_3NCO was investigated in some detail by Bamford and Bamford (3) in 1940. The flash photolysis of C_2H_5NCO has been used to study the spectrum of NCO (4), and the products of the flash photolysis of CH_3NCO have been examined briefly in this laboratory (5). Brief studies of the photolyses of *n*-butyl cyanate vapor and of several alkyl and aryl cyanates in the liquid phase have been described recently (6). One of our original objectives in the present work was to find a useful source of NCO radicals, and it was hoped that the photolysis of $CH_3CO.NCO$, by analogy with other acetyl compounds, might be suitable. The photolysis of C_2H_5NCO was studied for comparison after the somewhat unexpected behavior of the acetyl ester became apparent.

Experimental

Materials

$CH_3CO.NCO$ was prepared by reaction of CH_3COCl with AgNCO, and separated by distillation, collecting the fraction boiling at 80 °C at atmospheric pressure (7). Minor impurities (< 0.1%) were $CH_3CO.OCH_3$, CH_3CN, and CO_2, the latter forming in a slow dark reaction of the isocyanate at −78 °C. Pumping at −95 °C before each experiment removed all of the CO_2 and most of the acetate. The trace of CH_3CN, which is transparent down to ~1850 Å and which is also a reaction product, was not removed.

Ethyl isocyanate was obtained from Eastman Co., and gas chromatographic analysis showed no significant impurities after several trap-to-trap distillations. 2,3-Dimethyl butane was Phillip's Research grade, used after simple degassing. Azomethane was obtained from Merck, Sharp, and Dohme of Canada, Ltd., and used after degassing to remove traces of N_2, CH_4, and C_2H_6.

Vapor Pressures

Saturation vapor pressures of the 2 isocyanates, apparently not reported previously, were measured on a simple mercury manometer and are given by the equations

$$\log_{10} P_{CH_3CO.NCO} = 7.94 - 1813/T$$

and

$$\log_{10} P_{C_2H_5NCO} = 7.81 - 1620/T$$

(where P is in Torr and T in °K) based on data obtained from −33 to 10 °C and −52 to 5 °C for the acetyl and ethyl esters, respectively.

Absorption Spectra

Absorption spectra of the 2 isocyanates were measured on a Cary ultraviolet spectrophotometer at pressures of 29 and 40 Torr for the acetyl and ethyl esters, respectively, and are shown in Fig. 1. Woo and Liu (8) reported continuous absorption in ethyl isocyanate below a limit

---

[1]NRCC No. 10 907.

[2]NRCC Postdoctoral Fellow, 1966–1968. Present address: Shell Research Limited, Thornton Research Centre, Chester, England.

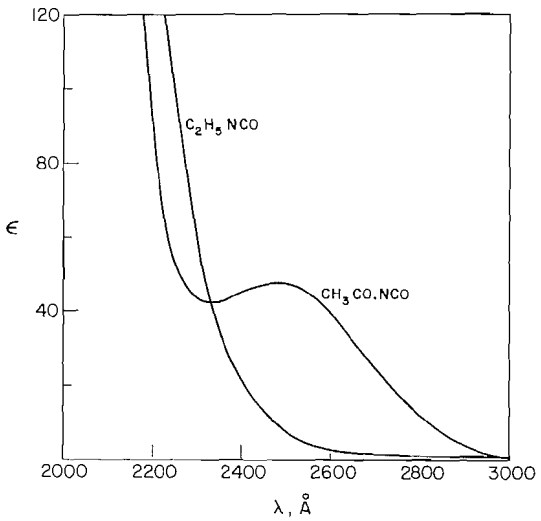

FIG. 1. Absorption spectra of acetyl and ethyl isocyanates. ε is the decadic molar extinction coefficient.

of 2480 Å. The spectrum of the acetyl ester had not been described before; the broad maximum at 2480 Å, which is absent in the alkyl isocyanates, may be ascribed to the acetyl carbonyl chromophore.

Apparatus

Photolyses were carried out in a conventional cylindrical quartz vessel, 5 cm in diameter, 10 cm long, and of about 200 cc volume, equipped with plane quartz windows. This was mounted in an air thermostat and attached to a vacuum line used for preparation and analysis, similar to those used previously in this laboratory (1). All photolyses were done at 25 °C.

Light Sources

Two light sources were employed, a Hanovia S-500 medium-pressure mercury arc, used with a Corning 7910 filter to cut off wavelengths below 2200 Å, and a flat-spiral cadmium resonance lamp operated at 271 °C with a current of 75 mA. The latter was used with a Hg-vapor – H_2-filter to remove traces of mercury resonance radiation, and with a gaseous Cl_2–$NiSO_4$–$CoSO_4$ combination of filters to remove the first Cd resonance line at 3261 Å and other light of longer wavelengths. The resulting light was examined with a grating spectrometer and found to be >99% monochromatic 2288 Å radiation. Quantum yield measurements were made with this light source, using azomethane as an actinometer (1), assuming $\Phi(N_2) = 1$. The relative transmitted light intensity was measured in these experiments by a suitably conditioned phototube with a platinum cathode (1).

Analysis

Products volatile at −196 °C (N_2, H_2, CO, CH_4) were removed by a Toepler pump, measured in a gas burette, and analyzed by gas chromatography on a 5A molecular sieve column at 28 °C. In the $CH_3CO.NCO$ photolysis, a fraction volatile at −160 °C (C_2H_4, C_2H_6) was removed and analyzed on a silica gel column at 28 °C. The remaining material, reagent and products (ketene, CH_3NCO, HCN, HNCO), was analyzed on a dinonyl phthalate column at 30 °C in an all-glass gas chromatograph, after partial fractionation at −120 or −95 °C to minimize complications arising from decomposition of the starting material, which occurred to some extent on every one of a number of columns that were tried.

In the C_2H_5NCO photolysis, C_4H_{10}, C_3H_8, C_2H_6, and C_2H_4 were removed at −120 °C and analyzed on a silica gel column at 50 °C, while the remaining reagents and products (HNCO, HCN, CH_3CN, CH_3NCO) were analyzed on a dinonyl phthalate column at 30 °C. All gas chromatogram peaks from both isocyanates were identified by retention times and by mass spectrometric analysis of effluent vapors, comparing with standard samples in all cases.

Results and Discussion

Photolysis of $CH_3CO.NCO$

Products from a typical experiment with the S-500 lamp (10 Torr isocyanate, 60 min irradiation), with approximate amounts in μmoles given in parentheses, were CH_2CO (31), CO (7), CO_2 (3), CH_3NCO (2), C_2H_4 (0.4), C_2H_6 (0.3), CH_4 (0.02), and N_2 (0.01). Rates of formation of the 3 hydrocarbons and CO showed a marked dependence on photolysis time, shown in Fig. 2; all other product yields were approximately proportional to time. All products increased roughly linearly with pressure of isocyanate from 2 to 23 Torr, presumably reflecting simply the increasing absorption of light.

The rather unexpected appearance of ketene as a major product of the photolysis would appear to be best explained by a molecular

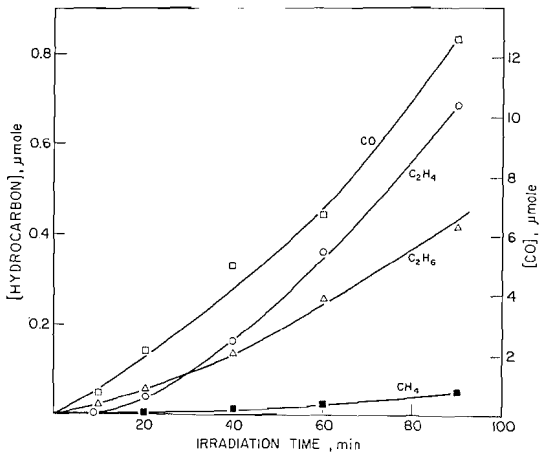

FIG. 2. Dependence of product yields on time of irradiation in the photolysis of $CH_3CO.NCO$. (Note different ordinate scale for CO on right-hand side.)

Can. J. Chem. Downloaded from www.nrcresearchpress.com by 210.87.254.105 on 09/05/12
For personal use only.

Can. J. Chem. Downloaded from www.nrcresearchpress.com by 210.87.254.105 on 09/05/12
For personal use only.

photodissociation

[1] $CH_3CO.NCO + h\nu \rightarrow CH_2CO + HNCO$

Isocyanic acid was not detected among the products, but tests showed that when it was added to $CH_3CO.NCO$, it could not be recovered, seeming to disappear in a reaction (probably co-polymerization) which yielded no volatile products. Certainly the elemental balance in the observed products demands the formation of HNCO or its stoichiometric equivalent. The radical-chain sequence

[2] $NCO + CH_3CO.NCO \rightarrow HNCO + CH_2CO.NCO$

[3] $CH_2CO.NCO \rightarrow CH_2CO + NCO$

could yield the same products as reaction [1], and to test this possibility, some photolyses were done with about 80 Torr of 2,3-dimethylbutane added. Production of C_2H_4 and C_2H_6 was completely suppressed, and that of CH_4 enhanced. All other products were reduced to about 2/3 of their original yields, but their ratios were unchanged. These observations appear to rule out the radical chain as a source of ketene, since NCO radicals should have reacted with the hydrocarbon, inhibiting the chain. The observed reduction in ketene and other products suggests quenching of an excited-molecule intermediate in reaction [1]. Further evidence against the radical chain is the quantum yield data obtained at 2288 Å, shown in Table I

Despite the considerable scatter in these data (which reflects the difficulty in the quantitative analysis of the small amounts of ketene formed at the low conversions ($\sim 1\%$) used in an attempt to minimize secondary photolysis), Φ(ketene) is clearly less than unity, and does not show the upward trend with increasing pressure of isocyanate that would be expected of a chain reaction. Yields of CO at 2288 Å were much higher, relative to those of ketene, than with the mercury arc. It is not certain whether this was a real change in the primary photolysis or whether secondary photolysis of ketene was more extensive at the shorter wavelength. Yields of other products at 2288 Å were too small to measure with any accuracy, and the photolysis at this wavelength was not pursued further.

TABLE I

Quantum yields of ketene and CO from the photolysis of $CH_3CO.NCO$ at 2288 Å

$CH_3CO.NCO$ pressure (Torr)	Φ(ketene)	Φ(CO)
9.8	0.90	0.69
10.6	0.98	0.69
13.9	1.00	0.67
17.7	0.58	0.51
32.4	0.85	0.63
33.7	0.76	0.74
35.0	†	0.72
37.4	†	0.80
40.6	†	0.63
	Ave. 0.85	Ave. 0.68

*Photolysis time was about 130 min and absorbed light intensity 3–9 × 10^{-10} einstein/l s.
†Not measured.

While it seems clear that reaction [1] describes the main course of the photolysis, there is evidence from the minor products observed that several other primary and secondary processes were also occurring. It is evident that ethylene is entirely a secondary product (see Fig. 2), and almost certainly comes from the photolysis of ketene and subsequent reaction of CH_2 radicals. The suppression of C_2H_4 production by 2,3-dimethylbutane supports this conclusion. Yields of CO, CH_4, and C_2H_6 also increased with increasing conversion, but to a lesser extent, and unlike C_2H_4, had appreciable initial values. The increase in CO is probably due to decomposition of ketene, while the source of the extra CH_4 and C_2H_6 is not clear. Other primary processes which must be considered are

[4] $CH_3CO.NCO + h\nu \rightarrow CH_3 + CO.NCO$

[5] $\rightarrow CH_3CO + NCO$

[6] $\rightarrow CH_3CO.N + CO$

[7] $\rightarrow CH_3NCO + CO$

[8] $\rightarrow CH_3CN + CO_2$

The production of CH_4 and C_2H_6, and the enhancement of the former and suppression of the latter by 2,3-dimethyl butane, provide good evidence for the presence of CH_3 radicals, presumably from reaction [4]. Evidence for NCO radicals in the system is less clear, since HNCO would be the product formed by hydrogen abstraction, and it could not be measured. If the combination of NCO radicals leads to N_2 and 2CO, as has been reasonably suggested in the past, then the very low yields of N_2 indicate a concentration of NCO much less than that of CH_3, assuming similar combination rates. It is possible that NCO could abstract H from $CH_3CO.NCO$ much faster than does CH_3, thus

Can. J. Chem. Downloaded from www.nrcresearchpress.com by 210.87.254.105 on 09/05/12
For personal use only.

reducing the NCO concentration. The CO.NCO radical formed in reaction [4] would probably decompose to CO and NCO, although nothing is known of its stability. If it abstracted H, the resulting HCO.NCO would probably decompose to HNCO and CO. Reaction [5] would yield NCO directly; there is no evidence for acetyl radicals in the system. It should be noted that the photon energy was probably sufficient to cause a primary dissociation to CH_3 + NCO + CO rather than reaction [4] or [5] (cf. acetone photolysis (9)).

Reaction [6] is suggested by analogy with the photolyses of HNCO and organic azides. The fate of the nitrene in the present system is not known. Similar nitrenes from the photolysis of azidoformates apparently do *not* rearrange to isocyanates (10), and for this reason reaction [7] is suggested as the probable source of the CH_3NCO observed in the present photolysis. Cross combination of CH_3 and NCO may be ruled out as an alternate source by the apparently low concentration of NCO noted earlier.

Finally, reaction [8] is postulated as the most likely source of the CO_2 observed. The same reaction also occurred slowly in the dark even with the isocyanate stored at −78 °C. For this reason, small amounts (<0.5%) of CH_3CN were usually present in the starting material, and it was impossible to say whether it was also produced in the photolysis. Small yields of CO_2 were undoubtedly formed in the photolysis, however.

The primary processes [4] to [8] were of very minor importance compared to reaction [1]. For photolysis with the S500 mercury arc, reactions [4], [7], and [8] may be estimated as about 2, 7, and 10% of reaction [1], based on yields of $CH_4 + 2C_2H_6$, CH_3NCO, and CO_2, respectively. The yield of CO might be thought to be a useful measure of the sum of reactions [4], [5], [6], and [8], but secondary photolysis of ketene became an important CO source at quite low conversions, and it is difficult to estimate. The quantum yields of reactions [5] and [6] are rather uncertain, but their sum is not more than 10% of reaction [1].

Photolysis of C_2H_5NCO

A series of experiments was done using the S-500 medium-pressure mercury arc with a 7910 Vycor filter, with pressures of isocyanate from about 4 to 30 Torr. Products from a typical experiment (13 Torr C_2H_5NCO, 60 min irradiation), with amounts in μmoles in parentheses, were C_2H_4 (2.16), CO (0.81), C_2H_6 (0.53), C_3H_8 (0.24), CH_4 (0.20), C_4H_{10} (0.07), and N_2 (0.001). Appreciable yields of HNCO were also observed, but quantitative analysis was not possible. All the products increased with increasing pressure, presumably due to increased absorption of light. The addition of 2,3-dimethyl butane reduced the yields of all products by roughly similar amounts, with a pressure of about 200 Torr causing a reduction of more than 50%. The addition of 1 Torr of oxygen reduced yields of C_2H_6, C_3H_8, and C_4H_{10} virtually to zero, and that of CH_4 by about 50%. Ethylene was approximately unaffected, while CO was about doubled. Addition of 3 Torr of nitric oxide also eliminated C_2H_6, C_3H_8, and C_4H_{10}, leaving CO and C_2H_4 almost unaffected.

All these observations point to a major primary process

[9] $$C_2H_5NCO + h\nu \rightarrow C_2H_4 + HNCO$$

which is analogous to reaction [1] in the $CH_3CO.NCO$ photolysis. The formation of CO seems best explained by another primary process

[10] $$C_2H_5NCO + h\nu \rightarrow CO + C_2H_5N$$

The alkane products and their suppression by NO and O_2 clearly indicate the presence of CH_3 and C_2H_5 radicals, and suggest a third primary process

[11] $$C_2H_5NCO + h\nu \rightarrow C_2H_5 + NCO$$

The source of CH_3 radicals, apparently in relatively large quantities, is not so obvious. Secondary reactions of ethylene with H or NCO from secondary photolysis of HNCO were considered, but were shown not to be a source of either CH_3 or C_2H_5 by experiments in which C_2D_4 was added to the photolysis system and no deuterium was found in the alkane products. The most probable source of CH_3 would seem to be decomposition of the nitrene formed in reaction [10]

[12] $$C_2H_5N \rightarrow CH_3 + H_2CN \text{ (or } H + HCN)$$

occurring as either a concerted part of reaction [10] or a subsequent decomposition. Such a reaction gains some support from the mechanism postulated for the reactions of N atoms with alkyl radicals (11). An alternative decomposition

[13] $$C_2H_5N \rightarrow CH_4 + HCN$$

Can. J. Chem. Downloaded from www.nrcresearchpress.com by 210.87.254.105 on 09/05/12
For personal use only.

might account for the incomplete suppression of CH_4 in the presence of O_2 and NO. There is some evidence that reactions analogous to [12] and [13] occur in the photolysis of CH_3NCO, yielding HCN and H_2 or 2H (5). In considering such decompositions, which are not a feature of liquid-phase nitrene chemistry, it should be noted that in the photolyses of isocyanates in the gas phase, the photon energies are probably much in excess of the RN—CO bond dissociation energy, and much of this excess energy will reside in the nitrene as electronic and vibrational excitation. It should also be noted that HCN was not observed as a product in the present system, but there seems to be great difficulty in detecting the relatively small amounts expected in the presence of the large excess of isocyanate and HNCO.

Reaction [11] generates equal numbers of C_2H_5 and NCO radicals, and one might expect that C_4H_{10} and N_2 should be about equal if the latter arose from combination of NCO radicals. As with the $CH_3CO.NCO$ photolysis, however, the much lower yield of N_2 suggests that NCO must disappear by abstracting H from the parent compound much faster than does C_2H_5; this is compatible with other evidence for a very strong H—NCO bond in isocyanic acid (1).

The photolysis of C_2H_5NCO with monochromatic 2288 Å radiation was studied briefly in order to obtain quantum yields. The quantum yield of ethylene is shown in Fig. 3, and is seen to decline steadily with increasing pressure from a low pressure limit of about 0.45. The other products showed a similar decline. The addition of 2,3-dimethyl butane also caused a considerable reduction in yields using the mercury arc, and it seems probable that collisional deactivation of an excited state, or states, of C_2H_5NCO is responsible for these pressure effects. The value of the quantum yield of ethylene and its decline with increasing pressure are strong evidence against a chain reaction analogous to reactions [2] and [3] as the source of HNCO and C_2H_4.

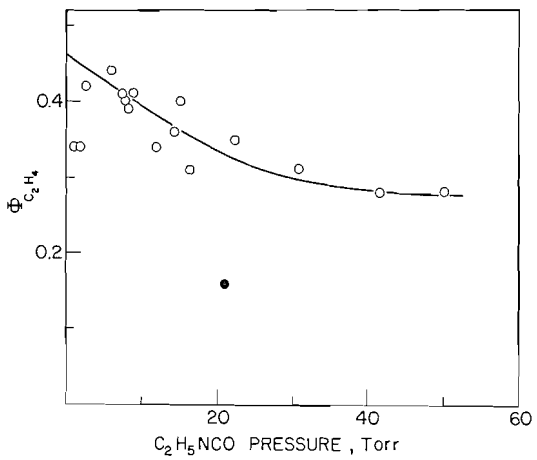

FIG. 3. Quantum yield of ethylene from the photolysis of C_2H_5NCO at 2288 Å ●; 180 Torr 2,3-dimethyl butane added.

Ethane and CO were also major products of the 2288 Å photolysis and were relatively more important than with the mercury arc. Accurate measurement of limiting low-pressure quantum yields were hampered by the relatively small amounts measured and, in the case of ethane, by an increase in yield with increasing conversion, perhaps due to photolysis of HNCO and subsequent secondary reactions. The initial limiting low-pressure quantum yield of CO was about 0.28, and that of C_2H_6 probably somewhat less. The minor products observed with the mercury arc were also formed at 2288 Å, but could not be measured with any accuracy.

It is clear that with both light sources, the molecular dissociation (reaction [9]) is the major primary process, but reactions [10] and [11] are relatively more important than their analogues in the photolysis of acetyl isocyanate. With the mercury arc, it may be estimated that reactions [10] and [11] each amounted to about 1/3 of reaction [9], while at 2288 Å they were somewhat more important.

General Conclusions

The photolyses of four R—NCO compounds have now been studied in the gas phase, with R = H (1, 2), CH_3 (3, 5), C_2H_5, and CH_3CO, and some general features may be noted.

(*a*) In every case it appears that both R—NCO and RN—CO bonds are dissociated. This leads to complex secondary reactions and complicates the use of isocyanates as sources of NCO radicals or nitrenes for kinetic studies. Organic azides, by contrast, appear on photolysis to dissociate much more cleanly at the RN—NN bond, and the difference in behavior must be ascribed to the much greater stability of the NCO radical relative to N_3.

(*b*) In the photolysis of the 2 higher isocyanates studied in the present work, molecular dissociations apparently become predominant. By analogy with the higher ketones, it seems reasonable to suggest that these dissociations are

essentially Norrish Type II processes, involving 6-membered transition states

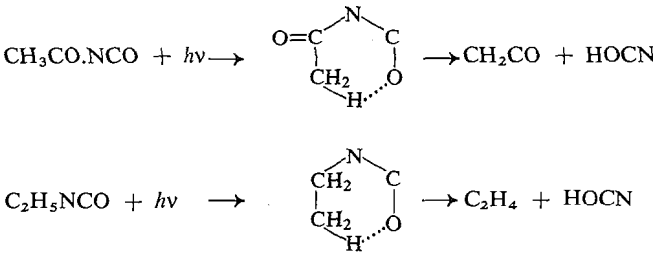

Cyanic acid, HOCN, is analogous to the enols formed in the Type II process in ketones and should rearrange rapidly at room temperature to the more stable HNCO isomer. It is interesting to note that formation of the postulated 6-membered rings requires bending of the NCO group in the excited state, presumably corresponding to an "opening" of the C=O double bond. There seems no reason to doubt that this Type II process is common to other isocyanate esters.

1. W. D. WOOLLEY and R. A. BACK. Can. J. Chem. **46**, 295 (1968).
2. J. N. BRADLEY, J. R. GILBERT, and P. SVEJDA. Trans. Faraday Soc. **64**, 911 (1968).
3. D. A. BAMFORD and C. H. BAMFORD. J. Chem. Soc. 30 (1941).
4. R. HOLLAND, D. W. G. STYLE, R. N. DIXON, and D. A. RAMSAY. Nature, **182**, 336 (1958).
5. R. A. BACK and D. W. L. GRIFFITHS. Unpublished results.
6. M. HARA, Y. ODAIRA, and S. TSUTSUMI. Tetrahedron Lett. 1641 (1967). M. HARA, T. FUJIMOTO, and Y. ODAIRA. Nippon Kagaku Zasshi **88**, 1091 (1967).
7. O. BILLETER. Ber. **36**, 3213 (1903).
8. S.-C. WOO and T.-K. LIU. J. Chem. Phys. 3, 544 (1935).
9. J. G. CALVERT and J. N. PITTS. Photochemistry. John Wiley and Sons, Inc., New York. 1966.
10. G. T. TISUE, S. LINKE, and W. LWOWSKI. J. Amer. Chem. Soc. **89**, 6303 (1967).
11. A. N. WRIGHT and C. A. WINKLER. Active nitrogen. Academic Press, Inc., New York. 1968.

Can. J. Chem. Downloaded from www.nrcresearchpress.com by 210.87.254.105 on 09/05/12
For personal use only.

Can. J. Chem. Downloaded from www.nrcresearchpress.com by 210.87.254.105 on 09/05/12
For personal use only.

Oxidation of hydrocarbons in the liquid phase: *n*-dodecane in a borosilicate glass chamber at 200 °C

B. D. Boss and R. N. Hazlett
Fuels Branch, Chemistry Division, Naval Research Laboratory, Washington, D.C. 20390

Received February 17, 1969

The 5-h oxidation of *n*-dodecane at 200 °C by air at 1 atm is reported for experiments in a borosilicate glass reaction chamber equipped with a gas bubbler. The rate of reaction was limited by the rate of oxygen diffusion from the gas phase due to the rapid reaction of dissolved oxygen. The reaction products were analyzed in aliquots taken periodically from the reaction chamber. Chemical analyses, gas–liquid phase chromatography (g.l.p.c.), tandem g.l.p.c.-mass spectroscopy, infrared, and ultraviolet were used to identify products accounting for 98% of the oxygen reacted. The isomer distribution of the dodecenes, dodecanols, and dodecanones formed, as well as the distribution of carboxylic acids, were determined. Three classes of intramolecular reaction products, cyclic ethers, cyclic hydrocarbons, and lactones, were detected. Many volatile products were detected. A filterable precipitate obtained after 10 h of oxidation was studied using infrared attenuated total reflectance techniques. A reaction mechanism is discussed based on current knowledge of other systems, the products identified, and the stoichiometry of the reaction.

Canadian Journal of Chemistry, 47, 4175 (1969)

An understanding of oxidation of hydrocarbons in the liquid phase is important in several fields of technology as well as being of considerable theoretical interest. Consequently, many investigations have dealt with this subject. The detailed mechanism of the early stages (1–12) and the general mechanism of later stages have been examined (4, 10, 13–16). Often the materials used are complex mixtures of hydrocarbons (13, 17, 18). In some studies, the effect of pertinent variables, such as the solid surface, have not been considered. The solvent effect is not completely understood at this time (3, 6, 11, 19).

An appropriate mechanism for *n*-alkane oxidation can be extracted from the current theory (simplified) of the mechanism of initial stages of oxidation of saturated hydrocarbons as follows (1, 2, 10–13, 20–23)

Initiation

[1] $2RH + O_2 \rightarrow 2R\cdot + H_2O_2$

[2] $RH + O_2 \rightarrow R\cdot + HO_2\cdot$

Propagation

[3] $R\cdot + O_2 \rightarrow RO_2\cdot$

[4] $RO_2\cdot + RH \rightarrow ROOH + R\cdot$

Branching

[5] $2ROOH \rightarrow RO_2\cdot + H_2O + RO\cdot$

[6] $ROOH \rightarrow RO\cdot + \cdot OH$

Termination

[7] $RO_2\cdot + R'CHOOR'' \rightarrow ROH + R'COR'' + O_2$

[8] $RO_2\cdot + R\cdot \rightarrow ROOR$

[9] $R\cdot + R\cdot \rightarrow R{-}R$

At low temperatures where hydroperoxide, $ROOH$, is relatively stable, we expect the predominant product in the initial stages of reaction to be ROOH along with some alcohols and ketones from reaction [7] in equal amounts. Reactions [5] and [6] rapidly become more important than reactions [1] and [2] as the end of an induction period is approached. In addition, hydrogen peroxide and dialkyl peroxides (12) should participate in chain branching processes. Reactions of RO· similar to those delineated for cyclohexane lead to ketones, alcohols, aldehydes, acids, and primary alkyl radicals.

[10] $RO\cdot \xrightarrow{-H\cdot} RO$

[11] $RO\cdot \xrightarrow{+H\cdot} ROH$

[12] $RO\cdot \rightarrow R'CHO + R''$

[13] $R'CHO \xrightarrow{O_2} \text{Acids}$

In this case alcohols and ketones are the predominant products for periods up to several hours at temperatures below 180 °C (2). Clearly reactions [10] through [12] produce free radicals which can continue the chain.

The work reported here is the initial phase of a study aimed at investigating aspects of the oxidation of simple mixtures of hydrocarbons. *n*-Dodecane was selected as the major component of the mixtures because its boiling point (216.3 °C) permits liquid-phase experiments at high temperatures in an open system and it is relatively stable to oxidation.

Can. J. Chem. Downloaded from www.nrcresearchpress.com by 210.87.254.105 on 09/05/12
For personal use only.

The oxidation of *n*-dodecane has been carried out in the liquid phase at 200 °C in a borosilicate glass chamber (24) at 1 atm of air. Initiation reactions ([1], [2]) were sufficiently rapid that enough air could not be supplied to simultaneously maintain an equilibrium oxygen concentration of 21% and maintain the *n*-dodecane as a bulk liquid (i.e., avoid the frothy state). Thus, the reaction was limited by the rate of oxygen diffusion from the gas phase. The gas exhaust contained 17.8% O_2. The reaction has been studied over a period of 5 h, and 98% of the absorbed oxygen has been accounted for in the products identified using gas–liquid phase chromatography (g.l.p.c.), g.l.p.c.-mass spectroscopy, infrared (i.r.), ultraviolet (u.v.), and chemical analyses. This thorough analysis allows us to suggest a macroscopic reaction mechanism based on the products identified, the stoichiometry of the reaction, and current knowledge of reaction mechanisms tested for similar systems.

Experimental

Reagents

n-Dodecane was obtained from Phillips Petroleum Co. as 99.7$^+$% pure grade. The material was passed through drierite, activated alumina, and silica gel to remove traces of polar impurities. The only major impurity identified by g.l.p.c. was *n*-hendecane (0.15%).

Apparatus

A diagram of the reaction vessel is presented in Fig. 1. The O-ring seal glands assure a tight fit. The chamber can be conveniently replaced with cylinders of various materials. The borosilicate glass chambers were prepared from different lots of glass stock and exposed to chromic acid cleaning solutions for 1 week followed by soaking and rinsing first in ammonia and then in distilled water. Collection tubes of drierite, of ascarite, and of borosilicate glass wool (cooled in dry ice – acetone) are connected to the chamber exhaust. The exhaust passes finally through a gas sampling valve in a Fisher Scientific Co. gas partitioner used to analyze the oxygen concentration. The reaction temperature was maintained by a heated, fluidized alumina bed.

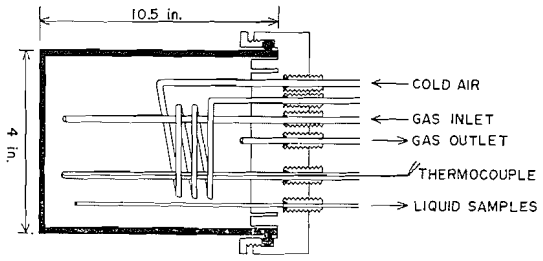

FIG. 1. Cylindrical reaction chamber with polytetrafluoroethylene cap and cooling coil; silicone rubber O-ring seals.

Reaction Conditions

The reaction chamber was maintained at 200.5 °C with oscillations of ±0.8 °C. The pressure was maintained at 10 mm above the generally prevailing 750 mm Hg atmospheric pressure. Dry air, with the CO_2 removed, was bubbled through the liquid at 260 cm^3 min^{-1}. Diffusion controlled kinetics (25) are expected (see discussion in introductory section).

The original charge of 325 ml of *n*-dodecane was sampled in seven 25-ml aliquots. Three runs were performed using air and one run was made with N_2 containing 160 ± 20 p.p.m. of O_2. In each case an analysis was made of all accessible products in the chamber and in the collection tubes.

A further experiment was performed at 200 °C using *n*-dodecane at air flow rates between 260 and 4500 cm^3 min^{-1}. In Fig. 2 the rate of accumulation of 4-, 5-, and 6-dodecanone is plotted as a function of flow rate. We conclude that to maintain the reaction in the kinetic region, at least 4000 cm^3 min^{-1} of air must be bubbled through the liquid with the configuration shown in Fig. 1. Thus it is not practical to perform experiments at 200 °C in the kinetic region and avoid a frothy state of the dodecane.

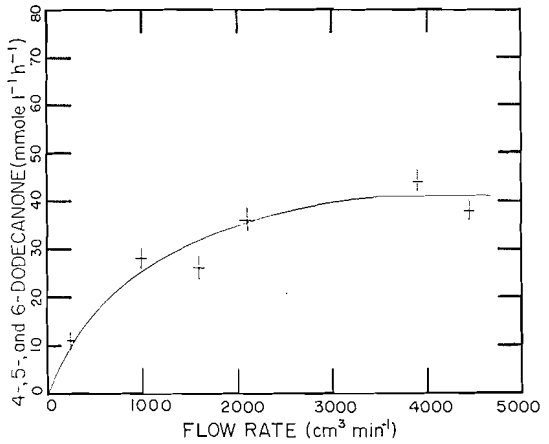

FIG. 2. Effect of air input flow rate on rate of formation of the combined ketones, 4-, 5-, and 6-dodecanone, at 200 °C. Measurements are made on randomly selected flow rates.

Chemical Tests

Hydroperoxide was determined by a minor variation of the colorimetric iodine method of Heaton and Uri (26). A spectrophotometric variation of Mair and Graupner's (27) method II was developed, but no dialkyl peroxide was detected in the product mix. No H_2O_2 was detected in a water extraction of the product mix. Carbonyl was determined by the very sensitive colorimetric method of Lappin and Clark (28). Acids and esters were determined according to American Society for Testing Materials test methods D974-58T (alcoholic KOH titration) and D94056T (saponification), respectively.

Chromatographic Analyses

Each liquid sample was analyzed by g.l.p.c. immediately after sampling (Fig. 3). In addition, chromatograms were

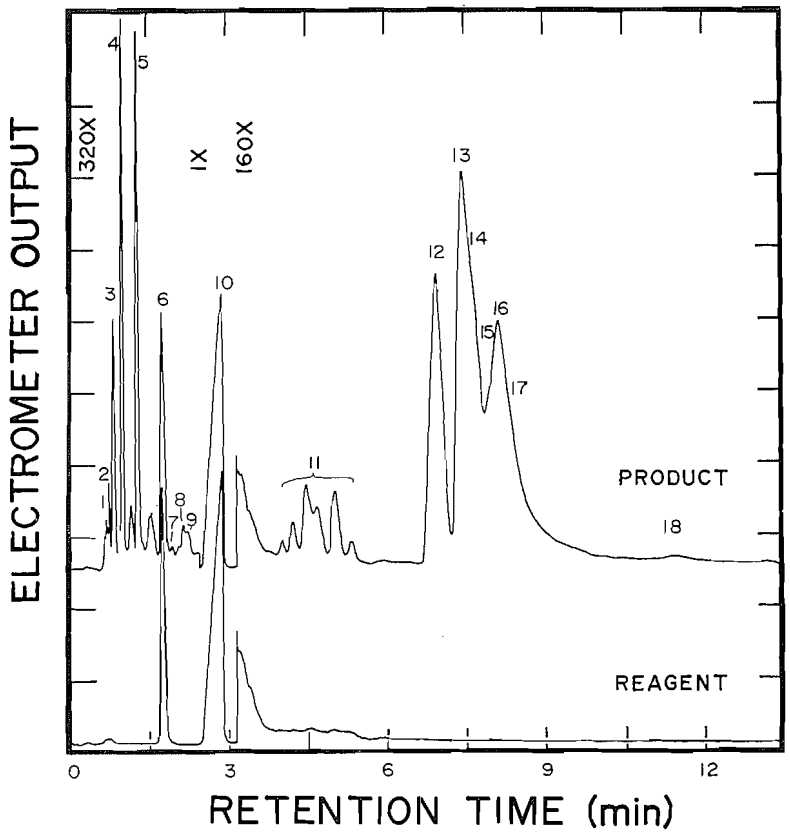

FIG. 3. Gas chromatograms of the *n*-dodecane starting material and of the reaction products after 5 h. Chromatographs obtained using a 100 ft × 0.020 in. i.d. DC-550 silicone oil support-coated open tubular column with a He carrier gas supplied at 35 p.s.i. (4 ml/min). The following temperatures were used: column, 126 °C; injector, 200 °C; flame ionization detector, 270 °C. The products were identified as follows: (1), *n*-hexane; (2), *n*-heptane; (3), *n*-octane; (4), *n*-nonane; (5), *n*-decane; (6), *n*-undecane; (7), decanone; (8), decanal; (9), C_{12} single ring alicyclics; (10), *n*-dodecane; (11), cyclic C_{12} ethers; (12), 6-, 5-, and 4-dodecanone; (13), 6- and 5-dodecanol; (14), 3-dodecanone; (15), 4-dodecanol; (16), 2-dodecanone; (17), 3-dodecanol; (18),2-dodecanol.

obtained on the liquid after reaction with benzoyl chloride (Fig. 4), and after reaction with hexamethyldisilazane (29) (Fig. 5). These derivative chromatograms were necessary to separate the dodecanol isomers from the dodecanone isomers by analyzing displacements of the alcohol peaks. Hydroperoxides do not interfere with the scheme presented here.

The distribution of the non-volatile carboxylic acids formed was determined by extraction of the reaction residue with 1 *N* KOH, neutralization with HCl, and formation of the methyl esters with a methanol–BF_3 reagent mixture (30). Chromatograms of this reaction mixture gave the distribution of the C_5 through C_{12} carboxylic acids. These acids were almost completely retained in the reaction chamber at 200 °C. Comparable treatment of a known acid mixture was used to verify the analysis.

Dodecenes were detected by bromination of the product mixture followed by g.l.p.c. under the conditions in Fig. 3 but with a column temperature of 150 °C. Peaks for monobromo-substituted dodecanes were detected and reaction with alcohols and ketones was observed. However, a set of dibromo dodecanes was eluted after a considerable time lag. Tests were made to identify, to measure quantitatively, and to establish any interference made by the alcohol and ketone products. No interferences were detected.

Mass Spectra

The mass spectra were obtained with a CH-4 Atlas mass spectrometer (with double ion source) fed by an F and M 810 gas chromatograph (31). The interface was a stainless steel capillary tube heated to 250 °C. The 200:1 exit split on the gas chromatograph effluent which was attained in this manner was effective for qualitative analysis purposes. Neither a polytetrafluoroethylene nor a sintered glass molecular separator (31) afforded adequate separation of the sample from the He carrier.

Absorption Spectra

Spectra of the product mixture in the i.r., u.v., and visible regions were obtained. A solid material which

Can. J. Chem. Downloaded from www.nrcresearchpress.com by 210.87.254.105 on 09/05/12
For personal use only.

Can. J. Chem. Downloaded from www.nrcresearchpress.com by 210.87.254.105 on 09/05/12
For personal use only.

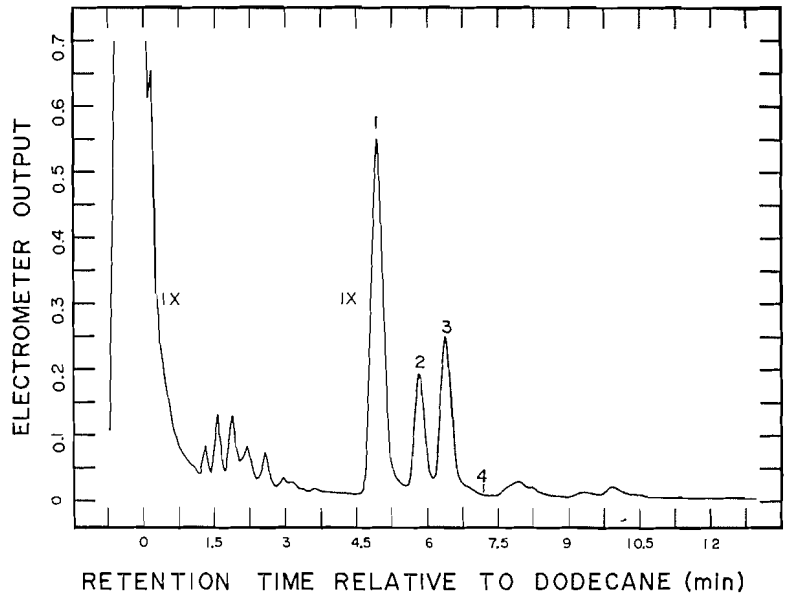

FIG. 4. Gas chromatogram of 5 h reaction products after reaction with benzoyl chloride. See Fig. 3 for the chromatograph conditions. The products are identified as follows: (1), 6-, 5-, and 4-dodecanone; (2), 3-dodecanone; (3), 2-dodecanone; (4), dodecanal.

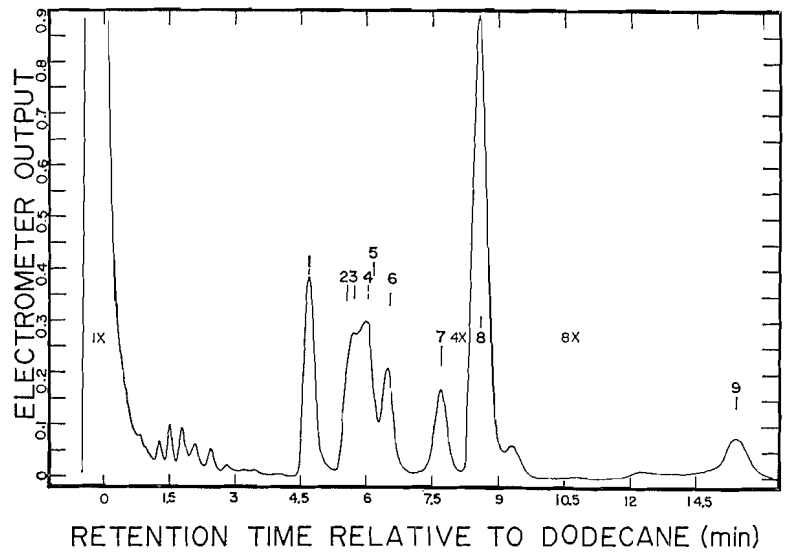

FIG. 5. Gas chromatogram of the 5 h reaction products after reaction with a silylating reagent. The conditions in Fig. 3 apply. The products are identified as follows: (1), 6-, 5-, and 4-dodecanone; (2), 3-dodecanone; (3), 6-, and 5-dodecanol derivatives; (4), 2-dodecanone; (5), a minor unidentified product; (6), 4-dodecanol derivative; (7), 3-dodecanol derivative; (8), 2-dodecanol derivative; (9), 1-dodecanol derivative.

Can. J. Chem. Downloaded from www.nrcresearchpress.com by 210.87.254.105 on 09/05/12
For personal use only.

TABLE I
Identification of products

Products*	Concentration (mmole l^{-1})	Methods of identification
C_1 through C_{11} *n*-paraffins	(108.0)†	g.l.p.c., mass spectra, and chemical tests
n-Nonane	10.2	g.l.p.c. and mass spectra
n-Decane	11.4	g.l.p.c. and mass spectra
n-Undecane	trace	g.l.p.c. and mass spectra
Dodecenes	41	g.l.p.c. and chemical tests
Pentanal through undecanal	(25.0)‡	g.l.p.c., i.r., mass spectra, and chemical tests
Pentanone through decanone	trace§	g.l.p.c., mass spectra, and chemical tests
Cyclic dodecanes	10	g.l.p.c. and mass spectra
Cyclic C_{12} ethers	23	g.l.p.c. and mass spectra
Lactones	6	i.r. and chemical tests
Dodecanols	183	g.l.p.c., i.r., mass spectra, and chemical tests
Dodecanones	100.5	g.l.p.c., i.r., u.v., mass spectra and chemical tests
Total carbonyl	125	Chemical tests
C_1–C_{12} carboxylic acids	32.5§	g.l.p.c. and chemical tests
Esters	23.0	Chemical tests
Hydroperoxides	8.6	Chemical tests
Carbon dioxide	3.0	Chemical tests
Water	256 ‖	Absorbtion

*Products were formed by the end of 5 h under the conditions specified in the text.
†Calculated from liquid phase and vapor trap materials by assuming additional loss of materials with low boiling points.
‡Based on the net carbonyl by assuming only trace amounts of C_5 through C_{10} ketones.
§Volatility or low concentration obscures complete identification of the series from C_1 through C_{12}.
‖Corrected for the capture of volatile polar products other than water.

precipitated after 10 h of oxidation was examined using i.r. attenuated total reflectance (a.t.r.) techniques on a Perkin–Elmer 457 dual grating spectrophotometer.

Results

The blank reaction using N_2 with 160 ± 20 p.p.m. O_2 contained 0.37 mmole l^{-1} of hydroperoxide as the only product detected after 5 h. Using air, numerous compounds were detected in a 5-h experiment as listed in Table I. The reaction consumed 9.4% of the *n*-dodecane starting material and at least 80% of the products have the same carbon backbone. The listed products account for consumption of 0.364 mole l^{-1} of oxygen. The exhaust contained 17.8% O_2. The oxygen uptake, as determined from the difference between the input and exhaust levels, was 0.370 mole l^{-1}. Thus 98% of the oxygen is accounted for. No induction period is observed for early products.

The starting material and reaction product mixture chromatograms are reproduced in Fig. 3. Intramolecular reaction products, cyclic C_{12} ethers, cyclic C_{12} hydrocarbons, and lactones (some of which are C_{12}) have been identified using combined information from mass spectra, g.l.p.c. and/or i.r. Some of the lactones appear

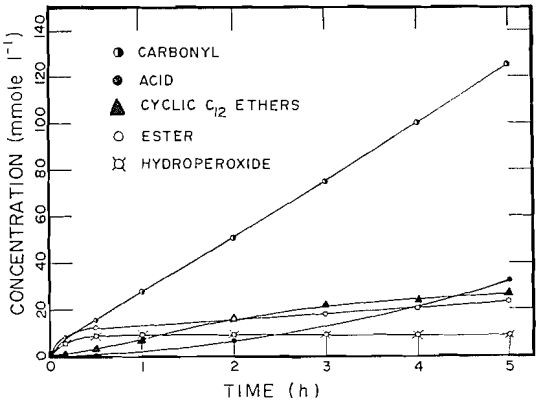

FIG. 6. Concentration of selected reaction products as a function of time under the conditions specified in the text.

from the i.r. absorption to be strained rings (i.e., less than 5-membered).

Concentrations of the major products determined by g.l.p.c. and chemical analysis are plotted in Figs. 6 and 7. The net carbonyl is the difference between the total carbonyl and the dodecanone concentration. Note that the net carbonyl concentration builds up at first and levels off rapidly. The peaks in the gas chromatograms which can

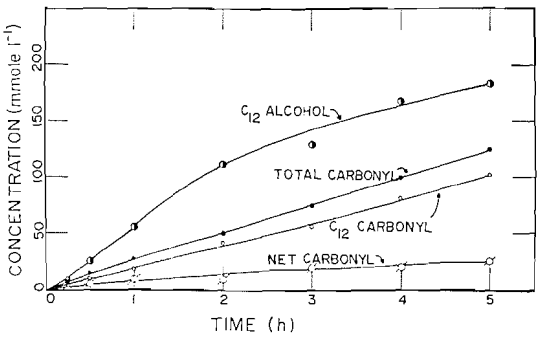

FIG. 7. Concentration of selected reaction products as a function of time under the conditions specified in the text.

be assigned to lower molecular weight aldehydes exhibit similar behavior.

It would be interesting to calculate the amount of water expected by accounting for all the hydrogen atoms in the product mixture. However, this would require a very accurate knowledge of all the volatile hydrocarbon products that escaped from the chamber. Thus, no such analysis was attempted.

Besides CO_2 and H_2O, insoluble products (gums) can form after considerable oxidation. No filterable material was detected after 5 h, but after 10 h a considerable amount was formed. This material was easily dissolved in acetone, coated on an a.t.r. plate, and dried for i.r. analysis. Significant absorption at 3460, 1790, 1650, 1180, 1050, and 1730 cm^{-1} indicate that this gum contains high concentrations of hydroxyl, acid, ester, and carbonyl groups. This information indicates that the gum contains highly polar molecules, some of which are capable of forming hydrogen bonds and possibly micelles (32).

Further details of the reaction were ascertained using g.l.p.c. The distributions of dodecanols, dodecanones, and carboxylic acids were examined. The distribution of C_5 to C_{12} straight chain monobasic acids relative to C_7 is as follows

Distribution of straight chain monobasic acids

No. of C	Relative amount	No. of C	Relative amount
5	5	9	7.5
6	9	10	4.5
7	10	11	0.9
8	9	12	0.4

Kudo *et al.* (15) have determined the isomer distributions for oxidation of *n*-decane under somewhat different conditions. Their observations are comparable to ours except that decanoic acid was relatively less plentiful than we observed for dodecanoic acid. Dawkins has noted the virtual absence of C_{11} acid among the oxidation products of *n*-dodecane (12).

The point of oxidative attack along the carbon chain is indicated by the data in Table II since the alcohols and ketones are abundant, relatively stable products. We conclude that the C-2 position is favored if the reasonable assumption is made that each of the 3 isomers determined in the combined C-4, -5, and -6 peak constitutes 1/3 of the total peak. Favored attack at C-2 was not observed in some studies performed in the kinetic reaction region by other workers (4, 8, 18, 23). Recent studies by Dawkins (13) tend to support preferential attack at C-2. Selectivity may be controlled by peroxy, alkoxy, and alkyl radical attacks on dodecane.

TABLE II

Isomers of dodecanol and dodecanone

Time*	Position of the functional group	% Isomer present	
		Dodecanones	Dodecanols
30 min	C-1	1.1±0.5†	—
	C-2	24.5±0.7	25.3±0.7
	C-3	19.0±0.7	18.2±0.7
	C-4, -5, -6	55.4±0.5	55.4±0.5
5 h	C-1	1.1±0.5	1.0±0.5
	C-2	25.5±0.7	25.4±0.7
	C-3	18.4±0.7	18.5±0.7
	C-4, -5, -6	55.0±0.5	55.1±0.5

*Under the conditions specified in the text.
†Dodecanal.

Dodecene was determined as 41 mmoles l^{-1}. The six isomers were distributed relative to the 4-dodecene isomer as follows

Relative distribution of dodecene isomers

Isomer	Relative amount	Isomer	Relative amount
1-C_{12}	2	4-C_{12}	10
2-C_{12}	5	5-C_{12}	6
3-C_{12}	12	6-C_{12}	2

This distribution is different from that found for the dodecanol and dodecanone isomers.

A close examination of the mass spectra of the eluted lighter-weight *n*-alkanes failed to detect

Can. J. Chem. Downloaded from www.nrcresearchpress.com by 210.87.254.105 on 09/05/12
For personal use only.

olefins. These analyses indicate the absence of any one such olefin above about 0.2 mmole l^{-1}.

Discussion

The data should be considered in the light of the restrictions associated with a bubbler reaction chamber operating under diffusion limited kinetics: loss of volatile products, possible vapor phase reactions, surface catalysis, and oxygen concentration gradient. In addition, taking samples of finite size (25 ml) changes the surface-to-volume ratio from 0.64 cm^{-1} at the beginning to 0.85 cm^{-1} at the end (24) of the experiment.

The limited mechanism scheme presented above provides an adequate, but simplified (11, 12) framework for the major course of the reaction. The absence of an observed induction period is the result of the time scale for sampling and the deficiency of oxygen in the experiment. Oxygen was limited to a steady rate perhaps 20 times below the kinetic rate. The considerable quantities of dodecene formed might be the result of the infrequent collisions of dodecyl radicals with O_2 molecules. The smaller alkyl radicals apparently formed few peroxy radicals for the same reason, but instead abstracted a hydrogen atom from the abundant dodecane solvent. We note the early appearance of hydroperoxides and the accumulation of considerable quantities of dodecanols and dodecanones. Similar isomer distributions for the dodecanols and dodecanones indicate a common precursor (i.e., hydroperoxide or peroxy radical). Though neither H_2O_2 nor dialkyl peroxides was detected, they still are likely to participate in chain initiation.

A slight leveling off of the dodecanol concentration indicates further reaction to form the ketone (1, 10). The series of short chain *n*-alkanes (C_6–C_{10} in the liquid phase, and C_4–C_8 from the vapor trap) and the series of aldehydes (C_5–C_{11} seen by the g.l.p.c. and measured as the net carbonyl) are reaction products predicted by the mechanism scheme for an alkoxy radical undergoing chain scission (reaction [12]). This reaction has been observed in hydroperoxide decomposition (33). The quantity of C_1–C_{11} *n*-alkanes cannot be accounted for by chain scission during acid formation from the ketone and/or alcohol (13). We estimate that the net carbonyl plus the carboxylic acids can account for the *n*-alkanes (allowing for loss of volatile components) in support of the above mechanism. Some decarbonylation of aldehydes seems likely. Further evidence that acids are formed by a later reaction (i.e., from aldehydes and/or esters) is the absence of an induction period for the formation of hydrocarbons, but a considerable time lag for acid formation.

There are two others features of the reaction to be discussed: the early formation of esters and the formation of intramolecular compounds. Intramolecular reaction products, cyclic hydrocarbons, cyclic ethers, and lactones, may be the result of vapor-phase reactions. A cyclic C_{12} hydrocarbon may form by the cyclization of a dodecyl free radical with loss of a hydrogen atom, while loss of water from dodecylhydroperoxide through a 5- or 6-membered transition state may account for cyclic ethers. Berry *et al.* (34) have determined a plausible mechanism in the gas phase. Both of these products appear early in the reaction. The method of formation of lactones is not clear at this time. Dodecene is a possible source.

Esters are an early product of the oxidation. Determined by saponification, the ester content does not include hydroperoxides, which decomposed to alcohols and ketones in alcoholic KOH. Lactones are included as esters. Esters are not the product of esterification between accumulated acid and alcohol molecules, since acids form only after a considerable time lag. Indeed, as water accumulates, esters are a likely source of acids by hydrolysis. To account for ester formation, rearrangement from an α-hydroperoxyketone has been suggested (35). The presence of this intermediate can be inferred by the accumulation of α-hydroxyketones (18). Further, we have observed absorption at 310 mμ which might be attributed to vicinal diketones.

Dawkins suggests that esters are formed by reaction of an alkoxy free radical with a *gem*-hydroperoxyalkyl free radical R′ĊOOHR″ to form the 3° ether hydroperoxide which can decompose to an ester. This would presumably yield esters early in the oxidation as we have noted. The reaction of a peracid (from aldehyde oxidation) with a ketone (12) can also yield an ester by the Baeyer–Villiger reaction.

Acknowledgments

We thank Dr. F. E. Saalfeld and Dr. Albert B. Harvey for guidance in obtaining and interpreting the mass and absorption spectra, respectively, and

Can. J. Chem. Downloaded from www.nrcresearchpress.com by 210.87.254.105 on 09/05/12
For personal use only.

Drs. H. W. Carhart and G. W. McLaren for advice and assistance. We especially thank a referee for his suggestion to search for dodecene products.

1. N. M. EMANUEL (*Editor*). The oxidation of hydrocarbons in the liquid phase. The Pergamon Press, Ltd., New York. 1965.
2. I. V. BEREZIN, E. T. DENISOV, and N. M. EMANUEL. The oxidation of cyclohexane. The Pergamon Press, Ltd., Oxford, England. 1966.
3. J. A. HOWARD and K. U. INGOLD. Can. J. Chem. **44**, 1119 (1966).
4. J. L. BENTON and M. M. WIRTH. Nature, **171**, 269 (1953).
5. J. BETTS and J. C. ROBB. Nature, **215**, 274 (1967).
6. L. SAJUS. *In* Oxidation of organic compounds. *Edited by* F. R. Mayo. Amer. Chem. Soc. Advan. Chem. Ser. 75. Washington, D. C. 1968. p. 59.
7. E. A. BLYUMBERG, YU. D. NORIKOV, and YE. S. SMIRNOV. Neft. **2**, 897 (1962).
8. G. V. KARPUKHINA and Z. K. MAIZUS. Neft. **2**, 901 (1962).
9. J. A. HOWARD and K. U. INGOLD. J. Amer. Chem. Soc. **90**, 1056 (1968). See also other papers by these authors.
10. N. M. EMANUEL, E. T. DENISOV, and Z. K. MAIZUS. Liquid phase oxidation of hydrocarbons. Plenum Press, New York. 1967.
11. F. R. MAYO. Accounts Chem. Res. **1**, 193 (1968). See also other papers by this author.
12. A. W. DAWKINS. Eur. Chem. News, Norm. Paraffins Suppl. 49 (1966).
13. I. V. BEREZIN, L. G. BEREZKINA, and T. A. NOSOVA. *In* The oxidation of hydrocarbons in the liquid phase. *Edited by* N. M. Emanuel. The Pergamon Press, Ltd., New York. 1965. p. 110.
14. S. KUDO, K. SHIMOMURA, K. NEGISHI, and K. FUKUI. Kogyo Kagaku Zasshi, **65**, 1379 (1962); Chem. Abstr. **58**, 6686*c* (1963).
15. S. KUDO, K. SHIMOMURA, and K. NEGISHI. Kogyo Kagaku Zasshi, **65**, 1372 (1962); Chem. Abstr. **58**, 6685*h* (1963).
16. F. G. SCHWARTZ and B. H. ECCLESTON. Bureau of Mines Report IC-8140. Bartlesville, Okla. 1962.
17. L. BAGNETTO. USAF Report APL-TDR-64-89, Pt. III. Phillips Petroleum Co., Bartlesville, Okla. 1966.
18. R. A. BROWN, M. I. KAY, J. M. KELLIHER, and W. A. DIETZ. Anal. Chem. **39**, 1805 (1967).
19. W. F. TAYLOR and T. J. WALLACE. Government Research and Laboratory Report AF33(615)-3575. Esso Research and Engineering Co., Linden, N.J. 1967.
20. G. SCOTT. Atmospheric oxidation and antioxidants. Elsevier Publ. Co., New York. 1965.
21. E. R. BELL, J. H. RALEY, F. F. RUST, F. H. SEUBOLD, and W. E. VAUGHAN. Discuss. Faraday Soc. **10**, 242 (1951).
22. J. P. WIBAUT and A. STRANG. Proc. Kon. Med. Akad. Wetensch. **54B**, 229 (1951).
23. K. I. IVANOV, V. K. SAVINOVA, and V. P. ZHAKHOVSKAYA. Dokl. Akad. Nauk SSSR, **72**, 903 (1950).
24. R. L. SHULER, J. A. KRYNITSKY, and H. W. CARHART. Naval Research Laboratory Report 5553. Washington, D.C. 1960.
25. V. V. VESELOV and Z. V. SIPEEVA. Zh. Prikl. Khim. **38**, 2043 (1965).
26. F. W. HEATON and N. URI. J. Sci. Food Agr. **9**, 781 (1958).
27. R. D. MAIR and A. J. GRAUPNER. Anal. Chem. **36**, 195 (1964).
28. G. R. LAPPIN and L. C. CLARK. Anal. Chem. **23**, 541 (1951).
29. C. C. SEELEY, R. BENTLEY, M. MAKITA, and W. W. WELLS. J. Amer. Chem. Soc. **85**, 2495 (1963).
30. M. LOURY. Rev. Fr. Corps. Gras, **14**, 383 (1967).
31. F. E. SAALFELD. Naval Research Laboratory Report 6525. Washington, D.C. 1967.
32. R. M. SCHIRMER. Research Division Report 5029-68R. Phillips Petroleum Co., Bartlesville, Okla. 1968.
33. A. G. DAVIES. Organic peroxides. Butterworths, London. 1961. p. 170.
34. T. BERRY, C. F. CULLIS, M. SAEED, and D. L. TRIMM. *In* Oxidation of organic compounds. *Edited by* F. R. Mayo. Amer. Chem. Soc. Advan. Chem. Ser. 76, 86 (1968).
35. N. M. EMANUEL. (*Editor*). The oxidation of hydrocarbons in the liquid phase. The Pergamon Press, Ltd., New York. 1965. p. 122.

Can. J. Chem. Downloaded from www.nrcresearchpress.com by 210.87.254.105 on 09/05/12
For personal use only.

Can. J. Chem. Downloaded from www.nrcresearchpress.com by 210.87.254.6 on 09/05/12
For personal use only.

Kinetics of the acetone-photosensitized addition of HBr to ethylene

K. T. WONG[1] AND D. A. ARMSTRONG
Chemistry Department, The University of Calgary, Calgary, Alberta

Received May 26, 1969

The kinetics of the acetone-sensitized photoaddition of HBr to ethylene are consistent with the free radical chain mechanism of Vaughan, Rust, and Evans. In the presence of excess propane the combination of bromine atoms (reaction [4]) is the main termination step, and bromoethyl radicals formed by the addition of bromine atoms to ethylene (reaction [2]) are collisionally stabilized. They undergo thermal decomposition (reaction [−2]) or abstract a hydrogen atom from hydrogen bromide (reaction [3*a*]) to form the product, ethyl bromide. The rate constant ratio, k_{-2}/k_{3a}, increases from 5.6×10^{18} molecules cm^{-3} at 15.3 °C to 11.5×10^{18} molecules cm^{-3} at 45.0 °C. This corresponds to $E_{-2} - E_{3a} = 4.5 \pm 0.5$ kcal $mole^{-1}$, and is in accord with the thermochemical data. Within experimental error, k_2 and k_{-2} are independent of propane pressure in the range 260 to 390 Torr. Also, $(2k_4[M]/k_2)^{\frac{1}{2}}$ is equal to $5.5 \pm 0.3 \times 10^8$ $cm^{3/2}$ $molecule^{-1/2}$ $s^{-1/2}$, independent of temperature over the range 15.3 to 45.0 °C, and $E_2 = 0.0 \pm 0.5$ kcal $mole^{-1}$. In the absence of propane, and at ethylene pressures in excess of 400 Torr, the combination and disproportionation of bromoethyl radicals is the main termination process (reaction [7]). The value of $k_{3a}/(2k_7)^{\frac{1}{2}}$ is $8.9 \pm 0.1 \times 10^{-10}$ $cm^{3/2}$ $molecule^{-1/2}$ $s^{-1/2}$ at 35.1 °C, in agreement with kinetic data for related reactions.

Canadian Journal of Chemistry, 47, 4183 (1969)

Introduction

During the past 15 years, extensive studies of the photochlorination of ethylene and its derivatives have contributed much to our understanding of the reactions of chloroethyl radicals (1–5). In contrast, few investigations of the analogous bromination and hydrobromination reactions have been reported, and there is a noticeable lack of information on bromoethyl radicals (6, 7).

The only kinetic investigation of the photobromination of ethylene appears to be that of Schmitz, Schumacher, and Jager (8), who confirmed its free radical chain mechanism in 1942. The chain character of the gas phase hydrobromination was established in the same year by Vaughan, Rust, and Evans (9). The kinetics of the latter reaction were not studied in detail, but thermodynamic considerations (10) show unequivocally that bromine atoms and bromoethyl radicals are the chain carriers. Since the same situation holds for the photobromination, the mechanisms of the 2 additions differ only in reactions [3*a*] and [3*b*] in the following reaction sequence

[1] $\quad X + h\nu \xrightarrow{I_a} \phi Br$

where X = HBr, Br_2, or a sensitizer

[2]/[−2] $\quad Br + C_2H_4 \rightleftarrows C_2H_4Br$

[3*a*] $\quad HBr + C_2H_4Br \rightarrow Br + C_2H_5Br$

[3*b*] $\quad Br_2 + C_2H_4Br \rightarrow Br + C_2H_4Br_2$

[4] $\quad Br + Br + M \rightarrow Br_2 + M$

[5] $\quad Br \xrightarrow{k_d}$ (Br on wall) $\rightarrow \frac{1}{2}Br_2$

[6] $\quad C_2H_4Br + Br \rightarrow C_2H_4Br_2$ or $C_2H_4 + Br_2$

[7] $\quad 2C_2H_4Br \rightarrow C_2H_4Br_2 + C_2H_4$ or $C_4H_8Br_2$

Armstrong and Spinks (11) studied the hydrobromination in 1959. Since their prime objective was to demonstrate the catalysis of gas phase chain addition reactions by ionizing radiation, they used ^{60}Co γ-rays as the initiating source. At ethylene pressures below 100 Torr, the reaction bore a strong resemblance to the photobromination. Similarities were: linear termination, attributed to reaction [5]; a negative temperature coefficient, ascribed to the occurrence of reaction [−2]; and a value of about 6×10^{-14} cm^3 $mole^{-1}$ s^{-1} for k_2. The only apparent discrepancy between the 2 sets of data lay in the values of $E_{-2} - E_{3a}$ and $E_{-2} - E_{3b}$, which were estimated to be 14 ± 2 and 6 ± 1 kcal $mole^{-1}$, respectively. Since Anderson and Van Artsdalen (12) had observed $k_{3c}/k_{3d} = 0.6$,

[3*c*] $\quad C_2H_5 + HBr \rightarrow C_2H_6 + Br$

[3*d*] $\quad C_2H_5 + Br_2 \rightarrow C_2H_5Br + Br$

independent of temperature over the range 35 to 90 °C, the difference was much larger than

[1]Present address: Chemistry Department, Northern Alberta Institute of Technology, Edmonton, Alberta.

Can. J. Chem. Downloaded from www.nrcresearchpress.com by 210.87.254.6 on 09/05/12
For personal use only.

expected, and the authors noted the need for more extensive studies to resolve this problem.

Kinetic and thermochemical data from related chemical systems now make it possible to reject the high value of $E_{-2} - E_{3a}$. From published heats of formation at 298 °K and 1 atm

$$\Delta H^0_f \text{ of } C_2H_5Br = -15.0 \pm 0.3 \quad \text{(ref. 13)}$$

$$\Delta H^0_f \text{ of } C_2H_4 = 12.5 \quad \text{(ref. 14)}$$

and

$$\Delta H^0_f \text{ of HBr} = -8.7 \text{ kcal mole}^{-1} \quad \text{(ref. 14)}$$

the heat of reaction [I]

[I] $$C_2H_4(g) + HBr(g) = C_2H_5Br(g)$$

is -18.8 ± 0.5 kcal mole^{-1}. The heat of reaction [3*a*] should not differ by more than 1 kcal mole^{-1} from that of reaction [3*c*], which is 10.5 kcal mole^{-1} (15). Thus, $\Delta H_2^0 = -8.3$[2] and $\Delta E_2^0 = -7.7$ kcal mole^{-1}. This was pointed out previously by Barker and Maccoll (16), whose value of

$$E_{-2} + E_{-3a} = 21.2 \text{ kcal mole}^{-1}$$

requires

$$E_{3a} \simeq 3.0 \text{ kcal mole}^{-1}$$

as shown on the energy level diagram in Fig. 1. By analogy with chlorine atom addition to ethylene (1, 2), E_2 is probably 0. In any case, it is most unlikely that E_2 exceeds E_{3a}, and, since

$$E_{-2} - E_{3a} = -\Delta E_2 + E_2 - E_{3a}$$

(see Fig. 1), values of $E_{-2} - E_{3a}$ larger than 8 kcal mole^{-1} can be excluded. Indeed, the high apparent value of

$$E_{-2} - E_{3a} = 14 \pm 2 \text{ kcal mole}^{-1}$$

implies that the radiation-induced addition cannot be explained purely on the basis of the foregoing free radical mechanism. Thus, there is an obvious need for further work on the kinetics of the hydrobromination reaction, and it was for this reason that the present study was undertaken. The main objectives were to provide kinetic verification of the Vaughan, Rust, and Evans mechanism (9), and to determine the conditions under which the various termination reactions occurred. A preliminary report of some of our results was published in 1966 (17).

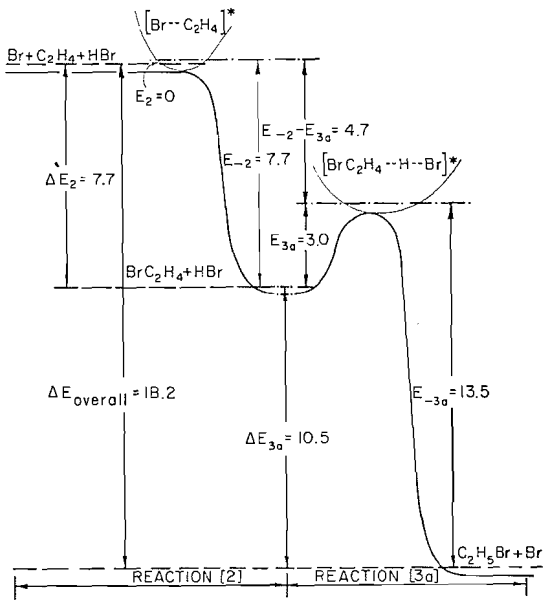

FIG. 1. Energy level diagram for reactions [2] and [3].

While this study was in progress, 3 other investigations of the hydrobromination were published. Abell's initial work (18*a*) was primarily concerned with the relative rates of addition of bromine atoms to different olefins and did not deal with the kinetics of the ethylene reaction per se. In a more recent publication with Field (18*b*), he has reported a study of the kinetics of the addition reaction at temperatures in the range 40–125 °C and pressures of 25–125 Torr. Their observations will be considered in the Results and Discussion sections below. Oldershaw and Cvetanović (19) showed that the hydrobromination of *cis*-1,2-dideuteroethylene was accompanied by a rapid isomerization. They interpreted this in terms of reactions [2*], [−2*], [8*], and [9*]

[2*]/[−2*] $$Br + C_2H_4 \rightleftarrows C_2H_4Br^*$$

[8*] $$C_2H_4Br^* + M \rightarrow C_2H_4 + Br + M$$

[9*] $$C_2H_4Br^* + M \rightarrow C_2H_4Br + M$$

The above presentation represents a slight generalization of their hypothesis, for they postu-

[2] Essentially the same result (-8.2 kcal mole^{-1}) is obtained from the data of ref. (14) by a similar treatment of reactions [II]

[II] $$Br_2(g) + C_2H_4(g) = C_2H_4Br_2(g)$$

and [3*b*]. We also note that Kerr and Lloyd (7) report $\Delta H_2^0 = -8.8$, based on thermodynamic data.

Can. J. Chem. Downloaded from www.nrcresearchpress.com by 210.87.254.6 on 09/05/12
For personal use only.

lated reactions [8*] and [9*] for M = HBr only. However, this generalization is necessary (3) and it follows that k_2 is a complex rate constant equal to

$$\frac{k_2^* \sum_M k_9^* [M]}{\sum_M k_8^* [M] + \sum_M k_9^* [M] + k_{-2}^*}$$

in the first approximation (a more complete treatment of the pressure dependence of k_2 is to be found in ref. 20).

It is clear from Oldershaw and Cvetanović's work and from the related observations on chloroethyl radicals, that an efficient deactivator, M, must be added to the reaction bath if the bromoethyl radicals are to be stabilized and brought to thermal energies. For this reason, most of our experiments at low ethylene pressures were conducted in the presence of 260 to 400 Torr of propane, which would be expected to have a high efficiency for deactivating $C_2H_4Br^*$ radicals. By contrast, HBr, which resembles krypton in terms of size and mass, should be relatively inefficient. As an illustration, it may be noted that krypton removes only ~ 2 kcal mole^{-1} of excess energy in the average collision with activated alkyl radicals, while C_3 and C_4 hydrocarbons remove $\geqslant 9$ kcal mole^{-1} (21). The addition of propane has a second simplifying effect in eliminating reaction [5] (see below).

One further point deserves comment here. At 2537Å, ethyl bromide has an extinction coefficient about twice that of HBr (22). Because of this, it was decided that a sensitizer, which absorbed at wavelengths longer than either of these molecules, should be used. This procedure avoided changes in the absorbed light intensity and rate of initiation during the course of a run and also provided a far more uniform absorbed light intensity than would have been possible with HBr as the light absorbing species. After preliminary trials of a number of compounds, acetone was chosen as the sensitizer. Its photolysis in the presence of HBr had been investigated in 1955 by Ridge and Steacie (23). During the course of this work, a more comprehensive study was published by Larson and O'Neal (24). Their results will be reviewed in the Discussion section.

Experimental

Materials

Matheson Co. anhydrous HBr of 99.8% purity was irradiated with a ^{60}Co γ-ray source as previously described (25) to remove impurities which were reactive to Br atoms. It was then sublimed through copper turnings to remove bromine, and further purified by several distillations from a trap at -120 °C to a trap cooled by liquid nitrogen. Philips research grade ethylene was degassed by bulb-to-bulb distillation and pumping. Matheson sulfur hexafluoride and ethyl chloride were treated in the same way. Spectrograde acetone was purchased from the Eastman Kodak Co. and thoroughly degassed by freeze–pump–thaw cycles before use.

Apparatus

The cylindrical quartz reaction cell was 10 cm long and had optically plane end windows. Its internal diameter was nominally 4.0 cm, and its volume 111.41 cm^3. It was connected to a mercury-free vacuum line and immersed in a thermostat tank which was regulated to within ± 0.03 °C. The tank and cell were mounted on a rugged optical bench.

Light from the Osram 100 W/2 high pressure mercury light source passed through a series of collimating quartz lenses, 2 filter glasses (Corning 0–53 and 7–54), and a 3×10^{-4} M K_2CrO_4 solution of 3 cm path length. The wavelengths of the emerging beam extended from 3050 to 3250 Å, with a maximum at 3125 Å. The incident light intensity was measured by a photometer, which had been calibrated against the ferri-oxalate actinometer (26). The absorbed light intensity, I_a, was calculated from the incident light intensity, I_0, and the acetone concentration in the reaction cell. The usual corrections were made for light losses in the cell windows, etc. (27). The effective extinction coefficient of acetone for the incident light spectrum was calculated to be 2.4 l mole^{-1} cm^{-1}, which compares well with an experimentally determined value of 1.97 for a similar light source (24). In a typical run, only about 0.7% of the light was absorbed over the length of the cell and I_a was taken to be uniform, within experimental error.

The absorbed light intensity was varied by using lamps of different output intensity, by changing the acetone pressure, or by changing the focal length of the first collimating lens. Care was taken to ensure that the light beam through the cell was homogeneous and parallel. It was defined by an iris diaphragm with a diameter only about 1 mm less than that of the cell. This procedure reduced the unirradiated volume of the cell to a minimum and avoided uncertainties caused by reactions of bromine atoms which diffused out of the light zone.

The rate of the overall addition (i.e., of reaction [1]) was measured by the decrease in pressure. For experiments to determine the light intensity dependence, the pressure was monitored with a Pyrex diaphragm gauge (28). For most other experiments, a Pyrex spiral gauge (Kern Chemical Corporation) with an optical lever was used. Both gauges were calibrated against a mercury manometer in an auxiliary vacuum system.

Procedure

For each experiment, the desired pressure of acetone vapor was admitted to a calibrated volume. This was isolated while the acetone vapor was pumped from the remainder of the system. The contents of the calibrated volume were then admitted to the reaction cell and flushed through the connecting tubes with measured

Can. J. Chem. Downloaded from www.nrcresearchpress.com by 210.87.254.6 on 09/05/12
For personal use only.

amounts of ethylene and HBr. This procedure gave reproducible rates. It was adopted after initial experiments showed that acetone and HBr reacted when condensed together at liquid nitrogen temperature (cf. ref. 24). When required, propane was introduced along with the HBr and ethylene. After all gases had been expanded into the reaction cell, the system was allowed to stand for about 25 min before photolysis commenced.

More extensive details of the apparatus and experimental procedures are given in ref. 22.

Results

The experiments fall into 3 categories: experiments with excess ethylene, experiments at ethylene pressures below 100 Torr with only the reactants present, and experiments at ethylene pressures below 100 Torr with propane and other added gases. Before presenting them under these 3 headings in sections (*iii*), (*iv*), and (*v*), we shall first describe the general features of the reaction.

(i) Reaction–Time Curves

Figure 2 shows plots of pressure decrease vs. time for experiments both with and without added propane. In each case, data are given for 2 almost identical experiments. The curves are typical of those used to obtain reaction rates, and they illustrate the precision which was achieved. The inset of Fig. 2 shows pressure changes recorded with the Kern spiral gauge for photolysis over 1 min periods followed by equal dark periods. The initial pressure rise, and the pressure decrease occurring after illumination ceased, are due to the heat liberated in the reaction (i.e., to the Budde–Draper effect). The induction periods observed in the reaction–time curves for continuous photolysis (main Fig. 2) are due mainly to this effect. It cannot be entirely eliminated, but in kinetic runs reaction conditions which caused the average temperature of the cell contents to rise by more than 2 °C above the thermostat temperature were avoided. Reaction rates were determined from the slopes of the reaction–time curves after about 10% reaction or, when possible (see below), from first order log plots for ethylene consumption.

When photolysis was continued until reaction ceased, the pressure drop corresponded to the initial pressure of the reactant present in stoichiometric deficiency. Analysis of the reaction mixture with an AEI type MS2 mass spectrometer confirmed that ethyl bromide was the only major product in systems both with and without added propane. No peaks of mass greater than the parent peak of ethyl bromide were detectable. Thus, C_4H_9Br and $C_2H_4Br_2$ can, at most, only be formed in trace quantities; also, the bromination of propane cannot be of any importance. Detection of "termination" or "initiation" products was not expected, since their partial pressures would have been of the order of 0.04 Torr in a total pressure of ~ 400 Torr.

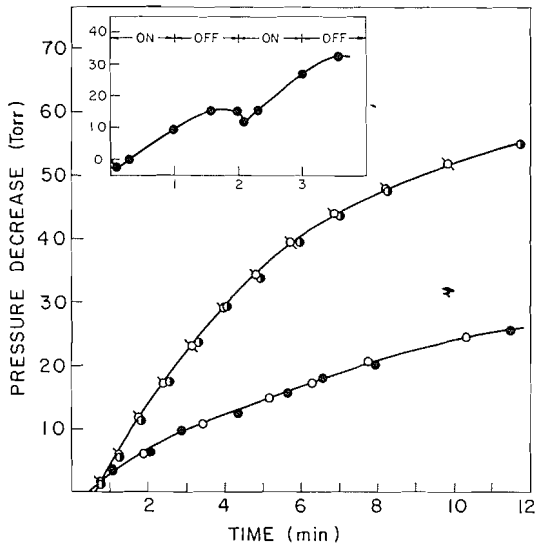

FIG. 2. Pressure decrease vs. time curves for reaction at 25.0 °C. Main figure: continuous illumination with points taken only after induction period. Inset: intermittent illumination; points taken to show the initial pressure increase and the pressure decrease after the light period. Both are caused by the Budde–Draper effect.

Symbol	Pressure, Torr HBr	C_3H_8	C_2H_4	$10^{-12}I_a$ (Photons cm^{-3} s^{-1})
◔	308	—	61.1	16.2
◑	307	—	61.5	15.5
○	62.7	263.8	58.1	8.26
●	61.7	259.1	56.6	8.28
●	441	—	61	8.40

(ii) The Effect of Light Intensity on Reaction Rate

Table I summarizes the intensity exponents for experiments under the 3 different sets of conditions mentioned above. They were derived from the least-squares slopes of log–log plots. Those shown in Fig. 3*a* are for experiments with HBr in excess, and the intensity exponents lie between 0.5 and 1.0. For all other conditions, the intensity exponents were close to 0.5, indicating that mutual termination was almost exclusive.

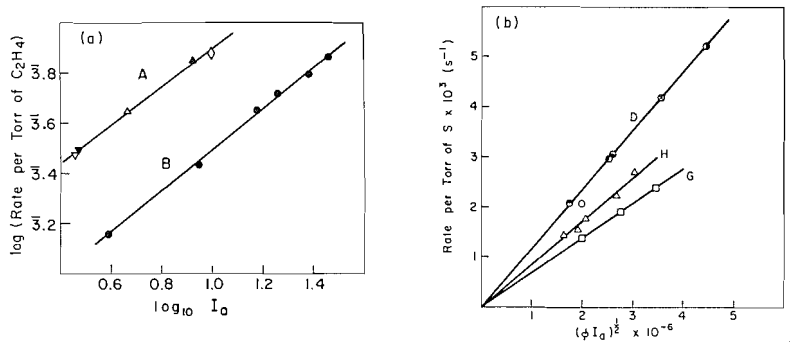

FIG. 3. Dependence of reaction rate on light intensity (*a*) $\log_{10}$ (reaction rate per Torr of C_2H_4) vs. $\log_{10}$ (absorbed light intensity) at 25 °C. Conditions for plots A and B are given in Table I, with more detailed data for plot A in Table II. (*b*) Reaction rate normalized with respect to *S* plotted as a function of $(\phi I_a)^{\frac{1}{2}}$. Conditions for plots D, H, and G are given in Table I, with more detailed data for plot D in Table II. S = C_2H_4 for plot D and S = HBr for plots H and G.

TABLE I

Intensity dependence of reaction rate

Reaction cell temperature (°C)	Pressure (Torr)				Intensity exponent	Plot*
	HBr	C_2H_4	C_3H_8	Total		
25.0	440	60	—	500	0.77±0.05	A
25.0	307	59	—	366	0.82±0.04	B
25.0	64	57	392	513	0.53±0.03	C
25.0	303	61	257	621	0.52±0.01	D
35.0	200	63	362	625	0.53±0.02	E
45.0	193	57	383	633	0.52±0.02	F
25.0	61	305	—	366	0.50±0.04	G
35.1	45	500	—	545	0.51±0.05	H

*See Fig. 3.

TABLE II

Complete data for plot A of Fig. 3*a* and plot D of Fig. 3*b*

Plot	Acetone pressure (Torr)	I_0*	ϕI_a*	Rate per Torr of C_2H_4 (s^{-1} × 10^3)	Symbol in Fig. 3
A	0.345	3.88	2.94	2.98	▽
	0.209	6.50	2.98	3.09	▼
	0.550	3.86	4.64	4.41	△
	0.209	18.60	8.51	7.02	▲
	0.961	4.76	10.00	7.58	◇
D	0.947	1.88	3.91	2.07	○
	0.963	9.60	20.21	5.21	◑
	0.926	2.33	6.43	2.99	◐
	0.426	3.28	3.06	2.08	◓
	0.945	3.28	6.81	3.05	◒
	1.88	3.10	12.77	4.21	⊗

*Arbitrary units.

Figure 3*b* shows a graph of reaction rate vs. $(\phi I_a)^{\frac{1}{2}}$ for the experiments of code numbers D, G, and H in Table I. The linearity confirms the dependence of reaction rate on $(\phi I_a)^{\frac{1}{2}}$. The acetone pressures and incident light intensities, I_0, used in obtaining the data for plot D of this figure and plot A of Fig. 3*a* are given in Table II. The data illustrate the fact that the intensity dependence is the same whether I_a is altered by changing I_0 or the acetone pressure over a factor

Can. J. Chem. Downloaded from www.nrcresearchpress.com by 210.87.254.6 on 09/05/12
For personal use only.

of 4. From this it may be concluded that acetone serves only as a photosensitizer and that it does not take part in the propagation or termination reactions. It may also be noted that in the absence of acetone, HBr–ethylene mixtures showed no measurable reaction after photolysis with our light system for periods of up to 1 h.

(iii) Experiments with Excess Ethylene

The reaction rate at 35.1 °C was studied as a function of ethylene pressure over the range 100 to 590 Torr with the HBr pressure held to 60 ± 6 Torr and the absorbed light intensity kept as close as possible to 2.9×10^{12} photons $cm^{-3}\ s^{-1}$. As shown in Fig. 4*a*, the reaction rate becomes independent of ethylene pressure above 380 Torr.

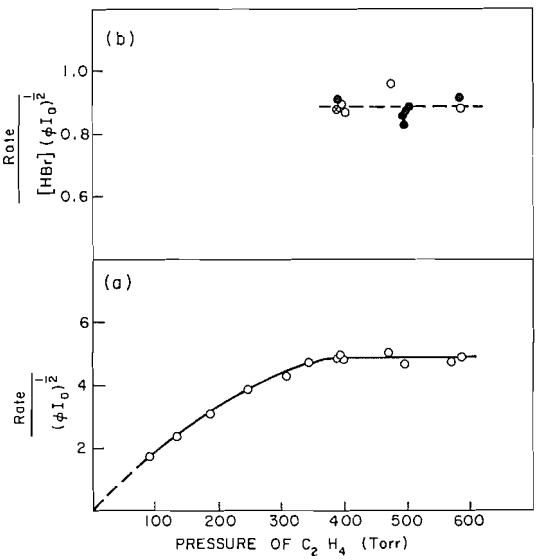

FIG. 4. Dependence of reaction rate on ethylene pressure at 35.1 °C; ethylene in excess. (*a*) Reaction rate $\times (\phi I_a)^{-\frac{1}{2}}$ for $I_a \simeq 2.9 \times 10^{12}$ photons $cm^{-3}\ s^{-1}$ and [HBr] = 60 ± 1 Torr, plotted against ethylene pressure. (*b*) Rate $\times (\phi I_a)^{-\frac{1}{2}} \times [HBr]^{-1}$ plotted vs. ethylene pressure. HBr pressure: 60 Torr, ○; 32 Torr, ⊗; 45 Torr (with I_a varied), ●.

From the linear plot of rate vs. HBr pressure in Fig. 5, the reaction is first order in HBr at high ethylene pressures. The empirical rate expression for experiments with ethylene in excess is therefore

$$[i] \qquad \frac{d[C_2H_5Br]}{dt} = k'[HBr]I_a^{\frac{1}{2}}$$

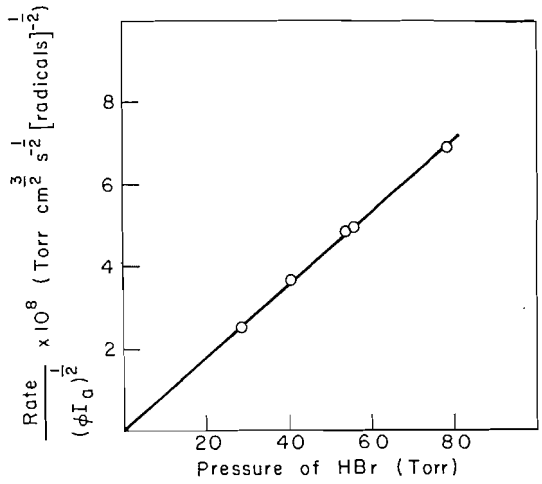

FIG. 5. Reaction rate $\times (\phi I_a)^{-\frac{1}{2}}$ plotted against HBr pressure. Temperature = 35.1 °C; ethylene pressure = 395 Torr.

(iv) Experiments at Ethylene Pressures Below 100 Torr with Only the Reactants Present

As the ethylene pressure is reduced below 400 Torr, the ethylene exponent increases (see Fig. 4*a*). Below 100 Torr it becomes unity. This was demonstrated by the fact that plots of initial reaction rate vs. ethylene pressure were linear. First order log plots showed that this dependence was maintained up to about 50% addition, beyond which there was a tendency for the rate to increase. A similar effect was observed by Field and Abell (18*b*) and attributed to the greater efficiency of ethyl bromide (than HBr and ethylene) as a deactivator of $C_2H_4Br^*$.

(v) Experiments at Ethylene Pressures Below 100 Torr with Propane and Other Added Gases

The effects of added gases on the reaction rate are illustrated in Table III, which summarizes the reaction rates observed in the presence of propane, sulfur hexafluoride, and ethyl chloride, each at 2 different pressures. The rate in their absence is shown for comparison. In each case, the reaction rate initially rises with added gas pressure and then falls as the added gas pressure is further increased.

In the presence of 260 to 400 Torr propane, the dependence on ethylene was again first order. The linearity of the first order log plots for these conditions was maintained up to at least 2 reaction half lives (see Fig. 6), showing that the effect of a growing concentration of ethyl bromide was

Can. J. Chem. Downloaded from www.nrcresearchpress.com by 210.87.254.6 on 09/05/12
For personal use only.

TABLE III

Dependence of reaction rate on pressure of added inert gases*

Pressure (Torr)			Rate per Torr of C_2H_4 ($s^{-1} \times 10^3$)
HBr	C_2H_4	Added gas [M]	
65.9	61.3	—	1.38
61.7	57.0	259(C_3H_8)	1.61
60.0	62.4	390(C_3H_8)	1.38
63.2	60.5	300(C_2H_5Cl)	2.37
62.1	59.9	382(C_2H_5Cl)	2.13
64.2	61.6	299(SF_6)	2.33
60.1	59.7	391(SF_6)	2.13

*$\phi I_a = 1.2 \times 10^{13}$ radicals cm^{-3} s^{-1}.

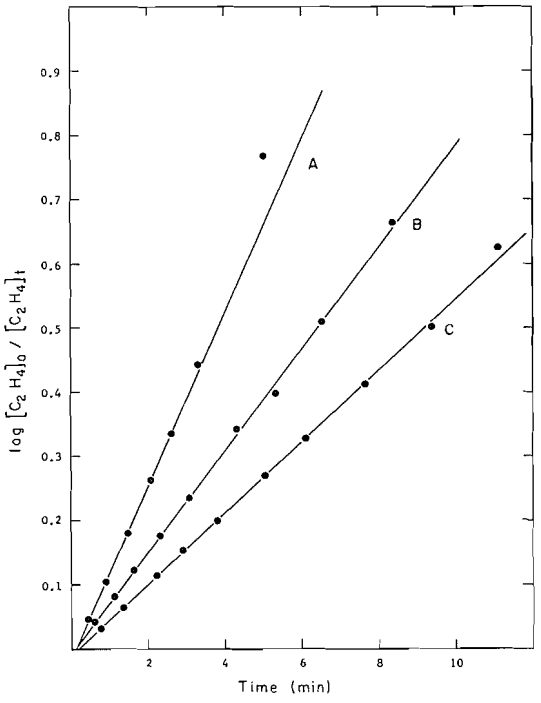

FIG. 6. First order plots for ethylene consumption at 25 °C in the presence of propane. HBr pressure, 300 Torr; C_2H_4 pressure, 61 Torr; C_3H_8 pressure, 257 Torr; ϕI_a, 20.2, 6.4_3, and $3.0_6 \times 10^{12}$ radicals cm^{-3} s^{-1} for A, B, and C, respectively.

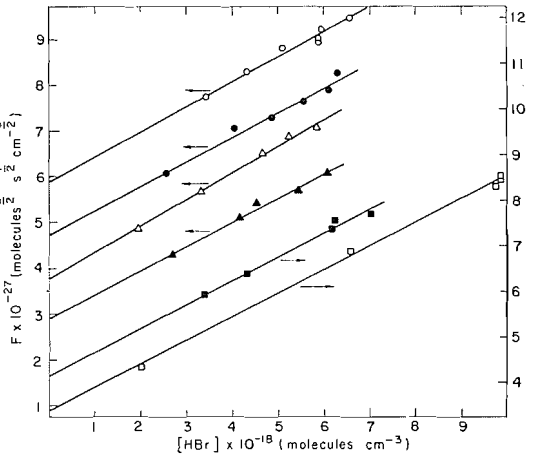

FIG. 7. Dependence of reaction rate on HBr concentration. Plot of $F = (\phi I_a)^{\frac{1}{2}}[C_2H_4][HBr]$/rate vs. [HBr]. Ethylene pressure ~60 Torr; C_3H_8 pressure (Torr) and temperature (°C) are, respectively: ○, 385 and 45.0; ●, 380 and 35.0; △, 390 and 25.0; ▲, 380 and 15.3; ■, 291 and 35.1; □, 259 and 25.0.

not as noticeable in the presence of propane. A similar behavior was observed at all of the temperatures used in this study, and as a general rule reaction rates were calculated from the slopes of such plots.

The dependence of reaction rate on HBr pressure, at fixed pressures of ethylene and propane, was investigated at 15.3, 25.0, 35.0, and 45.0 °C. The results are given in Fig. 7. The HBr dependence is complex, and the manner of presentation will be explained in the discussion.

The empirical rate expression for experiments in the presence of added propane is

$$[ii] \qquad \frac{d[C_2H_5Br]}{dt} = k''[C_2H_4]I_a^{\frac{1}{2}}f[HBr]$$

where $f[HBr]$ is a complex function of [HBr].

Discussion

A discussion of the photolysis of acetone in the present system is necessary before consideration of the chain reaction per se. The work of Larson and O'Neal (24) has shown that HBr is a highly efficient scavenger for triplet state

Can. J. Chem. Downloaded from www.nrcresearchpress.com by 210.87.254.6 on 09/05/12
For personal use only.

Can. J. Chem. Downloaded from www.nrcresearchpress.com by 210.87.254.6 on 09/05/12
For personal use only.

acetone molecules. The following reactions, in which A = acetone, were postulated to explain their results:

[A] $A + h\nu \xrightarrow{I_a} A_m^3$ (triplet, vibrationally active)

[B] $A_m^3 \rightarrow CH_3 + CH_3CO$

[C] $M + A_m^3 \rightarrow M + A_0^3$ (thermalized triplet)

[D] $HBr + A_0^3 \rightarrow CH_3C(OH)CH_3 + Br$

[E] $CH_3 + HBr \rightarrow CH_4 + Br$

[F] $CH_3CO + HBr \rightarrow CH_3CHO + Br$

[G] $CH_3C(OH)CH_3 + HBr \rightarrow CH_3CH(OH)CH_3 + Br$

[H] $Br +$ scavenger $\rightarrow$ Unreactive radical

Reactions [E] and [F] had previously been proposed by Ridge and Steacie (23). Like reaction [E], reaction [D] was estimated to have a rate constant equal to $6.6 \times 10^{-12} \times 10^{-1.1/\theta}$ cm^3 molecule^{-1} s^{-1}, and quenching of the acetone triplets by ethylene obviously could not compete with it, since the collision efficiency of the latter process is only $\simeq 2.6 \times 10^{-6}$ (29).

Larson and O'Neal also estimated

$$k_G \simeq 2 \times 10^{-12} \times 10^{-4.5/\theta} \text{ cm}^3 \text{ molecule}^{-1} \text{ s}^{-1},$$

which gives a lifetime of about 10^{-4} s for the 2-hydroxyisopropyl radicals at the HBr pressures employed in this study. Rotating sector experiments (22, 30) and other considerations show that the lifetimes of the chain centers in our system are of the order of 0.03 s or longer. Hence, it follows that reactions [I] and [J]

[I] $CH_3C(OH)CH_3 + Br \rightarrow CH_3CBr(OH)CH_3$

[J] $CH_3C(OH)CH_3 + C_2H_4Br \rightarrow CH_3CBr(OH)CH_3 + C_2H_4$

cannot be of any importance under present conditions. The situation for reaction [K]

[K] $CH_3CO + Br \rightarrow CH_2CO + HBr$

is less clear, since k_F is likely to be smaller than k_G. However, ϕ_{CH_3CO} will only be 0.1, or less, and discrepancies arising from the neglect of reaction [K] should not be serious. The foregoing mechanism leads to a quantum yield, ϕ, for bromine atoms equal to

$$2\phi_{\text{Isopropanol}} + \phi_{CH_3} + \phi_{CH_3CO}$$

and ϕ approaches 2 in the presence of bromine atom scavengers (24). To allow for some uncertainty, notably in the reactions of CH_3CO, we have taken $\phi = 1.7 \pm 0.3$. We assume this to be independent of temperature in the range 15 to 45 °C.

Returning to the results of this investigation, we may note from expression [*i*] of section (*iii*), that the data at ethylene concentrations in excess of 380 Torr are the most clear cut. The intensity exponent of 0.5, the lack of dependence on ethylene pressure, and the first order dependence on HBr all conform to expression [*iii*]

$$[iii] \qquad \frac{d[C_2H_5Br]}{dt} = k_{3a}\left(\frac{\phi I_a}{2k_7}\right)^{\frac{1}{2}}[HBr]$$

which is obtained when reaction [7] is the only significant termination reaction (11). The slope of the line in Fig. 5 gives

$$k_{3a}/(2k_7)^{\frac{1}{2}} = 8.9 \pm 0.1 \times 10^{-10} \text{ cm}^{3/2} \text{ molecule}^{-1/2} \text{ s}^{-1/2}$$

at 35.1 °C. Rearrangement of [*iii*] leads to

$$[iv] \qquad \frac{k_{3a}}{(2k_7)^{\frac{1}{2}}} = \frac{\text{Rate}}{(\phi I_a)^{\frac{1}{2}}[HBr]}$$

Figure 4b is a plot of the right hand side of expression [*iv*] against ethylene pressure, over the range 380 to 590 Torr. The above value of $k_{3a}/(2k_7)^{\frac{1}{2}}$ is seen to hold for all of the conditions shown on the figure.

Rotating sector experiments (1, 2) have led to rate constants of 2×10^{-11} and 3×10^{-11} cm^3 molecule^{-1} s^{-1}, respectively, for the combination plus disproportionation of the chlorethyl radicals Cl—CH_2—CH_2 and Cl—CHCl—CHCl. Because of the weaker bonding and slightly larger size of bromine atoms, one would expect a faster rate of disproportionation and a somewhat enhanced value of k_7 for Br—CH_2—CH_2 radicals. Taking

$$k_7 = 5 \times 10^{-11} \text{ cm}^3 \text{ molecule}^{-1} \text{ s}^{-1}$$

leads to

$$k_{3a} = 0.9 \times 10^{-14} \text{ cm}^3 \text{ molecule}^{-1} \text{ s}^{-1}$$

at 35.1 °C, which is consistent with 2.0×10^{-14} calculated for reaction [3*c*] at 35.0 °C from the data of Fettis, Knox, and Trotman-Dickenson (31).

Attention can now be given to the results observed at ethylene pressures below 100 Torr. The first order dependence on ethylene shows that addition of bromine atoms to the C=C bond is the main rate controlling process. Termination

Can. J. Chem. Downloaded from www.nrcresearchpress.com by 210.87.254.6 on 09/05/12
For personal use only.

must be by reactions [4] and [5] as was observed previously for the photobromination (8). The intensity exponents for code numbers A and B in Table I imply that both processes occur in the absence of propane, and that the proportion of termination by reaction [5] tends to decrease as the total pressure of reactants increases. This behavior is as expected, since the rate of reaction [5] is proportional to the diffusion coefficient of bromine atoms in the system and hence varies inversely with pressure. For the same reason, the addition of chemically inert gases to a system with constant light intensity and concentrations of the reactants should cause an increase in reaction rate until reaction [5] becomes negligible, and then a decrease, as the total concentration of third bodies (i.e., [M] in reaction [4]) is increased still further. This type of behavior is well documented for related systems (8, 32) and only a cursory investigation of the effects of C_2H_5Cl and SF_6 at $\sim$ 260 and $\sim$ 385 Torr was performed to establish that propane was not unique in its effect on this system. The results in Table III show the expected reduction in rate for high pressures of all 3 added gases. The initial enhancement in rate is in accord with the observations of Field and Abell (18*b*), and may be due, in fact, to the reduction in the rate of reaction [5]. However, in this system a large part of the enhancement is probably due to the greater efficiency of the added gases as moderators of $C_2H_4Br^*$ in reaction [9*], and the contributions of the 2 processes cannot be separated.

At 385 $\pm$ 5 Torr, propane gave a 50% lower rate than SF_6 or C_2H_5Cl. We attribute this to a better efficiency of propane as a third body in reaction [4], rather than to its failure as a deactivator of $C_2H_4Br^*$ or to the occurrence of the following reactions

$$[10]/[-10] \quad Br + C_3H_8 \rightleftarrows HBr + C_3H_7 \qquad \Delta H = 7.0 \text{ kcal mole}^{-1}$$

$$[11] \quad Br + C_3H_7 \rightarrow C_3H_7Br \text{ or } C_3H_6 + HBr$$

Reactions [10], [−10], and [11] lead to

$$[Br]_{ss} = \left(\frac{(\phi I_a)[HBr]}{2k_{11}K_{10}[C_3H_8]}\right)^{\frac{1}{2}}$$

and, if reaction [4] were unimportant, our apparent value of k_4 would in fact be $k_{11}K_{10}/(HBr)$. The data of refs. 14, 15, and 33 give

$$K_{10} = 6 \times 10^{-4} \text{ at } 298 \text{ °K}$$

and k_{11} should not exceed 6×10^{-11} cm^3 molecule^{-1} s^{-1}. Consequently, for our conditions of temperature and HBr concentration ($\sim 4 \times 10^{18}$ molecules ml^{-1}), $k_{11}K_{10}/[HBr]$ should be about 8×10^{-33} cm^6 molecule^{-2} s^{-1}, which is an order of magnitude smaller than would be expected for k_4, since Russell and Simons (34) observed

$$k_4 = 8 \times 10^{-32} \text{ cm}^6 \text{ molecule}^{-2} \text{ s}^{-1}$$

for iodine atoms combining in the presence of propane. The magnitude of $k_{11}K_{10}/[HBr]$ should also show a positive activation energy of 7 kcal mole^{-1} and vary inversely with [HBr]. The present data give no evidence for such trends in k_4. For these reasons, it is evident that reactions [10] and [11] do not contribute significantly to the termination reaction under the conditions of this study.

It can be shown (cf. ref. 1) that the intensity exponent of 0.77 for 440 Torr of HBr and 60 Torr of ethylene (See Table I*a*) corresponds to roughly equal proportions of mutual and linear termination. Comparison with the value of 0.52, which corresponds to over 90% termination by reaction [4], for a mixture containing 392 Torr of propane at a similar absorbed light intensity and total pressure, leads to the obvious conclusion that k_4 for M = HBr is at least a factor of 10 less than k_4 for M = C_3H_8. For this reason, the contribution of HBr as a third body in reaction [4] will be neglected in the subsequent analysis of the dependence of the reaction rate on HBr concentration.

The first order dependence on ethylene and mutual termination in the presence of propane (see expression [*ii*]) are both in accordance with expression [*v*]

$$[v] \quad \frac{d[C_2H_5Br]}{dt} = \left(\frac{\phi I_a}{2k_4[M]}\right)^{\frac{1}{2}} \frac{k_2[C_2H_4][HBr]}{[HBr] + k_{-2}/k_{3a}}$$

based on termination by reaction [4] (see ref. 11). It may be rearranged to

$$[vi] \quad \frac{(\phi I_a)^{\frac{1}{2}}[C_2H_4][HBr]}{\left(\frac{d[C_2H_5Br]}{dt}\right)} = \frac{(2k_4[M])^{\frac{1}{2}}}{k_2}\left(\frac{k_{-2}}{k_{3a}} + [HBr]\right)$$

Can. J. Chem. Downloaded from www.nrcresearchpress.com by 210.87.254.6 on 09/05/12
For personal use only.

TABLE IV

Rate constant ratios for experiments with propane present

Temperature (°C)	Pressure of $C_3H_8 + C_2H_4$ (Torr)	k_{-2}/k_{3a} (molecules $cm^{-3} \times 10^{-18}$)
15.3	440	5.6±0.6
25.0	445	6.5±0.3
35.0	445	8.7±0.8
45.0	445	11.5±1.0
25.0	320	6.5±0.3
35.1	350	8.2±0.7

Figure 7 shows values of F, the quantity on the left hand side of this expression, plotted against the HBr concentration for fixed pressures of propane and ethylene at temperatures of 15.3, 25.0, 35.0 and 45.0 °C. The magnitude of k_{-2}/k_{3a} calculated from the ratio of the slope to the intercept of each of the lines is given in Table IV. Since k_{3a} should not vary with pressure, any dependence of k_{-2} on pressure will be reflected in a pressure dependence of k_{-2}/k_{3a}. Analogy with other radical decompositions suggests that k_{-2} would be near its pressure dependent region under our conditions. For example, $P_{\frac{1}{2}}$ is estimated to be ~ 101 Torr for the acetyl radical at 235 °C (35), and ~ 110 Torr for C_2H_5CO at 42 °C (36). Due to practical limitations, the range of pressures shown in Table IV represents the maximum variation possible in this system with the present apparatus, and a meaningful estimate of $P_{\frac{1}{2}}$ for C_2H_5Br is impossible. However, the results for the 2 propane pressures at 25.0 and 35.0 °C imply that any pressure dependence of k_{-2} is minor, so that it is probably close to, if not equal to, its high pressure limiting value. Consistent with this is the fact that the Arrhenius plot for k_{-2}/k_{3a} in Fig. 8 gives

$$E_{-2} - E_{3a} = 4.5 \pm 0.5 \text{ kcal mole}^{-1}$$

which agrees within experimental error with the value predicted in Fig. 1. The above result is also in accord with

$$E_{-2} - E_{3b} = 6.1 \text{ kcal mole}^{-1}$$

obtained from the photobromination of ethylene in the presence of ~ 300 Torr of CF_2Cl_2 as moderating gas (8). Figure 8 also gives

$$A_{-2}/A_{3a} = 1.3 \times 10^{22} \text{ molecule cm}^{-3}$$

which is to be compared with

$$A_{-2}/A_{3b} = 0.8 \times 10^{22} \text{ molecule cm}^{-3}$$

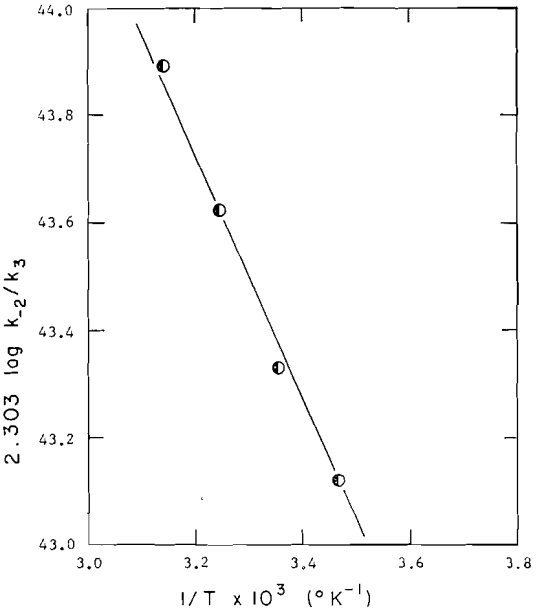

FIG. 8. Arrhenius plot of k_{-2}/k_{3a}.

The combined data for the bromination and hydrobromination lead to

$$k_{3a}/k_{3b} = 1.6 \exp(-1600/RT)$$

which has a value of 0.2 at 60 °C. The agreement of this value with the value of 0.6 for k_{3c}/k_{3d} at the same temperature from Anderson and Van Artsdalen (12) confirms the similarity of the mechanisms for the 2 chain reactions.

From expression [*vi*], it can be seen that the slopes of the lines in Fig. 7 correspond to the values of $(2k_4[M])^{\frac{1}{2}}/k_2$. For ethylene plus propane pressures of 440–445 Torr, there is some scatter, but all values of $(2k_4[M])^{\frac{1}{2}}/k_2$ for the temperature region 15.3 to 45.0 °C are accommodated within the range $5.5 \pm 0.3 \times 10^8$ $cm^{3/2}$ $molecule^{-1/2}$ $s^{-1/2}$. From the determined tem-

Can. J. Chem. Downloaded from www.nrcresearchpress.com by 210.87.254.6 on 09/05/12
For personal use only.

perature dependence of k_4 (22, 30), we conclude that $E_2 = 0.0 \pm 0.5$ kcal mole^{-1}.

Because of its complex nature, the dependence of k_2 on propane pressure is clearly of interest. The values of $(2k_4[M])^{\frac{1}{2}}/k_2$ for $\sim$ 330 Torr of ethylene plus propane at 25.0 and 35.0 °C are both 5.1×10^8, which is about 10% lower than the mean of those observed for $\sim$ 440 Torr, and in the opposite direction to that expected for a decrease in k_2. The intercepts of the 2 sets of data at 25.0 and 35.0 °C show a similar trend. Both observations can be explained by the reduction in $[M]^{\ddagger}$, if it is assumed that ethylene and propane have similar values of k_4. There is, therefore, no evidence for any significant change in k_2 over the limited range of propane pressures employed. This implies that effectively all $C_2H_4Br^*$ are deactivated by propane at 260 Torr (i.e., that $k_2 = k_2^*$ for these conditions). Confirmation of this may be obtained from studies of the isomerization:addition ratio for *cis*-1,2-dideuteroethylene in the presence and absence of propane.

Results obtained in the absence of propane and at low ethylene pressures lead to the conclusion that HBr is much less effective in deactivating $C_2H_4Br^*$ (17), and are in accord with the conclusions of Field and Abell (18*b*) as well as the observations of Oldershaw and Cvetanović (19). They will be reported in detail elsewhere. However, 3 points deserve immediate clarification. (*a*) We have not determined overall temperature dependences, only values of $E_{-2} - E_{3a}$. (*b*) Apart from the experiments in section (*iii*) of Results above, our work has been confined to conditions such that $k_{-2} \simeq k_{3a}[HBr]$, while Field and Abell's studies (18) have been done at conditions where $k_{-2} \gg k_{3a}[HBr]$. This difference and our previous comment (*a*) may contribute to some of the anomalies noted by them. (*c*) The rate of the linear termination process does not enter into the calculation of $E_{-2} - E_{3a}$. Hence, contrary to the statement on p. 754 of ref. 18*b*, the high apparent value of

$$E_{-2} - E_{3a} = 14 \text{ kcal mole}^{-1}$$

reported by Armstrong and Spinks (11) cannot be explained by a high activation energy E_5. In addition to this discrepancy, the chain lengths in the radiation-induced reaction are significantly longer than those observed for the photoinitiated reaction under comparable conditions. This implies that there is an enhanced catalysis of the radiation-induced reaction, possibly due to the creation of ions which are not produced in the photolysis. More detailed studies will be required to confirm this, but it is now quite clear that the results of Armstrong and Spinks cannot be used as a source of kinetic data for the free radical reaction.

Acknowledgments

The authors are grateful to the National Research Council of Canada for its financial support. One of us (K.T.W.) was the recipient of a studentship. D.A.A. wishes to express his gratitude to the University of Calgary for a sabbatical leave and to Atomic Energy of Canada, Chalk River Nuclear Laboratories, for a Visiting Scientist Appointment, 1968–1969. The assistance of Dr. A. M. Hogg, who kindly carried out the mass spectral analyses, is also acknowledged.

1. P. B. Ayscough, A. J. Cocker, F. S. Dainton, and S. Hirst. Trans. Faraday Soc. **58**, 295 (1962); **58**, 308 (1962).
2. G. Chiltz, P. Goldfinger, G. Huybrechts, G. Martens, and G. Verbeke. Chem. Rev. **63**, 388 (1963).
3. J. H. Knox and J. Riddick. Trans. Faraday Soc. **62**, 1 (1966).
4. J. H. Knox. Trans. Faraday Soc. **62**, 1206 (1966).
5. P. B. Ayscough, F. S. Dainton, and B. E. Fleischfresser. Trans. Faraday Soc. **62**, 1846 (1966).
6. R. J. Cvetanović. Advan. Photochem. **1**, 115 (1963).
7. J. A. Kerr and A. C. Lloyd. Quart. Rev. London, **22**, 549 (1968).
8. H. Schmitz, H. J. Schumacher, and A. Jager. Z. Phys. Chem. Frankfurt. **B 51**, 281 (1942).
9. W. E. Vaughan, F. F. Rust, and T. W. Evans. J. Org. Chem. **7**, 477 (1942).
10. F. R. Mayo and C. Walling. Chem. Rev. **26**, 351 (1940).
11. D. A. Armstrong and J. W. T. Spinks. Can. J. Chem. **37**, 1210 (1959).
12. H. C. Anderson and E. R. Van Artsdalen. J. Chem. Phys. **12**, 479 (1944).
13. (*a*) M. R. Lane, J. W. Linnett, and H. G. Oswim. Proc. Roy. Soc. London, Ser. A, **216**, 361 (1953). (*b*) P. Fowell, J. R. Lacher, and J. D. Park. Trans. Faraday Soc. **61**, 1324 (1965).
14. (*a*) S. W. Benson and J. H. Buss. J. Chem. Phys. **29**, 546 (1958). (*b*) Selected values of chemical thermodynamic properties. Natl. Bur. Stds. Circ. 500 (1952).
15. J. A. Kerr. Chem. Rev. **66**, 465 (1966).
16. R. Barker and A. Maccoll. J. Chem. Soc. 2839 (1963).
17. K. T. Wong and D. A. Armstrong. Chem. Commun. 353 (1966).
18. (*a*) P. I. Abell. Trans. Faraday Soc. **60**, 2214 (1964). (*b*) R. J. Field and P. I. Abell. Trans. Faraday Soc. **65**, 743 (1969).
19. G. A. Oldershaw and R. J. Cvetanović. J. Chem. Phys. **41**, 3639 (1964).

20. D. C. TARDY and B. S. RABINOVITCH. Trans. Faraday Soc. **64**, 1844 (1968).
21. (*a*) G. H. KOHLMAIER and B. S. RABINOVITCH. J. Chem. Phys. **38**, 1692 (1963); **38**, 1709 (1963). (*b*) Y. N. LIN and B. S. RABINOVITCH. J. Phys. Chem. **72**, 1726 (1968).
22. K. T. WONG. Ph.D. Thesis, The University of Calgary, Calgary, Alberta. 1966.
23. M. I. RIDGE and E. W. R. STEACIE. Can. J. Chem. **33**, 383 (1955).
24. C. W. LARSON and E. O'NEAL. J. Phys. Chem. **70**, 2475 (1966).
25. D. A. ARMSTRONG. Can. J. Chem. **40**, 1385 (1962).
26. (*a*) C. A. PARKER. Proc. Roy. Soc. London, Ser. A, **222**, 104 (1953). (*b*) C. T. HATCHARD and C. A. PARKER. Proc. Roy. Soc. London, Ser. A, **235**, 518 (1956).
27. J. G. CALVERT and J. N. PITTS. Photochemistry. John Wiley and Sons, Inc., New York. 1966.
28. A. MACCOLL. J. Chem. Soc. 965 (1955).
29. R. E. REBBERT and P. AUSLOOS. J. Amer. Chem. Soc. **87**, 5569 (1965).
30. K. T. WONG and D. A. ARMSTRONG. To be published.
31. G. C. FETTIS, J. H. KNOX, and A. F. TROTMAN-DICKENSON. J. Chem. Soc. 4177 (1960).
32. L. S. KASSEL. The kinetics of homogeneous gas reactions. The Chemical Catalogue Co., Inc., New York. 1932.
33. J. H. PURNELL and C. P. QUINN. J. Chem. Soc. 4049 (1964).
34. K. E. RUSSELL and J. SIMONS. Proc. Roy. Soc. London, Ser. A, **217**, 271 (1953).
35. E. O'NEAL and S. W. BENSON. J. Chem. Phys. **36**, 2196 (1962).
36. J. A. KERR and A. C. LLOYD. Trans. Faraday Soc. **63**, 2480 (1967).
37. S. W. BENSON. Foundations of chemical kinetics. McGraw-Hill Book Co., Inc., New York. 1960.

Can. J. Chem. Downloaded from www.nrcresearchpress.com by 210.87.254.6 on 09/05/12
For personal use only.

Some thermodynamic properties of the sulfolane–benzene and sulfolane–dichloromethane systems

R. L. BENOIT AND J. CHARBONNEAU
Department of Chemistry, University of Montreal, Montreal, Quebec
Received April 9, 1969

Molar excess free energies of the systems sulfolane–benzene and sulfolane–dichloromethane have been calculated from static vapor pressure measurements at 30.00 °C. Refractive indices, excess partial molar volumes of mixing, and enthalpies of mixing at infinite dilution of benzene and dichloromethane were also determined.

Les énergies libres molaires d'excès des systèmes sulfolane–dichlorométhane et sulfolane–benzène ont été calculées à partir de mesures statiques de pressions de vapeur, à 30.00 °C. Les indices de réfraction, les volumes molaires partiels d'excès de mélange, et les enthalpies de mélange à dilution infinie de benzène ou de dichlorométhane, ont aussi été déterminés.

Canadian Journal of Chemistry, 47, 4195 (1969)

Introduction

As part of a continuing study of binary systems involving sulfolane (TMS) (1), vapor pressure equilibrium data were obtained at 30.00 °C for the two binary systems of sulfolane with benzene and dichloromethane. Benzene was taken as representative of aromatics, and dichloromethane as representative of hydrogen bond donors involving the C—H link. Although refractive indices and densities were determined primarily as potential analytical methods, the latter data were used to calculate partial molar volumes. Finally, the heats of solution of the solutes at infinite dilution in sulfolane were also determined by calorimetry.

Experimental

(i) Chemicals

Sulfolane, kindly supplied by Shell Canada Ltd., was oxidized by air for 12 h at 180 °C. The liquid was then treated with activated charcoal and filtered. A distillation at 70 °C under a 0.5 mm vacuum yielded an ultraviolet transparent product.

Baker dichloromethane was treated successively with concentrated sulfuric acid and dilute sodium hydroxide, and then washed to neutrality with water. The product was stirred overnight over Drierite, filtered, and then subjected to a distillation from calcium hydride, using a 1 m high column filled with glass helices. The portion boiling at 39.85 °C, at 760 mm Hg, was retained.

Fisher high purity benzene was stirred overnight over Drierite, then filtered. The product was used without further purification.

(ii) Apparatus and Procedure

Density

Densities were determined at 30.00 ± 0.02 °C using a 25 ml capped picnometer, previously calibrated with conductivity water. This procedure, checked against KCl solutions, gave densities known to within 0.0001 g per ml. The samples were prepared by weight in approximately 10% steps, using 50 ml glass-stoppered flasks. The samples were kept at least 8 h in a constant temperature bath before measurement.

Refractive Index

An Abbe-type refractometer was used to determine refractive indices to 0.0001 with the temperature controlled at 30.00 ± 0.02 °C.

Vapor Pressure

Vapor pressure data were obtained by a static method previously described (1). Mole fractions were determined by weighing the samples of known composition before and after vapor pressure measurement. Assuming that sulfolane is non-volatile, the loss of weight corresponds to the second component.

Calorimetry

The same microcalorimeter was used as in a previous study (1). The paraffin oil used to prevent diffusion of the volatile component was replaced here by a glass cap containing mercury and a 1 cm layer of mercury, to facilitate mixing of the liquids.

TABLE I

Refractive indices of the TMS–C_6H_6 and TMS–CH_2Cl_2 systems at 30.00 °C

TMS (1) – C_6H_6 (2)		TMS (1) – CH_2Cl_2 (2)	
x_1	n_{12}	x_1	n_{12}
1.000	1.4813	1.000	1.4813
0.940	1.4830	0.903	1.4785
0.864	1.4848	0.842	1.4765
0.765	1.4873	0.805	1.4750
0.580	1.4912	0.663	1.4693
0.522	1.4923	0.587	1.4658
0.425	1.4943	0.504	1.4616
0.307	1.4960	0.353	1.4531
0.168	1.4967	0.243	1.4459
0.085	1.4964	0.197	1.4417
0.041	1.4959	0.072	1.4283
0.000	1.4949	0.000	1.4180

TABLE II

Densities and molar volumes of the mixtures at 30.00 °C

TMS (1) – C_6H_6 (2)			TMS (1) – CH_2Cl_2 (2)		
x_2	d_{12}	V_{12}	x_2	d_{12}	V_{12}
0.000	1.2626	95.2	0.000	1.2626	95.2
0.069	1.2400	94.6	0.091	1.2683	92.3
0.165	1.2070	93.8	0.158	1.2721	90.4
0.262	1.1724	93.1	0.195	1.2742	89.3
0.340	1.1443	92.5	0.337	1.2831	85.0
0.413	1.1175	92.0	0.413	1.2878	82.7
0.494	1.0858	91.5	0.496	1.2930	80.2
0.605	1.0119	90.9	0.647	1.3014	75.6
0.693	1.0058	90.5	0.757	1.3065	72.3
0.794	0.9624	90.2	0.803	1.3082	70.9
0.803	0.9587	90.1	0.928	1.3096	67.1
0.903	0.9139	89.9	0.932	1.3094	67.0
0.927	0.9029	89.9	1.000	1.3077	65.0
0.960	0.8870	89.9			
1.000	0.8681	90.0			

Results and Discussion

The refractive indices (n_{12}) of the mixtures and the pure components are summarized in Table I. Results of the density measurements (d_{12}) are given in Table II. Partial molar volumes ($\overline{V}_1$ and $\overline{V}_2$), believed to be accurate to 0.3% for CH_2Cl_2 and to 0.2% for C_6H_6 and TMS, were determined from molar volume plots (V_{12} vs. x_1) by the method of intercepts. Curves for the excess partial molar volumes ($V_1^E = \overline{V}_1 - V_1^0$) are illustrated in Fig. 1. There is a slight contraction over the whole concentration range, with maximum variation at low TMS concentrations.

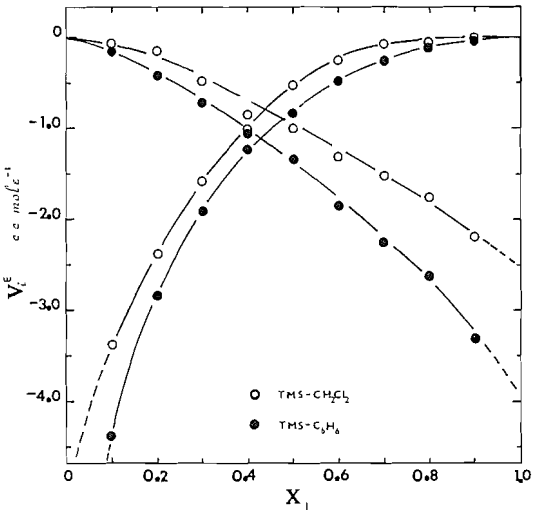

FIG. 1. Excess partial molar volumes of the components, for the TMS–C_6H_6 and TMS–CH_2Cl_2 mixtures at 30.00 °C.

TABLE III

Vapor pressures of the TMS–C_6H_6 and TMS–CH_2Cl_2 systems at 30.00 °C

TMS (1) – C_6H_6 (2)		TMS (1) – CH_2Cl_2 (2)	
x_2	P (mm Hg)	x_2	P (mm Hg)
1.000	118.5	1.000	524.1
0.966	115.8	0.962	503.6
0.945	113.6	0.944	493.3
0.914	112.0	0.908	473.9
0.877	109.5	0.861	447.7
0.818	106.6	0.815	421.6
0.776	103.7	0.792	408.7
0.728	100.8	0.761	392.0
0.696	98.5	0.712	362.3
0.652	95.7	0.648	325.3
0.623	94.0	0.548	270.1
0.593	91.7	0.515	252.7
0.508	84.5	0.492	240.5
0.471	81.3	0.437	211.7
0.404	73.9	0.373	178.6
0.381	72.5	0.288	136.5
0.332	65.3	0.264	124.8
0.283	59.0	0.252	118.3
0.240	52.8	0.180	84.3
0.183	43.0	0.117	54.1
0.135	33.3	0.054	25.4
0.041	10.8	0.000	0.02*
0.000	0.02*		

*Extrapolated value (1).

Results for the liquid–vapor equilibrium of sulfolane–benzene and sulfolane–dichloromethane mixtures are presented in Table III. The partial vapor pressures (p_1 and p_2) were determined by the method of Boissonnas (2), and are given in Table IV, together with the activity coefficients (γ_1 and γ_2).

The Redlich–Kister procedure (3) was used to give smoothed curves of ΔG^E against x_1 (Fig. 2).

TABLE IV

Partial pressures (mm Hg) and activity coefficients of the TMS–C_6H_6 and TMS–CH_2Cl_2 systems at 30.00 °C

x_1	P_t	p_1	p_2	γ_1	γ_2	$\ln(\gamma_1/\gamma_2)$
TMS (1) – C_6H_6 (2)						
1.00	0.02	0.0200	0.0	1.000	—	—
0.90	25.3	0.0180	25.3	1.002	2.140	−0.759
0.80	46.3	0.0165	46.2	1.029	1.952	−0.640
0.70	61.4	0.0150	61.4	1.071	1.727	−0.477
0.60	73.8	0.0136	73.8	1.130	1.558	−0.321
0.50	84.1	0.0122	84.0	1.211	1.419	−0.154
0.40	92.2	0.0109	92.2	1.356	1.297	0.044
0.30	99.0	0.0095	99.0	1.582	1.194	0.281
0.20	105.0	0.0080	105.0	1.993	1.107	0.581
0.10	110.9	0.0057	110.9	2.865	1.040	1.013
0.00	118.5	0.0000	118.5	—	1.000	—
TMS (1) – CH_2Cl_2 (2)						
1.00	0.02	0.0200	0.0	1.000	—	—
0.90	46.3	0.0180	46.2	0.999	0.882	0.124
0.80	93.4	0.0159	93.4	0.997	0.891	0.112
0.70	142.2	0.0139	142.2	0.991	0.904	0.092
0.60	192.9	0.0118	192.9	0.981	0.920	0.064
0.50	243.5	0.0097	243.5	0.972	0.929	0.045
0.40	297.2	0.0076	297.2	0.950	0.945	0.005
0.30	355.9	0.0054	355.9	0.897	0.970	−0.078
0.20	413.4	0.0034	413.4	0.848	0.986	−0.151
0.10	469.2	0.0016	469.2	0.796	0.995	−0.223
0.00	524.1	0.0000	524.1	—	1.000	—

Approximate values of the parameters B, C, and D were first obtained for the equation

$$[1]\quad \Delta G^E = RT x_1 (1 - x_1) \times [B + C(2x_1 - 1) + D(2x_1 - 1)^2]$$

through a plot of $\ln \gamma_1/\gamma_2$ vs. x_1. More accurate values were then selected by means of a program which allowed each coefficient to be varied by steps of 0.01 for C_6H_6 and 0.001 for CH_2Cl_2 and gave the corresponding root-mean-square (r.m.s.) deviation. The smallest r.m.s. deviations were found to correspond to the following sets of coefficients.

	Parameter values			
System	B	C	D	σ (cal mole^{-1})
TMS–C_6H_6	1.10	−0.34	0.19	2.65
TMS–CH_2Cl_2	−0.208	0.100	−0.035	0.335

The assumption that the vapor phase was ideal was checked using Schiebel's nomograph (4) and the critical constants of C_6H_6 and CH_2Cl_2. The values of the correction factors were found to be smaller than 1.01 for C_6H_6 and 1.03 for CH_2Cl_2.

The results of the calorimetric measurements are the average of two (CH_2Cl_2) or three (C_6H_6) determinations. As the C_6H_6 or CH_2Cl_2 mole fractions used are about 0.01, the heats of mixing can be considered approximately equal to the heats of solution at infinite dilution: $\Delta H^\infty = 0.080$ (C_6H_6), and -0.52 kcal mole^{-1} (CH_2Cl_2).

The volume contraction observed on mixing C_6H_6 or CH_2Cl_2 with TMS can either be attributed to structural effects, or to complex-forming interactions between solvent and solute molecules. For the TMS–C_6H_6 system, the positive excess Gibbs free energy, and the slightly endothermic heat of solution of C_6H_6 at infinite dilution, tend to indicate that the contraction is mainly due to structural factors. Other binary systems of benzene with oxygen-containing compounds, such as acetone (5), dimethylsulfoxyde (6), dioxan and diethylformamide (7), show this

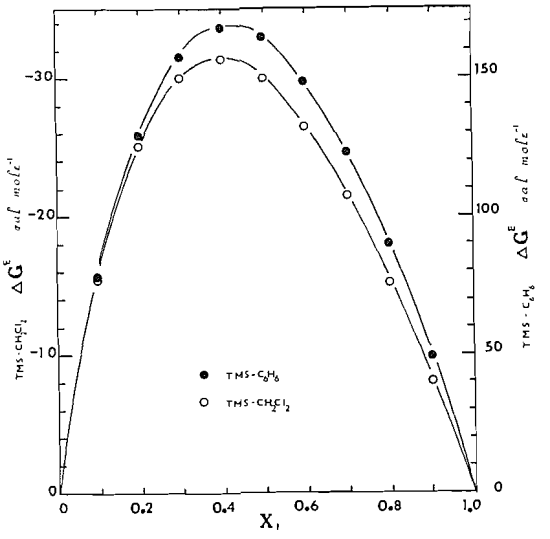

FIG. 2. Excess Gibbs free energy of the TMS–C_6H_6 and TMS–CH_2Cl_2 mixtures at 30.00 °C.

same tendency to a positive excess Gibbs free energy and an endothermic heat of mixing. The molar volumes of mixing have only been determined for the benzene–acetone system (5), where a volume contraction is also observed.

For the TMS–CH_2Cl_2 system, the excess Gibbs free energy is negative, and the heat of solution at infinite dilution of CH_2Cl_2 is exothermic. This suggests complex-forming interactions between solvent and solute molecules. Such complexes are known to exist in other binary systems of CH_2Cl_2 with a proton acceptor. Solid–liquid phase equilibria and infrared studies support the existence of complexes in the systems CH_2Cl_2–dioxan (8) and CH_2Cl_2–acetone (9). Although these complexes are weak, these systems exhibit somewhat larger heats of mixing at infinite dilution of CH_2Cl_2 than the CH_2Cl_2–TMS system (10).

Acknowledgments

The authors wish to express their gratitude to the National Research Council of Canada for a grant and a scholarship (J.C.) and to G. Choux for his continued interest in this work.

1. R. L. BENOIT and G. CHOUX. Can. J. Chem. **46**, 3215 (1968).
2. C. G. BOISSONNAS. Helv. Chim. Acta, **22**, 541 (1939).
3. O. REDLICH and A. KISTER. Ind. Eng. Chem. **40**, 345 (1948).
4. E. G. SCHIEBEL. Ind. Eng. Chem. **41**, 1076 (1949).
5. A. N. CAMPBELL, E. M. KARTZMARK and R. M. CHATTERJEE. Can. J. Chem. **44**, 1183 (1966).
6. J. KENTTAMAA, J. J. LINDBERG, and A. NISSEMA. Suom. Kem. **B33**, 189 (1960).
7. VON K. QUITZSCH. J. Prakt. Chem. **35**, (1, 2), 49 (1967).
8. J. R. GOATES, J. BEVAN, and N. F. MANGELSON. J. Phys. Chem. **67**, 2874 (1967).
9. R. E. KAGARISE. Spectrochem. Acta, **19**, 1371 (1963).
10. D. R. WINTERHALTER and H. C. VAN NESS. J. Chem. Eng. Data, **11**, 189 (1967).

Heat capacity of activation for the hydrolysis of methanesulfonyl chloride and benzenesulfonyl chloride in light and heavy water[1]

R. E. ROBERTSON[2], B. ROSSALL[3], S. E. SUGAMORI, AND L. TREINDL[4]
Division of Pure Chemistry, National Research Council of Canada, Ottawa, Canada

Received June 2, 1969

Rates of solvolysis of methanesulfonyl chloride and benzenesulfonyl chloride have been determined in H_2O and D_2O. The free energy, enthalpy, entropy, and heat capacity of activation were calculated. The exceptional accuracy of the data permitted an estimation of $d\Delta C_p^{\ddagger}/dT$ from a four parameter temperature dependence of the kinetic rates.

From these data we conclude that both sulfonyl chlorides hydrolyse by the same mechanism (S_N2) The change in R from CH_3 to C_6H_5 in RSO_2Cl did not alter $\Delta C_p^{\ddagger}$ but $\Delta S^{\ddagger}$ (20°) was changed from -8.32 to -13.25 cal deg^{-1} mole^{-1}, respectively. The significance of this difference is attributed to the probability of bond formation rather than to differences in solvent reorganization.

Canadian Journal of Chemistry, 47, 4199 (1969)

Can. J. Chem. Downloaded from www.nrcresearchpress.com by 210.87.254.40 on 09/05/12
For personal use only.

This paper is the first of a series reporting detailed studies of the hydrolysis of sulfonyl chlorides[5]. The experimental approach is the same as that applied in preceding studies on the halides and sulfonates: a careful examination of the effect of temperature and of isotopic substitution in the solvent on the temperature dependence of the rate of hydrolysis.

In the halide series we found a remarkable similarity in the values of the heat capacity of activation, $\Delta C_p^{\ddagger}$ (10), and in the differences in $\Delta G^{\ddagger}$ for hydrolysis in H_2O and D_2O over a range of structures for which it was reasonable to expect different degrees of bond-making in the activation process (11). These observations led to the conclusion that the S_N2 transition state was reached when the charge on the halide being displaced created interaction with the solvent equal to water–water interaction; i.e. the transition state corresponded to that degree of charge development where exothermic solvation of the quasi-halide was about to begin. Consequently, it followed that for a given temperature, the charge level ($\delta-$) on the chlorine atom, for example, is the same whether the ion is being displaced from allyl, ethyl, or methyl chloride. This in turn implies that the charge level on the anion at the transition state of an S_N2 displacement is independent of the degree of nucleophilic interaction. The evidence in favor of this conclusion derived from the similarity in $\Delta C_p^{\ddagger}$ values and from the limited range of $\delta_I\Delta H^{\ddagger} = \Delta H_{D_2O}^{\ddagger} - \Delta H_{H_2O}^{\ddagger}$ for S_N2 displacement for the hydrolysis of alkyl halides, is weakened by the possibility that the difference in the degree of bond-making at the transition state for the hydrolysis of the available halides is small, a possibility suggested by the uniformity of our kinetic solvent isotope effect (k.s.i.e.) values (10). To fill this deficiency we were led to examine the hydrolysis of the sulfonyl chlorides, since in this series there are good indications that a greater degree of nucleophilic overlap is required at the transition state (10, 12). We assumed that the nature of the activation process in the latter series is sufficiently similar in mechanism to that for the hydrolysis of alkyl halides, where some degree of bond-making is required, to provide an insight into the question of charge development on the anion and the associated solvent reorganization at the transition state for both systems.

In this first paper we report the results of a kinetic study for the hydrolysis of the first members of two series, methanesulfonyl chloride and benzenesulfonyl chloride.

The enhanced value of the kinetic solvent isotope effect found for the hydrolysis of these two reactants (k.s.i.e.(methanesulfonyl chloride) $= 1.568 \pm 0.006$, k.s.i.e.(benzenesulfonyl chloride) $= 1.564 \pm 0.006$, at 20°) compared with the corresponding value characterizing the hydrolysis of halides (k.s.i.e. = 1.20–1.25) together with the much higher selectivity ratio $k_{OH^-}/k_{H_2O} > 10^5$ (12) leaves little doubt that bond-making is more advanced at the transition state for the displacement of Cl^- from RSO_2Cl than from RCl. This

[1]NRCC No. 10 915.
[2]Present address: Chemistry Department, The University of Calgary, Calgary, Alberta.
[3]NRCC Postdoctoral Fellow, 1968–1969.
[4]NRCC Postdoctoral Fellow, 1965–1966.
[5]For references to previous work, see refs. 1–9.

Can. J. Chem. Downloaded from www.nrcresearchpress.com by 210.87.254.40 on 09/05/12
For personal use only.

does not exclude the possibility that certain sulfonyl chlorides may be found which react by an S_N1 mechanism (4, 13), but these appear to be exceptional. If changes in nucleophilic interaction at the transition state are accompanied by corresponding changes in the charge on the anion being displaced, then this should alter solvent reorganization about the quasi-anion. This fact should be reflected in the value of $\Delta C_p^{\ddagger}$, since this is the most sensitive indicator of solvent reorganization presently available. Further information reflecting relative degrees of solvent reorganization were expected from a comparison of $\Delta H^{\ddagger}$ and $\Delta C_p^{\ddagger}$ values for hydrolysis in H_2O and D_2O (11). While we recognize that $\Delta C_p^{\ddagger}$ is a sensitive indicator of the extent of solvent reorganization associated with ionogenic reactions in water, the interpretation of derived values is not simple and frequently the necessary data are lacking for any save the broadest conclusions. Not only must there be some basis for estimating probable initial state differences but in a comparison of $\Delta C_p^{\ddagger}$ values, either the rate data must be collected over the same temperature range or some allowance must be made for the fact that the structural stability of the initial state solvation shell decreases as the temperature increases. Further, the problem of deriving mechanistic information from a comparison of $\Delta C_p^{\ddagger}$ values is rendered more difficult by the complexity of the changes in water structure. Drost-Hansen (14) finds that the temperature dependence of the fluidity of water requires 5 terms in temperature to produce a good fit to the experimental points. The same complexities are likely to be found in the characterizing parameters for hydrolyses in water when rate data and initial state data can be determined with sufficient accuracy. However, as a balance for these potential difficulties, there is the operative fact that the effect of temperature on structural stability of the solvent in initial and transition states will be in the same direction leading to smaller differences.

The problem of initial state differences is inherent in any satisfactory interpretation of derived pseudo-thermodynamic parameters. Even if these data were available in the present instance, we should still face difficulties in application. Thus, only those solvation differences which relate directly to the solvent volume affected by the kinetic process are significant for the interpretation of $\Delta C_p^{\ddagger}$. As yet, the experimental problems associated with these questions have not been solved for the sulfonyl chlorides. These compounds range from being poorly soluble to practically insoluble in water. Therefore, we have assumed that the initial state differences are small compared with those arising between the initial and the transition state. The restriction imposed on interpretation by that area of ignorance was not considered sufficient to cancel out the advantage to be gained from comparing $\Delta C_p^{\ddagger}$ values.

Experimental

Methanesulfonyl chloride and benzenesulfonyl chloride were commercial samples. Methanesulfonyl chloride was redistilled (b.p. 161° at 730 mm Hg). Benzenesulfonyl chloride was vacuum distilled (b.p. 91° at 4 mm Hg) and zone refined. Excellent first order kinetics were found for both compounds.

D_2O was obtained either from Merck, Sharpe, and Dohme or from the A.E.C. of USA and was 99.8% D, as determined by density measurements. It was found necessary to subject the D_2O to a preliminary distillation from NaOD and thence through a Stuart–Wormwell still (15) having a quartz condenser. The cause of this difficulty was attributed to small amounts of impurities which were not identified.

Kinetic measurements on methanesulfonyl chloride were made by a conductance method using the traditional bridge system and rates were calculated by machine computation (10); benzenesulfonyl chloride hydrolyses were studied by the Auto-RAM system (16). Temperature control was better than ± 0.002°.

Hydrolysis of a sulfonyl chloride molecule in water produces 4 ions, 2 of which are protons

$$RSO_2Cl + H_2O \rightarrow RSO_3^- + 2H^+ + Cl^-$$

This is a particularly convenient system for a study dependent on accurate data and replicate determinations with a precision of ± 0.1% were usually found.

Results

The method of Clarke and Glew (17, 18) modified to treat kinetic data[6] was used to compute the pseudo-thermodynamic parameters. The temperature dependence of the rates was expressed by an equation of the general form.

$$[1] \quad \log_{10} k = A_1 + A_2/T + A_3 \log_{10} T + A_4 T + \cdots\cdots$$

Temperature–rate equations of the form of eq. [1] conveniently summarize these data within the limits of experimental error, permitting calculation of rates at any temperature with high accu-

[6]Photocopies of individual rate data may be obtained free of charge, upon request, from: Depository of Unpublished Data, National Science Library, National Research Council of Canada, Ottawa, Canada.

TABLE I

Empirical constants for a three-parameter fit to rate–temperature relation [1]

Compound	Solvent	A_1	$-A_2$	$-A_3$	$n_{T_1}{}^{T_2}$*
Methanesulfonyl chloride	H_2O	85.42441	7753.782	25.5127	40_1^{40}
	D_2O	85.82877	7847.273	25.6266	40_4^{43}
Benzenesulfonyl chloride	H_2O	89.12618	7284.232	27.1603	38_4^{25}
	D_2O	90.85547	7430.415	27.7379	39_4^{25}

*In $n_{T_1}{}^{T_2}$ n is the number of individual rate determinations, T_2, T_1 define the limits of the experimental temperature range.

TABLE II

Rates and pseudo-thermodynamic parameters for hydrolysis of benzenesulfonyl and methanesulfonyl chlorides in H_2O and D_2O

Compound	Solvent	T (°C)	$k_1 \times 10^4$ (s^{-1})	$\Delta H^{\neq}$ (cal $mole^{-1}$)	$-\Delta S^{\neq}$ (cal $mole^{-1}$ deg^{-1})	$-\Delta C_p{}^{\neq}$ (cal $mole^{-1}$ deg^{-1})
Methanesulfonyl chloride	H_2O	10	0.304	20 560 ± 17	6.49 ± 0.06	53 ± 1
		20	1.08	20 034 ± 8	8.32 ± 0.03	53 ± 1
		40	9.78	18 980 ± 29	11.80 ± 0.10	53 ± 1
	D_2O	10	0.190	20 925 ± 14	6.14 ± 0.05	53 ± 1
		20	0.687	20 396 ± 7	7.98 ± 0.02	53 ± 1
		40	6.49	19 337 ± 17	11.47 ± 0.06	53 ± 1
Benzenesulfonyl chloride	H_2O	10	6.35	17 485 ± 6	11.31 ± 0.02	56 ± 1
		20	18.67	16 926 ± 9	13.25 ± 0.03	56 ± 1
	D_2O	10	3.98	17 829 ± 7	11.03 ± 0.02	57 ± 2
		20	11.93	17 258 ± 11	13.01 ± 0.04	57 ± 2

racy. The corresponding constants are given in Table I.

The pseudo-thermodynamic parameters, derived from the empirical constants listed in Table I on the basis of the familiar assumptions of the transition state theory and the further assumption that $d\Delta C_p{}^{\neq}/dT \neq 0$, are given in Table II. An indication of the possible effect of assuming that $d\Delta C_p{}^{\neq}/dT \neq 0$ but that $d^2\Delta C_p{}^{\neq}/dT^2 = 0$ is indicated by the change in the corresponding terms with temperature as shown in Table III. The assumption ($d\Delta C_p{}^{\neq}/dT = 0$) is clearly an approximation accepted protempore as a consequence of the inadequate accuracy of the rates. It should be noted, that the value of $\Delta C_p{}^{\neq}$ at the midpoint of the temperature range will be the same for both equations, hence the effect of this approximation is unimportant where comparisons of $\Delta C_p{}^{\neq}$ values are made taking this fact into consideration.

Discussion

We have proceeded on the assumption that the mechanism of hydrolysis for the methanesulfonyl chloride and benzenesulfonyl chlorides is analogous to that for S_N2 displacement of halides from alkyl-carbon, the major difference being the requirement for a greater degree of bond-making to sulfur than to carbon. Thus Swain and Scott (12) report what might be called a "selectivity ratio" of $k_{OH^-}/k_{H_2O} = 7 \times 10^5$ for benzenesulfonyl chloride compared to the range about 10^3 for the primary halides (4, 9, 19). The effect of para-substitution on the rate of hydrolysis of this series in water is consistent with the requirements of an S_N2 mechanism (though Hedlund appears to reach a different conclusion (2)). However, successive methylation of the ring in benzenesulfonyl chloride can lead to a loss of sensitivity to the presence of alkali. Thus at 30° hydrolysis of 2,4,6-trimethylbenzenesulfonyl chloride in water has a mean rate of 1.66×10^{-4} s^{-1}, but only 1.73×10^{-4} s^{-1} in the presence of 0.004 *M* KOH (13). Such a loss of selectivity between OH^- and H_2O does not in itself signify the shift to an S_N1 mechanism as Vizgert would appear to assume; it may be no more than a reduction in the bond-making requirement. Other evidence would be required to support a claim of a shift in mechanism. There is no question that such substitution

Can. J. Chem. Downloaded from www.nrcresearchpress.com by 210.87.254.40 on 09/05/12
For personal use only.

Can. J. Chem. Downloaded from www.nrcresearchpress.com by 210.87.254.40 on 09/05/12
For personal use only.

TABLE III

Pseudo-thermodynamic parameters for the hydrolysis of methanesulfonyl chloride and benzenesulfonyl chloride in H_2O and D_2O, assuming $d^2\Delta C_c^*/dT^2 = 0$

Compound	Solvent	T (°C)	ΔG^* (cal mole^{-1})	ΔH^* (cal mole^{-1})	$-\Delta S^*$ (cal mole^{-1} deg^{-1})	$-\Delta C_p^*$ (cal mole^{-1} deg^{-1})	$d\Delta C_p^*/dT$ (cal mole^{-1} deg^{-2})
Methanesulfonyl chloride	H_2O	10	22 398 ± 1	20 562 ± 18	6.49 ± 0.06	54.1 ± 4.7	0.1 ± 0.4
		20	22 473 ± 1	20 028 ± 21	8.34 ± 0.07	52.7 ± 1.5	0.1 ± 0.4
		30	22 565 ± 1	19 507 ± 16	10.09 ± 0.05	51.4 ± 4.5	0.1 ± 0.4
	D_2O	10	22 663 ± 1	20 951 ± 9	6.05 ± 0.03	61.7 ± 1.9	0.7 ± 0.1
		20	22 734 ± 1	20 367 ± 7	8.07 ± 0.02	55.0 ± 0.6	0.7 ± 0.1
		30	22 824 ± 1	19 851 ± 5	9.81 ± 0.02	48.3 ± 1.0	0.7 ± 0.1
Benzenesulfonyl chloride	H_2O	10	20 689 ± 1	17 487 ± 7	11.31 ± 0.03	48.9 ± 3.7	−1.4 ± 0.8
		15	20 747 ± 1	17 224 ± 11	12.22 ± 0.04	55.9 ± 1.6	−1.4 ± 0.8
		20	20 811 ± 1	16 928 ± 11	13.25 ± 0.04	62.8 ± 5.0	−1.4 ± 0.8
	D_2O	10	20 951 ± 1	17 825 ± 8	11.04 ± 0.02	63.1 ± 4.3	1.3 ± 0.9
		15	21 009 ± 1	17 526 ± 12	12.09 ± 0.04	56.5 ± 1.6	1.3 ± 0.9
		20	21 072 ± 1	17 261 ± 11	13.00 ± 0.04	49.9 ± 5.1	1.3 ± 0.9

TABLE IV

Kinetic solvent isotope effects in terms of thermodynamic differences at 20°*

Compound	k_{H_2O}/k_{D_2O}	$\delta_I\Delta G^{\ddagger}$ (cal mole^{-1})	$\delta_I\Delta H^{\ddagger}$ (cal mole^{-1})	$\delta_I\Delta S^{\ddagger}$ (cal mole^{-1} deg^{-1})	$\delta_I\Delta C_p^{\ddagger}$ (cal mole^{-1} deg^{-1})
Methanesulfonyl chloride	1.568 ± 0.006	262 ± 2	362 ± 15	−0.34 ± 0.05	0 ± 2
Benzenesulfonyl chloride	1.564 ± 0.006	261 ± 2	332 ± 20	−0.24 ± 0.07	1 ± 3

*The values for H_2O are subtracted from the corresponding values found in D_2O, $\delta_I\Delta X^{\ddagger} = \Delta X_{D_2O}^{\ddagger} - \Delta X_{H_2O}^{\ddagger}$.

would alter the mechanism in the sense of reducing the requirements for bond-making at the transition state. If the 2,6-dimethyl substitution introduces sufficient steric hindrance to bond-making to permit an alternative mechanism (13), the difference is in kind (20) rather than degree (19, 21, 22).

Hall (4) suggests as an alternative to the normal three-center nucleophilic displacement the possibility of formation of a sulfonyl chloride hydrate

$$RSO_2Cl + H_2O \rightleftharpoons R{-}\overset{\displaystyle O}{\overset{\|}{S}}(OH)_2\,{}_{Cl} \rightarrow R{-}\overset{\displaystyle O}{\overset{\|}{S}}(OH)_2^{+} + Cl^-$$

and finds some support for this suggestion from k vs. σ plots based on Hedlund's rate data. Some years later, Jenkins and Hambly (9) returned to this hypothesis. As an alternative to the S_N2 mechanism for the hydrolysis of the sulfonyl chlorides they suggest that the preliminary step may be the formation of an addition compound of the solvent and the reactant. Such a complex has been advanced to account for the larger kinetic solvent isotope effect found in the case of neutral hydrolysis of acetic anhydride (23, 24). It should be noted that the corresponding term for the hydrolysis of the sulfonyl chlorides is much less (k.s.i.e.(25°) = 2.90 vs. 1.55), although the latter value is significantly larger than that for the hydrolysis of the primary halides (k.s.i.e.(ca. 90°) = 1.25). The difference in k.s.i.e. between values for the sulfonyl chlorides and for the alkyl halides is partly due to the differences in the experimental temperatures and hence in the relative stability of water structures in H_2O and D_2O, and in part to differences in the requirement for nucleophilic interaction. Conclusions based on much comparison are necessarily speculative. We have no way of knowing a priori whether the hydration of the proposed sulfonyl chloride hydrate and the corresponding complex with acetic anhydride would necessarily lead to similar k.s.i.e. values. There is no unambiguous proof of hydrate in either case; just working hypotheses, useful for the design of experiment and testing of results. As evidence against the formation of the proposed intermediate in the case of the solvolysis of benzenesulfonyl chloride, we may cite the failure of Bunton to find evidence of any such intermediate from studies in water containing ^{18}O (25).

In so far as they go, the derived parameters in Tables II and IV tend to confirm the conclusion based on k_{OH^-}/k_{H_2O} and k.s.i.e. values cited above in two respects: (*a*) the nucleophilic interaction is greater than that required for the corresponding S_N2 hydrolysis of the alkyl halides and (*b*) that solvent reorganization is about the same for both sulfonyl chlorides.

The first conclusion is supported by the larger value of $\delta_I\Delta H^{\ddagger} = \Delta H^{\ddagger}(D_2O) - \Delta H^{\ddagger}(H_2O)$ and about the same value of $\delta_I\Delta S^{\ddagger}$ and $\delta_I\Delta C_p^{\ddagger}$ for the sulfonyl chlorides compared to the corresponding values for the primary alkyl halides (11). For a wide range of the latter which react by an S_N2 mechanism, values of $\delta_I\Delta G^{\ddagger}$ have been found to lie in the range 150–200 cal, while $\delta_I\Delta H^{\ddagger}$ covers a somewhat wider range, 200–300 cal, compensating changes in $T\Delta S^{\ddagger}$ accounting for the difference. A similar comparison of data from Table IV shows that the values of $\delta_I\Delta G^{\ddagger}$ and $\delta_I\Delta H^{\ddagger}$ for the sulfonyl chlorides are about 100 cal higher than the corresponding terms for the primary alkyl halides while $\delta_I\Delta S^{\ddagger}$ and $\delta_I\Delta C_p^{\ddagger}$ remain about the same.

The small values of $\delta_I\Delta S^{\ddagger}$ and $\delta_I\Delta C_p^{\ddagger}$ suggest that for these systems, the solvent reorganization attending activation in H_2O and D_2O is about the same. It seems anomalous that there is an obvious difference in the size of RSO_2Cl, where R = CH_3 and C_6H_5, but no corresponding difference

Can. J. Chem. Downloaded from www.nrcresearchpress.com by 210.87.254.40 on 09/05/12
For personal use only.

TABLE V

A comparison of derived kinetic parameters

Compound RX	Temperature (°C)	$\Delta H^{\ddagger}$ (cal mole^{-1})	$-\Delta S^{\ddagger}$ (cal deg^{-1} mole^{-1})	$-\Delta C_p^{\ddagger}$ (cal deg^{-1} mole^{-1})
$MeSO_2Cl$	20	20 034	8.32	53
$C_6H_5SO_2Cl$	20	16 926	13.25	56
MeCl	50	25 250	8.64	49
$C_6H_5CH_2Cl$	50	20 420	12.23	39
EtBr	50	24 370	5.95	49
CH_2=$CHCH_2Br$	50	20 560	9.15	62

appears in $\Delta C_p^{\ddagger}$. Granted the absence of some undetected compensating factor, the simplest conclusion is that the corresponding solvent reorganization about CH_3 and C_6H_5 is small, the changes occurring close to the seat of reaction.

It is worth noting, however, that in spite of a similarity in solvent reorganization judged by the above criteria, the entropies of activation for the two sulfonyl chlorides are quite different. At 20° in H_2O, $\Delta S^{\ddagger}$ for the hydrolysis of methanesulfonyl chloride is -8.32 cal deg^{-1} mole^{-1} while a value of -13.25 cal deg^{-1} mole^{-1} is calculated for benzenesulfonyl chloride (equivalent to an energy difference of 1445 cal mole^{-1}) (8). We recognize that differences in this term ($\Delta S^{\ddagger}$) are less specific for solvent reorganization than the corresponding changes in $\Delta C_p^{\ddagger}$, at least for solvolysis in water. Undefined factors other than solvent reorganization are important in determining $\Delta S^{\ddagger}$, and for this reason entropies of activation have, so far, proven of limited value in characterizing solvolytic reactions (26, 27). Granted that solvent reorganization is about the same for the hydrolysis of methanesulfonyl and benzenesulfonyl chlorides, it is reasonable to inquire as to which stereochemical or electronic differences between the methyl and phenyl groups might account for such a variation in $\Delta S^{\ddagger}$. One possibility may arise from the fact that the distance between adjacent hydrogen atoms and the sulfonyl oxygen atoms will be smaller in the benzenesulfonyl chloride, see structures **1** and **2**. Hence, an interaction between these atoms would be more likely in benzenesulfonyl chloride than in methanesulfonyl chloride. In the transition state these interactions will be modified and hence the effect on the rotational entropy of the respective groups will change. We estimate this difference is likely to make a small contribution to $\Delta S^{\ddagger}$. Similarly initial state interaction of the

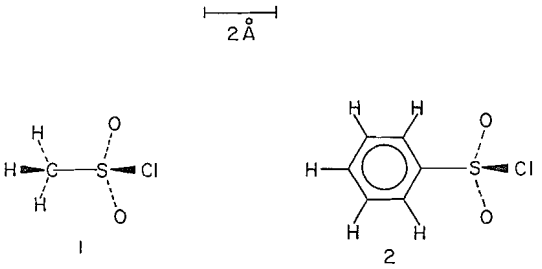

sulfonyl oxygens with water though small would tend to make $\Delta C_p^{\ddagger}$ more positive than -45 cal deg^{-1} mole^{-1} rather than more negative as observed (compare with $\Delta C_p^{\ddagger}$ for the hydrolysis of sulfonic esters (10)).

A much more likely source of difference in $\Delta S^{\ddagger}$ than changes in internal rotation is related to the nature of nucleophilic displacement and restrictions governing the initiation of a partial covalent bond at the transition state. Whereas for those reactants which can react by an S_N1 mechanism, increasing the size of the R group from which displacement occurs frequently leads to a positive shift in $\Delta S^{\ddagger}$ (28), just the opposite effect may be found where the S_N2 mechanism is operative. Displacement from a bridgehead carbon forms a special case; the S_N2 mechanism is unavailable and $\Delta S^{\ddagger}$ is very negative (29). In attempting to account for the relationship between nucleophilic reactivity and structure, entropy differences have, in many cases, been neglected, either explicitly (30) or implicitly through correlation of activation energy. In the present example such an approximation is clearly unjustified; a large entropy difference is found equivalent to about one-half of the enthalpy difference.

The general trend apparent in the pairs-comparison in Table V is that the introduction of a more polarizable R group reduces the enthalpy

Can. J. Chem. Downloaded from www.nrcresearchpress.com by 210.87.254.40 on 09/05/12
For personal use only.

Can. J. Chem. Downloaded from www.nrcresearchpress.com by 210.87.254.40 on 09/05/12
For personal use only.

of activation ($\Delta H^{\ddagger}$) and at the same time results in a more negative entropy of activation ($\Delta S^{\ddagger}$), the former being the dominant factor. Since the $\Delta C_p^{\ddagger}$ values are about the same, we can discount differences in solvent reorganization as providing an alternative explanation. Since the k.s.i.e. values are similar, and larger than found for the displacement of halogen from a series of saturated carbon atoms, the degree of bond-making at the transition state is about the same, appreciable but incomplete. Hence we are led to conclude that the observed differences in the value of $\Delta S^{\ddagger}$ is related in some way to the probability of establishing the required degree of nucleophilic overlap. In the unspecific terminology of "hard" and "soft" acids and bases (30, 31) water would be a "hard" base and methanesulfonyl chloride would be less polarizable than benzenesulfonyl chloride. A similar distinction marks the two other pairs given in Table V. Schwarzenbach and Schellenberg (32) have shown that a large entropy difference is found favoring (h–h) combinations as opposed to (h–s) combinations in the formation of certain ligands. A somewhat smaller entropy difference characterizes the pairs-comparison given in Table V. Hence we can conclude that a major part of this characteristic entropy difference is related to some intimate condition pertaining to bond formation. Since the same kind of a change is found for bond formation of the "hard" water with the halide examples presented in Table V, we think it probable that this probability factor associated with bond-making is likely to have much wider application in accounting for some of the remarkable changes in $\Delta S^{\ddagger}$ for S_N2 displacements. It is not our intention to develop this point further here, but we may draw attention to one question raised by such a claim. The $\Delta C_p^{\ddagger}$ for the solvolysis of isopropyl bromide is -59 cal deg^{-1} mole^{-1}, about the same as that for the hydrolysis of allyl bromide (-62 cal deg^{-1} mole^{-1}). While $\Delta S^{\ddagger}$ for the former is -1.4 cal deg^{-1} mole^{-1} at 50°, the corresponding value for the latter is -9.15 cal deg^{-1} mole^{-1} at the same temperature. It is probable that the former hydrolyses in water by an S_N1 mechanism and it might seem reasonable to assume that allyl bromide also reacts by the same mechanism. However, if our speculation about the negative $\delta_I\Delta S^{\ddagger}$ for the hydrolysis of the sulfonyl chlorides can be applied to the hydrolysis of the halides, then in spite of having a value of $\Delta C_p^{\ddagger}$ about the same as a compound which probably reacts by an S_N1 mechanism, the large negative shift in $\Delta S^{\ddagger}$ noted above indicates some degree of nucleophilic interaction in the activation process for the hydrolysis of allyl bromide.

Because of the high degree of precision and (presumably) accuracy possible in rate determinations for these systems, analysis of the temperature dependence of the rate data gave values of $d\Delta C_p^{\ddagger}/dT$ (Table III). The four-parameter analysis is sufficiently close to that of the three-parameter calculations that the values of $\Delta G^{\ddagger}$, $\Delta H^{\ddagger}$, and $\Delta S^{\ddagger}$ are unchanged. The values for $\Delta C_p^{\ddagger}$ at the midpoint of the temperature range are unaltered. The four-parameter analysis suggests that while the assumption $d\Delta C_p/dT = 0$ does not hold for these systems, the values obtained for $d\Delta C_p^{\ddagger}/dT$ are small.

We conclude by suggesting that the value of the results submitted here lies less in the indications that the hydrolysis of the two sulfonyl chlorides follow an S_N2 mechanism but rather in providing the experimental data to illustrate the kind of changes which characterize such a mechanism in the terms $\Delta C_p^{\ddagger}$, and the differential terms $\delta_I\Delta G^{\ddagger}$, $\delta_I\Delta H^{\ddagger}$, $\delta_I\Delta S^{\ddagger}$, and $\delta_I\Delta C_p^{\ddagger}$. The question of differences in $d\Delta C_p^{\ddagger}/dT$ is left in abeyance until we have further pertinent data for allied systems. In our view the most significant fact to emerge is an indication of the source of an important contribution to $\Delta S^{\ddagger}$ for nucleophilic displacement reactions.

1. G. Berger and S. C. J. Olivier. Rec. Trav. Chim. **46**, 516 (1927).
2. I. Hedlund. Ark. Kem. **14A**, 1 (1940).
3. A. F. Linetskaya and N. V. Sapoznikohova. J. Appl. Chem. USSR, Engl. Transl. **21**, 876 (1948).
4. H. K. Hall, Jr. J. Amer. Chem. Soc. **78**, 1450 (1956).
5. E. Tomilla and P. Hirsjärvi. Acta Chem. Scand. **5**, 659 (1951).
6. R. V. Vizgert. Zh. Obshch. Khim. **32**, 663 (1962).
7. R. V. Vizgert and E. K. Savchuk. Zh. Obshch. Khim. **34**, 3396 (1964).
8. R. Foon and A. N. Hambly. Aust. J. Chem. **15**, 668 (1962).
9. F. E. Jenkins and A. N. Hambly. Aust. J. Chem. **14**, 190 (1961); **14**, 205 (1961).
10. R. E. Robertson. Progr. Phys. Org. Chem. **4**, 213 (1967).
11. L. Treindl, R. E. Robertson, and S. E. Sugamori. To be published.
12. C. G. Swain and S. B. Scott. J. Amer. Chem. Soc. **75**, 246 (1953).
13. R. V. Vizgert. Zh. Obshch. Khim. **32**, 628 (1962).
14. L. Korson, W. Dröst-Hansen, and F. J. Millero. J. Phys. Chem. **73**, 34 (1969).

15. J. M. STUART and F. WORMWELL. J. Chem. Soc. 85, (1930).
16. R. E. ROBERTSON and S. E. SUGAMORI. To be published.
17. E. C. W. CLARKE and D. N. GLEW. Trans. Faraday Soc. **62**, 539 (1966).
18. L. J. BRUBACHER, L. TREINDL, and R. E. ROBERTSON. J. Amer. Chem. Soc. **90**, 4611 (1968).
19. G. H. FRISONE and E. R. THORNTON. J. Amer. Chem. Soc. **90**, 1211 (1968).
20. V. GOLD. J. Chem. Soc. 4633 (1956).
21. S. WINSTEIN, E. GRUNWALD, and H. W. JONES. J. Amer. Chem. Soc. **73**, 2700 (1951).
22. C. G. SWAIN. J. Amer. Chem. Soc. **70**, 1119 (1948).
23. A. R. BUTLER and V. GOLD. J. Chem. Soc. 2305 (1961).
24. C. A. BUNTON, N. A. FULLER, S. G. PERRY, and V. J. SHINER. J. Chem. Soc. 2918 (1963).
25. C. A. BUNTON. Private communication.
26. G. KOHNSTAM. Advan. Phys. Org. Chem. **5**, 121 (1967).
27. L. L. SCHALAGER and F. A. LONG. Advan. Phys. Org. Chem. **1**, 1, (1963).
28. A. G. EVANS and S. D. HAMANN. Trans. Faraday Soc. **47**, 25 (1951).
29. P. VAN R. SCHLEYER and R. N. NICHOLAS. J. Amer. Chem. Soc. **83**, 2700 (1961).
30. J. O. EDWARDS and R. G. PEARSON. J. Amer. Chem. Soc. **84**, 16 (1962).
31. R. G. PEARSON. Science, **151**, 172 (1966).
32. G. SCHWARZENBACH and M. SCHELLENBERG. Helv. Chim. Acta, **48**, 28 (1965).

Can. J. Chem. Downloaded from www.nrcresearchpress.com by 210.87.254.40 on 09/05/12
For personal use only.

Conductances, densities, and viscosities of concentrated solutions of lithium chlorate and of sodium chlorate in water–dioxane mixtures, at 25°

B. G. OLIVER[1] AND A. N. CAMPBELL
Department of Chemistry, University of Manitoba, Winnipeg, Manitoba

Received June 5, 1969

The conductances, densities, and viscosities of sodium chlorate and of lithium chlorate in the solvents 44.5% dioxane – 55.5% water and 64.5% dioxane – 35.5% water were determined, at 25 °C, almost up to saturation. The apparent molal volume of the electrolytes, calculated from the density data, was found to be greater in the dioxane–water solvents than it is in water, indicating a decrease in solvation in the mixed solvents. The relative viscosity increased as the dioxane content of the solvent increased, showing a larger ordering effect of the electrolytes as the solvent became less hydrogen bonded and less ordered. The equivalent conductance of both electrolytes was greatly reduced as the dioxane content of the solvent was increased, in accord with predictions based on solvent viscosity and dielectric properties. Also, sodium chlorate was found to be more associated than lithium chlorate in the mixed solvents.

Canadian Journal of Chemistry, 47, 4207 (1969)

Can. J. Chem. Downloaded from www.nrcresearchpress.com by 210.87.254.42 on 09/05/12
For personal use only.

We previously determined the conductances, densities, and viscosities of sodium chlorate at 25° and at 35° in 64.5% and 90% dioxane–water mixtures (1). To complete this work we have now extended our observations to include lithium chlorate in 64.5% dioxane and sodium and lithium chlorates in 44.5% dioxane. Very little work has been done on concentrated solutions of electrolytes in nonaqueous solvents, with one notable exception: Janz, Marcinkowski, and Ahmad (2) have studied concentrated solutions of silver nitrate in acetonitrile and benzonitrile.

Experimental

The experimental procedure and preparation of materials have been described previously (1). Because of the extremely hygroscopic nature of lithium chlorate, all solutions were prepared in a dry box.

We have used density determinations to obtain apparent molal volumes. This method is only permissible if the density determinations have a high degree of accuracy. We used Ostwald-type pyknometers, modified to our own design, of about 45 cc capacity. Two identical pyknometers were used, one serving as a counterpoise in the weighing procedure. The experimental pyknometer was kept, after removal from the thermostat, in the balance case for a fixed time before weighing. Only with such precautions can reproducible weighings be obtained. Our accuracy of density determination was ±0.0001 g/ml.

Results

Results are given in Tables I to IV.

TABLE I
Physical properties of water–dioxane solvents at 25 °C

Weight % dioxane	Density (g/ml)	Dielectric constant	Viscosity (cP)
0.0	0.99707	78.5	0.8903
44.5	1.0310	40.6	1.784
64.5	1.0366	23.4	1.923

Discussion

From the densities of the solutions given in Tables II and III, and those taken from refs. 1 and 5, the apparent molal volumes of the solutions were calculated, using the expression

$$\phi_v = \frac{1000}{cd_0}(d_0 - d) + \frac{M_2}{d_0}$$

where ϕ_v is the apparent molal volume, c is the concentration in mole per l, d_0 and d are the densities of the solvent and of the solution, respectively, and M_2 is the molecular weight of the solute. The ϕ_v values at rounded concentrations are given in Table IV.

The apparent molal volume is the result of 2 effects: the actual volume of the ions and the effect of the ions on the solvent. Ions with high surface charge tend to attract to themselves neighboring solvent dipoles and thus cause electrostriction of solvent molecules. This causes a decrease in the volume of the solvent in the immediate vicinity of the ion. It follows that the smaller lithium ion, with higher surface charge than the sodium ion, should have a smaller

[1]Present address: Rensselaer Polytechnic Institute, Troy, New York.

TABLE II

Conductances, densities, and viscosities of sodium and lithium chlorate in the solvent 44.5% dioxane – 55.5% water, at 25 °C

Concentration (mole/l)	Density (g/ml)	Relative viscosity (solvent = 1.00)	Specific conductance (mho/cm) × 10^3	Equivalent conductance (mho)
		Sodium chlorate		
0.0	1.0310	1.000	—	57.75*
0.01007	1.0316	1.004	0.5103	50.68
0.0995	1.0375	1.016	4.202	42.24
0.3900	1.0560	1.058	14.026	35.96
0.9837	1.0937	1.160	29.963	30.46
1.8817	1.1502	1.371	46.567	24.75
2.7354	1.2034	1.642	56.106	20.51
3.5404	1.2535	2.004	59.975	16.94
		Lithium chlorate		
0.0	1.0310	1.000	—	52.05†
0.01804	1.0318	1.004	0.7886	43.71
0.1101	1.0365	1.029	4.177	37.94
0.5262	1.0571	1.120	16.328	31.03
1.0103	1.0808	1.243	27.174	26.90
2.7484	1.1653	1.850	46.877	17.06
4.9544	1.2734	3.556	44.480	8.978
6.7555	1.3586	6.519	35.666	5.280
8.8705	1.4598	14.02	26.278	2.962

*Limiting equivalent conductance interpolated from the data of Accascina and D'Aprano (3).
†Limiting equivalent conductance interpolated from the data of Accascina, D'Aprano, and Triolo (4).

TABLE III

Conductances, densities, and viscosities of sodium and lithium chlorate in the solvent 64.5% dioxane – 35.5% water at 25 °C

Concentration (mole/l)	Density (g/ml)	Relative viscosity (Solvent = 1.00)	Specific conductance (mho/cm) × 10^3	Equivalent conductance (mho)
		Sodium chlorate		
1.5343	1.1336	1.510	21.156	13.79
2.0336	1.1646	1.762	24.315	11.96
		Lithium chlorate		
0.0	1.0366	1.000	—	43.10*
0.01571	1.0377	1.013	0.4827	30.73
0.1025	1.0421	1.045	2.478	24.18
0.4207	1.0583	1.180	8.350	19.85
1.0024	1.0876	1.448	15.746	15.71
1.9258	1.1336	2.087	21.222	11.02
3.4093	1.2065	4.065	20.498	6.012
6.0521	1.3347	15.37	12.064	1.993

*Limiting equivalent conductance from Campbell, Kartzmark, and Oliver (1).

apparent volume, and this is found to be the case. The increase in apparent molal volume with increasing concentration and with changing solvent (from water to water–dioxane) indicates a decrease in solvation in both cases.

The apparent molal volume of lithium chlorate, at a fixed concentration, increases in going from water to 44.5 % dioxane, passing through a maximum and then decreasing. The ϕ_v values for sodium chlorate also increase in the water–dioxane solvents and seem to be approaching a maximum in 64.5 % dioxane. Similar maxima were observed by Bateman for strontium chloride (6) and for barium chloride (7), in ethanol–water mixtures. Presumably, solvation decreases up to the maximum ϕ_v and then increases.

The change in apparent molal volume with solvent is much smaller for lithium chlorate than

Can. J. Chem. Downloaded from www.nrcresearchpress.com by 210.87.254.42 on 09/05/12
For personal use only.

TABLE IV

Apparent molal volumes of sodium and lithium chlorates in the solvents water, 44.5% dioxane – 55.5% water, and 64.5% dioxane – 35.5% water at 25 °C

	ϕ_v (ml/mole)					
	Water		44.5 % Dioxane		64.5 % Dioxane	
c (mole/l)	$NaClO_3$	$LiClO_3$	$NaClO_3$	$LiClO_3$	$NaClO_3$	$LiClO_3$
1.0	37.11	37.57	41.42	39.86	41.46	38.12
1.5	37.85	37.74	41.66	39.93	41.74	38.40
2.0	38.41	37.91	41.86	40.06	41.94	38.64
2.5	38.88	38.10	42.04	40.16	—	38.82
3.0	39.29	38.32	42.17	40.24	—	39.00
3.5	39.65	38.52	42.27	40.30	—	39.14
4.0	39.97	38.70	—	40.37	—	39.26
5.0	40.52	38.96	—	40.48	—	39.48
6.0	41.04	39.06	—	40.58	—	39.68
7.0	—	39.30	—	40.66	—	—
8.0	—	39.50	—	40.73	—	—

for sodium chlorate, indicating a stronger interaction between solute and solvent in the former case. Such a conclusion is in agreement with the work of Campbell, Kartzmark, and Maryk (8) who isolated the compound $LiClO_3 \cdot C_4H_8O_2$ but failed to observe any such compound with $NaClO_3$ in the corresponding ternary system $H_2O - C_4H_8O_2 - NaClO_3$.

Recently, viscosity has become an important method of characterizing ion–solvent interactions (9–11). The influence of a strong electrolyte upon the viscosity of a solvent is given (up to a concentration of about 0.1 M) by the Jones–Dole equation (12)

$$\eta/\eta_0 = 1 + A\sqrt{c} + Bc$$

where η/η_0 is the relative viscosity, c is the concentration in mole per l, and A and B are constants characteristic of the electrolyte. The coefficient A represents the contribution due to interionic electrostatic forces (13). The B coefficient represents the ion–solvent interaction and measures the order and disorder caused by the introduction of the ions into the solvent structure. The lithium and sodium ions have positive B coefficients in water and are thus structure ordering, whereas the chlorate ion has a negative B coefficient and is therefore structure disordering. The terms positive and negative hydration have been applied to the above phenomena (14).

Little work has been done on the viscosity of electrolytes in nonaqueous solvents, but Golek, Oristschenko, and Artentschenko (15) have studied the behavior of potassium iodide (a structure breaker which decreases the viscosity of water) in monohydric alcohols, glycol, and glycerol. They found that an increase in the concentration of potassium iodide in monohydric alcohols led to a large increase in viscosity, in glycol to little change in viscosity, and in glycerol to a large decrease in viscosity (negative viscosity). In this sequence, the number of hydroxyl groups in the alcohol molecule increases, the bonding between the molecules becomes more complex, and, correspondingly, the close-range order of the liquid increases. It thus appears that electrolytes have a larger ordering effect on those liquids that have the least ordered structure and, conversely, the greatest disordering effect on liquids with highly ordered structures.

Our experimental results are not sufficiently extensive to test the Jones–Dole equation and thus derive the B coefficients for the mixed solvents, but it is possible to make some qualitative statements about the ordering effects of sodium and lithium chlorates in these solvents. It is evident from Fig. 1 that the curve of relative viscosity for lithium chlorate lies above that of sodium chlorate, in all solvents studied, in agreement with the belief that lithium chlorate has a higher ordering effect (larger B coefficient) than sodium chlorate.

Moreover, the relative viscosities of sodium and lithium chlorates increase as the solvent changes from water to 44.5% dioxane to 64.5% dioxane (Fig. 1). The dioxane–water solvent must be less hydrogen bonded and less ordered than water because of the low dipole moment of

Can. J. Chem. Downloaded from www.nrcresearchpress.com by 210.87.254.42 on 09/05/12
For personal use only.

Can. J. Chem. Downloaded from www.nrcresearchpress.com by 210.87.254.42 on 09/05/12
For personal use only.

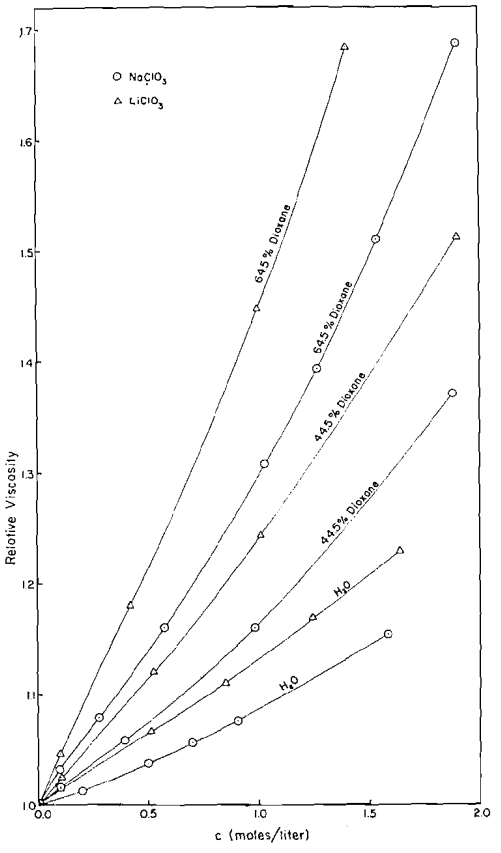

FIG. 1. Plot of relative viscosity of $NaClO_3$ and $LiClO_3$ in water, 44.5% dioxane, and 64.5% dioxane vs. c.

dioxane. Therefore, in agreement with Golek's results (15), the electrolytes should have a larger structure ordering effect and thus larger relative viscosities in the dioxane–water solvents.

The apparent molal volume results, viz., less solvation of the electrolytes in the dioxane–water mixtures, and the viscosity results (larger ordering effect of the electrolytes in the dioxane–water mixtures) are not incompatible. The apparent molal volume is affected by both short and long range interactions, while viscosity is affected by mainly short range effects.

The equivalent conductances of sodium and lithium chlorate in water, 44.5% dioxane, and 64.5% dioxane are plotted against the square root of concentration in Fig. 2. The data for the mixed solvents were taken from Tables II and III, and those for water from previous work (1, 5).

The equivalent conductances of sodium and lithium chlorates are greatly reduced in the dioxane–water solvents. Examination of Table I gives an obvious explanation. The mixed solvents are more than twice as viscous as water and their dielectric constants are much smaller.

Figure 2 also shows that the conductance curves of the 2 salts approach one another as the dioxane content of the solvent increases. In fact, the curve for lithium chlorate is well above that for sodium chlorate, in 90% dioxane (1). Since the apparent molal volume and viscosity results seem to indicate that the mobility of the lithium ion should be retarded more than that of the sodium ion, a possible explanation of this phenomenon may lie in higher ion association for sodium chlorate than for lithium chlorate, in the mixed solvents. This conclusion is supported by the work of Accascina, D'Aprano, and Triolo (4), who found sodium chlorate to be more highly associated than lithium chlorate in dilute solutions in water–dioxane.

The criteria for ion pair and triple ion aggregates, based on the Bjerrum and Fuoss–Kraus

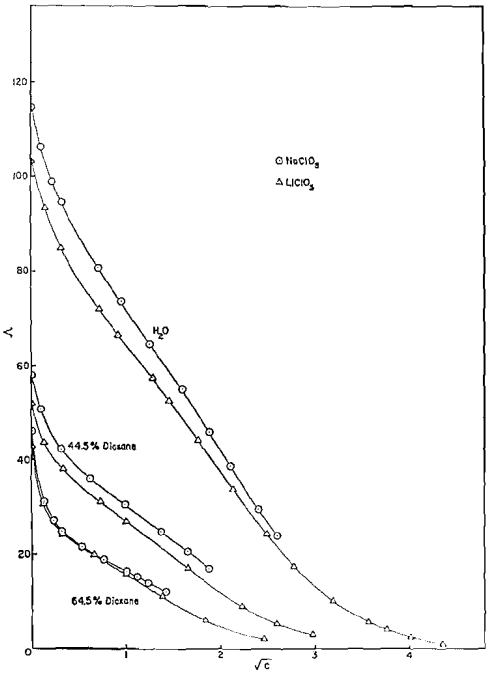

FIG. 2. Plot of equivalent conductance of $NaClO_3$ and $LiClO_3$ in water, 44.5% dioxane, and 64.5% dioxane vs. $\sqrt{c}$.

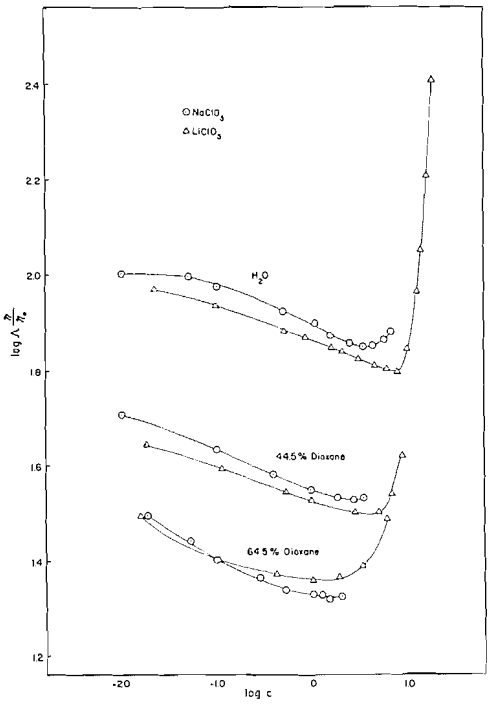

FIG. 3. Plot of log $\Lambda(\eta/\eta_0)$ of $NaClO_3$ and $LiClO_3$ in water, 44.5% dioxane, and 64.5% dioxane vs. log c.

scheme (16–18), which takes cognizance of the viscosity differences, are illustrated by the log $\Lambda(\eta/\eta_0)$ vs. log c graphs of Fig. 3. With increasing concentration, the log $\Lambda(\eta/\eta_0)$ curves show a minimum characteristic of triple-ion formation (19, 20). The minima in the log $\Lambda(\eta/\eta_0)$ curves shift to lower concentrations as the dielectric constant of the solvent decreases. This is in accord with the prediction for ionic interactions based on solvent dielectric properties.

1. A. N. CAMPBELL, E. M. KARTZMARK, and B. G. OLIVER. Can. J. Chem. **44**, 925 (1966).
2. G. J. JANZ, A. E. MARCINKOWSKI, and I. AHMAD. J. Electrochem. Soc. **112**, 104 (1965).
3. F. ACCASCINA and A. D'APRANO. Atti Accad. Sci. Lett. Arti Palermo **25**, 107 (1965).
4. F. ACCASCINA, A. D'APRANO, and R. TRIOLO. J. Phys. Chem. **71**, 3469 (1967).
5. A. N. CAMPBELL and W. G. PATERSON. Can. J. Chem. **36**, 1004 (1958).
6. R. L. BATEMAN. J. Amer. Chem. Soc. **71**, 2291 (1949).
7. R. L. BATEMAN. J. Amer. Chem. Soc. **74**, 5516 (1952).
8. A. N. CAMPBELL, E. M. KARTZMARK, and W. B. MARYK. Can. J. Chem. **44**, 935 (1966).
9. M. KAMINSKY. Discuss. Faraday Soc. **24**, 171 (1957).
10. E. R. NIGHTINGALE, JR. J. Phys. Chem. **63**, 1381 (1959).
11. E. R. NIGHTINGALE, JR. Chemical physics of ionic solutions. *Edited by* B. E. Conway and R. G. Barradas. John Wiley and Sons, Inc., New York. 1966. Chap. 7.
12. G. JONES and M. DOLE. J. Amer. Chem. Soc. **51**, 2950 (1929).
13. H. FALKENHAGEN and E. L. VERNON. Phys. Z. **33**, 140 (1932).
14. O. YA. SAMOILOV. Structure of aqueous electrolyte solutions and the hydration of ions. *Translated by* D. J. G. Ives. Consultants Bureau, New York. 1965.
15. A. S. GOLEK, A. W. ORISTSCHENKO, and A. I. ARTENTSCHENKO. Dokl. Akad. Nauk. S.S.S.R., No. 6, 453 (1954).
16. D. A. MACINNES. The principles of electrochemistry. Dover Publications, Inc., New York. 1961. p. 373.
17. N. BJERRUM. Det. Kegl. Dan., visden 9, 121 (1926).
18. R. M. FUOSS and C. A. KRAUS. J. Amer. Chem. Soc. **57**, 1 (1935).
19. H. STREHLOW and H. KOPP. Z. Elektrochem. **62**, 373 (1959).
20. K. H. STERN and E. S. AMIS. Chem. Rev. **59**, 1 (1959).

Can. J. Chem. Downloaded from www.nrcresearchpress.com by 210.87.254.42 on 09/05/12
For personal use only.

Can. J. Chem. Downloaded from www.nrcresearchpress.com by 210.87.254.105 on 09/05/12
For personal use only.

Studies of rhenium–carboxylate complexes. I. Tris(μ-*i*-butyrato)di(chlororhenium(III)) perrhenate

C. CALVO, N. C. JAYADEVAN, AND C. J. L. LOCK[1]

Department of Chemistry and Institute for Materials Research, McMaster University, Hamilton, Ontario

Received June 20, 1969

One of the compounds obtained by reacting rhenium(III) chloride with isobutyric acid while exposed to oxygen has been shown by single crystal X-ray diffraction to be tris(μ-*i*-butyrato)di(chlororhenium(III)) perrhenate. The crystals are monoclinic with lattice parameters $a = 8.980(5)$ Å, $b = 17.790(8)$ Å, $c = 15.361(8)$ Å, and $\beta = 114.4(1)°$. The space group is $P2_1/c$ and there are 4 formula units per cell. A total of 1729 independent reflections were examined and the structure was refined by full three dimensional least squares to an R value of 0.114. Two Re environments are found, one consisting of a dimer unit bridged by three carboxylate groups with a chlorine atom per rhenium and the other as a perrhenate group. This latter group, showing a mean Re—O distance of 1.74 Å, shares an oxygen atom with a Re in the dimer unit, and this Re—O bond length is 2.28 Å long. The structure consists of a packing of chains of alternate dimers and perrhenate groups running parallel to the *c* axis.

Canadian Journal of Chemistry 47, 4213 (1969)

Introduction

Taha and Wilkinson investigated the reaction of rhenium trichloride with carboxylic acids both in air and in oxygen-free (< 10 p.p.m.) nitrogen (1). The compound obtained in the absence of air

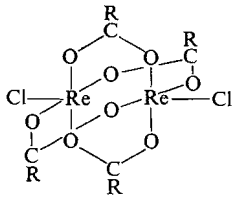

1

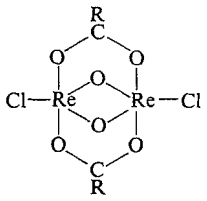

2

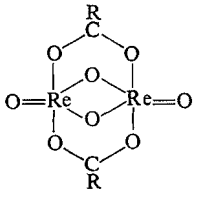

3

was postulated to be **1**, formally a compound of Re(III). The compounds obtained in the presence of air were postulated to be **2** and **3**, formally compounds of Re(IV) and Re(V), respectively. It has been shown (2, 3) that although the structure of **1** is basically correct, the compound has a very short Re—Re distance and this has been interpreted as indicating the presence of a very strong quadruple bond between the rhenium atoms in the dimer unit. It was of great interest to see whether strong metal–metal bonds were present in compounds **2** and **3**. In this paper we report our structural investigations of the μ-*i*-butyrato-complex supposedly of type **2**.

Experiments

Preparation

Rhenium(III) chloride[2] (2 g) was refluxed with isobutyric acid (25 ml) in a slow stream of oxygen which was dried by bubbling through concentrated sulfuric acid. After about 12 h, purple crystals formed and were filtered from the hot orange solution. The solid product was purified by repeated rapid crystallization from ethanol while under evacuation. Single crystals were prepared by recrystallization from chloroform. Attempts to crystallize the compound from acetone or ethanol solution in air always yielded a blue solid. The purple solid analyzed as C, 15.7%, H, 2.2%, O, 16.8%, and atoms Re:Cl, 1.4:1. $C_{12}H_{21}Cl_2O_{10}Re_3$ requires C, 15.1%, H, 2.2%, O, 16.8%, and atoms Re:Cl, 1.5:1. The suggested stoichiometry is confirmed by the successful structure analysis.

Analysis

C and H analyses were performed by the Galbraith Laboratories, Knoxville, Tennessee. Oxygen analyses were performed at the Microchemical Laboratories, Imperial College, London, by courtesy of Professor G. Wilkinson. The rhenium:chlorine atom ratio was determined by A. Guest using neutron activation analysis (4).

Infrared Spectra

The infrared absorption spectra were recorded on a Perkin–Elmer 337B spectrophotometer and are given in Table I. Powder samples dispersed as a mull in Nujol and mounted between potassium bromide plates, or dispersed in powdered potassium bromide and pressed in a disc, were used for recording spectra.

[1]To whom correspondence should be addressed.

[2]Obtained from the Shattuck Chemical Company, Denver, Colorado.

Can. J. Chem. Downloaded from www.nrcresearchpress.com by 210.87.254.105 on 09/05/12
For personal use only.

TABLE I

Infrared spectrum of $[Re_2(i\text{-}C_4H_7O_2)_3Cl_2]ReO_4$

ν (cm^{-1})	Intensity*	ν (cm^{-1})	Intensity*†
2950	s } v.b.	2970	m
2875	s }	2950	m
1480	vs	1480	vs
1463	s	1463	s
1430	s	1430	s
1385	s	1383	m
1370	s	1365	m
1300	s	1300	s
1171	m	1170	m
1096	s	1080	m
984	m		
971	sh	960	sh
952	s	940	s
908	s		
877	sh	887	s
850	s	835	s
765	w		
673	m	670	s
627	s		} not recorded
520	sh		
461	m		

*v.b. = very broad; s = strong; sh = shoulder; m = medium; w = weak.
†Results reported by Taha and Wilkinson (1) for the compound $Re_2(i\text{-}C_4H_7O_2)O_2Cl_2$.

Crystallography

The density of a few single crystals were determined by flotation in a mixture of di-iodomethane and tetrachloromethane, whose density was subsequently determined with a pycnometer.

Accurate unit cell parameters were determined from precession photographs of the [100] and [001] zones which were calibrated with a diffraction pattern from a TiO_2 single crystal (a = 4.5929(5) Å and c = 2.9591(3) Å (5)). The monoclinic angle β was measured from the spindle settings at which these two precession photographs were taken. The crystal data are shown in Table II. It was observed that reflections of the type $0k0$ with k odd were absent as were $h0l$ reflections with l odd. Thus, the space group was determined uniquely as $P2_1/c\text{–}C_{2h}^5$. A single crystal (0.1 × 0.1 × 0.1 mm^3) was used in taking the X-ray photographs. The equi-inclination Weissenberg method was used to record layers hnl (n = 0 to 6), the photographs being taken with Cu-K_α radiation. The $hk0$ and nkl (n = 0, 1, 2) layers were photographed by the precession method, using Mo-K_α radiation.

TABLE II

Crystal data for $[Re_2(i\text{-}C_4H_7O_2)_3Cl_2]ReO_4$

Parameter	Unit	Value
a	Å	8.980(5)
b	Å	17.790(8)
c	Å	15.361(8)
β	°	114.4 (1)
Vol	Å^3	2234
M		954.87
D_{measd}	g/cm^3	2.88 (2)
D_{calcd}	g/cm^3	2.84
Z		4

*Systematic absences, $0k0$, k odd; $h0l$, l odd. Space group, $P2_1/c\text{–}C_{2h}^5$.

Each layer was photographed 3 times using exposures involving time intervals differing by a factor of 3. The intensities were estimated visually and then corrected for Lorentz and polarization effects. All data obtained using copper radiation were corrected for absorption since otherwise errors of about 15% would have been introduced into the structure factors [μR = 1.66 for Cu-K_α and 0.08 for Mo-K_α]. For Mo-K_α radiation the absorption corrections would be negligible. These corrections were made assuming the crystal was a sphere of radius 0.05 mm.

Standard errors, σ, were assigned to each intensity and weights $w = 1/\sigma^2$ were used throughout the refinement. Greater weights were given to reflections which could be measured on all 3 films than to those which could be measured only on 1 or 2 films[3]. For unobserved reflections weights, calculated from $\sigma = 0.5\,F_{min}$ were used only when the calculated structure factor $|F_c| > 0.8\,F_{min}$, where F_{min} was the local minimum of the observed intensity. Otherwise they were given zero weight.

Solution of the Structure

The density required 12 rhenium atoms per unit cell and, if the structure proposed were correct (1), the cell must contain 6 dimeric groups per unit cell. Since the space group, $P2_1/c$, will generate 4 symmetry-related groups, one of the dimers must possess an element of symmetry and one must be in a general position. Thus, one of the dimers must have an inversion center. The Patterson function must show a rhenium–rhenium distance of the order of 2.5 to 3.4 Å, attributable to a dimer unit located at a center of symmetry together with a similar peak of double weight arising from the dimer in a general position. Otherwise the cell cannot contain 6 dimers of the type postulated in (1). These estimated distances were derived from known ReO separations and a range of assumed ReORe angles.

The two-dimensional Patterson maps for the 3 zero layer projections were readily soluble for the Re atoms. This solution was inconsistent with a dimeric unit placed on a center of symmetry. In addition the smallest Re—Re vector was 2.2 Å in length and indicated that the dimer in the general position must differ from that proposed by Taha and Wilkinson (1). The trial solution was obtained for the rhenium atom positions, however, and these positions were confirmed by an examination of the generalized Patterson maps using $h1l$ and $h2l$ reflections.

Structure factor calculations with these atomic positions gave, after one cycle of least-square refinement, an isotropic temperature factor B = 2.0 and the x, y, z coordinates Re(1): 0.073, 0.083, 0.126; Re(2): 0.191, 0.181, 0.372; Re(3): 0.141, 0.250, −0.027, and the overall residual error

$$R_1 = \frac{\sum|F_o - F_c|}{\sum|F_o|}$$

of 0.30. The 3 rhenium atoms in the asymmetric zone

[3]Thus $\sigma = 0.1\,F_o$ if $60 < F_o < 300$, $\sigma = 0.15\,F_o$ if $300 < F_o < 500$ or $40 < F_o < 60$, and $\sigma = 0.25\,F_o$ if $500 < F_o$ or $F_o < 40$.

TABLE III

Atomic parameters* for $[Re_2Cl_2(i\text{-}C_3H_7CO_2)_3]ReO_4$

Atom	Coordinates			B (Å)^2
	x	y	z	
Re(1)	0.07620(31)	0.08525(15)	0.12426(16)	†
Re(2)	0.19669(27)	0.17613(15)	0.36986(15)	†
Re(3)	0.13821(27)	0.25235(17)	0.46915(16)	†
Cl(3)	0.2861 (16)	0.2020 (11)	0.6176 (9)	5.17(32)
Cl(2)	0.3761 (18)	0.0931 (11)	0.4628 (10)	5.86(35)
O(13)	0.0413 (39)	0.1617 (25)	0.0430 (23)	5.23(84)
O(12)	0.1968 (39)	0.1183 (24)	0.2370 (22)	4.60(76)
O(11)	0.1837 (44)	0.0178 (27)	0.0931 (26)	6.06(91)
O(14)	−0.1148 (38)	0.0623 (24)	0.1218 (21)	4.29(75)
O(3C)	0.0035 (39)	0.3173 (24)	0.3558 (24)	4.75(81)
O(2C)	0.0573 (31)	0.2418 (20)	0.2593 (18)	2.57(59)
C(C1)	−0.0212 (58)	0.3046 (36)	0.2759 (33)	4.0 (10)
C(C2)	−0.1262 (62)	0.3453 (40)	0.1837 (37)	4.7 (12)
C(C3)	−0.2583 (84)	0.3015 (48)	0.1043 (47)	7.3 (17)
C(C4)	−0.1722 (80)	0.4169 (48)	0.2037 (46)	7.2 (17)
O(3A)	−0.0507 (38)	0.1849 (24)	0.4459 (23)	4.68(79)
O(2A)	0.0032 (38)	0.1113 (24)	0.3513 (22)	4.17(73)
C(A1)	−0.1137 (77)	0.1302 (45)	0.3887 (43)	6.3 (16)
C(A2)	−0.2554 (80)	0.0762 (46)	0.3727 (44)	6.8 (17)
C(A3)	−0.2328 (88)	0.0042 (51)	0.3135 (52)	8.4 (19)
C(A4)	−0.4080 (81)	0.1132 (49)	0.2972 (47)	7.5 (18)
O(3B)	0.3418 (34)	0.3171 (31)	0.4904 (20)	3.64(67)
O(2B)	0.3802 (35)	0.2502 (22)	0.3811 (20)	3.73(69)
C(B1)	0.3913 (58)	0.3026 (36)	0.4273 (32)	3.8 (11)
C(B2)	0.5072 (66)	0.3549 (42)	0.4118 (38)	4.8 (13)
C(B3)	0.6141 (74)	0.3310 (45)	0.3554 (43)	6.5 (16)
C(B4)	0.5413 (81)	0.4341 (51)	0.4310 (46)	7.4 (18)

Atom	U_{11}‡	U_{22}	U_{33}	U_{12}	U_{13}	U_{23}
Re(1)	1391(33)	330(38)	1077(28)	0(38)	485(23)	10(28)
Re(2)	1037(28)	330(38)	923(24)	−86(34)	351(21)	−71(25)
Re(3)	1083(28)	502(38)	994(26)	71(35)	467(21)	25(25)

*Estimated standard deviations in parentheses.
†Anisotropic thermal parameters used for rhenium atoms (Å)^2 × 10^4.
‡These values were obtained from $\beta_{ij} = 2\pi^2 b_i b_j U_{ij}$ where β_{ij}'s appear as a temperature effect through exp $[-(\beta_{11}h^2 + 2\beta_{12}hk + \ldots)]$ in the structure factor expression and b_i are the reciprocal lattice vectors.

consisted of 2 at a distance of 2.2 Å from each other, thus forming a dimer, while the third was at 3.8 Å from the nearest rhenium atom in the dimer. The nearest symmetry related pair of non-dimer atoms was at 4.6 Å. Thus there were 2 types of rhenium environments present in this structure; a pair of rhenium atoms were strongly bonded to each other while the third was either independent of the dimer or, at best, weakly bonded to it.

Electron density and difference syntheses based upon the signs determined for the structure factor for the contributions of the 3 rhenium atoms showed only 2 peaks that were large enough to be attributable to chlorine atoms. Ten more peaks had approximately half the chlorine peak heights and were attributed to oxygen atoms. Repeated structure factor calculations followed by difference Fourier syntheses revealed all 12 carbon atom positions. The positional parameters, isotropic temperature factors of all non-rhenium atoms, and anisotropic temperature factors for the rhenium atoms were varied in a full matrix least-square refinement, using the program MACLS written by J. S. Stephens. The minimum value obtained was $R_1 = 0.126$ and $R_2 = 0.150$, where R_2 is defined as

$$\left[\frac{\sum\omega(|F_o|^2 - |F_c|^2)}{\sum\omega|F_o|^2}\right]^{1/2}$$

The anomalous dispersion effects, tabulated by Cromer (6), show a significantly different value for Mo-K_α from that for Cu-K_α data. In the final stages of the refinement, the molybdenum data were modified to obtain pseudo observed structure factors that would have been obtained if copper radiation were employed. The atomic scattering factors of C, Cl, and O were obtained from the International tables for X-ray crystallography (7) while that for Re was taken from Cromer and Waber (8).

The positional and thermal parameters were subsequently refined to a minimum value of $R_1 = 0.114$ and $R_2 = 0.118$. In the final cycle of refinement no parameter changed by more than 1/3 of its estimated standard deviation. A difference synthesis obtained had no peaks higher than 1.8 e/Å^3 or lower than −1.6 e/Å^3. The final positional and thermal parameters are presented in Table III. The observed and calculated structure factors

Can. J. Chem. Downloaded from www.nrcresearchpress.com by 210.87.254.105 on 09/05/12
For personal use only.

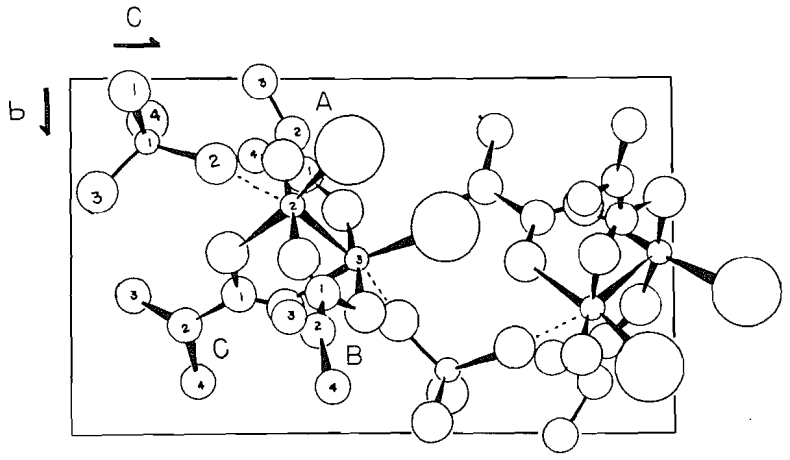

FIG. 1. The molecular packing of $[Re_2Cl_2(i\text{-}C_3H_7CO_2)_3](ReO_4)$ projected down the ***a*** axis. Atoms in order of decreasing size of circles are Cl, O, C, and Re. Full lines indicate bonds in the perrhenate group and dimer unit. Dotted lines indicate bonds between the perrhenate groups and the dimer units. A, B, C label the bridging carboxylate groups in the dimer unit. Of the small numbers 1 refers to the carboxylate carbon atom, 2 the α-carbon atom, and 3 and 4 the β-carbon atoms in each carboxylate group. The large numbers, 1–4, label the oxygen atoms in the perrhenate group.

are compared[4] in Table IV. Of the 1729 reflections examined, 1236 were observed. Each layer line was independently scaled and reflections observed on more than one film were averaged and assigned at random to one of the groups from which it originated.

Results and Discussion

The essential feature of the structure is the presence of a carboxylato-bridged rhenium dimer $[Re_2Cl_2(O_2CC_3H_7\text{-}i)_3]$ and a perrhenate group, ReO_4^-, per asymmetric unit of the unit cell, as shown in Fig. 1. Each dimeric unit has 3 bridging carboxylate groups and 1 chlorine atom on each rhenium atom. The other rhenium atom of the dimer and 1 oxygen atom of the perrhenate group completes a distorted octahedral arrangement of atoms around each rhenium atom. The dimeric unit is illustrated in Fig. 2. Two of the oxygen atoms of the ReO_4^- group are used to form a link between 2 otherwise independent dimer groups forming continuous chains. The compound is thus of interest, since it is the first of the series of compounds containing the strongly bonded Re_2 unit in addition to non-dimerized rhenium atoms. Since there are 2 ReO_4^- units

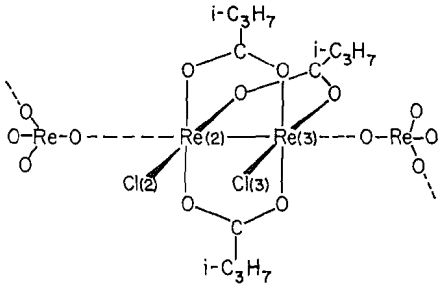

FIG. 2. The molecular geometry of the dimeric unit $[Re_2Cl_2(O_2CC_3H_7\text{-}i)_3]^+$.

associated with each dimer unit and 2 dimer groups associated with each ReO_4^-, the compound is properly called tris(μ-iso-butyrato)di-(chlororhenium(III)) perrhenate and the average formal oxidation number of rhenium is $4\frac{1}{3}$.

The bond distances and bond angles are listed in Table V. The numbering of atoms used refers to that in Fig. 1, which shows the packing of the molecule in the unit cell projected down the ***a*** axis. Within the dimer group the 2 rhenium atoms are separated by a distance of 2.259(3) Å. This distance is very similar to those observed in other dimeric Re(III) compounds where distances range from 2.20(2) to 2.241(7) Å (2, 3, 9–13), and lies well within the range 2.24 ± 0.10 Å predicted by Cotton (14) for a quadruple bond between the

[4]Table IV has been placed in the Depository of Unpublished Data. Photocopies may be obtained free of charge, upon request, from: Depository of Unpublished Data, National Science Library, National Research Council of Canada, Ottawa, Canada.

Can. J. Chem. Downloaded from www.nrcresearchpress.com by 210.87.254.105 on 09/05/12
For personal use only.

Can. J. Chem. Downloaded from www.nrcresearchpress.com by 210.87.254.105 on 09/05/12
For personal use only.

2 rhenium atoms. The quadruple bond is postulated to consist of one σ, two π, and one δ bond. An eclipsed rotomeric configuration was shown to be necessary for the formation of the δ bond. The Re—Re distance obtained for the present compound and the eclipsed configuration in the dimer unit is consistent with Cotton's model for a quadruple bond between the 2 rhenium atoms.

The 2 independent Re–Cl distances are 2.29(1), and 2.22(2) Å. These values are within the range of distances observed in $[Re_2Cl_8]^{2-}$ (11), $Re_2Cl_6[P(C_2H_5)_3]_2$ (9), and $ReCl_2CH_3CO_2(H)\cdot H_2O$ (12), thereby suggesting a similar type of bonding. The bond distances and angles within the carboxylate groups are similar to those observed in other compounds where the carboxylate group is known to bridge 2 metal atoms (15). Thus the β-carbon atom and the 2 oxygen atoms attached to the α-carbon atom in the carboxylate group form a plane, and pairs of them subtend angles of approximately 120° at the α-carbon atom. The angles subtended by pairs of the 3 carbon atoms bonded to the β carbon atom are close to the tetrahedral angle. The 6 independent rhenium atom to carboxylic oxygen distances do not differ significantly.

All the relevant least-squares planes (16) in the dimeric unit were calculated using the program PALS written by P. Ashmore for the CDC 6400 computer. Individual atoms forming a plane were given weights

$$\left[\frac{1}{a.b.c.\sigma(x).\sigma(y).\sigma(z)}\right]^{2/3}$$

where a, b, c, are cell constants, and $\sigma(x)$, $\sigma(y)$, $\sigma(z)$ are standard deviations of the atomic coordinates. The equations of these planes are shown in Table VI. The calculations show that the 2 rhenium atoms and the bridging carboxylate groups form 3 planes, 2 of them being coplanar (planes 2 and 3) and orthogonal to the other (plane 1). The chlorine atoms on each rhenium are coplanar (plane 6) with plane 1 but are slightly out of the plane containing the rhenium atom and the 3 carboxylic oxygen atoms bonded to it (about 0.6 Å). The non-bonded distance between the 2 chlorine atoms is 3.40(3) Å, slightly shorter than the sum of the Van der Waals radii (3.6 Å), and each rhenium–chlorine bond makes an average angle of 104.8(5)° to the rhenium–rhenium axis. These values are very similar to those obtained in $[Re_2Cl_8]^{2-}$ (11) and the deviation is probably caused by steric repulsion.

As remarked earlier, there is an oxygen atom from a perrhenate group at each end of the dimeric unit, almost colinear with the Re—Re axis at a distance of 2.28(4) Å. The distance is probably somewhat longer than other Re—O lengths observed (average 2.10 Å) although the errors in the reported bond lengths are usually quite large. There has been a suggestion that the long Re—Cl distance for the chlorine atom bonded axially and *trans* to the Re—Re bond in $Re_2(RCO_2)_4Cl_2$ indicates a bond which is considerably weaker than normal and, by implication, that this is related to the strong Re—Re bonding (2). A similar interpretation may be made for the long Re—O distance in our compound, but we feel that in this case the long distance is caused at least partly by repulsive non-bonded interactions between the oxygen of the perrhenate group and the oxygen atoms of the carboxylate groups and the chlorine atom attached to the rhenium atom. The non-bonded distances of the axial oxygen atom with the chlorine atoms and the carboxylic oxygen atom "*trans*" to it are

$$O(12)\text{—}Cl(2) = 3.20(4)\ Å$$

$$O(13)\text{—}Cl(3) = 3.15(4)\ Å$$

$$O(12)\text{—}O(2C) = 2.72(5)\ Å$$

$$O(13)\text{—}O(3C) = 2.78(4)\ Å$$

These values are of the same order as the sum of the Van der Waals radii (O + Cl = 3.2 Å and O + O = 2.8 Å, using Pauling's values (17)). The O—Re—O angles in the ReO_4^- groups are close to the tetrahedral angle except for a small increase in the angle subtended by the 2 oxygen atoms (O(11) and O(14)) not coordinated to the dimer unit. Probably the increase is caused by the repulsion of the non-bonded electrons on the oxygen atoms although the Re—O bond lengths involving these oxygen atoms are not significantly shorter than the others, and are comparable to those observed in $KReO_4$ (18).

The 2 oxygen atoms coordinated to the dimeric rhenium atoms help to form a chain of alternate dimer and ReO_4^- units running parallel to the *c* axis as shown in Fig. 1. These chains form a hexagonally closest packed arrangement when viewed in a cross section containing the *a* and *b*

axes. The packing of adjacent chains seems to be determined by the Van der Waals separation of the pair of ReO_4 tetrahedra related by the center of symmetries at 0, 0, 0, and 0, 1/2, 1/2.

The compound whose structure is described above is probably different from that obtained by Taha and Wilkinson for which they proposed the structure in **1**. We have duplicated the reaction conditions as far as possible, but failed to obtain the purple compound in any isolable amounts if the reaction is continued for more than 1 day. After this time, the major product is identical in composition to the orange compound they obtained (Part III of this series, to be published). The rhenium(III) chloride used in the original preparations was obtained by the thermal decomposition of rhenium pentachloride. We have used rhenium(III) chloride obtained by the same method as well as that bought from the Shattuck Company, Denver, Colorado, and obtained identical products. Stoichiometrically the difference is an additional oxygen atom in our compound at the expense of a chlorine atom. Analyses of the compound reported here were performed on single crystals, so differences in analysis might have been caused either by impurities in Taha and Wilkinson's compounds or by the compounds being different.

TABLE V

Bond distances and angles in $[Re_2Cl_2(O_2CC_3H_7\text{-}i)_3]ReO_4$

(*a*) Dimeric unit $[Re_2Cl_2(O_2CC_3H_7\text{-}i)_3]$

Bond	Designation, if any	Length (Å)	Bond	Designation, if any	Length (Å)
Re(3)—Re(2)		2.259(3)			
Re(3)— Cl(3)		2.29 (1)	Re(2)—Cl(2)		2.22 (2)
Re(3)— O(3)	A	1.99 (4)	Re(2)— O(2)	A	2.00 (4)
Re(3)— O(3)	B	2.07 (3)	Re(2)— O(2)	B	2.06 (3)
Re(3)— O(3)	C	2.02 (3)	Re(2)— O(2)	C	2.02 (2)
C(1)— O(3)	A	1.28 (7)	C(1)— O(2)	A	1.43 (7)
C(1)— O(3)	B	1.24 (5)	C(1)— O(2)	B	1.15 (6)
C(1)— O(3)	C	1.18 (3)	C(1)— O(2)	C	1.39 (7)
C(2)— C(1)	A	1.53(10)	C(2)— C(3)	A	1.63(11)
C(2)— C(1)	B	1.49 (9)	C(2)— C(3)	B	1.59 (8)
C(2)— C(1)	C	1.52 (6)	C(2)— C(3)	C	1.52 (8)
C(3)— C(4)	A	1.53 (8)			
C(3)— C(4)	B	1.45(11)			
C(3)— C(4)	C	1.43(11)			

Bonds	Designation, if any	Angle (deg)	Bonds	Designation, if any	Angle (deg)
Re(2)—Re(3)—Cl(3)		103.7 (5)	Re(3)—Re(2)—Cl(2)		105.9 (5)
Re(2)—Re(3)— O(3)	A	86.3(12)	Re(3)—Re(2)— O(2)	A	90.7(12)
Re(2)—Re(3)— O(3)	B	90.1(10)	Re(3)—Re(2)— O(2)	B	87.7(10)
Re(2)—Re(3)— O(3)	C	89.1(12)	Re(3)—Re(2)— O(2)	C	89.1 (9)
Cl(3)—Re(3)— O(3)	A	92.5(10)	Cl(2)—Re(2)— O(2)	A	93.7(11)
Cl(3)—Re(3)— O(3)	B	87.2 (9)	Cl(2)—Re(2)— O(2)	B	91.7(10)
Cl(3)—Re(3)— O(3)	C	166.8(13)	Cl(2)—Re(2)— O(2)	C	164.2(11)
O(3)— Re(3)— O(3)	AB	176.3(11)	O(2)—Re(2)— O(2)	AB	174.6(13)
O(3)— Re(3)— O(3)	AC	91.6(14)	O(2)—Re(2)— O(2)	AC	90.8(13)
O(3)— Re(3)— O(3)	BC	89.5(14)	O(2)—Re(2)— O(2)	BC	84.1(13)
Re(3)— O(3)— C(1)	A	130 (4)	Re(2)— O(2)— C(1)	A	123 (3)
Re(3)— O(3)— C(1)	B	111 (3)	Re(2)— O(2)— C(1)	B	116 (4)
Re(3)— O(3)— C(1)	C	125 (4)	Re(2)— O(2)— C(1)	C	130 (4)
O(3)— C(1)— O(2)	A	106 (5)	O(2)— C(1)— C(2)	A	119 (5)
O(3)— C(1)— O(2)	B	132 (5)	O(2)— C(1)— C(2)	B	107 (5)
O(3)— C(1)— O(2)	C	117 (4)	O(2)— C(1)— C(2)	C	112 (4)
C(1)— C(2)— C(3)	A	107 (6)	C(1)— C(2)— C(4)	A	106 (6)
C(1)— C(2)— C(3)	B	123 (5)	C(1)— C(2)— C(4)	B	132 (6)
C(1)— C(2)— C(3)	C	119 (5)	C(1)— C(2)— C(4)	C	111 (5)
C(3)— C(2)— C(4)	A	101 (5)			
C(3)— C(2)— C(4)	B	104 (6)			
C(3)— C(2)— C(4)	C	115 (5)			

Can. J. Chem. Downloaded from www.nrcresearchpress.com by 210.87.254.105 on 09/05/12
For personal use only.

TABLE V (*Concluded*)

(*b*) Monomeric unit [ReO_4]

Bond	Length (Å)	Bonds	Angle (deg)
Re(1)—O(11)	1.73(4)	O(11)—Re(1)—O(12)	109(2)
Re(1)—O(12)	1.72(3)	O(11)—Re(1)—O(13)	107(2)
Re(1)—O(13)	1.78(4)	O(11)—Re(1)—O(14)	119(2)
Re(1)—O(14)	1.75(3)	O(12)—Re(1)—O(13)	107(2)
		O(12)—Re(1)—O(14)	108(2)
		O(13)—Re(1)—O(14)	106(2)

(*c*) The bridging unit Re—O—Re

Bond	Length (Å)	Bonds	Designation, if any	Angle (deg)
O(12) —Re(2)	2.28(4)	Re(1)*—O(13)*—Re(3)		150.0(10)
O(12) —Re(1)	1.72(3)	O(13)*—Re(3) —Re(2)		169.9 (8)
		O(13)*—Re(3) — Cl(3)		87.1 (9)
O(13)*—Re(3)	2.28(4)	O(13)*—Re(3) — O(3)	A	91.2(16)
O(13)*—Re(1)*	1.78(4)	O(13)*—Re(3) — O(3)	B	92.5(14)
		O(13)*—Re(3) — O(3)	C	80.2(15)
		Re(1) —O(12) —Re(2)		145.0(10)
		O(12) —Re(2) —Re(3)		163.5 (9)
		O(12) —Re(2) — Cl(2)		90.4(10)
		O(12) —Re(2) — O(2)	A	86.2(15)
		O(12) —Re(2) — O(2)	B	93.9(14)
		O(12) —Re(2) — O(2)	C	74.8(13)

*These atoms are generated by the symmetry operation $(x, \frac{1}{2} - y, \frac{1}{2} + z)$ on the respective atomic coordinates in Table III.

TABLE VI

Weighted least-squares molecular planes*

Type of plane	Number	Equation
$Re_2O_2C(1)$	1	$0.8188x + 0.5576y + 0.1366z = 1.9780$
$Re_2O_2C(2)$	2	$0.2663x - 0.5696y + 0.7776z = 2.0838$
$Re_2O_2C(3)$	3	$0.3142x - 0.5360y + 0.7836z = 2.1919$
$Re_2Cl_2(4)$	4	$0.7996x + 0.5940y + 0.0876z = 1.8519$
Re_2O_4	5	$0.2913x - 0.5526y + 0.7808z = 2.1384$
$Re_2O_2Cl_2C$	6	$0.8031x + 0.5879y + 0.0963z = 1.8768$

*The orthogonal coordinate system corresponds to the crystallographic ***a b c**** axes.

Data from the infrared spectra of $[Re_2(i\text{-}C_4H_7O_2)_3Cl_2]ReO_4$ recorded using single crystals, powdered and dispersed in Nujol, are presented in Table I, together with data reported by Taha and Wilkinson (1) for $Re_2(i\text{-}C_4H_7O_2)_2O_2Cl_2$. It will be noticed that the spectra are very similar except in the region 750–1100 K, where Re—O stretches are normally found (19, 20). If Taha and Wilkinson's sample was identical to ours, but impure, we would expect to find that the spectra were identical except for possible extra bands in the spectrum for their sample. This does not appear to be the case and suggests that the compounds are different. An unambiguous decision cannot be made since many of the bands in the region 750–1100 K can be correlated if it is assumed that there is a zero shift of ~ 15–20 K in this region, although the good correlation above and below this region suggest such a shift is unlikely. No attempt has been made to assign the bands or to say which bands arise from the Re=O stretch, as bands from the complexed isobutyrate ion also occur in this region (1).

Conclusions

We conclude that our compound is another in

Can. J. Chem. Downloaded from www.nrcresearchpress.com by 210.87.254.105 on 09/05/12
For personal use only.

the series of rhenium(III) compounds which contain the remarkably stable Re_2 unit.

Acknowledgments

We wish to thank the National Research Council of Canada for financial support and one of us (N.C.J.) acknowledges the receipt of a Commonwealth Scholarship.

1. F. Taha and G. Wilkinson. J. Chem. Soc. 5406 (1963).
2. M. J. Bennett, W. K. Bratton, F. A. Cotton, and W. R. Robinson. Inorg. Chem. **7**, 1570 (1968).
3. C. Calvo, C. J. L. Lock, and R. Restivo. Part II. To be published.
4. W. Courrier, A. Guest, C. J. L. Lock, R. H. Tomlinson. Can. J. Chem. **46**, 2965 (1968).
5. D. T. Cromer and K. Herrington. J. Amer. Chem. Soc. **77**, 4708 (1955).
6. D. T. Cromer. Acta Cryst. **18**, 17 (1965).
7. International tables for X-ray crystallography. Vol. III. Kynoch Press, Birmingham. 1962. Table 3.3.1A.
8. D. T. Cromer and J. T. Waber. Acta Cryst. **18**, 104 (1965).
9. (*a*) M. J. Bennett, F. A. Cotton, B. M. Foxman, and P. F. Stokely. J. Amer. Chem. Soc. **89**, 2759 (1967). (*b*) F. A. Cotton and B. M. Foxman. Inorg. Chem. **7**, 2135 (1968).
10. V. G. Kuznetsov and P. A. Koz'min. Zh. Strukt. Khim. **4**, 55 (1963).
11. F. A. Cotton and C. B. Harris. Inorg. Chem. **4**, 330 (1965).
12. P. A. Koz'min, M. D. Surashkaya, and V. G. Kuznetsov. Zh. Strukt. Khim. **8**, 1107 (1967).
13. P. A. Koz'min, V. G. Kuznetsov, and Z. V. Popova. Zh. Strukt. Khim. **6**, 651 (1965).
14. F. A. Cotton. Inorg. Chem. **4**, 334 (1965).
15. S. Herzog and W. Kalies. Z. Chem. **8**, 81 (1968).
16. V. Shomaker, J. Waser, R. E. Marsh, and G Bergman. Acta Cryst. **12**, 600 (1959).
17. L. Pauling. The nature of the chemical bond. Cornell Univ. Press, Ithaca. 1942. p. 189
18. J. C. Morrow. Acta Cryst. **13**, 443 (1960).
19. C. A. Barraclough, J. Lewis, and R. S. Nyholm. J. Chem. Soc. 3552 (1959).
20. N. P. Johnson, C. J. L. Lock, and G. Wilkinson. J. Chem. Soc. 1054 (1964).

Can. J. Chem. Downloaded from www.nrcresearchpress.com by 210.87.254.105 on 09/05/12
For personal use only.

Can. J. Chem. Downloaded from www.nrcresearchpress.com by 210.87.254.5 on 09/05/12
For personal use only.

Cryoscopic studies with molten fluorides. I. Depression of the freezing point of calcium fluoride by alkaline-earth fluorides and oxides and calcium silicates[1]

H. KOJIMA[2] AND C. R. MASSON

Atlantic Regional Laboratory, National Research Council of Canada, Halifax, Nova Scotia

Received July 11, 1969

The depression of the freezing point of CaF_2 by BaF_2 and MgF_2 is ideal in the limit of low concentrations, and excess partial free energies of CaF_2 at finite concentrations are in accord with data for other systems. Limiting depressions due to SrF_2, CaO, and SrO are each approximately $\frac{1}{4}$, and due to BaO and MgO, $\frac{1}{2}$, of the ideal values. Calcium orthosilicate behaves ideally on the basis of 1 SiO_4^{4-} ion per molecule. For calcium metasilicate, the results are interpreted in terms of a distribution of fluorosilicate ions of general formula $(SiO_3)_nF^{(2n+1)-}$ in the melts. For Ca_3SiO_5, the depressions are complicated by the non-ideal behavior of oxygen ions. From the phase diagrams at low concentrations, CaO behaves ideally in $CaCl_2$, and MgO is ideal in MgF_2. The results are discussed in terms of possible formation of solid solutions in some of these systems.

Canadian Journal of Chemistry, 47, 4221 (1969)

Introduction

The depression of the freezing point (f.p.) of inorganic salts by substances such as silicates, phosphates, and borates which yield polymeric anions in solution, and structural conclusions derived from such studies, have been discussed by Førland (1). The object of the present work, which is part of a wider investigation of the constitution of polyionic melts, was to study the depression of the f.p. of CaF_2 by calcium silicates of varying CaO/SiO_2 ratios. Unexpected results with CaO alone as solute prompted a more detailed study, and depressions due to other alkaline earth oxides and the corresponding fluorides were also investigated.

Calcium fluoride was chosen as solvent because its heat of fusion has been determined calorimetrically (2), reliable data are available for the heat capacities of solid and liquid (2), and many phase diagrams (3) with CaF_2 as the main component, show the pure crystalline fluoride as primary phase.

Experimental

Materials

Calcium fluoride (B.D.H. "Extra Pure"), MgF_2 (Koch Light), SrF_2 and BaF_2 (B.D.H.) were purified by passing anhydrous HF through the melts in the apparatus described previously (4). The f.p.'s were 1423, 1261, 1473, and 1354 °C.

Calcium silicates with molar ratios CaO/SiO_2 of 1/1, 2/1, and 3/1 were prepared from $CaCO_3$ (B.D.H., AR) and SiO_2 (Mallinckrodt, AR) by repeated sintering at 1400–1410 °C and grinding. X-Ray diffraction of powdered specimens showed that the $CaSiO_3$ was pseudowollastonite and that the orthosilicate was γ-Ca_2SiO_4. No unreacted CaO or SiO_2 was detected in either product.

Strontium oxide was prepared from $SrCO_3$ (Hopkins and Williams) by heating in a stream of mixed H_2 (40%) and Ar (60%) at 1100 °C for 18 h (5). Barium oxide was prepared from $BaCO_3$ (Anachemia, Reagent) by heating at 1100 °C under high vacuum in a Pt container (5). Magnesium oxide (Mallinckrodt) was of reported purity 99.9%.

Apparatus and Procedure

Freezing points were determined by the method of thermal arrests with the apparatus described previously (6). Melts were held in graphite crucibles, 1 in. in diameter and 1.5 in. deep, equipped with a re-entrant well which housed the junction of the thermocouple. Crucibles were degassed at 1400–1450 °C in a separate apparatus before use. Approximately 11 g CaF_2 was used in each determination.

Temperatures were measured with a Pt/87% Pt - 13% Rh thermocouple calibrated periodically against copper, f.p. 1083.3 °C, supplied by the U.S. National Bureau of Standards. A Westronics potentiometric recorder with a full chart range of 2 mV was used to measure the electromotive force (e.m.f.). The recorder was calibrated after each series of measurements by a Leeds and Northrup potentiometer.

The temperature of the furnace was controlled by a Honeywell program controller, actuated by a second thermocouple located close to the winding. Linear cooling rates ranged from 1 to 3 °C per min. Too slow cooling often yielded indeterminate arrests at high concentrations of solute. Too rapid cooling occasionally resulted in supercooling. Each measurement reported is the mean of at least 3 determinations at a suitable rate. Melting points were reproducible to ±1.5 °C.

Results

The exact expression (7) for the temperature T

[1]NRCC No. 10 937.

[2]NRCC Postdoctorate Fellow, 1964–1966. Present address: Faculty of Engineering, Yamanashi University, Kofu-Shi, Japan.

at which pure solid component *1* crystallizes from a solution on cooling may be written

$$[1] \quad -R \ln a_{1(T)} = \frac{(T_0 - T)}{T} \times \left\{ \frac{\Delta H_f^0}{T_0} - A - \frac{B(T_0 - T)}{2} \right\} + A \ln \frac{T_0}{T}$$

where $a_{1(T)}$ is the activity of component *1*, at temperature T, relative to the supercooled liquid at the same temperature, ΔH_f^0 is the molar heat of fusion of pure component *1* at its melting point T_0, and A and B are constants in the equation

$$[2] \quad \Delta C_p = A + BT$$

where ΔC_p is the heat capacity of pure liquid component *1* less that of the crystalline solid at temperature T.

Various approximate forms of eq. [1] are found in the literature. As $T \rightarrow T_0$, the terms in A and B may be ignored and, for CaF_2 as solvent

$$[3] \quad \frac{1}{T} \simeq \frac{1}{T_0} - \frac{R}{\Delta H_f^0} \ln a_{CaF_2}$$

If the solute dissociates into ν foreign ions per molecule, and if the activity of CaF_2 can be replaced by its mole fraction N, eq. [3] becomes, in the limit (see also Appendix)

$$[4] \quad \frac{1}{T} \simeq \frac{1}{T_0} - \frac{\nu R}{\Delta H_f^0} \ln N_{CaF_2}$$

Alkaline-Earth Fluorides

Figure 1 shows the temperatures at which the first thermal arrests appeared on cooling. The solid lines correspond to ν = 1 and 1/4 in eq. [4]. Naylor's (2) value, 7100 cal/mole, was used for ΔH_f^0.

In the limit of low concentrations, the depressions due to MgF_2 and BaF_2 in Fig. 1 each correspond to 1 foreign ion, and that due to SrF_2, to 0.25 foreign ion per molecule of solute.

Activities of CaF_2 in its binary solutions with MgF_2 and BaF_2 were calculated by eqs. [1] and [2]. For CaF_2 in the range of temperatures under consideration, ΔC_p was obtained from the data of Naylor (2)

$$[5] \quad \Delta C_p = -1.93 - 0.0025T$$

Activities and activity coefficients calculated in this way are presented in Table I. For both systems, deviations from ideality are small over the range investigated.

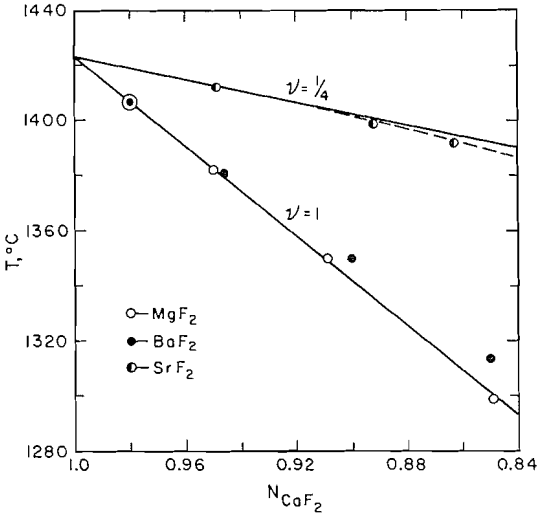

FIG. 1. Depression of the freezing point of CaF_2 by MgF_2, BaF_2, and SrF_2. The broken line corresponds to eq. [4′] in the Appendix, based on $n = 1/4$.

TABLE I

Activities of CaF_2 in its binaries with BaF_2 and MgF_2 at various temperatures

Mole fraction of CaF_2	Freezing point (°C)	a_{CaF_2}	γ_{CaF_2}
	(a) CaF_2–BaF_2		
1.000	1423		
0.980	1407	0.980	1.000
0.946	1381	0.947	1.001
0.900	1350	0.907	1.008
0.850	1313	0.858	1.010
	(b) CaF_2–MgF_2		
1.000	1423		
0.980	1407	0.980	1.000
0.950	1382	0.948	0.998
0.909	1350	0.907	0.997
0.849	1299	0.839	0.989

Alkaline-Earth Oxides

Figure 2 shows the results for MgO, CaO, SrO, and BaO as solutes. None of these systems approach ideal behavior in the accepted sense. At low concentrations, the depressions due to MgO and BaO each correspond to 1, rather than 2, foreign ion per molecule; that due to CaO corresponds approximately to ν = 1/4, while SrO shows intermediate behavior, with ν ≃ 1/2. The results for MgO show a minimum in the freezing curve near $T = 1370$ °C, $N_{CaF_2} = 0.93$.

Can. J. Chem. Downloaded from www.nrcresearchpress.com by 210.87.254.5 on 09/05/12
For personal use only.

Can. J. Chem. Downloaded from www.nrcresearchpress.com by 210.87.254.5 on 09/05/12
For personal use only.

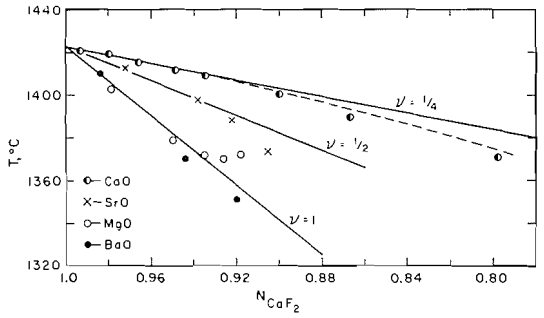

FIG. 2. Depression of the freezing point of CaF_2 by MgO, CaO, SrO, and BaO. Broken line corresponds to eq. [4′], based on $n = 1/4$.

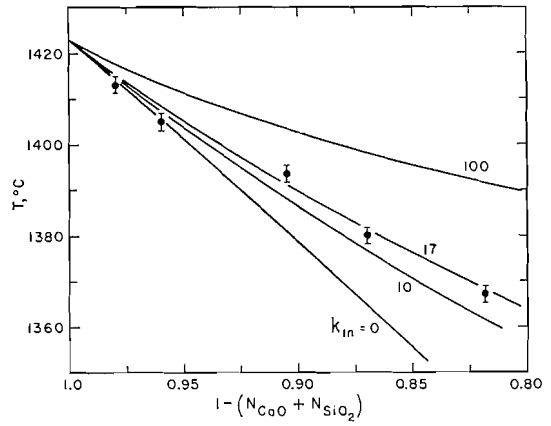

FIG. 3. Depression of the freezing point of CaF_2 by pseudowollastonite. The lines are calculated from eqs. [13] and [15] for various values of k_{1n}.

Calcium Silicates

The results for calcium silicates with molar ratio CaO/SiO_2 of 1/1 are shown in Fig. 3, and ratios of 2/1 and 3/1 in Fig. 4. Mole fractions of CaF_2 are expressed on the basis that CaF_2, CaO, and SiO_2 are components.

Discussion

Fluorides

The depressions due to MgF_2, SrF_2, and BaF_2 (Fig. 1) are in good agreement with values reported elsewhere (8, 9), although the absolute f.p. values are higher than those in previous studies, due to the higher purity of the materials in the present work.

Excess partial free energies of solution of CaF_2 in its binary solutions with MgF_2 and BaF_2, as calculated from the data in Table I, are plotted in Fig. 5 against the square of the mole fraction of solute. The slight negative departures from ideality associated with the smaller Mg^{2+} ion and the positive departures for the larger Ba^{2+} are in line with similar trends for the alkaline-earth fluorides in sodium fluoride, reported by Cantor (7), and for mixtures of the alkali fluorides themselves. Thus, LiF shows slightly negative, and KF slightly positive, deviations from ideality in NaF solutions (10).

The lower depressions for SrF_2 in CaF_2 (Fig. 1) are due to formation of solid solutions as concluded also by Delbove (9). This is supported by the work of Chernevskaya (11) and Chernevskaya and Anan'eva (12), who reported a complete series of solid solutions in this system. In line with this, it was noted in the present study that melts with SrF_2 as solute cooled to transparent solids,

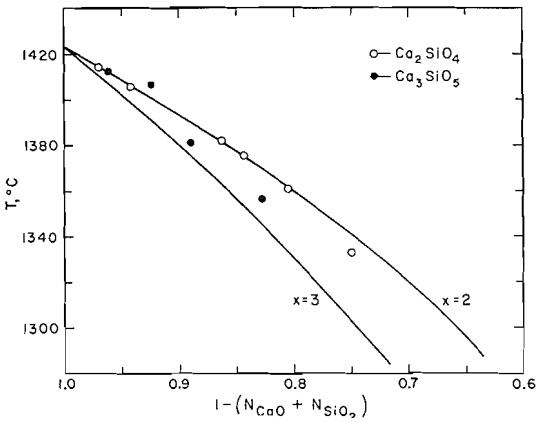

FIG. 4. Depression of the freezing point of CaF_2 by Ca_2SiO_4 and Ca_3SiO_5. The lines are calculated from eqs. [15] and [21] with $x = 2$ and 3.

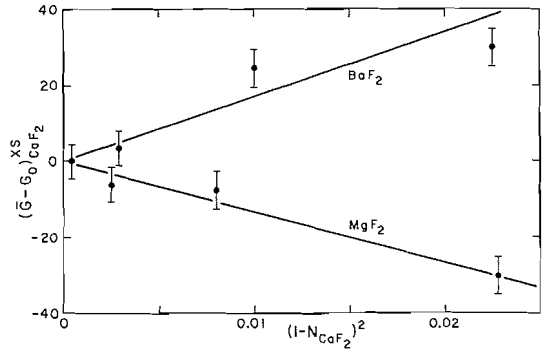

FIG. 5. Excess partial free energies of CaF_2 in its melts with BaF_2 and MgF_2 in the range 1299–1423 °C. The vertical lines correspond to an uncertainty of ± 1 °C in the freezing points.

Can. J. Chem. Downloaded from www.nrcresearchpress.com by 210.87.254.5 on 09/05/12
For personal use only.

in contrast to those with BaF_2 or MgF_2 which were milky or white.

Our results for the system CaF_2–SrF_2 indicate a value of 0.75 for the distribution coefficient ρ, the ratio of the concentration of solute in the solid to that in the liquid solution. This value, which does not vary with composition in the region investigated, is in reasonable agreement with the value of 0.705 reported by Delbove (9).

Oxides

The depressions due to CaO (Fig. 2) agree with those reported by Delbove (9) and Delbove *et al.* (13) and with the phase diagram as established by Mukerji (14), although our values of the f.p. are 4–10 °C higher. No evidence was found for the two-phase region of liquid immiscibility reported by Baak (15).

It has been shown recently (16) that solid solutions crystallize in the system CaF_2–CaO, and the relatively small depressions due to CaO must be attributed to this cause. The limiting value of 0.75 found for the distribution coefficient is in reasonable agreement with the value of 0.80 by Delbove *et al.* (13). This high value indicates that oxide ions readily substitute for fluoride ions in the CaF_2 lattice; two F^- ions are presumably replaced by one O^{2-} ion and a vacant anion site. A similar conclusion was reached by Baak (17) from studies of electrical conductivity and density.

All the oxides of Fig. 2 crystallize with the sodium chloride structure and might reasonably be expected to form solid solutions with CaF_2. The results are qualitatively in line with this expectation, the limiting depressions becoming greater as the cation becomes larger ($Ba^{2+} > Sr^{2+} > Ca^{2+}$) or smaller ($Mg^{2+} < Ca^{2+}$) than the Ca^{2+} ion.

An alternative, though less likely, interpretation is that the oxides MgO and BaO, for which $\nu \simeq 1$ in the limit, remain largely associated as ion pairs in the melt. Such an interpretation was used successfully by Lumsden (18) to predict the cryoscopic behavior of certain halides in fused nitrate media. In the present case, this would require a large increase in free energy when either BaO or MgO reacts with CaF_2. Available data do not allow these free energies to be estimated with sufficient accuracy to test this interpretation.

If the low depressions caused by the oxides in Fig. 2 were due to solid solutions, limiting depressions closer to ideality might be expected for CaO in $CaCl_2$ and MgO in MgF_2, as these solvents crystallize in the rutile structure and would not be expected to yield solid solutions with either CaO or MgO. This is borne out for MgO in MgF_2 by the data of Tomlinson and Welch (19) and of Delbove *et al.* (13), and for CaO in $CaCl_2$ by the data of Threadgill (20). The latter are shown in Fig. 6, where the line for $\nu = 1$ is based on Moore's (21) value of 6780 cal/mole for the heat of fusion of $CaCl_2$.

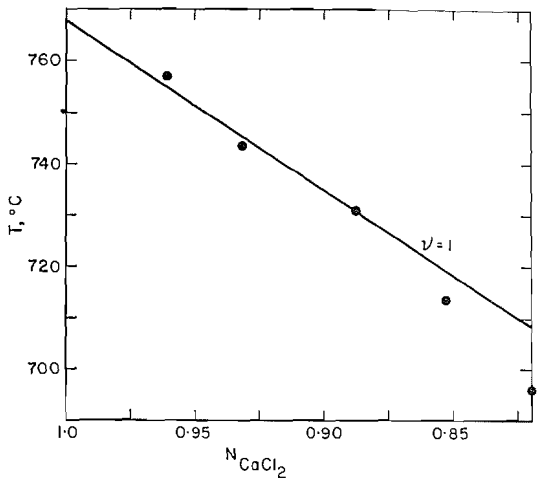

FIG. 6. Depression of the freezing point of $CaCl_2$ by CaO from the data of Threadgill (20).

Silicates

(a) The System CaF_2–$CaSiO_3$

Our results differ considerably from those of Baak and Olander (22) which correspond to $\nu = 1/3$ and were interpreted by them as evidence for cyclic $Si_3O_9^{6-}$ ions in the melt. Their results were in line with X-ray crystallographic data for pseudowollastonite, believed to have a ring structure (23). The discrepancy between our results and those of Baak and Olander is well beyond experimental error and amounts to 20 °C at the highest concentrations of solute. The reason for this discrepancy is at present unknown.

The results in Fig. 3 correspond, in the limit, to 1 foreign ion per molecule of $CaSiO_3$. The simplest anion which satisfies the tetrahedral coordination requirement of silicon and yields 1 foreign ion per molecule is SiO_3F^{3-} and the results are discussed below on the basis that such ions condense to yield linear chains of general formula $(SiO_3)_nF^{(2n+1)-}$ as the concentration of

Can. J. Chem. Downloaded from www.nrcresearchpress.com by 210.87.254.5 on 09/05/12
For personal use only.

silicate increases. Evidence for the presence of chains rather than rings in this system has been given by Mitchell (24). Buehler and Bues (25) showed the presence of PO_3F^{2-} ions in fluorophosphate melts by Raman spectroscopy, and concluded that anions with more than 1 fluorine atom were not formed.

Consider the self-condensation of SiO_3F^{3-} anions in a fluoride melt. Polyanions, each terminated by 1 fluorine atom, can be formed in the following steps

$$[1,1]\quad SiO_3F^{3-} + SiO_3F^{3-} = Si_2O_6F^{5-} + F^- \qquad k_{11}$$

$$[1,2]\quad SiO_3F^{3-} + Si_2O_6F^{5-} = Si_3O_9F^{7-} + F^- \qquad k_{12}$$

$$[1,3]\quad SiO_3F^{3-} + Si_3O_9F^{7-} = Si_4O_{12}F^{9-} + F^- \qquad k_{13}$$

etc.

It has been shown previously (26, 27) that polycondensation reactions of this nature can be treated by assuming that, as a first approximation, the equilibrium constants $k_{11}, k_{12}, k_{13}, \cdots k_{1n}$ are identical. The treatment is similar to that developed by Tobolsky and Eisenberg (28). The same assumption is made here. Strictly speaking, this assumption is valid only for linear polymers in the limit of high values of n. Refinement to include variation of k_{1n} with n for nonlinear polymers is possible on the basis of theoretical considerations developed elsewhere (29), but as the above model is tentative and the degree of branching unknown, this refinement is not considered to be warranted at present.

From eqs. [1,1], [1,2], [1,3], $\cdots$ and the above assumption, it follows that

$$[6]\quad N_{(SiO_3)_nF} = \left(\frac{k_{1n}N_{SiO_3F}}{N_{F'}}\right)^{n-1} N_{SiO_3F}$$

where N is the ion fraction of the species indicated. (In this and subsequent equations, the charge associated with each silicate ion is, for simplicity, omitted in expressions for ion fractions; fluoride and oxygen ions are denoted by F′ and O″.)

Hence, for the sum of the ion fractions of fluorosilicate ions

$$[7]\quad \sum_{n=1}^{\infty} N_{(SiO_3)_nF} = N_{SiO_3F}\sum_{n=1}^{\infty}\left(\frac{k_{1n}N_{SiO_3F}}{N_{F'}}\right)^{n-1} = N_{SiO_3F}\left(\frac{1}{1 - k_{1n}N_{SiO_3F}/N_{F'}}\right)$$

As fluoride and fluorosilicate are the only species of anion in the melt, their sum, in the Temkin formulation (30), equals unity.

$$[8]\quad \sum_{n=1}^{\infty} N_{(SiO_3)_nF} + N_{F'} = 1$$

From eqs. [7] and [8]

$$[9]\quad N_{SiO_3F} = \frac{1 - N_{F'}}{1 + k_{1n}\left(\frac{1}{N_{F'}} - 1\right)}$$

To use this expression, we must relate the mole fraction of CaF_2 to the ion fractions of the proposed constituents of the melt. The necessary relationship is

$$[10]\quad N_{CaF_2} = \frac{\text{moles } CaF_2 \text{ from fluoride} + \text{moles } CaF_2 \text{ from fluorosilicate}}{\text{moles } CaF_2 \text{ from fluoride} + \text{moles } CaF_2 \text{ from fluorosilicate} + \text{moles } SiO_2 \text{ from fluorosilicate} + \text{moles CaO from fluorosilicate}}$$

$$= \frac{\frac{1}{2}N_{F'} + \sum_{n=1}^{\infty}\frac{1}{2}N_{(SiO_3)_nF}}{\frac{1}{2}N_{F'} + \sum_{n=1}^{\infty}\frac{1}{2}N_{(SiO_3)_nF} + \sum_{n=1}^{\infty} nN_{(SiO_3)_nF} + \sum_{n=1}^{\infty} nN_{(SiO_3)_nF}}$$

From eqs. [8] and [10]

$$[11]\quad N_{CaF_2} = \tfrac{1}{2}/\left(\tfrac{1}{2} + 2\sum_{n=1}^{\infty} nN_{(SiO_3)_nF}\right)$$

From eq. [6] and the identity

$$\sum_{n=1}^{\infty} nx^{n-1} = (1 - x)^{-2}$$

we have, for the summation in the denominator of eq. [11]

$$[12]\quad \sum_{n=1}^{\infty} nN_{(SiO_3)_nF} = \frac{N_{SiO_3F}}{(1 - k_{1n}N_{SiO_3F}/N_{F'})^2}$$

Substituting for N_{SiO_3F} from eq. [9] and combining the result with eq. [11], we obtain

$$[13]\quad 1/N_{CaF_2} = 5 - 4N_{F'} + 4k_{1n}(1 - N_{F'})^2/N_{F'}$$

which yields $N_{F'}$ as a function of composition if k_{1n} is known.

By Temkin's law

$$[14]\quad a_{CaF_2} = N_{Ca^{2+}}N_{F'}^2$$

As Ca^{2+} is the only species of cation in the melt,

Can. J. Chem. Downloaded from www.nrcresearchpress.com by 210.87.254.5 on 09/05/12
For personal use only.

$N_{Ca^{2+}}$ is unity and eq. [3] for the depression of the f.p. becomes

$$[15] \qquad \ln N_{F'}^{\,2} = -\frac{\Delta H_f^{\,0}}{R}\left(\frac{1}{T} - \frac{1}{T_0}\right)$$

Values of $N_{F'}$ corresponding to arbitrary values of N_{CaF_2} were calculated by eq. [13] for various values of k_{1n}. These were substituted in eq. [15] to yield theoretical plots of f.p. against composition. Calculated curves for various values of k_{1n} are shown in Fig. 3. A value of $k_{1n} = 17 \pm 5$ fits the data within experimental error.

From this value of k_{1n}, the average chain length of the fluorosilicate ions may be calculated as a function of the composition of the melt. These details and the effect of other cations on the mean chain length will be given in a subsequent communication.

(b) The System CaF_2–Ca_2SiO_4

Our data agree with those of Mukerji (14) and of Gutt and Osborne (31).

For Ca_2SiO_4 and silicates with higher ratios of CaO/SiO_2, sufficient oxygen is available to satisfy the coordination requirement of silicon at all concentrations. Condensation of SiO_4^{4-} anions can occur in the following steps

$$[16,1] \qquad SiO_4^{4-} + SiO_4^{4-} = Si_2O_7^{6-} + O^{2-}$$

$$[16,2] \qquad SiO_4^{4-} + Si_2O_7^{6-} = Si_3O_{10}^{8-} + O^{2-}$$

$$[16,3] \qquad SiO_4^{4-} + Si_3O_{10}^{8-} = Si_4O_{13}^{10-} + O^{2-}$$

etc.

As before, it is assumed that the equilibrium constants k are identical. By a procedure analogous to that outlined above, it may be shown that

$$[17] \qquad \frac{1}{N_{SiO_2}} = 3 + \frac{N_{O''} + N_{F'}/2}{1 - N_{O''} - N_{F'}} - \frac{1}{2k}\left[\frac{2 - N_{F'}}{N_{O''}\left(\frac{1}{k} - 1\right) + 1 - N_{F'}}\right]$$

$$[18] \qquad \frac{1}{N_{CaF_2}} = 1 + \frac{2}{N_{F'}}\left\{2N_{O''}(k-1) + (1 - N_{F'})\left[2k\left(\frac{1 - N_{F'}}{N_{O''}} - 2\right) + 3\right]\right\}$$

and

$$[19] \qquad \frac{1}{N_{CaO}} = \frac{N_{O''}(3 - 2N_{O''} - 5N_{F'}/2) + 2k(1 - N_{O''} - N_{F'})^2}{(1 - N_{F'})^2 + (k-1)(1 - N_{O''} - N_{F'})^2}$$

Combination of eqs. [17] and [19] yields

$$[20] \qquad \frac{N_{CaO}}{N_{SiO_2}} = 2 - k + \frac{N_{O''}}{1 - N_{O''} - N_{F'}} + \frac{k(k-1)}{\left(k + \frac{N_{O''}}{1 - N_{O''} - N_{F'}}\right)}$$

From eqs. [18] and [20]

$$[21] \qquad N_{F'} = \frac{2(x+1)N_{CaF_2}}{(x-1) + (x+3)N_{CaF_2}}$$

where

$$[22] \qquad x = N_{CaO}/N_{SiO_2}$$

Equation [21] shows that the ion fraction of fluoride ion, and hence the depression of the f.p., is independent of k and depends only on the mole fraction of CaF_2 and the molar ratio CaO/SiO_2, a result which is self-evident if fluoride ions do not participate in the polymerization. In this case, no information can be obtained regarding the mean chain length of the polyions from measurements of the depression of the f.p. alone. The reason is, of course, that as polymerization proceeds and the number of silicate ions decreases, there is a corresponding increase in the number of free oxygen ions so that the number of foreign ions remains constant.

Substitution of $x = 2$ in eq. [21] gives, for melts which contain Ca_2SiO_4

$$[23] \qquad N_{CaF_2} = N_{F'}/(6 - 5N_{F'})$$

and combination of this result with eq. [15] yields the theoretical curve for the depression of the f.p. for all degrees of polymerization. As shown in Fig. 4, it is in good agreement with the experimental data.

Can. J. Chem. Downloaded from www.nrcresearchpress.com by 210.87.254.5 on 09/05/12
For personal use only.

Equation [23] was derived on the basis that oxygen and silicate ions behave ideally in CaF_2. As shown by the results for CaO, however, oxygen ions yield less than the ideal depression in this solvent. The good agreement of eq. [23] with the data suggests that oxygen ions are absent and the depression by Ca_2SiO_4 is due to SiO_4^{4-} ions alone. This is substantiated by the results for Ca_3SiO_5, as indicated below. It is also in line with previous conclusions (26) that Ca^{2+} ions cause almost complete depolymerization of silicate ions in melts near the orthosilicate composition.

(c) The System CaF_2–Ca_3SiO_5

Substitution of $x = 3$ in eq. [21] gives

$$[24] \qquad N_{CaF_2} = N_{F'}/(4 - 3N_{F'})$$

and combination with eq. [15] yields the theoretical curve in Fig. 4. In this case, the experimental depressions are less than predicted. As this system must contain excess oxygen ions, the result is undoubtedly due to the nonideal behavior of these ions discussed above.

Acknowledgments

The authors are grateful to Mrs. K. M. Castelliz, N. S. Technical College, who performed the X-ray diffraction measurements, and to S. G. Whiteway and I. B. Smith for valuable comments on the manuscript.

1. T. Førland. *In* Fused salts. *Edited by* B. R. Sundheim. McGraw-Hill Book Co., Inc., New York. 1964.
2. B. F. Naylor. J. Amer. Chem. Soc. **67**, 150 (1945).
3. E. M. Levin, C. R. Robbins, and H. F. McMurchie. Phase diagrams for ceramists. American Ceramic Society, Inc., Columbus, Ohio. 1964.
4. H. Kojima, S. G. Whiteway, and C. R. Masson. Can. J. Chem. **46**, 2968 (1968).
5. P. Ehrlich. *In* Handbook of preparative inorganic chemistry. Vol. 1. 2nd ed. *Edited by* G. Brauer. Academic Press Inc., New York. 1963.
6. H. B. Bell and C. R. Masson. J. Sci. Instrum. **41**, 389 (1964).
7. S. Cantor. J. Phys. Chem. **65**, 2208 (1961).
8. M. Rolin and M. Clausier. Rev. Int. Hautes Temp. Réfract. **4**, 39 (1967).
9. F. Delbove. Silicates Ind. **32**, 259 (1967).
10. M. Blander. Molten salt chemistry. Interscience Publishers, Inc., New York. 1964.
11. E. G. Chernevskaya. Opt. Spectrosc. **10**, 337 (1961).
12. E. G. Chernevskaya and G. V. Anan'eva. Fiz. Tverd. Tela, **8**, 216 (1966).
13. F. Delbove, C. Bourlange, and G. Petit. C.R. **260**, 6307 (1965).
14. J. Mukerji. Mem. Sci. Rev. Met. LX, 786 (1963); J. Amer. Ceram. Soc. **48**, 210 (1965).
15. T. Baak. Acta Chem. Scand. **8**, 1727 (1954).
16. W. W. Barker. Private communication.
17. T. Baak. Acta Chem. Scand. **9**, 1406 (1955).
18. J. Lumsden. Discuss. Faraday Soc. **32**, 97 (1961).
19. J. W. Tomlinson and B. J. Welch. J. Inorg. Nucl. Chem. **28**, 2131 (1966).
20. W. D. Threadgill. J. Electrochem. Soc. **112**, 632 (1965).
21. G. E. Moore. J. Amer. Chem. Soc. **65**, 1700 (1943).
22. T. Baak and A. Olander. Acta Chem. Scand. **9**, 1350 (1955).
23. J. W. Jeffrey. *In* The chemistry of cements. Vol. I. *Edited by* H. F. W. Taylor. Academic Press, Inc., New York. 1964. p. 138.
24. A. Mitchell. Trans. Faraday Soc. **63**, 1408 (1967).
25. K. Buehler and W. Bues. Z. Anorg. Allg. Chem. **308**, 62 (1961).
26. C. R. Masson. Proc. Roy. Soc. London, Ser. A, **287**, 201 (1965).
27. C. R. Masson. J. Amer. Ceram. Soc. **51**, 134 (1968).
28. A. V. Tobolsky and A. Eisenberg. J. Amer. Chem. Soc. **82**, 289 (1960).
29. S. G. Whiteway, I. B. Smith, and C. R. Masson. To be published.
30. M. Temkin. Acta Phys. URSS, **20**, 411 (1945).
31. W. Gutt and G. J. Osborne. Trans. Brit. Ceram. Soc. **65**, 521 (1966).
32. R. Haase. Z. Naturforsch. **8a**, 380 (1953).

Appendix

Dissociation of Solute

The term ν in eq. [4] represents the number of foreign ions per molecule of solute in the limit of low concentrations. Deviations from eq. [4] may be due to (*a*) neglect of heat capacity terms, (*b*) use of mole fractions in place of activities, and (*c*) apparent changes in ν with concentration.

The purpose of this note is to point out that deviations due to (*c*) may be larger than to either (*a*) or (*b*) and that, even when the number of foreign ions remains constant, ν as defined by eq. [4] may change appreciably with concentration.

Let S denote the number of moles of solute. Then

$$N_{CaF_2} = \frac{\text{moles } CaF_2}{\text{moles } CaF_2 + S}$$

If we assume that the solute dissociates into n foreign ions per molecule we may define

$$N'_{CaF_2} = \frac{\text{moles } CaF_2}{\text{moles } CaF_2 + nS}$$

The quantity N'_{CaF_2}, rather than N_{CaF_2}, is the correct quantity to be used in eq. [3] if the activity of CaF_2 is replaced by its mole fraction and dissociation of the solute is allowed. Thus, eq. [4] should be written

$$[4'] \qquad \frac{1}{T} \simeq \frac{1}{T_0} - \frac{R}{\Delta H_f^0} \ln N'_{CaF_2}$$

Comparison of eqs. [4] and [4′] shows that

$$\nu \ln N_{CaF_2} = \ln N'_{CaF_2}$$

This expression may also be derived from the equations of Haase (32).

Table II lists values of ν corresponding to various values of n and N_{CaF_2}. It is obvious that ν is only approximately the number of foreign ions per molecule of solute at finite concentrations. It tends to be too large when less than unity and too small when greater than unity.

The broken lines in Figs. 1 and 2 were calculated by eq. [4′] with $n = 1/4$. It is obvious that the solid lines corresponding to $\nu = 1/4$ in eq. [4] hold only in the limit of low concentrations and that deviations are due mainly to variations in ν with concentration.

TABLE II

Values of ν for various values of n, the number of foreign ions per molecule of solute

	ν for n =					
N_{CaF_2}	0.25	0.5	1	2	3	4
0.99	0.251	0.501	1	1.990	2.970	3.941
0.95	0.255	0.506	1	1.951	2.858	3.725
0.90	0.260	0.513	1	1.905	2.730	3.490
0.85	0.266	0.520	1	1.860	2.614	3.286
0.80	0.272	0.528	1	1.817	2.508	3.106

Can. J. Chem. Downloaded from www.nrcresearchpress.com by 210.87.254.5 on 09/05/12
For personal use only.

Hydrogen bonding in lidocaine salts. I. The $\overset{+}{N}H$ stretching band and its dependence on the associated anion[1]

GEORGE A. NEVILLE AND ZEPHYR R. REGNIER

Research Laboratories, Food and Drug Directorate, Department of National Health and Welfare, Ottawa, Canada

Received April 29, 1969

By means of deuterium exchange, the ν^{+}_{NH} band was identified in a series of lidocaine salts with varying anionic size. A value for the free $\overset{+}{N}$—H stretching frequency was obtained which permitted $\Delta\nu^{+}_{NH}$ to be related to anionic radius. Similar relationships were found for triethylamine and pyridinium salts using frequency data available in the literature. Four new lidocaine salts (HI, CF_3CO_2H, $HAsF_6$, and $HSbCl_6$) are reported.

Canadian Journal of Chemistry, 47, 4229 (1969)

Can. J. Chem. Downloaded from www.nrcresearchpress.com by 210.87.254.105 on 09/05/12
For personal use only.

Introduction

No critical analysis of the infrared spectra of salts of lidocaine (a tertiary aliphatic amine) has appeared in the literature. In publishing the infrared spectra of the hydrochloride monohydrate, styphnate, reineckate, tetraphenylborate, chloroplatinate, and methiodide salts of lidocaine, Rich and Chatten (1) commented briefly on the spectra in the context of their utility in the identification and differentiation of organic medicinal agents. Sandorfy and coworkers (2, 3) have conducted extensive infrared studies on the salts of various amines including triethylamine but limited the anions to the hydrohalides. Ebsworth and Sheppard have examined the di-, tri-, and tetra-methylammonium iodide salts (4), Nakanishi, Goto, and Ohashi have studied various amine hydrochloride salts (5), Nuttall, Sharp, and Waddington included trimethylammonium and pyridinium salts in their study of alkyl- and aryl-ammonium salts with a wide range of anions (6), and, most recently, Cook has made a detailed study of the infrared spectra of pyridinium salts having a wide range of anionic size (7).

In this paper we will limit our discussion to the variation in $\overset{+}{N}$—H stretching frequency (ν^{+}_{NH}) with eight different anions of varying size in the anhydrous series of lidocaine salts. By associating different anions with the same amine we can introduce a gradual change in hydrogen bond energy.

[1]Presented in part at the 51st Conference of the Chemical Institute of Canada, Vancouver, British Columbia, June 4, 1968.

Experimental

Spectra

Infrared spectra were obtained from a Perkin–Elmer Model 621 spectrometer whose calibration was periodically checked against indene. The spectra were produced from fluorolube mulls in NaCl windows over the range 4000–1350 cm^{-1} and from Nujol mulls in CsI windows over the range 1350–200 cm^{-1}. The enhanced band detail shown in Fig. 1 was achieved through the use of thicker mulls (approximately 5 times the quantity of solid usually employed for mull preparation) in conjunction with the variable expansion control of the spectrometer.

The mulls of hygroscopic salts and deuterio-salts were prepared under dry-box conditions (P_2O_5 and dry N_2).

Preparation of Salts

Lidocaine (m.p. 66–67°, Astra Pharmaceuticals Ltd.) was used without further purification for the preparation of all salts except the hydrochlorides.

Lidocaine hydrochloride monohydrate (m.p. 73–74.5°, Astra Pharmaceuticals Ltd.) was used without further treatment. The anhydrous hydrochloride was prepared from the monohydrate by drying over P_2O_5 at 55° in a mechanical pumping vacuum until constant melting at 123.5–125° was obtained. Literature melting values for the anhydrous hydrochloride are 128–129° (8) and 127–132° (9).

Lidocaine hydrobromide proved to be extremely hygroscopic. It was prepared by adding a slight molar excess of 47% aqueous hydrobromic acid to a lidocaine solution in a minimum volume of acetone. The mixture was reduced to a dry cake under water pump vacuum; then it was pulverized and dried over P_2O_5 at 55° in a mechanical pumping vacuum to obtain the constant melting range, 73.5–76.5°. The literature melting range for the anhydrous hydrobromide (127–132°) (9) appears to be erroneous since the same melting range was reported for the anhydrous hydrochloride.

Lidocaine hydrobromide monohydrate was prepared from the anhydrous salt by exposure to humid air. The gummy hygroscopic substance that quickly formed was kept over silica gel for several days during which it was progressively pulverized to a fine dry powder (m.p. 68–71°). The literature melting range for the hydrobromide monohydrate is 94–103° (9).

Can. J. Chem. Downloaded from www.nrcresearchpress.com by 210.87.254.105 on 09/05/12
For personal use only.

Anal. Calcd. for $C_{14}H_{25}O_2N_2Br$: C, 50.46; H, 7.56; N, 8.41. Found: C, 50.55, 50.58; H, 7.58, 7.60; N, 8.51, 8.51.

Lidocaine hydroiodide was prepared by addition of a slight molar excess of 49% aqueous hydrogen iodide to a concentrated aqueous solution of lidocaine. The pale yellow solid obtained by slow evaporation was recrystallized as a fluffy white solid from hot methyl ethyl ketone to which sufficient hexane was added to produce turbidity. The solid was dried as above in a pumping vacuum until a constant melting range (145.5–146.5°) was obtained.

Anal. Calcd. for $C_{14}H_{23}ON_2I$: C, 46.42; H, 6.40; N, 7.75. Found: C, 46.10, 45.90; H, 6.45, 6.44; N, 7.89, 7.66.

In contrast to the above halide salts, the hydroiodide does not form a hydrate.

Lidocaine hydrotrifluoroacetate was obtained by addition of a slight molar excess of trifluoroacetic acid to a concentrated aqueous solution of lidocaine. The crystals obtained by slow evaporation were recrystallized from mixed petroleum ether (boiling range 30–60°) – diethyl ether (1:1) and dried in a pumping vacuum to give solid, m.p. 138–139.5°.

Anal. Calcd. for $C_{16}H_{23}O_3N_2F_3$: C, 55.17; H, 6.66; N, 8.04. Found: C, 55.11, 54.84; H, 6.82, 6.52; N, 7.96, 7.91.

The infrared spectrum of the trifluoroacetate shows a strong band at 1685 cm^{-1} (asymmetric $\nu_{CO_2^-}$) and strong bands at 1200, 1170, 1160, 1130, and 1125 (sh) characteristic of the strong CF_3 stretching absorption reported for the range 1350–1120 cm^{-1} (10). The sharp, strong (s) to medium (m) peaks at 826 (s), 812 (m), 800 (s), 785 (m), and 767 (s) represent another band reported to involve the CF_3 group over the range 780–680 cm^{-1} (10).

Lidocaine hydronitrate was prepared by treating a concentrated aqueous solution of lidocaine with a slight molar excess of 1 *N* nitric acid. The solid which formed on slow evaporation was recrystallized from absolute ethanol and subjected to the usual pumping–drying until constant melting point (128–130°, decomp.) was observed. Literature melting data for the nitrate are 133–134°, decomp. (8) and 131–133° (9). The infrared spectrum shows strong bands at 1365 and 1340 cm^{-1} (asymmetric NO_3^- stretch).

Lidocaine hydrobisulfate was prepared by adding an equivalent amount of 1 *N* sulfuric acid for hydrobisulfate formation to a weighed sample of lidocaine dissolved in a minimum volume of water. The mixture was left under the hood to evaporate slowly, then it was subjected to the usual pumping vacuum until a constant melting range (196–200°) was obtained. The literature melting range for the hydrobisulfate is 210–212° (9). The infrared spectrum shows broad, medium intensity bands at 2877 and 2782 cm^{-1} (SO—H stretching) and strong bands at 1175 (asymmetric S—O stretching of $HOSO_3^-$), 1066 (symmetrical S—O stretching of $HOSO_3^-$), and 848 cm^{-1} (S—O(H) stretching).

Lidocaine hydrohexafluoroarsenate was prepared by treating lidocaine (0.64 g) dissolved in water (100 ml) in a polyethylene beaker with hexafluoroarsenic acid (0.75 g, $d_{25°}$ 1.902, Ozark-Mahoning Co.). After the mixture was heated on a steam bath, the salt was taken into solution by adding acetone (10 ml). The crystals which formed on cooling were collected and washed with water. The dry solid melted at 260–260.5°.

Anal. Calcd. for $C_{14}H_{23}ON_2AsF_6$: C, 39.63; H, 5.46; N, 6.60. Found: C, 39.93, 40.06; H, 5.66, 5.50; N, 6.57, 6.32.

Lidocaine hydrohexachloroantimonate was prepared by treating lidocaine.$HCl.H_2O$ (0.520 g) dissolved in chloroform (2 ml) with an equivalent quantity of antimony pentachloride (0.538 g, specific gravity 2.39). The yellow solid, which precipitated instantly, was collected and washed with chloroform after which it was subjected to the usual pumping–drying procedures until a constant melting range (177–180°) was obtained.

TABLE I

$\overset{+}{N}H$ and $\overset{+}{N}D$ stretching frequencies in lidocaine salts*

Salt	ν^+_{NH} (cm^{-1})	ν^+_{ND} (cm^{-1})	ν_H/ν_D
HCl	2590 b		
	2520 b, sh	*1900* b	1.33
	2450 b, sh		
$HCl.H_2O$	2640		
	2590 sh		
	2565 sh		
	2540		
	2510		
	2485		
	2470 sh		
	2460		
HBr		2067	
	2723	2016	1.34
	2690		
	2650 sh	1984 sh	
	2633	1972	1.33
		1935	
		1890	
$HBr.H_2O$	2690		
	2642		
	2623		
	2608		
	2547		
HI	2845	2150 b	1.32
	2778 sh		
	2743 sh		
	2713 sh		
	2658		
	2350		
CF_3CO_2H	2840	2190	1.30
	2760	2160 sh	
	2700 sh	2135	
	2567 sh	2123 sh	
	2505	2097	
	2360	2075	
	2325		
HNO_3	3015	2250	1.34
$H(HSO_4)$	3040	2233	1.36
	2630		
	2570		
	2540		
	2440		
$HSbCl_6$	3357 sp	2480 b	1.35
$HAsF_6$	3366 v sp	2502 b	1.35

*Center of gravity of band in italics; b, broad; sh, shoulder; sp, sharp; v sp, very sharp.

Can. J. Chem. Downloaded from www.nrcresearchpress.com by 210.87.254.105 on 09/05/12
For personal use only.

Figure 1 on p. 4231 should be as follows.

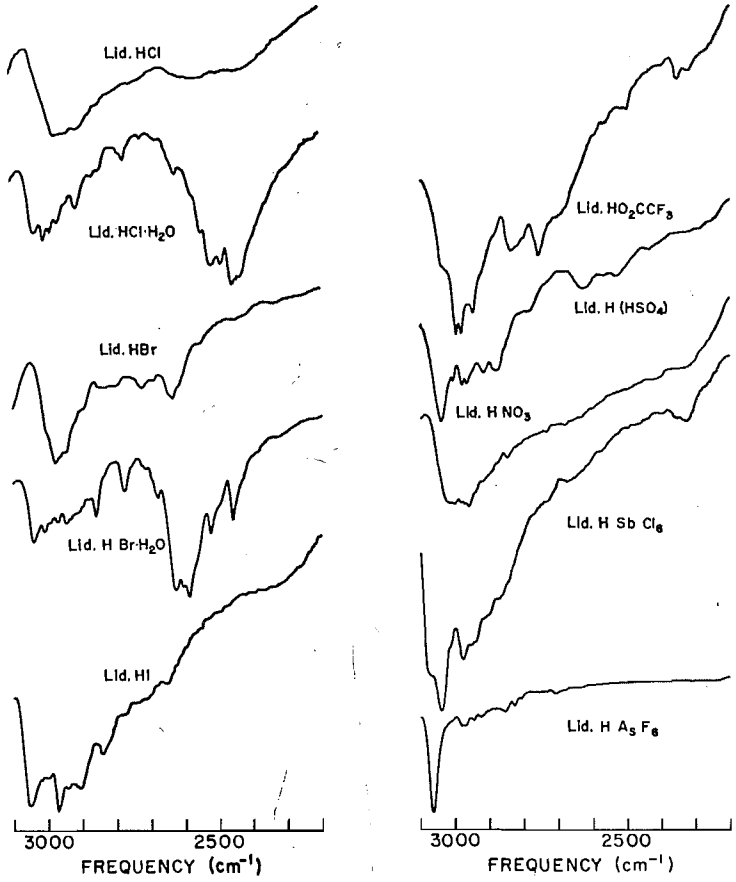

FIG. 1. Infrared spectra of lidocaine salts from 3100 to 2200 cm^{-1}.

Can. J. Chem. Downloaded from www.nrcresearchpress.com by 210.87.254.105 on 09/05/12
For personal use only.

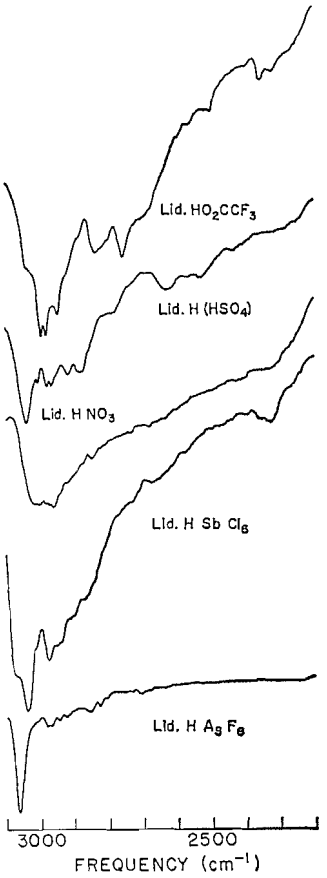

FIG. 1. Infrared spectra of lidocaine salts from 3100 to 2200 cm^{-1}.

Anal. Calcd. for $C_{14}H_{23}ON_2SbCl_6$: C, 29.51; H, 4.07; N, 4.92. Found: C, 29.24, 29.12; H, 4.12, 4.13; N, 5.17, 5.17.

Deuterium exchange of amide and ammonium hydrogen was effected in most of the salts by dissolving each salt (50–100 mg) in D_2O (1.0 ml) – DOAc (0.25 ml) and recovering the exchanged salt by mechanical pumping on a high-vacuum line. The deuteriotrifluoroacetate salt was prepared by treating lidocaine (free base) with D_2O and trifluoroacetic acid-*d*; the deuteriohexachloroantimonate salt was prepared by exchange in dimethyl sulfoxide with D_2O or in DOAc/D_2O with comparable results, and the deuterio-hexafluoroarsenate salt was prepared by exchange in acetone with D_2O. After initial heating to aid dissolution, each mixture was subjected to the pumping vacuum for 2–3 h while being heated at 100°. Infrared analysis showed that practically complete deuterium exchange was achieved under these conditions.

All melting points are reported as uncorrected and were obtained in sealed capillary tubes on a Thomas Hoover melting apparatus. The capillary tubes used for hygroscopic salts were prepared under dry-box conditions.

Carbon, hydrogen, and nitrogen analyses on the $HBr.H_2O$, HI, and $HSbCl_6$ salts were performed using an F & M Model 185 CHN analyzer. All other analyses reported were obtained from the Schwarzkopf Microanalytical Laboratory, 56-19 37th Ave., Woodside, N.Y. 11377.

TABLE II
Correlation of $\overset{+}{N}H$ stretching frequency with anionic radius in lidocaine salts

Salt	ν^{+}_{NH}* (cm^{-1})	$\Delta\nu$† (cm^{-1})	Anionic radius (Å)
HCl	2520	846	1.81
HBr	2678	688	1.95
HI	2845	521	2.16
CF_3CO_2H	2840	526	—
HNO_3	3015	351	2.62
$H(HSO_4)$	3040	326	2.92
$HSbCl_6$	3357	9	4.1
$HAsF_6$	3366	0	3.20

*Frequency for center of gravity of band.
†Frequency for free $\overset{+}{N}H$ stretching taken as 3366 cm^{-1}.

Outline of the Work

The spectra of the following salts of lidocaine were measured: hydrochloride, hydrochloride monohydrate, hydrobromide, hydrobromide monohydrate, hydroiodide, hydrotrifluoroacetate, hydronitrate, hydrobisulfate, hydrohexafluoroarsenate, and the hydrohexachloroantimonate. Spectra were also measured from the deuterio-analogs (amide ND and $\overset{+}{N}D$) of these salts. The frequency data for the ν^{+}_{NH} and ν^{+}_{ND} vibrations along with the frequency ratios are given in Table I. The spectral range, 3100–2700 cm^{-1}, of the normal salts has been reproduced in Fig. 1 to show the wealth and complexity of spectral detail.

The change in frequency ($\Delta\nu$) from that assumed for an $\overset{+}{N}H$ stretching vibration free of hydrogen bonding has been related to the ionic radius of the anion for each of the lidocaine salts (Table II and Fig. 2). The crystallographic data used for calculation of the ionic radii are given in Table III. Similar relationships were found for series of pyridinium and triethylamine salts using data obtained from the literature (Tables IV and V, Fig. 2). Upper limiting frequencies of 3366, 3300, and 3400 cm^{-1} were assumed for the free $\overset{+}{N}H$ stretching vibration in lidocaine, pyridinium, and triethylammonium salts, respectively.

Interpretation of the Spectra

The pronounced difference in the optimum quality of the spectra from lidocaine salts[2] (Fig. 1), as judged by band detail, between those of the hydrochloride and

[2]A referee has observed that some of the spectra appear to contain scattered light. This feature can be recognized from the gradual increase of apparent absorption toward higher frequencies and is dependent upon the particle size in the mull. The referee noted that the condition cannot always be helped by grinding in agreement with our experience, and did not wish to take exception to the quality of the spectra.

FOR ERRATA SEE
...1970.....p.390.....

Can. J. Chem. Downloaded from www.nrcresearchpress.com by 210.87.254.105 on 09/05/12
For personal use only.

TABLE III

Anionic radii derived from crystallographic data

	Crystallographic interatomic distance					Van der Waals radius		
Anion	Source	Symmetry	Bond	Length (Å)	Reference	Atom	Radius*	Calculated anionic radius (Å)
HF_2^-	H_nF_n	Zigzag polymer	F(H)...F	2.49	24			2.49
NO_3^-	$NaNO_3$	D_3	N—O	1.218	25	O	1.40	2.62
HSO_4^-	$KHSO_4$	C_1	S—O	1.52	26	O	1.40	2.92
AsF_6^-	$KAsF_6$	O_h	As—F	1.85	27	F	1.35	3.20
BCl_4^-	B_2Cl_4	D_{2d}	B—Cl	1.73	28	Cl	1.80	3.53
	BCl_3	D_{3h}	B—Cl	1.73	29			
$ZnCl_4^{2-}$	$(NH_4)_3ZnCl_5$	C_s	Zn—Cl	2.25	30	Cl	1.80	4.05
PF_6^-	$HPF_6.6H_2O$	O_h	P—F	1.73	31	F	1.35	4.08
$SbCl_6^-$	$SbCl_5$	D_{3h}	Sb—Cl	2.29 (basal)	32	Cl	1.80	4.1
			Sb—Cl	2.34 (apical)	32			
	$PhCOCl.SbCl_5$	O_h	Sb—Cl	2.29	33			
$SnCl_6^{2-}$	$(NH_4)_2SnCl_6$	O_h	Sn—Cl	2.41	34	Cl	1.80	4.21
$PbCl_6^{2-}$	$(NH_4)_2PbCl_6$	O_h	Pb—Cl	2.48	34	Cl	1.80	4.28
$SnBr_6^{2-}$	$(NH_4)_2SnBr_6$	O_h	Sn—Br	2.59	35	Br	1.95	4.54

*Van der Waals atomic radii are those derived by Pauling (ref. 23, p. 260).

Can. J. Chem. Downloaded from www.nrcresearchpress.com by 210.87.254.105 on 09/05/12
For personal use only.

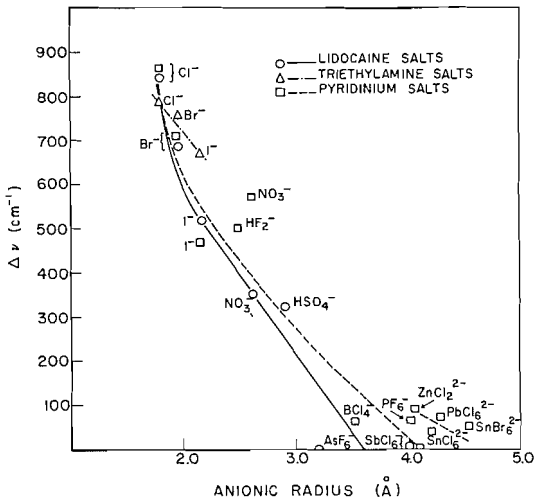

FIG. 2. Dependence of ν^{+}_{NH} on anionic radius in various salts.

hydrochloride monohydrate and between the hexachloroantimonate and the hexafluoroarsenate led us to suspect that the hydrochloride and hydrohexachloroantimonate salts were amorphous. Microscopic examination of these salts supported this hypothesis, the hydrochloride salt appearing as fragments of broken glass. X-Ray powder diffraction patterns, however, showed all four salts to be crystalline and confirmed the anhydrous nature of the hydrochloride relative to the monohydrated hydrochloride.

No attempt was made to disentangle and assign the generally poorly resolved C—H stretching bands near 3000 cm^{-1} arising from the N-ethyl substituents and the methyl substituents of the phenyl ring in these substituted ammonium salts. In this region overlapping occurs among ν_{CH_3} (asym) near 2960 ± 10 cm^{-1} (11), ν_{CH_3} (sym) near 2870 ± 10 cm^{-1} (11), ν_{CH_2} (asym) near 2930 cm^{-1} (11, 12) and those from the methyl groups of aromatic rings which usually give prominent bands near 2925 and 2865 cm^{-1} as well as variable intensity bands near 2975 and 2945 cm^{-1} (13). Although ν_{CH_2} (sym) for the CH_2 group next to nitrogen in tertiary amines is lowered from its value in hydrocarbons near 2850 cm^{-1} (11, 12) and appears near 2800 cm^{-1} (14), this effect is completely eliminated when the nitrogen acquires a positive charge in amine salts. In spite of the complexity of this region, the center of gravity of the ν^{+}_{NH} band could be located within it for the hydroiodide, hydrotrifluoroacetate, hydrobisulfate, and hydronitrate salts of lidocaine by careful comparison of the spectra from the normal salts and their deuterio-analogs. The frequency data for the ν^{+}_{NH} and ν^{+}_{ND} vibrations together with the frequency ratios are given in Table I.

The ν^{+}_{NH} band from the hydrochloride and hydrobromide of lidocaine is very broad and the center of gravity of the band shifts to higher frequency in the order Cl → Br → I. Both of these features were observed by Brissette and Sandorfy (3) from the spectra of the

TABLE IV

Correlation of $\overset{+}{N}H$ stretching frequency with anionic radius in triethylamine salts

Salt	ν^{+}_{NH}* (cm^{-1})	Δν† (cm^{-1})	Anionic radius (Å)
HCl	2613	787	1.81
HBr	2647	753	1.95
HI	2730	670	2.16

*Frequency data from Brissette and Sandorfy (3).

†Frequency for free $\overset{+}{N}H$ stretching assumed to be 3400 cm^{-1} (18).

TABLE V

Correlation of pyridinium $\overset{+}{N}H$ stretching frequency with anionic radius in various salts

Salt	ν^{+}_{NH}* (cm^{-1})	Δν†	Anionic radius (Å)
HCl	2439 (7)	861	1.81
HBr	2591 (7)	709	1.95
HI	2833 (7)	467	2.16
HNO_3	2730 (6)	570	2.62
$H(HF_2)$	2800 (6)	500	2.49
H_2ZnCl_4	3213 (7)	87	4.05
H_2PbCl_6	3230 (6)	70	4.28
$HBPh_4$	3230 (6)	70	—
HPF_6	3230 (6)	70	4.08
$HBCl_4$	3240 (6)	60	3.53
H_2SnBr_6	3251 (7)	49	4.54
H_2SnCl_6	3260 (7)	40	4.21
$HSbCl_6$	3300 (7)	0	4.1

*Numbers in parentheses are reference numbers.

†Frequency for free pyridinium $\overset{+}{N}H$ stretching taken as 3300 cm^{-1}.

hydrohalides of triethylamine, the frequency shift being in the reverse direction to that of the sharp bands between 2800 and 2400 cm^{-1} in primary and secondary amine salts. With increasing size of the anion from iodide to hexafluoroarsenate in the lidocaine salt series, the ν^{+}_{NH} frequency increases in the order $I^- \rightarrow CF_3CO_2^- \rightarrow NO_3^- \rightarrow HSO_4^- \rightarrow SbCl_6^- \approx AsF_6^-$ (Table I). While this shift to higher frequency with increasing size of anions is generally known and has been documented for salts of pyridine (6, 7), no demonstration of dependence of the ν^{+}_{NH} frequency on anionic size larger than the halides has been made for tertiary amines other than for salts of trimethylamine (6) as far as we know. Doubtless, other factors such as electronegativity, polarizability, crystal packing, and HY acid-strength are involved in the X—H...Y hydrogen bonding interaction, but this simple approach appears to offer a useful correlative procedure for an otherwise extremely complex bonding interaction.

The presence of multiple combination bands in the vicinity of the $\overset{+}{N}$—H stretching band is well displayed in the spectra from the monohydrated hydrochloride and hydrobromide salts and can also be seen on the low frequency side of the ν^{+}_{NH} band of the hydroiodide near 2500 cm^{-1}. Similar but weaker bands persist in the 2500 cm^{-1} region for the remaining salts of the series

Can. J. Chem. Downloaded from www.nrcresearchpress.com by 210.87.254.105 on 09/05/12
For personal use only.

with the exception of the hexafluoroarsenate and hexachloroantimonate salts where these bands appear to be absent. The presence of such multiple bands has been a controversial aspect of hydrogen bonding in amine salts. Sheppard (15) has reviewed the various explanations advanced in the literature for the low frequencies, and the broad and (sometimes) smooth contours observed for these bands under conditions of strong hydrogen bonding. More recently, from an analysis of band shifts, Brissette and Sandorfy (3) attributed the multiple band character seen in the ν^{+}_{NH} region in their study of tertiary amine hydrohalides to combination bands involving $\overset{+}{N}H$ deformation bands. Their interpretation is consistent with that arrived at by Bratož and Hadži (16) who demonstrated theoretically that anharmonicity in the stretching motion of a strongly bonded group (e.g. anion) gives rise to intense combination bands. For weak hydrogen bonding, they were also able to demonstrate theoretically that the combination effects could be reduced and that the ν^{+}_{NH} bands should be sharper and devoid of structure (16).

Discussion and Conclusions

The ν^{+}_{NH} band of the lidocaine salts varies in frequency from 2500 cm^{-1} in the hydrochloride to 3367 cm^{-1} in the hydrohexafluoroarsenate. The band is broad at low frequencies and becomes markedly sharper at the higher frequencies, culminating in a half width of 15 cm^{-1} for the hydrohexafluoroarsenate salt. Similar behavior has been observed and discussed by Sandorfy (hydrohalides of various amine salts) (2, 3), Nakanishi *et al.* (various amine hydrohalide salts) (5), Nuttall *et al.* (various trimethylammonium and pyridinium salts) (6), and recently by Cook (pyridinium salts) (7). Unfortunately only limited comparisons can be made since little ν^{+}_{NH} frequency data are available for salts of tertiary aliphatic amines with anions other than the halides (6). Nakanishi *et al.* (5) considered that the tetraphenylborate anion represented a case of free $\overset{+}{N}$—H stretching (near 3100 cm^{-1}); Nuttall *et al.* (6) regarded any trimethylammonium salt giving a strong ν^{+}_{NH} band near 3200 cm^{-1} to be free of hydrogen bonding; Mathieu and Poulet (17) questioned the degree of hydrogen bonding in the tetraphenylborates in particular and cited still higher frequencies (up to 3335 cm^{-1} with PF_6^-) from their study of unsubstitufed ammonium salts. For salts of pyridine, an aromatic tertiary amine, Nuttall *et al.* (6) considered those anions ($PbCl_6^{2-}$, ClO_4^-, BPh_4^-, BF_4^-, BCl_4^-, and PF_6^-) which gave ν^{+}_{NH} frequencies in the range 3230–3255 cm^{-1} to be free of hydrogen bonding[3] while Cook (7) has shown that both the reineckate and hexachloroantimonate salts of pyridine have a higher ν^{+}_{NH} frequency at 3300 cm^{-1}. In the lidocaine series, the $HSbCl_6$ and $HAsF_6$ salts give still higher ν^{+}_{NH} frequencies at 3357 and 3366 cm^{-1}, respectively, indicating weaker interionic interaction and a closer approximation to the condition of free $\overset{+}{N}$—H stretching. By comparing chemical shift values for the methylene protons from the series of lidocaine salts with those from the free base and the methiodide quaternary salt in DMSO-d_6 solution, we conclude that the tertiary amino nitrogen is strongly protonated and that $LidH^+...X^-$ is the correct model for all lidocaine salts (20).

The strong interaction between the nitrogen hydrogen and a small anion associated with an intense force field, appears to be responsible for the breadth, intensity, and low frequency that characterizes the ν^{+}_{NH} band. As the anion increases in size in the series Cl^-, Br^-, I^-, the force field weakens as the charge density decreases. For compounds containing polyatomic anions associated with weak peripheral force fields, the frequency increases until it appears that free $\overset{+}{N}$—H stretching is obtained as in the $HAsF_6$ salt. Lord and Merrifield, noting the striking breadth of X—H...Y bands in crystals, even at low temperatures, the near constancy of the band center[4] in tertiary amine hydrohalides, the structure of the bands, and the marked anharmonicity, considered such characterization to be incompatible with a simple electrostatic model of the hydrogen bond (21). Nevertheless, Lord and Merrifield showed a linear relationship between $\Delta\nu$ in stretching frequency vs. X—H...Y distance in various O—H...O strongly hydrogen bonded compounds. Similarly, Nakamoto, Margoshes, and Rundle (22) found approximately linear correlations between the N—H...Y distances and the N—H stretching frequencies in

[3]Recent crystallographic work has shown that no hydrogen bonding is found in any of the pyridinium (PyH^+) salts of PF_6^-, AsF_6^-, and SbF_6^- (18), whereas the interaction in pyridinium nitrate appears to be more correctly represented by the $PyH...NO_3^-$ model than by the $C_5H_5N...H—O—NO_2$ model (19).

[4]In succeeding years, it has been recognized that variations in the band center in tertiary amine hydrohalides are actually rather appreciable, e.g. see Tables II, IV, and V.

Can. J. Chem. Downloaded from www.nrcresearchpress.com by 210.87.254.105 on 09/05/12
For personal use only.

the systems N—H...F, N—H...O, N—H...Cl, and N—H...N.

Lacking crystallographic data for the series of lidocaine salts, we have correlated the difference in $\overset{+}{N}$—H stretching frequency ($\Delta\nu$) with the ionic radius of the respective anion (Fig. 2). The hydrohexafluoroarsenate salt was assumed to have free $\overset{+}{N}H$ stretching, and $\Delta\nu$ for the other salts was calculated on this basis. The ionic radii used for the halide anions are the crystal radii calculated by Pauling (ref. 23, p. 521) while those used for the polyatomic anions were derived by summation of crystallographically measured interatomic distances (Table III) and Van der Waals radii (ref. 23, p. 260) for the appropriate peripheral atoms of the anions. A very pleasing correlation is seen (Fig. 2) for the lidocaine salt series which suggests that the changes in ν^{+}_{NH} frequency are largely dependent on ionic size for constant anionic charge. Similar correlations were carried out for triethylamine and pyridinium salts (Fig. 2) using frequency data available in the literature (Tables IV and V). It is readily apparent from the data for the pyridinium salts that the doubly negatively charged anions constitute a class by themselves and that $\Delta\nu$ can be correlated with isoelectronic anions only. A similar correlation for a series of trimethylamine salts using the frequency data of Nuttall *et al.* (6) proved unsuccessful due to great scattering of points.

Acknowledgments

The authors wish to thank Dr. M. Przybylska and Mrs. H. M. Sheppard of the National Research Council of Canada, Ottawa, for the X-ray powder diffraction spectra and for helpful discussions concerning crystallographic data; Dr. R. N. Jones of the National Research Council of Canada, Ottawa, for his encouragement and suggestions for this work; Dr. H. S. Chang for preparing some of the salts (HBr, HI, HNO_3, $H(HSO_4)$, and CF_3CO_2H); Dr. Denys Cook for his interest in this work and for suggesting the preparation of the $HSbCl_6$ and $HAsF_6$ salts, and Mrs. Ruth Lane and Mr. Bruce Flann for the carbon, hydrogen, and nitrogen analyses on the F & M analyzer.

The gift of research samples of lidocaine and lidocaine hydrochloride monohydrate by Astra Pharmaceuticals (Canada) Ltd. is gratefully acknowledged.

1. N. W. Rich and L. G. Chatten. J. Pharm. Sci. **54**, 995 (1965).
2. B. Chenon and C. Sandorfy. Can. J. Chem. **36**, 1181 (1958).
3. C. Brissette and C. Sandorfy. Can. J. Chem. **38**, 34 (1960).
4. E. A. V. Ebsworth and N. Sheppard. Spectrochim. Acta, **13**, 261 (1959).
5. K. Nakanishi, T. Goto, and M. Ohashi. Bull. Chem. Soc. Jap. **30**, 403 (1957).
6. R. H. Nuttall, D. W. A. Sharp, and T. C. Waddington. J. Chem. Soc. 4965 (1960).
7. D. Cook. Can. J. Chem. **39**, 2009 (1961).
8. N. Löfgren. Xylocaine. Inaugural Dissertation, University of Stockholm, 1948. Reprinted by the Morin Press, Inc., Worcester, Mass., 1948. p. 60.
9. H. M. Koehler and J. J. Hefferren. J. Pharm. Sci. **53**, 1126 (1964).
10. N. B. Colthup, L. H. Daly, and S. E. Wiberley. Introduction to infrared and Raman spectroscopy. Academic Press, Inc., New York. 1964. p. 314.
11. J. J. Fox and A. E. Martin. Proc. Roy. Soc. London, Ser. A, **167**, 257 (1938).
12. J. E. Wiberley, S. C. Bunce, and W. H. Bauer. Anal. Chem. **32**, 217 (1960).
13. G. M. Badger and A. G. Moritz. Spectrochim. Acta, **15**, 672 (1959).
14. W. B. Wright, Jr. J. Org. Chem. **24**, 1362 (1959).
15. N. Sheppard. *In* Hydrogen bonding. *Edited by* D. Hadži. The Pergamon Press, Ltd., London. 1959. p. 85.
16. S. Bratož and D. Hadži. *In* Hydrogen bonding. *Edited by* D. Hadži. The Pergamon Press, Ltd., London. 1959. p. 111; J. Chem. Phys. **27**, 991 (1957).
17. J. P. Mathieu and H. Poulet. Spectrochim. Acta, **16**, 696 (1960).
18. R. F. Copeland, S. H. Conner, and E. A. Meyers. J. Phys. Chem. **70**, 1288 (1966).
19. A. J. Serewicz, B. K. Robertson, and E. A. Meyers. J. Phys. Chem. **69**, 1915 (1965).
20. G. A. Neville and D. Cook. J. Pharm. Sci. **58**, 636 (1969); and unpublished data.
21. R. C. Lord and R. E. Merrifield. J. Chem. Phys. **21**, 166 (1953).
22. K. Nakamoto, M. Margoshes, and R. E. Rundle. J. Amer. Chem. Soc. **77**, 6480 (1955).
23. L. Pauling. The nature of the chemical bond. 3rd ed. Cornell Univ. Press, Ithaca, N.Y. 1960.
24. M. Atoji and W. N. Lipscomb. Acta Cryst. **7**, 173 (1954).
25. R. L. Sass, R. Vidale, and J. Donohue. Acta Cryst. **10**, 567 (1957).
26. L. H. Loopstra and C. H. MacGillavry. Acta Cryst. **11**, 349 (1958).
27. R. B. Roof. Acta Cryst. **8**, 739 (1955).
28. M. J. Linevsky, E. R. Shull, D. E. Mann, and T. Wartik. J. Amer. Chem. Soc. **75**, 3287 (1953).
29. H. A. Levy and L. O. Brockway. J. Amer. Chem. Soc. **59**, 2085 (1937).
30. H. P. Klug and L. Alexander. J. Amer. Chem. Soc. **66**, 1056 (1944).
31. H. Bode and G. Teufer. Acta Cryst. **8**, 611 (1955).
32. S. M. Ohlberg. J. Amer. Chem. Soc. **81**, 811 (1959).
33. R. Weiss and B. Chevrier. Chem. Commun. 145 (1967).
34. G. Engel. Z. Krist. **90**, 341 (1935).
35. J. A. A. Ketelaar, A. A. Rietdijk, and C. H. Staveren. Rec. Trav. Chim. **56**, 907 (1937).

Can. J. Chem. Downloaded from www.nrcresearchpress.com by 210.87.254.42 on 09/05/12
For personal use only.

Electronic spectra of carbonato and oxalato ammine complexes of cobalt(III); average field model for singlet, triplet, and charge transfer bands[1]

V. S. SASTRI AND C. H. LANGFORD[2]
Department of Chemistry, Carleton University, Ottawa 1, Canada

Received May 22, 1969

The electronic spectra in ligand field (singlet and triplet) and charge transfer regions have been determined for a series of mixed carbonato and oxalato ammine complexes of Co(III). An average field model is shown to be quite adequate to complete interpretation of the spectra. The values of Δ appear to be dominated by σ bonding interactions. Full analysis of triplet bands reveals an abnormal C/B ratio which emphasizes the limitations to be placed on the interpretation of the values of parameters derived from first order perturbation theory parameterization of experimental spectra.

Canadian Journal of Chemistry, 47, 4237 (1969)

In the course of some kinetic studies[3], one of us had occasion to prepare a full series of carbonato and oxalato ammine complexes of Co(III) (1). The spectra of these complexes were recorded in singlet, triplet, and charge transfer regions. To our knowledge, the average field model (ref. 2, and earlier references cited therein), which treats the spectra of mixed nearly octahedral complexes in terms of the average of spectral parameters of the unmixed species, has not yet been subjected to test against such complete spectral data. Triplet bands have been recorded only comparatively rarely.

The first consequence of the analysis of the carbonato and oxalato ammine mixed systems was that the average field model proved successful to the usual degree. However, two dividends accrued. First, it emerged that the charge transfer bands in carbonato ammine complexes were readily interpretable. Second, the close analysis of triplet bands led to modification of the value of Δ (10 Dq) assigned to Co(III) and, in consequence, some modification of analysis of the evolution of Δ across the first transition series.

Experimental

Complexes were prepared by adaptation of standard procedures which have been described (1). Spectra in solution were recorded on a Cary 15 spectrophotometer. All measurements were made at room temperature. Spectral data for the spin forbidden bands were obtained with solutions nearly saturated with the complex. A sample spectrum is given in Fig. 1.

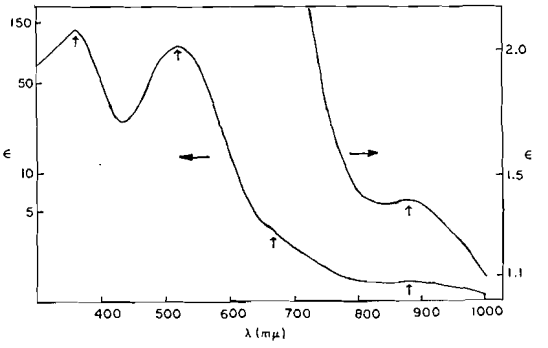

FIG. 1. Spectrum of $Co(NH_3)_4CO_3^+$ ion.

Results

Aqueous solution electronic spectral bands are recorded in Table I; assignments are indicated and calculated band maxima are given. The calculations are based on a best fit of the parameters Δ, B, and C to the spectra of $Co(NH_3)_6^{3+}$, $Co(CO_3)_3^{3-}$, and $Co(C_2O_4)_3^{3-}$, where Δ is the orbital energy difference between t_{2g} and e_g levels, B and C are the Racah interelectronic repulsion parameters[4]. For mixed complexes, weighted averages of the best fit values for $Co(NH_3)_6^{3+}$, $Co(CO_3)_3^{3-}$, or $Co(C_2O_4)_3^{3-}$ were used in the calculations. The energies of the levels of the d^6 system are taken to be (with respect to the free ion energy)

$$^1A_{1g}: \quad -2.4\Delta + 5B + 8C$$
$$^3T_{1g}: \quad -1.4\Delta + 5B + 5C$$
$$^3T_{2g}: \quad -1.4\Delta + 13B + 5C$$
$$^1T_{1g}: \quad -1.4\Delta + 5B + 7C$$
$$^1T_{2g}: \quad -1.4\Delta + 21B + 7C$$

[1]We acknowledge the financial support of the National Research Council of Canada.
[2]Alfred P. Sloan Foundation Research Fellow, 1968–1970.
[3]We are indebted to Professor G. M. Harris for his guidance of the synthetic work of V.S.S. and to Dr. H. Kelm for some samples of complexes.
[4]For an account of the development and significance of the parameters Δ, B, and C, see inter alia, ref. 3.

TABLE I

Singlet and triplet ligand field bands of Co(III) complexes

Complex	Electronic transition	Frequency (cm^{-1}) Calculated	Observed
$[Co(NH_3)_6]^{3+}$	$^1A_{1g} \rightarrow {}^1T_{1g}$	21 200	21 100
	$^1A_{1g} \rightarrow {}^1T_{2g}$	29 600	29 600
	$^1A_{1g} \rightarrow {}^3T_{1g}$	13 500	13 400
	$^1A_{1g} \rightarrow {}^3T_{2g}$	17 700	17 000
$[Co(NH_3)_5CO_3]^+$	$^1A_{1g} \rightarrow {}^1T_{1g}$	20 230	19 680
	$^1A_{1g} \rightarrow {}^1T_{2g}$	28 370	28 780
	$^1A_{1g} \rightarrow {}^3T_{1g}$	12 690	11 770
	$^1A_{1g} \rightarrow {}^3T_{2g}$	16 760	15 450
	c.t. band	—	42 910
$[Co(NH_3)_4CO_3]^+$	$^1A_{1g} \rightarrow {}^1T_{1g}$	19 280	19 150
	$^1A_{1g} \rightarrow {}^1T_{2g}$	27 200	27 780
	$^1A_{1g} \rightarrow {}^3T_{1g}$	11 840	11 380
	$^1A_{1g} \rightarrow {}^3T_{2g}$	15 800	14 950
	c.t. band	—	42 020
$[Co(NH_3)_2(CO_3)_2]^-$	$^1A_{1g} \rightarrow {}^1T_{1g}$	17 390	17 390
	$^1A_{1g} \rightarrow {}^1T_{2g}$	24 850	25 310
	$^1A_{1g} \rightarrow {}^3T_{1g}$	10 170	9 107
	$^1A_{1g} \rightarrow {}^3T_{2g}$	13 900	13 340
	c.t. band	—	40 320
$[Co(CO_3)_3]^{3-}$	$^1A_{1g} \rightarrow {}^1T_{1g}$	15 500	15 700
	$^1A_{1g} \rightarrow {}^1T_{2g}$	22 500	22 700
	$^1A_{1g} \rightarrow {}^3T_{1g}$	8 500	7 900
	$^1A_{1g} \rightarrow {}^3T_{2g}$	12 000	12 200
	c.t. band	—	38 460
$[Co(NH_3)_5C_2O_4]^+$	$^1A_{1g} \rightarrow {}^1T_{1g}$	20 400	20 300
	$^1A_{1g} \rightarrow {}^1T_{2g}$	28 600	29 200
	$^1A_{1g} \rightarrow {}^3T_{1g}$	12 700	12 300
	$^1A_{1g} \rightarrow {}^3T_{2g}$	16 800	15 500
$[Co(NH_3)_4C_2O_4]^+$	$^1A_{1g} \rightarrow {}^1T_{1g}$	19 600	19 700
	$^1A_{1g} \rightarrow {}^1T_{2g}$	27 500	28 800
	$^1A_{1g} \rightarrow {}^3T_{1g}$	11 500	11 900
	$^1A_{1g} \rightarrow {}^3T_{2g}$	15 300	15 300
$[Co(NH_3)_2(C_2O_4)_2]^-$	$^1A_{1g} \rightarrow {}^1T_{1g}$	18 300	18 000
	$^1A_{1g} \rightarrow {}^1T_{2g}$	25 800	26 300
	$^1A_{1g} \rightarrow {}^3T_{1g}$	10 300	10 400
	$^1A_{1g} \rightarrow {}^3T_{2g}$	14 000	14 000
$[Co(C_2O_4)_3]^{3-}$	$^1A_{1g} \rightarrow {}^1T_{1g}$	16 800	16 600
	$^1A_{1g} \rightarrow {}^1T_{2g}$	23 900	23 600
	$^1A_{1g} \rightarrow {}^3T_{1g}$	8 500	8 300
	$^1A_{1g} \rightarrow {}^3T_{2g}$	12 100	12 700

These formulas neglect off diagonal elements as is customary. Table II lists the relevant values of Δ, B, and C.

Discussion

Average Field Model

Note the modest but normal success of fit of calculated spectra to experimental spectra indicated in Table I. This indicates the reasonable success of an average field model when both singlet and triplet excitations are considered. Other examples indicate that this works only for *cis* complexes (4).

The Charge Transfer Bands

There is a linear relationship (Fig. 2) between the carbonato complex charge transfer (c.t.) energy and the ligand field (l.f.) bands with positive slope. This suggests assignment of the c.t. bands as ligand-to-metal. If the likely analogy between halide and oxygen donor ligands holds, this band is ligand $\pi \rightarrow$ metal e_g. It is noteworthy

Can. J. Chem. Downloaded from www.nrcresearchpress.com by 210.87.254.42 on 09/05/12
For personal use only.

TABLE II

Racah parameters and Δ values

Complex	Δ (cm^{-1})	B (cm^{-1})	C (cm^{-1})
$[Co(NH_3)_6]^{3+}$	25 000	524	3 825
$[Co(NH_3)_5CO_3]^{+}$	24 000	509	3 770
$[Co(NH_3)_4CO_3]^{+}$	23 000	495	3 720
$[Co(NH_3)_2(CO_3)_2]^{-}$	21 000	466	3 610
$[Co(CO_3)_3]^{3-}$	19 000	437	3 500
$[Co(NH_3)_5C_2O_4]^{+}$	24 300	511	3 873
$[Co(NH_3)_4C_2O_4]^{+}$	23 600	497	4 020
$[Co(NH_3)_2(C_2O_4)_2]^{-}$	22 300	467	4 018
$[Co(C_2O_4)_3]^{3-}$	20 900	443	4 113

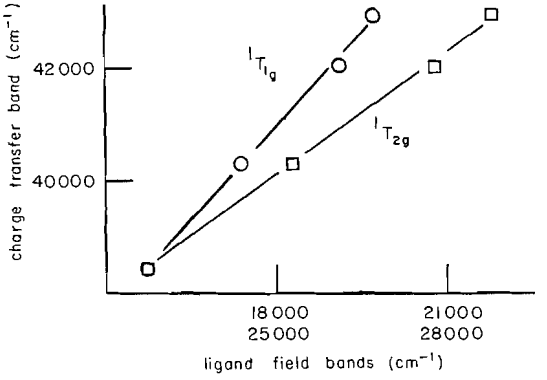

FIG. 2. Plot showing the linear relationship between charge transfer and ligand field energies.

that the slope of the correlation is almost unity between the $^1A_{1g} \rightarrow {}^1T_{1g}$ ligand field band and the c.t. band. The correlation slope is only 0.7 between $^1A_{1g} \rightarrow {}^1T_{2g}$ and c.t. bands but it is known (5) that the $^1T_{2g}$ state of $O_h d^6$ Co(III) has the configuration $t_{2g}{}^5e$ mixed significantly with $t_{2g}{}^4e^2$. We shall return to this point in the next section. At present, it seems fair to conclude that the linear relationship between the $\pi \rightarrow e_g$ c.t. transition energy and the $t_{2g} \rightarrow e_g$ ligand field transition energy strongly implies that *movement of the e_g levels dominates changes in both.* The e_g levels are σ^* and it would appear that changes from N to O donor ligands predominately change σ *bonding levels.* Δ appears to be determined by Δ_σ *not* Δ_π effects in the language of Wentworth and Piper (2).

The constancy implied for ligand π levels is an instance of the applicability of the independent ligand model (3).

The C/B Ratio and the Significance of Δ

It is usually assumed that the C/B ratio is approximately 4 as in the case of free ion spectra (3). When only the two singlet bands of Co(III) are measured, B is the only Racah parameter determinable and C is taken to equal $4B$. Since C is the parameter used to find Δ, this has led to Δ values lower by nearly 2000 cm^{-1} than those given here for $Co(NH_3)_6{}^{3+}$ and $Co(C_2O_4)_3{}^{3-}$. The discrepancy emerges when it is recognized that C/B ratios from the present analysis lie close to 8. The value of B usually obtained in a first order perturbation model may certainly be criticized. Usually, one calculates a B value from the $^1T_{1g}$–$^1T_{2g}$ splitting. This splitting is also influenced by $t_{2g}{}^5e_g$ mixing with $t_{2g}{}^4e_g{}^2$ in the $^1T_{2g}$ term. When only singlet bands are measured, the calculated B is low. Consequently, the estimated C is lower than the value given here and the value of Δ is also low. Such Δ values must be cautiously compared with those obtained where no estimate of B is required to get Δ. For example, a recent paper (6) compares Δ for Cr(III) and Co(III). It concludes that ligands with filled π levels which raise the π^* t_{2g} of the complex lead to decreasing Δ with increasing atomic number (or d″), that ligands without π symmetry orbitals are associated with constant Δ, and that ligands with empty π orbitals (acceptors) lead to increasing Δ. These results were taken to emphasize the importance of π interactions in a molecular orbital interpretation of Δ. In that paper, different parametrization schemes were used for different Co(III) complexes. Our results *do not* confirm the trends (Table III) which emphasize π interactions.

We do not wish to suggest that it is desirable to parameterize spectra of complexes in more elaborate terms or to make regular use of off diagonal elements. Other weaknesses in the approximation schemes of ligand field theory probably render additional sophistication nearly

Can. J. Chem. Downloaded from www.nrcresearchpress.com by 210.87.254.42 on 09/05/12
For personal use only.

TABLE III

Comparison of Δ values for d^6 and d^3 systems.

Ligand	Δ (cm^{-1}) Cr(III)*	Co(III)
$6NH_3$	21 600	25 000
$3C_2O_4^{2-}$	17 500	20 900
$3CO_3^{2-}$	—	19 000

*Values from ref. 3.

meaningless as the success of an assumed O_h symmetry for the present definitely non-octahedral complexes should indicate. Rather, the intention of these last paragraphs is to emphasize the critical requirement for consistent parameterization when different systems are to be compared.

1. V. S. SASTRI. Ph.D. Thesis, State University of New York at Buffalo, Buffalo, New York. 1966.
2. R. A. D. WENTWORTH and T. S. PIPER. Inorg. Chem. **4**, 709 (1965).
3. C. K. JORGENSON. Absorption spectra and chemical bonding in complexes. Addison–Wesley Publishing Co., Inc., Reading, Mass. 1962.
4. S. YAMADA, A. NAKAHARA, Y. SHIMURA, and T. TSUCHIDA. Bull. Chem. Soc. Jap. **28**, 222 (1955).
5. J. S. GRIFFITH. The theory of transition metal ions. Cambridge Univ. Press, London, England. 1961. p. 312.
6. J. ALEXANDER and H. B. GRAY. J. Amer. Chem. Soc. **90**, 4260 (1968).

Can. J. Chem. Downloaded from www.nrcresearchpress.com by 210.87.254.42 on 09/05/12
For personal use only.

Electrochemical generation of hydridopentamminerhodium(III) and its reaction with molecular oxygen

LESLIE E. JOHNSTON[1] AND JOHN A. PAGE
Department of Chemistry, Queen's University, Kingston, Ontario
Received July 8, 1969

The electrochemistry of $Rh(NH_3)_5OH^{2+}$ has been studied in a buffered ammoniacal solution. The polarographic reduction wave at the dropping mercury electrode had $E_{1/2}^0$ equal to -1.10 V (vs. saturated calomel electrode) in a 0.10 *M* NH_3 – 0.10 *M* NH_4ClO_4 electrolyte, and gross Hg cathode electrolysis at -1.19 V produced a stable $Rh(NH_3)_5H^{2+}$ hydride species. Both reductions were found to take place through a Rh(I) intermediate.

The reaction of the $Rh(NH_3)_5H^{2+}$ with molecular O_2 in the ammoniacal electrolyte was also studied. The product was demonstrated to be a stable $Rh(NH_3)_4(OH)(O_2H)^+$ hydroperoxo species.

Canadian Journal of Chemistry, 47, 4241 (1969)

Can. J. Chem. Downloaded from www.nrcresearchpress.com by 210.87.254.105 on 09/05/12
For personal use only.

Introduction

In a previous study (1), the electrochemical reduction of $RhPy_4Cl_2^+$ in aqueous pyridine was examined. The inability to demonstrate the formation of a Rh(III) hydride species paralleled the failure of the Wilkinson group (2–5) to chemically prepare a stable Rh(III) hydride in a similar medium. However, they were successful (6) in preparing $[Rh(NH_3)_5H]SO_4$ and this hydride was found to be stable in aqueous solution (7); this in turn prompted this electrochemical study of the rhodium(III) ammine system.

Gillard *et al.* (2) discussed the work done on the electrolytic reduction of $Rh(NH_3)_5Cl^{2+}$ and indicated that a 2 faradays per mole process at the dropping mercury electrode (d.m.e.) was consistent with diffusion data, although the coulometric studies by others indicated a 3 faradays per mole reduction. However, in the work reported here, the $Rh(NH_3)_5OH^{2+}$ complex and a buffered NH_3–NH_4ClO_4 electrolyte were used on account of the stability of the solution (8) and the absence of the pre-wave or maximum that was observed in polarography of solutions containing even minute amounts of chloride. A 2 faradays per mole reduction of $Rh(NH_3)_5OH^{2+}$ to stable $Rh(NH_3)_5H^{2+}$ has been characterized by coulometry, half-wave potential measurements, hydrogen ion consumption on gross electrolysis, and an identification of the reduced solution species.

The in situ generation of $Rh(NH_3)_5H^{2+}$ afforded an opportunity to study the reaction of the hydridic species with molecular O_2. Wilkinson (6, 7) has referred to a blue complex that results from the reaction of $Rh(NH_3)_5H^{2+}$ and O_2. More recently (9), Wilkinson has stated that the blue complex is likely aquotetramminerhodium (III)-μ-superoxoaquotetramminerhodium(III) formed from the initial product of the reaction, hydroperoxopentamminerhodium(III). This study, by a quantitative determination of the reaction stoichiometry and by examination of the product of the controlled potential reduction of the oxygen complex, shows that the initial reaction gives a stable hydroperoxo species.

Experimental

All potentials reported are in volts relative to a mercury calomel electrode used in conjunction with a 2.0 *M* $NaNO_3$ salt bridge. The reference electrode used throughout was a Metrohm EA-402 saturated KCl calomel electrode.

A three electrode system was used to record polarograms and to determine $E_{1/2}^0$ (1, 10) values and wave form parameters. This employed a Wenking Model 61 RS potentiostat to control the potential of the d.m.e. relative to a reference electrode in the working compartment of the cell. A Philbrick/Nexus Q3-A1P Stabilized Amplifier functioning as a current-to-voltage transducer (R = 100 kohm) was used to convert the polarographic current to a voltage suitable for display on a Hewlett–Packard Model 7100 B recorder (response time = 0.5 s). For normal polarography the potential was scanned manually; for $E_{1/2}^0$ and wave form parameter determination, the current was recorded as a function of time over a series of mercury drops at various fixed potentials on the rising part of the wave.

A conventional jacketed H-cell, thermostated at 25.0 °C and employing a frit/$NaClO_4$ agar gel to separate the working and counter compartments, was used. The d.m.e. had a flow rate of 1.401 mg s^{-1} with a drop time of 4.23 s at -1.20 V in a solution that was 0.851 m*M* in $Rh(NH_3)_5OH^{2+}$ and 0.1 *M* in each of NH_3 and

[1]Present address: Department of Chemistry, Erindale College, University of Toronto, Toronto 16, Ontario.

Can. J. Chem. Downloaded from www.nrcresearchpress.com by 210.87.254.105 on 09/05/12
For personal use only.

NH_4ClO_4, and with the ionic strength (μ) adjusted to 1.00 *M* with added $NaClO_4$.

Controlled potential coulometry was carried out as previously described (1). The electrolyte volume in the working electrode compartment of the cell varied between 75 and 100 ml, and the Hg cathode had an area of 19 cm^2. For the measurement of pH a Beckman Research pH meter was used with a Fisher 13-639-250 glass electrode and the calomel reference electrode used in conjunction with a 2.0 *M* $NaNO_3$ bridge. The meter was standardized against a borax solution, prepared according to the directions of the National Bureau of Standards from their sample 187*a* (pH = 9.180 at 25.0 °C).

All solutions for polarography and coulometry were deaerated with nitrogen gas. Before use, the N_2 (Matheson, purified) was passed through an acid vanadium(II) solution (10), scrubbed with water, then equilibrated with ammonia by passage through 3 successive towers filled with the appropriate supporting electrolyte.

All chemicals used were reagent grade. The starting material for preparation of rhodium salts was $[Rh(NH_3)_5Cl]Cl_2$ supplied by Johnson, Matthey Chemicals Limited (Lot B/6). The aquopentammine salt $[Rh(NH_3)_5H_2O](ClO_4)_3$ was prepared according to Bushnell, Lalor, and Moelwyn-Hughes (11) and a stock $Rh(NH_3)_5OH^{2+}$ solution was prepared by dissolution of this salt in NH_3–NH_4ClO_4 electrolyte (each 0.1 *M*). This stock solution was standardized coulometrically after perchloric acid fuming (1) (vanadium catalyst was not required in destroying the ammine complex). Typical analyses gave rhodium concentrations of 8.60 ± 0.03 m*M*. Solutions for polarography and electrolysis were prepared by volumetric dilution of this stock solution using standard NH_3 and NH_4ClO_4 solutions to provide the various concentrations and pH values desired; in all cases $NaClO_4$ solution was also added to give a total ionic strength of 1.00 *M*.

A sample of $[Rh(NH_3)_5H](ClO_4)_2$ was prepared according to Thomas, Osborn, Powell, and Wilkinson (7). The compound's infrared spectrum matched the ones reported. The method of Lebedinski (12) was used to prepare $[trans\text{-}Rh(NH_3)_4Cl_2]Cl$; this salt was then hydrolyzed in a 0.1 *M* NaOH electrolyte whereby complete conversion to $trans\text{-}Rh(NH_3)_4(OH)_2^+$ is affected according to Johnson, Basolo, and Pearson (13).

The ultraviolet and visible spectra were obtained on a Bausch and Lomb 505 Spectrophotometer using matched 10.0 or 1.0 cm quartz cells. During the controlled potential reduction, spectra were obtained by means of a flow connection to the electrolysis vessel. Solution from the vessel was circulated through 1.0 cm flow cells in the spectrophotometer by a peristaltic pump (LKB-Produkter Ab., Type 4912A, full speed flow ca. 8 ml/min) using neoprene tubing. The spectrum of the air-sensitive $Rh(NH_3)_5H^{2+}$ species was obtained by adding the perchlorate salt to deaerated supporting electrolyte in the electrolysis vessel (used as a dissolution vessel only) and circulating the resultant solution through the flow cell. This same flow cell arrangement was also used to follow the uptake of oxygen by the electrochemically generated $Rh(NH_3)_5H^{2+}$ species.

For the determination of the stoichiometry of the reaction between $Rh(NH_3)_5H^{2+}$ and O_2, the consumption of dissolved O_2 was followed polarographically. The $Rh(NH_3)_5H^{2+}$ was prepared by the reduction of $Rh(NH_3)_5OH^{2+}$ (> 1 m*M*) in a small, known volume of concentrated NH_3–NH_4ClO_4 electrolyte (each > 1 *M*). The electrolyses were carried out under N_2 using a Hg cathode controlled at −1.19 V; the cell was a 200 ml round-bottom flask with a Hg inlet at the bottom and ground glass fittings for the counter electrode compartment, reference probe, and N_2 dispersion tube. Stirring was by a magnetic stirring bar. When the reduction was judged complete, the Hg was withdrawn, then the N_2 inlet was removed and the electrolyzed solution diluted with O_2 saturated distilled water. The cell was completely filled so that no gas pockets remained over the solution, then it was completely sealed ($[NH_3] = [NH_4ClO_4] = 0.2\ M$ on dilution).

The solution was stirred for 4 h, the cell was then opened and the electrolyte immediately polarographed, yielding a reduction current due to excess O_2 ($E_{1/2}$ −0.05 and −1.1 V) and the Rh–O_2 complex ($E_{1/2}$ −0.33 and −1.03 V). The solution was then deaerated and again polarographed to determine the reduction current due to the Rh–O_2 complex. The decrease in current at −0.54 V was then proportional to the original concentration of unreacted O_2. The proportionality factor was determined by polarography of a solution prepared by diluting concentrated O_2-free supporting electrolyte with O_2-saturated distilled water. The O_2 content of the saturated distilled water was obtained from the solution temperature and solubility data (1.23 m*M* O_2 at 25 °C). A blank run performed in the absence of rhodium indicated that a 6% loss of oxygen was experienced in the course of the reaction.

Results

Polarographic Reduction of $Rh(NH_3)_5OH^{2+}$

A well defined cathodic wave was obtained in the NH_3–NH_4ClO_4 electrolyte. While it showed a limiting current plateau only over a small range of potential before the discharge of the supporting electrolyte, the measurements showed a linear relation between the limiting current and concentration of the $Rh(NH_3)_5OH^{2+}$. Diffusion control was demonstrated through the constancy of $i_l/h_{corr}^{1/2}$ (10) and a temperature coefficient for i_l of +1.4% $°C^{-1}$ over the range 5 to 30 °C.

The effect of ammonia concentration and pH on the half-wave parameter $E_{1/2}{}^0$ (1, 10) was

TABLE I

Variation of $E_{1/2}{}^0$ with NH_3 concentration*

$[NH_3]$ (moles l^{-1})	Slope† (mV)	$E_{1/2}{}^0$ (V)
0.10	−71.6	-1.10_0
0.50	−76.6	-1.10_3
1.00	−74.5	-1.11_0

*$[Rh(NH_3)_5OH^{2+}] = 0.851$ m*M*, $[NH_3] = [NH_4^+]$, pH = 9.35 ± 0.1, $\mu = 1.00\ M$ ($NaClO_4$).
†$E_{d.m.e.}$ vs. $\log\{i/(i_d - i)\} - 0.546 \log t$.

Can. J. Chem. Downloaded from www.nrcresearchpress.com by 210.87.254.105 on 09/05/12
For personal use only.

TABLE II

Variation of $E_{1/2}{}^0$ with pH*

pH	Slope† (mV)	αn	$E_{1/2}{}^0$ (V)
8.37	−73.0	0.744	-1.02_0
8.64	−73.8	0.736	-1.04_0
8.90	−72.5	0.748	-1.05_9
9.08	−72.0	0.754	-1.07_3
9.32	−71.0	0.760	-1.09_3
9.40	−80.3	0.674	-1.10_2
9.47	−66.7	0.812	-1.09_6
9.62	−67.6	0.800	-1.10_5
9.68	−76.3	0.709	-1.11_9
9.90	−69.0	0.785	-1.13_1
10.33	−70.2	0.772	-1.14_9

*$Rh(NH_3)_5OH^{2+}$ = 0.427 mM, pH < 9.4, $[NH_3]$ = 0.10; pH ≥ 9.4, $[NH_3]$ = 1.00; varying $[NH_4ClO_4]$ to give desired pH, μ = 1.00 M ($NaClO_4$).
†$E_{d.m.e.}$ vs. $\log\{i/(i_d - i)\} - 0.546 \log t$.

studied. At constant pH and variable ammonia concentration the $E_{1/2}{}^0$ values were relatively constant (Table I). A similar study at constant ammonia concentration showed a pH dependence of $E_{1/2}{}^0$ (Table II). For pH > 9.4 the variation of αn precluded analysis of the data. However, for pH < 9.4, αn was reasonably constant and a plot of $E_{1/2}{}^0$ vs. pH had a slope of −77.6 mV per pH unit (Fig. 1). For an average αn of 0.748, this gives a value of p equal to 0.98

$$\frac{d(E_{1/2}{}^0)}{d(pH)} = -\frac{0.05915}{\alpha n} p$$

and indicates that a fast reaction involving the uptake of one proton occurs prior to the electron transfer step.

Controlled Potential Reduction of $Rh(NH_3)_5OH^{2+}$

Gross electrolysis of the $Rh(NH_3)_5OH^{2+}$ complex was carried out on a mercury pool cathode controlled at −1.19 V in the NH_3–NH_4ClO_4 electrolyte (each 0.1 M). The electrolysis current decayed only to about 5% of the initial value and similar behavior was noted in reductions at −1.09 and −1.14 V. The net quantity of electricity used in the reductions was determined by extrapolation of the final linear portion of the coulogram back to zero time and a 2 faradays per mole reduction was indicated (Table III). It would appear that the relatively high background is due to a cyclic process involving the reduced rhodium species, for the supporting electrolyte by itself gave no such discharge. Presumably the reduced rhodium was oxidized in a slow reaction with the solvent, and this, in turn, reduced at the cathode. The small steady-state concentration of oxidized rhodium would result in the observed background current.

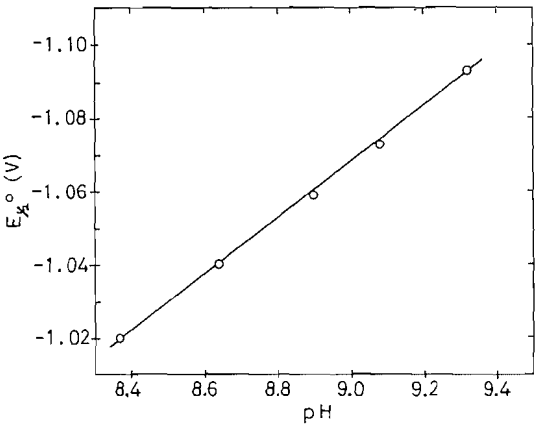

FIG. 1. Variation of $E_{1/2}{}^0$ with pH, $[Rh(NH_3)_5OH^{2+}]$ = 0.427 mM, $[NH_3]$ = 0.10, NH_4ClO_4 varied to control pH, μ = 1.00 M ($NaClO_4$); 25.0 °C.

Hydrogen ion consumption in the gross electrolysis was also studied by a titration technique. A series of reductions was carried out in which the pH of the electrolyte was maintained at its initial value by the addition of standard acid as necessary to replace the hydrogen ion consumed in the reduction. The pH was controlled within ±0.001 pH unit and titrations of about 5 ml of 0.02 M $HClO_4$ solution with a discrimination of 0.1 ml were typical.

To enhance the discrimination, these electrolyses were carried out in a relatively dilute NH_3–NH_4ClO_4 electrolyte at pH values somewhat removed from that of the optimum buffer capacity of the system. Three electrolyses were carried out at pH 8.45 and three at pH 8.60.

TABLE III

Coulometric reduction of $Rh(NH_3)_5OH^{2+}$*

Initial $Rh(NH_3)_5OH^{2+}$ (mM)	Electrolysis† (C)	n (faradays/mole Rh)
0.543	8.30	2.11
0.543	8.17	2.08
0.432	6.56	2.10
0.432	6.40	2.05
0.259	3.88	2.08
0.259	3.70	1.99

*Hg cathode at −1.19 V, T = 25 °C, 74.93 ml solution, $[NH_3]$ = $[NH_4{}^+]$ = 0.10, pH = 9.3, μ = 1.00 M ($NaClO_4$).
†Corrected for background.

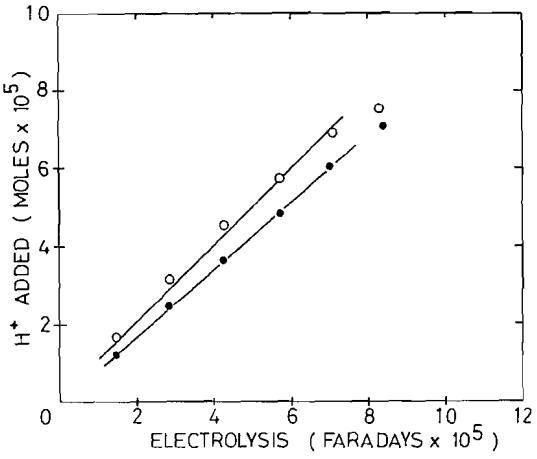

FIG. 2. Consumption of H^+ in reduction of $Rh(NH_3)_5OH^{2+}$. Initial $[Rh(NH_3)_5OH^{2+}] = 0.517$ mM, Hg cathode at -1.19 V, room temperature, 90.0 ml solution; ○, pH 8.45, $[NH_4^+] = 0.100$; ●, pH 8.60, $[NH_4^+] = 0.050$, varying $[NH_3]$ to give desired pH, $\mu = 0.100\ M$ ($NaClO_4$).

For each run, the moles of acid added were plotted against the quantity of electricity passed and typical plots are shown (Fig. 2). Good linearity was observed in each plot, except towards the end of the reductions. In the initial part of the reduction the background is negligible with respect to the total quantity of electricity passed, but at the end of the run the background effect would be the sole consumer of electricity. For the 6 runs, the observed slopes were 0.93 ± 0.09 moles H^+ consumed per faraday of electricity passed, corresponding to 1.8_6 moles H^+ consumed per mole of rhodium(III) reduced. This result is very close to the integral 2 expected for the formation of a $Rh(NH_3)_5H^{2+}$ product.

Characterization of the Reduced Species

The spectrum of the prepared $[Rh(NH_3)_5H](ClO_4)_2$ was obtained in the NH_3–NH_4ClO_4 electrolyte (both 0.4 M). Under the anaerobic conditions employed, 2 peaks were observed at 300 mμ ($\varepsilon = 300$) and 257 mμ ($\varepsilon = 400$).

The spectral changes during controlled potential reduction of a 2.36 mM $Rh(NH_3)_5H^{2+}$ solution in the same electrolyte were also followed. The final reduced solution had two absorption maxima at 300 mμ ($\varepsilon = 293$) and 257 mμ ($\varepsilon = 370$). However, the behavior during reduction depended upon the rate of mechanical stirring at the Hg cathode solution interface. With slow, steady stirring, spectra taken at intervals of time showed a clear-cut isobestic point at 326 mμ ($\varepsilon = 136$) throughout the reduction. Typically, in such cases the plot of ln i vs. t had a slope of -3×10^{-4} s^{-1} ($t_{1/2} = 2 \times 10^3$ s).

In contrast, with stirring that was much more vigorous than that normally employed, the isobestic point was not observed. The plots of ln i vs. t were only approximately linear but the initial slope was of the order of -3×10^{-3} s^{-1}. Typically, it was observed that the absorbance at 326 mμ increased from 0.32 to 0.38 over about the first 10 min of the reduction, then rapidly fell back to the original value. This behavior indicates that appreciable concentrations of some intermediate are present in the rapid electrolysis; this intermediate is presumably the first product of the electrode reaction, but does not build up to a detectable concentration in the slow reduction.

Nature of Product in $Rh(NH_3)_5H^{2+}$–O_2 Reaction

The reduction product of the gross electrolysis was observed to react readily with O_2. A peak grew at 237 mμ and an isobestic point was observed at 287 mμ as O_2 was introduced into the solution. The extinction coefficient at 237 mμ was 3800 l mole^{-1} cm^{-1} assigned on the basis of a clean complete reaction of the rhodium.

A polarographic reduction of the complex formed was observed after the excess O_2 was removed with N_2. The two polarographic steps found were of equal height, with $E_{1/2}$ values -0.33 and -1.03 V, respectively. The constancy of $i_l/h_{corr}^{1/2}$ indicated a diffusion controlled reduction.

This clean-cut behavior was important in that it permitted the polarographic determination of the stoichiometry of the $Rh(NH_3)_5H^{2+}$–O_2 reaction. The consumption of O_2 from a solution containing known concentrations of O_2 and $Rh(NH_3)_5H^{2+}$ was determined by the differential current measurement (vide supra) at -0.54 V, a potential where both O_2 and the Rh–O_2 complex are reduced under diffusion control. After applying the blank correction, the average found was 0.99 ± 0.07 mole of O_2 consumed per mole of $Rh(NH_3)_5H^{2+}$ (Table IV).

Gross reduction of this Rh–O_2 complex on a mercury cathode controlled at -0.70 V was carried out in the NH_3–NH_4ClO_4 electrolyte (each 1.0 M). The electrolysis proceeded smoothly to a negligible residual current (20–40 μA) and the quantity of electricity when corrected for background effects corresponded closely to 2

Can. J. Chem. Downloaded from www.nrcresearchpress.com by 210.87.254.105 on 09/05/12
For personal use only.

TABLE IV

Oxygen consumption by $Rh(NH_3)_5H^{2+}$

Initial $[Rh(NH_3)_5H^{2+}]$ (mM)	Initial $[O_2]$ (mM)	Final $[O_2]$ (mM)	O_2 loss (mM)	ΔO_2 (net) (mM)	O_2/Rh
0.268	1.06	0.76	0.06	0.24	0.90
0.265	1.05	0.72	0.06	0.27	1.02
0.530	1.03	0.47	0.06	0.50	0.94
0.526	1.03	0.40	0.06	0.57	1.08
					Ave. 0.99 ± 0.09

faradays per mole of rhodium (Table V). The spectrum of the product showed peaks at 302 mμ (ε = 123) and 345 mμ (ε = 93) and these match the spectrum of the prepared *trans*-$Rh(NH_3)_4(OH)_2^+$. After the reduction at −0.70 V was complete, a shift of the cathode potential to −1.20 V produced further reduction characterized by a high background current. The final solution had the same ultraviolet spectrum as $Rh(NH_3)_5H^{2+}$.

TABLE V

Coulometric reduction of rhodium–oxygen complex*

Initial [Rh] (mM)	Electrolysis† (C)	n (faradays/mole Rh)
0.591	10.18	1.98
0.591	10.23	1.99
0.469	8.13	2.00

*Hg cathode at −0.70 V, room temperature, 90.0 ml solution $[NH_3] = [NH_4^+] = 1.00$, pH = 9.3.
†Corrected for background.

The formation of the $Rh–O_2$ complex was also studied in an electrolyte of lower NH_3 concentration ($[NH_3] = [NH_4ClO_4] = 0.20$) and the rate was observed to be somewhat slower.

The $Rh–O_2$ complex was found to give an oxidation wave at a rotating platinum micro electrode with $E_{1/2} \approx +0.5$ V in the NH_3–NH_4ClO_4 electrolyte (each 1.0 M). Gross electrolysis at a platinum gauze anode controlled at +0.75 V showed an oxidation of approximately 1 faraday per mole of rhodium. During the electrolysis the solution became pink, but the color did not persist and had virtually disappeared at the end of the electrolysis (60 min).

In another reaction, the addition of 72% aqueous perchloric acid to the $Rh–O_2$ complex solution caused the solution to turn blue (absorption maximum, 556 mμ). As the acid concentration was increased from 1 to 40% (v/v), the extinction coefficient increased from 36 to 145 l $mole^{-1}$ cm^{-1}; at 40% $HClO_4$ the extinction coefficient was still increasing.

Discussion

This study shows that the electrochemical reduction of $Rh(NH_3)_5OH^{2+}$ proceeds to the hydridic species $Rh(NH_3)_5H^{2+}$. The reaction does not proceed directly to a Rh(III)–H species, for the shift of $E_{1/2}{}^0$ with pH indicates a unit involvement of hydrogen ion in the electrode process at the d.m.e. This may be accounted for by an equilibrium of the type

[1] $Rh(NH_3)_5OH^{2+} + H^+ \rightleftharpoons Rh(NH_3)_5H_2O^{3+}$

preceding the electron transfer step. Another valid interpretation of the pre-electrolysis equilibrium would be

[2] $Rh(NH_3)_5OH^{2+} \rightleftharpoons Rh(NH_3)_5{}^{3+} + OH^-$

but in both cases the initial product of the two-electron charge transfer would be a Rh(I) species

[3] $Rh(NH_3)_5H_2O^{3+} + 2e \rightarrow Rh(NH_3)_5H_2O^+$

or

$$Rh(NH_3)_5{}^{3+} + 2e \rightarrow Rh(NH_3)_5{}^+$$

and is the same result as was found in the electrochemical reduction of $RhPy_4Cl_2^+$ (1). The fate of this transient Rh(I) species was defined by the overall consumption of 2 moles of H^+ per mole of rhodium on gross electrolysis. This implies a bulk solution reaction of the sort

[4] $Rh(NH_3)_5H_2O^+ + H^+ \rightarrow Rh(NH_3)_5H^{2+} + H_2O$

or

$$Rh(NH_3)_5{}^+ + H^+ \rightarrow Rh(NH_3)_5H^{2+}$$

following the electrode reaction. This was substantiated by spectral studies that identified the Rh(III)–H as the final stable electrolysis product. The disappearance of the isobestic point upon

Can. J. Chem. Downloaded from www.nrcresearchpress.com by 210.87.254.105 on 09/05/12
For personal use only.

rapid electrolysis is also evidence for these steps, since under conditions of rapid electrolysis, reaction [4] is apparently too slow to consume the Rh(I) species as it is formed, so that the absorbance at 326 mμ is due to three complexes, not just two.

The stoichiometry of the Rh(III)H–O_2 reaction was important in establishing the nature of the product. Two obvious possibilities (9) are the simple hydroperoxo product that would require an exact 1:1 stoichiometry, and the dimerized μ-superoxo complex which would show (unfortunately) a near 1:1 combining ratio

[5] $Rh(III)H^{2+} + O_2 \rightarrow Rh(III)—O—O—H^{2+}$

[6] $8Rh(III)H^{2+} + 7O_2 + 4H^+ \rightarrow 4\{Rh(III)—\dot{O}—O—Rh(III)^{5+}\} + 6H_2O$

However, the choice between the two can be made unequivocally from the electrochemical behavior of the product which undergoes a clean 2 faradays per mole reduction at −0.70 V. The only reaction consistent with this would be the reduction of the hydroperoxo species

[7] $Rh(III)—O—O—H^+ + H^+ + 2e \rightarrow Rh(III)OH^{2+} + OH^-$

The reduction of the dimerized μ-superoxo complex would (fortunately) give a quite different relation. Wilkinson (9) has suggested that under some conditions the hydroperoxo complex may dimerize to give a blue superoxo complex and this may be the reaction that takes place upon acidification with $HClO_4$. The pink species formed on electrolysis of the hydroperoxo complex at +0.5 V may be a superoxo complex as well, since the oxidation required 1 faraday per mole of rhodium

[8] $Rh(III)—O—O—H^{2+} \rightarrow Rh(III)—\dot{O}—O—H^{3+} + e$

but in the alkaline medium the complex evidently decomposes.

The remaining ligands on the hydroperoxo complex are of interest. Since the reduction product was demonstrated to be *trans*-$Rh(NH_3)_4(OH)_2^+$, it is likely the hydroperoxo complex exists as *trans*-$Rh(NH_3)_4(OH)(O_2H)^+$. This is not surprising, for Wilkinson (6, 7) has demonstrated the *trans* labilizing power of the hydridic ligand

[9] $Rh(NH_3)_5H^{2+} + H_2O \rightleftharpoons Rh(NH_3)_4(H_2O)H^{2+} + NH_3$

and the hydroperoxo group probably has a stronger effect.

Acknowledgments

This study was supported by operating grants from the National Research Council of Canada and the Province of Ontario. The award of a National Research Council Scholarship to L. E. Johnston is also gratefully acknowledged.

1. L. E. Johnston and J. A. Page. Can. J. Chem. **47**, 2123 (1969).
2. R. D. Gillard, J. A. Osborn, and G. Wilkinson. J. Chem. Soc. 4107 (1965).
3. J. A. Osborn, R. D. Gillard, and G. Wilkinson. J. Chem. Soc. 3168 (1964).
4. B. N. Figgis, R. D. Gillard, R. S. Nyholm, and G. Wilkinson. J. Chem. Soc. 5189 (1964).
5. R. D. Gillard and G. Wilkinson. J. Chem. Soc. 3594 (1963).
6. J. A. Osborn, A. R. Powell, and G. Wilkinson. Chem. Commun. 461 (1966).
7. K. Thomas, J. A. Osborn, A. R. Powell, and G. Wilkinson. J. Chem. Soc. A, 1801 (1968).
8. S. C. Chan. Aust. J. Chem. **20**, 61 (1967).
9. G. Wilkinson. Private communication.
10. L. Meites. Polarographic techniques. 2nd ed. Interscience Publishers, Inc., New York. 1965.
11. G. W. Bushnell, G. C. Lalor, and E. A. Moelwyn-Hughes. J. Chem. Soc. A, 719 (1966).
12. Jacob Kleinberg (*Editor*). Inorganic syntheses. Vol. 7. McGraw-Hill Book Co., Inc., New York. 1963. p. 216.
13. S. A. Johnson, F. Basolo, and R. G. Pearson. J. Amer. Chem. Soc. **85**, 1741 (1963).

Can. J. Chem. Downloaded from www.nrcresearchpress.com by 210.87.254.105 on 09/05/12
For personal use only.

A ^{14}N nuclear magnetic resonance study on nitrogen–oxygen–halogen compounds

A. M. QURESHI, J. A. RIPMEESTER, AND F. AUBKE[1]

Department of Chemistry, The University of British Columbia, Vancouver 8, British Columbia

Received July 7, 1969

^{14}N nuclear magnetic resonance spectra of nitrogen oxides, fluorides, and oxyhalides have been recorded using direct measurement with a broad line nuclear magnetic resonance spectrometer. Also investigated are some nitrogen-containing fluoro- and oxo-cations in protonic solvents. Using the side band technique, fine structure due to ^{14}N–^{19}F spin–spin interaction could be resolved for nitrogen trifluoride, nitrogenoxide trifluoride, and nitrylfluoride.

Canadian Journal of Chemistry, 47, 4247 (1969)

Can. J. Chem. Downloaded from www.nrcresearchpress.com by 210.87.254.6 on 09/05/12
For personal use only.

Introduction

Due to an extremely poor natural sensitivity and quadrupole line broadening effects, ^{14}N nuclear magnetic resonance (n.m.r.) has found only limited use in spite of the high natural abundance of the ^{14}N isotope (99.635%). Whereas a fairly large number of spectra of organic compounds (1) have been recorded, only a very few studies are concerned with inorganic compounds (1, 2–5). For many inorganic nitrogen compounds, handling and corrosion problems exist. This has added to the fact that information is limited and agreement between different studies often poor.

The present study is concerned mainly with oxides, fluorides, and oxyhalides of nitrogen. The bonding in these compounds is subject to much discussion (6). Also included are nitrogen-containing heterocations in solution of strong protonic acids and dinitrogen tetroxide in solution of non-polar-oxygen-and-π-donor solvents. It was hoped to obtain a consistent series of ^{14}N chemical shifts of good accuracy to permit π-electron density calculations, currently in progress, using the molecular orbital method.

Of all published methods to record ^{14}N spectra (7), the method of Acrivos (8) seemingly promised the best resolution in order to resolve fine structure due to ^{14}N–^{19}F spin–spin interaction. Previous attempts (5) to observe fine structure had failed. Compared to the internuclear double resonance (INDOR) (9, 10) technique, a direct measuring method could be extended also to compounds without fluorine or protons attached to nitrogen.

[1]To whom correspondence should be addressed.

Experimental

Method

^{14}N resonances were recorded using a Varian DP60 spectrometer. A Varian 12 in. magnet provided the resonance field of about 13 000 G. The magnetic field was stabilized using a V-K 3506 flux stabilizer and swept using a V-K 3507 slow sweep unit. The frequency used was 4.000 MHz, provided by a V 4210 variable frequency r.f. unit stabilized by a crystal oscillator.

Two methods were used for recording the spectra. To resolve fine structure, the method of Acrivos was used with the modulation frequency and amplitude greater than the resonance line width. The modulation frequency generally used was 432 c.p.s. The ratio of the modulation amplitude to the modulation frequency $\beta = \gamma H \text{ mod}/\omega$ mod was equal to 1.54.

As can be seen in Fig. 1 it was not possible to phase out the centerband completely under this condition. The centerband, however, was of lesser intensity and also of opposite phase, so that reasonably well resolved absorption mode spectra could be obtained. This method has been found to give a higher resolution, because there is no line broadening arising from the finite modulation amplitude in the derivative method.

Chemical shifts were obtained by the sample replacement method, using the NO_3^- as a reference in a 4.5 *M* solution of NH_4NO_3 in 3 *M* aqueous HCl. The confidence limit is ±5 p.p.m. or better for most of the values obtained.

Samples were placed in 15 mm o.d. tubes for room temperature studies. For low temperature studies samples contained in ~10 mm o.d. tubes were placed in a Dewar containing slush baths as cooling agents. The sample tubes were made from Pyrex, quartz, or fluorocarbon resin depending on the system studied. The tubes were flame sealed or closed by teflon stem Fisher-Porter greaseless stopcocks and aluminum valves. Temperatures were monitored by placing a copper–constantan thermocouple next to the sample during the measurement. The accuracy of the temperature measurements was judged to be ±2.0 °C.

Materials and Preparative Methods

Nitrylfluoride and nitrogen trifluoride (Penninsular Chem. Research), nitrogendioxide (Matheson of Canada Ltd.), nitrosyl hydrogensulfate (Columbia Organic Chemicals), and tetrafluorohydrazine (Air Product Chemicals)

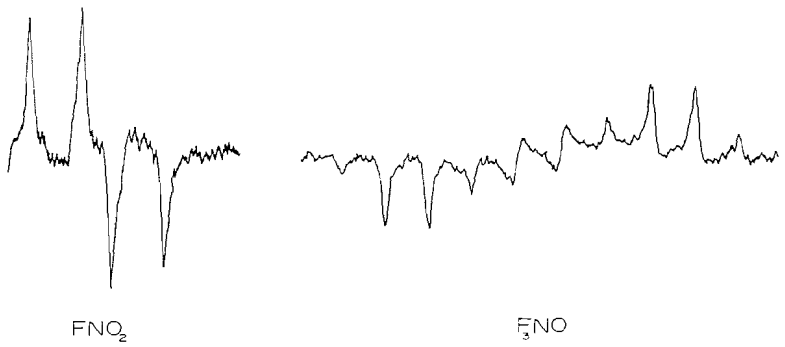

FIG. 1. ^{14}N–^{19}F fine structures.

were purchased, generally of research grade purity and further purified by vacuum distillation. Nitrosylchloride (ref. 11, p. 511), nitrosylbromide (ref. 11, p. 513), dinitrogenpentoxide (ref. 12, p. 83), chlorine(I) nitrate (ref. 12, p. 127), nitryl fluoride (13), nitrylchloride (14) and Cl_2O (15) (used in making chlorine nitrate) were all prepared using the literature methods. Nitrogen oxide trifluoride ONF_3 was obtained from Dr. J. M. Shreeve of the University of Idaho.

Nitronium- and nitrosonium-fluorosulfate, used as solutes to obtain the cations NO^+ and NO_2^+, were prepared by the interaction of nitric oxide (Matheson of Canada Ltd.) and nitrogendioxide with peroxydisulfuryl difluoride, $S_2O_6F_2$ (16). Details of this method together with solution studies in HSO_3F will be published later (17). The solutes ONF_2AsF_6 (18) and $N_2F_3AsF_6$ (19) were prepared from ONF_3 and N_2F_4, respectively, interacting with stoichiometric amounts of arsenic pentafluoride (Penninsular Chem. Research) as described. The products were characterized by their infrared spectra. Technical grade fluorosulfuric acid (Allied Chemical Corp.) was purified by double distillation in a nitrogen atmosphere. Solutions in anhydrous hydrogen fluoride (Matheson of Canada Ltd.) were prepared in Kel-F sample tubes using a monel metal vacuum line.

Where possible the purity was checked by infrared spectroscopy using a monel metal cell with silver chloride windows for gaseous samples. All solvents were of reagent grade purity and dried over molecular sieves.

Results and Discussion

The obtained ^{14}N chemical shifts together with previously reported values are listed in Table I. They now allow a more general discussion on trends of ^{14}N chemical shifts because the majority of the simple fluorides, oxides, and oxyhalides are listed together with a number of nitrogen containing ions. The chemical shifts of the two isomers of difluorodiazine are calculated on the basis of our value for nitrogen trifluoride. They had been determined originally by the double resonance technique (2) and were reported with NF_3 as a reference.

The agreement with previously reported chemical shifts is generally fair and often well within the reported confidence limits. Smaller discrepancies found for the oxyfluorides, FNO and FNO_2, are possibly caused by the extreme reactivity of the compounds. We have tried to eliminate the possible contamination due to wall reactions by using metal storage vessels and transfer systems and measuring the compounds in quartz tubes.

A large discrepancy is found for the chemical shift of the nitronium cation NO_2^+, apparently caused by the different ways in which the cation is produced. Kent and Wagner, who reported a chemical shift of 46 p.p.m., have used a 2:1 mixture of concentrated sulfuric acid and concentrated nitric acid, a mixture frequently used in preparative chemistry in aromatic substitution reactions. It must be regarded as very doubtful whether this procedure will lead to a quantitative formation of the NO_2^+ cation. An equilibrium of the following type is more likely

$$HNO_3 + 2H_2SO_4 \rightleftarrows NO_2^+ + 2HSO_4^- + H_3O$$

The reported ^{14}N chemical shift for 100% nitric acid is $+50 \pm 10$ p.p.m. upfield from NO_3^- in the ammonium nitrate reference and is relatively close to the above value.

Addition of sulfur trioxide to the sulfuric and nitric acid mixture will be expected to remove the H_3O^+ from the equilibrium and shift it gradually to the right side. This has been confirmed by us and was previously observed by Ogg and Ray in H_2SO_4 (21). The observed resonance signal is in

Can. J. Chem. Downloaded from www.nrcresearchpress.com by 210.87.254.6 on 09/05/12
For personal use only.

TABLE I

^{14}N chemical shifts δ(p.p.m.) from NO_3^-

Type of compounds	Compounds	Solvent	Temperature (°C)	$\delta^{14}N$ (p.p.m.) This work	$\delta^{14}N$ (p.p.m.) Reported	Reference
Nitrogen oxides	$ONNO_2$	Neat	−50		−67±10	4
	$ONNO_2$	Neat	−50		−302±10	4
	N_2O_4	CCl_4	−16 to −32	+15±3	11±10	4
	N_2O_4	$CHCl_3$	−30 to −58	+15.5 to +17.2		
	N_2O_4	C_6H_6	−20 to −42	+17.0 to +18.0		
	N_2O_4	CH_3NO	−18.5 to −56	+18.7 to +20.3		
	N_2O_4	$(CH_3)_2SO$	−19	+18.2		
	N_2O_4	CH_3COOH	−27 to −42	13.9 to 17.6		
	N_2O_4	HSO_3F	+25	+89		
	N_2O_5	$CHCl_3$	−25	+48±2	+60	22
					+48	21
	HNO_3	100%			50±10	34
					47.5±5	22
Nitrogen fluorides	NF_3	Neat	−152	+8	+6	5
	N_2F_4	Neat	−110	+35	+47.8	2
	cis-N_2F_2				−5.3	2
	trans-N_2F_2				−67.2	2
Nitrogen oxyhalides	ClNO	Neat	−20	−224±5	−207	35
	BrNO	Neat	−20	−352±5	−329	35
	FNO	Neat	−78	−116	−104	5
	FNO_2	Neat	−110	+81.6	+65	5
	$ClNO_2$	Neat	−20	+68	+63	35
	$ClONO_2$	Neat	−78	+43.6		
	F_3NO	Neat	−110	+131±5	+134	5
Nitrogen cations and anions	NO_2^+	HSO_3F	+25	+129	+46	3
	NO^+	HSO_3F	+25 and lower	Broad	+125	21
	NO_2^-	H_2O	+25	−250±10	−247	36
	NO_3^-	H_2O	+25	0		
	$N_2F_3^+$	Anhydrous HF	+25	−22		

all cases a single line, the position depends on the SO_3 concentration. The value of +125 p.p.m. by Ogg and Ray for a mixture of nitric acid in oleum is in good agreement with our reported chemical shift of +129 p.p.m.

The conclusion that Kent and Wagner's value is in error and the high field value of 125 p.p.m. is more probable had been reached previously by Witanowski (22). On the other hand, NO_2SO_3F has found to be highly soluble in fluorosulfuric acid and to behave as strong electrolyte, comparable to KSO_3F. Evidence for extensive ionic dissociation has been obtained even for concentrated solutions (16).

A similar exchange equilibrium is probably responsible for the chemical shift of +89 p.p.m., obtained when N_2O_4 is dissolved in HSO_3F. It is surprising that only one ^{14}N signal is observed, since the nitrosonium cation NO^+ should be a very likely reaction product in the solvolysis of the tetroxide and has indeed been found when H_2SO_4 is used as a solvent (20). However, all attempts to detect this species by ^{14}N n.m.r. have failed using $NOSO_3F$ in fluorosulfuric acid or $NOSO_4H$ in sulfuric acid even at concentrations up to 70–80% nitrosyl hydrogen sulfate. We conclude that the resonance signal is broadened by quadrupole effects beyond detectibility limits. No previous reports on this cation could be found.

Similarly, no signal due to the F_2NO^+ cation was found, using ONF_2AsF_6 as the solute and HSO_3F and HF as solvents. Here additional difficulties arise from the limited solubility at lower temperatures and from unresolved ^{14}N–^{19}F spin–spin interaction.

For the $N_2F_3^+$ cation in HF only a single signal was obtained. Both cations have been detected previously via ^{19}F n.m.r. (19, 23), suggesting that the greater natural sensitivity of the fluorine nucleus presents a great advantage for solution studies. The limits of ^{14}N n.m.r. in this respect are evident.

Attempts to observe solvent–solute interaction when N_2O_4 is dissolved in a variety of solvents (24) at various temperatures and concentrations

Can. J. Chem. Downloaded from www.nrcresearchpress.com by 210.87.254.6 on 09/05/12
For personal use only.

Can. J. Chem. Downloaded from www.nrcresearchpress.com by 210.87.254.6 on 09/05/12
For personal use only.

are also reported in Table I. All changes in chemical shifts with temperature and also with concentration are rather insignificant and within limits of error. It appears that ^{14}N n.m.r. is not a sensitive enough method to detect this interaction in O- and-π-donor solvents, even though sufficient evidence for this interaction exists.

Some emphasis was placed on the direct detection of fine structure due to ^{14}N–^{19}F spin–spin interaction. A previous report (5) fails to observe multiplets when employing the derivative method to record the spectrum. Such a fine structure will be detectable only where molecules are highly symmetrical, the electric field gradient sufficiently small, and the quadrupole broadening largely reduced. So, when applying the more sensitive side band technique (8), fine structure could be resolved for three molecules: nitrogen oxide trifluoride ONF_3, nitrogen trifluoride NF_3, both having C_{3v} symmetry, and nitrylfluoride FNO_2, with C_{2v} symmetry. The first two compounds show quartets of roughly 1:3:3:1 intensity; the last one shows a 1:1 doublet. The spectra of F_3NO and FNO_2 are shown in Fig. 1, the coupling constants are listed in Table II together with the corresponding constants obtained via ^{19}F n.m.r. In all cases, good agreement is found. Double resonance for NF_3 led to a value of 155 c.p.s., again comparable to our value of 158 c.p.s. The temperatures where fine structure could be found are listed for the three compounds in Table I.

TABLE II

^{14}N–^{19}F spin–spin interaction

Compound	$J(^{14}N$–$^{19}F)$ (c.p.s.)		Reference
	^{14}N n.m.r.	^{19}F n.m.r.	
ONF_3	134 ± 2	135.5	37
O_2NF	109 ± 5	112.5	38
NF_3	158 ± 5	160	39

Attempts to observe fine structure for FNO failed. This is not very surprising since the ^{19}F spectrum (25) is also found to show only one broad line.

The observed ^{14}N chemical shifts reveal a fairly wide spread (from −329 p.p.m. for BrNO to +35 p.p.m. for N_2F_4) for those compounds where a lone pair on nitrogen is found, whereas the remaining compounds give rise to chemical shifts in a much smaller range (from 0 p.p.m. for NO_3^- to +131 p.p.m. for ONF_3).

Interpretation of ^{14}N chemical shifts (1, 4, 5) have stressed the dominant role played by the paramagnetic contribution to the chemical shift. This contribution σ_p is directly proportional to $1/\Delta E$, where ΔE is the excitation energy from the electronic ground state to excited states (26, 27). The most accessible excited states for the first group of compounds arise from $n_N \rightarrow \pi^*$ and $n_N \rightarrow \sigma^*$ transitions. The observed order of chemical shifts $BrNO < O_2NNO < ONO^- < ClNO < FNO <$ *trans*-$N_2F_2 <$ *cis*-$N_2F_2 < N_2F_4$ indicates an increase of ΔE, explained by an increasing stabilization of the nitrogen lone pair with increasing electronegativity of the substituents around nitrogen as pointed out by Mason and van Bronswijk (5).

A more accurate correlation of observed $n_N \rightarrow \pi^*$ and $n_N \rightarrow \sigma^*$ transitions, however, seems not possible because these electronic transitions are often very weak, the maximum difficult to determine, and unambiguous assignments often not available (28). This holds true for the nitrosyl halides where the deep brown color of the chloride (29) and bromide indicates low energy transitions in contrast to the fluoride (30) where the lowest absorption is found at 3110 Å.

In this connection it is interesting to note that the ^{14}N chemical shift for FNO is not unusually low as predicted by Holmes *et al.* (25) when commenting on the unusually large downfield shift in the ^{19}F n.m.r. spectrum. (−479 p.p.m. from $CFCl_3$) of this compound. The explanation forwarded involved the combination of a low-lying repulsive state for FNO, detected in the emission spectrum (30), about 2.4 eV above the ground state, which should affect the ^{14}N chemical shift likewise. The ^{14}N chemical shift of −116 p.p.m. is in fact the highest of all XNO compounds.

When substituting the lone pair by an oxygen atom the ^{14}N chemical shifts are moved upfield. The range for XNO_2 compounds is very narrow, e.g. FNO_2 and $ClNO_2$ exhibiting shifts separated by only 13.6 p.p.m. The separation between the corresponding XNO compounds has been 108 p.p.m. The general trend whereby the resonance moves upfield with increasing electronegativity of X has been observed for alkyl and aryl derivatives previously (31–33) and is apparently found

for inorganic derivatives too, even though the differences are quite small. An empirical rationalization of this observation by Witanowski (22) may be extended to the values reported. The highest chemical shift value is found for ONF_3 in agreement with previous work (5) where also an interpretation can be found. A more detailed discussion of the significance of the ^{14}N chemical shifts for the compounds studied here will be made when our molecular orbital calculations are completed.

Acknowledgments

We wish to thank the National Research Council of Canada for financial support, and for a post-graduate scholarship to one of us (J.A.R.). One of the authors (A.M.Q.) wishes to thank the Government of Pakistan and the Canadian External Aid Office for a Colombo Plan Scholarship. We are also indebted to Dr. Joan Mason for helpful discussion and for making some of her unpublished results available to us for comparison. We are also very grateful to Professor J. M. Shreeve of the University of Idaho for a sample of F_3NO used in this study.

1. D. Herbison-Evans and R. E. Richards. Mol. Phys. **8**, 19 (1964).
2. J. H. Noggle, J. D. Baldeschwieler, and C. B. Colburn. J. Chem. Phys. **37**, 182 (1962).
3. J. E. Kent and E. L. Wagner. J. Chem. Phys. **44**, 3530 (1966).
4. L. O. Andersson and J. Mason. Chem. Commun. 99 (1968).
5. J. Mason and W. van Bronswijk. Chem. Commun. 357 (1969).
6. M. Green. *In* Developments in inorganic nitrogen chemistry. Vol. 1. Elsevier Publishing Coop. 1966.
7. J. W. Emsley, J. Feeney, and L. H. Sutcliffe. High resolution nuclear magnetic resonance spectroscopy. Vol. 2. The Pergamon Press, Ltd., 1966.
8. J. V. Acrivos. J. Chem. Phys. **36**, 1097 (1962).
9. E. B. Baker. J. Chem. Phys. **37**, 911 (1962).
10. J. D. Baldeschwieler and E. W. Randall. Proc. Chem. Soc. London, 303 (1969).
11. G. Brauer. Handbook of preparative inorganic chemistry. 2nd ed. Academic Press, Inc., 1963.
12. S. Y. Tyree, Jr. Inorganic synthesis. Vol. IX. McGraw-Hill Book Co., Inc., New York. 1967.
13. C. T. Ratcliffe and J. M. Shreeve. Chem. Commun. 674 (1966).
14. J. C. Bailar. Inorganic synthesis. Vol. IV. McGraw-Hill Book Co., Inc., New York.
15. C. J. Schack and C. B. Lindahl. Inorg. Nucl. Chem. Lett. **3**, 387 (1967).
16. F. B. Dudley and G. H. Cady. J. Amer. Chem. Soc. **79**, 513 (1957).
17. A. M. Qureshi and F. Aubke. To be published.
18. W. B. Fox, C. A. Wamser, R. Eibeck, D. K. Huggins, J. S. MacKenzie, and R. Juurik. Inorg. Chem. **8**, 1247 (1969).
19. A. R. Young and D. Moy. Inorg. Chem. **6**, 178 (1967). J. K. Ruff. J. Amer. Chem. Soc. **87**, 1140 (1965).
20. R. J. Gillespie and S. Wasif. J. Chem. Soc. 221 (1953).
21. R. A. Ogg and J. D. Ray. J. Chem. Phys. **25**, 1285 (1956).
22. M. Witanowski. J. Amer. Chem. Soc. **90**, 5683 (1968).
23. C. A. Wamser, W. B. Fox, B. Sukornick, J. R. Holmes, B. B. Stewart, R. Juurik, N. Vanderkooi, and D. Gould. Inorg. Chem. **8**, 1249 (1969).
24. C. C. Addison and J. C. Sheldon. J. Chem. Soc. 3142 (1958).
25. J. R. Holmes, B. B. Stewart, and J. S. Mackenzie. J. Chem. Phys. **37**, 2728 (1962).
26. A. Saika and C. P. Slichter. J. Chem. Phys. **22**, 26 (1954).
27. J. A. Pople. Mol. Phys. **7**, 301 (1963).
28. A. D. Walsh. J. Chem. Soc. 2266 (1953).
29. C. F. Goodeve and S. Katz. Proc. Roy. Soc. London, Ser. A, **172**, 432 (1939).
30. H. S. Johnston and H. J. Bertin, Jr. J. Mol. Spectrosc. **3**, 683 (1959).
31. M. Witanowski, T. Urbanski, and L. Stefaniak. J. Amer. Chem. Soc. **86**, 2569 (1964).
32. M. Witanowski and L. Stefaniak. J. Chem. Soc. B, 1061 (1967).
33. M. Witanowski and L. Stefaniak. J. Chem. Soc. B, 1065 (1967).
34. Y. Masuda and T. Kanda. J. Phys. Soc. Jap. **8**, 432 (1953).
35. J. Mason. Private communication.
36. B. E. Holder and M. P. Klein. J. Chem. Phys. **23**, 1956 (1955).
37. N. Bartlett, J. Passmore, and E. J. Wells. Chem. Commun. 213 (1966).
38. R. A. Ogg and J. D. Ray. J. Chem. Phys. **25**, 797 (1956).
39. E. L. Muetterties and W. D. Phillips. J. Amer. Chem. Soc. **81**, 1084 (1959).

Can. J. Chem. Downloaded from www.nrcresearchpress.com by 210.87.254.6 on 09/05/12
For personal use only.

Anodic behavior of silver in alkaline solutions

M. J. DIGNAM, H. M. BARRETT, AND G. D. NAGY[1]
Department of Chemistry, University of Toronto, Toronto 181, Ontario
Received August 28, 1968

Data, covering a range of pH and temperature, were obtained for the anodic oxidation of electropolished silver and the results compared with electrodes which had undergone repeated oxidation and reduction cycles. The behavior of the electrode is, in the main, complex, showing, for example, autopotential cycling under certain galvanostatic conditions (~3 μA/cm², 25 °C, 0.7 *N* NaOH), the period of oscillation being about ½ h. Several other hitherto unreported phenomena were also observed. The main conclusions reached are (*i*) that 2 different mechanisms are involved in the anodic formation of Ag_2O on silver electrodes in basic electrolytes resulting in 2 types of film, 1 mechanism involves a dissolution–precipitation process, the other possibly a direct interfacial reaction; (*ii*) that the reduction of anodically formed Ag_2O films either electrochemically or in hydrogen at 800 °C leaves behind a highly porous layer of silver metal; and (*iii*) that the limiting Ag_2O film thickness is probably determined by a diffusion process occurring within the film.

Canadian Journal of Chemistry, 47, 4253 (1969)

Can. J. Chem. Downloaded from www.nrcresearchpress.com by 210.87.254.6 on 09/05/12
For personal use only.

Introduction

To date, a considerable effort has been devoted to the study of the anodic behavior of silver (for reviews see refs. 1–5). Recent studies have been stimulated in large measure by applications of the Ag/AgO electrode in batteries of high energy-to-mass ratio (6–9). In addition, however, the system has intrinsic interest, as evidenced by the numerous theories which have been advanced to explain various features of the oxidation and reduction kinetics.

In relation to galvanostatic oxidation and reduction curves, the main processes occurring have been well established. Briefly, during oxidation from bare metal, Ag_2O is first formed on the electrode to a considerable thickness at a potential slightly above the reversible potential for the reaction, followed by conversion of the Ag_2O to AgO. Upon conversion of all the Ag_2O to AgO, oxygen is evolved. During reduction, AgO is first reduced to Ag_2O, which is subsequently reduced to metal.

The present paper is concerned principally with the growth of the Ag_2O film and its termination with the formation of AgO, the data being obtained for two types of electrodes. One type was first etched in nitric acid followed by cyclic anodic oxidation and cathodic reduction. This treatment was chosen for preliminary work primarily because most published data relate to this surface treatment. Most of the data reported here were obtained for electrodes prepared by electropolishing followed by reduction in hydrogen, and for conditions covering a range of pH and temperature.

Experimental

Apparatus

Two types of cells were used. For the cyclic oxidation and reduction experiments, the cell was of a standard two-compartment design, one compartment containing the test electrode and reference electrode with Luggin capillary (situated less than 0.5 mm from the electrode), the other a large area silver electrode with anodic oxide film. The cell was thermostated to within 0.1 °C and was grease free, employing KOH-lubricated standard tapered joints for connections. The electrolyte used was prepared from conductivity water of specific conductance approaching 7×10^{-7} ohm^{-1} cm^{-1} and reagent grade KOH. The stock solution was found to be 0.986 *N* in KOH and 0.077 *N* in K_2CO_3.

Galvanostatic runs were made employing a high voltage d.c. supply connected across the cell in series with a large resistor. Potential vs. time curves were measured using a strip chart recorder and cathode follower, or an oscilloscope (rise time < 0.1 μs) and camera.

Electropolished electrodes were investigated in the cell shown in Fig. 1. The Pyrex reaction cell was double walled in construction to permit easy temperature control. The electrodes, thermometer, and gas bubbling tube were mounted in a Lucite lid held by springs to the ground upper edge of the cell. A mercury – mercuric oxide reference electrode was immersed in a small compartment within the main cell compartment. The inner compartment and main cell compartment contained electrolyte of the same composition, and a capillary arm extended from the inner compartment terminating at a position close to the surface of the silver anode. The working cathode consisted of silver foil formed in the shape of an elliptical cylinder and coated electrochemically with silver oxide.

The electrolyte used in all cases was carbonate-free

[1]Present Address: Defence Research Board, Defence Research Establishment Ottawa, Ottawa 4, Canada.

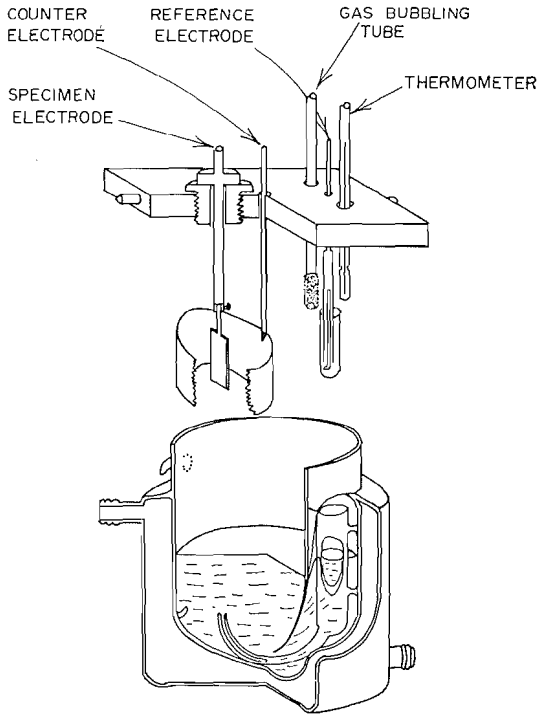

FIG. 1. Cell assembly.

sodium hydroxide. Care was taken to exclude CO_2 from the electrolyte, and to saturate freshly prepared electrolyte with Ag_2O.

The galvanostat used for the electropolished electrodes was constructed from operational amplifiers using conventional analogue computer circuits. Potentials were recorded either on a strip chart recorder or by employing an oscilloscope and polaroid camera, the recording systems being isolated by means of cathode followers.

Electrode Preparation

The test electrodes for the cyclic oxidation and reduction studies, were of dimensions 1.5 in. × 5/8 in. × 0.032 in., and were cut from a single piece of high purity silver (99.99%) obtained from Johnson, Matthey, and Mallory, Ltd. A length of 25 gauge silver wire was fused to a small tab at the top of the electrode. The electrodes were polished with numbers 1, 3/0, and 4/0 emery paper, etched in 1:1 aqueous nitric acid for 20 s, then rinsed well in conductivity water. This treatment left the surface of the electrode cream colored. The Ag/Ag_2O reference electrode and cathode were prepared in a similar manner and coated electrochemically with silver oxide.

The paddle-shaped, electropolished silver anodes, of dimensions 1/4 in. × 1 in. × 0.04 in., were punched from silver sheet stock from Johnson, Matthey, and Mallory (99.99% purity). The stem of each paddle was marked to create a level for immersion, then electropolished in a cyanide bath (35 g AgCN, 37 g KCN, and 38 g K_2CO_3 per l of water) (10) for 10 min. Following electropolishing, the majority of the electrodes were annealed in a stream of purified hydrogen for about 1 h at a temperature of 800 °C, cooled in hydrogen, then transferred to a CO_2-free desiccator. This procedure, which resulted in a bright, mirrorlike surface, gave the most reproducible kinetic results. Replacement of the hydrogen with nitrogen, annealing at lower temperatures, annealing for different times, mechanical buffing of the surface, and reduction in a furnace of a previously anodically oxidized electrode without intermediate acid washing or electropolishing were unable to surpass this preparation.

Other electrode preparations which were examined in some detail and which will be referred to in subsequent sections are summarized below, along with the main treatment outlined above, which will be referred to as Type I. (Type I, electropolished and annealed in hydrogen; Type II, electropolished only; Type III, electropolished, then anodically oxidized to completion of the Ag_2O film followed by reduction in hydrogen; Type IV, electropolished, anodically oxidized to completion of the Ag_2O film, then reduced electrochemically.)

The gases used for bubbling into the electrolysis chamber were at different times, carbon dioxide-free and water vapor-saturated nitrogen, oxygen, and air, with the choice having little or no effect on the results.

Typical Procedures for Electropolished Electrodes

To commence a run, the position of the silver electrode which was mounted in the cell holder was adjusted until the electrolyte–vapor interface coincided with the immersion mark. A box painted flat black was then lowered over the cell to exclude light, and the oxidation process initiated. On completion of a run, the specimen electrode was removed from the cell, rinsed, then dried (or rinsed and dipped in 1% nitric acid to remove the oxide, then rinsed and dried), placed in a desiccator and a new electrode mounted.

All potentials were measured against an Hg/HgO reference electrode in the same solution, but before recording, a potential of 0.244 V was added so that the zero of potential would correspond to the reversible potential for an unilluminated Ag/Ag_2O electrode. Insofar as formation of Ag_2O is concerned, therefore, the recorded potentials correspond to overpotentials.

Results

A. Cycled Electrodes

General Features of Galvanostatic Polarization Studies

Figure 2 shows a typical galvanostatic polarization curve. This curve shows the regions of Ag_2O formation (*A* to *D*), AgO formation (*E–F*), and oxygen evolution (*G–H*). The dip, *B*, and arrest, *C*, were most prominent at low apparent current densities and at higher temperatures. At low temperatures, the maximum at *A* was broader. For very high current densities, no dip or arrest could be detected. For a freshly etched electrode (one that had not been subjected to oxidation and reduction cycles), the potentials along the portion

Can. J. Chem. Downloaded from www.nrcresearchpress.com by 210.87.254.6 on 09/05/12
For personal use only.

TABLE I

Effect of succession of oxidation–reduction cycles and oxidation current on the charge and potential parameters for formation and reduction of Ag_2O films. (Apparent current density for reduction, 0.4 mA/cm²; 1 *N* KOH; 25 °C)

Cycle (or run) number	Apparent current density for oxidation (mA/cm²)	Charge passed		Potentials (V)	
		Oxidation (C)	Reduction (C)	Pt. A Fig. 1	Pt. B Fig. 1
1	0.40	7.45	6.90	0.060	0.058
2	0.40	8.55	8.26	0.025	0.020
3	0.40	8.08	7.97	0.026	0.022
4	0.08	11.82	11.82	0.020	0.016
5	0.77	7.53	7.47	0.035	0.030
6	0.04	13.36	13.20	0.015	0.013
8	0.08	11.23	11.37	0.020	0.017
9	0.77	8.45	8.42	0.032	0.030
15	0.40	12.59	12.74	0.030	0.025
16	0.08	14.81	14.86	0.025	0.019
17	0.77	10.99	10.98	0.032	0.029
18	0.04	15.68	15.64	0.022	0.018
19	0.04	16.04	16.17	0.020	0.020
20	0.04	18.16	18.22	0.030	0.023
21	0.77	14.26	14.64	0.033	0.028
22	0.77	12.42	12.60	0.030	0.023
23	0.77	10.91	10.63	0.033	0.030
24	0.77	9.10	9.29	0.038	0.033

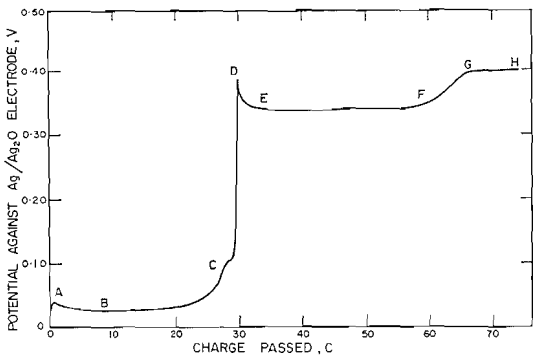

FIG. 2. Anodic polarization of Ag in *N* KOH at 25 °C. (Geometrical area of electrode, 12.6 cm²; apparent current density, 0.4 mA/cm².)

of the curve *AC* were substantially higher than those for a cycled electrode, the increase being as much as a factor of 2.

Charge Required to Complete Ag_2O Layer

Table I summarizes the data obtained for a succession of oxidation and reduction runs carried out on the same electrode at 25 °C. The oxidations were stopped when the potential reached 0.250 V, which is about 10 mV below the reversible potential for the Ag_2O/AgO couple. In all cases the reduction was carried out at an apparent current density of 0.4 mA/cm². The surface of the reduced electrode was observed to be darker than that for a freshly etched electrode, and remained so even after prolonged periods of hydrogen evolution. Because the charge passed for oxidation and reduction are in good agreement, it is reasonable to conclude that film formation and reduction took place with 100% current efficiency.

Examination of the Properties of Electrodes with Fully-Formed Ag_2O Films

Some properties of electrodes with fully-formed Ag_2O films (i.e., films formed under galvanostatic conditions to a potential of 0.250 V) were investigated in the course of obtaining the data in Table I. Two types of measurement were performed. In the first type, following completion of the Ag_2O layer as defined above, the cell was left on open circuit for a time period ranging from 3 min to 1000 h, then the same apparent current density as used to form the film was reapplied, the time being determined to charge the electrode once again to 0.250 V. The data for these experiments are summarized in Table II, insofar as the additional charge passed is concerned. The polarization curves on recharging the electrode gave rise to a hump similar to *C* of Fig. 2.

A second type of experiment was done in which, following formation of the Ag_2O layer at a high

Can. J. Chem. Downloaded from www.nrcresearchpress.com by 210.87.254.6 on 09/05/12
For personal use only.

TABLE II

Charge required to recharge "fully-formed" electrode to 0.250 V at the formation current density

Run number	Apparent current density for formation (mA/cm^2)	Time on open circuit	Additional charge required (C)
9	0.77	1017 h	0.095
10	0.04	3 min	0.004
		45 h	0.017
11	0.40	3 min	0.025
12	0.08	3 min	0.006
13	0.77	3 min	0.024
		2 h	0.037
		24 h	0.054
		41 h	0.058

TABLE III

Charge required to recharge "fully-formed" electrodes to 0.250 V at various apparent current densities. Formation current density was 0.77 mA/cm^2 for all 3 runs

Apparent current density (mA/cm^2)	Charge passed (C)		
	Run No. 27	Run No. 28	Run No. 29
0.77	14.36	11.91	10.18
0.40	0.053	0.065	—
0.08	0.085	0.044	—
0.04	0.061	0.038	0.22

current density (0.77 mA/cm^2) to a potential of 0.250 V, the cell was left on open circuit for 3 min, then repolarized to 0.250 V at a lower current density, allowed to decay on open circuit for 3 min once again, and so on. Table III summarizes the results for 3 such experiments, insofar as the charge passed is concerned.

Variation of Overpotential with Current Density for Successive Galvanostatic Conditions

Because of the large scatter in the measured potentials observed from run to run (see Table I) and the relatively small range of apparent current density used, it was not possible to determine the nature of the functional dependence of overpotential on current density from the data in Table I. The dependence was therefore determined during the course of a single oxidation run by increasing the current in 3 steps from 0.04 mA/cm^2 to 0.77 mA/cm^2, allowing only sufficient time for a steady potential to be established between steps. The process was repeated for various stages during the growth of the Ag_2O film. In order to make a correction for the slow rate of change of overpotential with charge passed, the overpotentials for each sequence of readings were extrapolated to a value for the charge passed lying at the midpoint of the particular sequence. The results of such measurements are summarized in Table IV.

Potential Decay Measurements

Open circuit potential decay measurements were obtained at various intervals during the formation of the Ag_2O film. Figure 3 illustrates a potential decay curve typical of those obtained for the region *B–C* of Fig. 2. The data are plotted in the manner of Morley and Wetmore (11), that is, in the form overpotential vs. $\log(t + \phi)$, where t is the elapsed time and ϕ is a constant chosen to linearize the initial portion of the decay. The decay of the final 20–30 mV was found invariably to give rise to an excellent linear plot on a potential vs. $\log(t)$ basis. For the particular run shown in Fig. 3, it appears probable that there is a change in the functional form of the decay at about 24 mV. This appears to be a general feature of all the decays, the position of the change varying somewhat in the range 20–30 mV.

Can. J. Chem. Downloaded from www.nrcresearchpress.com by 210.87.254.6 on 09/05/12
For personal use only.

Can. J. Chem. Downloaded from www.nrcresearchpress.com by 210.87.254.6 on 09/05/12
For personal use only.

TABLE IV

Functional dependence of overpotential on current density for Ag_2O formation at 25 °C. (Apparent current density range, 0.04 to 0.77 mA/cm^2; total charge passed for completion of Ag_2O film, 31.45 C)

Charge passed (C)	Dependence of η on I	Slope of curve (V or V cm^2/mA)	Potential range (mV)
2.73	Logarithmic	0.0137	21–39
4.63	"	0.0178	18–42
6.16	"	0.0182	19–43
7.27	"	0.0221	21–50
8.38	"	0.0200	26–52
11.40	"	0.0097	28–41
12.60	"	0.0087	26–38
15.53	"	0.0073	23–33
17.39	"	0.0069	26–35
19.55	"	0.0084	26–38
21.24	"	0.0069	26–36
23.64	"	0.0075	25–35
27.22	"	0.0094	24–37
29.50	*	—	—
30.05	Linear	0.00357	28–66
30.56	"	0.00731	28–95
30.88	†	—	—
31.27	†	—	—

*Rate of change of potential with current was too fast for $\eta \propto \log I$ but too slow for $\eta \propto I$.
†Rate of change of potential with current was too fast for $\eta \propto I$ and too slow for $\log \eta \propto I$.

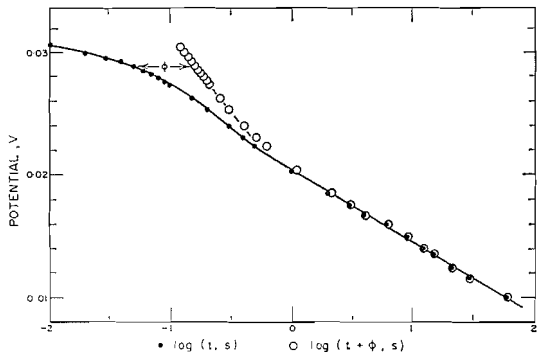

FIG. 3. Potential decay measurement for runs in which the current was interrupted near B of Fig. 2 (ϕ = 0.11 s).

The results of the measurements for the initial decay process in the region B–C are summarized in Fig. 4, in which the values for the potential decay slope (slope of potential vs. log (t)) and ϕ are plotted against the normalized charge passed. The potential decay slope for the second and slower portion of the decay was found to vary randomly from run to run between 0.004 and 0.0095 V, a period of from 4 to 8 h being required for the potential to reach essentially 0.

In order to elucidate the nature of the slow decay process, potential decay curves in the region B–C of Fig. 2 were obtained under conditions which were similar in all respects except for the resistance in parallel with the cell. For one run, a 50 kohm resistor was placed in parallel with the cell, whereas for another, the parallel resistance was that of the electrometer (about 10^{14} ohms). The potential decay slopes for the slow decay process were 0.00339 and 0.00405 V, respectively, for the 2 runs. Apparently a resistance of as low as 50 kohms across the cell has little or no effect on the rate of the slow potential decay, implying an effective electrode capacitance during the decay of about 2×10^4 μF, or more.

Potential decay measurements in the region C–D of Fig. 2 appear to give rise to 3 linear regions when plotted in the form potential vs. log ($t + \phi$). Figure 5 illustrates open circuit decays commencing from 150, 200, and 250 mV, respectively. The initial linear region appears to extend down to about 100 mV. From somewhat below 100 mV to approximately 20–25 mV, a second linear range is found with slope ranging from 0.019 to 0.023 V. The final decay took place with a slope in the range 0.007 to 0.009.

Effect of Stirring

Some experiments were carried out on cycled electrodes using a cell which permitted the effect of stirring on the electrode behavior to be examined. No significant dependence on either electrode potential or current efficiency for film

Can. J. Chem. Downloaded from www.nrcresearchpress.com by 210.87.254.6 on 09/05/12
For personal use only.

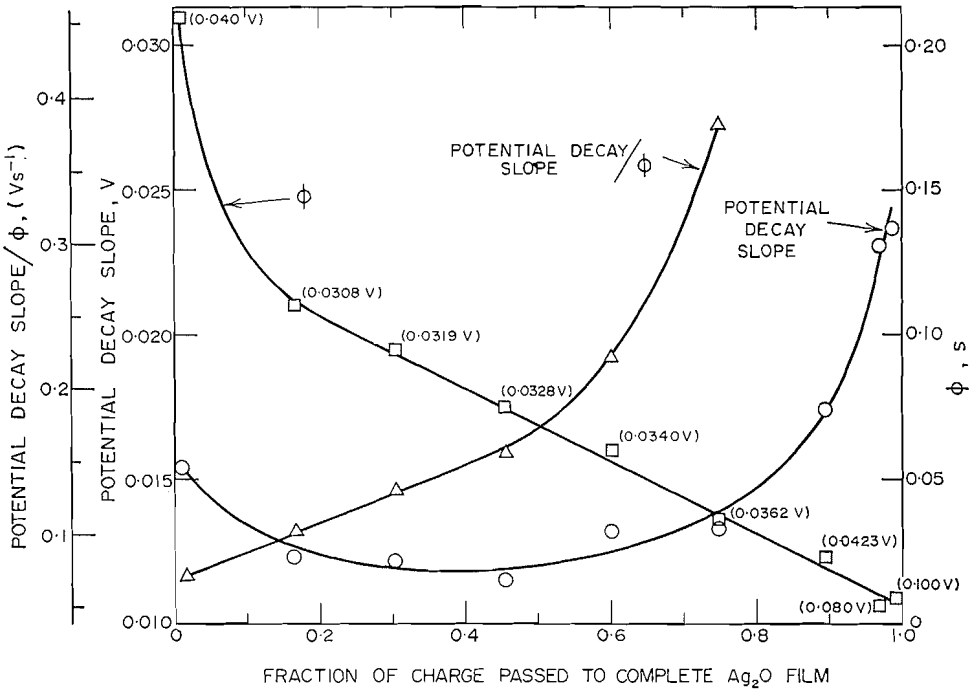

FIG. 4. Potential-decay-slope, ϕ, and potential-decay-slope $/\phi$ as functions of the fraction of charge passed to complete the Ag_2O film, for the initial decay process. (The bracketed numbers are the voltages from which the decays commenced.)

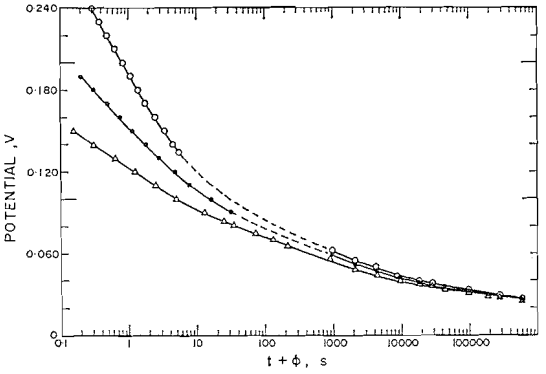

FIG. 5. Potential decay measurements for runs in which the current was interrupted in the region C–D of Fig. 2 (the 3 runs commenced from potentials of 0.150, 0.200, and 0.250 V).

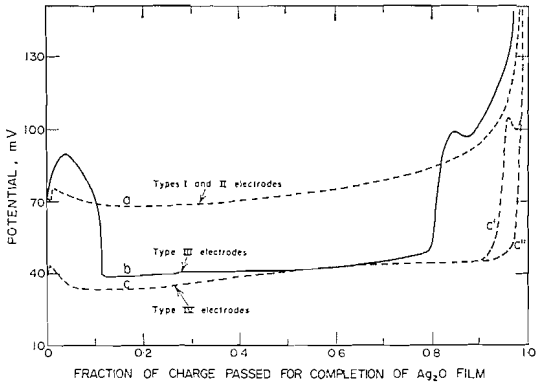

FIG. 6. Typical anodic polarization curves obtained for different electrode preparations (0.7 *N* NaOH, 27 °C, 0.25 mA/cm²).

formation on stirring could be detected, provided that the electrolyte was saturated with respect to Ag_2O.

B. Electropolished Electrodes

General Features of Galvanostatic Polarization Studies

In Fig. 6, three typical anodic polarization curves in 0.7 *N* NaOH are illustrated for 4 different types of electrode preparation. Curve (*a*) represents the usual behavior for Type I and Type II electrodes, curve (*b*), that for Type III electrodes, and (*c*), that for Type IV electrodes.

During runs designed to determine the variation of electrode potential with current density at low current densities, abrupt changes in potential

Can. J. Chem. Downloaded from www.nrcresearchpress.com by 210.87.254.6 on 09/05/12
For personal use only.

were observed. As the oxidizing current was increased in steps, a critical level would be reached at which a further increase in current led to an abrupt drop in the overpotential. The effect was reversible, so that on decreasing the current density once again the electrode potential resumed its initial higher value. This behavior is presented in greater detail in the section dealing with Tafel slopes.

A number of electrodes were observed to oscillate spontaneously between the above two potential levels under galvanostatic conditions. In extreme cases this oscillating occurred for the greater part of the galvanostatic run, as illustrated in Fig. 7. More frequently, however, only 1 to 3 of these cycles appeared just preceding the rise in potential to the Ag_2O/AgO level. It was found that stirring resulted in a reduction of the potential in the plateau regions, but had no effect in the valley regions.

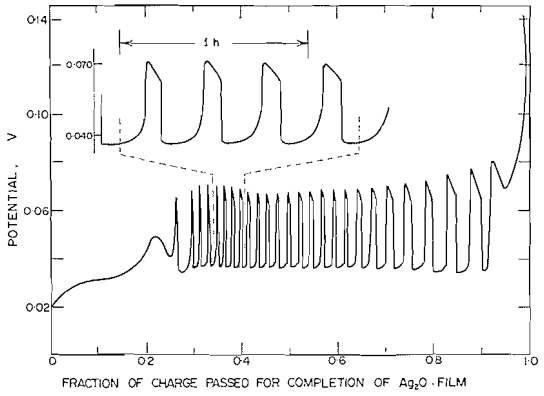

FIG. 7. Example of galvanostatic oxidation run exhibiting auto-oscillating of potential (0.7 *N* NaOH, 27 °C, 2.9 μA/cm²).

For measurements at low current densities, upon changing the current density, a period of about 1 h or more was required before the electrode potential achieved a constant value. The transition period was observed to increase with decreasing electrolyte concentration in the range 0.03 to 0.7 *N* NaOH, with Type I electrodes giving rise to the longest periods (3 or more h for 0.03 *N* NaOH). Type II electrodes gave rise to transition times lower by about a factor of 4. Type II electrodes were therefore used exclusively for the measurements at low concentrations, with Type I and Type II electrodes otherwise being used interchangeably.

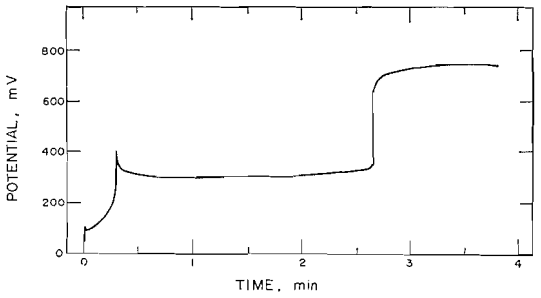

FIG. 8. Galvanostatic polarization curve for Type I electrode (0.7 *N* NaOH, 27 °C, 2.5 mA/cm²).

Charge Required to Complete Ag_2O Film

Figure 8 illustrates a typical galvanostatic polarization curve obtained for a Type I electrode at a relatively high current density (2.5 mA/cm²). The total charge passed for formation of Ag_2O is substantially less than that associated with the AgO plateau, a result found in general. At sufficiently high current density, no evidence of an Ag_2O plateau can be found. In order to determine the film thickness corresponding to completion of the Ag_2O plateau, galvanostatic polarization runs similar to that depicted in Fig. 8 were carried out on Type I, Type II, and Type III electrodes, the current being stopped, however, when the potential reached the peak between the Ag/Ag_2O and Ag_2O/AgO plateaus. The film was then reduced at 0.25 mA/cm² current density, the termination of the reduction process being signalled by an abrupt drop in electrode potential towards that for hydrogen evolution. The data collected in this manner for Type I and Type II electrodes are presented in Fig. 9. At low current

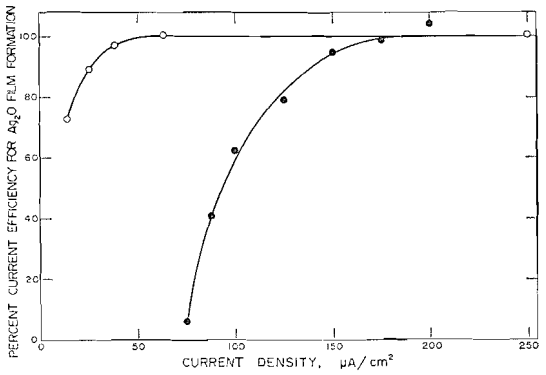

FIG. 9. Current efficiency for formation of Ag_2O films on Type I electrodes (0.7 *N* NaOH, 27 °C; ● and ○, in the presence and absence of electrolyte stirring, respectively).

densities, the current efficiency is less than 100%, increasing to 100% for currents of 0.062 mA/cm^2 or greater. For currents well above this value, film thicknesses were calculated from the charge passed during oxidation.

Film thicknesses were calculated using the bulk density (12) for Ag_2O (7.14 g/cm^3) and assuming unit roughness factor. The results for Type I electrodes are presented in Fig. 10.

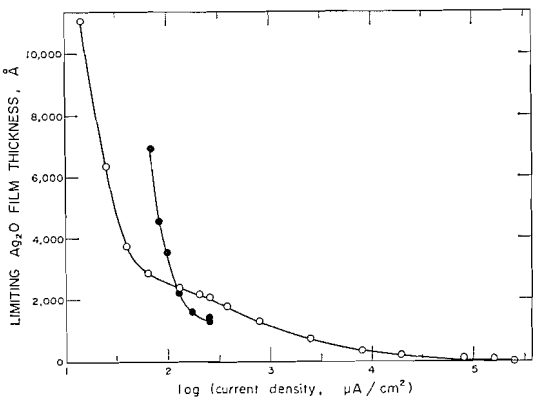

FIG. 10. Limiting thickness of Ag_2O film as a function of the formation current density for Types I and II electrodes (0.7 *N* NaOH, 27 °C; ● and ○, in the presence and absence of electrolyte stirring, respectively).

Ag_2O was found to form at 100% current efficiency on Type III electrodes at all current densities investigated. In other respects these electrodes gave irreproducible results which, in addition, were quite different from those for Type I and Type II electrodes.

Variation of Electrode Potential with Current Density, Film Thickness, and Electrolyte Concentration

Galvanostatic polarization curves for Type I electrodes polarized in 0.7 *N* NaOH at 27 °C are shown in Fig. 11. There is a pronounced dependence of overpotential on film thickness at high current densities, which decreases to essentially 0 at low current densities. At low current densities, it was therefore possible to determine the variation of overpotential with current density using the following procedure. A Type I or II electrode was anodically oxidized at 12 μA/cm^2 for a few hours. A succession of measurements were then made at different current densities as illustrated in Fig. 12. The behavior referred to earlier, in which, upon increasing the current density, the

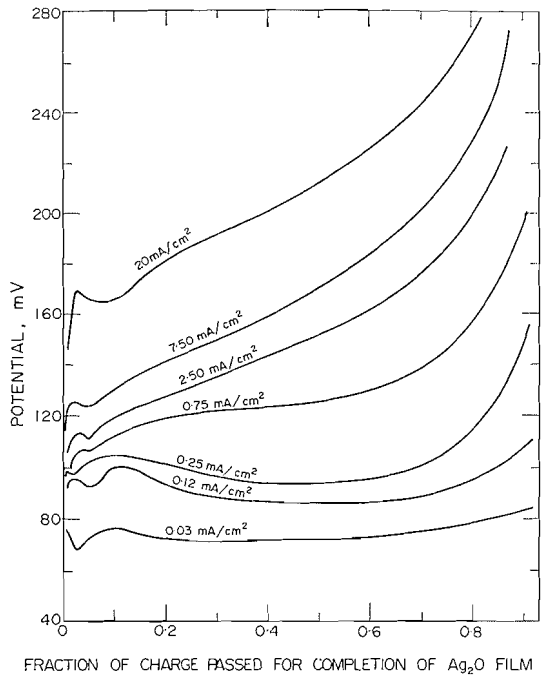

FIG. 11. Variation of galvanostatic polarization curve with current density (0.7 *N* NaOH, 27 °C).

potential first increases then decays to a value lying below the initial value, can be seen.

The results obtained from such runs are plotted in Tafel form in Fig. 13. The reproducibility of the data, both in connection with measurements made on a single Type I or II electrode and on comparing results for different electrodes, is evident.

In more dilute electrolytes a different behavior was observed. In the first instance it was noted that stirring the electrolyte caused a change in the steady-state potential. In Fig. 14, the variation of overpotential with electrolyte concentration and current density is illustrated, both in the absence and presence of stirring effected by agitation of the specimen electrode. The results for 0.7 *N* NaOH are taken from Fig. 13. At the lower concentrations, it is seen that a linear Tafel relationship is obtained only under conditions of stirring.

Influence of Stirring on Current Efficiency and Charge required to Complete Ag_2O Film

A few runs were carried out in a cell in which the electrolyte was stirred with a magnetic stirrer and, in addition, the electrode agitated through a

Can. J. Chem. Downloaded from www.nrcresearchpress.com by 210.87.254.6 on 09/05/12
For personal use only.

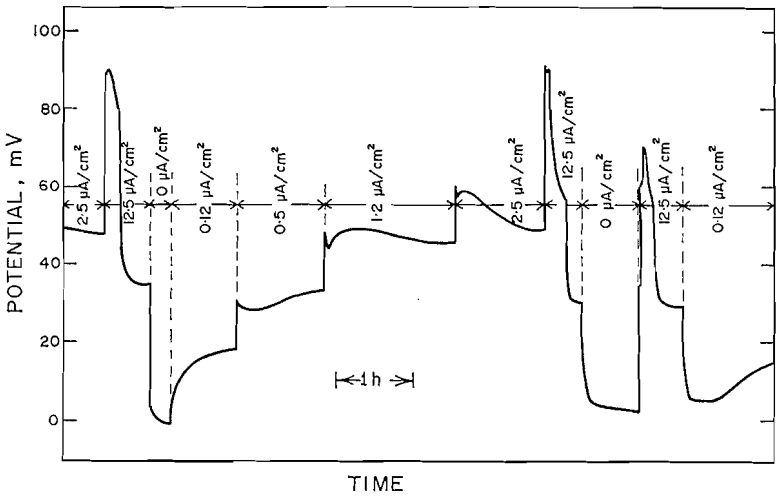

FIG. 12. Oxidation run for Type II electrode illustrating the current dependence of the overpotential for low current densities (0.13 *N* NaOH, 27 °C).

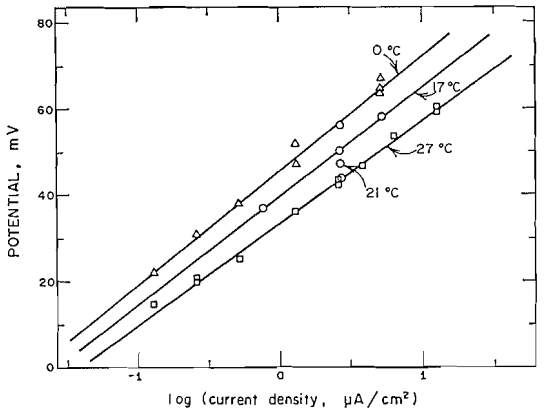

FIG. 13. Overpotential vs. the log of the current density for runs conducted in the manner illustrated in Fig. 12 (Types I and II electrodes; □, 0.70 *N* NaOH, 27 °C; △, 0.70 *N* NaOH, 0 °C; ○, 0.85 *N* NaOH, 0°, 17°, 21°, 27 °C).

TABLE V

Dependence of formation current efficiency on film thickness for 75 μA/cm² formation current density; 0.7 *N* NaOH, 25 °C

Film thickness (Å)	Mean current efficiency (%)
1575	6.3
2400	4.8
5850	7.8
6640	6.0

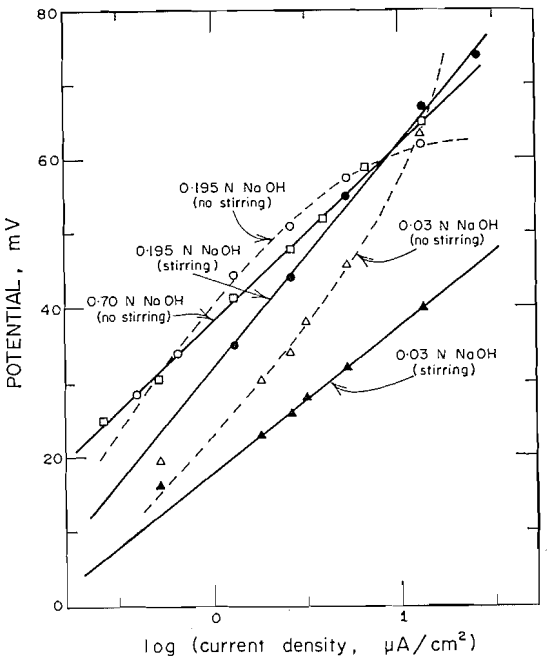

FIG. 14. Dependence of overpotential on current density at low current densities for different electrolyte concentrations and in the presence and absence of electrolyte stirring (Types I and II electrodes, 27 °C).

mechanical coupling to an electromagnetic vibrator. Data obtained in this manner are presented in Figs. 9 and 10, and in Table V. It is believed that all these data were obtained under conditions such that increasing the stirring rate would have only a small effect on the results. This opinion, however, is based solely on observing the variation in overpotential with the stirring rate. It

Can. J. Chem. Downloaded from www.nrcresearchpress.com by 210.87.254.6 on 09/05/12
For personal use only.

cannot be said with certainty, therefore, that the limit corresponding to high stirring rates was in fact achieved.

A further observation made during the course of these measurements was that films formed in the absence of stirring were dark brown or black in color and had a matt or semi-gloss appearance, whereas the films formed while stirring were light amber in color and transparent, even for films as thick as 7000 Å.

Discussion of Results

It is apparent from a number of different observations that at least 2 different mechanisms are operative during the anodic oxidation of silver in aqueous hydroxide solutions. We shall review the factors leading to this conclusion.

The most dramatic evidence is probably provided by the data of Fig. 7 in which, under galvanostatic conditions, the overpotential is seen to oscillate between 2 different levels differing from one another by about 40 mV. Again, from the data of Fig. 12, on increasing the current density above a certain critical value, the overpotential is seen to decrease abruptly, again by about 40 mV. Finally, from Fig. 9 it is apparent that the current efficiency for formation of Ag_2O in the current density range 60 to 200 $\mu A/cm^2$ is decreased by electrolyte stirring. This observation implies a mechanism which involves a dissolution–precipitation process similar to that proposed by Dirkse *et al.* (13), the solution species most likely being $Ag(OH)_2^-$ (solubility limit of $Ag(OH)_2^-$ in 1 *N* KOH solution is 1.9×10^{-4} g equiv./l (14)). The fact that current efficiencies do not go to 0 for conditions of rapid stirring, and furthermore that the films so produced have visual properties distinctly different from those formed in the absence of stirring, implies a parallel mechanism of film formation which does not involve dissolution–precipitation but rather formation of a compact film as a result of a direct interfacial reaction. The existence of a dual layer type of oxide film has also been reported previously by Briggs *et al.* (15).

In the following sections the electrode behavior is discussed on the premise that 2 mechanisms of the kind outlined above are indeed operative.

Charge Required to Complete Ag_2O Film

From Fig. 10, it can be seen that the effect of stirring on the limiting film thickness is to reduce

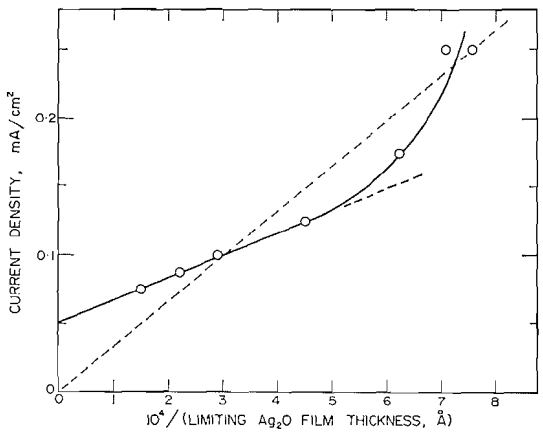

FIG. 15. Formation current density vs. reciprocal limiting film thickness for Type I electrodes under conditions of rapid electrolyte stirring (0.7 *N* NaOH, 27 °C).

it somewhat for current densities above about 12.5 $\mu A/cm^2$, while increasing it substantially for current densities below this value. Thus suppression of the precipitation process for Ag_2O formation has a very dramatic effect on the current dependence of the limiting film thickness only at very low current densities. It would seem therefore, that transport through the postulated "compact film", formed by the direct interface reaction, plays the major role in determining the limiting film thickness at high current densities, with the precipitated oxide assuming this role for very low current densities. Assuming, therefore, that in the presence of stirring the limiting film thickness is controlled by diffusion of some species (V centers, for example) through the compact oxide film, then the formation current density, i, should be a linear function of the reciprocal of the limiting film thickness, X. Referring to Fig. 15, it can be seen that the data do not conform well to such a relationship. A very much improved linear relationship is obtained by plotting i against $(X - A)^{-1}$ where A is a constant of the order of 600 Å. Some distortion, however, is not unexpected, because it is entirely possible that the stirring rate was insufficient to eliminate formation of oxide film by precipitation. The suggestion that the growth of the compact film is limited by diffusion remains, therefore, a reasonable one. The only immediate alternative explanations for the cessation of growth of the compact film are inapplicable to films which may be grown to a mean thickness of 7000 Å or more. Thus, a

Can. J. Chem. Downloaded from www.nrcresearchpress.com by 210.87.254.6 on 09/05/12
For personal use only.

Can. J. Chem. Downloaded from www.nrcresearchpress.com by 210.87.254.6 on 09/05/12
For personal use only.

mechanism such as proposed by Dirkse and Werkema (16), involving nucleation and 2-dimensional growth but leaving bare silver, is untenable for films of this thickness. Again, any mechanism based on a sudden change in one or more of the intrinsic film properties, such as its resistance, at best begs the question, as a credible mechanism for bringing about this change in a film 7000 Å thick must also be provided. Finally, rate control, by ion or electron transport through the film, of itself cannot account for the abrupt cessation of the growth of Ag_2O under galvanostatic conditions and at a potential below that for AgO formation. Under such conditions the potential should increase linearly with time, at least until the Ag_2O/AgO potential is reached. The growth of anodic oxide films on Al, Nb, and Ta behaves in this manner, film growth continuing in these instances far beyond the potential for oxygen evolution (17).

In the absence of stirring and at low current densities the limiting film thickness appears to be controlled by transport through the film formed by precipitation, as previously noted. Assuming diffusion of some species through the precipitated film to be the rate controlling process, i should be a linear funtion of X^{-1}. We may attempt to correct for the compact film by subtracting from X the thickness of the compact film, e.g. A. An excellent linear relationship is achieved on this basis for $A = 1810$ Å (cf. Fig. 16).

Tafel Slope Determinations

The 3 lines in Fig. 13 all have a slope of approximately 22 mV per decade which agrees closely both with the upper limit value found for cycled electrodes (7 to 22 mV, cf. Table IV) and with the potential decay slope (see Fig. 4) made in the same potential range[2].

For more dilute electrolyte concentrations, linear Tafel plots are not obtained in the absence of stirring (see Fig. 14), but only when measurements are made while stirring. The Tafel slope values lie in the range 20–30 mV per decade.

Because the Tafel slopes for electropolished electrodes were determined at low current densities and with stirring, they presumably apply to the electrochemical dissolution of silver as

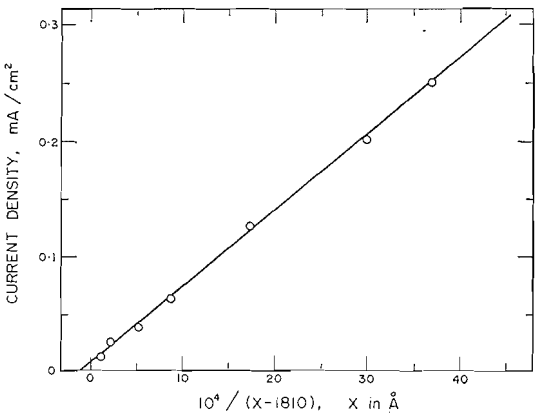

FIG. 16. Formation current density vs. $[X - 1810$ Å$]^{-1}$ for Type I electrodes in the absence of stirring (current densities < 0.25 mA/cm², 0.7 N NaOH, 27 °C).

$Ag(OH)_2^-$, the reaction occurring at the compact film–electrolyte interface. This account is consistent with the results obtained for the cycled electrodes in which the value of the potential-decay-slope/ϕ, which will be proportional to the reciprocal of the electrode capacitance for an electrode covered by a thick film (11), was found to vary approximately linearly with film thickness.

The high effective electrode capacitance associated with the slow decay (about 2×10^4 μF, or more) when combined with the assumption that it is determined by an interfacial or double layer capacitance of about 20 μF/cm² (which could only be the case if the oxide film were behaving as a good conductor during the decay) leads to an effective electrode area of about $2 \times 10^4/20 = 10^3$ cm², or more, and a roughness factor of about 10^2, or more. Surprisingly, a similar conclusion is reached in the section "Effect of electrode treatment". The high effective capacitance might, however, have a thermodynamic, rather than kinetic, origin.

Apparent Film "Resistivity"

At high current densities, the overpotential shows a definite upward rise with increasing film thickness, the rate of rise being approximately constant over a reasonable portion of the polarization curve. In Table VI, the slope of this nearly linear region in V/cm is recorded as a function of formation current density, and the ratio calculated in ohm cm. Apart from the very highest current densities, the ratio is approximately constant at 8×10^6 ohm cm (which is of

[2]For the relationship between the potential decay slope and the Tafel parameter, and also between the potential-decay-slope/ϕ and the electrode capacitance, see refs. 11 and 18–21.

TABLE VI

Calculation of apparent specific resistivity of film

Formation current density, i (mA/cm^2)	Rate of change of potential with film thickness, dV/dx (V/cm) $\times 10^{-5}$	Apparent specific resistivity of film, $(dV/dx)/i$ (ohm cm) $\times 10^{-6}$
162	2.83	1.75
19.7	0.580	2.95
7.61	0.502	6.67
2.47	0.227	9.19
0.75	0 038	5.07
0.375	0 0367	9.79
0.250	0 0246	9.84
0.200	0.0168	8.40

the same order as the electronic conductivity for Ag_2O reported by Le Blanc and Sachse (22), namely, 10^8 ohm cm).

The values at high current density may be brought into accord with the others if it is assumed that the conduction equation giving rise to the resistance term deviates from Ohm's law at high field strengths according to the equation

$$[1] \qquad i = \alpha|\exp \beta E - \exp(-\beta E)|$$

where α and β are temperature dependent constants and E, the field strength. Equation [1] is of the form normally assumed for high field ionic transport (17), in which case $\beta = \mu^*/kT$ where μ^* is the activation dipole or charge-activation distance product for ion migration. The required value of μ^* is about 35 eÅ, which is close to those obtained for the anodic oxidation of the valve metals (23). Thus it appears likely that at high current densities an ionic or electronic resistive term, associated with the film, makes an important contribution to the overpotential. This term might arise either in the "compact film" or in that formed by the precipitation reaction. Thus the resistive term might be associated with hydroxyl ion transport through the open pore structure of the precipitated oxide film.

Effect of Electrode Treatment

It is apparent that surface preparation plays a major role in the subsequent anodic behavior of silver electrodes (see Fig. 6). One might suppose that the large difference in overpotential observed for a freshly electropolished electrode, as compared with one which has been once oxidized and then electrochemically reduced, might be in some way related to the oscillating behavior exhibited in Fig. 7, or to the anomalous drop in potential on increasing the current, illustrated in Fig. 12. This appears very likely, however, as the surface treatment effect persists at current densities very much higher than those for which the other phenomena are observed. We examine, therefore, the possibility that the surface treatment effect arises solely as a result of a change in electrode surface area. Using the Tafel data of Fig. 13 in order to reconcile curves *a* and *c* of Fig. 6, a roughness factor of approximately 200 must be assumed for an electrode which is reduced electrochemically. For comparison purposes, polarization curves for electrodes etched in 1:1 nitric acid were similarly analyzed, and led to roughness factors of 15 to 20, in good agreement with those reported by Cahan *et al.* (24) for silver treated in this manner. There seems to be no reason, therefore, to reject the roughness factor value of 200 for electrochemically reduced electrodes. Such a high value could only be achieved through a porous structure for the metal surface, as observed by Burbank (25).

The effect of the reduction current density on the subsequent oxidation process can be seen in Table I. Runs 17 to 24 show that when the electrode is reoxidized at a current less than the reduction current, the charge passed to complete the Ag_2O film increases with successive oxidation cycles. When the electrode is reoxidized at a current greater than the reduction current, however, the converse is true. This is consistent with Wales' and Burbank's (4) observation concerning the dependence of the crystal size for the reduced metal upon current density.

On reoxidizing the electrochemically reduced metal to Ag_2O under current conditions, the porous metal will be oxidized first and at a very low current density, leading to a low overpotential. When the porous metal is completely converted to Ag_2O, some of the underlying "virgin" metal may oxidize, at a current density roughly 200 times that for the porous metal and hence at a higher overpotential. The potential plateau occurring just before the potential rises toward that for AgO formation (see Fig. 2 and Fig. 6, curve *c'*) has therefore a natural explanation in the above model. It explains the observation that, although formation at a lower current density results in an appreciable increase in the total amount of Ag_2O which may be formed, once a film is fully formed (i.e. an overpotential of 0.250 V is reached), attempts to increase the

Can. J. Chem. Downloaded from www.nrcresearchpress.com by 210.87.254.6 on 09/05/12
For personal use only.

Can. J. Chem. Downloaded from www.nrcresearchpress.com by 210.87.254.6 on 09/05/12
For personal use only.

film thickness by reducing the current density meet with remarkably little success (cf. Tables II and III).

Thus the termination of growth of Ag_2O on cycled electrodes is closely related to the filling in of a porous structure. The structure which is porous, however, is the metal substrate, not the forming oxide. In the absence of this porous structure, the film thickness appears to be limited by diffusion, the situation being complicated by the presence of more than 1 type of film material.

In the light of the above, the behavior of Type III electrodes (which are prepared by reduction in hydrogen for 1 h at 800 °C electrodes previously oxidized to completion of the Ag_2O film) is of interest. From Fig. 6 curve *b*, it can be seen that the electrode behaves initially in a similar manner to a freshly electropolished electrode (curve *a*) in that the overpotential is initially high. The potential soon drops, however, and subsequently matches fairly closely the behavior of electrochemically reduced electrodes. It would appear, therefore, that annealing at 800 °C leads to sintering of the porous metal only in a thin layer at the metal–hydrogen interface.

Clearly, the low current efficiency for formation of Ag_2O on electropolished electrodes (Types I and II) arises as a consequence of the silver dissolution mechanism. The postulate that Types III and IV and also cycled electrodes possess a highly porous surface layer of metal therefore provides an explanation for the fact that Ag_2O may be formed on these electrodes at close to 100% current efficiency, even at very low current densities and with electrolyte stirring, because the solution species will be formed within the cavities of the porous structure and will accordingly have little opportunity to escape into the bulk electrolyte before precipitating as oxide.

Summary

1. At least 2 different mechanisms are involved in the anodic formation of Ag_2O in basic electrolytes. One of these mechanisms involves a dissolution–precipitation process for the growth of the Ag_2O film, while another probably involves a direct interfacial reaction, leading to a compact film.

2. The reduction of anodically formed Ag_2O films, either electrochemically or in hydrogen at 800 °C, leaves behind a highly porous layer of silver metal.

3. Below 0.25 mA/cm^2, the anodic formation of Ag_2O on a smooth silver electrode (0.7 *N* aqueous NaOH) appears to be limited by the diffusion of some species (possibly OH^-, H^+, or H_2O) through the film formed by the dissolution–precipitation process. For these current densities, stirring greatly reduces the current efficiency for film formation, while at the same time greatly increasing the attainable limiting Ag_2O film thickness. The Tafel slope for the electrochemical dissolution process lies in the range 20 to 30 mV per decade of current.

4. Above 0.25 mA/cm^2, the anodic formation of Ag_2O on a smooth silver electrode appears to be limited by diffusion (and/or migration) of some species (possibly V centers and/or cation vacancies) through the underlying compact film. In this case, stirring reduces the limiting film thickness, presumably by suppressing the formation of the precipitated film. At these current densities, an overpotential, apparently resistive in nature, appears which corresponds to a mean film resistivity of the order of 10^7 ohm cm.

5. At low current densities, suppression of the precipitation mechanism for film formation leads to the growth of a film which is essentially transparent even for thickness as great as 7000 Å.

Acknowledgments

The authors wish to acknowledge their indebtedness to the late Professor F. E. W. Wetmore for initiating this research and for directing it in its early stages. They also wish to thank the National Research Council of Canada and the Department of University Affairs for supporting this research. Support in the form of scholarships from the Ontario Research Foundation (G.D.N.) and Canadian Industries Limited (H.M.B.) is also gratefully acknowledged.

1. T. P. DIRKSE. J. Electrochem. Soc. **106**, 453 (1959).
2. G. D. NAGY. Ph.D. Thesis, University of Toronto, Toronto, Ontario. 1963.
3. R. G. BARRADAS and G. H. FRASER. Can. J. Chem. **42**, 2488 (1964).
4. C. P. WALES and J. BURBANK. J. Electrochem. Soc. **112**, 13 (1965)
5. J. P. HOARE. Electrochemistry of oxygen. Interscience Publishers, Inc., New York. 1968. p. 211.
6. C. P. WALES. J. Electrochem. Soc. **109**, 1119 (1962).
7. C. P. WALES. J. Electrochem. Soc. **111**, 131 (1964).
8. T. P. DIRKSE. Electrochem. Tech. **4**, 163 (1966).
9. C. M. SHEPHERD and H. C. LANGELAN. J. Electrochem. Soc. **114**, 8 (1967).
10. L. I. GILBERTSON, 2nd, and O. W. FORTNER. Trans. Electrochem. Soc. **81**, 199 (1942).

11. H. R. MORLEY and F. E. W. WETMORE. Can. J. Chem. **34**, 359 (1956).
12. R. C. WEAST (*Editor*). Handbook of chemistry and physics. 43rd. ed. The Chemical Rubber Publishing Company, Cleveland. 1961–1962.
13. T. P. DIRKSE, D. DEWIT, and R. SHOEMAKER. J. Electrochem. Soc. **114**, 1196 (1967).
14. H. L. JOHNSON, F. CUTA, and A. B. GARRETT. J. Amer. Chem. Soc. **55**, 2311 (1933). G. BIEDERMANN and L. G. SILLEN. Acta Chem. Scand. **14**, 717 (1960).
15. G. W. D. BRIGGS, M. FLEISCHMANN, D. J. LAX, and H. R. THIRSK. Trans. Faraday Soc. **64**, 3120 (1968). Also, M. FLEISCHMANN, D. J. LAX, and H. R. THIRSK. Trans. Faraday Soc. **64**, 3128 (1968).
16. T. P. DIRKSE and C. J. WERKEMA. J. Electrochem. Soc. **106**, 88 (1959).
17. L. YOUNG. Anodic oxide films. Academic Press, Inc., New York. 1961.
18. G. ARMSTRONG and J. A. V. BUTLER. Trans. Faraday Soc. **29**, 1261 (1933).
19. A. FRUMKIN. Acta Physiochim. USSR, **18**, 23 (1943).
20. W. R. BUSING and W. KAUZMANN. J. Chem. Phys. **20**, 1129 (1952).
21. D. C. GRAHAME. J. Phys. Chem. **57**, 257 (1953).
22. M. LEBLANC and H. SACHSE. Phys. Z. **32**, 887 (1931).
23. M. J. DIGNAM. Can. J. Chem. **42**, 1155 (1964).
24. B. D. CAHAN, J. B. OCKERMAN, R. F. AMLIE, and P. RUETSCHI. J. Electrochem. Soc. **107**, 725 (1960).
25. J. P. BURBANK. Naval Research Laboratories, Washington. Report 6626. Dec. 20, 1967.

Can. J. Chem. Downloaded from www.nrcresearchpress.com by 210.87.254.6 on 09/05/12
For personal use only.

Can. J. Chem. Downloaded from www.nrcresearchpress.com by 210.87.254.105 on 09/05/12
For personal use only.

Infrared studies of the 1,3,5-trinitrobenzene – cyanide ion complex

A. R. NORRIS[1] AND H. F. SHURVELL
Department of Chemistry, Queen's University, Kingston, Ontario

Received June 16, 1969

Quantitative infrared studies have been made of the interactions of 1,3,5-trinitrobenzene and 1,3,5-trinitrobenzene-d_3 with cyanide ion in chloroform, deuterochloroform, and acetonitrile. Absorption bands assignable to the 1:1 complex have been characterized and attempts made to assign the absorptions to fundamental modes of the complex.

Canadian Journal of Chemistry, 47, 4267 (1969)

Introduction

Infrared studies have been reported on a wide variety of solid adducts precipitated from concentrated solutions containing an aromatic nitro compound and a suitable base (1–8). Although the infrared spectra are in accord with the formulation of these adducts as σ-complexes, this formulation receives much stronger support from proton nuclear magnetic resonance (n.m.r.) measurements (7, 9–11).

No attempt has so far been made to utilize infrared measurements to establish the stoichiometries of σ-complexes in solution or to analyze the spectra of the complexes in terms of their fundamental absorptions. We report here the results of our infrared investigations of the cyanide ion σ-complexes of 1,3,5-trinitrobenzene and 1,3,5-trinitrobenzene-d_3.

Experimental

Eastman 1,3,5-trinitrobenzene (TNB) was recrystallized several times from ethanol–water and dried to constant weight in vacuo over silica gel (m.p. 122 °C). 1,3,5-Trinitrobenzene-d_3 was prepared as described by Buncel and Symons (12), recrystallized from ethanol–water and dried in vacuo to constant weight (m.p. 120.5–121.5 °C). The deuterium content of the compound determined as described by Symons (13) was 91 ± 2% D.

Tetraphenylarsonium cyanide (TPAC) was prepared as described by Bosnich (14) and dried to constant weight in vacuo over phosphorous pentoxide.

Spectrograde chloroform and acetonitrile and Stohler Isotope Chemicals deuterochloroform (99.8%D) were used without further purification, but were stored over Linde Molecular Sieve once the bottles had been opened.

Spectra were run on a Beckman IR-10 grating instrument, a Perkin–Elmer Model 21 spectrophotometer equipped with a NaCl prism, and a Perkin–Elmer Eberr grating instrument. The latter two instruments were used primarily to check the accuracy of the peak positions as determined on the IR-10 and to resolve the fine structure associated with certain absorption bands near 3000, 1200, and 1050 cm^{-1}. Most of the quantitative data relates to work carried out on the IR-10.

Low-temperature spectra were recorded using a variable low-temperature cell unit (VLT-2 from Research and Industrial Instruments Co., London). The cell temperature was maintained at −31 ± 2 °C by adding sufficient finely-divided dry ice to the well of the low-temperature cell to keep the 50/50 (v/v) ethylene glycol – water mixture contained therein at its freezing point. The cell temperature was measured with a thermocouple (copper–constantan) inserted into one of the cell windows. Variable path length solution cells (FH-01) equipped with Teflon spacers were used in all the low-temperature work. Path lengths were determined both by the interference–fringe method (15) and the standard absorber method using benzene as the standard (16). Cell windows were of AgCl, CaF_2, and KRS-5, with AgCl being used most frequently. Since AgCl tends to deform under pressure, frequent checks on the path lengths were required when windows of this material were used.

Apparent molar extinction coefficients (ε_a) were calculated from the equation $\varepsilon_a = 1/Cl \log (I_0/I)$, where C is the concentration in moles l^{-1} and l is the path length in cm. Values of ε_a for 1,3,5-trinitrobenzene and tetraphenylarsonium cyanide were measured for solutions 10^{-1} to 10^{-2} M in cells of 0.005 to 0.020 cm path length. The molar extinction coefficients are dependent on the mode of operation of the spectrophotometer and the values quoted refer to measurements made at the normal setting of the IR-10 (nominal resolution ~4 cm^{-1}) and slow scan.

Solutions containing the complex were prepared by adding a known volume of pre-cooled solvent to weighed amounts of the two components contained in a test tube at −45 °C. When solution was complete a portion of the liquid was withdrawn using a cooled syringe and injected into the previously cooled cell. Indications are that in the transfer operation the temperature of the solution does not go above −20 °C. Recording of the spectrum was begun after the cell and contents had reached a constant temperature (~20 min). Spectra recorded on the Beckman IR-10 and the Perkin–Elmer 21 instruments were obtained using solvent alone in the reference beam.

Results

When solutions containing 1,3,5-trinitrobenzene (TNB) and tetraphenylarsonium cyanide

[1]To whom correspondence should be addressed.

Can. J. Chem. Downloaded from www.nrcresearchpress.com by 210.87.254.105 on 09/05/12
For personal use only.

(TPAC) at the concentrations required for infrared studies are prepared at room temperature, deep red solutions result which slowly turn brownish-red, and finally become deep brown in color. In typical experiments carried out at room temperature the first reaction is complete on mixing the two solutions while the secondary reaction has a half-life of from 10 to 20 min. As a result, the secondary reaction seriously interferes with attempts to obtain good infrared spectra of the deep red solutions.

While the rate of formation of the red color seems to be very rapid at all temperatures between 25 and -45 °C, the rate of the secondary reaction is dramatically reduced at lower temperatures. At 0 °C, for instance, with both reactants $\sim 0.07\ M$, $t_{\frac{1}{2}}$ for the decay reaction is approximately 9 h while at -30 °C, the solutions can be kept for up to 8 h with no evidence of a secondary reaction. The infrared spectra of these red solutions consist of many bands which, in the absence of the decomposition product, can be satisfactorily accounted for in terms of uncomplexed TNB and cyanide ion, a cyanide ion – TNB complex and tetraphenylarsonium ion. All the infrared evidence collected to date suggests that no changes occur in the absorptions characteristic of the tetraphenylarsonium ion as a result of complex formation[2]. The analysis which follows is, therefore, concerned with those absorptions which are characteristic of uncomplexed TNB, the cyanide ion – TNB complex and uncomplexed cyanide ion. We expect absorptions assigned to the cyanide ion – TNB complex to grow as the concentration of complex in solution is increased and to disappear as the solution is warmed and the secondary reaction begins.

For convenience of discussion, the changes which occur as a result of complex formation are discussed in terms of the fundamental vibrations of 1,3,5-trinitrobenzene as reported by Shurvell and co-workers (17, 18).

NO_2 vibrations

The infrared spectrum of 1,3,5-trinitrobenzene (TNB) is characterized by antisymmetric and symmetric stretching vibrations of the NO_2 group at 1550 and 1345 cm^{-1}, respectively, a symmetric NO_2 deformation vibration at 825 cm^{-1}, an out-of-plane bending vibration at 518 cm^{-1}, and an in-plane rocking vibration at 360 cm^{-1}. At -30 °C, the apparent molar extinction coefficients of the first two bands in $CHCl_3$ solution are 1740 and 1400 $M^{-1}\,cm^{-1}$, respectively.

As cyanide ion is added to a $CHCl_3$ solution containing a fixed concentration of TNB, the absorbances of the bands at 1550 and 1345 cm^{-1} decrease linearly and at a [cyanide]-to-[TNB] ratio of 1.8:1, the bands are completely absent (Fig. 1). The pronounced breaks in the two plots at a [cyanide]-to-[TNB] ratio near 1 suggests a one-to-one stoichiometry for the complex and a large equilibrium constant for the formation reaction (19).

Although a number of new bands appear in the 4000 to 300 cm^{-1} region as the bands at 1550 and 1345 cm^{-1} disappear, only the new bands at 1235 and 1190 cm^{-1}, having apparent molar extinction coefficients of 2200 and 1800 $M^{-1}\,cm^{-1}$, respectively, approach the intensities of the original NO_2 stretching vibrations. Though not shown in Fig. 1, the intensities of both the 1235

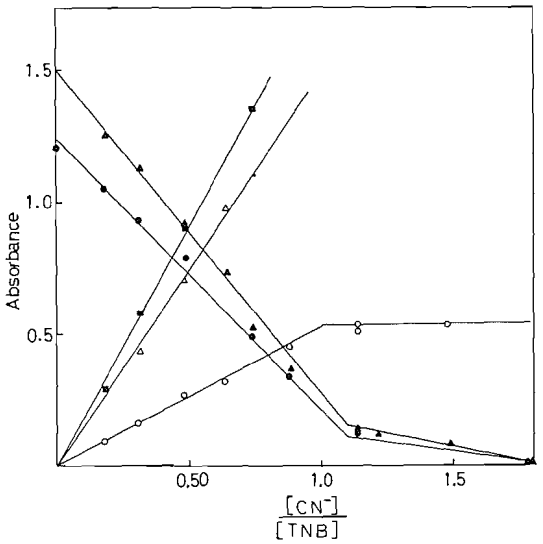

FIG. 1. Absorbances at different wave numbers vs. ratio of [cyanide]-to-[1,3,5-trinitrobenzene] in chloroform solutions at -30 °C containing a fixed concentration of 1,3,5-trinitrobenzene (0.084 M). Path length of cell, 0.010 cm. ■, 1235 cm^{-1}; △, 1190 cm^{-1}; ▲, 1550 cm^{-1}; ●, 1345 cm^{-1}; ○, 1050 cm^{-1}.

[2]Nuclear magnetic resonance studies of this complex formation reaction indicate little change in the positions of resonance absorption of the protons in the tetraphenylarsonium ion as a result of complex formation (11, 21).

Can. J. Chem. Downloaded from www.nrcresearchpress.com by 210.87.254.105 on 09/05/12
For personal use only.

and the 1190 cm^{-1} bands reach a maximum at a [cyanide]-to-[TNB] ratio slightly greater than 1.

The positions and intensities of the bands at 1235 and 1190 cm^{-1} do not change when TNB-d_3 is substituted for TNB; nor are the positions and intensities markedly affected by changing from $CHCl_3$ to $CDCl_3$ or CH_3CN as solvent.

Possible changes in the symmetric deformation vibration at 825 cm^{-1} could not be observed in $CHCl_3$, $CDCl_3$, or CH_3CN solution due to strong solvent absorption in this region.

On decomposition of the complex, bands reappear near 1550 and 1345 cm^{-1} as the bands at 1235 and 1190 cm^{-1} disappear (Fig. 2). In the final reaction mixture the band near 1550 cm^{-1} is usually split, and the band at 1345 cm^{-1} broadened (compared to TNB). Similar results are observed when TNB-d_3 is substituted for TNB. The split band near 1550 cm^{-1} and the broadened 1345 cm^{-1} band may indicate that the nitro groups in the product are not equivalent; or that different nitro-containing aromatic compounds are present in the system. Separation of the product(s) of the reaction has not yet been accomplished.

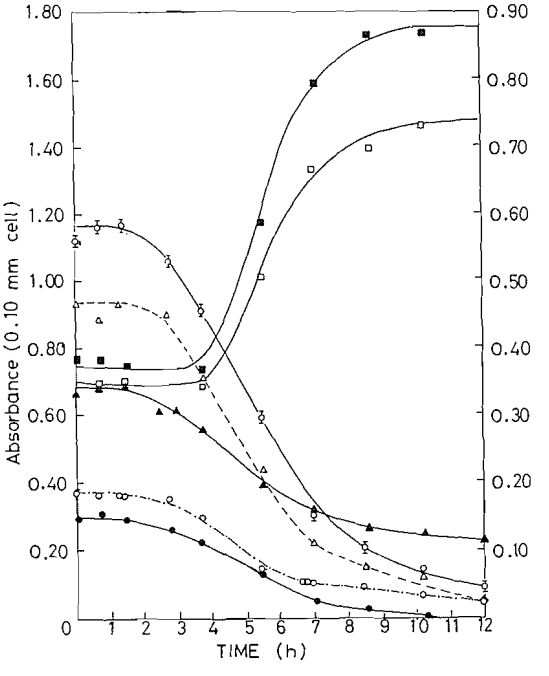

FIG. 2. Absorbances at different wave numbers as a function of time for chloroform solutions 0.054 M in tetraphenylarsonium cyanide and 0.079 M in 1,3,5-trinitrobenzene. Path length of cell, 0.010 cm. Temperature of solution varies from −30 to +30 °C over the 12 h period. Right hand ordinate: ■, 1545 cm^{-1}; □, 1345 cm^{-1}; ●, 1410 cm^{-1}; ▲, 1620 cm^{-1}. Left hand ordinate: ♀, 1235 cm^{-1}; △, 1190 cm^{-1}; ○, 1050 cm^{-1}.

CH Vibrations

The infrared spectrum of 1,3,5-trinitrobenzene is characterized by an antisymmetric stretching mode at 3108 cm^{-1} and a C—H in-plane bending mode at 1075 cm^{-1}. The apparent molar extinction coefficients of these two bands in $CHCl_3$ solution are 220 and 210 M^{-1} cm^{-1}, respectively, at −30 °C.

As cyanide ion is added to a $CHCl_3$ solution of fixed TNB concentration, the absorbance of the band at 3100 cm^{-1} decreases and at a [cyanide]-to-[TNB] ratio of 1.14:1, the band has virtually disappeared.

Studies in $CDCl_3$ solution at high ratios of [cyanide]-to-[TNB] indicate that in addition to the Φ_4As^+ absorptions at 3083, 3067, 3020, and 2990 cm^{-1} with apparent molar extinction coefficients of approximately 20 M^{-1} cm^{-1}, there is a new band at 3094 cm^{-1} with an apparent molar extinction coefficient of 30 M^{-1} cm^{-1}.

Because of strong new absorption bands which grow in at 1063 and 1050 cm^{-1} and which reach a maximum absorbance at a [cyanide]-to-[TNB] ratio slightly greater than 1 (Fig. 1), it is not possible to follow the disappearance of the C—H in-plane mode as increasing amounts of cyanide ion are added to the system. It seems clear, however, that the new bands at 1063 and 1050 cm^{-1} ($\varepsilon_a \sim 800$ M^{-1} cm^{-1}) are not the result of a shift in the 1075 cm^{-1} band to lower frequency, because a band near 1050 cm^{-1} is also generated when the cyanide ion complex is formed with TNB-d_3. The intensity of absorption of the 1050 cm^{-1} band in the TNB-d_3 complex with CN^- is, however, less than in the case of absorption by the TNB–CN^- complex. The C—D in-plane vibration occurs at 806 cm^{-1} in TNB-d_3, but we have been unable to locate this peak in the TNB-d_3 – cyanide ion complex because of strong solvent absorption by $CHCl_3$ and $CDCl_3$ in this region.

On decomposition of the complex, the bands at 1063 and 1050 cm^{-1} disappear completely (Fig. 2) and a band of reduced intensity (compared to TNB at the concentration of TNB initially present in the system) reappears at 3108 cm^{-1}.

C—C Vibrations

The C—C stretching vibrations of the benzene ring in TNB have been assigned to the peaks at

Can. J. Chem. Downloaded from www.nrcresearchpress.com by 210.87.254.105 on 09/05/12
For personal use only.

1625 and 1443 cm^{-1}, while the out-of-plane deformation, Φ-CCC, has been assigned to the band at 620 cm^{-1}. In chloroform solution the apparent molar extinction coefficients of the bands at 1625 and 1443 cm^{-1} are 330 and 60 M^{-1} cm^{-1}, respectively. The band at 620 cm^{-1} is masked by strong solvent absorption in all the solvents studied.

As a result of complete conversion of TNB to the TNB – cyanide ion complex, the band at 1625 cm^{-1} is replaced by a new band at 1615 cm^{-1}. The absorption of the 1615 cm^{-1} band at high $[CN^-]$-to-[TNB] ratios is almost twice as great as the absorption of the original 1625 cm^{-1} band. Much the same behavior is observed when the TNB-d_3 – cyanide ion complex is studied in $CHCl_3$; the shift in this case is from 1610 to 1600 cm^{-1}.

It has not been possible to study the changes in the absorption band at 1443 cm^{-1} as the [cyanide]/[TNB] ratio is increased, because the Φ_4As^+ ion absorbs much more strongly at 1445 cm^{-1} than does TNB at 1443 cm^{-1}. No new absorption bands were noted in the 1430–1470 cm^{-1} region, but at the concentrations of reactants employed in studying this region of the spectrum, new absorption bands with molar extinction coefficients of 20–40 M^{-1} cm^{-1} would not have been detected.

A broader, less intense band reappears at 1625 cm^{-1} when the complex decomposes.

CN Vibrations

The C—N stretching mode in TNB is found at 918 cm^{-1}, and in $CHCl_3$ solution has an apparent molar extinction coefficient of 200 M^{-1} cm^{-1}.

As a result of the complete conversion of TNB to the TNB – cyanide ion complex in $CHCl_3$ a broader, slightly more intense band with a maximum at 928 cm^{-1} replaces the original 918 cm^{-1} band. There is some indication that the new band is split, but the band was never completely resolved on the IR-10. The effect of solvent on the position and intensity of the 928 cm^{-1} band could not be ascertained due to strong absorption by both $CDCl_3$ and CH_3CN in this region.

Absorption in the 920–930 cm^{-1} region persists in the spectra of the solutions after decomposition has occurred, suggesting that ring-bonded nitro groups are present in the final product(s).

The CN stretching mode for cyanide ion is found at 2060 cm^{-1} in a KBr disk and in solutions of $CHCl_3$ or $CDCl_3$. The apparent molar extinction coefficient of this band in $CDCl_3$ is 30 M^{-1} cm^{-1}.

We earlier reported (20) that conversion of cyanide ion to the TNB – cyanide ion complex was accompanied by the disappearance of the band at 2060 cm^{-1} and the growth of a band at 2320 cm^{-1}. We have been unable, however, to obtain good quantitative data from either of these bands. This is due in part to the low molar extinction coefficient of the cyanide ion band at 2060 cm^{-1}, and to interference by carbon dioxide absorption in the band at 2320 cm^{-1}. We therefore regard the previous assignment of the band at 2320 cm^{-1} as suspect.

As a result of the decomposition reaction, the band at 2320 cm^{-1} disappears and is replaced by a broad absorption band with a maximum at 2210 cm^{-1}. At a constant TNB concentration the absorbance at 2210 cm^{-1} is proportional to the amount of TPAC added to the system, and the estimated ε_a at 2210 cm^{-1} is 75–95 M^{-1} cm^{-1}.

We have included in the above discussion all the new bands accompanying complex formation except for bands of medium intensity at 1410 cm^{-1} ($\varepsilon_a \sim 300$ M^{-1} cm^{-1}) and 1495–1505 cm^{-1} ($\varepsilon_a \sim 800$ M^{-1} cm^{-1}) and a very weak band at 1385 cm^{-1}. All three bands are unaffected in position or intensity by a change in solvent or by a change from TNB to TNB-d_3. Only the 1410 cm^{-1} band lies close to an absorption band of uncomplexed TNB (1443 cm^{-1}), but the complex band has an apparent molar extinction coefficient some 5 times greater. All three bands disappear completely when the TNB – cyanide ion complex decomposes (Fig. 2) and consequently are considered to be characteristic of the 1:1 complex.

Discussion

Proton n.m.r. studies (11, 21, 22) indicate that in deuterochloroform, acetone-d_6, acetonitrile-d_3, and dimethylsulfoxide-d_6, the predominant species formed by the interaction of 1,3,5-trinitrobenzene and cyanide ion is the σ-complex **1** The present infrared studies confirm the existence of a 1:1 complex in solution and this complex is postulated to be the same as that identified by proton n.m.r. studies (23).

The outstanding features of the infrared spectrum of this complex in chloroform, deuterochloroform, and acetonitrile are the absence of

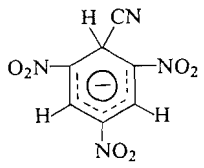

1

absorptions at 1540 and 1345 cm^{-1} and the presence of two very strong bands at 1230 and 1190 cm^{-1}. In addition, the complex shows moderately strong absorption bands at 1615, 1495–1505, 1063, and 1050 cm^{-1} and weak absorption bands at 3094, 1410, 1385, ~1150, and 928 cm^{-1}. Uncomplexed TNB shows two strong absorptions at 1540 and 1345 cm^{-1}, four very weak absorptions in the 1100–1300 cm^{-1} region, and no absorptions at 1495–1505, 1063, or 1050 cm^{-1}. The absorptions at 1495–1505, 1230, 1190, and 1050 cm^{-1} remain when TNB-d_3 is substituted for TNB in the complex.

One can attempt to rationalize the spectrum observed for the complex on the basis of two effects. One, associated with the changes in electron distribution within the molecule on going from TNB to the complex, will result in changes in force constants and give rise to changes in the normal vibration frequencies associated with the NO_2 groups and other normal modes. On this basis, one might expect to find the same number of bands (plus vibrations due to the CN group) in the infrared spectrum of the complex as in the infrared spectrum of TNB, though, in many cases, at different frequencies. The second effect is associated with the lowering of the symmetry from D_{3h} in TNB to approximately C_{2v} or C_s in the complex. This would be expected to effect a splitting of degenerate fundamentals and to make "allowed" the infrared inactive modes of TNB as illustrated in Table I. In the limit of C_s symmetry, one might expect to see 54 infrared and 54 Raman bands for the complex. The deviation from the D_{3h} selection rules and removal of degeneracy will depend, however, on how far the molecule deviates from D_{3h} symmetry. In the case of the nitro groups and the ring carbon atoms for instance, the symmetry is not completely removed in the complex, since these groups (atoms) are still arranged symmetrically with respect to each other. As a result, fewer than 54 infrared active modes may be observed.

A consideration of the infrared spectrum of the complex in the 4000–300 cm^{-1} region indicates that there are far too few infrared bands to accommodate a complex whose essential symmetry is either C_{2v} or C_s. For this reason we will consider the complex in terms of D_{3h} symmetry, taking into account the probable effects of added electron density which accompanies formation of the complex.

Since the increased electron density is primarily delocalized in the NO_2 groups of the complex (24), we expect the nitro group vibrations to be most affected as a result of complex formation. Transfer of negative charge to the nitro group will lead to a decreased N—O bond order and thus to a lowering of the symmetric and antisymmetric N—O stretching frequencies. Foster and Hammick (1) assigned bands at 1492 and 1291 cm^{-1} in potassium ethyl 1-methoxypicrate to N—O antisymmetric and symmetric stretches, respectively. The corresponding frequencies of the parent nitro compound were 1552 and 1343 cm^{-1}. Dyall and co-workers (4–6), in studies of Meisenheimer adducts of a series of picryl ethers, seem to concur with these assignments. They suggest further that the covalent structure **1** should show the characteristic bands of a ketal (25) at 1195–1158, 1143–1124, 1098–1063, and 1058–1038 cm^{-1} and consequently assign the strong bands of the adducts in the region 1300–1000 cm^{-1} to this source. Although the TNB–CN^- complex does possess a band in the 1495–1505 cm^{-1} region, its apparent molar extinction coefficient is smaller than those associated with the nitro group vibrations in TNB, and we prefer to assign the far more intense bands at 1235 and 1190 cm^{-1} to the antisymmetric and symmetric N—O stretching modes in the complex. In this connection we note that the apparent molar extinction coefficients of the 1235 and 1190 cm^{-1} bands are an order of magnitude greater than the apparent molar extinction coefficients of the bands characteristic of ketals (25) and that only the 1063 and 1050 cm^{-1} bands have apparent molar extinction coefficients in the range of those expected for a ketal.

The bands at 1163–1152 and 1063–1053 cm^{-1} in the Meisenheimer adducts of the picryl ethers have been assigned to out-of-plane and in-phase in-plane C—H deformations (4). In our system the new band at 1050 cm^{-1} is present in both the

Can. J. Chem. Downloaded from www.nrcresearchpress.com by 210.87.254.105 on 09/05/12
For personal use only.

Can. J. Chem. Downloaded from www.nrcresearchpress.com by 210.87.254.105 on 09/05/12
For personal use only.

TABLE I

Numbers of infrared- and Raman-active vibrations of 1,3,5-trinitrobenzene and the 1,3,5-trinitrobenzene – cyanide ion complex according to point groups D_{3h}, C_{2v}, and C_s

Species	Point group	Active species and correlation*	TNB vibrations		Additional C—C—N vibrations	
			Infrared	Raman	Infrared	Raman
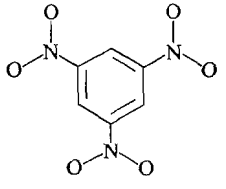	D_{3h}	$6A_1'$(R) $5A_2'$(—) $11E'$(i.r., R) $1A_1''$(—) $4A_2''$(i.r.) $5E''$(R)	15	22	—	—
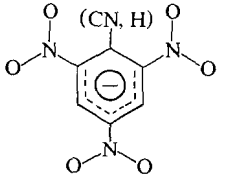	C_{2v}	$17A_1$(i.r., R) $16B_2$(i.r., R) $6A_2$(R) $9B_1$(i.r., R)	42	48	6	6
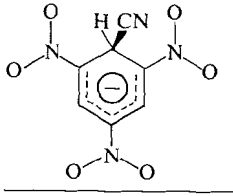	C_s	$33A_1'$(i.r., R) $15A''$(i.r., R)	48	48	6	6

*R for Raman active, i.r. for infrared active, — for inactive species.

TNB–CN^- complex and the TNB-d_3 – CN^- complex and consequently cannot be assigned to a C—H mode. As in the picryl ether adducts, the C—H stretching mode (3094 cm^{-1}) is extremely weak.

The ring stretching frequency of TNB at 1625 cm^{-1} shifts to lower frequency and increases slightly in intensity as a result of complex formation. In accord with the assignment of the band in this region as a ring stretching frequency, the TNB-d_3 – CN^- complex absorbs at slightly lower frequency than the TNB – CN^- complex.

Although some progress can be made in assigning the frequencies of the complex to various fundamental modes, none of the assignments is proved by the present information. The Raman spectrum of the complex would be particularly valuable in this context. Thus the Raman spectrum of TNB has very strong bands assigned to A_1' modes at 1365, 1184, 1002, and 825 cm^{-1} (Raman-active only), which appear not to have been made "allowed" in the complex. These bands should be present, however, in the Raman spectrum of the complex. On the other hand, E' modes appear in both the infrared and Raman spectrum of TNB, and shifts in frequencies of these bands on complex formation should be similar in both the Raman and infrared. Consequently the Raman spectrum of the complex might give support to our suggestion that the symmetry of the complex can be considered to remain approximately that of TNB and aid us in the assignment of frequencies. Raman studies in these systems are anticipated.

Acknowledgment

Financial support by the National Research Council of Canada is gratefully acknowledged.

1. R. Foster and D. Ll. Hammick. J. Chem. Soc. 2153 (1954).
2. R. A. Henry. J. Org. Chem. **27**, 2637 (1962).
3. R. C. Farmer. J. Chem. Soc. 3425 (1959).
4. L. K. Dyall. J. Chem. Soc. 5160 (1960).
5. L. K. Dyall. J. Chem. Educ. **43**, 663 (1966).
6. J. E. Dickeson, L. K. Dyall, and V. A. Pickles. Aust. J. Chem. **21**, 1267 (1968).
7. R. Foster and C. A. Fyfe. Rev. Pure Appl. Chem. Aust. **16**, 61 (1966).
8. A. Ya Kaminskii and S. S. Gitis. J. Gen. Chem. USSR, **34**, 3794 (1964).
9. E. Buncel, A. R. Norris, and K. E. Russell. Quart. Rev. London, 123 (1968).
10. M. R. Crampton. J. Chem. Soc. B, 1341 (1967).
11. E. Buncel, A. R. Norris, and W. Proudlock. Can. J. Chem. **46**, 2759 (1968).
12. E. Buncel and E. A. Symons. Can. J. Chem. **44**, 771 (1966).
13. E. A. Symons. Ph.D. Thesis, Queen's University, Kingston. 1969.
14. B. Bosnich. Ph.D. Thesis, Australian National University, Canberra. 1962.
15. N. B. Colthup, L. H. Daly, and S. E. Wiberly. Introduction to infrared and Raman spectroscopy. Academic Press, Inc., New York, N.Y. 1964. p. 62.
16. Barnes Engineering Company, Stamford, Conn. Catalog 1968.
17. H. F. Shurvell, J. A. Faniran, E. A. Symons, and E. Buncel. Can. J. Chem. **45**, 117 (1967).
18. H. F. Shurvell, A. R. Norris, and D. E. Irish. Can. J. Chem. **47**, 2515 (1969).
19. J. H. Yoe and A. L. Jones. Ind. Eng. Chem. Anal. Ed. **16**, 111 (1944). J. H. Yoe and A. E. Harvey, Jr. J. Amer. Chem. Soc. **70**, 648 (1948).
20. A. R. Norris. Can. J. Chem. **45**, 2703 (1967).
21. A. R. Norris. Can. J. Chem. **47**, 2895 (1969).
22. W. Proudlock. Unpublished results.
23. A. R. Norris. J. Org. Chem. **34**, 1486 (1969).
24. P. Caveng, P. B. Fischer, E. Heilbronner, A. L. Miller, and H. Zollinger. Helv. Chim. Acta, **50**, 848 (1967).
25. E. D. Bergmann and S. Pinchas. Rec. Trav. Chim. **71**, 161 (1952).

Can. J. Chem. Downloaded from www.nrcresearchpress.com by 210.87.254.105 on 09/05/12
For personal use only.

Electrical conductivity studies of fluorosulfuric acid and tetramethylammonium fluorosulfate in nitrobenzene

W. Reed, D. W. Secret, R. C. Thompson, and P. A. Yeats
Department of Chemistry, The University of British Columbia, Vancouver 8, British Columbia
Received July 17, 1969

Electrical conductivity data for solutions of tetramethylammonium fluorosulfate and fluorosulfuric acid in nitrobenzene are reported. The dissociation constant of the tetramethylammonium salt is 2.0×10^{-2} and the mobility of the fluorosulfate ion is 21.4. Although the conductivity data for solutions of fluorosulfuric acid could not be treated rigorously, it is shown that in dilute solutions, fluorosulfuric acid undergoes rather weak dissociation with a dissociation constant estimated to be less than 6×10^{-6}. This result is contrasted with earlier work which showed that nitrobenzene is fully protonated and dissociation into ions is complete when fluorosulfuric acid forms the bulk solvent.

Canadian Journal of Chemistry, 47, 4275 (1969)

Can. J. Chem. Downloaded from www.nrcresearchpress.com by 210.87.254.42 on 09/05/12
For personal use only.

Introduction

As a nonaqueous solvent, fluorosulfuric acid has proven extremely useful for the study of the protonation of very weak bases and in the study of cationic species which are unstable in more basic media (1, 2). In bulk, it provides the most strongly acidic medium of any simple liquid. Relatively little work has been devoted to the study of the acid strength of fluorosulfuric acid under the condition that it is present as a dilute solution in another solvent where, as was suggested previously (3), the acid strength may differ considerably from that of bulk fluorosulfuric acid. Under these conditions a measure of its acid strength is the extent to which it dissociates a proton. Previous work of this nature has involved studies of solutions of fluorosulfuric acid in protonic solvents. It has been reported to be fully dissociated in water (4), and in acetic acid, although no dissociation constant was measured, it has been shown to dissociate to a greater extent than perchloric acid (5). Even in the highly acidic medium, sulfuric acid, fluorosulfuric acid undergoes weak dissociation (3). The present work was undertaken in an effort to determine the acid strength of fluorosulfuric acid in a nonprotonic medium. Nitrobenzene was chosen as it has a reasonably high dielectric constant for an organic liquid and, moreover, previous work (6) has shown that it has a high enough proton affinity so that it is completely protonated when present as a dilute solution in fluorosulfuric acid.

For comparison, we have also used electrical conductivity measurements to determine the degree of dissociation of an ionic fluorosulfate, namely, tetramethylammonium fluorosulfate, in nitrobenzene.

Experimental

Preparation and Purification of Materials

Reagent grade nitrobenzene was washed successively with 1 *N* sulfuric acid and saturated sodium carbonate solution followed by continuous washing with water until the aqueous layer was colorless. The nitrobenzene was then stored over molecular sieve and finally doubly distilled under vacuum at 30 °C. Fluorosulfuric acid was purified by double distillation at atmospheric pressure as described previously (6). Tetramethylammonium fluorosulfate was prepared by reacting dry tetramethylammonium chloride with fluorosulfuric acid in a manner analogous to that used previously in the preparation of the alkali metal fluorosulfates (6). The product was recrystallized from water. Microanalyses were obtained in the microanalytical laboratory of the University of British Columbia.

Anal. Calcd. for $(CH_3)_4NFSO_3$: C, 27.74; H, 8.09; N, 6.97. Found: C, 27.71; H, 8.01; N, 7.02.

Electrical Conductivity Measurements

Cell resistances were measured at 25 ± 0.01° and 2000 cycles using a precision a.c. bridge described previously (7). The cell consisted essentially of 2 flasks of approximately 200 ml capacity, fitted with ground glass caps and joined by an electrode chamber containing 2 platinum electrodes which were coated with platinum black as described by Jones and Bollinger (8). The cell constant, determined using aqueous potassium chloride solution (9), was approximately 0.6 cm^{-1}. Electrode polarization effects were apparently not serious as periodic checks of solution resistances at 4000 cycles were found to be in satisfactory agreement with those obtained at 2000 cycles.

The nitrobenzene used in this work had a specific conductivity of $1–4 \times 10^{-8}$ ohm^{-1} cm^{-1} and was less than 1% of the conductivity observed for the most dilute solutions studied. The solution conductivities were corrected by subtracting the solvent conductivity from those of the solutions.

Preliminary studies on solutions of fluorosulfuric acid in nitrobenzene showed that the solutions are not stable indefinitely, particularly in regions of high concentration. Experiments in which fluorosulfuric acid, in the form of concentrated solutions in nitrobenzene (approximately 0.2 g per g nitrobenzene) which had been allowed to

TABLE I

Equivalent conductivities in nitrobenzene at 25 °C

Fluorosulfuric acid				Tetramethylammonium fluorosulfate	
Concentration, 10^2 *M*	Λ, ohm^{-1} cm^2 equiv.	Concentration, 10^2 *M*	Λ, ohm^{-1} cm^2 equiv.	Concentration, 10^4 *M*	Λ, ohm^{-1} cm^2 equiv.
Experiment 1		7.710	0.178	1.540	37.53
0.972	0.476	8.789	0.164	2.105	37.15
1.992	0.423	9.951	0.152	3.131	36.84
1.044	0.544	12.413	0.135	4.004	36.60
0.661	0.589	15.401	0.122	5.566	36.10
0.520	0.606	Experiment 2		6.284	35.54
1.635	0.461	1.816	0.449	7.664	35.61
3.282	0.315	1.079	0.518	8.376	35.43
3.630	0.292	0.772	0.572	9.359	35.20
4.055	0.273	0.446	0.651	9.660	35.11
5.788	0.213	3.116	0.326		

stand for several hours, was added to pure nitrobenzene in the conductivity cell did not give reproducible results. The procedure used in obtaining the results presented in Table I for solutions of fluorosulfuric acid over the concentration range 0.004 to 0.15 *M* avoided high concentrations and allowed for fairly rapid determinations of solution resistances.

The data given in Table I are presented in the order in which they were obtained. In experiment 1, approximately 15 ml of nitrobenzene were distilled directly into the conductivity cell. A dilute solution of fluorosulfuric acid in nitrobenzene (approximately 0.03 g acid per g nitrobenzene) was prepared in a weight dropper and the first 2 data points were obtained by making additions to the cell from this dropper. The next 3 points were obtained by making additions of pure nitrobenzene to the cell from a second weight dropper. The remaining points were obtained by adding pure fluorosulfuric acid to the cell from a third weight dropper. Resistance measurements were made 15 to 20 min after each addition to the cell, allowing time for mixing and the attainment of temperature equilibrium. Experiment 2 was performed in an analogous manner. A possible source of error in these experiments arises from the fact that, while every effort was made to minimize exposure of the contents of the cell to the atmosphere, the contents were exposed briefly during each addition and traces of atmospheric water entering the cell could affect the conductivity. The procedure employed allowed us to determine whether such errors are serious. The dilute region which was covered by the two experiments yields, apart from a single point corresponding to the first addition in experiment 1, a smooth conductivity vs. concentration curve with relatively small experimental scatter. If water impurities entering the cell during each addition were contributing significantly to the conductivity of the solution then data points obtained after 5 or 6 additions to the cell would not be expected to agree with those obtained on the first or second addition.

Fluorosulfuric acid and nitrobenzene are miscible in all proportions. To obtain conductivities of mixtures of the two over the entire range of composition the following procedure was used. The range 15 to 100 mole % nitrobenzene was covered by adding fluorosulfuric acid from a weight dropper to nitrobenzene in the cell. The range 0 to 45 mole % nitrobenzene was covered by adding nitrobenzene from a weight dropper to fluorosulfuric acid in the cell.

While visible–ultraviolet spectra of the solutions were not studied in this work, it was noted that the dilute solutions of fluorosulfuric acid in nitrobenzene were a very pale yellow, with the intensity increasing considerably in the higher concentration regions.

Solutions of tetramethylammonium fluorosulfate in nitrobenzene are stable and show no drift in conductivity with time. The solutions were obtained by making several additions from a weight dropper of a solution of the salt in nitrobenzene to nitrobenzene in the cell.

All solutions were made up by weight and where molarities are quoted these were calculated assuming a solution density of 1.1986 g/cc (10).

Molecular Weight Measurements

The molecular weight of fluorosulfuric acid in nitrobenzene was determined by the freezing-point depression method employing the conventional Beckmann technique. The cryoscope, which could be sealed to the atmosphere, was charged with a weighed amount of nitrobenzene in a drybox and opened to the atmosphere only momentarily during the addition of the solute. The solute, fluorosulfuric acid, was added in the form of a solution in nitrobenzene. Solutions in the cryoscope were stirred magnetically and temperatures were measured by a Leeds and Northrup capsule platinum resistance thermometer, calibrated by the National Research Council, Ottawa. Resistances were determined on a Guideline Potentiometer (Leeds and Northrup, Type 4363 A) with a standard 10 ohm resistance. The amount of supercooling was 0.5 to 0.9° and corrections were made for the amount of solvent frozen out. To test the accuracy of the apparatus and general procedure, the freezing points of solutions of benzil in nitrobenzene were determined. For freezing-point depressions over the range 0.05 to 1.3°, a plot of freezing-point depression vs. molality of benzil was linear

Can. J. Chem. Downloaded from www.nrcresearchpress.com by 210.87.254.42 on 09/05/12
For personal use only.

Can. J. Chem. Downloaded from www.nrcresearchpress.com by 210.87.254.42 on 09/05/12
For personal use only.

and corresponded to a molal freezing-point depression constant of 7.00, in good agreement with published values (11). This value of 7.00 was used in the subsequent calculation of the molecular weight of fluorosulfuric acid in nitrobenzene.

Results and Discussion

It is convenient to discuss first our results on solutions of tetramethylammonium fluorosulfate. Values of equivalent conductivity are tabulated in Table I. Electrical conductivity measurements have been reported on a number of alkylammonium salts in nitrobenzene (10, 12), where the authors used the method of Fuoss (13) to obtain values of Λ_0, the equivalent conductivity at infinite dilution, and K, the dissociation constant. Our data on tetramethylammonium fluorosulfate, treated in the same manner, yield values of 38.7 ohm^{-1} cm^2 equiv.$^{-1}$ for Λ_0 and 2.0×10^{-2} for K. The dissociation constant is comparable in magnitude to those reported for a number of tetraalkylammonium salts (10, 12). Employing the value 17.3 for the mobility (meaning here the equivalent conductivity at infinite dilution) of the tetramethylammonium cation (10) the mobility of the fluorosulfate ion is 21.4, agreeing favorably with the value 20.9 reported previously for the isoelectronic perchlorate ion (12). Woolf has estimated the mobility of the fluorosulfate ion in water to be 71, in close agreement with the value of 69 for the perchlorate ion in that solvent (4). In fluorosulfuric acid the fluorosulfate ion has an abnormally high mobility of 135, presumably due to its participation in a proton-transfer mechanism of conduction in fluorosulfuric acid (6).

We consider now the nature of solutions of fluorosulfuric acid in nitrobenzene. Since it is known that fluorosulfuric acid is extensively associated in the liquid state, freezing-point depression measurements on dilute solutions of the acid in nitrobenzene were made in order to determine whether any extensive association remains in solution. Results on 6 different concentrations in the range 7 to 32 g acid per kg nitrobenzene gave an average molecular weight of 103 ± 5 compared to the calculated value of 100, thus showing that the acid is essentially monomeric in solution.

Values of equivalent conductivity for dilute solutions of fluorosulfuric acid in nitrobenzene are given in Table I and plotted against the square root of the molarity, c, in Fig. 1. Although the simplest possible mode of dissociation of

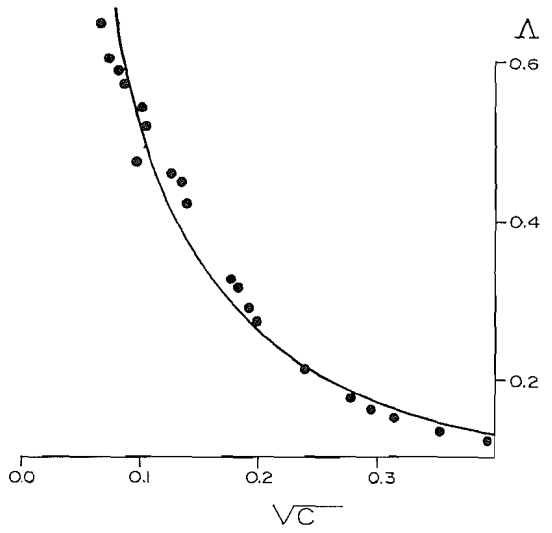

FIG. 1. Equivalent conductance (ohm^{-1} cm^2 equiv.$^{-1}$) vs. square root of molarity curve for fluorosulfuric acid in nitrobenzene. The solid line is calculated (see text).

fluorosulfuric acid in nitrobenzene is

[1] $$HSO_3F = H^+ + SO_3F^-$$

the possibility of the formation of triple ions according to

[2] $$SO_3F^- + HSO_3F = H(SO_3F)_2^-$$

cannot be neglected. Using a number of approximations, French and Roe (14) were able to account for the variation of the conductance of picric acid with concentration in a number of organic solvents by assuming processes analogous to those given in reactions [1] and [2]. Our data for dilute solutions of fluorosulfuric acid in nitrobenzene do not fit the expression developed by French and Roe. Ignoring reaction [2], the French and Roe equation becomes simply

[3] $$\Lambda = \Lambda_0 K_1^{1/2} c^{-1/2}$$

where K_1 is the dissociation constant for reaction [1] and Λ_0 is the equivalent conductivity at infinite dilution. Our data are in approximate agreement with a relationship of this form. In Fig. 1 the solid line was calculated using eq. [3] with $\Lambda_0 K_1^{1/2}$ equal to 0.052 ohm^{-1} cm$^{1/2}$ equiv.$^{-1/2}$. It would appear, then, that up to concentrations of 0.15 mole of fluorosulfuric acid per l of solution there is no significant amount of triple ion formation. Assuming that the dissociation of fluorosulfuric acid in nitro-

Can. J. Chem. Downloaded from www.nrcresearchpress.com by 210.87.254.42 on 09/05/12
For personal use only.

benzene is correctly given by reaction [1], it should be possible to determine the equilibrium constant from the conductivity data. Attempts to determine K_1 accurately are, however, hampered by the low equivalent conductivities observed, by the scatter in the experimental points, and by the fact that it is impossible to extrapolate the data to obtain Λ_0. It is possible, however, to estimate an upper limit for K_1. The minimum possible value that Λ_0 can have is 21.4 ohm^{-1} cm^2 equiv., the equivalent conductivity of the fluorosulfate ion at infinite dilution, and using this value for Λ_0 and the value 0.052 ohm^{-1} $cm^{1/2}$ $equiv.^{-1/2}$ for Λ_0 $K_1^{1/2}$, the maximum possible value for K_1 is 6×10^{-6}. This is qualitatively consistent with the observation that the equivalent conductivity values of solutions of fluorosulfuric acid in nitrobenzene are lower than those obtained by other workers for the weak electrolyte trimethylhydroxyammonium picrate, which has a dissociation constant of 1.7×10^{-5} (12).

In acid–base reactions of the type under consideration here the extent to which dissociation into free ions takes place depends not only on the relative acid–base strengths of the reactants but also on the properties of the bulk solvent, such as its dielectric constant and its ability to solvate the ions produced. As mentioned in the introduction, when fluorosulfuric acid forms the bulk medium, dissociation into free ions is complete, whereas when nitrobenzene forms the bulk solvent, only very weak dissociation takes place. The difference in the bulk dielectric constants of nitrobenzene and fluorosulfuric acid will account for only a part of this difference and may be estimated on a purely electrostatic basis as described by Bell (15). For 2 ions of opposite charge separated by a distance of 2 Å the dissociation constant will decrease by a factor of approximately 3×10^2 on going from a solvent of dielectric constant 120 (fluorosulfuric acid) to a solvent of dielectric constant 34.5 (nitrobenzene). It appears then that an important factor in accounting for the very weak dissociation of fluorosulfuric acid in nitrobenzene is that the ions produced, particularly the fluorosulfate ion, are relatively weakly solvated by the solvent. Conversely, the relatively high acidity of fluorosulfuric acid in bulk, and presumably also in solution in other protonic solvents, is due to a large extent to extensive solvation of the fluorosulfate ion through hydrogen-bonding to solvent molecules. The effect is also seen, but to a lesser degree, in the case of the dissociation of ionic fluorosulfates. Ionic fluorosulfates are fully dissociated in fluorosulfuric acid solutions (6), whereas, as shown in the present work, tetramethylammonium fluorosulfate is incompletely dissociated in nitrobenzene solution.

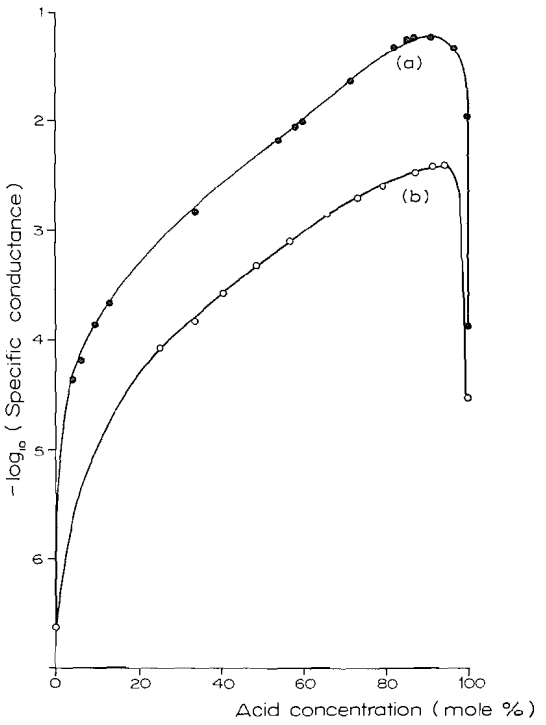

FIG. 2. Specific conductance (ohm^{-1} cm^{-1}) vs. mol % acid curves for: (*a*) HSO_3F–nitrobenzene mixtures, (*b*) HF–nitrobenzene mixtures (data taken from ref. 16).

Finally, specific conductivities of mixtures of fluorosulfuric acid and nitrobenzene over the entire range of compositions were measured and are presented graphically in Fig. 2, where they are compared with the findings of other workers (16) on the hydrogen fluoride–nitrobenzene system. Theoretical treatment of such results is difficult. It is interesting to note, however, that the general shape of the two curves, including the position of maximum conductance, is very similar. Over the entire range of compositions the fluorosulfuric acid – nitrobenzene mixtures give higher specific conductivities, reflecting a greater degree of dissociation of fluorosulfuric acid compared to hydrogen fluoride.

Acknowledgment

The authors wish to thank the National Research Council of Canada for financial support.

1. R. J. GILLESPIE. Accounts Chem. Res. 1, 202 (1968).
2. R. C. THOMPSON. *In* Inorganic sulphur chemistry. *Edited by* G. Nickless. Elsevier Publ. Co., Inc., Amsterdam. 1969. p. 587.
3. J. BARR, R. J. GILLESPIE, and E. A. ROBINSON. Can. J. Chem. **39**, 1266 (1961).
4. A. A. WOOLF. J. Chem. Soc. 2840 (1954).
5. R. C. PAUL, S. K. VAHISHT, K. C. MALHOTRA, and S. S. PAHIL. Anal. Chem. **34**, 820 (1962).
6. J. BARR, R. J. GILLESPIE, and R. C. THOMPSON. Inorg. Chem. **3**, 1149 (1964).
7. A. C. HARKNESS and H. M. DAGGETT, JR. Can. J. Chem. **43**, 1215 (1965).
8. G. JONES and D. M. BOLLINGER. J. Amer. Chem. Soc. **57**, 280 (1935).
9. J. E. LIND, J. J. ZWOLINEK, and R. M. FUOSS. J. Amer. Chem. Soc. **81**, 1557 (1959).
10. E. G. TAYLOR and C. A. KRAUS. J. Amer. Chem. Soc. **69**, 1731 (1947).
11. R. C. WEAST and S. M. SELBY (*Editors*). Handbook of chemistry and physics. 46th ed. Chemical Rubber Company, Cleveland, Ohio. 1965–66.
12. C. R. WITSCHONKE and C. A. KRAUS. J. Amer. Chem. Soc. **69**, 2472 (1947).
13. R. M. FUOSS. J. Amer. Chem. Soc. **57**, 488 (1935).
14. C. M. FRENCH and I. G. ROE. Trans. Faraday Soc. **49**, 314 (1953).
15. R. P. BELL. Acids and bases. Methuen and Co. Ltd., London, England. 1961.
16. L. QUARTERMAN, H. H. HYMAN, and J. J. KATZ. J. Phys. Chem. **65**, 90 (1961).

Can. J. Chem. Downloaded from www.nrcresearchpress.com by 210.87.254.42 on 09/05/12
For personal use only.

Can. J. Chem. Downloaded from www.nrcresearchpress.com by 210.87.254.105 on 09/05/12
For personal use only.

Isomers of bis(trifluoromethyl)phosphinomethylhydrazine, $(CF_3)_2PNHNHMe$ and $(CF_3)_2PN(Me)NH_2$

L. K. PETERSON AND G. L. WILSON
Department of Chemistry, Simon Fraser University, Burnaby 2, British Columbia

Received May 20, 1969

The synthesis of isomers of bis(trifluoromethyl)phosphinomethylhydrazine, $(CF_3)_2PNHNHMe$, **1**, and $(CF_3)_2PN(Me)NH_2$, **2**, and their characterization by infrared, nuclear magnetic resonance, and mass spectra, and by vapor phase molecular weight measurements are described. The significance of the formation of both isomers is discussed in terms of steric and electronic effects.

Canadian Journal of Chemistry, 47, 4281 (1969)

Discussion

The stepwise alkylation of methylhydrazine, which proceeds at the more alkylated of the 2 nitrogen atoms, has been rationalized in terms of the enhanced basicity of the methyl-nitrogen site (1). Substitution reactions of hydrazines with bis(trifluoromethyl)chloroarsine (2), however, give products indicative of reaction at the least alkylated site, a feature attributed to steric factors (2). In general, the reactions of trialkylsilylhydrazine, $R_3SiNHNH_2$, with chlorosilanes give mixtures of isomers, N,N- and N,N′-bis(trialkylsilyl)hydrazine (3); the presence of a bulky R group on silicon, such as *t*-butyl, results in exclusive formation of N,N′-isomers (3). A mixture of isomers was reported for the reaction of diphenylchlorophosphine with methylhydrazine, but separation was not achieved (4).

We have found that bis(trifluoromethyl)iodophosphine, $(CF_3)_2PI$, reacts at both nitrogen atoms of methylhydrazine, with equal preference, giving 2 isomeric compounds, N-methyl, N′-bis(trifluoromethyl)phosphinohydrazine, $MeNHNHP(CF_3)_2$, **1**, and N-methyl,N-bis(trifluoromethyl)phosphinohydrazine, $(CF_3)_2PN(Me)NH_2$, **2**. It appears that the enhanced basicity of the methyl nitrogen is compensated by steric interactions[1]. Alternatively, $(CF_3)_2PI$ may be insensitive to the differing basicities of the 2 nitrogen atoms, in the sense that the activation energies for the 2 possible 4-center intermediate complexes (**3**, **4**) may be quite similar.

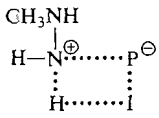

3

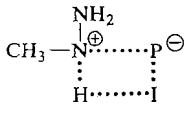

4

Compounds **1** and **2** were separated by vacuum fractionation, and were identified on the basis of infrared, nuclear magnetic resonance (n.m.r.), and mass spectra (parent peaks, M_{obs}, 214; M_{calcd}, 214; major fragments, MeNHNH and $CF_3PNHNHMe$), and by vapor phase molecular weight measurements. In addition, the overall reaction was essentially quantitative

$$(CF_3)_2PI + 2\ MeNHNH_2 \rightarrow \tfrac{1}{2}MeNHNHP(CF_3)_2 + \tfrac{1}{2}(CF_3)_2PN(Me)NH_2 + MeNHNH_2HI$$

Compound **1**, which could be obtained pure, has the higher melting point (35.5 ± 0.1 °C), in line with its more symmetrical molecular structure. The proton n.m.r. spectrum corresponded to the resonance absorptions of the N—CH_3 (at τ 7.37, $SiMe_4$ internal reference), MeN—H (τ 6.39) and PN—H protons (τ 5.70), the integrated intensity ratios being 3:1:1 (NCH_3:NH:NH). The N—H assignments were made by comparison with other members of a series of phosphinohydrazines (see Table I); on the basis of its electronegative character, the $(CF_3)_2P$ group must be linked with the nitrogen atoms bearing the least shielded proton.

The proton n.m.r. spectrum of compound **2** consisted of a doublet, indicative of the N—CH_3 absorption split by the spin $+\frac{1}{2}$, ^{31}P nucleus (τ, midpoint, 6.93; *J*(PNCH), 8.5 c.p.s.); and a

[1]Suggested by one of the referees.

Can. J. Chem. Downloaded from www.nrcresearchpress.com by 210.87.254.105 on 09/05/12
For personal use only.

TABLE I

Nuclear Magnetic resonance spectra* of phosphinohydrazines

(*a*) Proton spectra

	τ values			
Substituent†	$MeNHNHP(CF_3)_2$	$(CF_3)_2PNMeNH_2$	$Me_2NNHP(CF_3)_2$‡	$Me_2NNMeP(CF_3)_2$§
$-N(H)H$	—	6.15	—	—
$-N(H)CH_3$	6.39	—	—	—
$-N(H)P$	5.70	—	5.95	—
$-N(CH_3)CH_3$	—	—	7.50	7.50
$-N(CH_3)H$	7.37	—	—	—
$-N(CH_3)P$	—	6.93 (*J*, 8.5)	—	7.13 (*J*, 3.6)

(*b*) Fluorine spectra

	Values			
Substituent	$MeNHNHP(CF_3)_2$	$(CF_3)_2PNMeNH_2$	$Me_2NNHP(CF_3)_2$	$Me_2NNMeP(CF_3)_2$
$-P(CF_3)CF_3$	63.8 (*J*, 80)	60.6 (*J*, 84)	65.0‖ (*J*, 84)	61.5‖ (*J*, 82)

*The internal standards were $SiMe_4$ for the proton spectra and $CFCl_3$ for the fluorine spectra. Proton spectra are reported as τ values; fluorine spectra, in p.p.m. Coupling constants, *J*, are given in c.p.s.
†Protons and fluorines for which spectral values are given are indicated by italics.
‡Reference 5.
§Reference 6.
‖The fluorine spectra were re-run, on a re-calibrated instrument; literature values are: for $Me_2NNHP(CF_3)_2$, 63.5 p.p.m. (5); for $Me_2NNMeP(CF_3)_2$, 63.4 p.p.m. (6).

broad band for the NH_2 protons (τ 6.15; integrated ratios, NCH_3:NH_2, 3:2). The ^{19}F bands were simple doublets for both compounds, consistent with a splitting of the absorption due to 6 equivalent fluorines by coupling with the ^{31}P nucleus (compound **1**, midpoint, 63.8 p.p.m. above internal $CFCl_3$; *J*(PCF), 80.0 c.p.s.; compound **2**, midpoint, 60.6 p.p.m.; *J*(PCF), 84.3 c.p.s.).

The main features of the infrared spectra of compounds **1** and **2**, given in Tables II and III, are indicative of bands due to CF_3 (1100–1200 cm^{-1}), CH_3 (2800–3000 cm^{-1}), and NH or NH_2 (3300–3400 cm^{-1}). Compound **1** shows two

TABLE II

Infrared spectrum* of $MeNHNHP(CF_3)_2$

Frequency cm^{-1}	Intensity	Frequency cm^{-1}	Intensity
740	(9)	1485	shoulder
810	(17)	2250	(1)
978	(11)	2810	(8)
1110	(71)	2865	(13)
1158	(100)	2880	shoulder
1204	(84)	2925	shoulder
1270	shoulder	2970	(13)
1375	(3)	3008	shoulder
1440	shoulder	3340	(5)
1450	(7)	3428	(4)

*Intensities are quoted relative to the strongest band, at 1158 cm^{-1}, with a value of 100 arbitrary units.

TABLE III

Infrared spectrum* of $(CF_3)_2PNMeNH_2$

Frequency cm^{-1}	Intensity	Frequency cm^{-1}	Intensity
687	(24)	1470	(4)
835	(21)	1480	(4)
852	(23)	1605	(4)
868	(24)	2250	(2)
1010	(29)	2825	(7)
1035	shoulder	2880	shoulder
1111	(82)	2921	(13)
1148	(100)	2948	shoulder
1195	(86)	2995	shoulder
1280	(7)	3410	(2)
1425	shoulder		
1442	(5)		

*Intensities are quoted relative to the strongest band, at 1148 cm^{-1}, with a value of 100 arbitrary units.

N—H stretching modes, corresponding to the distinct PN—H and MeN—H groupings, at 3340 and 3428 cm^{-1}, respectively. Only one band at 3410 is found in compound **2**, in which the primary amino (NH_2) group is present.

Experimental

The experimental procedure has been described elsewhere (5).

Reaction of $(CF_3)_2PI$ with $MeNHNH_2$

Using a glass reaction vessel fitted with in situ filtration facilities, methylhydrazine (0.4550 g) was condensed onto a frozen solution of $(CF_3)_2PI$ (1.1952 g) in ether (5.1805 g); upon melting, a white precipitate was formed. After 1 h at room temperature, the products were filtered and separated by vacuum fractionation into $MeNHNHP(CF_3)_2$, **1** (0.3707 g, held at −33°), $(CF_3)_2PNMeNH_2$, **2** (0.43262 g, −63°), and ether (mainly held at −210°). A white residue of $MeNHNH_2HI$ (0.7796 g) remained. The overall yield of product was 91%. By repeated fractional condensation in vacuo, compound **1** was obtained pure (m.p. 35.5 ± 0.1°; b.p., 23.4°/6.60 mm). Compound **2** could not be freed from all traces of its isomer (b.p., ~23.2°/13.4 mm). Both compounds were identified by vapor phase molecular weight (*M*, calcd., 214; *M*, obsd., 215–219), by mass spectra (parent peak, obsd., 214; calcd., 214), by infrared (Tables II and III), and by n.m.r. measurements.

Acknowledgment

The authors gratefully acknowledge the financial support of the National Research Council of Canada.

1. R. L. Hinman J. Org. Chem. **23**, 1587 (1959).
2. L. K. Peterson and K. I. Thé. Can. J. Chem. **47**, 339 (1969).
3. R. West, M. Ishikawa, and R. E. Bailey. J. Amer. Chem. Soc. **88**, 4648 (1966).
4. R. P. Nielson and H. H. Sisler. Inorg. Chem. **2**, 753 (1963).
5. L. K. Peterson and G. L. Wilson. Can. J. Chem. **46**, 685 (1968).
6. L. K. Peterson, G. L. Wilson, and K. I. Thé. Can. J. Chem. **47**, 1025 (1969).

Adducts of oxovanadium(IV) dithiocarbamates

B. Jack McCormick

Department of Chemistry, West Virginia University, Morgantown, W.Va. 26506

Received May 12, 1969

Pyridine and 4-methylpyridine adducts of oxovanadium(IV) dithiocarbamates have been isolated and characterized as solids. It has been shown that the addenda can be removed under mild conditions with concomitant regeneration of the parent dithiocarbamate (DTC) complexes. Attempts to isolate dimethylsulfoxide adducts have not been successful, although spectral evidence suggests that adducts are formed in solution. A qualitative rationalization of the molecular orbital ordering and electronic spectral properties of the adducts is presented.

Canadian Journal of Chemistry, 47, 4283 (1969)

Introduction and Discussion

In a previous paper dealing with the isolation and characterization of several oxovanadium(IV) dithiocarbamate complexes, it was reported that rather significant spectral shifts occur in both the infrared and visible regions when the complexes

Can. J. Chem. Downloaded from www.nrcresearchpress.com by 210.87.254.105 on 09/05/12
For personal use only.

TABLE II

Infrared spectrum* of $MeNHNHP(CF_3)_2$

Frequency cm^{-1}	Intensity	Frequency cm^{-1}	Intensity
740	(9)	1485	shoulder
810	(17)	2250	(1)
978	(11)	2810	(8)
1110	(71)	2865	(13)
1158	(100)	2880	shoulder
1204	(84)	2925	shoulder
1270	shoulder	2970	(13)
1375	(3)	3008	shoulder
1440	shoulder	3340	(5)
1450	(7)	3428	(4)

*Intensities are quoted relative to the strongest band, at 1158 cm^{-1}, with a value of 100 arbitrary units.

TABLE III

Infrared spectrum* of $(CF_3)_2PNMeNH_2$

Frequency cm^{-1}	Intensity	Frequency cm^{-1}	Intensity
687	(24)	1470	(4)
835	(21)	1480	(4)
852	(23)	1605	(4)
868	(24)	2250	(2)
1010	(29)	2825	(7)
1035	shoulder	2880	shoulder
1111	(82)	2921	(13)
1148	(100)	2948	shoulder
1195	(86)	2995	shoulder
1280	(7)	3410	(2)
1425	shoulder		
1442	(5)		

*Intensities are quoted relative to the strongest band, at 1148 cm^{-1}, with a value of 100 arbitrary units.

N—H stretching modes, corresponding to the distinct PN—H and MeN—H groupings, at 3340 and 3428 cm^{-1}, respectively. Only one band at 3410 is found in compound **2**, in which the primary amino (NH_2) group is present.

Experimental

The experimental procedure has been described elsewhere (5).

Reaction of $(CF_3)_2PI$ with $MeNHNH_2$

Using a glass reaction vessel fitted with in situ filtration facilities, methylhydrazine (0.4550 g) was condensed onto a frozen solution of $(CF_3)_2PI$ (1.1952 g) in ether (5.1805 g); upon melting, a white precipitate was formed. After 1 h at room temperature, the products were filtered and separated by vacuum fractionation into $MeNHNHP(CF_3)_2$, **1** (0.3707 g, held at −33°), $(CF_3)_2PNMeNH_2$, **2** (0.43262 g, −63°), and ether (mainly held at −210°). A white residue of $MeNHNH_2HI$ (0.7796 g) remained. The overall yield of product was 91%. By repeated fractional condensation in vacuo, compound **1** was obtained pure (m.p. 35.5 ± 0.1°; b.p., 23.4°/6.60 mm). Compound **2** could not be freed from all traces of its isomer (b.p., ~23.2°/13.4 mm). Both compounds were identified by vapor phase molecular weight (*M*, calcd., 214; *M*, obsd., 215–219), by mass spectra (parent peak, obsd., 214; calcd., 214), by infrared (Tables II and III), and by n.m.r. measurements.

Acknowledgment

The authors gratefully acknowledge the financial support of the National Research Council of Canada.

1. R. L. Hinman J. Org. Chem. **23**, 1587 (1959).
2. L. K. Peterson and K. I. Thé. Can. J. Chem. **47**, 339 (1969).
3. R. West, M. Ishikawa, and R. E. Bailey. J. Amer. Chem. Soc. **88**, 4648 (1966).
4. R. P. Nielson and H. H. Sisler. Inorg. Chem. **2**, 753 (1963).
5. L. K. Peterson and G. L. Wilson. Can. J. Chem. **46**, 685 (1968).
6. L. K. Peterson, G. L. Wilson, and K. I. Thé. Can. J. Chem. **47**, 1025 (1969).

Adducts of oxovanadium(IV) dithiocarbamates

B. Jack McCormick

Department of Chemistry, West Virginia University, Morgantown, W.Va. 26506

Received May 12, 1969

Pyridine and 4-methylpyridine adducts of oxovanadium(IV) dithiocarbamates have been isolated and characterized as solids. It has been shown that the addenda can be removed under mild conditions with concomitant regeneration of the parent dithiocarbamate (DTC) complexes. Attempts to isolate dimethylsulfoxide adducts have not been successful, although spectral evidence suggests that adducts are formed in solution. A qualitative rationalization of the molecular orbital ordering and electronic spectral properties of the adducts is presented.

Canadian Journal of Chemistry, 47, 4283 (1969)

Introduction and Discussion

In a previous paper dealing with the isolation and characterization of several oxovanadium(IV) dithiocarbamate complexes, it was reported that rather significant spectral shifts occur in both the infrared and visible regions when the complexes

Can. J. Chem. Downloaded from www.nrcresearchpress.com by 210.87.254.105 on 09/05/12
For personal use only.

TABLE I

Analytical data for adducts*

Compound†	% carbon		% hydrogen		% nitrogen	
	Calcd.	Found	Calcd.	Found	Calcd.	Found
VOL_2A	34.2	35.4‡	4.44	4.63	10.9	11.0
VOL'_2A	41.1	41.3	4.82	4.42	9.58	10.1
VOL_2A'	36.0	37.6‡	4.78	4.73	10.5	10.5
VOL'_2A'	42.5	42.6	5.12	5.48	9.29	9.52

*Elemental analyses were done by Galbraith Laboratories, Knoxville, Tennessee.
†L and L′ are N,N-dimethyldithiocarbamate and pyrrolidine-N-carbodithioate, respectively; A and A′ are pyridine and 4-methylpyridine, respectively.
‡Carbon analyses on the methyl derivatives were consistently high.

are dissolved in pyridine or dimethylsulfoxide (1). These shifts were interpreted in terms of the addition of a solvent molecule to the sixth coordination position *trans* to the oxygen atom. The pyridine adduct of bis(N,N-dimethyldithiocarbamato)oxovanadium(IV) was isolated as a solid, but was not studied in detail. In view of the fact that very few of the adducts of oxovanadium(IV) complexes that have been so extensively studied in solution (2) have been prepared as solids, it seemed worthwhile to investigate solid adducts of oxovanadium(IV) dithiocarbamates more thoroughly.

Adducts of bis(N,N-dimethyldithiocarbamato)oxovanadium(IV) and bis(pyrrolidine-N-carbodithioato)oxovanadium(IV) with pyridine and 4-methylpyridine have been prepared as solids by straightforward synthetic procedures. Similar adducts of these and other oxovanadium(IV) dithiocarbamates with a variety of nitrogenous bases undoubtedly can be prepared by analogous techniques. The analytical data presented in Table I indicate that the adducts have the general formula $[VO(DTC)_2(base)]$.

It was shown previously that rather significant shifts in the C···N and V=O stretching frequencies result when the bis-dithiocarbamates are mulled with Nujol containing pyridine, and these shifts were interpreted in terms of the addition of pyridine to the sixth coordination position on the vanadium atom (1). The C···N and V=O stretching frequencies reported in Table II for the solid pyridine adducts are virtually identical to those reported earlier and the corresponding data for the 4-methylpyridine adducts is very similar to that obtained with pyridine. The infrared spectra clearly show bands attributable to coordinated pyridine and 4-methylpyridine (3). Of particular value are the strong bands near 1600 and 700 cm^{-1} in the pyridine complexes and near 1600, 800, and 715 cm^{-1} in the 4-methylpyridine complexes. Since the parent bis-dithiocarbamate complexes do not exhibit absorptions near these frequencies, the observance of these bands can be taken as good evidence for the presence of the addenda.

That addenda are rather weakly attached to the sixth coordination position of the bis-dithiocarbamates is shown by the ease with which coordinated pyridine and 4-methylpyridine can be removed. Removal can be effected by washing with a suitable solvent such as diethyl ether or by heating to 65–75° in vacuo for a period of ½ to 2 h. The gray compounds remaining after removal of the sixth ligand were shown to have infrared spectra which were *identical* to those of the parent bis-dithiocarbamates. A quantitative study was made of the weight loss that occurs when the pyridine adduct of bis(N,N-dimethyldithiocarbamato)oxovanadium(IV) is heated in vacuo (65° for 1.5 h). The weight loss corresponded to 1 mole of pyridine per mole of compound.

Since solutions of bis(dithiocarbamato)oxovanadium(IV) complexes in dimethylsulfoxide have optical spectra which are virtually identical to those measured in pyridine and 4-methylpyridine, and since pyridine and dimethylsulfoxide cause similar shifts in the C···N and V=O stretching frequencies (1), it is clear that dimethylsulfoxide forms adducts similar to those of pyridine and 4-methylpyridine. However, attempts to isolate such adducts have not been successful. The adducts are very soluble in dimethylsulfoxide and attempts to precipitate the desired compounds with reagents such as tetrahydrofuran have led to decomposition. Furthermore, it appears that the complexes slowly decompose in dimethylsulfoxide alone, and attempts to remove excess solvent by pumping have resulted in

Can. J. Chem. Downloaded from www.nrcresearchpress.com by 210.87.254.105 on 09/05/12
For personal use only.

TABLE II

Visible and infrared spectral data*

Compound†	$\bar{\nu}$ (V=O)	$\bar{\nu}$ (C···N)	$\bar{\nu}$ (base)‡	e_π*	b_1*
VOL_2	982	1546, 1539	—	17.6	16.0
VOL'_2	992	1510	—	17.8	16.5
VOL_2A	946	1518	1597, 700	13.2	16.5
VOL'_2A	950	1492	1600, 700	13.5	15.9
VOL_2A'	947	1511	1600, {800 / 790}§, 716	13.2	16.5
VOL'_2A'	944	1490	1610, 805, 716	13.3	~16.0

*Infrared data in cm^{-1}; optical spectral data in kilokaisers (kK).
†See Table I for symbols.
‡Frequencies characteristic of addenda A and A′ (see text).
§Doublet.

decomposition. Decomposition does not take place immediately, as indicated by the fact that addition of water to freshly prepared dimethylsulfoxide solutions results in the precipitation of the parent bis-dithiocarbamates.

Figure 1 shows the diffuse reflectance spectra obtained for the solid adducts. These spectra are very similar to the corresponding pyridine and dimethylsulfoxide solution spectra reported earlier (1), except for the shoulder at ca. 25 000 kK. This shoulder was not observed in the solutions.

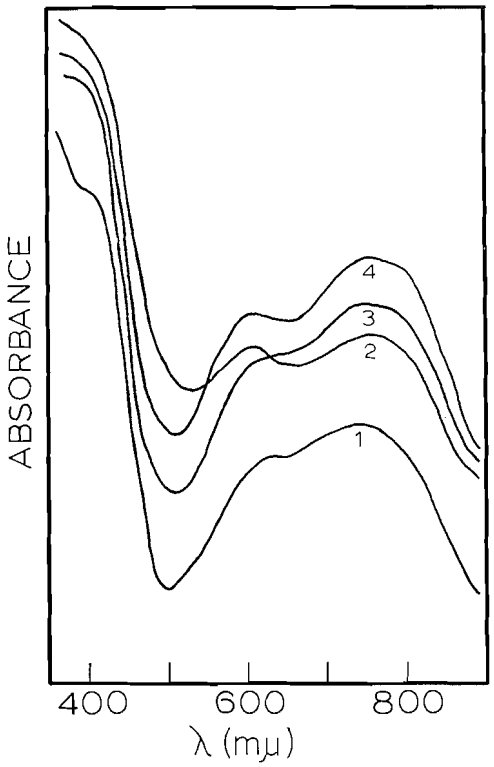

FIG. 1. Diffuse reflectance spectra of: **1**, VOL'_2A; **2**, VOL_2A; **3**, VOL'_2A'; **4**, VOL_2A'.

Our previous assignments of the optical bands of bis-dithiocarbamates were based on an inverted level scheme (4) in which the b_1* level lies below the e_π* level. It was suggested that such an inversion might result from π interactions between the vanadium atom and the equatorial sulfur ligands. Additional information bearing on the relative energies of the b_1* and e_π* levels is now available from the results of some recent molecular orbital calculations on $VO(H_2O)_5^{2+}$ by Vanquickenborne and McGlynn (5). It was shown that as the angle between the V—O axis and the 4 equatorial V—H_2O axes is increased from 90 to 105°, the b_1* and e_π* levels increase and decrease in stability, respectively, relative to the b_2 level. It is quite reasonable to expect that the O—V—S angles in the bis-dithiocarbamates are greater than 90°, since it has been shown that in other 5-coordinate dithiocarbamate complexes the metal atom is above the basal plane of the equatorial ligands (6–8). It should also be pointed out that O=V—O angles in VO(acetylacetonate)$_2$ are 106° (9). In view of these observations it is not difficult to understand the applicability of the inverted level scheme to the bis-dithiocarbamates, although it is difficult to assess the relative roles of π-bonding and O—V—S angle distortions from 90°.

Coordination of a sixth ligand to the bis-dithiocarbamates apparently displaces the sulfur atoms toward the oxygen atom with concomitant reduction of the O—V—S angles. This reduction results in the destabilization of the b_1* level relative to the e_π* level and renders the Ballhausen–Gray (10) scheme applicable to the adducts, as discussed previously (1).

Can. J. Chem. Downloaded from www.nrcresearchpress.com by 210.87.254.105 on 09/05/12
For personal use only.

The shoulder at ~25 000 kK in the adduct spectra is poorly defined, and further study will be necessary before the assignment of this band can be discussed.

Experimental

Bis (pyrrolidine - N - carbodithioato) oxovanadium (IV) and bis(N,N-dimethyldithiocarbamato)oxovanadium(IV) were prepared as described previously (1). Before use, all solvents and liquid reagents were deaerated with nitrogen, and all syntheses were carried out under an atmosphere of nitrogen.

In a typical preparation, 3 g of bis(pyrrolidine-N-carbodithioato)oxovanadium(IV) was treated with 20 ml of pyridine. The green precipitate which formed was separated by filtration and washed with five 30 ml portions of 1:1 pyridine–pentane mixtures. The adduct was dried first in a stream of dry nitrogen and then in vacuo for 10 h. Other adducts of nitrogenous bases were prepared similarly. The compounds were stored under dry nitrogen even though the air sensitivity of the adducts appears to be less than that of the parent compounds. Elemental analyses are given in Table I.

Reflectance spectra were measured with a Cary Model 14 spectrophotometer equipped with a Model 1411 reflectance attachment and a high intensity source (Cary Model 1471200) operating at 100 V. Infrared spectra were measured on Nujol mulls with a Beckman IR-8 spectrometer, and the reported frequencies are thought to be accurate to ± 2 cm^{-1}. Some pertinent spectral data are given in Table II.

Acknowledgments

The helpful comments of Mr. Irving Treitel and Prof. Harry Gray of the California Institute of Technology are gratefully acknowledged. This work was supported by the National Science Foundation through Grant No. GP-6671.

1. B. J. McCormick. Inorg. Chem. **7**, 1965 (1968).
2. J. Selbin. Chem. Rev. **65**, 153 (1965).
3. N. S. Gill, R. H. Nuttall, D. E. Scaife, and D. W. Sharp. J. Inorg. Nucl. Chem. **18**, 79 (1961).
4. J. Selbin. Coord. Chem. Rev. **1**, 293 (1966).
5. L. G. Vanquickenborne and S. P. McGlynn. Theoret. Chim. Acta, **9**, 390 (1968).
6. M. Colapietro, A. Domenicano, L. Scaramuzza, A. Vaciago, and L. Zambonelli. Chem. Commun. 583 (1967).
7. M. Bonamico, G. Dessy, A. Mugnoli, A. Vaciago, and L. Zambonelli. Acta Cryst. **19**, 886 (1965).
8. P. R. H. Alderman, P. G. Owston, and J. M. Rowe. J. Chem. Soc. 668 (1962).
9. R. P. Dodge, D. H. Templeton, and A. Zalkin. J. Chem. Phys. **35**, 55 (1961).
10. C. J. Ballhausen and H. B. Gray. Inorg. Chem. **1**, 111 (1962).

Ionization of liquid argon by X-rays: $\overline{W}$-value[1]

N. V. Klassen
Division of Applied Physics, National Research Council, Ottawa, Canada

AND

Werner F. Schmidt
Chemistry Department, Brookhaven National Laboratory, Upton, N.Y. 11973

Received August 18, 1969

Liquid argon at 87 °K was irradiated with 1.5 MeV X-rays. Saturation currents were achieved at low dose rates. The energy required to produce an ion pair ($\overline{W}_x$) was found to be 22.5 ± 3 eV, which is similar to the gas phase value.

Canadian Journal of Chemistry, 47, 4286 (1969)

A necessary quantity for the understanding of a radiolized system is the value of $\overline{W}$, the average energy required for the production of an ion pair in the system. In the gas phase, $\overline{W}$ can be determined by the saturation current method. In most liquids, field strengths exceeding the breakdown strength would be required to achieve saturation currents. Therefore, most investigators have tried to determine $\overline{W}$ by extrapolating ionization current measurements to infinite field strengths (1–3). The $\overline{W}$-values obtained in this way were substantially higher than the gas phase values.

In several liquified rare gases, Ar, Kr, Xe, the mobilities of excess electrons are high (4). Ionization currents in liquid argon have been investigated extensively using α particles. Because of the high linear energy transfer (l.e.t.) of α radiation it was impossible to obtain saturation currents.

[1]NRCC. No. 10 985.

Can. J. Chem. Downloaded from www.nrcresearchpress.com by 210.87.254.105 on 09/05/12
For personal use only.

The shoulder at ~25 000 kK in the adduct spectra is poorly defined, and further study will be necessary before the assignment of this band can be discussed.

Experimental

Bis (pyrrolidine - N - carbodithioato) oxovanadium (IV) and bis(N,N-dimethyldithiocarbamato)oxovanadium(IV) were prepared as described previously (1). Before use, all solvents and liquid reagents were deaerated with nitrogen, and all syntheses were carried out under an atmosphere of nitrogen.

In a typical preparation, 3 g of bis(pyrrolidine-N-carbodithioato)oxovanadium(IV) was treated with 20 ml of pyridine. The green precipitate which formed was separated by filtration and washed with five 30 ml portions of 1:1 pyridine–pentane mixtures. The adduct was dried first in a stream of dry nitrogen and then in vacuo for 10 h. Other adducts of nitrogenous bases were prepared similarly. The compounds were stored under dry nitrogen even though the air sensitivity of the adducts appears to be less than that of the parent compounds. Elemental analyses are given in Table I.

Reflectance spectra were measured with a Cary Model 14 spectrophotometer equipped with a Model 1411 reflectance attachment and a high intensity source (Cary Model 1471200) operating at 100 V. Infrared spectra were measured on Nujol mulls with a Beckman IR-8 spectrometer, and the reported frequencies are thought to be accurate to ± 2 cm^{-1}. Some pertinent spectral data are given in Table II.

Acknowledgments

The helpful comments of Mr. Irving Treitel and Prof. Harry Gray of the California Institute of Technology are gratefully acknowledged. This work was supported by the National Science Foundation through Grant No. GP-6671.

1. B. J. McCormick. Inorg. Chem. **7**, 1965 (1968).
2. J. Selbin. Chem. Rev. **65**, 153 (1965).
3. N. S. Gill, R. H. Nuttall, D. E. Scaife, and D. W. Sharp. J. Inorg. Nucl. Chem. **18**, 79 (1961).
4. J. Selbin. Coord. Chem. Rev. **1**, 293 (1966).
5. L. G. Vanquickenborne and S. P. McGlynn. Theoret. Chim. Acta, **9**, 390 (1968).
6. M. Colapietro, A. Domenicano, L. Scaramuzza, A. Vaciago, and L. Zambonelli. Chem. Commun. 583 (1967).
7. M. Bonamico, G. Dessy, A. Mugnoli, A. Vaciago, and L. Zambonelli. Acta Cryst. **19**, 886 (1965).
8. P. R. H. Alderman, P. G. Owston, and J. M. Rowe. J. Chem. Soc. 668 (1962).
9. R. P. Dodge, D. H. Templeton, and A. Zalkin. J. Chem. Phys. **35**, 55 (1961).
10. C. J. Ballhausen and H. B. Gray. Inorg. Chem. **1**, 111 (1962).

Ionization of liquid argon by X-rays: $\overline{W}$-value[1]

N. V. Klassen
Division of Applied Physics, National Research Council, Ottawa, Canada

AND

Werner F. Schmidt
Chemistry Department, Brookhaven National Laboratory, Upton, N.Y. 11973

Received August 18, 1969

Liquid argon at 87 °K was irradiated with 1.5 MeV X-rays. Saturation currents were achieved at low dose rates. The energy required to produce an ion pair ($\overline{W}_x$) was found to be 22.5 ± 3 eV, which is similar to the gas phase value.

Canadian Journal of Chemistry, 47, 4286 (1969)

A necessary quantity for the understanding of a radiolized system is the value of $\overline{W}$, the average energy required for the production of an ion pair in the system. In the gas phase, $\overline{W}$ can be determined by the saturation current method. In most liquids, field strengths exceeding the breakdown strength would be required to achieve saturation currents. Therefore, most investigators have tried to determine $\overline{W}$ by extrapolating ionization current measurements to infinite field strengths (1–3). The $\overline{W}$-values obtained in this way were substantially higher than the gas phase values.

In several liquified rare gases, Ar, Kr, Xe, the mobilities of excess electrons are high (4). Ionization currents in liquid argon have been investigated extensively using α particles. Because of the high linear energy transfer (l.e.t.) of α radiation it was impossible to obtain saturation currents.

[1]NRCC. No. 10 985.

Can. J. Chem. Downloaded from www.nrcresearchpress.com by 210.87.254.105 on 09/05/12
For personal use only.

Can. J. Chem. Downloaded from www.nrcresearchpress.com by 210.87.254.105 on 09/05/12
For personal use only.

Swan (5) extrapolated to infinite field strength and estimated $\overline{W}_\alpha$ in liquid argon to be 26 eV, similar to the gas phase value. Hutchinson (6) felt that $\overline{W}$ for liquid argon irradiated by γ rays was also similar to the gas phase value. Ullmaier (7) irradiated liquid argon with low energy X-rays and obtained $\overline{W}_x = 25.7 \pm 3$ eV. He found a definite l.e.t. effect of the X-ray energy on the ionization current. Furthermore, the liquid argon in his experiments appears to have been in contact with the atmosphere which would have allowed oxygen to dissolve in the liquid. In view of the importance of comparing $\overline{W}$-values in gases and liquids it seemed appropriate to investigate the ionization currents in liquid argon at low dose rates and low l.e.t. using energetic X-rays and excluding oxygen.

Experimental

X-Rays were obtained from a Van de Graaff by a beam of 1.5 MeV electrons impinging on a gold target. Two conductivity cells were used. Cell No. 1 was the metal cell of Hummel and Allen (8). It was slightly modified by filling the dead space around the collector electrode with ceresin wax. It had an electrode distance of 5.1 mm and an effective volume of 0.48 cm^3. Cell No. 2 was made of Pyrex. It had aluminum electrodes, 1.14 cm apart, and an effective volume of 3.6 cm^3. Both cells had guard rings which defined the effective cell volume. Commerical argon (Liquid Carbonic) was used without purification. The cells were evacuated to 10^{-2} Torr and filled with liquid argon. The assembly was held at 87 °K in a bath of liquid argon. A pressure of 1.4 atm of argon in the cell prevented bubble formation. Dosimetry was accomplished with an air ionization chamber (Electronic Instruments Limited, Model 37A) mounted in the radiation field in a fixed position relative to the cell. The ratio of the dose rates between the two positions was determined with the air chamber. The attenuation of the X-ray beam by the cell No. 2 assembly was determined by placing the air chamber inside a dummy cell. Attenuation by cell No. 1 was determined by irradiating a Fricke solution inside the cell. The absorbed dose rate in argon was calculated using mass energy absorption coefficients (9).

Results and Discussion

Figure 1 shows the ionization currents in liquid argon at various dose rates. The currents were independent of the polarity of the applied voltage. The current in the absence of radiation was negligible. At the lower dose rates, saturation currents were obtained at about 10 kV/cm. At the higher dose rates, saturation was not achieved at the highest voltage applied, demonstrating the effect of volume recombination. Corrections for

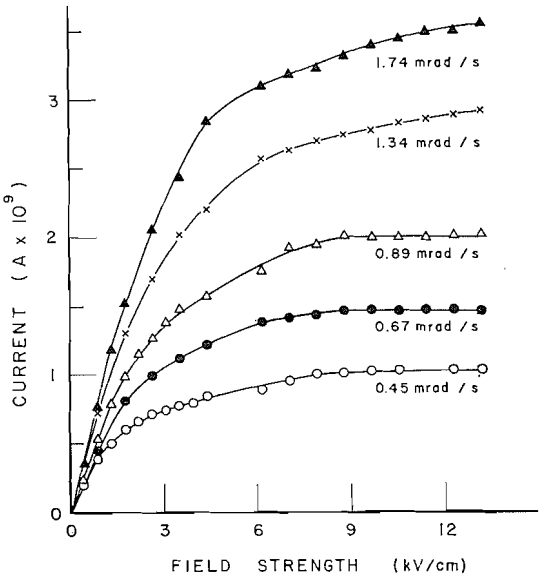

FIG. 1. Ionization current vs. electric field strength for liquid argon at several dose rates. The cell was Pyrex with 3.14 cm^2 aluminum electrodes spaced 1.14 cm apart.

current losses due to volume recombination can be made by plotting 1/current vs. 1/voltage^2. This plot yields a straight line which, on extrapolation to infinite voltage, gives the saturation current (10). The saturation current per unit dose rate obtained with this extrapolation agreed with the values determined at the lower dose rates.

The mean values of $\overline{W}_x$ were 22.3 eV with cell No. 1 and 22.7 eV with cell No. 2, determined with an estimated precision of ± 10%. This corresponds to G(total ionization) = 4.4 ± 0.4. Gas phase values for $\overline{W}$ range from 23.7 ± 1.4 to 27.9 ± 1.5 eV using X-ray and electron radiation (11).

The trapping of electrons by impurities, notably oxygen, should not have been a problem in this work since the results of Swan (12) suggest a mean capture distance of 1.4 cm at 10 kV/cm for electrons in liquid argon containing 1 p.p.m. oxygen. This conclusion was verified in the present work by observing the fast transient current generated by electrons when the X-ray beam was pulsed. This fast transient was partially removed by the addition of 100 p.p.m. oxygen and completely eliminated by 10 000 p.p.m. oxygen.

The fact that a saturation current can be achieved in liquid argon at relatively low electric

field strengths means that essentially all electrons escape geminate recombination. This is in contrast to liquid hydrocarbons in which most electrons are thermalized close to the parent positive ion and, therefore, undergo geminate recombination.

Acknowledgments

We are grateful to Dr. A. O. Allen for encouraging discussions. One of us (N.V.K.) wishes to thank the staff of the Chemistry Department of Brookhaven National Laboratory for the hospitality extended during his stay as a summer visitor in 1968.

1. S. LENKEIT and H. G. EBERT. Naturwiss. **51**, 237 (1964).
2. H. ULLMAIER. Z. Phys. **178**, 44 (1964).
3. J. MATHIEU, D. BLANC, P. CAMINADE, and J. P. PATAU. J. Chim. Phys. **64**, 1679 (1967).
4. L. S. MILLER, S. HOWE, and W. E. SPEAR. Phys. Rev. **166**, 871 (1968).
5. D. W. SWAN. Proc. Phys. Soc. **85**, 1297 (1965).
6. G. W. HUTCHINSON. Nature, **162**, 610 (1948).
7. H. A. ULLMAIER. Phys. Med. Biol. **11**, 95 (1966).
8. A. HUMMEL and A. O. ALLEN. J. Chem. Phys. **46**, 1602 (1967).
9. National Bureau of Standards Handbook 85. U.S. Dept. of Commerce, Washington, D.C. 1964.
10. J. BOOZ and H. G. EBERT. Z. Angew. Phys. **14**, 385 (1962).
11. J. BÖOZ and H. G. EBERT. Strahlenther. **120**, 7 (1963).
12. D. W. SWAN. Proc. Phys. Soc. **83**, 659 (1964).

A low temperature phase of $(NH_4)_2TeBr_6$[1]

A. K. DAS[2] AND I. D. BROWN[3]

Department of Physics, Hamilton College, McMaster University, Hamilton, Ontario

Received June 20, 1969

X-Ray diffraction has shown the existence of a low temperature tetragonal phase of $(NH_4)_2TeBr_6$ having space group $P4/mnc(D_{4h}^6)$ with $a = 7.501$, $c = 10.765$ Å.

Canadian Journal of Chemistry, 47, 4288 (1969)

Our previous X-ray diffraction study of ammonium hexabromotellurate(IV), $(NH_4)_2TeBr_6$ (1), confirmed that at room temperature the compound has the cubic K_2PtCl_6 structure first observed by Manojlević (2). Nakamura, Ito, and Kubo (3) using nuclear quadrupole resonance (n.q.r.) have observed that at -52 °C, $(NH_4)_2TeBr_6$ undergoes a phase transition to a structure with lower symmetry in which the bromine atoms are no longer all equivalent. We have observed that under the polarizing microscope, crystals of $(NH_4)_2TeBr_6$, cooled to below the phase transition, exhibit the extinction pattern characteristic of a non-cubic crystal. On warming above the transition temperature, the crystals revert to the cubic form in a manner which indicates that the transformation is rapid and reversible in nature. Many of the crystals are observed to be twinned in the low temperature phase, suggesting that the transformation in this case is probably "displacive" in the sense described by Buerger (4).

In order to study the symmetry and cell constants of $(NH_4)_2TeBr_6$ below the transition temperature, double exposure Weissenberg photographs were taken with CuKα radiation. One exposure was taken below the phase transition, the other at room temperature. In this way it was possible to make accurate measurements of the differences between the high and low temperature forms. Two separate crystals were examined, one oriented along the cubic [110] direction and the other along [100]. From these photographs, it was possible to measure the cell constants of the low temperature phase and assign its space group (see Table I).

The atomic positions in the low temperature structure can be inferred from the space group, from the splitting of the n.q.r. signal into two, and from the obvious general similarity with the cubic structure. Values of the atomic coordinates were not found, since the photographs were not suitable for making intensity measurements.

The proposed structure of the low temperature form of $(NH_4)_2TeBr_6$ lies somewhere between

[1]Taken in part from the M.Sc. thesis of A. K. Das, 1968.

[2]Present address: Department of Physics, Ranchi College, University of Ranchi, Ranchi 8, Bihar, India.
[3]Requests for reprints should be sent to this author.

Can. J. Chem. Downloaded from www.nrcresearchpress.com by 210.87.254.105 on 09/05/12
For personal use only.

field strengths means that essentially all electrons escape geminate recombination. This is in contrast to liquid hydrocarbons in which most electrons are thermalized close to the parent positive ion and, therefore, undergo geminate recombination.

Acknowledgments

We are grateful to Dr. A. O. Allen for encouraging discussions. One of us (N.V.K.) wishes to thank the staff of the Chemistry Department of Brookhaven National Laboratory for the hospitality extended during his stay as a summer visitor in 1968.

1. S. LENKEIT and H. G. EBERT. Naturwiss. **51**, 237 (1964).
2. H. ULLMAIER. Z. Phys. **178**, 44 (1964).
3. J. MATHIEU, D. BLANC, P. CAMINADE, and J. P. PATAU. J. Chim. Phys. **64**, 1679 (1967).
4. L. S. MILLER, S. HOWE, and W. E. SPEAR. Phys. Rev. **166**, 871 (1968).
5. D. W. SWAN. Proc. Phys. Soc. **85**, 1297 (1965).
6. G. W. HUTCHINSON. Nature, **162**, 610 (1948).
7. H. A. ULLMAIER. Phys. Med. Biol. **11**, 95 (1966).
8. A. HUMMEL and A. O. ALLEN. J. Chem. Phys. **46**, 1602 (1967).
9. National Bureau of Standards Handbook 85. U.S. Dept. of Commerce, Washington, D.C. 1964.
10. J. BOOZ and H. G. EBERT. Z. Angew. Phys. **14**, 385 (1962).
11. J. BÖOZ and H. G. EBERT. Strahlenther. **120**, 7 (1963).
12. D. W. SWAN. Proc. Phys. Soc. **83**, 659 (1964).

A low temperature phase of $(NH_4)_2TeBr_6$[1]

A. K. DAS[2] AND I. D. BROWN[3]

Department of Physics, Hamilton College, McMaster University, Hamilton, Ontario

Received June 20, 1969

X-Ray diffraction has shown the existence of a low temperature tetragonal phase of $(NH_4)_2TeBr_6$ having space group $P4/mnc(D_{4h}^6)$ with $a = 7.501$, $c = 10.765$ Å.

Canadian Journal of Chemistry, 47, 4288 (1969)

Our previous X-ray diffraction study of ammonium hexabromotellurate(IV), $(NH_4)_2TeBr_6$ (1), confirmed that at room temperature the compound has the cubic K_2PtCl_6 structure first observed by Manojlević (2). Nakamura, Ito, and Kubo (3) using nuclear quadrupole resonance (n.q.r.) have observed that at -52 °C, $(NH_4)_2TeBr_6$ undergoes a phase transition to a structure with lower symmetry in which the bromine atoms are no longer all equivalent. We have observed that under the polarizing microscope, crystals of $(NH_4)_2TeBr_6$, cooled to below the phase transition, exhibit the extinction pattern characteristic of a non-cubic crystal. On warming above the transition temperature, the crystals revert to the cubic form in a manner which indicates that the transformation is rapid and reversible in nature. Many of the crystals are observed to be twinned in the low temperature phase, suggesting that the transformation in this case is probably "displacive" in the sense described by Buerger (4).

In order to study the symmetry and cell constants of $(NH_4)_2TeBr_6$ below the transition temperature, double exposure Weissenberg photographs were taken with CuKα radiation. One exposure was taken below the phase transition, the other at room temperature. In this way it was possible to make accurate measurements of the differences between the high and low temperature forms. Two separate crystals were examined, one oriented along the cubic [110] direction and the other along [100]. From these photographs, it was possible to measure the cell constants of the low temperature phase and assign its space group (see Table I).

The atomic positions in the low temperature structure can be inferred from the space group, from the splitting of the n.q.r. signal into two, and from the obvious general similarity with the cubic structure. Values of the atomic coordinates were not found, since the photographs were not suitable for making intensity measurements.

The proposed structure of the low temperature form of $(NH_4)_2TeBr_6$ lies somewhere between

[1]Taken in part from the M.Sc. thesis of A. K. Das, 1968.

[2]Present address: Department of Physics, Ranchi College, University of Ranchi, Ranchi 8, Bihar, India.

[3]Requests for reprints should be sent to this author.

Can. J. Chem. Downloaded from www.nrcresearchpress.com by 210.87.254.6 on 09/05/12
For personal use only.

TABLE I
Crystal data for $(NH_4)_2TeBr_6$

Parameters	Value: Room temperature*	Value: Below transition temperature: Cubic setting	Value: Below transition temperature: Tetragonal setting
a (Å)	10.728 ± 0.003	10.606 ± 0.005	7.501 ± 0.005
c (Å)		10.765 ± 0.005	10.765 ± 0.005
Space group	$Fm3m(O_h^5)$	$C4/mcn(D_{4h}^6)$	$P4/mnc(D_{4h}^6)$
Atomic positions†	Te in 4(*a*) Br in 24(*e*) N in 8(*c*)		Te in 2(*a*) Br(1) in 4(*e*) Br(2) in 8(*h*) N in 4(*d*)

*See ref. 1.
†See ref. 5.

that of monoclinic K_2TeBr_6 (6) and the cubic form of $(NH_4)_2TeBr_6$. The principal change that occurs during the transformation is the rotation of the $TeBr_6^{2-}$ ion by a few degrees about the [001] direction. Although the anion is only required by the space group to have the symmetry D_{4h}, it is likely, by analogy with K_2TeBr_6, to retain the octahedral structure to a close approximation.

Acknowledgment

We acknowledge the financial support of the National Research Council of Canada for this work.

1. A. K. Das and I. D. Brown. Can. J. Chem. **44**, 939 (1966).
2. L. M. Manojlović. Bull. Inst. Nucl. Sci. "Boris Kidrich" Belgrade. 7, 79 (1957).
3. D. Nakamura, K. Ito, and M. Kubo. J. Amer. Chem. Soc. **84**, 163 (1962).
4. M. J. Buerger. Phase transformations in solids. *Edited by* R. Smoluchowski. J. Wiley and Sons, Inc., New York. 1951. p. 183.
5. International tables for X-ray crystallography. Vol. I. Kynoch Press, Birmingham, England. 1962.
6. I. D. Brown. Can. J. Chem. **42**, 2758 (1964).

The sign of the long-range spin–spin coupling constant between ^{19}F and the aldehydic ^1H in *p*-fluorobenzaldehyde: evidence for a negative Q_{CCHO}

T. Schaefer[1] and S. S. Danyluk
Division of Biological and Medical Research, Argonne National Laboratory, Argonne, Ill. 60439

Received June 16, 1969

The spin–spin coupling constant of -0.50 ± 0.03 Hz between the ^{19}F nucleus and the aldehydic proton in *p*-fluorobenzaldehyde contrasts with a positive coupling between ^{19}F and methyl protons in *p*-fluorotoluene derivatives. If the former coupling is dominated by a π electron mechanism, it implies a negative hyperfine interaction constant between the aldehydic proton and the aromatic π system.

Canadian Journal of Chemistry, 47, 4289 (1969)

Negative spin–spin coupling constants between methyl protons and ring protons in the para position, J_p^{H,CH_3}, in toluene derivatives (1) are consistent with a σ–π exchange mechanism (2, 3) in which

$$[1] \qquad J_p^{H,CH_3} \propto Q_{CH}\, Q_{CCH}$$

In eq. [1], $Q_{CH} < 0$ represents a hyperfine interaction between the proton in the C—H bond and an electron in a p_π orbital on the carbon atom. $Q_{CCH} > 0$ is the corresponding interaction

[1]Visiting summer scientist, 1968. Permanent address: University of Manitoba, Winnipeg, Manitoba.

Can. J. Chem. Downloaded from www.nrcresearchpress.com by 210.87.254.6 on 09/05/12
For personal use only.

TABLE I
Crystal data for $(NH_4)_2TeBr_6$

Parameters	Value: Room temperature*	Value: Below transition temperature: Cubic setting	Value: Below transition temperature: Tetragonal setting
a (Å)	10.728 ± 0.003	10.606 ± 0.005	7.501 ± 0.005
c (Å)		10.765 ± 0.005	10.765 ± 0.005
Space group	$Fm3m(O_h^5)$	$C4/mcn(D_{4h}^6)$	$P4/mnc(D_{4h}^6)$
Atomic positions†	Te in 4(*a*)		Te in 2(*a*)
	Br in 24(*e*)		Br(1) in 4(*e*)
	N in 8(*c*)		Br(2) in 8(*h*)
			N in 4(*d*)

*See ref. 1.
†See ref. 5.

that of monoclinic K_2TeBr_6 (6) and the cubic form of $(NH_4)_2TeBr_6$. The principal change that occurs during the transformation is the rotation of the $TeBr_6^{2-}$ ion by a few degrees about the [001] direction. Although the anion is only required by the space group to have the symmetry D_{4h}, it is likely, by analogy with K_2TeBr_6, to retain the octahedral structure to a close approximation.

Acknowledgment

We acknowledge the financial support of the National Research Council of Canada for this work.

1. A. K. Das and I. D. Brown. Can. J. Chem. **44**, 939 (1966).
2. L. M. Manojlović. Bull. Inst. Nucl. Sci. "Boris Kidrich" Belgrade. 7, 79 (1957).
3. D. Nakamura, K. Ito, and M. Kubo. J. Amer. Chem. Soc. **84**, 163 (1962).
4. M. J. Buerger. Phase transformations in solids. *Edited by* R. Smoluchowski. J. Wiley and Sons, Inc., New York. 1951. p. 183.
5. International tables for X-ray crystallography. Vol. I. Kynoch Press, Birmingham, England. 1962.
6. I. D. Brown. Can. J. Chem. **42**, 2758 (1964).

The sign of the long-range spin–spin coupling constant between ^{19}F and the aldehydic ^1H in *p*-fluorobenzaldehyde: evidence for a negative Q_{CCHO}

T. Schaefer[1] and S. S. Danyluk
Division of Biological and Medical Research, Argonne National Laboratory, Argonne, Ill. 60439

Received June 16, 1969

The spin–spin coupling constant of -0.50 ± 0.03 Hz between the ^{19}F nucleus and the aldehydic proton in *p*-fluorobenzaldehyde contrasts with a positive coupling between ^{19}F and methyl protons in *p*-fluorotoluene derivatives. If the former coupling is dominated by a π electron mechanism, it implies a negative hyperfine interaction constant between the aldehydic proton and the aromatic π system.

Canadian Journal of Chemistry, 47, 4289 (1969)

Negative spin–spin coupling constants between methyl protons and ring protons in the para position, J_p^{H,CH_3}, in toluene derivatives (1) are consistent with a σ–π exchange mechanism (2, 3) in which

$$[1] \qquad J_p^{H,CH_3} \propto Q_{CH}\, Q_{CCH}$$

In eq. [1], $Q_{CH} < 0$ represents a hyperfine interaction between the proton in the C—H bond and an electron in a p_π orbital on the carbon atom. $Q_{CCH} > 0$ is the corresponding interaction

[1]Visiting summer scientist, 1968. Permanent address: University of Manitoba, Winnipeg, Manitoba.

Can. J. Chem. Downloaded from www.nrcresearchpress.com by 210.87.254.40 on 09/05/12
For personal use only.

Can. J. Chem. Downloaded from www.nrcresearchpress.com by 210.87.254.40 on 09/05/12
For personal use only.

between the proton in the methyl group and the p_π electron on the bonded ring carbon atom. $Q_{CCH} \propto \cos^2 \theta$, where θ is the angle between the axis of the p_π orbital and the C—H bond, both projected on a plane perpendicular to the C—C bond.

Similarly, $|J_p^{H,CH_3}| < |J_p^{F,CH_3}|$ and $J_p^{F,CH_3} > 0$ in *p*-fluorotoluene derivatives (4) is consistent with a dominant π coupling mechanism for which

$$[2] \qquad J_p^{F,CH_3} \propto Q_{CF}\, Q_{CCH}$$

In eq. [2], $Q_{CF} > 0$ but is a composite term (5) which may vary considerably in magnitude (6).

Now *p*-fluorobenzaldehyde is almost certainly a planar molecule (7–9) with a barrier to reorientation of the formyl group sufficiently large (> 6 kcal/mole) so as to give a $Q_{CCHO} \approx 0$ ($\theta \approx 90°$) for a spin delocalization mechanism (9). Recent valence bond calculations (10) suggest the possibility of a spin polarization mechanism giving rise to $Q_{CCH} < 0$ when $\theta = 90°$, at least in aliphatic π electron radicals. Perhaps more to the point, an apparent negative Q value is found for the formyl proton in certain paramagnetic γ-formyl nickel(II) aminotroponeimine derivatives (11). In this case, $|Q_{CCHO}| \approx 1/6|Q_{CCH}|$, where Q_{CCH} is an average over θ for almost free rotation in toluene radical anions (12).

These considerations imply that for *p*-fluorobenzaldehyde, eq. [3] may be roughly applicable

$$[3] \qquad J_p^{F,CHO} \propto Q_{CF}\, Q_{CCHO}$$

From eq. [3], it would be predicted that $J_p^{F,CHO} < 0$ and is probably smaller in magnitude than J_p^{F,CH_3} in *p*-fluorotoluene derivatives. We find, indeed, that $J_p^{F,CHO} = -0.50$ Hz (see Experimental section), compared to $J_p^{F,CH_3} = 1.3$ Hz in 4-fluoro-2-iodotoluene (4).

The σ–π mechanism also depends on excitation energies to triplet states as well as on long-range mobile bond orders (3), so that a more detailed discussion of the relative magnitudes of J_p^{F,CH_3} and $J_p^{F,CHO}$ is probably not warranted at this time. A test of the proposed coupling mechanism may be devised by measuring $J_p^{F,CHO}$ in *p*-fluorobenzaldehyde derivatives in which bulky ortho substituents force the formyl group into a nonplanar configuration. $J_p^{F,CHO}$ should then increase algebraically and, if the degree of nonplanarity is sufficiently large, a spin delocalization (hyperconjugative overlap) mechanism will result in a positive $J_p^{F,CHO}$. The synthesis of the appropriate compounds is being attempted.

Experimental

A solution consisting of equal volumes of *p*-fluorobenzaldehyde, carbon disulfide, and tetramethylsilane was degassed by the freeze–pump–thaw technique. Proton magnetic resonance spectra were taken in the frequency sweep mode on a DA-60I Varian spectrometer. Double resonance experiments under conditions of weak irradiation were performed in the normal way (13, 14).

In Fig. 1*a*, the formyl proton resonance of *p*-fluorobenzaldehyde shows the expected pattern under conditions where $|J_p^{F,CHO}|$ is almost the same as $|J_m^{H,CHO}|$ (the stick diagram is intended to clarify this situation). The triplets arising from the small $J_o^{H,CHO}$ are clearly visible. The magnitudes of $J_m^{H,CHO}$ and $J_o^{H,CHO}$ could also be obtained from the ring proton spectrum in which the internal shift approaches 1 p.p.m.

In Fig. 1*b*, the low-field peaks of the meta ring protons (H_B) corresponding to net positive or zero spin states of the H_A protons, and to positive spin states of the fluorine nucleus, are being weakly irradiated. In Fig. 1*c*, the amplitude of the irradiating field is larger than in *b*. The high-field formyl proton peaks are affected. Note the unperturbed shape of the low-field triplet. Consequently,

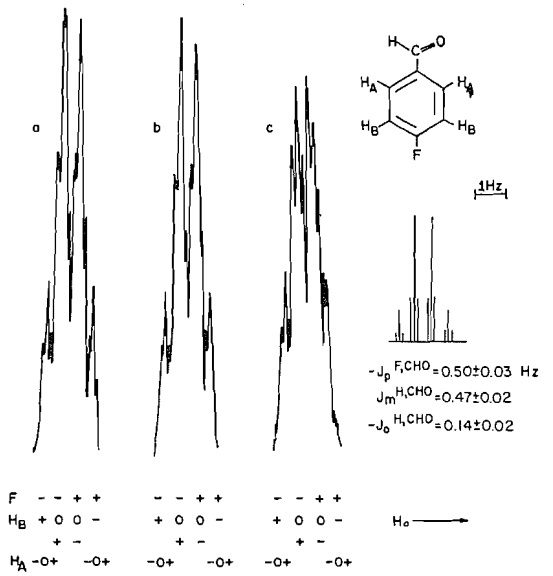

FIG. 1. The single proton resonance spectrum of the aldehydic proton in *p*-fluorobenzaldehyde is shown in *a*. Because the magnitudes of the spin–spin couplings to the 2 H_B protons and to the ^{19}F nucleus are very nearly equal, the aldehyde proton resonance appears as a basic 1:3:3:1 quartet, each of whose components are further split into a 1:2:1 triplet by the much smaller coupling of the 2 H_A protons. In *b* and *c* are shown double resonance spectra of the aldehydic proton under conditions described in the text (see experimental section). The spin states of the other nuclei are given with the convention that a positive sign under a low-field peak indicates a positive coupling to the aldehydic proton.

$J_o^{HF}/J_p^{F,CHO} < 0$. Because $J_o^{HF} > 0$ (15), it follows that $J_p^{F,CHO} < 0$. Other experiments indicate $J_o^{H,CHO} < 0$ in this molecule. In *p*-N,N-dimethylaminobenzaldehyde (16), as well as in a number of disubstituted benzaldehydes (17), it is known that $J_o^{H,CHO} < 0$.

1. G. KOTOWYCZ and T. SCHAEFER. Can. J. Chem. **44**, 2743 (1966).
2. H. M. MCCONNELL. J. Chem. Phys. **30**, 126 (1959).
3. M. J. S. DEWAR and R. C. FAHEY. J. Amer. Chem. Soc. **85**, 2704 (1963).
4. D. J. BLEARS, S. S. DANYLUK, and T. SCHAEFER. J. Chem. Phys. **47**, 5037 (1967).
5. M. KAPLAN, J. R. BOLTON, and G. K. FRAENKEL. J. Chem. Phys. **42**, 955 (1965).
6. A. HINCHLIFFE and J. N. MURRELL. Mol. Phys. **14**, 147 (1968).
7. F. A. L. ANET and N. AHMAD. J. Amer. Chem. Soc. **86**, 119 (1964).
8. S. FORSÉN and P. N. SKANCKE. *In* Selected topics in structure chemistry. *Edited by* P. Andersen, O. Bastiansen, and S. Furberg. Universitetsforlaget, Oslo, Norway. 1967.
9. A. H. MAKI and D. H. GESKE. J. Amer. Chem. Soc. **83**, 1852 (1961).
10. Z. LUZ. J. Chem. Phys. **48**, 4186 (1968).
11. D. R. EATON, A. D. JOSEY, and R. E. BENSON. J. Amer. Chem. Soc. **89**, 4040 (1967).
12. T. M. MCKINNEY and D. H. GESKE. J. Amer. Chem. Soc. **89**, 2806 (1967).
13. R. FREEMAN and W. A. ANDERSON. J. Chem. Phys. **37**, 2053 (1962).
14. R. KAISER. J. Chem. Phys. **39**, 2435 (1963).
15. W. B. MONIZ and E. LUSTIG. J. Chem. Phys. **50**, 1905 (1969).
16. S. S. DANYLUK, C. L. BELL, and T. SCHAEFER. To be published.
17. D. G. DEKOWALEWSKI and V. J. KOWALEWSKI. Mol. Phys. **9**, 331 (1965).

Effect of temperature on the spectrum of sulfur dioxide[1]

J. BROWN AND GEORGE BURNS

Department of Chemistry, University of Toronto, Toronto 181, Ontario

Received March 26, 1969

The effect of temperature on the ultraviolet spectrum of sulfur dioxide has been studied over the temperature range 20 to 1000 °C. The equilibrium constant for the reaction

$$SO_2 \rightleftharpoons (SO_2)$$

where (SO_2) is an isomeric form or an excited state of sulfur dioxide, has been obtained at several temperatures. The enthalpy change for the transition was found to be 4.1 ± 0.4 kcal mole^{-1}.

Canadian Journal of Chemistry, **47**, 4291 (1969)

Can. J. Chem. Downloaded from www.nrcresearchpress.com by 210.87.254.40 on 09/05/12
For personal use only.

The spectrum of sulfur dioxide in the region accessible to quartz optics shows 2 main regions of absorption, the first approximately between 3100 and 2500 Å and the second extending from about 2500 Å into the vacuum ultraviolet (u.v.). It is known (e.g. refs. 1–3) that as the temperature is raised the absorption bands are considerably weakened (being replaced by a continuous absorption in the far u.v.) but return to their original intensity when the gas is cooled. A thermal equilibrium has been postulated (2), viz.

$$SO_2 \rightleftharpoons (SO_2)$$

where (SO_2) is an isomeric form (2) or an electronically excited state (4) of sulfur dioxide. Recently, however, Hays and Pfeiffer (5) have postulated that non-ionic AB_2-type molecules with 14–18 valence electrons may have double minima in their ground state potential energy surfaces. They suggest, on the basis of molecular orbital calculations, that the "high temperature isomer of sulfur dioxide" may be a symmetrical form of SO_2 with a somewhat extended S—O bond distance and a bond angle of about 72°. In the present note, measurements of equilibrium constant have been obtained for the transition at a series of temperatures and the corresponding enthalpy change has been calculated.

Experimental

The apparatus employed for this investigation was originally intended for study of reactions by the technique of flash photolysis and kinetic spectroscopy and has been described many times previously (e.g. ref. 6). The reaction vessel was contained in a furnace which could obtain a maximum temperature of 1250 °C. The detector was a Hilger medium quartz spectrograph and exposures were made on Kodak Type No. 3 spectrographic analysis plates. Band intensities were measured on a Joyce Loebl microphotometer Model MKIIIC. Sulfur dioxide was supplied by the Matheson Company and was reported

[1]This work was supported in part by the Directorate of Chemical Sciences, Air Force Office of Scientific Research, Grant No. 506-69.

$J_o^{HF}/J_p^{F,CHO} < 0$. Because $J_o^{HF} > 0$ (15), it follows that $J_p^{F,CHO} < 0$. Other experiments indicate $J_o^{H,CHO} < 0$ in this molecule. In *p*-N,N-dimethylaminobenzaldehyde (16), as well as in a number of disubstituted benzaldehydes (17), it is known that $J_o^{H,CHO} < 0$.

1. G. KOTOWYCZ and T. SCHAEFER. Can. J. Chem. **44**, 2743 (1966).
2. H. M. MCCONNELL. J. Chem. Phys. **30**, 126 (1959).
3. M. J. S. DEWAR and R. C. FAHEY. J. Amer. Chem. Soc. **85**, 2704 (1963).
4. D. J. BLEARS, S. S. DANYLUK, and T. SCHAEFER. J. Chem. Phys. **47**, 5037 (1967).
5. M. KAPLAN, J. R. BOLTON, and G. K. FRAENKEL. J. Chem. Phys. **42**, 955 (1965).
6. A. HINCHLIFFE and J. N. MURRELL. Mol. Phys. **14**, 147 (1968).
7. F. A. L. ANET and N. AHMAD. J. Amer. Chem. Soc. **86**, 119 (1964).
8. S. FORSÉN and P. N. SKANCKE. *In* Selected topics in structure chemistry. *Edited by* P. Andersen, O. Bastiansen, and S. Furberg. Universitetsforlaget, Oslo, Norway. 1967.
9. A. H. MAKI and D. H. GESKE. J. Amer. Chem. Soc. **83**, 1852 (1961).
10. Z. LUZ. J. Chem. Phys. **48**, 4186 (1968).
11. D. R. EATON, A. D. JOSEY, and R. E. BENSON. J. Amer. Chem. Soc. **89**, 4040 (1967).
12. T. M. MCKINNEY and D. H. GESKE. J. Amer. Chem. Soc. **89**, 2806 (1967).
13. R. FREEMAN and W. A. ANDERSON. J. Chem. Phys. **37**, 2053 (1962).
14. R. KAISER. J. Chem. Phys. **39**, 2435 (1963).
15. W. B. MONIZ and E. LUSTIG. J. Chem. Phys. **50**, 1905 (1969).
16. S. S. DANYLUK, C. L. BELL, and T. SCHAEFER. To be published.
17. D. G. DEKOWALEWSKI and V. J. KOWALEWSKI. Mol. Phys. **9**, 331 (1965).

Effect of temperature on the spectrum of sulfur dioxide[1]

J. BROWN AND GEORGE BURNS

Department of Chemistry, University of Toronto, Toronto 181, Ontario

Received March 26, 1969

The effect of temperature on the ultraviolet spectrum of sulfur dioxide has been studied over the temperature range 20 to 1000 °C. The equilibrium constant for the reaction

$$SO_2 \rightleftharpoons (SO_2)$$

where (SO_2) is an isomeric form or an excited state of sulfur dioxide, has been obtained at several temperatures. The enthalpy change for the transition was found to be 4.1 ± 0.4 kcal mole^{-1}.

Canadian Journal of Chemistry, **47**, 4291 (1969)

Can. J. Chem. Downloaded from www.nrcresearchpress.com by 210.87.254.42 on 09/05/12
For personal use only.

The spectrum of sulfur dioxide in the region accessible to quartz optics shows 2 main regions of absorption, the first approximately between 3100 and 2500 Å and the second extending from about 2500 Å into the vacuum ultraviolet (u.v.). It is known (e.g. refs. 1–3) that as the temperature is raised the absorption bands are considerably weakened (being replaced by a continuous absorption in the far u.v.) but return to their original intensity when the gas is cooled. A thermal equilibrium has been postulated (2), viz.

$$SO_2 \rightleftharpoons (SO_2)$$

where (SO_2) is an isomeric form (2) or an electronically excited state (4) of sulfur dioxide. Recently, however, Hays and Pfeiffer (5) have postulated that non-ionic AB_2-type molecules with 14–18 valence electrons may have double minima in their ground state potential energy surfaces. They suggest, on the basis of molecular orbital calculations, that the "high temperature isomer of sulfur dioxide" may be a symmetrical form of SO_2 with a somewhat extended S—O bond distance and a bond angle of about 72°. In the present note, measurements of equilibrium constant have been obtained for the transition at a series of temperatures and the corresponding enthalpy change has been calculated.

Experimental

The apparatus employed for this investigation was originally intended for study of reactions by the technique of flash photolysis and kinetic spectroscopy and has been described many times previously (e.g. ref. 6). The reaction vessel was contained in a furnace which could obtain a maximum temperature of 1250 °C. The detector was a Hilger medium quartz spectrograph and exposures were made on Kodak Type No. 3 spectrographic analysis plates. Band intensities were measured on a Joyce Loebl microphotometer Model MKIIIC. Sulfur dioxide was supplied by the Matheson Company and was reported

[1]This work was supported in part by the Directorate of Chemical Sciences, Air Force Office of Scientific Research, Grant No. 506-69.

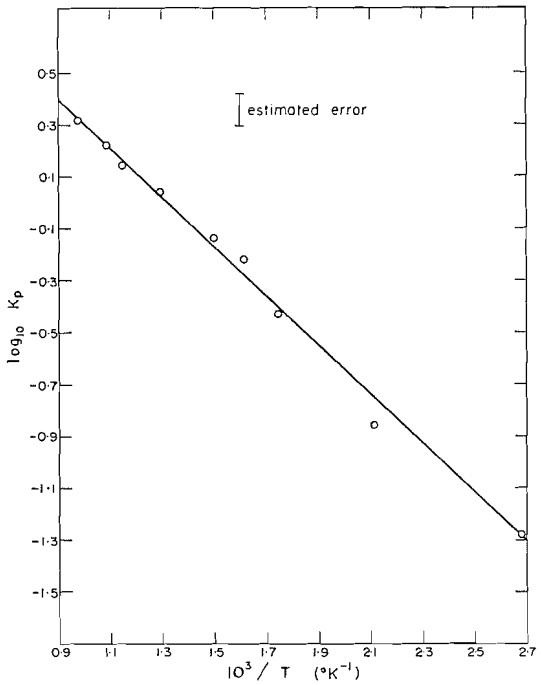

FIG. 2. Plot of logarithm of the equilibrium constant (K_P) against $1/T$. (Error estimated by comparing results obtained from all 4 calibration graphs and calculated by use of root-mean-square deviation formula.)

to have a purity of at least 99.98%. Pressures of the gas used throughout the experiment were of the order of mm and were measured on a glass Bourdon spoon gauge.

The effect of temperature on the absorption spectrum is shown on Fig. 1. It is readily observable that as the absorption bands of the system at 3000 Å become weakened with increasing temperature, there is a marked increase of continuous absorption at shorter wavelengths.

In order to calculate the enthalpy change accompanying the transition a plate was calibrated using known pressures of sulfur dioxide in the reaction vessel, at room temperature. The intensities of the absorption bands at 3131, 3088, 3043, and 3001 Å were measured on the microphotometer and graphs of $\log_{10}$ intensity (intensity being proportional to peak height) against concentration were drawn. Using the same plate, the absorption spectrum of sulfur dioxide (initial pressure 5 Torr) was photographed at a variety of temperatures up to 750 °C. The concentration of sulfur dioxide at each temperature was read from the calibration graphs. No significant change in the shape of the microphotometer trace was noted as the temperature was increased. The number of molecules in the ground vibrational state was calculated at each temperature, using the Boltzmann factor correction (exp $(-\Delta E/RT)$). The amount of sulfur dioxide present as isomer or in an electronically excited state (SO_2) was evaluated by difference. It was assumed that the amount of (SO_2) present at room temperature was zero. Since the rotational contour of a band changes with temperature the data were recalculated using the microdensitometer trace peak area rather than peak height. However, due probably to the low resolution of the spectrograph, no significant changes in the results obtained were noted. The equilibrium constant for the transition was calculated at each temperature, and a plot of $\log_{10} K_P$ (equilibrium constant) against $1/T$ was made (Fig. 2). The graph had a slope of $-0.9 \pm 0.1 \times 10^3$ (deg) which gave ΔH for the transition as 4.1 ± 0.4 kcal mole^{-1}. This result allows no conclusions to be drawn about the nature of (SO_2).

Professor N. Basco brought to our attention that, in general, in plate photometry it is difficult to separate unequivocally the continuum, which constitutes a base line, and peaks, which were used here to estimate SO_2 concentrations. For these reasons, plate photometric measurements of the type conducted here might be in error, especially if there is an appreciable overlap between various vibrational bands. However, in the present work, the vibrational bands seem to be well separated (Fig. 1), the continuum in the region in question (3000–3131 Å) is fairly weak (Fig. 1), and the calibration curves at wavelengths studied, as well as the plot in Fig. 2, produced good straight lines. For these reasons, we doubt that we can improve our results. However, we recognize that with superior equipment, it might be possible to do so.

Acknowledgments

This work was supported in part by the National Research Council of Canada and the Defence Research Board, Grant No. 9530–54. We wish also to thank Dr. R. B. Caton (Scarborough College, University of Toronto), who brought ref. 5 to our attention. It is a pleasure to express our gratitude to Prof. R. G. W. Norrish, F.R.S., upon whose advice this work was initiated.

1. K. WIELAND. Trans. Faraday Soc. **30**, 260 (1934).
2. R. G. W. NORRISH and G. A. OLDERSHAW. Proc. Roy. Soc. London, Ser. A, **249**, 498 (1959).
3. A. L. MYERSON, F. R. TAYLOR, and P. L. HANST. J. Chem. Phys. **26**, 1309 (1957).
4. P. A. GIGUÈRE and RODRIGUE SAVOIE. Can. J. Chem. **43**, 2357 (1965).
5. E. F. HAYES and G. V. PFEIFFER. J. Amer. Chem. Soc. **90** (18), 4773 (1968).
6. N. BASCO and R. G. W. NORRISH. Proc. Roy. Soc. London, Ser. A, **210**, 293 (1961).

Can. J. Chem. Downloaded from www.nrcresearchpress.com by 210.87.254.42 on 09/05/12
For personal use only.

Can. J. Chem. Downloaded from www.nrcresearchpress.com by 210.87.254.42 on 09/05/12
For personal use only.

PLATE I

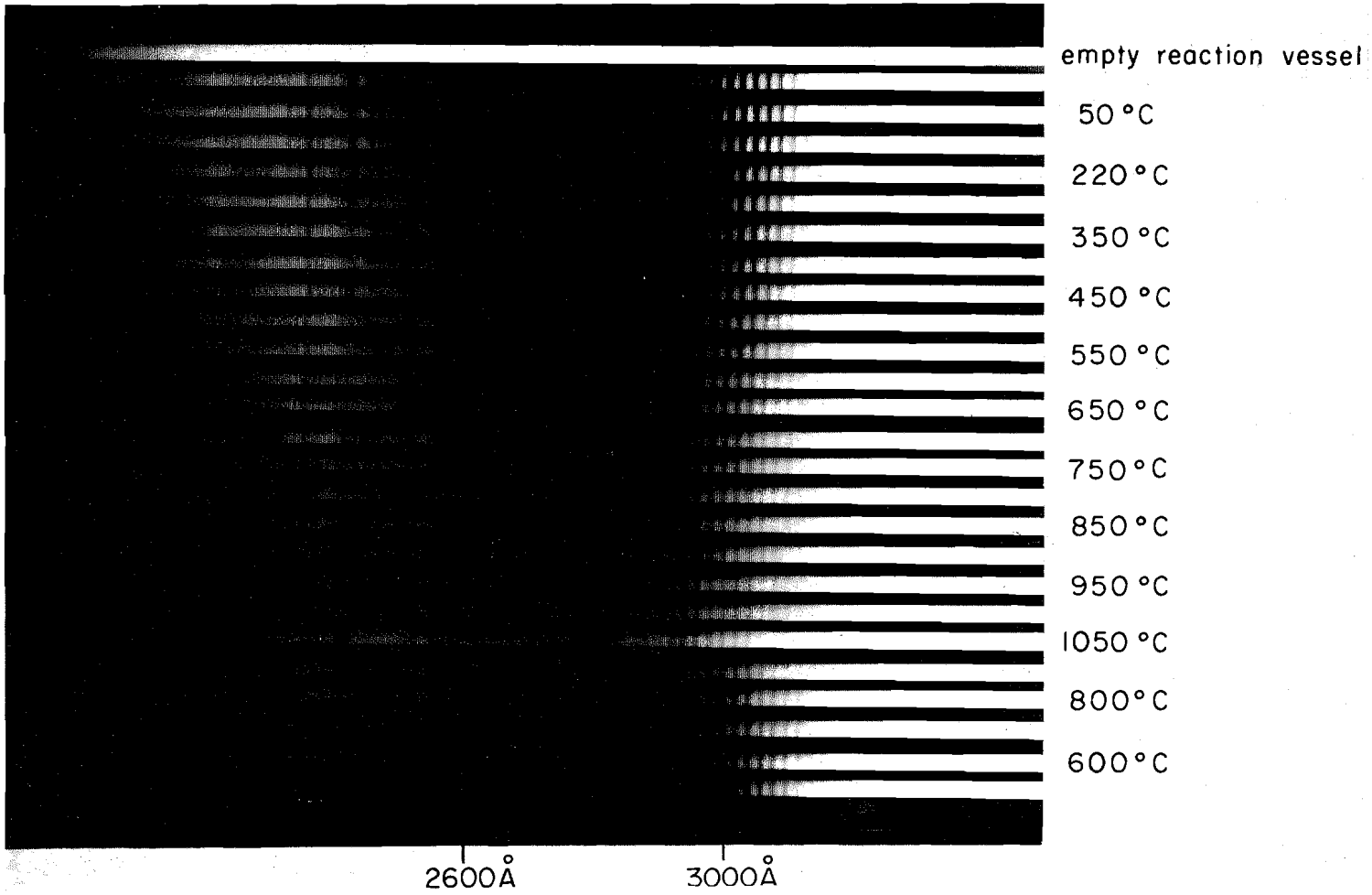

FIG. 1. Variation of spectrum of sulfur dioxide with temperature.

Erratum: Solvation thermodynamics of ions: free energies in water, ammonia, and fused LiCl–KCl eutectic

JAMES A. PLAMBECK
Department of Chemistry, University of Alberta, Edmonton, Alberta

Received August 6, 1969

(Ref.: Can. J. Chem. **47**, 1401 (1969))

Canadian Journal of Chemistry, **47**, 4293 (1969)

Can. J. Chem. Downloaded from www.nrcresearchpress.com by 210.87.254.40 on 09/05/12
For personal use only.

An error in ref. 19 has led to some incorrect values of $\Delta G_{CON}{}^{0}/z$ in LiCl–KCl in Table I. The correct values are: V^{3+}, 452.447; Cr^{3+}, 467.736; Fe^{3+}, 463.174. The points for these ions in Fig. 5 should be raised by the difference between the values just given and those in Table I. The paper is not otherwise affected.

Can. J. Chem. Downloaded from www.nrcresearchpress.com by 210.87.254.5 on 09/05/12
For personal use only.

Canadian Journal of Chemistry

Published by THE NATIONAL RESEARCH COUNCIL OF CANADA

VOLUME 47 DECEMBER 1, 1969 NUMBER 23

Photocycloaddition of 1,1-diphenylethylene to 2,3-dihydropyran

PAUL SERVÉ
The Department of Chemistry, Wright State University, Dayton, Ohio 45431

AND

HERBERT M. ROSENBERG AND R. RONDEAU
Air Force Materials Laboratory, Wright-Patterson Air Force Base, Ohio 45433

Received May 27, 1969

1,1-Diphenylethylene reacts with 2,3-dihydropyran on photolysis to yield two allylic addition products as well as cycloaddition product. The triplet state of 1,1-diphenylethylene is implicated in these reactions. The cycloaddition reaction is stereoselective and is thought to result from bond polarization of the reactants.

Canadian Journal of Chemistry, **47**, 4295 (1969)

In two previous papers (1,2) we reported the photocycloaddition of diphenylacetylene and stilbene to 2,3-dihydropyran. The symmetry properties of the reactants precluded observation of orientational preference in these cycloaddition reactions. We now report the photochemical reaction of 1,1-diphenylethylene (**1**) with 2,3-dihydropyran at 2537 and 3000 Å.

A solution of **1** in 2,3-dihydropyran was irradiated in a quartz vessel at 2537 or 3000 Å for 150 h. At the end of this period gas-liquid phase chromatography (g.l.p.c.) analysis showed no trace of **1**. Three major products accounting for 55% of the reaction were isolated and characterized as: 2-(1,1-diphenylethyl)-2*H*,5,6-dihydropyran (**2**), 20%; 4-(1,1-diphenylethyl)-4*H*,5,6-dihydropyran (**3**), 25%; and 7,7-diphenyl-2-oxabicyclo[4.2.0]octane (**4**), 55%. It is noteworthy that irradiation at 2537 or 3000 Å caused no deviation in the type products formed or the product distribution.

Mass spectral parent peaks established that the three major products were 1:1 adducts. Infrared (i.r.) and proton magnetic resonance (p.m.r.) spectral data shown in the Experimental section are consistent with the assigned structures. The coupling constant $J_{1,6} = 8.0$ c.p.s. for **4** provides evidence for *cis* ring fusion (3).

We note the apparent preference for *cis* ring fusion in photocycloaddition reactions to dihydropyran (1,2) in contrast to the frequent tendency toward *trans* ring fusion in cyclohexene adducts (4).

In order to obtain information concerning the reaction mechanism, sensitization experiments were performed. We found that the reaction was sensitized by benzophenone ($E_T = 69$ kcal) and the product distribution was not affected. The reaction could also be quenched by the addition of piperylene ($E_T = 58$ kcal). This demonstrated the involvement of the excited triplet state of **1** in the formation of the three major products.

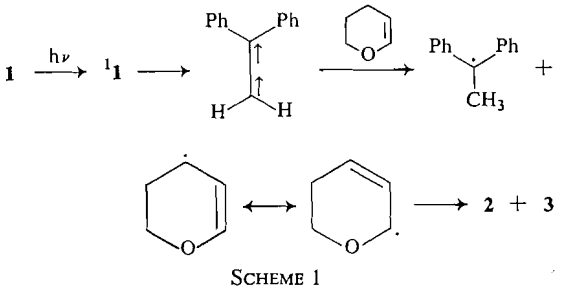

SCHEME 1

Formation of **2** and **3** is most readily accommodated by the reaction sequence (Scheme 1) in which allylic hydrogen abstraction by the

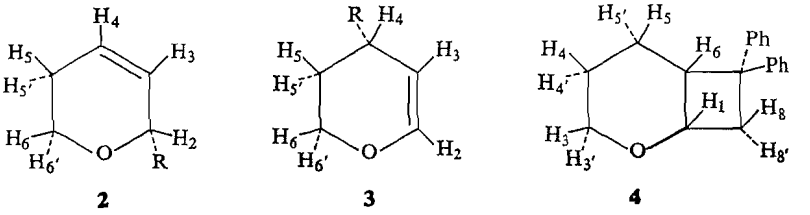

2 **3** **4**

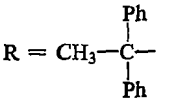

excited triplet (^{3}1) is followed by free radical combination.[1] Compound **4** is probably formed in a non-concerted cycloaddition reaction. There is no apparent steric basis for the orientational preference in the cycloaddition reaction which is contrary to the course that would be predicted for the initial formation of the more stable biradical. We postulate that bond polarization of the reacting species (Scheme 2) directs the initial attack, possibly via the formation of an excited state acceptor–donor complex (5), followed by intersystem crossing and ring closure to give the observed product. This hypothesis is speculative since we have no information regarding the charge distribution of the triplet olefin.

Experimental

Melting points are uncorrected. Photolyses were conducted in a Rayonet photochemical reactor at 2537, 3000, or 3500 Å. The i.r. spectra were obtained in a Perkin-Elmer Model 621 spectrophotometer. Mass spectra were obtained on a CEC-21-110 instrument. The g.l.p.c. was performed on a Varian Aerograph 1200 on 5 ft column packed with 3% SE30. The p.m.r. spectra were taken on a Varian DP-60-IL instrument.

Reaction of 1,1-Diphenylethylene with 2,3-Dihydropyran

A solution containing **1**, 3.6 g (0.02 mole) in 2,3-dihydropyran, 97 g (1.2 moles) was irradiated in a quartz vessel at 35° for 150 h at 3000 Å. At the end of the time no trace of **1** was observed by g.l.p.c. Three products were isolated by column chromatography on alumina (80–200 mesh). The following products in their order of elution were obtained with petroleum ether (b.p. 30–60°): **2**

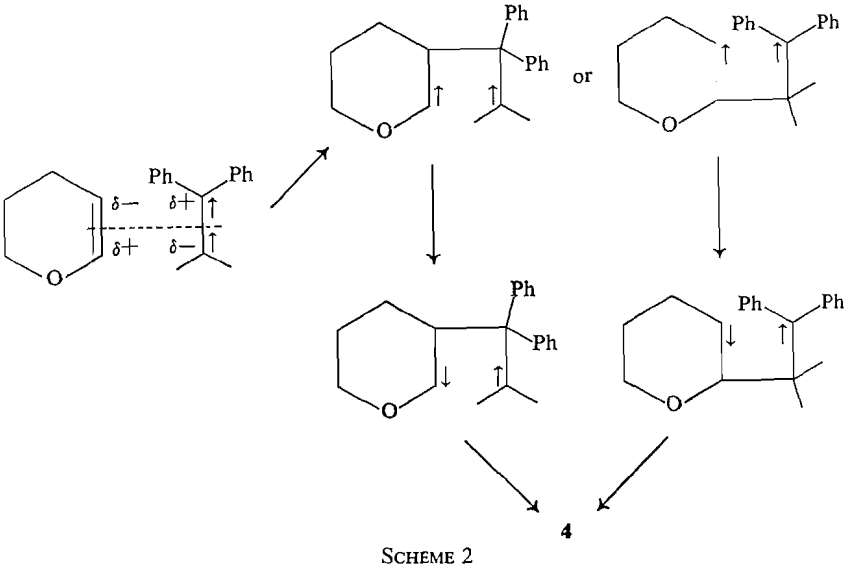

SCHEME 2

[1]We are indebted to the referees who noted the absence of reported examples of hydrogen abstraction by triplet olefins.

Can. J. Chem. Downloaded from www.nrcresearchpress.com by 210.87.254.5 on 09/05/12
For personal use only.

[.45 g (10%) m.p. 62–3°; *m/e*, 264; i.r. (thin film) 3030, 2930, 1610, 1600, 1110, 755, and 675 cm^{-1}; p.m.r. ($CDCl_3$) τ 2.8 (10H, multiplet, aromatic protons), 4.20 (1H, multiplet, H_4) 5.10 (1H, multiplet, H_2), 4.65 (1H, multiplet, H_3), 6.15 (2H, multiplet, H_6 and $H_{6'}$), 8.50 (2H, multiplet, H_5 and $H_{5'}$), 8.25, singlet, methyl protons)]; **3** [.55 g (15%); m.p. 77–8°; *m/e*, 264; i.r. (thin film) 3050, 2960, 1610, 1590, 1110, 735, and 675 cm^{-1}; p.m.r. ($CDCl_3$) τ 2.80 (10H, multiplet, aromatic protons), 3.75 (1H, doublet of doublets, H_2), 5.30 (1H, multiplet, H_3), 6.25 (2H, multiplet, H_6 and $H_{6'}$), 8.20 (1H, multiplet, H_4), 8.50 (2H, multiplet, H_5 and $H_{5'}$), 8.20 (3H, singlet, methyl protons) $J_{1,2}$ = 6Hz, $J_{1,3}$ = 2 Hz]; **4** [1.2 g (30%); m.p. 46–8°; *m/e*, 264; i.r. (thin film) 3090, 3060, 3010, 2930, 1600, 1110, 730, and 690 cm^{-1}; p.m.r. ($CDCl_3$) τ 2.90 (10H, multiplet, aromatic protons), 5.8 (1H, quartet, H_1), 6.4 (2H, multiplet, H_3 and $H_{3'}$), 6.8 (2H, multiplet, H_8 and $H_{8'}$), 7.3 (1H, multiplet, H_6), 8.4 (4H, multiplet, H_5 and $H_{5'}$, H_4 and $H_{4'}$), $J_{1,6}$ = 8 Hz; $J_{1,8'} = J_{1,8'}$ = 8.5 Hz; spin decoupling experiments demonstrated the following couplings (H_6–$H_{5'}$,H_6–$H_{5'}$,$J_{6,5} = J_{6,5'}$ = 7.5 Hz).

Attempted Sensitization of 1,1-Diphenylethylene with 2,3-Dihydropyran with Benzophenone

A solution containing 1,1-diphenylethylene, 1.8 g (0.01 mole) in 100 ml of 2,3-dihydropyran was divided into 2 equal portions. Benzophenone, 3.6 g (0.02 mole) was added to one portion. Both solutions were then irradiated at 3500 Å for 48 h. The reactions were monitored using g.l.p.c. The reaction in the vessel containing the added benzophenone was shown to have progressed to about 30% completion, while the unsensitized reaction showed no product formation.

Attempting Quenching of the Reaction of 1,1-Diphenylethylene with 2,3-Dihydropyran with Piperylene

A solution containing 1,1-diphenylethylene, 1.8 g (0.01 mole) in 100 ml of 2,3-dihydropyran was divided into 2 portions of 50 ml each. Piperylene, 3.2 g (0.05 mole) was added to one portion. The two solutions were irradiated in quartz vessels at 3000 Å for 48 h. The reaction was monitored by g.l.p.c. The unquenched reaction was 3.5 times as rapid as the quenched reaction.

1. H. M. Rosenberg and P. Servé. J. Org. Chem. **33**, 1653 (1968).
2. H. M. Rosenberg, R. Rondeau, and P. Servé. J. Org. Chem. **34**, 471 (1969).
3. I. Flemming and D. H. Williams. Tetrahedron, **23**, 2724 (1967).
4. P. de Mayo, S. T. Reed, and R. W. Yip. Can. J. Chem. **42**, 2828 (1964); Proc. Chem. Soc. **54**, (1963).
5. E. J. Corey, J. D. Bass, R. LeMahieu, and R. B. Mitra. J. Amer. Chem. Soc. **86**, 5570 (1964).

Can. J. Chem. Downloaded from www.nrcresearchpress.com by 210.87.254.5 on 09/05/12
For personal use only.

Can. J. Chem. Downloaded from www.nrcresearchpress.com by 84.22.46.98 on 09/08/12
For personal use only.

Total synthesis, stereochemistry, and lithium–ammonia reduction of (±)-4-demethylaristolone and (±)-5-epi-4-demethylaristolone

EDWARD PIERS, WILLIAM DE WAAL, AND RONALD W. BRITTON
Department of Chemistry, University of British Columbia, Vancouver 8, British Columbia

Received June 2, 1969

The total synthesis of (±)-4-demethylaristolone (**14**) and its epimer, (±)-5-epi-4-demethylaristolone (**15**) is described. The key step of this synthesis involves the intramolecular cyclization of the olefinic diazoketone **12**, which produces the two epimers, **14** and **15**, in a ratio of approximately 2:1, respectively. The stereochemistry of the two epimers is unambiguously determined. It is observed that the lithium–ammonia reduction of **14** gives a dihydro derivative **16** containing *trans*-fused six-membered rings, while, interestingly, a similar reduction of **15** affords the corresponding *cis*-fused decalone system **26**.

Canadian Journal of Chemistry, 47, 4299 (1969)

Very recently, we reported (1) the total synthesis of the racemic form of the sesquiterpenoid aristolone (**1**) (2–4). This synthesis, in which the key step involved the cupric sulfate catalyzed intramolecular cyclization of the diazoketone **2**, was based on a model study involving the preparation of (±)-4-demethylaristolone. The model study, which has already been reported in preliminary form (5), was undertaken primarily with the aim of determining whether or not the crucial cyclization of the type **2** → **1** would take place. That is, in order to initially avoid some of the stereochemical problems involved in the synthesis of aristolone itself, we first decided to prepare a diazoketone of the type **3**. Successful intramolecular cyclization of the latter would then eventually lead to aristolone-type compounds lacking the C-4 secondary methyl group. We report here the details of this model study which, in addition to demonstrating the feasibility of the proposed synthetic approach, also produced some interesting results regarding the lithium–ammonia reduction of the final products, (±)-4-demethylaristolone and (±)-5-epi-4-demethylaristolone.

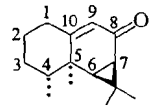

1

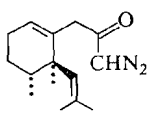

2

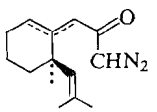

3

Alkylation of 2-methyl-6-*n*-butylthiomethylenecyclohexanone (**4**) (6) with methallyl chloride in *t*-butyl alcohol in the presence of potassium *t*-butoxide gave, after removal (6) of the *n*-butylthiomethylene blocking group from the product **5**, a 56% overall yield of 2-methyl-2-methallylcyclohexanone (**6**). Conversion of the latter into the desired 2-methyl-2-methylpropenylcyclohexanone (**7**) required isomerization of the olefinic double bond from the terminal position to the more highly substituted internal position. Although a number of different methods were attempted in order to carry out this transformation, it was eventually found that simple acid catalyzed isomerization was the most convenient. Thus, treatment of the methallyl compound **6** with *p*-toluenesulfonic acid in refluxing benzene for 3 days produced, in 77% yield, a mixture of compounds which, by gas–liquid chromatographic analysis, was shown to consist of approximately 80% of the desired isomerized ketone **7**, 17% of the starting material **6**, and 3% of an unidentified component. Careful fractionation of this mixture through a spinning band column allowed the isolation of nearly pure desired ketone **7**. The fact that simple double bond isomerization had taken place was shown clearly by the nuclear magnetic resonance (n.m.r.) spectra of compounds **6** and **7**. Thus, although the starting material **6** exhibited signals for two olefinic protons (τ 5.18 and 5.33) and one vinyl methyl group (τ 8.33), the product **7** showed signals for one olefinic proton (τ 4.74) and two vinyl methyl groups (τ 8.31 and 8.57).

In order to obtain, from ketone **7**, the diazoketone required to test the feasibility of the proposed intramolecular cyclization, the reaction of **7** with the modified Wittig reagent, triethyl phosphonoacetate (7), was attempted. This reaction proved very sluggish and even when high

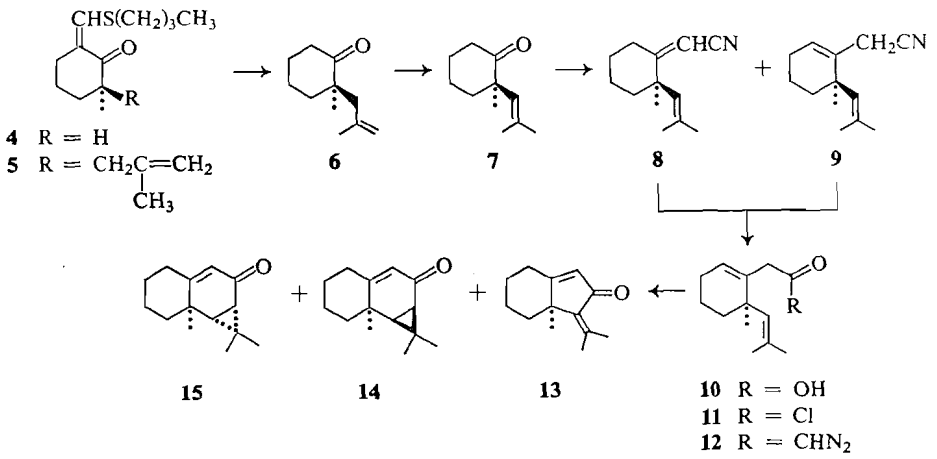

reaction temperatures were used, none of the desired product could be isolated. However, use of the sterically less demanding reagent, diethyl cyanomethylphosphonate (7), proved successful. Thus, reaction of the cyclohexanone **7** with this reagent in the presence of methylsulfinyl carbanion in dimethyl sulfoxide (8) at 100° for 15 h gave, in 95% yield, a mixture of the α,β-unsaturated nitrile **8** and the β,γ-unsaturated nitrile **9**, in a ratio of approximately 4:1, respectively. An analytical sample of the major compound (**8**) was obtained by preparative gas–liquid chromatography (g.l.c.) and gave spectral data in complete accord with the assigned structure. Furthermore, the n.m.r. spectrum of the mixture clearly showed that the other component of the mixture was indeed the β,γ-unsaturated isomer **9**.

Hydrolysis of the mixture of nitriles with potassium hydroxide in ethanol produced, in good yield, the β,γ-unsaturated carboxylic acid **10**. The fact that the double bond had now completely isomerized into the β,γ-position was clearly shown by the spectral data. The acid **10** exhibited no strong absorption in the ultraviolet (u.v.) spectrum and, in the n.m.r. spectrum, exhibited, in addition to the expected signals due to the angular methyl group and the methylpropenyl side chain, a two-proton multiplet at τ 7.09 (—CH_2COOH) and a one-proton triplet at τ 4.38 due to the γ-vinyl hydrogen. Although it is well known that equilibration of α,β- and β,γ-unsaturated carboxylic acids occurs in the presence of base (9), it is of interest to note that in the present case the equilibrium lies completely on the side of the β,γ-unsaturated isomer. One of the major factors contributing to this phenomenon may well be the $A^{(1,3)}$ strain (10) which would be associated with the exocyclic double bond in the α,β-unsaturated isomer. Presumably this is more severe than the $A^{(1,2)}$ strain (10) which is inherently present in the β,γ-unsaturated compound.

Treatment of the sodium salt of the carboxylic acid **10** with oxalyl chloride in benzene at room temperature gave the acid chloride **11**. The latter was quite unstable and readily cyclized to the cross-conjugated dienone **13**. In fact, when the acid chloride was allowed to stand at room temperature, or if it was gently warmed, a nearly quantitative yield of the dienone **13** was obtained. Therefore, even though special precautions were taken during the isolation of the crude acid chloride and even though the latter was reacted immediately with excess diazomethane, the resulting crude diazoketone **12** contained a considerable quantity of the bicyclic dienone **13**. Since no separation was affected at this stage, compound **13** was eventually isolated along with the demethylaristolones (*vide infra*). It is important to note that the n.m.r. spectrum of the crude diazoketone clearly showed that the olefinic double bond of this compound had remained in the β,γ-position with respect to the carbonyl group.

When the crude diazoketone **12** was heated with cupric sulfate in refluxing cyclohexane (11) for 2 h, a mixture of products was obtained. Analysis of the mixture by g.l.c. showed that it contained, in addition to a number of minor components, three major products, the cross-

Can. J. Chem. Downloaded from www.nrcresearchpress.com by 84.22.46.98 on 09/08/12
For personal use only.

Can. J. Chem. Downloaded from www.nrcresearchpress.com by 84.22.46.98 on 09/08/12
For personal use only.

conjugated dienone **13**, (±)-4-demethylaristolone (**14**), and (±)-5-epi-4-demethylaristolone (**15**), in a ratio of approximately 2:2:1, respectively. Treatment of this mixture with sodium hydroxide in hot aqueous ethanol for 10 min removed the minor components and gave a neutral product containing only the three compounds **13**, **14**, and **15**. Purification of this latter mixture by means of successive column chromatography on alumina and preparative g.l.c. allowed the isolation of all three components. The fact that the crucial cyclization had indeed taken place was clearly shown by the spectral data of the two cyclization products **14** and **15**. The major cyclization product, (±)-4-demethylaristolone (**14**), gave an u.v. maximum at 235 mμ and a strong carbonyl absorption at 6.10 μ in the infrared (i.r.). The n.m.r. spectrum, which was particularly instructive, exhibited a broad singlet at τ 4.32, due to the olefinic proton, and three sharp singlets at τ 8.70, 8.77, and 8.83 due to the three tertiary methyl groups. The minor cyclization product (±)-5-epi-4-demethylaristolone (**15**) was shown to be isomeric with **14** by means of a high resolution mass spectrometric measurement and gave spectral data very similar to that of compound **14**.

Having clearly shown that the initially proposed intramolecular cyclization of a diazoketone of the type **3** was a feasible process, we wished to unequivocally determine the stereochemistry of the two cyclization products, **14** and **15**. In order to accomplish this objective, we planned to convert the demethylaristolones into relatively simple decalone derivatives which, hopefully, could then be synthesized unambiguously.

Lithium–ammonia reduction of (±)-4-demethylaristolone (**14**) gave, in quantitative yield, (±)-9,10-dihydro-4-demethylaristolone (**16**). The fact that only the olefinic double bond had reduced and that the *gem* dimethylcyclopropyl moiety had been retained was clearly shown by the spectral data of the product **16**. The latter gave an u.v. absorption maximum at 212.5 mμ (see reference 12) and, in the n.m.r. spectrum, showed three sharp singlets due to the tertiary methyl groups, but gave no signal due to a vinyl proton. When compound **16** was again subjected to reduction with lithium in ammonia, the expected (13) substituted decalone **17** was obtained, again in virtually quantitative yield.

An unambiguous synthesis of the decalone **17** and subsequent correlation with the above reduction product would, of course, provide unequivocal proof for the stereochemistry of (±)-4-demethylaristolone (**14**). This synthesis was carried out as follows. Dehydrobromination of the known bromo ketone **18** (14) with a mixture of lithium bromide and lithium carbonate in hot dimethylformamide (15) afforded, in 90% yield, the octalone **19** (16). When the latter was reacted with isopropenylmagnesium bromide in the presence of cuprous chloride in tetrahydrofuran (17, 18), a mixture of products was obtained. Column chromatography of this mixture gave, in addition to a number of minor uncharacterized non-ketonic materials (presumably resulting from 1,2-addition of the Grignard reagent to the carbonyl of **19**), a 50% yield of the conjugate addition product **20**. It is noteworthy that the conjugate addition reaction was completely stereoselective, since a careful examination of the crude product of the reaction revealed that only one of the two possible epimeric 1,4-addition products was formed. Hydrogenation of the olefinic ketone **20** over Adams catalyst produced the decalone **17**, which was shown to be identical (m.p., mixed m.p., i.r.) with the decalone **17** obtained from the lithium–ammonia reduction of (±)-9,10-dihydro-4-demethylaristolone (**16**).

The stereochemical outcome of the above conjugate addition reaction requires comment. It has been proposed (19) that the conjugate introduction of a Grignard reagent to octalones of the type **19** must, for stereoelectronic reasons, take place via one (or both) of the two transition states **A** and **B**. Molecular models show that if stereoelectronic control is to be maintained in the boat-like transition state **B**, then the incoming Grignard reagent must approach the molecule in such a way that it is nearly eclipsed with the angular methyl group. The resulting torsional strain (20, 21) should override the steric hindrance (between the incoming isopropenyl group and the *syn*-axial hydrogens) present in transition state **A** and should ensure that the latter is favored over transition state **B**. Therefore, we fully expected that the cuprous chloride catalyzed 1,4-addition of isopropenylmagnesium bromide to octalone **19** would be highly stereoselective and, furthermore, predicted that the product should possess the stereochemistry depicted in **20**.

That the above prediction regarding the stereochemistry of **20** was correct was shown unambiguously as follows. Ketalization of **20** with

Can. J. Chem. Downloaded from www.nrcresearchpress.com by 84.22.46.98 on 09/08/12
For personal use only.

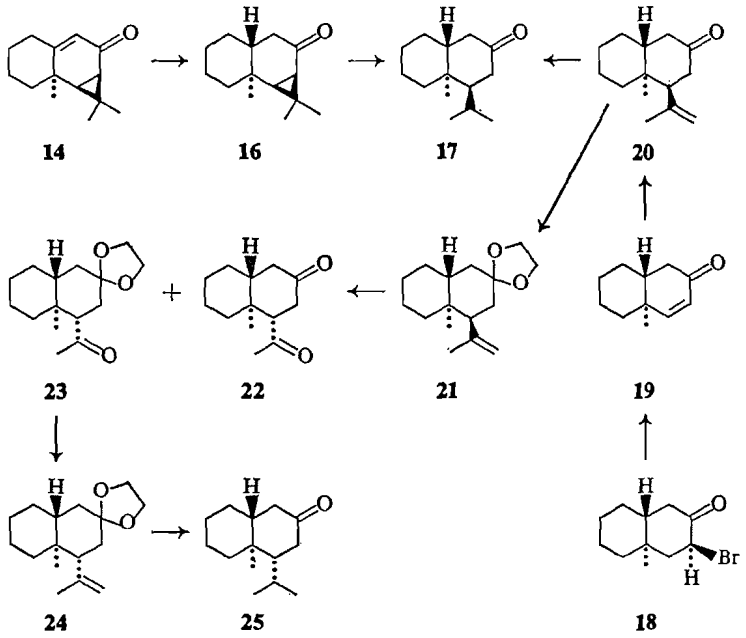

ethylene glycol afforded the crystalline ketal **21**, in 88% yield. Ozonolysis of this material, followed by column chromatography of the crude product, gave, in addition to the diketone **22**, the desired keto ketal **23**. The latter, upon reaction with methylenetriphenylphosphorane in dimethyl sulfoxide (8), gave a high yield of the olefinic ketal **24** which, on the basis of m.p., gas–liquid chromatographic retention time, and spectral data, was clearly different from, and therefore epimeric with, the olefinic ketal **21**. Successive hydrolysis and hydrogenation of compound **24** produced the decalone **25** which again was different from the decalone **17** obtained previously.

Obviously, the overall epimerization involved in the conversion of **21** into **24** required that the isopropenyl group was axial in the starting material **21**, and equatorial in the product **24**. The above stereochemical prediction was therefore correct and the stereochemistry of **20** was completely defined. This, in turn, unambiguously established the stereochemistry of (±)-4-demethylaristolone (**14**).

The lithium–ammonia reduction of (±)-5-epi-4-demethylaristolone (**15**) was also carried out. As in the case of the epimeric (±)-4-demethylaristolone (**14**), reduction of **15** was completely stereoselective and cleanly produced, in high yield, only one dihydro derivative (**26**). Lithium–

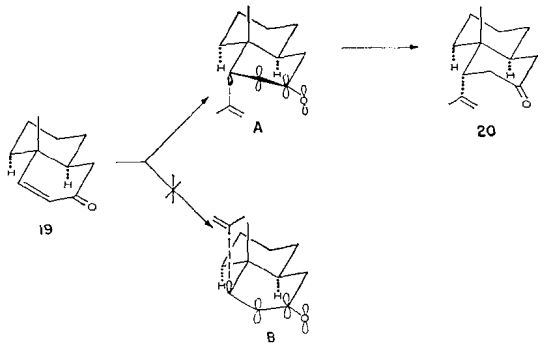

ammonia reduction of the latter afforded the substituted decalone **27**. Somewhat surprisingly, this decalone proved to be different from decalone **25**, the structure of which was unambiguously defined. This observation could only lead to the interesting conclusion that the lithium–ammonia reduction of (±)-5-epi-4-demethylaristolone (**15**) had produced a dihydro derivative with *cis*-fused six-membered rings. In contrast to the normal stereochemical outcome of reductions of this type (10, 22, 23) this is, to our knowledge, the

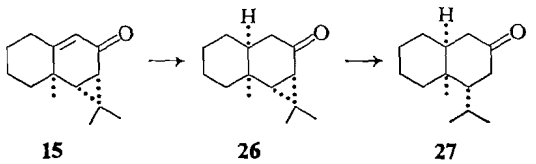

Can. J. Chem. Downloaded from www.nrcresearchpress.com by 84.22.46.98 on 09/08/12
For personal use only.

first recorded example of a lithium–ammonia reduction of a substituted $\Delta^{1(9)}$-octal-2-one which stereoselectively gave the corresponding *cis*-fused decalone derivative.

Experimental

General[1]

Melting points, which were determined on a Kofler block, and boiling points are uncorrected. Ultraviolet spectra were measured in methanol solution on either a Cary, model 14, or a Unicam, model SP.800, spectrophotometer. Routine i.r. spectra were recorded on a Perkin-Elmer Infracord model 137 spectrophotometer, while all comparison spectra were recorded on a Perkin-Elmer model 421 spectrophotometer. Nuclear magnetic resonance spectra were taken in deuterochloroform solution on Varian Associates spectrometers, model A-60 and/or model HA-100. Signal positions are given in the Tiers τ scale, with tetramethylsilane as an internal standard; the multiplicity, integrated peak areas, and proton assignments are indicated in parentheses. High resolution mass spectra were recorded on an AEI, type MS9, mass spectrometer. Gas–liquid chromatography was carried out on an Aerograph Autoprep, model 700. The following columns (10 ft × 1/4 in., unless otherwise stated) were employed, with the inert, supporting material being 60/80 mesh Chromosorb W in each case: Column A, 20% FFAP; Column B, 15% QF-1; Column C, 20% Apiezon J., Column D, 10% Apiezon J; Column E (10 ft × 3/8 in.), 30% FFAP; Column F (10 ft × 3/8 in.), 30% Carbowax 20 M; Column G (10 ft × 3/8 in.), 30% SE 30; Column H, 20% SE-30; Column I (10 ft × 3/8 in.), 30% Apiezon J. The specific column used, along with the column temperature and carrier gas (helium) flow-rate (in ml/min), are indicated in parentheses. Microanalyses were performed by Mr. P. Borda, Microanalytical Laboratory, University of British Columbia, Vancouver.

The procedure employed for isolation of reaction products consisted of thorough extraction with the specified solvent, washing the combined extracts first with water, then with saturated brine, and drying over either anhydrous magnesium sulfate or sodium sulfate. The solvent was removed from the filtered extracts by means of a rotary evaporator, under reduced pressure.

2-Methyl-2-methallyl-6-n-butylthiomethylene-cyclohexanone (5)

To a stirred solution of potassium-*t*-butoxide (140 g, 1.23 moles) in 1200 ml of dry *t*-butyl alcohol was added 77 g (0.363 mole) of 2-methyl-6-*n*-butylthiomethylenecyclohexanone (**4**) (6) and the resulting solution was stirred at room temperature for 10 min and then cooled to 0°. Freshly distilled methallyl chloride (174 g, 1.92 moles) was added and the reaction mixture was refluxed under an atmosphere of dry nitrogen for 2 h. After most of the solvent had been removed under reduced pressure, the residue was diluted with water and the product was isolated with ether. Distillation under reduced pressure afforded 78 g (70%) of the alkylated ketone **5**, b.p. 101–103° at 0.08 mm; n_D^{20} 1.4965; u.v. λ_{max} 280 mμ (ε = 12 100); i.r. (film), λ_{max} 5.98, 6.31, 10.92 μ.

Anal. Calcd. for $C_{16}H_{22}OS$: C, 72.12; H, 9.84; S, 12.03. Found: C, 72.07; H, 9.77; S, 11.94.

2-Methyl-2-methallylcyclohexanone (6)

A stirred solution of compound **5** (65.8 g, 0.25 mole) in 150 ml of 25% aqueous potassium hydroxide and 150 ml of ethylene glycol was refluxed, under an atmosphere of nitrogen, for 18 h. The reaction mixture was steam distilled until the distillate was clear. The distillate was saturated with salt and the product was extracted with ether. Distillation of the crude oil gave 33.3 g (80%) of the desired ketone **6**, b.p. 54–58° at 0.6 mm; n_D^{20} 1.4772; i.r. (film), λ_{max} 5.86, 6.10, 11.16 μ; n.m.r., τ 5.18, 5.33 (two multiplets, 2H, $=CH_2$), 8.33 (broad singlet, 3H, vinyl methyl), 8.92 (singlet, 3H, tertiary methyl).

Anal. Calcd. for $C_{11}H_{18}O$: C, 79.47; H, 10.91. Found: C, 79.67; H, 10.79.

2-Methyl-2-methylpropenylcyclohexanone (7)

A solution of the ketone **6** (36 g) and *p*-toluenesulfonic acid (460 mg) in 700 ml of dry benzene was refluxed under nitrogen for 3 days. The solution was cooled, washed with saturated aqueous sodium bicarbonate, washed with saturated brine, and the product was isolated in the normal manner. Distillation of the crude product gave 27.7 g (77%) of a clear oil, b.p. 59–62° at 0.8 mm. Gas–liquid chromatographic analysis (column A, 170°, 75) of this material indicated that it was a mixture, consisting of approximately 80% of the desired ketone **7**, 17% starting material **6**, and 3% of an unidentified compound. This mixture was subjected to fractional distillation through a spinning band column (stainless steel, 8 mm × 24 in.). The distillation was carried out at a pressure of 28 mm, and each fraction was submitted to gas–liquid chromatographic analysis (column A, 170°, 75). The initial, small fractions (1 and 2), b.p. 105–112°, consisted mainly of the unidentified impurity. Fractions 3, 4, and 5 (15.1 g, b.p. 112–116°) contained the desired ketone **7**, greater than 97% pure. Fraction 6 (3.3 g, b.p. 116–118°) contained approximately 80% of the desired product **7**, and 20% starting material **6**. The still-pot residue (6.4 g) consisted of a mixture of compounds **6** (85%) and **7** (15%). An analytical sample of 2-methyl-2-methylpropenylcyclohexanone (**7**) was collected by preparative g.l.c. (column A, 170°, 75) and exhibited n_D^{20} 1.4767; i.r. (film), 5.88 μ; n.m.r., τ 4.74 (multiplet, 1H, vinyl H), 8.31, 8.57 (doublets, 6H, vinyl methyls, J = 1.5, 1.2 Hz, respectively), 8.91 (singlet, 3H, tertiary methyl).

Anal. Calcd. for $C_{11}H_{18}O$: C, 79.47; H, 10.91. Found: C, 79.56; H, 11.10.

Reaction of Ketone 7 with Diethyl Cyanomethylphosphonate

A stirred suspension of sodium hydride (10.9 g, 0.454 mole) in dry dimethyl sulfoxide (220 ml) was slowly heated, under an atmosphere of nitrogen, to 75° and kept at this temperature until frothing had ceased (approximately 45 min). The solution was cooled to room temperature and a solution of diethyl cyanomethylphosphonate (80.5 g, 0.455 mole) in 150 ml of dimethyl sulfoxide was added. After stirring the reaction mixture for 10 min, a solution of ketone **7** (15.1 g, 0.091 mole) in 40 ml of dimethyl sulfoxide was added. The reaction was heated at 100° overnight, cooled, diluted with water,

[1]This general section is applicable to both the present paper and the succeeding paper (24).

Can. J. Chem. Downloaded from www.nrcresearchpress.com by 84.22.46.98 on 09/08/12
For personal use only.

and the product was isolated with petroleum ether (b.p. 30–60°). Distillation of the crude product gave 16.3 g (95%) of a clear oil, b.p. 84–87° at 0.15 mm. Analysis by g.l.c. (column B, 200°, 100) showed that this material was a mixture, containing approximately 80% of the α,β-unsaturated nitrile **8** and 20% of the β,γ-unsaturated nitrile **9**. An analytical sample of the major product was obtained by preparative g.l.c. (column B, 170°, 100) and exhibited n_D^{20} 1.5069; u.v., λ_{max} 219 mμ (ε = 10 900); i.r, (film), 4.55, 6.20 μ; n.m.r. τ 4.75 (singlet, 1H, =CHCN), 4.81 (multiplet, 1H, vinyl H), 8.28, 8.49 (doublets, 6H, vinyl methyls, J = 1.4, 1.3 Hz, respectively), 8.80 (singlet, 3H, tertiary methyl).

Mol. Wt. Calcd. for $C_{13}H_{19}N$: 189.152. Found (high resolution mass spectrometry): 189.150.

Although the minor product **9** was not isolated in pure form, the n.m.r. spectrum of the mixture of **8** and **9** clearly showed that the minor constituent was indeed the β,γ-unsaturated nitrile **9**. The mixture also gave satisfactory analytical data.

Anal. Calcd. for $C_{13}H_{19}N$: C, 82.48; H, 10.13. Found: C, 82.25; H, 10.35.

Preparation of Carboxylic Acid ***10***

To a solution of potassium hydroxide (75 g) in 390 ml of 95% ethanol was added 15.1 g (0.08 mole) of the mixture of nitriles **8** and **9**. The solution was refluxed under an atmosphere of nitrogen for 3 days. Most of the solvent was removed under reduced pressure, and the residue was diluted with water. The mixture was washed with ether and then acidified with dilute hydrochloric acid. The product was isolated in the normal manner with ether. Distillation of the crude product gave 10.9 g (65%) of the β,γ-unsaturated carboxylic acid **10**, b.p. 118–122° at 0.05 mm; n_D^{20} 1.5035; i.r. ($CHCl_3$), λ_{max} 2.9–4.1 (broad), 5.85 μ; n.m.r., τ 4.38 (triplet, 1H, γ-vinyl H), 4.95 (multiplet, 1H, vinyl H), 7.09 (multiplet, 2H, $-CH_2COOH$), 8.36, 8.40 (doublets, 6H, vinyl methyls, J = 1.5, 1.2 Hz, respectively), 8.87 (singlet, 3H, tertiary methyl).

Anal. Calcd. for $C_{13}H_{26}O_2$: C, 74.96; H, 9.68. Found: C, 74.80; H, 9.91.

Dienone ***13****, (±)-4-Demethylaristolone (****14****), and (±)-5-Epi-4-demethylaristolone (****15****)*

The β,γ-unsaturated carboxylic acid **10** (4.0 g, 20.6 mmoles) was dissolved in 0.1 *N* aqueous sodium hydroxide (22.6 mmoles), the water was removed under reduced pressure, and the residue was dried in a vacuum oven at 70°. To a stirred suspension of the resulting acid salt in 80 ml of cold (0°), dry benzene was added 6 drops of pyridine, followed by 28 ml of oxalyl chloride. The solution was stirred at room temperature for 30 min, filtered, and concentrated, under reduced pressure, at 40°. The crude acid chloride **11** [i.r. (film), λ_{max} 5.60 μ] thus obtained was immediately dissolved in 40 ml of dry ether and an excess of dry, alcohol-free ethereal diazomethane was added. After 30 min the solvent was removed under reduced pressure, affording the crude diazoketone **12**. The i.r. (film) spectrum showed λ_{max} 4.80, 6.16 μ. The n.m.r. spectrum of this crude material indicated that the olefinic double bond had remained in the β,γ-position relative to the carbonyl group. Furthermore, it was clear from the spectrum that the crude material contained a significant amount of the cross-conjugated dienone **13**.

The crude diazoketone was dissolved in 400 ml of cyclohexane and 8 g of anhydrous cupric sulfate was added. The resulting suspension was stirred vigorously and refluxed under an atmosphere of nitrogen for 2 h, at which time the i.r. absorption at 4.80 μ had disappeared. The suspension was cooled, filtered, washed with saturated aqueous sodium bicarbonate and with saturated brine, dried, and concentrated. Gas–liquid chromatographic analysis (column C, 200°, 85) of the resulting crude product (3.77 g) showed that it contained, in addition to a number of minor components of short retention time, three major components, **13**, **14**, and **15**, in a ratio of 2:2:1, respectively. The crude product was refluxed for 10 min in a mixture of ethanol (280 ml) and water (25 ml) containing 10 g of sodium hydroxide. The solution was concentrated under reduced pressure, the residue was diluted with water, and the neutral product was isolated with ether. Analysis of this crude product (2.32 g) by g.l.c. showed that all the minor components had been removed by this treatment, leaving only a mixture of the three major components **13**, **14**, and **15**. After partial separation of these compounds had been effected by column chromatography on Woelm neutral alumina, activity 1, an analytical sample of each compound was obtained by preparative g.l.c. (column C, 200°, 85).

The cross-conjugated dienone **13**, an oil, exhibited n_D^{20} 1.5408; u.v. λ_{max} 255 mμ (ε = 17 200); i.r. ($CHCl_3$), λ_{max} 5.98, 6.18 μ; n.m.r., τ 4.13 (broad singlet, 1H, vinyl H, width at half-height = 2 Hz), 7.68, 8.06 (singlets, 6H, vinyl methyls), 8.66 (singlet, 3H, tertiary methyl).

Anal. Calcd. for $C_{13}H_{18}O$: C, 82.05; H, 9.54. Found: C, 81.94; H, 9.72.

This compound could also be prepared by allowing the acid chloride **11** to stand at room temperature for 24 h, followed by distillation, b.p. 75° (bath temperature) at 0.2 mm. This product was identical with **13**, described above.

(±)-4-Demethylaristolone (**14**), an oil, exhibited the following spectral properties: u.v., λ_{max} 235 mμ (ε = 11 600); i.r. ($CHCl_3$), λ_{max} 6.10 μ; n.m.r., τ 4.32 (broad singlet, 1H, vinyl H), 8.70, 8.77, 8.83 (singlets, 9H, tertiary methyls).

Mol. Wt. Calcd. for $C_{14}H_{20}O$: 204.151. Found (high resolution mass spectrometry): 204.151.

The crystalline (±)-5-epi-4-demethylaristolone (**15**) was recrystallized from petroleum ether (b.p. 60–80°) and exhibited m.p. 86.5–87.5°; u.v. λ_{max} 232 mμ (ε = 11 700); i.r. ($CHCl_3$), λ_{max} 6.11 μ; n.m.r. τ 4.28 (singlet, 1H, vinyl H), 8.62, 8.65, 8.70 (singlets, 9H, tertiary methyls).

Mol. Wt. Calcd. for $C_{14}H_{20}O$: 204.151. Found (high resolution mass spectrometry): 204.150.

Preparation of Octalone ***19***

A stirred suspension of lithium bromide (1.1 g) and lithium carbonate (1.6 g) in 30 ml of dry dimethylformamide was heated, under an atmosphere of nitrogen, to 120°. A solution of the bromo ketone **18** (14) (1.5 g, 6.1 mmoles) in 30 ml of dry dimethylformamide was added and the mixture was heated at 120° for 1.75 h. The reaction mixture was cooled, filtered, diluted with water, and the product was isolated with *n*-heptane. Distillation

Can. J. Chem. Downloaded from www.nrcresearchpress.com by 84.22.46.98 on 09/08/12
For personal use only.

of the crude product gave 0.91 g (90%) of octalone **19** as a clear, colorless oil, b.p. 100° at 0.35 mm; n_D^{20} 1.5088 (lit. b.p. 69° at 0.1 mm; n_D^{26} 1.5006 (16)). Gas–liquid chromatographic analysis (column D, 200°, 85) of this material showed that it consisted of only one component; u.v. λ_{max} 229 mμ (ε = 9200); i.r. (film), λ_{max} 5.95, 6.16 μ; n.m.r., τ 3.33, 4.24 (pair of doublets, 2H, (O=C)CH=C*H* and (O=C)C*H*=CH, respectively, J = 9.8 Hz), 8.96 (singlet, 3H, tertiary methyl).

Preparation of Decalone ***20***

To a stirred, ice-cold 1 *M* solution (120 ml) of isopropenylmagnesium bromide in tetrahydrofuran was added 0.65 g of anhydrous cuprous chloride. A solution of octalone **19** (10.0 g, 0.061 mole) in 40 ml of tetrahydrofuran was added dropwise, over a period of 20 min. The reaction mixture was stirred for 2 h at 0° and then poured into 350 ml of aqueous ammonium chloride–ammonium hydroxide buffer (p*H* ≃ 8). The product was isolated by extraction with ether. Analysis by g.l.c. (column D, 180°, 80) revealed that the crude product (10.7 g, b.p. 99–103° at 0.5 mm) contained, in addition to a number of minor components, one major product (approximately 60% of the mixture). Chromatography of this mixture on Woelm neutral alumina (300 g) afforded, in the fractions eluted with 4:1 benzene–ether, 5.2 g (50%) of decalone **20**, as pale yellow crystals. A careful examination of the various chromatography fractions showed that **20** was the only carbonyl-containing compound present in the product. Recrystallization of **20** from hexane–ether afforded clear, colorless plates, m.p. 83–84°; i.r. (KBr), λ_{max} 5.88, 6.14, 11.25 μ; n.m.r., τ 5.08, 5.45 (multiplets, 2H, =CH_2), 8.23 (multiplet, 3H, vinyl methyl), 8.84 (singlet, 3H, tertiary methyl).

Anal. Calcd. for $C_{14}H_{22}O$: C, 81.49; H, 10.75. Found: C, 81.33; H, 10.69.

Lithium–ammonia Reduction of
*(±)-4-Demethylaristolone (**14**)*

To 50 ml of ammonia, which had been distilled from sodium metal, was added 70 mg of lithium metal, and the resulting blue solution was stirred, under an atmosphere of dry nitrogen, for 15 min. A solution of (±)-4-demethylaristolone (**14**) (100 mg) in 8 ml of anhydrous ether was added dropwise and the resulting solution was stirred for 1 h. After the reaction had been quenched with ammonium chloride, the ammonia was allowed to evaporate and the residual material was diluted with water. Isolation of the product with ether gave 90 mg (90%) of a clear, colorless oil. Gas–liquid chromatographic analysis (column C, 200°, 85) showed that this material consisted of nearly pure (±)-9,10-dihydro-4-demethylaristolone (**16**), the only impurity being a small amount of starting material (**14**). An analytical sample of compound **16**, an oil, was obtained by preparative g.l.c. (column C, 200°, 85); u.v., λ_{max} 212.5 mμ (ε = 5200); i.r. ($CHCl_3$), λ_{max} 6.00 μ; n.m.r., τ 8.35, 8.94 (pair of doublets, 2H, cyclopropyl protons, J = 8.0 Hz), 8.59, 8.87, 8.97 (singlets, 9H, tertiary methyls).

Mol. Wt. Calcd. for $C_{14}H_{22}O$: 206.167. Found (high resolution mass spectrometry): 206.166.

Preparation of Decalone ***17***

(a) By Hydrogenation of Decalone ***20***

Hydrogenation (platinum oxide, ethanol) of compound **20** was carried out at atmospheric pressure and room temperature. From 200 mg of **20**, there was obtained 182 mg (91%) of the crystalline decalone **17**. Recrystallization from *n*-hexane gave an analytical sample, m.p. 49–50°; i.r. ($CHCl_3$), λ_{max} 5.85 μ; n.m.r., τ 8.89 (singlet, 3H, tertiary methyl), 9.08, 9.17 (doublets, 6H, secondary methyls, J = 6.8 Hz).

Anal. Calcd. for $C_{14}H_{24}O$: C, 80.70; H, 11.61. Found: C, 80.95; H, 11.51.

(b) By Lithium–ammonia Reduction of
*(±)-9,10-Dihydro-4-demethylaristolone (**16**)*

The lithium–ammonia reduction of compound **16** was carried out by a procedure identical with that used for the reduction of (±)-4-demethylaristolone (**14**) (see above). From 60 mg of **16** there was obtained 58 mg of the crude crystalline decalone **17**. Recrystallization from *n*-hexane gave an analytical sample, m.p. 49–50°. This material was shown to be identical (m.p., mixed m.p., g.l.c. retention time, i.r. spectrum) with compound **17** obtained as described above.

Preparation of Ketal ***21***

A solution of the decalone **20** (3.1 g, 15 mmoles), ethylene glycol (3.72 g, 60 mmoles), and *p*-toluenesulfonic acid (50 mg) in 50 ml of dry benzene was refluxed under a Dean–Stark water separator for 20 h. The cooled solution was diluted with 50 ml of ether and washed with 50 ml of aqueous sodium bicarbonate. The organic layer was dried and concentrated, affording 3.93 g of colorless crystals. Recrystallization from *n*-hexane gave 3.31 g (88%) of the ketal **21** as colorless plates, m.p. 80–81°; i.r. ($CHCl_3$), λ_{max} 6.15, 9.07, 9.28, 11.18 μ; n.m.r., τ 5.01, 5.20 (multiplets, 2H, =CH_2), 6.10 (multiplet, 4H, —OCH_2CH_2O—), 8.13 (multiplet, 3H, vinyl methyl), 9.02 (singlet, 3H, tertiary methyl).

Anal. Calcd. for $C_{16}H_{26}O_2$: C, 76.75; H, 10.46. Found: C, 76.69; H, 10.39.

Ozonolysis of Ketal ***21***

A solution of 3.0 g (12 mmoles) of ketal **21** was dissolved in 150 ml of ethyl acetate and the solution was cooled in a dry ice–acetone bath. Ozone was bubbled through the solution until a blue color began to appear (approximately 15 min) and continued for a further 15 min. Platinum oxide (400 mg) was added and the reaction mixture was subjected to hydrogenation at room temperature and atmospheric pressure. After hydrogen uptake had ceased, the mixture was filtered and the filtrate was concentrated under reduced pressure. Gas–liquid chromatographic analysis (column B, 200°, 85) showed that the residual oil (2.63 g) consisted of three components. This material was subjected to column chromatography on Woelm neutral alumina (120 g). The first fraction (500 mg) showed no carbonyl absorption in its i.r. spectrum, and was not investigated further. The fractions eluted with 9:1 to 4:1 benzene–ether gave a total of 620 mg (21%) of the crystalline keto ketal **23** which, upon recrystallization from *n*-hexane, exhibited m.p. 74–74.5°; i.r. ($CHCl_3$), λ_{max} 5.88, 9.08, 9.28 μ; n.m.r., τ 6.06 (singlet, 4H, —OCH_2CH_2O—), 7.84 (singlet, 3H, —$COCH_3$), 9.09 (singlet, 3H, tertiary methyl).

Anal. Calcd. for $C_{15}H_{24}O_3$: C, 71.38; H, 9.59. Found: C, 71.15; H, 9.47.

Can. J. Chem. Downloaded from www.nrcresearchpress.com by 84.22.46.98 on 09/08/12
For personal use only.

The fractions from the above chromatography which were eluted with 4:1 to 7:3 benzene–ether afforded 1.0 g of oily crystals which were recrystallized from *n*-hexane to afford 840 mg (33%) of the diketone **22**, m.p. 95–95.5°; i.r. ($CHCl_3$), λ_{max} 5.85 μ; n.m.r., τ 7.80 (singlet, 3H, $-COCH_3$), 8.83 (singlet, 3H, tertiary methyl).

Anal. Calcd. for $C_{13}H_{20}O_2$: C, 74.95; H, 9.67. Found: C, 74.98; H, 9.89.

Preparation of Ketal ***24***

To a solution of methylenetriphenylphosphorane (1.27 g, 4.5 mmoles) in 6 ml of dimethyl sulfoxide was added a solution of the keto ketal **23** (225 mg, 0.9 mmole) in 10 ml of dimethyl sulfoxide. The resulting solution was heated at 100° for 6 h, cooled, and poured into 25 ml of cold water. Isolation of the product with pentane gave 203 mg (91%) of the crystalline ketal **24** which, upon recrystallization from *n*-hexane, exhibited m.p. 76–77°; i.r. ($CHCl_3$), λ_{max} 6.14, 9.08, 9.28, 11.18 μ; n.m.r., τ 5.05, 5.34 (multiplets, 2H, $=CH_2$), 6.04 (singlet, 4H, $-OCH_2-CH_2O-$), 8.26 (multiplet, 3H, vinyl methyl), 9.17 (singlet, 3H, tertiary methyl).

Anal. Calcd. for $C_{16}H_{26}O_2$: C, 76.75; H, 10.46. Found: C, 77.00; H, 10.45.

Preparation of Decalone ***25***

A solution of the ketal **24** (186 mg, 0.75 mmole) in a mixture of acetone (5 ml) and 10% hydrochloric acid (5 ml) was heated on a steam bath until most of the acetone had distilled. The product was isolated from the cooled reaction mixture by extraction with ether. The crude product [156 mg; i.r. (film), λ_{max} 5.85, 6.14, 11.20 μ] thus obtained was not purified further, but was subjected directly to hydrogenation (platinum oxide, ethanol) at atmospheric pressure and room temperature. Distillation of the crude hydrogenation product gave 110 mg of pure decalone **25** as a clear, colorless oil, b.p. 95° at 0.1 mm; n_D^{20} 1.4965; i.r. (film), λ_{max} 5.85 μ; n.m.r., τ 9.01 (singlet, 3H, tertiary methyl), 9.12, 9.18 (doublets, 6H, secondary methyls, $J = 6.5$ Hz).

Anal. Calcd. for $C_{14}H_{24}O$: C, 80.70; H, 11.61. Found: C, 80.63; H, 11.49.

*Lithium–ammonia Reduction of (±)-5-Epi-4-demethylaristolone (**15**)*

The lithium–ammonia reduction of **15** was carried out in a manner identical with that described previously for the reduction of (±)-4-demethylaristolone (**14**). From 100 mg of compound **15** there was obtained 90 mg of crude product, consisting nearly entirely of the dihydro derivative **26**. An analytical sample of the latter, an oil, was obtained by preparative g.l.c. (column C, 200°, 85); u.v., λ_{max} 210 mμ (ε = 4800); i.r. ($CHCl_3$), λ_{max} 5.99 μ; n.m.r., τ 8.43, 9.04 (pair of doublets, 2H, cyclopropyl protons, $J = 8$ Hz), 8.71, 8.74, 8.87 (singlets, 9H, tertiary methyls).

Mol. Wt. Calcd. for $C_{14}H_{22}O$: 206.167. Found (high resolution mass spectrometry): 206.167.

Lithium–ammonia Reduction of Compound ***26***

Reduction of 60 mg of compound **26**, *via* a procedure identical with that described previously for the reduction of **14**, gave 55 mg of crude crystalline material. Recrystallization from *n*-hexane afforded an analytical sample of the decalone **27**, m.p. 50.5–51°; i.r. ($CHCl_3$), λ_{max} 5.88 μ; n.m.r., τ 8.87 (singlet, 3H, tertiary methyl), 9.08, 9.16 (doublets, 6H, secondary methyls, $J = 6.5$ Hz).

Mol. Wt. Calcd. for $C_{14}H_{24}O$: 208.183. Found (high resolution mass spectrometry): 208.182.

Acknowledgments

We are grateful for financial support from the National Research Council of Canada and from the University of British Columbia Committee on Research. A National Research Council of Canada studentship (to W. de. W.) is gratefully acknowledged.

1. E. Piers, R. W. Britton, and W. de Waal. Can. J. Chem. **47**, 831 (1969).
2. T. Kariyone and S. Naito. J. Pharm. Soc. Japan, **75**, 1511 (1955).
3. S. Furukawa and N. Soma. J. Pharm. Soc. Japan, **81**, 559 (1961); S. Furukawa, K. Oyamada, and N. Soma. J. Pharm. Soc. Japan, **81**, 565 (1961); S. Furukawa. J. Pharm. Soc. Japan, **81**, 570 (1961).
4. G. Buchi, F. Greuter, and T. Tokoroyama. Tetrahedron Letters, 827 (1962).
5. E. Piers, W. de Waal, and R. W. Britton. Chem. Commun. 188 (1968).
6. R. E. Ireland and J. A. Marshall. J. Org. Chem. **27**, 1615 (1962).
7. W. S. Wadsworth and W. D. Emmons. J. Amer. Chem. Soc. **83**, 1733 (1961).
8. E. J. Corey and M. Chaykovsky. J. Amer. Chem. Soc. **87**, 1345 (1965), and references therein.
9. R. R. Rando and W. von E. Doering. J. Org. Chem. **33**, 1671 (1968).
10. F. Johnson. Chem. Rev. **68**, 375 (1968).
11. M. M. Fawzi and C. D. Gutsche. J. Org. Chem. **31**, 1390 (1966), and references therein.
12. W. G. Dauben and G. H. Berezin. J. Amer. Chem. Soc. **89**, 3449 (1967).
13. W. G. Dauben and J. T. Deviny. J. Org. Chem. **31**, 3794 (1966).
14. J. A. Marshall, N. Cohen, and K. R. Arenson. J. Org. Chem. **30**, 762 (1965).
15. E. J. Corey and A. G. Hortmann. J. Amer. Chem. Soc. **87**, 5736 (1965).
16. R. B. Woodward, F. Sondheimer, O. Taub, K. Heusler, and W. M. McLamore. J. Amer. Chem. Soc. **74**, 4223 (1952).
17. H. O. House, R. A. Latham, and C. D. Slater. J. Org. Chem. **31**, 2667 (1966).
18. E. Piers and R. J. Keziere. Can. J. Chem. **47**, 137 (1969).
19. J. A. Marshall and N. H. Andersen. J. Org. Chem. **31**, 667 (1966).
20. M. Cherest, H. Felkin, and N. Prudent. Tetrahedron Letters, 2199 (1968).
21. M. Cherest and H. Felkin. Tetrahedron Letters, 2205 (1968).
22. G. Stork and S. D. Darling. J. Amer. Chem. Soc. **86**, 1761 (1964).
23. M. J. T. Robinson. Tetrahedron **21**, 2475 (1965).
24. E. Piers, R. W. Britton, and W. de Waal. Can. J. Chem. This issue.

Can. J. Chem. Downloaded from www.nrcresearchpress.com by 210.87.254.6 on 09/05/12
For personal use only.

Annelation of 2,3-dimethylcyclohexanone. Synthetic proof for the stereochemistry of the sesquiterpene aristolone

EDWARD PIERS, RONALD W. BRITTON, AND WILLIAM DE WAAL
Department of Chemistry, University of British Columbia, Vancouver 8, British Columbia

Received June 2, 1969

An efficient annelation of 2,3-dimethylcyclohexanone is described. The key step of this process involves the reaction of the enol lactone **16** with methyllithium, under carefully controlled conditions. The completely stereoselective conversion of the sesquiterpene (−)-aristolone (**1**) into the levorotatory decalone **22***b* is described. Comparison of the latter with the unambiguously synthesized racemic decalone **22***a* conclusively establishes the relative stereochemistry of aristolone (**1**).

Canadian Journal of Chemistry, 47, 4307 (1969)

The relative and absolute stereochemistry of the sesquiterpene aristolone (1,2) has been proposed (3) as shown in formula **1**. However, even though two independent and entirely different total syntheses of the racemic form of this interesting natural product have recently been reported (4,5), the stereochemical proposal (3) has not as yet received synthetic verification, since both of the syntheses were stereochemically ambiguous. For example, in the synthesis reported by the present authors (5), the key step involved the cupric sulfate catalyzed intramolecular cyclization of the olefinic diazoketone **2**. This reaction was not completely stereoselective, since it produced not only (±)-aristolone (**1**), but also the isomeric (±)-6,7-epi-aristolone (**3**). Therefore, although the stereochemistry of the crucial synthetic intermediate **2** was clearly and unambiguously determined (5), the above synthesis did not unequivocally establish the total relative stereochemistry of aristolone (**1**). We have therefore obtained direct independent synthetic evidence which fully corroborates the stereochemical assignment (3) of this sesquiterpene.

Previously, in a model study (6,7) we had shown that (±)-4-demethylaristolone (**4**) gave, upon reduction with lithium in ammonia, a near quantitative yield of (±)-9,10-dihydro-4-demethylaristolone (**5**). The latter, when again subjected to lithium–ammonia reduction, afforded the substituted decalone **6**. Furthermore, we had also shown (6,7) that the cuprous chloride catalyzed conjugate addition of isopropenylmagnesium bromide to the octalone **7** gave, completely stereoselectively, the decalone **8** which, upon hydrogenation, produced compound **6**, identical with that obtained from the lithium–ammonia reduction of **5**.

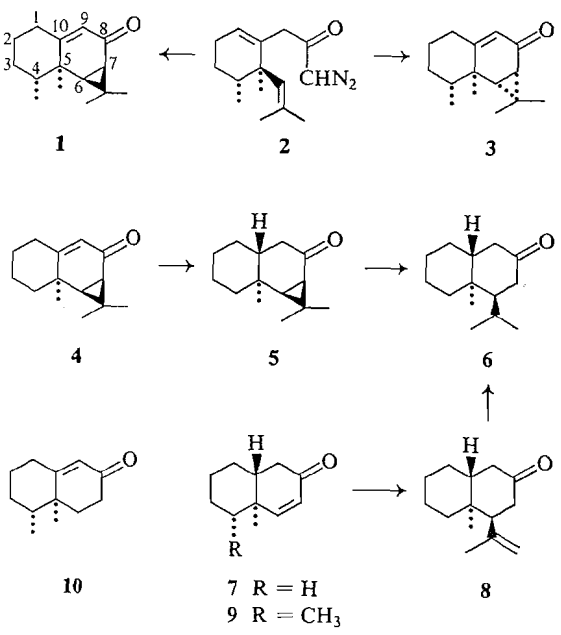

1 **2** **3**
4 **5** **6**
10 **7** R = H, R = CH_3 **8**

From the foregoing, it was clearly apparent that a similar series of reactions involving aristolone (**1**) and the octalone **9** would provide unambiguous synthetic proof for the relative stereochemistry of the natural product. It appeared highly unlikely that the presence of an extra (equatorial) methyl group (**1** and **9** as compared with **4** and **7**, respectively) would alter the stereochemical outcome of either the lithium–ammonia reduction (of **1**) or the conjugate addition of isopropenylmagnesium bromide (to **9**).

The first synthetic objective, then, was the octalone **10**, which presumably could be readily converted by standard reactions into the required isomeric compound **9**. One obvious way

Can. J. Chem. Downloaded from www.nrcresearchpress.com by 210.87.254.6 on 09/05/12
For personal use only.

to prepare **10** would be to carry out the Robinson annelation (8) of 2,3-dimethylcyclohexanone with methyl vinyl ketone or its equivalent. In fact, Ourisson and co-workers (4) had already reported this reaction, although no yield was given by these workers. We attempted the Robinson annelation of 2,3-dimethylcyclohexanone with both methyl vinyl ketone and 4-diethylamino-2-butanone methiodide under a variety of experimental conditions, but were unable to obtain the annelated material in yields exceeding approximately 15%. Furthermore, the octalone which was obtained consisted, in each case, of a mixture of two epimers in a ratio of approximately 3:2, making it extremely difficult to obtain a reasonable quantity of the desired octalone **10** in a pure state. Therefore, since the Robinson annelation did not appear to be a particularly efficient method for the preparation of **10**, we considered alternative routes to this compound.

During our work on the total synthesis of (±)-aristolone (5) we had observed that alkylation of 2,3-dimethyl-6-*n*-butylthiomethylenecyclohexanone (**11**) with methallyl chloride produced, in high yield, a mixture of *cis*- (**12**) and *trans* - 2,3 - dimethyl - 2 - methallyl - 6 - *n* - butylthiomethylenecyclohexanone (**13**), in a ratio of approximately 4:1, respectively. The fairly high stereoselectivity of this process encouraged us to consider a preparation of **10** which was based upon alkylation of **11**. This approach proved to be very satisfactory.

Alkylation of compound **11** with ethyl 3-bromopropionate in the presence of potassium-*t*-butoxide in *t*-butyl alcohol (9) proved to be a very facile reaction and produced, in 86% yield, a mixture of the keto esters **14**. Removal of the *n*-butylthiomethylene blocking group from the latter was accomplished in the normal way (9) (potassium hydroxide in hot aqueous diethylene glycol) and was accompanied by hydrolysis of the ester group. The product, a mixture of keto acids **15**, was obtained in 90% yield.

When the mixture of keto acids **15** was refluxed in acetic anhydride containing sodium acetate (see ref. 10), there was produced, in 85% yield, a crystalline material which consisted of a mixture of the two epimeric enol lactones **16** and **17**. The ratio of the two epimers, as judged by the nuclear magnetic resonance (n.m.r.) spectrum of the mixture, was approximately 9:1, respectively. The major, desired epimer **16** could readily be obtained in 80% yield from the mixture by careful recrystallization of the latter from *n*-hexane. An analytical sample of **17** was obtained from the mother liquors of recrystallization by means of preparative gas–liquid chromatography (g.l.c.). Both **16** and **17** exhibited spectral data which was in complete accord with the assigned structures.

Although, in order to convert the enol lactone **16** into the required octalone **10**, we investigated the use of a number of different reagents,[1] it was eventually found that methyllithium was the most convenient and gave the most consistent results. Thus, reaction of **16** with methyllithium in dry ether at −25° for 1.75 h, followed by successive acidic hydrolysis and base-catalyzed aldol cyclization afforded, in addition to a small amount (10%) of starting material (in the form of the keto acid **15**, *cis* epimer) a 70% yield of the desired octalone. The overall yield of pure octalone **10**, based on 2,3-dimethylcyclohexanone, was, therefore, approximately 30%, obviously a considerable improvement over the Robinson annelation method.

It should be noted that the success of the reaction of the enol lactone **16** with methyllithium depended, to a large extent, upon a judicious choice of the reaction temperature and reaction time. That is, use of reaction temperatures greater than −25°, or use of longer reaction times, resulted in the formation of a considerable amount of alcohol-containing product, presumably due to "di-addition" of methyllithium to the enol lactone. On the other hand, milder reaction conditions (lower temperatures, shorter reaction times) resulted in the recovery of fairly copious amounts of starting material, in the form of the corresponding keto acid (**15**, *cis* epimer).

Reduction of the octalone **10** with lithium in ammonia in the presence of ethanol (see ref. 16) gave, in 75% yield, the decalol **18** which, upon oxidation with Jones reagent (17) gave the decalone **19**. The latter exhibited infrared (i.r.) spectrum and gas–liquid chromatographic retention times identical with those of the (+)-antipode of **19**, which had previously been prepared, via a lengthy synthetic sequence, by Djerassi and coworkers (18).[2] This comparison conclusively showed that the initial alkylation of compound

[1]For previous examples of annelation via enol lactones, see refs. 11–15, inclusive.

[2]We are very grateful to Professor Djerassi for a small sample of this compound.

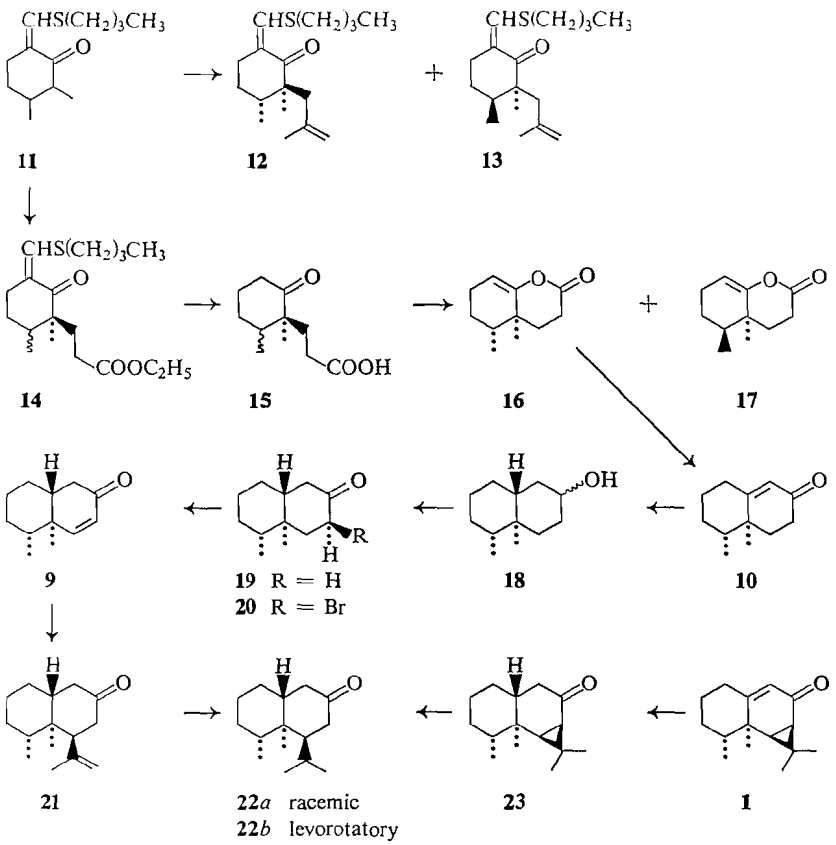

11 with β-bromopropionate had been stereoselective in the desired sense and that, therefore, our synthetic intermediates indeed possessed a *cis* stereochemistry with respect to the two methyl groups.

Bromination of the decalone **19** with bromine in acetic acid (19) afforded the known (4) bromo ketone **20**. Dehydrobromination of the latter with a mixture of lithium bromide and lithium carbonate in hot dimethylformamide (20) gave, in 86% yield, a mixture of compounds which contained, in addition to a number of minor components, the desired octalone **9** as the major (80%) constituent. This material was isolated from the mixture by means of preparative g.l.c., and showed the expected spectral properties. Of particular pertinence was the ultraviolet (u.v.) spectrum, which exhibited a maximum at 230 mμ, and the n.m.r. spectrum, which showed the vinyl protons as an AB pair of doublets (J = 10 Hz) at τ 2.88 and 4.11.

When the octalone **9** was reacted with isopropenylmagnesium bromide in the presence of cuprous chloride in tetrahydrofuran (7), the decalone **21** was produced as the only conjugate addition product.[3] Hydrogenation of **21** over Adams catalyst afforded the racemic decalone **22*a***.

Lithium–ammonia reduction of (−)-aristolone (**1**)[4] gave, in high yield, (+)-9,10-dihydroaristolone (**23**). The latter gave an u.v. absorption maximum at 213 mμ (see ref. 21) and, in the n.m.r. spectrum, showed no signal due to a vinyl proton, thus clearly demonstrating that only the olefinic double bond had reduced. When compound **23** was again reduced with lithium in ammonia, the expected (22) levorotatory decalone **22*b*** was obtained in virtually quantitative yield. This compound gave spectra (i.r., n.m.r.)

[3]For a discussion regarding the stereochemical outcome of the conversion of **9** into **21**, see ref. 7.

[4]We are very grateful to Professor A. Marsili and to Professor F. Sorm for generous samples of authentic (−)-aristolone.

Can. J. Chem. Downloaded from www.nrcresearchpress.com by 210.87.254.6 on 09/05/12
For personal use only.

Can. J. Chem. Downloaded from www.nrcresearchpress.com by 210.87.254.6 on 09/05/12
For personal use only.

and gas–liquid chromatographic retention times identical with those of the racemic decalone **22***a* obtained as outlined above. Since, by analogy with previous work (7), the stereochemistry of **22***a* was completely defined, this comparison provided unambiguous synthetic evidence for the stereochemistry of aristolone (**1**).

Experimental[5]

*Alkylation of 2,3-Dimethyl-6-n-butylthiomethylene-cyclohexanone (**11**) with Ethyl 3-Bromopropionate*

The *n*-butylthiomethylene derivative **11** (5) (100 g, 0.44 mole) was added to 1800 ml of dry *t*-butyl alcohol containing 144 g (1.4 moles) of potassium *t*-butoxide and the resulting solution was stirred at room temperature for 10 min. Ethyl 3-bromopropionate (250 g, 1.38 mole) was added slowly from a dropping funnel. The alkylation was exothermic and, after the addition was complete, the reaction mixture was stirred for an additional 15 min. Most of the solvent was removed under reduced pressure and the residue was diluted with water. Isolation of the product with ether gave an oil which, upon distillation under reduced pressure, afforded 124 g (86%) of the keto ester **14** (mixture of epimers); b.p. 190–195° at 0.2 mm; n_D^{20} 1.5261; u.v., λ_{max} 311 mμ (ε = 14 900); i.r. (film), λ_{max} 5.79, 6.03, 6.52 μ.

Anal. Calcd. for $C_{18}H_{30}O_3S$: C, 66.22; H, 9.26. Found: C, 66.14; H, 9.33.

*Preparation of Keto Acid **15***

To a solution of the above alkylated material (**14**) (124 g, 0.38 mole) in 600 ml of diethylene glycol was added 600 ml of 25% aqueous potassium hydroxide, and the resulting solution was refluxed, under an atmosphere of nitrogen, for 18 h. The solution was cooled, diluted with water, and extracted twice with ether. The ether extracts were discarded. The aqueous layer was acidified with 6 *N* hydrochloric acid, and the product was extracted with ether. Distillation of the crude material afforded 67.5 g (90%) of the keto acid **15** (mixture of epimers) as a clear viscous oil; b.p. 142–147° at 0.15 mm; n_D^{20} 1.4868; i.r. (film), λ_{max} 2.7–4.2 (very broad), 5.78, 5.85 μ.

Anal. Calcd. for $C_{11}H_{18}O_3$: C, 66.64; H, 9.15. Found: C, 66.83; H, 9.07.

*Preparation of Enol Lactones **16** and **17***

A solution of the mixture of keto acids **15** (64 g, 0.32 mole) in 1400 ml of acetic anhydride containing 14 g of anhydrous sodium acetate was refluxed under an atmosphere of nitrogen for 2 h. The acetic anhydride was removed under reduced pressure, and the residual material was diluted with water. Isolation of the product with ether, followed by distillation, gave 49 g (85%) of crystalline material; b.p. 90–94° at 0.15 mm. This material, as judged by its n.m.r. spectrum, consisted of a mixture of the enol lactones **16** and **17**, in a ratio of approximately 9:1, respectively. Recrystallization of this mixture from *n*-hexane produced pure **16** (40 g). An analytical sample of **16** was obtained by vacuum sublimation and exhibited m.p. 51–51.5°; i.r. (CS_2), λ_{max} 5.72, 5.98 μ; n.m.r., τ 4.72 (triplet, 1H, vinyl H, J = 3.5 Hz), 8.97 (singlet, 3H, tertiary methyl), 9.04 (doublet, 3H, secondary methyl, J = 6.0 Hz).

Anal. Calcd. for $C_{11}H_{16}O_2$: C, 73.30; H, 8.95. Found: C, 73.60; H, 8.93.

An analytical sample of the minor epimer **17**, an oil, was obtained from the mother liquors of the above recrystallization by means of preparative g.l.c. (column E, 225°, 200) and exhibited n_D^{20} 1.4910; i.r. (film) λ_{max} 5.71, 5.98 μ; n.m.r., τ 4.68 (triplet, 1H, vinyl H, J = 4.0 Hz), 8.79 (singlet, 3H, tertiary methyl), 9.04 (doublet, 3H, secondary methyl, J = 6.5 Hz).

Mol. Wt. Calcd. for $C_{11}H_{16}O_2$: 180.115. Found (high resolution mass spectrometry): 180.113.

*Preparation of Octalone **10***

A solution of the crystalline enol lactone **16** (19.6 g, 0.11 mole) in 200 ml of dry ether was cooled to −25° by means of an external carbon tetrachloride–dry ice slush bath. An ethereal solution of methyllithium (75 ml, 2.35 M) was added over a period of 3 min, and the resulting solution was stirred at −25°, under an atmosphere of dry nitrogen, for 1.75 h. The reaction mixture was poured into dilute hydrochloric acid and the product was extracted with ether. To the crude, oily product thus obtained was added a solution of potassium hydroxide (16 g) in 120 ml of water and 1000 ml of methanol, and the solution was refluxed under an atmosphere of nitrogen for 2 h. The methanol was removed under reduced pressure, the residue was diluted with water, and the neutral product was isolated by extraction with ether. Distillation of the crude yellow oil thus obtained gave 13.5 g (70%) of the octalone **10**; b.p. 96–99° at 0.2 mm; n_D^{20} 1.5155; u.v., λ_{max} 240 mμ (ε = 12 100); i.r. (film), λ_{max} 5.98, 6.19 μ; n.m.r., τ 4.33 (broad singlet, 1H, vinyl H), 8.90 (singlet, 3H, tertiary methyl), 9.09 (unresolved multiplet,[6] 3H, secondary methyl).

Anal. Calcd. for $C_{12}H_{18}O$: C, 80.85; H, 10.18. Found: C, 80.96; H, 10.29.

The basic aqueous layer from the above extraction was acidified with concentrated hydrochloric acid and the acidic product was isolated by extraction with ether. Distillation of the crude product provided 2.1 g (10%) of a carboxylic acid (**15**, *cis* epimer) which, upon treatment with sodium acetate in refluxing acetic anhydride, as described above, gave the enol lactone **16**.

*Preparation of Decalol **18***

To a solution of 6 g of lithium metal in 1500 ml of liquid ammonia was slowly added, from a dropping funnel, a solution of the octalone **10** (15 g, 0.084 mole) in 100 ml of anhydrous ether. After 1 h, 16 ml of anhydrous ethanol was added and the reaction mixture was allowed to stir for an additional 1.5 h. The reaction was then quenched by careful addition of excess ethanol, and the ammonia was allowed to evaporate. The residual

[5]For general information, see preceding paper (ref. 7).

[6]In the n.m.r. spectrum of each of the compounds **9**, **10**, **18**, **19**, and **20**, the signal due to the secondary methyl group appeared as a broad band, with very little resolution. Presumably, this was due to virtual coupling (see ref. 23).

Can. J. Chem. Downloaded from www.nrcresearchpress.com by 210.87.254.6 on 09/05/12
For personal use only.

material was diluted with saturated brine and the product was isolated by extraction of the mixture with ether. Distillation of the crude product afforded 11.5 g (75%) of the decalol **18**, b.p. 86–90° at 0.2 mm, as a clear, viscous oil which resisted crystallization. An analytical sample, collected by preparative g.l.c. (column F, 250°, 200), exhibited n_D^{20} 1.4944; i.r. (film), λ_{max} 3.01, 9.54 μ; n.m.r., τ 6.40 (broad signal, 1H, —C*H*OH), 9.24 (unresolved multiplet, 3H, secondary methyl), 9.29 (singlet, 3H, tertiary methyl).

Anal. Calcd. for $C_{12}H_{22}O$: C, 79.06; H, 12.16. Found: C, 79.03; H, 11.97.

Preparation of Decalone ***19***

Standard chromic acid solution (17) was added to a solution of the decalol **18** (8.7 g, 0.048 mole) in acetone (200 ml) at 0° until the orange color persisted. Isopropyl alcohol was added to destroy the excess oxidizing reagent, and the solution was evaporated under reduced pressure. The residual material was diluted with water and the product was extracted with ether. Distillation of the crude oil gave 7 g (81%) of the decalone **19**; b.p. 83–86° at 1.0 mm; n_D^{20} 1.4943; i.r. (film), λ_{max} 5.84 μ; n.m.r., τ 9.08 (singlet, 3H, tertiary methyl), 9.13 (unresolved multiplet, 3H, secondary methyl).

Anal. Calcd. for $C_{12}H_{20}O$: C, 79.94; H, 11.18. Found: C, 80.21; H, 11.24.

This compound exhibited i.r. spectrum and gas–liquid chromatographic retention time (column G, 245°, 190) identical with those of the (+)-antipode of **19**, which had been previously prepared by Djerassi and co-workers (18).

Preparation of the Bromo Ketone ***20***

A solution of bromine (4.7 g, 29.5 mmoles) in glacial acetic acid (40 ml) was added slowly, at room temperature, to a stirred glacial acetic acid (40 ml) solution of the decalone **19** (5.3 g, 29.5 mmoles). After the addition was complete, the solution was stirred for an additional 30 min and then poured into ice-cold water. The resultant mixture was extracted with ether. The combined ether extracts were washed twice with water, then with saturated aqueous sodium bicarbonate until free of acid, and finally with saturated brine. Recrystallization of the crude crystalline product from ether afforded 5.6 g (72%) of the bromo ketone **20**. An analytical sample was obtained by vacuum sublimation and exhibited m.p. 132–133° [lit. m.p. 132–133° (4)]; i.r. ($CHCl_3$), λ_{max} 5.80 μ; n.m.r., τ 5.22 (pair of doublets, 1H, —CHBr, J = 6.5 Hz and 13.5 Hz), 8.98 (singlet, 3H, tertiary methyl), 9.10 (unresolved multiplet, 3H, secondary methyl).

Anal. Calcd. for $C_{12}H_{19}OBr$: C, 55.61; H, 7.37; Br, 30.83. Found: C, 55.68; H, 7.48; Br, 31.02.

Preparation of Octalone ***9***

A stirred suspension of lithium bromide (0.3 g) and lithium carbonate (0.4 g) in 6 ml of dry dimethylformamide was heated to 120°, under an atmosphere of nitrogen. The bromo ketone **20** (0.57 g, 2.2 mmoles) was added and the reaction mixture was stirred at 120° for 75 min. The suspension was cooled and filtered. The filtrate was diluted with water and the product was isolated with *n*-heptane. Distillation of the crude oil gave 0.34 g (86%) of a clear, colorless oil, b.p. 100° (bath temperature) at 0.4 mm. Analysis of this material by g.l.c. (column F, 250°, 240) showed that it was a mixture consisting of approximately 80% of the desired octalone **9**, 5% of the isomeric octalone **10** (on the basis of g.l.c. retention time only), and some minor unidentified components. The desired compound **9** was isolated by preparative g.l.c. (column F, 250°, 240) and exhibited n_D^{20} 1.5122; u.v., λ_{max} 230 mμ (ε ≈ 9400); i.r. (film), λ_{max} 5.97, 6.15 μ; n.m.r., τ 2.88 (doublet, 1H, β-vinyl H, J = 10 Hz), 4.11 (doublet, 1H, α-vinyl H, J = 10 Hz), 9.03 (unresolved multiplet, 3H, secondary methyl), 9.07 (singlet, 3H, tertiary methyl).

Anal. Calcd. for $C_{12}H_{18}O$: C, 80.85; H, 10.18. Found: C, 80.83; H, 10.16.

Preparation of Decalone ***21***

To a stirred solution of isopropenylmagnesium bromide (0.29 g, 2 mmoles) in 2 ml of dry tetrahydrofuran was added approximately 6 mg of anhydrous cuprous chloride and the resulting mixture was cooled to 0°. A solution of the octalone **9** (0.1 g, 0.56 mmoles) in tetrahydrofuran (4 ml) was added by means of a syringe, and the reaction mixture was stirred, under an atmosphere of nitrogen, at 0° for 15 min and then refluxed for 1 h. The cooled reaction mixture was poured slowly into rapidly stirred, ice-cold dilute hydrochloric acid, and the product was isolated by extraction with ether. Distillation of the crude product gave 110 mg (89%) of a clear oil, b.p. 100° (bath temperature) at 0.4 mm. Gas–liquid chromatographic analysis (column G, 245°, 190) of this material showed that it contained, in addition to a number of minor components, approximately 80–85% of the desired decalone **21**. The latter was isolated by preparative g.l.c. (column G, 245°, 190) and showed n_D^{20} 1.5147; i.r. (film), λ_{max} 5.87, 6.15, 11.22 μ; n.m.r., τ 5.10, 5.36 (unresolved multiplets, 2H, $=CH_2$, width at half-height ≃ 4.5 and 3.5 Hz, respectively), 8.24 (unresolved multiplet, 3H, vinyl methyl, width at half-height ≃ 3 Hz), 9.00 (singlet, 3H, tertiary methyl), 9.12 (poorly resolved doublet, 3H, secondary methyl).

Anal. Calcd. for $C_{15}H_{24}O$: C, 81.76; H, 10.98. Found: C, 81.99; H, 11.08.

Preparation of Decalone ***22a***

Hydrogenation of the decalone **21** was carried out in ethanol, at atmospheric pressure and room temperature, over Adams catalyst. From 50 mg of **21** there was obtained a quantitative yield of decalone ***22a*** as a crystalline solid. Recrystallization from *n*-hexane afforded an analytical sample; m.p. 49–51°; i.r. (CS_2), λ_{max} 5.87 μ; n.m.r., τ 9.02 (singlet, 3H, tertiary methyl), 9.06, 9.17 (doublets, 3H and 6H, respectively, secondary methyls, J = 6.8 Hz).

Mol. Wt. Calcd. for $C_{15}H_{26}O$: 222.198. Found (high resolution mass spectrometry): 222.198.

*(+)-9,10-Dihydroaristolone (****23****)*

Small pieces of freshly cut lithium metal (210 mg) were added to 150 ml of liquid ammonia which had been distilled from sodium metal. The resulting solution was stirred for 30 min. A solution of (−)-aristolone (**1**) (300 mg) in 25 ml of dry ether was added and the reaction mixture was stirred for 45 min. After the reaction had been quenched by careful addition of excess dry ammonium chloride, the ammonia was allowed to evaporate under a stream of nitrogen. The residual material was

diluted with saturated brine and the product was isolated by extraction with ether. Distillation of the crude product gave 275 mg (92%) of (+)-9,10-dihydroaristolone (**23**) as a clear colorless oil; b.p. 100° (bath temperature) at 0.1 mm; $[\alpha]_D^{24}$ + 7° (*c*, 0.76 in methanol); u.v., λ_{max} 213 mμ (ε = 4300); i.r. (film), λ_{max} 5.98 μ; n.m.r., τ 8.36 (doublet, 1H, —C^7H, *J* = 8 Hz), 8.70 (doublet, 1H, —C^6H, *J* = 8 Hz), 8.59, 8.83, 9.08 (singlet, 9H, tertiary methyls), 8.99 (doublet, 3H, secondary methyl, *J* = 6 Hz).

Mol. Wt. Calcd. for $C_{15}H_{24}O$: 220.183. Found (high resolution mass spectrometry): 220.182.

Preparation of (−)-Decalone 22b

The lithium–ammonia reduction of (+)-9,10-dihydroaristolone (**23**) was carried out by a procedure identical with that described above for the reduction of (−)-aristolone. From 120 mg of **23**, there was obtained 110 mg (91%) of the crystalline (−)-decalone **22***b*. Recrystallization from *n*-hexane provided an analytical sample; m.p. 80–82°; $[\alpha]_D^{24}$ −30° (*c*, 0.59 in methanol). This material gave spectra (i.r., n.m.r.) and gas–liquid chromatographic retention times (column H, 210°, 90; column I, 260°, 200) identical with those of the racemic decalone **22***a*, prepared as described previously.

Mol. Wt. Calcd. for $C_{15}H_{26}O$: 222.198. Found (high resolution mass spectrometry): 222.197.

Acknowledgments

We are grateful for financial support from the National Research Council of Canada and from the University of British Columbia Committee on Research. A National Research Council of Canada Studentship (to W. de W.) is gratefully acknowledged.

1. T. KARYYONE and S. MAITO. J. Pharm. Soc. Japan, **75**, 1511 (1955).
2. S. FURUKAWA and N. SOMA. J. Pharm. Soc. Japan, **81**, 559 (1961); S. FURUKAWA, K. OYAMADA, and N. SOMA. J. Pharm. Soc. Japan, **81**, 565 (1961); S. FURUKAWA. J. Pharm. Soc. Japan, **81**, 570 (1961).
3. G. BUCHI, F. GREUTER, and T. TOKOROYAMA. Tetrahedron Letters, 827 (1962).
4. C. BERGER, M. FRANCK-NEUMANN, and G. OURISSON. Tetrahedron Letters, 3451 (1968).
5. E. PIERS, R. W. BRITTON, and W. DE WAAL. Can. J. Chem. **47**, 831 (1969).
6. E. PIERS, W. DE WAAL, and R. W. BRITTON. Chem. Commun. 188 (1968).
7. E. PIERS, W. DE WAAL, and R. W. BRITTON. Can. J. Chem. This issue.
8. E. D. BERGMANN, D. GINSBERG, and R. PAPPO. Organic reactions. Vol. 10. John Wiley & Sons, Inc., New York. 1959. p. 179.
9. R. E. IRELAND and J. A. MARSHALL. J. Org. Chem. **27**, 1615 (1962).
10. H. MINATO and T. NAGASAKI. J. Chem. Soc. C, 1866 (1966).
11. R. B. WOODWARD, F. SONDHEIMER, D. TAUB, K. HEUSLER, and W. M. MCLAMORE. J. Amer. Chem. Soc. **74**, 4223 (1952).
12. P. WIELAND, H. UEBERWASSER, G. ANNER, and K. MIESCHER. Helv. Chim. Acta, **36**, 1231 (1953).
13. L. B. BARKLEY, M. W. FARRAR, S. W. KNOWLES, H. RAFFELSON, and Q. E. THOMPSON. J. Amer. Chem. Soc. **76**, 5014 (1954).
14. E. J. COREY, H-J. HESS, and S. PROSKOW. J. Amer. Chem. Soc. **85**, 3979 (1963).
15. C. A. HENRICK, E. BOHME, J. A. EDWARDS, and J. H. FRIED. J. Amer. Chem. Soc. **90**, 5926 (1968).
16. J. A. MARSHALL, N. COHEN, and K. R. ARENSON. J. Org. Chem. **30**, 762 (1965).
17. K. BOWDEN, I. M. HEILBRON, E. R. H. JONES, and B. C. L. WEEDON. J. Chem. Soc. 39 (1946).
18. L. H. ZALKOW, F. X. MARKLEY, and C. DJERASSI. J. Amer. Chem. Soc. **82**, 6354 (1960).
19. M. YANAGITA and A. TAHARA. J. Org. Chem. **18**, 792 (1953).
20. E. J. COREY and A. G. HORTMANN. J. Amer. Chem. Soc. **87**, 5736 (1965).
21. W. G. DAUBEN and G. H. BEREZIN. J. Amer. Chem. Soc. **89**, 3449 (1967).
22. W. G. DAUBEN and J. T. DEVINY. J. Org. Chem. **31**, 3794 (1966).
23. N. S. BHACCA and D. H. WILLIAMS. Applications of nuclear magnetic resonance spectroscopy in organic chemistry. Holden–Day, Inc., San Francisco, 1964, p. 36.

Can. J. Chem. Downloaded from www.nrcresearchpress.com by 210.87.254.6 on 09/05/12
For personal use only.

ortho-Diquaternary aromatic compounds. II. Synthesis and spectral properties of β,β′-dihydroxy-2,3-di-*t*-butylnaphthalene and related crowded aromatics

L. R. C. BARCLAY, G. R. NIXON,[1] H. M. FOOTE,[1] AND S. L. BARCLAY
Department of Chemistry, Mount Allison University, Sackville, New Brunswick

Received June 20, 1969

Cyclialkylation of naphthalene with 2,2,5,5-tetramethyltetrahydrofuranone yielded 2-keto-1,1,4,4-tetramethyl-1,2,3,4-tetrahydroanthracene (**1**). Selenium dioxide oxidation of **1** yielded the corresponding diketone (**3**) and periodate cleavage of **3** yielded 2,3-naphthalene-diisobutyric acid (**4**). Hydride reduction of the dimethyl ester (**6**) of **4** yielded the diol, β,β′-dihydroxy-2,3-di-*t*-butylnaphthalene (**7**). The relative chemical shifts of aromatic protons of 1,2,4,5-tetraalkylbenzenes containing *gem* dimethyls are rationalized in terms of compression effects exerted by the bulky *ortho* groups. Nuclear magnetic resonance and ultraviolet spectral results for the *ortho* di-*t*-butyl aromatic derivatives **4**, **6**, and **7** are compared to the model cyclic compounds **1** and anhydride (**5**) of **4** in terms of the strain caused by bond angle deformations in the side chains.

Canadian Journal of Chemistry, 47, 4313 (1969)

Can. J. Chem. Downloaded from www.nrcresearchpress.com by 210.87.254.105 on 09/05/12
For personal use only.

Introduction

There have been several syntheses and interesting studies of the chemistry and properties of *ortho*-di-*t*-butylbenzenes (1). The chemical and physical properties of naphthalene are also modified by crowding of substituents. For example, there is ample evidence of such steric effects by substituents at the 1- and 8-positions due to *peri* interactions (2). Compression effects (*peri*) in 1,4-di-*t*-butylnaphthalene are reflected in nuclear magnetic resonance (n.m.r.) spectra by deshielding of the *peri* hydrogens (3) and increased rate of hydrogenation of the substituted ring (4). A recent communication (5) reported significant ultraviolet (u.v.) spectral perturbations in the 1,8-di-*t*-butylnaphthalenes.

The first synthesis of a condensed aromatic system containing adjacent *t*-butyl groups was the synthesis of the crowded heteroaromatic compound, 2,3-di-*t*-butylquinoxaline, by de-Groot and Wynberg (6). X-Ray analysis of this compound (7) indicated some bond stretching and significant bond angle deformation (10°) between the *t*-butyl groups. 1,2,4,5-Tetra-*t*-butylbenzene also exhibited bond angle deformation (10°) due to repulsion of the *t*-butyl groups but the *planarity* of the benzene ring was not affected (8).

A synthesis of naphthalene containing adjacent *t*-butyl groups has not yet been reported. The continuing interest in strained aromatic systems prompted us to investigate methods of synthesizing naphthalenes containing adjacent *t*-butyl groups. The Friedel–Crafts cyclialkylation method (9) using 2,2,5,5-tetramethyltetrahydrofuranone does not lead directly to hydrocarbons. Nevertheless, this method produces suitable model compounds containing functional groups in the side chains. Cyclization at these groups permit a comparison between the crowded *ortho* diquaternary aromatic compounds and the cyclic analogues.

Discussion of Results

Cyclialkylation of naphthalene with 2,2,5,5-tetramethyltetrahydrofuranone yielded 2-keto-1,1,4,4-tetramethyl-1,2,3,4-tetrahydroanthracene (**1**). The structure of **1** was confirmed by its n.m.r. spectrum (Table I). Any possibility of **1** being the 1,2-isomer, 3-keto-1,1,4,4-tetramethyl-1,2,3,4-tetrahydrophenanthrene[2] (**2**), was ruled out by comparison of the n.m.r. spectra of the two compounds. The ketone (**1**) and the various products derived from it showed the typical AA′BB′ symmetrical multiplet in the aromatic proton region expected of 2,3-disubstitution (Table I). On the other hand, the 1,2-isomer (**2**) showed distinctly different absorption in the aromatic proton region. The absorption of H-5 in isomer **2** was shifted down field by approximately 0.9 τ compared to the multiplet for **1**. The effect is attributed to strong *peri* interaction or compression effect on H-5 by the *gem* dimethyl

[1]Recipient of National Research Council of Canada Scholarships.

[2]This isomer (m.p. 113–114°) was synthesized by an unambiguous route from α-(1-naphthyl)isobutyric acid. Details on this will be published separately.

TABLE I

Nuclear magnetic resonance absorption spectra

Compound	Chemical shifts(τ)*	Multiplicity	Relative area	Assignment
2-Keto-1,1,4,4-tetramethyl-1,2,3,4-tetrahydroanthracene (**1**)	8.58	singlet	5.87	$C(CH_3)_2$ (4)
	8.42	singlet	6.00	$C(CH_3)_2$ (1)
	7.28	singlet	1.94	$-CH_2-$
	2.36	AA′BB′	6.00	aromatic H's
	2.13	and singlet	—	—
3-Keto-1,1,4,4-tetramethyl-1,2,3,4-tetrahydrophenanthrene (**2**)	8.65	singlet	5.95	$C(CH_3)_2$ (1)
	8.19	singlet	6.15	$C(CH_3)_2$ (4)
	7.31	singlet	1.80	$-CH_2-$
	2.32	multiplet	5.05	aromatic H's-6,7,8,9,10
	1.51	multiplet	0.95	aromatic H-5
2,3-Dioxo-1,1,4,4-tetramethyl-1,2,3,4-tetrahydroanthracene (**3**)	8.37	singlet	11.9	$2\times C(CH_3)_2$
	2.32	AA′BB′	6.00	aromatic H's
	2.14	and singlet	—	—
Anhydride (**5**)	8.16	singlet	11.9	$2\times C(CH_3)_2$
	2.33	AA′BB′ multiplet	3.86	aromatic H's-5,6,7,8
	2.04	singlet	2.14	aromatic H's-1,4
Dimethyl ester (**6**)	8.24	singlet	11.8	$2\times C(CH_3)_2$
	6.63	singlet	5.90	$2\times -OCH_3$
	2.39	AA′BB′ multiplet	3.86	aromatic H's-5,6,7,8
	2.06	singlet	2.14	aromatic H's-1,4
Diol (**7**)	8.48	singlet	11.9	$2\times C(CH_3)_2$
	7.76	singlet	2.00	$2\times -OH$
	6.21	singlet	3.80	$2\times -CH_2-$
	2.42	AA′BB′ multiplet	4.10	aromatic H's-5,6,7,8
	2.00	singlet	1.90	aromatic H's-1,4

*Measurements were determined in $CDCl_3$ containing TMS; concentrations were 0.50 molar.

group on carbon-4. Comparable shifts were observed for *peri* protons in 1,4-di-*t*-butylnaphthalene (3).

Selenium dioxide oxidation of the ketone **1** yielded the yellow diketone (**3**) which gave the expected n.m.r. spectrum (Table I). Periodic acid oxidation of the diketone (**3**) yielded an acid which was readily converted into the cyclic anhydride (**5**) or, by diazomethane, into the dimethyl ester (**6**). Lithium aluminum hydride reduction of **6** afforded the diol (**7**).

The n.m.r. spectra of **5**, **6**, and **7** were consistent with these structures (Table I). These spectra were normal in the aromatic region and comparable to that of the starting ketone (**1**). This indicates that the aromatic rings of the compounds are not significantly distorted from the preferred planar configuration. The n.m.r. spectra showed no evidence for enhanced double bond fixation in these compounds. Such bond fixation is known to shift the n.m.r. absorption of the naphthalene hydrogens towards the olefinic hydrogen region (10, 11). In contrast, the hydrogens of the substituted ring in **5**, **6**, and **7** showed a slight shift (approximately 0.1 p.p.m.) *downfield* relative to **1**. There has been considerable discussion on the effect of crowding on the n.m.r. spectra of crowded aromatics (1). It is of interest

Can. J. Chem. Downloaded from www.nrcresearchpress.com by 210.87.254.105 on 09/05/12
For personal use only.

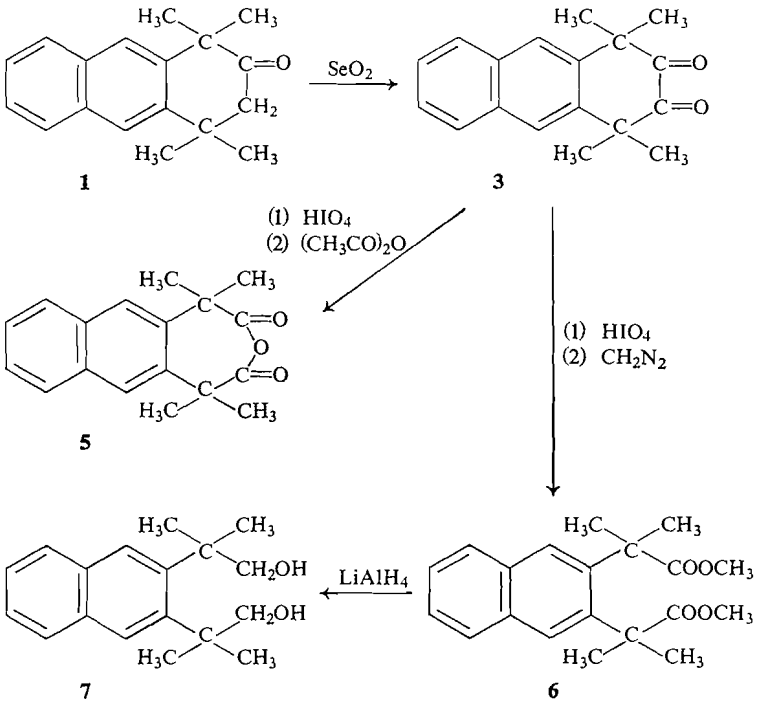

1 3 5 6 7

to our present study to attempt an empirical rationalization of the chemical shifts of aromatic protons in various crowded aromatic systems in terms of compression forces (3).

In the initial part of the n.m.r. study, the chemical shifts of aromatic protons in a series of 1,2,4,5-symmetrically substituted aromatic hydrocarbons bearing *gem* dimethyl groups are compared to those of the crowded but planar (8) hydrocarbon 1,2,4,5-tetra-*t*-butylbenzene (**12**) (see Table II). The variation in chemical shifts can reasonably be accounted for in terms of comparative van der Waals or compression forces exerted on the aromatic hydrogens by the bulky *ortho* substituents. The downfield shift (approximately 0.3 to 0.4 p.p.m.) of the aromatic proton resonances in octamethyloctahydroanthracene (**11**) compared to octamethyl- and decamethylhydrindacene (**8** and **9**) can be attributed to more compression interaction exerted by the *gem* dimethyls of a six membered ring (**11**) than by those of a five membered ring in **8** and **9**. 1,2,4,5-Tetra-*t*-butylbenzene exhibits the largest shift; 0.58 p.p.m. relative to tetraisopropylbenzene (**10**) and 0.51 p.p.m. relative to the model compound (**11**). Presumably this is a reflection of the increased compression exerted by the crowded *ortho*-*t*-butyls in **12** on the aromatic protons.[3]

Variations in the compression forces can similarly account for chemical shift differences of compressed aromatic hydrogens (1 and 4) in the substituted aromatic ring of the naphthalene derivatives, **1**, **3**, **5**, **6**, and **7**. In Table III the downfield shifts of the compressed hydrogens (1 and 4) relative to the hydrogens of the unsubstituted ring are compared for the series. The diol **7** shows the maximum downfield shift for hydrogens 1 and 4 (24.6 c.p.s.). This compound probably has the maximum compression of these hydrogens as a result of maximum crowding between the substituted *t*-butyl groups. The compression effect is progressively less in the

[3]B. V. Cheney (17) has shown that magnetic deshielding of aromatic protons by steric interactions is not only dependent upon the separation of the interacting hydrogens. The steric shift observed for various structural types was much better correlated to the component of the hydrogen–hydrogen repulsive force along the H—C bond axis. Nevertheless, in the present series of aromatic compounds of closely related structures, there is some justification for qualitatively relating the deshielding of aromatic protons to the expected compression forces.

Can. J. Chem. Downloaded from www.nrcresearchpress.com by 210.87.254.105 on 09/05/12
For personal use only.

TABLE II

Compression effects on chemical shifts of aromatic protons of 1,2,4,5-tetra-substituted benzenes

	Hydrocarbon	Chemical shifts* (τ)
8	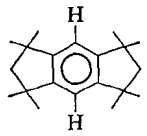	3.16
9	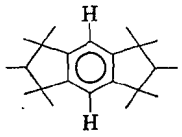	3.09
10	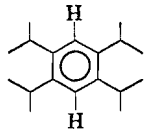	2.85
11	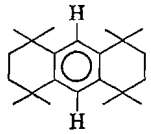	2.78
12	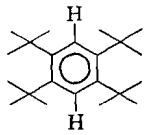	2.27

*Measurements were determined in $CDCl_3$ containing TMS; concentrations were 0.4 molar.

ester (**6**) and the cyclic anhydride (**5**). The result in the latter case indicates that crowding and the resulting repulsion between the groups can be partially relieved by cyclization.

Electronic spectra of *o*-di-*t*-butylbenzene systems are characterized by loss of the usual vibrational fine structure typical of benzenoid hydrocarbons in the 240–280 mμ region. This effect has been observed for certain highly substituted naphthanoid hydrocarbons such as 1,2,3,4-tetramethylnaphthalene (12) but not in 1,4-di-*t*-butylnaphthalene (3) or even in 2,3-di-*t*-butylquinoxaline (6). On the other hand, *peri* di-*t*-butyl groups cause a very significant alteration in the naphthalene spectrum through bathochromic shifts and loss of fine structure (5). The geometry of naphthalene brings substituents at the 1,8-positions in close proximity to each other in space even when compared to *ortho* substituents.

TABLE III

Chemical shift differences* between aromatic hydrogens 1 and 4, and 5, 6, 7, and 8 of 2,3-di-*t*-butylnaphthalene derivatives

Compound	Δ c.p.s.
1	12.3
3	11.0
5	15.9
6	18.4
7	24.6

*The differences were estimated by measuring the downfield shift of the singlet due to H-1 and H-4 relative to the centre of the symmetrical multiplet for H's 5,6,7, and 8. The results were for $CDCl_3$ solutions (Table I). The same trend was shown in CCl_4 solution but compound 7 was not sufficiently soluble in CCl_4 to complete the series.

This could result in more crowding in 1,8-di-*t*-butylnaphthalene than in compounds bearing adjacent *tertiary* butyl groups.

The u.v. spectra of the anhydride (**5**), dimethylester (**6**), diol (**7**), and starting ketone (**1**), the model for comparison, are compared in Fig. 1. Only minor differences were noticed in the strong band near 230 mμ. The dimethylester (**6**) and diol (**7**) exhibited a similar loss of fine structure in the regions near 320 and 280 mμ. This provides an interesting comparison with the same effect observed in the benzene series (9) which has been the subject of considerable speculation. As pointed out before (1, 9), the alteration in the spectra due to two adjacent *t*-butyl groups is only slight compared to that for a seriously distorted aromatic system. The

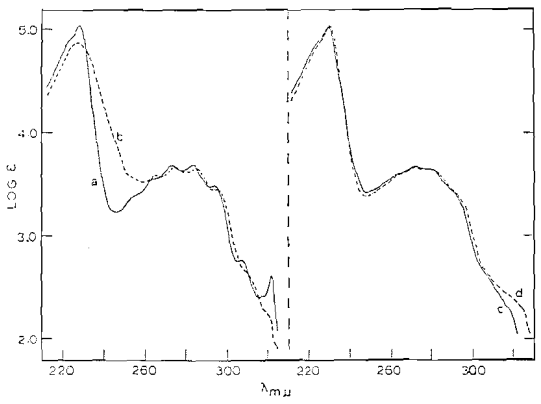

FIG. 1. Ultraviolet spectra of: (*a*) ——— 2-keto-1,1,4,4 - tetramethyl - 1,2,3,4 - tetrahydroanthracene (**1**); (*b*) --- 2,3-naphthalenediisobutyric anhydride (**5**); (*c*) ——— dimethyl ester (**6**); (*d*) --- β,β′-dihydroxy-2,3-di-*t*-butyl-naphthalene (**7**).

Can. J. Chem. Downloaded from www.nrcresearchpress.com by 210.87.254.105 on 09/05/12
For personal use only.

Can. J. Chem. Downloaded from www.nrcresearchpress.com by 210.87.254.105 on 09/05/12
For personal use only.

loss of fine structure in 2,3-di-*t*-butylnaphthalene derivatives (**6** and **7**) is not attributed to out-of-plane warping of the aromatic rings in the ground state because this is not consistent with the n.m.r. evidence (Table III). Qualitatively the perturbations of the aromatic fine structure in the u.v. spectra follows the same trend as observed in the comparison of aromatic hydrogens 1 and 4 in the n.m.r. spectra. The small spectral changes are undoubtedly to be associated with the angle deformations due to repulsions between *t*-butyl groups and not to a warped or puckered aromatic ring. Angle deformations probably provide the driving force for cyclizations of various derivatives of *o*-di-*t*-butylbenzene (13). It is of interest to find that the anhydride (**5**) exhibits fine structure in the u.v. (especially in the 280 mμ region, Fig. 1). This is to be expected if the angle deformation is at least partially relieved on cyclization.

Experimental

Ultraviolet spectra were recorded in cyclohexane on a Perkin–Elmer Model 202 Spectrophotometer. Nuclear magnetic resonance spectra were recorded on a Varian A-60 spectrometer in deuterochloroform containing tetramethylsilane as internal standard. Infrared (i.r.) spectra were recorded on a Perkin–Elmer Infracord Model 137 in potassium bromide pellets. Melting points were determined by the capillary method on a Thomas Hoover apparatus and are uncorrected. Elemental analyses were determined by Dr. C. Daessle, Montreal. Samples of aromatic hydrocarbons **8**, **9**, **10**, and **11** were available from earlier syntheses (14).

2-Keto-1,1,4,4-tetramethyl-1,2,3,4-tetrahydroanthracene (1)

Naphthalene (45 g, 0.35 mole) and 2,2,5,5-tetramethyltetrahydrofuranone (15) (50 g, 0.35 mole) were dissolved in 375 ml of carbon disulfide in a 1 l flask equipped with a stirrer, thermometer, reflux condenser, and gas trap. Commercial anhydrous aluminum chloride (94 g, 0.71 mole) was added to the above solution over a 5 min period while the temperature of the reaction mixture was maintained below 45°. The resulting reaction mixture was stirred at room temperature for 8 h. By the end of this time, the reaction mixture had separated into 2 layers, a carbon disulfide layer which contained unreacted naphthalene (21 g) and a lower thick complex layer. The complex layer was poured into ice water, the organic material extracted with ethyl ether, and the extract dried over anhydrous sodium sulfate. Distillation of the solvent left a dark amorphous residue. This product was heated at 200°/1 mm in a Späth tube and 25.6 g (29%) of crude crystalline material distilled. Recrystallization of this from petroleum ether gave 13 g of colorless crystals; m.p. 84–85°. Sublimation raised the melting point to 88–89°. The i.r. spectrum showed carbonyl absorption at 1710 cm^{-1}. The n.m.r. and u.v. spectral results are given in the Discussion.

Anal. Calcd. for $C_{18}H_{20}O$: C, 85.71; H, 7.94. Found (mass spectrum, 252): C, 85.68, 85.88; H, 8.02, 8.18.

The above synthesis of **1** was accompanied by the formation of rearrangement byproducts analogous to those reported in the benzene series (16). Details on such rearrangements will be published separately. In subsequent runs to prepare **1**, the progress of the cyclialkylation was followed by working up aliquots and analyzing for **1** by vapor phase chromatography (v.p.c.) using an F and M Model 500 instrument. Suitable separations were obtained on a 6 ft × ¼ in. column containing 5% apiezon on Chromosorb W and programming from 100 to 275°.

2,3-Dioxo-1,1,4,4-tetramethyl-1,2,3,4-tetrahydroanthracone (3)

2-Ketotetramethyltetrahydroanthracene (**1**) (12.8 g, 0.0508 mole) was dissolved in 110 ml of dioxane, selenium dioxide (5.99 g, 0.0532 mole) added, and the reaction mixture stirred while heating under reflux for 43 h. The precipitated selenium was filtered, the solvent distilled under reduced pressure, and the residue crystallized from petroleum ether to yield yellow crystals (10.8 g, 80%). Sublimation gave yellow crystals; m.p. 120–121°. The (i.r.) spectrum showed carbonyl absorption at 1725 cm^{-1}. The u.v. spectrum had maxima at 225 mμ (ε 87 393), 275 mμ (ε 4829), 286.6 mμ (ε 4132), 307 mμ (ε 1348), 323 mμ (ε 556). The n.m.r. spectral results are shown in Table I.

Anal. Calcd. for $C_{18}H_{18}O_2$: C, 81.20; H, 6.77. Found: C, 81.31, 81.13; H, 6.91, 6.77.

2,3-Naphthalenediisobutyric Acid, Anhydride (5), and Dimethyl Ester (6)

The above diketone (**3**) (10.0 g, 0.0396 mole) was dissolved in a solution containing 69 ml of dioxane and 36 ml of water. Periodic acid dihydrate (12.96 g, 0.0480 mole) was added and the reaction mixture was heated in a constant temperature bath at 60° ± 0.5° for 10 h. The solvent was distilled at 80° under reduced pressure. The residue was dissolved in ethyl ether and the ether solution extracted with 8% sodium hydroxide. The alkaline extract was boiled with decolorizing charcoal, filtered, and the solution acidified with hydrochloric acid to yield the crude acid (11.4 g, 96%). Recrystallization from 1:1 acetone–methanol yielded colorless prisms, m.p. 198° (decomposition). The i.r. spectrum exhibited carbonyl absorption at 1710 cm^{-1}. The u.v. spectrum (CH_3OH solution) had maxima at 230 mμ (ε 74 100) and 273.5 mμ (ε 3740).

A sample of the dicarboxylic acid (0.50 g) was heated under reflux in 5 ml of acetic anhydride for 3 h. The acetic anhydride was distilled under reduced pressure to give a quantitative yield of brown crystalline solid. Sublimation gave colorless crystals; m.p. 161–162°. The i.r. spectrum exhibited carbonyl bands at 1780 and 1740 cm^{-1} attributed to the anhydride (**5**). The u.v. and n.m.r. results are given in the Discussion.

Anal. Calcd. for $C_{18}H_{18}O_3$: C, 76.54; H, 6.45. Found: C, 76.33, 76.51; H, 6.54, 6.47.

The dicarboxylic acid (8.00 g, 0.027 mole) was dissolved in 400 ml of ethyl ether and to this solution was added a freshly prepared ethereal solution of diazomethane until the yellow color of diazomethane persisted.

The reaction mixture was stored in the refrigerator overnight, then extracted with 5% sodium hydroxide to recover unreacted acid. The ether solution was dried, the solvent distilled, and the residue recrystallized from petroleum ether to give 6.64 g (76%) of product; m.p. 123–124°. Sublimation yielded colorless crystals, m.p. 123.5–124°. The i.r. spectrum exhibited ester carbonyl absorption at 1725 cm^{-1}. The u.v. and n.m.r. spectral results are given in the Discussion.

Anal. Calcd. for $C_{20}H_{24}O_4$: C, 73.14; H, 7.37; O, 19.49. Found: C, 73.07, 72.85; H, 7.36, 7.16; O, 19.57, 19.99.

β,β′-*Dihydroxy-2,3-di-t-butylnaphthalene (7)*

A solution of the above dimethyl ester (**6**) (5.00 g, 0.0153 mole) in 200 ml of ethyl ether was added dropwise to an ethereal solution containing 2.3 g of lithium aluminum hydride and the mixture was heated under reflux in a nitrogen atmosphere for 24 h. The reaction mixture was slowly added to crushed ice and made acidic with hydrochloric acid. The residue obtained from working up the ether solution was recrystallized from petroleum ether to yield 3.22 g (78%) colorless crystals; m.p. 100.5–101.5°. The i.r. spectrum showed hydroxyl absorption at 3450 cm^{-1}. Carbonyl absorption was absent. The u.v. and n.m.r. spectral results are given in the Discussion.

Anal. Calcd. for $C_{18}H_{24}O_2$: C, 79.37; H, 8.90; O, 11.75. Found: C, 79.16, 79.39; H, 8.59, 8.60; O, 12.25, 12.01.

Acknowledgments

Financial support of this work provided by the National Research Council of Canada is gratefully acknowledged. We thank Dr. W. Hübel, European Research Associates, Brussels, for a sample of 1,2,4,5-tetra-*t*-butylbenzene.

1. E. M. Arnett, J. C. Sanda, J. M. Bollinger, and M. Barber. J. Amer. Chem. Soc. **89**, 5389 (1967), and references reported therein.
2. V. Balasubramaniyan. Chem. Rev. **66**, 567 (1966).
3. R. W. Franck and K. Yanagi. J. Org. Chem. **33**, 811 (1968).
4. H. van Bekkum, T. J. Nieuwstad, J. van Barneveld, and B. M. Wepster. Tetrahedron Letters, **24**, 2269 (1967).
5. R. W. Franck and E. G. Leser. J. Amer. Chem. Soc. **91**, 1577 (1969).
6. A. de Groot and H. Wynberg. J. Org. Chem. **31**, 3954 (1966).
7. G. J. Visser, A. Vos, A. de Groot, and H. Wynberg. J. Amer. Chem. Soc. **90**, 3253 (1968).
8. A. van Bruijnsvoort, L. Eilermann, H. van der Meer, and C. H. Stam. Tetrahedron Letters, **21**, 2527 (1968).
9. L. R. C. Barclay, C. E. Milligan, and N. D. Hall. Can. J. Chem. **40**, 1664 (1962).
10. M. P. Cava, B. Hwang, and J. P. Van Meter. J. Amer. Chem. Soc. **85**, 4032 (1963).
11. C. A. Coulson and M. D. Poole. Tetrahedron **20**, 1859 (1964).
12. W. L. Mosby. J. Amer. Chem. Soc. **75**, 3348 (1953).
13. A. W. Burgstahler and M. O. Abdel-Rahman. J. Amer. Chem. Soc. **85**, 173 (1963).
14. L. R. C. Barclay, J. W. Hilchie, A. H. Gray, and N. D. Hall. Can. J. Chem. **38**, 94 (1960).
15. H. A. Bruson, F. W. Grant, and E. Bobko. J. Amer. Chem. Soc. **80**, 3633 (1958).
16. F. W. Grant, L. Ames, and E. Chaitman. J. Org. Chem. **26**, 1299 (1961); R. H. Young. M.Sc. Thesis, Mount Allison University, Sackville, N.B. (1963).
17. B. V. Cheney. J. Amer. Chem. Soc. **90**, 5386 (1968).

Can. J. Chem. Downloaded from www.nrcresearchpress.com by 210.87.254.105 on 09/05/12
For personal use only.

Can. J. Chem. Downloaded from www.nrcresearchpress.com by 210.87.254.105 on 09/05/12
For personal use only.

Influence of Lewis acids on the Diels–Alder reaction. II. Rearrangement of 1- and 1,4-substituted diethyl 7-oxabicyclo[2·2·1]2,5-heptadiene-2,3-dicarboxylate adducts to 4- and 4,6-substituted diethyl 3-hydroxyphthalates[1]

A. W. McCulloch,[2] B. Stanovnik,[3] D. G. Smith, and A. G. McInnes
Atlantic Regional Laboratory, National Research Council of Canada, Halifax, Nova Scotia

Received June 25, 1969

Direct formation of 4- or 4,6-alkyl and aryl substituted diethyl 3-hydroxyphthalates from the correspondingly substituted Diels–Alder adducts of 2- or 2,5-substituted furans and diethyl acetylenedicarboxylate is promoted by $AlCl_3$ in CH_2Cl_2 at room temperature. The first adduct of 2,5-diphenylfuran to be isolated has been obtained from the same reaction at −20°. The aromatic compounds can be obtained alternatively by treating the adducts with BF_3 or H_2SO_4: where the adducts can be prepared by conventional means this two-step procedure has resulted in greatly improved yields. Adducts of furan and furfuryl alcohol are similarly converted to substituted phenols. HCl effected conversion only in the case of adducts carrying a bridgehead aryl substituent; in all other cases HCl added to the substituted double bond. The mechanism of the adduct rearrangement is discussed.

Canadian Journal of Chemistry, 47, 4319 (1969)

Introduction

Suitably substituted Diels–Alder adducts provide the most versatile route by which a benzene ring may be formed while simultaneously introducing substituents (1). The adducts usually possess a six-membered carbocyclic ring containing one or two double bonds and may have in addition a 1,4-bridge consisting of one or two carbon atoms or a heteroatom. Aromatization is induced by dehydrogenation (2), dehydrohalogenation (3), deamination (4), pyrolytic elimination of substituents (5), or a 1,4-bridge (6), or fission of a 1,4-oxygen bridge followed by loss of H_2O (7). Less general procedures for the annelation of readily available molecules to benzene rings include the catalytic trimerization of acetylenes (8), the reaction of pyrylium salts with nitromethane (9), or triphenylphosphinemethylene (10), the condensation of pyrones with Grignard reagents (11), the ketovinylation of β-dicarbonyl compounds followed by intramolecular cyclization or further reaction with β-chlorovinyl ketones (12), and the reaction of enamines with esters of acetylenedicarboxylic acid (13).

In preliminary communications (14,15) we reported that Lewis acids produced an enormous increase in the rate of formation of 1- and 1,4-substituted diethyl 7-oxabicyclo[2·2·1]2,5-heptadiene-2,3-dicarboxylates (**1**) from suitably substituted furans and diethyl acetylenedicarboxylate (DEAD), and also promoted the rearrangement of these adducts to 4- and 4,6-substituted derivatives of diethyl 3-hydroxyphthalate (**2**). Reactions using ethyl propiolate behaved similarly (15). Subsequently, other workers have reported that the dimethyl ester corresponding to **1** (R_1 = 4-methoxyphenyl; R_2 = H) rearranged to the analogue of **2** (R_1 = 4-methoxyphenyl; R_2 = H) in the presence of warm acetic acid (16).[4]

This paper discusses in full the mechanism and experimental conditions for the conversion of **1** to **2**. The derivatives **2** prepared in this way, with one exception **2***a*, contain *three different types* of substituents, one of which is a phenolic hydroxyl group. Diels–Alder reactions using dienes such as 2-acetoxyfuran (17), 1,4-diacetoxybutadiene (5), and substituted 4-hydroxy-α-pyrones (18) have been used previously to introduce a phenolic hydroxyl substituent, but these methods seem to be of limited scope as compared to our method. The substituent migrations which occur in the transformation of **1** to **2**, although not particularly new from a chemical standpoint, are nevertheless the first to be reported in the direct formation of benzene derivatives from Diels–Alder adducts. High yields of **2** and the possibility of increasing the number of types of substituents

[1]Issued as NRCC No. 10925.
[2]NRCC Postdoctorate Fellow, 1965–1966.
[3]NRCC Postdoctorate Fellow, 1964–1965.

[4]During the final stages of preparation of this manuscript Vogel and co-workers published (30) an account of work closely related to that previously reported by us (14,15) and by Ayres and Smith (16). Their work involved acid-catalyzed rearrangement of a variety of methyl or methoxyl-substituted oxanorbornadienes. The spectral data reported for compounds analogous to **2***b* and **2***e* are in full agreement with our own data.

Can. J. Chem. Downloaded from www.nrcresearchpress.com by 210.87.254.105 on 09/05/12
For personal use only.

TABLE I

Proton magnetic resonance data for **1**, **2**, and derivatives

Compound	τ							$J_{p,q}$(Hz)			Sub-spectra; other resonances
	OCH_2CH_3(J = 7.0)	OH*	R_1, R_2	H_1	H_4	H_5	H_6	4,5	4, 6	5,6	
1*a*	5.74(q)†, 8.69(t)			4.34(m)		2.78(m)					A(H_1) X(H_6) X′(H_5) A′(H_4) $J_{4,5} + J_{4,6}$ = 2.1 Hz
1*b*‡	5.70(q), 5.77(q), 8.68(t), 8.72(t)		8.23(CH_3, d)		4.44(q)	2.83(m)		2.1	0.1	5.3	A(H_5) B(H_6) X(H_4) $\Delta\nu_{5,6}$ = 12.5; $J_{H5,CH3}$ = 0.4 Hz
1*c*	5.70(q), 5.75(q), 8.68(t), 8.69(t)	7.0(s)	5.74(CH_2, s)		4.34(q)	2.85(m)		2.2	0.1	5.0	A(H_5) B(H_6) X(H_4) $\Delta\nu_{5,6}$ = 10.8 Hz
1*d*	5.76(q), 5.92(q), 8.73(t), 8.93(t)		2.60(C_6H_5, m)		4.19(q)						A(H_5) B(H_6) X(H_4) $J_{4,5} + J_{4,6}$ = 2.2 Hz; H_5,H_6 in C_6H_5 multiplet
1*e*‡	5.74(q), 8.68(t)		8.20($2CH_3$, s)			3.05(s)					
1*f*	5.92(q), 8.93(t)		2.50($2C_6H_5$, m)			2.40(s)					
2*a*	5.71(q), 5.73(q), 8.63(t), 8.67(t)	−0.33(s)			2.50 − 3.10(m)						A(H_4) B(H_5) C(H_6)
2*b*‡	5.63(q, 4H), 8.63(t), 8.65(t)	−0.83(s)	7.78(CH_3, d)		2.91(q)			8.7			A(H_4) B(H_5)§ $\Delta\nu_{4,5}$ = 19.2; $J_{H5,CH3}$ = 0.4 Hz
2*d*	5.62(q), 5.97(q), 8.67(t), 9.04(t)	−1.07(s)	2.66(C_6H_5, s)		2.75(q)			8.7			A(H_4) B(H_5)§ $\Delta\nu_{4,5}$ = 19.8 Hz
2*e*‡	5.63(q), 5.64(q), 8.60(t), 8.65(t)	−1.01(s)	7.77, 7.80 ($2CH_3$, s)			2.85(s)					$J_{H5,CH3}$ = 0.4 Hz
2*f*‖	5.58(q), 5.92(q), 8.67(t), 9.05(t)	−1.58(s)	2.55($2C_6H_5$ + H_5, m)								
3	5.48(q), 8.53(t)	−0.80(s)			2.61(q)			8.7			A(H_4) B(H_5)§ $\Delta\nu_{4,5}$ = 15.2; $J_{H4,CH2}$ < 0.2 Hz 4.83 τ (CH_2, s)
4*g*¶		3.20(s)	7.46, 7.66 ($2CH_3$, s)			2.64(s)					
4*h***			7.43, 7.65 ($2CH_3$, s)			2.42(s)					5.92 τ (OCH_3, s)
4*i*¶		2.08(s)	2.50($2C_6H_5$, m)			2.21(s)					
5	5.68(q), 5.70(q), 8.68(t, 6H)					2.82(s)					7.63, 7.84 τ ($2CH_3$, s); 7.74 τ ($OCOCH_3$, s)
6**		1.43(s), 4.73(t), 5.50(t)				3.17(s)					5.23, 5.52 τ ($2CH_2$, d); 7.78, 7.87 τ ($2CH_3$, s)

*Hydroxyl protons were replaceable by deuterium.
†s = singlet; d = doublet; t = triplet; q = quartet; m = multiplet. Average τ values are reported for multiplets.
‡References in parentheses give parameters for dimethyl ester and diacid of **1***b* (27, 28, 30), **1***e* (28, 30), and **2***b*, *e* (30), as well as dimethyl ester of **1***a* (26).
§H_5 occurs at lower field than H_4 in **2***b* and **2***d*; H_4 is at lower field than H_5 in **3**.
‖Diethyl 3-methoxy-4,6-diphenylphthalate (acetone-d_6): 5.64(q), 5.96(q), 8.66(t), 9.03(t) (OCH_2CH_3); 6.55(OCH_3, s); 2.60(11 aromatic H,m).
¶At 50°.
Acetone-d_6 (4***h*); DMSO-d_6 (**6**).

TABLE II

Overall yields of **2** and **3** obtained at room temperature from dienes and DEAD directly in the presence of $AlCl_3$,* or from **1** by treatment with BF_3† or H_2SO_4

Diene	Reaction product	Addends + $AlCl_3$ Time (h)	Addends + $AlCl_3$ Yield %	**1** + BF_3 or H_2SO_4 Time (h)	**1** + BF_3 or H_2SO_4 Yield %
Furan	**2***a*	—	—	50	45
2-Methylfuran	**2***b*	72	50	0.4	90
2-Phenylfuran	**2***d*	1	50	0.2	90
2,5-Dimethylfuran	**2***e*	72	45	0.4	90
2,5-Diphenylfuran	**2***f*	1	65	0.2	40‡
Furfuryl alcohol	**3**	—	—	3.0	35

*Reactions were carried out in CH_2Cl_2 and were 0.1 *M* in addends and $AlCl_3$.
†Reactions were carried out in CH_2Cl_2 and were 0.3 *M* in **1**: the solutions were treated with excess BF_3 or H_2SO_4.
‡**1***f* could only be isolated in 40% yield but was converted to **2***f* quantitatively. Overall yield is therefore 40%.

suggests that our procedure should prove generally useful for the synthesis of a large number of benzene derivatives which would be difficult by more conventional routes.

Our studies on the formation of **1** in the presence of Lewis acids are not relevant to the present work and will therefore be published separately.

Results and Discussion

The proton magnetic resonance (p.m.r.) spectral evidence used in the structural elucidation of the compounds discussed below is detailed in Table I.

Preparation and Structures of 1

Thermal condensation of the addends (19) enabled the adducts **1***a–e* to be isolated in excellent yield. However, attempts to prepare **1***f* by heating the addends at temperatures up to 180° in a sealed tube were unsuccessful. Indeed no adducts of 2,5-diphenylfuran have been reported previously, and this can undoubtedly be attributed to a reduction in diene character as a result of extensive π-delocalization due to coplanarity of the aromatic and furan rings. Conversion of the addends to crystalline **1***f* was, however, promoted by $AlCl_3$ (see Experimental).

The structures of **1***a–f* were established from their p.m.r. spectra although their identity was quite clear from their mode of formation. Compounds **1***a*, *e*, and *f* belong to the symmetry group C_s and consequently gave characteristic p.m.r. signals for two chemically equivalent olefinic hydrogens, bridgehead substituents, and carbethoxy groups. The aromatic hydrogens in **1***f* gave a complex multiplet (ABCDE system? - due to asymmetry at C_1 and C_4), and the olefinic and bridgehead hydrogens of **1***a* an AXX'A' spectrum. The unsymmetrical adducts **1***b*, *c*, and *d*, on the other hand, gave characteristic ABX systems for the two olefinic and bridgehead hydrogens as well as signals for the bridgehead substituents and two chemically non-equivalent carbethoxy groups. An interesting example of long-range spin–spin coupling across five bonds (20) (J_{H_5,CH_3} = 0.4 Hz) was observed in **1***b*.

Preparation and Structures of 2

Adducts **1***a–f* rearranged in the presence of BF_3 or H_2SO_4 in CH_2Cl_2 to compounds of type **2** or to compound **3** (see Table II).

The p.m.r. and infrared (i.r.) spectra of **2***a* and the observation that it gave 3-hydroxyphthalic acid on saponification establishes the structure as diethyl 3-hydroxyphthalate.

The unsymmetrical tetra-substituted benzene derivatives gave p.m.r. signals with chemical shifts, multiplicities, and intensities consistent with the numbers and types of hydrogens shown in structures **2***b*, **2***d*, and **3**. Each compound gave a characteristic AB pattern for two *ortho* coupled aromatic hydrogens. In two compounds, the proton giving rise to the low-field half of the AB pattern was long-range coupled (21) to the benzylic methyl (**2***b*) or methylene (**3**) hydrogens, while in all three, the proton giving rise to the high-field part of the AB system had a chemical shift consistent with the presence of an *ortho* phenolic hydroxyl group (22). A proton *ortho* to

Can. J. Chem. Downloaded from www.nrcresearchpress.com by 210.87.254.105 on 09/05/12
For personal use only.

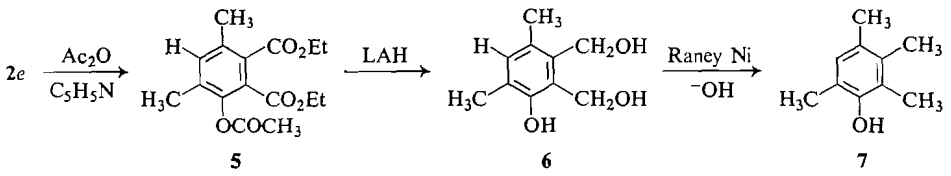

5 6 7

SCHEME 1

a carbonyl function would give a signal at lower field (ca. τ 2.0) (22). This evidence together with the known structures of **1***b*, *c*, and *d* and the fact that **1***a* gave diethyl 3-hydroxyphthalate (**2***a*), requires that the compounds be diethyl 6-methyl-3-hydroxyphthalate (**2***b*), diethyl 6-phenyl-3-hydroxyphthalate (**2***d*), and 7-carbethoxy-6-hydroxyphthalide (**3**). The i.r. spectra were consistent with these structures. The structure of **3** was confirmed by its saponification to the known 7-carboxy-6-hydroxyphthalide (23).

The structure of **2***e* was established from the following evidence: (*a*) it could be converted to isodurenol (**7**) via Scheme 1; (*b*) i.r. studies on a 0.005 *M* solution of **2***e* in CCl_4 indicated intramolecular hydrogen bonded hydroxyl and ester carbonyl groups as well as a free ester carbonyl group; (*c*) it could be converted to an anhydride (**4***g*) and the phenolic hydroxyl group of this compound could be methylated (**4***h*); and (*d*) the p.m.r. spectra of **2***e*, **4***g*, **4***h*, and **7** contained signals with characteristic chemical shifts, multiplicities, and intensities for each proton type. From (*b*), (*c*), and (*d*) it can be deduced that the phenolic hydroxyl and two carbethoxy groups in **2***e* have the same relative orientation as in diethyl 3-hydroxyphthalate (**2***a*). This structural feature together with (*a*) establishes that the two methyl substituents on C_2 and C_3 of isodurenol (**7**) must have been derived from the two carbethoxy groups of **2***e*. It follows that the two remaining methyl substituents at C_4 and C_6 of isodurenol must have been the original methyl substituents which were observed in (*d*) for **2***e*. We can, therefore, state unambiguously that **2***e* is diethyl 4,6-dimethyl-3-hydroxyphthalate and **4***g* and **4***h* are 4,6-dimethyl-3-hydroxy- and 3-methoxyphthalic anhydride. Compound **6** must be 2,3-dihydroxymethyl-4,6-dimethylphenol.

The single aromatic hydrogen in **2***e*, **4***g*, and **4***h* is long-range coupled to about the same extent with both methyl substituents (21) but is not similarly coupled to the methoxyl hydrogens (24) in **4***h*. These observations provide strong evidence that the aromatic hydrogen is *ortho* to both methyl substituents in all these compounds and confirms their structures by an alternative procedure.

The structure of the *m*-terphenyl derivative (**2***f*) was established in a similar manner to that of **2***e* [see (*b*), (*c*), and (*d*) above]. The 11 aromatic hydrogens in **2***f* covered the range from τ 2.3 to 2.7 and no characteristic signal was observed for a single aromatic hydrogen deshielded by an *ortho* carbonyl function (ca. τ 2.0) (22). This evidence, together with the structure of the adduct (**1***f*) from which **2***f* is produced, requires that the latter be diethyl 4,6-diphenyl-3-hydroxyphthalate and **4***i* be 4,6-diphenyl-3-hydroxyphthalic anhydride.

Optimum Conditions for the Formation of 2a, b, d, e, and f and 3

Table II lists the yields of benzene derivatives (**2** or **3**) formed either directly by a one-step synthesis from the addends in the presence of $AlCl_3$ or indirectly via Diels–Alder adducts (**1**) through the action of BF_3 or H_2SO_4.

When alkyl-substituted furans or 2-phenylfuran were used as the diene component in the one-step synthesis, yields of **2** were only about 50%; no aromatic compound was formed in the case of furan or furfuryl alcohol. The lack of reaction or low yields could be attributed to extensive diene polymerization caused by $AlCl_3$ and/or precipitation of insoluble diene-$AlCl_3$ complexes. One or other of these side reactions became more dominant if the $AlCl_3$ concentration was increased. Attempts to replace $AlCl_3$ with excess BF_3 or BCl_3 also led to lower yields of product indicating that these Lewis acids also promote the side reactions. The latter were less important in the case of 2,5-diphenylfuran where yields of **2***f* as high as 75% were obtained when the addends and $AlCl_3$ were equimolar.

The side reactions could be reduced or eliminated, and the scope of the synthetic procedure increased, by first converting the addends to the

Can. J. Chem. Downloaded from www.nrcresearchpress.com by 210.87.254.105 on 09/05/12
For personal use only.

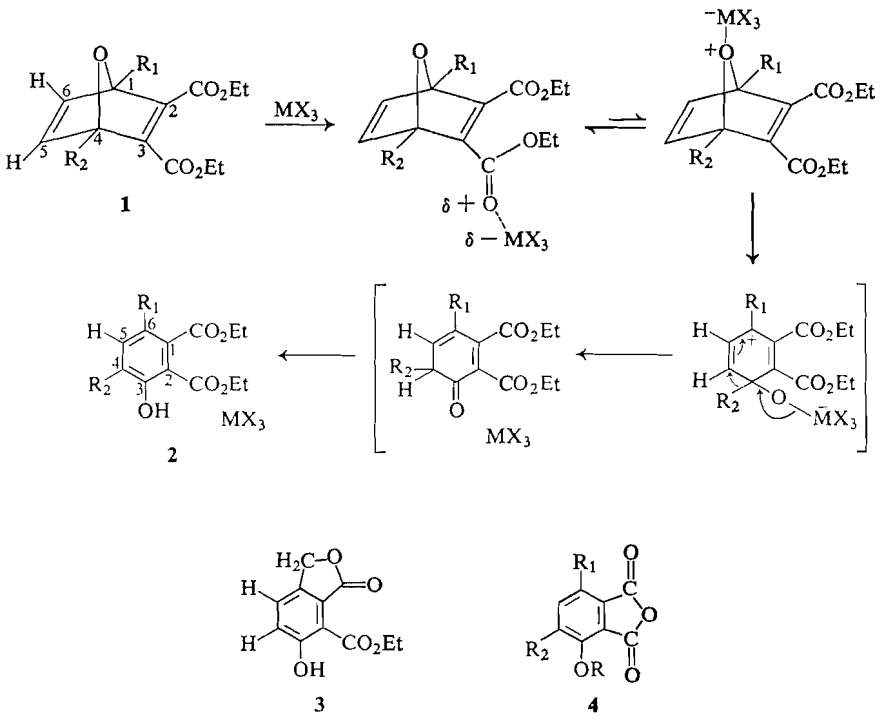

a) $R_1 = R_2 = H$ *d*) $R_1 = C_6H_5$; $R_2 = H$ *g*) $R_1 = R_2 = CH_3$; $R = H$
b) $R_1 = CH_3$; $R_2 = H$ *e*) $R_1 = R_2 = CH_3$ *h*) $R_1 = R_2 = R = CH_3$
c) $R_1 = CH_2OH$; $R_2 = H$ *f*) $R_1 = R_2 = C_6H_5$ *i*) $R_1 = R_2 = C_6H_5$; $R = H$

Scheme 2

corresponding Diels–Alder adduct (**1**) in the absence of Lewis acid. The adducts (**1***a–e*) could be obtained in about 95% yield and rearranged in the presence of excess BF_3 or H_2SO_4 to the corresponding benzene derivatives (**2***a*, *b*, *d*, *e* and **3**). Essentially quantitative yields (>90%) of **2***b*, *d*, and *e* could be obtained, while **2***a* and **3** were isolated in about 40% yield. Since the adduct (**1***f*) can only be isolated in about 40% yield in the presence of $AlCl_3$ the two-step procedure for forming **2***f* is inferior to the direct method although acid promotes quantitative conversion to the aromatic compound.

In the one-step procedure, rates of conversion to alkyl-substituted derivatives of **2** were slower by a factor of about 70 than for the aryl-substituted derivatives.

Boron trichloride could be used in place of BF_3 or H_2SO_4 in the two-step method, but reaction times were increased by a factor of 20 if $SnCl_4$ was used. Aluminium chloride does, of course, catalyze the rearrangement of **1** to **2** but is much less soluble in the CH_2Cl_2 solution of the adduct and in some cases precipitation of adduct-$AlCl_3$ complexes occurs.

While H_2SO_4 is generally effective as a catalyst for the rearrangement of **1** to **2** or **3**, halogen acids are not. Although anhydrous HCl effects quantitative conversion of **1***d* and **1***f* to **2***d* and **2***f*, it adds (*cis* and *trans*) to the 2,3-double bond of **1***a*, *b*, *c*, and *e*. The structures of the products and mechanisms of the addition reactions of some of these adducts (**1**) will be reported in full elsewhere.

The structures of the aromatic compounds (**2**) formed from the adducts (**1**) suggest the mechanism of rearrangement outlined in Scheme 2. Coordination or protonation of the bridge oxygen in the adduct will induce bridge cleavage which is followed by migration of the unsubstituted double bond and substituent geminal to the complexed or protonated oxygen atom. Enolization then yields **2**. Where $R_2 = H$, bridge cleavage may be followed by elimination of this proton and double bond migration.

Can. J. Chem. Downloaded from www.nrcresearchpress.com by 210.87.254.105 on 09/05/12
For personal use only.

Can. J. Chem. Downloaded from www.nrcresearchpress.com by 210.87.254.105 on 09/05/12
For personal use only.

Substituents at the bridgehead, e.g. methyl or phenyl, will facilitate reaction by inductive and resonance stabilization of the carbonium ion formed on bridge cleavage. Consequently, excellent yields of **2** were obtained from adducts carrying these substituents at the bridgehead. Moreover, the rates of conversion of phenyl-substituted adducts to the corresponding derivatives of diethyl 3-hydroxyphthalate were greater than those for alkyl-substituted adducts (see Table II). This indicates that resonance stabilization of the transition state is more significant than inductive stabilization, as would be expected. In the case of the aryl-substituted compounds the rate of HCl-promoted bridge cleavage must be greater than that of HCl addition to the double bond while the reverse is true of the alkyl-substituted derivatives.

Rearrangement of the adducts of furan (**1***a*) and furfuryl alcohol (**1***c*), which lack substituents at the bridgehead, to **2***a* and **3** occurs more slowly and lower yields are obtained. The adduct of dimethyl acetylenedicarboxylate and 2,2′-bifuryl has been reported to be stable to acid (25). In view of our results, it seems probable that cleavage of the oxygen bridge of this compound might be induced by BF_3 or H_2SO_4.

Experimental

The p.m.r. spectra were obtained on a Varian A-60A spectrometer equipped with a V-6058A spin-decoupler using $CDCl_3$ as solvent (unless stated otherwise) and tetramethylsilane as internal standard. The i.r. spectra were recorded on either a Perkin–Elmer model 521 or 237 spectrometer.

Chromatographic separations were carried out on Mallinckrodt silicic acid (100–150 mesh) using $CHCl_3$ as eluant.

Preparation of ***1****a–e in the Absence of Lewis Acid*

The following adducts were prepared in the absence of solvent from the appropriate furan and diethyl acetylenedicarboxylate at 100° by the method of Alder *et al.* (19). Essentially quantitative conversion (>95%) of addends to adduct occurred in 4 h and the adducts were obtained in a pure state by chromatography.

1*a* ($\eta_d^{23} = 1.4795$), **1***b* ($\eta_d^{19} = 1.4749$), **1***c* ($\eta_d^{23} = 1.4971$), **1***d* ($\eta_d^{19} = 1.5240$) and **1***e* ($\eta_d^{19} = 1.4680$) were obtained as yellow oils.

Preparation of ***1****f in the Presence of Lewis Acid*

Two solutions containing 2,5-diphenylfuran (0.2 *M*) and DEAD (0.2 *M*) plus $AlCl_3$ (0.28 *M*) in CH_2Cl_2 were prepared separately, cooled to −20° and mixed. After 1 h at this temperature the reaction was stopped by washing the dark red reaction solution with water to remove the Lewis acid. After drying and removing the solvent the residue was triturated with petroleum ether to remove starting materials and leave the adduct as an insoluble residue.

1*f* was obtained as needles from ether–petroleum ether in 40% yield, m.p. 103–104°.

Direct Formation of 2b, d, e, and f from Furans and DEAD in the Presence of $AlCl_3$

The experimental procedure was the same as given above for the preparation of **1***f* except that all 3 reagents were equimolar, and the solutions were allowed to stand at room temperature until no further reaction occurred.

The reaction products were purified by chromatography or crystallization. Yields of **2** prepared in this way are given in Table II. This procedure can not be used with furan or furfuryl alcohol because of side reactions.

Using excess BF_3 or BCl_3 in place of $AlCl_3$ caused extensive diene polymerization which reduced the yields of **2**.

2*b* was obtained as a yellow oil, $\eta_d^{19} = 1.5083$. Characteristic i.r. absorptions (liquid film): hydrogen bonded (1675 cm^{-1}) and free (1735 cm^{-1}) carbonyl functions, and hydrogen bonded hydroxyl group (broad band with maximum at 3100 cm^{-1}).

2*d* was obtained as a yellow–orange oil, $\eta_d^{19} = 1.5630$. Characteristic i.r. absorptions (liquid film): hydrogen bonded (1675 cm^{-1}) and free (1730 cm^{-1}) carbonyl functions.

2*e* was obtained as a yellow oil, $\eta_d^{19} = 1.5186$. Characteristic i.r. absorptions (0.005 *M* in CCl_4): hydrogen bonded (1673 cm^{-1}) and free (1731 cm^{-1}) carbonyl functions, and hydrogen bonded hydroxyl group (measured after deuteration, at 2340 cm^{-1}).

Saponification of **2***e* with 1 *N* KOH followed by acidification gave an acid which was sublimed at 140–145° and 0.01 mm pressure to yield **4***g* in virtually quantitative yield, m.p. 178–179°. Characteristic i.r. absorptions (KBr disc): anhydride carbonyls (1760 and 1830 cm^{-1}) and phenolic hydroxyl (3450 cm^{-1}).

4*g* was converted to **4***h* with diazomethane in ether and the latter crystallized as colorless prisms from this solvent, m.p. 151–152°. Characteristic i.r. absorptions (KBr disc): anhydride carbonyls (1770 and 1845 cm^{-1}).

2*f* was obtained from methanol as colorless plates, m.p. 128–129°.

Anal. Calcd. for $C_{24}H_{22}O_5$ (mol. wt. 386): C, 73.83; H, 5.68; O, 20.49. Found (390 (osmometer)): C, 73.83; H, 5.76; O, 20.37. In ethanol $\lambda\lambda_{max}$ 232 (ε 33 500), 330 (ε 6 500) mμ; 0.025 *N* NaOH in 96% ethanol 254 (ε 22 900), 287 (ε 10 700), 365 (ε 9 900) mμ. Characteristic i.r. absorptions (0.005 *M* in CCl_4): hydrogen bonded (1665 cm^{-1}) and free (1732 cm^{-1}) carbonyl functions, and hydrogen bonded hydroxyl group (measured after deuteration at 2320 cm^{-1}).

2*f* was converted to diethyl 3-methoxy-4,6-diphenylphthalate with diazomethane in ether and crystallized from ethanol as needles, m.p. 96°.

Anal. Calcd. for $C_{25}H_{24}O_5$ (mol. wt. 404): C, 74.24; H, 5.98; O, 19.78. Found (399 (osmometer)): C, 74.13; H, 5.89; O, 19.74. In ethanol $\lambda\lambda_{max}$ 245 (ε 29 600), 294 (ε 4 150) mμ. Characteristic i.r. absorption (KBr disc): ester carbonyl (1730 cm^{-1}).

2*f* was converted to **4***i* by heating it with acetic acid saturated with HBr in a sealed tube at 110–125° for 7 h. **4***i* crystallized from the acetic acid solution on cooling

Can. J. Chem. Downloaded from www.nrcresearchpress.com by 210.87.254.105 on 09/05/12
For personal use only.

and was recrystallized from CCl_4 as needles, m.p. 190–191°.

Anal. Calcd. for $C_{20}H_{22}O_4$ (mol. wt. 316): C, 75.94; H, 3.82; O, 20.83. Found (317 (osmometer)): C, 75.24; H, 3.97; O, 20.68. In ethanol $\lambda\lambda_{max}$ 237 (ε 26 200), 300 (ε 6 370), and 355 (ε 6 300) mμ. Characteristic i.r. absorptions (KBr disc): anhydride carbonyls (1750 and 1830 cm^{-1}) and phenolic hydroxyl (3450 cm^{-1}).

Preparation of 2a, b, d, e, and f and of 3 from the Corresponding Adducts 1

(a) In the Presence of BF_3

Solutions of the adducts in CH_2Cl_2 (0.33 *M*) were cooled in ice while saturating with BF_3 and then allowed to stand at room temperature. The reactions were stopped by removing the Lewis acid with water and the reaction products purified by chromatography or crystallization.

(b) In the Presence of H_2SO_4

Solutions of the adducts in CH_2Cl_2 were cooled in ice and a slight molar excess of concentrated H_2SO_4 added dropwise with stirring. After standing at room temperature the reactions were worked up as in (*a*).

The yields of **2** prepared in (*a*) and (*b*) are given in Table II.

2*a* was obtained as a yellow oil.

Saponification of **2***a* gave 3-hydroxyphthalic acid. Recrystallization from water gave colorless needles which on slow heating had m.p. 195–196° [reported m.p. for 3-hydroxyphthalic anhydride is 198–199° (29)]. The p.m.r. and i.r. spectra of this material were identical to those of an authentic sample of 3-hydroxyphthalic acid prepared by diazotization of 3-aminophthalic acid.

3 was obtained as colorless prisms from benzene–petroleum ether, m.p. 179–179.5°. Characteristic i.r. absorptions (KBr disc): α,β-unsaturated γ-lactone (1750 cm^{-1}) and ester (1728 cm^{-1}) carbonyls, and phenolic hydroxyl (broad band with maximum at 3200 cm^{-1}).

Saponification of **3** gave the free acid (90%), crystallized from acetone as colorless prisms, m.p. 216–217° [lit. (23) m.p. 212–213°].

Action of Hydrogen Chloride on 1d and 1f

When solutions of **1***d* or **1***f* (0.1 *M*) in CH_2Cl_2 were saturated with hydrogen chloride and left standing for 10 min at room temperature they were quantitatively (>95%) converted to **2***d* and **2***f*.

Conversion of 2e to Isodurenol

2*e* (8.38 g) was acetylated in 15 min at 100° with acetic anhydride (5.5 ml) in pyridine (10 ml). After working up in usual manner, **5** was obtained as a viscous oil (9.22 g, 95% yield). Characteristic i.r. absorption (liquid film): ester (1730 cm^{-1}) and phenolic acetate (1770 cm^{-1}) carbonyls.

Without further purification **5** (7.3 g) was reduced with $LiAlH_4$ (3 g) in ether (260 ml) in a nitrogen atmosphere. After standing for 1 h at room temperature and at reflux for a further 2 h the excess $LiAlH_4$ was destroyed by adding ethyl acetate (45 ml). The reaction solution was then worked up in the usual manner to yield a residue of **6** which crystallized from petroleum ether–ethyl acetate as cream colored needles (2.12 g, 50% yield), m.p. 125–128°. Characteristic i.r. absorption (KBr disc): hydroxyl (broad band, with maxima at 3350 and 3100 cm^{-1}).

6 (500 mg) was dissolved in 5% NaOH (135 ml) and Raney alloy (6 g) added in small portions with mechanical agitation. After standing for 1 h at room temperature, the mixture was heated for a further 1 h on a steam bath. The solution was then cooled, filtered, and acidified with concentrated hydrochloric acid. A colorless precipitate was collected by filtration and subsequently crystallized from petroleum ether to give **7** as colorless needles (298 mg, 72%), m.p. 79.5–81.5°. No depression in m.p. was observed on admixing with authentic isodurenol (**7**), and the i.r. and p.m.r. spectra of the synthetic material were identical to those of an authentic sample of isodurenol.

Acknowledgments

We have to acknowledge the excellent technical assistance of Mrs. M. G. Flack and Mr. J. van Ingen.

1. J. SAUER. Angew. Chem. Intern. Ed. **5**, 211 (1966).
2. E. BERGMANN, L. HASKELBERG, and F. BERGMANN. J. Org. Chem. 7, 303 (1942); K. ALDER and J. HAYDN. Ann. **570**, 201 (1950).
3. P. E. HOCH. J. Org. Chem. **26**, 2066 (1961).
4. M. F. FEGLEY, N. M. BORTNICK, and C. H. MCKEEVER. J. Amer. Chem. Soc. **79**, 4736 (1957).
5. R. K. HILL and R. M. CARLSON. Tetrahedron Lett. 1157 (1964); J. Org. Chem. **30**, 2414 (1965).
6. C. F. H. ALLEN. Chem. Reviews, **37**, 209 (1945); **62**, 653 (1962).
7. J. A. NORTON. Chem. Reviews, **31**, 470 (1942).
8. E. F. LUTZ. J. Amer. Chem. Soc. **83**, 2551 (1961); W. HERWIG, M. METLESICS, and H. ZEISS. J. Amer. Chem. Soc. **81**, 6203 (1959); F. W. HOOVER, O. W. WEBSTER, and C. T. HANDY. J. Org. Chem. **26**, 2234 (1961).
9. K. DIMROTH, G. BRÄUNINGER, and G. NEUBAUER. Chem. Ber. **90**, 1364 (1957); K. DIMROTH, G. NEUBAUER, H. MÖLLENKAMP, and G. OOSTERLOO. Chem. Ber. **90**, 1668 (1957).
10. G. MÄRKL. Angew. Chem. Intern. Ed. **1**, 511 (1962).
11. R. GOMPPER and O. CHRISTMANN. Chem. Ber. **94**, 1795 (1961).
12. N. K. KOCHETKOV, L. J. KUDRYASHOV, and T. M. SENCHENKOVA. Zh. Obshch. Khim. **29**, 650 (1959); Chem. Abstr. **54**, 395a. N. K. KOCHETKOV, L. J. KUDRYASHOV, and B. P. GOTTICH. Tetrahedron, **12**, 63 (1961).
13. C. F. HUEBNER and E. DONOGHUE. J. Org. Chem. **28**, 1732 (1963).
14. A. W. MCCULLOCH, B. STANOVNIK, and A. G. MCINNES. Chem. in Canada. 1966. Oct. p. 46.
15. A. W. MCCULLOCH and A. G. MCINNES. Chem. in Canada, 1967. Sept. p. 51.
16. D. C. AYRES and J. R. SMITH. Chem. Commun. 886 (1967); J. Chem. Soc. C, 2737 (1968).
17. M. P. CAVA, C. L. WILSON, and C. J. WILLIAMS. J. Amer. Chem. Soc. **78**, 2303 (1956).
18. J. D. BU'LOCK and H. G. SMITH. J. Chem. Soc. 502 (1960).
19. O. DIELS and K. ALDER. Ann. **490**, 243 (1931); K. ALDER and H. F. RICKERT. Chem. Ber. **70B**, 1354 (1937).
20. K. TORI and M. OHTSURU. Chem. Commun. 886 (1966).

21. H. ROTTENDORF and S. STERNHELL. Australian J. Chem. **17**, 1315 (1964); S. STERNHELL. Rev. Pure Appl. Chem. **14**, 15 (1964).
22. J. W. EMSLEY, J. FEENEY, and L. H. SUTCLIFFE. High resolution nuclear magnetic resonance spectroscopy. Vol. 2. Pergamon Press. p. 757.
23. C. A. BUEHLER, A. V. SLACK, D. A. SHIRLEY, P. A. SANGUINETTI, and S. H. FREY. J. Amer. Chem. Soc. **73**, 2347 (1951).
24. S. FORSÉN. J. Phys. Chem. **67**, 1740 (1963).
25. R. GRIGG, P. ROFFEY, and M. V. SARGENT. J. Chem. Soc. C, 2327 (1967).
26. R. P. GANDHI and V. K. CHADHA. Chem. Commun. 552 (1968); H. PRINZBACH, M. ARGUELLES, and E. DRUCKREY. Angew. Chem. Intern. Ed. 5, 1039 (1966).
27. E. PAYO, L. CORTÉS, J. MANTECON, C. RIVAS, and G. DE PINTO. Tetrahedron Lett. 2415 (1967).
28. H. PRINZBACH, P. VOGEL, and W. AUGE. Chimia (Aarau), 469 (1967).
29. D. S. PRATT and G. A. PERKINS. J. Amer. Chem. Soc. **40**, 219 (1918).
30. P. VOGEL, B. WILLHALM, and H. PRINZBACH. Helv. Chim. Acta, **52**, 584 (1969).

Can. J. Chem. Downloaded from www.nrcresearchpress.com by 210.87.254.105 on 09/05/12
For personal use only.

Can. J. Chem. Downloaded from www.nrcresearchpress.com by 210.87.254.42 on 09/05/12
For personal use only.

Dibenzo[*a*,*d*]cycloheptene and related compounds. II.[1] The synthesis of some 11-substituted dibenzo[*b*,*e*]azepin-6-one, 5-substituted dibenzo[*a*,*d*]cycloheptene, and 12-substituted dibenzo[*a*,*d*]cyclooctene derivatives

K. Ackermann, J. Chapuis, D. E. Horning, G. Lacasse, and J. M. Muchowski[2]
Bristol Laboratories of Canada, Candiac, Quebec

Received July 16, 1969

The synthesis of several 11-substituted-5,6-dihydro-11*H*-dibenzo[*b*,*e*]azepin-6-ones, and an improved method of preparing 5-cyano-10,11-dihydro-5*H*-dibenzo[*a*,*d*]cycloheptene and 12-cyano-5,6,7,12-tetrahydrodibenzo[*a*,*d*]cyclooctene are described.

A description of the synthesis of epoxides from diaryl ketones and dimethylsulfonium methylide by a modified technique is given.

The nuclear magnetic resonance spectra of several of the 11-substituted dibenzo[*b*,*e*]azepin-6-ones are interpreted on the basis of a slow interconversion between diastereomeric boat conformers in which the C-11 substituent is quasi axial or quasi equatorial.

Canadian Journal of Chemistry, 47, 4327 (1969)

In connection with the synthesis of some compounds of potential pharmacological utility, we recently found it necessary to have available large amounts of the nitriles **1** (n = 2, 3) and **2**. The 7-membered nitrile **1** (n = 2) is well known, and has been prepared from the corresponding chloride and silver cyanide (2) or cuprous cyanide (3). The 8-membered nitrile (n = 3) has

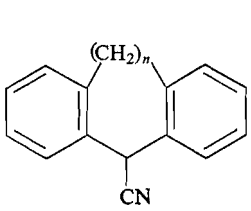

1

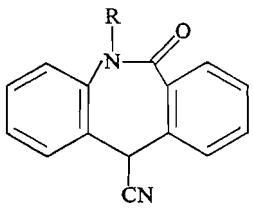

2

apparently been prepared in the same way with silver cyanide, but it was not characterized (4). When these methods were applied to the synthesis of derivatives of **2**, mixtures which contained only moderate amounts of the desired materials were obtained. The solution to this problem was based on the observation that the epoxide **4** (n = 2) could be prepared in variable yield from dibenzosuberone (**3**, n = 2) and dimethylsulfonium methylide at 30–50°. This was doubly surprising in view of the known instability (5) of this ylid, and also because of a recently reported (6) failure to observe the formation of **4** (n = 2) from **3** (n = 2) and dimethylsulfonium methylide or dimethyloxosulfonium methylide. A careful study of the conditions for the reaction of dimethylsulfonium methylide with **3** (n = 2) in dimethyl sulfoxide (DMSO), showed that at 30–50°, the yields of **4** were not reproducible, and that at temperatures of ca. 15° no trace of product was ever observed. With these observations as a basis, it was found that **4** (n = 2) could be best produced by the addition of an excess (50%) of trimethylsulfonium iodide, in one or two portions at room temperature, to a slurry of sodium hydride in DMSO containing the dissolved ketone. There was no necessity to generate the dimethylsulfinyl carbanion as an ylid forming reagent; this observation was to be expected on the basis of work published several years ago by Franzen and Driesen (7). By this method, excellent yields of **4** (n = 2, 3) and the dibenzo[*b*,*e*]azepine derivatives **5** could be prepared in a matter of a few hours (see Table I). The epoxides were then converted to the nitriles by a classical sequence involving rearrangement of the epoxides to the aldehydes **6**, followed by dehydration (with hot acetic anhydride) of the oximes **7** obtained therefrom, to the nitriles **2** (see Table III). Dehydration of the oxime **7** (R = H) was exceptional in that the primary product was the imide **2** (R = CH_3CO; infrared (i.r.) absorptions at 1710 and 1687 cm^{-1}); hydrolysis to the nitrile **2** (R = H) was easily accomplished in refluxing aqueous acetonitrile.

[1]For Part I see ref. 1.

[2]To whom correspondence concerning this paper should be addressed.

TABLE I

Yields and physical properties of the epoxides*

Compound	Yield (%)†	Reaction time (h)	Melting point (°C)	Crystallization solvent	% Calculated C	% Calculated H	% Calculated N	% Found C	% Found H	% Found N
4 (n = 2)	90	3.5‡	76–78	Alcohol	86.45	6.35	—	86.17	6.45	—
4 (n = 3)	98	3	Oil§	—	—	—	—	—	—	—
5 (R = H)	74–86‖	4	222–224	Acetonitrile	75.93	4.67	5.90	75.69	4.73	6.09
5 (R = CH_3)	74–80	4	116–117	Hexane	76.47	5.22	5.57	76.48	5.26	5.52

*The synthesis of other epoxides has been examined in a cursory way; e.g. benzophenone and benzaldehyde gave 85% 1,1-diphenyl oxirane and 55% phenyl oxirane respectively. Enolizable aldehydes and ketones have not been investigated.
†Unless specified otherwise, the yields refer to those of the purified products, here and in tables following.
‡This compound decomposed after a few days at room temperature or after ca. one month at 0°.
§We have not yet succeeded in obtaining this compound in crystalline form. Attempts to effect its purification by molecular distillation resulted in partial or complete rearrangement to the aldehyde. The epoxide was, therefore, not characterized.
‖An extra equivalent of sodium hydride was added to convert the lactam to its sodium salt.

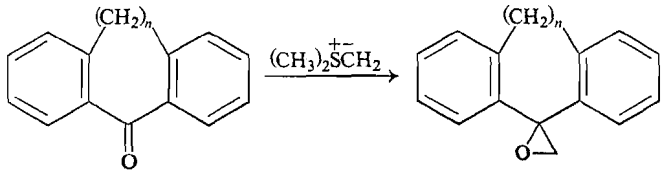

3 **4**

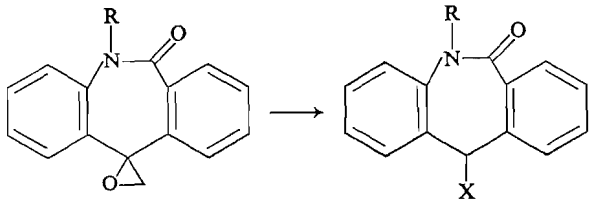

5

6 X = CHO
7 X = CHNOH
8 X = COOH

An analogous series of transformations beginning with the epoxides **4** (n = 2 and 3) gave 5-cyano-10,11-dihydro-5*H*-dibenzo[*a*,*d*]cycloheptene (**1**, n = 2; see Table II) and 12-cyano-5,6,7,12-tetrahydrodibenzo[*a*,*d*]cyclooctene (**1**, n = 3) respectively. When the sequence **3** to **1** was effected without purification of the intermediates, the overall yields of the nitriles **1** (n = 2) and **1** (n = 3) were 55 and 70% respectively, based on the ketones **3** (n = 2 and 3). This represents the most efficient and convenient synthesis of these compounds which has been published to date.

The oxidation of the aldehydes **6** to the carboxylic acids **8** was only moderately successful (see Table III). Nevertheless, this was found to be the most reliable method of preparing these compounds.

The i.r. and nuclear magnetic resonance (n.m.r.) spectra of the dibenzo[*b*,*e*]azepine derivatives[3] described above, are listed in Tables IV and V respectively. The i.r. spectral data were unexceptional and therefore require no comment. The n.m.r. spectra, on the other hand, were especially interesting since several of the *N*-substituted dibenzo[*b*,*e*]azepine derivatives showed two well separated resonances for the C-11 proton (in most, but not all cases, the *N*-substituent showed two closely spaced absorptions). The data presented in Table VI ("B" series) showed that the relative intensity of these absorptions was markedly dependent on

[3]The n.m.r. spectra of the dibenzo[*a*,*d*]cycloheptene and cyclooctene derivatives will be discussed in a forthcoming publication.

Can. J. Chem. Downloaded from www.nrcresearchpress.com by 210.87.254.42 on 09/05/12
For personal use only.

TABLE II

Yields and properties of some dibenzo[a,d]cycloheptene and dibenzo[a,d]cyclooctene derivatives

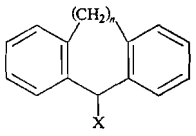

n	X	Yield (%)	Reaction time (h)	Melting point (°C)	Crystallization solvent	% Calculated			% Found		
						C	H	N	C	H	N
2	CHO	87–92	2	77–78*	Ether	86.45	6.35	—	86.50	6.44	—
3	CHO	90	2	87.5–89.5†	Hexane	86.40	6.83	—	86.45	6.86	—
2	CHNOH	90	3.5–5	165–166‡	Hexane: benzene (1:1)	80.98	6.37	5.90	80.85	6.40	5.85
3	CHNOH	90	5	166–169	Benzene: cyclohexane (1:1)	81.24	6.82	5.57	81.37	6.69	5.56
2	CN	55§	2‖	87–89	Cyclohexane: pet. ether (b.p. 35–60°); 1:1	—	—	—	—	—	—
3	CN	70§	2	190–192**	Cyclohexane	87.50	6.48	—	87.50	6.53	—

*Stable for several months at 0°.
†Sublimed at 75°/0.001 mm before analysis.
‡Only one isomer was characterized, here and for the oximes following.
§Yield based on starting ketone.
‖Mixed melting point undepressed; see ref. 2.
**Sublimed at 110°/0.001 mm before analysis.

TABLE III

Yields and properties of some 11-substituted 5,6-dihydro-11*H*-dibenzo[b,e]azepin-6-ones

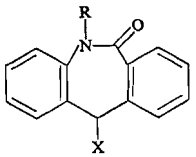

X	R	Yield (%)	Reaction time (h)	Melting point (°C)	Crystallization solvent	% Calculated			% Found		
						C	H	N	C	H	N
CHO	H	68–84*	3.5	243–245	Acetonitrile	75.93	4.67	5.90	76.00	4.79	6.06
CHNOH	H	80	4	242–243	Methanol	71.41	4.80	11.11	71.40	4.92	10 98
CN	CH_3CO	80	5	172–174	Cyclohexane: benzene (1:2)	73.90	4.38	10.14	74.25	4.38	10.21
CN	H	76†	28	262–263	Ethanol	71.93	4.75	11.19‡	72.18	4.38	11.17
COOH	H	51	—	221–223	Acetonitrile	71.14	4.37	5.53	71.13	4.50	5.55
CHO	CH_3	87–92	3	159–160	Benzene: ether (3:1)	76.47	5.22	5.57	76.59	5.26	5.54
CHNOH	CH_3	85	3.5	181–182	Benzene	72.16	5.30	10 52	72.19	5.34	10 58
CN	CH_3	77	4.5	171–172	Benzene	77.40	4.87	11.28	77.53	4.89	11.18
COOH	CH_3	53–65	—	197–198	Acetonitrile	71.90	4.90	5.24	71.61	5.10	5.41
CO_2CH_3	CH_3	80–88	20§	186–188	Methanol	72.58	5.37	4.98	72.44	5.59	5.16

*Solvent, tetrahydrofuran.
†Yield based on oxime; the imide was usually not isolated, but deacetylated directly with 1:1 aqueous acetonitrile at reflux temperature.
‡Calculated for $C_{15}H_{10}ON_2 \cdot 0.9\ H_2O$. The n.m.r. spectrum indicated the presence of 0.85 moles of water; see Table V.
§A solution consisting of 6 ml of methanol and 0.09 ml of concentrated sulfuric acid for each gram of the carboxylic acid, was heated under reflux for the indicated period.

the solvent polarity and the C-11 substituent. These phenomena are interpreted as another case of slow (on the n.m.r. time scale) interconversion of diastereomeric boat conformers in which the C-11 substituent is quasi axial or quasi equatorial, like that described recently by Lansbury *et al.* (8) and others (9, 10) for similar systems. A particularly informative spectrum was observed for the 5-methyl-11-methoxy dibenzazepinone (**9**). In DMSO-d_6 the methine

Can. J. Chem. Downloaded from www.nrcresearchpress.com by 210.87.254.42 on 09/05/12
For personal use only.

TABLE IV

Infrared spectra of some dibenzo[*b*,*e*]azepine derivatives

R	X	Medium	Frequency in cm^{-1} NH	CN	O ‖ —C—	O ‖ —C—N—	Other
*"A" Series**							
H	—	Nujol	3171	—	—	1661	—
CH_3	—	$CHCl_3$	—	—	—	1633	—
*"B" Series**							
H	CHO	Nujol	3177	—	1715	1651	2732†
CH_3	CHO	$CHCl_3$	—	—	1720	1637	2731†
CH_3CO	CN	$CHCl_3$	—	2250	1709	1685	—
H	CN	Nujol	3171	2246	—	1657	3485‡
CH_3	CN	$CHCl_3$	—	2247	—	1640	—
H	COOH	Nujol	3274, 3220 3170	—	1701	1635	2483§
CH_3	COOH	Nujol	—	—	1721	1614	2548§
CH_3	CO_2CH_3	$CHCl_3$	—	—	1738	1640	—

* *A* = 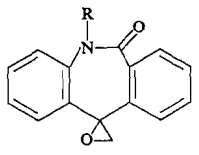 ; *B* = 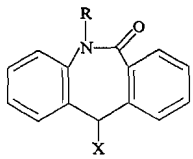

†Aldehyde C—H stretching absorption.
‡Water of crystallization.
§O—H Stretching absorption for carboxylic acid dimer.

protons showed two singlets at δ 5.31 and 5.67, while the methoxyl groups appeared as two singlets at δ 3.16 and 3.56. The integrated intensities of the two high field resonances, i.e. δ 5.31 and 3.16, for the methine and methoxyl protons respectively, indicated that these absorptions were due to the same and least abundant isomer. This isomer was assigned the quasi axial configuration **9***b*, on the expectation that an axially oriented methoxyl group would lie in the positive shielding region above the plane of the aromatic rings (11). Identical conclusions have been reached by Lansbury *et al.* (8) for 7-methoxy-7,12-dihydropleiadene and by Childs and Winstein (10) for the epimeric dibenzohomotropyl methyl ethers, and these results give much weight to our assignment. On the basis of the above information, for those compounds listed in Table VI ("B" series) which showed two signals for the C-11 proton, the axial configuration was assigned to that isomer having the C-11 proton resonance at higher field (i.e. H equatorial).

There were several interesting observations to be made from the data given in Tables V and VI ("B" series). Firstly, for those compounds which showed restricted inversion, the quasi axial isomer represented an appreciable fraction of the mixture. Indeed, when the 11-substituent was chlorine, the axial configuration was actually the

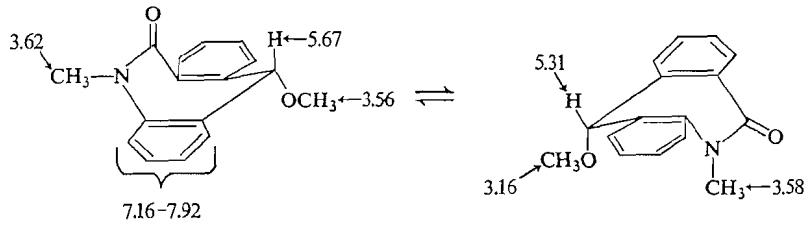

9a *9b*

Can. J. Chem. Downloaded from www.nrcresearchpress.com by 210.87.254.42 on 09/05/12
For personal use only.

TABLE V

Nuclear magnetic resonance spectra of some dibenzo[b,e]azepine derivatives

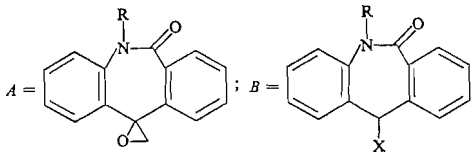

R	X	Solvent	Chemical shifts in p.p.m. (δ) from tetramethylsilane* —N—CH_3	C-11	Aromatic hydrogens	NH	Other
"A" Series							
H	—	DMSO-d_6: $CDCl_3$ (9:1)	—	—	7.13–8.10	10.75	3.07, 3.63†‡
CH_3	—	$CDCl_3$	3.63	—	7.02–8.05	—	3.08, 3.64†§
"B" Series							
H	CHO	CF_3COOH: $CDCl_3$ (9:1)	—	5.08‖	7.32–8.28	10.38	9.95**
CH_3	CHO	$CDCl_3$	3.47	4.50	7.17–8.10	—	9.85**
$COCH_3$	CN	$CDCl_3$	—	4.85, 5.75	7.28–8.22	—	3.05, 3.10††
H	CN	DMSO-d_6	—	6.00	7.28–8.05	10.92	3.37‡‡
CH_3	CN	$CDCl_3$	3.67, 3.72	4.90, 5.50	7.22–8.05	—	—
H	COOH	CF_3COOH: $CDCl_3$ (9:1)	—	5.15	7.32–8.05	10.35	—
CH_3	CO_2CH_3	$CDCl_3$	3.50 or 3.65§§	4.70	7.13–8.02	—	3.50 or 3.65§§

*All absorptions, except those due to the aromatic hydrogens and the epoxide —CH_2—, were singlets.
†Epoxide —CH_2—.
‡These absorptions were broad.
§In pyridine, the high field absorption was a clearly visible AB quartet (J_{AB} = 6.1 c.p.s.), and the low field absorption was an AB quartet (J_{AB} = 5.4 c.p.s.) partially obscured by the *N*-methyl peak. In $CDCl_3$ the epoxide methylenes were singlets for this compound.
‖This proton resonates at δ 5.24 in DMSO-d_6.
**Aldehyde —CH—.
††Acetyl methyl absorptions.
‡‡Water of crystallization; 0.85 H_2O.
§§One singlet due to the *N*-methyl and the other due to the *O*-methyl hydrogens.

preferred one. This was not especially surprising, since Lansbury *et al.* have shown (8) that the axial configuration is favored over the equatorial in the dihydropleiadene series. Secondly, all the *N*-unsubstituted compounds in the "B" series (Tables V and VI) had only one sharp resonance for the C-11 proton. In those cases where a comparison was made, the position of this absorption was about halfway between the corresponding peaks in the *N*-methyl compounds. This would seem to indicate that these *N*-unsubstituted compounds are undergoing rapid inversion at the temperature of the measurement (37°). However, such a conclusion is unjustified in the absence of variable temperature studies. Whatever the explanation, it is indeed curious that the nitrogen substituent should have such a profound effect on the n.m.r. spectra of these compounds. Lastly, two of the *N*-methyl dibenzazepinones (Table V, "B" series), e.g. X = CHO and CO_2CH_3, also showed only a sharp singlet for the C-11 proton. Once again, without variable temperature spectra, a choice between fast inversion and configurational homogeneity cannot be made, but the high field position of the methine resonance may well be an implication of the latter.

The n.m.r. spectra of both epoxides (Tables V and VI, "A" series) showed evidence of restricted inversion. In as much as spiro fusion, such as is present in these epoxides, might, like a double bond, slow down the rate of inversion (e.g. compare refs. 9 and 12), this would also tend to implicate rapid inversion of the *N*-unsubstituted compounds discussed above.

Experimental

The melting points were determined in a Gallenkamp melting point apparatus and are not corrected. The i.r. spectra were measured in chloroform (unless specified otherwise) on a Perkin–Elmer 237-B grating spectrophotometer. The n.m.r. spectra were recorded at 60 Mc.p.s. on a Varian A-60A spectrometer at ca. 37°

Can. J. Chem. Downloaded from www.nrcresearchpress.com by 210.87.254.42 on 09/05/12
For personal use only.

TABLE VI

Conformational composition of some dibenzo[*b*,*e*]azepine derivatives at 37°

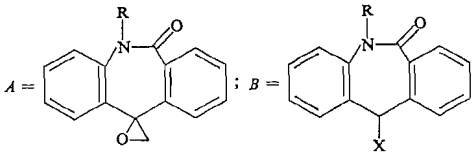

R	X	Solvent	Chemical shifts: C_{11}—H δe	C_{11}—H δa*	Other δe	Other δa	Conformational composition (%)† e	a
	"A" Series							
H	—	DMSO-d_6	—	—	3.60‡	3.08‡	24§	76§
		Pyridine: DMSO-d_6(1:1)	—	—	3.51	2.77	22	78
CH_3	—	$CDCl_3$	—	—	3.64	3.07	6	94
		DMSO-d_6	—	—	3.68	3.18	21	79
		Pyridine	—	—	2.96	2.43	9	91
	"B" Series							
CH_3	OCH_3‖·¶	$CDCl_3$	5.07	5.45	3.65[a]	3.25[a]	77	23[b]
		DMSO-d_6	5.31	5.67	3.56	3.16	60	40[b]
H	OCH_3‖·¶	DMSO-d_6	5.37		3.29		?	
H	OH‖·[c]	DMSO-d_6	5.82		—	—	?	
CH_3	OH‖·[c]	DMSO-d_6	5.62	5.93	—	—	90	10
CH_3	Cl‖·[d]	$CDCl_3$	5.83	6.33	—	—	19	81
		DMSO-d_6	6.55	6.76	—	—	8	92
H	CN	DMSO-d_6	6.00		—	—	?	
CH_3	CN	DMSO-d_6	5.83	6.18	—	—	53.5	46.5
		$CDCl_3$	4.90	5.50	—	—	83	17
$COCH_3$	CN	$CDCl_3$	4.85	5.75	—	—	68	32
		DMSO-d_6	5.88	6.72	—	—	54	46

*a = axial; e = equatorial.
†Determined from the integrated areas of the methine resonance in the "B" series and the methylene resonance in the "A" series.
‡Refers to the epoxide —CH_2— throughout the "A" series.
§Orientation of epoxide —CH_2—.
‖These compounds were prepared in connection with other work (13) and were fully characterized.
¶Prepared from the chloro compounds and methanolic sodium methoxide.
[a]Methoxyl absorptions. In $CDCl_3$, the *N*-methyl peak is unresolved and absorbs at δ 3.65. In DMSO-d_6 the *N*-methyl group appears as two peaks at δ 3.58 (a) and 3.62 (e).
[b]The isomeric composition determined from the methoxyl absorptions was within 1% of the value obtained from the methine absorptions.
[c]Prepared from the corresponding ketones by reduction with sodium borohydride in methanol.
[d]Prepared from the alcohol and thionyl chloride.

(probe temperature). The chemical shifts are recorded as p.p.m. (δ) from internal tetramethylsilane, with tetramethylsilane taken as zero.

Dibenzosuberone was purchased from the Aldrich Chemical Company. 5,6,7,12-Tetrahydrodibenzo[*a*,*d*]cycloocten-12-one was prepared according to the method of Winthrop *et al.* (14). 5,6-Dihydro-11*H*-dibenzo[*b*,*e*]azepine-6,11-dione was prepared by the method of Caronna and Palazzo (15) in 85–90% yield.

5-Methyl-5,6-dihydro-11H-dibenzo[b,e]azepine-6,11-dione

This compound has previously been prepared by the alkylation of the sodium salt of the dioxo compound with methyl iodide. The anion was generated with sodamide in refluxing toluene (16). We have found that the sodium salt is more conveniently generated with sodium hydride in dimethyl formamide at room temperature. The addition of an excess of methyl iodide to this salt produced the *N*-methyl compound in yields of 85–90%.

Preparation of the Epoxides

A 250 ml three-necked flask containing a magnetic stirring bar, and fitted with a thermometer, a gas inlet, and a calcium chloride drying tube, was flame dried. A flow of purified dry nitrogen was initiated through the apparatus and 1.28 g of a 56% dispersion of sodium hydride in mineral oil (29.9 mmoles)[4] were placed in the flask. The sodium hydride was twice washed with petroleum ether (b.p. 35–60°) to remove the mineral oil, and then 75 ml of dry dimethyl sulfoxide and 19.3 mmoles of the ketone were added. The mixture was stirred to effect solution of the ketone, and then 6.0 g of trimethylsulfonium iodide were added all at once (for larger scale reactions the salt was sometimes added in two equal

[4]When the ketone was 5,6-dihydro-11*H*-dibenzo[*b*,*e*]azepine-6,11-dione, an extra equivalent of sodium hydride was added to convert the lactam to its sodium salt.

Can. J. Chem. Downloaded from www.nrcresearchpress.com by 210.87.254.42 on 09/05/12
For personal use only.

Can. J. Chem. Downloaded from www.nrcresearchpress.com by 210.87.254.42 on 09/05/12
For personal use only.

portions because of excess frothing). After stirring for the specified time (see Table I) at room temperature, the solution was poured into a large excess of cold water containing a little sodium chloride. The mixture was extracted with benzene (or the product was collected by filtration if it crystallized), the extract was washed well with water, dried over sodium sulfate, and then evaporated *in vacuo*. The residue was then crystallized from the solvent indicated in Table I.

Rearrangement of the Epoxides

To a solution of the epoxide (27 mmoles) in 150 ml of anhydrous dichloromethane or tetrahydrofuran, were added 1.6 ml of boron trifluoride etherate. The solution was stirred at room temperature for the specified time (see Tables II and III), then washed with sodium carbonate solution (10%), with water, and then it was dried over sodium sulfate. The solvent was removed *in vacuo*, and the residue was crystallized from the solvent indicated in the Tables.

Preparation of the Nitriles

The aldehyde (42.2 mmoles), hydroxylamine hydrochloride (3.57 g, 51.5 mmoles), dry pyridine (40 ml), and dry ethanol (160 ml) were heated under reflux for the times indicated in Tables II and III and then the solvent was removed *in vacuo*. The residue was taken up in dichloromethane, washed with 10% hydrochloric acid, then with water, and finally dried over sodium sulfate. The solvent was removed *in vacuo* and the residue was crystallized from a suitable solvent.

For the preparation of the nitriles, the oximes were not purified, but used directly in the manner indicated below.

Oxime (30.3 mmoles) and 150 ml of acetic anhydride were heated at reflux temperature for the times indicated in Tables II and III. The acetic anhydride was then removed *in vacuo*, and the residue was taken up in dichloromethane, extracted with 5% sodium carbonate solution, and then with water. The dichloromethane was dried over sodium sulfate, evaporated *in vacuo*, and the residue was crystallized from a suitable solvent.

In the preparation of 11-cyano-5,6-dihydro-11*H*-dibenzo[*b*,*e*]azepin-6-one the primary product was the 5-acetyl derivative (see text). Deacetylation was effected by heating a solution of the imide in 1:1 aqueous acetonitrile (20 ml/g) at reflux for 28 h. The major portion of the product crystallized when the solution had cooled to room temperature; the remainder was recovered by evaporation of the mother liquor and crystallization of the residue.

In the case of 5-cyano-10,11-dihydro-5*H*-dibenzo[*a*,*d*]-cycloheptene, the crude cyanide was taken up in the minimum amount of benzene and placed on a dry packed column of Fluka neutral alumina (act. II, 30–50 g of alumina/g of crude nitrile). The product was eluted with benzene and appeared in the first few fractions of the eluant. This chromatography was necessary to remove an orange-colored impurity.

Oxidation of the Aldehydes to the Carboxylic Acids

The aldehyde was dissolved in glacial acetic acid (10 ml/g for **6** (R = CH_3), or 120 ml/g for **6** (R = H) and titrated with 0.649 *M* sodium dichromate in 2.5 *M* sulfuric acid at a rate such that the reaction temperature did not exceed 30°. A 10% excess of the oxidant was used for **6** (R = CH_3) and a 2% excess for **6** (R = H). When the addition was completed, the mixture was stirred at room temperature for ½ h, and then poured into a large volume of cold water. The product was extracted into dichloromethane, the extract was washed well with water, dried over sodium sulfate, and then evaporated *in vacuo*. The residue was crystallized from a suitable solvent (see Table III).

1. D. E. Horning and J. M. Muchowski. Can. J. Chem. **46**, 3665 (1968).
2. M. A. Davis, S. O. Winthrop, J. Stewart, F. A. Sunahara, and F. Herr. J. Med. Chem. **6**, 251 (1963).
3. C. van der Stelt, A. Haasjes, H. M. Tersteege, and W. Th. Nauta. Rec. Trav. Chim. **84**, 1466 (1965).
4. M. A. Davis, S. O. Winthrop, R. A. Thomas, F. Herr, M-P. Charest, and R. Gaudry. J. Med. Chem. **7**, 88 (1964).
5. E. J. Corey and M. Chaykovsky. J. Amer. Chem. Soc. **87**, 1353 (1965).
6. M. A. Davis, F. Herr, R. A. Thomas, and M-P. Charest. J. Med. Chem. **10**, 627 (1967).
7. V. Franzen and H. E. Driesen. Chem. Ber. **96**, 1881 (1963).
8. P. T. Lansbury, J. F. Bieron, and A. J. Lacher. J. Amer. Chem. Soc. **88**, 1482 (1966).
9. W. Tochtermann, G. Schnabel, and A. Mannschreck. Ann. Chem. **705**, 169 (1967).
10. R. F. Childs and S. Winstein. J. Amer. Chem. Soc. **89**, 6348 (1967).
11. L. M. Jackman. Applications of n.m.r. spectroscopy in organic chemistry. The Pergamon Press Inc., London, 1959. p. 125.
12. A. Ebnother, E. Jucker, and A. Stoll. Helv. Chim. Acta, **48**, 1237 (1965).
13. K. Ackermann and J. M. Muchowski. Unpublished observations.
14. S. O. Winthrop, M. A. Davis, F. Herr, J. Stewart, and R. Gaudry. J. Med. Chem. **6**, 130 (1963).
15. G. Caronna and S. Palazzo. Gazz. Chim. Ital. **83**, 533 (1953).
16. A. E. Drukker, C. I. Judd, J. M. Spoerl, and F. E. Kaminski. J. Heterocycl. Chem. **2**, 283 (1965).

Can. J. Chem. Downloaded from www.nrcresearchpress.com by 210.87.254.40 on 09/05/12
For personal use only.

Thermal [2 + 3] cycloaddition of imino compounds to 3-aroylaziridines. Synthesis of imidazolidines

J. W. LOWN, J. P. MOSER, AND R. WESTWOOD[1]
Department of Chemistry, University of Alberta, Edmonton, Alberta

Received July 31, 1969

3-Aroylaziridines react with a variety of imines and aryl-*N*-sulfonylimines in refluxing benzene to give imidazolidines in excellent yield. The orientation of the [2 + 3] cycloaddition of the intermediate azomethine ylids to the C=N double bond was proven by synthesis of specifically 5-deuterated imidazolidines. The reactions provide a convenient new general synthesis of imidazolidines.

Canadian Journal of Chemistry, 47, 4335 (1969)

Many substituted aziridines will undergo thermal cleavage of the 2-3 bond to an azomethine ylid intermediate, and subsequent [2 + 3] cycloaddition can take place to the acetylenic bond and to activated alkenes, in many and stereospecifically (1–14).

We have reported the analogous thermally induced additions of 3-aroylaziridines to the polarized carbonyl bond of diphenylcyclopropenone with the formation of 4-aroyl-4-oxazolines (15) and to the C=S double bond of aryl isothiocyanates to form 4-aroyl-5-arylimino-4-thiazolines (16). In a continuing study of these additions to heteromultiple bonds, we report the [2 + 3] cycloaddition of 3-aroylaziridines to activated imino compounds which provides a new synthesis of imidazolidines.

Treatment of 3-benzoyl-1-isopropyl-2-phenylaziridine with an equimolar quantity of benzalaniline in refluxing toluene for 16 h, followed by chromatographic separation on alumina afforded the imidazolidine **1** as a white crystalline solid in 24% yield, m.p. 182°. The nuclear magnetic resonance (n.m.r.) spectrum of **1** shows the isopropyl methyl groups are non-equivalent, indicating proximity to an asymmetric center in accordance with the proposed structure. While the initial product consisted of an isomeric mixture corresponding to *cis* and *trans* arrangement of protons at the 4 and 5 positions as shown by the n.m.r. spectrum, only the isomer described above could be obtained in solid form. This was assigned the *cis* geometry at the 4,5 positions on the basis of an 8 Hz coupling constant for the AB

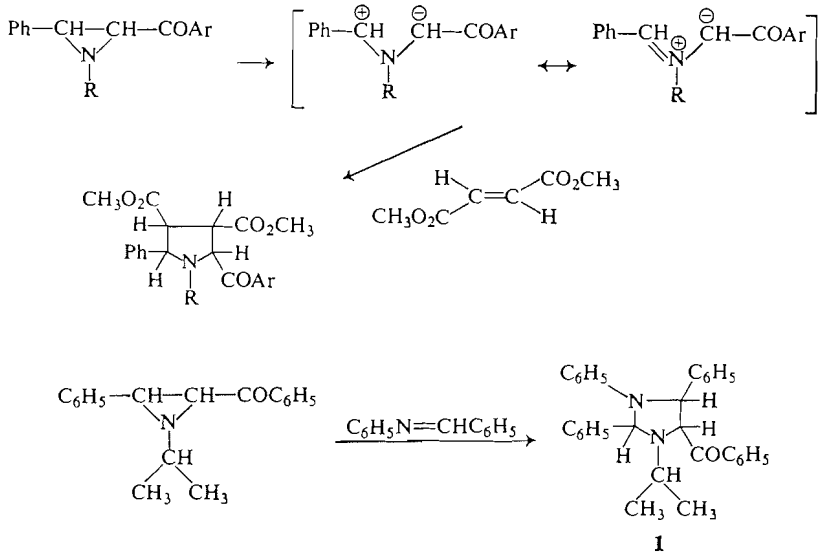

1

[1]NRCC Postdoctoral Fellow, 1967–1969.

Can. J. Chem. Downloaded from www.nrcresearchpress.com by 210.87.254.40 on 09/05/12
For personal use only.

TABLE I

1-Alkyl-2,4-diaryl-5-aroyl-3-(*N*-arylsulfonyl)-imidazolidines (**9**)

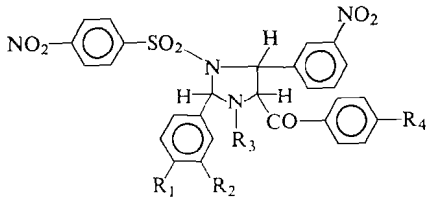

							Observed					Calculated				
No.	R_1	R_2	R_3	R_4	Melting point (°C)	Yield %	C	H	N	S	Imidazole fragment ion	C	H	N	S	Imidazole fragment ion
a	H	H	CH_3	H	94–95	93	60.71	4.60	9.49	5.57	383.1272	60.82	4.86	9.78	5.60	383.1270
b	H	H	CH_3	CH_3	172	41	61.85	4.51	9.39	5.47	397.1424	61.44	4.47	9.55	5.47	397.1426
c	H	H	$(CH_3)_2CH$	H	159–160	61.5	61.95	4.84	9.57	5.27	411.1581	61.97	4.81	9.33	5.34	411.1583
d	H	H	$(CH_3)_2CH$	CH_3	156–157	58	62.32	4.84	9.01	4.96	425.1737	62.50	4.92	9.11	5.21	425.1739
e	H	NO_2	$(CH_3)_2CH$	H	173–175	51	59.91	4.62	10.24	4.74	456.1437	59.61	4.56	10.22	4.97	456.1434
f	H	H	$C_6H_5CH_2$	H	165–166	84	64.69	4.24	8.35	5.15	459.1584	64.79	4.35	8.64	4.94	459.1587
g	H	H	$C_6H_5CH_2$	CH_3	169	57	64.87	4.97	8.27	4.91	473.1741	65.24	4.56	8.45	4.84	473.1739
h	H	H	C_6H_{11}	H	160–161	94	63.73	5.09	8.53	5.40	451.1898	63.74	5.04	8.74	5.10	451.1896
i	H	H	C_6H_{11}	CH_3	165–167	54	64.33	5.54	8.54	4.75	465.2048	64.19	5.33	8.56	4.90	465.2052
j	NO_2	H	C_6H_{11}	H	183–184.5	14.5	59.91	4.62	10.24	4.61	496.1752	59.55	4.56	10.22	4.68	496.1747
k	H	NO_2	C_6H_{11}	H	112–113	80	59.85	4.68	9.98	4.58	496.1748	59.55	4.56	10.21	4.68	496.1747
l	H	H	C_6H_{11}	NO_2	160–161	79	59.83	4.93	9.38	4.49	496.1748	59.55	4.56	10.21	4.68	496.1747
m	CH_3O	H	C_6H_{11}	H	162–164	63	63.08	5.35	8.17	4.76	481.2000	62.67	5.11	8.35	4.78	481.2002
n	H	H	C_6H_{11}	CH_3O	152–153	34	62.58	5.39	8.16	4.78	481.1999	62.67	5.11	8.35	4.78	481.2002

Can. J. Chem. Downloaded from www.nrcresearchpress.com by 210.87.254.40 on 09/05/12
For personal use only.

quartet due to these protons in the n.m.r. spectrum (8). This configuration of **1** is evidently quite stable since no epimerization occurred, and no deuterium was incorporated at the 5 position upon refluxing **1** with deuterium oxide containing potassium carbonate. Specifically 5-deuterated imidazolidines could however be synthesized by a different method (*vide infra*).

Similarly, benzalaniline reacted with 3-*p*-anisoyl-1-cyclohexyl-2-phenylaziridine to give imidazolidine **2**

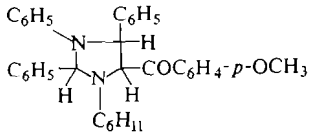

2

Addition of the more reactive *N*-(*m*-nitrobenzal)-*p*-nitrobenzenesulfonamide (**3**) to 3-benzoyl-1-cyclohexyl-2-phenylaziridine in refluxing benzene proceeded smoothly to give the imidazolidine **4** m.p. 160–161° in 94% yield.

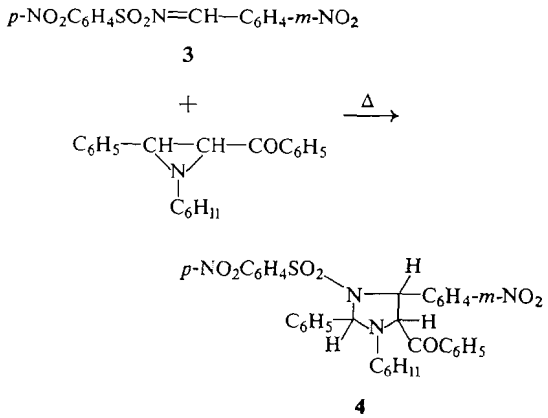

4

The scope of this new synthesis of imidazolidines was then explored. Several *N*-sulfonylimines were prepared by condensation of arylsulfonamides with the methyl acetal of *m*-nitrobenzaldehyde, following a method previously used by Kresze *et al.* (17, 18).

Excellent yields of imidazolidines were obtained by reaction of these sulfonylimines with a variety of aziridines containing different 2 and 3 substituents and with *N*-substituents of cyclohexyl, isopropyl, methyl, and benzyl. The sulfonylimines **3** and **5** gave excellent yields; **6** and **7** gave good to excellent yields, while **8**, containing

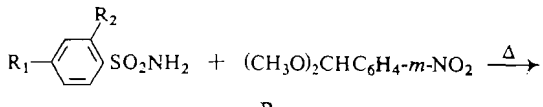

3 $R_1 = NO_2$, $R_2 = H$
5 $R_1 = -C{\equiv}N$, $R_2 = H$
6 $R_1 = Cl$, $R_2 = NO_2$
7 $R_1 = Cl$, $R_2 = H$
8 $R_1 = CH_3$, $R_2 = H$

an electron releasing substituent in the arylsulfonyl group, was an exception and gave only poor yields. The analytical and spectral data on the product imidazolidines are summarized in Tables I–IV. Table V contains the analytical data on the new aryl-*N*-sulfonylimines.

The molecular ion cannot be observed in the high resolution mass spectrum of these imidazolidines. Fragmentation to the ion of the 5-aroylimidazole, although in low abundance relative to the aroyl ion, was highly characteristic of these compounds (see Tables I and III).

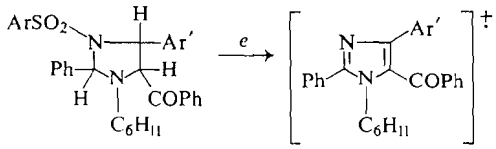

Three distinct structural and spectral problems connected with this synthesis of imidazolidines, required solution, namely, (*i*) orientation of addition, (*ii*) dependence of product configuration on the stereochemistry of the aziridine, i.e., possible stereospecificity of the reaction, and (*iii*) unambiguous assignment of the imidazolidine ring proton magnetic resonances, which consisted of one sharp singlet in the region of 6.0 δ and two weakly coupled broad singlets at higher field in the region of 5.5 and 5.1 δ.

The question of orientation of addition, i.e., whether the products are of type **9** or **10** is not a trivial one, since Huisgen has pointed out that in 1,3-dipole addition reactions, one may not safely

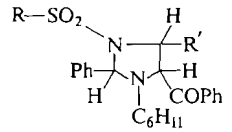

9

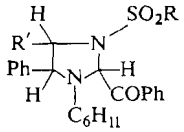

10

Can. J. Chem. Downloaded from www.nrcresearchpress.com by 210.87.254.40 on 09/05/12
For personal use only.

TABLE II

Spectroscopic properties of 1-alkyl-2,4-diaryl-5-aroyl-3-*N*-arylsulfonylimidazolidines (**9**)

No.	Infrared spectrum $CHCl_3$ (C=O)	Nuclear magnetic resonance spectrum $[(CD_3)_2SO]\delta$							
		Aryl protons	Ring proton 2	Ring proton 5	Ring proton 4	2-Aryl substituent	5-Aroyl substituent	*N*-Substituents	
a	1690	7.0–8.3(18H)m	5.80(1H)s	5.13(1H)s	4.93(1H)s	—	—	2.09(3H)s CH_3	
b	1693	6.9–8.1(17H)m	4.64(1H)s	4.84 AB quartet	5.62 (J = 8 Hz)		2.18(3H)s CH_3	1.93(3H)s CH_3	
c	1681	7.0–8.4(18H)m	5.84(1H)s	5.16(1H)s	4.98(1H)s	—	—	0.70, (3H)d; 0.58 (3H)d J = 6 Hz $(CH_3)_2CH$—	2.46–3.07(1H)m J = 6 Hz $(CH_3)_2CH$—
d	1677	7.0–8.4(17H)m	6.04(1H)s	5.30(1H)s	5.11(1H)s	—	2.37(3H)s CH_3	0.83(3H)d J = 6 Hz 0.72(3H)d J = 6 Hz $(CH_3)_2CH$—	2.61–3.65(1H)m $(CH_3)_2CH$
e	1684	7.0–8.5(17H)m	6.20(1H)s	5.53(1H)s	5.24(1H)s	—	—	0.83(6H)d J = 4.5 Hz $(CH_3)_2CH$—	2.76–3.12(1H)m $(CH_3)_2CH$—
f	1690	6.7–8.3(23H)m	5.68(1H)s	5.07(1H)s	4.73(1H)s	—	—	3.25–3.81(2H)m Ph—CH_2	—
g	1687	6.7–8.3(22H)m	5.13(1H)s	4.86 AB quartet	5.84 (J = 8 Hz)	—	2.36(3H)s CH_3	3.48–4.10(2H)m Ph—CH_2	—
h	1681	7.1–8.9(18H)m	6.09(1H)s	5.39(1H)s	5.13(1H)s	—	—	0.37–1.87(10H)m C_6H_{11}	—
i	1675	7.2–8.6(17H)m	6.07(1H)s	5.33(1H)s	5.08(1H)s	—	2.40(3H)s CH_3	0.58–1.90(10H)m C_6H_{11}	—
j	1680	7.2–8.6(18H)m	6.19(1H)s	5.50(1H)s	5.16(1H)s	—	—	0.49–1.91(10H)m C_6H_{11}	—
k	1681	7.0–8.5(17H)m	6.04(1H)s	5.35(1H)s	5.01(1H)s	—	—	0.25–1.80(10H)m C_6H_{11}	—
l	1693	7.2–8.3(17H)m	6.02(1H)s	5.43(1H)s	5.22(1H)s	—	—	0.30–1.90(10H)m C_6H_{11}	2.9–3.3(1H)m 1-cyclohexyl CH
m	1680	7.27–8.50(17H)m	6.06(1H)s	5.37(1H)s	5.13(1H)s	3.79(3H)s —OCH_3	—	0.48–1.81(10H)m C_6H_{11}	—
n	1674	6.70–8.60(17H)m	6.13(1H)s	5.33(1H)s	5.12(1H)s	—	3.92(3H)s —OCH_3	0.38–1.90(10H)m C_6H_{11}	

Can. J. Chem. Downloaded from www.nrcresearchpress.com by 210.87.254.40 on 09/05/12
For personal use only.

TABLE III

1-Cyclohexyl-2,4-diaryl-5-aroyl-3-(*N*-arylsulfonyl)-imidazolidines (**9**)

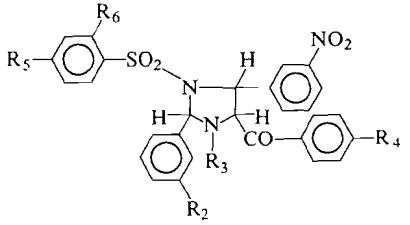

							Observed						Calculated					
No.	R_2	R_4	R_5	R_6	Melting point (°C)	Yield %	C	H	N	Cl	S	Imidazole fragment ion	C	H	N	Cl	S	Imidazole fragment ion
o	H	H	CH_3	H	Oil	13	68.96	6.10	6.86	—	5.00	451.1898	68.95	5.80	6.89	—	5.26	451.1896
p	H	H	Cl	NO_2	155–157	62	60.51	4.64	7.98	5.54	4.81	451.1898	60.45	4.63	8.30	5.25	4.75	451.1896
q	H	H	Cl	H	163–164	85	65.00	5.20	6.74	5.30	4.91	451.1903	64.80	5.11	6.67	5.60	5.09	451.1896
r	H	H	C≡N	H	181–182	72	67.86	4.98	9.31	—	5.05	515.1740*	67.72	5.20	9.03	—	5.00	515.1753
s	H	CH_3	Cl	NO_2	168–169	10.5	61.13	4.78	8.17	4.86	4.84	465.2046	60.99	4.83	8.13	5.15	4.65	465.2052
t	H	CH_3	C≡N	H	193–194	76.5	67.92	5.65	8.70	—	4.95	515.1740*	68.11	5.39	8.82	—	5.05	515.1753
u	H	NO_2	Cl	H	171.5–173	54.5	60.60	4.75	8.30	5.57	4.84	496.1748	60.47	4.63	8.30	5.25	4.75	496.1747
v	NO_2	H	C≡N	H	180–182	93	63.15	5.14	10.65	—	4.83	496.1753	63.14	4.70	10.52	—	4.82	496.1747
												560.1611*						560.1604

*Fragment ion corresponding to loss of 5-aroyl moiety.

Can. J. Chem. Downloaded from www.nrcresearchpress.com by 210.87.254.40 on 09/05/12
For personal use only.

TABLE IV

Spectroscopic properties of 1-cyclohexyl-2,4-diaryl-5-aroyl-3-*N*-aryl-sulfonylimidazolidines (**9**)

	Infrared	Nuclear magnetic resonance spectrum [$(CD_3)_2SO$]δ							
No.	(C=O) $CHCl_3$	Aryl protons	Ring proton 2	Ring proton 5	Ring proton 4	3-*N*-Aryl-sulfonyl substituent	5-Aroyl substituent	1-*N*-substituent	
o	1683	7.0–8.3(18H)m	6.10(1H)s	5.26(1H)s	5.02(1H)s	2.42(3H)s $CH_3C_6H_4SO_2$—	—	0.40–1.90 (10H) m C_6H_{11}	2.99–3.53 (1H) m $C_5H_{10}CH$—N
p	1682	7.1–8.5(17H)m	6.31(1H)s	5.53(1H)s	5.31(1H)s	—	—	0.36–2.02 (10H) m C_6H_{11}	—
q	1680	7.2–8.3(18H)m	5.97(1H)s	5.28(1H)s	4.95(1H)s	—	—	0.50–1.87 (10H) m C_6H_{11}	—
r	1677	7.1–8.5(18H)m	5.98(1H)s	5.27(1H)s	5.03(1H)s	—	—	0.33–1.83 (10H) m C_6H_{11}	—
s	1674	7.2–8.3(16H)m	6.02(1H)s	5.38(1H)s	5.13(1H)s	—	2.37(3H)s CH_3	0.50–1.93 (10H) m C_6H_{11}	—
t	1673	6.9–8.1(17H)m	5.90(1H)s	5.21(1H)s	4.89(1H)s	—	2.32(3H)s CH_3	0.24–1.66 (10H) m C_6H_{11}	—
u	1688	7.1–8.3(17H)m	5.90(1H)s	5.34(1H)s	4.91(1H)s	—	—	0.31–1.85 (10H) m C_6H_{11}	—
v	1690	7.2–8.4(17H)m	6.13(1H)s	5.42(1H)s	5.07(1H)s	—	—	0.37–1.81 (10H) m C_6H_{11}	—

TABLE V

Aryl-*N*-sulfonylimines

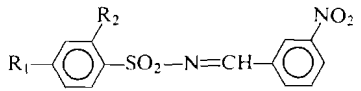

R_1	R_2	Melting point (°C)	Yield (%)	C	H	N	Cl	S	Molecular ion (found)	C	H	N	Cl	S	Molecular ion (calcd.)
CH_3	H	120–122	83*	55.18	4.22	8.81	—	10.75	304.0519	55.25	3.98	9.21	—	11.03	304.0518
Cl	NO_2	152.5–154	91†	42.20	2.40	11.37	9.92	9.03	368.9814	42.23	2.18	11.37	9.59	8.67	368.9807
Cl	H	163–164	81.5†	48.06	2.78	8.59	10.87	9.68	323.9972	48.08	2.80	8.63	10.92	9.87	323.9972
C≡N	H	136–137	57†	53.32	2.82	13.25	—	10.16	315.0310	53.32	2.88	13.32	—	10.16	315.0314

*From benzene/hexane.
†From ethyl acetate.

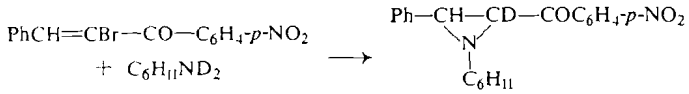

11

predict the orientation of addition on the basis of assignment of nucleophilic and electrophilic centers in the 1,3-dipole (19).

1-Cyclohexyl-3-deutero-2-phenyl-3-*p*-nitrobenzoylaziridine (**11**) was prepared by the reaction of 2-bromo-2-*p*-nitrobenzoyl-1-phenylethylene with cyclohexylamine-ND_2 in anhydrous ether. Examination of the integral of the aziridine ring protons in the n.m.r. spectrum showed, by comparison with the protium compound, about 50–60% deuterium incorporation at the 3-position.

Reaction of **11** with the sulfonylimine **3** gave an imidazolidine corresponding to **12** in structure.

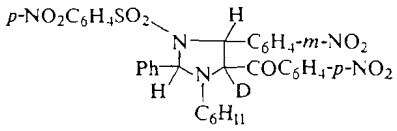

12

The n.m.r. spectrum of **12** showed a sharp singlet at 6.0 δ (1H), now assignable to the 2 proton; and two broad and weakly coupled singlets at 5.43 (0.75H) and 5.22(1H) δ now assigned unambiguously to the 5 and 4 imidazolidine ring protons respectively in **12**. An examination of several integrals showed an average of 24% deuterium incorporation in **12**.

The possible dependence of the course of the [2 + 3] cycloaddition on the stereochemistry of the aziridine was examined by reacting the *N*-sulfonylimine **3** in separate experiments with stereoisomerically pure samples of *cis*- and *trans*-3-benzoyl-1-cyclohexyl-2-*m*-nitrophenylaziridine.

In both cases the only product isolated in good yield was the imidazolidine **13**.

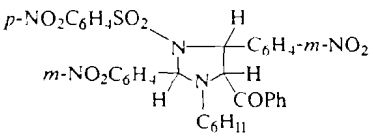

13

The n.m.r. spectrum showed a sharp singlet for the 2-imidazolidine proton at 6.04 δ and two broadened and weakly coupled singlets for the 4 and 5 protons at 5.01 and 5.35 δ respectively, and was therefore assigned the *trans* arrangement for the 4,5 protons because the small coupling constant is characteristic of *trans* coupling in a five membered ring (8).

Similarly reaction of *N*-(*m*-nitrobenzal)-*p*-cyanobenzenesulfonamide **5** with either *cis*- or *trans*-3-benzoyl-1-cyclohexyl-2-*m*-nitrophenylaziridine gave only the *trans* imidazolidine **14**.

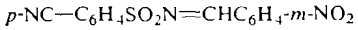

5

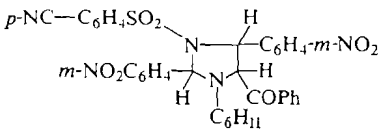

14

It seems probable that in these reactions, the [2 + 3] cycloaddition is stereospecific, but in the case of *cis*-imidazolidines is usually followed by post isomerization to the more stable *trans*-imidazolidine, as has been observed in other [2 + 3] cycloadditions with aziridines (1).

All the imidazolidines listed in Tables I and III which show small or zero 4,5 proton coupling have accordingly been assigned the *trans* configuration. The n.m.r. spectra of the imidazolidines obtained from *N*-benzyl and *N*-methylaziridines were different from the majority of the compounds listed in Tables I–IV, consisting of singlet at about 5.1 δ flanked by a strongly coupled AB quartet centered at ca. 4.9 and 5.8 δ with a coupling constant ($J \approx 8$ Hz) characteristic of *cis* vicinal proton coupling. An opposite orientation of addition of the azomethine ylids derived from these aziridines to the sulfonylimines was possible. Therefore 1-benzyl-3-deutero-2-phenyl-3-toluoylaziridine (**15**) was prepared as shown. Integration of the n.m.r. spectrum of **15** confirmed 71% deuterium incorporation in the 3-position of **15**. Reaction of **15** with the *N*-sulfonylimine **3** afforded an imidazolidine to which structure **16** was assigned unambiguously.

Can. J. Chem. Downloaded from www.nrcresearchpress.com by 210.87.254.40 on 09/05/12
For personal use only.

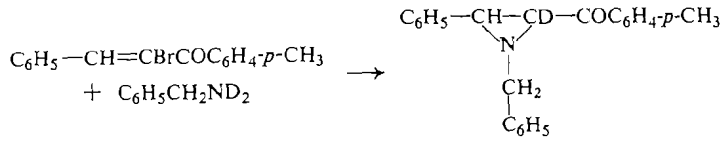

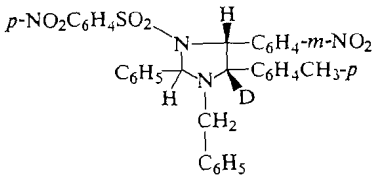

16

The n.m.r. spectrum of **16** showed a singlet at 5.13 (1H) δ and an AB quartet centered at 4.86(0.7H) and 5.84(1H) δ, $J = 8$ Hz, and integration confirmed 29% deuterium incorporation in the 5-position of **16**. Therefore the orientation of addition of all the *N*-sulfonylimines to the 3-aroylaziridines is the same. The exceptional line positions for the heterocycle **16** and similar compounds derived from *N*-methylaziridine is attributed to screening factors operating in *cis* 4,5 configuration of the imidazolidine ring.

Imidazolidines are rare in the chemical literature and very few general syntheses exist (20–23). The principal method of synthesis consists of reaction of aldehydes with 1,2 diamines.

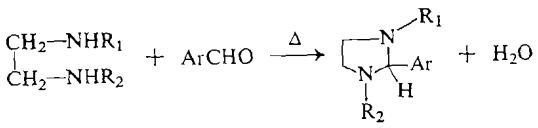

The [2 + 3] cycloaddition reactions described in this paper provide a convenient and versatile general synthesis of imidazolidines which nicely complements the existing routes in allowing for a wide variety of substituents in the imidazolidine ring.

Experimental

Melting points were determined on a Fisher–Johns apparatus and are uncorrected. Infrared spectra were recorded on a Perkin–Elmer model 421 spectrophotometer, and only the principal, sharply defined peaks are reported. Nuclear magnetic resonance spectra were recorded on Varian A-60 and A-100 analytical spectrometers. The spectra were measured on approximately 10–15% (w/v) solutions in $CDCl_3$, with tetramethylsilane as a standard. Line positions are reported in p.p.m. from the reference. Absorption spectra were recorded in 'spectro'-grade solvents on a Beckman DB recording spectrophotometer. Mass spectra were determined on an Associated Electrical Industries MS-9 double focussing high resolution mass spectrometer. The ionization energy, in general, was 70 eV. Peak measurements were made by comparison with perfluorotributylamine at a resolving power of 15 000. Kieselgel DF-5 (Camag, Switzerland) and Eastman Kodak precoated sheets were used for thin layer chromatography. Microanalyses were carried out by Dr. D. Daesslé, Organic Microanalysis Ltd., Montreal, Quebec and by Mrs. D. Mahlow of this department.

Reaction of 3-Benzoyl-1-isopropyl-2-phenylaziridine with Benzalaniline

A solution of 2.65 g (0.01 mole) of 3-benzoyl-1-isopropyl-2-phenylaziridine (16) and 1.81 g (0.01 mole) of benzalaniline in 15 ml of dry benzene was heated under reflux for 16 h when a deep orange color developed. The solution was passed down a column of Fisher alumina. Elution with benzene afforded one main fraction which upon evaporation of the solvent *in vacuo* gave a yellow gum, from which crystallized as a white powder, 5-benzoyl-1-isopropyl-2,3,4-triphenyl-(*cis*-4,5)-imidazolidine, 1.05 g (24% yield), m.p. 182°.

Anal. Calcd. for $C_{31}H_{30}N_2O$ (mol. wt. 446.2358): N, 6.27. Found (mol. wt. (mass spectrum) 446.2356): N, 6.20.

Infrared spectrum: ν_{max} (film): 1680 cm^{-1} (C=O). Nuclear magnetic resonance spectrum $\delta_{TMS}(CDCl_3)$: 0.85 and 1.15 (3H each, doublets $J = 6.5$ Hz, $(CH_3)_2CH$); 2.81–3.35 (1H, septet, $J = 6.5$ Hz, $(CH_3)_2CH$); AB quartet centered at 4.76 and 5.33 (2H, $J = 8$ Hz, 4 and 5 protons) 5.82 (1H, singlet, 2 proton); 6.60–8.40 (multiplet, 20H, aromatic protons).

A solution of 0.350 g (0.0008 moles) of 5-benzoyl-1-isopropyl-2,3,4-triphenylimidazolidine and 46 mg of potassium carbonate in a mixture of 10 ml of dry tetrahydrofuran and 3 ml of deuterium oxide was heated under reflux for 24 h, allowed to cool, and the organic material extracted with benzene. The combined extract was evaporated and the exchange process repeated with fresh deuterium oxide. Finally the recovered imidazolidine was purified by recrystallization from methanol m.p. 182°. An examination of the n.m.r. spectrum confirmed there had been no epimerization or deuterium incorporation.

Reaction of 3-p-Anisoyl-1-cyclohexyl-2-phenylaziridine with Benzalaniline

A solution of 3.35 g (0.01 mole) of 3-*p*-anisoyl-1-cyclohexyl-2-phenylaziridine (24) and 1.81 g (0.01 mole) of benzalaniline in 15 ml of dry benzene was heated under reflux for 48 h. The white solid which had precipitated 0.100 g (11% yield on the basis of unrecovered benzalaniline) was collected and purified by recrystallization from a large volume of benzene m.p. 182–184°, representing 5-*p*-anisoyl-1-cyclohexyl-2,3,4-triphenylimidazolidine.

Anal. Calcd. for $C_{35}H_{36}N_2O_2$ (mol. wt. 516.2777): C,

Can. J. Chem. Downloaded from www.nrcresearchpress.com by 210.87.254.40 on 09/05/12
For personal use only.

Can. J. Chem. Downloaded from www.nrcresearchpress.com by 210.87.254.40 on 09/05/12
For personal use only.

81.36; H, 7.03; N, 5.42. Found (mol. wt. (mass spectrum) 516.2773): C, 81.24; H, 6.96; N, 5.62.

Infrared spectrum ν_{max} ($CHCl_3$): 1677 cm^{-1} (C=O). Nuclear magnetic resonance spectrum $\delta_{TMS}(CDCl_3)$: 0.74–2.17 (10H, multiplet, cyclohexyl protons); 2.54–3.10 (1H, multiplet CH—N<); 3.73 (3H, singlet, —OCH_3); 5.51 (2H, singlet, 4,5 protons); 6.34 (1H, singlet, 2 proton); 6.38–7.80 (19H, multiplet, aromatic protons).

Preparation of Aryl-N-sulfonylimines

(i) m-Nitrobenzaldehyde Methyl Acetal

It was prepared in 85% yield by the method of Claisen (25), b.p. 139°/5 mm (lit. b.p. 145–146°/9 mm).

(ii) Preparation of N-(m-Nitrobenzal)-p-nitrobenzenesulfonamide

The following general method of preparation of this and similar aryl-*N*-sulfonylimines listed in Table V is due to Kresze *et al.* (18).

A mixture of 7.6 g (0.038 mole) of *p*-nitrobenzenesulfonamide and 8.2 g (0.042 mole) of *m*-nitrobenzaldehyde methyl acetal was heated to 150° until no more methanol was evolved. About 5 ml of 1:1 benzene/nitrobenzene mixture was added and the solution concentrated to ca. 20 ml and allowed to cool when the residue crystallized. The pure aryl-*N*-sulfonylimine was obtained by recrystallization from a 1:1 mixture of *o*-xylene and dimethylformamide in 84% yield, m.p. 212–214° (lit. 210–212° (18)).

General Method of Preparation of 1-Alkyl-2,4-diaryl-5-aroyl-3-(N-arylsulfonyl)-imidazolidines

The following experimental procedure is typical and was used to prepare all 22 imidazolidines listed in Tables I and III.

5-Benzoyl-1-cyclohexyl-3-(N-p-nitrobenzenesulfonyl)-4-m-nitrophenyl-2-phenylimidazolidine

A suspension of 1.53 g (0.005 mole) of 3-benzoyl-1-cyclohexyl-2-phenylaziridine and 1.68 g (0.005 mole) of *N*-(*m*-nitrobenzal)-*p*-nitrobenzenesulfonamide in 100 ml of dry benzene was stirred and heated under reflux for 24 h during which time the aryl-*N*-sulfonylimine gradually went into solution. The solvent was removed *in vacuo* and the residual yellow oil induced to crystallize as a pale yellow crystalline solid, 3.01 g (94% yield), m.p. 161–162°. The product was decolorised by treatment with charcoal in benzene and then purified by recrystallization from 3:2 hexane/benzene giving a white solid, m.p. 160–161°.

Anal. Calcd. for $C_{34}H_{32}N_4O_7S$: C, 63.74; H, 5.04; N, 8.74; S, 5.10. Found: C, 63.73; H, 5.09; N, 8.53; S, 5.40.

Mass spectrum calcd. for $C_{28}H_{25}N_3O_3$ (imidazole fragment ion): 451.1896. Found: 451.1898. Infrared spectrum ν_{max} ($CHCl_3$): 1681 cm^{-1} (C=O). Nuclear magnetic resonance spectrum δ_{TMS} ($(CD_3)_2SO$): 0.37–1.87 (10H, multiplet, cyclohexyl protons); 5.13 (1H, singlet, 4 proton); 5.39 (1H, singlet, 5 proton); 6.09 (1H, singlet, 2 proton); 7.1–8.7 (18H, multiplet, aromatic protons).

Preparation of 1-Cyclohexyl-2-phenyl-3-deutero-3-p-nitrobenzoylaziridine

(a) 2-Bromo-2-p-nitrobenzoyl-1-phenylethylene

A slurry of 4.13 g (0.01 mole) of 1,2-dibromo-1-phenyl-2-*p*-nitrobenzoylethane and 1.410 g (0.011 mole) of potassium acetate in 500 ml of 95% ethanol was heated under reflux for 12 h. The resulting pale yellow solution was evaporated to ca. 30 ml poured into 500 g of ice water and the organic material extracted with ether. The combined ether extract was dried ($MgSO_4$) and evaporated to give a pale yellow oil which readily solidified on cooling. Crystallization from benzene/heptane gave 2-bromo-2-*p*-nitrobenzoyl-1-phenylethylene, 2.1 g (63% yield), m.p. 108°.

Infrared spectrum ν_{max} ($CHCl_3$): 1670 (α,β unsaturated ketone) 1600 (C=C stretching); 1540 and 1350 cm^{-1} (aromatic —NO_2). Nuclear magnetic resonance spectrum $\delta_{TMS}(CDCl_3)$: 7.15 (singlet, 1H, —CH); 7.3–8.5 (multiplet, 9H, aromatic protons). Mass spectrum showed molecular ion at 331.

This material had previously been reported by Weygand as a pale yellow oil (26).

(b) Reaction of 2-Bromo-2-p-nitrobenzoyl-1-phenylethylene with Cyclohexylamine-ND_2

A solution of 2.495 g (0.05 mole) of redistilled dry cyclohexylamine (27) in 25 ml of anhydrous ether was shaken vigorously with 3 ml of deuterium oxide (99.97%), separated, and the ethereal layer washed with further quantities of deuterium oxide (5 × 1 ml), then removed and dried ($MgSO_4$). The ether solution was filtered directly into a dried ($MgSO_4$) solution of 1.66 g (0.005 mole) of 2-bromo-2-*p*-nitrobenzoyl-1-phenylethylene in 100 ml of ether. The mixture was stirred at room temperature for 24 h before being filtered to remove the precipitated cyclohexylamine hydrobromide 0.7 g; (78% of theoretical). The filtrate was washed with water and dried ($MgSO_4$). Evaporation of the ether gave a pale yellow oil which after trituration with hexane gave the solid aziridine 1.26 g (72% yield) pure enough for further use.

Mass spectrum: *m/e* 349 (3%); (undeuterated material $M-1$); *m/e* 350 (44%) (undeuterated material M); *m/e* 351 (40%) (deuterated material M'); *m/e* 352 (9%) (deuterated material, $M'+1$).

Nuclear magnetic resonance spectrum $\delta_{TMS}(CDCl_3)$: 1.0–2.0 (multiplet, 10H, cyclohexyl protons); 2.5 (multiplet, 1H, $C_5H_{10}CHN$); 3.2 and 3.55 (2 broad singlets 1.35 H; aziridine ring protons); 7.0–8.5 (multiplet, 9H, aromatic protons). The integral indicates about 60% deuterium incorporation of the 3 position.

Reaction between 1-Cyclohexyl-2-phenyl-3-deutero-3-p-nitrobenzoylaziridine and N-(m-Nitrobenzal)-p-nitrobenzenesulfonamide

Reaction of 0.329 g (0.93 mmole) of 1-cyclohexyl-2-phenyl-3-deutero-3-*p*-nitrobenzoylaziridine (containing about 60% deuterium incorporation) and 0.314 g (0.93 mmole) of *N*-(*m*-nitrobenzal)-*p*-nitrobenzenesulfonamide in the manner described in the general procedure above gave 1-cyclohexyl-5-deutero-3-(*N*-*p*-nitrobenzenesulfonyl)-4-*m*-nitrophenyl-5-*p*-nitrobenzoylimidazolidine in 41.3% yield, m.p. 160–161°. Examination of the n.m.r. spectrum showed the position and extent of deuterium incorporation. The product was identical in all other respects to the protium analogue listed in Table I.

Nuclear magnetic resonance spectrum: $\delta_{TMS}(CDCl_3)$: 0.30–1.90 (10H, multiplet, cyclohexyl protons); 2.9–3.3 (1H, multiplet, CH—N); 5.22 (1H broad singlet, 4-ring proton); 5.43 (0.7H, broad singlet, 5 ring proton); 6.02

Can. J. Chem. Downloaded from www.nrcresearchpress.com by 210.87.254.40 on 09/05/12
For personal use only.

(1H, sharp singlet, 2-ring proton); 7.2–8.3 (17H, multiplet, aromatic proton).

Averaging of 6 integrals confirmed 24–25% deuterium incorporation at position 5.

cis- and trans-3-Benzoyl-1-cyclohexyl-2-m-nitrophenylaziridines

A solution of 50 g (0.121 mole) of 3-*m*-nitrophenyl-2,3-dibromopropiophenone (28) in 500 ml of benzene at 0° was treated dropwise with stirring with a solution of 35.9 g (0.363 mole) of cyclohexylamine in 100 ml of benzene. The mixture was stirred at room temperature for 24 h, the precipitated cyclohexylamine hydrobromide was collected, and the filtrate washed with water (3 × 100 ml) and dried ($MgSO_4$). The solvent was evaporated and the residual oil treated with 50 ml of benzene and 100 ml of heptane and chilled when 6.5 g of *cis*-3-benzoyl-1-cyclohexyl-2-*m*-nitrophenylaziridine, m.p. 124–126° (17% yield), precipitated.

Anal. Calcd. for $C_{21}H_{22}N_2O_3$ (mol. wt. 350.1630): C, 72.00; H, 6.29; N, 8.00. Found (mol. wt. (mass spectrum) 350.1630): C, 71.70; H, 6.17; N, 8.02.

Infrared spectrum ν_{max} ($CHCl_3$): 1680 cm^{-1} (C=O of *cis* isomer). Nuclear magnetic resonance spectrum $\delta_{TMS}(CDCl_3)$: 1.00–2.05 (10H, multiplet, cyclohexyl); AB quartet centered at 3.44 and 3.24, $J = 7$ Hz (2H, *cis* 2,3 protons (30)); 7.2–8.3 (9H, multiplet, aromatic protons).

The filtrate from the above separation was treated with a further 100 ml of heptane and kept at 0° for 4 weeks when 17.5 g (41.4% yield) of *trans*-3-benzoyl-1-cyclohexyl-2-*m*-nitrophenylaziridine, m.p. 82–84°, was obtained.

Mol. wt. Calcd. for $C_{21}H_{22}N_2O_3$: 350.1630. Found (mass spectrum): 350.1630. Infrared spectrum ν_{max} ($CHCl_3$): 1663 cm^{-1} (C=O of *trans* isomer). Nuclear magnetic resonance spectrum $\delta_{TMS}(CDCl_3)$: 0.89–2.02 (10H, multiplet, cyclohexyl protons); 2.30–2.87 (1H, multiplet, CH—N); 3.64 (2H, singlet, *trans* 2,3 protons (30)); 7.3–8.3 (9H, multiplet, aromatic protons).

Reaction of N-(m-Nitrobenzal)-p-nitrobenzenesulfonamide with Stereoisomerically pure cis- and trans-3-Benzoyl-1-cyclohexyl-2-m-nitrophenylaziridines

(*a*) Reaction of 1.68 g (0.005 mole) of *N*-(*m*-nitrobenzal)-*p*-nitrobenzenesulfonamide and 1.75 (0.005 mole) of *cis*-3-benzoyl-1-cyclohexyl-2-*m*-nitrophenylaziridine in the manner described in the general procedure above gave 2.73 g (80% yield) of 5-benzoyl-1-cyclohexyl-2,4-di(*m*-nitrophenyl)-3(-*N*-*p*-nitrobenzenesulfonyl)-imidazolidine, m.p. 112–113°.

(*b*) A similar reaction of 1.68 g (0.005 mole) of *N*-(*m*-nitrobenzal)-*p*-nitrobenzenesulfonamide and 1.75 g (0.005 mole) of *trans*-3-benzoyl-1-cyclohexyl-2-*m*-nitrophenylaziridine gave the identical imidazolidine, 2.61 g (76.5% yield), m.p. 111–112°.

Reaction of N-(-m-Nitrobenzal)-p-cyanobenzenesulfonamide with Stereoisomerically pure cis- and trans-3-Benzoyl-1-cyclohexyl-2-m-nitrophenylaziridine

(*a*) Reaction of 1.662 g (0.0053 mole) of *N*-(*m*-nitrobenzal)-*p*-cyanobenzene sulfonamide and 1.846 g (0.0053 mole) of *cis*-3-benzoyl-1-cyclohexyl-2-*m*-nitrophenylaziridine in the manner described in the general procedure above gave 3.25 g (93% yield) of 5-benzoyl-3-(*N*-*p*-cyanobenzenesulfonyl)-1-cyclohexyl-2,4-di(*m*-nitrophenyl)-imidazolidine, m.p. 180–182°.

(*b*) A similar reaction of 0.784 g (0.0025 mole) of *N*-(*m*-nitrobenzal)-*p*-cyanobenzenesulfonamide and 0.871 g (0.0025 mole) of *trans*-3-benzoyl-1-cyclohexyl-2-*m*-nitrophenylaziridine gave the identical imidazolidine 1.257 g (68% yield), m.p. 180–182°.

Preparation of 1-Benzyl-3-deutero-3-p-toluoyl-2-phenylaziridine

A solution of 7.64 g (0.070 mole) of redistilled dry benzylamine in 70 ml of anhydrous ether was shaken vigorously with 9 ml of deuterium oxide (99.97%), separated, and the organic layer washed with further quantities of deuterium oxide (4 × 3 ml), then removed and dried ($MgSO_4$). The ether solution was filtered directly into a dried ($MgSO_4$) solution of 4.30 g (0.014 mole) of 2-bromo-2-*p*-toluoyl-1-phenylethylene (26) in 200 ml of ether. The mixture was stirred at room temperature for 24 h before being filtered to remove the precipitated benzylamine hydrobromide ca. 1 g. The filtrate was washed with water and dried ($MgSO_4$). Evaporation of the ether gave a yellow oil which upon trituration with 2:1 heptane/benzene gave 1-benzyl-3-deutero-3-*p*-toluoyl-2-phenylaziridine 2.105 g (45% yield), m.p. 108–110° (lit. (29) m.p. 113–114°). Examination of the n.m.r. spectrum showed the position and extent of deuterium incorporation. The aziridine was identical in all other respects to the protium compound.

Nuclear magnetic resonance spectrum $\delta_{TMS}(CDCl_3)$: 2.30 (3H, singlet, aryl CH_3); 3.30 (1.3H, multiplet, aziridine ring protons). AB quartet centered at 3.73 and 4.05, $J = 14$ Hz (2H, $PhCH_2$); 7.0–8.0 (14H, multiplet, aromatic protons). Averaging of integrations confirmed 71% deuterium incorporation in position 3.

Reaction between 1-Benzyl-3-deutero-3-p-toluoyl-2-phenylaziridine and N-(m-Nitrobenzal)-p-nitrobenzenesulfonamide

Reaction of 0.290 g (0.89 mmole) of 1-benzyl-3-deutero-3-*p*-toluoyl-2-phenylaziridine (71% deuterium incorporation) and 0.300 g (0.89 mmole) of *N*-(*m*-nitrobenzal)-*p*-nitrobenzene sulfonamide in the manner described in the general procedure above gave 1-benzyl-5-deutero-3-(*N*-*p*-nitrobenzenesulfonyl)-4-*m*-nitrophenyl-5-*p*-toluoylimidazolidine, 0.231 g (39.3% yield), m.p. 160°. Examination of the n.m.r. spectrum showed the position and extent of deuterium incorporation. The product was identical in all other respects to the protium analogue listed in Table I.

Nuclear magnetic resonance spectrum: δ_{TMS} ($(CD_3)_2SO$): 2.36 (3H, singlet, aryl CH_3); 3.48–4.10 (2H, quartet, $J = 15$ Hz, $PhCH_2$); AB quartet centered at 4.86 (0.7H) and 5.84 (1H), $J = 8$ Hz, (now assigned unambiguously to the 5 and 4 imidazolidine ring protons respectively); 5.13 (1H, singlet, 2 proton); 6.7–8.3 (22H, multiplet, aromatic protons). Averaging of the integrations confirmed 29% deuterium incorporation in position 5.

Acknowledgments

This research was supported by a National

Research Council of Canada grant to J. W. Lown. We thank Mr. R. Swindlehurst and Dr. A. Hogg for the n.m.r. and mass spectra.

1. P. B. WOLLER and N. H. CROMWELL. J. Heterocycl. Chem. **5**, 579 (1968).
2. H. W. HEINE and R. PEAVY. Tetrahedron Lett. 3123 (1965).
3. B. K. CAMPBELL and K. N. CAMPBELL. J. Org. Chem. **9**, 178 (1944).
4. R. HUISGEN, W. SCHEER, G. SZEIMIES, and H. HUBER. Tetrahedron Lett. 397 (1966).
5. G. H. COLEMAN and G. P. WAUGH. Proc. Iowa State Acad. Sci. **40**, 115 (1933); Proc. Iowa State Acad. Sci. **49**, 286 (1942).
6. A. PADWA and L. HAMILTON. Tetrahedron Lett. 4363 (1965).
7. VON R. V. CAPELLER, R. GRIOT, M. HARING, and T. WAGNER-JAUREGG. Helv. Chim. Acta, **40**, 1652 (1957).
8. H. W. HEINE, R. E. PEAVY, and A. J. DURBETAKI. J. Org. Chem. **31**, 3924 (1966).
9. H. W. HEINE, A. B. SMITH, and J. D. BOWER. J. Org. Chem. **33**, 1097 (1968).
10. A. PADWA and L. HAMILTON. J. Heterocycl. Chem. **4**, 118 (1967).
11. A. PADWA and W. EISENHARDT. Chem. Commun. **7**, 380 (1968).
12. R. HUISGEN, W. SCHEER, and H. HUBER. J. Amer. Chem. Soc. **89**, 1753 (1967).
13. S. OIDA and E. OHKI. Chem. Pharm. Bull. (Tokyo). **16**, 764 (1968).
14. H. W. HEINE and R. HENZEL. J. Org. Chem. **34**, 171 (1969).
15. J. W. LOWN, R. K. SMALLEY, and G. DALLAS. Chem. Commun. 1543 (1968).
16. J. W. LOWN, G. DALLAS, and T. W. MALONEY. Can. J. Chem. **47**, 3557 (1969).
17. G. KRESZE and R. ALBRECHT. Chem. Ber. **97**, 490 (1964).
18. G. KRESZE, R. ALBRECHT, and B. MLAKAR. Chem. Ber. **97**, 483 (1964).
19. R. HUISGEN. Angew. Chem. Int. Ed. Engl. **2**, 565 (1963).
20. R. J. FERM and J. L. RIEBSOMER. Chem. Rev. **54**, 593 (1954).
21. K. HOFMANN. *In* Imidazole and its derivatives. The chemistry of heterocyclic compounds. *Editor* A. Weissberger, Interscience Publishers, Inc., New York. 1953. p. 242.
22. E. S. SCHIPPER and A. R. DAY. *In* Heterocyclic compounds. *Editor* R. C. Elderfield. Vol. 5. John Wiley and Sons, Inc., New York. 1957. p. 245.
23. R. M. ACHESON. An Introduction to the Chemistry of Heterocyclic Compounds. 2nd ed. Interscience Publishers, Inc., New York. 1967. p. 308.
24. J. W. LOWN, R. K. SMALLEY, G. DALLAS, and T. W. MALONEY. Can. J. Chem. In press.
25. L. CLAISEN. Chem. Ber. **31**, 1016 (1898).
26 C. WEYGAND. Ann. Chem. **459**, 99 (1928).
27. D. B. DENNEY and M. A. GREENBAUM. J. Amer. Chem. Soc. **79**, 3701 (1957).
28. E. SORGE. Chem. Ber. **35**, 1068 (1902).
29. N. H. CROMWELL and H. HOEKSEMA. J. Amer. Chem. Soc. **71**, 708 (1949).
30. A. E. POHLAND, R. C. BADGER, and N. H. CROMWELL. Tetrahedron Lett. 4369 (1965).

Can. J. Chem. Downloaded from www.nrcresearchpress.com by 210.87.254.40 on 09/05/12
For personal use only.

Can. J. Chem. Downloaded from www.nrcresearchpress.com by 210.87.254.6 on 09/05/12
For personal use only.

Alkoxycarbenes from the thermolysis of silyl ketals

A. G. Brook and P. J. Dillon
Department of Chemistry, University of Toronto, Toronto 181, Ontario

Received June 13, 1969

It is shown that α,α-dimethoxybenzylsilanes thermally rearrange to give methoxysilanes and phenylmethoxycarbene; the latter species has been trapped by a variety of reagents. The rearrangement involves retention of configuration at an asymmetric silicon center. While α,α-dimethoxyethylsilanes eliminate methanol when heated, methoxybenzhydrylsilanes rearrange to methoxysilane and diphenylcarbene but monomethoxybenzylsilanes or 2-silyldioxolanes do not thermally rearrange up to 250°.

Canadian Journal of Chemistry, 47, 4347 (1969)

The thermolysis of methoxypolysilanes has been reported to produce divalent organosilicon (silylene) species (1,2). It seemed possible that

$$MeOSiMe_2—(SiMe_2)_n—SiMe_2OMe \xrightarrow{\Delta} MeOSiMe_2—(SiMe_2)_n—OMe + :SiMe_2$$

α-alkoxyalkylmonosilanes might similarly undergo this sort of reaction to produce carbenes, and indeed, since this work was completed, Atwell *et al.* have reported such behavior on thermolysis of (dimethoxymethyl)trimethoxysilane (3).

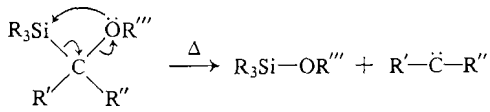

α-Alkoxyalkylsilanes are generally difficult to synthesize, but a convenient source was found to be the ketals **1** of acylsilanes, which could be prepared either from the dithiane precursors (4,5) of the acylsilanes by reaction in methanol over several days with a mixture of mercuric

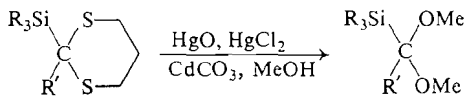

1

a R_3Si = Ph_3Si; R′ = Ph
b R_3Si = Ph_3Si; R′ = Me
c R_3Si = (+)-1-NpPhMeSi; R′ = Ph

chloride, mercuric oxide, and anhydrous cadmium carbonate, or from the dioxolanes **2**,

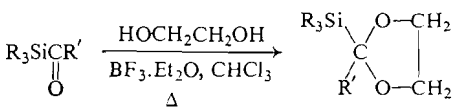

2

a R_3Si = Ph_3Si; R′ = Ph
b R_3Si = Ph_3Si; R′ = Me

prepared from the acylsilanes and ethylene glycol in hot chloroform containing boron trifluoride etherate.

Attempts to prepare simple ketals using boron trifluoride etherate and alcohols were not successful. Details of the compounds prepared will be found in the Experimental section.

While the dioxolanes of acetyl and benzoyltriphenylsilane were thermally stable to at least 250°, it was found that the dimethoxy ketals, when pyrolyzed at 150–200°, readily decomposed in one of two ways. Where there was hydrogen α to the carbon bearing the alkoxy groups, e.g. **1***b*, methanol was thermally eliminated and an enol ether was formed. This type of reaction has been

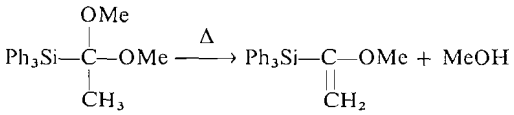

1*b*

observed previously (6). However, with α,α-dimethoxybenzylsilanes, which lack α-hydrogen, the thermolysis gave high yields of alkoxysilane, consistent with the elimination of an alkoxycarbene. Subsequent studies were devoted to

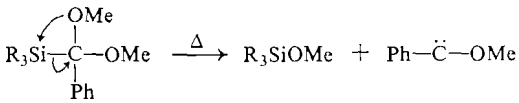

demonstrating the formation of the carbene by carrying out the thermolysis in the presence of suitable carbene traps.

When α,α-dimethoxybenzyltriphenylsilane (**1***a*) was heated at 170° in the presence of diphenylacetylene, 1-methoxy-1,2,3-triphenylcyclopropene (**3**) was evidently formed since the reaction product, when treated with gaseous

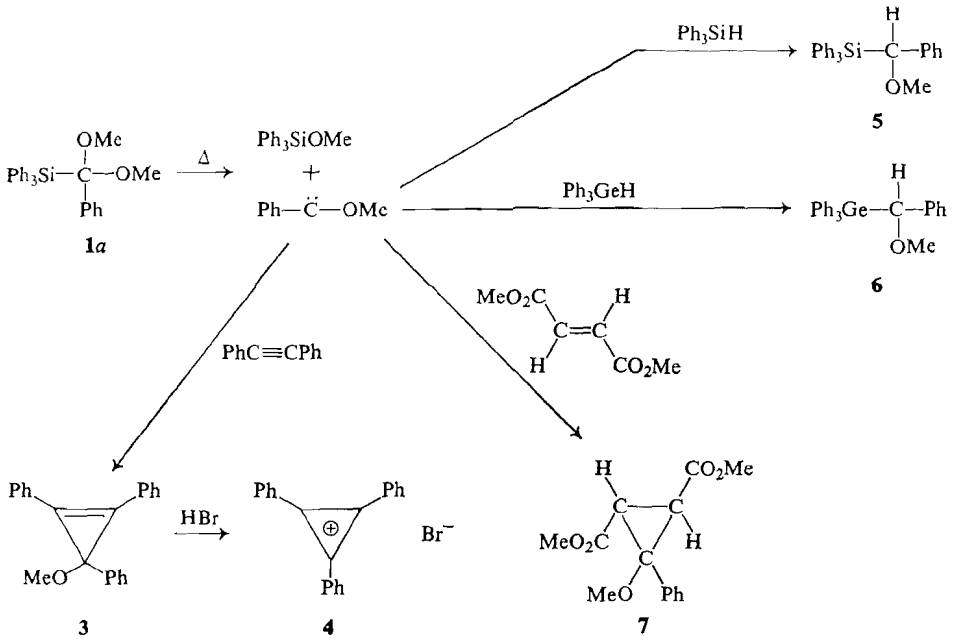

hydrogen bromide, gave triphenylcyclopropenium bromide (**4**) (7). The relatively low yield of **4** is probably due to a competitive thermal decomposition since no **4** was obtained when the thermolysis was carried out at 190°.

When the dimethoxy compound **1***a* was heated to 190° in the presence of about two equivalents of triphenylsilane, a 61% yield of α-methoxybenzyltriphenylsilane (**5**) was obtained; similarly, when heated in the presence of triphenylgermane, α-methoxybenzyltriphenylgermane (**6**) was isolated in 75% yield.

Finally, when **1***a* was heated in dimethyl fumarate, triphenylmethoxysilane and a compound believed to be the substituted cyclopropane **7** were obtained, the latter in 55% yield. The nuclear magnetic resonance (n.m.r.) spectrum of this compound showed two 1-proton doublets ($J = 3$ c.p.s.) at δ 2.88 and 2.90 p.p.m. attributable to the diastereotopic *trans* hydrogens, and three 3-proton singlets at δ 3.01, 3.40, and 3.70 p.p.m., corresponding to the methoxy group and the two diastereotopic methyl ester functions. There was no evidence for the formation of the *cis*-cyclopropane derivative.

These results are consistent with a thermal rearrangement of the α,α-dimethoxybenzylsilane resulting in the formation of triphenylmethoxysilane and phenylmethoxycarbene, which subsequently inserts either into a multiple bond or into an Si—H or Ge—H bond. Studies by Seyferth *et al.* have demonstrated the susceptibility of Si—H and Ge—H bonds toward insertion by dihalocarbenes (8) and the insertion of electronegatively-substituted carbenes into multiple bonds is also well-documented (9). The rearrangement closely parallels the known thermal rearrangements of silanecarboxylate and germanecarboxylate esters in which an alkoxysilane or -germane and carbon monoxide are formed (10,11).

$$R_3M{-}\overset{\overset{O}{\|}}{C}{-}OMe \xrightarrow{\Delta} R_3MOMe + :CO \qquad M = Si, Ge$$

It appeared to be of interest to establish the stereochemistry of the rearrangement at an asymmetric silicon atom. When optically active (+)-α,α-dimethoxybenzyl-1-naphthylphenylmethylsilane of known absolute configuration[1] and assumed 100% optical purity was thermally rearranged, the (−)-1-naphthylphenylmethyl-

[1]The absolute configuration of the dithiane precursor and hence of the α,α-dimethoxy compound is known both from its method of formation from (−)-R_3Si^*—Cl with 2-lithio-2-phenyl-1,3-dithiane (inversion) and also from the known configuration of its hydrolysis product (+)-benzoyl-1-naphthylphenylmethylsilane, established previously (12,13).

Can. J. Chem. Downloaded from www.nrcresearchpress.com by 210.87.254.6 on 09/05/12
For personal use only.

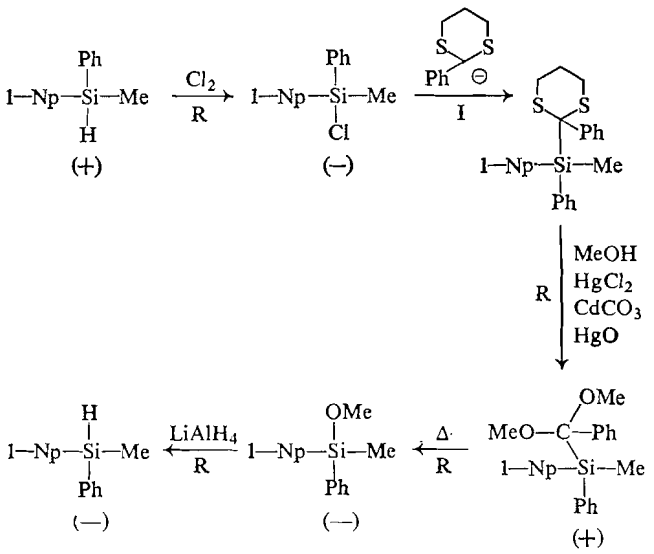

R = retention; I = inversion

methoxysilane of known configuration (14), obtained in 87% yield, was 95% optically pure indicating that the reaction had occurred with high stereospecificity and involved retention of configuration at silicon as anticipated for a 1,2-rearrangement of this type.

Compared to dimethoxyalkylsilanes, monomethoxy compounds appear to rearrange much less readily. Thus α-methoxybenzyltriphenylsilane was formed at 190° from the reaction of phenylmethoxycarbene with triphenylsilane with little evidence of further reaction, and even when heated at 250° for 4 days, while some decomposition occurred, there was no evidence of triphenylmethoxysilane formation. Similarly, after being heated at 315° for 45 min, starting material was recovered in good yield. However, when α-methoxybenzhydrylmethyldiphenylsilane, prepared by refluxing a solution of the corresponding bromide in methanol–carbon tetrachloride, was heated to 250° in the presence of air, methyldiphenylmethoxysilane and benzophenone were formed, suggesting rearrangement of the compound to methoxysilane and diphenylcarbene; the reaction of diphenylcarbene with oxygen to form benzophenone is well known (15).

$$Ph_2MeSi—CPh_2OMe \xrightarrow{\Delta} Ph_2MeSiOMe + Ph_2C: \xrightarrow{O_2} Ph_2CO$$

This rearrangement is not likely to prove a very useful route to carbenes because of the relatively high temperatures involved but we are investigating its utility for substituted cyclopropane synthesis. However, it is another interesting example of a now common type of rearrangement like the silylcarbinol to silyl ether rearrangement (16) or the acylsilane to siloxycarbene photochemical interconversion (17) which involves, with retention stereochemistry, the formation of a silicon–oxygen bond and the cleavage of a silicon–carbon bond.

The fact that dimethoxyalkylsilanes rearrange much more readily than the monoalkoxysilane may be explained, at least in part, by the anticipated extra stability of methoxyphenylcarbene relative to phenylcarbene because of the possibility of sharing lone pair electrons on oxygen with the carbenoid carbon (18).

$$Ph—\ddot{C}—\ddot{O}—Me \longleftrightarrow Ph—\overset{-}{\ddot{C}}=\overset{+}{O}—Me$$

Experimental

Preparation of α,α-Dimethoxybenzyltriphenylsilane (1a)

In a typical experiment, 3.4 g (7.5 mmoles) of 2-triphenylsilyl-2-phenyl-1,3-dithiane, 8.1 g (37.5 mmoles) of mercuric oxide, 4.05 g (15 mmoles) of mercuric chloride, 3.9 g (22.5 mmoles) of anhydrous cadmium carbonate, and 175 ml of methanol were refluxed under an atmosphere of dry nitrogen for 84 h. Filtration, evaporation, and recrystallization from hexane gave 2.53 g (83%) of a white solid, m.p. 163–163.5 °C, with the following spectral data: n.m.r. (CCl_4) δ 3.23 (6H singlet), 7–8 p.p.m.

Can. J. Chem. Downloaded from www.nrcresearchpress.com by 210.87.254.6 on 09/05/12
For personal use only.

(20H multiplet); infrared (i.r.) (CCl_4) 3.52 (—OMe), 6.90 (C—Ph), 7.00, 9.05 μ(Si—Ph).

Anal. Calcd. for $C_{27}H_{26}O_2Si$: C, 78.98; H, 6.38. Found: C, 79.42; H, 6.46.

Preparation of (+)-α,α-Dimethoxybenzyl-1-naphthylphenylmethylsilane (1c)

This compound was prepared in an analogous manner to the above. The product was recrystallized several times from hexane to give a colorless solid, m.p. 135.5–136.5°, $[\alpha]_D^{25} = 46.1°$ (*c* 6.83, chloroform); n.m.r. (CCl_4) δ 0.73 (3H singlet), 3.22 (3H singlet), 3.27 (3H singlet), 6.8–8.0 p.p.m. (17H multiplet); i.r. (CCl_4) 3.52 (—OMe), 6.92 (C—Ph), 7.00, 9.05 μ (Si—Ph).

Anal. Calcd. for $C_{26}H_{26}O_2Si$: C, 78.35; H, 6.58. Found: C, 78.50; H, 6.59.

Preparation of α,α-Dimethoxyethyltriphenylsilane (1b)

This compound was prepared at room temperature but in an otherwise identical manner. Work-up gave a compound, m.p. 113–114°, that was very susceptible to hydrolysis and thermolysis. The n.m.r. (CCl_4) δ 1.41 (3H singlet), 3.19 (6H singlet), 7–8 p.p.m. (15H multiplet); i.r., 3.50 (—OMe), 7.00, 9.05 μ (Si—Ph). Since recrystallization led to partial decomposition, an accurate analysis could not be obtained.

Preparation of 2-Triphenylsilyl-2-phenyl-1,3-dioxolane (2a)

Benzoyltriphenylsilane (1.25 g, 3.42 mmoles) and 10 ml of ethylene glycol were added in 25 ml of chloroform to a refluxing solution of 5 ml of boron trifluoride etherate in 50 ml of chloroform. After 1 h, the mixture was extracted with 5% hydrochloric acid, dried over anhydrous magnesium sulfate, filtered, evaporated under reduced pressure, and the resulting solid was recrystallized from hexane to give 1.20 g (86%) of product, m.p. 212–213°; n.m.r. (CCl_4) δ 3.5–4.0 (4H multiplet), δ 7.1–7.7 p.p.m. (20H multiplet); i.r. (CCl_4) 6.90 (C—Ph), 7.00, 9.05 μ (Si—Ph).

Anal. Calcd. for $C_{27}H_{24}O_2Si$: C, 79.37; H, 5.93. Found: C, 79.06; H, 5.91.

Preparation of 2-Triphenylsilyl-2-methyl-1,3-dioxolane (2b)

This compound was prepared analogously to the 2-phenyl compound, using acetyltriphenylsilane in place of benzoyltriphenylsilane: m.p. 138–139.5°; n.m.r. (CCl_4) δ 1.35 (3H singlet), 3.4–4.0 (4H multiplet), 7.1–7.8 p.p.m. (15H multiplet).

Anal. Calcd. for $C_{22}H_{22}O_2Si$: C, 76.26; H, 6.40. Found: C, 76.00; H, 6.41.

Thermolysis of α,α-Dimethoxybenzyltriphenylsilane with Triphenylsilane

In a typical experiment, 0.494 g (1.2 mmoles) of **1***a* was heated at 190° with 0.59 g (2.3 mmoles) of triphenylsilane for 27 min. Chromatography of the reaction mixture on silica gel and elution with carbon tetrachloride gave triphenylmethoxysilane (91%), identified by spectrum and mixture melting point while benzene elution yielded α-methoxybenzyltriphenylsilane (**5**). Recrystallization from methanol gave a 61% yield of product, m.p. 148.5–149.5°. The mixture melting point with an authentic sample (19) was not depressed; n.m.r. (CCl_4) δ 3.30 (3H singlet), 4.65 (1H singlet), 7–8 p.p.m. (20H multiplet).

Anal. Calcd. for $C_{26}H_{24}OSi$: C, 82.06; H, 6.36. Found: C, 81.79; H, 6.46.

Thermolysis of α,α-Dimethoxybenzyltriphenylsilane in Triphenylgermane

Thermolysis of 0.37 g (0.9 mmole) of α,α-dimethoxybenzyltriphenylsilane in 0.27 g (0.9 mmole) of triphenylgermane gave 0.23 g (86%) of triphenylmethoxysilane and 0.29 g (75%) of α-methoxybenzyltriphenylgermane (**6**), m.p. 144–145°; n.m.r. (CCl_4) δ 3.30 (3H singlet), 4.85 (1H singlet), 7–8 p.p.m. (20H multiplet).

Anal. Calcd. for $C_{26}H_{24}OGe$: C, 73.47; H, 5.69. Found: C, 73.33; H, 5.72.

Thermolysis of α,α-Dimethoxybenzyltriphenylsilane with Diphenylacetylene

A mixture of 0.34 g (0.8 mmole) of **1***a* and 0.15 g (0.8 mmole) of diphenylacetylene was heated under nitrogen at 170° for 25 min. The crude melt, whose n.m.r. spectrum showed strong signals at δ 3.58 p.p.m. (Ph_3SiOMe) and 3.31 p.p.m. (methoxytriphenylcyclopropene?) was then dissolved in diethyl ether and HBr gas was bubbled into the solution. The white precipitate was collected to give 0.08 g (29%) of triphenylcyclopropenium bromide, **4**, m.p. 269.5–272°, (lit. (6) 269–271°), whose ultraviolet (u.v.) spectrum was very similar to that previously reported: u.v. (95% EtOH) λ_{max} 317 (ε 24 600), 302 (30 400), 287 (24 200), 230 (32 800), and 223 mμ (36 400). Triphenylmethoxysilane (0.18 g, 75%) was recovered by chromatography of the filtrate. Attempts to isolate the proposed cyclopropene intermediate were unsuccessful.

Thermolysis of α,α-Dimethoxybenzyltriphenylsilane with Dimethyl Fumarate

A mixture of 1.25 g (3.0 mmoles) of **1***a* and 0.44 g (3.0 mmoles) of dimethyl fumarate was heated at 185° for 30 min. Separation of the triphenylmethoxysilane (0.78 g, 89%), unreacted fumarate, and cyclopropyl product was accomplished by column chromatography (silica gel column, and elution with carbon tetrachloride, then benzene, and finally chloroform–benzene, 1:1), followed by fractional distillation. The carbene-trapped product was then recrystallized from carbon tetrachloride–hexane to give 0.44 g (55%) of a white solid, m.p. 76–77°; n.m.r. (CCl_4) δ 2.88, 2.90, $J = 3$ c.p.s. (two doublets for the two *trans* hydrogens) 3.01 (3H singlet), 3.40 (3H singlet), 3.70 (3H singlet), 7.32 (5H multiplet); i.r. (CCl_4) 3.51 (—OMe), 5.76 (ester carbonyl), 6.90 μ (C—Ph).

Anal. Calcd. for $C_{14}H_{16}O_5$: C, 63.63; H, 6.10. Found: C, 63.26; H, 6.15.

Thermolysis of α,α-Dimethoxyethyltriphenylsilane

A 0.20 g sample of **1***b* (0.58 mmole) was heated at 140° for 7 min. After pumping to dryness, a white solid, 1-triphenylsilyl-1-methoxyethene, m.p. 118–121° was obtained quantitatively; n.m.r. (CCl_4) δ 3.56 (3H singlet), 4.40 (1H doublet, $J = 2$ c.p.s.), 4.89 (1H doublet, $J = 2$ c.p.s.) 7.1–8 p.p.m. (15H multiplet); i.r. (CCl_4) 3.50 (—OMe), 7.00, 9.03 (Si—Ph), 11.20 μ (C=C).

Anal. Calcd. for $C_{21}H_{20}OSi$: C, 79.70; H, 6.37. Found: C, 79.65; H, 6.28.

Can. J. Chem. Downloaded from www.nrcresearchpress.com by 210.87.254.6 on 09/05/12
For personal use only.

Thermolysis of (+)-α,α-Dimethoxybenzyl-1-naphthylphenylmethylsilane

Thermolysis of 0.55 g (1.4 mmoles) of **1***c* ($[\alpha]_D^{25}$ = 46.1° (*c* 6.83, $CHCl_3$)) at 200° for 90 min gave a reaction mixture that was chromatographed on silica gel to give 0.34 g (89%) of pure (−)-1-naphthylphenylmethylmethoxysilane, $[\alpha]_D^{25} = -16.4°$ (*c* 4.70, pentane), [lit. (14) $[\alpha]_D^{25} = -17.2°$ (pentane)]. No attempt was made to isolate other products.

Thermolysis of α-Methoxybenzyltriphenylsilane

A small sample (0.05 g, 0.13 mmole) of α-methoxybenzyltriphenylsilane was heated at 240° for 65 h. An n.m.r. spectrum showed that starting material remained as well as some decomposition products; there was no evidence of formation of triphenylmethoxysilane. A similar experiment at 315° for 45 min showed that very little of the starting material had decomposed, and that again, no triphenylmethoxysilane was formed.

Preparation of α-Methoxybenzhydrylmethyldiphenylsilane

A solution of 2.0 g (4.5 mmoles) of bromobenzhydrylmethyldiphenylsilane in 40 ml of methanol and 60 ml of carbon tetrachloride was refluxed for 2 h. Partial evaporation and cooling gave 1.3 g (72%) of white solid, m.p. 149°; n.m.r. ($CDCl_3$) δ 0.35 p.p.m. (3H singlet), 3.05 p.p.m. (3H singlet), 7–8 p.p.m. (20H multiplet); i.r. ($CHCl_3$), 3.51 μ (—OMe).

Anal. Calcd. for $C_{27}H_{26}OSi$: C, 82.23; H, 6.59. Found: C, 82.10; H, 6.24.

Thermal Rearrangement of α-Methoxybenzhydrylmethyldiphenylsilane

A 2.0 g sample of compound was heated in a sealed tube containing air at 250° for 18 h. The crude brown liquid product showed the following spectral data: n.m.r. ($CDCl_3$) δ 0.55 p.p.m., 3.45 p.p.m. (ratio 1:1) 7–8 p.p.m. (multiplets); i.r. ($CHCl_3$) 3.53 (—OMe), 6.01 μ (C=O).

When the experiment was repeated in an open tube while oxygen was bubbled into the molten material, the i.r. band at 6.01 μ was stronger. Treatment of 1 g of the reaction product with 0.5 g of 2,4-dinitrophenylhydrazine in 15 ml of DMSO gave after 2 h 0.2 g of crude phenylhydrazone which after recrystallization gave 0.1 g of benzophenone-2,4-dinitrophenylhydrazone, m.p. and mixture m.p. 242–244°.

Methyldiphenylmethoxysilane (20)

To 5.8 g (25 mmoles) of methyldiphenylchlorosilane in 30 ml dry ether were added 1.5 g of methanol and 2.8 g of pyridine. After 1 h stirring, and filtration of the insoluble pyridine hydrochloride, the solution was distilled to yield 4.4 g (76%) of methyldiphenylmethoxysilane, b.p. 80° at 5 mm; n.m.r. ($CDCl_3$) δ 0.55 p.p.m. (3H, singlet), 3.45 p.p.m. (3H, singlet), 7–8 p.p.m. (10H, multiplet); i.r. (CCl_4) 3.53 μ.

Acknowledgments

This research was supported by the National Research Council of Canada. We are indebted to Dr. Geoffrey Chivers for assistance.

1. W. H. Atwell and D. R. Weyenberg. J. Amer. Chem. Soc. **90**, 3438 (1968).
2. W. H. Atwell and D. R. Weyenberg. J. Organometal. Chem. **5**, 594 (1966).
3. W. H. Atwell, D. R. Weyenberg, and J. G. Uhlmann. J. Amer. Chem. Soc. **91**, 2025 (1969).
4. A. G. Brook, J. M. Duff, P. F. Jones, and N. R. Davis. J. Amer. Chem. Soc. **89**, 431 (1967).
5. E. J. Corey, D. Seebach, and R. Freedman. J. Amer. Chem. Soc. **89**, 434 (1967).
6. A. Johannissian and E. Akunian. Bull. Univ. Etat R.S.S. Arménie, **5**, 245 (1930); Chem. Abstr. **25**, 921 (1931).
7. R. Breslow and C. Yuan. J. Amer. Chem. Soc. **80**, 5991 (1958).
8. D. Seyferth, R. Damrauer, J. Yick-Pui Miu, and T. Jula. J. Amer. Chem. Soc. **90**, 2944 (1968).
9. W. Kirmse. Carbene chemistry. Academic Press, London. 1964.
10. A. G. Brook. J. Amer. Chem. Soc. **77**, 4827 (1955).
11. A. G. Brook and H. Gilman. J. Amer. Chem. Soc. **76**, 77 (1954).
12. A. G. Brook and W. W. Limburg. J. Amer. Chem. Soc. **85**, 832 (1963).
13. A. G. Brook, C. M. Warner, and W. W. Limburg. Can. J. Chem. **45**, 1231 (1967).
14. L. Sommer and H. Fujimoto. J. Amer. Chem. Soc. **90**, 982 (1968).
15. W. Kirmse, L. Horner, and H. Hoffmann. Ann. **618**, 19 (1958).
16. A. G. Brook, G. E. Legrow, and D. M. MacRae. Can. J. Chem. **45**, 239 (1967).
17. A. G. Brook and J. M. Duff. J. Amer. Chem. Soc. **89**, 454 (1967).
18. R. Gleiter and R. Hoffmann. J. Amer. Chem. Soc. **90**, 5457 (1968).
19. A. G. Brook and D. G. Anderson. Unpublished studies.
20. J. W. Ryan. J. Amer. Chem. Soc. **84**, 47 (1962).

Can. J. Chem. Downloaded from www.nrcresearchpress.com by 210.87.254.6 on 09/05/12
For personal use only.

Can. J. Chem. Downloaded from www.nrcresearchpress.com by 210.87.254.105 on 09/05/12
For personal use only.

The synthesis of silyl- and germyldiazoalkanes via tosylhydrazones

A. G. Brook and Peter F. Jones
Lash Miller Chemical Laboratories, University of Toronto, Toronto 181, Ontario, Canada

Received December 27, 1968

Tosylhydrazones have been prepared from acylsilanes and -germanes. These may be converted in excellent yield by *n*-butyllithium to the metalloidal diazoalkanes under milder conditions than are required for the analogous carbon compounds. The diazoalkanes are far more stable than their carbon counterparts. These results, together with spectral shifts noted for the silyl and germyl compounds, are interpreted in terms of $d\pi$–$p\pi$ bonding between the diazo group and the metalloid atom.

Canadian Journal of Chemistry, 47, 4353 (1969)

The recent appearance in the literature (1–6) of a number of short communications on the preparation of silyldiazoalkanes reflects the interest currently being shown in these compounds. However, all these methods are somewhat restricted in scope due to the non-availability of suitable starting materials. It seemed to us that the best (and only general) route to silyl- and germyldiazoalkanes was, with the wide spectrum of acylmetalloids available in this laboratory (7), via the use of tosylhydrazones (eg. [1]).

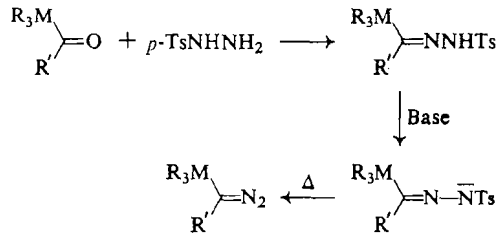

[1]

Prior to this work, few studies had been made on the synthesis of the "classical" ketone derivatives from acylmetalloids. Benzoyltriphenylsilane, the first acylsilane, was found (8) to give a phenylhydrazone, while 2,4-dinitrophenylhydrazones were prepared (9) from some low molecular weight acylmetalloids. We have found that tosylhydrazones may be prepared in good yield in the case of alkyl ketones ($R_3MCOAlk$) simply by heating the ketone and *p*-tosylhydrazine together under reflux in alcohol. However, on the attempted extension of this method to the aryl ketone benzoyltriphenylsilane, only a low yield of the desired tosylhydrazone was obtained, accompanied by extensive formation of silanol and benzaldehyde. In this case, attack of the hydroxylic solvent at silicon appears to be competitive with tosylhydrazone formation due to the lower reactivity of the carbonyl group in aryl ketones. A similar decomposition has been noted (8) in the attempted preparation of an oxime of this ketone. This difficulty has now been easily circumvented by heating the aryl ketone and *p*-tosylhydrazine together in a minimal volume of glacial acetic acid. Table III of the Experimental section lists the tosylhydrazones prepared in this study.

A preferred method for the generation of carbenes in carbon chemistry is the pyrolysis (10) of tosylhydrazone anions. The diazoalkanes obtained *in situ* decompose smoothly to carbenes in aprotic media at the elevated (ca. 150°) temperature employed, thus avoiding the necessity of isolating these explosive compounds. However, the use of this technique for the generation of silylcarbenes has been found to suffer from competing attack of the base employed (methoxide ion) at silicon, resulting in reduced yields of products derived from silylcarbenes. Thus the decomposition of acetyltriphenylsilane tosylhydrazone anion in refluxing diglyme gave vinyltriphenylsilane, the carbene rearrangement product and, in addition, considerable triphenylsilanol, arising from hydrolysis of triphenylmethoxysilane during workup (eq. [2]). Similarly,

[2]

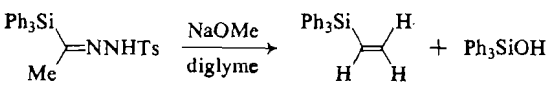

in the pyrolysis of benzoyltriphenylsilane tosylhydrazone in dimethyl sulphoxide, none of the desired (11) benzoylsilane was isolated, and only its decomposition products, triphenylsilanol and benzaldehyde, were observed (eq. [3]). Benzoyltriphenylsilane was found to completely decompose under similar conditions.

TABLE I

The conversion of tosylhydrazones to diazoalkanes via their sodium salts*

R_3M	R′	Conditions	% Recovered tosylhydrazone	% Yield of diazoalkane†
Ph_3Si	Me	70°; 90 min	45	31
Ph_3Si	Ph	70°; 120 min	19	25
Ph_3Si	C_6H_4-*p*-Cl	75°; 90 min	—	31
Ph_3Si	C_6H_4-*p*-F	80°; 150 min	13	29
Me_3C	Ph	70°; 150 min	65	77‡

*The general reaction was: $R_3M(R')C{=}NNHTs \xrightarrow[\text{pyridine}]{\text{NaOMe}} R_3M(R')C{=}N_2$.

†Yield of crystallized, purified diazoalkane (based on the tosylhydrazone consumed).
‡Yield of crude red oil obtained after removal of tosylhydrazone.

[3] $Ph_3Si(Ph)C{=}NNHTs \xrightarrow[\text{DMSO}]{\text{NaOMe}} Ph_3SiCOPh + Ph_3SiOH + PhCHO$

To avoid these problems the direct isolation of silyldiazoalkanes and their decomposition under base-free conditions has been sought. Initial work was centered on the decomposition of the sodium salts of the tosylhydrazones. In their pioneering study Bamford and Stevens (12) showed that under mild conditions in ethanolic sodium ethoxide, the stabilized aryldiazoalkanes could be produced. Farnum (13) reported an improvement in the synthesis with the use of pyridine as solvent. However, non-stabilized alkyldiazoalkanes could not be prepared, since the parent tosylhydrazone salts showed no decomposition under the mild conditions employed. Using Farnum's conditions, it was found, in complete contrast to the carbon compounds, that this method can be used for the preparation of *both* alkyl- and arylsilyldiazoalkanes. Unfortunately the method suffers from incomplete conversion to silyldiazoalkanes, up to 50% recovered tosylhydrazone being obtained with the silyl–alkyl compounds, as shown in Table I. However, the extent of conversion does indicate an unexpected stability of the silyldiazoalkanes.

Excellent conversions of tosylhydrazones to diazoalkanes have been obtained using the decomposition of the lithium salts. Kaufman and co-workers have reported (14) that lithium salts of tosylhydrazones decompose at a lower temperature than the corresponding sodium salts. The metalloid compounds behave similarly, since treatment at room temperature of the tosylhydrazones in tetrahydrofuran with *n*-butyllithium gives complete conversion to the corresponding diazoalkane. Details are given in Table V in the experimental section. These results again reflect an unusual stability of silyl- and germyldiazoalkanes, since it is reported (14) that temperatures of 80–120° are required to effect decomposition of the solid lithium salts in carbon compounds.

As indicated above by their ease of formation, the metalloidal diazoalkanes do in fact possess striking stability. These compounds, which are yellow-orange in color in contrast to the characteristic red carbon compounds, may be readily purified by recrystallization and appear to be indefinitely stable on storage at room temperature. This behaviour may be contrasted to the notorious instability of carbon diazoalkanes such as 2-diazopropane, Me_2CN_2, which is reported (15) to have a half-life of 3 h at 0°.

Diazoalkanes are considered (16) to be a hybrid of 2 major resonance forms (I and II).

$$R_2C{=}\overset{+}{N}{=}\overset{-}{N} \leftrightarrow R_2\overset{-}{C}{-}\overset{+}{N}{\equiv}N$$
I II

Diazoketones and -esters are said to owe their increased stability to delocalization of charge by the carbonyl group (16).

$$R'{-}\underset{\underset{O}{\|}}{C}{-}\overset{-}{C}R{-}\overset{+}{N}{\equiv}N \leftrightarrow R'{-}\underset{\underset{-O}{|}}{C}{=}CR{-}\overset{+}{N}{\equiv}N$$

The aryl group of aryldiazoalkanes plays a similar stabilizing role. The increased stability of diazoalkanes on replacement of carbon by silicon is therefore surprising at first thought, since it is in apparent contradiction to the expected destabilization of contributors of type II due to the greater

Can. J. Chem. Downloaded from www.nrcresearchpress.com by 210.87.254.105 on 09/05/12
For personal use only.

Can. J. Chem. Downloaded from www.nrcresearchpress.com by 210.87.254.105 on 09/05/12
For personal use only.

inductive release arising from the lower electronegativity of silicon. However, silicon in addition to acting as a sigma-donor can act as a pi-acceptor since, unlike carbon, it possesses energetically available empty d orbitals capable of interaction with, and stabilization of, the adjacent carbanion centre. Similar arguments have

$$R_3Si{-}CR{=}\overset{+}{N}{=}\overset{-}{N} \leftrightarrow R_3Si{-}\overset{-}{C}R{-}\overset{+}{N}{\equiv}N \leftrightarrow R_3\overset{-}{Si}{=}CR{-}\overset{+}{N}{\equiv}N$$

I IIa IIb

been advanced (17) to explain the unexpected stability of carbanions adjacent to silicon. This $d\pi$–$p\pi$ ground state interaction, which alters so noticeably the stability of these compounds, is also reflected by changes in their spectral properties. In the ultraviolet (u.v.) region, the lower ground-state energy leads to an increased energy requirement for promotion to the excited state. The low energy transition responsible for the characteristic red color of diazoalkanes undergoes a hypsochromic shift, shown visually by the color change to yellow–orange, on replacement of carbon by a metalloid atom. The u.v. spectral data are given in Table II for representative compounds of the two general classes studied. Model carbon compounds containing the trityl group could not be prepared, due to the failure of both acetyltriphenylmethane and benzoyltriphenylmethane (β-benzopinacolone) to give tosylhydrazone derivatives, even under conditions more vigorous than those used successfully for the conversion of the analogous acylmetalloids. This inertness is presumably a result of steric factors. It was decided that diazoalkanes containing the *t*-butyl group would provide the best alternative, since the parent carbonyl compounds are known (14, 18) to give tosylhydrazones which may be readily converted to the diazo compounds.

TABLE II

Ultraviolet maxima in cyclohexane and position of diazo stretching band in carbon tetrachloride for R_3MCN_2R'

R_3M	R′	λ_{max}(mμ) in ultraviolet region	Wavelength (μ) in infrared region
Ph_3Si	Ph	440	4.89
Ph_3Ge	Ph	451	4.90
Me_3C	Ph	501	4.92
Ph_3Si	Me	426	4.89
Me_3C	Me*	490	4.90

*Prepared by the pyrolysis of the dry lithium salt of the tosylhydrazone (reference 14).

The suggested increased contribution of resonance form II to the hybrid would be predicted to lead to an increase in the triple bond character of the N—N bond. Such an effect should be, and is, observable in the infrared (i.r.) spectrum by a shift of the diazo stretching band to higher energy. Significant data are given in Table II. The above results are very similar to those found (19) in the isoelectronic azide system, where substitution of adjacent carbon by silicon or germanium results in increased N—N i.r. stretching frequency and a hypsochromic shift of the low energy u.v. band.

Extensive work has been carried out on the 1,3-cycloaddition reactions of these compounds, together with their decomposition to carbenes and diazonium ions. This will be reported in a future paper.

Experimental

All reactions were carried out under an atmosphere of nitrogen. The nuclear magnetic resonance (n.m.r.) spectra were measured on a Varian A60 instrument, the i.r. spectra on a Perkin–Elmer 237B, and the u.v. spectra on a Perkin–Elmer Model 350.

Preparation of Acetyltriphenylsilane Toluene-p-sulphonylhydrazone

A mixture of 5.0 g (0.0166 mole) of acetyltriphenylsilane and 3.10 g (0.0166 mole) of toluene-*p*-sulphonylhydrazine was heated under reflux for 2 h in 100 ml of ethanol acidified by 20 drops of glacial acetic acid. During the course of the reaction an initial clear solution was obtained, which later deposited a white precipitate. This was filtered off to give 6.08 g (78%) of tosylhydrazone, m.p. 188–190° with decomposition.

Preparation of Benzoyltriphenylsilane Toluene-p-sulphonylhydrazone

Separate solutions of 2.2 g (0.0061 mole) of benzoyltriphenylsilane and 1.1 g (0.0059 mole) of toluene-*p*-sulphonylhydrazine, each dissolved in the minimal volume of hot glacial acetic acid, were mixed, and heated to boiling. Cooling precipitated a white solid, which was filtered off, washed with aqueous acetic acid and water, and then oven-dried to give 3.15 g (98%) of the crude tosylhydrazone, m.p. 170–180°. Recrystallization from methanol–benzene gave 2.35 g (73%) of product, m.p. 187–191° with decomposition.

The remainder of the tosylhydrazones were similarly prepared by one of the two methods given. Details are shown in Table III. The n.m.r. spectral data are given in Table IV.

Attempted Preparations of β-Benzopinacolone Toluene-p-sulphonylhydrazone

An equimolar mixture of β-benzopinacolone and

TABLE III

The preparation of tosylhydrazones*

R_3M	R′	Method†	Melting point‡	% Yield	Analysis: Calcd. (%) C	H	N	Found (%) C	H	N
Ph_3Si	Me	A	188–190° dec.	78	68.90	5.57	5.95	69.06	5.81	5.86
Ph_3Si	Et	B	183–185° dec.	82	69.38	5.82	5.78	69.38	5.82	5.70
Ph_3Si	CH_2Ph	A	187–189° dec.	52	72.49	5.53	5.13	72.72	5.55	5.17
Ph_3Si	Ph	B	187–191° dec.	73	72.16	5.30	5.26	72.12	5.12	5.24
Ph_3Si	C_6H_4-*p*-F	B	196–200° dec.	57	69.81	4.94	5.09	69.86	4.95	5.02
Ph_3Si	C_6H_4-*p*-Cl	B	200–203° dec.	71	67.76	4.80	4.94	67.91	4.78	4.88
Ph_3Si	C_6H_4-*p*-Br	B	203–205° dec.	31	62.85	4.45	4.58	62.79	4.29	4.49
Me_3Si	Ph§	B	124–125° dec.	58	58.92	6.40	8.09	59.24	6.48	7.97
Ph_3Ge	Me	A	162–164° dec.	86	62.95	5.09	5.44	62.65	5.17	5.41
Ph_3Ge	Ph	B	188–190° dec.	97	66.59	4.89	4.85	66.90	4.89	4.85
Me_3C	Ph	B	161–162°	77	65.43	6.71	8.48	65.40	6.94	8.47
Me_3C	Me‖	A	156–158°	71	—	—	—	—	—	—

*The general reaction was: $R_3M(R')C{=}O + p\text{-}TsNHNH_2 \rightarrow R_3M(R')C{=}NNHTs.$

†A: ethanol. B: acetic acid. (See text).
‡Samples recrystallized from ethanol- or methanol-benzene.
§Material decomposes on standing at room temperature.
‖Literature m.p. 155° (reference 12).

TABLE IV

Nuclear magnetic resonance data for tosylhydrazones*

R_3M	R′	δ (p.p.m.; $CDCl_3$,)
Ph_3Si	Me	8.53 (s, 1 H), 7.8–7.1 (multiplet, 19 H), 2.41 (s, 3 H), 1.83 (s, 3 H)
Ph_3Si	Et†	7.75–7.05 (multiplet, 19 H), 2.40 (s, 3 H), 2.23 (q, 2 H, J = 7.5 c.p.s.), 0.72 (t, 3 H, J = 7.5 c.p.s.)
Ph_3Si	CH_2Ph	8.16 (s, 1 H), 7.6–6.7 (multiplet, 24 H), 3.61 (s, 2 H), 2.40 (s, 3 H)
Ph_3Si	Ph	7.93 (s, 1 H), 7.7–6.7 (multiplet, 24 H), 2.45 (s, 3 H)
Ph_3Si	C_6H_4-*p*-F	7.98 (s, 1 H), 7.7–6.75 (multiplet, 23 H), 2.45 (s, 3 H)
Ph_3Si	C_6H_4-*p*-Cl	7.96 (s, 1 H), 7.7–7.1 (multiplet, 19 H), 6.98 (AA′BB′, q, 4 H), 2.46 (s, 3 H)
Ph_3Si	C_6H_4-*p*-Br	7.92 (s, 1 H), 7.7–6.5 (multiplet, 23 H), 2.43 (s, 3 H)
Me_3Si	Ph†	7.85–6.8 (multiplet, 9 H), 2.41 (s, 3 H), 0.08 (s, 9 H)
Ph_3Ge	Me	8.25 (s, 1 H), 7.8–7.1 (multiplet, 19 H), 2.38 (s, 3 H), 1.88 (s, 3 H)
Ph_3Ge	Ph	7.95 (s, 1 H), 7.4–6.7 (multiplet, 24 H), 2.38 (s, 3 H)
Me_3C	Ph†	7.85–6.75 (multiplet, 9 H), 2.45 (s, 3 H), 1.04 (s, 9 H)
Me_3C	Me†	7.61 (AA′BB′, q, 4 H), 2.43 (s, 3 H), 1.75 (s, 3 H), 1.02 (s, 9 H)

*The general structure was: $R_3M(R')C{=}NNHSO_2$–C$_6$H$_4$–Me.

†In these cases the NH singlet was not observed in chloroform-*d*. The i.r. spectra of all compounds showed a single =NH stretching band in the 3.04–3.10 μ region, and several —SO_2— stretching bands with two bands in the 7.25–7.50 μ region, and a strong single band at about 8.60 μ.

toluene-*p*-sulphonylhydrazine was heated under reflux in ethanol for 15 h. The ketone was recovered in 94% yield. When equimolar amounts of the two reagents were heated to boiling in glacial acetic acid and then allowed to stand overnight, the ketone was quantitatively recovered.

Attempted Preparation of Acetyltriphenylmethane Toluene-p-sulphonylhydrazone

A mixture of 0.58 g (0.002 mole) of acetyltriphenylmethane and 0.38 g (0.002 mole) of toluene-*p*-sulphonylhydrazine was heated under reflux for 24 h in 50 ml of ethanol acidified with glacial acetic acid. Evaporation gave an oily solid, whose i.r. spectrum showed a strong carbonyl band. Recrystallization from ethanol gave 0.34 g (59%) of recovered ketone, m.p. 132–140°.

The Pyrolysis of the Sodium Salt of Acetyltriphenylsilane Toluene-p-sulphonylhydrazone

A mixture of 0.36 g (0.00078 mole) of the tosylhydra-

Can. J. Chem. Downloaded from www.nrcresearchpress.com by 210.87.254.105 on 09/05/12
For personal use only.

TABLE V

The conversion of tosylhydrazones to diazoalkanes via their lithium salts*

				Analysis					
				Calcd. (%)			Found (%)		
R_3M	R′	% Yield	Melting point	C	H	N	C	H	N
Ph_3Si	Ph	73	150–151°†§	79.77	5.36	7.44	80.21	5.32	7.23
Ph_3Si	C_6H_4-*p*-F	63	143–144°†	76.12	4.85	7.10	76.14	4.83	7.13
Ph_3Si	C_6H_4-*p*-Cl	71	143–145°†	73.07	4.66	6.82	73.16	4.73	6.80
Ph_3Si	C_6H_4-*p*-Br	56	146–147°†	65.92	4.20	6.15	65.60	4.39	6.28
Ph_3Si	Me	82	82–84°‡	76.38	5.77	8.91	76.02	5.79	8.52
Ph_3Si	Et	72	72–73°‡	76.76	6.14	8.53	76.33	6.08	8.46
Ph_3Si	CH_2Ph	48	65–67°‡	79.95	5.68	7.17	79.97	5.83	7.11
Ph_3Ge	Ph	65	153–154°†	71.31	4.79	6.66	71.20	4.63	6.57
Me_3Si	Ph	73	67–68° (2mm)‖	63.10	7.41	14.72	63.27	7.42	14.66

*The general reaction was: $R_3M\!\!>\!\!C\!\!<\!\!R' \!=\! NNHTs \xrightarrow[THF]{n\text{-}BuLi} R_3M\!\!>\!\!C\!\!<\!\!R' \!=\! N_2$.

†Recrystallization solvents were ethanol–benzene.
‡Recrystallization solvent was pentane.
§Literature m.p. 150–151° (reference 14).
‖Boiling point (pressure).

zone and 0.041 g (0.00078 mole) of sodium methoxide was heated under reflux for 30 min in 15 ml of diglyme. The mixture was poured into water and extracted with hexane. After drying over magnesium sulphate, evaporation of the organic layer gave an oil, which was chromatographed on silica gel. Elution with carbon tetrachloride gave 0.075 g (30%) of vinyltriphenylsilane, m.p. 50–58°. Recrystallization from ethanol raised the m.p. to 67–68°. A mixed m.p. with an authentic sample was undepressed. Further elution with benzene gave 0.10 g (46%) of triphenylsilanol, m.p. 152–155°.

The Pyrolysis of the Sodium Salt of Benzoyltriphenylsilane Toluene-p-sulphonylhydrazone in Dimethyl Sulphoxide

A mixture of 0.20 g (0.00038 mole) of the tosylhydrazone and 0.024 g (0.00044 mole) of sodium methoxide was heated under nitrogen in 5 ml of dimethyl sulphoxide (dried over calcium hydride) at up to 145° for 15 min. The mixture was poured into water and extracted with ether. An oil was obtained upon workup of the organic layer, which smelled strongly of benzaldehyde. An i.r. spectrum confirmed the presence of benzaldehyde and also triphenylsilanol. None of the expected benzoyltriphenylsilane could be detected.

In a separate experiment, 0.20 g of benzoyltriphenylsilane was heated to 150° with 0.010 g of sodium methoxide in 5 ml of dimethyl sulphoxide for 15 min. The mixture was poured into water and extracted with ether. The colorless oil obtained from evaporation of the organic layer was shown by its i.r. spectrum to be a mixture of benzaldehyde and hexaphenyldisiloxane. None of the starting ketone could be observed.

In contrast to the above, when 0.15 g of benzoyltriphenylsilane was heated in 5 ml of dimethyl sulphoxide at up to 150° for 15 min in the absence of base, the ketone was recovered in 87% yield.

The Preparation of Triphenylsilylphenyldiazomethane using Sodium Methoxide in Pyridine

A mixture of 2.0 g (0.00376 mole) of benzoyltriphenylsilane toluene-*p*-sulphonylhydrazone and 0.20 g (0.00370 mole) of sodium methoxide in 50 ml of dry pyridine was heated by means of an oil bath at up to 70° for 2 h. The resulting orange mixture was poured into water and extracted with pentane. A white solid which precipitated from the organic layer was removed to give 0.38 g (19%) of crude recovered tosylhydrazone, m.p. 155–170°. Recrystallization from methanol raised the m.p. to 186–190°. The orange pentane filtrate was dried over magnesium sulphate and the solvent was evaporated. The resulting solid was recrystallized from pentane–benzene to give 0.30 g (25% based on tosylhydrazone consumed) of orange diazoalkane, m.p. 146–150°. A further recrystallization from pentane–benzene raised the m.p. to 150–152°.

Details are given in Table I of the other tosylhydrazones converted to diazoalkanes by this method.

The Preparation of 1-Triphenylsilyl-1-diazoethane using n-Butyllithium

To a solution of 9.40 g (0.02 mole) of acetyltriphenylsilane toluene-*p*-sulphonylhydrazone in 300 ml of anhydrous tetrahydrofuran, cooled to 0°, was added 12.5 ml (0.02 mole) of *n*-butyllithium solution. The mixture was stirred in the dark at room temperature for 46 h and then was filtered. Ether was added to the filtrate, which was then washed with water, dried over sodium sulphate, and evaporated to give a yellow solid. Recrystallization from a minimal volume of pentane gave 5.12 g (82%) of yellow diazoalkane, m.p. 82–84°.

Results of the other reactions of this class are given in Table V. Details of the u.v. and i.r. spectra of these compounds are given in Table VI. Table VII gives the n.m.r. data for the diazoalkanes.

Can. J. Chem. Downloaded from www.nrcresearchpress.com by 210.87.254.105 on 09/05/12
For personal use only.

TABLE VI

Infrared and ultraviolet data for diazoalkanes R_3MCN_2R'

R_3M	R′	Diazo stretching band in infrared (μ, CCl_4 solvent)	Ultraviolet spectrum in cyclohexane λ_{max} (mμ) (ε)*
Ph_3Si	Me	4.89	426 (56), 253 (4,800), 224 (s, 27,500), 220 (29,900), 207 (41,000)
Ph_3Si	Et	4.89	426 (59), 255 (7,900), 221 (s, 37,600)
Ph_3Si	CH_2Ph	4.89	424 (47), 258 (7,120), 220 (s, 35,000)
Ph_3Si	Ph	4.89	440 (68), 308 (s, 2,000), 280 (s, 13,150), 222 (31,200)
Ph_3Si	C_6H_4-*p*-F	4.88	438 (81), 309 (s, 2,550), 276 (17,150), 221 (s, 34,500), 209 (44,500), 200.5 (s, 38,900), 196 (s, 29,400), 192.5 (s, 20,600)
Ph_3Si	C_6H_4-*p*-Cl	4.88	441 (95), 320 (s, 2,270), 287 (23,200), 222 (35,600)
Ph_3Si	C_6H_4-*p*-Br	4.88	437 (95), 289 (19,400), 222 (37,000)
Ph_3Ge	Ph	4.90	451 (71), 284 (12,800), 217 (s, 32,200)
Me_3C	Ph	4.92	501
Me_3C	Me	4.90	490

*s = shoulder.

TABLE VII

Nuclear magnetic resonance data in carbon tetrachloride for R_3MCN_2R'

R_3M	R′	δ (p.p.m.)
Ph_3Si	Me	7.8–7.2 (multiplet, 15 H), 1.80 (s, 3 H)
Ph_3Si	Et	7.7–7.1 (multiplet, 15 H), 2.80 (q, 2 H, J = 7.5 c.p.s.), 1.05 (t, 3 H, J = 7.5 c.p.s.)
Ph_3Si	CH_2Ph	7.7–6.9 (multiplet, 20 H), 3.30 (s, 2 H)
Ph_3Si	Ph	7.75–6.8 (multiplet, 20 H)
Ph_3Si	C_6H_4-*p*-F	7.8–7.3 (multiplet, 15 H), 6.87 (d, 4 H, J = 6.5 c.p.s.)
Ph_3Si	C_6H_4-*p*-Cl	7.8–7.3 (multiplet, 15 H), 6.97 (AA′BB′ q, 4 H)
Ph_3Si	C_6H_4-*p*-Br	7.2–7.1 (multiplet, 15 H), 6.93 (AA′BB′ q, 4 H)
Me_3Si	Ph	7.2–6.7 (multiplet, 5 H), 0.16 (s, 9 H)
Ph_3Ge	Ph	7.7–6.66 (multiplet, 20 H)

Acknowledgments

The research was supported by the National Research Council of Canada.

1. M. F. Lappert and J. Lorberth. Chem. Commun. 836 (1967).
2. U. Schöllkopf and N. Rieber. Angew. Chem. **79**, 906 (1967).
3. D. Seyferth, A. W. Dow, H. Menzel, and T. C. Flood. J. Amer. Chem. Soc. **90**, 1080 (1968).
4. K. D. Kaufmann, B. Auräth, P. Träger, and K. Rühlmann. Tetrahedron Letters, 4973 (1968).
5. K. D. Kaufmann and K. Rühlmann. Z. Chem. **8**, 262 (1968).
6. M. F. Lappert and J. S. Poland. Chem. Commun. 156 (1969).
7. A. G. Brook. Advan. Organometal. Chem. **7**, 95 (1968).
8. A. G. Brook. J. Amer. Chem. Soc. **79**, 4373 (1957).
9. A. G. Brook, J. M. Duff, Peter F. Jones, and N. R. Davis. J. Amer. Chem. Soc. **89**, 431 (1967).
10. L. Friedman and H. Shecter. J. Amer. Chem. Soc. **81**, 5513 (1959).
11. R. Oda, M. Mieno, and Y. Hayashi. Tetrahedron Letters, 2363 (1967).
12. W. R. Bamford and T. S. Stevens. J. Chem. Soc. 4735 (1952).
13. D. G. Farnum. J. Org. Chem. **28**, 870 (1963).
14. G. Kaufman, F. Cook, H. Shecter, J. Bayless, and L. Friedman. J. Amer. Chem. Soc. **89**, 5736 (1967).
15. A. C. Day, P. Raymond, R. M. Southam, and M. C. Whiting. J. Chem. Soc. (C) 467 (1966).
16. H. Zollinger. Diazo and azo chemistry, Interscience Publishers, Inc., New York. 1961. Chapt. 3.
17. G. A. Gornowicz and R. West. J. Amer. Chem. Soc. **90**, 4478 (1968).
18. G. M. Kaufman, J. A. Smith, G. G. Vander Stouw, and H. Shecter. J. Amer. Chem. Soc. **87**, 935 (1965).
19. R. West and J. S. Thayer. Inorg. Chem. **3**, 889 (1964).

Can. J. Chem. Downloaded from www.nrcresearchpress.com by 210.87.254.105 on 09/05/12
For personal use only.

Can. J. Chem. Downloaded from www.nrcresearchpress.com by 210.87.254.105 on 09/05/12
For personal use only.

Studies related to Bute Inlet wax[1]. The identity of norphytane, pristane, and bute hydrocarbon

TIKAM C. JAIN AND ROBERT J. STRIHA[2]
Department of Chemistry, University of Victoria, Victoria, British Columbia
Received June 20, 1969

Spectral and gas–liquid chromatographic evidence is presented to confirm the identity of pristane with norphytane and bute hydrocarbon.

Canadian Journal of Chemistry, 47, 4359 (1969)

Bute Inlet wax is a dark colored semi-solid which appears mysteriously during extremely cold winters on the water of Bute Inlet situated on the west coast of British Columbia. Recently we reported (1) on the isolation of a hydrocarbon, $C_{19}H_{40}$, from this source which was proven to be 2,6,10,14-tetramethylpentadecane (pristane) (**1**). Sörensen (2,3) established the identity of pristane with norphytane **1** on the basis of their physical constants and infrared (i.r.) spectra.[3] In view of the significance of pristane in organic geochemical work (4,5), coupled with our own work on bute hydrocarbon (1), it was desirable to execute a more rigorous comparison of pristane[4] with an authentic specimen of norphytane and bute hydrocarbon.

Norphytane required for this work was prepared[5] in the manner described in Scheme 1. The mass spectrum of norphytane (Table I) was identical with the corresponding spectra of pristane and bute hydrocarbon. Finally, gas–liquid chromatographic behavior of these three hydrocarbons (Table II) conclusively established their structural identity.

Experimental

All melting points and boiling points are uncorrected; melting points were determined on a Kofler hot stage. Infrared spectra were recorded with a Perkin–Elmer Infracord Model 337, calibrated with polystyrene film.

TABLE I

Important peaks (in order of decreasing mass) in the mass spectra of $C_{19}H_{40}$

	$\%\Sigma_{27}$		
m/e	Bute hydrocarbon	Pristane	Norphytane
268	1.10	1.27	1.19
183	4.65	4.79	4.58
113	4.46	4.54	4.46
85	5.14	5.28	5 30
71	12.33	12.12	12.14
57	14.70	12.56	12.78
43	10.12	10.19	10 40
41	4.53	4.48	4.65

Nuclear magnetic resonance (n.m.r.) spectra were obtained with Varian Associates Model HA-60 spectrometer. The mass spectra were measured with Hitachi–Perkin–Elmer RMU-6E single-focus mass spectrometer using an ionizing energy of 70 eV and a source temperature of 250°. Gas–liquid chromatographic analyses were carried out on a Perkin–Elmer Gas Chromatograph Model 810 (with flame ionization detector) equipped with 6 ft × 0.25 in. columns with helium as a carrier gas. Thin-layer chromatographic determinations were carried out on alumina and silica plates; the spots were developed by exposure to I_2 vapor. The microanalyses were performed by Schwarzkopf Microanalytical Laboratory, New York.

Phytol (2)

Commercially available phytol, 75% pure by gas–liquid chromatography (g.l.c.), was purified by column chromatography on silica gel followed by fractional distillation. The fraction boiling at 170–185° (bath)/0.25 mm was g.l.c. pure (> 99%) phytol (**2**) obtained as a colorless liquid; ν_{max} (film): 3340, 1670, 1375, 1365, and 1000 cm^{-1}; τ ($CDCl_3$): 9.14 (12H, doublet, J = 5.6 Hz), 8.35 (3H, singlet), 8.07 (2H, broad multiplet), 7.59 (1H, singlet), 5.91 (2H, doublet, J = 7.0 Hz), 4.62 (1H, broad multiplet); mass spectrum: *m/e* ($\%\Sigma_{29}$): 296 (1.09, M^+), 278 (0.47, M—H_2O).

Anal. Calcd. for $C_{20}H_{40}O$: C, 81.00; H, 13.60. Found: C, 80.49; H, 13.61.

Phytyl Acetate (3)

Freshly distilled phytol (**2**) turns light yellow on

[1]Presented at the VIth International Symposium on the Chemistry of Natural Products (Steroids and Terpenes), Mexico City, April 21–25, 1969.
[2]N.R.C.C. Postgraduate Scholar, 1968–present.
[3]Besides these two publications (2,3), we are unaware of any other report concerning this aspect.
[4]From K & K Laboratories, Inc., U.S.A.
[5]Because of the lack of precise experimental details in the literature (2), a full account of our modified procedures is given in the experimental part of this paper. However, a different procedure for synthesis of pristane from phytol has been recently reported by Kates (6).

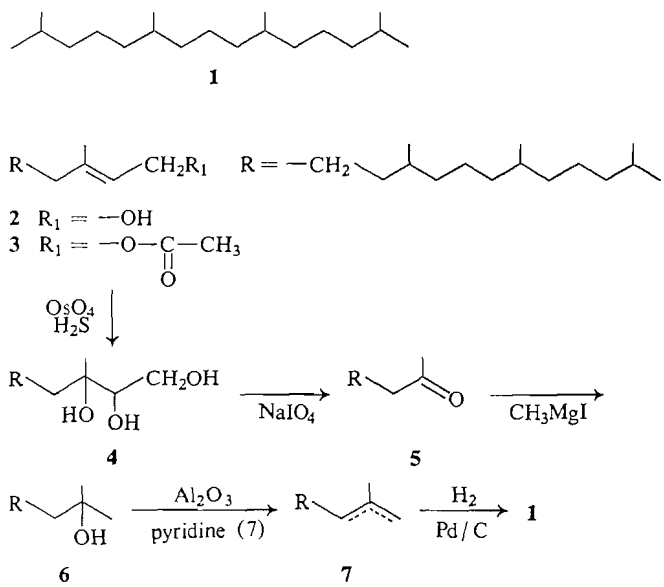

SCHEME 1

standing due to aerial oxidation. It was converted into its relatively more stable acetoxy derivative (Ac_2O–pyridine method). Phytyl acetate (**3**) was distilled[6] at 145–146°/0.25 mm as a clear liquid;[7] ν_{max} (film): 1740 (acetoxy carbonyl), 1670 (>C=C<), 1375, and 1360 cm^{-1} (*gem*-dimethyl); τ ($CDCl_3$): 9.14 (12H, doublet, J = 5.5 Hz), 8.79 (broad singlet), 8.33 (3H, broad singlet), 8.03 (3H, singlet), 5.45 (2H, broad doublet, J = 7.2 Hz), 4.5–4.8 (1H, broad multiplet).

Anal.[8] Calcd. for $C_{22}H_{42}O_2$: C, 78.04; H, 12.50. Found: C, 79.44; H, 12.95.

Phytane-1,2,3-triol (4)

A solution of OsO_4 (1 g) in 1:1 ether–petroleum ether (60 ml) was slowly added in two portions to a magnetically stirred solution of phytyl acetate (**3**) (1.3 g) dissolved in ether–petroleum ether (1:1, 40 ml) containing anhydrous pyridine (3 ml), and the reaction mixture was stirred at room temperature for 4 days in the dark. The bulk of the solution was concentrated to ca. 25 ml and the solid osmic ester was collected, dissolved in benzene–methanol (1:1, 120 ml), and the solution saturated with H_2S with cooling. The brownish–black precipitate was filtered off and washed with benzene (10 ml). The solvent was removed *in vacuo* and the residual gum [1.25 g; ν_{max} (film): 3450 (hydroxyl), 1745 cm^{-1} (acetate)] was hydrolyzed by refluxing in aqueous methanolic KOH. The reaction mixture was worked up in the usual manner yielding phytane-1,2,3-triol [**4**], crystallised from acetone–acetonitrile to give white crystals, m.p. 56–57°; ν_{max} ($CHCl_3$): 3445, 1210, 1086 cm^{-1} (hydroxyl); τ ($CDCl_3$): 9.13 (12H, doublet, J = 5.6 Hz), 8.85 (singlet), 5.8–6.7 (broad, 6-proton band reduced to a 3-proton multiplet after exchange with D_2O).

Anal. Calcd. for $C_{20}H_{42}O_3$: C, 72.67; H, 12.81. Found: C, 72.70; H, 12.68.

$NaIO_4$ Oxidation of Phytane-1,2,3-triol (4)

A solution of $NaIO_4$ (360 mg dissolved in 1 ml H_2O and diluted with 9 ml MeOH) was slowly added to the triol **4** (233 mg) dissolved in MeOH (9 ml) and the reaction mixture was set aside for 24 h at room temperature in the dark. The solvent was removed *in vacuo* and the residue diluted with water (30 ml) and extracted with Et_2O (3 × 20 ml). The combined extract was washed with brine solution (2 × 15 ml), dried over Na_2SO_4, and the solvent removed under suction, to yield a yellow oil (208 mg). Filtration through a column of silica gel (4.2 g) in petroleum ether (50 ml) afforded a clear mobile liquid (188 mg), b.p. 194–197° (bath)/8.5 mm; ν_{max} (film): 1717 cm^{-1} (acyclic ketone); τ ($CDCl_3$): 9.13 (12H, doublet, J = 5.7 Hz), 7.89 (3H, singlet), 7.61 (2H, broad triplet).

Anal. Calcd. for $C_{18}H_{36}O$: C, 80.52; H, 13.52. Found: C, 79.65; H, 13.05.

The ketone **5** was further characterized by its semicarbazone, m.p. 65–67° (lit. (8) m.p. 66–67°).

Grignard Addition to the Ketone 5

A solution of ketone **5** (219 mg) in dry ether (15 ml) was added in N_2 atmosphere to 5 equivalents of MeMgI (prepared from 125 mg Mg and 740 mg MeI) and the

[6]Attempted purification by column chromatography on alumina invariably led to its hydrolysis.

[7]The homogeneity of each liquid intermediate was rigorously checked by t.l.c. and g.l.c. [cf. experimental details given in reference (2)].

[8]A better analysis on this g.l.c. pure specimen could not be obtained presumably due to its tendency towards partial hydrolysis on standing. However, its mass spectrum displayed a weak molecular ion peak at *m/e* 338 with an intense peak at *m/e* 278 due to M—CH_3COOH fragment.

Can. J. Chem. Downloaded from www.nrcresearchpress.com by 210.87.254.105 on 09/05/12
For personal use only.

TABLE II

Retention times relative to nonadecane

Sample	DEGS*	MPS oil†	APL‡	MPS gum§
Nonadecane	1.00	1.00	1.00	1.00
Pristane	0.52	0.42	0.43	0.58
Norphytane	0.52	0.42	0.44	0.58
Bute hydrocarbon	0.52	0.42	0.44	0.58

*Diethyleneglycolsuccinate (DEGS) at 188° with 35 ml of helium/min.
†Methylphenylsilicone oil (MPS oil) at 189° with 23.5 ml of helium/min.
‡Apiezon L (APL) at 227° with 22 ml of helium/min.
§Methylphenylsilicone gum (MPS gum) at 237° with 30 ml of helium/min.

mixture was stirred at room temperature for 1 h. Ether was removed with a swift current of nitrogen and replaced with anhydrous benzene (40 ml) and the reaction mixture was refluxed for 24 h. The mixture was then cooled and rapidly acidified with saturated aqueous NH_4Cl. The product was extracted with ether (3 × 30 ml) and the combined ether extract was washed with brine (15 ml), dried, and evaporated to yield the alcohol **6** (245 mg); ν_{max} (film): 3390 cm^{-1} (hydroxyl). There was apparently some dehydration during the work up, evidenced by a band at 910 cm^{-1} in its i.r. spectrum. Consequently, the product was used as such without any further purification for subsequent reaction.

Dehydration of the Alcohol 6

The crude alcohol **6** (245 mg) was mixed with pyridine-treated alumina (2%) and heated in an atmosphere of nitrogen at 150–170° for 1 h (7). The reaction mixture was slurried with ether, filtered, and dried over Na_2SO_4. Removal of solvent *in vacuo* furnished a mobile liquid (200 mg) which was filtered through a column of silica gel and then distilled at 175° (bath)/7.0 mm to give a mixture[9] of hydrocarbons **7** (158 mg); ν_{max} (film): 1652, 1380, 1365, 1173, 1154, and 886 cm^{-1}.

Anal. Calcd. for $C_{19}H_{38}$: C, 85.63; H, 14.37. Found: C, 85.51; H, 14.42.

Norphytane (1)

A solution of hydrocarbons **7** (80 mg) in absolute ethanol (20 ml) containing 10% Pd/C (20 mg) was stirred at room temperature under H_2 until absorption ceased. The catalyst was removed by filtration and the filtrate was evaporated under reduced pressure to give norphytane **1** in quantitative yield; no coloration with tetranitromethane; distilled over sodium at 165–170° (bath)/7.0 mm as a clear liquid; ν_{max} (film): 1385, 1365, 1170, and 1155 cm^{-1}; τ ($CDCl_3$): 9.14 (18H, doublet, J = 5.8 Hz), 8.78 (22H, singlet); overall yield: 85% based on triol **4**.

Anal. Calcd. for $C_{19}H_{40}$: C, 84.98; H, 15.02. Found: C, 85.09; H, 14.70.

[9]Careful integration of the olefinic signals in the n.m.r. spectrum revealed the presence of norphytene-1 and norphytene-2 in the ratio of 3:7.

Acknowledgments

The authors are indebted to the National Research Council of Canada and the UVIC Research Committee for financial support of this research.

1. T. C. Jain, G. L. Owen, and R. J. Striha. Phytochem. **8**, 785 (1969).
2. J. S. Sörensen and N. A. Sörensen. Acta Chem. Scand. **3**, 939 (1949).
3. J. Pliva and N. A. Sörensen. Acta Chem. Scand. **4**, 846 (1950).
4. H. J. Nicholas. In Biogenesis of natural compounds. P. Bernfeld, Ed. Pergamon Press, New York. 1967. p. 866 and references cited therein.
5. J. G. Bendoraitis, B. L. Brown, and L. S. Hepner. Anal. Chem. **34**, 49 (1962).
6. M. Kates, C. N. Joo, B. Palameta, and T. Shier. Biochem. **6**, 3329 (1967).
7. E. Von Rudloff. Can. J. Chem. **39**, 1860 (1961).
8. F. G. Fischer. Ann. **464**, 69 (1928).

Can. J. Chem. Downloaded from www.nrcresearchpress.com by 210.87.254.105 on 09/05/12
For personal use only.

Can. J. Chem. Downloaded from www.nrcresearchpress.com by 210.87.254.6 on 09/05/12
For personal use only.

threo- and *erythro*-β-Hydroxy-DL-aspartic acids

CLIFTON W. JONES, III,[1] DONALD E. LEYDEN, AND CHARLES H. STAMMER[2]
Department of Chemistry, University of Georgia, Athens, Georgia 30601

Received May 1, 1969

An improved procedure for the synthesis of *threo*- and *erythro*-β-hydroxy-DL-aspartic acids is described. An nuclear magnetic resonance study of both diastereomers indicated that the *threo* isomer exists primarily as the conformer having *anti* carboxyl groups while the *erythro* compound prefers a conformation with *gauche* carboxyl functions. Possible reasons for this anomaly are presented.

Canadian Journal of Chemistry, 47, 4363 (1969)

During the pursuit of intermediates useful in the synthesis of cycloserine analogs, we became interested in the diastereomers of racemic β-hydroxyaspartic acid (HAA). The synthesis of these isomers was carried out using a reaction path described by Miller (*1*); i.e., the treatment of *cis*- and *trans*-epoxysuccinic acids with ammonia, with some considerable modification of the actual procedure. The sodium salt of *cis*-epoxysuccinic acid, which was obtained directly from the oxidation of maleic acid, was treated with concentrated ammonium hydroxide without the troublesome prior conversion to the free acid as was done by the early workers. This resulted in a considerable saving of time and an increased yield of the *threo* amino acids. The *erythro* isomer was also prepared by this modified procedure, and, even though the product had the expected physical properties, we found that it was impure. The melting points of these highly polar amino acids are very poor indices of purity since partial decomposition always occurs during heating. Dimethyl sulfite esterification of the recrystallized *erythro* amino acid gave a dimethyl ester which consistently contained excess nitrogen by elemental analysis. Apparently, an ammonium salt was coprecipitated with the acid when it was isolated from the amination reaction mixture by acidification. Since recrystallization failed to remove this, the amino acid was placed on a strongly basic anion exchange resin (Amberlite IRA-400) and eluted with acetic acid. Pure erythro-DL-HAA was obtained which gave derivatives having the correct nitrogen content.[3]

Having the pure diastereomers in hand, we investigated their nuclear magnetic resonance (n.m.r.) spectra in D_2O where only the H_α, H_β protons were detectable. Previous investigations of amino acid n.m.r. spectra (*3*) indicated that the size of the vicinal coupling constant, $J_{\alpha,\beta}$, might allow us to estimate which rotational conformation of HAA is preferred. Both cysteine and histidine (*3d*) had $J_{\alpha,\beta}$ values consistent with the Karplus relationship (*4*), but those for β-hydroxy amino acids, threonine, and *allo*-threonine are somewhat anomalous (*3f*); i.e., assuming that the preferred rotomer will have the carboxyl and β-substituents *anti*, the *threo* isomer should show $J_{\alpha,\beta} \sim 3$ and *erythro* isomer should have $J_{\alpha,\beta} \sim 11$ c.p.s., whereas the observed values are 3.8 and 3.6 c.p.s., respectively. A similar "anomaly" was reported in connection with the *N*,β-dimethylleucines and *N*-methylisoleucine (*5*). Reports by Pachler (*3a,b*) on aspartic acid and by Alberty and co-workers (*6a*), Gawron and co-worker (*6b*), and Pachler (*3a*) on malic acid indicated, however, that these dicarboxylic acids do indeed exist preferably with the carboxyl groups in the *anti* conformation. We were led, therefore, to expect that *threo*-HAA might have a small $J_{\alpha,\beta}$ (see TA, Chart 1) while that of the *erythro* isomer would be large (see EA, Chart 1). Tables I and II show that *erythro*-HAA does not conform to these expectations, but *threo*-HAA does.

When the staggered conformations for these amino acids (T = *threo*, E = *erythro*, R = H) are examined (Chart 1), the small $J_{\alpha,\beta}$ of the *threo* acid suggests that conformers TA and TB having H_α and H_β *gauche* are very largely preferred over TC. It follows from the conformer populations (Table II), that the equilibrium constant for the formation of TA + TB from TC is approximately 99, which corresponds

[1]Abstracted from the Master of Science thesis presented to the University of Georgia Graduate School by C. W. Jones, III, in June, 1968.

[2]To whom inquiries should be addressed.

[3]Early workers who obtained *erythro*-DL-HAA by acidification of its ammoniacal solutions undoubtedly had an impure product; cf. (*2*).

TABLE I

$J_{\alpha,\beta}$, ν_α, ν_β, and conformer populations at various pH's for *erythro*-β-hydroxy-DL-aspartic acid

pH	$J_{\alpha,\beta}$(c.p.s.)	ν_α†	ν_β†	Conformer populations* EA	EB + EC
1.00	2.8	480	492	0.02	0.98
2.96	3.0	426	459	0.04	0.96
3.65	3.1	424	453		
4.05	3.2	415	445	0.05	0.95
4.65	3.3	409	437		
6.82	3.4	407	432	0.07	0.93
7.75	3.4	404	432		
8.18	3.5	402	431		
9.25	3.6	392	428	0.09	0.91
9.70	3.8	357	411		
10.20	4.0	348	409	0.13	0.87
12.85	4.3	343	409		
13.30	4.3	343	409	0.15	0.85

*Calculated by the method of K. Pachler (9) using $J_g = 2.6$ and $J_{anti} = 13.6$. When these couplings were calculated using the electronegativities of the substituents, $J_g = 2.2$ and $J_{anti} = 11.4$. The use of these values made only slight changes in the rotomer populations.
†100 Hz values.

TABLE II

$J_{\alpha,\beta}$, ν_α, ν_β, and conformer populations at high and low pH for *threo*-β-hydroxy-DL-aspartic acid

pH	$J_{\alpha,\beta}$(c.p.s.)	ν_α†	ν_β†	Conformer populations* TC	TA + TB
1.00	2.7	468	504	0.01	0.99
13.20	2.7	359	434	0.01	0.99

*See Table I.
†100 Hz values.

(7) to a ΔG of -2.72 kcal/mole. In order to calculate the enthalpy change for this equilibrium, we must take into account the fact that *two* of the possible conformers have a small $J_{\alpha,\beta}$ while only one has a large $J_{\alpha,\beta}$. The rotamers having the small coupling are favored probability-wise and ΔS for the equilibrium can be equated (7) to R ln 2. Using similar arguments for the *erythro* isomer, the thermodynamic parameters (see Table III) for the equilibrium formation of EB + EC (conformations with gauche protons) from EA were also calculated. These results show that the EB + EC mixture is strongly favored even though both of these conformations have *gauche* carboxyl groups. The overwhelmingly favored conformation (TA) of the *threo* isomer[4] has *anti* carboxyl functions and the question as to why the *anti* conformation is favored in one isomer and disfavored in the other is complex and cannot be completely explained at this time. As the pH of the solutions is increased, increasing electrostatic repulsion between the negatively charged carboxyl groups will cause the anti-conformers (EA and TA) to be favored. Since $J_{\alpha,\beta}$ of the *threo* isomer underwent essentially no change with pH, it most probably exists in both acid and base as the *anti* conformer, TA. The *erythro* compound should show a considerable increase in $J_{\alpha,\beta}$ as the pH rises since conformer EA should become more prevalent. The small change from 2.8 to only 4.3 c.p.s. concurrent with a pH increase of approximately 12 units shows that the concentration of EA does increase, but not to a predominant level. An n.m.r. study of both *threo*- and *erythro*-HAA in basic D_2O solution at temperatures between 30 and 90° showed essentially no change in $J_{\alpha,\beta}$ consistent

[4]TA is doubly favored because it allows a hydroxyl–amine hydrogen bond but lacks the carboxyl–carboxyl *gauche* interaction of TB.

Can. J. Chem. Downloaded from www.nrcresearchpress.com by 210.87.254.6 on 09/05/12
For personal use only.

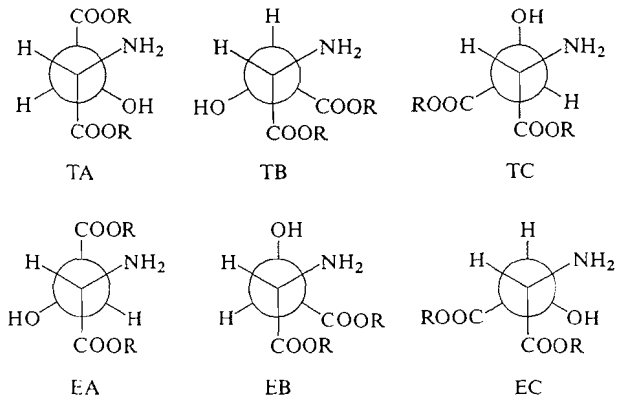

CHART 1

TABLE III
Thermodynamic parameters

	p*H*	*K*	Δ*G*(kcal/mole)	Δ*H*(kcal/mole)
threo-HAA TC ⇌ TA + TB	1.00 and 13.20	99	−2.72	−2.31
erythro-HAA	2.96	24	−1.88	−1.46
EA ⇌ EB + EC	13.30	5.75	−1.03	−0.62

with the small Δ*H* associated with these equilibria. The addition of Cd^{++} and Zn^{++} to solutions of these isomers also caused no change in $J_{\alpha,\beta}$ but did cause some shift in ν_α and ν_β.

In the course of the work on *erythro*-HAA, we determined pK_{a_1} (4.05) and pK_{a_2} (9.75) for the equilibria shown in Scheme 1. A plot of ν_α and ν_β vs. p*H* as shown in Fig. 1 allowed assignment of the more downfield doublet to H_β since this absorption underwent the larger diamagnetic shift (22 vs. 15 c.p.s.) during the first ionization, while H_α shifted more (44 vs. 17 c.p.s.) during the second. None of this information could be obtained for *threo*-HAA due to its very low solubility in water at ambient temperature.

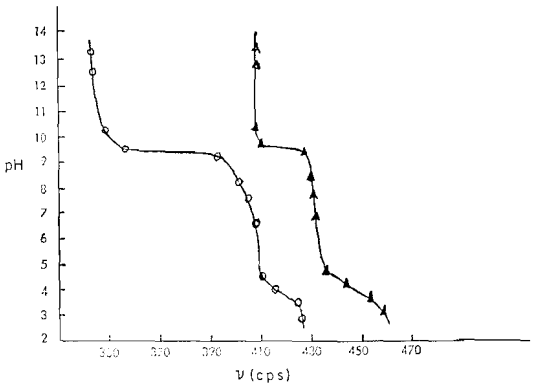

FIG. 1. Plot of p*H* versus ν(c.p.s., 100 Hz values) for *erythro*-HAA. ○—○, H_α values; ▲—▲, H_β values.

Experimental

Spectral Measurements

The proton magnetic resonance spectra were recorded using a Varian HA-100 high resolution n.m.r. spectrometer. Chemical shift measurements were made by the usual side band technique. Sodium-3-(trimethylsilyl)-propanesulfonate (tms*) was the internal reference compound. The ambient temperature of the sample compartment was 29 ± 2 °C. The precision of the chemical shift measurement was estimated to be better than ±0.01 p.p.m.

Measurement of pK_a Values

Measurements of p*H* were made at room temperature using a Leeds and Northrup Model No. 7403-A1 line operated expanded scale p*H* meter equipped with Model 124 138 miniature electrode assembly and standardized

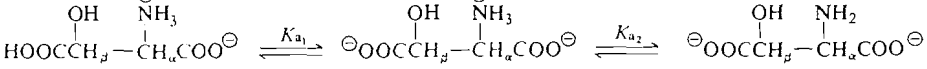

SCHEME 1

Can. J. Chem. Downloaded from www.nrcresearchpress.com by 210.87.254.6 on 09/05/12
For personal use only.

Can. J. Chem. Downloaded from www.nrcresearchpress.com by 210.87.254.6 on 09/05/12
For personal use only.

using National Bureau of Standard buffers. No corrections were made for glass electrode errors at either p*H* extreme. The pK_a values of the compounds in D_2O were determined by potentiometric titration, using a semi-automatic recording device previously described. The titrant used was standard 6 *M* CO_2-free potassium deuteroxide solution. The KOD solution was prepared by reacting reagent grade potassium metal with CO_2-free D_2O (99.8%) in a nitrogen atmosphere. A layer of ether covered the D_2O to slow the reaction rate. The ether was removed by warming the KOD solution with hot water while passing a stream of nitrogen over the surface.

Infrared (i.r.) spectra were recorded on either a Perkin–Elmer Infracord Model 137 or Model 237-B. Melting points were taken on a Nalge–Axelrod apparatus and are corrected. Radial paper chromatography was carried out on 31-cm Whatman No. 1 circles having a 1 cm center hole. Compounds were visualized using ninhydrin (N). A substance having an R_f of 0.5 in the MPW system and located with ninhydrin is reported as R_f^{MPW} 0.5 (N). The solvent systems were as follows: MPW was methyl ethyl ketone:pyridine:water, 20:5:8; BAW was butanol:-acetic acid:water, 4:1:5 (upper phase); MAW was methyl ethyl ketone:acetic acid:water, 20:5:8.

erythro-β-*Hydroxy*-DL-*aspartic Acid*

A solution of 79.0 g (0.60 mole) *trans*-epoxysuccinic acid (8) in 2 l of concentrated ammonium hydroxide was heated to 40–50° for 25 h. The solution was evaporated to dryness on a rotary evaporator to remove residual ammonia and the residue was dissolved in sufficient water to make a 3% solution (w/v). The solution was placed on a column (6.5 × 65.0 cm) containing 2 pounds of Amberlite IRA-400 anion exchange resin (OH^- cycle) and eluted with 10% acetic acid. The combined acidic eluate was evaporated to dryness using a rotary evaporator and the resulting amino acid was crystallized from a 1:1 water:ethanol mixture giving 41.0 g (46%); i.r. (KBr) 3436 (O—H), 1710, and 1690 cm^{-1} (C=O); R_f^{MPW} 0.20 (N), R_f^{MAW} 0.64 (N).

threo-β-*Hydroxy*-DL-*aspartic Acid*

The disodium salt of *cis*-epoxysuccinic acid was prepared from 116 g (1 mole) maleic acid by the method of Payne and Williams (8). The crude salt was dissolved in 3.5 l conc. ammonium hydroxide and the solution was heated to 40–50° for 10 h. The reaction mixture was concentrated *in vacuo* to a heavy syrup and 700 ml of water was added. The solution was acidified to p*H* 3 with concentrated hydrochloric acid and kept at 5° for 12 h. The first crop, weighing 113.4 g, was filtered, washed with cold water, and dried *in vacuo*, over phosphorous pentoxide. The second crop, weighing 18.8 g, was obtained from the concentrated filtrate after cooling. The combined crude product was recrystallized from water giving a total of 66.0 g (44%) of *threo*-HAA; i.r. (nujol) 2.95 (O—H), 5.2, and 6.0 μ (C=O); R_f^{MPW} 0.21 (N), R_f^{BAW} 0.20 (N), R_f^{MAW} 0.42 (N).

Anal. Calcd. for $C_4H_7NO_2$: C, 32.23; H, 4.73; N, 9.38. Found: C, 32.19; H, 4.89; N, 9.35.

erythro-β-*Hydroxy*-DL-*aspartic Acid Dimethyl Ester Hydrochloride*

A solution of dimethylsulfite in methanol was prepared by the addition of 34 ml (0.48 mole) thionyl chloride to 230 ml of ice-cold methanol stirred magnetically. To this solution was added 23.0 g (0.15 mole) *erythro*-HAA and the mixture was refluxed 6 h. The solution was evaporated on a rotary evaporator, and the residue was redissolved in ca. 100 ml of methanol and the solution again evaporated to dryness. This process was repeated twice to remove excess hydrogen chloride. The resulting solid was pumped mechanically for 2 h and dissolved in a minimum amount of hot methanol. The solution was cooled and diluted with ether until crystals appeared. Slow dilution with ether as crystallization proceeded gave 25.0 g (76%) of crude *erythro*-β-hydroxy-DL-aspartic acid dimethyl ester hydrochloride; m.p. 148–151°; i.r. (KBr) 3240 ($\overset{+}{N}H_3$), 1750 cm^{-1} (C=O); n.m.r. (D_2O) δ 4.85 and 4.75 (d, 2, J = 2.8 Hz, H_β, H_α), and 3.83 p.p.m. (s, 6, —OCH_3); R_f^{MPW} 0.90 (N). A sample recrystallized three times from methanol–ether for analysis melted at 152–153°.

Anal. Calcd. for $C_6H_{12}ClNO_5$: C, 33.73; H, 5.66; N, 6.56. Found: C, 33.49; H, 5.78; N, 6.71.

threo-β-*Hydroxy*-DL-*aspartic Acid Dimethyl Ester Hydrochloride*

The procedure for synthesis of the *threo* ester hydrochloride was the same as that described for the *erythro* isomer; yield 31.7 g (96%); m.p. 134–136°; i.r. (nujol) 3.05 (O—H), 3.20 ($\overset{+}{N}H_3$), 5.70, and 5.75 μ (C=O); n.m.r. (D_2O) δ 4.91 and 4.48 (d, 2, J = 3.0 Hz, H_α, H_β) 3.88 (s, 3, —OCH_3), and 3.84 p.p.m. (s, 3, —OCH_3); R_f^{MPW} 0.91 (N), R_f^{MAW} 0.78 (N). Recrystallization of the crude product from methanol–ether gave an analytical sample.

Anal. Calcd. for $C_6H_{12}ClNO_5$: C, 33.73; H, 5.66; N, 6.56; Cl, 16.60. Found: C, 33.95; H, 5.69; N, 6.85; Cl, 16.53.

1. M. Miller. J. Med. Chem. **6**, 233 (1963).
2. T. Kaneko and H. Katsura. Bull. Chem. Soc. Japan, **36**, 899 (1963); Y. Liwschitz, Y. Rabinson, and A. Haber. J. Chem. Soc. 3589 (1962).
3. (*a*) K. Pachler. Z. Anal. Chem. **224**, 211 (1967); (*b*) K. Pachler. Spectrochim. Acta, **19**, 2085 (1963); (*c*) H. Ogura, Y. Arata, and S. Fujiwara. J. Mol. Spectrosc. **23**, 76 (1967); (*d*) R. Martin and R. Mathur. J. Amer. Chem. Soc. **87**, 1065 (1965); (*e*) S. Fujiwara and Y. Arata. Bull. Chem. Soc. Japan, **37**, 344 (1964); (*f*) F. Taddei and L. Pratt. J. Chem. Soc. 1553 (1964); (*g*) O. Jardetzsky and C. Jardetzsky. J. Biol. Chem. **223**, 383 (1958).
4. M. Karplus. J. Amer. Chem. Soc. **85**, 2870 (1963).
5. J. Shoji, K. Tori, and H. Otsuka. J. Org. Chem. **30**, 2772 (1965).
6. (*a*) R. A. Alberty and P. Bender. J. Amer. Chem. Soc. **81**, 542 (1959); (*b*) O. Gawron and T. P. Fondy. J. Amer. Chem. Soc. **83**, 3634 (1961).
7. E. L. Eliel, N. L. Allinger, S. J. Angyal, and G. A. Morrison. Conformational analysis. Interscience Publishers, Ltd., New York, 1965. Pp. 10–11.
8. G. Payne and P. Williams. J. Org. Chem. **24**, 54 (1959).
9. K. Pachler. Spectrochim. Acta, **20**, 581 (1964).

Can. J. Chem. Downloaded from www.nrcresearchpress.com by 210.87.254.5 on 09/05/12
For personal use only.

Reaction of methyl azidoformate with norbornene[1]

A. C. OEHLSCHLAGER, R. S. MCDANIEL, A. THAKORE, P. TILLMAN, AND L. H. ZALKOW[2]
Department of Chemistry, Simon Fraser University, Burnaby 2, British Columbia
AND
Department of Chemistry, Oklahoma State University, Stillwater, Oklahoma

Received July 11, 1969

The thermal reaction of methyl azidoformate and norbornene has been found to proceed via 1,3-dipolar-cycloaddition yielding *exo* triazoline adduct, **15***a*. Thermal decomposition of the triazoline results in the loss of nitrogen and the formation of at least 5 products. The major products of the thermal decomposition in decalin were 3-carbomethoxy-3-azatricyclo(3.2.1.$0^{2,4}$ ^{exo})octane, **18***a*, and *N*-carbomethoxy-2-norbornimine, **20**. In addition, *syn*-2-norbornene-7-methyl carbamate, **21**, and 3-carbomethoxy-3-azatricyclo(3.2.1.$0^{2,3}$ ^{endo})octane, **19***a*, were isolated. The thermal decomposition of the triazoline adduct is considered to proceed by a multi-step mechanism. The first step is considered to involve heterolytic cleavage of the N_3—N_4 bond to give a zwitterion which may lead to products or rearrange *via* carbon–carbon bond cleavage to give a diazoalkyl imine.

Canadian Journal of Chemistry, 47, 4367 (1969)

Introduction

The thermal and photochemical reaction of ethyl azidoformate (**1**) with several acyclic and monocyclic alkenes has been investigated in detail by Lwowskii and co-workers (2). Thus, both the thermal and photolytic reaction of **1** with cyclohexene (**2**) gave approximately the same distribution of products consisting of aziridine, (**3**), urethanes (**4**–**7**), and 3,3′-biscyclohexenyl (**8**). Nearly the same product distribution was also observed from the base catalyzed decomposition of *N*-*p*-nitrobenzenesulfonoxyurethan (**9**) in cyclohexene. These observations, coupled with the observation that the rate of thermal decomposition of **1** in cyclohexene and cyclohexane was identical, led these workers to formulate the

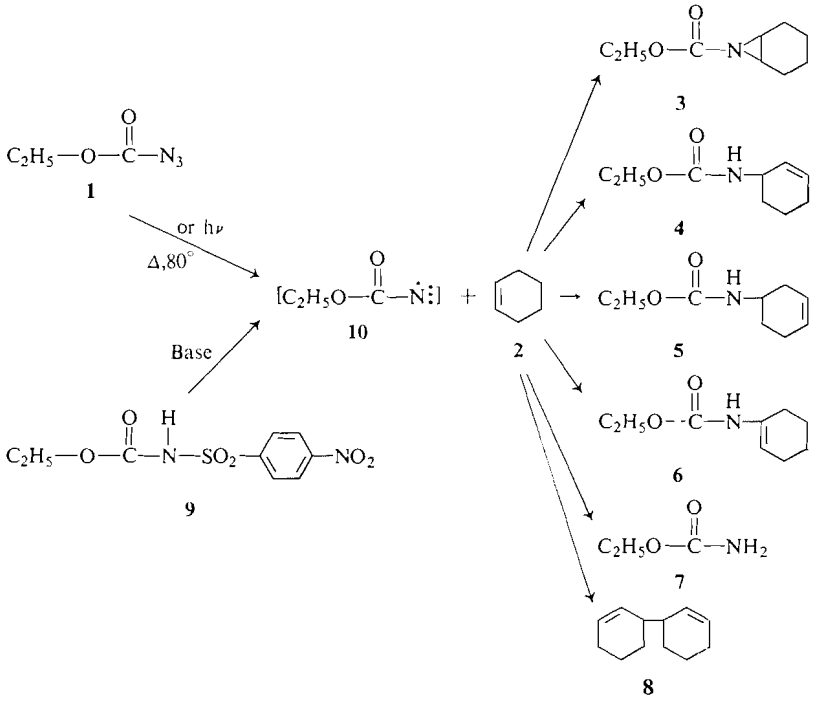

[1]For a preliminary account of this work see ref. 1.
[2]Present address: School of Chemistry, Georgia Institute of Technology, Atlanta, Georgia.

Can. J. Chem. Downloaded from www.nrcresearchpress.com by 210.87.254.5 on 09/05/12
For personal use only.

reaction of **1**, with cyclohexene as proceeding to carboethoxynitrene (**10**) prior to reaction with the carbon–carbon double bond. A further test of this mechanism would be to determine the molecular order to azide decomposition with respect to alkene.[3]

An observation that the reaction was zero order in alkene and first order in azidoformate would support the nitrene mechanism. If however the reaction was found to be first order in alkene and azidoformate, initial reaction between the azido group and alkene would be indicated.

The latter has been found to be the case in the reactions of aryl azides (**11**) and alkenes. In all cases reported thus far the thermal reaction proceeds by initial 1,3-dipolar cycloaddition of the azido group to the alkene to produce 1,2,3-Δ^2-triazolines (**12**), which may thermally decompose under the conditions of the reaction to give aziridines, imines, and products of molecular rearrangement (4, 5).

For the relatively thermally stable aryl azides, the 1,3-dipolar cycloaddition reaction with alkenes has a lower activation energy than nitrene generation (6). Conjugation, angle strain, and the presence of α heteroatoms have all been found to increase the reactivity of alkenes toward the 1,3-dipolar cycloaddition by aryl azides (7). The rate of azide–alkene addition is also increased by electron-withdrawing substituents on the azido group (8).

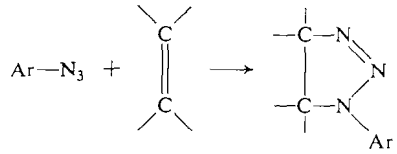

11 **12**

The apparent intervention of carboalkoxynitrenes in the reactions of azidoformates with unstrained alkenes prompted our investigation of methyl azidoformate (**13***a*) with an angle strained alkene, norbornene (**14**). Both the angle strain present in the alkene and the electron-withdrawing effect of the carbomethoxy group of the azide could be expected to facilitate a reaction via 1,3-dipolar cycloaddition. Since this mode of reaction was indeed observed we have

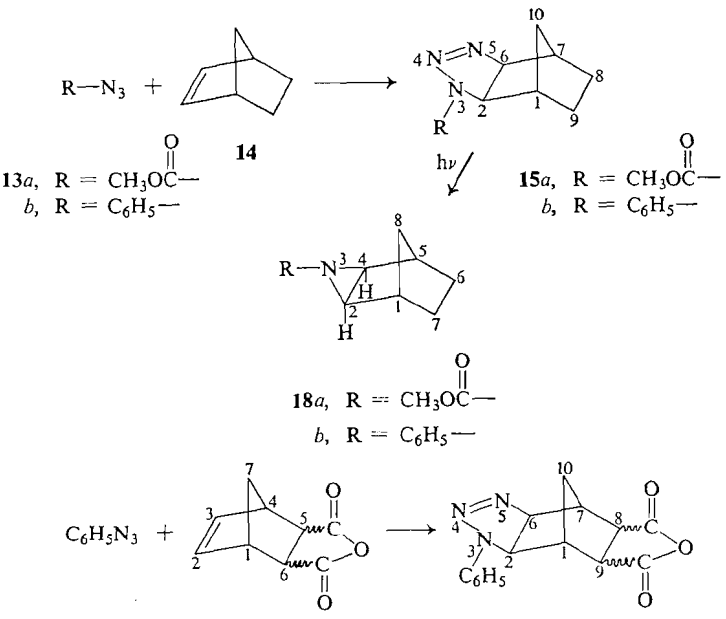

13*a*, R = $CH_3OC(=O)$—
b, R = C_6H_5—

14

15*a*, R = $CH_3OC(=O)$—
b, R = C_6H_5—

18*a*, R = $CH_3OC(=O)$—
b, R = C_6H_5—

16

[3]Breslow and co-workers (3) have shown that the thermal decomposition of octadecylazidoformate in olefinic solvents obeys first order kinetics but the molecularity of the azide decomposition with respect to olefin was not determined.

TABLE I

Rates and activation parameters for the addition of methylazidoformate to norbornene in 1,4-dioxane

Temperature (°C)	$k \times 10^5$ (l mole^{-1} s^{-1})	$\Delta H^{\ddagger}$ (kcal/mole)	$\Delta S^{\ddagger}$ (cal/mole deg)
39.65±0.02	3.93±0.01		
40.80±0.02	4.30±0.03	15.0	−30.0
49.75±0.1	8.41±0.03		
59.30±0.01	17.20±0.01		
71.40±0.05	39.9 ±0.5		

been able to study in some detail the thermal decomposition of the 1,2,3-Δ^2-triazoline adduct initially formed. The thermal decomposition of this triazoline is compared with the thermolysis of the triazoline adducts obtained from the reaction of phenyl azide (**13***b*) with norbornene (9*a*) and *cis-exo*-norbornene-5,6-dicarboxylic anhydride (**16**) (9*b*).

Methyl azidoformate and norbornene react slowly at 40–50 °C in hydrocarbon solvent. A typical reaction at this temperature took several days and gave good yields (70%) of a low-melting solid. The nuclear magnetic resonance (n.m.r.) spectrum of this solid revealed a methoxyl resonance (δ 3.80) and a two hydrogen AB quartet with doublets (J = 8.5 Hz) centered at δ 3.53 and 4.43.

A two hydrogen AB quartet would be expected for the C-2 and C-6 hydrogens of either the triazoline, **15***a*, or the oxazoline, **17**, both of which are reasonable on mechanistic grounds. The n.m.r. spectrum of the known triazoline, **15***b*, contains a two proton AB quartet due to the C-2 and C-6 hydrogens with doublets (J = 9.3 Hz) centered at δ 3.65 and 4.51 (10).

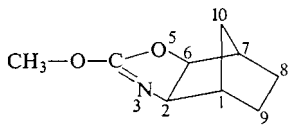

17

The observation that the solid product isolated evolves nitrogen when heated in an inert solvent indicates the triazoline structure **15***a* is correct. That a 1,3-dipolar cycloaddition of methyl azidoformate (**13***a*) and norbornene (**14**) had occurred was further substantiated by a kinetic study of the reaction.

The rates of addition of **13***a* to **14** were determined at different concentrations of norbornene and at different temperatures by infrared (i.r.) spectroscopy. The reaction was found to be first order in both azidoformate and norbornene. Thus graphs of second order plots of $1/C$ (azide) vs. time were linear over at least two half lives. The rate constants reported were determined graphically and are average values of two or more determinations. The enthalpy and entropy of activation were determined by least squares treatment of log k/T vs. $1/T$ using values in Table I. The standard deviation was found to be 0.013.

The relatively small enthalpy of the activation and strongly negative entropy of activation observed in the present addition are indicative of a 1,3-dipolar cycloaddition. The addition of phenyl azide to norbornene has been found (10) to have similar activation parameters ($\Delta H^{\ddagger}$ = 15.2 kcal/mole and $\Delta S^{\ddagger}$ = −29 cal/mole deg).

The triazoline ring in **15***a* is assumed to be fused *exo*. There is ample precedent for the addition of organic azides to norbornene from the least hindered *exo* side (11). Indeed no *endo* addition of organic azides to norbornenes has yet been detected. There is no reason to suspect a different course of addition in the present reaction. Furthermore, photolytic elimination of nitrogen from **15***a* gives exclusively one product which is assigned the *exo* aziridine structure, **18***a* (12).

Thermal decomposition of the *exo* triazoline **15***a* in dry decalin at 113.5° for 3 days gave a mixture that n.m.r., thin-layer chromatography (t.l.c.), and gas–liquid phase chromatography (g.l.p.c.) analyses showed to have 5 components (see Table II). The principle components, **18***a*, **19***a*, **20**, and **21** were isolated by a combination of g.l.p.c. and column chromatography. Compound **22** could not be isolated in a pure state but

Can. J. Chem. Downloaded from www.nrcresearchpress.com by 210.87.254.5 on 09/05/12
For personal use only.

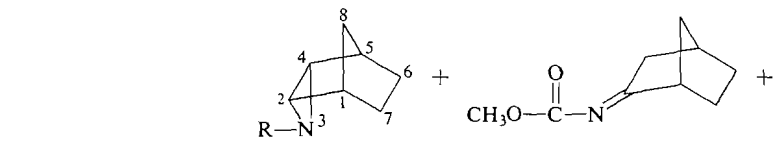

15*a* → **18***a* + **19***a*, R = $CH_3O-\overset{O}{\overset{\|}{C}}$ **20**
b, R = C_6H_5-

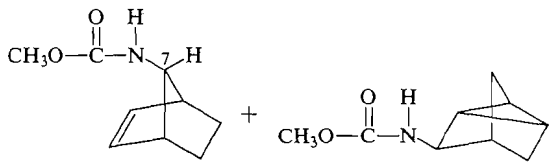

21 **22**

TABLE II

Products from decomposition of **15***a* in decalin

Component	%
exo Aziridine **18***a*	51.7
Imine **20**	36.1
endo Aziridine **19***a*	6.7
Unsaturated carbamate **21**	4.7
Unknown **22**	0.8

is probably the cyclopropyl isomer of **21** (9*a*). Analysis of the pyrolysate by g.l.p.c. after prolonged (24 h) heating showed there was no change in the product composition. Therefore the interconversion of products is not appreciable at the reaction temperature.

The i.r. spectrum of **18***a* was devoid of N—H absorptions and also of C=N absorption. Comparison of the n.m.r. spectra of **18***a* with the bicyclic *exo* aziridine (**18***b*) which was obtained from the photolysis of triazoline, **15***b*, (9*a*) showed basic similarities. A low field singlet was present in both cases and was attributed to the hydrogens attached to carbons bearing nitrogen. In **18***a* this occurred at δ 2.46 and in **18***b* at δ 2.10. A high field doublet (J = 9.5 Hz) at δ 0.73 in the n.m.r. of **18***a* is attributable to the *anti*-C_8-hydrogen, and a doublet of triplets (J = 9.5 and 1.8 Hz) at δ 1.51 is attributable to the *syn*-C_8-hydrogen. These signals are characteristic of 3-azatricyclo(3,2,1,$0^{2,4\text{-}exo}$)octanes (13).

Since we obtained the corresponding *endo* aziridine **19***a* (see below) in the thermal decomposition of **15***a*, we were able to establish its absence in the photolytic decomposition. If any *endo* triazoline were present in **15***a*, its photolysis should have given the *endo* aziridine **19***a*.

The *endo* aziridine (**19***a*) was isolated from the pyrolysate by preparative gas chromatography. The n.m.r. spectrum of **19***a* exhibited 4 distinct signals in the ratio of 3:2:2:6 in the direction of stronger field. Specifically, the signals appeared as follows: a singlet centered at δ 3.58 assigned to the methoxyl hydrogens; a triplet (J = 2.0 Hz) at δ 3.0 assigned to the hydrogens attached to carbon bearing nitrogen at C-2 and C-4; a broad symmetrical peak at δ 2.37 assigned to the two bridgehead hydrogens, and a complex pattern at δ 0.96–1.82 corresponding to the three methylene groups of the norbornyl ring system. The spectrum was very similar to that of the known (9*a*) *endo* aziridine (**19***b*). The absence of N—H stretching bands and of bands due to C=N stretching in the i.r. spectrum of **19***a* supports the proposed structure.

The imine, **20**, was identified by its hydrolysis to 2-norbornanone and methyl carbamate. The 2-norbornanone was characterized by the mixture melting point of its 2,4-dinitrophenylhydrazone with that of an authentic derivative.

The unsaturated carbamate **21** was isolated by gas chromatography and characterized by its n.m.r. and i.r. spectra. The i.r. spectrum of **21** showed an absorption at 3300 cm^{-1} (N—H). The n.m.r. spectrum of **21** contained signals in the ratio 2:3:1:1:2:4 in the direction of stronger field. Two olefinic hydrogens appeared as a symmetrical triplet (J = 2.9 Hz) centered at δ

Can. J. Chem. Downloaded from www.nrcresearchpress.com by 210.87.254.5 on 09/05/12
For personal use only.

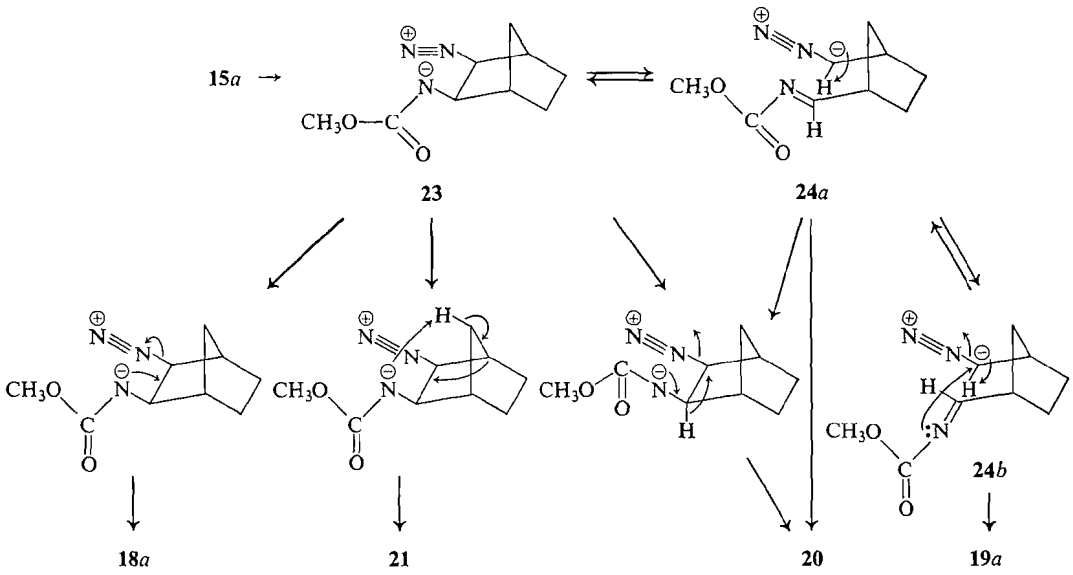

5.85. The hydrogen attached to nitrogen (exchanged with D_2O) gave a broad peak at δ 5.06. The hydrogen attached to carbon (C-7) bearing nitrogen appeared at δ 3.58 as a singlet.

The unsaturated carbamate, **21**, was reduced with H_2 over PtO_2 to give norbornane-7-methylcarbamate which was in turn hydrolyzed to 7-norbornamine, which when treated with acetic anhydride gave the 7-acetamidonorbornane. The 7-acetamidonorbornane prepared in this manner was identical to an authentic sample (14) and different from both 2-*exo*- and 2-*endo*-acetamidonorbornanes by g.l.p.c.

The pyrolysis of azide adducts of norbornene gives principally *exo* aziridines and imines. Recent investigations (9) have shown that, in addition to these products, varying amounts of Wagner–Meerwein rearranged and *endo* aziridine products were also formed. The production of the primary and minor products of pyrolysis of azide–norbornene adducts such as **15***a* is satisfactorily explained by the mechanism advanced below.

We consider the thermal decomposition of **15***a* to proceed *via* initial heterolytic cleavage of the N_3—N_4 bond of **15***a* (**15***a* → **23**) followed by carbon–carbon bond cleavage to give **24**. Each of these intermediates may lead to products as shown. The proposal for initial N_3—N_4 bond cleavage is based on the observation that the thermal decomposition of **15***a* is accelerated in more polar solvents (see Table III). This parallels the behavior noted in the decomposition of **15***b* (9*a*) and several related triazolines (5, 15, 16). The direction of N_3—N_4 heterolysis is considered by others (15, 16*a–d*) and ourselves (9) to involve formation of a negative charge on N-3 of the triazoline since electron withdrawing substituents at this position aid the pyrolysis reaction in analogous systems.

TABLE III

Relative rates of decomposition of triazoline **15***a* in different solvents

Solvent	Temperature (°C)	$t_{\frac{1}{2}}$ (min)
$(C_6H_5)_2C_2H_4$	71.40±0.05	4.68×10^4
Triglyme	71.40±0.05	3.98×10^2
DMSO	71.40±0.05	6.54×10
Decalin	113.5 ±0.2	9.09×10^2

These data lead to the formulation of the initial species generated during the decomposition of **15***a* as **23**. Once formed, **23** may lose nitrogen to form the *exo* aziridine, **18***a*, the imine, **20**, and Wagner–Meerwein rearrangement products of which the carbamate, **21**, has been identified.

Alternatively, carbon–carbon bond cleavage may occur in **23** to produce **24**. Reformation of the carbon–carbon bond in **24** could produce **23** or an isomeric structure in which the vicinal

Can. J. Chem. Downloaded from www.nrcresearchpress.com by 210.87.254.5 on 09/05/12
For personal use only.

nitrogen groups are *cis–endo*.[4] Any reclosure which produces an *endo*-carbomethoxy substituted nitrogen at C-2 could give rise to the *endo* aziridine **19***a* by loss of nitrogen.

Baldwin has put forward a scheme involving species analogous to **23** and **24** to account for the formation of **25** from the decomposition of **15***b* in the presence of phenyl isocyanate (17).

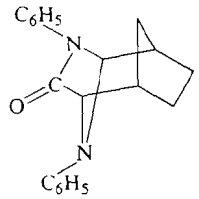

25

Furthermore, in our studies of the pyrolysis of **15***b*, which also produces a small amount of *endo* aziridine (**19***b*), we noted the appearance of an i.r. absorption at 2175 cm^{-1} during the pyrolysis (160°). This absorption is clearly in the region expected for intermediates such as **23** and **24**. It was observed to appear early in the reaction and decrease in intensity as the reaction proceeded (9*a*). Similar measurements during the decomposition of **15***a* were inconclusive.

The determination of $\Delta H^{\neq}$ and $\Delta S^{\neq}$ for the thermal decomposition of **15***a* was not attempted since the rate of nitrogen evolution was not strictly first order. During the later stages of the reaction, nitrogen evolution showed a positive deviation from first order kinetics. This type of deviation could mean that the generation of **23** and/or **24***a* is faster than their conversion to nitrogen and products (9*a*, 16*c*). Since there are other interpretations which may be placed on this result and since we were unsuccessful in detecting i.r. absorptions in the 2000–2500 cm^{-1} region for **23** or **24***a* during the pyrolysis in an i.r. hot cell, the evidence for these as stable intermediates is at present only circumstantial.

Comparison of the *exo-endo* aziridine ratio resulting from the thermal decomposition of triazolines **15***a* (15.7:6.7), **15***b* (49:9) (9*a*), and **16** (24:76) (9*b*) reveals that in norbornene triazolines **15***a* and **15***b*, the substituent on N-3 has only a small effect. The rather pronounced increase in *endo* aziridine formation in the case of **16** may be attributed to the enhancement of carbon–carbon bond cleavage during the pyrolysis of this triazoline, because of the stabilization of the incipient negative charge at C-6 by the electron-withdrawing anhydride groups (9*b*). Since Baldwin *et al.* (17) obtained a 60% yield of **25** in the pyrolysis of **15***b* in phenyl isocyanate and only 9% of *endo* aziridine **19***b* was isolated from pyrolysis of **15***b* in decalin, it is clear that the amount of *endo* aziridine formation may not be an accurate measure of the amount of C—C bond cleavage which is involved in the thermolysis of these triazolines. Assuming that a greater amount of carbon–carbon bond cleavage does occur in **16** than in **15***a* and **15***b*, it is still rather difficult to explain the *predominance* of *endo* aziridine from the pyrolysis of **16**.

The pathway from **15***a* to the *endo* aziridine **19***a* is not clear at present; it may involve conversion of **24***b* to the *endo–cis* analogue of **23** followed by loss of nitrogen and aziridine ring closure. Alternatively the *endo* triazoline might be formed from **24***b* by intramolecular 1,3-dipolar cycloaddition of the diazoalkane and imine groups. This could then undergo decomposition to **19***a* in a manner similar to the **15***a* → **23** → **18***a* conversion. Since diazoalkanes and imines combine in 1,3-dipolar cycloadditions only at moderate rates (18) and the triazoline products would be unstable at the reaction temperature, it seems reasonable that if the *endo* triazoline were involved in the production of the *endo* aziridine **19***a*, it would be difficult to detect. It is also not clear if the **23** → **24** reaction is reversible and if the imine **20** is formed via **23** as shown or also via **24**.

Experimental

Carbon and hydrogen analysis was performed by Midwest Microlabs, Inc., Indianapolis, Indiana. All thin layer chromatograms were developed in iodine vapor. Melting points were determined by a Fisher-Johns melting point apparatus and are uncorrected. Infrared spectra were recorded with a Unicam S.P. 200 i.r. spectrophotometer or a Beckman IR-5A spectrophotometer. Nuclear magnetic resonance spectra were recorded on Varian A-60 n.m.r. spectrometers with TMS as an internal standard. Analysis by g.l.p.c. was done using an Aerograph HiFi chromatograph and preparative work was done using an Aerograph autoprep 700 chromatograph. Gas–liquid phase chromatographic columns used were a 5 ft × 1/8 in. column with 20% XF-1150 on 60–80 Mesh Chrom

[4]It is of course possible for reformation of the carbon–carbon bond of **24** to occur in such a way that the vicinal nitrogen groups are *trans* in two possible orientations. There is no way *a priori* to determine if this is a significant process since the zwitterions thus formed would also be expected to lead to the products observed.

Can. J. Chem. Downloaded from www.nrcresearchpress.com by 210.87.254.5 on 09/05/12
For personal use only.

Can. J. Chem. Downloaded from www.nrcresearchpress.com by 210.87.254.5 on 09/05/12
For personal use only.

W for analysis, a 10 ft × 1/4 in. Craig's polyester column, and a 5 ft × 1/2 in. column with 20 in. XF-1150 on 60–80 Mesh Chrom W for preparative work.

*Preparation of 3-Carbomethoxy-3,4,5-triazatricyclo-(5.2.1.0^{2,6})dec-4-ene (**15a**)*

Methyl azidoformate (19, 20) (0.11 moles, 11 g) was added to 0.12 moles (14.2 g) of norbornene (Aldrich) dissolved in 80 ml of 30–60° petroleum ether. The solution was refluxed (45°) for several days until the azide peak in the i.r. spectrum had disappeared. A white solid (**15**a) was obtained in 70% yield which after recrystallization from *n*-hexane melted at 35.0–35.5 °C. Nuclear magnetic resonance data: δ 0.93–1.73 (m, 6, C-8, C-9, C-10); 2.55 (m, 1, C-1); 2.68 (m, 1, C-7); 3.80 (s, 3, OCH_3); 3.53 (d, 1, J = 8.5 Hz, C-2); 4.43 (d, 1, J = 8.5 Hz, C-6).

Pyrolysis of **15**a at 71.4 °C in diphenylethane, triglyme, and dimethyl sulfoxide gave 93–98% of the theoretical amount of nitrogen.

*Thermal Decomposition of 3-Carbomethoxy-3,4,5-triazotricyclo(5.2.1.0^{2,6})-4-decene (**15a**) in Decalin*

A 1 g sample of the triazoline, **15**a, was thermally decomposed at 113.5 °C in 10 ml of freshly distilled decalin under anhydrous conditions. After 72 h, a sample of the pyrolysate was injected onto the 1/8 in. XF 1150 column.

After 120 h, a second sample was analyzed by g.l.p.c. and found to be unchanged. Water was mixed with the remaining pyrolysate and the mixture was left for 24 h at room temperature. The appearance of norcamphor and methyl carbamate as well as the marked decrease in the amount of imine was shown by g.l.p.c.

Separation of the Products of Thermal Decomposition

The decalin was removed by distillation under vacuum and a portion of the remaining fraction was chromatographed on neutral alumina. The fractions collected were analyzed by g.l.p.c. and those showing the greatest enrichment in a particular component were used in isolating the pure components by preparative g.l.p.c.

*3-Carbomethoxy-3-azatricyclo(3.2.1.0$^{2,3\ endo}$)octane (**19a**)*

The *endo* aziridine, **19***a*, was isolated by g.l.p.c. and had a retention time of 4.8 min. Nuclear magnetic resonance (CCl_4): δ 0.96–1.82 (m, 6, C-6, C-7, C-8); 2.37 (s, 2, C-1, C-5); 3.0 (t, 2, J = 2.0 Hz, C-2, C-4) (9*a*); 3.58 (s, 3, OCH_3). Infrared (film): no peaks due to N—H or C=N. Mass Spectrum Calcd.: M, 167; M/M + 1, 13.6. Found: M, 167; M/M + 1, 14.0.

*syn-2-Norbornene-7-methyl Carbamate (**21**)*

Column chromatography of 3.11 g of the pyrolysate on 50 g of Woehm neutral alumina gave 0.78 g of **18***a* upon elution with 0.5 l of 95:5 petroleum ether – diethyl ether. Elution with 0.5 l of 9:1 petroleum ether – diethyl ether gave 0.24 g of a mixture of **21** and **18***a*. Elution with 0.5 l of 6:4 petroleum ether – diethyl ether gave 0.18 g of **21**. After distillation of the last fraction (b.p. 0.5 mm/70–75 °C) under vacuum, **21** showed by i.r.: ν_{max}(film) 3300 (N—H), 1725 (amide I), and 1520 (amide II) cm^{-1}; n.m.r. (CCl_4): δ 5.85 (t, 2, J = 2.0 Hz, C-2, C-3); 2.78 (s, 2, C-1, C-4); 3.72 (s, 3, OCH_3); 5.06 (s, 1, N—H); 3.58 (s, 1, C-7); 0.8–1.9 (m, 4, C-5, C-6).

Anal. Calcd. for $C_9H_{13}NO_2$: C, 64.65; H, 7.87. Found: C, 64.70; H, 7.81.

Conversion of syn-2-Norbornene-7-methyl Carbamate to 7-Acetamidonorbornane

A solution of 0.70 g of **21** in 2 cc of methyl acetate was stirred under an H_2 atmosphere with 0.30 g of PtO_2. After hydrogen uptake (≈ 10 cc) ceased, the solution was filtered and the catalyst washed with 5 cc of methyl acetate. Evaporation of the solvent *in vacuo* gave 0.66 g of norbornane-7-methyl carbamate, m.p. 79–80.5 °C after recrystallization from petroleum ether in the cold; ν_{max}(KBr) 3260 (NH), 1725, 1690 (amide I), 1540 (amide II), and 1265 (C—O) cm^{-1}; n.m.r. (CCl_4): δ 5.15 (s, 1, N—H); 3.57 (s, 3, OCH_3); 3.45 (s, 1, C-7); 1.0–2.2 (m, 10, C-1 to C-6).

A 2 cc aqueous solution of sodium hydroxide (6 *N*) containing 50 mg of dihydro-**21** was refluxed for 4 h. The solution was cooled and extracted with two 10 cc portions of petroleum ether. The petroleum ether extract was stirred with 0.6 g of acetic anhydride for 0.5 h, then sufficient aqueous sodium bicarbonate was added to destroy the excess acetic anhydride. The petroleum ether portion was separated from the aqueous layer and dried over anhydrous magnesium sulfate. Evaporation of the petroleum ether gave 35 mg of an oil. Gas chromatographic analysis of this oil on a 10 ft × 0.25 in. Craig's polyester column at 180 °C using a flow rate of 90 ml/min revealed two peaks in the ratio of 8:2 eluted at 12.5 and 23.5 min respectively. The larger peak was identical to dihydro-**21** upon mixed injection. The smaller peak was identical to 7-acetamido norbornane (14) upon mixed injection and different from both 2-*exo*- and 2-*endo*-acetamidonorbornanes (14), whose retention times under these conditions were 27.3 and 26.0 min respectively.

*3-Carbomethoxy-3-azatricyclo(3.2.1.0$^{2,3\ exo}$)octane (**18a**)*

The *exo* aziridine, **18***a*, was isolated by g.l.p.c. The sample was identical in all respects with a sample prepared by photolysis of **15***a*. A solution of 1.2 g of **15***a* in 125 cc of spectral grade cyclohexane was irradiated for 2 h with a Hanovia 200 W. mercury vapor lamp through a Pyrex filter. Evaporation of the solvent gave an oil which after distillation (b.p. 10 mm, 78–80 °C) under vacuum gave 0.58 g of aziridine **18***a*, n.m.r. (CCl_4): δ 0.73 (d, 1, $J_{8a,8s}$ = 9.5 Hz, C-8s); 2.40 (s, 2, C-1, C-5); 2.46 (s, 2, C-2, C-4); 3.51 (s, 3, OCH_3).

*N-Carbomethoxy-2-norbornimine (**20**)*

The imine, **20**, was isolated from the pyrolysis mixture by g.l.p.c. Nuclear magnetic resonance (CCl_4): δ 1.9 (m, 6, C-6, C-7); 2.05 (quartet, 2, C-3); 2.50 (s, 1, C-4); 2.72 (s, 1, C-1); 3.60 (s, 3, OCH_3). Infrared (film) data showed the absence of any N—H bonds.

A 0.330 g sample of the pyrolysis mixture was shaken with D_2O. The n.m.r. spectrum of the organic layer showed the disappearance of the signal at δ 3.60. The sample was dissolved in 50 cc of methanol containing 500 mg of 2,4-dinitrophenylhydrazine. The methanol was evaporated *in vacuo* and the mixture chromatographed on acid washed alumina using benzene as the eluent.

Evaporation of the solvent gave 0.317 g of the 2,4-dinitrophenylhydrazone of norbornanone, m.p. 128–129 °C. After recrystallization from ethanol, the derivatives melted at 130–131 °C, (lit. (21) m.p. 129.5–130.5 °C). The mixed m.p. (130–131°) with an authentic sample (m.p. 130–131°) prepared from norbornanone (Aldrich) was undepressed.

Kinetic Method for Rates of Addition of Azides to ***14***

The 2100–2200 cm^{-1} region of the i.r. was chosen for following the addition reactions. In this region the maximum difference in the magnitude of the extinction of azides and the olefin and products occurred. The i.r. measurements were taken using matched fixed thickness solution cells. The transmittance of 0.05 and 0.250 mm fixed thickness solution cells containing 0.2 *M* norbornene, 0.2 *M* products, and solvent, differed by less than 0.009 transmittance unit in this region. The transmittances of a solution of known azide concentration were measured and plots of azide concentration vs. log transmittance were linear. The transmittance of each sample from the kinetic experiments was measured and the concentration of azide was determined by graphical interpolation on a log transmittance vs. concentration plot. A plot of log transmittance vs. azide concentration was made for each solvent used.

Determination of Rates of Addition of Methyl Azidoformate to Norbornene

Separate solutions 0.2 *M* in norbornene and 0.2 *M* in azide in the appropriate solvent were made up just before use. Equal volumes (1.0 cc) of each solution were pipetted into precooled (in dry ice) ampules which were immediately sealed and stored at dry ice – acetone bath temperatures until they were immersed in a thermostatted bath. Duplicate ampules were periodically removed from the bath and placed in a dry ice – acetone bath to quench the reaction. After all ampules for a given experiment had been frozen, each ampule was thawed and immediately (within 5 min) analyzed by i.r.

Reactions were followed to at least 85% completion. Runs lasted from 8 to 100 h and usually involved a transmittance change of 0.5 transmittance unit.

*Kinetic Determination of the Pyrolysis of Triazoline (****15****a)*

A solution of 0.997 g of triazoline, **15***a*, in 50 ml of freshly distilled solvent was made while passing pure dry nitrogen through the liquid for 1 h at room temperature. The solution was kept in a sealed bottle.

The reaction was carried out in a glass reaction vessel immersed in an oil bath maintained at constant temperature (±0.15 °C). The measurements of gas evolution were made with the aid of a thermostatted 100 ml gas burette attached to the reaction vessel by a glass capillary. The results were reproducible to within ± 2% as shown by graphic and computer analysis.

A typical run was carried out by placing 20 ml of solvent into the reaction vessel and allowing it to come to equilibrium while flushing the system with dry nitrogen. To start a run, 10 ml of the triazoline solution was injected with a syringe into the reaction vessel. The system was sealed after 1 min and the volume of nitrogen evolved was recorded as a function of time. Plots of log $(V_\infty/V_\infty - V_t)$ vs. t, and log V_t vs. t gave smooth curves which exhibited divergence from linearity (9*a*). The $t_{\frac{1}{2}}$ values are recorded in Table III for various solvents.

Acknowledgments

A. C. O. wishes to thank the National Research Council of Canada and the Simon Fraser University Research Fund for partial support of this work. R. S. M. wishes to thank the National Research Council of Canada 1967–1968 Bursary.

1. A. C. Oehlschlager, P. Tillman, and L. H. Zalkow. Chem. Commun. 596 (1965).
2. W. Lwowskii and T. W. Mattingly, Jr. J. Amer. Chem. Soc. **87**, 1947 (1965).
3. T. J. Prosser, A. F. Marcantonio, C. A. Genge, and D. S. Breslow. Tetrahedron Lett. 2483 (1964).
4. P. Scheiner. Tetrahedron, **24**, 349, 2757 (1967).
5. R. Huisgen, R. Grashey, and J. Sauer. *In* The chemistry of alkenes. S. Patel (*Editor*). Interscience Publishers, Inc., London. 1964. Chapter 11.
6. R. Walker and W. A. Waters. J. Chem. Soc. 1632 (1962).
7. A. S. Bailey and J. E. White. J. Chem. Soc. (B) 819 (1966).
8. P. Scheiner, J. H. Shomaker, S. Deming, W. J. Libbey, and G. P. Nowack. J. Amer. Chem. Soc. **87**, 306 (1965).
9. (*a*) R. S. McDaniel and A. C. Oehlschlager. Tetrahedron, **25**, 1381 (1969). (*b*) R. L. Hale and L. H. Zalkow. Tetrahedron, **25**, 1392 (1969).
10. R. Huisgen, R. Grashey, J. M. Vernon, and R. Kunz. Tetrahedron, **24**, 3311 (1965).
11. K. Alder and G. Stein. Ann. Chem. **501**, 1 (1933); Am. Chem. **515**, 165 (1935).
12. P. Scheiner. J. Org. Chem. **30**, 7 (1965).
13. K. Tori, K. Kitahonoki, Y. Takano, H. Tanida, and T. Tsuji. Tetrahedron Lett. 869 (1965).
14. L. H. Zalkow and A. C. Oehlschlager. J. Org. Chem. **28**, 3303 (1963).
15. A. L. Logothetis. J. Amer. Chem. Soc. **87**, 749 (1965).
16. (*a*) A. C. Oehlschlager and L. H. Zalkow. J. Org. Chem. **30**, 4205 (1965). (*b*) A. G. Anastassiou. J. Org. Chem. **31**, 1131 (1966). (*c*) K. D. Berlin, L. A. Wilson, and L. M. Raff. Tetrahedron, **23**, 965 (1967). (*d*) K. D. Berlin and R. Ranganathan. Tetrahedron, **25**, 793 (1969).
17. J. E. Baldwin, G. V. Kaiser, and J. A. Romersberger. J. Amer. Chem. Soc. **87**, 4114 (1965).
18. P. K. Kudaba. Tetrahedron, **22**, 2453 (1966).
19. M. O. Forester and H. E. Fierz. J. Chem. Soc. **93**, 81 (1908).
20. W. Lwowskii and T. W. Mattingly, Jr. J. Amer. Chem. Soc. **87**, 1953 (1965).
21. H. Kwart and L. Kaplan. J. Amer. Chem. Soc. **76**, 4079 (1954).

Can. J. Chem. Downloaded from www.nrcresearchpress.com by 210.87.254.5 on 09/05/12
For personal use only.

Preparation and properties of the hydroxyindole-3-carboxylic acids[1]

ROSANGELA MARCHELLI,[2] O. HUTZINGER, AND R. A. HEACOCK
Atlantic Regional Laboratory, National Research Council of Canada, Halifax, Nova Scotia

Received June 5, 1969

A procedure for the synthesis of the 4-, 5-, 6-, and 7-hydroxyindole-3-carboxylic acids starting from the corresponding 4-, 5-, 6-, and 7-benzyloxyindoles respectively has been devised. The benzyloxyindoles are converted to mixtures of their 1- and 3-carbethoxy derivatives by the action of ethyl chloroformate on their Grignard reagents. The hydroxyindole-3-carboxylic acids are then obtained by the alkaline hydrolysis and debenzylation of the benzyloxy-3-carbethoxyindoles.

Canadian Journal of Chemistry, 47, 4375 (1969)

Can. J. Chem. Downloaded from www.nrcresearchpress.com by 210.87.254.6 on 09/05/12
For personal use only.

In view of their importance in biology and medicine [cf. review by Cerletti (1)], the metabolism of indole compounds in plants and animals has been the subject of extensive studies in the past. In recent years the importance of the hydroxyindoles (cf. 2, 3), has also been recognized.

Whilst a considerable amount of research has been carried out on the metabolism of 3-indolylacetic acid (cf. 4, 5), very little has been reported on the metabolism of indole-3-carboxylic acid. Acheson and King reported that the urine of rats which had been fed or injected intraperitoneally with indole-3-carboxylic acid, contained the original acid (ca. 20%), the corresponding glucuronide, and 6-hydroxyindole-3-carboxylic acid (6). These authors further reported that oxidation of indole-3-carboxylic acid with a model hydroxylating system (Fe^{2+}, ascorbic acid, EDTA, oxygen) (cf. 7, 8) gave 5- and 6-hydroxyindole-3-carboxylic acid, indole, anthranilic acid, *N*-formylanthranilic acid, and a number of unidentified products. In other instances the oxidation of indole compounds with this system [i.e. indole (9), tryptophan (9) and skatole (10)], has resulted in the formation of all 4 hydroxyindole derivatives, hydroxylated in the benzene moiety of the indole ring, together with other products produced by oxidation of the pyrrole ring.

Before reinvestigating the hydroxylation of indole-3-carboxylic acid, it was desirable to have available authentic samples of the 4-, 5-, 6-, and 7-hydroxyindole-3-carboxylic acids. The synthesis of these 4 compounds is described in this paper.

R_f Values have been reported for both 5- and 6-hydroxyindole-3-carboxylic acids (6, 11, 12), but as far as the authors are aware the unambiguous syntheses of neither these two acids nor the 4- and 7-hydroxyindole-3-carboxylic acids have been reported.

The syntheses of these 4 acids have now been achieved, starting from the corresponding authentic benzyloxyindoles, which are available commercially. Since the reactions of the indole Grignard reagent with both ethyl chloroformate and carbon dioxide [i.e. methods which introduce a COOR group into the 3-position of the indole ring system where R = C_2H_5 or H respectively (cf. 13)] have recently been the subject of extensive studies in these laboratories (14, 15), it was decided to apply one of these methods to the syntheses of the 4-, 5-, 6-, and 7-hydroxyindole-3-carboxylic acids. Preliminary experiments suggested that the route via the ester was the more promising. The benzyloxyindoles were converted into their Grignard reagents and the subsequent reactions with ethyl chloroformate carried out at low temperatures and for relatively short periods of time.

Preliminary thin-layer chromatographic (t.l.c.) analysis of the reaction mixtures indicated that they invariably consisted of mixtures of 3 major components: the benzyloxy-1-carbethoxyindole, the benzyloxy-3-carbethoxyindole, and unchanged starting material. Their presence was confirmed by gas–liquid chromatography (g.l.c.). It was not possible to separate efficiently the reaction mixtures into their individual components by fractional crystallization, but satisfactory separations could be achieved using preparative scale t.l.c.

The reaction between the indole Grignard reagent and ethyl chloroformate proceeded satisfactorily at 0° with the 4-, 5-, and 6-isomers, but was carried out at 20° in the case of the 7-isomer

---

[1]Issued as NRCC No. 10933.
[2]NRCC Postdoctoral Fellow 1967–1969.

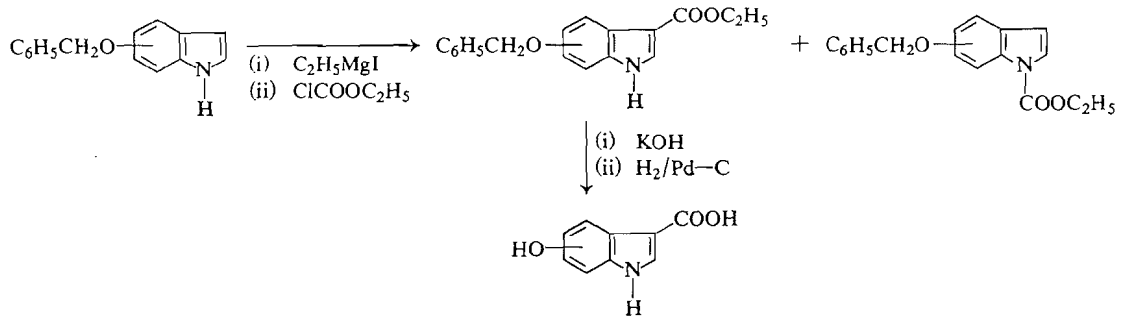

in view of the apparent insolubility of the 7-benzyloxyindole Grignard reagent in the reaction mixture at the lower temperature.

The position of the carbethoxy group in each of the major products was established by their infrared (i.r.) spectra. The carbonyl stretching peak of the 3-esters consistently occurred at lower frequencies (ca. 1670 cm^{-1}) than those of the 1-esters (ca. 1740 cm^{-1}) (cf. 14, 16). The typical N—H stretching peak at 3300–3200 cm^{-1} was also absent in the spectra of the 1-esters. Restricted rotation probably accounts for the fact that two peaks (at 1760 and 1730 cm^{-1}) are observed in the carbonyl region of the i.r. spectrum of 7-benzyloxy-1-carbethoxyindole. The 3-carbethoxy derivatives react slowly with Ehrlich's reagent on heating, whereas the 1-carbethoxy derivatives do not react with this reagent [cf. analogous behavior of 1- and 3-carbethoxyindole with Ehrlich's reagent (14)].

The benzyl group was easily removed from the 4 isomeric benzyloxy-3-carbethoxyindoles hydrogenolytically to give the corresponding 3-carbethoxyhydroxyindoles. The proton magnetic resonance (p.m.r.) spectra of these compounds confirmed that they were in fact substituted in the 3-position. The signals due to the indole 2-protons were observed as singlets (after exchange of the N—H protons with D_2O) at low field, in DMSO-d_6 [cf. Jardine and Brown (17)]. The chemical shifts of these signals and the fact that no significant secondary couplings were observed with any of the protons in the six-membered ring, confirmed that it was the indole 2-proton and not the indole 3-proton that was being observed.

The benzyloxyindole-3-carboxylic acids were readily obtained by hydrolysis of the corresponding benzyloxy-3-carbethoxyindoles with alcoholic potassium hydroxide. However, in the case of the 4-isomer it was impossible to prevent the formation of some decarboxylated product at the same time. In this case the decarboxylation reaction was presumably aided by steric assistance of the 4-benzyloxy group.

The benzyloxyindole-3-carboxylic acids were smoothly debenzylated by catalytic hydrogenation to give the desired hydroxyindole-3-carboxylic acids in high yield. The hydroxyindole-3-carboxylic acids are all high melting colorless crystalline solids, stable in the solid state; 7-hydroxyindole-3-carboxylic acid however, appears to be unstable in solution and is difficult to recrystallize without loss.

Experimental

The melting points were determined on a Thomas–Hoover capillary melting point apparatus and are uncorrected. Infrared, ultraviolet (u.v.), and p.m.r. spectra were recorded on Perkin–Elmer model 237, Beckman DK-2, and Varian A-60-A instruments respectively. The mass spectral data were obtained on a Consolidated Electrodynamics Corp. 21-110B mass spectrometer. A controlled temperature probe was used for introduction of the sample directly into the source.

Benzyloxy-1- and -3-Carbethoxyindoles

Preparation

A solution of the benzyloxyindole[3] (2.2 g, 0.01 moles) in anhydrous ether (50–75 ml) was added dropwise at 5°,[4] during 15–20 min, to the Grignard reagent, prepared from magnesium turnings (0.48 g, 0.02 moles) and ethyl iodide (3.2 g, 0.02 moles) in anhydrous ether (10 ml) (cf. ref. 18). The solution was boiled under reflux for 45 min to complete the formation of the indole Grignard reagent. The solution was cooled to 10°,[5] and ethyl chloroformate (1.2 g, 0.011 moles) added dropwise, with stirring, during 10 min. The resulting reaction mixture was cooled to 0°

[3]5-Benzyloxyindole was obtained from the Aldrich Chemical Co. and 4-, 6-, and 7-benzyloxyindoles were obtained from the Regis Chemical Co.

[4]Room temperature in the case of 7-benzyloxyindole.

[5]0° in the case of 6-benzyloxyindole.

Can. J. Chem. Downloaded from www.nrcresearchpress.com by 210.87.254.6 on 09/05/12
For personal use only.

Can. J. Chem. Downloaded from www.nrcresearchpress.com by 210.87.254.6 on 09/05/12
For personal use only.

TABLE I

Experimental data for benzyloxycarbethoxyindoles

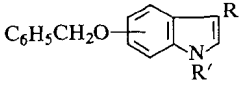

Isomer	Grignard reaction products	Melting point (°C)	Yield* (%)	Analyses (%) or *mass measurement on molecular ion:* Found† C	H	N	Spectral data: Infrared‡ (cm^{-1}) 3500–3100	1800–1600	Ultraviolet§ λ_{max} (mμ)
4-	R = $COOC_2H_5$; R′ = H	117–118	40	73.57	5.84	4.77	3235(s);3125(w)	1675(s)	277;[235];208
	R = H; R′ = $COOC_2H_5$	78–80	25	73.55	5.87	4.81	—	1740(s)	[297];289;[257];250;217
5-	R = $COOC_2H_5$; R′ = H	142–144	25	73.11	5.70	4.65	3200(s)	1670(s)	281;238
	R = H; R′ = $COOC_2H_5$	58–59	46	*295.1209*	—	—	—	1740(s)	[305];295;[265];238
6-	R = $COOC_2H_5$; R′ = H	131–132(d)‖	20	73.44	5.76	4.43	3235(s)	1665(s)	[302];274;[228];216
	R = H; R′ = $COOC_2H_5$	Oil	20	*295.1206*	—	—	—	1735(s)	264;[242];[234];229
7-	R = $COOC_2H_5$; R′ = H	166–167	18	73.04	5.93	4.54	3300(s);3140(w)	1665(s)	286;[230]
	R = H; R′ = $COOC_2H_5$	Oil	26	*295.1206*	—	—	—	1760(s);1730(s)	[300];291;[258];250;224

*Starting material (20–37%) was recovered in all cases.
†Calcd. for $C_{18}H_{17}NO_3$ (295.12084): C, 73.22; H, 5.76; N, 4.74.
‡In Nujol; as a thin film for 6- and 7-benzyloxy-1-carbethoxyindole: (s) = strong; (w) = weak.
§In methanol solution; shoulders in parentheses.
‖(d) = With decomposition.

TABLE II

Retention times of compounds present in the Grignard reaction mixtures

Compounds in the reaction mixture	Retention times (min) for isomers			
	4-	5-	6-	7-
Benzyloxyindole	1.58	2.50	2.00	0.42
Benzyloxy-1-carbethoxyindole	3.17	4.67	3.15	0.62
Benzyloxy-3-carbethoxyindole	8.12	14.25	2.48*	4.33

*Isothermal determination at 275°.

and the stirring continued for a further 15 min. The reaction mixture was poured into ice-water and extracted with ether (3 × 50 ml). The combined ether extracts were washed with saturated aqueous sodium bicarbonate, dried (Na_2SO_4), and concentrated to dryness *in vacuo*. The reaction products (which contained some unchanged starting material) were separated by preparative t.l.c. Glass plates (100 × 20 cm), coated with silica gel HF-254 (Merck; thickness, 0.9 mm) were used. In the case of the 7-benzyloxy isomer the developing solvent used was benzene – carbon tetrachloride (13:7). In all other cases the plates were developed twice in the same direction with cyclohexane – diisopropyl ether mixtures (a 1:1 mixture was used for the first development and a 4:1 mixture was used for the second run). Under these conditions each plate could initially be loaded with up to ca. 0.5 g of the solid mixture of reaction products. A total of 4 plates was used for each reaction mixture. The separated products were located on the developed chromatoplates by observing them in u.v. light. The bands of silica containing the individual components were scraped from the plates and the products obtained by extraction of the silica with ethanol (300 ml) at room temperature. The filtered ethanol extracts were concentrated to dryness *in vacuo* and the crude products recrystallized from suitable solvents, usually benzene – light petroleum or benzene for the 3-carbethoxy and 1-carbethoxy derivatives respectively. Details of the yields of the products obtained and their physical properties are given in Table I.

Gas–liquid Chromatography

A Varian Aerograph model 204, dual column instrument, fitted with two hydrogen-flame ionization detectors; a 6 ft × 1/8 in. stainless-steel column (5% SE-30 on 60–80 Chromosorb W) was used; the injector and detector temperatures were maintained at 275 and 300° respectively; the nitrogen carrier gas flow rate was 30 ml/min and the hydrogen flow rate was 27 ml/min. The column was maintained at 225° during the determination of the relative retention times of the compounds obtained from the reaction mixture. The values are reported in Table II.

3-Carbethoxyhydroxyindoles

The benzyloxy-3-carbethoxyindole (0.5 g) in methanol (100 ml) was shaken with palladium-on-charcoal (5%; 0.25 g) in a hydrogen atmosphere at room temperature for 1 h. The hydrogenation mixture was filtered through Celite 545 (Fisher) and the filtrate evaporated to dryness *in vacuo*. The crude 3-carbethoxyhydroxyindole so obtained was recrystallized from water containing a small amount of ethanol. The properties of the products are reported in Table III.

Benzyloxyindole-3-carboxylic Acids

A solution of the benzyloxy-3-carbethoxyindole (0.2 g) in a mixture of 1-propanol (30 ml), ethanol (3 ml), and 2 *N* aqueous potassium hydroxide[6] (14 ml) was heated at the temperatures and for the periods specified in Table IV. The solution was then evaporated to small bulk *in vacuo*, diluted with water, extracted with ether (3 × 20 ml), and the ether extracts discarded. The p*H* of the aqueous solution was adjusted to 3 with hydrochloric acid and extracted with ether (3 × 30 ml). The combined, dried (Na_2SO_4) ether extracts were evaporated to dryness *in vacuo* to give the benzyloxyindolecarboxylic acid, which, when recrystallized from aqueous ethanol, had the properties listed in Table IV.

Hydroxyindole-3-carboxylic Acids

A solution of the benzyloxyindole-3-carboxylic acid (0.25 g) in methanol[7] (50 ml) containing a palladium-on-charcoal catalyst (5%; 0.125 g)[8] was shaken in a hydrogen atmosphere at room temperature and under atmospheric pressure for 1 h. The reaction mixture was filtered through Celite 545 (Fisher) and concentrated to dryness *in vacuo*. The crude products were purified by recrystallization from a suitable solvent. The physical properties of the pure compounds and solvent of crystallization are given in Table V.

Thin-layer Chromatography

Glass plates (20 × 20 cm), precoated with silica gel F_{254} (Merck; thickness, 0.25 mm), were used throughout this investigation. The solvent systems used in the separations of the various groups of products and the R_f values of the individual compounds are given in Table VI. The colors given by the compounds with Ehrlich's reagent (after the sprayed plates had been heated at 125° for 10 min) are also reported in Table VI.

Acknowledgments

The authors wish to express their thanks to

[6]The same quantity of 1 *N* sodium hydroxide solution was used in the case of 4-benzyloxy-3-carbethoxyindole.

[7]A mixture of methanol and ethyl acetate was used to dissolve the 4-isomer.

[8]The catalyst was moistened with water before it was added to the solution to minimize the potential fire hazard.

Can. J. Chem. Downloaded from www.nrcresearchpress.com by 210.87.254.6 on 09/05/12
For personal use only.

Can. J. Chem. Downloaded from www.nrcresearchpress.com by 210.87.254.6 on 09/05/12
For personal use only.

TABLE III

Experimental data for 3-carbethoxyhydroxyindoles

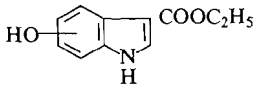

Isomer	Melting point* (°C)	Yield (%)	Analyses (%)† Found C	H	N	Spectral data: Infrared‡ (cm^{-1}) 3500–3100	1800–1600	Ultraviolet§ λ_{max} (mμ) Neutral	Alkaline	p.m.r.‖ 2-proton (τ value)
4-	155–156	68	64.52	5.45	6.73	3300(m);3125(b)	1620(s)	297;235;212	[310];[250]	1.98
5-	185–186	70	64.41	5.65	6.63	3330(b); 3200(b)	1650(s);1625(m)	[300];281;237	325;266;[250];[242]	2.07
6-	174–176(d)	60	64.47	4.92	6.58	3300(b); 3175(b)	1650(s);1625(s)	[304];275;[226]	[318];284;[240]	2.17
7-	188(d)	70	64.59	5.18	6.75	3350(m);3170(b)	1650(s)	292;233;208	317;[241]	2.13

*(d) = With decomposition.
†Calcd. for $C_{11}H_{11}NO_3$: C, 64.38; H, 5.40; N, 6.83.
‡In Nujol; (b) = broad; (s) = strong; (m) = medium.
§In methanol; a few drops of 2 *N* potassium hydroxide were added for the measurements in alkaline solution; shoulders in parentheses.
‖In dimethylsulfoxide-d_6. A singlet is observed after the solution has been shaken with D_2O to exchange the N–H protons.

TABLE IV

Experimental data for benzyloxyindole-3-carboxylic acids

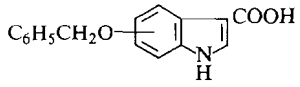

Isomer	Reaction time: Hours at 75°	Days at room temperature	Melting point (°C)	Yield (%)	Analyses (%)* Found C	H	N	Spectral data: Infrared† (cm^{-1}) 3500–3100	1800–1600	Ultraviolet‡ λ_{max} (mμ)
4-	0.5	1	254	75	72.37	5.06	4.94	3130(m)	1680(s)	280;[230];210
5-	5	1	203–204(d)§	90	71.92	4.64	5.12	3370(m)	1665(s)	[305];277;236;213
6-	1	3	185–187(d)§	75	72.10	5.10	5.01	3310(w);3135(m)	1645(s)	[300];[290];273;[230];216
7-	3	1	189–190(d)§	80	71.54	4.67	5.38	3420(m);3380(m)	1660(s)	277;210

*Calcd. for $C_{16}H_{13}NO_3$: C, 71.91; H, 4.86; N, 5.24.
†In Nujol; (w) = weak; (m) = medium; (s) strong.
‡In methanol solution; shoulders in parentheses.
§(d) = with decomposition.

Can. J. Chem. Downloaded from www.nrcresearchpress.com by 210.87.254.6 on 09/05/12
For personal use only.

TABLE V

Experimental data for hydroxyindole-3-carboxylic acids

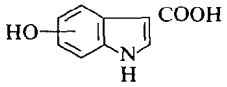

Isomer*	Melting point** (°C)	Yield (%)	Analyses (%)† Found C	H	N	Spectral data: Infrared‡ (cm^{-1}) 1800–1600	Ultraviolet§: Neutral λ_{max} (ε_{max})	Ultraviolet§: Alkaline λ_{max}
4-	240	85	61.12	3.94	7.76	1625(s);1630(s) (sh)	286(6,925);[235](13,650);211(46,950)	280
5-	187	77	60.85	3.86	7.98	1625(s);1630(s)	[305](6,925);281(8,875);[245](15,250); 237(16,100);213(41,350)	323;[241]
6-	229	70	61.66‖	3.97	7.73	1625(s);1650(s)	[305](5,450);274(8,175); [230](17,700);214(25,200)	312;[280];[235]
7-	230	65	60.95	4.05	7.83	1645(s)	282(5,350);[235](15,025);[208](32,725)	[335];295;[245]

*Solvents of crystallization [isomer(solvent)]: 4-, (ethanol/water); 5-, (benzene/ethanol); 6-, (ethanol/water); 7-, (5% ethanol in water).
†Calcd. for $C_9H_7NO_3$: C, 61.01; H, 3.98; N, 7.91.
‡In Nujol; (s) = strong; (sh) = shoulder. Very broad peaks occur in the OH/NH stretching region (3500–2700 cm^{-1}), probably due to hydrogen bonding in the solid state.
§In 95% ethanol; λ_{max} (mμ); shoulders in square brackets; extinction coefficients in parentheses. A few drops of 2 *N* potassium hydroxide were added for the measurements in alkaline solution.
‖It has proved difficult to obtain a satisfactory microanalytical value for carbon in the case of 6-hydroxyindole-3-carboxylic acid. However, the acid is chromatographically homogeneous and mass measurement of the molecular ion confirms the molecular formula. (Calcd.: 177.0425. Found: 177.0424.)
**With decomposition.

TABLE VI

Thin-layer chromatographic data for indole compounds investigated

Compound name	R_f Values in solvent system*				Color reaction with Ehrlich's reagent
	S_1	S_2	S_3	S_4	
4-Benzyloxyindole	0.44	0.87	0.84	0.71	Blue
4-Benzyloxy-1-carbethoxyindole	0.68	0.89	—	0.60	Colorless†
4-Benzyloxy-3-carbethoxyindole	0.04	0.43	0.53	0.01	Blue
3-Carbethoxy-4-hydroxyindole	—	0.68	0.67	—	Blue
4-Benzyloxyindole-3-carboxylic acid	—	—	0.14	—	Blue
4-Hydroxyindole-3-carboxylic acid	—	—	0.03	—	Blue
5-Benzyloxyindole	0.36	0.87	—	0.61	Purple
5-Benzyloxy-1-carbethoxyindole	0.61	—	—	0.49	Colorless†
5-Benzyloxy-3-carbethoxyindole	0.05	0.58	—	0.02	Mauve
3-Carbethoxy-5-hydroxyindole	0.01	0.42	—	—	Mauve
5-Benzyloxyindole-3-carboxylic acid	0.00	0.19§	—	—	Purple
5-Hydroxyindole-3-carboxylic acid‡	0.00	0.13§	—	—	Purple
6-Benzyloxyindole	0.36	0.90	—	0.61	Violet
6-Benzyloxy-1-carbethoxyindole	0.65	0.96	—	0.55	Colorless†
6-Benzyloxy-3-carbethoxyindole	0.02	0.45	—	0.02	Pale violet
3-Carbethoxy-6-hydroxyindole	—	0.21	—	—	Mauve
6-Benzyloxyindole-3-carboxylic acid	—	0.16	0.35	—	Mauve
6-Hydroxyindole-3-carboxylic acid‡	—	0.17	0.23	—	Blue
7-Benzyloxyindole	0.68	—	0.87	0.84	Violet
7-Benzyloxy-1-carbethoxyindole	0.62	—	0.87	0.45	Pale grey
7-Benzyloxy-3-carbethoxyindole	0.09	—	0.70	0.03	Pale violet
3-Carbethoxy-7-hydroxyindole	—	—	0.20	—	Blue
7-Benzyloxyindole-3-carboxylic acid	—	—	0.15	—	Blue
7-Hydroxyindole-3-carboxylic acid	—	—	0.06	—	Blue

*S_1 = Diisopropyl ether – cyclohexane (1:4); S_2 = diisopropyl ether; S_3 = diisopropyl ether – chloroform (1:1); S_4 = benzene – carbon tetrachloride (13:7).

†A colorless spot on a yellow background was observed.

‡The R_f values of samples of 5- and 6-hydroxyindole-3-carboxylic acid (prepared by the method described above) were determined on paper (ascending development) using both isopropanol – ammonia – water (8:1:1) and *n*-butanol – acetic acid – water (8:2:2) as running solvents. The values obtained (0.26 and 0.20) and (0.76 and 0.73) respectively are comparable to those previously reported in the literature (6, 11, 12).

§A better separation of 5-benzyloxyindole-3-carboxylic acid and 5-hydroxyindole-3-carboxylic acid can be achieved with a diisopropyl ether – dimethylformamide (4:1) solvent system. These two acids have R_f values of 0.32 and 0.12 respectively in the system.

Mr. J. van Ingen for recording the p.m.r. spectra; to Mr. D. J. Embree for recording the mass spectra, and to Dr. W. D. Jamieson for useful discussions of the latter.

1. A. CERLETTI. Progr. Drug Res. **2**, 227 (1960).
2. J. B. JEPSON. *In* The clinical chemistry of monoamines. *Edited by* H. Varley and A. H. Gowenlock. Elsevier Publishing Co., Inc., Amsterdam. 1963. p. 107.
3. V. ERSPARMER. Handbook of experimental pharmacology. Vol. XIX. 5-Hydroxytryptamine and related indolealkylamines. Springer-Verlag, Berlin. 1966.
4. F. WIGHTMAN. Can. J. Bot. **40**, 689 (1962).
5. P. E. PILET and TH. GASPAR. Le catabolisme auxinique. Masson et Cie, Paris, 1968.
6. R. M. ACHESON and L. J. KING. Biochim. Biophys. Acta, **71**, 643 (1963).
7. S. UDENFRIEND, C. T. CLARK, J. AXELROD, and B. B. BRODIE. J. Biol. Chem. **208**, 731 (1954).
8. B. B. BRODIE, J. AXELROD, P. A. SHORE, and S. UDENFRIEND. J. Biol. Chem. **208**, 741 (1954).
9. E. EICH and H. ROCHELMEYER. Pharm. Acta Helv. **41**, 109 (1966).
10. R. A. HEACOCK and M. E. MAHON. Can. J. Biochem. Physiol. **41**, 2381 (1963).
11. M. D. ARMSTRONG, K. N. F. SHAW, M. J. GORTATOWSKI, and H. SINGER. J. Biol. Chem. **232**, 17 (1958).
12. D. M. SMITH, R. M. PAUL, E. G. MCGEER, and P. L. MCGEER. Can. J. Biochem. Physiol. **37**, 1493 (1959).
13. R. A. HEACOCK and S. KAŠPÁREK. Advan. Heterocycl. Chem. **10**, 43 (1969).
14. S. KAŠPÁREK and R. A. HEACOCK. Can. J. Chem. **44**, 2805 (1966).
15. S. KAŠPÁREK and R. A. HEACOCK. Can. J. Chem. **45**, 771 (1967).
16. F. MILLICH and E. I. BECKER. J. Org. Chem. **23**, 1096 (1958).
17. R. V. JARDINE and R. K. BROWN. Can. J. Chem. **41**, 2067 (1963).
18. F. P. DOYLE, W. FERRIER, D. O. HOLLAND. M. D. METHA, and J. H. C. NAYLER. J. Chem. Soc. 2853 (1956).

Can. J. Chem. Downloaded from www.nrcresearchpress.com by 210.87.254.6 on 09/05/12
For personal use only.

Can. J. Chem. Downloaded from www.nrcresearchpress.com by 210.87.254.40 on 09/05/12
For personal use only.

Lanthanum ion catalysis of nucleophilic displacement reactions of monoesters of methyl phosphonic acid

R. J. WITHEY[1]

Chemical Defence Experimental Establishment, Porton Down, Nr. Salisbury, Wilts., England

Received February 24, 1969

The catalytic effects of lanthanum ion on the rate of hydrolysis of *p*-nitrophenyl hydrogen methylphosphonate in aqueous solution at p*H* >7.0 are reported. Increases in rate by a factor of about 3.6×10^4 have been observed. No such catalysis was found for diesters of methylphosphonic acid.

Canadian Journal of Chemistry, 47, 4383 (1969)

Introduction

As long ago as 1938, Bamann and his collaborators investigated the catalysis of the hydrolysis of monoesters of phosphonic acid by metal ions (1). Since then many papers have been published on this subject by this group (2–14) and some conclusions about the mechanisms for the catalytic effects were described. Most of this work was carried out in heterogeneous conditions and, for mechanistic purposes, any interpretation of the experimental data is extremely complicated because of the two phases which are present. The catalytic effect of metal ions on the hydrolysis of various phosphorus esters has been reviewed recently (15) and suggests that the available data on heterogeneous metal ion catalysis does not allow any meaningful conclusions about the reaction mechanism.

Butcher and Westheimer (16) have also investigated the catalytic cleavage of phosphate esters in the presence of lanthanum hydroxide gel but their mechanistic interpretations demand the involvement of β-substituents in the ester group and cannot therefore be extrapolated to include phosphorus esters with less complicated structures.

Szabo (17) has described some investigations of the catalytic cleavage of cyclic 5′,6′ glucose phosphates (**1**) by Ba^{++} and La^{+++}. Increases in the rate of hydrolysis of (**1**) of the order of ×35 to $\times 10^3$ at p*H* 8.0 were observed (18). The 1000 fold increase in rate which was observed in the case of La^{+++} by Szabo is in agreement with the values previously reported by Bamann and Westheimer.

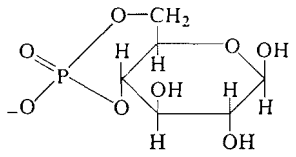

1

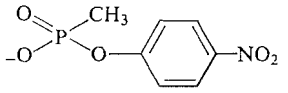

2

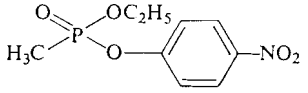

3

In this paper the hydrolysis of *p*-nitrophenyl hydrogen methylphosphonate, which is analogous to **1**, was examined in aqueous solution at 70° and at p*H*'s between 7.3 and 9.0 in the presence and absence of added lanthanum ions. The diester, ethyl *p*-nitrophenyl methylphosphonate **3**, was also examined to ascertain whether the catalysis by lanthanum ion was specific for substrates having P—O^- functions.

Experimental

The kinetic experiments which were carried out were as follows:

(*a*) Hydrolysis rates for *p*-nitrophenyl hydrogen methylphosphonate in water at 70.0 ± 0.1° and p*H*'s 7.19, 7.88, 8.51 (obtained by diluting 0.1 *M* tris buffer and adding NaCl to maintain an ionic strength of 0.1.) Measurement of the uncatalyzed hydrolysis rate was essential in order to estimate the catalytic activity of lanthanum. Since exploratory investigations revealed that these rates were extremely slow (half-lives of the order of

[1]Present address: Research Laboratories, Food and Drug Directorate, Department of National Health & Welfare, Ottawa, Canada.

Can. J. Chem. Downloaded from www.nrcresearchpress.com by 210.87.254.40 on 09/05/12
For personal use only.

two to three months) reactions were followed for a period of not less than six months.

(*b*) Hydrolysis rates for *p*-nitrophenyl hydrogen methylphosphonate in water at 50.0 ± 0.05° with 0.5 to 1.0 *M* NaOH in the presence and absence of lanthanum. It was hoped that at more basic p*H*'s the faster hydrolysis rates would allow greater facility in assessing the lanthanum catalytic effect.

(*c*) The lanthanum ion catalysed hydrolysis of *p*-nitrophenyl hydrogen methylphosphonate was studied at 79, 70, and 37° in the p*H* range 7.19 to 8.51 and with from 0.5 to 10 molar equivalents of lanthanum relative to an ester concentration of 5×10^{-4} *M*.

(*d*) The effect of lanthanum ion on the rate of nucleophilic attack by hydroxide ion and pyridine-2-aldoxime methyl methanesulphonate (P2S) at p*H* 7.5 on ethyl *p*-nitrophenyl methylphosphonate was measured. The object of this study was, first, to see if lanthanum ion catalyzed the hydrolysis of neutral phosphate esters and secondly to see if lanthanum formed a complex with the nucleophile so as to reduce the effective concentration of the nucleophilic anion. The nucleophile P2S was chosen because of its high activity towards phosphorus compounds.

Materials and Methods

p-Nitrophenyl hydrogen methylphosphonate (28), ethyl *p*-nitrophenyl methylphosphonate (27), and P2S (24) were prepared by the standard procedures and purified by distillation or recrystallization before use. *p*-Nitrophenyl hydrogen methylphosphonate was recrystallized and had m.p. 90 to 91°.

Anal. Calcd. for $C_7H_8NO_5P$: C, 38.73; H, 3.71; N, 6.45; P, 14.27. Found: C, 38.68; H, 3.79; N, 6.43; P, 14.20.

Ethyl *p*-nitrophenyl methylphosphonate was distilled at 0.1 mm and the fraction boiling at 125–126° was collected.

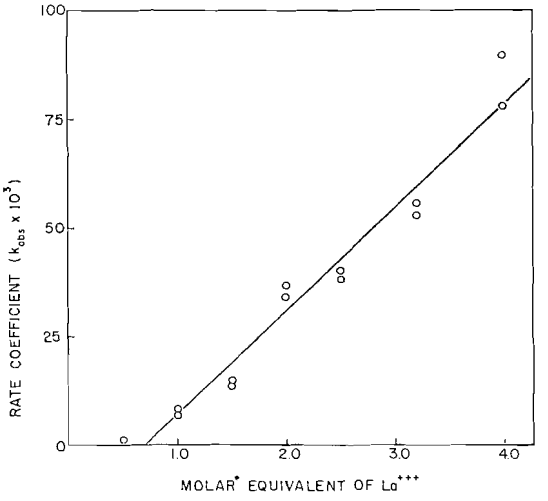

FIG. 1. First order rate coefficient plotted against $[La^{+++}]$ for the hydrolysis of *p*-nitrophenyl methylphosphonate at 70.0° and p*H* 7.60. *One molar equivalent $\equiv 5 \times 10^{-4}$ moles.

Anal. Calcd. for $C_9H_{12}NO_5P$: C, 44.09; H, 4.93; N, 5.71; P, 12.63. Found: C, 44.12; H, 5.01; N, 5.68; P, 12.71.

Pyridine-2-aldoxime methyl methanesulphonate was recrystallized and had m.p. 154–155°.

Anal. Calcd. for $C_8H_{12}N_2O_4S$: C, 41.37; H, 5.21; N, 12.06. Found: C, 41.42; H, 5.15; N, 12.11.

For the measurement of hydrolysis rates the concentration of ester substrate was usually about 5×10^{-4} *M*. Lanthanum ion solutions were prepared by dissolving lanthanum nitrate, $La(NO_3)_3 \cdot 6H_2O$, laboratory reagent grade purchased from B.D.H., in water and the solution was brought to the required p*H* before use.

Cleavage of the *p*-nitrophenyl group was followed at 400 millimicrons with a Unicam S.P.600 spectrophotometer. It was ascertained that, in the concentration range used throughout, Beer–Lamberts law was obeyed. In each hydrolysis reaction which was studied the stoichiometric release of one mole of *p*-nitrophenol per mole of substrate was observed.

Solutions of the reactants were prepared and aliquots pipetted into glass ampoules which were sealed under nitrogen and then placed in a thermostat bath at the required temperature. Tris buffer was used to maintain p*H*. Since this buffer has a relatively large p*H*-temperature coefficient, p*H* measurements of the reactant solutions at the operating temperature were carried out with a Radiometer type TTTIc in conjunction with the recommended special high temperature electrodes G.202BH and K4016.

Results

Rate data is presented in Tables I to V. A plot of the first order rate coefficient against the molar concentrations of lanthanum ion for the catalyzed hydrolysis of *p*-nitrophenyl hydrogen methylphosphonate at 70 °C and p*H* 7.6 is presented in Fig. 1.

TABLE I

Basic hydrolysis of *p*-nitrophenyl hydrogen methylphosphonate at 70°

p*H*	7.19	7.88	8.51
$10^4 k_1$ (hrs^{-1})	3.45	4.43	4.45
$t_{1/2}$ (hrs)	2009	1569	1558

TABLE II

Basic hydrolysis of *p*-nitrophenyl hydrogen methylphosphonate at 50°

[Ester] $\times 10^5$ moles	$[La^{+++}]$ $\times 10^5$ moles	$[OH^-]$ moles	k_{obs} $\times 10^3$ min^{-1}	$10^3 k_2$ l $moles^{-1}$ min^{-1}
7.0	0	0.50	6.010	12.02
7.0	0	0.75	9.945	13.26
7.0	0	1.00	15.27	15.27
7.0	7.0	0.50	6.355	12.71
7.0	7.0	0.75	10.125	13.50
7.0	7.0	1.00	14.99	14.99

Can. J. Chem. Downloaded from www.nrcresearchpress.com by 210.87.254.40 on 09/05/12
For personal use only.

TABLE III

Lanthanum catalyzed hydrolysis of *p*-nitrophenyl hydrogen methylphosphonate

Temperature T °C	pH*	Molar equivalents† of La^{+++}	k_1 min^{-1}
79.0	7.30	1	2.637×10^{-2}
79.0	7.30	2	6.488×10^{-2}
79.0	7.30	2	6.667×10^{-2}
79.0	7.30	1	2.140×10^{-2}
79.0	7.30	1	1.718×10^{-2}
79.0	7.30	1	1.730×10^{-2}
70.0	7.60	0.5	13.89×10^{-4}
70.0	7.60	1.0	7.67×10^{-3}
70.0	7.60	1.0	7.54×10^{-3}
70.0	7.60	1.5	13.83×10^{-3}
70.0	7.60	1.5	14.67×10^{-3}
70.0	7.60	2.0	36.80×10^{-3}
70.0	7.60	2.0	34.10×10^{-3}
70.0	7.60	2.5	40.30×10^{-3}
70.0	7.60	2.5	38.20×10^{-3}
70.0	7.60	3.2	55.58×10^{-3}
70.0	7.60	3.2	53.00×10^{-3}
70.0	7.60	4.0	89.60×10^{-3}
70.0	7.60	4.0	78.00×10^{-3}
37.0	8.0	6.0	3.011×10^{-3}
37.0	8.0	6.0	3.323×10^{-3}

*The pH of the tris buffer solution was measured at the operating temperature.
†The lanthanum ion concentration is reported in molar equivalents with respect to the substrate concentration which was always about 5×10^{-4} moles.

TABLE IV

Hydrolysis of ethyl *p*-nitrophenyl methylphosphonate at 50° and pH 9.0

[Ester] $\times 10^5$ moles	[La^{+++}] $\times 10^4$ moles	$10^3 k_1$ min^{-1}
6.699	0.000	9.94
7.311	3.656	10.23
6.699	6.699	10.07
7.311	14.62	11.18

TABLE V

Effect of lanthanum ion on the nucleophilic attack of P2S on ethyl *p*-nitrophenyl methylphosphonate* at pH 7.50 and 25°

[La^{+++}] $\times 10^3$ moles	$10^3 k_1$ min^{-1}
0	15.56
0	15.47
0	15.36
2.985	15.89
2.985	15.91

*The concentration of substrate was 8.954×10^{-5} moles and of pyridine-2-aldoxime methyl methanesulphonate was 8.954×10^{-3} moles.

Discussion

An anionic charge near a reaction center precludes facile interaction with nucleophiles so that the reactivity of *p*-nitrophenyl hydrogen methylphosphonate **2** towards hydroxide ion is predictably poor at alkaline pH on electrostatic grounds. No kinetic data are available for the alkaline hydrolysis of monoesters of methylphosphonic acid although Larsen (19) claims that the hydrolysis of dialkyl methyl phosphonofluoridates, in strongly alkaline conditions, results only in the release of one mole of acid per mole of substrate.

More information on the analogous dialkyl phosphate ester hydrolysis has been reported and Westheimer and his co-workers (20–22) found that the monoanion substrate species was relatively unreactive. In the case of dimethyl phosphate (see Table VI) the hydrolysis rate in alkaline solution was observed to be slow and first order in hydroxide ion which is consistent with the generalization (23) that alkaline lability in dialkyl hydrogen phosphates occurs only when the molecule contains an hydroxyl group in proximity to the phosphonyl function.

TABLE VI

Alkaline hydrolysis rates for dialkyl phosphate esters

Substrate	Temperature	pH	First order rate coefficient min^{-1}	Reference
Dibenzyl phosphate	75.6	5.85	0.25×10^{-5}	20
Dimethyl phosphate	124.9	>13	5×10^{-6}	22
Di-*p*-nitrophenyl-phosphate	25	>13	6×10^{-6}	27

The results for the hydrolysis of *p*-nitrophenyl hydrogen methylphosphonate, which are given in Table I, indicate a very slow cleavage of the ester group. The values of the observed first order rate coefficient are of the same order of magnitude as those previously reported for the electrostatically analogous dialkyl phosphate esters (see Table VI).

Excellent linear first order plots were obtained for these reactions but in a plot of the logarithm of the observed first order rate coefficient against pH, the points did not fall on a straight line.

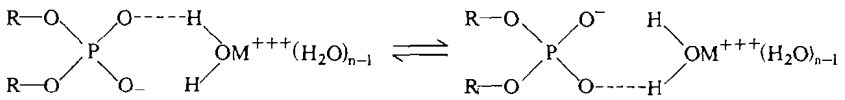

FIG. 2. Resonance structures involving hydrogen bonding.

However, the line of maximum slope that could be drawn through these points had a slope of only 0.15. In contrast, for runs carried out at pH > 13 (see Table II), the slope for a similar plot was found to be 1.29 ± 0.15. While the latter data does not allow the conclusion that the kinetic mechanism at pH > 13 is first order in hydroxide ion it, nevertheless, suggests a change in the mechanism of nucleophilic cleavage of the ester group as the pH increases.

The results in Table II indicate clearly that no enhancement of the hydrolysis rate for *p*-nitrophenyl hydrogen methylphosphonate, at pH > 13 and 50° in the presence of lanthanum ion, could be detected. According to Vickery (25), lanthanum ions exist in solution in at least three different forms depending on the pH:

$$La^{+++} \rightleftharpoons La(OH)^{++} \rightleftharpoons La(OH)_2^{+} \xrightarrow[\text{Increasing pH}]{}$$

In addition to the above species Lewis (26) has suggested that hydrolysis equilibria may involve polynuclear forms like $La[La(OH)_3]^{+++}$. Unfortunately, no evidence is available which allows an unambiguous assignment of the ionic state of lanthanum ion at alkaline pH. Certainly each of the complex forms, described above, would be hydrated in aqueous solution and the actual charge on the cation would be modified by hydration sheath field effects. A reduction in the net charge per mole of lanthanum, which occurs as the pH increases, would be expected to reduce the catalytic activity if any of the proposed mechanisms for lanthanum ion catalysis (*vide infra*) are valid.

The results for the lanthanum ion catalysis of the hydrolysis of *p*-nitrophenyl hydrogen methylphosphonate, which are presented in Table III, show the remarkably high catalytic activity for this cation. The highest concentration of lanthanum ion that we were able to obtain, which appeared to be a homogeneous solution at pH 7.8, was about 5×10^{-3} M.

At this concentration observed rates were too fast at 70° to allow good kinetic analysis without radical changes in the experimental method, but from extrapolation of the line of best fit through the points in Fig. 1 the rate should be about 0.221 min^{-1}. If this is compared with the uncatalyzed rate of 3.72×10^{-4} h^{-1}, at the same temperature and pH, it can be deduced that lanthanum at a concentration of 5×10^{-3} M would increase the hydrolysis rate by a factor of 35,600.

Westheimer (16) and Bamann (14) have shown that lanthanum hydroxide gel can increase the hydrolysis rate of the anionic species of diesters of phosphonic acid by a factor of one thousand. Westheimer suggests a mechanism which involves the catalytic species $La(OH)^{++}$ and its interaction with β-substituents on the ester group. Bamann also suggests that the catalytic species is $La(OH)^{++}$ although he implies that it behaves as a general acid catalyst.

The explanation by Szabo (17) for the metal ion catalytic hydrolysis of 5′6′ glucose phosphate **1** involves the hydrogen bonding of hydrated metal ions (Ba^{++} or La^{+++}) to give resonance structures like those in Fig. 2. If the catalytic mechanism does involve the formation of such complexes it would appear that two effects can operate which increase the nucleophilic susceptibility of the phosphorus atom, viz:

(*i*) The resonance structures lead to a delocalization of the integral charge on P—O^-;

(*ii*) The proximity of the positive charge on the metal ion to the phosphorus atom would polarize the substrate and make the phosphorus atom more electrophilic. Thus cleavage of the P—O-alkyl group by nucleophilic displacement is then feasible.

Whether the suggestion that one of the water molecules in the hydration sheath of the catalytic lanthanum ion can act as a "carrier" of lanthanum and its cationic charge to the substrate or whether lanthanum acts as a general acid catalyst cannot be decided until further examination of the reaction system.

The study of the reactivity of ethyl-*p*-nitrophenyl methylphosphonate toward hydroxide ion and pyridine-2-aldoxime methyl methanesulphonate, in the pH range 7 to 9 and in the presence

Can. J. Chem. Downloaded from www.nrcresearchpress.com by 210.87.254.40 on 09/05/12
For personal use only.

and absence of lanthanum ion was of importance for two reasons. First it was necessary to determine whether catalysis by the lanthanum ion was operative only with phosphorus esters having an anionic charge and secondly to see if, in the reaction of the substrate with a nucleophile other than hydroxide ion, lanthanum ions were capable of co-ordinating or complexing oximate anions so as to reduce the concentration of active nucleophile in the reaction system.

The results, presented in Table IV and V, show clearly that neither the rate of attack by $OH^{\ominus}$ nor oximate ions is altered in the presence of lanthanum ion. Spectrophotometric investigations showed no change for the ultraviolet absorption of P2S in the absence and presence of equimolar lanthanum ions.[2]

Acknowledgment

Thanks are due to Dr. B. C. Barrass of this Establishment who provided samples of the substrates and P2S.

1. E. BAMANN and M. MEISENHEIMER. Ber. **71**, 1711, 1980, 2086, 2233 (1938).
2. E. BAMANN. Angew. Chem. **52**, 186 (1939).
3. E. BAMANN and E. NOWOTNY. Ber. **81**, 451, 455, 463 (1948).
4. (*a*) E. BAMANN, F. FISCHLER, and H. TRAPMANN. Biochem. Z. **325**, 313 (1954).
   (*b*) E. BAMANN, F. FISCHLER, and H. TRAPMANN. Biochem. Z. **326**, 89 (1954).
5. E. BAMANN, F. FISCHLER, and H. TRAPMANN. Biochem. Z. **326**, 161, 237 (1955).
6. E. BAMANN and H. TRAPMANN. Ber. **88**, 199 (1955).
7. E. BAMANN and A. SCHEGRAF. Biochem. Z. **326**, 507 (1955).
8. E. BAMANN, H. TRAPMANN, and A. SCHEGRAF. Ber. **88**, 1726 (1955).
9. E. BAMANN, J. RICHL, and R. NICOLAI. Biochem. Z. **328**, 12 (1956).
10. E. BAMANN, L. F. SANCHEZ, and H. TRAPMANN. Ber. **88**, 1846 (1955).
11. E. BAMANN, A. ROTHER, and H. TRAPMANN. Naturwiss. **43**, 326 (1956).
12. E. BAMANN, A. ROTHER, and H. TRAPMANN. Naturwiss. **44**, 232 (1957).
13. E. BAMANN, M. STEBER, H. TRAPMANN, and J. BRAUN KASNY. Naturwiss. **44**, 328 (1957).
14. E. BAMANN and W. D. MUTTERLEIN. Ber. **91**, 1322 (1958).
15. T. C. BRUICE and S. J. BENKOVIC. Bio-organic mechanisms. Vol. II, W. A. Benjamin Inc., New York, 1966. p. 61.
16. W. W. BUTCHER and F. H. WESTHEIMER. J. Amer. Chem. Soc. 77, 2420 (1955).
17. L. SZABO. Symposium on Organo Phosphorus Chemistry, Toulouse, September, 1965.
18. Notes Techniques, Contribution à l'étude du mechanisme de l'hydrolyses des phosphates cycliques hexa atomiques, by C. Hetzer, Publications scientifiques et techniques du Ministère de l'air No. N.T. 153 (1966).
19. L. LARSON. Acta Chem. Scand. **11**, 1131 (1957).
20. F. H. WESTHEIMER and KUMAMOTO. J. Amer. Chem. Soc. **77**, 2515 (1955).
21. F. H. WESTHEIMER. Chem. Soc. Spec. Publ. No. 8, 1 (1957).
22. F. H. WESTHEIMER and KUMAMOTO. J. Amer. Chem. Soc. **78**, 4858 (1956).
23. A. R. TODD and D. M. BROWN. J. Chem. Soc. 52 (1952).
24. N. H. CREASEY and A. L. GREEN. J. Pharm. and Pharmacol. **11**, 485 (1959).
25. R. C. VICKERY. Chemistry of the lanthanons. Butterworths, 1953. 213.
26. D. C. L. LEWIS. Chem. and Ind. 1238 (1957).
27. R. F. HUDSON and L. KEAY. J. Chem. Soc. 2463 (1956).
28. K. A. PETROV, R. A. BAKSOVA, L. V. KHORKHOYANU, L. P. SINOGEIKINA, and T. V. SKUDINA. Zh. Obshch. Khim. **35**, 723 (1965).

[2]The P2S solutions were equimolar with respect to lanthanum ion in the sense that the oxime was considered to be fully ionized and the ratio of the actual molar concentrations was assessed on the basis that one mole of La^{+++} was equivalent to three moles of P2S.

Can. J. Chem. Downloaded from www.nrcresearchpress.com by 210.87.254.40 on 09/05/12
For personal use only.

Can. J. Chem. Downloaded from www.nrcresearchpress.com by 210.87.254.6 on 09/05/12
For personal use only.

Norditerpene alcohols in the bark of *Thuja plicata* Donn

H. H. QUON[1] AND ERIC P. SWAN[2]

Canada Department of Fisheries and Forestry, Forest Products Laboratory, Vancouver 8, B.C.

Received May 6, 1969

The neutral extractives from the bark of western red cedar (*Thuja plicata* Donn) contained, among other components, three alcohols. One was the known diterpene alcohol, isopimarinol, the other two were the new $\Delta^{8(14),15}$-4α- and $\Delta^{8(14),15}$-4β-hydroxy-18-norisopimaradienes. The syntheses of these two alcohols are described. The greater amount of the 4α compound found in nature, and its relative ease of synthesis compared to the 4β isomer, showed it to be formed preferentially.

Canadian Journal of Chemistry, 47, 4389 (1969)

Introduction

The extraction of the outer bark of western red cedar (*Thuja plicata* Donn) with petroleum ether yielded 2.6% (1) of an oil. This has been fractionated and the neutral portion examined chromatographically. This paper describes the characterization and syntheses of three components of the neutral fraction.

Discussion

The neutral fraction of the petroleum ether solubles contained seven components as shown by thin-layer chromatography (t.l.c.). Three of these were new compounds (one ketone and two alcohols), two were known compounds, and the remainder were a hydrocarbon mixture and a fat mixture. One of the known compounds was isopimarinol[3] (**1**), a compound previously isolated from *Cryptomeria japonica* (3), and the other known compound was the ubiquitous β-sitosterol. The identity of **1** was the key to the structures of the two new alcohols. Compound **1** had an infrared (i.r.) spectrum identical with one from the material previously isolated from sugi (3). Comparison with a synthetic sample prepared by reduction of methyl isopimarate (**2**) showed identical nuclear magnetic resonance (n.m.r.) and undepressed mixture melting point. Compound **3** and **4** had spectra similar to **1**, except for the absence of the signals from the methylene carrying the hydroxyl group. The evidence supporting the formulation of compound **3** as $\Delta^{8(14),15}$-4α-hydroxy-18-norisopimaradiene and compound **4** as $\Delta^{8(14),15}$-4β-hydroxy-18-norisopimaradiene is now presented.

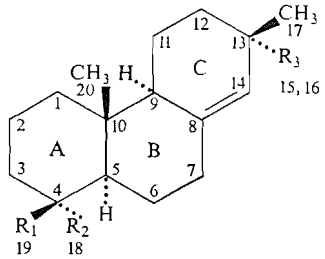

R_3 = vinyl
1 $R_1 = CH_3$; $R_2 = CH_2OH$
2 $R_1 = CH_3$; $R_2 = COOCH_3$
3 $R_1 = CH_3$; $R_2 = OH$
4 $R_1 = OH$; $R_2 = CH_3$

R_3 = ethyl
5 $R_1 = CH_3$; $R_2 = OH$
6 $R_1 = OH$; $R_2 = CH_3$
7 $R_1 + R_2 = CH_2$
8 $R_1 = CH_3$; $R_2 = CH_2OH$

The ultraviolet (u.v.) spectra of **1**, **3**, and **4** showed a single maximum at 209 mμ as expected from the unconjugated double bonds. The i.r. spectra showed bands at about 3080, 1640, 1410, 1000, and 906 cm^{-1}, attributed to a vinyl group and about 1660 and 820 cm^{-1} from a trisubstituted double bond. Hydroxyl group absorption in the near i.r. spectra of **1** was at 3642 cm^{-1}. Compounds **5** and **6**, which were the dihydroderivatives of **3** and **4**, absorbed at 3612 cm^{-1} and 3615 cm^{-1}. These data showed that **1** contained a primary hydroxyl group, and that **5** and **6** contained a tertiary hydroxyl group. Extinction coefficients calculated were 61, 30, and 41, respectively, and Bellamy (4) stated that primary alcohols absorbed at 3642 cm^{-1} and tertiary alcohols at 3618 cm^{-1} with extinction coefficients of 70 and 45.

[1]Graduate student, Department of Chemistry, Simon Fraser University, Burnaby, B.C.

[2]To whom enquiries should be addressed at the laboratory.

[3]We are following the nomenclature of Edwards and Rosich (2) who gave the names isopimarane and derivatives to compounds formerly called sandaracopimarane and derivatives.

Can. J. Chem. Downloaded from www.nrcresearchpress.com by 210.87.254.6 on 09/05/12
For personal use only.

The n.m.r. spectra of **1**, **3**, and **4** showed an ABX signal centered at 4.8 and 5.7 δ from the three protons of a monosubstituted double bond. The position of these signals suggested the $\Delta^{8(14),15}$ isopimaradiene configuration (2,5). However, Edwards and Rosich have shown similar vinyl absorption patterns from $\Delta^{8(9),15}$ pimaradiene and its 18- or 19-derivatives (2). These compounds also showed a broad singlet at about 5.2 δ arising from the proton on a trisubstituted double bond. The spectrum of compound **1** had a quartet from the C-18 methylene centered at 3.2 δ, and this indicated the equatorial configuration (6). Compounds **1**, **3**, and **4** each had three sharp singlets attributed to methyl groups. Since these were not coupled, the methyl groups were therefore all tertiary and the hydroxyl groups of **3** and **4** were probably on position 4. The absence of a signal from a proton on a carbinol in the spectra of **3** and **4** downfield from the methylene protons, showed that the hydroxyl groups were not secondary in these compounds.

The axial methyl groups at C-10 were at about 0.77 δ in the spectra of **1** and **3**. The signal shifted downfield to about 0.95 δ in **4**, showing an interesting effect with changes in structure. Table I shows the positions of the signals from the other two (C-17 and C-19) methyl groups in these compounds. These data indicated that compounds **3** and **4** were norditerpenes with the isopimaradiene configuration.

TABLE I

Chemical shifts of methyl groups in δ

Compound	C-20	C-19	C-17
1	0.79	0.86	1.02
3	0.75	1.08	1.02
4	0.91	1.13	1.01

Parent ion peaks in the low-resolution mass spectra of **1** and **3** to **6** were all visible at the calculated molecular weight. Empirical formulae were confirmed by high-resolution spectra of **1**, **5**, and **6**. The initial fragmentation mode appeared similar in all compounds; *i.e.* an initial loss of a methyl group (perhaps C-17), and loss of water in **3** and **4**. Table II summarizes the spectral data.

It was decided to synthesize the dihydroderivatives (compounds **5** and **6**) of compounds **3** and **4**. The synthesis of **5** was similar to the synthesis of $\Delta^{8(14)}$-4α-hydroxy-18-norpimarene by Grant *et al.* (7). Dihydroisopimaric acid was decarboxylated with lead tetraacetate (6) to a mixture of olefins and an acetoxy substituted compound. The desired product, the $\Delta^{4(19),8(14)}$ olefin **7** was separated by column chromatography on silver nitrate–alumina. Compound **7** was epoxidized (8) and then reduced with lithium aluminium hydride to give $\Delta^{8(14)}$-4α-hydroxy-18-norisopimarene (**5**). Compound **5** was identical (t.l.c. on silver nitrate–silica gel, mixture melting point, n.m.r. spectra) with the product from the hydrogenation of **3**.

The above mixture of hydrocarbons (from the decarboxylation of dihydroisopimaric acid) were examined on the gas chromatograph. They had the same retention times, on two different columns, as the mixture of hydrocarbons obtained from the dehydration of **5** and **6**. These data showed that the location of the hydroxyl group in **5** and **6**, and thus **3** and **4**, was on C-4.

Compound **6**, the dihydro derivative of **4**, was synthesized by the same method as used for the preparation of 4α- and 4β-hydroxy-18-norhibaene from erythroxylol A by Martin and Murray

TABLE II

Major peaks in the low resolution mass spectra*

Compound **1**	Compound **3**	Compound **4**	Compound **5**	Compound **6**
m/e	*m/e*	*m/e*	*m/e*	*m/e*
288 (15)	274 (50)	274 (44)	276 (5)	276 (6)
273 (11)	259 (22)	259 (36)	258 (6)	258 (6)
257 (54)	256 (50)	241 (15)	247 (42)	247 (20)
220 (15)	241 (42)	202 (15)	229 (21)	191 (12)
177 (17)	189 (53)	189 (49)	191 (12)	163 (16)
161 (34)	161 (44)	161 (49)	163 (24)	147 (16)
131 (42)	135 (97)	133 (47)	147 (15)	139 (19)
105 (63)	121 (45)	121 (71)	139 (17)	121 (100)
91 (64)	109 (83)	95 (50)	121 (75)	95 (65)
	95 (61)	81 (73)	95 (46)	81 (72)
			81 (50)	

*Starting from the parent ion peak, with the peak height in parentheses relative to a *m/e* 43 ion of 100 percent.

Can. J. Chem. Downloaded from www.nrcresearchpress.com by 210.87.254.6 on 09/05/12
For personal use only.

(9). Partial hydrogenation of **1** gave **8** which was reacted with chromium trioxide in acetic acid. The major product was the putative aldehyde. The t.l.c. in two solvent systems showed both **5** and **6** as minor products. The latter was isolated in 1% yield. Other evidence supporting structure **4** was the similarities for it (and **3**) with the spectral data reported (7) for the 4α- and 4β-hydroxy-18-norhibaenes. Thus the methyl group resonance reported in Table I for **4** agreed within 0.06 δ with the data for 4α-hydroxy-18-norhibaene, and within 0.05 δ for **3** and the 4β-isomer.

Experimental

Melting points were uncorrected. Infrared spectra were taken of carbon tetrachloride solutions with Perkin–Elmer 421 and Beckman DK-2 spectrophotometers. Nuclear magnetic resonance spectra were taken in deuteriochloroform solutions containing tetramethylsilane (δ = 0) with Varian A-60 or HA-100 instruments. Low-resolution mass spectra were taken on an Atlas CH-4 and high-resolution mass spectra on an AEI-MS9 double-focusing spectrometer. Thin-layer chromatography was on Merck silica gel G with dichloromethane developing solvent and nitric–sulphuric acid detecting reagent unless otherwise noted. Petroleum ether was the 65–100° fraction.

Isolation of Compounds

Petroleum ether solubles (3.60 g) from the extraction of western red cedar bark (1) were placed on a column (5 × 40 cm) of Woelm alumina (activity III). The column was eluted with petroleum ether for the first 400 ml, followed by mixtures of petroleum ether containing increasing amounts of benzene (10% more every 200 ml); fractions were collected every 50 ml and examined by t.l.c. Fractions 1–4, 498 mg, contained a straight-chain hydrocarbon mixture which was not examined further. Fractions 5–6, 71 mg, contained a fat also not examined. Fractions 11–12, 33 mg, contained an unknown ketone (m.p. 50°, λ_{max} 267 mμ) whose structure has not yet been determined. Fraction 13–16, 43 mg, contained compound **4**. Fractions 17–20, 54 mg, contained compound **1**. Fractions 21–24, 62 mg, contained compound **3**. Fractions 25–28, 85 mg, contained β-sitosterol, m.p. 137°, mixture m.p. undepressed with an authentic sample, also identical t.l.c. R_f values. Yields quoted above were those obtained after the compound had been purified via preparative-layer chromatography. Compounds **1**, **3**, **4**, in ethanol absorbed at 209 mμ in the ultraviolet (u.v.) region. They all had a vinyl signal in their n.m.r. spectra, with the AB portion centered at 4.80 δ and the X at 5.70 δ, with $J_{AB} = 2$, $J_{AX} = 10$, and $J_{BX} = 18.5$ Hz: also a broad singlet at 5.15 δ (W 1/2, 3.5 Hz) from the proton on C-14. Other spectral data are summarized in Tables I and II.

Isopimarinol (1)

Compound **1** $[\alpha]_D$ − 1.5° (*c*, 0.2 ethanol) had identical i.r. and n.m.r. spectra with isopimarinol, m.p. 43–45°, mixture m.p. undepressed with a sample synthesized by reduction of methyl isopimarate $[\alpha]_D$ − 7.9° (*c*, 1 ethanol); both had R_f 0.26.

Calcd. (mass spectrum) for $C_{20}H_{32}O$: 288.245303. Found: 288.243135.

$\Delta^{8(14),15}$-4α-Hydroxy-18-norisopimaradiene (3) and $\Delta^{8(14)}$-4α-Hydroxy-18-norisopimarene (5)

Compound **3** had R_f 0.20, spectra very similar to **1** (except methylene components) and crystallized from ethanol–water to needles, m.p. 100–101°. Compound **3** (20 mg) in ethanol (5 ml) plus platinum oxide (5 mg) was treated with hydrogen at 2 atm and room temperature for 10 min. After isolation, the product **5** crystallized as needles from acetone–water, m.p. 93–95°. Both **3** and **5** had similar R_f values and colour reactions (purple) on the chromatoplate. On silver nitrate–silica gel G plates, however, **3** hardly moved from the origin whilst **5** had R_f 0.2.

Calcd. (mass spectrum) for $C_{19}H_{32}O$ (**5**): 276.245303. Found: 276.244319.

$\Delta^{8(14),15}$-4β-Hydroxy-18-norisopimaradiene (4) and $\Delta^{8(14)}$-4β-Hydroxy-18-norisopimarene (6)

Compound **4** had R_f 0.31, spectra similar to **3**, and did not crystallize. It was hydrogenated to **6**, as above, which crystallized from ethanol–water as plates, m.p. 82–84°. R_f values were again similar; on the argentous plate, **6** had R_f 0.5 and **4** had 0.1.

Calcd. (mass spectrum) for $C_{19}H_{32}O$ (**6**): 276.245303. Found: 276.243768.

Synthesis of $\Delta^{8(14)}$-4α-Hydroxy-18-norisopimarene (5)

Dihydroisopimaric acid (1.5 g) in dry benzene (45 ml) and pyridine (3 ml) under nitrogen was treated with lead tetraacetate (3.26 g) with stirring at room temperature for 1 h and refluxing for 3 h. The mixture was filtered, the filtrate was washed with water, and the solvent was evaporated to yield a yellow oil (1.20 g) which was placed on a column of silver nitrate–silica gel (40 g, 10%). The column was first eluted with 1 l of petroleum ether to yield a fraction (330 mg) of an oil believed to be a mixture of $\Delta^{3,8(14)}$- and $\Delta^{4(5),8(14)}$-18-norisopimaradienes. Elution of the column with 1 l of ether–petroleum ether (1:9) gave the desired crude **7** (345 mg), recognized from the *exo*-methylene signals in its i.r. (890 cm^{-1}) and n.m.r. (4.40, 4.68 δ broad singlets) spectra. Further elution of the column with ether–petroleum ether (2:8) gave an unknown product containing an acetoxy group. The crude **7** was purified on a similar column to give pure $\Delta^{4(19),8(14)}$-18-norisopimaradiene (245 mg), R_f = 0.75 on argentous plates (petroleum ether developed) vs. R_f 0.95 for the first fraction eluted from the column.

Compound **7** (113 mg) in chloroform (8 ml) was treated with *m*-chloroperbenzoic acid (86 mg) at about 0° for 1 day. Removal of the acid left the crude epoxide (86 mg) which was dissolved in ether (5 ml) and added to a stirred solution of lithium aluminium hydride (120 mg) in ether (10 ml). The mixture was refluxed under nitrogen for 2 h and worked up in the usual manner. The product, 71 mg recrystallized from ethanol–water, had m.p. 91–94°, undepressed on admixture with **5**; i.r. and n.m.r. spectra and chromatographic behaviour all identical to **5**. Its mass spectrum is given in Table II.

Syntheses of $\Delta^{8(14)}$*-4β-Hydroxy-18-norisopimarene (6)*

Compound **8** (650 mg), chromium trioxide (200 mg), acetic acid (15 ml), and water (0.50 ml) were stirred 2 h at room temperature. The reaction mixture was taken up in ether and washed with sodium bicarbonate. After ether evaporation, the product (0.475 g) was fractionated chromatographically on a small column of silica gel (10 g) with petroleum ether going to ether as the eluant. Concentration of the fractions and further chromatographic purification of the appropriate ones on preparative layer plates of silica gel G (dichloromethane eluant) gave crude **6** (7 mg), m.p. 83–85°, mixture m.p. undepressed. The identity was confirmed by R_f values in two t.l.c. systems, and the position of the methyl groups signals in the n.m.r. spectrum of the synthesized **6**.

Dehydration of ***5*** *and* ***6*** *and Gas-liquid Chromatography*

Compound **5** (14 mg) and compound **6** were each treated with phosphoryl chloride (0.5 ml) and pyridine (1.5 ml) in sealed tubes at 125° for 3.5 h. The products were isolated in the usual manner and examined with the aid of the gas chromatograph. Compounds **5** and **6** both gave the same mixture of three hydrocarbons, believed to be the $\Delta^{3,8(14)}$-, $\Delta^{4,8(14)}$-, and $\Delta^{4(18),8(14)}$-18-norisopimaradienes. The same 3 were isolated from the decarboxylation of dihydroisopimaric acid by lead tetraacetate above. Gas chromatographic columns used were 5′ × 1/8″ 25% SE-30 on Gas Chrom. Q (4.3, 4.8, 5.2) at 225°, and 5′ × 1/8″ 3% OV-1 on Gas Chrom. Q (4.8, 5.9, 6.5) at 175°, retention time in min for the 3 hydrocarbons are given in parentheses. Nitrogen carrier gas at 25 ml/min was used and the flame ionization detector was at 300°. The 3 olefins from each experiment also had the same R_f values on silver nitrate impregnated thin-layer plates.

Acknowledgments

We thank Dr. O. E. Edwards, National Research Council, Ottawa, for the gift of isopimaric acid. Also, Dr. S. Nagahama for the i.r. spectra of **1**.

1. E. P. Swan. Forest Prod. J. **13**, 195 (1963).
2. O. E. Edwards and R. S. Rosich. Can. J. Chem. **46**, 1113 (1968).
3. S. Nagahama. Chem. Soc. Japan Bull. **37**, 886 (1964).
4. L. J. Bellamy. The infrared spectra of complex molecules. J. Wiley and Sons, New York, 1964. p. 98.
5. E. Wenkert, A. Afonso, P. Beak, R. W. J. Carney, P. W. Jeffs, and J. D. McChesney. J. Org. Chem. **30**, 713 (1965).
6. A. Gaudemer, J. Polonsky, and E. Wenkert. Soc. Chim. France Bull. 407 (1964).
7. P. K. Grant, C. Huntrakul, and D. R. J. Sheppard. Aust. J. Chem. **20**, 969 (1967).
8. J. W. Huffman and P. G. Arapakos. J. Org. Chem. **30**, 1604 (1965).
9. A. Martin and R. D. H. Murray. J. Chem. Soc. C, 2529 (1968).

Can. J. Chem. Downloaded from www.nrcresearchpress.com by 210.87.254.6 on 09/05/12
For personal use only.

Can. J. Chem. Downloaded from www.nrcresearchpress.com by 210.87.254.105 on 09/05/12
For personal use only.

Absolute configuration of conhydrine[1]

G. FODOR[2] AND E. BAUERSCHMIDT[3]
Department of Chemistry, Laval University, Quebec 10, Quebec

AND

J. CYMERMAN CRAIG
Department of Pharmaceutical Chemistry, University of California, San Francisco, California 94122

Received June 16, 1969

Catalytic hydrogenation of optically active 2-pyridyl ethylcarbinol (**1**) formed the alkaloid conhydrine (**2**) stereospecifically. Application of the von Braun reaction gave conversion of (+)-conhydrine into *R*-(−)-3-octyl benzoate and of (−)-conhydrine into the *S*-(+)-antimer. Both the relative and absolute configuration of the two asymmetric centers in natural (+)-conhydrine have been determined by the combined use of optical rotatory dispersion (o.r.d.) and circular dichroism (c.d.). The results are in agreement with other physical and chemical evidence.

Canadian Journal of Chemistry, 47, 4393 (1969)

The alkaloid conhydrine was isolated from *Conium maculatum* and natural (+)-conhydrine was oxidized to L-(−)-pipecolic acid (1). The relative configuration of the two asymmetric centres in conhydrine is regarded as *erythro* on the basis of chemical evidence (2, 3) identifying the octan-3,4-diol obtained from (±)-conhydrine by Hofmann degradation and hydrogenation of the methine base (4) with racemic *erythro*-octan-3,4-diol.

Since this work was done on the racemic alkaloid, and the conclusions are based on assumptions regarding the stereochemistry of the intermediate steps, it was desirable to obtain further evidence concerning the configuration of the carbinol carbon. This has now been achieved both by chemical means and by the o.r.d.–c.d. method previously applied (5) to the configuration of the sedridine and allosedridine alkaloids.

The catalytic hydrogenation of optically active (+)-2-pyridyl ethylcarbinol (**1**) under conditions identical to those used (6*a*) for the reaction forming sedridine gave, by asymmetric induction, (+)-conhydrine (**2**) as the major product (6*b*).

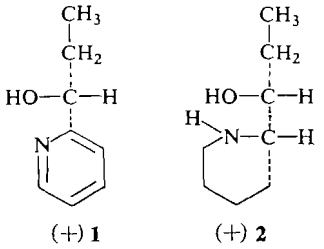

(+) **1** (+) **2**

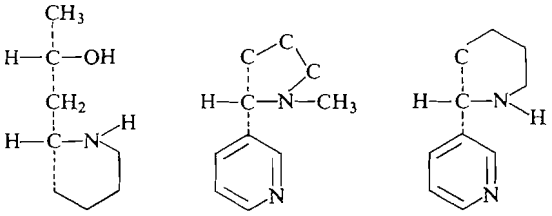

(+) **3** (−) **4** (−) **5**

N,*O*-Dibenzoyl-(+)-conhydrine (**6**) was subjected to the von Braun reaction (7, 8) with phosphorus pentabromide, giving levorotatory 4,8-dibromo-3-octyl benzoate[4] (**7**). Hydrogenolysis led to (−)-3-octyl benzoate (**8**), the infrared (i.r.) and nuclear magnetic resonance (n.m.r.) spectra of which were superimposable to those of the benzoate from natural (9*a*)

[1]Supported by research grant HE-5881 from the National Institutes of Health, U.S. Public Health Service to one of us (J.C.C.) and by Grant No. A-2839 of the National Research Council of Canada to the other (G.F.). This joint paper forms part XV of the series "Optical rotatory dispersion and absolute configuration" and it also belongs to the series on the "Applications and mechanism of the von Braun reaction."

[2]Present address: Department of Chemistry, West Virginia University, Morgantown, W.Va. 26506.

[3]Present address: Department of Chemistry, University of Virginia, Charlottesville, Va. 22903.

[4]*N*-4-(3-benzoxy-8-bromooctyl)-benzimidoyl bromide (**9**), was, however, the main product of the von Braun reaction unlike in the case of sedridine. Hydrolysis led to 3-benzoxy-4-benzamido-8-bromo-octane (**10**) as proven by n.m.r. and analytical data. Hydrogenolysis of this latter afforded 3-benzoxy-4-benzamido octane (**11**). Detailed study of the mechanism and steric course of the von Braun reaction will be presented in forthcoming papers.

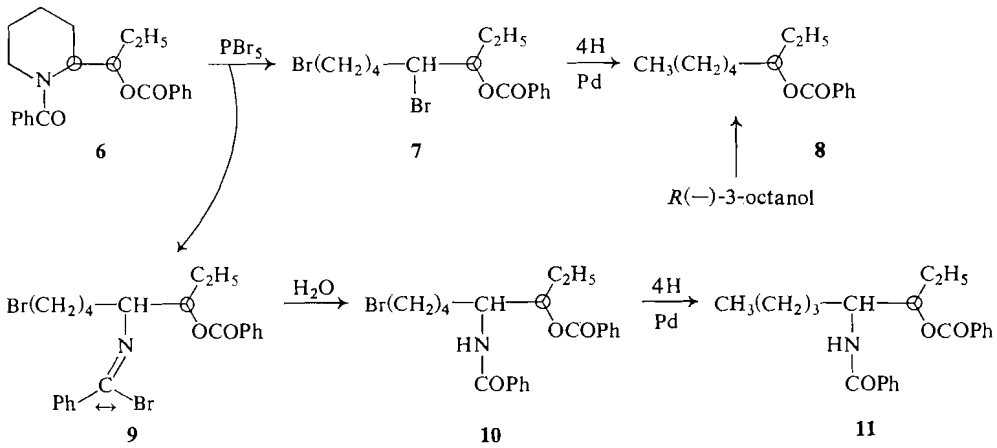

(+)-3-octanol of *S*-configuration (9*b*) while the sense of optical rotation was the opposite.

Since the absolute configuration of the latter is known (9*b*), natural (+)-conhydrine has the *R*-configuration at the carbinol carbon of the side-chain. This direct method of chemical correlation has been applied formerly to the degradation of *N*,*O*-dibenzoyl sedridine to *S*-(+)-2-octanol (8).

The o.r.d. curve for (+)-conhydrine (Fig. 1) showed a positive Cotton effect centred around 200 mμ (confirmed by a positive c.d. maximum at

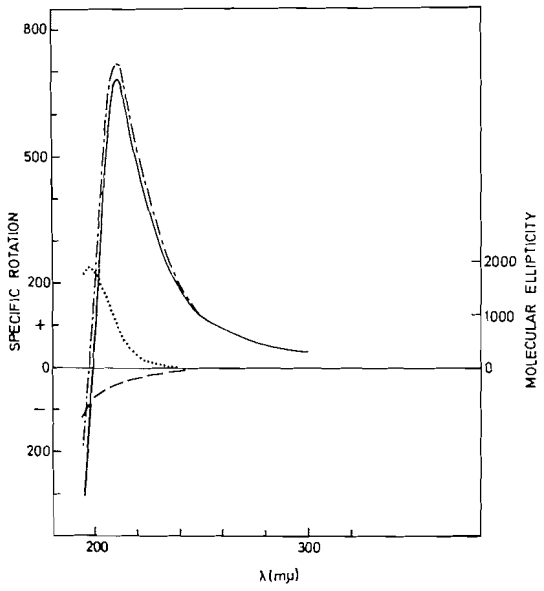

FIG. 1. (+)-Conhydrine, o.r.d. curves of base (—), hydrochloride (- - -), base–hydrochloride (—. —. —. —.); c.d. curve of base (. . . .).

that wavelength), which is due to the n → σ* transition of the non-bonding electrons of nitrogen and oxygen. Below 210 mμ, the curve descends steeply. However, the hydrochloride of (+)-conhydrine gave a plain negative curve (Fig. 1) while its c.d. was zero down to 195 mμ. Since protonation of the nitrogen is known (10) to remove the n → σ* transitions, shifting it into the low wavelength region of the σ → σ* transition, the curve of the hydrochloride is due to the n → σ* transition of the oxygen (11) and indicates the asymmetric centre in the side-chain to have the L-configuration, as found (12) for L-(−)-heptan-3-ol.

Subtraction of the curve for the hydrochloride from that of the base gives a curve very similar to, and slightly more intense than, that of the base, descending steeply below 210 mμ, (Fig. 1) and showing the same positive Cotton effect.

This indicates the absolute configuration of the asymmetric centre in the piperidine ring to be L, and is confirmed by the positive c.d. shown by (+)-conhydrine, identical in sign with that given by (+)-sedridine (5) and by *R*-(−)-coniine (13) both of which are known to give *S*-(−)pipecolic acid on oxidation (1) and thus to be members of the L-series for the asymmetric centre in the piperidine ring.

The absolute configuration of (+)-conhydrine is thus correctly given as **1** from o.r.d. and c.d. evidence, in complete agreement with the direct chemical evidence presented in this paper and in earlier work. As required by this conclusion, the o.r.d. and c.d. curves of (+)-conhydrine are the mirror images of those obtained (5) from (+)-allosedridine (**3**).

Can. J. Chem. Downloaded from www.nrcresearchpress.com by 210.87.254.105 on 09/05/12
For personal use only.

TABLE I
Ultraviolet spectra (in ethanol)

Compound	λ_{max}mμ (log ε)		
2-Pyridyl ethylcarbinol (**1**)	257 (3.30)	262 (3.33)	269 (3.24)
2-Picoline (15)	256 (3.4)	262 (3.5)	269 (3.3)
3-Picoline (15)	257 (3.3)	263 (3.4)	270 (3.3)
Nicotine (**4**)		262 (3.46)	
Nornicotine (16)		262 (3.47)	
Anabasine (17)		261 (3.46)	

The chromophore in (+)-2-pyridyl ethylcarbinol (**1**) is very similar to that in nicotine (3), being made up of the intense $\pi \rightarrow \pi^*$ transitions of the pyridine ring together with the (very much less intense) $n \rightarrow \sigma^*$ transitions of the non-bonding electrons of oxygen or nitrogen. This similarity is reflected in the almost identical ultraviolet (u.v.) absorption spectra (14) of 2-pyridyl ethylcarbinol (**1**), nicotine (**4**), 2-picoline, and 3-picoline (15), anabasine (**5**), and nor-nicotine (16) (Table I). It is significant that (−)-2-pyridyl ethylcarbinol gives an o.r.d. and c.d. spectrum which is almost the same as that given (17) by natural (−)-nicotine (**4**) and (−)-anabasine (**5**). Since (−)-nicotine has been assigned the *S*-configuration with reference to both L-proline (18*a*) and L-serine (18*b*) and (−)-anabasine has been related to L-pipecolic acid (19), it follows that (+)-2-pyridyl ethylcarbinol (**1**) has the *R*-configuration as shown.

This is in agreement with the fact that the conversion (+)**1** → (+)**2** does not alter the configuration of the carbinol carbon in the side-chain, known to be *R* in (+) **2** from the evidence reported above.

Experimental

The o.r.d. and c.d. curves were measured at 25° in 95% ethanol on a JASCO or Jouan spectropolarimeter. Rotations are given below only for (*1*) the highest and lowest wavelengths measured, and (*2*) peaks and troughs. The c.d. is recorded (20) in molecular ellipticity units, θ.

(+)-Conhydrine

The following values were obtained: α_D +9.3° (*c*, 3 in ethanol); o.r.d. (*c*, 0.492) α_{300} + 40.7°, α_{212} + 681°, α_{195} − 305°; c.d. $[\theta]_{240}$ 0, $[\theta]_{198}$ + 1917, $[\theta]_{195}$ + 1772.

Hydrochloride of (+)-Conhydrine

The following values were obtained: o.r.d. (*c*, 0.618 in 95% ethanolic 0.1 *N* HCl) α_{300} 0, α_{195} − 121.5°.

O,N-Dibenzoylconhydrine (6)

Dextrorotatory conhydrine (**2**) (1.43 g, 0.01 mole) was dissolved in dry pyridine (20 ml) and benzoyl chloride (3.51 g, 0.0255 mole) added after cooling with ice and stirring. The mixture was allowed to reach room temperature within 2 h and then was kept for another 24 h at 25°. This mixture was poured on ice cold 20% H_2SO_4 (100 ml), the precipitated yellowish dibenzoate taken up in chloroform (50 ml), and the acidic solution extracted five times with a total of 200 ml chloroform. The combined extracts were washed with a saturated sodium chloride solution, then 3 times with a total of 50 ml 5% sodium hydrogen carbonate solution, finally dried ($MgSO_4$) and evaporated to give 3.1 g (88%) of crude dibenzoylconhydrine. Recrystallization from 80% aqueous methanol (50 ml) afforded a pure product (2.6 g, 74%) m.p. 133–134%. The following data was obtained – i.r.: 2900, 1720 (benzoic ester); 1625 (N—CO), 1440, 1275 (ester C—O stretch) 710, 690 (aromatic); n.m.r.: multiplet δ, 7.45 (10H), 0.95 C—Me (triplet); α_D − 13° (*c*, 3 in chloroform).

Anal. Calcd. for $C_{22}H_{25}NO_3$: C, 75.18 H, 7.17 O, 13.66 N, 3.99. Found: C, 75.51 H, 6.81 O, 13.13 N, 4.52.

Treatment of (−)-Dibenzoylconhydrine with Phosphorus Pentabromide

Procedure A

(−)-Dibenzoylconhydrine (**6**) (2.6 g, 0.074 mole) and phosphorus tribromide (1.99 g, 0.07 mole) were dissolved in tetrachloromethane (10 ml) and a few drops of chloroform. Bromine (1.18 g, 0.074 mole) in CCl_4 (5 ml) was then added and the reddish colored solution evaporated on a Rotavapor at 25° to dryness. Distillation was begun under 20 mm pressure until the oil bath reached 100°, to give a fraction consisting mainly of phosphorus oxybromide and benzonitrile, as indicated by the i.r. bands at 1780 and 2100 cm^{-1}, respectively. Water decomposes the former to afford benzoic acid which was collected by filtration and identified, while the latter was taken up in ether (20 ml), and redistilled. An oil pump was used to collect the higher boiling products, under 1 mm pressure from 100–160°, a bromine-containing oil (1 g) distilled. The i.r. indicated the presence of some benzonitrile (2000 cm^{-1}) together with an ester (1720 and 1273 cm^{-1}) and a weak amide band appeared around 1620 cm^{-1}. It was levorotatory ($\alpha_D^{20} \sim 9.7°$) in chloroform; the concentration is uncertain because of benzonitrile as contamination. The n.m.r. spectrum resembles one obtained by similar treatment of dibenzoylsedridine (8).

Redistillation under 10^{-2} mm from a Späth tube gave a nearly colorless oil, dibromoester (**7**) (700 mg), (i.r.: 1725 and 1275 cm^{-1}), free of benzonitrile (which was collected in the liquid nitrogen trap). This fraction was

Can. J. Chem. Downloaded from www.nrcresearchpress.com by 210.87.254.105 on 09/05/12
For personal use only.

Can. J. Chem. Downloaded from www.nrcresearchpress.com by 210.87.254.105 on 09/05/12
For personal use only.

subjected to catalytic hydrogenation in ethanol (50 ml) at atmospheric pressure and 25° over Pd/charcoal (0.5 g) and barium hydroxide octahydrate (1 g). The consumption of hydrogen amounted to 2 moles within 2 h. The solution was then filtered and evaporated to dryness, the residual oil taken up in chloroform (15 ml), washed with 0.1 *N* HCl (2 ml) and water (10 ml), dried ($MgSO_4$), and evaporated again leaving behind a colorless oil (500 mg) free of bromine. The n.m.r. showed the presence of 5 protons (7.8 δ), a deshielded H around 4.2 δ, and the terminal methyl at 1.1 δ. The i.r. showed an ester CO at 1720 cm^{-1}. The spectra were superimposable with those of authentic 3-octyl benzoate. The latter was prepared from natural (9*a*) (+)-3-octanol (240 mg, 0.002 mole) dissolved in dry pyridine (2 ml) and stirred with benzoyl chloride (300 mg, 0.0021 mole) at 25° for 24 h. Pyridine was removed on a Rotavapor and the product was extracted with chloroform (20 ml), washed with 0.1 *N* H_2SO_4 (5 ml), water (5 × 2 ml), 20% potassium hydrogen carbonate (5 ml), dried ($MgSO_4$), and finally the solvent removed; α_D^{20} + 6.8° (*c*, 2 in chloroform) (9*c*). The product of degradation showed α_D^{20} − 6.2° (*c*, 2 in chloroform).

Hydrolysis of the benzoate (**8**) was carried out by refluxing for 6 h with 10% methanolic (10 ml) potassium hydroxide. Evaporation of the solvent gave potassium benzoate together with 3-octanol. The salt was precipitated by adding dry ether (20 ml) and removing the solvent again. The residual colorless oil gave an i.r. spectra: 3390 (OH), 2950, 2880 (CH), 1470 (deformation), and 1270 cm^{-1} (C—O stretch) and n.m.r. spectra superimposable to those of an authentic specimen of *S*-(+)-3-octanol we obtained by courtesy of Professor Y. R. Naves (University of Lausanne); α_D^{20} − 8.9° (*c*, 2 in chloroform). An authentic specimen (9*a*) showed α_D^{20} + 8.97° ($CHCl_3$). The allophanate has m.p. 185°, as recorded by Dr. Naves in a previous publication for 3-octyl allophanate.

Procedure B

(+)-Dibenzoylconhydrine (5.6 g, 0.0169 mole, α_D^{20} + 12.8° (*c*, 3 in dimethyl formamide)) prepared from (−)-conhydrine in the same way as was its antimer from natural conhydrine was mixed in a 20 ml flask with phosphorus tribromide (3.32 g, 0.015 g mole) and bromine (2.55 g, 0.016 mole) was added. The reddish colored mixture was distilled *in vacuo* from the same flask essentially as described for Procedure A. After a first fraction (800 mg) consisting mainly of phosphorus oxybromide (b.p. below 80°, 20 mm) was obtained, distillation gave (+) **7**, together with benzonitrile (b.p. below 120°, 30–50 μ) and a viscous liquid (2.48 g, b.p. 120–170°). The lower boiling fraction when worked up as in Procedure A yielded some dextrorotatory octyl benzoate (**8**). The solution of the higher boiling fraction in ether (50 ml) was washed with ice-cold 10% potassium hydrogen carbonate solution (20 ml), dried ($MgSO_4$) and the solvent removed. The product was then purified by thin-layer chromatography (Silicagel/HF, 0.8 mm) using benzene and ethyl acetate (3:1). The main fraction of crystals, m.p. 107–108°, obtained after recrystallization from hexane proved to be 8-bromo-4-benzamido-3-octyl benzoate.

Anal. Calcd. for $C_{22}H_{26}BrNO_3$: C, 61.25; H, 6.63; Br, 17.56. Found: C, 61.78; H, 6.72; Br, 17.33.

The i.r. spectrum showed peaks at: 3380 (NH); 3010, 2290 (C—H); 1720 (CO ester); 1660 (CO amide); 1580 (amide II); 1270 (C—O stretch); 710 cm^{-1} (aromatic). The n.m.r. spectrum (on δ scale) showed: multiplet, 8.2–7.3 (10H) (aromatic); multiplet, 5.2 (1H) probably H-3; multiplet, 4.4 (2H) assigned to CH_2Br; multiplet, 2.1–1.6 (various methylenes); and a triplet at 1.0 δ (CH_3). The pseudotriplet at 3.32 δ corresponding to 2H disappears after catalytic hydrogenolysis over Pd/C in ethanol (20 ml) so the bromine was terminal, hence the benzamido group was attached to C-4 in the bromoamide. The methyl region increased from 3H to 6H after hydrogenolysis which is consistent with the structure of 4-benzamido-3-octyl benzoate; α_D^{20} + 32.6° (*c*, 3 in chloroform).

Anal. Calcd. for $C_{22}H_{27}NO_3$: C, 74.75; H, 7.70; N, 3.96. Found: C, 74.35; H, 6.65; N, 4.11.

(−)-2-Pyridyl Ethylcarbinol

This carbinol was obtained in crystalline form for the first time by Y. K. Wang, m.p. 25°. α_D − 72.9° (*c*, 2.0 in ethanol). The c.d. showed: *c*, 0.08 in 95% ethanol)$[\theta]_{280}$ 0, $[\theta]_{272}$ − 230, $[\theta]_{264}$ − 530, $[\theta]_{258}$ − 530, $[\theta]_{238}$ − 3000, $[\theta]_{220}$ − 1060 (sh), $[\theta]_{207}$ + 2100. α_D − 65° was reported earlier (6*b*) for this carbinol. However, checking its optical purity by integration of the diastereotopic n.m.r. signal of its acetyl mandelic ester, indicated an 93% optical purity. The product prepared for the present work α_D − 72.9 is therefore optically pure.

Acknowledgments

The authors wish to express their gratitude to Mr. Y. K. Wang, M.Sc., Laval University, who repeated some of Dr. Bauerschmidt's experiments and who is continuing the preparative work with conhydrine.

1. R. Willstätter. Ber. **34**, 3166 (1901).
2. R. K. Hill. J. Amer. Chem. Soc. **80**, 1609 (1958).
3. J. Sicher and M. Tichy. Coll. Czech. Chem. Comm. **23**, 2081 (1958).
4. E. Späth and E. Adler. Monatsh. **63**, 127 (1933).
5. H. C. Beyerman, L. Maat, J. C. Craig, R. P. K. Chan, and S. K. Roy. Unpublished results. See also, J. C. Craig. 5th Symposium on the chemistry of natural products (IUPAC), London, July 8, 1968; Abstract No. A1, p. 1.
6. (*a*) G. A. Cooke and G. Fodor. Can. J. Chem. **46**, 1105 (1968); (*b*) G. Fodor and E. Bauerschmidt. J. Heterocycl. Chem. **5**, 205 (1968).
7. J. von Braun. Ber. **38**, 2339 (1905).
8. G. Fodor and D. Butruille. Chem. Ind. (London), 1437 (1968).
9. (*a*) Y. R. Naves. Helv. Chim. Acta, **26**, 168, 169, 1035 (1943); (*b*) P. A. Levene and A. Walti. J. Biol. Chem. **94**, 593 (1932); (*c*) Schimmel & Co. Chem. Zentralbl. I, 1973 (1913).
10. E. Tannenbaum, E. M. Coffin, and A. J. Harrison. J. Chem. Phys. **21**, 311 (1953).
11. A. J. Harrison, B. J. Cederholm, and M. A. Terwilliger. J. Chem. Phys. **30**, 355 (1959).
12. J. C. Craig and S. K. Roy. Tetrahedron **21**, 1847 (1965).

13. J. C. CRAIG, W. E. PEREIRA, JR., and A. R. PINDER. Unpublished results.
14. M. L. SWAIN, A. EISNER, C. F. WOODWARD, and B. A. BRICE. J. Amer. Chem. Soc. **71**, 1341 (1949).
15. H. V. DAENIKER. Helv. Chim. Acta, **35**, 1955 (1952).
16. G. BIGLANO. Ann. Chim. (Rome), **49**, 1299 (1959).
17. J. C. CRAIG and S. K. ROY. Tetrahedron **21**, 401 (1965).
18. (*a*) P. KARRER and R. WIDMER. Helv. Chim. Acta, **8**, 364 (1925); (*b*) C. S. HUDSON and A. NEUBERGER. J. Org. Chem. **15**, 24 (1950).
19. R. LUKES, A. A. AROJAN, J. KOVAŘ, and K. BLAHA. Coll. Czech. Chem. Comm. **27**, 751 (1962).
20. C. DJERASSI and E. BUNNENBERG. Proc. Chem. Soc. 299 (1963).

Can. J. Chem. Downloaded from www.nrcresearchpress.com by 210.87.254.105 on 09/05/12
For personal use only.

Synthèse et propriétés de la *tert*-butyl-5 diméthyl-3,3 cycloheptanone

JEAN-CLAUDE RICHER ET ROBERT BISSON[1]
Département de Chimie, Université de Montréal, Montréal, P.Q.

Reçu le 5 mai 1969

La *tert*-butyl-5 diméthyl-3,3 cycloheptanone a été synthétisée à partir de la *tert*-butyl-4 diméthyl-2,2 cyclohexanone; la stéréochimie de sa réduction par divers agents a été déterminée. Pour fins de comparaison, la *tert*-butyl-5 diméthyl-2,2 cycloheptanone a aussi été préparée en utilisant la *tert*-butyl-4 cyclohexanone comme produit de départ.

Canadian Journal of Chemistry, 47, 4399 (1969)

Can. J. Chem. Downloaded from www.nrcresearchpress.com by 210.87.254.6 on 09/05/12
For personal use only.

Introduction

Alors que la réduction des alkylcyclohexanones a fait l'objet de nombreuses communications (1) peu de travaux sur les cycloheptanones correspondantes ont été effectués (2–7). Il apparaissait intéressant, dans le cadre de nos travaux sur la stéréochimie des additions sur des systèmes cycliques (8), de déterminer si l'introduction sur la *tert*-butyl-5 cycloheptanone d'un groupe *gem*-diméthyle en position 3 provoquerait lors de la réduction de cette molécule (**1***a*) une stéréosélectivité plus élevée que celle observée lors de la réduction (6, 7) de la *tert*-butyl-4 cycloheptanone non substituée (**1***b*). Les résultats obtenus lors de la synthèse et de la réduction de **1***a* font l'objet du présent travail.

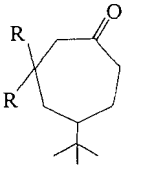

1

a R = CH_3
b R = H

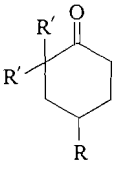

2

a R = *tert*-Bu; R′ = CH_3
b R = H; R′ = CH_3
c R = *tert*-Bu; R′ = H

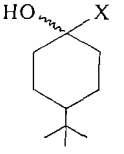

3

a X = CN
b X = CH_2—NH_2
c X = CH_2—$\overset{\oplus}{N}H_3$ $Cl^{\ominus}$
d X = C(=CH_2)—CH_3

Résultats et discussion

Synthèse des tert-butyl-5 diméthyl-2,2 cycloheptanone (4a) et diméthyl-3,3 cycloheptanone (1a)

La réaction directe de la *tert*-butyl-4 diméthyl-2,2 cyclohexanone (**2***a*) avec le diazométhane pour conduire à la *tert*-butyl-5 diméthyl-3,3 cycloheptanone (**1***a*) a été tentée; cette réaction comme celle rapportée par Mousseron et Manon (9) sur la diméthyl-2,2 cyclohexanone **2***b* ne conduit qu'à peu d'agrandissement de cycle et le produit obtenu avec un faible rendement n'a pu être purifié. Les cyanohydrines **3***a* sont facilement obtenues à partir de la cétone **2***a*, suivant la technique de Bélanger (10); la présence dans le spectre de résonance magnétique nucléaire (r.m.n.) du mélange réactionnel de quatre pics dus à des groupes méthyles permet d'une part de réaliser que les deux cyanohydrines isomères se sont formées et d'autre part de préciser que l'une forme 83% du total. Par analogie avec les résultats de Gravel (11), il est permis de supposer que le produit prépondérant de la réaction correspond à une entrée axiale du réactif sur la cétone. La réduction des cyanohydrines brutes (**3***a*) par $LiAlH_4$ conduit aux aminoalcools **3***b* correspondants isolés sous forme de chlorhydrates **3***c*; l'existence des deux isomères attendus pour ces aminoalcools est mise en évidence par la présence dans leur spectre r.m.n. de deux pics dus aux groupements *tert*-butyles. La désamination nitreuse de ces aminoalcools fournit un mélange réactionnel qui d'après la chromatographie en

[1]Les résultats rapportés dans cette communication sont extraits du mémoire soumis par M. BISSON, en vue de l'obtention du grade de Maître ès-Sciences, Faculté des Sciences, Université de Montréal.

Les récherches qui font l'objet de la présente étude ont été appuyées en partie par le Conseil de Récherches pour la Défense du Canada, subvention numéro 9530-61.

Can. J. Chem. Downloaded from www.nrcresearchpress.com by 210.87.254.6 on 09/05/12
For personal use only.

phase gazeuse (c.p.g.) contiendrait sept produits; la cétone **1***a* formerait 55% du total. La formation de **1***a* en prépondérance pouvait être prévue, quelle que soit la stéréochimie de l'aminoalcool **3***b* utilisé, par un simple examen des conformations privilégiés. La cétone **1***a* est isolée à l'état pur par l'intermédiaire de sa semicarbazone et sa structure est confirmée par le fait que quatre atomes de deutérium peuvent être introduits lors de sa deutération (12) par l'intermédiaire de son énamine **5**.

Pour fins de comparaison, la *tert*-butyl-5 diméthyl-2,2 cycloheptanone (**4***a*) a été préparée à partir de la *tert*-butyl-4 cyclohexanone (**2***c*) en mettant à profit les méthodes d'extension de cycles préconisées par Julia et Guereny (13) et Johnson *et al.* (14). La condensation de **2***c* avec le bromure d'*iso*propénylmagnésium conduit aux alcools tertiaires **3***d* qui seraient présents d'après la c.p.g. dans le rapport 60/40; le traitement de ces alcools par l'hypobromite de *tert*-butyle (14) fournit un mélange réactionnel duquel les cétones bromées **4***b* peuvent être isolées. Leur hydrogénolyse selon les indications de Julia et Guereny (13) mène quantitativement à la cétone désirée **4***a* dont la structure est confirmée par la fixation de deux atomes de deutérium lors de sa deutération (12).

Sur la réduction de la tert-butyl-5 diméthyl-3,3 cycloheptanone (1a)

La réduction de la cétone **1***a* par le sodium dans l'éthanol conduit à un mélange des deux alcools **6***a* et **7***a* qui peuvent être obtenus à l'état pur par recristallisations de leurs *p*-interbenzoates **6***b* et **7***b*. La c.p.g. appliquée aux alcools **6***a* et **7***a* n'a donné dans nos mains aucun résultat satisfaisant; les éthers triméthylsilanés **6***c* et **7***c* préparés d'après la méthode de Sweeley *et al.* (15) peuvent toutefois être très bien séparés et des expériences connexes ont permis de montrer que la transformation en éther est quantitative.

La cétone **1***a* a été réduite par divers agents réducteurs et les produits obtenus analysés par la méthode décrite plus haut; les résultats sont consignés dans le tableau I. Ces résultats montrent d'une part que la réduction par le sodium et l'éthanol conduit normalement au produit le plus stable **7***a*; d'autre part les résultats obtenus lors de la réduction par les hydrures complexes permettent de mettre en évidence qu'en passant à un hydrure plus volumineux la quantité de l'alcool le moins stable **6***a*, provenant d'une réduction de la cétone par sa face la plus dégagée (8) est formé en quantités croissantes. Les temps relatifs de rétention en c.p.g. des produits **6***c* et **7***c* de même que les résultats obtenus lors des réductions permettent après un examen attentif des modèles moléculaires, de suggérer les structures des alcools épimères; si l'on admet pour la cétone **1***a* la conformation "chaise tordue" (16) qui permet de fixer le groupe *tert*-butyle dans une position équatoriale tout en minimisant les intéractions du groupe *gem*-diméthyle d'une part avec le cycle et d'autre part avec le group carbonyle, l'alcool cis, **6***a*, aurait un groupement hydroxyle en position pseudo axiale alors que dans l'alcool *trans* **7***a*, ce groupe serait en position pseudo équatoriale.

TABLEAU I

Stéréochimie de la réduction de la cétone **1***a*

Agent réducteur	Références	Pourcentage alcool **6***a*/**7***a**
$Al(OiPr)_3$†	(20)	38/62
$Al(OiPr)_3$‡	(21)	57/43
H_2/Pt	(22)	46/54
Na/EtOH		45/55
$NaBH_4/iPrOH$	(23)	55/45
$LiAlH_4/Et_2O$	(24)	60/40
$LiAl(OtBu)_3H/THF$	(25)	70/30

*Les pourcentages indiqués sont les moyennes d'au moin trois essais.
†Réactions équilibrées.
‡Contrôle cinétique.

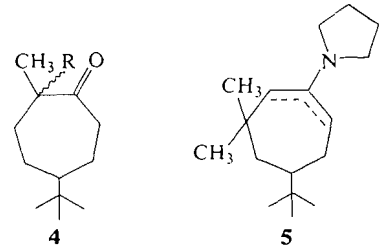

4 **5**

a R = CH_3
b R = CH_2Br

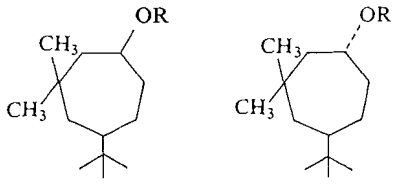

6 **7**

a R = H *b* R = CO—C_6H_4—NO_2—*p* *c* R = $Si(CH_3)_3$

Les résultats obtenus au cours du présent

travail permettent donc de noter que l'introduction du groupement *gem*-diméthyle en position 3 semble conférer à la molécule une rigidité conformationnelle que la cétone **1***b* ne possède pas, ce qui permet dans certains cas d'effectuer des réductions plus sélectives.

Partie expérimentale

Les spectres infrarouges (i.r.) ont été pris à l'aide d'un appareil Beckman, Modèle IR 8, à double faisceau pour des solutions chloroformiques, dans des cellules de chlorure de sodium de 0.1 mm d'épaisseur. Les spectres de r.m.n. ont été pris sur un spectromètre modèle JNM-C-60 H (Jeolco); les déplacements chimiques, δ, sont exprimés en partie par millions et se réfèrent au tétraméthylsilane utilisé comme référence interne. Les spectres de masse ont été pris sur un spectromètre modèle RMU-6D (Hitachi) à température ambiante; l'énergie du faisceau ionisant est de 70 e*V*. Les points de fusion ont été mesurés à l'aide d'un appareil "Hot Stage Apparatus" (Reichert); ils ne sont pas corrigés. Les indices de réfraction ont été mesurés à l'aide d'un réfractomètre Abbe (Carl Zeiss). Les analyses en c.p.g. ont été effectuées avec des chromatographes F et M, modèle 852 et 700 à ionisation de flamme. Les conditions d'analyse sont suivant la colonne utilisée : colonne de polyester de Craig à 15% sur chromosorb W 30–60 mesh, de 10 p, maintenue à 170° et utilisant un courant d'hélium de 80 ml par min; une colonne de Zonyl E-7 à 10% sur chromosorb W, 80–100 mesh, de 10 p, maintenue à 160° et utilisant un courant d'hélium de 60 ml par min ou une colonne de SE-30 à 9% sur Chromport XXX, 80–90 mesh, de 12 p maintenue à 160° et utilisant un courant d'hélium de 55 ml par min.

1. Synthèse de la tert-butyl-5 diméthyl-3,3 cycloheptanone (1a)

1.1 Les cyanohydrines 3a

Utilisant le protocole expérimental décrit par Belanger (10), une solution de bisulfite de sodium dans 55 ml l'eau distillée est ajoutée, sous bonne agitation et à un rythme tel que la température ne dépasse par 5°, à un mélange de 11.3 g de cyanure de sodium dans 55 ml d'eau distillée et de 28.8 g de *tert*-butyl-4 diméthyl-2,2 cyclohexanone (**2***a*). L'addition terminée, le mélange est agité à la température ambiante pendant 2 h et extrait à l'éther à la manière habituelle pour fournir 33 g (100% du rendement théorique) de produits bruts. Les cyanohydrines **3***a* montrent dans leur spectre i.r., la présence de bandes hydroxyle à 3410 et —C≡N à 2210 cm^{-1}. Le spectre r.m.n. de ce mélange déterminé dans le benzène, montre la présence du groupe *tert*-butyle à 0.74 p.p.m., de 4 singulets à 0.81, 0.96, 1.06, et 1.16 p.p.m. correspondants aux groupements méthyles en position 2 et les 2 groupes hydroxyles des alcools tertiaires apparaissent à 2.53 et 2.78 p.p.m.

1.2 Les aminoalcools 3b

Suivant les indications de Gravel (11) une solution de 24.9 g de cyanohydrines **3***a* dans 135 ml d'éther est ajoutée goutte à goutte à 0° à une suspension de 9.2 g d'hydrure de lithium et d'aluminium en suspension dans 200 ml d'éther. Le mélange réactionnel est agité à reflux pendant 21 h et le complexe décomposé par addition successivè à 0° de 12 ml d'eau, 9 ml d'une solution de soude 6 *N*, et de 30 ml d'eau. L'extraction des produits à la manière habituelle permet d'isoler 22.8 g (76% du rendement théorique) de chlorhydrate (**3***c*) d'aminoalcools fondant entre 235–242 °C et présentant dans le spectre i.r. déterminé dans la Nujol des bandes à 3300, 3070, 1625, 1585, 1510, 1368, et 1040 cm^{-1}.

Le spectre r.m.n. de ces dérivés, déterminé dans l'acide trifluoroacétique, montre la présence de pics à 0.89 et 1.02 p.p.m. (*tert*-butyles) et à 1.04 et 1.16 p.p.m. (*gem*-diméthyles). Les aminoalcools **3***b* régénérés de leur chlorhydrate fondent, après recristallisation de l'éther de pétrole, entre 102 et 112 °C et montrent dans l'i.r. des bandes à 3435, 1370, 1040, et 1005 cm^{-1} ; leur spectre r.m.n. présente des bandes à 0.82 et 0.84 p.p.m. (*tert*-butyles) et 0.87 et 1.07 p.p.m. (*gem*-diméthyles).

1.3 Désamination nitreuse

S'inspirant de la méthode décrite par Gravel (11), 34.2 g de chlorhydrate **3***e* sont dissous dans 575 ml d'eau distillée. A cette solution, 1.43 ml d'une solution *N* de soude sont d'abord ajoutés pour libérer l'aminoalcool, puis 247 ml d'acide acétique glaciale pour obtenir une solution d'aminoalcool dans l'acide acétique à 25%. A ce mélange 28 g de nitrite de sodium dissous dans 115 ml d'eau sont ajoutés lentement à 0°. L'addition terminée le mélange réactionnel est agité à 0° pendant 3 h, puis alcalinisé par addition à 0° d'une solution de soude 6 *N* puis légèrement acidifié par addition d'acide acétique glaciale et extrait à l'éther à la manière habituelle pour obtenir 25.4 g d'un liquide qui, après distillation sous pression réduite, est transformé en semicarbazone selon la méthode de Durocher (17). Après deux recristallisations fractionnées d'un mélange méthanol–éthanol, 8.5 g de prismes blancs fondant à 198° (décomposition) sont isolés. L'entraînement à la vapeur de la semicarbazone pure, mise en suspension dans une solution aqueuse contenant 14.5 g d'acide oxalique, conduit après les extractions habituelles à 6.3 g (95% de rendement) de produit cétonique. La distillation de ce produit brut utilisant une colonne Vigreux de 8 cm donne comme fraction de coeur 5.5 g d'un liquide incolore possédant les caractéristiques suivantes : n_D^{26}, 1.4631; p.c. : 134 °C/20 mm Hg ; i.r., bandes à 1692 (carbonyle) et 1368 cm^{-1} (*tert*-butyle) ; r.m.n. (solution benzénique), bandes à 0.72 p.p.m. (*tert*-butyle), à 0.81 et 0.84 p.p.m. (*gem*-diméthyle); spectre de masse, pic parent à *m/e* de 196. La dinitrophénylhydrazone, préparée à la manière habituelle, fond à 153–154 °C (éthanol) ; i.r. bandes à 3040, 1618, 1592, 1368, et 1335 cm^{-1} ; r.m.n. ($CDCl_3$), pics à 0.85 (*tert*-butyle), 0.87 et 1.06 p.p.m. (*gem*-diméthyle) et à 7.74, 8.06, et 8.85 (protons aromatiques); spectre de masse, pic parent à *m/e* de 376. La deutération selon les indications de Fuchs (12) à l'aide de 0.4 g de cétone **1***a*, de 0.16 g de pyrollidine, et 15 ml de benzène traités 8 fois par 0.5 ml d'oxyde de deuterium contenant des traces d'anhydride acétique conduit, après extraction à la méthode habituelle, à la cétone **1***a* deutériée contenant dans son spectre i.r. des bandes dans la région de 2220 à 2200 cm^{-1} et dans son spectre de masse des pics à 196 (100%), 197 (166%), 198 (248%), 199 (292%), et 200 (258%).

Can. J. Chem. Downloaded from www.nrcresearchpress.com by 210.87.254.6 on 09/05/12
For personal use only.

Can. J. Chem. Downloaded from www.nrcresearchpress.com by 210.87.254.6 on 09/05/12
For personal use only.

2. Synthèse de la tert-butyl-5 diméthyl-2,2 cycloheptanone (4a)

2.1 Tert-butyl-4 isopropenyl-1 cyclohexanol (3c)

Au réactif de Grignard préparé selon les indications de Normant (18) dans le tétrahydrofuranne et à partir de 3.6 g de magnésium et 18.2 g de bromo-2 propène, une solution de 17.9 g de *tert*-butyl-4 cyclohexanone (**2***c*) est ajoutée tout en maintenant la température à 0°. Le mélange est ensuite chauffé à reflux pendant 2 h, puis hydrolysé par addition goutte à goutte à 0° d'une solution de chlorure d'ammonium et extrait à l'éther à la manière habituelle pour fournir 23 g d'une huile montrant dans son spectre i.r. des vibrations caractéristiques à 3400 (hydroxyle) et 1710 cm^{-1} (cétone qui n'a pas réagie). Une analyse en c.p.g. (Zonyl E-7) du produit brut de la réaction révèle la présence de 3 produits principaux soit 52 et 35% respectivement, des 2 isomères de l'alcool **3***d* et 4% de cétone (**2***e*) qui n'a pas réagi.

2.2 Bromométhyl-2 tert-butyl-5 méthyl-2 cycloheptanone (4b)

Selon une technique expérimentale modifiée inspirée de Johnson *et al.* (14) 8.6 g d'alcool **3***d* sont mis en solution dans 205 ml de chloroforme débarassé de toute trace d'alcool et 10 g d'hypobromite de *tert*-butyle à 90% (d'après un dosage iodomidrique) préparé selon la méthode de Geneste et Kergomard (19) sont ajoutés ; le mélange est agité à 50–55° à l'abri de la lumière pendant 38 h puis filtré sur 80 g d'alumine neutre (colonne de 50 mm de diamètre) pour isoler, après évaporation du chloroforme, 10 g d'un liquide qui est chromatographié sur 900 g de gel de silice. L'élution de la colonne avec un mélange d'éther de pétrole contenant 3% d'éther anhydre permet d'isoler 2.2 g des bromocétones **4***b* pures à au moins 90% d'après la c.p.g. Ces composés p.e. 82–84°/0.04 mm Hg ; n_D^{25} 1.4988 ; test de Beilstein positif ; i.r.: bandes à 1695 (carbonyle) et à 1368 cm^{-1} (*tert*-butyle); r.m.n. (benzène) pics à 0.66 et 0.67 p.p.m. (*tert*-butyle), 0.94 et 1.02 (méthyle en position 2), et entre 2.86 et 3.72 (bromométhyle).

2.3 Hydrogénolyse des bromocétones 4b

Selon la procédure décrite par Julia et Guereny (13), 0.75 g de bromocétone **4***b*, 2.2 g de zinc en poudre, 10 ml d'acide acétique glaciale, et 2 ml d'acide bromhydrique à 48% sont chauffés à reflux pendant 3 h. Le mélange réactionnel est filtré, versé dans un excès d'ammoniaque à 50% et extrait à l'éther. Les fractions éthérées, lavées à la manière habituelle fournissent 0.55 g (100% de rendement) d'un liquide brun montrant dans son spectre i.r. une forte vibration à 1700 cm^{-1}. La distillation fractionnée permet d'isoler comme fraction de coeur un liquide montrant dans la c.p.g. (polyester de Craig) un seul pic (dans les conditions utilisées il a été démontré que la cétone isomère **1***a* peut être détectée). La cétone **4***a* : p.e., 130–131°/16 mm Hg ; n_D^{25} 1.4631; i.r., bandes à 1695 (vibration C=O) et 1368 cm^{-1} (*tert*-butyle) ; spectre r.m.n., pics à 0.71 p.p.m. (*tert*-butyle), à 0.89 et 1.08 p.p.m. (*gem*-diméthyle) et entre 1.90 et 2.55 p.p.m. massif intégrant pour les deux protons en position 7 ; spectre de masse, pic parent à *m/e* de 196. La dinitrophénylhydrazone de cette cétone fond à 147–149° (éthanol); i.r., bandes à 3300, 1618, 1592, 1368, et 1335 cm^{-1} ; spectre r.m.n. ($CDCl_3$), pics à 0.83 p.p.m. (*tert*-butyle), à 1.13 et 1.25 p.p.m. (*gem*-diméthyle), et à 7.73, 8.06, et 8.86 p.p.m. (protons aromatiques) ; spectre de masse, pic parent à *m/e* de 376. La deutériation (12) effectuée sur 200 mg de cétone en présence de 100 mg de pyrollidine dans 25 ml de benzène anhydre après 6 échanges à l'aide de 0.5 ml d'eau lourde fournit une cétone contenant dans son spectre i.r. une bande à 2170 cm^{-1} et une diminution sensible de l'intégration dans la région de 1.90 et 2.50 p.p.m. du spectre r.m.n. Le spectre de masse de cette cétone deutériée montre des pics à *m/e* de 196 (100%), 197 (50%), et 198 (23%).

3. Tert-butyl-5 diméthyl-3,3 cycloheptanols (6a et 7a)

3.1 Préparation

La réduction de 5 g de cétone **1***a* par 13 g de sodium et 28 ml d'éthanol absolu conduit, après extraction et distillation à 142°/16 mm de mercure, à 4.41 g (87% du rendement théorique) d'un liquide visqueux incolore dont le spectre i.r. montre une forte absorption à 3350 cm^{-1} et dont le spectre r.m.n. montre 4 singulets dans la région des méthyles. La réaction de 7.7 g de chlorure de *p*-nitrobenzoyle dans 37 ml de pyridine avec 3.7 g des alcools **6***a* et **7***a* conduit après extractions à la manière habituelle à 6.3 g de solide. Plusieurs recristallisations fractionnées dans l'éthanol permettent de recueillir deux types de produits cristallins ; le *p*-nitrobenzoate **6***b* sous forme de paillettes : p.f., 119–120° ; i.r., bandes à 1710, 1525, 1350, 1280, 1105, et 1100 cm^{-1} ; r.m.n., bandes à 0.87 p.p.m. (*tert*-butyle), à 0.95 et 1.11 p.p.m. (*gem*-diméthyle), entre 4.80 et 5.24 p.p.m. (proton carbinolique), et à 8.25 p.p.m. protons aromatiques ; le *p*-nitrobenzoate *trans* (**7***b*) : p.f., 111–112 °C (p.f. mixte avec le précédent 100°) ; i.r., bandes à 1710, 1538, 1320, 1280, 1112, et 1095 cm^{-1} ; r.m.n., bandes à 0.86 p.p.m. (*tert*-butyle), à 1.06 p.p.m. (*gem*-diméthyle), entre 4.85 et 5.24 p.p.m. (proton carbinolique), et à 8.25 p.p.m. (protons aromatiques) ; spectre de masse, pic parent à *m/e* de 347. La saponification de 0.80 g du *p*-nitrobenzoate **6***b* à l'aide de 0.2 g d'hydroxyde de potassium dans 8 ml de méthanol et 2 ml d'eau, conduit à 0.3 g d'un liquide **6***a*, p.e., 70°/0.06 mm Hg ; n_D^{25}, 1,4713 ; i.r., bandes à 3625, 3450, 1368, 1020, et 980 cm^{-1} ; r.m.n. ($CDCl_3$) bandes à 0.81 p.p.m. (*tert*-butyle), à 0.92 et 0.95 p.p.m. (*gem*-diméthyle), à 1.45 p.p.m. (proton hydroxylique), et entre 3.55 et 4.00 p.p.m. (proton carbinolique); spectre de masse, pic parent à *m/e* de 198. De la même manière la saponification de 0.80 g de *p*-nitrobenzoate *trans* **7***b* fournit 0.3 g de l'alcool **7***a*, p.e., 69°/0.96 mm Hg ; n_D^{25}, 1.4708 ; i.r., bandes à 3650, 3625, 1368, 1006, et 1007 cm^{-1} ; r.m.n., pics à 0.80 p.p.m. (*tert*-butyle), à 0.87 et 0.98 p.p.m. (*gem*-diméthyle), à 1.47 p.p.m. (hydroxyle), et entre 3.40 et 3.90 p.p.m. (proton carbinolique); spectre de masse, pic à *m/e* de 198. Lorsque le mélange des deux alcools **6***a* et **7***a* est traité selon la méthode Sweeley *et al.* (15) avec l'hexaméthyldisilazane et le triméthylchlorosilane en milieu pyridine anhydre, les dérivés **6***c* et **7***c* ainsi obtenus peuvent être séparés sur la colonne de SE 30. Ces dérivés triméthylsilyl **6***c* et **7***c* semblent être stables si gardés à l'abri de l'humidité puisque l'analyse en c.p.g. à différents intervalles de temps d'un même mélange a toujours donné des résultats constants. Afin de vérifier que la formation des dérivés triméthylsilanés est quantitative pour chacun des iso-

mères, 2 mélanges d'alcool **6***a* et **7***a* de compositions connues ont été préparés par pesée, traités avec les réactifs de silylation et analysés en c.p.g. (SE 30) ; des mélanges contenant respectivement 60.7% **6***a*/39.3% **7***a* et 33.8% **6***a*/65.2% **7***a* montraient par analyse en c.p.g. de leurs dérivés silanés des compositions de 61.3/38.7 et 35.6/64.4.

3.2 Réduction de la cétone ***1****a*

Les méthodes de réduction utilisées correspondent aux méthodes standards et les références appropriées sont indiquées dans le tableau I.

Remerciements

Les auteurs remercient vivement le Conseil National de Récherches du Canada pour l'aide financière apportée. Ils remercient aussi la compagnie Dow Chemicals du Canada pour un généreux échantillon de *tert*-butyl-4 cyclohexanone.

L'un de nous (J.C.R.) tient à exprimer sa profonde gratitude au Dr. Pierre Maroni et à Mlle Marthe Benoit de la Faculté des Sciences de Toulouse pour l'accueil et l'aide qui lui ont été accordés durant la préparation de ce manuscrit.

1. A. V. KAMERNISTSKY et A. A. AKHREM. Tetrahedron **18**, 705 (1962).
2. W. HÜCKEL et J. WÄCHTER. Ann. **672**, 62 (1964).
3. M. GAUCHOT et G. CAUQUIL. C. R. **190**, 642 (1930).
4. J. W. HUFFMAN et J. E. ENGLE. J. Org. Chem. **26**, 3116 (1961).
5. W. HÜCKEL et O. HONECKER. Ann. **678**, 10, (1964).
6. M. MÜHLSTADT, R. BORSDORF, et F. J. STRUBER. Tetrahedron Letters, 1879 (1966).
7. D. D. ROBERTS. J. Org. Chem., **30**, 4375 (1965).
8. J. C. RICHER. J. Org. Chem. **30**, 324 (1965).
9. M. MOUSSERON et G. MANON. Bull. Soc. Chim. France, 392 (1949).
10. P. BELANGER. Mémoire de Maîtrise, Faculté des Sciences, Université de Montréal (1963).
11. D. GRAVEL. Thèse de Doctorat, Faculté des Sciences, Université de Montréal (1962).
12. B. FUCHS. Communication personnelle.
13. S. JULIA et C. GUERENY. Bull. Soc. Chim. France, 2994 (1965).
14. C. R. JOHNSON, C. J. CHEER, et D. J. GOLDSMITH. J. Org. Chem. **29**, 3320 (1964).
15. C. C. SWEELEY, R. BENTLEY, M. MAKITA, et W. W. WELLS. J. Amer. Chem. Soc. **85**, 2497 (1963).
16. O. H. WHEELER et E. G. RODRIGUEZ. J. Org. Chem. **29**, 718 (1964).
17. J. G. DUROCHER. Mémoire de Maîtrise, Faculté des Sciences, Université de Montréal (1961).
18. H. NORMANT. Bull. Soc. Chim. France, 1764 (1959).
19. J. M. GENESTE et A. KERGOMARD. Bull. Soc. Chim. France, 471 (1963).
20. E. L. ELIEL et R. S. RO. J. Amer. Chem. Soc. **79**, 5992 (1951).
21. A. L. WILD. *Dans* Organic reactions. Vol. II. R. Adams (Editor). John Wiley and Sons, Inc., New York, 1946. p. 73.
22. S. WINSTEIN et N. J. HOLNESS. J. Amer. Chem. Soc. **77**, 5562 (1955).
23. D. M. S. WHEELER et J. W. HUFFMAN. Experientia **16**, 516 (1960).
24. D. S. NOYCE et L. J. DOLBY. J. Org. Chem. **26**, 3619 (1961).
25. H. C. BROWN et R. F. MCFARLIN. J. Amer. Chem. Soc. **72**, 252 (1956).

Can. J. Chem. Downloaded from www.nrcresearchpress.com by 210.87.254.6 on 09/05/12
For personal use only.

Decomposition of lauroyl, decanoyl, and octanoyl peroxides in solution

J. E. GUILLET
Department of Chemistry, University of Toronto, Toronto, Ontario

AND

J. C. GILMER
Research Laboratories, Tennessee Eastman Company, Kingsport, Tennessee

Received April 17, 1969

The thermal decomposition from 50 to 250° of lauroyl, decanoyl, and octanoyl peroxides in solution in a high molecular weight hydrocarbon was studied. These peroxides are convenient sources of C-11, C-9, and C-7 straight-chain aliphatic free radicals, whose reactions may be considered as models for the higher molecular weight radicals formed during thermal cracking of polyolefins.

The ratio of disproportionation to combination for these radicals is about 0.2, which is very similar to the values obtained for lower alkyl radicals in the gas phase. This ratio appears to be relatively independent of temperature. Intramolecular chain transfer, which results in the isomerization of the radical, occurs at the higher temperatures, and the process has an apparent activation energy of about 2 kcal per mole.

The product distribution indicates that at reaction temperatures up to 250° a statistically random distribution of alkyl radicals is never achieved in solution. Since the radicals are formed in pairs, they tend to react with each other rather than with radicals formed from other peroxide molecules. This is demonstrated by the near absence of cross-combination products when two different peroxides are decomposed in the same solution simultaneously at 70°. At 250°, some cross-product is formed but less than one-fifth of the amount expected if the radicals were uniformly distributed in the solution. The activation energy for the formation of cross-product is of the same order as that for diffusion. The significance of these results in terms of the classical picture of "cage reactions" is discussed.

Canadian Journal of Chemistry, 47, 4405 (1969)

Can. J. Chem. Downloaded from www.nrcresearchpress.com by 210.87.254.5 on 09/05/12
For personal use only.

Introduction

Diacyl peroxides have been used for many years as sources of free radicals for the initiation of various radical reactions, such as vinyl polymerization. Early studies of the decomposition of such peroxides indicated a relatively straightforward mechanism by which the diacyl peroxide broke down by scission of the oxygen–oxygen bond to give acyloxy radicals

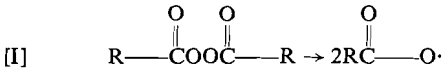

[I] $$R{-}\overset{O}{\overset{\|}{C}}{-}O{-}O{-}\overset{O}{\overset{\|}{C}}{-}R \rightarrow 2R\overset{O}{\overset{\|}{C}}{-}O\cdot$$

The acyloxy radicals were assumed to be unstable and to break down to give two alkyl radicals and two molecules of carbon dioxide

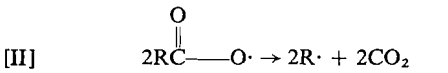

[II] $$2R\overset{O}{\overset{\|}{C}}{-}O\cdot \rightarrow 2R\cdot + 2CO_2$$

There was some evidence that the splitting out of carbon dioxide might take place simultaneously with the initial scission. On the basis of such a mechanism, Szwarc (1) used the decomposition of acetyl peroxide as a convenient source of free methyl radicals to study relative reactivities in solution. Propionyl and heptanoyl peroxides were used as sources of free ethyl (2) and hexyl (3) radicals in similar studies.

In the present work, studies of the decomposition of the higher diacyl peroxides were made to obtain a better understanding of the reactions of linear C-7, C-9, and C-11 alkyl radicals in solution. Of particular interest was the question of whether these species could be used as models for longer chain hydrocarbon radicals, such as those formed in the polymerization of ethylene and other olefins, and in the thermal and oxidative degradation of long-chain hydrocarbons.

Theory

The scheme of diacyl peroxide decomposition exemplified by eqs. [I] and [II] is now known to be a considerable oversimplification. Based on the very thorough studies of De Tar and coworkers, (4–6) it is now known that the major reactions occurring can best be explained by the following kinetic scheme:

[1] $$(RCOO)_2 \rightarrow [2RCOO\cdot]$$
[2] $$\rightarrow [RCOO\cdot + R\cdot] + CO_2$$
[3] $$\rightarrow [2R\cdot] + 2CO_2$$
[4] $$[2R\cdot] \rightarrow 2R\cdot$$
[5] $$\rightarrow R{-}R$$

[6] $\rightarrow R'CH_3 + R''CH{=}CH_2$

[7] $[RCOO\cdot + R\cdot] \rightarrow R\cdot + RCOO\cdot$

[8] $\rightarrow RCOOR$

[9] $\rightarrow RCOOH + R'CH{=}CH_2$

[10] $[2RCOO\cdot] \rightarrow 2RCOO\cdot$

[11] $\rightarrow (RCOO)_2$

[12] $RCOO\cdot \rightarrow R\cdot + CO_2$

[13] $R\cdot + SH \rightarrow RH + S\cdot$

[14] $RCOO\cdot + SH \rightarrow RCOOH + S\cdot$

[15] $2S\cdot \rightarrow S{-}S$

[16] $\rightarrow S'CH_3 + S''CH{=}CH_2$

where S = solvent molecule, R′ = R minus 1 methylene, R″ = R minus 2 methylenes, S′ = S minus 1 methylene, S″ = S minus 2 methylenes. In the above scheme, the terms in brackets denote components or reactions occurring within the solvent "cage", within the broad meaning of the term as defined by Noyes (7–10). It was shown by De Tar and co-workers (4–6) that these so-called "geminate cage" reactions represent at least 50% of the total decomposition products. The present study confirms that over half the total reaction may be considered to take place within a solvent "cage" which is a modification of the type envisaged by Frank and Rabinowitch (11) even at temperatures as high as 250°.

In addition to the reactions listed above, secondary reactions occur, such as the addition of a free radical to the olefins formed in reactions [6], [9], and [16], and radical attack on the peroxide molecule to give induced decomposition. De Tar and Weis (5) showed that the latter reaction represents only a small fraction of the total, even at quite high peroxide concentrations, and the analytical results of the present study confirm this.

Experimental

In the present work the objective was to study these reactions in hydrocarbon media at temperatures up to 250°. This necessitated the use of a high boiling hydrocarbon solvent, and heavyweight mineral oil (Primol D) was selected. At temperatures above 100° the rate of decomposition of the peroxides became very rapid and special techniques were necessary to make sure that most of the reaction was taking place at the desired temperature. Three methods were tried: (*1*) the peroxide solution was dropped into a stirred reactor containing mineral oil, (*2*) the mineral oil solution of the peroxide was dropped onto the surface of an aluminum block at a controlled temperature, and (*3*) the mineral oil solution was pumped through a heated capillary tube. Method (*3*) proved to be the most convenient and reliable and was used for most of the work.

Lauroyl, decanoyl, and octanoyl peroxides were obtained from Lucidol Corporation. Lauroyl and decanoyl peroxides were purified by recrystallizing them twice from pentane and drying them under high vacuum at 25°. Peroxide assay combined with infrared (i.r.) and gas chromatography measurements on the decomposition products indicated that the purity of the compounds was greater than 99%. Octanoyl peroxide was received as a 50% solution in mineral oil and was used without further purification.

Primol D is a completely saturated, branched hydrocarbon, which boils above 300° and has a viscosity of 125 cp at 25° and 3 cp at 250°. It was shown to contain no oxygen or unsaturation by i.r. analysis. For these experiments it was purified by heating it at 250° under 1 mm pressure for 3 h and then cooling under a blanket of nitrogen.

Thermal decomposition rates for the three peroxides were determined using 0.5% w/v solutions in mineral oil. Studies of product distribution were made by decomposing 10% w/v solutions of the peroxides in mineral oil. Thermal decompositions at temperatures below 100° were carried out in glass vials sealed under nitrogen after thorough degassing of the peroxide solutions. The vials were heated in thermostatted aluminum blocks. Decompositions above 100° were carried out using the procedure described by Guillet *et al.* (12). The degassed solution was pumped through a stainless steel capillary 20 in. long and 0.016 in. internal diameter. The volume of the heated part of the capillary was 0.0640 cc. A syringe pump (50 ml capacity) driven by a synchronous motor was used to pump the solution through the capillary. The rate of pumping could be varied widely by changing the frequency of the a.c. voltage applied to the motor. After passing through the heated zone, the solution was chilled in a water condenser and collected in sample vials.

Analyses of the decomposition products were carried out by gas chromatography using a thermal conductivity detector. In most of the work a Micro-Tek model GC-2500 PT programmed-temperature unit was used with a 4 ft × 1/4 in. column packed with 5% Silicone SE30 on Chromosorb W. A linear program rate from 50 to 300° was used for analysis of the decomposition products. At 300° the mineral oil solvent came off the column in about 10 min. Analyses for saturated and unsaturated hydrocarbons were performed on a 4 ft × 1/4 in. column packed with 20% Carbowax 20M on Chromosorb W. After several analyses the mineral oil was removed from the column by backflushing. The analyses were made on the basis of area percentage, using known hydrocarbons for calibration.

Lauric, decanoic, and octanoic acids were determined by titration in alcohol solutions with 0.025 *N* alcoholic sodium hydroxide using phenolphthalein indicator.

Results

Rate of Thermal Decomposition

The first-order rate constants for the thermal decomposition of the three peroxides were fitted to the Arrhenius equation by regression analysis. The frequency factors and activation energies obtained are listed in Table I.

It is apparent that the peroxides decompose at

Can. J. Chem. Downloaded from www.nrcresearchpress.com by 210.87.254.5 on 09/05/12
For personal use only.

TABLE I

Arrhenius parameters for peroxide decompositions*

Peroxide	Frequency factor (A) × 10^{-15}	Activation energy (E_a), kcal/mole
Octanoyl	9.9±1.1	32.5±1.2
Decanoyl	2.7±0.4	31.5±1.4
Lauroyl	21.7±3.3	32.9±1.4

*95% Confidence limits (2σ) based on regression equation.

nearly identical rates. A modified Arrhenius plot of the experimental data and the regression lines is given in Fig. 1 using the half life, $\tau = (0.6932/k)$, in place of the first-order rate constant, k. The activation energies are believed to be quite reliable because of the wide temperature range over which the rates were studied. With 5-phenylvaleryl peroxide De Tar and Weis (5) showed that the first-order rate constants were unchanged over a 600-fold variation in peroxide concentration. The three peroxides studied in this work appear to behave in the same manner, at least over the range of concentrations used. The values of the rate constants and activation energies obtained are almost identical to those reported previously by Ray (13) and Doehnert and Mageli (14).

Thermal Decomposition Products

The results of the study of the product distribution obtained by thermally decomposing solutions of lauroyl peroxide at temperatures from 50 to 257° are summarized in Table II. The most surprising aspect of these results is that the amount of docosane, usually considered to be formed exclusively in the solvent "cage", increases with temperature, whereas the amount of "noncage" product, undecane, decreases. The amount of ester produced is almost independent of temperature, whereas the amount of lauric acid produced appears to decrease as the temperature increases. The concentration of a sixth

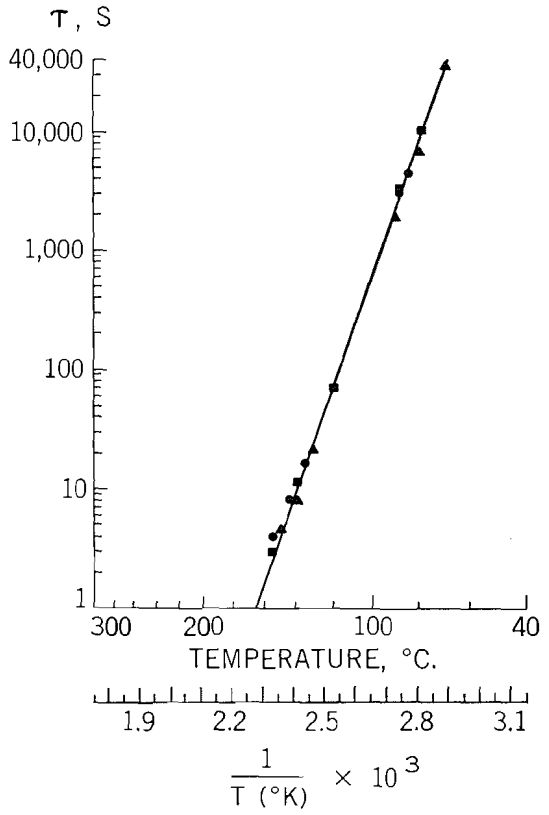

FIG. 1, Half-life τ of diacyl peroxides as function of reciprocal temperature measured in 1% solutions in Primol D; ▲ lauroyal peroxide; ● decanoyl peroxide; ■ octanoyl peroxide.

product, which appears in only very small amounts at low temperatures, increases significantly as the temperature is raised. Its retention time is slightly less than that of docosane. A similar product is formed in the decomposition of decanoyl peroxide or octanoyl peroxide and, in the latter case, has been isolated by gas chromatography and identified by i.r. studies as a

TABLE II

Decomposition products of lauroyl peroxide (moles product/mole peroxide × 100)

Decomposition temperature, °C	Acid	Ester	1-Undecene	Undecane	Docosane	Isodocosane
50.0	16.5	7.5	7.0	114	25.6	0.27
75.2	15.3	9.2	8.5	102	30.8	0.44
96.5	12.3	9.6	11.9	92.7	34.7	0.65
148	16.3	7.1	15.9	72.3	43.1	1.5
184	8.6	8.0	15.0	66.9	48.1	2.5
222	7.6	5.8	16.9	65.0	50.0	3.6
257	7.8	7.0	17.1	60.8	50.0	3.9

Can. J. Chem. Downloaded from www.nrcresearchpress.com by 210.87.254.5 on 09/05/12
For personal use only.

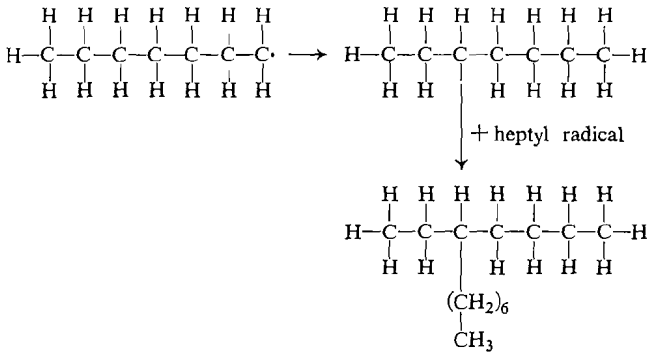

SCHEME 1

branched isomer of tetradecane, formed presumably by the reaction shown in Scheme 1. This intramolecular hydrogen abstraction reaction has been generally accepted as the basis for the formation of short-chain branches in polyethylene. This then represents an interesting experimental verification of the actual occurrence of such reactions. The same features are shown in the product distributions for the thermal decomposition of decanoyl and octanoyl peroxides, listed in Tables III and IV.

The amount of the combination products octadecane and tetradecane increases with temperature, whereas the amount of the "noncage" products nonane and heptane decreases. The theory of "cage" dissociation processes as formulated by Noyes (7) suggests that the probability of escape from the solvent "cage" should increase with temperature because of the decrease in density and viscosity of the medium. The increased yield of the combination products as the temperature is raised is in apparent contradiction to this theory, if it is true that all of the combination takes place as a "geminate cage" reaction.

It occurred to us that, since lauroyl and decanoyl peroxides decompose thermally at nearly identical rates, a study of the amount of cross-combination product formed when mixtures of the two are heated would give an indication of the number of radicals combining outside the "cage". Accordingly, 25 mmoles of each peroxide was dissolved in 19.0 ml of Primol D and heated at various temperatures until reaction was complete. The results are summarized in Table V.

The data in column 5, Table V, express the

TABLE III

Decomposition products of decanoyl peroxide (moles product/mole peroxide × 100)

Decomposition temperature, °C	Acid	Ester	1-Nonene	Nonane	Octadecane	Isoöctadecane
151	14.7	11.7	12.7	61.0	41.9	2.5
183	11.0	10.4	14.0	59.4	46.5	3.8
221	7.8	9.5	14.6	56.3	48.5	4.5
255	7.5	9.1	13.2	49.8	52.3	5.3

TABLE IV

Decomposition products of octanoyl peroxide (moles product/mole peroxide × 100)

Decomposition temperature, °C	Acid	Ester	1-Heptene	Heptane	Tetradecane	Isotetradecane
150	—	9.2	12.3	74.0	35.6	2.3
222	19.7	7.3	12.5	57.6	44.0	3.8
257	19.4	5.9	14.3	60.0	43.1	4.4

Can. J. Chem. Downloaded from www.nrcresearchpress.com by 210.87.254.5 on 09/05/12
For personal use only.

Can. J. Chem. Downloaded from www.nrcresearchpress.com by 210.87.254.5 on 09/05/12
For personal use only.

TABLE V

Thermal decomposition of equimolar mixtures of lauroyl and decanoyl peroxide

Temperature, °C	Relative peak areas			Amount of "noncage" combination, %
	C-18	C-20	C-22	
76.5	9.7	0.50	10.0	4.9
96.5	17.5	0.92	16.0	5.4
152	20.7	1.82	21.5	8.3
183	12.8	1.95	16.7	12.4
262	19.9	3.60	21.20	16.1

results in terms of the amount of cross-product formed as a percentage of the amount expected if all the radicals formed in the decomposition were randomly distributed throughout the solution. The relatively small value (16.1%) at 262° indicates how poorly the system approximates this random distribution, even at temperatures where the peroxide is decomposing in about 10 ms. This value will be equivalent to the actual percentage of radicals combining outside the "cage". The data from Table V can be used to estimate the actual amount of "cage" recombination occurring at various temperatures. When this is done, the results shown in Tables VI and VII are obtained

TABLE VI

"Cage" recombination of C-11 radicals

Decomposition temperature °C	Moles docosane/mole peroxide	
	Measured	Corrected for "random" recombination
50.0	25.6	25.6
75.2	30.8	29.3
96.5	34.7	32.8
148	43.1	39.5
184	48.1	42.1
222	50.0	43.0
257	50.0	42.0

TABLE VII

"Cage" recombination of C-9 radicals

Decomposition temperature °C	Moles octadecane/mole peroxide	
	Measured	Corrected for "random" recombination
151	41.9	38.4
183	46.5	40.7
221	48.5	41.5
255	52.3	43.9

for lauroyl and decanoyl peroxides, respectively. It is apparent that the amount of "cage" recombination increases with temperature up to about 150°, after which only a slight increase is observed which may not be outside the experimental error. Similarly, the total amount of "noncage" products decreases with temperature up to 150° and then remains constant at about 35%.

A similar increase in "cage" recombination of methyl radicals from acetyl peroxide with temperatures increasing from 40 to 100° was observed by Braun *et al.* (15). This increase was attributed to a mechanism involving the separation of acetoxy radicals followed by decarboxylation to give methyl radicals which undergo "geminate diffusive recombination." The increase in combination with temperature is due to an activation energy of about 6.6 kcal/mole for the decarboxylation reaction, which becomes, in a sense, the rate controlling step. This mechanism appears to give a satisfactory explanation of the product distribution for acetyl peroxide. However, it has been well established (16–19) that the ester formed in the decomposition, if formed from an optically active diacyl peroxide, will retain configuration in both the alcohol and acyloxy groups. This would appear to preclude the formation of the ester by diffusive recombination of an alkyl and an acyl radical as proposed by Braun and co-workers (15), since the free alkyl group would be expected to lose configuration if it had any appreciable lifetime as a free radical. It would appear, therefore, that the ester must be formed either in a single step during the initial decomposition or by a reaction involving geminate diffusive recombination of two acyloxy radicals by the following kinetic scheme:

[17] $$\left[\begin{matrix}\text{O}\\ \|\\ 2\text{RC}\text{—O}\cdot\end{matrix}\right] \longrightarrow \begin{matrix}\text{O}\\ \|\\ \text{RCOR}\end{matrix} + \text{CO}_2$$

This reaction would require an appreciable activation energy in order to explain the fact that, with the higher diacyl peroxides, the yield of ester is much less than that for the combination of the two alkyl radicals. Recent studies on the decomposition of acetyl peroxide by isotopic tracer methods (20) confirm the intramolecular nature of the processes leading to both the ester and the recombination product of the primary alkyl radical.

Can. J. Chem. Downloaded from www.nrcresearchpress.com by 210.87.254.5 on 09/05/12
For personal use only.

An Arrhenius plot of the amount of "random" combination taking place (from Table V) indicates an apparent activation energy of 2.6 kcal/mole. However, this probably does not represent the actual temperature coefficient for escape from the solvent "cage" since the probability of one free radical meeting another before chain transfer to solvent occurs is included in this.

Intramolecular Chain Transfer

A similar activation energy (2.0 kcal) is shown for the process involving intramolecular chain transfer (Scheme 1) to give a branched-chain combination product. This indicates that no intramolecular chain transfer takes place within the time interval (10^{-9} s) for "geminate cage" recombination; once the radical escapes from the immediate vicinity of the "cage", it has an appreciable lifetime during which intramolecular chain transfer will compete with chain transfer to solvent and reaction with another free radical.

Disproportionation/Combination Ratio

Estimates of the amount of disproportionation of alkyl radicals (reaction [6]) is complicated by the fact that alkenes can be formed both by reaction [6] and by the disproportionation of an alkyl radical with an acyloxy radical (reaction [9]) which is presumably a primary "cage" reaction. At low temperatures the amount of acid formed is greater than the amount of alkene, indicating that it is formed by another process, possibly by hydrolysis with traces of moisture. (The original peroxides and solutions contained less than 0.2% acid based on the peroxide.) The amount of acid reported in this work is higher than that shown by De Tar and Weis (4). In view of the uncertainty regarding the mechanism of formation of acid, the disproportionation/combination ratio can be reported only as maximum and minimum limits, assuming either absence or occurrence of reaction [9]. However, we feel that the maximum values are probably the more significant.

These limits are given in Table VIII for temperatures ranging from 50 to 260°. At temperatures of 180° and above, the values range from 0.2 to 0.3, which is of the order of magnitude expected from gas phase studies.

Role of the Solvent

In this work it has been assumed that most of the reactions with the solvent will be described by reactions [13] and [15]. That there is little combination of alkyl radicals with solvent is indicated by the material balances, which indicate that, in most cases, greater than 95% of all the alkyl radicals can be accounted for by the products listed in Tables II–IV.

TABLE VIII

Disproportionation/combination ratio for alkyl radicals

Temperature, °C	C-11 Radicals		C-9 Radicals		C-7 Radicals	
	Max.	Min.	Max.	Min.	Max.	Min.
50.0	0.27	0	—	—	—	—
75.2	0.28	0	—	—	—	—
96.5	0.34	0	—	—	—	—
148	0.37	0	0.30	0	0.35	—
184	0.31	0.13	0.30	0.07	—	—
222	0.34	0.19	0.30	0.14	0.28	0
257	0.34	0.19	0.25	0.11	0.33	0

Conclusion

We conclude from the present study that the thermal decomposition of the higher diacyl peroxides can be explained on the basis of a modified "cage" process in which ester and possibly acid are formed in a concerted or one-step process, probably within the original solvent "cage". About 10% of all the molecules decomposing give ester or acid by this mechanism. The acyloxy radicals, if formed in the initial decomposition of the peroxide, decarboxylate rapidly to give alkyl radicals which recombine exclusively by a "geminate cage" process at relatively low temperatures (50°). At higher temperatures, up to 16% of the radicals recombine after escape from the immediate vicinity of the "cage". The apparent activation energy for this process is 2.6 kcal/mole, which is of the same order as that for diffusion. The amount of "geminate cage" combination varies from about 46% at low temperatures to 65% at 260°; the remaining 35–54% of the radicals escape the immediate vicinity of the "cage". At low temperatures these react exclusively with solvent. At higher temperatures they may isomerize by intramolecular chain transfer or react with other alkyl radicals. When two alkyl radicals react, they may either disproportionate or combine, the ratio of the rate constants for these two reactions being 0.2–0.3.

The relatively high proportion of geminate cage processes (46–65%) in the higher diacyl peroxides relative to those observed in diacetyl peroxide (20–40%) is to be expected from the

larger size of the radicals produced. Since the enthalpy of decomposition is very similar for all diacyl peroxides, the separation velocity of the larger radical fragments will be much lower, and hence the probability of their escape from the "cage" will be significantly reduced.

Acknowledgments

The authors acknowledge many helpful discussions with H. W. Coover, Jr., and the assistance of M. F. Meyer and T. R. Walker in determining the thermal decomposition rates.

1. M. Szwarc. J. Polym. Sci. 16, (1955).
2. J. Smid and M. Szwarc. J. Amer. Chem. Soc. **78**, 3322 (1956).
3. D. F. De Tar and D. V. Wells. J. Amer. Chem. Soc. **82**, 5839 (1960).
4. D. F. De Tar and C. Weis. J. Amer. Chem. Soc. **78**, 4296 (1956).
5. D. F. De Tar and C. Weis. J. Amer. Chem. Soc. **79**, 3041 (1957).
6. D. F. De Tar and R. C. Lamb. J. Amer. Chem. Soc. **81**, 122 (1959).
7. R. M. Noyes. J. Chem. Phys. **22**, 1349 (1954).
8. R. M. Noyes. J. Chem. Phys. **23**, 1982 (1955).
9. R. M. Noyes. J. Amer. Chem. Soc. **77**, 2042 (1955).
10. R. M. Noyes. J. Amer. Chem. Soc. **78**, 5486 (1956).
11. J. Frank and E. Rabinowitch. Trans. Faraday Soc. **30**, 120 (1934).
12. J. E. Guillet, T. R. Walker, M. F. Meyer, J. P. Hawk, and E. B. Towne. Ind. Eng. Chem. Prod. Res. and Develop. **3**, 257 (1964).
13. N. H. Ray. J. Chem. Soc. 4023 (1960).
14. D. F. Doehnert and O. L. Mageli. Chem. Abstr. **53**, 18535 (1959).
15. W. Braun, L. Rajbenbach, and F. R. Eirich. J. Phys. Chem. **66** 1951 (1962).
16. D. F. De Tar and C. Weis. J. Amer. Chem. Soc. **79**, 3045 (1957).
17. F. D. Greene. J. Amer. Chem. Soc. **77**, 4869 (1955).
18. M. S. Kharasch, J. Kuderna, and W. Nudenburg. J. Org. Chem. **19**, 1283 (1954).
19. F. D. Greene, H. P. Stein, C. -C. Chu, and F. M. Vine. J. Amer. Chem. Soc. **86**, 2080 (1964).
20. J. C. Martin and J. Taylor. J. Amer. Chem. Soc. **89**, 6904 (1967).

Can. J. Chem. Downloaded from www.nrcresearchpress.com by 210.87.254.5 on 09/05/12
For personal use only.

Anomeric deoxy and unsaturated methyl pentofuranosides and pentopyranosides[1]

R. U. LEMIEUX, K. A. WATANABE[2], AND A. A. PAVIA[3]
Department of Chemistry, University of Alberta, Edmonton, Alberta

Received May 5, 1969

Both the anomers for methyl 2,3-dideoxy-D-*glycero*-pent-2-enofuranoside were characterized and hydrogenated to the corresponding methyl 2,3-dideoxy-D-*glycero*-pentofuranosides. The similar compounds were prepared in the pyranoside ring form but in the L-*glycero* configuration. The anomeric forms for methyl 3-deoxy-L-*erythro*-pentopyranoside are reported together with a number of their derivatives of interest for the study of solvation effects on conformational equilibria (21). The molar rotations of the deoxy and unsaturated glycosides are discussed as are the conformational properties of the various compounds.

Canadian Journal of Chemistry, 47, 4413 (1969)

Can. J. Chem. Downloaded from www.nrcresearchpress.com by 210.87.254.40 on 09/05/12
For personal use only.

In a previous communication (1), the preparation of the four stereoisomeric methyl 4,6-*O*-benzylidene-2,3-dideoxy-D-hex-2-enopyranosides was accomplished, in each case, by opening of the epoxide ring of a parent 2,3-anhydro derivative to the corresponding iodohydrin which was treated with either *p*-toluenesulfonyl (tosyl) or methanesulfonyl (mesyl) chloride in pyridine. We wish to report a modified procedure which allowed the preparation of the anomeric forms both for methyl 2,3-dideoxy-D-*glycero*-pent-2-enofuranoside (**4***c* and **9***c*) and for methyl 2,3-dideoxy-L-*glycero*-pent-2-enopyranoside (**17***c* and **18***c*).

Methyl 5-*O*-benzoyl-2,3-dideoxy-β-D-*glycero*-pent-2-enofuranoside (**9***a*) was first prepared by reaction of 3,5-di-*O*-benzoyl-D-*erythro*-pent-1-enofuranose with methanol (2). The β-D-configuration was later assigned by an alternative synthesis (3,4) involving reduction of methyl 5-*O*-benzoyl-2,3-di-*O*-tosyl-β-D-ribofuranoside by the method of Tipson and Cohen (5). The physical constants and nuclear magnetic resonance (n.m.r.) spectrum reported for **9***a* indicate that this compound was not pure. Also, the n.m.r. signal for H_2 was erroneously assigned to H_1. It is of interest to note that several 2′,3′-unsaturated nucleosides have been prepared (6–10).

The 5-*O*-benzoyl derivative (**1***a*) of the readily available methyl 2,3-anhydro-α-D-lyxofuranoside (11) was treated with sodium iodide in acetone in the presence of acetic acid and sodium acetate as described previously (1). The spectrum of the sirupy product (**2***a*) required high purity. That the epoxide opening followed the normal course (attack at the 3-position) for a 2,3-anhydrofuranoside (12,13) was established by benzoylation of the iodohydrin **2***a* to **2***c* followed by hydrogenolysis to yield crystalline methyl 2,5-di-*O*-benzoyl-3-deoxy-α-D-*threo* pentofuranoside (**3**). This 3-deoxy structure was required since the anomeric proton (singlet at τ 4.85) was not appreciably coupled to either of the methylene protons at τ 7.35 and 8.05. The quartet at τ 5.35 was assigned to H_2 and the spacings indicated 6.5 Hz coupling with the methylene proton (H_3) at τ 7.35, and 1.6 Hz coupling with that (H_3) at τ 8.05. Spin decoupling also showed the methylenic protons to be coupled with a signal forming part of a multiplet (H_4, H_5, and $H_{5'}$) centered at τ 5.5 and assigned to H_4.

Following the previously reported procedure for the reduction of iodohydrins to olefins (1), namely, treatment of the iodohydrin **2***a* with tosyl chloride in boiling pyridine gave only furfuryl benzoate. However, when the *O*-tosyl derivative was treated with tetraethylammonium chloride in pyridine in the presence of zinc dust, an 82% yield of pure crystalline 2,3-unsaturated furanoside **4***a* was readily obtained.

Essentially the same sequence of reactions was carried out in the β-series starting with methyl 2,3-anhydro-β-D-lyxofuranoside (**5***c*) (11). The n.m.r. examination of the product obtained upon treatment of the sirupy 5-*O*-benzoyl derivative (**5***a*) with sodium iodide in the usual manner showed that the nucleophilic attack had occurred at the 2-position as readily as at the 3-position to

[1]Presented at the Symposium on Unsaturated Sugars, 155th National Meeting, American Chemical Society, San Francisco, California, March 31–April 5, 1968, Abstracts of Papers C34.

[2]Postdoctorate Fellow, 1966–1968. Present address, Sloan–Kettering Institute for Cancer Research, Rye, N.Y.

[3]Postdoctorate Fellow, 1967–1968. Present address, Ecole Nationale Supérieure de Chimie, Montpellier, France.

Can. J. Chem. Downloaded from www.nrcresearchpress.com by 210.87.254.40 on 09/05/12
For personal use only.

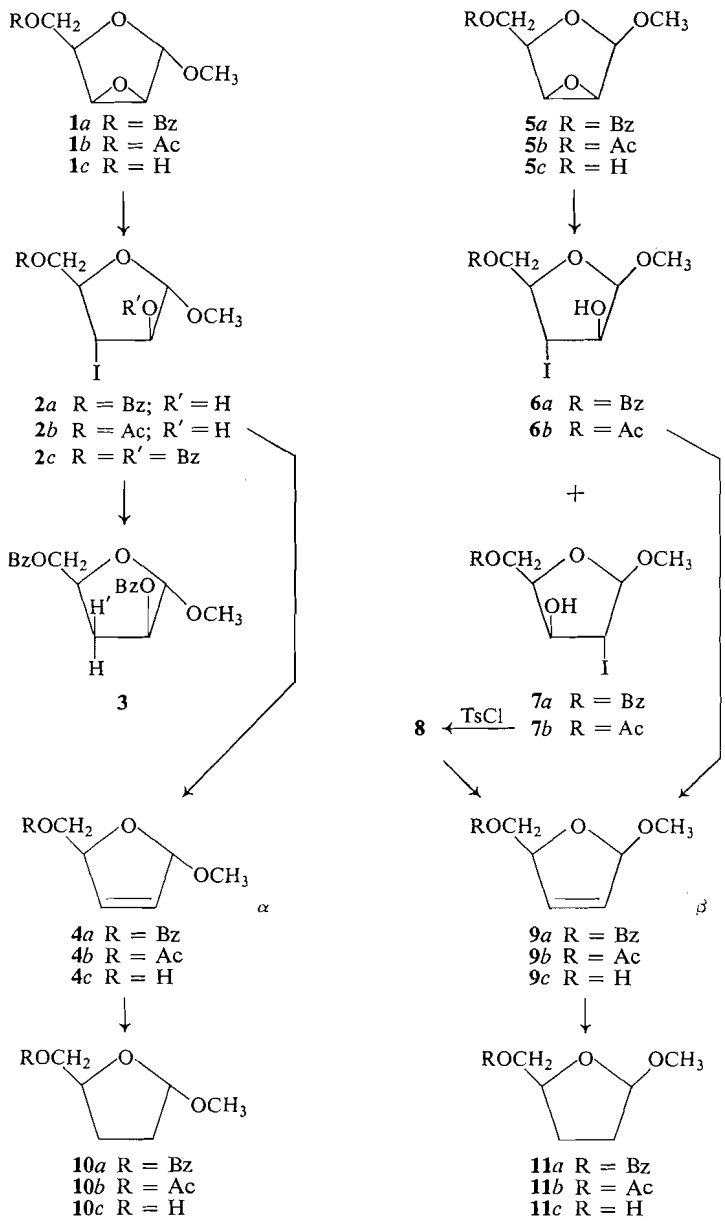

form compounds **6***a* and **7***a*. This was evident from the presence of two signals of about equal intensity for methoxy groups in the n.m.r. spectrum of the product and from the fact the product gave an over 71% yield of the olefin **9***a*.

The acetyl derivative **5***b* also gave an about equimolar mixture of the iodohydrins (**6***b* and **7***b*). On treatment of this mixture with tosyl chloride in pyridine, a crystalline product was obtained in 31% yield together with furfuryl acetate. The structure of this crystalline compound (**8**) was assigned as methyl 5-*O*-acetyl-2-deoxy-2-iodo-3-*O*-tosyl-β-D-xylofuranoside on the basis of n.m.r. analysis. The signal for the anomeric proton (pyridine-d_5 at 100 MHz) was a sharp singlet at τ 5.30, that for H_2 a doublet at τ 5.12 (spacing 4.3 Hz), and that for H_3 a quartet τ 4.81 ($J_{2,3}$ = 4.3 and $J_{3,4}$ = 9.3 Hz). The small

Can. J. Chem. Downloaded from www.nrcresearchpress.com by 210.87.254.40 on 09/05/12
For personal use only.

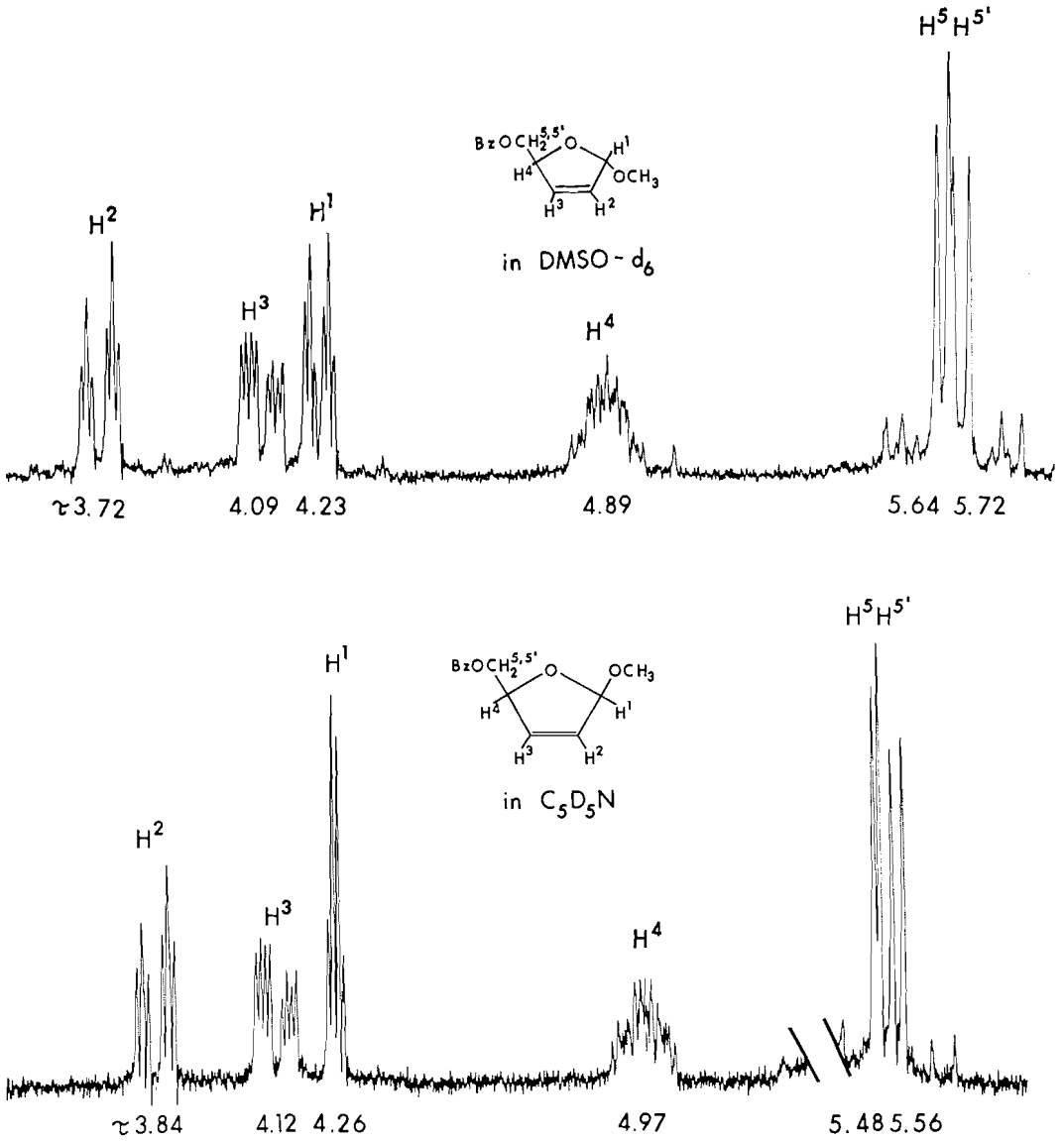

FIG. 1. The n.m.r. spectra at 100 MHz of methyl 5-*O*-benzoyl-2,3-dideoxy-α-D-*glycero*-pent-2-enofuranoside (**4***a*) and its β-anomer (**9***a*).

coupling constant (<0.5 Hz) for $J_{1,2}$ requires a *trans*-relationship for these two hydrogens. Therefore, as expected and as was confirmed by the quartet signal for H_3, C_2 was inverted in the formation of this iodohydrin. The large coupling of 9.3 Hz for H_3 and H_4 which are in *cis*-relationship on the furanoside ring is noteworthy. Extensive opening of the epoxide ring at C_2 as well as C_3 is rare (12,13). However, a result similar to that presented above was obtained on treating **5***b* with benzyl mercaptide ion (14,15). Dick and Jones (16) have recently concluded from a study of the epoxide ring opening of methyl 2,3-anhydro-4-azido-4-deoxypentopyranosides that the direction of opening could not, in some cases, be accounted for by consideration of only steric and inductive effects. A proper appreciation of these phenomena requires a consideration of the

Can. J. Chem. Downloaded from www.nrcresearchpress.com by 210.87.254.40 on 09/05/12
For personal use only.

TABLE I

Nuclear magnetic resonance parameters for 2,3-unsaturated methyl pentosides

Compound	Chemical shifts (τ)						Approximate coupling constants* (Hz, ±0.2)										Solvent
	H_1	H_2	H_3	H_4	H_5	$H_{5'}$	$J_{1,2}$	$J_{1,3}$	$J_{1,4}$	$J_{2,3}$	$J_{2,4}$	$J_{3,4}$	$J_{3,5}$	$J_{4,5}$	$J_{4,5'}$	$J_{5,5'}$	
α-D-Furanoside																	
4*a*	4.23	3.72	4.09	4.89	5.64	5.72	1.2	−1.2	4.4	6.0	−1.2	2.3	~0	3.7	4.5	−12.0	DMSO-d_6
4*b*	4.24	3.77	4.09	5.00	5.70	6.00	1.2	−1.2	4.4	6.0	−1.2	2.3	~0	3.8	5.4	−11.8	DMSO-d_6
4*c*	4.24	3.74	4.11	5.20	6.53	6.53	1.2	−1.2	4.4	6.0	−1.2	2.3	~0	5.2	—	—	DMSO-d_6
β-D-Furanoside																	
9*a*	4.26	3.84	4.12	4.97	5.48	5.56	1.2	−1.2	1.2	6.0	−1.2	2.2	~0	3.8	5.3	−12.0	Pyridine-d_5
9*b*	4.29	3.90	4.15	5.13	5.73	5.87	1.2	−1.2	1.2	6.0	−1.2	2.2	~0	4.2	6.0	−11.5	Pyridine-d_5
9*c*	4.09	3.49	3.89	5.11	6.32	6.32	1.2	−1.2	1.2	6.0	−1.2	2.2	~0	5.5	—	—	DMSO-d_6
α-L-Pyranoside																	
23*a*	5.05	4.05	3.90	4.57	6.05	6.17	2.1	−0.9	2.0	10.5	−1.2	2.2	—	5.5	7.5	−11.0	DMSO-d_6
23*b*	5.25	4.23	4.11	4.78	6.35	6.20	1.5	−1.2	1.2	11.5	−1.2	2.3	<0.5	6.0	8.5	−10.5	CCl_4
23*c*	5.19	4.28	4.03	5.85	6.30	6.53	2.1	−1.1	1.1	10.0	−2.0	2.0	−1.0	5.7	9.4	−10.0	DMSO-d_6
β-L-Pyranoside																	
27*a*	5.00	3.60	3.44	4.70	5.72	5.94	2.3	<0.3	~0	10.4	~0	4.4	−1.3	1.3	2.8	−13.2	Pyridine-d_5
27*b*	5.26	4.11	4.02	5.20	5.98	6.29	2.0	<0.3	~0	10.0	~0	3.8	−0.7	1.2	3.0	−13.0	CCl_4
27*c*	5.19	4.21	4.01	6.24	6.13	6.42	2.6	−0.8	~0	10.0	<0.5	4.0	−1.0	1.8	3.0	−11.5	DMSO-d_6

*The signs given to these coupling constants are assumed.

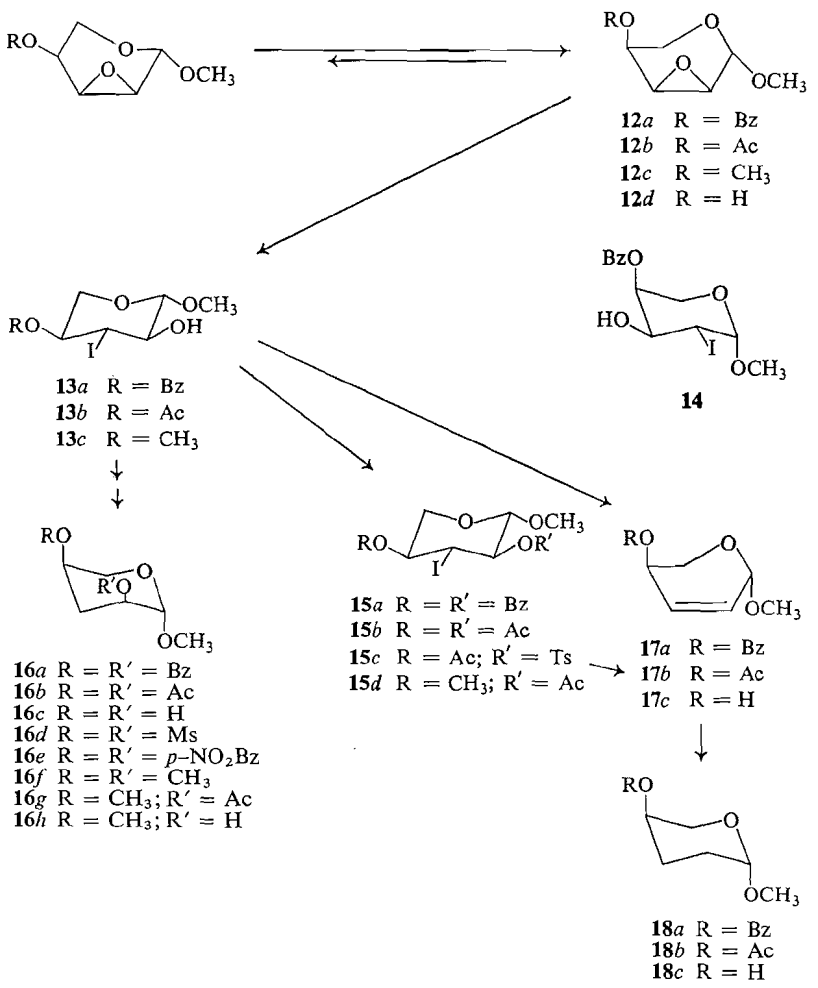

nucleophile as well as the epoxide and it is apparent that strongly nucleophilic reagents are either not as sensitive to differences in the electronegativities of the carbons of the epoxide group or actually prefer the more electronegative center. Methyl 5-*O*-acetyl-β-D-*glycero*-pent-2-enofuranoside (**9***b*) was readily obtained from **8** as a colorless liquid.

The mixture of iodohydrins (**6***a* and **7***a*) on tosylation followed by reduction as described above for the formation of **4***a* gave crystalline methyl 5-*O*-benzoyl-2,3-dideoxy-β-D-*glycero*-pent-2-enofuranoside (**9***a*); 71% yield; m.p. 62–63° (sharp); $[\alpha]_D^{25}$ −102° (chloroform), −104° (dichloromethane). The literature values (2,3) are m.p. 40–46°; $[\alpha]_D$ −98° [in chloroform (4) or in dichloromethane (2)]. The physical constants of the α-anomer (**4***a*) are remarkably similar; m.p. 61–62°; $[\alpha]_D^{25}$ −100° (in chloroform), −102° (in dichloromethane). That these compounds are in fact different and anomeric is clear from the n.m.r. spectra shown in Fig. 1. For the α-anomer (**4***a*), of the seven solvents used, only dimethylsulfoxide-d_6 brought about a complete separation of the signals for H_1 and H_3. The n.m.r. parameters for **4***a* and its β-anomer (**9***a*) are given in Table I. The assignments of the signals for H_2 and H_3 are based on the assumption that, as always found in glycosidic structures, the anomeric proton is more weakly coupled with a vicinal proton (because of the electron withdrawing effect of two oxygen atoms at C_1) than are the other ring protons in a similar geometric relationship. For both anomers, as

Can. J. Chem. Downloaded from www.nrcresearchpress.com by 210.87.254.40 on 09/05/12
For personal use only.

Can. J. Chem. Downloaded from www.nrcresearchpress.com by 210.87.254.40 on 09/05/12
For personal use only.

seen in Table I, $J_{1,3}$ and $J_{2,4}$ are equal at -1.2 Hz. This result indicates that the dihedral angles defined by H_1 and H_2 and by H_3 and H_4 in each case are near equal and in the range 50 to 55° using the relationship shown in eq. [1] provided

$$[1] \quad J = 3.9\cos^2\phi - 2.6 \quad (0° \leq \phi \leq 90°)$$

by Garbisch (17) for the coupling of allylic protons. On this basis, the dihydrofuran rings in these compounds must be near planar as is indicated by molecular models. For both anomers, one of the vicinal coupling constants ($J_{1,2}$ or $J_{3,4}$) is 1.2 Hz and the other is 2.2–2.3 Hz. For the reason stated above, the smaller value is assigned to $J_{1,2}$. Thus, for both anomers the signal at lowest field is assigned to H_2. This procedure is supported by the fact that both $J_{1,3}$ and $J_{2,4}$ are also -1.2 Hz for methyl 4-*O*-acetyl-2,3-dideoxy-α-L-*glycero*-pent-2-enopyranoside (**23***b*) and for this compound $J_{1,2} = 1.5$ Hz and $J_{3,4} = 2.3$ Hz as established unequivocally by spin-decoupling. It may be noted that, for 2,3-unsaturated pyranosides, the signal for H_2 is to higher field than that for H_3 (see below and reference 1). It is of interest to note that the long range couplings $J_{1,4}$ for the 1,4-*trans*-α-anomers (**4**) are much larger, 4.4 Hz, than those, 1.2 Hz for the 1,4-*cis*-β-anomers (**9**).

The 4-*O*-acetyl derivatives of both the known α (19) and β (18,19) anomers for methyl 2,3-anhydro-L-ribopyranoside were treated with sodium iodide in the usual manner (1) to provide the iodohydrins. Assuming diaxial opening of the oxide ring from the compounds in half-chair conformation, the ground-state for attack in 3-position would be that depicted in **12***b* for the β-compound. High yields (>90%) of the 3-iodocompound were obtained from both the acetate (**12***b*) and the benzoate (**12***a*). The yield of the 2-iodobenzoate (**14**) was only 5%. The n.m.r. spectrum of **12***b* required $J_{4,5} = J_{4,5'} \simeq 4$ Hz and indicates that the compound is largely in the half-chair conformation wherein H_4 is in near gauche relationship with both the hydrogens at C_5. $J_{3,4}$ was about 2.5 Hz and $J_{5,5'}$ about -13 Hz. This latter coupling is in the range expected for the compound in this conformation (1).

In the case of α-anhydride, the conformation appears to be close to that depicted in formula **19***b* with the 4-acetoxy group in *quasi*-equatorial orientation. This was indicated by the fact that the rough quartet observed for H_4 collapsed to a clean quartet (τ 4.87) with spacings of 8.5 and 3.3 Hz when the signals for H_2 and H_3, both at about τ 6.50, were spin-decoupled. Therefore, diaxial opening of the epoxide ring with attack by iodide at the 3-position would require a change in conformation. Although a high yield of the 3-iodo compound was obtained from the acetate (**19***b*), about equal amounts of the 2- and 3-iodo derivatives were obtained from the benzoate **19***a*. This may result from a greater resistance by the benzoyloxy group to accept the *quasi*-axial orientation of the alternate half-chair conformation which can lead to diaxial opening. It should be noted that here, as for the analogous furanoside compounds considered earlier, extensive attack at the 2-position was observed only when the methoxyl group was *cis* to the oxygen of the anhydro ring so that a 1,2-*trans*-product was obtained. The n.m.r. spectra of the benzoates (**12***a* and **19***a*) gave almost identical patterns for the ring protons as did the corresponding acetates (**12***b* and **19***b*). It is of interest to note that for

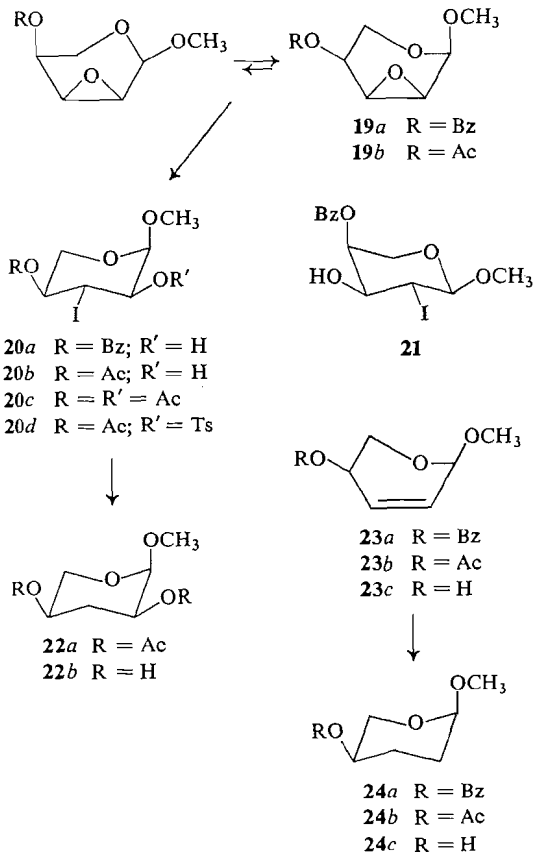

TABLE II

Physical properties of methyl 2,3-dideoxypentosides

Compound	Chemical shifts (τ)*				Solvent	$[\alpha]_D^{25}$¶	$[M]_D^{25}$
	H_1	H_4	Methoxyl	Acetyl			
β-D-Furanoside							
11*a*	—	—	—	—	—	−73	−172
11*b*	5.14†	—	6.75	7.98	CCl_4	−99	−172
11*c*	—	—	—	—	—	−128	−169
α-D-Furanoside							
10*a*	—	—	—	—	—	+88	+208
10*b*	5.08†	—	6.74	8.0	CCl_4	+119	+207
10*c*	—	—	—	—	—	+147	+194
α-L-Pyranoside							
24*a*	5.45‡	5.00§	6.65	—	CCl_4	−85	−201
24*b*	5.53‡	5.30§	6.68	8.01	CCl_4	−105	−180
24*c*	5.62‡	—	6.83	—	D_2O	−131	−173
β-L-Pyranoside							
18*a*	5.35‡	5.00‖	6.65	—	CCl_4	+115	270
18*b*	5.48‡	5.32‖	6.70	7.98	CCl_4	+141	245
18*c*	5.60‡	—	6.86	—	D_2O	+168	223

*Tetramethylsilane as internal standard with carbon tetrachloride and as external standard with deuterium oxide.
†Quartet with spacings of about 2 and 4 Hz.
‡Triplet with spacings of 2 to 3 Hz.
§Broad multiplet.
‖Unresolved narrow signal.
¶*c*, 1.5 in chloroform.

both anomeric pairs of the anhydrides, the anomeric effect plays a significant role in determining conformation. This was especially surprising in the case of the β-anomers since, by the methoxy group becoming *quasi*-axial, the acetoxy group must approach closely the oxygen of the anhydride ring.

The iodohydrins (**13***b* and **20***b*) were tosylated and these treated with tetraethylammonium chloride in pyridine in the presence of zinc dust to provide the olefins (**17***b* and **23***b*) in excellent yield. Deacetylation provided the anomeric methyl 2,3-dideoxy-L-*glycero*-pent-2-enopyranosides (**17***c* and **23***c*). The n.m.r. parameters for these compounds are reported in Table I together with those for the 4-*O*-benzoates (**17***a* and **23***a*). The coupling constants which are apparent from the spacings observed clearly require a large predominance of the conformations shown for the compounds with R = Ac or Bz. This follows especially from a consideration of the magnitudes of $J_{2,4'}$ $J_{5,5'}$ and $J_{4,5'}$. According to the Garbisch relationship (17), the values for $J_{1,3}$ suggest that the anomeric protons of the β-anomers are more in the *quasi*-axial orientation than are those of the α-anomers. It is evident that, as found for the corresponding 2,3-anhydro compounds which are also expected to be in half-chair conformations, the anomeric effect controls the conformations of these olefins.

The alcohols of both the 2-enofuranosides (**4***c* and **9***c*) and the 2-enopyranosides (**23***c* and **17***c*) were readily hydrogenated to provide the anomeric forms for methyl 2,3-dideoxy-D-*glycero*-pentofuranoside (**10***c* and **11***c*) and methyl 2,3-dideoxy-L-*glycero*-pentopyranoside (**24***c* and **18***c*) respectively. From the n.m.r. parameters given in Table II, it is evident that for the 2,3-dideoxypyranosides the anomeric effect controls the conformational equilibria.

It is of interest to note (Table II) that neither acetylation nor benzoylation of a given anomer for a 2,3-dideoxyfuranoside changed the molar rotation appreciably. Therefore, following the line of interpretation presented by Brewster (20) to account for optical rotation, it is apparent that the contributions to rotation by the hydroxymethyl group is not affected by acylation. Application of Brewster's rules as elaborated for pyranoside structures to these furanosides yields molar rotations of 230 for the α-anomer and −180 for the β-anomer, values that are in excellent agreement with those observed, 194 and −169, respectively, if it is assumed that the furanose rings favor conformations for both anomers that have the methoxy group in *quasi*-axial orientation in accordance with expectations based on the anomeric effect.

According to Brewster (20), it can be expected that the conformational units defined by the

Can. J. Chem. Downloaded from www.nrcresearchpress.com by 210.87.254.40 on 09/05/12
For personal use only.

Can. J. Chem. Downloaded from www.nrcresearchpress.com by 210.87.254.40 on 09/05/12
For personal use only.

substituents at C_1 and C_4 with the endocyclic double bonds of the 2,3-unsaturated furanosides (**4***c* and **9***c*) make important contributions to rotation. For the α-D-anomer (**4***c*), following Brewster, two such contributions can be assigned each of about −130°. Also, a strong contribution of +105° from the conformational unit defined by the methoxy group and C_1 to ring-oxygen group can be expected. On this basis only, a molar rotation of −155° is indicated. The observed rotation was −102°. In the case of the β-anomer (**9***c*) (observed molar rotation = −202), the contributions arising from the conformational units defined by the C_1 and C_4 substituents with double bond should nearly cancel. Thus, a rotation of −105° would be indicated disregarding all contributions other than that arising from the methoxy group. Since other contributions to rotation can be expected to be *relatively* small, these considerations provide a basis for appreciating why both anomers are levorotatory. It should be noted, however, that the nature of the substituent at C_5 has, for these unsaturated compounds, a considerable influence on rotation. Indeed, for the 5-*O*-benzoyl derivatives, the anomers **4***a* and **9***a* differ little in rotation.

The molar rotations of the 2-enopyranosides, as seen in Table III, are very dependent on the nature of the substituent at C_4. The strong levorotations for all the compounds listed likely arise mainly for reasons similar to those noted above for the 2-enofuranosides.

TABLE III

Rotations in chloroform of 2,3-unsaturated methyl pentosides and their *O*-acyl derivatives

	$[\alpha]_D^{25}$	$[M]_D^{25}$
α-D-Furanoside		
4*a*	−100°	−234
4*b*	−91	−157
4*c*	−78	−102
β-D-Furanoside		
9*a*	−102	−239
9*b*	−103	−177
9*c*	−155	−202
α-L-Pyranoside		
23*a*	−180	−421
23*b*	−148	−254
23*c*	−129	−168
β-L-Pyranoside		
17*a*	−187	−438
17*b*	−135	−232
17*c*	−108	−141

The main reason for undertaking these syntheses was to obtain the anomeric methyl 3-deoxy-L-*erythro*-pentopyranosides **16***c* and **22***b* by way of hydrogenolyses of the iodohydrins **13** and **20**. The effect of solvent on the conformational equilibria for the β-L-pentoside (**16***c*) has already been reported (21). An accompanying paper (22) reports the relative effects on conformational equilibria observed in changing the substituents at the 2 and 4 positions. These compounds are reported herein and include the dibenzoate, diacetate, dimesylate, di-*p*-nitrobenzoate, di-*O*-methyl, 4-*O*-methyl, and 2-*O*-acetyl-4-*O*-methyl derivatives of methyl 3-deoxy-β-L-*erythro*-pentopyranoside (**16***c*). The diacetate (**22***a*) of methyl 3-deoxy-α-L-*erythro*-pentopyranoside (**22***b*) is also reported.

The methyl 2,3-dideoxypentopyranosides **18***c* and **24***c* were desired for an extension of these studies and a discussion of the effect of solvent on their rotations is reserved for a communication related to solvent effects on the conformational equilibria of methyl 2,3,4-trideoxy-β-L-pentopyranoside (*dextro*-2-methoxypyran).

Experimental

*Methyl 2,3-Anhydro-α-D-lyxofuranoside (**1***c*)*

Methyl 2-*O*-methanesulfonyl-α-D-xylofuranoside (11) (70 g, 0.29 mole; obtained from 58.5 g of methyl 3,5-*O*-isopropylidene-α-D-xylofuranoside) was dissolved in absolute methanol (140 ml) and cooled to 0°. To the stirred solution was added freshly prepared 2 *M* methanolic sodium methoxide (158 ml, 0.316 mole) at such a rate that the temperature was maintained at 0°. After 3 days at this temperature the reaction mixture was filtered through Celite. The filtrate was neutralized with acetic acid (8 ml) then evaporated to dryness under reduced pressure. The residue was dissolved in water (50 ml) and extracted with chloroform (3 × 100 ml). The extracts were dried over magnesium sulfate and evaporated to dryness under reduced pressure. Crystallization occurred during evaporation of the chloroform. The residue was recrystallized from benzene (about 100 ml). A first crop was obtained (31.0 g) as colorless, long needles, m.p. 82–83°. A second crop (6.6 g), m.p. 75–79°, was obtained from the mother liquor, giving a total yield of 92.0%.

*Methyl 2,3-Anhydro-5-O-benzoyl-α-D-lyxofuranoside (**1a**)*

Compound **1***c* (29.2 g, 0.2 mole) was dissolved in pyridine (100 ml) and treated with benzoyl chloride (30 ml). After 3 h at room temperature, the mixture was poured onto an ice-water mixture (ca 1000 ml). The solid was collected and recrystallized from ethanol as colorless needles, (48.0 g, 96%); m.p. 88–90°, $[\alpha]_D^{25}$ + 42.6° (*c*, 2.32 in chloroform).

Anal. Calcd. for $C_{13}H_{14}O_5$: C, 62.40; H, 5.60. Found: C, 62.58; H, 5.66.

Can. J. Chem. Downloaded from www.nrcresearchpress.com by 210.87.254.40 on 09/05/12
For personal use only.

Methyl 5-O-Benzoyl-3-deoxy-3-iodo-α-D-arabino-furanoside (2a)

1*a* (25 g, 0.1 mole) was treated with sodium iodide (75 g, 0.5 mole), sodium acetate (4.1 g, 0.05 mole) and acetic acid (120 ml) in acetone (500 ml) at reflux temperature for 20 h. The orange solution was evaporated to dryness and the residue was partitioned between water (500 ml) and chloroform (500 ml). The aqueous layer was again washed with chloroform (500 ml). The combined organic extracts were washed with 0.1 *M* sodium thiosulfate and with water (each 500 ml), dried over sodium sulfate, and evaporated to a sirup under reduced pressure. The sirup (38 g, quantitative yield), $[\alpha]_D^{25}$ + 73.1° (*c*, 1.58 in chloroform), could not be crystallized, but examination by thin layer chromatography (t.l.c.) and n.m.r. spectroscopy showed it to be homogeneous.

Methyl 2,5-Di-O-benzoyl-3-deoxy-α-D-threo-pentofuranoside (3)

2*a* (1.56 g) was treated with benzoyl chloride (0.53 ml) in pyridine (2 ml) at room temperature overnight. The reaction mixture was worked up in the usual way, giving the sirupy dibenzoate of the iodohydrin (**2***c*).

The dibenzoate (**2***c*) (1.47 g, 0.003 mole) was dissolved in methanol (25 ml) and hydrogenated with 5% palladium on charcoal (0.22 g) in the presence of triethylamine (0.65 g). After 75 min, the mixture was filtered through Celite and the filtrate was evaporated to dryness. The residue was taken up in chloroform and washed with water. The organic layer was dried over magnesium sulfate and evaporated to dryness. The crystalline residue was recrystallized from ether–Skellysolve B. The yield (first crop) was 0.756 g (70%); m.p. 89–89.5°, $[\alpha]_D^{25}$ + 36.7° (*c*, 1.05 in chloroform).

Anal. Calcd. for $C_{20}H_{20}O_6$: C, 67.40; H, 5.67. Found: C, 67.10; H, 5.63.

Methyl 5-O-Benzoyl-α-D-glycero-pent-2-enofuranoside (4a)

2*a* (38 g, 0.1 mole) was treated with *p*-toluenesulfonyl chloride (21 g, 0.11 mole) in pyridine (100 ml) at 0° for 3 days. The reaction mixture was diluted with an ice-water mixture (600 ml) and extracted with chloroform (2 × 200 ml). The extracts were washed with saturated sodium bicarbonate solution and water then dried over sodium sulfate. Evaporation of the chloroform left a sirup (53.5 g, quantitative yield) which could not be crystallized, but examination by t.l.c. and n.m.r. showed that the sirup was practically pure.

The above compound (53.5 g, 0.1 mole) was dissolved in pyridine (150 ml). Tetraethylammonium chloride (1.66 g, 0.01 mole) and zinc dust (16 g, 0.25 mole) were added and the mixture was refluxed for 20 min. Residual zinc was collected and washed with a small amount of pyridine. The combined pyridine solutions were evaporated to dryness. The residue was suspended in water (200 ml) and extracted with ether (4 × 100 ml), and the extracts were dried over sodium sulfate and evaporated to dryness. The crystalline residue was recrystallized from a small amount of ether. The yield of colorless needles after two recrystallizations was 16.5 g (70.5%); m.p. 61–62°, $[\alpha]_D^{25}$ −100° (*c*, 1.25 in chloroform), −102° (*c*, 1.24 in methylene chloride).

Anal. Calcd. for $C_{13}H_{14}O_4$: C, 66.67; H, 5.98. Found: C, 66.38; H, 5.97.

The mother liquors from the two recrystallizations were evaporated to a dry brown solid. The solid was suspended in ether (20 ml) and filtered through an alumina column (1.7 × 4 cm). The column was washed with ether (20 ml), and the filtrate and washings were combined and evaporated. Colorless needles remained and were recrystallized from ether–Skellysolve B to yield 2.6 g (11.1%) of needles; m.p. 59.5–60°, alone or admixed with the first crop.

Methyl 5-O-Benzoyl-β-D-glycero-pent-2-enofuranoside (9a)

The epoxide (**5***c*) (11) (1.46 g, 0.01 mole) was quantitatively benzoylated in the usual way, giving **5***a* as a sirup; $[\alpha]_D^{25}$ −48.9° (*c*, 1.88 in chloroform). This (2.5 g) was refluxed for 6 h in acetone (50 ml) with sodium iodide (7.5 g), sodium acetate (0.41 g), and acetic acid (12 ml), then worked up as usual. The n.m.r. spectrum of the sirupy product showed two signals for methoxyl groups at $\tau \sim 5.5$, indicating that the product consisted of two compounds.

The mixture, without further purification, was treated with *p*-toluenesulfonyl chloride (2.1 g) in pyridine (15 ml) for 3 days at 0°. The dark sirup obtained (4.8 g) was triturated well with Skellysolve B (10 ml). The solvent was decanted and the residue was dissolved in pyridine (30 ml) and refluxed for 20 min with tetraethylammonium chloride 1.65 g) and zinc dust (16 g). Zinc was removed and washed with a small amount of pyridine and the combined filtrate and washings were evaporated to dryness to a dark sirup which was covered with Skellysolve B (10 ml) and stored overnight at 0°. Crystals separated which were gathered and redissolved in ether (20 ml). The ether solution was filtered through a bed of alumina (1.7 × 4 cm) and the alumina was washed with ether (20 ml). The filtrate and washings were combined and evaporated to dryness, whereupon colorless needles were obtained. After one recrystallization from ether–Skellysolve B, the yield of **9***a* was 1.67 g (71.4%); m.p. 62–63°, $[\alpha]_D^{25}$ = −102° (*c*, 1.1 in chloroform), −104° (*c*, 1.23 in methylene chloride; lit. m.p. 40–46° (2,3), $[\alpha]_D^{20}$ −98° both in chloroform (4) and in methylene chloride (2). The mixed m.p. with **4***a* was 37–44°.

Anal. Calcd. for $C_{13}H_{14}O_4$: C, 66.67; H, 5.98. Found: C, 66.25; H, 5.74.

Methyl 5-O-Acetyl-2,3-anhydro-α-D-lyxofuranoside (1b)

1*c* (2.92 g, 0.02 mole) (11) was acetylated in pyridine (5.5 ml) with acetic anhydride (3 ml) at room temperature overnight. The reaction mixture was poured onto an ice-water mixture (50 ml) and extracted with chloroform (5 × 10 ml). After being dried over magnesium sulfate, the extracts were evaporated to dryness under reduced pressure. The residual long, colorless needles were recrystallized from a small amount of ethanol. Yield, 3.70 g (98.4%); m.p. 73–75°, $[\alpha]_D^{25}$ + 64.2° (*c*, 1.84 in chloroform).

Anal. Calcd. for $C_8H_{12}O_5$: C, 51.06; H, 6.38. Found: C, 51.00; H, 6.45.

Methyl 5-O-Acetyl-α-D-glycero-pent-2-enofuranoside (4b)

1*b* (2.66 g, 0.014 mole) was treated with sodium iodide (10.5 g), sodium acetate (0.57 g), and acetic acid (17 ml) in acetone (70 ml) at reflux temperature for 20 h, then the mixture was worked up as usual. The iodohydrin **2***b* was

Can. J. Chem. Downloaded from www.nrcresearchpress.com by 210.87.254.40 on 09/05/12
For personal use only.

obtained as a slightly yellowish sirup; 4.21 g (95.2%), $[\alpha]_D^{25}$ +78.3° (*c*, 4.1 in chloroform). The n.m.r. spectroscopy and examination by t.l.c. showed it to be homogeneous.

This sirup was treated with *p*-toluenesulfonyl chloride (3.46 g, 0.018 mole) in pyridine for 3 days at 4°. The product (7.30 g) isolated as a sirup was, without purification, dissolved in pyridine (15 ml) and refluxed for 20 min with tetraethylammonium chloride (0.23 g, 0.0014 mole) and zinc dust (2.3 g). The zinc was gathered and washed with a small amount of pyridine. The combined filtrate and washings were worked up as usual and purified by distillation; 1.92 g (79.8%); b.p. 47–47.5° (0.1 mm Hg), m.p. 0–2°, $[\alpha]_D^{25}$ −91° (*c*, 4.9 in chloroform), n_D^{23} = 1.4502.

Anal. Calcd. for $C_8H_{12}O_4$: C, 55.81; H, 7.03. Found: C, 56.25; H, 6.94.

*Methyl 5-O-Acetyl-2-deoxy-2-iodo-3-O-(p-toluenesulfonyl)-β-D-xylofuranoside (**8**)*

Acetylation of **5***c* (11) (1.50 g, 0.0104 mole) afforded **5***b* (1.88 g, 96.2%) as a sirup, which was, without further purification, refluxed in acetone (50 ml) with sodium idiode (7.5 g), sodium acetate (0.41 g), and acetic acid (12 ml) for 6 h. The product, 2.12 g (67%), isolated in the usual manner, was a mixture of two isomers (**6***b* and **7***b*) (n.m.r.). The mixture was dissolved in pyridine (15 ml) and treated with *p*-toluenesulfonyl chloride (1.6 g, 0.008 mole) for 3 days at 4°. The reaction mixture was poured onto an ice-water mixture (70 ml) and extracted with chloroform (3 × 30 ml). The extracts were dried over sodium sulfate then evaporated to dryness under reduced pressure. Pyridine was removed from the residue by repeated azeotropic distillation with ethanol. The semi-crystalline residue, 2.5 g (79%), was covered with a small amount of ethanol and kept at −7° for 3 h. Crystalline cubes deposited and were washed with a small amount of cold ethanol, 0.99 g (31.4%); m.p. 117–118°.

For analyses, a small amount of the compound was recrystallized from ethanol; m.p. 118–119°, $[\alpha]_D^{25}$ −80.7° (*c*, 3.4 in chloroform).

Anal. Calcd. for $C_{15}H_{19}O_7SI$: C, 38.31; H, 4.08; I, 26.98. Found: C, 38.27; H, 3.94; I, 26.95.

*Methyl 5-O-Acetyl-β-D-glycero-pent-2-enofuranoside (**9***b*)*

A mixture of **8** (4.70 g, 0.01 mole), tetraethylammonium chloride (0.17 g, 0.001 mole), and zinc dust (1.66 g) in pyridine (20 ml) was refluxed for 20 min. The product was isolated in the usual manner, purified by distillation to provide a colorless liquid, 1.21 g (70.3%); b.p. 49° (0.4 mm Hg), $[\alpha]_D^{25}$ −103° (*c*, 1.99 in chloroform), n_D^{23} = 1.4473.

Anal. Calcd. for $C_8H_{12}O_4$: C, 55. 81; H, 6.98. Found: C, 56.12; H, 7.06.

*Methyl 2,3-Anhydro-4-O-benzoyl-β-L-ribopyranoside (**12***a*)*

Benzoylation of **12***d* (18,19) and recrystallization from ethanol gave an analytical sample as colorless needles; m.p. 108–108.5°, $[\alpha]_D^{25}$ −22.4° (*c*, 2.78 in chloroform).

Anal. Calcd. for $C_{13}H_{14}O_5$: C, 62.40; H, 5.60. Found: C, 62.23; H, 5.31.

*Methyl 4-O-Benzoyl-3-deoxy-3-iodo-β-L-xylopyranoside (**13***a*) and Methyl 4-O-Benzoyl-2-deoxy-2-iodo-β-L-arabinopyranoside (**14**)*

12*a* (5.0 g, 0.02 mole) was mixed with sodium iodide (15 g, 0.1 mole), sodium acetate (0.84 g, 0.01 mole), acetic acid (24 ml), and acetone (100 ml) and refluxed for 20 h. The reaction mixture was worked up as usual and the semi-solid residue (7.6 g, quantitative yield) was recrystallized from ethanol (60 ml) to give **13***a* as colorless needles, 6.27 g (82.9%); m.p. 158–159°, $[\alpha]_D^{25}$ +113° (*c*, 1.44 in chloroform).

Anal. Calcd. for $C_{13}H_{15}O_5I$: C, 41.29; H, 3.99; I, 33.56. Found: C, 41.42; H, 3.95; I, 33.34.

The mother liquor of the above recrystallization was evaporated to dryness. Upon triturating the sirupy residue with cold ethanol (5 ml), crystals (m.p. 84–86°) separated, which were recrystallized from a small amount of ethanol (2.5 ml). Colorless needles of methyl 4-*O*-benzoyl-2-deoxy-2-iodo-β-L-arabinopyranoside (**14**) were obtained, 377 mg (5%); m.p .96–97°, $[\alpha]_D^{25}$ +144° (*c*, 2.32 in chloroform). Mixed m.p. with **13***a*, 68–76°.

Anal. Calcd. for $C_{13}H_{15}O_5I$: C, 41.29; H, 3.99. Found: C, 41.40; H, 4.01.

*Methyl 4-O-Benzoyl-β-L-glycero-pent-2-enopyranoside (**17***a*)*

13*a* (1.89 g, 0.005 mole) was treated with *p*-toluenesulfonyl chloride (1.29 g, 0.0063 mole) in pyridine (5 ml) for 3 days at room temperature. The mixture was poured onto an ice-water mixture (50 ml) and was extracted with chloroform (3 × 25 ml). The combined extracts were dried over sodium sulfate and evaporated.

The residue was mixed with pyridine (20 ml) containing tetraethylammonium chloride (0.083 g, 0.0005 mole) and zinc dust (0.83 g). The mixture was heated to reflux for 20 min, cooled, and filtered. The filtrate was evaporated to dryness and the residue was suspended in water (25 ml); then extracted with ether (3 × 25 ml). The combined ether extracts were dried over sodium sulfate and evaporated. A small amount of pyridine was removed from the residue by repeated azeotropic distillation with ethanol until fine needles were obtained. The crystalline residue was dissolved in ether (3 ml) and decolorized by filtration through an alumina column (2 × 2 cm) and the column was washed with ether (10 ml). Upon evaporation of the combined ethereal solutions and recrystallization of the residual colorless needles from ethanol, the product 0.86 g (75%) had the following properties, m.p. 58–59.5°, $[\alpha]_D^{25}$ −187° (*c*, 2.03 in chloroform).

Anal. Calcd. for $C_{13}H_{14}O_4$: C, 66.67; H, 5.98. Found: C, 66.56; H, 6.12.

*Methyl 2,4-Di-O-benzoyl-3-deoxy-3-iodo-β-L-ribopyranoside (**15***a*)*

Benzoylation of **13***a* in the usual manner and recrystallization of the product from ethanol gave colorless leaflets; m.p. 143–144°, $[\alpha]_D^{25}$ +55.0° (*c*, 1.64 in chloroform).

Anal. Calcd. for $C_{20}H_{19}O_6I$: C, 49.80; H, 3.98; I, 26.31. Found: C, 49.67; H, 4.04; I, 26.34.

*Methyl 2,4-Di-O-benzoyl-3-deoxy-β-L-erythropentopyranoside (**16***a*)*

15*a* (723 mg, 0.0015 mole) was hydrogenated in ethyl acetate (20 ml) with 5% palladium on charcoal (200 mg) in the presence of diethylamine (0.1 ml). After the consumption of hydrogen had ceased, the mixture was filtered the filtrate was evaporated to dryness to a sirup, which then was dissolved in chloroform (25 ml). The chloroform solution was, after being washed with water (3 × 25 ml) and dried over sodium sulfate, evaporated to dryness to a sirup. The sirup was dissolved in benzene (1 ml) and the

Can. J. Chem. Downloaded from www.nrcresearchpress.com by 210.87.254.40 on 09/05/12
For personal use only.

solution was absorbed on an alumina column(1.2 × 4 cm) then eluted with benzene (50 ml). The eluate was evaporated to a colorless sirup to a constant weight (452 mg, 84.6%); $[\alpha]_D^{25}$ +100° (*c*, 1.70 in chloroform). The n.m.r. spectrum of this sirup was identical with that of the product formed on benzoylation of methyl 3-deoxy-β-L-*erythro*-pentopyranoside (**16***c*) as described below.

Anal. Calcd. for $C_{20}H_{20}O_6$: C, 67.40; H, 5.67. Found: C, 67.54; H, 6.08.

*Methyl 4-O-Acetyl-3-deoxy-3-iodo-*β*-L-xylopyranoside (13b)*

12*b* (18,19) (1.88 g, 0.01 mole) was treated with sodium iodide (7.5 g, 0.05 mole), sodium acetate (0.41 g, 0.005 mole) and acetic acid (12 ml) in acetone (50 ml) at reflux temperature for 6 h. The mixture was worked up in the usual manner. The product was recrystallized from a small amount of ethanol to yield 3.01 g (95.3%); m.p. 145–145.5°, $[\alpha]_D^{25}$ +10.7° (*c*, 3.28 in chloroform).

Anal. Calcd. for $C_8H_{13}O_5I$: C, 30.38; H, 4.11. Found: C, 30.44; H, 4.05.

Acetylation of **13***b* with acetic anhydride in pyridine gave methyl 2,4-di-*O*-acetyl-3-deoxy-3-iodo-β-L-xylopyranoside (**15***b*) as colorless leaflets; m.p. 141–141.5°, $[\alpha]_D^{25}$ +39.4° (*c*, 3.2 in chloroform).

Anal. Calcd. for $C_{10}H_{15}O_6I$: C, 33.54; H, 4.22. Found: C, 33.70; H, 4.04.

*Methyl 3-Deoxy-*β*-L-erythro-pentopyranoside (16c)*

15*b* (10.4 g, 0.029 mole) was dissolved in hot methanol (300 ml) containing triethylamine (3.6 g), and hydrogenated with 5% palladium on charcoal catalyst (1.25 g). After the theoretical amount of hydrogen was consumed, the catalyst was removed by filtration. The filtrate was evaporated to dryness. The residue was dissolved in ether. Insoluble triethylammonium iodide was filtered off and the filtrate was evaporated to yield 4.2 g (69.7%) of a colorless sirup. Examination by t.l.c. showed that deacetylation had occurred during hydrogenolysis.

The above sirup (450 mg) was dissolved in absolute methanol (6 ml). Sodium methoxide in methanol (3 ml), prepared by dissolving sodium (0.5 g) in methanol (100 ml), was added and the mixture was set aside for 1 h. The reaction mixture was neutralized with Dowex 50 (H^+), filtered and evaporated to a sirup. The residue was purified by chromatography on a Celite column (23), then by distillation (70–80° bath temperature at 0.05 mm Hg). The product had $[\alpha]_D^{25}$ +94.5° (*c*, 10.5 in water). The examination by t.l.c. and n.m.r. spectroscopy showed it to be homogeneous. The same product was obtained on deacylation of the crystalline *p*-nitrobenzoyl derivative (**16***e*).

Anal. Calcd. for $C_6H_{10}O_4$: C, 48.65; H, 8.16. Found: C, 48.72; H, 8.22.

*Methyl 2,4-Di-O-acetyl-3-deoxy-*β*-L-erythro-pentopyranoside(16b)*

Prepared by acetylation of the pure **16***c* obtained from **16***e* and isolated as a distilled sirup; $[\alpha]_D^{25}$ +117° (*c*, 1.78 in chloroform).

Anal. Calcd. for $C_{10}H_{16}O_6$: C, 51.72; H, 6.93. Found: C, 51.93; H, 7.12.

*Methyl 3-Deoxy-2,4-di-O-methanesulfonyl-*β*-L-erythro-pentopyranoside (16d)*

Prepared from **16***c* in the usual manner and recrystallized from ethanol; m.p. 101.5–102°, $[\alpha]_D^{25}$ +73.1° (*c*, 1.04 in chloroform).

Anal. Calcd. for $C_8H_{16}O_8S_2$: C, 31.58; H, 5.29. Found: C, 31.54; H, 5.16.

*Methyl 3-Deoxy-2,4-di-O-(p-nitrobenzoyl)-*β*-L-erythro-pentopyranoside (16e)*

Treatment of **16***c* with recrystallized *p*-nitrobenzoyl chloride in pyridine gave a crystalline product which was recrystallized from ether; m.p. 123.5–124.5°, $[\alpha]_D^{25}$ +51.2° (*c*, 1.30 in chloroform).

Anal. Calcd. for $C_{20}H_{18}O_{10}N_2$: C, 53.82; H, 4.06. Found: C, 53.63; H, 4.23.

*Methyl 3-Deoxy-2,4-di-O-methyl-*β*-L-erythro-pentopyranoside (16f)*

Methyl 3-deoxy-β-L-*erythro*-pentopyranoside (**16***c*, 200 mg) was dissolved in 6 ml of freshly distilled methyl iodide and gently refluxed for 6 h. Freshly prepared silver oxide (1.39 g) was added in 10 equal portions at 0.5 h intervals to the continuously stirred solution. The heating was continued for 1 h after the final addition, then the silver oxide was removed by filtration and washed with 15 ml of diethyl ether. After solvent removal, the slightly yellow liquid residue was twice distilled under vacuum to give a colorless liquid b.p. (25 mm), 80–85° (180 mg, yield 75%) with the n.m.r. parameters consistent with the assigned structure (22). The three methyl groups gave singlets at τ 4.7, 4.75, and 4.81 in $CDCl_3$. The specific rotations, $[\alpha]_D^{25}$, were +86.2° (*c*, 0.9 in chloroform) and +94.0° (*c*, 1 in water).

Anal. Calcd. for $C_8H_{16}O_4$: C, 54.54; H, 9.14. Found: C, 54.51; H, 9.05.

*Methyl 2,3-Anhydro-4-O-methyl-*β*-L-ribopyranoside (12c)*

Methyl 2,3-anhydro-β-L-ribopyranoside (10 g) was *O*-methylated using 30 ml of freshly distilled methyl iodide as described above. On solvent removal, crystalline material was obtained and recrystallized from ethanol to give 7.50 g (68%); m.p. 74–75°, $[\alpha]_D^{25}$ +3.6 (*c*, 1.2 in chloroform) and −10.6 (*c*, 1.3 in water). The n.m.r. spectrum (60 MHz in $CDCl_3$) showed two sharp methoxy signals at τ 6.50 and 6.53 and the anomeric singlet at τ 5.18.

*Methyl 3-Deoxy-3-iodo-4-O-methyl-*β*-L-xylopyranoside (13c)*

A solution of 7.5 g of **12***c*, 27.2 g of sodium iodide, 2 g of sodium acetate, and 50 ml of acetic acid in 50 ml of acetone was refluxed overnight. A crystalline product was isolated in the usual manner (1). After recrystallization from ethanol, the yield was 12.6 g, m.p. 94.5–95.5°. The signals for the two methyl groups in the n.m.r. spectrum (in $CDCl_3$ at 60 MHz) were at τ 6.45 and 6.49. The anomeric proton produced a doublet at τ 5.83 with a spacing of ~ 6.5 Hz.

*Methyl 2-O-Acetyl-3-deoxy-3-iodo-4-O-methyl-*β*-L-xylopyranoside (15d)*

Compound **13***c* 7.5 g was acetylated using pyridine and acetic anhydride in the usual manner to afford a crystalline product. After recrystallization from ethanol, the yield was 7.6 g; m.p. 125.5–126.5°. The n.m.r. spectrum (in $CDCl_3$ at 60 MHz) showed the presence of the two methoxy groups, τ 6.54 and 6.61 and the acetoxy group signal at τ 6.91. The anomeric proton produced a doublet at τ 5.89 with a spacing of 7 Hz.

Can. J. Chem. Downloaded from www.nrcresearchpress.com by 210.87.254.40 on 09/05/12
For personal use only.

Methyl 2-O-Acetyl-3-deoxy-4-O-methyl-β-L-erythro-pentopyranoside (16g)

The above iodo-compound (**15***d*) (7.5 g) was dissolved in 100 ml of methanol containing 4 ml of triethylamine and shaken in an hydrogen atmosphere with 1 g of 5% palladium on charcoal. After the uptake of hydrogen ceased, the catalyst was removed by filtration and the filtrate evaporated to dryness. The residue was extracted with benzene, the benzene solution was washed with water, then with sodium thiosulfate, and finally with water. After drying with sodium sulfate, the solvent was removed to give a colorless syrup. The n.m.r. spectrum (22) required a high state of purity. The specific rotations, $[\alpha]_D^{25}$, were +94.8° (*c*, 1.3 in water) and +81.1° (*c*, 1.4 in CCl_4).

Methyl 3-Deoxy-4-O-methyl-β-L-erythro-pentopyranoside (16h)

Deacetylation of the foregoing methyl 2-*O*-acetyl-3-deoxy-4-*O*-methyl-β-L-*erythro*-pentopyranoside with 0.5% sodium methoxide solution at room temperature gave the desired methyl 3-deoxy-4-*O*-methyl-β-L-*erythro*-pentopyranoside in 95% yield. After short-path distillation (at about 0.5 mm with a bath temp. 50°) the specific rotations, $[\alpha]_D^{25}$, were +131° (*c*, 1.6 in chloroform), +144° (*c*, 1.4 in dichloroethane), and +83.5° (*c*, 1.4 in dimethylsulfoxide). The n.m.r. spectrum is discussed in the accompanying publication (22).

Anal. Calcd. for $C_7H_{14}O_4$: C, 51.85; H, 8.69. Found: C, 51.85; H, 8.72.

Methyl 4-O-Acetyl-3-deoxy-3-iodo-2-O-(p-toluenesulfonyl)β-L-xylopyranoside (15c)

The iodohydrin (**13***b*) (3.16 g, 0.01 mole) was treated with *p*-toluenesulfonyl chloride (2.10 g, 0.011 mole) in pyridine (20 ml) for 44 h at room temperature. The reaction mixture was worked up as usual whereupon a crystalline product was obtained (4.70 g, quantitative yield). A small amount was recrystallized from ethanol; m.p. 131–132.5°, $[\alpha]_D^{25}$ −60° (*c*, 2.51 in chloroform) and found to possess an n.m.r. spectrum consistent with the assigned structure.

Methyl 4-O-Acetyl-β-L-glycero-pent-2-enopyranoside (17b)

The foregoing crude **15***c* (4.5 g) was dissolved in pyridine (20 ml) and refluxed for 20 min with tetraethylammonium chloride (0.16 g) and zinc dust (1.6 g). The product was a colorless liquid, 1.28 g (78%); $b.p._{0.5}$ 56°, n_D^{22} 1.4582, $[\alpha]_D^{25}$ −135° (*c*, 1.56 in chloroform).

Anal. Calcd. for $C_8H_{12}O_4$: C, 55.81; H, 7.03. Found: C, 56.33; H, 7.26.

Methyl 2,3-Anhydro-4-O-benzoyl-α-L-ribopyranoside (19a)

Benzoylation of methyl 2,3-anhydro-α-L-ribopyranoside, m.p. 83–84.5°, $[\alpha]_D^{25}$ −160° (*c*, 2.1 in chloroform) (19), provided colorless needles; m.p. 80–81°, $[\alpha]_D^{25}$ −172° (*c*, 2.53 in chloroform).

Anal. Calcd. for $C_{13}H_{14}O_5$: C, 62.40; H, 5.60. Found: C, 62.66; H, 5.40.

Methyl 4-O-Benzoyl-α-L-glycero-pent-2-enopyranoside (23a)

The foregoing benzoate **19***a* (2.50 g, 0.01 mole) was treated with sodium iodide (7.5 g) in acetone (50 ml) with sodium acetate (0.41 g) and acetic acid (12 ml) for 6 h. A mixture containing **20***a* and **21** in approximately equal amounts was obtained as a sirup in quantitative yield.

The mixture, without purification, was dissolved in pyridine (30 ml) and treated with *p*-toluenesulfonyl chloride (2.1 g, 0.011 mole) at room temperature for 3 days. The dark product obtained was refluxed in pyridine (20 ml) containing tetraethylammonium chloride (0.166 g) and zinc dust (1.66 g) for 20 min. The product, 1.66 g (71%), was isolated in the usual manner, and after distillation, $b.p._{0.05}$ 95°, was found to have m.p. 14–15°, $[\alpha]_D^{25}$ −180° (*c*, 1.71 in chloroform).

Anal. Calcd. for $C_{13}H_{14}O_4$: C, 66.67; H, 5.98. Found: C, 66.82; H, 5.91.

Methyl 4-O-Acetyl-3-deoxy-3-iodo-α-L-xylopyranoside (20b)

Methyl 2,3-anhydro-α-L-ribopyranoside (2.92 g, 0.02 mole) (18), m.p. 83–84.5°, $[\alpha]_D^{25}$ −160° (*c*, 2.1 in chloroform), was acetylated in the usual way, giving **19***b* in quantitative yield. This product was treated with sodium iodide in acetone in the presence of sodium acetate and acetic acid as usual. A colorless, crystalline product which appeared to be homogeneous by t.l.c. and n.m.r. examinations, was obtained in quantitative yield. For analysis a small amount was recrystallized from ethanol; m.p. 125–126°, $[\alpha]_D^{25}$ −109° (*c*, 2.2 in chloroform).

Anal. Calcd. for $C_8H_{13}O_5I$: C, 30.40; H, 4.14. Found: C, 30.73; H, 4.47.

The n.m.r. spectrum in $CDCl_3$ showed two sharp singlets for the methoxy and acetoxy groups at τ 6.58 and 7.80, respectively. The anomeric proton gave a doublet (spacing 3.0 Hz) at τ 5.40 and H_3 a triplet (spacings 10.3 Hz) at τ 5.88.

Methyl 2,4-Di-O-acetyl-3-deoxy-3-iodo-α-L-xylopyranoside (20c)

Acetylation of **20***b* in pyridine–acetic anhydride provided a crystalline product; m.p. 89.5–90.5°. The n.m.r. spectrum in $CDCl_3$ showed singlets at τ 6.60 (methoxy) and τ 7.82 and 7.87 (acetoxy). The signal for the anomeric proton was a doublet (spacing 3.2 Hz) at τ 5.30 and H_3 was a triplet (spacings 10.6 Hz) at τ 5.72.

Methyl 3-Deoxy-α-L-erythro-pentopyranoside (22b)

The above diacetate (**20***c*) was hydrogenolized as described above for the preparation of its β-anomer. The product was a sirup which, on deacetylation using sodium methoxide in methanol provided the title compound; m.p. 95.5–96° with $[\alpha]_D^{25}$ −157° (*c*, 0.9 in water), −120° (*c*, 0.9 in chloroform).

The n.m.r. spectrum in D_2O at 100 MHz (TMS external) showed a doublet for H_1 (τ 4.90, spacing 3.5 Hz), a triplet for the axial-H_5 (τ 6.16, spacings 10.2 Hz), the equatorial-H_3 was a multiplet centered at τ 7.41, and the axial-H_3 appeared as a sextet centered at τ 7.89. The following approximate coupling constants were established by double irradiation, $J_{3a,3e} = 11.4$, $J_{3e,4} = J_{3e,2} = 4.5$, $J_{3a,4} = J_{3a,2} = 10.5$, and $J_{3e,5e} = 1.7$ Hz. The methoxy signal was at τ 6.10.

Methyl 4-O-Acetyl-3-deoxy-3-iodo-2-O-(p-toluenesulfonyl)-α-L-xylopyranoside (20d)

Treatment of **20***b* (3.16 g, 0.01 mole) with *p*-toluene-

Can. J. Chem. Downloaded from www.nrcresearchpress.com by 210.87.254.40 on 09/05/12
For personal use only.

sulfonyl chloride (2.10 g, 0.011 mole) in pyridine (20 ml) for 44 h at room temperature gave a crystalline product in quantitative yield. A small quantity was recrystallized from ethanol; m.p. 116–117°, $[\alpha]_D^{25}$ −60° (*c*, 2.5 in chloroform).

Anal. Calcd. for $C_{15}H_{19}O_7SI$: C, 38.31; H, 4.08. Found: C, 38.02; H, 3.78.

Methyl 4-O-Acetyl-α-L-glycero-pent-2-enopyranoside (23b)

The crude product obtained in the above experiment was dissolved in pyridine and treated with tetraethylammonium chloride (0.16 g) and zinc dust (1.6 g) for 20 min at reflux temperature. The product was a colorless liquid, 1.19 g (69.2%); b.p.$_{0.5}$ 52.0°, $[\alpha]_D^{25}$ −148° (*c*, 1.32 in chloroform) n_D^{22} 1.4560.

Anal. Calcd. for $C_8H_{12}O_4$: C, 55.81; H, 7.03. Found: C, 55.68; H, 7.15.

Methyl 2,3-Dideoxy-β-L-glycero-pent-2-enopyranoside (17c)

The acetate (**17***b*) (5.0 g, 0.0287 mole) dissolved in absolute methanol (75 ml) was treated with 2 *M* sodium methoxide in methanol (5 ml) for 1 h at room temperature. The alkaline solution was neutralized to p*H* 6.8 with acetic acid and the solvent evaporated under reduced pressure. The residue was extracted with ethyl acetate. The ethyl acetate was removed and upon distillation of the colorless residue, there was obtained a colorless liquid (b.p. $_{0.07}$ 38.5°; 3.53 g, 93.3%) which crystallized to long needles; m.p. 44° $[\alpha]_D^{25}$ −108° (*c*, 1.5 in chloroform).

Anal. Calcd. for $C_6H_{10}O_3$: C, 55.38; H, 7.96. Found: C, 55.28; H, 7.66.

Methyl 2,3-Dideoxy-β-L-glycero-pentopyranoside (18c) and Derivatives

The foregoing olefin (**17***c*) (2.87 g, 0.022 mole) was dissolved in absolute methanol (30 ml) and hydrogenated in the presence of 5% palladium on charcoal catalyst (280 mg). The hydrogen uptake ceased within 2 h. The catalyst was filtered and washed with small amount of methanol. The combined filtrate and washings were evaporated and the residue was distillated. A colorless liquid was obtained; b.p.$_{0.1}$ 51.0°, 2.44 g (84%), $[\alpha]_D^{30}$ +168° (*c*, 1.5 in chloroform), n_D^{22} 1.4529.

Anal. Calcd. for $C_6H_{12}O_3$: C, 54.55; H, 9.09. Found: C, 54.31; H, 9.11.

Derivatives: Methyl 4-O-benzoyl-2,3-dideoxy-β-L-*glycero*-pento-pyranoside (**18***a*); b.p.$_{0.07}$ 92.0°, $[\alpha]_D^{25}$ +115° (*c*, 1.7 in chloroform), n_D^{22} 1.5173.

Anal. Calcd. for $C_{13}H_{16}O_4$: C, 66.08; H, 6.83. Found: C, 66.08; H, 6.84.

Methyl 4-O-acetyl-2,3-dideoxy-β-L-*glycero*-pentopyranoside (**18***b*); b.p.$_{0.07}$ 50.0°, $[\alpha]_D^{25}$ +141° (*c*, 1.8 in chloroform), n_D^{22} 1.4418.

Methyl 2,3-Dideoxy-α-L-glycero-pent-2-enopyranoside (23c) and Derivatives

The title compound b.p.$_{0.07}$ 40°, $[\alpha]_D^{25}$ −129° (chloroform), was obtained by deacetylation of **23***b* in the manner described above for the preparation of **17***c* from **17***b*.

Anal. Calcd. for $C_6H_{10}O_3$: C, 55.38; H, 7.96. Found: C, 55.18; H, 8.02.

Hydrogenation of **23***c* as described for the preparation of **18***c* provided methyl 2,3-dideoxy-α-L-*glycero*-pentopyranoside (**24***c*); b.p.$_{0.1}$ 48°, $[\alpha]_D^{25}$ −131° (*c*, 1.3 in chloroform), n_D^{22} 1.4550.

Anal. Calcd. for $C_6H_{12}O_3$: C, 54.55; H, 9.09. Found: C, 54.27; H, 8.99.

Benzoylation of **24***c* gave methyl 4-*O*-benzoyl-2,3-dideoxy-α-L-*glycero*-pentopyranoside (**24***a*); b.p. $_{0.07}$ 90°, $[\alpha]_D^{25}$ −85° (*c*, 2.0 in chloroform), n_D^{22} 1.5193.

Anal. Calcd. for $C_{13}H_{16}O_4$: C, 66.08; H, 6.83. Found: C, 66.04; H, 6.93.

Acetylation of **24***c* gave methyl 4-*O*-acetyl-2,3-dideoxy-α-L-*glycero*-pentopyranoside (**24***b*); b.p.$_{0.5}$ 52°, $[\alpha]_D^{25}$ −105° (*c*, 1.8 in chloroform), n_D^{22} 1.4429.

Anal. Calcd. for $C_8H_{14}O_4$: C, 55.17; H, 8.05. Found: C, 54.98; H, 8.18.

Methyl 2,3-Dideoxy-α-D-glycero-pent-2-enofuranoside (4c) and Derivatives

Deacetylation of **4***b* provided the title compound **4***c*; b.p.$_{0.07}$ 38°, $[\alpha]_D^{25}$ −78° (*c*, 2.5 in chloroform), n_D^{21} 1.4656.

Anal. Calcd. for $C_6H_{10}O_3$: C, 55.38; H, 7.96. Found: C, 55.19; H, 8.04.

Hydrogenation of **4***c* as described for the preparation of **18***c* gave methyl 2,3-dideoxy-α-D-*glycero*-pentofuranoside (**10***c*); b.p.$_{0.07}$ 40°, $[\alpha]_D^{25}$ +147° (*c*, 1.5 in chloroform), n_D^{22} 1.4460.

Anal. Calcd. for $C_6H_{12}O_3$: C, 54.55; H, 9.09. Found: C, 55.68; H, 8.95.

Benzoylation of **10***c* gave methyl 5-*O*-benzoyl-2,3-dideoxy-α-D-*glycero*-pentofuranoside (**10***a*); b.p.$_{0.07}$ 95°, $[\alpha]_D^{25}$ +88° (*c*, 1.5 in chloroform), n_D^{22} 1.5108.

Anal. Calcd. for $C_{13}H_{16}O_4$: C, 66.08; H, 6.83. Found: C, 66.17; H, 6.87.

Acetylation of **10***c* gave methyl 5-*O*-acetyl-2,3-dideoxy-α-D-*glycero*-pentofuranoside (**10***b*); b.p.$_{0.07}$ 41.5°, $[\alpha]_D^{25}$ +119° (*c*, 1.5 in chloroform), n_D^{22} 1.4368.

Anal. Calcd. for $C_8H_{14}O_4$: C, 55.17; H, 8.05. Found: C, 55.38; H, 8.23.

Methyl 2,3-Dideoxy-β-D-glycero-pento-2-enofuranoside (9c) and Derivatives

Deacetylation of **9***b* provided the title compound **9***c*; b.p.$_{0.07}$ 36°, $[\alpha]_D^{25}$ −155° (*c*, 2.4 in chloroform), n_D^{23} 1.4667.

Anal. Calcd. for $C_6H_{10}O_3$: C, 55.38; H, 7.96. Found: C, 55.22; H, 7.91.

Hydrogenation of **9***c* as described for the preparation of **18***c* gave methyl 2,3-dideoxy-β-D-*glycero*-pentofuranoside (**11***c*); b.p.$_{0.07}$ 38°, $[\alpha]_D^{25}$ −128° (*c*, 1.5 in chloroform), n_D^{22} 1.4446.

Anal. Calcd. for $C_6H_{12}O_3$: C, 54.55; H, 9.09. Found: C, 54.29; H, 9.03.

Benzoylation of **11***c* gave methyl 5-*O*-benzoyl-2,3-dideoxy-β-D-*glycero*-pentofuranoside (**11***a*); b.p.$_{0.07}$ 94°, $[\alpha]_D^{25}$ −73° (*c*, 1.8 in chloroform), n_D^{22} 1.5098.

Anal. Calcd. for $C_{13}H_{16}O_4$: C, 66.08; H, 6.83. Found: C, 66.01; H, 6.87.

Acetylation of **11***c* gave methyl 5-*O*-acetyl-2,3-dideoxy-β-D-*glycero*-pentofuranoside (**11***b*); b.p.$_{0.07}$ 41°, $[\alpha]_D^{25}$ −99° (*c*, 1.5 in chloroform), n_D^{22} 1.4340.

Anal. Calcd. for $C_8H_{14}O_4$: C, 55.17; H, 8.05. Found: C, 54.99; H, 8.18.

Acknowledgments

The support of a National Research Council of Canada Grant A-172 to R.U.L. and the provision of microanalyses and nuclear magnetic resonance spectra by the Department of Chemistry, University of Alberta are gratefully acknowledged.

1. R. U. LEMIEUX, E. FRAGA, and K. A. WATANABE. Can. J. Chem. **46**, 61 (1968).
2. R. K. NESS and H. G. FLETCHER, JR. J. Org. Chem. **28**, 435 (1963).
3. J. HILDESHEIM, J. CLEOPHAX, and S. D. GERO. Tetrahedron Letters, 1685 (1967).
4. J. CLEOPHAX, J. HILDESHEIM, and S. D. GERO. Bull. Soc. Chim. France, 4111 (1967).
5. R. S. TIPSON and A. COHEN. Carbohyd. Res. **1**, 338 (1965).
6. C. L. STEVENS, N. A. NIELSEN, and P. BLUMBERGS. J. Amer. Chem. Soc. **86**, 3592 (1964).
7. J. P. HORWITZ, J. CHUA, I. L. KLUNDT, M. A. DAROOGE, and M. NOEL. J. Amer. Chem. Soc. **86**, 1896 (1964).
8. J. P. HORWITZ, J. CHUA, M. A. DAROOGE, and M. NOEL. Tetrahedron Letters, 2725 (1964).
9. J. P. HORWITZ, J. CHUA, M. A. DAROOGE, M. NOEL, and I. L. KLUNDT. J. Org. Chem. **31**, 205 (1966).
10. J. R. MCCARTHY, JR., M. J. ROBINS, L. B. TOWNSEND, and R. K. ROBINS. J. Amer. Chem. Soc. **88**, 1549 (1966).
11. B. R. BAKER, R. E. SCHAUB, and J. H. WILLIAMS. J. Amer. Chem. Soc. **77**, 7 (1955).
12. R. E. SCHAUB and M. J. WEISS. J. Amer. Chem. Soc. **80**, 4683 (1958).
13. R. E. PARKER and N. S. ISAACS. Chem. Rev. **59**, 737 (1959).
14. G. CASINI and L. GOODMAN. J. Amer. Chem. Soc. **85**, 235 (1963).
15. G. CASINI and L. GOODMAN. J. Amer. Chem. Soc. **86**, 1427 (1964).
16. A. J. DICK and J. K. N. JONES. Can. J. Chem. **45**, 2879 (1967).
17. E. W. GARBISCH, JR. J. Amer. Chem. Soc. **86**, 5561 (1964).
18. J. HONEYMAN. J. Chem. Soc. 990 (1946).
19. S. MUKHERJEE and A. R. TODD. J. Chem. Soc. 969 (1947).
20. J. H. BREWSTER. J. Amer. Chem. Soc. **81**, 5483 (1959).
21. R. U. LEMIEUX and A. A. PAVIA. Can. J. Chem. **46**, 1453 (1968.)
22. R. U. LEMIEUX and A. A. PAVIA. Submitted.
23. R. U. LEMIEUX, C. T. BISHOP, and G. E. PELLETIER. Can. J. Chem. **34**, 1365 (1956).

Can. J. Chem. Downloaded from www.nrcresearchpress.com by 210.87.254.40 on 09/05/12
For personal use only.

Can. J. Chem. Downloaded from www.nrcresearchpress.com by 210.87.254.40 on 09/05/12
For personal use only.

Solvation effects on conformational equilibria. Studies related to the conformational properties of 2-methoxytetrahydropyran and related methyl glycopyranosides[1]

R. U. LEMIEUX, A. A. PAVIA,[2] J. C. MARTIN,[3] AND K. A. WATANABE[4]
Department of Chemistry, University of Alberta, Edmonton, Alberta

Received May 5, 1969

Further evidence is presented (8) that changes in optical rotation at the D-line of sodium which occur with changes in solvent largely reflect changes in conformational equilibria.

Changes in the nuclear magnetic resonance spectrum of 4,4,5,5-tetradeuterio-2-methoxytetrahydropyran and in the rotation of s(+)-2-methoxytetrahydropyran with changes in solvent are interpreted to show that solvents capable of donating a hydrogen to a hydrogen bond have an effect on the magnitude of the anomeric effect which is greater than that resulting from the change in the dielectric constant of the solvent. In the case of methyl 2-deoxypyranosides with the methoxy group in axial orientation, water appears to have an especially profound influence in stabilizing that orientation of the methyl group which brings it into *gauche* relationship with both the C_2-grouping and the anomeric hydrogen; that is, counter to the anomeric effect.

The methyl 2-deoxy-β-L-*erythro*-pentopyranoside was synthesized from di-*O*-acetyl-L-arabinal by way of an iodomethoxylation. Deuterolysis of the resulting 1,2-*trans*-acetylated methyl 2-deoxy-2-iodopentosides is shown to proceed in one case with extensive inversion of configuration and with extensive retention in the other case and offers a route to the preparation of 2-deoxy-2-deuterio-*erythro*-pentose with a high proportion (>75%) of the diastereoisomer with the *arabino*-configuration.

Canadian Journal of Chemistry, 47, 4427 (1969)

We wish to report synthetic routes to the α- and β-anomers of methyl 2-deoxy-2-deuterio-L-*arabino*-pentopyranoside and s-*dextro*-2-methoxytetrahydropyran(methyl 2,3,4-trideoxy-β-L-pentopyranoside).

Di-*O*-acetyl-L-arabinal (**1**) on treatment with iodine in methanol solution containing silver acetate following the directions of Lemieux and Fraser-Reid (1) yields approximately 1:1 mixture of methyl di-*O*-acetyl-2-deoxy-2-iodo-α-L-*arabino*-pyranoside (**2**) and methyl di-*O*-acetyl-2-deoxy-2-iodo-β-L-*ribo*-pyranoside (**3**). The *arabino*-isomer was isolated by crystallization. The *ribo*-isomer (**3**) was obtained only as a syrup of about 90% purity. However, catalytic hydrogenolysis of this compound followed by deacetylation gave a crystalline methyl 2-deoxy-β-L-*erythro*-pentopyranoside (**4***a*). Similar hydrogenolysis of the α-L-*arabino*-iodo compound (**2**) provided crystalline methyl di-*O*-acetyl-2-deoxy-α-L-*erythro*-pentopyranoside (**5***a*).

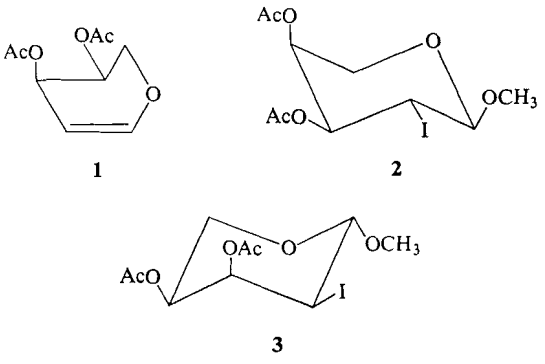

1 **2** **3**

Lemieux and Levine (2) showed that deuterolysis using palladium on charcoal as catalyst went with very high degree of retention of configuration from methyl 2-deoxy-2-iodo-β-D-glucopyranoside, whereas extensive inversion occurred with methyl 2-deoxy-2-iodo-α-D-mannopyranoside. The iodo compounds **2** and **3** were subjected to deuteriolysis in methanol. Replacement of the equatorial iodine of the *arabino* compound **2** proceeded with a high degree of retention, whereas the equatorial iodine of the isomeric *ribo* compound **3** was replaced with extensive inversion of the configuration. That is, both compounds **2** and **3** provided the 2-deoxy-2-deuterioglycoside with the *arabino* configuration (>75% yield). Evidently this procedure can

[1]Presented by R. U. L. at the Karl Pfister Lecture, Massachusetts Institute of Technology, Cambridge, Mass., November 15, 1968.

[2]University of Alberta Postdoctoral Fellow, 1967–1968. Present address: École Nationale Supérieure de Chimie, Montpellier, France.

[3]Canada Council Postdoctoral Fellow, 1968–1969. Present address: Université de Lyon, Département de Chimie Organique, Lyon, France.

[4]University of Alberta Postdoctoral Fellow, 1966–1968. Present address: Sloan-Kettering Institute for Cancer Research, Rye, N.Y.

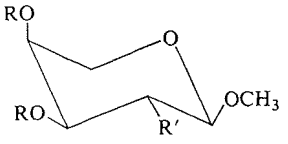

4

	R	R′
a	Ac	H
b	H	H
c	Ms	H
d	CH_3	H
e	Ac	D
f	H	D

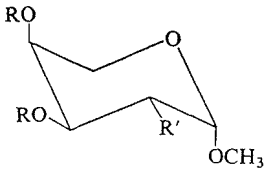

5

	R	R′
a	Ac	H
b	H	H
c	H	D
d	Ts	H

be used to provide 2-deoxy-D-ribose with either deuterium or tritium at the 2-position mainly in the *arabino*-configuration.

The configurations of the deuterated deoxypentopyranosides were established by nuclear magnetic resonance (n.m.r.) spectroscopy in deuterium oxide. The signal for the anomeric proton both for compounds **4***e* and **4***f* is in the form of a doublet with spacings of 8.5 and 7.3 Hz, respectively, indicating a *trans*-relationship between the hydrogens at positions 1 and 2. In the case of compound **5***c*, the spacings of the doublet for the anomeric proton was 3.0 Hz, both in deuterium oxide and deuteriochloroform. The optical purity seemed as great as that for compound **4***f* and probably better than 80%. The configuration for compound **5***c* was established by hydrolysis to provide the 2-deoxy-2-deuterio-L-arabinose. The n.m.r. spectrum of the compound in deuterium oxide showed the presence of the two pyranose and two furanose forms identified by Lemieux and Anderson (3). Thus, the quartet centered at τ 4.78, with spacings of 8.2 and 3.0 Hz, assigned to the anomeric proton of the α-pyranose form for 2-deoxy-D-ribose(2-deoxy-D-*erythro*-pentose) was now present in the spectrum for the 2-deoxy-2-deuteriopentose (**8**) as a doublet with a spacing of 9.0 Hz. This requires the hydrogens at positions 1 and 2 in **8** to be in *trans* relationship. Therefore, the hydrogens at positions 2 and 3 in compound **5***c* are in *trans* relationship and the compound has the *arabino*-configuration shown. It is planned to extend these studies and to establish the stereochemical routes of the deuteriolysis more precisely by use of mass spectroscopy.

The above routes for the preparation of the methyl 2-deoxy-α- and β-L-*erythro*-pentopyranosides were examined primarily to provide these compounds for studies on the effect of solvents on their conformations (4). Also, the use of these compounds to prepare optically active 2-methoxy-tetrahydropyran was of interest. Tosylation of the impure methyl 2-deoxy-β-L-*erythro*-pentopyranoside (**5***b*) provided the crystalline ditosylate (**5***d*) which was readily converted to the 6-methoxy-5,6-dihydro[2*H*]pyran (**6**). This compound was not characterized but converted directly to S-*dextro*-2-methoxytetrahydropyran (**7**), $[\alpha]_D$ + 157°(carbon tetrachloride), which had an infrared (i.r.) spectrum identical to the well-known racemic mixture (5).

In order to gain a better appreciation of the effects of solvent change on the optical rotation of the above 2-methoxytetrahydropyran and its 5-hydroxy derivative [namely, methyl 2,3-dideoxy-β-L-*glycero*-pentopyranoside (6)], the 4,6-ethylidene derivatives of both the α (**11***a*) and β (**11***b*) anomers for methyl 2,3-dideoxy-D-*erythro*-hexopyranoside were prepared. These compounds were prepared by hydrogenation of the α (**10***a*) and β (**10***b*) forms, respectively, of methyl 4,6-ethylidene-2,3-dideoxy-D-*erythro*-hex-2-enopyranoside. The latter compounds were synthesized from the known anomers for methyl

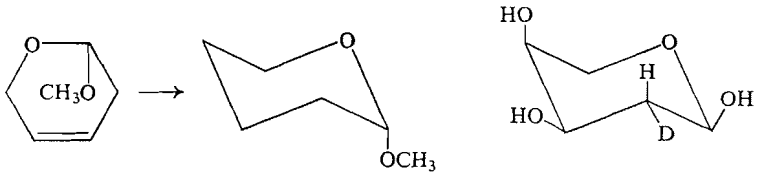

6 7 8

Can. J. Chem. Downloaded from www.nrcresearchpress.com by 210.87.254.40 on 09/05/12
For personal use only.

Can. J. Chem. Downloaded from www.nrcresearchpress.com by 210.87.254.40 on 09/05/12
For personal use only.

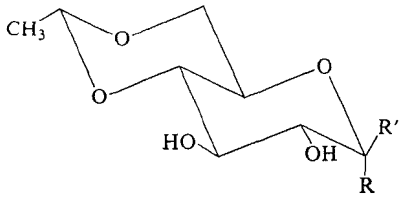

9

a R = OCH_3; R′ = H
b R = H; R′ = OCH_3

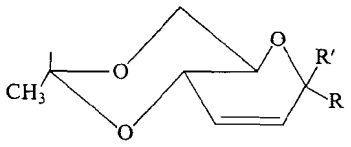

10

a R = OCH_3; R′ = H
b R = H; R′ = OCH_3

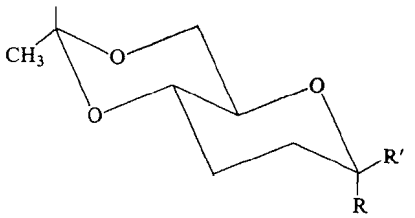

11

a R = OCH_3; R′ = H
b R = H; R′ = OCH_3

4,6-ethylidene-D-glucopyranoside (compounds **9***a* and **9***b*) respectively following the recently published (7) procedures for the corresponding 4,6-benzylidene derivatives of the methyl glucopyranosides. In order to provide further evidence in support of our contention (8) that changes in rotation which occur on changing solvent are largely related to changes in conformation, compounds of fixed conformation were prepared, namely, the 4,6-*O*-ethylidene derivatives of 1,2-dideoxy-D-*arabino*-hexopyranose (**16**) and 1,2,3-trideoxy-D-*erythro*-hexopyranose (**15**). These compounds were synthesized by hydrogenation of tri-*O*-acetyl-D-glucal (**12**) followed by deacetylation of the products **13***a* and **14***a* as described by Gray and Barker (9). As described in the experimental, in our hands, the course of the hydrogenation in the presence of diethylamine did not provide **14***a* as the major product. As expected, as seen in Table III, the rotations of compounds **15** and **16** are virtually insensitive to change in solvent.

A main purpose of this research was to investigate the possible effect of solvation phenomena on the apparent magnitude of the anomeric effect. For example, if the origin of the anomeric effect is indeed the result of dipole interactions between lone pairs of electrons on the oxygen atoms of the acetal linkage of glycosides or between those of the oxygen and halogen atoms of α-haloethers (10), then changes in the dielectric constant should tend to favor the more polar conformer (11,12). However, as suggested by Lemieux and Morgan (13), in view of the apparent occurrence of the "reverse anomeric effect", the engagement of the lone pair electrons of an acetal linkage in hydrogen bonds can be

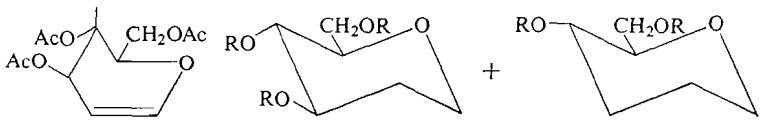

12 **13** **14**

a R = Ac
b R = H

a R = Ac
b R = H

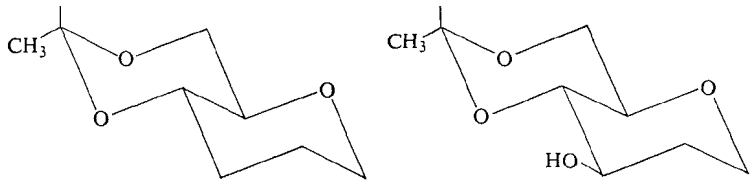

15 **16**

Can. J. Chem. Downloaded from www.nrcresearchpress.com by 210.87.254.40 on 09/05/12
For personal use only.

TABLE I

Nuclear magnetic resonance parameters of 2-methoxytetrahydropyran-4,4,5,5-d_4*

Solvent	τ H_2	τ H_3	τ H_3'	τ H_6	τ H_6'	$J_{2,3} + J_{2,3'}$	$J_{2,3}$	$J_{2,3'}$	$J_{3,3'}$	$J_{6,6'}$	τ OCH_3
CCl_4	5.67(t)	8.41(A)	8.52(B)	6.38(A)	6.69(B)	6.4	—	—	—	11.5	6.82(s)
C_6D_6	5.58(t)	8.25 to	8.85(m)	6.29(A)	6.67(B)	6.5	—	—	—	12.0	6.75(s)
CS_2	5.62(t)	8.44(A)	8.55(B)	6.34(A)	6.63(B)	6.6	—	—	—	11.8	6.77(s)
$CDCl_3$	5.50(t)	8.32(A)	8.45(B)	6.17(A)	6.52(B)	7.2	4.1	3.1	12.0	12.0	6.63(s)
CD_3COCD_3	5.57(t)	8.25 to	8.70(m)	6.27(A)	6.60(B)	7.1	—	—	—	11.5	6.73(s)
CH_3OD	5.65(t)	8.50(A)	8.64(B)	6.32(A)	6.60(B)	7.3	2.6	4.7	12.8	11.5	—
DMSO-d_6	5.57(t)	8.25 to	8.65(m)	6.30(A)	6.58(B)	7.0	—	—	—	11.5	6.75(s)
CD_3CN	5.67(q)	8.52(A)	8.68(B)	6.35(A)	6.68(B)	7.4	2.7	4.7	12.8	11.5	6.81(s)
D_2O	5.13(q)	8.27(A)	8.03(B)	5.89(A)	6.17(B)	8.4	5.8	2.6	13.5	12.0	6.34(s)

*Abbreviations used are: (s), singlet; (t), triplet; (q), quadruplet; (A), A part of AB or ABX System; (B), B part of AB or ABX System; (m), multiplet.

Can. J. Chem. Downloaded from www.nrcresearchpress.com by 210.87.254.40 on 09/05/12
For personal use only.

expected to lead to a change in the dipoles about these atoms and thereby influence the magnitude of the anomeric effect. For example, Lemieux and Saluja (14) have found that N-protonation of *N*-(tetra-*O*-acetyl-α-D-glycopyranosyl) imidazole with trifluoroacetic acid or N-methylation to the quaternary salt provides an important driving force for the imidazole residue to adopt the equatorial orientation. Certainly, the demonstration that specific solvation effects can substantially alter conformational equilibria is of basic importance for the appreciation of the interactions involved in enzyme–substrate complexing phenomena which may lead to stereoelectronic situations more favorable for reaction than are provided in the absence of such interactions. It was, therefore, desired to compare changes in conformation for 2-methoxytetrahydropyran with change in solvent both by n.m.r. and optical rotation. The n.m.r. data could be expected to provide information on chair–chair conformational change whereas the optical rotatory data would, following Brewster's rules for the anticipation of optical rotation (15), provide information on the effect of solvent on the orientation of the methoxy grouping relative to the pyranose ring.

$$HOCH_2—C\equiv C—CH_2—CH(OCH_3)_2$$

17

D_2 ↓ Pd/C

CH_3OH ↓ H^+

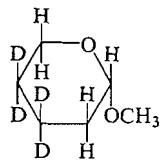

18

In order to obtain n.m.r. data on 2-methoxytetrahydropyran which was useful for the assessment of the coupling constants of H_2 with the geminal hydrogens at the 3-position, it was required to eliminate the virtual coupling of H_2 with the hydrogens at the 4-position which are only weakly chemically shifted from those at the 3-position. This was accomplished by replacement of the two C_4-hydrogens by deuterium atoms. Thus, 3-pentyn-5-ol-l-al-dimethyl-acetal (**17**) (16) was deuterated with deuterium over palladium on charcoal. The resulting 3,3,4,4-tetradeuteriopentane-5-ol-l-al-dimethyl-acetal was cyclized in methanolic hydrogen chloride to the desired 4,4,5,5-tetradeuterio-2-methoxytetrahydropyran (**18**). As expected, sharp signals were obtained for the hydrogens at the 2-, 3-, and 6-positions. The n.m.r. parameters for the product (**18**) in a variety of solvents are reported in Table I.

In order to attach a significance in terms of the populations of the two chair conformations for 2-methoxytetrahydropyran of the coupling constants of H_2 with H_3 and $H_{3\varepsilon'}$, it is necessary to evaluate the coupling constants $J_{aa} + J_{ae}$ and $J_{ee} + J_{ea}$ in order to apply the relationship $n(J_{aa} + J_{ae}) + (1 - n)(J_{ea} + J_{ee}) =$ observed sum of coupling constants where n is the fraction of the compound with the methoxy group in equatorial orientation. The individual coupling constants are known for the anomeric pair of the methyl 2-deoxy-D-*arabino*-hexopyranosides as a result of the preparation of three of the 2-deuterio-derivatives (2). The values found for these compounds in deuterium oxide wherein a high degree of conformational purity is expected, were $J_{aa} = 9.9, J_{ae} = 1.9, J_{ea} = 3.9$, and $J_{ee} = 1.4$ Hz, respectively. These values are expected to represent closely those existing for 2-methoxytetrahydropyran in view of the close structural similarities between these compounds. On this basis and assuming that only chair forms are present, the effects of solvent on the population of the conformer with the methoxy group in equatorial orientation are given in Table II. It is seen that there is not a simple relationship between dielectric constant and the equilibrium constant for this conformational change. Although the results show an increase in the presumably more polar equatorial form with increasing solvent polarity, the marked effect of chloroform as compared to the much more polar dimethylsulfoxide is noteworthy especially since chloroform like methanol and water is capable of donating its hydrogen to a hydrogen bond (17). Chloroform molecules can be expected to form weak hydrogen bonds with the oxygens of acetal linkage and, perhaps, thereby stabilize the less stable form of 2-methoxytetrahydropyran which has the methoxy group in equatorial orientation. This effect by chloroform has also been noted in the case of a number of glycosides (4).

The conclusion that hydrogen bonding can influence the strength of the anomeric effect is

Can. J. Chem. Downloaded from www.nrcresearchpress.com by 210.87.254.40 on 09/05/12
For personal use only.

TABLE II

Effect of solvent on the conformational equilibrium for 2-methoxytetrahydropyran

Solvent	Dielectric* constant	Percentage with equatorial 2-methoxy group	
		N.m.r.	Optical rotation†
CCl_4	2.2	17	23
C_6D_6	2.3	18	—
CS_2	2.6	20	—
$CDCl_3$	4.8	29	38
$(CD_3)_2CO$	21	28	28
CH_3OD	32	31	39
$(CD_3)_2SO$	36	26	34
CD_3CN	38	32	—
D_2O	78	48	78

*See reference 33.
†In non-deuterated solvent, the molar rotations found are reported in Table III.

supported by the following studies of the effect of solvent on the rotations of 2-methoxytetrahydropyran derivatives with the methoxy group in axial orientation. Examination of the rotations given in Table III for a variety of compounds with an axial methoxy group at the anomeric center of fixed chair conformation shows that change in solvent has relatively little effect *except* for water and it is therefore concluded that water has a particularly strong ability to affect the orientation of the methoxy group.

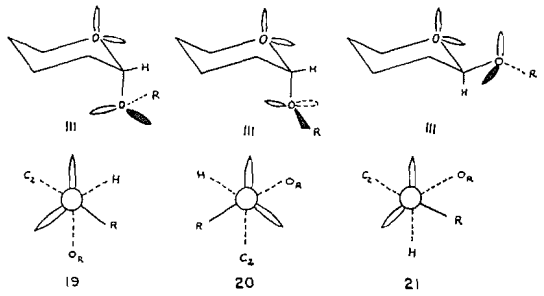

19 20 21

It was pointed out several years ago that both for reasons of steric effects and of the anomeric effect, an aglycon (10,18) should tend to adopt the conformation shown in **19** when in axial orientation and that depicted by **21** when in equatorial orientation. Indeed, X-ray crystallographic studies (19–21) in a number of glycosidic structures have found the aglycons in these orientations which are those to which Brewster (15) assigned the value of $\pm 105°$ as their contribution to molar rotation for methyl glycosides in water. As is seen in the projections, the C—O_r bond is in *gauche*-relationship with an orbital for an unshared pair of electrons of the OR group in both the anomers. However, it can be seen from the conformational formulas that the equatorial OR group has an orbital parallel and opposing an orbital of the ring oxygen[5] and that such a dipole interaction is avoided in the axially oriented anomer.

There is to date no accurate way to establish, in solution, the relative importance of other staggered orientations for the aglycon about the anomeric center. However, the dipole moment of each conformer may be calculated by the bond moment (26) and are estimated to be 0.0, 1.84, 1.84, 1.84, 1.84, and 2.60 Debye (D) units for conformers **22**, **23**, **24**, **25**, **26**, and **27**, respectively. For the axial conformer, that (**24**) which has the methyl group oriented under the ring, can be expected to have a negligible existence. As seen in Table II, we estimate the mole fractions of the two chairs to be $n_{22} + n_{23} = 0.82$ and $n_{25} + n_{27} = 0.18$ with benzene as solvent. For the present purposes, it can be assumed that the equilibrium constant for the chair–chair equilibrium also applies to the equilibria which separate the various conformers of a given chair. On this basis, the concentration of **27** relative to these

[5]Hutchins, Kopp, and Eliel (22) have recently suggested that this interaction be termed the "rabbit ear effect." We consider the term "anomeric effect" first introduced in 1961 with reference to the establishment of the phenomenon through n.m.r. studies of conformation and studies of anomerization equilibria (10,23) to be of historical interest and recommend that it be maintained. The possibility that the effect may arise at least in part from such dipole interactions was clearly envisaged by Edward (24) and discussed by Kabayama and Patterson (25); Lemieux (10) designated the interaction by the term *e*//*e*.

Can. J. Chem. Downloaded from www.nrcresearchpress.com by 210.87.254.40 on 09/05/12
For personal use only.

TABLE III

Effects of solvent on optical rotation

Solvent	Dielectric constant		15*	16*	10*	11*a**	28	7*
$CHCl_3$	4.2	$[M]_D^{25}$ (in $CHCl_3$)	1.8	−38	270	258	173	167
CCl_4	2.3	Δ[*M*]†	+0.3	0.6	—	+3	+3	+15
CH_3COCH_3	21	Δ[*M*]†	−0.2	+0.4	—	−7	—	+10
CH_3OH	32	Δ[*M*]†	—	+0.1	−6	−1	0	−1
CH_3CN	39	Δ[*M*]†	−1.1	1.0	+17	−5	—	—
$(CH_3)_2NCHO$	36	Δ[*M*]†	—	−0.2	+14	−3	—	+3
CH_3SOCH_3	45	Δ[*M*]†	+0.1	+5	−5	+2	—	4
H_2O	78	Δ[*M*]†	+0.2	−5	−24	−40	−25	−40

*The compounds have the following structures:

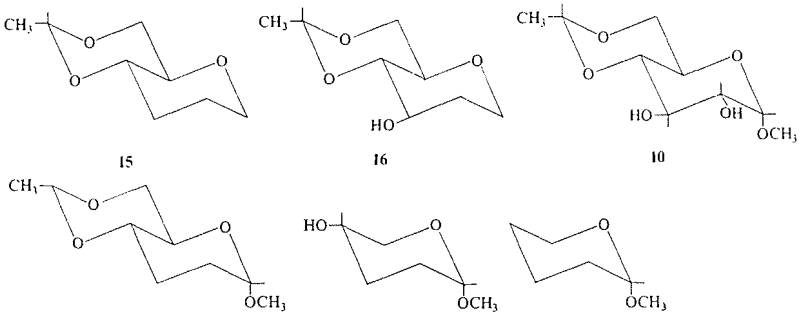

15 16 10

11*a* 28 (6) 7

†Δ[*M*] refers to the difference between the rotation in the solvent indicated to the left and that in chloroform.

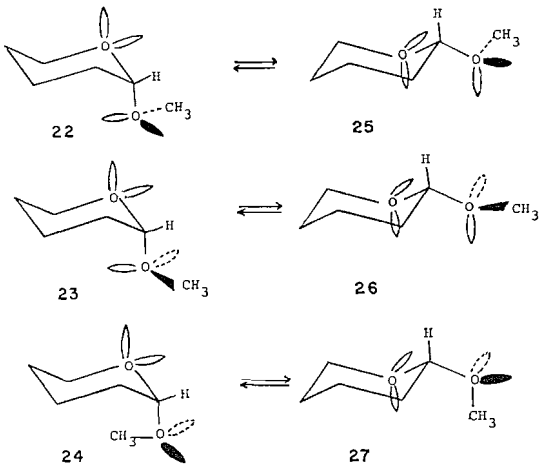

22 25

23 26

24 27

of **23**, **25**, and **24** must be small. Therefore, we expect the square of the moment of 2-methoxytetrahydropyran in benzene to be approximately $0.82 \times 0.82 \times 0 + 0.82 \times 0.18 \times 1.84^2 + 0.18 \times 1.84^2 = 1.09$. The dipole moment, 1.06 D, thus estimated is in good agreement with that found, 1.16 D (27).

The changes in rotation noted above for compounds **11***a* and methyl 2,3-dideoxy-α-D-*glycero*-pentopyranoside are (Table III) taken as evidence that for these 2-deoxy-α-pyranosides, there exists a substantial abundance of at least another conformer. Since that conformer which would have the methyl group *gauche* to both the O_r and C_2 must be highly strained, the conformation (**20**) which has the methyl group in *gauche* orientation with C_2 and H_1 must be expected to be that which is most stable next to conformation **19**. The fact that the conformer **20** has an *e*//*e* interaction, whereas **19** has none, may provide the clue to apparent stabilization of **20** by water. Thus, by virtue of its dihydric structure, water may form a bridge between the two parallel and opposing orbitals and thereby cause an effective cancelling of what may be termed the *exo*-anomeric effect. Such considerations are of obvious interest to the eventual understanding of α-glucosidase action.

The effect of hydration on aglycon orientation was also evident from the changes in rotation given in Table III for s-*dextro*-2-methoxytetrahydropyran (**7**) and related compounds. The α- and β-anomers of 2,3-dideoxy-4,6-*O*-ethylidene-D-*erythro*-hexopyranoside **11***a* and **11***b*, respectively, and the 1,2,3-trideoxy-4,6-*O*-ethylidene-D-*erythro*-pyranoside (**15**) were prepared to

TABLE IV

Molar rotations of methyl 2,3-dideoxy-4,6-*O*-ethylidene-D-erythropyranosides and s-*dextro*-2-methoxytetrahydropyran

Solvent	**11***a**	**11***b**	**7*** Calculated	**7*** Observed	ΔM
$CHCl_3$	258	−152	227	167	60
CCl_4	261	−144	240.5	182	58.5
CH_3COCH_3	251	−152	231	177	54
CH_3OH	257	−155	224	166	58
CH_3CN	253	−153	250.9	—	—
DMF	245	−141	—	170	—
DMSO	260	−142	229	171	58
H_2O	218	−144†	183	127	56

*The compounds have the following structures:

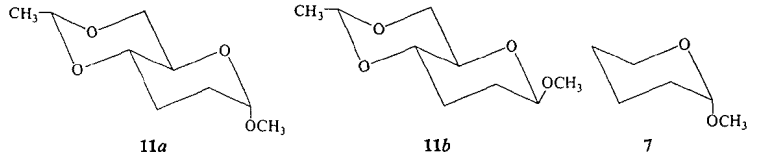

11*a* **11***b* **7**

†Calculated by extrapolation of values of methanol–water mixtures.

provide a basis for a rationalization of the optical rotatory change of **7** with changes in solvent. As expected (15), the rotation of **15** was near zero. The rotation of **11***b* could not be determined in water. However, it was found for several compounds that the rotation in water could be found by extrapolation of values found in mixtures of methanol and water. The rotations of **11***a*, **11***b*, and **7** in a variety of solvents are given in Table IV. Using the rotation of **11***a* for **7** in the 2-axial conformation and that for **11***b* for that of **7** in the other chair form, the calculated rotations for **7** using the chair–chair equilibria determined by n.m.r. and reported in Table II are listed in Table IV. It is seen that in all cases, there exists a difference of $57 \pm 3°$ between the calculated rotation and that observed. Although this discrepancy cannot be explained at this time, it seems most probable that it arose from a 15% racemization of **7** in the course of its preparation.

Assuming that changes in conformation are the most important factor causing changes in rotation and considering the general variation of rotation rather than particular experimental values, the proportions of conformers of **7** may be estimated. It can be anticipated (15,28) that the s-*dextro*-2-methoxytetrahydropyran (**7**) in conformation **22** will have a molar rotation of +205 and +105° in conformation **25**. If we assume that only these conformations prevail, the proportions of conformer **25** in the variety of solvents shown in Table II are obtained using the rotations listed in Table III. As it appears in Table II, the discrepancy between the proportions of conformers estimated by n.m.r. and by optical rotation may be explained by the partial racemization of **7** and the presence, mainly in water, of amounts of conformers involving rotation about CH_3O—C bond. It can be pointed out that change in solvent does not appreciably affect the molar rotation of the methyl 2,3-dideoxy-4,6-*O*-ethylidene-β-D-*erythro* hexopyranoside (**11***b*) (see Table IV).

The special effect of water on the rotation of compounds with the methoxy group in axial orientation is therefore readily apparent in both s-*dextro*-2-methoxytetrahydropyran and the bicyclic compound (**11***a*). These results confirm our general contention that specific solvation effects can play an important role in determining conformational equilibria. Clearly these conclusions have an important bearing on the conformational properties in water of important α-glucopyranoside structures as represented by starch, glycogen, several antibiotics, etc. In view of the marked changes in rotation which can occur for an α-D-hexopyranoside on changing solvent and which occur as a result of changes in the relative populations of conformers involving the aglycon, the proposal (29) that the rotation of ethyl 2,3,6-trideoxy-α-D-*threo*-hexopyranoside in water requires the compound to exist largely in the 1C-conformation is without basis.

Can. J. Chem. Downloaded from www.nrcresearchpress.com by 210.87.254.40 on 09/05/12
For personal use only.

Can. J. Chem. Downloaded from www.nrcresearchpress.com by 210.87.254.40 on 09/05/12
For personal use only.

Experimental

Methyl 3,4-Di-O-Acetyl-2-deoxy-2-iodo-α-L-arabinopyranoside (2)

Di-*O*-acetyl-L-arabinal (di-*O*-acetyl-1,2-dideoxy-L-*erythro*-pent-1-enopyranose (**1**) (30), 4.3 g, was dissolved in 200 ml of dry methanol containing 5.5 g of silver acetate. The mixture was maintained at 0° and 5.0 g of iodine were added over a period of 10 min with continuous stirring. After an additional h, the silver salts were removed by filtration, washed with methanol and the filtrate evaporated *in vacuo*. The residue was dissolved in chloroform, washed successively with water, saturated sodium bicarbonate solution, thiosulfate solution, water, and dried over sodium sulfate. Evaporation gave a semi-solid residue, 7.2 g, whose n.m.r. spectrum showed it to be a 1:1 mixture of the α and β iodo-compounds **2** and **3**, respectively. Successive recrystallizations from ether–petroleum ether provided the title compound, m.p. 100–101.5°. The n.m.r. spectrum in $CDCl_3$ showed singlets at τ 7.89 and 7.95 (acetyls) and τ 6.46 (methoxy). The signal for the anomeric proton (H_1) was a doublet at τ 5.50 with a spacing of 8.2 Hz. The signals for H_3 and H_4 were superimposed at τ 4.90.

Methyl 3,4-Di-O-acetyl-2-deoxy-α-L-erythro-pentopyranoside (4a)

Compound **2**, 11 g, was dissolved in 120 ml of methanol containing 4 g of triethylamine and hydrogenated at normal pressure using 1.8 g of 5% palladium on charcoal. After the hydrogen uptake had ceased the catalyst and the methanol were removed. The solid residue was dissolved in benzene and the solution was washed successively with water, sodium thiosulfate, water, and dried over sodium sulfate. Evaporation gave a crystalline product which was recrystallized from ether–petroleum ether to give 4.5 g of the title compound, m.p. 73.5–74°, $[\alpha]_D^{25}$ −22.7° (*c*, 0.9 in chloroform) and +4.3° (*c*, 0.9 in water).

Anal. Calcd. for $C_{10}H_{16}O_6$: C, 51.72; H, 6.89. Found: C, 52.00; H, 6.96.

The n.m.r. parameters are given in Table V.

Methyl 2-Deoxy-α-L-erythro-pentopyranoside (4b)

Deacetylation of **4***a* with 0.5% sodium methoxide solution at room temperature gave a theoretical yield, m.p. 101–102° (sublimes), $[\alpha]_D^{25}$ −169° (*c*, 1.03 chloroform) and −50° (*c*, 1.15 water).

Anal. Calcd. for $C_6H_{12}O_4$: C, 48.64; H, 8.10. Found: C, 48.68; H, 8.15.

The n.m.r. parameters are given in Table V.

Methyl 2-Deoxy-β-L-erythro-pentopyranoside (5b)

The sirupy residue from the isolation of the iodo-compound **2** was found by n.m.r. to be an approximately 9:1 mixture of compounds **3** and **2**, respectively. This mixture was hydrogenated in the same manner as described above for the preparation of **4***a* and the product was deacetylated as described for the preparation of **4***b*. Chromatography on a dry-packed silica gel column and using a 1:4 mixture of acetone and chloroform provided the title compound (**5***b*) after **4***b* had been eluted. Purification was achieved by recrystallization from ether–petroleum ether, m.p. 85.5–86.5°, $[\alpha]_D^{25}$ +197° (*c*, 1.25 in water), +201° (*c*, 1.36 in chloroform), +192° (*c*, 0.96 in dimethylsulfoxide).

The 100 MHz spectrum in deuterium oxide (TMS external) showed a triplet at τ 4.69 (spacings 3.0 Hz) for H_1, the methoxy signal at τ 6.22 and the multiplet for H_2 and H_3 centered at τ 7.16.

Methyl 2-Deoxy-3,4-di-O-mesyl-α-L-erythro-pentopyranoside (4c)

To a solution of 450 mg (0.003 ml) of **4***b* in 4 ml of pyridine chilled to 0°, 1 g (0.007 mole) of methanesulfonyl chloride. The reaction mixture was worked up as usual after 30 min to give, after recrystallization from ethanol, 700 mg of the title compound, m.p. 99–100°.

Anal. Calcd. for $C_8H_{14}O_8S$: C, 31.57; H, 5.25. Found: C, 31.32; H, 5.37.

The n.m.r. parameters are given in Table V.

Methyl 2-Deoxy-3,4-di-O-methyl-α-L-erythro-pentopyranoside (4d)

Compound **4***b*, 550 mg, was dissolved in 10 ml of pure anhydrous methyl iodide and, to stirred refluxing solution, 1.9 g of freshly prepared silver oxide was added in 10 equal portions over 30 min intervals. After refluxing an additional h, the product was isolated in the usual manner. Thin-layer chromatography revealed three components and purification required preparative gas chromatography on a 20% Carbowax column with a column temperature of 120° using an F&M Prepmaster Model 776. The main component, which also had the longest retention time, was assigned the structure **4***d* on the basis of its n.m.r. spectrum (see Table V).

It is noteworthy that both the 2-deoxy and 3-deoxy methyl *erythro*-pentopyranosides prepared in the course of this research exhibited pronounced instability in acid media. The by-products formed in the above methylation are believed to be isomers of **4***d* and their formation could not be avoided.

Methyl 2-Deoxy-2-deuterio-α-L-arabino pentopyranoside (4f)

The pure methyl di-O-acetyl-2-deoxy-2-iodo-α-L-arabinopyranoside (**2**) was deuterolyzed under the same conditions as used for the hydrogenolysis of **2** to provide **4***a* except that the deuterium gas was employed. The crystalline product (**4***e*) melted at 73–74.5° closely similar to that of compound **4***a*. The n.m.r. spectrum in dimethylsulfoxide-d_6 showed an intense doublet for the anomeric proton with a spacing of 8.5 Hz. As seen in Table V, the undeuterated compound (**4***a*) showed a quartet for this signal with coupling constants (calculated) of 8.5 and 2.6 Hz. The compound was evidently contaminated to an extent of 20 to 25% of the *ribo*-isomer in view of the presence of a low intensity doublet (spacing 2.6 Hz) centered at the same position as the above more intense doublet.

Deacetylation of **4***e* as described for the deacetylation of **4***a* provided the title compound (**4***f*), contaminated 20 to 25% by the *ribo*-isomer. The n.m.r. spectrum in deuterium oxide showed the main anomeric doublet with a spacing of 7.3 Hz. On changing the solvent to deuteriochloroform, the spacing diminished to 2.7 Hz.

Compound **4***f*, 120 mg, in 2 ml of 0.1 *N* aqueous sulfuric acid was maintained at 50° for 4.5 h in which time

Can. J. Chem. Downloaded from www.nrcresearchpress.com by 210.87.254.40 on 09/05/12
For personal use only.

TABLE V

Nuclear magnetic resonance parameters for methyl 2-deoxy-α-L-*erythro*-pentopyranosides and derivatives*

				Chemical shift†							Coupling constants (Hz)								
Compound	R	R′	Solvent	H_1	H_2'	H_2	H_3	H_4	H_5'	H_5	$J_{1,2'}$‡	$J_{1,2'}$‡	$J_{2',2}$§	$J_{2',3}$	$J_{2,3}$	$J_{3,4}$	$J_{4,5}$	$J_{4,5'}$	$J_{5',5}$§
4*c*	Mesyl	Mesyl	$CDCl_3$	5.52	7.86	7.86	5.05	5.15	5.82	6.4	6.4	3.1	—	—	—	—	2.4	5.0	−12.7
4*c*	Mesyl	Mesyl	DMSO-d_6	5.52	8.22	7.9	5.09	5.15	5.99	6.36	8.0	2.5	∼−12.7	∼10.5	∼4.7		1.5	3.5	−13.2
4*a*	Acetyl	Acetyl	$CDCl_3$	5.6	∼8.05		5.03	4.95	5.99	6.47	7.4	3.2	—	—	—	—	2.0	3.4	−12.8
4*a*	Acetyl	Acetyl	DMSO-d_6	5.51	∼8.15		4.95	5.02	6.11	6.39	8.5	2.6	—	—	—	—	1.8	3.0	−13.0
4*d*	Methyl	Methyl	CCl_4	5.72	8.08	8.25	6.55	6.75	6.02	6.75	6.8	3.1	−12.8	8.7	4.5	—	—	—	—
4*d*	Methyl	Methyl	$CDCl_3$	5.6	8.02	8.02	∼6.5		5.81	—	7.0	3.5	−12.7	—	4.0	—	—	3.6	∼−12.3
4*d*	Methyl	Methyl	DMSO-d_6	5.7	8.21	8.39	∼6.6		6.03	—	8.4	2.6	−12.5	—	—	—	—	3.1	−12.5
4*d*	Methyl	Methyl	D_2O‖	6.08	8.57	8.91	∼6.85	∼6.9	6.44	—	8.5	2.6	−12.2	—	—	—	—	3.0	−13.0
4*b*	H¶	H	$CDCl_3$	5.37	8.13	7.93	6.10	∼6.4	∼6.4		3.0	3.0	−14.2	3.6	4.5	—	—	—	—
4*b*	H	H	D_2O**	6.12	∼8.85	∼8.65	∼6.75		6.7	7.07	7.6	2.9	∼−12.2	—	—	—	1.8	∼3.5	∼−12.2

*The compounds have the following general structure:

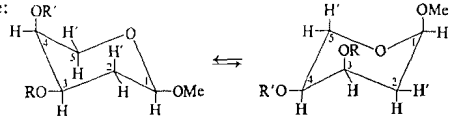

†The chemical shifts are expressed in τ values from TMS as internal standard unless otherwise specified.

‡These values (±0.2 Hz) were calculated from the X part of an AB (2,2′) X(1) system. It is noteworthy that the shape of the H_1 signal was very dependent of the chemical shift of 2 and 2′. In some cases, although the H_1 axial was a triplet, the real coupling constant differed from the spacing by 2 to 3 Hz. In some of the compounds, the calculated $J_{1,2'}$ values agreed well with those derived from the 2-deuterated derivative.

§Assumed to be negative.

‖Pyrazine as internal standard (τ 1.65 versus TMS as external standard).

¶As previously reported (8), the coupling constants, $J_{1,2}$ and $J_{1,2'}$, of the β-anomer are 2.9 Hz, both in $CDCl_3$ and in D_2O.

**TMS as external standard.

Can. J. Chem. Downloaded from www.nrcresearchpress.com by 210.87.254.40 on 09/05/12
For personal use only.

the observed rotation increased from −2.8° to a constant value of +2.27°. Thin-layer chromatographic examination (silica gel, 3:7 methanol–benzene) showed the presence of a compound with R_f about half that of the starting material which was present in trace amount. The solution was neutralized with barium carbonate and the product isolated in the usual manner. The sirup was twice exchanged with deuterium oxide before the determination of its n.m.r. spectrum in this solvent at 100 MHz (TMS external). The spectrum showed signals at τ 4.45 (multiplet), 4.76 (doublet, spacing 3.2 Hz), and 5.22 (doublet, spacing 9.0 Hz). In the spectrum of 2-deoxy-D-ribose under the same conditions, these signals were present but the 2 higher-field signals were in the form of a triplet (spacing 3.6 Hz) and a quartet (spacings 8.2 and 3.0 Hz). The signal at τ 5.22 was assigned to the α-pyranose form (30) and the 9.0 Hz spacing for **4***f* requires the *arabino*-configuration for the main component (75–80%).

Methyl 2-Deoxy-2-deuterio-β-L-arabino-pentopyranoside (5c)

The impure **3**, as mentioned above for the preparation of **5***b*, was deuterolyzed as described for the preparation of **4***e* and **5***c* was obtained from this product as described in the preparation of **5***b*. The melting points of **5***b* and the title compound (**5***c*) were the same. The spacing of the doublet for the anomeric hydrogen at τ 4.69 was 3.0 Hz. Hydrolysis of this glycoside as described above for α-anomer (**4***f*) gave a product with an n.m.r. spectrum in deuterium oxide virtually identical to that of 2-deoxy-2-deuterio-L-*arabino*-pentose obtained from **4***f*. The sugar possessed less of the *ribo*-isomer as evidenced by a much lower intensity of signal corresponding to the anomeric proton of this compound. Thus, the stereoselectivity in the deuterolysis of **3** with inversion of the reacting center was greater than that for **2** which proceeded mainly (75–80%) with retention.

Methyl 2-Deoxy-di-O-(p-toluenesulfonyl)-β-L-erythro-pentopyranoside (5d)

Methyl 2-deoxy-β-L-*erythro*-pentopyranoside containing a small amount of its α-anomer (5.6 g, 0.038 mole) was dissolved in pyridine (25 ml) and treated with *p*-toluenesulfonyl chloride (15.3 g, 0.08 mole) for 2 h at room temperature. The reaction mixture was poured into an ice-water mixture (250 ml) and extracted with 2 × 200 ml of chloroform. The chloroform layer was washed with sodium carbonate solution (2 × 30 ml) then with water, dried over sodium sulfate, and evaporated to dryness. The solid residue was recrystallized 3 times from ethanol. Colorless, fine needles, m.p. 110–111°, $[\alpha]_D^{25}$ 117° (*c*, 1.8 in chloroform) were obtained. These constants were not changed by further recrystallization. The n.m.r. signal ($CDCl_3$ as solvent) showed the presence of the two *p*-toluenesulfonyl groups (singlet with relative intensity 6 at τ 7.55), the methoxy group (singlet of relative intensity 3 at τ 6.72).

dextro-2-Methoxytetrahydropyran (7) (Methyl 2,3,4-Trideoxy-β-L-pentopyranoside)

A mixture of the ditosylate (**5***d*), 6.84 g, sodium iodide, 113 g, zinc dust, 53 g, and *N,N*-dimethylformamide, 190 ml, was refluxed for 2 h without stirring. Fractional distillation at atmospheric pressure using a spinning-band column provided a 25 ml first fraction which contained over 95% of the optical activity. This fraction was diluted with 25 ml of water. The resulting solution and two 25 ml volumes of water were successively extracted with Skellysolve B (20 ml) until the three aqueous solutions were devoid of optical activity. Six extractions were required. The combined extracts were dried and hydrogenated within 1 h at atmospheric pressure in the presence of 5% palladium on charcoal. The catalyst was removed and the solution was concentrated to about 2.5 ml using a spinning-band column for fractional distillation. The distillate boiled in the range 66–67° and was optically inactive. The undistilled fraction was applied to a 20% butanediol succinate column at 65° for preparative gas chromatography using an F&M Prepmaster Model 776. In this way, the title compound (**7**) was purified to the extent that its i.r. spectrum in carbon tetrachloride was superimposable on that of an authentic sample of the racemic 2-methoxytetrahydropyran under the same conditions for measurement. The rotations of the compound in a variety of solvents is given in Table III.

The 6-methoxy-5,6-dihydro[2*H*]pyran intermediate **6** was not isolated for characterization.

Methyl 2,3-Dideoxy-4,6-O-ethylidene-α-D-erythro-hexopyranoside (11a)

Methyl 2,3-anhydro-4,6-*O*-ethylidene-α-D-allopyranoside was converted to methyl 2-deoxy-4,6-*O*-ethylidene-2-iodo-α-D-altropyranoside and this compound tosylated following the procedures described by Lemieux, Fraga, and Watanabe (7) for the sample reactions starting with methyl 2,3-anhydro-4,6-*O*-benzylidene-α-D-allopyranoside. Neither of the compounds crystallized. The tosylated iodohydrin appeared pure but some of the 2,3-unsaturated compound (**10***a*) was present in the product isolated from the tosylation. In order to complete the reduction, this product, 17.5 g, was heated with 0.64 g of tetraethylammonium chloride, 6.4 g of zinc dust, and 100 ml of pyridine at the reflux temperature for 40 min. The product (**10***a*) isolated in the usual manner, was not purified but hydrogenated in the presence of 5% palladium on charcoal in methanol (30 ml) which contained 6 ml of triethylamine. Although **10***a* was not highly pure, the n.m.r. parameters were consistent with the assigned structure as was ascertained by comparison with those of the corresponding 4,6-*O*-benzylidene compound (7). After the hydrogenation, the solvents were removed *in vacuo* and the residue dissolved in water for extraction with benzene. The benzene was removed by distillation at atmospheric pressure and the product purified by distillation at about 15 mm (bath temperature 60°). The yield was 3.0 g of a colorless liquid which gave an n.m.r. spectrum in $CDCl_3$ in complete accord with the assigned structure (**11***a*). The signal for H_1 (unresolved triplet) at τ 5.37 was partly overlapped by the quartet (spacing 5.0 Hz) for the acetal hydrogen of the ethylidene group centered at τ 5.23. The relative intensity of the group of signals in the range τ 5.9 to 6.8 (which includes a sharp signal of relative intensity three for the methoxy group at τ 6.67) was that expected for seven hydrogens (H_4, H_5, $2H_6$, and OCH_3). A multiplet in the range τ 8.08 to τ 8.30 had the relative intensity (4) required for the ethylene group. The methyl signal of the ethylidene group was a doublet (spacing 5.0 Hz) at τ 8.69. The optical rotations in a number of solvents are given in Table IV.

Can. J. Chem. Downloaded from www.nrcresearchpress.com by 210.87.254.40 on 09/05/12
For personal use only.

*Methyl 2,3-Dideoxy-4,6-O-ethylidene-β-D-erythro-hexopyranoside (**11b**)*

As was previously observed for the reaction of methyl 2,3-anhydro-4,6-*O*-benzylidene-β-D-allopyranoside (7), the reaction of methyl 2,3-anhydro-4,6-*O*-ethylidene-β-D-allopyranoside with sodium iodide proceeded with attack at both the 2 and 3 positions. The mixture of these iodohydrins was tosylated as described above and the product was hydrogenated directly under conditions described for the preparation of the α-anomer (**11a**). The product, isolated in the usual manner, was purified by chromatography on silica gel using 3% acetone in chloroform as eluant. After recrystallization from Skellysolve B, the compound (**11b**) melted at 65.5–66.5° and provided an n.m.r. spectrum in $CDCl_3$ in complete accord with the assigned structure. Thus, the ethylidene group provided a quartet (spacing 5.0 Hz) at τ 5.25 and a doublet (spacing 5.0 Hz) at τ 8.66. The methoxy group gave its signal at τ 6.50. In accordance with the axial orientation for H_1 and the strong virtual coupling to be expected between H_1 and the hydrogens at C_3, the signal for H_1 was broad multiplet centered at about τ 5.52. Also, the ethylene group produced a broad multiplet (as compared to the α-anomer) in the range τ 7.8 to 8.6.

The molar rotations of this compound in various solvents are listed in Table IV.

4,4,5,5-Tetradeuterio-2-methoxytetrahydropyran

Freshly distilled 1-methoxy-2-butene-3-yne was converted to pent-3-yne-5-ol-1-al dimethyl acetal following the directions prescribed by Weygand and Leube (16). The latter compound (14 g, 0.1 mole) was reacted with deuterium over 5% palladium on charcoal in 50 ml of ethyl acetate for 7 h at 50 p.s.i. Removal of the catalyst and solvent left a residue which was distilled under reduced pressure [b.p. 70° (1.2 mm)], n_D^{25} = 1.4325. Gas chromatography indicated a high state of purity as did the n.m.r. spectrum which was in general agreement with that expected for 3,3,4,4-tetradeuteriopentane-5-ol-1-al dimethylacetal.

The foregoing compound (0.5 g) was dissolved in dry methanol, 5 ml, containing a small amount (1%) of hydrogen chloride. After 3 h, the reaction was complete as evidenced by the appearance of peak in the gas chromatogram with a retention time equal to that of 2-methoxytetrahydropyran. After neutralization with sodium methoxide, the product (b.p. 124°, n_D^{25} 1.4234) was obtained by distillation at atmospheric pressure. High purity was evident from the gas chromatogram on a 15 ft, 1/4 in. (o.d.) column of diethyleneglycol succinate polyester on Chromosorb at 85°. Also, the n.m.r. spectrum (see Table I) were in good agreement (allowing for the deuteration) with that provided with an authentic sample of 2-methoxytetrahydropyran. The mass spectrum gave the required parent peak at *m/e* 120 and the most important fragments were at *m/e* 90, 89, 61, and 58 in accordance with the fragmentation pattern described by Isser and coworkers (32).

*Tri-O-acetyl-1,2-dideoxy-D-arabino-hexopyranose (**13a**) and Di-O-acetyl-1,2,3-trideoxy-D-erythro-hexopyranose (**14a**)*

These compounds were prepared from 3,4,6-tri-*O*-acetyl-D-glucal (**12**) following the directions reported by Gray and Barker (9). In our experience, based on a gas chromatographic investigation of the product using silicone rubber on Chromosorb at 175°, the dideoxy compound was the main product regardless of the catalyst solvent or presence of diethylamine. The maximum yields of the trideoxy compound was about 20% and were achieved using either platinum or palladium catalysts in ethyl acetate containing diethylamine. In absence of the amine, the yields of this product were less than 5%. Gray and Baker reported yields in order of 85%. The compounds were separated by fractional distillation at 0.7 mm pressure. Compound **13a**, $[\alpha]_D^{25}$ = 33° (*c*, 0.8 in carbon tetrachloride) distilled at 129–130° and **14a**, $[\alpha]_D^{25}$ = 23° (*c*, 0.9 in carbon tetrachloride), at 89–90°.

The structures of the products were confirmed by the following n.m.r. parameters obtained at 100 MHz in hexadeuteriobenzene.

For the dideoxy compound **13a**, the chemical shifts (τ values) were 7.10, 6.48, 8.2–8.6, 8.2–8.6, 5.06, 4.91, 6.81, 5.73, 5.93, 8.27, 8.31, and 8.25 for H_1, H_1', H_2, H_2', H_3 (axial), H_4, H_5, H_6, and H_6', and three acetoxy groups, respectively. First-order coupling constants could be established employing spin decoupling; namely, 11.5, 11.5, 3.6, 4.9, 2.0, 9.5, 9.5, 4.9, 2.5, and 12.0 for $J_{1,1'}$, $J_{1,2}$, $J_{1,2'}$, $J_{1',2'}$, $J_{3,4}$, $J_{4,5}$, $J_{5,6}$, $J_{5,6'}$, and $J_{6,6'}$, respectively.

For the trideoxy compound **14a**, the chemical shifts were 6.93, 6.28, 5.27, 6.66, 5.74, 5.85, 8.22, and 8.19 for H_1, H_1', H_4, H_5, H_6, H_6', and two acetoxy groups, respectively. The first-order coupling constants that could be determined were 11.0, 10, 3.7, 4.3, 2.0, 1.4, 10.0, 5.0, 2.7, and 12, for $J_{1,1'}$, $J_{1,2}$, $J_{1,2'}$, $J_{1',2}$, $J_{1',2'}$, $J_{1',3'}$, $J_{4,5}$, $J_{5,6}$, $J_{5,6'}$, and $J_{6,6'}$, respectively.

Compound **13a** was deacetylated to provide a crystalline product (**13b**) m.p. 79–80° (lit. (9), 76–77°), $[\alpha]_D$ = 14.0° (*c*, 1 in water). Deacetylation of **14a** gave a sirup (**14b**) b.p. 62–63° (0.7 mm), $[\alpha]_D^{25}$ = 40° (*c*, 0.6 in water). The n.m.r. spectra in deuterium oxide were in complete agreement with the assigned structures. In the case of **13b**, the signals of H_6 and $H_{6'}$ were at τ 5.96 and 5.78 and $J_{6,6'}$ = 12.0, $J_{5,6}$ = 5.7, $J_{5,6'}$ = 2.4 Hz were estimated. For **16b**, the signals for H_6 and $H_{6'}$ were at τ 6.02 and 5.80; $J_{6,6'}$ = − 12.0, $J_{5,6}$ = 6.0, and $J_{5,6'}$ = 2.7 Hz were estimated.

The 4,6-*O*-ethylidene derivatives of **13b** and **14b** were prepared in the usual manner using 1,1-dimethoxyethane in the presence of *p*-toluenesulfonic acid. The product (**15**), obtained from **13b**, was purified by preparative gas chromatography using a silicone rubber on Chromosorb column (15 ft × 1/4 in. diam.) at 175°. The n.m.r. spectrum required high purity and the assigned structure. Its optical rotations in the variety of solvents are presented in Table III.

The product **16**, obtained from **14b**, was crystallized in ethyl acetate–petroleum ether and has m.p. 55–56°. The n.m.r. spectrum required the assigned structure and its optical rotation in a variety of solvents are listed in Table III.

Acknowledgments

The authors are indebted to the National Research Council of Canada for generous support

of this research through Grant T-172 to R.U.L. and to the Corn Products Research Foundation for additional financial assistance. The n.m.r. spectra were provided by this Department of Chemistry under the supervision of G. Bigam. Mrs. E. Fraga provided valuable technical assistance.

1. R. U. LEMIEUX and B. FRASER-REID. Can. J. Chem. **43**, 1460 (1965).
2. R. U. LEMIEUX and S. LEVINE. Can. J. Chem. **42**, 1473 (1964).
3. R. U. LEMIEUX and L. ANDERSON. In preparation.
4. R. U. LEMIEUX and A. A. PAVIA. Can. J. Chem. This issue.
5. R. PAUL and S. TCHELITCHEFF. Bull. Soc. Chim. Fr. 869 (1956).
6. R. U. LEMIEUX, K. A. WATANABE, and A. A. PAVIA. Can. J. Chem. This issue.
7. R. U. LEMIEUX, E. FRAGA, and K. A. WATANABE. Can. J. Chem. **46**, 61 (1968).
8. R. U. LEMIEUX and A. A. PAVIA. Can. J. Chem. **46**, 1453 (1968).
9. G. R. GRAY and R. BARKER. J. Org. Chem. **32**, 2764 (1967).
10. R. U. LEMIEUX. *In* Molecular rearrangements. Part 2. *Edited by* Paul de Mayo. Interscience Publishers. 1964. p. 738.
11. R. U. LEMIEUX and J. W. LOWN. Can. J. Chem. **42**, 893 (1964).
12. C. B. ANDERSON and D. T. SEPP. J. Org. Chem. **32**, 607 (1967).
13. R. U. LEMIEUX and A. R. MORGAN. Can. J. Chem. **43**, 2205 (1965).
14. R. U. LEMIEUX and S. SALUJA. Can. J. Chem. In preparation.
15. J. H. BREWSTER. J. Amer. Chem Soc. **81**, 5483 (1959).
16. F. WEYGAND and H. LEUBE. Chem. Ber. 1915 (1956).
17. R. D. GREEN and J. S. MARTIN. J. Amer. Chem. Soc. **90**, 3659 (1968).
18. R. U. LEMIEUX. Abstract of papers, Amer. Chem. Soc. **135**, 5E (1959).
19. H. M. BERGMANN and S. H. KIM. Acta Cryst. **24**, 897 (1968).
20. S. C. CHU and G. A. GEFFREY. Acta Cryst. **23**, 1038 (1967).
21. J. H. ROBERTSON and B. SHELDUCH. Acta Cryst. **19**, 820 (1965).
22. R. O. HUTCHINS, L. D. KOPP, and E. L. ELIEL. J. Amer. Chem. Soc. **90**, 7174 (1968).
23. R. U. LEMIEUX and N. J. CHU. Abstracts of Papers, Amer. Chem. Soc. **133**, 31N (1958).
24. J. T. EDWARD. Chem. and Ind. (London), 1102 (1955).
25. M. A. KABAYAMA and D. PATTERSON. Can. J. Chem. **36**, 563 (1958).
26. C. P. SMYTH. Dielectric behavior and structure. McGraw Hill Book Co. Inc., New York. 1955. p. 253, 301.
27. V. GREY and J. BARTSCH. Liebigs Ann. Chem. **712**, 201 (1968).
28. R. U. LEMIEUX and J. C. MARTIN. In preparation.
29. A. B. FOSTER, R. HARRISON, J. LEHMANN, and J. M. WEBBER. J. Chem. Soc. 4471 (1963).
30. M. GEHRKE and F. X. AICHNER. Chem. Ber. **60**, 918 (1927).
31. R. U. LEMIEUX, R. K. KULLNIG, H. J. BERNSTEIN, and W. G. SCHNEIDER. J. Amer. Chem. Soc. **80**, 6098 (1958).
32. S. J. ISSER, A. M. DUFFIED, and C. DJERASSI. J. Org. Chem. **33**, 2266 (1968).
33. R. C. WEAST. Handbook of chemistry and physics. Chemical Rubber Company, 1969. p. E57.

Can. J. Chem. Downloaded from www.nrcresearchpress.com by 210.87.254.40 on 09/05/12
For personal use only.

Substitutional and solvation effects on conformational equilibria. Effects on the interaction between opposing axial oxygen atoms[1]

R. U. LEMIEUX AND A. A. PAVIA[2]
Department of Chemistry, University of Alberta, Edmonton, Alberta
Received May 5, 1969

Evidence based both on nuclear magnetic resonance and rotation data primarily obtained from methyl 3-deoxy-β-L-*erythro*-pentopyranoside and a number of its derivatives is interpreted to show that the electrostatic repulsion between the oxygen atoms at the 2 and 4 positions is substantially less when these oxygens are linked to acyl groups than when in the form of either methyl ethers or as hydroxyl groups hydrogen bonded to solvent. Also, experimental evidence is presented which requires the hydrogen bridge between two axially disposed hydroxyl groups to be substantially strengthened by hydrogen bonding of the free hydroxyl by solvent.

Canadian Journal of Chemistry, 47, 4441 (1969)

Can. J. Chem. Downloaded from www.nrcresearchpress.com by 210.87.254.5 on 09/05/12
For personal use only.

The purpose of this communication is to report on substitutional and solvation effects on chair–chair conformational equilibria which involve in one conformation an interaction between two oxygen atoms in opposing axial orientation. Profound effects are noted which have an important bearing on the notion that so-called non-bonded interaction free energies can be assigned to such interactions without reference to the kind of compound or to the conditions of the experiment.

As seen in Table I, the coupling constants estimated for the di-*O*-acyl derivatives (**1***b*, **1***c*, and **1***d*) of methyl 3-deoxy-β-L-*erythro*-pentopyranoside (**1***a*) require these compounds to exist largely in the C-1 conformation which has both the acyloxy groups in axial and opposing orientation. That this situation is maintained for solvents of such diverse polarity and chemical nature as carbon tetrachloride, chloroform, acetonitrile, and water in the case of the diacetate is particularly interesting. In all cases, appreciable (0.5–1.7 Hz) long range coupling was observed for the equatorial $H_{5'}$ and related by spin-decoupling to a hydrogen at the 3-position and expected to be the equatorial $H_{3'}$. This coupling together with the small chemical shift between H_3 and $H_{3'}$ [deshielding of H_3 by the methoxy group (1)] supports the evidence provided by the coupling constants that the compounds are in the chair conformation indicated.

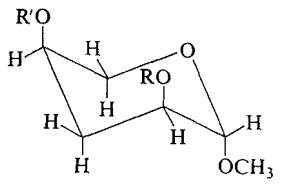

1

a R = R′ = H
b R = R′ = CH_3CO
c R = R′ = *p*-$O_2NC_6H_4CO$
d R = R′ = CH_3SO_2
e R = R′ = CH_3
f R = Ac; R′ = CH_3
g R = H; R′ = CH_3

The main driving force for the compounds **1***b* to **1***d* to adopt the C-1 conformation must be the anomeric effect (2) which favors the axial orientation for the methoxy group. The *gauche* interaction between the C-1 and C-2 substituents in the alternate (1-C) conformation must also be important (3) in this regard, especially for the dimesylate **1***d*. Since the compounds **1***c* and **1***d* maintain the C-1 conformation in dimethylsulfoxide as well as in chloroform and this is also the case for the diacetate **1***b* when dissolved either in deuterium oxide or deuteriochloroform; it is abundantly clear that the preference for the C-1 conformation is not appreciably affected by the dielectric constant of the solvent. An electrostatic attraction between the acyloxy groups could be invoked to explain these results. However, a consideration of molecular models indicates this to be a highly improbable event for 1,3-diaxially disposed acyloxy groups. Most likely, the C-1 conformation is largely adopted because of a weak repulsion which does not effectively oppose

[1]Presented by R. U. L. at the Karl Pfister Lecture, Massachusetts Institute of Technology, Cambridge, Mass., November 15, 1968.
[2]University of Alberta Postdoctoral Fellow, 1967–1968. Present address: École Nationale Supérieure de Chimie, Montpellier, France.

Can. J. Chem. Downloaded from www.nrcresearchpress.com by 210.87.254.5 on 09/05/12
For personal use only.

TABLE I

The n.m.r. parameters for methyl di-*O*-acyl-3-deoxy-β-L-*erythro*-pentopyranosides*

Compound	R	R′	Solvent	Coupling constants (H_z)										Chemical shifts†				
				$J_{1,2}$	$J_{3',5'}$	$J_{4,5}$	$J_{4,5'}$	$J_{5,5'}$	$J_{2,3}$	$J_{2,3'}$	$J_{3,3'}$	$J_{3,4}$	$J_{3',4'}$	$\tau_{5'}$	$\tau_5-\tau_{5'}$	τ_3	$\tau_{3'}-\tau_3$	τ_5
1*b*	Acetyl		CCl_4	2.7	1.5	2.7	2.9	−12.5	—	—	—	—	—	6.50	0.34	—	< ±0.1	—
			$CDCl_3$	2.8	1.5	2.6	2.8	−12.5	—	—	—	—	—	6.40	0.30	—	< ±0.1	—
			CD_3CN	3.0	1.7	2.7	3.4	−12.7	—	—	—	—	—	6.45	0.36	—	< ±0.1	—
			D_2O†	2.8	1.5	2.4	2.4	−12.8	—	—	—	—	—	6.95	0.31	—	< ±0.1	—
1*c*	Benzoyl		DMSO-d_6	—	0.5	3	3	−13.0	—	—	—	—	—	6.15	0.20	—	< ±0.1	—
1*d*	Mesyl		$CDCl_3$	3.0	0.7	2.7	3.7	−12.9	—	—	—	—	—	6.24	0.25	—	< ±0.1	—
			DMSO-d_6	3.3	1.0	3.0	4.0	−12.8	—	—	—	—	—	6.37	0.24	—	< ±0.1	—
	p-Nitrobenzoyl		$CDCl_3$	2.0	0.5	2	2	−12.8	—	—	—	—	—	6.62	0.24	—	< ±0.1	—
1*e*	CH_3	CH_3	CCl_4	6.7	—	—	—	—	5.0	11.0	−12.5	4.5	11	—	—	8.73	1.01	—
			$CDCl_3$	5.7	—	—	—	—	—	—	—	—	—	—	—	8.62	0.75	—
			DMSO-d_6	6.5	—	—	—	—	4.7	10.4	−12.5	—	10	—	—	8.73	1.02	—
			D_2O	5.0	—	—	—	—	5.0	8.0	−12.0	—	8	—	—	9.01	0.73	—
1*f*	Ac	CH_3	CCl_4	5.5	—	—	—	—	5.0	8.0	—	—	—	—	0.6	8.43	0.64	6.75
			D_2O	<3	—	2.5	3.3	−12.2	—	—	—	—	—	—	0.25	7.6	< ±0.2	5.97

*The general structure is:

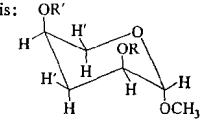

†From TMS as internal standard except for D_2O where pyrazine was used as internal standard and set at τ 2.00.

TABLE II

The n.m.r. parameters for methyl 3-deoxy-β-L-*erythro*-pentopyranoside and derivatives*

Compound	R	R′	Solvent	$J_{1,2}$‡	Chemical shifts (τ)†			
					$\delta_{3'}$	$\delta_{3'}-\delta_3$	$\delta_{5'}$	$\delta_{5'}-\delta_5$
1*a*	H	H	$CDCl_3$	2.2	8.0	$<\pm0.1$	6.4	0.3
			acetone-d_6	3.2	8.30	0.32	6.6	0.4
			pyridine-d_5	4.35	7.97	0.37	–	–
			DMSO-d_6	5.6	8.62	0.61	6.9	0.6
			D_2O§	6.0	7.93	0.68	6.1	0.55
1*g*	H	CH_3	CCl_4	2.2	8.1	$<\pm0.1$	6.3	$<\pm0.1$
			DMSO-d_6	6.0	8.63	0.78	6.83	0.7
			D_2O‖	5.2	8.95	0.61	7.13	0.5

*The general structure:

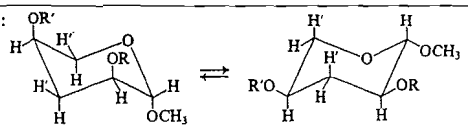

1 (C-1) 1 (1-C)

†Chemical shifts are in τ-values from TMS as internal standard unless otherwise specified.
‡The *J*-values (approx. coupling constants) are expressed in Hz.
§TMS as external standard.
‖Pyrazine as internal standard (τ 2.00).

the non-bonded interactions in the alternate chair. The main interaction between the oxygen atoms in opposing axial orientation must be coulombic repulsion between the unshared pairs of electrons. As will be seen below, these repulsions appear minimized by the presence of strongly electron attracting substituents such as are the acyl groups in compounds **1***b* to **1***d*.

Examination of the nuclear magnetic resonance (n.m.r.) data reported in Table I reveals that, in all solvents studied, the repulsion between the two methoxy groups in compound **1***e* is sufficiently large to effectively overcome the non-bonded interactions in the 1-C conformation. This follows from the magnitudes of the coupling constants of hydrogens in *trans*-relationship on the pyranose ring ($J_{1,2}$, $J_{2,3'}$, and $J_{3',4}$). Thus a substantial increase in the repulsion between the oxygen atoms in axial orientation exists for this compound as compared to those of the di-*O*-acyl analogs unless this change substantially reduces the anomeric effect and the repulsion between the 1- and 2-substituents in *gauche* relationship. This latter possibility is not likely in view of the results obtained for compound **1***f* wherein the 2-substituent is acetoxy and the 4-substituent is methoxy. As for compound **1***e*, the conformational equilibrium favors the 2,4-diequatorial conformer in carbon tetrachloride, a solvent of low dielectric constant. However, in water, the 2,4-diaxial conformer is preferred for **1***f* as is clearly evident from the magnitudes of the coupling constants $J_{1,2}$, $J_{4,5}$, and $J_{4,5'}$. It is known that water has a special ability to weaken the anomeric effect (2). Nevertheless, these results appear best explained by a more *evident* stabilization of a weak coulombic repulsion between an axial acetoxy and an opposing axial methoxy group than when both groups are methoxy and the repulsion is greater. We, therefore, contend that the more electron-rich oxygen atoms of the methyl ether groupings exert a stronger repulsion than that between the relatively much more electron deficient ether oxygens of the acyloxy group when these oxygens are in opposing axial orientation. This conclusion found strong support in the following observations on the solvent effects on the conformational equilibria for the compounds listed in Table II.

The n.m.r. data in Table II require that the diol **1***a* favors the C-1 conformation in solvents which do not form strong hydrogen bonds with the hydrogens of the hydroxyl groups. However, the engagement of these hydroxyl groups in hydrogen bonds with strong proton-accepting solvents such as pyridine, dimethylsulfoxide, and water leads to predominance of the 1-C conformation. This is evident both from the changes in the magnitudes of the coupling of H_1 with H_2 and of the rotations of the solutions (Table III).

It is not possible to arrive at precise knowledge of the equilibria for this conformational change

Can. J. Chem. Downloaded from www.nrcresearchpress.com by 210.87.254.5 on 09/05/12
For personal use only.

TABLE III

Approximate fraction (n) of methyl 3-deoxy-β-L-*erythro*-pentopyranoside in the 1-C conformation

Solvent	$J_{1,2}$ Hz	n (n.m.r.)*	$[\alpha]_D^{25}$	n (rotation)†	Dielectric constant‡
$CDCl_3$	2.2	0	142°	0	4.2
C_6D_6	2.8	0.16	—	—	2.3
$(CD_3)_2CO$	3.2	0.26	131°	0.23	21
CD_3CN	3.4	0.32	127°	0.31	39
C_5D_5N	4.35	0.57	113°	0.60	12.3
$(CD_3)_2SO$	5.6	0.90	99°	0.90	36
D_2O	6.0	1	94°	1	78

*Estimated from the expression $nJ_{1,2}^{D_2O} + (1 - n)J_{1,2}^{CDCl_3}$ = observed $J_{1,2}$.
†Estimated from the expression $n[\alpha]_D^{D_2O} + (1 - n)[\alpha]_D^{CDCl_3}$ = specific rotation taken at the concentration of the n.m.r. solution.
‡At 25° in the absence of deuteration.

in the various solvents. Nevertheless, for purposes of discussion, it is of interest to compare the n.m.r. and rotation data on the assumption that the compound is totally in the C-1 conformation in D_2O. On this basis, the fraction of the compound in the 1-C conformation in each of the solvents is calculated as shown in Table III. The excellent agreement between the estimates based on the n.m.r. and rotation data (4) requires the interpretation attached to these data. Furthermore, following Brewster's rules for the calculation of rotations for methyl glycopyranosides (5), the rotation of **1***a* in the C-1 conformation is expected to be 205° and that in the 1-C conformation, 155° and these values are in close correspondence to the molar rotations found in $CDCl_3$ (210°) and in D_2O (140°). It is known (2) that changes in solvent can affect the magnitude of the contributions made by the methoxy group through changes in the relative contributions of the asymmetric conformation units that arise from rotation about the C_1 to OCH_3 bond. These changes, however, are not so large as to obscure the present conclusions that, in contrast to the acylation of the hydroxyl groups of **1***a*, the engagement of both the hydroxyl groups in strong intermolecular hydrogen bonds depletes the C-1 conformation which has the two oxygen atoms in axial orientation.

It is not reasonable to expect the ability of a proton-accepting solvent to destabilize the C-1 conformation to be related to space demand by the solvent molecules hydrogen bonded to opposing axial hydroxyl groups since the resulting complex should not be more space demanding than, for example, the mesyl group. Instead, we propose that the hydrogen bonding of both hydroxyls with solvent (ROH- -S) increases the negative charge on the oxygen atoms through polarization of the O—H bond (RO←H←S) to such an extent that the repulsion of the C—O bond dipoles in opposing axial orientation becomes adequately large to force the compound from the 1-C to the C-1 conformation. It is, of course, not possible to know what the effect of two non-hydrogen bonded hydroxyl groups would be. Clearly in non-basic solvents such as chloroform, the C-1 conformation is stabilized by an intramolecular hydrogen bridge (6) and this intramolecular hydrogen bond will undoubtedly form in the absence of conditions (such as in dimethylsulfoxide and water) which compel intermolecular hydrogen bonding. The following studies of the effect of adding dimethylsulfoxide to solutions of **1***a* in ethylene chloride on the conformational equilibria require that the repulsion between two opposing axial hydroxyl groups be greater because of their external hydrogen bonding than that hypothetical situation wherein both such external solvation and intramolecular hydrogen bonding are absent.

The n.m.r. data in Table II for **1***g* in carbon tetrachloride require the compound to be largely in the C-1 conformation which has the 2- and 4-substituents in axial orientation. This conformation must also be preferred in ethylene chloride. The 1-C conformation is required for **1***g* in dimethyl sulfoxide in view of $J_{1,2} = 6.0$ Hz.

The breaking of the intramolecular hydrogen bond between the C_2—OH and the C_4—OCH_3 groups in methyl 3-deoxy-4-*O*-methyl-β-L-*erythro*-pentopyranoside (**1***g*), which helps maintain the compound in the C-1 conformation when dissolved in dry ethylene chloride, by addition of dimethylsulfoxide, leads to a decrease in specific rotation as seen in Fig. 1. This decrease in rotation is in good agreement with that expected from Brewster's rules for a change in the conformational equilibrium favoring the C-1 conformation in ethylene chloride to that favoring the 1-C

Can. J. Chem. Downloaded from www.nrcresearchpress.com by 210.87.254.5 on 09/05/12
For personal use only.

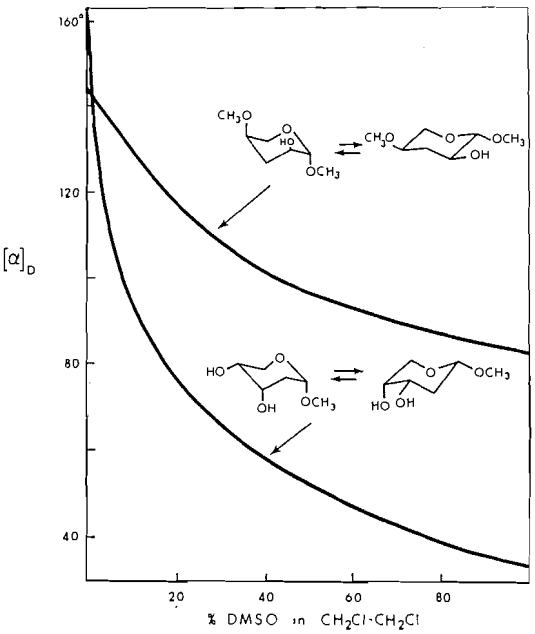

FIG. 1. Effect of increasing concentration of dimethylsulfoxide on the specific rotations at 25° of solutions (about 1%) of methyl 4-*O*-methyl-3-deoxy-β-L-*erythro*-pentopyranoside and of methyl 2-deoxy-α-D-*erythro*-pentopyranoside in ethylene chloride.

conformation in dimethylsulfoxide, the conclusion reached through the n.m.r. studies. It is therefore evident that the repulsion between the C_4—OCH_3 group in axial orientation with the C_2-hydroxyl hydrogen bonded to dimethylsulfoxide is sufficiently strong to require the 1-C conformation as was the case for the di-*O*-methyl derivative (**1***e*). Methyl 2-deoxy-α-D-*erythro*-pentopyranoside behaved in a similar manner and the shapes of these curves are as expected for such phenomena. It may be noted at this point that the pronounced initial changes in rotation on adding dimethylsulfoxide to a solution of the latter compound render this compound interesting as a probe for the study of hydrogen bonding phenomena. It is envisaged, for example, that competition of this compound with other alcohols for dimethylsulfoxide in the range of 2 to 5% in ethylene chloride as measured by the changes in rotation will yield a new approach to the establishment of relative strengths of hydrogen bonds with dimethylsulfoxide or other proton acceptor. These possibilities are under investigation.

The plots shown in Fig. 2 for the effect on rotation of adding dimethylsulfoxide to solutions of the diols shown in ethylene chloride are of extreme importance to this investigation. For the reasons already outlined, the initial numerical increases in rotation are assigned to an increase of that conformation which has the two hydroxyl groups in axial and opposing orientations. This type of plot was also observed in this laboratory for methyl 3-*O*-methyl-β-L-xylopyranoside and for 1,2,3-trideoxy-D-*erythro*-hexopyranoside and seems general for β-diol structures for which intramolecular hydrogen bonding is effective in solvents like ethylene chloride or carbon tetrachloride but which assume an alternate conformation in dimethylsulfoxide wherein both hydroxyls are bonded to solvent.[3] A detailed discussion of this phenomena is reserved for a forthcoming publication (7) where the relative effects of *para* substitution on pyridines used as bases will be described together with thermodynamic analyses of temperature effects. The general conclusions reached confirm the conclusion that at low (~7 moles of dimethylsulfoxide per mole of diol at 1% concentrations of diol) concentrations of dimethylsulfoxide the intramolecularly hydrogen bonded form is at higher concentrations than in pure ethylene chloride. We conclude this behavior to arise from a strengthening of the hydrogen bridge through hydrogen bonding of the remaining free hydroxyl. This result is in line with the above-made contention that the engagement of the hydrogen of an hydroxyl group in a hydrogen bond with a base results in a polarization of the H—O bond in the direction of the oxygen atom. Thus, the oxygen atom becomes a relatively better hydrogen acceptor in hydrogen bond formation. Also, it is at once apparent why the dipole interaction between two opposing axial hydroxyl groups both bonded to solvent is substantially greater than when both the hydroxyl groups are acylated by electron withdrawing acyl groups. These observations likely have a

[3]The data presented in Figure 2 for 1,2-*O*-isopropylidene-β-D-sorbopyranose was the first observation of this phenomenon in experiments by D. Detert in collaboration with R. U. Lemieux and J. A. Mills. A further point of interest was the observation that, for the diol the coupling constant for H_3 and OH_3 was 7.6, 6.5, and 5.0 Hz in 10% v/v, 40% v/v dimethylsulfoxide-d_6-benzene-d_6 mixtures and in dimethylsulfoxide-d_6, respectively. In contrast, H_5 and OH_5 were coupled by 5.0, 5.5, and 6.0 Hz, respectively. The high coupling of H_3 with OH_3 at the lowest concentrations of dimethylsulfoxide indicates that it is the OH_3 proton which is involved in the hydrogen bridge between O_3 and O_5 in the C-1 conformation where the 3-hydroxyl hydrogen defines a dihedral angle of 180° with H_3.

Can. J. Chem. Downloaded from www.nrcresearchpress.com by 210.87.254.5 on 09/05/12
For personal use only.

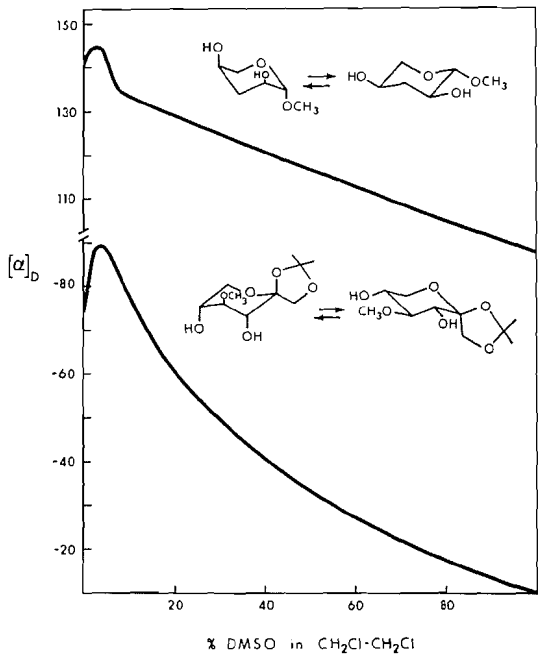

FIG. 2. Effect of increasing concentration of dimethylsulfoxide on the specific rotations at 25° of solutions (about 1%) of methyl 3-deoxy-β-L-*erythro*-pentopyranoside and of 1,2-*O*-isopropylidene 4-*O*-methyl-β-D-sorbopyranoside in ethylene chloride.

bearing on such facts as the A-value of the hydroxyl group being larger in deuterium oxide (1.25 kcal/mole) than in carbon tetrachloride (1.0 kcal/mole) and greater in both cases to the A-value of the acetoxy group (0.66 kcal/mole) (8). Also, the repulsion between the hydroxyl groups in *trans*-1,2-cyclohexanediol appeared to increase when the solvent was changed from deuteriochloroform to deuterium oxide (3). The greater preference for the anomeric hydroxyl group of aldopyranoses to occupy the equatorial rather than the axial orientation on changing the solvent from pyridine to water is probably at least in part a result of changes in the dipoles about the anomeric center as a result of the hydrogen bonding of the hydroxyl group with the solvent. As seen in Table III, such equilibria are more sensitive to the chemical nature of the solvent than on the dielectric constant. Similar specific solvation effects were demonstrated to influence the magnitude of the anomeric effect (2).

As a result of these studies, we conclude that meaningful conformational analyses involving non-bonded interactions between atoms which have unshared pairs of electrons will require a consideration of the substituents on these atoms either as chemically bonded groups or as solvates whether or not these substituents are sterically disposed for appreciable interaction. Furthermore, we contend to have gained evidence that the polarizations which occur as a result of an hydroxyl group becoming hydrogen bonded to a proton acceptor render the oxygen atom a better proton acceptor for hydrogen-bond formation. Such *hydrogen-bond conjugation* can conceivably be of importance as a force which originates in an anionic center for the organization of macromolecules into specific conformations as are known to exist for proteins and nucleic acids. Certainly, the results require the proton-accepting power of a solute in aqueous solution to be extended by this *hydrogen-bond conjugation* to influence the structure of the water beyond its immediate environment.

Experimental

The optical rotations were measured with an automatic Perkin Elmer 141 polarimeter using a thermostatted 10 cm tube. The solvents were purified by distillation and stored over Linde 4A molecular sieve. All solutions were made up and handled using syringes under strictly anhydrous conditions. The experimental points from which the curves in Figs. 1 and 2 were drawn did not deviate from the values provided by the width of line presented and were highly reproducible.

The preparations and further characterizations of the compounds **1***a* to **1***g* are reported in a separate communication (9). The 1,2-*O*-isopropylidene-4-*O*-methyl-β-D-sorbopyranose (Fig. 2) was prepared as described by Ohle and Just (10). The pure material melted at 118–119°, $[\alpha]_D$ −74° (*c*, 1 in ethylene chloride).

Acknowledgment

This research was supported by grant A-172 to R.U.L. from the National Research Council of Canada.

1. R. U. LEMIEUX and J. D. STEVENS. Can. J. Chem. **43**, 2059 (1965).
2. R. U. LEMIEUX, A. A. PAVIA, J. C. MARTIN, and K. A. WATANABE. Can. J. Chem. This issue.
3. R. U. LEMIEUX and J. W. LOWN. Can. J. Chem. **42**, 893 (1964).
4. R. U. LEMIEUX and A. A. PAVIA. Can. J. Chem. **46**, 1453 (1968).
5. J. H. BREWSTER. J. Amer. Chem. Soc. **81**, 5483 (1959).
6. R. U. LEMIEUX and S. LEVINE. Can. J. Chem. **42**, 1473 (1964).
7. R. U. LEMIEUX and J. BREWER. In preparation.
8. R. A. L. ANET. J. Amer. Chem. Soc. **84**, 1053 (1962).
9. R. U. LEMIEUX, K. A. WATANABE, and A. A. PAVIA. Can. J. Chem. This issue.
10. H. OHLE and F. JUST. Ber. **68**, 601 (1935).

Can. J. Chem. Downloaded from www.nrcresearchpress.com by 210.87.254.5 on 09/05/12
For personal use only.

Can. J. Chem. Downloaded from www.nrcresearchpress.com by 210.87.254.42 on 09/05/12
For personal use only.

Auto-oxidation of tetrakis-(*p*-dimethylaminophenyl)-ethylene

R. M. ELOFSON AND K. F. SCHULZ
Research Council of Alberta

AND

R. B. SANDIN
Department of Chemistry, University of Alberta, Edmonton, Alberta

Received April 3, 1969

Tetrakis-(*p*-dimethylaminophenyl)-ethylene (**1**) dissolved in benzene and a small amount of acetic acid is oxidized by air and in time sets to a gel. The reaction products are formaldehyde, formylated and demethylated substances, peroxides, and there is evidence for the formation of polymeric peroxides. The latter are believed to bring about the gelation. The oxidation of **1** is autocatalyzed by a complex between oxygen and **1** in the presence of acetic acid.

Canadian Journal of Chemistry, 47, 4447 (1969)

Introduction

Tetrakis - (*p* - dimethylaminophenyl) - ethylene (**1**) can be oxidized by two one-electron transfers by a variety of reagents such as chlorine, silver nitrate, ferric chloride, and lead tetraacetate to the dication (**2**). Buckles and Meinhardt (1) have made a careful study of the halogen arylated ethylene complexes and have established the ionic character of these complexes. In non-aqueous solvents, **1** and iodine undergo a reversible one-electron transfer to produce a cation radical (2,3). In aqueous solvents, **1** and iodine afford the diiodide.

$$[(CH_3)_2NC_6H_4]_2C = C[C_6H_4N(CH_3)_2]_2$$

1

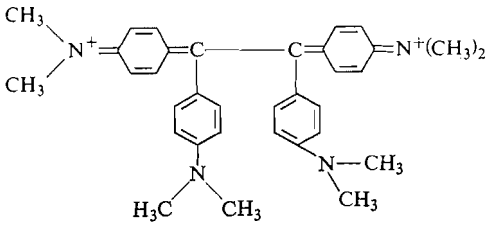

2

The air oxidation of **1** has been examined by the present authors, using a variety of chemical and physical techniques, and with consistent results. It is felt that the results are pertinent to the work of Conant and Bigelow (4) in which they have shown that the associated free radicals (the ethane) from *sym-p,p'*-tetramethyldiaminohexaphenylethane and *p,p,p',p'*-octomethyltetraminohexaphenylethane on exposure to oxygen decompose with the evolution of formaldehyde. It is also felt that the present results are pertinent to the extensive work carried out by Horner and co-workers (5). The latter work has been discussed by Walling (6). Again it may be that the air oxidation of **1** is relevant to what has been shown for the oxidation of the electron rich *N,N,N',N'*-octamethyltetraminoethylene (**3**), (7).

Experimental

Tetrakis-(p-dimethylaminophenyl)-ethylene (1)

This material was prepared according to Willstätter and Goldman (8) and was purified by three recrystallizations from benzene.

Oxidation of 1

A solution of 4.0 g of **1** in 200 ml of benzene and 20 drops of acetic acid was allowed to stand in air at room temperature and in the absence of light for 48 h. At the end of this time the reaction mixture had become a green gel which was broken up with a stirring rod, washed with benzene, filtered, and air-dried to give 3.0 g of solid material A. On standing the solid became black and evolved formaldehyde which was collected in water and characterized as the dimedon derivative, m.p. 193–194°. A mixture melting point with an authentic sample of the dimedon formaldehyde derivative showed no depression. No satisfactory solvent was found for the purification of A. The black product A has been known to evolve formaldehyde for long periods of time (up to 2 mos).

Anal. Found for sample A: C, 76.20; H, 6.64; N, 9.48; O, 7.60.[1]

A second preparation gave a sample, B, which was air-dried for 1 week, was green in color, and evolved formaldehyde, in air, dried over phosphorous pentoxide.

Anal. Found for sample B: C, 74.90; H, 6.57; N, 11.03; O, 8.09.[1]

[1]Microanalyses by Micro-Tech Laboratories, Inc., Skokie, Illinois.

Can. J. Chem. Downloaded from www.nrcresearchpress.com by 210.87.254.42 on 09/05/12
For personal use only.

Many oxidation experiments were carried out and attempts to perform the experiment in the absence of air or acetic acid, and in the presence of octyl alcohol instead of acetic acid, afforded no gel and no change in color of the solution. Also, no gelation occurred when ionol, an inhibitor of free radical chain reactions, was added to the system benzene, acetic acid, and olefin **1**. However, ionol did not inhibit the air oxidation of **1**, in glacial acetic acid, to the dication. Addition of potassium bromide to the glacial acetic acid oxidation mixture afforded a good yield of $\mathbf{1}^{++}\ 2Br^-$. Oxidation in glacial acetic acid was relatively slow, compared with oxidation in the system benzene–acetic acid.

Hydrolysis and Infrared Spectroscopy of Product B

Sample B showed strong infrared (i.r.) absorption at 1670 cm^{-1}. Sample B (5 g) was refluxed with 150 ml of 10% sulfuric acid for 16 h to afford 0.0067 mole of formic acid, identified by a Duclaux distillation and recovered from the first 50 ml of distillate. The peak at 1670 cm^{-1} in the i.r. had decreased to approximately 26% of the original and further refluxing decreased the peak slightly.

Reaction with Raney Nickel

Product B and its hydrolysis derivative from the above experiment were insoluble in the common organic solvents. However, both materials dissolved and no significant change occurred in the i.r. absorption spectra, when they were suspended in isopropyl alcohol and refluxed with Raney Nickel W-2 catalyst (9).

Mass Spectra

A sample of B was examined with a mass spectrometer (A.E.I. type MS9) with a source temperature of 270° and ionizing voltage of 70 eV. Sharp peaks were found at *m/e* 448, 462, 476, 490, 504, 518, 532, 546, and 560. Examination of the 476 and 532 peaks with high resolution indicated the formulas, $C_{31}H_{32}N_4O$ and $C_{33}H_{32}N_4O_3$, respectively. The original olefin had a single strong peak at *m/e* of 504 and a weak peak at *m/e* of 490.

Optical Spectra

Compound **1** (0.8 g) was dissolved in benzene (100 ml) and acetic acid (10 drops) was added. The solution was kept in the dark and exposed to air. Examination of the aliquots taken at various time intervals showed no change in the intensities of the main absorption bands at 300 mμ ($\varepsilon = 48\,750$) and 375 mμ ($\varepsilon = 25\,000$) over a period of 31 h. However, a hypsochromic shift in the absorption became discernable after 23 h and became definite after 31 h, at which time the absorption occurred at 295 mμ and 365 mμ. After 47 h gelation occurred and the supernatant liquid showed maxima at 293 mμ and 360 mμ.

The above experiments were repeated with dilute solutions of **1** and under conditions of controlled oxidation. The olefin (50 mg) was dissolved in benzene (10 ml) and the solution was swept with purified nitrogen. Acetic acid (3 drops) was added and the spectrum shown in Fig. 1, curve *1* was obtained. The solution was now saturated with oxygen for 0.5 h and curve *2* resulted. Curve *3* was obtained by flushing the cell with oxygen for 1.5 h. At this point the cell was sealed and after 35 min curve *4* resulted. Curve *5* was obtained after 17 h and resaturation of the solution with oxygen restored the spectrum of curve *3*. Curve *6* is the spectrum of a solution of the diiodide of **1** in benzene and acetic acid. Pentane was added to the solution corresponding to curve *5* and this afforded a solid which showed formanilide structure in the i.r. spectra. Omission of acetic acid in the above experiment gave a very wide band from 525 mμ to 650 mμ, and of very low intensity, and which we believe is an olefin, oxygen charge transfer band.

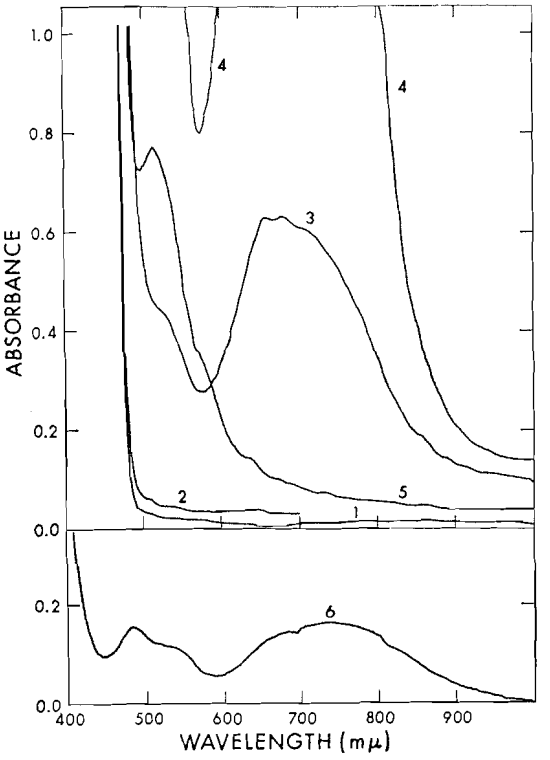

FIG. 1. Absorption spectra: (*1*) compound **1** (50 mg) in benzene (10 ml) and acetic acid (3 drops) and under nitrogen; (*2*) solution swept with oxygen for 0.5 h; (*3*) solution saturated with oxygen (after 1.5 h flushing) and sealed; (*4*) absorption spectrum 35 min after sealing the cell; (*5*) absorption spectrum 17 h after sealing; (*6*) diiodide of **1** (1.38 mg) in benzene (20 ml) and acetic acid (0.5 ml).

Polarographic Studies

In acetonitrile the olefin **1** produced a well-defined anodic wave at +0.25 V vs. saturated calomel electrode (s.c.e.). One gram of **1** was dissolved in 50 ml of benzene containing 5 drops of acetic acid. A 2 ml aliquot taken at zero time when mixed with 15 ml of 0.1 *M* tetrabutylammonium perchlorate, produced no other wave than the anodic wave. After oxidation for 375 min a 2 ml aliquot produced as well as the anodic wave, a mixed anodic cathodic wave at −0.12 V and a much larger cathodic wave at −0.8 to −0.9 V vs. s.c.e. (Fig. 2).

Pyrolysis Experiments

A sample of B was heated to 200° in a sealed tube. Aliquots were chromatographed on a molecular sieve

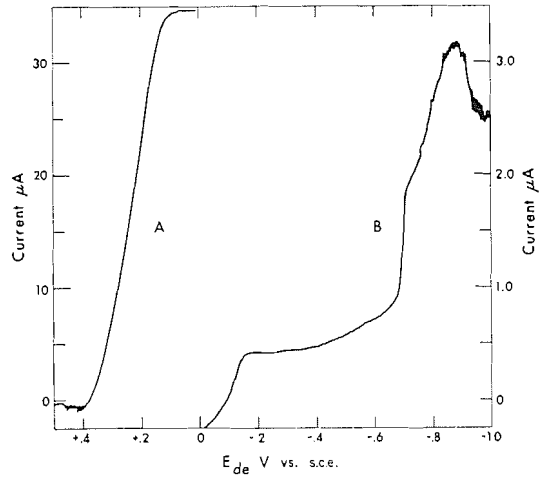

FIG. 2. Polarogram of **1** in 0.1 *M* $(C_4H_9)_4NClO_4$ in acetonitrile and oxidized for 375 min. (*A*) Anodic wave of **1**. (*B*) Waves of peroxides.

(13 × Linde) column. Hydrogen was detected but no other gases.

One gram of **1** was dissolved in 100 ml of benzene and 10 drops of acetic acid added. After standing in the air for 24 h a 5 ml aliquot was withdrawn and mixed with 10 ml of pentane. An i.r. spectrum on the resulting precipitate showed the presence of the formyl group at 1670 cm^{-1}. When the precipitate was heated between 150–200° for 5 min the intensity of the formyl peak increased. Sample B heated on a spatula in a flame burned with a mild explosion.

Oxygen Uptake Experiments

Oxygen uptake was followed manometrically using a Warburg apparatus, Model #66691, made by Precision Scientific Co., Chicago, Illinois. Reaction vessels No. 66703 and manometers No. 66693 were used throughout. A variable induction time was followed by an accelerating rate of oxygen uptake. Furthermore, the oxygen uptake rates were the same for pure oxygen and air, and remained so until near exhaustion of the oxygen in the sealed air reaction vessel. At this point the rate in air fell behind the rate of uptake in the pure oxygen containing vessel (Fig. 3). It is to be noted that in the pure oxygen, over 200 μmoles of oxygen have reacted with only 118 μmoles of **1**, implying secondary reactions (see Discussion). When catechol was added to the system no oxygen uptake occurred. When the acetic acid was reduced to a 1:5 mole ratio, the oxygen uptake was very slow. In pure acetic acid, slow absorption of oxygen occurred at a rate corresponding to that of the induction period (see Fig. 4). It was also found that in the latter case oxidation to the dication (**2**) had occurred and the oxidation corresponded quantitatively to the uptake of oxygen. Also, no evidence of the oxidation of methyl groups could be detected by i.r. analysis. At concentrations of acetic acid comparable to that of the olefin (**1**), the rates of oxygen uptake were roughly independent of acid concentration.

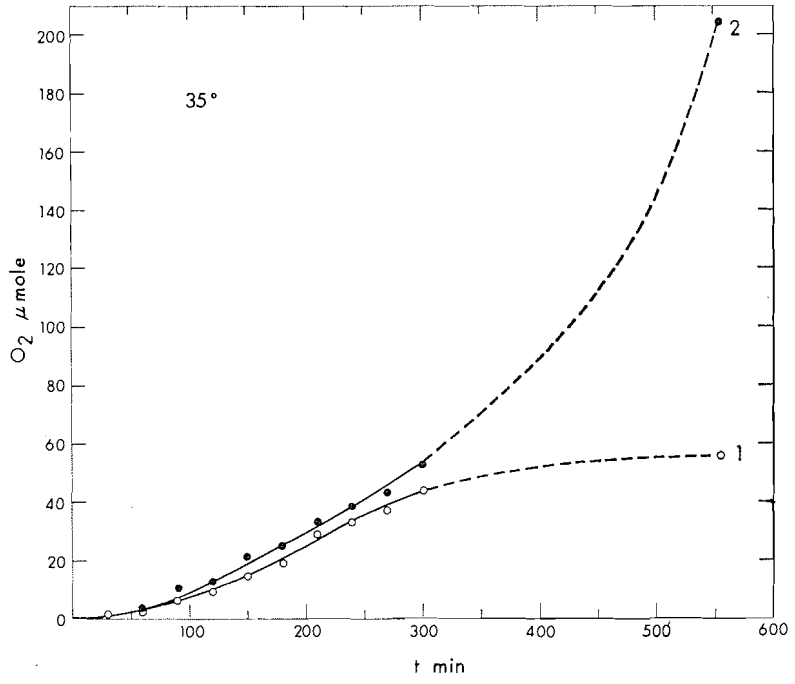

FIG. 3. Oxygen uptake rate: (*1*) olefin **1** (119 μmole) and acetic acid (64 μmole) in 2.8 cm^3 benzene and in air; (*2*) olefin **1** (199 μmole) and acetic acid (64 μmole) in 2.8 cm^3 benzene and in oxygen. All temperatures at 25°.

Can. J. Chem. Downloaded from www.nrcresearchpress.com by 210.87.254.42 on 09/05/12
For personal use only.

Can. J. Chem. Downloaded from www.nrcresearchpress.com by 210.87.254.42 on 09/05/12
For personal use only.

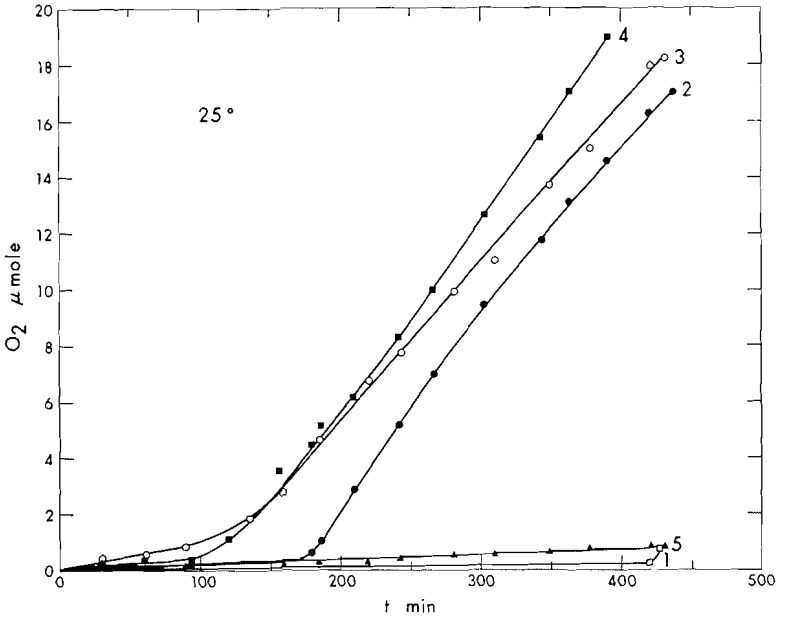

FIG. 4. Oxygen uptake rate: olefin **1** in different amounts of acetic acid and in 2.8 cm³ benzene: (*1*) acetic acid (24 μmole) in air; (*2*) acetic acid (94 μmole) in air; (*3*) acetic acid (140 μmole) in air; (*4*) acetic acid (94 μmole) in oxygen; (*5*) pure acetic acid (44 mmole) in air. All temperatures at 25°.

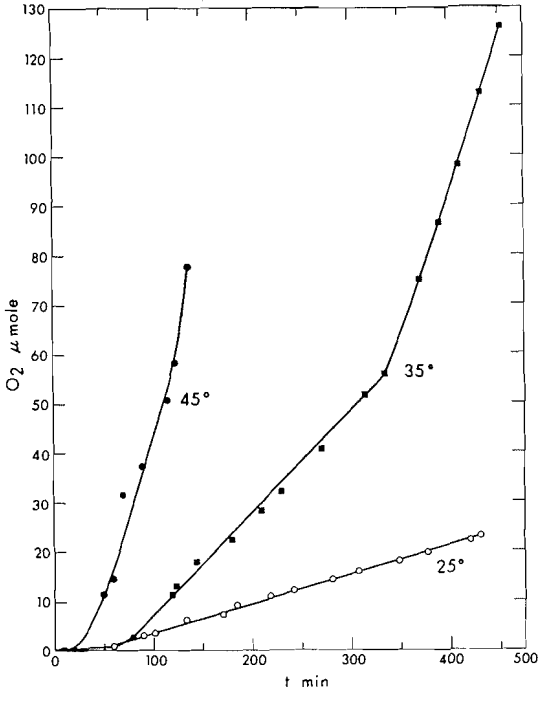

FIG. 5. Oxygen uptake at different temperatures. Olefin **1** (119 μmole) in acetic acid (71 μmole) and benzene (2.8 cm³) and in air.

The induction periods continued to vary in a disconcerting fashion.

The rates of oxygen uptake were dependent on temperature as shown by the results of Fig. 5. These results show an increasing rate of oxygen uptake at a single temperature and a greater increase in rate between 45° and 35° than between 35° and 25°.

Electron Spin Resonance Spectra

Measurements were made with a Varian Model 4500, fitted with a TE102 100 kc cavity and a 100 kc modulation attachment. Sample B showed electron spin resonance (e.s.r.) absorption to the extent of 1.5×10^{18} spins/g of freshly dried solid. The signal consisted of 2 overlapping lines of widths 31.5 and 12.6 G with g values of 2.0071 and 2.0029, respectively. The number of spins dropped rapidly with time at first but reached a steady state (up to 1 year) at about 3.2×10^{17} spins/g.

In the experiment described under polarography the sample taken at 645 min had 1.4×10^{16} spins/ml. After 1175 min the solution had 2.4×10^{16} spins/ml. After gelation had occurred (2400 min) the supernatant liquid still contained free radicals but less than 2×10^{15} spins/ml.

Nuclear Magnetic Resonance Spectra

Measurements were made with an Hitachi Model R20 nuclear magnetic resonance (n.m.r.) spectrometer at 60 Mc, and tetramethylsilane was used as internal reference. Olefin **1** (0.2 g) was dissolved in C_6D_6 (10 ml) in a 20 ml Erlenmeyer flask and left open to the air. After an aliquot was taken for n.m.r. analysis (*A*) acetic acid (1 drop) was added and aliquots for measurements were taken after

Can. J. Chem. Downloaded from www.nrcresearchpress.com by 210.87.254.42 on 09/05/12
For personal use only.

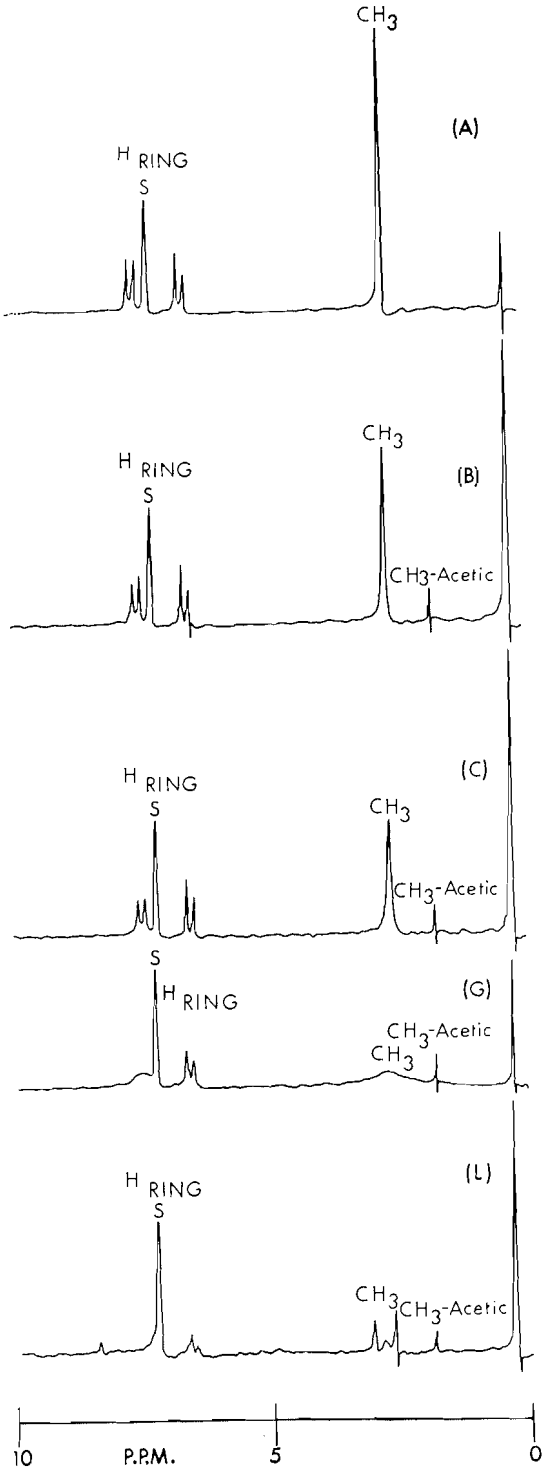

FIG. 6. Nuclear magnetic resonance spectra of reaction mixtures of **1** (0.2 g) in C_6D_6 (10 ml) and acetic acid (one drop) at (*A*) before acetic acid and after acetic acid at (*B*) 3 min, (*C*) 20 min, (*G*) 240 min, (*L*) 4200 min. S denotes C_6H_6 impurity in C_6D_6.

3 (*B*), 20 (*C*), 50 (*D*), 90 (*E*), 170 (*F*), 240 (*G*), 390 (*H*), 420 (*I*), 480 (*J*), 2800 (*K*), 4200 (*L*) min, (Fig. 6).

Discussion

The facile air oxidation of **1** in benzene containing a small amount of acetic acid, and which affords a gel, is undoubtedly a free radical chain reaction. This is demonstrated by the independence of the reaction to oxygen pressure, except at very low concentrations of oxygen. The occurrence of definite but variable induction periods, followed by an increasing rate of oxygen uptake, is also suggestive of a free radical chain reaction (Fig. 4). Moreover, the inhibiting action shown by catechol and ionol indicates a free radical chain mechanism.

Formaldehyde is the only reaction product which has been definitely determined. However, the presence of certain functional groups was established. The formanilide group in the solid reaction material was determined by i.r. spectroscopy. There was strong i.r. absorption at 1670 cm^{-1}. The compound formanilide absorbs at 1673 cm^{-1}. The formyl group was also determined as formic acid by a Duclaux distillation. Demethylated products were considered to be present as a direct result of formaldehyde evolution. Moreover, the optical spectra indicated a hypsochromic shift due to demethylation and (or) formylation.

Polarographic studies indicated the presence of the peroxide function. The cathodic wave at -0.8 to -0.9 V vs. s.c.e. corresponds to what would be expected for a hydroperoxide wave (Fig. 2). The lower wave at -0.12 V may be associated with some oxygen complex of **1**, which is also revealed in the visible spectrum (Fig. 1). The present authors believe that some of the peroxide function is involved in a polymeric peroxide structure and that this may possibly account for the gelation which occurs and which is reproducible. An indication of a possible polymeric peroxide structure is the solubilization which occurs with Raney Nickel treatment. This type of polymeric peroxide would be different from previously isolated addition polymeric

Can. J. Chem. Downloaded from www.nrcresearchpress.com by 210.87.254.42 on 09/05/12
For personal use only.

peroxides (10, 11), since it would be a condensation polymeric peroxide. It is significant that no appreciable change occurred in the i.r. absorption spectra with the Raney Nickel treatment. This supports the view that polymer formation and not formylation was responsible for gelation. In this connection it may also be significant that a sample of the supernatant liquid taken after gelation and mixed with pentane afforded a precipitate which showed intense formyl i.r. absorption, and which was more intense than the i.r. absorption for the solid sample B.

The polymer presumably decomposes in the mass spectrometer to afford a series of formylated and demethylated compounds with mass spectra peaks at *m/e* 448, 462, 476, 490, 504, 518, 532, 546, and 560. The compounds $C_{31}H_{32}N_4O$ and $C_{33}H_{32}N_4O_3$, whose formulae were determined by high resolution mass spectrometry might be formulated as **4** or **5** or their isomers.

From the similarity of the optical spectra of **1** to that of the diiodide under the same conditions (Fig. 1 and ref. 2) we favor a similar complex (cation radical) of **1** with oxygen. The *g* values of the e.s.r. signals which are low and at 2.0029 are suggestive of the cation radical of **1** (2). The broader e.s.r. signals at *g* equal to 2.0071, are probably due to radicals with the electron on oxygen rather than carbon, although these values are low for true peroxy or alkoxy radicals (12).

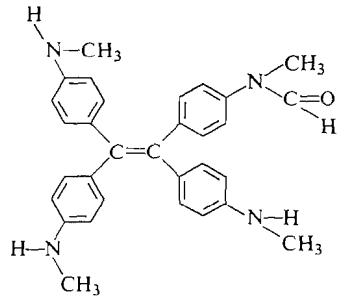

m/e 476

4

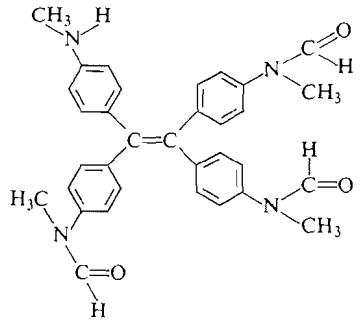

m/e 532

5

A plausible primary oxidation mechanism involves the formation of a cation radical and is shown by Scheme 1*a* and *b*.

Compound **1** + O_2 ⇄ **1** ..... O_2

1 ..... O_2 + HOAc ⇄ $\mathbf{1}^{\cdot+}$ + $\cdot O_2H$ + OAc^-

SCHEME 1*a*

1 .... O_2 + HOAc ⇄

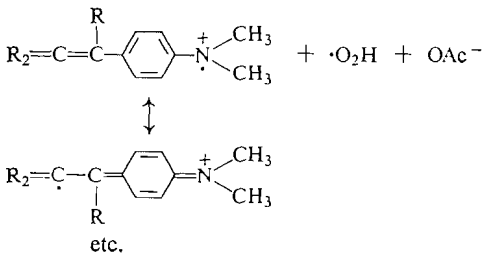

6

R = $(CH_3)_2NC_6H_4^-$

SCHEME 1*b*

It is possible that the small amount of acetic acid adjusts the polarity in favor of **6** and not the separated ion pair (13). Whatever its nature, **6** (the cation radical) disappears under anaerobic conditions to form oxidation products (Fig. 1). Addition of oxygen brings about the reappearance of **6** and from the time course of the formation of **6** (Fig. 1) the reaction must be autocatalytic.

It is interesting that the formulation of the cation radical of **1** is similar to the structures of the dimethylaminophenyl substituted methyl radicals studied by Conant and Bigelow (4). There must be delocalization of the odd electron of $\mathbf{1}^{\cdot+}$ and interaction with the electrons of the C—H bonds of the side chain to account for the reactivity of the C—H bond and which affords such products as formaldehyde and peroxides.

The n.m.r. spectra (Fig. 6) show that line broadening of the spectra occurred almost immediately upon mixing. This is characteristic of the presence of the cation radical **6** in exchange with the parent compound **1** (14). It is to be noted

Can. J. Chem. Downloaded from www.nrcresearchpress.com by 210.87.254.42 on 09/05/12
For personal use only.

that the presence of free radicals is apparent by the n.m.r. technique much sooner than by the conventional e.s.r. experiment. The broadening of all the n.m.r. signals is suggestive of extensive electron delocalization in the free radical. As the oxidation proceeds, broadening increases up to 24 h for some of the aromatic signals. However, at this time, non-broadened signals due to nonparamagnetic products are apparent. Further developments in this direction are impeded by precipitation of products from solution. This experiment leaves little doubt concerning the formation of the ion radical **6** and that it is a key intermediate in the oxidation of **1**. It is possible that **6** is also the intermediate in the oxidation of **1** in pure acetic acid. The complex $\mathbf{1}^{\cdot+} + \cdot O_2H + OAc^-$ would then become $\mathbf{1}^{++} + O_2H^- + OAc^-$. We conclude therefore that oxidation to the dication or oxidation of side chains depends on the polarity of the system.

The insertion of 4 *p*-phenylene groups into the structure of the electron rich *N,N,N',N'*-octamethyltetraaminoethylene (**3**) gives rise to the structure of compound **1** with lowered electron donor strength. This lowering is indicated by the high degree of reversibility shown in the oxidation of **1** by iodine in non-aqueous solvents, and in which an equilibrium exists between $\mathbf{1}^{++}$, $\mathbf{1}^{\cdot+}$, **1**, and elementary iodine. It is also known that **1** adds two atoms of sodium in ether (15), and thereby shows some acceptor character. Compound **3** does not react with lithium in diethylamine (16).

It is quite probable that the relatively higher electron "richness" of **3** accounts for certain differences in the chemical behavior of **1** and **3**. Compound **3** undergoes auto-oxidation in the presence of protonic compounds, emits chemiluminescence and affords high yields of products which involve a cleavage of the C=C bond (7).

In the present work, no split products such as Michler's ketone have been detected in the solid polymer or in the solid from the filtrate. The oxidation of **1** affords side chain products and the molecular skeleton remains intact. The oxidation of **3** lacks an induction period and is dependent on oxygen pressure (17). The reverse of this is indicated for the oxidation of **1**. Very interesting is the fact that ionol, an inhibitor of free radical chain reactions, is an effective catalyst for the oxidation of **3** in cyclohexane (7). Catechol and ionol, on the other hand, prevent the uptake of oxygen in the system compound **1**, benzene, and acetic acid.

While the oxidation of **1** in benzene and acetic acid is a free radical chain reaction, and the oxidation of **3** in hexane and octanol apparently is not (17), the reactions may resemble each other under certain conditions. Thus, according to Urry and Sheeto (7), when dilute solutions of **3** in decane and octanol at $-25°$, or in dioxane at 0°, are shaken with oxygen, an e.s.r. signal develops in 20 min and remains constant for about 2 h, which implies a steady state of chain carrying radicals. Also, Urry and Sheeto oxidized **3** in methanol-d_4 and found a broadening of the n.m.r. spectrum. This is probably indicative of free radical reactions, although the authors did not comment on this fact. Again, it is interesting that Kuwata and Geske (18) found that strong e.s.r. signals occurred during the controlled potential oxidation of **3**.

We believe that the final oxidation products of **1** involve reactions which are similar to those studied by Horner and his students (5,6). One example of this similarity is the formation of the product $C_6H_5N(CH_3)CH_2OOCH_2(CH_3)NC_6H_5$, which Horner found and investigated, and which on pyrolysis gave rise to hydrogen and formanilide. We have found that the pyrolysis of product B increased the formanilide band in the i.r. and also afforded hydrogen. At this time a discussion of a probable mechanism for side chain oxidation is not warranted. It should be mentioned that Horner *et al.* noted that the auto-oxidation of dimethylaniline initiated by benzoyl peroxide afforded a series of reactions as shown

$$(CH_3)_2N{-}C_6H_5 \xrightarrow{O_2} \text{complex}$$

$$\xrightarrow{O_2} C_6H_5N(CH_3)CH_2OOH \rightarrow C_6H_5NHCH_3 + CH_2O$$

$$C_6H_5N(CH_3)CH_2OOH + H^+ \rightarrow C_6H_5N(CH_3)CH_2OO{-}CH_2(CH_3)NC_6H_5.$$

SCHEME 2

in Scheme 2. Since **1** is polyfunctional with respect to this series of reactions, polymer formation, as indicated by gelation, results.

Acknowledgments

We are very grateful for the continued help and encouragement given to us by Professor Harry Gunning. We appreciate very much the

discussions we have had with Drs. W. A. Ayer, R. J. Crawford, D. Darwish, K. Kopecky, and D. Tanner. We are much indebted to Dr. A. M. Hogg, Mr. A. I. Budd, and Mr. J. Olekszyk for the determinations and interpretation of mass spectra. Thanks are due to Mr. John F. Fryer for the pyrolysis experiments. We acknowledge with thanks the financial aid (R.B.S.) of the National Research Council of Canada.

1. R. E. BUCKLES and N. A. MEINHARDT. J. Amer. Chem. Soc. **74**, 1171 (1952).
2. D. H. ANDERSON, R. M. ELOFSON, H. S. GUTOWSKY, S. LEVINE, and R. B. SANDIN. J. Amer. Chem. Soc. **83**, 3157 (1961).
3. R. M. ELOFSON, D. H. ANDERSON, H. S. GUTOWSKY, R. B. SANDIN, and K. F. SCHULZ. J. Amer. Chem. Soc. 85, 2622 (1963).
4. J. B. CONANT and N. BIGELOW. J. Amer. Chem. Soc. **53**, 676 (1931).
5. L. HORNER and E. SCHWENK. Angew. Chem. **61**, 411 (1945); L. HORNER and H. JUNKERMAN. Ann. Chem. **591**, 53 (1955).
6. C. WALLING. Free radicals in solution. John Wiley and Sons, New York, N. Y. 1957. p. 590.
7. W. H. URRY and J. SHEETO. Photochem. and Photobiol. **4**, 1067 (1965); R. W. HOFFMANN. Angew. Chem. Int. Ed. **7**, 754 (1968); N. WIBERG. Angew. Chem. Int. Ed. **7**, 766 (1968); see also F. MCCAPRA. Quart. Rev., London, **20**, 506 (1966) and references cited.
8. R. WILLSTÄTTER and M. GOLDMAN. Ber. **39**, 3775 (1906).
9. R. MOZINGO. *In* Organic syntheses. Coll. Vol. III, John Wiley and Sons, Inc., New York, N.Y. 1955. p. 181.
10. (*a*) F. A. BOVEY and I. M. KOLTHOFF. J. Amer. Chem. Soc. **69**, 2143 (1947); (*b*) A. A. MILLER and F. R. MAYO. J. Amer. Chem. Soc. **78**, 1017 (1956).
11. C. E. BARNES, R. M. ELOFSON, and G. D. JONES. J. Amer. Chem. Soc. **72**, 210 (1950).
12. K. U. INGOLD and J. R. MORTON. J. Amer. Chem. Soc. **86**, 3400 (1964).
13. E. M. KOSOWER. Physical organic chemistry. John Wiley and Sons, Inc., New York, N.Y. 1968. p. 189 and following.
14. E. DE BOER and C. MACLEAN. J. Chem. Phys. **44**, 1334 (1966).
15. W. SCHLENK and E. BERGMANN. Ann. Chem. **463**, 40 (1928).
16. N. WIBERG and J. W. BUCHLER. Unpublished work.
17. A. FLETCHER and C. A. HELLER. J. Catalysis **6**, 263 (1966).
18. K. KUWATA and D. H. GESKE. J. Amer. Chem. Soc. **86**, 2101 (1964).

Can. J. Chem. Downloaded from www.nrcresearchpress.com by 210.87.254.42 on 09/05/12
For personal use only.

Can. J. Chem. Downloaded from www.nrcresearchpress.com by 210.87.254.105 on 09/05/12
For personal use only.

Etude du comportement thermique de l'alcool diméthyl allylique

CLAUDE ROUX[1] ET FRANÇOISE KATZANEVAS
Institut Français du Caoutchouc, Paris, France

Reçu le 15 mai 1969

Le comportement à la chaleur de certains monométhylbuténols a été étudié, sur les produits chromatographiquement purs, en milieu neutre. Le méthyl-3 butène-2 ol, dont la structure peut être rattachée à celle de l'alcool allylique par substitution, possède un comportement particulier. Il subit, en effet, la déshydratation à partir de 140 °C et conduit à la formation d'isoprène, du dimère et du trimère de ce diène et à un polymère dont la structure est, en majorité, celle du polyisoprène 1,4 et 3,4, la structure 1,4 étant prédominante.

Canadian Journal of Chemistry, 47, 4455 (1969)

Introduction

Le mécanisme de la biosynthèse du caoutchouc naturel et des isoprénoides met en jeu des pyrophosphates d'alcényle de structure simple: les pyrophosphates de méthyl-3 butène-2 yle et méthyl-3 butène-3 yle.

Le premier motif des chaînes polyisopréniques serait alors dû au pyrophosphate de méthyl-3 butène-2 yle et tous les motifs suivants au pyrophosphate de méthyl-3 butène-3 yle (1). Dans un milieu différent un autre mécanisme pouvant être envisagé (2).

Il nous a paru intéressant d'étudier le comportement des alcools insaturés correspondant au radical alcényle des pyrophosphates indiqués et, en particulier, la stabilité thermique en milieu neutre.

Ces deux alcools sont le méthyl-3 butène-2 ol et le méthyl-3 butène-3 ol dont les formules semi-développées:

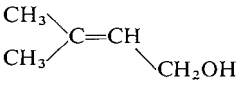

Méthyl-3 butène-2 ol

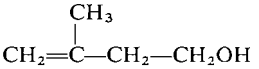

Méthyl-3 butène-3 ol

mettent en évidence l'analogie partielle de structure avec le motif polyisoprénique unitaire:

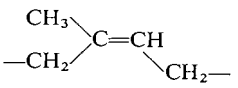

Partie expérimentale

Synthese des Alcools

Méthyl-3 butène-3 ol

Cet alcool a été préparé selon la méthode de Lynen *et al.* (3) et d'Eggerer et Lynen (4), avec un rendement voisin de 40% par rapport au chlorure de méthallyle de départ:

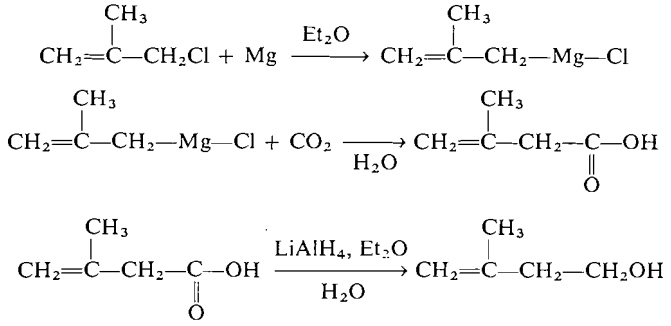

[1]Adresse actuelle: Département de Chimie, Université de Montréal, Montréal, Canada.

Pour éviter la réduction par l'hydrure de lithium aluminium, il est possible de traiter le dérivé organomagnésien par le trioxane à ébullition pendant 72 h; on obtient ainsi directement l'alcool après hydrolyse et le rendement est amélioré d'environ 9% par rapport à la réduction.

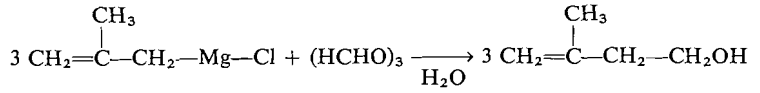

Méthyl-3 butène-2 ol

Trois méthodes ont été utilisées pour la synthèse de cet alcool:

(i) A partir d'acide méthyl-3 butène-2 oique (commercial)

Pour avoir un rendement quantitatif dans un temps raisonnable, il faut tout d'abord sécher l'acide organique parfaitement; on y parvient facilement par extraction azéotropique de l'eau par le benzène; les autres méthodes de dessication ne donnant que des résultats médiocres.

Estérification de l'acide organique par un fort excès de méthanol anhydre en présence d'acide sulfurique en quantité catalytique:

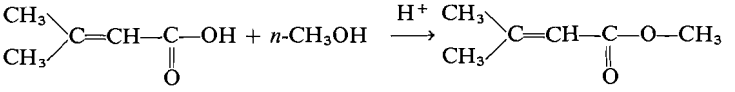

L'ester est ensuite réduit par l'hydrure de lithium aluminium avec un rendement supérieur à celui de la réduction directe de l'acide d'environ 18%.

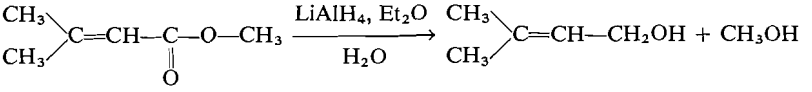

Le rendement moyen sur différentes opérations est de l'ordre de 88% par rapport à l'acide de départ.

(ii) A partir d'isoprène (Claisen)

L'isoprène peut fixer l'acide chlorhydrique en donnant selon les conditions de température, les deux chlorures suivants:

Vers 0 °C on obtient préférentiellement le chlorure tertiaire:

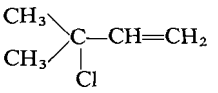

Vers 15–20 °C on obtient préférentiellement le chlorure primaire:

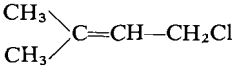

La réaction a été effectuée à partir d'acide chlorhydrique concentré en excès (20% en mole), par simple agitation rapide de l'isoprène et de l'acide aqueux.

Ce chlorure a été transformé en acétate par la méthode préconisée par Halsall et Hands (5).

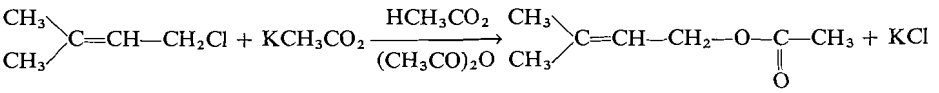

La saponification de cet ester par la soude dissoute dans le méthanol conduit à l'alcool désiré.

Le rendement par rapport à l'isoprène mis en oeuvre est faible et voisin de 11%.

(iii) A partir de méthyl-2 butène-3 ol-2 (commercial)

Vers −20 °C l'action du tribromure de phosphore sur ce carbinol conduit au bromo-1 méthyl-3 butène-2 et non pas au bromo-3 méthyl-3 butène (6)

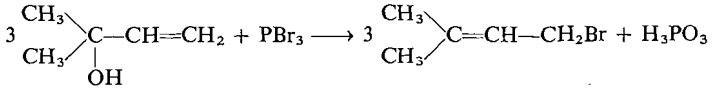

Can. J. Chem. Downloaded from www.nrcresearchpress.com by 210.87.254.105 on 09/05/12
For personal use only.

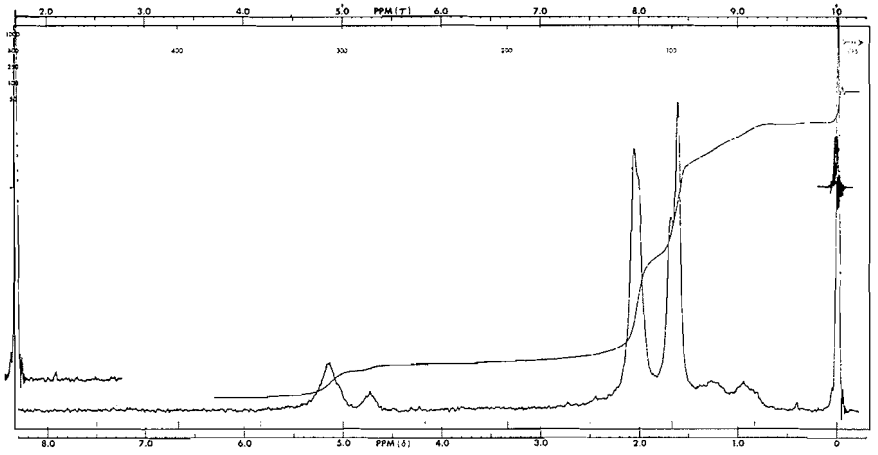

FIG. 1. Spectre r.m.n. du polymère.

Ce bromure primaire traité de la même façon que le chlorure obtenu dans la méthode précédente a fourni l'acétate dont nous avons tiré l'alcool avec des rendements très voisins.

La pureté de ces alcools a été vérifiée par chromatographie en phase gazeuse (c.p.g.) sur une colonne de dix pieds dont la phase liquide stationnaire est constituée de silicones, le gaz vecteur étant l'hélium.

Ces deux alcools avaient été rectifiés plusieurs fois sur colonne à distiller à bande tournante dont l'efficacité théorique est de soixante-dix plateaux.

Les spectres de résonance magnétique nucléaire (r.m.n.) ont été effectués sur appareil Varian A60, en utilisant comme solvant le tétrachlorure de carbone.

Les spectres d'absorption infra-rouge (i.r.) ont été effectués sur appareil Beckmann IR 8, à partir de films de polymère obtenus de solutions.

Les masses moléculaires moyennes en nombre ont été déterminées par tonométrie sur appareil Mechrolab, le solvant utilisé étant soit le chloroforme, soit le benzène.

Les réactions concernant la stabilité des alcools sont faites en tubes scellés, en étuve régulée à ± 1 °C sur les produits purs.

Résultats et Discussion

Il a été constaté que dans des conditions identiques, seul le méthyl-3 butène-2 ol subissait une transformation.

Parmi les produits de la réaction, il a été possible d'isoler les mélanges ou corps suivants, certains identifiés par comparaison avec des témoins en c.p.g. et spectrographie i.r.:

(*a*) de l'eau;

(*b*) un mélange de deux diènes (p.e.$_{760}$ 35–40 °C), dont l'un est de l'isoprène;

(*c*) un mélange des alcools suivants: méthyl-3 butène-2 ol non réagi et méthyl-3 butène-3 ol (p.e.$_{760}$ 128–136 °C);

(*d*) un mélange de deux hydrocarbures (p.e.$_{760}$ 178–182 °C) de formule $(C_5H_{10})_n$ non identifié, mais pouvant correspondre à une dimérisation de l'isoprène ($n = 2$);

(*e*) un liquide (p.e.$_{50}$ 178–180 °C) pouvant correspondre à un trimère ($n = 3$);

(*f*) des traces d'un corps à odeur terpénique très prononcée;

(*g*) un polymère solide.

Parmi les deux diènes, l'un est l'isoprène, l'autre ne peut être, par élimination–déduction, que du méthyl-3 butadiène-1,2 ou diméthylallène dissymétrique (à partir du méthyl butane on ne peut déduire que deux diènes, l'un conjugué, l'autre cumulé).

L'étude en r.m.n. du polymère obtenu a donné les résultats suivants: analogie avec un polymère obtenu par polymérisation thermique de l'isoprène (7). La fig. 1 représente le spectre r.m.n. de ce polymère.

En spectrographie i.r. (7), la même analogie a été constatée. La fig. 2 représente le spectre i.r. de ce polymère.

Les masses moléculaires moyennes en nombre Mn, obtenues à différentes températures de réaction sont données dans le tableau I.

TABLEAU I

Masses moléculaires moyennes en nombre du polymère

Température °C	Mn
140	3,330
150	4,530
180	3,270
200	3,290

Can. J. Chem. Downloaded from www.nrcresearchpress.com by 210.87.254.105 on 09/05/12
For personal use only.

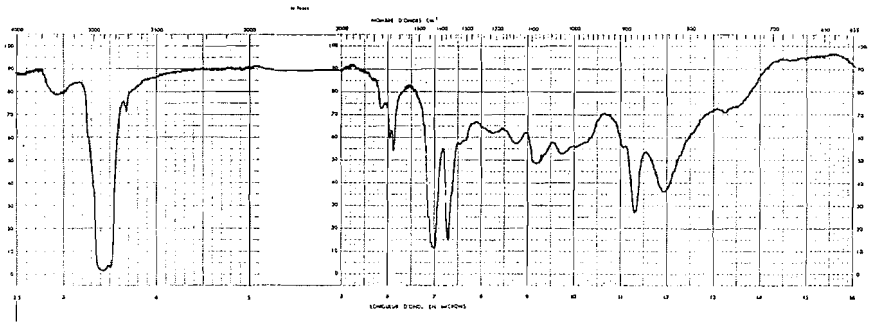

FIG. 2. Spectre i.r. du polymère.

Mécanisme

Pour expliquer la déshydratation de cet alcool, en milieu neutre, l'hypothèse de réarrangement de l'alcool primaire en alcool tertiaire fut envisagée: la facilité de déshydratation des alcools augmente avec la substitution (8). Cette hypothèse fut abandonnée après vérification que le carbinol correspondant (méthyl-2 butène-3 ol-2) ne subissait pas la déshydratation dans les mêmes conditions.

Dans cette réaction qui peut être qualifiée de *Thermique* (en effet, seule l'énergie thermique intervient), l'hypothèse d'un transfert électronique (9) n'est pas à rejeter; elle donne une représentation assez concrète de la réaction, un transfert à six centres pouvant être envisagé:

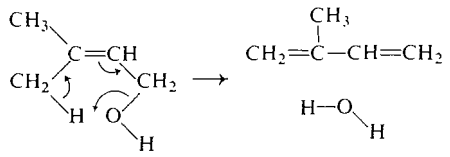

La présence supposée de méthyl-3 butadiène-1,2 (en mélange avec l'isoprène, structure du polymère obtenu) pourrait être attribuée:

(i) Soit à une isomérisation qui a été constatée,

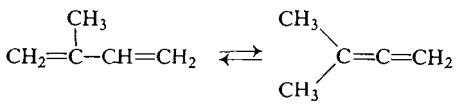

mais dans d'autres conditions (10).

(ii) Soit à une déshydratation du méthyl-3 butène-2 ol, selon un autre mécanisme, peut-être moins favorisé que le transfert à six centres, et qui serait à quatre centres.

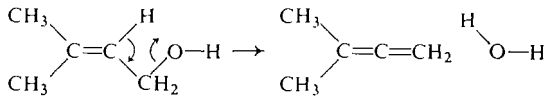

Conclusion

De ces deux alcools, seul celui de structure allylique subit la déshydratation dans les conditions indiquées.

L'étude du comportement des autres isomères se poursuit, en particulier celle du méthyl-2 butène-2 ol dans lequel la double liaison carbone–carbone occupe la même position que dans le méthyl-3 butène-2 ol.

1. F. LYNEN et U. Henning. Angew. Chem. **72** (22), 820 (1960).
2. R. CHÉRITAT, M. BILLUART, R. PAUTRAT, et J. F. PAULET. Institut Français du Caoutchouc. Travaux non publiés.
3. F. LYNEN, H. EGGERER, U. HENNING, et I. KESSEL. Angew. Chem. **70**, 738 (1958).
4. H. EGGERER et F. LYNEN. Ann. 630, 58 (1960).
5. T. G. HALSALL et A. R. HANDS. J. Chem. Soc. **32**, 51 (1961).
6. V. GRIGNARD. Précis de chimie organique, 3ème éd. Masson et Cie, Paris, 1949. p. 248.
7. J. P. KISTLER, G. FRIEDMANN, et B. KAEMPF. Bull. Soc. Chim. no. 12, 4759 (1967).
8. V. GRIGNARD. Précis de Chimie organique, 3ème éd. Masson et Cie, Paris, 1949. p. 297.
9. J. MATHIEU et J. VALLS. Bull. Soc. Chim. 1509 (1957).
10. V. GRIGNARD. Précis de Chimie Organique, 3ème éd. Masson et Cie, Paris, 1949. p. 126.

Can. J. Chem. Downloaded from www.nrcresearchpress.com by 210.87.254.105 on 09/05/12
For personal use only.

Can. J. Chem. Downloaded from www.nrcresearchpress.com by 210.87.254.40 on 09/05/12
For personal use only.

Steroids and steroidases. IX.[1] Activation parameters and the mechanism of base- and enzyme-catalyzed isomerizations of androst-5-ene-3,17-dione. The nature of the active center of the $\Delta^5 \rightarrow \Delta^4$-3-ketosteroid isomerase of *Pseudomonas testosteroni*[2]

J. Bryan Jones and Donald C. Wigfield

Lash Miller Chemical Laboratories, Department of Chemistry, University of Toronto, Toronto 5, Ontario

Received May 28, 1969

Determination of the activation parameters for the acid-, base-, and enzyme-catalyzed isomerizations of androst-5-ene-3,17-dione has revealed that the facility of the enzymic process is mainly due to an extremely low enthalpy of activation of 5.0 kcal mole^{-1}. Further circumstantial evidence regarding the nature of the reacting groups at the active center has also been obtained, and a mechanism of enzyme action is proposed employing tyrosine and histidine as the principal amino acids responsible for catalyzing the isomerization.

Canadian Journal of Chemistry, 47, 4459 (1969)

Introduction

The $\Delta^5 \rightarrow \Delta^4$-3-ketosteroid isomerase of *Pseudomonas testosteroni* is, at the present time, probably the most intensively studied of the enzymes of steroid metabolism, particularly from the mechanistic viewpoint (1). One of the reasons for the interest in this enzyme is that it is the most active yet discovered, having a molecular activity of 16.7×10^6 for the isomerization of androst-5-ene-3,17-dione (**1**) to androst-4-ene-3,17-dione (**2**). The rate of enzymic isomerization is several orders of magnitude greater than those of the related acid- or base-catalyzed processes, and in order to gain an insight into the reasons for the vastly greater efficiency of the enzymic isomerization, the determinations of the activation parameters for the 3 types of catalyses were undertaken.

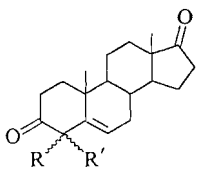

1

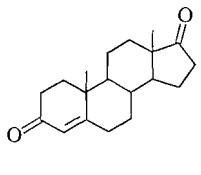

2

Experimental

Compounds

The criteria of purity applied, the methods and analytical instrumentation used, specifications of the chromatographic supplies, solvents, etc. were as described previously (2).

*Androst-5-ene-3,17-dione (**1**, R,R′ = H)*

This compound was prepared by a Pfitzner–Moffatt oxidation of 3β-hydroxy-androst-5-en-17-one (2).

*4,4-Dideuterioandrost-5-ene-3,17-dione (**1**, R,R′ = D)*

Androst-5-ene-3,17-dione (100 mg) in methanol-*d* (1.5 ml) was heated under reflux for 36 h. The solution was then concentrated to half-volume by rotary evaporation at 20° and on cooling the resulting solution to −20°, deuterated androst-5-ene-3,17-dione (65 mg) crystallized out. Thin-layer chromatographic (t.l.c.) and infrared (i.r.) analyses showed traces only of isomerized androst-4-ene-3,17-dione contaminants. Deuterium elemental analysis[3] indicated 4.80 atom% excess of deuterium which corresponds overall to 80% exchange of two hydrogen atoms. From the relative intensities of the mass spectral peaks at *m/e* 286, 287, 288, and 289 respectively, the deuterated androst-5-ene-3,17-dione sample was estimated to consist of unchanged starting material **1** (R,R′ = H) (8.9%); **1** (R = H,R′ = D) (25.2%); the required dideutero compound **1** (R,R′ = D) (63.2%); and a trideutero compound (2.8%). That the main exchange had occurred at C-4 and not elsewhere in the molecule was confirmed by the kinetic isotope effect of 4.1 observed for the acid-catalyzed isomerization reaction.

Phenolic Compounds

2-, 3-, and 4-Hydroxypyridine, phenol, and *p*-nitrophenol were obtained commercially (Aldrich or B.D.H.) and were recrystallized to constant melting point and until each sample showed only a single spot on t.l.c. analysis.

3,4-Dinitrophenol

This compound was prepared by nitration of *m*-nitrophenol (2.5 g) with 6 *N* nitric acid (3). Separation of the desired product from 2,3-dinitrophenol and 2,5-dinitrophenol was achieved by the fractional crystallization procedure recommended (3). Chromatography of

[1]For Part VIII of this series, see J. B. Jones and J. M. Zander (20).

[2]Reported in part at the 50th Canadian Chemical Conference, Toronto, June 1967 and at the 5th I.U.P.A.C. International Symposium on the Chemistry of Natural Products, London, July 1968.

[3]Performed by Mr. J. Nemeth, Urbana, Illinois.

Can. J. Chem. Downloaded from www.nrcresearchpress.com by 210.87.254.40 on 09/05/12
For personal use only.

the product so obtained on Florisil with benzene – ether (1:1) elution yielded 3,4-dinitrophenol, pale yellow needles from benzene (0.45 g) m.p. 133–134° (lit. (3) m.p. 134°); i.r. ($CHCl_3$) ν_{max} 3597 and 1344 cm^{-1}.

Imidazole (Eastman White Label)

This compound was recrystallized twice from benzene prior to use to give needles m.p. 89.5–90°.

General Isomerization Kinetics Procedures

All isomerizations and treatment of data[4] were carried out as described previously (4). As before all runs were carried out at least twice and the reproducibility was ±3% except for the variable temperature enzyme catalyzed reactions. For the latter the errors were within the limits ±6%.

Base-catalyzed Isomerizations of Androst-5-ene-3,17-dione by Aqueous Sodium Hydroxide Solutions of Varying pH

A 40% (w/v) stock solution of sodium hydroxide in CO_2-free distilled water was prepared and was then stored in an air-tight polyethylene bottle. Successive dilutions of this solution with CO_2-free distilled water gave solutions with p*H* within the desired range of 10.5–12.0. To avoid the involvement of activity coefficients the p*H* of each solution was determined directly with a p*H* meter. Kinetic data were obtained with 3.0 ml reaction volumes of the following composition: aqueous sodium hydroxide solution of known p*H* (2.95 ml), methanolic 0.05% androst-5-ene-3,17-dione solution (0.05 ml). Absorbance measurements were taken against a control cuvette containing no steroid.

The pseudo first order rate constants calculated for the various p*H* values are recorded in Table I.

C-4 Deuterium Kinetic Isotope Effect for Base-catalyzed Isomerizations of Androst-5-ene-3,17-dione

Kinetic data were obtained as described above using an aqueous sodium hydroxide solution of p*H* 10.0 as the catalyst. The pseudo first order rate constants for androst-5-ene-3,17-dione and the deuterated sample containing 63.2% of 4,4-dideuterioandrost-5-ene-3,17-dione were 0.148 and 0.046 min^{-1} respectively.

Determinations of the Activation Parameters for the Acid-, Base-, and Enzyme-catalyzed Isomerizations of Androst-5-ene-3,17-dione

Acid- and base-catalyzed isomerization studies were carried out on solutions composed of 2.95 ml of aqueous hydrochloric acid p*H* 0.88, or 0.05 *M* Tris[5] – HCl buffer solution p*H* 8.82, respectively, to which was added 0.05 ml of an 0.05% methanolic androst-5-ene-3,17-dione solution. Rates were measured at ~5° intervals between 15 and 40°. The enzyme-catalyzed reactions were studied as described previously (4) and the initial isomerization rates were determined at ~5° intervals in the range 15–30°. All temperatures were measured with a U.S. National Bureau of Standards thermometer and are accurate to within ±0.03°; a correction was made for the small temperature differential between the thermostatted bath and the reaction cell jacket.

For the acid- and base-catalyzed isomerizations, the pseudo first order rate constants obtained were converted to the appropriate second order rate constants using the p*H* of the solutions as a guide to the respective hydrogen ion and hydroxide ion concentrations. The relative initial rates of enzymic isomerization were converted to the respective first order rate constants using the value of 16.7×10^6 for the molecular activity[6] of the isomerase at 25° (1). The relevant data are quoted in Table II. Arrhenius plots gave good straight lines in each case and the activation parameters were calculated by the standard methods (5, 6) and are recorded in Table III.

Catalysis by Hydroxypyridines, Phenols, and Imidazole

The data on the effect of 2-, 3-, and 4-hydroxypyridine, phenol, *p*-nitro-, and 3,4-dinitrophenol, and of imidazole on the isomerization of **1** (R,R′ = H) to **2** were obtained with 3.0 ml reaction volumes made up of 0.05 *M* Tris – HCl buffer solution p*H* 8.58 (2.90 ml) containing the catalyst (0.14 μmole ml^{-1}) and methanolic substrate solution (0.81 μmole ml^{-1}; 0.10 ml). The pseudo first order rate constants k'_{cat} describing the net effect of the catalysts were obtained by subtraction of the rate constant of the uncatalyzed isomerization determined under the same conditions. The results are summarized in Table IV.

Results and Discussion

A prerequisite to any meaningful comparison of the acid-, base-, and enzyme-catalyzed processes is a knowledge of the rate determining step for each isomerization pathway.

The mechanism of the acid-catalyzed isomerization of Δ^5-3-ketosteroids has been studied by Nes and his co-workers (7) who showed the reaction to be first order with respect to both steroid and to hydrogen ion concentrations, and by Malhotra and Ringold (8) who observed a primary deuterium kinetic isotope effect of 4.1 when the C-4 hydrogen atoms of the substrate were replaced by deuterium. These data support the mechanism proposed (8) in which protonation of the C-3 carbonyl group is followed by rate determining loss of a C-4 hydrogen during the enolization step. The enzyme catalyzed isomerization was similarly shown to proceed with rate

[4]Typical sets of data for each type of isomerization condition are recorded in the Ph.D. thesis of D. C. Wigfield, University of Toronto, 1967.

[5]Tris(hydroxymethyl)aminomethane.

[6]The molecular activity (16.7×10^6) can be regarded as the first order rate constant for the rate determining step of the formation of products from the enzyme-**1** (R,R′ = H) complex at 25° at p*H* 7.0 (1). The arbitrary first order rate constants k' obtained at various temperatures were converted to the true relative rate constants k by multiplication by $16.7 \times 10^6/k'_{25°}$.

Can. J. Chem. Downloaded from www.nrcresearchpress.com by 210.87.254.40 on 09/05/12
For personal use only.

determining C-4β proton loss,[7] the deuterium kinetic isotope effect being 5.35 (8).

Analogous mechanism of action studies had not been carried out on the base-catalyzed reaction partly due to the complications of multiple product formation encountered initially (7). However the subsequent delineation of satisfactory conditions for base-mediated isomerizations (4) enabled a mechanistic study of the process to be carried out.

The previous data on base isomerizations of androst-5-ene-3,17-dione (**1**, R,R′ = H) and other Δ^5-3-keto steroids, had demonstrated a first order dependence on the steroid concentration (4). In order to determine the order of reaction with respect to the hydroxide ion, the p*H* dependence of the pseudo first order rate constant for androst-5-ene-3,17-dione isomerization was determined. Aqueous sodium hydroxide solutions, rather than buffer solutions of the same p*H*, were used in order to avoid any possible influence by the components of the buffer. The data obtained are summarized in Table I. The restriction of the p*H* range studied to 10.61–11.72 was dictated by two factors: at p*H* values > 12.0 the half-life of the reaction (~10 s) was too small for accurate measurements to be made and at p*H* < 10.0, the possibility of multiple product formation existed. A plot of $\log_{10}k'$ against p*H* gave a straight line (Fig. 1) of unit slope, thus showing the reaction to be first order with respect to the hydroxide ion. Thus both the acidic and basic catalytic processes are second order overall.

The next aspect of the base catalysis mechanism considered was the identification of the rate determining step. While it might have been anticipated that, in common with the acid- and enzyme-catalyzed reaction, this would be loss of a C-4 proton during enolization, it was obviously necessary to establish this point before attempting a comparison of the three processes. For this purpose, 4,4-dideuterioandrost-5-ene-3,17-dione (**1**, R,R′ = D) was required. The method which had proven satisfactory for C-4 deuteration of 17β-hydroxyandrost-5-en-3-one, *viz.* heating the Δ^5-3-ketone in D_2O–diglyme (8), caused extensive isomerization of **1** to **2** before deuteration at C-4 was sufficiently complete.[8] This difficulty was obviated by deuteration of **1** (R,R′ = H) in methanol-*d* under reflux. That the sample obtained was predominantly (63.2%) the dideuterated compound **1** (R,R′ = D) was established by the deuterium elemental and mass spectral analytical results, and by the deuterium kinetic isotope effect of 4.1 observed for the acid catalyzed isomerization reaction. These data are in excellent agreement with those reported by

TABLE I

Rates of isomerization of androst-5-ene-3,17-dione as a function of p*H**

p*H*	k' (min^{-1})
10.61	0.29
11.02	0.79
11.28	1.3
11.55	2.8
11.72	3.5

*All measurements taken at 25° with a steroid concentration of 0.03 μmole ml^{-1} using aqueous sodium hydroxide solutions of appropriate p*H*.

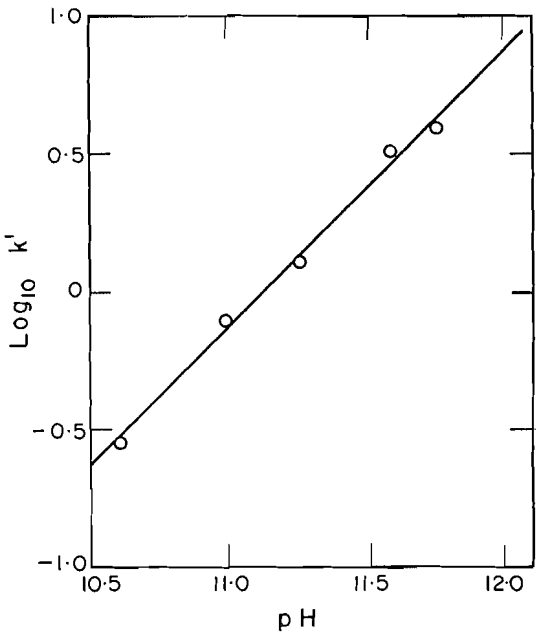

FIG. 1. Plot of $\log_{10}k'$ against p*H* for the base-catalyzed isomerization of androst-5-ene-3,17-dione.

[7]Disappointingly, the data on the stereospecificity of proton abstraction, mechanism of action etc. for mammalian isomerases (9–11) do not parallel those established for the *P. testosteroni* enzyme.

[8]Torgov and his co-workers have also reported isomerization to be a problem in this solvent mixture (11).

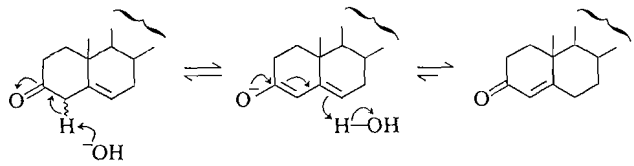

FIG. 2. The mechanism of base-catalyzed isomerization of Δ^5-3-ketones.

Malhotra and Ringold (8) for the analogous 17β-hydroxy substrates.[9]

The k_H/k_D ratio observed for the base-catalyzed isomerizations of **1** (R,R′ = H) and **1** (R,R′ = D) was 3.2 thus establishing that, as for the acid and enzyme reactions, loss of the C-4 hydrogen atom is the rate determining step. The initial runs were carried out in Tris – HCl buffer solutions of p*H* 8.82 (which provided an optimum rate of reaction for measurement purposes) and the data obtained indicated that deuterium–hydrogen exchange prior to isomerization might be occurring at a significant rate. Re-examination of the isomerization in aqueous sodium hydroxide solution of p*H* 10.0 confirmed this view and when the results were treated in the usual first order manner, a plot was obtained that curved upwards until eventually a straight line was obtained whose slope was equal to that observed previously for the isomerization of the non-deuterated substrate. The effect of this competitive C-4 deuterium exchange reaction was minimized by taking readings every few seconds for the first 3 min of the reaction. The first order plot based on such measurements afforded a relatively straight line from which the kinetic isotope effect value of 3.2 was obtained. The fact that this value is slightly smaller than the 4.1 obtained for the acid-catalyzed process is probably due, at least in part, to our inability to eliminate completely the effect of the C-4 exchange process. The total data are consistent with the mechanism proposed in Fig. 2. Removal of a C-4 hydrogen by a hydroxide ion gives the enolate anion which can reprotonate either at C-4 to regenerate the starting material, or at C-6 to give the product. In view of the observed facility of the deuterium exchange process, it seems likely that the intermediate enolate anion may pick up a proton at C-4 and C-6 with comparable ease. At first sight this result might seem to contradict the results of Ringold and Malhotra (8, 12) who have shown that in *t*-butyl alcohol, the enolate anion preferentially reprotonates at C-4 whereas the neutral enol selectively picks up a hydrogen atom at C-6 under conditions of kinetic control. However in the present work the enolate anion was generated in aqueous solution in which it would be expected to be better solvated, and hence more stable, than in *t*-butyl alcohol.

In order to determine the activation parameters for the isomerizations catalyzed by acid, base, and enzyme, the rates were measured at various temperatures. The acid- and base-catalyzed rates of isomerization of androst-5-ene-3,17-dione were measured at 5° intervals between 15 and 40°, and the pseudo first order rate constants obtained were converted to the corresponding second order rate constants by dividing by the hydrogen ion and hydroxide ion concentrations[10] respectively. The corresponding measurements on the enzyme-catalyzed reaction were carried out in the temperature range 15–30°. At temperatures greater than 30° the enzyme began to show the effects of heat denaturation. That such inactivation was a reversible process was demonstrated by keeping the enzyme at 40° for 30 min, and then reassaying it at 25°. No detectable loss of activity was apparent. The

[9]The deuteration patterns of the substrates used by Malhotra and Ringold (8) and in this investigation are very similar, thus enabling direct comparisons to be made of the kinetic isotope effects observed in this and the previous (8) investigation. In neither study have the k_H/k_D values been corrected for the presence of non-C-4 deuterated species in the samples assayed.

[10]These were calculated from the p*H* of the reaction solution. 0.05 *M* Tris – HCl buffer p*H* 8.82 was used as the base-catalyst since the range of isomerization rates was optimized at this p*H* (aqueous sodium hydroxide solution of the same p*H* could not be used since multiple product formation was observed under such conditions (4)). The catalytic effects of the components of the buffer solution on the rate of reaction were not taken into account. This is not considered to affect the validity of the data since (*a*) the buffer used was a dilute one and (*b*) the comparison of dilute Tris – HCl and sodium hydroxide solutions as catalysts in the isomerization and deuterium exchange experiments of **1** (R,R′ = D) showed them to be indistinguishable in their activities.

Can. J. Chem. Downloaded from www.nrcresearchpress.com by 210.87.254.40 on 09/05/12
For personal use only.

TABLE II

Rate constants for the isomerization of androst-5-ene-3,17-dione at different temperatures*

T (°C)	k'	k
(a) Acid (pH 0.88) catalysis		
14.71	0.054 (min^{-1})	0.41 (l $mole^{-1}$ min^{-1})
19.65	0.086	0.65
24.92	0.135	1.02
29.24	0.194	1.47
34.66	0.293	2.22
39.34	0.405	3.07
(b) Base (pH 8.82) catalysis		
14.71	0.227 ($min^{-1} \times 10^2$)	344 (l $mole^{-1}$ min^{-1})
19.65	0.339	513
24.92	0.458	693
29.24	0.643	973
34.66	0.890	1350
39.34	1.060	1600
(c) Enzyme (pH 7.0) catalysis†		
14.71	0.044 (min^{-1})	1.17×10^7 (min^{-1})
19.65	0.053	1.41×10^7
24.92	0.063	1.67×10^7
29.24	0.071	1.88×10^7

*Data obtained with 1.6% aqueous methanol solutions and a steroid concentration of 0.05 μmole ml^{-1}.
†Reversible inactivation of the enzyme occurred at temperatures > 30°.

TABLE III

Activation parameters for the isomerization of androst-5-ene-3,17-dione*

Parameter	Acid	Catalyst base	Enzyme
Activation energy E_A†	14.6±0.1	12.0±0.1	5.6±0.1
Enthalpy of activation ΔH^*†	14.0±0.1	11.4±0.1	5.0±0.1
Entropy of activation ΔS^*‡	−19.6±0.4	−15.5±0.4	−16.8±0.4
Free energy of activation ΔG^*†	19.8±0.1	16.0±0.1	10.0±0.1
Temperature coefficient Q_{10}	2.29	1.97	1.37

*Calculated at 25° from the data recorded in Table II and Fig. 3.
†In kcal $mole^{-1}$.
‡In cal deg^{-1} $mole^{-1}$.

relative rate constants obtained from the rate data were converted to true first order rate constants using the value of 16.7×10^6 obtained by Talalay (1) for the molecular activity of the enzyme with androst-5-ene-3,17-dione as the substrate.

The results are summarized in Table II from which it is seen that the relative rates of isomerizations catalyzed by acid, base, and enzyme are in the approximate ratio 1:700: 1.7×10^7. This demonstrates very dramatically the efficiency of the enzyme relative to the chemical catalysts.

The activation parameters for the three processes were calculated from the appropriate Arrhenius equations. The Arrhenius plots all gave good straight lines (Fig. 3) and the values of the various parameters[11] are recorded in Table III.

From these results it is clear that the great

[11]A preliminary account of these results has been published (13).

Can. J. Chem. Downloaded from www.nrcresearchpress.com by 210.87.254.40 on 09/05/12
For personal use only.

Can. J. Chem. Downloaded from www.nrcresearchpress.com by 210.87.254.40 on 09/05/12
For personal use only.

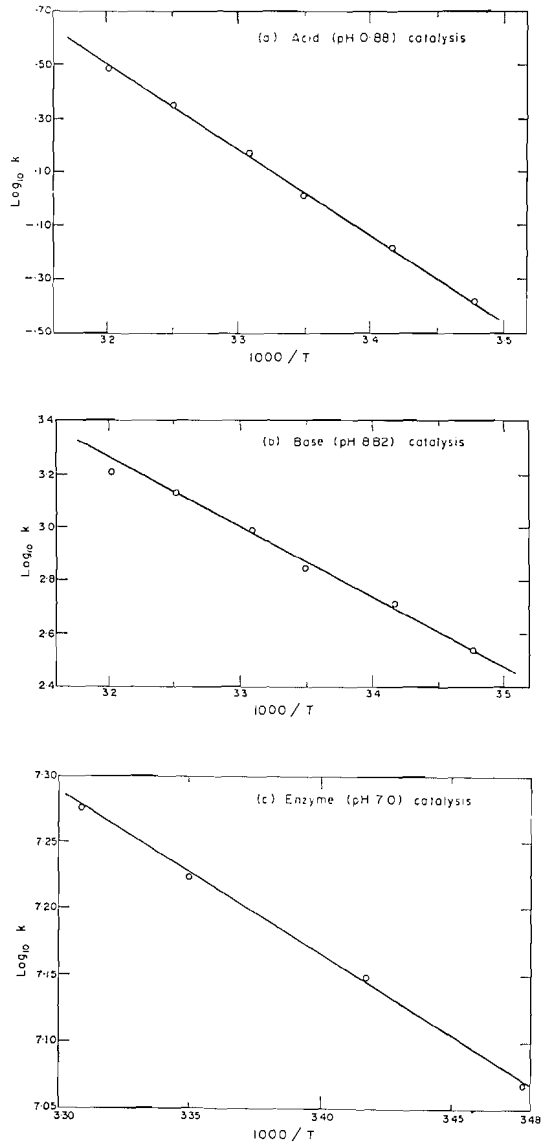

FIG. 3. Arrhenius plots for the isomerizations of androst-5-ene-3,17-dione.

TABLE IV

Catalysis of the isomerization of androst-5-ene-3,17-dione by model compounds*

Catalyst	pK_a	k'_{cat}†
2-Hydroxypyridine	11.62‡	0
4-Hydroxypyridine	11.09‡	7
Phenol	9.98‡	31
3-Hydroxypyridine	8.72‡	150
p-Nitrophenol	7.15‡	13
3,4-Dinitrophenol	5.42§	13
Imidazole		9
Imidazole and phenol		30

*All measurements taken at 25° in 0.05 *M* Tris – HCl buffer solution of p*H* 8.58 with a steroid concentration of 0.03 μmole ml^{-1}.
†k'_{cat}(min^{-1} × 10^5) is defined as the difference in *pseudo* first order rate constant between the catalyzed and non-catalyzed isomerizations.
‡Reference 16.
§Reference 17.

facility of the enzymic process is mainly due to its extremely low enthalpy of activation of 5.0 kcal mole^{-1}. This low value indicates that the C-4β-H bond cleavage in the rate determining step is accompanied by an energetically compensating bond formation. This is in accord with the mechanism proposed by Malhotra and Ringold (8) (Fig. 4). The entropy of activation of −16.8 e.u. is also consistent with this type of mechanism since the rate determining step involves charge development in the transition state.

Attention was then directed towards further attempts to identify the acidic and basic groups at the active center. As was recently pointed out (4), the fluorescence (1) and nitration (14) results of Talalay and his co-workers and data on 17-deoxy-substrates (4) make the phenolic group of a tyrosine residue an attractive candidate for the acidic group designated as HA. In order to assist in evaluating the validity of this suggestion, the catalytic effects of various phenols, particularly those of the hydroxypyridine type found to be so effective in catalyzing glucose mutarotation (15), were measured. The results, which are summarized in Table IV, showed that the

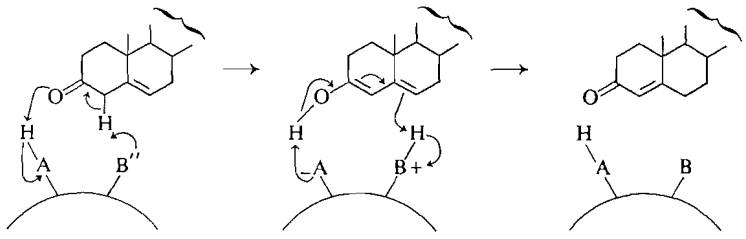

FIG. 4. Mechanism of isomerase action proposed by Malhotra and Ringold (8).

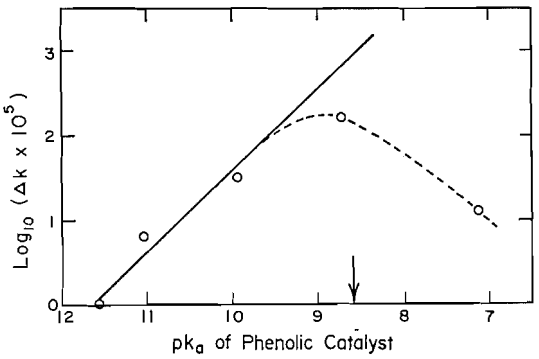

FIG. 5. Brønsted catalysis plot for the phenol-catalyzed isomerizations of androst-5-ene-3,17-dione. The arrow indicates the pH of the Tris – HCl buffered reaction medium.

catalytic effects were small and indicated that the isomerization was subject to general acid catalysis by phenols. A plot of the logarithm of the rate constants against the pK_a of the phenols (Fig. 5) showed that the Brønsted catalysis law was obeyed, provided that the proportion of the phenol present as the conjugate base was not significant. When the rate constants, corrected for the proportions of the phenolic catalysts present as the conjugate bases at pH 8.58, were used in the Brønsted law calculations, a linear plot was again obtained and its slope of 0.67 confirmed that the isomerization was relatively sensitive to general acid-catalysis by phenols.[12] No special rate accelerations ascribable to the bifunctional nature of the hydroxypyridines were detected, and the effects of the ring nitrogen atoms were manifested only in their overall influence on the pK_a of the compound.

The above results thus indicate that a phenolic group can assist in the isomerization of Δ^5-3-ketones but that phenolate anions are insufficiently powerful bases to act as general base-catalysts (cf. ref. 18). These data are thus consistent with the postulate (4) that the phenolic group of a tyrosine residue may well be the acidic group responsible for full or partial protonation of the carbonyl group of the substrate during enzyme-catalyzed isomerization.

[12]Although the linearity of such a plot is strongly indicative of predominant general acid-catalysis, a referee has correctly pointed out that variable pH and concentration studies would be required before it could be unequivocally stated that the contribution of general base-catalysis to the overall rate was insignificant.

With regard to the nature of the basic catalytic group B (Fig. 4), the body of evidence pointing to the presence of an imidazole group of a histidine residue at the active center is substantial (1, 14). In fact Talalay (1) has proposed an elegant mechanism in which he suggested that the imidazole group could act as the complete protonating–deprotonating unit responsible for the hydrogen transfer. Whether or not the geometry of the transition states involved would be favorable to such a situation is open to debate and our analysis, based on the use of Dreiding models, suggests that although the initial removal of the C-4 proton could occur as proposed by Talalay, the subsequent transfer of this hydrogen to C-6 would require considerable puckering of the steroid skeleton. Furthermore, since such a mechanism represents an essentially bimolecular reaction in contrast to the termolecular situation implied in the Malhotra and Ringold postulate (Fig. 4), imidazole itself should be capable of at least partial simulation of the enzymic process by acting as a bifunctional catalyst.[13] That imidazole, alone or mixed with phenol, is in fact (Table IV) not a very effective catalyst would appear to weigh against the Talalay mechanism. We feel that it is more probable that the imidazole group of the active center histidine is in fact the basic group responsible for the removal of the C-4 proton and its subsequent transfer to C-6, and the mechanism we consider to be most consistent with all the present and previous data (1, 4, 8, 14) is shown in Fig. 6. The involvement of both a tyrosine phenolic group (pK_a ~ 10–11 (19)) and a histidine imidazole function (pK_a ~ 6–7 (19)) as the catalytic groups, rather than the imidazole residue alone, is further supported by the pH-activity profile of the enzyme (1) which shows a flat maximum in the pH range 6–9. The decrease in activity at pH > 9 can be rationalized in terms of this mechanism, since the increasing predominance of the phenolate anion as the pH is increased, would correspondingly reduce the contribution to the overall catalytic process made by the carbonyl protonation step. However, obviously several other equally valid rationalizations for the effect of high pH on the enzyme can be put forward.

Experiments involving substrate analogues

[13]This would again be analogous to the hydroxypyridine catalysis of the mutarotation of glucose (15).

Can. J. Chem. Downloaded from www.nrcresearchpress.com by 210.87.254.40 on 09/05/12
For personal use only.

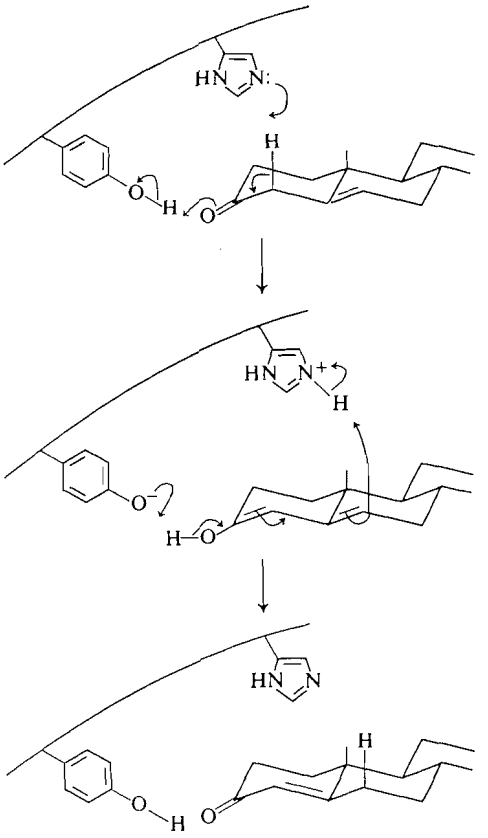

FIG. 6. Mechanism of isomerase action most compatible with currently available data.

designed to react irreversibly with the basic or nucleophilic amino acid residues of the active center are in progress, and it is hoped that the data obtained will help to clarify the roles of histidine and tyrosine in the enzymic process, and also provide information on their orientation with respect to rings A and B of the substrates.

Acknowledgments

We thank the National Research Council of Canada for their generous support and the Canadian Universities Foundation for the award (to D.C.W.) of a Commonwealth Scholarship.

1. P. TALALAY. Ann. Rev. Biochem. **34**, 347 (1965).
2. J. B. JONES and D. C. WIGFIELD. Can. J. Chem. **44**, 2517 (1966).
3. M. A. F. HOLLEMAN and M. G. WILHELMY. Rec. Trav. Chim. **21**, 432 (1902).
4. J. B. JONES and D. C. WIGFIELD. Can. J. Chem. **46**, 1459 (1968).
5. S. GLASSTONE, K. J. LAIDLER, and H. EYRING. The theory of rate processes. McGraw-Hill Book Co., Inc., New York. 1941. p. 199.
6. J. E. LEFFLER and E. GRUNWALD. Rates and equilibria of organic reactions. J. Wiley and Sons, Inc., New York. 1963. p. 71.
7. W. R. NES, E. LOESER, R. KIRDANI, and J. MARSH. Tetrahedron, **19**, 299 (1963).
8. S. K. MALHOTRA and H. J. RINGOLD. J. Amer. Chem. Soc. **87**, 3228 (1965).
9. H. WERBIN and I. L. CHAIKOFF. Biochim. Biophys. Acta, **82**, 581 (1964).
10. D. K. FUKUSHIMA, H. L. BRADLOW, T. YAMAUDI, A. YAGI, and D. KOERNER. Steroids, **11**, 541 (1968).
11. I. V. TORGOV, G. M. SEGAL, and T. S. FRADKINA. 5th I.U.P.A.C. Intern. Symp. Chem. Natural Products. London, July 1968, Abstracts D14.
12. H. J. RINGOLD and S. K. MALHOTRA. Tetrahedron Lett. 669 (1962).
13. J. B. JONES and D. C. WIGFIELD. J. Amer. Chem. Soc. **89**, 5294 (1967).
14. O. M. COLVIN and P. TALALAY. Fed. Proc., **27**, 523 (1968).
15. C. G. SWAIN and J. F. BROWN. J. Amer. Chem. Soc. **74**, 2538 (1952).
16. Dictionary of organic compounds. J. R. A. POLLOCK and R. STEVENS (*Editors*). 4th ed. Eyre and Spottiswood Ltd., London. 1965.
17. R. A. ROBINSON, M. M. DAVIS, M. PAABO, and V. E. BOWER. J. Res. Natl. Bur. Stds., **64A**, 347 (1960).
18. J. F. BUNNETT and L. A. RETALLICK. J. Amer. Chem. Soc. **89**, 423 (1967).
19. D. D. PERRIN. Dissociation constants of organic bases in aqueous solutions. Butterworth and Co., London. 1965. pp. 385–387, 402–404.
20. J. B. JONES and J. M. ZANDER. Can. J. Chem. **47**, 3501 (1969).

Can. J. Chem. Downloaded from www.nrcresearchpress.com by 210.87.254.40 on 09/05/12
For personal use only.

Can. J. Chem. Downloaded from www.nrcresearchpress.com by 210.87.254.42 on 09/05/12
For personal use only.

Synthesis of olivomycose (2,6-dideoxy-3-*C*-methyl-L-*arabino*-hexose)

E. H. WILLIAMS, W. A. SZAREK, AND J. K. N. JONES
Department of Chemistry, Queen's University, Kingston, Ontario

Received July 10, 1969

Oxidation of methyl 4,6-*O*-benzylidene-2-deoxy-α-L-*arabino*-hexopyranoside (**1**) with ruthenium tetroxide gave the 3-ketone **2** in high yield. A Wittig reaction between methylenetriphenylphosphorane and compound **2** gave methyl 4,6-*O*-benzylidene-2,3-dideoxy-3-*C*-methylene-α-L-*erythro*-hexopyranoside (**3**), which was hydrated by the oxymercuration–demercuration procedure to afford methyl 4,6-*O*-benzylidene-2-deoxy-3-*C*-methyl-α-L-*arabino*-hexopyranoside (**4**). The reaction of compound **4** with *N*-bromosuccinimide gave methyl 4-*O*-benzoyl-6-bromo-2,6-dideoxy-3-*C*-methyl-α-L-*arabino*-hexopyranoside (**5**) in high yield. Treatment of compound **5** with lithium aluminium hydride followed by acid-catalyzed hydrolysis of the resultant product, gave L-olivomycose (**6**).

L'oxydation par le tétroxyde de ruthénium du méthyl 4,6-*O*-benzylidène-2-désoxy-α-L-*arabino*-héxopyranoside (**1**) conduit avec un très bon rendement à la cétone **2**. Une réaction de Wittig entre le composé **2** et le méthylènetriphénylphosphorane donne le méthyl 4,6-*O*-benzylidène-2,3-didésoxy-3-*C*-méthylène-α-L-*érythro*-héxopyranoside (**3**), qui par hydratation par la réaction d'oxymercuration–démercuration donne le méthyl 4,6-*O*-benzylidène-2-désoxy-3-*C*-méthyl-α-L-*arabino*-héxopyranoside (**4**). Par réaction de **4** avec la *N*-bromosuccinimide on obtient avec un trés bon rendement le méthyl 4-*O*-benzoyl-6-bromo-2,6-didésoxy-3-*C*-méthyl-α-L-*arabino*-héxopyranoside (**5**). Le traitement de **5** avec l'hydrure de lithium et d'aluminium conduit, après hydrolyse acide du mélange réactionnel, au L-olivomycose (**6**).

Canadian Journal of Chemistry, **47**, 4467 (1969)

Introduction

Olivomycose is a branched-chain sugar which occurs as its 4-*O*-acetyl and 4-*O*-isobutyryl derivatives in olivomycin, a mixture of antibiotics produced by *Streptomyces olivoreticuli* (1). The 4-*O*-acetyl derivative is a component also of the carcinostatic antibiotic chromomycin A_3, and has been named chromose B (2). On the basis of nuclear magnetic resonance (n.m.r.) and chemical evidence, the structure of 2,6-dideoxy-3-*C*-methyl-L-*arabino*-hexose (**6**) was assigned to olivomycose; the sugar is, therefore, epimeric with L-mycarose at C-3. Syntheses of DL-epimycarose from non-carbohydrate precursors have been reported (3). We describe now the preparation of the L-enantiomer from 2-deoxy-L-*arabino*-hexose, a synthesis which corroborates the structure and stereochemistry previously assigned to olivomycose.

Results and Discussion

2-Deoxy-L-*arabino*-hexose, commonly known as 2-deoxy-L-glucose, can be prepared from 3,4,5,6-tetra-*O*-acetyl-1,2-dideoxy-1-nitro-L-*arabino*-hex-1-enitol by the method of Sowden and Fischer (4), which involves selective hydrogenation of the ethylenic bond, using palladium black as catalyst, and acid hydrolysis of the *aci*-salt of the resultant 1,2-dideoxy-1-nitroalditol (Nef reaction). In the present work two modifications of this procedure were employed; the double bond in 3,4,5,6-tetra-*O*-acetyl-1,2-dideoxy-1-nitro-L-*arabino*-hex-1-enitol was selectively reduced with sodium borohydride (5), and the de-*O*-acetylated product was converted into 2-deoxy-L-*arabino*-hexose by oxidative denitration with potassium permanganate (6). Methyl 2-deoxy-α-L-*arabino*-hexopyranoside was prepared from the free sugar, by the method described by Hughes *et al.* (7) for the D-enantiomer, and then treated with benzaldehyde and zinc chloride to give methyl 4,6-*O*-benzylidene-2-deoxy-α-L-*arabino*-hexopyranoside (**1**) (8).

Oxidation of compound **1** with ruthenium tetroxide, according to the improved procedure of Lawton *et al.* (9), afforded methyl 4,6-*O*-benzylidene-2-deoxy-α-*erythro*-hexopyranosid-3-ulose (**2**) (8) in 84% yield. The D-enantiomer of the 3-ketone **2** has been prepared from methyl 4,6-*O*-benzylidene-2-deoxy-α-D-*arabino*-hexopyranoside using chromium trioxide in pyridine (10), ruthenium tetroxide (11), and methyl sulfoxide – acetic anhydride (12) as oxidants; a 90% yield of the ketone was reported with the last procedure. In our hands, however, treatment of compound **1** with methyl sulfoxide – acetic anhydride gave an approximately 1:1 mixture of **2** and another compound; the two components

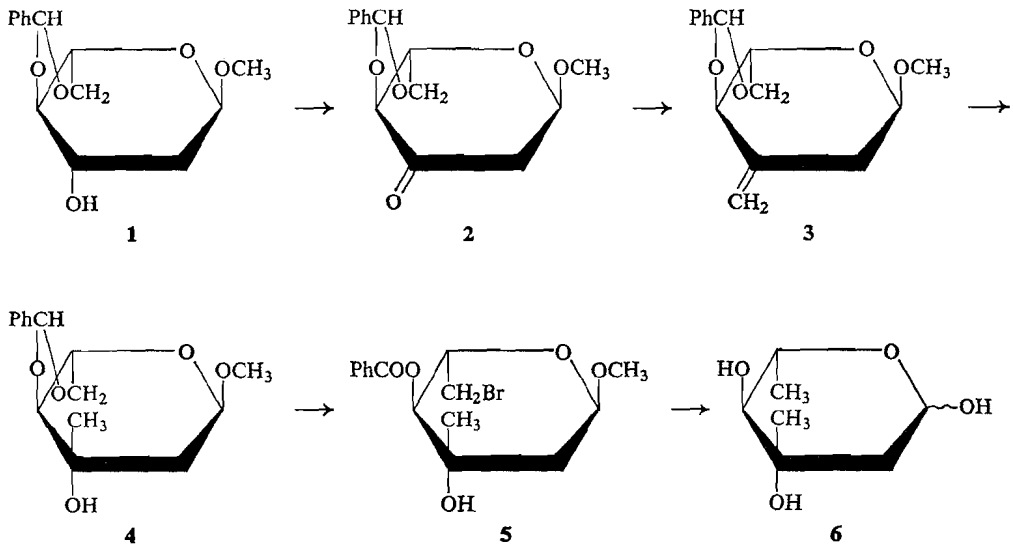

could be separated by chromatography on silica gel, with 3:7 ethyl acetate – chloroform as eluent. The new compound was formulated as methyl 4,6-*O*-benzylidene-2-deoxy-3-*O*-(methylthio)-methyl-α-L-*arabino*-hexopyranoside on the basis of spectroscopic and chemical evidence. Its n.m.r. spectrum in chloroform-*d* showed a 2-proton singlet at τ 5.18 that may be assigned to the protons of an —OCH_2S— group, and a 5-proton multiplet in the region τ 7.5–8.1 that may be assigned to an *S*-methyl group and the two protons at C-2. Treatment with mercuric chloride and cadmium carbonate in aqueous acetone regenerated the starting compound **1**. The formation of (methylthio)methyl ethers, by treatment of carbohydrate derivatives with methyl sulfoxide – acetic anhydride, has been reported previously (13).

It has been shown (8) that addition of methylmagnesium iodide to methyl 4,6-*O*-benzylidene-2-deoxy-α-L-*erythro*-hexopyranosid-3-ulose (**2**) is highly stereoselective giving predominantly the axially-oriented tertiary alcohol (Fig. 1*a*). In compound **2** attack by the Grignard reagent from the side resulting in the formation of the axial alcohol is sterically more favorable than attack from the side resulting in the formation of the equatorial alcohol; considerable steric interaction would be expected between the attacking species and the axial methoxyl group at C-1 in the latter route. The addition product was converted then into L-mycarose (2,6-dideoxy-3-*C*-methyl-L-*ribo*-hexose) (8). L-Olivomycose is epimeric with L-mycarose at C-3. Brown *et al.* (14) have reported that the hydration of many cyclic and bicyclic olefins by the oxymercuration–demercuration procedure gives predominantly the tertiary alcohol formed by addition of water to the tertiary center from the less hindered side. The procedure provides a convenient route to isomeric alcohols epimeric with those obtained from a Grignard synthesis, since the addition of alkyl Grignard reagents to related ketones gives predominantly the tertiary alcohol formed by addition of the alkyl group from the less hindered side. Thus, application of the oxymercuration–demercuration procedure to methyl 4,6-*O*-benzylidene-2,3-dideoxy-3-*C*-methylene-α-L-*erythro*-hexopyranoside (**3**) afforded methyl 4,6-*O*-benzylidene-2-deoxy-3-*C*-methyl-α-L-*arabino*-hexopyranoside (**4**) in 72% yield (see Fig. 1*b*). The branched-chain unsaturated sugar **3** was obtained by the reaction of methylenetriphenylphosphorane with the 3-ketone **2** according to the procedure described by Lance and Szarek (15). The infrared (i.r.) spectrum of compound **4** in carbon tetrachloride ($c < 0.005$ *M*) showed strong absorption at 3640 cm^{-1}, unlike the spectrum of methyl 4,6-*O*-benzylidene-2-deoxy-3-*C*-methyl-α-D-*ribo*-hexopyranoside (10), which showed strong absorption at 3538 cm^{-1}. The low O—H stretching frequency observed for the latter compound was considered to indicate the presence of 1,3-diaxial, hydrogen-bonded interaction (16).

Can. J. Chem. Downloaded from www.nrcresearchpress.com by 210.87.254.42 on 09/05/12
For personal use only.

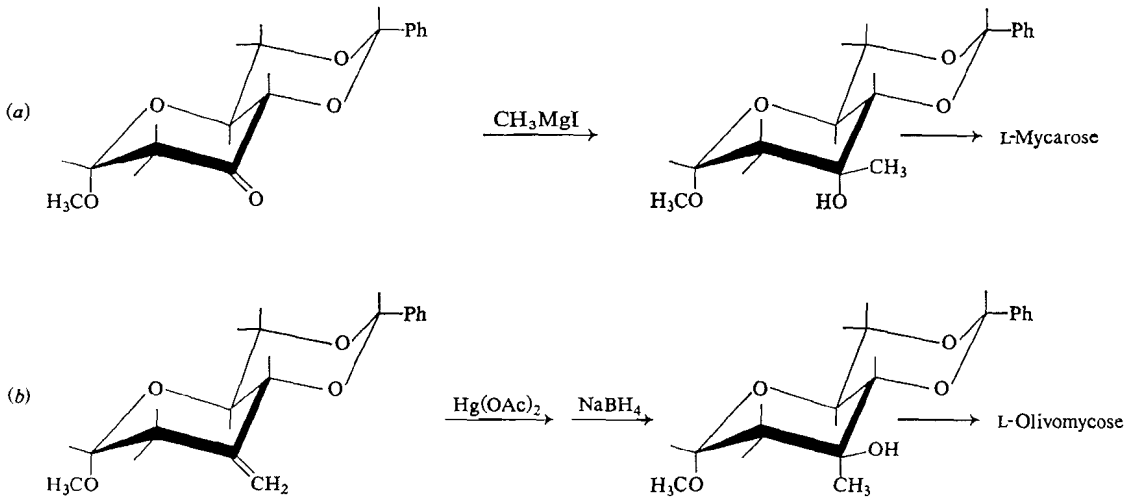

FIG. 1. (*a*) Addition of methylmagnesium iodide to methyl 4,6-*O*-benzylidene-2-deoxy-α-L-*erythro*-hexopyranosid-3-ulose (**2**) (8); (*b*) hydration of methyl 4,6-*O*-benzylidene-2,3-dideoxy-3-*C*-methylene-α-L-*erythro*-hexopyranoside (**3**) by the oxymercuration–demercuration procedure.

Such interaction does not arise in compound **4** with the *arabino* configuration. The preparation of the D-enantiomer of **4**, by reduction with lithium aluminium hydride of one of the *spiro*-epoxides produced in the reaction of methyl 4,6-*O*-benzylidene-2-deoxy-α-D-*erythro*-hexopyranosid-3-ulose with diazomethane, has been reported (17).

The benzylidene ring in compound **4** was opened by treatment with *N*-bromosuccinimide in boiling carbon tetrachloride (18) to give methyl 4-*O*-benzoyl-6-bromo-2,6-dideoxy-3-*C*-methyl-α-L-*arabino*-hexopyranoside (**5**). When compound **5** was heated with lithium aluminium hydride in tetrahydrofuran at reflux temperature, debromination and debenzoylation occurred to give a product which afforded the crystalline free sugar (**6**) by acid-catalyzed hydrolysis. The physical constants of **6** were in good agreement with those reported previously (1) for L-olivomycose.

Experimental

Melting points were determined on a Fisher–Johns melting point apparatus and are uncorrected. Optical rotations were measured with a Perkin–Elmer model 141 automatic polarimeter at 21 ± 2°. Infrared spectra were measured on a Beckman-IR5A spectrophotometer. The n.m.r. spectra were determined at 60 MHz in chloroform-*d* and tetramethylsilane as internal standard. Thin-layer chromatography (t.l.c.) was performed with Silica Gel G as the adsorbent. The developed plates were air dried, sprayed with 5% ethanolic sulfuric acid and heated at about 150°. The term "petroleum ether" refers to the fraction of b.p. 60–80°. Paper chromatography was carried out by the descending method at room temperature on Whatman No. 1 filter paper in butan-1-ol:ethanol:water, 3:1:1 (v/v). The sugars were detected by spraying the chromatograms with a 1:1 mixture of vanillin (1% in ethanol) and perchloric acid (3% in water) and heating (19).

Methyl 4,6-O-Benzylidene-2-deoxy-α-L-arabino-hexopyranoside (1)

To a stirred solution of 3,4,5,6-tetra-*O*-acetyl-1,2-dideoxy-1-nitro-L-*arabino*-hex-1-enitol (4) (20 g) in diglyme (100 ml) and ethanol (200 ml), a solution of sodium borohydride (15 g) in ethanol (200 ml) was added dropwise over a period of 15 min. Stirring was continued at room temperature for 1 h; carbon dioxide was bubbled into the mixture during the reaction. The reaction mixture was filtered, and the filtrate was diluted with chloroform (500 ml) and washed with water. Evaporation of the solvent gave a residue, which was recrystallized from ether to yield 3,4,5,6-tetra-*O*-acetyl-1,2-dideoxy-1-nitro-L-*arabino*-hexitol (15.5 g, 78%), m.p. 90–91°; $[\alpha]_D$ −28.2° (*c*, 2.0 in chloroform). Sowden and Fischer (4) report m.p. 91–92° and $[\alpha]_D^{26}$ +29.4° (*c*, 2.5 in chloroform) for the D-enantiomer.

3,4,5,6-Tetra-*O*-acetyl-1,2-dideoxy-1-nitro-L-*arabino*-hexitol (15 g) was dissolved in *M* aqueous sodium hydroxide solution (300 ml). To the solution was added *M* magnesium sulfate (165 ml) and then water to a final volume of 3 l. A solution of potassium permanganate (4 g) in water (400 ml) was added dropwise, with stirring, to the mixture, cooled in an ice–water bath, over a period of 3 h. Stirring was continued at 0–5° for 30 min, and then at room temperature for 1 h. The mixture was filtered, and the filtrate was concentrated to a volume of 500 ml and passed through Rexyn-101 (H^+) and Duolite A-4 (OH^-) ion-exchange resins. Concentration of the eluate

Can. J. Chem. Downloaded from www.nrcresearchpress.com by 210.87.254.42 on 09/05/12
For personal use only.

Can. J. Chem. Downloaded from www.nrcresearchpress.com by 210.87.254.42 on 09/05/12
For personal use only.

gave a colorless, chromatographically homogeneous (paper chromatography) syrup (6 g, 89%) with the same R_f as an authentic sample of 2-deoxy-L-*arabino*-hexose.

Methyl 2-deoxy-α-L-*arabino*-hexopyranoside was prepared from 2-deoxy-L-*arabino*-hexose, by the method described by Hughes *et al.* (7) for the D-enantiomer, and then converted into methyl 4,6-*O*-benzylidene-2-deoxy-α-L-*arabino*-hexopyranoside (**1**) as reported previously (8).

Methyl 4,6-O-Benzylidene-2-deoxy-α-L-erythro-hexopyranosid-3-ulose (2)

This compound was prepared by oxidation of methyl 4,6-*O*-benzylidene-2-deoxy-α-L-*arabino*-hexopyranoside (**1**) (1 g) with a mixture of ruthenium dioxide and potassium metaperiodate in chloroform, in the presence of potassium carbonate, by the procedure described by Lawton *et al.* (9). The crystalline product was recrystallized from ether–petroleum ether to give white needles (0.8 g, 84%), whose physical constants were the same as those reported previously (8) for compound **2**.

Methyl 4,6-O-Benzylidene-2,3-dideoxy-3-C-methylene-α-L-erythro-hexopyranoside (3)

To a solution of methylenetriphenylphosphorane [prepared, as described by Lance and Szarek (15), from methyltriphenylphosphonium bromide (1.4 g) and sodium amide (0.21 g)] in ether (10 ml) was added dropwise, with stirring and at reflux temperature, a solution of ketone **2** (0.7 g) in ether (10 ml). When addition was complete, the mixture was filtered, and the filtrate was concentrated to dryness; the residue was extracted several times with hot petroleum ether. Evaporation of the solvent gave a syrup, which was chromatographed on silica gel, with 3:7 ethyl acetate–petroleum ether as eluent, to yield a crystalline product. Recrystallization from ethanol–water gave compound **3** (0.45 g, 69%), m.p. 120°; $[\alpha]_D$ −137.3° (*c*, 1.0 in ethanol); n.m.r. data: τ 2.34–2.8 (5-proton multiplet, aromatic H's), 4.35 (-proton singlet, benzylidene-methine H), 4.78–5.15 (2-proton multiplet, 2 vinyl H's), 5.15–5.3 (1-proton multiplet, H-1), 6.66 (3-proton singlet, OMe), 7.38–7.58 (2-proton multiplet, 2H-2's).

Anal. Calcd. for $C_{15}H_{18}O_4$: C, 68.7; H, 6.9. Found: C, 68.9; H, 7.3.

Methyl 4,6-O-Benzylidene-2-deoxy-3-C-methyl-α-L-arabino-hexopyranoside (4)

Compound **3** (0.40 g) was added with stirring to a mixture of mercuric acetate (0.516 g) in water (2.5 ml) and tetrahydrofuran (2 ml). The reaction mixture was stirred for 30 min at room temperature, and then 3 *M* sodium hydroxide (3.5 ml) followed by a solution of 0.5 *M* sodium borohydride in 3 *M* sodium hydroxide (2 ml) were added. The mixture was filtered, and the filtrate was extracted several times with chloroform. The extracts were washed with water, dried over magnesium sulfate, and concentrated to yield a crystalline product. Recrystallization from ethanol–water gave compound **4** (0.30 g, 72%), m.p. 77–79°; $[\alpha]_D$ −100° (*c*, 0.2 in ethanol). Flaherty *et al.* (17) report m.p. 79–79.5° and $[\alpha]_D$ +122° (ethanol) for the D-enantiomer.

The i.r. spectrum of compound **4** in carbon tetrachloride ($c < 0.005$ *M*) showed strong absorption at 3640 cm^{-1}; n.m.r. data: τ 2.37–2.78 (5-proton multiplet, aromatic H's), 4.42 (1-proton singlet, benzylidene-methine H), 5.15–5.36 (1-proton multiplet, H-1), 6.65 (3-proton singlet, OMe), 7.57–7.74 (1-proton, OH), 7.95–8.12 (2-proton multiplet, 2H-2's), 8.53 (3-proton singlet, C-3 Me).

Methyl 4-O-Benzoyl-6-bromo-2,6-dideoxy-3-C-methyl-α-L-arabino-hexopyranoside (5)

A solution of compound **4** (0.20 g) and *N*-bromosuccinimide (0.14 g) in carbon tetrachloride (20 ml) containing barium carbonate (0.70 g) was heated at reflux temperature with vigorous stirring for 1 h. The reaction mixture was filtered, and the filtrate concentrated to a syrup, which was chromatographed on silica gel, with 3:4 ethyl acetate–petroleum ether as eluent, to yield a crystalline product. Recrystallization from ether–petroleum ether gave compound **5** (0.22 g, 86%), m.p. 115°; $[\alpha]_D$ −66.2° (*c*, 0.2 in chloroform); λ_{max} (Nujol) 5.72 (OBz), 6.2, 14.0 μm (Ph); n.m.r. data: τ 1.83–2.05, 2.33–2.75 (multiplets, 5 protons, aromatic H's), 4.97 (1-proton doublet, $J_{4,5}$ 10 Hz, H-4), 5.06–5.24 (1-proton multiplet, H-1), 6.6 (3-proton singlet, OMe), 7.42 (1-proton singlet, OH), 7.85–8.0 (2-proton multiplet, 2H-2's), 8.55 (3-proton singlet, C-3 Me).

Anal. Calcd. for $C_{15}H_{19}O_5Br$: C, 50.0; H, 5.3; Br, 22.3. Found: C, 50.3; H, 5.4; Br, 22.0.

2,6-Dideoxy-3-C-methyl-L-arabino-hexose (Olivomycose) (6)

A mixture of compound **5** (0.20 g) and lithium aluminium hydride (0.30 g) in tetrahydrofuran (20 ml) was heated at reflux temperature for 6 h. The product was isolated in the usual manner, and chromatographed on silica gel, with ethyl acetate as eluent, to yield a syrup (0.060 g); λ_{max} (film) 2.8–2.9 μm (OH), no absorption attributable to benzoate. The t.l.c. (2:3 ethyl acetate–petroleum ether) showed the presence of a major component with R_f 0.2, and a small amount of a component which migrated slightly faster.

A solution of the syrup obtained above (0.050 g) in 0.2 *N* sulfuric acid (3 ml) was kept overnight at room temperature. The solution was neutralized with Duolite A-4 (OH^-) ion-exchange resin and concentrated to yield a crystalline product. Recrystallization from ethyl acetate–petroleum ether gave olivomycose (**6**) (0.030 g, 55%), m.p. 102–103°; $[\alpha]_D$ −13.8° (initial), −22.2° (after 20 min and after 2 h) (*c*, 1.0 in water). For olivomycose m.p. 103–106° and $[\alpha]_D^{26}$ −13° (immediately after dissolution), −22° (after 20 min and 1.5 h) (*c*, 1.1 in H_2O) have been reported (1).

Acknowledgments

The authors thank the National Research Council of Canada and the Department of University Affairs in the Province of Ontario for financial support of this research. We also acknowledge the counsel of Dr. G. B. Howarth.

1. (*a*) Y. A. Berlin, S. E. Esipov, M. N. Kolosov, M. M. Shemyakin, and M. G. Brazhnikova. Tetrahedron Letters, 1323, 3513 (1964); (*b*) Y. A.

BERLIN, S. E. ESIPOV, M. N. KOLOSOV, and M. M. SHEMYAKIN. Tetrahedron Letters, 1431, 1643 (1966); (*c*) Y. A. BERLIN, S. E. ESIPOV, M. N. KOLOSOV, and V. A. KRIVORUCHKO. Khim. Prir. Soedin. **3**, 405 (1967), Chem. Abstr. **68**, 96060*x* (1968).
2. M. MIYAMOTO, Y. KAWAMATSU, M. SHINOHARA, K. NAKANISHI, Y. NAKADAIRA, and N. S. BHACCA. Tetrahedron Letters, 2371 (1964).
3. (*a*) F. KORTE, U. CLAUSSEN, and K. GÖHRING. Tetrahedron, **18**, 1257 (1962); (*b*) D. M. LEMAL, P. D. PACHT, and R. B. WOODWARD. Tetrahedron, **18**, 1275 (1962); (*c*) H. GRISEBACH, W. HOFHEINZ, and N. DOERR. Ber. **96**, 1823 (1963).
4. J. C. SOWDEN and H. O. L. FISCHER. J. Amer. Chem. Soc. **69**, 1048 (1947).
5. (*a*) A. I. MEYERS and J. C. SIRCAR. J. Org. Chem. **32**, 4134 (1967); (*b*) W. A. SZAREK, D. G. LANCE, and R. L. BEACH. Chem. Commun. 356 (1968).
6. (*a*) H. SHECHTER and F. T. WILLIAMS. J. Org. Chem. **27**, 3699 (1962); (*b*) H. H. BAER and M. C. T. WANG. Can. J. Chem. **46**, 2793 (1968).
7. I. W. HUGHES, W. G. OVEREND, and M. STACEY. J. Chem. Soc. 2846 (1949).
8. G. B. HOWARTH and J. K. N. JONES. Can. J. Chem. **45**, 2253 (1967).
9. B. T. LAWTON, W. A. SZAREK, and J. K. N. JONES. Carbohyd. Res. **10**, 456 (1969).
10. B. FLAHERTY, W. G. OVEREND, and N. R. WILLIAMS J. Chem. Soc. 398 (1966).
11. P. J. BENYON, P. M. COLLINS, P. T. DOGANGES, and W. G. OVEREND. J. Chem. Soc. 1131 (1966).
12. A. ROSENTHAL and P. CATSOULACOS. Can. J. Chem. **46**, 2868 (1968).
13. (*a*) J. L. GODMAN and D. HORTON. Carbohyd. Res. **6**, 229 (1968); (*b*) J. S. JEWELL and W. A. SZAREK. Tetrahedron Letters, 43 (1969).
14. (*a*) H. C. BROWN and P. GEOGHEGAN, JR. J. Amer. Chem. Soc. **89**, 1522 (1967); (*b*) H. C. BROWN and W. J. HAMMAR. J. Amer. Chem. Soc. **89**, 1524 (1967); (*c*) H. C. BROWN, J. H. KAWAKAMI, and S. IKEGAMI. J. Amer. Chem. Soc. **89**, 1525 (1967).
15. D. G. LANCE and W. A. SZAREK. Carbohyd. Res. **10**, 306 (1969).
16. R. J. FERRIER, W. G. OVEREND, G. A. RAFFERTY, H. M. WALL, and N. R. WILLIAMS. Proc. Chem. Soc. 133 (1963).
17. B. FLAHERTY, W. G. OVEREND, and N. R. WILLIAMS. Chem. Commun. 434 (1966).
18. S. HANESSIAN. Carbohyd. Res. **2**, 86 (1966).
19. A. P. MACLENNAN, H. M. RANDALL, and D. W. SMITH. Anal. Chem. **31**, 2020 (1959).

Can. J. Chem. Downloaded from www.nrcresearchpress.com by 210.87.254.42 on 09/05/12
For personal use only.

Addition of pseudohalogens to unsaturated carbohydrates. III. Synthesis of 3-deoxy-3-*C*-nitromethyl-D-allose, a branched-chain nitro sugar[1]

W. A. SZAREK, J. S. JEWELL, I. SZCZEREK,[2] AND J. K. N. JONES
Department of Chemistry, Queen's University, Kingston, Ontario

Received June 24, 1969

Addition of nitryl iodide to 3-deoxy-1,2:5,6-di-*O*-isopropylidene-3-methylene-α-D-*ribo*-hexofuranose (**2**), followed by treatment of the product with sodium borohydride, gave crystalline 3-deoxy-1,2:5,6-di-*O*-isopropylidene-3-*C*-nitromethyl-α-D-allofuranose (**3**); the branched-chain unsaturated sugar (**2**) was prepared by way of a Wittig reaction with 1,2:5,6-di-*O*-isopropylidene-α-D-*ribo*-hexofuranos-3-ulose (**1**). Acid-catalyzed hydrolysis of **3** afforded 3-deoxy-3-*C*-nitromethyl-D-allose, which exists predominantly in the β-D-furanose form (**4**).

L'addition d'iodure de nitryle au 3-deoxy-1,2:5,6-di-*O*-isopropylidène-3-methylene-α-D-*ribo*-hexofuranose (**2**), le produit obtenu étant traité au borohydrure de sodium, donne le 3-desoxy-1,2:5,6-di-*O*-isopropylidène-3-*C*-nitromethyl-α-D-allofuranose cristallisé (**3**); le sucre à double liaison exocyclique (**2**) a été préparé par réaction de Wittig par le 1,2:5,6-di-*O*-isopropylidène-α-D-*ribo*-hexofuranos-3-ulose (**1**). L'hydrolyse catalysée par les acides de **3** conduit au 3-desoxy-3-*C*-nitromethyl-D-allose, qui existe de manière prédominante sous la forme β-D-furanose (**4**).

Canadian Journal of Chemistry, 47, 4473 (1969)

Introduction

Branched-chain sugars may be divided into two groups, according to whether branching occurs in the carbon chain by substitution of hydrogen (Type A) or of a hydroxyl group (Type B)

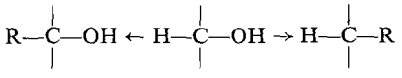

Type A Type B

Those found in plants are of Type A, whereas those produced by micro-organisms are of both types. Several methods are available for the synthesis of branched-chain sugars of Type A, but only a few syntheses of Type B sugars have been reported (3, 4). Recently the application of the Wittig reaction with phosphonoacetic acid trimethyl ester (5) and alkylidene phosphoranes (6) to keto sugar derivatives to afford branched-chain unsaturated carbohydrates was described; the former condensation products are readily converted into saturated branched-chain sugars (Type B) having a free terminal primary hydroxyl function. A Wittig reaction between diethyl cyanomethylphosphonate and a keto sugar gave a branched-chain unsaturated carbohydrate containing a nitrile group; reduction of this compound afforded a branched-chain amino sugar (7).

Two other recently reported routes to Type B branched-chain sugars involve the application of the oxo reaction to unsaturated carbohydrates (8), and the synthesis of cyanodeoxy sugars by the opening of carbohydrate epoxides (9). The preparation of branched-chain dinitro sugar derivatives, namely methyl 4,6-*O*-benzylidene-2,3-dideoxy-3-nitro-2-nitroalkyl-β-D-glucopyranosides and methyl 4,6-*O*-benzylidene-2,3-dideoxy-3-nitro-2-nitroalkyl-β-D-galactopyranosides, by Michael addition has been reported also (10). In continuation of our studies on the addition of pseudohalogens to unsaturated carbohydrate derivatives (1, 2), we have now prepared a branched-chain (Type B) nitro sugar, 3-deoxy-3-*C*-nitromethyl-D-allose (**4**), by way of the addition of nitryl iodide to the branched-chain unsaturated sugar **2**. The olefinic substrate (**2**) had been used previously for the synthesis of a Type B branched-chain sugar by a photochemical addition reaction (11).

Results and Discussion

Oxidation of 1,2:5,6-di-*O*-isopropylidene-α-D-glucofuranose with methyl sulfoxide – acetic anhydride (12) gave 1,2:5,6-di-*O*-isopropylidene-α-D-*ribo*-hexofuranos-3-ulose (**1**), which was obtained in crystalline form in 54% yield by distillation of its crystalline hydrate (13). Reaction of methylenetriphenylphosphorane with

[1]For part I in this series, see ref. 1, and for part II, see ref. 2.

[2]Permanent address: Institute of Organic Chemistry, Polish Academy of Sciences, Warsaw 42, Poland.

Can. J. Chem. Downloaded from www.nrcresearchpress.com by 210.87.254.42 on 09/05/12
For personal use only.

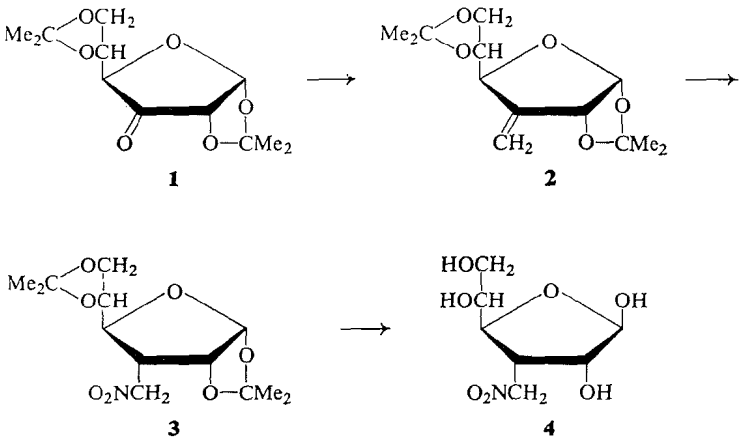

1 2

3 4

the 3-ketone (**1**) afforded the branched-chain unsaturated sugar, 3-deoxy-1,2:5,6-di-*O*-isopropylidene-3-methylene-α-D-*ribo*-hexofuranose (**2**). The Wittig reaction was performed in ether, and involved preparing the ylid in liquid ammonia with sodium amide as the base, and then replacing the ammonia by ether (6).

Nitryl iodide (prepared *in situ* by the reaction of silver nitrite and iodine in ether solution) has been shown to add to unsaturated sugars to produce β-nitro iodides; sugars which contain terminal unsaturated linkages form 2-iodo-1-nitro-adducts (1, 2). The new derivatives are frequently unstable on standing, but are converted readily into α-nitroolefins by sodium hydrogen carbonate in boiling benzene. The double bonds in the latter compounds can be selectively reduced with sodium borohydride. In the present work, reaction of compound **2** with nitryl iodide in ether gave a syrup, which on treatment with sodium borohydride in methanol afforded crystalline 3-deoxy-1,2:5,6-di-*O*-isopropylidene-3-*C*-nitromethyl-α-D-allofuranose (**3**). The *allo* configuration for compound **3** was assigned by nuclear magnetic resonance (n.m.r.) spectroscopy. The spectrum of compound **3** itself in chloroform-*d* was of little value in establishing the configuration, but a solution in deuterium oxide containing a small proportion of NaOD gave a spectrum which could be assigned, with the aid of spin decoupling, to the nitronate anion **3***a* (Fig. 1). The spectrum showed a 1-proton doublet at τ 3.85 attributable to H-3′ with $J_{3',3} = 7.5$ Hz, and a 1-proton doublet at τ 4.05 attributable to H-1 with $J_{1,2} = 3.8$ Hz. Irradiation of H-1 caused the triplet centered at τ 5.02 to collapse to a doublet with a splitting of 4.8 Hz. The triplet was assigned, therefore, to H-2, and the coupling constant $J_{2,3} = 4.8$ Hz. In 1,2:5,6-di-*O*-isopropylidene-α-D-allofuranose and its derivatives, the signal for H-2 is a triplet, and values of ca. 4 Hz for $J_{2,3}$ have been reported (5, 11), unlike 1,2-*O*-isopropylidene-α-D-*xylo*-hexofuranose derivatives, in which the coupling between H-2 and H-3 is very small and results in the spectral pattern for H-2 being a doublet (14). The 1-proton multiplet at τ 6.85 in the spectrum of **3***a* was assigned to H-3, since the signal simplified to a quartet with splittings of 4.8 and 10.0 Hz ($J_{3,4}$) on irradiation of H-3′. Irradiation of H-2 also caused the multiplet to collapse to a quartet, in addition to causing the H-1 doublet to appear as a broad band. The value for $J_{3,4}$ is significantly larger than the range of values observed for $J_{3,4}$ (2.7–3.0 Hz) in 1,2-*O*-isopropylidene-α-D-*xylo*-hexofuranose derivatives (14). After acidification of the sodium nitronate solution with hydrochloric acid or acetic acid, compound **3** could be recovered. If DCl in deuterium oxide was used for acidification, both the hydrogens at C-3′ in **3** were exchanged by deuterium atoms.

Acid-catalyzed hydrolysis of compound **3** with Rexyn-101 resin (H^+) gave 3-deoxy-3-*C*-nitromethyl-D-allose (**4**) as a glass. The n.m.r. spectrum (Fig. 2) of the equilibrium solution in deuterium oxide at ambient temperature (30°) had 3 readily discernible signals of total intensity one, which could be assigned to anomeric protons. These signals were a doublet at τ 4.53 with a

Can. J. Chem. Downloaded from www.nrcresearchpress.com by 210.87.254.42 on 09/05/12
For personal use only.

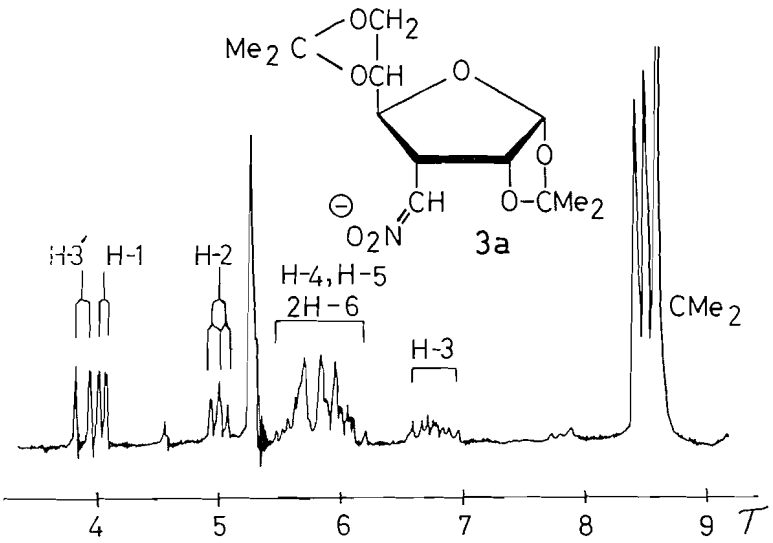

FIG. 1. The 60 MHz n.m.r. spectrum of 3-*C*-(*aci*-nitromethyl)-3-deoxy-1,2:5,6-di-*O*-isopropylidene-α-D-allofuranose sodium in deuterium oxide (sodium 4,4-dimethyl-4-silapentane-1-sulfonate as internal standard).

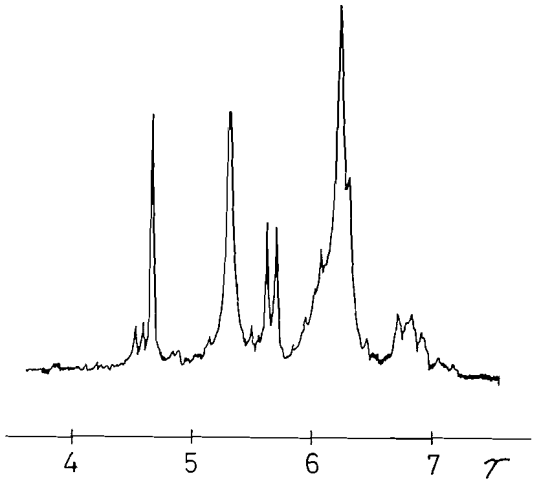

FIG. 2. The 60 MHz n.m.r. spectrum of 3-deoxy-3-*C*-nitromethyl-D-allose (**4**) in deuterium oxide (sodium 4,4-dimethyl-4-silapentane-1-sulfonate as internal standard).

splitting of 4.3 Hz, a singlet at τ 4.62, and a doublet at τ 4.87 with a splitting of 3.2 Hz; the relative intensities were 16:79:5. The n.m.r. spectrum of D-allose itself in deuterium oxide has been determined previously (15, 16); integration of the anomeric signals in the spectrum obtained at 40° (16) showed that the mixture contained 5% of the α-D-furanose, 7% of the β-D-furanose, 16% of the α-D-pyranose, and 71% of the β-D-pyranose forms. The spacing for the anomeric doublet of the predominant β-D-allopyranose form was 8.2 Hz (15). Evidently, the presence of the singlet at τ 4.62 in the spectrum of 3-deoxy-3-*C*-nitromethyl-D-allose suggests that the compound exists predominantly in the β-D-furanose form (**4**) in aqueous solution (17). Further evidence for the presence of the furanose form(s) was provided by the observation that the hydrolysis product gave, on a paper chromatogram, a substance which reacted with a spray reagent based upon the liberation of formaldehyde by acidified metaperiodate solution (18).

Experimental

Melting points are uncorrected and were determined with a Fisher–Johns apparatus. Optical rotations were measured using a Perkin–Elmer model 141 automatic polarimeter at 21 ± 2°. Thin-layer chromatography (t.l.c.) was performed on Brinkmann pre-coated aluminium sheets with silica gel as the sorbent in the following solvent systems (v/v): (A) chloroform – ether, 3:1; (B) ether – ethyl acetate, 3:2. The developed plates were air dried, sprayed with 5% ethanolic sulfuric acid, and heated at about 150°. Paper chromatography was carried out by the descending method on Whatman No. 1 filter paper in 1-butanol – ethanol – water, 3:1:1. Infrared (i.r.) spectra were recorded on a Beckmann-IR5A spectrophotometer. Nuclear magnetic resonance spectra were measured on a Varian T-60 spectrometer in chloroform-*d* with tetramethylsilane (τ 10.00) as internal standard, unless otherwise stated; coupling constants were measured at 250 or 100 Hz sweep widths.

Can. J. Chem. Downloaded from www.nrcresearchpress.com by 210.87.254.42 on 09/05/12
For personal use only.

Can. J. Chem. Downloaded from www.nrcresearchpress.com by 210.87.254.42 on 09/05/12
For personal use only.

1,2:5,6-Di-O-isopropylidene-α-D-ribo-hexofuranos-3-ulose (1)

A solution of 1,2:5,6-di-*O*-isopropylidene-α-D-glucofuranose (13.0 g) in methyl sulfoxide (75 ml) and acetic anhydride (50 ml) was left for 24 h at room temperature. The reagents were removed by evaporation at low temperature (19), and the residue was distilled, b.p. 104°/0.02 Torr. Trituration of the distillate with water gave the crystalline hydrate of **1** (13). Distillation of this product afforded **1** as a clear syrup which crystallized spontaneously (6.9 g, 54%), m.p. 39–40°, $[\alpha]_D$ +139° (*c*, 1.0 in chloroform); λ_{max} (KBr) 5.61 (C=O), 7.20 μm (CMe_2).

3-Deoxy-1,2:5,6-di-O-isopropylidene-3-methylene-α-D-ribo-hexofuranose (2)

Methyltriphenylphosphonium bromide (10.7 g) was added to a solution of sodium amide (0.80 g) in liquid ammonia (100 ml) under nitrogen. Anhydrous ether (125 ml) was added, and the ammonia removed by evaporation. To the bright yellow solution of methylenetriphenylphosphorane was added dropwise with stirring a solution of compound **1** (5.6 g) in anhydrous ether. The reaction mixture was stirred for 2 h, and then filtered. The filtrate was washed with dilute sulfuric acid and water, and concentrated to give a clear syrup which was extracted with petroleum ether (100 ml). The solvent was evaporated, and compound **2** was obtained as a syrup by distillation (3.4 g, 60%), b.p. 71–72°/0.02 Torr, $[\alpha]_D$ +75° (*c*, 1.0 in chloroform); R_f 0.85 (solvent A), 0.68 (solvent B); λ_{max} (KBr) 6.05 (C=C), 7.31 μm (CMe_2); n.m.r. data: τ 4.22 (1-proton doublet, $J_{1,2}$ = 3.8 Hz, H-1), 4.45–4.65 (2-proton multiplet, 2 vinyl H's), 5.19 (1-proton doublet, H-2), 5.30–6.22 (4-proton multiplets, H-4, H-5, 2H-6's), 8.50, 8.58, 8.63 (3-, 3-, and 6-proton singlets, CMe_2).

Anal. Calcd. for $C_{13}H_{20}O_5$: C, 60.9; H, 7.9. Found: C, 60.9; H, 8.1.

3-Deoxy-1,2:5,6-di-O-isopropylidene-3-C-nitromethyl-α-D-allofuranose (3)

Compound **2** (3.80 g) was added portionwise to a stirred mixture of freshly prepared silver nitrite (2.6 g) and iodine (4.05 g) in anhydrous ether (50 ml), and stirring was continued for 6 h at room temperature in the dark. The reaction mixture was filtered, and the filtrate was concentrated to a dark red syrup. To a solution of this material in methanol (25 ml) was added with stirring sodium borohydride (ca. 1.5 g). After 1 h, the solution was treated with acetic acid until the p*H* was 6. Concentration of the solution gave a syrup which crystallized from water. Recrystallization from ethanol – water gave compound **3** as needles (2.30 g, 51%), m.p. 86–87°, $[\alpha]_D$ +80° (*c*, 1.0 in chloroform); R_f 0.56 (solvent A), 0.66 (solvent B); λ_{max} (KBr) 6.45 (C—NO_2), 7.30 μm (CMe_2); n.m.r. data: τ 4.18 (1-proton doublet, $J_{1,2}$ = 3.8 Hz, H-1), 5.06–5.36 (3-proton multiplets, H-2 and CH_2NO_2), 5.72–6.50 (4-proton multiplets, H-4, H-5, 2H-6's), 7.20 (1-proton multiplet, H-3).

Anal. Calcd. for $C_{13}H_{21}NO_7$: C, 51.5; H, 7.0; N, 4.6. Found: C, 51.1; H, 6.9; N, 4.7.

3-Deoxy-3-C-nitromethyl-D-allose (4)

Compound **3** (300 mg) in water (10 ml) was stirred with 2 g of Rexyn-101 resin (H^+) at 60° for 4 h. The resin was then removed by filtration, and the filtrate was shaken briefly with a small amount of Duolite A-4 resin (OH^-) to remove any trace of acid. Concentration of the solution gave a colorless glass (203 mg), $[\alpha]_D$ +42° (constant, during 24 h) (*c*, 1.0 in water). Paper chromatography showed the presence of only one substance, $R_{rhamnose}$ 1.3, with *p*-anisidine hydrochloride (20) and a formaldehyde-detecting spray reagent (18). The n.m.r. spectrum is shown in Fig. 2; the i.r. spectrum (film) had a broad band centered at 3.07 μm (OH) and a broad band centered at 6.42 μm (C—NO_2).

Anal. Calcd. for $C_7H_{13}NO_7 \cdot \frac{1}{2}H_2O$: C, 36.2; H, 6.1; N, 6.1. Found: C, 36.8; H, 5.9; N, 5.8.

Acknowledgments

The authors thank the National Research Council of Canada and the Department of University Affairs in the Province of Ontario for financial support of this research.

1. W. A. SZAREK, D. G. LANCE, and R. L. BEACH. Chem. Commun. 356 (1968); Carbohyd. Res. Soc. To be published.
2. J. S. JEWELL and W. A. SZAREK. To be published
3. W. G. OVEREND. Chem. Ind. (London), 342 (1963).
4. L. HOUGH and A. C. RICHARDSON. *In* Rodd's chemistry of carbon compounds. Vol. I. Part F. *Edited by* S. Coffey. Elsevier Publishing Co., Amsterdam. 1967. pp. 529–543.
5. A. ROSENTHAL and L. (BENZING) NGUYEN. Tetrahedron Lett. 2393 (1967). A. ROSENTHAL and P. CATSOULACOS. Can. J. Chem. **46**, 2868 (1968).
6. D. G. LANCE and W. A. SZAREK. Carbohyd. Res. **10**, 306 (1969).
7. A. ROSENTHAL and D. A. BAKER. Tetrahedron Lett. 397 (1969).
8. A. ROSENTHAL and H. J. KOCH. J. Amer. Chem. Soc. **90**, 2181 (1968). A. ROSENTHAL. Advan. Carbohyd. Chem. **23**, 59 (1969).
9. N. R. WILLIAMS. Chem. Commun. 1012 (1967). B. E. DAVIDSON, R. D. GUTHRIE, and A. T. MCPHAIL. Chem. Commun. 1273 (1968).
10. H. H. BAER and K. S. ONG. Can. J. Chem. **46**, 2511 (1968).
11. J. S. JEWELL and W. A. SZAREK. Tetrahedron Lett. 43 (1969).
12. W. SOWA and G. H. S. THOMAS. Can. J. Chem. **44**, 836 (1966).
13. P. J. BEYNON, P. M. COLLINS, and W. G. OVEREND. Proc. Chem. Soc. 342 (1964).
14. R. J. ABRAHAM, L. D. HALL, L. HOUGH, and K. A. MCLAUCHLAN. J. Chem. Soc. 3699 (1962).
15. R. U. LEMIEUX and J. D. STEVENS. Can. J. Chem. **44**, 249 (1966).
16. S. J. ANGYAL and V. A. PICKLES. Carbohyd. Res. **4**, 269 (1967).
17. S. J. ANGYAL. Angew. Chem. **81**, 172 (1969). J. D. STEVENS and H. G. FLETCHER, JR. J. Org. Chem. **33**, 1799 (1968).
18. T. NASH. Biochem. J. **55**, 416 (1953). J. K. N. JONES, M. B. PERRY, and W. SOWA. Can. J. Chem. **41**, 2712 (1963).
19. D. HORTON and J. S. JEWELL. Carbohyd. Res. **2**, 251 (1966).
20. L. HOUGH, J. K. N. JONES, and W. H. WADMAN. J. Chem. Soc. 1702 (1950).

Branched-chain sugar nucleosides. IV. 9-(3-Deoxy-3-*C*-"hydroxymethyl"-β(and α)-D-allofuranosyl and ribofuranosyl)adenine

ALEX ROSENTHAL AND MATEJ SPRINZL
Department of Chemistry, University of British Columbia, Vancouver, British Columbia

Received June 25, 1969

Hydroboration followed by alkaline hydrogen peroxide oxidation of 1,2:5,6-di-*O*-isopropylidene-3-*C*-methylene-α-D-*ribo*-hexofuranose (**2**) yielded 3-deoxy-3-*C*-"hydroxymethyl"-1,2:5,6-di-*O*-isopropylidene-α-D-allofuranose (**3**) and partially hydrolyzed **3** in a total yield of 88%. Compound **3** was hydrolyzed selectively to the 1,2-monoisopropylidene derivative **5**, which was converted via benzoylation followed by acetolysis into the 1,2-diacetate **7**. Condensation of the latter compound with chloromercuri-*N*-benzoyladenine in the presence of titanium tetrachloride, followed by deblocking with methanolic sodium methoxide, yielded 9-(3-deoxy-3-*C*-"hydroxymethyl"-β(and α)-D-allofuranosyl)adenine in yields of 44 and 4% respectively, based on **7**. The over-all yield of **10** based on **3** is 20%. Sodium metaperiodate oxidation of **10**, followed by sodium borohydride reduction of the *aldehydo*-derivative, afforded 9-(3-deoxy-3-*C*-"hydroxymethyl"-β-D-ribofuranosyl)adenine (**11**) in 81% yield.

Direct acetolysis of **3**, followed by conversion of the mixture of peracetates into a mixture of glycosyl chlorides, and finally condensation of the latter with **8** gave the blocked crystalline β-D-nucleoside **9** in an over-all yield of about 9%, based on **3**. Subsequent unblocking of **9** gave a nucleoside having the same physical constants as **10**.

Canadian Journal of Chemistry, 47, 4477 (1969)

Can. J. Chem. Downloaded from www.nrcresearchpress.com by 210.87.254.42 on 09/05/12
For personal use only.

In continuation of our studies on the synthesis of branched-chain sugar nucleosides (1–3) we now wish to report the synthesis of two nucleosides having a hydroxymethyl group on C-3 of the furanosyl ring. The starting material for this research was 1,2:5,6-di-*O*-isopropylidene-α-D-*ribo*-hexofuranos-3-ulose (**1**) which was converted into the branched-chain unsaturated sugar 1,2:5,6-di-*O*-isopropylidene-3-*C*-methylene-α-D-ribofuranose (**2**) by application of a Wittig reaction to **1** (3). It was envisaged that hydroboration of the methylene group on C-3 of **2** might give the desired product. Previous workers (4, 5) have reported the application of the hydroboration reaction (6) to carbohydrates containing either a terminal or endocyclic double bond to yield hydration products in low yield. Both in the general field and in the few carbohydrates investigated hydroboration was found to proceed in an *anti*-Markownikov manner. When the hydroboration reaction (4, 5) was first applied to **2** using a stoichiometric amount of diborane then only a negligible yield of the diborane-unsaturated sugar adduct was formed. However, when a very large excess of diborane was allowed to react with **2** followed by an immediate alkaline hydrogen peroxide oxidation of the adduct, then two compounds **3** and **4** in the ratio of 3:1 were formed in 88% yield. These substances were separated by column chromatography. Compounds **3** and **4** showed identical H-2 resonances (triplet) thus confirming that each was formed via hydroboration. Because of the much slower thin-layer chromatography (t.l.c.) mobility of **4** than that of **3** it was reasoned that a partial hydrolysis of **3** might have occurred during the reaction or work-up of **3**. This postulation was confirmed by carrying out a selective hydrolysis of **3** and **4** to afford an identical substance **5** from each. The structure of **3** was readily ascertained from its proton magnetic resonance (p.m.r.) spectrum. As already indicated above the H-2 signal of **3** appears as a triplet (two overlapping doublets) at τ 5.28 showing that H-2 is coupled to H-3 and to H-1. Because H-2 of the glucofuranose derivatives (in which H-3 is *trans* to H-2) gives a doublet (no measurable or less than 0.7 Hz coupling between H-2 and H-3) (7), it was inferred that H-2 and H-3 of **3** must be in a *cis* orientation. This is supported by the fact that the H-2 signal of 1,2:5,6-di-*O*-isopropylidene-α-D-allofuranose is a triplet. Therefore, **3** is undoubtedly 3-deoxy-3-*C*-"hydroxymethyl"-1,2:5,6-di-*O*-isopropylidene-α-D-allofuranose. Compound **3** was readily converted into its crystalline *p*-bromobenzenesulfonate derivative.

Benzoylation of **5** in the usual way afforded 1′,5,6-tri-*O*-benzoyl-3-deoxy-3-*C*-"hydroxymethyl"-1,2-*O*-isopropylidene-α-D-allofuranose (**6**) in 88% yield. Acetolysis of the latter with acetic anhydride – acetic acid – sulfuric acid gave

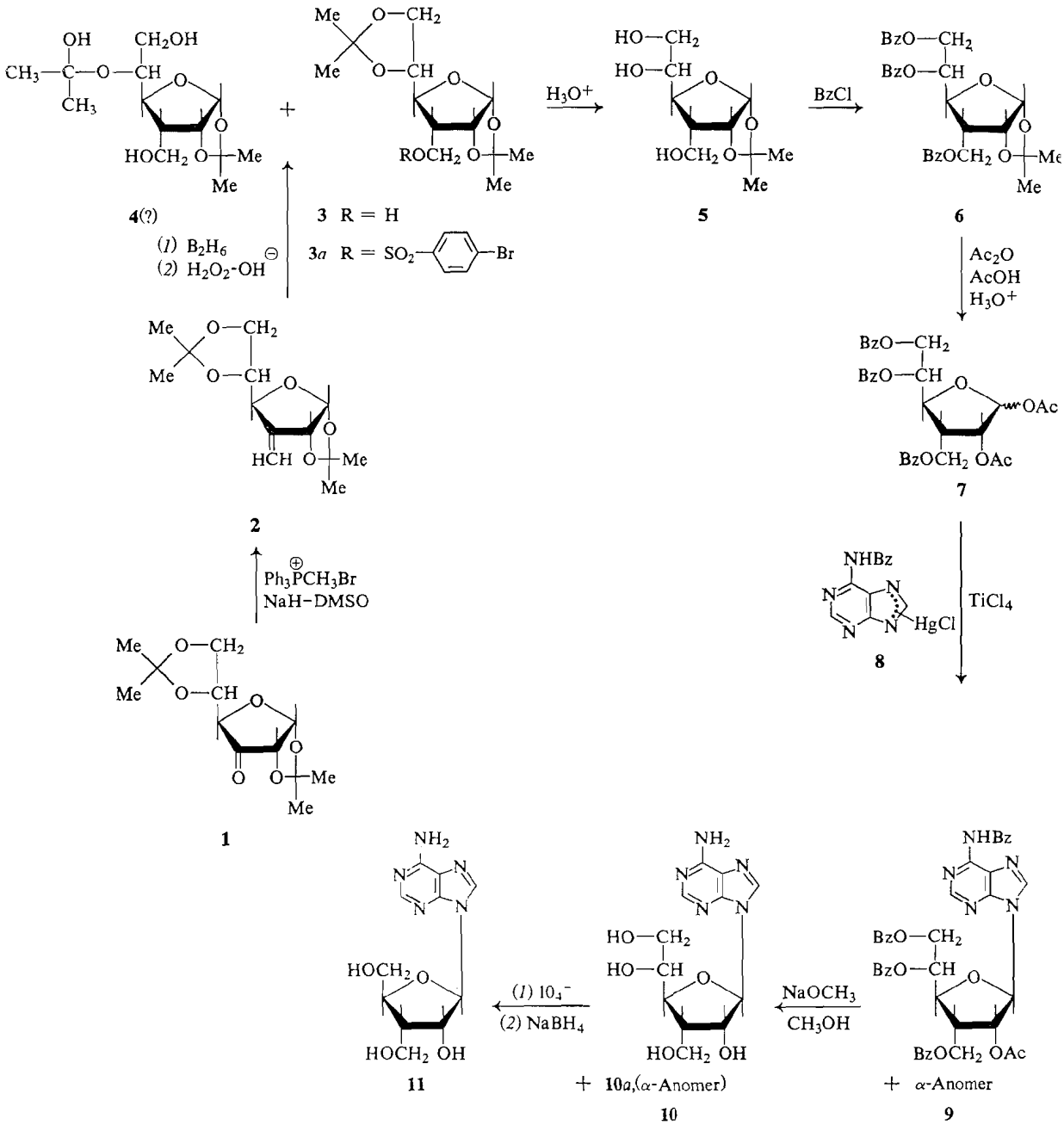

the anomeric mixture of diacetates **7** in 65% yield. Condensation of **7** with 6-benzamidochloromercuripurine (**8**) by the titanium tetrachloride method (1) gave a mixture of blocked nucleosides **9** which was immediately unblocked with methanolic sodium methoxide to give a mixture of the β-D (and α-D)-nucleosides **10** in the ratio of 11:1. Fractional crystallization of this mixture from 80% methanol–water afforded crystalline 9-(3-deoxy-3-*C*-"hydroxymethyl"-β-D-allofuranosyl)adenine (**10**) in 44% yield, based on the diacetate **7**. After the solvent from the

Can. J. Chem. Downloaded from www.nrcresearchpress.com by 210.87.254.42 on 09/05/12
For personal use only.

Can. J. Chem. Downloaded from www.nrcresearchpress.com by 210.87.254.42 on 09/05/12
For personal use only.

mother liquor was evaporated to dryness, the residue was partially separated by gradient elution chromatography on Dowex 1 × 2 (OH^-) resin (5) using water, followed by aqueous methanol as developers, to afford pure β-D-anomer and a mixture of the α-D- and β-D-anomers (**10**). The latter was separated by preparative paper chromatography to yield the syrupy α-D-anomer of **10** in about 4% yield.

The assignment of structure of both anomers of **10** was based on ultraviolet (u.v.), optical rotatory dispersion (o.r.d.), and p.m.r. spectra. Such evidence, although not unequivocal when only one anomer is available, as in our first investigation (1), is more definitive for the proof of structure of both anomers **10** because a comparison of the physical measurements of both could be made. For example, as expected, **10***a* gave a positive Cotton effect whereas **10** showed the normal negative Cotton effect. From a mechanistic viewpoint, it is surprising that branched-chain sugars having either a hydroxyethyl or methyl group on C-3 gave only the β-D-anomeric nucleoside (1, 3) whereas the hydroxymethyl analogue reported herein afforded both anomers.

In order to prepare the ribo nucleoside **11**, the β-D-allo-nucleoside (**10**) was degraded by sodium metaperiodate to the *aldehydo* nucleoside. The latter was immediately reduced with sodium borohydride to yield crystalline 9-(3-deoxy-3-*C*-"hydroxymethyl"-β-D-ribofuranosyl)adenine (**11**) in 81% yield. In the latter nucleoside, nuclear magnetic resonance (n.m.r.) evidence (H-1 gave a doublet having $J_{1,2} = 2$ Hz) substantiates the β-anomeric configuration of **11** and of **10**.

In an attempt to increase the over-all yield of **10** from **3**, the latter was subjected to fewer steps as outlined below. Acetolysis of **3** followed by treatment of the resulting mixture of peracetates with anhydrous hydrogen chloride in ether gave a mixture of glycosyl halides. This mixture was not purified but was condensed with **8** to afford a mixture of compounds. The main fluorescing component of this mixture was separated by preparative t.l.c. on silica gel to yield a crystalline blocked nucleoside in an overall yield of about 9% which was deblocked with methanolic sodium methoxide affording a non-crystalline nucleoside having the same R_f and u.v. spectrum as that of an authentic sample of **10**. The low yield of **9** might be ascribed to the fact that acetolysis of **3** probably yielded both the allopyranose and allofuranose peracetates because of ring opening during the reaction (t.l.c. of the peracetate mixture showed at least three components and n.m.r. revealed three low field signals that might be attributed to three anomeric hydrogens of three different peracetates); the allofuranose peracetates on treatment with hydrogen chloride would be converted into a mixture of allofuranosyl chlorides but the α-allopyranose peracetate would be unaffected since it is known that only the β-pyranose peracetate reacts with anhydrous hydrogen chloride in ether.

In an attempt to shed additional light on the chemistry of branched-chain sugars, the blocked branched-chain sugar **3** was unblocked by two different routes. In the first method, when **3** or **7** was subjected to acetolysis followed by treatment with methanolic sodium methoxide, a mixture of four distinct compounds (as evidenced by paper chromatography) was formed. When the major component having the highest R_f was separated by preparative chromatography and allowed to stand in water, it surprisingly gave a complex mixture of substances which could not be separated. In the second procedure **3** was hydrolyzed with dilute acid to give a mixture of three substances, two of which only had the same R_f as those obtained by acetolysis and saponification of **3**.

Experimental

General considerations were similar to those previously described (1, 3). Silica gel G was used in the t.l.c. For column chromatography Silica gel Woelm 100–200 mesh, activity grade II, was used.

Hydroboration Followed by Alkaline Hydrogen Peroxide Oxidation of 1,2:5,6-Di-O-isopropylidene-3-C-methylene-α-D-ribo-hexofuranose (2) to Yield 3-Deoxy-3-C-"hydroxymethyl"-1,2:5,6-di-O-isopropylidene-α-D-allofuranose (3)

Into a solution of compound **2** (3) (1.3 g, 0.005 mole) in anhydrous tetrahydrofuran (16 ml) was slowly bubbled a large excess of commercial diborane for 4 h at room temperature. It is essential that the tetrahydrofuran be saturated with diborane. In preliminary experiments a stoichiometric amount of diborane gave a negligible yield of product in which diborane had added to the olefinic double bond of the sugar. After the reaction mixture was cooled to 0° a 50% aqueous mixture of tetrahydrofuran (5 ml) was added dropwise with vigorous stirring, followed by the addition of 2 *N* sodium hydroxide (15 ml) and then 30% hydrogen peroxide (8 ml). The reaction mixture was allowed to come to room temperature and stirred for a further 0.5 h. After the solvent was removed under reduced pressure, the residue was

Can. J. Chem. Downloaded from www.nrcresearchpress.com by 210.87.254.42 on 09/05/12
For personal use only.

dissolved in 40 ml water and the aqueous solution extracted with 4 × 20 ml of ether. The combined ether extracts were dried over magnesium sulfate, filtered, and evaporated under reduced pressure to afford 1.23 g (88%) of a syrup. An aliquot of this product was separated by preparative t.l.c. on silica gel G using a 1:1 mixture of benzene–ethyl acetate as developer into two components having R_f's of 0.5 and 0.2 in the ratio of 3:1. The faster moving component (**3**) was a syrup, $[\alpha]_D^{22}$ + 103° (*c* 2, chloroform), τ($CDCl_3$), 4.25 (d, $J_{1,2}$ = 4 Hz, H-1), 5.28 (t, H-2), 6.1 (m), 6.95 (peak due to H of OH), 7.9 (m, H-3), 8.6 (two isopropylidene groups). The slower moving fraction **4** had $[\alpha]_D^{22}$ + 96° (*c* 1, chloroform) and τ($CDCl_3$) 4.25 (d, $J_{1,2}$ = 4 Hz, H-1), 5.28 (t, H-2), 6.25 (m), 6.95 (s, due to OH), 7.9 (m, H-3), 8.4–8.9 (two isopropylidene groups). Selective hydrolysis (1) of **3** and of **4** using 0.1 *N* sulfuric acid yielded the same compound **5**, described in a subsequent section.

*1-O-p-Bromophenylsulfonyl-3-deoxy-3-C-"hydroxymethyl"-1,2:5,6-di-O-isopropylidene-*α-D-*allofuranose (3a)*

An amount (0.137 g) of **3** in anhydrous pyridine (0.5 ml) was allowed to react with freshly recrystallized *p*-bromophenylsulfonyl chloride (0.141 g) at room temperature for 1 h. After adding 10 ml water, the solid precipitate was removed by filtration and recrystallized from methanol to yield 0.186 g (76%) of **3***a*, m.p. 101–102°; $[\alpha]_D^{22}$ + 71° (*c* 1, chloroform); R_f 0.35 (10:1 benzene–ethyl acetate); τ($CDCl_3$) (100 Mc) 2.25 (m, phenyl), 4.28 (d, $J_{1,2}$ = 3.8 Hz, H-1), 5.38 (t, H-2), 5.7–6.5 (m), 7.7 (m, H-3), 8.65 (two isopropylidene groups).

Anal. Calcd. for $C_{19}H_{25}BrO_8S$: C, 46.25; H, 4.93; Br, 16.20; S, 6.50. Found: C, 46.21; H, 5.14; Br, 16.41; S, 6.72.

*3-Deoxy-3-C-"hydroxymethyl"-1,2-O-isopropylidene-*α-D-*allofuranose (5)*

Selective hydrolysis (1) of the mixture of **3** and **4** (1.12 g) using 0.1 *N* sulfuric acid gave 0.89 g (95%) of **5**, $[\alpha]_D^{22}$ + 75° (*c* 1, chloroform); R_f 0.45 (3:1 benzene–methanol); τ($CDCl_3$), 4.2 (d, $J_{1,2}$ = 3.5 Hz, H-1), 5.22 (t, H-2), 5.8–6.4 (m), 7.8 (m, H-3), 8.55 (d, one isopropylidene group).

*1,5,6-Tri-O-benzoyl-3-deoxy-3-C-"hydroxymethyl"-1,2-O-isopropylidene-*α-D-*allofuranose (6)*

Benzoylation of 0.7 g of **5** in the usual way gave 1.22 g (88%) of **6** which was purified by column chromatography on silica gel using 10:1 benzene–ethyl acetate as developer. Compound **6** was crystallized from chloroform, m.p. 80–81°; $[\alpha]_D^{22}$ + 24° (*c* 3, chloroform); τ($CDCl_3$) 2–2.5 (m, phenyl), 4.1 (d, $J_{1,2}$ = 3.8 Hz, H-1), 5.15 (t, H-2), 5.2–5.7 (m), 7.8 (m, H-3), 8.5 (d, isopropylidene group).

Anal. Calcd. for $C_{31}H_{30}O_9$: C, 68.12; H, 5.53. Found: C, 68.89; H, 5.69.

*1,2-Di-O-acetyl-1,5,6-tri-O-benzoyl-3-deoxy-3-C-"hydroxymethyl"-*β*(and* α*-)-*D*-allofuranose (7)*

The benzoate **6** (1.10 g) was acetolyzed for 3 days in the usual way (1, 3) to afford 0.77 g (65%) of **7** as a syrup, $[\alpha]_D^{22}$ 0° (*c* 2, chloroform); R_f 0.4 (10:1 benzene–ethyl acetate); τ($CDCl_3$) 1.9–2.5 (m, phenyl groups), 3.90 (s, H-1; ratio of β:α anomer, about 5:1).

*9-(3-Deoxy-3-C-"hydroxymethyl"-*β*-(and* α*-)-*D*-allofuranosyl)adenine (10)*

A mixture of 0.59 g (0.001 mole) of **7**, 0.530 g (0.001 mole) of 6-benzamidochloromercuripurine (**8**), 0.3 g of Celite, and 25 ml of anhydrous xylene was freed of moisture by distilling off the xylene under reduced pressure. To the residue were then added 20 ml of ethylene dichloride and 5 ml of the solvent was distilled off. To the reaction mixture, which was kept under reflux, was then added dropwise a solution of 1,2-dichloroethane (3 ml) and titanium tetrachloride (0.12 ml) and the resulting solution refluxed for 4 h. The cooled reaction mixture was poured with stirring into 25 ml saturated sodium bicarbonate, stirred for a further 0.5 h, filtered, and the Celite cake washed with 3 × 20 ml chloroform. The chloroform extract was washed with 30% aqueous potassium iodide (10 ml) and then water (2 × 20 ml), dried over magnesium sulfate, filtered, and evaporated to dryness. The residue was dissolved in 15 ml methanol, norited, and evaporated to dryness. Extraction of the residue with boiling petroleum ether (30–60°) left the solid blocked nucleoside **9** (0.42 g, 56%), R_f 0.3 (1:2 benzene–ethyl acetate) and τ($CDCl_3$), 0.7 (m), 1.4 (m), 2.0 (m), 2.5 (m), 3.9 (s), 5.3 (m), 7.9 (m).

The blocked nucleoside **9** (0.42 g) was allowed to react with 0.1 *N* methanolic sodium methoxide and the product worked-up as described previously (3) to give after crystallization from 80% aqueous methanol 0.118 g (67%) of the β-D-anomer (**10**), m.p. 238°, $[\alpha]_D^{22}$ −12° (*c* 2, water); λ_{max} (H_2O) 261 (ε = 12 600); R_f (adenine), 0.68 on Whatman No. 1 paper (water as developer); τ(D_2O) (60°), 4.1 (d, $J_{1',2'}$ = 3 Hz, H-1'); $[\phi]_{269}$ −390°, $[\phi]_{259}$ 0°, $[\phi]_{245}$ +145° (*c* 0.003, water).

Anal. Calcd. for $C_{12}H_{17}N_5O_5$: C, 46.30; H, 5.50; N, 22.50. Found: C, 46.24; H, 5.66; N, 22.70.

The mother liquor from the above recrystallization was evaporated to dryness and the residue then dissolved in 20 ml water. The aqueous solution was twice extracted with 10 ml portions of ether. The aqueous layer which showed the presence of three fluorescent materials was applied to 10 ml (1 cm diam) of a column of Dowex 1 × 2 (OH^-) resin. Fractionation of the zones was achieved as described previously (3, 8) using water followed by 30% methanol and finally 60% aqueous methanol (each about 100 ml). From the 30% methanol eluant there was obtained an additional amount of 0.023 g of β-D-nucleoside **10**. The α-D-anomer **10***a*, contaminated with a little β-D-anomer, was obtained from the 60% aqueous methanol eluant. This mixture was separated by preparative paper chromatography using water as developer to afford 0.0124 g (4%) of α-D-anomer **10***a*, having R_{Ad} = 0.85; λ_{max} (H_2O) 258 (ε = 11 800); $[\alpha]_D^{22}$ = +24° (*c* 1, water). The o.r.d. curve of the α-D-anomer showed a positive Cotton effect in the region of 260 mμ. An attempt to convert syrupy α-D-anomer **10***a* into crystalline material led to accidental loss of all material.

Sodium Metaperiodate Oxidation and Reduction of the β-D-*allo-Nucleoside **10** to Yield 9-(3-Deoxy-3-C-"hydroxymethyl"-*β*-*D*-ribofuranosyl)adenine (11)*

The β-D-nucleoside **10** (0.155 g) was degraded by a previously described procedure (3) to yield on recrystallization 0.113 g (81%) of ribo nucleoside **11**, m.p. 213–214°; $[\alpha]_D^{22}$ −26° (*c* 1, water); λ_{max} (H_2O) 261 (ε =

Can. J. Chem. Downloaded from www.nrcresearchpress.com by 210.87.254.42 on 09/05/12
For personal use only.

13 400); R_{Ad} 0.96; τ(methyl sulfoxide-d_6) (100 Mc), 1.66 (s, H-2), 1.94 (s, H-8), 2.83 (s, NH_2), 4.18 (d, $J_{1,2} = 2$ Hz, H-1), 4.42 (d), 4.86 (m), 5.52 (m), 6.00 (m), 6.4 (m), 7.68 (m, H-3′, near methyl sulfoxide peak).

Anal. Calcd. for $C_{11}H_{15}N_5O_4$: C, 46.97; H, 5.36; N, 24.90. Found: C, 46.94; H, 5.37; N, 24.75.

Direct Conversion of **3** *into* β-D-*allo-Nucleoside* **10**

An amount of 0.47 g of branched-chain sugar **3** was subjected to acetolysis in the usual way (3) to yield 0.48 g (67%) of a mixture of at least 3 peracetates. The R_f's of the major components of the mixture were 0.62 and 0.55 using 1:1 benzene–ethyl acetate; $[\alpha]_D^{22}$ 0° (*c* 2, $HCCl_3$); τ($CDCl_3$) 3.9 (s), 4.0 (small peak), 4.75 (d, $J_{1,2} = 5$ Hz). The ratio of these peaks was about 4:1:2. Preparative t.l.c. of an aliquot of the peracetates gave two components having different n.m.r.'s (the faster moving component showed H-1 as a singlet at τ 3.90 whereas the slower component exhibited the doublet at τ 4.75).

An aliquot of the mixture of peracetates (0.100 g) was allowed to react with anhydrous hydrogen chloride in ether (20 ml) at room temperature for 1 day. After the solvent was removed under reduced pressure 5 ml of anhydrous toluene was added to the residue and the solvent again removed under vacuum. The resulting glycosyl halide was dissolved in anhydrous xylene and allowed to react under reflux conditions for 5 h and the product worked-up in the usual way (2). Thin-layer chromatography of the product (1:2 benzene–ethyl acetate) revealed 5 spots. Preparative t.l.c. of the mixture on silica gel G gave 9-(1,2,5,6-tetra-*O*-acetyl-β-D-allofuranosyl)-6-benzamidopurine 0.015 g (9%); R_f 0.4. This nucleoside was recrystallized from methanol, m.p. 135–135°; $[\alpha]_D^{22}$ −18° (*c* 1, $CHCl_3$); λ_{max} (ethanol) 262 mμ (ε 6400).

Anal. Calcd. for $C_{26}H_{29}O_{20}N_5$: N, 12.15. Found: N, 12.20.

The above blocked nucleoside was allowed to react with sodium methoxide according to the method previously described, λ_{max} (H_2O) 261; R_f (adenine) 0.68 (compared directly with authentic **10** on the same sheet of paper).

Attempts to Prepare Unblocked Branched-chain Sugars of Compound **3**

The mixture of peracetates described in the previous section was separated into 2 components by preparative t.l.c. on silica gel G and each component (0.050 g) was then deacetylated with methanolic sodium methoxide. Paper chromatographic examination using ethyl acetate, pyridine, water 8:2:2 as developer revealed that each fraction gave 4 identical spots having R_{Gl} 1.1, 1.4, 1.6, and 2.8. The fastest moving zone was eluted with water (0.015 g) and had $[\alpha]_D^{22}$ + 46° (*c* 1, water). Rechromatography of this zone after standing for several days showed that this component had changed into a mixture of compounds which were poorly resolved. Attempts to crystallize this compound were unsuccessful. The same complicated mixture of compounds (by paper chromatography) was obtained when compound **7** was treated with methanolic sodium methoxide.

When compound **3** (0.270 g) was hydrolyzed with 1% sulfuric acid (5 ml) at 60° for 1.5 h and the product worked-up in the usual way, 3 major components having R_{Gl} of 1.1, 1.4, and 1.86 were obtained.

Acknowledgments

This work was supported in part by the National Research Council of Canada and by a University of British Columbia Research Grant. We thank Dr. L. D. Hall for many helpful discussions of the n.m.r. The authors also thank the U.S. National Cancer Institute (Grant CA-08382) for carrying out biological tests of the nucleosides.

1. A. ROSENTHAL and L. NGUYEN. J. Org. Chem. **34**, 1029 (1969).
2. A. ROSENTHAL, M. SPRINZL, and H. J. KOCH. Can. J. Chem. **47**, 3263 (1969).
3. A. ROSENTHAL and M. SPRINZL. Can. J. Chem. **47**, 3941 (1969).
4. M. L. WOLFROM, K. MATSUDA, F. KOMITSKY, JR., and T. E. WHITELEY. J. Org. Chem. **28**, 3551 (1963).
5. H. PAULSEN and H. BEHRE. Carbohyd. Res. **2**, 81 (1966).
6. H. C. BROWN, K. J. MURRAY, L. J. MURRAY, J. A. SNOVER, and G. ZWEIFUL. J. Amer. Chem. Soc. **82**, 4233 (1960).
7. R. J. ABRAHAM, L. D. HALL, L. HOUGH, and K. A. MCLAUCHLAN. J. Chem. Soc. 3699 (1962).
8. A. P. MARTINEZ, W. W. LEE, and L. GOODMAN. J. Org. Chem. **34**, 92 (1969).

Can. J. Chem. Downloaded from www.nrcresearchpress.com by 210.87.254.5 on 09/05/12
For personal use only.

Tautomérie des composés chloroacylés d'aminobenzothiazoles à l'état solide

E. COSTAKIS ET P. CANONNE
Département de Chimie, Université Laval, Québec 10, Québec

ET

G. TSATSAS
Laboratoire de Chimie Pharmaceutique, Université d'Athènes, 104, rue Solonos, Athènes, Grèce

Reçu le 5 Juin, 1969

Nous rapportons la séparation, par recristallisation, des deux formes tautomères, imido et amido, des dérivés chloroacetylés et α-chloropropionylés de l'amino-2 benzothiazole. Le choix du solvant permet non seulement l'obtention de l'une ou de l'autre forme séparément, mais aussi le passage de l'une à l'autre.

La structure de chaque forme tautomère a été déterminée au moyen de leurs spectres infrarouges et ultraviolets.

The isolation by crystallization of the tautomeric imido and amido forms of the chloroacetyl and α-chloropropionyl-2 aminothiazoles is reported. A judicious choice of solvents leads to the separation of one or the other tautomer and also allows interconversions.

The structure of each form has been determined from the corresponding ultraviolet and infrared spectra.

Canadian Journal of Chemistry, 47, 4483 (1969)

Dès 1926, Hunter et son collaborateur (1*a*, *b*) ont montré que l'aminobenzothiazole et ses dérivés existent sous deux formes tautomères (I) et (II).

Dans une étude récente sur la tautomérie des composés hétérocycliques par spectroscopie infrarouge (i.r.) et ultraviolet (u.v.), Peresleni et ses collaborateurs ont prouvé un tel équilibre tautomère pour les dérivés acylés et alcoylés de l'amino-2 thiazole, de l'amino-2 benzothiazole, (2*a*) de l'amino-2 thiazoline (2*b*,*c*), et de l'amino-2 thiazolone-4 (2*d*); ils constatèrent aussi que les deux formes tautomères sont présentes dans le même cristal bien que l'examen cristallographique n'ait montré qu'une seule forme cristalline (2*b*).

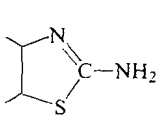

I

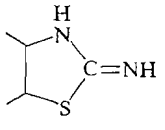

II

Nous avons également remarqué durant nos travaux (3) sur les dérivés de l'aminobenzothiazole que ces composés chloroacylés se présentent dans la plupart des cas, indépendamment de leur mode de préparation mais selon les moyens de recristallisation, sous deux formes cristallines donnant la même analyse élémentaire mais ayant des points de fusion et des spectres différents.

Dans le présent mémoire, nous établissons que ces formes cristallines différentes d'un dérivé chloroacylé de l'aminobenzothiazole sont deux tautomères et appartiennent aux structures imido et amido de l'équilibre tautomère (III et IV).

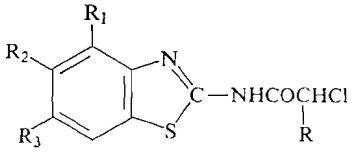

III

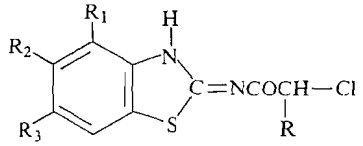

IV

Un exemple, entre-autres, l'(α-chloropropionylamino)-2 benzothiazole (R = CH_3, $R_1 = R_2 = R_3 = H$), par recristallisation dans le mélange benzène–éther de pétrole s'obtient sous deux formes cristallines, que nous avons séparé mécaniquement, et dont les points de fusion sont: 114–115 (*a*) et 124–125 °C (*b*). Par nouvelle cristallisation dans un autre solvant de l'une des deux formes cristallines on obtient de nouveau, presque toujours, un mélange de deux

Can. J. Chem. Downloaded from www.nrcresearchpress.com by 210.87.254.5 on 09/05/12
For personal use only.

TABLEAU I

	Composés				Spectres infrarouges§						Spectres ultraviolets‖	
					Type III*			Type IV*				
No.	R	R_1	R_2	R_3	C=O cm^{-1}	C=C cm^{-1}	C=N cm^{-1}	C=O cm^{-1}	C=C cm^{-1}	C=N cm^{-1}	λ_{max} mμ	ε_{max}
1	CH_3	H	H	H	1720	1605	1566	1680	1608	1560	210,278	24.440, 18.540
2	H	H	H	H	1715	1600	1565	1675	1605	1562	207,277	20.860, 16.100
3	H	H	H	CH_3O	1710	1615	1580	1670	1620	1560	217,308	23.000, 19.000
4	H	H	H	C_2H_5O	1715	1605	1583	1670	1612	1560	216,308	27.940, 22.000
5	H	H	H	Cl	—	—	—	1678	1603	1558	210,280	24.500, 20.000
6	H	Cl	H	H	1690	1598	1556	—	—	—	218,285,304	23.900, 20.000, 18.400
7	H	H	CH_3	CH_3	1730	1610	1556	—	—	—	210,284,305	24.200, 19.100, 18.100
8†					—	—	—	1630	1588	1518	215,314	20.660, 22.700
9‡					—	—	—	1640	1590	1510	215,313	20.250, 22.200

*Les deux types de structures sont:

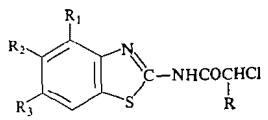

III

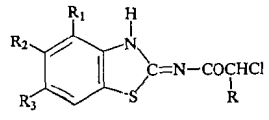

IV

†(α-Chloropropionylimino)-2 methyl-3 benzothiazoline.
‡(Chloroacetylimino)-2 methyl-3 benzothiazoline.
§Les spectres i.r. dans KBr.
‖Dans éthanol 95%.

Can. J. Chem. Downloaded from www.nrcresearchpress.com by 210.87.254.5 on 09/05/12
For personal use only.

tautomères *a* et *b* ayant les mêmes points de fusion 114–115 et 124–125 °C.

En outre, par recristallisation des deux formes dans le cyclohexane et pour l'exemple choisi, on parvient à un seul composé solide *b* de point de fusion 124–125 °C tandis que par l'utilisation d'une grande quantité d'éther de pétrole on parvient au composé solide *a* de point de fusion 114–115 °C.

L'analyse élémentaire de ces deux substances donne la même formule brute, néanmoins, les spectres infrarouges à l'état solide sont très différents.[1]

En effet, les spectres i.r. présentent dans la région de 1500 à 1720 cm^{-1}, pour les deux formes *a* et *b*, trois bandes intenses, mais la position de chacune est différente pour chaque tautomère. Ainsi pour la forme *a*, on trouve ces trois bandes à 1720, 1605, et 1566 cm^{-1} et pour la forme *b* elles sont fortement déplacées et se trouvent respectivement à 1680, 1608, et 1560 cm^{-1}. Nous pensons que la forme *a* correspond au tautomère ayant la structure amido. Nous attribuons la bande à 1720 cm^{-1} à l'absorption caractéristique du groupement carbonyle légèrement déplacée vers des fréquences plus élevées, la bande à 1605 cm^{-1} au noyau aromatique, et la bande à 1566 cm^{-1} à la liaison C=N du cycle thiazolique (6).

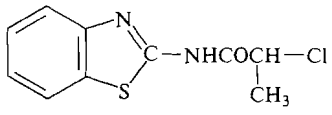

V

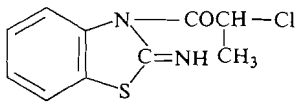

VI

La forme *b* correspond au tautomère ayant la structure imido. Nous attribuons par conséquent la bande 1680 cm^{-1} à l'absorption du groupement fonctionnel imido (C=N—C=O) (3*b*), la bande 1608 cm^{-1} au noyau benzénique, et enfin la bande à 1560 cm^{-1} à l'absorption du (C=N) exocyclique.

[1]Nous avons exclu la possibilité de formation de deux isomères (V) et (VI) car l'acylation conduit seulement aux dérivés exocycliques de l'azote contrairement à l'alkylation qui fournit les composés alkylés en position 3 sur l'azote cyclique (2,4,5).

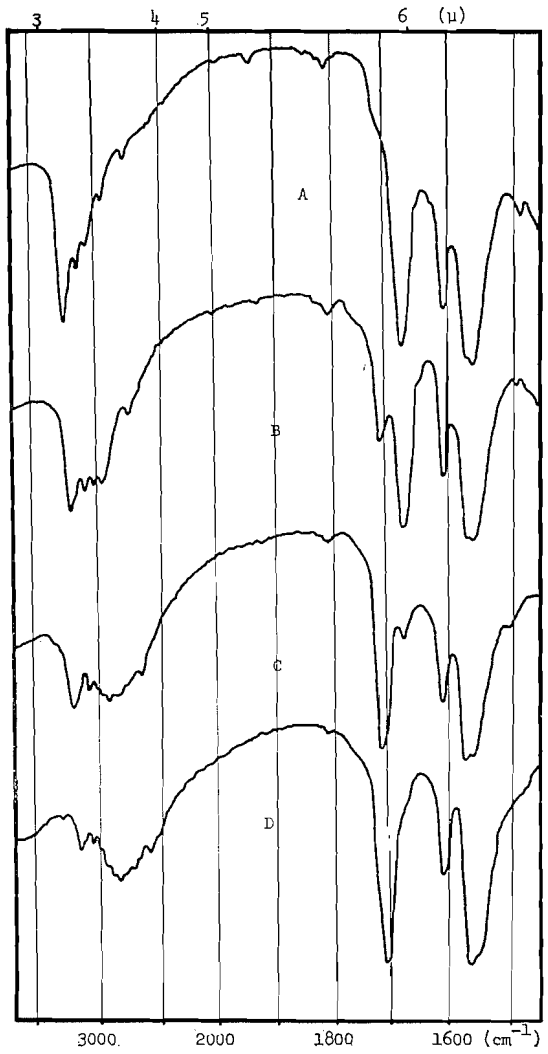

FIG. 1. Spectres i.r. dans KBr de l'(α-chloropropionylamino)-2 benzothiazole A: forme imido, D: forme amido, B et C mélanges des deux formes.

Dans la Fig. 1 nous rapportons quatre spectres i.r. à l'état solide (dans KBr) qui illustrent ces données. Les spectres A et D correspondent respectivement à la forme imido et amido pures tandis que les spectres B et C sont des mélanges des deux tautomères tels qu'obtenus par recristallisations.

Par comparaison nous avons dressé dans le tableau I: (*i*) Les valeurs de trois bandes caractéristiques de la forme imido pour le (α-chloropropionylimino)-2 methyl-3 benzothiazoline (**8**) et le (chloroacetylamino)-2 methyl-3 benzothiazoline (**9**). (*ii*) Les valeurs de trois bandes

caractéristiques de la forme amido d'une part et de la forme imido d'autre part pour les dérivés chloroacylés qui montrent les mêmes facilités de séparation des deux formes tautomères que l'(α-chloropropionylamino)-2 benzothiazole; en l'occurence, le (chloroacetylamino)-2 methoxy-6 benzothiazole (**3**), le (chloroacetylamino)-2 ethoxy-6 benzothiazole (**4**), et le (chloroacetylamino)-2 benzothiazole (**2**). (*iii*) Les valeurs spectrales des trois autres dérivés chloroacylés dont malgré les nombreuses tentatives de recristallisation dans différents solvants nous n'avons isolé qu'une forme cristalline. Nous les avons classés d'après les bandes caractéristiques de leurs spectres i.r. pris dans KBr. Il est vraisemblable que les deux formes existent à l'état solide si nous nous référons aux spectres u.v. (Fig. 4) soit que dans ces cas particuliers la résolution soit faible, soit que l'une des deux formes prédomine.

Leurs spectres i.r. pris en solution dans le chloroforme et le dioxanne, rapportés à la Fig. 2, laissent prévoir l'existence des deux formes, si on

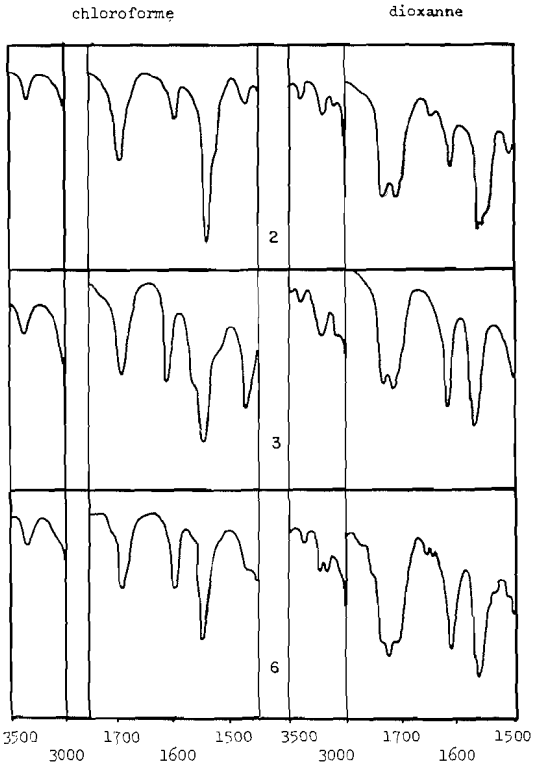

FIG. 2. Spectres i.r. des composés **2**, **3**, et **6** en solution dans le dioxanne et dans le chloroforme.

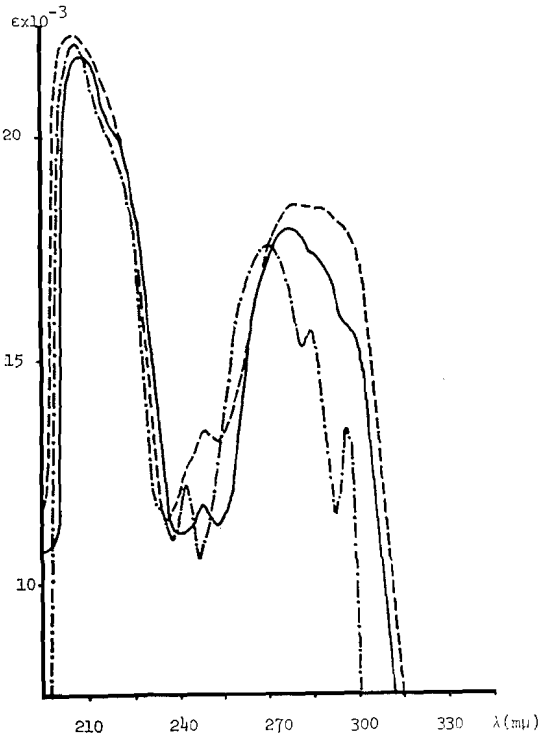

FIG. 3. Spectre u.v. de composé **1**; —— dans l'éthanol; - . - . - . dans le *n*-hexane; - - - - - dans HCl *N*/10.

les compare dans les composés **2** et **3** que nous avons démontré précédemment peuvent être un mélange des deux tautomères.

Les spectres u.v. de ces mêmes composés résumés au tableau I sont représentés par les Figs. 3–5, dans trois solvants différents. Nous remarquons d'une part que la (chloroacetylamino)-2 methylbenzothiazoline **9** de structure imino bien caractéristique présente un maximum d'absorption dans la région 313 mμ lequel de même que le coefficient d'absorption (ε_{max} 22 200–22 220) est peu modifié sous l'influence de la polarité du solvant (2*b*).

D'autre part les composés **1–4** qui par cristallisation ont donné les deux formes cristallines, comme nous l'avons montré par l'analyse i.r., voient leurs maxima d'absorption se déplacer vers le visible avec la polarité du solvant (Fig. 3): nous attribuons l'absorption aux longueurs d'ondes plus élevées à la présence de la forme imido (système conjugué (—C=N—C=O) tandis que l'absorption aux plus faibles longueurs d'ondes à la forme amido (—N=C—NH—

Can. J. Chem. Downloaded from www.nrcresearchpress.com by 210.87.254.5 on 09/05/12
For personal use only.

Can. J. Chem. Downloaded from www.nrcresearchpress.com by 210.87.254.5 on 09/05/12
For personal use only.

C=O). Nous sommes par conséquent tentés de faire une correlation entre la possibilité de séparer les deux formes cristallines et le déplacement des maxima de ces substances sous l'influence de solvants; à l'inverse à considérer, la Fig. 4 qui montre un faible déplacement de maxima du composé **5** comme nous l'avons mentionné, la séparation de deux formes cristallines ne s'est pas révélée possible. Toutefois nous ne pouvons pas conclure à l'inexistence de deux formes tautomères.

Enfin dans le spectre de résonance magnétique nucléaire (r.m.n.) de l'(α-chloropropionyl-amino)-2 benzothiazole le signal de NH amido se manifeste à 660 c.p.s. et celui de NH imido à 627 c.p.s. Malheureusement la faible solubilité de ces composés dans tous les solvants ne nous a pas permis d'en effectuer une étude comparative.

Partie expérimentale

Les points de fusion ont été déterminés avec un appareil à tubes capillaires et sont rapportés non corrigés. Les spectres i.r. ont été enregistrés sur un spectrophotomètre Beckmann IR-4, vérifiés avec un film de polystyrène, pris soit l'état solide soit en pastilles de KBr en dispersion dans le nujol; aussi en solution dans le $CHCl_3$, CCl_4, et dioxanne. Les spectres u.v. ont été déterminés sur un appareil Beckmann DK-1 dans l'alcool, cyclohexane et HCl *N*/10.

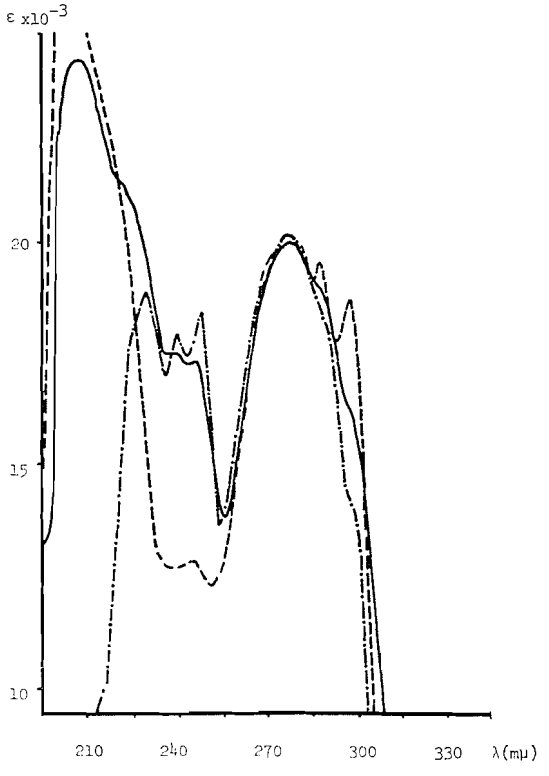

FIG. 4. Spectre u.v. de composé **5**; —— dans l'éthanol; - . - . - . dans le cyclohexane; - - - - dans HCl *N*/10.

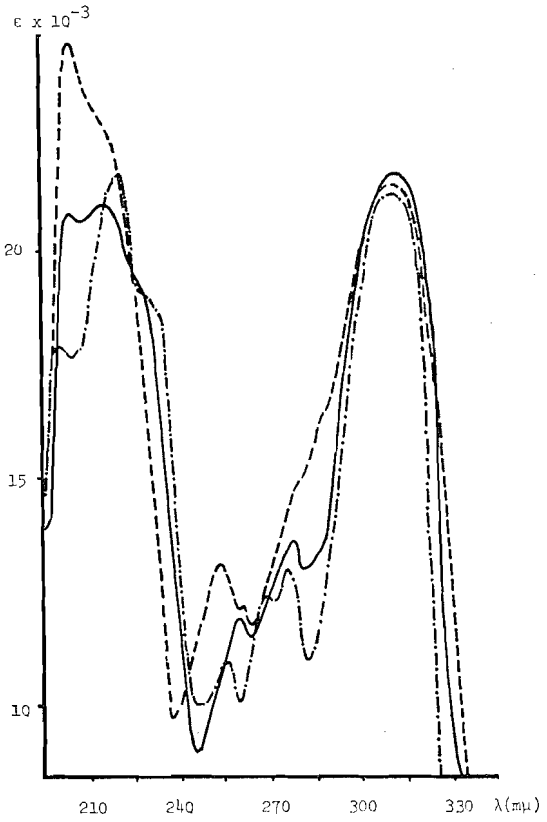

FIG. 5. Spectre u.v. de composé **9**; —— dans l'éthanol; - . - . - . dans le cyclohexane; - - - - dans HCl *N*/10.

Préparations des (chloroacylamino)-2 benzothiazoles

Méthode A. A une solution de 0.1 mole d'amino-2 benzothiazole dans 200 ml de $CHCl_3$ on met 0.11 mole de Na_2CO_3 dans 75 ml d'eau sous agitation magnétique puis on ajoute goutte à goutte une solution de 0.11 mole de chlorure de chloroacide dissout dans 20 ml d'éther anhydre (durant 30 min). Le mélange est filtré et lavé à l'eau. Les eaux mères sont décantées et la couche chloroformique est ensuite lavée à l'acide chlorohydrique 5%, $NaCO_3$ 5% puis à l'eau. On sèche sur Na_2SO_4 anhydre, on évapore le chloroforme et on récupère encore une petite quantité du dérivé chloroacylèque l'on rejoint au composé déjà recueilli par filtration.

Méthode B. A une solution de 0.1 mole d'amino-2 benzothiazole dans 15 ml de benzène anhydre sous agitation magnétique, on ajoute goutte à goutte pendant 30 min 0.12 mole de chlorure de chloroacide dissout dans 30 ml

Can. J. Chem. Downloaded from www.nrcresearchpress.com by 210.87.254.5 on 09/05/12
For personal use only.

de benzène anhydre (7, 8). On continue l'agitation pendant 1 h en chauffant (65–70 °C) puis à reflux et on évapore le 1/3 du solvant; on refroidit, on décante, on lave au bicarbonate de sodium, puis à l'eau, on sèche sur P_2O_5.

Méthode C. A une solution de 0.065 mole d'amino-2 benzothiazole dans 100 ml d'acétone contenant 13.6 g de CH_3COONa anhydre on ajoute goutte à goutte pendant 15–20 min 0.075 mole de chlorure de chloroacide (9). On maintient l'agitation et chauffe à 60 °C durant 1 h; on refroidit, puis ajoute 25 ml de HCl 5 *N* et 100 ml d'eau. Le mélange est filtré, lavé à l'eau puis séché sur P_2O_5.

*(α-Chloropropionylamino)-2 benzothiazole (**1**)*

Préparé selon les méthodes A (rendement 45%) et B (rendement 70%). Par recristallisation dans le mélange benzène–éther de pétrole on obtient deux formes cristallines (*a*) p.f. 114–115 °C et (*b*) 124.5 °C. Par recristallisation dans le cyclohexane on obtient p.f. 124.5 °C. Par recristallisation dans une grande quantité d'éther de pétrole on obtient p.f. 114–115 °C.

Anal. calc. pour $C_{10}H_9ON_2ClS$: C, 49.89; H, 3.77; N, 11.63; Cl, 14.73; S, 13.33. Trouvé (*a*): C, 49.73; H, 3.67; N, 11.61; Cl, 14.77; S, 13.27; (*b*): C, 49.73; H, 3.92; N, 11.56; Cl, 14.70; S, 13.25.

*(Chloroacetylamino)-2 benzothiazole (**2**)*

Préparé selon les méthodes A (rendement 48%), B (rendement 96%), et C (rendement 85%). Par recristallisation dans le mélange des solvants benzène–éther de pétrole on obtient deux formes p.f. 158–160 °C et p.f. 168–170 °C; CH_3COOH aqueux: p.f. 158–160 °C; cyclohexane: p.f. 168–170 °C. (Lit.: p.f. 156 °C (8), 158–159 °C (9), 167 °C (7).)

*(Chloroacetylamino)-2 methoxy-6 benzothiazole (**3**)*

Préparé selon les méthodes B (rendement 85%) et C (rendement 81%). Par recristallisation dans le mélange des solvants benzène–éther de pétrole ou toluène–éther de pétrole on obtient deux formes: p.f. 164–166 °C et p.f. 180–182 °C; CH_3COOH aqueux: p.f. 174 °C; cyclohexane: p.f. 180–182 °C (lit.: p.f. 188 °C (8)).

*(Chloroacetylamino)-2 éthoxy-6 benzothiazole (**4**)*

Préparé selon les méthodes B (rendement 78%) et C (rendement 84%). Par recristallisation dans le mélange des solvants benzène–éther de pétrole on obtient deux formes: p.f. 180–181 °C et p.f. 185–186 °C; CH_3COOH aqueux: p.f. 186 °C; éther de pétrole: p.f. 180 °C (lit.: p.f. 174 °C (8); p.f. 169–170 °C (9)).

*(Chloroacetylamino)-2 chloro-6 benzothiazole (**5**)*

Préparé selon les méthodes B (rendement 76%) et C (rendement 86%). Par recristallisation dans le mélange des solvants benzène–éther de pétrole ou toluène–éther de pétrole on obtient une seule forme: p.f. 212–213 °C. (Lit.: p.f. 212 °C (9).)

*(Chloroacetylamino)-2 chloro-4 benzothiazole (**6**)*

Préparé selon les méthodes B (rendement 68%) et C (rendement 80%). Par recristallisation dans le mélange benzène–éther de pétrole; p.f. 186.8 °C. (Lit.: p.f. 182 °C (8).)

*(Chloroacetylamino)-2 dimethyl-5,6 benzothiazole (**7**)*

Préparé selon la méthode C (rendement 88%). Par recristallisation dans le mélange benzène–éther de pétrole au toluène–éther de pétrole on obtient une seule forme; p.f. 244° avec décomposition.

Anal. calc. pour $C_{11}H_{11}ON_2SCl$: C, 51.88; H, 4.36; N, 11.01; Cl, 13.91. Trouvé: C, 51.93; H, 4.18; N, 11.04; Cl, 14.00.

Imino-2 methyl-3 benzothiazoline

A une solution de 15 g d'amino-2 benzothiazole dans 50 ml d'éthanol absolu on ajoute 15 ml de CH_3I et on porte à reflux pendant 3 h. Après refroidissement on filtre et on lave avec de l'éther anhydre (rendement 90%), on prend 15 g de ce sel, le dissout à chaud dans l'eau puis on ajoute une solution de NaOH à 15% pour le rendre fortement basique. Après refroidissement on filtre on lave à l'eau et on sèche, rendement 83% p.f. 123–124 °C. (Lit.: p.f. 123 °C (10) après recristallisation des benzène–éther de pétrole.)

*(α-Chloropropionylimino)-2 methyl-3 benzothiazoline (**8**)*

Préparé selon la méthode A (rendement 94%). Recristallisation dans le mélange benzène–éther de pétrole p.f. 98–99 °C.

Anal. calc. pour $C_{11}H_{11}ON_2SCl$: C, 51.87; H, 4.36; N, 11.00; S, 12.58; Cl, 13.92. Trouvé: C, 52.00; H, 4.16; N, 11.08; S, 19.66; Cl, 14.09.

*(Chloroacétylimino)-2 methyl-3 benzothiazoline (**9**)*

Préparé selon la méthode A (rendement 94%). Recristallisation dans le mélange benzène–éther de pétrole: p.f. 159–160 °C.

Anal. calc. pour $C_{10}H_9ON_2SCl$: C, 49.89; H, 3.77; N, 11.64; S, 13.32; Cl, 14.73. Trouvé: C, 49.42; H, 4.05; N, 11.81; S, 13.35; Cl, 14.88.

Remerciements

Nous remercions le Conseil National de Recherches pour l'aide financière apportée sous forme de subventions et l'Université Laval pour l'octroi d'une bourse post-doctorale à l'un de nous (E.C.).

1. (*a*) R. F. Hunter. J. Chem. Soc. 1385 (1926). (*b*) R. F. Hunter et M. A. Wali. J. Chem. Soc. 1513 (1937).
2. (*a*) Yu. N. Sheinker, E. M. Peresleni, N. P. Zosimova, et Yu. I. Pomerantsev. Zhur. Fiz. Khim. **33**, 2096 (1959); Russ. J. Phys. Chem. 303 (1959). (*b*) E. M. Peresleni, Yu. N. Sheinker, N. P. Zosimova, et Yu. I. Pomerantsev. Zhur. Fiz. Khim. **37**, 2713 (1963); Russ. J. Phys. Chem. 1466 (1963). (*c*) E. M. Peresleni et Yu. N. Sheinker. Russ. J. Phys. Chem. 1167 (1964). (*d*) E. M. Peresleni, Yu. N. Sheinker, et N. P. Zosimova. Russ. J. Phys. Chem. 488 (1965).
3. E. Costakis et G. Tsatsas. Sous presse.
4. T. Wagner-Jauregg et E. Helmert. Ber. **75B**, 935 (1942).
5. C. F. H. Allen et J. A. Vanallan. J. Org. Chem. **13**, 603 (1948).
6. L. J. Bellamy. The infra-red spectra of complex molecules. 2nd ed. John Wiley and Sons, New York, 1958. Pp. 270, 271.
7. G. Tsatsas et N. Vassiliadou. Bull. Soc. Chim. France, 736 (1962).
8. P. N. Bhargava et P. Ram. Bull. Chem. Soc. Japan, **38** (3), 339 (1965).
9. E. Habicht. U.S. Patent No. 2 952 687 (Sept. 13, 1960); Chem. Abstr. **55**, 4534 (1961).
10. R. F. Hunger. J. Chem. Soc. 1932 (1926), 139 (1930).

Can. J. Chem. Downloaded from www.nrcresearchpress.com by 210.87.254.40 on 09/05/12
For personal use only.

Ring B conformation in 9,10-dihydroanthracenes by nuclear magnetic resonance[1]

F. GARCIA JIMENEZ, M. C. PEREZAMADOR, AND J. R. ALCAYDE[2]
Instituto de Química, Universidad Nacional Autónoma de México, México D. F., México

Received March 14, 1969

The nuclear magnetic-resonance data of some 9,10-dihydroanthracenes with substituents on the aromatic rings allow the assignment of a pseudoboat conformation for the central ring. The dihedral angle formed by the two planes in the molecule changes according to the substituents.

Canadian Journal of Chemistry, 47, 4489 (1969)

The conformation of the central ring in some 9,10-dihydroanthracenes has been studied by several workers. It appears that some of these compounds have a pseudoboat conformation, with the molecule folded about the axis through the methylenes of the central ring, and a dihedral angle of 145° as in 9,10-dihydroanthracene (1), while others have a planar structure (2). The present paper is a contribution to the study of this problem.

The 9,10-dihydroanthracenes studied (2,6-dimethoxy-2,3,6,7-tetramethoxy- and 1,2,3,5,6,7-hexamethoxy-9,10-dihydroanthracene) were obtained by the Robinson's method (3), with some minor modifications, starting with the corresponding substituted benzyl alcohol. No 9,10-dihydroanthracene was obtained applying the same method with 5-bromo- and 5-chloroveratryl alcohol.

The 2,6-dimethoxy-9,10-dihydroanthracene (m.p. 245°) has not been reported in the literature. The spectroscopic data are consistent with the assigned structure, which was also confirmed by converting the product into 2,6-dimethoxyanthracene (4).

Discussion

The preparation of 9,10-dihydroanthracenes by this method is strongly dependent both on the nature and the position of the aromatic substituents. The high degree of selectivity is remarkable since the attack always occurs at positions *para* to the methoxyl groups. The low yield (10%) obtained with 3,4,5-trimethoxy benzyl alcohol, and the negative results with 5-bromo- and 5-chloro-veratryl alcohol and particularly in cases where the substituents are in close proximity to the reactive sites in the molecule provide support for this explanation.

Nuclear Magnetic Resonance Data Analysis

In the 9,10-dihydroanthracenes the signals of the aliphatic protons at C_9 and C_{10} correspond to an A–B system with different coupling constants and variable chemical shifts depending on the substituents. The chemical shifts for axial and equatorial protons as well as the mean chemical shifts may be explained by a combination of electronic and stereoelectronic effects.

In 9,10-dihydroanthracene itself there is only one signal for the methylene protons at 3.87 p.p.m. (5). This has been explained by a rapid interconversion between two extreme boat conformations (6). In 2,6-dimethoxy-9,10-dihydroanthracene, the introduction of two methoxyl groups in positions 2 and 6 reduces the rate of interconversion and the differences between the axial and the equatorial protons are now evident. The axial protons absorb at 3.51 and 3.73 p.p.m. and the equatorial protons at 4.67 and 4.87 p.p.m. (Table I). This difference is due to the shielding of the axial hydrogens by the aromatic magnetic fields. Considering that positions 2 and 6 are relatively far away from the hydrogens in 9 and 10, the steric effect of the two methoxyl groups seems remarkable.

With two more methoxyl groups in positions 3 and 7 (in 2,3,6,7-tetramethoxy-9,10-dihydroanthracene), the electromagnetic effect increases

[1]Contribution No. 280 from the Instituto de Química, Universidad Nacional Autónoma de México, México 20, D. F.

[2]J. R. Alcayde, B.Sc. Thesis. Universidad Nacional Autónoma de México.

TABLE I

Coupling constants and chemical shifts of some 9,10-dihydroanthracenes

Compound	J (c.p.s.)	Chemical shift (p.p.m.) A*	Chemical shift (p.p.m.) B*	ΔA–B	Mean chemical shift (p.p.m.)	Reference
9,10-Dihydroanthracene	0	3.87		0	3.87	5
2,6-Dimethoxy-9,10-dihydroanthracene	13.5	3.51, 3.62	3.73–4.67, 4.87 4.77	1.15	4.19	—
2,3,6,7-Tetramethoxy-9,10-dihydroanthracene	13.5	3.63, 3.50	3.37–4.60, 4.83 4.72	1.20	4.11	—
2,3,4,6,7,8-Hexamethoxy-9,10-dihydroanthracene	13.5	3.87, 3.96	4.09–4.32, 4.56 4.44	0.48	4.20	—
9-Terbutyl-9,10-dihydroanthracene	19	3.79	4.23	0.44	4.01	7
9,10-Diterbutyl-9,10-dihydroanthracene	0	3.94		0	3.94	7

*A = axial protons; B = equatorial protons.

the difference between the axial and the equatorial protons (3.63, 3.37, and 4.60, 4.83). In addition, there is an increased shielding both for axial and equatorial protons which results in a smaller mean chemical shift.

The introduction of two more methoxyl groups in positions 1 and 5 (in 1,2,3,5,6,7-hexamethoxy-9,10-dihydroanthracene) causes a different kind of effect which cannot be readily explained in terms of shielding due to substituents as in the above mentioned case. The interaction of the substituents with the equatorial protons in 9 and 10 forces the molecule to an even more planar conformation, thereby increasing the dihedral angle formed by the two halves of the molecule. The difference between the axial and the equatorial protons is thus diminished (3.87, 4.09 and 4.32, 4.56) together with the total electromagnetic shielding. This is also observed in 9-*tert*-butyl-9,10-dihydroanthracene (7).

The steric effect can be anticipated to become more critical with an increase in temperature and therefore the difference between the chemical shifts of the equatorial and the axial protons should therefore decrease. In agreement with this expectation we have found experimentally that the difference in the chemical shifts between axial and equatorial protons in 1,2,3,5,6,7-hexamethoxy-9,10-dihydroanthracene is diminished by 2 c.p.s. between −20 and 55°.

From the nuclear magnetic resonance (n.m.r.) spectra analysis it may be deduced that in the 9,10-dihydroanthracenes the chemical shifts of the axial and the equatorial protons is largely dependent on the dihedral angle formed by the two planes in the molecule. This angle is variable and dependent on the substituents, particularly in positions 1,4,5,8,9, and 10.

Experimental[3]

2,6-Dimethoxy-9,10-dihydroanthracene

m-Methoxy benzyl alcohol (5 g) was mixed with 20 ml of Lucas reagent (8), followed by 5 drops of acetic acid. The mixture was stirred for 12 h at room temperature. It was then diluted with water and extracted with ethyl acetate. Evaporation of the solvent left a dark yellow oil which was chromatographed on SiO_2, eluting with 80:20 ethyl acetate–hexane. The crystalline fraction yielded white crystals (495 mg) of m.p. 245° (sealed tube); λ_{max} 207, 230, 282, and 289 mμ (ε, 29 200, 15 900, 2740, and 2740); ν_{max} 2990, 2930, 2915, 2860, and 2830; 1610, 1575, 1495, 1472, and 1415; 1285, 1250, 1200, 1143, 1095, 1074, 1040; 930, 867, 820, 800, 785, 752, 730, 710, and 700 cm^{-1}; n.m.r. spectrum: 3.62 (2H, doublet, J = 13 c.p.s.) and 4.77 (2H, doublet, J = 13 c.p.s.); 3.75 (6H, singlet); ABX system, 6.64 (2H, multiplet, J = 8 and 2.5 c.p.s.), 6.9 (2H, doublet, J = 2.5 c.p.s.), 7.29 (2H doublet, J = 8 c.p.s.).

[3]Melting points were determined in a Kofler block and are uncorrected. The infrared spectra were run in a Perkin–Elmer 521 spectrometer, in KBr. The ultraviolet spectra were determined in a Perkin–Elmer 450 spectrophotometer, in hexane solution. The n.m.r. spectra were run in a Varian A-60 spectrometer using TMS as internal standard. The elemental analysis was carried out by Dr. Franz Pascher, Bonn, Germany.

Can. J. Chem. Downloaded from www.nrcresearchpress.com by 210.87.254.40 on 09/05/12
For personal use only.

Anal. Calcd. for $C_{16}H_{16}O_2$: C, 79.97; H, 6.71; O, 13.32. Found: C, 80.08; H, 6.30; O, 13.91.

2,6-Dimethoxyanthracene

To 100 mg of 2,6-dimethoxy-9,10-dihydroanthracene were added 500 mg of lead oxide (litharge) and the mixture heated at 200° for 5 h. The reaction product was sublimed *in vacuo*, yielding pale yellow crystals (40 mg) which, when recrystallized from ethyl acetate, afforded white crystals of m.p. 260° (lit. (4) 257°, from benzene); the ultraviolet spectrum is in agreement with that reported for the product (4).

2,3,6,7-Tetramethoxy-9,10-dihydroanthracene

Veratryl alcohol (2 g) was mixed with 10 ml of concentrated hydrochloric acid and stirred for a few minutes. The thick paste so formed was filtered and washed with water, resulting in 1.540 g of white crystals, m.p. 220–224°. These were recrystallized from ethyl acetate raising the m.p. to 227° (lit. (3) 227°, from benzene); ν_{max} 2995, 2950, 2934, and 2908; 1675, 1603, 1584, 1500, 1457, 1390, and 1340; 1180–1270, 1130, 1080, 1015; 990, 935, 865, and 838 cm^{-1}; n.m.r. spectrum: 3.5 (2H, doublet, J = 13 c.p.s.) and 4.72 (2H, doublet, J = 13 c.p.s.): 3.82 (12H, singlet): 6.84 (4H, singlet).

1,2,3,5,6,7-Hexamethoxy-9,10-dihydroanthracene

3,4,5-Trimethoxy benzyl alcohol (2 g) was mixed with 10 ml of concentrated hydrochloric acid and stirred for 1 h. The reaction mixture was diluted with water and extracted with ethyl acetate. After evaporation of the solvent an orange oil was obtained. This oil crystallized from ethanol–water yielding 200 mg of white crystals with m.p. 199–201° (lit. (9) 202–203°, from ethanol). No change in the m.p. was observed after recrystallization from ethyl acetate; ν_{max} 3000, 2960, 2937, and 2833; 1710, 1570, 1490, 1464, 1450, 1430, 1400, and 1332; 1287, 1192, 1160, 1115, 1057, and 1033; 990, 960, 910, and 850 cm^{-1}; n.m.r. spectrum: 3.96 (2H,doublet, J = 13 c.p.s.) and 4.44 (2H, doublet, J = 13 c.p.s.); 3.78 (6H, singlet); 3.82 (6H, singlet), and 3.99 (6H, singlet); 7.26 (2H, singlet).

1. W. G. Ferrier and J. Iball. Chem. Ind. 1296 (1945).
2. Y. Yannoni, A. P. Krukonis, and J. Silvermann. Science, **148**, 231 (1965).
3. G. M. Robinson. J. Chem. Soc. **107**, 267 (1915).
4. D. W. Cameron, R. I. T. Cromartie, D. G. I. Kingston, and G. B. V. Subramanian. J. Chem. Soc. IV, 4565 (1964).
5. Varian NMR spectra catalog. spectrum No. 307.
6. W. B. Smith and B. A. Shoulders. J. Phys. Chem. **69**, 2022 (1965).
7. W. Carruthers and G. E. Hall. J. Chem. Soc. B, 861 (1966).
8. R. L. Shriner, R. C. Fuson, and D. Y. Curtin. The systematic identification of organic compounds. 4th Edition. John Wiley and Sons, Inc., New York, 1956. p. 117.
9. N. L. Drake and W. B. Tuemmler. J. Am. Chem. Soc. 77, 1204 (1955).

Concerning the problems involved with use of external references for variable temperature chemical shift measurements[1]

B. J. Blackburn,[2] Frank E. Hruska,[3] and Ian C. P. Smith
Biochemistry Laboratory, National Research Council of Canada, Ottawa 7, Canada

Received July 10, 1969

The importance of making bulk susceptibility corrections to nuclear magnetic resonance chemical shifts measured versus an external reference is emphasized. The special significance of this correction for variable temperature studies is demonstrated by comparing data obtained with external and internal references for uridine-5′-phosphate. Opposite trends in chemical shift and inaccurate activation energies can result.

En utilisant une référence externe en résonance magnétique nucléaire pour déterminer et comparer des déplacements chimiques, il est très important de tenir compte de l'effet dû à la susceptibilité magnétique. Nous nous sommes servi de l'uridine-5′-phosphate et de références internes et externes pour bien démontrer l'importance de cette correction, spécialement lorsqu'on varie la température. Nous soulignons également la possibilité de variations de déplacements chimiques en sens opposés et la mise en garde contre le danger d'obtenir des énergies d'activation inexactes si de telles corrections ne sont pas appliquées.

Canadian Journal of Chemistry, 47, 4491 (1969)

The use of external reference compounds for measurement of nuclear magnetic resonance (n.m.r.) chemical shifts is becoming increasingly widespread (1–4). This is principally to avoid

[1]NRCC No. 10930.
[2]NRCC Postdoctoral Fellow, 1968–1970.
[3]NRCC Visiting scientist, summer 1969. Permanent address: Department of Chemistry, University of Winnipeg, Winnipeg, Manitoba.

Can. J. Chem. Downloaded from www.nrcresearchpress.com by 210.87.254.40 on 09/05/12
For personal use only.

Anal. Calcd. for $C_{16}H_{16}O_2$: C, 79.97; H, 6.71; O, 13.32. Found: C, 80.08; H, 6.30; O, 13.91.

2,6-Dimethoxyanthracene

To 100 mg of 2,6-dimethoxy-9,10-dihydroanthracene were added 500 mg of lead oxide (litharge) and the mixture heated at 200° for 5 h. The reaction product was sublimed *in vacuo*, yielding pale yellow crystals (40 mg) which, when recrystallized from ethyl acetate, afforded white crystals of m.p. 260° (lit. (4) 257°, from benzene); the ultraviolet spectrum is in agreement with that reported for the product (4).

2,3,6,7-Tetramethoxy-9,10-dihydroanthracene

Veratryl alcohol (2 g) was mixed with 10 ml of concentrated hydrochloric acid and stirred for a few minutes. The thick paste so formed was filtered and washed with water, resulting in 1.540 g of white crystals, m.p. 220–224°. These were recrystallized from ethyl acetate raising the m.p. to 227° (lit. (3) 227°, from benzene); ν_{max} 2995, 2950, 2934, and 2908; 1675, 1603, 1584, 1500, 1457, 1390, and 1340; 1180–1270, 1130, 1080, 1015; 990, 935, 865, and 838 cm^{-1}; n.m.r. spectrum: 3.5 (2H, doublet, J = 13 c.p.s.) and 4.72 (2H, doublet, J = 13 c.p.s.): 3.82 (12H, singlet): 6.84 (4H, singlet).

1,2,3,5,6,7-Hexamethoxy-9,10-dihydroanthracene

3,4,5-Trimethoxy benzyl alcohol (2 g) was mixed with 10 ml of concentrated hydrochloric acid and stirred for 1 h. The reaction mixture was diluted with water and extracted with ethyl acetate. After evaporation of the solvent an orange oil was obtained. This oil crystallized from ethanol–water yielding 200 mg of white crystals with m.p. 199–201° (lit. (9) 202–203°, from ethanol). No change in the m.p. was observed after recrystallization from ethyl acetate; ν_{max} 3000, 2960, 2937, and 2833; 1710, 1570, 1490, 1464, 1450, 1430, 1400, and 1332; 1287, 1192, 1160, 1115, 1057, and 1033; 990, 960, 910, and 850 cm^{-1}; n.m.r. spectrum: 3.96 (2H,doublet, J = 13 c.p.s.) and 4.44 (2H, doublet, J = 13 c.p.s.); 3.78 (6H, singlet); 3.82 (6H, singlet), and 3.99 (6H, singlet); 7.26 (2H, singlet).

1. W. G. Ferrier and J. Iball. Chem. Ind. 1296 (1945).
2. Y. Yannoni, A. P. Krukonis, and J. Silvermann. Science, **148**, 231 (1965).
3. G. M. Robinson. J. Chem. Soc. **107**, 267 (1915).
4. D. W. Cameron, R. I. T. Cromartie, D. G. I. Kingston, and G. B. V. Subramanian. J. Chem. Soc. IV, 4565 (1964).
5. Varian NMR spectra catalog. spectrum No. 307.
6. W. B. Smith and B. A. Shoulders. J. Phys. Chem. **69**, 2022 (1965).
7. W. Carruthers and G. E. Hall. J. Chem. Soc. B, 861 (1966).
8. R. L. Shriner, R. C. Fuson, and D. Y. Curtin. The systematic identification of organic compounds. 4th Edition. John Wiley and Sons, Inc., New York, 1956. p. 117.
9. N. L. Drake and W. B. Tuemmler. J. Am. Chem. Soc. 77, 1204 (1955).

Concerning the problems involved with use of external references for variable temperature chemical shift measurements[1]

B. J. Blackburn,[2] Frank E. Hruska,[3] and Ian C. P. Smith
Biochemistry Laboratory, National Research Council of Canada, Ottawa 7, Canada

Received July 10, 1969

The importance of making bulk susceptibility corrections to nuclear magnetic resonance chemical shifts measured versus an external reference is emphasized. The special significance of this correction for variable temperature studies is demonstrated by comparing data obtained with external and internal references for uridine-5′-phosphate. Opposite trends in chemical shift and inaccurate activation energies can result.

En utilisant une référence externe en résonance magnétique nucléaire pour déterminer et comparer des déplacements chimiques, il est très important de tenir compte de l'effet dû à la susceptibilité magnétique. Nous nous sommes servi de l'uridine-5′-phosphate et de références internes et externes pour bien démontrer l'importance de cette correction, spécialement lorsqu'on varie la température. Nous soulignons également la possibilité de variations de déplacements chimiques en sens opposés et la mise en garde contre le danger d'obtenir des énergies d'activation inexactes si de telles corrections ne sont pas appliquées.

Canadian Journal of Chemistry, 47, 4491 (1969)

The use of external reference compounds for measurement of nuclear magnetic resonance (n.m.r.) chemical shifts is becoming increasingly widespread (1–4). This is principally to avoid

[1]NRCC No. 10930.
[2]NRCC Postdoctoral Fellow, 1968–1970.
[3]NRCC Visiting scientist, summer 1969. Permanent address: Department of Chemistry, University of Winnipeg, Winnipeg, Manitoba.

Can. J. Chem. Downloaded from www.nrcresearchpress.com by 210.87.254.105 on 09/05/12
For personal use only.

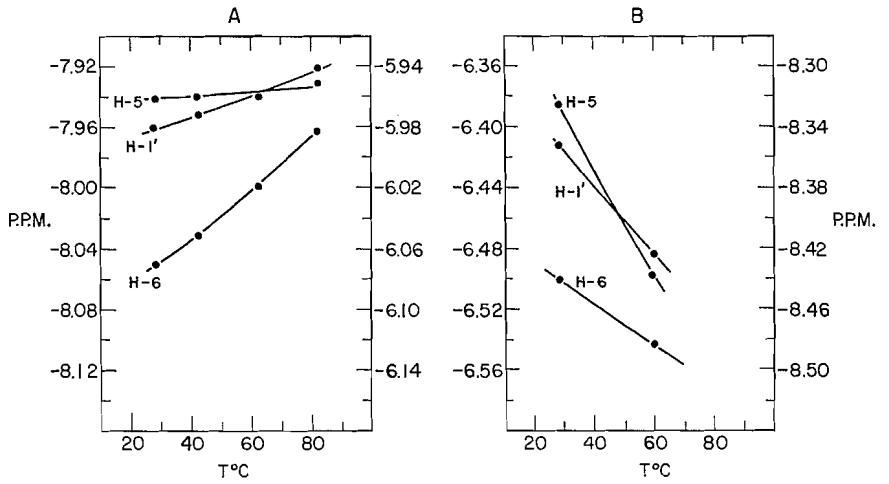

FIG. 1. The chemical shift of the H-5, H-6, and H-1′ protons of uridine-5′-monophosphate as a function of temperature: (*A*) relative to internal DSS; (*B*) relative to external TMS (4). The shift of the H-6 proton is given by the extreme scales; the shifts of the H-5 and H-1′ protons are given by central scales. In (*A*) the uridine-5′-monophosphate was 0.1 *M* in D_2O, p*D* 7.0, the DSS was 0.15 *M*, and the spectra were obtained on a Varian HA-100 spectrometer operating in frequency sweep mode. In (*B*) the uridine-5′-monophosphate was 0.045 *M* in D_2O, p*D* 6.3.

contamination of the samples and is particularly important for biologically significant compounds. The chemical shifts so measured should, however, be corrected for bulk magnetic susceptibility effects if the data are to be meaningfully compared with those of other workers. If variable temperature measurements are made, *changes* in the correction for a given solvent–external reference pair *must* be considered. Even at fixed temperatures, variations due to different capillaries and to different solvent systems are important.

Problems arising from the use of external references are demonstrated vividly in recent studies of the temperature dependence of the proton chemical shifts of nucleosides, nucleotides, and oligonucleotides (4, 5). For example, in Fig. 1, we show the temperature dependence for the protons at positions 5, 6, and 1′ in uridine-5′-monophosphate. The data in Fig. 1*A* were obtained by measurement relative to the internal reference sodium 3-(trimethylsilyl)-propanesulfonate (DSS); those of Fig. 1*B* are taken from the published work of Ts'O *et al.* (4) and were measured relative to an external capillary of tetramethylsilane (TMS). It is clear from Fig. 1 that the trends of the chemical shifts are opposite in direction. These opposing trends, which are a consequence solely of the choice of reference, can lead to errors in the interpretation of the chemical shift data. In Fig. 2*A*, we present the temperature dependence for the following proton shifts: (*1*) external hexamethyldisiloxane, (HMS), relative to the methyl resonance of aqueous DSS, δ (HMS–DSS), (*2*) external HMS relative to the methyl protons of aqueous ethyl alcohol, δ (HMS–EA), and (*3*) external TMS relative to aqueous tetramethylammonium bromide, δ (TMS–TMAB). In each instance, temperature elevation from 5 to 60 °C results in increased shielding of the external reference relative to the internal reference in excess of 0.1 p.p.m. In Fig. 2*B* are shown the chemical shift data for DSS relative to the methyl protons of ethyl alcohol, δ (DSS–EA), both dissolved in the same aqueous solution. Only a slight temperature dependence is observed.

Figure 2 suggests that the variations of the apparent chemical shift of the external reference with temperature are due mainly to changes in the bulk susceptibility of the surrounding heavy water solution. When these corrections are applied to the data in Fig. 1*B*, they follow the same trend as those in Fig. 1*A*. This demonstrates the importance of either using an internal reference, or making bulk susceptibility corrections with an

Can. J. Chem. Downloaded from www.nrcresearchpress.com by 210.87.254.105 on 09/05/12
For personal use only.

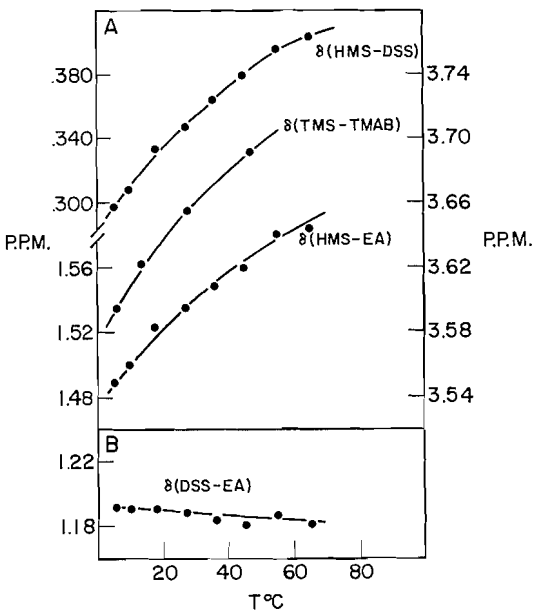

FIG. 2. (*A*) Shift of external HMS relative to internal aqueous DSS [δ(HMS–DSS), upper left-hand scale], shift of external HMS relative to methyl resonance of aqueous ethyl alcohol [δ(HMS–EA), lower left-hand scale], and the shift of external TMS relative to aqueous tetramethylammonium bromide [δ(TMS–TMAB), right-hand scale], all as a function of temperature. (*B*) Shift of internal DSS relative to methyl resonance of ethyl alcohol as a function of temperature in aqueous solution. A positive shift indicates a resonance at higher field. All solutions were in D_2O, p*D* 7.0 ± 0.2. Concentrations were: DSS, 0.15 *M*; EA, 0.05 *M*; TMAB, 0.01 *M*. Spectra were measured on a field-swept Varian A60A n.m.r. instrument with calibrated sweep.

external reference, when variable temperature measurements are made; otherwise, incorrect trends and calculated activation energies will result.[4]

The procedure for making such corrections is simple. The n.m.r. data for the compound of interest are obtained under the desired conditions using a reference compound in a concentric external capillary. The sample is then replaced by a solution of similar composition, but with the compound of interest substituted by an internal reference. The chemical shift of the external reference relative to the internal reference is then added algebraically to the shift of the compound of interest relative to the external reference, thus yielding the chemical shift of the compound of interest relative to the internal reference. To ensure that the susceptibility of the compound of interest makes no contribution to this correction, the procedure should be followed for at least two concentrations of the compound of interest.

1. I. C. P. SMITH, T. YAMANE, and R. G. SHULMAN. Sci. **159**, 1360 (1968).
2. F. E. HRUSKA and S. S. DANYLUK. Biochem. Biophys. Acta, **157**, 238 (1968).
3. K. D. KOPPLE and M. OHNISHI. J. Amer. Chem. Soc. **91**, 962 (1969).
4. P. O. P. TS'O, N. S. KONDO, M. P. SCHWEIZER, and D. P. HOLLIS. Biochem. **8**, 997 (1969).
5. I. C. P. SMITH, B. J. BLACKBURN, and T. YAMANE. Can. J. Chem. **47**, 513 (1969).

[4]It should be emphasized that in (4), the effect of variable susceptibility was taken into account in interpretation of the data. We use the results of reference (4) only to demonstrate our point.

2-Acetamido-2-deoxy-D-*glycero*-D-*gulo*-heptose[1]

D. T. WILLIAMS[2] AND M. B. PERRY
Biochemistry Laboratory, National Research Council of Canada, Ottawa, Canada

Received July 14, 1969

3,4,5,6,7-Pentaacetoxy-D-*gluco*-1-nitro-1-heptene with methanolic ammonia afforded crystalline 2-acetamido-1,2-dideoxy-1-nitro-D-*glycero*-D-*gulo*-heptitol which was converted via a modified Nef reaction to 2-acetamido-2-deoxy-D-*glycero*-D-*gulo*-heptose.

Canadian Journal of Chemistry, 47, 4493 (1969)

A previous paper (1) recorded the synthesis of the epimeric 2-acetamido-2-deoxyheptoses derived from D-mannose, D-galactose, and D-talose but at the time that this work was done the derivatives from D-glucose could not be readily made owing to experimental difficulties experienced in trying to effect the condensation of

[1]Issued as NRCC No. 10923.
[2]NRCC Postdoctoral Fellow 1967–1969.

Can. J. Chem. Downloaded from www.nrcresearchpress.com by 210.87.254.105 on 09/05/12
For personal use only.

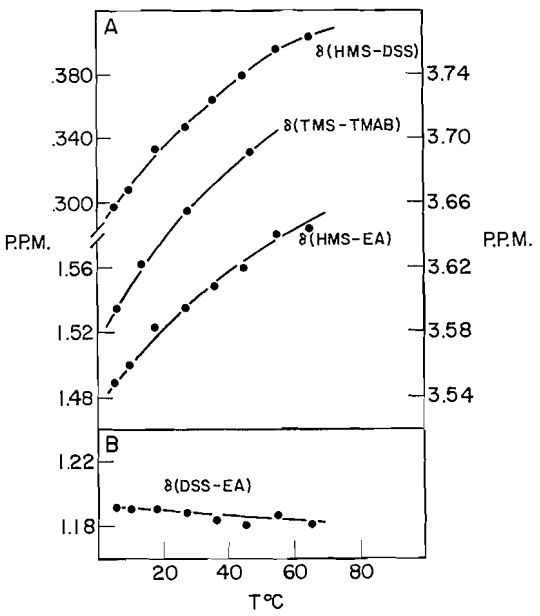

FIG. 2. (*A*) Shift of external HMS relative to internal aqueous DSS [δ(HMS–DSS), upper left-hand scale], shift of external HMS relative to methyl resonance of aqueous ethyl alcohol [δ(HMS–EA), lower left-hand scale], and the shift of external TMS relative to aqueous tetramethylammonium bromide [δ(TMS–TMAB), right-hand scale], all as a function of temperature. (*B*) Shift of internal DSS relative to methyl resonance of ethyl alcohol as a function of temperature in aqueous solution. A positive shift indicates a resonance at higher field. All solutions were in D_2O, p*D* 7.0 ± 0.2. Concentrations were: DSS, 0.15 *M*; EA, 0.05 *M*; TMAB, 0.01 *M*. Spectra were measured on a field-swept Varian A60A n.m.r. instrument with calibrated sweep.

external reference, when variable temperature measurements are made; otherwise, incorrect trends and calculated activation energies will result.[4]

The procedure for making such corrections is simple. The n.m.r. data for the compound of interest are obtained under the desired conditions using a reference compound in a concentric external capillary. The sample is then replaced by a solution of similar composition, but with the compound of interest substituted by an internal reference. The chemical shift of the external reference relative to the internal reference is then added algebraically to the shift of the compound of interest relative to the external reference, thus yielding the chemical shift of the compound of interest relative to the internal reference. To ensure that the susceptibility of the compound of interest makes no contribution to this correction, the procedure should be followed for at least two concentrations of the compound of interest.

1. I. C. P. SMITH, T. YAMANE, and R. G. SHULMAN. Sci. **159**, 1360 (1968).
2. F. E. HRUSKA and S. S. DANYLUK. Biochem. Biophys. Acta, **157**, 238 (1968).
3. K. D. KOPPLE and M. OHNISHI. J. Amer. Chem. Soc. **91**, 962 (1969).
4. P. O. P. TS'O, N. S. KONDO, M. P. SCHWEIZER, and D. P. HOLLIS. Biochem. **8**, 997 (1969).
5. I. C. P. SMITH, B. J. BLACKBURN, and T. YAMANE. Can. J. Chem. **47**, 513 (1969).

[4]It should be emphasized that in (4), the effect of variable susceptibility was taken into account in interpretation of the data. We use the results of reference (4) only to demonstrate our point.

2-Acetamido-2-deoxy-D-*glycero*-D-*gulo*-heptose[1]

D. T. WILLIAMS[2] AND M. B. PERRY
Biochemistry Laboratory, National Research Council of Canada, Ottawa, Canada

Received July 14, 1969

3,4,5,6,7-Pentaacetoxy-D-*gluco*-1-nitro-1-heptene with methanolic ammonia afforded crystalline 2-acetamido-1,2-dideoxy-1-nitro-D-*glycero*-D-*gulo*-heptitol which was converted via a modified Nef reaction to 2-acetamido-2-deoxy-D-*glycero*-D-*gulo*-heptose.

Canadian Journal of Chemistry, 47, 4493 (1969)

A previous paper (1) recorded the synthesis of the epimeric 2-acetamido-2-deoxyheptoses derived from D-mannose, D-galactose, and D-talose but at the time that this work was done the derivatives from D-glucose could not be readily made owing to experimental difficulties experienced in trying to effect the condensation of

[1]Issued as NRCC No. 10923.
[2]NRCC Postdoctoral Fellow 1967–1969.

Can. J. Chem. Downloaded from www.nrcresearchpress.com by 210.87.254.42 on 09/05/12
For personal use only.

Can. J. Chem. Downloaded from www.nrcresearchpress.com by 210.87.254.42 on 09/05/12
For personal use only.

D-glucose with nitromethane. Following the finding of conditions leading to the successful condensation of D-glucose with nitromethane to yield 1-deoxy-1-nitro-D-*glycero*-D-*ido*-heptitol and 1-deoxy-1-nitro-D-*glycero*-D-*gulo*-heptitol (2), the preparation of 2-acetamido-2-deoxy-D-*glycero*-D-*gulo*-heptose and 2-acetamido-2-deoxy-D-*glycero*-D-*ido*-heptose from these derivatives, became a possibility.

Acetylation of 1-deoxy-1-nitro-D-*glycero*-D-*ido*-heptitol (2) afforded 2,3,4,5,6,7-hexa-*O*-acetyl-1-deoxy-1-nitro-D-*glycero*-D-*ido*-heptitol which on refluxing in benzene solution in the presence of sodium bicarbonate afforded 3,4,5,-6,7-pentaacetoxy-D-*gluco*-1-nitro-1-heptene. The 3,4,5,6,7-pentaacetoxy-D-*gluco*-1-nitro-1-heptene with saturated methanolic ammonia afforded a mixture of the 2-acetamido-1,2-dideoxy-1-nitro-heptitols from which the major component, 2-acetamido-1,2-dideoxy-1-nitro-D-*glycero*-D-*gulo*-heptitol was obtained crystalline in 70% yield. This derivative underwent a modified (3) Nef (4) reaction to yield 2-acetamido-2-deoxy-D-*glycero*-D-*gulo*-heptose. The identity of the heptose was established by the identification of 2-acetamido-2-deoxy-gulitol (5) as the major product produced by borohydride reduction of the major compound produced by the action of one mole portion of metaperiodate on one mole part of the 2-acetamido-2-deoxyheptose (1, 6).

The mother liquors remaining after the removal of the 2-acetamido-1,2-dideoxy-1-nitro-D-*glycero*-D-*gulo*-heptitol, contained presumably a mixture of 2-acetamido-1,2-dideoxy-1-nitro-D-*glycero*-D-*gulo*-heptitol and 2-acetamido-1,2-dideoxy-1-nitro-D-*glycero*-D-*ido*-heptitol and, when subjected to the modified Nef reaction, the mixture afforded 2-acetamido-2-deoxy-D-*glycero*-D-*gulo*-heptose and 2-acetamido-2-deoxy-D-*glycero*-D-*ido*-heptose which were separated by cellulose column chromatography. The 2-acetamido-2-deoxy-D-*glycero*-D-*ido*-heptose could not be obtained in a completely pure state but after treatment with one mole part of metaperiodate it gave a major product which on borohydride reduction afforded 2-acetamido-2-deoxyiditol (5), thus establishing the identity of the heptose.

Experimental

Paper chromatography was performed by the descending method on Whatman No. 1 filter paper using either (*a*) pyridine–ethyl acetate–water (2:5:5 v/v, top layer) or (*b*) 1-butanol–ethanol–water (3:1:1 v/v) as the mobile phase. Compounds were detected with either alkaline silver nitrate (7) or *p*-anisidine hydrochloride (8) spray reagents and their rates of movement are quoted relative to D-glucose (R_G).

Gas–liquid partition chromatography was carried out using a Hewlett-Packard 402 gas chromatograph with a hydrogen flame detector and fitted with glass U tubes (4 ft × 6 mm × 3 mm i.d.) packed with 10% (w/w) neopentylglycol sebacate polyester on 80–100 mesh acid washed Chromosorb W. Development was made with helium at a flow rate of 90 ml/min and a column temperature of 245 °C, and retention times are quoted relative to hexa-*O*-acetyl-D-glucitol (T_G).

Melting points were determined on a hot stage and are corrected. Optical rotations were determined at 22 °C with a Perkin–Elmer 141 polarimeter. Solutions were concentrated under reduced pressure below 40 °C.

2,3,4,5,6,7-Hexa-O-acetyl-1-deoxy-1-nitro-D-*glycero*-D-*ido-heptitol*

1-Deoxy-1-nitro-D-*glycero*-D-*ido*-heptitol (2) (3 g) in acetic anhydride (25 ml) was treated with one drop of concentrated sulfuric acid and the mixture was heated for 35 min on a boiling water bath. The cooled reaction mixture was poured into an ice and water mixture (200 ml) and the product was extracted with chloroform in the usual way. The product crystallized from benzene and after recrystallization from ethanol, gave pure crystalline 2,3,4,5,6,7-hexa-*O*-acetyl-1-deoxy-1-nitro-D-*glycero*-D-*ido*-heptitol (5 g; 82%) which had m.p. 85–87 °C and $[\alpha]_D$ + 53.5° (*c*, 3.6 in chloroform).

Anal. Calcd. for $C_{19}H_{27}NO_{14}$: C, 46.24; H, 5.51; N, 2.83. Found: C, 46.23; H, 5.59; N, 2.67.

The 2,3,4,5,6,7-hexa-*O*-acetyl-1-deoxy-1-nitro-D-*glycero*-D-*ido*-heptitol was converted in the usual way (2), in almost quantitative yield to 3,4,5,6,7-pentaacetoxy-D-*gluco*-1-nitro-1-heptene having m.p. and mixture m.p. 106–107 °C.

2-Acetamido-1,2-dideoxy-1-nitro-D-*glycero*-D-*gulo-heptitol*

3,4,5,6,7-Pentaacetoxy-D-*gluco*-1-nitro-1-heptene (5 g) was suspended in methanol (50 ml) and dry ammonia gas was bubbled through the solution until all the solid material had dissolved. The mixture was kept at 0 °C for 24 h and, after aeration to remove most of the volatile material, a crystalline mass was obtained which after collection, and recrystallization from ethanol, gave pure 2-acetamido-1,2-dideoxy-1-nitro-D-*glycero*-D-*gulo*-heptitol (2.23 g, 69%) which had m.p. 142–143 °C and $[\alpha]_D$ + 7.5° (*c*, 2.7 in water).

Anal. Calcd. for $C_9H_{18}N_2O_8$: C, 38.30; H, 6.43; N, 9.92. Found: C, 38.80; H, 6.70; N, 10.06.

On paper chromatography the product gave a single silver nitrate-positive spot which had R_G 2.70 (solvent *a*) and R_G 2.50 (solvent *b*).

2-Acetamido-2-deoxy-D-*glycero*-D-*gulo-heptose*

2-Acetamido-1,2-dideoxy-1-nitro-D-*glycero*-D-*gulo*-heptitol (1.25 g) was dissolved in a solution of $Ba(OH)_2 \cdot 8H_2O$ (1.4 g) in water (22 ml) and the solution was added dropwise with stirring to an ice cold solution of con-

centrated sulfuric acid (2.3 g) in water (9.6 ml). After 30 min, the reaction mixture was neutralized ($BaCO_3$), filtered, and the filtrate was concentrated to a syrup (0.96 g) which paper chromatography (solvent *a*) showed to be essentially a single compound having R_G 1.23. It was the only material detected by *p*-anisidine hydrochloride but the silver nitrate spray revealed the presence of several very minor impurities. The 2-acetamido-2-deoxy-D-*glycero*-D-*gulo*-heptose, obtained chromatographically pure by cellulose column chromatography using 1-butanol one half saturated with water as the mobile phase, had $[\alpha]_D$ $-45° \rightarrow -53°$ (*c*, 0.87 in water; equilibrium value).

Anal. Calcd. for $C_9H_{17}NO_7$: C, 43.03; H, 6.82; N, 5.58. Found: C, 42.76; H, 6.65; N, 5.45.

*Degradation of 2-Acetamido-2-deoxy-*D*-glycero-*D*-gulo-heptose to 2-Acetamido-2-deoxy-*D*-gulitol*

2-Acetamido-2-deoxy-D-*glycero*-D-*gulo*-heptose (39 mg) in water (1 ml) was treated with sodium metaperiodate (34 mg) in water (3 ml) and after 2 h, sodium borohydride (50 mg) was added. The mixture after acidification with acetic acid was concentrated to dryness and the residue was acetylated in the usual manner (5). Gas–liquid chromatographic analysis of the product gave a chromatogram with a major peak (ca. 95%) having T_G 3.33 corresponding in retention time with 1,3,4,5,6-penta-*O*-acetyl-2-acetamido-2-deoxy-D-gulitol and very minor peaks having T_G 0.36, 0.85, and 1.80. The major peak is distinguished from 1,3,4,5,6-penta-*O*-acetyl-2-acetamido-2-deoxy-D-iditol which had T_G 3.10.

*2-Acetamido-2-deoxy-*D*-glycero-*D*-ido-heptose*

The mother liquors remaining after the removal of 2-acetamido-1,2-dideoxy-1-nitro-D-*glycero*-D-*gulo*-heptitol from the product of the action of ammonia on 3,4,5,6,7-pentaacetoxy-D-*gluco*-1-nitro-1-heptene were concentrated to a syrup (ca. 1 g) which was subjected to the modified Nef reaction, in the way described above for the synthesis of 2-acetamido-2-deoxy-D-*glycero*-D-*gulo*-heptose, to yield a product (0.8 g) which on paper chromatography showed two major components having R_G 1.23 and 2.10 (solvent *a*).

The above product was separated by cellulose column chromatography using 1-butanol one half saturated with water as the mobile phase to yield pure 2-acetamido-2-deoxy-D-*glycero*-D-*gulo*-heptose (0.3 g) having R_G 1.23 (solvent *a*) and 2-acetamido-2-deoxy-D-*glycero*-D-*ido*-heptose (0.35 g) having R_G 2.10 (solvent *a*) which was contaminated with small amounts of unknown impurities having similar chromatographic mobilities. Attempts to purify the heptose via its 2,5-dichlorophenylhydrazone derivative were unsuccessful. A portion of the 2-acetamido-2-deoxy-D-*glycero*-D-*ido*-heptose fraction (20 mg) was oxidized with periodate and the product reduced in the way described for 2-acetamido-2-deoxy-D-*glycero*-D-*gulo*-heptose gave a fully acetylated final product which on gas–liquid chromatography gave a major peak (T_G 3.10) corresponding with 1,3,4,5,6,7-penta-*O*-acetyl-2-acetamido-2-deoxy-D-iditol together with minor components having T_G 0.85 and 1.70 which were not identified.

1. C. F. GIBBS, D. T. WILLIAMS, and M. B. PERRY. Can. J. Chem. **47**, 1479 (1969).
2. D. T. WILLIAMS and M. B. PERRY. Can. J. Chem. **47**, 2763 (1969).
3. C. SATOH and A. KIYOMOTO. Chem. Pharm. Bull. Tokyo, **12**, 615 (1964).
4. J. U. NEF. Ann. Chem. **280**, 263 (1894).
5. M. B. PERRY and A. C. WEBB. Can. J. Biochem. **46**, 1163 (1968).
6. N. J. ANTIA and M. B. PERRY. Can. J. Chem. **38**, 1917 (1960).
7. W. E. TREVELYAN, D. P. PROCTER, and J. S. HARRISON. Nature, **166**, 444 (1950).
8. L. HOUGH, J. K. N. JONES, and W. H. WADMAN. J. Chem. Soc. 1702 (1950).

Lignans of western red cedar (*Thuja plicata* Donn). IX. Plicatinaphthalene

HAROLD MACLEAN AND B. F. MACDONALD

Department of Fisheries and Forestry, Canadian Forestry Service, Forest Products Laboratory, Vancouver 8, B.C.

Received June 27, 1969

The last of nine lignans detectable by thin-layer chromatography in the hot-water soluble extractives of western red cedar (*Thuja plicata* Donn) heartwood has been determined as 6-hydroxy-2(hydroxymethyl)-7-methoxy-4-(3′,4′-dihydroxy-5′-methoxyphenyl)-3-naphthoic acid lactone (plicatinaphthalene **2**) by spectrometric methods, by degradation studies of derivatives, and by preparation of its trimethyl ether derivative **3** from dehydroanhydropicropodophyllin by opening of the methylenedioxy group with boron trichloride.

Canadian Journal of Chemistry, 47, 4495 (1969

Introduction

Previous work has elucidated the structural relationship of eight lignans present in the heartwood of western red cedar (*Thuja plicata* Donn), two of which were 4-aryltetrahydronaphthalenes, five were substituted dibenzyl butyrolactones, and the eighth was a 4-aryl-α-naphthol lactone (1). All of these lignans have the usual guaiacyl substitution pattern in the A ring with either a monomethylated pyrogallyl or syringyl pattern

Can. J. Chem. Downloaded from www.nrcresearchpress.com by 210.87.254.42 on 09/05/12
For personal use only.

centrated sulfuric acid (2.3 g) in water (9.6 ml). After 30 min, the reaction mixture was neutralized ($BaCO_3$), filtered, and the filtrate was concentrated to a syrup (0.96 g) which paper chromatography (solvent *a*) showed to be essentially a single compound having R_G 1.23. It was the only material detected by *p*-anisidine hydrochloride but the silver nitrate spray revealed the presence of several very minor impurities. The 2-acetamido-2-deoxy-D-*glycero*-D-*gulo*-heptose, obtained chromatographically pure by cellulose column chromatography using 1-butanol one half saturated with water as the mobile phase, had $[\alpha]_D$ $-45° \rightarrow -53°$ (*c*, 0.87 in water; equilibrium value).

Anal. Calcd. for $C_9H_{17}NO_7$: C, 43.03; H, 6.82; N, 5.58. Found: C, 42.76; H, 6.65; N, 5.45.

*Degradation of 2-Acetamido-2-deoxy-*D*-glycero-*D*-gulo-heptose to 2-Acetamido-2-deoxy-*D*-gulitol*

2-Acetamido-2-deoxy-D-*glycero*-D-*gulo*-heptose (39 mg) in water (1 ml) was treated with sodium metaperiodate (34 mg) in water (3 ml) and after 2 h, sodium borohydride (50 mg) was added. The mixture after acidification with acetic acid was concentrated to dryness and the residue was acetylated in the usual manner (5). Gas–liquid chromatographic analysis of the product gave a chromatogram with a major peak (ca. 95%) having T_G 3.33 corresponding in retention time with 1,3,4,5,6-penta-*O*-acetyl-2-acetamido-2-deoxy-D-gulitol and very minor peaks having T_G 0.36, 0.85, and 1.80. The major peak is distinguished from 1,3,4,5,6-penta-*O*-acetyl-2-acetamido-2-deoxy-D-iditol which had T_G 3.10.

*2-Acetamido-2-deoxy-*D*-glycero-*D*-ido-heptose*

The mother liquors remaining after the removal of 2-acetamido-1,2-dideoxy-1-nitro-D-*glycero*-D-*gulo*-heptitol from the product of the action of ammonia on 3,4,5,6,7-pentaacetoxy-D-*gluco*-1-nitro-1-heptene were concentrated to a syrup (ca. 1 g) which was subjected to the modified Nef reaction, in the way described above for the synthesis of 2-acetamido-2-deoxy-D-*glycero*-D-*gulo*-heptose, to yield a product (0.8 g) which on paper chromatography showed two major components having R_G 1.23 and 2.10 (solvent *a*).

The above product was separated by cellulose column chromatography using 1-butanol one half saturated with water as the mobile phase to yield pure 2-acetamido-2-deoxy-D-*glycero*-D-*gulo*-heptose (0.3 g) having R_G 1.23 (solvent *a*) and 2-acetamido-2-deoxy-D-*glycero*-D-*ido*-heptose (0.35 g) having R_G 2.10 (solvent *a*) which was contaminated with small amounts of unknown impurities having similar chromatographic mobilities. Attempts to purify the heptose via its 2,5-dichlorophenylhydrazone derivative were unsuccessful. A portion of the 2-acetamido-2-deoxy-D-*glycero*-D-*ido*-heptose fraction (20 mg) was oxidized with periodate and the product reduced in the way described for 2-acetamido-2-deoxy-D-*glycero*-D-*gulo*-heptose gave a fully acetylated final product which on gas–liquid chromatography gave a major peak (T_G 3.10) corresponding with 1,3,4,5,6,7-penta-*O*-acetyl-2-acetamido-2-deoxy-D-iditol together with minor components having T_G 0.85 and 1.70 which were not identified.

1. C. F. GIBBS, D. T. WILLIAMS, and M. B. PERRY. Can. J. Chem. **47**, 1479 (1969).
2. D. T. WILLIAMS and M. B. PERRY. Can. J. Chem. **47**, 2763 (1969).
3. C. SATOH and A. KIYOMOTO. Chem. Pharm. Bull. Tokyo, **12**, 615 (1964).
4. J. U. NEF. Ann. Chem. **280**, 263 (1894).
5. M. B. PERRY and A. C. WEBB. Can. J. Biochem. **46**, 1163 (1968).
6. N. J. ANTIA and M. B. PERRY. Can. J. Chem. **38**, 1917 (1960).
7. W. E. TREVELYAN, D. P. PROCTER, and J. S. HARRISON. Nature, **166**, 444 (1950).
8. L. HOUGH, J. K. N. JONES, and W. H. WADMAN. J. Chem. Soc. 1702 (1950).

Lignans of western red cedar (*Thuja plicata* Donn). IX. Plicatinaphthalene

HAROLD MACLEAN AND B. F. MACDONALD

Department of Fisheries and Forestry, Canadian Forestry Service, Forest Products Laboratory, Vancouver 8, B.C.

Received June 27, 1969

The last of nine lignans detectable by thin-layer chromatography in the hot-water soluble extractives of western red cedar (*Thuja plicata* Donn) heartwood has been determined as 6-hydroxy-2(hydroxymethyl)-7-methoxy-4-(3′,4′-dihydroxy-5′-methoxyphenyl)-3-naphthoic acid lactone (plicatinaphthalene **2**) by spectrometric methods, by degradation studies of derivatives, and by preparation of its trimethyl ether derivative **3** from dehydroanhydropicropodophyllin by opening of the methylenedioxy group with boron trichloride.

Canadian Journal of Chemistry, 47, 4495 (1969

Introduction

Previous work has elucidated the structural relationship of eight lignans present in the heartwood of western red cedar (*Thuja plicata* Donn), two of which were 4-aryltetrahydronaphthalenes, five were substituted dibenzyl butyrolactones, and the eighth was a 4-aryl-α-naphthol lactone (1). All of these lignans have the usual guaiacyl substitution pattern in the A ring with either a monomethylated pyrogallyl or syringyl pattern

Can. J. Chem. Downloaded from www.nrcresearchpress.com by 210.87.254.105 on 09/05/12
For personal use only.

Can. J. Chem. Downloaded from www.nrcresearchpress.com by 210.87.254.105 on 09/05/12
For personal use only.

in the pendant C ring. The last lignan component of the hot-water soluble extractives detectable by thin-layer chromatography (t.l.c.) (2) is now shown to be a derivative of plicatin (**1**) (3) in which the two tertiary hydroxyls have been removed and the B ring aromatized to a naphthalene nucleus (**2**). This component has been given the trivial name plicatinaphthalene.

This compound was recovered from the hot-water soluble components by extraction with chloroform. A trituration of the recovered chloroform solubles with petroleum ether followed by benzene removed the thujaplicins and other terpenoids (2), and the residue was chromatographed on polyamide powder followed by microcrystalline cellulose to yield crystalline plicatinaphthalene (**2**).

The structure of plicatinaphthalene was inferred by spectrometric identification. The molecular weight of 368 was determined by low-resolution mass spectrometry. This spectrum was similar to plicatinaphthol (1) in that the molecular ion was the only major peak, all others being less than 8%, indicative of the stable aromatic system of the compound (4). Also similar to plicatinaphthol, the compound was nearly insoluble in deuteriochloroform, but with ethanol of crystallization was sufficiently soluble in deuterioacetone to confirm all protons as to species and number by nuclear magnetic resonance (n.m.r.) spectrum. Ultraviolet (u.v.) and infrared (i.r.) spectra are in agreement with the proposed structures for plicatinaphthalene and its derivatives. Here again similarities with plicatinaphthol (1) exist in that the lactone ring appeared at lower wave number, 1735 cm^{-1}, than usually found for lactones.

Plicatinaphthalene was crystallized from ethanol, dichloromethane and spontaneously from acetone-d_6, being least soluble in the former and most soluble in the latter. Crystals from ethanol changed from transparent to opaque at 158–160°, began discoloring at 240° and melted with decomposition between 248–254°. The transition at 158–160° was indicated as resulting from ethanol of crystallization, since crystals dried at 100° under vacuum for 3 h, when dissolved in acetone-d_6, recrystallized from the acetone-d_6 during the n.m.r. spectral run giving a strong spectrum of ethanol and acetone-d_5 (5) superimposed on a weaker spectrum of plicatinaphthalene. A second n.m.r. spectrum run in pyridine showed the plicatinaphthalene–ethanol ratio was 1:1 in the crystals from ethanol which had also been dried at 100° under vacuum for 3 h. Crystals which had been heated beyond the 158–160° transition point were much less soluble in acetone-d_6 and showed only the spectrum of plicatinaphthalene.

Plicatinaphthalene recrystallized from dichloromethane and dried at 100° under vacuum for up to 7 h, melted at 158–160° with foaming, recrystallized on the melting point stage between 180 and 210°, and melted with discoloration and decomposition as for crystals from ethanol. When the melting point of this compound was taken on a Mettler FP-1 (automatic melting point determination) at 0.2°/min its melting point was recorded at 157.4°. The presence of dichloromethane in the crystals before, and its absence after, the primary melt was shown by use of the C—Cl band of dichloromethane at 735 cm^{-1} in comparative i.r. spectra. The spontaneously recrystallized material from the n.m.r. spectrum in acetone-d_6 underwent identical melting characteristics as for dichloromethane. Here again the presence of the acetone-d_6 before the transition point at 158–160°, and its absence after, was shown by detection and disappearance of a carbonyl band at 1695 cm^{-1} in comparative i.r. spectra.

If any of the three crystallization products are heated to 200° and allowed to cool, then on reheating no phase change occurs at 158°, but only melting with decomposition at 248–254°. From the above data, it would seem that plicatinaphthalene undergoes a monotropic phase change (6) at 157.4° with release of the solvent from which it has been crystallized, followed by a crystal change to its more stable form and finally melting with decomposition at 248–254°. In the case of ethanol it becomes only opaque, but in the case of the other two solvents in which it is more soluble, an actual melting takes place at the first transition point.

The n.m.r. spectra of a trimethyl (**3**) and a triacetyl (**5**) derivative confirmed the presence of two methoxyl and three hydroxyl groups in the original plicatinaphthalene andw ere confirmatory both as to species and number of protons required for each compound. The spectrum of the trimethyl ether derivative (**3**) was extremely simple owing to the lack of coupling, all peaks being singlets whose width at half-height indicated less than one Hz coupling in the *para* and *peri* aromatic positions, the *meta* protons of the

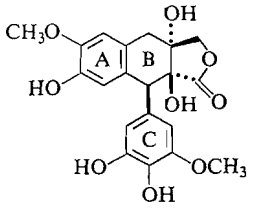

1

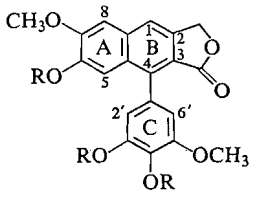

2 R = H 4 R = C_2H_5
3 R = CH_3 5 R = Ac

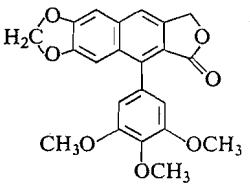

6

symmetrical pendant ring being a sharp 2-proton singlet. A similar situation existed in the triacetyl derivative (**5**) spectrum except that the latter two protons (C-2′, C-6′) were present as doublets owing to the magnetic asymmetry in ring C introduced by the acetyl groups.

Mass spectrum of the trimethyl derivative (**3**) gave a molecular ion of 410 as the base peak, an M-15 of 30% indicating loss of a methyl group from one of the methoxyl groups and an M-30 peak of 5%, probably loss of two methyl groups. Many other peaks occurred, but none were greater than 4% as would be expected from the stabilized aromatic nucleus (4).

Final proof of structure of plicatinaphthalene trimethyl ether (**3**), which identified the position of the lactone ring, was provided by its partial synthesis from podophyllotoxin obtained from podophyllin resin (7). Podophyllotoxin was epimerized to picropodophyllin by sodium acetate (8), thence to apopicropodophyllin, and finally to the naphthalene derivative, dehydroanhydropicropodophyllin (**6**) (9). The methylenedioxy ring of the latter compound was opened with boron trichloride and remethylated with diazomethane to yield trimethyl plicatinaphthalene (**3**), identical with the natural methylated derivative by n.m.r. and i.r. spectroscopy.

The substitution pattern of the pendant ring C was established by alkaline permanganate oxidation of a triethyl ether derivative (**4**) with subsequent detection of 3,4-diethoxy-5-methoxybenzoic acid by paper chromatography and t.l.c. The substitution pattern of the A ring and additional proof of structure for plicatinaphthalene (**2**) were shown by its preparation from plicatin (**1**) by aromatization with phosphorous oxychloride (11). To ensure that plicatinaphthalene was not an artifact being produced by the mild organic acid conditions of the hot-water extraction procedure, plicatin was refluxed for 8 h in aqueous acetic acid at p*H* 3 and for 6 h in glacial acetic acid and did not produce any plicatinaphthalene detectable by chromatography.

Experimental

The following equipment and materials were used: melting points, Fisher–Johns heated block (uncorrected); i.r. spectra, Perkin–Elmer 521 grating spectrometer (KBr disks); u.v. spectra, Beckman DK-2 spectrophotometer (ethanol); n.m.r., Varian HA-100 (tetramethylsilane $\delta = 0$ as internal standard in the solvents shown); low-resolution mass spectrum, Atlas CH-4, University of British Columbia. The t.l.c. values were obtained with silica gel G (Merck) as adsorbent, benzene–ethanol–acetic acid (90:10:1) as developer, with u.v. light followed by nitric acid–sulphuric acid (1:1) spray and heat as detector. Paper chromatograms were developed with 2% aqueous acetic acid and detected with potassium ferricyanide-ferric chloride reagent (mixed 1% solutions).

Plicatinaphthalene (2)

The aqueous layer from a hot-water extract of western red cedar heartwood (1 kg moisture-free basis) was extracted with chloroform (3 × 500 ml). After evaporation of the chloroform solvent the residue (6.8 g) was triturated with petroleum ether (65–110°) (150 ml) and then with benzene (150 ml) to remove thujaplicins, thujic acid, methyl thujate, and other terpenoids. The remainder (3 g) was dissolved in benzene–formic acid (9:1) and chromatographed on a polyamide (Woelm) column (3 cm × 40 cm), eluting with the same solvent. The fractions were monitored by t.l.c. The band between R_f 0.16 and 0.24 was further chromatographed on a cellulose column using water as the eluting solvent to yield, after recrystallization from ethanol, 6-hydroxy-2-(hydroxymethyl)-7-methoxy-4-(3′,4′-dihydroxy-5′-methoxyphenyl)-3-naphthoic acid lactone (plicatinaphthalene) (120 mg), $C_{20}H_{16}O_7$; t.l.c. R_f 0.16, and papergram R_f 0.14; u.v. blue fluorescent; m.p., crystals become opaque at 158–160°, discoloration began at 240° and finally melted with decomposition at 248–254°. Crystals from dichloromethane, melted (Mettler FP-1) 157.4° (see Discussion in text).

The spectra gave: λ_{max} in mμ (log ε), 259 (4.36) (shifting to 278 mμ in alkaline media), 315 (3.88), 356 (3.64); ν_{max} 3380 (broad hydroxyl), 1735 (lactone) cm^{-1}; n.m.r. plicatinaphthalene with ethanol of crystallization in deuterioacetone from which plicatinaphthalene crystallized out during the spectral run (all plicatinaphthalene peaks were singlets), 8.20, 7.55, 7.39 (1H each-phenols, quenched overnight by deuterium exchange with the

Can. J. Chem. Downloaded from www.nrcresearchpress.com by 210.87.254.105 on 09/05/12
For personal use only.

Can. J. Chem. Downloaded from www.nrcresearchpress.com by 210.87.254.105 on 09/05/12
For personal use only.

solvent), 7.74, 7.31, 7.10 (1H each, C-1, C-5, and C-8), 6.39 (2H, C-2′ and C-6′), 5.28 (2H, lactone methylene), 3.96 and 3.75 (3H each, methoxyls), and the remainder of spectrum consisted of large peaks for ethanol and acetone-d_5 (5). No additional protons were detected when the spectrum was offset 400 Hz. Total protons: 16; mass spectrum (low-resolution), parent ion = base peak 368, all other peaks were less than 8%.

Trimethyl Plicatinaphthalene (3)

Plicatinaphthalene (100 mg) was dissolved in methanol (40 ml) with warming. On cooling, excess diazomethane in ether (5 ml) was added each h for 5 h at room temperature with stirring and allowed to stand overnight. The product (t.l.c. R_f 0.71) was recrystallized from ethanol to yield 2-(hydroxymethyl)-6,7-dimethoxy-4-(3′,4′,5′-trimethoxyphenyl)-3-naphthoic acid lactone, (**3**) (50 mg), $C_{23}H_{22}O_7$, m.p. 238–239 °C.

The spectra gave: λ_{max} in mμ (log ε), 258.5 (4.60), 315 (3.85), and 350 (3.57); ν_{max}, no hydroxyl band, 1746 (lactone) cm^{-1}; n.m.r. (deuteriochloroform) (all peaks are sharp singlets), 7.66, 7.15, and 7.10 (1H each, C-1, C-5 and C-8) 6.58 (2H, C-2′ and C-6′), 5.34 (2H, lactone methylene), 4.02, 3.94, and 3.77 (3H each, C-6, C-7 and C-4′ methoxyls), and 3.82 δ (6H, C-3′ and C-5′ methoxyls); mass spectrum, parent ion = base peak 410, M-15 (30%), M-30 (5%), remaining peaks were all less than 4 percent.

Triacetyl Plicatinaphthalene (5)

Plicatinaphthalene (85 mg) was dissolved with warming in acetic anhydride (10 ml) and left standing for 3 h. The reaction mixture was heated on a steam bath for 1 h, *p*-toluenesulphonic acid (25 mg) added, and the mixture heated for an additional h. It was cooled overnight and added slowly to ice water (200 ml) with stirring. After filtering, the crude acetate was purified by recrystallization from dichloromethane to yield 2-(hydroxymethyl)-6-acetoxy-7-methoxy-4-(3′,4′-diacetoxy-5′-methoxyphenyl)-3-naphthoic acid lactone (**5**) (30 mg), $C_{26}H_{22}O_{10}$, t.l.c. R_f 0.61, m.p., 221–222 °C.

The n.m.r. spectrum (deuterioacetone) gave: 7.98, 7.54, 7.43 (1H each, singlets, C-1, C-5, C-8), 6.98 and 6.77 (1H each, doublets, J = 1 Hz, C-2′ and C-6′), 5.40 (2H, singlet, lactone methylene), 3.96 and 3.81 (3H each, singlets, methoxyls), 2.28 and 2.23 δ (3H and 6H, singlets, acetyls).

Triethyl Plicatinaphthalene (4)

Plicatinaphthalene (220 mg) in dry acetone (100 ml) containing anhydrous potassium carbonate (5 g) was treated with diethyl sulfate (1 ml per h) for 3 h on 2 consecutive days. After filtration and solvent removal, the product was purified on an alumina column by benzene to ethanol gradient elution to yield, after crystallization from ethanol, 6-ethoxy-2-(hydroxymethyl)-7-methoxy-4-(3′,4′-diethoxy-5-methoxyphenyl)-3-naphthoic acid lactone (**4**) (126 mg); t.l.c. R_f 0.80; m.p. 210–211°.

Permanganate oxidation and detection of 3,4-diethoxy-5-methoxy benzoic acid was carried out as previously described (10).

Synthesis of Trimethyl Plicatinaphthalene (3) from Podophyllin Resin

Podophyllotoxin was extracted from crude podophyllin resin (7). Podophyllotoxin (5 g) was dissolved in absolute ethanol (100 ml) containing anhydrous sodium acetate (1 g) and refluxed overnight (8). Hot water (200 ml) was added and the solution brought to a boil. On cooling, picropodophyllin (3.5 g) precipitated. The crude picropodophyllin (3.5 g) was converted to apopicrodophyllin (2.07 g) and thence to dehydroanhydropicropodophyllin (**6**) (1.6 g) by the method of Schrecker and Hartwell (9).

The methylenedioxy ring of dehydroanhydropicropodophyllin (**6**) (150 mg) was opened with boron trichloride and remethylated with diazomethane as previously described (1) to form 2-(hydroxymethyl)-6,7-dimethoxy-4-(3′,4′,5′-trimethoxyphenyl)-3-naphthoic acid lactone (**3**) (82 mg), which on recrystallization from ethanol (32 mg) was identical by mixture melting point, i.r. and n.m.r. spectra with trimethyl plicatinaphthalene (**3**).

Preparation of Plicatinaphthalene (2) from Plicatin (1)

Plicatin (15 mg), dissolved in pyridine (5 ml), was treated with $POCl_3$ (5 ml) and left overnight at room temperature. The reaction mixture was added dropwise to water (40 ml) which was then extracted with ethyl acetate (3 × 50 ml). After solvent removal, the residue showed 2 products by paper chromatography, R_f 0.77 (plicatin) and R_f 0.14 (plicatinaphthalene) which was confirmed by its naphthalene u.v. spectrum.

1. H. MacLean and B. F. MacDonald. Can. J. Chem. **47**, 457 (1969).
2. H. MacLean and K. Murakami. Can. J. Chem. **44**, 1544 (1966).
3. R. J. Swan, W. Klyne, and H. MacLean. Can. J. Chem. **45**, 319 (1967).
4. J. H. Beynon, R. A. Saunders, and A. F. Williams. The mass spectra of organic molecules. Elsevier Publ. Co., Ltd., London. 1968. p. 129.
5. N. S. Bhacca, L. F. Johnson, and J. N. Shoolery. N.M.R. Spectra Catalog, Vols. 1 and 2. Spectra 14 and 388. Varian Associates, Palo Alto, Calif. 1962–1963.
6. E. E. Jelley. *In* Technique of organic chemistry. Vol. I, Part I, 2nd Edition. Physical methods of organic chemistry. *Edited by* A. Weissburger. Interscience Publishers, Inc., New York. 1949. p. 886.
7. J. L. Hartwell and W. E. Detty. J. Amer. Chem. Soc. **72**, 246 (1950).
8. J. L. Hartwell and A. W. Schrecker. J. Amer. Chem. Soc. **73**, 2910 (1951).
9. A. W. Schrecker and J. L. Hartwell. J. Amer. Chem. Soc. **74**, 5676 (1952).
10. H. MacLean and B. F. MacDonald. Can. J. Chem. **45**, 739 (1967).
11. L. F. Fieser and M. Fieser. Reagents for organic synthesis. John Wiley & Sons, Inc., New York. 1967. p. 879.

Aromatic nucleophilic substitutions. Reactions of chloro- and nitro-substituted benzenes

P. S. RADHAKRISHNAMURTI AND JANARDAN SAHU
Department of Chemistry, Khallikote College, Berhampur (Ganjam), Orissa, India

Received May 12, 1969

The kinetics of the reaction of 2,4-dinitro-1-chlorobenzene with various aromatic bases to give 2,4-dinitrodiphenylamines have been studied in alcohol, alcohol–acetonitrile, alcohol–dimethylformamide, and alcohol – dimethyl sulfoxide mixtures. No base catalysis has been observed under these conditions. ρ Values have been computed. In the reaction of *o*-chloro- and *p*-chloronitrobenzene with hydroxide in 50% dimethyl sulfoxide, the reactivity of both the isomers has been found to be identical, in contradiction to the previously reported observations.

Canadian Journal of Chemistry, **47**, 4499 (1969)

Can. J. Chem. Downloaded from www.nrcresearchpress.com by 210.87.254.6 on 09/05/12
For personal use only.

Introduction

Singh and Peacock (1,2) were the earliest workers to study the reaction of 2,4-dinitro-1-chlorobenzene with amines in alcohol as solvent. The reactions have been found to be second order and there was no base catalysis reported. Other important workers in the field were Blanksma and Schreinemachers (3), Brady and Cropper (4), Rheinlander (5), and van Opstall (6) who arrived at similar conclusions. LeRoux *et al.* (7) and Bennett and Vernon (8) have studied the simplest of all nucleophilic displacements with these compounds; viz, when the reagent is a halide ion, either isotopically distinguished from, as in the former case, or chemically different from the halogen present in the organic compound, as in the latter case. The work was extended to the fluoro derivative and other bases like pyridine and picolines by Chapman and co-workers (*9a–e*) who arrived at similar conclusions as the previous investigators did with the chloro derivatives. Kingsbury (10) and Suhr (11) studied the action of dipolar aprotic solvents in the reaction of benzylamine with these halides. The speed can be attributed to the fact that DMSO molecules in, or arranged about, the transition state for a reaction in DMSO – methanol mixtures, lower the free energy of the transition state relative to that for a reaction in pure methanol.

Bunnett and Pruitt (12) studying the reaction of 2,4-dinitro-1-chlorobenzene with piperidine in 80% dioxan – water observed only an uncatalyzed reaction as did all the previous investigators. But, subsequently, Ross *et al.* (*13a–f*) have published a series of papers questioning the validity of postulating a simple uncatalyzed reaction for this amine reaction and confirmed that, with a series of aliphatic amines in various solvents, this reaction is catalyzed by bases. In their work on aniline with 2,4-dinitro-1-chlorobenzene in ethanol and in ethanol – ethyl acetate (50%), Ross and Kuntz (14) found that, due to charge transfer complexing, there is a decrease in the measured rate constant with an increase in concentration of the base. No sure choice can be made between the two alternatives: the first, that aniline and 2,4-dinitro-1-chlorobenzene are in equilibrium with a charge transfer complex and that concurrently they react to form products; the second, that the two reagents are in equilibrium with a complex which decomposes to products. It is clearly seen from the previous work that, though plausible explanations have been advanced to account for all the results both in terms of the one step mechanism and the two step intermediate complex mechanisms, it is best to conclude that no definite choice can be made between the two possibilities.

The present investigation is intended to study the effect of dipolar aprotic solvents like acetonitrile, dimethylformamide, and dimethyl sulfoxide under perfectly homogeneous conditions and also to correlate structure and reactivity in a systematic manner. Absence or presence of amine catalysis is also investigated.

Experimental

Materials

All the bases and the substrates used were obtained from British Drug House (B.D.H.) and were purified and distilled before use. The physical constants of the compounds are as follows: 2,4-dinitro-1-chlorobenzene, m.p. 52 °C; aniline, b.p. 183 °C; *p*-toluidine, m.p. 45 °C; *m*-toluidine, b.p. 199 °C; *p*-chloroaniline, m.p. 70 °C;

TABLE I

Rate constants for aromatic nucleophilic substitutions (solvent, alcohol; substrate, 2,4-dinitro-1-chlorobenzene; temperature, 50 ± 0.02 °C)

Concentration of substrate (M)	Base	Concentration of base (M)	k(l mole^{-1} min^{-1}) × 10^3
0.02494	Aniline	0.02612	14.18
0.02570	Aniline	0.05115	15.55
0.02474	Aniline	0.07660	14.48
0.02476	*p*-Toluidine	0.07560	39.40
0.02510	*m*-Toluidine	0.07525	20.87
0.02498	*p*-Chloroaniline	0.07590	3.591
0.02493	*m*-Chloroaniline	0.07580	1.161

TABLE II

Rate constants for aromatic nucleophilic substitutions (solvent, alcohol – acetonitrile (80:20% v/v); substrate, 2,4-dinitro-1-chlorobenzene; temperature, 50 ± 0.02 °C)

Concentration of substrate (M)	Base	Concentration of base (M)	k(l mole^{-1} min^{-1}) × 10^3
0.02490	Aniline	0.02500	8.536
0.02478	Aniline	0.05000	8.459
0.02461	Aniline	0.07505	9.035
0.02488	*p*-Toluidine	0.07620	34.240
0.02523	*m*-Toluidine	0.07545	11.470
0.02481	*p*-Chloroaniline	0.07445	2.757
0.02533	*m*-Chloroaniline	0.07565	1.003

and *m*-chloroaniline, b.p. 230 °C. Acetonitrile, dimethylformamide, and dimethyl sulfoxide were of B.D.H. A.R. grade and were used without further purification. Alcohol was of absolute grade. Second order rate constants were calculated by using the least squares method.

Preparation of Indicator and Solutions

Ferric alum indicator, potassium thiocyanate, and silver nitrate solutions required for kinetic studies were prepared using standard procedures (15).

Procedure

The solution of the substrate and the base in the mixed solvent after attaining the required temperature was mixed in a narrow mouthed stoppered bottle. Five ml aliquots of the reaction mixture were quenched in standard silver nitrate solution at different intervals of time and the excess of silver nitrate solution determined by Volhard's method (16).

Results and Discussion

We have studied this reaction with 2,4-dinitro-1-chlorobenzene and a series of substituted aromatic primary amines and in some cases with different concentrations of amines in alcohol as solvent. We find that there is no amine catalysis and the reactions are straightforward second order reactions within the concentration ranges studied.

The concentration ranges are 0.025 to 0.075 M for the amine, but as against the reported homogeneous reactions with aliphatic amines, there has been extensive precipitation of the product with all the aromatic amines studied towards the last stages of the reaction, and the precipitate is found to be insoluble in excess alcohol or water but soluble in dimethyl sufoxide, dimethylformamide, and acetonitrile. The rate constants have been computed from the initial percentages in all cases for the purpose of comparison. To this date this is the first case of a report of precipitation with alcohol as solvent in these reactions.

Hence to have homogeneous conditions, the kinetics were studied in 80:20% (v/v) mixtures of alcohol with acetonitrile, dimethylformamide, and dimethyl sulfoxide. Perfect homogeneity has been found in all cases. The reactivity is alcohol – dimethyl sulfoxide > alcohol – dimethylformamide > alcohol > alcohol – acetonitrile. The rate constants are given in Tables I–IV.

Can. J. Chem. Downloaded from www.nrcresearchpress.com by 210.87.254.6 on 09/05/12
For personal use only.

TABLE III

Rate constants for aromatic nucleophilic substitutions (solvent, alcohol – DMF (80:20% v/v); substrate, 2,4-dinitro-1-chlorobenzene; temperature, 50 ± 0.02 °C)

Concentration of substrate (M)	Base	Concentration of base (M)	$k \times 10^3$ (l mole^{-1} min^{-1})
0.02522	Aniline	0.02575	17.93
0.02522	Aniline	0.05065	18.05
0.02522	Aniline	0.07560	17.48
0.02498	*p*-Toluidine	0.07410	58.76
0.02500	*m*-Toluidine	0.07550	24.68
0.02522	*p*-Chloroaniline	0.07585	4.249

TABLE IV

Rate constants for aromatic nucleophilic substitutions (solvent, alcohol – DMSO (80:20% v/v); substrate, 2,4-dinitro-1-chlorobenzene; temperature, 50 ± 0.02 °C)

Concentration of substrate (M)	Base	Concentration of base (M)	k(l mole^{-1} min^{-1}) $\times 10^3$
0.02523	Aniline	0.02498	23.97
0.02526	Aniline	0.05050	22.50
0.02503	Aniline	0.07670	23.86
0.02486	*p*-Toluidine	0.07525	76.17
0.02530	*m*-Toluidine	0.07560	28.11
0.02493	*p*-Chloroaniline	0.07515	5.943

A plot of log k vs. pK_a shows linearity. A plot of log k vs. σ shows linearity with the rate constants obtained in pure alcohol, alcohol – acetonitrile, alcohol – dimethylformamide, and alcohol – dimethyl sulfoxide mixtures. The ρ values are −2.74, −2.77, −2.90, and −2.82 for alcohol and mixed solvents respectively. This shows that bond formation is an important feature in these reactions. Electron releasing groups in the base are accelerating the process. It is pertinent to point out that as alcohol is used as solvent, the amine – alcohol interaction will not cause significant disturbance in the nucleophilic aromatic displacements studied. The reactions are consistently slower in the alcohol – acetonitrile mixtures than in pure alcohol. It can be rationalized that as the reaction is a dipole–dipole reaction, an increase in dielectric constant increases the kinetic rate. This seems to be true except in the case of acetonitrile mixtures. Alternatively, the higher reaction rate in alcohol – dimethyl sulfoxide mixtures is due to the special solvent effect due to DMSO. A major portion of the solvent effect can be associated with the dramatic influence of DMSO upon the solvation shell geometry.

Table V shows that there is no amine catalysis. Increase of concentration of the amine does not cause much change in the rate.

In the latter case there has been an increase of 6% which can be taken to be either a small general co-solvent effect or it can be safely remarked that as far as weak bases like aromatic primary amines are concerned, there does not seem to be any amine catalysis as found earlier for the stronger aliphatic amines by Ross and co-workers. Our investigations are confirmed by the very recent work of Ross in systems containing hydroxylic solvents (17).

In addition we wish to record some interesting observations on the hydroxide reactions with *o*-chloronitrobenzene and *p*-chloronitrobenzene in 50% aqueous dimethyl sulfoxide at 80 °C. "It has long been known that for displacements with primary and secondary amines, *o*-nitrohalobenzenes react more rapidly than *p*-nitrohalobenzenes, but, that, in substitutions which do not involve the removal of a proton, as in reactions with alkoxides or thiophenoxides, it is the *p*-nitrohalobenzenes which react more rapidly." (18). This statement needs revision on the basis of the present work. Hydroxide reactions

Can. J. Chem. Downloaded from www.nrcresearchpress.com by 210.87.254.6 on 09/05/12
For personal use only.

TABLE V

Second order rate constants (l mole^{-1} min^{-1} × 10^3) for 2,4-dinitro-1-chlorobenzene – aniline reaction at 50 ± 0.02 °C

Solvent	Concentration (M)	k
100% Alcohol	1:1 (0.02494 : 0.02612)	14.18
	1:2 (0.02570 : 0.05115)	15.55
	1:3 (0 02475 : 0 07660)	14.48
Alcohol – acetonitrile (80:20 % v/v)	1:1 (0 02490 : 0 02500)	8.536
	1:2 (0.02478 : 0.05000)	8.459
	1:3 (0 02461 : 0 07505)	9.035
Alcohol – DMSO (80:20 % v/v)	1:1 (0 02523 : 0 02498)	23.97
	1:2 (0 02526 : 0 05050)	22.50
	1:3 (0 02503 : 0 07670)	23.86
Alcohol – DMF (80:20 % v/v)	1:1 (0.02522 : 0 02575)	17.93
	1:2 (0 02522 : 0.05065)	18.05
	1:3 (0.02522 : 0.07560)	17.48

in dimethyl sulfoxide at 80 °C show that the *o*- and *p*-nitrohalobenzenes react with identical rates. With *n*-butylamine neither isomer reacts. The reactions were facile in 1:10 stoichiometry. The rates were almost identical for *ortho* and *para* isomers and *m*-chloronitrobenzene did not even react under these conditions. It was also found when 1-nitro-2,5-dichlorobenzene was subjected to the same reaction in dimethyl sulfoxide, there was substitution of one of the chlorines yielding 1-nitro-5-chloro-2-hydroxybenzene. When 1-nitro-3,4-dichlorobenzene was hydrolyzed similarly, it yielded 1-nitro-3-chloro-4-hydroxybenzene, confirming that a chlorine at the *meta* position does not get hydrolyzed. The rate constants are 10 times higher than those for *o*-chloro- and *p*-chloronitrobenzenes as seen from Table VI.

TABLE VI

Second order rate constants (l mole^{-1} min^{-1} × 10^3) at 80 ± 0.02 °C in 50% aqueous dimethyl sulfoxide

Compound	k
1-Nitro-2-chlorobenzene	1.541
1-Nitro-4-chlorobenzene	1.563
1-Nitro-2,5-dichlorobenzene	15.710
1-Nitro-3,4-dichlorobenzene	16.150

1. A. SINGH and D. H. PEACOCK. J. Chem. Soc. 1410 (1935).
2. A. SINGH and D. H. PEACOCK. J. Phys. Chem. **40**, 669 (1936).
3. BLANKSMA and SCHREINEMACHERS. Rec. Trav. Chim. **52**, 428 (1933).
4. O. L. BRADY and F. R. CROPPER. J. Chem. Soc. 507 (1950).
5. A. H. RHEINLANDER. J. Chem. Soc. 3099 (1923).
6. H. J. VAN OPSTALL. Rec. Trav. Chim. **52**, 901 (1933).
7. J. J. LEROUX, C. S. LU, S. SUGDEN, and R. W. K. THOMSON. J. Chem. Soc. 586 (1945).
8. BENNETT and VERNON. J. Chem. Soc. 1783 (1938).
9. (*a*) N. B. CHAPMAN and C. W. REES. J. Chem. Soc. 1190 (1954); (*b*) R. R. BISHOP, E. A. S. CAVELL, and N. B. CHAPMAN. J. Chem. Soc. 437 (1952); (*c*) E. A. S. CAVELL and N. B. CHAPMAN. J. Chem. Soc. 3392 (1953); (*d*) N. B. CHAPMAN and R. E. PARKER. J. Chem. Soc. 3301 (1951); (*e*) N. B. CHAPMAN, R. E. PARKER, and P. W. SOANES. J. Chem. Soc. 2109 (1954).
10. C. A. KINGSBURY. J. Org. Chem. **29**, 3262 (1964).
11. H. SUHR. Chem. Ber. **97**, 3277 (1964).
12. J. F. BUNNETT and K. M. PRUITT. Elisha Mitchell Sci. Soc. **73**, 297 (1957).
13. (*a*) S. D. ROSS and M. FINKELSTEIN. J. Amer. Chem. Soc. **79**, 6547 (1957); (*b*) S. D. ROSS and R. C. PETERSEN. J. Amer. Chem. Soc. **80**, 2447 (1958); (*c*) S. D. ROSS. J. Amer. Chem. Soc. **80**, 5319 (1958); (*d*) S. D. ROSS. J. Amer. Chem. Soc. **81**, 2113 (1959); (*e*) S. D. ROSS, M. FINKELSTEIN, and R. C. PETERSEN. J. Amer. Chem. Soc. **81**, 5336 (1959); (*f*) S. D. ROSS, J. E. BARRY, and R. C. PETERSEN. J. Amer. Chem. Soc. **83**, 2133 (1961).
14. S. D. ROSS and I. KUNTZ. J. Amer. Chem. Soc. **76**, 3000 (1954).
15. A. I. VOGEL. Quantitative inorganic analysis. Longmans, Green and Co., Ltd., London. 1961. pp. 258, 259, and 265.
16. A. I. VOGEL. Quantitative inorganic analysis. Longmans, Green and Co., Ltd., London. 1961. p. 264.
17. S. D. ROSS, M. FINKELSTEIN, and R. C. PETERSEN. J. Amer. Chem. Soc. **90**, 6411 (1968).
18. S. D. ROSS. Progress in physical organic chemistry. Vol. I. Interscience Publishers, Inc., New York. 1963. p. 65.

Can. J. Chem. Downloaded from www.nrcresearchpress.com by 210.87.254.6 on 09/05/12
For personal use only.

Photo-addition of indene and acrylonitrile: orientation and stereochemistry of the cycloadducts

R. M. BOWMAN AND J. J. MCCULLOUGH
Department of Chemistry, McMaster University, Hamilton, Ontario
AND
J. S. SWENTON
Department of Chemistry, The Ohio State University, Columbus, Ohio

Received June 24, 1969

The cyclobutanes obtained on photosensitized cyclo-addition of indene and acrylonitrile have been reinvestigated and the structures formerly assigned (1) have been unambiguously confirmed. The photo-addition of indene and cyanoacetylene has been shown to smoothly afford a single adduct, 7-cyano-2,3-benzobicyclo[3.2.0]hepta-2,6-diene.

Canadian Journal of Chemistry, **47**, 4503 (1969)

Can. J. Chem. Downloaded from www.nrcresearchpress.com by 210.87.254.6 on 09/05/12
For personal use only.

In earlier papers (1) we reported that indene and acrylonitrile react on acetophenone sensitization to yield a small amount of indene dimer and two isomeric nitrilic adducts. The latter were assigned structures **1***a* and **1***b* on the basis of their mode of formation and interconvertibility by strong base. The stereochemistry was tentatively assigned from the nuclear magnetic resonance (n.m.r.) spectra (**1***b*). Recently in connection with studies on the photochemistry of a carbomethoxy benzonorcaradiene, the nitriles **1***a* and **1***b* were used for structural correlation (2). During the course of this study it was deemed advisable to confirm the location of the nitrile group chemically, since the photoproduct from the benzonorcaradiene appeared to be without precedent. Furthermore, the discovery that cyanoacetylene adds to indene furnished a chemical method of establishing with certainty the stereochemistry of the nitrile group.

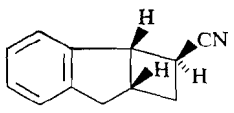

1*a* m.p. 49°

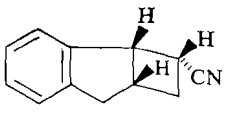

1*b* m.p. 70°

The orientation of the nitrile group was established by degradation of the nitrile, m.p. 47–50° as shown in Scheme 1. The key step in this sequence was ring-opening of the cyclobutyl carbinyl iodide **4***a* on reaction with magnesium (3) to afford 2-allylindane. The degradation product proved to be identical with a 2-allylindane prepared by coupling 2-indanyl magnesium iodide and allyl bromide.

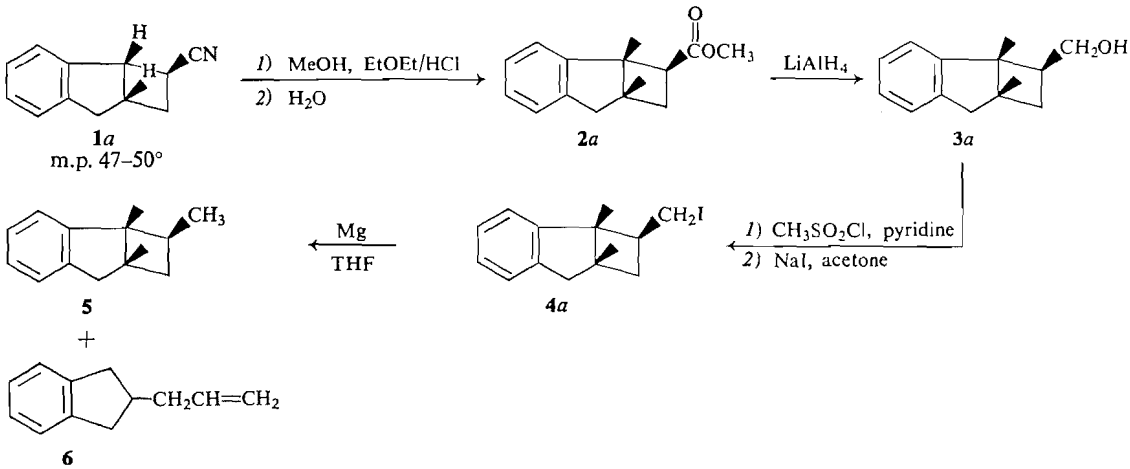

SCHEME 1

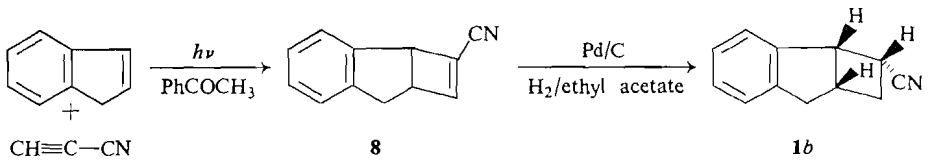

SCHEME 2

There still remained the problem as to the stereochemistry of the nitrile groups in the cycloadducts. The tentative assignment of stereochemistry made on the basis of the n.m.r. spectra (**1***b*) earlier was further supported by the methoxy resonance positions of the esters **2***a* and **2***b*. While **2***a* showed the methoxy singlet at 6.23 τ, the resonance in the ester **2***b* occurred at 6.58 τ suggestive of shielding by the aromatic ring.

A rational approach to elucidation of the configuration at C-7 would involve addition of indene to cyanoacetylene to afford the cyanocyclobutene having the same carbon skeleton as **1***a* and **1***b*. Since ample precedent exists for hydrogenation involving addition from the less hindered side to afford the *endo*-nitrile, the success of this method depended on the ease and direction of the cyanoacetylene addition.

On photolysis of a mixture of indene and cyanoacetylene in ethanol using a Corex filter (or with acetophenone as sensitizer and a Pyrex filter), a single product was formed, at a somewhat slower rate than the adducts of indene and acrylonitrile (**1***b*). The progress of the reaction was followed by vapor phase chromatography (v.p.c.), and one new peak appeared. On termination of the photolysis, chromatography on silica gel afforded the adduct, m.p. 80–81°, molecular ion of *m/e* 167 and infrared (i.r.) band at 2210 cm^{-1} (nitrile). In the n.m.r. spectrum (CCl_4, 100 Mc.p.s.), peaks appeared at 2.7–3.1 τ, multiplet, area 4 (aromatics); 2.38 τ, singlet, area 1 (vinylic); 5.54 τ, doublet, area 1 (methine); and at 6.7–7.1 τ, multiplet, area 2 (methylene).

The spectral data are consistent with the structure of the required cyanocyclobutene **8**. Hydrogenation of **8** at 1 atm in ethyl acetate gave a quantitative yield of **1***b*, m.p. and mixed m.p. 67–68°, identical by i.r. and n.m.r. spectra. Obtaining **1***b* as the only product in the hydrogenation established both the position of the nitrile group in the cyclobutene **8**, and the *cis* stereochemistry (4) of **1***b*, see Scheme 2.

It is interesting that the adducts formed in the acrylonitrile– and cyanoacetylene–indene additions have the orientation which would result from closure of the more stable biradical intermediate (5). In the cyanoacetylene case, the electronic structure of the cyano-group is such that it can stabilize an adjacent vinyl radical, while retaining conjugation with the π-system of the C≡C linkage.

We also report that the adducts **1***a* and **1***b* formed so efficiently in the sensitized addition of indene and acrylonitrile, are formed in the direct irradiation. They are accompanied by the isomeric 6-cyanobenzobicyclo[3.2.0]hept-2-enes, and cyanoethylindenes (1). Separation of the cyclobutanes from this reaction mixture is difficult if not impossible by chromatography alone, and was achieved by oxidizing the indenes with permanganate, followed by chromatography of the cyanocyclobutane mixture and fractional crystallization of the solid isomers. The operations are described in the Experimental.

Experimental

Except where stated otherwise, the instruments and materials described previously were used (**1***b*). Gas chromatography was performed at 165° using a 5 ft × 1/8 in. column of 5% QF-1 on Chromosorb W, with helium at 30–35 ml/min as carrier gas.

*Conversion of exo-7-Cyano-2,3-benzobicyclo[3.2.0]hept-2-ene (**1a**) to exo-7-Carbomethoxy-2,3-benzobicyclo[3.2.0]hept-2-ene (**2a**)*

A 270 ml mixture of anhydrous ether–methanol (200:70) was saturated with dry hydrogen chloride. 5.0 g (0.029 mole) of nitrile **1***a* added, and the reaction mixture magnetically stirred at 0° for 8 h. After cautious addition of 200 ml of water the mixture was allowed to warm to room temperature over a period of 3 h. The reaction mixture was then poured into 1 l of cold water, the organic layer separated, and the aqueous layer extracted, 3 × 75 ml of ether. The organic layers were combined, dried over $CaSO_4$, and the ether distilled to yield 5.66 g of crude ester. Purification by v.p.c. (5% PDEAS on 60–80 Chromosorb W—10 ft × 1/4 in.—150°) yielded a colorless liquid ester. The n.m.r. spectrum (CCl_4) exhibited the aromatic protons as a singlet, 2.71 τ (4H); a low field broad absorption, 6.03 τ (1H); the methoxy group, 6.23 τ (3H); and complex structured absorption from 6.46–8.38 τ (6H).

Can. J. Chem. Downloaded from www.nrcresearchpress.com by 210.87.254.6 on 09/05/12
For personal use only.

Can. J. Chem. Downloaded from www.nrcresearchpress.com by 210.87.254.6 on 09/05/12
For personal use only.

exo-7-Carboxy-2,3-benzobicyclo[3.2.0]hept-2-ene (7a)

Hydrolysis of the *exo*-ester (**2a**) followed by chromatography on deactivated silica gel and recrystallization from hexane:methylene chloride yielded a crystalline acid, m.p. 85–87°.

Anal. Calcd. for $C_{12}H_{12}O_2$: C, 76.57; H, 6.43. Found: C, 76.46; H, 6.43.

Conversion of endo-7-Cyano-2,3-benzobicyclo[3.2.0]hept-2-ene to Ester 2b and Acid 7b

The conversion of **1b**–**2b** and subsequent hydrolysis to **7b** were analogous to the transformations **1a**–**2a** and **2a**–**7a**. The prominent features of the n.m.r. spectrum of **2b** were aromatic absorption centered at 3.00 τ (4H); a broad peak centered at 6.00 τ (1H); the methoxy resonance appeared as a singlet at 6.58 τ overlapping a structured absorption (6.43–6.83 τ), the total area being 4H; and two broad structured absorptions centered at 7.10 τ (3H) and 7.76 τ (2H). Hydrolysis of the ester yielded an acid which was recrystallized from hexane/methylene chloride to yield a white crystalline material, m.p. 141–143°.

Anal. Calcd. for $C_{12}H_{12}O_2$: C, 76.57; H, 6.43. Found: C, 76.56; H, 6.44.

$LiAlH_4$ Reduction of exo-7-Carbomethoxy-2,3-benzobicyclo[3.2.0]hept-2-ene (2a)

The crude ester, 5.66 g (0.028 mole), obtained from hydrolysis of the corresponding nitrile in 50 ml of anhydrous ether was added dropwise to a slurry of 1.5 g of $LiAlH_4$ in 250 cc of anhydrous ether. The mixture was refluxed for 5 h followed by decomposition of the excess hydride and reduction complex by cautious addition of 6.0 ml of water. Filtration of the solution followed by distillation of the ether afforded 5.06 g of light yellow oil. Crystallization of the oil from hexane yielded a total of 4.0 g (0.023 mole) of **3a** as white needles, m.p. 55.0–56.5°.

Anal. Calcd. for $C_{12}H_{12}O$: C, 82.72; H, 8.10. Found: C, 82.76; H, 8.19.

Conversion of Alcohol 3a to Iodide 4a

Reaction of 3.3 g (0.02 mole) of alcohol **3a** with methane sulfonyl chloride in pyridine at 0° in the usual manner afforded after work-up 5.0 g of crude mesylate as a light yellow oil. The mesylate without further purification was refluxed for 10 h in 200 ml of acetone containing 20 g of sodium iodide. After filtration of the solid and evaporation of the acetone, the residue was transferred to a separatory funnel with 100 ml of water and 150 ml of ether. The organic layer was washed with 100 ml of 10% $NaHSO_3$, 10% $NaHCO_3$, and saturated NaCl. The yellow oil obtained after drying of the organic layer and removal of solvent was chromatographed on silica gel to 4.54 g (85%) of a nearly colorless oil which slowly darkened on standing.[1]

Anal. Calcd. for $C_{12}H_{13}I$: C, 50.70; H, 4.58; I, 44.71. Found: C, 51.05; H, 4.65; I, 43.85.

Reaction of Iodide 4a with Magnesium in Tetrahydrofuran

The general procedure of Hill *et al.* (3) was utilized. In a typical procedure, the Grignard was refluxed for 3 h followed by quenching with water. Vapor phase chromatographic analysis (10% SE-30 on 60–80 Chromosorb P—10 ft × 1/4 in.—120°) showed two major reaction products. The ratio of the two products was dependent upon reaction conditions varying from 1:3 to 1:1 in two different runs. The material of lower retention time was identified as *exo*-7-methyl-2,3-benzobicyclo[3.2.0]hept-2-ene on the basis of its i.r., n.m.r., and mass spectra. The material of longer retention time was identified as 2-allylindane by comparison of its i.r. and n.m.r. spectrum with that of an authentic sample synthesized by the procedure below.

2-Iodoindane

The 2-iodoindane was prepared in 65% purified yield by iodide displacement of the mesylate of 2-indanol as in the **3a**–**4a** conversion. Recrystallization from hexane yielded white crystals, m.p. 52–53°. The n.m.r. spectrum showed the aromatic protons as a singlet at 2.91 τ (4H), the methine hydrogen as a pentuplet centered at 5.46 τ (1H, J = 6 c.p.s.), and the benzylic protons as a doublet centered at 6.66 τ (4H, J = 6 c.p.s.).

Anal. Calcd. for C_9H_9I: C, 44.30; H, 3.72; I, 52.20. Found: C, 44.29; H, 3.74; I, 52.16.

2-Allylindane

The mixture of 2-iodoindane, 1.16 g (4.8 mmoles), and magnesium, 0.15 g (6.5 mmoles), in 25 ml of anhydrous ether was stirred at room temperature for 1 h during which the Grignard reagent formed. The solution was heated to reflux and 1.1 g (6.3 mmoles) of allyl bromide in 5 ml of ether were added dropwise. After 30 min reflux the reaction mixture was poured into 100 ml of 5% HCl. Work-up in the usual manner afforded a light yellow liquid from which the 2-allylindane was isolated in 31% yield by preparative v.p.c. (10% SE-30 on 60–80 Chromosorb P—10 ft × 1/4 in.—120°). Prominent bands in the i.r. were the double bond absorption at 6.07 μ, and the bands at 10.09 and 10.95 μ characteristic of a monosubstituted ethylene. The n.m.r. spectrum showed the aromatic protons as a singlet, 2.97 τ (4H), complex vinyl absorption from 3.83–4.58 τ (1H), two structured signals centered at 4.90 and 5.13 τ having an area of 2H, and structured absorption from 6.70–8.0 τ (7H).

Anal. Calcd. for $C_{12}H_{14}$: C, 91.08; H, 8.92. Found: C, 90.93; H, 8.83.

Cyanoacetylene

Cyanoacetylene was prepared in 70–85% yield by phosphorus pentoxide dehydration of propiolamide in the manner described by Murahashi *et al.* (6). Decalin was the reaction medium and the cyanoacetylene was swept from the reaction flask in a slow stream of nitrogen and collected in a wide U-tube cooled in dry ice – acetone. The colorless solid had m.p. 7–8° and λ_{max} (EtOH) mμ(log ε_{max}) 210 (2.20), 219 (2.24), 229 (2.00), and 243 (0.78).

Photocondensation of Indene and Cyanoacetylene

Cyanoacetylene (4.60 g; 0.090 mole) and indene (1.03 g; 0.009 mole) in 95% ethanol (400 ml) were irradiated in the usual manner for 4 h (1*b*). A Corex sleeve was used. Monitoring by v.p.c. indicated that one major volatile component was formed. The solvent was evaporated and the residue taken up in ether and filtered through

[1]This decomposition apparently precluded an accurate analysis.

Can. J. Chem. Downloaded from www.nrcresearchpress.com by 210.87.254.6 on 09/05/12
For personal use only.

Celite. The crude product was chromatographed on silica gel (2.5 × 38 cm). Benzene was used as eluent throughout and 100 ml fractions were collected. Fraction 1 contained residual indene (590 mg) and fractions 6–9 contained a gum (116 mg) which gave a single peak on gas–liquid chromatography with a retention time of 2.8 min. The combined fractions 6–9 afforded colorless prisms (81 mg) m.p. 80–81°, from light petroleum (b.p. 30–60°). The i.r. spectrum (KBr) showed bands at 2210 (nitrile) and 1575 (C=C) cm^{-1}, while the n.m.r. spectrum (see above) and the mass spectrum (molecular ion *m/e* 167 and strong peaks at *m/e* 116 and 115) showed the product to be cyano-2,3-benzobicyclo[3.2.0]-hepta-2,6-diene.

Anal. Calcd. for $C_{12}H_9N$: C, 86.18; H, 5.44; N, 8.38. Found: C, 86.05; H, 5.45; N, 8.27.

Acetophenone Sensitized Photo-addition of Indene and Cyanoacetylene

A solution of indene (1.03 g; 0.009 mole), cyanoacetylene (4.60 g; 0.090 mole), and acetophenone (1.00 g; 0.0083 mole) in benzene (300 ml) was irradiated in the usual way for 3 h using a Pyrex filter. Chromatography as described in the previous experiment gave the cyanocyclobutene **8**, m.p. 80–81° (from light petroleum) (180 mg), found in fractions 4–6. Fractions 7–12 contained a yellow oil, which contained **8** plus adducts of the latter with indene and benzene, detected by ions of *m/e* 283 and 245 respectively in the mass spectrum.

Hydrogenation of the Indene – cyanoacetylene Photo-adduct

The cyanocyclobutene **8**, from the above addition reactions, (51 mg) in ethyl acetate (10 ml) was hydrogenated at atmospheric pressure and ambient temperature over 10% palladium on charcoal catalyst (10 mg), (Matheson, Coleman and Bell). Hydrogen uptake (6.9 ml, theoretical 6.7 ml) was complete in 5 min, and v.p.c. on the filtered solution showed one peak, retention time 4.2 min. Evaporation gave *cis*-7-cyano-2,3-benzobicyclo-[3.2.0]hept-2-ene as needles, m.p. 67–67.5° from light petroleum, (46 mg, 90%). This was identical with the higher-melting adduct from the sensitized indene – acrylonitrile reaction (1), by mixed m.p. (67–68°) and i.r. and n.m.r. spectra comparison.

Anal. Calcd. for $C_{12}H_{11}N$: C, 85.16; H, 6.57; N, 8.28. Found: C, 85.29; H, 6.64; N, 8.16.

Isolation of the Cyclobutane Adducts from the Direct Irradiation of Indene and Acrylonitrile

Indene (5.50 g; 0.0477 mole) and acrylonitrile (30.0 g; 0.566 mole) in 95% ethanol (1 l) were irradiated for 4.5 h precisely as described previously (1*b*), except that a Corex sleeve was used. The reaction mixtures from two runs were combined and evaporated. The residue was freed from indene and polymer by filtration through a 2.5 × 30 cm column of silica gel; benzene eluted the indene, and the adducts were eluted with 1:1 benzene – ether. The adduct mixture from the latter fractions was dissolved in *tert*-butyl alcohol (100 ml) and water (100 ml) was added; this mixture was stirred at ambient temperature while carbon dioxide was bubbled through. A total of 3.5 g of potassium permanganate was added, in 0.5 g portions at 10 min intervals. The mixture was acidified (litmus) with 10% H_2SO_4, and sodium bisulfite was added until all the precipitate dissolved. The organic layer was separated, and the aqueous phase was extracted with ether (3 × 50 ml). The combined organic solutions were washed with water, 10% Na_2CO_3 solution, and finally water, and dried ($MgSO_4$). On evaporation, 2.8 g of oil were obtained, which showed 3 components on v.p.c., retention times 3.1, 3.4, and 4.2 min, ratio (by areas) 25:10:65, respectively. This ratio was unchanged by further permanganate treatment. The mixture was chromatographed on a 3 × 75 cm column of silica gel, which was eluted with benzene – light petroleum (9:1) (3 l), then with benzene; 200 ml fractions were collected. Fractions 23–25 contained the 3.1 min component (66 mg); 26–30 (327 mg) were mixtures of all three components and the component of retention time 4.2 min was found in fractions 31–37. Fractions 23–25 were combined and crystallized twice from light petroleum, b.p. 30–60°, to afford *trans*-7-cyano-2,3-benzobicyclo-[3.2.0]hept-2-ene (1*a*), m.p. and mixed m.p. 48–50°. Fractions 31–37 were oily, but on repeated crystallization from light petroleum, b.p. 30–60°, *cis*-7-cyano-3-benzobicyclo[3.2.0]hept-2-ene, m.p. and mixed m.p. 68–70°, was obtained. The mother liquors from these crystallizations (of the *cis*-compound) gave an oil on evaporation; this oil had an n.m.r. spectrum very similar to that reported for 6-cyano-benzobicyclo[3.2.0]hept-2-ene (1*b*), and had a retention time of 4.2 min, the same as the *cis*-7-cyano-compound.

Acknowledgments

The McMaster group thanks the Imperial Oil Co., Ltd., and the National Research Council of Canada for financial support. J. S. S. wishes to acknowledge an unrestricted research grant from the Eli Lilly Co., Indianapolis, Indiana.

1. (*a*) J. J. McCullough and C. W. Huang. Chem. Commun. 815 (1967). (*b*) J. J. McCullough and C. W. Huang. Can. J. Chem. **47**, 757 (1969).
2. J. S. Swenton and A. J. Krubsack. J. Amer. Chem. Soc. **91**, 786 (1969).
3. E. A. Hill, H. G. Richey, and T. R. Rees. J. Org. Chem. **28**, 421 (1963).
4. (*a*) H. O. House. Modern synthetic reactions. W. A. Benjamin Inc., New York, N.Y. 1965. p. 16. (*b*) B. Franzus, W. C. Baird, Jr., N. F. Chamberlain, T. Hines, and E. I. Snyder. J. Amer. Chem. Soc. **90**, 3721 (1968).
5. N. J. Turro and P. D. Bartlett. J. Org. Chem. **30**, 1849 (1965).
6. S. Murahashi, T. Takizawa, S. Kurioka, and S. Maekawa. Nippon Kagaku Zasshi, **77**, 1689 (1956); Chem. Abstr. **53**, 5763*g* (1959).

Can. J. Chem. Downloaded from www.nrcresearchpress.com by 210.87.254.40 on 09/05/12
For personal use only.

Une nouvelle méthode de synthèse des peptides de la cystine

BERNARD MARINIER ET MICHÈLE BÉRUBÉ
Research Laboratories, Frank W. Horner Limited, Montréal, Québec

Reçu le 13 août 1969

La synthèse du glutathion oxydé à partir de l'acide djenkolique illustre une nouvelle méthode de préparation des peptides de la cystine. L'oxydation par le brome d'un peptide de l'acide djenkolique constitue l'étape essentielle et originale de cette méthode.

The synthesis of oxidized glutathione from djenkolic acid is used to expose a new method of preparation of cystine peptides. The brominative oxidation of a djenkolic acid peptide is the essential and original step of this method.

Canadian Journal of Chemistry, 47, 4507 (1969)

Jusqu'à présent, deux méthodes ont été utilisées pour synthétiser les peptides cycliques de la cystine. La première date de la synthèse de l'oxytocine par du Vigneaud et ses collaborateurs en 1954 (1): elle consiste à utiliser des cystéines protégées par des groupes benzyles durant la synthèse peptidique proprement dite, puis, à la fin, à éliminer les groupes protecteurs et à provoquer la cyclisation par oxydation des groupes SH en disulfure. Le rendement de ces dernières opérations est généralement assez bas à cause de la formation de polymères. D'autres chercheurs, notamment Zervas *et al.* (2), Hiskey et Smith (3), et Kamber et Rittel (4) utilisèrent avec des succès divers le groupe protecteur trityle pour protéger le SH des cystéines, mais le principe de la méthode demeura toujours le même et consiste à utiliser des cystéines durant la synthèse peptidique puis à les oxyder en cystine, avec ou sans formation de thiols, à la fin de la synthèse.

La deuxième méthode consiste à utiliser un peptide dissymétrique non cyclique de la cystine et à cycliser par formation d'une liaison peptidique. Cette méthode semble cependant n'avoir été mise en pratique qu'une seule fois (5) car on démontra très tôt qu'un peptide ou un dérivé dissymétrique non cyclique de la cystine est peu stable et tend à se décomposer en un mélange de peptides ou de dérivés symétriques (6).

L'acide djenkolique (**1**) est un mercaptal obtenu par la condensation de la formaldéhyde avec la cystéine (7). Bien que semblable à la cystine, cette molécule est beaucoup plus stable de sorte

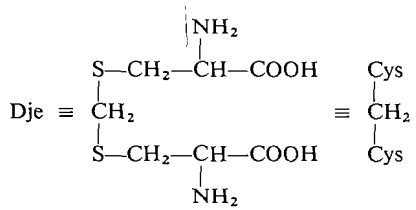

1

que la préparation de dérivés dissymétriques stables est possible (8) ainsi que celle de peptides dissymétriques. L'hypothèse de travail fut que la cyclisation de tels peptides par formation d'une liaison peptidique fournirait des composés qui, par élimination du méthylène central et oxydation consécutive, donnerait des peptides cycliques de la cystine. Cette communication montre un premier point, à savoir qu'il est possible de préparer un peptide symétrique de la cystine à partir du peptide symétrique correspondant de l'acide djenkolique.

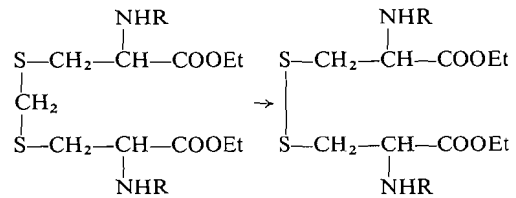

1*a* R = Cbo— **2** R = Cbo—
3 R = C_6H_5CO— **4** R = C_6H_5CO—

Cbo— = $C_6H_5CH_2OCO$—

Pour éliminer le méthylène central, une hydrolyse ne put être utilisée mais on trouva

Can. J. Chem. Downloaded from www.nrcresearchpress.com by 210.87.254.40 on 09/05/12
For personal use only.

qu'une oxydation par le brome (9) pouvait dans certaines conditions effectuer la transformation avec des rendements très satisfaisants. Ainsi, le dicarbobenzoxy-L-djenkolate de diéthyle (**1***a*) fut traité par un équivalent de brome dans le chloroforme anhydre, puis le composé d'addition formé fut hydrolysé par l'eau ou le bicarbonate de sodium pour donner le dicarbobenzoxy-L-cystinate de diéthyle (**2**) avec un rendement de 76% et, en prolongeant le temps d'hydrolyse, le dibenzoyl-L-djenkolate de diéthyle (**3**) fut transformé en dibenzoyl-L-cystinate de diéthyle (**4**) avec un rendement de 77%.

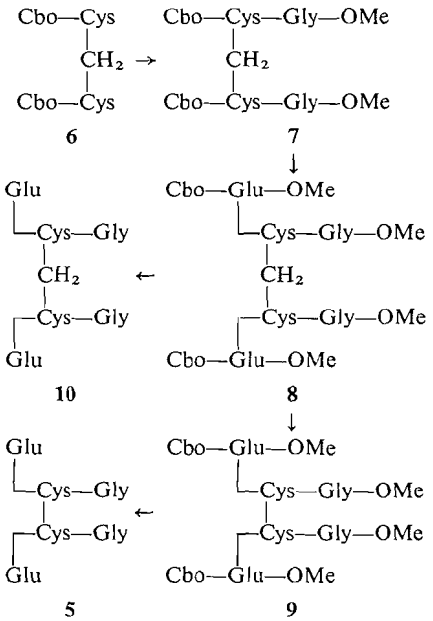

La synthèse du glutathion oxydé (**5**), un peptide naturel non cyclique de la cystine, fut ensuite entreprise. L'acide dicarbobenzoxy-L-djenkolique (**6**) (8) fut d'abord condensé avec 2 équivalents de glycinate de méthyle par la méthode des anhydrides mixtes (10) pour donner avec un rendement de 95% le tripeptide dicarbobenzoxy-L-djenkolyl-bis(glycinate de méthyle) (**7**). Ce tripeptide fut débarrassé de ses groupes carbobenzoxy par HBr dans l'acide acétique (11) puis condensé avec le carbobenzoxy-L-glutamate d'α-monométhyle (12) par la méthode des anhydrides mixtes: le pentapeptide bis-γ-L-[*N*-carbobenzoxy-L-glutamyl-α-(*O*-méthyl)]-L-djenkolyl-bis(glycinate de méthyle) (**8**) fut obtenu avec un rendement de 84%. Ce pentapeptide fut traité par le brome dans le chloroforme anhydre puis le complexe bromé fut hydrolysé par le bicarbonate de sodium en milieu hétérogène durant 20 h pour donner le pentapeptide correspondant de la cystine **9** avec un rendement de 68.5%. L'enlèvement des groupes protecteurs de ce peptide au moyen d'une saponification suivie d'une scission des groupes carbobenzoxy par HBr dans l'acide acétique donna le dibromhydrate du glutathion oxydé ne montrant qu'une seule tache à la chromatographie sur papier. Le peptide libre **5** fut obtenu en filtrant la solution aqueuse ajustée au p*H* 2.85 à travers une colonne de Séphadex G-10. Le rendement de ces dernières opérations fut de 69% ce qui donne un rendement global de 38% à partir de l'acide djenkolique. Le peptide contient les acides aminés constituants Glu, Cys, et Gly dans le rapport attendu et son indice de rotation est de −94° (litt., −93.9° (13); −92.8° (14)). A la chromatographie sur papier, il ne donne qu'une seule tache ayant le même R_f que le produit commercial et donne un test de disulfure positif (15).

L'analogue **10** du glutathion oxydé contenant de l'acide djenkolique au lieu de la cystine fut aussi préparé en effectuant la même séquence de réactions sur le pentapeptide **8**. Cet analogue qui fut obtenu avec un rendement global de 57% donne un indice de rotation de −34.2° mais un R_f identique à celui du glutathion oxydé. De plus, à l'analyse il ne donne pas uniquement de l'acide glutamique, de la glycine, et de la cystéine mais aussi de l'acide djenkolique, de l'acide thiazolidine-carboxylique-4 et un inconnu, ces trois derniers produits étant caractéristiques de l'hydrolyse de l'acide djenkolique en tube scellé; l'addition de la cystéine à ces trois produits donne le rapport Glu:Cys:Gly attendu.

La synthèse d'un peptide cyclique de la cystine via son analogue contenant de l'acide djenkolique est présentement en cours.

Remerciements

Nous remercions le Conseil National de Recherches du Canada qui a subventionné ce travail, les docteurs F. L. Chubb et L. Erichomovitch pour diverses suggestions, et le Dr. N. A. Attalah de l'Université McGill qui a effectué les analyses d'acides aminés.

1. V. du Vigneaud, C. Ressler, J. M. Swan, C. W. Roberts, et P. G. Katsoyannis. J. Amer. Chem. Soc. **76**, 3115 (1954).

2. L. ZERVAS, I. PHOTAKI, A. COSMATOS, et D. BOROVAS. J. Amer. Chem. Soc. **87**, 4922 (1965).
3. R. G. HISKEY et R. L. SMITH. J. Amer. Chem. Soc. **90**, 2677 (1968).
4. B. KAMBER et W. RITTEL. Helv. Chim. Acta, **51**, 2061 (1968).
5. R. G. HISKEY et E. L. SMITHWICK, JR. J. Amer. Chem. Soc. **89**, 437 (1967).
6. A. P. RYLE et F. SANGER. Biochem. J. **60**, 535 (1955); R. E. BENESCH et R. BENESCH. J. Amer. Chem. Soc. **80**, 1666 (1958); L. ZERVAS, L. BENOITON, E. WEISS, M. WINITZ, et J. P. GREENSTEIN. J. Amer. Chem. Soc. **81**, 1729 (1959); H. N. RYDON et F. O. DOS S. P. SERRÃO. J. Chem. Soc. 3638 (1964).
7. M. D. ARMSTRONG et V. DU VIGNEAUD. J. Biol. Chem. **168**, 373 (1947).
8. B. MARINIER et P. PENEV. Can. J. Chem. **45**, 1253 (1967).
9. B. GAUTHIER. Ann. pharm. franç. **12**, 281 (1954).
10. J. R. VAUGHAN, JR. et R. L. OSATO. J. Amer. Chem. Soc. **74**, 676 (1952).
11. D. BEN-ISHAI et A. BERGER. J. Org. Chem. **17**, 1564 (1952).
12. G. H. L. NEFKENS et R. J. F. NIVARD. Rec. Trav. Chim. **83**, 199 (1964).
13. J. M. JOHNSON et C. VOEGTLIN. J. Biol. Chem. **75**, 703 (1927).
14. C. BERSE, R. BOUCHER, et L. PICHÉ. Can. J. Chem. **37**, 1733 (1959).
15. G. TOENNIES et J. J. KOLB. Anal. Chem. **23**, 823 (1951).

Sulfene[1]

J. F. KING, P. DE MAYO, AND D. L. VERDUN[2]
Department of Chemistry, University of Western Ontario, London, Ontario

Received September 15, 1969

Evidence indicating the existence of sulfene ($CH_2{=}SO_2$) as a discrete species in the gas phase is presented.

Canadian Journal of Chemistry, **47**, 4509 (1969)

The existence of sulfene ($CH_2{=}SO_2$) as a transitory intermediate has been deduced from the evidence of product analysis[3] and rate studies (3). We now report experiments in the gas phase which provide independent support for the intermediacy of sulfene and further define its properties.

We have recently employed flash thermolysis (1) for the generation of sulfenes (1, 4), but though it was concluded that the sulfene was probably formed in those instances, it rapidly underwent the further reactions illustrated in Scheme 1. To gain further evidence for this scheme and to investigate the possibility of producing sulfene under conditions sufficiently mild that we might trap the sulfene outside the hot zone of the apparatus, we have studied the flash thermolysis of chlorosulfonylacetic acid (**1**). Using the previously described apparatus (1)[4] and trapping the products on a cold-finger coated with methanol and cooled with liquid nitrogen, we found (see Scheme 2) that **1** was converted to formaldehyde (isolated as dimethoxymethane) in good yield at 940°. This observation is consistent with, and presumably analogous to, the formulation proposed in Scheme 1. At 640° a relatively low yield of dimethoxymethane (~8%) was obtained, the major product being methanesulfonyl chloride (~50%). The most significant result from the viewpoint of the question of sulfene formation, however, was a small but reproducible yield (2.6%) of methyl methanesulfonate. The workup and identification of the products of the reaction were carried out following a procedure which was shown by control experiments to lead to no methyl methanesulfonate by reaction of methanol with the methanesulfonyl chloride. That at least half of the methyl methanesulfonate arose from sulfene was rigorously established by using methanol-*d* as the trapping agent. In two such runs the methyl methanesulfonate produced was found to contain 50.4 and 63.0% of $CH_2DSO_2OCH_3$, the remainder being $CH_3SO_2OCH_3$; the methanesulfonyl chloride contained 3.0 and 3.3% CH_2DSO_2Cl in the same runs. These results require that a species capable of supplying

[1](*a*) Flash Thermolysis. Part 2. Reference 1 is to be considered as Part 1 in the series. (*b*) Organic Sulfur Mechanisms. Part 6.
[2]Holder of NRCC Scholarships, 1967–1969.
[3]For a summary of this argument see the review by Opitz (2).
[4]This technique has been elegantly used by Hedaya and his colleagues (5) for the generation of other unstable species, e.g. cyclobutadiene.

Can. J. Chem. Downloaded from www.nrcresearchpress.com by 210.87.254.40 on 09/05/12
For personal use only.

2. L. ZERVAS, I. PHOTAKI, A. COSMATOS, et D. BOROVAS. J. Amer. Chem. Soc. **87**, 4922 (1965).
3. R. G. HISKEY et R. L. SMITH. J. Amer. Chem. Soc. **90**, 2677 (1968).
4. B. KAMBER et W. RITTEL. Helv. Chim. Acta, **51**, 2061 (1968).
5. R. G. HISKEY et E. L. SMITHWICK, JR. J. Amer. Chem. Soc. **89**, 437 (1967).
6. A. P. RYLE et F. SANGER. Biochem. J. **60**, 535 (1955); R. E. BENESCH et R. BENESCH. J. Amer. Chem. Soc. **80**, 1666 (1958); L. ZERVAS, L. BENOITON, E. WEISS, M. WINITZ, et J. P. GREENSTEIN. J. Amer. Chem. Soc. **81**, 1729 (1959); H. N. RYDON et F. O. DOS S. P. SERRÃO. J. Chem. Soc. 3638 (1964).
7. M. D. ARMSTRONG et V. DU VIGNEAUD. J. Biol. Chem. **168**, 373 (1947).
8. B. MARINIER et P. PENEV. Can. J. Chem. **45**, 1253 (1967).
9. B. GAUTHIER. Ann. pharm. franç. **12**, 281 (1954).
10. J. R. VAUGHAN, JR. et R. L. OSATO. J. Amer. Chem. Soc. **74**, 676 (1952).
11. D. BEN-ISHAI et A. BERGER. J. Org. Chem. **17**, 1564 (1952).
12. G. H. L. NEFKENS et R. J. F. NIVARD. Rec. Trav. Chim. **83**, 199 (1964).
13. J. M. JOHNSON et C. VOEGTLIN. J. Biol. Chem. **75**, 703 (1927).
14. C. BERSE, R. BOUCHER, et L. PICHÉ. Can. J. Chem. **37**, 1733 (1959).
15. G. TOENNIES et J. J. KOLB. Anal. Chem. **23**, 823 (1951).

Sulfene[1]

J. F. KING, P. DE MAYO, AND D. L. VERDUN[2]
Department of Chemistry, University of Western Ontario, London, Ontario

Received September 15, 1969

Evidence indicating the existence of sulfene ($CH_2{=}SO_2$) as a discrete species in the gas phase is presented.

Canadian Journal of Chemistry, **47**, 4509 (1969)

The existence of sulfene ($CH_2{=}SO_2$) as a transitory intermediate has been deduced from the evidence of product analysis[3] and rate studies (3). We now report experiments in the gas phase which provide independent support for the intermediacy of sulfene and further define its properties.

We have recently employed flash thermolysis (1) for the generation of sulfenes (1, 4), but though it was concluded that the sulfene was probably formed in those instances, it rapidly underwent the further reactions illustrated in Scheme 1. To gain further evidence for this scheme and to investigate the possibility of producing sulfene under conditions sufficiently mild that we might trap the sulfene outside the hot zone of the apparatus, we have studied the flash thermolysis of chlorosulfonylacetic acid (**1**). Using the previously described apparatus (1)[4] and trapping the products on a cold-finger coated with methanol and cooled with liquid nitrogen, we found (see Scheme 2) that **1** was converted to formaldehyde (isolated as dimethoxymethane) in good yield at 940°. This observation is consistent with, and presumably analogous to, the formulation proposed in Scheme 1. At 640° a relatively low yield of dimethoxymethane (~8%) was obtained, the major product being methanesulfonyl chloride (~50%). The most significant result from the viewpoint of the question of sulfene formation, however, was a small but reproducible yield (2.6%) of methyl methanesulfonate. The workup and identification of the products of the reaction were carried out following a procedure which was shown by control experiments to lead to no methyl methanesulfonate by reaction of methanol with the methanesulfonyl chloride. That at least half of the methyl methanesulfonate arose from sulfene was rigorously established by using methanol-*d* as the trapping agent. In two such runs the methyl methanesulfonate produced was found to contain 50.4 and 63.0% of $CH_2DSO_2OCH_3$, the remainder being $CH_3SO_2OCH_3$; the methanesulfonyl chloride contained 3.0 and 3.3% CH_2DSO_2Cl in the same runs. These results require that a species capable of supplying

[1](*a*) Flash Thermolysis. Part 2. Reference 1 is to be considered as Part 1 in the series. (*b*) Organic Sulfur Mechanisms. Part 6.
[2]Holder of NRCC Scholarships, 1967–1969.
[3]For a summary of this argument see the review by Opitz (2).
[4]This technique has been elegantly used by Hedaya and his colleagues (5) for the generation of other unstable species, e.g. cyclobutadiene.

Can. J. Chem. Downloaded from www.nrcresearchpress.com by 210.87.254.40 on 09/05/12
For personal use only.

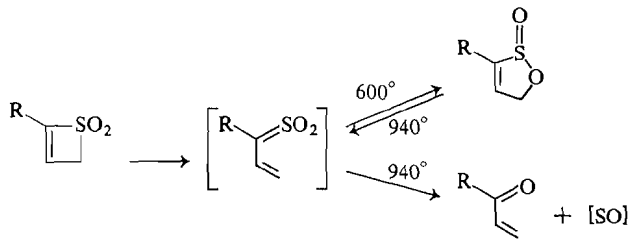

R = H or Ph

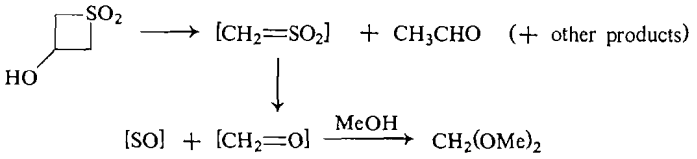

SCHEME 1

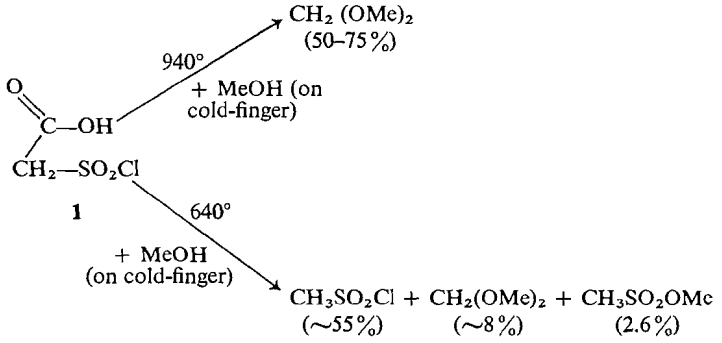

SCHEME 2

the structural unit CH_2SO_2 in a reaction with methanol-*d* at 77 °K be formed in the hot zone of the apparatus and travel to the cold-finger and react there. The only reasonable CH_2SO_2-supplying species in this experiment is sulfene itself, which must therefore be a discrete, volatile compound capable of existence for a finite period of time.[5]

In all likelihood the undeuterated ester is also formed from the sulfene, the proton arising ultimately from the hydrogen chloride produced in the reaction. The small proportion of the deuterium in the methanesulfonyl chloride may arise by reaction of sulfene with DCl formed by the exchange between HCl and CH_3OD. This in turn suggests that at least part of the CH_3SO_2Cl derives from sulfene and hydrogen chloride, though whether or not this is the major source of the sulfonyl chloride cannot be ascertained at present. By summing the yields of methyl methanesulfonate, dimethoxymethane, and CH_2DSO_2Cl we obtain the value of 12% as the probable minimum conversion to sulfene in the reaction. Because of the uncertainty surrounding the origin of the CH_3SO_2Cl and also of certain

[5]The mass spectra of the samples of methyl methanesulfonate from the runs with methanol-*d* clearly show the absence of any significant amount (i.e. less than 2%) of $CHD_2SO_2OCH_3$. The formation of $CH_2DSO_2OCH_3$ in the absence of a significant amount of $CHD_2SO_2OCH_3$ is the key piece of evidence supporting the intermediacy of sulfene, and this conclusion is not dependent on arguments based on control experiments; the latter experiments, however, are strongly suggestive and form the basis for the comments in the final paragraph.

Can. J. Chem. Downloaded from www.nrcresearchpress.com by 210.87.254.40 on 09/05/12
For personal use only.

other materials produced in the reaction, notably a modest amount of an intractable material perhaps derived by polymerization of sulfene, the above estimate of the extent of sulfene formation is almost certainly highly conservative.

Acknowledgment

This work was supported by the Petroleum Research Fund, administered by the American Chemical Society.

1. C. L. McIntosh and P. de Mayo. Chem. Commun. 32 (1969).
2. G. Opitz. Angew. Chem. Inter. Ed. **6**, 107 (1967).
3. J. F. King and T. W. S. Lee. J. Amer. Chem. Soc. In press.
4. J. F. King, K. Piers, D. J. H. Smith, C. L. McIntosh, and P. de Mayo. Chem. Commun. 31 (1969).
5. E. Hedaya, R. D. Muller, D. W. McNeil, P. F. D'Angelo, and P. Schissel. J. Amer. Chem. Soc. **91**, 1875 (1969).

Can. J. Chem. Downloaded from www.nrcresearchpress.com by 210.87.254.40 on 09/05/12
For personal use only.

Photochemistry of imines: concerning the formation of dihydrophotodimers from *N*-diphenylmethylenebenzylamine

Bert Fraser-Reid, Angus McLean, and E. W. Usherwood

Received September 10, 1969

Department of Chemistry, University of Waterloo, Waterloo, Ontario

When alcohol solutions of *N*-diphenylmethylenebenzylamine (**1***d*) are irradiated in the presence of benzophenone with light of intensity ~200 W there is predominant formation of the *unsymmetrical* dihydrophotodimer (**4**) and no symmetrical dimers are detected. The dihydromonomer (**2***d*) is also produced. However, when a more intense light source (450 W) is used *no dimer of any sort* is formed although the dihydromonomer is still produced. The formation of the unsymmetrical dihydrodimer (**4**) cannot be attributed entirely to secondary reactions of the dihydromonomer (**2***d*) since irradiation of the latter produces both symmetrical (**7**) and unsymmetrical (**4**) dihydrodimers in the ratio 1:2.

Canadian Journal of Chemistry, 47, 4511 (1969)

Recently, Okada and co-workers (1) reported that irradiation of *N*-benzoyldiphenylketimine (**1***a*) in alcoholic solvent led to quantitative reduction of the C—N double bond to give the corresponding amide, **2***a*. In order to explain these results, they (1) sought precedent in a report by Fischer (2) which stated that benzophenone sensitized irradiation of *N*-diphenylmethylenebenzylamine (**1***d*) in alcohol had also caused reduction of the C—N double bond, the amine **2***d* formed thereby being the only product reported (2). It was therefore suggested (1) that the carbonyl group of **1***a* provided "intramolecular chemical sensitization" for the reduction (**1***a* to **2***a*) in the same manner that benzophenone provided *intermolecular* chemical sensitization for the reduction of **1***d* to **2***d* (2).

In a recent examination of the mechanism of photoreduction of aryl *N*-alkylimines, Padwa (3) also cited Fischer's report (2), and noted that a number of imines with the general structure **1** (and including **1***a* and **1***d*) were "photoreduced to the corresponding amine(s) as opposed to (the) dihydrophotodimer(s)". It was further

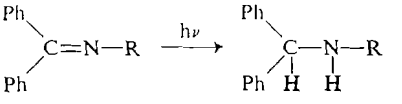

1 **2**

a R = —COC_6H_5
b R = —COC_6H_4-*p*-Cl
c R = —COC_6H_4-*p*-OCH_3
d R = —$CH_2C_6H_5$

suggested that this unusual result could be accommodated in the framework of the general mechanism of photoreduction being proposed (3).

In the light of the foregoing (1–3), and in view of the interest in the photochemistry of these and related systems (4, 5), we are prompted to report that *there are conditions*[1] *in which irradiation of*

[1]Ethanol or *i*-propanol solutions of the amide (**1***a* to **1***c*) or imine prepared as indicated in Table I, were irradiated in a Rayonet Photochemical reactor (R.P.R. −100) using a pyrex vessel (40 cm × 2 cm) equipped with a water-cooled finger and 350 mμ medium pressure lamps. Use of the 254 mμ medium pressure lamps had no effect on the reaction. The reaction was stopped when the infrared absorption for C=N had disappeared.

other materials produced in the reaction, notably a modest amount of an intractable material perhaps derived by polymerization of sulfene, the above estimate of the extent of sulfene formation is almost certainly highly conservative.

Acknowledgment

This work was supported by the Petroleum Research Fund, administered by the American Chemical Society.

1. C. L. McIntosh and P. de Mayo. Chem. Commun. 32 (1969).
2. G. Opitz. Angew. Chem. Inter. Ed. **6**, 107 (1967).
3. J. F. King and T. W. S. Lee. J. Amer. Chem. Soc. In press.
4. J. F. King, K. Piers, D. J. H. Smith, C. L. McIntosh, and P. de Mayo. Chem. Commun. 31 (1969).
5. E. Hedaya, R. D. Muller, D. W. McNeil, P. F. D'Angelo, and P. Schissel. J. Amer. Chem. Soc. **91**, 1875 (1969).

Can. J. Chem. Downloaded from www.nrcresearchpress.com by 210.87.254.5 on 09/05/12
For personal use only.

Photochemistry of imines: concerning the formation of dihydrophotodimers from *N*-diphenylmethylenebenzylamine

Bert Fraser-Reid, Angus McLean, and E. W. Usherwood

Received September 10, 1969

Department of Chemistry, University of Waterloo, Waterloo, Ontario

When alcohol solutions of *N*-diphenylmethylenebenzylamine (**1***d*) are irradiated in the presence of benzophenone with light of intensity ~200 W there is predominant formation of the *unsymmetrical* dihydrophotodimer (**4**) and no symmetrical dimers are detected. The dihydromonomer (**2***d*) is also produced. However, when a more intense light source (450 W) is used *no dimer of any sort* is formed although the dihydromonomer is still produced. The formation of the unsymmetrical dihydrodimer (**4**) cannot be attributed entirely to secondary reactions of the dihydromonomer (**2***d*) since irradiation of the latter produces both symmetrical (**7**) and unsymmetrical (**4**) dihydrodimers in the ratio 1:2.

Canadian Journal of Chemistry, 47, 4511 (1969)

Recently, Okada and co-workers (1) reported that irradiation of *N*-benzoyldiphenylketimine (**1***a*) in alcoholic solvent led to quantitative reduction of the C—N double bond to give the corresponding amide, **2***a*. In order to explain these results, they (1) sought precedent in a report by Fischer (2) which stated that benzophenone sensitized irradiation of *N*-diphenylmethylenebenzylamine (**1***d*) in alcohol had also caused reduction of the C—N double bond, the amine **2***d* formed thereby being the only product reported (2). It was therefore suggested (1) that the carbonyl group of **1***a* provided "intramolecular chemical sensitization" for the reduction (**1***a* to **2***a*) in the same manner that benzophenone provided *intermolecular* chemical sensitization for the reduction of **1***d* to **2***d* (2).

In a recent examination of the mechanism of photoreduction of aryl *N*-alkylimines, Padwa (3) also cited Fischer's report (2), and noted that a number of imines with the general structure **1** (and including **1***a* and **1***d*) were "photoreduced to the corresponding amine(s) as opposed to (the) dihydrophotodimer(s)". It was further

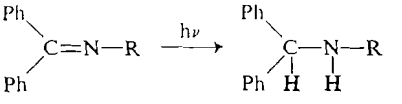

1 **2**

a R = —COC_6H_5
b R = —COC_6H_4-*p*-Cl
c R = —COC_6H_4-*p*-OCH_3
d R = —$CH_2C_6H_5$

suggested that this unusual result could be accommodated in the framework of the general mechanism of photoreduction being proposed (3).

In the light of the foregoing (1–3), and in view of the interest in the photochemistry of these and related systems (4, 5), we are prompted to report that *there are conditions*[1] *in which irradiation of*

[1]Ethanol or *i*-propanol solutions of the amide (**1***a* to **1***c*) or imine prepared as indicated in Table I, were irradiated in a Rayonet Photochemical reactor (R.P.R. −100) using a pyrex vessel (40 cm × 2 cm) equipped with a water-cooled finger and 350 mμ medium pressure lamps. Use of the 254 mμ medium pressure lamps had no effect on the reaction. The reaction was stopped when the infrared absorption for C=N had disappeared.

Can. J. Chem. Downloaded from www.nrcresearchpress.com by 210.87.254.5 on 09/05/12
For personal use only.

TABLE I

Photoproducts from irradiation of *N*-diphenylmethylenebenzylamine under a variety of reaction conditions

Reactants*	Ratio of photoproducts†			
	$PhCHNHCHPh_2$ | Ph_2CNHCH_2Ph **4**	$PhCHNHCHPh_2$ | $PhCHNHCHPh_2$ (*dl* + *meso*) **7**	$PhCH_2NHCHPh_2$ **2***d*	$PhCHNHCHPh_2$ | Ph_2COH **3**
(a) $Ph_2C{=}NCH_2Ph$(1.5) + Ph_2CO(0.43)‡ **1***d*	4.5	absent	1	3
(b) $PhCH{=}NCHPh_2$(1.5) + Ph_2CO(0.43)‡ **8**	absent	2.5	1	<0.1
(c) $Ph_2C{=}NCHPh_2$(0.25) + Ph_2CO(0.010)§ **1***d*	absent	absent	present	not detected
(d) $Ph_2C{=}NCHPh_2$(0.25) + Ph_2CO(0.010)‖ **1***d*	0.6	absent	1	<0.1
(e) $Ph_2CHNHCH_2Ph$(1.5) + Ph_2CO(0.43)‡ **2***d*	0.6¶	0.3¶	1	1.1
(f) $Ph_2CHNHCH_2Ph$(0.75) + Ph_2CO(0.43)‡ **2***d* + $Ph_2C{=}NCH_2Ph$ (0.75) **1***d*	1	—	1	0.7

*Weights in g dissolved in 50 ml of ethanol or *i*-propanol are in parenthesis.
†Based on total weight of all fractions from preparative layer chromatograms, benzophenone being excluded. Benzene was solvent and zones were detected by ultraviolet light. Compounds (R_f): 4 and 7 (0.60); 3 (0.50); 3*d* (0.30).
‡Rayonet reactor used.
§Hanovia 450 W lamp used.
‖Hanovia 200 W lamp used.
¶The ratio of dimers 4 and 7 in the fraction was determined by integrating the signals at τ 6.85 and 6.40 respectively.

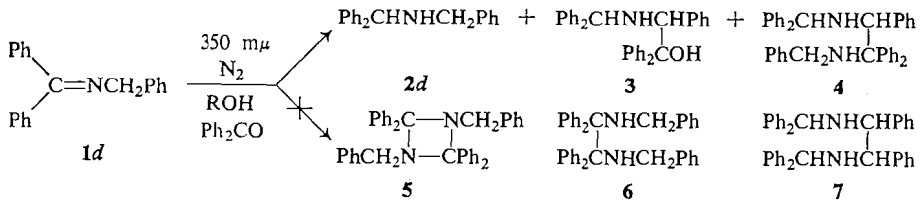

imine **1***d leads to predominant formation of a dihydrophotodimer.*

Our studies support the report (1) that irradiation[1] of **1***a* causes quantitative conversion to the saturated amide (**2***a*). Similarly, **1***b* and **1***c* are converted to **2***b* and **2***c* respectively. Absence of the hoped for photodimers was considered due to the steric unfavorability of the tetraphenylethane linkage that would have to be forged, and in order to test this hypothesis, the structural *N*-alkyl equivalent of amide **1***a*, namely imine **1***d*, was irradiated[1] in the presence of benzophenone. The residue obtained on evaporation of the solution contained apart from benzophenone, three components *A*, *B*, and *C*, which were fractionated on a preparative layer chromatogram (Table I, entry (a)). Component *A* was identical to the product of catalytic hydrogenation of imine **1***d*; i.e. it was amine **2***d*,[2] however, it represented only 12% of the total fractions *A* + *B* + *C*. Component *B*, readily identified as **3**,[3] constituted 35% of the total fractions.

The major photoproduct, component *C*, had a molecular weight[4] which required it to be dimeric[3] but an exchangeable proton in the nuclear magnetic resonance (n.m.r.) spectrum dispensed with azetidines such as **5**, claimed to be produced on irradiation of some Schiff's bases (4). A 2-line pattern at τ 5.55 and 5.70 and a 4-line pattern centered at τ 6.85, both sets being of equal intensity, eliminated **6**. There remained only two possibilities, **4** or **7**, and of these **4** is clearly favored by the n.m.r. data. The remote possibility that a phenomenal conformation of **7** might accommodate the observed spectrum was discounted since both patterns of protons were not coupled. Hence photoproduct *C* is formulated as **4**, and all the n.m.r. signals can be conveniently assigned: τ 5.55, benzhydryl methine proton; τ 5.70, other methine proton; τ 6.85, an AB system (J_{AB} = 12.6 Hz) arising from benzylic protons made non-equivalent by barriers to free rotation (7).

However, in order to substantiate this assignment, a sample of **7** was sought by irradiation[1] of imine **8**, (c.f. 3) an isomer of **1***d*. The photoproduct (Table I, entry (*b*)) contained a dimer in 58% yield which was also obtainable by aluminum-amalgam induced coupling of **8** (8). It was therefore the desired dimer (**7**) and its n.m.r. spectrum was distinguished from that of component *C* in that instead of the 4-line pattern at τ 6.85, it (**7**) displayed a 2-proton singlet at τ 6.40.

When the irradiation was carried out using the same concentrations of reactants, and a 450 W Hanovia lamp as described by Padwa (3), dimer **4** was indeed not detected although the monomer (**2***d*) was produced (Table I, entry (c)). However when the same concentration of reactants was irradiated using a *200* W Hanovia lamp (whose intensity is nearer to that of the Rayonet source), dimer **4** was in fact formed, although its ratio was considerably reduced (Table I, entry (d)). Comparison of entries (a) and (d) indicate that there is a marked effect on the ratio of photodimer (**4**) to monomer (**2***d*) when the concentration of sensitizer is varied. However the crucial absence of photodimer **4** when the 450 W Hanovia lamp is used (compare entries (c) and (d)) indicate that the light intensity effect is a real one and therefore that the photochemical behavior of **1***d* is very sensitive to the radiation source.

Conceivably, the principal reaction pathway could be via reduction of **1***d* to **2***d*; the latter on further irradiation could react to give **3** and **4**. However, this possibility is unappealing in view of entry (c), Table I; apart from the unfavorable ratio in which **3** and **4** are produced there, the symmetrical dimer (7) is seen to constitute 1/3 of the total dimeric photoproduct whereas it is usually (entries (a) and (d)) absent. Again the possibility of photoaddition of amine **2***d* to imine

[2]For the hydrochloride of **2***d* m.p. and mixed m.p. = 265–267° (*2a*).

[3]All new compounds gave satisfactory micro analyses and spectral data.

[4]Osmometry: 566. Base peak *m/e* = 272 ($M^+/2$) characteristic of diamines such as **4** (6).

Can. J. Chem. Downloaded from www.nrcresearchpress.com by 210.87.254.5 on 09/05/12
For personal use only.

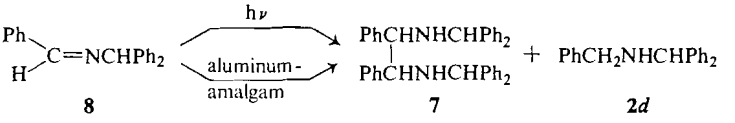

8 7 2*d*

1*b* (entry (f); Table I) is also unlikely to be the only reaction pathway to **4**, in view of the product ratios.

In order to be comprehensive, a mechanistic interpretation of the photochemistry of *N*-diphenylmethylenebenzylamine (**1***d*) must account for the formation of the novel unsymmetrical dimer **4**. Studies designed to investigate the mode of formation of **4** and the origin of the intensity effect are underway and will be reported upon in due course.

Acknowledgments

We are grateful to the National Research Council of Canada and the Ontario Department of University Affairs for financial assistance. The investigation was greatly facilitated by loan of a T-60 n.m.r. spectrometer to the Chemistry Department by Varian Associates of Toronto.

1. T. OKADA, M. KAWANISI, and H. NOZAKI. Tetrahedron Lett. 927 (1969).
2. (*a*) M. FISCHER. Chem. Ber. **100**, 3599 (1967); (*b*) M. FISCHER. Tetrahedron Lett. 5273 (1966).
3. (*a*) A. PADWA, W. BERGMARK, and D. PASHAYAN. J. Amer. Chem. Soc. **91**, 2653 (1969); (*b*) A. PADWA, W. BERGMARK, and D. PASHAYAN. J. Amer. Chem. Soc. **90**, 4458 (1968).
4. R. O. KAN and R. L. FUREY. J. Amer. Chem. Soc. **90**, 1666 (1968).
5. S. G. COHEN and N. STEIN. J. Amer. Chem. Soc. **91**, 3690 (1969), and references cited therein.
6. H. BUDZIKIEWICZ, C. DJERASSI, and D. H. WILLIAMS. Interpretation of mass spectra of organic compounds. Holden–Day Inc., San Francisco, California, 1964. p. 63.
7. W. L. MEYER and R. B. MEYER. J. Amer. Chem. Soc. **85**, 2170 (1963).
8. H. THIES, H. SCHONENBERGER, and K. H. BAUER. Archive der Pharmazie, **293**, 67 (1960).

Can. J. Chem. Downloaded from www.nrcresearchpress.com by 210.87.254.5 on 09/05/12
For personal use only.

Can. J. Chem. Downloaded from www.nrcresearchpress.com by 210.87.254.105 on 09/05/12
For personal use only.

Canadian Journal of Chemistry

Published by THE NATIONAL RESEARCH COUNCIL OF CANADA

VOLUME 47 DECEMBER 15, 1969 NUMBER 24

Influence de la structure du prépolymère sur la température de transition vitreuse de polyuréthanes réticulés

GUY PERRAULT

Centre Canadien de Recherches et Perfectionnement des Armes, Québec, Québec

Reçu le 5 mai, 1969

Une étude a été faite de l'influence de la structure du prépolymère sur la température de transition vitreuse (T_g) de polyuréthanes élastomériques réticulés. Ces prépolymères sont des polysébaçates obtenus à partir d'une famille d'alkyl-N bis(hydroxy-2 alkyl)amines. Ils permettent, en variant les substituants alkyls, d'étudier l'effet d'allongement des chaînes latérales (C_1 à C_{18}) et l'effet d'addition d'interactions *gauches* au sein de la chaîne. Les résultats mettent en évidence que dans ce système, l'effet d'addition des interactions *gauches*, est plus importante que l'effet d'allongement des substituants latéraux. T_g est augmenté de 9 °C par interaction *gauche* introduite dans un segment de diol. La comparaison est faite avec d'autre systèmes.

The influence of prepolymer structure on glass transition temperatures (T_g) of cross-linked polyurethanes has been studied with polysebacates from a homologous family of N-substituted bis(2-hydroxyalkyl)amines. The tertiary amine segments have made it possible to study the effect of lengthening the side chains (C_1–C_{18}) and inserting *gauche* interactions in the polymeric chain. The results show that in this system, adding *gauche* interactions has more effect on T_g than lengthening the side chains. Each time a *gauche* interaction is introduced in the diol segments, T_g increases by 9 °C. Comparisons with other systems are also presented.

Canadian Journal of Chemistry, 47, 4515 (1969)

Introduction

Plusieurs relations ont été proposées pour relier la structure moléculaire des homopolymères et des copolymères à leur température de transition vitreuse (T_g) (1–7). De ces approches, il est possible d'anticiper un minimum de T_g pour un minimum d'énergie en conformations gauches des segments, c'est-à-dire un minimum de rigidité de la chaîne, causé par un minimum dans la barrière de potentiel aux rotation internes, et pour une quantité maximisée de groupes latéraux à longue chaîne, c'est-à-dire pour un maximum de volume libre au sein du réseau.

Toutefois, ces concepts ne s'appliquent pas directement aux élastomères réticulés. En particulier dans le cas des polyuréthanes réticulés, plusieurs facteurs influencent le T_g. Notons l'effet de la concentration des groupes uréthanes (8, 9), l'effet du degré de réticulation (10), de la nature de l'agent de cuisson ainsi que maintes autres composantes (11). Cependant, il est à noter, comme le font remarquer certains auteurs (8), que la structure des produits initiaux, entre autres le prépolymère, a très peu d'effet sur les propriétés de l'élastomère final.

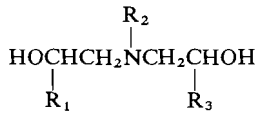

1

Une famille de prépolymères, des polysébaçates de la diisopropanolamine substituée sur l'azote (**1**; $R_1 = R_3 = CH_3$, R_2 = alkyl) avait déjà été utilisée pour étudier l'effet de la basicité d'un azote au sein de la chaîne polymérique sur les propriétés de l'élastomère (12).

Au cours d'expériences subséquentes, il est apparu que ce système pouvait être utilisé pour étudier à la fois l'effet de l'allongement d'une chaîne latérale (**1**, R_2) sur le T_g de l'élastomère réticulé, et l'effet d'introduction de conformations *gauches* (**1**, R_1 et R_3). Il est en effet facile de constater en se référant aux projections (Newman) de la liaison α,β à l'azote que si les radicaux R_1 et R_3 sont des groupes méthyle où éthyle des interactions *gauches* CH_3—N ou O—N seront

introduites augmentant la rigidité de la chaîne. La Fig. 1 représente ces interactions pour les deux

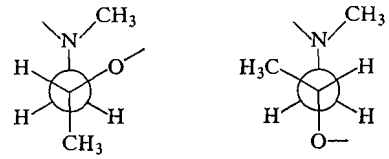

FIG. 1. Interaction *gauche* introduite par un substituant méthyle.

conformations les plus stables dans le cas d'un substituant méthyle. Il semblait donc qu'en travaillant dans des conditions constantes, il serait possible d'évaluer l'effet de structure du prépolymère.

Les polysébaçates de ces produits ont été préparés et les polyuréthanes obtenus dans des conditions expérimentales constantes. Quelques dérivés supplémentaires (**2** et **3**) ont été ajoutés à cette série pour fin de comparaison.

Partie Experimentale

La préparation et les propriétés de la plupart des diols ont déjà été publiées (13–15). Le méthyl-3 pentanediol-1,5 (**2**) est disponible commercialement. Deux nouvelles amines ont été préparées selon la méthode déjà décrite (13) par condensation de l'époxy-2,3 butane sur l'amine primaire correspondante, ce sont la méthyl-N bis-(hydroxy-3 butyl)-2 amine (**3**, R = CH_3) (*Eb*: 85–87 °C/0.1 mm).

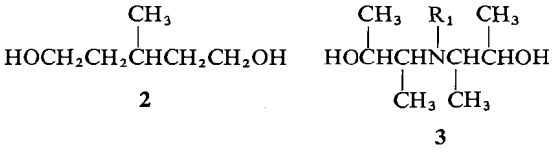

2 **3**

Anal. Calcd. pour $C_9H_{21}O_2N$ (**3**, R = CH_3): C, 61.67; H, 12.08; N, 7.99. Trouvé: C, 61.34; H, 11.79; N, 8.01.

Pour l'hexyl-N bis(hydroxy-3-butyl)-2 amine (**3**, R = C_6H_{13}) (*Eb*: 65–68 °C/0.05 mm).

Anal. Calcd. pour $C_{14}H_{31}O_2N$ (**3**, R = C_6H_{13}): C, 68.52; H, 12.73; N, 5.90. Trouvé: C, 68.36; H, 12.84; N, 5.90.

Les analyses élémentaires ont été faites par Organic Microanalyses à Montréal.

Les polysébaçates ont été préparés en vrac par chauffage à 175 °C durant quatre h, d'une mole d'acide sébacique et de 1.3 mole de diol. Un barbotage constant d'azote a été maintenu pour agiter le mélange et entraîner l'eau formée au travers d'une colonne Vigreux qui sert à condenser les vapeurs de diol. Après ce temps, le chauffage a été continué à la même température sous pression réduite (<0.1 mm) durant quatre h additionnelles afin d'enlever l'excès de diol et les traces d'eau. Ces conditions expérimentales ont été adoptées afin d'atteindre un compromis entre un poids moléculaire trop bas et un nombre d'acidité trop élevé, et aussi pour éviter l'uniformisation des propriétés des polysébaçates par équilibration. Les poids moléculaires (M_n) des polysébaçates (Tableau I) ont été déterminés par analyse des fonctions hydroxylées (16). La correction a été faite pour le nombre d'acidité qui se situe entre 0 et 5, la grande majorité des produits étant autour de 1.

Les polyuréthanes ont été obtenus par cuisson sous vide à 60 °C durant 48 h, d'une mole de polysébaçate, deux moles de polyol Niax LHT 240 (Union Carbide Chemicals) et un excès de 10% de l'agent de cuisson, soit le diisocyanate de tolyle (TDI), soit un diisocyanate polymérique, le DDI-1410, (General Mills Company).

Les températures de transition vitreuse (T_g) et le contenu énergétique de la transition des polysébaçates on été mesurées sur un calorimètre à balayage thermique différentiel (DSC 1B de Perkin–Elmer) calibré avec de l'octane, du décane et du dodécane entre −90 et 0 °C. Le taux de chauffage du DSC a été fixé à 5 °C par min. Un taux de 10 °C par min ne provoquait pas de variation sensible dans la température de transition. La température de transition a été prise au point de rencontre entre le prolongement de la ligne de base et l'extrapolation du début du pic de transition. Un exemple représentatif est reproduit à la Fig. 2 avec le polyuréthane du polysébaçate de propyl-N (hydroxy-2 propyl,hydroxy-2 éthyl)amine (**1**, $R_1 = CH_3$, $R_2 = C_3H_7$, R_3 = H).

Le contenu énergétique de la transition des polysébaçates d'hexyl-N bis(hydroxy-2 alkyl)amine a été évalué par le décalage de la ligne de base avant et après la transition, tel qu'illustré à la Fig. 3 avec le polysébaçate d'hexyl-N-bis(hydroxy-2-propyl)amine (**1**, $R_1 = R_3 = CH_3$, $R_2 = C_6H_{13}$). Ce décalage a été divisé par le nombre de mole d'échantillon utilisé pour pouvoir établir facilement la relation avec les interactions butane-*gauche* qui sont en kcal/mole.

La reproductibilité des températures de transition vitreuse est de ±3 °C. Une variation de ±10% sur la quantité de TDI fait varier le T_g de ±1 °C. La même variation sur la quantité de DDI amène des fluctuations de ±3 °C. Une cuisson de quatre jours au lieu de deux jours, n'influence pas de façon notable le T_g de sorte qu'il est permis de supposer que la cuisson est complète

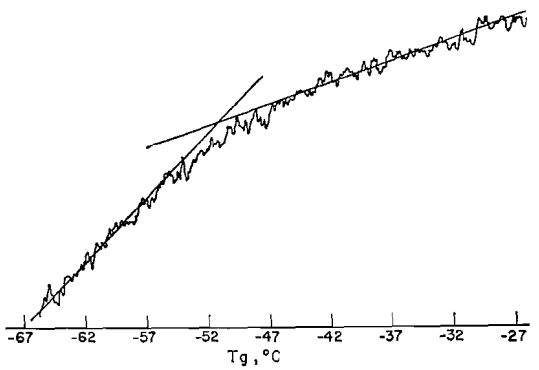

FIG. 2. Détermination du T_g du polyuréthane obtenu avec le polysébaçate de propyl-N (hydroxy-2 propyl, hydroxy-2-éthyl)amine (**1**, $R_1 = CH_3$, $R_2 = C_3H_7$, R_3 = H).

Can. J. Chem. Downloaded from www.nrcresearchpress.com by 210.87.254.105 on 09/05/12
For personal use only.

TABLEAU I
Propriétés des différents polymères

Polysébaçates des diols **1**			Propriétés des polysébaçates		T_g, °C, des polyuréthanes	
R_1	R_2	R_3	M_n	Température de transition °C	TDI	DDI
C_2H_5	CH_3	C_2H_5	2010	−55	−31	−40
"	C_3H_7	"	1600		−45	
"	C_6H_{13}	"	1750	−62	−47	−42
"	C_8H_{17}	"	950		−46	
"	$C_{12}H_{25}$	"	2230	−61	−37	−47
"	$C_{16}H_{33}$	"	2300	−48	−44	−48
"	$C_{18}H_{37}$	"	2155		−31	−48
CH_3	CH_3	CH_3	1870	−52	−38	−41
"	C_6H_{13}	"	3120	−57	−55	−50
"	$C_{12}H_{25}$	"	4090	−50	−25	−50
H	CH_3	H	1800	−72	−58	−59
"	C_6H_{13}	"	1770	−73	−66	−56
"	$C_{12}H_{25}$	"	4300		−51	−55
C_2H_5	CH_3	CH_3	1080	−62	−27	−38
"	C_3H_7	"	1920		−34	
"	C_6H_{13}	"	1680	−59	−36	−40
"	C_8H_{17}	"	1630		−38	
"	$C_{12}H_{25}$	"	2040	−58	−42	−49
C_2H_5	CH_3	H	950	−67	−33	−38
"	C_3H_7	"	1510		−35	
"	C_6H_{13}	"	1530	−69	−32	−40
"	C_8H_{17}	"	1720		−50	
"	$C_{12}H_{25}$	"	2295	−55	−51	−48
CH_3	CH_3	"	1790	−63	−40	−49
"	C_3H_7	"	1910		−50	
"	C_6H_{13}	"	2540	−69	−50	−47
"	C_8H_{17}	"	1965		−58	
"	$C_{12}H_{25}$	"	2450	−56	−47	−48
Polysébaçate du diol **2**			1770	−68	−55	
Polysébaçates des diols **3**						
	$R_1 = CH_3$			−37	−20	
	$R_1 = C_6H_{13}$			−39	−22	

après deux jours. De plus, une variation de ±20% dans le poids moléculaire du polysébaçate provoque une fluctuation au hasard de ±3 °C. Tout ceci permet de s'attendre à une précision de ±3 °C sur les T_g.

Resultats et Discussion

Les T_g mesurés pour les polyuréthanes sont rassemblés au Tableau I. L'examen de ce tableau peut être séparé en quatre parties, la première considérant l'effet des chaînes latérales et la seconde, l'effet d'introduction de conformations *gauches*. Une troisième section mentionne un résultat sur l'effet de mobilité de l'azote, et finalement une quatrième section compare les transitions mesurées sur les polyesters initiaux à celles des polyuréthanes.

Effet des Chaînes Latérales

Vu la complexité des systèmes d'élastomères réticulés, et la très grande variété de causes qui puissent venir influencer le T_g de chacun des produits individuellement, il est préférable de profiter du nombre relativement élevé de produits disponibles et d'examiner les tendances des T_g moyens. Soulignons que ces moyennes ne sont pas matématiquement consistantes et qu'il ne faut pas attacher trop d'importance aux valeurs absolues de ces moyennes. Leur rapport relatif a l'avantage toutefois, de refléter les tendances du Tableau I en éliminant les déviations trop grandes. Il est cependant possible en n'utilisant que le Tableau I de suivre l'argumentation.

Ainsi si la moyenne des T_g du Tableau I est calculée pour tous les produits ayant la même chaîne latérale en R_2, les résultats du Tableau II sont obtenus. Il apparaît alors à l'examen de ce tableau, que la chaîne latérale a un léger effet sur le T_g.

Dans le cas des polyuréthanes cuits au TDI, le T_g passe par un minimum pour une chaîne de

Can. J. Chem. Downloaded from www.nrcresearchpress.com by 210.87.254.105 on 09/05/12
For personal use only.

Can. J. Chem. Downloaded from www.nrcresearchpress.com by 210.87.254.105 on 09/05/12
For personal use only.

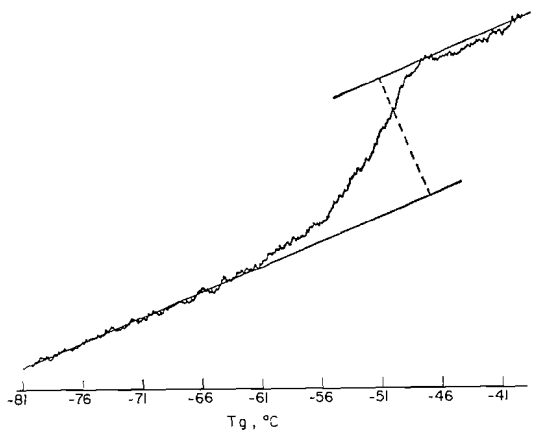

FIG. 3. Contenu énergétique de la transition du polysébaçate d'hexyl-N bis(hydroxy-2 propyl)amine (**1**, $R_1 = R_3 = CH_3$, $R_2 = C_6H_{13}$).

TABLEAU II

Moyenne des T_g selon l'allongement de R_2 (**1**)

R_2	T, polyesters (°C)	T_g, polyuréthanes, (°C)	
		TDI	DDI
CH_3	−62	−38	−44
C_3H_7		−41	
C_6H_{13}	−65	−48	−46
C_8H_{17}		−48	
$C_{12}H_{25}$	−56	−42	−50
$C_{16}H_{33}$	−48	−44	−48
$C_{18}H_{37}$		−31	−48

6 à 8 atomes, et la diminution maximale de T_g qu'il est possible d'obtenir en variant la longueur de R_2 est de 10 °C. Pour les polyvinyles non-réticulés avec groupes alkoxydes latéraux de différentes longueurs, il a été rapporté aussi, un minimum de T_g pour une chaîne latérale de 6–8 atomes (17*a*); toutefois dans ce cas la diminution est de 50 °C. Il faut remarquer cependant qu'avec les polyvinyles la chaîne latérale se répète à tous les deux atomes de carbone tandis que dans le système élastomérique adopté ici, il n'y a qu'une chaîne latérale par segment de diol dans le prépolymère. Ceci amène une dilution de l'effet global. Ajoutons que dans le cas des polymères sans réticulation, le T_g des polyméthylmétacrylate diminue continuellement à mesure que la chaîne latérale est allongée jusqu'à 12 atomes de carbone (17*b*).

Avec le DDI comme agent de cuisson, le minimum de T_g est atteint pour une chaîne longue de 12 atomes et l'effet total n'est que de 6 °C. Dans ce cas, l'agent de cuisson est plus gros que le TDI, les chaînes se trouvent encore plus diluées dans le réseau et leur effet est plus petit.

Effet d'Introduction des Interactions Gauches

Au Tableau III, la moyenne des T_g a été faite cette fois pour illustrer l'effet des interactions *gauches*, c'est-à-dire selon la nature des substituants R_1 et R_3.

Dans le cas de la cuisson au TDI, le minimum de T_g est atteint lorsqu'il n'y a pas de conformations *gauches* ajoutées dans la chaîne par les substituants R_1 et R_3 soit lorsque R_1 et R_3 sont des hydrogènes. L'effet total pour cette série de produits est de 23° entre le T_g des produits sans conformation *gauche* et le T_g des produits les plus influencés par ces conformations.

Avec le DDI, évidemment le minimum de T_g est atteint avec la même série de produits ($R_1 = R_3 = H$) mais l'effet total n'est que de 15 °C. Encore une fois la diminution de l'effet total est attribuable au grossissement de l'agent de cuisson.

Il est à souligner ici qu'un T_g moyen de −58 °C est obtenu pour l'ensemble des produits où aucune interaction *gauche* additionnelle n'est introduite à l'aide des substituants R_1 et R_3. Si une conformation *gauche* est introduite

TABLEAU III

Moyenne des T_g °C selon les conformations *gauches* introduites dans les diols **1**

Substituants		T, poylsébaçates (°C)	T_g, polyuréthanes (°C)	
R_1	R_3		TDI	DDI
CH_3	CH_3	−53	−40	−47
CH_3	C_2H_5	−60	−35	−42
C_2H_5	C_2H_5	−57	−40	−45
CH_3	H	−63	−49	−48
C_2H_5	H	−64	−40	−42
H	H	−72	−58	−57

Can. J. Chem. Downloaded from www.nrcresearchpress.com by 210.87.254.105 on 09/05/12
For personal use only.

(R_1 = CH_3 ou C_2H_5, R_3 = H) par segment de diol, le T_g moyen devient de -45 °C, et si deux interactions *gauches* sont ajoutées, (R_1 = R_3 = CH_3 ou C_2H_5) le T_g passe à -39 °C. Il était donc intéressant de confirmer cette tendance avec des produits homologues qui permettent l'introduction d'un plus grand nombre d'interactions *gauches* par segment de diol. Cette possibilité se présente avec les polysébaçates d'alkyl-N bis-(hydroxy-3-butyl)-2 amines (**3**) qui permettent l'introduction de 4 interactions *gauches* par segment de diol comme le montre la Fig. 4 pour

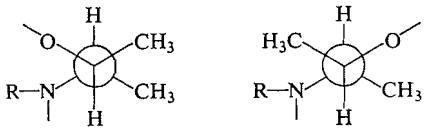

FIG. 4. Deux interactions *gauches* introduites par liaison en α, β de l'azote pour les produits **3**.

une des 2 liaisons C—C en α,β de l'azote dans les conformations les plus stables. Avec le polyuréthane de ces produits, donc pour 4 interactions *gauches* le T_g est de -21 °C. L'ensemble donne une augmentation du T_g de 9 °C par conformation *gauche* introduite.

Effet de la Mobilité de l'Azote

En théorie, il était plausible de prévoir que l'azote tertiaire au sein de la chaîne pourrait par sa mobilité, diminuer la rigidité de la chaîne et concourir à la baisse du T_g.

Pour obtenir tout au moins une indication sur cette hypothèse, le polyuréthane du polysébaçate de méthyl-N-bis(hydroxy-2-éthyl)amine (**1**, R_1 = R_3 = H, R_2 = CH_3) a été comparé au polyuréthane du polysébaçate de méthyl-3-pentanediol-1,5 (**2**). Il est à remarquer que ces 2 produits ont exactement la même structure sauf que l'atome d'azote est remplacé par un carbone dans le second cas. Les T_g obtenus, $-58°$ pour le produit azoté et $-55°$ pour l'autre, indique que cet effet, s'il existe, n'est pas très grand.

Polyesters

Afin de vérifier à l'aide d'une approche différente la relation entre le T_g et la rigidité de la chaîne soit le nombre de conformation *gauche*, la température de transition à basse température a été mesurée sur un certain nombre de polyesters (*cf.* Tableau I). Il est à noter que la nature de cette transition des polyesters n'a pas été déterminée, et qu'il se peut qu'il ne s'agisse pas d'une transition vitreuse.

Les moyennes ont été faites comme dans le cas des polyuréthanes; elles se trouvent aussi aux Tableaux II et III. D'après les tendances générales des résultats, soit température de transition minimum pour une chaîne de 6 atomes, de même que pour l'absence d'interaction *gauche* (R_1 = R_3 = H), il est plausible de supposer que cette température de transition mesurée pour les polyesters est associée aux mêmes transformations physiques que le T_g mesuré pour les polyuréthanes.

Or s'il est posé que les interactions *gauches* introduites par les substituants R_1 et R_3 ont le même contenu énergétique que les interactions *gauches* butane ou pentane (18), soit respectivement 0.8 kcal/mole pour l'interaction entre deux CH_3 et 0.5 kcal/mole entre un CH_2 et un CH_3, il devrait y avoir une relation linéaire entre l'énergie de la transition et l'énergie des interactions *gauches*. L'hypothèse sur l'énergie des interactions *gauches* a d'ailleurs été vérifiée par résonance magnétique nucléaire (15). La Fig. 5 reproduit cette relation pour l'énergie de transition telle que mesurée par calorimétrie. Les résultats de ces mesures sont compilés au Tableau IV. Cette relation confirme tout au moins que la transition mesurée est associée à un changement de mobilité des segments de chaîne qui contiennent les interactions *gauches* introduites par les substituants R_1 et R_3.

Conclusions

En se plaçant dans des conditions idéales, il est possible de mettre en évidence des effets de structure du prépolymère sur le T_g d'élastomères

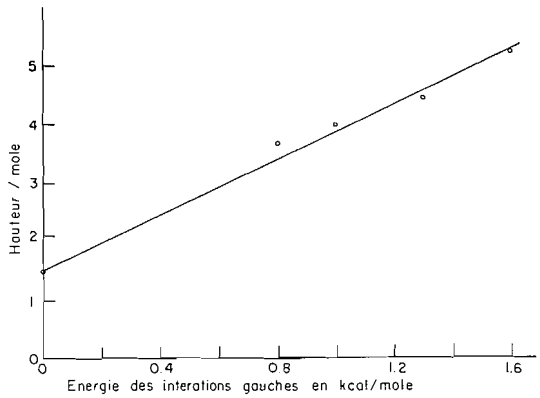

FIG. 5. Relation entre l'énergie de transition mesurée et l'énergie des interactions *gauches* calculée pour les polysébaçates d'hexyl-N bis(hydroxy-2 alkyl)amines.

TABLEAU IV

Energie de transition des polysébaçates des diols **1**, $R_2 = C_6H_{13}$

Substituants		Hauteur/ mole	Energie des conformations *gauches* introduites (kcal/mole)
R_1	R_3		
H	H	1.5	0
H	C_2H_5	1.9	0.5
H	CH_3	3.7	0.8
C_2H_5	C_2H_5	4.0	1.0
C_2H_5	CH_3	4.4	1.3
CH_3	CH_3	5.3	1.6

réticulés. Avec le modèle choisi, l'effet des interactions *gauches* amène des variations de 9 °C par interaction introduite dans un segment de diol. Il a été possible d'augmenter le T_g de 36 °C en changeant les substituants du diol qui ne se trouve qu'à une concentration de 8 équivalents par 100 équivalents de réactifs initiaux. Par contre, l'effet d'allongement d'une chaîne latérale n'est que de 10 °C. Cet effet est maximale pour une chaîne de 6 à 8 atomes de carbone.

Remerciements

Tous mes remerciements s'adressent à Mlle M. Talbot qui a synthétisé les produits et à Yves Giguère qui a préparé les polyuréthanes et mesuré la plupart des T_g. L'assistance du groupe du Dr. R. MacDonald et de M. Bédard nous a aussi été profitable. Je tiens aussi à remercier le Dr. M. Tremblay pour son encouragement.

1. W. A. Lee and J. H. Sewell. J. Appl. Polym. Sci. **12**, 1397 (1968).
2. D. P. Wyman. J. Appl. Polym. Sci. **11**, 1439 (1967).
3. J. M. Barton. Communication A12, 7, Symposium International de Chimie Macromoléculaire. Toronto. 1968; cf. Tech. Reports 66292, 67187, 67298 et 68257, Royal Aircraft Establishment, Farnborough, England.
4. E. A. Dimarzio and J. H. Gibbs. J. Polym. Sci. **40**, 121 (1959).
5. R. A. Hayes. J. Appl. Polym. Sci. **5**, 318 (1961).
6. G. Kanig. Kolloid-Z. Polym. **190**, 1 (1963).
7. A. J. Kovacs. Advan. Polym. Sci. **3**, 394 (1963).
8. (*a*) Y. S. Lipatov, Y. Y. Kerchas, V. G. Sinyavskii, et N. A. Lapatnikov. Rubber Chem. Tech. **41**, 537 (1968); (*b*) J. Polym. Sci. USSR, **9**, 1502 (1968).
9. T. L. Smith and A. B. Magnusson. J. Polym. Sci. **42**, 391 (1960).
10. S. Loshaek. J. Polym. Sci. **15**, 391 (1955).
11. J. H. Saunders and K. C. Frisch. Polyurethanes, chemistry and technology. Vol. XVI. Interscience Publishers, Inc., New York. 1962. p. 261.
12. J. L. Boivin. Can. J. Chem. **36**, 1405 (1958).
13. G. Perrault. Can. J. Chem. **45**, 1063 (1967).
14. G. Perrault. Can. J. Chem. **46**, 2021 (1968).
15. G. Perrault. Can. J. Chem. **46**, 3762 (1968).
16. V. V. Korshak et S. V. Vinogradova. Polyesters. *Traduit par* B. J. Hazzard. The Pergamon Press, Ltd., New York. 1965. p. 187.
17. (*a*) J. Lal and K. W. Scott. J. Polym. Sci. Part C, 113 (1965). (*b*) S. S. Rogers and L. Mandelkern. J. Phys. Chem. **61**, 985 (1957).
18. M. Hanack. Conformation theory. Academic Press, Inc., New York. 1965. pp. 31 et 33.

Can. J. Chem. Downloaded from www.nrcresearchpress.com by 210.87.254.105 on 09/05/12
For personal use only.

Catalytic reduction of dimethylsulfoxide by molecular hydrogen using rhodium(III) complexes

B. R. JAMES, F. T. T. NG (MISS), AND G. L. REMPEL
Department of Chemistry, University of British Columbia, Vancouver 8, British Columbia
Received June 30, 1969

Dimethylsulfoxide is reduced by molecular hydrogen under mild conditions to dimethylsulfide and water in the presence of rhodium(III) complexes as catalysts. The kinetics of the systems using $RhCl_3.3H_2O$ and *cis*-$RhCl_3(Et_2S)_3$ have been investigated, and a mechanism involving reduction of coordinated dimethylsulfoxide in a rhodium(III) hydride complex is postulated. The catalytic efficiency of the systems decreases slowly due to the production of inactive rhodium(I) species.

Canadian Journal of Chemistry, 47, 4521 (1969)

Can. J. Chem. Downloaded from www.nrcresearchpress.com by 210.87.254.5 on 09/05/12
For personal use only.

Introduction

We have recently been interested in the homogeneous hydrogenation of olefinic substrates using platinum metal complexes (1–3), and have found that catalytic activity is very dependent on the solvent medium used. The activity of rhodium chloride complexes was very much enhanced in the coordinating aprotic solvent N,N-dimethylacetamide (DMA) (1). As part of these general studies, we attempted to investigate catalytic activity in dimethylsulfoxide (DMSO); it soon became clear that a hydrogenation reaction occurred in the *absence* of any organic substrate. This has been shown to be a catalytic reduction of the solvent and these studies are described in this paper. DMSO has come to be widely used as an advantageous medium for inorganic chemical reactions because of its ability to dissolve fairly high concentrations of many inorganic solutes (4, 5), and has been used extensively as an oxidizing agent in organic synthesis (5, 6). A few Group III–V main group halides have been shown to reduce DMSO (6); most transition metal halides form coordination compounds (7), although niobium and tantalum pentahalides do abstract the oxygen atom of the sulfoxide to form the corresponding oxyhalide and halogen substituted sulfides (8). The present investigation shows that molecular hydrogen can be activated by rhodium(III) complexes for reduction of DMSO to dimethylsulfide (DMS) and is considered important in view of the present extensive use of this solvent.

Experimental

Rhodium(III) trichloride was obtained as $RhCl_3.3H_2O$ from Platinum Chemicals. Dimethyl and diethylsulfides were Eastman Organic chemicals and were used without further purification. The cyclo-octene was obtained from K and K Laboratories. 1,2,3-trichlotris(diethylsulfide) rhodium(III) (9) and the cyclo-octene complex, $[(C_8H_{14})_2RhCl]_2$ (10), were prepared according to the literature. Prepurified H_2 was obtained from Canadian Liquid Air Co. and was passed through a Deoxo catalytic purifier before use. Deuterium was obtained as C.P. grade (99.5%) from Matheson Co. DMSO (Baker Analyzed grade) was purified by storing over CaH_2 under N_2 for long periods, followed by distillation under reduced pressure; it was collected onto Linde 4A molecular sieve and stored under N_2.

The kinetics of the hydrogenation reactions were studied by measuring the rate of gas uptake at constant pressure using the apparatus and procedure described earlier (11). The initial concentration of Rh(III) in these experiments was in the range 0.01–0.03 *M*. The partial pressure of H_2 was varied from 130–800 mm. The solubility of H_2 in DMSO is quite small but was determined to be about 6×10^{-5} *M* atm^{-1} at 80 °C. Dimethylsulfide and water, the products from the H_2 reduction of DMSO, were separated from the reaction mixture by distillation and identified in the distillate by gas chromatography using a dinonyl phthalate column. The water was also readily detected and estimated by the ^1H nuclear magnetic resonance spectrum of the distillate (Varian A.60, TMS external standard). Visible and ultraviolet spectra were recorded on a Perkin–Elmer 202 spectrophotometer, and infrared spectra were recorded on a Perkin–Elmer 137 spectrophotometer using Nujol mulls or KBr disks.

Results

Stoichiometry

The visible absorption spectrum of a solution of $RhCl_3.3H_2O$ in DMSO changed slowly with time at room temperature, presumably due to equilibration between complexes. This change could be accomplished rapidly by heating to 80°, and the steady spectrum of the orange solution showed absorption maxima at 360 mμ (ε 380) and 435 mμ (ε 270). Such solutions were found to absorb hydrogen at measurable rates from 70–90°. Figure 1 shows such an uptake at 80° for

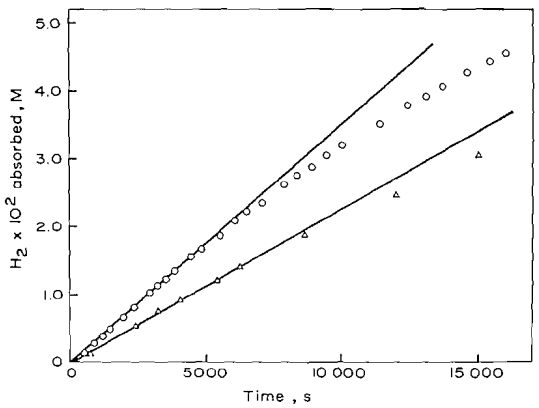

FIG. 1. Rate plots at 80°, 746 mm H_2, DMSO solution: Δ, 0.02 *M* $RhCl_3.3H_2O$; ○, 0.02 *M* $RhCl_3(Et_2S)_3$.

a 0.02 *M* Rh(III) solution; a linear uptake plot is observed for about 3 h and then the rate falls off very slowly. There is no obvious stoichiometric relationship between the H_2 uptake and the rhodium used; an uptake was followed up to 1.0 *M* of H_2 for a solution 0.03 *M* in Rh. In the absence of rhodium complex, there was no measureable uptake over 3 h. No reactions other than equilibration were observed between $RhCl_3.3H_2O$ and DMSO in the absence of H_2 under the conditions of the kinetic experiments.

The visible absorption spectra of solution samples taken during the linear uptake region were unchanged from that of the starting solution, showing that the reaction is catalytic with respect to Rh(III); no Rh(III) hydride species were detected.

Analysis for the reaction products in solution, after the reaction in which 1.0 *M* H_2 had been consumed, gave dimethylsulfide and water, both about 1 mole for each mole of H_2 absorbed. The overall reaction which occurs in the presence of $RhCl_3.3H_2O$ is thus

[1] $$(CH_3)_2SO + H_2 \rightarrow (CH_3)_2S + H_2O$$

A similar catalyzed reaction has been observed using the complex *cis*-$RhCl_3(Et_2S)_3$, although the linear rates are somewhat greater for this system (Fig. 1). The initial equilibrated $RhCl_3(Et_2S)_3$/DMSO solution showed absorption maxima at 370 mμ (ε 500) and 430 mμ (ε 300).

The gradual fall-off in the hydrogenation rate is paralleled by a decrease in the intensity of the orange solutions, and after a 15 h experiment with the trichloride system the final solution is yellow, showing a single absorption maximum at 390 mμ (ε 425) indicating likely formation of the Rh(I) state (1, 12). This solution is stable in air for many hours at room temperature, but on heating to 80° under oxygen overnight an orange solution again results with the characteristic 2-peak spectrum of a Rh(III) species (λ_{max} 380 mμ, ε 410; λ_{max} 430 mμ, ε 300).

Kinetics

The H_2-uptake plots were analyzed by measuring the rates in the long linear region. Tables I and II summarize the kinetic data obtained for the

TABLE I

Kinetic data for the $RhCl_3.3H_2O$ system (80°, unless otherwise stated)

[Rh] *M*	H_2 mm	$[H_2] \times 10^5$ *M*	Linear rate $\times 10^6$ $M\,s^{-1}$	*k* $M^{-1}\,s^{-1}$
0.005	746	6.0	0.54	1.80
0.01	746	6.0	1.02	1.70
0.02	746	6.0	2.28	1.89
0.03	746	6.0	3.50	1.94
0.03	804	6.5	3.83	1.96
0.03	486	3.9	2.72	2.30
0.03	236	1.9	1.36	2.37
0.03	746	6.0	3.63	2.01[a]
0.03	746	6.0	4.30	2.39[b]
0.02	746	6.0	2.30	1.91[c]
0.03	742	~6.0	5.25	2.93[d]
0.03	749	~6.0	1.86	1.03[e]
0.03	751	~6.0	0.91	0.50[f]

[a] D_2 gas.
[b] *p*-Toluene sulfonic acid 0.1 *M* (a strong acid).
[c] 0.1 *M* DMS.
[d] 85°.
[e] 75°.
[f] 70°.

Can. J. Chem. Downloaded from www.nrcresearchpress.com by 210.87.254.5 on 09/05/12
For personal use only.

TABLE II

Kinetic data for the $RhCl_3(Et_2S)_3$ system (80°, unless otherwise stated)

[Rh] M	H_2 mm	$[H_2] \times 10^5$ M	Linear rate $\times 10^6$ $M\,s^{-1}$	k $M^{-1}\,s^{-1}$
0.005	746	6.0	1.04	3.56
0.01	746	6.0	2.10	3.50
0.015	746	6.0	2.92	3.24
0.02	746	6.0	3.68	3.07
0.01	814	6.5	2.20	3.37
0.01	628	5.0	1.69	3.35
0.01	383	3.1	1.07	3.47
0.01	135	1.1	0.35	3.22
0.01	746	6.0	2.0	3.33[a]
0.01	746	—	4.20[b]	—
0.01	746	—	4.60[c]	—
0.01	737	~6.0	4.30	7.16[d]
0.01	742	~6.0	3.10	5.16[e]
0.01	749	~6.0	1.40	2.34[f]
0.01	751	~6.0	1.00	1.67[g]

[a] 2.2 M H_2O.
[b] 20% (volume) H_2O.
[c] 40% (volume) H_2O.
[d] 90°.
[e] 85°.
[f] 75°.
[g] 70°.

$RhCl_3.3H_2O$ system and the $RhCl_3(Et_2S)_3$ system, respectively. The rate is first order in rhodium and hydrogen, and the data have been fitted to the rate law

$$[2] \qquad -d[H_2]/dt = k[Rh(III)][H_2]$$

to obtain the k values listed in the Tables. For the trichloride system, k was independent of added dimethylsulfide (0.1 M) although the linear rate fell off much more rapidly for this experiment; there was no significant dependence on acid and there was no measurable kinetic isotope effect within experimental error using deuterium gas. The addition of up to 2.2 M H_2O had no effect on k for the diethylsulfide system; higher concentrations of water (up to 40% by volume) increased the rate by a factor of about 2.5.

Discussion

The Reduction Reaction

The rate law for the reaction together with spectroscopic data show that hydrogen reacts with a rhodium(III) species to give an intermediate which is then decomposed to DMS, water, and the initial rhodium(III) complex. In polar solvents such as water and ethanol, reactions of molecular hydrogen with rhodium(III) complexes can give rise to intermediate hydrides formed through heterolytic splitting of the H_2 molecule (1, 13)

$$[3] \qquad Rh(III) + H_2 \underset{k_{-1}}{\overset{k_1}{\rightleftharpoons}} Rh(III)H + H^+$$

(ligands omitted)

In the highly polar DMSO (dielectric constant 49 at 20°) this is again likely to be the rate determining step. Such reactions show little measurable isotope effect (1, 14). We have, of course, no rate data on the dependence on the DMSO concentration but, since the hydride intermediate contains coordinated DMSO, the most obvious subsequent step is its rapid decomposition to the products with regeneration of the rhodium catalyst

$$[4] \qquad HRh(III)(DMSO) \xrightarrow[\text{fast}]{H^+} DMS + H_2O + Rh(III)$$

The essential independence of k on acid is consistent with the back reaction [3] not competing with reaction [4].

Johnson and Walton (15) have isolated the complex $RhCl_3(DMSO)_3$ from solutions of the trichloride trihydrate in DMSO, and it is likely that this is the species present in our equilibrated solutions of the trichloride salt; also, according to Gutmann (16), the donor strength of DMSO is greater than for water, the concentration of which will be a maximum of about 0.1 M (3 times the rhodium concentration). $RhCl_2H(DMSO)_3$ is the most likely intermediate produced in reaction [3].

The detailed path of reaction [4] is uncertain.

Can. J. Chem. Downloaded from www.nrcresearchpress.com by 210.87.254.5 on 09/05/12
For personal use only.

DMSO complexes of transition metals are well known with coordination generally being through the oxygen atom (17). However, complexes of platinum(II), palladium(II), and iridium(III) have been shown to contain DMSO bonded through the sulfur atom (18); these conclusions were originally drawn from infrared spectra, particularly in the S—O stretching region, but have been verified by X-ray work. The cation $Pd(DMSO)_4^{2+}$ contains both sulfur-bonded and oxygen-bonded ligands (19). Johnson and Walton (15) draw no definite conclusion from far infrared data about the bonding in the $RhCl_3(DMSO)_3$ complex, but the existence of the strong S—O band at 1120 cm^{-1} in a sample that we made strongly suggests (20) bonding of the DMSO through the sulfur atom. Sulfur appears the likely donor atom in a rhodium(II) acetate – DMSO complex (21). Rhodium is on the border line of the class *a* – class *b* metals (22); in the thiocyanate complex $[Rh(SCN)_6]^{3-}$ however, bonding is through the "softer" sulfur atom (23). A plausible mechanism for reaction [4] can be written assuming sulfur bonding

[5] 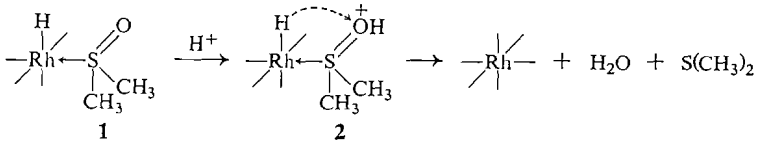

1 2

Protonation of the basic oxygen atom (24) would give **2**. Nucleophilic attack by the coordinated hydride (a typical insertion reaction of an unsaturated moiety into a metal–hydride bond (25)) would lead to elimination of water and dimethylsulfide, either free or coordinated depending on the stability of rhodium dimethylsulfide complexes. The constancy of the initial reaction rate and visible spectrum indicates that the DMS is not coordinated in this region. In the system with added DMS the more rapid fall-off in rate suggests that DMS may well coordinate as its concentration builds up (see later discussion). No effect is observed by the addition of up to 2.2 *M* water; water therefore does not cause the retardation in rate and is also unlikely to be coordinated to the rhodium at this concentration. Little can be said about the increase in rate at the high water concentration; aquo complexes may be involved, and also the solubility of hydrogen is some 10 times greater in water (26) than in DMSO.

An interesting possibility for the overall reduction reaction is that intermediate **2** is formed directly in a single concerted step by the approach of a H_2 molecule to the rhodium–DMSO complex; the heterolytic splitting of the H_2 molecule would be "built into" such a mechanism which would be indistinguishable from the kinetic point of view.

The diethylsulfide system is about twice as active at 80° as the trichloride system; the visible absorption spectrum shows a different rhodium(III) complex is initially present in solution and it must have coordinated diethylsulfide. This system was investigated primarily to see if rhodium complexes containing such sulfur ligands were less active than those derived from $RhCl_3.3H_2O$; diethylsulfide will be a somewhat stronger donor ligand than dimethylsulfide. The conclusion is that the fall-off in rate is not due to coordination of dimethylsulfide to *trivalent* rhodium. The activation parameters for the trichloride and diethylsulfide systems were estimated from good Arrhenius plots to be $\Delta H^{\ddagger} = 27.0 \pm 1$ kcal $mole^{-1}$, $\Delta S^{\ddagger} = +18 \pm 3$ e.u.; $\Delta H^{\ddagger} = 16.8 \pm 0.5$ kcal $mole^{-1}$, $\Delta S^{\ddagger} = -9 \pm 1$ e.u., respectively. The significance of the difference is not clear but it may be related to a difference in the charges of the reacting complexes. In the diethylsulfide system, for example, cationic species of the type $[RhCl_2(Et_2S)(DMSO)_3]^+$ could be present. In some related systems in dimethylacetamide, in which $RhCl_3.3H_2O$ and $RhCl_3(Et_2S)_3$ have been reduced to rhodium(I) complexes through rhodium(III) hydride intermediates, the diethylsulfide system again showed a lower enthalpy of activation and a more unfavorable entropy factor (1).

The Fall-Off in Catalytic Activity

Rhodium(III) hydride complexes readily dissociate into rhodium(I) species (1, 27, 28)

[6] $$Rh(III)H \rightarrow Rh(I) + H^+$$

The experimental data strongly indicate that in the region of lower rate some rhodium(I) com-

Can. J. Chem. Downloaded from www.nrcresearchpress.com by 210.87.254.5 on 09/05/12
For personal use only.

Can. J. Chem. Downloaded from www.nrcresearchpress.com by 210.87.254.5 on 09/05/12
For personal use only.

plexes are present. Reaction [6] is a fast reaction (1) and hence the production of rhodium(I) will depend on the comparative rates of the decomposition of the hydride according to reaction [6] and its reaction with DMSO according to a reaction such as [5]. Production of rhodium(I) could be more favorable at higher concentrations of dimethylsulfide since this ligand is expected to stabilize the lower valent state (more class *b* character). Attempts to isolate a pure inorganic complex at the end of a long reaction, when the presence of rhodium(I) is indicated, have not been successful, and we can find no reports on the production of rhodium(I) alkyl sulfide complexes. However, an isolated impure orange solid gave strong infrared bands at 1120, 1020, and 980 cm^{-1}. The first is attributed to the S—O stretch of a sulfur-bonded DMSO (20) and the latter two may be assigned to CH_3 rocking modes of coordinated DMSO or DMS (20). Rhodium(I) is likely to bond through the sulfur atom of DMSO.

The kinetic data could also be consistent with a rate determining hydrogen reduction to rhodium(I) through reactions [3] and [6], followed by a rapid oxidation of the rhodium(I) by DMSO. However, DMSO complexes of low valent transition metals such as manganese(II) (17), ruthenium(II) (29), and iridium(I) (3) are known and also our final reaction solutions appear to contain rhodium(I), so such a mechanism seems unlikely and we strongly favor reaction through a rhodium(III) hydride. Solutions of the complex $[(C_8H_{14})_2RhCl]_2$ containing the labile cyclooctene ligand (10) also showed no redox reaction with DMSO at 80°.

The observation that the final yellow solution was oxidized slowly by oxygen back to rhodium(III) suggested that use of a hydrogen/oxygen mixture might prevent the slow fall off in reaction rate. In an experiment using a mixture of 500 mm H_2 and 250 mm O_2 with 0.03 *M* $RhCl_3.3H_2O$, the initial rate was that expected for the reaction in the absence of oxygen; however, the rate now showed autocatalytic behavior before reaching a steady rate of 1.3×10^{-5} *M* s^{-1}, some 3 times faster than the initial rate, and showed no signs of falling off over a 3 h period. It is of interest that Trocha-Grimshaw and Henbest (30) have recently reported that solutions of $RhCl_3$ or $H[Cl_4Rh(DMSO)_2]$ in hot isopropanol/water mixtures catalyze the air oxidation of DMSO to dimethyl sulfone although no mechanism was suggested. We find that solutions of $RhCl_3.3H_2O$ in DMSO showed no reactivity towards oxygen (80°, 1 atm O_2) and it seems likely that the alcoholic medium is necessary to furnish intermediate hydride species (31). These workers state that hydrides are the most effective catalysts. Rhodium(I) complexes are known to activate molecular oxygen through an oxidative addition reaction (32) and these could well be produced from the rhodium(III) hydrides according to reaction [6]. Hence, from these considerations, it seemed possible that the increase in rate of gas uptake in our experiment using the hydrogen/oxygen mixture might be due to an induced catalytic oxidation through the rhodium(III) hydride intermediates or the slowly produced rhodium(I) species. And indeed, isolation of the products from further reactions using such mixtures yielded mainly dimethyl sulfone (readily identified by infrared and melting point) and only small amounts of dimethylsulfide and water, confirming the catalytic oxidation. The fact that neither our initial rhodium(III) solutions nor our final rhodium(I) solutions from the hydrogenation experiments showed any catalytic activity towards oxygen indicates that rhodium(III) hydrides may be directly involved as the oxygen carriers. No catalytic oxidation was observed using solutions of $[(C_8H_{14})_2RhCl]_2$ in DMSO, although we have found that this complex does activate molecular oxygen in other solvents (33).

Acknowledgment

Grateful acknowledgment is made to the National Research Council of Canada for support of this research.

1. B. R. James and G. L. Rempel. Discuss. Faraday Soc. **46**, 48 (1968).
2. B. R. James, F. T. T. Ng, and G. L. Rempel. Inorg. Nucl. Chem. Lett. **4**, 197 (1968).
3. B. R. James and N. A. Memon. Can. J. Chem., **46**, 217 (1968).
4. H. L. Schläfer and W. Schaffernicht. Angew. Chem. **72**, 618 (1960).
5. Proc. Intra-Science Symposium on DMSO, Santa Monica, 1967. Quart. Rep. Sulfur Chem. **3**, (2) (1968).
6. W. W. Epstein and F. W. Sweat. Chem. Rev. **67**, 247 (1967).
7. DMSO: reaction medium and reactant. Crown-Zellerbach Corp., Camus, Washington. June, 1962.
8. D. B. Copley, F. Fairbrother, K. H. Grundy, and A. Thompson. J. Less-Common Metals, **6**, 407 (1964).
9. J. E. Fergusson, J. D. Karen, and S. Seevaratnam. J. Chem. Soc. 2627 (1965).
10. L. Porri, A. Lionelli, G. Allegra, and A. Immirza. Chem. Commun. 336 (1965).

11. B. R. JAMES and G. L. REMPEL. Can. J. Chem. **44**, 233 (1966).
12. B. N. FIGGIS. Introduction to ligand fields. 2nd ed. Interscience Publishers, Inc., New York. 1967. p. 315.
13. J. A. OSBORN, F. H. JARDINE, J. F. YOUNG, and G. WILKINSON. J. Chem. Soc. A, 1711 (1966).
14. J. F. HARROD and J. HALPERN. Can. J. Chem. **37**, 1933 (1959).
15. B. F. G. JOHNSON and R. A. WALTON. Spectrochim. Acta, **32**, 1853 (1966).
16. V. GUTMANN. Papers presented at Conf. Non-Aqueous Solvent Chemistry (Hamilton, Ontario. 1967); Coord. Chem. Rev. **2**, 239 (1967).
17. V. GUTMANN. Quart. Rep. Sulfur Chem. **3**, 169 (1968) and refs. therein.
18. W. KITCHING and C. J. MOORE. Inorg. Nucl. Chem. Lett. **4**, 691 (1968) and refs. therein.
19. B. B. WAYLAND and R. F. SCHRAMM. Chem. Commun. 1465 (1968).
20. F. A. COTTON, R. FRANCIS, and W. D. HORROCKS. J. Amer. Chem. Soc. **64**, 1534 (1960).
21. S. A. JOHNSON, H. R. HUNT, and H. M. NEWMANN. Inorg. Chem. **2**, 960 (1963).
22. S. ARHLAND, J. CHATT, and N. R. DAVIES. Quart. Rev. **12**, 265 (1958).
23. H. M. SCHMIDTKE. J. Amer. Chem. Soc. **87**, 2522 (1965).
24. J. R. HOLMES, D. KIVELSON, and W. C. DRINKARD. J. Amer. Chem. Soc. **84**, 4677 (1962).
25. R. F. HECK. Adv. Chem. Series. Vol. 49. Amer. Chem. Soc., Washington, D.C. 1965. p. 181.
26. R. WEIBE and V. L. GADDY. J. Amer. Chem. Soc. **56**, 76 (1934).
27. B. R. JAMES. Coord. Chem. Rev. **1**, 505 (1966).
28. A. SACCO, R. UGO, and A. MOLES. J. Chem. Soc. A, 1670 (1966).
29. A. D. ALLEN, F. BOTTOMLEY, R. O. HARRIS, V. P. REINSALU, and C. V. SENOFF. J. Amer. Chem. Soc. **89**, 5595 (1967).
30. J. TROCHA-GRIMSHAW and H. B. HENBEST. Chem. Commun. 1035 (1968).
31. F. BASOLO and R. G. PEARSON. Mechanisms of inorganic reactions. 2nd ed. John Wiley and Sons, Inc., New York. 1967. p. 595.
32. J. P. COLLMAN. Accounts Chem. Res. **1**, 136 (1968); J. BLUM, H. ROSENMAN, and E. D. BERGMAN. Tetrahedron Lett. 3665 (1967).
33. B. R. JAMES and F. T. T. NG. To be published.

Can. J. Chem. Downloaded from www.nrcresearchpress.com by 210.87.254.5 on 09/05/12
For personal use only.

Effect of an external heavy atom on the photochemistry of monofluorobenzene vapor

A. Cook, G. P. Semeluk, and I. Unger
Department of Chemistry, University of New Brunswick, Fredericton, New Brunswick

Received June 30, 1969

Spectrofluorometric techniques have been used to study the effect of added xenon on the singlet and triplet yields of monofluorobenzene vapor excited by 2670, 2520, and 2470 Å radiation. For each wavelength examined, the fluorescent yield was found to decrease with increasing xenon pressure and plots of $1/\Phi_f$ vs. P_{Xe} are linear. The sensitized emission of biacetyl technique was used to determine triplet yields. The effect of xenon on the emission yield of biacetyl excited directly at 4358 Å was also examined and it was found that xenon reduced the phosphorescent yield of biacetyl. Plots of $1/\Phi_p$ vs. P_{Xe} were found to be linear, for all cases of sensitized as well as directly excited emission. At 2470 Å both the fluorescence yield and the triplet yield initially increase with increasing Xe pressure, but when the Xe pressure exceeds about 30 Torr the behavior at this wavelength is the same as it is at the other two wavelengths.

The data suggest that xenon enhances intersystem crossover in both monofluorobenzene (FB) and biacetyl (BiA). The important process in the former is $^1FB + Xe \rightarrow {}^3FB + Xe$, while in the latter is $^3BiA + Xe \rightarrow BiA + Xe$. A mechanism consistent with the experimental observation is presented.

Canadian Journal of Chemistry, 47, 4527 (1969)

Can. J. Chem. Downloaded from www.nrcresearchpress.com by 210.87.254.5 on 09/05/12
For personal use only.

Introduction

Singlet–triplet transitions may be enhanced by the presence of either an internal heavy atom (1) or an external heavy atom (2). The former is generally referred to as McClure enhancement, while the latter is usually called Kasha enhancement. Robinson (3) has shown that Xe, present as a solvent, will promote intersystem crossover in the solid phase. Wilkinson and co-workers (4, 5) and Cundall and Voss (6) have noted the same phenomenon with Xe dissolved in liquids. A recent gas phase study (7) has shown that Xe quenches the singlet state of small aromatic molecules, presumably because of promotion of singlet to triplet crossover.

This paper describes the results of an investigation of the effect of Xe on the singlet and triplet yields of monofluorobenzene excited at 2470, 2520, and 2670 Å. Monofluorobenzene was chosen as the test molecule since it does not show any appreciable dissociation when irradiated by 2520 and 2670 Å radiation, and since its basic photochemistry in this spectral region is now fairly well understood (8–11). Since monofluorobenzene does not show any phosphorescent emission in the gas phase, it was necessary to use an indirect technique (sensitized emission of biacetyl (12)) to measure triplet yields. It was therefore necessary to determine the effect of Xe on triplet biacetyl molecules. This was accomplished by irradiating biacetyl directly at 4358 Å and following the emission yield as a function of Xe pressure.

Experimental

The fluorobenzene used in this study was obtained from the Aldrich Chemical Company and shown by vapor phase chromatography to have an impurity content $\leqslant 0.02$ mole %. The biacetyl, also obtained from Aldrich, was stored in a blackened bulb. The "Research Grade" xenon obtained from Matheson had the quoted impurities: nitrogen, 2 p.p.m.; oxygen, 1 p.p.m.; krypton, 10 p.p.m. Both the fluorobenzene and biacetyl as well as the xenon were used without further purification.

The high vacuum line employed in this study was grease and Hg free, using Hoke packless diaphragm metal valves exclusively. Emission measurements were made on a modified Aminco-Bowman Spectrophotofluorometer (SPF) (13). The entrance slit of the excitation monochromator was set at 0.5 mm and the exit slits on this monochromator were 1.0, 0.5, and 1.0 mm. This slit combination provides an optimum light intensity, with a concomitant band pass of 70 Å.

The light source was a 200 W xenon–mercury compact arc lamp operated on a d.c. power supply, both supplied by American Instrument Company, Incorporated (Aminco). Fluorescence and sensitized emission were detected by means of an E.M.I. 6256B (S 13 response) photomultiplier tube. The signal generated by this tube was amplified and then recorded by a Moseley 7030 AM X–Y recorder. Absorption measurements were performed with an R.C.A. 935 single stage phototube, the signal being read on a Keithley Instruments Model 410, micro-microammeter. The cell used in this study was a flow-through cuvette type, 1 cm × 1 cm and 4.6 cm high, polished on all four sides (Aminco Number 4–8115). All experiments were carried out at room temperature $\simeq 27$ °C.

Quantum yields of fluorescence and of sensitized emission were obtained by a technique in which a calibration factor for the system was determined based on the accurately determined quantum yield of a reference material (9). In this case, benzene and benzene–biacetyl mixtures were used as the reference materials.

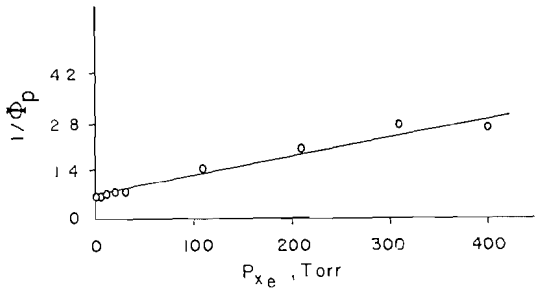

FIG. 1. Variation of $1/\Phi_p$ as a function of P_{Xe}. P_{BIA} = 5 Torr, λ_{ex} = 4358 Å.

Results and Discussion

The addition of Xe to 5 Torr of BiA excited at 4358 Å results in a decrease in the emission yield of BiA. A plot of $1/\Phi_p$ vs. [Xe] is linear (see Fig. 1) and obeys the relationship

$$[1] \qquad 1/\Phi_p = 6.67 + 292\,[Xe]$$

Addition of Xe to FB excited at 2670 and 2520 Å decreases the fluorescent yield, giving a linear dependence of $1/\Phi_f$ on [Xe] (see Fig. 2 and Table I). The relationship obeyed, for λ_{ex} = 2670 Å, is

$$[2] \qquad 1/\Phi_f = 4.67 + 53.9[Xe]$$

while for λ_{ex} = 2520 Å, the relationship is

$$[3] \qquad 1/\Phi_f = 4.3 + 55[Xe]$$

When the excitation wavelength is 2470 Å, addition of Xe up to a partial pressure of 30 Torr causes a rise in the fluorescent yield. Beyond this pressure the fluorescent yield has the same behavior as that noted at 2670 and 2520 Å (see Table I). For λ_{ex} = 2470 Å and Xe pressures

TABLE I

Variation of $1/\Phi_f$ as a function of P_{Xe}

$1/\Phi_f$*	P_{Xe}, Torr*	$1/\Phi_f$†	P_{Xe}, Torr†
3.97	0	12.45	5.27
4.29	5.06	11.14	10.68
4.37	10.12	11.05	20.41
4.31	15.18	12.27	30.35
4.38	20.24	14.19	49.55
4.71	50.34	13.21	99.55
4.79	100.34	20.44	313.55
4.71	202.34	23.13	421.25
5.06	303.34	23.25	528.25
5.83	505.34		

*λ_{ex} = 2520 Å, P_{FB} = 10.08 Torr; $1/\Phi_f$ = 4.30 + 55[Xe].
†λ_{ex} = 2470 Å, P_{FB} = 10.21 Torr; $1/\Phi_f$ = 11.60 + 444[Xe].

greater than 30 Torr, the applicable equation is

$$[4] \qquad 1/\Phi_f = 11.6 + 444[Xe]$$

Fluorescent yields reported here are based on the fluorescent yield of benzene equal to 0.18 (14).

Addition of Xe to mixtures of 10 Torr of FB and 5 Torr BiA irradiated at 2670 and 2520 Å causes the sensitized emission of BiA to decrease (see Fig. 3 and Table II). Plots of $1/\Phi_p$ vs. [Xe] are linear and obey the following equations

$$[5] \qquad 1/\Phi_p = 4.1 + 5.2 \times 10^2[Xe] \qquad \lambda_{ex} = 2670 \text{ Å}$$

$$[6] \qquad 1/\Phi_p = 3.5 + 7.65 \times 10^2[Xe] \qquad \lambda_{ex} = 2520 \text{ Å}$$

For an exciting wavelength of 2470 Å, initial addition of Xe to mixtures of FB and BiA results in an increase in the sensitized emission yield of BiA. Addition of Xe, beyond a pressure of

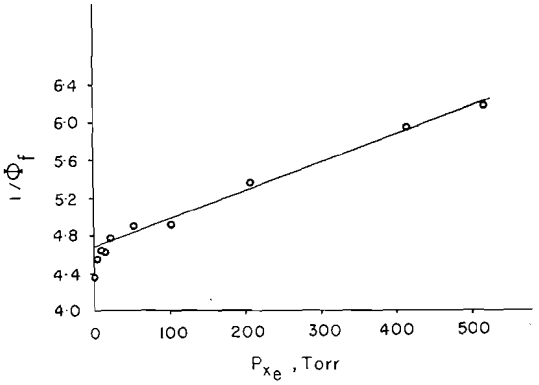

FIG. 2. Variation of $1/\Phi_f$ as a function of P_{Xe}. P_{FB} = 10 Torr, λ_{ex} = 2670 Å.

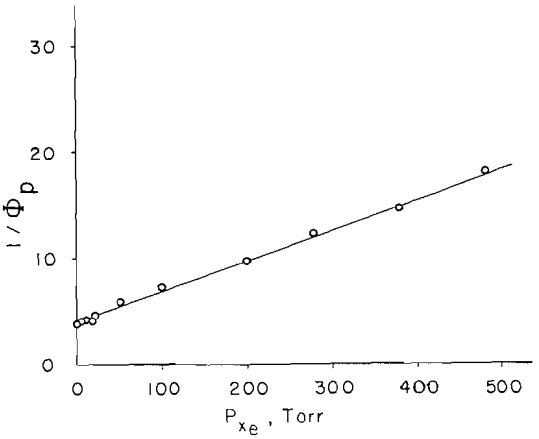

FIG. 3. Variation of $1/\Phi_p$ as a function of P_{Xe}. P_{FB} = 10 Torr, P_{BIA} = 5 Torr, λ_{ex} = 2670 Å.

Can. J. Chem. Downloaded from www.nrcresearchpress.com by 210.87.254.5 on 09/05/12
For personal use only.

Can. J. Chem. Downloaded from www.nrcresearchpress.com by 210.87.254.5 on 09/05/12
For personal use only.

TABLE II
Variation of $1/\Phi_p$ as a function of P_{Xe}

$1/\Phi_p$*	P_{Xe}, Torr*	$1/\Phi_p$†	P_{Xe}, Torr†
2.60	0	15.21	0
3.87	5	15.88	5.92
4.29	10	15.41	12.05
4.41	15	5.45	23.37
4.96	20	5.60	35.00
7.35	50.9	4.72	56.20
7.52	101.9	3.98	104.20
9.81	201.9	5.86	206.20
17.00	301.9	9.96	308.20
		8.05	410.40

*λ_{ex} = 2520 Å, P_{FB} = 9.88 Torr, P_{BiA} = 5.00 Torr; $1/\Phi_p = 3.5 + 765[Xe]$.
†λ_{ex} = 2470 Å, P_{FB} = 10.98 Torr, P_{BiA} = 5.63 Torr; $1/\Phi_p = 3.9 + 237[Xe]$.

30 Torr, causes the sensitized emission yield to decrease according to the equation

$$[7] \qquad 1/\Phi_p = 3.9 + 2.37 \times 10^2[Xe]$$

The data are summarized in Table II. The triplet yields given here are based on the triplet yield of benzene equal to 0.63 (15).

The photochemical behavior of BiA excited at 4358 Å is well known (16) and is adequately described by reactions [8] through [12′] below. Data obtained in the presence of xenon indicate that only one additional reaction, [12′], need be considered.

[8] $\quad BiA + h\nu \rightarrow {}^1BiA^I$
[9] $\quad {}^1BiA^I \rightarrow {}^3BiA^I$
[10] $\quad {}^1BiA^I \rightarrow BiA + h\nu_f$
[11] $\quad {}^3BiA^I \rightarrow BiA + h\nu_p$
[12] $\quad {}^3BiA^I \rightarrow BiA$
[12′] $\quad {}^3BiA^I + Xe \rightarrow BiA + Xe$

In the above scheme Arabic numerals represent spin multiplicity, Roman numeral I represents the first excited state. The reaction

$$ {}^1BiA^I + Xe \rightarrow {}^3BiA^I + Xe$$

need not be considered since intersystem crossover in BiA is almost 100% efficient (17). Steady state treatment of the above scheme yields for the phosphorescent emission efficiency of BiA

$$[13] \quad 1/\Phi_p = \frac{k_{11} + k_{12}}{k_9 k_{11}}(k_{10} + k_9) + \frac{k_{12'}}{k_9 k_{11}}(k_9 + k_{10})[Xe]$$

Equation [13] predicts that a plot of $1/\Phi_p$ vs. [Xe] should be linear with slope $= k_{12'}(k_9 + k_{10})/k_9 k_{11}$, which is confirmed experimentally (see Fig. 1). It has been shown that $k_9 \gg k_{10}$ (18), thus the slope of the line in eq. [13] becomes $k_{12'}/k_{11}$. Since k_{11} has been given as $10^2\ s^{-1}$ (18), this yields

$$k_{12'} = 4.64 \times 10^{-17}\ \text{mole}^{-1}\ \text{cc}\ s^{-1}$$

For systems involving FB and Xe, as well as FB, Xe, and BiA, the following additional reactions must be considered

[14] $\quad FB + h\nu \rightarrow {}^1FB^I$
[15] $\quad {}^1FB^I \rightarrow FB + h\nu'$
[16] $\quad {}^1FB^I \rightarrow {}^3FB^I$
[16′] $\quad {}^1FB^I + Xe \rightarrow {}^3FB^I + Xe$
[17] $\quad {}^1FB^I + FB \rightarrow 2FB$
[18] $\quad {}^3FB^I \rightarrow FB$
[19] $\quad {}^1FB^I + BiA \rightarrow {}^1BiA^{II} + FB$
[20] $\quad {}^3FB^I + BiA \rightarrow {}^3BiA^I + FB$
[21] $\quad {}^1BiA^{II} \rightarrow$ Dissociation
[22] $\quad {}^1BiA^{II} + M \rightarrow {}^1BiA^I + M$

The symbols used in these have the same meaning as previously, but Roman numeral II indicates the second excited state, and M represents any molecule capable of accepting vibrational energy. The evidence for the occurrence of most of the above reactions has been adequately discussed previously and rate constants for the various steps at different exciting wavelengths have also been given (11). In the absence of BiA, steady state treatment gives for the fluorescent yield of FB

$$[23] \quad 1/\Phi_f = \frac{k_{15} + k_{17}[FB] + k_{16} + k_{16'}[Xe]}{k_{15}}$$

At constant [FB], eq. [23] predicts that plots of $1/\Phi_f$ vs. [Xe] should be linear with slope $k_{16'}/k_{15}$. The experimental evidence (Fig. 2 and Table I) shows that this is indeed the case. Since k_{15} has been previously evaluated (11), $k_{16'}$ may be determined from the data. Values of $k_{16'}$ at various exciting wavelengths are listed in Table III.

TABLE III
Summary of values of rate constants for various exciting wavelengths

λ_{ex}, Å	$k_{16'}$, mole^{-1} cc s^{-1}	$k_{12'}$, mole^{-1} cc s^{-1}
2670	3.14×10^{-12}	1.45×10^{-16}
2520	4.02×10^{-12}	2.44×10^{-16}
2470	3.76×10^{-12}	6.77×10^{-17}

In the presence of BiA, eq. [24] is obtained for the sensitized emission yield of BiA.

$$[24] \qquad \frac{1}{\Phi_p} = \frac{(k_{11} + k_{12} + k_{12'}[\mathrm{Xe}])(k_{15} + k_{17}[\mathrm{FB}] + k_{16} + k_{16'}[\mathrm{Xe}] + k_{19}[\mathrm{BiA}])}{k_{11}(k_{16} + k_{16'}[\mathrm{Xe}])}$$

Since $k_{16} \gg k_{16'}[\mathrm{Xe}]$ even at high pressures of Xe, eq. [24] may be reduced to

$$[25] \qquad \frac{1}{\Phi_p} = \frac{(k_{11} + k_{12} + k_{12'}[\mathrm{Xe}])(k_{15} + k_{17}[\mathrm{FB}] + k_{16} + k_{19}[\mathrm{BiA}])}{k_{11}k_{16}}$$

which suggests a linear dependence of $1/\Phi_p$ on [Xe] at constant pressures of FB and BiA. The experimental evidence (Fig. 3 and Table II) confirms this. Equation [25] also yields

$$[26] \qquad \text{Slope/intercept} = \frac{k_{12'}}{k_{11} + k_{12}}$$

The values of k_{11} and k_{12} have been determined (18), and thus values of $k_{12'}$ for various exciting wavelengths can be calculated, these are given in Table III.

The fluorescent yield and the sensitized emission yield both increase initially on addition of Xe when the exciting wavelength is 2470 Å. A possible explanation for these phenomena could be the vibrational deactivation of very hot $^1FB^I$ molecules by collisions of the "second kind" (19), which would prevent them from dissociating and hence increase the singlet and triplet yields.

Acknowledgments

The authors gratefully acknowledge a grant from the Associated Alumni of the University of New Brunswick towards the purchase of the instrumentation used in this study, and other financial assistance from the National Research Council of Canada.

1. D. S. McClure. J. Chem. Phys. **17**, 905 (1949).
2. M. Kasha. J. Chem. Phys. **20**, 71 (1952).
3. G. W. Robinson. J. Mol. Spectrosc. **6**, 58 (1961).
4. A. R. Horrocks and F. Wilkinson. Proc. Roy. Soc. **A306**, 257 (1968).
5. A. R. Horrocks, A. Kearvell, K. Tickle, and F. Wilkinson. Trans. Faraday Soc. **62**, 3393 (1966).
6. R. B. Cundall and A. J. R. Voss. Chem. Commun. 902 (1968).
7. C. S. Burton and W. A. Noyes, Jr. J. Chem. Phys. **49**, 1705 (1968).
8. D. F. Evans. J. Chem. Soc. 2753 (1959).
9. I. Unger. J. Phys. Chem. **69**, 4284 (1965).
10. D. Phillips. J. Phys. Chem. **71**, 1839 (1967).
11. M. MacBeath, G. P. Semeluk, and I. Unger. J. Phys. Chem. **73**, 995 (1969).
12. W. A. Noyes, Jr. and I. Unger. Advan. Photochem. **4**, 49 (1966).
13. F. W. Ayer, F. Grein, G. P. Semeluk, and I. Unger. Ber. Bunsenges. Phys. Chem. **72**, 282 (1968).
14. W. A. Noyes, Jr., W. A. Mulac, and D. A. Harter. J. Chem. Phys. **44**, 2100 (1966).
15. W. A. Noyes, Jr. and D. A. Harter. J. Chem. Phys. **46**, 674 (1967).
16. W. A. Noyes, Jr., G. B. Porter, and J. E. Jolley. Chem. Rev. **56**, 49 (1956).
17. G. B. Porter. J. Chem. Phys. **32**, 1587 (1960).
18. W. A. Noyes, Jr. and H. Okabe. J. Amer. Chem. Soc. **79**, 801 (1957).
19. P. Seybold and M. Gouterman. Chem. Rev. **65**, 413 (1965).

Can. J. Chem. Downloaded from www.nrcresearchpress.com by 210.87.254.5 on 09/05/12
For personal use only.

Can. J. Chem. Downloaded from www.nrcresearchpress.com by 210.87.254.42 on 09/05/12
For personal use only.

An analytical method for determining rate constants using a periodical irradiation technique

W. KAWAKAMI[1] AND H. S. ISBIN

Department of Chemical Engineering, University of Minnesota, Minneapolis, Minnesota 55455

Received June 16, 1969

A new analytical method is presented for the determination of rate constants using a periodical irradiation technique. This method is applicable to reactions which have both a first and a second order termination for the chain radical concentration, and is illustrated for the radiolysis of aqueous solutions of chloral hydrate by ^{137}Cs γ rays. The apparent rate constant of first order termination, and the mean chain life time of the chain radical were determined to be 1.10 s^{-1}, and 0.25 s for 400 rad/min, at 22 °C, respectively.

Canadian Journal of Chemistry, 47, 4531 (1969)

Noyes and Leighton (1) discussed the graphical method of determination of rate constants based on the rotating sector method. Melville (2), Bartlett and Swain (3–5), and Matheson, Auer, Bevilaqua, and Hart (6) applied this method to polymerization reactions. Freeman, Van Cleave, and Spinks (7) examined the radiolysis of aqueous solution of chloral hydrate by this method. They found a mean chain life time of about 0.1 s for 21 rad/min of γ rays of ^{60}Co. On the other hand, Lotz and Schmidt (8) determined the rate constant of the first order termination of this reaction by measuring the increasing rate of the reaction rate at the initial stage of irradiation. They found the apparent rate constant to be 2.35 s^{-1} and a mean chain life time to be 0.2 s for 430 rad/min of X-rays at 20 °C.

Shepp (9) applied the rotating sector method to reactions which have a first and a second order termination and determined the rate constants of the photolysis of acetone using a graphical method. This method, however, requires knowing the value of the ratio of first-to-second order termination reaction rates. Measurement of the ratio is difficult, and may not be possible for polymerization reactions.

The purpose of this paper is to report an analytical method by which rate constants can be determined when a periodical irradiation experiment is carried out together with continuous irradiation experiments. In this method it is not necessary to know the ratio of both termination rates. Hence, it is applicable to determination of rate constants of polymerization reactions which have both a first and second order termination.

[1]On leave from the Takasaki Radiation Chemistry Research Establishment, Japan Atomic Energy Research Institute, Takasaki, Gumma, Japan. Present address: Japan Atomic Energy Research Institute, Takasaki Radiation Chemistry Research Establishment, Watanuki-machi, Takasaki, Gumma-ken, Japan.

Theory

The chain reaction to be considered is as follows

Initiation

$$M \xrightarrow{\sim\sim} R\cdot$$

Reaction rate $= GI$

Propagation

$$R\cdot + D \xrightarrow{k_1} R\cdot + C$$

Reaction rate $= k_1[R\cdot][D] \equiv K[R\cdot]$

Termination

$$R\cdot + S \xrightarrow{k_2} \text{Stable byproduct}$$

Reaction rate $= k_2[R\cdot][S] \equiv k[R\cdot]$

$$2R\cdot \xrightarrow{l} \text{Stable byproduct}$$

Reaction rate $= l[R\cdot]^2$

where M and D are reactants, C is the product, and S is a scavenger. The concentrations of M, D, and S are assumed to be constant. R· is the chain carrier radical and, for convenience, the concentration will be designated by n. G is a constant, I is the dose rate, k_1, k_2, and l are rate constants, K and k are the apparent rate constants.

Continuous Irradiation

The chain radical concentration is given by

$$[1] \qquad \frac{dn}{dt} = GI - kn - 2ln^2$$

Can. J. Chem. Downloaded from www.nrcresearchpress.com by 210.87.254.42 on 09/05/12
For personal use only.

The rate of production of the product at steady state is termed X and is expressed by

$$[2] \qquad X = Kn = A[(1 + BI)^{\frac{1}{2}} - 1]$$

where

$$A = Kk/4l$$

$$B = 8lG/k^2$$

Periodical Irradiation

Consider a periodical exposure of the solution to a radiation field which is varied between two limits. The concentration of the chain radical at ith high and low dose rate intervals at time t are

$iT \leqslant t < iT + \eta T$ (ith high dose rate interval)

$$[3] \qquad \frac{dn}{dt} = GI_1 - kn - 2ln^2$$

$iT + \eta T \leqslant t < (i + 1)T$

(ith low dose rate interval)

$$[4] \qquad \frac{dn}{dt} = GI_2 - kn - 2ln^2$$

where T is the period, η is the fraction of the period that the dose rate is I_1, and i is an integer representing the number of periods. Introducing

$$Y = X/A$$

$iT \leqslant t < iT + \eta T$

$$[5] \qquad \frac{dY}{dt} = \frac{k}{2}(a - Y)(a + 2 + Y)$$

$iT + \eta T \leqslant t < (i + 1)T$

$$[6] \qquad \frac{dY}{dt} = \frac{k}{2}(b - Y)(b + 2 + Y)$$

where

$$a = (1 + BI_1)^{\frac{1}{2}} - 1$$

$$b = (1 + BI_2)^{\frac{1}{2}} - 1$$

When

$$i \gg 1$$

$iT \leqslant t < iT + \eta T$

$$[7] \quad \ln\left(\frac{a + 2 + Y}{a - Y}\right) = k(a + 1)(t - iT) + \ln\left(\frac{a + 2 + M}{a - M}\right)$$

$iT + \eta T \leqslant t < (i + 1)T$

$$[8] \quad \ln\left(\frac{Y + b + 2}{Y - b}\right) = k(b + 1)(t - iT - \eta T) + \ln\left(\frac{N + b + 2}{N - b}\right)$$

where N and M are initial values of Y at the low and high dose rate intervals, and are given by solutions of the following equations

$$[9] \qquad \left(\frac{a + 2 + N}{a - N}\right)\left(\frac{a - M}{a + 2 + M}\right) = u^k$$

$$[10] \qquad \left(\frac{M + 2 + b}{M - b}\right)\left(\frac{N - b}{N + b + 2}\right) = v^k$$

where

$$u = \exp[\eta(a + 1)T]$$

$$v = \exp[(1 - \eta)(b + 1)T]$$

The overall reaction rate which corresponds to the average reaction rate over one period, $\bar{Y}$, should be expressed by

$$[11] \quad \bar{Y} = \frac{1}{T}\int_{iT}^{(i+1)T} Y\,dt = \frac{2}{kT}\ln\left[\left(\frac{M + a + 2}{N + a + 2}\right)\left(\frac{N + b + 2}{M + b + 2}\right)\right] + \eta a + (1 - \eta)b$$

Rearranging eq. [11]

$$[12] \qquad \left(\frac{M + a + 2}{N + a + 2}\right)\left(\frac{N + b + 2}{M + b + 2}\right) = w^k$$

where

$$w = \exp\left[\frac{T}{2}(\bar{Y} - \eta a - (1 - \eta)b)\right]$$

A and B can be determined by continuous irradiation experiments and $\bar{Y}$ can be obtained by periodical irradiation experiments, where I_1, I_2, η, and T are known. Since a and b can be calculated, k is determined from eqs. [9], [10], and [12].

Experimental

The method described in this paper was applied to the radiolysis of aqueous solutions of chloral hydrate. Although the mechanism of this reaction has not been clearly established, the reaction rate is reported to be expressed by the same function of dose rate (8, 11, 12) as shown in eq. [2]. Since the dose rate dependency of reaction rate has an important meaning in this method,

Can. J. Chem. Downloaded from www.nrcresearchpress.com by 210.87.254.42 on 09/05/12
For personal use only.

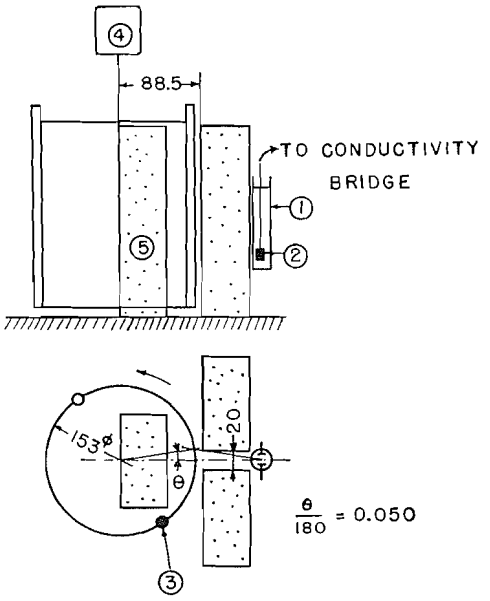

FIG. 1. Experimental apparatus. (1) reactor (20 mm$^{\phi}$, 50 cc Pyrex glass), (2) electrodes (tungsten, cell constant = 0.27 cm^{-1}), (3) source (^{137}Cs, 900 Ci, 10 mm$^{\phi}$ × 200 mm), (4) motor for rotating the source, (5) shielding leads (50 × 100 × 200 mm^3).

this reaction is considered to be applicable for the examination of this method.

The experimental apparatus is shown in Fig. 1. All experiments were carried out in the presence of dissolved oxygen (9–11) at 22 °C. The concentration of hydrochloride, which is the main product, is determined by measuring the specific conductivity (8, 10–13). Chloral hydrate from the Mallinckrodt Co. was used without further purification. The water used was distilled from alkaline potassium permanganate solution. The initial concentration of chloral hydrate was 1.0 mole/l.

The dose rate at high and low dose rate intervals was 400 and 0.0 rad/min, respectively. The value of η, determined by the geometry (Fig. 1), was 0.050, and the period was varied from 0.2 to 30 s.

Results and Discussions

The results for the continuous irradiation experiments are shown in Fig. 2. In this figure, the curve according to an approximate equation is also shown, from which A and B have been evaluated as 0.45 × 10^{-5} mho/cm min and 0.10 min/rad, respectively. These values agree very well with the results of McIntosh, Eager, and Spinks (12), using the conversion factor of 3.49 moles per l of acid per mho per cm.

The experimental results are listed in Table I together with values of k calculated by using the

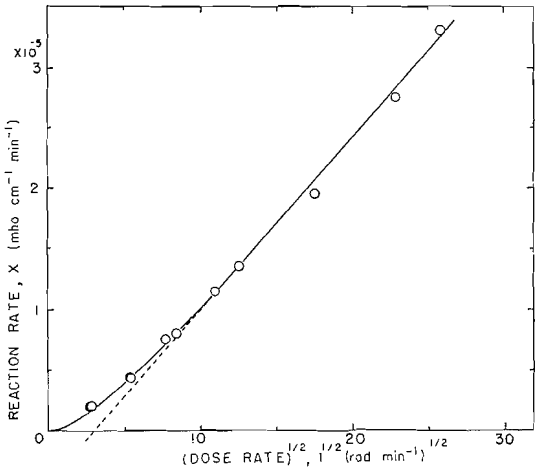

FIG. 2. Rate of formation of hydrochloric acid under continuous irradiation vs. (dose rate)$^{1/2}$. The solid line is based on eq. [2], and the dotted line is based on $X = A(BI)^{1/2} - A$; ○ denotes measured value.

method described in this paper. k is determined to be 1.10 s^{-1} by taking the average of the calculated values, except Runs 1, 2, 6, and 11.

In Fig. 3, the results for the periodical irradiation experiments are shown. The curve in the figure is based on eq. [11], using $B = 0.10$ min/rad, $k = 1.10$ s^{-1}, $I_1 = 400$ rad/min, $I_2 = 0.0$ rad/min, and $\eta = 0.050$. When the initiation rate G is known, l and K can be determined from the following relations

$$l = \frac{k^2 B}{8G}$$

$$K = \frac{kAB}{2G}$$

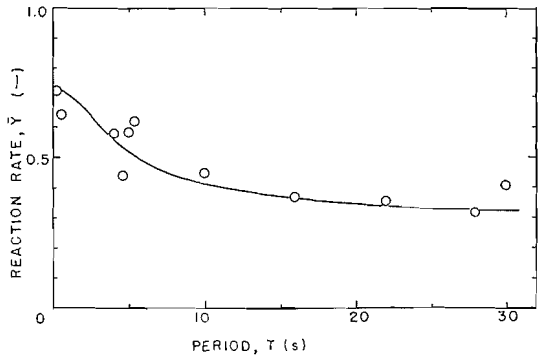

FIG. 3. Effect of periodical irradiation of the solution with ^{137}Cs γ-rays. The solid line is based on eq. [11], ○ denotes measured value.

TABLE I

Periodical irradiation of aqueous solution of chloral hydrate: summary of experimental data and calculated values of k

Run No.	Period T(s)	Reaction rate $\bar{Y}$(—)	k* (s^{-1})	k† (s^{-1})
1	0.2	0.718	4.13	—
2	0.54	0.640	4.54	—
3	4.0	0.580	0.92	1.23
4	4.6	0.437	1.89	1.98
5	5.0	0.585	0.71	0.97
6	5.4	0.649	0.46	0.76
7	10.0	0.448	0.81	0.85
8	16.0	0.367	0.98	0.98
9	22.0	0.352	0.84	0.84
10	28.0	0.311	1.33	1.32
11	30.0	0.405	0.37	0.38

*The solutions of eqs. [9], [10], and [12].
†Based on eq. [16].

An approximation method for determining k is shown below.

Introducing

$$y = 1/(M + a + 2)$$

$$x = 1/(N + a + 2)$$

into eqs. [9], [10], and [12]

$$[13] \qquad y = u^k x - \frac{u^k - 1}{2(a + 1)}$$

$$[14] \qquad y = w^{-k} x + \frac{1 - w^{-k}}{a - b}$$

$$[15] \qquad y = (vw)^{-k} x + \frac{1 - (vw)^{-k}}{a + b + 2}$$

are obtained.

When $u^k \gg 1$, and $v^k \gg 1$, which are realized for longer period experiments

$$x = 1/(2a + 2)$$

and

$$y = 1/(a + b + 2)$$

Hence, from eq. [14], k is given by

$$[16] \qquad k = \frac{1}{T} \frac{2 \ln \left[\frac{(a + b + 2)^2}{4(a + 1)(b + 1)} \right]}{\bar{Y} - \eta a - (1 - \eta) b}$$

The approximate values of k based on eq. [16] are also listed in Table I.

The chain radical life time τ is defined (1) by

$$\tau = \frac{\text{No. of radicals per unit vol.}}{\text{No. of radicals disappearing per unit vol. per unit time}}$$

At steady state with continuous irradiation, τ is calculated by

$$[17] \qquad \tau = n/GI = \frac{2}{k(a + 2)}$$

Using eq. [17], the chain life time at 400 rad/min is found to be 0.25 s.

For reactions in which k is zero, by considering eqs. [18], [19], and [20] instead of eqs. [2], [7], and [8], I/K can be determined. This is equivalent to the method of Noyes and Leighton.

$$[18] \qquad X = F\sqrt{I}$$

$$[19] \qquad \frac{dX}{dt} = \frac{2I}{K}(c - X)(c + X)$$

$$[20] \qquad \frac{dX}{dt} = \frac{2I}{K}(d - X)(d + X)$$

where

$$F = K\left(\frac{G}{2}\right)^{\frac{1}{2}}$$

$$c = F\sqrt{I_1}$$

$$d = F\sqrt{I_2}$$

Acknowledgments

The authors appreciate the exchange arrangements made by the Takasaki Radiation Chemistry Research Establishment, Japan Atomic Energy Research Institute, and the University of Minnesota, and one of the authors wishes to thank Tomomichi Kasamatsu and Masaaki Takehisa for their encouragement.

1. W. A. Noyes and P. A. Leighton. The photochemistry of gases. Reinhold Publ. Corp., New York. 1941.

Can. J. Chem. Downloaded from www.nrcresearchpress.com by 210.87.254.42 on 09/05/12
For personal use only.

2. H. W. MELVILLE. Proc. Roy. Soc. **A163**, 511 (1937).
3. P. D. BARTLETT and C. G. SWAIN. J. Amer. Chem. Soc. **67**, 2273 (1945).
4. P. D. BARTLETT and C. G. SWAIN. J. Amer. Chem. Soc. **68**, 2377 (1946).
5. P. D. BARTLETT and C. G. SWAIN. J. Amer. Chem. Soc. **68**, 2381 (1946).
6. M. S. MATHESON, E. A. AUER, E. B. BEVILAQUA, and E. J. HART. J. Amer. Chem. Soc. **71**, 497 (1949).
7. G. R. FREEMAN, A. B. VAN CLEAVE, and J. W. T. SPINKS. Can. J. Chem. **32**, 322 (1954).
8. A. P. LOTZ and K. SCHMIDT. Nature, **201**, 493 (1964).
9. A. SHEPP. J. Chem. Phys. **24**, 939 (1956).
10. G. R. FREEMAN, A. B. VAN CLEAVE, and J. W. T. SPINKS. Can. J. Chem. **31**, 1164 (1953).
11. W. KAWAKAMI, K. YOSHIDA, and T. SUGO. Preprint of the 30th Annual Meeting of Soc. of Chem. Eng., Japan. 297 (1965).
12. R. G. MCINTOSH, R. L. EAGER, and J. W. T. SPINKS. Can. J. Chem. **42**, 2033 (1964).
13. H. L. ANDREWS and P. A. SHORE. J. Chem. Phys. **18**, 1165 (1950).

Can. J. Chem. Downloaded from www.nrcresearchpress.com by 210.87.254.42 on 09/05/12
For personal use only.

Can. J. Chem. Downloaded from www.nrcresearchpress.com by 210.87.254.42 on 09/05/12
For personal use only.

Kinetics of the reaction of methyl iodide with sulfite and thiosulfate ions in aqueous solution[1]

R. A. HASTY[2] AND S. L. SUTTER
Pacific Northwest Laboratory, Battelle Memorial Institute, Richland, Washington 99352

Received June 30, 1969

The rate of reaction of methyl iodide with sulfite ion is determined. In addition, the rate of reaction of methyl iodide with thiosulfate ion is reexamined and the rate of reaction of methyl iodide with bisulfite ion is estimated. A pronounced effect of ionic strength on the reaction rate in the methyl iodide – sulfite ion system is observed, this effect does not occur in the methyl iodide – thiosulfate ion system. The second order reaction rate constant and activation energy for the reaction of methyl iodide with the respective nucleophiles are: SO_3^{2-}, 4.4×10^{-2} M^{-1} s^{-1}, 18.6 kcal $mole^{-1}$; HSO_3^-, 1×10^{-3} M^{-1} s^{-1}, 18.4 kcal $mole^{-1}$; and $S_2O_3^{2-}$, 3.1×10^{-2} M^{-1} s^{-1}, 19.4 kcal $mole^{-1}$.

Canadian Journal of Chemistry, 47, 4537 (1969)

Introduction

The reaction of methyl iodide with nucleophiles such as sulfite, bisulfite, sulfate, or thiosulfate ions presents an opportunity to compare and correlate the reactivity with non-kinetic properties of these nucleophiles. The reaction of methyl iodide is the simplest of the nucleophilic displacement reactions of the alkyl halides and should be the most easily understood. Excellent correlation of the reaction rate constant with the oxidative dimerization potential (1) is obtained with a number of nucleophiles (2–4). Fluoride ion is the only exception to the correlation. The reaction rate of methyl iodide with thiosulfate ion has been reported (3, 4) and is reexamined in this work. The determination of the rates of reaction of sulfite, bisulfite, and thiosulfate ions with methyl iodide are reported in this paper. In addition, the effect of ionic strength on the reaction rate is determined for both the thiosulfate ion and sulfite ion reaction with methyl iodide. The comparison of the two reactions presents an extreme contrast in two reactions which in most aspects are very similar.

Experimental

The gas chromatographic system utilized in this study has been described (5). The preparation of methyl iodide solutions and the details of the kinetic measurements are also reported. The only unusual feature of the chromatographic separation and detection of the gas which exits from the reaction vessel containing acidic solutions (pH 4.5) from observations reported earlier is the appearance of the chromatographic peak due to SO_2. The elution of SO_2 from the chromatographic column occurs after the elution of O_2 and before the elution of CH_3I. A small caustic scrubber removes SO_2 from the gas stream. Methyl iodide is not removed by this scrubber.

Sodium sulfite, sodium bisulfite, and sodium thiosulfate, reagent grade, are used without purification to prepare the reaction solution. The total sulfite or thiosulfate concentrations of the reaction solutions are determined by titration with potassium iodate standard solutions in the presence of carbon tetrachloride. The disappearance of iodine from the carbon tetrachloride layer is taken to be the end point of the titration.

The determination of the rate of reaction of methyl iodide in very dilute solutions (ca. 10^{-8} M) has been described (5). The rate of disappearance of methyl iodide from the reaction solution, k_{obsd}, and the total amount of methyl iodide which is sparged from the reaction vessel are determined for at least four flow rates of the sparge gas. The rate of reaction of methyl iodide in the solution is obtained from a graphical representation of $(1/k_{obsd})$ vs. the amount of methyl iodide recovered from the reaction vessel.

Results

Preliminary experiments at 24.70 °C, a pH of 12.05, and 0.020, 0.040, and 0.080 M sulfite ion gave 0.84×10^{-3}, 1.65×10^{-3}, and 3.3×10^{-3} s^{-1} for the pseudo first order reaction of methyl iodide. This demonstrates that the rate expression is first order with respect to the sulfite ion concentration. Although these measurements are not obtained at constant ionic strength ($\mu = 0.11$, 0.17, and 0.29, respectively), subsequent measurements at constant ionic strength verify the conclusion. The lack of an ionic strength effect in these preliminary results is attributed to the small variation of ionic strength coupled with the experimental uncertainties. The rate expression is also first order with respect to the methyl iodide

[1]This paper is based on work performed under United States Atomic Energy Commission Contract AT(45-1)–1830.

[2]Present address: Department of Chemistry, Montana State University, Bozeman, Montana.

TABLE I

Rate constant of methyl iodide – sulfite and – bisulfite ion reaction at 24.73 ± 0.03 °C, and ionic strength and pH dependence

pH	[NaCl] (*M*)	[Na_2SO_4] (*M*)	Total SO_3^{2-} HSO_3^- (*M*)	μ	$k_2 \times 10^2$ (M^{-1} s^{-1})
11.65	0	0.100	0.0480	0.47	3.80
11.50	0.255	0.075	0.0481	0.62	3.40
11.55	0.150	0.100	0.0468	0.62	3.52
11.70	0	0.150	0.0476	0.62	3.57
11.70	0	0.103	0.0973	0.62	3.4
11.90	0	0	0.0742	0.32	3.9
11.75	0.10	0	0.0872	0.41	3.7
11.8	0.20	0	0.0944	0.51	3.5
11.7	0.50	0	0.0965	0.81	3.0
8.5	0.027*	0	0.053	0.30	3.9
8.0	0.038*	0	0.073	0.19	3.5
7.5	0.049*	0	0.066	0.24	3.2
7.12	0.060*	0	0.061	0.23	2.4
4.5	0	0	0.10	0.10	<0.4†
4.45	0	0	4.68	4.68	0.064

*NaCl formed by neutralization of NaOH with HCl.
†Estimate of rate constant only, higher HSO_3^- concentration needed (see next row).

concentration, as demonstrated by the exponential decrease of methyl iodide concentration from the reaction vessel.

The effects of pH, chloride ion concentration, and ionic strength on the reaction rate are determined. The results of these measurements are given in Table I. Hydrochloric acid is added in some experiments to partially neutralize the sodium hydroxide and obtain solutions of a desired pH. In order to determine the effect of chloride ion on the rate of reaction, the chloride ion concentration is varied. The second order reaction rate constant is reduced ca. 30% in these experiments. Since this reduction in the observed rate constant could be due either to the increase in chloride ion concentration or to the increased ionic strength of the solution, sodium sulfate is added to adjust the ionic strength of the solutions. These results demonstrate that the rate constant is decreased as the ionic strength of the solution is increased. They are displayed in Fig. 1.

The temperature dependence of the sulfite and bisulfite reactions with methyl iodide are determined from the measurement of the reaction rate of methyl iodide at 33 and 49 °C and are reported in Table II.

The rate of reaction of methyl iodide with sodium thiosulfate is determined at constant and variable ionic strength. The results of these measurements are reported in Table III.

Discussion

Thiosulfate, sulfite, and bisulfite ions react with methyl iodide by a simple displacement mechanism (S_N2). The kinetics of these processes are straight forward as are most displacement reac-

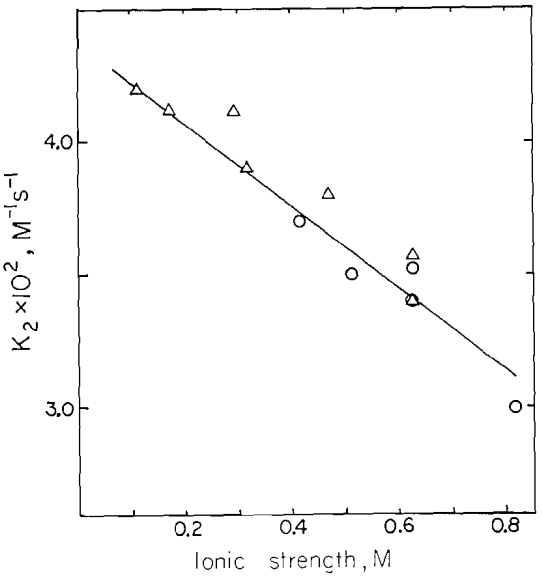

FIG. 1. Reaction rate constant for the methyl iodide – sulfite ion reaction as a function of ionic strength, △, Na_2SO_4 added; ○, NaCl and NaCl–Na_2SO_4 mixtures added.

Can. J. Chem. Downloaded from www.nrcresearchpress.com by 210.87.254.42 on 09/05/12
For personal use only.

TABLE II

Rate constant of methyl iodide – sulfite ion reaction at a pH of 12.1 ± 0.1, temperature dependence

$\Sigma[SO_3^{2-}]$ (M)	$k_r \times 10^3$ (s^{-1})	$k_2 \times 10^2$ ($M^{-1}\,s^{-1}$)	T (°C)	μ
0.0020	0.83	41.5	49.10	0.058
0.0037	1.57	42	49.11	0.064
0.0078	3.5	45	49.11	0.076
0.0214	1.78	8.3	33.35	0.11
0.0488	4.2	8.7	33.30	0.20
0.0089	0.77	8.6	33.80	0.079

TABLE III

Rate constant of methyl iodide – sodium thiosulfate reaction in 0.052 N sodium hydroxide solution

$[S_2O_3^{2-}]$ (M)	Ionic strength*	$k_r \times 10^3$ (s^{-1})	$k_2 \times 10^2$ ($M^{-1}\,s^{-1}$)
Temperature, 24.70 ± 0.02 °C			
0.0996	0.65	3.16	3.2
0.0505	0.65	1.51	3.0
0.0254	0.65	0.76	3.0
0.0103	0.65	0.31	3.0
0.0498	0.20	1.51	3.0
0.0500	0.35	1.58	3.2
0.0504†	0.15	1.70	3.4
0.0301†	0.165	0.96	3.2
Temperature, 33.28 ± 0.02 °C			
0.0251	0.20	2.0	8.0
0.03705	0.20	2.71	7.3
Temperature, 49.04 ± 0.04 °C			
0.00489	0.20	1.95	40.0
0.00292	0.20	0.99	34.0
0.00739	0.20	2.96	40.0

*Ionic strength adjusted by the addition of sodium sulfate.
†pH of 9.0 compared to 12.2 for 0.052 N sodium hydroxide solutions.

tions which involve methyl iodide (1, 3, 6). The only complication is the hydrolysis by hydroxide ion in the case of the slower reactions. The rate of reaction can be generalized in the form

$$[1] \quad -\frac{d[CH_3I]}{dt} = k_2[CH_3I][N] + k_h[CH_3I][OH^-]$$

where N represents the nucleophile.

In the case of the sulfite ion as the nucleophile, the sulfite–bisulfite equilibria profoundly affects the observed rate of reaction of methyl iodide as shown in Table I. In the case of the sulfite–bisulfite equilibria, the term which involves the nucleophile in eq. [1] is separated into two parts and the term which involves hydroxide is neglected.

$$[2] \quad -\frac{d[CH_3I]}{dt} = k_2'[CH_3I][N](x) + k_2''[CH_3I][N](1-x)$$

where [N] is the total sulfite–bisulfite ion concentration and x is the sulfite ion fraction of the total. In theory, the fraction of sulfite ion can be calculated from the dissociation constant (6) of bisulfite ion of 5.6×10^{-8} but, in practice, the ionic strength is too high to permit reliable estimation of the activity coefficients of bisulfite or sulfite ions. Reasonable agreement between the observed decrease in reaction rate and the fraction of sulfite ion is obtained when values of the activity coefficient calculated by the formula cited by Conway (7) are employed.

Although the bimolecular reaction rate constant for sulfite ion with methyl iodide can be

Can. J. Chem. Downloaded from www.nrcresearchpress.com by 210.87.254.42 on 09/05/12
For personal use only.

Can. J. Chem. Downloaded from www.nrcresearchpress.com by 210.87.254.42 on 09/05/12
For personal use only.

determined, the bimolecular reaction rate constant for bisulfite ion with methyl iodide can only be approximated. At a pH of 4.5, the sulfite ion composes approximately 1% of the total bisulfite–sulfite concentration when the equilibrium constant is considered and activity coefficients are estimated as before. Thus, the bimolecular reaction rate constant for bisulfite ion with methyl iodide of 0.064 M^{-1} min^{-1} is only an upper limit. It should be noted that this value is close to that predicted by the Edwards correlation (1). The high ionic strength of the bisulfite solutions which is required because of the low reactivity of bisulfite ion with methyl iodide also requires that caution be used when stating this reaction rate constant.

In the case of thiosulfate ion, the dissociation constant of bithiosulfate ion (6) is 10^{-2}. The bithiosulfate ion is less than 1% of the thiosulfate concentration at pH greater than 4.

The effect of ionic strength is first noted in the studies which involved the dependence of reaction rate of sulfite–bisulfite with methyl iodide upon the pH. Extension of the ionic strength studies is made for both the sulfite and thiosulfite reaction with methyl iodide at high pH to preclude the formation of other species. The two reactions, i.e., sulfite – methyl iodide and thiosulfate–methyl iodide, although quite similar (both are reactions of dinegatively-charged ion with a dipole reaction and both have the same order-of-magnitude reaction rate constant), exhibit extremely contrasting dependence upon ionic strength.

The thiosulfate – methyl iodide reaction rate constant is $(3.1 \pm 0.1) \times 10^{-2}$ M^{-1} s^{-1} at 24.70 °C which is in excellent agreement with previously reported values (3, 4) at much higher methyl iodide concentrations (10^{-2} M compared to 10^{-8} M in this work). The reaction rate constant is independent of ionic strength up to an ionic strength of 0.65.

In contrast, the sulfite ion – methyl iodide reaction rate constant is very strongly dependent upon ionic strength of the solution as shown in Fig. 1. The Hückel extension of the Debye–Hückel treatment for activity coefficients (ref. 8, p. 229) to include a second term $b\mu$, where b is a constant which is related to the dielectric saturation of the medium and μ is the ionic strength of the medium, is an attempt to explain the effect of ionic strength on ion–dipole reactions. The relationship can then be derived that

$$\log k\mu = \log k_0 + \Delta b\mu \quad [3]$$

where k is the reaction rate constant (at ionic strength μ or zero) and Δb is the difference of the constant, b, between the transition state and the reactants. For Δb much less than unity the expression can be written as

$$k\mu = k_0 + \Delta b\mu \quad [4]$$

Normally Δb is small and there is little or no dependence of the rate constant of an ion–dipole reaction on the ionic strength as in the case of the thiosulfate – methyl iodide reaction. In the case of the sulfite – methyl iodide reaction, Δb is sufficiently large to cause the decrease of reaction rate constant for the sulfite – methyl iodide reaction to be nearly as large as in ion–ion reactions (ref. 8, p. 219).

An alternative quantitative treatment such as proposed by Amis (9) results in too small a predicted decrease of the reaction rate constant for the sulfite – methyl iodide reaction (10% decrease going from ionic strength of 0 to 1 as compared to ca. 40% decrease observed). Perhaps the principal reason for the poor quantitative correlation is the inability to accurately estimate values of the dielectric constant and distance of closest approach of the ion and dipole.

Extrapolation of the rate constant presented in Fig. 1 in accord with eq. [4] gives the bimolecular reaction rate constant at zero ionic strength and 24.7 °C to be 4.4×10^{-2} M^{-1} s^{-1}.

The activation energies of the reaction are summarized in Table IV. For the thiosulfate – methyl iodide reaction the activation energy of 19.44 ± 0.89 kcal $mole^{-1}$ is somewhat higher

TABLE IV

Summary of Arrhenius parameters for various nucleophiles

Nucleophile	k_2 at 25 °C (mole l^{-1} s^{-1})	$\log_{10} A$ (mole l^{-1} s^{-1})	E_a (kcal $mole^{-1}$)
SO_3^{2-}	4.4×10^{-2}	12.3	18.6 ± 0.6
HSO_3^-	1×10^{-3}	10.5	~ 18.4
$S_2O_3^{2-}$	$(3.1 \pm 0.1) \times 10^{-2}$	12.75	19.4 ± 0.9

but in agreement with 18.88 kcal mole^{-1} previously reported. The activation energy of the sulfite – methyl iodide reaction is 18.6 $\pm$ 0.6 kcal mole^{-1}. The activation energy of the bisulfite – methyl iodide reaction is ca. 18.4 kcal mole^{-1} but, because of the uncertainty of the sulfite ion contribution, this value is only an approximation.

1. J. O. EDWARDS. J. Amer. Chem. Soc. **76**, 1540 (1954).
2. E. A. MOELWYN-HUGHES. Proc. Roy. Soc. Ser. A, **220**, 386 (1953). R. H. BATHGATE and E. A. MOELWYN-HUGHES. J. Chem. Soc. 2647 (1938). E. A. MOELWYN-HUGHES. J. Chem. Soc. 779 (1959). B. W. MARSHALL and E. A. MOELWYN-HUGHES. J. Chem. Soc. 7119 (1965). R. A. OGG. J. Amer. Chem. Soc. **60**, 2000 (1938). G. C. LALOR and E. A. MOELWYN-HUGHES. J. Chem. Soc. 2201 (1965).
3. A. SLATOR. J. Chem. Soc. **85**, 1286 (1904).
4. E. A. MOELWYN-HUGHES. Proc. Roy. Soc. Ser. A, **196**, 540 (1949).
5. R. A. HASTY. J. Chem. Phys. **73**, 317 (1969).
6. L. G. SILLEN and A. E. MARTELL. Stability constants of metal–ion complexes. Special Publication No. 17, Chem. Soc. London. 1964.
7. B. E. CONWAY. Electrochemical data. Elsevier Publishing Co., New York. 1952. p. 102.
8. K. J. LAIDLER. Chemical kinetics. 2nd ed. McGraw-Hill Book Co., Inc., New York. 1968.
9. E. S. AMIS. Kinetics of chemical change in solution. The MacMillan Company, New York. N.Y. 1949. pp. 165–174.

Can. J. Chem. Downloaded from www.nrcresearchpress.com by 210.87.254.42 on 09/05/12
For personal use only.

Can. J. Chem. Downloaded from www.nrcresearchpress.com by 188.143.235.115 on 09/06/12
For personal use only.

Chelate-exchange titrimetry in nonaqueous solvents. I. Determination of dithizone and metal dithizonates

PETER GREY AND G. C. B. CAVE
Department of Chemistry, McGill University, Montreal, Quebec

Received[1] December 7, 1967

A new spectrophotometric titration method is proposed for determination of the amounts of metal chelates present in nonaqueous solvents. The titrant is a standard solution of a chelating agent which quantitatively displaces the chelate anion of the metal chelate. The method is exemplified by the titration of μg amounts of the dithizonates of Ag, Pb, Cu(II), Cd, Zn, and In in chloroform, both in the absence and the presence of free dithizone. Some binary and ternary mixtures were also successfully analyzed for the individual metal dithizonates. The titrant was a standard solution of sodium diethyldithiocarbamate in ethanol. Precision and accuracy were good. The preparation and analysis of the metal dithizonates are described. New titrimetric procedures are also proposed and shown to be satisfactory for determination of the free dithizone content of a chloroform solution.

Canadian Journal of Chemistry, 47, 4543 (1969)

Introduction

The present work demonstrates that a chelating agent in a nonaqueous solvent can be a useful titrant for metal chelates present in low dielectric-constant solvents. The overall reaction is the quantitative replacement of the chelate anion of the undissociated metal chelate by the titrant. The term chelate-exchange titration seems appropriate. The example studied is the spectrophotometric titration of μg amounts of the dithizonates of Ag, Pb, Cu(II), Cd, Zn, and In in chloroform; the titrant was sodium diethyldithiocarbamate in ethanol. The initial presence of free dithizone in the chloroform solution was found not to affect the accuracy of the results.

Růžička and Starý (1) were the first to suggest the possibility of using chelate-exchange titrations, in particular for the determination of the metal content of the organic solvent phase from a solvent extraction procedure. Extraction of metals as neutral, undissociated chelates into low dielectric-constant solvents is widely used as a separation procedure. The choice of dithizonates for the present study was dictated by the wide use of dithizone in solvent extractions.

In analytical chemistry, chelating agents have been used chiefly as selective precipitants for metals present in aqueous solution. Their use as titrants has not been widely exploited, and apparently not at all when the sample for titration was a metal chelate in a low dielectric-constant solvent. Brummet and Hollweg (2) quantitatively formed, with a given metal salt, a metal chelate in 4:1 benzene–methanol by addition of a chelating agent. They then determined the liberated hydrogen ions by a conventional potentiometric titration. Underwood and Underwood (3) determined metal 8-hydroxyquinolates by a conductometric titration with potassium methoxide in ethylenediamine. Chelating agents have also been used as titrants in spectrophotometric titrations of metals, mostly in aqueous solutions. For example, aminocarboxylic acids have been widely used as titrants in aqueous solutions (4, 5). Several workers (6–10) have titrated metal ions directly with organic chelating agents, in nonaqueous solvents. However, they used ionizing solvents which dissolved and dissociated the metal salt prior to titration. Accordingly, their technique differs in an important way from the proposed chelate-exchange method.

Experimental

Apparatus

Spectrophotometric Titration Assembly

A Beckman Model DU manual spectrophotometer with a conventional tungsten lamp source was used, but the Beckman cell compartment was replaced by a specially constructed one.

The special cell compartment was made of nonmagnetic material and was light tight. Its shape and dimensions duplicated those of the conventional Beckman compartment for cells of 100 mm path length. It accommodated one 65 ml rectangular glass titration cell of path length 50 mm, flanked by 2 hollow rectangular copper tanks through which constant-temperature water was circulated. The temperature of the thermostatted solution in the cell was measured with a copper–constantan thermocouple. However, close temperature control would be

[1]Revision received July 24, 1969.

Can. J. Chem. Downloaded from www.nrcresearchpress.com by 188.143.235.115 on 09/06/12
For personal use only.

unnecessary in many practical titrations. The shutter opening of the Beckman phototube compartment was covered with a thin, fused-silica plate which prevented any organic solvent vapors from entering the phototube compartment.

A 1 in. × 1/8 in. disk of silicone elastomer was countersunk in the removable lid of the cell compartment and covered a hole bored vertically through the center of the lid. Through this disk, a platinum–rhodium needle which served as the buret tip was inserted so that the tip of the needle was below the surface of the solution for titration.

A calibrated 1 ml Koch microburet with a detachable tip and a Luer joint at the tip was used to deliver the titrant. This buret had a 2-way Teflon stopcock and a 60 ml reservoir for titrant. The glass capillary tip normally supplied with the buret was replaced by a stiff platinum–rhodium hypodermic needle 2 in. long and 28 standard gauge bore. This needle was fitted with a Kel-F Luer joint to provide a direct, tight fitting connection to the buret[2].

Titration cells were of 2 capacities. For macrotitrations, a 65 ml rectangular glass cell was used. For microtitrations, a conventional cuvet, 10 mm × 10 mm × 45 mm high, was used in a Plexiglass frame that fitted snugly between the 2 copper tanks that comprized the thermostat in the cell compartment.

The macro and micro cells had covers to prevent evaporation of solvent. Each cover consisted of a sandwich of 1/8 in. silicone elastomer between two 1/8 in. aluminum plates bolted together. Coincident holes bored through the centers of the aluminum plates, but not through the elastomer, allowed the buret needle and the thermocouple wires to be passed through the silicone septum into the titration cell. A thin smear of silicone grease placed along the top edge of the cell prior to a titration provided an effective seal between the cell and this cover.

Stirring of the solution during a titration was with a conventional magnetic stirrer mounted immediately under the cell compartment. For the macro cell, a 1/2 in. Teflon-coated magnetic bar was used, and for the micro cell, a specially made 1/4 in. bar.

Glassware

All volumetric glassware was calibrated with the solvent used.

Red, low-actinic glass 50 ml and 100 ml volumetric flasks and 125 ml separatory funnels with Teflon stopcocks were used for solutions of dithizone and metal dithizonates.

Glassware that had contained nonaqueous solutions of metal dithizonates and metal 8-hydroxyquinolates was found to have a thin adhering film of the metal chelate that was very difficult to remove by customary washing techniques. An effective washing technique was the following. The glassware was rinsed first with acetone, then with water. It was then filled with a warm 4:1 mixture of concentrated sulfuric acid – concentrated nitric acid, and left for 1 h. After draining, it was thoroughly rinsed, first with ion-exchanged water, then with absolute alcohol. It was air dried for ordinary use; but for studies with very dry solvents, dry nitrogen was used instead of air.

Reagents

Solvents

Chloroform and carbon tetrachloride were Analar grade, further purified according to the method of Biddle (11). To the final chloroform distillate, 1% of ethanol was added as a preservative.

Methanol (Fisher) and ethanol (Gooderham and Worts) were absolute grade, used without further purification.

Benzene was Fisher "Spectranalysed" grade. Further purification was unnecessary; purified dithizone was not measurably oxidized by this solvent sample, over a period of 1 month.

Solids

Diphenylthiocarbazone (dithizone) was Fisher reagent grade, further purified before use. The major impurity was the oxidation product, diphenylthiocarbadiazone. Purification was carried out entirely in subdued light and in low-actinic glassware. The method of Mathre and Sandell (12) was used, with Barnes' modification (13) that the sulfur dioxide was added as a saturated aqueous solution, instead of as a gas. For a product of highest purity, the above procedure had to be carried out in its entirety 3 times; 4 times were used in the present work. The product was stable when stored in a tightly stoppered bottle in the dark. Its purity was determined by 2 methods: (*i*) gravimetric determination of sulfur as $BaSO_4$, after oxidation of the solid sample with a mixture of concentrated nitric acid and solid potassium chlorate (14) (Anal. Calcd. S in $C_{13}H_{12}N_4S$, 12.51%. Found: 12.48 ± 0.06%); (*ii*) spectrophotometric titration of a solution of the sample in benzene, the titrant being a 4×10^{-4} *M* standard solution of silver nitrate in a 1:20 methanol–benzene solvent. The procedure is original, and is given below. The product assayed 99.93 ± 0.22% dithizone by this method.

Sodium diethyldithiocarbamate was Fisher reagent grade, further purified by 2 recrystallizations from ethanol. The product was collected on a glass frit, washed with ice-cold ethanol, and dried in vacuo over Drierite for a week (15). Its purity was determined by 2 methods: (*i*) gravimetric determination of sodium as Na_2SO_4 by a conventional procedure (16) (Anal. Calcd. Na in $C_5H_{10}NS_2Na$: 13.42%. Found: 13.39 ± 0.08%); (*ii*) gravimetric determination of the diethyldithiocarbamate radical by precipitation with cupric ion (17) (Anal. Calcd. $C_5H_{10}NS$: 86.58%. Found: 86.56 ± 0.19%).

Dithizonates of Ag(I), Pb, Cu(II), Cd, Zn, and In were prepared by following the procedure described by Mathre and Sandell (12) for the preparation of lead dithizonate. The starting materials were specially purified metal salts and purified dithizone; the chloroform and carbon tetrachloride solvents were also purified as described above. The final products were dried in a stream of dry nitrogen in a dry-box, then in vacuo over potassium hydroxide for 2 weeks in the dark. All the operations were carried out in subdued light, and the vessels were of red, low-actinic glass. The prepared solids were stable when stored in tightly stoppered bottles in the dark.

The purity of the prepared metal dithizonates was determined by 2 methods.

[2]Needles fitted with joints were obtained from the Hamilton Company, Whittier, California.

Can. J. Chem. Downloaded from www.nrcresearchpress.com by 188.143.235.115 on 09/06/12
For personal use only.

(*i*) Assay for the metal, after decomposition of the chelate by wet oxidation with a 1:1 mixture of concentrated nitric acid and 30% (vol.) hydrogen peroxide (18). At least 3 such treatments were found necessary for complete decomposition, with evaporation of the solution to moist dryness after each treatment; 4 treatments were used as a precaution. Even then, decomposition of indium dithizonate was incomplete; evaporation to fumes of concentrated sulfuric acid was a necessary additional step. Because the zinc assay was by polarography, decomposition of its dithizonate was by a different method, namely 4 evaporations to moist dryness with aqua regia; the sodium stannate present as a preservative in the hydrogen peroxide would have interfered in the polarographic analysis.

(*ii*) Spectrophotometric titration of the dithizone liberated on treating the lead, zinc, cadmium, and indium dithizonates with acid. Thus, the solid sample was mechanically shaken for 6–12 h with 50 ml of 0.1 *N* hydrochloric acid containing 1% of a saturated aqueous solution of sulfur dioxide and 50 ml of benzene in a low-actinic glass flask. The sulfur dioxide prevented air oxidation of the liberated dithizone (13). The dithizone in an aliquot of the benzene phase was then titrated with a 4×10^{-4} *M* standard solution of silver nitrate in a 1:20 methanol–benzene mixture. The detailed procedure is given below. In the case of silver dithizonate, the dithizone was liberated for titration by using a 6% solution of potassium iodide in 0.25 *N* sulfuric acid, as recommended by Irving and Ramakrishna (19). Chloroform solutions of primary and secondary dithizonates of copper(II) were not decomposed by diluted acid. Therefore, a gravimetric analysis supplanted the spectrophotometric titration; the sulfur was determined as $BaSO_4$, after oxidation of the chelate.

The results of the analyses of the metal dithizonates by the 2 procedures described above are given in Table I.

Standard Solutions

(a) Sodium diethyldithiocarbamate, 2.5×10^{-3} M in Ethanol

A 0.025 *M* stock solution of sodium diethyldithiocarbamate in ethanol was prepared from a weighed amount of the purified, dried salt. Working standard solutions were prepared by 10- and 100-fold dilution of the stock solution with ethanol and were standardized by a spectrophotometric titration procedure described below. All solutions were freshly prepared each day, because they were found to deteriorate with time.

(b) Metal dithizonates, 5×10^{-5} N in Chloroform

Standard solutions were prepared in chloroform from accurately weighed amounts of the prepared salts. Preparations were done in subdued lighting, and solutions were kept in red, low-actinic glassware. Aliquots of the standard solutions were taken in replicate for standardization by the following methods: (*i*) For dithizonates of Pb, Cd, Zn, and In, the aliquot was shaken with 0.1 *N* hydrochloric acid. The aqueous phase, containing the metal, was separated and after conventional treatment it was assayed polarographically for the metal. (*ii*) For primary and secondary dithizonates of copper(II), the aliquot was evaporated to dryness. The residue was decomposed by wet oxidation with a 1:1 mixture of concentrated nitric acid and 30% hydrogen peroxide by following the procedure described above for the assaying of solid metal dithizonates for the metal. The final

TABLE I

Analysis of metal dithizonates

Metal dithizonate	Analytical method for the metal	Metal, %			Dithizonate radical, %			Purity of metal dithizonate,‡ %
		Calcd.	Found*	*s*†	Calcd.	Found	*s*†	
AgHDz	Gravimetric, as AgCl	29.73	29.61	0.03	70.27	70.13	0.13	99.74
$Pb(HDz)_2$	Gravimetric, as $PbSO_4$	28.87	28.75	0.10	71.13	70.90	0.24	99.70
	Gravimetric, as $PbCrO_4$		28.80	0.05				
$Cd(HDz)_2$	Electrolytic	18.04	17.88	0.05	81.96	81.60	0.31	99.89
	Volumetric, by EDTA		17.93	0.07				
$Zn(HDz)_2$	Volumetric, by $K_4Fe(CN)_6$	11.35	11.27	0.08	88.65	88.52	0.20	99.79
	Volumetric, by EDTA		11.20	0.08				
$In(HDz)_3$	Gravimetric, as In_2O_3	13.03	12.86	0.04	86.97	87.00	0.22	99.83
CuDz	Electrolytic	20.00	19.91	0.03	10.09§	10.08§	0.11§	99.93
	Gravimetric, as α-benzoin oximate		19.93	0.08				
$Cu(HDz)_2$	Electrolytic	11.08	10.94	0.02	11.18§	11.15§	0.14§	99.90
	Gravimetric, as α-benzoin oximate		10.98	0.08				

*Mean of 5 determinations.
†Standard deviation, based on 4 degrees of freedom.
‡Based on the assay result for the dithizonate radical, in the preceding column.
§These values are for % sulfur, rather than % dithizonate as above.

residue was taken up with 2 ml of concentrated hydrochloric acid, evaporated to moist dryness, and then taken up with 0.1 *N* hydrochloric acid. The copper was determined colorimetrically by using zinc dibenzyldithiocarbamate (20). (*iii*) For silver dithizonate, the aliquot was shaken with a 6% solution of potassium iodide in 0.25 *N* sulfuric acid. The aqueous phase, containing the silver, was separated and evaporated to dense fumes. The cooled residue was processed by a conventional procedure, and a final nitrate solution was assayed polarographically for silver (21).

Analytical Procedures

General Procedure for Chelate-Exchange Titrations (Procedure I)

In the present investigation, the procedure has been applied to the titration of metal dithizonates in chloroform with standard solutions of sodium diethyldithiocarbamate in ethanol. However, it apparently is of rather general validity for nonaqueous chelate-exchange titrations.

The Beckman spectrophotometer with the special cell housing was used. For some titrations the wavelength chosen was 615 mμ, the absorbance peak for free dithizone; for others it was the absorbance peak of the metal dithizonate being titrated.

The spectrophotometric blank was purified chloroform in the titration cell. The spectrophotometer was adjusted for this blank prior to the titration, and checked for absence of drift by reinserting the blank after the titration.

The 1 ml Koch microburet was rinsed and filled with titrant (sodium diethyldithiocarbamate in ethanol). An aliquot of the chloroform solution of the metal dithizonate for analysis was transferred by pipet into the 65 ml titration cell and then diluted to 50 ± 2 ml with purified chloroform.

Stirring with the magnetic stirrer was adjusted to a rapid rate and was continuous throughout the titration. The sandwich cover of the titration cell (with thermocouple leads in place when registration of temperature was required) was placed on the cell and the lid of the compartment was put in place. The microburet was clamped in position, with the platinum–rhodium needle pushed through the silicone elastomer septum of the compartment lid and the cell cover so that the needle tip dipped into the solution for titration.

Titrations were performed with the cell compartment thermostatted at 25 °C. However, for purely practical titrations, close control of temperature was unnecessary; variations of ± 3 °C did not affect the results.

Constant increments of titrant were added, and the absorbance was read after each addition. Since the total volume of titrant was only about 0.25 ml, it was unnecessary to apply a dilution correction to the absorbance readings.

A plot of absorbance vs. volume of titrant gave the titration graph. The equivalence point was found by extrapolation of the 2 straight line arms of the graph. By drawing these arms by eye, a satisfactory estimate of the equivalence point was obtained. However, in the present work, the equivalence point was found by algebraic solution of the least-squares equations for the 2 straight line arms of the graph.

Titrations were also performed in the 4.5 ml titration cell. The sample volume was 2.5 ml. The procedure was that used for the 65 ml cell, except that the cell was housed in the Plexiglass frame mentioned above, and also it was necessary to correct the absorbance readings for dilution of the sample by the titrant.

Spectrophotometric Titration of Dithizone Solutions (Procedure II)

A rapid, accurate method was developed for the determination of dithizone in benzene.

Reagent grade silver nitrate was recrystallized twice from water, dried at 110 °C, then for 15 min at 225 °C. This product was used as a primary standard.

An 8×10^{-3} *M* stock standard solution of silver nitrate in methanol was prepared, and an aliquot was diluted 20-fold with benzene to provide the working standard solution. All solutions were stored in red, low-actinic glassware. The stock solution was stable for at least a month. The working solution was prepared fresh daily, because its titer was found to decrease significantly after about 48 h.

For the titration, a 100 μl sample of the benzene solution of dithizone was transferred to the 65 ml titration cell by using a calibrated, self-filling micropipet reserved exclusively for dithizone solutions. Fifty ml of benzene were added. The 1 ml Koch microburet contained the working standard solution of silver nitrate in 1:2 methanol–benzene. The titration was carried out by following Procedure I, above. The spectrophotometric blank was benzene. The wavelength setting was 618 mμ, at which the molar absorptivity of dithizone was 3.47×10^4 and that of silver dithizonate was negligibly small.

Standardization of Diethyldithiocarbamate Solutions (Procedure III)

A rapid, accurate method was developed for the standardization of ethanol solutions of sodium diethyldithiocarbamate.

A 1.8×10^{-4} *M* standard solution of copper(II) nitrate in ethanol was prepared from British Drug Houses electrolytic grade metal, which was the primary standard. The weighed metal was dissolved in 1:1 nitric acid and the solution was evaporated to moist dryness. The residue was dissolved in water and the solution again evaporated to moist dryness. The residue was dissolved and diluted to volume with ethanol.

A measured aliquot of the standard solution of copper(II) nitrate was transferred to the 65 ml titration cell and diluted to 50 ml with ethanol. The 1 ml Koch microburet contained the sodium diethyldithiocarbamate solution to be standardized.

The titration was carried out by following Procedure I, above. The spectrophotometric blank was ethanol. The wavelength setting was 435 mμ, which was the absorption peak of copper diethyldithiocarbamate in ethanol.

Tests for Equilibrium

In the titration of the metal dithizonates in chloroform by sodium diethyldithiocarbamate, tests confirmed that equilibrium existed at each stage of the titration. Thus, increments of a standard solution of the titrant, corresponding to 0.5, 1.0, and 1.5 equivalents of metal dithizonate taken, were added to the latter solution in the titration cell thermostatted at 25 °C. Absorbance measurements were made over a 2 h period. For the metal dithi-

Can. J. Chem. Downloaded from www.nrcresearchpress.com by 188.143.235.115 on 09/06/12
For personal use only.

zonates studied, namely those of Ag, Pb, Cu(II), Cd, Zn, and In, equilibrium was reached almost instantaneously, and the absorbance readings remained constant thereafter for the 2 h period.

Choice of Wavelength

Titrations of the metal dithizonates were conducted at 2 wavelengths in the visible region. One was at the absorption peak of the metal dithizonate, and the other was at 615 mμ, which is a peak of dithizone. The diethyldithiocarbamates of sodium and of the titrated metals other than copper absorb only in the ultraviolet region; the use of this region is not explored in the present paper.

Results and Discussion

Standarization of Sodium Diethyldithiocarbamate Solutions

The precision and accuracy of the proposed method were measured. Aliquots of a 1.8×10^{-4} *M* standard solution of $Cu(NO_3)_2$ in ethanol were titrated against 2.5×10^{-3} and 2.3×10^{-4} *M* standard solutions of sodium diethyldithiocarbamate in ethanol by following Procedure III, above. The results are given in Table II, and a typical titration graph is shown in Fig. 1. Both the precision and the accuracy are good.

Standardization of Dithizone Solutions

Heretofore, the so-called extractive titration with silver nitrate (12, 19, 22) apparently was the only method available for the standardization of dithizone solutions. The presently proposed method avoids the disadvantages of the extractive titration method and is rapid and convenient to use.

The titer of the 8×10^{-3} *M* standard stock solution of silver nitrate in methanol was measured by high-frequency titrimetry (23), at intervals over a period of a month. When the standard solution was stored in low-actinic glassware, the total change over the month was less than 0.1%; when stored in ordinary glassware, it was about 0.6%. The standard working solution was prepared by dilution of the 8×10^{-3} *M* stock solution with benzene in the ratio 1:20. This solution was prepared fresh daily for use. Over a 12 h period, the titer changed by less than 0.1%. Over a 30 day period it changed by about 1%.

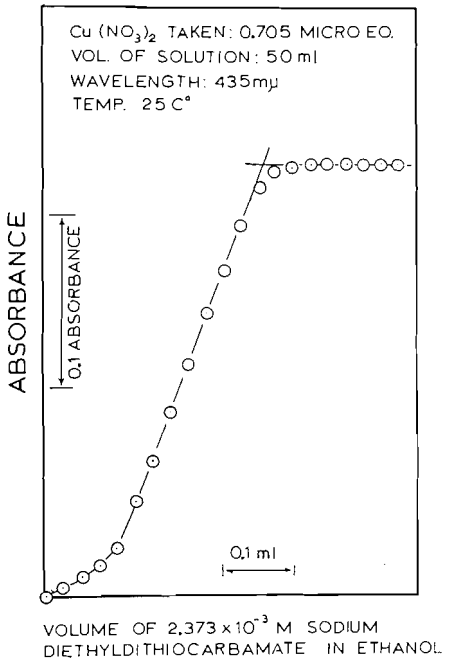

FIG. 1. Typical titration graph for the standardization of an ethanol solution of sodium diethyldithiocarbamate with copper(II) nitrate in ethanol.

The precision and accuracy of the proposed method were measured. Thus, aliquots of a 2×10^{-3} *M* standard stock solution of dithizone in benzene were diluted with benzene to provide 2×10^{-4} and 2×10^{-5} *M* standard solutions. The molarities of these 3 standard solutions were checked by measuring their absorbances at

TABLE II

Precision and accuracy of standardization of ethanol solutions of sodium diethyldithiocarbamate by spectrophotometric titration*

Aliquot of Cu solution taken ml	*M*, titrant		
	Found†	*s*‡	Taken§
1.98 ±0.02	2.346×10^{-3}	0.015×10^{-3}	2.373×10^{-3}
0.197±0.002	2.344×10^{-4}	0.029×10^{-4}	2.373×10^{-4}

*Sample solution, 1.762×10^{-4} *M* standard solution of copper(II) nitrate in ethanol; titrant, sodium diethyldithiocarbamate in ethanol; initial volume of solution, 50 ml; path length, 50 mm; wavelength, 435 mμ.
†Mean of 10 determinations.
‡Standard deviation of *M* found, based on 9 degrees of freedom.
§Calculated on the basis of the sodium diethyldithiocarbamate reagent being 100% pure.

Can. J. Chem. Downloaded from www.nrcresearchpress.com by 188.143.235.115 on 09/06/12
For personal use only.

TABLE III

Precision and accuracy of standardization of benzene solutions of dithizone, by spectrophotometric titration*

Dithizone M	Solution 1 $M \times 10^3$	Solution 2 $M \times 10^4$	Solution 3 $M \times 10^5$
Found†	1.915	1.926	1.918
s‡	(0.034)	(0.031)	(0.026)
Calcd. from absorbance	1.923	1.920	1.929
Calcd. from wt. of dithizone taken§	1.927	1.927	1.927

*Titrant, 4.013×10^{-4} M standard solution of $AgNO_3$ in 1:20 methanol–benzene; initial volume, 50 ml; path length, 50 mm; wavelength, 618 mμ.
†Mean of 11 determinations.
‡Standard deviation of M found.
§Based on the dithizone being 100% pure.

TABLE IV

Chelate-exchange titration of metal dithizonates in chloroform, with standard solutions of sodium diethyldithiocarbamate in ethanol, at 25 °C

Dithizonate	Dithizonate taken (μeq) Macro*	Micro*	Initial molar ratio (Dithizone/metal dithizonate)	Wavelength (mμ)	Dithizonate found† (μeq) Macro		Micro	
AgHDz	0.2286	0.02286	0	615	0.231	(0.0088)	0.0233	(0.0011)
				465	0.230	(0.0092)	0.0466‡	(0.0008)
			2	615	0.234	(0.0033)	0.0235	(0.0012)
				465	0.234	(0.0065)	0.0471‡	(0.0006)
			4	615	0.237	(0.0063)	0.0241	(0.0012)
				465	0.236	(0.0042)	0.0479‡	(0.0012)
$Pb(HDz)_2$	0.2286	0.02286	0	615	0.231	(0.0070)	0.0228	(0.0011)
				510	0.226	(0.0056)	0.0222	(0.0010)
			2	615	0.229	(0.0068)	0.0224	(0.0012)
				510	0.240	(0.0087)	0.0226	(0.0009)
			4	615	0.226	(0.0104)	0.0225	(0.0010)
				510	0.233	(0.0046)	0.0220	(0.0012)
$In(HDz)_3$	0.2811	0.02811	0	615	0.278	(0.011)	0.0274	(0.0010)
				510	0.278	(0.0070)	0.0268	(0.0010)
			3	615	0.275	(0.0084)	0.0263	(0.0014)
				510	0.282	(0.0092)	0.0272	(0.0010)
			6	615	0.278	(0.0056)	0.0268	(0.0012)
				510	0.271	(0.0073)	0.0267	(0.0009)
$Cu(HDz)_2$	0.2618	—	0	615	0.263	(0.010)		
				545	0.268	(0.0064)		
			4	615	0.261	(0.0062)		
				545	0.270	(0.0100)		
$Cd(HDz)_2$	0.2840	—	0	615	0.286	(0.0074)		
				518	0.280	(0.0067)		
			4	615	0.278	(0.0051)		
				518	0.276	(0.0082)		
$Zn(HDz)_2$	0.2946	—	0	615	0.290	(0.0059)		
				530	0.279	(0.0066)		
			4	615	0.286	(0.0082)		
				530	0.287	(0.0100)		

*Nominal molarity of titrant in ethanol, 2.4×10^{-3} M (macrotitrations), 2.4×10^{-4} M (microtitrations); initial volume of solution in titration cell, 50 ml (macro), 2.5 ml (micro); path length of titration cell, 50 mm (macro), 10 mm (micro).
†Mean of 6 determinations in the case of macrotitrations of Ag, Pb, and In; mean of 4 determinations in the case of macrotitrations of Cu, Cd, and Zn, and in the case of all microtitrations. Standard deviations, in parentheses, are for $N - 1$ degrees of freedom.
‡0.04572 μeq. dithizonate taken.

Can. J. Chem. Downloaded from www.nrcresearchpress.com by 188.143.235.115 on 09/06/12
For personal use only.

Can. J. Chem. Downloaded from www.nrcresearchpress.com by 188.143.235.115 on 09/06/12
For personal use only.

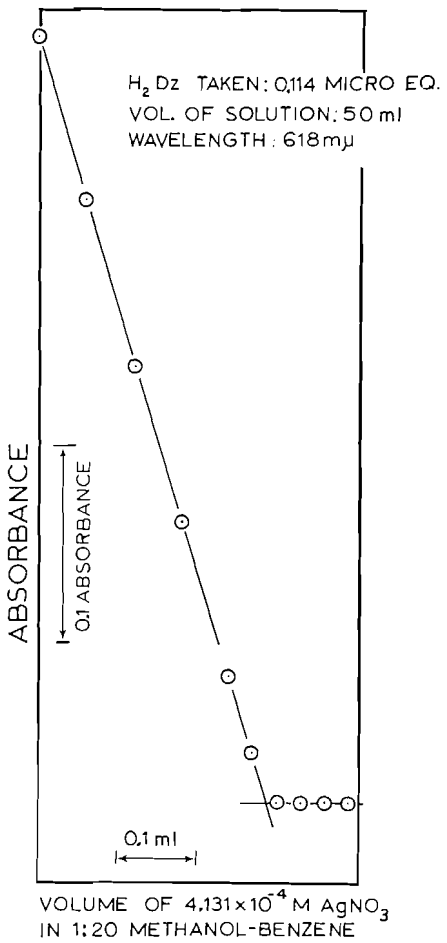

FIG. 2. Typical titration graph for the standardization of a benzene solution of dithizone with a standard solution of $AgNO_3$ in 1:20 methanol–benzene.

618 mμ, the molar absorptivity of dithizone being known. Replicate aliquots, 0.1 ml for the 2×10^{-3} *M* solution, 1 ml and 10 ml, respectively, for the other 2 solutions, were diluted to 50 ml with benzene. The resulting solutions were titrated by Procedure II, using a 4×10^{-4} *M* standard solution of silver nitrate in 1:20 methanol–benzene. The results are in Table III. A typical titration graph is shown in Fig. 2.

The precision of the method is good. Based on the dithizone reagent being 100% pure, the accuracy also is good; dithizone purity has been noted above. The molarities of the dithizone solutions as found from the measured absorbances at 618 mμ merely provide confirmation of the values given for the concentrations of the standard solutions.

Titration of Metal Dithizonates with Sodium Diethyldithiocarbamate

Aliquots of 5×10^{-5} *N* standard solutions of the primary dithizonates of Ag, Pb, Cu(II), Cd, Zn, and In in chloroform were separately titrated in replicate against a standard solution of sodium diethyldithiocarbamate in ethanol. For titrations in the 65 ml cell, 5 ml aliquots were diluted to 50 ml with chloroform; for titrations in the 4.5 ml cell, 0.5 ml aliquots were diluted to 2.5 ml. The general procedure for chelate-exchange titrations (Procedure I) was used. The metal dithizonates had been purified and analyzed (Table I). The titrant had been standardized by Procedure III. The titrations were performed at 2 wavelengths: (*i*) 615 mμ, the absorption peak of free dithizone in chloroform; (*ii*) the absorption peak of the primary metal dithizonate.

The titration results are in Table IV. Typical titration graphs for titrations performed at the absorption peak of the metal dithizonate are shown in Fig. 3. Also shown in this figure is a titration graph typical of all titrations performed at 615 mμ.

The degree of curvature in the titration graph around the end point decreased in the order

$$Ag > Zn \approx Cd > Pb > In > Cu$$

The dithizonates of Hg(II), Bi, Co(II), and Ni gave titration graphs with such excessive curvature that the arms could not be extrapolated to a precise intersection point. Their study was therefore not pursued.

In applications of chelate-exchange titrimetry, an initial excess of dithizone may be present in the nonaqueous solution of the metal dithizonate. Table IV shows that precision and accuracy are good up to at least a 4-fold initial excess of dithizone over metal dithizonate, and 6-fold in the case of indium. At the sample concentrations used, an excess of dithizone greater than 4-fold produced absorbance readings greater than 2, except for indium. The 4-fold initial excess of dithizone increased very slightly the curvature of the silver dithizonate titration graph; the increase in curvature was still less for the other metals, and least for copper(II).

In exploratory studies, several binary and

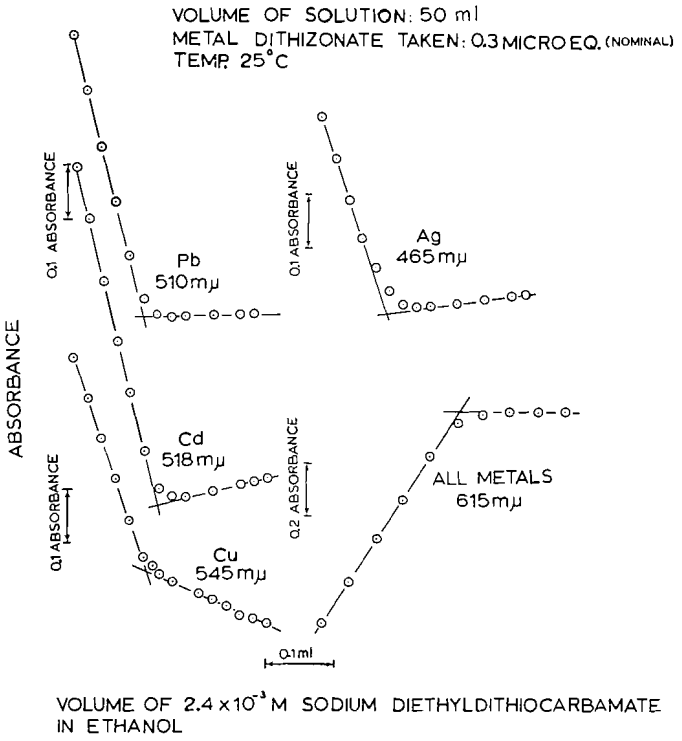

FIG. 3. Typical titration graphs for the chelate-exchange titration of metal dithizonates in chloroform with a standard solution of sodium diethyldithiocarbamate in ethanol.

TABLE V

Chelate-exchange titrations of mixtures of metal dithizonates in chloroform, with standard solutions of sodium diethyldithiocarbamate in ethanol, at 25 °C*

Dithizonates mixture†	Wavelength (mμ)	Dithizonate Taken (μeq)	Dithizonate Found‡ (μeq)	Standard deviation	% difference
Pb	570	0.3070	0.300	0.014	−2.2
Pb + Ag		0.5922	0.603	0.016	1.8
In	510	0.3736	0.363	0.012	−2.8
In + Pb		0.6806	0.676	0.0050	−0.7
Cu	530	0.2618	0.269	0.010	2.8
Cu + Zn		0.5412	0.552	0.011	2.0
Cu	518	0.2618	0.234	0.014	−10.6
Cu + Cd		0.5458	0.544	0.0080	−0.3
Cu	465	0.2618	0.260	0.0096	−0.8
Cu + Ag		0.5200	0.530	0.0060	2.0
Cu	530	0.2618	0.265	0.015	1.3
Cu + Zn		0.5564	0.596	0.017	7.0
Cu + Zn + Cd		0.8404	0.861	0.0076	2.4
Cu	510	0.2618	0.260	0.012	−0.6
Cu + Pb		0.5688	0.600	0.015	5.6
Cu + Pb + Zn		0.8634	0.850	0.0063	−1.6
Cu	510	0.2618	0.267	0.010	1.8
Cu + Pb		0.5688	0.565	0.013	−0.7
Cu + Pb + Ag		0.8540	0.906	0.0066	6.1

*Molarity of titrant in ethanol, 2.803×10^{-3} *M* (binary), 2.536×10^{-3} *M* (ternary); initial volume of solution in titration cell, 50 ml; path length of titration cell, 50 mm.
†Tabulated in the order in which the end points occurred.
‡Mean of 3 determinations. Standard deviations are for 2 degrees of freedom.

Can. J. Chem. Downloaded from www.nrcresearchpress.com by 188.143.235.115 on 09/06/12
For personal use only.

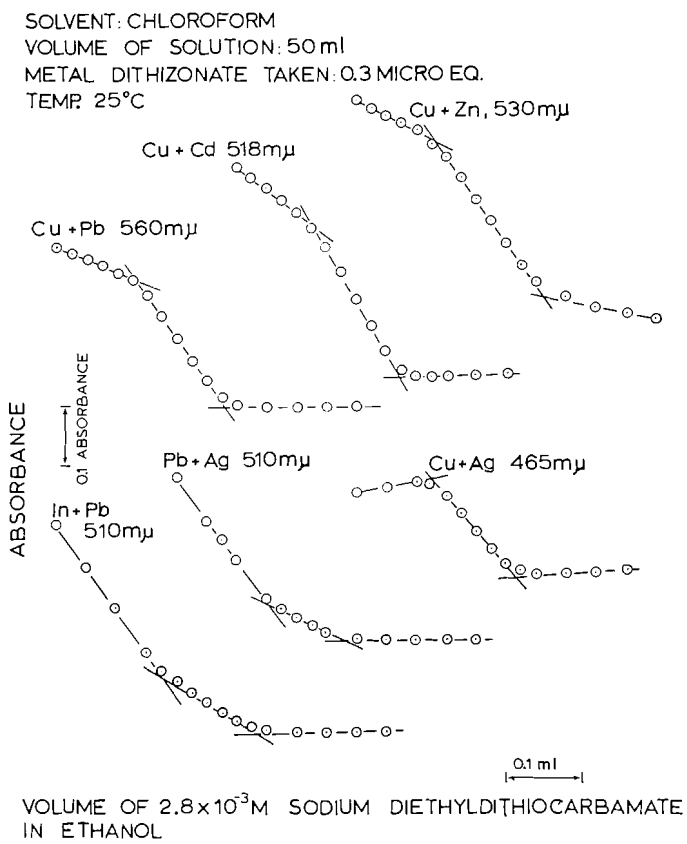

FIG. 4. Typical titration graphs for the chelate-exchange titration of binary mixtures of metal dithizonates in chloroform with a standard solution of sodium diethyldithiocarbamate in ethanol.

ternary mixtures of metal dithizonates in chloroform were titrated against sodium diethyldithiocarbamate in ethanol. The following 1:1 or 1:1:1 mixtures gave indefinite end points due to the curvature of the arms of the titration graph: Ag–Zn, Ag–Cd, Zn–Cd, Zn–Pb, Ag–Zn–Cd, Ag–Zn–Pb, Ag–Zn–Cu, Ag–Cd–Pb, and Zn–Cd–Pb. However, the mixtures listed in Table V gave satisfactory end points; but only equi–equivalent ratios were studied.

Typical titration graphs for mixtures are shown in Figs. 4 and 5. In these figures, the metals are listed in the order of appearance of their end points.

In the titration of a mixture, 1 wavelength was in general found to give much sharper end points than other possible choices. For example, for ternary mixtures, the best wavelength was that of the absorption peak of the second metal dithizonate titrated. All the graphs in Figs. 4 and 5 are for the best wavelength.

Factors Affecting the Shape of Titration Graphs

In the absence of side reactions, sodium dithizonate would be a product of the titrations. Its existence was not proven in the present work. However, the titrated solutions were green at the end point and absorbed strongly at 615 mμ, the peak for dithizone. Moreover, Fig. 3 shows no change immediately after the end point, and the absorptivity calculated therefrom agrees reasonably well with that of dithizone.

If the dithizonate product and reactant are NaHDz and $M(HDz)_n$ respectively, then one of the factors that would determine the slope of the first arm of the titration graph would be

$$a_{NaHDz} - a_{M(HDz)_n}/n$$

where a denotes molar absorptivity. This quantity was approximately calculated for the titration graphs of single metal dithizonates, on the basis of available data. The absorptivities of the metal dithizonates in chloroform had been measured

Can. J. Chem. Downloaded from www.nrcresearchpress.com by 188.143.235.115 on 09/06/12
For personal use only.

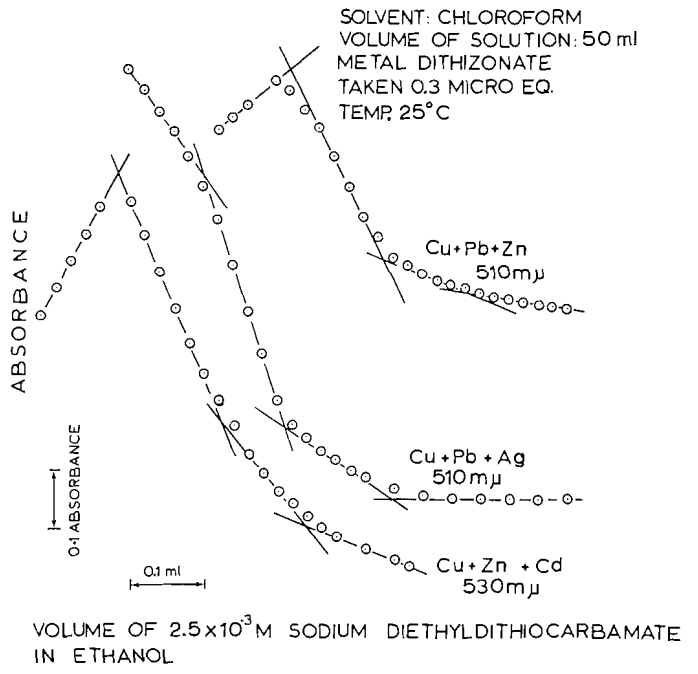

FIG. 5. Typical titration graphs for the chelate-exchange titration of ternary mixtures of metal dithizonates in chloroform with a standard solution of sodium diethyldithiocarbamate in ethanol.

in this laboratory, but instead of the unavailable absorptivity of sodium dithizonate, that of dithizone in benzene was used. The calculated values differed by about 50% from the values read from the titration graphs. Moreover, the nonzero slopes of the second arms of the titration graphs for copper and cadmium in Fig. 3 were not explained; zinc also had a nonzero slope.

In the titration of binary mixtures, the ratio of the slopes of the first and second arms of the titration graphs (Fig. 4) were in moderate agreement with values calculated from absorptivities as outlined above; but the absolute slopes were out by 50–100%. Finally, in the titration of ternary mixtures, the slopes of the arms of the titration graphs are anomalous with respect to the titration graphs of single metals.

The nature of the species participating in these chelate-exchange reactions, including intermediates and adducts, together with the relevant equilibrium constants, are required before the titration graphs can satisfactorily be predicted.

Acknowledgments

We are grateful to the National Research Council of Canada for financial support and to the Province of Quebec for a scholarship to one of us (P.G.).

1. J. RŮŽIČKA and J. STARÝ. Talanta, **14**, 909 (1967).
2. B. D. BRUMMET and R. M. HOLLWEG. Anal. Chem. **28**, 448 (1956).
3. E. E. UNDERWOOD and A. L. UNDERWOOD. Talanta, **3**, 249 (1960).
4. J. B. HEADRIDGE. Photometric titrations. The Pergamon Press, Ltd., New York. 1961.
5. G. SCHWARZENBACH. Complexometric titrations. Interscience Publishers, Inc., New York. 1957.
6. W. G. BOYLE, JR. and R. J. ROBINSON. Anal. Chem. **30**, 958 (1958).
7. T. L. MARPLE, G. MATSUYAMA, and L. W. BURDETT. Anal. Chem. **30**, 937 (1958).
8. I. T. TAKAHASHI and R. J. ROBINSON. Anal. Chem. **32**, 1350 (1960).
9. R. K. BEHM and R. J. ROBINSON. Anal. Chem. **35**, 1010 (1963).
10. P. LE GOFF and B. TRÉMILLON. Bull. Soc. Chim. 350 (1964).
11. D. A. BIDDLE. Ind. Eng. Chem., Anal. Ed. **8**, 99 (1936).
12. O. B. MATHRE and E. B. SANDELL. Talanta, **11**, 295 (1964).
13. H. BARNES. Analyst, **72**, 469 (1947).
14. Treatise on analytical chemistry. Vol. 12, Part II. *Edited by* I. M. Kolthoff and P. J. Elving. Interscience Publishers, Inc., New York. 1965.
15. H. BODE. Z. Anal. Chem. **142**, 414 (1954).
16. Scott's standard methods of chemical analysis. Vol. I, 6th ed. *Edited by* N. H. FURMAN. D. Van Nostrand Co. Inc., New York. 1962.

Can. J. Chem. Downloaded from www.nrcresearchpress.com by 188.143.235.115 on 09/06/12
For personal use only.

17. J. B. DUBSKY. Mikrochem. **28**, 145 (1940).
18. Y. TSUCHITANI, Y. TOMITA, and K. UENO. Talanta, **9**, 1023 (1962).
19. H. IRVING and R. S. RAMAKRISHNA. Analyst, **85**, 40 (1960).
20. R. I. MARTENS and R. E. GITHENS. Anal. Chem. **24**, 991 (1952).
21. G. C. B. CAVE and D. N. HUME. Anal. Chem. **24**, 588 (1952).
22. O. A. WEBER and V. B. VOUK. Analyst, **85**, 40 (1960).
23. P. GREY and G. C. B. CAVE. Can. J. Chem. **42**, 770 (1964).

Can. J. Chem. Downloaded from www.nrcresearchpress.com by 188.143.235.115 on 09/06/12
For personal use only.

Can. J. Chem. Downloaded from www.nrcresearchpress.com by 210.87.254.40 on 09/05/12
For personal use only.

Chelate-exchange titrimetry in nonaqueous solvents. II. Determination of 8-quinolinol and metal 8-quinolinates

PETER GREY AND G. C. B. CAVE
Department of Chemistry, McGill University, Montreal, Quebec

Received[1] December 7, 1967

Chelate-exchange titrimetry has been applied to the determination of μg amounts of some metal 8-quinolinates in benzene. The titrant was a standard solution of diphenylthiocarbazone in benzene. Accuracy and precision were good in the cases of Pb, Cu(II), Cd, Zn, and In. Very slow reaction rates made titrations of Ag and Ni impracticable, and chelate-exchange was negligible in the case of Co(II). A new titrimetric method is also shown to be precise and accurate for the determination of free 8-quinolinol in benzene; the titrant was a standard solution of $Cu(NO_3)_2$ in ethanol.

Canadian Journal of Chemistry, 47, 4555 (1969)

Introduction

In a previous communication (1), a new type of titrimetric analysis was described, namely, the spectrophotometric titration of a metal chelate in a low dielectric-constant solvent with a standard solution of a chelating agent in a nonaqueous solvent. It was exemplified by the titration of some metal dithizonates in chloroform with a standard solution of sodium diethyldithiocarbamate in ethanol.

In the present investigation, the method has been applied to the determination of μg amounts of metal 8-quinolinates in benzene by titration with a standard solution of diphenylthiocarbazone in benzene. New features, not observed in the previous metal dithizonate titration, were evident in the present systems. In particular, some limitations of the general method of chelate-exchange titrimetry are exemplified and studied in detail. The larger values of the equilibrium constants and the faster reaction rates of the metal dithizonate – sodium diethyldithiocarbamate systems made a study of these factors less convenient in this system than in the present system.

Experimental

Apparatus

The spectrophotometric titrations were performed by using the previously described apparatus (1) without modification. The macro titration cells were 65 ml, the micro cells, 4.5 ml.

All glassware was specially cleaned, and volumetric glassware was calibrated, in the manner previously described (1). Red, low-actinic glass 50 ml and 100 ml volumetric flasks and 125 ml separatory funnels with Teflon stopcocks were used for the light sensitive solutions of diphenylthiocarbazone, 8-quinolinol, and the metal 8-quinolinates.

[1]Revision received July 24, 1969.

Reagents

Solvents

Benzene was Fisher "Spectranalysed" grade. Further purification was found to be unnecessary; purified dithizone was not measurably oxidized by this solvent sample, over a period of 1 month. For some experiments, the benzene was dried before use by percolation twice through fresh columns of silica gel, followed by treatment with calcium hydride (2). Water was not found in the dried product by a Karl Fischer potentiometric titration (3).

Ethanol was "absolute" reagent grade, used without further purification.

Water was purified by distillation, followed by passage through a 46 cm long column of Fisher "Rexyn" 1-300 research grade, mixed-bed ion-exchange resin. The metal content of the product was found to be negligible on testing with diphenylthiocarbazone in carbon tetrachloride.

Carbon tetrachloride was Analar grade, further purified as previously described (1).

Solids

Diphenylthiocarbazone (hereafter called dithizone) was reagent grade, further purified by using a previously described procedure (1). The product was stored in a tightly stoppered bottle in the dark.

8-Quinolinol (hereafter called oxine) was reagent grade, further purified by recrystallization from ethanol, followed by vacuum sublimation of the product at 100 ± 1 °C (4). The sublimed crystals were dried in vacuo over Drierite for 2 weeks in the dark and then stored in the dark. They assayed 100 ± 0.2% by a conventional bromometric method (5). The m.p. was 75.6–76.1 °C; lit. 75.8 °C (6).

The oxinates of Ag, Pb, Cu(II), Cd, Zn, Co(II), Ni(II), and In were prepared according to the respective procedures described by Hollingshead (7). The starting materials were the purified oxine and reagent grade metal salts that were further purified by standard methods. The purity of these starting materials was checked by analysis.

Each of the prepared metal oxinates was analyzed for metal content and for oxine content. For the metal assays, replicate samples were decomposed with a mixture of concentrated nitric acid and 30% hydrogen peroxide as previously described (1) for the decomposition

Can. J. Chem. Downloaded from www.nrcresearchpress.com by 210.87.254.40 on 09/05/12
For personal use only.

of metal dithizonates. Whereas the dithizonates required repetitive treatment with the mixture in order to effect complete decomposition, the oxinates needed only one treatment. The assay methods were conventional ones; they are tabulated along with the analytical results in Table I. The oxine content of the metal oxinate was determined on a separate sample by a colorimetric procedure described below (Procedure I). Results are in Table I.

Standard Solutions

Standard solutions of dithizone, 1×10^{-3} *M*, were prepared in benzene and stored in red, low-actinic glassware. These solutions were standardized against a standard solution of silver nitrate in ethanol by using a previously described spectrophotometric titration procedure (1).

Standard solutions of oxine in benzene were prepared from accurately weighed amounts of the analyzed solid. They were standardized by Procedure II, below.

Standard stock solutions of the metal oxinates in benzene were prepared as saturated solutions at 25 °C. From these solutions, standard 5×10^{-5} *N* working solutions were prepared in benzene and standardized. In the case of zinc, cadmium, and nickel oxinates, the "Spectranalysed" grade benzene contained enough water to have produced the less soluble dihydrates of the metal oxinates. These dihydrates become anhydrous only at 130 °C, the drying temperature used in the preparation of the solids. Therefore, in order to get sufficiently high concentrations, the standard solutions of these oxinates were prepared with the specially dried benzene, in a dry box flushed with dry nitrogen.

Miscellaneous Reagents

Sodium hydroxide, used in the preparation of cadmium dithizonate, was prepared from reagent grade sodium chloride by passage through a column of Amberlite IRA-410 resin in the hydroxide form (10). The product was stored in polypropylene.

Ammonia and hydrochloric acid were reagent grade, further purified by conventional distillation into previously steamed polyethylene bottles. The products, after adjustment of pH where necessary, were shown to be free from heavy metals by shaking them with a carbon tetrachloride solution of dithizone.

Nitric acid and sulfuric acid were Nichols reagent grade, used without further purification. Each new bottle of acid was tested for metals with dithizone, after appropriate initial treatment. In every case, the metal content introduced by these acids during an analysis that employed them was less than the standard deviation for that analytical method.

The other reagents were reagent grade, used without further purification.

Standardization of Metal Oxinate Solutions

Aliquots of each standard solution were evaporated to dryness. Except for lead, zinc, and cadmium, the residues were then decomposed by the 1:1 mixture of concentrated nitric acid and 30% hydrogen peroxide used in the analysis of the solids. Decomposition of lead oxinate was unnecessary. For zinc and cadmium oxinates, decomposition was effected by repeated use of aqua regia; the sodium stannate present as a preservative in the hydrogen peroxide would have interfered in the subsequent polarographic analysis for zinc and cadmium.

The subsequent treatment of the residues depended on the metal, as follows

Silver

The residue was dissolved in water, the solution carefully neutralized with ammonia, then diluted to volume with a 1:1 mixture of 1 *M* potassium nitrate and 1 *M* potassium thiocyanate, and the silver determined by polarography (13).

Lead

The residue was both dissolved and diluted to volume with 0.1 *N* hydrochloric acid, and the lead determined polarographically after addition of gelatin as a maximum suppressor.

Copper(II)

The residue was dissolved in concentrated hydrochloric acid and the solution evaporated to dryness. The residue was dissolved in 0.1 *N* hydrochloric acid, and the copper

TABLE I

Analysis of solid metal oxinates

Metal oxinate	Analytical method	Metal assays, % metal		Oxinate assays, % oxinate	
		Calcd.	Found*	Calcd.	Found*
$PbOx_2$	Gravimetric, as $PbSO_4$ (8)	41.82	41.73±0.14	58.18	58.22±0.11
	Gravimetric, as $PbCrO_4$ (8)		41.80±0.07		
$ZnOx_2$	Titrimetric, with $K_4Fe(CN)_6$ (8)	18.48	18.45±0.08	81.52	81.54±0.11
	Titrimetric, with EDTA (9)		18.54±0.07		
$CdOx_2$	Electrolytic (8)	28.04	28.01±0.06	71.96	71.94±0.13
	Titrimetric, with EDTA (9)		27.95±0.09		
$CuOx_2$	Electrolytic (8)	18.06	18.06±0.03	81.94	81.88±0.15
	Gravimetric, with α-benzoin oxime (8)		18.11±0.08		
$InOx_3$	Gravimetric, as In_2O_3 (8)	20.97	20.95±0.02	79.05	79.09±0.15
$AgOx \cdot HOx$	Gravimetric, as AgCl (8)	28.46	28.55±0.04	71.49	71.40±0.13
$CoOx_2$	Electrolytic (8)	16.97	16.94±0.06	83.06	83.07±0.10
$NiOx_2$	Gravimetric, with dimethylglyoxime (8)	16.92	16.89±0.08	83.08	83.01±0.13

*Mean of 5 assays. The values after the ± signs are the standard deviations.

Can. J. Chem. Downloaded from www.nrcresearchpress.com by 210.87.254.40 on 09/05/12
For personal use only.

extracted with four 5 ml portions of a 1% solution of zinc dibenzyldithiocarbamate in carbon tetrachloride (11). The combined organic phases were diluted to volume, and the absorbance was read at 435 mμ.

Cadmium

The residue was treated and analyzed by the procedure used for lead oxinate.

Zinc

The residue was both dissolved and diluted to volume with a 1:1 mixture of 1 *M* ammonia – 1 *M* ammonium chloride, and the zinc determined polarographically after addition of gelatin as a maximum suppressor.

Nickel

After solution of the residue in concentrated ammonium hydroxide, the nickel was determined colorimetrically at 445 mμ by the dimethylglyoxime method (15).

Cobalt

The cobalt in the dissolved residue was determined colorimetrically, by the conventional nitroso-R-salt method (14).

Indium

The residue was both dissolved and diluted to volume with 2.5 *N* hydrochloric acid which contained 4% of hydrazine hydrochloride, 20 ml of a saturated aqueous solution of sodium formate per 100 ml of solution, and 0.04% starch. The indium was then determined by polarography (12).

Colorimetric Determination of Oxine in a Metal Oxinate (Procedure I)

Use was made of the quantitative conversion of oxine and metal oxinates into H_2Ox^+ ions in 0.1 *N* hydrochloric acid. This ion has two absorption peaks, one at 358 mμ ($a \sim 1660$) and another at 252 mμ ($a \sim 43\,000$) (16). The colorimetric analysis described here is essentially that proposed by Deterding and Harding (17) for the determination of magnesium oxinate.

Replicate 0.1 g samples of the solid were both dissolved and diluted to volume with 0.1 *N* purified hydrochloric acid, in red, low-actinic 100 ml volumetric flasks. An aliquot was diluted exactly 20-fold with 0.1 *N* hydrochloric acid, in a similar flask. Its absorbance was read against 0.1 *N* hydrochloric acid, at 358 mμ in a 10 mm cuvet. The calibration curve was prepared from standard solutions of the purified oxine reagent (as primary standard) in 0.1 *N* hydrochloric acid. Beer's law was obeyed.

Spectrophotometric Titration of Oxine Solutions (Procedure II)

The method was similar to that previously developed for the determination of the dithizone content of chloroform solutions (1), except that the titrant was copper(II) nitrate in ethanol.

A 2×10^{-3} *M* standard solution of copper(II) nitrate in ethanol was prepared from British Drug Houses electrolytic grade metal, which was the primary standard. The weighed metal was dissolved in 1:1 nitric acid, and the solution was evaporated to moist dryness. The residue was dissolved in water, and the solution was again evaporated to moist dryness. The residue was dissolved and diluted to volume with ethanol.

The titration apparatus and procedure were identical to those reported for the determination of dithizone (1). Thus, an aliquot of the oxine solution in benzene was pipetted into a 65 ml titration cell and diluted to 50 ml with benzene. It was then titrated with the 2×10^{-3} *M* standard solution of copper(II) nitrate in ethanol. The spectrophotometric blank was benzene. The wavelength was set at 420 mμ, the absorption peak of copper(II) oxinate in benzene; the molar absorptivity was 5900. The products of the titration were undissociated nitric acid and copper(II) oxinate.

General Procedure for Chelate-Exchange Titrations (Procedure III)

Titrations of metal oxinates, except those of zinc and cadmium, were carried out by using the apparatus and procedure previously described (1) for the titration of metal dithizonates, but in the present case, the titrant was dithizone and the solvent was benzene.

For a macrotitration, a 5 ml aliquot of a 5×10^{-5} *N* solution of the metal oxinate in benzene was diluted to 50 ± 0.2 ml with benzene in the 65 ml titration cell; for a microtitration, a 0.5 ml aliquot was diluted to 2.5 ± 0.01 ml in the 4.5 ml cell. These solutions were thermostatted at 25 °C for titration. The small dilution tolerances of ±0.2 ml and ±0.01 ml were chosen so as to permit use of the data for other, theoretical purposes not reported here; for practical titrations, tolerances of ±2 ml and ±0.1 ml are suggested. Temperature control, also, was to enable other, theoretical use to be made of the data; otherwise, variations of at least ±3 °C could be tolerated during a titration.

The titrants were 1×10^{-3} *M* (macro) and 1×10^{-4} *M* (micro) standard solutions of dithizone in benzene. Titrations were conducted in a dark room lit only by a 40 W red light bulb placed near the titration apparatus. This light source was shown not to change the titer of the dithizone solutions over an 8 h period.

Chelate-Exchange Titration of Zinc and Cadmium Oxinates (Procedure IV)

Procedure III was followed, except for the program used to introduce the titrant. For titrations at 618 mμ, where only dithizone absorbs, an accurately measured excess of titrant was added all at once to the metal oxinate solution in the titration cell; usually about 50% excess was added. The resulting solution was allowed to stand for 20 min, thermostatted at 25 °C for cadmium and 42 °C for zinc. Then several measured increments of titrant were added in the usual way from the microburet, in order to obtain points for the second branch of the titration graph. Because the slope and the absorbance of the first branch were 0, extrapolation of the second branch back to the volume-of-titrant axis gave the end point.

For titrations at the wavelength of the absorption peak of the metal dithizonate, the titration was essentially as in Procedure III. The titration was begun by adding a few increments of titrant over a 10 min period, in order to obtain the first branch of the titration graph. Then a measured excess of titrant was added all at once, in order to carry the titration well past the end point. The reaction was then left for 20 min. Finally, a few additional increments were added at the normal rate, in order to obtain the second branch of the titration graph.

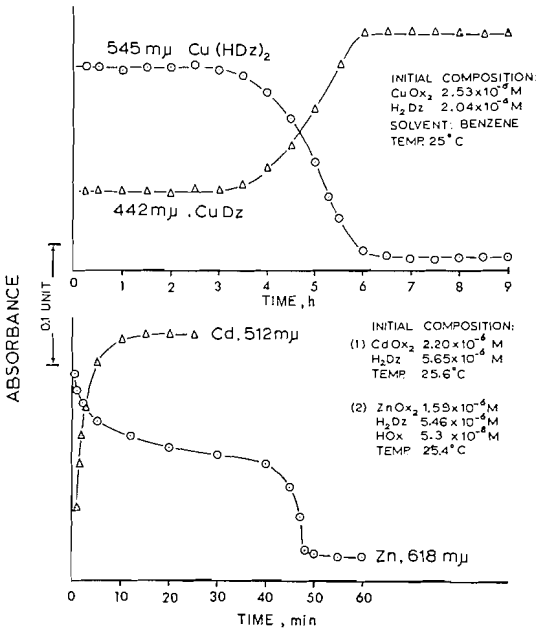

FIG. 1. Reaction rates in benzene for some metal oxinates with dithizone, at 25 °C.

Tests for Equilibrium

Benzene solutions of dithizone were mixed separately with benzene solutions of the oxinates of lead, copper(II), and indium, in the molar ratios 2:1, 1:1, and 1:2. In all cases, constant absorbance readings were obtained almost instantaneously, and no change was observed thereafter over a 2 h period. However, the copper(II) system was not in equilibrium. In Fig. 1, absorbance readings for the copper oxinate – dithizone system are shown over a 9 h period. One curve shows the absorbance readings at 545 mμ, which is the absorption peak of primary copper(II) dithizonate. The other curve is at 442 mμ, which is an absorption peak of secondary copper(II) dithizonate. Advantage was taken of the essentially constant absorbance readings over the first 2 h to perform titrations that proved to be entirely reliable. An explanation of the rate curves will be given elsewhere.

The reactions of dithizone with zinc and cadmium oxinates were too slow for direct titrations to be useful; rate curves for them are also in Fig. 1. The reaction mechanisms were not sought in the present work. Due to the slowness of these rates, a modified form of Procedure III was necessary for titrations and it is given in Procedure IV. It gave entirely satisfactory results, although it is somewhat inconvenient.

The reactions of dithizone with silver(I) oxinate and with nickel oxinate were much slower than with zinc oxinate; titrations were impracticable. Finally, dithizone apparently did not react at all with cobalt(II) oxinate.

Results and Discussion

Determination of Oxine in Solutions

The precision and accuracy of Procedure II, above, were measured. A 10^{-2} *M* standard stock solution of oxine in benzene was prepared from an accurately weighed amount of the purified solid, which assayed 100 ± 0.2%. Standard working solutions were prepared by accurate dilution of the stock solution with benzene. Aliquots of these working solutions were diluted to 50 ml with benzene, then were titrated spectrophotometrically at 420 mμ against a 2×10^{-3} *M* standardized solution of copper(II) nitrate in ethanol by following Procedure II. The results are in Table II. Precision and accuracy evidently are good.

A typical titration graph is shown in Fig. 2. For the data in Table II, the first break was taken as the end point. This first break occurred when the molar ratio of copper to oxine was 1:2; the second break occurred when this ratio was 1:1. The slope of the first branch corresponded to the molar absorptivity of $CuOx_2$. Therefore, it is proposed that the first break represents the formation of $CuOx_2$. The further addition of an equal amount of copper(II) nitrate led to the second break, at which the absorbance was 1/2

TABLE II

Determination of oxine in stock benzene solutions by spectrophotometric titration at 25 °C with a standard solution of copper(II) nitrate in ethanol*

Aliquot of oxine solution ml	*M*, taken 1.070×	*M*, found†	Standard deviation
0.196 ± 0.001	10^{-2}	1.066×10^{-2}	0.020×10^{-2}
1.000 ± 0.004	10^{-3}	1.059×10^{-3}	0.014×10^{-3}
1.998 ± 0.007	10^{-4}	1.053×10^{-4}	0.013×10^{-4}

*Molarity of $Cu(NO_3)_2$ solution, 2.080×10^{-3} *M*; volume of solution for titration, 50 ml; spectrophotometric path length, 50 mm; wavelength, 420 mμ.
†Mean of 5 determinations.

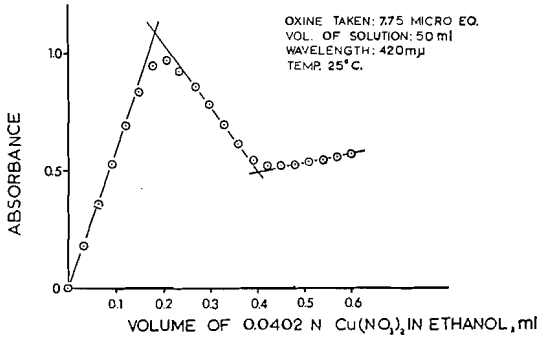

FIG. 2. Typical titration graph for the standardization of a benzene solution of oxine with a standard solution of copper(II) nitrate in ethanol.

Can. J. Chem. Downloaded from www.nrcresearchpress.com by 210.87.254.40 on 09/05/12
For personal use only.

TABLE III

Chelate-exchange titrations of metal oxinates in benzene with standard solutions of dithizone in benzene, at 25 °C*

Oxinate	Metal oxinate taken, μeq. Macro	Micro	Initial molar ratio (HOx/metal oxinate)	Metal oxinate found, μeq. Macro 618 mμ	Macro *X* mμ†	Micro 618 mμ	Micro *X* mμ†
$PbOx_2$	0.3020	0.03020	0	0.295	0.304	0.0300	0.0302
			25	0.299	0.308	0.0305	0.0308
			50	0.298	0.304	—	—
			100	0.297	0.309	0.0307	0.0304
				(25×10^{-6})‡		(1.8×10^{-6})	
$CdOx_2$	0.2204	0.01102	0	0.223	0.222	0.0112	0.0111
			25	0.224	0.222	0.0112	0.0112
			50	0.224	0.224	—	—
			100	0.227	0.226	0.0113	0.0113
				(18×10^{-6})		(0.15×10^{-6})	
$ZnOx_2$‖	0.1592	0.01592	0	0.161	0.164	0.0163	0.0164
			§	0.159	0.163	0.0161	0.0165
			50	0.161	0.168	0.0162	0.0164
				(10×10^{-6})		(0.25×10^{-6})	
$CuOx_2$	¶	0.03463	0			0.0347	0.0349
			42.6			0.0351	0.0362
			106.6			0.0364	0.0376
						(0.95×10^{-6})	
$InOx_3$	0.2656	0.02656	0	—	0.118	—	0.0119
			20	—	0.142	—	0.0144
			50	—	0.149	—	0.0151
				(14×10^{-6})		(0.24×10^{-6})	

*Nominal molarity of titrant, 1×10^{-3} *M* (macro), 1×10^{-4} *M* (micro); nominal normality of metal oxinate solution, 5×10^{-6} *N* (macro), 1×10^{-5} *N* (micro); volume of solution for titration, 50 ml (macro), 2.5 ml (micro); spectrophotometric path length, 50 mm (macro), 10 mm (micro). Each analytical result is the mean of 5 determinations.
†*X* = 517, 512, 528, 545, and 505 for Pb, Cd, Zn, Cu, and In oxinates, respectively.
‡Numbers in parentheses are pooled variances for the preceding set of values.
§Initial molar ratio was 30 for the macro- and 10 for the micro-titrations.
‖Titrated at 42 °C.
¶For macrotitrations, see Table IV.

that for the first break. It is suggested that the second break may therefore be due to the conversion of $CuOx_2$ into $[CuOx^+, NO_3^-]$ ion pairs.

Titration of Metal Oxinates by Dithizone

The results of replicate macro- and micro-titrations of the oxinates of Pb, Cu(II), Cd, Zn, and In are given in Table III. As noted there, the titrations were performed both at the absorption peak of the particular metal oxinate, and also at 618 mμ, the absorption peak of free dithizone. In addition, the effect of the initial presence of free oxine on the accuracy and precision of the results was studied. For that purpose, the initial molar ratio of free oxine to metal oxinate was varied between 0 and 100.

In Fig. 3, typical titration graphs for copper(II) oxinate vs. dithizone titrant are shown for 2 wavelengths, 618 mμ, where dithizone absorbs, and 545 mμ, where copper(II) dithizonate absorbs. The general shapes of these graphs are typical of those obtained for the other metal oxinates studied, although there were minor differences. For example, in the case of titrations at 618 mμ, the slope of the first branch of the graph was characteristic of the metal. Thus, the slope for zinc and cadmium was 0 because their

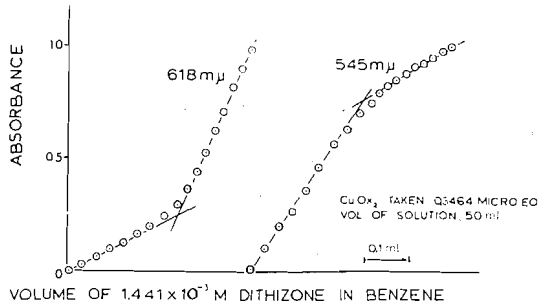

FIG. 3. Typical titration graphs for the titration of copper(II) oxinate in benzene with a standard solution of dithizone in benzene, at 25 °C.

Can. J. Chem. Downloaded from www.nrcresearchpress.com by 210.87.254.40 on 09/05/12
For personal use only.

TABLE IV

Comparison of 2 methods for estimation of the end point in the chelate-exchange titration of copper(II) oxinate in benzene with a standard solution of dithizone in benzene, at 25 °C*

Initial molar ratio ($HOx/CuOx_2$)	$CuOx_2$ found, μeq.				Variance, $\times 10^6$			
	Least squares		Manual†		Least squares		Manual†	
	618 mμ	545 mμ	618 mμ	545 mμ	618 mμ	545 mμ	618 mμ	545 mμ
0	0.344	0.348	0.343	0.350	29	17	31	58
10.7	0.347	0.350	0.346	0.351	8.2	2.5	0.75	11
21.3	0.349	0.354	0.349	0.352	19	14	6.2	43
42.6	0.351	0.360	0.353	0.362	8.7	29	2.2	25
85.3	0.357	0.371	0.359	0.370	12	26	54	1.6
106.6	0.366	0.375	0.367	0.374	16	42	5.1	35

*Molarity of titrant, 1.365×10^{-3} *M*; normality of copper(II) oxinate solution, 6.926×10^{-5} *N*; volume of solution for titration, 50 ml; amount of copper(II) oxinate taken for titration, 0.3463 μeq. Each analytical result is the mean of 5 titrations.
†The manual method consisted in drawing the "best" lines through the titration points and reading their intersection points.

dithizonates have negligible absorbance at 618 mμ, whereas the corresponding slopes for copper and lead were positive but different. Curvature of the first branch of the indium graph for 618 mμ dictated that titrations be performed at 505 mμ, where its dithizonate strongly absorbs.

Statistical Treatment of the Titration Data

The data for statistical analysis are drawn from Tables III and IV; but some sets of variances have been pooled because they were homogeneous, and to avoid redundancy some molar ratios of oxine to metal oxinate are omitted in the cases of Pb, Cd, and Zn.

In all the statistical tests, the 5% level of significance was used.

Method of End Point Determination

End points for all the titrations were found as follows: the least-squares lines for the 2 linear branches of the titrations graph were solved algebraically for their intersection point. In the case of copper, this method was supplemented by observing the intersection point of the 2 lines drawn manually as nearly as possible through the points on each arm of the titration graph.

The mean values ($n = 5$) and the corresponding variances of the end points found for copper by the 2 methods are given in Table IV. The application of Bartlett's criterion (18) showed that the variances of the least-squares method were homogeneous when various ratios of oxine to copper oxinate were used, while those of the manual method were not.

For each of the other metals also, variances of the end point found by the least-squares method were homogeneous when various ratios of oxine to metal oxinate were taken. Moreover, the variances of the end point were homogeneous for all metals titrated, when similar amounts of metal were taken. It is concluded that the nature of the metal, and the amount of free oxine initially present in the solution for titration, had no significant effect on the precision of the titrations.

Effect of Initial Free Oxine

An expected application of these chelate-exchange titrations is the determination of metal oxinates extracted from aqueous solutions. Some free oxine would be coextracted. Therefore, it was necessary to determine whether or not free oxine, initially present in the solution for titration, affected the accuracy of the result. Therefore, the relevant data for each metal in Tables III and IV were treated by a conventional analysis-of-variance technique for a 2-stage grouping. Thus, estimates were obtained for (*i*) the variance (σ_{HOx}^2) due to the effect of oxine, (*ii*) the variance (σ_λ^2) due to wavelength, and (*iii*) the variance (σ_r^2) due to random fluctuations. These values are exemplified in Table V for the copper system.

It was concluded from the statistical analysis that the initial presence of free oxine had a significant effect on the value of the end point in the cases of copper and indium, but not in the cases of lead, cadmium, and zinc. A correction factor is described below which was successfully applied to the determination of copper in the presence of oxine.

It is possible quantitatively to explain (*i*) the large discrepancy between the amount of indium taken and the amount found as shown in Table III, and (*ii*) the significant effect of initial free

Can. J. Chem. Downloaded from www.nrcresearchpress.com by 210.87.254.40 on 09/05/12
For personal use only.

TABLE V

Statistical treatment of data for copper(II) oxinate titrations*

$CuOx_2$ taken, μeq.	Number of (HOx)/($CuOx_2$) ratios used	$\sigma_r^2 \times 10^6$	$\sigma_{HOx}^2 \times 10^6$	$\sigma_\lambda^2 \times 10^6$	Degrees of freedom σ_r†	σ_{HOx}‡	σ_λ§
0.3463	6	19.9	91.1	9.8	48	10	1
0.03463	3	0.956	1.14	0.57	24	4	1

*The basic data are in Table III.
†σ_r^2 is variance due to random fluctuations.
‡σ_{HOx}^2 is variance due to the effect of oxine.
§σ_λ^2 is variance due to wavelength.

oxine on the end point. Our studies have shown that in this and other chelate-exchange titrations, mixed chelates are formed. In the case of indium, the formation constants for these mixed chelates, and also the overall formation constant for the titration, have been calculated and found to be relatively low. These calculations are to be presented elsewhere.

Effect of the Choice of Wavelength

Each metal had been titrated in replicate at 2 different wavelengths; the data are in Table III. These data had been incorporated in the statistical analysis described in the preceding section. From that analysis of variance, it was concluded in every case that the end points obtained at the 2 wavelengths were not significantly different from one another for a given molar ratio of initial oxine to metal oxinate. Moreover, the variances for all the macrotitrations in Table III had been shown to be homogeneous; similarly for all the microtitrations. Therefore it was concluded that the precision of the titrations was independent of the wavelength used.

Correction Factor for Initial Oxine in Copper Titrations

It was concluded above that oxine initially present affected the accuracy of a copper titration. In Fig. 4 are plots of % error in the determination of copper, vs. the initial molar ratio of free oxine to copper oxinate, for 2 wavelengths and for 2 different amounts of copper. The points are the experimental data, from Tables III and IV. The broken lines are regression lines calculated by least squares. A regression analysis confirmed their linearity.

In practice, an approximate but satisfactory value for the free oxine content of the copper oxinate solution may be obtained by either of 2 convenient methods: (*i*) titration of a separate sample of the copper oxinate solution with a

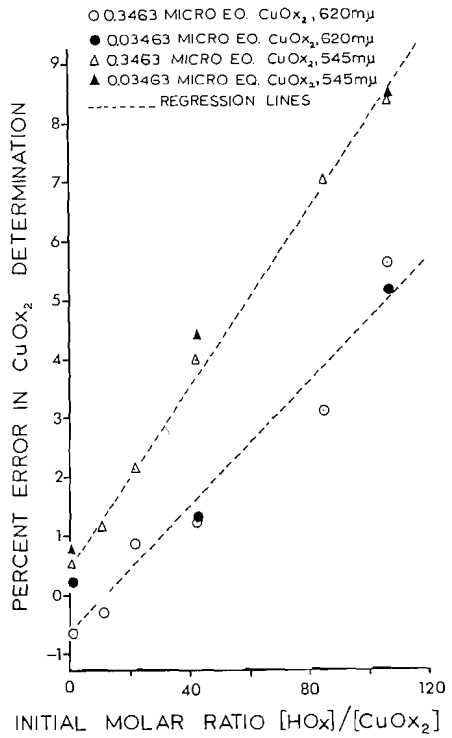

FIG. 4. Correction curves for the titration of benzene solutions of copper oxinate with a standard solution of dithizone in benzene in the initial presence of free oxine, at 25 °C.

standard solution of copper(II) nitrate in ethanol, at 420 mμ as prescribed in Procedure II; (*ii*) direct measurement of the absorbance at 315 mμ of the copper oxinate solution, where oxine has a peak and where copper(II) oxinate absorbs much less. From either measurement, and from the value found by titration for the copper oxinate content of the solution, a first approximation may be obtained for the molar ratio of initial oxine to copper oxinate. From the regression line in Fig. 4, an approximate value for the % error

Can. J. Chem. Downloaded from www.nrcresearchpress.com by 210.87.254.40 on 09/05/12
For personal use only.

may then be obtained. By iteration, the initial result for the copper content may then be corrected to the necessary degree.

The Slopes of the Titration Graphs

The shapes of the titration graphs depend on the nature of the participating species, including mixed complexes and adducts, and on their formation constants. This information for selected systems will be the subject of a separate report. However, it should be noted here that in Fig. 3, the titration graphs for copper(II) oxinate, the corresponding rate curves in Fig. 1, and the titration graph in Fig. 2 are explained by the coexistence in these nonequilibrium systems of primary and secondary copper(II) dithizonates. Thus, in Fig. 3 the first arm of the graph represents the conversion of copper(II) oxinate into a mixture of secondary and primary dithizonates, with the primary dithizonate predominating and quantitatively replacing the secondary dithizonate as the titration proceeds. After the end point, the slope of the second arm of the titration graph corresponds accurately to the measured absorptivity of dithizone.

Acknowledgments

We are grateful to the National Research Council of Canada for financial support and to the Province of Quebec for a scholarship to one of us (P.G.).

1. P. Grey and G. C. B. Cave. Can. J. Chem. This issue.
2. P. W. Perryman. Analyst, **70**, 45 (1945).
3. E. G. Almy, W. C. Griffin, and C. S. Wilcox. Ind. Eng. Chem. Anal. Ed. **12**, 392 (1940).
4. R. G. Charles and A. Langer. J. Phys. Chem. **63**, 603 (1959).
5. H. R. Fleck, F. V. Greenane, and A. M. Ward. Analyst, **59**, 325 (1934).
6. J. J. Fox. J. Chem. Soc. 1124 (1910).
7. R. G. W. Hollingshead. Oxine and its derivatives. Vols. I and II. Butterworths, London. 1954.
8. Scott's standard methods of chemical analysis. Vol. I., 6th ed. *Edited by* N. H. Furman. D. Van Nostrand Company, Inc., New York. 1962.
9. N. Strafford. Analyst, **78**, 733 (1953).
10. J. H. Yoe and H. J. Koch. Trace analysis. John Wiley and Sons, Inc., New York. 1957. p. 83.
11. R. I. Martens and R. E. Githens. Anal. Chem. **24**, 991 (1952).
12. G. W. C. Milner. Analyst, **76**, 488 (1951).
13. G. C. B. Cave and D. N. Hume. Anal. Chem. **24**, 588 (1952).
14. K. J. McNaught. Analyst, **67**, 97 (1942).
15. M. P. Rollet. C. R. **183**, 212 (1926).
16. R. Näsänen, P. Lumme, and A. Mukula. Acta Chem. Scand. **5**, 1199 (1951).
17. H. C. Deterding and R. G. Taylor. Ind. Eng. Chem. Anal. Ed. **18**, 127 (1946).
18. Biometrika tables for statisticians. Vol. I, 3rd ed. *Edited by* E. S. Pearson and H. O. Hartley. Cambridge University Press. 1966. p. 63.

Can. J. Chem. Downloaded from www.nrcresearchpress.com by 210.87.254.40 on 09/05/12
For personal use only.

Can. J. Chem. Downloaded from www.nrcresearchpress.com by 210.87.254.40 on 09/05/12
For personal use only.

Mössbauer spectra of toluene-3,4-dithiolene and *cis*-1,2-bistrifluoromethyl-1,2-ethylenedithiolene complexes of iron(III)

T. BIRCHALL
Department of Chemistry, McMaster University, Hamilton, Ontario

Received August 11, 1969

The Mössbauer spectra of a number of dithiolene complexes of iron have been examined at 77 °K. The data obtained are discussed in relation to the known structural data.

Canadian Journal of Chemistry, 47, 4563 (1969)

Introduction

Transition metals form many and varied complexes with the bidentate sulfur ligands dithiocarbamate and 1,2-dithiolate. Mössbauer spectroscopy has been used to study complexes of these ligands with iron, and much useful information about the structure and nature of the bonding has been obtained (1–5). Continuing the earlier studies (4, 5), data on complexes of iron with the toluene-3,4-dithiolene and bistrifluoromethyl-1,2-dithiolene ligands are reported.

Experimental

The Mössbauer spectra were recorded on an apparatus previously described (6). All chemical shifts are relative to sodium nitroprusside taken as zero. As only small quantities of the compounds were available (20–50 mg) the samples were packed into holders made by drilling an appropriately-sized hole in 1/16 in. lead sheet in an attempt to achieve 10 mg of iron/cm^2. This resulted in rather small sample areas with the consequence that long counting periods were necessary to obtain a spectrum. Spectra at room temperature were often barely detectable and even at liquid nitrogen temperature, the resonance absorption often only amounted to 1–3% of the total counts. Only data obtained at liquid nitrogen temperature are reported here and these are thought to be accurate to ±0.03 mm/s.

Results and Discussion

All the data are summarized in Table I. The chemical shifts (δ) are typical of iron(III) and differ little from the shifts of analogous compounds reported earlier (5). These are then, apart from **7** and **8**, presumably also five-coordinate complexes. The toluene-3,4-dithiolene series has been arranged in order of decreasing quadrupole splitting which is also the order of increasing chemical shift. However, apart from the Δ value for compound **7**, these variations are for the most part within the experimental error. There appears to be no correlation between the strength of the nitrogen base occupying the fifth coordination site and either of the Mössbauer parameters. In the case of the 4-aminopyridine complex, **7**, it is felt that the quadrupole splitting is significantly smaller than that for the other toluene-3,4-dithiolene complexes, **1**–**6**. A similar effect was noted in the corresponding maleonitrile series (5)

TABLE I

Mössbauer parameters of some 1,2-dithiolene complexes of iron

Compound		Chemical shift, δ mm/s	Quadrupole splitting, Δ mm/s
Number	Formula		
1	$[(C_6H_5)_4P]$ $[Fe(S_2C_6H_3.CH_3)_2.\beta\text{-pic}]$	0.62	3.18
2	$[(C_6H_5)_4P]$ $[Fe(S_2C_6H_3.CH_3)_2.py]$	0.62	3.10
3	$[(C_6H_5)_4P]$ $[Fe(S_2C_6H_3.CH_3)_2.quin]$	0.62	3.10
4	$[(C_6H_5)_4P]$ $[Fe(S_2C_6H_3.CH_3)_2.\gamma\text{-pic}]$	0.63	3.09
5	$[(C_6H_5)_4P]$ $[Fe(S_2C_6H_3.CH_3)_2.\text{iso-quin}]$	0.63	3.05
6	$[(C_6H_5)_4P]$ $[Fe(S_2C_6H_3.CH_3)_2.\alpha\text{-pic}]$	0.63	3.03
7	$[(C_6H_5)_4P]$ $[Fe(S_2C_6H_3.CH_3)_2.4\text{-}NH_2\text{-py}]$	0.64	2.85
8	$[(C_6H_5)_4P]$ $[Fe(S_2C_2(CF_3)_2)_2.o\text{-phen}]$	0.60	1.97
9	$[(C_2H_5)_4N]$ $[Fe(S_2C_2(CF_3)_2)_2.py]$*	0.59	2.61
10	$[(C_6H_5)_4P]$ $[Fe(S_2C_2(CF_3)_2)_2.(C_2H_5)_3P]$	0.46	2.49
11	$[(C_2H_5)_4N]$ $[Fe(S_2C_2(CF_3)_2)_2.NO]$*	0.28	2.11

*Data taken from ref. 5.

Can. J. Chem. Downloaded from www.nrcresearchpress.com by 210.87.254.40 on 09/05/12
For personal use only.

and, again, strongly suggests that the lone pair of the free NH_2 group of one unit is forming a weak donor bond to the vacant sixth position of the iron atom of another unit, as shown in Fig. 1. In this way every iron atom achieves essentially six-coordination, though the Fe——NH_2 bond is probably very long. Only an X-ray structure determination could confirm this. The effect of six-coordination is seen in compound **8**, where the quadrupole splitting of 1.97 mm/s is considerably lower than the value obtained for the five-coordinate pyridine adduct i.e., 2.61 mm/s (5). This indicates a more symmetric environment

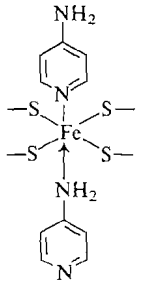

FIG. 1. Donor bond of NH_2 group to Fe of another unit.

at the iron. The quadrupole splitting in compound **8** is nevertheless still large. Recent X-ray structure determinations on the ions $\{Co[S_2C_2(CN)_2]_2$-(*o*-phen)$\}^-$ and $\{Co[S_2C_6H_3.CH_3]_2$(*o*-phen)$\}^-$ indicate that the arrangement about the cobalt is octahedral in both complexes (7). In addition it was found that the Co—S bond *trans* to a nitrogen atom is shorter by $\sim$ 0.035 Å than when *trans* to another sulfur. One would expect the $\{Fe[S_2C_2(CF_3)_2]_2$(*o*-phen)$\}^-$ to have a similarly distorted structure and a considerable quadrupole splitting would be expected from a formally d^5 iron in this environment, even if there was no extensive π-delocalization onto the ligands.

Comparison of the data for compounds **9–11** illustrates the effect of electron delocalization from the metal to the ligand upon the Mössbauer parameters. Strong π-type interactions result in a decrease in chemical shift as 3d electrons are removed from the iron nuclear environment. This is the result of a decrease in screening of the "s" electrons from the nuclear charge and a resultant increase in "s" electron density. Since $\delta r/r$ is negative for ^{57}Fe (ref. 8, p. 54), a decrease in chemical shift means an increase in "s" electron density. One can immediately arrange ligands in order of π-bonding capabilities with a decreasing ability to accept electrons via π-bonding in the series NO > Et_3P > Py. The substituted pyridines and quinolines are identical in this respect, showing no variation in chemical shift.

Removal of electron density from the metal in the above manner also has a marked influence on the quadrupole splitting, which decreases as the degree of π back-donation increases. While the change in quadrupole splitting might be a direct consequence of the back donation of electrons onto the axial ligand in the case of the triethylphosphine complex, this is probably not so for the nitrosyl compound. A quite different situation pertains in the nitrosyl compound as compared to compounds **9** and **10** (Table I). $\{Fe(pyridine)$-$[S_2C_2(CN)_2]_2\}^-$ has spin $S = 3/2$ (9) and it is probable that compounds **9** and **10** have the same electronic arrangements. The nitrosyl complex **11** has an extra electron, supplied by the NO group which in itself would markedly affect the asymmetry at the iron nucleus. In addition, the strong π-bonding to the NO antibonding orbitals results in a complete change in the molecular orbital scheme to give a diamagnetic complex (10). All of these factors undoubtedly contribute to the lower quadrupole splitting.

Comparison of the Mössbauer parameters for the toluene-3,4-dithiolene series with the other dithiolenes (5) reveals that the series reported here exhibit a much larger quadrupole splitting than all others, except perhaps those involving the tetrachlorobenzene-1,2-dithiolene ligand. Table II lists the Mössbauer parameters for the five-coordinate pyridine adducts and one notes a 25% increase in quadrupole splitting down the series with virtually no change in chemical shift. The same ordering of ligands has been noted by

TABLE II

Mössbauer parameters of some iron dithiolene adducts with pyridine

Compound	Chemical shift, δ mm/s	Quadrupole splitting, Δ mm/s
$[Fe(S_2C_2(CN)_2)_2.py]^-$*	0.59	2.41
$[Fe(S_2C_2(CF_3)_2)_2.py]^-$*	0.59	2.61
$[Fe(S_2C_6Cl_4)_2.py]^-$*	0.59	3.02
$[Fe(S_2C_6H_3.CH_3)_2.py]^-$	0.62	3.10

*Data from ref. 5.

Can. J. Chem. Downloaded from www.nrcresearchpress.com by 210.87.254.40 on 09/05/12
For personal use only.

McCleverty *et al.* (10) for similar series and is taken as being indicative of an increase in acceptor ability of the dithiolene ligand. One would have to argue that a synergic mechanism operates, to replace by stronger σ bonds, electron density that is removed by a π mechanism in order to explain the constant chemical shift. However in the $[S_2C_2(CF_3)_2]$ series discussed above and in many other complexes, notably the nitroprussides (ref. 8, p. 258), it is found that strong π back-donation lowers the chemical shift indicating that the electron density removed is not replaced by a synergic mechanism. Clearly we must look elsewhere for an explanation.

The constant values for the chemical shift in these complexes indicates that no marked changes in electronic environment are occurring at the iron nucleus. The variation in asymmetry must be looked for in subtle changes in molecular structure. Unfortunately the crystal structures of very few of these compounds have been reported. Rae (11) has reported the structure of the dianionic $Fe(NO)[S_2C_2(CN)_2]_2$ and Hamilton and Bernal (12) that of the dimeric $[(n\text{-}C_4H_9)_4N][FeS_2C_2(CN)_2]_2$ complex. Both complexes have iron atoms in five-coordinate square pyramidal situations; four sulfurs and one NO group in the former and five sulfurs in the latter case. The iron – basal sulfur distances are 2.26–2.29 and 2.20–2.28 Å, respectively. In the former case (11) the variation in Fe—S distances is barely outside the standard deviations but in the dimeric maleonitrile complex, the differences are significant and a field gradient at the ion would be expected from such a situation.

Of more interest are the displacements of the Fe above the basal plane of sulfurs. These are 0.51 and 0.36 Å, respectively. Such a significant difference would have a pronounced effect on the symmetry at the iron and on the disposition of the nonbonding sulfur lone pairs which would, in turn, influence the iron environment. This change in structure has also been noted in analogous cobalt systems (13). Gray and co-workers (13) summarize the structures of some square planar, four-coordinate, and square pyramidal, five-coordinate cobalt dithiolene complexes of varying overall charge. The height of the cobalt above the basal plane varies considerably in these complexes, while the Co—S distances remain virtually constant. Unfortunately, information on a series of iron–dithiolene complexes such as those listed in Table II is not available. Such a study appears to be essential for a complete understanding of the Mössbauer data.

Acknowledgments

The author wishes to thank the National Research Council of Canada for financial support. All samples were kindly supplied by Dr. J. A. McCleverty, University of Sheffield, whose help is gratefully acknowledged.

1. E. Frank and C. R. Abeledo. Inorg. Chem. **5**, 1453 (1966).
2. R. L. Martin and A. H. White. Inorg. Chem. **6**, 712 (1967).
3. H. H. Wickman and A. M. Trozzolo. Inorg. Chem. **7**, 63 (1968).
4. T. Birchall, N. N. Greenwood, and J. A. McCleverty. Nature, **215**, 625 (1967).
5. T. Birchall and N. N. Greenwood. J. Chem. Soc. A, 286 (1969).
6. T. Birchall. Can. J. Chem. **47**, 1351 (1969).
7. G. P. Khare, C. G. Pierpont, and R. Eisenberg. Chem. Commun. 1692 (1968).
8. V. I. Goldanskii and R. H. Herber. Chemical applications of Mössbauer spectroscopy. Academic Press, Inc., New York. 1968.
9. J. A. McCleverty, J. Locke, and N. Connelly. Unpublished results.
10. J. A. McCleverty, N. M. Atherton, J. Locke, E. J. Wharton, and C. J. Winscom. J. Amer. Chem. Soc. **89**, 6082 (1967).
11. A. I. M. Rae. Chem. Commun. 1245 (1967).
12. W. C. Hamilton and I. Bernal. Inorg. Chem. **6**, 2003 (1967).
13. M. J. Baker-Hawkes, Z. Dori, R. Eisenberg, and H. B. Gray. J. Amer. Chem. Soc. **90**, 4253 (1968).

Photochemical and thermal isomerizations of *cis*- and *trans*-cinnamic acids, and their photostationary state[1]

MARTIN B. HOCKING
Exploratory Research Laboratory, Dow Chemical of Canada, Limited, Sarnia, Ontario
Received May 13, 1969

cis-Cinnamic acid was prepared photochemically from the *trans* isomer according to a published method, but was isolated by vacuum distillation. The photostationary state of these acids has been determined for moderately concentrated solutions of each isomer exposed to unfiltered ultraviolet. The position of the *cis–trans* thermal equilibrium approached from all *cis*- and from all *trans*-isomers has been tested without solvent and found to lie at, or very close to, 100% *trans*. Kinetic examination of the rates of these isomerizations shows that they fit a kinetic expression of the form $-d[cis]/dt = k[cis][H^+]$.

Canadian Journal of Chemistry, 47, 4567 (1969)

Can. J. Chem. Downloaded from www.nrcresearchpress.com by 210.87.254.42 on 09/05/12
For personal use only.

Introduction

This investigation was initiated primarily to determine the proportion of *cis*-cinnamic acid formed by heating the *trans*-acid, and whether or not vacuum distillation could separate this mixture. Even though the *cis–trans* thermal equilibrium of the cinnamic acids lies well on the side of the *trans*-acid, because of the large boiling point difference (*trans*, 300 °C; *cis*, 265 °C), it was thought that an equilibrium mixture could possibly be separated by distillation.

The two isomeric cinnamic acids were required initially to establish the position of the thermal equilibrium by experiment, and to determine temperatures at which the rate of equilibration was sufficiently fast to be useful. *cis*-Cinnamic acid was prepared by a published photochemical method (1), which led to our determination of the photostationary state for cinnamic acid using unfiltered ultraviolet irradiation.

Photochemical isomerizations of cinnamic acids have received considerable attention. Sunlight has been used in a number of experiments (2–4) on *trans*-cinnamic acid with the predominant result being a cyclobutane-type dimerization to truxillic or truxinic acids; however, the formation of small amounts of the *cis* isomer was also observed (4). The early ultraviolet irradiation work of Stoermer (5, 6) of benzene solutions of *trans*-cinnamic acid yielded fair conversions to the *cis* (m.p. 68 °C). He found that irradiation of *cis*-cinnamic acid yielded a proportion of the two lower stability allotropes (m.p. 42 and 58 °C) of *cis*-cinnamic acid which he was unable to isolate (5).

Vaidya (1) used unfiltered ultraviolet irradiation in his more recent photochemical preparations of *cis*-cinnamic acid. Using a saturated methanolic solution of the *trans*-acid, yields of 25 to 30% of the m.p. 42 °C allotrope were isolated by trituration and fractional crystallization of the irradiated solution. Comparison of the photochemical results of ultraviolet irradiation with the results observed in sunlight has led to the empirical suggestion that the different products are solely due to the different relative intensities of short and long wavelength radiation (7). Most recently, Lindenfors (8, 9) has used ultraviolet irradiation to prepare ring substituted monochloro- and dichloro-*cis*-cinnamic acids from the corresponding *trans*-compounds using an ion exchange resin for isolation.

Thermal isomerizations of cinnamic acid or its derivatives have not been as frequently investigated as the photochemical transformations. Noyce and his co-workers (10) have carefully measured the rates of aqueous sulfuric acid catalyzed isomerizations of *cis*-cinnamic acid and conclude that the kinetics are first order in cinnamic acid. Neat thermal isomerizations have previously been reported only for the *cis*-methyl ester. Kistiakowsky and Smith (11) have determined the rate constants for the vapor phase isomerization of the *cis*-ester to the *trans* at several temperatures in the range 202 to 387 °C and conclude from the magnitude of these that the "... mechanism ... is essentially different from the mechanical rotation around the double bond. ..."

Results and Discussion

Preparation of cis-Cinnamic Acid

The procedure used to prepare *cis*-cinnamic acid was that reported by Vaidya (1), which

[1]Contribution No. 171.

Can. J. Chem. Downloaded from www.nrcresearchpress.com by 210.87.254.42 on 09/05/12
For personal use only.

involved ultraviolet irradiation of a saturated methanolic solution of the *trans*-isomer and fractional crystallization of the solvent extracted *cis*-isomer. Analysis of the *cis*- and *trans*-cinnamic acid mixtures obtained during the preparations and isomerizations was by integration of the respective vinylic proton resonances in nuclear magnetic resonance (n.m.r.) spectra of the mixtures (details are given in Experimental). A complication in the irradiation step of our preparations was the formation of a significant proportion of ester, a finding noted by others (9, 12), at least in sunlight. Stoermer and Ladewig (13) claimed that ester formation occurred only if traces of strong mineral acid were present, and Lindenfors (9) suggested that even in its absence, the catalytic effect of the glass vessel would be sufficient to bring this about. The latter author also found very little effect on the rate or equilibrium of photolytic isomerizations with large changes in the solvent dielectric; however, the photolytic instability of acetonitrile (14) unfortunately made its use inappropriate. In our photostationary state experiments with cold methanol solutions, no esterification took place. Apart from the temperature and the somewhat more dilute solutions, the latter experiments were identical to the preparative ones and are an indication of one way in which ester formation may be avoided.

Isolation of *cis*-cinnamic acid formed on irradiation by trituration and crystallization was attempted several times but was found to be relatively ineffective. From a *cis*-acid content of 39% obtained in one irradiation experiment, a trituration and crystallization gave an improvement of only 14% in the *cis*-content of the crystals obtained. Because of the limited effectiveness of this technique, vacuum distillation of the *cis*-acid from irradiated material was tried. The success of vacuum distillation for isolation of the *cis*-cinnamic acid was measured in two ways. The first was the significant improvement of *cis* concentration found in the distillate, even without a packed column. This yielded initially a 37% improvement which, upon successive distillations, dropped to 14 and 9%. The total amount of *cis*-cinnamic acid remained constant, however, indicating that no isomerization occurred during distillation.

The m.p. 42 °C allotrope of *cis*-cinnamic acid is the predominant form usually isolated on simple recovery of the *trans*-isomer after ultraviolet irradiation (1, 5). Some of this allotrope may have crystallized from an initial fraction of the distillate, but the m.p. 58 °C allotrope was the main product. It is surprising, though, that this is so since the allotrope melting at 68 °C is the only one previously reported to have crystallized from a distillate (15). The m.p. 58 °C form was converted to the m.p. 68 °C form as confirmation of the identity of the former.

Photostationary State

A solution of *trans*-cinnamic acid in a quartz flask was irradiated with unfiltered ultraviolet to determine whether or not a higher equilibrium proportion of *cis*-isomer was obtainable in this way than by irradiation with only the longer wavelength ultraviolet used by Vaidya. The data of Lindenfors (9) have indicated a decreasing *cis*-isomer concentration at the photostationary state with increasing wavelength of the ultraviolet radiation.

Using 0.002 and 0.003 *M* solutions in water and 313 mμ irradiation Vaidya (1) obtained photostationary equilibria of 75 and 72% *cis*-isomer, respectively, approached from both all *cis*- and all *trans*-cinnamic acid. Lindenfors (9), using water-filtered ultraviolet on 0.00423 *M* solutions in benzene, ethanol, or formic acid obtained a photoequilibrium of 82% *cis*-isomer, approached from the all *trans*-isomer side only. Our result of 60% *cis*-isomer at photoequilibrium (Table VII) in unfiltered ultraviolet, for a 0.27 *M* solution in methanol approached from pure *trans*- and pure *cis*-isomer, is somewhat lower than the earlier figures. Vaidya's result, a higher concentration yielding lower *cis* concentration at photoequilibrium, has been noted for the photostationary states of other olefins (16). It therefore indicates a real trend in this system which may in part explain the lower [*cis*] equilibria in our experiments carried out at much higher concentrations. The variation in wavelengths, different solvents, and different spectral profiles for the lamps used are probably also important variables contributing to this difference. Use of an appropriate sensitizer might greatly enhance the *cis*-isomer proportion at equilibrium (17).

Thermal Isomerizations

Purified *trans*-cinnamic acid failed to yield any *cis*-isomer when heated at 257.5, 200, and 143.5 °C for extended periods of time. It is estimated that

Can. J. Chem. Downloaded from www.nrcresearchpress.com by 210.87.254.42 on 09/05/12
For personal use only.

if 1% or more *cis*-isomer were present it would have been detected.

To determine whether or not the absence of the *cis*-isomer on heating of the *trans*-isomer was due to the position of the equilibrium or merely to inadequate conditions for attaining it, similar experiments at 182, 163.5, and 143.5 °C were conducted with *cis*-cinnamic acid. Less than 0.7% of *cis*-acid was present at thermal equilibrium in all of the runs but data from intermediate aliquots indicated that the *cis*-to-*trans* isomerization proceeded quite smoothly (see Experimental).

When the data were plotted as a first order reaction the plots showed a definite upward curvature. On second order coordinates a good straight line fit could be obtained for the data up to 70% isomerization, but beyond this the rates were faster than that predicted by the initial straight line. At this stage a number of mathematical tests of reaction order were applied in an objective attempt to differentiate between first and second order, but these too gave an *apparently* ambiguous conclusion (Table I). Also an attempt to obtain a computer fit of the data to first or second order coordinates, either to complete reaction (Table II) or through the region of reasonable visual fit to 70% isomerization, failed to sharply define the order. However, the manual plots, the tests of reaction order, and the evident bowing of the data in opposite senses for the computer-obtained best lines all suggested that an order intermediate between first and second was operative in these isomerizations.

On these bases it was assumed that a three-halves order expression [1], which upon integration yields eq. [2]

$$[1] \qquad \frac{-\mathrm{d}[cis]}{\mathrm{d}t} = k[cis]^{3/2}$$

$$[2] \qquad 2[cis]^{-1/2} = kt + C$$

might apply. When the cinnamic acid isomerization data were plotted on coordinates of $[cis]^{-1/2}$ vs. time, quite good straight lines at all three temperatures up to about 90% isomerization were obtained (Fig. 1). In fact, comparison of the fit, the intercepts, and the errors in the slopes by computer showed that the three-halves order plots generally fitted better to 90% conversion than the first or second order plots did to only 70% conversion. Table II gives the overall comparison on the basis of 90% isomerization and a comparison of the 50% isomerization slopes with those of 90%. For the three-halves order computer plot at 143.5 °C the % error in the slope is not so markedly improved over the plots with other orders, but in four other criteria, the fit, the extent to which the points show a definite trend from the line (bowing), the minimization of the deviation from the theoretical intercept, and in the smallest change in the slope when

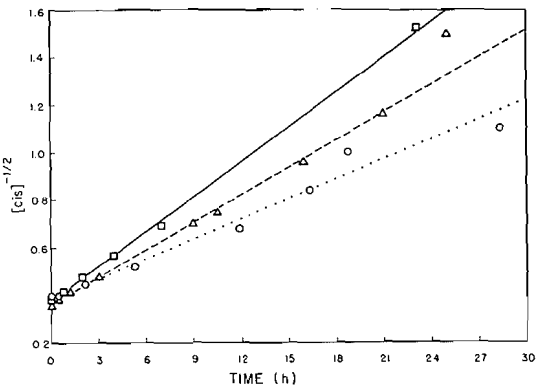

FIG. 1. Three-halves order plots of the thermal isomerization of *cis*-cinnamic acid; ○, 143.5 °C, time axis multiplied by 10; △, 163. 5 °C, time axis multiplied by 3; □, 182.0 °C.

TABLE I

Order of reaction by various tests

Determination method	Reference	Order "n" for isomerization at 143.5 °C	163.5 °C	182.0 °C
Plot* of t/f vs. t Slope = $n/2$	18, 19	1.46	1.82	1.74
Plot of log (rate) vs. log (conc.) Slope = n	18, 20	1.18	1.54	1.72
Fractional-life period method†	18, 20	1.39	1.57	1.70

*t = time, f = fraction reacted.
†Average of four determinations over the inclusive range 0.3 to 0.6 reacted is the value given.

Can. J. Chem. Downloaded from www.nrcresearchpress.com by 210.87.254.42 on 09/05/12
For personal use only.

TABLE II

Calculated plots of *cis*- to *trans*-cinnamic acid isomerizations*

	Value								
	First order plots			Three-halves order plots			Second order plots		
Parameter	143.5 °C	163.5 °C	182.0 °C	143.5 °C	163.5 °C	182.0 °C	143.5 °C	163.5 °C	182.0 °C
Fit†	0.0772	0.0416	0.0662	0.0466	0.0091	0.0161	0.511	0.501	0.916
Intercept‡	−0.0377	−0.0328	−0.0807	0.396	0.374	0.375	0.805	0.757	0.253
Slope	−0.00347	−0.0161	−0.0503	0.00268	0.0122	0.0493	0.0249	0.124	0.662
Error in slope§	2.67×10^{-4}	5.91×10^{-4}	3.30×10^{-3}	1.61×10^{-4}	1.29×10^{-4}	8.01×10^{-4}	1.77×10^{-3}	7.12×10^{-3}	4.56×10^{-2}
% Error in slope	7.85	3.67	6.55	6.00	1.06	1.62	7.10	5.74	6.89
Rate constant‖ (mole$^{-1/2}$ l$^{1/2}$ s^{-1})	—	—	—	$7.44\pm0.45\times10^{-7}$	$3.39\pm0.04\times10^{-6}$	$1.37\pm0.02\times10^{-5}$	—	—	—

*Coordinates of form log $(1-f)$ vs. t for first order, $c^{-1/2}$ vs. t for three-halves order, and $1/(1-f)$ vs. t for second order, where f is fraction isomerized, t is time in h (abscissa), and c is concentration of *cis*-cinnamic acid (moles/l).

†Standard deviation of points about the line. The first order deviations must be multiplied by 2 and the second order deviations by 0.2 to compare with the three-halves order deviations in order to equalize the effect of the relative magnitudes of the ordinates involved.

‡The theoretical intercepts are 0 for first order, 0.374 for three-halves order, and 1 for second order. The actual intercepts given here must be multiplied by the same factors as the "fit" for equitable comparisons.

§One standard deviation.

‖See Discussion.

TABLE III

Deviations from ideality of calculated plots of *cis*-cinnamic acid isomerizations*

	Value								
	First order plots			Three-halves order plots			Second order plots		
Parameter	143.5 °C	163.5 °C	182.0 °C	143.5 °C	163.5 °C	182.0 °C	143.5 °C	163.5 °C	182.0 °C
Fit	0.154	0.083	0.132	0.047	0.009	0.016	0.256	0.251	0.458
Bowed	Yes	Yes	Yes	No	Slight	Slight	Yes	Yes	Yes
Intercept deviation	0.075	0.065	0.161	0.022	0.000	0.001	0.039	0.049	0.149
% error in slope	7.85	3.67	6.55	6.00	1.06	1.62	7.10	5.74	6.89
% change in slope†	+38.6	+41.6	+65.6	−6.7	−5.7	−7.5	−40.2	−45.5	−55.0

*Deviations calculated, incorporating the differing intercepts and the different relative magnitudes of the ordinates (Table II), so that the smaller the number the closer is the agreement with theory.

†Calculated by taking the difference between the calculated slope to 90% reaction from the calculated slope to 50% reaction and dividing this difference by the 90% slope.

Can. J. Chem. Downloaded from www.nrcresearchpress.com by 210.87.254.42 on 09/05/12
For personal use only.

plotted to differing extents of reaction, the improvement is well demonstrated at all temperatures (Table III). Therefore, the isomerization of neat *cis*-cinnamic acid at these temperatures is considered to proceed by three-halves order kinetics.

In order to rationalize the three-halves order in terms of a plausible reaction path, one can introduce a first-order dependence of the isomerization rate on the concentration of hydrogen ion in the system. From the expression for the dissociation of a weak acid, eq. [3], the hydrogen ion concentration is defined by eq. [4].

$$[3] \qquad K_{\text{diss.}} = \frac{[\text{H}^+][cis^-]}{[cis]}$$

$$[4] \qquad [\text{H}^+] = K_{\text{diss.}}{}^{1/2}\,[cis]^{1/2}$$

$$[5] \qquad \frac{-\text{d}[cis]}{\text{d}t} = k'[cis]\cdot[\text{H}^+]$$

Substitution of eq. [4] into eq. [5], the appropriate expression for a first-order dependence of the rate on concentration of both *cis*-acid and hydrogen ion, yields an expression [6]

$$[6] \qquad \frac{-\text{d}[cis]}{\text{d}t} = k'K_{\text{diss.}}{}^{1/2}[cis]^{3/2}$$

which is analogous to the experimentally determined expression [1] with $k = k'K_{\text{diss.}}{}^{1/2}$. The constant of integration in eq. [2] is, at time zero, $2\,[cis_0]^{-1/2}$ and, since $[cis_0]$ for 100% *cis*-cinnamic acid liquid is about 7.15 moles/l (21), C has a calculated value of 0.748 moles$^{-1/2}$ l$^{1/2}$. Because the three-halves order data of Table II are from plots of $[cis]^{-1/2}$ vs. t, the slopes and intercepts quoted represent $\frac{1}{2}k$ and $\frac{1}{2}C$, respectively. Thus, the rate constants for use with eq. [2] are $1.49 \pm 0.09 \times 10^{-6}$, $6.78 \pm 0.07 \times 10^{-6}$, and $2.74 \pm 0.04 \times 10^{-5}$ moles$^{-1/2}$ l$^{1/2}$ s^{-1} at 143.5, 163.5, and 182.0 °C, respectively, while the experimentally-determined values for C are 0.792, 0.748, and 0.750, in very good agreement with the calculated value.

All the preceding mathematical interpretation has been based, for simplicity of treatment and understanding, on the substitution of eq. [4] for $[\text{H}^+]$ in the rate expression. To be rigorously correct the gradually increasing contribution of hydrogen ion from the dissociation of *trans*-cinnamic acid must also be taken into account. By dividing the *trans*-isomer dissociation equation by that of the *cis*, eq. [3], and substituting the quantity $([cis_0] - [cis])$ for $[trans]$ in the resulting expression, with rearrangment we obtain the concentration equivalence eq. [7]

$$[7] \qquad [trans^-] = \frac{K_{\text{diss}.t}}{K_{\text{diss}.c}}\cdot[cis^-]\cdot\frac{[cis_0]-[cis]}{[cis]}$$

$$[8] \qquad [\text{H}^+] = [cis^-] + [trans^-]$$

Substitution of eq. [7] in eq. [8] and squaring gives us eq. [9]

$$[9] \qquad [\text{H}^+]^2 = K_{\text{diss}.t}\,[cis_0] + (K_{\text{diss}.c} - K_{\text{diss}.t})\,[cis]$$

which expresses the hydrogen ion concentration yielded by both *cis*- and *trans*-cinnamic acids in terms of only the *cis* concentration. Equation [9] can be verified by substituting the concentration equivalence $[cis_0] - [trans]$ for $[cis]$.

When the values obtained for the concentration of hydrogen ion using eq. [9] are compared with those obtained using the simple eq. [3], good correspondence is demonstrated to 50% isomerized (Table IV). Only when $[\text{H}^+]$ ap-

TABLE IV

Hydrogen ion concentration in mixtures of *cis*- and *trans*-cinnamic acids*

% *cis*	[*cis*] moles/l	Calculated $[\text{H}^+] \times 10^2$ moles/l: $K_{\text{diss}.c}{}^{1/2}[cis]^{1/2}$	Calculated $[\text{H}^+] \times 10^2$ moles/l: Equation [9]	% $[\text{H}^+]$ from *cis*†
100	7.15	3.16	3.16	100
75	5.37	2.74	2.86	93
50	3.58	2.23	2.50	80
25	1.79	1.58	2.09	67
0	0.0	0.0	1.58	0

*Calculated using the *aqueous* dissociation constants for *cis*- and *trans*-cinnamic acids.
†Calculated using the expression $\frac{[cis^-]}{[cis]} = \frac{K_{\text{diss}.c}}{K_{\text{diss}.t}}\frac{[trans^-]}{[trans]}$

Can. J. Chem. Downloaded from www.nrcresearchpress.com by 210.87.254.42 on 09/05/12
For personal use only.

proaches zero does the discrepancy become serious. It should be pointed out that the approximation of $[H^+]$ by using expression [3] lies only in interpretation and explanation of the three-halves order kinetics which, if $[H^+]$ of eq. [9] were used, would still give terms in $[cis]^{3/2}$. The latter course yields a very much more complicated rate expression since $[H^+]$ of eq. [9] is solved by a power series. Subsequent integration of this can be accomplished but the result makes plotting or mechanistic interpretation next to impossible.

An Arrhenius plot of the rate constants derived from the slopes of the three-halves order plots (Fig. 2) yields an activation energy of 28.5 ± 0.7 kcal/mole (one standard deviation) with a preexponential factor of 1.3×10^9 $mole^{-1/2}\, l^{1/2}\, s^{-1}$. This compares with a value of 24.0 ± 1.0 kcal/mole derived by Noyce *et al.* (10).

Noyce and co-workers (10) found 50% sulfuric acid catalyzed isomerizations of *cis*-cinnamic acid at 70 °C to be first order in cinnamic acid, with a rate constant of 4.13×10^{-5} s^{-1}. In their study, the high concentration of hydrogen ion evidently removed the dependence of the rate of isomerization upon its concentration, making the latter system essentially pseudo-first order. However, they have found also a first order dependence of the rate constant k (eq. [10])

$$[10] \quad \frac{-d[cis]}{dt} = k \cdot [cis] = k' \cdot [a_{H^+}] \cdot [cis]$$

upon the activity of the hydrogen ion and from their data, one can obtain a value of 1.91×10^{-8} $mole^{-1}\, l\, s^{-1}$ for the concentration independent rate constant k' at 70 °C.

An extrapolation of the Arrhenius equation for neat *cis*-cinnamic acid isomerization permits a comparison of the rate constant at 70 °C with that of strong acid catalyzed isomerization by Noyce *et al.* The rate constant obtained, 7.85×10^{-10} $mole^{-1/2} l^{1/2} s^{-1}$, when divided by $(K_{diss.})^{1/2}$ for *cis*-cinnamic acid[2] becomes 6.65×10^{-8} $mole^{-1}\, l\, s^{-1}$. Although our experimental conditions for the kinetic investigations are quite different from those of Noyce *et al.*, the fact that the rate constants are of the same order of magnitude is an indication that the same mechanism is operative in the two systems.

[2] $K_{diss.}^{25°} = 1.4 \times 10^{-4}$ for *cis*-cinnamic acid in an aqueous system. It may be significantly different for non-aqueous acid at 70 °C.

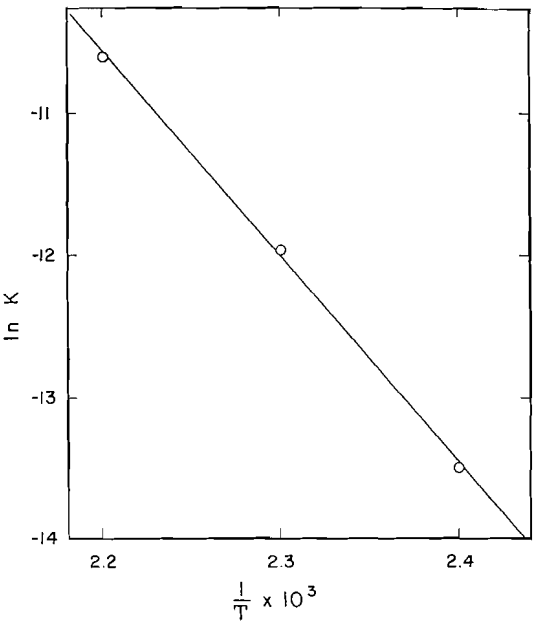

FIG. 2. Arrhenius plot of *cis*-cinnamic acid thermal isomerizations.

Thermal isomerization of methyl *cis*-cinnamate in the vapor phase was reported by Kistiakowsky and Smith (11) to proceed with a specific rate of 3.44×10^{-6} s^{-1} at 292 °C, relatively much slower than our neat free acid isomerizations. Hence, the credibility of our data when compared with a system which would be expected to show less facile isomerization is high.

The dependence of the rate of the thermal isomerization of the neat acid upon hydrogen ion activity can be rationalized by assuming that isomerization is preceded by a rate-determining protonation of the double bond, **1**, or of the carbonyl group, **2**, of *cis*-cinnamic acid followed by single bond rotation to the conformer required to yield *trans*-cinnamic acid prior to proton elimination.

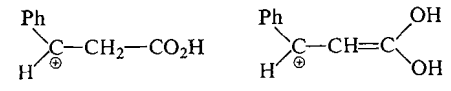

1

2

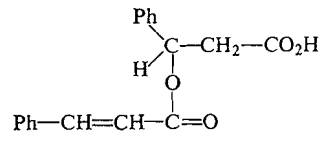

3

Can. J. Chem. Downloaded from www.nrcresearchpress.com by 210.87.254.42 on 09/05/12
For personal use only.

Since *cis*-cinnamic acid is four times more highly dissociated than the *trans* acid, 1.4×10^{-4} vs. 3.5×10^{-5} for $K_{diss.}$, respectively (15), the *cis*-acid is not only the initial source of hydrogen ions but continues to be the predominant source to more than 70% isomerization (see Table IV). This may be, in part, the explanation for the long term validity of the substitution $[H^+] = K_{diss.}[cis]^{-1/2}$.

The likelihood of β-lactone intermediacy in this isomerization is low because an α,β-unsaturated acid cannot be made to form a β-lactone (22), and S_N2 displacement by an available nucleophile has been shown (23) to be the mode of opening. In this case the only available nucleophile, cinnamate anion, would yield intermolecular esters, which are not observed. Even if transitory β-lactone intermediacy was a fact, since it is fixed in conformation, the substituents cannot epimerize. Intermolecular ester formation, **3**, from intermediates **1** or **2**, even though there is established precedence (24), is probably not occurring here because no ester is observed.

Noyce and co-workers (10) concluded as a result of their kinetic studies that the intermediate **4**, formed by the addition of

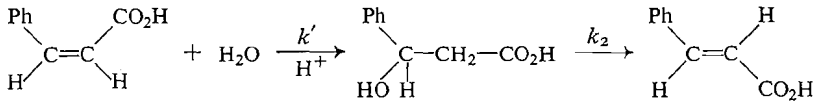

4

water across the double bond, was involved in the isomerization. In the present system involvement of this intermediate can be ruled out. The much lower rates observed in the neat than in the aqueous system must be attributable either to the involvement of a different intermediate (i.e. **1** or **2**) or to the very significantly lower hydrogen ion concentrations in the neat isomerizations, or to both factors.

Experimental

trans-Cinnamic acid used was reagent grade material supplied by Eastman Kodak, unless otherwise stated. Melting points and boiling points were not corrected. Infrared (i.r.) spectra were obtained on a Perkin–Elmer model 337 spectrometer. Nuclear magnetic resonance (n.m.r.) spectra were obtained at room temperature in deuteriochloroform on a Varian A60 instrument, the sweep width of which was routinely calibrated, except where otherwise indicated. Shifts are reported in p.p.m. from internal tetramethylsilane and coupling constants in c.p.s. Ultraviolet irradiations were performed using an unfiltered Hanovia 325 W high pressure quartz mercury arc lamp (model 65A-10 4¼ in. arc length) no more than 2–3 in. from the irradiated vessel. The apparatus for the irradiation experiments was wrapped with aluminum foil leaving a 6 in. opening top and bottom. To the top opening a 6 in. air exhaust hose was fitted which partially cooled and vented the whole apparatus.

Preparation of cis-Cinnamic Acid

(a) Without Water Cooling, Work-up by Successive Solvent Trituration or Crystallization

A solution of *trans*-cinnamic acid (100 g) in warm dry methanol (480 ml) was placed in a quartz flask fitted with a water condenser and drying tube ($CaSO_4$) and irradiated at the boiling point for 100 h. The residual oily crystals remaining on removal of the solvent consisted of 49% *trans*- and 39% *cis*-acids, with 7% *trans*- and 5% *cis*-methyl esters (determined by n.m.r.). Isomerization was achieved without esterification in photostationary state experiment (see below). Trituration of this residue with cold petroleum ether (p.e., 3 × 80 ml) and evaporation of the solvent yielded a yellow oil (11.7 g), which comprised most of the total ester content, plus a small amount of the *cis*-acid (i.r. and n.m.r.). Trituration of the solid residue from above with hot p.e. (5 × 80 ml) yielded 13.5 g of crystals on evaporation of the solvent. Recrystallization of the latter from p.e. (150 ml) with a trace of ether yielded a first crop (3.0 g; 53% *cis*-acid) melting at 72–82 °C with prior sintering, and a second crop (1.0 g) melting at 45–75 °C.

In another preparative experiment, when 270 g of *trans*-cinnamic acid had been irradiated, the residue on solvent evaporation and ester removal by cold trituration was fractionally crystallized from ethanol (1500 ml). After four crops of crystals (last crop, 19 g, melting at 115–129 °C) the residue (70 g) consisted of 44% *cis*-acid (n.m.r.).

(b) Without Water Cooling, Effect of Pyrex vs. Quartz on Isomerization Rate

A solution of *trans*-cinnamic acid (380 g) dissolved in warm methanol (900 ml) was divided into three equal portions. One portion was irradiated in a new Pyrex flask, one in an internally frosted (etched) Vycor flask, and one in a new transparent fused quartz flask. Isomerization progress at roughly equal irradiation intensities was as follows: Pyrex, 2 days, 4% *cis*; 9 days, 21% *cis*; etched Vycor, 2 days, no *cis*; quartz, 4 days, 21% *cis*; 7 days, 35% *cis*.

(c) Fractional Distillation

After a preliminary small scale vacuum distillation was found to considerably enhance the proportion of *cis* in the distillate with very little loss of total *cis* content by thermal isomerization to the *trans*, this was the method by which isolation of the *cis*-isomer was carried out. In all the distillations described below, an unpacked,

TABLE V

(*a*) Distillation of 103 g of acid, consisting of about 45% *cis*-isomer at 0.05 mm Hg

			Analysis* (%)			
			Methyl cinnamate		Cinnamic acid	
Fraction	Boiling point (°C)	Amount and description	*cis*	*trans*	*cis*	*trans*
1		7 g yellow oil	(30)	(55)	(15)	0
2	100–104.5	12.5 g oily crystals	(8)	(10)	82	0
3	104.5–107	37 g crystals	0	0	75	25
4	107	8 g crystals	—	—	—	—
Residue	> 107		0	0	28	72

*Approximations in parentheses.

(*b*) Distillation of 93 g of acid, consisting of about 77% *cis*-isomer

			Analysis* (%)			
			Methyl cinnamate		Cinnamic acid	
Fraction	Boiling point (°C)	Amount and description	*cis*	*trans*	*cis*	*trans*
1	90–100/0.1 mm	4.5 g oily crystals	—	—	—	—
2	100–104/0.1 mm	6.5 g oily crystals	(3)	(6)	91	0
3	103–104/0.1–0.05 mm	25 g crystals	—	—	91.5	8.5
4	103/0.05 mm	15 g crystals	—	—	—	—

*Approximations in parentheses.

(*c*) Distillation of 33 g of acid, consisting of about 91% *cis*-isomer at 0.03 mm Hg

			Analysis (%) cinnamic acid	
Fraction	Boiling point (°C)	Amount and description	*cis*	*trans*
1	93–103	0.5 g oily crystals	—	—
2	103–104	5.3 g crystals	99	1
3	104–106	5.8 g crystals	99–100	0
4	102–106	6.0 g crystals	99–100	0
5	103–106	5.3 g crystals	98	2
6	103	11.2 g oil	93	7

vacuum-jacketed column (35 × 1 cm) was used, and the distilland was kept below 145 °C, usually in the range 130–140 °C to avoid significant *cis* isomerization. Details of three successive distillations of enriched *cis*-acid fractions are given in Table V.

From the last distillation, fraction 4 melted at 34–40 °C, and fraction 5 at 49–55 °C. A portion of fraction 5 was recrystallized from p.e. to a constant m.p. (3 times) of 58–60 °C. Melting points of 32, 42, 58, and 68 °C are quoted (25) for the four crystalline polymorphic forms of *cis*-cinnamic acid. Confirmation that the recrystallized material was 58 °C melting point acid and not the impure 68 °C melting point acid was obtained by conversion of a small finely ground sample of the 58 °C m.p. acid to the 68 °C m.p. one. The sample was sealed in a glass tube and cooled to −196 °C for 15 min, then allowed to warm to room temperature for 15 min before opening (26). The m.p. was now 64–66 °C. Attempts to use sunlight for conversion of the 58 °C m.p. to the 68 °C m.p. acid (27) in quartz for 12 days gave material which partly melted at 187 °C and the remainder at 232–233 °C, probably a mixture of truxinic and/or truxillic acids (28). In Pyrex, 12 days of sunlight yielded material melting partly at 66–72 °C, partly at 130–135 °C, and the remainder at 170–200 °C from the *cis*. This was probably a mixture of 68 °C m.p. *cis*- and *trans*-cinnamic acids, plus some β-truxinic acid (lit. m.p. for the latter two compounds are 135 and 206 °C, respectively (28)).

Nuclear Magnetic Resonance Spectra and Analysis of Cinnamic Acids and Esters

The coupling between the two vinylic protons of the cinnamic acids yielded a doublet for each (29) in both the *cis*- (J = 12.5 c.p.s.) and the *trans*-isomers (J = 16 c.p.s.), the coupling of either of which was not significantly changed on esterification (cf. ref. 29). The aromatic proton resonance gave a multiplet 26 cycles wide for the *trans* (centered at 7.45 p.p.m.) and two groups of multiplets over a total of 33.5 cycles for the *cis* (centered at 7.47 p.p.m.), again unchanged on esterification. The remaining shifts are tabulated below.

Analysis of acid mixtures was accomplished by integra-

Can. J. Chem. Downloaded from www.nrcresearchpress.com by 210.87.254.42 on 09/05/12
For personal use only.

TABLE VI

Nuclear magnetic resonance spectra

Proton assignment	Shifts (p.p.m.)			
	cis-Cinnamic acid	Methyl *cis*-cinnamate	*trans*-Cinnamic acid	Methyl *trans*-cinnamate
α-Vinylic	5.93	5.88	6.45	6.40
β-Vinylic	7.05	7.00	7.83	7.78
Carboxyl or ester	11.80	3.60	—	3.73

tion of the *cis*- and *trans*-vinylic proton resonances and calculation of the proportions of each present from these integrals. In acid–ester mixtures, integrals were obtained for the *cis*- and *trans*-ester methyl resonances. Where more than 2 or 3% of one or both esters were present with the acids, the figure obtained for a one proton equivalence from the methyl integrals was subtracted from the respective vinylic integrals, a procedure necessary because, though the ester vinylic protons gave visibly distinct bands from the acid vinylic protons, they were not sufficiently so for accurate separate integration on a 500 cycles sweep width. No account was taken of the higher molecular weight of the esters in the calculation of percentages from the integrals; hence the percentages in the acid–ester mixtures represent mole %. At no time was there any sign of the formation of truxinic or truxillic acids in the solution ultraviolet or thermal isomerizations.

Photostationary State of the Cinnamic Acids

A solution of *cis*-cinnamic acid (2 g) in dry methanol (50 ml) was placed in a fused quartz test tube fitted with a water-cooled Pyrex cold finger reaching to the bottom of the solution, a short thermometer, and a drying tube ($CaSO_4$). An identical parallel experiment was set up using 2 g of *trans*-cinnamic acid. The two tubes were irradiated equidistant from the ultraviolet source for 3 days and aliquots were withdrawn, concentrated by boiling off some of the methanol, and analyzed by n.m.r. for the proportions of *cis* and *trans* present. The solution temperature was kept at 14 °C during the whole period of irradiation. No esters were formed during these experiments (see refs. 7 and 9). Progress of the isomerization is shown in Table VII.

TABLE VII

Photostationary state of cinnamic acid in methanol

Irradiation time (h)	% *cis* acid present	
	From all *cis*	From all *trans*
0	99.0	0
24	54.0	52.0
48	57.7	58.3
72	60.2	59.0

Thermal Isomerizations of the Cinnamic Acids

(a) trans-Cinnamic Acid

The commercial material (50 g) was wastefully recrystallized from ethanol (100 ml) and dried at 80 °C for 24 h, yielding colorless cinnamic acid (26 g), m.p. 134–136 °C. Portions of this recrystallized material (6 g) were placed in three stoppered test tubes, which were then heated in the vapor–liquid equilibrium of boiling flasks of diphenyl (257.5 °C), diethyl malonate (200.0 °C), and amyl acetate (143.5 °C). Aliquots were then removed from each of these tubes at intervals during a total time of 49 h for the 257.5 °C bath and 336 h for both the 200 °C and the 143.5 °C baths, and examined for the presence of *cis*-cinnamic acid by n.m.r. There was none present in any aliquot.

An aliquot from the *trans*-acid heated at 257.5 °C for 7½ h still crystallized (yellow crystals) but an aliquot after 23 h cooled to a brown glass without crystallizing. At 200 and 143.5 °C, even after 336 h heating, the aliquots of *trans*-acid still crystallized, though the crystals were brown.

(b) cis-Cinnamic Acid

In a way similar to the isomerization experiments of the *trans* species above, three approximately 1 g portions of *cis*-cinnamic acid were isomerized. One was carried out at 143.5 °C, as previously with the *trans*, and the others in the liquid–vapor equilibria of boiling cyclohexanol (163.5 °C) and ortho-dichlorobenzene (182.0 °C), temperatures being measured before and after a run with the same calibrated thermometer. With aliquots from the 163.5 °C run containing less than 10% of either isomer, analysis was sharpened by use of a computer of average transients attachment on the n.m.r. and using from 20 to 50 scans of the area of interest, before integrating. The last two aliquots of the 163.5 °C run were determined on a Varian HA 100 instrument and are estimated to be reliable to ± 0.1% *cis*-acid. The progress of these isomerizations is summarized in Table VIII. There was no evidence of any dimerization.

In calculations and plots of the above data it was found that the last point in each run deviated considerably from the norm set by the others, and in the 182 °C run had obviously been taken some time after complete isomerization. Consequently, these points and in addition the 75 and 98 h points for the 163.5 °C run which also showed significant deviation (possibly because of some sublimation of *cis*-acid from the small amount remaining at this extent of reaction) were omitted for the kinetic calculations. Concentration calculations to convert the above data into moles/l were made using 7.15 moles/l as the concentration of neat liquid *cis*-cinnamic acid at 133 °C, having allowed for the slightly higher density of *cis*-cinnamic acid. The concentration of liquid *trans*-cinnamic acid at 133 °C, calculated from a density measurement of Weger (21) is 7.13 moles/l, but for

Can. J. Chem. Downloaded from www.nrcresearchpress.com by 210.87.254.42 on 09/05/12
For personal use only.

TABLE VIII

Thermal isomerizations of *cis*-cinnamic acid

143.5 °C Run		163.5 °C Run		182.0 °C Run	
Heating time, h	% *cis*-cinnamic	Heating time, h	% *cis*-cinnamic	Heating time, h	% *cis*-cinnamic
0.0	90.3	0.0	98.8	0.0	97.0
1.0	89.2	0.25	96.7	0.58	82.3
3.0	88.2	0.50	93.8	1.0	73.8
21.0	69.0	1.0	92.3	2.0	61.4
52.0	51.3	2.0	86.3	4.0	43.8
118.0	29.7	4.0	77.3	7.0	29.4
164.0	19.5	9.0	61.0	23.17	6.0
188.0	13.9	27.0	28.6	47.17	0
284.0	11.6	32.0	25.1		
380.0	1	48.0	15.3		
		63.0	10.4		
		75.0	5.9		
		98.0	3.4		
		145.0	0.7		

simplification of the calculations here was taken as the same as *cis*-acid.

Acknowledgments

The author thanks E. C. Clarke to whom he is indebted for assistance with all the IBM 360 (model 30) computer-based calculations and for the use of his polynomial regression program. He also thanks H. D. Mak and J. P. Heeschen for obtaining the n.m.r. spectra required for this work, and C. G. Carlson, H. W. Quinn, and J. G. Smith for many helpful discussions.

1. B. K. VAIDYA. Proc. Roy. Soc. A, **129**, 299 (1930).
2. J. BERTRAM and R. KURSTEN. J. Prakt. Chem. **51**, 316 (1895).
3. J. BERTRAM and R. KURSTEN. Ber. **28**, 368 (1895).
4. A. W. K. DE JONG. Chem. Weekbl. **26**, 270 (1929).
5. R. STOERMER. Ber. **42**, 4865 (1909).
6. R. STOERMER. Ber. **44**, 666 (1911).
7. C. ELLIS and A. A. WELLS. The chemical action of ultraviolet rays. *Revised by* F. F. Heyroth. Reinhold Publishing Corp., N.Y. 1940. p. 482.
8. S. LINDENFORS. Arkiv. Kem. **10**, 561 (1957).
9. S. LINDENFORS. Arkiv. Kem. **12**, 267 (1958).
10. D. S. NOYCE, P. A. KING, F. B. KIRBY, and W. I. REED. J. Amer. Chem. Soc. **84**, 1632 (1962).
11. G. B. KISTIAKOWSKY and W. R. SMITH. J. Amer. Chem. Soc. **57**, 269 (1935).
12. G. SIAMICIAN and P. SILBER. Ber. **35**, 4128 (1902).
13. R. STOERMER and H. LADEWIG. Ber. **47**, 1803 (1914).
14. D. E. MCELCHERAN, M. J. H. WIJNEN, and E. W. R. STEACIE. Can. J. Chem. **36**, 321 (1958).
15. I. HEILBRON, A. H. COOK, H. M. BUNBURY, and D. H. HEY. Dictionary of organic compounds. 4th ed. Eyre and Spottiswoode, Ltd., London. 1965. p. 711.
16. A. A. ZIMMERMAN, C. M. ORLANDO, JR., and M. H. GIANNI. J. Org. Chem. **34**, 73 (1969), and refs. cited therein.
17. R. SEARLE, J. L. R. WILLIAMS, D. E. DEMEYER, and J. C. DOTY. Chem. Commun. 1165 (1967).
18. A. A. FROST and R. G. PEARSON. Kinetics and mechanism. 2nd ed. John Wiley and Sons, Inc., New York. 1961. pp. 43–47.
19. G. M. MULLET and C. R. NODDINGS. Science, **138**, 1346 (1962).
20. K. B. WIBERG. Physical organic chemistry. John Wiley and Sons, Inc., New York. 1964. pp. 308, 309.
21. F. WEGER. Ann. **221**, 73 (1883).
22. R. B. WAGNER and H. D. ZOOK. Synthetic organic chemistry. John Wiley and Sons, Inc., New York. 1953. p. 534.
23. E. S. GOULD. Mechanism and structure in organic chemistry. Henry Holt and Company, New York. 1959. p. 345.
24. M. B. HOCKING. Can. J. Chem. **47**, 821 (1969).
25. E. H. RODD. Chemistry of carbon compounds. Vol. III B. Elsevier Publishing Co., New York. 1953. p. 997.
26. H. STOBBE. Ber. **44**, 2744 (1911). H. STOBBE and C. SCHÖNBURG. Ann. **402**, 226 (1914). See also Beilstein IX, 1st suppl., p. 236.
27. C. LIEBERMANN. Ber. **42**, 1031 (1909). H. STOBBE, Ber. **52**, 666 (1919). See also Beilstein IX, 593.
28. E. H. RODD. Chemistry of carbon compounds. Vol. II A. Elsevier Publishing Co., New York. 1953. p. 64.
29. E. O. BISHOP and R. E. RICHARDS. Mol. Phys. **3**, 114 (1960).

Can. J. Chem. Downloaded from www.nrcresearchpress.com by 210.87.254.42 on 09/05/12
For personal use only.

Infrared spectra of aqueous sodium benzoates and salicylates in the carboxyl-stretching region: chelation in aqueous sodium salicylates

G. E. DUNN AND R. S. MCDONALD
Department of Chemistry, the University of Manitoba, Winnipeg 19, Manitoba
Received June 9, 1969

Infrared spectra in the frequency region 1300–1760 cm^{-1} are reported for 41 substituted sodium benzoates and 10 substituted sodium salicylates in deuterium oxide solution, and for 9 substituted salicylic acids in chloroform and carbon tetrachloride solutions. Carboxylate stretching frequencies of benzoates and salicylates correlate poorly with substituent constants, but the asymmetric frequencies of benzoates and salicylates correlate well with each other, and the asymmetric frequencies of benzoates correlate well with the asymmetric frequencies of the corresponding nitrobenzenes. It is suggested that, among substituted aromatic compounds, group vibrations which couple with the ring vibrations may correlate well with similar vibrations of other groups, but not with coupled vibrations of different symmetry, uncoupled vibrations, or substituent constants. Chelation in chloroform solutions of salicylic acid dimers can be detected by its influence on substituent effects, but infrared spectra provide no good evidence for chelation in aqueous sodium salicylates.

Canadian Journal of Chemistry, **47**, 4577 (1969)

Can. J. Chem. Downloaded from www.nrcresearchpress.com by 210.87.254.40 on 09/05/12
For personal use only.

There are a number of interesting problems concerning the ionization of benzoic acids which can be attacked by means of infrared spectrophotometry. Well-known examples are provided by the numerous correlations which have been made between the infrared absorptions corresponding to O—H and C=O stretching vibrations of carboxylic acids and interactions of the carboxyl group with other functional groups in the same molecule (substituent effects and chelation), in identical molecules (dimerization), or in different molecules (solvation and ionization).

Since molecular vibration frequencies are governed by atomic masses and the shape of the potential energy well in which they find themselves, it is to be expected that the carboxyl O—H and C=O stretching frequencies will be altered when these atoms form hydrogen bonds to other groups. Thus, it is not surprising to find that the O—H frequency decreases by about 500 cm^{-1} when benzoic acid in carbon tetrachloride dimerizes, or by about 200 cm^{-1} when it chelates with an *o*-methoxy group. Similarly, the C=O frequency decreases by about 50 cm^{-1} on dimerization, or chelation with an *o*-hydroxy group (1).

Also, it is to be expected that benzoic acid substituents too remote from the carboxyl group to chelate with it may alter the carboxyl frequencies by changing the electron densities in the bonds through inductive and resonance effects. Not only are such frequency changes observed, but both the O—H and C=O stretching frequencies of benzoic acids in carbon tetrachloride have been shown to be linearly related to the Hammett σ-constants, and therefore to the pK's of the acids in water (1–7). This is somewhat surprising, since ionization constants reflect substituent effects on the free-energy difference between the acid and its anion, both solvated by water. It might be reasonable to guess that the electronic displacements produced by a meta or para substituent on the solvated benzoic acid molecule could have parallel effects on the carboxyl stretching frequencies and the free energy of the acid. Then, if substituents were to have no effect, or a parallel but quantitatively different effect, on the free energy of the anion, ionization constants and carboxyl frequencies of the solvated acids would be linearly related. This leads to the expectation that, if solvent effects are small, constant, or proportional to frequency, the carboxyl frequencies of benzoate ions should be constant or linearly related to pK. Until very recently there has been no data to test this hypothesis.

A related problem is that of the abnormally large dissociation constant of salicylic acid in water. This is commonly attributed to stabilization of the monoanion by an intramolecular hydrogen bond (chelation) between the carboxylate oxygen and the ortho phenolic group. The infrared spectrum of salicylic acid in carbon tetrachloride and other nonpolar solvents shows the decrease in O—H and C=O frequencies expected for chelation (8–13), but this is hardly helpful. What is required is that chelation should

Can. J. Chem. Downloaded from www.nrcresearchpress.com by 210.87.254.40 on 09/05/12
For personal use only.

stabilize the anion more than the acid, and that this relationship should persist in aqueous solution where chelation will encounter severe competition from intermolecular hydrogen bonding with the solvent. It is perhaps not unreasonable that such should be the case, since the negative charge on the anionic oxygens should increase chelation, but this has never been adequately demonstrated by experiment.

Information pertinent to both of these problems might be obtained from the spectra of substituted benzoic acids and their salts in aqueous solution but when the present work was begun, no such data were available. In the interim, Lindberg has reported spectra of 21 substituted benzoates in aqueous solution (14). The scarcity of such data is no doubt due in part to the opacity of water to infrared radiation of the frequencies characteristic of carboxyl stretching vibrations. However, deuterium oxide is sufficiently transparent in the range 1700–1300 cm^{-1} to permit examination of substituent effects on carbon–oxygen stretching frequencies in aqueous solution, and the present work reports the absorption spectra of 41 benzoic and 10 salicylic acids in this region. Unfortunately, most of the acids are not sufficiently soluble in deuterium oxide to produce C=O absorptions which would penetrate the solvent absorption, so the investigation was confined to the much more soluble sodium salts. In a number of cases, it was necessary to use ^{18}O-enriched salts in order to identify the carbon–oxygen frequencies conclusively.

Experimental

Materials

All the benzoic acids were commercial products except *m*-methoxybenzoic acid. It was synthesized by methylation of *m*-hydroxybenzoic acid with dimethyl sulfate. The preparations of 4- and 5-methoxysalicylic acids have been previously described (15), as have those of 4- and 5-fluoro- and 4-bromosalicylic acids (16). The other salicylic acids were commercial products, as were nitrobenzene, *o*- and *p*-nitrophenol, sodium benzoate, and sodium salicylate. Sodium *p*-hydroxybenzoate was prepared by dissolving *p*-hydroxybenzoic acid in the theoretical amount of 0.4 *M* aqueous sodium hydroxide, evaporating the water, and drying the residue at 100° for 24 h.

Solvents

Carbon tetrachloride was purified by refluxing it with 5% aqueous sodium hydroxide for 3 h, washing with water, then with concentrated sulfuric acid 3 times or until colorless, again with water, and drying over first calcium chloride then magnesium sulfate. It was distilled, and distillate collected between 76.0 and 76.2°.

Chloroform was purified from its alcohol stabilizer by the method of Fieser (17) and stored in the dark over chromatographic alumina. Under these conditions, it will keep for a few weeks without developing any spurious absorptions in either the infrared or ultraviolet regions. Spectra of benzoic acids obtained in this solvent and in hydrocarbon-stabilized chloroform (Matheson, Coleman, and Bell) were identical, so that the latter solvent was used in much of the work.

Potassium bromide was International Crystal Laboratories Spectrograde, and heavy water was certified by the supplier (Merck, Sharpe, and Dohme of Canada) to be 99.7 mole % deuterium oxide.

^{18}O-Labelled Benzoates

Labelling of the carboxyl group with ^{18}O was accomplished by hydrolyzing the acid chlorides in water containing 42.1 atom % ^{18}O according to the supplier (Yeda Research and Development Co. Ltd., Rehovoth, Israel). The acid chlorides were prepared by refluxing the appropriate acids in a 10-fold excess of thionyl chloride and distilling off the thionyl chloride, then the substituted benzoyl chloride, under vacuum. About 20 μl or 20–30 mg (0.15 mmol) of the acid chloride was transferred to a small flask with standard taper joint which was immediately placed on a vacuum line, cooled in liquid nitrogen, and evacuated. Then about 1 g of ^{18}O-labelled water was distilled into the flask from an adjacent bulb on the vacuum line, the flask was closed off and heated in a boiling water bath for 0.5 to 16 h. The short time was used for salicylic acid to minimize decarboxylation; longer times were required for hydrolysis of some of the solid chlorides. The ^{18}O-water storage bulb was then frozen in liquid nitrogen and the labelled water was distilled back into it from the reaction flask. The flask was removed from the vacuum line and 1 ml of a 0.20 *M* solution of sodium hydroxide in D_2O was added to it. The resulting solution was used to record the spectrum.

The amino-, hydroxy-, and thiohydroxy-benzoic acids could not be converted to their chlorides by the above procedure, so they were not labelled. Salicylic acid was converted to its chloride by the method of Kahovec and Kohlrausch (18).

Spectra

All spectra were recorded by a Perkin–Elmer double-beam, grating spectrophotometer, Model 337, equipped with expanded scale readout attachment coupled to a Brown recording potentiometer. The instrument was used at its smallest slit width, scanning at 39 cm^{-1}/min and recording at 40 s/in. Since both frequency and chart speed are linear with respect to time, this produced a recorder trace of about 26 cm^{-1}/in. For spectra of D_2O solutions, the indene peaks at 1797.7 and 1288.0 cm^{-1} were used to calibrate the scale for each sample by beginning a scan with indene in a 0.1 mm cell, recording from 1850 to 1700 cm^{-1}, then replacing indene by sample, recording to 1300 cm^{-1}, restoring the indene and recording to 1250 cm^{-1}, all without stopping the scan. Frequencies calculated by interpolation were reproducible to 0.3 cm^{-1} and should be accurate to $\pm$ 1 cm^{-1}. They are reported to the nearest cm^{-1}. Spectra in carbon tetrachloride and chloroform were calibrated by the same procedure using the polystyrene peaks at 1844.0 and 1601.2 cm^{-1}. These are not as sharp as the indene peaks, so the reproducibility of frequency is reduced to about 0.5 cm^{-1}.

Samples of benzoates and salicylates in deuterium oxide were prepared by making 0.15 *M* solutions of the acids in

Can. J. Chem. Downloaded from www.nrcresearchpress.com by 210.87.254.40 on 09/05/12
For personal use only.

a 0.20 *M* solution of sodium hydroxide in deuterium oxide. The dianions of the hydroxybenzoates were obtained by the same procedure, using 1.0 *M* sodium hydroxide solution. Samples were scanned in 0.05 mm cells with calcium fluoride windows. Frequencies at the absorption peaks were the same with either deuterium oxide or air in the reference beam. Spectra of the substituted salicylic acids were recorded at concentrations such that the monomer and dimer absorptions were about equally intense. This was found to require concentrations of about 1.5×10^{-3} *M* in carbon tetrachloride or 2.5×10^{-3} *M* in chloroform. These solutions were scanned in a 5 mm cell with sodium chloride windows.

Results

Figure 1 shows the spectrum of sodium benzoate in deuterium oxide through the region 1350–1650 cm^{-1}. The upper solid line shows sodium benzoate and the dotted line shows ^{18}O-labelled sodium benzoate, both run against air. Since the carboxyl oxygens are only about 40% labelled, the spectra of labelled and unlabelled acids are not resolved, but the peaks at 1548 and 1390 cm^{-1} are seen to be broadened on the low-frequency side, showing that these are absorptions by the carbon–oxygen bonds. The lower solid line was obtained by scanning a 0.15 *M* solution of the labelled benzoate against a 0.09 *M* solution of unlabelled benzoate in the reference beam, so that most of the absorption by solvent and unlabelled salt cancels out. The carbon–oxygen peaks have shifted to 1538 and 1380 cm^{-1}, respectively, a decrease in frequency of 10–11 cm^{-1}. While this may not be a satisfactory method of determining isotopic shifts,

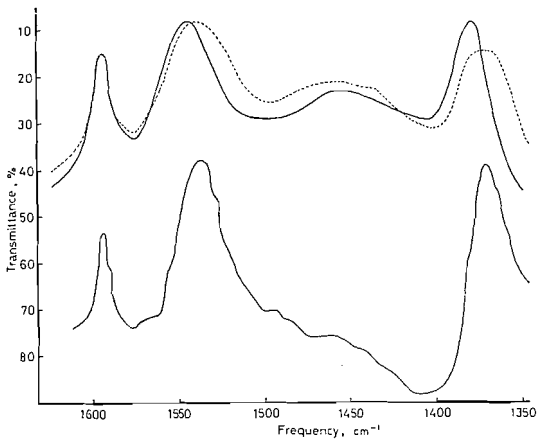

FIG. 1. Infrared spectra of sodium benzoate in deuterium oxide. Upper solid line, unlabelled salt; dashed line, salt containing 40% of ^{18}O; lower solid line, salt containing 40% ^{18}O vs. 60% of its concentration of unlabelled salt.

because the solution contains a mixture of benzoates containing zero, one, and two ^{18}O atoms, the peak broadening is quite adequate to ensure correct identification of the carbon–oxygen frequencies.

Edsall first assigned the carbon–oxygen stretching frequencies in the carboxylate ion (19). He studied the Raman spectra of a number of dicarboxylic acids and their salts and found a band near 1400 cm^{-1} in all the salts, which he assigned to the

$$[O\cdots\underset{|}{C}\cdots O]^-$$

symmetric stretching frequency by analogy with the corresponding 1380 cm^{-1} peak of the nitro group. Similarly, an infrared band near 1580 cm^{-1} was assigned to the asymmetric stretching frequency. Gore, Barnes, and Petersen found corresponding peaks at 1410 and 1560 cm^{-1} in the infrared spectra of sodium acetate in deuterium oxide solution (20), and Erlich found peaks at 1412 and 1550 cm^{-1} for sodium polymethacrylate in the same solvent (21).

The symmetric and asymmetric peaks for sodium benzoate were found in thin films at 1411 and 1554 cm^{-1} by Davies and Jones (22), in potassium bromide pellets at 1413 and 1554 cm^{-1} by Stimson (23), and in Nujol mulls at 1413 and 1552 cm^{-1} by Green, Kynaston, and Lindsey (24). The last-named authors found these bands at 1392 and 1544 cm^{-1} in the Raman spectrum of aqueous sodium benzoate. Chapman, Lloyd, and Prince found the symmetric and asymmetric infrared absorptions of aqueous sodium benzoate at 1395 and 1553 cm^{-1}, respectively (25). Subsequently, in a study of sodium benzoate in deuterium oxide, Hoshino, Hosoya, and Nagakura found infrared absorptions at 1599 and 1550 cm^{-1} and assigned the one at 1599 cm^{-1} to the asymmetric carboxylate vibration (26). Figure 1 shows that this assignment is incorrect; the 1599 cm^{-1} peak (we find it at 1595 cm^{-1}) is not produced by a carbon–oxygen bond since it is not affected by ^{18}O labelling. On the basis of the earlier assignments, we attribute the carboxylate peaks at 1391 and 1548 cm^{-1} in Fig. 1 to the symmetric and asymmetric

$$[O\cdots\underset{|}{C}\cdots O]^-$$

stretching frequencies, respectively.

Carbon–oxygen stretching absorptions were found at similar frequencies in the spectra of all

TABLE I

Infrared frequencies of substituted sodium benzoates in deuterium oxide solution

Compound	Substituent	Infrared frequency (cm^{-1})									
					CO_2^-						
		Aromatic			Asymmetric				Symmetric		
1	H*		1595		1548				1391		
	para										
2	O^-		1590		1567	1511†		1503	1381		
3	NH_2	1609		1588	1533				1385		
4	OH	1607	1596		1542				1386		
5	OMe	1606	1594		1541			~1470	1388		
6	OEt*	1607	1595		1542	~1515			1389		
7	*t*-Bu*	1609	1588		1538				1391		
8	Me	1609	1590		1542				1389		
9	*i*-Pr	1607	1589		1541				1390		
10	C_6H_5*	~1604	1590	1576	1540				1390		
11	F*	1609			1554				1390		
12	Cl		1593		1548				1393		
13	Br		1591		1547				1392		
14	I		1588		1544				1391		
15	CF_3	1601			1558	~1515			1395	1328	
16	CN		1595		1553				1387		
17	NO_2*	1615			1575	1525			1392	1349	1312
	meta										
18	O^-			1573	1540			1475	1423	1386	
19	NH_2		1592		1554			1442		1390	
20	Me	1604	1594		1552				~1425	1390	
21	OH		~1590		1551			~1475	1423	1388	
22	OMe		1597		1555			1469	1437	1388	
23	Cl		1592		1554				1420	1384	
24	Br		1589		1551				1415	1383	
25	NO_2*	1616	1599		1562	1532		1477	1435	1386	1355
	ortho										
26	O^-		1591		1555	1534†		1471	1446	1401	
27	NH_2	1612	1579		1541			1485	1454	1382	
28	OH*	1618	1589		1546			1476	1459	1377	
29	OMe*	1603	1587		1556	1490		1468	1439	1400	
30	OEt	1602	1587		1557			~1475	~1450	1400	
31	Et	1602	1575		1553					1406	
32	Me*	1603	1579	1561	1551				~1445	1405	
33	C_6H_5		1599		1555	1480		1452		1400	
34	F*	1614	1596		~1561			~1485	~1455	1392	
35	Cl*		1581		~1570‡			~1475	~1435	1401	
36	Br		1580		‡			~1475	~1435	1401	
37	I		1575		‡			~1470	~1430	1399	
38	SH	1590	1577		1551	1467		1437	1430	1393	
39	CF_3*		1574		‡	~1490				1402	
40	CN	1604	1588		1566	~1485		~1445		1388	
41	NO_2*		1590		1570‡	1529		1479		1387	1343

*Frequencies identified by ^{18}O labelling.
†Identification of the carboxylate frequency is uncertain.
‡There is only one intense, unsymmetrical peak in the 1500–1600 cm^{-1} region. In the *o*-Cl and *o*-NO_2 cases ^{18}O labelling produces a shoulder at ~1570 cm^{-1}, which suggests that the aromatic and asymmetric carboxylate frequencies are not resolved.

the substituted benzoates; 1377–1406 cm^{-1} for symmetric and 1533–1566 cm^{-1} for asymmetric vibrations. They are recorded in Table I. In 14 cases, the carbon–oxygen stretching bands were identified by ^{18}O labelling. These are indicated by asterisks in Table I. In most cases, the remaining spectra resembled the spectrum of one of the labelled acids with a chemically similar substituent so closely that the peaks could be identified without labelling.

Lindberg has reported frequencies for 16 of the benzoates in Table I (14). For a few substituents (H, *p*-NH_2, *p*-OMe), these agree closely with our values, but in most cases Lindberg's frequencies for both carboxylate and non-carboxylate vibrations are 3–5 cm^{-1} less than ours. The out-

Can. J. Chem. Downloaded from www.nrcresearchpress.com by 210.87.254.40 on 09/05/12
For personal use only.

Can. J. Chem. Downloaded from www.nrcresearchpress.com by 210.87.254.40 on 09/05/12
For personal use only.

standing exception is the salicylate ion, for which Lindberg's frequencies are all 6–9 cm^{-1} greater than ours. This is unfortunate, since it tends to confuse deductions concerning chelation in salicylates. However, our salicylate values can not be the result of an error arising from a bad sample or a single bad measurement, since 10 substituted salicylates from a wide variety of sources were examined and the frequencies for sodium salicylate are in excellent agreement with the others. For example, the asymmetric frequency for salicylate is precisely that predicted by the Hammett relationship from the substituted salicylates. It will, therefore, be assumed for the purposes of this paper that the frequencies reported here are at least internally consistent.

The peak at 1595 cm^{-1} in Fig. 1 is no doubt the same as the one found by Hoshino, Hosoya, and Nagakura at 1599 cm^{-1} and by Chapman, Lloyd, and Prince at 1602 cm^{-1}. The latter authors attribute it to a carbon–carbon stretching vibration (25). Such bands have been observed by many workers in a great variety of aromatic compounds, and their intensities are very sensitive to the nature of substituents on the aromatic nucleus. All the benzoates, salicylates, and salicylic acids examined in this work have from one to three bands in the 1575–1620 cm^{-1} region which we have listed in the tables under the heading "aromatic" without any other justification than that they are not carboxylate or nitro absorptions. Their intensities are highly variable, being weakest in the *m*-substituted acids and strongest in the *o*-substituted ones. The *o*-chloro-, *o*-bromo-, *o*-iodo-, and *o*-nitro-benzoates show only one very intense peak, with small low-frequency shoulders in the region 1500–1600 cm^{-1}, which is very probably a superposition or combination of aromatic and asymmetric carboxylate absorptions, since it is broadened by ^{18}O labelling. We could find no correlation of these aromatic frequencies with substituent or ionization constants. Most benzoates had peaks between the symmetric and asymmetric ones. These are not important for the purpose of this work and are listed for information only.

The spectrum of sodium salicylate is of particular interest in connection with the expected intramolecular hydrogen bonding of the salicylate ion. Green, Kynaston, and Lindsey found the asymmetric stretching frequency of sodium salicylate in Nujol mull at 1582 cm^{-1} but were not able to

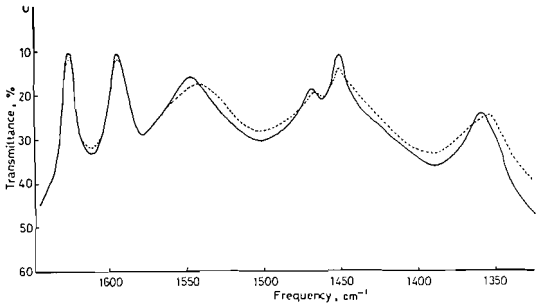

FIG. 2. Infrared spectra of sodium salicylate in deuterium oxide. Solid line, unlabelled salt; dashed line, salt containing 40% of ^{18}O.

decide between peaks at 1407 and 1376 cm^{-1} for the symmetric stretching frequency (24). Chapman, Lloyd, and Prince examined sodium salicylate in deuterium oxide and found peaks at 1621, 1593, and 1377 cm^{-1} (25). They assigned the 1377 and 1621 cm^{-1} peaks to the symmetric and asymmetric carboxylate stretching frequencies, respectively, and the one at 1593 cm^{-1} to an aromatic stretch. Our spectra of deuterium oxide solutions of sodium salicylate unlabelled and labelled with ^{18}O are shown in Fig. 2. It is seen that the carbon–oxygen stretching frequencies are at 1376 and 1546 cm^{-1}, and we assign these to the symmetric and asymmetric frequencies, respectively. The broad peak at 1546 cm^{-1} is not mentioned by Chapman, Lloyd, and Prince, but it is in the region where all the other substituted benzoates have asymmetric carboxylate absorptions, and ^{18}O-substitution produces a distinct broadening on its low-frequency side, whereas the peaks at 1617 and 1589 cm^{-1} are not affected at all. These are probably both aromatic stretching frequencies. Spectra of the substituted salicylates resembled that of the parent compound sufficiently to make assignment of the carboxylate stretching frequencies possible without labelling. They are recorded in Table II.

The spectra of most of the salicylic acids from which the above salicylates were derived have not been reported previously, so they were recorded in carbon tetrachloride and chloroform. The latter solvent was used because the nitrosalicylic acids were not sufficiently soluble in carbon tetrachloride to produce satisfactory spectra. The results are reported in Table III. Edsall first assigned the aliphatic carboxylic acid peaks near 1720 and 1670 cm^{-1} in nonpolar solvents to the C=O stretching frequencies of the

TABLE II

Infrared frequencies of substituted sodium salicylates in deuterium oxide solution

	Infrared frequency (cm^{-1})								
				CO_2^-					
Substituent	Aromatic			Symmetric			Asymmetric		
H	1617	1589	1546	1476	1459		1376		
4-OMe	1620	1589	1537		1448		1370	1337	
4-F	1624	1596	1550		~1442		1375		
4-Br	1610	1579	1544		1425		1378		
4-NO_2	1629		1566	1526	1475	1436	~1396	1354	~1310
5-OMe	1626	1586	1558		1485	1432	1370		
5-F	1628	1596	1559		~1475	~1433	1368		
5-Cl	1618	1584	1552		1472	1422	1367		
5-I	1610	1579	1548		~1465	~1415	1366		
5-NO_2	1625	1599	1564		~1480	~1440	~1392		

TABLE III

Carbonyl frequencies of substituted salicylic acids

	Infrared frequencies (cm^{-1})			
	Monomer in		Dimer in	
Substituent	$CHCl_3$	CCl_4	$CHCl_3$	CCl_4
H	1691	1696	1664	1663
4-OMe	1678	1687	1653	1652
4-F	1692	1698	1664	1662
4-Br	1691	1697	1665	1663
4-NO_2	1705	*	1678	*
5-OMe	1693	1699	1669	1667
5-F	1698	1702	1669	1667
5-Br	1694	1700	1671	1667
5-NO_2	1702	*	*	*

*Not sufficiently soluble to give a measurable frequency.

monomeric and dimeric forms of the acid, respectively (27), and this assignment has been amply confirmed by other workers. Brooks, Eglinton, and Morman found the monomeric and dimeric frequencies of a large series of benzoic acids in carbon tetrachloride in the regions 1737–1760 cm^{-1} and 1691–1715 cm^{-1}, respectively (6). They also studied a series of 21 alkyl- and aryl-substituted salicylic acids and found the monomer and dimer absorptions to be shifted to the regions 1668–1703 and 1640–1670 cm^{-1}, respectively (12). Our values of 1696, 1663 cm^{-1} for salicylic acid in carbon tetrachloride may be compared with 1698, 1663 cm^{-1} by Brooks and co-workers, or 1696, 1662 cm^{-1} by Josien and co-workers (7) for the same acid in the same solvent.

Discussion

Benzoates and Nitrobenzenes

Considered by itself, the carboxylate group consists of two carbon–oxygen bonds back-to-back on the same carbon atom. Consequently, the two carbon–oxygen vibrations of the same symmetry are strongly coupled and give rise to two widely separated vibration frequencies, the average of which represents the hypothetical uncoupled carbon–oxygen vibration. In these respects, the carboxylate group resembles the carbon dioxide molecule and, as in that molecule, the composite vibrations are commonly labelled "symmetric" and "antisymmetric". Strictly speaking, of course, these terms are not applicable to the carboxylate vibrations because the carboxylate group is not an isolated unit but is attached through its carbon to another molecular moiety. In the case of the benzoates, these terms are particularly inappropriate because the other moiety is the aromatic nucleus, which is composed of atoms having masses and bond strengths similar to those of the carboxylate group and vibrating in modes some of which have the same symmetry as the carboxylate vibrations. It is, therefore, to be expected that there will be some coupling between the carboxylate and aromatic ring vibrations.

How these multi-nuclear vibrations will be affected by substituents on the aromatic ring is difficult to predict. Empirically, many good correlations have been found between substituent constants and frequencies of vibrations, such as carbonyl, which are largely insulated from the aromatic ring by mass, bond strength, or symmetry considerations (8). On the other hand, no such correlations are known between substituent constants and aromatic ring vibrations. Hence, if it is assumed that carboxylate frequencies will have characteristics of both the carbonyl and aromatic ring vibrations, it may be too optimistic

Can. J. Chem. Downloaded from www.nrcresearchpress.com by 210.87.254.40 on 09/05/12
For personal use only.

Can. J. Chem. Downloaded from www.nrcresearchpress.com by 210.87.254.40 on 09/05/12
For personal use only.

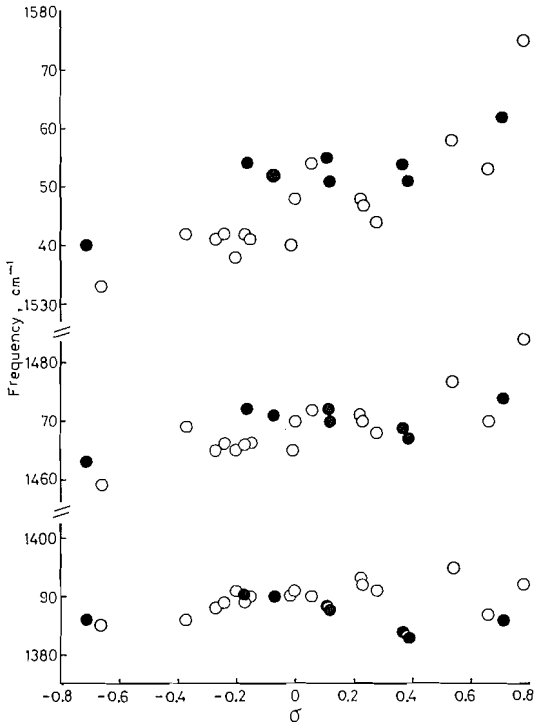

FIG. 3. Infrared frequency of benzoates vs. σ. Upper series, asymmetric frequencies; lower series, symmetric frequencies; middle series, average of symmetric and asymmetric frequencies. ○ are *p*-substituents; ● are *m*-substituents.

to expect a good correlation between substituent constants and carboxylate frequencies.

Figure 3, where the symmetric and asymmetric frequencies, and the average of these, are plotted against Hammett's σ (28) for 24 *m*- and *p*-substituted benzoates, shows that the correlation is, in fact, not good. Although there is a tendency for frequency to increase with increasing σ in all 3 cases, the scatter is large. The correlation is better for the asymmetric frequencies (correlation coefficient, $r_{\nu_{as}\sigma_{mp}} = 0.80$; $\rho = 20.2 \pm 3.2$) than the symmetric ones ($r_{\nu_s\sigma_{mp}} < 0.01$, $\rho = 1.0 \pm 1.7$), but this is largely because the frequency spread is larger in the former case. In fact, the Hammett relationship predicts the symmetric frequencies with a standard error of $\pm 3\ cm^{-1}$ compared to $\pm 5\ cm^{-1}$ for the asymmetric ones, but the range of frequencies covered is only $9\ cm^{-1}$ for the symmetric as compared to $42\ cm^{-1}$ for the asymmetric frequencies. Averaging the symmetric and asymmetric frequencies produces no improvement ($r_{\nu_{ave}\sigma_{mp}} = 0.72$; $\rho = 9.8 \pm 2.0$), and the symmetric and asymmetric frequencies do not correlate with each other ($r_{\nu_s\nu_{as}} < 0.01$).

Lindberg, using 14 substituents of which 10 are the same as ours, also found the asymmetric frequencies to give a poor fit to the Hammett relationship, and the symmetric frequencies a worse one (14). Among the asymmetric frequencies, he observed a tendency for meta and para points to fall on separate lines. This tendency is not evident in our data. The scatter of the 8 meta points is particularly bad ($r_{\nu_{as}\sigma_m} = 0.56$) so that the fit is improved somewhat when they are omitted ($r_{\nu_{as}\sigma_p} = 0.84$; $\rho = 21.6 \pm 3.6$) but there is little evidence for a separate line. Lindberg also suggested that *p*-substituents having unshared electron pairs on the atom next to the aromatic ring (+M substituents) fall on a separate line from other *p*-substituents. This was a tentative proposal, because his substituents included only 2 without unshared pairs. Eight of our 16 *p*-substituents are not of the +M type and they show little evidence of forming a separate line ($r_{\nu_{as}\sigma_p} = 0.88$; $\rho = 27.4 \pm 5.5$).

If the poor fit of the benzoate frequencies to the Hammett relationship is the result of mixing of the carboxylate and aromatic ring vibrations as postulated above, the nitro group should show a similar behavior. Nitro and carboxylate groups have the same symmetry and very nearly the same force constants, mass, and size. The only major difference between the two groups is the charge on the carboxylate group.

Stretching frequencies of aromatic nitro groups have been examined by a number of workers. Brown plotted the frequencies of 5 *m*- and 5 *p*-substituted nitrobenzenes in chloroform against σ and found a fair correlation for asymmetric frequencies but a poor one for symmetric frequencies (29). Kross and Fassel used 15 *p*-substituted nitrobenzenes and found a better correlation of the asymmetric frequencies with σ^- than with σ (30). On the other hand, Yates and Thompson found a better correlation of the asymmetric frequencies of 11 *m*- and *p*-substituted nitrobenzenes with σ^+ than with σ (47). Katritzky and Simmons published an extensive list of aromatic nitro frequencies in chloroform (31), but did not attempt a correlation with substituent constants. Twenty-two of Katritzky's substituents are the same as ours, so it is possible to compare benzoate frequencies in aqueous solution with nitrobenzene frequencies in chloro-

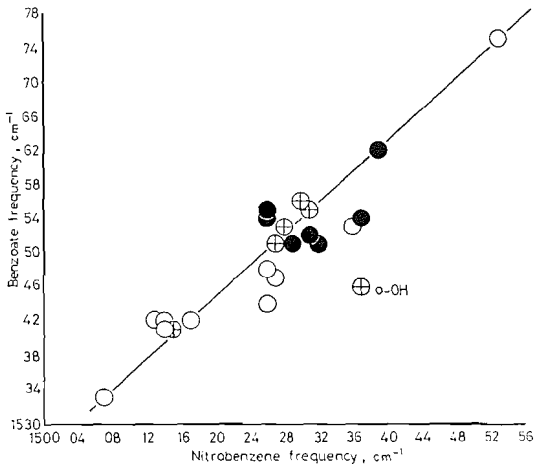

FIG. 4. Asymmetric frequencies of benzoates vs. those of nitrobenzenes. ○ are *p*-substituents; ● are *m*-substituents; ⊕ are *o*-substituents. Frequencies of *p*-substituted nitrobenzenes are from ref. 30; those of *o*- and *m*-substituted nitrobenzenes, from ref. 31.

form. The comparison has to be confined to asymmetric frequencies, however, because the range of symmetric frequencies is too small to permit reliable correlation.

Figure 4 shows a fairly good correlation between the asymmetric benzoate and nitro frequencies, not only for *m*- and *p*-substituents, but (excepting *o*-hydroxy) for *o*-substituents as well ($r_{\nu_{CO_2},\nu_{NO_2}} = 0.92$; $\nu_{CO_2} \pm 3 = 0.91\nu_{NO_2} + 162$). Excluding ortho, or ortho and meta, substituents have almost no effect on the correlation. It is apparent that substituent effects on the asymmetric vibration frequencies are similar for the aromatic carboxylate and nitro groups, but different from those on other vibrations more effectively insulated from the aromatic ring.

A possible reason for the different substituent effects on insulated and uninsulated vibrations might be that substituents exert their influence through different blends of polar and resonance effects in the two cases. This interpretation is encouraged by the observation of Kross and Fassel (30) and Yates and Thompson (47) that asymmetric nitro frequencies fit σ^- or σ^+ better than σ, and by Rao's successful use of combinations of σ, σ^-, and σ^+ in some correlations (8). A convenient method for testing this hypothesis has recently been provided by Swain and Lupton, who have separated the polar and resonance contributions to substituent effects in the form of field and resonance parameters, $\mathcal{F}$ and $\mathcal{R}$ (32). These can be recombined in any proportion appropriate to the system under investigation. Correlation with vibration frequencies take the form

$$\nu = f\mathcal{F} + r\mathcal{R} + \nu_0$$

which can be solved for f and r, the field and resonance weighting factors, and ν_0, the frequency of the unsubstituted parent compound.[1] Clearly, the blend of $\mathcal{F}$ and $\mathcal{R}$ will be different for *m*- and *p*-substituents so that these must be treated separately.

For *p*-substituted benzoates, the multiple correlation coefficient is $r_{\nu_{as}\mathcal{F}\mathcal{R}} = 0.83$ and the standard error in the calculated ν_{as} is 4 cm^{-1}. For *m*-substituted benzoates, the figures are $r_{\nu_{as}\mathcal{F}\mathcal{R}} = 0.46$, standard error in ν_{as} = 4 cm^{-1}. Comparison of these numbers with those given earlier for the correlation with σ ($r_{\nu_{as}\sigma_p} = 0.84$; $r_{\nu_{as}\sigma_m} = 0.56$) shows that the correlation with $\mathcal{F}$ and $\mathcal{R}$ is no better than that with σ. The same is true for Katritzky's nitrobenzene frequencies, whether for *p*-substituents ($r_{\nu_{as}\mathcal{F}\mathcal{R}} = 0.86$; $r_{\nu_{as}\sigma_p} = 0.92$) or *m*-substituents ($r_{\nu_{as}\mathcal{F}\mathcal{R}} = 0.82$; $r_{\nu_{as}\sigma_m} = 0.81$). Evidently vibration frequencies in the functional groups of benzoates or nitrobenzenes do not correlate well with any blend of polar and resonance effects.[2]

Apparently there is a fundamental difference in substituent effects between insulated and uninsulated frequencies. The fact that it is the insulated frequencies which correlate well with substituent constants seems to suggest that substituent effects on equilibria and rates are also largely localized in the bonds undergoing reaction.

Salicylates and Salicylic Acids

When this investigation was begun, it was hoped that the correlation between carboxylate vibration frequencies and substituent constants might be good enough to permit detection of

[1]In order to apply Swain and Lupton's computer program (ref. 32, footnote 32) to infrared frequencies, it is necessary to convert it to double precision form, or else to replace ν by some function of frequency with the same number of digits and decimal places as $\mathcal{F}$ and $\mathcal{R}$; for example, $\nu \times 10^{-3} - 1$.

[2]For nitrobenzenes this conclusion is weakened by the correlations found with σ^- (30) and σ^+ (47). The discrepancy is due, in part, to the different choice and limited number of substituents used in each case, but mainly to disagreement among the various workers concerning the asymmetric nitro frequencies of *p*-nitrophenol and *p*-nitroanisole.

Can. J. Chem. Downloaded from www.nrcresearchpress.com by 210.87.254.40 on 09/05/12
For personal use only.

Can. J. Chem. Downloaded from www.nrcresearchpress.com by 210.87.254.40 on 09/05/12
For personal use only.

chelation between carboxylate and phenolic groups of salicylates in aqueous solution. However, as has been pointed out above, this did not prove to be the case. The correlations of salicylate frequencies with σ ($r_{\nu_{as}\sigma_{mp}} = 0.81$; $r_{\nu_{s}\sigma_{mp}} = 0.58$) are neither better nor worse than those of benzoates.

On the other hand, the correlation of asymmetric salicylate frequencies with asymmetric benzoate frequencies is considerably better ($r_{\nu_{as}\nu_{as}} = 0.92$), suggesting that the poor correlations of both salicylate and benzoate frequencies with substituent constants are caused by the same factors, most probably coupling of the carboxylate and ring frequencies.

The carbonyl frequencies of benzoic acids in carbon tetrachloride have been shown to give good correlations with σ; for the monomer, Rao *et al.* (8) report $r_{\nu_m\sigma_{mp}} = 0.96$, and for the dimer, $r_{\nu_d\sigma_{mp}} = 0.99$. The correlations for salicylic acids in chloroform are also good ($r_{\nu_m\sigma_{mp}} = 0.93$; $r_{\nu_d\sigma_{mp}} = 0.94$) but not quite as good as those for the benzoic acids. The possibility that the decrease in correlation coefficient is caused by chelation will be considered in the next section.

Chelation in Salicylic Acids and Salicylate Anions

It is a well known fact that salicylic acid is a much stronger acid than benzoic acid or its *m*- and *p*-hydroxy derivatives, and the increased acidity is commonly attributed to chelation between the *o*-phenolic group and the carboxyl oxygen. That such chelation exists in crystalline salicylic acid and in solutions of salicylic acid in nonpolar solvents is demonstrated by a wide variety of evidence based on data from X-ray crystallography, infrared and ultraviolet absorption spectroscopy, vapor pressures, and other physical properties (references quoted in refs. 16 and 33). The fact that the carbonyl vibration frequencies of the substituted salicylic acids in chloroform reported in Table III are almost uniformly 48 cm^{-1} less for the monomers and 35 cm^{-1} less for the dimers than the corresponding frequencies of benzoic acids (6) may be taken as additional evidence for chelation in the salicylic acids. Hydroxyl groups in the *m*- and *p*-positions of benzoic acid have no such effect on the carbonyl frequency (5, 34).

Chelation between the phenolic hydroxyl and the carbonyl groups of substituted salicylic acids should influence the correlation between carbonyl frequencies and substituent effects by providing a second path through which the substituent can influence the frequency; namely, through the chelate hydrogen bond. Jaffe (35) has proposed that such dual path substituent effects can be handled by an extension of the Hammett equation which, for vibration frequencies, would take the form

$$\nu = \rho_1\sigma + \rho_2\sigma^- + \nu_0$$

where $\rho_1\sigma$ refers to the carboxyl group and $\rho_2\sigma^-$ to the phenolic group. He suggests that this 2-parameter equation may be considered to give a better correlation than the usual 1-parameter Hammett equation if ρ_2 turns out to be significant at the 95% confidence level or better, when the correlation coefficient between σ referred to the carboxyl group and σ^- referred to the phenolic group is 0.9 or less for the substituents used. For our salicylic acid substituents $r_{\sigma\sigma^-} = 0.61$, so they are suitable for studying the contribution by $\rho_2\sigma^-$ to the vibration frequency. Application of the monomer data to the 2-parameter equation yields $\rho_1 = 25.7 \pm 4.1$ cm^{-1}; $\rho_2 = -4.3 \pm 3.1$ cm^{-1}. Obviously, substituent influence on the monomer vibration frequencies through the chelate pathway is small compared to that through the direct one. Student's *t*-test on ρ_2 and its standard deviation indicate that it is significant only at the 80% confidence level. For the dimer frequencies, transmission through chelation is more important: $\rho_1 = 26.4 \pm 2.5$ cm^{-1}; $\rho_2 = -7.9 \pm 3.0$ cm^{-1}. The *t*-test on ρ_2 indicates significance at greater than 97.5% confidence level.

Why dimerization should increase the importance of chelation on the substituent effect is not clear.[3] Table III shows that changing solvent from carbon tetrachloride to chloroform decreases the monomer frequency by 5–6 cm^{-1} for all the salicylic acids, whereas it increases the dimer frequency by 1–2 cm^{-1}. Similar, but larger (7–17 cm^{-1}) solvent shifts are found in benzoic acids and are attributed to intermolecular hydrogen bonding of monomer with chloroform (6). Possibly such intermolecular hydrogen bonding

[3]Evidence that a fit to the 2-parameter equation does have physical significance is found in the fact that when the equation is applied to the carbonyl frequencies of benzoic acids, either monomer or dimer (6), where no chelation is possible, ρ_2 never differs from zero at more than 50% confidence level.

Can. J. Chem. Downloaded from www.nrcresearchpress.com by 210.87.254.40 on 09/05/12
For personal use only.

in salicylic acid monomers reduces the importance of chelation.

Although chelation of salicylic acids in nonpolar solvents is generally accepted, there is less agreement about chelation in hydroxylic solvents where intermolecular hydrogen bonding with solvent may compete with chelation. From the abundant literature on the subject, one may quote examples of contradictory views by several recent workers. Among those favoring retention of the intramolecular hydrogen bond of salicylic acid in aqueous solution are Scheraga and co-workers, from the temperature dependence of pK (36), and Prince and co-workers, on the basis of infrared spectra (25). On the other hand, Puar and Grunwald concluded from the rates of proton exchange that chelation of salicylic acid in methanol solution is negligible (37).

Whatever the extent of chelation in aqueous solutions of salicylic acid, it is clear that in order to account for the great acidity of salicylic acid, chelation must be much stronger in aqueous salicylate monoanion. Here the evidence is very meager. Voroshin and Vlasov interpreted the ultraviolet spectra of salicylic acid and sodium salicylate in alcohol as showing that the acid "has a strong intramolecular hydrogen bonding which is retained even during salt formation" (38), but their data can be interpreted otherwise. Scheraga and co-workers concluded from the temperature dependence of pK that the intramolecular hydrogen bond is about equally strong in aqueous salicylic acid and sodium salicylate (36). Dunn and Kung could find no transmission by chelation of substituent effects on the ionization of salicylic acids in aqueous solution (33) although Dunn and Penner did find such transmission in benzene solution (16). This leaves the infrared data of Chapman, Lloyd, and Prince (25) as apparently the only substantial evidence (other than that from acidity) for intramolecular hydrogen bonding of salicylate monoanion in aqueous solution.

Chapman, Lloyd, and Prince based their interpretation on the observation that the asymmetric frequency of a strongly hydrogen-bonded carboxylate group is uniformly about 35 cm^{-1} higher than that of a non-hydrogen-bonded carboxylate group (39). They reported the asymmetric stretching frequency of sodium salicylate in deuterium oxide solution at 1621 cm^{-1} and, by comparing this with their asymmetric frequency for sodium benzoate, 1553 cm^{-1}, they concluded that aqueous sodium salicylate is strongly chelated. However, as has been pointed out above, the assignment of the 1621 cm^{-1} frequency to the asymmetric carboxylate vibration is incorrect. This is probably a ring-stretching frequency, and the asymmetric stretching frequency is found at 1546 cm^{-1}, at no great displacement from that of benzoate at 1548 cm^{-1}. The same is true of all the substituted salicylates shown in Table II; the asymmetric frequency of a salicylate is only a few cm^{-1} different from that of the corresponding benzoate.

Our own data do not provide any evidence for intramolecular hydrogen bonding of salicylate monoanion in water. Among the infrared data, the only systematic relationships we have are the correlation between the asymmetric stretching frequencies of salicylates and benzoates, and of benzoates and nitrobenzenes. The parallelism between salicylate and benzoate frequencies argues against chelation in salicylates, but the correlation is perhaps not good enough to permit a firm conclusion. In the benzoate–nitrobenzene correlation, the fact that ortho as well as meta and para substituents fit the linear relationship suggests that, as would be expected, steric as well as electronic substituent effects are similar for the carboxylate and nitro groups. In Fig. 4, however, the *o*-hydroxy point falls well outside the spread of the other points from the line. The salicylate frequency can not be seriously in error because, as was pointed out above, it is consistent with those of all the substituted salicylates in Table II. Apparently this one point is anomalous. The interesting question then is, which frequency is anomalous? Is the nitro frequency abnormally high or is the benzoate frequency abnormally low? If the anomaly is attributed to chelation, then it would appear to be *o*-nitrophenol which is anomalous, because it is generally believed that *o*-nitrophenol is chelated in nonpolar solvents (40–42) and that chelation increases the asymmetric frequency of the carboxylate group (39). It would follow, then, that the salicylate anion in aqueous solution is less chelated than is *o*-nitrophenol in chloroform.

Bellamy has suggested that symmetric nitro frequencies are more sensitive to ortho effects than are the asymmetric ones (43). Examination of the symmetric frequency values for *o*-substituted benzoates in Table I at first seems to

TABLE IV

Infrared frequencies of benzoates and nitrobenzenes in various media

Compound	Mode	Frequencies (cm^{-1}) in KBr	CCl_4	D_2O	1:2 D_2O–methanol
Sodium benzoate	Asymmetric	1550		1548	
	Symmetric	1415		1391	
Sodium *p*-hydroxybenzoate	Asymmetric	1547		1542	
	Symmetric	1416		1386	
Sodium salicylate	Asymmetric	1577		1546	
	Symmetric	1373		1377	
Nitrobenzene	Asymmetric	1524*	1532	1527	1528
	Symmetric	1348	1348	1358	1351
p-Nitrophenol	Asymmetric	1500	1527	1513†	1511†
				1502	1500
	Symmetric	1342	1345	1344	1341
o-Nitrophenol	Asymmetric	1535	1540	‡	1521
	Symmetric	1335	1332	~1339‡	1338

*Neat liquid.
†Two peaks are found in the asymmetric region; no assignment is attempted.
‡Not sufficiently soluble to give a measurable frequency.

suggest that the same may be true for benzoates. Most *o*-substituents increase the symmetric frequency, possibly by forcing the carboxylate group out of the plane of the ring, while *o*-hydroxy and *o*-amino substituents decrease the symmetric frequency, presumably by chelating with the carboxylate group. However, comparison of the frequencies of *o*-substituted anions with those of the corresponding *p*-substituted ones shows a parallel trend. In fact, if the O^- substituent (which will be abnormal because of strong coulomb effects in the dianion) is omitted, there is a surprisingly good correlation between the symmetric frequencies of *o*- and *p*-substituted benzoates, with the spread of ortho frequencies about three times that of the para. Consequently, the data could better be taken to indicate that ortho symmetric vibration frequencies are more sensitive to electronic effects than are the para, as is the case with many reaction rates (44). However, in view of the poor correlation of symmetric benzoate frequencies with either substituent constants or nitrobenzene frequencies, it seems unwise to base any conclusions about structure on this analysis.

Some additional data for comparison of *o*-nitrophenol and salicylate monoanion are presented in Table IV. There it is seen that in the solid state or in carbon tetrachloride solution, where chelation is believed to be strong (24, 42), a *p*-hydroxy substituent has only a small effect on the symmetric and asymmetric frequencies of both benzoate and nitrobenzene, but an *o*-hydroxy substituent produces a pronounced increase in the asymmetric frequency and decrease in the symmetric frequency of both groups. This behavior is believed to be characteristic of chelation in carboxylate ions (39). The effect is larger in the benzoates (30 cm^{-1}) than in the nitrobenzenes (13 cm^{-1}), consistent with the stronger chelation expected for the negatively charged carboxylate group. In deuterium hydroxide solution, however, the *o*-hydroxy group produces no such dramatic frequency changes. Since *o*-nitrophenol is generally believed to be unchelated in hydroxylic solvents (45, 46), the implication is that the same is true of sodium salicylate.

It may be concluded, then, that the infrared data of Fig. 4 and Table IV show that any intramolecular hydrogen bond of sodium salicylate in water is considerably weaker than that of *o*-nitrophenol in carbon tetrachloride or chloroform. Although the infrared data do not provide any positive evidence for chelation of salicylate monoanion in water, they are not convincing enough to exclude it entirely either. However, they do suggest that such chelation is surprisingly weak to produce the well known large effect on the ionization constant of the acid.

Can. J. Chem. Downloaded from www.nrcresearchpress.com by 210.87.254.40 on 09/05/12
For personal use only.

Acknowledgments

This work was supported by a grant and a scholarship from the National Research Council of Canada. The authors are grateful to Dr. P. J. Krueger and Dr. G. S. Hammond for helpful discussions, and to the California Institute of Technology for hospitality and the use of their computer services during a leave spent there by one of us.

1. L. J. BELLAMY. The infrared spectra of complex molecules. Methuen and Co., Ltd., London. 1958.
2. M. S. FLETT. Trans. Faraday Soc. **44**, 767 (1948).
3. J. D. S. GOULDEN. Spectrochim. Acta, **6**, 129 (1954).
4. H. A. LLOYD, K. S. WARREN, and H. M. FALES. J. Amer. Chem. Soc. **88**, 5544 (1966).
5. M. JOSIEN, D. PELTIER, and A. PICHEVIN. C. R. **235**, 1206 (1952).
6. C. J. W. BROOKS, G. EGLINTON, and J. F. MORMAN. J. Chem. Soc. 106 (1961).
7. D. PELTIER, A. PICHEVIN, P. DIZABO, and M. JOSIEN. C. R. **248**, 1148 (1959).
8. C. N. R. RAO and R. VENKATARAGHAVAN. Can. J. Chem. **39**, 1757 (1961).
9. A. E. MARTIN. Nature, **166**, 474 (1950).
10. G. V. L. N. MURTY and T. R. SHESHADRI. Proc. Indian Acad. Sci. Sect. A, **19**, 17 (1944).
11. W. F. FORBES, A. R. KNIGHT, and D. L. COFFEN. Can. J. Chem. **38**, 728 (1960).
12. C. J. W. BROOKS, G. EGLINTON, and J. F. MORMAN. J. Chem. Soc. 661 (1961).
13. F. E. MURRAY and S. SUNDARAM. Can. J. Chem. **39**, 1625 (1961).
14. B. J. LINDBERG. Acta Chem. Scand. **22**, 571 (1968).
15. G. E. DUNN, E. G. JANZEN, and W. RODEWALD. Can. J. Chem. **46**, 2905 (1968).
16. G. E. DUNN and T. L. PENNER. Can. J. Chem. **45**, 1699 (1967).
17. L. J. FIESER. Experiments in organic chemistry. D. C. Heath and Co., New York. 1957.
18. L. KAHOVEC and K. W. F. KOHLRAUSCH. Z. Phys. Chem. Frankfurt, **B38**, 119 (1937).
19. J. T. EDSALL. J. Chem. Phys. **5**, 508 (1937).
20. R. C. GORE, R. B. BARNES, and E. PETERSEN. Anal. Chem. **21**, 382 (1949).
21. G. ERLICH. J. Amer. Chem. Soc. **76**, 5263, 5268 (1954).
22. M. DAVIES and R. L. JONES. J. Chem. Soc. 120 (1954).
23. M. M. STIMSON. J. Chem. Phys. **22**, 1942 (1954).
24. J. H. S. GREEN, W. KYNASTON, and A. S. LINDSEY. Spectrochim. Acta, **17**, 486 (1961).
25. D. CHAPMAN, D. R. LLOYD, and R. H. PRINCE. J. Chem. Soc. 550 (1964).
26. S. HOSHINO, H. HOSOYA, and S. NAGAKURA. Can. J. Chem. **44**, 1961 (1966).
27. J. T. EDSALL. J. Chem. Phys. **4**, 1 (1936).
28. H. C. BROWN and Y. OKAMOTO. J. Amer. Chem. Soc. **80**, 4979 (1958).
29. J. F. BROWN. J. Amer. Chem. Soc. **77**, 6341 (1955).
30. R. D. KROSS and V. A. FASSEL. J. Amer. Chem. Soc. **78**, 4225 (1956).
31. A. R. KATRITZKY and P. SIMMONS. Rec. Trav. Chim. **79**, 361 (1960).
32. C. G. SWAIN and C. LUPTON. J. Amer. Chem. Soc. **90**, 4329 (1968).
33. G. E. DUNN and F. L. KUNG. Can. J. Chem. **44**, 1261 (1966).
34. M. S. FLETT. J. Chem. Soc. 962 (1951).
35. H. H. JAFFE. J. Amer. Chem. Soc. **76**, 4261 (1954).
36. J. HERMANS, S. J. LEACH, and H. A. SCHERAGA. J. Amer. Chem. Soc. **85**, 1390 (1963).
37. M. S. PUAR and E. GRUNWALD. J. Amer. Chem. Soc. **89**, 4403 (1967).
38. E. M. VOROSHIN and V. G. VLASOV. J. Gen. Chem. USSR Engl. Transl. **30**, 2976 (1960).
39. L. EBERSON. Acta Chem. Scand. **13**, 203 (1959); **13**, 211 (1959); **13**, 224 (1959).
40. A. W. BAKER and A. T. SHULGIN. J. Amer. Chem. Soc. **80**, 5358 (1958).
41. R. J. FRANCEL. J. Amer. Chem. Soc. **74**, 1265 (1952).
42. H. HOYER. Chem. Ber. **86**, 1016 (1953).
43. L. J. BELLAMY. Advances in infrared group frequencies. Methuen, London. 1968.
44. R. W. TAFT, JR. *In* Steric effects in organic chemistry. *Edited by* M. S. Newman. John Wiley and Sons, Inc., New York. 1956. p. 649.
45. J. F. COETZEE and G. R. PADMANABHAN. J. Phys. Chem. **69**, 3193 (1965).
46. L. B. MAGNUSSON, C. A. CRAIG, and C. POSTMUS. J. Amer. Chem. Soc. **86**, 3958 (1964).
47. K. YATES and A. A. THOMPSON. Can. J. Chem. **45**, 2997 (1967).

Can. J. Chem. Downloaded from www.nrcresearchpress.com by 210.87.254.40 on 09/05/12
For personal use only.

Can. J. Chem. Downloaded from www.nrcresearchpress.com by 210.87.254.42 on 09/05/12
For personal use only.

Nature of the coordination bond in metal complexes of substituted pyridine derivatives. IV. Skeletal vibration spectra and the substituent effect upon the coordination bond of the pyridine complex of zinc(II) ion

PATRICK T. T. WONG[1] AND D. G. BREWER
Department of Chemistry, University of New Brunswick, Fredericton, New Brunswick

Received June 20, 1969

Far infrared spectra of the complexes $Zn(pyridine)_2X_2$, where X = Cl or Br, have been investigated in the region 350–20 cm^{-1}. Eight infrared-active skeletal modes of these complexes have been observed, and a tentative assignment of these absorption bands has been made. The previous investigation of the effect of substituents upon the coordination bond of the copper–pyridine complex has been extended to the zinc–pyridine complex in the present paper. It was found that the relative zinc–pyridine bond strength, affected by the substituents, is determined by both the relative σ-contribution and π-contribution to the bond, rather than mainly by the σ-contribution as in the system of copper complexes. The force constants associated with the zinc–pyridine coordination bond of a series of 4-substituted pyridine complexes have been calculated by a normal coordinate treatment described in previous papers in this series.

Canadian Journal of Chemistry, 47, 4589 (1969)

Introduction

The infrared spectra of zinc–halide complexes of pyridine in the low frequency region (700–200 cm^{-1}) have been studied recently (1, 2), and two of the infrared-active zinc–halide modes and one of the infrared-active zinc–pyridine modes have been observed. However, no infrared spectra of these complexes below 200 cm^{-1} have been reported thus far. The present work has been undertaken to extend the far infrared spectra of these complexes to 20 cm^{-1}, in order to establish all the infrared-active skeletal vibrations of the pyridine complexes of zinc chloride and zinc bromide.

The substituent effects upon the coordination bond strength, as well as the magnitude of the π-bonding contribution to this bond, in dichlorobis(pyridine)copper(II) have been previously reported (3, 4). It has been found that both the σ- and π-bonding contributions to the coordination bond are influenced considerably by the nature of the substituents on the fourth position of the pyridine ring. The magnitude of π-bonding in the metal–pyridine bond seems to depend more on the properties of the substituents than on those of the metal ions themselves. For instance, the π-bonding ability of zinc(II) ion is much lower than that of copper(II) ion (5); but, when these two metal ions coordinate with 4-substituted pyridines of electron attracting groups, almost the same amount of π-bonding exists in the coordination bond of the analogous complexes of these two metals (3). Since the relative magnitude of σ-bonding is much stronger than that of π-bonding in the copper(II) complexes of 4-substituted pyridines (5), the change in the π-bonding strength due to the substituents does not appreciably affect the relative magnitude of the total M—N (ligand) bond strength among these copper complexes. The relative metal–ligand bond strength of a series of 4-substituted pyridine complexes of copper(II) ion is therefore mainly determined by the relative σ-bonding ability of these substituted pyridines.

An attempt has been made to study the substituent effect upon both the σ- and π-contribution to the total metal–pyridine bond strength in the present work. A metal ion with both lower σ-bonding ability and lower π-bonding ability, (viz. zinc(II) ion) has been selected for this purpose. Moreover, the effect of the substituents upon the metal–halogen bond of the zinc–pyridine complex has also been examined.

In previous papers (4, 6), normal coordinate calculations have been made for a series of metal complexes of substituted pyridines with a simplified model in which only a 1:1 complex had been considered. In the present work, in addition to performing this same normal coordinate treatment for a series of zinc(II) complexes of substituted pyridines, a normal coordinate analysis,

[1]Present address: National Research Council, Division of Chemistry, Ottawa, Canada.

Can. J. Chem. Downloaded from www.nrcresearchpress.com by 210.87.254.42 on 09/05/12
For personal use only.

taking the tetrahedral skeletal sites into account, has been made for zinc(II)–pyridine complex, and will be reported separately (17).

Experimental

The reagents and the preparation of the zinc complexes, ZnL_2Cl_2, where L = pyridine, 4-methylpyridine, 4-carbinylpyridine, 4-acetylpyridine, 4-pyridinecarboxamide, 4-carbomethoxypyridine, and 4-cyanopyridine, have been reported elsewhere (3). The method for the preparation of the pyridine complex of zinc bromide, $ZnPy_2Br_2$ (Py = pyridine), was similar to that for zinc chloride.

Anal. Calcd. for $ZnPy_2Br_2$: C, 34.83; H, 3.41; N, 6.77; Zn, 15.81. Found: C, 34.94; H, 3.51; N, 6.70; Zn, 16.00.

The infrared spectra of the complexes in the region of 4000–400 cm^{-1} were recorded on a Perkin–Elmer Model 521 spectrometer under conditions which have been described in a previous paper of this series (4).

The far infrared spectra in the 400 cm^{-1} – 20 cm^{-1} region were recorded on a Perkin–Elmer Model 301 spectrometer. The complexes were recorded as mulls in Nujol with low-density polyethylene windows. The spectra in Figs. 1 and 2 were replotted by means of an IBM 360 computer from the % transmittance scale measured by the instrument on a linear optical density scale, after subtracting the stray light and the background absorption.

Results and Discussion

I. The Skeletal Vibration Spectra of Pyridine–Zinc Complexes

The infrared spectra in the 400–20 cm^{-1} region of dichlorobis(pyridine)zinc(II) and dibromobis(pyridine)zinc(II) are shown in Figs. 1 and 2, respectively, and the maximum absorption frequencies are listed in Table I. It has been reported that the lowest internal fundamental frequency of the pyridine molecule is 374 cm^{-1} (7), and that this band is shifted toward higher frequency by coordination of pyridine with metal ions (4, 8). Therefore the absorption bands in Figs. 1 and 2 are obviously not due to the internal fundamentals of the pyridine molecule.

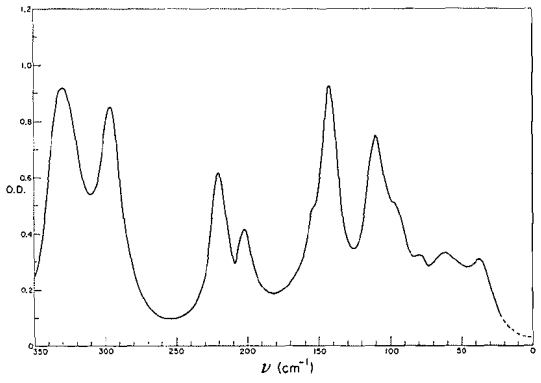

FIG. 1. Infrared spectra (350–20 cm^{-1}) of dichlorobis(pyridine)zinc(II) complex.

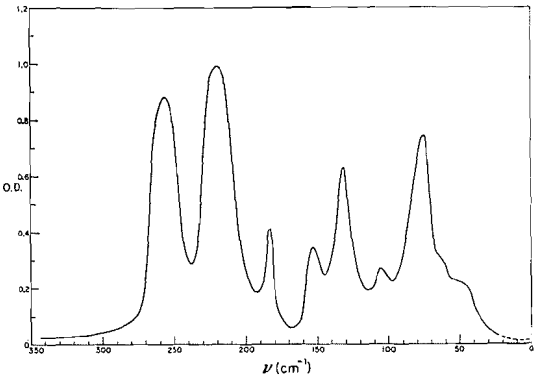

FIG. 2. Infrared spectra (350–20 cm^{-1}) of dibromobis(pyridine)zinc(II) complex.

TABLE I

The frequencies maximum absorption in the 400–20 cm^{-1} region of pyridine complexes of zinc halides, $ZnPy_2X_2$

Mode	Frequency (cm^{-1}) X = Cl	X = Br
ν_1	324.6	255.8
ν_2	292.4	219.2
ν_3	219.2	(219.2)*
ν_4	201.1	183.1
ν_5	152.6	153.1
ν_6	142.4	131.2
ν_7	109.6	76.8
ν_8	100.6	104.4
ν_9	79.5	63.0
ν_{10}	62.0	53.0

*Masked by ν_2.

Porai-Koshits *et al.* (9) have studied the structure of this pyridine complex of zinc chloride and reported that the molecule has a tetrahedral configuration, with 2 pyridine molecules and 2 chlorine atoms at the 4 tetrahedral sites. A similar structure for the zinc bromide complex has also been reported (1). This skeletal structure of the complexes belongs to C_{2v} symmetry. Neglecting the perturbations of the other complex molecules in the unit cell, 8 normal vibrations ($4A_1 + 2B_1 + 2B_2$) are expected to be infrared-active, of which 5 normal modes ($2A_1 + 2B_1 + 1B_2$) are halogen-sensitive.

However, it is seen in the spectrum of the pyridine complex of zinc chloride that there are 7 halogen-sensitive bands (324.6, 292.4, 201.1, 142.4,

Can. J. Chem. Downloaded from www.nrcresearchpress.com by 210.87.254.42 on 09/05/12
For personal use only.

109.6, 79.5, and 62.0 cm^{-1}), which shift to lower frequencies in the spectrum of the analogous complex of zinc bromide (255.8, 219.2, 183.1, 131.2, 76.8, 63.0, and 53.0 cm^{-1}, respectively). Apparently, some of these halogen-sensitive bands belong to lattice modes, which are expected in this frequency region, and are sensitive to the molecular mass of the complex molecules.

The two higher frequency bands (ν_1 and ν_2) are assigned to Zn—X stretching modes, since the frequency ratio of these bands in the zinc chloride complex relative to the zinc bromide complex is about 0.77. This has been used as a guide to the magnitude of the halogen dependence of the metal–halogen stretching frequencies for the tetrahedral metal chlorides and bromides with the first row transition metal ions (10). This also indicates that the coupling of the metal–halogen vibrations is insignificant, as has been observed by several authors (1, 2, 11).

Comparing the spectra in Figs. 1 and 2 with those of the complexes of zinc halides and other metal halides (12–14), the halogen-sensitive bands at 201.1, 109.6, and 79.5 cm^{-1} (zinc chloride) and 183.1, 76.8, and 63.0 cm^{-1} (zinc bromide) are assigned to X—M—X bending modes. In the spectra of a series of metal chloride complexes, a band at a similar position to the ν_9 mode in the pyridine – zinc chloride complex has been assigned to the Cl—M—Cl bending mode or to the lattice vibration (12). In the present work, the assignment of this band to the X—M—X bending mode is preferred, since, having regard for the ratio of the square root of the molecular masses of the complexes of zinc chloride and bromide, the frequency of this mode in the chloride complex shifts to too low a frequency in the spectrum of the bromide complex. The frequencies of this mode in both the pyridine complexes of zinc chloride and zinc bromide are even lower than those of the corresponding bands in the 4-methylpyridine complexes (15).

The ν_6 and ν_{10} modes are also halogen-sensitive and the frequencies of these two bands shift to lower frequencies in the sequence Cl > Br. However, it is different from the other halogen-sensitive bands in that the shift is related to the molecular mass of the complexes of zinc chloride and bromide. The frequency ratios (the chloride complex to the bromide complex) also are close to the inverse ratio of the square root of the molecular masses. The same relationship is also observed between these bands in the pyridine complexes and in those of the 4-methylpyridine complexes (15). Therefore, these bands are reasonably assigned to lattice modes.

It has been observed (1, 2, 16) that for a series of complexes MX_2–nL, where L is a pyridine derivative, the frequencies of the M—L modes are at approximately the same position for the analogous chloro-, bromo-, and iodo-complexes with a given central metal. For the tetrahedral dichlorobis(pyridine derivatives)metal complexes, the spectra are characterized by two strong M—Cl stretching bands and one medium M—L stretching band in the 400–200 cm^{-1} region. The spectra of the zinc–pyridine complexes have the same characteristics, and thus the ν_3 and ν_5 modes are assigned to the M—L stretching vibrations and ν_8 to the L—M—L bending mode, respectively. Although the ν_3 mode of the zinc bromide complex does not appear in the spectrum (since it probably overlaps with the strong Zn—Br stretching band), the assignment of the ν_3 band to M—L stretching agrees with those reported in the literature recently (1, 2) and is comparable with the assignment in the spectra of 4-methylpyridine complexes of zinc chloride and zinc bromide (15).

A weak band ($\sim$35 cm^{-1}) in the spectrum of the pyridine – zinc chloride complex is probably due to a lattice vibration and is not observed in the spectrum of the pyridine – zinc bromide complex.

II. Effect of Substituents upon the Coordination Bond

The infrared spectra in the region 350–150 cm^{-1} have been measured for a series of zinc complexes of the type $Zn(4\text{-R-pyridine})_2Cl_2$ (R = CH_3, CH_2OH, H, $COCH_3$, $CONH_2$, $COOCH_3$, and CN) and the maximum absorption frequencies are listed in Table II. The spectra of all these zinc complexes of 4-substituted pyridines have features similar to those of the zinc – pyridine complex, viz., they are characterized by two strong metal–chlorine stretching bands and two medium metal–nitrogen (ligand) stretching bands in this region. Therefore, it can be reasonably assumed that the substituents on the fourth position of the pyridine ring do not change the stereoconfiguration of the zinc complexes (1).

It is seen from Table II that the M—Cl stretching frequencies of the pyridine complex are affected considerably by the substituents on the

TABLE II

The metal–halogen and metal–pyridine stretching frequencies of the zinc complexes of substituted pyridines

Complex	Absorption bands (cm^{-1})			
	ν(M—Cl)	ν(M—Cl)	ν(M—N)	ν(M—N)
$Zn(4\text{-}CH_3Py)_2Cl_2$	333.4	301.7	238.2	192.4
$Zn(4\text{-}CH_2OHPy)_2Cl_2$	310.9	293.9	232.9	173.3
$ZnPy_2Cl_2$	324.6	292.4	219.2	152.6
$Zn(4\text{-}COCH_3Py)_2Cl_2$	336.3	298.2	—	204.6
$Zn(4\text{-}CONH_2Py)_2Cl_2$	328.5	294.3	227.5	209.9
$Zn(4\text{-}COOCH_3Py)_2Cl_2$	329.0	298.2	229.9	203.6
$Zn(4\text{-}CNPy)_2Cl_2$	337.3	299.2	214.8	176.3

fourth position of the pyridine ring. On the whole, analogous to the case of the copper(II) complexes (4), the zinc–chlorine stretching frequencies shift to higher frequencies due to the effects of both electron-releasing substituents and electron-attracting substituents. This phenomenon is apparently due to the delocalized nature of the coordination bonds in the complexes (4), and the same interpretation as for the copper complexes can be applied to the present case.

However, the substituent effect on the metal–halogen stretching frequency of the zinc–pyridine complex is not as straightforward as in the case of the copper–pyridine complex. As shown in Table II, there is an exception in that one of the zinc–chlorine frequencies of the 4-carbinylpyridine complex, in which the CH_2OH is an electron-releasing group, is even lower than that of the pyridine complex. This is probably due to the fact that the dπ–dπ zinc-to-chlorine bond is much weaker than the zinc–chlorine σ-bond, since the π-bonding ability of zinc is much weaker than that of copper (5). Therefore, only a small increase in the electron density on the zinc atom results from the effect of the weakly electron-releasing group, CH_2OH, and this does not provide enough dπ–dπ bonding to overcome the decreased bond strength of the zinc–chlorine σ-bond.

The zinc–nitrogen stretching frequencies of the zinc–pyridine complex are also shifted by the effects of the substituents on the fourth position of the pyridine ring. These effects, as expected, are larger than those on the zinc–chlorine stretching frequencies, since the former ones are more directly involved in any shifts in electron density due to the substituent. The effects of electron-releasing groups on the zinc–nitrogen stretching frequency are similar to the effects of these same groups on the copper–nitrogen stretching mode (4).

The effects of electron-attracting substituents on the Zn—N (ligand) stretching frequencies of the Zn–pyridine complexes are, however, quite different from those in the Cu–pyridine complex. In the copper complexes (4), the M—N stretching frequencies shift to lower frequencies due to the effects of electron-attracting substituents, and increasingly stronger electron-attracting groups give a lower M—N stretching frequency. In the case of the zinc complexes, the converse is true, except for the CN group, which leaves the M—N stretching frequency unchanged. Therefore, the relationship between the electron-attracting ability of the substituents and the M—N stretching frequencies, as observed in the case of the copper complexes, is no longer valid. Since the M—N stretching frequency correlates to the M—N bond strength (3, 4, 6), these differences between the zinc and copper complex systems may be interpreted as being due to the different nature of their bonding. It has been reported (5) that the σ-bonding contribution in the zinc complexes is much weaker than that in the analogous copper complexes, and, for ordinary complexes, or complexes of substituted pyridine with electron-releasing groups in the fourth position of the pyridine ring, the π-contribution in the zinc complexes is also very much weaker. In fact, with zinc, this π-contribution is smaller than in the analogous complexes of any of the first-row transition metals. However, as we have indicated, this π-bonding ability is no longer characterized by the metal ions themselves, but by the nature of the substituted groups (3). It turns out that for a given

Can. J. Chem. Downloaded from www.nrcresearchpress.com by 210.87.254.42 on 09/05/12
For personal use only.

TABLE III

F matrix on the basis of the symmetry coordinates

A_1 species

f_1	f_2	0	f_3	0	f_4	0	f_5	f_6	f_7										
	f_8	f_9	0	0	f_{10}	f_{11}	f_{12}	0	f_{13}										
		f_{14}	0	f_{15}	0	f_{16}	f_{17}	f_{18}	f_{19}										
			f_{20}	0	0	0	0	f_{21}	f_{22}										
				f_{23}	0	0	0	f_{24}	f_{25}										
					f_{26}	0	f_{27}	0	f_{28}										
						f_{29}	f_{30}	0	f_{31}										
(Symmetrical)							f_{32}	0	f_{33}										
								f_{34}	f_{35}										
									f_{36}										
										Zero									
										f_1	f_2	f_3	f_4	0	f_5	0	f_6	f_7
											f_8	f_9	f_{10}	f_{11}	0	0	f_{12}	f_{13}
												f_{14}	0	f_{15}	0	f_{16}	f_{17}	f_{18}
													f_{19}	0	0	0	f_{20}	f_{21}
														f_{22}	0	0	f_{23}	f_{24}
										Zero					f_{25}	0	0	0
											(Symmetrical)					f_{26}	0	0
																	f_{27}	f_{28}
																		f_{29}

B_2 species

electron-attracting substituent, the π-bond in the zinc and copper systems is comparable and increases as electron-attracting ability of the substituent increases. However, the σ-bond in the copper complexes is so strong that any small change in π-bonding does not give a significant change in the total bond strength. Therefore, the relative total bond strength in these copper complexes follows the same trend as would be expected for just the σ-bonding contribution. On the other hand, in the zinc complexes the σ-bonding is relatively very weak, and the π-bonding is strongly influenced by electron-attracting substituents. Therefore, the π-bond in these zinc complexes makes a significant contribution to the total bond strength. The R_π values (3) show that the π-bond strength in the zinc complexes of 4-substituted pyridine with $-CONH_2$, $-COCH_3$, and $-COOCH_3$ as substituents is about double that in the pyridine complex. Therefore, the higher M—N frequencies and the increased total coordination bond strength of the zinc complexes with these substituted pyridines over that with pyridine itself are understandable. The M—N frequency of the 4-cyanopyridine zinc complex is the only one which has the same magnitude as that of pyridine complex, although the π-bond strength in the former is about 3 times higher than that in the latter. This is probably due to the extremely weak σ-bond in the 4-cyanopyridine complex. A rough calculation, using the stability constants of the pyridinium ion and the 4-cyanopyridinium ion (3), shows that the σ-bonding ability of 4-cyanopyridine is only about 0.04% that of pyridine. The compensation due to the increase in π-bonding, and the decrease in the σ-bonding caused by the substitution of a CN group on the fourth position of pyridine, gives the observed total bond strength in the zinc-4-cyanopyridine complex.

The symmetrical M—N stretching frequency of the 4-acetylpyridine is not observed in the spectrum. However, the asymmetrical M—N stretching and the M—Cl stretching frequencies of this complex are very similar to those of the 4-carbo-

TABLE VI

Metal–nitrogen (ligand) stretching force constants

Complex	Force constant dyn/cm × 10^{-5}
$Zn(4\text{-}CH_3Py)_2Cl_2$	1.08
$Zn(4\text{-}CH_2OHPy)_2Cl_2$	0.935
$Zn(Py)_2Cl_2$	0.653
$Zn(4\text{-}COCH_3Py)_2Cl_2$	(0.774)*
$Zn(4\text{-}CONH_2Py)_2Cl_2$	0.750
$Zn(4\text{-}COOCH_3Py)_2Cl_2$	0.774
$Zn(4\text{-}CNPy)_2Cl_2$	0.623

*Frequency data incomplete, see Table II.

Can. J. Chem. Downloaded from www.nrcresearchpress.com by 210.87.254.42 on 09/05/12
For personal use only.

Can. J. Chem. Downloaded from www.nrcresearchpress.com by 210.87.254.42 on 09/05/12
For personal use only.

TABLE VII

Fundamental vibrational frequencies of zinc complexes of 4-substituted pyridines

Description	Frequency (cm^{-1})							
	$Zn(4\text{-}CH_3Py)_2Cl_2$		$Zn(4\text{-}CH_2OHPy)_2Cl_2$		$Zn(Py)_2Cl_2$		$Zn(4\text{-}COCH_3Py)_2Cl_2$	
	Obsd.	Calcd.	Obsd.	Calcd.	Obsd.	Calcd.	Obsd.	Calcd.
A_1 species								
ν(M—N)	238.2	238.0	232.9	232.6	219.2	218.8	—	237.5
ν_{6a}, ring, R-sensitive	554.0	638.0	610.0	553.3	676.0	774.2	661.0	520.2
ν_1, ring, β(C—M)	1033	908.0	1032	874.4	1016	991.6	1028	865.5
ν_{12}, ring	1034	1037	1049	1008	1043	1045	1055	1009
ν_{18}, ν(C—R), β(C—H)	1211	1160	1190	1149	3025	3043	1159	1147
ν_{9a}, β(C—H)	1231	1227	1221	1222	1217	1217	1216	1218
R-sensitive	1425	1403	1419	1420	1423	1346	—	1418
ν_{19a}, ν(C—C), ν(C—N)	1507	1523	1502	1478	1491	1506	1495	1484
ν_{8a}, ν(C—C)	1630	1614	1619	1648	1609	1604	1613	1639
B_2 species								
ν(M—N)	192.4	250.0	173.3	224.5	152.6	308.1	204.6	217.6
ν_{15}, R-sensitive	421.0	423.8	430.0	403.8	1162	1117	420.0	405.4
ν_{6b}, ring	721.0	775.1	712.0	772.4	690.0	779.4	750.0	771.5
ν_{18b}, β(C—H)	1098	1075	1099	1045	1155	1153	1088	1036
ν_3, β(C—H)	1120	1145	1113	1129	1220	1301	—	1125
ν_{14}, ν(C—C), ν(C—N)	1330	1342	1340	1339	1359	1393	1324	1338
ν_{19}, ν(C—C), ν(C—N), β(C—R), β(C—H)	1432	1398	1430	1390	1487	1513	1422	1389
ν_{8b}, ν(C—C)	1618	1550	1560	1544	1566	1714	1552	1544

Can. J. Chem. Downloaded from www.nrcresearchpress.com by 210.87.254.42 on 09/05/12
For personal use only.

TABLE VII (*Concluded*)

Description	Frequency (cm^{-1})					
	$Zn(4\text{-}CONH_2Py)_2Cl_2$		$Zn(4\text{-}COOCH_3Py)_2Cl_2$		$Zn(4\text{-}CNPy)_2Cl_2$	
	Obsd.	Calcd.	Obsd.	Calcd.	Obsd.	Calcd.
A_1 species						
ν(M—N)	227.5	227.1	229.9	229.2	214.8	214.5
ν_{6a}, ring, R-sensitive	650.0	512.4	—	488.2	565.0	527.9
ν_1, ring, β(C—M)	1030	864.5	1031	861.5	1029	905.8
ν_{12}, ring	1055	1005	1056	929.0	1063	1012
ν_{18}, ν(C—R), β(C—H)	1150	1146	1170	1143	1212	1194
ν_{9a}, β(C—H)	1219	1218	1215	1216	1224	1235
R-sensitive	1395	1417	1436	1415	1430	1383
ν_{19a}, ν(C—C), ν(C—N)	1502	1483	1500	1487	1547	1529
ν_{8a}, ν(C—C)	1618	1639	1618	1633	1617	1646
B_2 species						
ν(M—N)	209.9	217.0	203.6	210.8	176.3	246.3
ν_{15}, R-sensitive	405.0	405.0	430.0	407.6	492.0	436.3
ν_{6b}, ring	760.0	771.5	762.0	772.0	663.0	791.3
ν_{18b}, β(C—H)	1089	1036	1080	1038	1120	1149
ν_3, β(C—H)	1118	1125	1123	1125	—	1216
ν_{14}, ν(C—C), ν(C—N)	1328	1338	1368	1338	1326	1363
ν_{19b}, ν(C—C), ν(C—N), β(C—R), β(C—H)	1421	1389	1421	1391	1419	1458
ν_{8b}, ν(C—C)	1553	1544	1561	1546	1553	1600

Can. J. Chem. Downloaded from www.nrcresearchpress.com by 210.87.254.42 on 09/05/12
For personal use only.

methoxylpyridine complex. The normal coordinate analysis in Section III shows that a calculated value of 237 cm^{-1} of this mode is obtained if a similar M—N stretching force constant to that of the 4-carbomethoxylpyridine complex is used.

III. Normal Coordinate Analysis

In previous papers (4, 6) a 1:1 complex model has been used for the normal coordinate analysis of a series of metal complexes of substituted pyridine derivatives. The calculated results agreed with the observed ones satisfactorily, since only very weak coupling between the skeletal modes was indicated by a clear separation of the halogen-sensitive bands from the metal–nitrogen (ligand) bands.

In the present work, as a preliminary step, the same 1:1 complex model is used for the normal coordinate treatment of the systems of the zinc-(II) – substituted pyridine complexes. Again, only 21 in-plane vibrations are calculated.

Since the results of the previous studies showed that the coupling between the M—N (ligand) vibration and the internal substituted-pyridine modes is also very weak, a further refinement of the normal coordinate analysis for the skeletal modes, considering the substituted-pyridines as point masses, has been attempted. Full details of this analysis and the comparison of the results obtained by these 2 methods are reported elsewhere (17).

For the 1:1 complex model of the zinc complexes, the internal coordinates, the symmetry coordinates, and the **G** matrix constructed on the basis of these coordinates, are similar to those described previously (4, 6). To construct the **F** matrix, shown in Table III, the modified Urey–Bradley force field (4) is used. The force constants of the C—H stretching modes are not included in this **F** matrix, and have been removed by the high-frequency separation method (18). The corresponding elements of the **F** matrix are given[2] in Tables IV and V.

Removal of 7 of the 9 redundancies is accomplished by the coordinates transformations (4). Two remaining redundant conditions are again left in the secular equations as a check on the calculation.

[2]Tables IV and V have been placed in the Depository of Unpublished Data. Photocopies may be obtained free of charge, upon request, from: Depository of Unpublished Data, National Science Library, National Research Council of Canada, Ottawa, Canada.

The molecular parameters used in this calculation are similar to those listed in a previous paper (4), except r_6, which is 2.06 Å. In view of the transferability of the Urey–Bradley force constants and the small change in the spectra of the zinc complexes compared with those of the copper complexes, the force constants related to the internal vibrations of the ligands in this calculation are identical with those of the copper complexes (4). Only the metal–nitrogen (ligand) stretching force constants are refined in this calculation and are listed in Table VI.

The eigenvalues of the secular equation of the zinc complexes obtained by the **QR** transformation (19) compare favorably with the observed ones, as shown in Table VII. These results show that the Urey–Bradley force constants of the ligands of the copper complexes (4) are transferable to the zinc systems, except the carbon–metal bending force constants and some of the ring vibrational force constants, leading to lower calculated frequencies of the ν_1 mode of the zinc complexes than the observed ones.

As expected, the resulting zinc–nitrogen (ligand) stretching force constants of this series of zinc complexes give the same order as that of the zinc–nitrogen (ligand) stretching frequencies, viz.

$$CH_3Py > CH_2OHPy > COOCH_3Py > CONH_2Py > Py > CNPy$$

Therefore the conclusion reached in the previous paper (4), that the magnitude of the metal–ligand stretching frequency can be used as a measure of the coordination bond strength for copper complexes of pyridine derivatives, is also valid for the zinc complexes of 4-substituted pyridines.

Acknowledgments

We wish to thank Dr. E. Whalley and Dr. M. Falk of the National Research Council of Canada for the use of their instruments and Mr. M. Sears for the preparation of the pyridine – zinc bromide complex.

1. R. H. H. Clark and C. S. Williams. Inorg. Chem. **4**, 350 (1965).
2. C. W. Frank and L. B. Rogers. Inorg. Chem. **5**, 615 (1966).
3. P. T. T. Wong and D. G. Brewer. Can. J. Chem. **46**, 131 (1968).
4. P. T. T. Wong and D. G. Brewer. Can. J. Chem. **46**, 139 (1968).
5. D. G. Brewer and P. T. T. Wong. Can. J. Chem. **44**, 1407 (1966).

6. D. G. BREWER, P. T. T. WONG, and M. C. SEARS. Can. J. Chem. **46**, 3137 (1968).
7. R. ISAAC, F. F. BENTLEY, H. S. STERNGLAND, W. C. COBURN, JR., C. V. STEPHENSON, and W. S. WILCOX. Appl. Spectrosc. **17**, 90 (1963).
8. N. S. GILL, R. H. HUTTALL, D. E. SCAIFE, and D. W. A. SHARP. J. Inorg. Nucl. Chem. **18**, 79 (1961).
9. M. A. PORAĬ-KOSHITS, L. D. ATOVMYAN, and G. N. TISHCHENKO. Zh. Strukt. Khim. **1**, 337 (1960).
10. R. J. H. CLARK and T. M. DUNN. J. Chem. Soc. 1196 (1963).
11. R. J. H. CLARK and C. S. WILLIAMS. Chem. Ind. London, 1317 (1964).
12. A. SALATINI and L. SACCONI. J. Amer. Chem. Soc. **86**, 17 (1964).
13. M. L. DELWANLLE. C. R. **240**, 2132 (1955).
14. K. NAKAMOTO. Infrared spectra of inorganic and coordination compounds. John Wiley and Sons, Inc., New York. 1963.
15. M. C. SEARS and D. G. BREWER. To be published.
16. M. GOLDSTEIN, E. F. MOONEY, A. ANDERSON, and H. A. GELBIE. Spectrochim. Acta, **21**, 105 (1965).
17. PATRICK T. T. WONG. To be published.
18. E. B. WILSON, JR., J. C. DECINS, and P. C. CROSS. Molecular vibrations. McGraw-Hill Book Company, Inc., New York. 1955. p. 74.
19. J. G. F. FRANCIS. Comput. J. **4**, 265 (1961).

Can. J. Chem. Downloaded from www.nrcresearchpress.com by 210.87.254.42 on 09/05/12
For personal use only.

Can. J. Chem. Downloaded from www.nrcresearchpress.com by 210.87.254.40 on 09/05/12
For personal use only.

Solvent reorganization for hydrolysis with hydrogen participation[1]

Y. INOMOTO[2], R. E. ROBERTSON, AND G. SARKIS[3]

Received July 24, 1969

A study of the rates of hydrolysis of 3-Me-2-butyl bromide and methanesulfonate in water leads to values of ΔC_p^* of -80 and -40 cal deg^{-1} mole^{-1}, respectively. The product was about 85–95 % *t*-pentanol, the remainder being olefin. The value of ΔC_p^* for the solvolysis of the methanesulfonate in D_2O was -44 cal deg^{-1} mole^{-1}. The kinetic solvent isotope effect (k.s.i.e.) for the latter was unusually low (k.s.i.e. = 1.047 at 5 °C and 1.025 at 25 °C). Deuteration at C-3 led to a reduction in the rate of hydrolysis by a factor of about 2.25. This is consistent with an activation process involving "hydrogen participation" as previously reported by Winstein and Takahashi for solvolysis of the corresponding tosylate in acetic acid. In contrast to the latter work, the reaction in water appears to be uncomplicated.

Canadian Journal of Chemistry, 47, 4599 (1969)

Introduction

In extending our examination of solvent reorganization accompanying the hydrolysis of solutes giving evidence of neighboring group participation (1), we report here the results of such a study involving hydrogen participation for the hydrolysis of 3-methyl-2 butyl methanesulfonate in H_2O and D_2O and the corresponding bromide in H_2O. Evidence for hydrogen participation for the solvolysis of this latter compound in acetic acid was discussed previously by Winstein and Takahashi (2), although they regarded the participation of hydrogen under their conditions as somewhat marginal. Because of this estimate, a question was raised as to the effect a change in solvent would have on the mechanism. Acetic acid is not a good ionizing solvent and is a weak nucleophile, while water is a good ionizing solvent and a fair nucleophile. At the time the work was initiated there was some uncertainty as to whether secondary halides hydrolyzed in water by an S_N1, S_N2, or mixed mechanism. If the mechanism were S_N1, the better ionizing solvent would render hydrogen participation less important than in acetic acid; if S_N2, then the $\Delta C_p^{\neq}$ value should reflect this fact. Our criterion at that time was that $\Delta C_p^{\neq}$ for hydrolytic displacement of a halide by an S_N2 mechanism would have a value of about -55 cal deg^{-1} mole^{-1}, while for reaction by an S_N1 mechanism the corresponding value would be -80 cal deg^{-1} mole^{-1}. As a result of this study and related work we now recognize that this latter criterion involves an oversimplification and probably a misconception as well.

[1]NRCC No. 10949.
[2]NRCC Postdoctoral Fellow, 1966—1967.
[3]NRCC Postdoctoral Fellow, 1966—1968.

Experimental

3-Methyl-2-butyl Methanesulfonate

This compound was prepared by the method of Tipson (3) from pure methylisopropylcarbinol and purified by double distillation under reduced pressure (0.1 mm Hg) with a bath at 60–65 °C: n_D^{25} 1.4305; neutralization equivalent 165.1, Calcd. 166.2.

Anal. Calcd. for $C_6H_{14}O_3S$: C, 43.33; H, 8.49. Found: C, 43.19; H, 8.30.

The sample proved to be kinetically pure from estimation of solvolytic behavior in water.

3-Methyl-2-butyl Bromide

This compound was prepared by the method used by Cason and Corrcia (4) for synthesizing 3-bromopentane, with slight modification. The crude product was purified by the method of Bailey and Hirsch (5). A mixture of 300 ml of dimethyl sulfoxide, 33.3 g (0.323 mole) NaBr, and 62.4 g (0.258 mole) of 3-methyl-2-butyl *p*-toluenesulfonate was stirred at room temperature for 64 h. The reaction mixture was distilled directly under reduced pressure (ca. 15 mm Hg; bath, 55–65 °C) and distillate boiling between 32–39 °C (50 mm Hg) collected. The distillate was stirred with 30 ml water at room temperature for 2 h. The water layer was extracted once with 50 ml ether, the combined ether extract and organic layer being shaken with 50 ml concentrated HCl for 2 min. The ethereal solution was washed with ice-water, then with cold saturated $NaHCO_3$ solution, twice with H_2O, and then dried over $CaCl_2$. Two distillations gave 6.0 g (12 %) of pure material: b.p. 39–40° (55 mm) (lit. (5) b.p. 49.8–51.0° (75 mm)); n_D^{24} 1.4452.

Anal. Calcd. for $C_5H_{11}Br$: C, 39.75; H, 7.34; Br, 52.91. Found: C, 39.71; H, 7.17; Br, 52.82.

Vapor phase chromatography (v.p.c.) of the sample gave but 1 peak, using a 20 wt. % polypropylene oxide on Chromosorb W column with a He flow rate of 60 cc/min. Retention time was 37.5 min. The compound was shown to be kinetically pure by the use of a large scale Guggenheim plot (6).

Solvent

H_2O was distilled and passed through an ion exchange column containing Fisher Rexyn-1-300. D_2O was obtained from Merck, Sharpe, and Dohme or Atomic Energy Commission of Canada. This was redistilled

TABLE I

Products of hydrolysis in water ($CaCO_3$ present)

Substrate	Solvolysis temperature (°C)	Product yield (%)	
		2-Me-2-butene	*t*-Pentanol
3-Me-2-Bu-mesylate	2	5.4	94.6
	22	6.3	93.7
3-Me-2-Bu-bromide	35	6.7	93.3
	51	16.6	83.4

from sodium, then from $NaDSO_4$ through a scaled-down Stuart–Wormwell still (7) where the hot vapors and condensate contacted only quartz.

Analysis of Products

The analysis of products was done by vapor phase chromatography and also by direct titration of the olefin produced. A mixture of 0.6–0.7 mmole of the compound, 5 ml of water, and sufficient precipitated calcium carbonate to neutralize the acid were placed together with a small magnetic stirring bar in a sealed tube and allowed to react for 20 half-lives. The sealed tubes were thoroughly cooled in an ice bath prior to opening for analysis. Analyses were done in quadruplicate.

Olefin Determination

The content of the olefin in the solvolysis products was determined by an iodometric back titration of the excess bromine (8). To the solvolytic mixture was added 2.5 cc of carbon tetrachloride and 5 cc of water. The resulting mixture was kept at 0 °C for 10 min. Two cc of a 0.2 *N* solution of bromine in carbon tetrachloride was then added to the mixture, which was kept at 0 °C for another 10 min with occasional shaking.

The mixture was titrated, after addition of 2.5 cc of 20% potassium iodide solution, with 0.1 *N* standard sodium thiosulfate, using starch as an indicator. The yield of olefin was calculated by averaging the results for 3 separate solvolysis mixtures.

Vapor Phase Chromatography

A Poropack Q (80–100 mesh) column was used at 120° for olefin separation and 180° for the alcohols. The kind and amounts of solvolytic products are listed in Table I.

In the absence of calcium carbonate, the olefin yield increased by about 10% in the case of the methanesulfonate, some 1,2 as well as 2,3 isomer being found (v.p.c.), with a corresponding decrease in alcohol. This was regarded as an artifact, and since it became apparent that the reaction probably followed an S_N1 mechanism, the question of product was not pursued. The fact that the products found for hydrolysis in water were simpler than those reported by Winstein and Tagahashi (2) is not surprising if allowance is made for the difference in solvent properties.

Kinetics

Rates were determined by a conductance method, in stirred Queen type cells (9) using either a conventional bridge (10) or, in the later part of the work, our Auto-RAM system (11). Temperature control and measurement, and calculations were the same as previously reported (11).

Results and Discussion

Average rate data for the hydrolysis of the methanesulfonate in H_2O and D_2O are given in Table II; corresponding data for the hydrolysis of the bromide in H_2O are given in Table III.

The temperature dependence of the rate in each case was fitted by a least-mean-square method to an equation of the form

$$[1] \quad \log_{10} k = \frac{A}{T} + B \log T + C$$

The corresponding equations are as follows

3-Methyl-2-butyl bromide in H_2O

$$[2] \quad \log_{10} k = \frac{-10628.888}{T} - 40.03150 \log T + 130.60409$$

3-Methyl-2-butyl mesylate in H_2O

$$[3] \quad \log_{10} k = \frac{-7030.13779}{T} - 18.89552 \log T + 67.64076$$

3-Methyl-2-butyl mesylate in D_2O

$$[4] \quad \log_{10} k = \frac{-7300.50548}{T} - 20.99025 \log T + 73.72049$$

Quasi-thermodynamic parameters (10) characterizing the reactions based on transition state assumptions and on the approximation that $d\Delta C_p^{\ddagger}/dT = 0$ are given in Table IV. It is recognized that the latter approximation is least

Can. J. Chem. Downloaded from www.nrcresearchpress.com by 210.87.254.40 on 09/05/12
For personal use only.

TABLE II

Average rate data for the hydrolysis of 3-methyl-2-butyl methanesulfonate in H_2O and D_2O

H_2O			D_2O		
Temperature (°C)	$10^4 k$ (s^{-1}) Obsd.	Calcd.*	Temperature (°C)	$10^4 k$ (s^{-1}) Obsd.	Calcd.*
1.163	0.8745 ± 0.0020	0.8736	3.797	1.289 ± 0‡	1.240
1.651	0.9381 ± 0.0020	0.9380	5.012	1.472 ± 0.001	1.474
3.897	1.296 ± 0.001	1.297	7.112	1.977 ± 0.001	1.980
5.891	1.721 ± 0.002	1.719	8.365	2.364 ± 0.002	2.355
7.936	2.282 ± 0.003	2.284	12.409	4.064 ± 0.001	4.066
10.421	3.193 ± 0.006	3.203	14.287	5.203 ± 0.006	5.205
15.454	6.229 ± 0†	6.216	21.879	13.53 ± 0.013	13.56
18.338	8.986 ± 0.013	8.973	24.808	19.34 ± 0.038	19.30
20.590	11.87 ± 0†	11.87	(25.000)		19.75
21.923	13.98 ± 0.010	14.00			
23.398	16.73 ± 0.033	16.72			
25.502	21.45 ± 0.010	21.49			
(25.000)		20.22			

*Equation [1].
†Two cells gave identical results.
‡Four cells gave identical results.

TABLE III

Average* rate data for the hydrolysis of 3-methyl-2-butyl bromide in H_2O

Temperature (°C)	$10^4 k$ (s^{-1}) Obsd.	Calcd.
22.746	0.5756 ± 0.0010	0.5758
24.812	0.7740 ± 0.0014	0.7734
25.00	—	0.793
27.011	1.053 ± 0 001	1.052
29.109	1.399 ± 0.004	1.402
31.161	1.845 ± 0.001	1.845
33.020	2.357 ± 0.004	2.356
33.023	2.359 ± 0.003	2.358
35.692	3.321 ± 0.008	3.322
38.820	4.912 ± 0.011	4.913
41.611	6.892 ± 0.011	6.896
41.623	6.911 ± 0 023	6.905
44.686	9.921 ± 0.020	9.913
46.744	12.58 ± 0.04	12.57
48.748	15.77 ± 0 003	15.76
49.822	17.71 ± 0.02	17.75
50.784	19.72 ± 0.04	19.74
50.787	19.77 ± 0.02	19.75

*Average of 4 determinations.

important about the center of the experimental temperature range.

Winstein and Takahashi (2) have discussed the mechanism of solvolysis of 3-methyl-2-butyl tosylate in acetic acid in terms of two independent processes, (*a*) anchimerically unassisted solvolysis and (*b*) a mechanism in which the tertiary hydrogen provides neighboring group assistance. Evidence based on a comparison of k_H/k_D for the solvolysis of the corresponding methanesulfonate (MeS) in water indicates a similar anchimeric assistance occurs in the present study. An approximate value of the rate of solvolysis of $(CH_3)_2CDCH(MeS)CH_3$ at 25.5° is 1.04×10^{-3} s^{-1} for 91% D; the corresponding value for the protium compound is 2.145×10^{-3} s^{-1}. These values lead to about the same value of the k_H/k_D ratio for the methanesulfonate as was found for the solvolysis of the tosylate in two solvents (Table V). Having due regard for the fact that the methanesulfonate is a somewhat poorer leaving group than the tosylate ($k_{Tos}/k_{MeS} = 3.4$ at 25 °C for solvolytic displacement from isopropyl (10)), it will be apparent from Table V that the degree of anchimeric assistance is just about the same for hydrolysis in water as for the tosylate under much poorer ionizing conditions but possibly conditions favoring such interaction. It would appear that the products of hydrolysis in water are simpler than for reaction in acetic acid, the major product being the tertiary alcohol (Table I). This is consistent with a transition state involving hydrogen participation and the transfer of the tertiary H to C-2 with attack of a water molecule on C-3 to yield the tertiary alcohol, subsequent to the transition state.

The fact that accurate rates, a very low k.s.i.e. (below), and about the same value of $\Delta C_p^{\ddagger}$ was obtained in D_2O as in H_2O confirm that in this reaction the "neighboring hydrogen" was not exchanging with the solvent in the activation process. However, two facts in connection with the

Can. J. Chem. Downloaded from www.nrcresearchpress.com by 210.87.254.40 on 09/05/12
For personal use only.

TABLE IV

Quasi-thermodynamic values for the hydrolysis of 3-methyl-2-butyl X

X	Medium	Temperature (°C)	$\Delta H^{\ddagger}$ (cal mole^{-1})	$\Delta S^{\ddagger}$ (cal deg^{-1} mole^{-1})	$\Delta C_p^{\ddagger}$ (cal deg^{-1} mole^{-1})
Br^-	H_2O	25	24.313	4.27	82 ± 1
		50	23.014	−2.288	
$^-O-\overset{O}{\overset{\|}{S}}(=O)-Me$	H_2O	25	20.371	−2.513	40 ± 3
		50	19.383	−5.69	
$^-O-\overset{O}{\overset{\|}{S}}(=O)-Me$	D_2O	25	20.376	−2.57	44 ± 3

TABLE V

Comparison of k_H/k_D values for the solvolysis of 3-methyl-2-butyl X

X$^-$	Solvent	Temperature (°C)	k_H/k_D Experimental	k_H/k_D Estimated*
MeS (91% D)†	H_2O	10.42	2.04	—
		25	2.06	2.25
Tos	80% EtOH	25	2.05	2.14
Tos	AcOH	25	2.26	2.26

*For 100% deuteration.

†The loss of deuterium occurred during the synthesis since exchange under solvolytic conditions would have made rate determination unreliable and was not expected in any case (12). However, the presence of 9% of the protonated impurity would increase the rate by a small but indeterminate degree depending on the extent of the reaction prior to time $t = 0$. The ratio given is therefore a lower limit.

solvolytic studies in D_2O remain unexplained. The kinetic solvent isotope effect for the solvolysis of the methanesulfonate (from smoothed data, eqs. [3], [4]) was found to be 1.047 at 5.00 °C and 1.024 at 25.00 °C. These values are somewhat lower than those previously found for the solvolysis of the sulfonates (average value 1.09)[4]. In addition, we were unable to find conditions which would give reproducible rates for the solvolysis of the 3-methyl-2-Br-butane in D_2O; in the majority of attempts the change in resistance with time did not appear to conform to a first order relationship. None of these difficulties was apparent in our results in H_2O for either the bromide or the methanesulfonate, or for the latter in D_2O. The possibility of exchange of deuterium in the case of 3-methyl-2-butyl bromide was recognized as a possibility but not proven.

[4]Robertson and Laughton (13) reported a value of k.s.i.e. = 1.046 for the hydrolysis of neopentyl methanesulfonate. It is probable that this reaction is accompanied by rearrangement but this possibility was not confirmed.

The argument that the solvolytic displacement of X from 3-methyl-2-butyl X, in water, occurs by a single mechanism has been used previously (14, 15) and may be summarized as follows. If solvolysis occurs by two mechanisms, it is improbable that each will have the same temperature coefficient, hence the one having the higher coefficient will become successively more important as the temperature increases. This trend will add a positive component to $\Delta C_p^{\ddagger}$ and the resultant $\Delta C_p^{\ddagger}$ will be less negative than "normal". Clearly such a criterion depends on our ability to define the limits of normality for the type of reaction under consideration. This positive effect on $\Delta C_p^{\ddagger}$ is quite different from that resulting from impurities. Thus, the presence of a faster reacting impurity in the case of crotyl chloride resulted in a spurious value of $\Delta C_p^{\ddagger}$ of -130 cal deg^{-1} mole^{-1} (14). The 91% deuterated mesylate, in the present study, gave an apparent $\Delta C_p^{\ddagger} < -100$ cal deg^{-1} mole^{-1}, compared to a real value of about -45 cal deg^{-1} mole^{-1}.

Can. J. Chem. Downloaded from www.nrcresearchpress.com by 210.87.254.40 on 09/05/12
For personal use only.

TABLE VI

Comparison of $\Delta C_p^{\ddagger}$ values for hydrolysis in water

Compound	$\Delta C_p^{\ddagger}$ (cal deg^{-1} mole^{-1})	Reference	Compound	$\Delta C_p^{\ddagger}$ (cal deg^{-1} mole^{-1})	Reference
3-Me-2-butyl bromide	−80	This work	*t*-Butyl chloride	−83	18
3-Br-2-Me-2-butanol	−77	1	2,2-Dichloropropane	−75	19
2-Cl-ethyl methyl sulfide	−71	1	*trans*-γ-Methyl allyl chloride	−82	15
4-Br-butyl methyl ether	−46	1	2,2-Dibromopropane	−81	19
α-Br-isobutyrate	−78	17	Isopropyl bromide	−59	20
			Cyclohexyl bromide	−59	10
			Cyclopentyl bromide	−68	10

These latter results illustrate the sensitivity of $\Delta C_p^{\ddagger}$ to certain types of reactive impurities. No evidence of such an impurity was detected in the protium compounds, hence the large negative value of $\Delta C_p^{\ddagger}$ (-80 cal deg^{-1} mole^{-1}) for the solvolysis of 3-methyl-2-butyl bromide in water was taken as evidence of extensive solvent reorganization in the activation process and similar to values found for molecules reacting by an S_N1 mechanism (Table VI). Values of $\Delta C_p^{\ddagger}$ for the hydrolysis of the secondary halides, isopropyl, cyclohexyl, and cyclopentyl bromides are included. From this comparison it is clear that the $\Delta C_p^{\ddagger}$ value found here for the hydrolysis of the 3-Me-2-butyl bromide is more negative than the corresponding value found for some secondary bromides and in the same range as values found for halides which probably react unambiguously by an S_N1 mechanism. Following the argument given above, and in contrast with the conclusion reached by Winstein and Takahashi (2) for the solvolysis of the corresponding tosylate in acetic acid, it seems unlikely that the solvolysis of this halide occurs in water by mixed kinetics. The same conclusion seems equally likely for the mechanism of solvolysis of the corresponding methanesulfonate where $\Delta C_p^{\ddagger} = -40 \pm 3$ cal deg^{-1} mole^{-1} for solvolysis in water. The corresponding value for solvolysis in D_2O is -44 ± 3 cal deg^{-1} mole^{-1}.

These latter values lie very close to those for the hydrolysis of isopropyl benzenesulfonate and methanesulfonate. If anchimeric assistance predicates solvent reorganization associated with an S_N1 mechanism in the hydrolysis of the bromide, it is even more likely to do so with the solvolysis of the sulfonates. This seemingly inevitable conclusion raises an anomaly. In previous papers we have accounted for the more negative values of $\Delta C_p^{\ddagger}$ which characterize the S_N1 displacement of halides from tertiary carbon in terms of the requirement for additional solvent reorganization about the quasi-cation (10). It seemed logical that the same reasoning apply to the value of -80 cal deg^{-1} mole^{-1} found for the displacement of the bromide in this study, compared to a value of about -50 which characterizes displacement from primary halides and -60 for secondary halides. Why then should there be no corresponding difference between the value of $\Delta C_p^{\ddagger}$ for the hydrolysis of methyl methanesulfonate (-35 cal deg^{-1} mole^{-1}) and that for isopropyl methanesulfonate (-35 cal deg^{-1} mole^{-1}), or for 3-Me-2-butyl methanesulfonate ($\Delta C_p^{\ddagger} = -44$ cal deg^{-1} mole^{-1})? One possible suggestion is that the presence of the sulfonic group localizes the breakdown of water structure, an interpretation which is consistent at least with the reduced kinetic solvent isotope effects which characterize the hydrolysis of this series of compounds (16). The similarity in the products (Table I) for the hydrolysis of bromides and methanesulfonates is consistent with the creation of some common intermediate which can react with adjacent water molecules. Neither reason provides a necessary and sufficient condition to explain the difference in $\Delta C_p^{\ddagger}$. Intuitively we feel that if the bromide reacts by an S_N1 mechanism, as seems likely on the above evidence, then the methanesulfonate does so as well. This leaves the lack of sensitivity of $\Delta C_p^{\ddagger}$ to an expected change in mechanism of solvolysis in the sulfonate series

Can. J. Chem. Downloaded from www.nrcresearchpress.com by 210.87.254.40 on 09/05/12
For personal use only.

Can. J. Chem. Downloaded from www.nrcresearchpress.com by 210.87.254.40 on 09/05/12
For personal use only.

an open question. This conclusion led to a reconsideration of our criterion (admittedly based on a limited number of examples) that the hydrolysis of halides reacting by an S_N1 mechanism (Table VI) is normally characterized by much more negative values of $\Delta C_p^{\ddagger}$ than those reacting by an unambiguous S_N2 mechanism. Quite aside from the problem raised above with respect to the $\Delta C_p^{\ddagger}$ for the hydrolysis of the secondary sulfonates, there are the intermediate values of $\Delta C_p^{\ddagger}$ already noted for the unassisted solvolysis of secondary halides. For the purposes of this paper, we note that the $\Delta C_p^{\ddagger}$ value determined for the 3-methyl-2-butyl bromide here implies extensive solvent reorganization at the transition state characteristic of those halides reacting by an S_N1 mechanism. The more general problem will be dealt with in a forthcoming paper (21).

Some years ago, Hoffmann proposed that the value of the rate ratio k_{Tos}/k_{Br} be used as a criterion of mechanism, though he omitted to specify the limits which define any particular mechanism (22). In the presence of a strong nucleophile and a poor ionizing medium, this ratio may be less than unity. Under good ionizing conditions and with favorable structure, values greater than 1000 are found. The ratio obtained here for $k_{Mes}/k_{Br} = 25.5$, which is equivalent to $k_{Tos}/k_{Br} = 53$, i.e., about 1/2 the value given for displacement from isopropyl, but well above the value of the ratio (17–5) which characterizes the hydrolysis of primary compounds in water.

Whatever the quantitative utility of this ratio in terms of mechanistic distinction, there is undoubted value to be gained from examining the probable reasons for variation in this ratio and relating these to other criteria of mechanism. Hoffmann notes that the value of the k_{Tos}/k_{Br} ratio for gas phase dehydrohalogenation follow a similar pattern to that found for solvolysis, the difference being that the activation energies in solution are reduced by about 1/2 and there is some indication that the spread of the values may be reduced as well. In the gas phase, the ratio apparently reflects the ability of an R-group to support the partial or total loss of an electron, coupled to the relative advantage the "electronically versatile" tosylate has over bromide to accommodate the complementary acquisition of charge. This intrinsic difference revealed in the gas phase experiments provides a quantitative answer to the curious fact that while $\Delta S^{\ddagger}$ for a series of sulfonates showed a wider change for $(\Delta S^{\ddagger}_{isopropyl} - \Delta S^{\ddagger}_{ethyl})$ than for the corresponding halides, the $\Delta C_p^{\ddagger}$ values showed just the opposite tendency (20). Thus, $(\Delta S^{\ddagger}_{isopropyl} - \Delta S^{\ddagger}_{ethyl})$ for the hydrolysis of mesylate is 8.3 e.u., and for bromide is 4.6 e.u. The corresponding values[5] for $(\Delta S_I^{\ddagger} - \Delta S_{ethyl}^{\ddagger})$ from the present study are 6.6 e.u. for the mesylate and 3.68 e.u. for the bromide. In both systems, the value of $\Delta C_p^{\ddagger}$ for the hydrolysis of the sulfonates are about the same, while the value of the $\Delta\Delta C_p^{\ddagger}$ for the bromides are, respectively, -10 and -32 cal deg^{-1} $mole^{-1}$. We know of no reason to question the assumption that $\Delta C_p^{\ddagger}$ is a more sensitive indicator of solvent reorganization than $\Delta S^{\ddagger}$, at least for hydrolysis in water. Hence, the above comparison points to the existence of important factors, other than solvent reorganization, which contribute to $\Delta S^{\ddagger}$. For solutes which react by an S_N1 mechanism, these factors seem to be related to the ease with which the solute becomes thermally activated. In this connection, it is probable that the nature of the solvent as well as the solute is significant in determining $\Delta S^{\ddagger}$, but a detailed study designed to relate the properties of the solute to variations in $\Delta S^{\ddagger}$ has yet to be made. An indication of the possibility of individual difference may be gained from a consideration of the variation in k_{Tos}/k_{Br} reported by Hoffmann (22) for the solvolysis of the 2-pentyl compounds: k_{Tos}/k_{Br} has the values 498 in formic acid, 105 in water, 73 in ethanol. For the neophyl series ($PhMe_2CCH_2X$) the corresponding values are 14 – 106. The corresponding $Y + 3$ values (23) which purport to measure the relative ionizing power of the solvent are 5.05, 6.49, and 0.97; the lack of correlation with the latter solvent property is obvious. Hoffmann suggests that these anomalies and others he discusses may be related to a desolvation of the nonclassical carbonium ion formed in the transition state. Our interpretation would be to attribute the difference to variations in the charge distribution which determines the initiation of exothermic solvation or of more specific interaction with the quasi-cation, individually. This is implied in Hoffmann's postulate that "the faster an S_N1 (E_1) reaction, the more ionic its transition state". This statement is consistent with the requirement that the more

[5] $\Delta S_I^{\ddagger}$ is for 3-Me-2-butyl methanesulfonate.

diffuse the charge, the higher the charge level required on the ion as a whole to exceed solvent–solvent interaction, and to result in secondary solvent–cation interaction leading to the completion of the reaction. The fact that those structures which release electrons better, solvolyze faster was established early in the work of Ingold and his co-workers (24) and is related to the inherent hypothetical $\Delta F_g^{\ddagger}$ (22). A graded series of increasingly reactive structures would probably show a parallel increase in $\Delta S_g^{\ddagger}$, as we have already noted.

We disagree with Hoffmann's conclusion that the more polar solvent necessarily favors the more polar transition state. It is a recognized fact that a reactant with structural characteristics which favor an S_N1 mechanism will show a very strong rate dependence on the ionizing properties of the solvent. Water is a better ionizing solvent than acetic acid, but the values of the k_{Tos}/k_{Br} ratio are higher in the latter. The relation of charge level to ionizing properties cannot be resolved by a simple hypothesis because at the transition state not only solvation properties, but also nucleophilic properties of the solvent are involved, as well as charge distribution and steric considerations of the quasication. The tosyl group undoubtedly disperses charge better than the bromide, thus facilitating both the S_N1 and S_N2 mechanism. In the S_N2 displacement of the sulfonic group from a primary carbon, the spare electrons on the oxygen provide available sites for solvent interaction; thus nucleophilic displacement is achieved with less requirement for overlap, an inference supported by the relative α-deuterium isotope effects (25).

From these observations, we are led to conclude that while the k_{Tos}/k_{Br} ratio forms an interesting basis for inspection, it should be regarded as a supplementary indication of possible mechanistic difference, the common lot of most comparable tests.

It would be simple to conclude on the basis of the above evidence that hydrogen participation in the hydrolysis of 3-Me-2-butyl bromide is characterized by solvent reorganization characteristic of an S_N1 mechanism. Neighboring group participation has been shown previously to result in reduced (as well as enhanced) values of the kinetic solvent isotope effect (26). The example reported here may be regarded as a further example of the same phenomenon. Obviously, to draw attention to such similarity is not equivalent to providing a satisfactory explanation, and further work will be required in this area.

1. M. J. Blandamer, H. S. Golinkin, and R. E. Robertson. J. Amer. Chem. Soc. **91**, 2678 (1969).
2. S. Winstein and J. Takahashi. Tetrahedron Lett. **2**, 316 (1958).
3. R. S. Tipson. J. Org. Chem. **9**, 235 (1944).
4. J. Cason and J. S. Corrcia. J. Org. Chem. **26**, 3645 (1961).
5. W. J. Bailey and S. S. Hirsch. J. Org. Chem. **28**, 2894 (1963).
6. R. E. Robertson. Can. J. Chem. **33**, 1536 (1955).
7. J. M. Stuart and F. Wormwell. J. Chem. Soc. 85 (1930).
8. E. D. Hughes, C. K. Ingold, and S. Shapiro. J. Chem. Soc. 225 (1936).
9. L. Hakka, A. Queen, and R. E. Robertson. J. Amer. Chem. Soc. **87**, 161 (1965).
10. R. E. Robertson. Progr. Phys. Org. Chem. **4**, 213 (1967).
11. R. E. Robertson and S. E. Sugamori. J. Amer. Chem. Soc. In Press.
12. N. C. Deno, H. J. Peterson, and G. S. Saines. Chem. Rev. **59**, 7, (1959).
13. R. E. Robertson and P. M. Laughton. Can. J. Chem. **35**, 1319 (1957).
14. G. Kohnstam. Advan. Phys. Org. Chem. **5**, 121 (1967).
15. L. J. Brubacher, L. Treindl, and R. E. Robertson. J. Amer. Chem. Soc. **90**, 4611 (1968).
16. P. M. Laughton and R. E. Robertson. Can. J. Chem. **34**, 1714 (1956).
17. B. N. Hendy and R. E. Robertson. Can. J. Chem. **45**, 2071 (1967).
18. E. A. Moelwyn-Hughes, R. E. Robertson, and S. E. Sugamori. J. Chem. Soc. 1965 (1965).
19. A. Queen and R. E. Robertson. J. Amer. Chem. Soc. **88**, 1363 (1966).
20. R. L. Heppolette and R. E. Robertson. Can. J. Chem. **44**, 677 (1966).
21. W. M. J. Strachan and R. E. Robertson. To be published.
22. M. W. R. Hoffmann. J. Chem. Soc. 6753 (1965).
23. S. Winstein and E. Grunwald. J. Amer. Chem. Soc. **70**, 848 (1948).
24. C. K. Ingold. Structure and mechanism of organic chemistry. Cornell Univ. Press, Ithaca, N.Y. 1953. Chap. VII.
25. A. J. Llewellyn, R. E. Robertson, and J. M. W. Scott. Can. J. Chem. **38**, 222 (1960).
26. P. M. Laughton and R. E. Robertson. Can. J. Chem. **39**, 2155 (1961).

Can. J. Chem. Downloaded from www.nrcresearchpress.com by 210.87.254.40 on 09/05/12
For personal use only.

Can. J. Chem. Downloaded from www.nrcresearchpress.com by 210.87.254.40 on 09/05/12
For personal use only.

Organoantimony compounds. II. Studies on tetraphenylantimony(V) derivatives[1,2]

R. G. GOEL
Department of Chemistry, University of Guelph, Guelph, Ontario

Received July 11, 1969

Tetraphenylantimony halides, pseudohalides, carboxylates, nitrate, sulfate, selenate, and chromate have been synthesized. The infrared spectra, molecular weights, and electrical conductances of these compounds have been investigated to elucidate the chemical constitution. The compounds have molecular, monomeric constitution in benzene solutions. Infrared results indicate that with the exception of the acetate and the oxalate, all the compounds have 5-coordinate structures. The acetate is 6-coordinate in the solid state and 5-coordinate in bromoform or chloroform solution. The oxalate is indicated to be 6-coordinate in the solid state as well as in chloroform solution. The electrical conductivities of the bromide, chloride, thiocyanate, trifluoroacetate, and the nitrate in nitromethane correspond to those of 1:1 electrolyte. The conductivities of the other compounds indicate little dissociation in this solvent.

Canadian Journal of Chemistry, 47, 4607 (1969)

Introduction

The first tetraphenylstibonium compound, Ph_4SbBr, was reported by Chatt and Mann (1). Since then other tetraphenylantimony derivatives have been described in the literature (2). By analogy with tetraphenylphosphonium and tetraphenylarsonium acid derivatives, the analytical applications of tetraphenylantimony derivatives have also been explored. The tetraphenylphosphonium and arsonium halides and nitrates are known to have ionic constitution (3). However, the chemical constitution of the analogous antimony derivatives has not been established. Investigations were therefore initiated in this laboratory to establish the nature of tetraphenylantimony acid derivatives. While this work was in progress X-ray crystallographic studies on tetraphenylantimony methoxide (4) and hydroxide (5) were reported. The X-ray studies have shown that both the compounds have molecular, trigonal bipyramidal structures.

Very recently, studies on some tetraphenylantimony–acetylacetonate (6, 7) and –oxinates (7, 8) have also appeared. In these compounds an octahedral configuration around the antimony atom is indicated. In this paper the results of infrared spectral, electrical conductance, and molecular weight studies on tetraphenylantimony halides, pseudohalides, carboxylates, nitrate, sulfate, selenate, chromate, and the oxalate are reported.

[1]For part I of this series, see ref. 17.

[2]Presented in part at the 52nd Annual Conference of Chemical Institute of Canada, Montreal. May 26–28, 1969.

Experimental

Preparations

Tetraphenylantimony bromide was prepared by the method of Willard, Perkins, and Blicke (9). Other tetraphenylantimony derivatives were prepared by the reaction of the bromide with the appropriate silver salt, using benzene or methanol as the solvent. After removing the solvent the solid residue was recrystallized from petroleum ether or a mixture of benzene and petroleum ether. The compounds were characterized by elemental analyses, molecular weight determinations, infrared spectra, and melting points.

Measurements

Infrared spectra were recorded on a Beckman Model IR-12 double beam spectrophotometer. Solid samples were prepared as mulls in Nujol or halocarbon oil and the spectra were obtained using KRS-5 and polyethylene windows. Spectra of the solutions were obtained using silver chloride or potassium bromide demountable liquid cells. Spectra of the solid samples were measured in the 4000 to 200 cm^{-1} region. The spectra in solutions were measured only in selected frequency regions. The electrical conductivities were measured with a Yellow Springs Instrument Co. Inc. Model 31 conductivity bridge. A conductance cell with bright platinum electrodes and a ground glass stopper was used. The cell constant was determined by use of standard aqueous solutions of potassium chloride.

The molecular weights were determined with a Hitachi–Perkin–Elmer Model 115 vapor osmometer. Melting points were measured with a Gallenkamp melting point apparatus in glass melting point tubes with one open end. Elemental analyses were carried out by Dr. A. B. Gygli, Microanalytical Laboratory, Toronto.

Solvents

Analytical and spectrograde solvents from Fisher, Baker, or Matheson Coleman and Bell were used without further purification. In the conductance measurements, the conductance of the solvent was measured in each case and corrections to the observed conductances were made.

TABLE I
Analytical data

Compound	Analysis (%) Found C	Found H	Calcd. C	Calcd. H	Molecular weight* Found	Molecular weight* Calculated	Melting point (°C)
Ph_4SbBr	56.08	3.77	56.54	3.92	511	510	210–213
Ph_4SbCl	61.90	4.62	61.92	4.30	457	465	204–205
Ph_4SbF	63.36	4.36	64.16	4.50	448	449	165
$Ph_4Sb(N_3)$†	60.50	4.68	61.04	4.28	472	472	191
$Ph_4Sb(CNO)$	63.78	4.39	63.58	4.27	475	472	206
$Ph_4Sb(SCN)$	61.79	4.23	61.48	4.13	486	488	226–228
$Ph_4Sb(CH_3COO)$	63.60	4.87	63.83	4.74	486	489	129–131
$Ph_4Sb(CCl_3COO)$	53.66	3.46	52.73	3.38	588	591	103–104
$Ph_4Sb(CF_3COO)$	58.25	3.86	57.49	3.71	545	543	164–165
$Ph_4Sb(NO_3)$	58.41	4.12	58.54	4.10	500	492	179
$(Ph_4Sb)_2SO_4$	60.07	4.32	60.27	4.21	954	956	231
$(Ph_4Sb)_2SeO_4$	57.46	4.07	57.49	4.02	1011	1003	228–230
$(Ph_4Sb)_2CrO_4$	58.94	4.24	59.06	4.13	993	976	165
$(Ph_4Sb)_2C_2O_4$	63.95	4.44	63.35	4.25	968	948	237

*Solvent: benzene; concentration range: 10^{-2}–10^{-3} mole/kg.
†Percentage N: found, 8.90; calcd., 9.10.

Results and Discussion

The compounds are nonhygroscopic and soluble in organic solvents such as methanol, nitromethane, benzene, chloroform, and carbon disulfide. About half of the compounds are also soluble in petroleum ether. With the exception of the chromate, the compounds are stable under ordinary conditions. The chromate decomposes slowly at room temperature and on exposure to light. However, it can be stored in a refrigerator without any decomposition.

Molecular Weight and Conductance

The analytical and molecular weight data and melting points of the investigated compounds are recorded in Table I. The molecular weight data clearly show that all the compounds exist as molecular and monomeric species in benzene.

The electrical conductances of these compounds were measured in nitromethane at 25 °C in the concentration range of 10^{-3} to 10^{-4} M. The equivalent conductances, Λ_e, as a function of the square root of the concentration in equivalents per l., $\sqrt{c}$, are shown in Figs. 1, 2, and 3. The plots of Λ_e against $\sqrt{c}$ for tetraphenylantimony bromide, chloride, nitrate, thiocyanate, and the trifluoroacetate give straight lines. The equivalent conductances of these compounds occur in the same range as observed for tetraphenylarsonium chloride in nitromethane. Thus the above compounds can be considered as 1:1 electrolyte in nitromethane. However, the observed conductances of tetraphenylantimony fluoride, cyanate, azide, acetate, and trichloroacetate are significantly lower than those of tetraphenylarsonium chloride. Also, the

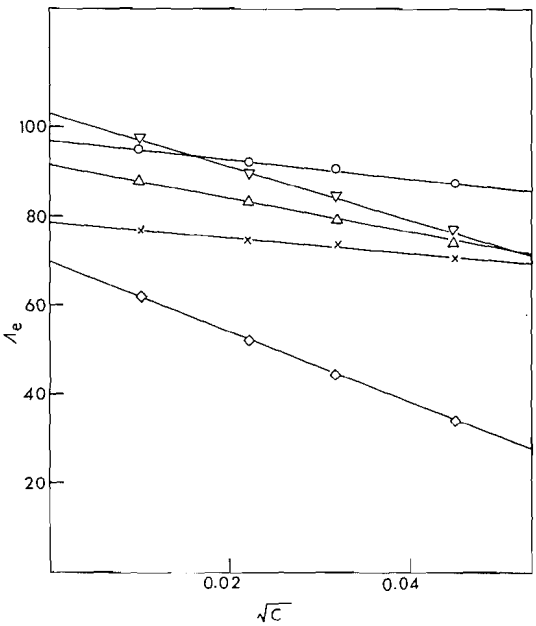

FIG. 1. Equivalent conductances of Ph_4SbX compounds in nitromethane solutions at 25° vs. square roots of concentrations in equivalents per l. Δ, Ph_4SbBr; ◇, Ph_4SbCl; ▽, $Ph_4Sb(SCN)$; ×, $Ph_4Sb(CF_3COO)$; ○, $Ph_4Sb(NO_3)$.

Can. J. Chem. Downloaded from www.nrcresearchpress.com by 210.87.254.40 on 09/05/12
For personal use only.

Can. J. Chem. Downloaded from www.nrcresearchpress.com by 210.87.254.40 on 09/05/12
For personal use only.

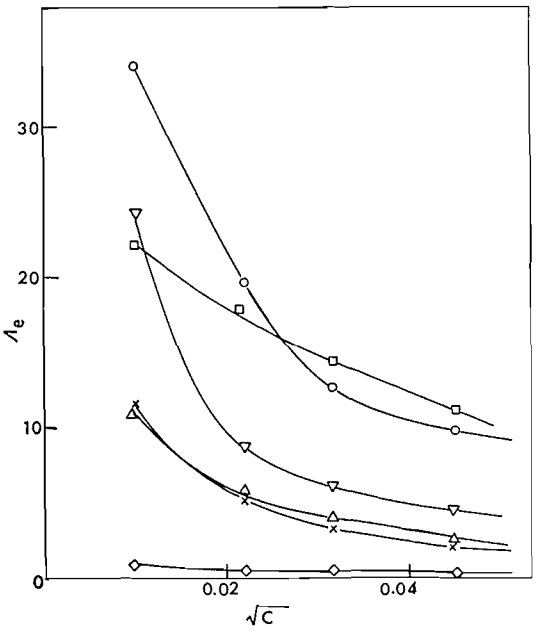

FIG. 2. Equivalent conductances of Ph_4SbX compounds in nitromethane solutions at 25° vs. square roots of concentrations in equivalents per l. ◇, Ph_4SbF; □, $Ph_4Sb(N_3)$; ○, $Ph_4Sb(CNO)$; ▽, $Ph_4Sb(CH_3COO)$; Δ, $Ph_4Sb(CCl_3COO)$; ×, $Ph_4Sb(OH)$.

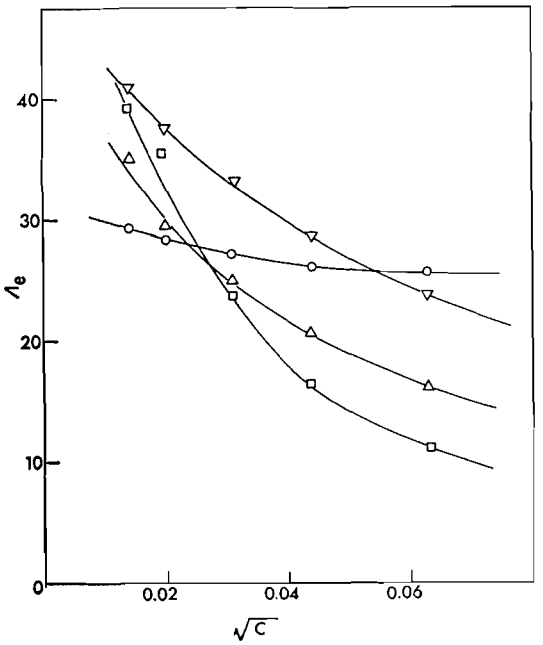

FIG. 3. Equivalent conductances of $(Ph_4Sb)_2X$ compounds in nitromethane solutions at 25° vs. square roots of concentrations in equivalent per l. ▽, $(Ph_4Sb)_2SO_4$; Δ, $(Ph_4Sb)_2SeO_4$; □, $(Ph_4Sb)_2CrO_4$; ○, $(Ph_4Sb)_2C_2O_4$.

plots of the Λ_e against $\sqrt{c}$ are not straight lines. The conductance data of these compounds thus indicate a small degree of dissociation in nitromethane. In fact, the conductivities of the fluoride are so low that it may be considered to be a nonelectrolyte in nitromethane. Since the molecular structure of tetraphenylantimony hydroxide has been established, the conductances of this compound were measured to provide a comparison. The plot of Λ_e against $\sqrt{c}$ for the hydroxide is also shown in Fig. 2. The conductances of the trichloroacetate are found to be very close to those of the hydroxide.

The equivalent conductance of a 10^{-3} *M* solution of a uni–bivalent electrolyte in nitromethane has been reported (10) to be 80 Ω^{-1} cm^{-2} $equiv.^{-1}$. The observed conductances of tetraphenylantimony sulfate, selenate, chromate, and the oxalate are significantly lower. Also, the plots of Λ_e against $\sqrt{c}$ do not give straight lines. Thus, all four $(Ph_4Sb)_2X$ compounds appear to behave as weak electrolytes in nitromethane.

Infrared Spectra

The infrared spectroscopic results provide further support for the molecular constitution of these compounds. The infrared spectra of all the compounds show almost identical absorption bands due to the phenyl groups. The absorption bands due to the anion groups can therefore be assigned with confidence. The observed absorption frequencies associated with the anion group, X, in the Ph_4SbX compounds are listed in Table II. In the case of the acetate and haloacetates, only the (COO) stretching frequencies are listed. In the spectra of tetraphenylantimony fluoride, a strong absorption band is observed at 400 cm^{-1}. This band does not occur in the spectrum of the bromide or the chloride and it can be assigned to the (Sb—F) stretching frequency. The Sb—F stretching frequency in trimethylantimony difluoride (11) occurs at 475 cm^{-1}, and the Sb—OH stretching frequency in tetraphenylantimony hydroxide (5) is reported at 528 cm^{-1}. The antimony–halogen stretching frequency in the spectra of the bromide and chloride are not observed in the 4000–250 cm^{-1} region.

The absorption bands due to the N_3, CNO, and SCN groups compare very well with those reported (12) for other covalent organometallic pseudohalides. The frequencies of the cyanate

TABLE II

Observed infrared absorption frequencies associated with the X group in Ph_4SbX compounds

Compound	Frequency* (cm^{-1})	Assignment
Ph_4SbF	400 (s)	(Sb—F) str.
$Ph_4Sb(N_3)$	2045 (s)	(N—N—N) asym. str.
	1328 (m)	(N—N—N) sym. str.
	636 (w)	(N—N—N) bend
$Ph_4Sb(NCO)$	2180 (s)	(C—N) str.
	640 (m)	(NCO) bend
$Ph_4Sb(NCS)$	2040 (s)	(C—N) str.
	795 (w)	(C—S) str.
	480 (w)	(N—C—S) bend
$Ph_4Sb(OOCCH_3)$	1555 (m); 1625† (s)	(COO) asym. str.
	1395 (m); 1370† (s)	(COO) sym. str.
$Ph_4Sb(OOCCCl_3)$	1700 (s)	(COO) asym. str.
	1315 (s)	(COO) sym. str.
$Ph_4Sb(OOCCF_3)$	1700 (s)	(COO) asym. str.
	1400 (s)	(COO) sym. str.
$Ph_4Sb(NO_3)$	1465 (s)	NO_2 asym. str.
	1300 (s)	NO_2 sym. str.
	1010 (m)	NO str.
	818 (m)	out-of-plane rock
	715 (m)	NO_2 bend

*Measured in the solid state; m = medium, s = strong, w = weak.
†Measured in bromoform solution.

and the thiocyanate indicate that both the cyanate and the thiocyanate groups are involved in bonding through the nitrogen atom (12, 13).

In the infrared spectrum of tetraphenylantimony acetate in the solid state, the (COO) symmetric and asymmetric stretching frequencies occur at 1395 and 1555 cm^{-1}, respectively. However, in bromoform or chloroform solutions these frequencies are observed at 1370 and 1625 cm^{-1}, respectively. In the solid state the C—O—O stretching frequencies are of the same order as reported for the free acetate ion or bidentate acetate ligand (14). However, C—O—O stretching frequencies in solution are as expected for monodentate acetate group (14). The spectrum of the solid tetraphenylantimony acetate can best be interpreted in terms of a 6-coordinate structure. The ionic structure can be ruled out in view of the conductance and molecular weight data and the solubility of this compound in hot petroleum ether. The significant increase in the difference between the C—O—O asymmetric and symmetric stretching frequencies in the chloroform or bromoform solution suggests a 5-coordinate structure in solution. The observed solid state infrared spectra of tetraphenylantimony trifluoro- and trichloro-acetate and tetraphenylantimony nitrate are consistent with 5-coordinate structures containing a unidentate X group (11, 15, 16).

The infrared absorption frequencies due to the anion group, X, in the tetraphenylantimony sulfate, selenate, chromate, and the oxalate are listed in Table III. The spectra of the sulfate, selenate, and the chromate, clearly indicate that the tetrahedral symmetry of the anion group, X, has been reduced to at least C_{2v}. The spectral data indeed are in accord with the presence of bridging X groups (11, 17). Although in the case of the tetraphenylantimony sulfate only 3 stretching frequencies due to the sulfate group can be assigned with confidence, the spectra of the selenate and the chromate clearly show 4 strong, well resolved bands which can be assigned to the stretching frequencies due to the coordinated selenate or chromate group (11, 17). Similarly, in the low frequency region 4 absorption frequencies due to the selenate or chromate group are observed. In this region only 3 frequencies can be assigned to the sulfate group, the fourth frequency in the 470–450 cm^{-1} region is presumably masked by the strong phenyl band in

Can. J. Chem. Downloaded from www.nrcresearchpress.com by 210.87.254.40 on 09/05/12
For personal use only.

TABLE III

Observed infrared absorption frequencies* of the X group in $(Ph_4Sb)_2X$ compounds

Frequency (cm^{-1})			
$(Ph_4Sb)_2SO_4$	$(Ph_4Sb)_2SeO_4$	$(Ph_4Sb)_2CrO_4$	$(Ph_4Sb)_2C_2O_4$
1240 (s)	936 (s)	950 (s)	1625 (s)
1122 (s)	890 (s)	920 (s)	1310 (w)
955 (s)	795 (s)	830 (s)	788 (m)
622 (w)	775 (s)	780 (s)	375 (w)
612 (m)	470 (m)	408 (m)	
600 (w)	410 (m)	376 (m)	
	400 (s)	352 (w)	
	370 (m)	330 (w)	

*Measured in the solid state; m = medium; s = strong; w = weak.

this region. The possibility of the lowering of the anion group symmetry due to the solid state effects can be ruled out, because no significant change was observed in the anion group stretching frequencies when spectra were recorded in carbon disulfide solutions.

The infrared spectrum of tetraphenylantimony oxalate shows only one O—C—O stretching frequency at 1625 cm^{-1}. The other absorption bands which can be assigned to the oxalate group are observed at 1310, 788, and 375 cm^{-1}. The spectrum of the tetraphenylantimony oxalate thus differs significantly with that of triphenylantimony oxalate (17), which shows 2 strong (O—C—O) stretching bands at 1740 and 1655 cm^{-1} and for which a 5-coordinate bridging structure is proposed. The oxalate frequencies in tetraphenylantimony oxalate correspond to the presence of either a free oxalate ion or a symmetrical oxalate group functioning as bichelate ligand (18). In view of the conductance and molecular weight data, the coordinated structure containing a symmetrical bichelate oxalate group and a 6-coordinate antimony atom is more probable than an ionic structure. The infrared spectrum of chloroform solution of this compound also shows only 1 absorption band due to (O—C—O) stretching vibration, and the position of this band is not changed in solution. Therefore, unlike the tetraphenylantimony acetate, the structure of the tetraphenylantimony oxalate does not change in solution.

Regarding the infrared frequencies associated with the antimony–carbon stretching vibrations, no definite assignments can be made due to the presence of the phenyl absorption bands. A recent study (19) of the vibrational spectra of triphenyl compounds of the main group V elements indicates that in the case of triphenylantimony, the (Sb—C) stretching vibrations occur below 300 cm^{-1}. However, due to overlap with the phenyl ring vibrations the assignments cannot be made unequivocally. Absorption frequencies due to the antimony–ligand stretching vibrations could not be identified in any compound with the exception of tetraphenylantimony fluoride. These frequencies are most likely to occur near 300 cm^{-1} or lower, and again due to the presence of the phenyl bands no conclusion can be reached about them.

In conclusion, the results of this study indicate that the tetraphenylantimony derivatives investigated are nonionic and monomeric in benzene. The electrical conductances in nitromethane show a significant degree of ionization in the case of the bromide, chloride, thiocyanate, trifluoroacetate, and the nitrate. This indicates appreciable ionic character of the Sb—X bond in these compounds. The conductances of the fluoride, azide, cyanate, acetate, trichloroacetate, sulfate, selenate, chromate, and the oxalate do not show any significant ionization in nitromethane, and in these compounds the Sb—X bond can be described as being more covalent. With the exception of the acetate and the oxalate, all the compounds appear to have a 5-coordinate structure in the solid state. The acetate appears to have a 6-coordinate structure in the solid state, but a 5-coordinate structure in solution. The oxalate appears to be 6-coordinate in the solid state as well as in solution. The reason for this difference in the mode of coordination of the carboxylate group is not clear at present. The

Can. J. Chem. Downloaded from www.nrcresearchpress.com by 210.87.254.40 on 09/05/12
For personal use only.

difference between the constitution of the tetraphenylantimony acid derivatives and the corresponding phosphorus and arsenic halides and nitrates is in accord with the reported (20, 21) differences in the properties of tertiary organometallic dihalides, R_3MX_2, (R = methyl or phenyl, M = group VB atom) of the group VB elements. However, the structural aspects of organometallic derivatives of group VB elements have not been extensively investigated, and further experimental studies are required in order to rationalize the stereochemistry of organometallic derivatives of group VB elements in the +5 oxidation state.

Acknowledgments

The author gratefully acknowledges the financial support from the National Research Council of Canada and the Department of Education, Province of Ontario. Thanks are also due to Robert Boynton for assistance in the experimental part of the investigation.

1. J. CHATT and F. G. MANN. J. Chem. Soc. 1184 (1940).
2. H. E. AFFSPRUNG and H. E. MAY. Anal. Chem. **32**, 1164 (1960).
3. A. R. DAVIS, J. W. MACKLIN, and R. A. PLANE. J. Chem. Phys. **50**, 1478 (1969) and references therein.
4. K. SHEN, W. E. MCEWEN, S. J. LAPLACA, W. C. HAMILTON, and A. P. WOLF. J. Amer. Chem. Soc. **90**, 6685 (1968).
5. A. L. BEAUCHAMP, M. J. BENNETT, and F. A. COTTON. J. Amer. Chem. Soc. **91**, 297 (1969).
6. H. A. MEINEMA and J. G. NOLTES. J. Organometal. Chem. Amsterdam, **16**, 257 (1969).
7. Y. MATSUMURA and R. OKAWARA. Inorg. Nucl. Chem. Lett., **4**, 521 (1968).
8. H. A. MEINEMA, MRS. E. RIVAROLA, and J. G. NOLTES. J. Organometal. Chem. Amsterdam, **17**, 71 (1969).
9. H. H. WILLARD, L. R. PERKINS, and F. F. BLICKE. J. Amer. Chem. Soc. **70**, 737 (1948).
10. C. M. HARRIS, R. S. NYHOLM, and D. J. PHILLIPS. J. Chem. Soc. 4379 (1960).
11. H. C. CLARK and R. G. GOEL. Inorg. Chem. **5**, 998 (1966).
12. J. S. THAYER and R. WEST. Advan. Organometal. Chem. **5**, 169 (1967).
13. A. H. NORBURY and A. I. P. SINHA. J. Chem. Soc. A, 1598 (1968).
14. N. F. CURTIS. J. Chem. Soc. A, 1579 (1968).
15. P. B. SIMONS and W. A. G. GRAHAM. J. Organometal. Chem. Amsterdam, **10**, 457 (1967).
16. E. V. VAN DEN BERGHE, G. P. VAN DER KELEN, and J. ALBRECT. Inorg. Chim. Acta, **2**, 89 (1968).
17. R. G. GOEL, P. N. JOSHI, D. R. RIDLEY, and R. E. BEAUMONT. Can. J. Chem. **47**, 1423 (1969).
18. N. F. CURTIS. J. Chem. Soc. A, 1584 (1968).
19. K. SHOBATAKE, C. POSTMUS, J. R. FERRARO, and K. NAKAMOTO. Appl. Spectrosc. **23**, 12 (1969).
20. A. D. BEVERIDGE, G. S. HARRIS, and F. INGLIS. J. Chem. Soc. A, 520 (1966).
21. M. H. O'BRIEN, G. O. DOAK, and G. G. LONG. Inorg. Chim. Acta, **1**, 34 (1967).

Can. J. Chem. Downloaded from www.nrcresearchpress.com by 210.87.254.40 on 09/05/12
For personal use only.

Thermal expansion and structure in water and aqueous solutions

LOREN G. HEPLER
Department of Chemistry, University of Lethbridge, Lethbridge, Alberta
Received July 17, 1969

The thermodynamic equation $(\partial C_P/\partial P)_T = -T(\partial^2 V/\partial T^2)_P$ is used as a basis for relating thermal expansion to structure (at several temperatures and pressures) of water and "normal" liquids. Similar considerations lead to a relation between the sign of $(\partial^2 \overline{V}_2{}^0/\partial T^2)_P$ for solutions and classification of solutes as structure-making or structure-breaking.

Canadian Journal of Chemistry, 47, 4613 (1969)

Can. J. Chem. Downloaded from www.nrcresearchpress.com by 210.87.254.42 on 09/05/12
For personal use only.

A variety of evidence has led to the view that water is a partly "structured" liquid that can be loosely described as a sort of partly broken down ice. Possibly the simplest useful description of liquid water, is that in which the water is pictured as being a mixture of two species; one a bulky icelike species with relatively low density and the other a denser species that is formed by breaking (or bending) the hydrogen bonds that maintain the ice-likeness of the bulky species. Since both increasing temperature and increasing pressure would have the effect of increasing the fraction of the dense species at the expense of the bulky species, this simple model can account qualitatively for the maximum in density, the unusually high heat capacity, and several other properties of water. Some of the properties of aqueous solutions have also been interpreted in terms of the "structure-making" or "structure-breaking" characteristics of various solutes. This paper is concerned with the relation between these structural ideas and the thermal expansion of water and of aqueous solutions.

Partial molal heat capacities of aqueous electrolytes are commonly negative. An early explanation (for example, Lewis and Randall (1)) that is consistent with other properties of aqueous electrolytes is that these solutes break up the bulky aggregates and thereby decrease the effective heat capacity of the water. Since increasing pressure would also break up the bulky aggregates, the same reasoning suggests that the heat capacity of pure water should decrease with increasing pressure. We therefore expect $(\partial C_P/\partial P)_T$ to be negative and use the thermodynamic equation

$$[1] \qquad \left(\frac{\partial C_P}{\partial P}\right)_T = -T\left(\frac{\partial^2 V}{\partial T^2}\right)_P$$

in predicting that $(\partial^2 V/\partial T^2)_P$ for water is positive. Because increasing temperature also breaks up the bulky aggregates, we expect that the magnitude of $(\partial C_P/\partial P)_T$ should decrease with increasing temperature, which requires that $T(\partial^2 V/\partial T^2)_P$ should also decrease with increasing temperature. Similarly, we expect that $T(\partial^2 V/\partial T^2)_P$ should decrease with increasing pressure. Since a variety of evidence suggests that D_2O is a more structured liquid than is H_2O, we also expect that the magnitude of $(\partial C_P/\partial P)_T$ and thence $T(\partial^2 V/\partial T^2)_P$ would be larger for D_2O than for H_2O.

Kell (2) has tabulated values of density (ρ) and coefficient of thermal expansion ($\alpha = (1/V)(\partial V/\partial T)_P$) for H_2O(liquid) at 1 atm. over a range of temperatures. These values have been used with the equation

$$[2] \qquad \left(\frac{\partial^2 V}{\partial T^2}\right)_P = \frac{M}{\rho}\left[\alpha^2 + \left(\frac{\partial \alpha}{\partial T}\right)_P\right]$$

in which M represents the molecular weight, to obtain values of $(\partial^2 V/\partial T^2)_P$ and thence the values of $T(\partial^2 V/\partial T^2)_P$ that are shown in Fig. 1. Densities of D_2O(liquid) tabulated by Kell (2) also lead to the (molar) values of $T(\partial^2 V/\partial T^2)_P$ that are shown in Fig. 1. Here it might be noted that small irregularities in $(\partial^2 V/\partial T^2)_P$ for D_2O in the ranges of 35–45 and 65–75 °C have been smoothed in constructing the figure. Specific volumes tabulated by Kell and Whalley (3) have been used in calculating the (slightly smoothed) values of $T(\partial^2 V/\partial T^2)_P$ for H_2O(liquid) under pressures of 200 and 1000 bars as also shown in Fig. 1.

The curves in Fig. 1 show the predicted differences in $T(\partial^2 V/\partial T^2)_P$ for H_2O and D_2O at 1 atm. and confirm the predicted effect of pressure on H_2O. At higher temperatures the values of $T(\partial^2 V/\partial T^2)_P$ increase very slightly

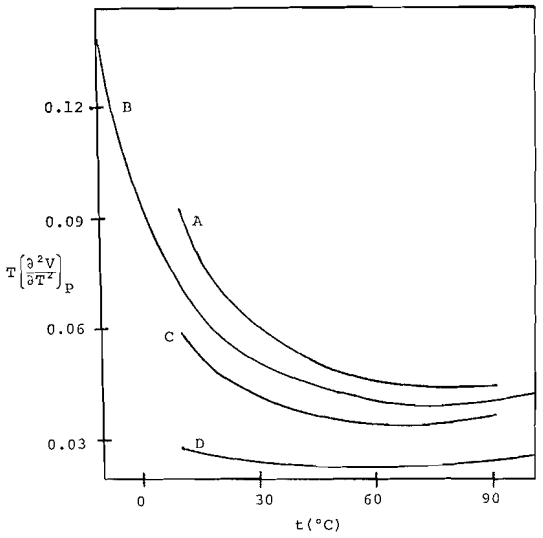

FIG. 1. Thermal expansion data: *A* (D_2O, 1 atm); *B* (H_2O, 1 atm); *C* (H_2O, 200 bars); *D* (H_2O, 1000 bars).

with increasing temperature, in contrast with the decrease observed at lower temperatures that was predicted earlier on the basis of structural arguments. This slight increase of $T(\partial^2 V/\partial T^2)_P$ at higher temperatures can be rationalized as follows.

According to the structural model described earlier, water becomes more like a normal liquid as the temperature (or pressure) increases. In order to ascertain what constitutes "normal" variation of volume with temperature, density data for a number of liquids (*n*-heptane, diethylether, CCl_4, ethanol, benzene, and mercury) have been used to obtain corresponding values of $T(\partial^2 V/\partial T^2)_P$ over a range of temperatures. Although the highest values (for ether and heptane) of $T(\partial^2 V/\partial T^2)_P$ are some 500 times the smallest values (for Hg), the temperature dependence of this quantity falls within the relatively narrow range of an increase of about 1–2% per degree. At 100 °C we find that $T(\partial^2 V/\partial T^2)_P$ for water is increasing by only about 0.2% per degree, and even at 140 °C the increase is still less than 0.5% per degree. Thus we see that the volumetric behavior of water, even at high temperature, is still consistent with a structural model in which it is assumed that increasing temperature and pressure break down structure and cause water to approach "normal" behavior.

Extension of the approach described here to aqueous solutions should contribute to understanding of structure-making/breaking by various solutes. We begin by differentiating the thermodynamic equation of state $(\partial H/\partial P)_T = V - T(\partial V/\partial T)_P$ with respect to n_2 (P, T, and n_1 constant) and then with respect to T (n_1, n_2, and P constant) to obtain

$$[3] \qquad \left(\frac{\partial \bar{C}_P}{\partial P}\right)_T = -T\left(\frac{\partial^2 \bar{V}_2}{\partial T^2}\right)_P$$

Since present considerations are limited to consequences of solute–solvent interactions, we choose to apply eq. [3] to partial molal properties of the solute at infinite dilution as indicated subsequently by the superscript zero.

As already mentioned, partial molal heat capacities of electrolytes are commonly negative. The common explanation (1) in terms of structure-breaking leads to the prediction that $(\partial \bar{C}_P{}^0/\partial P)_T$ should be positive. On the basis of this reasoning and eq. [3], it is seen that structure-breaking solutes should have negative $(\partial^2 \bar{V}_2{}^0/\partial T^2)_P$. Similar reasoning shows that positive $(\partial^2 \bar{V}_2{}^0/\partial T^2)_P$ should be associated with structure-making solutes.

Although interpretation of the experimental data is not entirely certain, a variety of evidence (4–6) suggests that alcohols (in dilute solutions) are structure-making solutes. On this basis and our reasoning concerning the sign of $(\partial \bar{C}_P/\partial P)_T$, we expect that $(\partial^2 \bar{V}_2{}^0/\partial T^2)_P$ should be positive for aqueous alcohols. The most obvious confirmation of this expectation is the figure presented by Alexander (7) in which $\bar{V}_2{}^0$ values for methanol, ethanol, *i*-propanol, *i*-butanol, and *i*-pentanol are plotted against temperature (0–60 °C). Franks and Smith (4)[1] have obtained $\bar{V}_2{}^0$ values for the four isomeric butanols at four temperatures (0.5–40 °C), while Friedman and Scheraga (8) have reported $\bar{V}_2{}^0$ values for nine alcohols at four temperatures (1–50 °C). All of the $\bar{V}_2{}^0$ vs. temperature curves for alcohols (4, 7, 8) are of the general shape illustrated in Fig. 2, with the positive $(\partial^2 \bar{V}_2{}^0/\partial T^2)_P$ expected for structure-makers.

Dunn's measurements (9) have led to $\bar{V}_2{}^0$ values for NaCl, KBr, KCl, $BaCl_2$, and $CaCl_2$ at eight temperatures from 0.5 to 65 °C. The general shape of graphs of $\bar{V}_2{}^0$ against T is shown

[1]References to earlier work, with particular emphasis on volumetric properties, are cited in this paper.

Can. J. Chem. Downloaded from www.nrcresearchpress.com by 210.87.254.42 on 09/05/12
For personal use only.

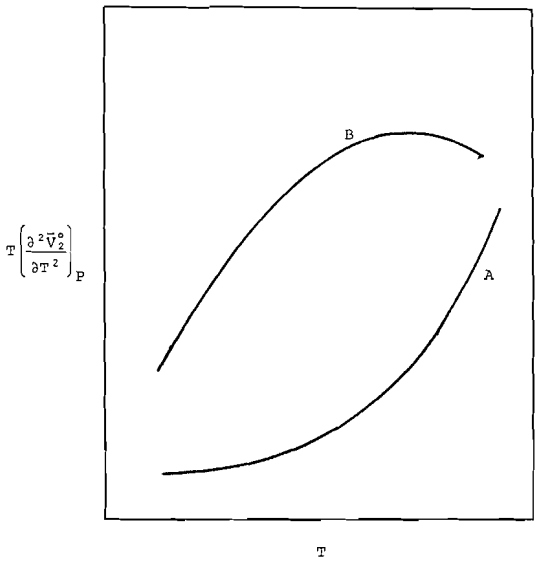

FIG. 2. Typical thermal expansion data for aqueous solutes: Curve *A* is associated with structure-making solutes and curve *B* with structure-breaking solutes.

in Fig. 2, with $(\partial^2 \bar{V}_2^0/\partial T^2)_P$ negative as expected for structure-breaking solutes. Bull and Breese (10) have recently published a graph of apparent molal volume of KCl (dilute solution) against temperature that is in agreement with the general shape of the curve in Fig. 2 based on Dunn's data (9). Data from Ellis (11, 12) for LiCl, NaCl, KCl, CsCl, $MgCl_2$, $CaCl_2$, $SrCl_2$, and $BaCl_2$ up to 200 °C also lead to negative $(\partial^2 \bar{V}_2^0/\partial T^2)_P$. Other data from Millero (13) confirm that $(\partial^2 \bar{V}_2^0/\partial T^2)_P$ is negative for most aqueous salt solutions. Thus the volumetric data indicate that these electrolytes should be regarded as structure-breaking solutes in water. We also conclude from the high temperature data that water at temperatures well above the normal boiling point is still sufficiently structured that structure-breaking solutes can "find" structure to break.

Gopal and Siddiqi (14) have reported $\bar{V}_2^0$ values for four tetraalkylammonium iodides (methyl, ethyl, propyl, and butyl) at temperatures ranging from 25–80 °C. Values of $(\partial^2 \bar{V}_2^0/\partial T^2)_P$ are positive, indicating that these solutes are all net structure-makers, as previously suggested on other grounds for some R_4NX compounds. The magnitude of $(\partial^2 \bar{V}_2^0/\partial T^2)_P$ increases in going from methyl to ethyl to propyl to butyl compounds in this series. This is consistent with the idea that structure-making is in the form of "iceberg" formation about the hydrocarbon parts of these ions, with the extent of structure-making increasing as the amount of hydrocarbon increases. Millero and Drost-Hansen (15) have previously pointed out that volumetric properties of aqueous alcohols and tetraalkylammonium salts are similar, with both having volumetric properties different from those of most electrolytes.

The $\bar{V}_2^0$ values for aqueous urea, given by Stokes (16), show that $(\partial^2 \bar{V}_2^0/\partial T^2)_P$ is negative, which indicates that urea should be regarded as a structure-breaking solute.

Masterton (17) has reported $\bar{V}_2^0$ data for benzene, methane, ethane, and propane in aqueous solution at several temperatures. For benzene, $(\partial^2 \bar{V}_2^0/\partial T^2)_P$ is very close to zero. The resulting conclusion that benzene is neither a strong structure-maker nor a strong structure-breaker may be explained in terms of a balance between iceberg formation and structure-breaking due to poor fit of planar benzene molecules into the partly tetrahedral structure of water. Masterton's data (17) indicate that $(\partial^2 \bar{V}_2^0/\partial T^2)_P$ values are negative for methane, ethane, and propane. Thus the approach developed in this paper leads to the conclusion that these solutes are structure-breakers in aqueous solution. On the basis of different reasoning, Masterton (17) has previously suggested a "breaking down of the cage-like structure of water molecules around the aliphatic hydrocarbon molecules". Thus both this paper and Masterton disagree with the common idea that methane, ethane, and propane are net structure-makers as a result of iceberg formation about the solute molecules.

Although classification of solutes as structure-makers or -breakers has proven useful in several connections, it must be recognized that the entire concept of structure in water and aqueous solutions is only partly satisfactory (18). One problem is that we are unable to be entirely specific about the structure that is being made or broken by various solutes or as a result of changes in temperature and pressure. A further difficulty is that we have no unambiguous numerical measure of structure-making/breaking. Therefore, it should not be surprising that there are disagreements between conclusions based on different approaches. A similar situation is known in connection with the useful but poorly

Can. J. Chem. Downloaded from www.nrcresearchpress.com by 210.87.254.42 on 09/05/12
For personal use only.

Can. J. Chem. Downloaded from www.nrcresearchpress.com by 210.87.254.42 on 09/05/12
For personal use only.

defined concept of hydration number, where it is common for different approaches to lead to different numbers.

Since the conclusion of this paper concerning classification of alcohols and the larger tetraalkylammonium ions as structure-makers is in agreement with several earlier workers, no detailed comments on these solutes are required. On the other hand, several earlier workers have concluded that $(CH_3)_4N^+$ and possibly $(C_2H_5)_4N^+$ ions are structure-breakers, in contrast to our conclusion that these ions are structure-makers. Similarly, the present conclusion that urea is a structure-breaker is contrary to conclusions of some earlier workers.

First, we consider the reliability of the data (14) we have used for the R_4N^+ salts. Since the most dilute solutions investigated were about 0.05 *M*, the extrapolation to infinite dilution to obtain desired $\overline{V}_2^0$ values is of considerable importance. Gopal and Siddiqi (14) did these extrapolations "as required" by Masson's equation with empirical limiting slope based on their own data for solutions more concentrated than about 0.05 *M*. Redlich and Meyer (19) have shown the inadequacies of this extrapolation procedure and have also shown how such extrapolations should be done in accord with the Debye–Huckel theory. Accurate measurements on R_4NX compounds (only at 25°) reported by Conway, Verrall, and Desnoyers (20) show that Gopal and Siddiqi (14) used incorrect slopes (wrong sign for three of their four solutes!) for extrapolation to infinite dilution. Although we conclude that the accuracy of the reported (14) $\overline{V}_2^0$ values is not high, it is likely that these values do lead to the correct sign for $(\partial^2 \overline{V}_2^0/\partial T^2)_P$ for the larger R_4N^+ ions. On the other hand, it is possible that the reported values lead to an incorrect sign for $(\partial^2 \overline{V}_2^0/\partial T^2)_P$ for aqueous $(CH_3)_4NI$. Further measurements are required to settle this uncertainty.

The conclusion in this paper [assuming that the available data lead to the correct sign for $(\partial^2 \overline{V}_2^0/\partial T^2)_P$] that $(CH_3)_4NI$ is a structure-maker is in disagreement with some earlier workers. For example, Gopal and Siddiqi (14) have concluded from the concentration dependence of their apparent molar volumes that this solute is a structure-breaker, but it is the present author's opinion that their interpretation should have given greater consideration to solute–solute interactions and may therefore be mistaken. Other evidence that $(CH_3)_4N^+$ ion is a structure-breaker comes from results of conductance (21) and viscosity (22) measurements, although a Referee has suggested that the viscosity data might also be interpreted to indicate that $(CH_3)_4N^+$ is a structure-maker.

Conway and Laliberté (23) have reported $\overline{V}_2^0$ values for NaF, NaCl, NaBr, $(C_2H_5)_4Br$, and $(C_4H_9)_4Br$ in both H_2O and D_2O at 25 °C. They concluded from their results that the first three salts are structure-breakers and the latter two salts are structure-makers, in agreement with conclusions of this paper. Similar accurate data for $(CH_3)_4N^+$ halides and also other electrolytes with charges greater than ± 1 will be useful.

Earlier workers (24–28) are in poor agreement as to whether urea should be classed as a structure-maker or structure-breaker, although the most recent work (28) and some earlier workers are in agreement with our conclusion that urea is a structure-breaker. Further, the inadequate logic leading to an earlier suggestion (26) that urea is a structure-maker has been pointed out (18).

A Referee has pointed out that Krishnan and Friedman (29) have found evidence for a "saturation" effect in structure-making by alcohols and R_4N^+ ions. That is, structure-making does not increase without limit as hydrocarbon size increases. The same Referee has also suggested that diffusion data from Witherspoon and Sarat (30) can be interpreted to support the idea presented in this paper that the gaseous hydrocarbons are structure-breakers.

Acknowledgments

The author is grateful to Brian Dunford, Robert Goldberg, and Frank Millero for helpful discussions.

1. G. N. Lewis and M. Randall. Thermodynamics. McGraw-Hill Book Co., Inc., New York. 1923.
2. G. S. Kell. J. Chem. Eng. Data, **12**, 66 (1967).
3. G. S. Kell and E. Whalley. Phil. Trans. Roy. Soc. **258a**, 565 (1965).
4. F. Franks and H. T. Smith. Trans. Faraday Soc. **64**, 2962 (1968).
5. E. M. Arnett, W. G. Bentrude, J. J. Burke, and P. McC. Duggleby. J. Amer. Chem. Soc. **87**, 1541 (1965). E. M. Arnett and D. R. McKelvey. J. Amer. Chem. Soc. **87**, 1393 (1965).
6. G. L. Bertrand, F. J. Millero, C. H. Wu, and L. G. Hepler. J. Phys. Chem. **70**, 699 (1966).
7. D. M. Alexander. J. Chem. Eng. Data, **4**, 252 (1959).

8. M. E. FRIEDMAN and H. A. SCHERAGA. J. Phys. Chem. **69**, 3795 (1965).
9. L. A. DUNN. Trans. Faraday Soc. **64**, 2951 (1968).
10. H. B. BULL and K. BREESE. J. Phys. Chem. **72**, 1817 (1968).
11. A. J. ELLIS. J. Chem. Soc. A, 660 (1966).
12. A. J. ELLIS. J. Chem. Soc. A, 1579 (1966).
13. F. J. MILLERO. Private communication.
14. R. GOPAL and M. A. SIDDIQI. J. Phys. Chem. **72**, 1814 (1968).
15. F. J. MILLERO and W. DROST-HANSEN. J. Phys. Chem. **72**, 1758 (1968).
16. R. H. STOKES. Aust. J. Chem. **20**, 2087 (1967).
17. W. L. MASTERTON. J. Chem. Phys. **22**, 1830 (1954).
18. A. HOLTZER and M. F. EMERSON. J. Phys. Chem. **73**, 26 (1969).
19. O. REDLICH and D. M. MEYER. Chem. Rev. **64**, 221 (1964).
20. B. E. CONWAY, R. E. VERRALL, and J. E. DESNOYERS. Trans. Faraday Soc. **62**, 1 (1966).
21. R. L. KAY and D. F. EVANS. J. Phys. Chem. **70**, 2325 (1966).
22. R. L. KAY, T. VITUCCIO, C. ZAWOYSKI, and D. F. EVANS. J. Phys. Chem. **70**, 2336 (1966).
23. B. E. CONWAY and L. H. LALIBERTÉ. J. Phys. Chem. **72**, 4317 (1968).
24. J. A. RUPLEY. J. Phys. Chem. **68**, 2002 (1964).
25. J. M. TSANGARIS and R. B. MARTIN. Arch. Biochem. Biophys. **112**, 267 (1965).
26. M. ABU-HAMDIYYAH. J. Phys. Chem. **69**, 2720 (1965).
27. G. G. HAMMES and R. SCHIMMEL. J. Amer. Chem. Soc. **89**, 442 (1967).
28. H. S. FRANK and F. FRANKS. J. Chem. Phys. **48**, 4746 (1968).
29. C. V. KRISHNAN and H. L. FRIEDMAN. J. Phys. Chem. **73**, 1572 (1969).
30. P. A. WITHERSPOON and D. N. SARAT. J. Phys. Chem. **69**, 3752 (1965).

Can. J. Chem. Downloaded from www.nrcresearchpress.com by 210.87.254.42 on 09/05/12
For personal use only.

Chloryl compounds. Part II. Chloryl hexafluoroarsenate and chloryl fluoride[1]

H. A. CARTER, W. M. JOHNSON, AND F. AUBKE
Department of Chemistry, The University of British Columbia, Vancouver 8, British Columbia

Received June 30, 1969

The infrared and Raman spectra of chloryl hexafluoroarsenate have been obtained. The observed vibrations have been interpreted in terms of an ionic compound $ClO_2^+AsF_6^-$, where strong cation–anion interaction results in a symmetry lowering of the AsF_6^- ion. The compound together with chloryl fluoride produces the chloronium cation ClO_2^+(solv) in solution of fluorosulfuric acid. The solvolysis of $FClO_2$ is studied by conductometry and ^{19}F nuclear magnetic resonance (n.m.r.) in order to elucidate the observed anion–cation interaction for ClO_2AsF_6 more fully. ^{19}F n.m.r. studies of $FClO_2$ and related molecules have been used to discuss the bonding in chloronium compounds.

Canadian Journal of Chemistry, 47, 4619 (1969)

Can. J. Chem. Downloaded from www.nrcresearchpress.com by 210.87.254.5 on 09/05/12
For personal use only.

Introduction

A limited number of chloryl compounds have been known for some time (1). They can be easily divided into 2 groups. Chloryl fluoride, $FClO_2$ (2), and its reaction products with strong Lewis acids such as BF_3, AsF_5, and SbF_5 (3–5) are colorless, moderately reactive compounds. On the other hand, chloryl fluorosulphate, ClO_2SO_3F (3, 5), and dichloryl trisulfate, $(ClO_2)_2S_3O_{10}$ (6), are deep red colored solids at room temperature and are highly reactive compounds. The red color in these compounds fades to a faint yellow at liquid air temperature. (Similar behavior is found for chlorine dioxide.) All substances have been postulated to contain the chloronium cation, ClO_2^+ (3, 7, 8). Such a cation has recently been found to exist in a solution of fluorosulfuric acid (9) when ClO_2SO_3F and $(ClO_2)_2S_3O_{10}$ were used as solutes. The cation is red colored.

The present study is intended to resolve the apparent contradiction regarding the chloronium cation in the solid state by extending the solution studies to the colorless compounds $FClO_2$ and ClO_2AsF_6, and by studying the vibrational spectra of ClO_2AsF_6 and ClO_2SbF_6. No detailed structural investigation on any one of the solid compounds has yet been reported. Only the infrared (i.r.) and Raman spectra of $FClO_2$ (10, 11), have been well investigated. Assignment of 5 bands in the i.r. spectrum of Cl_2FAsF_6 as being due to the ClO_2^+ cation has been briefly mentioned in a recent paper (12) but no discussion of these bands has yet been published.

It was found necessary also to record the ^{19}F nuclear magnetic resonance spectrum of ClO_2F together with a number of related molecules, and to discuss the bonding in this molecule on the basis of the presently available information.

[1]For Part I, see ref. 9.

Experimental

General

All volatile materials were handled in a monel metal vacuum line. The solids were transferred in a dry box containing a purified nitrogen atmosphere. All chloryl compounds encountered in this investigation were found to be hygroscopic and highly reactive. They explode violently on contact with oxidizable material.

Materials

Elemental fluorine (Allied Chemical Corp.) was purified from HF by passing the gas in a metal flow system over sodium fluoride. Arsenic pentafluoride (Peninsular Chemical Research) and antimony pentafluoride (Alpha Inorganic Chemical Corp.) were purified by trap-to-trap distillation. Chlorine dioxide was prepared from $KClO_3$ and H_2SO_4 in the presence of oxalic acid (15). Chloryl fluoride was prepared using 2 methods: (*a*) reaction of $KClO_3$ with BrF_3 in monel metal reactors according to Woolf (5), (*b*) direct fluorination of chlorine dioxide at −50 °C in a quartz apparatus (16). Method (*a*) was found to be safe but yields a slightly impure yellowish product. Method (*b*) yields a very pure, colorless product but involves all the hazards of handling ClO_2. The purity of ClO_2F was checked on the basis of the i.r. spectrum.

Chloryl hexafluoro-arsenate and -antimonate were prepared by reacting a very slight excess of chloryl fluoride with a known amount of pentafluoride in a ~100 ml thin-wall monel, 2-part reactor, equipped with a Hoke valve according to Woolf (5). The reaction was followed by weight changes. The ClO_2AsF_6 was purified by high vacuum sublimation.

Solutions of $FClO_2$ in fluorosulfuric acid were prepared by distilling purified chlorylfluoride in a metal vacuum line from a storage vessel into a weighing burette kept at −80 °C and containing a known quantity of doubly distilled HSO_3F. This stock solution was used for addition to the acid in the conductivity cell.

Infrared Spectra

The i.r. spectra were recorded on a Perkin–Elmer 457 Grating Infrared Spectrophotometer in the region of

TABLE I

Infrared and Raman spectra of ClO_2AsF_6 and $KAsF_6$; infrared spectrum of ClO_2SbF_6 (cm^{-1})*

ClO_2AsF_6		ClO_2SbF_6,	$KAsF_6$	
Infrared	Raman	Infrared	Infrared	Raman
1293 s	1296 w	1304 s	698 s	692 s
1280 s	1281 w	1291 s	382 br	580 ms
1080 w	1045 s	1050 ms		375 ms
1045 s	725 w	720 s, br		
817 w	684 s	680 s, br		
725 s, br	572 s	585 ms		
685 s, br	518 m	510 ms		
563 s	370 s	490 ms		
515 s				
382 s				
372 s, sh				

*s = sharp, w = weak, m = medium, sh = shoulder, br = broad.

4000–250 cm^{-1}. Silver chloride and KSR-5 windows were used (Harshaw Chemicals). Due to the high reactivity of the chloryl compounds, no mulling agents were used.

Raman Spectra

A Cary 81 Spectrophotometer equipped with a Spectra Physics Model 125 laser as a source of exciting light was used. The solid samples were contained in flat-bottom Pyrex tubes (6 mm o.d.).

Conductivity Measurements

Fluorosulfuric acid (Allied Chemical Co.) was purified by double distillation under nitrogen atmosphere. This technique and the design of the conductivity cells have been described by Barr *et al.* (19). A Wayne Kerr Universal Bridge B 221A was used for the measurements. The cells were contained in a constant temperature oil bath of 25.00 ± 0.01 °C with a Sargent Thermonitor Model ST.

^{19}F n.m.r. Spectra

These were obtained with a Varian HR100 spectrometer. The ClO_2F samples were contained in quartz tubes using $CFCl_3$ in quartz capillaries as an external standard.

Results and Discussion

A. The Vibrational Spectrum of ClO_2AsF_6

The recorded absorption frequencies for the infrared spectra of ClO_2AsF_6 and ClO_2SbF_6 and the Raman spectrum of ClO_2AsF_6 are listed in Table I, together with the frequencies for $KAsF_6$.

The interpretation of the spectra will be restricted to the hexafluoroarsenate for the following reasons: (1) the compound can be purified by sublimation, (2) the formation of polyanions is unlikely, (3) the AsF_6^- ion has been well characterized previously (12, 20–22, 24). Possible molecular structures for ClO_2AsF_6 are (*a*) an ionic solid $ClO_2^+AsF_6^-$, (*b*) a molecular 1:1 adduct $ClO_2F.AsF_5$ with bridging over F, and (*c*) the same, with bridging over oxygen.

For model (*a*) the chloronium cation would be isoelectronic to sulfur dioxide, the symmetry C_{2v}, with 3 vibrational modes i.r.- as well as Raman-active. This is confirmed by the findings shown in Table II. The vibration ν_3 is similar to that of SO_2(s) (25*c*), which is split into 2 i.r.- and Raman-active components by the crystalline field. Noteworthy is that the average stretching frequencies for the ClO_2 group are lower than that for SO_2: $\bar{\nu}_{SO_2} = 1233\ cm^{-1}$ vs. $\bar{\nu}_{ClO_2} = 1166\ cm^{-1}$ (i.r.) or 1168 cm^{-1} (Raman) in ClO_2AsF_6. This is unexpected considering the increase in nuclear charge on chlorine. The same vibrations are slightly shifted for the ClO_2SbF_6 spectrum by about 8 to 10 cm^{-1} to higher wavenumbers. Similar shifts have been known to occur for similar complexes containing the NO^+ cation, (26) and have been explained as being due to anion–cation interaction. Some chlorine–oxygen stretching vibrations are listed in Table III together with the SO_2 values.

For a corresponding AsF_6^- anion with O_h symmetry, 2 infrared-active vibrations, ν_3 (F_{1u}) and ν_4 (F_{1u}) are expected together with 3 Raman-active vibrations, ν_1 (A_{1g}), ν_2 (E_g), and ν_5 (F_{2g}).

The observed i.r. spectrum apparently does not confirm these expectations. Not only are the 2 expected vibrations ν_3 and ν_4 shifted, compared to the generally accepted positions of 700–690 and 392 cm^{-1}, but the region of strong absorption reveals a shoulder at 725 cm^{-1} and a broad 685 cm^{-1} absorption. (A similar observation has

Can. J. Chem. Downloaded from www.nrcresearchpress.com by 210.87.254.5 on 09/05/12
For personal use only.

TABLE II

Frequencies (cm^{-1}) and tentative assignments of ClO_2^+ and AsF_6^-

ClO_2^+ in ClO_2AsF_6		ClO_2^+ in ClO_2SbF_6,	SO_2(s),*	Assignment
Infrared	Raman	Infrared	Infrared	$ClO_2^+(C_{2v})$
1045	1045	1050	1147	ν_1 (A_1)
515	518	510	521	ν_2 (A_1)
1293, 1280	1296, 1281	1304, 1291	1330, 1308	ν_3 (B_1)

AsF_6^- in ClO_2AsF_6		SbF_6^- in ClO_2SbF_6,	AsF_6^- in $KAsF_6$		Assignment
Infrared	Raman	Infrared	Infrared	Raman	$AsF_6^-(O_h)$
(685)†	684	(680)	—	692	ν_1 (A_{1g})
(563)	572	(585)	—	580	ν_2 (E_g)
725	(725)	720	698	—	ν_3 (F_{1u})
382	—	—	382	—	ν_4 (F_{1u})
(372)	370	—	—	375	ν_5 (F_{2g})
—	—	—	—	—	ν_6 (F_{2u})

*Reference 25 *c*.
†Frequencies in parentheses are forbidden for AsF_6^- with O_h symmetry.

TABLE III

ClO_2^- stretching frequencies (cm^{-1})

		ClO_2 frequencies			
Compound	Method	Asymmetric	Symmetric	Average	Reference
$Na^+ClO_2^-$ (s)	Raman	832	804	818	This work
ClO_2 (g)	Infrared	1111	943	1027	25*a*
$FClO_2$ (l)	Raman	1253	1097	1175	11
ClO_2AsF_6 (s)	Infrared	1293, 1280	1045	1166	This work
ClO_2AsF_6 (s)	Raman	1296, 1281	1045	1168	This work
ClO_2SbF_6 (s)	Infrared	1304, 1291	1050	1174	This work
[SO_2] (s)	Infrared	1330, 1308	1147	1233	25*b*
$K^+ClO_3^-$ (s)	Infrared	960	910	935	25*c*

been made by Clark and O'Brien for the i.r. spectrum of $(CH_3)_3SnAsF_6$ (23), where the AsF_6 group acts as a bridging group and the symmetry appears to be lowered to D_{4h}.) ν_4 appears to be split into a doublet and, in addition, a reasonably strong absorption at 563 cm^{-1}, which is not found in the ClO_2SbF_6 spectrum, is observed. It must therefore be due to the AsF_6^- group.

The Raman spectrum also shows more vibrations than expected. Again all positions are slightly shifted to lower frequencies. From the position of the expected E_g mode, ν_2, at 572 cm^{-1}, it is concluded that it is identical with the observed 563 cm^{-1} vibration in the infrared spectrum. The occurrence of the ν_2 vibration in the i.r. region has been reported previously for $NF_4^+AsF_6^-$ (20), $AsCl_4^+AsF_6^-$ (44), and $ClF_2^+AsF_6^-$ (21). The interpretation of the 563 cm^{-1} vibration as ν_2 presents a departure from the assignment in ref. 12. All reported frequencies agree quite well with ours. The 725 cm^{-1} vibration is also weakly Raman active, and the possibility that this vibration is a combination mode seems rather unlikely. From these findings, it seems safe to say that the symmetry of the AsF_6 group is lowered considerably from expected O_h to possible C_{2v} symmetry, causing a partial breakdown in the selection rules and general shift of all frequencies in comparison with other AsF_6 compounds. The tentative assignment of the observed frequencies is shown in Table II. The reason for the observed symmetry lowering can be seen in appreciable anion–cation interaction, already reflected in the shifts of the ClO stretching vibrations (Table III).

Anion–cation interaction is not too surprising for these compounds, and is also found in 2

Can. J. Chem. Downloaded from www.nrcresearchpress.com by 210.87.254.5 on 09/05/12
For personal use only.

TABLE IV

Specific conductivities, κ, of KSO_3F, $KAsF_6$, ClO_2AsF_6, and ClO_2F at various concentrations

Molality × 10^2	κ × 10^4 (Ω^{-1} cm^{-1})				
	KSO_3F	$KAsF_6$	ClO_2AsF_6	ClO_2F	γ
0.00	1.085	1.127	1.318	1.329	
0.25	7.0	6.8	4.0	7.0	1.00
0.50	13.6	9.8	6.5	13.2	0.97
0.75	19.7	12.3	13.2	19.5	0.99
1.00	25.8	14.5	16.2	26.1	1.01
1.50	38.0	21.7	22.5	44.1	1.16
2.00	50.0	24.3	27.3	61.0	1.22
2.50	62.5	27.7	31.8	75.8	1.21
3.00	72.7	33.3	36.0	90.2	1.24
3.50	84.9	37.3	40.0	104.7	1.23
4.00	97.0	40.5	43.6	118.9	1.23
4.50	106.8	45.1	47.3	133.0	1.24

reported structures based on X-ray diffraction for ICl_2SbCl_6 (27) and BrF_2SbF_6 (28), resulting in a distorted octahedral environment for antimony.

In conclusion, a strictly ionic formulation of ClO_2AsF_6 is not supported by the infrared and Raman spectrum, unless allowance is made for appreciable anion–cation interaction and a subsequent lowering of symmetry for the AsF_6^- ion. This model explains the observed spectrum quite well.

Noteworthy also is that the ClO stretching frequencies for $FClO_2$ do not show a similar wide split to the corresponding stretching frequencies of ClO_2AsF_6, but the values of $\bar{\nu}_{ClO_2}$ are almost identical for all chloryl compounds. In similar systems, e.g. FNO (29) vs. $NOAsF_6$ (26), FNO_2 (30) vs. NO_2SbF_6 (31), and F_3NO (17) vs. F_2NOAsF_6 (13, 14), stretching frequencies are substantially raised on complexation.

B. Solution Studies

The solvent HSO_3F was selected since previous work on the ClO_2^+ cation had shown that this ion is capable of existence in this solvent (9).

The solutes are all soluble and behave as bases in this solvent. The solutions are highly conducting. Specific conductivities of various concentrations are listed in Table IV. The solutions of ClO_2AsF_6 are yellow to reddish colored, the color being characteristic for the ClO_2^+ cation; the solute $KAsF_6$ gives rise to a colorless solution. However, whereas $KAsF_6$ is only moderately soluble, the limiting molality being 5.0×10^{-2} at 25.0 °C, the ClO_2 compound is soluble to a far greater degree, up to 1–2 *M*. Both solutions are conducting, and are remarkably similar. The specific conductivity plots vs. molality are shown in Fig. 1. The specific conductances of the ClO_2AsF_6 solutions are slightly higher than the ones for $KAsF_6$, whereas the situation was reversed when ClO_2SO_3F and KSO_3F were compared as solutes (9). The electronic absorption spectrum indicates the formation of the ClO_2^+ cation as expected. The differences in solubilities and conductivities for the 2 solutes are unexpected. Since the concentration ranges were found to be too low for meaningful Raman and

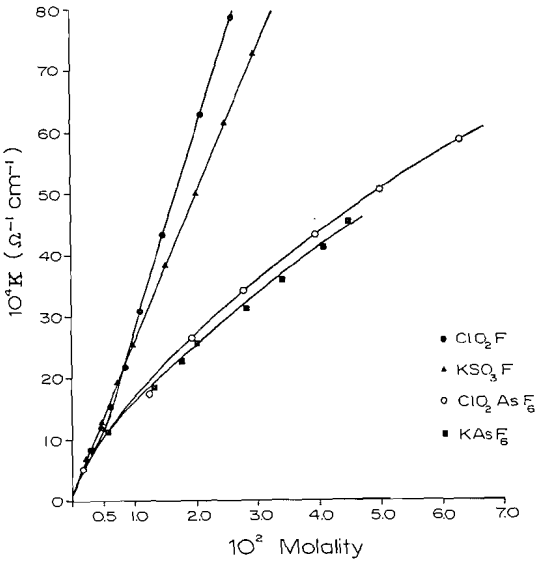

Fig. 1. Plot of specific conductivity vs. molality.

Can. J. Chem. Downloaded from www.nrcresearchpress.com by 210.87.254.5 on 09/05/12
For personal use only.

Can. J. Chem. Downloaded from www.nrcresearchpress.com by 210.87.254.5 on 09/05/12
For personal use only.

^{19}F n.m.r. studies, greater attention was focussed on the solvolysis of $FClO_2$ in fluorosulfuric acid.

Solutions of ClO_2F in HSO_3F were red colored and highly conducting. The ultraviolet–visible absorption spectrum agrees well with the reported one (9) and the ^{19}F n.m.r. spectrum indicates the presence of HF as the only fluorine-containing species besides the solvent. The γ values, defined as the number of moles of fluorosulfate anions produced per mole of solute, are higher than the reference KSO_3F values, which is not unexpected since KF has also been found to be more conducting than KSO_3F (19) (because HF behaves as a weak base in HSO_3F). In addition, $FClO_2$ prepared according to Woolf (5) was used in this part of the study, and the preparation of the solution in a Pyrex container may have resulted in side reactions and a very slightly higher conductivity value. At concentrations below 10^{-2} M, γ values (32) slightly less than 1 are obtained. This is very likely due to the presence of SO_3 as an impurity in the HSO_3F which behaves as an acid in this solvent system (19). The solvolysis can be formulated as follows

$$FClO_2 + HSO_3F \rightarrow ClO_2^+(solv) + HF + SO_3F^-$$

$$HF + HSO_3F \rightleftarrows H_2F^+ + SO_3F^-$$

This would result in γ values > 1.0. The described solvolysis was studied previously by Schmeisser and Fink (4), who postulated the equilibrium

$$FClO_2 + HSO_3F \rightleftarrows HF + ClO_2SO_3F$$

It is reasonable to assume that in dilute solutions, HF and ClO_2SO_3F will be solvolyzed and the equilibrium shifted to the right.

It is interesting to note that the colorless chloryl compounds gave rise to a red colored ClO_2^+ cation. Considering the fact that SO_2 is colorless, the ClO_2^+, isoelectronic but colored, needs some explanation. The absorption spectrum of ClO_2^+ shows an absorption maximum at 2700 Å with a molar extinction coefficient of 1950, and a shoulder at about 3300 Å. In addition, strong absorption occurs at 2200 Å. Since the expected ground state for ClO_2^+ would be $^1A_1$, the 2 bands of the lower energy region can be assigned as due to the transitions $^1A_1 \rightarrow {}^1B_1$ and $^1A_1 \rightarrow {}^1B_2$, using the model proposed by Walsh (33) for triatomic molecules. The former is of lower energy, and by branching off into the visible region, this transition, involving the antibonding b_1'' orbital, is responsible for the color. Transitions into the same orbital are largely responsible for the color of ClO_2 (33). Since the energy spacing is similar, the angle OClO, 117.4°, for ClO_2 (34) is not too different from an expected angle of $\sim 120°$ for ClO_2^+ (the angle for SO_2 is found to be 119.5°) (35). Such a similarity is expected. ClO_2^+-containing solutions are also faintly yellow colored at liquid air temperature as shown for the red chloryl compounds and chlorine dioxide.

The corresponding absorption bands for SO_2 have been observed at 3740 and 2940 Å (36), but they are of far lower intensity (ε_{max} for the stronger band is ~ 400) and do not reach into the visible region. The low energy transitions of ClO_2 are also far higher in intensity than corresponding SO_2 bands.

The concept of isoelectronic molecules can, it seems, be applied to suggest similar molecular structures. However, an extension to electronic transitions and color should be done with extreme care. The absence of any color in ClO_2AsF_6 and ClO_2SbF_6 indicates that the interaction between the ClO_2^+ cation and fluorine in the AsF_6^- or SbF_6^- anion may involve the b_1'' orbital, which is weakly bonding for O—O but antibonding for O—Cl. The degree of interaction will affect the overall Cl—O bond order and the bond strength, as reflected in the differences in $\bar{\nu}_{Cl-O}$, the average stretching frequency. Such a model, whereby the b_1'' orbital takes part in bonding, can be invoked to explain the bonding in $FClO_2$. Even though the exact structure is not known, vibrational spectroscopy (11) provides some idea about this molecule. The symmetry appears to be C_s. The ClO stretching force constant has been found to be 9.07 mdyn/Å compared to 6.9 for the ClO_2 (37) molecule. The Cl—F force constant of 2.53 mdyn/Å, however, is the smallest reported. The overall bonding situation, short and strong element–oxygen bond, usually weak and long element–fluorine bond, becomes reminiscent of the situation in FNO (38) and FNO_2 (39) as well as for O_2F_2 (40) and O_2F (41) where the observed element–fluorine bonds are found to be longer than the normal single bonds.

In addition, extremely low field chemical shifts in the ^{19}F nuclear magnetic resonance spectrum have been found for these fluorides. We have therefore recorded the spectrum and compared it to the chemical shift values of the isoelectronic

TABLE V

^{19}F nuclear magnetic resonance chemical shifts for $FClO_2$ and selected fluorides

Molecule	^{19}F Chemical shift*	Reference
O_2F_2	−865	45*a*
ONF	−479	45*b*
O_2NF	−394	45*c*
ONF_3	−366	18
$FClO_2$	−328	This work
$FClO_3$	−284	This work
F_2SO	−71	This work
F_2SO_2	−30	This work

*In p.p.m. from the external standard $CFCl_3$.

molecule, SOF_2, and the odd-electron molecule fluorides. The results are shown in Table V.

The spectrum was taken at −80 °C and consisted of a broad, unresolved signal due to spin–quadrupole interaction with the isotopes Cl^{35} and Cl^{37} Only for the highly symmetrical $FClO_3$ with C_{3v} symmetry is fine structure detectable (42). The chemical shift of −328 p.p.m. is indeed very low, the lowest reported for fluorine attached to a second period element and lower than the value for SOF_2. Since the ultraviolet–visible spectrum of $FClO_2$ (16) gives no evidence for any low lying excited states, fluorine appears to be highly deshielded.

The description of the bonding in all these compounds can be based on a description of the O_2F_2 bonding by Lipscomb (40). It is seen to involve a high-lying singly occupied antibonding π^* orbital of O_2 and a singly occupied $2p$ orbital on fluorine resulting in a highly delocalized multicenter bonding. These ideas have been extended by Spratley and Pimentel (41) and the bonding type has been labelled $[\pi^*–p]$ bonding. Preliminary attempts to describe this bond type in a more quantitative manner have been reported (43), but no completely satisfactory bonding description is available at the present. There seems no doubt, however, that the bonding in $FClO_2$ is very similar in principle to the bonding of the other odd electron molecule fluorides and O_2F_2. It is therefore feasible that this interaction is retained when $FClO_2$ reacts with AsF_5 and SbF_5, causing no alteration in the ClO bond order as evidenced by the vibrational spectrum.

Attempts to investigate the vibrational spectra of the red chloryl compounds have not been too successful since these compounds are far more reactive. No satisfactory spectra have yet been obtained.

Acknowledgment

We wish to thank the National Research Council of Canada for financial support of this project.

1. M. Schmeisser and K. Brandle. Advan. Inorg. Chem. Radiochem. **5**, 41 (1963).
2. H. Schmitz and H. J. Schumacher. Z. Anorg. Allg. Chem. **249**, 238 (1942).
3. M. Schmeisser and F. L. Ebenhöch. Angew. Chem. **66**, 230 (1954).
4. M. Schmeisser and W. Fink. Angew. Chem. **69**, 780 (1957).
5. A. A. Woolf. J. Chem. Soc. 4113 (1954).
6. H. A. Lehmann and G. Krueger. Z. Anorg. Allg. Chem. **274**, 141 (1953).
7. A. A. Woolf. Advan. Inorg. Chem. Radiochem. **9**, 217 (1966).
8. A. A. Woolf. J. Chem. Soc. A, 401 (1967).
9. H. A. Carter, A. M. Qureshi, and F. Aubke. Chem. Commun. 1461 (1968).
10. A. J. Arvia and P. J. Aymonino. Spectrochim. Acta, 1449 (1963).
11. D. F. Smith, G. M. Begun, and W. H. Fletcher. Spectrochim. Acta, **20**, 1763 (1964).
12. K. O. Christe and W. Sawodny. Inorg. Chem. **8**, 212 (1969).
13. C. A. Wamser, W. B. Fox, B. Sukornick, J. R. Holmes, B. B. Stewart, N. Vanderkooi, and D. Gould. Inorg. Chem. **8**, 1249 (1969).
14. K. O. Christe and W. Maya. Inorg. Chem. **8**, 1253 (1969).
15. G. Brauer. Handbook of preparative inorganic chemistry. Academic Press, Inc., New York. 1963.
16. J. E. Sicre and H. J. Schumacher. Z. Anorg. Allg. Chem. **286**, 232 (1956).
17. W. B. Fox, J. L. MacKenzie, N. Vanderkooi, B. Sukorvik, C. A. Wamser, J. R. Holmes, R. E. Eibeck, and B. B. Stewart. J. Amer. Chem. Soc. **88**, 2604 (1966).
18. N. Bartlett, J. Passmore, and E. J. Wells. Chem. Commun. 213 (1966).
19. J. Barr, R. J. Gillespie, and R. C. Thompson. Inorg. Chem. **3**, 1149 (1964).
20. K. O. Christe, J. P. Guertin, A. E. Pavlath, and W. Sawodny. Inorg. Chem. **6**, 533 (1967).
21. K. O. Christe and W. Sawodny. Inorg. Chem. **6**, 313 (1967).
22. G. M. Begun and A. C. Rutenberg. Inorg. Chem. **6**, 2212 (1967).
23. H. C. Clark and R. J. O'Brien. Inorg. Chem. **8**, 1020 (1963).
24. J. Binenboym, H. Selig, and J. Shamir. J. Inorg. Nucl. Chem. **30**, 2863 (1968).
25. (*a*) A. H. Nielsen and P. J. H. Woltz. J. Chem. Phys. **20**, 1878 (1952). (*b*) R. N. Wiener and E. R. Nixon. J. Chem. Phys. **25**, 175 (1956). (*c*) N. Duveau. Bull. Soc. Chim. France, **10**, 374 (1943).
26. D. W. A. Sharp and J. Thorley. J. Chem. Soc. 3557 (1963).
27. C. G. Vonk and E. H. Wiebenga. Acta Cryst. **12**, 859 (1959).
28. A. J. Edwards and G. R. Jones. Chem. Commun. 1304 (1967).

Can. J. Chem. Downloaded from www.nrcresearchpress.com by 210.87.254.5 on 09/05/12
For personal use only.

29. P. J. H. WOLTZ, E. A. JONES, and A. H. NIELSEN. J. Chem. Phys. **20**, 378 (1952).
30. R. E. DODD, J. A. ROLFE, and L. A. WOODWARD. Trans. Faraday Soc. **52**, 145 (1956).
31. D. COOK, S. J. KUHN, and G. A. OLAH. J. Chem. Phys. **33**, 1669 (1960).
32. R. C. THOMPSON. *In* Inorganic sulphur chemistry. *Edited by* G. Nickless. Elsevier Publ. Co., Inc., Amsterdam. 1968. p. 587.
33. A. D. WALSH. J. Chem. Soc. 2266 (1953).
34. J. C. BAIRD, J. RASTRUP-ANDERSON, and G. R. BIRD. Bull. Amer. Phys. Soc. **2**, 99 (1956).
35. D. KIVELSON. J. Chem. Phys. **22**, 904 (1954).
36. N. C. METROPOLIS and H. BEUTLER. Phys. Rev. **58**, 1078 (1940).
37. S. SMITH and J. W. LINNETT. Trans. Faraday Soc. **52**, 891 (1956).
38. D. W. MAGNUSON. J. Chem. Phys. **19**, 1071 (1951).
39. A. C. LEGION and D. J. MILLEN. J. Chem. Soc. A, 1737 (1968).
40. R. H. JACKSON. J. Chem. Soc. 4585 (1962).
41. R. D. SPRATLEY and G. C. PIMENTEL. J. Amer. Chem. Soc. **88**, 2394 (1966).
42. J. BACON, R. J. GILLESPIE, and J. W. QUAIL. Can. J. Chem. **41**, 3063 (1963).
43. S. J. TURNER and R. D. HARCOURT. Chem. Commun. 4 (1967).
44. J. WEIDLEIN and K. DEHNICKE. Z. Anorg. Allg. Chem. **337**, 113 (1965).
45. (*a*) J. W. NEBGEN, F. J. METZ, and W. B. ROSE. J. Amer. Chem. Soc. **89**, 3118 (1967). (*b*) J. R. HOLMES, B. B. STEWART, and J. S. MACKENZIE. J. Chem. Phys. **37**, 2728 (1962). (*c*) R. S. DRAGO. Physical methods in inorganic chemistry. Reinhold Publ. Corp., New York. 1967. p. 252.

Can. J. Chem. Downloaded from www.nrcresearchpress.com by 210.87.254.5 on 09/05/12
For personal use only.

Can. J. Chem. Downloaded from www.nrcresearchpress.com by 210.87.254.40 on 09/05/12
For personal use only.

Reactions of hexacarbonylrhenium(I) perchlorate with phosphines and other ligands

E. W. ABEL
Department of Chemistry, University of Bristol, Bristol, England

AND

S. P. TYFIELD
Department of Chemistry, University of Toronto, Toronto, Ontario

Received July 23, 1969

Hexacarbonylrhenium perchlorate, $[Re(CO)_6]ClO_4$, reacts on heating above 120° with 1,2-bis(diphenylphosphino)ethane and with triphenylphosphine to form respectively $[Re(CO)_4(Ph_2C_2H_4PPh_2)]ClO_4$ and *trans*-$Re(CO)_3(PPh_3)_2Cl$. The stereochemistry of *trans*-$Re(CO)_3(PPh_3)_2Cl$ was established by dipole moment and infrared measurements. Other phosphines failed to yield clean products. The reactions of phosphines and other ligands with $[Re(CO)_6]ClO_4$ are discussed, in particular the reaction with triphenylphosphine in which the perchlorate is reduced to chloride and incorporated by rhenium to form *trans*-$Re(CO)_3(PPh_3)_2Cl$.

Canadian Journal of Chemistry, 47, 4627 (1969)

Introduction

The substitution reactions of the neutral (1), and to a lesser extent, the anionic metal carbonyls (2) have received considerable attention, but little work has been reported of the reactions of the metal carbonyl cations (3). The first binary metal carbonyl cation $[Re(CO)_6]^+$ was reported by Hieber and Kruck in 1961 (4). Hitherto the investigation of the lability and extent of carbonyl substitution of $[Re(CO)_6]^+$ by both neutral and ionic ligands has been limited to the substitution by a tridentate arsine, v-triars, to form $[Re(CO)_3$-v-triars$]^+$ (5), by several carbonylate anions to form mixed metal–metal carbonyls (6), and by $H_2{}^{18}O$ in acid media whereupon oxygen exchange occurs (7). The reactions of the perchlorate salt of $[Re(CO)_6]^+$ with a number of phosphorus(III). and other ligands are described. Part of this work has been previously reported (8).

Results

The reaction of hexacarbonylrhenium perchlorate with 1,2-bis(diphenylphosphino)ethane (diphos) produced, on heating in cyclohexanone above 120°, the substituted carbonyl cation $[Re(CO)_4$diphos$]ClO_4$. Alternatively this salt may be obtained by high pressure carbonylation of *cis*-$Re(CO)_3$(diphos)Cl in the presence of aluminum chloride, followed by precipitation of the perchlorate from an aqueous-methanol solution. Recently an analogous carbonylation reaction has been used to prepare some $[Re(CO)_4L_2]^+$ cations, where L_2 is an olefin–phosphine chelating ligand (9).

The $[Re(CO)_4$diphos$]ClO_4$ is a white, air stable salt (1:1 electrolyte in nitrobenzene). Its infrared spectrum in the terminal carbonyl stretching region consists of four bands characteristic of octahedral *cis*-$ML_2(CO)_4$ (10) species. There are also present bands assignable to uncoordinated perchlorate (11) at 1100 (s, broad), 937 (w), and 634 cm^{-1} (m).

In contrast, triphenylphosphine reacts in diglyme or cyclohexanone with $[Re(CO)_6]ClO_4$ to form a neutral complex, the previously unreported *trans*-$Re(CO)_3(PPh_3)_2Cl$. The *cis* isomer is well known (12). The product was characterized by elemental analysis, conductimetry, dipole moment measurements, mass and infrared spectroscopy, and a molecular weight determination.

The stoichiometry of the triphenylphosphine reaction was found to be as follows

$$[Re(CO)_6]ClO_4 + 5\ PPh_3 \rightarrow Re(CO)_3(PPh_3)_2\ Cl + 2\ CO + CO_2 + 3\ PPh_3O$$

The carbon dioxide was estimated by absorption by lithium hydroxide, and the triphenylphosphine oxide produced was determined spectrophotometrically in acetonitrile by use of the intense ν_{P-O} absorption at 1185 cm^{-1}.

The source of the chlorine in the product is the perchlorate, which was confirmed by using ^{36}Cl labelled perchlorate. A radiochemical count of the product showed that incorporation of ^{36}Cl

Can. J. Chem. Downloaded from www.nrcresearchpress.com by 210.87.254.40 on 09/05/12
For personal use only.

was essentially quantitative. This confirms that in the absence of chlorine containing solvents, there was no other source of chlorine present in the starting material besides perchlorate.

The reactions of other phosphines, such as trisdimethylaminophosphine, triethyl and tri-*n*-butyl phosphines, as well as trimethyl and triphenyl phosphites with $[Re(CO)_6]ClO_4$ were studied. In no case was it possible to isolate clean products, although their identity could be tentatively assigned by comparison with the products of the reaction of the ligands with $Re(CO)_5Cl$. Among the products obtained from the latter reactions were *trans*-$Re(CO)_3(Tdp)_2Cl$ and *cis*-$Re(CO)_2L_3Cl$, where L is $P(OPh)_3$, PPh_2Me, and PPh_2H. Phosphorus trichloride failed to react with $[Re(CO)_6]ClO_4$.

The reaction with aliphatic nitrogen ligands, namely piperidine and tetramethylethylenediamine, resulted in the isolation of rhenium carbonyl. With both pyridine and α,α'-bipyridyl a variety of products was obtained, of which rhenium carbonyl and respectively *cis*-$Re(CO)_3py_2Cl$ or *cis*-$Re(CO)_3BipyCl$ were isolated. Continued refluxing of $Re(CO)_5Cl$ with pyridine failed to yield a dicarbonyl derivative, $Re(CO)_2py_3Cl$.

Discussion

It was considered at the outset of this study that the $[Re(CO)_6]^+$ cation would react in an analogous manner to the isoelectronic neutral tungsten hexacarbonyl, suitably modified by the presence of a formal positive charge on rhenium. It appears that the higher metal carbonyl stretching frequencies (13, 14) and the lower intensity of the T_{1u} vibration (15) of $[Re(CO)_6]^+$ compared with $W(CO)_6$ are consistent with poorer metal–carbonyl π back donation for the cation (16). This has recently been substantiated by a Raman intensity study (17). If the metal–carbonyl bond fission is crucial in carbonyl substitution reactions, then the $[Re(CO)_6]^+$ would be more readily substituted than $W(CO)_6$ on the basis that reduced M—CO π-bonding corresponds to reduced overall M—CO bonding (16). In fact it was found that $[Re(CO)_6]^+$ was reluctant to lose carbon monoxide and required forcing conditions, as does tungsten hexacarbonyl. However, it is not possible to meaningfully compare the reactivities of $[Re(CO)_6]^+$ and $W(CO)_6$ without kinetic data, which was not obtainable due to the absence of a suitable solvent for $Re(CO)_6ClO_4$. These results prompted us to study the whole vibrational spectrum of $[Re(CO)_6]^+$, which we have already reported (18). This work yielded the surprising result that the tungsten–carbon stretching force constants were almost identical.

The perchlorate anion was chosen because of its poor tendency to complex, stability to reduction (19), and ease of isolation of $[Re(CO)_6]ClO_4$. The salt is thermally stable, only exploding on heating above 180°. It may be kept indefinitely in air or light and is hygroscopic. It was dried before use.

The reaction between diphos and $[Re(CO)_6]ClO_4$ is analogous to that of $W(CO)_6$ (20) to form $[Re(CO)_4diphos]ClO_4$. With triphenylphosphine or any other unidentate phosphorus (III) ligand, a neutral rhenium pentacarbonylchloride derivative is formed. The stoichiometry of the triphenylphosphine reaction indicates that the phosphine is largely responsible for the reduction of perchlorate, but carbon dioxide is formed, presumably by oxidation of displaced carbon monoxide. When triphenylphosphine and sodium perchlorate were heated in diglyme under analogous reaction conditions (130°, 2–3 h in N_2 atmosphere), both phosphine oxide and chloride ion were detected, but the reaction is slow. Diglyme is not oxidized under these conditions. This suggests that the rhenium complex may be important in the perchlorate reduction. The involvement of rhenium is possible in view of the fact that triphenylphosphine oxide may be complexed to rhenium carbonyl chloride (21) and tungsten hexacarbonyl (22), and the oxide can be displaced from the tungsten complex by PPh_3. Further perchlorate complexes are known for a number of metals (23). The reaction of triphenylphosphine oxide with $[Re(CO)_6]ClO_4$ failed to produce a stable product, although carbon monoxide was displaced.

A reaction scheme for the PPh_3 reaction remains unresolved, although several plausible paths may be suggested in the light of further observations. Firstly, *trans*-$[Re(CO)_4(PPh_3)_2]ClO_4$, a possible reaction intermediate, reacts under analogous conditions to those used for $[Re(CO)_6]ClO_4$ with PPh_3 to form *trans*-$Re(CO)_3(PPh_3)Cl$. Attempts to prepare *trans*-$[Re(CO)_4(PPh_3)_2]ClO_4$ by using a stoichiometric amount of PPh_3 with $[Re(CO)_6]ClO_4$ resulted in

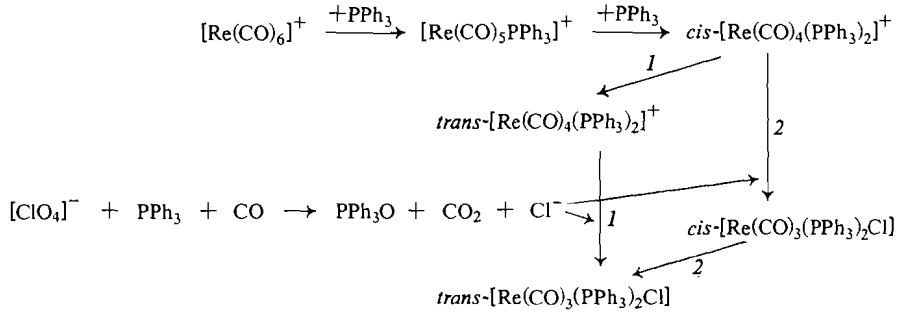

SCHEME 1

the incomplete conversion to the *trans*-chloride. Further, if *cis*-$Re(CO)_3(PPh_3)_2Cl$ is heated with triphenylphosphine under the same conditions, thermal isomerization to the *trans* isomers occurs, as is reported for the iodide (24).

Scheme 1 is tentatively proposed. Either or both routes *1* or *2* may be involved.

The reactions of trimethyl and triphenyl phosphites, trisdimethylaminophosphine (Tdp), and several alkyl phosphines with $[Re(CO)_6]ClO_4$ appear to occur analogously to the triphenylphosphine reaction to produce substituted rhenium chlorocarbonyl complexes. Although these compounds were not isolated, their identity was established by comparison with the infrared spectra of the products of the reaction of the ligands with $Re(CO)_5Cl$. With triphenylphosphite both *cis*-$Re(CO)_2(P(OPh)_3)_3Cl$ and *cis*-$Re(CO)_3[P(OPh)_3]_2Cl$ are obtained, as is reported for the reaction with $Re(CO)_5I$ (24). All the chlorocarbonyl products contained *cis* configuration of carbonyls with the one exception of trisdimethylaminophosphine reacting with $Re(CO)_5Cl$ and $[Re(CO)_6]ClO_4$ to form *trans*-$Re(CO)_3(Tdp)_2Cl$. This has a similar infrared spectrum to *trans*-$Re(CO)_3(PPh_3)_2Cl$ and a well resolved 1:2:1 triplet proton resonance, consistent with the *trans* disposition of phosphines (25).

The stereochemistry of *trans*-Re $CO)_3(PPh_3)_2$-Cl was elucidated from its infrared spectrum and dipole moment. There are three isomers of $Re(CO)_3(PPh_3)_2Cl$ which are, in terms of the carbonyls, one *cis* and two *trans* isomers (**1**, **2**, and **3**). The *cis* and the *trans* isomers may be distinguished by inspection of their infrared-active carbonyl stretching absorptions. The *cis* should give rise to three strong bands (2 A' + A''), while the *trans* forms should show two strong bands ($A_1 + B_1$) and a higher energy band of low intensity (A_1). (See Figs. 1 and 2).

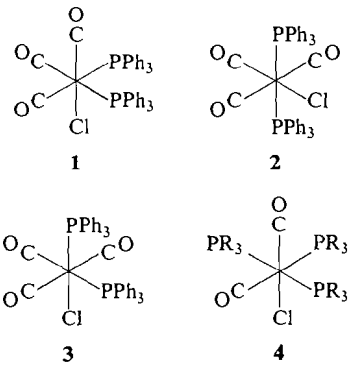

The rhenium–chlorine stretching vibration may be used to distinguish the two *trans* isomers. It has been noted that the metal–chlorine stretching frequency in octahedral (26 and references therein) and square planar complexes (27 and references therein) is markedly influenced

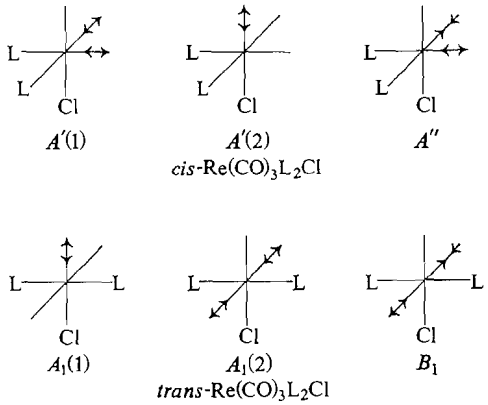

FIG. 1. Normal modes of stretching vibrations of *cis*- and *trans*-$Re(CO)_3L_2Cl$.

Can. J. Chem. Downloaded from www.nrcresearchpress.com by 210.87.254.40 on 09/05/12
For personal use only.

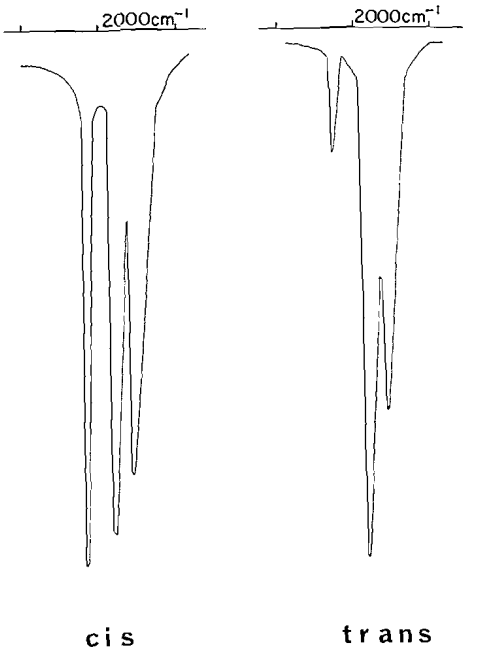

FIG. 2. Chloroform solution spectra of *cis*- and *trans*-$Re(CO)_3(PPh_3)_2Cl$.

by the *trans* ligand. For example the Pt—Cl stretching band is reduced in the order of *trans* ligand CO > R_3P. The effect is appreciable, so that for the $[PtLCl_3]^-$ (27), $\nu_{Pt-Cl} = 322$ cm^{-1} (Cl *trans* to CO), $\nu_{Pt-Cl} = 279$ cm^{-1} (Cl *trans* to PPh_3). A comparison of the ν_{Re-Cl} of *cis*- and *trans*-$[Re(CO)_3(PPh_3)_2Cl]$ and $Re(CO)_5Cl$ (28) at 281, 275, and 294 cm^{-1}, respectively, indicates that the unique carbonyl of the *trans* isomer is *trans* to a chlorine rather than the phosphine, that is, type **2**.

The stereochemistry is confirmed by a dipole moment study, Table I. The dipole moment of *trans*-$Re(CO)_3(PPh_3)_2Cl$ is close to that of $Re(CO)_5Cl$ (3.4 and 2.5 D, respectively) when compared to that of *cis*-$Re(CO)_3(PPh_3)_2Cl$ (7.2 D). By Chatt's method of estimating dipole moments (29), the isomer type **2** is the only form consistent with a dipole moment of the same magnitude as $Re(CO)_5Cl$. Both *cis* (type **1**) and the other *trans* isomer (type **3**) would have greater values. The corresponding manganese complexes have been studied by Angelici *et al.* (30). It is interesting to note that *trans* complexes of manganese are readily formed from their *cis* isomers whereas, with the notable exception of *cis*-$Re(CO)_3(PPh_3)_2Cl$,

TABLE I

Dipole moments of some rhenium carbonyl halide complexes

Complex	Dipole moment in benzene D (± 0.5)
$Re(CO)_5Cl$	3.04
$Re(CO)_5Br$	3.24
cis-$Re(CO)_3(P(OPh)_3)_2Cl$	5.22
cis-$Re(CO)_3(PPh_3)_2Cl$	7.27
trans-$Re(CO)_3(PPh_3)_2Cl$	2.54

the rhenium *cis* complexes are found not to isomerize or else to be further substituted to *cis*-$Re(CO)_2L_3Cl$, type **4**.

Similarly, the *cis* configuration of *cis*-$Re(CO)_2(PPh_2H)_3Cl$ was established by infrared spectroscopy to have a configuration of type **4**. The values of ν_{CO} and ν_{ReCl} are presented in Tables II and III.

The proton nuclear magnetic resonance (n.m.r.) of *cis*-$Re(CO)_3(PPh_2Me)_2Cl$ (31 and references therein) and *cis*-$Re(CO)_3(PPh_2H)_2Cl$ (32) give rise to symmetrical doublets as expected for simple splitting of the hydrogen resonances by a single ^{31}P nucleus, supporting the type **1** stereochemistry. *cis*-$Re(CO)_3(P(OMe)_3)_2Cl$ gives a symmetric triplet band in which the outer resonances are more intense than the central resonance, as is noted for *cis*-$Mo(CO)_4(P(OMe)_3)_2$ (33). ^{31}P spectra were precluded by the low solubility of the complexes.

The mass spectra of *cis*- and *trans*-$Re(CO)_3(PPh_3)_2Cl$ were run to see if there was any difference in the cracking pattern. In fact, the spectra are identical. Very strong peaks for PPh_3 and PPh_3O are obtained with faint peaks at high mass for some rhenium-containing fragments. There are no molecular ions (P) observed, but $(P—CO)^+$, $(P—2CO)^+$, $(Re(PPh_3)Cl)^+$, and $Re(\langle\bigcirc\!\!\bigcirc\!\!\bigcirc\!\!\bigcirc\rangle_P)^+$ are of appreciable intensity. Further, there are weak peaks at *m/e* 744 (P − 300), 666 $(744 - C_6H_6)^+$, 588 $(666 - C_6H_6)^+$, and 538 $(Re(CO)_2(PPh_3)_2Cl)^+$.

The various stereochemistries of the rhenium chlorocarbonyl complexes prepared in this study may be rationalized in terms of the *trans* directive effect of ligands which favor the formation of *cis* carbonyl complexes (1, 12), and the steric effect of the substituting ligands which favor the

Can. J. Chem. Downloaded from www.nrcresearchpress.com by 210.87.254.40 on 09/05/12
For personal use only.

TABLE II

Infrared ν_{CO} frequencies of some rhenium carbonyl complexes in chloroform (cm^{-1})

Complex	Infrared frequencies†			
$[Re(CO)_4diphos]ClO_4$	2110 (m)	2027 (s)	2017 (s)	1997 (s)
cis-$Re(CO)_3(PPh_3)_2Cl$	2040 (s)	1959 (s)	1903 (s)	
trans-$Re(CO)_3(PPh_3)_2Cl$	2049 (w)	1954 (s)	1904 (s)	
cis-$Re(CO)_3(PPh_2Me)_2Cl$	2036 (s)	1958 (s)	1898 (s)	
cis-$Re(CO)_3(PPh_2H)_2Cl$	2042 (s)	1968 (s)	1906 (s)	
cis-$Re(CO)_3(diphos)Cl$	2038 (s)	1958 (s)	1906 (s)	
cis-$Re(CO)_3(PBu^n_3)_2Cl$	2026 (s)	1941 (s)	1890 (s)	
cis-$Re(CO)_3(P(OMe)_3)_2Cl$	2051 (s)	1979 (s)	1916 (s)	
cis-$Re(CO)_3(P(OPh_3)_2)Cl$	2061 (s)	1996 (s)	1934 (s)	
trans-$Re(CO)_3(Tdp)_2Cl$	2036 (w)	1941 (s)	1894 (s)	
cis-$Re(CO)_3(TMED)Cl$*	2031 (s)	1924 (s)	1884 (s)	
cis-$Re(CO)_3(C_5H_{11}N)_2Cl$	2025 (s)	1913 (s)	1885 (s)	
cis-$Re(CO)_2(PPh_2H)_3Cl$	1963 (s)	1860 (s)		
cis-$Re(CO)_2(PPh_2Me)_3Cl$	1952 (s)	1842 (s)		
cis-$Re(CO)_2(P(OPh)_3)_3Cl$	1986 (s)	1934 (s)		

*TMED = tetramethylethylenediamine, $Me_2NC_2H_4NMe_2$.
†s = strong, m = medium, w = weak.

TABLE III

Rhenium–chlorine stretching vibrations of $Re(CO)_5Cl$ and substituted complexes

Complex	Stretching vibration frequencies* (cm^{-1})	
$Re(CO)_5Cl$	294 (m)	287 (sh)
cis-$Re(CO)_3(PPh_3)_2Cl$	281 (m)	275 (sh)
trans-$Re(CO)_3(PPh_3)_2Cl$	275 (m)	268 (sh)
cis-$Re(CO)_3(PPh_2Me)_2Cl$	286 (m)	277 (sh)
cis-$Re(CO)_3(PPh_2H)_2Cl$	274 (m)	270 (sh)
trans-$Re(CO)_3(Tdp)_2Cl$	271 (m)	266 (sh)
cis-$Re(CO)_2(PPh_2H)_3Cl$	270 (m)	264 (sh)

*In Nujol mulls; m = medium, sh = shoulder.

formation of stable, *trans* disubstituted tricarbonyl chloride complexes, particularly for triphenylphosphine. The reason for the formation of rhenium carbonyl on reaction with nitrogen ligands remains unclear at present.

Experimental

Infrared spectra were recorded on Perkin–Elmer 225 and 247 spectrophotometers, ^1H n.m.r. spectra were recorded on Varian A60 and HA-100 spectrophotometers using TMS as an internal reference for $CDCl_3$ solutions. Elemental analyses were carried out by the Microanalytical Laboratory of Bristol University. Melting points are uncorrected and determined by means of an electrothermal melting point apparatus. Conductivities were measured in AnalaR nitrobenzene by use of a Cambridge conductivity bridge. Dipole moments in benzene and mass spectral results were determined by ICI Petrochemical and Polymer Laboratories, Runcorn.

All reactions were conducted under a nitrogen atmosphere.

Hexacarbonylrhenium perchlorate was prepared from pentacarbonylrhenium, aluminum trichloride, and carbon monoxide using methods in literature (4, 5). The $[Re(CO)_6]ClO_4$ was precipitated from chilled water by the addition of 60% perchloric acid, washed with ether, and dried in vacuo. Yields were high (90%).

The other reagents used were commercial samples or were prepared according to methods in literature.

A. Preparation of 1,2-Bis(diphenylphosphino)-ethanetetracarbonylrhenium(I) Perchlorate

(*i*) Hexacarbonylrhenium perchlorate (0.5 g, 1 mole) and 1,2-bis(diphenylphosphino ethane) (0.88 g, 2 moles) were heated (120°, 1 h) in cyclohexanone (15 ml). The product was precipitated by the addition of ether and recrystallized from acetone–ether.

Anal. Calcd. for $C_{30}H_{24}O_8P_2ClRe$: C, 45.2; H, 3.0; O, 16.1. Found: C, 45.15; H, 3.3; O, 15.8.

$\Lambda_{0.001\ M}(C_6H_5NO_2) = 19.5\ ohm^{-1}\ cm^2\ mole^{-1}$. It decomposes at 205° without exploding. The salt is soluble in polar solvents including chloroform, insoluble in benzene, carbon tetrachloride, and ether. It appears to be indefinitely stable in air.

(*ii*) *cis*-Chloro-1,2-bis(diphenylphosphino)ethanetricarbonylrhenium (1 g, 1 mole) and aluminum trichloride (1 g, 6 moles) with benzene (3 ml) were autoclaved with carbon monoxide (350 atm) for 30 h (75°). The product was hydrolyzed and extracted with chilled water (15 ml), washed with ether, and recrystallized from acetone–ether (0.6 g, 53% yield).

Anal. Calcd. for $C_{30}H_{24}O_8P_2ClRe$: C, 45.2; H, 3.0. Found: C, 45.6; H, 3.0.

B. Preparation of trans-Chlorobis(triphenylphosphine)-tricarbonylrhenium

(*i*) Hexacarbonylrhenium perchlorate (0.4 g, 1 mole) and triphenylphosphine (1.2 g, 5 moles) in diglyme (10 ml) were heated (130°, 2–3 h) until carbon monoxide ceased to evolve and product precipitated out. The reaction is slow to start and results in the gradual dissolution of starting materials, which eventually dissolve completely. The white product was collected on cooling,

Can. J. Chem. Downloaded from www.nrcresearchpress.com by 210.87.254.40 on 09/05/12
For personal use only.

TABLE IV

Reaction of hexacarbonylrhenium perchlorate with phosphines and phosphites

Ligand, L	Solvent	Product
$P(OPh)_3$, $P(OMe)_3$ PEt_3, PBu_3^n, PPh_2H, PPh_2Me	—	*cis*-$Re(CO)_3L_2Cl$ + *cis*-$Re(CO)_2L_3Cl$
PCl_3	—	No reaction
$P(NMe_2)_3$	—	*trans*-$Re(CO)_3L_2Cl$
PPh_3O	Diglyme	Unidentified products
$AsPh_3$	Diglyme	*cis*-$Re(CO)_3L_2Cl$
$C_5H_{11}N$, $(Me_2NCH_2—)_2$	—	$Re_2(CO)_{10}$
C_5H_5N, $C_{10}H_8N_2$	—	$Re_2(CO)_{10}$ + *cis*-$Re(CO)_3L_3Cl$

TABLE V

^1H n.m.r. spectra of some substituted rhenium carbonyl complexes

Complex	Parameter	Value†	J_{PH} (c.p.s.)
$[Re(CO)_4diphos]ClO_4$*	τ_{CH_2}	6.55 (d)	17.6
cis-$Re(CO)_3(PPh_2H)_2Cl$	τ_{PH}	3.74 (d)	370.5
	τ_{Ph}	2.75 (m)	
cis-$Re(CO)_3(PPh_2Me)_2Cl$	τ_{CH_3}	8.1 (d)	7.9
	τ_{Ph}	2.74 (m)	
cis-$Re(CO)_3(P(OMe)_3)_2Cl$	τ_{CH_3}	6.30 (t) (2:1:2)	11.0
trans-$Re(CO)_3(Tdp)_2Cl$	τ_{CH_3}	7.30 (t) (1:2:1)	5.0

*$PhNO_2$ solution.
†d = symmetric doublet, m = multiplet, t = symmetric triplet.

washed with ether (15 ml), recrystallized from chloroform–pentane (0.49 g, 54% yield).

Anal. Calcd. for $C_{39}H_{30}O_3P_2ClRe$: C, 56.4; H, 3.6; Cl, 4.3. Found: C, 55.9; H, 3.9.

The solid decomposes above 230°. Molecular weight found[1] 829.6, required 829.8. $\Lambda_{0.001\ M}(C_6H_5NO_2)$ = 0.33 $ohm^{-1}\ cm^2\ mole^{-1}$.

(*ii*) *trans*-Bis(triphenylphosphine)tetracarbonylrhenium perchlorate (0.25 g, 1 mole), prepared by the literature method (34), and triphenylphosphine (0.29 g, 4 moles) were reacted under the same conditions as (*i*).

Found: C, 55.7; H, 3.4; Cl, 4.3.

(*iii*) *cis*-Chlorobis(triphenylphosphine)tricarbonylrhenium (0.3 g, 1 mole) and triphenylphosphine (0.2 g, 2 moles) were heated (150°) under nitrogen or in vacuo for 2 h. The product was washed with ether (10 ml) and recrystallized from chloroformpentane.

Found: C, 55.8; H, 3.5.

C. Reaction of Hexacarbonylrhenium Perchlorate with Other Ligands

The reaction of hexacarbonylrhenium perchlorate with a variety of phosphines and phosphites, that only yield infrared spectral evidence of the nature of the products, are listed in Table IV. The reactions of several other ligands are included. Authentic rhenium carbonyl chloride derivatives were prepared from chloropentacarbonylrhenium by treatment with excess ligand in diglyme (12, 24).

The unreported $Re(CO)_3L_2Cl$ complexes prepared from $Re(CO)_5Cl$ were characterized. Infrared and ^1H n.m.r. results are reported in Tables II, III, and V. Elemental analyses of complexes are given in Table VI.

D. The Investigation of the Reaction of Triphenylphosphine with Hexacarbonylrhenium Perchlorate

(i) Production of Triphenylphosphineoxide

The quantity of PPh_3O produced in *B*(*i*) was determined by use of the intense P—O stretching vibration ($\nu_{P—O}$ = 1185 cm^{-1}, CH_3CN solution). After the reaction *B*(*i*), for which PPh_3 was checked to be free of PPh_3O, the diglyme solution was dried in vacuo and the solid dissolved in acetonitrile. Comparison with a standard plot of intensity of the band vs. concentration showed that approximately 3 ± 0.5 moles of PPh_3O were produced per mole of $[Re(CO)_6]ClO_4$.

(ii) Production of Carbon Dioxide

The CO_2 evolved in reaction *B*(*i*) was estimated gravimetrically by absorption on Lithasorb (LiOH). Approximately 1.0 ± 0.1 mole of CO_2 was collected per mole of $[Re(CO)_6]ClO_4$.

(iii) Incorporation of ^{36}Cl into trans-$Re(CO)_3(PPh_3)_2Cl$

The reaction *B*(*i*) was repeated using a sample of ^{36}Cl labelled perchlorate, obtained by equilibrating $K^{36}ClO_4$ (from the Radiochemical Centre, Amersham) with $[Re(CO)_6]ClO_4$ in nitromethane. $[Re(CO)_6]^{36}ClO_4$ was obtained by taking the filtered nitromethane solution to dryness in vacuo. The product was counted in acetonitrile solution. After repeating reaction *B*(*i*) with $[Re(CO)_6]^{36}ClO_4$, the product precipitated on cooling, and was washed with ether, dried in vacuo, and counted in acetonitrile solution.

Specific activities were recorded using a 20th Century

[1]Analyses done in Microanalytical Laboratory, Imperial College, London.

Can. J. Chem. Downloaded from www.nrcresearchpress.com by 210.87.254.40 on 09/05/12
For personal use only.

TABLE VI

Elemental analyses of $Re(CO)_3L_2Cl$ complexes prepared from $Re(CO)_5Cl$

Ligand	Melting point (°C)	Configuration of $Re(CO)_3L_2Cl$	Analysis							
			Found, %				Calculated, %			
			C	H	Cl	N	C	H	Cl	N
PPh_2Me	158–159	*cis*	49.55	3.2	4.9	—	49.3	3.7	5.0	—
PPh_2H	165–166	*cis*	48.5	3.2	5.2	—	47.8	3.3	5.2	—
$P(NMe_2)_3$	130 (decomp.)	*trans*	28.55	5.9	5.9	13.5	28.5	5.7	5.6	13.3
$C_5H_{11}N$	225 (decomp.)	*cis*	33.4	5.0	7.7	6.0	32.8	4.7	7.45	5.9
$(Me_2NCH_2-)_2$	235 (decomp.)	*cis*	26.1	3.9	8.2	6.5	25.6	3.8	8.2	6.6

TABLE VII

Specific activity of precursor $[Re(CO)_6]ClO_4$ and product *trans*-$Re(CO)_3(PPh_3)_2Cl$*

Experiment No.	Specific activity†	
	$[Re(CO)_6]ClO_4$	*trans*-$Re(CO)_3(PPh_3)_2Cl$
1	6.52	6.23
2	6.43	6.12

*Background (acetonitrile) = 26 counts min^{-1}.
†Unit = counts min^{-1} g^{-1} of chloride × 10^{-5}.

Electronics G.M. liquid counter type DM6. The detector assembly was supplied by a Phillips high voltage unit type PW4022, and the output from a rate meter, type 4042, was displayed on a Phillips Electronic Counter, type 4032. Results are given in Table VII. Mean percentage ^{36}Cl incorporation is found to be 95.3%.

Acknowledgments

The authors wish to thank the S.R.C. London, England, for a Research Studentship (S.P.T.) and Dr. D. T. Thompson of ICI Petrochemical and Polymers Research Laboratory, Runcorn, England, for dipole moment and mass spectral measurements.

1. (*a*) F. A. COTTON and G. WILKINSON. Advanced inorganic chemistry. 2nd ed. Interscience Publishers, Inc., New York. 1966. (*b*) G. R. DOBSON, I. W. STOLZ, and R. K. SHELINE. Advan. Inorg. Chem. Radiochem. **8**, 1 (1966). (*c*) T. A. MANUEL. Advan. Organometal. Chem. **3**, 181 (1965).
2. R. B. KING. Advan. Organometallic Chem. Amsterdam, **2**, 157 (1964).
3. E. W. ABEL and S. P. TYFIELD. Advan. Organometal. Chem. Amsterdam. In press.
4. W. HIEBER and T. KRUCK. Angew. Chem. **73**, 580 (1961); Z. Naturforsch. **16b**, 709 (1961).
5. R. S. NYHOLM, M. R. SNOW, and M. H. B. STIDDARD. J. Chem. Soc. 6564 (1965).
6. T. KRUCK, M. HÖFLER, and K. NOACK. Chem. Ber. **99**, 1153 (1966).
7. E. L. MUETTERTIES. Inorg. Chem. **4**, 1841 (1965).
8. E. W. ABEL and S. P. TYFIELD. Chem. Commun. 485 (1968).
9. L. V. INTERRANTE and G. V. NELSON. Inorg. Chem. **7**, 2059 (1968).
10. (*a*) L. E. ORGEL. Inorg. Chem. **1**, 25 (1962). (*b*) D. M. ADAMS. Metal–ligand and related vibrations. Edward Arnold and Co., London. 1968.
11. R. J. HATHAWAY and A. E. UNDERHILL. J. Chem. Soc. 3091 (1961).
12. E. W. ABEL and G. WILKINSON. J. Chem. Soc. 1501 (1959).
13. E. W. ABEL, R. A. N. MCLEAN, S. P. TYFIELD, P. S. BRATERMAN, A. P. WALKER, and P. J. HENDRA. J. Mol. Spectrosc. **30**, 29 (1969).
14. J. M. SMITH and L. H. JONES. J. Mol. Spectrosc. **20**, 248 (1966).
15. T. L. BROWN and D. J. DARENSBOURG. Inorg. Chem. **6**, 971 (1967).
16. E. W. ABEL. Quart. Rev. 133 (1963).
17. P. J. HENDRA and M. M. QURASHI. J. Chem. Soc. A, 2963 (1968).
18. E. W. ABEL, R. A. N. MCLEAN, M. G. NORTON, and S. P. TYFIELD. Chem. Commun. 900 (1968).
19. H. TAUBE. J. Chem. Ed. **45**, 452 (1968).
20. J. CHATT and H. R. WATSON. J. Chem. Soc. 4980 (1961).
21. U. SARTORELLI, F. CANZIANI, and F. ZINGALES. Inorg. Chem. **5**, 2233 (1966).
22. F. CANZIANI, F. ZINGALES, and U. SARTORELLI. Gazz. Chim. Ital. **94**, 841 (1964).
23. (*a*) S. F. PAVKOVIC and D. W. MEEK. Inorg. Chem. **4**, 1091 (1965) and references therein. (*b*) P. M. TREICHEL and G. WERBER. Inorg. Chem. **4**, 1098 (1965). (*c*) J. LEWIS, R. S. NYHOLM, and G. A. RODLEY. Nature, **207**, 72 (1965). (*d*) P. PAULING, G. B. ROBERTSON, and G. A. RODLEY. Nature, **207**, 73 (1965).
24. M. FRENI, P. GIUSTO, and P. ROMITI. J. Inorg. Nucl. Chem. **29**, 761 (1969).
25. R. B. KING. Inorg. Chem. **2**, 936 (1963).
26. M. S. LUPIN and B. L. SHAW. J. Chem. Soc. A, 741 (1968).
27. R. J. GOODFELLOW, P. L. GOGGIN, and D. A. DUDDELL. J. Chem. Soc. A, 504 (1968).
28. M. A. BENNETT and R. J. H. CLARKE. J. Chem. Soc. 5560 (1964).
29. (*a*) J. CHATT. Proc. Chem. Soc. 318 (1962). (*b*) J. CHATT, R. S. COFFEY, and G. L. SHAW. J. Chem. Soc. 7391 (1965). (*c*) J. CHATT and B. L. SHAW. J. Chem. Soc. A, 1437 (1966).
30. R. J. ANGELICI, F. BASOLO, and A. J. POË. J. Amer. Chem. Soc. **85**, 2215 (1963).
31. R. G. GOODFELLOW. Chem. Commun. 114 (1968).
32. J. G. SMITH and D. T. THOMPSON. J. Chem. Soc. A, 1694 (1967).
33. M. LENZI and R. POILBLANC. C.R. **C263**, 674 (1966).
34. T. KRUCK and M. HÖFLER. Chem. Ber. **96**, 3035 (1963).

Can. J. Chem. Downloaded from www.nrcresearchpress.com by 210.87.254.40 on 09/05/12
For personal use only.

Spin–lattice relaxation of 1,2-dichloroethane in different solvents[1]

E. BOCK
Parker Chemistry Laboratory, University of Manitoba, Winnipeg, Manitoba

AND

E. TOMCHUK
Department of Physics, University of Winnipeg, Winnipeg, Manitoba

Received June 11, 1969

The spin–lattice relaxation time of the 1,2-dichloroethane molecule has been determined in 6 different nonmagnetic or weakly magnetic solvents at 20 °C, *viz*: deuterated benzene, carbon disulfide, deuterated 1,2-dichloroethane, carbon tetrachloride, and deuterated chloroform. From the experimental results the relaxation rate in infinitely dilute solution, the so called intramolecular relaxation rate, was determined for each solvent. It was found that the observed intramolecular relaxation rate could be successfully interpreted as arising solely from a dipole–dipole relaxation mechanism. It was further found that the individual differences in the value of the intramolecular spin–lattice relaxation rate of the 1,2-dichloroethane molecule in different solvents could be accounted for in terms of weak complex formation between the solute and solvent molecules.

Canadian Journal of Chemistry, **47**, 4635 (1969)

Can. J. Chem. Downloaded from www.nrcresearchpress.com by 210.87.254.42 on 09/05/12
For personal use only.

Introduction

A number of workers have reported on the anomalous dielectric behavior (enhanced relaxation times and electric dipole moments) of the 1,2-dichloroethane molecule in aromatic and highly polarizable solvents (1–4). All of the work on the microdynamical behavior of the 1,2-dichloroethane molecule in different solvents reported heretofore has been carried out employing dielectric relaxation studies. We thought it, therefore, not inappropriate to repeat and in some cases, to extend some of the earlier investigations using an entirely different method of investigation from the usual dielectric relaxation method, viz. the pulsed nuclear magnetic relaxation method. We are aware of only one paper in the literature, a paper by Linder (5), in which an attempt was made to study the motional properties of the 1,2-dichloroethane molecule in the liquid state. We have reasons to believe that Linder's data are in error. Thus, he reports a spin–lattice relaxation time for pure liquid 1,2-dichloroethane of 0.8–0.6 s in the temperature region from room temperature to the melting point, 234 °K. Furthermore, he attributes the very considerable scatter of his experimental results to the action of light on his samples of 1,2-dichloroethane. We, on the other hand, find that the spin–lattice relaxation time of a carefully degassed sample of liquid 1,2-dichloroethane over the same temperature region varies between 8.35 s at 20 °C and 3.0 s at the melting point, and that of a liquid sample saturated with air has a relaxation time of ~2.6 s at room temperature. Moreover, we did not detect any effect of light on the relaxation time of the sample, not even after the latter was exposed for several h to a mercury ultraviolet lamp or a 500 W projection lamp. Since Linder has not given any details regarding the purity of his molecules or preparation of samples (indeed it is not clear from his description of his experimental procedure whether he did remove dissolved oxygen from his samples), we are not able to give any explanation for the observed discrepancy except to note that any paramagnetic impurity would tend to lower the spin–lattice relaxation time, and that therefore any lowering of the spin–lattice relaxation time may be taken as a certain indication of the presence of impurities in the sample.

In an earlier paper we reported on the spin–lattice relaxation time of 1,2-dichloroethane in deuterated benzene and carbon disulfide (6). In this paper we have extended our earlier work and report on the spin–lattice relaxation of 1,2-dichloroethane molecule in 4 additional solvents, viz. chloroform-*d*, acetone-d_6, 1,2-dichloroethane-d_4, and carbon tetrachloride.

Experimental

Solvents

All deuterated solvents (isotopic purity 99–99.5%) were obtained from Merck, Sharp, and Dohme of Canada, Ltd. and were used without further purification.

[1]Presented in part at the XXII International Congress of Pure and Applied Chemistry, Sydney, Australia. August 20–27, 1969.

TABLE I

Extrapolated values of T_1^{-1} for 1,2-dichloroethane molecule in different solvents, and the viscosity, η, dipole moment, μ, and density, d, of the different solvents at 20 °C

Solvent	$T_{0_1}^{-1}$ ($s^{-1} \times 10^2$)	η (cP)	μ (D)	d (g/cm^3)	δ* ($s^{-1} \times 10^2$)
Benzene-d_6	3.19	0.652	0	0.8790	0.44
Chloroform-d	5.77	0.563	1.01	1.4916	0.58
Acetone-d_6	4.92	0.325	2.86	0.7908	0.49
1,2-Dichloroethane-d_4	7.94	0.833	1.6	1.2564	0.42
Carbon tetrachloride	5.27	0.965	0	1.5942	0.71
Carbon disulfide	1.44	0.367	0	1.2628	0.72

*δ is the standard deviation from the straight-line plot of the experimental data.

The carbon disulfide, Fisher certified reagent, was purified using a standard purification method (7). The carbon tetrachloride, *spectro-quality reagent*, was obtained from Matheson, Coleman, and Bell Co., and was used without further purification.

Solute

The 1,2-dichloroethane was obtained from Eastman Organic Chemicals. It was redistilled once under reduced pressure and stored in a dark bottle.

Apparatus and Procedure

The spin–lattice relaxation time of all samples was determined at 20 ± 0.1 °C on a PS-60A NMR Specialties pulsed nuclear magnetic resonance (n.m.r.) spectrometer using a 180–90° pulse sequence (8). All experimental solutions were carefully degassed by repeated (8 or more) freeze–pump–thaw cycles. Further details of the experimental procedure are described elsewhere (6, 9).

Results and Discussion

The experimental results are summarized in Table I. Included in this Table are the pertinent properties of the different solvents, containing protons in natural abundance, viz. viscosity, electric dipole moment, and density. Also included is the standard root-mean-square deviation, δ, of the experimental points from a straight-line plot of the form $T_1^{-1} = T_{0_1}^{-1} + Cx$, where T_1^{-1} is the reciprocal of the measured spin–lattice relaxation time T_1, $T_{0_1}^{-1}$ is the reciprocal of the extrapolated value of T_1^{-1}, i.e. the intramolecular contribution to the relaxation rate, C is a constant, and x the mole fraction of the solute in solution. The extrapolated value of T_1^{-1}, $T_{0_1}^{-1}$, was then used, following a slightly modified method of Powles (10) to calculate a molecular reorientation time, τ_r. The modification consisted of treating all protons in the calculation of the constant A in eq. [1], below, as equivalent protons. This modification is applicable in all those cases where an average response only is recorded from chemically shifted protons, as pointed out by Goldammer and Zeidler (11)

$$[1] \qquad T_{0_1}^{-1} = A\tau_r$$

$$[2] \qquad A = \frac{\hbar^2\gamma^4}{2n}\sum_{i=1,i\neq j}^{n}\sum_{j=1,i\neq j}^{n} d_{ij}^{-6}$$

Here $\hbar$ is Planck's constant; γ, magnetogyric ratio of the proton; n, number of protons per molecule; and d_{ij}, distance between proton i and proton j.

The required structural data for the calculation of d_{ij} were taken from the literature (12). The thus calculated values of τ_r are summarized in Table II. From a perusal of Table II it is clear that the different values of τ_r in the different solvents cannot be accounted for solely in terms of the different viscosities of the various solvents. Thus, acetone has a viscosity which is somewhat lower than that of CS_2, yet τ_r in acetone is approximately 3 times that in CS_2. In order to facilitate the comparison of the different τ_r values we have "normalized" the latter by the following procedure. The τ_r value in CS_2, a liquid which we regard for the sake of this comparison as an "inert" liquid, was multiplied by the ratio of the viscosity of a particular solvent to that of carbon disulfide. The resulting value, designated as τ_r' in Table II, may then be regarded as the reorientation time that the solute molecule would have if in the absence of solute–solvent interactions its reorientation were hindered by viscous forces only. Such an analysis of the experimental data is a reasonable one, since it is expected on the basis of the simple Debye theory for disorientation of electric dipoles that τ_r be proportional to the viscosity of the medium, η (13). It is true that more elaborate expressions for τ_r have been proposed from time to time in the literature (14), in which the bulk viscosity is replaced by a so-called empirical viscosity and which, in addition, con-

Can. J. Chem. Downloaded from www.nrcresearchpress.com by 210.87.254.42 on 09/05/12
For personal use only.

TABLE II
Summary of derived or calculated results

Solvent	τ_r ($s \times 10^{12}$)	τ_r' ($s \times 10^{12}$)	$\Delta\Delta G^*$ (cal/mole)	$\frac{2\mu_A\mu_B}{r^3}$ (cal/mole)
Benzene-d_6	3.43	2.80	120	—
Chloroform-d	6.29	2.40	560	240
Acetone-d_6	5.35	1.40	785	740
1,2-Dichloroethane-d_4	8.62	3.56	516	400
Carbon tetrachloride	5.74	4.15	189	—
Carbon disulfide	1.57	1.57	—	—

tain a structure factor which reflects the role of the solvent. However, in the absence of any detailed knowledge of either the empirical viscosity or the structural factor, it may be permissible to analyze the data in terms of the albeit approximate but much simpler Debye expression. The corrected, or normalized, values of τ_r may now be used to further analyze the experimental data. Thus according to Eyring's theory of rate processes, the relaxation time of a process is connected with the activation free energy ΔG^* for that process by the expression

$$[3] \qquad \tau = Ae^{\Delta G^*/RT}$$

Here ΔG^* is the free energy of activation; R, the gas constant; T, the absolute temperature; and A, a constant. If it is assumed that both reorientation times, τ_r, the measured reorientation time, and τ_r', the corrected reorientation time, obey an expression of the form of eq. [3], then the ratio of τ_r/τ_r' should yield the difference between the free energy of activation for the 2 reorientation processes, viz. the reorientation process that actually takes place in the particular solvent and the reorientation process which would take place in the same solvent if the processes were governed only by the viscosity of the solvent. The values of the difference in the free energy of activation for the 2 processes, designated as $\Delta\Delta G^*$, calculated with the aid of eq. [3] are summarized in Table II. It is interesting to note that the largest values of $\Delta\Delta G^*$ are found for those solvents the molecules of which possess permanent electric dipole moments, and that the values of the $\Delta\Delta G^*$'s roughly parallel the magnitude of the electric dipole moment of the solvent molecules. Moreover, if a rough estimate is made of the solute–solvent electric dipole–dipole interaction energy using the well known expression

$$[4] \qquad 2\mu_A\mu_B/r^3 = E$$

where μ_A and μ_B are the dipole moment of the solute and solvent molecule, respectively, and r is the distance between the 2 interacting dipoles, there results an interaction energy which is very nearly equal to the difference in the activation free energy $\Delta\Delta G^*$ of the 2 processes. (See last column of Table II.)

The values of r in eq. [4] were estimated from the known densities of the various liquids, assuming close packing of the spheres in the liquid. From the rather close agreement of the $\Delta\Delta G^*$ values and the dipole–dipole interaction energy values, it would appear that the main retarding mechanism of molecular reorientation of polar molecules in a polar solvent is the dipole–dipole interaction between the dipole moments of the solute and solvent molecules.

The calculated values of $\Delta\Delta G^*$ for the 2 nonpolar solvents, i.e., benzene and carbon tetrachloride, may be rationalized in terms of specific solute–solvent interactions in the case of benzene, and in terms of the large bond polarizability of the C—Cl bond and the relatively large number of such bonds per molecule in the case of the carbon tetrachloride.

That benzene in particular, and aromatic solvents in general, interact with the 1,2-dichloroethane molecule is well known. Thus, Chitoku and Higasi (1) concluded from their work on the dielectric relaxation of 1,2-dichloroethane in

TABLE III
Comparison of dielectric, τ_D, and magnetic, τ_r, relaxation times of 1,2-dichloroethane in different solvents

Solvent	τ_r (ps)	τ_D (ps)	η (cP)
Benzene	3.43	3.69	0.652
Carbon disulfide	1.57	—	0.367
Hexane	—	1.56*	0.308
Carbon tetrachloride	5.74	2.15	0.965
Cyclohexane	—	2.16	0.965

*Viscosity corrected value.

Can. J. Chem. Downloaded from www.nrcresearchpress.com by 210.87.254.42 on 09/05/12
For personal use only.

benzene, *p*-xylene, and other nonpolar solvents, that the *gauche* conformer of 1,2-dichloroethane forms a 1:1 complex with aromatic solvents. There are also a number of infrared studies (15) and dipole moment studies (1) which support this conclusion, viz., that aromatic solvents do interact preferentially with the 1,2-dichloroethane molecule. Our results, obtained by yet another method, are in general agreement with these conclusions.

In the case of carbon tetrachloride it is not too difficult to imagine that the extra hindrance to molecular reorientation of the 1,2-dichloroethane molecule arises from dipole – induced-dipole type of interaction, or, in general, as the result of the polarizability of the C—Cl bond. From nuclear magnetic resonance work on chemical shifts of different haloethanes and other molecules in different solvents, including CCl_4, it is known that CCl_4 is far from being an inert solvent. Thus McClellan and Nicksic (16), who investigated the chemical shift of a large number of haloethanes in CCl_4, conclude that these molecules i.e., the haloethanes, exhibit not only self-association, but that they also form loose complexes with the CCl_4 by perhaps forming hydrogen bonds between the chlorine atoms of the CCl_4 and the protons of the haloethane molecules. Our results support both of these conclusions. For we do find that both the molecular reorientation time and $\Delta\Delta G^{\ddagger}$ are exceptionally large when deuterated 1,2-dichloroethane is used as the solvent, and that in the case of CCl_4 both of these quantities are significantly larger than is the case for CS_2.

In conclusion, it is interesting to note that our values for the molecular reorientation time in benzene and carbon disulfide are in fair agreement with those reported by Chitoku and Higasi (1) which they derived from dielectric relaxation studies, viz., 3.43×10^{-12} s and 3.69×10^{-12} s, respectively, for benzene and 1.57×10^{-12} s and 1.56×10^{-12} s, respectively, for carbon disulfide, where the last quoted value represents the "viscosity corrected" value of Chitoku and Higasi in *n*-hexane solution. The close agreement between our values and those obtained by dielectric relaxation methods suggests that the intramolecular nuclear magnetic relaxation mechanism is dominated by the dipole–dipole relaxation mechanism and that other mechanisms such as spin–rotation relaxation mechanisms are of minor importance. Although our values of τ_r for benzene and carbon disulfide are in fair agreement with the dielectric relaxation results of Chitoku and Higasi, it is only proper to also point out that there is no agreement between our value of τ_r in CCl_4 (5.74×10^{-12} s) and their value (2.15×10^{-12} s) in the same solvent. We confess that we are at a loss to explain this discrepancy. Intuitively, one would expect that collisions between CCl_4 and 1,2-dichloroethane molecules, because of the large polarizability of the C—Cl bond, would be much more "sticky" than collisions between a cyclohexane molecule and a 1,2-dichloroethane molecule, and we would therefore expect that the reorientation time of the 1,2-dichloroethane molecule in CCl_4 should be much longer than in cyclohexane. However, Chitoku and Higasi, who measured the dielectric relaxation of 1,2-dichloroethane molecule in both solvents, found almost identical reorientation times, viz., 2.15×10^{-12} s in CCl_4 and 2.16×10^{-12} s in cyclohexane.

Acknowledgments

We thank Dr. T. Schaefer for helpful discussions. We also gratefully acknowledge the financial assistance of the National Research Council of Canada.

1. K. Chitoku and K. Higasi. Bull. Chem. Soc. Jap. **40**, 733 (1967).
2. H. Muller. Phys. Z. **34**, 689 (1933).
3. M. Kubo. Bull. Inst. Phys. Chem. Res. Tokyo, **13**, 1221 (1934).
4. A. Neckel and H. Volk. Z. Elektrochem. **62**, 1104 (1958).
5. S. Linder. J. Chem. Phys. **26**, 900 (1957).
6. E. Bock and E. Tomchuk. Can. J. Chem. **47**, 2301 (1969).
7. E. Bock. Can. J. Chem. **45**, 2761 (1967).
8. A. Laukien. Handbuch der Physik. Vol. XXXVIII. Springer-Verlag, Berlin. 1958. p. 20.
9. E. Bock and E. Tomchuk. Can. J. Chem. **47**, 2167 (1969).
10. J. G. Powles. Ber. Bunsenges, Phys. Chem., **67**, 328 (1963).
11. E. V. Goldammer and M. D. Zeidler, Ber. Bunsenges. Phys. Chem. **73**, 4 (1969).
12. Tables of interatomic distances and configuration in molecules and ions. Special Publication No. 11. The Chemical Society, London. 1958.
13. P. Debye. Polar molecules. Dover Publications, Inc., New York. 1948.
14. E. Fischer. Phys. Z. 645 (1939).
15. A. Wada and Y. Morino. J. Chem. Phys. **22**, 1276 (1954).
16. A. L. McClellan and S. W. Nicksic. J. Phys. Chem. **69**, 446 (1965).

Can. J. Chem. Downloaded from www.nrcresearchpress.com by 210.87.254.42 on 09/05/12
For personal use only.

Salting-in and salting-out of polar nonelectrolytes

J. E. DESNOYERS AND F. M. ICHHAPORIA
Département de Chimie, Université de Sherbrooke, Sherbrooke, Québec
Received July 14, 1969

The solubility of toluene and benzaldehyde was measured in NaBr and $(n\text{-Pr})_4$NBr aqueous solutions at 25 °C, and the solubility of benzoic acid and nitrobenzene was measured in the same systems at 10, 25, and 40 °C. The apparent molal volumes of the four nonelectrolytes were also determined from the densities of the saturated aqueous solutions.

The volumes of mixing of the nonelectrolytes in water are all negative but become less so as their polarity increases. With the exception of benzoic acid, the salting-out by NaBr and the salting-in by $(n\text{-Pr})_4$NBr both decrease with increasing polarity of the nonelectrolytes. Both salting effects increase with temperature. These trends can be explained with existing theories of salting-out and salting-in.

Canadian Journal of Chemistry, 47, 4639 (1969)

Can. J. Chem. Downloaded from www.nrcresearchpress.com by 210.87.254.105 on 09/05/12
For personal use only.

Introduction

In previous studies (1, 2) on the solubility of nonelectrolytes in salt solutions, the influence of ionic hydration and size of the nonelectrolytes were investigated; it was suggested that the salting-out effect was primarily electrostatic in nature, while salting-in by hydrophobic ions was caused mainly by structural hydration attractive forces. More recent work (3–5) on structural interaction in aqueous electrolyte solutions has shown that solvent-induced attractive forces exist between two hydrophobic solutes and repulsive forces between an hydrophobic solute and an hydrophilic one. Consequently, it is most probable that structural interactions are also involved in the salting-out of nonelectrolytes by hydrophilic salts.

Most of the recent studies on the salting effects have been restricted to nonpolar nonelectrolytes. Apart from the compilations of Long and McDevit (6), few correlations between the salting effects and the polarity of the nonelectrolyte have been attempted, especially in the case of hydrophobic salts. In order to establish meaningful relations, it is important that the polar nonelectrolytes be similar in nature and size and have low solubilities (to minimize self-interactions (6)). The four benzene derivatives, i.e., toluene, benzoic acid, benzaldehyde, and nitrobenzene, should fulfil these conditions. As typical hydrophilic and hydrophobic salts, sodium bromide and tetrapropylammonium bromide were chosen. The temperature dependence of the salting constants were also determined in two cases (nitrobenzene and benzoic acid).

To determine the effective size of the nonelectrolytes in solution, their apparent molal volumes were measured from the density of the saturated solutions.

Experimental

Tetrapropylammonium bromide, sodium bromide, and benzoic acid were of Baker Analyzed Reagent Grade and were used as such after drying under vacuum for 24 h. The nonelectrolytes, nitrobenzene, benzaldehyde, and toluene, were all redistilled, and the fractions collected were those boiling respectively at 210.8 (nitrobenzene), 178.1 (benzaldehyde), and 110.6 °C (toluene).

The salt solutions were saturated with the nonelectrolytes at 25 °C by vigorously agitating them with an excess of nonelectrolyte for 20 h in a constant temperature bath maintained at 25.0 ± 0.1 °C. After equilibrium had been reached, the agitation was stopped and the saturated solutions were left in the bath for another 4 h to attain complete phase separation of the excess nonelectrolyte. Aliquots of the saturated solution were then pipetted out and diluted 1:1, care being taken to submerge the tip of the pipette below the surface of the water to minimize liquid surface exposure. In the case of the saturated solution of benzoic acid, the excess acid was removed by filtration in a specially designed closed system immersed in the bath.

Refractive index measurements using a Waters Model R-4 Laboratory Differential Refractometer were carried out to determine the concentration of the various saturated solutions. Salt solutions of the same concentration as those containing the nonelectrolytes were used in the reference cell, and the rate of flow through both cells was maintained constant. The salting-out by NaCl and the salting-in by $(n\text{-Pr})_4$NBr of benzene were carried out as a check of the technique and the salting-out constant for NaCl and the salting-in constant for $(n\text{-Pr})_4$NBr were, within experimental error, identical with those obtained earlier by an ultraviolet absorption method (2).

The solubilities of the nonelectrolytes in water at 25 °C were determined by extrapolation from a plot of changes of refractive index as a function of known concentration of the solution. From this method, the solubilities obtained at 25 °C are: 0.0588 (toluene), 0.192 (nitrobenzene), 0.757 (benzaldehyde), and 0.337 g/100 ml of water (benzoic acid). As a check of the solubility of benzoic acid, the saturated solution was titrated against standardized

TABLE I

Solubility ratio S/S_0 of benzene derivatives

		S/S_0							
			φCOOH				φNO$_2$		
Salt	c moles l^{-1}	φCH$_3$ 25 °C	10 °C	25 °C	40 °C	φCHO 25 °C	10 °C	25 °C	40 °C
NaBr	0.2	0.942	0.944	—	—	—	—	0.960	0.946
	0.4	—	—	0.889	0.863	0.902	0.921	0.912	—
	0.6	0.849	0.839	0.830	0.810	0.862	0.880	0.863	0.841
	0.8	0.806	0.794	0.778	0.755	0.817	0.846	0.825	0.797
(n-Pr)$_4$NBr	0.2	—	1.331	—	—	—	—	—	1.159
	0.3	1.511	1.510	1.606	1.662	1.259	1.162	1.219	1.254
	0.4	1.684	1.744	1.820	2.004	1.380	1.193	1.288	—
	0.5	1.907	—	2.094	2.301	1.483	1.260	1.372	1.429

NaOH solution. The value (0.331 g/100 ml) agrees satisfactorily with that obtained from the refractive index. The probable error in the determination of solubilities is of the order of 1 to 2%. In all the measurements water was redistilled from an alkaline permanganate solution using an all-glass still and was equilibrated with atmospheric CO_2.

The densities of the saturated solutions, containing a slight excess of nonelectrolyte, were determined with a densimeter (3). Although this technique is in principle capable of high precision ($\pm$ 2 × 10^{-6}g ml^{-1}), the accuracy of the derived apparent molal volume ϕ_v is limited by the uncertainty in the solubility concentration and by the rate of evaporation of the volatile nonelectrolytes. The uncertainty in ϕ_v is probably of the order of $\pm$ 0.05 ml mole^{-1}.

Results and Discussion

The influence of the salt concentration c on the solubility ratio S/S_0 can be expressed at low salt concentration by the relation

$$[1] \qquad \ln S/S_0 = k_s c$$

As written, a positive value for the salting constant k_s indicates salting-in and a negative one, salting-out. The solubility ratios of the four nonelectrolytes studied are given in Table I and the derived k_s in Table II along with the molar and apparent molal volumes and the solubilities of the nonelectrolytes. The molar volume of benzoic acid in the liquid state is not known. The apparent molal volume of benzoic acid was therefore determined in nitrobenzene with a pycnometer. This apparent molal volume is, inside experimental error, independent of concentration and may therefore be taken as the molar volume of "liquid benzoic acid" at 25 °C.

As expected, the volume of mixing, $\Delta V = \bar{V}_{NE} - V$ are all negative and become less so as the polarity of the nonelectrolyte increases. This behavior is consistent with the view that the volume of mixing of nonelectrolytes in water is related to the hydrophobic hydration of the nonelectrolytes (7, 8); as the polarity of the nonelectrolyte increases, the hydrophobic character decreases and so does ΔV.

The salting-out and the salting-in of nonelectrolytes decrease as the dipole moment of the nonelectrolyte increases with the exception of benzoic acid; benzoic acid has the largest salting-out and salting-in constants in spite of the fact that it is much more polar than toluene. The size of the molecules cannot be responsible for this apparent anomaly since all four nonelectrolytes have very similar partial molal volumes. A more plausible explanation is that benzoic acid ionizes in water and that the benzoate ion is much more soluble than the neutral molecule. Any factor which will influence the ionization constant of benzoic acid will consequently also influence its solubility. The present data would therefore suggest that the ionization of benzoic acid decreases in the presence of NaBr and increases with (n-Pr)$_4$NBr. This conclusion is supported by the work of Lucas (9, 10) who has studied the ionization of weak acids and bases in electrolyte solutions and has observed similar trends.

The variation of the salting-out constant ($k_{so} = -k_s$) of the three aprotic nonelectrolytes with their dipole moment is in the order predicted by most electrostatic theories. For example, Conway, Desnoyers, and Smith (1) and Desnoyers and Jolicoeur (4) have suggested that the limiting k_{so} should have two contributions. The first term takes into account the removal, by ions, of water

Can. J. Chem. Downloaded from www.nrcresearchpress.com by 210.87.254.105 on 09/05/12
For personal use only.

Can. J. Chem. Downloaded from www.nrcresearchpress.com by 210.87.254.105 on 09/05/12
For personal use only.

TABLE II

Salting-in, salting-out, and volume of mixing of benzene derivatives

Compound	$\mu_0 \times 10^{18}$ e.s.u.	Temperature °C	k_s (NaBr) Exp.*	k_s (NaBr) Calcd.	k_s† $(n\text{-Pr})_4\text{NBr}$	$\phi_v \simeq \bar{V}_{NE}$‡ ml mole^{-1}	V‡ ml mole^{-1}	ΔV ml mole^{-1}	Solubility g/100 ml
ϕCH_3	0.4	25	−0.271	−0.397	1.29	97.71	106.28	−8.57	0.058_8
$\phi COOH$	1.64	10	−0.290		1.37				
		25	−0.310	−0.381	1.52	98.77	104.96	−6.19	0.334
		40	−0.352		1.71				
ϕCHO	2.76	25	−0.253	−0.337	0.77	96.08	101.03	−4.95	0.75_7
ϕNO_2	3.98	10	−0.207		0.47				
		25	−0.238	−0.275	0.64	97.71	102.71	−5.00	0.192
		40	−0.282		0.73				

*Error = ±0.005.
†Error = ±0.01.
‡Error = ±0.05.

Can. J. Chem. Downloaded from www.nrcresearchpress.com by 210.87.254.105 on 09/05/12
For personal use only.

molecules from their solvent role and is proportional to the volume of the hydrated ion, V_h

$$[2] \qquad k_{hyd} = V_h/1000$$

The second term allows for the distribution of nonelectrolytes and solvent molecules beyond the radius r_h of the hydrated ion; the ion will preferentially attract the more polar molecules.

$$[3] \qquad k_{elect} = \frac{(Ze)^2}{2000\varepsilon_0{}^2 kTr_h}\left(\overline{V}_{NE}\varepsilon_0 - \frac{9}{2}P_{NE}\right)$$

where ε_0 is the dielectric constant of water and $\overline{V}_{NE}$ is the partial molal volume of the nonelectrolyte. The total molar polarization P_{NE} of the nonelectrolyte is related to the dipole moment μ_0 of the nonelectrolyte by an approximate form of the Kirkwood–Onsager theory

$$[4] \qquad \frac{9}{2}P_{NE} \simeq \frac{2}{9}\frac{\pi N}{kT}(n^2 + 2)^2\mu_0{}^2$$

where n is the refractive index of the nonelectrolyte.

Using a reasonable value for the hydration number of NaBr, 4.8 (4), the mean parameters V_h and r_h may be estimated (4). Therefore, from the known $\overline{V}_{NE}$ and μ_0 (Table II), the k_s of the four nonelectrolytes may be estimated at 25 °C and are given in Table II. Although the absolute values do not agree too well, the correct trend with increasing polarity is predicted for the aprotic nonelectrolytes. It therefore seems that the salting-out theory of Conway *et al.* (1) can be used as a rough guide for the salting-out of polar nonelectrolytes.

We should bear in mind, however, that the above treatment ignores all structural interactions, and it has been well established (4, 5) that important structural repulsive forces exist between an hydrophobic (nonelectrolyte) and an hydrophilic solute (electrolyte). This structural hydration contribution is in the same direction as the hydrophilic hydration contribution to k_s (eq. [2]), and it is difficult to distinguish between the two. It is suspected, however, that the high specificity of salting-out to the nature of the ions can be to a large extent attributed to structural interactions.

With the exception of benzoic acid, the salting-in of polar nonelectrolytes by $(n\text{-Pr})_4\text{NBr}$ decreases with the polarity of the nonelectrolyte. This supports the suggestion (2) that salting-in is caused by hydrophobic attractive forces. Short-range attractive forces (van der Waals, charge–dipole, etc.) between the large ions and the nonelectrolytes cannot be the main reason for salting-in, since they usually become more important as the polarity of the nonelectrolyte increases; an increasing k_s with polarity would then be expected. On the other hand, if hydrophobic hydration is involved, the order is predicted correctly; a polar nonelectrolyte will increase the structure of water less than the equivalent nonpolar one and structural salting-in will be less.

The thermodynamic functions of transfer from water to electrolyte solutions are often derived from solubility data (6). Since the solubility ratio S/S_0 is equal to f_0/f (the ratio of the activity coefficients of the nonelectrolyte in water and in the electrolyte solutions) the free energy of transfer is given by

$$[5] \qquad \Delta G_t = -RT \ln \frac{f_0}{f} = -RT \ln \frac{S}{S_0} = -RTk_s c$$

Also, from the Gibbs–Helmholtz equation, the heat of transfer is

$$[6] \qquad \Delta H_t = RT^2 \frac{\mathrm{d}k_s c}{\mathrm{d}T}$$

These functions are not true functions of transfer since the nonelectrolytes are at equal activities in both systems, rather than at equal concentrations. Still, they should not differ too significantly and should yield at least the correct order of magnitude and sign. The ΔH_t estimated from the temperature dependence of k_s were found to be

ϕCOOH–NaBr	− 360	cal mole^{-1}
ϕNO_2–NaBr	− 400	cal mole^{-1}
ϕCOOH–$(n\text{-Pr})_4$NBr	+1900	cal mole^{-1}
ϕNO_2–$(n\text{-Pr})_4$NBr	+1500	cal mole^{-1}

The large positive ΔH_t associated with salting-in are typical of hydrophobic interactions. When a nonelectrolyte is dissolved in water, the structure of water is increased and the heat of solution is negative. However, a solution containing hydrophobic ions is already more structured than water,

and less ordering needs to take place during the dissolution of a nonelectrolyte. The heat of solution will therefore be less exothermic than in water and a positive ΔH_t will result.

A similar simple model cannot be used for the interpretation of ΔH_t from water to alkali halide solutions. Direct calorimetric measurements of ΔH_t of ethyl acetate, nitromethane, and acetic acid (11, 12) from water to alkali halide solutions show that ΔH_t can be positive or negative depending on the particular system studied, and it seems that other factors in addition to structural hydration changes contribute to ΔH_t.

Recently, some of the theories of liquids, e.g. the scaled-particle theory (13), the two-structure model of Ben–Naim (14, 15) and Ben–Naim and Egel–Thal (16), have been successfully applied to the solution of simple gases in electrolyte solutions. These theories account for the dependence of the solubility on salt concentration and for the thermodynamic functions of transfer. It would be most useful to test these theories for a large number of combinations of nonelectrolytes (gases, liquids, and solids) and electrolytes. For example, CsCl sometimes salts-in nonelectrolytes (9, 11), while electrostatic theories predict that this electrolyte should always salt-out nonelectrolytes. Careful solubilities and thermodynamic functions of transfer measurements would also be warranted for a larger variety of salts before the nature of the electrolyte–nonelectrolyte interactions can be fully understood.

Acknowledgment

We are grateful to the National Research Council of Canada for financial assistance.

1. B. E. Conway, J. E. Desnoyers, and A. C. Smith. Phil. Trans. Roy. Soc. London, Ser. A, **256**, 389 (1964).
2. J. E. Desnoyers, G. E. Pelletier, and C. Jolicœur. Can. J. Chem. **43**, 3232 (1965).
3. J. E. Desnoyers and M. Arel. Can. J. Chem. **45**, 359 (1967).
4. J. E. Desnoyers and C. Jolicœur. Modern aspects of electrochemistry. Vol. 5. *Edited by* J. O'M. Bockris and B. E. Conway. Plenum Press, New York. 1969. p. 1.
5. J. E. Desnoyers, M. Arel, G. Perron, and C. Jolicœur. J. Phys. Chem. **73**, 3346 (1969).
6. F. A. Long and W. F. McDevit. Chem. Rev. **51**, 119 (1952).
7. F. Franks and D. J. G. Ives. Quart. Rev. London, **20**, 1 (1966).
8. M. E. Friedman and H. A. Scheraga. J. Phys. Chem. **69**, 3795 (1965).
9. M. Lucas. Bull. Soc. Chim. 178 (1966).
10. M. Lucas. Bull. Soc. Chim. 43 (1967).
11. J. H. Stern and A. Hermann. J. Phys. Chem. **71**, 306 (1967); **71**, 309 (1967).
12. J. H. Stern, J. P. Sandstrom, and A. Hermann. J. Phys. Chem. **71**, 3623 (1967).
13. S. K. Shoor and K. E. Gubbins. J. Phys. Chem. **73**, 498 (1969).
14. A. Ben-Naim. J. Phys. Chem. **69**, 1922 (1965); **69**, 3240 (1965); **69**, 3245 (1965).
15. A. Ben-Naim. J. Phys. Chem. **71**, 1137 (1967).
16. A. Ben-Naim and M. Egel-Thal. J. Phys. Chem. **69**, 3250 (1965).

Can. J. Chem. Downloaded from www.nrcresearchpress.com by 210.87.254.105 on 09/05/12
For personal use only.

Can. J. Chem. Downloaded from www.nrcresearchpress.com by 210.87.254.105 on 09/05/12
For personal use only.

Dielectric studies. Part XXV. Methoxy group rotation in anisole and three para-substituted anisoles

D. B. FARMER
The Donnan Laboratories, University of Liverpool, Liverpool, England

AND

S. WALKER
Chemistry Department, Lakehead University, Port Arthur, Ontario

Received June 12, 1969

The dielectric absorption at several microwave frequencies of anisole, *p*-methylanisole, and *p*-bromoanisole in the solvent *p*-xylene, and *p*-dimethoxybenzene in the solvent cyclohexane has been investigated at 4 to 6 temperatures. Anisole, *p*-methylanisole, and *p*-dimethoxybenzene were all found to relax mainly by methoxy group rotation, whereas the relaxation process in *p*-bromoanisole was very largely molecular relaxation. In the literature, considerable divergence exists for the analyses of the dielectric data of anisole and substituted anisoles into contributions from two relaxation times and the magnitude of the weight factors governing each relaxation process. Such divergencies have been explored and justifiable analyses established for these systems where the weight factors governing the relaxation processes are shown to be roughly of the same order as those estimated from group moment data. The weight factor for molecular relaxation in the pure liquid appears considerably greater than that for a dilute solution of it in a non-polar solvent.

Canadian Journal of Chemistry, 47, 4645 (1969)

Introduction

Results of dielectric studies on anisole, trifluoromethoxybenzene, and methoxypentafluorobenzene in the solvent cyclohexane at a single temperature have been reported previously and their significance discussed (1). It was found in all the above molecules that there was a contribution to the total dielectric absorption from methoxy or trifluoromethoxy group rotation. It was decided to carry out a further study of molecules containing methoxy groups, particularly on those where group rotation should be the predominant relaxation process, with a view to obtaining more precise values for group relaxation and to establish these values better by work at a variety of temperatures.

A number of previous studies has been carried out on aromatic methoxy compounds (2–4), and a detailed study of four such compounds is now reported. Serious discrepancies exist amongst different workers with respect to analysis of the anisole data which justify its re-examination. *p*-Methylanisole has been chosen for examination, since group moment calculations suggest it may relax predominantly by methoxy group relaxation which would, of course, lead to more accurate group relaxation parameters. *p*-Dimethoxybenzene presented an interesting case where both the methoxy groups have the possibility of relaxing, while *p*-bromoanisole merits examination since, from assessment from group moments, it would appear to have a large weight factor (C_1) for molecular relaxation, and, hence, analysis of its dielectric data would help to assess the validity of group moment calculation of the C values for these aromatic methoxy compounds.

Experimental

Apparatus

The apparatus and techniques employed have been described previously (5, 6) and the errors assessed (7). The dielectric constant (ε') and loss factor (ε'') were determined by a bridge method at 70.0, 35.11, 23.98, 16.20, 9.313, and 6.700 GHz. The static dielectric constant (ε_0) was measured with a heterodyne beat apparatus at 2 MHz.

Purification of Materials

The commercially available liquids were dried prior to distillation, then distilled using a (30 theoretical plates) spinning band column and a small center fraction collected. *p*-Dimethoxybenzene was recrystallized twice from petroleum ether and then dried. The observed boiling and melting points compared well with literature values, and the compounds were shown to have no detectable impurities by gas–liquid chromatography.

Results

The evaluation of the high frequency dielectric constant (ε_∞), distribution coefficient (α), mean relaxation time (τ_0), discrete relaxation times (τ_1

TABLE I

Dielectric constant and loss data for anisole, *p*-methylanisole, and *p*-bromoanisole in the solvent *p*-xylene and for *p*-dimethoxybenzene in the solvent cyclohexane at specified weight fractions (ω_2)*

Solute	Solvent	Temperature (°C)	Frequency (GHz)	ε'	ε''	ε'_{calcd}	ε''_{calcd}
Anisole ($\omega_2 = 0.09125$)	*p*-Xylene	15	35.11	2.32_4	0.041_4	2.33_0	0.044_9
			23.98	2.34_4	0.055_9	2.35_1	0.054_7
			16.20	2.37_6	0.061_6	2.36_9	0.059_4
			9.313	2.40_6	0.054_1	2.39_7	0.052_8
			6.70	2.42_3	0.042_7	2.41_0	0.045_1
Anisole ($\omega_2 = 0.10531$)	*p*-Xylene	25	35.11	2.32_7	0.055_3	2.32_9	0.056_0
			23.98	2.34_5	0.065_3	2.34_9	0.064_7
			16.20	2.37_3	0.066_2	2.37_4	0.066_0
			9.313	2.40_8	0.055_5	2.40_4	0.055_6
			6.70	2.41_8	0.047_0	2.41_7	0.047_0
Anisole ($\omega_2 = 0.10531$)	*p*-Xylene	40	35.11	2.30_7	0.055_1	2.31_3	0.055_2
			23.98	2.32_4	0.060_4	2.33_4	0.061_2
			16.20	2.35_8	0.060_9	2.35_7	0.059
			9.313	2.38_6	0.045_6	2.38_3	0.046^3
			6.70	2.39_2	0.037_2	2.39_2	0.036^3
Anisole ($\omega_2 = 0.09502$)	*p*-Xylene	50	35.11	2.29_0	0.047_8	2.29_4	0.048_7^7
			23.98	2.31_0	0.052_0	2.31_2	0.051_1
			16.20	2.33_3	0.047_7	2.33_1	0.047_0
			9.313	2.34_8	0.035_9	2.34_9	0.034_5
			6.70	2.35_7	0.025_6	2.35_5	0.026_7
Anisole ($\omega_2 = 0.09125$)	*p*-Xylene	60	35.11	2.27_0	0.045_9	2.27_5	0.046_1
			23.98	2.29_8	0.045_2	2.29_1	0.045_7
			16.20	2.31_2	0.042_1	2.30_6	0.040_2
			9.313	2.32_5	0.030_0	2.32_1	0.028_9
			6.70	2.32_4	0.021_9	2.32_6	0.022_4
p-Methylanisole ($\omega_2 = 0.09835$)	*p*-Xylene	15	70.0	2.30_9	0.027_4	2.31_4	0.027_6
			35.11	2.33_3	0.043_5	2.33_0	0.043_7
			23.98	2.34_6	0.052_3	2.34_6	0.051_2
			16.20	2.36_2	0.052_7	2.36_5	0.054_1
			9.313	2.39_4	0.048_6	2.39_1	0.048_0
p-Methylanisole ($\omega_2 = 0.09216$)	*p*-Xylene	25	70.0	2.29_9	0.025_5	2.29_9	0.024_0
			35.11	2.31_1	0.038_6	2.31_4	0.039_6
			23.98	2.33_0	0.045_3	2.32_8	0.046_6
			16.20	2.34_5	0.050_3	2.34_6	0.048_4
			9.313	2.37_0	0.039_8	2.36_9	0.040_6
p-Methylanisole ($\omega_2 = 0.09216$)	*p*-Xylene	32.5	70.0	2.27_4	0.028_4	2.29_2	0.024_6
			35.11	2.31_1	0.038_4	2.30_8	0.039_8
			23.98	2.32_4	0.043_7	2.32_4	0.045_1
			16.20	2.33_8	0.044_2	2.34_1	0.044_4
			9.313	2.35_6	0.036_1	2.36_1	0.034_3
p-Methylanisole ($\omega_2 = 0.09216$)	*p*-Xylene	40	70.0	2.26_9	0.029_7	2.27_6	0.029_5
			35.11	2.30_6	0.042_5	2.29_7	0.042_9
			23.98	2.31_9	0.045_5	2.31_3	0.044_8
			16.20	2.33_5	0.040_4	2.32_9	0.041_1
			9.313	2.34_1	0.031_8	2.34_5	0.030_0
p-Methylanisole ($\omega_2 = 0.09216$)	*p*-Xylene	50	70.0	2.25_6	0.028_4	2.26_0	0.028_5
			35.11	2.28_1	0.040_9	2.28_0	0.041_1
			23.98	2.30_4	0.042_4	2.29_6	0.042_3
			16.20	2.31_3	0.037_6	2.31_1	0.037_7
			9.313	2.32_4	0.027_1	2.32_5	0.026_4
p-Methylanisole ($\omega_2 = 0.09835$)	*p*-Xylene	60	70.0	2.23_4	0.032_8	2.24_8	0.031_4
			35.11	2.27_6	0.040_5	2.27_1	0.042_4
			23.98	2.28_9	0.041_2	2.28_7	0.041_6
			16.20	2.30_4	0.036_4	2.30_1	0.035_4
			9.313	2.31_0	0.025_1	2.31_2	0.023_9

Can. J. Chem. Downloaded from www.nrcresearchpress.com by 210.87.254.105 on 09/05/12
For personal use only.

TABLE I *(Concluded)*

Solute	Solvent	Temperature (°C)	Frequency (GHz)	ε'	ε''	ε'_{calcd}	ε''_{calcd}
p-Bromoanisole ($\omega_2 = 0.04912$)	*p*-Xylene	15	35.11	2.29_2	0.024_4	2.29_8	0.024_8
			23.98	2.30_5	0.033_6	2.30_3	0.033_3
			16.20	2.31_6	0.042_0	2.31_2	0.043_3
			9.313	2.33_6	0.059_9	2.33_1	0.058_5
			6.70	2.34_6	0.065_9	2.34_8	0.066_7
p-Bromoanisole ($\omega_2 = 0.04970$)	*p*-Xylene	25	35.11	2.28_3	0.025_7	2.28_5	0.026_3
			23.98	2.29_0	0.035_6	2.29_1	0.035_0
			16.20	2.30_4	0.045_0	2.30_0	0.045_3
			9.313	2.32_6	0.060_1	2.32_2	0.060_6
			6.70	2.33_8	0.067_7	2.34_0	0.066_9
p-Bromoanisole ($\omega_2 = 0.04970$)	*p*-Xylene	40	35.11	2.26_5	0.027_9	2.26_0	0.028_7
			23.98	2.26_8	0.038_4	2.26_7	0.038_0
			16.20	2.28_1	0.048_6	2.27_9	0.048_0
			9.313	2.30_3	0.059_4	2.30_3	0.059_6
			6.70	2.32_0	0.062_4	2.32_2	0.062_3
p-Bromoanisole ($\omega_2 = 0.04970$)	*p*-Xylene	50	35.11	2.25_1	0.030_0	2.24_7	0.030_0
			23.98	2.25_8	0.039_6	2.25_5	0.038_6
			16.20	2.27_1	0.047_2	2.26_7	0.047_8
			9.313	2.29_0	0.058_4	2.29_2	0.057_8
			6.70	2.30_5	0.059_0	2.31_1	0.058_5
p-Bromoanisole ($\omega_2 = 0.04912$)	*p*-Xylene	60	35.11	2.23_2	0.029_8	2.22_9	0.030_4
			23.98	2.23_7	0.039_3	2.23_7	0.038_9
			16.20	2.25_0	0.046_8	2.25_0	0.047_2
			9.313	2.27_5	0.055_7	2.27_5	0.054_5
			6.70	2.28_8	0.052_3	2.29_2	0.053_6
p-Dimethoxybenzene ($\omega_2 = 0.05818$)	Cyclohexane	15	70.0	2.06_5	0.028_1	2.07_1	0.027_5
			35.11	2.08_5	0.041_9	2.08_8	0.043_2
			23.98	2.09_3	0.049_9	2.10_4	0.049_2
			16.20	2.12_9	0.049_4	2.12_3	0.049_7
			9.313	2.14_7	0.039_4	2.14_5	0.040_8
p-Dimethoxybenzene ($\omega_2 = 0.06586$)	Cyclohexane	25	70.0	2.05_5	0.033_7	2.06_5	0.032_7
			35.11	2.08_5	0.048_0	2.08_8	0.049_7
			23.98	2.10_2	0.053_4	2.10_6	0.053_6
			16.20	2.13_3	0.050_4	2.12_6	0.050_6
			9.313	2.14_8	0.039_6	2.14_7	0.037_9
p-Dimethoxybenzene ($\omega_2 = 0.06751$)	Cyclohexane	40	70.0	2.04_1	0.035_6	2.04_6	0.035_5
			35.11	2.07_7	0.049_4	2.07_2	0.050_1
			23.98	2.10_0	0.050_4	2.09_1	0.050_7
			16.20	2.11_8	0.045_4	2.10_9	0.044_4
			9.313	2.12_1	0.031_6	2.12_4	0.030_6
p-Dimethoxybenzene ($\omega_2 = 0.05818$)	Cyclohexane	50	70.0	2.00_7	0.031_9	2.02_0	0.032_0
			35.11	2.05_3	0.040_4	2.04_4	0.041_7
			23.98	2.05_9	0.041_1	2.05_9	0.040_0
			16.20	2.07_8	0.033_1	2.07_2	0.033_4
			9.313	2.08_4	0.022_3	2.08_2	0.022_1

*ε' and ε'' are the measured values, while ε'_{calcd} and ε''_{calcd} are the values estimated from τ_1, τ_2, and C_1 values in Table II.

and τ_2), weight factors (C_1 and C_2), and dipole moment (μ) has been described previously (6).

The dielectric constant and loss data are presented in Table I. The experimental values of ε' and ε'' are compared with those calculated from the Budó equations (7, 8) using the τ_1, τ_2, and C_1 values given by computer analysis. These values are listed in Table II, together with the mean relaxation time, weight fraction, dipole moment, static and high frequency dielectric constant, and distribution coefficient.

Discussion

Studies of the dielectric absorption of anisole have all indicated that the observed mean relaxation time is too short to be attributed solely to a

Can. J. Chem. Downloaded from www.nrcresearchpress.com by 210.87.254.105 on 09/05/12
For personal use only.

TABLE II

Relaxation times (in ps), distribution parameter (α), static dielectric constant (ε_0), dielectric constant at very high frequency (ε_∞), and dipole moment (μ) for solutions of weight fraction ω_2 at temperature t (°C) for molecules containing methoxy groups

t (°C)	ω_2	τ_0	τ_1	τ_2	C_1	α	ε_0	ε_∞	μ (D)
				Anisole/p-xylene					
15	0.09125	10.8	(79)*	9.6	0.15	0.04	2.4439	2.31_0	1.19
25	0.10531	9.0	(40)*	8.0	0.15	0.03	2.4445	2.29_8	1.19
40	0.10531	7.7	14	6.8	0.15	0.01	2.4047	2.27_8	1.15
50	0.09502	6.7	11	5.8	0.15	0	2.3629	2.25_8	1.13
60	0.09125	5.8	12	4.9	0.15	0	2.3321	2.23_4	1.14
15	0.09125	10.8	$13._3$	9.1	0.33				
25	0.10531	9.0	$14._6$	7.0	0.33				
40	0.10531	7.7	$11._4$	5.9	0.33				
50	0.09502	6.7	$9._6$	5.1	0.33				
60	0.09125	5.8	$9._2$	4.3	0.33				
				p-Methylanisole/p-xylene					
15	0.09835	9.7				0.03	2.4246	2.31_1	1.20
25	0.09216	9.0				0.02	2.3924	2.29_2	1.19
32.5	0.09216	7.8				0	2.3762	2.28_5	1.16
40	0.09216	6.3				0.02	2.3569	2.26_4	1.19
50	0.09216	5.9				0	2.3341	2.24_9	1.17
60	0.09835	5.2				0	2.3196	2.23_4	1.16
				p-Bromoanisole/p-xylene					
15	0.04912	32.2	39	$9._1$	0.8_4	0.09	2.4474	2.29_1	2.31
25	0.04970	27.1	31	$7._4$	0.8_8	0.06	2.4235	2.27_7	2.28
40	0.04970	21.9	27	$8._9$	0.7_9	0.06	2.3865	2.25_1	2.28
50	0.04970	19.4	23	$5._7$	0.8_5	0.05	2.3633	2.23_6	2.27
60	0.04912	17.4	21	$6._6$	0.8_0	0.05	2.3362	2.21_7	2.26
				p-Dimethoxybenzene/cyclohexane					
15	0.05818	8.3				0.04	2.1683	2.06_1	1.69
25	0.06586	6.9				0.04	2.1634	2.04_8	1.69
40	0.06751	5.7				0	2.1345	2.03_2	1.67
50	0.05818	4.9				0	2.0886	2.00_5	1.67

*These values are much too long but are discussed in text.

molecular relaxation process and that there is a contribution to the total dielectric absorption from methoxy group rotation (2, 3, 9). This contribution would appear to be quite large since the τ_0 value in decalin is 10.8×10^{-12} s at 20 °C (2) compared with our interpolated value in *p*-xylene at 20 °C of about 10×10^{-12} s; thus, about a fourfold increment in the macroscopic viscosity in decalin has produced only a slight increment in the observed relaxation time. Furthermore, measurements on anisole in the highly viscous solvent nujol ($\eta = 211$ cP at 20 °C) yielded a mean relaxation time of 19.5×10^{-12} s (2), again indicating that the weight factor for methoxy group rotation predominates, since any appreciable contribution from molecular relaxation would have the effect of considerably lengthening the mean relaxation time.

In order to determine the success of the analysis of dielectric data into group and molecular relaxation times of a molecule, it would be useful to have an accurate assessment of the weight factors calculated from group moment data. For mono-substituted benzene compounds a check on the validity of the data employed in estimating C_1 is obtained by the determination of the weight factor data of para-substituted derivatives of the parent compound, for if C_1 (experimental) is approximately equal to C_1 (calculated) in these compounds, then this would support the initial C_1 calculation, providing the para-substituents chosen do not lead to appreciable mutual conjugation between the 2 substituent positions. Generally, C_1 values in the literature are quoted without any reason being given for the change in C_1 from one compound to a fairly similar compound. In addition, many erroneous results exist which require further explanation. For example, Forest and Smyth (3) find that the C_1 value for anisole in benzene at 20 °C is 0.2, but Klages and

Can. J. Chem. Downloaded from www.nrcresearchpress.com by 210.87.254.105 on 09/05/12
For personal use only.

Can. J. Chem. Downloaded from www.nrcresearchpress.com by 210.87.254.105 on 09/05/12
For personal use only.

Zentek (10) report a C_1 value of 0.8 for anisole in the same solvent at the same temperature. Clearly one of these results must be in considerable error. Further, Grubb and Smyth obtained a value of ~ 0.4 for anisole in Nujol (2), while Vaughan, Roeder, and Provder (11) quoted ~ 0.75 for liquid anisole. An attempt will now be made to justify both the observed relaxation times and C_1 values for anisole, *p*-methylanisole, and *p*-bromoanisole.

C_1 for anisole may be calculated from group moments. The dipole moment of a para-substituted anisole, where the moment of the para-substituent is in a direction parallel to the long axis and away from the ring, may be related to the moments of the mono-substituted compound by the equation

$$\mu_{p\text{-Xanisole}} = [(\mu_{\text{anisole}})^2 + (\mu_{C_6H_5X})^2 + 2\mu_{\text{anisole}} \cdot \mu_{C_6H_5X} \cdot \cos\theta]^{\frac{1}{2}}$$

where θ is the angle formed by the total dipole moment vector of the anisole molecule and that of the chlorobenzene molecule, where the latter moment lies on the long axis. When X = Cl, since the dipole moments of *p*-chloroanisole and chlorobenzene are 2.32 and 1.58 D, respectively (12, 13), and our experimental value for anisole is 1.19 D, then the angle subtended on the long axis towards the ring is 67° 40′, which leads to a C_1 value of 0.15. From the group moment data of Forest and Smyth (3), however, a C_1 value of 0.43 results. Thus there is a fair degree of latitude in the calculated value.

The values of τ_1 and τ_2 obtained from the computer analysis, with C_1 fixed at 0.15, are listed in Table II. With such a small weight factor on the molecular relaxation process, the τ_1 values are fairly inaccurate. However, an analysis for a $C_1 = 0.33$ (see Table II) leads to more satisfactory τ_1 values which are slightly less than to be expected for molecular relaxation of a molecule of this size and shape. From the molecular size, the τ_1 value might be expected to lie between that of bromobenzene and iodobenzene, the values for which are, respectively, 14- and 18 $\times 10^{-12}$ s at 15 °C in *p*-xylene (14). The value of C_1 is within 0.1 of that calculated from the Forest and Smyth group moment data (3). In our experience, C_1 values as obtained from an analysis of dielectric data are rarely accurate to better than ± 0.1. It would seem that for anisole, a C_1 value of 0.3 ± 0.15 would account for both extremes of calculated values and the one obtained from the dielectric data.

p-Methylanisole has been chosen because the methyl group moment is directed into the ring and opposes the resultant fixed component of the moment from the anisole part of the molecule on the long axis so this molecule would be expected to have more internal rotation than anisole, i.e., C_2 should be greater for *p*-methylanisole. Since the mean relaxation times of *p*-methylanisole are shorter than that of anisole at four temperatures and the molecular relaxation time of anisole is considerably shorter than that of *p*-methylanisole, the results bear out this point of view. Calculations based on our group moment data indicate that the intramolecular relaxation predominates and therefore the mean relaxation time tends to that of the group relaxation time τ_2. It is evident from Table II that the mean relaxation times of *p*-methylanisole are not appreciably longer than the group relaxation times of anisole. The observed relaxation time of 9.0 $\times 10^{-12}$ s for *p*-methylanisole in *p*-xylene at 25 °C is to be compared with a molecular relaxation time of 23 $\times 10^{-12}$ s for *p*-bromotoluene (14), a molecule which Courtald models indicate is slightly less in size. That there is a large contribution from group relaxation to the total dielectric absorption in *p*-methylanisole is thus supported by this appreciable difference in the two relaxation times.

For *p*-bromoanisole, group moment calculations give a C_1 value of 0.76, suggesting that this molecule will relax predominantly by molecular rotation. This is borne out by the long mean relaxation time value which is, for example, at 25 °C, $\tau_0 = 27 \times 10^{-12}$ s in *p*-xylene. Analysis of the data in terms of two relaxation times gave an average C_1 value of 0.83, which compares well with the calculated value. The τ_2 values, while not very accurate owing to the small weight factor on this process, are of the same order of magnitude for group rotation in anisole and *p*-methylanisole.

p-Dimethoxybenzene was studied in cyclohexane at four temperatures, and a mean relaxation time of 6.9 $\times 10^{-12}$ s was obtained at 25 °C which compares with a τ_2 value of 6.4 $\times 10^{-12}$ s for anisole in cyclohexane at 25 °C (10). Previous workers have examined *p*-dimethoxybenzene in benzene at 20 °C and obtained values of 9.7 $\times 10^{-12}$ and 6.2 $\times 10^{-12}$ s (3, 4). An excellent log

Can. J. Chem. Downloaded from www.nrcresearchpress.com by 210.87.254.105 on 09/05/12
For personal use only.

τ_0 T vs. $1/T$ plot was obtained from the data in Table II and helped to establish our mean relaxation time values. It would seem likely that group rotation is the predominant relaxation process present in *p*-dimethoxybenzene. *p*-Bromoanisole, a molecule just less in size than *p*-dimethoxybenzene, has a molecular relaxation time of 31×10^{-12} s in *p*-xylene at 25 °C, and hence the observed short relaxation time of *p*-dimethoxybenzene would suggest that group relaxation is the principal one in this compound, as is also borne out by the small or zero α values. For the case where the end groups are freely rotating, Williams (15) has shown that the resultant dipole moment (μ) is related to the group dipole moment (μ_g) and the angle (θ) that they subtend with the long axis of the molecule by the equation $\mu = \sqrt{2}\,\mu_g \sin\theta$. For *p*-dimethoxybenzene, the methoxy group moment is 1.2 D, and θ, derived from the group moment calculations in anisole, is 67° 40′ and therefore, by substitution in the above equation, $\mu = 1.6$ D, which is in good agreement with the observed value of 1.7 D.

In conclusion, it would seem that to obtain convincing analyses of dielectric data into contributions from 2 relaxation times, it is preferable to employ several frequencies (as widely spaced as feasible) and carry out the examination at a few temperatures to establish consistent behavior. Further, it is desirable to examine a variety of molecules with varying C_2 contributions and justify the magnitude of the C_2 values obtained from the analyses by group moment calculations, although establishment of more precise group moments is desirable. For anisole, *p*-methylanisole, and *p*-bromoanisole, the experimental and calculated C_2 values are of a similar order of magnitude, while the linear log τ_0 T vs. $1/T$ plots help to establish the consistency of the dielectric data.

It is difficult to reconcile our C_1 of 0.3 ± 0.15 for anisole in *p*-xylene with that of ~ 0.75 for the pure liquid obtained by Vaughan, Roeder, and Provder (11) and recently confirmed by Garg and Smyth (16). It would seem, however, that the appreciable difference in C_1 value between that for pure liquid anisole and that for a dilute solution of it in a non-polar solvent is genuine and worthy of more detailed study.

Acknowledgment

We wish to thank Mr. B. K. Morgan for invaluable technical assistance.

1. D. B. Farmer, A. Holt, and S. Walker. J. Chem. Phys. **44**, 4116 (1966).
2. E. L. Grubb and C. P. Smyth. J. Amer. Chem. Soc. **83**, 4873 (1961).
3. E. Forest and C. P. Smyth. J. Amer. Chem. Soc. **86**, 3474 (1964).
4. D. M. Roberti and C. P. Smyth. J. Amer. Chem. Soc. **82**, 2106 (1960).
5. W. F. Hassell, M. D. Magee, S. W. Tucker, and S. Walker. Tetrahedron, **20**, 2137 (1964).
6. D. B. Farmer and S. Walker. Tetrahedron, **22**, 111 (1966).
7. M. D. Magee and S. Walker. Trans. Faraday Soc. **62**, 3093 (1966).
8. A. Budó. Phys. Z. **39**, 706 (1938).
9. E. Fischer. Z. Naturforsch. **9a**, 909 (1954).
10. G. Klages and A. Zentek. Z. Naturforsch. **16a**, 1016 (1961).
11. W. E. Vaughan, S. B. W. Roeder, and T. Provder. J. Chem. Phys. **39**, 701 (1963).
12. A. L. McClellan. Tables of experimental dipole moments. W. H. Freeman and Co., San Francisco. 1963.
13. J. W. Smith. Electric dipole moments. Butterworths Scientific Publications Ltd., London. 1955.
14. W. F. Hassell. Ph.D. Thesis, University of Aston, Birmingham, England. 1966.
15. J. W. Williams. Z. Phys. Chem **138**, 75 (1928).
16. S. K. Garg and C. P. Smyth. J. Chem. Phys. **46**, 373 (1967).

Can. J. Chem. Downloaded from www.nrcresearchpress.com by 210.87.254.6 on 09/05/12
For personal use only.

Bromine chloride clathrate gas hydrate[1]

D. N. GLEW AND D. A. HAMES
Exploratory Research Laboratory, Dow Chemical of Canada, Limited, Sarnia, Ontario

Received August 13, 1969

Bromine chloride hydrate, prepared free of excess halogen, has been analyzed directly to give the formula $BrCl \cdot 7.77 \pm 1.58\ H_2O$. The halogen is found to be bromine-rich in the hydrate and bromine-deficient in the aqueous solution at 5 °C. Aqueous solutions in equilibrium with the hydrate between 1 and 15 °C have been analyzed and yield the bromine chloride hydrate enthalpy of fusion 10 450 ± 860 cal/mole which leads to the formula $BrCl \cdot 7.28 \pm 0.60\ H_2O$. It is concluded that bromine chloride forms a normal clathrate-type gas hydrate of formula $BrCl \cdot 7.34\ H_2O$, and that the frequently quoted formula $BrCl \cdot 4\ H_2O$ is wrong.

Canadian Journal of Chemistry, 47, 4651 (1969)

Introduction

The formula of chlorine hydrate is $Cl_2 \cdot 7.27\ H_2O$ (1) and that of bromine hydrate is $Br_2 \cdot 8.4\ H_2O$ (2), whereas an early study of bromine chloride hydrate gives the formula $BrCl \cdot 4H_2O$ (3). It is probable that bromine chloride forms a clathrate hydrate similar to those of chlorine and bromine so that the reported water content of the bromine chloride hydrate appears to be erroneously low. Since the molar volume of bromine chloride is not very different from that of chlorine or bromine we would expect BrCl molecules either to fill the medium sized cavities of the cubic structure Type-I hydrate lattice (4) giving a formula $BrCl \cdot 7.66H_2O$, or to fill the two larger types of cavities in the tetragonal lattice (5) giving the formula $BrCl \cdot 8.6H_2O$.

The use at low temperatures of aqueous bromine chloride or "bromine chloride water" as a brominating agent is limited by the formation of bromine chloride hydrate below 18 °C (3). In this study the maximum bromine chloride concentration attainable in the presence of the hydrate has been measured over the temperature range 1 to 15 °C. In addition, the equilibrium Br/Cl atomic ratio has been determined for both the hydrate and aqueous phases.

Experimental

Materials

Bromine chloride with a Br/Cl atomic ratio 0.9969 was prepared by the weighed addition of 99.99 wt. % liquid chlorine to 99.98 wt. % purified grade bromine, both supplied by The Dow Chemical Company. The bromine chloride was used in liquid form to minimize composition changes. Water was laboratory distilled.

[1]Contribution No. 175.

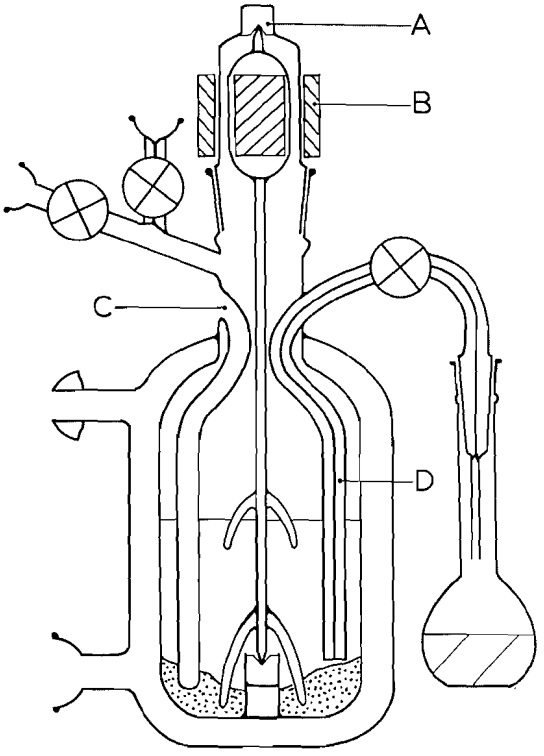

FIG. 1. Magnetic stirred hydrate cell.

Apparatus

The thermostatted cell of about 500 ml volume used for all experiments is shown in Fig. 1. The stirrer, mounted on Teflon bearings A, is driven by a composite copper–steel armature sealed into the glass casing at the upper end of the shaft. The armature is rotated inductively by stator B. Cell temperatures, constant to ±0.01 °C, were maintained by the circulation of thermostatted glycol–water through the outer jacket. The cell temperature was measured differentially with respect to a stainless steel block within the thermostat using a 5-junction copper–constantan thermocouple contained

Can. J. Chem. Downloaded from www.nrcresearchpress.com by 210.87.254.6 on 09/05/12
For personal use only.

in thermowell C. The temperature of the stainless steel block was measured using a standardized platinum resistance thermometer and Mueller bridge.

Method

(a) Hydrate–Solution Equilibration and Analysis

In order to suppress the hydrolysis of aqueous bromine chloride (6), all experiments were carried out in *M*/40 sulfuric acid solutions. Approximately 250 ml of the *M*/40 sulfuric acid were added to the weighed cell, dissolved air was removed by evacuation, and the cell reweighed. The cell was returned to its normal position, liquid from the thermostat at 5 °C was circulated through the cooling jacket, and the cell liquid stirred.

Bromine chloride samples of between 10 and 20 cm^3 were frozen at −80 °C in a small, weighed, evacuated container, and the weighed bromine chloride was added to the cell via the upper 12/2 hemispherical joint.

In the first day, the cell was shaken vigorously 3 or 4 times, the circulating liquid temperature was increased progressively until only a small quantity of the hydrate remained, and this temperature was maintained until all traces of liquid bromine chloride had disappeared. The cell was cooled slowly to between 2 and 3 °C below the operating temperature and maintained there overnight. The cell temperature was then increased to the preselected operating level, and aqueous samples were withdrawn and analyzed for both halogens at regular intervals until equilibrium was obtained.

A small helium pressure differential of 15 Torr above atmospheric, applied to the cell at the lower 12/5 hemispherical joint, was used to express 5–10 ml samples of aqueous bromine chloride via sampling tube *D* into a weighed 50 ml volumetric flask containing 25 ml *M*/5 NaOH. The flask was weighed, 4 ml formic acid added to reduce the halogen to halide ion, and the solution made up to volume and reweighed. Weighed aliquots were titrated potentiometrically for bromide and chloride ions with *M*/10 $AgNO_3$ using a Beckman pH meter with Ag wire indicator and calomel reference electrodes (7). End points were improved by adding 10 drops 1% aqueous Dowfax 9N-40 and approximately 3 mole % 1-propanol. To allow for the systematic effect of the well-known late bromide end point in mixed bromide–chloride titrations (8), the method was standardized using a series of 9 mixtures in which the Br/Cl ionic ratio was varied over the range 0.7 to 1.7. All halogen concentrations are expressed as molality *m*, mole/1000 g water.

(b) Hydrate Formula Determination

After the attainment of equilibrium, the aqueous phase was expressed from the cell via *D*, leaving the drained solid hydrate with some adhering mother liquor. The hydrate was dissolved by the weighed addition to the cell of 250 ml *M*/20 HNO_3 at about 5 °C, and final concentrations of bromine chloride and sulfate ion were determined. The final solution was removed from the cell and weighed. The sulfate ion level was used to calculate the amount of mother liquor adhering to the hydrate, based on the assumption that no sulfate is incorporated into the bromine chloride hydrate lattice. Water in the hydrate was calculated as the total weight of water, minus the weight of water adhering to the hydrate, minus the weight of water from the *M*/20 HNO_3. Bromine chloride in the hydrate was calculated as the total weight of bromine chloride after dissolution of the hydrate, minus the weight of bromine chloride in the solution adhering to the hydrate, allowing for the weight of bromine chloride in the gas phase.

Solutions were analyzed for sulfate ion by the addition of a known excess of *M*/200 $BaCl_2$, filtration of matured barium sulfate precipitate, and back-titration of the excess barium with *M*/100 ethylenediaminetetraacetic acid disodium salt using Eriochrome black T indicator. The EDTA reagent was standardized with known calcium solutions.

Results and Discussion

The hydrate formed initially on the stirrer at the gas–liquid interface, appearing as a finely divided light orange precipitate which gradually changed into a dark red crystalline solid with continuous stirring for 24 h. On the surface of any liquid bromine chloride, a coherent, thin, and impervious hydrate layer formed which entrapped the bromine chloride and inhibited its dissolution into the aqueous phase. To ensure complete dissolution of all liquid bromine chloride the aqueous solution was heated slowly until only few hydrate crystals remained and then was cooled slowly to grow hydrate crystals without reprecipitation of liquid bromine chloride. The cell was cooled just below and then increased to the operating temperature to take advantage of the more rapid approach to equilibrium from subsaturation (9). Without these precautions we were unable to dissolve all of the liquid bromine chloride despite continuous vigorous stirring for 3 weeks. It is apparent that the method of preparation used by Anwar–Ullah (3) will invariably yield a hydrate contaminated by excess liquid bromine chloride and will give a hydrate formula too rich in bromine chloride and deficient in water.

The first 3 columns of Table I show the variation with temperature of the total halogen (bromine plus chlorine) molality, m_2, and the Br/Cl ratio for the aqueous phase in equilibrium with solid bromine chloride hydrate. Columns 4 and 5 show the Br/Cl ratio and the water/halogen mole ratio for the hydrate in equilibrium with the aqueous phase at 5 °C. The final 2 columns show the mass balance for the experiment giving a comparison of the bromine chloride and water as determined by analysis relative to their initial values.

The measurements at 5 °C establish that the

TABLE I

Aqueous solution equilibrium with bromine chloride hydrate

	Solution phase		Hydrate phase		Mass balance	
Temperature (°C)	Halogen molality m_2 (mole/1000 g H_2O)	Br/Cl ratio	Br/Cl ratio	H_2O/halogen ratio	BrCl recovered (%)	H_2O recovered (%)
1.14	0.819	0.87	—	—	—	—
3.08	0.896	0.94	—	—	—	—
5.01	1.071	0.89	1.18	9.99	97.3	99.2
4.98	1.020	0.89	1.21	6.19	96.2	99.2
4.99	1.027	0.92	1.21	9.31	98.5	99.3
4.99	1.044	0.90	1.19	6.81	84.7	97.6
4.98	0.928	0.92	1.24	6.42	98.6	98.5
5.04	0.929	0.95	1.16	7.88	97.9	99.0
9.99	1.311	—	—	—	—	—
15.00	2.073	1.05	—	—	—	—

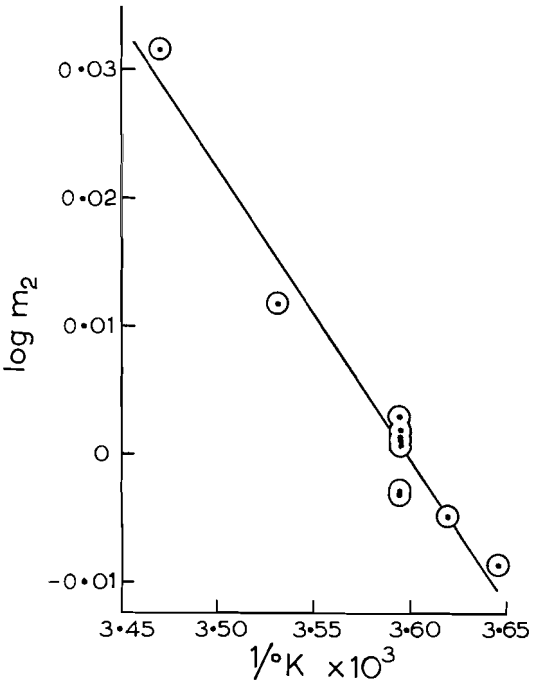

FIG. 2. Temperature dependence of the aqueous bromine chloride molality m_2 in equilibrium with the hydrate.

bromine chloride is bromine-rich in the hydrate phase and is bromine-deficient in the aqueous phase, although all experiments started with liquid bromine chloride having a Br/Cl ratio of 0.9969. The 6 independent direct analyses of the hydrate give the mean formula and standard error $BrCl \cdot 7.77 \pm 1.58\ H_2O$.

In Fig. 2, a plot of log m_2 against the reciprocal of the absolute temperature is presented where the straight line, evaluated by the method of least squares, is given by

$$[1] \qquad \log m_2 = -2284/T + 8.216_4$$

from which the standard error on a single determination is found to be 6.5%. From eq. [1] we find that the standard enthalpy of fusion of solid bromine chloride hydrate to give aqueous bromine chloride is $\Delta H^0(h \rightarrow l_1) = 10\,450 \pm 860$ thermochemical cal/mole. Assuming that the gaseous bromine chloride heat of solution in water $\Delta H^0(g \rightarrow l_1)$ is equal to its heat of reaction with ice to form hydrate $\Delta H^0(s_1 g \rightarrow h)$, as is found for both chlorine and bromine (10), we can obtain a second water/halogen ratio for the bromine chloride hydrate from $\Delta H^0(h \rightarrow l_1)/1436.3$ giving the formula $BrCl \cdot 7.28 \pm 0.60\ H_2O$, in agreement with our value by direct analysis. In conclusion, a weighted mean formula $BrCl \cdot 7.34 H_2O$, with an error of less than $0.60 H_2O$, is obtained from the two independent methods of determination and shows that bromine chloride forms a normal clathrate-type gas hydrate (4, 5).

Acknowledgment

The authors wish to thank Dr. J. F. Mills of The Dow Chemical Company, Midland, Michigan for his assistance in this work.

1. K. W. ALLEN. J. Chem. Soc. 4131 (1959).
2. E. M. J. MULDERS. Ph.D. Thesis, Technical University of Delft, Holland. 1937.

Can. J. Chem. Downloaded from www.nrcresearchpress.com by 210.87.254.6 on 09/05/12
For personal use only.

3. S. ANWAR-ULLAH. J. Chem. Soc. 1176 (1932).
4. L. PAULING and R. E. MARSH. Proc. Nat. Acad. Sci. U.S. **38**, 112 (1952).
5. K. W. ALLEN and G. A. JEFFREY. J. Chem. Phys. **38**, 2304 (1963).
6. N. N. GREENWOOD. *In* Mellor's comprehensive treatise on inorganic and theoretical chemistry. Supplement II, Part 1. Longmans, Green, and Co., Ltd., London. 1956.
7. A. J. MARTIN. Anal. Chem. **30**, 233 (1958).
8. H. A. LAITINEN. Chemical analysis. McGraw-Hill Book Co., Inc., New York. 1960.
9. D. N. GLEW. Can. J. Chem. **38**, 208 (1960).
10. D. N. GLEW. J. Phys. Chem. **66**, 605 (1962).

Can. J. Chem. Downloaded from www.nrcresearchpress.com by 210.87.254.6 on 09/05/12
For personal use only.

Can. J. Chem. Downloaded from www.nrcresearchpress.com by 210.87.254.5 on 09/05/12
For personal use only.

Metal chelates of 2-(2′-thienyl)-8-hydroxyquinoline: anomalous ratios of formation constants

A. CORSINI AND E. J. BILLO[1]

Department of Chemistry, McMaster University, Hamilton, Ontario

Received July 30, 1969

The ligand 2-(2′-thienyl)-8-hydroxyquinoline has been synthesized and the solution stability of some of its metal chelates determined. The finding that $\log K_1 < \log K_2$ is attributed to strong steric interaction between the 2-substituent and coordinated water on addition of the first ligand. This interaction results in distortion toward tetrahedral geometry. Previously unexplained data for other 2-substituted 8-hydroxyquinolines have been interpreted in terms of this effect.

Canadian Journal of Chemistry, **47**, 4655 (1969)

Introduction

Successive stepwise formation constants of metal complexes usually decrease in a regular manner with increasing coordination of the metal ion, owing primarily to statistical, electrostatic, and steric effects. These effects have been discussed by Rossotti (1) and Manning (2 and references therein). In some instances, the ratio of successive formation constants, K_n/K_{n+1}, can provide valuable information about the nature of the complex. Large values of the ratio are indicative of changes in the stereochemistry of the metal ion and of π-bonding and steric packing effects (1, 3). Small values (i.e., $K_n \leqslant K_{n+1}$) have been attributed to changes in ground state configuration of the metal ion and steric interactions (1, 4). In the special case of bis complexes of dimethylglyoxime, the small values have been attributed to hydrogen bonding (5, 6).

During a study of new potentially terdentate ligands, 2-(2′-thienyl)-8-hydroxyquinoline (THQ) was prepared. In the present report, the findings obtained with this ligand in its reactions with selected metal ions are summarized. The unusually small values of K_1/K_2 have been explained in terms of steric interactions between coordinated water and the first incoming ligand. Examples from the literature are cited to show that this effect occurs with several ligands containing suitable substituents close to donor atoms.

Experimental

Microanalyses were by Alfred Bernhardt, Elbach über Engelskirchen, West Germany.

2-(2′-Thienyl)-8-hydroxyquinoline

To an ether solution (200 ml) containing 17 g of thiophene, a 1.6 *M* solution (125 ml) of *n*-butyllithium in hexane was added dropwise. An ether solution (200 ml) of 32 g of 8-methoxyquinoline (7) was added over 1 h. The mixture was stirred for 2 h and water (300 ml) was added. The ether layer and ether extracts of the aqueous phase were evaporated, leaving a deep red oil. Oxidation of this oil on boiling (15 min) with nitrobenzene (100 ml) and removal of excess nitrobenzene under reduced pressure yielded 2-(2′-thienyl)-8-methoxyquinoline, b.p. 230 °C/8 mm Hg, which rapidly crystallized on cooling. Yield, 33 g. Recrystallization from ether gave yellow needles, m.p. 110–111 °C.

2-(2′-Thienyl)-8-methoxyquinoline (17.5 g) in 48% HBr (150 ml) was refluxed for 24 h. The hydrobromide of THQ, which crystallized on cooling, was dissolved in warm water. Neutralization yielded 6.0 g of THQ, which formed colorless needles from ethanol, m.p. 71.5–72.0 °C.

Anal. Calcd. for $C_{13}H_9ONS$: C, 68.68; H, 4.00; N, 6.16; S, 14.11. Found: C, 68.97; H, 3.71; N, 6.28; S, 14.35.

The mass spectrum (ionization potential, 80 eV; ionizing current 50 μA) gave the correct molecular weight and the infrared spectrum showed absorption bands in the characteristic regions. The proton nuclear magnetic resonance spectrum (60 Mc, HMDS internal standard, dioxane solvent) showed that substitution occurred in the 2-position. The resonance assigned to the alpha hydrogen in 8-hydroxyquinoline (8) is absent in the spectrum of the thienyl derivative. Also, splitting of the H_A resonance by H_x is absent.

All common laboratory chemicals were of suitable purity for the purpose intended. Reagent-grade dioxane was purified as described elsewhere (9). Stock solutions (0.01 *M*) of metal ions were prepared from the perchlorate salts and standardized by accepted EDTA methods. For qualitative tests with metal ions, an ethanolic solution of THQ (0.1%) was used. Standard solutions of THQ in dioxane were used for potentiometric titrations.

In screening tests with 29 metal ions, 11 ions reacted with THQ in borate buffer (pH 10), and only 5 (Cu(II), Hg(II), Pd(II), Fe(III), Rh(III)) reacted in acetate buffer (pH 5). THQ is much more selective than 8-hydroxyquinoline and merits consideration as an analytical reagent.

Solid metal chelates were prepared by addition of an excess of THQ (in dioxane) to an aqueous solution of the metal ion, and dropwise addition of NaOH solution until

[1]Present address: Department of Chemistry, Boston College, Chestnut Hill, Massachusetts 02167.

TABLE I

Formation constants of proton and metal-ion complexes of 2-(2′-thienyl)-8-hydroxyquinoline in 50% v/v dioxane–water at 25 °C, $\mu = 0.1$

Ion	$\log K_1$	$\log K_2$	$\log \beta_2$
H^+	$\log K_{OH} = 11.66 \pm 0.01$*	$\log K_{NH} = 1.48 \pm 0.03$†	
Co(II)	5.83 ± 0.01	7.08 ± 0.03	12.91 ± 0.01
Ni(II)	5.94 ± 0.01	6.77 ± 0.03	12.70 ± 0.01
Cu(II)	8.84 ± 0.01	11.01 ± 0.06	19.85 ± 0.01
Zn(II)	6.61 ± 0.02	8.38 ± 0.02	14.99 ± 0.01
Cd(II)	6.15 ± 0.02	7.03 ± 0.03	13.19 ± 0.01

*The limits are standard deviations.
†Determined spectrophotometrically.

precipitation occurred. The chelates were digested for 1–2 h, washed with 20% v/v dioxane–water and dried overnight at 60 °C in vacuo.

Anal. Calcd. for $Co(C_{13}H_8ONS)_2$: C, 61.05; H, 3.15; N, 5.47; S, 12.53. Found: C, 62.59; H, 3.60; N, 5.39; S, 11.90.

Anal. Calcd. for $Ni(C_{13}H_8ONS)_2$: C, 61.09; H, 3.15; N, 5.48; S, 12.54. Found: C, 60.84; H, 3.31; N, 5.59; S, 12.33.

Anal. Calcd. for $Cu(C_{13}H_8ONS)_2$: C, 60.51; H, 3.11; N, 5.43; S, 12.42. Found: C, 62.10; H, 3.24; N, 5.20; S, 11.65.

Anal. Calcd. for $Zn(C_{13}H_8ONS)_2$: C, 60.30; H, 3.11; N, 5.41; S, 12.38. Found: C, 61.08; H, 3.22; N, 5.18; S, 11.94.

The magnetic susceptibilities of the Ni(II) and Co(II) complexes were determined at room temperature by the Guoy method. $Hg[Co(CNS)_4]$ was used as a standard. The molar susceptibilities were corrected for diamagnetism of the ligands using Pascal's constants (10). For the Ni(II) and Co(II) complexes, U_{eff} was 3.21 and 4.50 B.M., respectively.

Absorption spectra of the Ni(II) and Co(II) complexes (in 50% v/v dioxane–water) were taken in the range 250–750 mμ, with a Cary Model 14 spectrophotometer.

All equilibrium measurements were made in 50% v/v dioxane–water at 25 °C and $\mu = 0.10$ ($NaClO_4$). Ligand protonation constants (Table I) were determined potentiometrically and spectrophotometrically (Hitachi Perkin–Elmer 139 spectrophotometer) using the equations

$$\log K_{OH} = p_cH + \log \frac{\bar{n}_H}{1 - \bar{n}_H}$$

and

$$\log K_{NH} = p_cH + \log \frac{A_{HL} - A}{A - A_{H_2L^+}}$$

Chelate formation constants (Table I) were determined potentiometrically essentially as described elsewhere (9). The general equations of Hearon and Gilbert (11) were used for calculation of $\bar{n}$, [L] data. The stepwise formation constants were calculated from this data by a linear least-squares fit of the equation

$$\frac{\bar{n}}{(1 - \bar{n})[L]} = \frac{(2 - \bar{n})[L]}{(1 - \bar{n})} \cdot K_1K_2 + K_1$$

to the $\bar{n}$, [L] data, where values of $\bar{n}$ used were restricted to the ranges 0.2–0.8 and 1.2–1.8.

For all titrations, a ligand-to-metal molar ratio of 6:1 was used. The pH range of complex formation was 4–5 for Cu(II) and 6–7 for the other metal ions. Because of the possibility of metal-ion hydrolysis, which would lead to erroneous results, the titrations were repeated at a molar ratio of 20:1. No significant change in the formation constants was obtained, showing that hydrolysis was not an interfering factor.

For potentiometric measurements, the correction factor for converting pH-meter readings to $-\log [H^+]$ in the solvent medium used was -0.08 ± 0.01; p_cK_w was 15.33 ± 0.02. These values are in close agreement with previously reported values (12, 13).

Results and Discussion

The second protonation constant, $\log K_{NH}$, of THQ is considerably lower than the corresponding constant for 8-hydroxyquinoline (Tables I and II). The large decrease (2.7 log units) is the result of sterically inhibited solvation of the protonated nitrogen by the thiophene ring. Comparable decreases in basicity have been observed for 2-phenyl-8-hydroxyquinoline (17) and 2-(*o*-hydroxyphenyl)quinoline (15).

Two features of the chelate formation constants are of interest. First, the overall formation constants, $\log \beta_2$, are 3 to 7 units smaller than the formation constants of the corresponding 8-hydroxyquinoline chelates, and 1.8 to 2.5 log units smaller than those of the similar ligand, 2-phenyl-8-hydroxyquinoline (Tables I and II). This lower stability is due partly to differences in basicity in donor atoms, and partly to steric interference to coordination by the thiophene group[2]. The latter effect is well illustrated by molecular models. Failure of the sulfur atom to coordinate is not surprising since the thienyl

[2]The enhanced selectivity of THQ is due to these basicity and steric effects.

Can. J. Chem. Downloaded from www.nrcresearchpress.com by 210.87.254.5 on 09/05/12
For personal use only.

TABLE II

Formation constants of some 2-substituted 8-hydroxyquinoline chelates in 50% v/v dioxane–water, at 25 °C, $\mu \leq 0.1$

2-Substituent	H^+		Ni(II)		Cu(II)		Zn(II)		Cd(II)	
	log K_{OH}	log K_{NH}	log K_1	log K_2	log K_1	log K_2	log K_1	log K_2	log K_1	log K_2
—H	11.20*	4.16*	10.50*	9.77	13.29*	12.61	9.45*	8.70	9.43*	7.68
$-CH_3$	11.83†	4.63	9.35†	8.91	12.43†	12.46	9.89†	9.22	9.18†	8.21
$-C_2H_5$	11.86†	4.47	8.69†	9.05	12.05†	11.28	9.66†	9.30	8.66†	8.31
—*n*-C_3H_7	11.95†	4.44	9.01†	9.46	12.06†	11.81	8.96†	10.49	8.84†	8.70
—*n*-C_4H_9	12.07†	4.41	9.18†	9.89	12.05†	12.23	9.75†	10.24	9.28†	8.98
$-C_6H_5$	11.87‡	2.07	7.1‡	7.4	10.2‡	12.1	7.8‡	9.7	—	—

*References 14 and 15.
†Reference 16.
‡Reference 17, conditional constants in this reference were corrected by Schroder's procedure (18).

sulfur in 2-(2'-thienyl)pyridine is a very weak donor (19).

Second, for each metal ion, log K_2 > log K_1 (Table I). This unusual feature is also the result of sterically inhibited coordination. Williams *et al.* (20, 21) and Irving and Mellor (4) have observed that in the series 1,10-phenanthroline, 2-methyl- and 2,9-dimethyl-1,10-phenanthroline, the first formation constant for the Cu(II) chelate decreases markedly (despite increasing ligand basicity), while the second formation constant is less sensitive to substitution. In the mono-complex, steric interaction occurs between the methyl substituent(s) and one or more water molecules remaining in the coordination plane of the Cu(II) ion. This interaction causes distortion of the structure of the mono-ligand complex from a square-planar toward a tetrahedral arrangement, in which the interaction is reduced. The distortion results in a decrease in log K_1. Substitution of the second ligand on the distorted structure occurs without any serious decrease in stability. As the degree of steric interaction is increased, the separation between the two formation constants decreases. In the case of the THQ complexes, the steric interaction is very large and the first formation constant is considerably smaller than the second.

The data of Table II, collected from the literature, support this hypothesis. Values of log K_1 and log K_2 are listed for several 2-alkyl-8-hydroxyquinolines and for 2-phenyl-8-hydroxyquinoline. With increasing size of the 2-alkyl substituent, the separation between log K_1 and log K_2 decreases until in most cases, log K_1 < log K_2. The effect is even more pronounced with the 2-phenyl derivative.

Although the difference between log K_1 and log K_2 varies in magnitude with the size of the substituent, it should not be assumed that the effect is the direct result of solely the steric effect. An enthalpy effect arising from a sterically forced change in coordination number must also be considered. If the mono-ligand species is tetrahedral, its formation from the hexa-aquo complex would involve the breaking of 4 M—H_2O bonds, while addition of the second ligand would involve the rupture of only 2 such bonds. The net result would be to cause a separation between the log K_1 and log K_2 values in the direction observed.

Examination of molecular models indicates that the occurrence of negative values of log K_1/K_2 for substituted phenylazo-5-pyrazolones (22–24) may also originate from a steric effect of the type described above. Recently, Snavely *et al.* reported the same steric effect for the similarly substituted 3-pyrazolones (25). It was found that the Ni(II) and Co(II) complexes of meta and para substituted azo-5-pyrazolones are precipitated from aqueous solution as $ML_2(H_2O)_2$, while complexes of the ortho substituted derivatives do not appear to contain water of hydration. In the present work, elemental[3], thermal[4], and infrared analyses indicated that the chelates of Co, Ni, Cu, and Zn with THQ are anhydrous. Formation of non-hydrated, presumably 4-coordinate solid complexes is consistent with a pseudo-tetrahedral configuration in solution.

[3]The elemental analyses, although not particularly good, do suggest on an overall basis the absence of water in the solid complexes.

[4]No loss in weight was observed on drying the complexes at 150 °C. The dihydrates of the bis-8-hydroxyquinoline complexes of Cu(II), Ni(II), Co(II), and Zn(II) lose water at or below this temperature (26).

Can. J. Chem. Downloaded from www.nrcresearchpress.com by 210.87.254.5 on 09/05/12
For personal use only.

Can. J. Chem. Downloaded from www.nrcresearchpress.com by 210.87.254.5 on 09/05/12
For personal use only.

In order to obtain more positive information on the solution structure of the complexes, an attempt was made to determine the magnetic moments of the Ni(II) and Co(II) complexes of THQ in solution; however, the solubility of these complexes in the usual non-polar solvents proved to be too low to yield meaningful results. Accordingly, the (room temperature) magnetic moments of the solids were measured. Since $U_{eff} = 3.21$ B.M. for the Ni(II) complex of THQ, a planar structure for the solid can be eliminated. The magnetic moment is not inconsistent with an octahedral or tetragonal structure, but these structures can be ruled out on the basis of the 2:1 stoichiometry of the isolated compound. The magnetic moment is lower than expected (3.6–4.0 B.M.) for true tetrahedral Ni(II) complexes (27), but Sacconi and co-workers (28, 29) have found that the magnetic moments of Ni(II) complexes in a distorted tetrahedral environment are also lower (e.g., $U_{eff} = 3.34$ B.M. for bis(N-isopropylsalicylaldiminato)nickel(II). For the solid Co(II) complex of THQ, $U_{eff} = 4.50$ B.M. This value is in agreement with the value (4.47) for the bis(N-butylsalicylaldiminato)cobalt(II) complex, which is tetrahedral (30, 31), and is within the range (4.3-4.8 B.M.) observed for tetrahedral Co(II) complexes (27). The value is well above the range (2.4–2.8 B.M.) found for square and tetragonal complexes (32). An octahedral structure can be eliminated on the basis of stoichiometry.

Although the magnetic moments indicate a tetrahedral or distorted tetrahedral structure for the solid complexes, they do not necessarily reflect the structure of the species in solution, and in this regard should be interpreted with caution. Unfortunately, no information on the solution structure of the Ni(II) or Co(II) complexes could be obtained from the ultraviolet and visible absorption spectra. The spectra, which were similar, exhibited a very intense band ($\varepsilon \sim 2 \times 10^4$) at 300 mμ, a shoulder ($\varepsilon \sim 5 \times 10^3$) at 340 mμ and a shoulder ($\varepsilon \sim 1 \times 10^3$) at 400 mμ. These bands originate from the bound ligand. The spectra are featureless from about 450 to 750 mμ and provide no evidence to support the solution structure.

Finally, the same steric effect proposed in the present work to explain the values of log K_1/K_2 for the solution complexes of 2-substituted-8-hydroxyquinolines has recently been found in solid complexes. Chia and Livingstone (33) have reported that in the complexes of 2-methyl-8-methylthioquinoline, the 2-methyl group causes severe steric hindrance to other ligands in a square plane; magnetic moments and reflectance spectra indicated pseudo tetrahedral configuration about the metal ion.

Acknowledgments

We wish to thank the National Research Council of Canada for the financial support of this study. The authors are grateful to the referees for their critical comments and helpful suggestions.

1. F. J. C. Rossotti. *In* Modern coordination chemistry. *Edited by* J. Lewis and R. G. Wilkins. Interscience Publishers, Inc., New York. 1960. Chap. 1.
2. P. G. Manning. Can. J. Chem. **44**, 3057 (1966).
3. H. Irving and D. H. Mellor. J. Chem. Soc. 5222 (1962).
4. H. Irving and D. H. Mellor. J. Chem. Soc. 5237 (1962).
5. R. G. Charles and H. Freiser. Anal. Chim. Acta, **11**, 101 (1954).
6. K. Burger and I. Ruff. Talanta, **10**, 329 (1963).
7. F. E. King and J. A. Sherred. J. Chem. Soc. 415, 1942.
8. L. W. Reeves and K. O. Stromme. Can. J. Chem. **39**, 2318 (1961).
9. H. Freiser, R. G. Charles, and W. D. Johnston. J. Amer. Chem. Soc. **74**, 1383 (1952).
10. B. N. Figgis. *In* Modern coordination chemistry. *Edited by* J. Lewis and R. G. Wilkins. Interscience Publishers, Inc., New York. 1960. p. 403.
11. J. Z. Hearon and J. B. Gilbert. J. Amer. Chem. Soc. **77**, 2594 (1955).
12. S. Takamoto, Q. Fernando, and H. Freiser. Anal. Chem. **37**, 1249 (1965).
13. H. M. N. H. Irving and U. S. Mahnot. J. Inorg. Nucl. Chem. **30**, 1215 (1968).
14. R. L. Stevenson and H. Freiser. Anal. Chem. **39**, 1354 (1967).
15. W. D. Johnston and H. Freiser. J. Amer. Chem. Soc. **74**, 5239 (1952).
16. H. Kaneko and K. Ueno. Bull. Chem. Soc. Jap. **39**, 1910 (1966).
17. W. D. Johnston and H. Freiser. Anal. Chim. Acta, **11**, 201 (1954).
18. K. H. Schroder. Acta Chem. Scand. **20**, 1401 (1966).
19. K. Kahmann, H. Sigel, and E. Erlenmeyer. Helv. Chim. Acta, **47**, 1754 (1964).
20. B. R. James and R. J. P. Williams. J. Chem. Soc. 2007 (1961).
21. B. R. James, M. Parris, and R. J. P. Williams. J. Chem. Soc. 4630 (1961).
22. F. A. Snavely, W. C. Fernelius, and B. P. Block. J. Amer. Chem. Soc. **79**, 1028 (1957).
23. F. A. Snavely, B. D. Krecker, and C. G. Clark. J. Amer. Chem. Soc. **81**, 2337 (1959).
24. F. A. Snavely and B. D. Krecker. J. Amer. Chem. Soc. **81**, 4199 (1959).
25. F. A. Snavely, D. A. Sweigart, C. H. Yoder, and A. Terzis. Inorg. Chem. **6**, 1831 (1967).
26. M. Borrel and R. Paris. Anal. Chim. Acta, **4**, 267 (1950).

27. N. S. GILL and R. S. NYHOLM. J. Chem. Soc. 3997 (1959).
28. L. SACCONI, M. CIAMPOLINI, and U. CAMPIGLI. Inorg. Chem. **4**, 407 (1965).
29. M. R. FOX, P. L. ORIOLI, E. C. LINGAFELTER, and L. SACCONI. Acta Cryst. **17**, 1159 (1964).
30. L. SACCONI, M. CIAMPOLINI, F. MAGGIO, and F. P. CAVASINO. J. Amer. Chem. Soc. **84**, 3246 (1962).
31. E. FRASSON and C. PANATTONI. Z. Krist. **116**, 154 (1961).
32. F. A. COTTON and G. WILKINSON. Advanced inorganic chemistry. Interscience Publishers, Inc., New York. 1966. pp. 870–73, 882–84.
33. P. S. K. CHIA and S. E. LIVINGSTONE. Aust. J. Chem. **21**, 339 (1968).

Can. J. Chem. Downloaded from www.nrcresearchpress.com by 210.87.254.5 on 09/05/12
For personal use only.

Can. J. Chem. Downloaded from www.nrcresearchpress.com by 210.87.254.5 on 09/05/12
For personal use only.

Adsorption of gases on 4A synthetic zeolite

R. J. HARPER, G. R. STIFEL[1], AND R. B. ANDERSON
Department of Chemical Engineering, McMaster University, Hamilton, Ontario

Received July 30, 1969

Equilibrium data are presented for the adsorption of permanent gases and C_1 and C_2 hydrocarbons on Linde 4A synthetic zeolite from 50 °C down to the boiling point of the adsorbate or to a temperature at which the rate was very slow. The Freundlich equation often fits isotherms accurately; however, these linear logarithmic plots seem to be only portions of a more general non-linear relationship. Generalized Polanyi plots did not yield a unique characteristic curve for individual adsorbates at different temperatures nor for groups of adsorbates; nevertheless, these plots are useful in estimating the relative strength of adsorption of gases. Ar, O_2, CH_4, and C_2H_6 were the least strongly adsorbed, followed in order of increasing strength by N_2, CO, CO_2, and C_2H_2. Ethylene was strongly but anomalously adsorbed. For the gases studied, the quadrupole moment seems to be the principal factor determining strong adsorption.

Canadian Journal of Chemistry, 47, 4661 (1969)

Introduction

Molecular sieves of the aluminosilicate type have been widely studied because of their interesting structural and adsorptive properties and their practical use in separative processes and catalysis. Barrer has made major contributions in studies of natural zeolite minerals, the preparation of new types of molecular sieves, and the structures and adsorption properties of natural and synthetic zeolites; his earlier work has been summarized (1–3). Type A synthetic zeolites have been available commercially since 1954 and have found extensive practical use in separation, drying, and purification of gases. Many papers have described the behavior of these zeolites in separative processes, but detailed adsorption studies of single permanent gases and C_1- and C_2-hydrocarbons have been less comprehensive. The most extensive investigations of this type were made by Breck and co-workers (4–6). Russian workers have investigated adsorption on Type A sieves, notably Dubinin *et al.* (7–10), Kel'tsev and co-workers (11–14), Kiselev and co-workers (15–17), and Kvitkovskii and co-workers (18, 19).

Most of the present data were obtained in a study of rates of adsorption of permanent gases and C_1- and C_2-hydrocarbons on 4A sieves. Equilibrium adsorption data are presented for N_2, O_2, CO, CO_2, Ar, CH_4, C_2H_6, C_2H_4, and C_2H_2 from 50 °C down to about the boiling point of the gases or to temperatures at which the adsorption was so slow that equilibrium required longer than 24 h.

[1]Present address: Uniroyal Research Center, Guelph, Ontario.

Type A zeolite contains approximately spherical cavities of 11.4 Å diameter at the center of each unit cell, each cavity being connected in a cubic arrangement with 6 similar cavities by rings of 8 oxygen atoms forming a restricted opening 4.2 Å in diameter. The 4A sieve studied in the present paper contain sodium as the exchangeable cation. The 8 sodium ions per cavity are located near the apertures and decrease their diameter to about 3.5 Å.

Experimental

A sample of 4A molecular sieve powder was supplied by the Linde Division of Union Carbide. To avoid difficulties in handling this fine powder in evacuation and adsorption measurements, the zeolite was compressed to form an aggregate of sufficient strength for the present purposes by the following procedure: the powder was immersed in water for 1 day, dried in air at 120 °C, and then pressed in a 1-in. die at about 12 000 p.s.i. for 2 or 3 min. The large pellet was then crushed and sieved to yield aggregates varying in size from 1 to 2 mm. The sample was dried in air at 350 °C for 36 h, placed in an adsorption tube and evacuated at 450 °C for 12 h. Adsorption data are given per gram of sample after this treatment. Evacuations at 450 °C for several days yielded the same rate and equilibrium data. At the end of this heating period and at the start of the adsorption experiments, the pressure in the vacuum system was less than 10^{-5} Torr. The same sample of adsorbent was used for a number of adsorption measurements.

Adsorption measurements were made in a Pyrex volumetric system, similar to the Brunauer, Emmett, and Teller apparatus (20) but also equipped with a manostat and a calibrated burette. Dead space in the sample bulb was determined using helium at −196, −118, −98, −78, −37, 0, 30, and 50 °C. Appropriate plots of these data were made assuming a fraction of the volume was at room temperature and the remainder at the temperature of the bath. Deviations from the linear plots, which indicated significant adsorption of helium, were found

TABLE I

Values of Freundlich exponent, n

Temperature (°C)	n								
	O_2	Ar	CH_4	N_2	CO	C_2H_6	C_2H_4	C_2H_2	CO_2
−196	0.010								
−183	0.021								
−160	0.031, 0.14								
−118	0.27, 0.85	0.37							
−101		0.77							
− 78	0.85	0.94	0.15	0.18	0.12			0.033	0.036
− 37	0.91	0.97		0.65	0.20		0.041	0.043	0.090
0	0.95	0.99	0.96	0.87	0.39, 0.67	0.073	0.020	0.091	0.096
30	0.94	0.89	0.95	0.90	0.77	0.18	0.014	0.10	0.10
50	0.93	0.86	0.98						

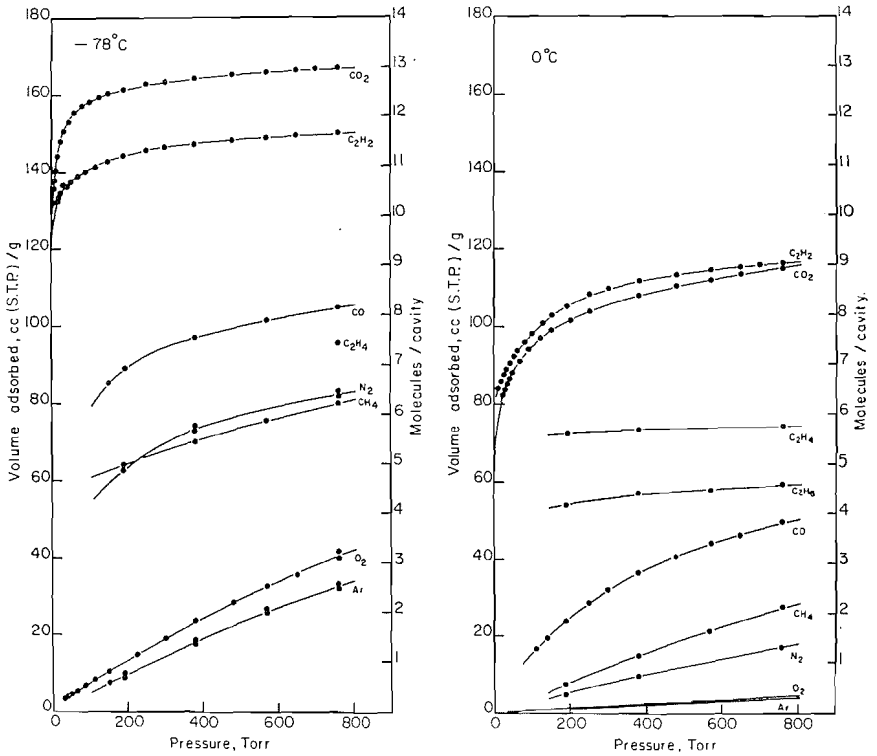

FIG. 1. Adsorption isotherms on 4A molecular sieve at −78 and 0 °C.

only at −196 °C, and the dead space factors at temperatures below −118 °C were obtained by extrapolation. Corrections for non-ideality of adsorbates were made. Adsorption measurements were accurate to about ±0.1 cc. Gases of purity better than 99.8% were obtained from Matheson of Canada, Ltd., and Canadian Liquid Air Co., Ltd. They were condensed or frozen in traps in the adsorption system at −196 °C, evacuated, and subsequently distilled into storage bulbs. Helium was passed through activated carbon at −196 °C.

Temperatures were maintained by liquid baths; those of liquid nitrogen, liquid oxygen, acetone – dry ice with CO_2 bubbled through the mixture, and ice could be maintained at constant temperatures without difficulty. Intermediate temperatures were obtained at the melting points of organic compounds: isopentane, −162 °C; ethanol, −119 °C; methanol, −102 °C; chloroform, −65 °C; ethylene dichloride, −37 °C. The solid phase was maintained by periodically adding liquid nitrogen and stirring. Temperatures were measured by a chromel–alumel thermocouple and could be maintained within ±1 °C of the values quoted above for long periods of time. Temperatures of 30 and 50 °C were maintained with water baths.

Can. J. Chem. Downloaded from www.nrcresearchpress.com by 210.87.254.5 on 09/05/12
For personal use only.

TABLE II
Isosteric heats of adsorption on 4A molecular sieve

Volume adsorbed (cc (S.T.P.)/g)	Isosteric heats (kcal/mole)						
	O_2	Ar	CH_4	N_2	CO	C_2H_2	CO_2
5	3.4	3.6	4.0	5.7	8.0		
10	3.3	3.5	3.9	5.15	7.4		
30	3.1	3.2	3.55	4.2	6.0		
50		2.8	3.35	3.8	5.1		
70		2.4	3.1	3.5	4.3	10.3	
90		2.1	2.8	3.3	3.3	9.35	8.4
110						8.6	8.1
130							8.0
150							7.9

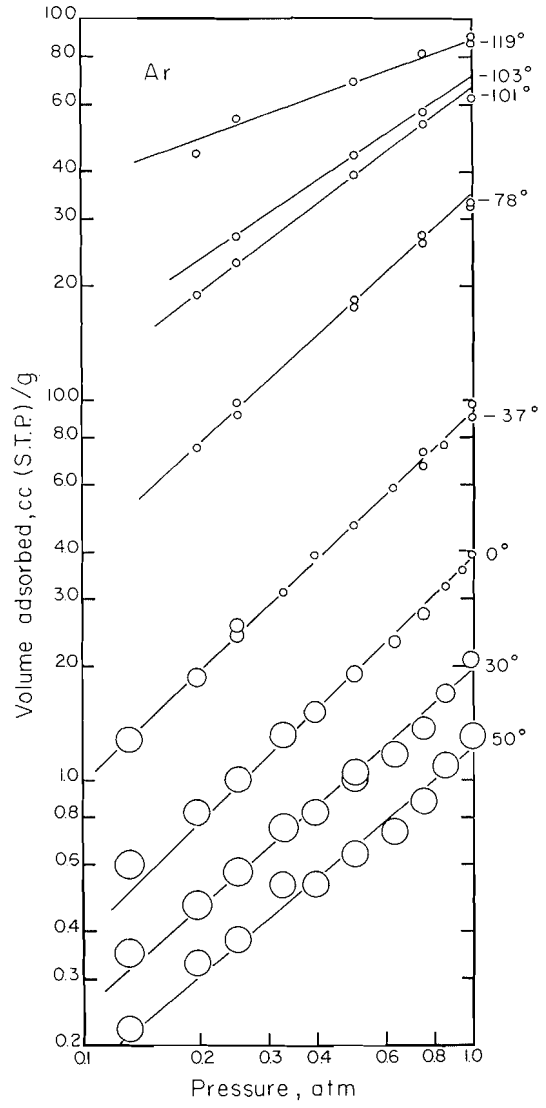

FIG. 2. Logarithmic plots of isotherms for argon on 4A molecular sieve.

Time required for equilibration varied from minutes to 24 or more hours. For argon at −195 °C and 0.2 atm, the apparatus failed after 65 days, when 133 cc (S.T.P.)/g had been adsorbed. In this case only, the equilibrium value, 176 cc (S.T.P.)/g, was estimated by matching this partial rate curve with others for argon at higher temperatures. The leak rate in the adsorption system was zero, except in a few instances when stopcock grease failed, usually because the ambient temperature exceeded 35 °C.

Results

Adsorption isotherms were determined in the following temperature ranges: N_2, −118 to 30 °C; O_2, −196 to 50 °C; CO, −118 to 50 °C; CO_2, −78 to 50 °C; Ar, −196 to 50 °C; CH_4, −78 to 50 °C; C_2H_6, 0 to 50 °C; C_2H_4, −78 to 30 °C; and C_2H_2, −78 to 50 °C. The lowest temperatures were usually determined by either the vapor pressure or slow rate of equilibration. Hysteresis was not observed in any of the isotherms. Isotherms at −78 and 0 °C are presented in Fig. 1. All of the isotherms are plotted logarithmically in Figs. 2, 3, and 4. Many are rather accurately represented by the Freundlich isotherm, $V = kp^n$, where V is amount adsorbed, k and n are constants, and p the pressure of adsorbate. Values for n are given in Table I. Some isotherms could be approximated by 2 linear portions, and in this case both slopes are given.

Isosteric heats of adsorption are presented in Table II. Evaluation of heats of adsorption from isotherms of nearly rectangular shape was difficult and often the experimental data did not extend to low enough pressures; therefore, data are not reported over the entire range of adsorbates, temperatures, and amounts adsorbed. Isobars at 1 atm are presented in Fig. 5, where the amount adsorbed is plotted as the fraction of the pore volume filled by adsorbate. The method of

Can. J. Chem. Downloaded from www.nrcresearchpress.com by 210.87.254.5 on 09/05/12
For personal use only.

Can. J. Chem. Downloaded from www.nrcresearchpress.com by 210.87.254.5 on 09/05/12
For personal use only.

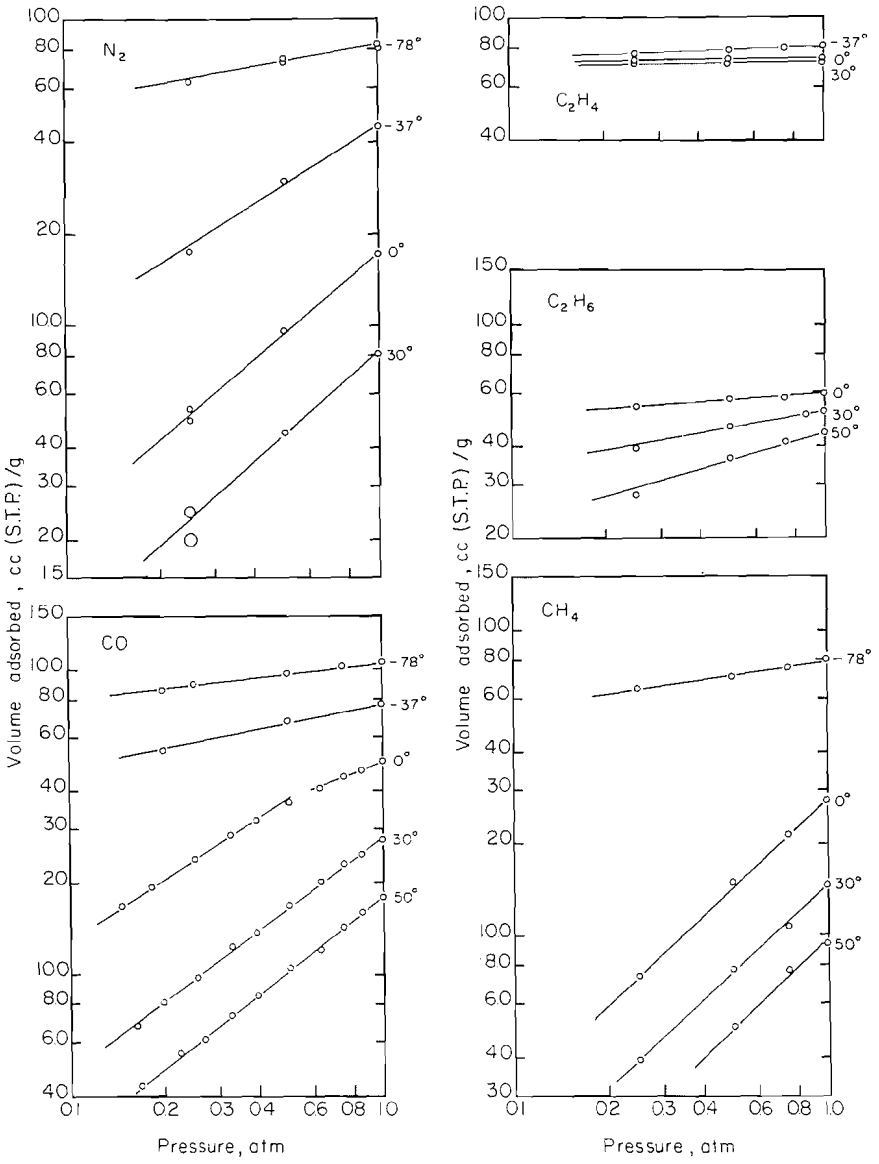

FIG. 3. Logarithmic plots of isotherms for nitrogen, carbon monoxide, methane, ethylene, and ethane on 4A molecular sieve.

estimating pore volume and adsorbate density is described in the next section.

Discussion

The A zeolites are interesting adsorbents because they are crystalline and their structure has been established (4, 5). From the unit cell dimension, 12.32 Å, and the density of the hydrated zeolite, 1.99 g/cm^3, the number of unit cells per gram of dehydrated 4A sieve is calculated as 3.454×10^{20}, close to the value reported by Dubinin (21). Each unit cell contains a large, essentially spherical cavity of 11.4 Å diameter and 776 Å^3 volume. The six passages of 4.2 Å diameter connecting the cavities of adjacent unit cells contribute 38 Å^3 to the accessible volume to yield a total of 814 Å^3. Hence the pore volume is 0.281 cc/g anhydrous 4A zeolite.

Can. J. Chem. Downloaded from www.nrcresearchpress.com by 210.87.254.5 on 09/05/12
For personal use only.

Most of our adsorption data are presented as cc(S.T.P.)/g and molecules per cavity; 100 cc(S.T.P.)/g is equivalent to 7.785 molecules per cavity. In the present work the largest number of molecules per cavity was 15. Other adsorption data are presented as the fraction of the pore volume filled by adsorbate, with the adsorbate assumed to have the density of the liquid at the normal boiling point and to pack in the cavities the same as in the liquid. Of course, neither of these assumptions is correct; however, the "fraction of pore volume filled" provides a useful index for comparing data.

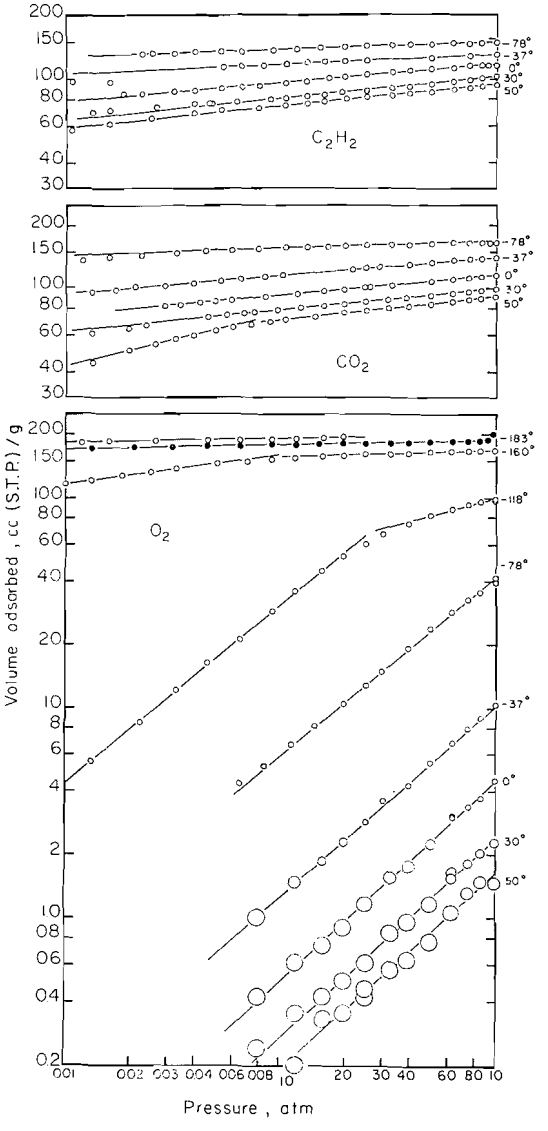

FIG. 4. Logarithmic plots of isotherms for oxygen, carbon dioxide, and acetylene on 4A molecular sieve.

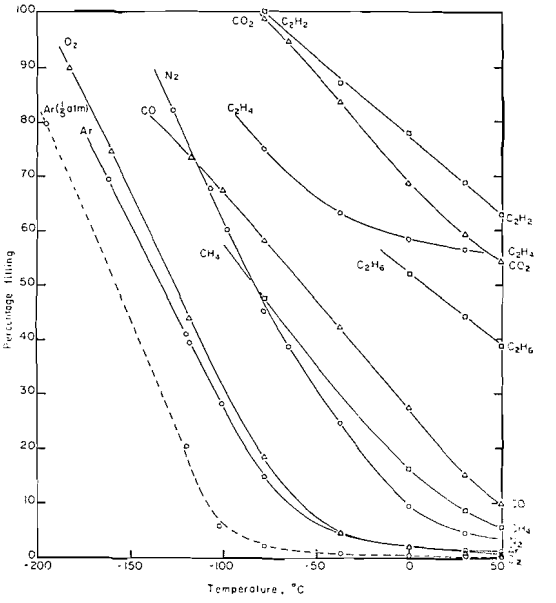

FIG. 5. Adsorption isobars on 4A molecular sieve, where volume adsorbed is expressed as fractional filling of pores assuming the density of adsorbate equals the density of liquid at its normal boiling point. Solid curves for 1 atm; broken curve for 1/5 atm.

All of the isotherms reported in this paper are plotted logarithmically in Figs. 2 to 4, because these plots are frequently linear and because of economy of presentation. Although some isotherms are accurately represented by the Freundlich equation, the linear logarithmic plots often seem to be portions of a sigmoidal curve with a small slope at high pressures and low temperatures, changing to a larger slope at lower pressures or higher temperatures, and in some cases assuming a slightly smaller slope at low pressures or high temperatures. The shape of the Polanyi plots, to be described subsequently, is consistent with this postulate. On linear coordinates, the initial portions of the argon isotherms from 0 to 50 °C are linear but extrapolate to 0.2 cc(S.T.P.)/g at zero pressure; however, above 50 cm Hg these argon isotherms bend upward slightly. All other isotherms seem to extrapolate to the origin. Linear isotherms have been reported for argon and other rare gases on A and X sieves at −78 °C and higher temperatures (22–27), and the Freundlich equation has

Can. J. Chem. Downloaded from www.nrcresearchpress.com by 210.87.254.5 on 09/05/12
For personal use only.

been generally satisfactory for rare gases on molecular sieves (28–30).

Nitrogen and methane isotherms are approximately linear at 0 °C and above, values of n being about 0.90 and 0.95, respectively. However, carbon monoxide isotherms have considerable curvature, even at 50 °C ($n = 0.80$). For the 5A zeolite, Freundlich exponents have been reported to increase from 0.895 to 1.0 as temperature is increased from −78 °C (31). In the present work, methane and nitrogen adsorb in equal amounts at −78 °C, but more methane is adsorbed at 0 °C; however, the adsorption of carbon monoxide exceeds N_2 and CH_4 at all temperatures. On NaX zeolites in the range −120 to −60 °C, more nitrogen was adsorbed than argon and the nitrogen isotherm had more curvature (32). Thus, for gases with boiling points in the range −195 to −161 °C, the adsorption on the 4A sieve does not follow the observations made for activated carbons, where the amount adsorbed at a given temperature and pressure increases with decreasing boiling point of adsorbate.

Gases with boiling points near −78 °C, carbon dioxide, ethane, ethylene, and acetylene, yielded nearly rectangular isotherms with the Freundlich exponent n at 30 °C having values of 0.10, 0.18, 0.014, and 0.10, respectively. This result is not unexpected, because in comparing argon and ethane on a reduced temperature basis, −78 °C for argon corresponds to +121 °C for ethane. Nearly rectangular isotherms have been reported for acetylene on A and X sieves at 0–40 °C (33). In the present work acetylene and CO_2 are adsorbed in the largest amounts in the range −78 to +50 °C, followed by ethylene and ethane. Ethylene adsorption decreases slowly with increasing temperature, the values of n remain small to 30 °C, and rate curves (34) show anomalies. These results suggest that a chemisorption process possibly accompanied by polymerization may occur to an increasing extent with increasing temperature. However, ethylene was quantitatively desorbed at 50 °C and essentially zero pressure (liquid N_2 trap) and mass spectrometric analysis of the desorbed gas showed only ethylene.

For adsorption isobars and generalized Polanyi plots in Figs. 5, 6, and 7, respectively, the amount adsorbed is given as the percentage of the pore space filled assuming that the adsorbate has the density of normal liquid at its boiling point and that packing in the pores is the same as in the liquid. For all of the isobars, the amount adsorbed decreased with increasing temperature, as expected for equilibrium data, and no maxima were observed as has been reported for adsorption for fixed periods of time (35). For gases with appreciable rates of adsorption at temperatures near their boiling points, the percentage filling of pore volume approached 100: argon, 80; oxygen, 90; and carbon dioxide and acetylene, about 100. The isobars for ethylene decreased less rapidly with temperature than expected, and this anomalous behavior has been considered earlier.

Dubinin, *et al.* (9, 10) reported that on CaA and NaX sieves the molar volume of some adsorbates was near the molar volume of the liquid and for others widely different. Barrer and Gibbons (36) found that the sorption, calculated as normal liquid, on synthetic faugasite at saturation pressure corresponded satisfactorily to the volume of the larger cavities. Nevertheless, small strongly adsorbed molecules can apparently penetrate the sodalite cages of some zeolites (37) and this phenomenon may occur to a limited extent in the present work.

A generalized Polanyi equation has been shown to correlate adsorption data on charcoal reasonably well (38–40), and the method of Grant and Manes (40) was applied to the present data on the 4A zeolite. The characteristic curve in terms of volume of adsorbate as a function of the adsorption potentials, ϕ, per unit volume of adsorbate, where

$$\phi = (RT/V) \ln p_0/p$$

is plotted, assuming that the density of adsorbate equals the density of liquid at the boiling point. Here V is the molar volume based on this density, and p is the pressure of adsorbate. The values of vapor pressure, p_0, were estimated from a plot of $\log p_0$ vs. T^{-1}, extrapolated above the critical temperature where necessary (40).

For the 4A zeolite, the generalized Polanyi plots do not yield unique characteristic curves for each adsorbate nor a general curve for all gases, as shown for oxygen and acetylene in Fig. 6. For each gas the curves for different temperatures have the same shape but are displaced. Other estimates of molar volume of adsorbate (38) or no volume correction generally led to no improvement. The plots for C_2H_2 lie significantly to the right of those for O_2.

Can. J. Chem. Downloaded from www.nrcresearchpress.com by 210.87.254.5 on 09/05/12
For personal use only.

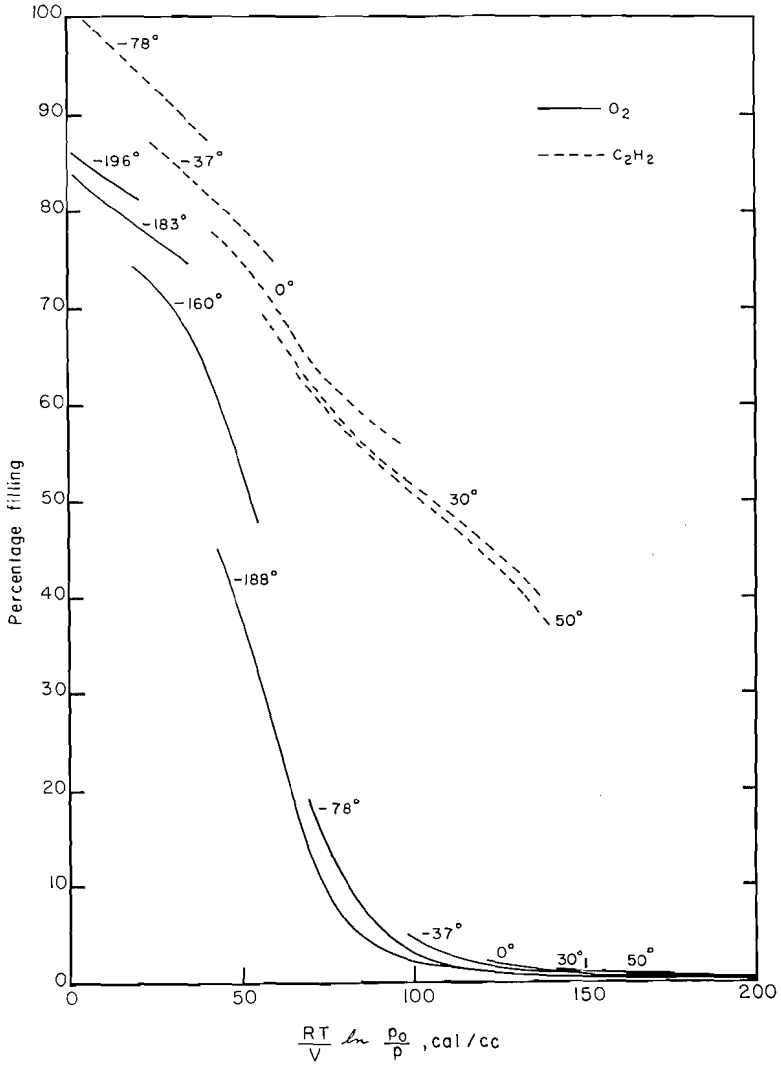

FIG. 6. Generalized Polanyi plots for oxygen and acetylene on 4A molecular sieve. See Fig. 5 for significance of vertical scale.

Despite the failure of the Polanyi plots to provide unique characteristic curves for individual adsorbates or groups of adsorbates, these plots are a useful way of comparing adsorption data on a single graph. For example, the conclusion that acetylene is more strongly adsorbed than oxygen at a given fractional filling can be made unambiguously from Fig. 6. The characteristic curves could be represented by bands having a width of ± 5 to 10% of the fractional filling. However, we have chosen to pass curves through points for pressures from 0.25 to 1.0 atm as shown in Fig. 7. At a fractional filling of pores of 0.4, the adsorption potentials per unit volume increased in the following order

$$Ar < O_2 < C_2H_6 \cong CH_4 < N_2 < CO < CO_2 < C_2H_2$$

with ethylene behaving anomalously. The fact that the generalized Polanyi equation correlates adsorption data on charcoal better than on the 4A molecular sieve might have been anticipated, as adsorption on charcoal is relatively nonspecific

Can. J. Chem. Downloaded from www.nrcresearchpress.com by 210.87.254.5 on 09/05/12
For personal use only.

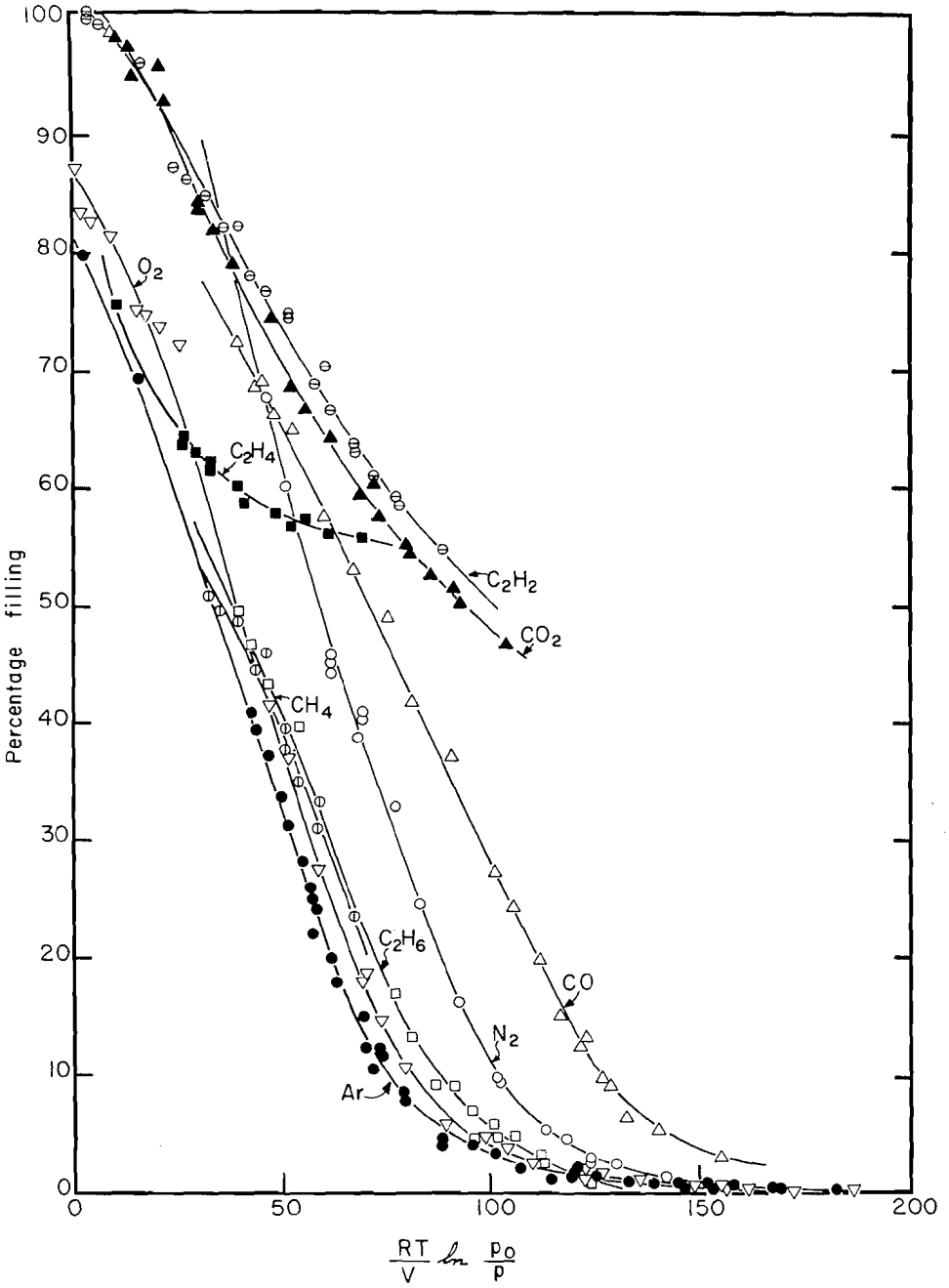

FIG. 7. Generalized Polanyi plots for all adsorbates on 4A molecular sieve. Curves are based only on data for 0.25 to 1.0 atm. See Fig. 5 for significance of vertical scale.

Can. J. Chem. Downloaded from www.nrcresearchpress.com by 210.87.254.5 on 09/05/12
For personal use only.

compared with adsorption on zeolites; furthermore, the pores in charcoal are larger so that packing of molecules is a less serious problem. Because the greatest number of molecules adsorbed per large cavity is only about 15, the number that can be packed in a cavity at different temperatures may vary significantly.

From Fig. 7 and Table II, the adsorption of C_2H_2, CO_2, C_2H_4 (from 0 to 50 °C), CO, and N_2 seems to be stronger than O_2, Ar, CH_4, and C_2H_6. The first group of molecules have moderately large quadrupole moments and CO also has a small dipole moment. Correlations between polarizability and heats of adsorption, heats of adsorption minus heats of liquefaction, or adsorption potential per unit volume were poor. The enthalpies and potentials for gases having quadrupole and dipole moments lay significantly above a curve through data for O_2, Ar, CH_4 and, for potentials, C_2H_6. Barrer and Gibbons (36) have attributed the strong adsorption of CO_2 and NH_3 on X-type sieves to quadrupole and dipole moments, respectively. The strongly adsorbed molecules also have double or triple bonds. The adsorption of CO_2 is the most rapid of the gases studied in the present paper, and CO_2 is also rapidly and strongly adsorbed on coal (41, 42). On amorphous silica–alumina adsorbed CO_2 yields a characteristic infrared spectrum which has been suggested as an index for cracking activity (43). The surfaces of A and X sieves are polar and large electrical fields have been postulated near the exchangeable cations. However, the apparent correlation between adsorption and quadrupole and dipole moments may not be an adequate explanation of the present observation, because specific interactions between highly charged sites and molecules containing multiple bonds might be expected.

Surface areas were not estimated from adsorption isotherms, because the basic premises of surface area determination do not hold for A, X, and Y zeolites and some other microporous solids (44). Specifically, the initial part of the adsorption isotherm is not limited by the number of molecules required to cover the surface but by the number that fills the pore volume. Thus, the areas of the large cavities plus channels of A and X zeolites calculated from structural data are about 1200 and 1400 m^2/g compared with gas adsorption values of 600 to 900 m^2/g that are often quoted (5, 45, 46).

Acknowledgments

The authors are pleased to acknowledge fellowship and operating funds furnished by the National Research Council of Canada.

1. R. M. Barrer. Quart. Rev. London, **3**, 293 (1949).
2. R. M. Barrer. Proc. Symp. Colston Res. Soc. **10**, 6 (1958).
3. R. M. Barrer. Brit. Chem. Eng. **4**, 267 (1959).
4. T. B. Reed and D. W. Breck. J. Amer. Chem. Soc. **78**, 5972 (1956).
5. D. W. Breck, W. G. Eversole, R. M. Milton, T. B. Reed, and T. L. Thomas. J. Amer. Chem. Soc. **78**, 5963 (1956).
6. D. W. Breck. J. Chem. Educ. **41**, 678 (1964).
7. M. M. Dubinin. Dokl. Akad. Nauk SSSR, **138**, 866 (1961).
8. M. M. Dubinin, M. M. Vishuyakova, E. D. Zaverina, E. G. Zhukovskaya, E. A. Leont'ev, V. M. Luk'yanovich, and A. I. Sarakhov. Izv. Akad. Nauk SSSR, Otd. Khim. Nauk, 396 (1961).
9. M. M. Dubinin, E. G. Zhukovskaya, and K. O. Murdinaa. Izv. Akad. Nauk SSSR, Ser. Khim. **4**, 620 (1966).
10. M. M. Dubinin and E. G. Zhukovskaya. Dokl. Akad. Nauk SSSR, **156**, 404 (1964).
11. Zh. A. Dzharylkapova, N. V. Kel'tsev, and N. S. Torocheschnikov. Tr. Mosk. Khim. Tekhnol. Inst. No. **35**, 158 (1961).
12. Z. A. Zhukova and N. V. Kel'tsev. Razdelenie i Anal. Uglevodorodnykh Gazov, Akad. Nauk SSSR, Inst. Neftekhim. Sin. Sb. Statei, 134 (1963).
13. Yu. I. Shumyatskii, N. V. Kel'tsev, and N. S. Torocheschnikov. Tr. Mosk. Khim. Tekhnol. Inst. No. **48**, 242 (1965).
14. I. B. Grudnikov, N. V. Kel'tsev, and N. S. Torocheschnikov. Tr. Mosk. Khim. Tekhnol. Inst. No. **56**, 130 (1967).
15. A. V. Kiselev, Yu. A. El'tekov, and V. N. Semenova. Sin. Tseolity, Poluch. Issled. i Primen. Akad. Nauk SSSR, Otd. Khim. Nauk, 218 (1962).
16. B. G. Aristov, A. V. Kiselev, Ya. V. Mirskii, L. F. Pavlova, and R. S. Petrova. Khim. i Tekhnol. Topl. Masel, **7**, No. 8, 7 (1962).
17. A. V. Kiselev and A. A. Lopatkin. Kinet. i Katal. **5** (1), 183 (1964).
18. L. N. Kvitkovskii and S. R. Sergienko. Dokl. Akad. Nauk SSSR, **147**, 1399 (1962).
19. L. N. Kvitkovskii. Neftekhim. Akad. Nauk Ukr. SSR, Inst. Khim. Vysokomol. Soedin. 39 (1964).
20. P. H. Emmett. Advan. Colloid Sci. **1**, 1 (1942).
21. M. M. Dubinin. Izv. Akad. Nauk SSSR, Ser. Khim. 209 (1964).
22. S. Kitani and J. Takada. J. Nucl. Sci. Technol. (Tokyo), **2**, 51 (1965).
23. L. I. Kazarnovskaya and N. M. Dykhno. Tr. Vses. Nauch. Issled. Inst., Kislorod. Mashinostr. No. **9**, 170 (1965).
24. S. A. Stern and F. S. DiPaolo. J. Vac. Sci. Technol. **4**, 347 (1967).
25. R. M. Barrer and J. H. Petropoulos. Surface Sci. **3**, 126 (1965).
26. B. G. Aristov and A. V. Kiselev. Zh. Fiz. Khim. **41**, 3133 (1967).
27. R. D. Ackley and W. E. Browning, Jr. U.S. At. Energy Comm. CF-61-2-32, 12 pp. 1961.
28. J. Rozenberg and H. Kahan. Comm. Energ. At. (France), Rapp. CEA-R 3366, 18 pp. 1967.

29. F. T. TURNER and M. FEINLEIB. Trans. 8th. AVS Vac. Symp. The Pergamon Press, Inc., New York. 1962. p. 300.
30. E. N. MARTINSON, B. I. PLECHEV, and YU. T. PUTYANTIN. Prib. i Tekh. Eksp. **4**, 154 (1965).
31. I. YASUMOTO. Nippon Kagaku Zasshi, **86**, 1084 (1965).
32. B. G. ARISTOV and A. V. KISELEV. Kolloid. Zh. **29**, 749 (1967).
33. N. V. KEL'TSEV, V. I. MYAKINIENKOV, and N. S. TOROCHESCHNIKOV. Khim. Prom. 813 (1964).
34. R. J. HARPER, G. R. STIFEL, and R. B. ANDERSON. Unpublished data.
35. T. H. THOMAS and R. L. MAYS. *In* Physical methods in chemical analysis. Vol. 4. *Edited by* W. G. Berl. Academic Press, Inc., New York. 1961. pp. 45–97.
36. R. M. BARRER and R. M. GIBBONS. Trans. Faraday Soc. **61**, 948 (1965); **59**, 2569 (1963); **59**, 2875 (1963).
37. R. M. BARRER and A. F. DENNY. J. Chem. Soc. 4684 (1964).
38. W. K. LEWIS, E. R. GILLILAND, B. CHERTOW, and W. P. CADOGAN. Ind. Eng. Chem. **42**, 1326 (1950).
39. R. J. GRANT, M. MANES, and S. B. SMITH. Amer. Inst. Chem. Eng. J. **8**, 403 (1962).
40. R. J. GRANT and M. MANES. Ind. Eng. Chem. Fundamentals, **3**, 221 (1964).
41. S. P. NANDI and P. L. WALKER, Jr. Fuel, **43**, 385 (1964).
42. R. B. ANDERSON. J. BAYER, and L. J. E. HOFER. Fuel, **44**, 443 (1965).
43. J. B. PERI. J. Phys. Chem. **70**, 3168 (1966).
44. M. M. DUBININ. J. Colloid Interface Sci. **23**, 487 (1967).
45. T. G. LAMOND and H. MARSH. Carbon, **1**, 281 (1964).
46. D. J. C. YATES. Can. J. Chem. **46**, 1695 (1968).

Can. J. Chem. Downloaded from www.nrcresearchpress.com by 210.87.254.5 on 09/05/12
For personal use only.

Can. J. Chem. Downloaded from www.nrcresearchpress.com by 210.87.254.42 on 09/05/12
For personal use only.

Fluorocarbon-bridged di(tertiary phosphine) complexes of Group VIB metal carbonyls

W. R. CULLEN, D. F. DONG, AND J. A. J. THOMPSON
Department of Chemistry, University of British Columbia, Vancouver 8, British Columbia

Received June 11, 1969

A series of complexes of the general formula $(C_6H_5)_2PC{=}CP(C_6H_5)_2(CF_2)_nM(CO)_4$, n = 2, 3, or 4; M = Cr, Mo, or W have been prepared. The properties of the new complexes, in particular their infrared spectra, are discussed.

Canadian Journal of Chemistry, 47, 4671 (1969)

Introduction

It is well known that di(tertiary phosphines) such as **1** react with the hexacarbonyls of chromium, molybdenum, and tungsten to displace 2 carbon monoxide groups and give the tetracarbonyl complex (e.g., Reaction [1]) (1)

[1] 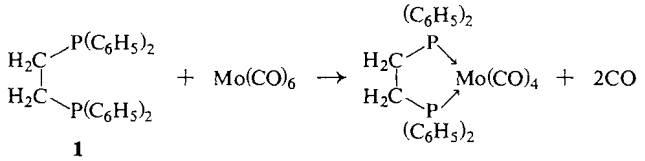

1

In the course of investigations of the complexing abilities of the fluorocarbon-bridged di(tertiary phosphines) ffos (**2***a*), and $f_6$fos (**2***b*) (2–5)

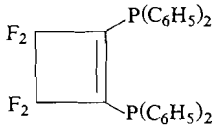

2*a*

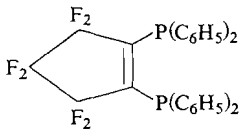

2*b*

we have found that there are two main products from the reactions of these ligands with iron carbonyls. These have the formulae[1] (P—P)Fe(CO)$_3$ and (P—P)Fe$_2$(CO)$_6$ and, using ffos as an example, the structures **3** and **4**, respectively (5, 6)

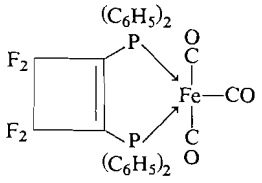

3

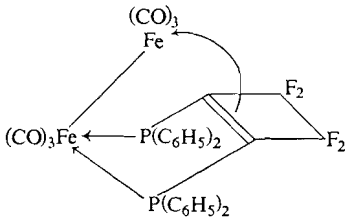

4

The yield of the Fe$_2$(CO)$_6$ compound is much lower when $f_6$fos is used and thus it was of interest to find what would happen when the ring size was further increased. For this reason, $f_8$fos, **5**, has been synthesized (see below) and found to react

[1]In this paper the symbol P—P is used to indicate a chelating di(tertiary phosphine).

Can. J. Chem. Downloaded from www.nrcresearchpress.com by 210.87.254.42 on 09/05/12
For personal use only.

TABLE I

Analytical data for (P—P)M(CO)$_4$ complexes

Compound	Color	Melting point (°C)	Preparative method	Yield (%)	Analyses (%) Found C	H	F	P	Calcd. C	H	F	P
ffosW(CO)$_4$	Yellow	205–210*	*A*	56	48.9	2.8	9.6	7.8	48.6	2.6	9.6	7.8
$f_6$fosCr(CO)$_4$	Orange-brown	188–191*	*C*	84	56.2	3.0	15.8	—	56.0	2.8	16.1	—
$f_6$fosCr(CO)$_4\cdot\frac{1}{2}C_6H_6$	Dark red	186*			57.9	3.4	15.1	—	57.9	3.1	15.3	—
$f_6$fosMo(CO)$_4$	Yellow	192*	*B*	80	52.8	2.8	15.2	—	52.7	2.7	15.2	—
$f_6$fosMo(CO)$_4\cdot\frac{1}{2}C_6H_6$	Red	197–201*			54.4	3.2	—	—	54.6	2.9	—	—
$f_6$fosMo(CO)$_4\cdot\frac{1}{2}C_6H_{12}$	Orange-red	192–195*			54.5	3.4	14.1	—	54.4	3.3	14.4	—
$f_6$fosW(CO)$_4$	Yellow	216–217*	*A*	75	47.3	2.5	13.4	—	47.2	2.4	13.6	—
$f_6$fosW(CO)$_4\cdot\frac{1}{2}C_6H_6$	Orange-red	215–217*			49.4	2.6	12.6	—	49.2	2.6	13.0	—
$f_8$fosCr(CO)$_4$	Amber (red-black)†	208–210	*A*	55	53.7	2.7	20.5	8.0	53.8	2.7	20.0	8.2
$f_8$fosMo(CO)$_4$	Orange (dark red)†	201–203	*B*	62	51.1	2.9	18.6	7.8	50.9	2.5	18.9	7.7
$f_8$fosW(CO)$_4$	Orange (dark red)†	210–212	*A*	50	45.8	2.2	17.6	—	45.9	2.3	17.1	—

*With decomposition.
†Color of benzene solvate in parentheses.

Can. J. Chem. Downloaded from www.nrcresearchpress.com by 210.87.254.42 on 09/05/12
For personal use only.

with iron carbonyls to give a compound analogous to **3** but not to **4** (7). In order to see if this result can be explained by an increase or decrease in the donor–acceptor abilities of the new phosphine ligands, the compounds $(P—P)M(CO)_4$ (M = Cr, Mo, W) have been synthesized to examine their infrared spectra in the carbonyl stretching region. This paper is also an expansion of an investigation of complexes of Group VIB metals briefly described in an earlier publication (2).

Experimental

The hexacarbonyls, $M(CO)_6$ (M = Cr, Mo, W), were obtained commercially and used without further purification. The di(tertiary phosphines), 1,2-bis(diphenylphosphino)tetrafluorocyclobutene (ffos), and 1,2-bis(diphenylphosphino)hexafluorocyclopentene ($f_6$fos) were prepared from published procedures (4, 8). 1,2-Bis(diphenylphosphino)octafluorocyclohexene ($f_8$fos) was prepared as described below.

Infrared spectra were obtained using a Perkin–Elmer Model 457 Grating Spectrometer and were calibrated against polystyrene and cyclohexane. ^1H and ^{19}F nuclear magnetic resonance (n.m.r.) spectra were recorded on Varian Associates' A-60 and HA-100 instruments, respectively. Microanalyses were performed by the Pascher Mikro-analytisches Laboratorium, Bonn, West Germany and by Mr. P. Borda of this Department.

Preparation of (P—P)M(CO)$_4$

Three general methods of preparation of the new complexes are outlined below. The method used for a specific complex is shown in Table I.

Method A

A benzene solution (15–20 ml) containing a 1:1 mole ratio of ligand to hexacarbonyl was heated at 150 °C in an evacuated Carius tube for 17 to 46 h. At the end of the reaction period the initially orange or colorless solution had become deep red (except for ffosW(CO)$_4$, which was amber). The reaction solution was filtered to remove any suspended impurities and then solvent was removed at reduced pressure. The resulting yellow-to-red solid was dissolved in benzene and recrystallized by addition of hexane or by slow evaporation of the solvent.

Method B

A solution of the hexacarbonyl (~1 mmole) and the ligand (1 mmole plus a 10% excess) in toluene or cyclohexane was refluxed under a nitrogen atmosphere for 3–7 h. The solvent was removed to give a red solid which was redissolved in benzene. The solution was filtered and crystals of the benzene solvate were obtained by the addition of hexane to the solution or by slow evaporation of solvent.

Method C

An acetone solution (15 ml) containing approximately equimolar amounts of ligand and hexacarbonyl was irradiated by ultraviolet light (100 W Hanovia lamp 10 cm from the tube) for 18 h in a sealed Carius tube. The contents of the tube were evaporated to dryness and dissolved in hot benzene. The solution was filtered and the solvent allowed to evaporate slowly to afford crystals of the product.

Reaction of $f_6$fos with $[C_6H_3(CH_3)_3]W(CO)_3$

The tungsten compound (0.38 g, 1 mmole) and $f_6$fos (0.54 g, 1 mmole) were refluxed in cyclohexane for 14 h. No reaction products were detected. The tungsten compound (0.38 g, 1 mmole) and $f_6$fos (2 mmole) in benzene solution were heated (150°) in a sealed tube (20 h). The solvent was removed, and the solid residue chromatographed on Fluorisil. The main product, identified as $f_6$fosW(CO)$_4$ (0.23 g, 27%) eluted as a red band using 30% benzene in petroleum ether. Only trace amounts of other products were isolated.

1,2-Bis(diphenylphosphino)octafluorocyclohexene, ($f_8$fos)

Diphenylphosphine (3.72 g, 20 mmoles) and decafluorocyclohexene (2.62 g, 10 mmoles) were heated (100°) in a sealed Carius tube for 21 h. The gummy orange-red reaction product was extracted from the tube with benzene (100 ml). The orange solution was filtered to remove unidentified solid impurities and the solvent was removed at reduced pressure. Trituration of the oil thus obtained under petroleum ether (b.p. 30–60°) initiated solidification. The crude solid was recrystallized from hexane to yield 3 g (50%) of orange, crystalline product, m.p. 135°.

Anal. Calcd. for $C_{30}H_{20}F_8P_2$: C, 60.6; H, 3.4. Found: C, 61.1; H, 3.6.

Principal infrared bands (CCl_4 solution) were: 3080(w), 3060(w), 1485(w), 1435(m), 1340(m), 1315(w), 1215(s), 1195(vs), 1175(vs), 1163(vs), 1113(vs), 1090(m), 1070(w), 1035(vs), 980(s), 694(s). The ^{19}F n.m.r. spectrum ($CHCl_3$ solution, $CFCl_3$ internal standard) shows two poorly resolved, equal-area resonances at 101 (triplet) and 135 p.p.m. (multiplet) upfield from $CFCl_3$.

Results and Discussion

Three of the new Group VIB carbonyl derivatives described here were prepared in good yield using the previously unreported 1,2-bis(diphenylphosphino)octafluorocyclohexene, $f_8$fos, **5** (Reaction [2]). The preparation and properties of this ligand warrant some comment as they differ somewhat from those of the better-known ffos and $f_6$fos. Unlike the latter ligands, which can be prepared by simply mixing the reactants at room temperature or below (2, 8), the cyclohexene derivative is obtained in about 50% yield by heating the phosphine and olefin at 100° or higher (Reaction [2])

[2] 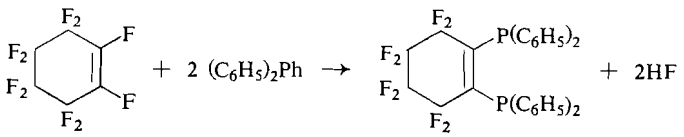

5

[3] 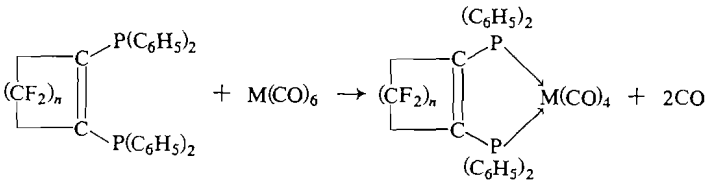

Recently, Stockel, Megson, and Beachem (9, see also (10)) reported that perfluorocyclohexene and 1,2-dichlorooctafluorocyclohexene do not give phosphobetaines when reacted with tertiary phosphines. In comparison, the 4- and 5-membered ring systems reacted readily. The difference in reactivity was attributed to lack of double-bond strain in the cyclohexene ring. A similar argument in the present case can be made.

F_8fos is a bright-orange, crystalline, air-stable solid. In solution it is indefinitely stable to light or air[2]. To our knowledge this is the first reported case of a so highly colored simple phosphine. In contrast, both ffos and $f_6$fos are white and the $(C_6H_{11})_2P$ analog (11) pale yellow.

The three fluorocarbon-bridged ligands could all form complexes by using the double bond alone (no known examples) or by acting as a chelating phosphine (reaction [3] (2, 5)) or both (4). However, as is also reported for the related ligand $(C_6H_5)_2PCH{=}CHP(C_6H_5)_2$, **6** (12), we have found that they act only as chelating ligands when reacted with Group VIB carbonyls. Thus the complexes $(P{-}P)M(CO)_4$ (M = Cr, Mo, W) have been prepared by reaction of the ligand with the hexacarbonyl in hydrocarbon solvent (reaction [3]). Where M = Cr and W, complete reaction occurred only when the reactants in benzene solution were heated to 150° in sealed evacuated Carius tubes. The greater lability of the carbonyl groups of $Mo(CO)_6$, which has been well documented in the literature, enabled us to prepare the corresponding $Mo(CO)_4$ derivatives by refluxing the reactants in toluene for a few hours. One of the complexes, $f_6$fosCr$(CO)_4$, was prepared by ultraviolet irradiation of an acetone solution of the reactants for several hours.

The new complexes are highly colored, stable, and crystalline. Other $(P{-}P)M(CO)_4$ derivatives are white or yellow (1). The complexes of $f_6$fos and $f_8$fos are somewhat unusual in their ability to form extremely strong solvates which, in the case of the $f_6$fos derivatives, analyze well for the general formula $(P{-}P)M(CO)_4\frac{1}{2}S$ (M = Cr, Mo, W; S = benzene, cyclohexane, chloroform). On heating, all solvates lose solvent at about 30° below their melting or decomposition points. The light colored unsolvated complexes of $f_6$fos were obtained by vacuum sublimation at moderately high temperatures. The $f_8$fos analogues of Mo and W formed similar dark red solvates with benzene and could be obtained unsolvated as bright-orange plates by recrystallization from boiling *n*-heptane. Only $f_8$fosCr$(CO)_4$ could be desolvated by treatment in vacuo at refluxing toluene temperatures.

All the new complexes reported here are stable in most solvents. However, it was noted that the $Mo(CO)_4$ derivatives decomposed in the space of a few hours in carbon tetrachloride, the decomposition being easily followed by the appearance of new bands in the infrared carbonyl stretching region. Both the chromium and tungsten derivatives were stable indefinitely in this solvent. We cannot explain this anomaly at the present time but it may involve an oxidative addition reaction similar to that known for MCl_4 (M = Ge, Sn) with (bipy)$Mo(CO)_4$ (13).

Chatt and Watson (14) reported some years ago that the mesitylene metal tricarbonyls reacted with di(tertiary phosphines). They obtained, in addition to the expected dicarbonyl derivatives $(P{-}P)_2M(CO)_2$, considerable amounts of the tetracarbonyl compound, $(P{-}P)M(CO)_4$, and suggested that carbonyl groups on one molecule could exchange with ligand on another. In the present investigation there was no reaction between mesitylenetungsten tricarbonyl and $f_6$fos in refluxing cyclohexane. However, when the reaction was run in benzene solution in a sealed tube at 150°, the main product was the tetracarbonyl compound $f_6$fosW$(CO)_4$ with very little, if any, $(f_6fos)_2W(CO)_2$ being formed.

Infrared Spectra

The infrared spectra of the new complexes in

[2]The color was first believed to be due to contamination. However, chromatography on a Fluorisil column and repeated crystallization wrought no change.

Can. J. Chem. Downloaded from www.nrcresearchpress.com by 210.87.254.42 on 09/05/12
For personal use only.

Can. J. Chem. Downloaded from www.nrcresearchpress.com by 210.87.254.42 on 09/05/12
For personal use only.

the carbonyl stretching region are listed in Table II. The spectra of complexes of related saturated (**1**) and unsaturated (**6**) ligands are also given for comparison.

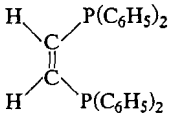

6

Firstly, it is to be noted that there is very little difference between the carbonyl spectra of the two hydrocarbon bridged ligands. It has been suggested that the complexes of **1** have slightly higher frequencies than those of **6**, indicating a slightly higher π-acceptor strength for **1** (12). However, comparison is being made here between spectra run in different solvents. The spectrum of $C_2H_4[P(C_6H_5)_2]_2Mo(CO)_4$ has been reported in hydrocarbon solvent as being 2028, 1932, 1919, and 1906 cm^{-1} (15). Thus it seems that the inductive effect in the sp^2 carbon atoms and the presence of the unsaturated bridging system have little effect. However, the spectra of the fluorocarbon bridged species are at higher wavenumber than the others. This seems to indicate that it is the inductive effect of the fluorine atoms in the bridge which is responsible for the apparent increase in π-acceptor strength.

Secondly, there is no significant difference in the spectra of the complexes of the fluorocarbon bridged ligands, apart from the extra band of the $f_6$fos complexes which is discussed below. Thus, any difference in reactivity of the fluorocarbon ligands is unlikely to arise because of donor–acceptor differences. This leaves geometrical factors (including ring strain) as the main cause. The spectra of the compounds (P—P)$Fe(CO)_3$ (P—P = **2***a*, **2***b*, **5**, or **1**) show this same trend (5, 7); that is, the fluorocarbon bridged complexes have almost identical spectra which occur at higher wave numbers than the hydrocarbon bridged compounds.

Thirdly, the spectrum of $f_6$fos$Fe(CO)_3$ shows four bands, one more than that expected for a compound with C_{2v} symmetry (5). This same feature is seen in the $M(CO)_4$ complexes of $f_6$fos where four bands are predicted yet five are observed. Dobson (16) has found six carbonyl stretching bands in the spectrum of (DTO)$Cr(CO)_4$ (DTO = $(CH_3)_3CSC_2H_4SC(CH_3)_3$) and has made the suggestion that another species such as a 5-coordinate one, in which one end of the ligand is dissociated, is present in solution. It is possible that the extra band in the chromium $f_6$fos complex is due to a similar phenomenon; however, we are not happy with this explanation, especially since the "explanation" would presumably need to be used to account for the extra band in *all* the $f_6$fos complexes. The complex **7** contains two 5-membered rings, one of which is shown to be

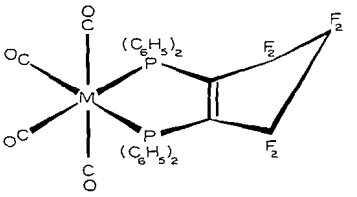

7

puckered; the other could be also. It is possible that the combination of these two puckered rings could give rise to two distinct isomers in solution which have a long enough lifetime to be detected by infrared spectroscopy. Two 5-membered rings seem to be necessary since the ffos and $f_8$fos complexes show no unusual features. However, geometrical considerations such as the bite of the ligand which could stabilize certain conformations should not be ignored completely. It is also possible that the cyclopentene ring in a complex such as **7** can exist as two conformers with different energies, such as the planar–bent forms suggested for certain cyclobutanes (17). If the lifetime of any conformer in solution was short, then n.m.r. experiments would show only the average chemical shift of the fluorine atoms, as was found to be the case.

The extra bands observed by Dobson may have a similar origin, since two isomers are possible for rings containing two coordinated sulfur atoms. One of these is shown in projection in **8**. The energy barrier to interconversion of the two forms, which should be detectable by n.m.r. studies, would be small (18).

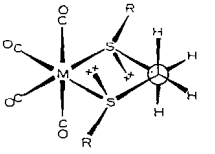

8

Can. J. Chem. Downloaded from www.nrcresearchpress.com by 210.87.254.42 on 09/05/12
For personal use only.

TABLE II

Carbonyl infrared bands for (P—P)M(CO)$_4$ complexes

	Infrared frequency* (cm^{-1})				
(P—P)M(CO)$_4$	ffos†‖	f$_6$fos†	f$_8$fos†	$C_2H_4(P(C_6H_5)_2)_2$‡	$C_2H_2(P(C_6H_5)_2)_2$§
(P—P)Cr(CO)$_4$	2021 (m)	2025 (m)	2028 (s)	2009	2011
	1936 (s)	1943 (m)	1943 (s)	1914	1915
	1919 (vs)	1939 (s, sh)	1919 (vs)	1899	1902
		1918 (s)			
	1911 (vs)	1912 (s, sh)	1907 (m, sh)	1877	1886
(P—P)Mo(CO)$_4$	2034 (m)	2036 (s)	2034 (m)	2020	2022
	1945 (s)	1952 (s)	1949 (m)	1919	1925
	1931 (vs)	1948 (s, sh)	1929 (vs)	1907	1925
		1925 (s)			
	1921 (vs)	1921 (s, sh)		1881	1897
(P—P)W(CO)$_4$	2028 (m)	2032 (s)	2032 (m)	2016	2022
	1939 (s)	1945 (s)	1943 (m)	1912	1920
		1940 (s, sh)			
	1921 (vs, sh)	1920 (s)	1923 (s)	1901	1906
	1917 (vs)	1914 (s, sh)	1915 (sh)	1876	1890

*s = strong, m = medium, w = weak, sh = shoulder, v = very.
†C_6H_{12} solution, this work.
‡From ref. 14, $C_2H_4Cl_2$ solution.
§From ref. 12, C_6H_6 solution.
‖Cr and Mo complexes are known compounds (2) and were prepared again for comparison purposes.

Lastly, additional evidence that the complexes possess a normal chelate structure was garnered from the C—F stretching region in the infrared. Spectra in this region (1300–1000 cm^{-1}) were nearly identical with those of the free ligands. Any loss of symmetry would have resulted in obvious changes in band number and distribution.

Acknowledgment

The authors are grateful to the Defence Research Board of Canada for financial support.

1. G. R. DOBSON, I. W. STOLZ, and R. K. SHELINE. Advan. Inorg. Chem. Radiochem. **8**, 1 (1966).
2. W. R. CULLEN, P. S. DHALIWAL, and C. J. STEWART. Inorg. Chem. **6**, 2256 (1967).
3. W. R. CULLEN, D. A. HARBOURNE, B. V. LIENGME, and J. R. SAMS. J. Amer. Chem. Soc. **90**, 3293 (1968).
4. W. R. CULLEN, D. A. HARBOURNE, B. V. LIENGME, and J. R. SAMS. Inorg. Chem. **8**, 95 (1969).
5. W. R. CULLEN, D. A. HARBOURNE, B. V. LIENGME, and J. R. SAMS. Inorg. Chem. **8**, 1464 (1969).
6. F. W. B. EINSTEIN and J. TROTTER. J. Chem. Soc. A, 824 (1967).
7. W. R. CULLEN, J. R. SAMS, and J. A. J. THOMPSON. Unpublished results.
8. W. R. CULLEN, D. S. DAWSON, and P. S. DHALIWAL. Can. J. Chem. **45**, 683 (1967).
9. R. F. STOCKEL, F. MEGSON, and M. T. BEACHEM. J. Org. Chem. **33**, 4395 (1968).
10. S. E. ELLZEY. Can. J. Chem. **47**, 1251 (1969).
11. R. F. STOCKEL. Can. J. Chem. **46**, 2625 (1968).
12. R. B. KING and C. A. EGGERS. Inorg. Chim. Acta, **2**, 33 (1968).
13. W. R. KUMMER and W. A. G. GRAHAM. Inorg. Chem. **7**, 310 (1968).
14. J. CHATT and H. R. WATSON. J. Chem. Soc. 4980 (1961).
15. G. R. DOBSON and L. W. HOUK. Inorg. Chim. Acta, **1**, 287 (1967).
16. G. R. DOBSON. Inorg. Chem. **8**, 90 (1969).
17. J. B. LAMBERT and J. D. ROBERTS. J. Amer. Chem. Soc. **87**, 3884 (1965); **87**, 3891 (1965).
18. E. W. ABEL, R. P. BUSH, F. J. HOPTON, and C. R. JENKINS. Chem. Commun. 58 (1966).

Can. J. Chem. Downloaded from www.nrcresearchpress.com by 210.87.254.42 on 09/05/12
For personal use only.

Can. J. Chem. Downloaded from www.nrcresearchpress.com by 210.87.254.6 on 09/05/12
For personal use only.

Synthesis of some organophosphorus compounds: a study of the electron spin resonance spectra of the free radical anions formed by the reactions of 4,4′-bis(diphenylphosphine)biphenyl with alkali metals

MAHDY H. HNOOSH[1] AND RALPH A. ZINGARO
Chemistry Department, Texas A&M University, College Station, Texas 77843

Received June 16, 1969

By the halogen–lithium interconversion method, 4,4′-bis(diphenylphosphine)biphenyl (**1**) was prepared. Under different reaction conditions, mono- and di-oxygenated products were obtained. An attempt to prepare **1** by the Grignard reagent method failed to give the expected product but

$$C_6H_5(OH)(O)PC_6H_4C_6H_4P(O)(OH)C_6H_5$$

was obtained. Bis(diphenylamine)phenylphosphine was also prepared. Tetraphenyldiphosphine monoxide resulted from an attempt to prepare N-diphenylaminodiphenylphosphine. The mechanism of this reaction is discussed. Infrared spectroscopy, elemental analysis, and activation analysis for the determination of oxygen content were performed for the identification of the above compounds.

Reactions of **1** with sodium–potassium alloy in tetrahydrofuran (THF) and 1,2-dimethoxyethane (DME) gave a radical anion which was identified by its electron spin resonance spectra at different temperatures.

Canadian Journal of Chemistry, 47, 4679 (1969)

Introduction

The utilization of the halogen–lithium interconversion method (1) has been found to be useful for the synthesis of a variety of organometallic compounds. Curtis and Allred (2) have utilized the reaction between *n*-butyl lithium and the corresponding halogenated biphenyl for the preparation of the compounds 4-$(CH_3)_3MC_6H_4C_6H_5$ and 4,4′-$(CH_3)_3MC_6H_4C_6H_4M(CH_3)_3$, where M = Si, Ge, or Sn.

Cowley and Hnoosh (3) reported the preparation of 4,4′-$(CH_3)_2P$—$C_6H_4C_6H_4$—$P(CH_3)_2$. Both investigations also included electron spin resonance (e.s.r.) studies of the free radical anions formed by the reduction of these compounds with alkali metals.

In the present investigation the preparation of the compound 4,4′-$(C_6H_5)_2PC_6H_4C_6H_4P(C_6H_5)_2$ is reported and its reactions with alkali metals in tetrahydrofuran (THF) and 1,2-dimethoxyethane (DME) have been studied by e.s.r. spectroscopy. The interest in the e.s.r. study of the latter compound lies in the comparison with that of triphenylphosphine (4) and its oxide (3), where a phenyl group has been shown to cleave from the phosphorus atom in their reactions with alkali metals in the same solvents.

Sisler and Smith (5) reported the preparation of N-diphenylaminodiphenylphosphine by means of the reaction of chlorodiphenylphosphine with sodium diphenylamine produced by the reaction of diphenylamine with NaH in diglyme. In this work a similar approach has been used for the preparation of bis(diphenylamino)phenylphosphine. In addition, an attempt to prepare $[(C_6H_5)_2N](C_6H_5)_2P$ under different conditions from those previously reported (5) resulted in the formation of the unexpected product, tetraphenyldiphosphine monoxide $(C_6H_5)_2P$—$P(O)(C_6H_5)_2$. This reaction appears to be similar to that reported for the production of tetraphenyldiphosphine dioxide by the reaction of diphenylphosphine chloride in the presence of a tertiary amine like diethylaniline (6).

Experimental

Reagents

All the chemical reagents used in this work were obtained from the usual commercial sources. *n*-Butyl lithium was in the form of a hexane solution. It was pumped from the storage container into the reaction vessel under a pressure of dry nitrogen in order to avoid atmospheric contamination. 4,4′-Dibromobiphenyl was used following recrystallization from butanol. Sodium hydride was used in the form of a 50% dispersion in oil. Diethylene glycol dimethyl ether (diglyme) was dried over CaH_2 and distilled prior to its use. THF and DME were purified by distillation after drying over CaH_2 and potassium metal.

The sodium–potassium alloy which was used in the

[1]Present address: Ashland Chemical Co., Research Center, P.O. Box 1503, Houston, Texas 77001.

Can. J. Chem. Downloaded from www.nrcresearchpress.com by 210.87.254.6 on 09/05/12
For personal use only.

reduction of 4,4′-bis(diphenylphosphine)biphenyl was prepared by mixing proper amounts of sodium and potassium metals after they were first cleaned by treatment with benzene and then ether. They were sublimed by heating under vacuum in the reaction apparatus used for free radical generation.

Apparatus

All infrared spectra were recorded on a Beckman Model IR-12 spectrometer using KBr pellets. The e.s.r. spectra were measured using the X-band of a Varian V-4502-15 e.s.r. spectrometer.

Oxygen determinations were performed using the neutron activation and analysis system at the Activation Analysis Research Lab., Texas A&M University. Weighed amounts of dry primary standard grade benzoic acid in polyethylene vials were used as standards. The unknown samples and standards were subjected to the same experimental conditions. The other elemental analyses were performed by the Galbraith Laboratories, Inc., Knoxville, Tennessee.

Preparation of 4,4′-Bis(diphenylphosphine)biphenyl, 4,4′-$(C_6H_5)_2PC_6H_4C_6H_4P(C_6H_5)_2$

To 31.2 g (0.1 mole) of 4,4′-dibromobiphenyl dissolved in 200 ml of anhydrous ether contained in a 1 l three-necked flask, equipped with a mechanical stirrer, a reflux condenser, and dropping funnel, 12.8 g (0.2 mole) of *n*-butyl lithium (in hexane) was added dropwise, with stirring, under an atmosphere of dry nitrogen at room temperature. The lithium exchange reaction was essentially complete after 30 min. Chlorodiphenylphosphine, $(C_6H_5)_2PCl$, (22.05 g, 0.2 mole) was added dropwise to the lithium compound. After 3 min the brown color began to fade and a yellowish precipitate formed The reaction was slightly exothermic. The mixture was stirred for 2 h after completion of the $(C_6H_5)_2PCl$ addition. It was then refluxed for 2 h and allowed to cool under nitrogen. The reaction mixture was hydrolyzed with saturated aqueous ammonium chloride solution. The ether layer plus washings were dried overnight over anhydrous sodium sulfate. The ether solution was then evaporated under reduced pressure, and the brown-yellow product was recrystallized first from ethanol and then from a mixture of ether and petroleum ether. This resulted in a yield of 51.2% of white crystals which melted at 195 °C.

Anal. Calcd. for $(C_6H_5)_2P—C_6H_4C_6H_4—P(C_6H_5)_2$: C, 82.76; H, 5.37; P, 11.87. Found: C, 82.79; H, 5.52; P, 11.67.

In this reaction it was found that if the conditions were changed slightly, different products were formed. In one run, all steps up to the hydrolysis were carried out in a similar manner. The reaction flasks, while hot, were opened to the air and hydrolyzed with saturated ammonium chloride solution with stirring. Evaporation of the organic layer yielded another quantity of solid product. The solid product from the water layer was recrystallized from ethanol and then *n*-butanol. The white crystals melted at 205–206 °C.

The analysis is in agreement with a stoichiometry which suggests the compound 4,4′-bis(diphenylphosphine)biphenyl monoxide.

Anal. Calcd. for 4,4′-$(C_6H_5)_2PC_6H_4C_6H_4P(O)(C_6H_5)_2$: C, 80.29; H, 5.23; P, 11.62. Found: C, 80.26; H, 5.18; P, 11.62.

A second solid was obtained from the organic layer which was recrystallized first from ethanol and then *n*-butanol; m.p. 265–266 °C. The analysis suggests the compound 4,4′-bis(diphenylphosphine oxide)biphenyl.

Anal. Calcd. for 4,4′-$(C_6H_5)_2(O)PC_6H_4C_6H_4P(O)(C_6H_5)_2$: C, 77.97; H, 5.05; P, 11.30. Found: C, 77.49; H, 5.49; P, 11.01.

Activation analysis for oxygen gave 5.54%, compared with the calculated value of 5.68%.

An attempt to prepare 4,4′-bis(diphenylphosphine)biphenyl by the use of Grignard reagent in THF with I_2 to catalyze the reaction resulted in the formation of 4,4′-bis(diphenylphosphoric acid)biphenyl, 4,4′-$C_6H_5(OH)(O)P—C_6H_4C_6H_4—P(O)(OH)C_6H_5$, which was identified by chemical analysis, infrared spectrum, and molecular weight determination.

Preparation of Bis(diphenylamino)phenylphosphine $[(C_6H_5)_2N_2]PC_6H_5$

A solution of 33.8 g, (0.2 mole) of diphenylamine in 150 ml of dry (over CaH_2) diethylene glycol dimethyl ether (diglyme) was added to a suspension of 14 g of NaH (50% dispersion in oil) in 300 ml of diglyme. When the evolution of hydrogen was over, 18 g (0.1 mole) of $C_6H_5PCl_2$ was added, with stirring, to the mixture. The solution was warmed to 110 °C and kept at this temperature for 2 h. The solid reaction product (sodium chloride) was filtered hot, and washed with dry ether. The filtrate and the ether washings were combined and the solvents removed under reduced pressure. The residue was recrystallized from ethanol and then ether. The resulting crystals melted at 139–140 °C.

Anal. Calcd. for $[(C_6H_5)_2N]_2PC_6H_5$: C, 81.02; H, 5.67; P, 7.01; N, 6.30. Found: C, 80.27; H, 5.74; P, 7.54; N, 6.25.

This compound was found to be exceedingly sensitive to air and moisture. On standing, even in a desiccator, the crystals turned yellow and then bluish green.

Attempts to prepare diphenylaminodiphenylphosphine $[(C_6H_5)_2N](C_6H_5)_2P$ as reported (5) with slightly different conditions resulted in the formation of tetraphenyldiphosphine monoxide. The diphenylamine was added to the NaH suspension dropwise at room temperature. After the addition of $(C_6H_5)_2PCl$ the mixture was refluxed for about 2 h. Then the precipitate was filtered, while hot, in the atmosphere. The organic solvent was evaporated under reduced pressure and the product was recrystallized from ethanol and then ether. The compound melted at 122 °C and the yield was 17.2%.

The elemental analysis fits the stoichiometry of the compound

$$(C_6H_5)_2P—\overset{\overset{O}{\|}}{P}(C_6H_5)_2$$

Determination of the oxygen content by oxygen analysis gave very good results compared with the calculated value.

Anal. Calcd. for $(C_6H_5)_2P—PO(C_6H_5)_2$: C, 74.61; H, 5.18; P, 16.06; O, 4.15. Found: C, 74.82; H, 4.96; P, 15.90; O, 4.20.

The Reactions of 4,4′-Bis(diphenylphosphine)biphenyl with Alkali Metals

These reactions with alkali metals were carried out in an apparatus specially designed for this purpose which

Can. J. Chem. Downloaded from www.nrcresearchpress.com by 210.87.254.6 on 09/05/12
For personal use only.

was connected to a vacuum line of conventional design. The compound was permitted to react in the reaction bulb after the metals were heated and condensed as shiny mirrors on this bulb and after the solvent was distilled under vacuum into the same bulb. Samples were taken after various times and at various temperatures.

Results and Discussion

I. Syntheses and Infrared Spectra

During the synthesis of 4,4′-bis(diphenylphosphine)biphenyl it was noted that two kinds of products, the monoxide and the dioxide, were obtained when the reaction mixture was opened to air and hydrolyzed while hot, immediately following the reflux period. The stability of this compound toward oxidation is not surprising in view of the fact that each phosphorus atom bears three aryl substituents. The formation of a monoxide is quite unusual and further illustrates the oxidative stability of this molecule. The formation and isolation of the stable monoxide suggests that this species may be the first one formed during the atmospheric oxidation process.

A comparison of the infrared spectra of the unoxygenated compound and that of the oxygenated products has been made. The absorption band of principal interest is the fundamental P—O stretching vibration, ν_s(P—O). Zingaro and Hedges reported P—O stretching frequencies of a number of organophosphine oxides (7). These were found over the range 1144–1206 cm^{-1}. Kuchen and Buchwalt (8) reported P—O stretching frequencies for tetraphenyl diphosphine dioxide at 1180 cm^{-1}. In the present study strong bands have been observed at 1196 and 1190 cm^{-1} for the di- and monoxide, respectively. These bands were absent in the infrared spectrum of the unoxygenated compound.

Attempts to prepare 4-diphenylphosphinebiphenyl in the same manner, i.e., by the halogen–lithium interconversion reaction, failed to give the desired product. It appears that the reaction of mono-halogenated biphenyl with *n*-butyl lithium proceeds with difficulty, or not at all. This may be due to the fact that the carbon–bromine bond is much stronger than when there is present another C—Br bond in the opposite position (4′) on the biphenyl. The failure of this reaction may also be due to the extreme sensitivity of the product toward oxygen and water.

In the attempt to prepare the 4,4′-bis(diphenylphosphine)biphenyl via the Grignard reagent using I_2 as a catalyst, the desired product was not formed. As described in the experimental part, 4,4′-bis(phenylphosphonic acid)biphenyl was obtained. This means that the chlorodiphenylphosphine underwent cleavage of one phenyl group and then reacted with 4,4′-dibromobiphenyl. This was followed by hydrolysis and oxidation. However, the mechanism of this unusual reaction remains indefinite. The infrared spectrum also shows the principal absorption bands expected for this molecule, including ν_s(P—O) at 1183 cm^{-1} and ν_s(P—O—H) at 1131 cm^{-1}.

Attempts to prepare the compound

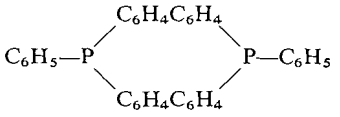

by the reaction of $C_6H_5PCl_2$ with 4,4′-dibromobiphenyl by the halogen–lithium interconversion method resulted in a very low yield of noncrystalline solid which may be a polymer of the following type.

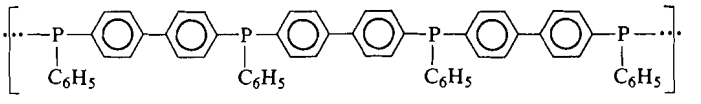

The material was formed in very small quantities and was found to be exceedingly insoluble in the usual organic solvents.

The reaction of diphenylamine with chlorodiphenylphosphine proceeded as expected. The synthesis of diphenylaminodiphenylphosphine $[(C_6H_5)_2N](C_6H_5)_2P$ was accomplished in the manner described (5) by the following reaction sequence.

$$(C_6H_5)_2NH + NaH \xrightarrow{\text{Diglyme}} (C_6H_5)_2NNa + H_2$$

$$(C_6H_5)_2NNa + (C_6H_5)_2PCl \longrightarrow [(C_6H_5)_2N](C_6H_5)_2P + NaCl$$

In this reaction the addition of the diphenylamine solution to the NaH suspension was not carried

Can. J. Chem. Downloaded from www.nrcresearchpress.com by 210.87.254.6 on 09/05/12
For personal use only.

out dropwise, but both reagents were mixed together completely prior to the reaction. When the addition was carried out in a dropwise manner without heat, the expected product was not obtained. The product obtained was tetraphenyldiphosphine monoxide. Comparison of the infrared spectrum of this compound with that for the dioxygenated compound (8) showed that the spectra are essentially superimposible. Both possess a strong absorption band for the P—O stretching frequency in the region of 1180 cm^{-1}.

The manner of the formation of tetraphenyl diphosphine monoxide is similar to that reported by Quin and Anderson (6) who utilized phosphinous chlorides for the formation of the phosphorus–phosphorus bond. They reported a similar case in which they obtained tetraphenyldiphosphine dioxide from the reaction of chlorodiphenylphosphine in the presence of an amine like diethylaniline, a very small amount of water, and air.

In the present case, as in that reported by Quin and Anderson, in order to account for the formation of the diphosphine monoxide it was necessary to assume that both hydrolytic and oxidative reactions are involved

$$2(C_6H_5)_2PCl + 2(C_6H_5)_2NH + H_2O + 0.5\ O_2 \rightarrow (C_6H_5)_2\overset{\overset{O}{\|}}{P}—P(C_6H_5)_2 + 2(C_6H_5)_2NH_2Cl$$

The diphenylamine hydrochloride was isolated and unequivocally characterized.

In the present study, when the amine solution was added dropwise to the sodium hydride without heat, it did not react. When the chlorodiphenylphosphine was added, the amine probably functioned as a catalyst in the formation of the diphosphine. In the case just referred to (6), it was reported that the amine plays a vital role as no coupling occurs in its absence. In this process, phosphorus–phosphorus bond formation precedes the hydrolysis and oxidation steps, and the amine is involved in the coupling reaction, but in a manner different from that of metals when they participate in coupling reactions since the amine cannot function as a reducing agent. It is quite possible that an amine–phosphinous chloride complex, similar to those which have been reported to form between amines and phosphorus trihalides (9) is first formed. The complex is susceptible to attack by a second molecule of phosphinous chloride, with displacement of the amine (10). The intermediate which forms would be of the type

$$[(C_6H_5)_2\ddot{P}—\overset{+}{P}(C_6H_5)_2Cl]Cl^-$$

which is easily hydrolyzed and oxidized. It is to be noted that in this process the same kind of atom is involved, first in electrophilic, and then in nucleophilic behavior.

It is difficult to account for monoxide formation without the formation of any dioxide. The stability of the monoxide may be the most important factor. Resonance among the following structures may explain this stability

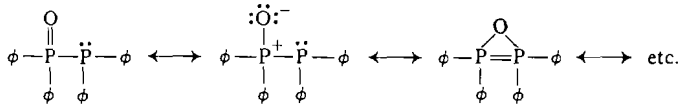

The preparation of bis(diphenylamino)phenylphosphine proceeded in the manner expected. This compound is very sensitive to moisture and oxygen. The sensitivity toward oxidation is to be expected because of the availability of unbonded electron pairs on both the nitrogen and phosphorus atoms.

II. Electron Spin Resonance Studies of the Reactions of 4,4′-Bis(diphenylphosphine)-biphenyl with Alkali Metals in THF and DME

These reactions proceeded similarly with lithium, sodium, potassium, and sodium–potassium (NaK) alloy in both THF and DME. When each reaction started, a purple color developed. This color intensified as the reaction mixture was permitted to stand for longer times in contact with the alkali metal as the solution warmed to room temperature. At the latter temperature the color became deep violet.

The sample prepared by the reaction of this compound with sodium–potassium alloy in THF gave the best resolved e.s.r. spectrum. This spectrum, Fig. 1, which was recorded at temperatures between −65 and −10 °C consists of 23

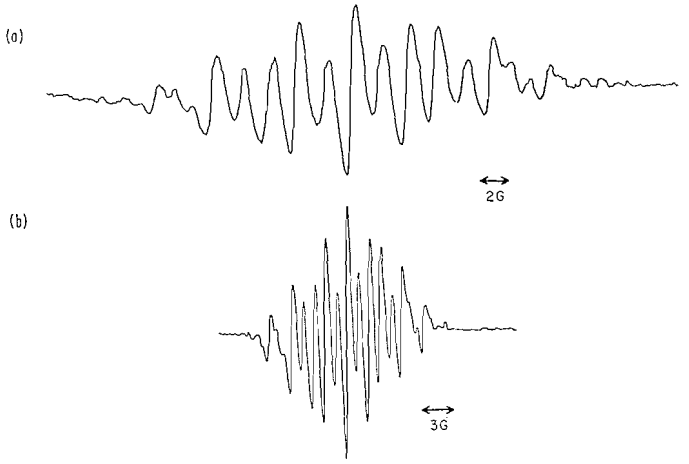

FIG. 1. Electron spin resonance spectrum of the free radical anion formed by the reaction of 4,4′-bis(diphenylphosphine)biphenyl with sodium–potassium alloy in THF: *a*, at −10 °C; *b*, at −65 °C.

lines. The overlap of the lines reduces the number of the lines from the expected 105 to 23. According to the hyperfine splitting constants and relative line intensities, these lines arise from the interaction of the unpaired electron of the radical anion with three different sets of equivalent nuclei. First, there is a triplet with a hyperfine splitting constant of 3.05 G which arises from the interaction with 2 phosphorus nuclei (spin of 1/2). These 3 lines have relative intensities of 1:2:1. Each of these 3 lines splits into 7 as a result of the interaction with a set of 6 equivalent protons. The hyperfine splitting constant of the splitting is 2.05 G and the relative line intensities are 1:6:15:20:15:6:1. The resultant lines each split into 5 lines of relative intensities 1:4:6:4:1, having a hyperfine splitting constant of 1.02 G. This is caused by the interaction with 4 equivalent protons. The 4 lines at both extreme ends of the spectrum almost disappear because of their low intensities.

The 6 equivalent protons are those on 2 phenyl groups. They are the 2 in the ortho position and the 1 in the para position of each phenyl group. The ortho and para positions in the phenyl group usually have very similar electron densities as in triphenylphosphine (4) and its oxide (3). Since each phenyl group should be attached to a separate phosphorus atom, this means that the reaction of this compound with alkali metals resulted in cleavage of 1 phenyl group from each phosphorus atom. The set of 4 equivalent protons which caused the quintet splitting are on the biphenyl part of the molecule, namely, at positions 9, 14, 23, and 26. This analysis suggests the following radical–anion structure

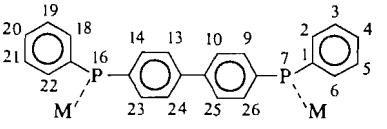

The resolution of the e.s.r. spectrum appeared to be temperature dependent. As the temperature of the sample was raised to room temperature, the resolution of the spectrum decreased, particularly in the middle portion of the spectrum. In this poorly resolved spectrum, Fig. 2, the central lines became broader and, as a result, some lines disappeared. However, additional splitting appeared, especially for those lines at the extreme ends of the spectrum. This additional splitting is in the form of a quintet which is caused by the interaction of a set of four equivalent protons. The hyperfine splitting constant of this quintet is 0.4 G and the relative intensities

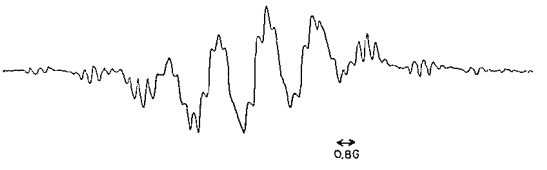

FIG. 2. Electron spin resonance spectrum of the free radical anion formed by the reaction of 4,4′-bis(diphenylphosphine)biphenyl with sodium–potassium alloy in THF at room temperature.

Can. J. Chem. Downloaded from www.nrcresearchpress.com by 210.87.254.6 on 09/05/12
For personal use only.

are 1:4:6:4:1. These protons are believed to be in positions 10, 13, 24, and 25. No alkali metal splitting was observed.

Acknowledgments

The authors express their appreciation for financial support to the Robert A. Welch Foundation of Houston, Texas, and to the United States Atomic Energy Commission, contract AT-(40-1)-2733.

1. R. G. JONES and H. GILMAN. Organic reactions. Vol. VI. John Wiley and Sons, Inc., New York. 1951. Chap. VII.
2. M. D. CURTIS and A. L. ALLRED. J. Amer. Chem. Soc. **87**, 2554 (1965).
3. A. H. COWLEY and M. H. HNOOSH. J. Amer. Chem. Soc. **88**, 2595 (1966).
4. A. D. BRITT and E. T. KAISER. J. Phys. Chem. **69**, 2775 (1965).
5. H. H. SISLER and NATHAN L. SMITH. J. Org. Chem. **26**, 611 (1961).
6. L. D. QUIN and H. G. ANDERSON. J. Amer. Chem. Soc. **86**, 2090 (1964).
7. R. A. ZINGARO and R. M. HEDGES. J. Phys. Chem. **65**, 1132 (1961).
8. W. KUCHEN and H. BUCHWALT. Ber. **91**, 2871 (1958).
9. (*a*) R. R. HOLMES. J. Phys. Chem. **64**, 1295 (1960). (*b*) R. R. HOLMES. J. Amer. Chem. Soc. **82**, 5285 (1960).
10. A. BURG. J. Amer. Chem. Soc. **83**, 2226 (1961).

Can. J. Chem. Downloaded from www.nrcresearchpress.com by 210.87.254.6 on 09/05/12
For personal use only.

Can. J. Chem. Downloaded from www.nrcresearchpress.com by 210.87.254.105 on 09/05/12
For personal use only.

Infrared studies on rotational isomerism. IV. 2-Cyanoethanol

MICHEL SCHNEIDER AND PAUL A. GIGUÈRE
Département de Chimie, Université Laval, Québec, Québec

Received August 22, 1969

From the infrared spectra of the vapor measured between 4000 and 200 cm^{-1}, 2-cyanoethanol was found to exist as *gauche* and *trans* isomers in roughly equal proportions around 100 °C. The *gauche* form is the more stable of the two, as in 2-chloro- and 2-bromo-ethanol, but the enthalpy difference is less than half as large; at most 0.7 kcal $mole^{-1}$. This indicates some weak (about 1 kcal $mole^{-1}$) intramolecular hydrogen bonding between the OH group and the π electrons of the C≡N bond.

In the solid, two distinct crystalline phases have been observed. Crystal II, consisting of *gauche* molecules only, is normally obtained; for instance by annealing the vitreous solid from low temperature deposition of the vapor. Crystal I, which contains the two isomers, may be obtained irreversibly from the melt of crystal II under controlled conditions.

On the other hand there was no indication in the spectra of a cyclic tautomer as suggested recently.

Les spectres infrarouges de la vapeur pris entre 60 et 140 °C ont confirmé la présence dans le 2-cyanoéthanol ($CN—CH_2—CH_2—OH$) de deux isomères de rotation, le *gauche* et le *trans*, en proportions à peu près égales. L'isomère *gauche* est le plus stable des deux, comme dans le 2-chloro- et le 2-bromo-éthanol; cependant la différence d'enthalpie est moins de la moitié de ceux-ci, soit 0.7 kcal $mole^{-1}$ tout au plus. Ceci doit être attribué à une liaison hydrogène intramoléculaire faible (environ 1 kcal $mole^{-1}$) entre le groupe OH et les électrons π de la liaison C≡N.

Tout commele 2-chloroéthanol, le 2-cyanoéthanol peut exister sous deux phases cristallines distinctes. La phase normale (II) faite de molécules *gauches* seulement, peut se transformer par fusion ménagée en une phase métastable (I) qui contient les deux isomères.

Par ailleurs on ne trouve dans les spectres aucune indication d'une forme tautomère cyclique telle que proposée récemment.

Canadian Journal of Chemistry, 47, 4685 (1969)

Introduction

Continuing this series of investigations on rotational isomerism in the 2-substituted ethanols (1), we have considered next 2-cyanoethanol, also called hydracrylonitrile, ethylene cyanohydrin or, as a derivative of propane, 3-hydroxypropanenitrile, or β-hydroxypropionitrile. Published information on the molecular configuration of this compound is scanty and in part contradictory. An early Raman study of the liquid (2) has led to no definite conclusion in that respect. Electron diffraction by the vapor (3) has been interpreted in terms of one isomer only, the *trans*. In contrast the two isomers were found to be present in dilute solutions in carbon tetrachloride (4), the *gauche* being only slightly more stable (by 0.14 ± 0.03 kcal $mole^{-1}$). Since stabilization by solvent could be suspected in that case, it seemed desirable to apply the spectroscopic methods to the free molecule.

Experimental

The commercial product (Hopkins and Williams) was distilled repeatedly under 13–15 Torr pressure in a current of dry nitrogen until the final middle fraction passing at 106–107 °C was colorless and pure as shown by the absorption spectrum. It could be kept in that condition for a few weeks if stored in the cool, in a dark flask under nitrogen atmosphere. Because of its low volatility, of the order of 0.1 Torr at room temperature, a 10 m multiple reflection cell heated electrically was used, as described previously (5). The liquid sample kept at 50 °C in a side flask was entrained in a current of dry nitrogen. The spectra were recorded at various temperatures of the vapor cell from 70 to 140 °C. Above that range, decomposition became noticeable as shown in particular by the bands of ammonia in the 700–1100 cm^{-1} region and the C=O bands at 1700–1800 cm^{-1}.

Discussion of Results

The main evidence for the two rotational isomers in the vapor of 2-cyanoethanol comes, of course, from the O—H bands at 3 μ. These consist of two overlapping doublets (Fig. 1) of which that at higher frequency, 3682/3674 cm^{-1}, increases in intensity with temperature. Accordingly it must belong to the less stable isomer and, logically, to the "free" OH group of the *trans*, as in 2-chloro- and 2-bromo-ethanol (5). Further confirmation of this comes from the P- and R-branch separation calculated as explained below. The average frequency difference of some 38 cm^{-1} between the O—H stretching of the two isomers (compared with 15 cm^{-1} in CCl_4 solution

Can. J. Chem. Downloaded from www.nrcresearchpress.com by 210.87.254.105 on 09/05/12
For personal use only.

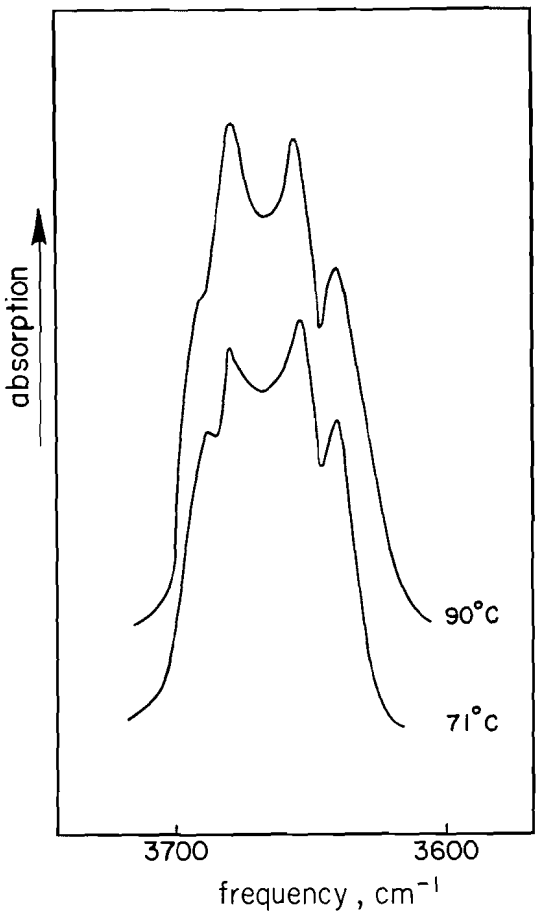

FIG. 1. The O—H stretching bands of 2-cyanoethanol vapor.

(4)) is of the same magnitude as in the 2-haloethanols. However, as explained before, for that type of molecule, this parameter is not a direct measure of the importance of the hydrogen bond. Because the spectra of the deuterated alcohol CN—CH_2—CH_2—OD are not available, identification of the other OH modes must rest on analogy with related molecules. Thus the band at 1332 cm^{-1} in the midst of the CH_2 wagging group is assigned tentatively to the OH bending of the *gauche* isomers. The corresponding *trans* mode is probably lying around 1170 cm^{-1} among the CH_2 twisting bands. As for the OH torsions, only that of the *gauche* molecule could be identified, namely with the 296 cm^{-1} band which also shows a marked temperature effect.

The spectra of the liquid and the vapor in the region from 4000 to 1500 cm^{-1} have the same general appearance as those of 2-chloro- and 2-bromo-ethanol, except of course for the C—N stretching band near 2260 cm^{-1}. The latter shows no sign of any doubling in the vapor, even at the higher temperature of our measurements, 140 °C. Therefore, it is not affected by rotational isomerism as may be gathered from the geometry. Surprisingly, its intensity in the vapor spectra is quite low; less than 10% of that of the strongest bands. This peculiarity has already been noticed in other molecules with a cyano group near to an oxygen atom (6). On the other hand, the C—CN vibrational frequency at 990 cm^{-1} in the *gauche* isomer is shifted down by some 50 cm^{-1} in the *trans* isomer (Table I). The present assignment agrees with that of Fujiyama *et al.* for succinonitrile (7). It is further confirmed by our force constant calculations (8). In a recent study of the related molecules X—CH_2—CH_2—CN (where X = Cl, Br, and I) Wyn-Jones and Orville-Thomas (9) concluded that the C—C and the C—CN stretching modes are strongly coupled. Accordingly they assigned to them the bands at 984 and 907 cm^{-1}, respectively, assuming they have the same frequency in the two rotational isomers. We doubt if these two modes are strongly coupled since their force constants and bond lengths are fairly different. Assignment of the other experimental frequencies was made by analogy with the other 2-substituted ethanols. The various bending modes of the skeleton, in particular those of the CCN group, were identified first in the solid phase spectra, as explained below.

Enthalpy Difference

The spectra of 2-cyanoethanol vapor do not lend themselves as well as those of the 2-haloethanols to intensity measurements. Indeed, the characteristic bands of the rotational isomers are either rather weak, poorly developed (e.g. the CCC bending mode of the *trans* conformer), or overlapped (e.g. the C—CN stretching of the *gauche*). Eventually the O—H stretching bands had to be used in spite of their strong overlap. Optical density measurements lead to a value of $\Delta H = 0.7$ kcal $mole^{-1}$ with a large estimated uncertainty; viz. $\pm$ 0.3 kcal $mole^{-1}$. From the near equal intensity of the two doublets in the temperature range covered here (Fig. 1), it might be concluded that the two isomers are present in roughly equal amounts. However, this is

Can. J. Chem. Downloaded from www.nrcresearchpress.com by 210.87.254.105 on 09/05/12
For personal use only.

TABLE I

Vibrational spectra of 2-cyanoethanol*

Raman liquid	Infrared Liquid	Infrared Vapor	Assignments
		3682 m, 3674 s	O—H stretching (*t*)
	3420 s	3647 s, 3633 m	O—H stretching (*g*)
2995, 2973, 2934 vs	2960, 2940, 2905 s	2976 s, 2952, 2901 s	C—H stretching
2250 vs	2255 s	2262 w	C—N stretching
1496, 1474 s	1473 w	1420 w	CH_2 scissoring
1416 m	1414 s	1395, 1386, 1375 s	CH_2 wagging
1380 vw	1385 m	1332 m	OH bending (*g*)
1327 vs, 1293 w	1325 m, 1300 w	1312 m	CH_2 wagging
1248 m	1245 m	1221, 1210 m	CH_2 twisting
1205 vw	1185 m	1190, 1175 m	CH_2 twisting
1060 m	1061 vs	1076 vs, 1063 vs, 1045 w	C—O stretching
	1030 w	1030 m, 1015 w	C—C stretching
1010 w			
995 w	996 w	990 w	C—CN stretching (*g*)
940?	942 w	948, 939, 932 m	C—CN stretching (*t*)
851 vs	850 m	859 m	CH_2 rocking (*g*)
829 vs	830 w	834 m	CH_2 rocking (*t* and *g*)
	750 vw	720 vw	CH_2 rocking (*t*)
577 m	580 m	573, 560 m	CCC bending (*g*)
524 m			CCC bending (*t*)
391 w	390 m	392 s	CCO bending (*g*)
376 s	376 m	380 s	CCN bending (*g*)
		305 s	CCO bending (*t*)
	600 m	296 s	OH torsion (*g*)
	280 vw		CCN bending (*t*)
217 m	215 vw		CCN bending (*g*)
170 vw	~184 w		CCN bending (*t*)
	~148 w		C—C torsion (*g*)
	126?		C—C torsion (*t*)

*Frequencies in cm^{-1}; s = strong, m = medium, w = weak, v = very, *t* = *trans*, *g* = *gauche*.

assuming that the absorption coefficients are about the same for both isomers. Not to be overlooked, also, is the possibility of nonbonded *gauche* isomers which will be even more important here than in the 2-haloethanols, in view of the still weaker intramolecular hydrogen bonds. For these reasons we consider the above value of ΔH as a maximum. The much lower value, 0.14 kcal $mole^{-1}$, found in dilute CCl_4 solutions (4) confirms the existence of an appreciable solvent effect. Recently Fletcher (10) has reported surprisingly strong interactions between so-called inert solvents and various alcohols in dilute solutions.

By analogy with succinonitrile (11) and the 1–2 halocyanoethanes (9), for which the *trans* form is the most stable, it is clear that in 2-cyanoethanol the *gauche* form is stabilized by some interaction of the OH group with the CN group. The latter is well known to be a fairly good proton acceptor through the lone pair orbital along the C≡N bond. In the present case, however, the geometry is much less favorable. Presumably the OH group points towards the cyanogen carbon so that the π electrons of the latter may be visualized as the acceptor. Considering that in 1–2 chlorocyanoethane the *trans* isomer is more stable by 0.38 kcal $mole^{-1}$ (9), we estimate the energy of the intramolecular hydrogen bond in 2-cyanoethanol as 1 kcal $mole^{-1}$ at the most. The weakness of this hydrogen bond is further confirmed by the low frequency of the OH torsion mode in the *gauche* isomer, 296 cm^{-1}, not much above that of methanol, 270 cm^{-1} (12).

The present conclusion on rotational isomers in 2-cyanoethanol raises a question about the electron diffraction study (3) which detected only the less stable conformer, the *trans*. Here the uncertainty as to temperature of the vapor in the diffractometer is of little consequence in view of the low ΔH of isomerization. Interference from certain diffraction centers is always a possibility with such rather complex molecules. Still, it is surprising that the radial distribution curve shows no indication whatsoever of a maximum near 2.95 Å, the expected O . . . CN distance in the *gauche* molecule. Using the bond lengths and angles found or assumed by Yamaha, we have calculated the moments of inertia of the *trans* isomer (Table II). The same parameters were used for the *gauche*, with an azimuthal angle of 65°, close to that found by microwave for the 2-haloethanols (13). From these data the separation of the P and R branches of vibrational bands were calculated by the usual method (14). The results, 12 cm^{-1} for the *trans* and 16 cm^{-1} for the *gauche* isomer, agree satisfactorily with the

Can. J. Chem. Downloaded from www.nrcresearchpress.com by 210.87.254.105 on 09/05/12
For personal use only.

experimental ones. The barrier to internal rotation about the C—C bond, estimated from the reduced moments of inertia (Table II), was 3.1 kcal mole^{-1} based on a torsional frequency of 130 cm^{-1} for the *gauche* molecule, and 3.6 kcal mole^{-1} using a frequency of 115 cm^{-1} for the *trans*. The latter is probably too high, which may account for the discrepancy.

TABLE II

Moments of inertia of 2-cyanoethanol (in g cm^2 × 10^{-40})

Isomer	I_A	I_B	I_C	$I_{red.}$
trans	19.17	223.35	236.17	20.40
gauche	45.92	151.09	182.15	15.41

Spectra of the Solid Phases

As in general with hydroxylic compounds, the solid obtained by rapid cooling of the liquid 2-cyanoethanol was vitreous in nature. Crystalline spectra could be obtained by slow cooling, down to about −80 °C, of a liquid film between plates of NaCl, AgCl, CsBr, or polyethylene. Usually crystallization occurred after 30–60 min at that temperature. The crystal thus obtained, hereafter called crystal II after the accepted convention,[1] showed the infrared bands of the *gauche* isomer only, as expected. Now, since 2-chloroethanol was found to crystallize in a second form, crystal I, we tried to reproduce the same phenomenon in the cyano alcohol. This was achieved eventually by annealing a film of the vitreous solid between two windows of polyethylene at liquid nitrogen temperature. Around −87 °C a new form of crystal appeared as a white powder. Its far infrared spectrum revealed more bands than in crystal II. As experienced before, phase I turned out to be much more difficult to prepare on a crystalline support of the ionic type, e.g. NaCl, CsBr, etc. Details of the experimental procedure as well as the temperature relationships will be reported elsewhere.

Assignment of the various bands in crystal I (Table III) is based on the spectra of the liquid which is known to contain both *trans* and *gauche* isomers. The major differences between the two crystalline spectra occur at low frequency, especially below 350 cm^{-1}. The new bands were very useful in assigning the various bending modes of the skeleton; e.g. the CCN out-of-plane and the torsional modes. In the middle infrared the broad band at 649 cm^{-1} was assigned to OH torsion on the basis of a strong temperature effect; indeed, it is shifted by some 25 cm^{-1} to lower frequency at −90 °C. The multiplet structure may be due to combinations with lattice modes or again to different crystallographic sites for the OH groups. Unaccountably two bands are missing in the spectra of crystal I, namely the CCC bending and the C—CN stretching of the *trans* isomer. The former was detected only in the Raman spectrum of the liquid, and the latter is extremely weak even in the liquid, for some unknown reason. Finally, it may be noted that the relative intensities of the crystal I bands are practically the same as in the liquid, contrary to crystal II.

The Presumed Cyclic Tautomer

Matsui and Ishimoto (15) have reported spectroscopic data indicating that in the ω-cyanoalkanols, the electrophilic hydrogen of the hydroxyl group may lead to cyclization through the cyano group. In particular, in the case of 2-cyanoethanol they have observed in the infrared spectrum of the liquid at room temperature a medium intensity band at 1772 cm^{-1} which they assigned to the C=N stretching mode of a cyclic iminolactone tautomer, **2**, supposedly in equilibrium with **1**. We have never observed such an

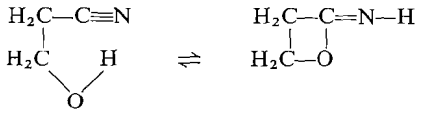

1 **2**

absorption band in the pure compound. Only at higher temperature in the vapor, when decomposition set in, did the C=O bands gradually emerge in that region. Incidentally, the spectra of 3-cyanopropanol and 4-cyanobutanol published by the Japanese authors also show a band at 1770 cm^{-1} besides the stronger ones at 1695 and 1676 cm^{-1}, respectively, which they correctly assigned to the C=N stretching. Furthermore, tautomer **2**, if present in appreciable concentration, should exhibit some other characteristic bands contrary to observations. Therefore, we conclude that the available data provide no

[1]By mistake this convention was not observed in our previous paper (5).

Can. J. Chem. Downloaded from www.nrcresearchpress.com by 210.87.254.105 on 09/05/12
For personal use only.

TABLE III

Spectra of the solid phases of 2-cyanoethanol*

Raman, crystal II	Infrared			Assignments
	Crystal II	Crystal I	Glassy	
3347 s 3219 s 3205 s	3330 s 3250 sh 3083 sh	3220 s 3150 sh	3200 s	O—H stretching
2994 2970 2961 s 2928 2910	2987 w 2970 w 2960 m 2929 w 2908 m 2880 w	2995 w 2964 m 2938 w 2905 m 2845 w	2960 m 2940 w 2905 m	C—H stretching
2245 2251 m	2246 m	2251 m		C≡N stretching
1482 s	1502 m 1463 m	1469 m	1468 m	CH_2 scissoring
1420 w 1408 w	1420 m 1405 m	1415 m 1405 m	1411 m	CH_2 wagging
1380 s	1374 w	1380 1370	1377 w	OH bending
1258 s	1257 1217 s	1241 m	1241 m	CH_2 twisting (g)
		1205 1194 vw	1191 vw	CH_2 twisting (t)
1068 s	1070 1061 s	1070 s 1060 s	1055 s	C—O stretching (g)
		1052 1045 s	1055 s	C—O stretching (t)
1040 m	1041 1032 w	1040 1031 w		C—C stretching
998 m	997 m	999 m	997 m	C—CN stretching (g)
			941 vw	C—CN stretching (t)
850 vs 828	850 s 830 m	849 m 830 m 825 m	850 m 830 m	CH_2 rocking (g)
		725 w		CH_2 rocking (t)?
	618 s	649 m	650 m	OH torsion
584 w	583 s	583 579 s	580 m	CCC bending (g)
392 m 384 m 379 m	395 s 383 s	398 m 393 m 379 m	390 370 m	CCO bending (g)
	340 m	296 w 278 m	264 w	CCN bending (t)
214 s	216 w	230 w 216 w	220 w	CCN bending (g)
		172 w	185 w	CCN bending (t)
155 w 135 w	137 s	143 s	140 sh	C—C torsion
101 m	104 vs	115 vs 102 vs	120 s	Librations ?
87, 71 60, 37		85, 62 47	70	Lattice modes

*See footnote of Table I for meaning of abbreviations.

ground for postulating cyclic tautomerism in 2-cyanoethanol.

Acknowledgments

The authors wish to acknowledge the financial assistance from the National Research Council of Canada. In the early part of this investigation the junior author (M. S.) held a NRCC fellowship. The authors are grateful to Dr. Paul Buckley for his sustained interest.

1. P. BUCKLEY and P. A. GIGUÈRE. Can. J. Chem. **45**, 397 (1967).
2. K. W. F. KOHLRAUSCH and G. P. YPSILANTI. Z. Phys. Chem. B**29**, 274 (1935).
3. M. YAMAHA. Bull. Chem. Soc. Japan, **29**, 876 (1956).
4. P. J. KRUEGER and H. D. METTEE. Can. J. Chem. **43**, 2888 (1965).
5. P. BUCKLEY, P. A. GIGUÈRE, and M. SCHNEIDER. Can. J. Chem. **47**, 901 (1969).
6. R. E. KITSON and N. E. GRIFFITH. Anal. Chem. **24**, 334 (1952).
7. T. FUJIYAMA, K. TOKUMARU, and T. SHIMANOUCHI. Spectrochim. Acta, **20**, 415 (1964).
8. M. SCHNEIDER. Ph.D. Thesis, Université Laval, Québec. 1969.
9. E. WYN-JONES and W. J. ORVILLE-THOMAS. J. Chem. Soc. A**1**, 101 (1966).
10. A. N. FLETCHER. Abs. Phys. 019, 157th ACS National Meeting, Minneapolis, 1969.
11. W. E. FITZGERALD and G. J. JANZ. J. Mol. Spectrosc. **1**, 49 (1957).
12. D. G. BURKHARD and D. M. DENNISON. J. Mol. Spectrosc. **3**, 299 (1959).
13. R. G. AZRAK. Symp. Mol. Structure Spectrosc., Columbus, Ohio, 1968.
14. S. L. GERHARD and D. M. DENNISON. Phys. Rev. **43**, 197 (1933).
15. H. MATSUI and S. ISHIMOTO. Tetrahedron Lett. 1827 (1966).

Can. J. Chem. Downloaded from www.nrcresearchpress.com by 210.87.254.105 on 09/05/12
For personal use only.

Coordination compounds of olefins with anhydrous silver salts. IV. Complexes with some endocyclic monoolefins[1]

H. W. QUINN AND R. L. VANGILDER
Exploratory Research Laboratory, Dow Chemical of Canada, Limited, Sarnia, Canada

Received June 25, 1969

A study has been made of the changes in the infrared and nuclear magnetic resonance (n.m.r.) spectra of cyclopentene, cyclohexene, cycloheptene, and *cis*-cyclooctene, and of their 1-methyl-substituted analogues upon formation of the silver tetrafluoroborate complexes, $AgBF_4 \cdot 2$olefin. Based on the perturbation of the double bond stretching frequency in the olefin, the order of decreasing strength of the silver ion – olefin interaction is cyclopentene > cyclohexene > *cis*-cyclooctene ≈ cycloheptene.

Canadian Journal of Chemistry, 47, 4691 (1969)

Can. J. Chem. Downloaded from www.nrcresearchpress.com by 210.87.254.105 on 09/05/12
For personal use only.

Introduction

Endocyclic monoolefins produce, in general, more stable silver ion complexes than do the corresponding *cis*-2-olefins (1, 2). The difference has been attributed to the effect of ring strain upon the π basicity of the olefin and thus upon the strength of the coordinate bond (1). Distribution studies with aqueous $AgNO_3$ (1) have produced the order of increasing complex stability

cyclopentene > cycloheptene
> cyclohexene > *cis*-cyclooctene

By contrast, the order obtained by a gas chromatographic technique employing $AgNO_3$ dissolved in ethylene glycol (2) is

cis-cyclooctene > cycloheptene
> cyclopentene > cyclohexene

The difference has been attributed in part (2) to differences in the physical state of the systems or to the different solvents employed.

Our earlier studies (3, 4) of the silver tetrafluoroborate complexes of acyclic monoolefins have indicated a relationship between the low frequency shift of the double bond stretching vibration and the strength of the silver ion – olefin coordinate bond. The present study was undertaken with the aim of establishing, by use of the above criterion, a relative order of strength of the coordinate bond between $AgBF_4$ and the cycloolefins having from 5 to 8 carbon atoms in the ring, and a comparison of that order with those reported earlier for the relative stability of the complexes. The investigation has involved determination of complex stoichiometry and of the changes in the infrared and n.m.r. spectra of the olefins upon complexing.

[1]Contribution No. 173.

Experimental

Anhydrous silver tetrafluoroborate was prepared from silver fluoride and boron trifluoride as previously described (3) or purchased from Peninsular Chemical Research Inc., Gainesville, Florida. The purchased material was thoroughly degassed to remove traces of hydrogen fluoride and stored under petroleum ether.

Cyclopentene and cyclohexene were Phillips Research Grade and Pure Grade materials, respectively. The other olefins were obtained either from Columbia Organic Chemical Company or from Aldrich Chemical Company with 95 mole% minimum purity. When required for satisfactory determination of spectral shifts, the olefin was purified by preparative-scale gas chromatography.

Determination of Complex Stoichiometry

(a) Cyclopentene

Anhydrous $AgBF_4$ (2.969 g, 15.25 mmoles) was exposed at 25 °C to cyclopentene vapor in equilibrium with its liquid in a reservoir at 0 °C (130 Torr). After 16 h, the olefin uptake was 1.900 g (27.94 mmoles) yielding the system of stoichiometry $AgBF_4 \cdot 1.829C_5H_8$. The temperature of the olefin reservoir was raised to 24 °C (olefin pressure = 366 Torr) and over 24 h an additional 0.861 g (12.66 mmoles) was absorbed yielding $AgBF_4 \cdot 2.773C_5H_8$. The temperature dependence of the complex dissociation pressure was determined between 0 and 30 °C for the latter system employing a mercury manometer read to ± 0.01 mm with a cathetometer. The dissociation pressure of the complex with an olefin: silver mole ratio of 2:1 or less was too low to be measured with this technique.

A 1.930 g (9.91 mmoles) sample of $AgBF_4$ exposed at 25 °C to cyclopentene vapor in equilibrium with liquid in a reservoir at 24 °C over a period of 4 days absorbed 1.913 g (28.13 mmoles) C_5H_8 to yield $AgBF_4 \cdot 2.834C_5H_8$. Upon cooling the reservoir at 0 °C for 20 h and at −80 °C for 6 h, 0.565 g (8.31 mmoles) olefin was removed from the system to leave a complex of stoichiometry $AgBF_4 \cdot 1.997C_5H_8$.

(b) Cyclohexene

$AgBF_4$ (0.396 g, 2.03 mmoles) was exposed at 25 °C

over a period of 4 days to cyclohexene vapor in equilibrium with its liquid at 0 °C (25 Torr). The salt absorbed 0.316 g (3.85 mmoles) olefin to yield $AgBF_4 \cdot 1.893C_6H_{10}$.

(c) Other Olefins

Infrared and n.m.r. spectra of $CDCl_3$ solutions of the olefin–$AgBF_4$ systems indicate the 2:1 olefin:silver ratio for the most stable complex with each olefin. Beyond the 2:1 stoichiometry, the infrared spectrum has bands corresponding to uncomplexed olefin and the proton chemical shifts in the n.m.r. spectrum are smaller, indicative of averaging of the spectra of complexed and free olefin molecules (4).

Spectroscopic Studies

The infrared spectra were obtained from fluorolube and Nujol mulls or $CDCl_3$ solutions of the complexes on either a Beckman IR-9 or a Perkin–Elmer 221 recording spectrophotometer employing cells with KBr windows. The n.m.r. spectra of deuterochloroform solutions of the complexes were recorded with a Varian A60 proton resonance spectrometer and the chemical shifts are expressed in c.p.s. with respect to tetramethylsilane as an internal standard.

Results and Discussion

Stoichiometry of Complexes

As has been observed with the cycloolefin complexes of $AgNO_3$ (5–7) and $AgClO_4$ (7, 8), the most stable complexes of $AgBF_4$ with the endocycloolefins have an olefin:silver ion mole ratio of 2:1. Cyclopentene has been found also to form the much less stable 3:1 complex which at 25 °C has an equilibrium dissociation pressure of about 206 Torr (the saturation vapor pressure of C_5H_8 at 25 °C is 280 Torr). For the dissociation equilibrium

$$AgBF_4 \cdot 3C_5H_8(s) \rightleftharpoons AgBF_4 \cdot 2C_5H_8(s) + C_5H_8(g)$$

the dissociation pressure equation, $\log P$ (Torr) $= 12.727 - 3105/(273.2 + t\,(°C))$ (over the range 0–30 °C), yields values for the standard enthalpy change and standard entropy change (at 25 °C and 1 international atm. pressure) of 14.20 ± 0.04 kcal mole^{-1} and 45.05 ± 0.01 cal mole^{-1} degree^{-1}, respectively. The $\log P$ vs. $1/T$ dissociation line for the 3:1 complex intersects the saturation vapor pressure line for cyclopentene, as defined by its Antoine equation (9), at about 40 °C.

The 3:1 complexes have not been detected with the other cycloolefins studied but it must be observed that the pursuit of them has not been diligent.

Infrared Spectra

The spectra of the complexes are quite analogous to those of the free olefins with the largest frequency shifts being observed for the double bond stretching mode (shift to lower frequency) and the out-of-plane deformation mode at about 700 cm^{-1} for the olefinic hydrogens (shift to higher frequency). The latter shift amounts to 59 cm^{-1} for cyclopentene and 33 cm^{-1} for cyclohexene (4). With the complexes of the other cycloolefins, the complexity of this region of the spectrum of the Nujol mulls made it impossible to accurately define the deformation band. With the $CDCl_3$ solution, there was strong solvent absorption in this region.

In Table I are reported the double bond stretching frequencies, $\nu_{C=C}$, for the olefins in $CDCl_3$ solution and for the complexes either in solution or as Nujol mulls or both. The study has included the parent hydrocarbons from cyclopentene to *cis*-cyclooctene, their 1-methyl-substituted analogues, and the 3-methyl- and 4-methyl-cyclohexenes.

There appears to be little dependence of $\nu_{C=C}$ for the complexed olefin upon the anion of the silver salt. For the cyclopentene and cyclohexene complexes the values of $\nu_{C=C}$ are quite comparable to those obtained from the Raman spectra of aqueous $AgNO_3$ solutions of the olefins (10). Similarly, the value of $\nu_{C=C}$ from the Nujol mull of $AgBF_3 \cdot 2C_6H_{10}$ is essentially identical to that obtained from the mull of $AgClO_4 \cdot 2C_6H_{10}$ (8). On the basis of the $\Delta\nu_{C=C}$ values from the solution spectra, the order of relative perturbation of the double bond by the silver ion appears to be

cyclopentene > cyclohexene
> *cis*-cyclooctene ≈ cycloheptene

The difference between the $\Delta\nu_{C=C}$ values for the latter two olefins is not greater than the uncertainty in the values themselves.

As has been observed with the acyclic olefins (3, 4), methyl substitution at the double bond results in a stronger interaction between the olefin and silver ion as evidenced by the greater perturbation in $\nu_{C=C}$ upon complex formation. This effect is undoubtedly due to an increase in the π basicity of the olefin as a result of the electron releasing inductive effect of the methyl substituent. Despite this evidence for stronger coordinate bonding, the 1-methyl-substituted cycloolefins have been reported (1, 2, 11) to form less stable complexes than do the parent hydrocarbons, presumably as a result of the steric effect of the

Can. J. Chem. Downloaded from www.nrcresearchpress.com by 210.87.254.105 on 09/05/12
For personal use only.

TABLE I

Infrared and n.m.r. data from spectra of cycloolefins and their $AgBF_4$ complexes

Olefin	Double bond stretching frequency (cm^{-1})				Chemical shift of olefinic protons (c.p.s.)		
	$\nu_{C=C_{olefin}}$	$\nu_{C=C_{complex}}$		$\Delta\nu_{C=C}$			
		Solution	Mull	Solution	ν_o*	ν_c*	$\Delta\nu$
Cyclopentene	1617	1542	1538	75	344	396	52
Cyclohexene	1655	1587	1583	68	339	389	50
Cycloheptene	1650	1588	1587	62	347	396	49
cis-Cyclooctene	1652	1588	1588	64	337	376	39
1-Methylcyclopentene	1645	1562		83	317	358	41
1-Methylcyclohexene	1672	1595		77	323	358	35
1-Methylcycloheptene	1669	1595		74	333	374	41
1-Methyl-*cis*-cyclooctene	1672	1597		75	322	356	34
3-Methylcyclohexene	1650	1585		65	334	386	52
4-Methylcyclohexene	1655	1588		67	339	386	47

*ν_o and ν_c represent n.m.r. chemical shift of olefinic protons in olefin and complex, respectively.

substituent group. With the 1-methyl-substituted cycloolefins, the order of relative double bond perturbation, i.e. of $\Delta\nu_{C=C}$, upon complexation is

1-methylcyclopentene > 1-methylcyclohexene
> 1-methyl-*cis*-cyclooctene ≈ 1-methylcycloheptene

identical to the order shown by the parent hydrocarbons.

The difference between the relative magnitude of the double bond perturbation upon complexation and the order of complex stability previously observed may be largely attributable to steric effects. While the double bond perturbation may be a measure of the strength of the interaction between the olefin and silver ion and closely related to the enthalpy change upon complexation (3), the complex stability will be more directly related to the free energy change which reflects the contribution of steric effects to the entropy change.

The relative magnitude of $\Delta\nu_{C=C}$ for 3-methyl- and 4-methyl-cyclohexene parallels the calculated relative basicity of the double bond in 3-methyl- and 4-methyl-cycloolefins (11), but it is the inverse of the relative stability of the $AgNO_3$ complexes as determined by the gas chromatographic technique (12).

Nuclear Magnetic Resonance Spectra

In Table I are recorded the values of the chemical shift for the olefinic protons in both free and complexed olefins. The greater shielding of these protons in cyclohexene and *cis*-cyclooctene than cyclopentene and cycloheptene parallels the ^{13}C chemical shifts for the trigonal carbon atoms (13). As has been observed with other olefins (4), formation of the silver ion complex results in a deshielding of the olefinic protons by about 30–50 c.p.s. There was also observed upon complexing a deshielding of the methylene protons adjacent to the double bond of about 10 c.p.s. in the parent cycloolefin and of 10–20 c.p.s. in the 1-methyl-substituted olefins, the magnitude of the latter increasing with increasing ring size. Similarly, the protons of the 1-methyl substituents were deshielded by about 20 c.p.s.

An attempt to relate the magnitude of the deshielding of the olefinic protons to the strength of the coordinate bond for either series of cycloolefins would produce a quite different order of relative bond strength from that obtained from the values of $\Delta\nu_{C=C}$. Since with the 1-methyl-substituted olefins the proton deshielding upon complexing is smaller than with the parent compounds while, on the other hand, the change in the double bond stretching frequency is greater, it is obvious that both sets of data cannot be used satisfactorily for determination of relative bond strengths. It is our view that the infrared data provide a better basis for such an assessment. As has been discussed previously (4), the deshielding of the olefinic protons as a result of the σ-component of the coordinate bond is at least partially compensated by a shielding effect produced by the π-component involving metal d-electrons. The fact of net deshielding indicates a stronger

Can. J. Chem. Downloaded from www.nrcresearchpress.com by 210.87.254.105 on 09/05/12
For personal use only.

σ- than π-component. Others have suggested also that this is the case (1). The observed smaller deshielding with the 1-methyl-substituted olefins is probably a result of asymmetric positioning of the silver ion with respect to the double bond which places it closer to the 2-carbon thereby permitting more effective d-electron shielding at C_2 than at C_1 (4).

Acknowledgments

The authors acknowledge with gratitude the contributions of H. D. Mak of this laboratory and of D. J. Peterson of the Analytical Laboratory, Dow Chemical of Canada, Limited who have obtained the n.m.r. and infrared spectra, respectively.

1. J. G. TRAYNHAM and J. R. OLECHOWSKI. J. Amer. Chem. Soc. **81**, 571 (1959).
2. M. A. MUHS and F. T. WEISS. J. Amer. Chem. Soc. **84**, 4697 (1962).
3. H. W. QUINN and D. N. GLEW. Can. J. Chem. **40**, 1103 (1962).
4. H. W. QUINN, J. S. MCINTYRE, and D. J. PETERSON. Can. J. Chem. **43**, 2896 (1965).
5. W. D. JONES. J. Chem. Soc. 1808 (1954).
6. A. C. COPE, D. C. MCLEAN, and N. A. NELSON. J. Amer. Chem. Soc. **77**, 1628 (1955).
7. A. E. COMYNS and H. J. LUCAS. J. Amer. Chem. Soc. **79**, 4339 (1957).
8. H. HOSOYA and S. NAGAKURA. Bull. Chem. Soc. Jap. **37**, 249 (1964).
9. F. D. ROSSINI, B. J. MAIR, and A. J. STREIFF. Hydrocarbons from petroleum. Reinhold Publishing Corp., New York. 1953. p. 206.
10. H. J. TAUFEN, M. J. MURRAY, and T. F. CLEVELAND. J. Amer. Chem. Soc. **63**, 3500 (1941).
11. W. H. PRITCHARD and W. J. ORVILLE-THOMAS. Theoret. Chim. Acta, **3**, 426 (1965).
12. E. GIL-AV and J. HERLING. J. Phys. Chem. **66**, 1208 (1962).
13. G. B. SAVITSKY and K. NAMIKAWA. J. Phys. Chem. **68**, 1956 (1964).

Can. J. Chem. Downloaded from www.nrcresearchpress.com by 210.87.254.105 on 09/05/12
For personal use only.

Can. J. Chem. Downloaded from www.nrcresearchpress.com by 210.87.254.40 on 09/05/12
For personal use only.

Some new tetrakis(*p*-tolyl)cyclobutadiene molybdenum complexes

A. EFRATY[1]
Department of Chemistry, University of Waterloo, Waterloo, Ontario

Received June 2, 1969

Tetrakis(*p*-tolyl)cyclobutadiene molybdenum dicarbonyl bromide dimer and (tetrakis(*p*-tolyl)cyclobutadiene)(cyclopentadienyl)molybdenum carbonyl bromide were prepared and their structures studied by proton magnetic resonance. An improved synthesis of tetraphenylcyclobutadiene molybdenum dicarbonyl bromide dimer is also described.

Canadian Journal of Chemistry, 47, 4695 (1969)

Introduction

Tetraphenylcyclobutadiene molybdenum dicarbonyl bromide dimer (**1**; R = Ph) was originally prepared by Maitlis and Games (1) and characterized as a tetraphenylcyclobutadiene molybdenum tricarbonyl bromide dimer, **2**. Recently, however, this compound has been shown, by a crystal structure study (2), to contain a tetraphenylcyclobutadiene ring, bromine bridges, and two carbonyl groups per molybdenum atom. Moreover, a relatively short Mo—Mo distance was detected which together with the reported diamagnetism of this compound suggested a strong metal–metal interaction. In this work additional information in support of structure (**1**; R = To = *p*-tolyl) is presented; also the structure of (tetrakis(*p*-tolyl)cyclobutadiene)(cyclopentadienyl)molybdenum carbonyl bromide (**3**; R = To) is discussed.

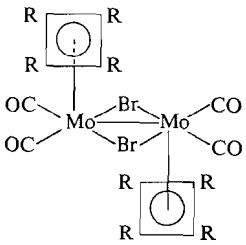

1

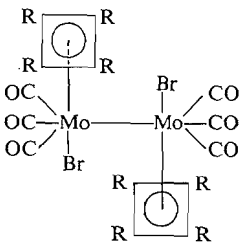

2

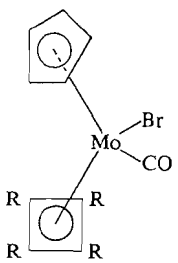

3

Results and Discussion

The molybdenum complex (**1**; R = Ph), on which the crystal structure study was performed (2), was isolated from the reaction of tetraphenylcyclobutadienepalladium bromide dimer with molybdenum hexacarbonyl in refluxing *p*-xylene. Under these conditions the product was obtained in 18% yield after 10 min of reaction. A similar reaction carried out in boiling benzene for a period of 67 h was previously reported (1) to afford only 7% yield of (**1**; R = Ph). The infrared spectrum of (**1**; R = Ph), isolated here, was identical to that of the material originally reported (1) and the proton magnetic resonance (p.m.r.) spectrum consisted of a singlet at 2.76 τ due to the phenyl protons.

Tetrakis(*p*-tolyl)cyclobutadiene molybdenum dicarbonyl bromide dimer (**1**; R = To) was prepared in 14% yield from tetrakis(*p*-tolyl)cyclobutadienepalladium bromide dimer and molybdenum hexacarbonyl by an exactly analogous reaction. The infrared spectrum of (**1**; R = To) showed two carbonyl stretching bands of similar intensity at 1965 and 2020 cm^{-1} as expected for a dicarbonyl compound of this nature, and the p.m.r. spectrum consisted of an AB quartet pattern centered at 2.94 τ and a singlet at 7.69 τ due

[1]Present address: Department of Chemistry, University of Georgia, Athens, Georgia, U.S.A.

Can. J. Chem. Downloaded from www.nrcresearchpress.com by 210.87.254.40 on 09/05/12
For personal use only.

to the AA'BB' and methyl protons of the *p*-tolyl groups.

Another novel molybdenum complex whose structure was investigated was the (tetrakis-(*p*-tolyl)cyclobutadiene)(cyclopentadienyl) molybdenum carbonyl bromide (**3**; R = To). This complex was prepared by the method previously reported (3) for (**3**; R = Ph). The infrared spectrum of (**3**; R = To) was similar to that of (**3**; R = Ph) and showed one carbonyl stretch at 1984 cm^{-1}. The p.m.r. spectrum contained three sharp singlets at 3.0, 4.7, and 7.8 τ due to the AA'BB' *p*-tolyl, cyclopentadienyl, and methyl protons, with the expected intensity ratio of 16:5:12, respectively. The absence of an AB quartet pattern in the p.m.r. spectrum of (**3**; R = To) was at first surprising since all the known tetrakis(*p*-tolyl)cyclobutadiene metal complexes (4–7) appear to contain this characteristic splitting pattern. However, a sharp singlet for the AA'BB' *p*-tolyl protons implied the presence of equivalent *p*-tolyl groups as expected of a tetrakis(*p*-tolyl)cyclobutadiene ring.

Experimental

Cyclopentadienylmolybdenum tricarbonyl dimer (8), tetraphenylcyclobutadienepalladium bromide dimer (9), and tetrakis(*p*-tolyl)cyclobutadienepalladium bromide dimer (10) were prepared by known procedures. All reactions were carried out under oxygen free nitrogen. Infrared spectra were measured on a Nujol mull; and p.m.r. spectra were obtained in deuterochloroform solution with tetramethylsilane as internal reference. Melting points were determined in evacuated capillaries but are not corrected. Light petroleum refers to the fraction of b.p. 30–60°.

*Tetraphenylcyclobutadiene molybdenum dicarbonyl bromide dimer (**1**; R = Ph)*

Molybdenum hexacarbonyl (2.0 g, 7.6 mmoles) was added slowly to a refluxing suspension of tetraphenylcyclobutadienepalladium bromide dimer (1.0 g, 0.8 mmole) in *p*-xylene (50 ml) over a 5 min period. Reflux was continued for an additional 5 min, then the reaction mixture was filtered hot and the filtrate reduced in volume to 5 ml. This solution was chromatographed on an alumina column prepared using light petroleum. An orange band which was eluted with light petroleum–benzene (1:1) mixture gave, after the evaporation of the solvents and recrystallization from dichloromethane and ethanol, red crystals of (**1**; R = Ph) (0.16 g, 18%), m.p. 283° decomp. (lit. (1) 280° decomp).

The infrared spectrum showed two strong terminal carbonyl bands at 1975 and 2025 cm^{-1} (lit. (1) 1976 and 2026 cm^{-1}). The p.m.r. spectrum consisted of a singlet at 2.76 τ. This sample was analyzed by X-ray diffraction (2).

*Tetrakis(p-tolyl)cyclobutadiene molybdenum dicarbonyl bromide dimer (**1**; R = To)*

This complex was prepared in 14% yield by the same procedure described for (**1**; R = Ph). The m.p. was 233–235° decomp.

Anal. Calcd. for $C_{68}H_{56}O_4Br_2Mo_2$: C, 63.40; H, 4.37; Br, 12.41; mol. wt., 1289. Found: C, 63.34; H, 4.40; Br, 12.20; mol. wt., 1333 (osmometric in CH_2Cl_2).

The infrared spectrum showed two strong terminal carbonyl bands at 1965 and 2020 cm^{-1}, and the p.m.r. spectrum consisted of an AB quartet centered at 2.92 τ (2.74, 2.87, 2.97, and 3.11 τ; J_{AB} = 8 c.p.s.) and a singlet at 7.69 τ with the intensity ratio of 4:3.

*Tetrakis(p-tolyl)cyclobutadiene)(cyclopentadienyl) molybdenum carbonyl bromide (**3**; R = To)*

Tetrakis(*p* - tolyl)cyclobutadienepalladium bromide dimer (1.20 g, 0.9 mmole) and cyclopentadienylmolybdenum tricarbonyl dimer (0.7 g, 2.9 mmoles) were refluxed and stirred in benzene (50 ml) for a period of 48 h. The hot reaction mixture was filtered; the filtrate reduced in volume to 10 ml and then chromatographed on an alumina column prepared using light petroleum. Excess molybdenum dimer was removed with benzene and then a pale orange band was rapidly eluted with ether. The orange ether solution was taken to dryness and the solid obtained recrystallized from methanol–dichloromethane mixture to afford (**3**; R = To) (0.07 g, 6%), m.p. 286–288° decomp.

Anal. Calcd. for $C_{38}H_{33}OBrMo$: C, 66.90; H, 4.88; Br, 11.72; mol. wt., 681. Found: C, 66.61; H, 4.92; Br, 11.60; mol. wt., 662 (osmometric in CH_2Cl_2).

The infrared spectrum showed a strong terminal carbonyl band at 1984 cm^{-1} and the p.m.r. spectrum consisted of three singlets at 3.0, 4.71, and 7.80 τ with intensity ratio 16:5:12.

Acknowledgments

The author wishes to thank the University of Waterloo for supporting this work and to Dr. A. J. Carty for his help.

1. P. M. Maitlis and M. L. Games. Chem. Ind. London, 1624 (1963).
2. M. Mathew and G. J. Palenik. Can. J. Chem. **47**, 705 (1969).
3. P. M. Maitlis and A. Efraty. J. Organometal. Chem. Amsterdam, **4**, 172 (1965).
4. A. Efraty and P. M. Maitlis. Tetrahedron Lett. 4025 (1966).
5. A. Efraty and P. M. Maitlis. J. Amer. Chem. Soc. **89**, 3744 (1967).
6. D. F. Pollock and P. M. Maitlis. Can. J. Chem. **44**, 2673 (1966).
7. D. F. Pollock, A. Efraty, and P. M. Maitlis. Unpublished results.
8. R. G. Hayter. Inorg. Chem. **2**, 1031 (1963).
9. P. M. Maitlis and M. L. Games. Can. J. Chem. **42**, 183 (1964).
10. A. Efraty. Ph.D. Dissertation, McMaster University, Hamilton, Ontario. 1968.

Dielectric and nuclear magnetic resonance properties of a clathrate hydrate of cyclopropane[1]

Y. A. MAJID, S. K. GARG, AND D. W. DAVIDSON
Division of Applied Chemistry, National Research Council of Canada, Ottawa, Canada

Received July 3, 1969

Dielectric relaxation data and proton magnetic resonance spectra are given for the structure I clathrate hydrate of cyclopropane. Vapor pressures have been measured along the structure I – structure II – gas equilibrium line missing from the recent phase diagram of Hafemann and Miller.

Canadian Journal of Chemistry, 47, 4697 (1969)

Can. J. Chem. Downloaded from www.nrcresearchpress.com by 210.87.254.105 on 09/05/12
For personal use only.

Although cyclopropane was expected (1) to form a clathrate hydrate, the formation of solid in the cyclopropane–water system has been studied only very recently. Hafemann and Miller (2) have now provided a phase diagram based on vapor pressure measurements. Their data (circles in Fig. 1) showed 4 stable quadruple points and the existence of 2 hydrates which were identified as clathrate hydrates of von Stackelberg's (3) structures I and II. In systems with excess water, structure I (HI) was found to be stable below −16.0 °C and again above 1.5°; structure II (HII) at intermediate temperatures.

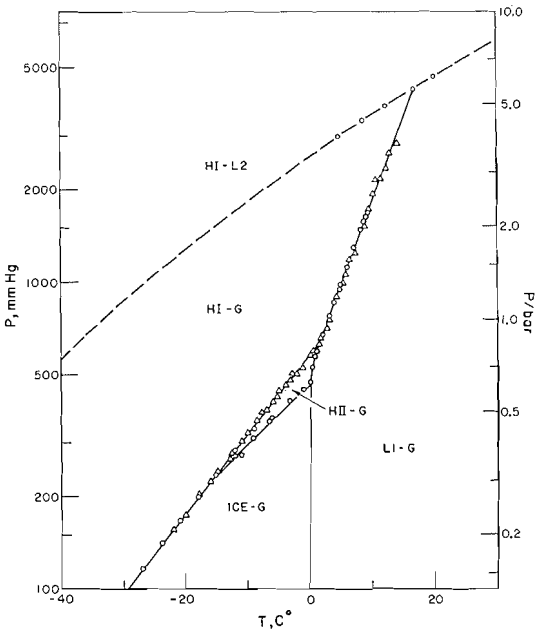

FIG. 1. Phase diagram of the cyclopropane–water system. ○, data from ref. 2; △, this work.

From dielectric, p.m.r., and composition measurements, we had concluded before we were aware of the work of Hafemann and Miller (2) that cyclopropane forms a structure I hydrate. We outline these results here, together with vapor pressure measurements which, combined with the previous ones (2), define the region of stability of structure II.

Hydrate for all measurements was prepared at about 0 °C from deaerated conductivity water and gaseous cyclopropane (Matheson, vapor phase chromatographic impurity less than 0.1%) at a pressure of about 44 p.s.i.a. The reaction vessel was vigorously shaken for about a day. Analyses of the volume of gas evolved when hydrate was thermally decomposed gave compositions within a few percent of $C_3H_6 \cdot 7\frac{2}{3}H_2O$, the composition of a structure I hydrate with all the large, but none of the small, cages occupied by cyclopropane.

Vapor pressures were measured with powdered samples, initially almost completely structure I hydrate, heated at an average rate of 0.1° per min. Some of our data, along with the more precise data of Hafemann and Miller (2), are shown in Fig. 1. The only significant difference lies in the region between −16 and 1.5°, where the previous data define the HII–ice–gas equilibrium line; ours, the HI–HII–gas line. This difference is attributable to the higher cyclopropane content of our samples. The limited field of stability of HII is bounded by these lines and the short HII–LI–gas line. Although trimethylene oxide is known (4) to form hydrates of the same 2 structures, there is no evidence of a low temperature bound to the stability of either.

The upper quadruple point (16.2°, 5.6 bar) of the cyclopropane–water system is some 11° higher than that for the propane–water system (5.4°,

[1]NRCC No. 10 924.

TABLE I

Dielectric parameters of cyclopropane hydrate

Temperature (°C)	ε_0 (exp)	ε_∞ (exp)	α	τ_0 (exp) (s)	ε_0 (ass)	τ_0 (corr) (s)	δ
−32.4	52.8	2.9	0.06	1.3×10^{-4}	63.0	1.6×10^{-4}	0.003
−49.6	51.2	2.8_6	0.10	5.7×10^{-4}	67.5	7.7×10^{-4}	0.005
−66.8	57.2	2.8_5	0.16	2.7×10^{-3}	72.8	3.7×10^{-3}	0.004
−83.7	55.6	2.8_4	0.21	1.1×10^{-2}	78.9	1.7×10^{-2}	0.005

5.5 bar) (5), which should give cyclopropane an advantage in the hydrate formation stage in processes under development for the desalination of sea water (see, for example, ref. 6). Propane forms a structure II hydrate only (5). Its largest van der Waals diameter (~6.3 Å) is too large to enable propane to fit into the 14-hedral cages of structure I which can, however, readily accommodate cyclopropane (maximum diameter ~5.3 Å).

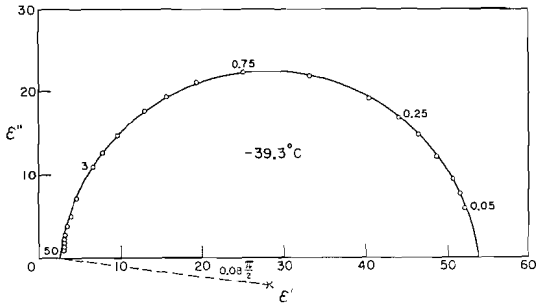

FIG. 2. Complex permittivity locus of cyclopropane hydrate. Frequencies are in kHz.

The complex permittivity loci of structure I hydrate pressed into disks (Fig. 2 shows an example) were well defined at temperatures between −30 and −100 °C. The shapes are similar to those of other structure I hydrates, the Cole–Cole circular arc parameters α which approximately describe the shapes being intermediate between those found for ethylene oxide hydrate (7) and for the hydrates of argon and nitrogen (8). At relatively high frequencies consistent departures from the Cole–Cole representation took the form of a steeper approach to the ε' axis. This behavior is commonly observed in the clathrate hydrates and suggests the presence of a number of discrete closely-grouped reorientational relaxation times instead of the continuous distribution to which the Cole–Cole arc corresponds. A general treatment of relaxation of water molecules in solids with nonequivalent water sites and orientations (9) predicts as many as 10 discrete relaxation times in structure I hydrates.

A few of the dielectric results are given in Table I. The differences between the measured static permittivities, ε_0 (exp), and those expected, ε_0 (ass), for structure I hydrates of nonpolar molecules have been used to estimate corrections to the relaxation times for the presence of small air gaps making up a fraction δ of sample thickness (8).

The Arrhenius energy of relaxation (~10 kcal mole^{-1} at temperatures above −70 °C) is appreciably higher than for other structure I hydrates where relatively high populations of Bjerrum defects appear to be produced by interaction with polar guest molecules (ethylene oxide, trimethylene oxide) or by occasional substitution of lattice water molecules by small hydrate-forming molecules (argon, nitrogen) (8). As for the case of argon and nitrogen, the (extrapolated) value of the relaxation time τ_0 at 0 °C (~15 μs) is very similar to that of ice I (22 μs).

Figure 3 shows typical derivative curves of the proton magnetic resonance absorption signal of samples in sealed tubes, measured at 16 MHz as previously described (10). The narrow and wide lines clearly defined at all temperatures between −196 and −10 °C, arise from the protons of cyclopropane and water, respectively. The relative intensity and width of the narrow lines show that all cyclopropane molecules are executing rapid, effectively isotropic rotation within their cages. Thus, for a Gaussian line shape, the second moment of the narrow component at −196°, corrected for modulation broadening, is 3.7 G^2, that estimated by the method previously described (10) for rapidly rotating cyclopropane in a rigid water lattice, 3.6 G^2. The experimental value at −30° is 2.6 G^2.

Can. J. Chem. Downloaded from www.nrcresearchpress.com by 210.87.254.105 on 09/05/12
For personal use only.

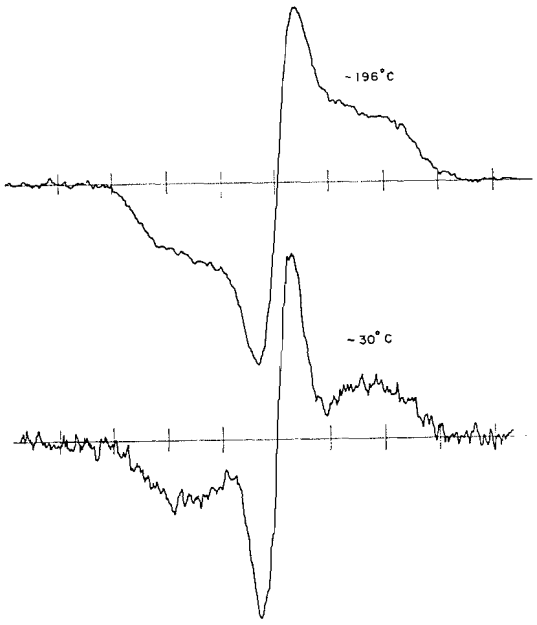

FIG. 3. Derivative curves of ^1H absorption lines. Scale lines are 5 G apart. Radio frequency field 6 mG, modulation field 0.85 G, time constant 3 s, sweep rate 2 G/min.

The wide line characterizes the rigid water lattice until it begins to narrow at about $-20°$. As in the similar case of SF_6 hydrate (10), line narrowing by diffusion of water molecules appears not to occur at such a low temperature as in hexagonal ice, a result which supports the interstitial mechanism of diffusion in ice (11).

1. M. VON STACKELBERG. Naturwiss. **36**, 327 (1949).
2. D. R. HAFEMANN and S. L. MILLER. J. Phys. Chem. **73**, 1392 (1969).
3. M. VON STACKELBERG and H. R. MÜLLER. Z. Elektrochem. **58**, 25 (1954).
4. R. E. HAWKINS and D. W. DAVIDSON. J. Phys. Chem. **70**, 1889 (1966).
5. H. H. REAMER, F. T. SELLECK, and B. H. SAGE. J. Petrol. Technol. **4**, No. 8, 197 (1952).
6. V. C. WILLIAMS, C. L. ROY, H. SMITH, JR., O. B. BATTLE, J. A. HUNTER, W. W. RINNE, and S. S. VERIKIOS. Development of propane hydrate desalting process. U.S. Office of Saline Water, R. and D. Progress Report 373. Washington, D.C. 1968.
7. D. W. DAVIDSON and G. J. WILSON. Can. J. Chem. **41**, 1424 (1963).
8. S. R. GOUGH, E. WHALLEY, and D. W. DAVIDSON. Can. J. Chem. **46**, 1673 (1968).
9. D. W. DAVIDSON. Unpublished results.
10. Y. A. MAJID, S. K. GARG, and D. W. DAVIDSON. Can. J. Chem. **46**, 1683 (1968).
11. L. ONSAGER and L. K. RUNNELS. J. Chem. Phys. **50**, 1089 (1969).

Spectra of Co(II) in molten nitrates and dimethyl sulfone

K. W. FUNG AND K. E. JOHNSON
Department of Chemistry, University of Saskatchewan, Regina Campus, Regina, Saskatchewan

Received June 30, 1969

The electronic spectrum of Co(II) in $LiNO_3$–KNO_3, $AgNO_3$–KNO_3, and dimethyl sulfone containing excess $LiNO_3$–KNO_3 resembles that of the dodecahedral $[Co(NO_3)_4]^{2-}$ ion and parameters for this symmetry and the approximation T_d are calculated. $Co(ClO_4)_2$ yields an octahedral species in dimethyl sulfone.

Canadian Journal of Chemistry, **47**, 4699 (1969)

The spectrum of $CoCl_2$ dissolved in $LiNO_3$–KNO_3 eutectic melt was obtained by Gruen (1). He compared the single band in the visible region (extinction coefficient approximately 100) with the more intense system of bands, resembling those of $CoCl_4^{2-}$, obtained on adding a large excess of chloride and deduced that Co(II) was octahedrally coordinated by nitrate (1), perhaps by four nitrate groups (2). Recently, Duffy and Ingram (3) drew attention to the similarity of the spectra of Co(II) in KNO_3–$Ca(NO_3)_2$ glass, of $[CH_3(C_6H_5)_3As]_2[Co(NO_3)_4]$ (4) and, for the visible region, of Co(II) in $LiNO_3$–KNO_3 melt. The $[Co(NO_3)_4]^{2-}$ ion was shown to contain four bidentate nitrates giving a dodecahedral coordination to Co(II) (5). As reported elsewhere (6), the spectra of Co(II) in several sulfate melts are similar and can be successfully accounted for in terms of D_{2d} symmetry. Here we report our findings, including the near infrared spectra for $Co(NO_3)_2$ in several systems.

Experimental

Anhydrous cobalt nitrate was prepared according to Addison and Logan (7). $LiNO_3$–KNO_3, $NaNO_3$–KNO_3, and KNO_3–$AgNO_3$ eutectics were prepared by fusing

Can. J. Chem. Downloaded from www.nrcresearchpress.com by 210.87.254.105 on 09/05/12
For personal use only.

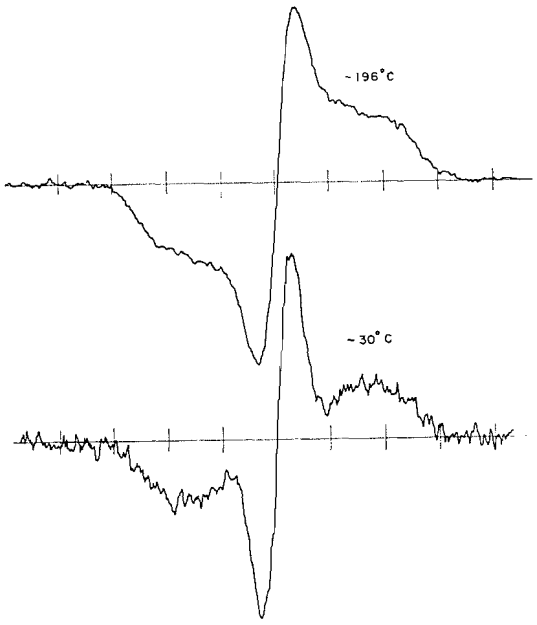

FIG. 3. Derivative curves of ^1H absorption lines. Scale lines are 5 G apart. Radio frequency field 6 mG, modulation field 0.85 G, time constant 3 s, sweep rate 2 G/min.

The wide line characterizes the rigid water lattice until it begins to narrow at about $-20°$. As in the similar case of SF_6 hydrate (10), line narrowing by diffusion of water molecules appears not to occur at such a low temperature as in hexagonal ice, a result which supports the interstitial mechanism of diffusion in ice (11).

1. M. VON STACKELBERG. Naturwiss. **36**, 327 (1949).
2. D. R. HAFEMANN and S. L. MILLER. J. Phys. Chem. **73**, 1392 (1969).
3. M. VON STACKELBERG and H. R. MÜLLER. Z. Elektrochem. **58**, 25 (1954).
4. R. E. HAWKINS and D. W. DAVIDSON. J. Phys. Chem. **70**, 1889 (1966).
5. H. H. REAMER, F. T. SELLECK, and B. H. SAGE. J. Petrol. Technol. **4**, No. 8, 197 (1952).
6. V. C. WILLIAMS, C. L. ROY, H. SMITH, JR., O. B. BATTLE, J. A. HUNTER, W. W. RINNE, and S. S. VERIKIOS. Development of propane hydrate desalting process. U.S. Office of Saline Water, R. and D. Progress Report 373. Washington, D.C. 1968.
7. D. W. DAVIDSON and G. J. WILSON. Can. J. Chem. **41**, 1424 (1963).
8. S. R. GOUGH, E. WHALLEY, and D. W. DAVIDSON. Can. J. Chem. **46**, 1673 (1968).
9. D. W. DAVIDSON. Unpublished results.
10. Y. A. MAJID, S. K. GARG, and D. W. DAVIDSON. Can. J. Chem. **46**, 1683 (1968).
11. L. ONSAGER and L. K. RUNNELS. J. Chem. Phys. **50**, 1089 (1969).

Spectra of Co(II) in molten nitrates and dimethyl sulfone

K. W. FUNG AND K. E. JOHNSON

Department of Chemistry, University of Saskatchewan, Regina Campus, Regina, Saskatchewan

Received June 30, 1969

The electronic spectrum of Co(II) in $LiNO_3$–KNO_3, $AgNO_3$–KNO_3, and dimethyl sulfone containing excess $LiNO_3$–KNO_3 resembles that of the dodecahedral $[Co(NO_3)_4]^{2-}$ ion and parameters for this symmetry and the approximation T_d are calculated. $Co(ClO_4)_2$ yields an octahedral species in dimethyl sulfone.

Canadian Journal of Chemistry, **47**, 4699 (1969)

The spectrum of $CoCl_2$ dissolved in $LiNO_3$–KNO_3 eutectic melt was obtained by Gruen (1). He compared the single band in the visible region (extinction coefficient approximately 100) with the more intense system of bands, resembling those of $CoCl_4^{2-}$, obtained on adding a large excess of chloride and deduced that Co(II) was octahedrally coordinated by nitrate (1), perhaps by four nitrate groups (2). Recently, Duffy and Ingram (3) drew attention to the similarity of the spectra of Co(II) in KNO_3–$Ca(NO_3)_2$ glass, of $[CH_3(C_6H_5)_3As]_2[Co(NO_3)_4]$ (4) and, for the visible region, of Co(II) in $LiNO_3$–KNO_3 melt. The $[Co(NO_3)_4]^{2-}$ ion was shown to contain four bidentate nitrates giving a dodecahedral coordination to Co(II) (5). As reported elsewhere (6), the spectra of Co(II) in several sulfate melts are similar and can be successfully accounted for in terms of D_{2d} symmetry. Here we report our findings, including the near infrared spectra for $Co(NO_3)_2$ in several systems.

Experimental

Anhydrous cobalt nitrate was prepared according to Addison and Logan (7). $LiNO_3$–KNO_3, $NaNO_3$–KNO_3, and KNO_3–$AgNO_3$ eutectics were prepared by fusing

Can. J. Chem. Downloaded from www.nrcresearchpress.com by 210.87.254.42 on 09/05/12
For personal use only.

Can. J. Chem. Downloaded from www.nrcresearchpress.com by 210.87.254.42 on 09/05/12
For personal use only.

TABLE I

Spectra of Co(II) in molten nitrates and dimethyl sulfone

Compound	Solvent	Temperature (°C)	Symmetry	ν (kK)	ε_{max}	$f \times 10^4$	Excited state*		Predicted ν (kK)	Parameters†	
							T_d or O_h	D_{2d}		Name	Value
$Co(NO_3)_2$	$LiNO_3$–KNO_3	156	D_{2d}, D_{2d}	4.50	0.89	0.02	$^4T_2$(F)	^4E, $^4B_2$	4.78	Δ	4.78
				8.26	6.48	1.39	$^4T_1$(F)	^4E	7.16	B	0.859
								$^4A_2$	9.36	C	1.57
				12.44	2.80	0.29	$^2T_1$, ^2E	$^2(A_1, A_2, B_1, E)$	12.44	η	2.21
				17.87	65.22	8.53	$^4T_1$(P)	^4E	17.87	β	0.89
				20.08	35.03	4.93		$^4A_2$	20.08		
$Co(NO_3)_2$	$AgNO_3$–KNO_3	156	T_d, D_{2d}	4.50	2.00	0.06	$^4T_2$(F)	^4E, $^4B_2$	4.82	Δ	4.82
				8.33	13.53	3.12	$^4T_1$(F)	^4E	7.03	B	0.869
								$^4A_2$	9 36	C	1.53
				12.43	9.80	1.39	$^2T_1$, ^2E	$^2(A_1, A_2, B_1, E)$	12.43	η	2.59
				17.89	72.26	11.27	$^4T_1$(P)	^4E	17.89	β	0.91
				20.48	31.00	3.66		$^4A_2$	20.48		
$Co(ClO_4)_4$	Dimethyl sulfone	128	O_h	4.78	1.28	0.0072	$^4T_2$(F)‡		5.53	Δ	6.26
				6.28	1.70	0.0164				B	0.867
				12.19	0.25	0.0029	$^4A_2$(F)		11.79	β	0.91
				17.80	8.79	0.0720	$^4T_1$(P)		17.80		
				20.10	2.72	0.0359					

*cf. ref. 6.
†Δ is the crystal field splitting, B and C are Racah parameters, β = B(complex)/B(free ion), η = D_{2d} splitting.
‡The splitting of this band is unexpected but it may arise from interaction with ligand vibrations.

Can. J. Chem. Downloaded from www.nrcresearchpress.com by 210.87.254.42 on 09/05/12
For personal use only.

together dry reagent grade salts and bubbling dry nitrogen through the melts. Spectra were recorded with a Beckman DK-2A spectrophotometer as discussed previously (6, 8) and were analyzed into Gaussian components by the method of Chatt *et al.* (9).

Cobalt perchlorate and dimethyl sulfone were prepared according to Liu *et al.* (10).

Results

Figure 1 shows the spectrum of Co(II) in $LiNO_3$–KNO_3 and $AgNO_3$–KNO_3 eutectic melts. A stable solution of $Co(NO_3)_2$ in $NaNO_3$–KNO_3 was not obtainable. Figure 2 shows the spectra obtained for dimethyl sulfone solutions of $Co(NO_3)_2$ and $Co(ClO_4)_2$ alone and with added $LiNO_3$–KNO_3. Details of all the bands are collected in Table I.

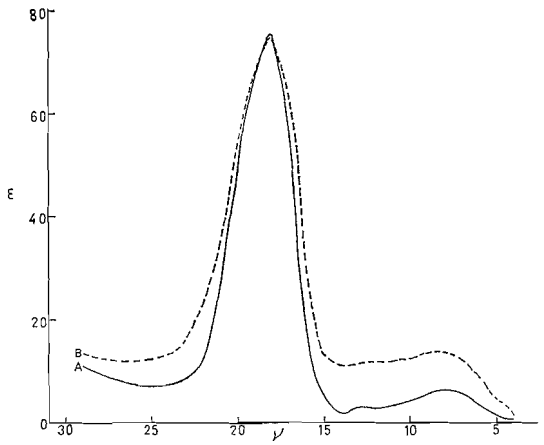

FIG. 1. Spectrum of $Co(NO_3)_2$ in *A*, $LiNO_3$–KNO_3 and *B*, $AgNO_3$–KNO_3, both at 156 °C.

Discussion

The molten salt spectra do indeed resemble those of Co(II) in KNO_3–$Ca(NO_3)_2$ glass (3), the $[Co(NO_3)_4]^{2-}$ ion (4, 5) and the sulfate melts (6) and may be assigned to a first approximation in tetrahedral symmetry or, more precisely, in dodecahedral symmetry, with the parameters listed in Table I.

The intensity of the visible band in $LiNO_3$–KNO_3 is somewhat lower than that recorded by Gruen (1), but he did not start from anhydrous $Co(NO_3)_2$.

$Co(ClO_4)_2$ dissolved in dimethyl sulfone gave rise to a typical octahedral spectrum (11) which was unaffected by the addition of $LiClO_4$, but changed to the dodecahedral spectrum on adding $LiNO_3$–KNO_3. On the other hand, $Co(NO_3)_2$ in dimethyl sulfone gave a dodecahedral spectrum, but of intermediate intensity which increased to

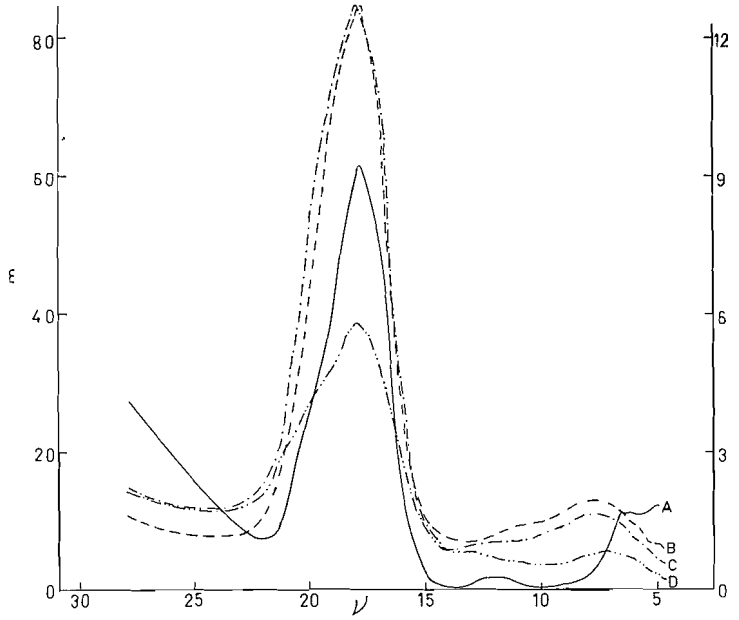

FIG. 2. Spectra of *A*, $Co(ClO_4)_2$ (right-hand ordinate); *B*, $Co(ClO_4)_2$ + $LiNO_3$–KNO_3; *C*, $Co(NO_3)_2$ + $LiNO_3$–KNO_3; and *D*, $Co(NO_3)_2$ (*B*, *C*, and *D* left-hand ordinate). All in dimethyl sulfone at 128 °C.

the usual value (largest $\varepsilon_{max} \sim 80$) on adding $LiNO_3$–KNO_3. This could mean either the formation of $[Co(NO_3)_4]^{2-}$ and octahedral $Co(DMSO_2)^{2+}$ or of a dodecahedral cationic complex on the addition of $Co(NO_3)_2$ to dimethyl sulfone.

A comparison with the sulfate melts (6) places nitrate as a slightly weaker ligand than sulfate ($\Delta_{NO_3^-} = 4.8$ kK vs. $\Delta_{SO_4^{2-}} = 5.1$ kK) and with less tendency toward covalent bonding ($\beta_{NO_3^-} = 0.90$ vs. $\beta_{SO_4^{2-}} = 0.74$).

Acknowledgment

This work was supported by the National Research Council of Canada.

1. D. M. GRUEN. J. Inorg. Nucl. Chem. **4**, 74 (1957).
2. D. M. GRUEN. *In* Fused salts. *Edited by* B. R. Sundheim. McGraw-Hill Book Co., Inc., New York. 1964.
3. J. A. DUFFY and M. D. INGRAM. J. Amer. Ceram. Soc. **51**, 544 (1968).
4. F. A. COTTON, D. M. L. GOODGAME, and R. H. SODERBERG. Inorg. Chem. **2**, 1162 (1963).
5. F. A. COTTON and J. G. BERGMAN. J. Amer. Chem. Soc. **86**, 2941 (1964).
6. J. R. DICKINSON and K. E. JOHNSON. In press.
7. C. C. ADDISON and N. LOGAN. Adv. Inorg. Chem. Radiochem. **6**, 71 (1964).
8. K. E. JOHNSON, J. R. MACKENZIE, and J. N. SANDOE. J. Chem. Soc. 2644 (1968).
9. J. CHATT, L. E. ORGEL, and G. A. GAMLEN. J. Chem. Soc. 486 (1958).
10. C. H. LIU, J. HASSON, and G. P. SMITH. Inorg. Chem. **7**, 2244 (1968).
11. J. R. DICKINSON and K. E. JOHNSON. In press.

Mesure directe de la constante d'ionisation de l'ammoniac liquide entre −77 et −36 °C

MAURICE RENAUD
Département de Génie métallurgique, Ecole Polytechnique, Montreal, Québec

Reçu le 13 juin, 1969

La constante d'ionisation de l'ammoniac liquide a été mesurée à l'aide d'une pile de concentrations entre −77 et −36 °C. Sur ce domaine de température, le pK passe de 33.1 ± 0.3 à −36 °C à 37.8 ± 0.3 à −77 °C. Les valeurs mesurés confirment celles calculées à partir des valeurs thermodynamiques de l'ammoniac liquide, de l'ion ammonium et de l'ion amidure. L'expression $pK = 9.0 + 5.7\,(10^3/T)$ rend bien compte des valeurs du pK de l'ammoniac liquide sur le domaine de température étudié.

The ionization constant of liquid ammonia has been measured with a concentration cell between −77 and −36 °C. Between these temperatures, pK increased from 33.1 ± 0.3 at −36 °C to 37.8 ± 0.3 at −77 °C. These measured data confirm those calculated with thermodynamic values of liquid ammonia, ammonium ion, and amide ion. The formula $pK = 9.0 + 5.7\,(10^3/T)$ can represent the values of the pK of liquid ammonia for the studied temperatures.

Canadian Journal of Chemistry, 47, 4702 (1969)

Introduction

L'ammoniac liquide est un solvant capable de dissoudre des quantités notables de sels ioniques. Comme par ailleurs il est très basique et que de ce fait il ne réagit pas avec la plupart des métaux, divers auteurs ont envisagé son emploi, soit pour obtenir les métaux les plus électronégatifs par voie humide, soit pour réaliser des piles à fortes différences de potentiel.

Bien que son pK soit une des propriétés qui confèrent le plus d'originalité à l'ammoniac liquide, la littérature n'en signale qu'une mesure, celle réalisée par Pleskov et Monoszon (1) en 1935. Nous avons donc cherché à mesurer le pK dans tout le domaine de température pour lequel l'ammoniac est liquide à pression ordinaire.

Pour effectuer nos mesures nous avons utilisé une pile de concentrations semblable à celle décrite par Pleskov et Monoszon (1). Elle est constituée de deux électrodes à hydrogène en platine platiné trempant dans deux compartiments séparés par une paroi de verre fritté

$$H_2/Pt/NH_4Cl_{am} \;||\; KNH_{2am}/Pt/H_2$$

compartiment a ||compartiment b

Principe des Mesures

Les électrodes à hydrogène en platine platiné

Can. J. Chem. Downloaded from www.nrcresearchpress.com by 210.87.254.42 on 09/05/12
For personal use only.

the usual value (largest $\varepsilon_{max} \sim 80$) on adding $LiNO_3$–KNO_3. This could mean either the formation of $[Co(NO_3)_4]^{2-}$ and octahedral $Co(DMSO_2)^{2+}$ or of a dodecahedral cationic complex on the addition of $Co(NO_3)_2$ to dimethyl sulfone.

A comparison with the sulfate melts (6) places nitrate as a slightly weaker ligand than sulfate ($\Delta_{NO_3^-} = 4.8$ kK vs. $\Delta_{SO_4^{2-}} = 5.1$ kK) and with less tendency toward covalent bonding ($\beta_{NO_3^-} = 0.90$ vs. $\beta_{SO_4^{2-}} = 0.74$).

Acknowledgment

This work was supported by the National Research Council of Canada.

1. D. M. GRUEN. J. Inorg. Nucl. Chem. **4**, 74 (1957).
2. D. M. GRUEN. *In* Fused salts. *Edited by* B. R. Sundheim. McGraw-Hill Book Co., Inc., New York. 1964.
3. J. A. DUFFY and M. D. INGRAM. J. Amer. Ceram. Soc. **51**, 544 (1968).
4. F. A. COTTON, D. M. L. GOODGAME, and R. H. SODERBERG. Inorg. Chem. **2**, 1162 (1963).
5. F. A. COTTON and J. G. BERGMAN. J. Amer. Chem. Soc. **86**, 2941 (1964).
6. J. R. DICKINSON and K. E. JOHNSON. In press.
7. C. C. ADDISON and N. LOGAN. Adv. Inorg. Chem. Radiochem. **6**, 71 (1964).
8. K. E. JOHNSON, J. R. MACKENZIE, and J. N. SANDOE. J. Chem. Soc. 2644 (1968).
9. J. CHATT, L. E. ORGEL, and G. A. GAMLEN. J. Chem. Soc. 486 (1958).
10. C. H. LIU, J. HASSON, and G. P. SMITH. Inorg. Chem. **7**, 2244 (1968).
11. J. R. DICKINSON and K. E. JOHNSON. In press.

Mesure directe de la constante d'ionisation de l'ammoniac liquide entre −77 et −36 °C

MAURICE RENAUD
Département de Génie métallurgique, Ecole Polytechnique, Montreal, Québec

Reçu le 13 juin, 1969

La constante d'ionisation de l'ammoniac liquide a été mesurée à l'aide d'une pile de concentrations entre −77 et −36 °C. Sur ce domaine de température, le pK passe de 33.1 ± 0.3 à −36 °C à 37.8 ± 0.3 à −77 °C. Les valeurs mesurés confirment celles calculées à partir des valeurs thermodynamiques de l'ammoniac liquide, de l'ion ammonium et de l'ion amidure. L'expression $pK = 9.0 + 5.7\,(10^3/T)$ rend bien compte des valeurs du pK de l'ammoniac liquide sur le domaine de température étudié.

The ionization constant of liquid ammonia has been measured with a concentration cell between −77 and −36 °C. Between these temperatures, pK increased from 33.1 ± 0.3 at −36 °C to 37.8 ± 0.3 at −77 °C. These measured data confirm those calculated with thermodynamic values of liquid ammonia, ammonium ion, and amide ion. The formula $pK = 9.0 + 5.7\,(10^3/T)$ can represent the values of the pK of liquid ammonia for the studied temperatures.

Canadian Journal of Chemistry, 47, 4702 (1969)

Introduction

L'ammoniac liquide est un solvant capable de dissoudre des quantités notables de sels ioniques. Comme par ailleurs il est très basique et que de ce fait il ne réagit pas avec la plupart des métaux, divers auteurs ont envisagé son emploi, soit pour obtenir les métaux les plus électronégatifs par voie humide, soit pour réaliser des piles à fortes différences de potentiel.

Bien que son pK soit une des propriétés qui confèrent le plus d'originalité à l'ammoniac liquide, la littérature n'en signale qu'une mesure, celle réalisée par Pleskov et Monoszon (1) en 1935. Nous avons donc cherché à mesurer le pK dans tout le domaine de température pour lequel l'ammoniac est liquide à pression ordinaire.

Pour effectuer nos mesures nous avons utilisé une pile de concentrations semblable à celle décrite par Pleskov et Monoszon (1). Elle est constituée de deux électrodes à hydrogène en platine platiné trempant dans deux compartiments séparés par une paroi de verre fritté

$$H_2/Pt/NH_4Cl_{am} \;||\; KNH_{2am}/Pt/H_2$$

compartiment a ||compartiment b

Principe des Mesures

Les électrodes à hydrogène en platine platiné

Can. J. Chem. Downloaded from www.nrcresearchpress.com by 210.87.254.6 on 09/05/12
For personal use only.

étant réversibles dans l'ammoniac liquide (2) la tension mesurée aux bornes de la pile s'écrit

$$[1]\quad U_a - U_b = \frac{RT}{F}[\ln x.y - \ln K] + E_j$$

où x est l'activité des ions NH_4^+ dans le compartiment a, y est l'activité des ions NH_2^- dans le compartiment b, E_j est le potentiel de jonction entre les deux compartiments

$$[2]\quad pK = \frac{F}{2.303RT}[(U_a - U_b) - E_j] - \log x.y$$

$U_a - U_b$ étant mesuré aux bornes de la cellule il faut déterminer E_j et log $x.y$ pour pouvoir calculer pK.

Sachant que

$$NH_4^+, Cl^- \rightleftharpoons NH_4^+ + Cl^- \qquad \text{avec } K = 1.2 \times 10^{-3} \text{ à } -34\,^\circ\text{C} \quad (3)$$

et

$$K^+, NH_2^- \rightleftharpoons K^+ + NH_2^- \qquad \text{avec } K = 1 \times 10^{-4} \text{ à } -40\,^\circ\text{C} \quad (4)$$

Nous avons effectué les mesures avec des concentrations en chlorure d'ammonium et en amidure de potassium suffisamment faibles pour que ces sels soient à peu de chose près entièrement dissociés.

Le calcul du potentiel de jonction n'a pu être fait que pour la température de $-34\,^\circ$C. A cette température les conductivités équivalentes limites des ions mis en jeu sont celles portées au Tableau I.

TABLEAU I

Mesure directe de la constante d'ionisation de l'ammoniac liquide entre -77 et $-36\,^\circ$C

Ions	Conductivités équivalentes limites Ω^{-1} cm^{-1} equiv.$^{-1}$	
NH_4^+	142	(5)
K^+	177	(6)
NH_2^-	166	(6)
Cl^-	171	(7)

En posant que le gradient d'activité des ions au travers de la paroi poreuse est linéaire l'expression générale [3] devient [4].

$$[3]\quad E_j = -\frac{RT}{F}\int_a^b \sum_i \frac{t_i}{Z_i}\frac{da_i}{a_i}$$

$$[4]\quad E_j = \frac{RT}{F}\frac{11y + 29x}{343y - 313x}\ln\frac{343\,y}{313\,x}$$

Le rapport des conductivités équivalentes limites des ions K^+ et NH_4^+ varient peu en fonction de la température: de 1.25 à $-34\,^\circ$C à 1.38 à $-65\,^\circ$C (8). Nous considérerons donc que la valeur du potentiel de jonction est constante sur tout le domaine de température considéré.

Technique Expérimentale

La solution de chlorure d'ammonium est obtenue par dissolution dans l'ammoniac liquide d'une masse connue de sel. Celle d'amidure de potassium l'est par décomposition catalytique d'une solution de concentration connue de potassium dans l'ammoniac liquide.

Pour obtenir une solution de concentration connue de potassium, on distille sous vide un volume connu de ce métal. Pour ce faire on opère en deux étapes: premièrement on fait condenser une goutelette de potassium dans un tube capillaire dont on connaît le diamètre. Après avoir mesuré la longueur de la goutelette on scelle le tube capillaire entre celle-ci et la réserve de métal. Il ne reste plus alors qu'à distiller cette goutelette dans le compartiment b de la cellule de mesure.

Cette série d'opérations effectuées on condense de l'ammoniac dans la cellule. Après quelques heures, voir un jour ou deux la solution de potassium s'est entièrement transformée en une solution d'amidure par décomposition catalytique au contact du noir de platine des électrodes (9).

Pendant toute la durée de l'expérience la cellule est immergée dans un bain de méthanol dont la température est maintenue constante à $\pm 0.5\,^\circ$C.

Résultats

Les mesures ont été effectuées avec des solutions de concentrations suivantes: compartiment a, 8×10^{-5} mole de NH_4Cl/l; compartiment b, 2×10^{-5} mole de KNH_2/l.

Comme à ces concentrations-ci le coefficient d'activité calculé par la théorie de Debye et Hückel est pratiquement égal à 1 nous considérons que les activités des ions sont égales à leurs concentrations.

Par ailleurs, pour tenir compte des constantes d'ionisation des sels utilisés nous écrivons

$$\log x.y = -9 \pm 0.2$$

A l'aide de ces valeurs nous pouvons calculer le potentiel de jonction donné par [4]

$$E_j = 2\text{ mV}$$

Le tableau II réunit les mesures expérimentales $U_a - U_b$ lues à ± 3 mV et les valeurs du pK déduites de l'expression [5]

$$[5]\quad pK = 5.04\frac{10^3}{T}[(U_a - U_b) - 2 \times 10^{-3}] + 9$$

Can. J. Chem. Downloaded from www.nrcresearchpress.com by 210.87.254.6 on 09/05/12
For personal use only.

TABLEAU II

Mesure directe de la constante d'ionisation de l'ammoniac liquide entre −77 et −36 °C

θ, °C à ± 0.5 °C	$10^3/T$ °K^{-1}	$U_a - U_b$, V à ± 0.003 V	pK à ± 0.3
−77.0	5.10	1.121	37.8
−76.0	5.07	1.134	37.9
−73.0	5.00	1.124	37.3
−68.5	4.89	1.129	36.8
−64.5	4.79	1.115	35.8
−57.0	4.63	1.132	35.4
−50.5	4.49	1.121	34.2
−46.0	4.40	1.128	34.0
−36.0	4.22	1.133	33.1

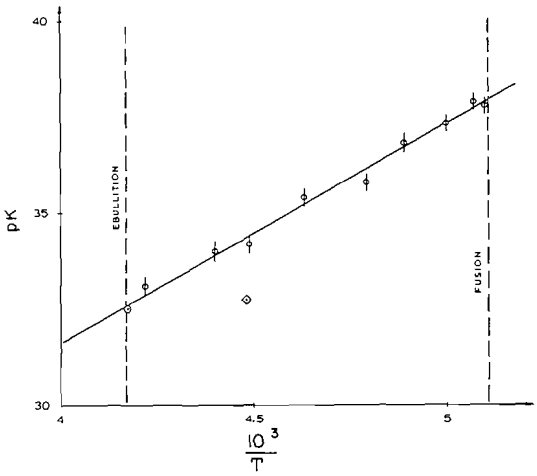

FIG. 1. pK vs. $1/T$; ⊕, nos mesures; ◇, mesure de Pleskov et Monoszon; ⊙, valeur calculée par Coulter *et al.* (10).

La Fig. 1 représente les valeurs du pK portées en fonction de $1/T$. On y remarque que la valeur mesurée par Pleskov et Monoszon à −50 °C (1) se place nettement au-dessous de nos résultats alors que celle calculée par Coulter *et al.* (10) se trouve confirmée.

En utilisant la méthode des moindres carrés on obtient l'expression [6] qui représente la droite passant au mieux à travers tous les points expérimentaux portés sur la Fig. 1

$$[6] \qquad pK = 9.0 + 5.7(10^3/T)$$

Cette expression permet de calculer les fonctions thermodynamiques de la réaction d'ionisation. On obtient $\Delta H^0 = 26$ kcal mole^{-1} et $\Delta S^0 = -41$ cal mole^{-1} deg^{-1}. Ces valeurs sont en accord avec celles mesurées calorimétriquement $\Delta H^0 = 26.1$ kcal mole^{-1} (11) et $\Delta S^0 = -40.1$ cal mole^{-1} deg^{-1} (10).

La relation [6] peut donc être retenue pour exprimer le pK de l'ammoniac liquide sur le domaine de température considérée.

Remerciement

Ce travail a été réalisé à l'Ecole Polytechnique de Montréal grâce à l'octroi de recherche A-4705 du Conseil National de Recherches du Canada.

1. V. A. PLESKOV et A. M. MONOSZON. J. Phys. Chem. USSR, **6**, 513 (1935).
2. W. J. JOLLY et C. J. HALLADA. Liquid ammonia. *Dans* Nonaqueous solvent systems. *Editeé par* T. C. Waddington. Academic Press, Inc., New York. 1967.
3. J. J. LAGOWSKI. Chemistry, **41**, 10 (1968).
4. G. CHARLOT et B. TREMILLON. Les réactions chimiques dans les solvants et les sels fondus. Gauthier-Villars, Paris. 1963.
5. H. A. LAITINEN et C. E. SHOEMAKER. J. Amer. Chem. Soc. **72**, 4975 (1950).
6. W. W. HAWES. J. Amer. Chem. Soc. **55**, 4422 (1933).
7. V. F. HNIZDA et C. A. KRAUS. J. Amer. Chem. Soc. **71**, 1565 (1949).
8. J. B. GILL. J. Chem. Soc. 5730 (1965).
9. T. J. SWIFT, S. B. MARKS et W. G. SAYRE. J. Chem. Phys. **44**, 2797 (1966).
10. L. V. COULTER, J. R. SINCLAIR, A. G. COLE et G. C. ROPER. J. Amer. Chem. Soc. **81**, 2986 (1959).
11. H. D. MULDER et F. C. SCHMIDT. J. Amer. Chem. Soc. **73**, 5575 (1951).

Can. J. Chem. Downloaded from www.nrcresearchpress.com by 210.87.254.6 on 09/05/12
For personal use only.

Studies on complex compounds. VI. Coordination compounds of copper and biologically active cyclohexylamine derivatives[1]

C. H. MISRA, SURENDRA S. PARMAR[2], AND J. P. BARTHWAL[3]

Department of Pharmacology and Therapeutics, King George's Medical College, Lucknow University, Lucknow-3, India

Received[4] October 16, 1968

Five complexes of copper(II) chloride and different cyclohexylamine derivatives were synthesized, the copper:ligand ratios are 1:2. These complexes were characterized by analyses, infrared (700–3500 cm^{-1}) and visible spectra, and conductance. The results have indicated participation of nitrogen atom adjacent to the cyclohexyl ring in coordination.

Canadian Journal of Chemistry, 47, 4705 (1969)

Can. J. Chem. Downloaded from www.nrcresearchpress.com by 210.87.254.105 on 09/05/12
For personal use only.

Initial antibacterial and antifungal evaluation of mercury coordination compounds of the biologically active amines have indicated facilitation of the activity of mercuric chloride on coordination (1). Such facilitation could presumably account for the interference with cellular metabolism of the organisms (2) by the inhibition of certain enzyme system(s) by organo mercury compounds. Our continuing interest in the coordination compounds (3–5) and the greater affinity of the bivalent copper for nitrogen and oxygen to facilitate ready formation of coordination compounds with ammonia, alkyl and aryl substituted amines, heterocyclic bases, amino acids, amino phenols, and other nitrogen and oxygen containing compounds led us to examine the possibility of the synthesis of the complexes of cupric chloride with pharmacologically active cyclohexylamine derivatives. Complexes of copper with cyclohexylamines have not so far been reported. It is hoped that the investigations with such coordination compounds will prove useful in the elucidation of the role of complex formation in their activity in the central nervous system (6).

Experimental

Materials

The cyclohexylamine derivatives used in the present study were N-cyclohexyl-β-alanine, N-(2-hydroxyethyl)-cyclohexylamine, N-(2-cyanoethyl)cyclohexylamine, 2-cyclohexylamino-1-phenylethanol, and N-(3-aminopropyl)cyclohexylamine. Cupric chloride, as $CuCl_2.2H_2O$, was analytical grade. Absolute ethanol and purified anhydrous cyclohexanol (7) were used throughout these experiments.

Analyses

The copper content of the complexes was estimated gravimetrically as thiocynate (8) or as the pyridine complex (9). Chlorine content was assayed gravimetrically (3). The nitrogen content of these coordination compounds was determined by well known combustion methods.

Preparation and Properties of the Copper Complexes

The preparation of the copper coordination compounds and determination of their conductance, absorption spectra, and the infrared spectra were carried out following the methods reported earlier (8, 10). All complexes reported in Table I were stable at room temperature. No change of the nature of these complexes could be observed on heating up to 120° except for the complex obtained from N-(3-aminopropyl)cyclohexylamine, which is highly hygroscopic in nature.

Results and Discussion

Conductance measurements (Table I) have indicated the electrolytic nature of all the complexes which presumably give three ions in ethanol (11) except the one synthesized from N-(3-aminopropyl)cyclohexylamine. The higher molar conductance of dichloro-bis[N-(3-aminopropyl)cyclohexylamine]copper(II) dihydrate as compared to that of a non-electrolyte may presumably account for solvolysis (12, 13) caused by the absorption of the moisture. The characteristic absorption of these complexes suggests a square planar configuration. The observed analytical data and the presence of an intense OH stretching vibration bands in the infrared spectra (Table II) provide further support for this structure in the absence of experiments with the use of deuterium to establish the exact nature of water in these complexes.

[1]This investigation was supported, in part, by the Indian Council of Medical Research, New Delhi, and the State Medical Research Council, Lucknow, U.P.

[2]To whom correspondence should be addressed.

[3]Pool Officer of the Council of Scientific and Industrial Research, Government of India, New Delhi.

[4]Revision received July 17, 1969.

Can. J. Chem. Downloaded from www.nrcresearchpress.com by 210.87.254.105 on 09/05/12
For personal use only.

TABLE I

Compounds	Melting points* (°C)	Analyses: Calculated (%) N	Cl	Cu	Found (%) N	Cl	Cu	Molar conductance (mho)	Absorption spectra†‡: Wavelength (mμ)	Extinction coefficient (log ε)	Solvent used
$\left[\bigcirc\!\!-NH.CH_2CH_2COOH\right]_2CuCl_2.2H_2O$	176	5.46	13.82	12.39	5.55	13.8	12.01	59.47	705	1.74	Ethanol
$\left[\bigcirc\!\!-NH.CH_2CH_2OH\right]_2CuCl_2$	172	6.65	16.88	15.1	5.58	16.93	15.0	64.00	697.5	2.47	Cyclohexanol
$\left[\bigcirc\!\!-NH.CH_2CH_2C{\equiv}N\right]_2CuCl_2.2H_2O$	142–144	11.8	14.93	13.38	11.35	14.50	13.2	56.47	700	2.195	Cyclohexanol
$\left[\bigcirc\!\!-NH.CH_2.\underset{\displaystyle OH}{\underset{|}{CH}}-\bigcirc\right]_2CuCl_2$	172	4.89	12.4	11.1	4.75	12.16	11.3	45.02	680	1.90	Ethanol
$\left[\bigcirc\!\!-NH.CH_2.CH_2.CH_2.NH_2\right]_2CuCl_2.2H_2O$ §	98–100	11.61	14.71	13.16	11.07	14.6	13.0	8.02	630	2.30	Ethanol

*Melting points were taken in open capillary tubes and are graphically corrected.
†All the copper complexes were used at a final concentration of 1×10^{-3} *M* in absolute ethanol.
‡Measurements checked with Hitachi Perkin–Elmer UV-VIS Spectrophotometer.
§Hygroscopic in nature.

TABLE II

Frequencies and assignments for copper complexes of cyclohexylamine derivatives

Frequency* (cm^{-1})					
1	2	3	4	5	Assignment
3447 m	—	3383 m	—	3398 m	Asymmetric and symmetric vibration of lattice water
3083 sh	3138 s	3124 sh	3178 m	3178 m	NH stretching vibration
1683 vs	1630 w	1601 s	1590 vw	1601 s	Asymmetric NH deformation
1415 s	1437 s	1420 b	—	1451 s	NH degenerate deformation
1445 sh	1451 sh	1440 b	1451 s	1462 sh	CH_2 scissoring
2942 vs	2921 vs	2902 vs	2902 s	2902 vs	CH_2 stretching vibration of cyclohexyl ring
2846 s	2825 s	2813 sh	2852 m	2810 s	
1335 w	1379 w	1379 m	—	1379 w	C–N stretching for secondary amine
1316 sh	1335 w	1322 w	—	1283 w	
		1316 w	—	1328 vw	
1574 w 1638 vs	—	1663 vs	—	1601 s	H–O–H bending mode and COO^- stretching vibration
—	—	2472 m 2437 m	—	—	C=N stretching vibration

*sh = shoulder; s = sharp; m = medium; vs = very sharp; w = weak; vw = very weak; b = broad; 1 = dichloro-bis(N-cyclohexyl-β-alanine)copper(II) dihydrate; 2 = dichloro-bis[N-(2-hydroxyethyl)cyclohexylamine]copper(II); 3 = dichloro-bis[N-(2-cyanoethyl)cyclohexylamine]copper(II) dihydrate; 4 = dichloro-bis(2-cyclohexylamino-1-phenylethanol)copper(II); 5 = dichloro-bis[N-(3-aminopropyl)-cyclohexylamine]copper(II) dihydrate.

Acknowledgments

The authors wish to express their thanks to Professors S. N. Shukla and K. P. Bhargava for their advice and encouragement and to Drs. Nitya Anand and S. C. Agarwal of the Central Drug Research Institute, Lucknow, for providing facilities for microanalysis and infrared absorption measurements, respectively. Grateful acknowledgment is made to the Indian Council of Medical Research for providing financial assistance to one of us (C.H.M.), to Dr. Richard P. Germann of the Abbott Laboratories, Development Division, North Chicago, Illinois, for the generous supply of cyclohexylamine derivatives, and to the Perkin–Elmer Corporation, Norwalk, Connecticut, for the generous gift of a Hitachi Perkin–Elmer UV-VIS spectrophotometer.

1. S. S. Parmar and C. H. Misra. To be published.
2. S. M. A. Smolt, C. W. Kreke, and E. S. Cook. J. Biol. Chem. **224**, 999 (1957).
3. C. H. Misra, S. S. Parmar, and S. N. Shukla. J. Inorg. Nucl. Chem. **28**, 147 (1966).
4. C. H. Misra, S. S. Parmar, and S. N. Shukla. J. Inorg. Nucl. Chem. **29**, 2589 (1967).
5. C. H. Misra, S. S. Parmar, and S. N. Shukla. Can. J. Chem. **46**, 2685 (1968).
6. S. S. Parmar, C. H. Misra, and J. P. Barthwal. To be published.
7. R. W. Crowe and C. P. Smyth. J. Amer. Chem. Soc. **73**, 5406 (1951).
8. C. H. Misra, S. S. Parmar, and S. N. Shukla. Can. J. Chem. **45**, 2459 (1967).
9. A. I. Vogel. Quantitative inorganic analysis. Longman Green and Co., Ltd., London. 1962. p. 499.
10. C. H. Misra, Surendra S. Parmar, and R. C. Arora. Inorg. Nucl. Chem. Lett. **3**, 603 (1967).
11. R. Blackhouse, M. E. Foss, and R. S. Nyholm. J. Chem. Soc. 1714 (1957).
12. L. Ricocoboni. Atti, Ist Veneto Sci. Lett. Arti, **96**, 183 (1937).
13. A. B. Thomas and E. C. Rochow. J. Inorg. Nucl. Chem. **4**, 205 (1957).

Erratum: Electrochemiluminescence of carbazole

K. S. V. Santhanam, R. N. O'Brien, and A. D. Kirk

University of Victoria, Victoria, British Columbia

Received June 16, 1969

(Ref.: Can. J. Chem. **47**, 1355 (1969))

Canadian Journal of Chemistry, 47, 4707 (1969)

On page 1358, column 2 sentence 8 should read "The bonding levels are full" instead of "Both bonding and antibonding levels are full".

Reference 14 on page 1359 in the bibliography section is superfluous and should be deleted.

Can. J. Chem. Downloaded from www.nrcresearchpress.com by 210.87.254.105 on 09/05/12
For personal use only.

Isolation of the initial step in the thermal decomposition of di-*tert*-butyl peroxide

C. K. YIP AND H. O. PRITCHARD
Centre for Research in Experimental Space Science, York University, Downsview, Ontario

Received September 2, 1969

The thermal decomposition of di-*tert*-butyl peroxide in the presence of propane has been studied at total pressures up to 100 atm. At the highest propane concentrations, the major product of the decomposition is *tert*-butyl alcohol, and extrapolation to infinite propane pressure indicates that the initial step in the peroxide decomposition is exclusively the formation of two *tert*-butoxy radicals. The activation energy for the abstraction of hydrogen from propane by *t*-BuO radicals is discussed.

Canadian Journal of Chemistry, 47, 4708 (1969)

Can. J. Chem. Downloaded from www.nrcresearchpress.com by 210.87.254.105 on 09/05/12
For personal use only.

In the gas-phase thermal decomposition of di-*tert*-butyl peroxide, it is generally accepted that the reaction takes place, by and large, through the sequence

[1] DTBP → 2 *t*-BuO

[2] *t*-BuO → CH_3 + CH_3COCH_3

so that the overall process is

[1*a*] DTBP → $2CH_3$ + $2CH_3COCH_3$

A selection of pertinent references is collected together in ref. 1. The presence of the *tert*-butoxy radical should lead to the formation of *tert*-butyl alcohol via

[3] *t*-BuO + RH → *t*-BuOH + R etc.

but in the gas-phase decomposition, the relative rate constants and concentrations are such that less than 1% of the *t*-BuO radicals are able to abstract to form the alcohol (2). However, in the presence of more reactive substrates, such as ethylenimine (3), acetaldehyde, acrolein (4), and hydrogen chloride (5), considerable stabilization of the *tert*-butoxy radical via reaction [3] has been observed; nitric oxide has also been used to trap the *t*-BuO radical (6). The formation of *t*-BuOH is well known in the liquid-phase decomposition of the peroxide (7, 8). However, it has never been proved that reaction [1] is the sole mechanism of the decomposition, and since there are two other channels [1*a*] and

[1*b*] DTBP → *t*-BuO + CH_3 + CH_3COCH_3

which differ very little in endothermicity from channel [1] itself (9), it is important to try to establish whether such two-bond or three-bond processes contribute to the overall reaction.

Experimental

The purification of di-*tert*-butyl peroxide has been described previously (1). Propane was of Research Grade, supplied by Phillips Petroleum Company; the principal impurity was stated to be ethane. The material was subjected to normal degassing procedures, with extended pumping at 77 °K, and the product was free from any impurities detectable by mass-spectrometric or gas-chromatographic techniques.

The reactions were carried out in the manner described previously (1, 10) by condensing about 10^{-4} mole of the peroxide together with the required quantity of propane into a 10 cc Hoke stainless steel pressure vessel. The vessel, sealed by a needle valve, was heated for the required time in an oil bath, after which the reaction was quenched by cooling the vessel. The contents were then transferred to the vacuum system and the bulk of the propane removed by carefully controlled distillation using two LeRoy stills. The residue was then transferred by vacuum technique to the inlet of a gas phase chromatograph and the yields of acetone and *tert*-butyl alcohol were determined using a 4 m column packed with Porapak P at 90 °C; no detectable decomposition of the peroxide occurred during the analytical procedure.

Results and Discussion

The critical temperature of propane is 96 °C, and thus to ensure a homogeneous system, experiments were performed only above the critical point, at 100.4, 112.0, and 124.0 °C. Each experiment was taken to about 5% peroxide decomposition and the results are plotted in Fig. 1 in the form [acetone]/[*t*-BuOH] produced vs. $[C_3H_8]^{-1}$. In view of the experimental difficulties in separating quantitatively some 5×10^{-6} mole of acetone/alcohol mixture from some 10^{-1} mole of propane by distillation, we regard each of the three sets of data as an acceptable straight line passing through the origin. Hence we conclude that at infinite propane pressure, when all the *t*-BuO radicals will be trapped by reaction [3], no acetone is formed, and so the two-bond and three-bond breaking channels [1*a*] and [1*b*] can be discounted.

If these two mechanisms are ignored, inspection of the reaction scheme [1], [2], [3] shows that the slopes of the plots in Fig. 1 are simply k_2/k_3, from which we find that when T = 100.4, 112.0, 124.0 °C, k_2/k_3 = 0.51, 0.89, 1.23 mole l^{-1}, respectively, corresponding roughly to $E_2 - E_3$ =

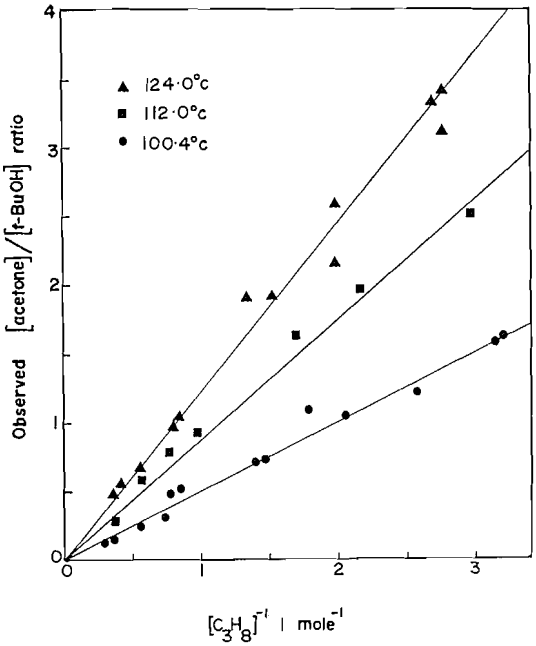

FIG. 1. Variation of the [Acetone]/[*t*-BuOH] ratio as a function of propane pressure in the range 10–100 atm.

11.0 kcal/mole. It is generally agreed that the activation energy E_2 for the dissociation of the *t*-BuO radical is pressure dependent (6, 11–13), but there is little consistency amongst the actual values of E_2 that have so far been determined. At low pressures, usually in the fall-off region, values from 11 to 17 kcal have been quoted (3, 11), and at infinite pressure, values of 15.5 and 22.8 kcal have been suggested (6, 11). Hence, it is not possible at this stage to quote a value for E_3, but we observe that our data is consistent with other data in the literature to the extent that when RH = toluene (8), $E_2 - E_3 = 11.3$ kcal/mole, and it is well known that both propane and toluene exhibit very similar activation energies in abstraction reactions with a variety of free radicals.

Finally, we note that the measurement of [acetone + *t*-BuOH] production leads to rate constants for reaction [1], and within the limited accuracy of this experiment (±20%) the observed values for k_1 are independent of pressure up to the highest pressures used at each of the three temperatures; the independence of k_1 on pressure was only established up to 15 atm in our previous work (1).

1. D. H. SHAW and H. O. PRITCHARD. Can. J. Chem. **46**, 2721 (1968).
2. L. BATT and S. W. BENSON. J. Chem. Phys. **36**, 895 (1962).
3. R. K. BRINTON and D. H. VOLMAN. J. Chem. Phys. **20**, 25 (1952).
4. D. H. VOLMAN and R. K. BRINTON. J. Chem. Phys. **20**, 1764 (1952).
5. M. FLOWERS, L. BATT, and S. W. BENSON. J. Chem. Phys. **37**, 2662 (1962).
6. M. J. YEE QUEE and J. C. J. THYNNE. Trans. Faraday Soc. **63**, 2970 (1967).
7. J. H. RALEY, F. F. RUST, and W. E. VAUGHAN. J. Amer. Chem. Soc. **70**, 1336 (1948).
8. J. H. T. BROOK. Trans. Faraday Soc. **53**, 327 (1957).
9. D. CLARK and H. O. PRITCHARD. J. Chem. Soc. 2136 (1956).
10. D. H. SHAW, B. K. DUNNING, and H. O. PRITCHARD. Can. J. Chem. **47**, 669 (1969).
11. P. GRAY, R. SHAW, and J. C. J. THYNNE. Progr. React. Kinet. **4**, 63 (1967).
12. H. HERSHENSON and S. W. BENSON. J. Chem. Phys. **37**, 1889 (1962).
13. M. F. R. MULCAHY and D. J. WILLIAMS. Aust. J. Chem. **17**, 1291 (1964).

Free radical halogenation of deuteriochloroform

DENNIS D. TANNER, MELVYN W. MOSHER[1], AND N. J. BUNCE[2]
Department of Chemistry, University of Alberta, Edmonton, Alberta

Received July 14, 1969

The vapor phase chlorination and bromination of deuteriochloroform has been carried out in the presence of the corresponding hydrogen halide. The halogenations demonstrated the reversibility of the abstraction reaction by atomic bromine while the chlorination reactions failed to show any evidence for a reversible abstraction.

Canadian Journal of Chemistry, 47, 4709 (1969)

As part of a series of studies of reversible free radical abstractions of hydrogen from saturated carbon (1–3), we have reinvestigated the vapor phase chlorination and bromination of chloroform. Both these halogenations have previously been indicated, on kinetic evidence (4, 5), to involve reversible abstraction of a hydrogen

[1]University of Alberta Postdoctoral Fellow, 1967–1969.
[2]Killam Memorial Postdoctoral Fellow, 1967–1969.

Can. J. Chem. Downloaded from www.nrcresearchpress.com by 210.87.254.105 on 09/05/12
For personal use only.

TABLE II

Frequencies and assignments for copper complexes of cyclohexylamine derivatives

Frequency* (cm^{-1})					
1	2	3	4	5	Assignment
3447 m	—	3383 m	—	3398 m	Asymmetric and symmetric vibration of lattice water
3083 sh	3138 s	3124 sh	3178 m	3178 m	NH stretching vibration
1683 vs	1630 w	1601 s	1590 vw	1601 s	Asymmetric NH deformation
1415 s	1437 s	1420 b	—	1451 s	NH degenerate deformation
1445 sh	1451 sh	1440 b	1451 s	1462 sh	CH_2 scissoring
2942 vs	2921 vs	2902 vs	2902 s	2902 vs	CH_2 stretching vibration of cyclohexyl ring
2846 s	2825 s	2813 sh	2852 m	2810 s	
1335 w	1379 w	1379 m	—	1379 w	C–N stretching for secondary amine
1316 sh	1335 w	1322 w	—	1283 w	
		1316 w	—	1328 vw	
1574 w 1638 vs	—	1663 vs	—	1601 s	H–O–H bending mode and COO^- stretching vibration
—	—	2472 m 2437 m	—	—	C=N stretching vibration

*sh = shoulder; s = sharp; m = medium; vs = very sharp; w = weak; vw = very weak; b = broad; 1 = dichloro-bis(N-cyclohexyl-β-alanine)copper(II) dihydrate; 2 = dichloro-bis[N-(2-hydroxyethyl)cyclohexylamine]copper(II); 3 = dichloro-bis[N-(2-cyanoethyl)cyclohexylamine]copper(II) dihydrate; 4 = dichloro-bis(2-cyclohexylamino-1-phenylethanol)copper(II); 5 = dichloro-bis[N-(3-aminopropyl)-cyclohexylamine]copper(II) dihydrate.

Acknowledgments

The authors wish to express their thanks to Professors S. N. Shukla and K. P. Bhargava for their advice and encouragement and to Drs. Nitya Anand and S. C. Agarwal of the Central Drug Research Institute, Lucknow, for providing facilities for microanalysis and infrared absorption measurements, respectively. Grateful acknowledgment is made to the Indian Council of Medical Research for providing financial assistance to one of us (C.H.M.), to Dr. Richard P. Germann of the Abbott Laboratories, Development Division, North Chicago, Illinois, for the generous supply of cyclohexylamine derivatives, and to the Perkin–Elmer Corporation, Norwalk, Connecticut, for the generous gift of a Hitachi Perkin–Elmer UV-VIS spectrophotometer.

1. S. S. Parmar and C. H. Misra. To be published.
2. S. M. A. Smolt, C. W. Kreke, and E. S. Cook. J. Biol. Chem. **224**, 999 (1957).
3. C. H. Misra, S. S. Parmar, and S. N. Shukla. J. Inorg. Nucl. Chem. **28**, 147 (1966).
4. C. H. Misra, S. S. Parmar, and S. N. Shukla. J. Inorg. Nucl. Chem. **29**, 2589 (1967).
5. C. H. Misra, S. S. Parmar, and S. N. Shukla. Can. J. Chem. **46**, 2685 (1968).
6. S. S. Parmar, C. H. Misra, and J. P. Barthwal. To be published.
7. R. W. Crowe and C. P. Smyth. J. Amer. Chem. Soc. **73**, 5406 (1951).
8. C. H. Misra, S. S. Parmar, and S. N. Shukla. Can. J. Chem. **45**, 2459 (1967).
9. A. I. Vogel. Quantitative inorganic analysis. Longman Green and Co., Ltd., London. 1962. p. 499.
10. C. H. Misra, Surendra S. Parmar, and R. C. Arora. Inorg. Nucl. Chem. Lett. **3**, 603 (1967).
11. R. Blackhouse, M. E. Foss, and R. S. Nyholm. J. Chem. Soc. 1714 (1957).
12. L. Ricocoboni. Atti, Ist Veneto Sci. Lett. Arti, **96**, 183 (1937).
13. A. B. Thomas and E. C. Rochow. J. Inorg. Nucl. Chem. **4**, 205 (1957).

Erratum: Electrochemiluminescence of carbazole

K. S. V. Santhanam, R. N. O'Brien, and A. D. Kirk

University of Victoria, Victoria, British Columbia

Received June 16, 1969

(Ref.: Can. J. Chem. **47**, 1355 (1969))

Canadian Journal of Chemistry, 47, 4707 (1969)

On page 1358, column 2 sentence 8 should read "The bonding levels are full" instead of "Both bonding and antibonding levels are full".

Reference 14 on page 1359 in the bibliography section is superfluous and should be deleted.

Can. J. Chem. Downloaded from www.nrcresearchpress.com by 210.87.254.5 on 09/05/12
For personal use only.

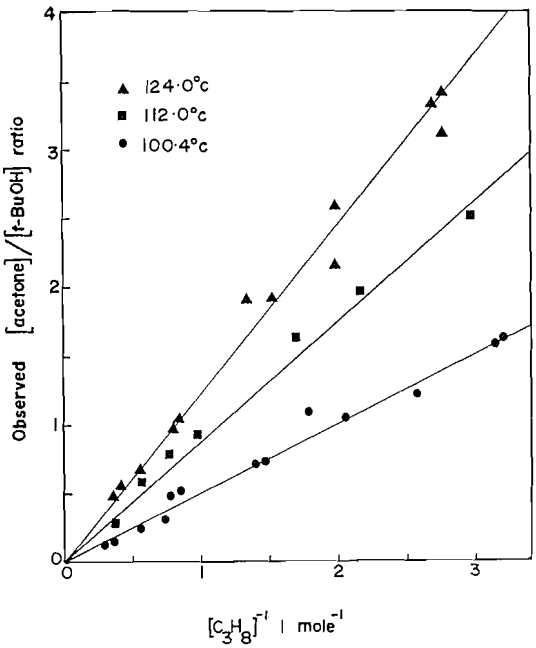

FIG. 1. Variation of the [Acetone]/[*t*-BuOH] ratio as a function of propane pressure in the range 10–100 atm.

11.0 kcal/mole. It is generally agreed that the activation energy E_2 for the dissociation of the *t*-BuO radical is pressure dependent (6, 11–13), but there is little consistency amongst the actual values of E_2 that have so far been determined. At low pressures, usually in the fall-off region, values from 11 to 17 kcal have been quoted (3, 11), and at infinite pressure, values of 15.5 and 22.8 kcal have been suggested (6, 11). Hence, it is not possible at this stage to quote a value for E_3, but we observe that our data is consistent with other data in the literature to the extent that when RH = toluene (8), $E_2 - E_3 = 11.3$ kcal/mole, and it is well known that both propane and toluene exhibit very similar activation energies in abstraction reactions with a variety of free radicals.

Finally, we note that the measurement of [acetone + *t*-BuOH] production leads to rate constants for reaction [1], and within the limited accuracy of this experiment (±20%) the observed values for k_1 are independent of pressure up to the highest pressures used at each of the three temperatures; the independence of k_1 on pressure was only established up to 15 atm in our previous work (1).

1. D. H. SHAW and H. O. PRITCHARD. Can. J. Chem. **46**, 2721 (1968).
2. L. BATT and S. W. BENSON. J. Chem. Phys. **36**, 895 (1962).
3. R. K. BRINTON and D. H. VOLMAN. J. Chem. Phys. **20**, 25 (1952).
4. D. H. VOLMAN and R. K. BRINTON. J. Chem. Phys. **20**, 1764 (1952).
5. M. FLOWERS, L. BATT, and S. W. BENSON. J. Chem. Phys. **37**, 2662 (1962).
6. M. J. YEE QUEE and J. C. J. THYNNE. Trans. Faraday Soc. **63**, 2970 (1967).
7. J. H. RALEY, F. F. RUST, and W. E. VAUGHAN. J. Amer. Chem. Soc. **70**, 1336 (1948).
8. J. H. T. BROOK. Trans. Faraday Soc. **53**, 327 (1957).
9. D. CLARK and H. O. PRITCHARD. J. Chem. Soc. 2136 (1956).
10. D. H. SHAW, B. K. DUNNING, and H. O. PRITCHARD. Can. J. Chem. **47**, 669 (1969).
11. P. GRAY, R. SHAW, and J. C. J. THYNNE. Progr. React. Kinet. **4**, 63 (1967).
12. H. HERSHENSON and S. W. BENSON. J. Chem. Phys. **37**, 1889 (1962).
13. M. F. R. MULCAHY and D. J. WILLIAMS. Aust. J. Chem. **17**, 1291 (1964).

Free radical halogenation of deuteriochloroform

DENNIS D. TANNER, MELVYN W. MOSHER[1], AND N. J. BUNCE[2]
Department of Chemistry, University of Alberta, Edmonton, Alberta

Received July 14, 1969

The vapor phase chlorination and bromination of deuteriochloroform has been carried out in the presence of the corresponding hydrogen halide. The halogenations demonstrated the reversibility of the abstraction reaction by atomic bromine while the chlorination reactions failed to show any evidence for a reversible abstraction.

Canadian Journal of Chemistry, 47, 4709 (1969)

As part of a series of studies of reversible free radical abstractions of hydrogen from saturated carbon (1–3), we have reinvestigated the vapor phase chlorination and bromination of chloroform. Both these halogenations have previously been indicated, on kinetic evidence (4, 5), to involve reversible abstraction of a hydrogen

[1]University of Alberta Postdoctoral Fellow, 1967–1969.
[2]Killam Memorial Postdoctoral Fellow, 1967–1969.

Can. J. Chem. Downloaded from www.nrcresearchpress.com by 210.87.254.42 on 09/05/12
For personal use only.

TABLE I

Photobromination of deuteriochloroform with bromine in the presence of hydrogen bromide

	Reactants			Products	
Reaction	$CDCl_3$* (mmoles)	HBr (mmoles)	Br_2 (mmoles)	$CHCl_3$† (atom %)	$CBrCl_3/CHCl_3$
2	7.59	83	2.14	65	1.18
3	7.28	83	1.86	65	2.38
4	8.10	83	3.78	32	0.36

*0.31 atom % ^1H.
†Analyzed by n.m.r.; total of $CHCl_3$ + $CDCl_3$ vs. CCl_3Br was determined by gas–liquid phase chromatography.

atom from chloroform by the halogen atom as in reaction [1].

[1] $$HCCl_3 + X^{\cdot} \rightleftharpoons HX + {}^{\cdot}CCl_3$$

In order to attempt to demonstrate chemically the reversibility of hydrogen abstraction, deuteriochloroform was halogenated in the vapor phase in the presence of a large excess of the corresponding hydrogen halide, and the recovered chloroform was analyzed by nuclear magnetic resonance (n.m.r.) for the ^1H which it should incorporate if reaction [1] is reversible. The reactions were carried out at the ambient temperature and initiated photolytically by the use of two 200 W tungsten lamps placed a few inches from the reaction chamber, a 3.3 l Pyrex glass bulb.

When deuteriochloroform (7.3 mmoles), initially containing 0.31 atom % ^1H, was chlorinated by elemental chlorine (2.5 mmoles) in the presence of 62.2 mmoles hydrogen chloride, n.m.r. analysis of the recovered deuteriochloroform showed no detectable increase in ^1H content when all the chlorine had reacted. This result suggests that if any reversible hydrogen abstraction occurs in this system, its extent must be below the level of detection for our experiment. Furthermore, this result is not unexpected, since simple bond energy calculations indicate that the reverse of reaction [1] is endothermic by some[3] 12 (7.5) kcal/mole (6, 7).

Similar calculations for the bromination of chloroform give for the reversal reaction $\Delta H \sim -3\ (-8)$ kcal/mole. Sullivan and Davidson (5) have proposed that the thermally initiated bromination of chloroform is completely reversible with the overall equilibrium constant $K = [CCl_3Br]\,[HBr]/[CHCl_3]\,[Br_2] \simeq 2$.

Deuteriochloroform was, therefore, photobrominated with molecular bromine in the presence of hydrogen bromide. The chloroform recovered after the reaction was analyzed for incorporation of ^1H (Table I).

The results given in Table I show that, unlike the case of chlorination of deuteriochloroform, bromination of this substrate involves a considerable degree of reversible hydrogen abstraction. Although reversible hydrogen abstraction has long been recognized as being important in free-radical brominations (3, 5, 8–10, and references cited in (10)), this is, to our knowledge, only the second occasion (11) on which it has been demonstrated chemically.

Experimental

Materials

Deuteriochloroform was from Columbia Chemical Corporation and contained 0.31 atom % of ^1H. Chlorine, hydrogen bromine, and hydrogen chloride were obtained from Matheson Chemical. Molecular bromine, reagent grade, was from the Shawinigan Chemical Co. All materials were distilled before use.

Gas Phase Bromination of Deuteriochloroform in the Presence of Hydrogen Bromide

Three 3.3 l evacuated bulbs were filled with hydrogen bromide to a pressure of 154 mm Hg. The hydrogen bromide was frozen and a mixture of deuteriochloroform and bromine (7.59 mmoles, 2.14 mmoles, reaction [2]; 7.28 mmoles, 1.86 mmoles, reaction [3]; 8.10 mmoles, 3.78 mmoles, reaction [4]) was vacuum transferred into each of the bulbs in turn. The reaction bulbs were degassed, the contents allowed to warm in the dark until the contents had vaporized, and then allowed to stand 30 min. The bulbs were irradiated with two 200 W incandescent lamps placed 3 in. from the reaction. One bulb (reaction [4]) was irradiated 4.5 days while the other two were irradiated for 8 days.

After the irradiation was stopped the bromine color

[3]The values in parentheses were calculated from data given in ref. 6.

Can. J. Chem. Downloaded from www.nrcresearchpress.com by 210.87.254.42 on 09/05/12
For personal use only.

was still pronounced. The bulbs were placed in a methanol slush (−98°) and the hydrogen bromide removed by distillation. The remaining material was vacuum transferred into a small flask. Methylene chloride was added as a standard and the amount of hydrogen incorporation was determined by comparison of the n.m.r. singlet of the hydrogens of methylene chloride to the singlet for the hydrogen of chloroform. The amount of total chloroform and product, bromotrichloromethane, was determined from the area ratios of these materials to that of the standard on a 10 ft. × 1/4 in. SE-30 gas–liquid phase chromatographic column programmed from 50 to 120°. The results are shown in Table I.

Gas Phase Chlorination of Deuteriochloroform in the Presence of Hydrogen Chloride

Hydrogen chloride was placed in two 3.3 l evacuated bulbs to a pressure of 350 mm Hg. Molecular chlorine (62 ml, standard temperature and pressure) was transferred into each bulb and frozen. Deuteriochloroform (7.3 mmoles, reaction [5]; 7.6 mmoles, reaction [6]) was vacuum transferred into the bulb and the contents of the bulbs degassed and allowed to warm in the dark until the material had completely vaporized. The bulbs were irradiated with two 200 W incandescent lamps placed 2 in. from the reaction mixture until the chlorine color had disappeared plus an additional 3 h. Isolation and analysis of the organic material from each reaction vessel was carried out in the same manner as above. No increase in the ^1H content of the deuteriochloroform was detected.

Acknowledgment

The financial support of this work by the National Research Council of Canada and the University of Alberta is gratefully acknowledged.

1. D. D. Tanner and N. J. Bunce. J. Amer. Chem. Soc. **91**, 3028 (1969).
2. N. J. Bunce and D. D. Tanner. J. Amer. Chem. Soc. In press.
3. D. D. Tanner, D. Darwish, M. W. Mosher, and N. J. Bunce. J. Amer. Chem. Soc. In press.
4. G. M. Schwab and U. Heyde. Z. Phys. Chem. **B8**, 147 (1930).
5. J. H. Sullivan and N. Davidson. J. Chem. Phys. **19**, 143 (1951).
6. S. W. Benson. J. Chem. Phys. **43**, 2044 (1965).
7. T. L. Cottrell. The strengths of chemical bonds. 2nd ed. Butterworths, London. 1958.
8. R. E. Pearson and J. C. Martin. J. Amer. Chem. Soc. **85**, 3142 (1963).
9. H. R. Anderson, H. A. Scheraga, and E. R. Van Artsdaler. J. Chem. Phys. **21**, 1258 (1953).
10. C. Walling, A. L. Rieger, and D. D. Tanner. J. Amer. Chem. Soc. **85**, 3129 (1963).
11. K. B. Wiberg and L. H. Slaugh. J. Amer. Chem. Soc. **80**, 3033 (1958).

Spectrofluorometric studies. VI. Photochemistry of toluene vapor excited in the 2480–2660 Å region

S. L. Lem, G. P. Semeluk, and I. Unger

Department of Chemistry, University of New Brunswick, Fredericton, New Brunswick, Canada

Received July 18, 1969

The fluorescent yields and triplet yields of toluene vapor as a function of exciting wavelengths and pressure have been determined. The sensitized emission of biacetyl technique was used to determine triplet yields. The sums of fluorescent yield and triplet yield at 2660, 2600, and 2540 Å are near unity. The data reported here confirm recently published results on toluene wherein the *cis–trans* isomerization of olefins technique was used as a triplet probe.

Canadian Journal of Chemistry, **47**, 4711 (1969)

Of the several methods for detecting triplet states of those molecules which do not phosphoresce in the gas phase, the two most commonly used are the *cis–trans* isomerization of olefins technique first described by Cundall and co-workers (1, 2) and the sensitized emission of biacetyl technique (3). The advantages and disadvantages of these two techniques have been discussed (4). Recently (5) toluene triplet yields determined by the Cundall method, as well as fluorescent yields, have been reported for excitation in the 2480–2668 Å region. The results of a similar study using the biacetyl technique to determine triplet yields are reported herein.

Fluorometric grade toluene and benzene obtained from the Hartman–Leddon Company were used without further purification. Biacetyl, obtained from the Aldrich Chemical Company, was purified by bulb-to-bulb distillation and stored in a blackened bulb. The studies were carried out in a mercury- and grease-free high vacuum line, equipped with Hoke packless diaphragm metal valves. All emission measurements were performed on a modified Aminco–Bowman

Can. J. Chem. Downloaded from www.nrcresearchpress.com by 210.87.254.42 on 09/05/12
For personal use only.

was still pronounced. The bulbs were placed in a methanol slush (−98°) and the hydrogen bromide removed by distillation. The remaining material was vacuum transferred into a small flask. Methylene chloride was added as a standard and the amount of hydrogen incorporation was determined by comparison of the n.m.r. singlet of the hydrogens of methylene chloride to the singlet for the hydrogen of chloroform. The amount of total chloroform and product, bromotrichloromethane, was determined from the area ratios of these materials to that of the standard on a 10 ft. × 1/4 in. SE-30 gas–liquid phase chromatographic column programmed from 50 to 120°. The results are shown in Table I.

Gas Phase Chlorination of Deuteriochloroform in the Presence of Hydrogen Chloride

Hydrogen chloride was placed in two 3.3 l evacuated bulbs to a pressure of 350 mm Hg. Molecular chlorine (62 ml, standard temperature and pressure) was transferred into each bulb and frozen. Deuteriochloroform (7.3 mmoles, reaction [5]; 7.6 mmoles, reaction [6]) was vacuum transferred into the bulb and the contents of the bulbs degassed and allowed to warm in the dark until the material had completely vaporized. The bulbs were irradiated with two 200 W incandescent lamps placed 2 in. from the reaction mixture until the chlorine color had disappeared plus an additional 3 h. Isolation and analysis of the organic material from each reaction vessel was carried out in the same manner as above. No increase in the ^1H content of the deuteriochloroform was detected.

Acknowledgment

The financial support of this work by the National Research Council of Canada and the University of Alberta is gratefully acknowledged.

1. D. D. TANNER and N. J. BUNCE. J. Amer. Chem. Soc. **91**, 3028 (1969).
2. N. J. BUNCE and D. D. TANNER. J. Amer. Chem. Soc. In press.
3. D. D. TANNER, D. DARWISH, M. W. MOSHER, and N. J. BUNCE. J. Amer. Chem. Soc. In press.
4. G. M. SCHWAB and U. HEYDE. Z. Phys. Chem. **B8**, 147 (1930).
5. J. H. SULLIVAN and N. DAVIDSON. J. Chem. Phys. **19**, 143 (1951).
6. S. W. BENSON. J. Chem. Phys. **43**, 2044 (1965).
7. T. L. COTTRELL. The strengths of chemical bonds. 2nd ed. Butterworths, London. 1958.
8. R. E. PEARSON and J. C. MARTIN. J. Amer. Chem. Soc. **85**, 3142 (1963).
9. H. R. ANDERSON, H. A. SCHERAGA, and E. R. VAN ARTSDALER. J. Chem. Phys. **21**, 1258 (1953).
10. C. WALLING, A. L. RIEGER, and D. D. TANNER. J. Amer. Chem. Soc. **85**, 3129 (1963).
11. K. B. WIBERG and L. H. SLAUGH. J. Amer. Chem. Soc. **80**, 3033 (1958).

Spectrofluorometric studies. VI. Photochemistry of toluene vapor excited in the 2480–2660 Å region

S. L. LEM, G. P. SEMELUK, AND I. UNGER

Department of Chemistry, University of New Brunswick, Fredericton, New Brunswick, Canada

Received July 18, 1969

The fluorescent yields and triplet yields of toluene vapor as a function of exciting wavelengths and pressure have been determined. The sensitized emission of biacetyl technique was used to determine triplet yields. The sums of fluorescent yield and triplet yield at 2660, 2600, and 2540 Å are near unity. The data reported here confirm recently published results on toluene wherein the *cis–trans* isomerization of olefins technique was used as a triplet probe.

Canadian Journal of Chemistry, **47**, 4711 (1969)

Of the several methods for detecting triplet states of those molecules which do not phosphoresce in the gas phase, the two most commonly used are the *cis–trans* isomerization of olefins technique first described by Cundall and co-workers (1, 2) and the sensitized emission of biacetyl technique (3). The advantages and disadvantages of these two techniques have been discussed (4). Recently (5) toluene triplet yields determined by the Cundall method, as well as fluorescent yields, have been reported for excitation in the 2480–2668 Å region. The results of a similar study using the biacetyl technique to determine triplet yields are reported herein.

Fluorometric grade toluene and benzene obtained from the Hartman–Leddon Company were used without further purification. Biacetyl, obtained from the Aldrich Chemical Company, was purified by bulb-to-bulb distillation and stored in a blackened bulb. The studies were carried out in a mercury- and grease-free high vacuum line, equipped with Hoke packless diaphragm metal valves. All emission measurements were performed on a modified Aminco–Bowman

Can. J. Chem. Downloaded from www.nrcresearchpress.com by 210.87.254.6 on 09/05/12
For personal use only.

TABLE I

Summary of fluorescent and triplet yields of toluene at various exciting wavelengths

λ_{ex} (Å)	P_T (Torr)	P_{BIA} (Torr)	Φ_t	Φ_f	$\Phi_f + \Phi_t$	Φ_f/Φ_t
2660	20.2	5.4	0.66	0.34	1.00	0.51
2600	20.2	5.3	0.67	0.37	1.04	0.55
2540	19.4	5.6	0.66	0.28	0.94	0.42
2480	20.8	5.4	0.26	0.13	0.39	0.50
2450	10.2–23.9	0	—	0.08	—	—
2510	10.5–20.2	0	—	0.28	—	—

TABLE II

Stern–Volmer relations between fluorescence yields and concentrations of toluene and of biacetyl at 20 Torr toluene*

λ_{ex} (Å)	Equation of line	Pressure range (Torr)
2570	$1/\Phi_f = 2.63 + 1.21 \times 10^2$ [T]	2.5–23.6
2600	$1/\Phi_f = 2.24 + 5.35 \times 10^2$ [T]	2.2–23.6
2630	$1/\Phi_f = 2.37 + 1.85 \times 10^2$ [T]	2.6–24.0
2660	$1/\Phi_f = 2.29 + 3.55 \times 10^2$ [T]	2.9–24.7
2480	$1/\Phi_f = 8.25 + 6.53 \times 10^4$ [BiA]	0.1–5.4
2540	$1/\Phi_f = 3.98 + 3.67 \times 10^4$ [BiA]	0.1–5.6
2600	$1/\Phi_f = 2.82 + 3.45 \times 10^4$ [BiA]	0.1–5.4
2660	$1/\Phi_f = 2.59 + 3.48 \times 10^4$ [BiA]	0.1–5.4

*All concentrations are in units of moles l^{-1}.

spectrophotofluorometer. Experimental details have been given previously (6). It must be noted that the band pass for the current work was approximately 70 Å, whereas Burton and Noyes (5) used a band pass of 32 Å.

Fluorescent yields and triplet yields, corrected for self-quenching and singlet quenching by BiA, of toluene vapor, excited at four different wavelengths, are given in Table I. The fluorescent yields reported in this study are based on the value 0.18 (7) for the fluorescent yield of benzene. From Table I, it is seen that the fluorescent yields obtained in this study are between 10 and 20% higher than those reported by Burton and Noyes (5). This difference is possibly due to the difference of viewing geometry used in the two studies. Our cells have a 1 cm path, with the viewing zone (between 0.45 and 0.55 cm from the incident "face" of the vapor) defined by a careful selection of three appropriately sized and placed non-reflecting apertures placed between the cell and the monochromator. Burton and Noyes used a 5.3 cm path T-cell, viewing the emission from a window 1.5 cm diameter at a distance of 1.5 cm from the inside of the incident face of the cell. In the event that Beer's Law is not strictly obeyed, or that the extinction coefficients of the benzene calibrant and toluene differ significantly, the calculated yields tend to be somewhat lower than true yields and the discrepancy is more pronounced for longer absorption paths (8).

Our triplet yields were calculated from a value of 0.63 (9) (instead of 0.72) for the triplet yield of benzene, and are substantially in agreement with those recently reported (5), although they appear to be 10% lower because of this choice. Since there is some disagreement in the literature regarding the *cis–trans* branching ratio of the *cis*-butene-2, (10–12) but substantial agreement about the biacetyl yield, there is reason to prefer the lower triplet yield of benzene and indirectly, therefore, the lower triplet yields for toluene. It is also evident that choosing the higher yield of benzene would lead to the conclusion that the sum of singlet and triplet yields are larger than unity at several wavelengths. Our data confirm the observation (5) that the singlet-to-triplet ratio is independent of exciting wavelength (see Table I), and support the conclusion that intersystem crossover and fluorescence occur from the lower vibrational levels of the excited singlet.

The summary of Stern–Volmer relations listed

Can. J. Chem. Downloaded from www.nrcresearchpress.com by 210.87.254.6 on 09/05/12
For personal use only.

in Table II indicate that although there is some self-quenching in toluene for excitation above 2540 Å, this is a 100-fold smaller than quenching by biacetyl.

Acknowledgments

The authors gratefully acknowledge the financial assistance from the Associated Alumni of the University of New Brunswick and from the National Research Council of Canada.

1. R. B. CUNDALL and D. G. MILNE. J. Amer. Chem. Soc. **83**, 3902 (1961).
2. R. B. CUNDALL, F. J. FLETCHER, and D. G. MILNE. J. Chem. Phys. **39**, 3536 (1963).
3. H. ISHIKAWA and W. A. NOYES, JR. J. Chem. Phys. **37**, 583 (1962).
4. W. A. NOYES, JR. and I. UNGER. Advan. Photochem. **4**, 49 (1966).
5. C. S. BURTON and W. A. NOYES, JR. J. Chem. Phys. **49**, 1705 (1968).
6. F. W. AYER, F. GREIN, G. P. SEMELUK, and I. UNGER. Ber. Bunsenges. Phys. Chem. **72**, 282 (1968).
7. W. A. NOYES, JR., D. A. HARTER, and W. A. MULAC. J. Chem. Phys. **44**, 2100 (1966).
8. J. L. DURHAM, G. P. SEMELUK, and I. UNGER. Can. J. Chem. **46**, 3177 (1968).
9. W. A. NOYES, JR. and D. A. HARTER. J. Chem. Phys. **46**, 674 (1967).
10. (*a*) G. A. HANINGER, JR. and E. K. C. LEE. J. Phys. Chem. **71**, 3104 (1967); (*b*) E. K. C. LEE, H. O. DENSCHLAG, and G. A. HANINGER, JR. J. Chem. Phys. **48**, 4547 (1968).
11. S. SATO, K. KIKUCHI, and M. TANAKA. J. Chem. Phys. **39**, 239 (1963).
12. R. B. CUNDALL and F. J. FLETCHER, and D. G. MILNE. Trans. Faraday Soc. **60**, 1146 (1964).

Erratum: N-Chlorination of secondary amides. II. Effects of substituents on rates of N-chlorination

E. W. C. W. THOMM AND M. WAYMAN

Department of Chemical Engineering and Applied Chemistry, University of Toronto, Toronto 181, Ontario

Received October 1, 1969

(Ref. Can. J. Chem. **47**, 3289 (1969))

Canadian Journal of Chemistry, **48**, 4713 (1970)

On p. 3295, the footnote ‡ of Table V should read "In amide series $R_1\overset{\overset{O}{\|}}{C}NHR_2$", not "In amide series $R_1\overset{\overset{O}{|}}{C}NHCH_3$".

On p. 3296, the ordinate legends of Figs. 1 and 2 should both read "log k (k in (mole/ls)$^{-1}$)".

Can. J. Chem. Downloaded from www.nrcresearchpress.com by 210.87.254.6 on 09/05/12
For personal use only.

Can. J. Chem. Downloaded from www.nrcresearchpress.com by 210.87.254.40 on 09/05/12
For personal use only.

Observation of a large dose rate effect on the ozone yield in the radiolysis of gaseous oxygen[1]

A. W. BOYD, C. WILLIS, AND R. CYR
Physical Chemistry Branch, Chalk River Nuclear Laboratories, Atomic Energy of Canada Limited, Chalk River, Ontario

AND

D. A. ARMSTRONG
Department of Chemistry, The University of Calgary, Calgary, Alberta

Received September 22, 1969

The ozone yield from the radiolysis of gaseous oxygen has been measured to be $G(O_3) = 12.8 \pm 0.6$ at 10^{26}–10^{27} eV g^{-1} s^{-1} and to be $G(O_3) = 6.2 \pm 0.6$ at 10^{16} eV g^{-1} s^{-1}. The latter result depends on a new determination of the stoichiometry of the oxidation of iodide by ozone. It is proposed that the difference in yields between the two dose rates is due to differences in ion-recombination processes.

Canadian Journal of Chemistry, 47, 4715 (1969)

Introduction

The yield of ozone from the radiolysis of gaseous oxygen has been proposed (1) as an optical dosimeter for use in pulse radiolysis studies where optical observations of transients are made. Ghormley, Hochanadel, and Boyle (1) report the ozone yield to be $G(O_3) = 13.8 \pm 0.7$ at a dose rate of 6×10^{25} eV g^{-1} s^{-1} and suggest that this is not significantly different from the yield observed at low dose rates (2, 3).

To confirm their conclusions we have determined the ozone yield in the radiolysis of oxygen at both high and low dose rates. We have compared the yield of ozone from the radiolysis of oxygen with the yield of nitrogen from the radiolysis of nitrous oxide at both 10^{26}–10^{27} eV g^{-1} s^{-1} and at 10^{16} eV g^{-1} s^{-1}.

Our value for $G(O_3)$ at the high dose rates agrees within experimental error with that of Ghormley *et al.* (1). However, both our low dose rate work and the re-examined data of other workers (2, 3) give yields of ozone that are significantly lower than the high dose rate values.

It is important to explain the difference in yields between the two dose rates before the acceptance of the system as a dosimeter.

Experimental

A Febetron 705 pulsed electron accelerator was used for high dose rate irradiations and a Gammacell 220 for low dose rate irradiations. The silica irradiation cells and experimental procedures have already been described (4, 5). The dose absorbed in the cells was measured by nitrous oxide dosimetry using $G(N_2) = 12.4$ for the high dose rates (6, 7) and $G(N_2) = 10.0$ for the ^{60}Co γ dose rates (8). The dose rate obtained with the Febetron was varied by using a scattering foil (9) and placing the irradiation cell at various distances from it.

We employed both optical and chemical procedures for ozone determination. The optical method is essentially that described by Sears and Sutherland (3), except that a 10 cm absorption cell and a Perkin–Elmer 450 spectrophotometer were used. The extinction coefficient of ozone at 254 mμ is 135 cm^{-1} at standard temperature and pressure. This was established absolutely by DeMore and Raper (10) who measured the pressure increase on decomposition of ozone to oxygen.

For low doses and low oxygen pressures the above method does not have enough sensitivity. In these cases the ozone was determined by the iodide method. Potassium iodide solution phosphate buffered at pH 7 was introduced into the cooled reaction cell immediately after irradiation. The amount of I_3^- formed was determined by measuring the absorbance at 358 mμ and reference to a calibration curve prepared using standard iodine–iodide solutions. Comparison of the optical and iodide methods for identical irradiations shows that under these conditions one molecule of ozone produces 1.52 ± 0.05 molecules of I_3^-. The stoichiometry of the iodide method at various pH's has been previously discussed. Byers and Saltzmann (11), assuming a stoichiometry of 1:1 for neutral solutions, obtain a ratio of O_3:I_3^- of 1.54:1 for 1 *N* alkaline solution. Ingols, Fetner, and Eberhardt (12) give the stoichiometry at pH 9 to be 1:1 but at pH 2 give O_3:I_3^- to be approximately 1:2. Neither of these determinations can be considered absolute. However, if the latter (12) determination at pH 9 is correct and can

[1]A.E.C.L. No. 3486.

Can. J. Chem. Downloaded from www.nrcresearchpress.com by 210.87.254.40 on 09/05/12
For personal use only.

be applied to the 1 *N* alkaline solution of Byers and Saltzmann, then in neutral iodide their (11) result would give O_3:I_3^- of 1:1.54. This agrees well with our value for this ratio.

Results

The amount of ozone formed under various conditions is shown in Fig. 1. The Febetron results are for single irradiation pulses. Analyses were complete within 10 min after irradiation and on further standing there was no significant decrease in the measured optical density for at least 30 min. At both temperatures, the yields per unit dose were independent of pressure (in the range 30 to 800 Torr) and of dose rate (in the range 10^{26} to 2×10^{27} eV g^{-1} s^{-1}). The slope of the best line through the results gives $G(O_3) = 12.8 \pm 0.6$.

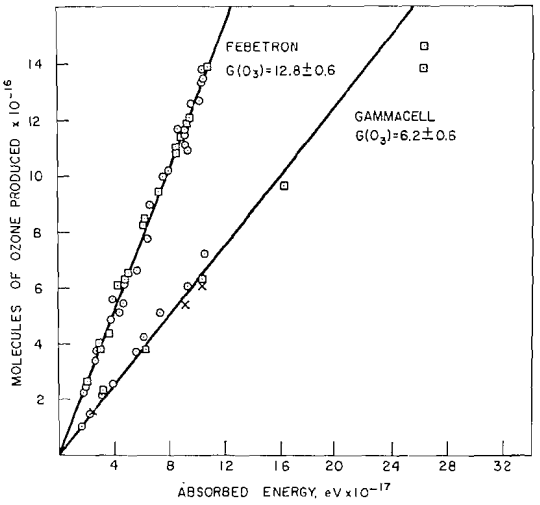

FIG. 1. Amount of ozone produced in the radiolysis of oxygen under various conditions. Febetron results: ○, 298 °K; □, 195 °K; Gamma cell results: ○, taken from ref. 2 both for 77 and 195 °K; □, taken from ref. 3 both for 77 and 195 °K; ×, present work at 77 °K. The units for both molecules of ozone and absorbed dose for the Febetron results must be multiplied by 10, i.e., the maximum absorbed energy is 1.12×10^{19} eV.

The lower line in Fig. 1 gives the amount of ozone formed in the radiolysis of oxygen at low dose rates ($\sim 10^{16}$ eV g^{-1} s^{-1}). Included are values taken directly from the paper of Sears and Sutherland (3) and also from the work of Johnson and Warman (2), who determined ozone by the iodide method at pH 7, assuming a stoichiometry of 1:1. The values of these latter authors have been corrected to $G(N_2) = 10.0$ instead of the value they used of $G(N_2) = 12.5$ for the nitrous oxide dosimeter (8) at this low dose rate and also for the stoichiometry observed by us for the iodide method of ozone determination. The line drawn represents the best slope and corresponds to an initial yield of $G(O_3) = 6.2 \pm 0.6$. The only values discordant with this are those of Sears and Sutherland (3) for irradiations at 77 °K with doses above 2×10^{18} eV g^{-1} which give $G(O_3) = 10.5 \pm 0.5$. These are outside the range of values plotted in Fig. 1.

Discussion

The present yield of $G(O_3) = 12.8 \pm 0.6$ for the radiolysis of oxygen at Febetron dose rates does not seriously disagree with that of Ghormley, Hochanadel, and Boyle (1) ($G(O_3) = 13.8 \pm 0.7$). Our value may be more reliable because the geometry of their cells made it difficult to calculate the integrated mean dose over the effective light path.

Of much greater significance is the difference of a factor of about 2 between the yields at Febetron dose rates and those at ^{60}Co γ-ray dose rates. A possible explanation of this difference lies in different ion-combination reactions at the two dose rates.

The principal ions formed in the irradiation of oxygen are O_2^+ and e with a small proportion of O^+ (13). Dissociative excitation leads to the formation of O atoms and all oxygen atoms formed in the system react with O_2 to give O_3, at least at reasonably low doses.

[1] $$O + 2O_2 \rightarrow O_3 + O_2$$

Electrons can undergo a three body attachment to yield O_2^-

[2] $$e + 2O_2 \rightarrow O_2^- + O_2$$

At 10^{27} eV g^{-1} s^{-1} the lifetime of the positive ions with respect to neutralization is 5×10^{-9} s. Thus the actual lifetime of the ions will closely follow the irradiation pulse and ion recombination reactions such as reaction [3] will be predominant

[3] $$O_2^+ + O_2^- \rightarrow 2O + O_2$$

All such recombination processes are highly exothermic and will almost certainly produce two oxygen atoms per event. Thus the yield of ozone from ionic precursors will be $2G(e)$.

As we have previously pointed out (4), at low

dose rates O_2^- will undergo a charge transfer reaction with ozone

[4] $$O_2^- + O_3 \rightarrow O_2 + O_3^-$$

The rate constant for this reaction, k_4 equals 3×10^{-10} cm^3 molecule^{-1} s^{-1} (14), so that all electrons captured by oxygen in reaction [2] will be transferred to ozone at ozone concentrations above 0.1 p.p.m. (i.e. 3×10^{12} molecules cm^{-3}) for dose rates of 10^{16} eV g^{-1} s^{-1}. The typical mean ion lifetime at these dose rates is of the order of 10^{-2} s.

For these conditions, then, the main neutralization reaction must involve the O_3^- ion. A possible neutralization reaction is

[5] $$O_2^+(nO_2) + O_3^- \rightarrow O_3 + (n+1)O_2$$
$$\text{or} \quad O + (n+2)O_2$$

If this is so then at low dose rates there will be no net contribution to the ozone yield from ionic processes and $G(O_3)$ should correspond to the yield of oxygen atoms from dissociative excitation. The extent of clustering of O_2^+ will be greater at low dose rates and this could also account for the lack of dissociative neutralization in reaction [5]. At high dose rates the yield is enhanced by the contribution from ion combination processes discussed above. This increase should be equal to twice the ion yield. From $W_{O_2} = 30.6$ eV per ion pair (15 and references therein, 16), G(ion pair) = 3.27 and $G(O_3)$ for Febetron conditions should equal [low dose yield + $2G(e)$] = 6.2 + 6.55 = 12.75, which is in good agreement with the observed value.

It may be noted that various additives which have electron scavenging capabilities have no significant effect on the yields of ozone at low dose rates (3), in agreement with the above conclusion. Preliminary experiments show that at Febetron dose rates both SF_6 and cyclo-C_4F_8 reduce the ozone yield to close to $G(O_3) = 6.0$.

Further work on this system is in progress and will be reported later. However, it is already clear that the yield of ozone, $G(O_3) = 12.0$–13.0 at Febetron dose rates, is correct and that the difference between it and the low dose rate yields is due to changes in ion combination reactions.

Acknowledgments

D.A.A. wishes to thank A.E.C.L. for a Visiting Scientist's appointment and the University of Calgary for sabbatical leave (1968–1969).

1. J. GHORMLEY, C. HOCHANADEL, and J. BOYLE. J. Chem. Phys. **50**, 419 (1969).
2. G. R. A. JOHNSON and J. M. WARMAN. Discuss. Faraday Soc. **37**, 87 (1964).
3. J. T. SEARS and J. N. SUTHERLAND. J. Phys. Chem. **72**, 1166 (1968).
4. C. WILLIS, A. W. BOYD, and D. A. ARMSTRONG. Can. J. Chem. **47**, 3783 (1969).
5. C. WILLIS, A. W. BOYD, and O. A. MILLER. Can. J. Chem. **47**, 3007 (1969).
6. C. WILLIS, O. A. MILLER, A. E. ROTHWELL, and A. W. BOYD. Advan. Chem. Ser. **81**, 539 (1968).
7. A. W. BOYD, C. WILLIS, and O. A. MILLER. Can. J. Chem. **47**, 351 (1969).
8. T. J. SWORSKI and F. T. JONES. J. Phys. Chem. **70**, 1546 (1966).
9. A. W. BOYD, C. WILLIS, O. A. MILLER, and A. E. ROTHWELL. Advan. Chem. Ser. **82**, 456 (1968).
10. W. B. DEMORE and O. RAPER. J. Phys. Chem. **68**, 412 (1964).
11. D. H. BYERS and B. E. SALTZMANN. Adv. Chem. Ser. **21**, 93 (1959).
12. R. S. INGOLS, R. H. FETNER, and W. H. EBERHARDT. Adv. Chem. Ser. **21**, 102 (1959).
13. Mass spectral data tables. American Petroleum Inst. Research Project 44.
14. R. C. FEHSENFELD, A. L. SCHMELTEKOPF, H. I. SCHIFF, and E. E. FERGUSON. Planetary Space Sci. **15**, 373 (1967).
15. R. COOPER and R. M. MOORING. Aust. J. Chem. **21**, 2417 (1968).
16. G. G. MEISELS. J. Chem. Phys. **41**, 51 (1964).

Can. J. Chem. Downloaded from www.nrcresearchpress.com by 210.87.254.40 on 09/05/12
For personal use only.